PDF Output of CLIC (clustering by inferred co-expression)

Dataset:

Num of genes in input gene set: 20

Total number of genes: 16493

CLIC PDF output has three sections:

1) Overview of Co-Expression Modules (CEMs)

- Heatmap shows pairwise correlations between all genes in the input query gene set.
- Red lines shows the partition of input genes into CEMs, ordered by CEM strength.
- Each row shows one gene, and the brightness of squares indicates its correlations with other genes.
- Gene symbols are shown at left side and on the top of the heatmap.

2) Details of each CEM and its expansion CEM+

- Top panel shows the posterior selection probability (dataset weights) for top GEO series datasets.
- Bottom panel shows the CEM genes (blue rows) as well as expanded CEM+ genes (green rows).
- Each column is one GEO series dataset, sorted by their posterior probability of being selected.
- The brightness of squares indicates the gene's correlations with CEM genes in the corresponding dataset.
- CEM+ includes genes that co-express with CEM genes in high-weight datasets, measured by LLR score.

3) Details of each GEO series dataset and its expression profile:

- Top panel shows the detailed information (e.g. title, summary) for the GEO series dataset.
- Bottom panel shows the background distribution and the expression profile for CEM genes in this dataset.

Overview of Co-Expression Modules (CEMs) with Dataset Weighting

Num of Genes in Query Geneset: 20. Num of CEMs: 0.

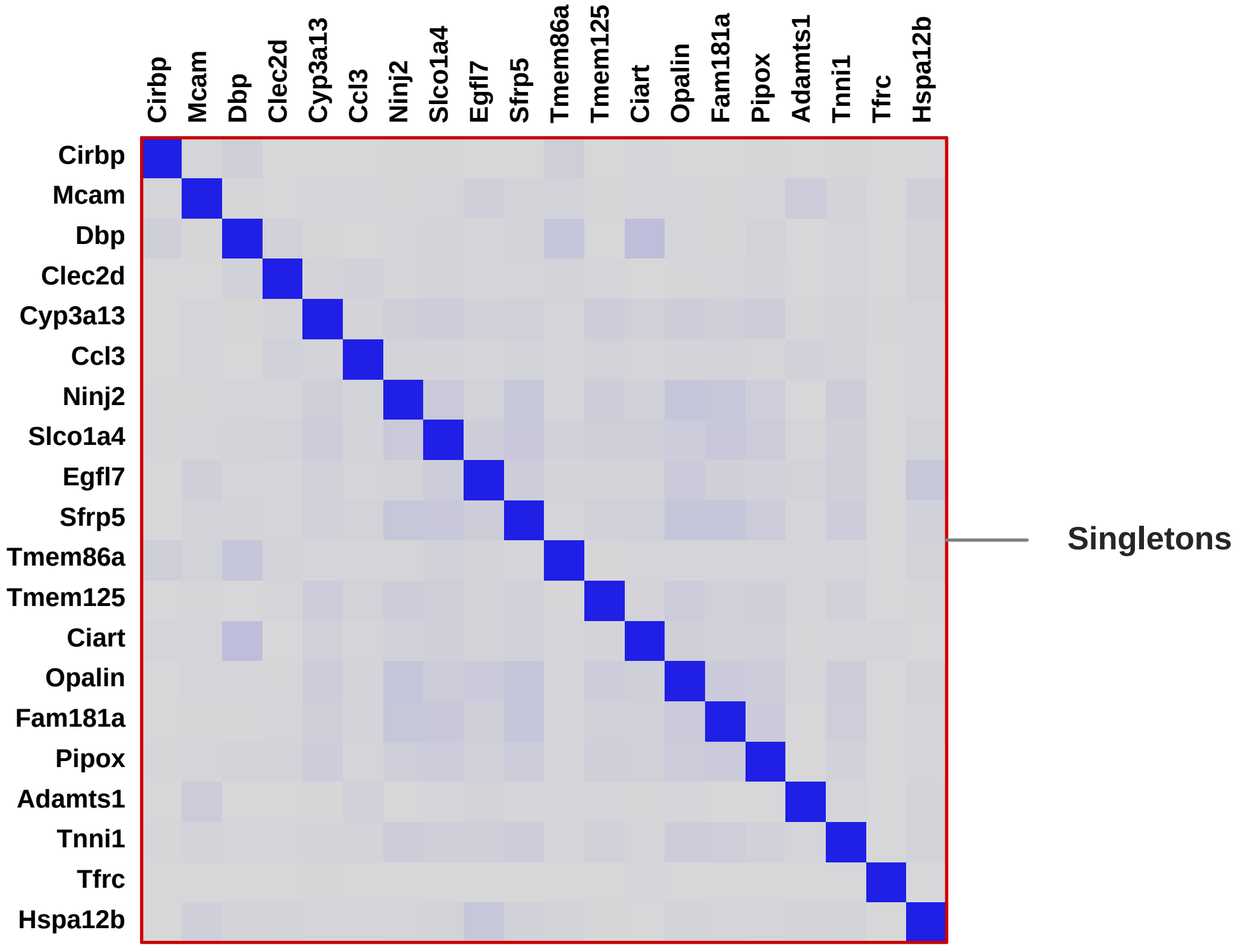

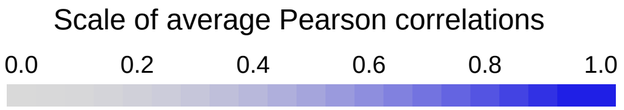

GEO Series "GSE10071" Expression Profiles

Num of samples in this series: 10

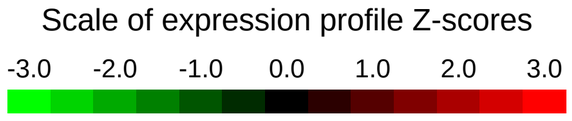

GEO Link:	http://www.ncbi.nlm.nih.gov/geo/query/acc.cgi?acc=GSE10071
Status:	Public on Jan 04 2008
Title:	NUP98-NSD1 links H3K36 methylation to Hox-A gene activation and leukaemogenesis
Organism:	Mus musculus
Experiment type:	Expression profiling by array
Platform:	GPL1261
Pubmed ID:	17589499
Summary & Design:	**Summary:** Nuclear receptor-binding SET domain protein 1 (NSD1) prototype is a family of mammalian histone methyltransferases (NSD1, NSD2/MMSET/WHSC1, NSD3/WHSC1L1) that are essential in development and are mutated in human acute myeloid leukemia (AML), overgrowth syndromes, multiple myeloma and lung cancers. In AML, the recurring t(5;11)(q35;p15.5) translocation fuses NSD1 to nucleoporin-98 (NUP98). Here, we present the first characterization of the transforming properties and molecular mechanisms of NUP98-NSD1. We demonstrate that NUP98-NSD1 induces AML in vivo, sustains self-renewal of myeloid stem cells in vitro, and enforces expression of the HoxA7, HoxA9, HoxA10 and Meis1 proto-oncogenes. Mechanistically, NUP98-NSD1 binds genomic elements adjacent to HoxA7 and HoxA9, maintains histone H3 Lys 36 (H3K36) methylation and histone acetylation, and prevents EZH2-mediated transcriptional repression of the Hox-A locus during differentiation. Deletion of the NUP98 FG-repeat domain, or mutations in NSD1 that inactivate the H3K36 methyltransferase activity or that prevent binding of NUP98-NSD1 to the Hox-A locus precluded both Hox-A gene activation and myeloid progenitor immortalization. We propose that NUP98-NSD1 prevents EZH2-mediated repression of Hox-A locus genes by colocalizing H3K36 methylation and histone acetylation at regulatory DNA elements. This report is the first to link deregulated H3K36 methylation to tumorigenesis and to link NSD1 to transcriptional regulation of the Hox-A locus. **Keywords:** expression analysis **Overall design:**

Background corr dist: KL-Divergence = 0.0759, L1-Distance = 0.0227, L2-Distance = 0.0009, Normal std = 0.4842

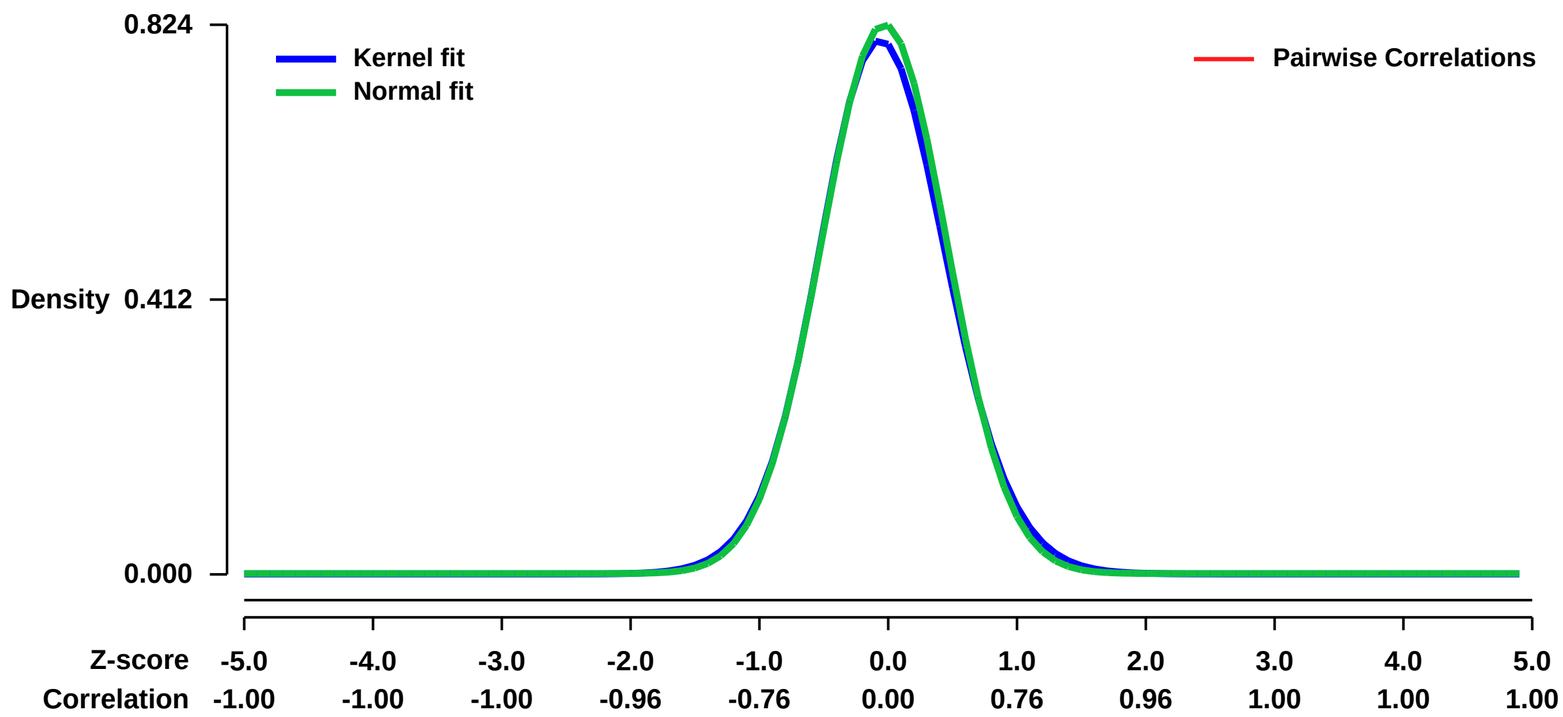

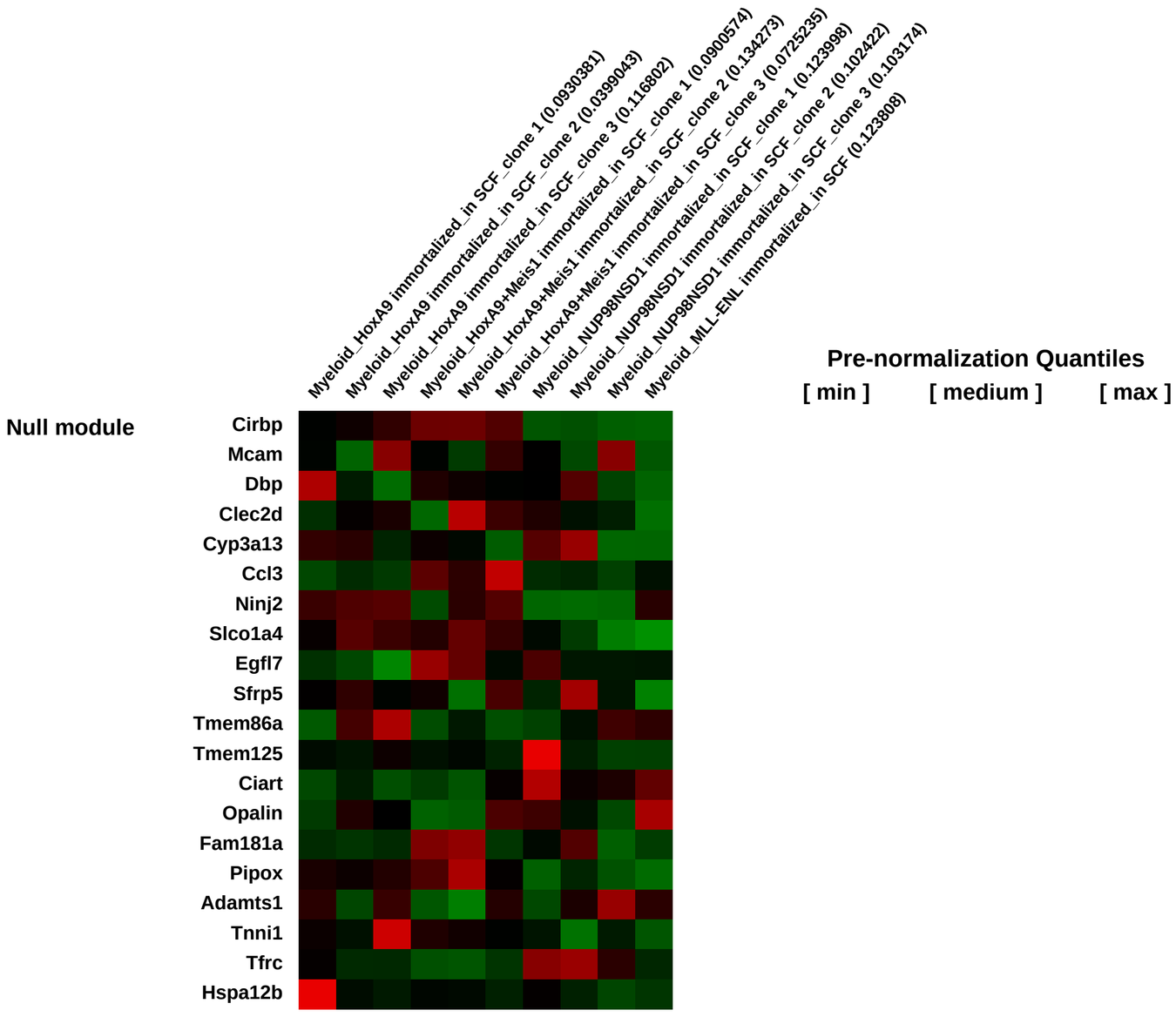

GEO Series "GSE10113" Expression Profiles

Num of samples in this series: 12

Scale of expression profile Z-scores

-3.0 -2.0 -1.0 0.0 1.0 2.0 3.0

GEO Link:	http://www.ncbi.nlm.nih.gov/geo/query/acc.cgi?acc=GSE10113
Status:	Public on Dec 28 2009
Title:	Comparison of gene expression pattern between Wild-type and Hypb knockout embryo yolk sacs
Organism:	Mus musculus
Experiment type:	Expression profiling by array
Platform:	GPL1261
Pubmed ID:	20133625
Summary & Design:	**Summary:** This study aimed at exploring the physiological function of mammalian HYPB by means of knockout mouse model. Homogenous disruption of mouse Hypb gene leads to embryonic lethality at E10.5-E11.5. Severe vascular defects were observed in the Hypb-/- embryos, yolk sac and placenta.In the mutant embryo and yolk sac, disorganized and abnormally dilated capillaries cannot be remodeled into large blood vessels or intricate networks. Thus, our results suggest that the mammalian HYPB HMT plays an important role in embryonic vascularization. **Keywords:** knockout, mouse embryo development, angiogenesis, yolk sac, E9.0, E10.5 **Overall design:** To systematically examine and compare gene expression patterns between Hypb+/+ and Hypb-/- embryos at the global genome-level, we use the Affymetrix GeneChip´fi mouse genome 430 2.0 arrays. We choose to use E9.0 and E10.5 yolk sacs for analysis because at E9.0 this early stage Hypb-/- embryos did not show severe visible mutant phenotype, and at E10.5 this antemortem stage Hypb-/- embryos show mang lethal mutant phenotypes. For comparison, four independently derived yolk sacs were pooled for each genotype of the two development stages, and three biological repeats were performed.

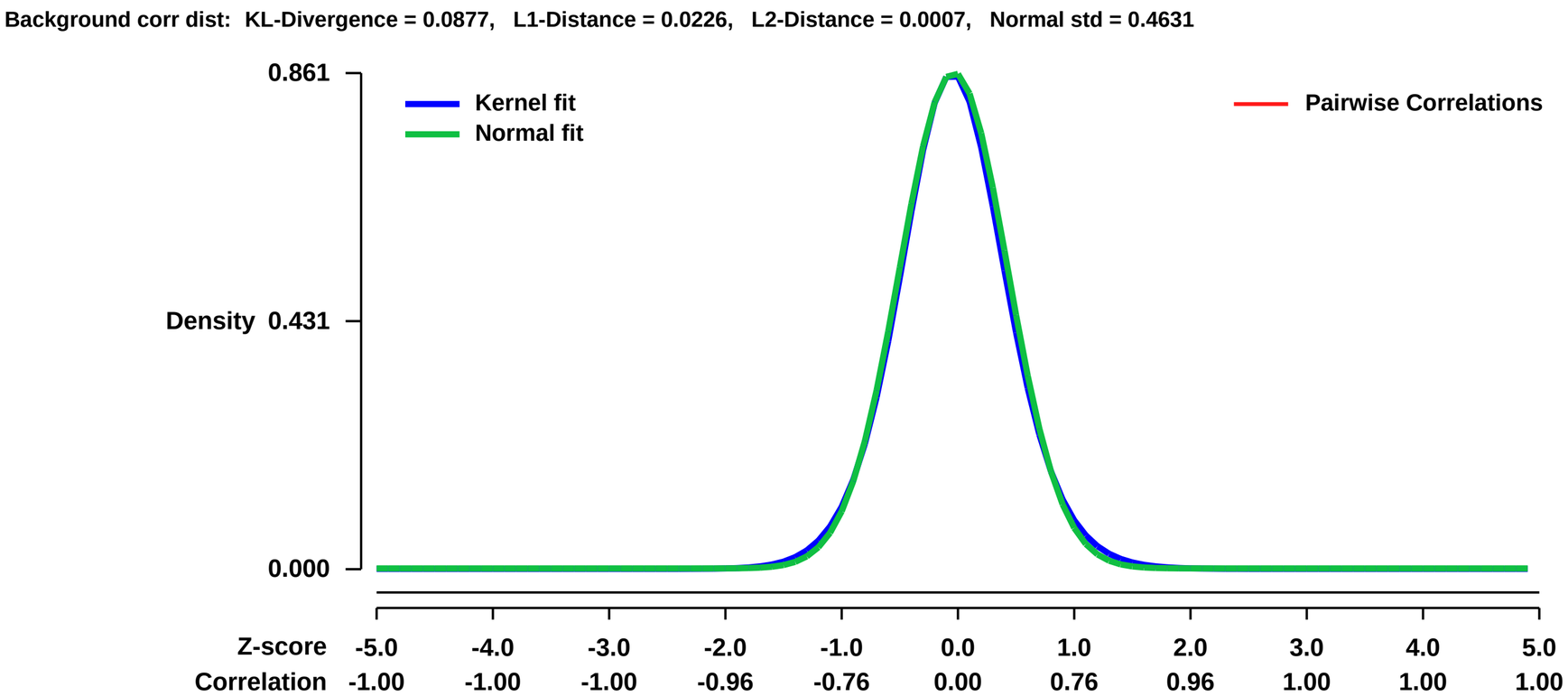

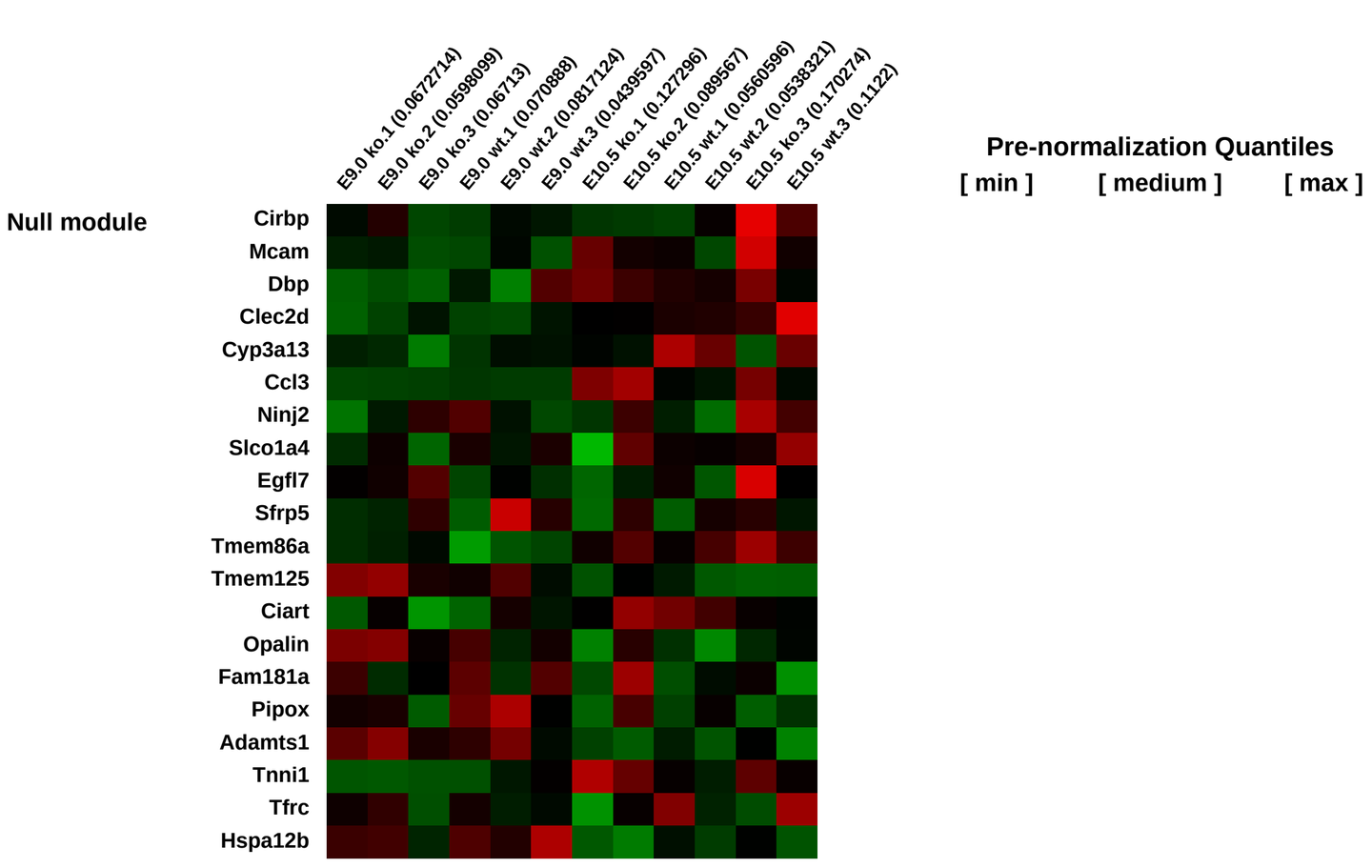

GEO Series "GSE10162" Expression Profiles

Num of samples in this series: 6

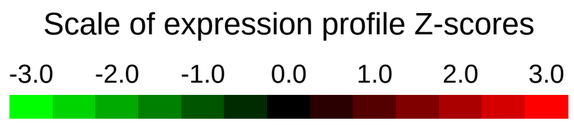

GEO Link:	http://www.ncbi.nlm.nih.gov/geo/query/acc.cgi?acc=GSE10162
Status:	Public on Apr 03 2008
Title:	Transcriptional Adaptation to Clcn5 Knockout in Proximal Tubules of the Mouse Kidney
Organism:	Mus musculus
Experiment type:	Expression profiling by array
Platform:	GPL1261
Pubmed ID:	18349385
Summary & Design:	**Summary:** Dent disease has multiple defects attributed to proximal tubule malfunction including low molecular weight proteinuria, aminoaciduria, phosphaturia and glycosuria. In order to understand the changes in kidney function of the Clc5 transporter gene knockout mouse model of Dent disease, we examined gene expression profiles from proximal tubules of mouse kidneys. Overall 720 genes are expressed differentially in the proximal tubules of the Dent Clcn5 knockout mouse model compared to those of control wild type mice. The fingerprint of these gene changes may help us to understand the phenotype of Dent disease. Keywords: gene knockout, mouse, Clcn5, Dent’s disease **Overall design:** 3 microarrays each of wild type and knockout mouse proximal tubule were processed

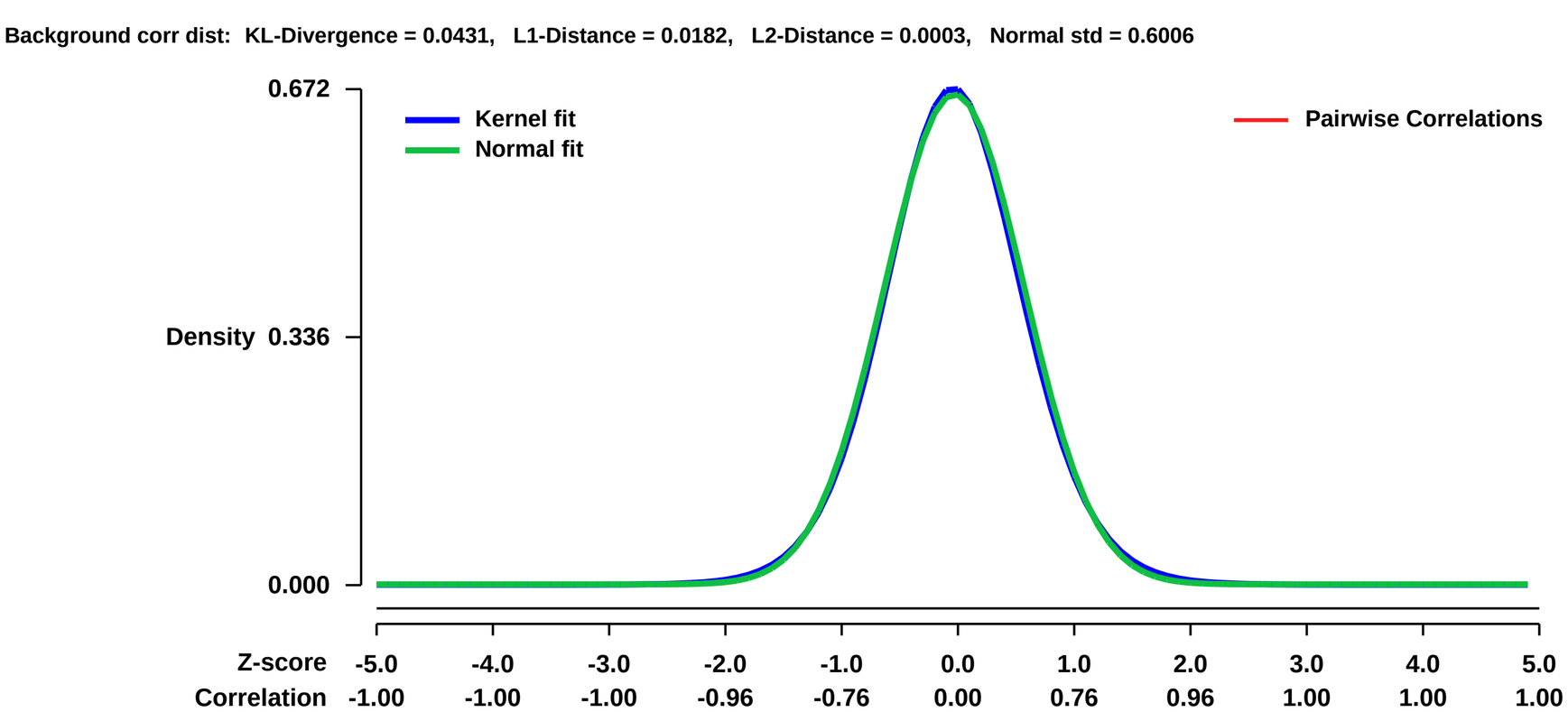

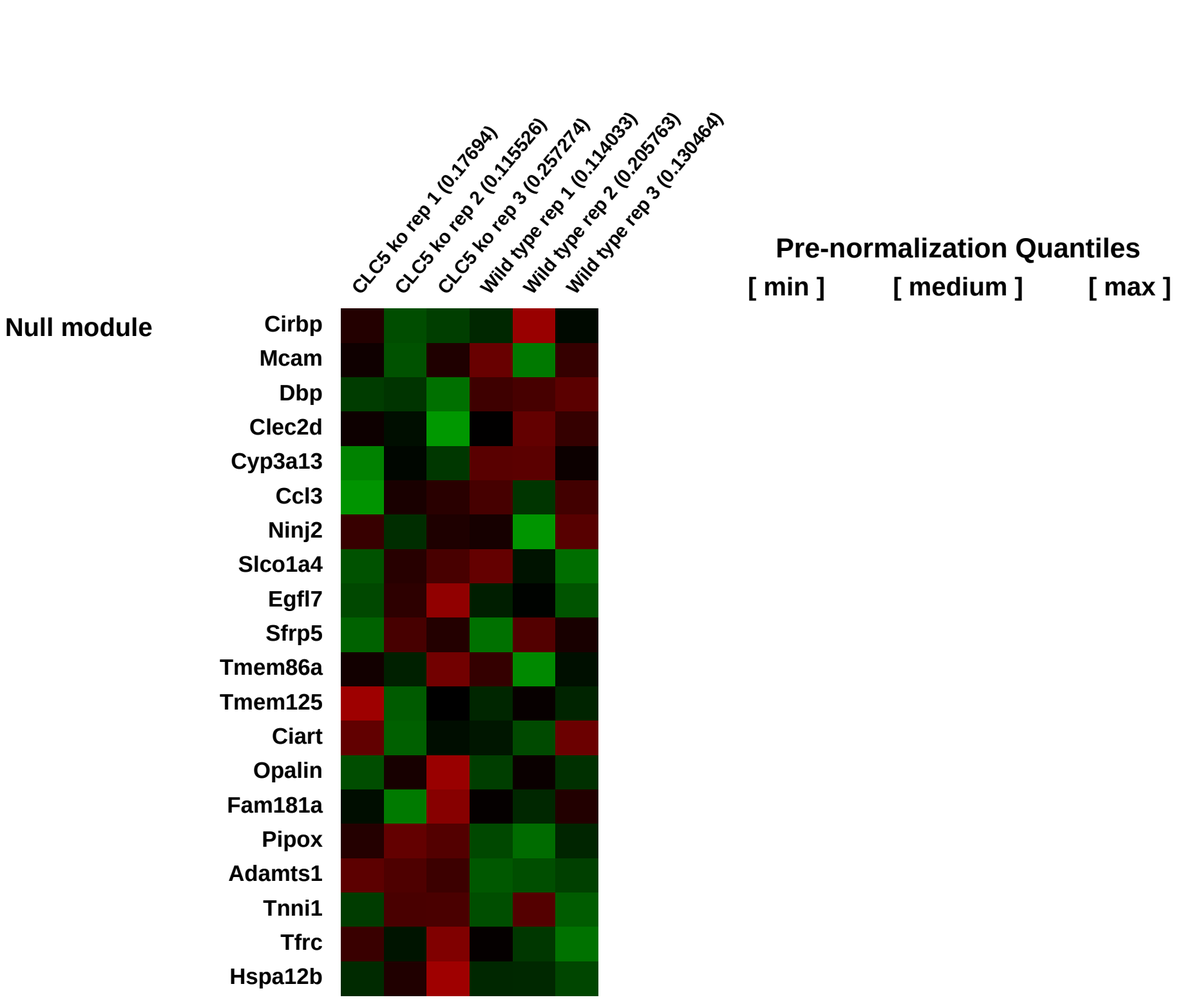

GEO Series "GSE10167" Expression Profiles

Num of samples in this series: 6

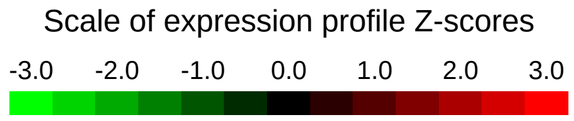

GEO Link:	**http://www.ncbi.nlm.nih.gov/geo/query/acc.cgi?acc=GSE10167**
Status:	**Public on Jan 15 2008**
Title:	**Microarray Analysis of Treacher Collins Syndrome**
Organism:	**Mus musculus**
Experiment type:	**Expression profiling by array**
Platform:	**GPL1261**
Pubmed ID:	**18246078**
Summary & Design:	**Summary:** **The object of this study was to identify genes transcriptionally upregulated and downregulated in response to Tcof1 haploin-sufficiency during mouse embryogensis** **Keywords: mouse embryo, littermates, Tcof1, Treacher Collins sydnrome, comparative hybridisation** **Overall design:** **Total RNA was extracted from 3 E8.5 wild-type and 3 E8.5 Tcof1+/- littermate embryos using the RNeasy Mini Protocol for Isolation of Total RNA from Animal Tissues (Qiagen) according to the manufacturerâ s protocol. RNA quality and quantity was determined using the Bioanalyser. To generate targets for microarray analysis, total RNA (100 ng) from each wild-type and mutant embryo was amplified using Two-Cycle Target Labeling (Affymetrix) according to the manufacturerâ s instructions. Biotinylated target cRNAs (20 ¸…g) from the 3 wild-type and 3 Tcof1+/- embryos were hybridised to separate GeneChip´fi Mouse Genome 430 2.0 arrays (Affymetrix), following standard Affymetrix procedures.**

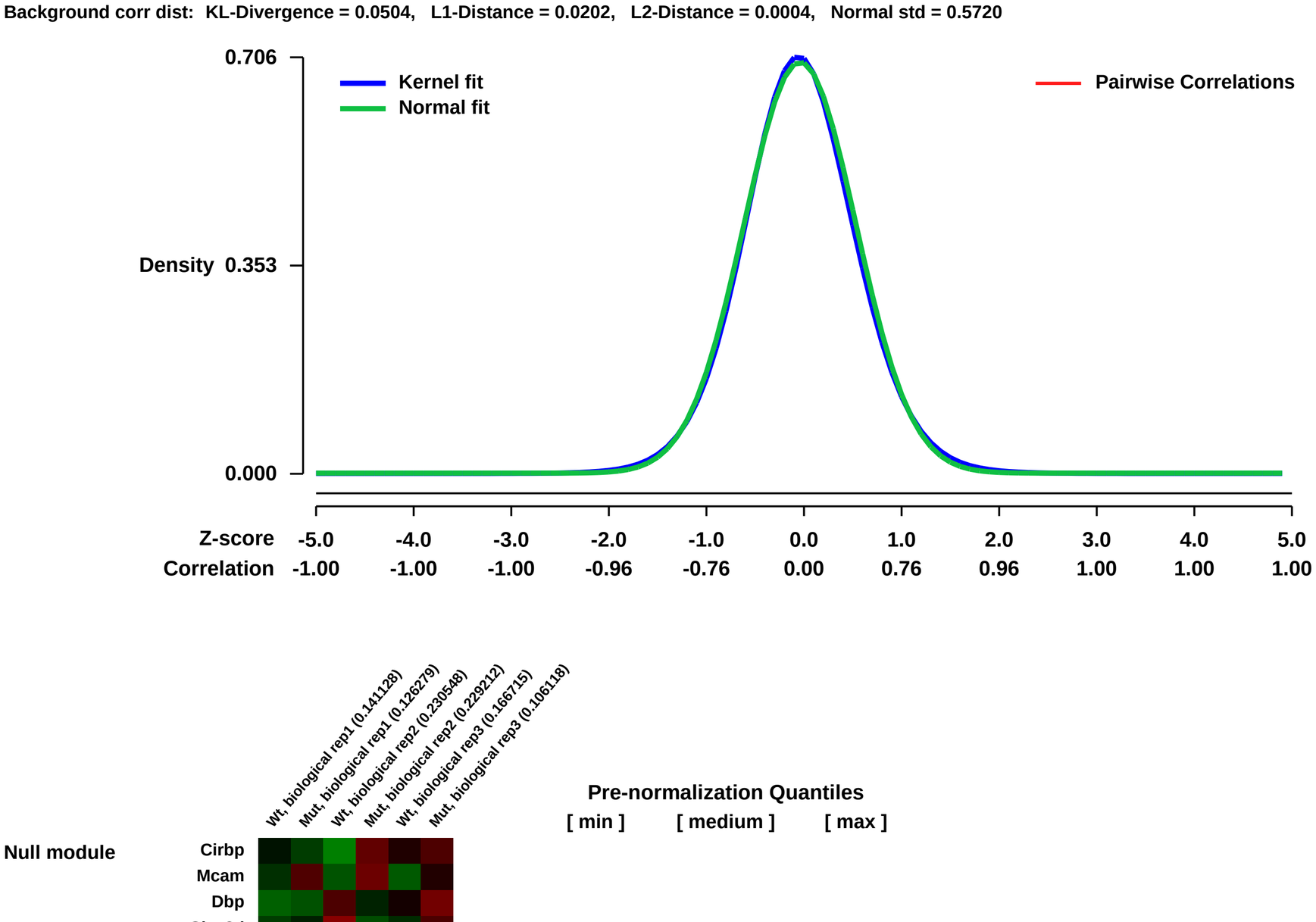

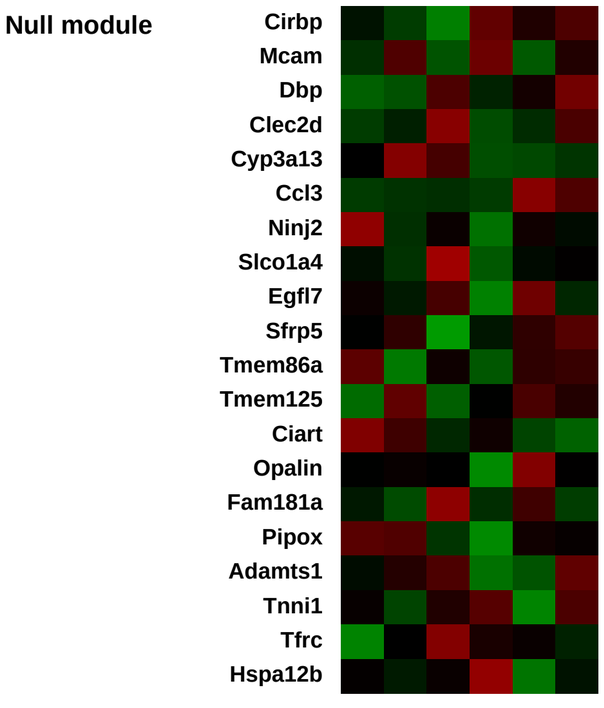

GEO Series "GSE10175" Expression Profiles

Num of samples in this series: 6

Scale of expression profile Z-scores

-3.0 -2.0 -1.0 0.0 1.0 2.0 3.0

GEO Link:	http://www.ncbi.nlm.nih.gov/geo/query/acc.cgi?acc=GSE10175
Status:	Public on Jan 16 2008
Title:	Comparison of gene expression in the epidermis of Tcfap2c mutant and control skin at embryonic day 16.5
Organism:	Mus musculus
Experiment type:	Expression profiling by array
Platform:	GPL1261
Pubmed ID:	18353300
Summary & Design:	**Summary:** The development of the epidermis, a stratified squamous epithelium, is dependent on the regulated differentiation of keratinocytes. Differentiation begins with the initiation of stratification, a process tightly controlled through proper gene expression. AP-2‚Ä° is expressed in skin and previous research suggested a pathway where p63 gene induction results in increased expression of AP-2‚Ä° which in turn is responsible for induction of K14. This study uses a conditional gene ablation model to further explore the role of AP-2‚Ä° in skin development. Mice deficient for AP-2‚Ä° exhibited delayed expression of p63, K14, and K1, key genes required for development and differentiation of the epidermis. In addition, microarray analysis of E16.5 skin revealed delayed expression of additional late epidermal differentiation genes: filaggrin, repetin and secreted Ly6/Plaur domain containing 1, in mutant mice. The genetic delay in skin development was further confirmed by a functional delay in the formation of an epidermal barrier. These results document an important role for AP-2‚Ä° in skin development, and reveal the existence of regulatory factors that can compensate for AP-2‚Ä° in its absence. **Keywords:** genetic modification **Overall design:** Skin samples were collected from 3 Tcfap2c and 3 control animals at embryonic day 16.5.

Background corr dist: KL-Divergence = 0.0410, L1-Distance = 0.0179, L2-Distance = 0.0003, Normal std = 0.6117

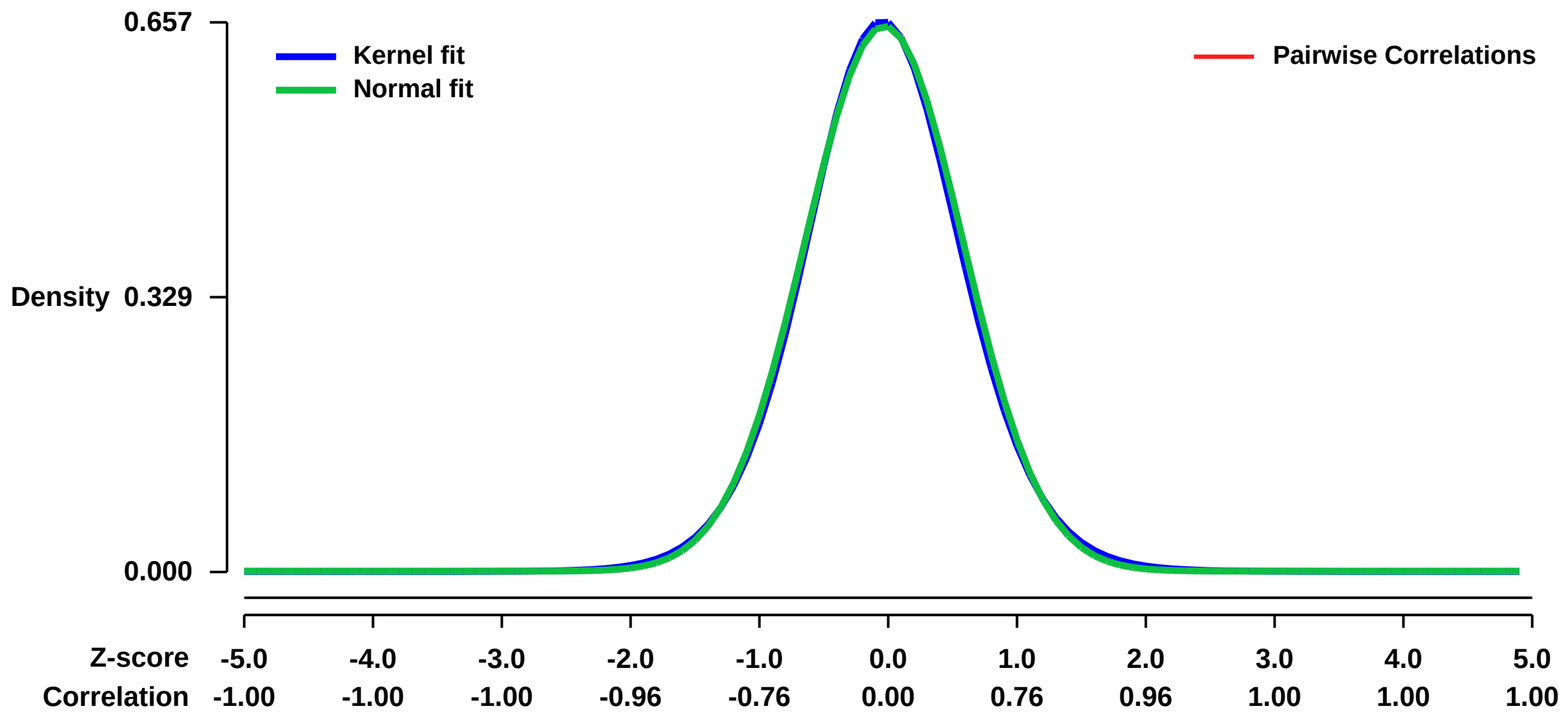

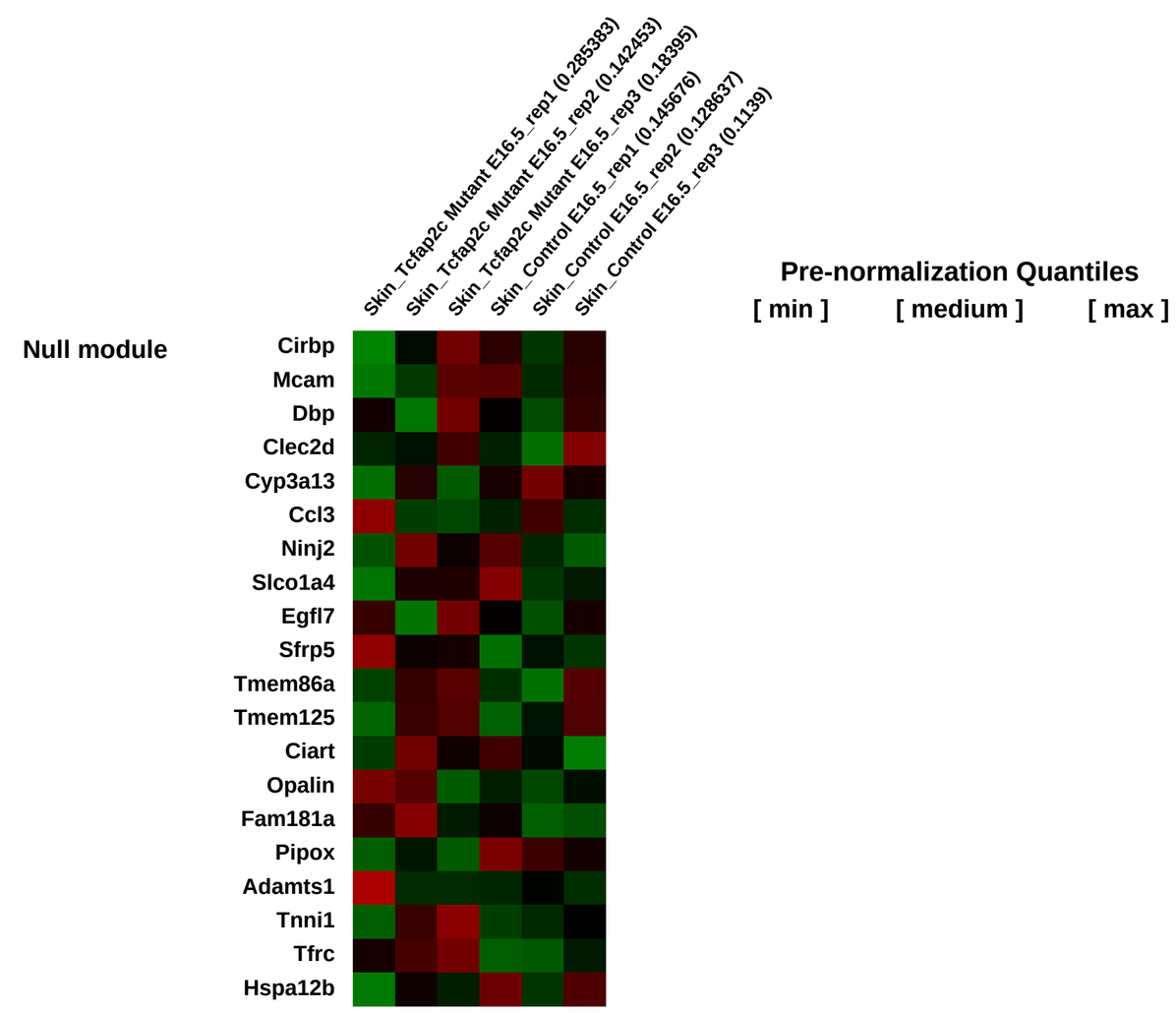

GEO Series "GSE10176" Expression Profiles

Num of samples in this series: 6

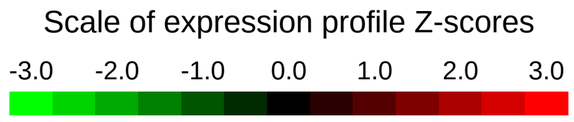

GEO Link:	http://www.ncbi.nlm.nih.gov/geo/query/acc.cgi?acc=GSE10176
Status:	Public on Jan 16 2008
Title:	Inducible repositioning of genes to the inner nuclear membrane
Organism:	Mus musculus
Experiment type:	Expression profiling by array
Platform:	GPL1261
Pubmed ID:	18272965
Summary & Design:	**Summary:** Nuclear compartmentalization appears to play an important role in regulating metazoan genes. While studies on immunoglobulin (Ig) and other loci have correlated positioning at the nuclear lamina with gene repression, the functional consequences of this compartmentalization remain untested. We devised an approach for inducible tethering of genes to the inner nuclear membrane (INM) and demonstrate with 3D DNA-ImmunoFISH, repositioning of chromosomal regions to the nuclear lamina. Relocalization requires mitotic nuclear envelope breakdown and reformation. Tethering leads to the accumulation of lamin and INM proteins but not to association with pericentromeric heterochromatin or nuclear pore complexes. Recruitment of genes to the INM can result in their transcriptional repression. Using DamID we show that as is the case for our model system, inactive Ig loci at the nuclear periphery are contacted by INM and lamina components. We propose that such molecular interactions are used to compartmentalize and limit the accessibility of Ig loci. **Keywords: Inducible** **Overall design:** We used microarray to analyze the transcription status of genomic regions are inducibly tethered to the INM

Background corr dist: KL-Divergence = 0.0247, L1-Distance = 0.0189, L2-Distance = 0.0005, Normal std = 0.7016

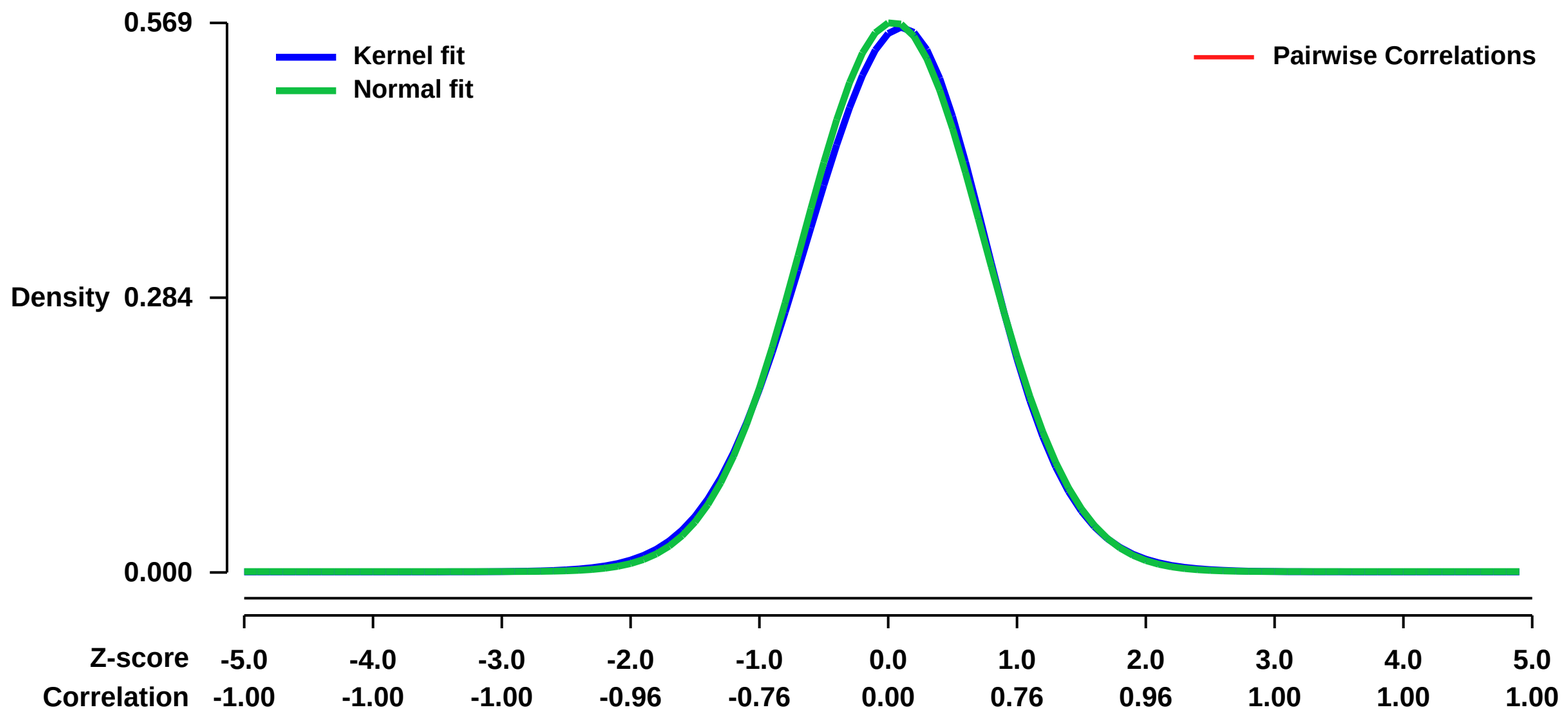

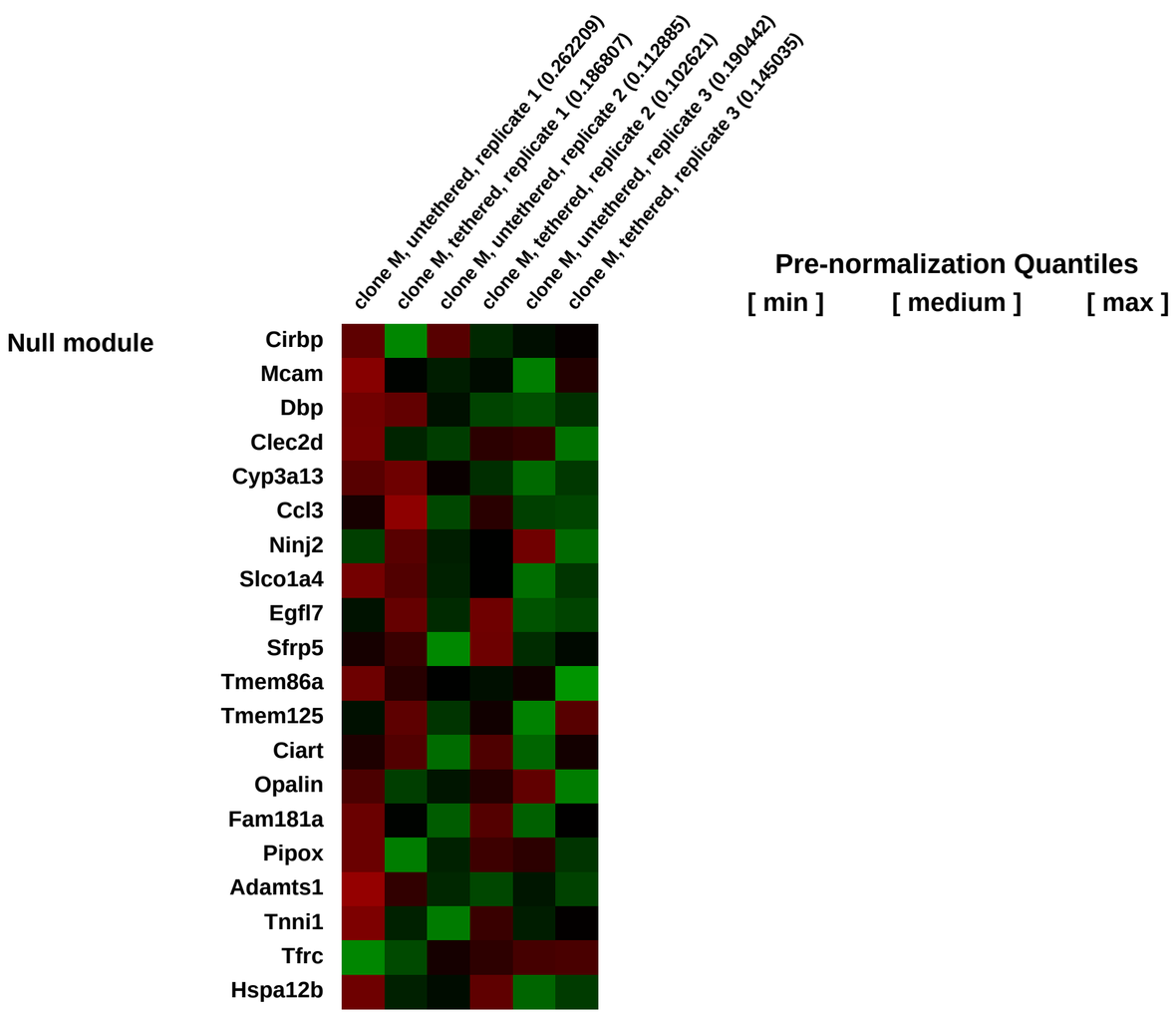

GEO Series "GSE10182" Expression Profiles

Num of samples in this series: 7

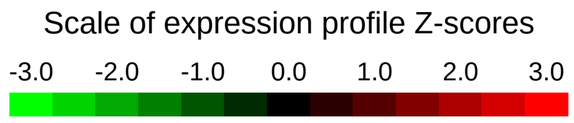

GEO Link:	http://www.ncbi.nlm.nih.gov/geo/query/acc.cgi?acc=GSE10182
Status:	Public on Mar 15 2008
Title:	MDP- and Pam3CSK4-induced genes in naˆflve and tolerant macrophages
Organism:	Mus musculus
Experiment type:	Expression profiling by array
Platform:	GPL1261
Pubmed ID:	18261938
Summary & Design:	**Summary:** **Most of the genes were self-tolerized by Pam3CSK4 and MDP but there was no or minimal cross-tolerization.** **The transcriptome induced via Nod2 stimulation is greatly expanded in TLR2-tolerant macrophages.** **Keywords: self and cross tolerance by MDP or Pam3CSK4** **Overall design:** **Genes induced by Pam3CSK4 or MDP were selected based on a three-fold increase over expression levels in unstimulated macrophages.** **Tolerized genes are defined as genes downregulated more than 2-fold in tolerant macrophages stimulated with Pam3CSK4 or MDP.**

Background corr dist: **KL-Divergence = 0.0435, L1-Distance = 0.0246, L2-Distance = 0.0007, Normal std = 0.6065**

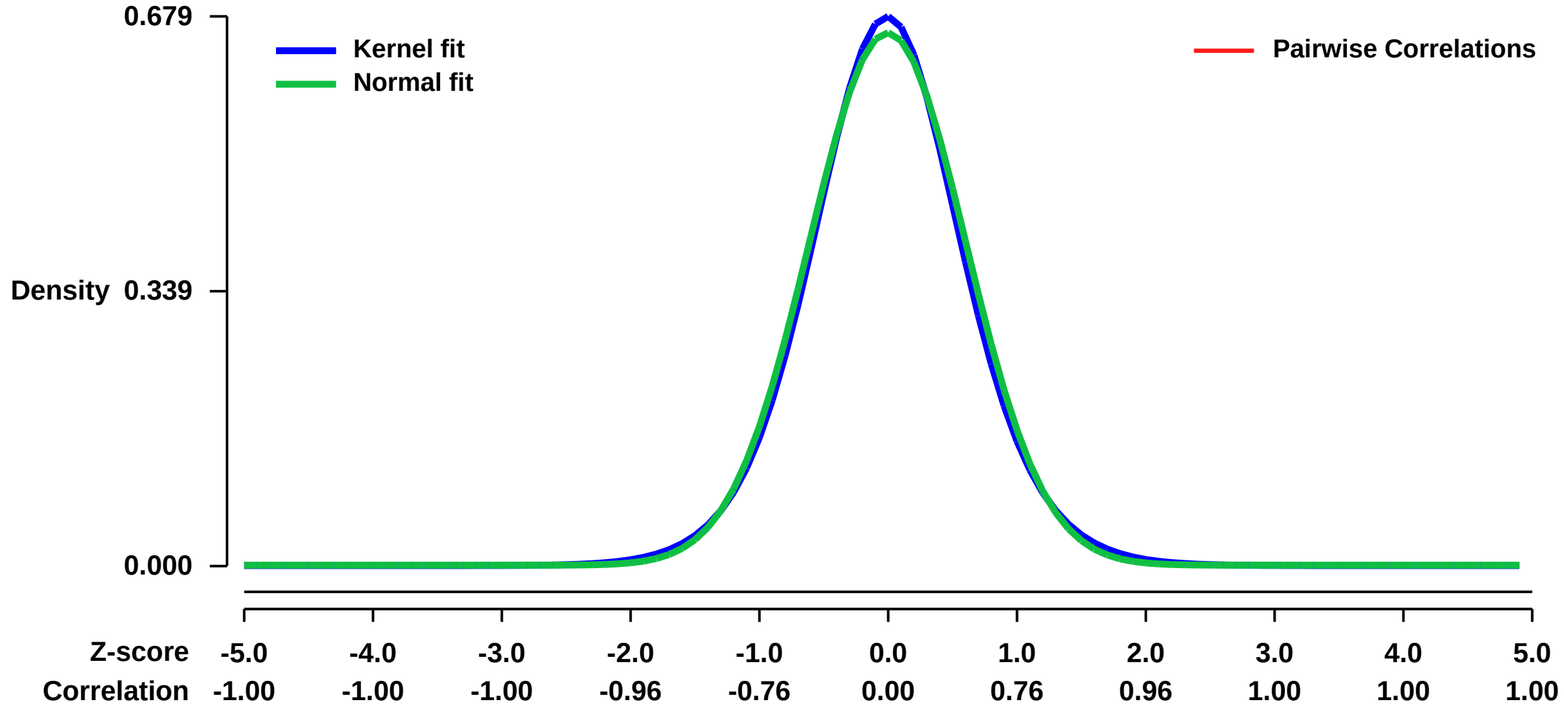

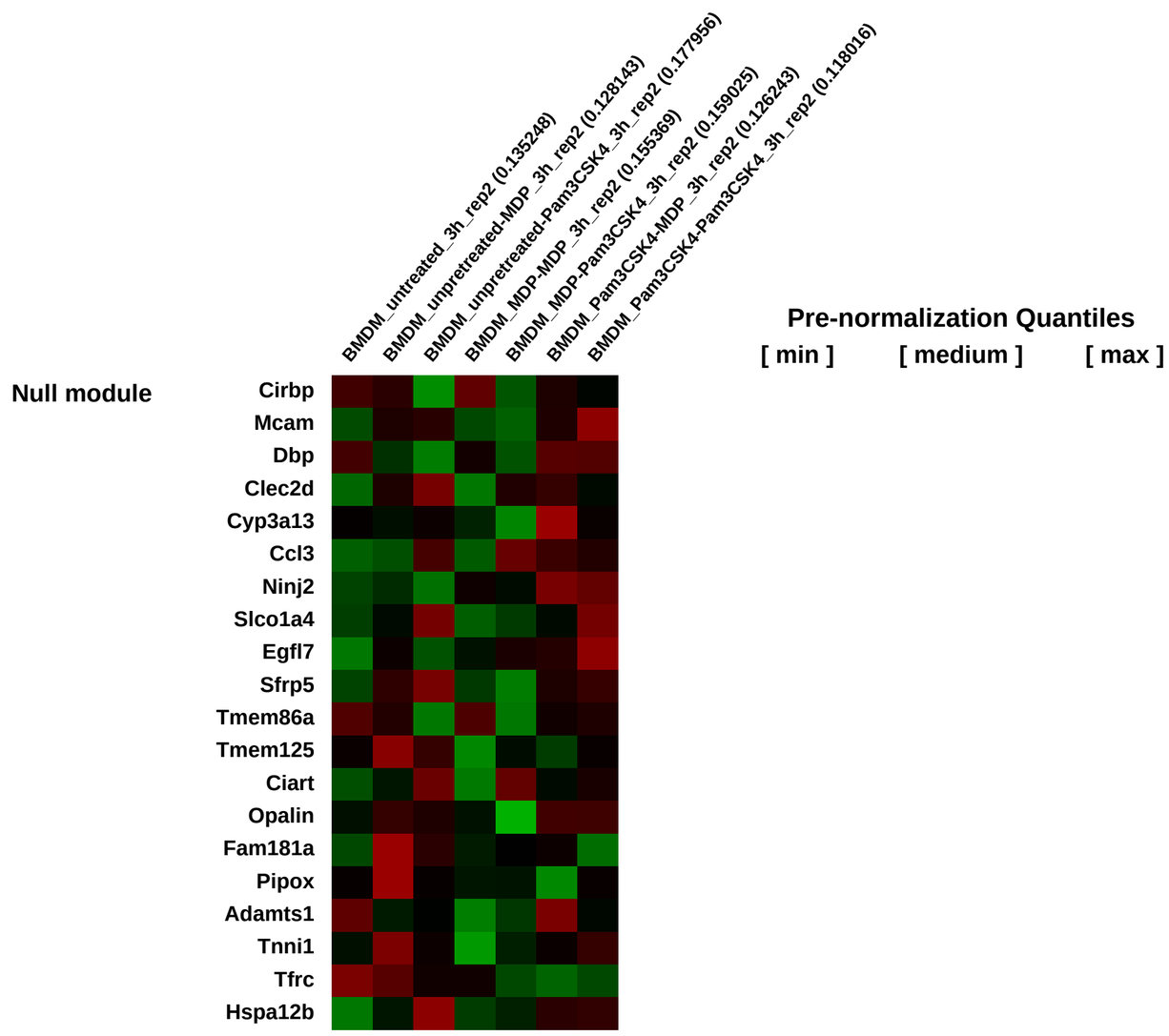

GEO Series "GSE10192" Expression Profiles

Num of samples in this series: 24

Scale of expression profile Z-scores

-3.0 -2.0 -1.0 0.0 1.0 2.0 3.0

GEO Link:	http://www.ncbi.nlm.nih.gov/geo/query/acc.cgi?acc=GSE10192
Status:	Public on Jan 15 2009
Title:	PPAR Controls Gene Expression in MSC Cells
Organism:	Mus musculus
Experiment type:	Expression profiling by array
Platform:	GPL1261
Pubmed ID:	19115254
Summary & Design:	**Summary:** Rosiglitazone (Rosi), a member of the thiazolidinedione class of drugs used to treat type 2 diabetes, activates the adipocyte-specific transcription factor peroxisome proliferator-activated receptor gamma (PPARg). This activation causes bone loss in animals and humans, at least in part due to suppression of osteoblast differentiation from marrow mesenchymal stem cells (MSC). In order to identify mechanisms by which PPARg2 suppresses osteoblastogenesis and promotes adipogenesis in MSC, we have analyzed the PPARg2 transcriptome in response to Rosi. A total of 4,252 transcriptional changes resulted when Rosi (1 uM) was applied to the U-33 marrow stromal cell line, stably transfected with PPARg2 (U-33/g2), as compared to non-induced U-33/g2 cells. Differences between U-33/g2 and U-33 cells stably transfected with empty vector (U-33/c) comprised 7,928 transcriptional changes, independent of Rosi. Cell type-, time- and treatment-specific gene clustering uncovered distinct patterns of PPARg2 transcriptional control of MSC lineage commitment. The earliest changes accompanying Rosi activation of PPARg2 included adjustments in morphogenesis, Wnt signaling, and immune responses, as well as sustained induction of lipid metabolism. Expression signatures influenced by longer exposure to Rosi provided evidence for distinct mechanisms governing the repression of osteogenesis and stimulation of adipogenesis. Our results suggest interactions that could lead to the identification of a â masterâ regulatory scheme controlling osteoblast differentiation. **Keywords:** rosiglitazone, PPARgamma, microarray, time course, gene expression, stem cells **Overall design:** U-33/g2 and U-33/c cells were cultured in the presence or absence of Rosi and gene expression was monitored at three different time points (2, 24, 72h) after exposure to the agonist. Each time point corresponds to a separate stage of Rosi-treated U-33/g2 cell conversion from the osteoblast-like phenotype to the adipocyte-like phenotype and includes induction (2h), intermediate alterations in phenotype progression (24h), and a terminally differentiated adipocytic with completely suppressed osteoblastic phenotype (72h). The experiment is a full factorial design performed in replicate.

Background corr dist: KL-Divergence = 0.0462, L1-Distance = 0.0784, L2-Distance = 0.0103, Normal std = 0.6400

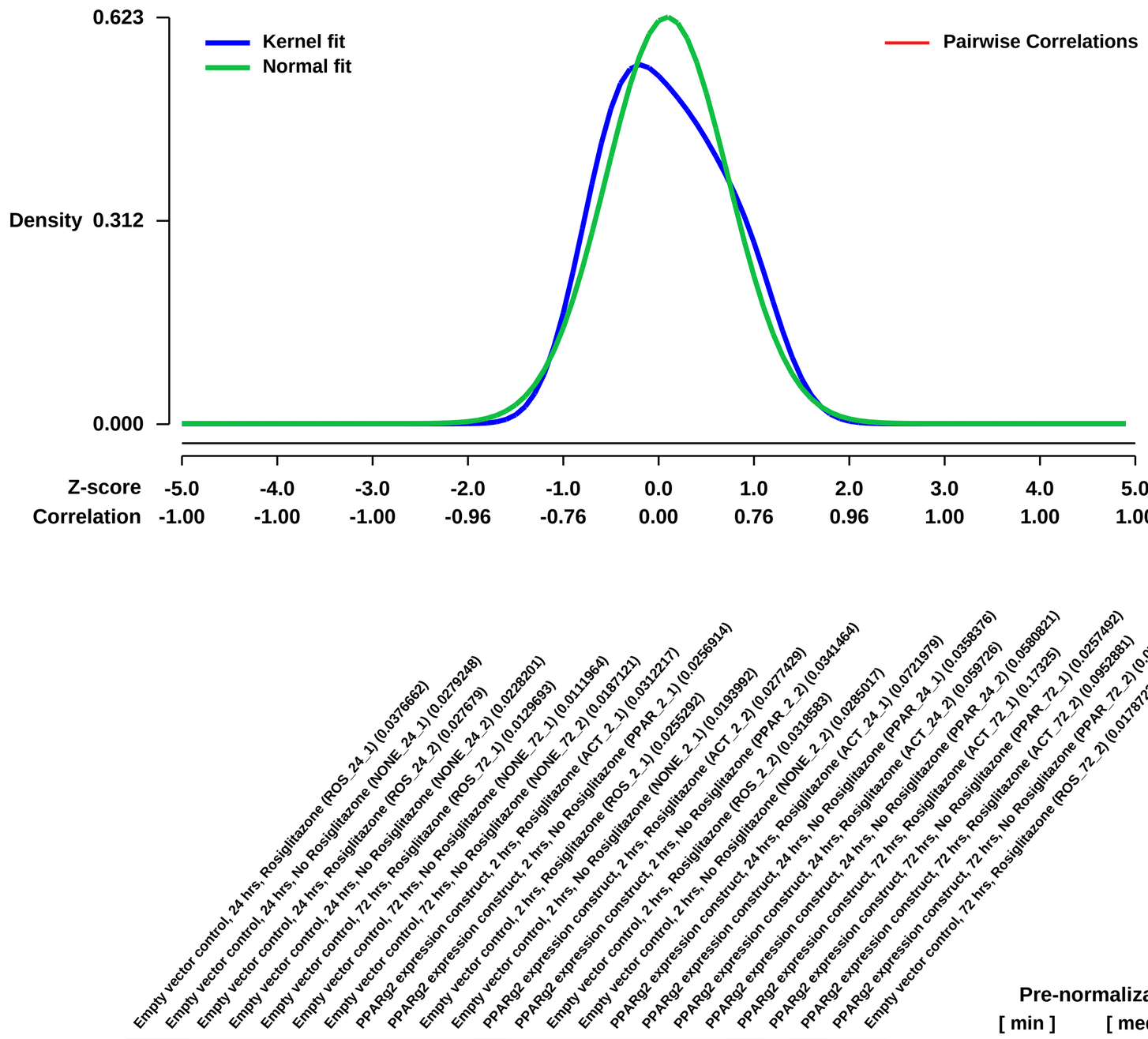

GEO Series "GSE10202" Expression Profiles

Num of samples in this series: 8

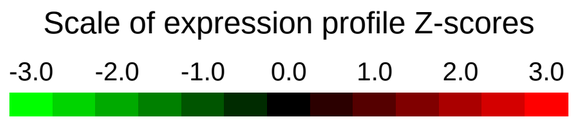

GEO Link:	http://www.ncbi.nlm.nih.gov/geo/query/acc.cgi?acc=GSE10202
Status:	Public on Jan 25 2008
Title:	Striatal gene expression data from 22-month-old CHL2 mice and control mice.
Organism:	Mus musculus
Experiment type:	Expression profiling by array
Platform:	GPL1261
Pubmed ID:	17519223
Summary & Design:	**Summary:** Achieving a mechanistic understanding of disease and initiating preclinical therapeutic trials necessitate the study of huntingtin toxicity and its remedy in model systems. To allow the engagement of appropriate experimental paradigms, Huntingtonâ s disease (HD) models need to be validated in terms of how they recapitulate a particular aspect of human disease. In order to examine transcriptome-related effects of mutant huntingtin, we compared striatal mRNA profiles from seven genetic mouse models of disease to that of postmortem human HD caudate using microarray analysis. Transgenic models expressing short N-terminal fragments of mutant huntingtin (R6/1 and R6/2 mice) exhibited the most rapid effects on gene expression, consistent with previous studies. Although changes in the brains of knock-in models of HD took longer to appear, 15-month and 22-month CHL2Q150/Q150, 18-month HdhQ92/Q92 and 2-year-old YAC128 animals also exhibited significant HD-like mRNA signatures. When the affected genes were compared across models, a robust concordance was observed. Importantly, changes concordant across multiple lines mice were also in excellent agreement with the mRNA changes seen in human HD caudate. Although it was expected that the expression of full-length huntingtin transprotein might result in unique gene expression changes compared to those caused by expression of an N-terminal huntingtin fragment, no discernable differences between full-length and fragment models were detected. There was, however, an overall concordance between transcriptomic signature and disease stage. We thus conclude that the transcriptional changes of HD can be modelled in several available lines of transgenic mice, comprising lines expressing both N-terminal and full-length mutant huntingtin proteins. The combined analysis of mouse and human HD transcriptomes provides an important chronology of mutant huntingtin's gene expression effects. **Keywords:** genetic modification **Overall design:** Striatal samples from 4 CHL2 Q150/Q150 mutant mice and 4 age-matched wild-type mice.

Background corr dist: KL-Divergence = 0.0644, L1-Distance = 0.0182, L2-Distance = 0.0003, Normal std = 0.5164

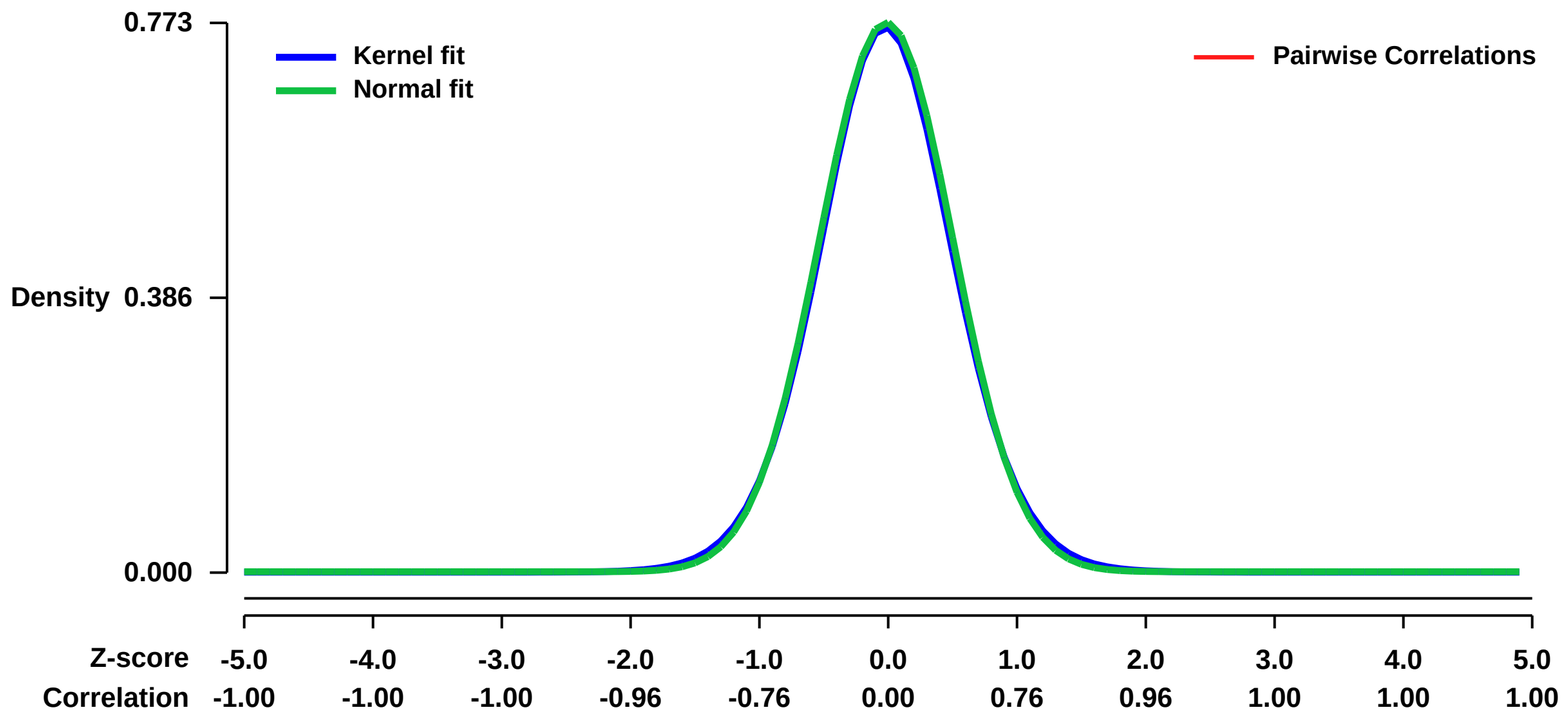

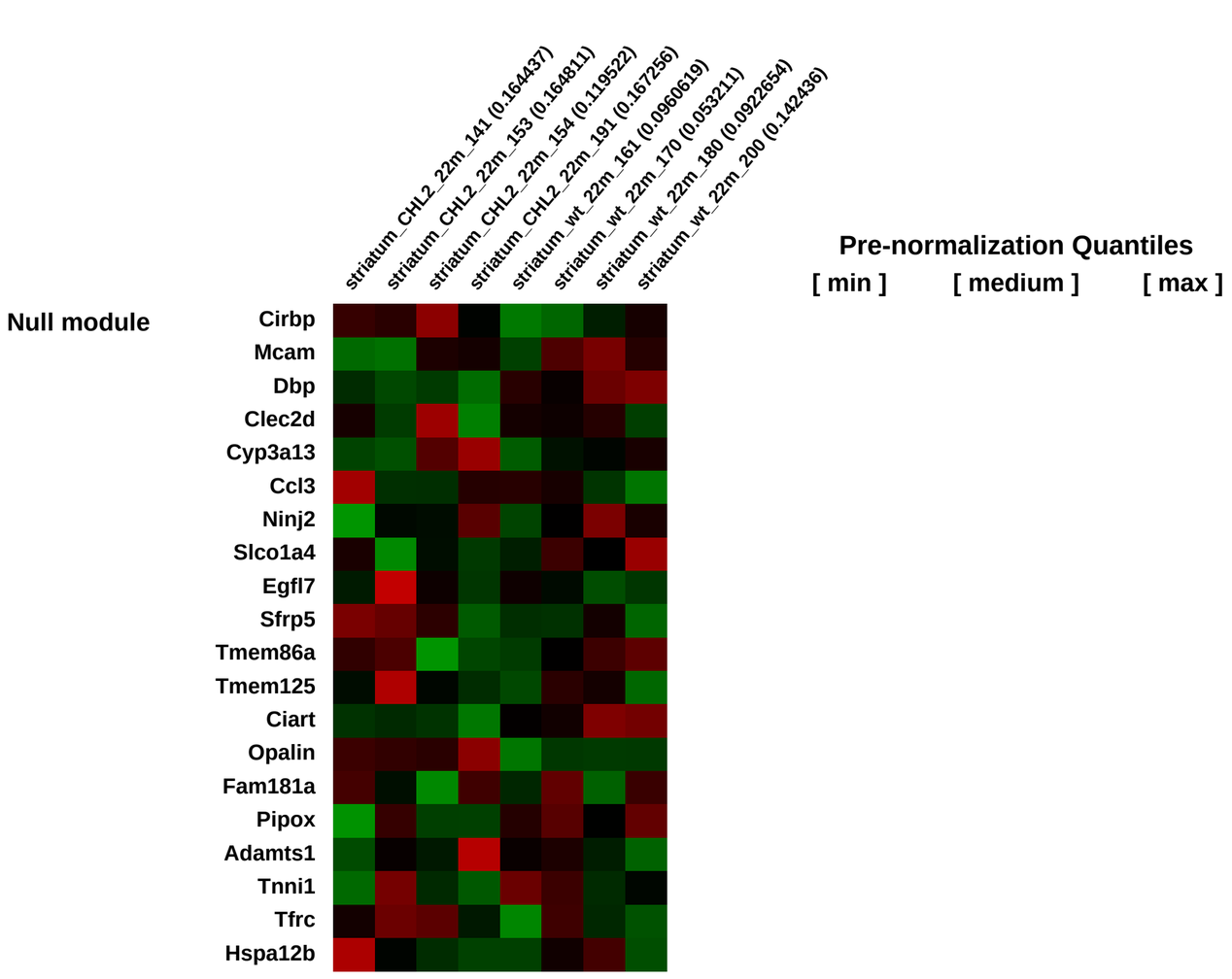

GEO Series "GSE10210" Expression Profiles

Num of samples in this series: 16

Scale of expression profile Z-scores

-3.0 -2.0 -1.0 0.0 1.0 2.0 3.0

GEO Link:	http://www.ncbi.nlm.nih.gov/geo/query/acc.cgi?acc=GSE10210
Status:	Public on Jul 14 2008
Title:	Gene expression analysis of embryonic stem cells expressing VE-cadherin (CD144) during endothelial differentiation
Organism:	Mus musculus
Experiment type:	Expression profiling by array
Platform:	GPL1261
Pubmed ID:	18498633
Summary & Design:	**Summary:** Endothelial differentiation occurs during normal vascular development in the developing embryo. Mouse embryonic stem (ES) cells were used to further define the molecular mechanisms of endothelial differentiation. By flow cytometry a population of VEGF-R2 positive cells was identified as early as 2.5 days after differentiation of ES cells, and a subset of VEGF-R2 + cells, that were CD41+ positive at 3.5 days. A separate population of VEGF-R2+ stem cells expressing the endothelial-specific marker CD144 (VE-cadherin) was also identified at this same time point. Microarray analysis of >45,000 transcripts was performed on RNA obtained from cells expressing VEGF-R2, CD41, and CD144. **Keywords:** expression analysis **Overall design:** We identified four populations of cells; cells expressing VEGF-R2 (day 2.5), CD41 expressing cells (day 3.5), cells expressing CD144 (VE-Cadherin, day 3.5), and cells expressing CD144 (day 6.5). In addition to this, we have also obtained the negative control cells at each time such as VEGF-R2 (day 2.5) negative, CD41 negative (day 3.5), CD144 negative (VE-Cadherin, day 3.5), and negative CD144 (day 6.5). RNA for the microarray experiments were obtained in duplicate from two separately conducted experiments using the murine embryonic stem cells..

Background corr dist: KL-Divergence = 0.0996, L1-Distance = 0.0266, L2-Distance = 0.0013, Normal std = 0.4386

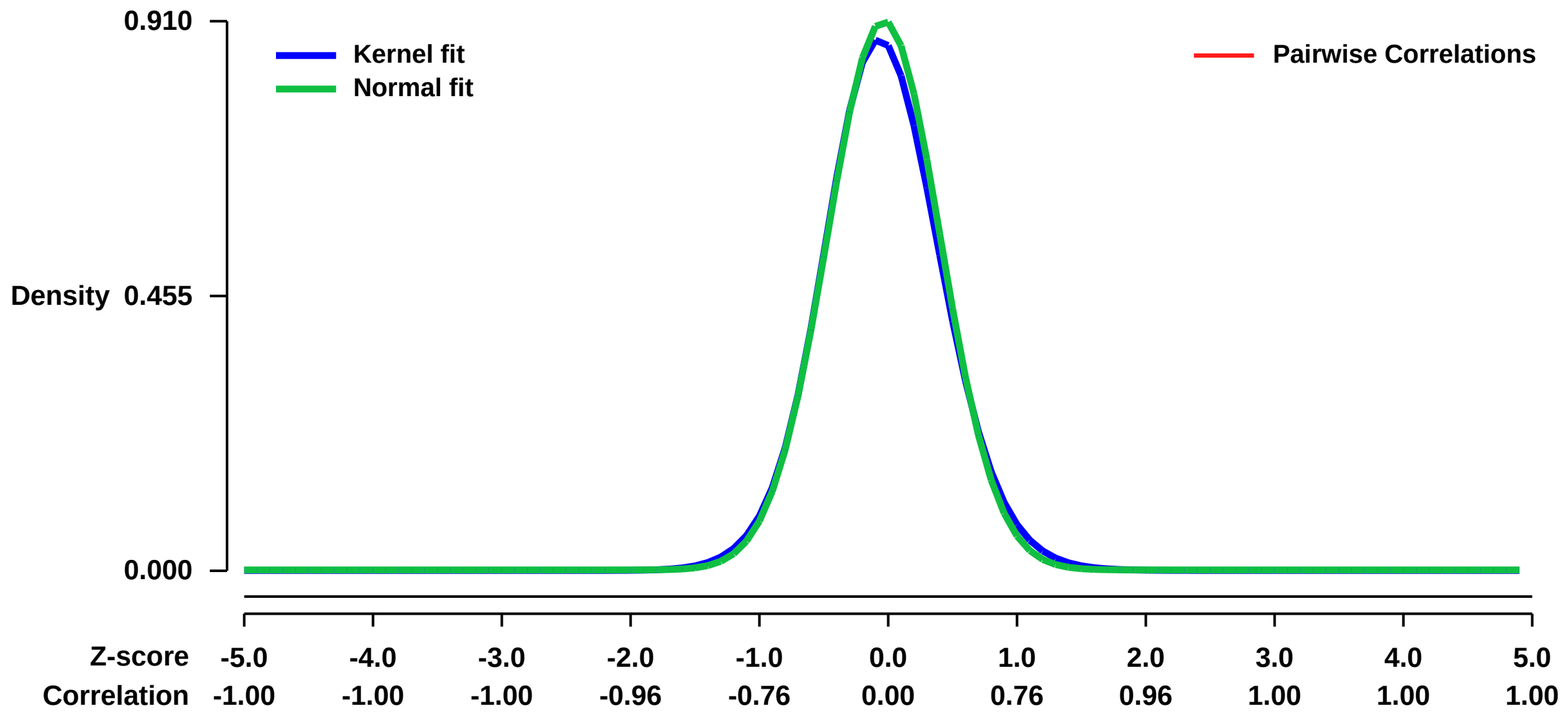

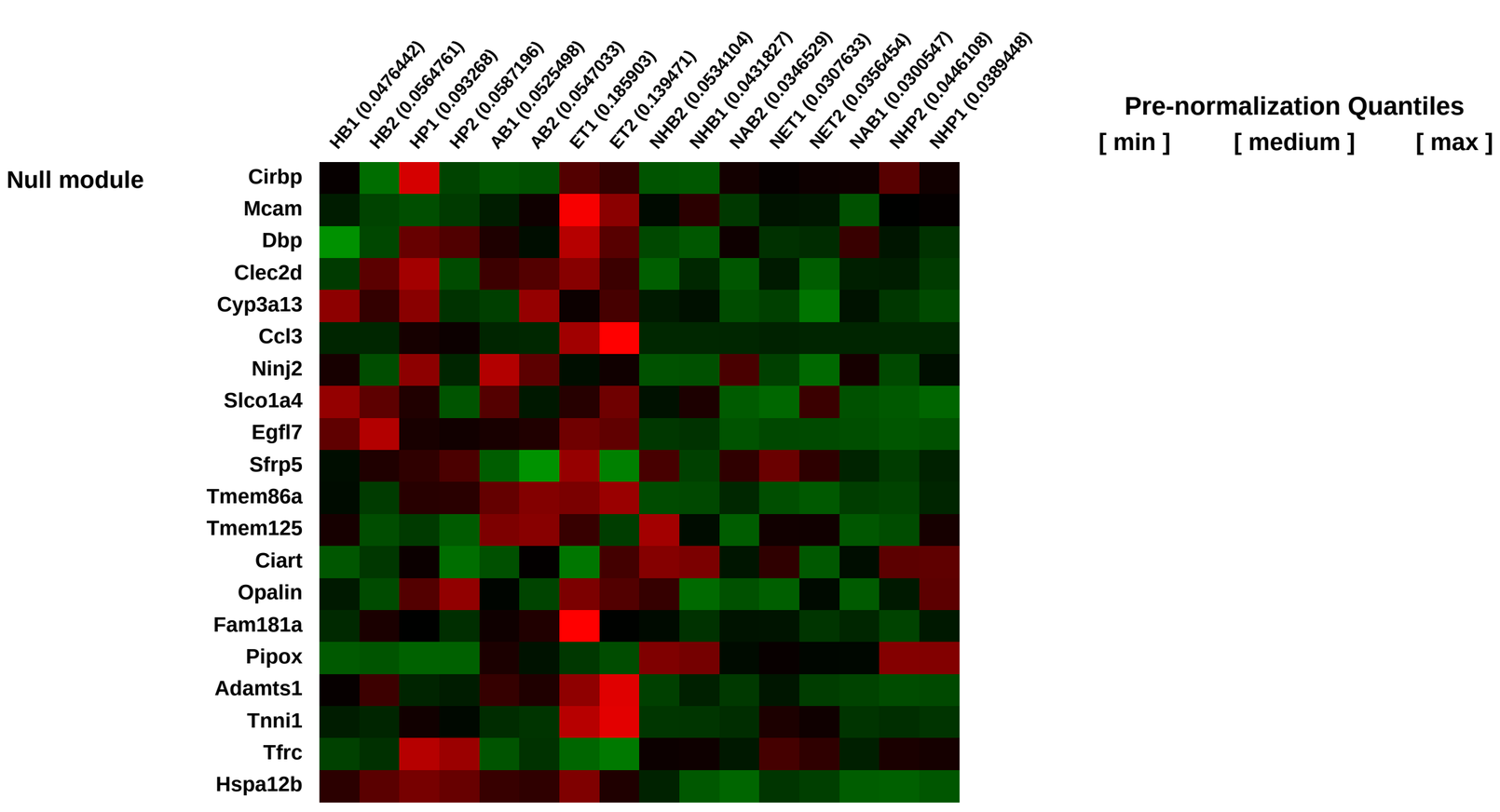

GEO Series "GSE10216" Expression Profiles

Num of samples in this series: 6

Scale of expression profile Z-scores

-3.0 -2.0 -1.0 0.0 1.0 2.0 3.0

GEO Link:	http://www.ncbi.nlm.nih.gov/geo/query/acc.cgi?acc=GSE10216
Status:	Public on Jan 30 2008
Title:	Emx2 knock-out urogenital epithelium
Organism:	Mus musculus
Experiment type:	Expression profiling by array
Platform:	GPL1261
Pubmed ID:	20962046
Summary & Design:	**Summary:** Series of samples studying effect of knock out Emx2 in urogenital epithelium of mouse embryos at E10.5. **Keywords: repeated sample** **Overall design:** The epithelial cells of the gonadal primordium were obtained by Laser Microdissection System. The specimens prepared from three individuals were mixed as one pool. There are three experimental replicates in each genotype, 3-pools of wild-type and 3-pools of Emx2 KO mouse.

Background corr dist: KL-Divergence = 0.0463, L1-Distance = 0.0207, L2-Distance = 0.0005, Normal std = 0.5877

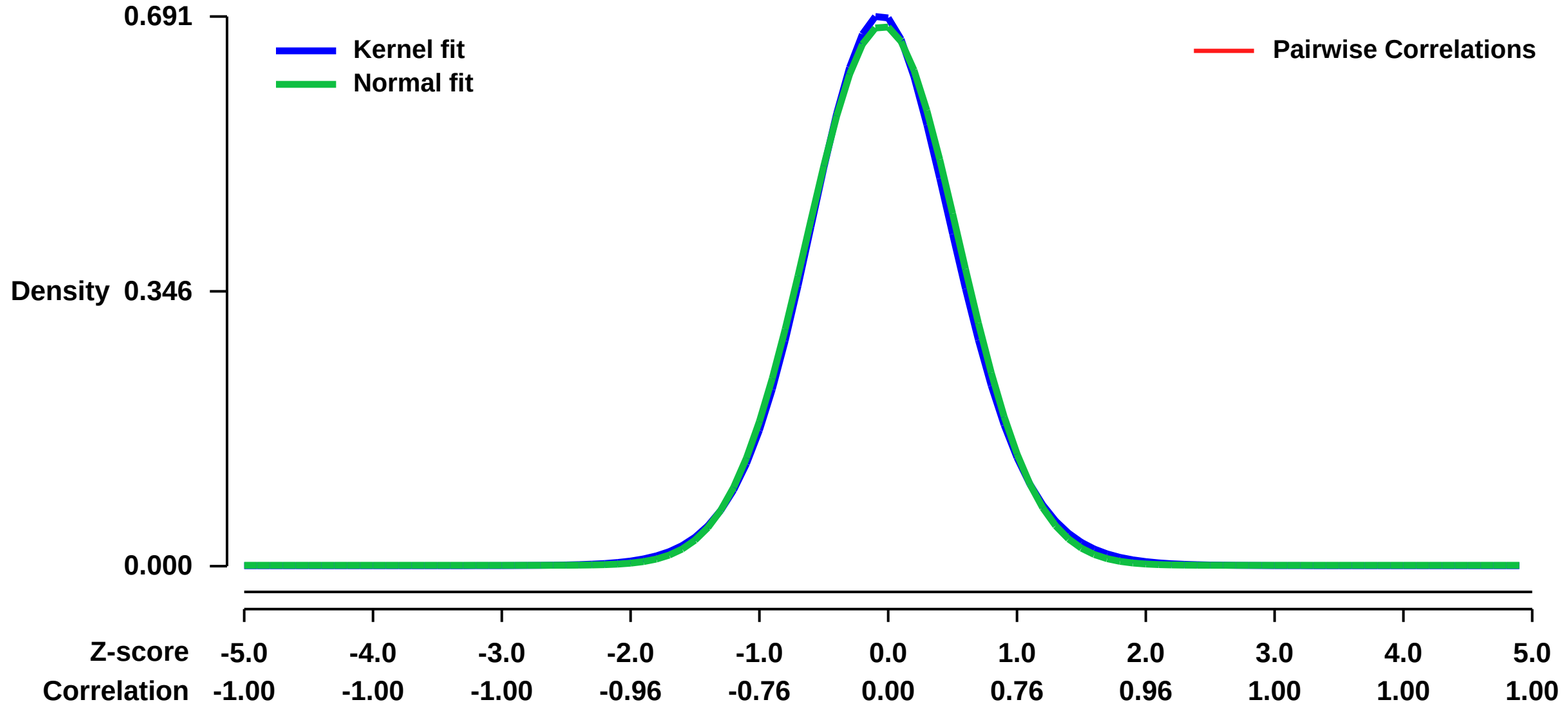

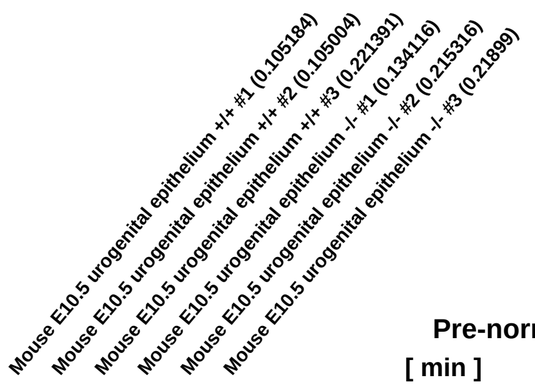

Pre-normalization Quantiles

[min] [medium] [max]

Null module

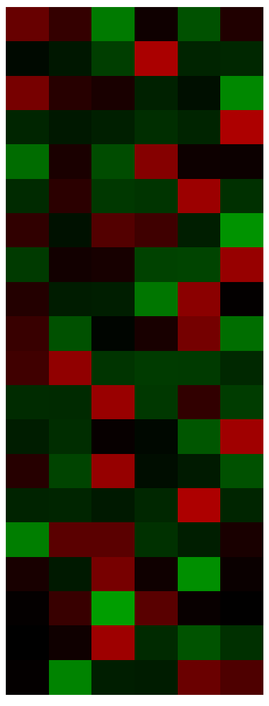

GEO Series "GSE10239" Expression Profiles

Num of samples in this series: 12

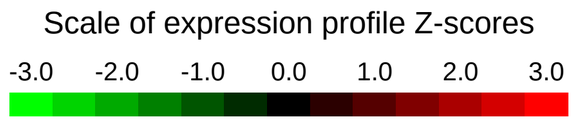

GEO Link:	http://www.ncbi.nlm.nih.gov/geo/query/acc.cgi?acc=GSE10239
Status:	Public on Jan 23 2008
Title:	Functional and Genomic Profiling of Effector CD8 T Cell Subsets
Organism:	Mus musculus
Experiment type:	Expression profiling by array
Platform:	GPL1261
Pubmed ID:	18316415
Summary & Design:	**Summary:** Using killer cell lectin-like receptor G1 as a marker to distinguish terminal effector cells from memory precursors, we found that despite their diverse cell fates both subsets possessed remarkably similar gene expression profiles and functioned as equally potent killer cells. However, only the memory precursors were capable of making IL-2 thus defining a novel effector cell that was cytotoxic, expressed granzyme B, and produced inflammatory cytokines in addition to IL-2. This effector population then differentiated into long-lived protective memory T cells capable of self-renewal and rapid re-call responses. Mechanistic studies showed that cells that continued to receive antigenic stimulation during the later stages of infection were more likely to become terminal effectors. Importantly, curtailing antigenic stimulation towards the tail-end of the acute infection enhanced the generation of memory cells. These studies support the decreasing potential model of memory differentiation and show that the duration of antigenic stimulation is a critical regulator of memory formation **Keywords:** Infection Type **Overall design:** An important question in memory development is understanding the differences between effector CD8 T cells that die versus effector cells that survive and give rise to memory cells. In this study we provide a comprehensive phenotypic, functional and genomic profiling of terminal effectors and memory precursors, towards better understanding the generation of these subsets. The two effector subsets were FACS purified during the early expansion phase (Days 4-5 post-infection) and extensively analyzed for their phenotypic (eg. CD127, CD62L, CD27, Bcl-2, Granzyme B, etc.) and functional properties (cytokine production, cytotoxicity, homeostatic proliferation, recall proliferation), and gene expression profiles (by genome-wide microarray analyses). Mechanistic studies involving the extent of proliferation and duration of antigen stimulation on memory differentiation potential of effectors were also performed using adoptive transfer techniques.

Background corr dist: KL-Divergence = 0.0430, L1-Distance = 0.0323, L2-Distance = 0.0019, Normal std = 0.5846

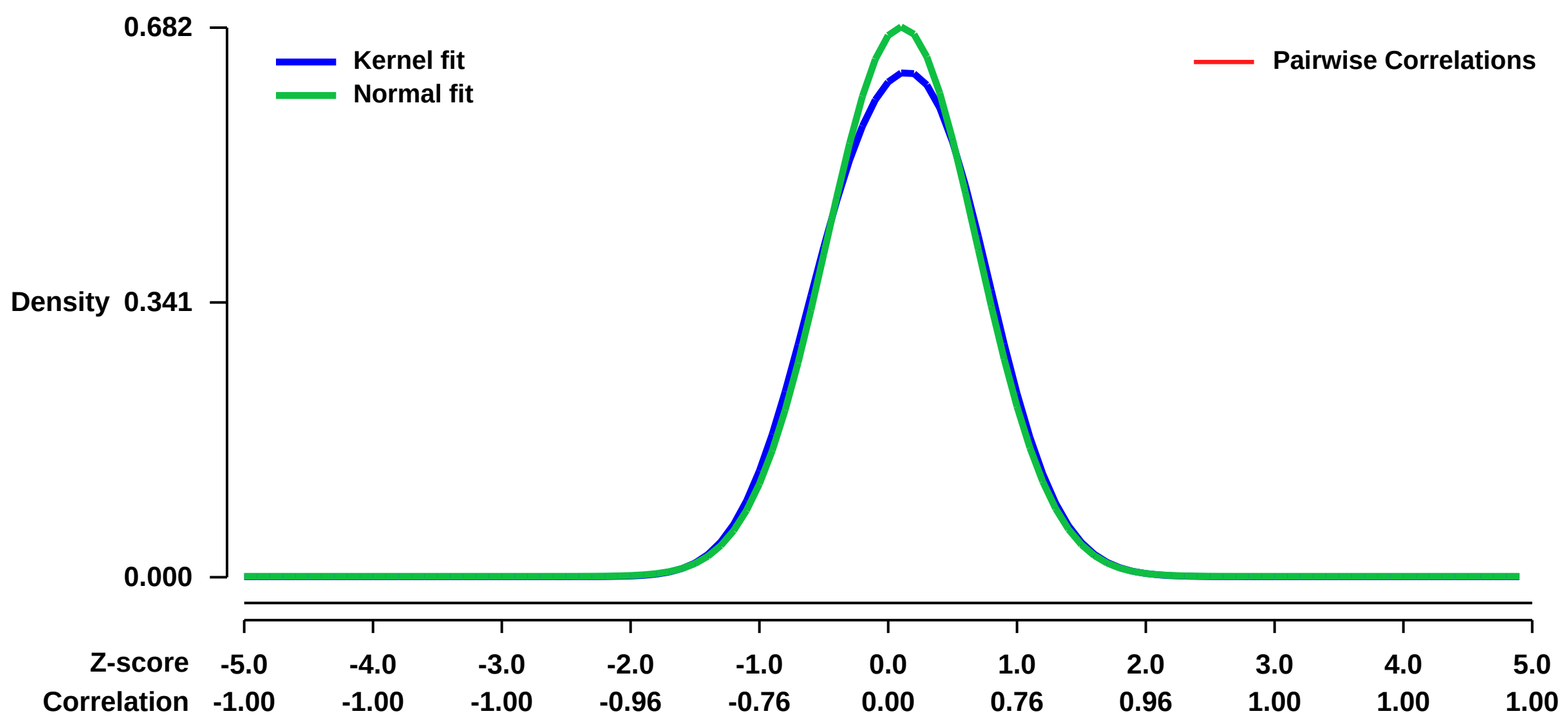

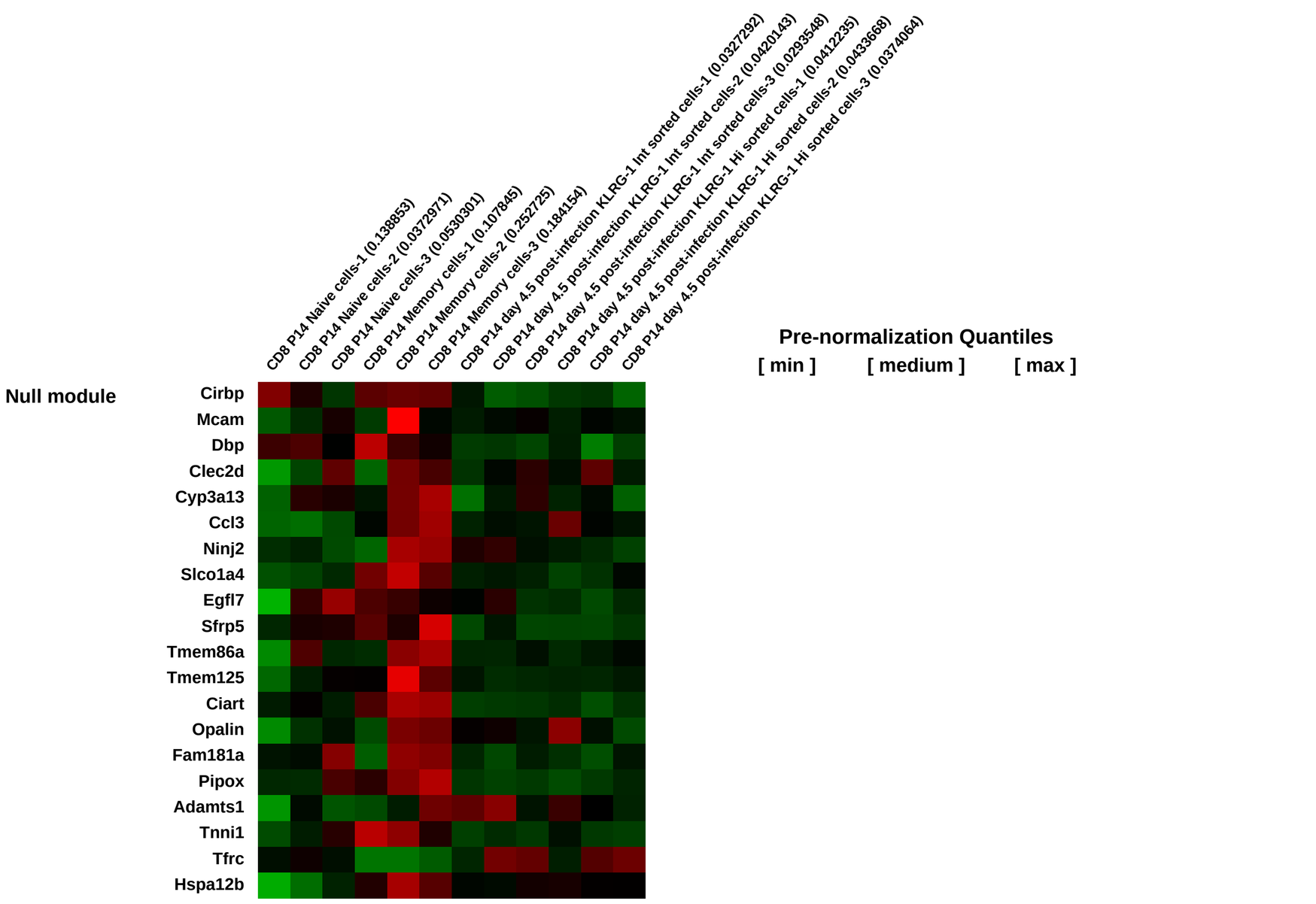

GEO Series "GSE10273" Expression Profiles

Num of samples in this series: 9

Scale of expression profile Z-scores

-3.0 -2.0 -1.0 0.0 1.0 2.0 3.0

GEO Link:	**http://www.ncbi.nlm.nih.gov/geo/query/acc.cgi?acc=GSE10273**
Status:	**Public on Jan 26 2008**
Title:	**Convergent molecular pathways that induce immunoglobulin light-chain recombination**
Organism:	**Mus musculus**
Experiment type:	**Expression profiling by array**
Platform:	**GPL1261**
Pubmed ID:	**18280186**
Summary & Design:	**Summary:** **Productive rearrangement of the immunoglobulin heavy chain locus triggers a major developmental checkpoint that promotes limited clonal expansion of pre-B cells, culminating in cell cycle arrest and rearrangement of the kappa (¸”) or lambda (¸») light-chain loci. B lineage cells lacking the related transcription factors IRF-4 and IRF-8 undergo a developmental arrest at the cycling pre-B cell stage and are blocked for light-chain recombination. Using Irf-4,8-/- pre-B cells we demonstrate that two pathways converge to synergistically drive light-chain rearrangement, a process that is not simply activated by cell cycle exit. One pathway is directly dependent on IRF-4, whose expression is elevated by pre-BCR signaling. IRF-4 targets the ¸” 3â† and ¸» enhancers to increase locus accessibility and positions a kappa allele away from pericentromeric heterochromatin. The other pathway is triggered by attenuation of IL-7 signaling and results in activation of the ¸” intronic enhancer via binding of the transcription factor, E2A. Intriguingly, IRF-4 regulates the expression of CXCR4 and promotes the migration of pre-B cells in response to the chemokine CXCL12. We propose that IRF-4 coordinates the two pathways regulating light-chain recombination by positioning pre-B cells away from IL-7 expressing stromal cells.** **We used microarrys to identify the changes in gene expression under different levels of the cytokine IL-7 and after rescue of genetic defect.** **Keywords: growth conditions and rescue** **Overall design:** **IRF4,8 null pre-B cells were cultures in the indicated conditions prior to RNA isolation and hybridization to Affymetrix arrays.**

Background corr dist: KL-Divergence = 0.0485, L1-Distance = 0.0228, L2-Distance = 0.0005, Normal std = 0.5808

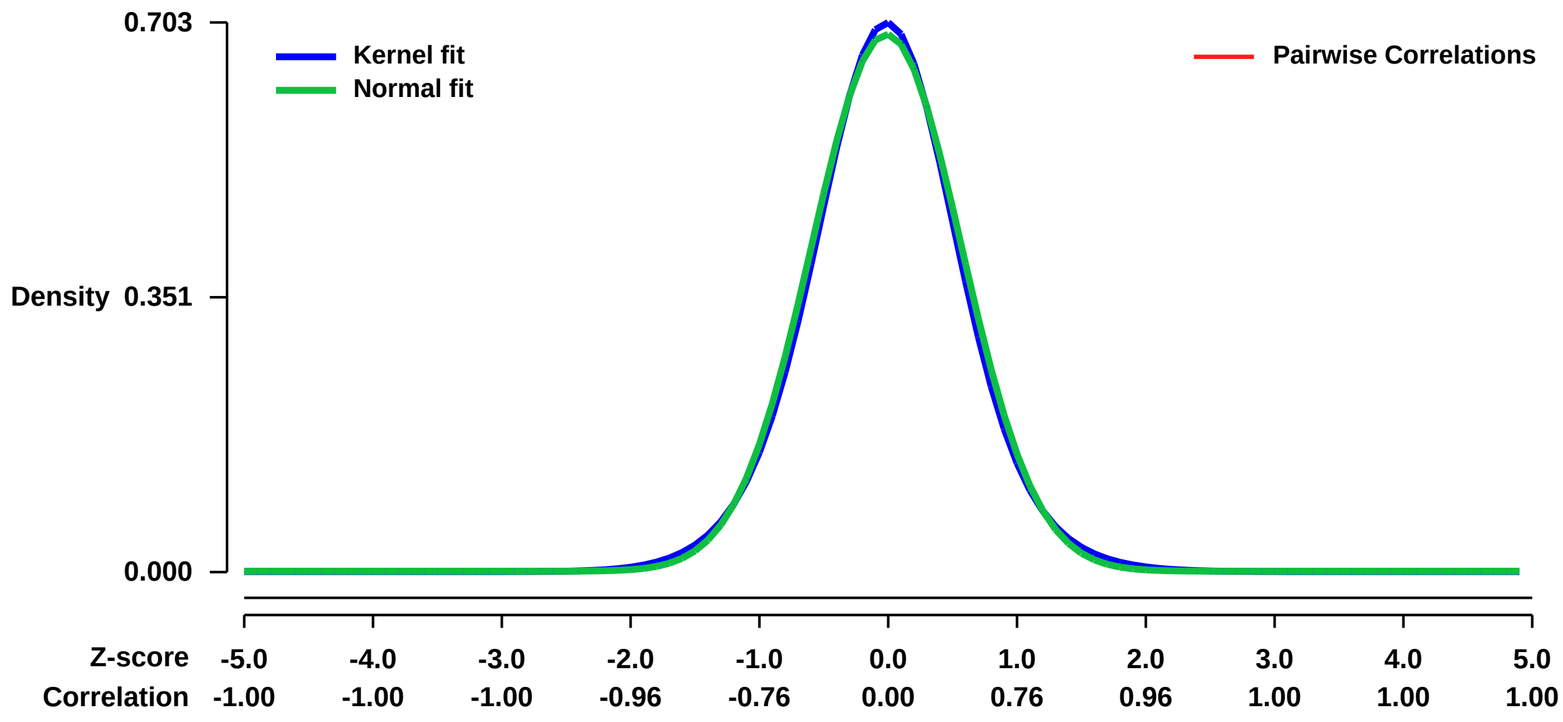

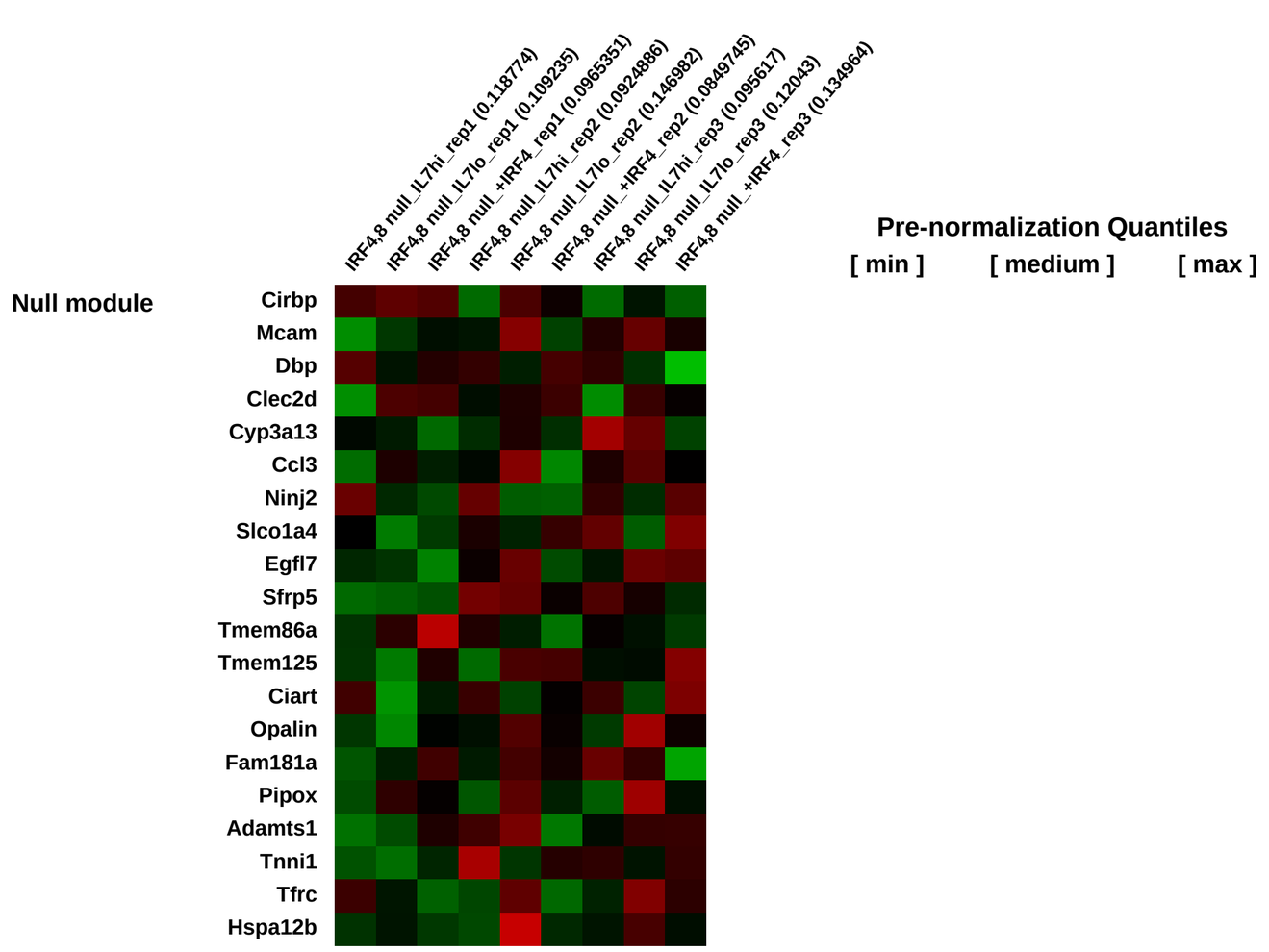

GEO Series "GSE10285" Expression Profiles

Num of samples in this series: 8

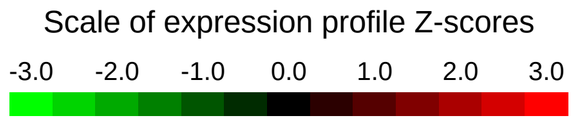

GEO Link:	**http://www.ncbi.nlm.nih.gov/geo/query/acc.cgi?acc=GSE10285**
Status:	**Public on Feb 24 2009**
Title:	**Role of Transglutaminase 2 in Liver Injury via Crosslinking and Silencing of Transcription Factor, Sp1**
Organism:	**Mus musculus**
Experiment type:	**Expression profiling by array**
Platform:	**GPL1261**
Pubmed ID:	**19208340**
Summary & Design:	**Summary:** **Gene expression of Ethanol-treated hepatocytes from WT and transglutaminase 2 knockout mice** **Keywords: transglutmianse 2** **Overall design:** **8 of Samples were analysed (its replicates are included)**

Background corr dist: **KL-Divergence = 0.0486, L1-Distance = 0.0293, L2-Distance = 0.0012, Normal std = 0.5776**

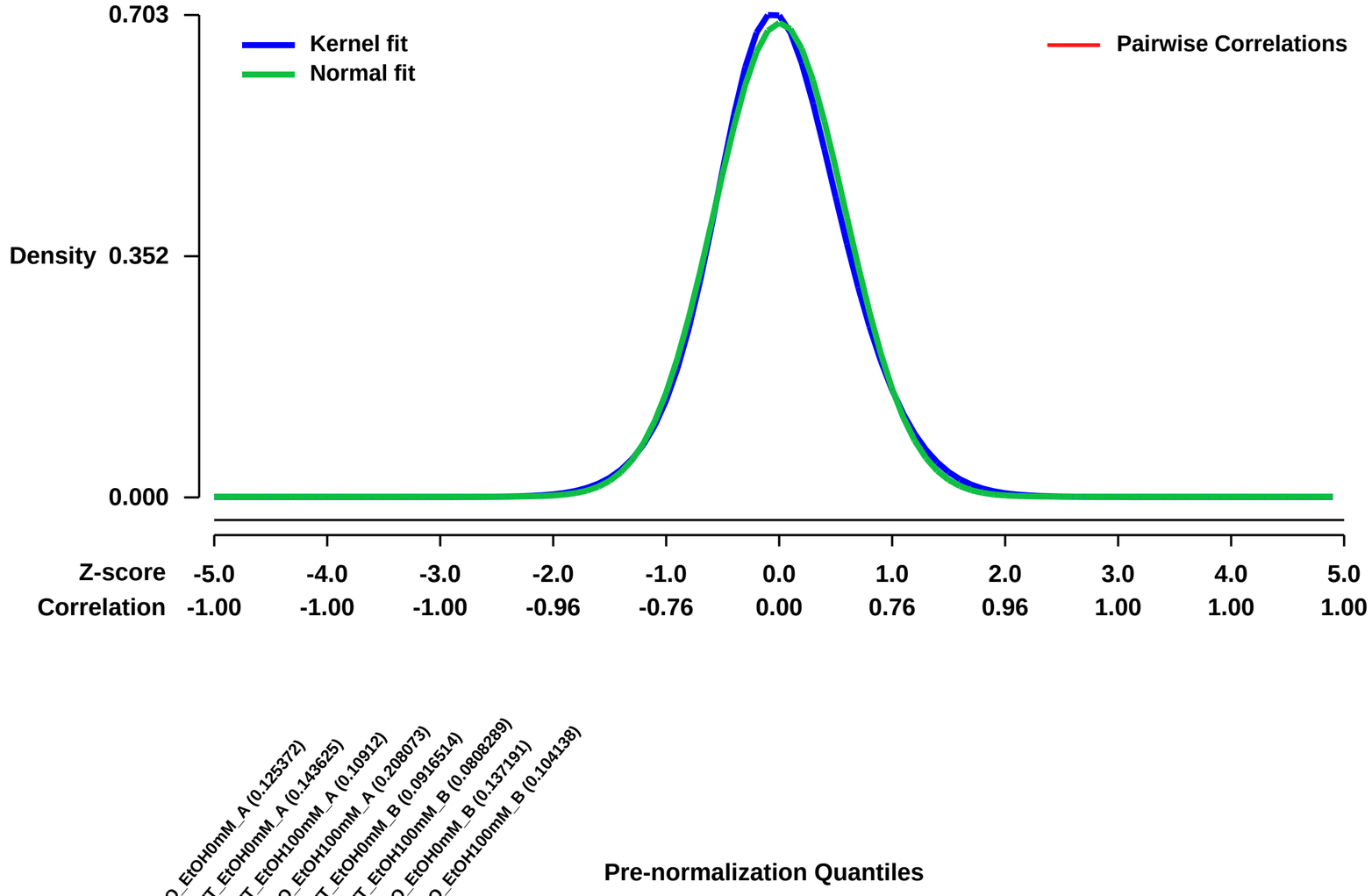

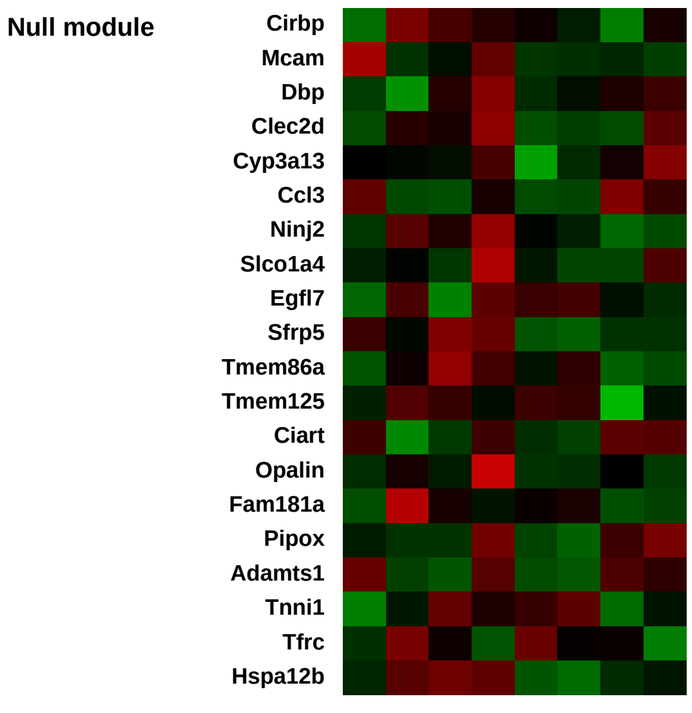

GEO Series "GSE10290" Expression Profiles

Num of samples in this series: 24

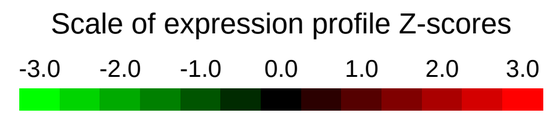

GEO Link:	http://www.ncbi.nlm.nih.gov/geo/query/acc.cgi?acc=GSE10290
Status:	Public on Nov 15 2008
Title:	Gene expression analyses of PR action in the mammary gland of ovariectomized mice
Organism:	Mus musculus
Experiment type:	Expression profiling by array
Platform:	GPL1261
Pubmed ID:	18687774
Summary & Design:	**Summary:** Beyond demonstrating a critical role for progesterone receptor signaling in normal mammary epithelial proliferation, the progesterone receptor knockout mouse disclosed the progesterone receptor along with its effector pathways as key determinants of mammary neoplastic progression. Despite these advances, however, further progress in our mechanistic understanding of progesteroneâ s involvement in mammary morphogenesis and tumorigenesis is contingent upon defining the essential effector pathways responsible for transducing the progesterone signal into a mammary proliferative and/or pro-survival response. Toward this goal, a judiciously chosen acute progesterone treatment regimen together with microarray methods was applied to the mammary gland of the normal mouse to uncover new effectors that operate immediately downstream of the progesterone mammary signal. Examination of the resultant progesterone-responsive transcriptome disclosed â inhibitor of differentiation or DNA binding 4â (Id4) as a molecular target acutely induced by progesterone in the murine mammary epithelium. **Keywords: time course** **Overall design:** Microarray analysis was performed on mammary tissue total RNA obtained from ovariectomized mice previously treated with progesterone for 4, 16, 28, and 76 hours. For each hormone treatment time-point, mammary gland microarray data from sesame oil (vehicle) treated mice was included as controls. Total mammary gland RNA from each time-point and treatment group was interrogated using the Affymetrix GeneChip Mouse Genome 430 2.0 Array. For a given time-point and treatment group, three sets of mice (5 mice in each set) were used for gene expression profiling; mammary RNA pooled from each set was hybridized to one microarray chip. Therefore, a total of 15 mice (or 3 microarray chips) were used per time-point and treatment group.

Background corr dist: KL-Divergence = 0.2584, L1-Distance = 0.0529, L2-Distance = 0.0067, Normal std = 0.2993

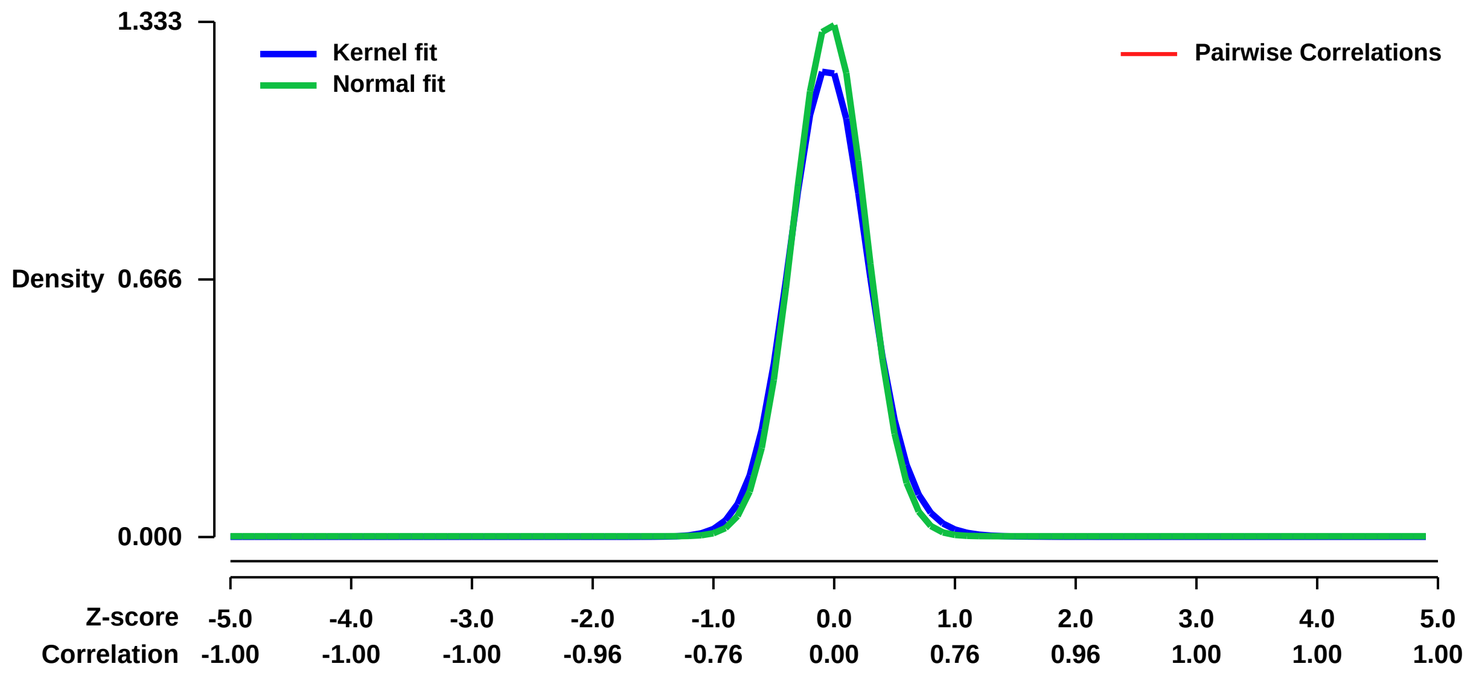

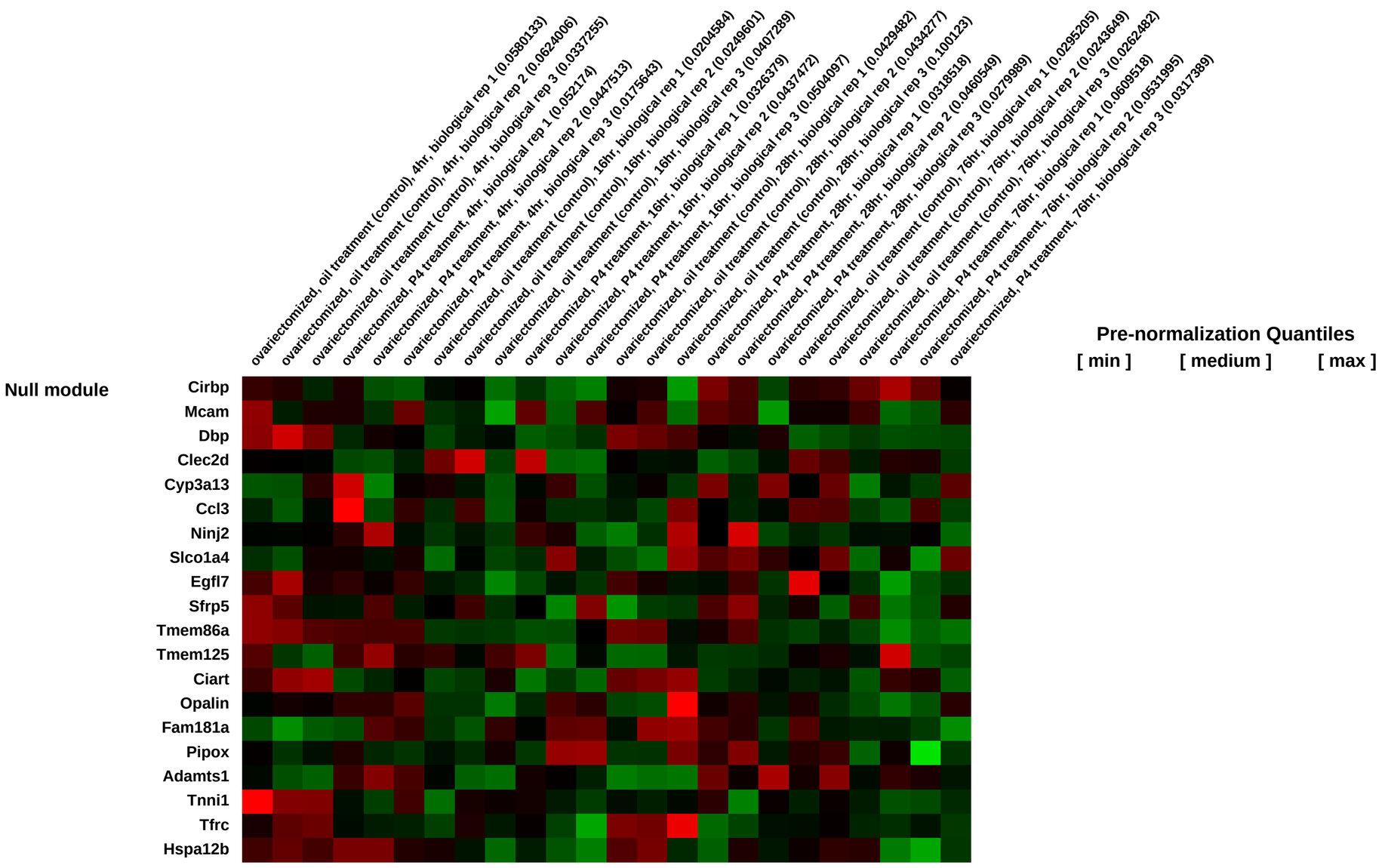

GEO Series "GSE10343" Expression Profiles

Num of samples in this series: 18

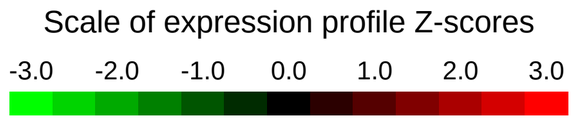

GEO Link:	http://www.ncbi.nlm.nih.gov/geo/query/acc.cgi?acc=GSE10343
Status:	Public on Feb 02 2008
Title:	Murine Acute Lung Injury
Organism:	Mus musculus
Experiment type:	Expression profiling by array
Platform:	GPL1261
Pubmed ID:	19136373
Summary & Design:	**Summary:** With advances in supportive therapy in the last two decades, mortality rates from ALI/ARDS have improved somewhat, but remain around 30 to 40% with significant morbidity in survivors. Several promising treatments are in various stages of evaluation, but many have failed to prove beneficial in large randomized clinical trials (RCT). The first definitive step forward in ALI therapeutics occurred recently as a result of a large RCT demonstrating a mortality decrease from 40 to 31% with the use of low-volume ventilation strategies. From this, it is clear that the opportunity for successful intervention in ALI exists. However, therapeutic advances remain frustrated by the lack of complete understanding of ALI pathophysiology. This stresses the importance of integrating basic and clinical research of the molecular pathogenesis of this disease. The conclusions of a recent National Heart, Lung, and Blood Institute (NHLBI) Working Group on ALI support this type of research as a priority for future investigations of ALI. One of the areas of research given priority by this ALI Working Group is the issue of ALI severity progression and the role of cells of innate immunity in this process. Currently, the processes that determine which ALI patients progress to ARDS and which do not are unclear. As with many phenotype differences, there is most likely a genetic component involved. The basis for this has been demonstrated. For example, a surfactant protein B (SP-B) polymorphism appears to increase a patientâ s risk of developing ALI from pneumonia. Additionally, a polymorphism in the promoter region of the gene for interleukin-6 (IL-6) has been associated with a poor prognosis in patients with ARDS. Understanding the intracellular processes of these genes and the cells expressing them in ALI progression could lead to the identification of molecular markers of ALI severity and eventually to the development of targeted therapies. An examination of genetically uniform animals will provide a clearer insight into the interaction between immune cells in ALI progression as well as guide future human experiments. **Keywords:** Time Series Design, ALI - acute lung injury, ARDS - acute respiratory distress syndrome, CLP - cecal ligation and puncture **Overall design:** Specific Aim 1. We will prospectively collect and bank RNA from peripheral blood CD4+ T lymphocytes (Th1 and Th2 subsets) and platelets from cecal ligation and puncture-treated BALB/c mice using a negative selection technique. Specific Aim 2. Four mice will undergo whole blood sampling at each of 3 time points (t = 0, 24, and 48 hours). Time 0 represents the point of CLP. Specific Aim 3. The temporal series of 3 cell types pooled within each time point will be expression profiled (3 time points x 3 cell types x MOE430A array = 9 profiles) in order to generate a map of potential cell-cell interactions and a prioritization model for examining these further.

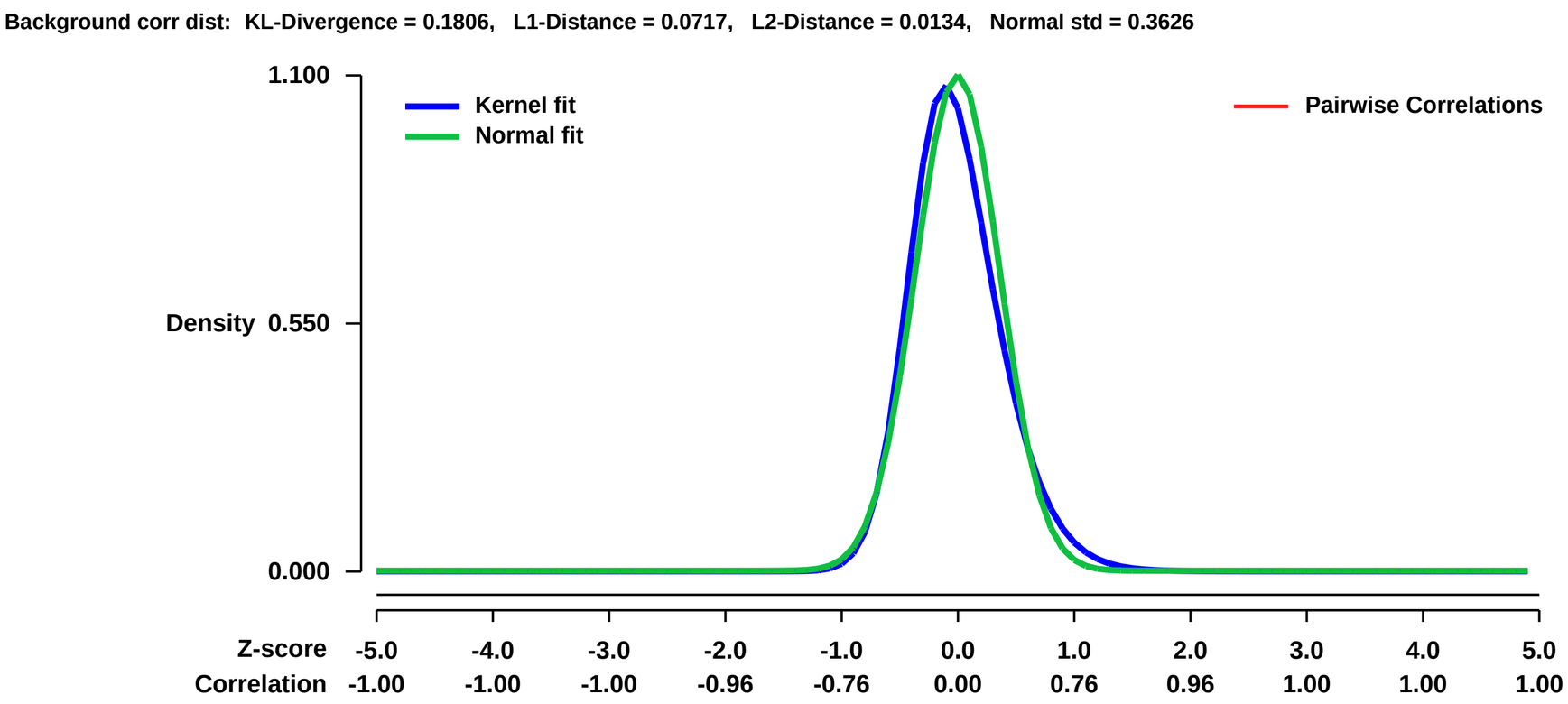

GEO Series "GSE10344" Expression Profiles

Num of samples in this series: 6

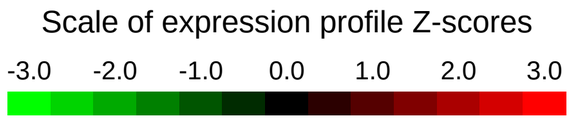

GEO Link:	**http://www.ncbi.nlm.nih.gov/geo/query/acc.cgi?acc=GSE10344**
Status:	**Public on Dec 31 2008**
Title:	**Expression data from garlic-fed mouse**
Organism:	**Mus musculus**
Experiment type:	**Expression profiling by array**
Platform:	**GPL1261**
Pubmed ID:	
Summary & Design:	**Summary:** **Garlic is a popular flavor enhancer in modern cuisines. Although anti-atherosclerotic, anti-proliferative, hypolipidemic and chemopreventative effects of garlic are known for a long time, the mechanisms of garlic as a dietary supplement ramain largely unknown.** **We used microarrays to analyze the global programme of gene expression in control (cellulose) and garlic-fed mice and identified erythropoietic and heme biosynthetic genes that could, in part, be responsible for the pleiotropic effects of garlic on health** **Keywords: diet, garlic** **Overall design:** **8-week old male C57BL/6J mice were divided into two diet groups and maintained at an SPF facility. Mice were fed (ad libitum) a special diet (Yeh and Yeh, 1994) with 4% cellulose (Control group, 3 mice) or 4% lyophilized raw garlic powder (Treatment group, 3 mice). At the end of the 15-week treatment, spleen organs were used for RNA isolation and arraying.**

Background corr dist: **KL-Divergence = 0.0471, L1-Distance = 0.0191, L2-Distance = 0.0004, Normal std = 0.5847**

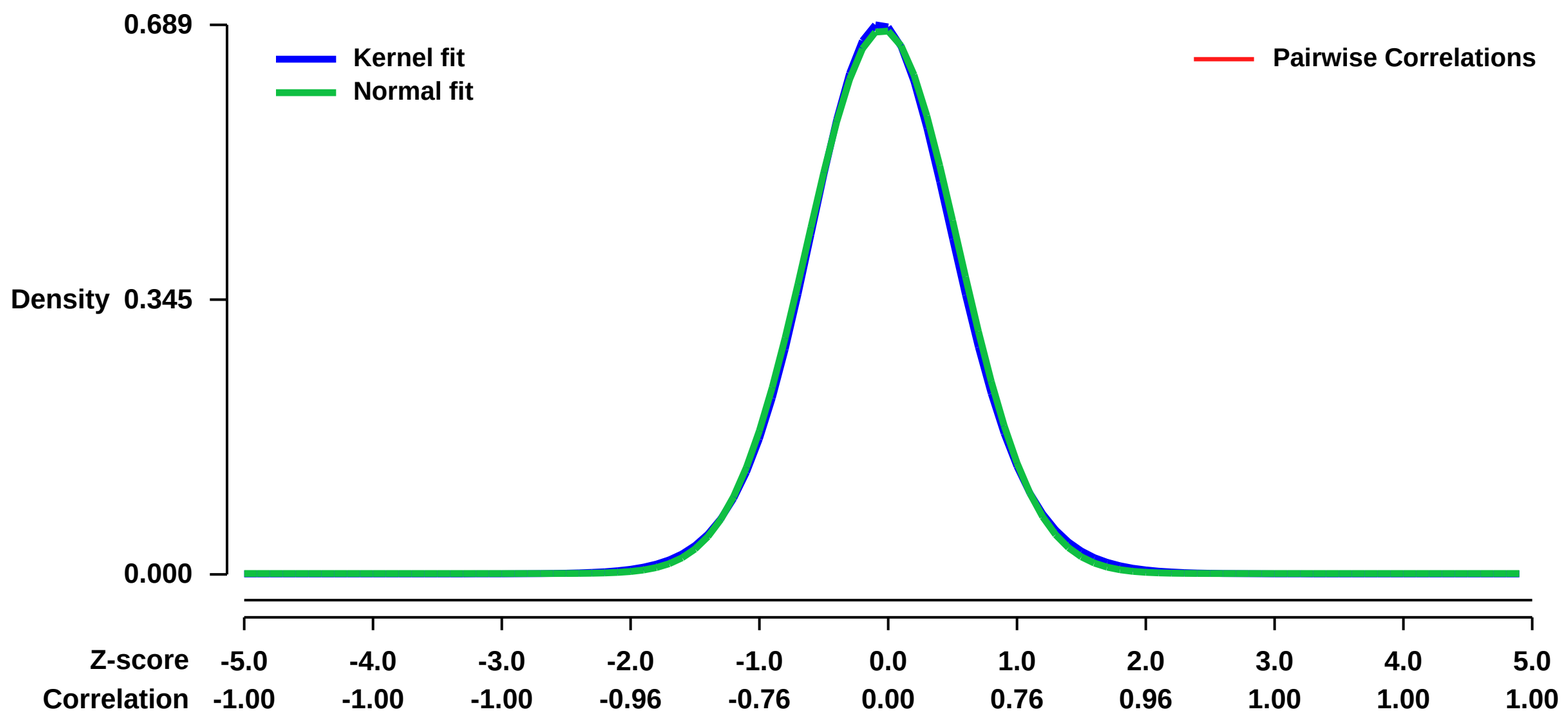

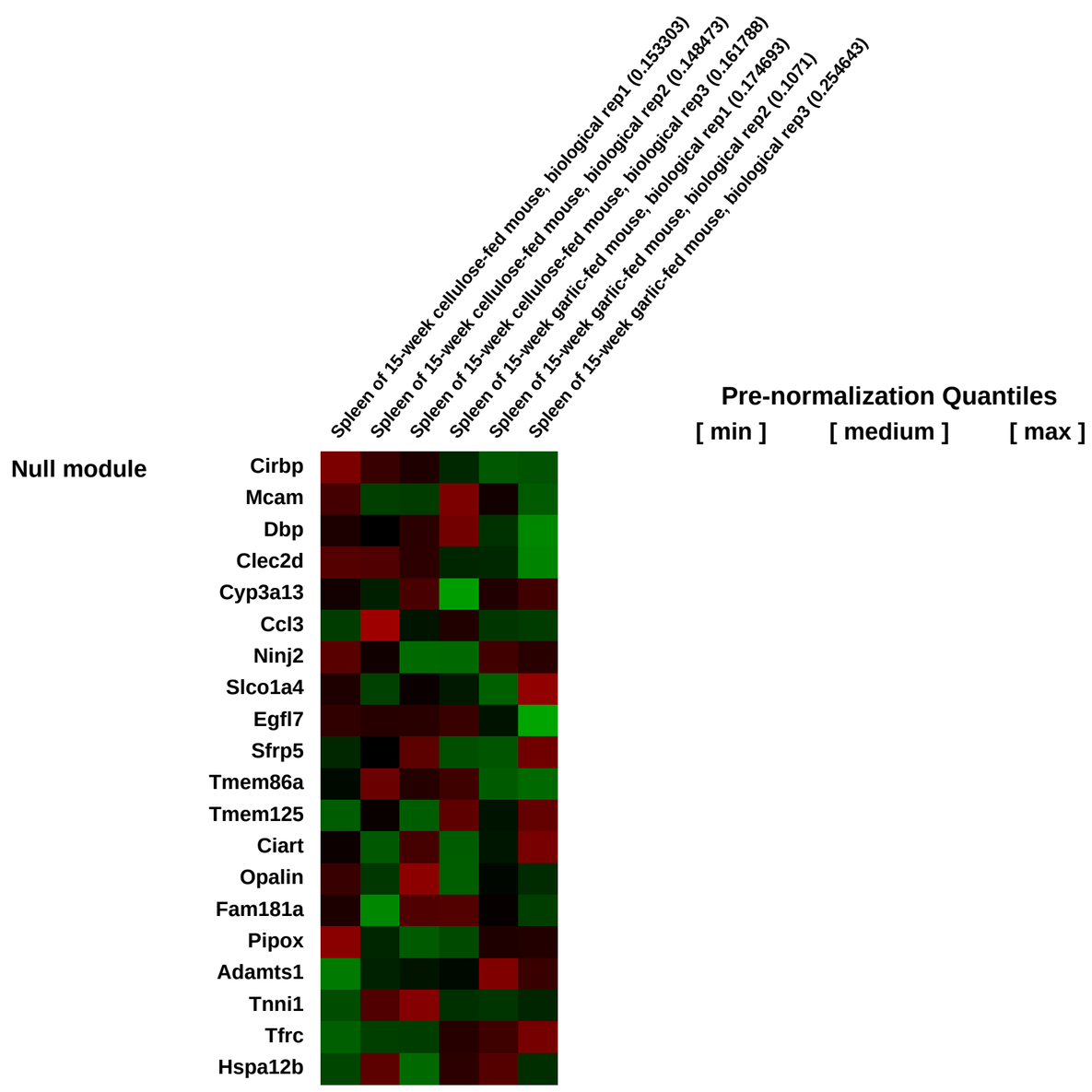

GEO Series "GSE10516" Expression Profiles

Num of samples in this series: 6

Scale of expression profile Z-scores

-3.0 -2.0 -1.0 0.0 1.0 2.0 3.0

GEO Link:	http://www.ncbi.nlm.nih.gov/geo/query/acc.cgi?acc=GSE10516
Status:	Public on Feb 15 2008
Title:	Identification of genes controlled by LMX1B in the developing mouse hindlimb bud
Organism:	Mus musculus
Experiment type:	Expression profiling by array
Platform:	GPL1261
Pubmed ID:	18351676
Summary & Design:	**Summary:** A control vs. genetic knockout experiment aimed at determining what RNAs are upregulated or downregulated in e11.5 mouse proximal limb tissue lacking the Lmx1b gene. Because Lmx1b is required for dorsal-ventral patterning of the limb, this screen gives insight into what putative downstream targets of Lmx1b contribute to dorsal-ventral patterning. **Keywords:** Genetic allele comparison **Overall design:** The proximal portion of e11.5 hindlimb buds (~500um) was used for RNA extraction. Each array was hybridized with pooled cRNAs from both hindlimb buds of three embryos (6 hindlimbs/sample).

Background corr dist: KL-Divergence = 0.0438, L1-Distance = 0.0172, L2-Distance = 0.0003, Normal std = 0.5963

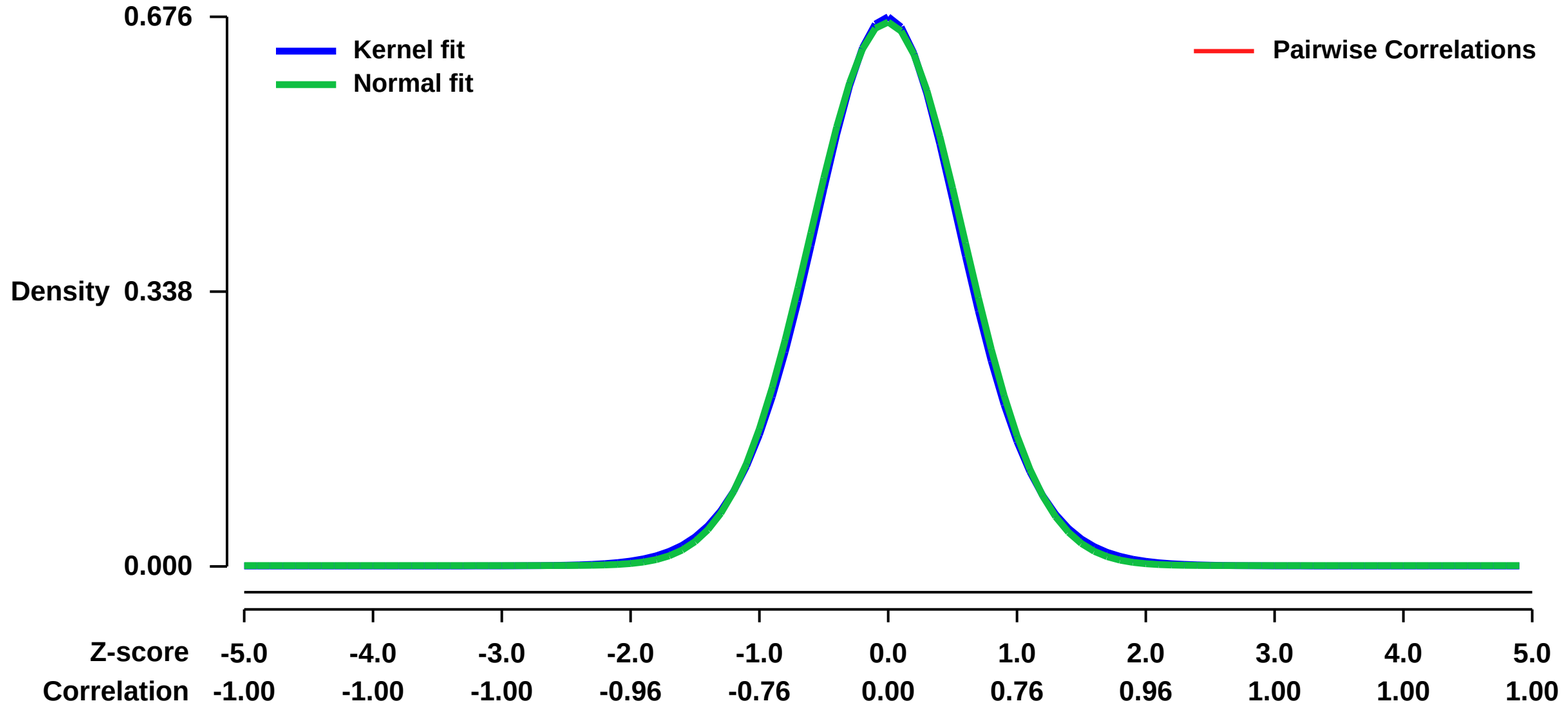

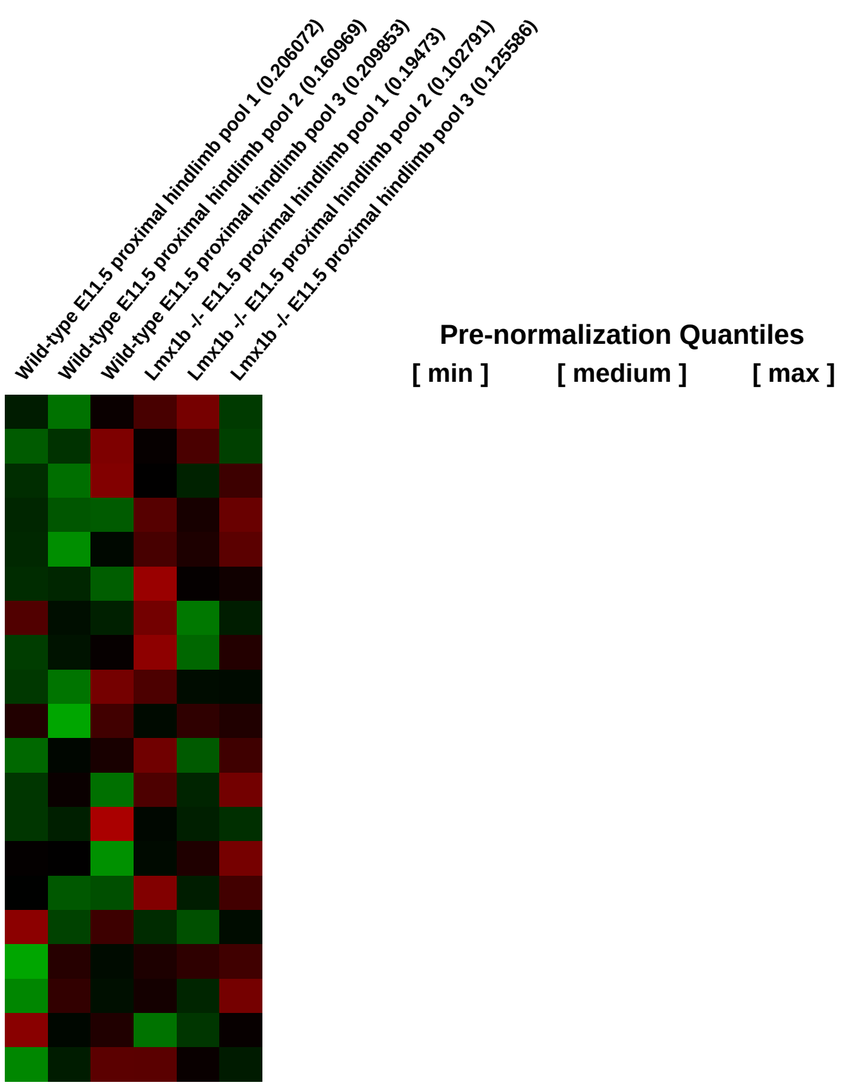

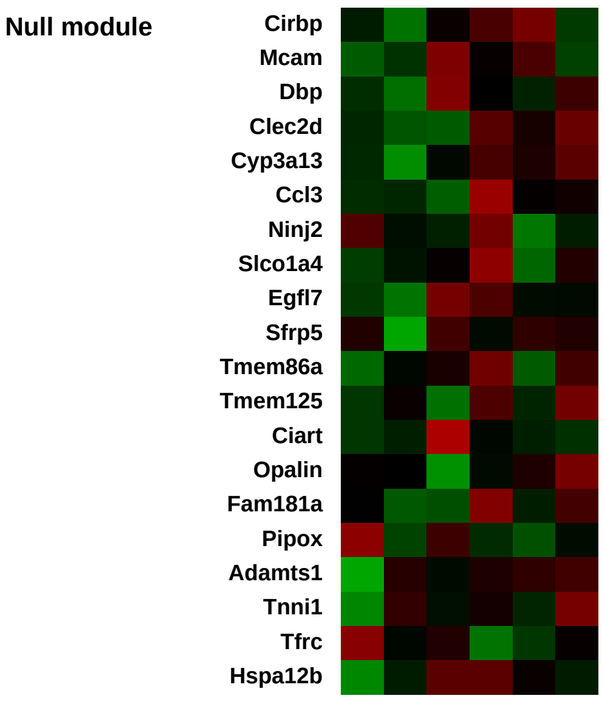

GEO Series "GSE10528" Expression Profiles

Num of samples in this series: 6

Scale of expression profile Z-scores

-3.0 -2.0 -1.0 0.0 1.0 2.0 3.0

GEO Link:	http://www.ncbi.nlm.nih.gov/geo/query/acc.cgi?acc=GSE10528
Status:	Public on Feb 15 2008
Title:	The retinal transcriptional response to light damage
Organism:	Mus musculus
Experiment type:	Expression profiling by array
Platform:	GPL1261
Pubmed ID:	15872101
Summary & Design:	**Summary:** Transcriptional profiles were compared between dark adapted and light damaged BALBc (albino) mouse retinas. **Keywords: stress response** **Overall design:** BALBc mice were dark adapted for one week. To produce light damage a subset of the mice were then exposed to 6,000 lux white fluorescent light for 6 hours. Retinas were collected for RNA extraction 24 hours after light damage.

Background corr dist: KL-Divergence = 0.0225, L1-Distance = 0.0186, L2-Distance = 0.0004, Normal std = 0.7206

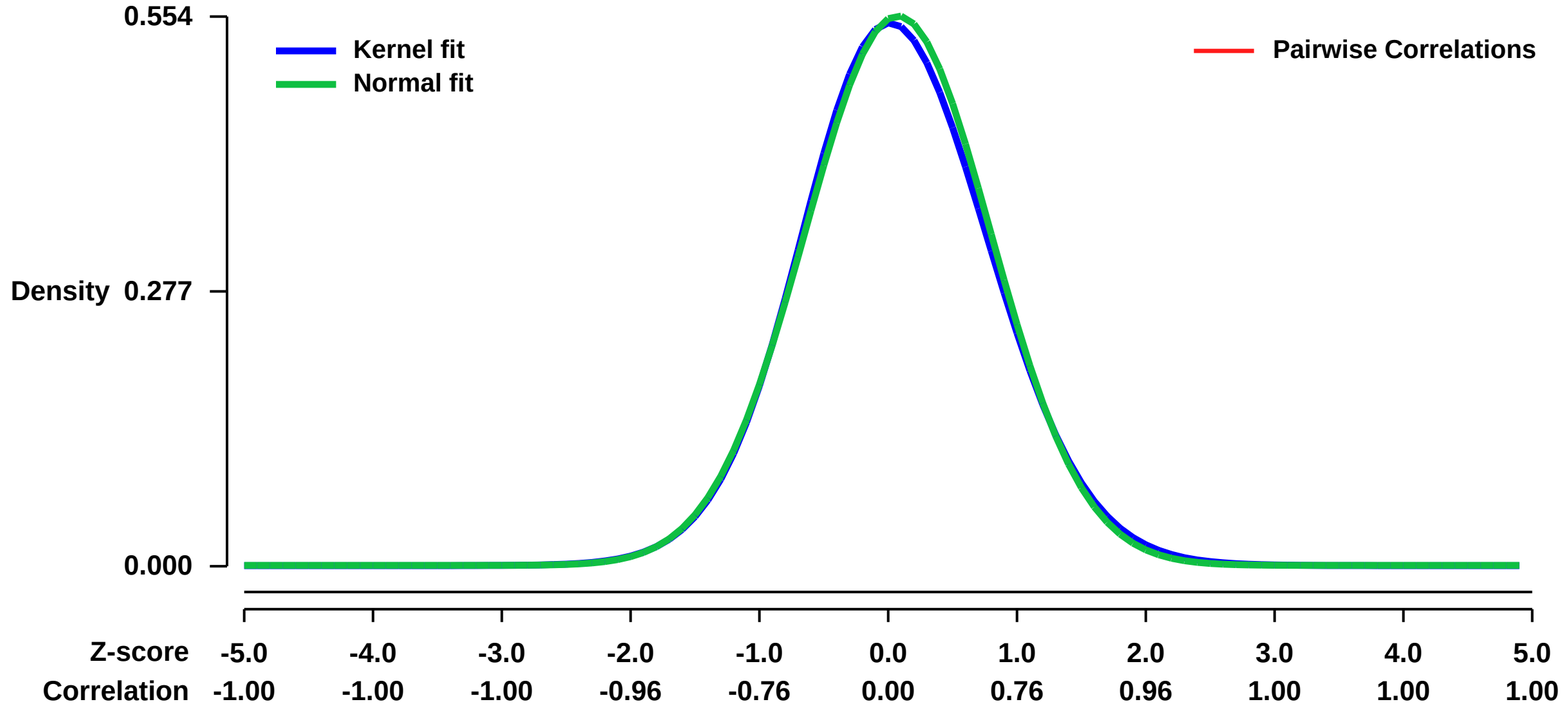

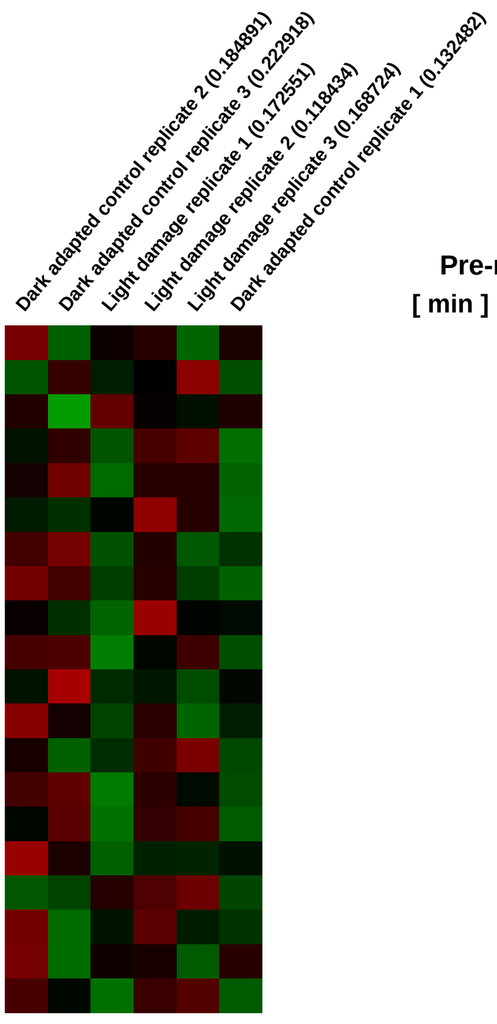

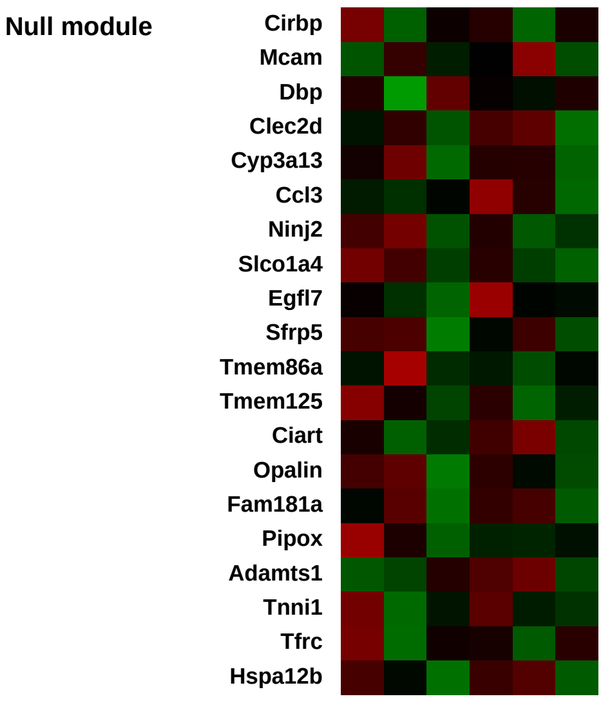

GEO Series "GSE10535" Expression Profiles

Num of samples in this series: 6

Scale of expression profile Z-scores

-3.0 -2.0 -1.0 0.0 1.0 2.0 3.0

GEO Link:	http://www.ncbi.nlm.nih.gov/geo/query/acc.cgi?acc=GSE10535
Status:	Public on Feb 21 2008
Title:	Retinal transcripts level alteration in the prCAD -/- mouse, a model for retinal degeneration
Organism:	Mus musculus
Experiment type:	Expression profiling by array
Platform:	GPL1261
Pubmed ID:	15872101
Summary & Design:	**Summary:** This experiment was designed to identify transcripts that exhibit changes in abundance in the context of retinal degeneration by comparing transcript levels in adult wild type and prCAD -/- mouse retinas. **Keywords: genetic mutant analysis** **Overall design:** Retinas were dissected from ~4 weeks old mice. Retinas from 3 prCAD knockout mice or wild type 129 mice were pooled for each sample and 3 replicate of wild type and mutant samples were analysed.

Background corr dist: KL-Divergence = 0.0328, L1-Distance = 0.0125, L2-Distance = 0.0001, Normal std = 0.6456

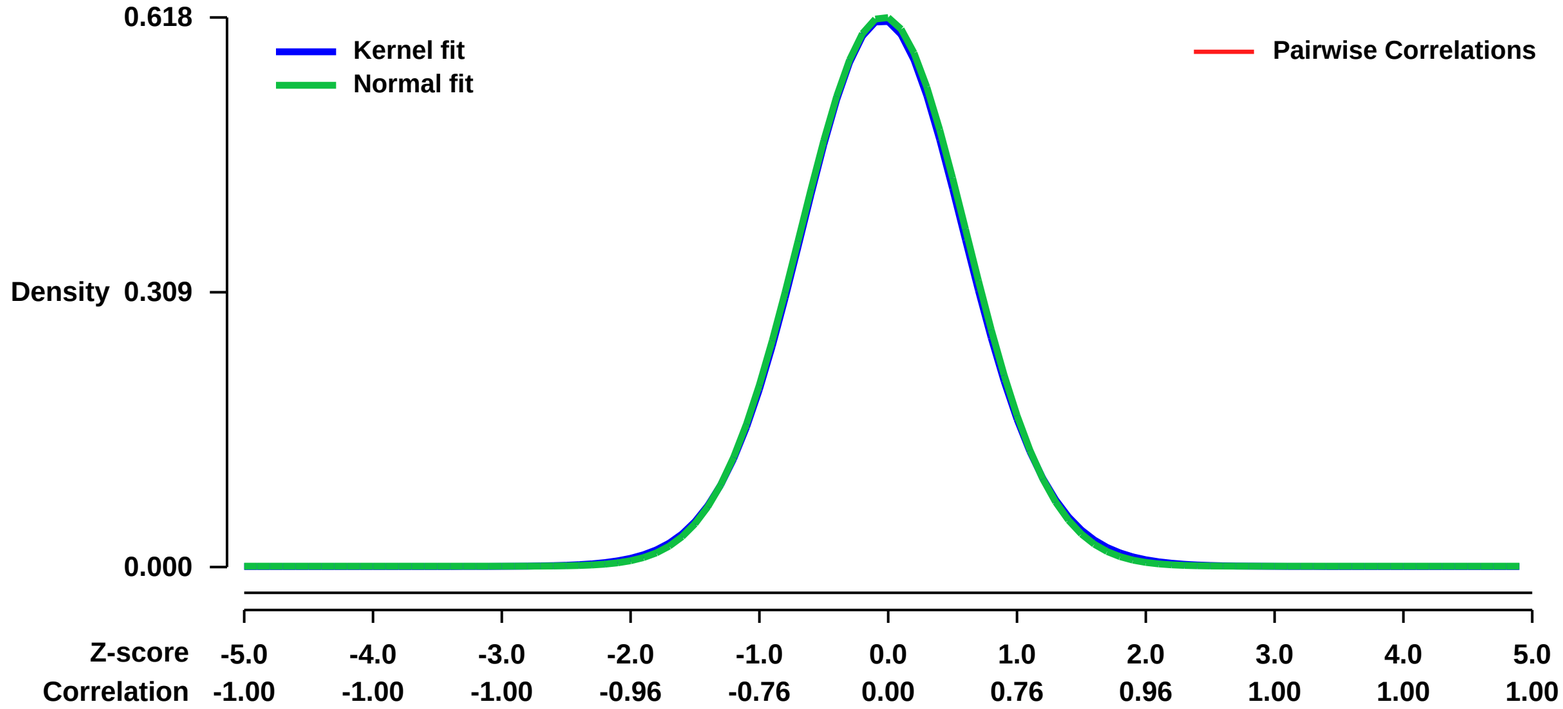

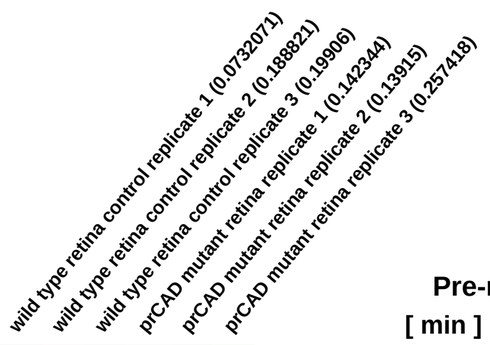

Pre-normalization Quantiles

[min] [medium] [max]

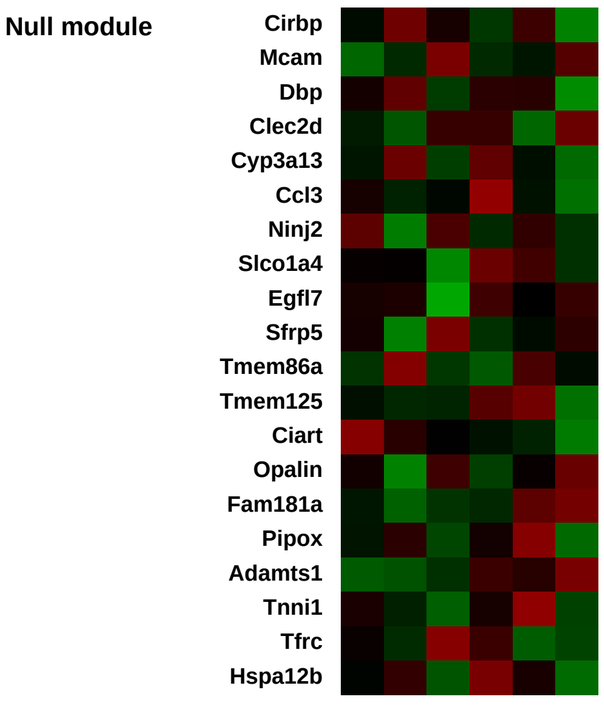

GEO Series "GSE10552" Expression Profiles

Num of samples in this series: 6

Scale of expression profile Z-scores

-3.0 -2.0 -1.0 0.0 1.0 2.0 3.0

GEO Link:	http://www.ncbi.nlm.nih.gov/geo/query/acc.cgi?acc=GSE10552
Status:	Public on Dec 31 2008
Title:	Genome wide expression analysis in AtT-20 cells following Dnmt1 knockdown
Organism:	Mus musculus
Experiment type:	Expression profiling by array
Platform:	GPL1261
Pubmed ID:	18922972
Summary & Design:	**Summary:** Efficient and sustained knockdown of DNMT1 transcript and protein was achieved using a consecutive transfection protocol in the mouse pituitary adenoma cell line, AtT-20. Genome wide microarray analysis identified 91 transcripts that were significantly differentially expressed relative to cells treated with a non-targeting control. **Keywords: Differential expression** **Overall design:** AtT-20 cells were repeatedly treated with 20 nM siRNA (siDNMT1 or siNT) over an eight day period. After eight days total RNA was extracted and prepared for microarray analysis. The procedure was repeated three times independently.

Background corr dist: KL-Divergence = 0.0482, L1-Distance = 0.0201, L2-Distance = 0.0004, Normal std = 0.5806

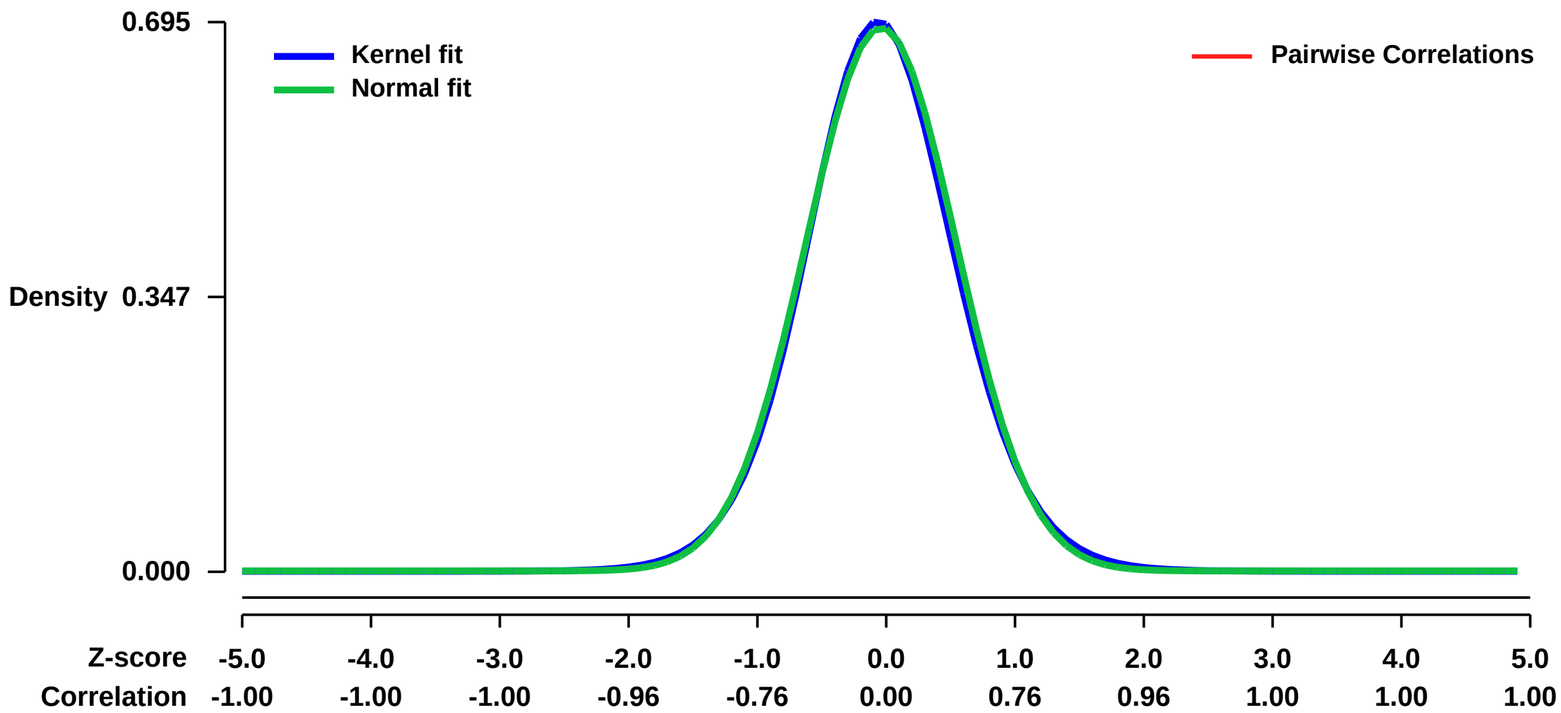

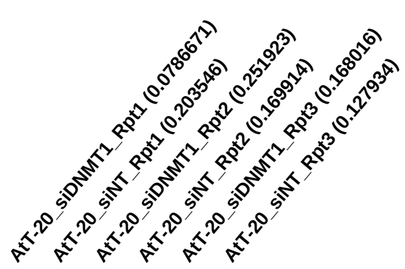

Pre-normalization Quantiles

[min] [medium] [max]

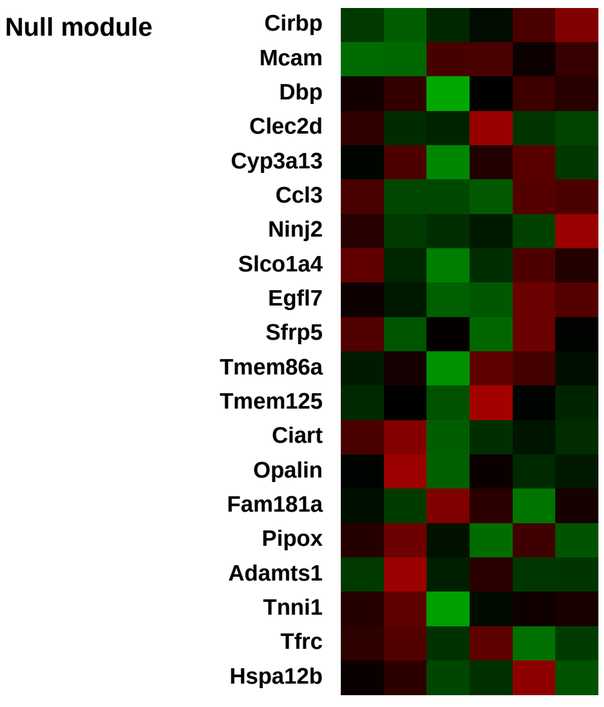

GEO Series "GSE10556" Expression Profiles

Num of samples in this series: 6

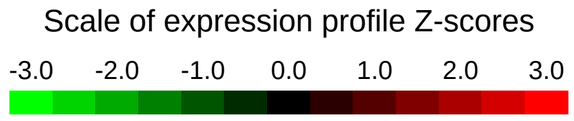

GEO Link:	http://www.ncbi.nlm.nih.gov/geo/query/acc.cgi?acc=GSE10556
Status:	Public on Nov 07 2008
Title:	Comparision of expression profile between wild-type and Slc39a13 knockout chondrocytes
Organism:	Mus musculus
Experiment type:	Expression profiling by array
Platform:	GPL1261
Pubmed ID:	18985159
Summary & Design:	**Summary:** In order to explore molecules whose expression is controlled by Slc39a13, we investigated gene expression profiling of primary chondrocyte isolated from wild-type and Slc39a13 knockout mice. **Keywords: knockout vs wild-type** **Overall design:** wild-type vs Slc39a13 knockout

Background corr dist: KL-Divergence = 0.0339, L1-Distance = 0.0199, L2-Distance = 0.0004, Normal std = 0.6472

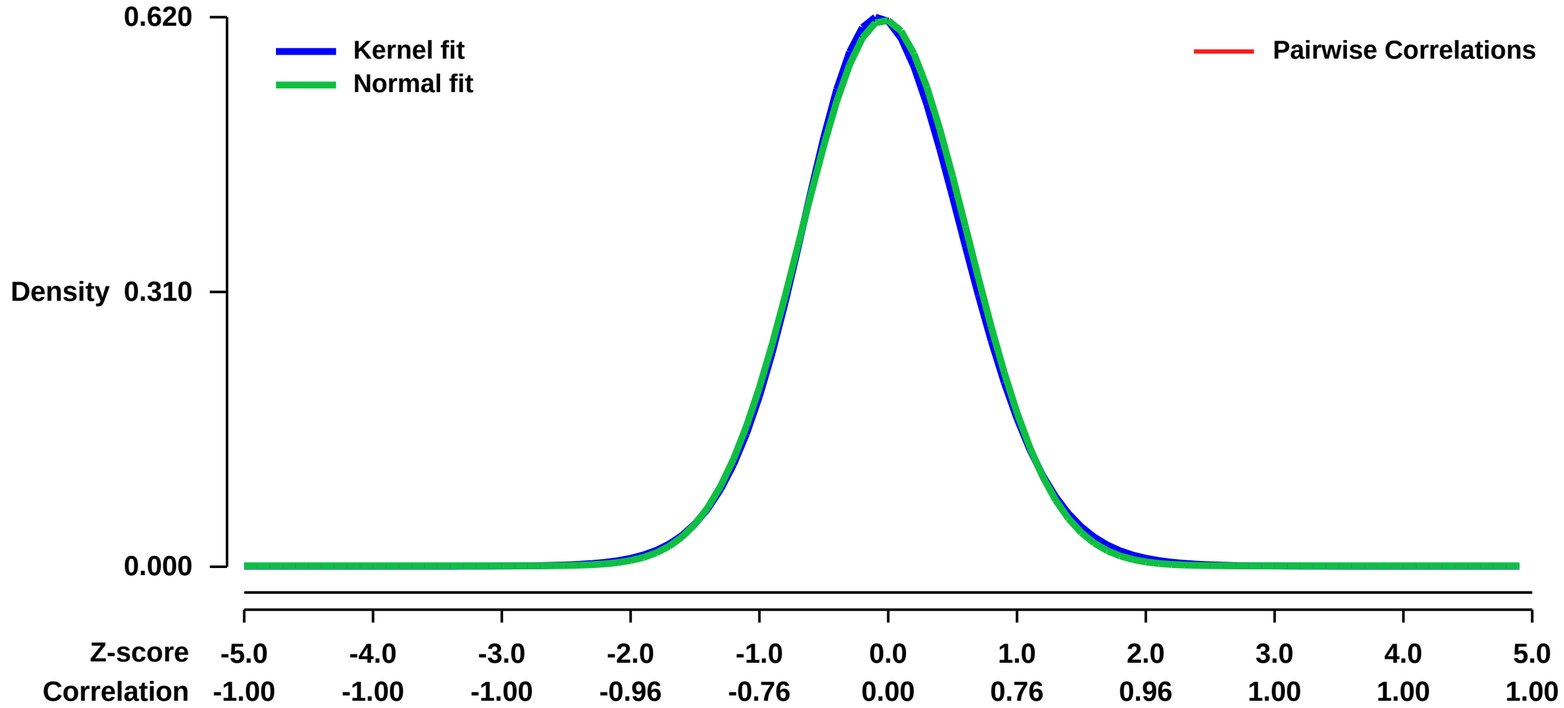

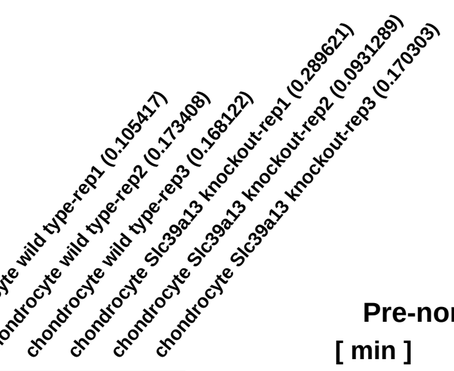

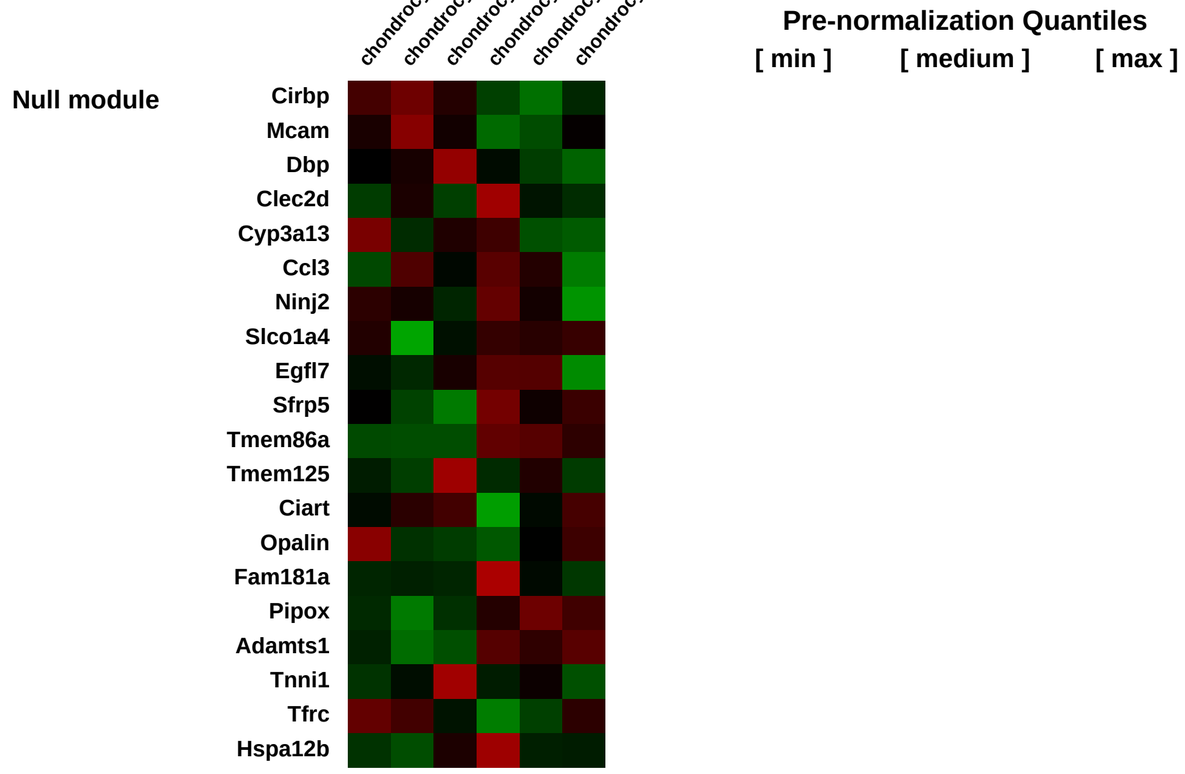

GEO Series "GSE10587" Expression Profiles

Num of samples in this series: 6

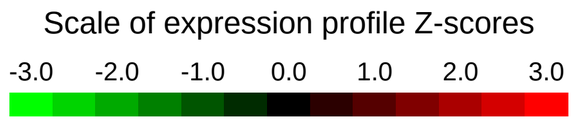

GEO Link:	http://www.ncbi.nlm.nih.gov/geo/query/acc.cgi?acc=GSE10587
Status:	Public on Feb 19 2009
Title:	Gene expression in stria vascularis of mice lacking Slc26a4 and heterzygous controls before the onset of hearing.
Organism:	Mus musculus
Experiment type:	Expression profiling by array
Platform:	GPL1261
Pubmed ID:	
Summary & Design:	**Summary:** Determination of differential expression of genes in the stria vascularis of pendrin (Slc26a4) heterozygous and knockout mice before the onset of hearing at postnatal day 10 (P10). **Keywords:** differential expression under disease state **Overall design:** A total of Six samples of stria vascularis RNA obtained from P10 mice were analyzed. Triplicates from pendrin (Slc26a4) heterozygous and knockout mice were run and analyzed.

Background corr dist: KL-Divergence = 0.0370, L1-Distance = 0.0201, L2-Distance = 0.0004, Normal std = 0.6322

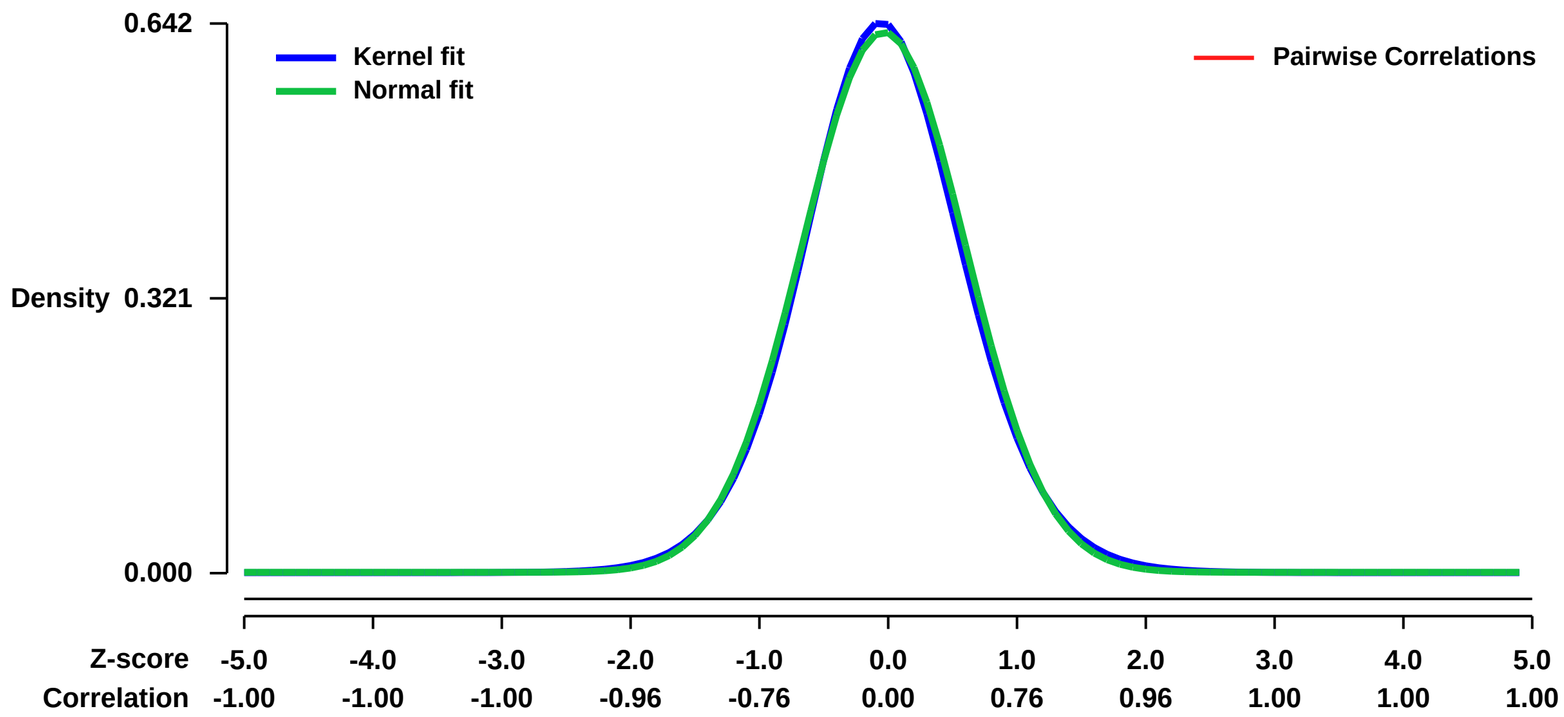

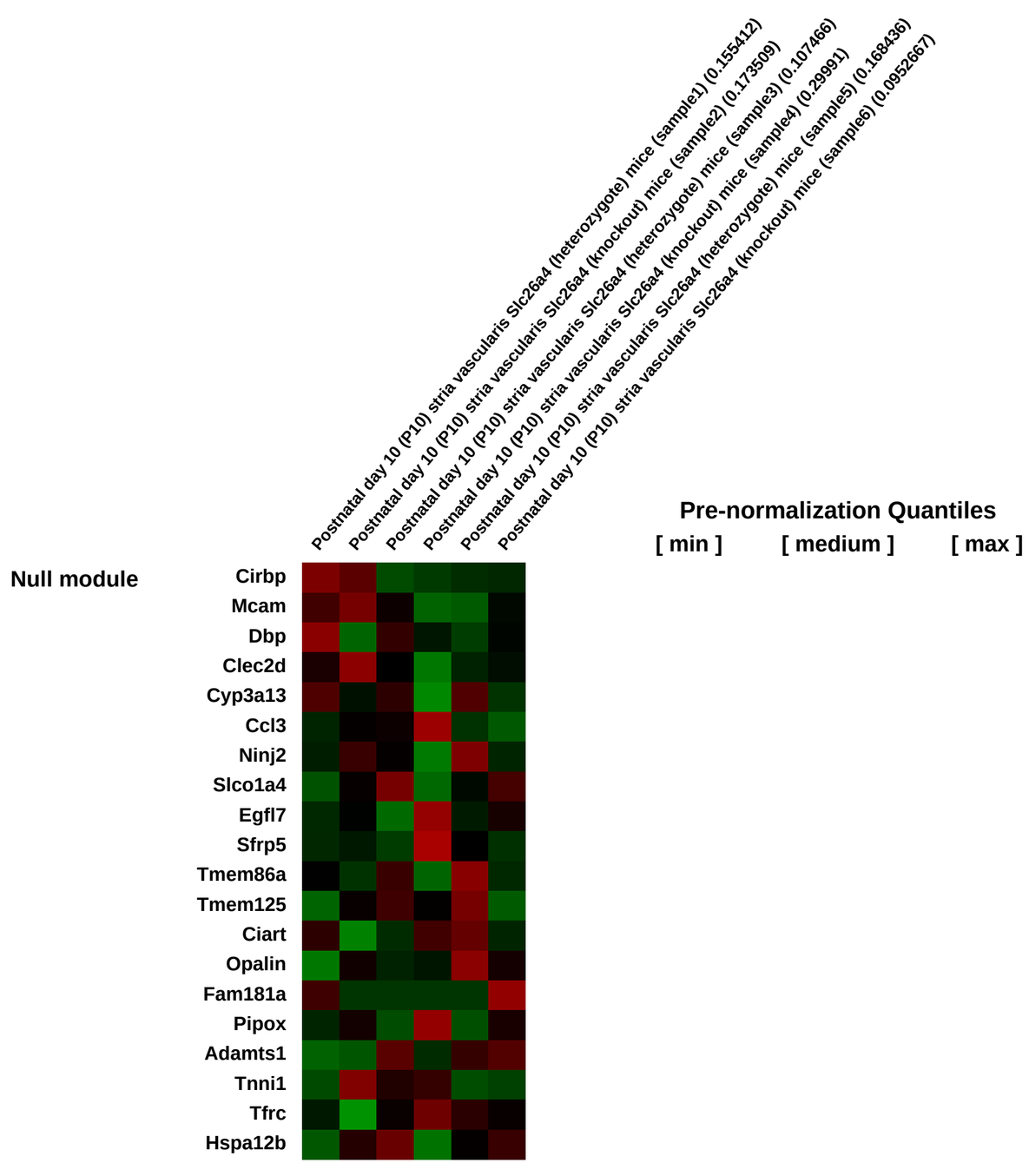

GEO Series "GSE10589" Expression Profiles

Num of samples in this series: 6

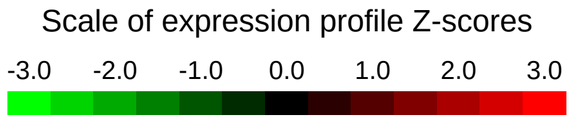

GEO Link:	http://www.ncbi.nlm.nih.gov/geo/query/acc.cgi?acc=GSE10589
Status:	Public on Feb 19 2009
Title:	Comparison of gene expression between the thyroid of mice lacking Slc26a4 and heterzygous controls.
Organism:	Mus musculus
Experiment type:	Expression profiling by array
Platform:	GPL1261
Pubmed ID:	19692489
Summary & Design:	**Summary:** Determination of differential expression of genes in the thyroid of pendrin (Slc26a4) heterozygous and knockout mice at a time point corresponding to maximal thyroid gland activity, postnatal day 15 (P15). **Keywords:** Differential expression under disease state **Overall design:** A total of Six samples of thyroid RNA obtained from P15 mice were analyzed. Triplicates from pendrin (Slc26a4) heterozygous and knockout mice were run and analyzed.

Background corr dist: KL-Divergence = 0.0392, L1-Distance = 0.0183, L2-Distance = 0.0004, Normal std = 0.6178

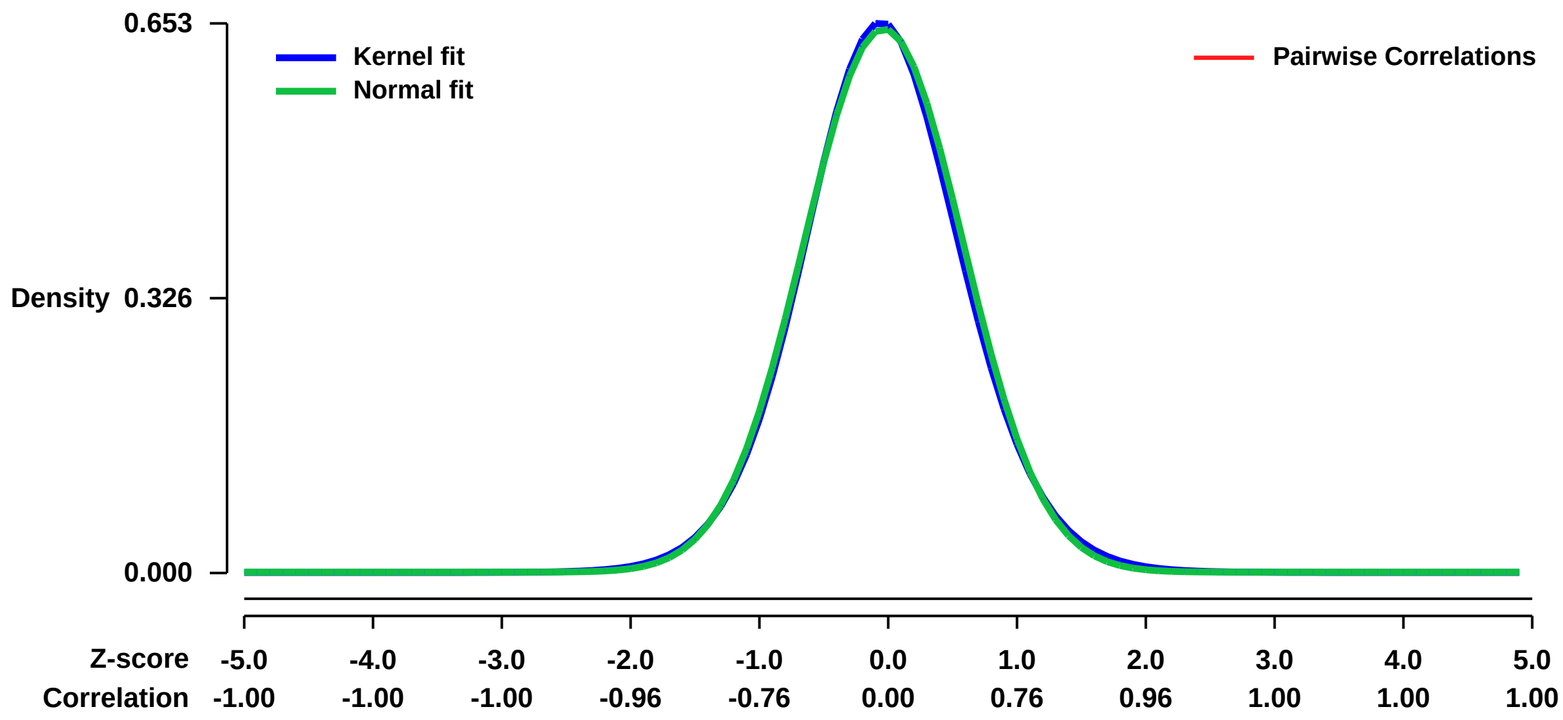

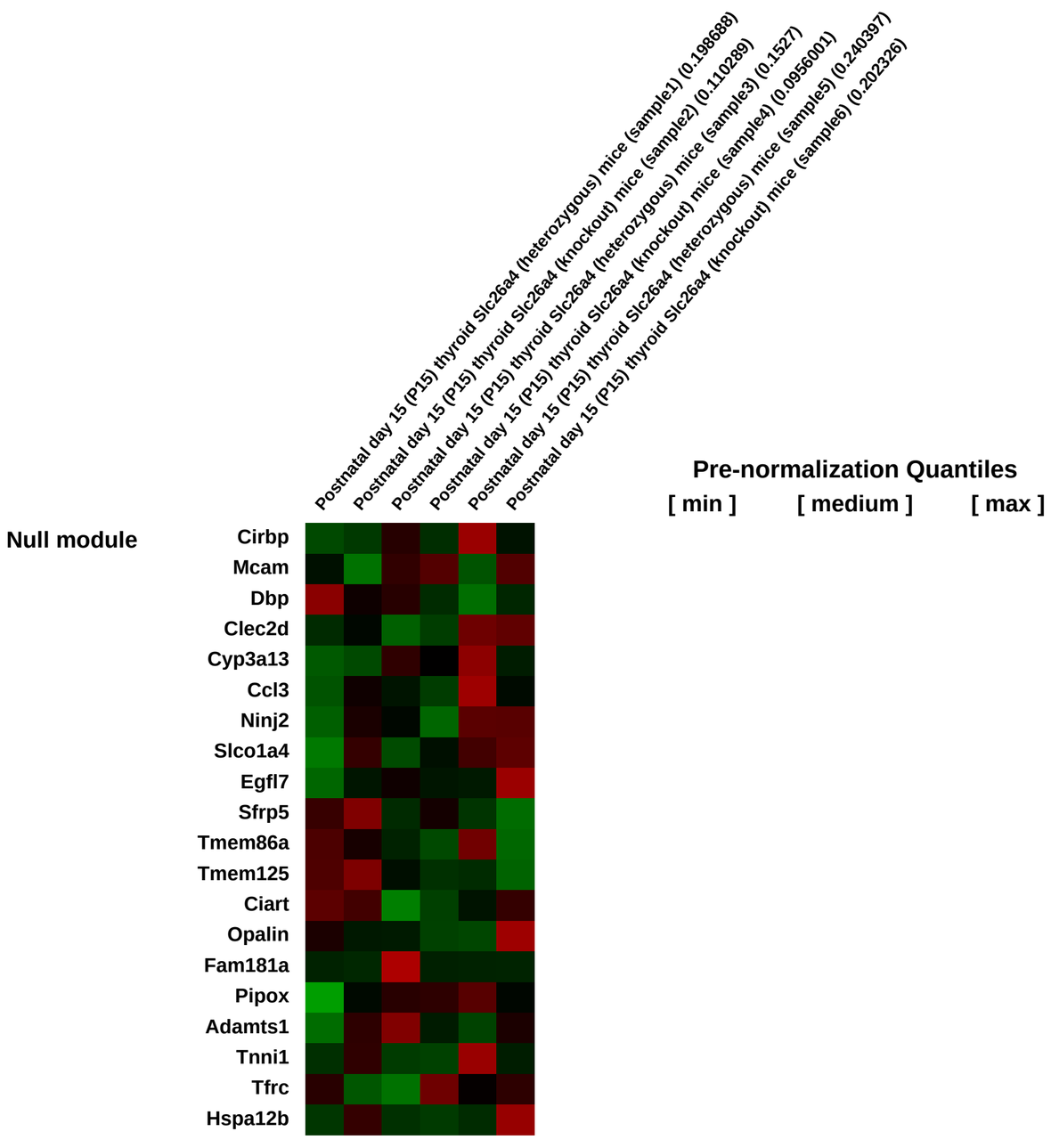

GEO Series "GSE10634" Expression Profiles

Num of samples in this series: 16

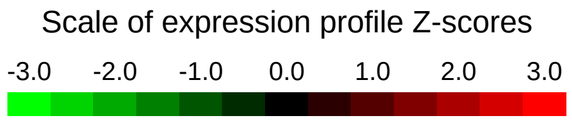

GEO Link:	http://www.ncbi.nlm.nih.gov/geo/query/acc.cgi?acc=GSE10634
Status:	Public on Oct 01 2008
Title:	Aquaporin-11 knockout effect on kidney
Organism:	Mus musculus
Experiment type:	Expression profiling by array
Platform:	GPL1261
Pubmed ID:	18606867
Summary & Design:	**Summary:** **Aquaporin-11 (AQP11), a new member of the aquaporin family, is localized in the endoplasmic reticulum (ER). Aqp11â /â mice neonatally suffer from polycystic kidneys derived from the proximal tubule. Its onset is proceeded by the vacuolization of ER. However, the mechanism for the formation of vacuoles and the development of cysts remain to be clarified. Here, we show that Aqp11â /â mice and polycystic kidney disease animals share a common pathogenic mechanism of cyst formation.** **Keywords: Geneexpression profile of Aqp11 knokout mouse kidney** **Overall design:** **Aqp11+/â mice, originally generated in a 129/SvEvBrd background (4), were back-crossed 10â 11 times to a C57/BL6 background. Heterozygous mice were interbred to obtain knockout (Aqp11â /â) and wild-type littermates (Aqp11+/+). The genotypes of offsprings were analyzed by PCR using tail DNA as a template. All animal experiments were approved by the Animal Care Committee of the University of Tokyo. One-week-old mice were sacrificed by cervical dislocation. Kidneys were rapidly excised on ice, washed in ice-cold phosphate-buffered saline, immersed in RNAlater (Ambion) and stored at â 20´℃. Total RNA was isolated using TRIzol Reagent (Invitrogen) and cleaned up using an RNeasy minikit with DNase treatment (Qiagen). The RNA quality and quantity were examined by agarose-gel electrophoresis and a spectrophotometer (GE Healthcare). Five pairs of Aqp11+/â mice were interbred, and we obtained 7 Aqp11+/+ and 9 Aqp11â /â offsprings. Three micrograms of total RNA obtained from each kidney was individually reverse-transcribed, amplified, and labeled using GeneChip One-Cycle Target Labeling and Control Reagent package (Affymetrix) according to the manufacturerâ s protocol. Labeled cRNA was hybridized to GeneChip Mouse Genome 430 2.0 Array (Affymetrix) (a total of 16 samples on 16 different arrays). The arrays were washed, stained using Fluidics Station (Affymetrix), and then scanned with the GeneChip Scanner (Affymetrix). Data collection was performed using GeneChip Operating Software (Affymetrix). The quality of collected data was checked by scatter plot analysis.**

Background corr dist: KL-Divergence = 0.1852, L1-Distance = 0.0379, L2-Distance = 0.0028, Normal std = 0.3436

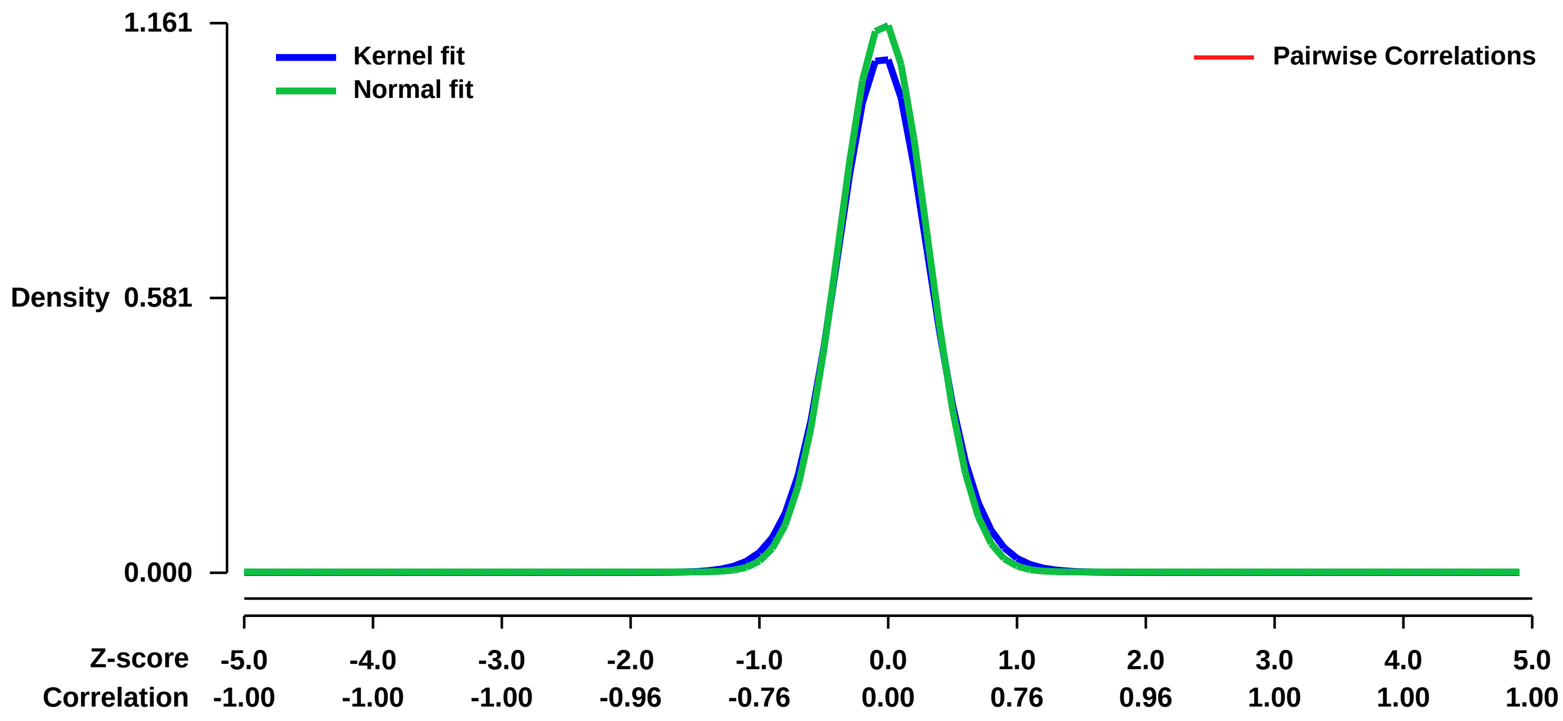

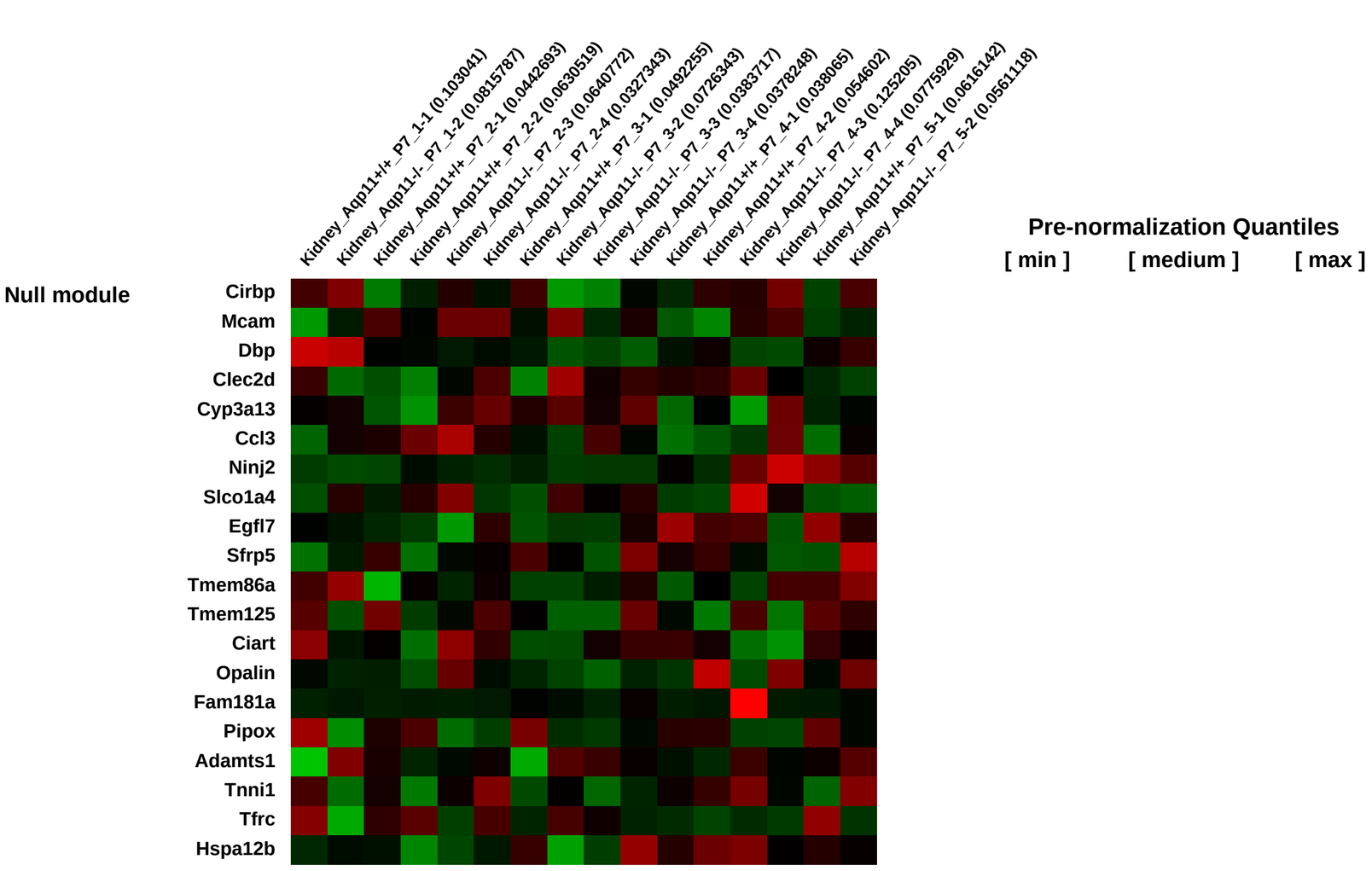

GEO Series "GSE10644" Expression Profiles

Num of samples in this series: 18

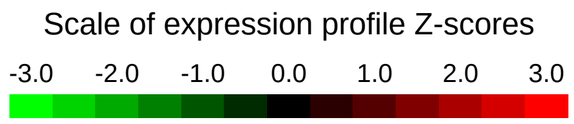

GEO Link:	**http://www.ncbi.nlm.nih.gov/geo/query/acc.cgi?acc=GSE10644**
Status:	**Public on Sep 15 2008**
Title:	**Characteristic Transcriptional Profiling of Rhythmic mRNA Expression in the Murine Distal Colon**
Organism:	**Mus musculus**
Experiment type:	**Expression profiling by array**
Platform:	**GPL1261**
Pubmed ID:	**18848557**
Summary & Design:	**Summary:** **To identify a cohort of rhythmically expressed genes in the murine Distal Colon,microarrays were used to measure gene expression over a 24-hour light/dark cycle.The rhythmic transcripts were classified according to expression patterns, functions and association with physiological and pathophysiological processes of the colon including motility, colorectal cancer formation and inflammatory bowel disease.** **Keywords: time series** **Overall design:** **Mice were maintained for 2 weeks on a 12 hour light/dark (LD) cycle (lights on 7 AM, lights off 7 PM) prior to all experiments. For the reference experiment, mice had ad libitum access to food. Samples were collected every four hours, at 0400, 0800, 1200, 1600, 2000 and 2400, starting 1 hour after the lights went on. Total RNA was isolated by modified guanidinium thicyanate-phenol-chloroform extraction method and was treated with DNase I (Promega, Madison, WI) at 37 oC for 30 minutes.Hybridizations and Scaning were done as per Affymetrix techniques. Three MOE 430 plus 2.0 chips were used per time point.**

Background corr dist: KL-Divergence = 0.1192, L1-Distance = 0.0315, L2-Distance = 0.0018, Normal std = 0.4077

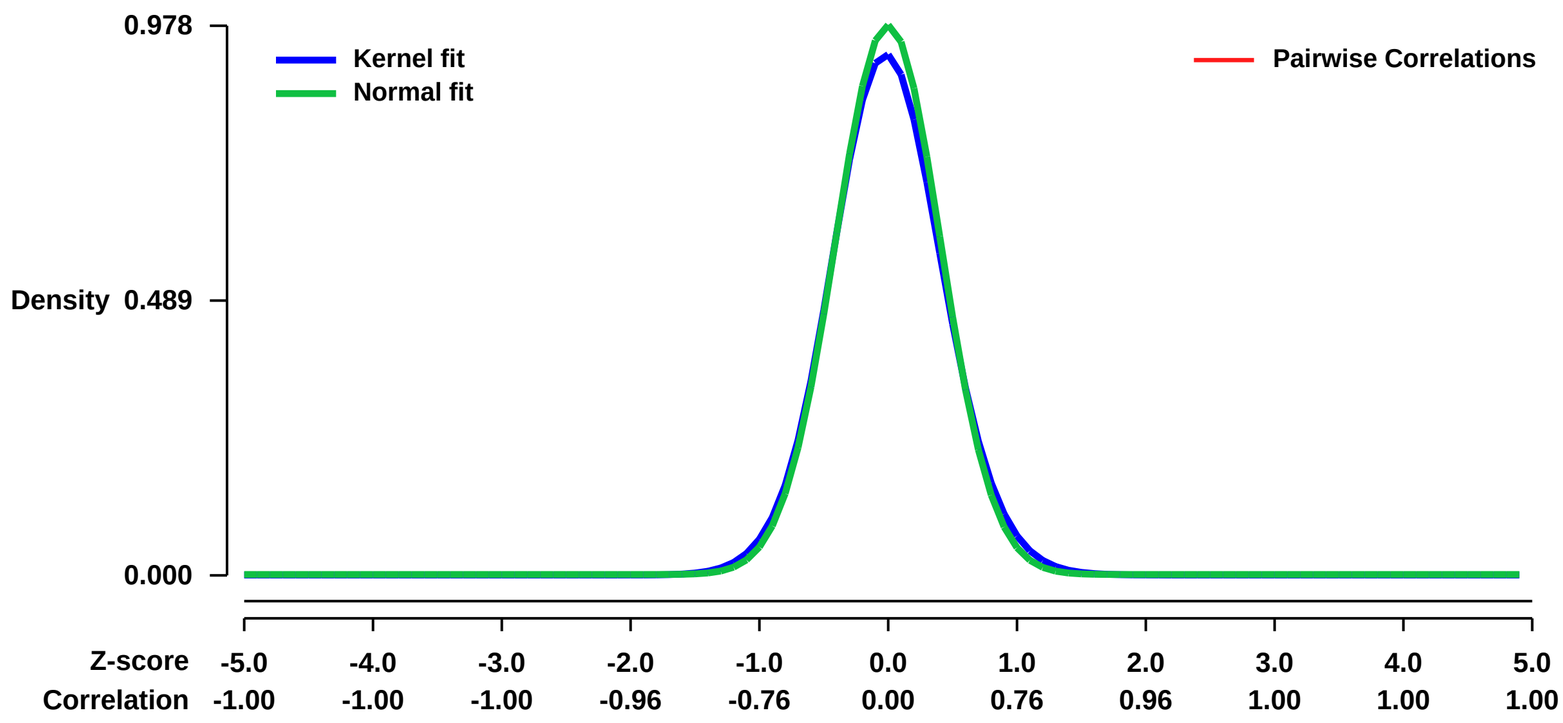

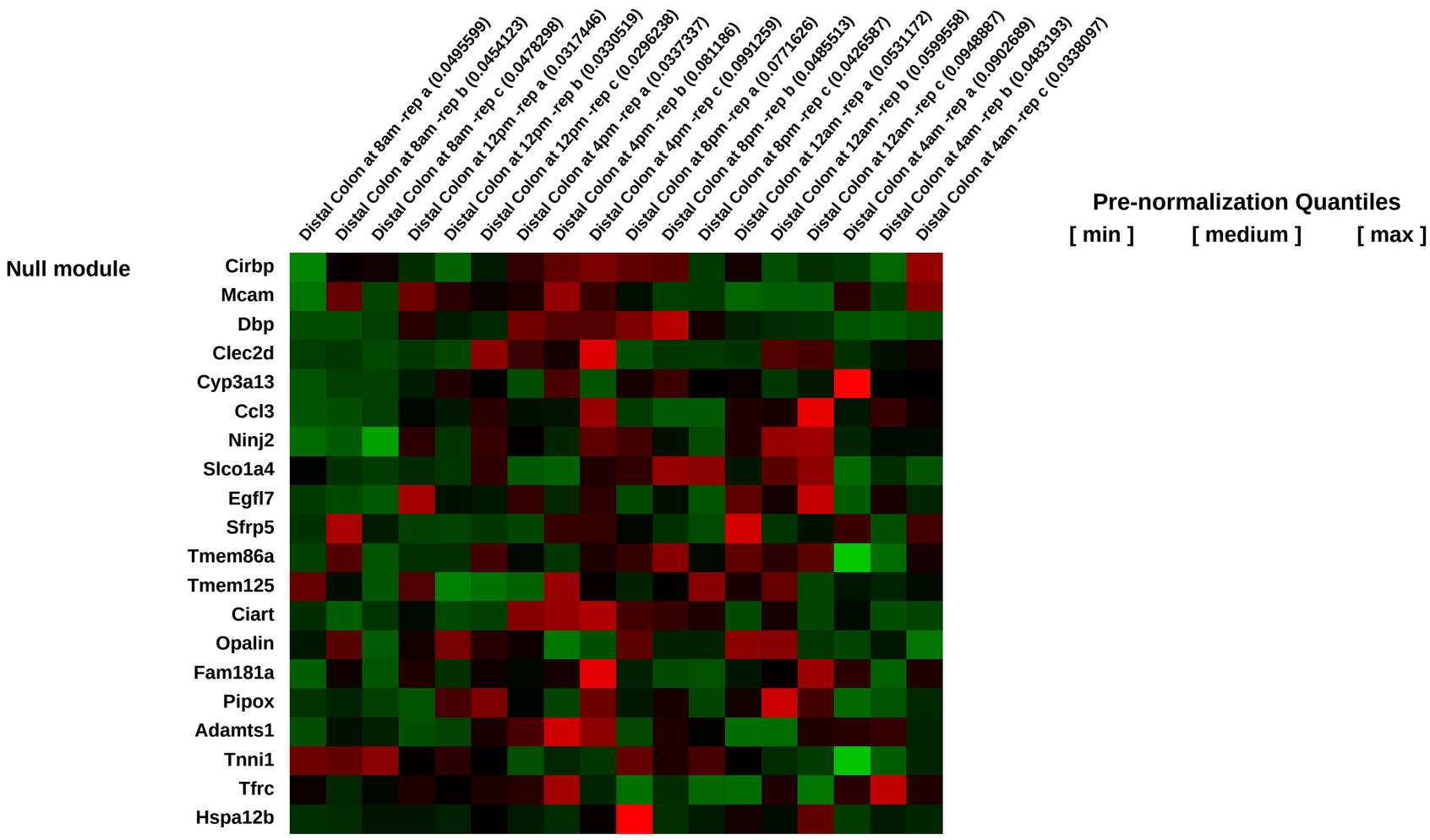

GEO Series "GSE1074" Expression Profiles

Num of samples in this series: 12

Scale of expression profile Z-scores

-3.0 -2.0 -1.0 0.0 1.0 2.0 3.0

GEO Link:	http://www.ncbi.nlm.nih.gov/geo/query/acc.cgi?acc=GSE1074
Status:	Public on Mar 11 2004
Title:	Strain-dependent effects of alcohol on early mouse embryos
Organism:	Mus musculus
Experiment type:	Expression profiling by array
Platform:	GPL1261
Pubmed ID:	17200951
Summary & Design:	**Summary:** **EXPERIMENT: Microarray expression profiles derived from the cranial neural folds (headfold) of neurulation-stage mouse embryos 3.0h after maternal alcohol exposure on 8 d.p.c.** **ANIMAL MODEL: Pregnancies from 2 substrains of C57BL/6 mice that differ in relative risk of Fetal Alcohol Syndrome (FAS): C57BL/6J (B6J) high-risk condition, and C57BL/6NCrl (B6N) low-risk condition.** **EXPOSURE: Dams dosed with ethanol (EtOH) by intraperitoneal injection at 2.9 g EtOH per kg body weight. Controls received vehicle (saline) alone. A third group of dams received EtOH + 4.0 mg/kg PK11195, a specific high-affinity ligand to the 18 KDa mitochondrial peripheral benzodiazepine receptor site.** **INTERVAL: High blood alcohol content must be sustained in dams for several hours to invoke FAS and is traditionally accomplished by a double injection of EtOH 4.0h apart. Since these embryos were harvested for genetic analysis 1h before dams would have gotten the second alcohol injection, the interval represents a snapshot of the critical response, prior to the second maternal injection that invokes greater risk. Counter-exposure to PK11195 significantly lowers the adverse response of B6J embryos to EtOH.** **PLATFORM: Two independent assays run. The first dataset (PE), run April 2002 â January 2003, used samples pooled from 2 litters (PE) and the platform was a two-channel MPS621 array (http://www.lifesciences.perkinelmer.com/). This platform has 4800 sequence-verified gene elements derived from over 50 different human cDNA libraries reflecting a variety of well-annotated cellular processes and disease pathways. The second dataset (AF), run between May 2005 â November 2005, used samples pooled from 1 litter and the platform was Affymetrix GeneChip´fi Mouse Genome 430A 2.0 Array (http://www.affymetrix.com/). The MG430A 2.0 platform has 45,102 oligonucleotide probe cells representing approximately 14,000 well-characterized genes in the draft mouse genome assembly. The corresponding GEO samples are GSM12218 - GSM12227 for the two-channel PE arrays, and GSM136067 - GSM136078 for the one-channel AF arrays.** **Keywords = fetal alcohol syndrome** **Keywords = alcohol-related birth defects** **Keywords = EtOH** **Keywords = PK11195** **Keywords = embryo** **Keywords = strain differences** **Keywords: Ordered** **Overall design:** **Assay of early mouse embryos during pathogenesis of Fetal Alcohol Syndrome (FAS). Replicate RNA samples were arrayed by one-channel oligonucleotide (Affymetrix) or two-channel cDNA (Perkin-Elmer) platforms.**

Background corr dist: **KL-Divergence = 0.0731, L1-Distance = 0.0209, L2-Distance = 0.0005, Normal std = 0.4915**

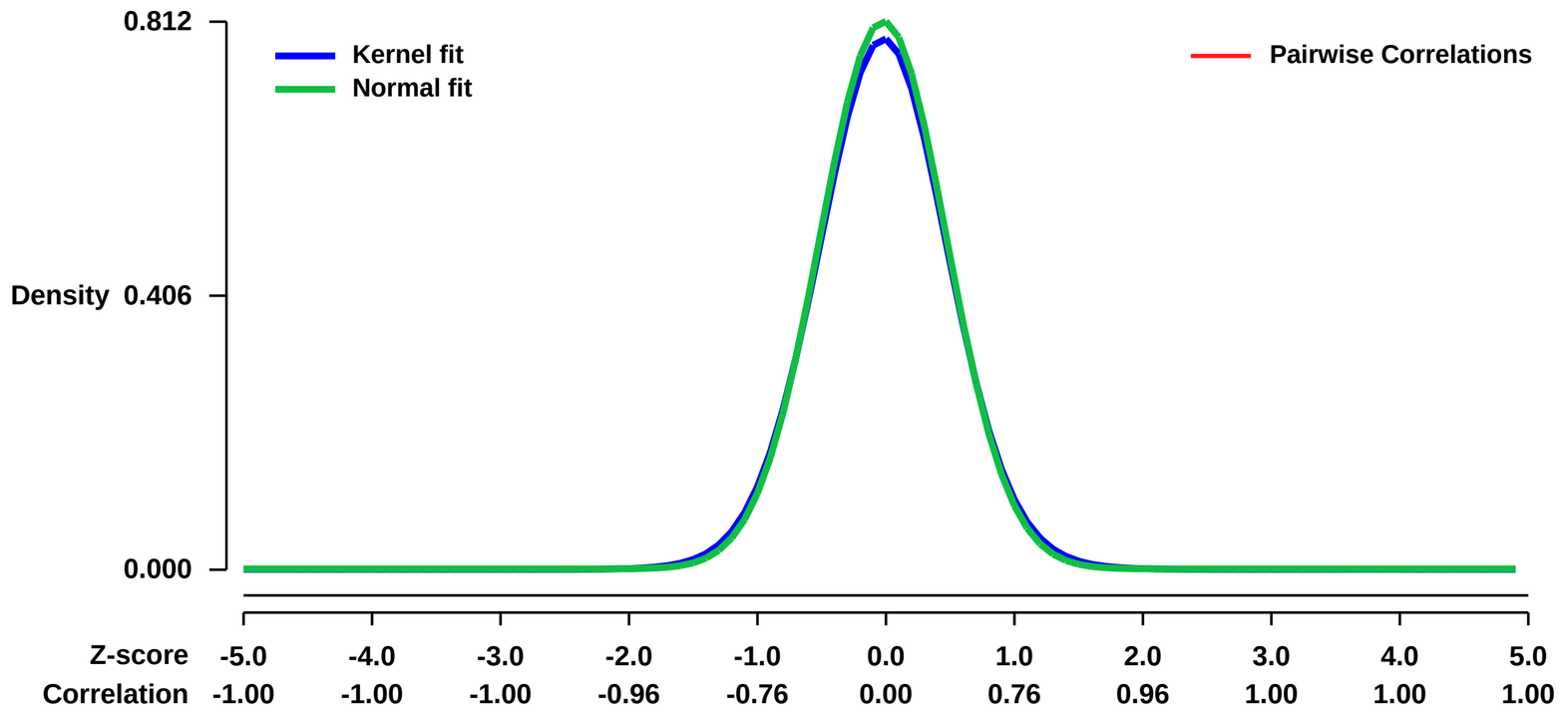

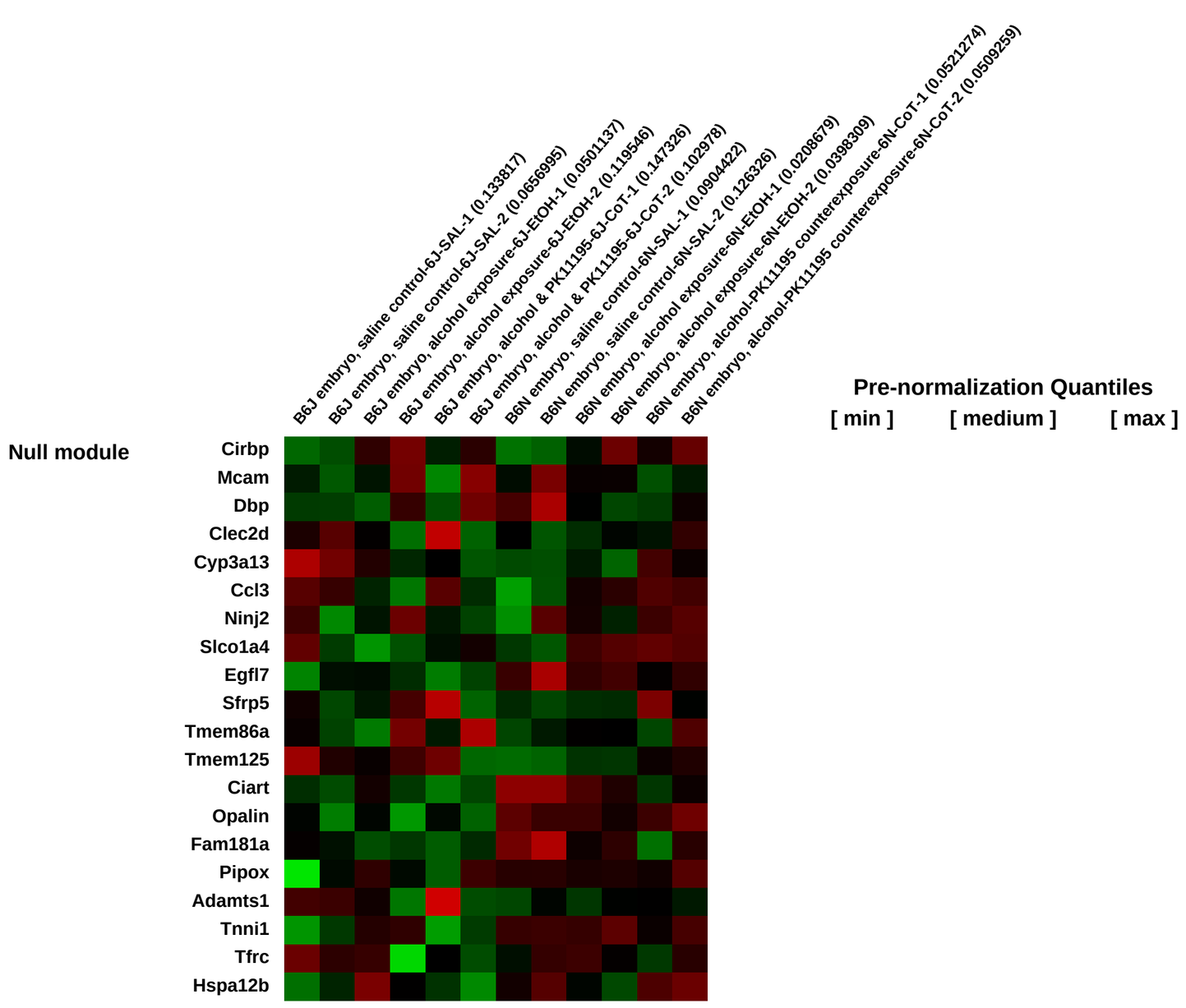

GEO Series "GSE10740" Expression Profiles

Num of samples in this series: 6

Scale of expression profile Z-scores

-3.0 -2.0 -1.0 0.0 1.0 2.0 3.0

GEO Link:	http://www.ncbi.nlm.nih.gov/geo/query/acc.cgi?acc=GSE10740
Status:	Public on Mar 06 2008
Title:	Expression data from the colon of wild-type and Slc9a3 (NHE3)-deficient mice
Organism:	Mus musculus
Experiment type:	Expression profiling by array
Platform:	GPL1261
Pubmed ID:	18467500
Summary & Design:	**Summary:** Na+/H+ exchanger 3 (NHE3) provides a major route for intestinal Na+ absorption. It has been considered as a target of proinflammatory cytokines and enteropathogenic bacteria and impaired NHE3 expression and/or activity may be responsible for inflammation-associated diarrhea. We used microarray analysis to detail the global programme of colonic gene expression in the absence of functional NHE3. Keywords: knockout effect **Overall design:** Whole colon was dissected from 6-8 week old NHE3-deficient mice and their wild-type littermates and total RNA isolated for microarray analysis using Affymetrix murine MOE430 2.0 arrays

Background corr dist: KL-Divergence = 0.0390, L1-Distance = 0.0210, L2-Distance = 0.0005, Normal std = 0.6231

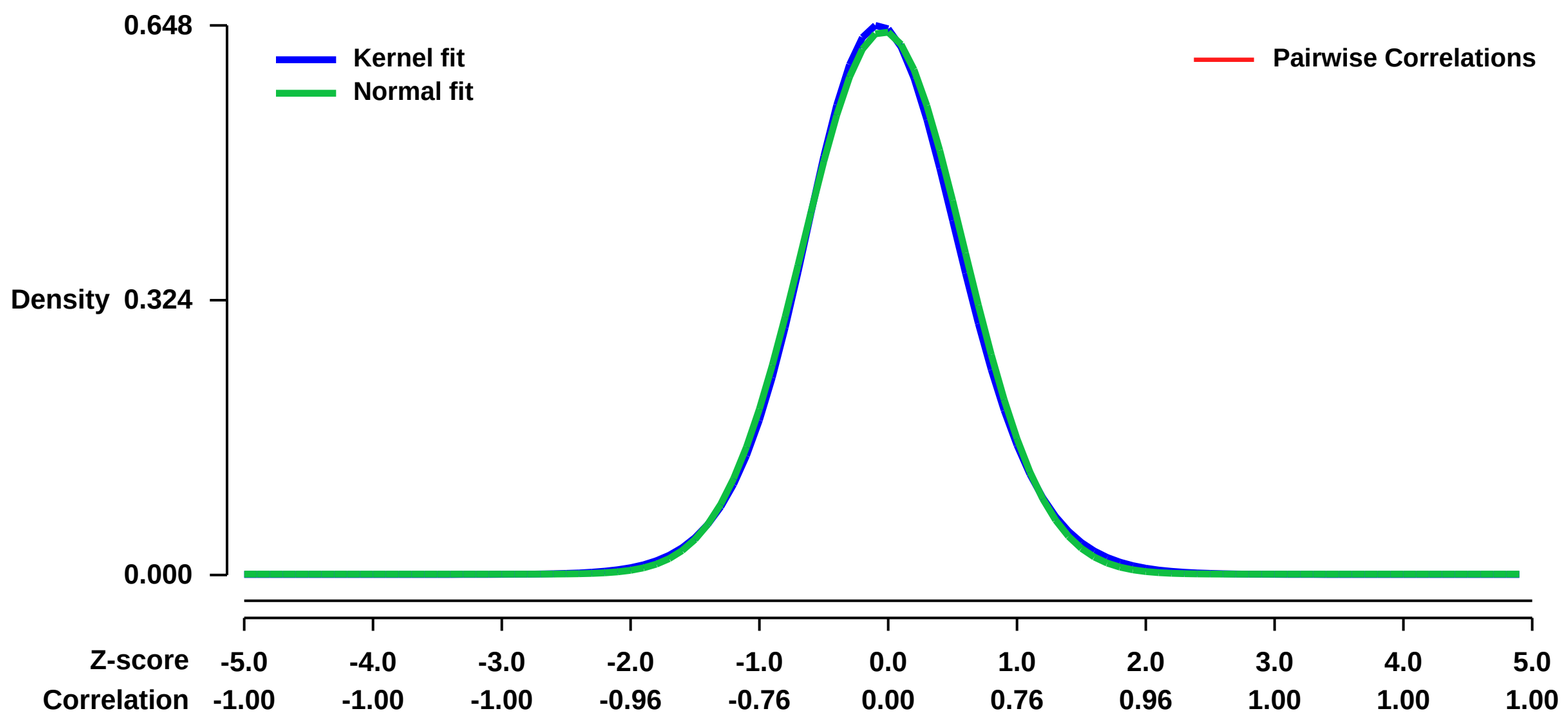

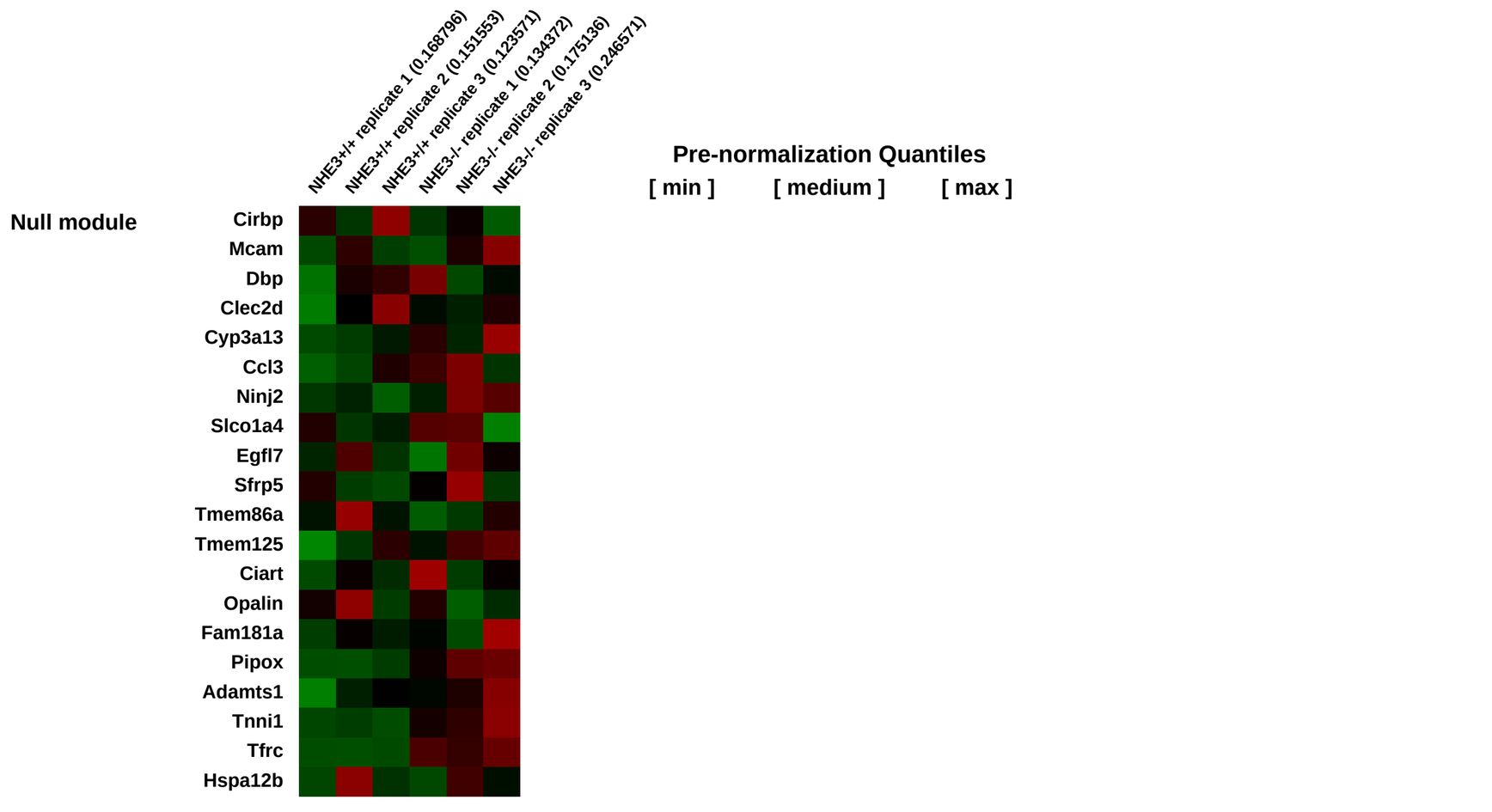

GEO Series "GSE10765" Expression Profiles

Num of samples in this series: 12

Scale of expression profile Z-scores

-3.0 -2.0 -1.0 0.0 1.0 2.0 3.0

GEO Link:	http://www.ncbi.nlm.nih.gov/geo/query/acc.cgi?acc=GSE10765
Status:	Public on Mar 08 2008
Title:	Expression data from MALP-2-stimulated macrophages from wild-type, IRAK-2-/- and IRAK-1-/IRAK-2-/- mice
Organism:	Mus musculus
Experiment type:	Expression profiling by array
Platform:	GPL1261
Pubmed ID:	18438411
Summary & Design:	**Summary:** **IL-1R-associated kinases (IRAKs) participate in Toll-like receptor (TLR) signal transduction. MALP-2 is a TLR2 ligand, and stimulation of macrophages with MALP-2 activates expression of various genes including proinflammatory cytokines.** **We used microarrays to examine influence of IRAK-2 or IRAK-1/IRAK-2 deficiency in MALP-2-inducible gene expression.** **Keywords: Time course after MALP-2 stimulation** **Overall design:** **Peritoneal macrophages from wild-type, IRAK-2-/- and IRAK-1/IRAK-2 mice were stimulated with MALP-2 for 0, 2, 4, and 8 hours, followed by RNA extraction. Then hybridization on affymetrix microarrays was performed.**

Background corr dist: **KL-Divergence = 0.0314, L1-Distance = 0.0844, L2-Distance = 0.0107, Normal std = 0.7991**

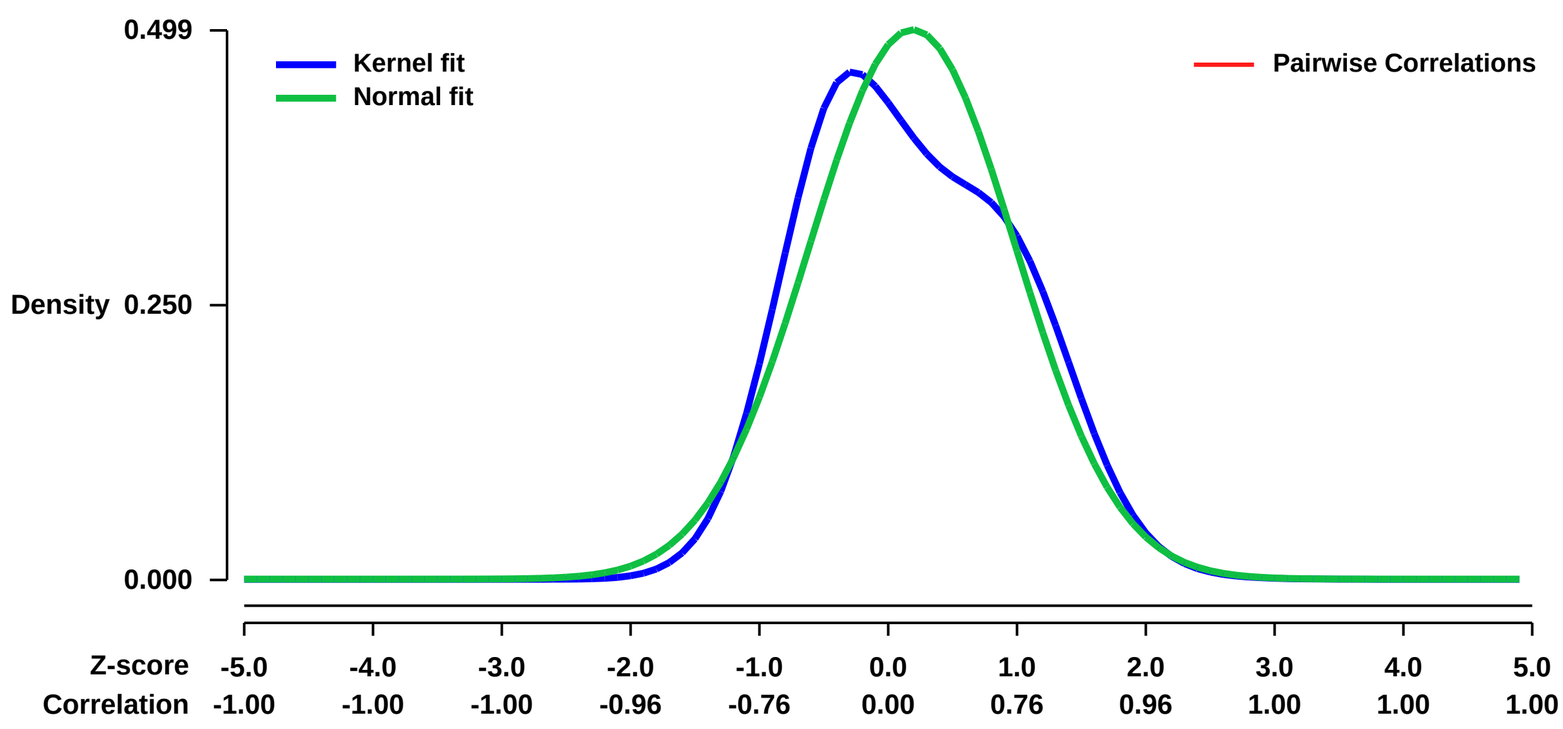

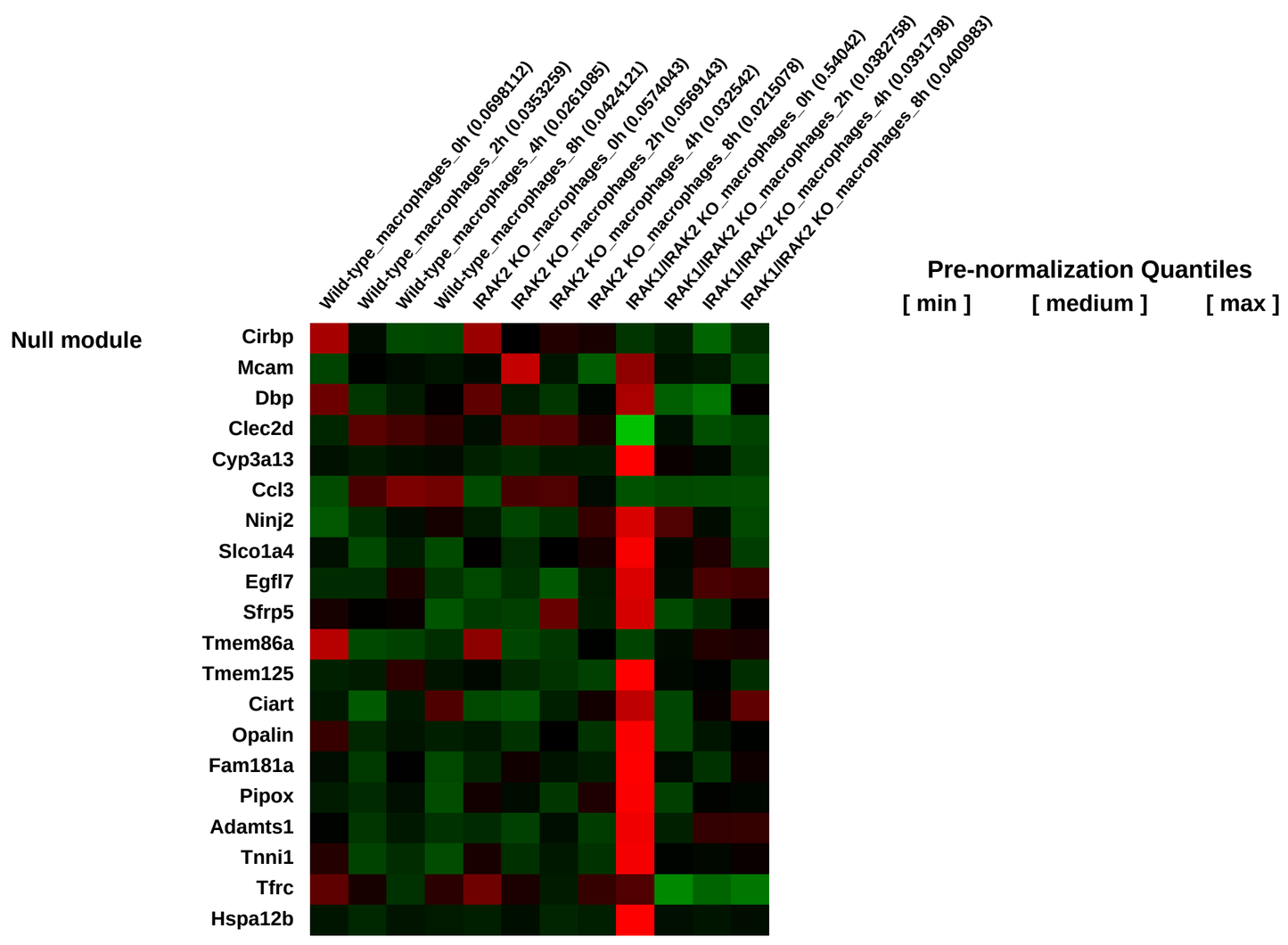

GEO Series "GSE10849" Expression Profiles

Num of samples in this series: 6

Scale of expression profile Z-scores

-3.0 -2.0 -1.0 0.0 1.0 2.0 3.0

GEO Link:	**http://www.ncbi.nlm.nih.gov/geo/query/acc.cgi?acc=GSE10849**
Status:	**Public on Mar 04 2009**
Title:	**Caveolin-1 Knockout Hearts**
Organism:	**Mus musculus**
Experiment type:	**Expression profiling by array**
Platform:	**GPL1261**
Pubmed ID:	**18719368**
Summary & Design:	**Summary:** **Hearts Lacking Caveolin-1 Develop Hypertrophy with Normal Cardiac Substrate Metabolism** **Keywords: gene knockout** **Overall design:** **3 wild types, 3 knockouts**

Background corr dist: **KL-Divergence = 0.0216, L1-Distance = 0.0174, L2-Distance = 0.0003, Normal std = 0.7235**

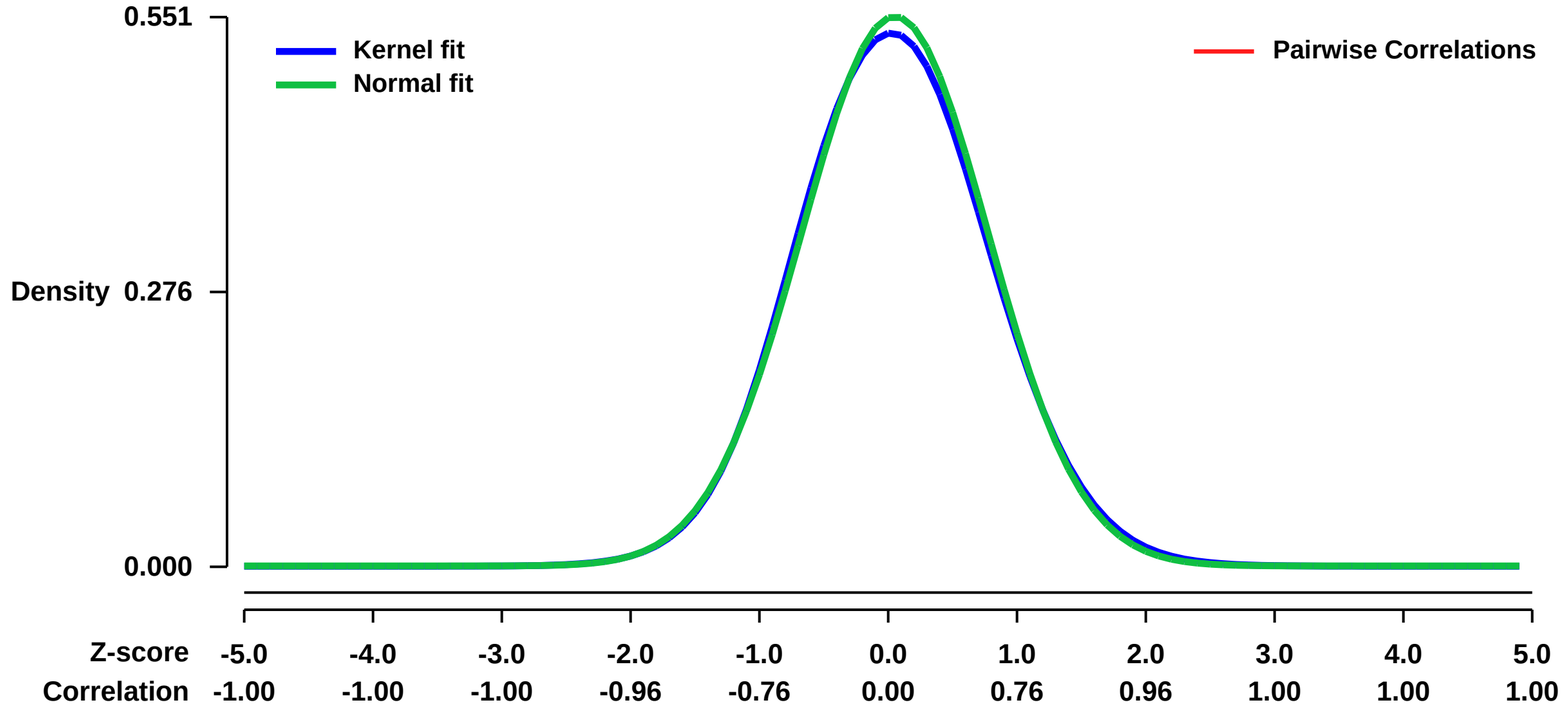

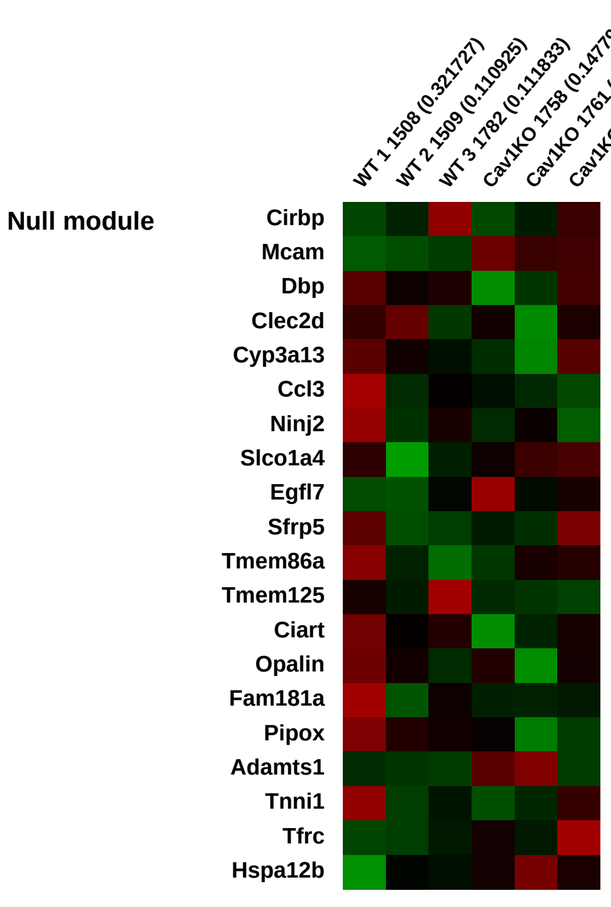

GEO Series "GSE10895" Expression Profiles

Num of samples in this series: 8

Scale of expression profile Z-scores

-3.0 -2.0 -1.0 0.0 1.0 2.0 3.0

GEO Link:	**http://www.ncbi.nlm.nih.gov/geo/query/acc.cgi?acc=GSE10895**
Status:	**Public on Nov 06 2008**
Title:	**Expression study of liver smaples of 2-days old Mfp2 knockout mice as compared to wild type**
Organism:	**Mus musculus**
Experiment type:	**Expression profiling by array**
Platform:	**GPL1261**
Pubmed ID:	**18773970**
Summary & Design:	**Summary:** **Study on gene expression in multifunctional protein 2 deficient mice. Liver samples of two days old mice in normal conditions are used. In total 8 arrays were hybridized corresponding to 4 KO mice and 4 WT mice Results: Cholesterol synthesis is induced and ppar alpha targets also differentially expressed between KO and WT.** **Keywords: Knockout gene expression study; genetic modification** **Overall design:** **Liver samples, 4 KO mice and 4 WT mice**

Background corr dist: **KL-Divergence = 0.0772, L1-Distance = 0.0214, L2-Distance = 0.0006, Normal std = 0.4812**

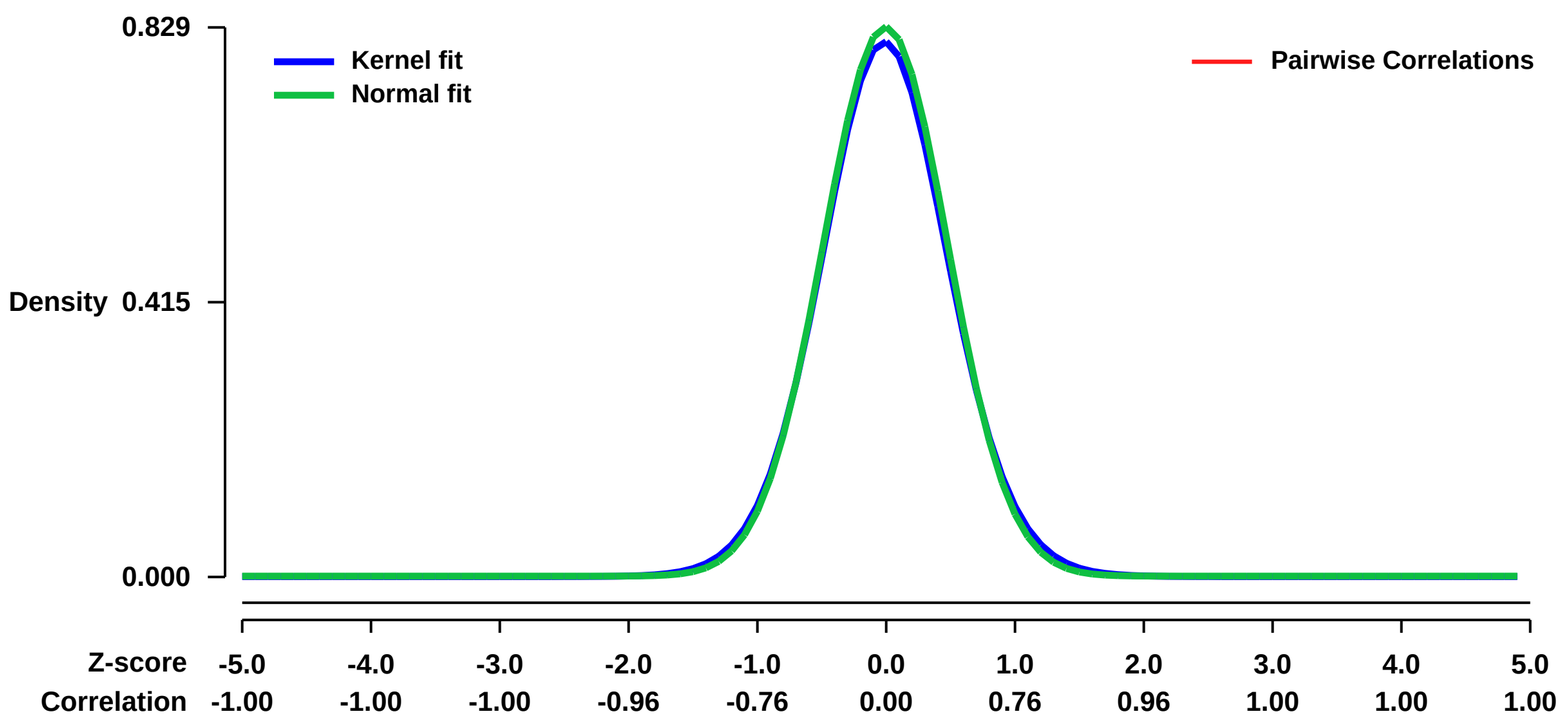

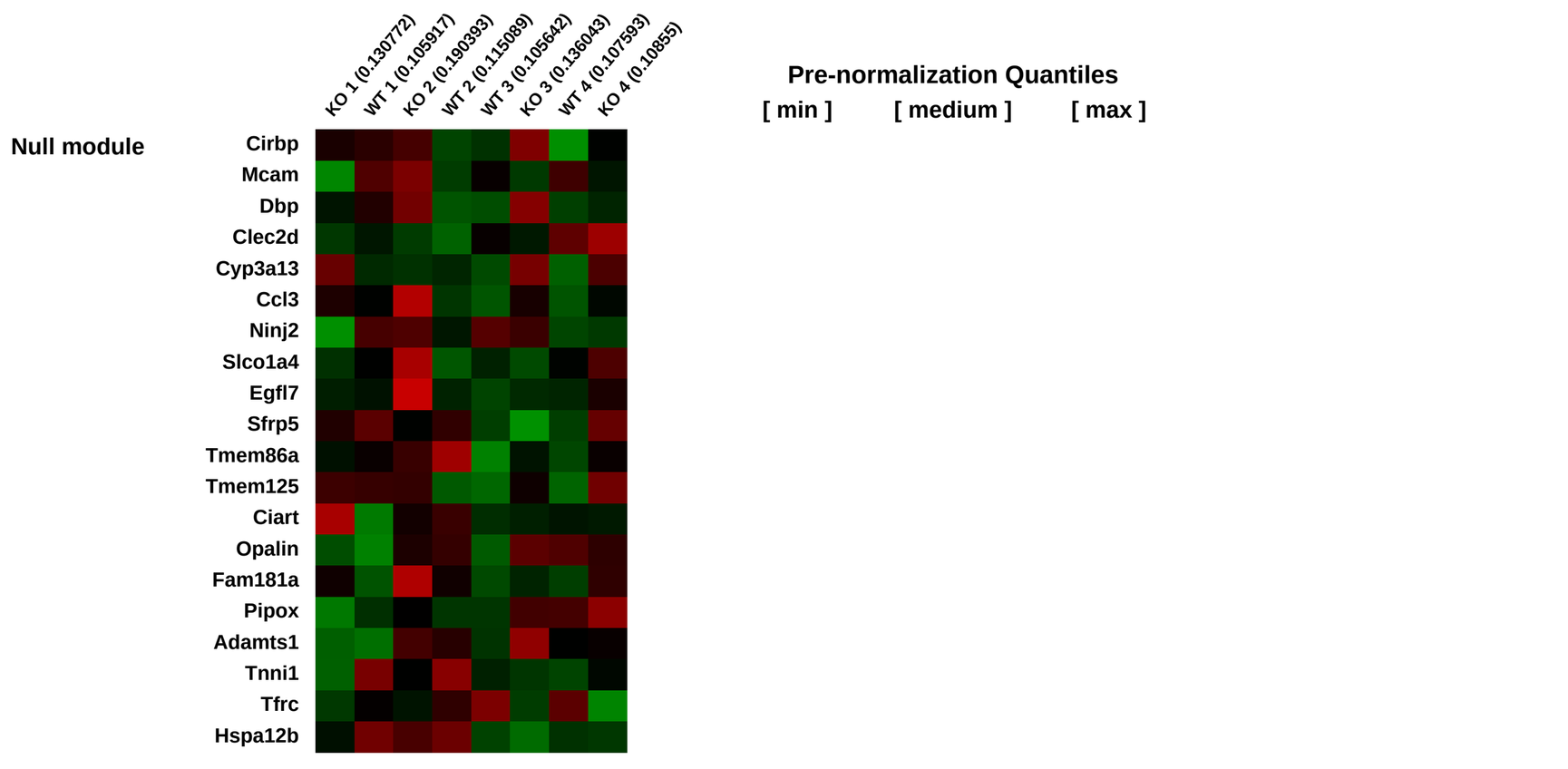

GEO Series "GSE10902" Expression Profiles

Num of samples in this series: 6

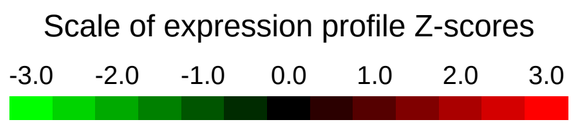

GEO Link:	http://www.ncbi.nlm.nih.gov/geo/query/acc.cgi?acc=GSE10902
Status:	Public on Jun 06 2008
Title:	Differential expression between FHL2-/- and WT MEFs.
Organism:	Mus musculus
Experiment type:	Expression profiling by array
Platform:	GPL1261
Pubmed ID:	19018287
Summary & Design:	**Summary:** The LIM-only protein FHL2 acts as a transcriptional modulator that positively or negatively regulates multiple signaling pathways. We recently reported that FHL2 cooperates with CBP/p300 in the activation of ^-catenin/TCF target gene cyclin D1. In this paper, we demonstrate that FHL2 is associated with the cyclin D1 promoter at the TCF/CRE site, providing evidence that cyclin D1 is a direct target of FHL2. We show that deficiency of FHL2 greatly reduces the proliferative capacity of spontaneously immortalized mouse fibroblasts which is associated with decreased expression of cyclin D1 and p16INK4a, and hypophosphorylation of Rb. Reexpression of FHL2 in FHL2-null fibroblasts efficiently restores cyclin D1 levels and cell proliferative capacity, indicating that FHL2 is critical for cyclin D1 activation and cell growth. Moreover, ectopic cyclin D1 expression is sufficient to override growth inhibition of immortalized FHL2-null fibroblasts. Gene expression profiling revealed that FHL2 deficiency triggers a broad change of the cell cycle program that is associated with downregulation of several G1/S and G2/M cyclins, E2F transcription factors and DNA replication machinery, thus correlating with reduced cell proliferation. This change also involves downregulation of the negative cell cycle regulators, particularly INK4 inhibitors, which could counteract the decreased expression of cyclins, allowing cells to grow. Our study illustrates that FHL2 can act on different aspects of the cell cycle program to finely regulate cell proliferation. **Keywords:** mouse embryonic fibroblasts derived from FHL2-/- and WT mouse embryos (14.5 days) **Overall design:** Two biological genotypes, FHL2-/- and WT MEF cells. Three spontaneously immortalized clones of each genotype were analyzed using Affymetrix arrays.

Background corr dist: KL-Divergence = 0.0204, L1-Distance = 0.0119, L2-Distance = 0.0002, Normal std = 0.7307

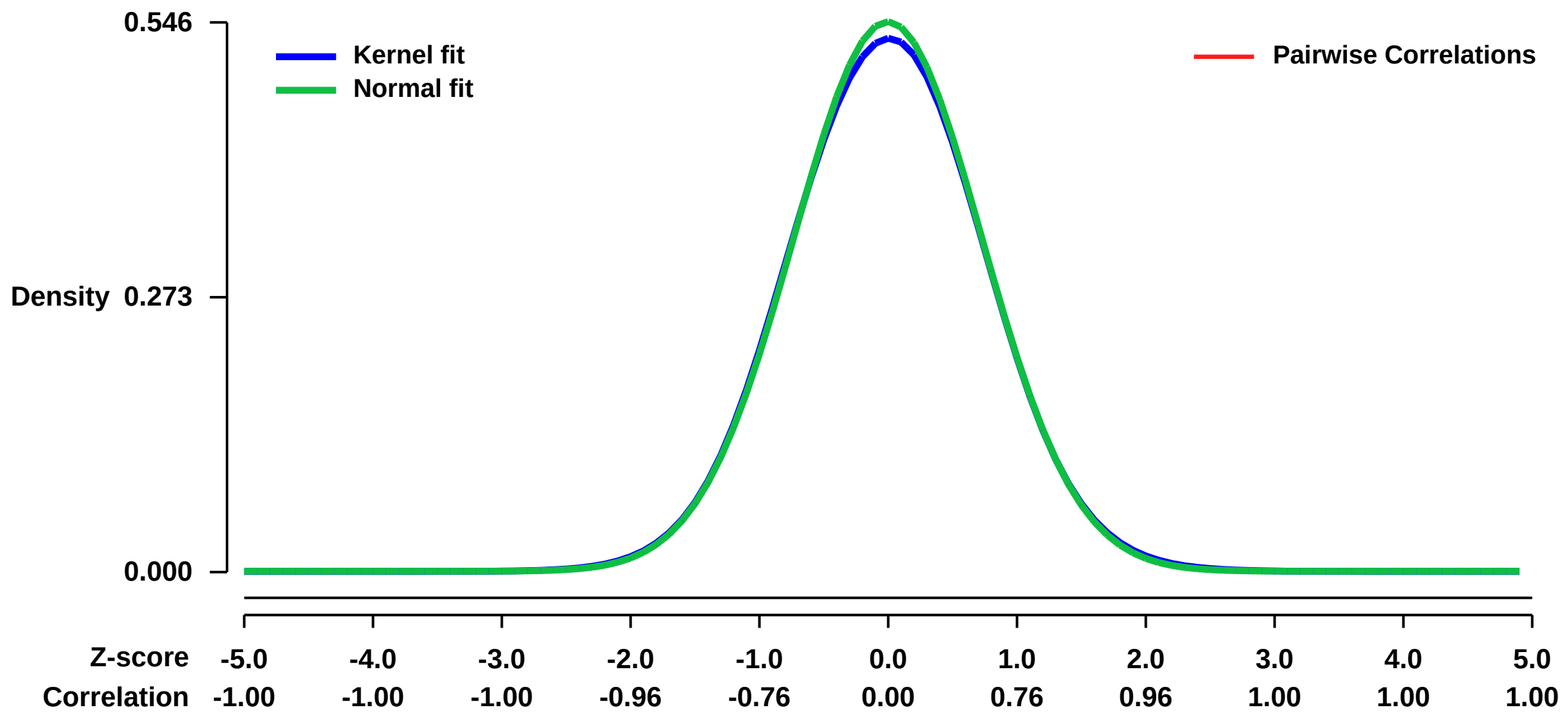

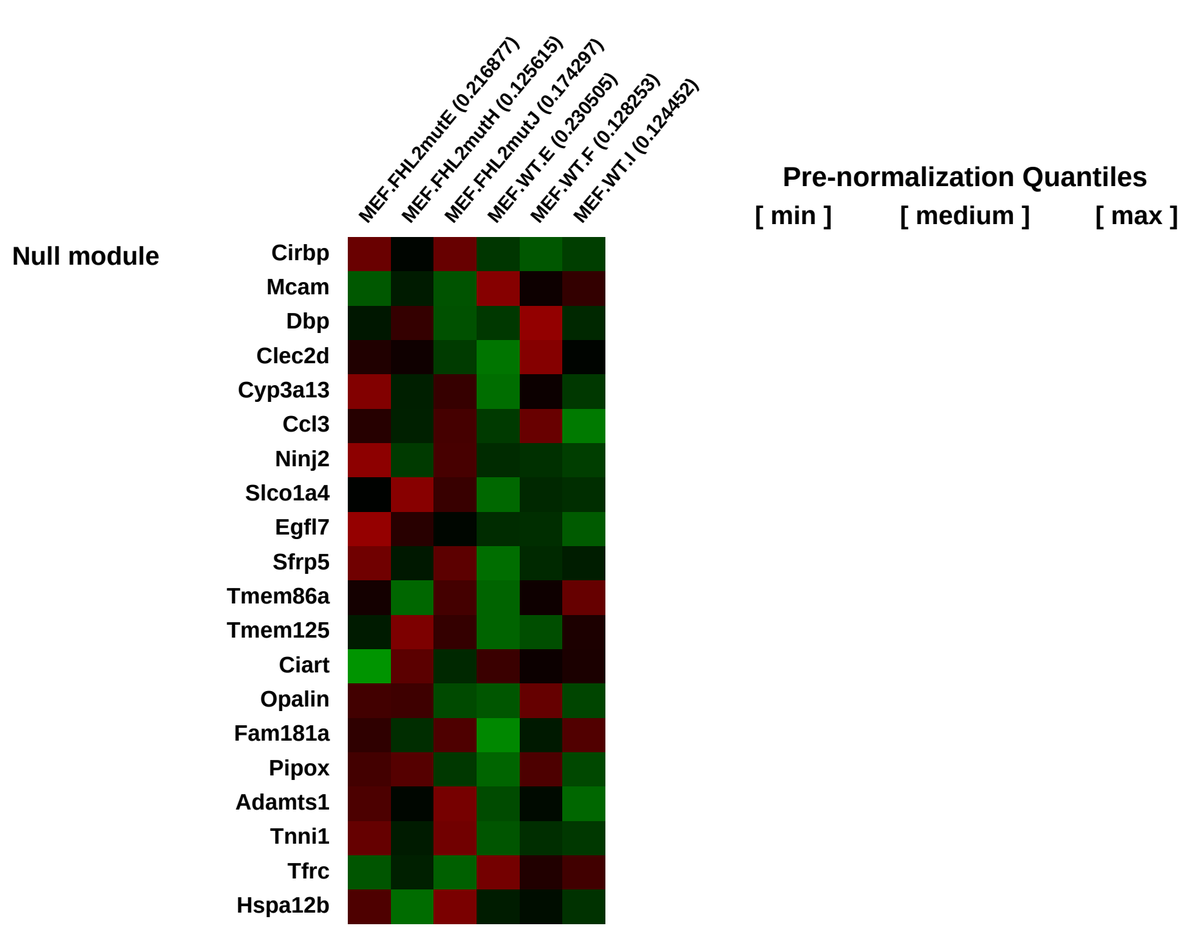

GEO Series "GSE10904" Expression Profiles

Num of samples in this series: 6

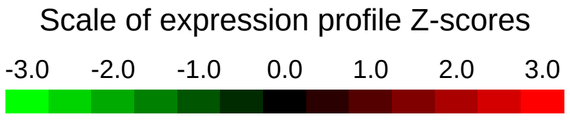

GEO Link:	http://www.ncbi.nlm.nih.gov/geo/query/acc.cgi?acc=GSE10904
Status:	Public on Apr 30 2008
Title:	Expression data from wildtype and alb/cre liver-conditional Pdss2 knockout mutant mice
Organism:	Mus musculus
Experiment type:	Expression profiling by array
Platform:	GPL1261
Pubmed ID:	18437205
Summary & Design:	**Summary:** Utilizing M. musculus as a model of mitochondrial dysfunction provides insight into cellular adaptations which occur as a consequence of genetic alterations causative of human disease. We characterized genome-wide expression profiles of liver-conditional knockout mice for Pdss2 compared with loxP controls. Our goal was to detect concordant changes among clusters of genes that comprise defined metabolic pathways utilizing gene set enrichment analysis. Keywords: Wildtype vs mutant comparison as a method for studying contributors to disease processes. **Overall design:** Liver from three biological replicates each of wildtype and coenzyme Q biosynthetic mutant M. musculus were used as sources of total RNA for hybridization to Affymetrix whole-genome microarrays. Comparison of the data was intended to reveal metabolic pathway alterations downstream of the mutation.

Background corr dist: KL-Divergence = 0.0183, L1-Distance = 0.0199, L2-Distance = 0.0005, Normal std = 0.7615

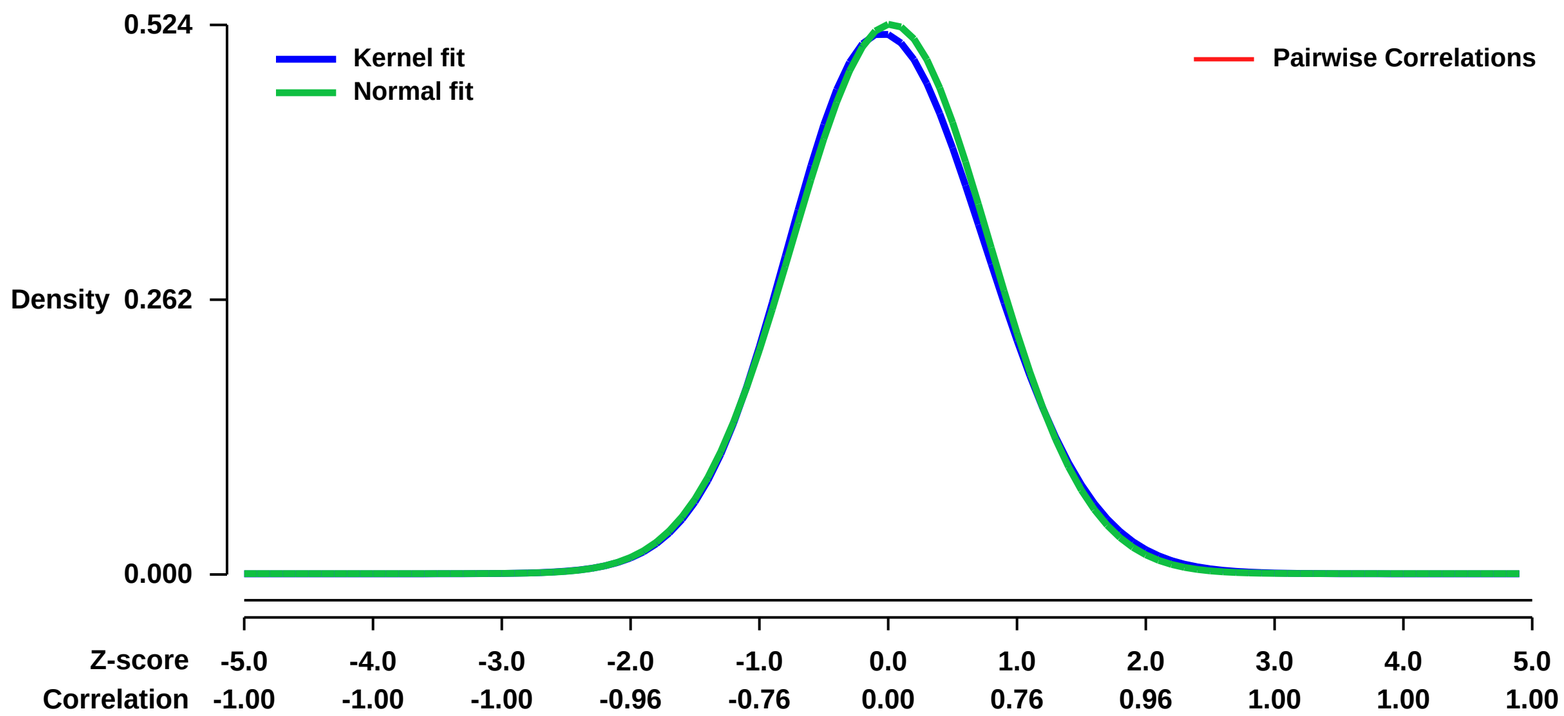

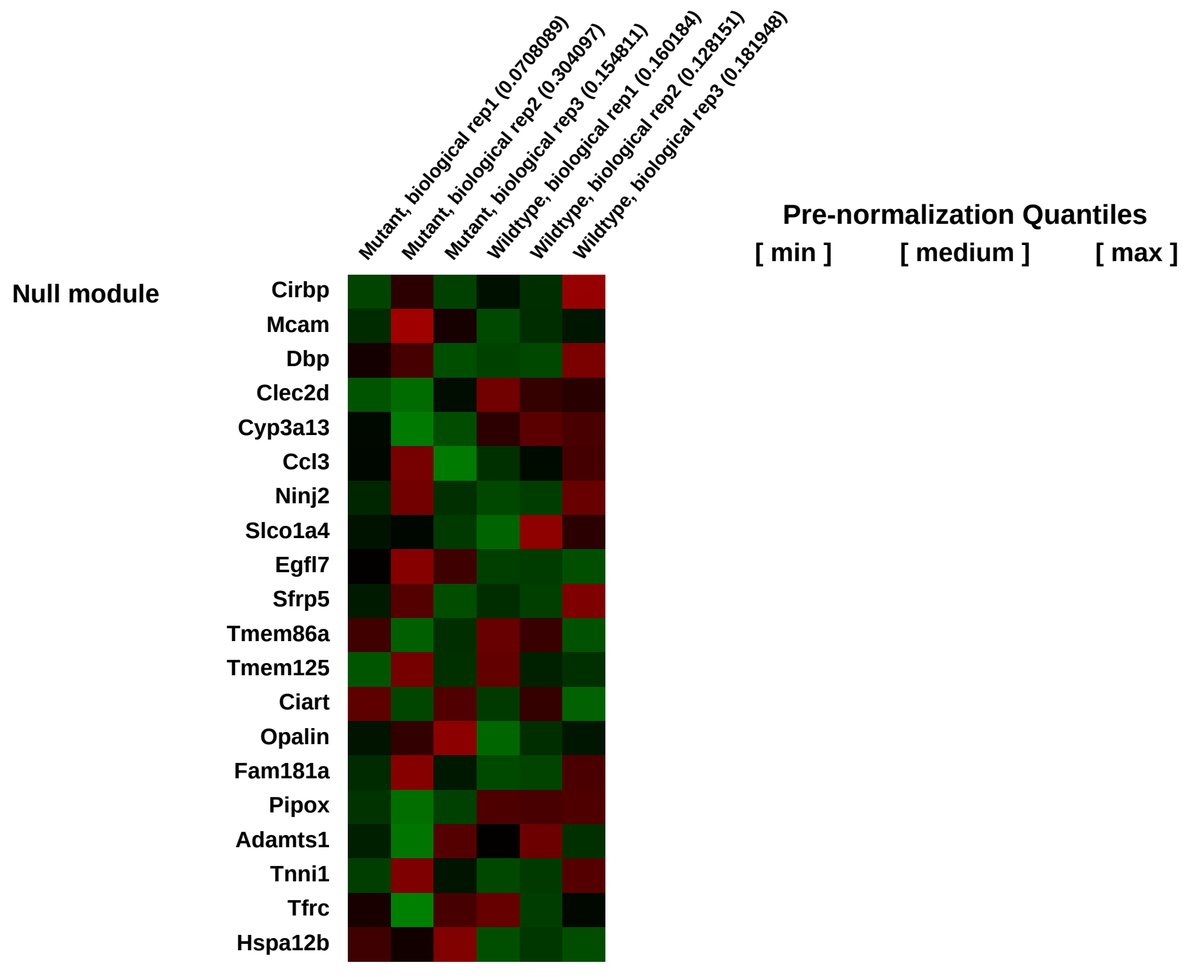

GEO Series "GSE10913" Expression Profiles

Num of samples in this series: 6

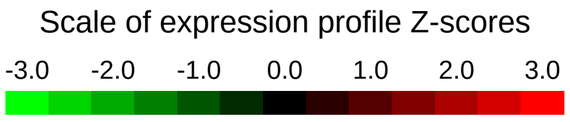

GEO Link:	http://www.ncbi.nlm.nih.gov/geo/query/acc.cgi?acc=GSE10913
Status:	Public on Mar 21 2008
Title:	Bmp2 Is Critical for the Murine Decidual Response
Organism:	Mus musculus
Experiment type:	Expression profiling by array
Platform:	GPL1261
Pubmed ID:	17515606
Summary & Design:	**Summary:** The role of bone morphogenetic protein 2 (Bmp2)in regulating the transformation of the uterine stroma during embryo implantation in the mouse was investigated by the conditional ablation of Bmp2 in the uterus using the (PR-cre) mouse. **Keywords: Genetic modification** **Overall design:** Bmp2 gene ablation was confirmed by real-time PCR analysis in the PR-cre; Bmp2fl/fl (termed Bmp2d/d) uterus. While littermate controls average 0.9 litter of 6.2 ´– 0.7 pups per month, Bmp2d/d females are completely infertile. Analysis of the infertility indicates that whereas embryo attachment is normal in the Bmp2d/d as in control mice, the uterine stroma is incapable of undergoing the decidual reaction to support further embryonic development. Recombinant human BMP2 can partially rescue the decidual response, suggesting that the observed phenotypes are not due to a developmental consequence of Bmp2 ablation. Microarray analysis demonstrates that ablation of Bmp2 leads to specific gene changes, including disruption of the Wnt signaling pathway, Progesterone receptor (PR) signaling, and the induction of prostaglandin synthase 2 (Ptgs2). Taken together, these data demonstrate that Bmp2 is a critical regulator of gene expression and function in the murine uterus.

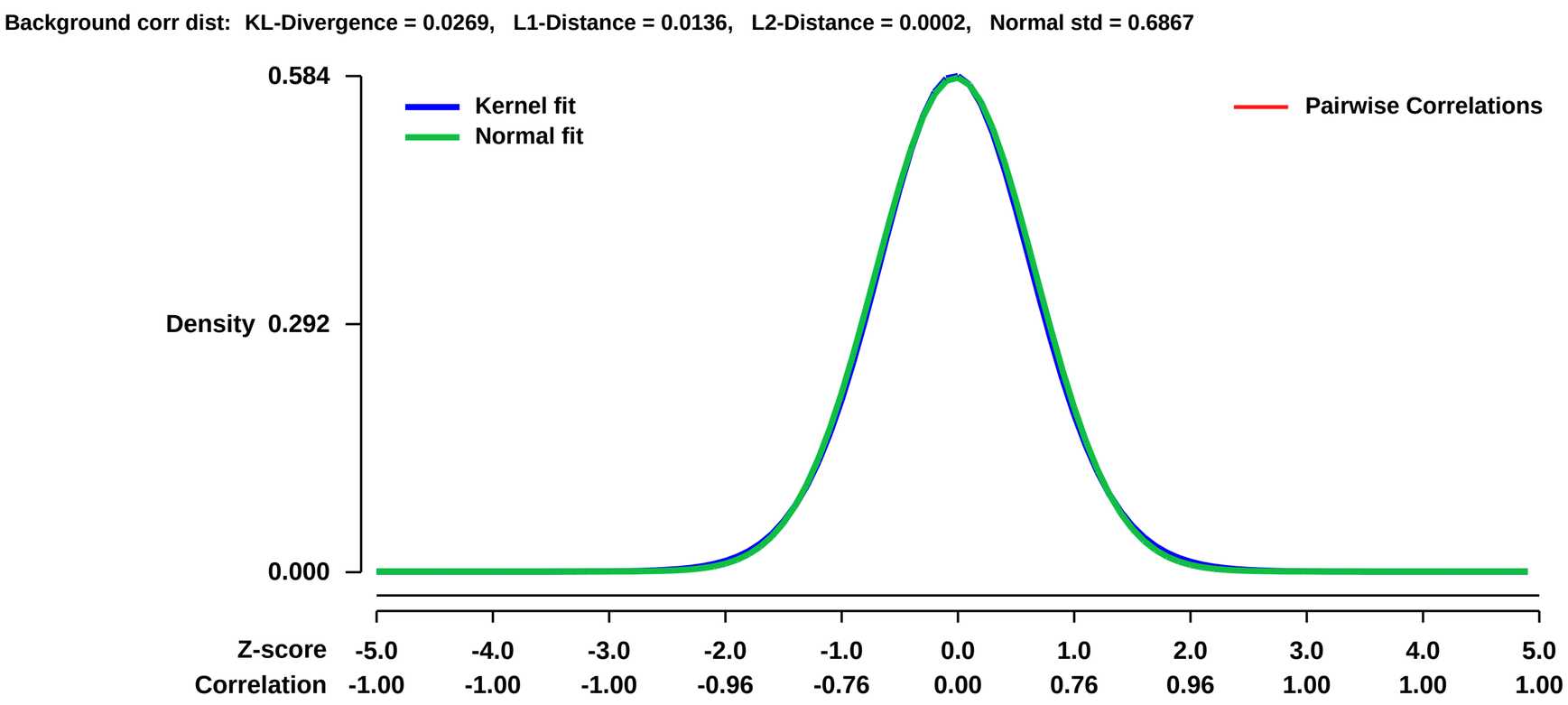

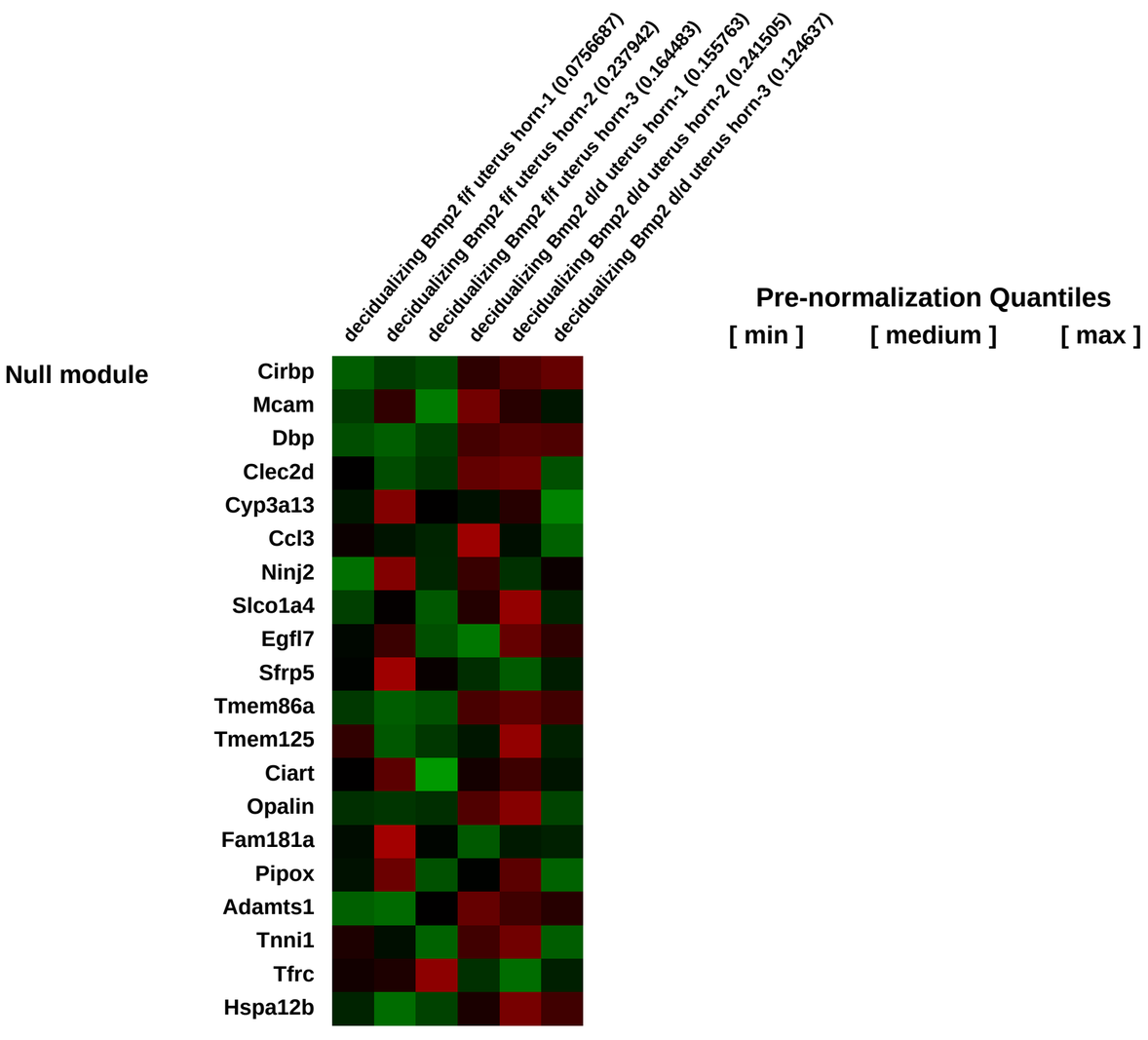

GEO Series "GSE10954" Expression Profiles

Num of samples in this series: 8

Scale of expression profile Z-scores

-3.0 -2.0 -1.0 0.0 1.0 2.0 3.0

GEO Link:	http://www.ncbi.nlm.nih.gov/geo/query/acc.cgi?acc=GSE10954
Status:	Public on May 31 2008
Title:	Transcription Profiling of Lung Adenocarcinomas of c-Myc-Transgenic Mice
Organism:	Mus musculus
Experiment type:	Expression profiling by array
Platform:	GPL1261
Pubmed ID:	18498649
Summary & Design:	**Summary:** The transcriptional regulator c-Myc is the most frequently deregulated oncogene in human tumors. Targeted overexpression of this gene in mice results in distinct types of lung adenocarcinomas. By using microarray technology, alterations in the expression of genes were captured based on a female transgenic mouse model in which, indeed, c-Myc overexpression in alveolar epithelium results in the development of bronchiolo-alveolar carcinoma (BAC) and papillary adenocarcinoma (PLAC). In this study, we analyzed exclusively the promoters of induced genes by different in silico methods in order to elucidate the c-Myc transcriptional regulatory network. Keywords: c-myc transgenic versus non-transgenic **Overall design:** For gene expression analysis, RNA was isolated from lung tissue of either 16 c-Myc-transgenic or 16 non-transgenic control female mice. Identical amounts of RNA from 4 individuals of one group were pooled, such that 4 pools of 4 mice per group could be analyzed. Each pool was analysed in one microarray experiment.

Background corr dist: KL-Divergence = 0.0694, L1-Distance = 0.0187, L2-Distance = 0.0004, Normal std = 0.5027

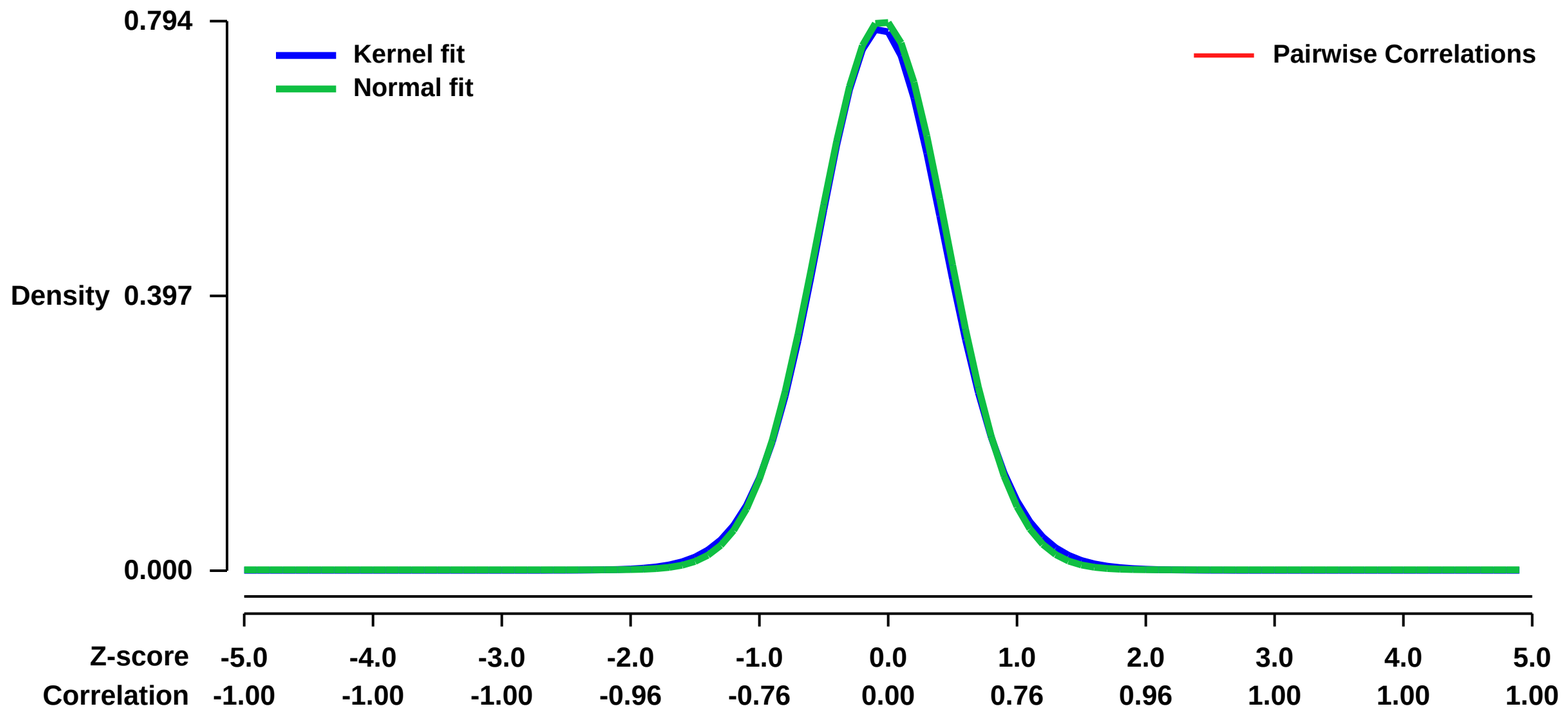

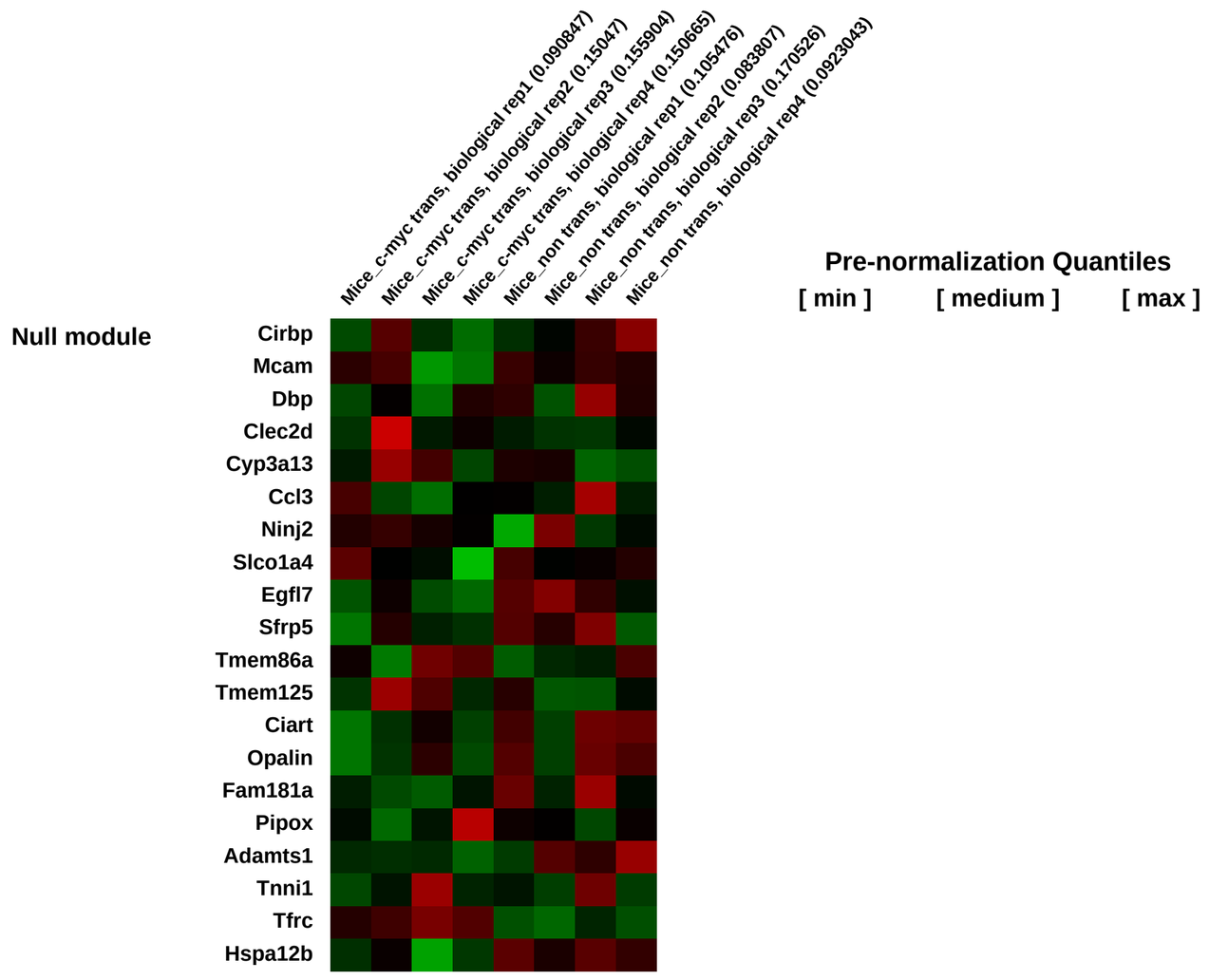

GEO Series "GSE10965" Expression Profiles

Num of samples in this series: 8

Scale of expression profile Z-scores

-3.0 -2.0 -1.0 0.0 1.0 2.0 3.0

GEO Link:	http://www.ncbi.nlm.nih.gov/geo/query/acc.cgi?acc=GSE10965
Status:	Public on Mar 29 2008
Title:	Comparison of the transcriptional profiles of the retinal pigmental epithelium/choroid from young and old mice
Organism:	Mus musculus
Experiment type:	Expression profiling by array
Platform:	GPL1261
Pubmed ID:	18523633
Summary & Design:	**Summary:** To characterize underlying changes in the retinal pigment epithelium (RPE)/choroid with age, we produced gene expression profiles for the RPE/choroid and compared the transcriptional profiles of the RPE/choroid from young and old mice. The changes in the aged RPE/choroid suggest that the tissue has become immunologically active. Such phenotypic changes in the normal aged RPE/choroid may provide a background for the development of age-related macular degeneration. **Keywords: age-related change** **Overall design:** We compared the gene expression of retinal pigmental epithelium/choroid from young and old animals. There were 4 samples from young mice and 4 samples from old mice. Each sample contained 4 retinal pigmental epithelium/choroid from 2 animals

Background corr dist: **KL-Divergence = 0.0376, L1-Distance = 0.0149, L2-Distance = 0.0002, Normal std = 0.6113**

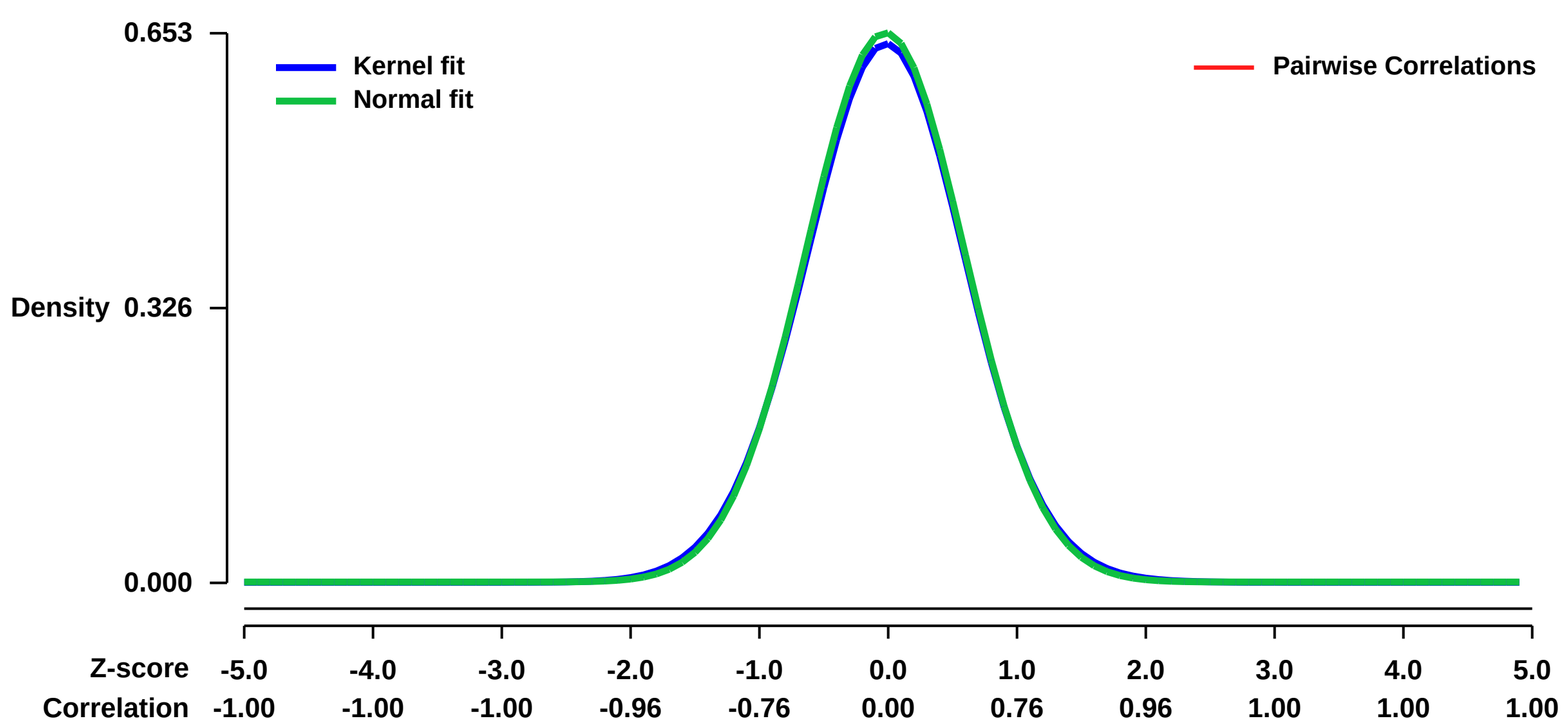

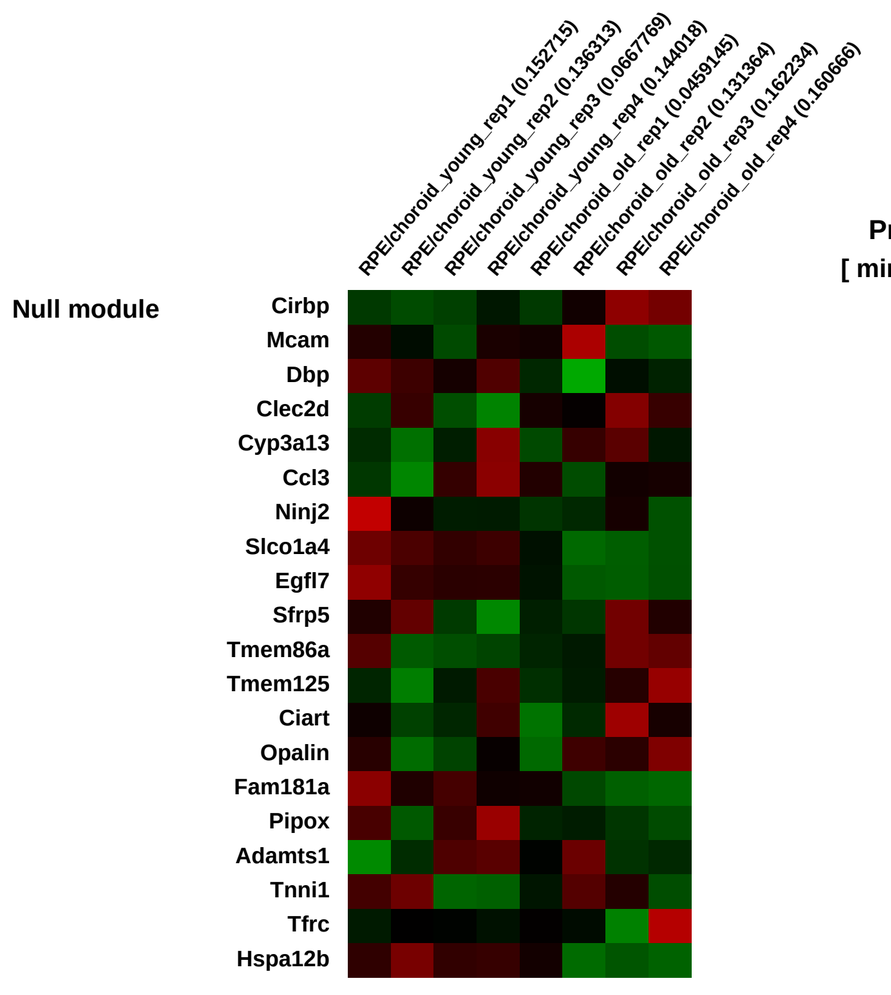

GEO Series "GSE10970" Expression Profiles

Num of samples in this series: 12

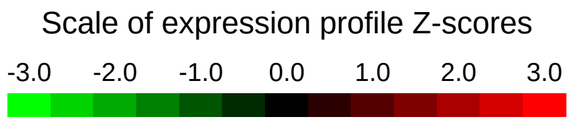

GEO Link:	http://www.ncbi.nlm.nih.gov/geo/query/acc.cgi?acc=GSE10970
Status:	Public on Mar 05 2009
Title:	Efficient Array-based Identification of Novel Cardiac Genes through Differentiation of Mouse ESCs
Organism:	Mus musculus
Experiment type:	Expression profiling by array
Platform:	GPL1261
Pubmed ID:	18478100
Summary & Design:	**Summary:** Cardiac disease accounts for the largest proportion of adult mortality and morbidity in the industrialized world. However, progress toward improved clinical treatments is hampered by an incomplete understanding of the genetic programs controlling early cardiogenesis. To better understand this process, we set out to identify genes whose expression is enriched within early cardiac fated populations, obtaining the transcriptional signatures of mouse embryonic stem cells (mESCs) differentiating along a cardiac path. We compared the RNA profiles of cardiac precursors cells (CPCs) with time-matched non-CPCs and undifferentiated mESCs, using a transgenic mESC line harboring an Nkx2-5 cardiac-specific regulatory sequence driving green fluorescent protein (GFP) to facilitate selection of CPCs. Approximately 24% (43/176) of the transcripts enriched in the CPC population have known roles in cardiac function or development. Importantly, we evaluated the biological relevance of a subset 31/133 (23%) of the remaining candidate genes by in situ hybridization and report that all were expressed in key cardiac structures during cardiogenesis (embryonic day, E7.5 - 9.5), many of which were previously uncharacterized. These data demonstrate the power of mESC differentiation to model specific developmental processes and provide a valuable resource that may be mined to further elucidate the genetic programs underlying cardiogenesis. **Keywords:** time course, differentiated cardiac cell fate **Overall design:** Cells from day 6 were then sorted using the BD Biosciences FACSAriaâ¢ Cell sorting system into GFP+ and GFP- fractions into RLT buffer (RNeasy, Qiagen). This sorting separates cells into two groups reflecting their differentiation into those fated to a non-cardiac lineage (GFP negative) and to a cardiac lineage (GFP positive).

Background corr dist: KL-Divergence = 0.0937, L1-Distance = 0.0404, L2-Distance = 0.0035, Normal std = 0.4542

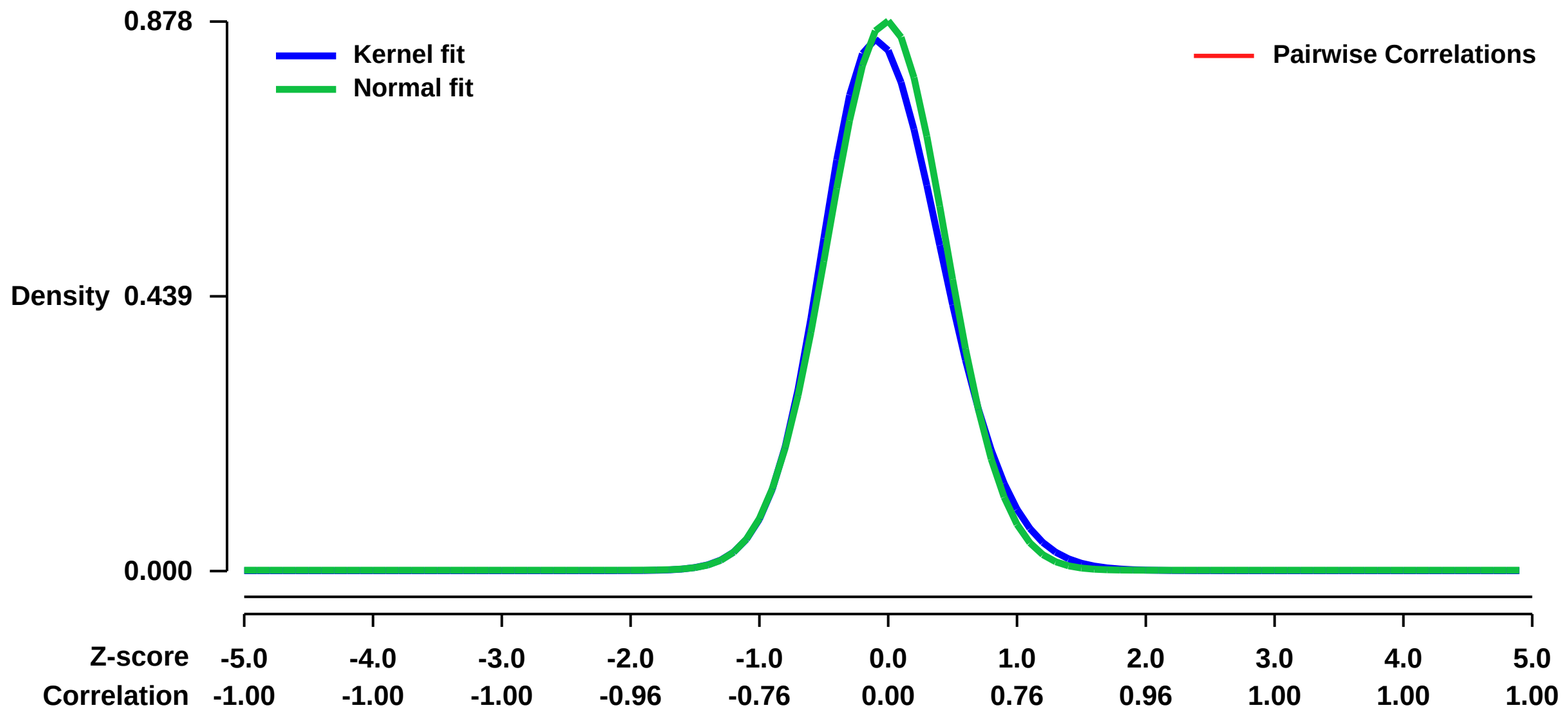

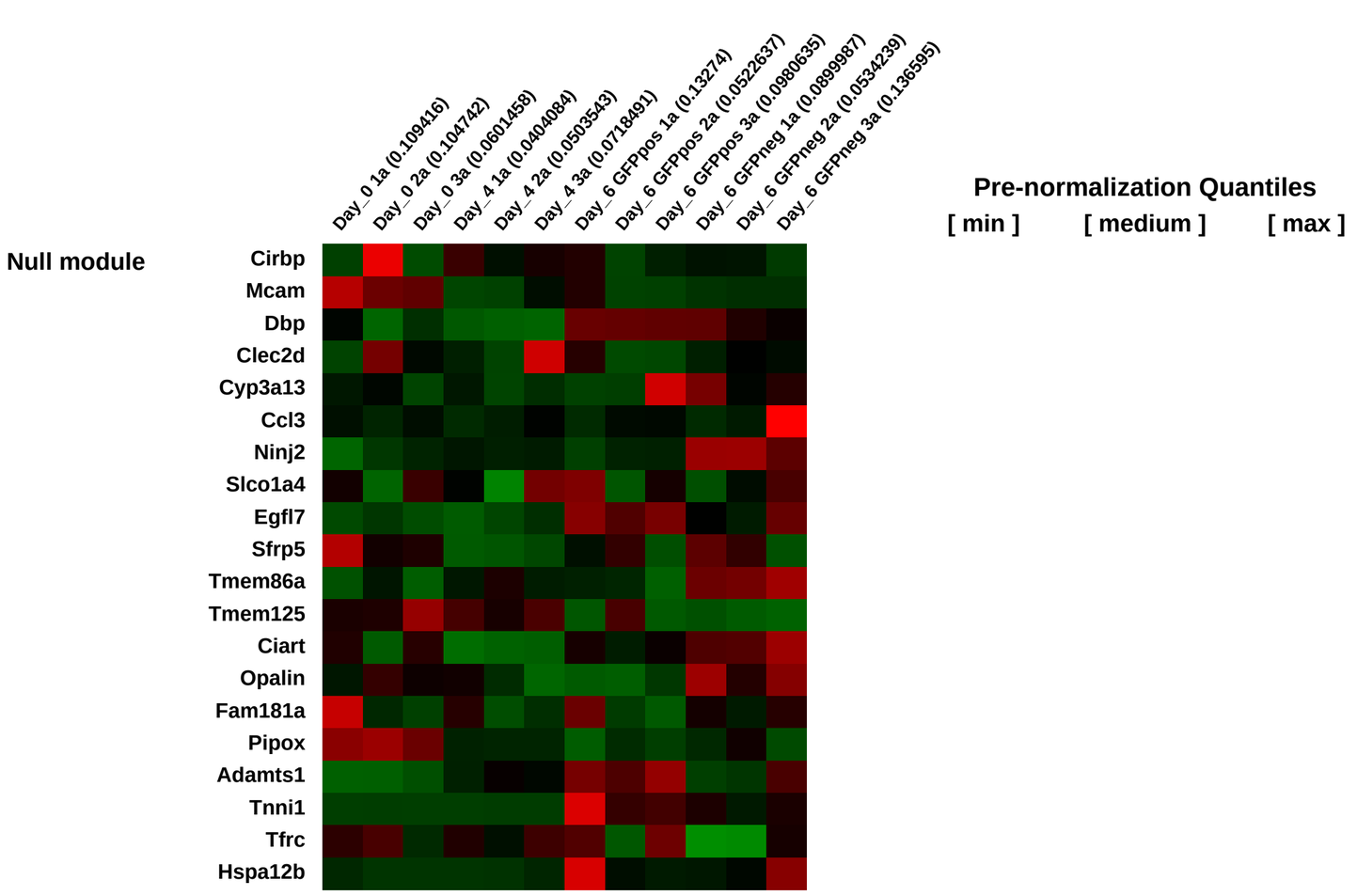

GEO Series "GSE10989" Expression Profiles

Num of samples in this series: 6

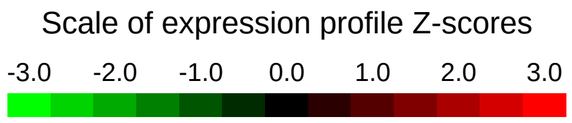

GEO Link:	**http://www.ncbi.nlm.nih.gov/geo/query/acc.cgi?acc=GSE10989**
Status:	**Public on Dec 22 2010**
Title:	**Expression data of cystic renal epithelial tissue from mice deficient for fumarate hydratase.**
Organism:	**Mus musculus**
Experiment type:	**Expression profiling by array**
Platform:	**GPL1261**
Pubmed ID:	
Summary & Design:	**Summary:** **Fumarate hydratase (FH) mutations cause hereditary leiomyomatosis and renal cell cancer (HLRCC). We have conditionally inactivated the murine ortholog (Fh1) in renal tubular epithelial cells in order to generate an in vivo model of HLRCC. Fh1 knockout mice recapitulates important aspects of HLRCC including the development of renal cysts that overexpress hypoxia inducible factor alpha (Hifa) and Hif-target genes.** **We used microarrays to detail the global programme of gene expression underlying cyst development in Fh1 knockout mice and identified distinct classes of up-regulated genes during this process.** **Keywords: gene expression, comparison (wild-type n=3 vs knockout n=3)** **Overall design:** **Renal epithelial tissue was macro-dissected from Fh1 knockout mice and sex-matched litter mate control disease-free animals for RNA extraction and hybridization on Affymetrix microarrays.**

Background corr dist: KL-Divergence = 0.0186, L1-Distance = 0.0758, L2-Distance = 0.0076, Normal std = 0.9701

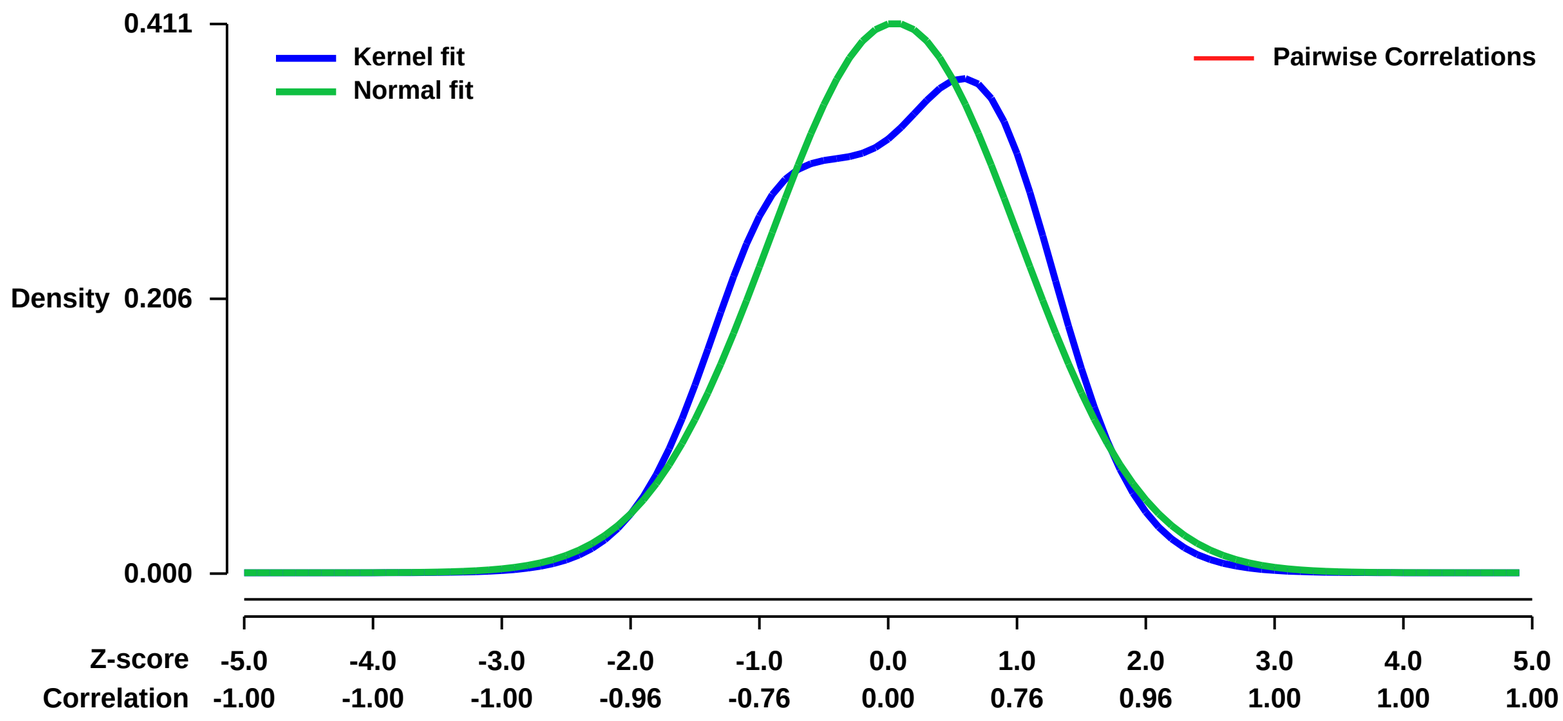

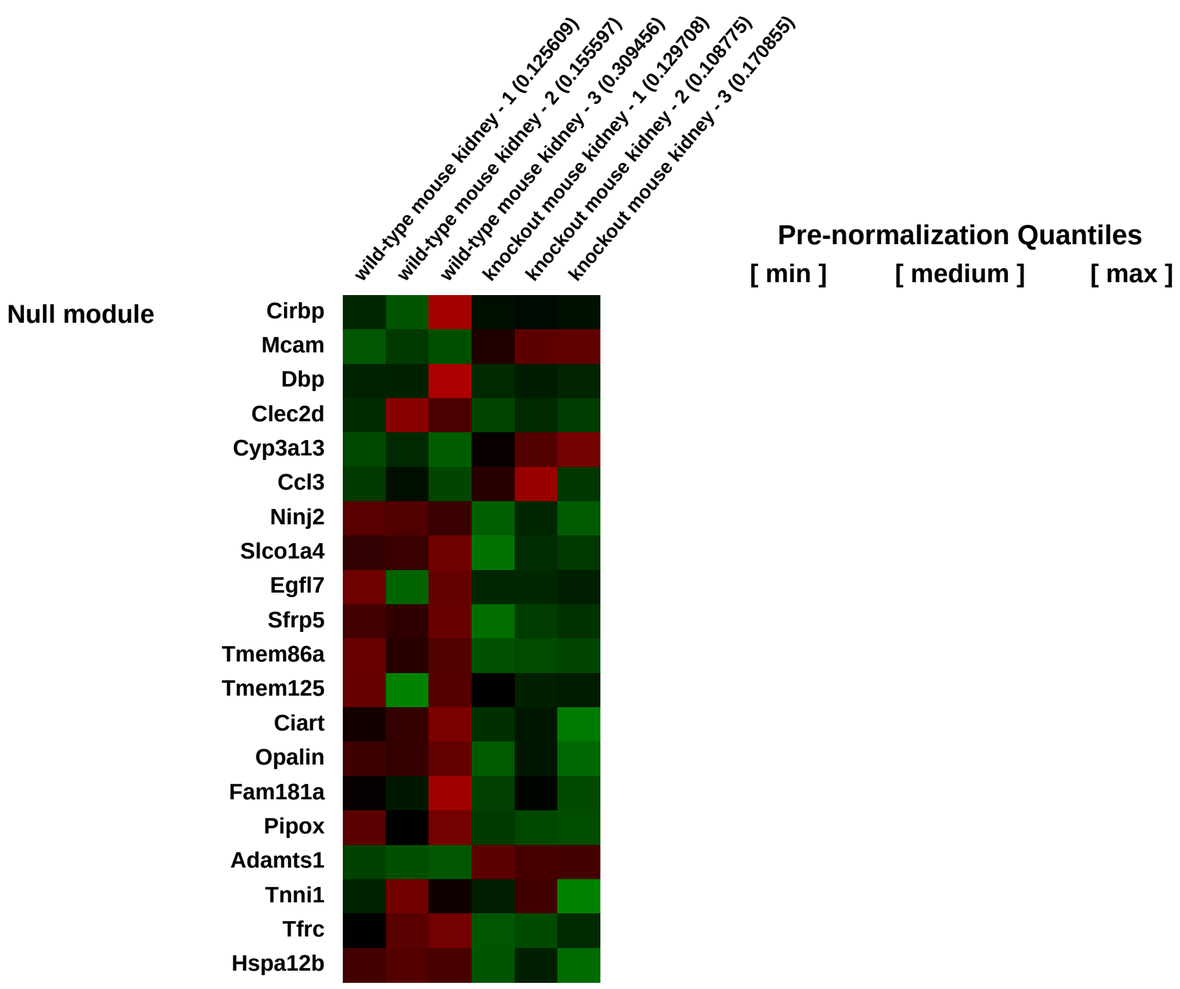

GEO Series "GSE11013" Expression Profiles

Num of samples in this series: 6

Scale of expression profile Z-scores

-3.0 -2.0 -1.0 0.0 1.0 2.0 3.0

GEO Link:	http://www.ncbi.nlm.nih.gov/geo/query/acc.cgi?acc=GSE11013
Status:	Public on Nov 30 2009
Title:	Gene expression rates in a mouse model for Potocki-Lupski Syndrome
Organism:	Mus musculus
Experiment type:	Expression profiling by array
Platform:	GPL1261
Pubmed ID:	18469339
Summary & Design:	**Summary:** To identify gene(s) that are modified in their relative expression levels in the Potocki-Lupski Syndrome mouse model and map to the rearranged region, i.e. possible candidate genes at the source of the PTLS-like phenotypes shown by the PTLS mouse, we comp **Keywords: disease model, expression profiling** **Overall design:** We profiled the hippocampi of three Dp(11)17/+ and three wild type males, all six in a pure C57BL/6-Tyr c-Brd genetic background.

Background corr dist: KL-Divergence = 0.0399, L1-Distance = 0.0164, L2-Distance = 0.0003, Normal std = 0.6127

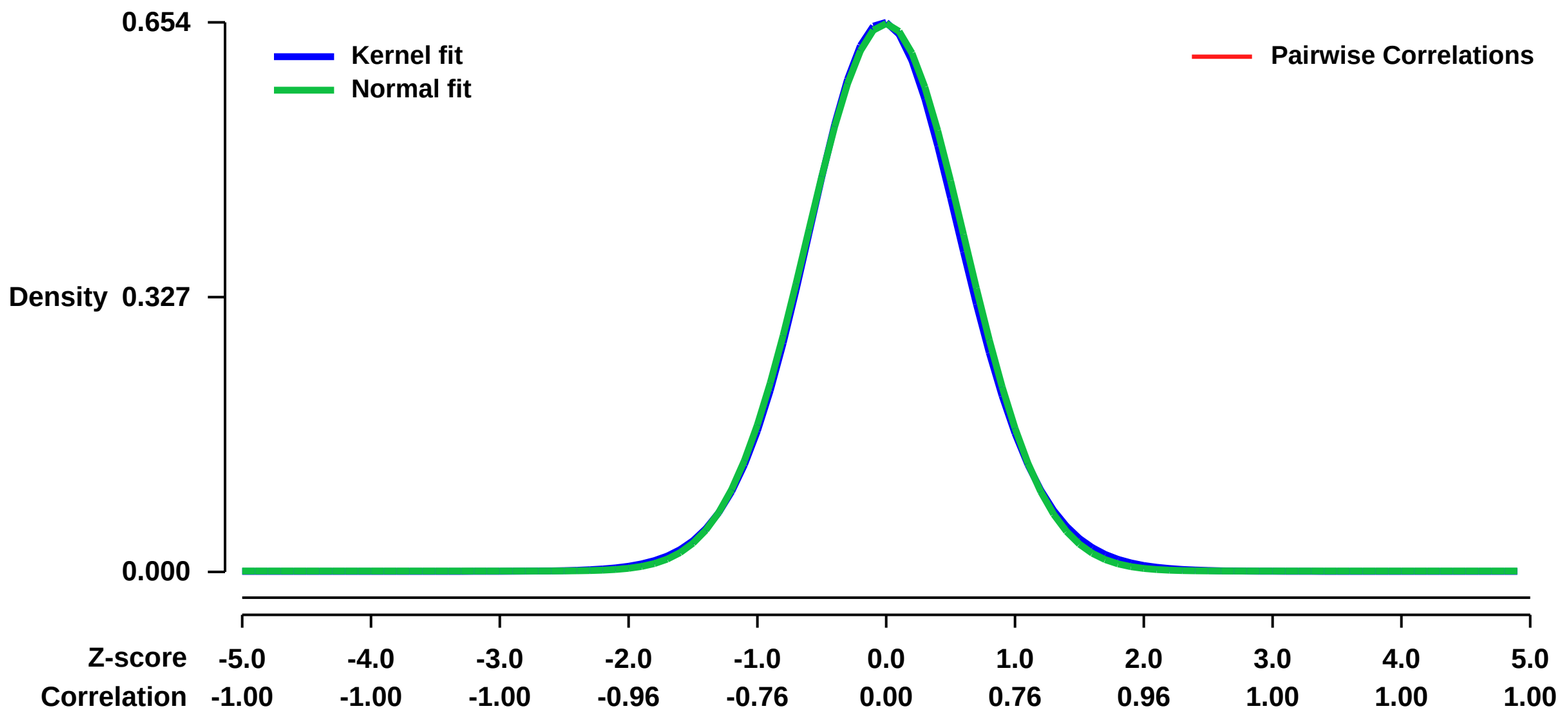

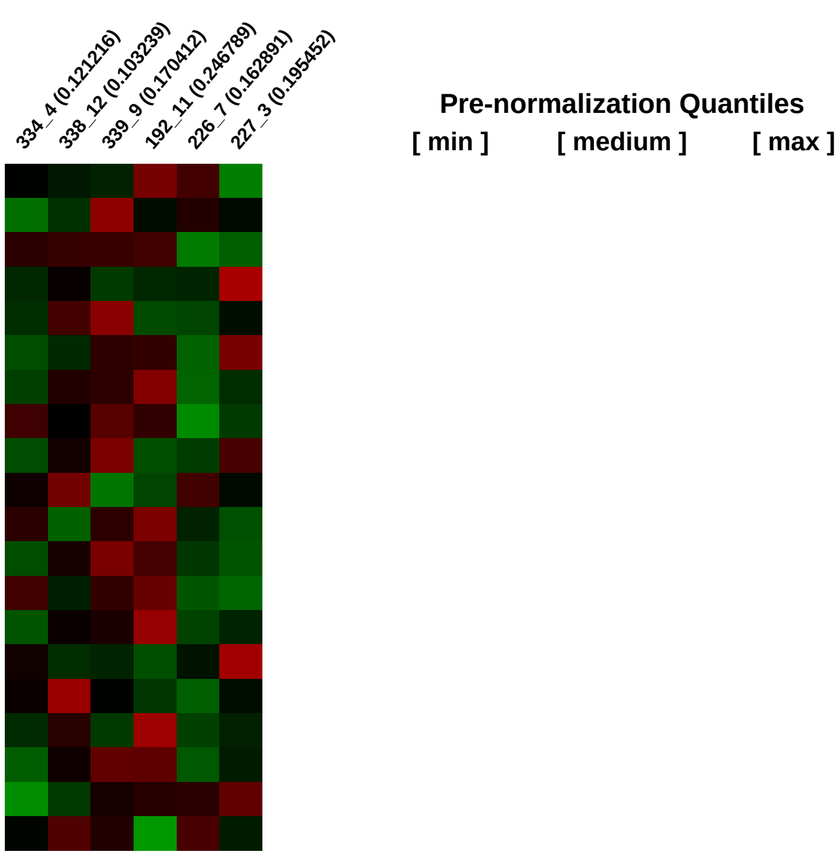

GEO Series "GSE11035" Expression Profiles

Num of samples in this series: 6

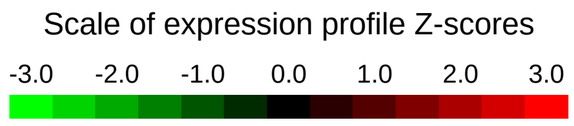

GEO Link:	http://www.ncbi.nlm.nih.gov/geo/query/acc.cgi?acc=GSE11035
Status:	Public on Jun 01 2008
Title:	Effect of 5HTT knockout and heterozygosity in whole mouse lung
Organism:	Mus musculus
Experiment type:	Expression profiling by array
Platform:	GPL1261
Pubmed ID:	19426553

Summary & Design:

Summary:
Rationale: While modulation of the serotonin transporter (5HTT) has shown to be a risk factor for pulmonary arterial hypertension for almost 40 years, there is a lack of in vivo data about the broad molecular effects of pulmonary inhibition of 5HTT. Previous studies have suggested effects on inflammation, proliferation, and vasoconstriction. The goal of this study was to determine which of these were supported by alterations in gene expression in serotonin transporter knockout mice. Methods: Eight week old normoxic mice with a 5-HTT knock-out (5HTT-/-) and their heterozygote(5HTT+/-) or wild-type(5HTT+/+) littermates had right ventricular systolic pressure(RVSP) assessed, lungs collected for RNA, pooled, and used in duplicate in Affymetrix array analysis. Representative genes were confirmed by quantitative RT-PCR and western blot. Results: RVSP was normal in all groups. Only 124 genes were reliably changed between 5HTT-/- and 5HTT+/+ mice. More than half of these were either involved in inflammatory response or muscle function and organization; in addition, some matrix, heme oxygenase, developmental, and energy metabolism genes showed altered expression. Quantitative RT-PCR for examples from each major group confirmed changes seen by array, with an intermediate level in 5HTT+/- mice. Conclusions: These results for the first time show the in vivo effects of 5HTT knockout in lungs, and show that many of the downstream mechanisms suggested by cell culture and ex vivo experiments are also operational in vivo. This suggests that the effect of 5HTT on pulmonary vascular function arises from its impact on several systems, including vasoreactivity, proliferation, and immune function.

Keywords: Genetic modification

Overall design:
Comparison of whole lung total RNA from pools of wild-type, heterozygote, and knockout 5HTT mice to determine the pulmonary effects of loss of 5HTT expression.

Background corr dist: KL-Divergence = 0.0496, L1-Distance = 0.0187, L2-Distance = 0.0004, Normal std = 0.5747

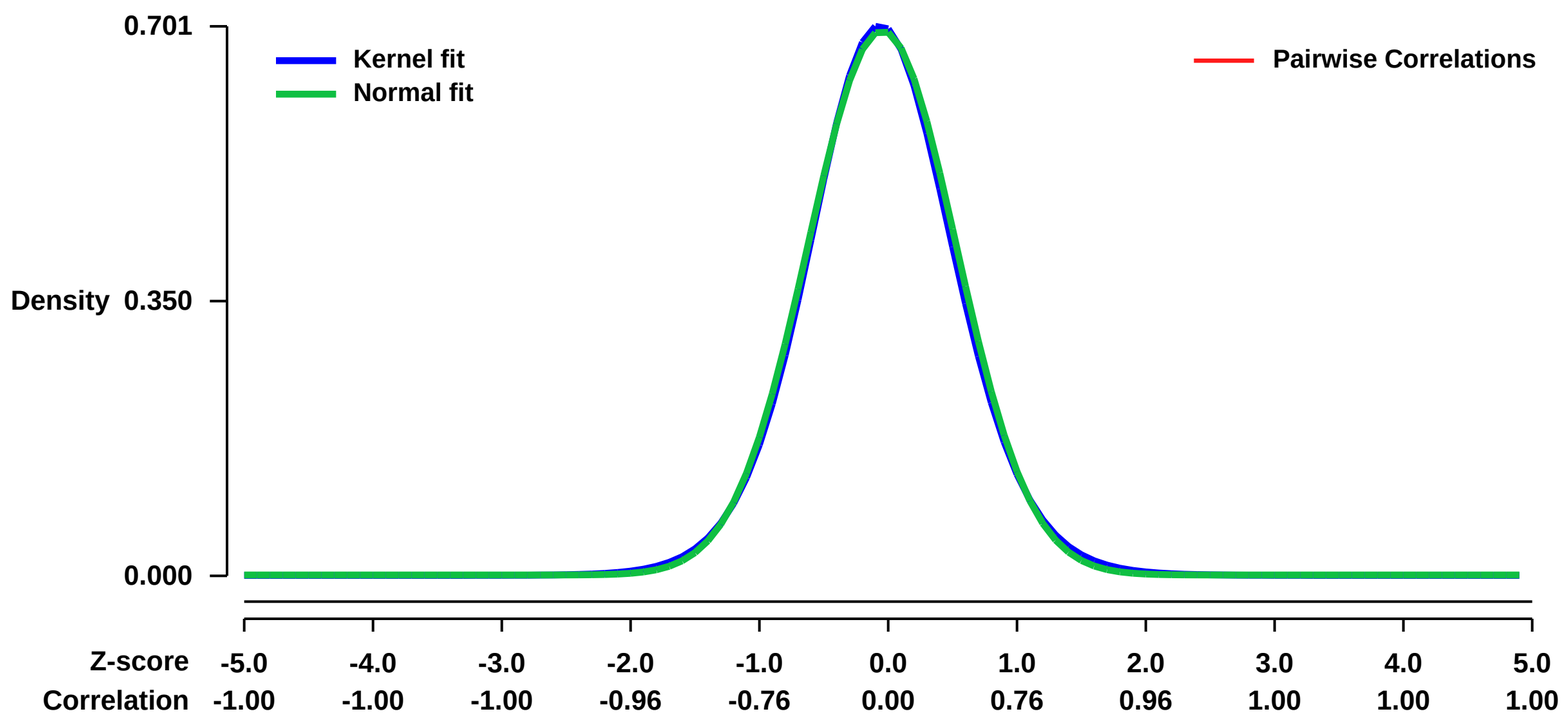

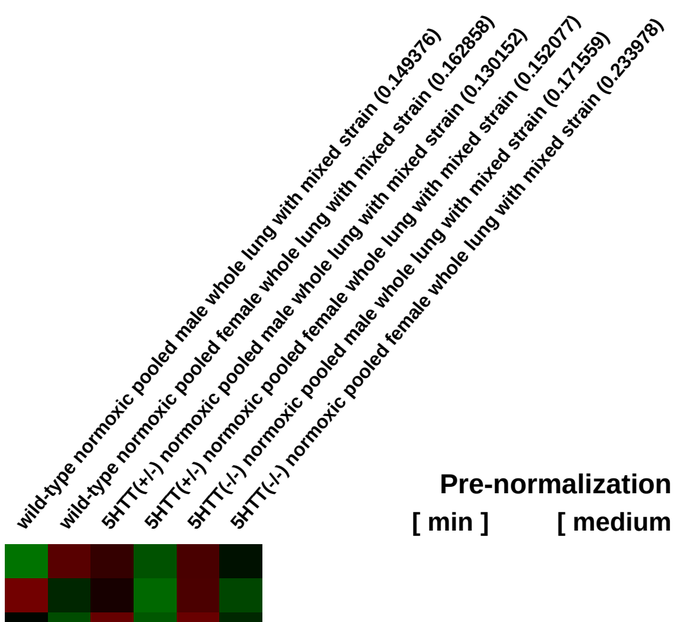

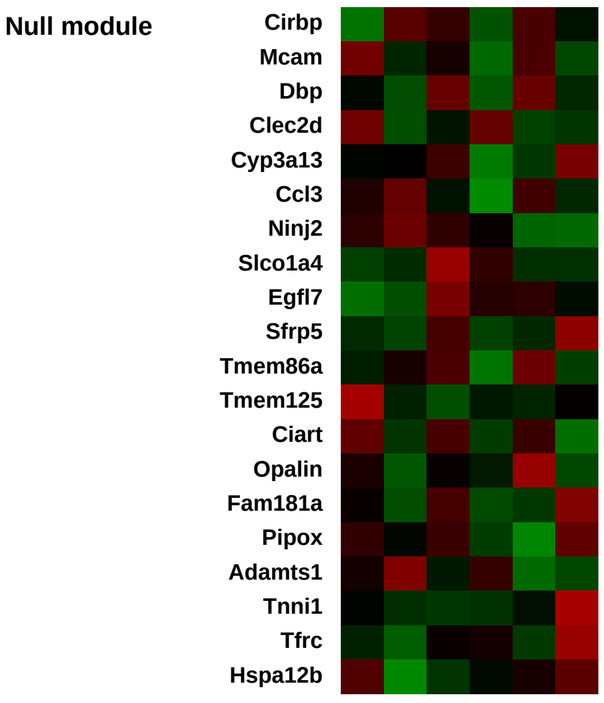

GEO Series "GSE11141" Expression Profiles

Num of samples in this series: 21

Scale of expression profile Z-scores

-3.0 -2.0 -1.0 0.0 1.0 2.0 3.0

GEO Link: http://www.ncbi.nlm.nih.gov/geo/query/acc.cgi?acc=GSE11141

Status: Public on Apr 12 2008

Title: Effects of NgR overexpression on the developing and mature forebrain (backm-affy-mouse-433094)

Organism: Mus musculus

Experiment type: Expression profiling by array

Platform: GPL1261

Pubmed ID:

Summary & Design:

Summary:
The lack of axonal growth after injury in the adult central nervous system (CNS) is partly due to the presence of growth-inhibitory molecules associated with myelin and the intrinsic growth-state of the injured neurons. To date, three inhibitors have been identified in myelin: Myelin- Associated Glycoprotein (MAG), Nogo A, and Oligodendrocyte-Myelin glycoprotein (OMgp). These three proteins all appear to be located in the periaxonal surface of the myelin membrane placing them in an optimal location to mediate axon-glial interaction. In addition, the three proteins have been shown to bind the same neuronal receptor, known as the Nogo-66 receptor (NgR). It has been hypothesized that inhibition of NgR may be a strategy to increase regeneration, plasticity and functional recovery of the lesioned central nervous system. Strong NgR mRNA expression is observed in the hippocampal pyramidal cell layers (CA1-3) and the granular layer of the dentate gyrus. It has been shown that animals exposed to entorhinal lesions show a biphasic regulation of NgR in the hippocampus, suggesting a tightly regulated mechanism mediated by this receptor. We have access to a transgenic model to over-express NgR in forebrain hippocampal neurons. Preliminary results have shown a phenotypic response in behavior and some molecular markers, as result of NgR overexpression. Knowledge of what genes are reacting in this novel transgenic model may provide insights into what pathways are affected by NgR to control synaptic plasticity in normal animals and during injury.

We have access to a bitrasgenic conditional mouse model to everexpress the NgR receptor in forebrain neurons, through the CamKII promoter. This conditional model uses the tetracycline transactivator (tTA), which is expressed through the CamKII promoter. Upon removal of doxycycline, the TetOp target gene becomes active and over-expression of NgR in cells with an active CaMKII promoter is achieved.

We will determine gene expression patterns in the dentate gyrus of transgenic animals engineered to over-express NgR through the CamKII promoter (present in several forebrain areas), and upon removal of doxyxycline.

We hypothesize that over-expression of NgR in the hippocampus inhibits synaptic plasticity, thereby suppressing the formation of new synapses necessary for the formation of memory.

EXPERIMENT 1

- Effects of NgR overexpression in the mature forebrain -

1) Experimental group: Bitrasgenic + water: Overexpresses NgR in forebrain neurons. In this group, doxyxycline was removed from the drinking water in adult animals. All the control groups were aged matched.

2) Control group: Bitransgenic + doxy: Should control for leakage by the TetOp target gene, or for any effects mediated by doxycycline, as compared to other control groups.

3) Control group: Monotransgenic + water: Should control for any leakage mediated by the TetOp target gene, as compared to other control groups.

4) Control group: Monotrangenic + water: Should control for leakage by the TetOp target gene, or for any effects mediated by doxycycline, as compared to other control groups.

EXPERIMENT 2

- Effects of NgR overexpression in the developing forebrain -

We will also analyze the effects of NgR overexpression in bitransgenic animals raised on water. In these animals, the NgR transgene is expressed in the forebrain upon activation of the CamKII promoter. Since neuronal differentiation and neuronal pathways are being formed during development, we anticipate that NgR overexpression (de)effects in these animals will be markedly different to those observed in adult animals.

1) Bitransgenic + water (through entire lifespan): The animals in this group were never treated with doxycycline, and therefore expressed the NgR transgene upon activity of the CamKII promoter.

2) Monotransgenic + water: This control group will control for leakage by the Tet Op gene, or for effects of the tTA expression.

Keywords: NgR, forebrain, development

Overall design:

Background corr dist: KL-Divergence = 0.2830, L1-Distance = 0.0577, L2-Distance = 0.0084, Normal std = 0.2873

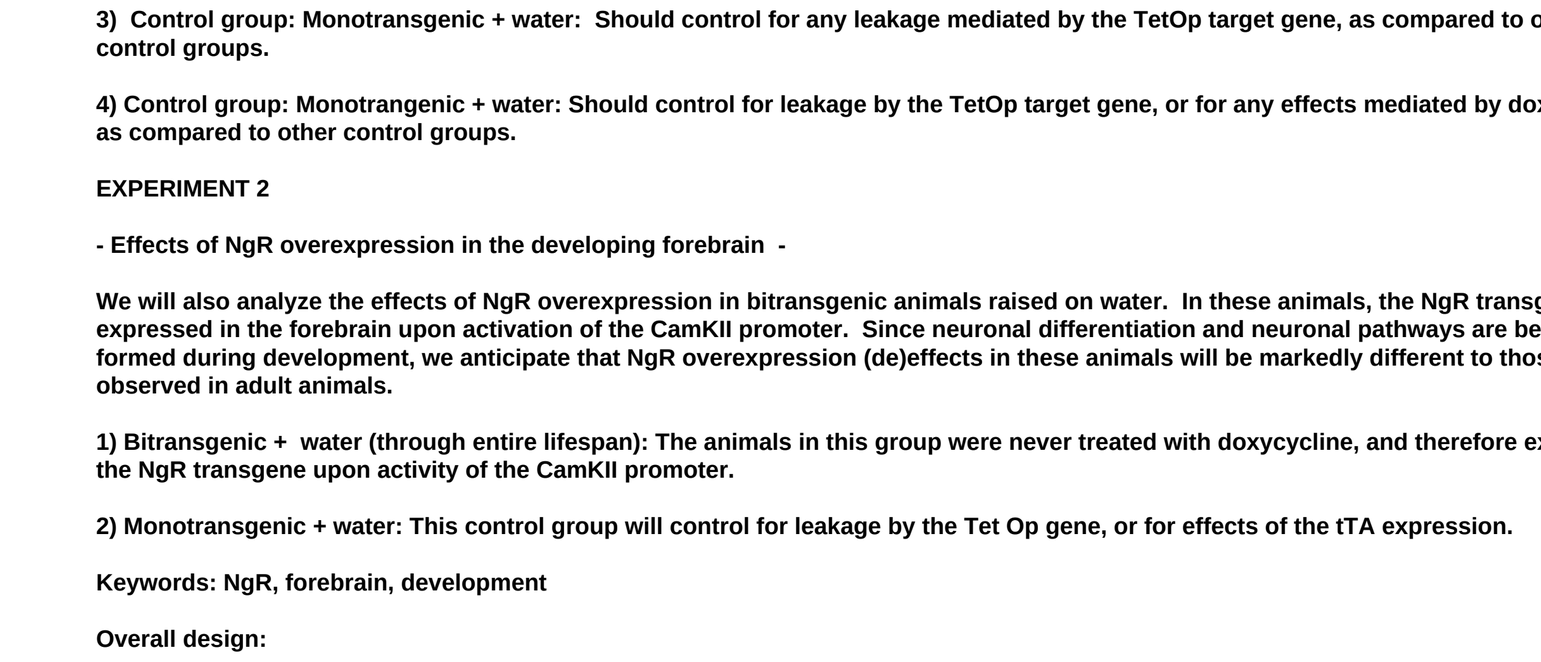

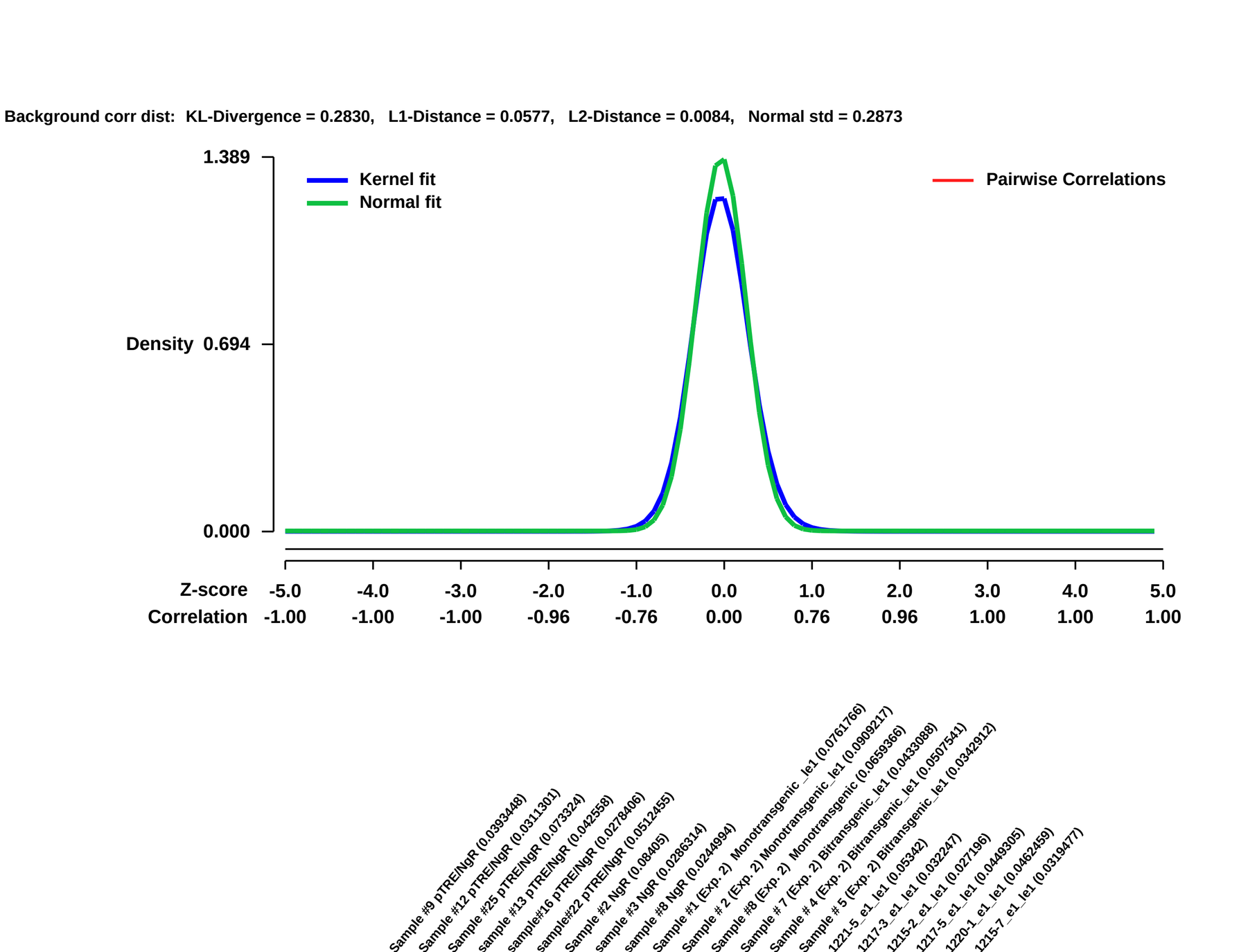

GEO Series "GSE11147" Expression Profiles

Num of samples in this series: 6

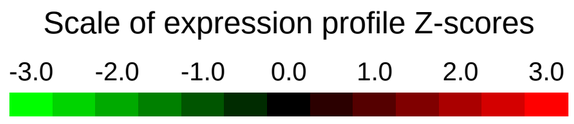

GEO Link:	**http://www.ncbi.nlm.nih.gov/geo/query/acc.cgi?acc=GSE11147**
Status:	**Public on Apr 12 2008**
Title:	**Hippocampus of HuD overexpressor mice (perro-affy-mouse-309741)**
Organism:	**Mus musculus**
Experiment type:	**Expression profiling by array**
Platform:	**GPL1261**
Pubmed ID:	

Summary & Design:

Summary:
Post-transcriptional mechanisms play an important role in the control of gene expression. RNA-binding proteins are key players in the post-transcriptional control of many neural genes and they participate in multiple processes, from RNA splicing and mRNA transport to mRNA stability and translation. Our laboratory has developed the first mouse model overexpressing a RNA-binding protein, the ELAV-like protein HuD, in the CNS under the control of the CaMKinII alpha promoter. Initial behavioral characterization of the mice revealed that they had significant learning deficits together with abnormalities in prepulse inhibition (PPI). At the molecular level, we found that the expression of the growth-associated protein GAP-43, one of the targets of HuD, was increased in the hippocampus of HuD transgenic mice. To characterize these mice further and to evaluate the utility of these animals in understanding human diseases, we propose to use DNA microarray methods.

To characterize the pattern of gene expression in the hippocampus of HuD overexpressor mice

Based on the behavioral and molecular properties of our HuD transgenic mice we hypothesize that these animals may be good models for the studying the basis of learning disabilities and of diseases that show deficits in PPI such as fetal alcohol syndrome and schizophrenia.

All mice are in C57BL/6 background and are male approximately 30 days old. Animals are bred and sacrificed according to our approved animal protocol. Brains will be rapidly dissected on ice, quickly frozen and stored at -80C until analysis. Frozen brains will be embedded in OCT and shipped to the DNA microarray facility at Duke University where LCM was performed. Dentate granule cells from control and HuD transgenic mice will be isolated by Susan Su, who will also perform RNA isolation and the first round of RNA amplification. For our first experiment, we want to examine the pattern of gene expression in the hippocampus of 2 transgenic mice and 2 non-transgenic littermates.

Keywords: HuD, hippocampus

Overall design:

Background corr dist: **KL-Divergence = 0.0495, L1-Distance = 0.0217, L2-Distance = 0.0005, Normal std = 0.5777**

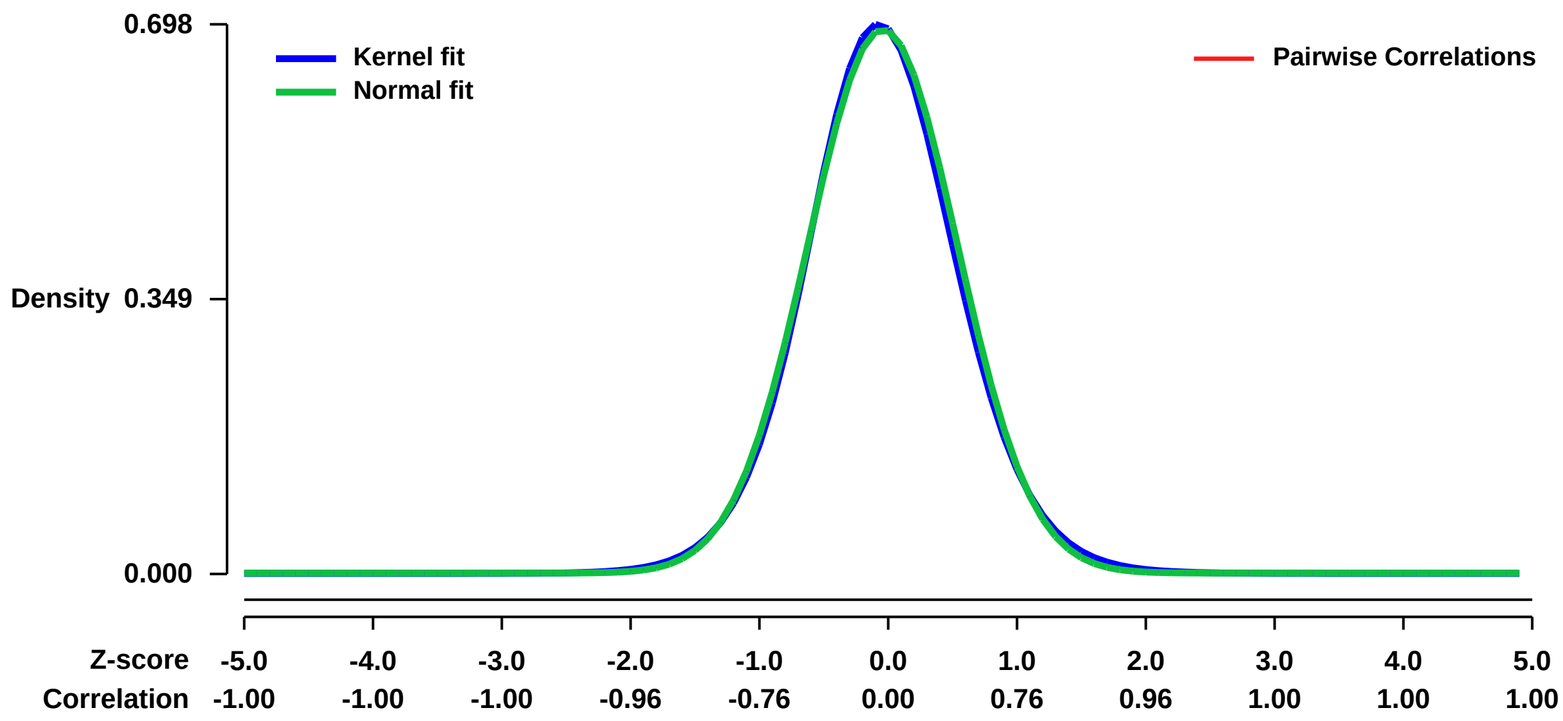

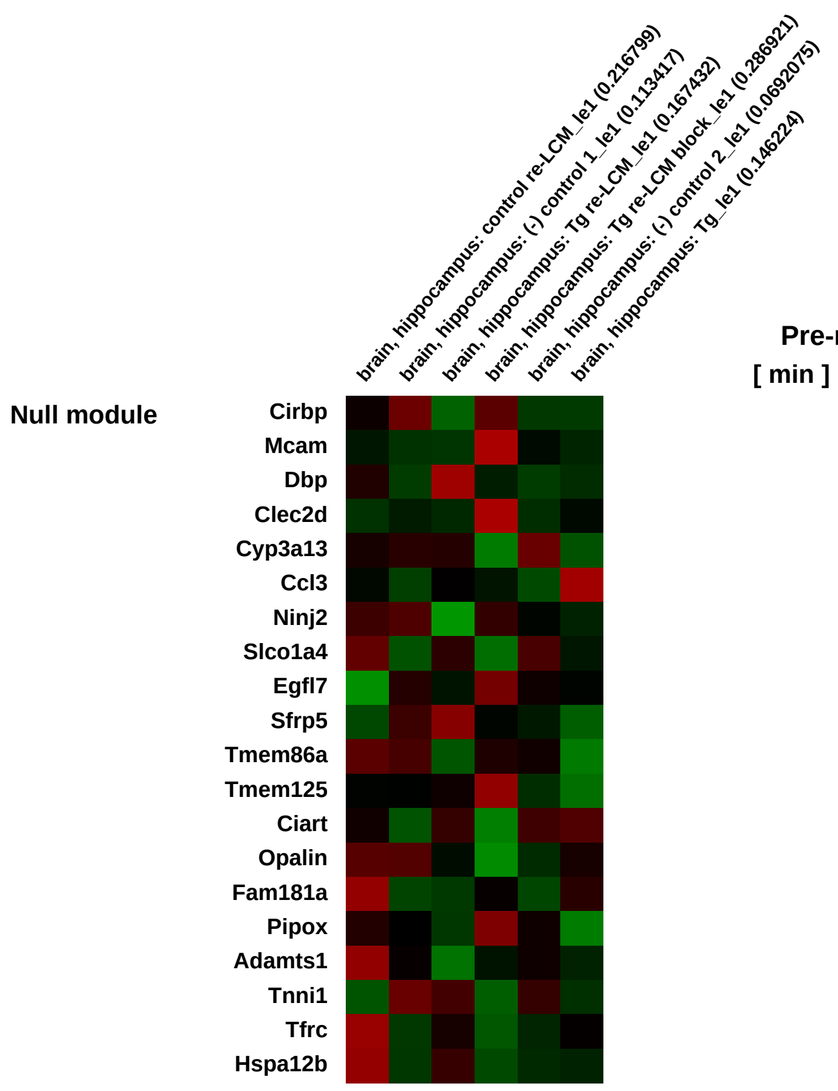

GEO Series "GSE11148" Expression Profiles

Num of samples in this series: 6

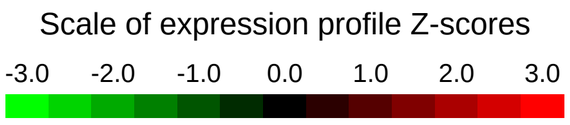

GEO Link:	**http://www.ncbi.nlm.nih.gov/geo/query/acc.cgi?acc=GSE11148**
Status:	**Public on Apr 12 2008**
Title:	**Polytopic protease downregulation effect on the brain (rogae-affy-arabi-492460)**
Organism:	**Mus musculus**
Experiment type:	**Expression profiling by array**
Platform:	**GPL1261**
Pubmed ID:	
Summary & Design:	**Summary:** **Regulation of AD-related genes. Presenilins are intramembrane polytopic proteases. These proteases are critical proteins in pathogenesis of Alzheimer's disease. The function of other polytopic proteases expressed in brains is unknown. Proteins that may potentially interact with PS pathway are of interest to elucidate.** **In this project we will determine gene expression patterns in the brains of mice with altered expression of polytopic protease.** **We hypothesize that family of polytopic proteases expressed in brain may potentially interact with presenilin pathway.** **We will examine 4 RNA samples isolated from brains of mice with significant downregulation of polytopic protease and control animals.** **Total RNA was extracted, purified according to the manufacturer's protocol and stored at -80C.** **Keywords: polytopic protease, brain** **Overall design:**

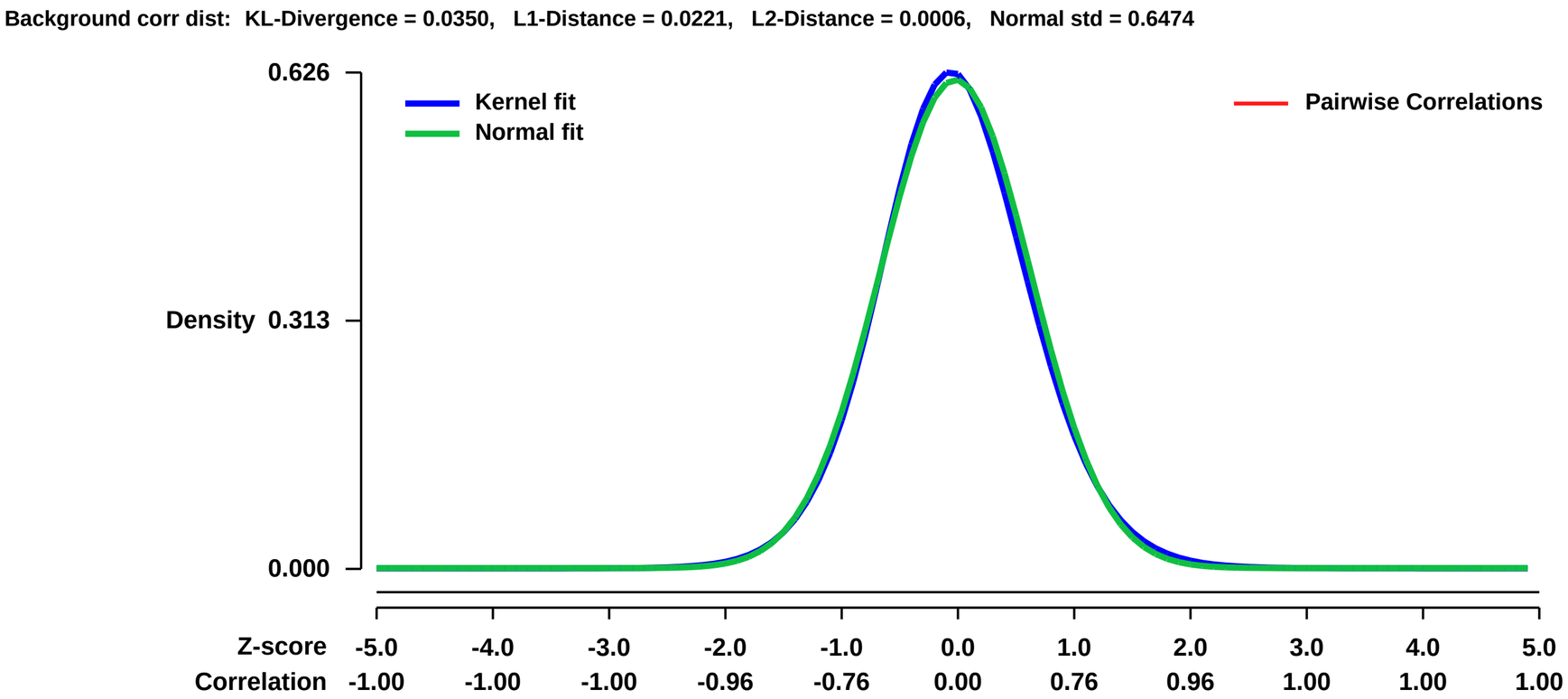

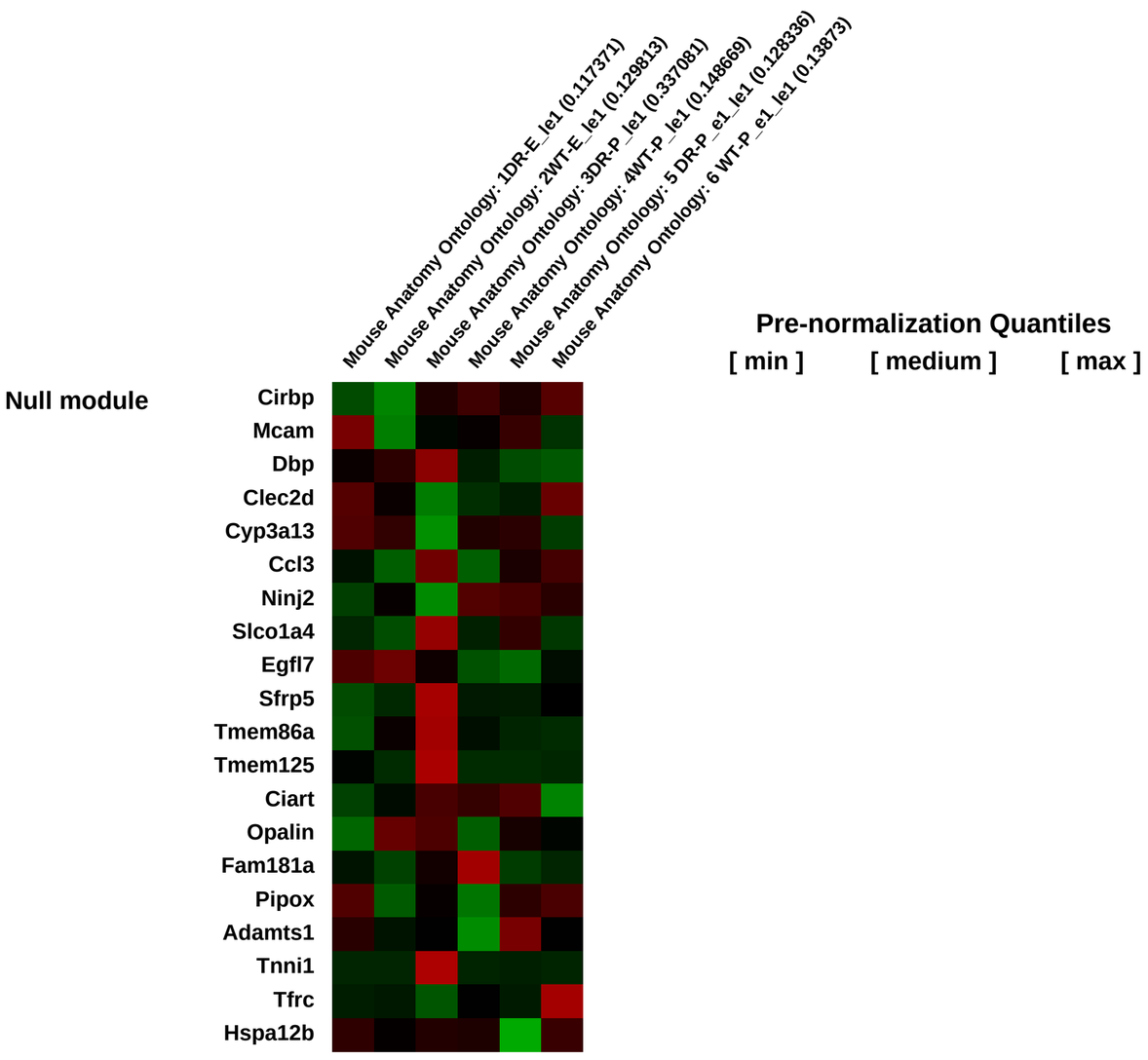

GEO Series "GSE11149" Expression Profiles

Num of samples in this series: 8

Scale of expression profile Z-scores

-3.0 -2.0 -1.0 0.0 1.0 2.0 3.0

GEO Link:	http://www.ncbi.nlm.nih.gov/geo/query/acc.cgi?acc=GSE11149
Status:	Public on May 06 2008
Title:	Cranial neural crest cells of E11.5 wild type and FAK mutants (valle-affy-mouse-480721)
Organism:	Mus musculus
Experiment type:	Expression profiling by array
Platform:	GPL1261
Pubmed ID:	
Summary & Design:	**Summary:** **Cranial neural crest cells (NCC) give rise to the majority of the cartilage, bone, connective tissue, and sensory ganglia in the head, and also participate in the remodeling of the cardiac outflow tract and pharyngeal arch arteries during cardiovascular development. Our preliminary results show that targeted deletion of focal adhesion kinase (FAK) in murine NCC results in cardiovascular and craniofacial alterations, resembling human congenital heart diseases The objective of this project is to elucidate the underlying mechanisms by which FAK mediates NCC function during development.** **Compare gene expression in cranial neural crest cells of E11.5 wild type and FAK mutants.** **FAK is a tyrosine kinase that transduces integrin and growth factor signaling pathways. Abnormal growth factor signaling leads to cardiovascular malformations caused by deficient cardiac NCC function. However, a direct role for FAK in NCC morphogenesis has not been demonstrated. We will test the hypothesis that FAK is a downstream target of essential growth factor signaling in cranial neural crest cells during development.** **1) Generate E11.5 mouse embryos that are either control (FAK+/flox) or NCC specific FAK knockout (Wnt1Cre;FAKflox/flox). 2) Determine genotype by PCR. 3) Dissect head and torax from the different genotypes. 4) Obtain NCC from dissected tissue by magnetic cell sorting using p75 antibody. 5) Prepare total RNA from speciments. We will pool the NCC from 3 different embryos of the same genotype, and send total RNA to TGEN for probe preparation, hybridization and array result analysis.** **Keywords: other** **Overall design:**

Background corr dist: KL-Divergence = 0.0453, L1-Distance = 0.0369, L2-Distance = 0.0019, Normal std = 0.6042

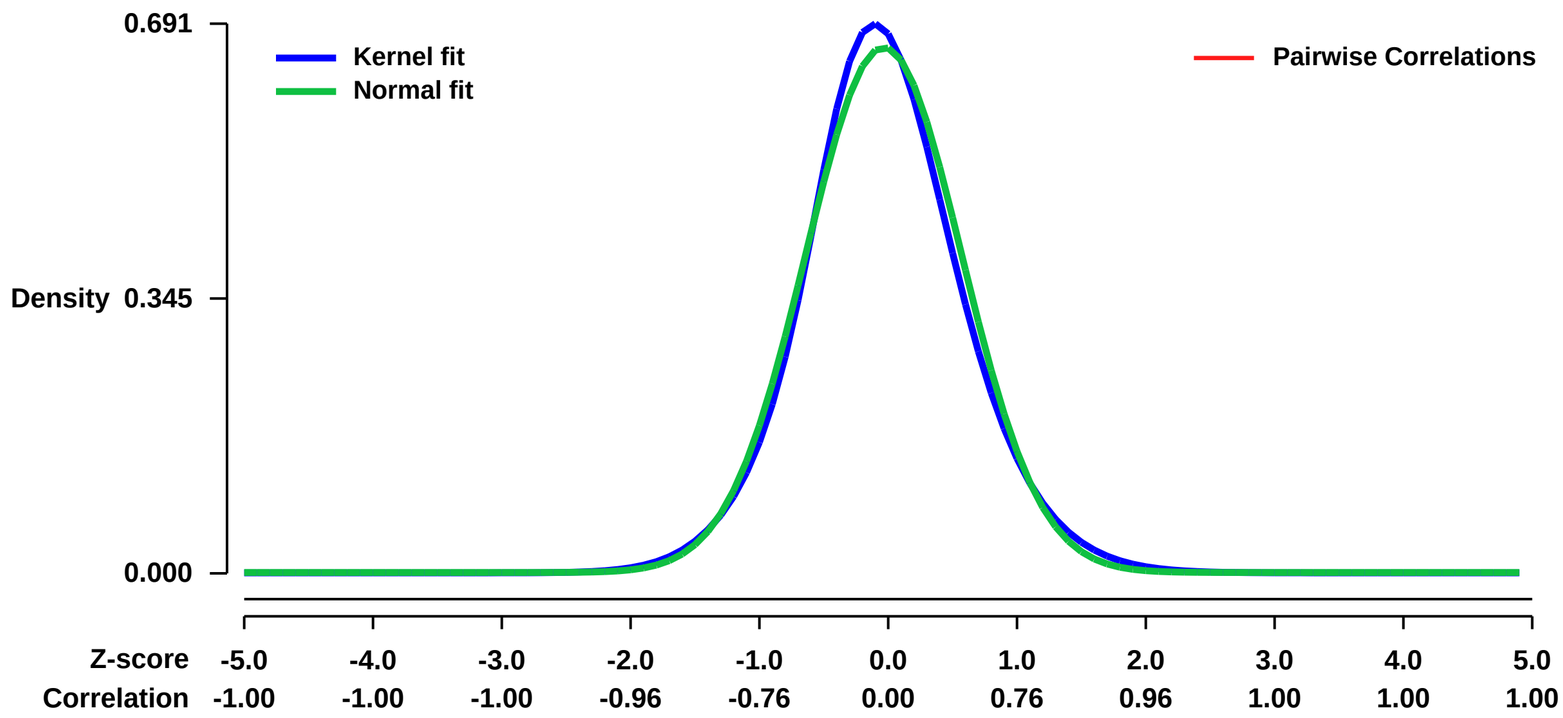

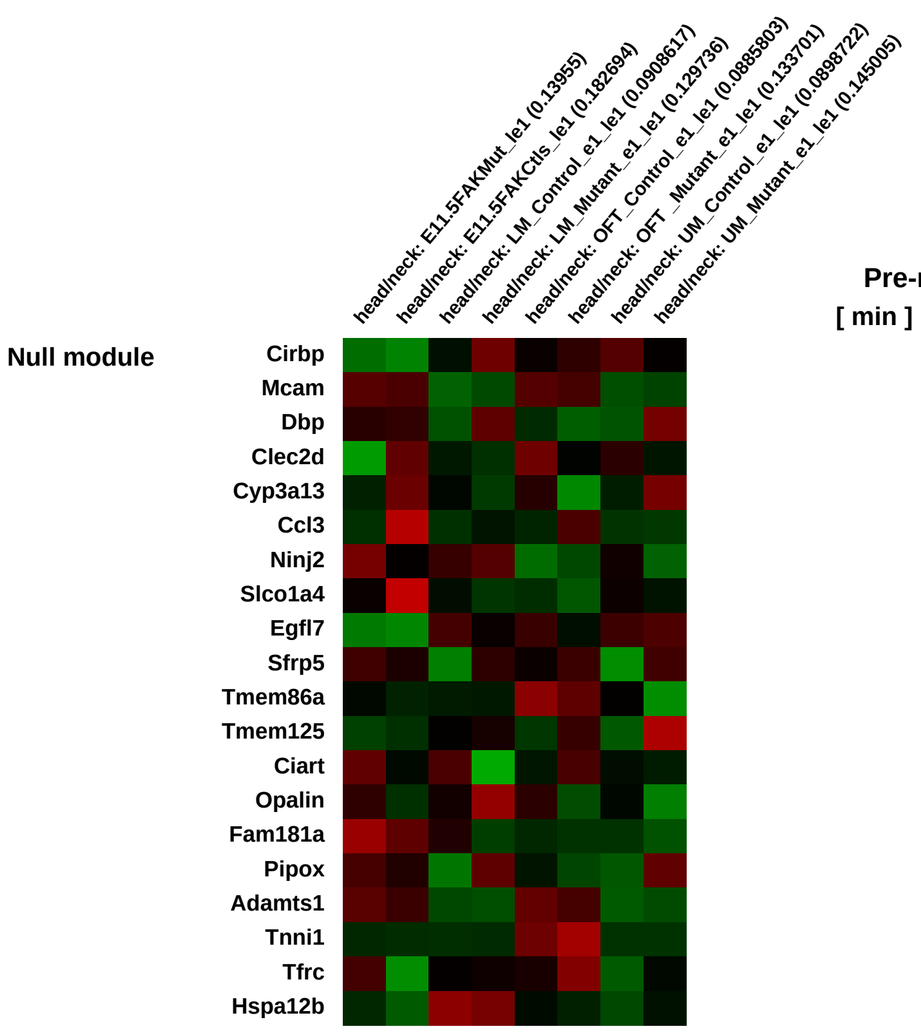

GEO Series "GSE11161" Expression Profiles

Num of samples in this series: 6

Scale of expression profile Z-scores

-3.0 -2.0 -1.0 0.0 1.0 2.0 3.0

GEO Link:	**http://www.ncbi.nlm.nih.gov/geo/query/acc.cgi?acc=GSE11161**
Status:	**Public on Apr 17 2008**
Title:	**Gene expression profiles of neonatal bladder samples. (GUDMAP Series ID: 19)**
Organism:	**Mus musculus**
Experiment type:	**Expression profiling by array**
Platform:	**GPL1261**
Pubmed ID:	
Summary & Design:	**Summary:** **The long term objective is to create an encyclopedia of the expression levels of all genes in multiple components of the developing bladder. The central thesis is straightforward. The combination of microdissected tissues and FACS sorted cells plus microarray analysis offers a powerful, efficient and effective method for the creation of a global gene expression atlas of the developing urogenital system. Microarrays with essentially complete genome coverage can be used to quantitate expression levels of every gene. The ensuing rapid read-out provides an expression atlas that is more sensitive, more economical and more complete than would be possible by in situ hybridizations alone. The data submitted here represents the gene expression profiles of FACS sorted newborn bladder cells and compares two distinct cell populations of smooth muscle cells since both of these populations contain EGFP from a SMGA (Actg2) promoter shown to be expressed only in smooth muscle cells.** **Gene expression comparison from developing regions of the mouse postnatal day 2 urogenital system.** **Overall design:** **Bladder cells were FACS sorted from newborn double transgenic mice expressing EGFP under the control of a SMGA promoter and EYFP under the control of a SMAA promoter. Total RNA was isolated and underwent 2-round amplification (Epicentre´fi Biotechnologies) for gene expression analysis using the Affymetrix MOE430 microarray chip.**

Background corr dist: KL-Divergence = 0.0443, L1-Distance = 0.0332, L2-Distance = 0.0016, Normal std = 0.6073

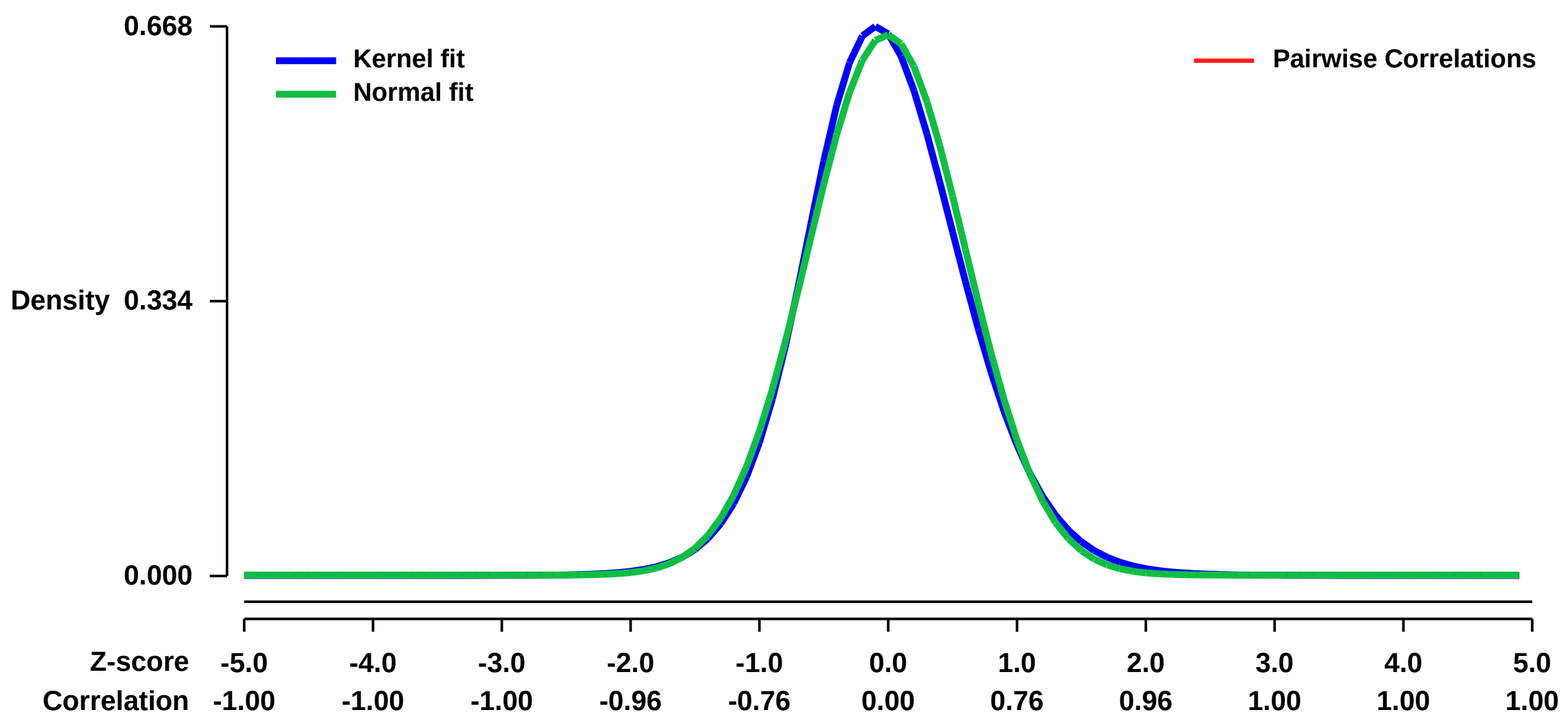

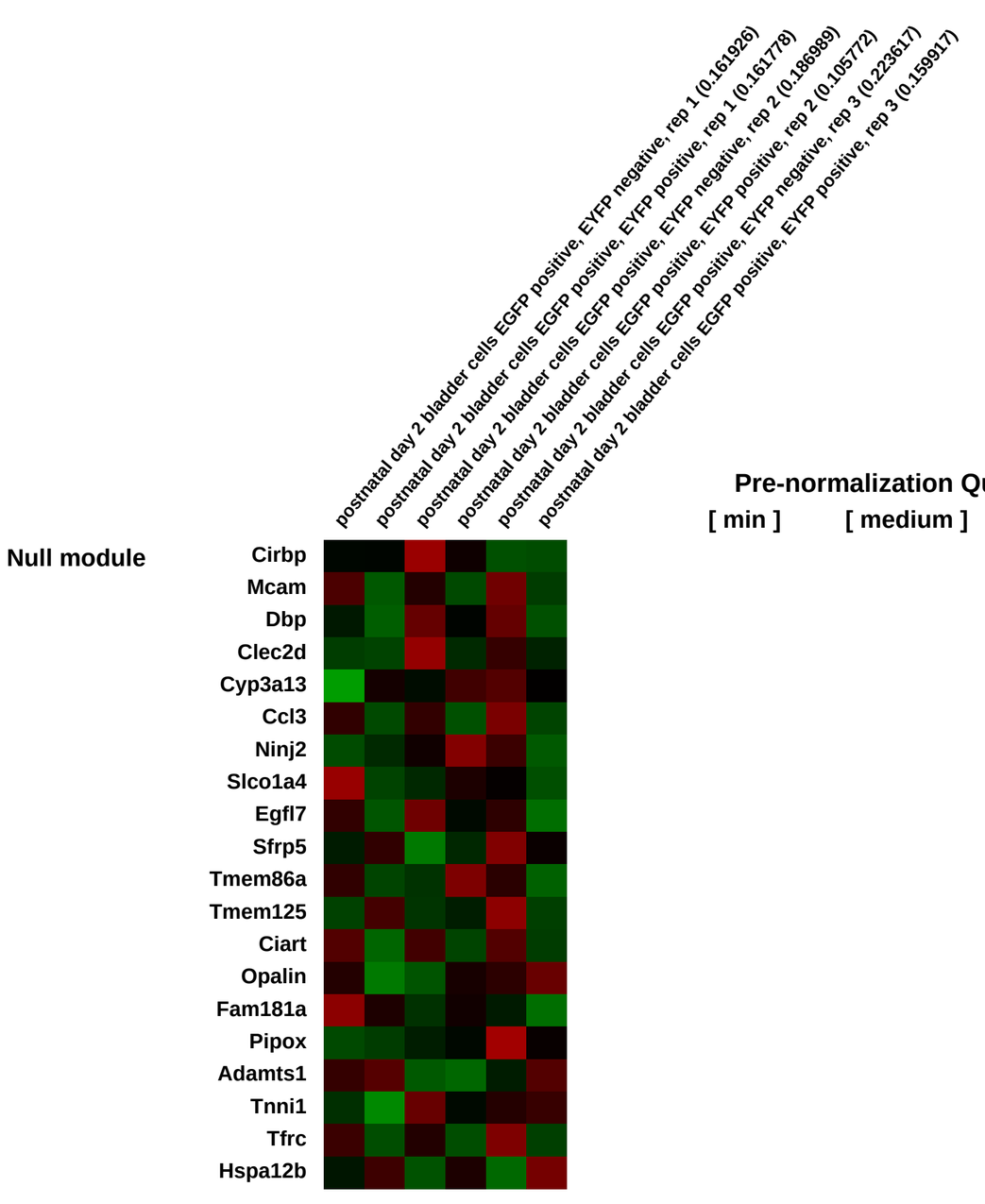

GEO Series "GSE11165" Expression Profiles

Num of samples in this series: 6

Scale of expression profile Z-scores

-3.0 -2.0 -1.0 0.0 1.0 2.0 3.0

GEO Link:	http://www.ncbi.nlm.nih.gov/geo/query/acc.cgi?acc=GSE11165
Status:	Public on Apr 15 2008
Title:	Genes regulated by GATA6 in the lung
Organism:	Mus musculus
Experiment type:	Expression profiling by array
Platform:	GPL1261
Pubmed ID:	18536717
Summary & Design:	**Summary:** Epithelial organs including the lung are known to possess regenerative abilities through activation of endogenous stem cell populations but the molecular pathways regulating stem cell expansion and regeneration are not well understood. Here we show that Gata6 regulates the temporal appearance and number of bronchioalveolar stem cells (BASCs) in the lung leading to the precocious appearance of BASCs and concurrent loss in epithelial differentiation in Gata6 null lung epithelium. This expansion of BASCs is the result of a dramatic increase in canonical Wnt signaling in lung epithelium upon loss of Gata6. Expression of the non-canonical Wnt receptor Fzd2 is down-regulated in Gata6 mutants and increased Fzd2 or decreased ¸†-catenin expression rescues, in part, the lung epithelial defects in Gata6 mutants. During lung epithelial regeneration, we show that canonical Wnt signaling is activated in the niche containing BASCs and forced activation of Wnt signaling leads to a dramatic increase in BASC numbers. Moreover, Gata6 is required for proper lung epithelial regeneration and postnatal loss of Gata6 leads to increased BASC expansion and decreased differentiation. Together, these data demonstrate that Gata6 regulated Wnt signaling controls the balance between stem/progenitor expansion and epithelial differentiation required for both lung development and regeneration. **Keywords:** gene targets in knockout mouse model **Overall design:** 3 replicates of each condition-wild-type and GATA6 null tissue. 6 total samples.

Background corr dist: KL-Divergence = 0.0496, L1-Distance = 0.0769, L2-Distance = 0.0084, Normal std = 0.7206

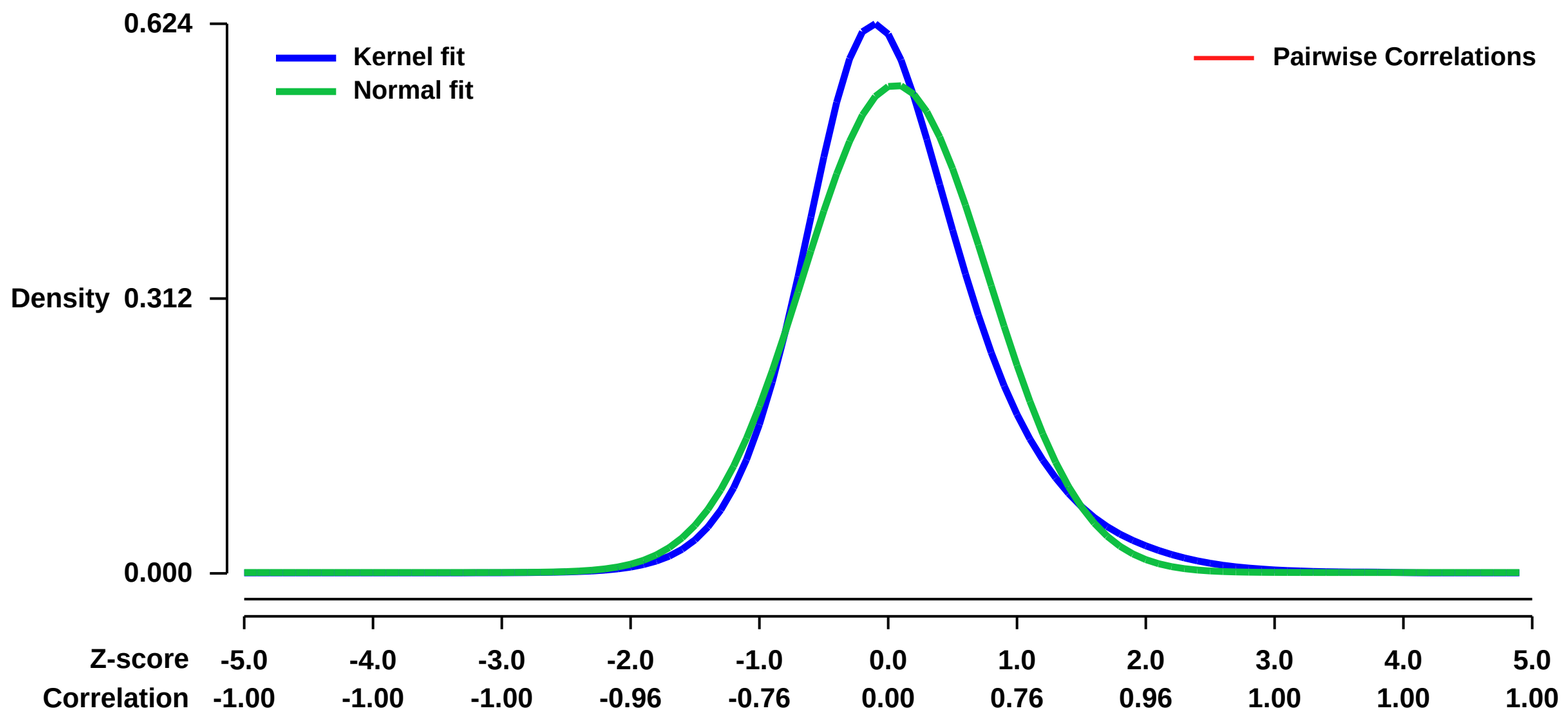

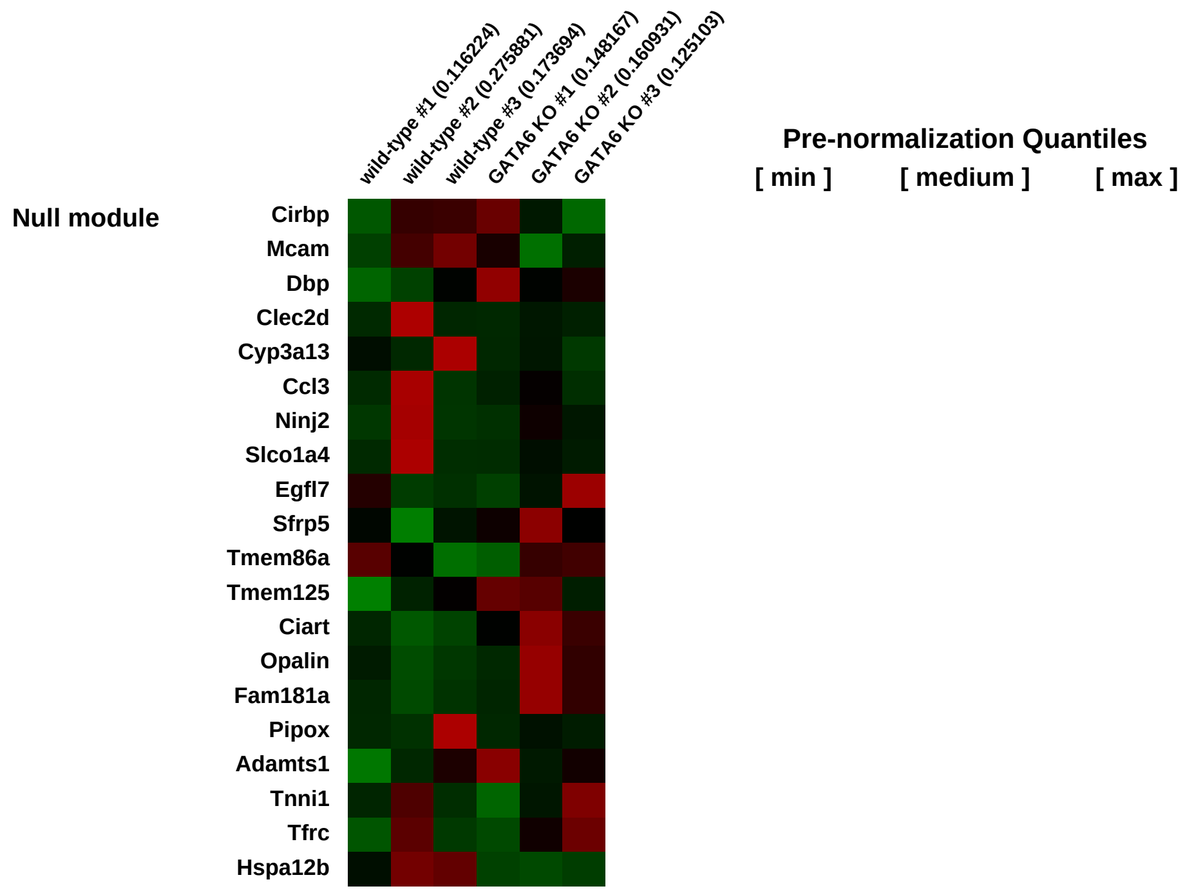

GEO Series "GSE11186" Expression Profiles

Num of samples in this series: 33

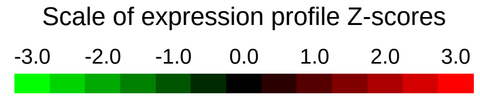

GEO Link:	http://www.ncbi.nlm.nih.gov/geo/query/acc.cgi?acc=GSE11186
Status:	Public on Jul 17 2009
Title:	Expression profiling of mouse dorsal skin during hair follicle cycling
Organism:	Mus musculus
Experiment type:	Expression profiling by array
Platform:	GPL1261
Pubmed ID:	19629164
Summary & Design:	**Summary:** Hair follicles undergo recurrent cycling of controlled growth (anagen), regression (catagen), and relative quiescence (telogen) with a defined periodicity. Taking a genomics approach to study gene expression during synchronized mouse hair follicle cycling, we discovered that, in addition to circadian fluctuation, CLOCK-regulated genes are also modulated in phase with the hair growth cycle. During telogen and early anagen, circadian clock genes are prominently expressed in the secondary hair germ, which contains precursor cells for the growing follicle. Analysis of Clock and Bmal1 mutant mice reveals a delay in anagen progression, and the secondary hair germ cells show decreased levels of phosphorylated Rb and lack mitotic cells, suggesting that circadian clock genes regulate anagen progression via their effect on the cell cycle. Consistent with a block at the G1 phase of the cell cycle, we show a significant upregulation of p21 in Bmal1 mutant skin. While circadian clock mechanisms have been implicated in a variety of diurnal biological processes, our findings indicate that circadian clock genes may be utilized to modulate the progression of non-diurnal cyclic processes. **Overall design:** To investigate the molecular control of hair follicle cycling, we profiled mRNA expression in mouse dorsal skin at multiple representative time points in the synchronized second postnatal hair growth cycle and in a depilation-induced hair growth cycle. For profiling of second synchronized and depilation-induced hair growth cycle, the same upper-mid region of dorsal skin was excised from C57BL/6 mice at representative postnatal days (P). The time points for second hair growth cycle are classified into different phases of the hair growth cycle based on established morphological guidelines as follow: early anagen (P23, P25), mid anagen (P27), late anagen (P29, P34), early catagen (P37, P39), mid catagen (P41), and telogen (P44). Depilation-induced hair growth cycle by applying wax/rosin mixture on the dorsal skin of seven-week old mice (all follicles in telogen) was performed on mice. The corresponding phases of the hair growth cycle at number of days following depilation (D) is as follow: early anagen (D3), mid anagen (D5), late anagen (D8, D12), and early catagen (D17). For each time point, multiple biological replicates were profiled, with each mouse dorsal skin separately hybridized to an Affymetrix array.

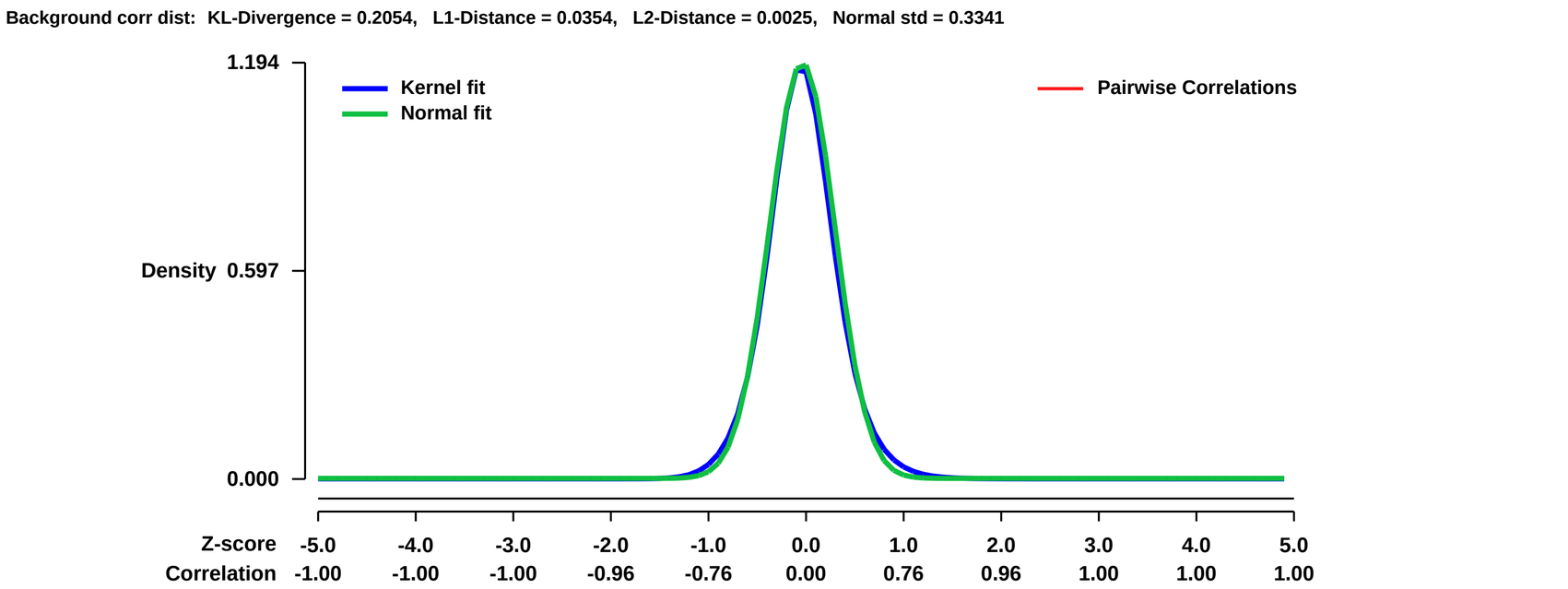

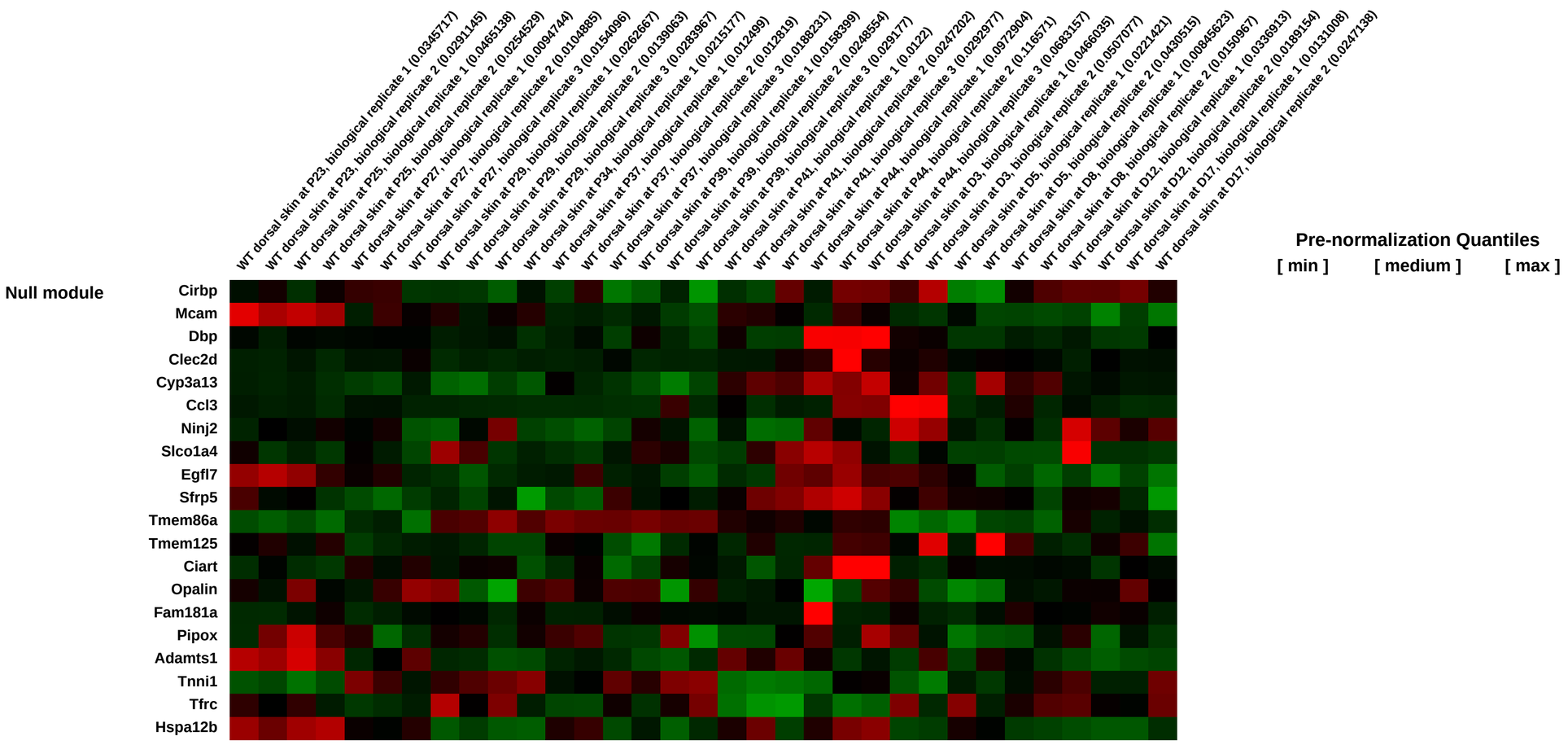

GEO Series "GSE11207" Expression Profiles

Num of samples in this series: 6

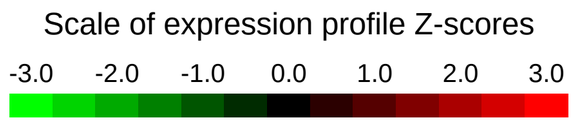

GEO Link:	**http://www.ncbi.nlm.nih.gov/geo/query/acc.cgi?acc=GSE11207**
Status:	**Public on Apr 19 2008**
Title:	**Dorsal root ganglion (katz-affy-mouse-210210)**
Organism:	**Mus musculus**
Experiment type:	**Expression profiling by array**
Platform:	**GPL1261**
Pubmed ID:	
Summary & Design:	**Summary:** **The molecular identity of touch sensation is still largely unknown. We choose an extrem and very specific example, touch sensation of pennis glan, to study this problem. It's known from previous retro-grade labeling result that only one DRG in rat innervate the pennis glan, which makes it idea for microarry analysis.** **To clone the mechanosensory receptor specifically or highly expressed in the primary sensory neurons innervating pennis glan.** **There is a specific mechanosensory receptor in the primary sensory neurons innervating pennis glan.** **1. Retrograde labeling the innervating nerve by DiI** **2. Dissect DRGs, dissociate neurons and pick up the fluorescent cells.** **3. Pool around 20 positive cells and 50 control cells (big diameter neuron and small to medium diameter neuron respectively), purify total RNA.** **4. Two rounds of amplification** **5. Affymetrix analysis** **Keywords: dorsal root ganglion, touch sensatiion** **Overall design:**

Background corr dist: KL-Divergence = 0.0479, L1-Distance = 0.0281, L2-Distance = 0.0010, Normal std = 0.5894

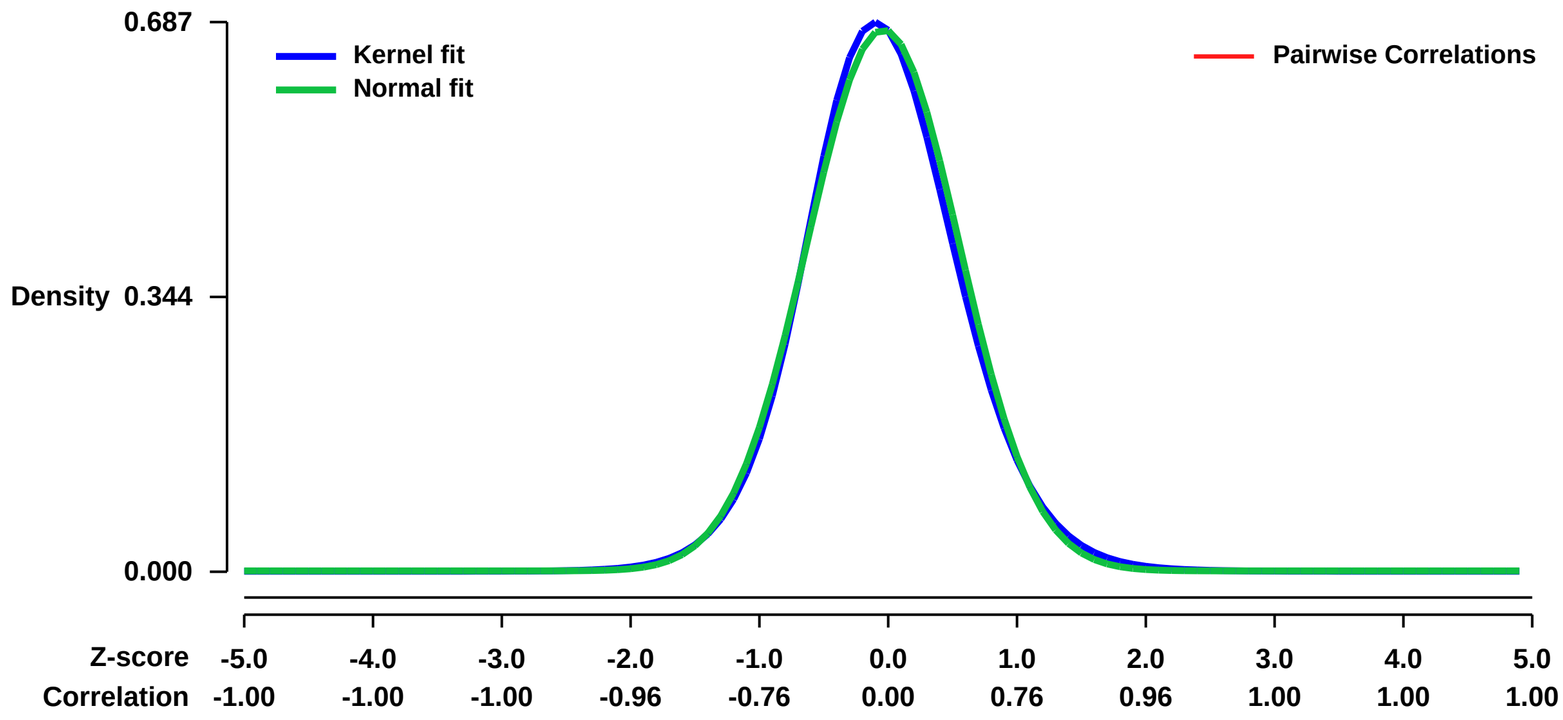

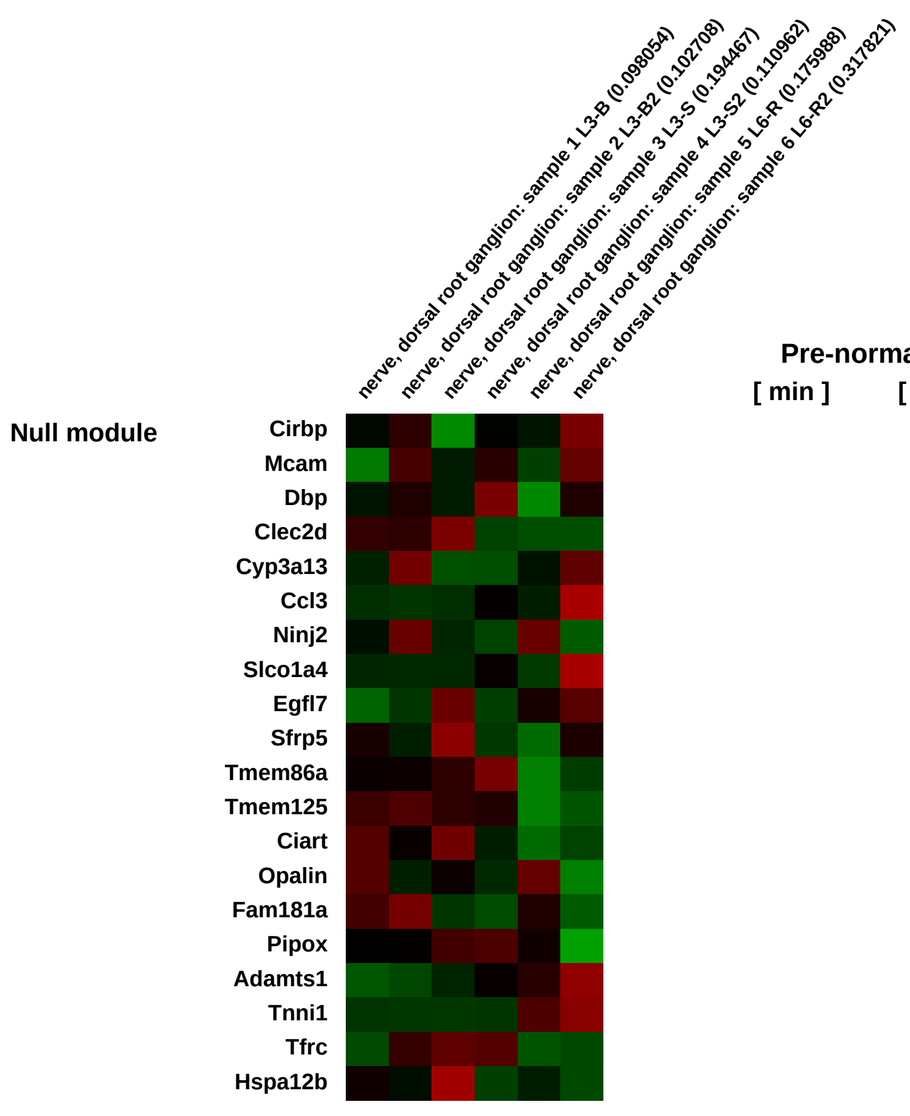

GEO Series "GSE11258" Expression Profiles

Num of samples in this series: 24

Scale of expression profile Z-scores

-3.0 -2.0 -1.0 0.0 1.0 2.0 3.0

GEO Link:	**http://www.ncbi.nlm.nih.gov/geo/query/acc.cgi?acc=GSE11258**
Status:	**Public on Sep 24 2008**
Title:	**Npas4-regulated genes in mouse hippocampal neurons**
Organism:	**Mus musculus**
Experiment type:	**Expression profiling by array**
Platform:	**GPL1261**
Pubmed ID:	**18815592**
Summary & Design:	**Summary:** **we performed a DNA microarray experiment to identify activity-regulated genes that are misregulated in the absence of Npas4.** **Keywords: Primary neuron culture, depolarization, activity-dependent, Npas4** **Overall design:** **We infected mouse hippocampal neurons with lentivirus expressing Npas4-RNAi or control-RNAi @ 3 DIV and depolarized the neurons @ 8 DIV with 50 mM of KCl for 0, 1, 3 or 6 hours. Neurons were lysed, mRNA isolated and hybridized to Affymetrix arrays. Data were collected from 3 independent experiments.**

Background corr dist: **KL-Divergence = 0.2486, L1-Distance = 0.0389, L2-Distance = 0.0028, Normal std = 0.3070**

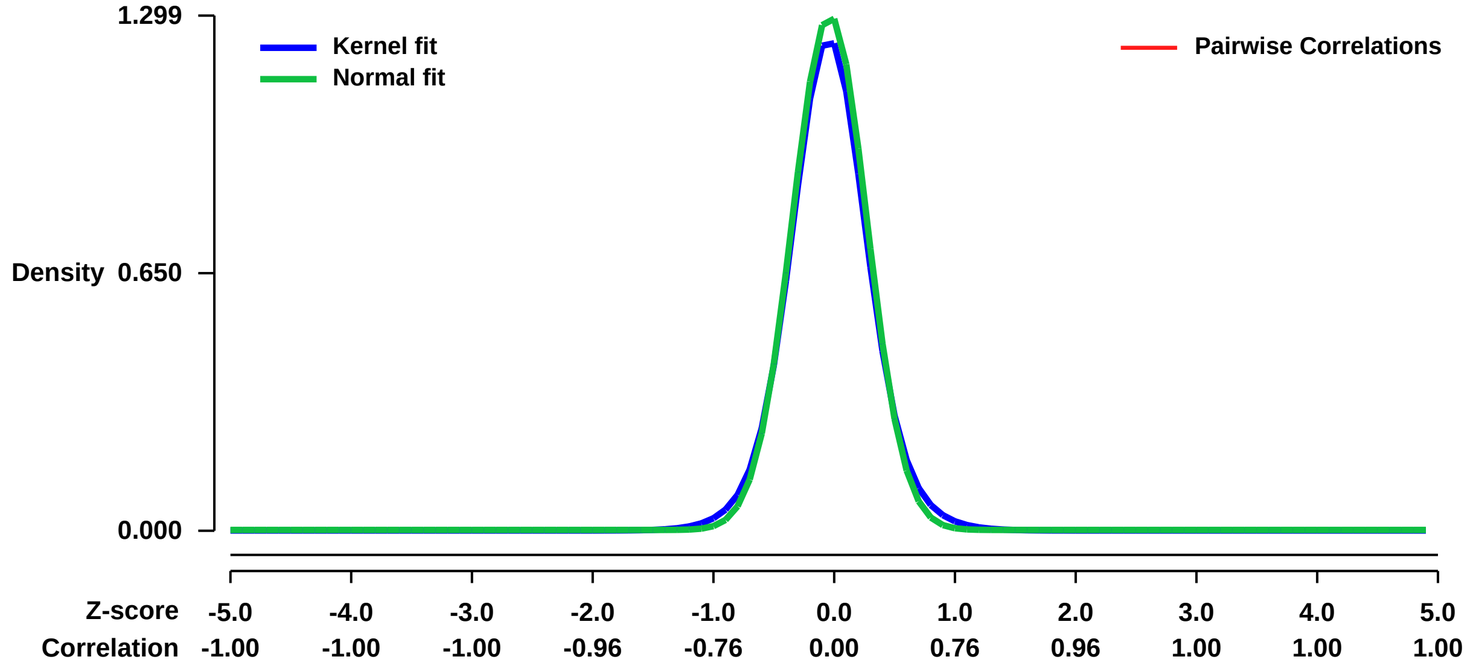

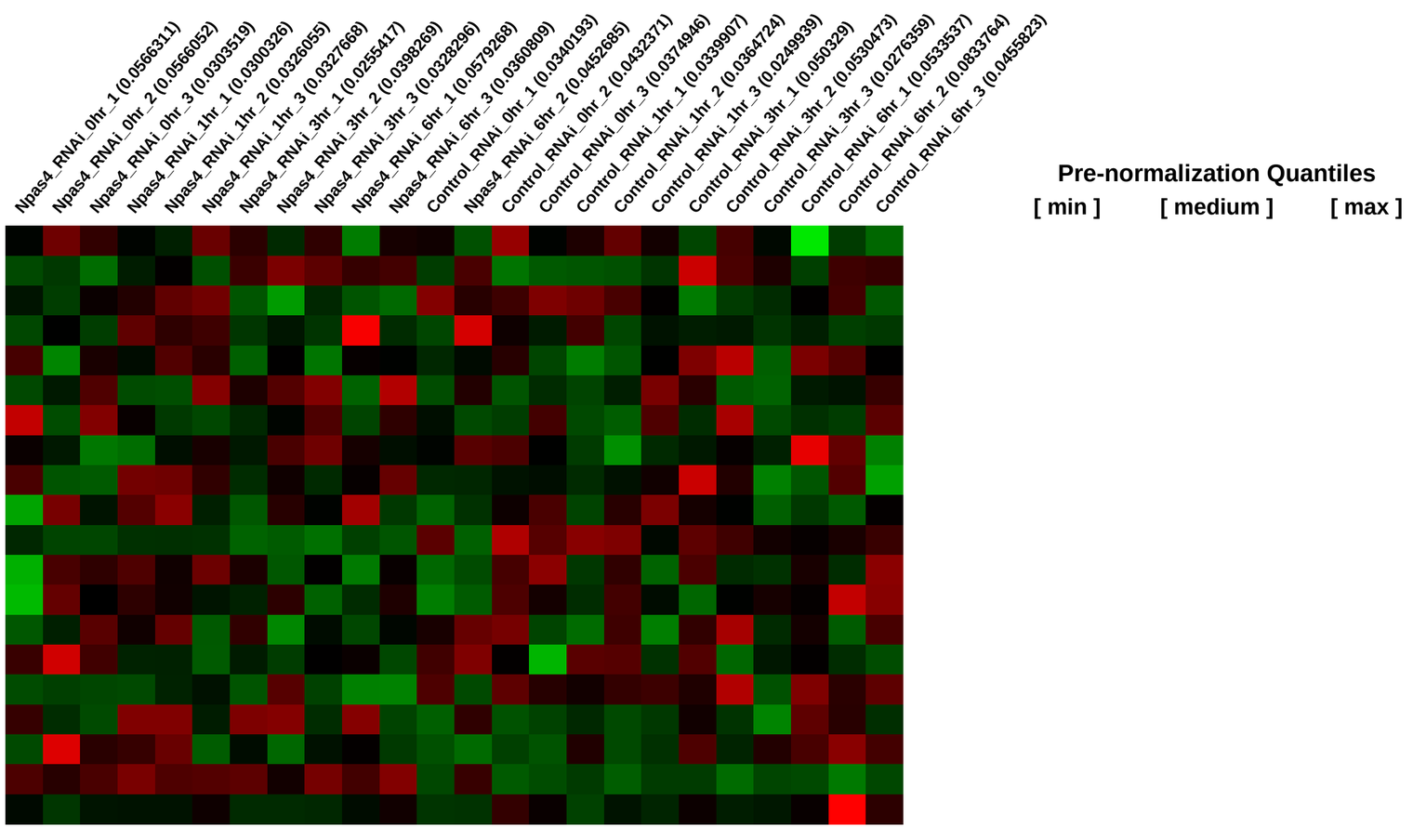

GEO Series "GSE11276" Expression Profiles

Num of samples in this series: 6

Scale of expression profile Z-scores

-3.0 -2.0 -1.0 0.0 1.0 2.0 3.0

GEO Link:	**http://www.ncbi.nlm.nih.gov/geo/query/acc.cgi?acc=GSE11276**
Status:	**Public on Nov 01 2010**
Title:	**Comparison of adult intact naive C57Bl/6 Nogo-A KO versus WT spinal cord**
Organism:	**Mus musculus**
Experiment type:	**Expression profiling by array**
Platform:	**GPL1261**
Pubmed ID:	
Summary & Design:	**Summary:** **Nogo-A localized on myelin adaxonal membrane in the adult CNS is well known for its role as neurite outgrowth inhibitor following a lesion. Nogo-A KO mice show enhanced regenerative/compensatory fiber growth following CNS lesion. However, changes undergoing in their intact CNS have not been studied. Moreover, Nogo-A in the intact adult CNS in also expressed in some neuronal subpopulations, e.g. in the hippocampus, olfactory bulbs and dorsal root ganglia.** **We compared the intact adult CNS (spinal cord) of Nogo-A KO mice in order to identify: potential compensating molecules which could be interesting new inhibitory neurite outgrowth candidates, possible molecules involved in the up to now not yet clarified downstream signalling pathway of Nogo-A, additional new functions for myelin or neuronal Nogo-A in the intact adult CNS.**
	Keywords: gene expression, Nogo-A KO, spinal cord, adult, naive, unlesioned
	Overall design: **Spinal cords from 3 adult C57Bl/6 wild type and Nogo-A KO mice have been explanted. Total RNA has been extracted and processed for hybridization on Mouse 430 2.0 Affymetrix GeneChips. Following scanning and first analysis with MAS 5.0, further analysis was performed by GeneSpring 7.2 (Silicon Genetics, Redwood City, CA). A present call filter (2 out of 3 present calls in at least one out of the different studied conditions) was applied. Normalization was run per chip as well as per gene to the median of the control replicates. Data were statistical restricted through a 1-way Anova (p=0.05). A final threshold of =1.2 folds of increase or decrease in the expression level of each single transcript was applied. Regulated transcripts have been assigned to functional categories according to GeneOntology as well as literature and database mining (Pubmed and Bioinformatics Harvester EMBL Heidelberg).**

Background corr dist: **KL-Divergence = 0.0322, L1-Distance = 0.0218, L2-Distance = 0.0006, Normal std = 0.6601**

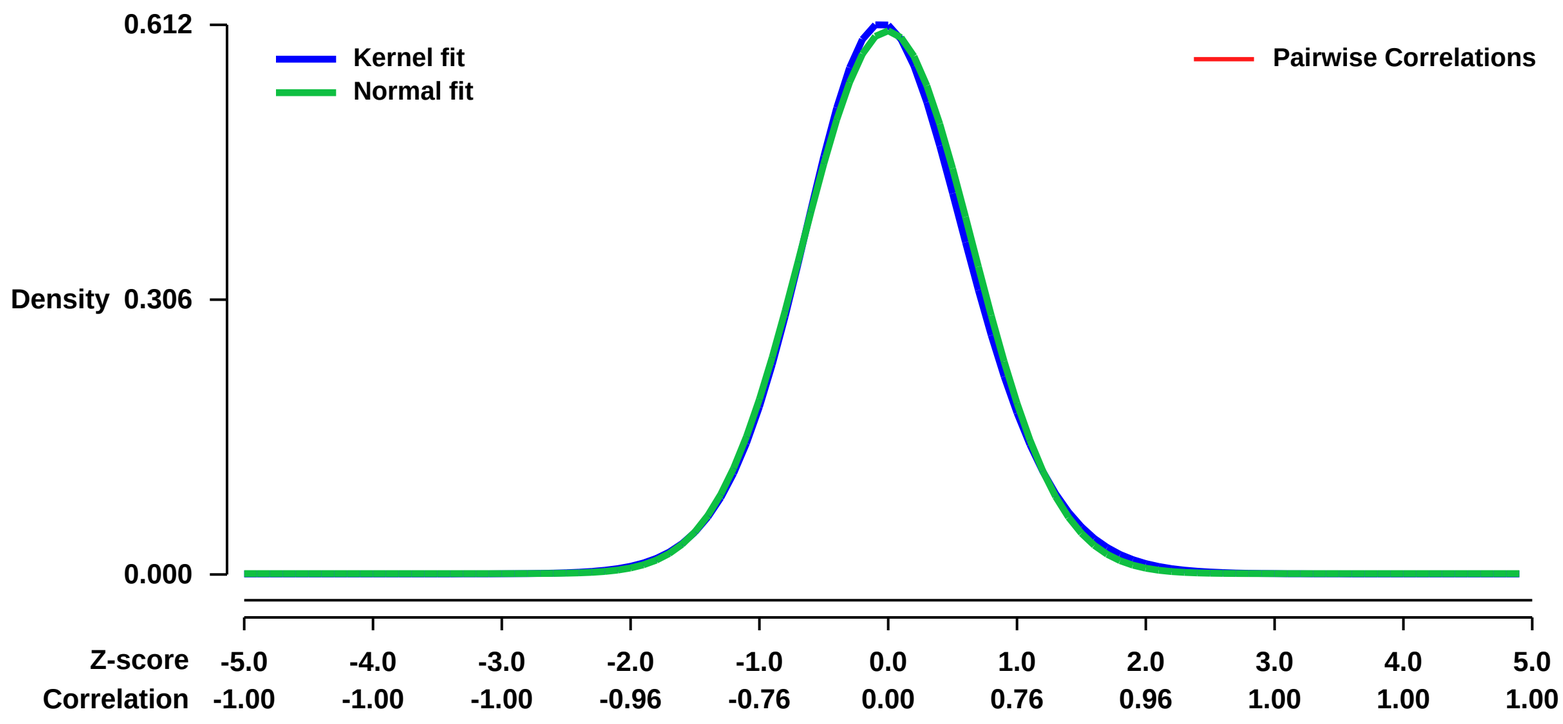

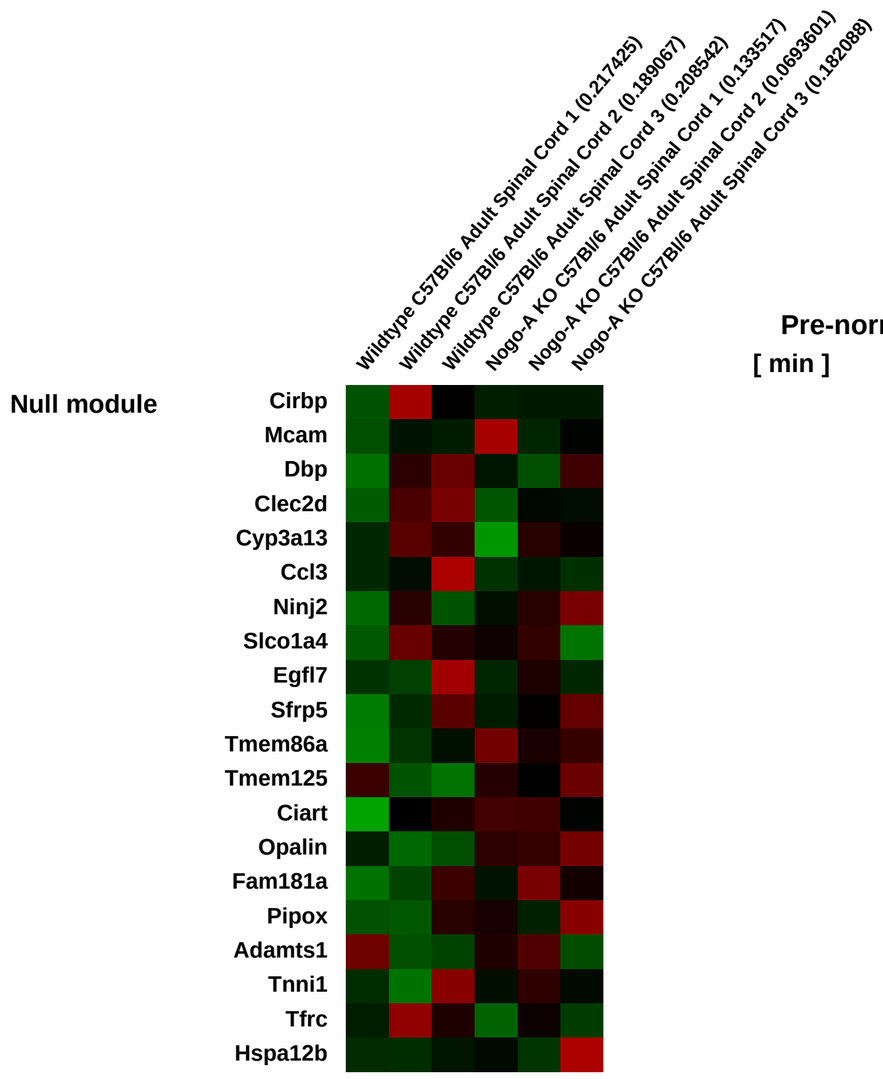

GEO Series "GSE11287" Expression Profiles

Num of samples in this series: 6

Scale of expression profile Z-scores

-3.0 -2.0 -1.0 0.0 1.0 2.0 3.0

GEO Link:	http://www.ncbi.nlm.nih.gov/geo/query/acc.cgi?acc=GSE11287
Status:	Public on May 01 2008
Title:	Keap1-dependent gene expression determined in the liver using conditional Keap1 knockout mice vs. genetic control mice
Organism:	Mus musculus
Experiment type:	Expression profiling by array
Platform:	GPL1261
Pubmed ID:	18417483
Summary & Design:	**Summary:** To compare hepatic gene expression in conditional Keap1 knockout (Alb-Cre:Keap1(flox/-)) and genetic control mice. Disruption of Keap1-mediated repression of Nrf2 signaling was expected to result in increased expression of Nrf2-regulated genes. **Keywords: comparative expression profiling** **Overall design:** Hepatic gene expression was compared in conditional Keap1 knockout and genetic control mice (Alb-Cre:Keap1(flox/+)) mice. Male 9 week old mice were used, n=3/group.

Background corr dist: KL-Divergence = 0.0460, L1-Distance = 0.0177, L2-Distance = 0.0003, Normal std = 0.5880

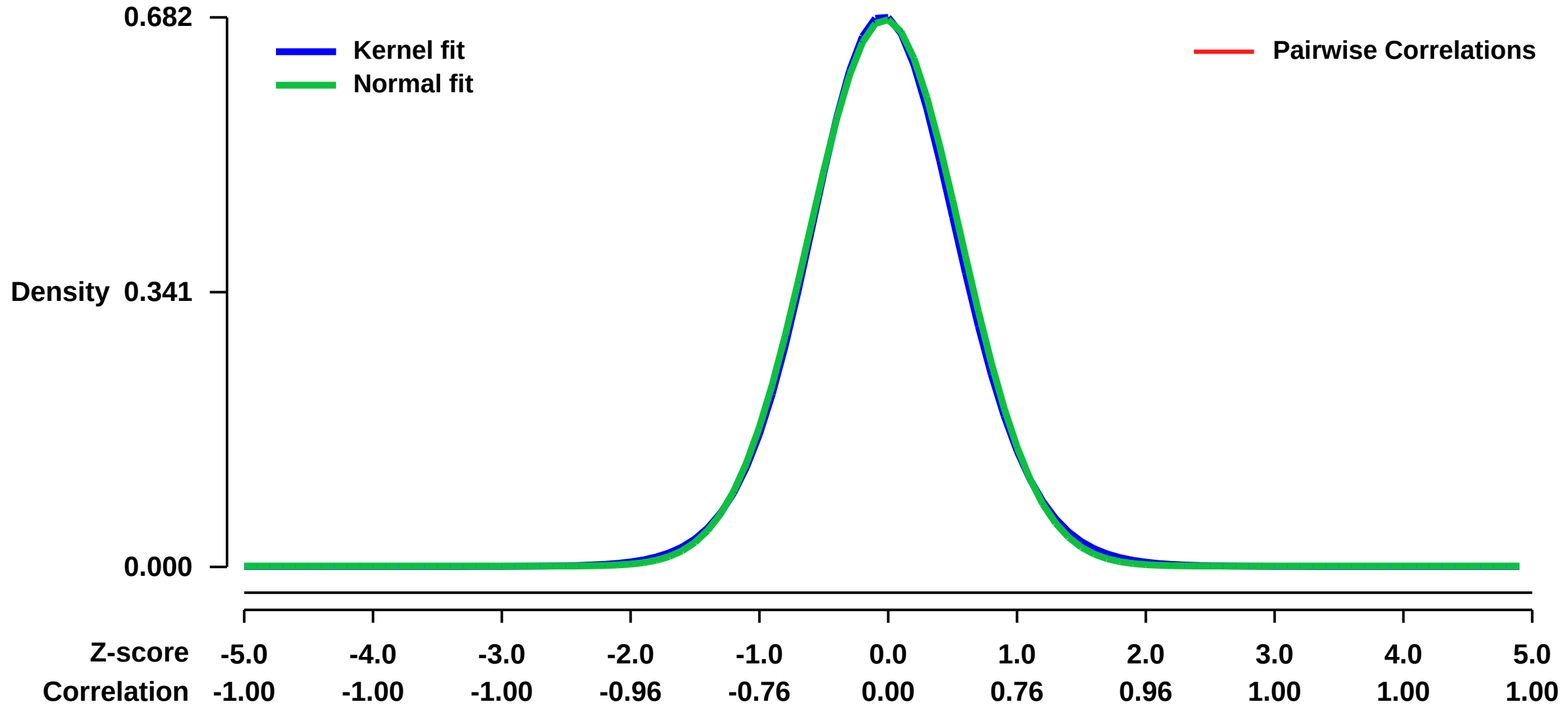

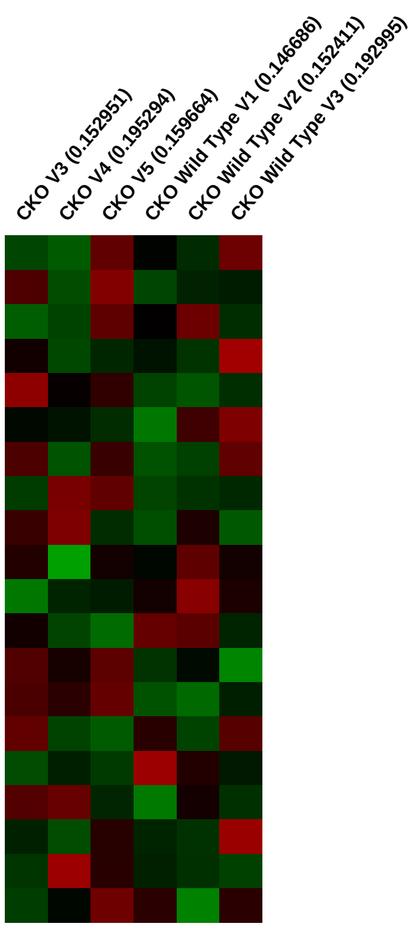

GEO Series "GSE11343" Expression Profiles

Num of samples in this series: 19

Scale of expression profile Z-scores

-3.0 -2.0 -1.0 0.0 1.0 2.0 3.0

GEO Link:	http://www.ncbi.nlm.nih.gov/geo/query/acc.cgi?acc=GSE11343
Status:	Public on May 10 2008
Title:	Rosiglitazone Treatment Reduces Diabetic Neuropathy in STZ treated DBA/2J mice
Organism:	Mus musculus
Experiment type:	Expression profiling by array
Platform:	GPL1261
Pubmed ID:	18583417
Summary & Design:	**Summary:** Diabetic Neuropathy (DN) is a common complication of diabetes. Currently, there is no drug treatment to prevent or slow the development of DN. Rosiglitazone (Rosi) is a potent insulin sensitizer and may also slow the development of DN by a mechanism independent of its effect on hyperglycemia. A two by two design was used to test the effect of Rosi treatment on the development of DN. Streptozotocin-induced diabetic DBA/2J mice were treated with Rosi. DN and oxidative stress were quantified, and gene expression was profiled using the Affymetrix Mouse Genome 430 2.0 microarray platform. An informatics approach identified key regulatory elements activated by Rosi. Diabetic DBA/2J mice developed severe hyperglycemia, DN and elevated oxidative stress. Rosi treatment did not affect hyperglycemia but did reduce oxidative stress and prevented development of thermal hypoalgesia. Two novel transcription factor binding modules were identified that may control genes correlated to changes in DN following Rosi treatment: SP1F_ZBPF and EGRF_EGRF. Rosi treatment reduced oxidative stress and DN independent of its insulin sensitizing effects. Gene expression profiling identified two novel targets activated by Rosi treatment. These targets may be useful in designing drugs with the same efficacy as Rosi in treating DN but with fewer undesirable effects. **Keywords: disease and treatment analysis** **Overall design:** Affymetrix chips were run on five mice from each group. One chip (in the Control group) failed quality control measures and was excluded.

Background corr dist: KL-Divergence = 0.0893, L1-Distance = 0.0337, L2-Distance = 0.0021, Normal std = 0.4560

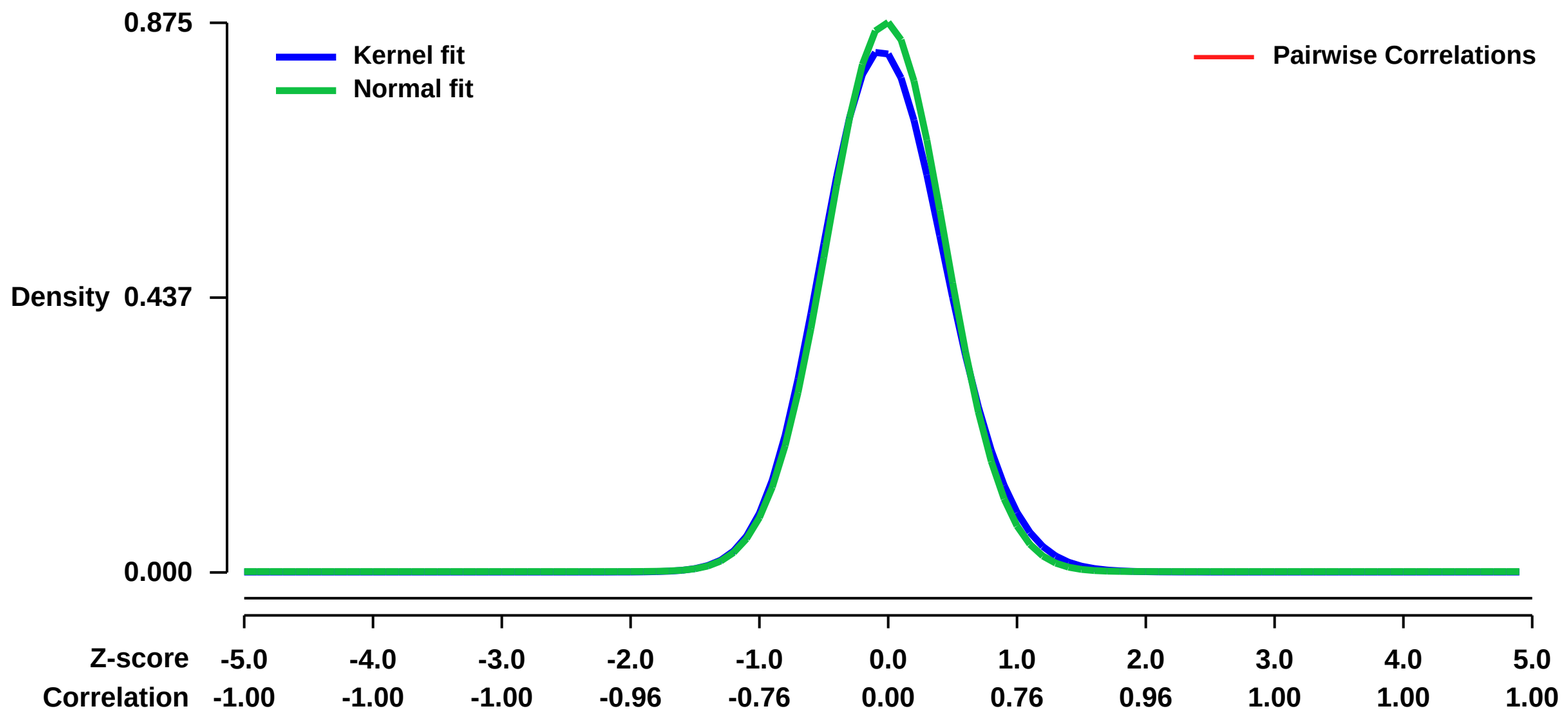

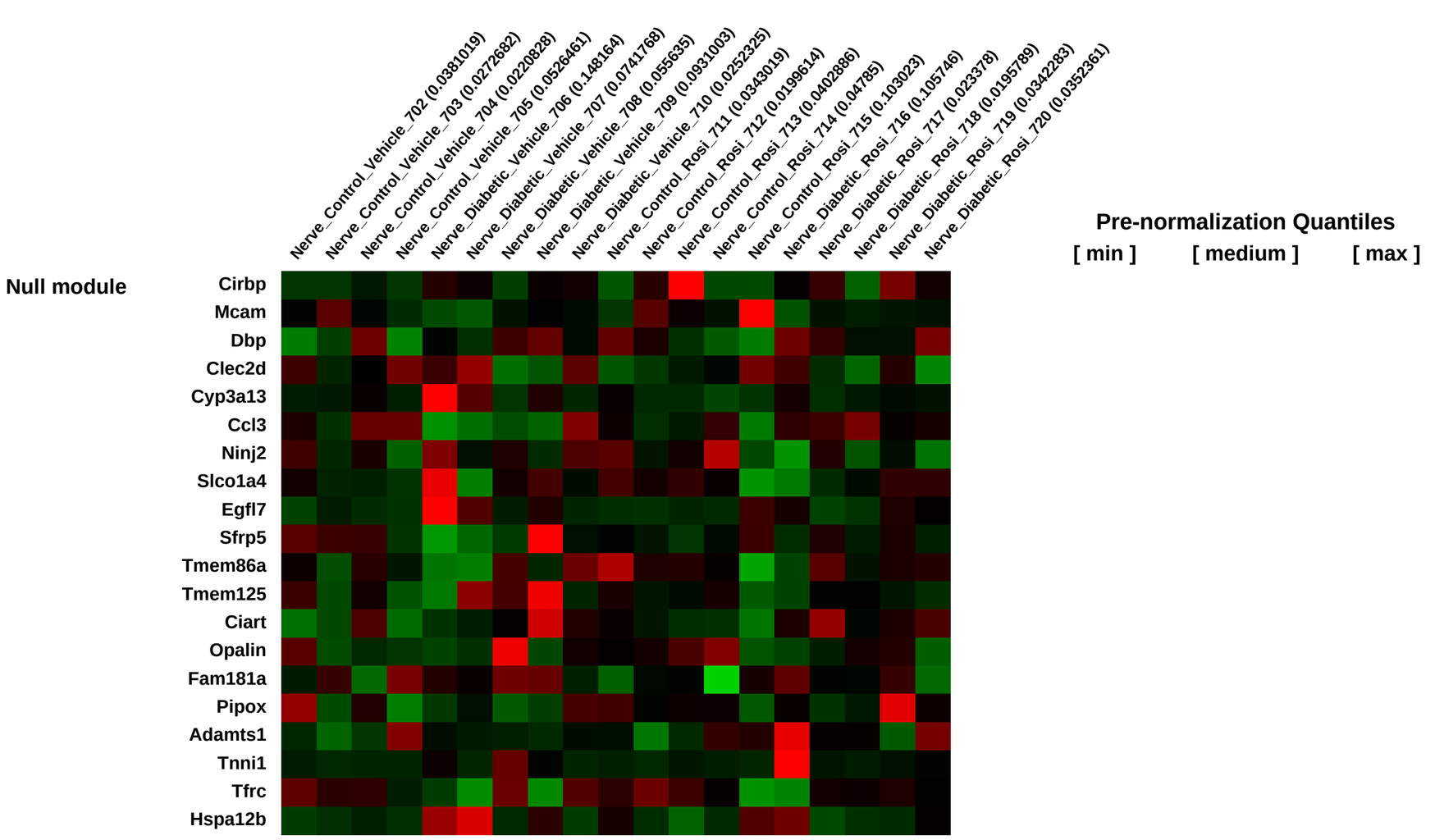

GEO Series "GSE11356" Expression Profiles

Num of samples in this series: 9

Scale of expression profile Z-scores

-3.0 -2.0 -1.0 0.0 1.0 2.0 3.0

GEO Link:	**http://www.ncbi.nlm.nih.gov/geo/query/acc.cgi?acc=GSE11356**
Status:	**Public on May 06 2008**
Title:	**Expression data from early and adult stages of mouse development**
Organism:	**Mus musculus**
Experiment type:	**Expression profiling by array**
Platform:	**GPL1261**
Pubmed ID:	
Summary & Design:	**Summary:** **DNA repair genes have been shown to be expressed in the early stages of mammalian development probably to reduce possible replication errors and genotoixc damages. Several birth defects and some cancers are due to inappropriate or defective DNA repair machinery indicating that a right activity of DNA repair genes in the early stages of fetal development are essential for an appropriate DNA function. Neuroblastoma (NB), an embryonal tumor deriving from neural crest cells (NCCs) is diagnosed in about 30% of patients within the first year of life. Moreover, several reports show that NB can be detected in foetus and in neonatal period.** **To assess gene expression profiling of DNA repair genes during early stage of development, we performed a genome-wide analysis of Neural Crest cells (NCCs) generating a gene expression database that can help to better understand the gene(s) involved in both genetic and cancer diseases. We found 11 genes involved in DNA repair activity during mouse embryo development overexpressed in early stages. Six out 11 were never been described in mouse embryology.** **Keywords: time course** **Overall design:** **Mouse embryos were collected at successive stages of early and adult development stages for RNA extraction and hybridization on Affymetrix microarrays. We sought to obtain homogeneous populations of NCCs by Laser Capture Microdissection (LCM) from embryos and adult in order to analyze DNA repair genes during mouse development. To that end, we collected cells at three time-points: at embryonal stage of 8.5 dpc: E8.5 (neural tube closure); at embryonal stage of 13.5dpc: E13.5 (dorsal root ganglion); at adult stage of 3 months postnatal: P90 (adrenal medulla).**

Background corr dist: KL-Divergence = 0.0700, L1-Distance = 0.0501, L2-Distance = 0.0047, Normal std = 0.5213

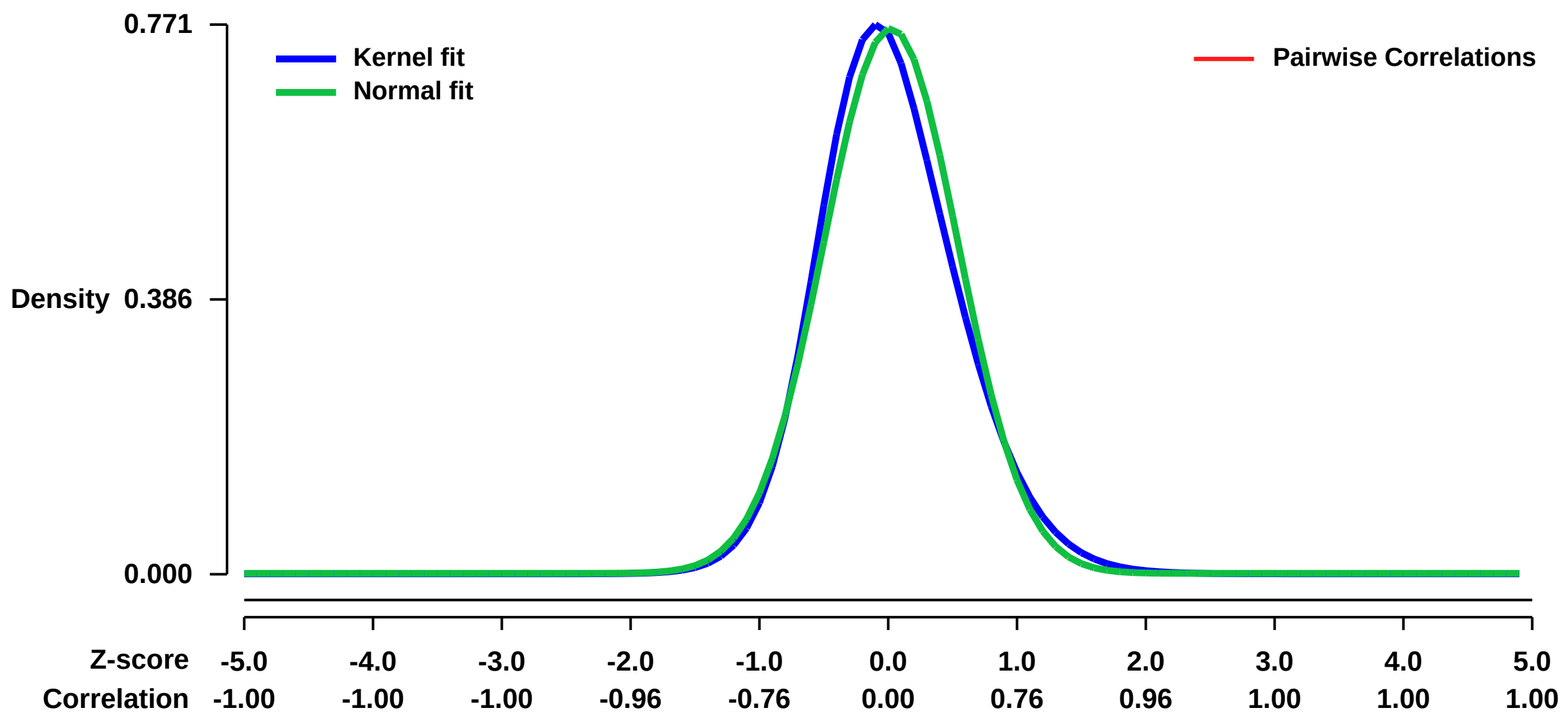

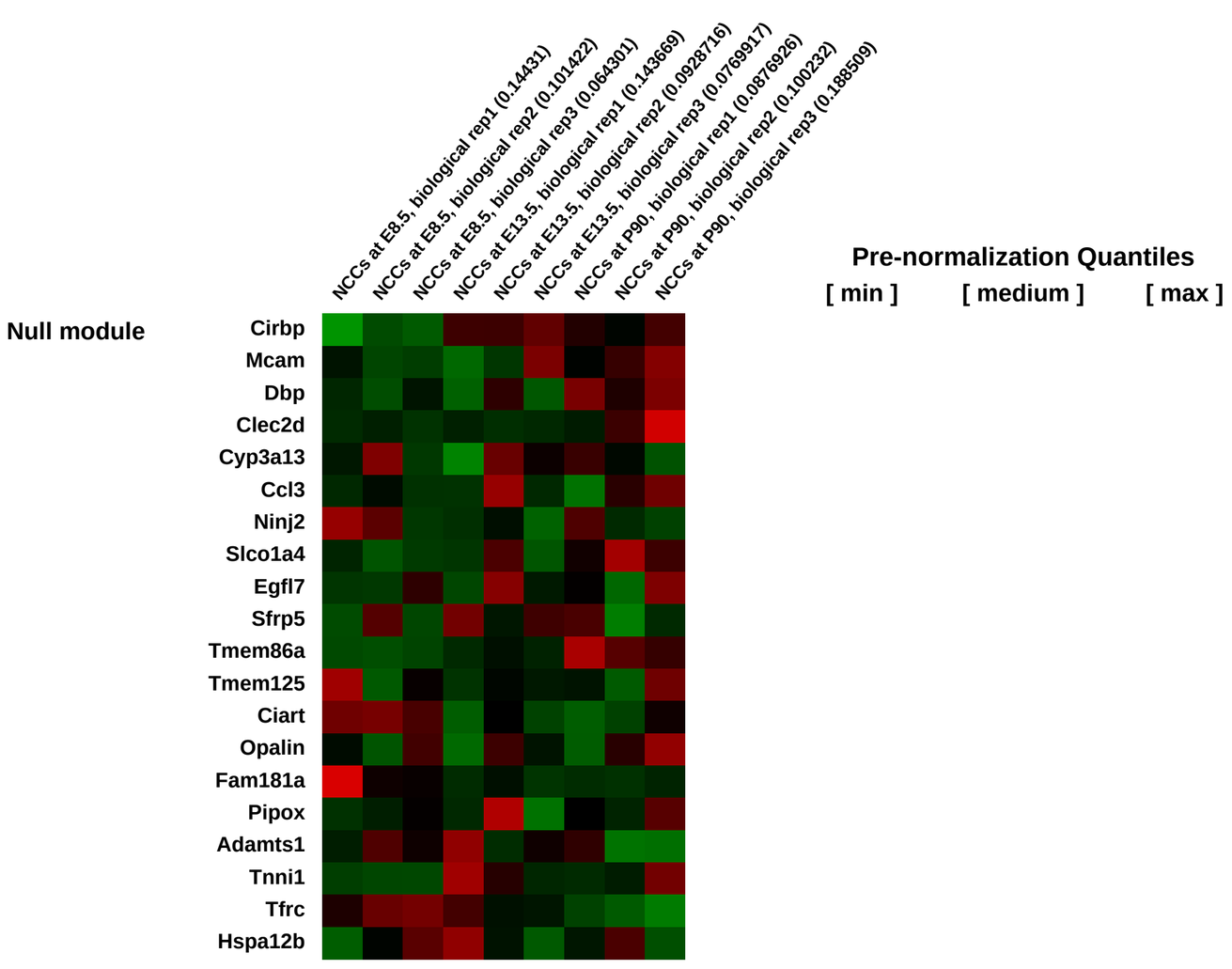

GEO Series "GSE11419" Expression Profiles

Num of samples in this series: 6

Scale of expression profile Z-scores

-3.0 -2.0 -1.0 0.0 1.0 2.0 3.0

GEO Link:	**http://www.ncbi.nlm.nih.gov/geo/query/acc.cgi?acc=GSE11419**
Status:	**Public on Jul 12 2010**
Title:	**GeneChip expression profiling of Glud1 (glutamate dehydrogenase 1) transgenic mice**
Organism:	**Mus musculus**
Experiment type:	**Expression profiling by array**
Platform:	**GPL1261**
Pubmed ID:	**20529287**
Summary & Design:	**Summary:** **Glud1 (glutamate dehydrogenase 1) transgenic mice release more excitatory neurotransmitter glutamate to synaptic cleft throughout lifespan and show signs of accelerated aging.** **Here we compared transcriptomic profiles of these animals to their wild-type counterparts. The hippocampus was used for the analysis.** **Keywords: transgenic analysis** **Overall design:** **Three Glud1 transgenic mice vs. three age-matched wide-type mice. Age: 9-month-old. Tissue: hippocampus.**

Background corr dist: **KL-Divergence = 0.0484, L1-Distance = 0.0189, L2-Distance = 0.0004, Normal std = 0.5788**

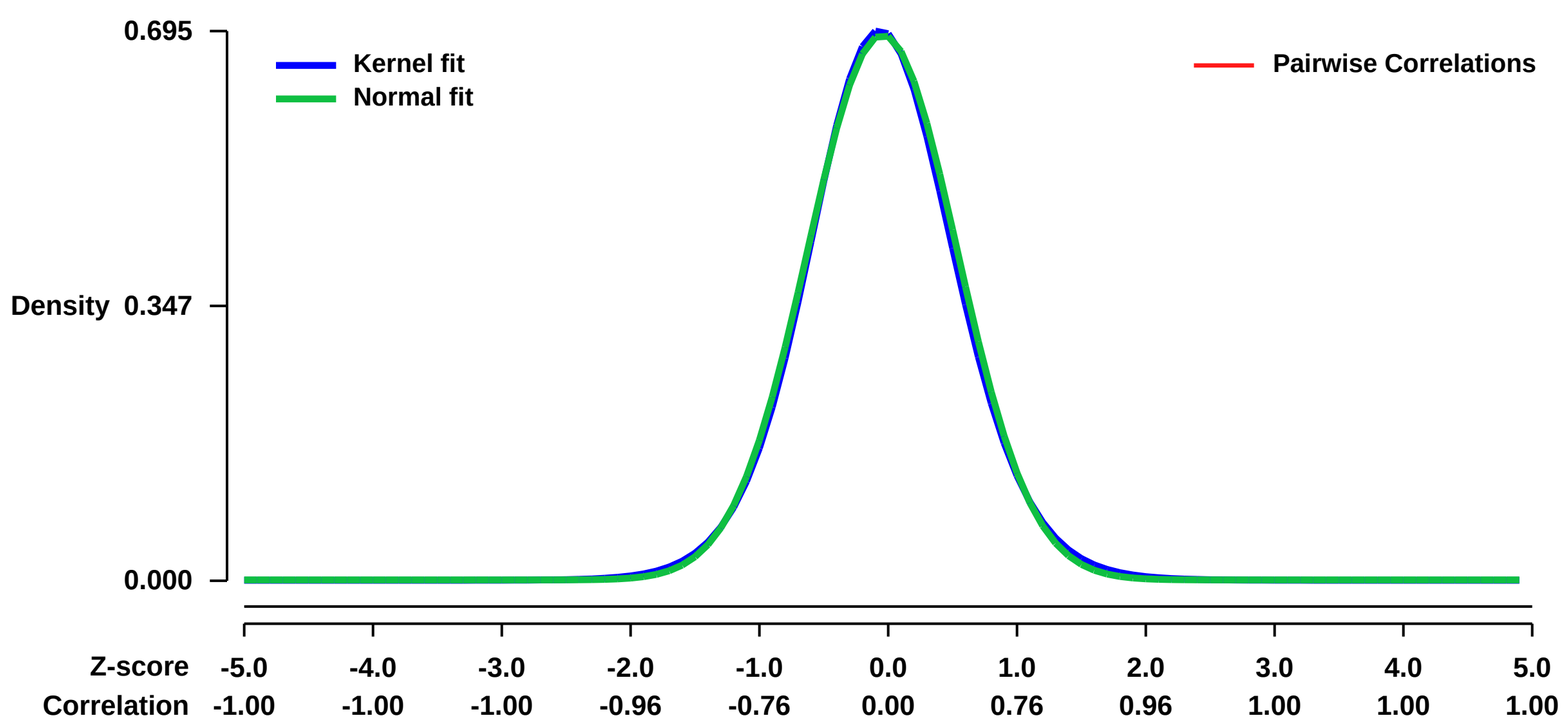

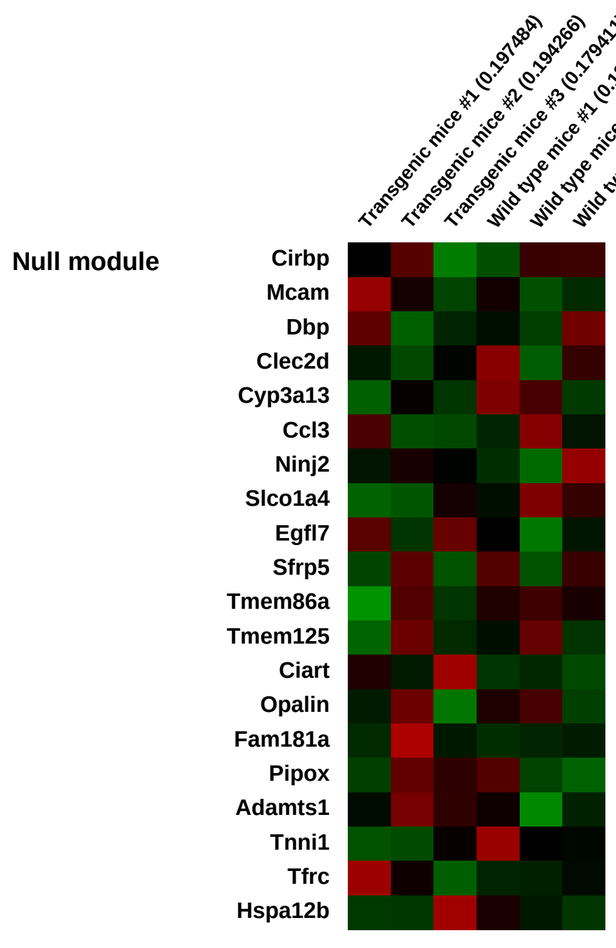

GEO Series "GSE11434" Expression Profiles

Num of samples in this series: 10

Scale of expression profile Z-scores

-3.0 -2.0 -1.0 0.0 1.0 2.0 3.0

GEO Link:	http://www.ncbi.nlm.nih.gov/geo/query/acc.cgi?acc=GSE11434
Status:	Public on May 15 2008
Title:	Ventilator-induced lung injury in C57BL\6 mice
Organism:	Mus musculus
Experiment type:	Expression profiling by array
Platform:	GPL1261
Pubmed ID:	19447895
Summary & Design:	**Summary:** This study was undertaken to examine differential gene expression across the whole genome during short-term ventilator-induced lung injury in mice, a commonly used model of acute lung injury, as compared with spontaneous ventilation. **Keywords: Disease state analysis** **Overall design:** Mice were anesthetized with isoflurane followed by ketamine/xylaxine. Saline (0.25 ml) was given every hour ip. A tracheotomy tube was placed and the mice were ventilated with an initial peak airway pressure of 20 cmH2O approximating a tidal volume of 20 ml/kg and without end-expiratory pressure. Ventilation was continued for 3h. Tidal volume was not adjusted. Body temperature was monitored with a digital rectal thermometer and maintained at 37C with a heating table and external heating lamp. Control mice were treated identically, but were not mechanically ventilated (i.e. breathed spontaneously). There were 5 biological relicates in each group.

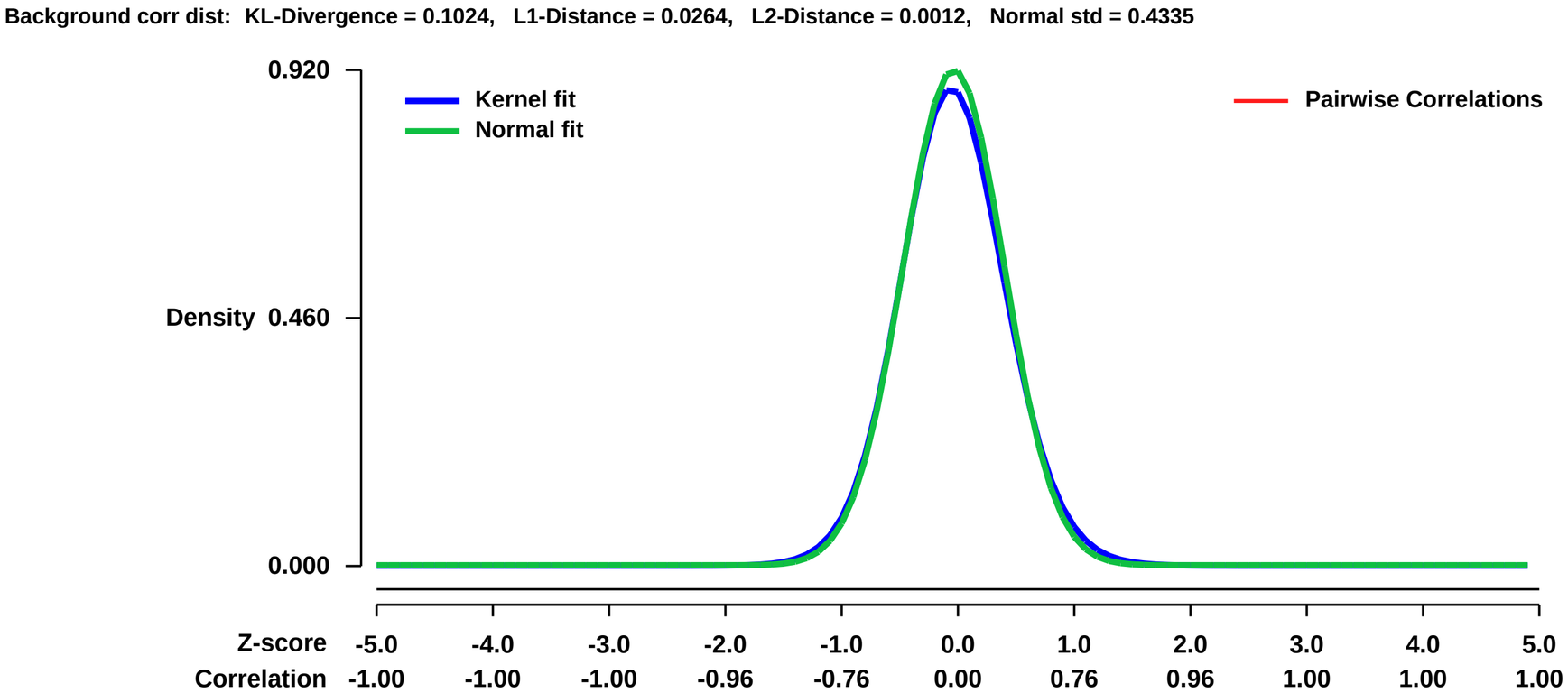

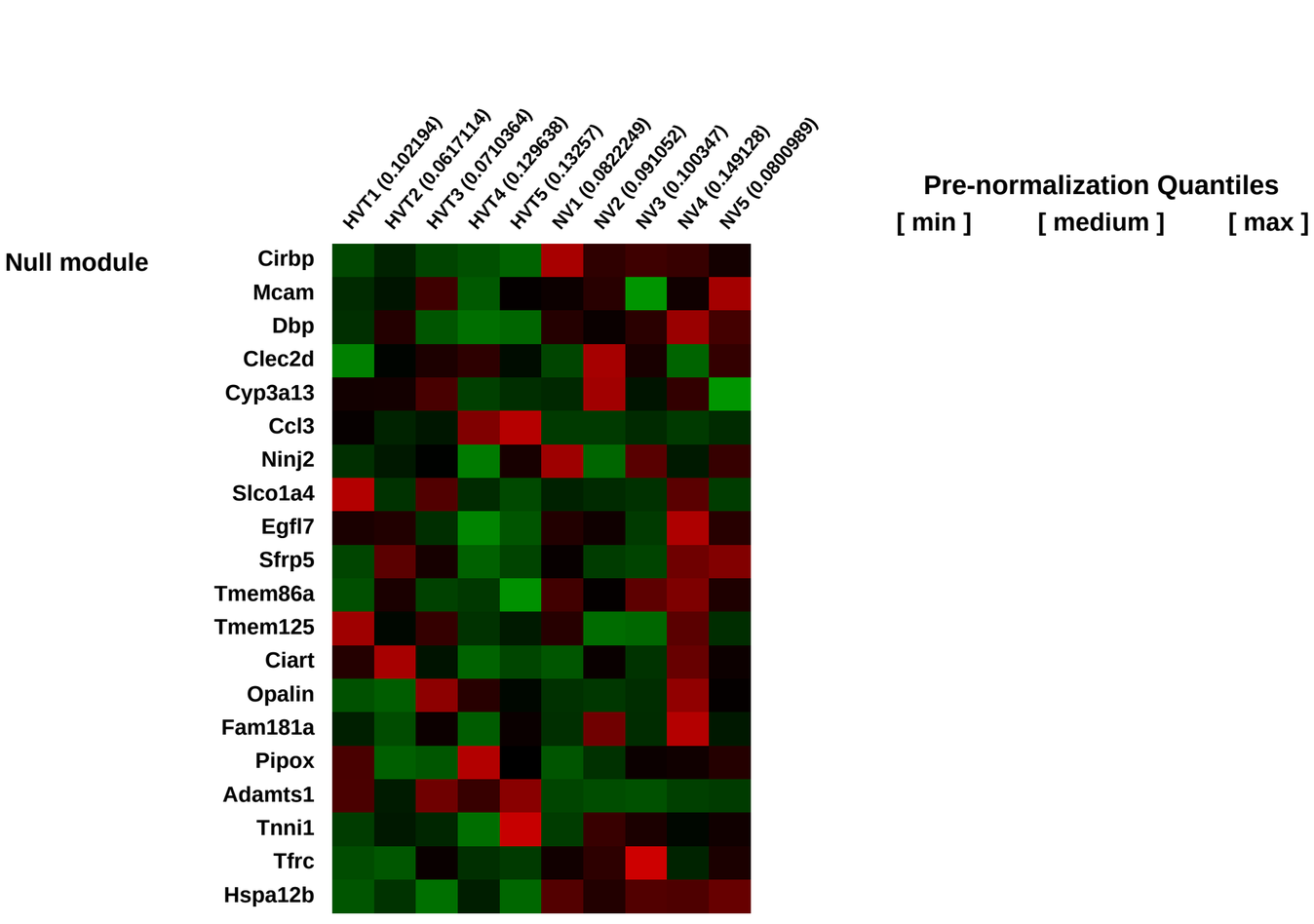

GEO Series "GSE11443" Expression Profiles

Num of samples in this series: 6

Scale of expression profile Z-scores

-3.0 -2.0 -1.0 0.0 1.0 2.0 3.0

GEO Link:	**http://www.ncbi.nlm.nih.gov/geo/query/acc.cgi?acc=GSE11443**
Status:	**Public on May 17 2008**
Title:	**Choroid plexus function in B10.pl WT mice versus B10.PL RAG-/- mice (carri-affy-mouse-302760)**
Organism:	**Mus musculus**
Experiment type:	**Expression profiling by array**
Platform:	**GPL1261**
Pubmed ID:	
Summary & Design:	**Summary:** **Previous work has led us to examine the differences in the choroid plexus function in B10.pl WT mice versus B10.PL RAG-/- mice. We believe that there is a difference between those that are normal functioning and those that are lymphocyte deficient.** **To determine the gene expression profile of the choroid plexus in wild type mice as compared to those that are lymphocyte deficient.** **We hypothesize that there is altered expression in the genes that mediate cellular adhesion in choroid plexus from wild type mice as compared to those that are lymphocyte deficient.** **8-10 week old animals (age and sex matched) were injected with Evan's blue post anesthetization. After waiting an hour the animals were euthanized and their brains were extracted and placed in RNALater for 24 hours. The brains were then sliced sagitally**
	Keywords: RAG mutant, choroid plexus
	Overall design:

Background corr dist: KL-Divergence = 0.0359, L1-Distance = 0.0301, L2-Distance = 0.0012, Normal std = 0.6517

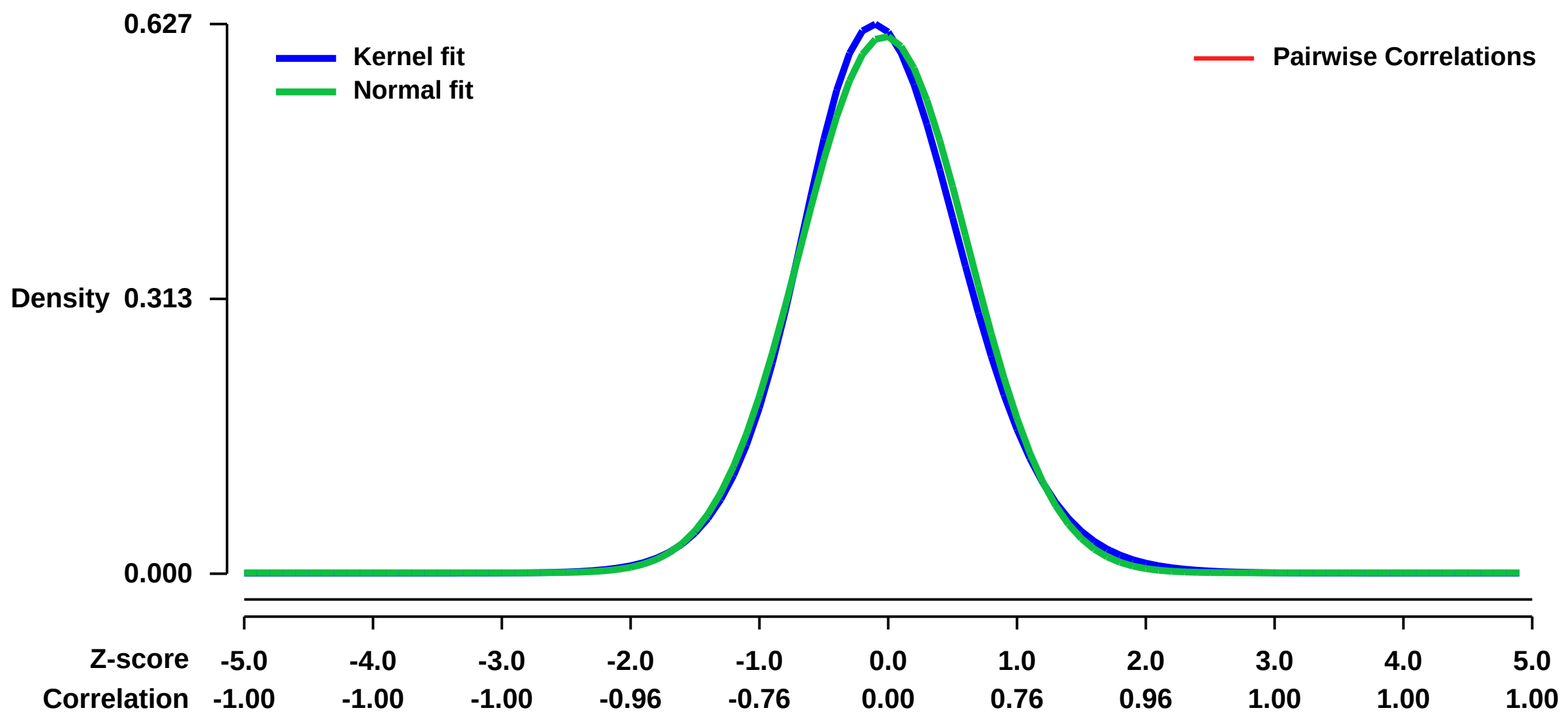

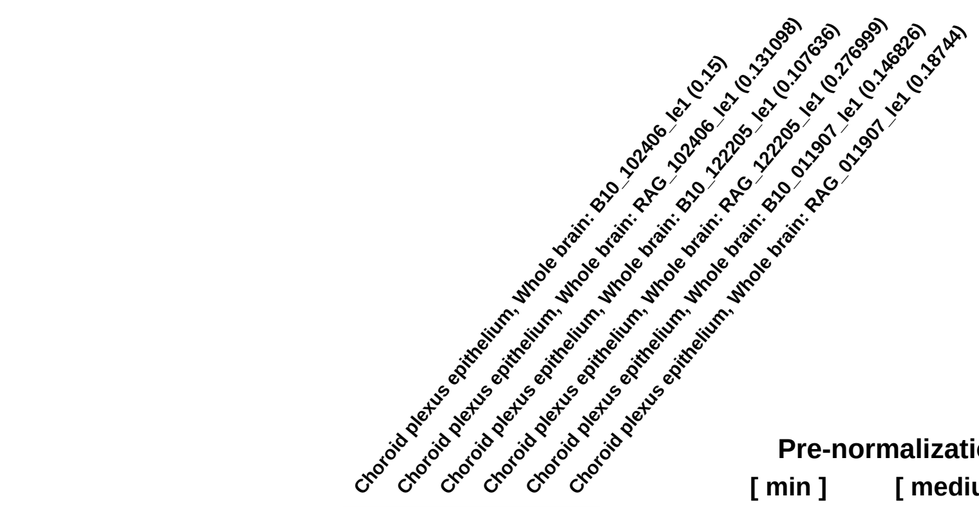

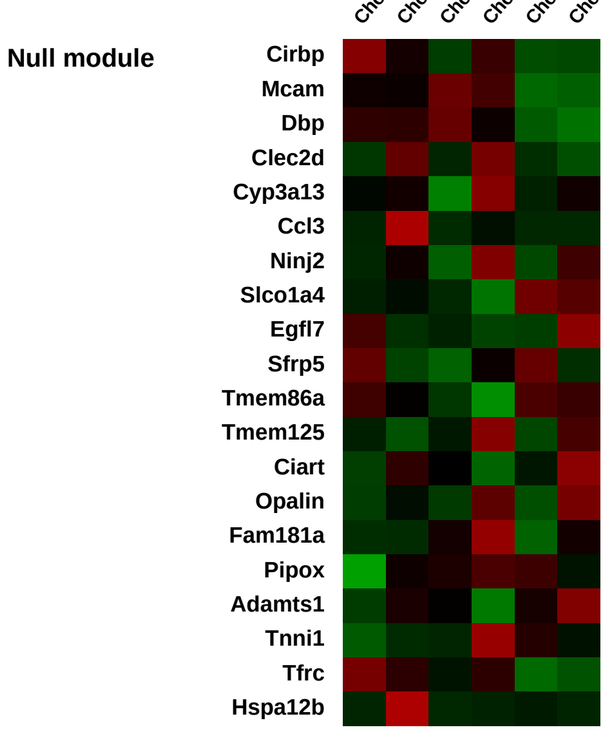

GEO Series "GSE11484" Expression Profiles

Num of samples in this series: 6

Scale of expression profile Z-scores

-3.0 -2.0 -1.0 0.0 1.0 2.0 3.0

GEO Link:	http://www.ncbi.nlm.nih.gov/geo/query/acc.cgi?acc=GSE11484
Status:	Public on Nov 15 2008
Title:	Gene expression analysis of ctrl_islets versus VhlhKO_islets
Organism:	Mus musculus
Experiment type:	Expression profiling by array
Platform:	GPL1261
Pubmed ID:	19056893
Summary & Design:	**Summary:** Understanding the nature of the various glucose-derived signals for insulin secretion (both triggering and amplifying) is essential for gaining insight into the functional failure of the beta-cells in diabetes and the development of drugs for correcting this problem. The beta-cells uniquely couple changes in cellular metabolism to electrical activity and thus insulin release. In mice, beta-cell specific deletion of the von Hippel-Lindau (VHL) tumor suppressor protein leads to the activation of a HIF transcription program that includes genes involved in glycolysis, suppression of mitochondrial activity and lactate production. This reprogramming of cellular metabolism results in abnormal insulin secretion properties. **Overall design:** Three batches of isolated islets from each genotype where used for RNA isolation and Affymetrix measurements.

Background corr dist: KL-Divergence = 0.0441, L1-Distance = 0.0255, L2-Distance = 0.0008, Normal std = 0.6009

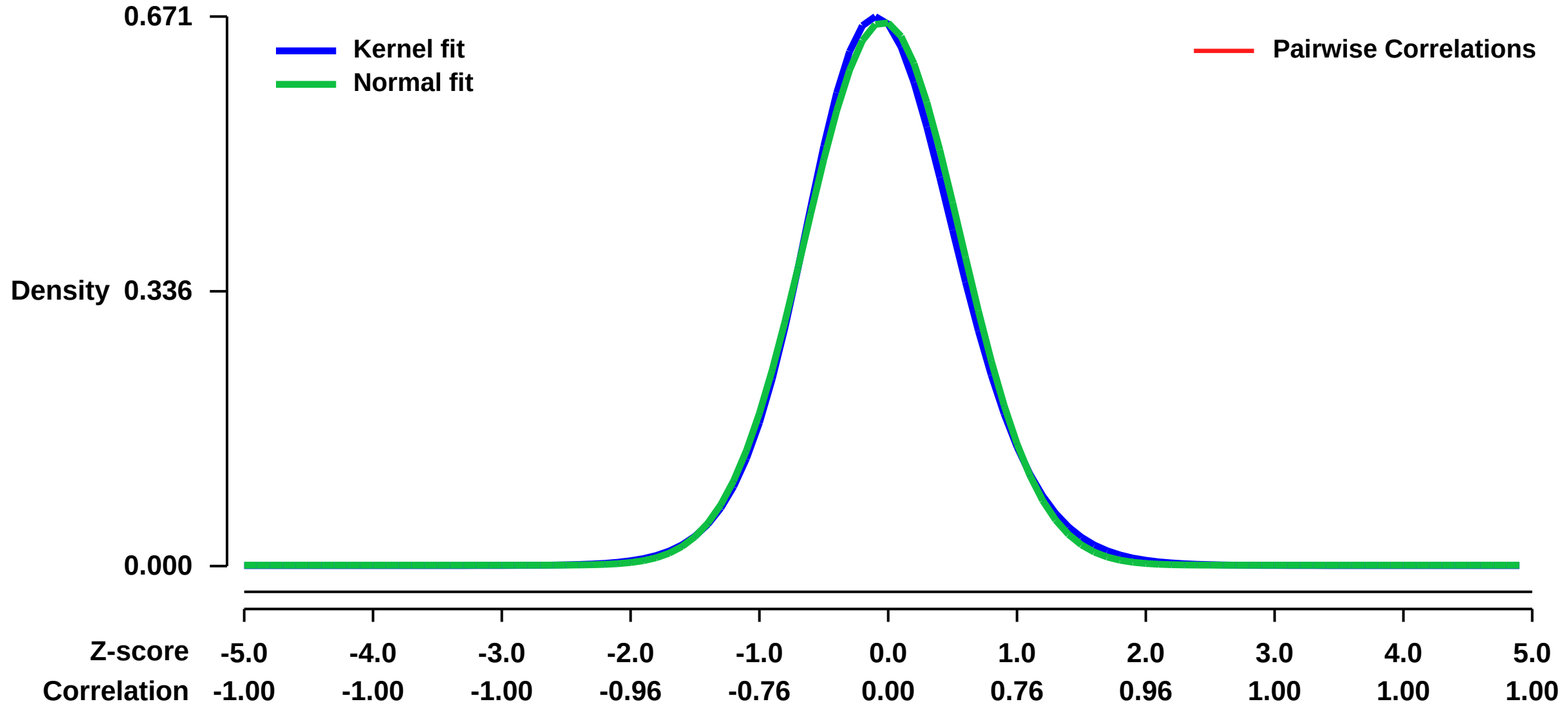

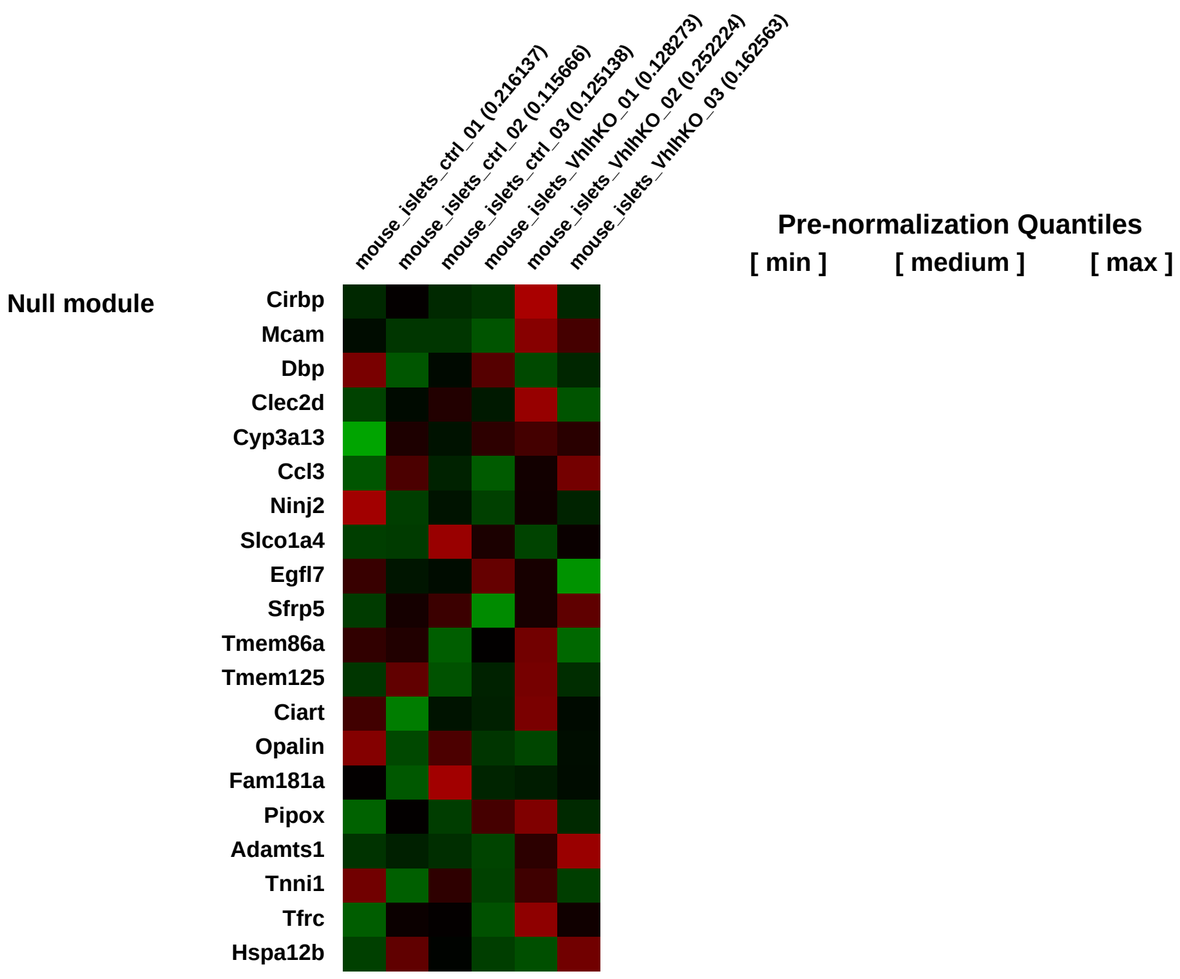

GEO Series "GSE11494" Expression Profiles

Num of samples in this series: 16

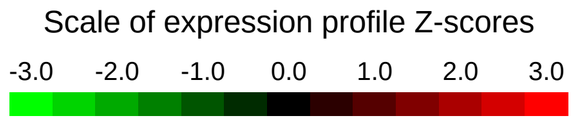

GEO Link:	http://www.ncbi.nlm.nih.gov/geo/query/acc.cgi?acc=GSE11494
Status:	Public on Jul 01 2009
Title:	Innate immune response of murine nasal-associated lymphoid tissue (NALT) to Streptococcus pyogenes infection.
Organism:	Mus musculus
Experiment type:	Expression profiling by array
Platform:	GPL1261
Pubmed ID:	19243434
Summary & Design:	**Summary:** Streptococcus pyogenes is a major causative agent of tonsillitis or pharyngitis in children, which can lead to more invasive infections and noninfectious sequellae. S. pyogenes can persist in tonsils, while one-third of children treated with antibiotics continue to shed streptococci and have recurrent infections. Mouse nasal-associated lymphoid tissue (NALT) is functionally analogous to human oropharangeal lymphoid tissues. The innate immune responses of naˆflve cells from a mucosal site to S. pyogenes is not well described; therefore, we infected C57BL/6 mice intranasally with 108 CFU S. pyogenes. Transcriptional responses by NALT after S. pyogenes infection were analyzed by Affymetrix microarray and quantitative RT-PCR. Wild-type S. pyogenes induces transcription of both type I and IFN-gamma-responsive genes, pro-inflammatory genes, and acute phase response plasma proteins within 24h after infection. Invasion of NALT and the induction of the interferon response were not dependent on expression of anti-phagocytic M1 protein. However, infection with an attenuated, less invasive mutant indicated that a robust innate response by NALT is significantly influenced by intra-NALT bacterial load. Granulocytic populations of NALT, cervical lymph nodes and spleen were discriminated by characteristic surface and intracellular markers. Intranasal infection induces systemic release of neutrophils and a substantial influx of neutrophils into NALT at 24h, which decline by 48h after infection. Macrophages do not significantly increase in S. pyogenes-infected NALT. Intranasal infection of IFN-gamma -/- (GKO) C57BL/6 mice did not lead to systemic dissemination of wild type S. pyogenes, despite reduced expression of IFN-gamma-responsive mRNAs in NALT. Infected GKO mice had an unregulated influx of neutrophils into NALT compared to immunocompetant mice and mice treated with an anti-IFN-gamma antibody more rapidly cleared S. pyogenes from NALT. Thus, IFN-gamma-induced responses have a suppressive influence on early clearance of this pathogen from NALT. **Keywords:** disease state analysis **Overall design:** C57BL/6 mice (6-10 weeks old), 4 per group, were infected intranasally with log-phase Streptococcus pyogenes, 2 to 4 x 10^8 CFU per 15 ´µl of pyrogen-free PBS. Sham-infected mice were administered 15 ´µl of the same PBS. Mice were infected with wild type strain 90-226 (Cue 1998), a 90-226 strain containing an in-frame deletion of M1 protein (90-226 delta emm1) (Zimmerlein 2005) or an attenuated 90-226 which lacks both M1 and SCPA proteins (90-226att). NALT was collected from mice at 24h after infection and stored in RNAlater until RNA could be purified).

Background corr dist: KL-Divergence = 0.2816, L1-Distance = 0.0637, L2-Distance = 0.0111, Normal std = 0.2873

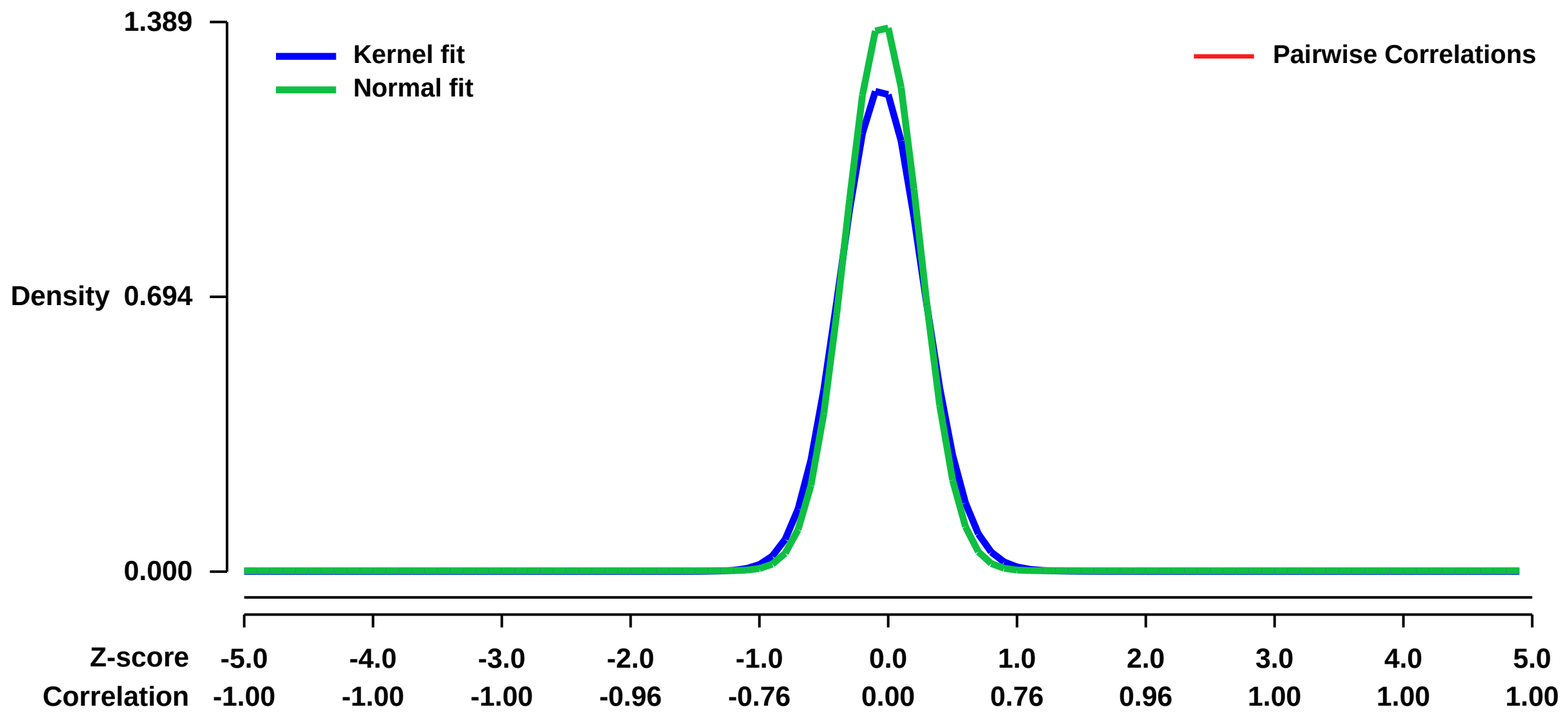

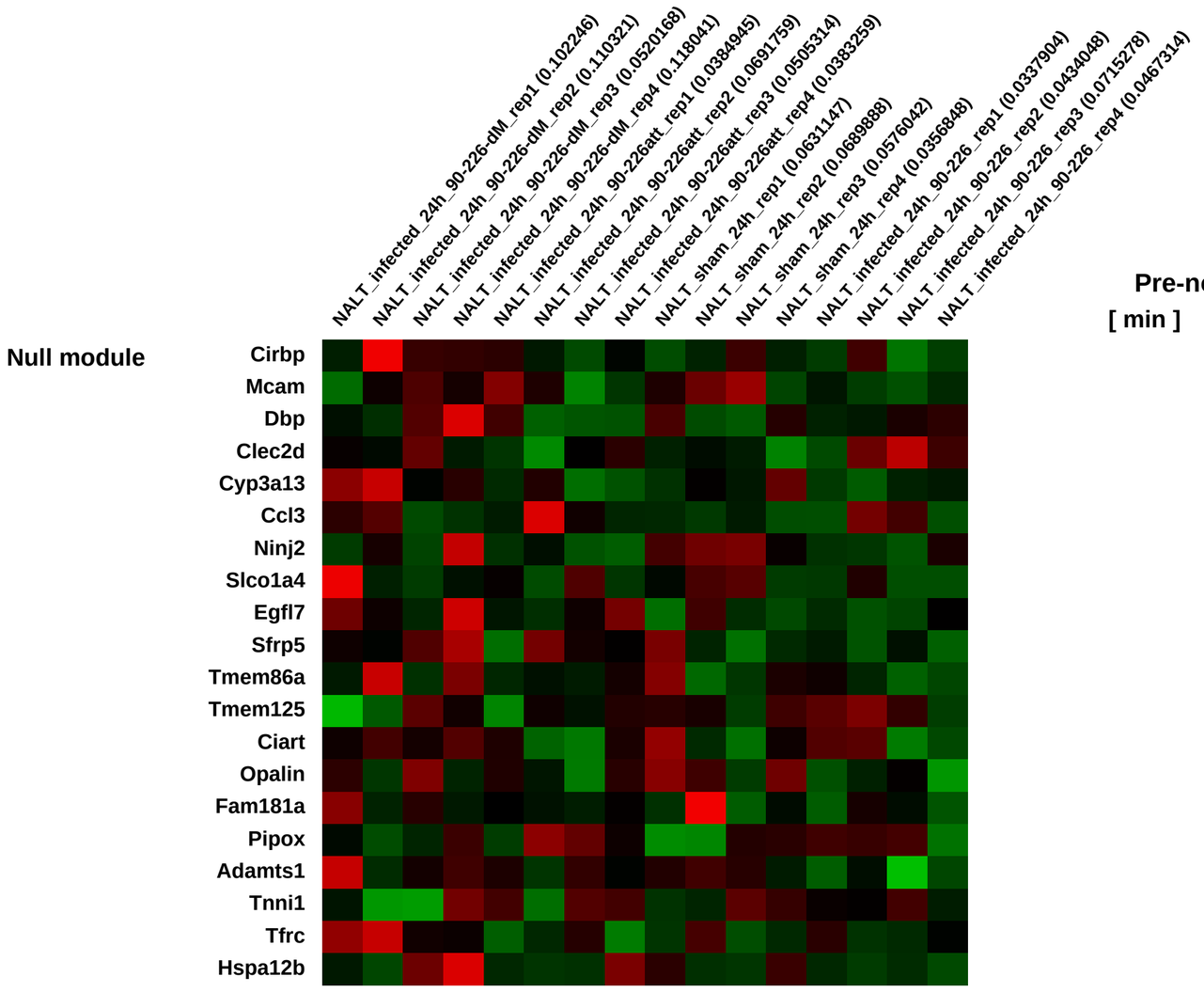

GEO Series "GSE11496" Expression Profiles

Num of samples in this series: 16

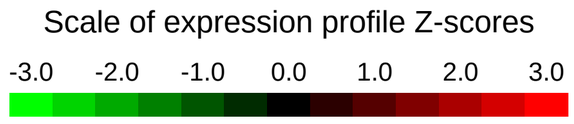

GEO Link:	http://www.ncbi.nlm.nih.gov/geo/query/acc.cgi?acc=GSE11496
Status:	Public on Nov 10 2009
Title:	Expression data from Gcn2 wild-type and knockout mouse liver perfused with or without methionine
Organism:	Mus musculus
Experiment type:	Expression profiling by array
Platform:	GPL1261
Pubmed ID:	19509078
Summary & Design:	**Summary:** In eukaryotes, regulation of mRNA translation enables a fast, localized and finely tuned expression of gene products. Within the translation process, the first stage of translation initiation is most rigorously modulated by the actions of eukaryotic initiation factors (eIFs) and their associated proteins. These 11 eIFs catalyze the joining of the tRNA, mRNA and rRNA into a functional translation complex. Their activity is influenced by a wide variety of extra- and intracellular signals, ranging from global, such as hormone signaling and unfolded proteins, to specific, such as single amino acid imbalance and iron deficiency. Their action is correspondingly comprehensive, in increasing or decreasing recruitment and translation of most cellular mRNAs, and specialized, in targeting translation of mRNAs with regulatory features such as a 5â terminal oligopyrimidine tract (TOP), upstream open reading frames (uORFs), or an internal ribosomal entry site (IRES). In mammals, two major pathways are linked to targeted mRNA translation. The target of rapamycin (TOR) kinase induces translation of TOP and perhaps other subsets of mRNAs, whereas a family of eIF2 kinases does so with mRNAs containing uORFs or an IRES. TOR targets translation of mRNAs that code for proteins involved in translation, an action compatible with its widely accepted role in regulating cellular growth. The four members of the eIF2 kinase family increase translation of mRNAs coding for stress response proteins such as transcription factors and chaperones. Though all four kinases act on one main substrate, eIF2, published literature demonstrates both common and unique effects by each kinase in response to its specific activating stress. This suggests that the activated eIF2 kinases regulate the translation of both a global and a specific set of mRNAs. Up to now, few studies have attempted to test such a hypothesis; none has been done in mammals. We use array analysis to determine the global mRNA shift into polysomes following a stress response, and to compare the translational response following activation of GCN2 versus PERK, two of the four eIF2alpha kinases. **Overall design:** Gcn2 wild-type or knockout mouse liver were perfused with complete amino acids media or media lacking methionine for RNA extraction and hybridization of Affymetrix microarrays. RNA was extracted from unfractionated liver samples and polysome fraction of samples separated on sucrose density gradient. To minimize biological variations, we pooled RNA from two perfused liver samples to use in each array analysis. The conditions were total and polysome fraction of Gcn2+/+, +Met or -Met; total and polysome fraction of Gcn2-/-, +Met or -Met. Each array analysis was done in duplicate.

Background corr dist: KL-Divergence = 0.2327, L1-Distance = 0.0508, L2-Distance = 0.0061, Normal std = 0.3119

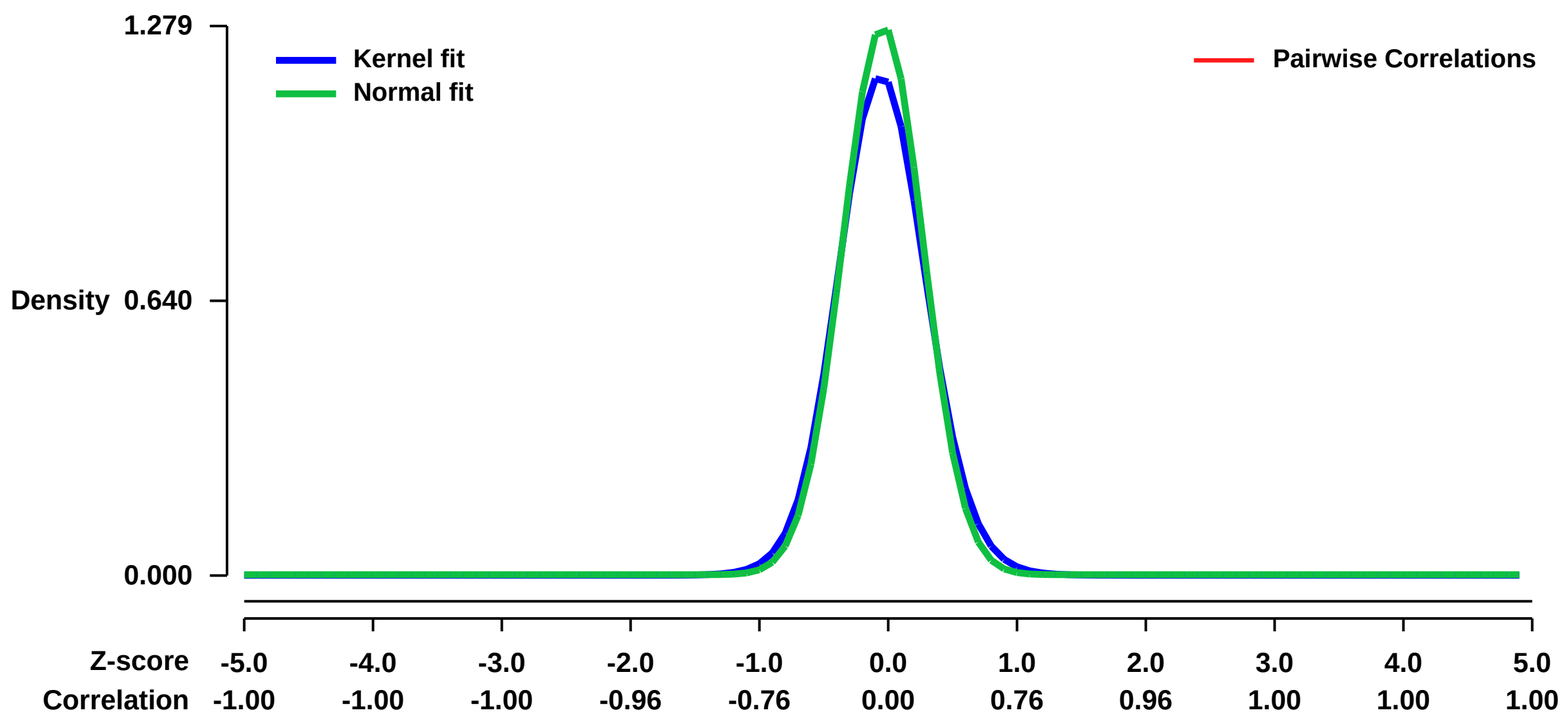

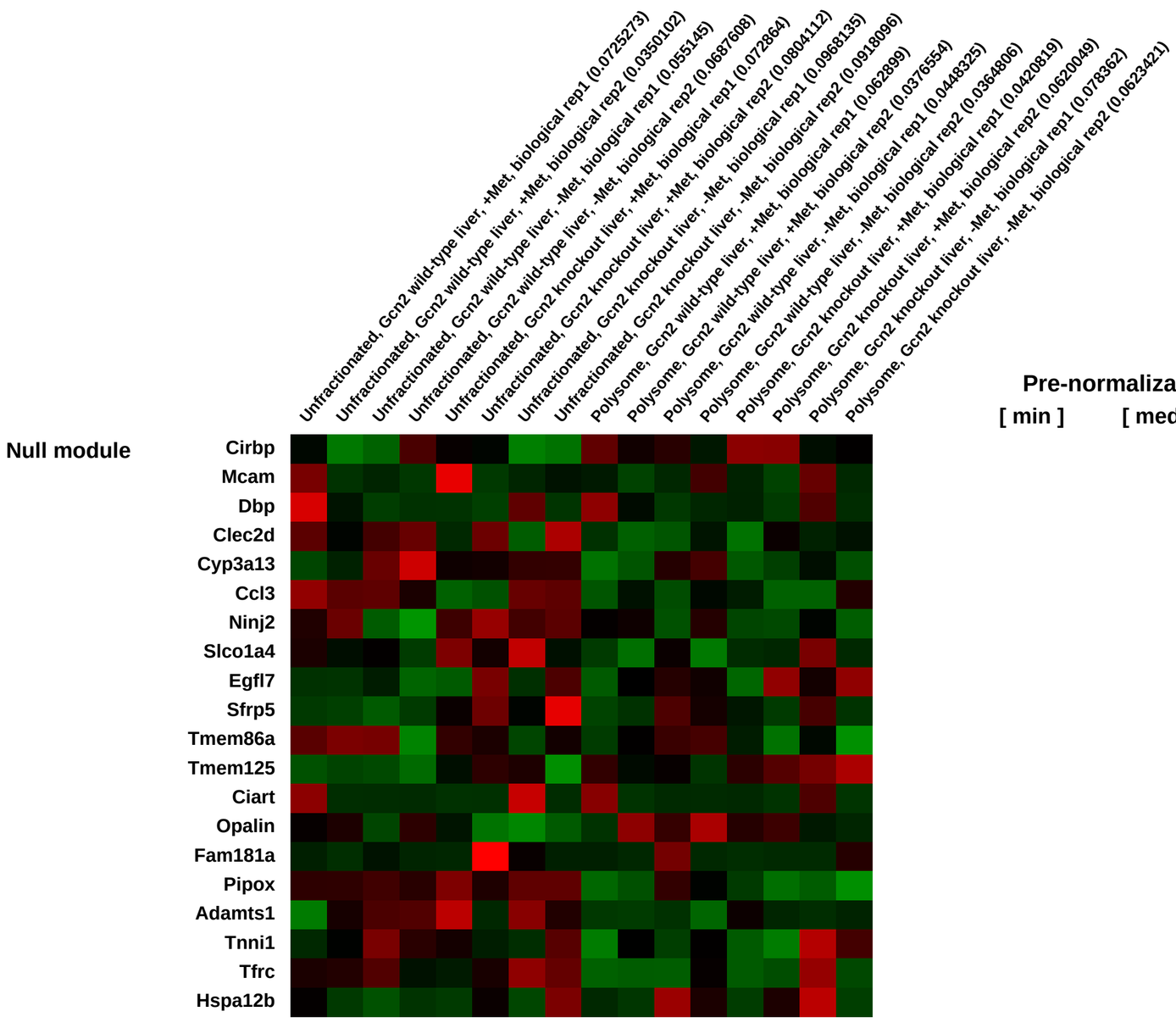

Null module

GEO Series "GSE11628" Expression Profiles

Num of samples in this series: 12

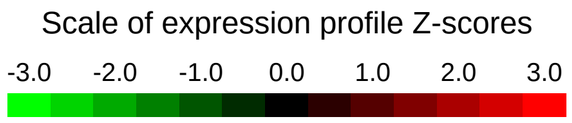

GEO Link:	**http://www.ncbi.nlm.nih.gov/geo/query/acc.cgi?acc=GSE11628**
Status:	**Public on Dec 31 2009**
Title:	**Wnt & LIF signalling in mESC**
Organism:	**Mus musculus**
Experiment type:	**Expression profiling by array**
Platform:	**GPL1261**
Pubmed ID:	
Summary & Design:	**Summary:** **The molecular processes underlying the properties of ESC are yet unknown even when it's well established that LIF/STAT3 is neccesary for the maintenance of pluripotency. Other pathways as Wnt are may be implicated in the regulation of the biological mechanisms in mESC. Work model: D3-ES cultivated with or without LIF and treated with chronic (7 days) low doses (50nM) of GSK3 ¸† inhibitor (lithium).** **We used microarrays to detail the global profile of gene expression to identified different groups of up and down-regulated genes in the work model.** **Overall design:** **mESC cultivated as it has been defined in the work model were prepared for RNA extraction and hybridization on Affymetrix microarrays. We analyzed 3 independent experiments per replicate, and we did three replicates per sample.**

Background corr dist: **KL-Divergence = 0.0952, L1-Distance = 0.0254, L2-Distance = 0.0010, Normal std = 0.4504**

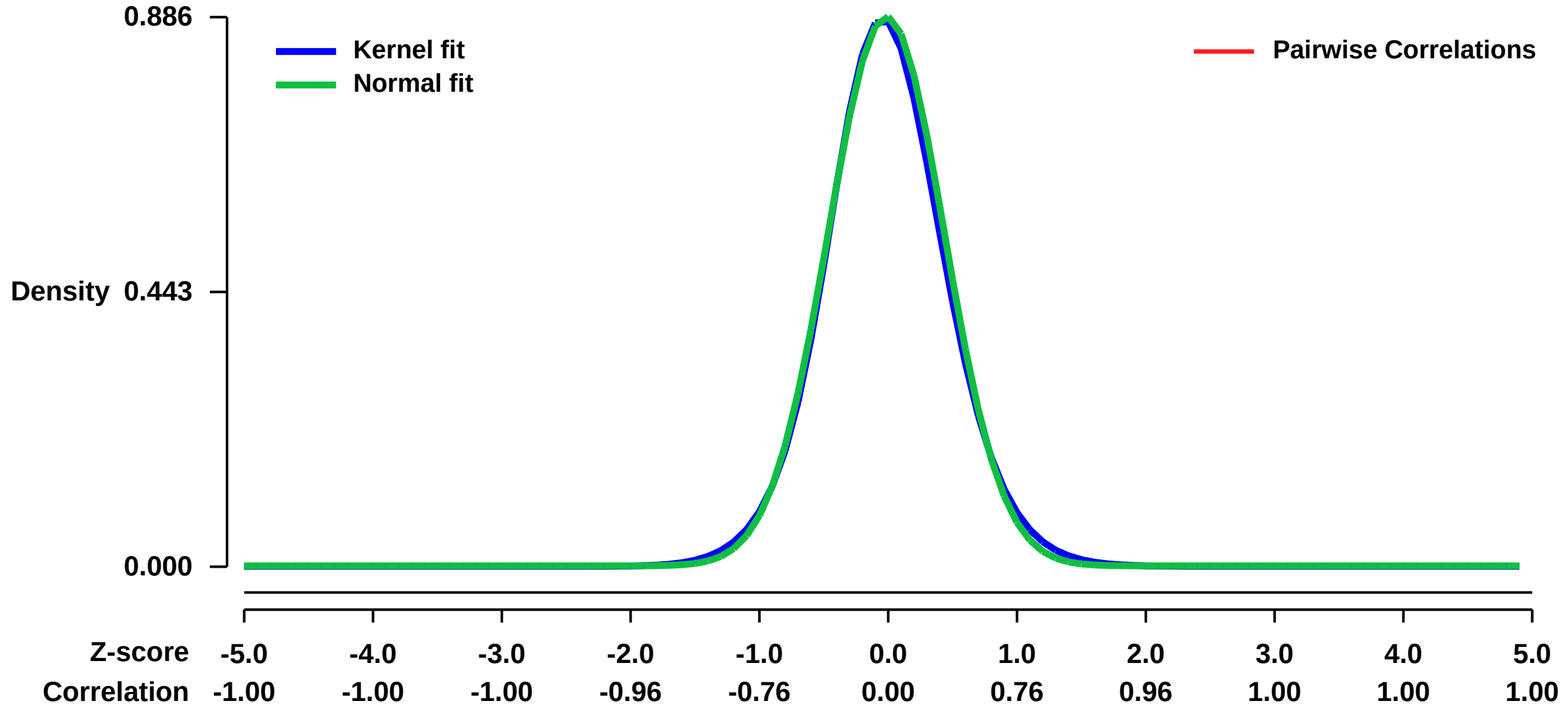

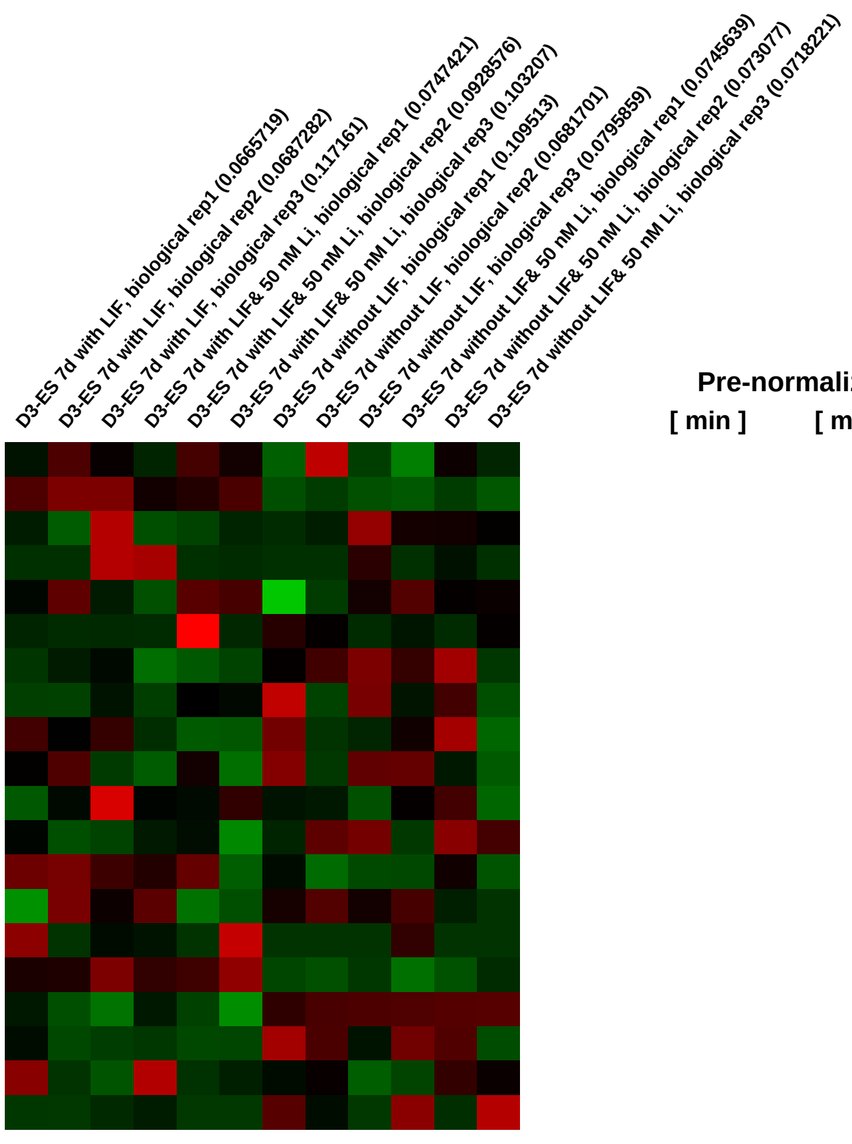

GEO Series "GSE11664" Expression Profiles

Num of samples in this series: 10

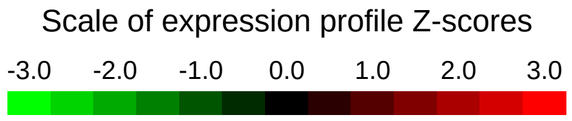

GEO Link:	http://www.ncbi.nlm.nih.gov/geo/query/acc.cgi?acc=GSE11664
Status:	Public on Jun 05 2008
Title:	gene expression of CTCF-depleted mouse oocyte
Organism:	Mus musculus
Experiment type:	Expression profiling by array
Platform:	GPL1261
Pubmed ID:	18614575
Summary & Design:	**Summary:** CTCF is a multifunctional nuclear factor involved in epigenetic regulation. We have used transgenic RNA interference to deplete maternal stores of CTCF from growing mouse oocytes, and identified the potential target genes **Overall design:** We profiled the global gene expression in the wild type and CTCF-depleted GV oocytes, and identified a set of target genes.

Background corr dist: KL-Divergence = 0.1157, L1-Distance = 0.0232, L2-Distance = 0.0009, Normal std = 0.4149

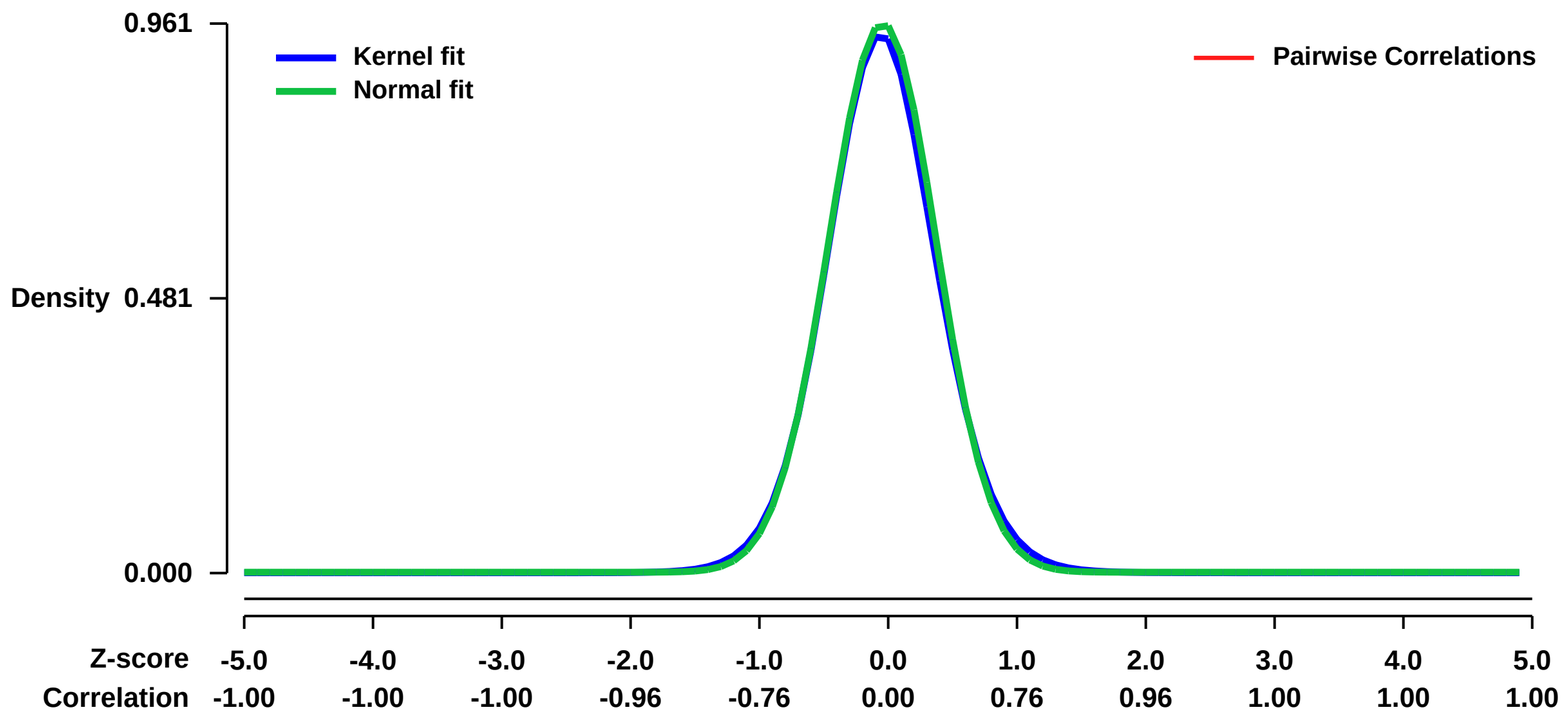

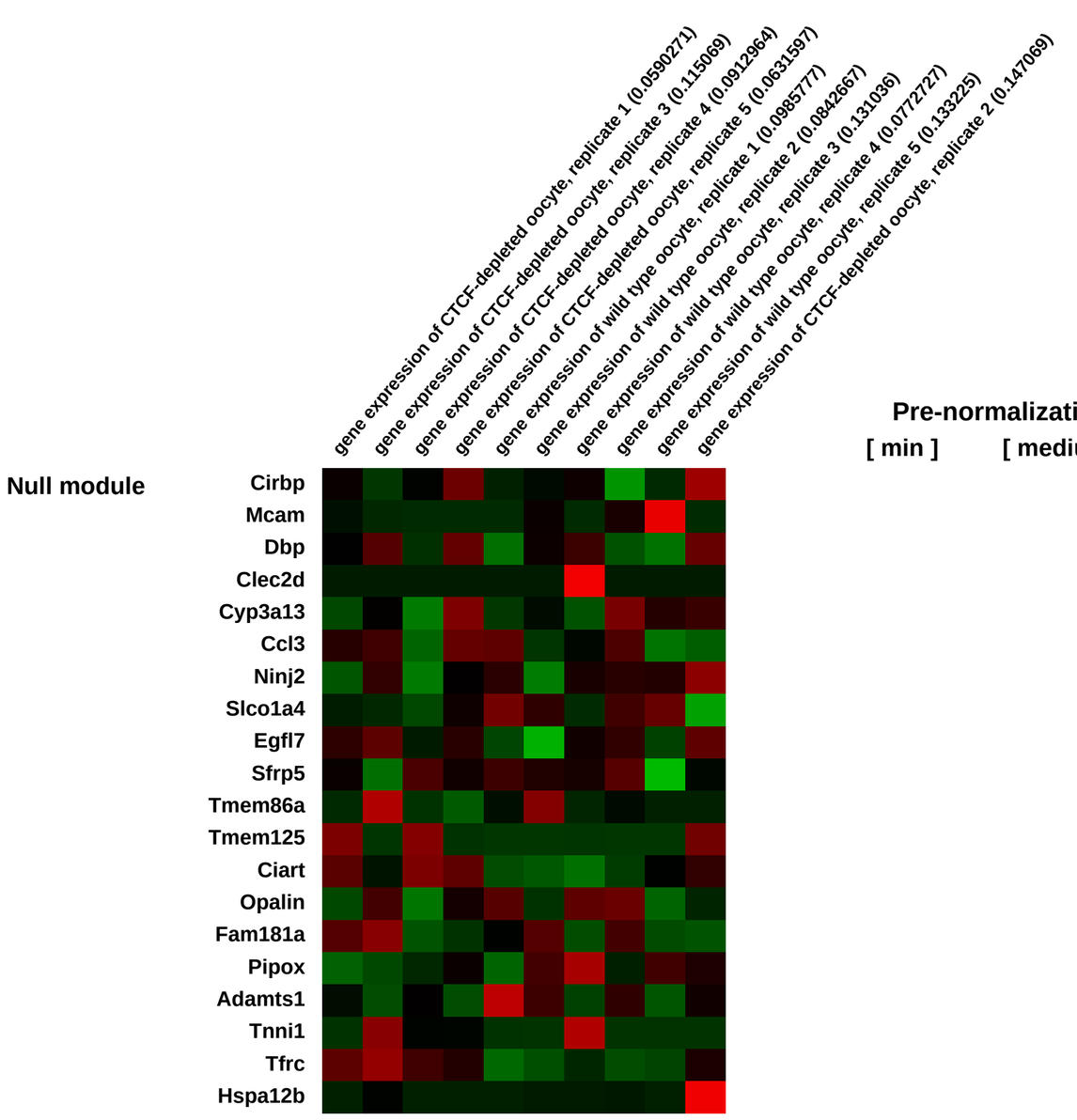

GEO Series "GSE11679" Expression Profiles

Num of samples in this series: 25

Scale of expression profile Z-scores

-3.0 -2.0 -1.0 0.0 1.0 2.0 3.0

GEO Link:	http://www.ncbi.nlm.nih.gov/geo/query/acc.cgi?acc=GSE11679
Status:	Public on Oct 08 2008
Title:	Gene expression changes related to postnatal handling
Organism:	Mus musculus
Experiment type:	Expression profiling by array
Platform:	GPL1261
Pubmed ID:	18836535
Summary & Design:	**Summary:** Postnatal handling in rodents leads to decreased anxiety-like behavior in adulthood. We used microarrays to look at gene expression differences in the CA1 region of the hippocampus in female mice subjected to postnatal handling compared to controls. **Overall design:** Balb c/J offspring were briefly separated from mothers for 15 minutes each morning on postnatal days 1-14 (handled group) or left undisturbed. At 8 weeks of age mice were tested in the open-field and light-dark behavioral paradigms to verify a handling-induced behavioral phenotype. 2 weeks after behavioral testing, animals were sacrificed and the CA1 region was microdissected. CA1 regions were stored at -20C in RNA later. RNA was extracted from 8 samples (4 handled and 4 non-handled) using Trizol. RNA was extracted from second group of animals (7 handled and 10 non-handled) using Qiagen RNA/DNA columns. All total RNA samples were double round amplied and labeled using standard Affymetrix protocols and hybridized to Mouse 430_2.0 arrays in parallel.

Background corr dist: KL-Divergence = 0.1846, L1-Distance = 0.0311, L2-Distance = 0.0015, Normal std = 0.3522

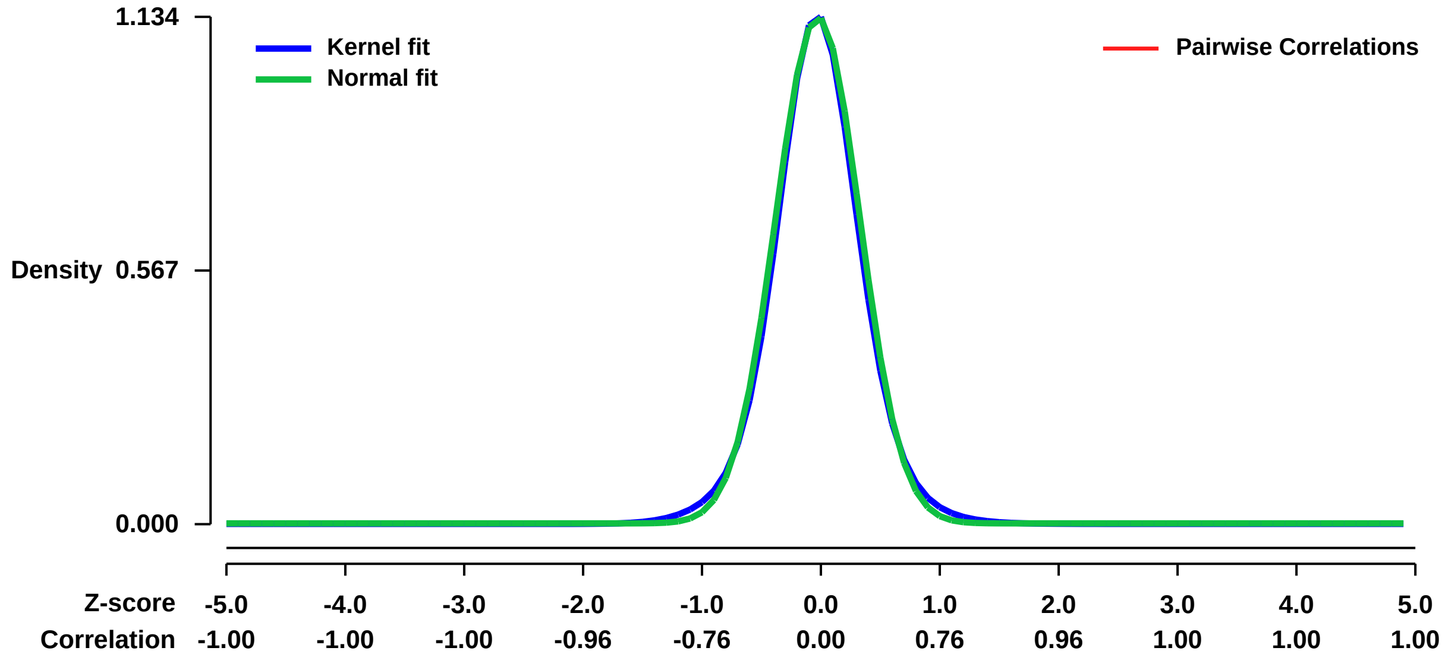

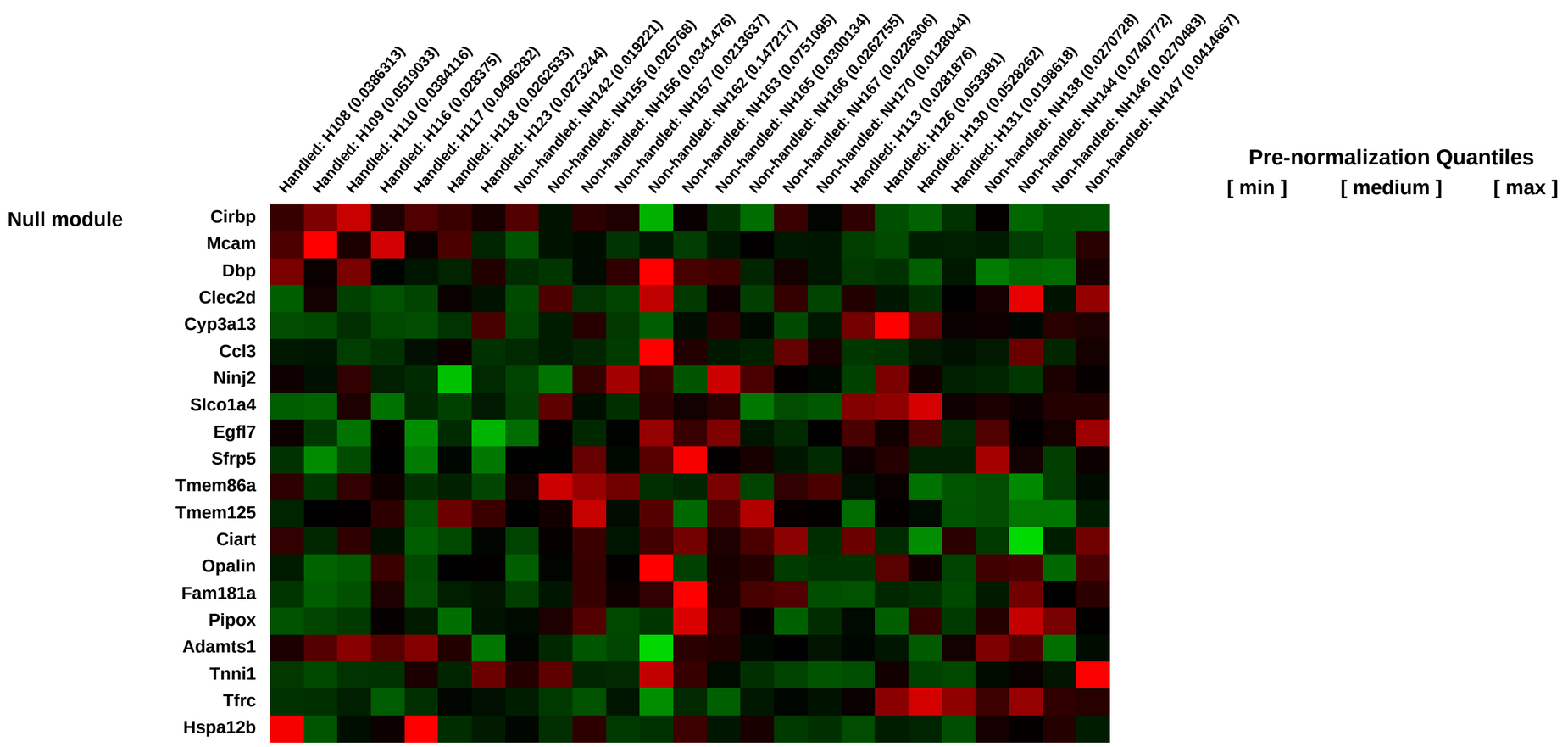

GEO Series "GSE11680" Expression Profiles

Num of samples in this series: 10

Scale of expression profile Z-scores

-3.0 -2.0 -1.0 0.0 1.0 2.0 3.0

GEO Link:	http://www.ncbi.nlm.nih.gov/geo/query/acc.cgi?acc=GSE11680
Status:	Public on Oct 08 2008
Title:	Gene expression differences between high and low exploratory genetically identical mice
Organism:	Mus musculus
Experiment type:	Expression profiling by array
Platform:	GPL1261
Pubmed ID:	18836535
Summary & Design:	**Summary:** Genetically identical inbred mice exhibit substantial stable individual variability in exploratory behavior. We used microarrays to look at gene expression differences in the hippocampus in female mice separated by stable differences in exploratory behavior **Overall design:** Balb c/J offspring were briefly separated from mothers for 15 minutes each morning on postnatal days 1-14 (handled group) or left undisturbed. At 8 weeks of age mice were tested in the open-field and light-dark behavioral paradigms to verify a handling-induced behavioral phenotype. 2 weeks after behavioral testing, animals were sacrificed and the CA1 region was microdissected. CA1 regions were stored at -20C in RNA later. RNA was extracted from 8 samples (4 handled and 4 non-handled) using Trizol. RNA was extracted from second group of animals (7 handled and 10 non-handled) using Qiagen RNA/DNA columns. All total RNA samples were double round amplied and labeled using standard Affymetrix protocols and hybridized to Mouse 430_2.0 arrays in parallel.

Background corr dist: KL-Divergence = 0.1115, L1-Distance = 0.0448, L2-Distance = 0.0044, Normal std = 0.4277

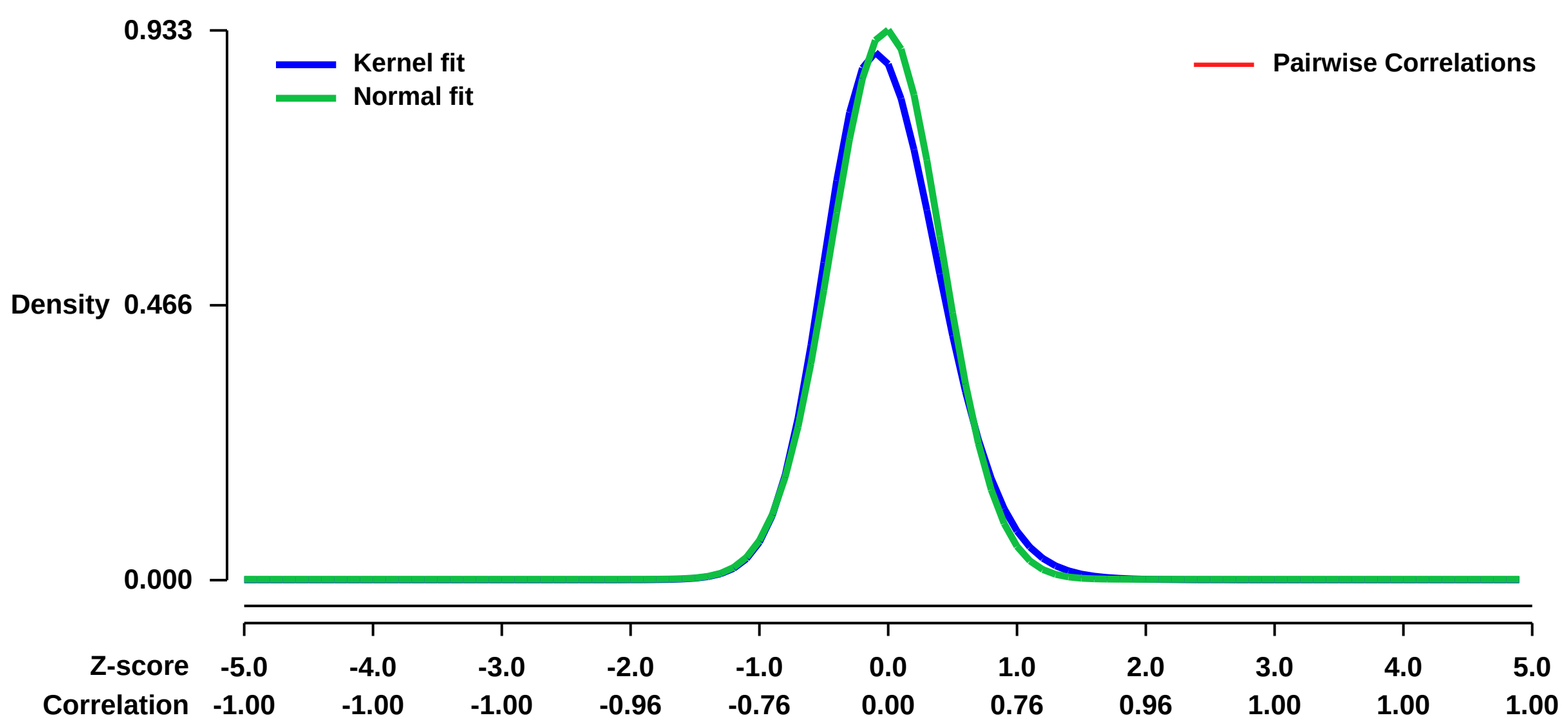

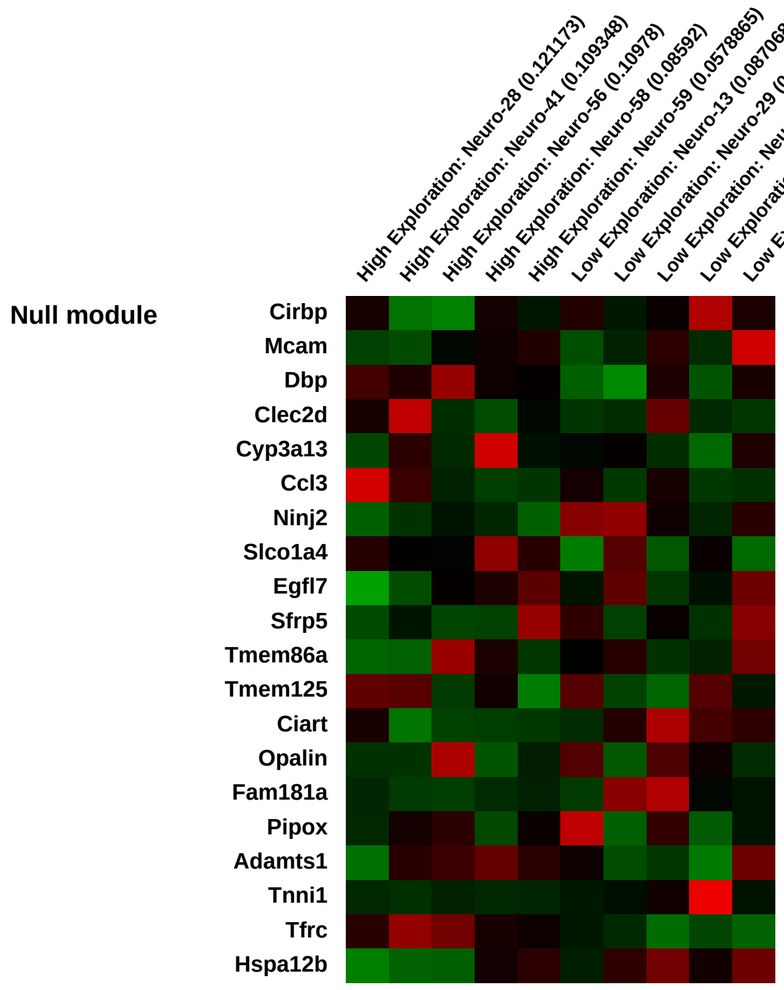

GEO Series "GSE11684" Expression Profiles

Num of samples in this series: 16

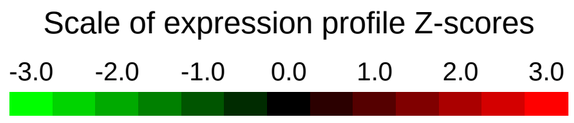

GEO Link:	http://www.ncbi.nlm.nih.gov/geo/query/acc.cgi?acc=GSE11684
Status:	Public on Nov 10 2009
Title:	Expression data from Perk wild-type and knockout mouse liver perfused without or with 2,5-di-tert-butylhydroquinone
Organism:	Mus musculus
Experiment type:	Expression profiling by array
Platform:	GPL1261
Pubmed ID:	19509078

Summary & Design:

Summary:
In eukaryotes, regulation of mRNA translation enables a fast, localized and finely tuned expression of gene products. Within the translation process, the first stage of translation initiation is most rigorously modulated by the actions of eukaryotic initiation factors (eIFs) and their associated proteins. These 11 eIFs catalyze the joining of the tRNA, mRNA and rRNA into a functional translation complex. Their activity is influenced by a wide variety of extra- and intracellular signals, ranging from global, such as hormone signaling and unfolded proteins, to specific, such as single amino acid imbalance and iron deficiency. Their action is correspondingly comprehensive, in increasing or decreasing recruitment and translation of most cellular mRNAs, and specialized, in targeting translation of mRNAs with regulatory features such as a 5â terminal oligopyrimidine tract (TOP), upstream open reading frames (uORFs), or an internal ribosomal entry site (IRES). In mammals, two major pathways are linked to targeted mRNA translation. The target of rapamycin (TOR) kinase induces translation of TOP and perhaps other subsets of mRNAs, whereas a family of eIF2 kinases does so with mRNAs containing uORFs or an IRES. TOR targets translation of mRNAs that code for proteins involved in translation, an action compatible with its widely accepted role in regulating cellular growth. The four members of the eIF2 kinase family increase translation of mRNAs coding for stress response proteins such as transcription factors and chaperones. Though all four kinases act on one main substrate, eIF2, published literature demonstrates both common and unique effects by each kinase in response to its specific activating stress. This suggests that the activated eIF2 kinases regulate the translation of both a global and a specific set of mRNAs. Up to now, few studies have attempted to test such a hypothesis; none has been done in mammals.

We use array analysis to determine the global mRNA shift into polysomes following a stress response, and to compare the translational response following activation of GCN2 versus PERK, two of the four eIF2alpha kinases.

Keywords: stress response, comparative genomic

Overall design:
Perk wild-type or knockout mouse liver were perfused without or with 2,4-di-tert-butylhydroquinone (tBuHQ) for RNA extraction and hybridization of Affymetrix microarrays. RNA was extracted from unfractionated liver samples and polysome fraction of samples separated on sucrose density gradient. To minimize biological variations, we pooled RNA from two perfused liver samples to use in each array analysis. The conditions were total and polysome fraction of Perk+/+, -tBuHQ or +tBuHQ; total and polysome fraction of Perk-/-, -tBuHQ or +tBuHQ. Each array analysis was done in duplicate.

Background corr dist: KL-Divergence = 0.2098, L1-Distance = 0.0435, L2-Distance = 0.0042, Normal std = 0.3267

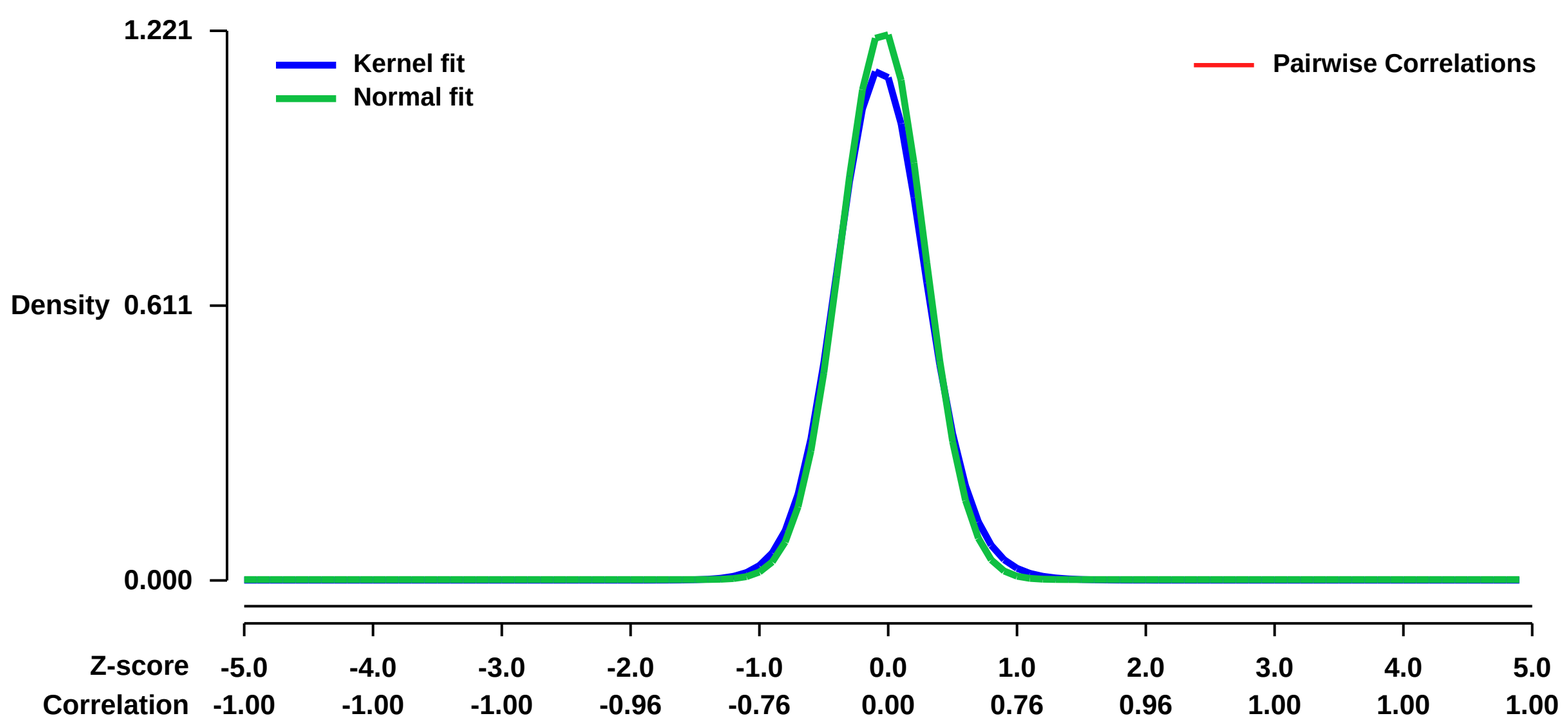

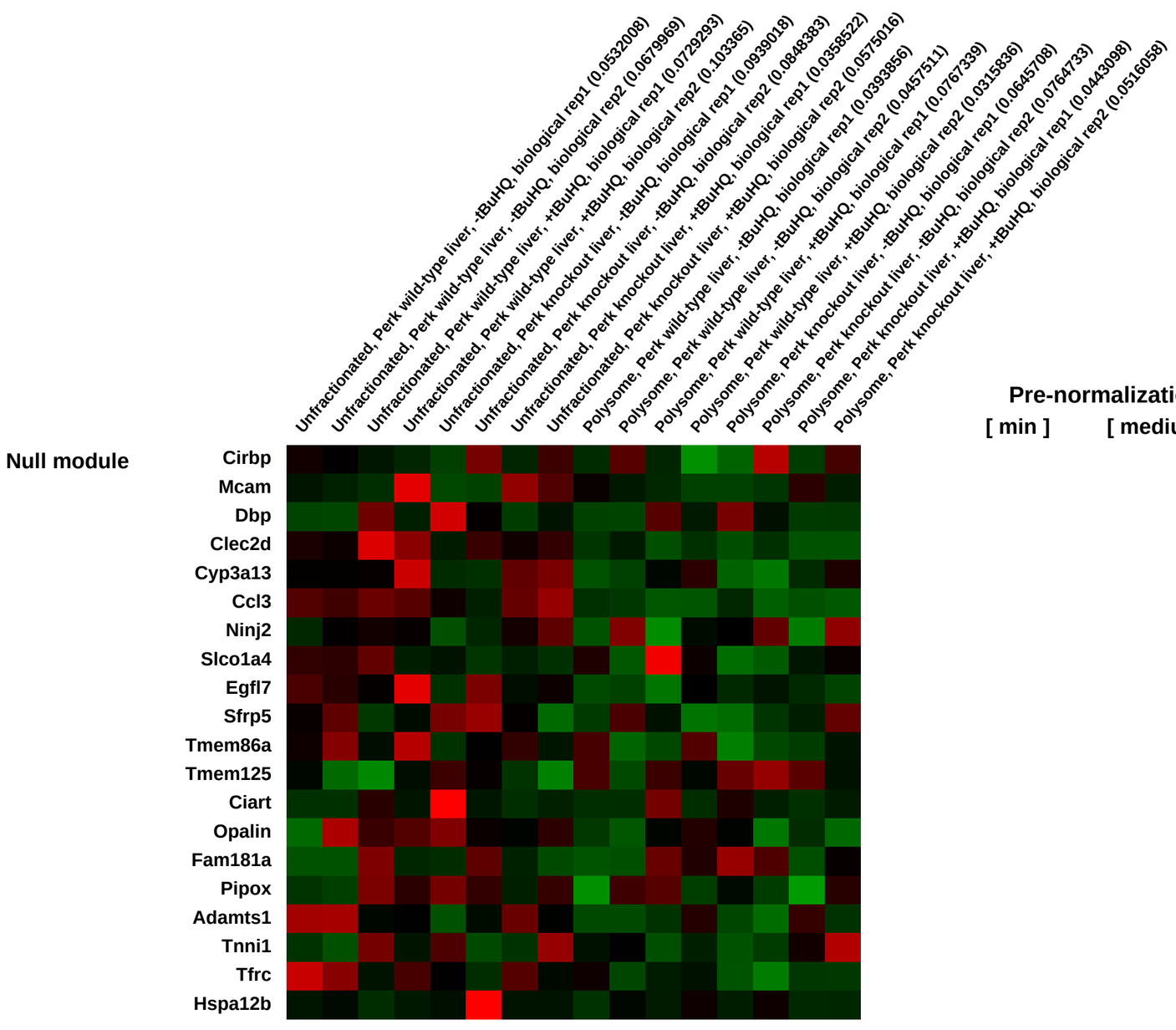

GEO Series "GSE11698" Expression Profiles

Num of samples in this series: 6

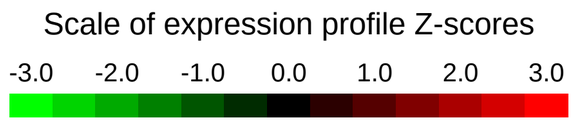

GEO Link:	http://www.ncbi.nlm.nih.gov/geo/query/acc.cgi?acc=GSE11698
Status:	Public on Aug 22 2008
Title:	Microarray of Trex1 WT and Trex1 KO hearts on RAG2KO background
Organism:	Mus musculus
Experiment type:	Expression profiling by array
Platform:	GPL1261
Pubmed ID:	18724932
Summary & Design:	**Summary:** Heart ventricle tissue was harvested from Trex1/RAG2 DKO mice and from Trex1WT/RAG2KO littermate controls. RNA was extracted, and an Affymetrix Mouse 430 2.0 gene chip analysis was performed. **Overall design:** Three pairs of littermates are included: 779/780, 4184/4185, and 4192/4193.

Background corr dist: KL-Divergence = 0.0476, L1-Distance = 0.0187, L2-Distance = 0.0004, Normal std = 0.5822

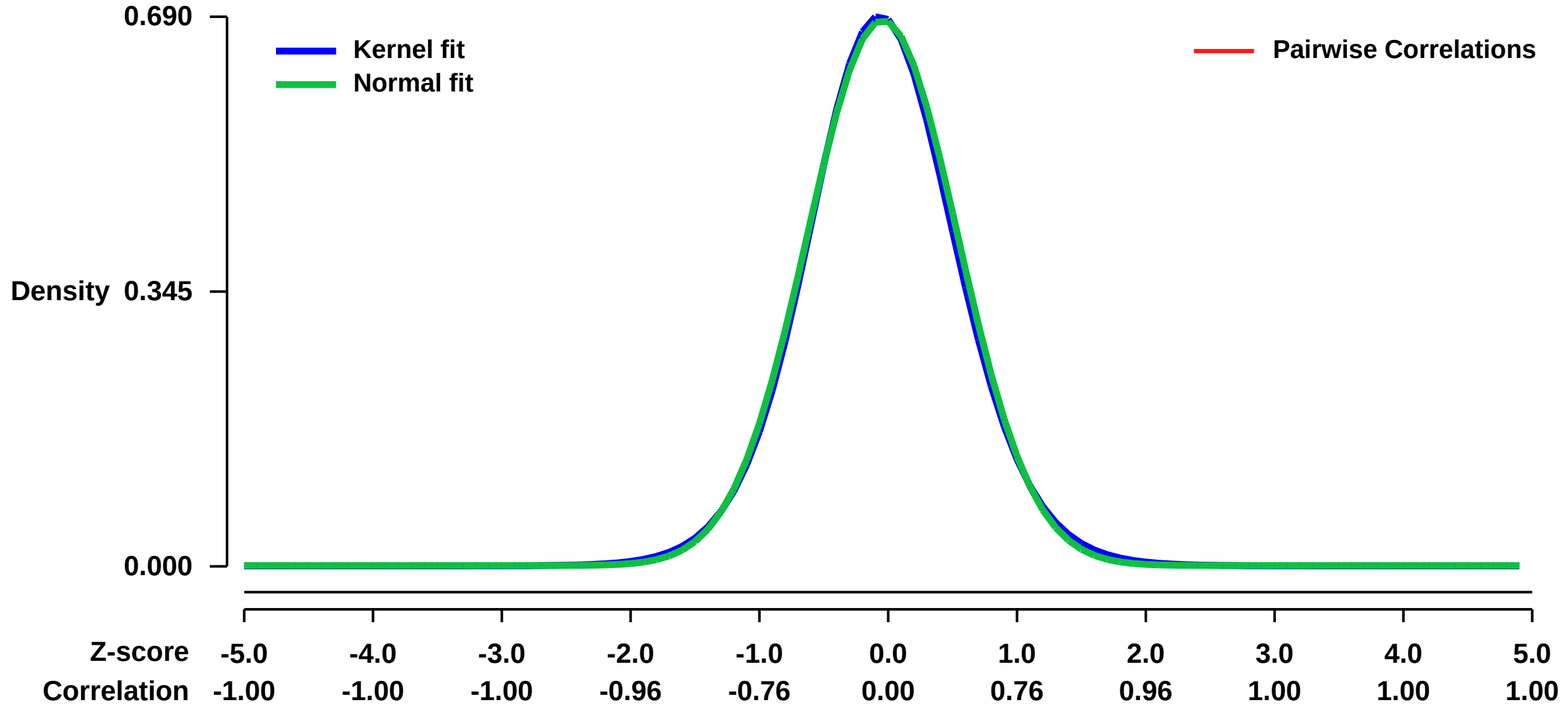

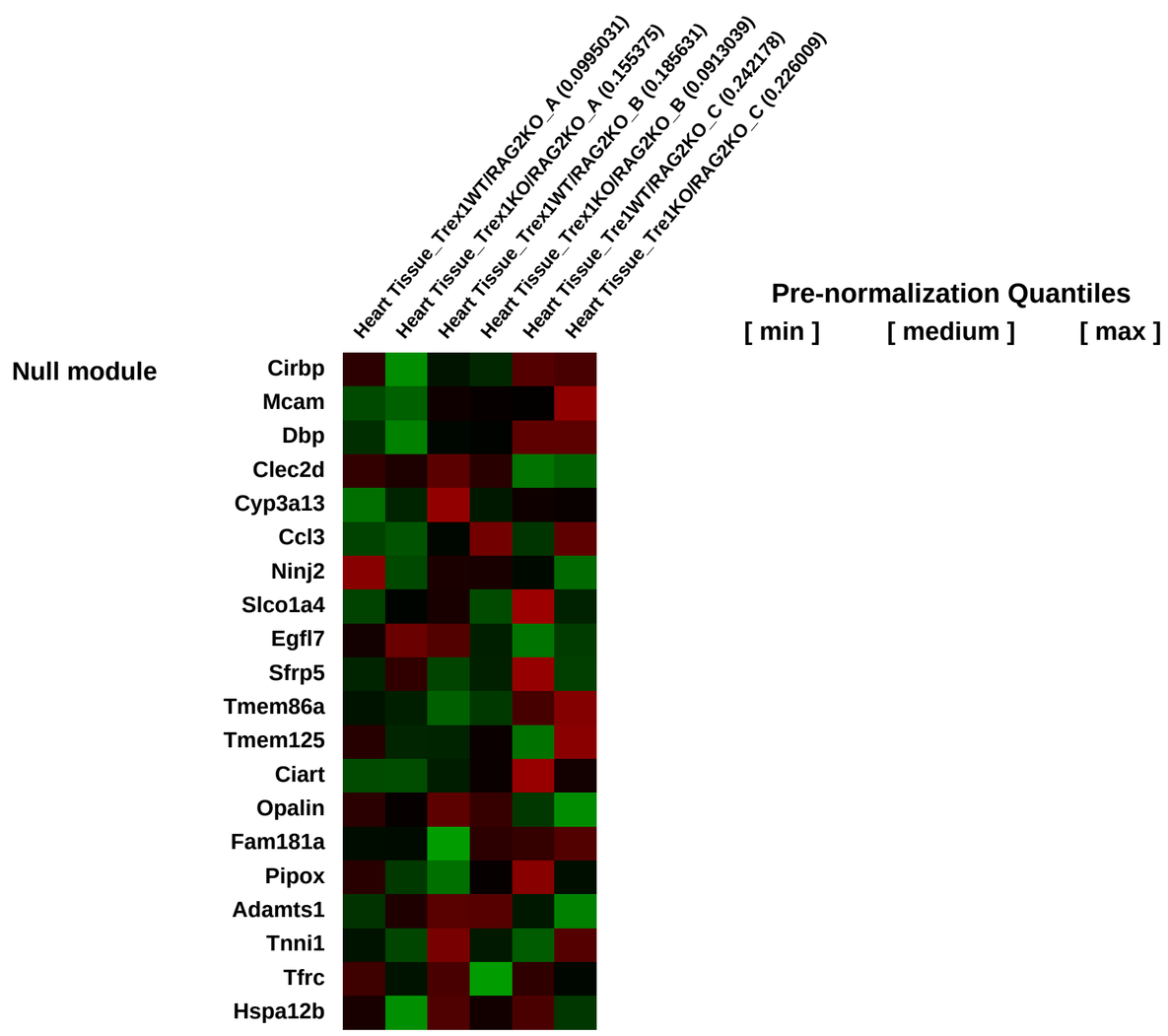

GEO Series "GSE11759" Expression Profiles

Num of samples in this series: 6

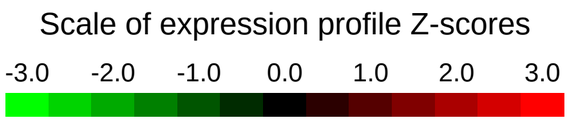

GEO Link:	http://www.ncbi.nlm.nih.gov/geo/query/acc.cgi?acc=GSE11759
Status:	Public on Dec 01 2008
Title:	Role of HNF4alpha in the adult colon
Organism:	Mus musculus
Experiment type:	Expression profiling by array
Platform:	GPL1261
Pubmed ID:	19898610
Summary & Design:	**Summary:** **Background & Aims: HNF4¿– is an important transcriptional regulator of hepatocyte and pancreatic function. Hnf4¿– deletion is embryonically lethal with severe defects in visceral endoderm formation, liver maturation and colon development. However, the precise role of this transcription factor in maintaining homeostasis of the adult intestine remains unclear. Herein, we aimed to elucidate the adult intestinal functions of Hnf4¿–. Methods: A conditional intestinal epithelial Hnf4¿– knockout mouse was generated. Histological abnormality of the colonic mucosa was assessed by immunodetection and Western. Changes in global gene expression and biological network were analyzed. Results: Hnf4¿– intestine null mice developed normally until reaching young adulthood. Crypt distortion became apparent in the Hnf4¿– null colon at 3 months of age followed by focal areas of crypt dropout, increased immune cell infiltrates, crypt hyperplasia and early signs of polyposis later in life. A gene profiling analysis identified cell death and cell cycle related to cancer as the most significant sets of genes altered in the Hnf4¿– colon null mice. Expression levels of the tight junction proteins claudin 4, 8 and 15 were altered early in the colon epithelium of Hnf4¿– mutants and correlated with increased barrier permeability to a molecular tracer that does not normally penetrate normal mucosa. Conclusion: These observations support a functional role for Hnf4¿– in protecting the colonic mucosa against the initiation of the changes resembling inflammatory bowel diseases and polyp formation.** **Overall design:** **HNF4alpha was conditionally knockout in the mouse epithelial colon with the villin CRE. A total of 3 control and 3 mutant littermates individuals were sacrificed at 1 year of age. The colon was harvested and Total RNA was isolated from each individuals. Each RNA sample was independently used to generate probes to screen affymetrix chips.**

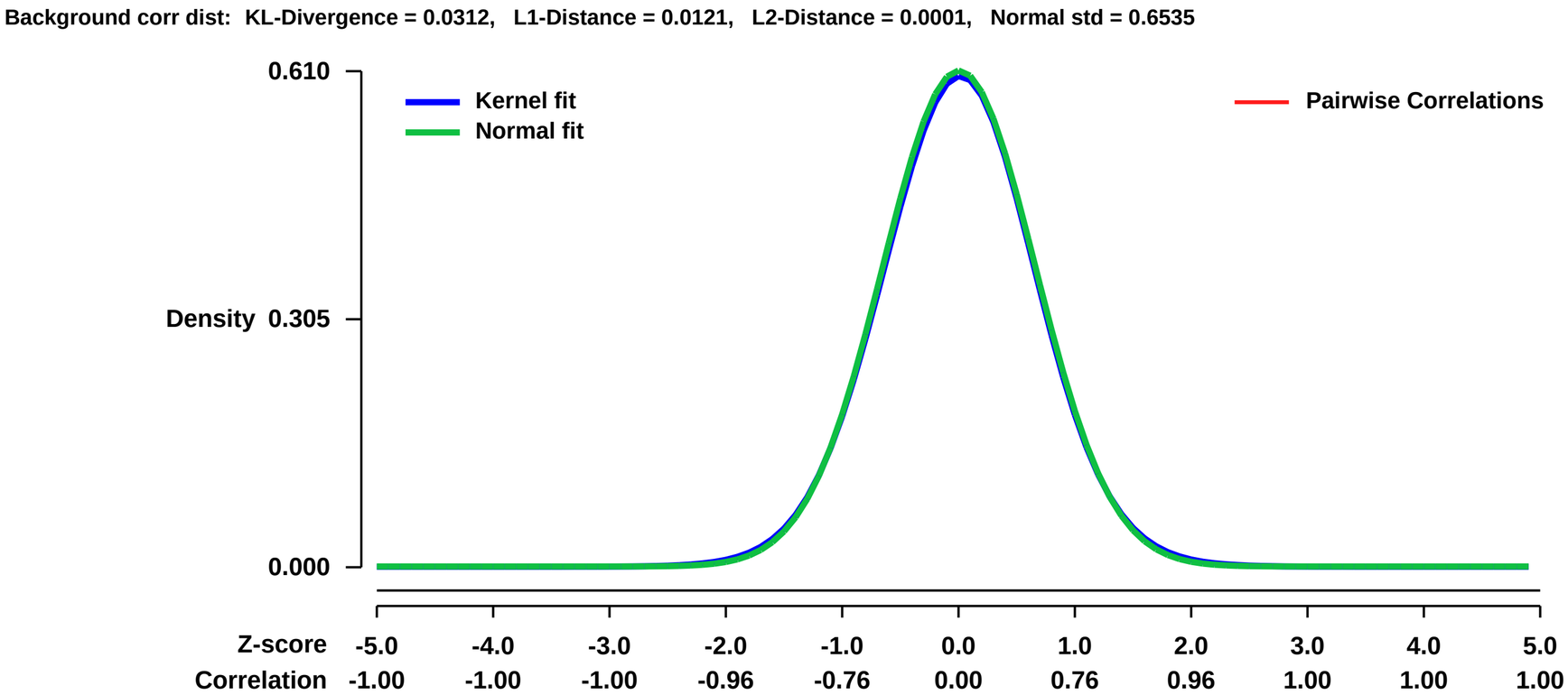

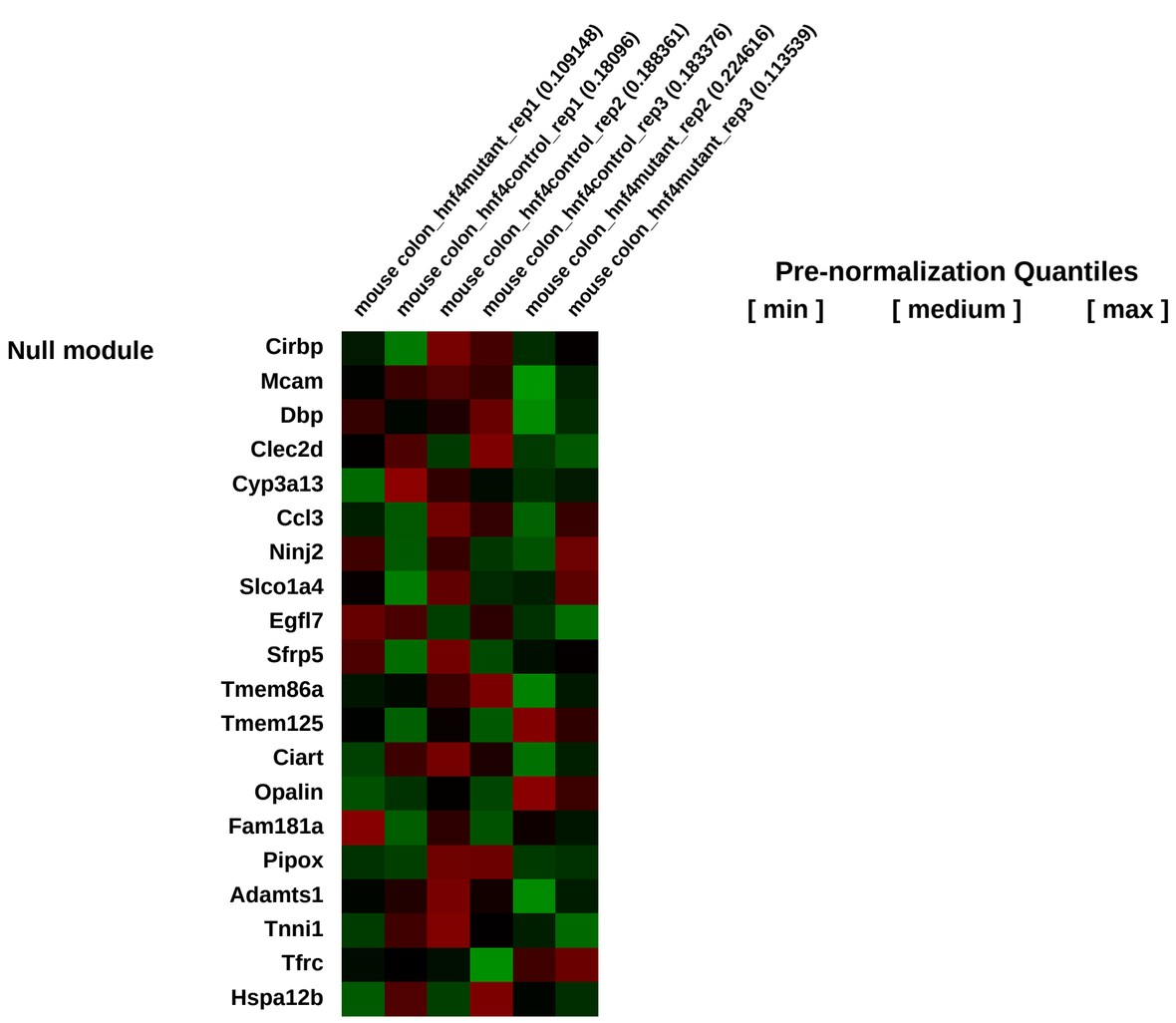

GEO Series "GSE11777" Expression Profiles

Num of samples in this series: 6

Scale of expression profile Z-scores

-3.0 -2.0 -1.0 0.0 1.0 2.0 3.0

GEO Link:	http://www.ncbi.nlm.nih.gov/geo/query/acc.cgi?acc=GSE11777
Status:	Public on Jun 13 2008
Title:	Microarray data of mouse fetal liver
Organism:	Mus musculus
Experiment type:	Expression profiling by array
Platform:	GPL1261
Pubmed ID:	18552213
Summary & Design:	**Summary:** Iron is essential for all cells but is toxic in excess, so iron absorption and distribution are tightly regulated. Serum iron is bound to transferrin and primarily enters erythroid cells via receptor-mediated endocytosis of the transferrin receptor (Tfr1). Tfr1 is essential for developing erythrocytes and reduced Tfr1 expression is associated with anemia. The transcription factors STAT5A/B are activated by many cytokines, including erythropoietin. Stat5a/b-/- mice are severely anemic and die perinatally, but no link has been made to iron homeostasis. To study the function of STAT5A/B in vivo, we deleted the floxed Stat5a/b locus in hematopoietic cells with a Tie2-Cre transgene. These mice exhibited microcytic, hypochromic anemia, as did lethally irradiated mice transplanted with Stat5a/b-/- fetal liver cells. Flow cytometry and RNA analyses of erythroid cells from mutant mice revealed a 50% reduction in Tfr1 mRNA and protein. We detected STAT5A/B binding sites in the first intron of the Tfr1 gene and found that expression of constitutively active STAT5A in an erythroid cell line increased Tfr1 levels. Chromatin immunoprecipitation experiments confirmed the binding of STAT5A/B to these sites. We conclude that STAT5A/B is an important regulator of erythroid progenitor iron uptake via its control of Tfr1 transcription. **Keywords:** genetic modification **Overall design:** Isolated Ter119-positive fetal liver cells from three to five E14.5 embryos of the same genotype were combined, and total RNA was extracted using TRIzol reagent (Life Technologies) with two additional ethanol precipitations. RNA quality was verified using an Agilent Bioanalyzer (Agilent Technologies). Microarray analyses were performed using Affymetrix Mouse Genome 430 2.0 array GeneChips (Affymetrix). Up- and down-regulated genes were selected based on P values of <0.05 and fold changes of >1.5 or -1.5 as assessed by ANOVA using Partek Pro software (Partek). To determine specific pathways, gene pathway analysis was obtained using the statistically significant gene list (P<0.05) represented on the chip.

Background corr dist: KL-Divergence = 0.0431, L1-Distance = 0.0190, L2-Distance = 0.0004, Normal std = 0.5998

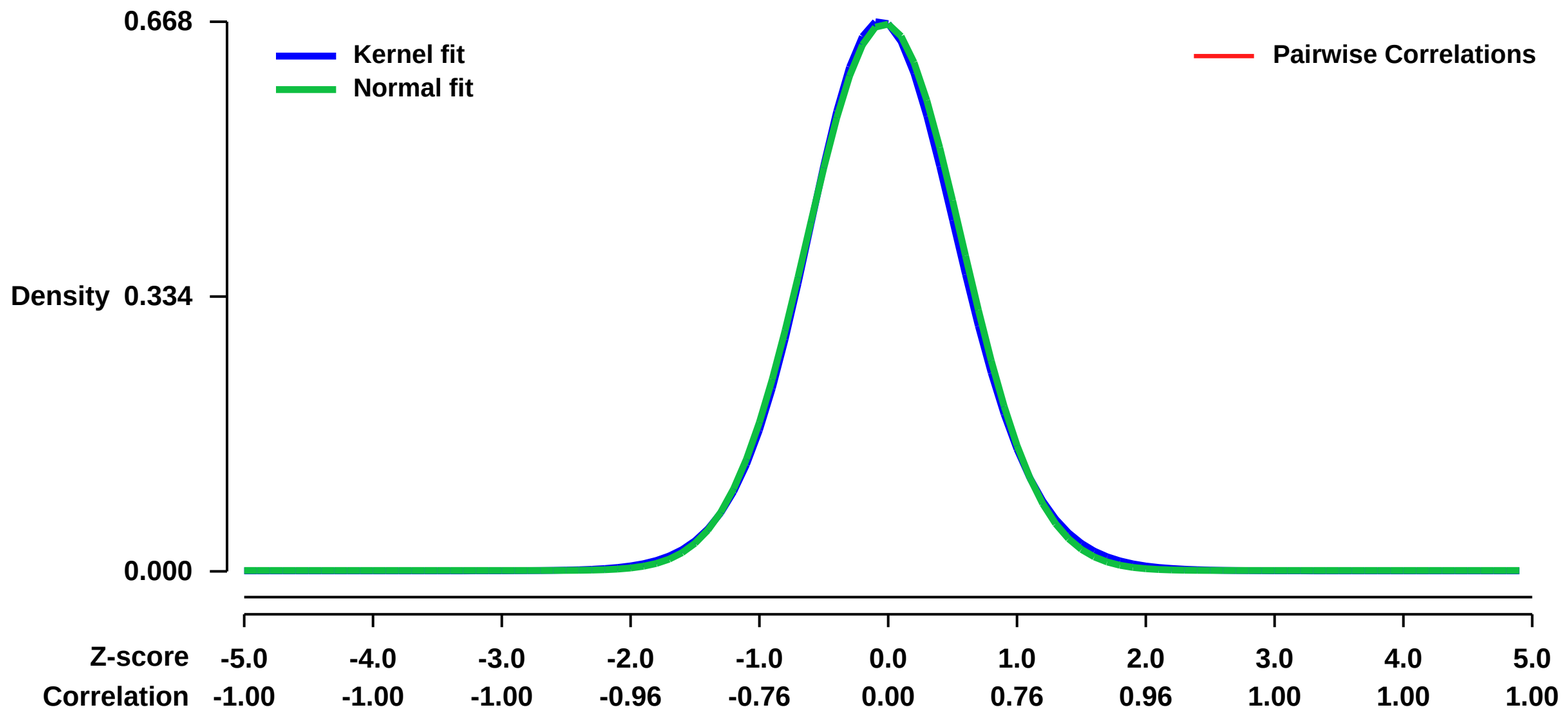

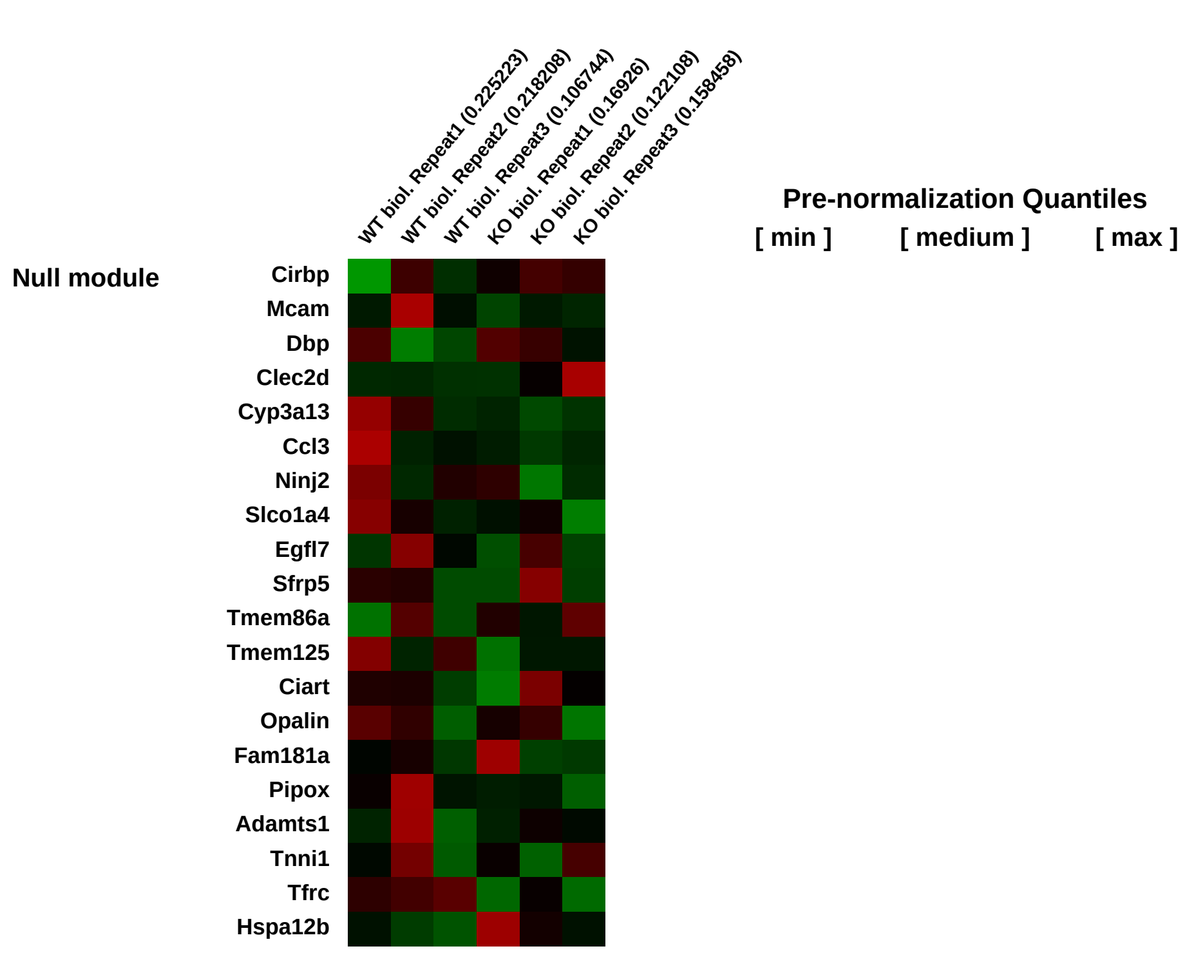

GEO Series "GSE11796" Expression Profiles

Num of samples in this series: 18

Scale of expression profile Z-scores

-3.0 -2.0 -1.0 0.0 1.0 2.0 3.0

GEO Link:	http://www.ncbi.nlm.nih.gov/geo/query/acc.cgi?acc=GSE11796
Status:	Public on Apr 17 2009
Title:	ligand-activated and -unactivated AHR in wiltype and mutant hepatoma cells
Organism:	Mus musculus
Experiment type:	Expression profiling by array
Platform:	GPL1261
Pubmed ID:	19654925
Summary & Design:	**Summary:** Starting with our early global expression analyses of TCDD-treated human hepatoma cells {Puga, 2000 4679 /id}, the AHR transcriptional induction profile has been extensively studied, whether activated by TCDD, B[a]P or in the absence of exogenous ligands (reviewed in {Frericks, 2007 5618 /id}). In addition to using prior knowledge to integrate expression profiles into the AHR gene target network, we performed a new set of expression profile analyses of wild type Hepa-1c1c7 and c35 cell lines and compared the responses in naˆflve cells with responses in TCDD or B[a]P exposed cells for 8 hours. Results of our expression array studies are in close agreement with current knowledge. **Overall design:** Three biological replicates were each performed for wildype naˆflve cells (DMSO), TCDD activated cells, and B[a]P activated cells, and for c35 (AHR mutant) naˆflve cells (DMSO), TCDD activated cells, and B[a]P activated cells.

Background corr dist: KL-Divergence = 0.0767, L1-Distance = 0.0883, L2-Distance = 0.0132, Normal std = 0.5635

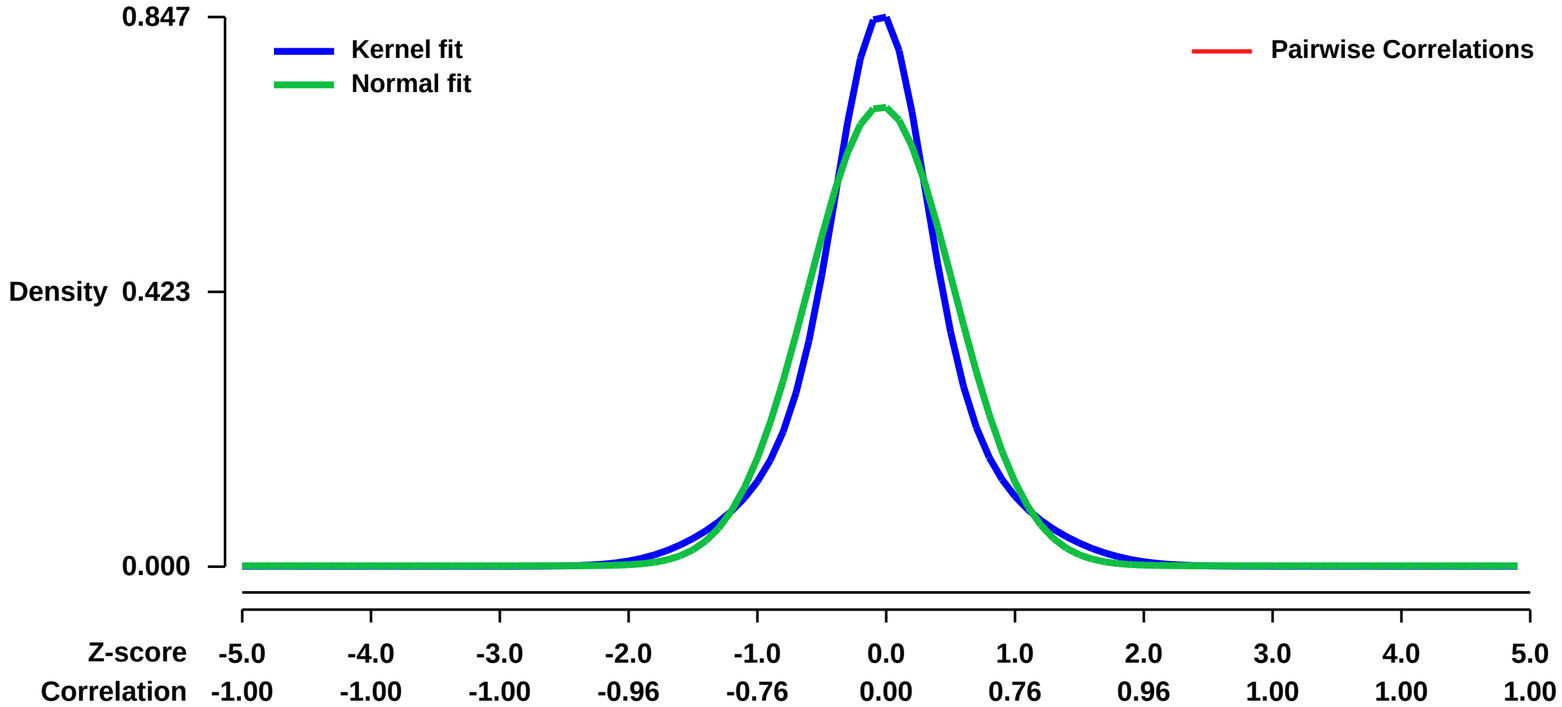

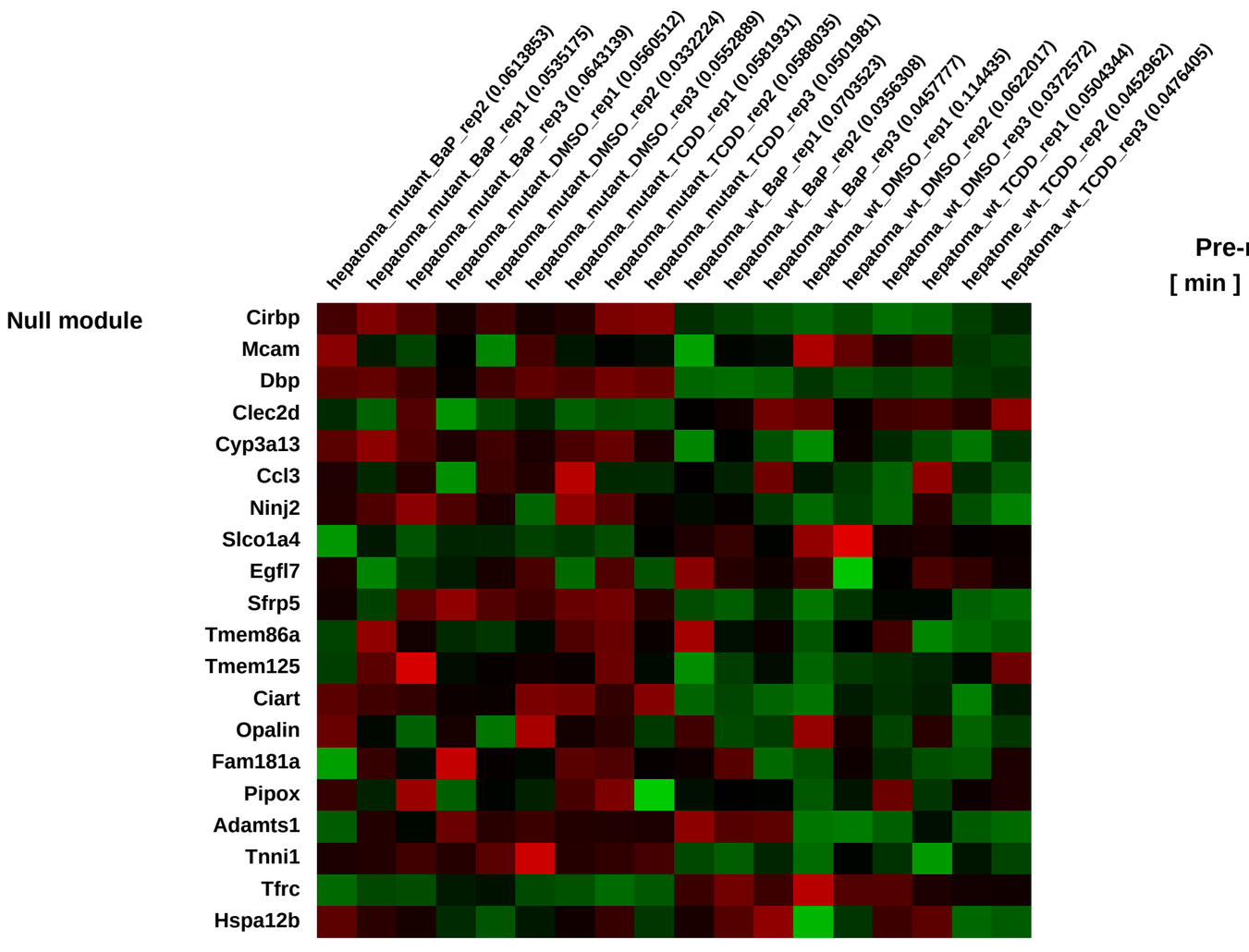

GEO Series "GSE11804" Expression Profiles

Num of samples in this series: 12

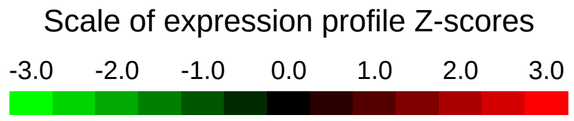

GEO Link:	**http://www.ncbi.nlm.nih.gov/geo/query/acc.cgi?acc=GSE11804**
Status:	**Public on Jun 18 2008**
Title:	**Pharmacological regulation of skeletal muscle gene expression**
Organism:	**Mus musculus**
Experiment type:	**Expression profiling by array**
Platform:	**GPL1261**
Pubmed ID:	**18674809**
Summary & Design:	**Summary:** **Exercise activates serine/threonine kinase AMPK and transcriptional factor PPARdelta that re-model metabolism and endurance capacity of skeletal muscle. Whether and how synthetic activation of these molecules regulated muscle gene signature is unknown.** **We have conducted skeletal muscle microarrays from mice treated with AMPK agoinst (AICAR), PPARdelta agonist (GW1516) or the combination of the two drugs to investigate the individual and interactive effects of the two on muscle genes.** **Keywords: Pharmacology study** **Overall design:** **C57Bl/6J mice were treated with Vehicle, AICAR, GW1516 and the combination of two drugs for 6 days, followed by collection of quadriceps for gene expression analysis.**

Background corr dist: KL-Divergence = 0.1790, L1-Distance = 0.0427, L2-Distance = 0.0040, Normal std = 0.3470

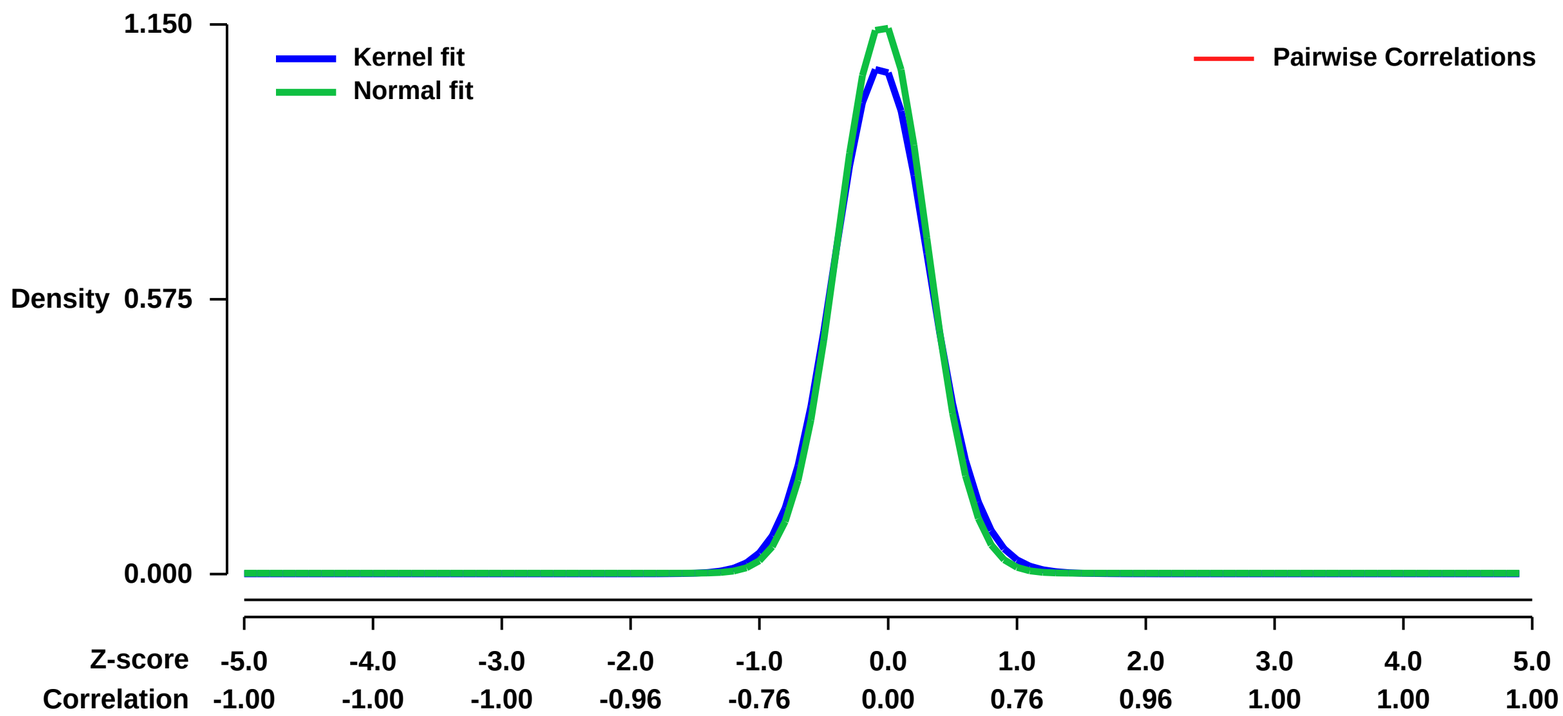

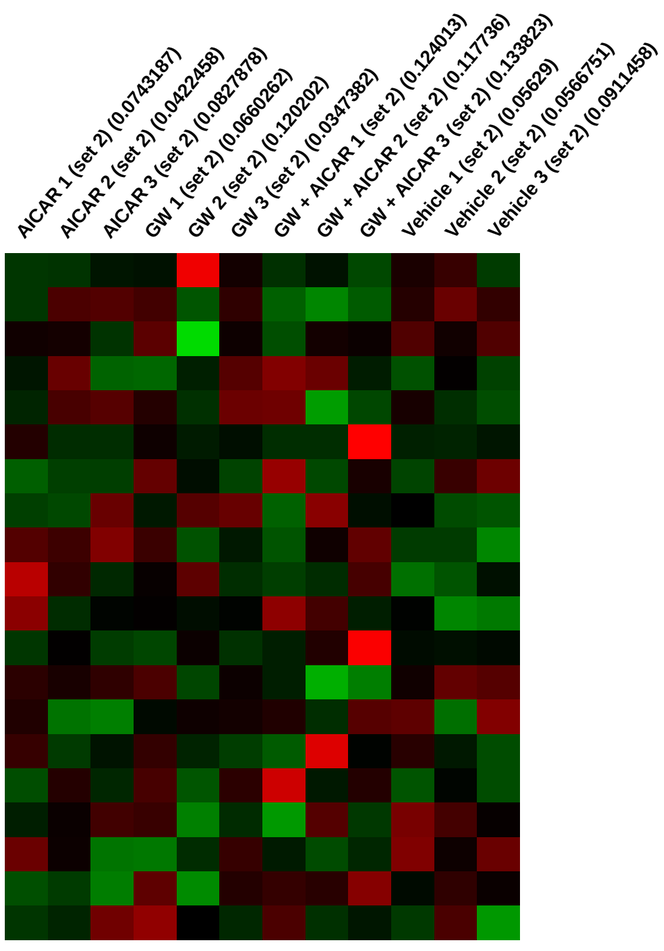

GEO Series "GSE11818" Expression Profiles

Num of samples in this series: 6

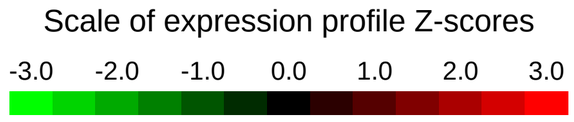

GEO Link:	http://www.ncbi.nlm.nih.gov/geo/query/acc.cgi?acc=GSE11818
Status:	Public on Jun 20 2008
Title:	Selective miRNA disruption in Tregs leads to uncontrolled autoimmunity
Organism:	Mus musculus
Experiment type:	Expression profiling by array
Platform:	GPL1261
Pubmed ID:	18725525
Summary & Design:	**Summary:** A new Treg-specific, FoxP3-GFP-hCre BAC transgenic was crossed to a conditional Dicer knock-out mouse strain to analyze the role of microRNAs (miRNA) in the development and function of regulatory T cells (Tregs). Although thymic Tregs developed normally in this setting, the cells showed evidence of altered differentiation and dysfunction in the periphery. Dicer-deficient Treg lineage cells failed to remain stable as a subset of cells down-regulated the Treg-specific transcription factor, FoxP3, while the majority expressed altered levels of multiple genes and proteins (including Neuropilin 1, GITR and CTLA-4) associated with the Treg fingerprint. In fact, a significant percentage of the Treg lineage cells took on a Th memory phenotype including increased levels of CD127, IL-4, and interferon-g. Importantly, Dicer-deficient Tregs lost suppression activity in vivo; the mice rapidly developed fatal systemic autoimmune disease resembling the FoxP3 knockout phenotype. These results support a central role for miRNAs in maintaining the stability of differentiated Treg function in vivo and homeostasis of the adaptive immune system. **Overall design:** Lymph node CD4+YFP+ T cells from FoxP3-GFP-hCre x ROSA26R-YFP Dicerwt/lox (Het) and FoxP3-GFP-hCre x ROSA26R-YFP Dicerlox/lox (KO) mice were isolated by flow cytometry. Triplicate GeneChips were used for each T cell population.

Background corr dist: KL-Divergence = 0.0337, L1-Distance = 0.0497, L2-Distance = 0.0029, Normal std = 0.7485

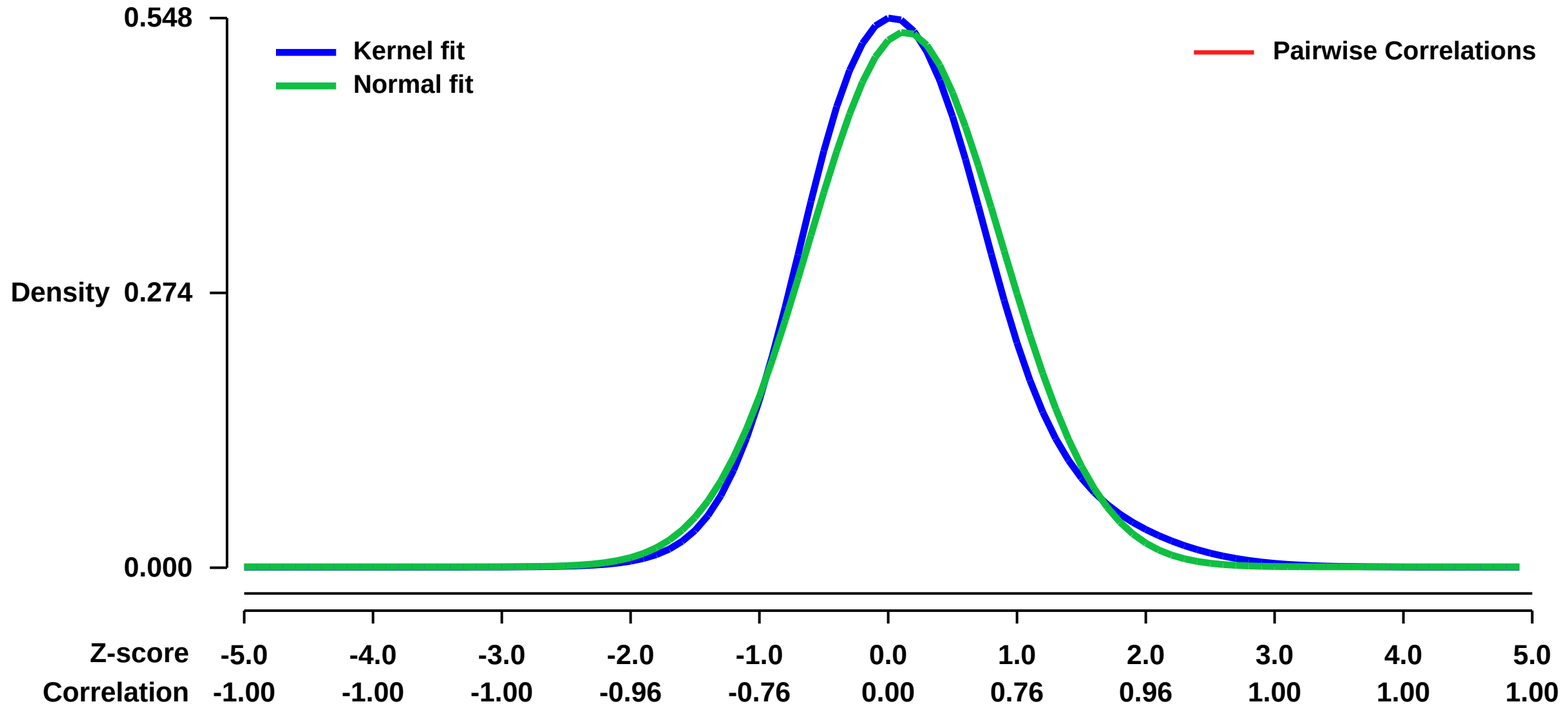

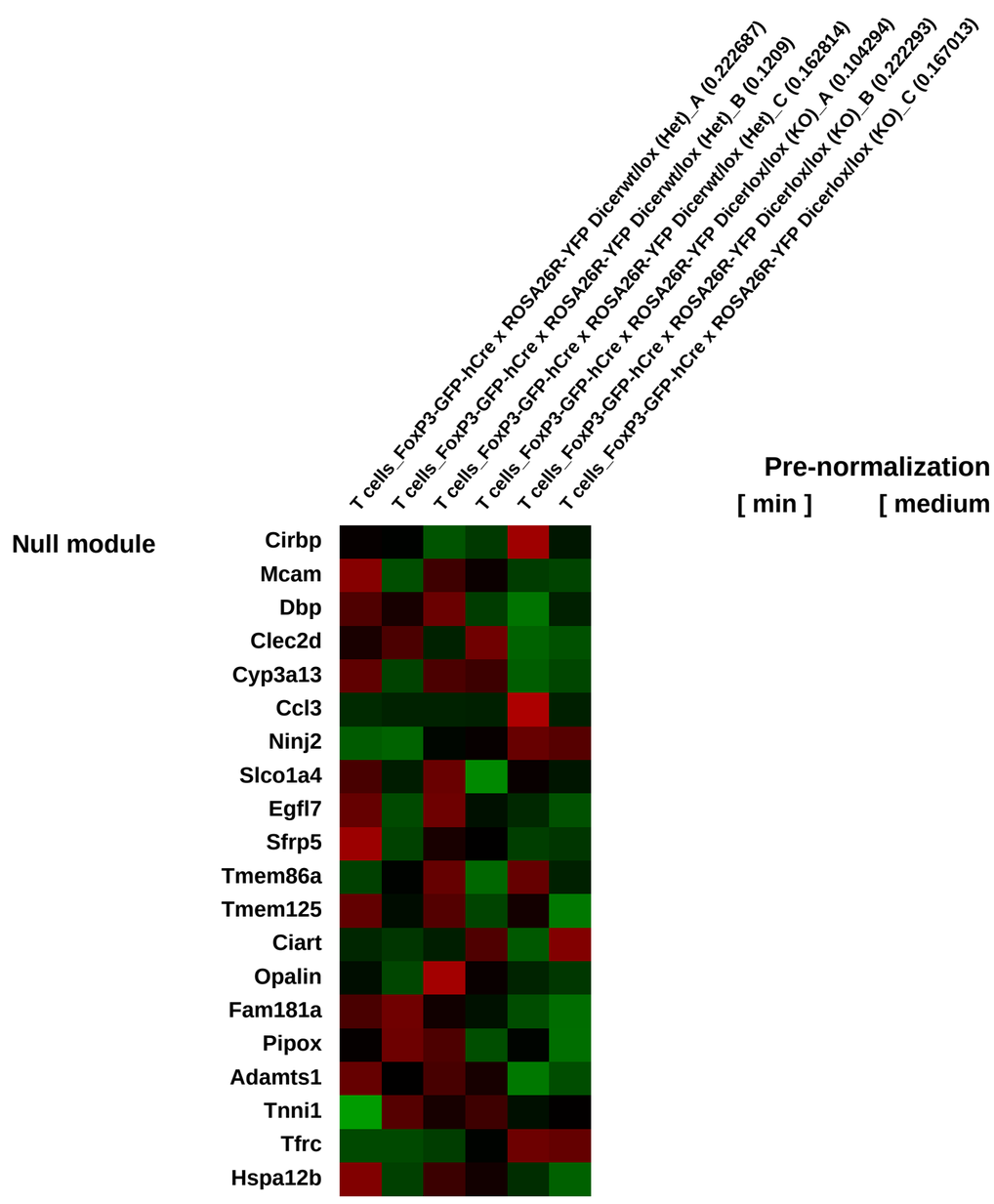

GEO Series "GSE11862" Expression Profiles

Num of samples in this series: 6

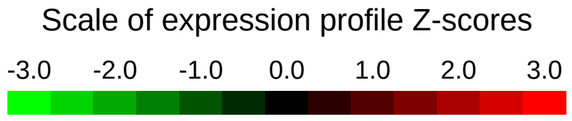

GEO Link:	http://www.ncbi.nlm.nih.gov/geo/query/acc.cgi?acc=GSE11862
Status:	Public on Sep 01 2008
Title:	Early Gene expression changes after axonal injury
Organism:	Mus musculus
Experiment type:	Expression profiling by array
Platform:	GPL1261
Pubmed ID:	19284657
Summary & Design:	**Summary:** We used optic nerve injury as a model to study early signaling events in the neuronal soma following axonal injury. Optic nerve injury results in the selective death of retinal ganglion cells (RGCs). The time course of cell death takes place over a period of days with the earliest detection of RGC death at about 48 hr post injury. We hypothesized that in the period immediately following axonal injury, there are changes in the soma that signal surrounding glia and neurons and that start programmed cell death. In the current study, we investigated early changes in cellular signaling and gene expression that occur within the first 6 hrs post optic nerve injury. We detected differences in phosphoproteins and gene expression within this time period that we used to interpret temporal events. Our studies revealed that the entire retina has been signaled by the RGC soma within 30 min after optic nerve injury and that pathways that modulate cell death are likely to be active in RGCs within 6 hrs following axonal injury **Keywords: Stress Response** **Overall design:** In the treated animals, axons of the optic nerve were crushed with fine forceps for 10 sec, 1 mm posterior to the globe, under direct visualization, within an intact meningeal sheath. Controls were contralateral eyes from the same animals in each group that had not been injured. After 6 hr eyes were enucleated and processed for tissue sectionin

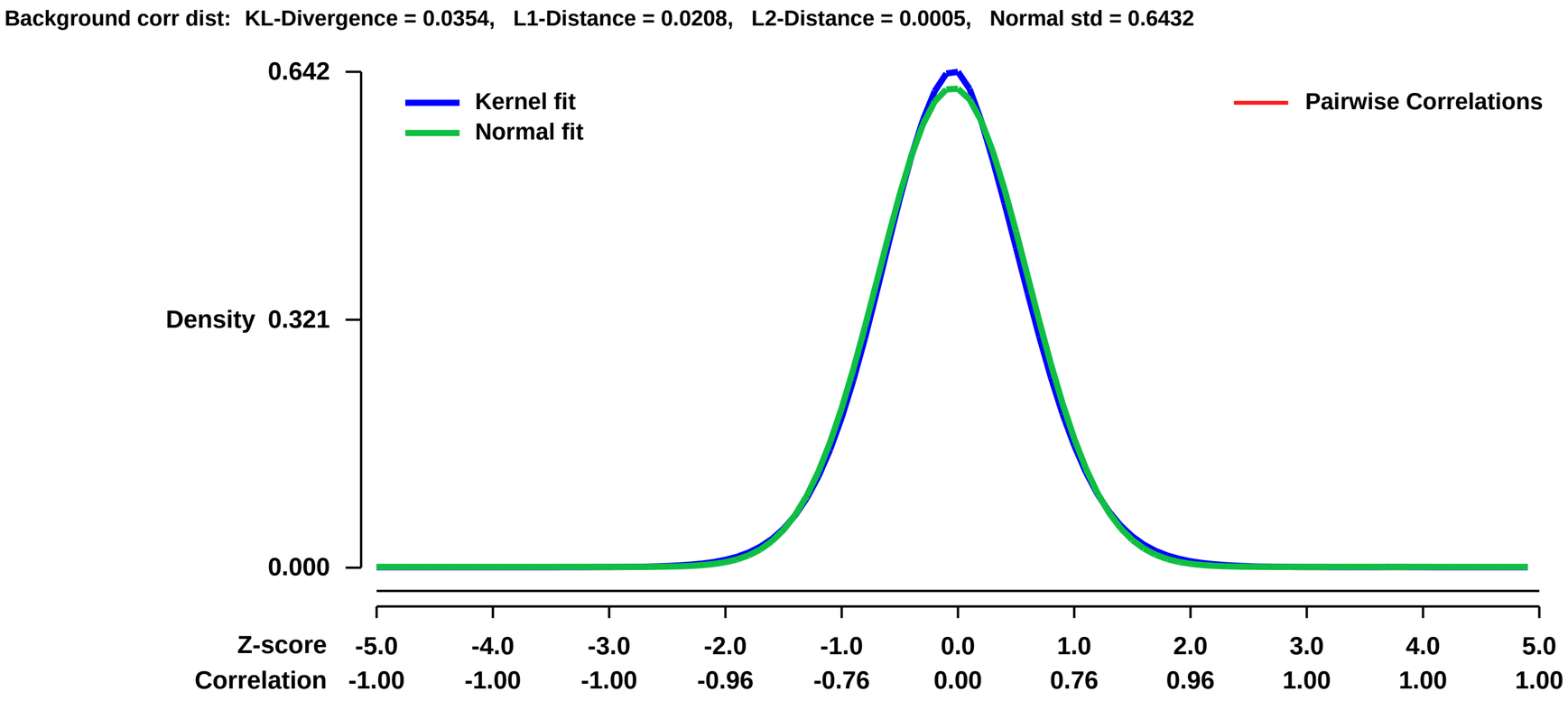

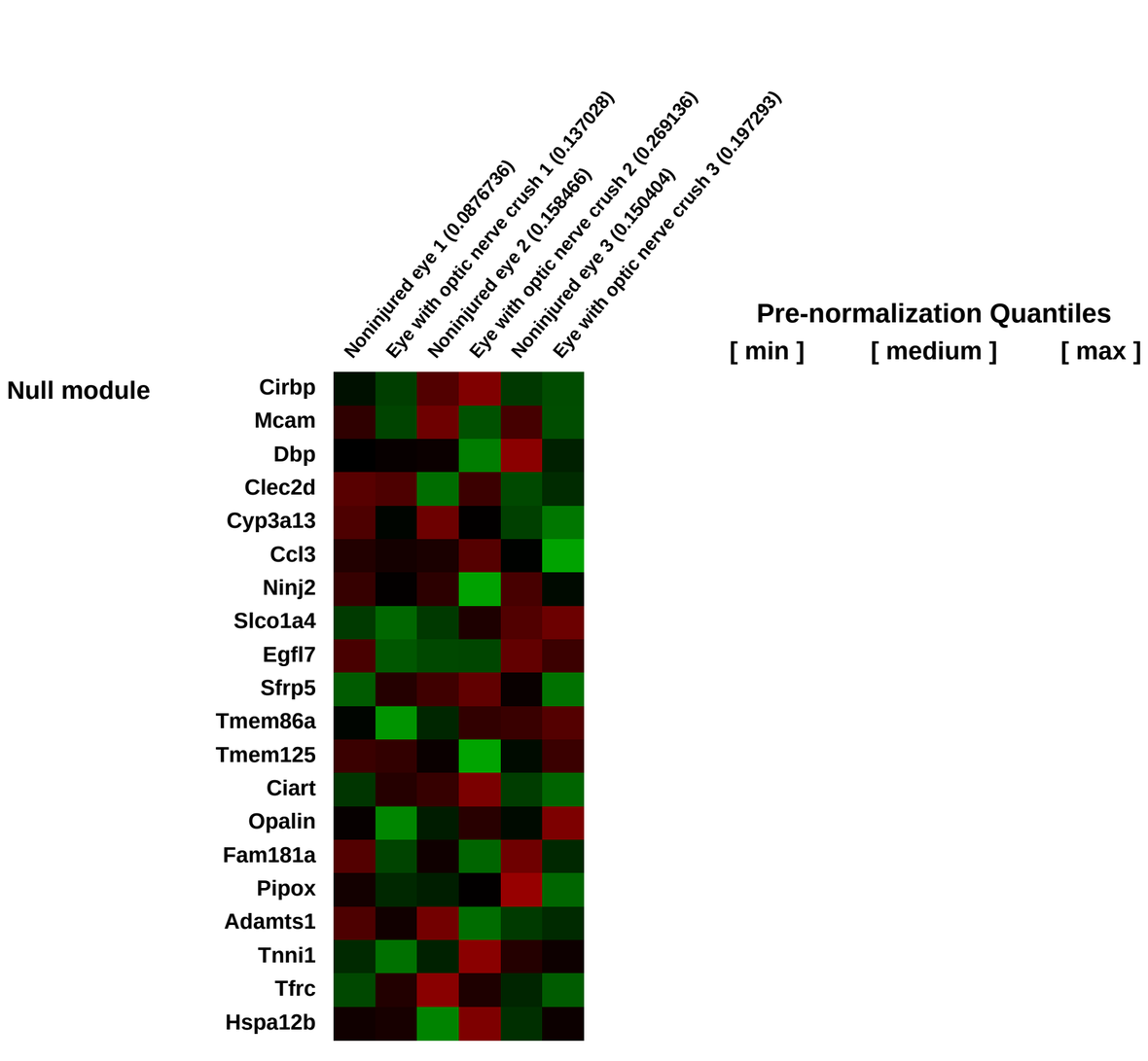

GEO Series "GSE11870" Expression Profiles

Num of samples in this series: 6

Scale of expression profile Z-scores

-3.0 -2.0 -1.0 0.0 1.0 2.0 3.0

GEO Link:	http://www.ncbi.nlm.nih.gov/geo/query/acc.cgi?acc=GSE11870
Status:	Public on Jul 23 2008
Title:	Gene expression changes in primary aortic endothelial cells during expression of dominant negative PPAR gamma (V290M).
Organism:	Mus musculus
Experiment type:	Expression profiling by array
Platform:	GPL1261
Pubmed ID:	18676352
Summary & Design:	**Summary:** Ligand-mediated activation of the nuclear hormone receptor PPAR gamma lowers blood pressure and improves glucose tolerance in humans. Two naturally occurring mutations (P467L, V290M) in the ligand binding domain of PPAR gamma have been described in humans that lead to severe insulin resistance and hypertension. Experimental evidence suggests that these mutant versions of PPAR gamma act in a dominant negative fashion. To better understand the molecular mechanisms underlying PPAR gamma action in the vasculature, we determined the global gene expression profile in primary aortic endothelial cells in response to endothelial cell specific expression of a dominant negative isoform of PPAR gamma (V290M). **Overall design:** We generated transgenic mice specifically targeting expression of dominant negative human PPAR gamma to the endothelium using an endothelial-specific promoter (vascular endothelial cadherin or CDH5). Primary aortic endothelial cells were isolated from 10 non-transgenic and 10 EC-DN mice by Dominion Pharmakine (http://www.pharmakine.com/). For each group, 5 cultures of cells were established. Each culture was derived from 2 mice and remained separate from the other cultures. Cellular RNA was prepared using conventional methods and quality was assessed using the Bioanalyzer 2100 (Agilent Technologies). For the microarray hybridizations, RNA from 3 of the cultures in each group was used. All the microarray procedures were conducted at the University of Iowa DNA Core facility using standard Affymetrix protocols. In brief, approximately 50 ng of total RNA was used as input to a two-step amplification procedure (NuGen, http://www.nugeninc.com/) to generate biotin-labeled RNA fragments for hybridization to the Affymetrix GeneChip Mouse Genome 430 2.0 array.

Background corr dist: KL-Divergence = 0.0338, L1-Distance = 0.0226, L2-Distance = 0.0006, Normal std = 0.6536

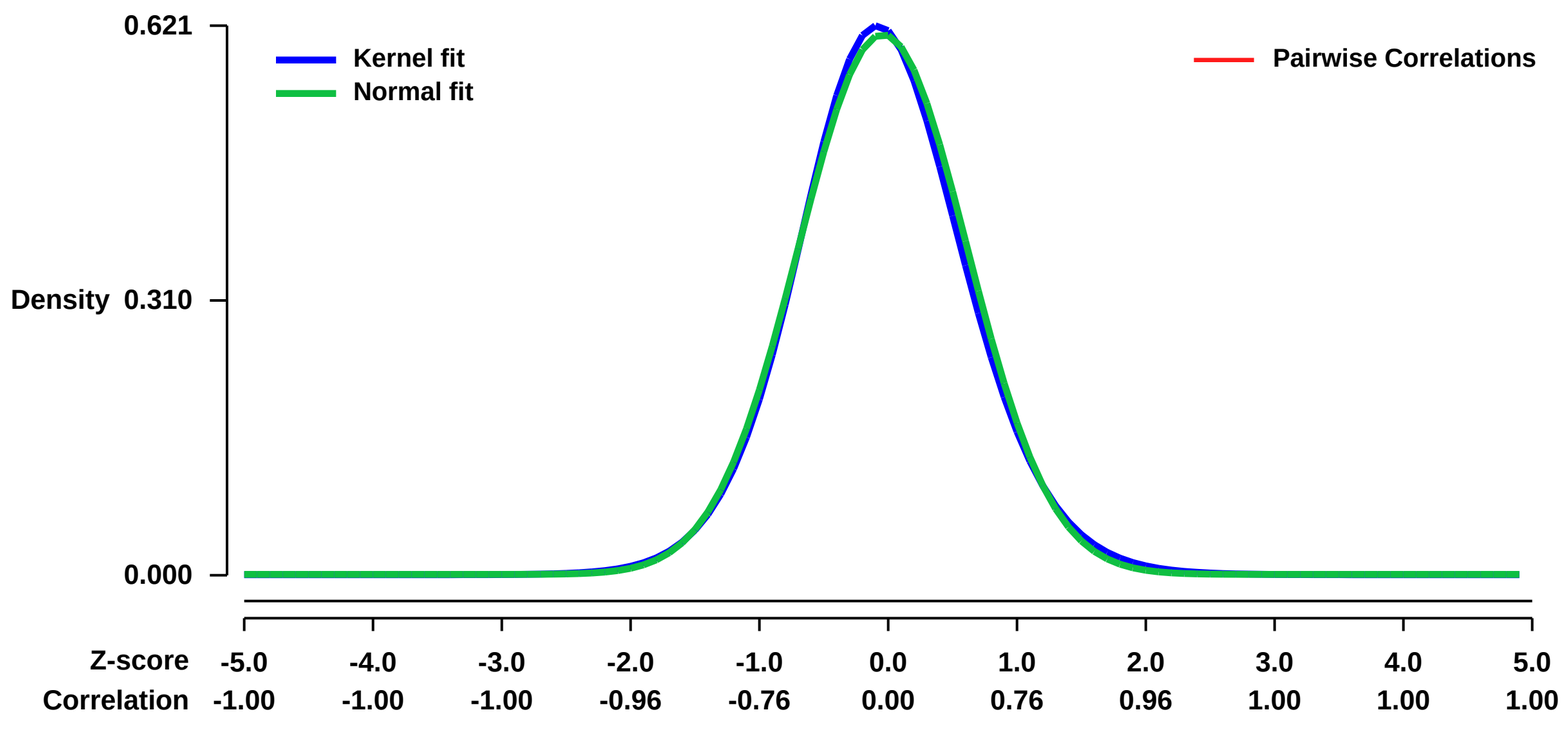

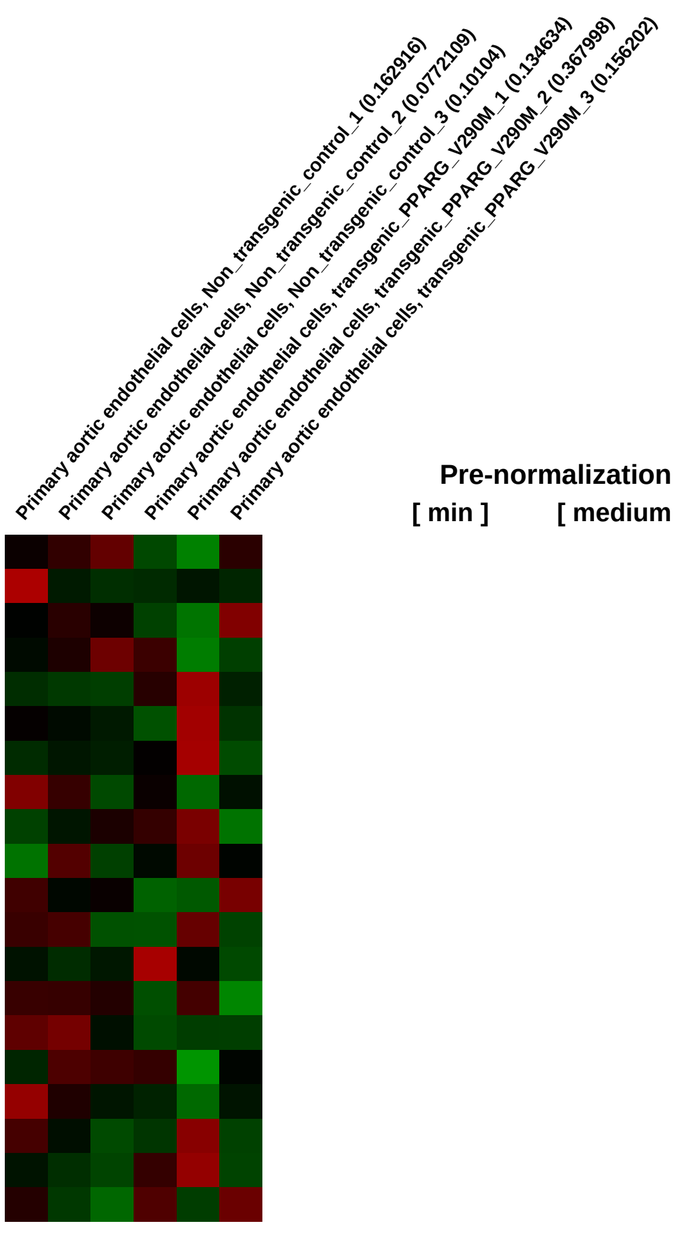

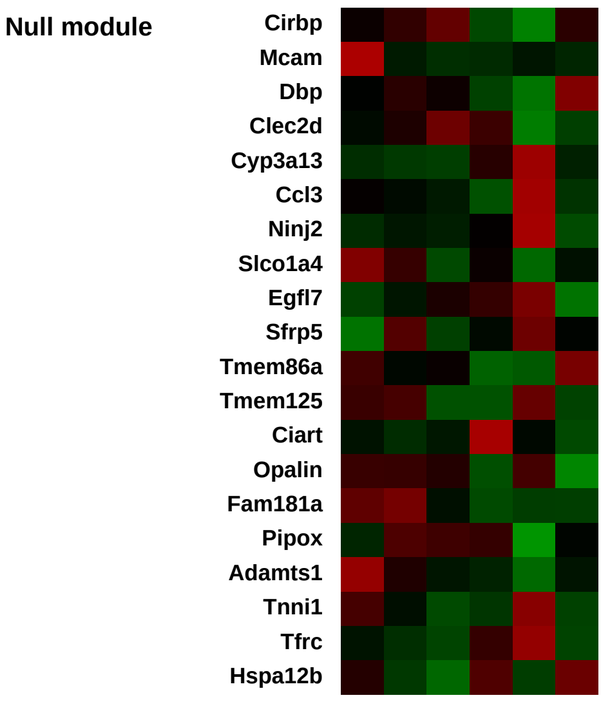

GEO Series "GSE11973" Expression Profiles

Num of samples in this series: 6

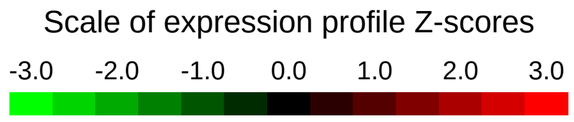

GEO Link:	http://www.ncbi.nlm.nih.gov/geo/query/acc.cgi?acc=GSE11973
Status:	Public on Jul 31 2008
Title:	Wild-type cultured neutrophils versus miR-223 null cultured neutrophils
Organism:	Mus musculus
Experiment type:	Expression profiling by array
Platform:	GPL1261
Pubmed ID:	18668037
Summary & Design:	**Summary:** This array analysis is to study the regulation of target messagesâ expression in in vitro cultured murine neutrophils versus miR-223 null neutrophils. Culture media was SILAC-IMDM for MS analysis. **Overall design:** Wild-type cultured neutrophils versus miR-223 null cultured neutrophils

Background corr dist: KL-Divergence = 0.0336, L1-Distance = 0.0241, L2-Distance = 0.0006, Normal std = 0.6585

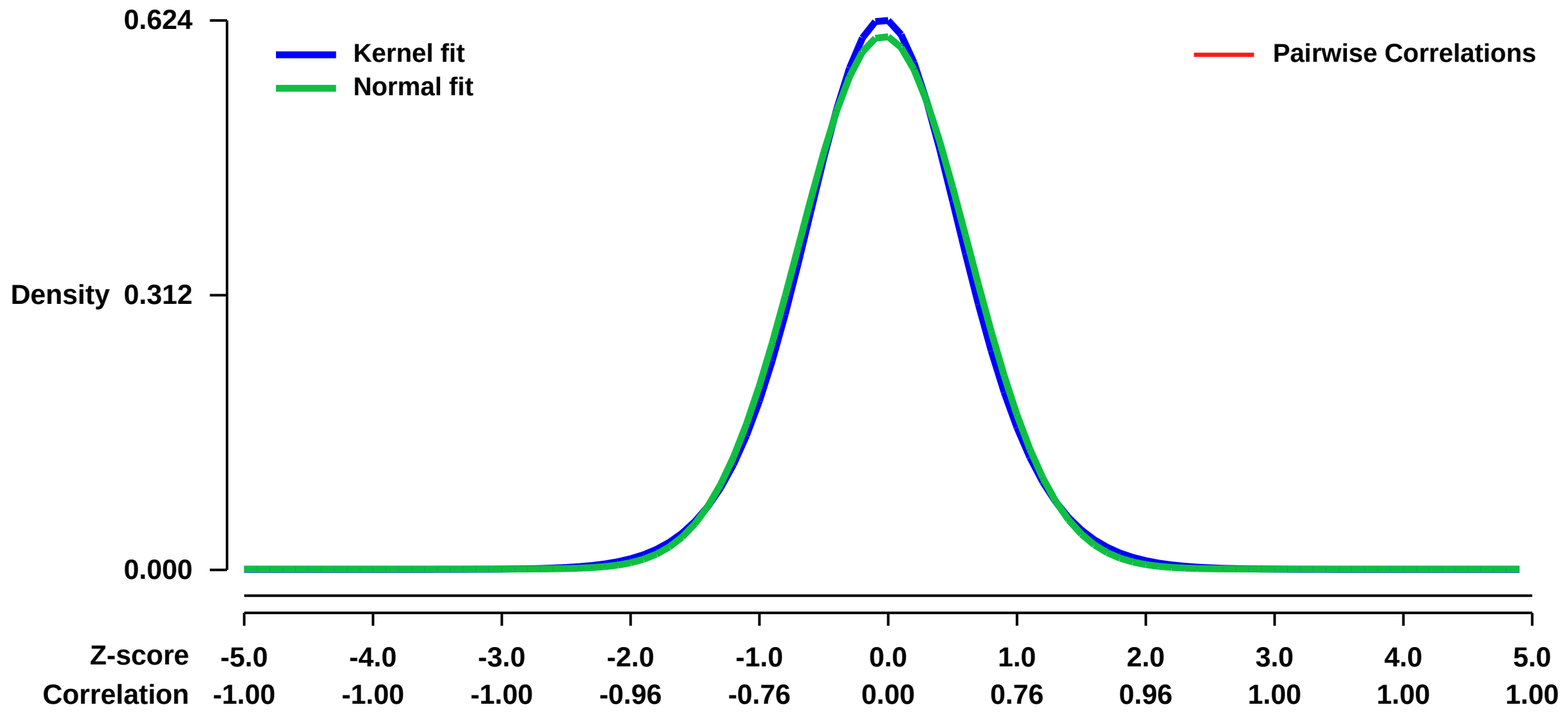

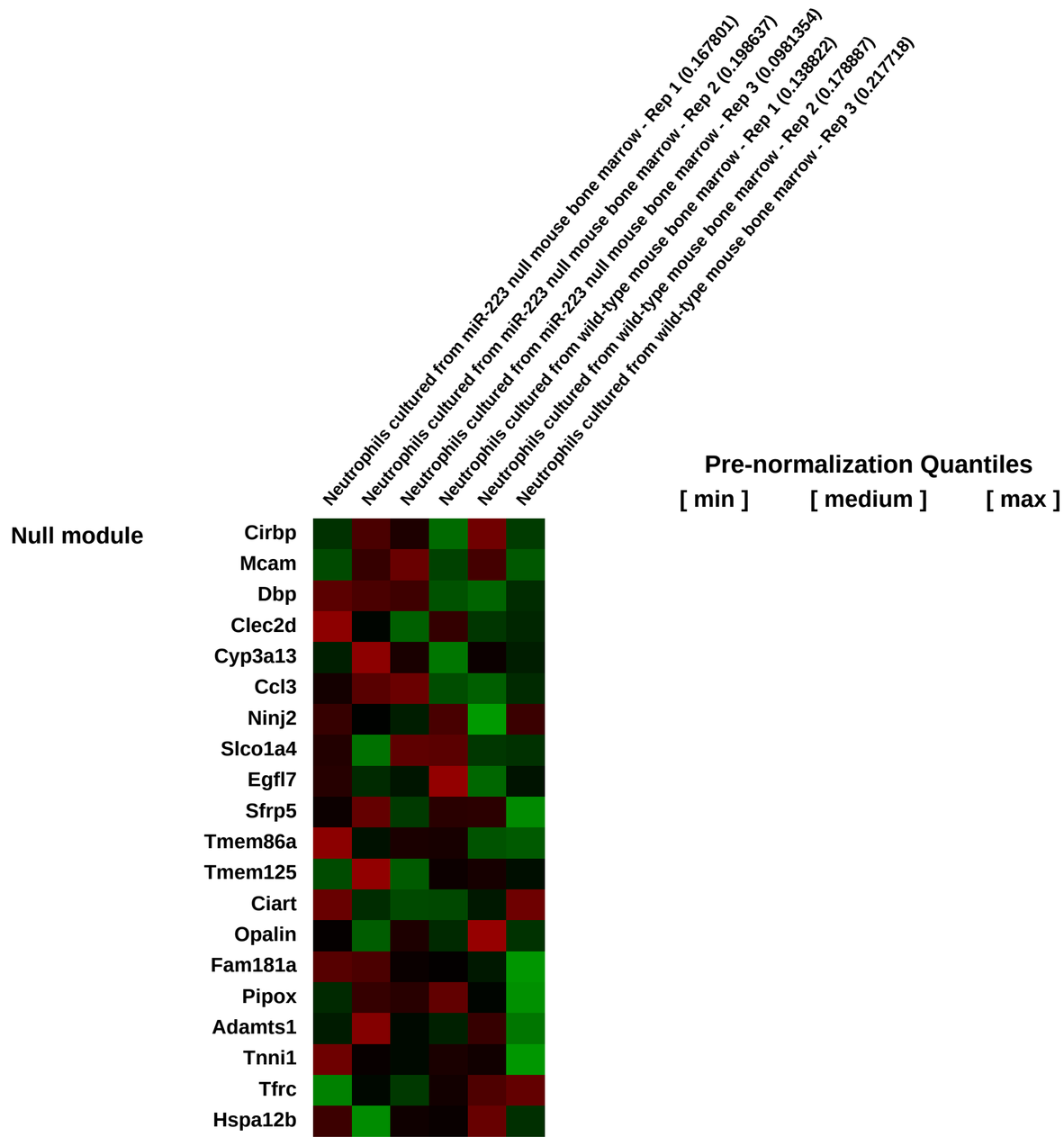

GEO Series "GSE11981" Expression Profiles

Num of samples in this series: 8

Scale of expression profile Z-scores

-3.0 -2.0 -1.0 0.0 1.0 2.0 3.0

GEO Link:	**http://www.ncbi.nlm.nih.gov/geo/query/acc.cgi?acc=GSE11981**
Status:	**Public on Sep 12 2008**
Title:	**Gene expression profiling of HhAntag-treated pancreatic xenografts**
Organism:	**Mus musculus**
Experiment type:	**Expression profiling by array**
Platform:	**GPL1261**
Pubmed ID:	**18754008**
Summary & Design:	**Summary:** **Four vehicle-treated and four HhAntag-treated pancreatic xenograft tumors were profiled for gene expression changes using Affymetrix U133 Plus 2.0 and Affymetrix Mouse Genome 430 2.0 arrays.** **Keywords: comparative gene expression, hedgehog, hh** **Overall design:** **A primary human pancreatic tumor xenograft (1051178-A) was established by direct implantation of surgical material into female CD1 nu/nu mice of 6-8 weeks of age. Tumors were serially passaged into larger cohorts of mice for efficacy testing and subsequently distributed into tumor volume-matched cohorts upon tumors reaching between 200 to 350 mm3. HhAntag was resuspended in 0.5% methyl-cellulose, 0.2% Tween-80 (MCT) and administered orally twice daily at 75 mg/kg from a 10 mg/ml suspension. MCT alone served as vehicle control. Tumor xenografts (4/group) were excised following 21 days of dosing and RNA was extracted. Preparation of complementary RNA, Human Genome U133 Plus 2.0 array and Mouse Genome 430 2.0 array hybridizations, and subsequent data analysis were carried out using Affymetrix protocols, with signal intensities being determined by the MAS5.0 algorithm.**

Background corr dist: KL-Divergence = 0.0855, L1-Distance = 0.0227, L2-Distance = 0.0007, Normal std = 0.4633

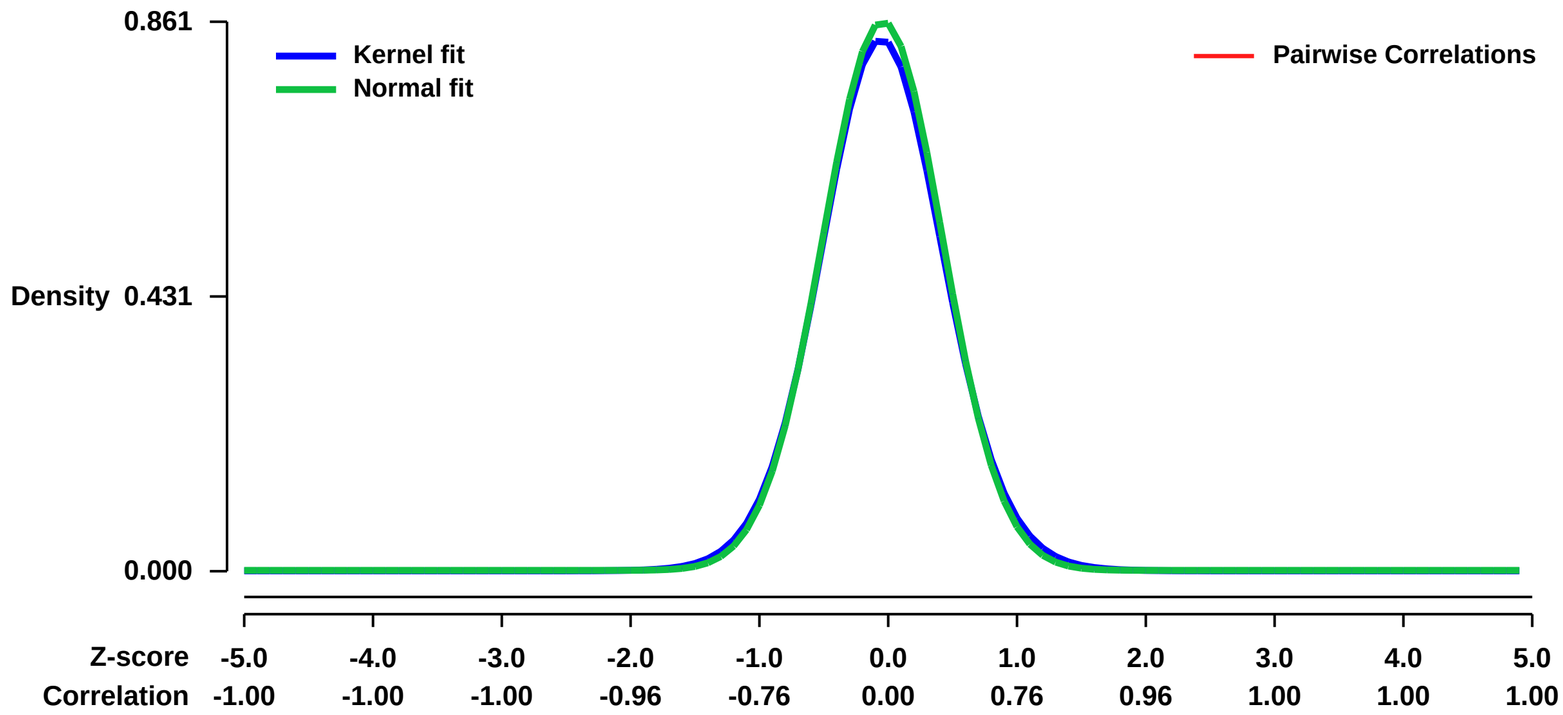

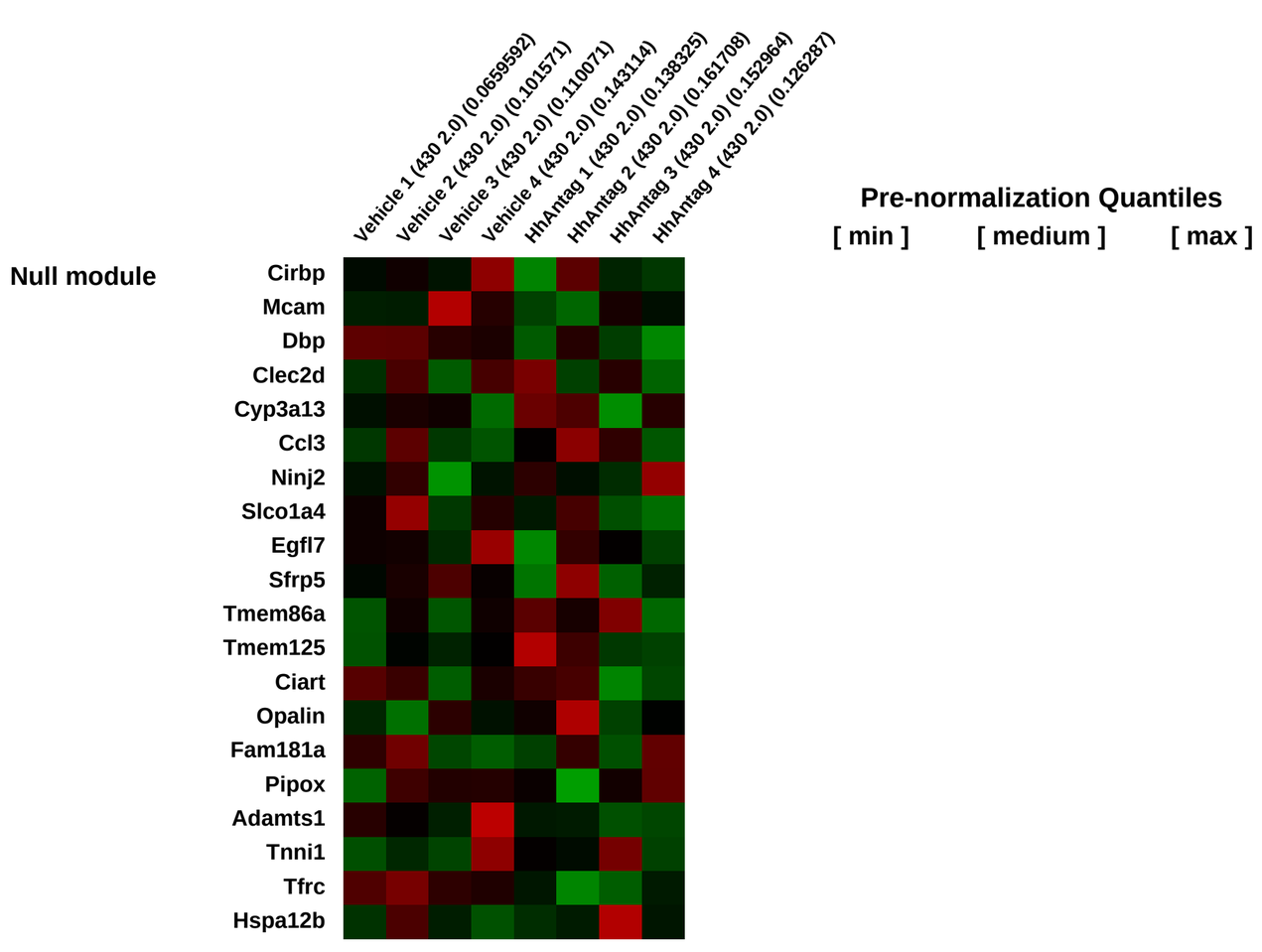

GEO Series "GSE12001" Expression Profiles

Num of samples in this series: 6

Scale of expression profile Z-scores

-3.0 -2.0 -1.0 0.0 1.0 2.0 3.0

GEO Link:	http://www.ncbi.nlm.nih.gov/geo/query/acc.cgi?acc=GSE12001
Status:	Public on Jul 31 2008
Title:	Wild-type neutrophils and miR-223 null neutrophils
Organism:	Mus musculus
Experiment type:	Expression profiling by array
Platform:	GPL1261
Pubmed ID:	18668037
Summary & Design:	**Summary:** **This array analysis is to study the regulation of target messagesâ expression in murine neutrophils versus miR-223 null neutrophils.** **Overall design:** **Three arrays for wild-type neutrophils and miR-223 null neutrophils**

Background corr dist: **KL-Divergence = 0.0437, L1-Distance = 0.0189, L2-Distance = 0.0004, Normal std = 0.5982**

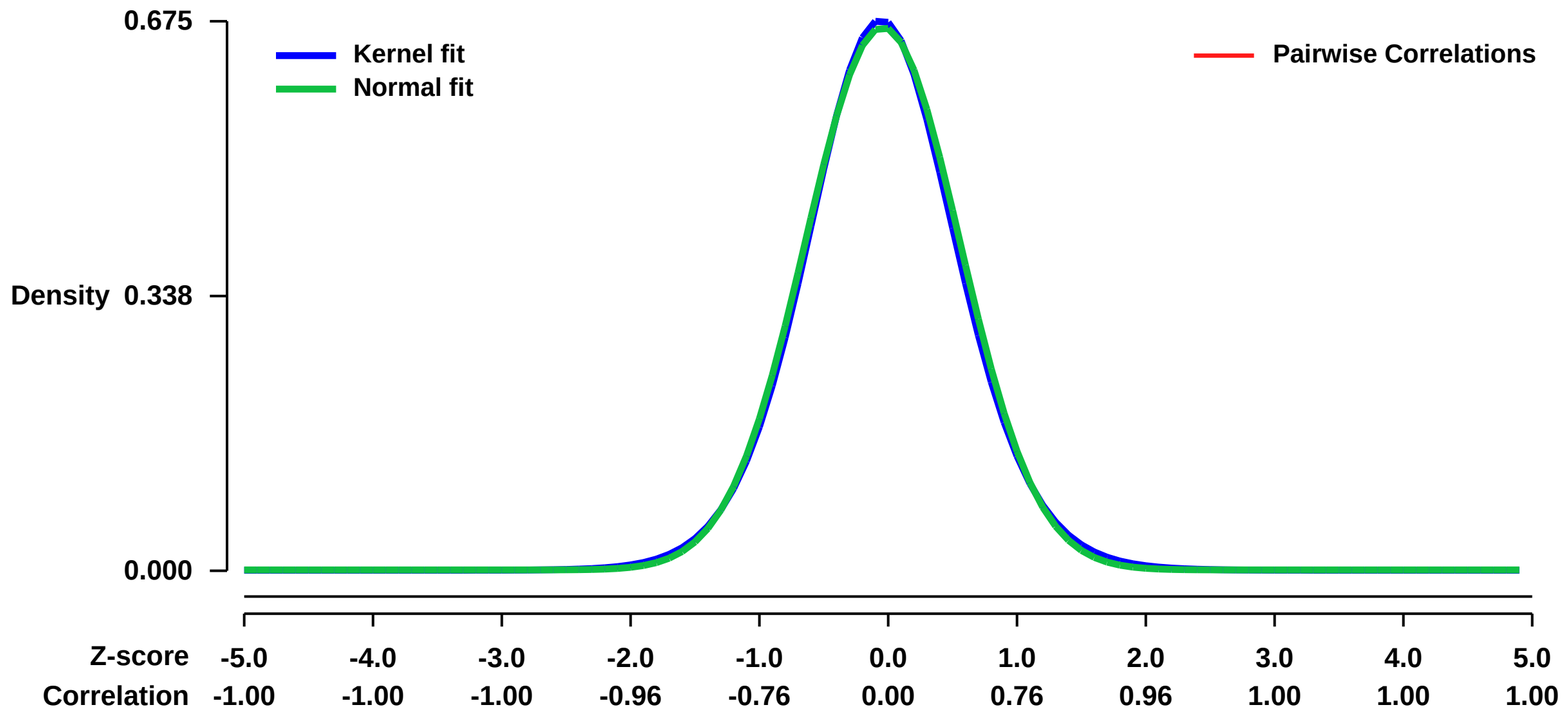

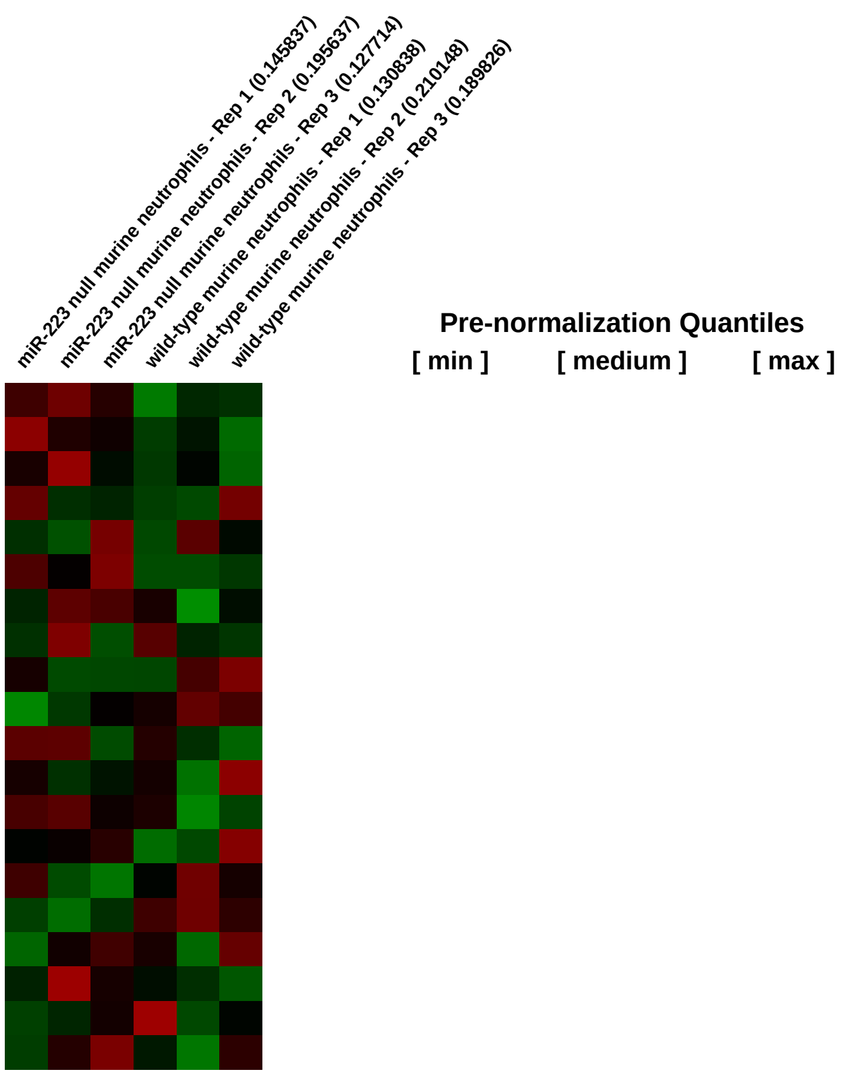

GEO Series "GSE12049" Expression Profiles

Num of samples in this series: 6

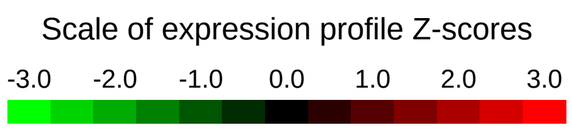

GEO Link:	http://www.ncbi.nlm.nih.gov/geo/query/acc.cgi?acc=GSE12049
Status:	Public on Jul 10 2008
Title:	Expression data from laminin alpha 2 chain deficient mice vs wild type
Organism:	Mus musculus
Experiment type:	Expression profiling by array
Platform:	GPL1261
Pubmed ID:	18611855
Summary & Design:	**Summary:** Mutations in the gene encoding laminin a2 chain cause congenital muscular dystrophy, MDC1A. In skeletal muscle, laminin a2 chain binds at least two receptor complexes; the dystrophin-glycoprotein complex and integrin a7b1. To gain insight into the molecular mechanisms underlying this disorder, we performed gene expression profiling of laminin a2 chain deficient mouse limb muscle. One of the down-regulated genes encodes a protein called calcium and integrin binding protein 2 (Cib2) whose expression and function is unknown. However, the closely related Cib1 has been reported to bind integrin allb and may be involved in outside-in-signaling in platelets. Since Cib2 might be a novel integrin a7b1 binding protein in muscle, we have studied Cib2 expression in the developing and adult mouse. Cib2 mRNA is mainly expressed in the developing central nervous system and in developing and adult skeletal muscle. In skeletal muscle Cib2 colocalizes with integrin a7B subunit at the sarcolemma and at the neuromuscular- and myotendinous junctions. Finally, we demonstrate that Cib2 is a calcium binding protein that interacts with integrin a7Bb1D. Thus, our data suggest a role for Cib2 as a cytoplasmic effector of integrin a7Bb1D signaling in skeletal muscle **Keywords: disese state analysis** **Overall design:** Skeletal muscle (all hind limb skeletal muscle) from 4-weeks old laminin alpha 2 chain deficient mice and 4-weeks old wild type mice were isolated individually and RNA were extracted and hybridized on Affiymetrix microarrys. Three biological replicates from each group were analyzed.

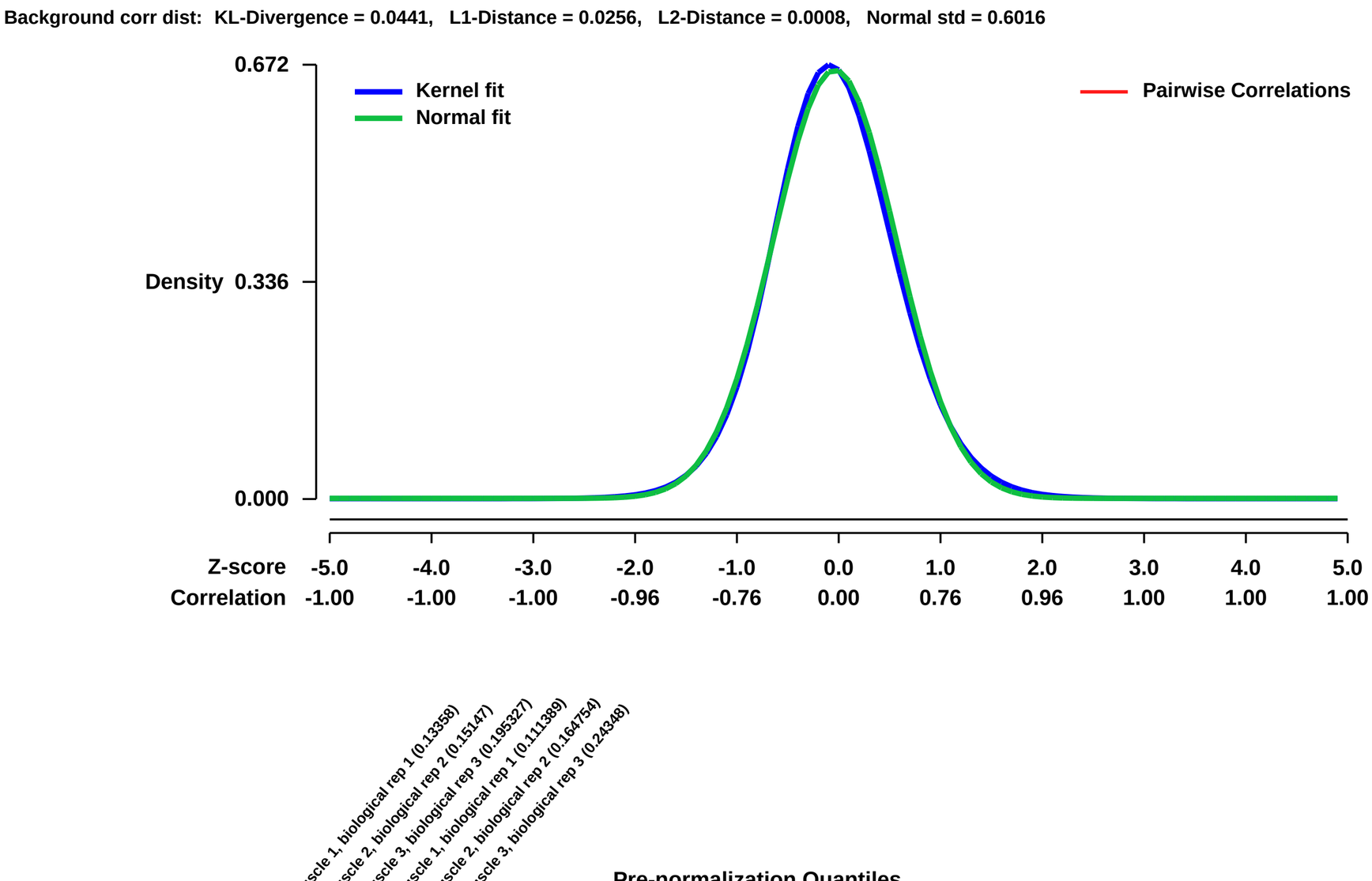

GEO Series "GSE12078" Expression Profiles

Num of samples in this series: 8

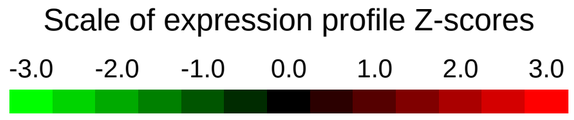

GEO Link:	**http://www.ncbi.nlm.nih.gov/geo/query/acc.cgi?acc=GSE12078**
Status:	**Public on Jul 18 2008**
Title:	**Ctr9 knockdown in mouse ES cells**
Organism:	**Mus musculus**
Experiment type:	**Expression profiling by array**
Platform:	**GPL1261**
Pubmed ID:	**19345177**
Summary & Design:	**Summary:** **To monitor global transcript changes after Paf1C depletion we transfected ESCs with esiRNA targeting Ctr9 and control esiRNA (Luc).** **Overall design:** **4 replicates of esiRNA tranfection controls (luciferase esiRNA) and 4 replicates of Ctr9 esiRNA tranfection samples**

Background corr dist: **KL-Divergence = 0.0399, L1-Distance = 0.0419, L2-Distance = 0.0022, Normal std = 0.6455**

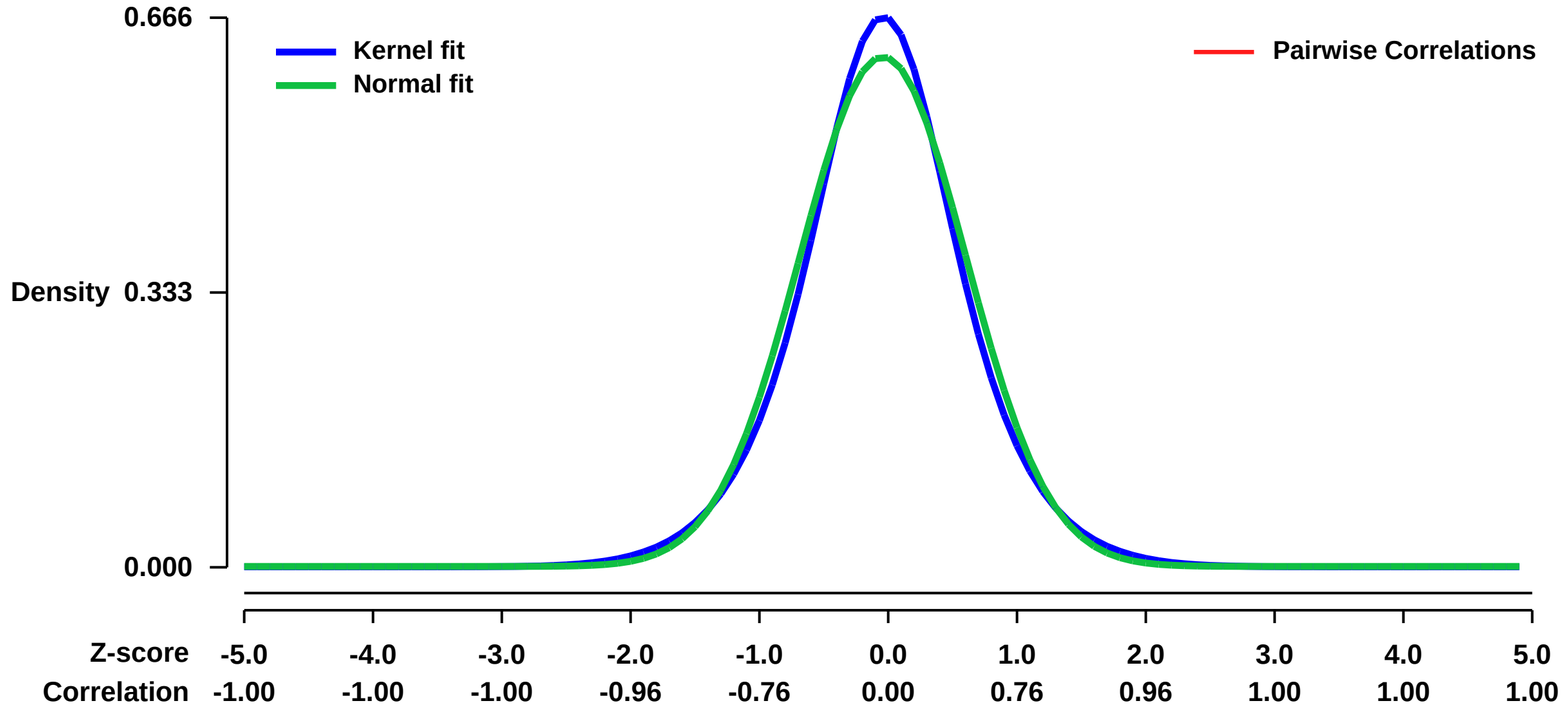

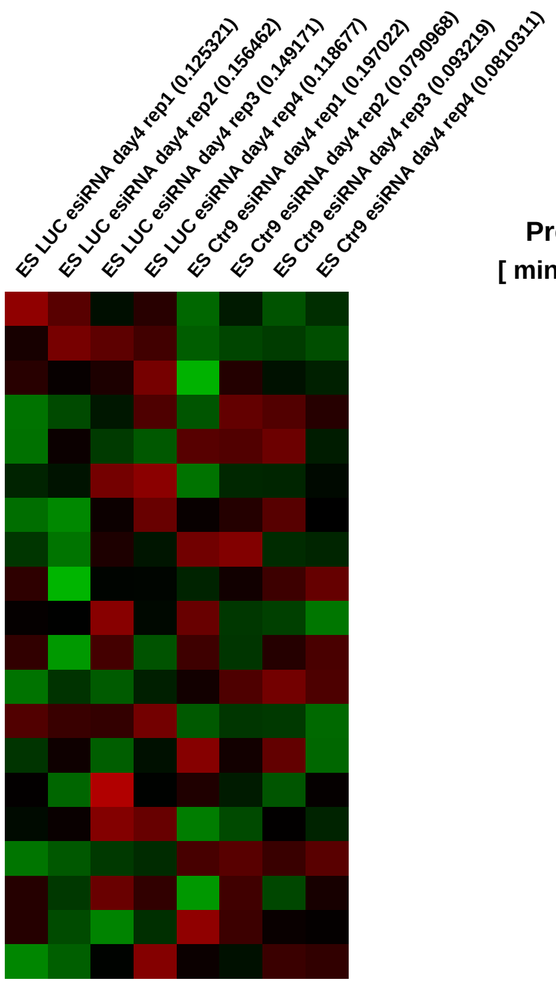

GEO Series "GSE12333" Expression Profiles

Num of samples in this series: 6

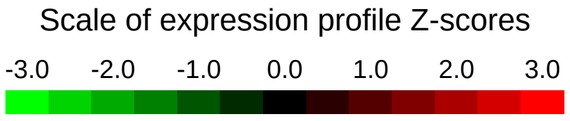

GEO Link:	http://www.ncbi.nlm.nih.gov/geo/query/acc.cgi?acc=GSE12333
Status:	Public on Aug 04 2009
Title:	Retinoic Acid Delivery within Embryoid Bodies Induces an Early Streak Phenotype in vitro
Organism:	Mus musculus
Experiment type:	Expression profiling by array
Platform:	GPL1261
Pubmed ID:	19162317
Summary & Design:	**Summary:** During embryogenesis, cell specification and tissue formation is directed by the concentration and temporal presentation of morphogens, and similarly, pluripotent embryonic stem cells differentiate in vitro into various phenotypes in response to morphogen treatment. Embryonic stem cells are commonly differentiated as three dimensional spheroids called embryoid bodies (EBs); however, differentiation within EBs is typically heterogeneous and disordered. Here we show that spatiotemporal control of microenvironmental cues embedded directly within EBs enhances the homogeneity, synchrony and organization of differentiation. Degradable polymer microspheres releasing retinoic acid within EBs induce the formation of cystic spheroids closely resembling the early streak mouse embryo, with an exterior of visceral endoderm enveloping an epiblast layer. These results demonstrate that controlled morphogen presentation to stem cells more efficiently directs cell differentiation and tissue formation, thereby improving developmental biology models and enabling the development of regenerative medicine therapies and cell diagnostics. **Overall design:** Triplicate control and experiment EBs were processed for microarray.

Background corr dist: KL-Divergence = 0.0339, L1-Distance = 0.0253, L2-Distance = 0.0007, Normal std = 0.6623

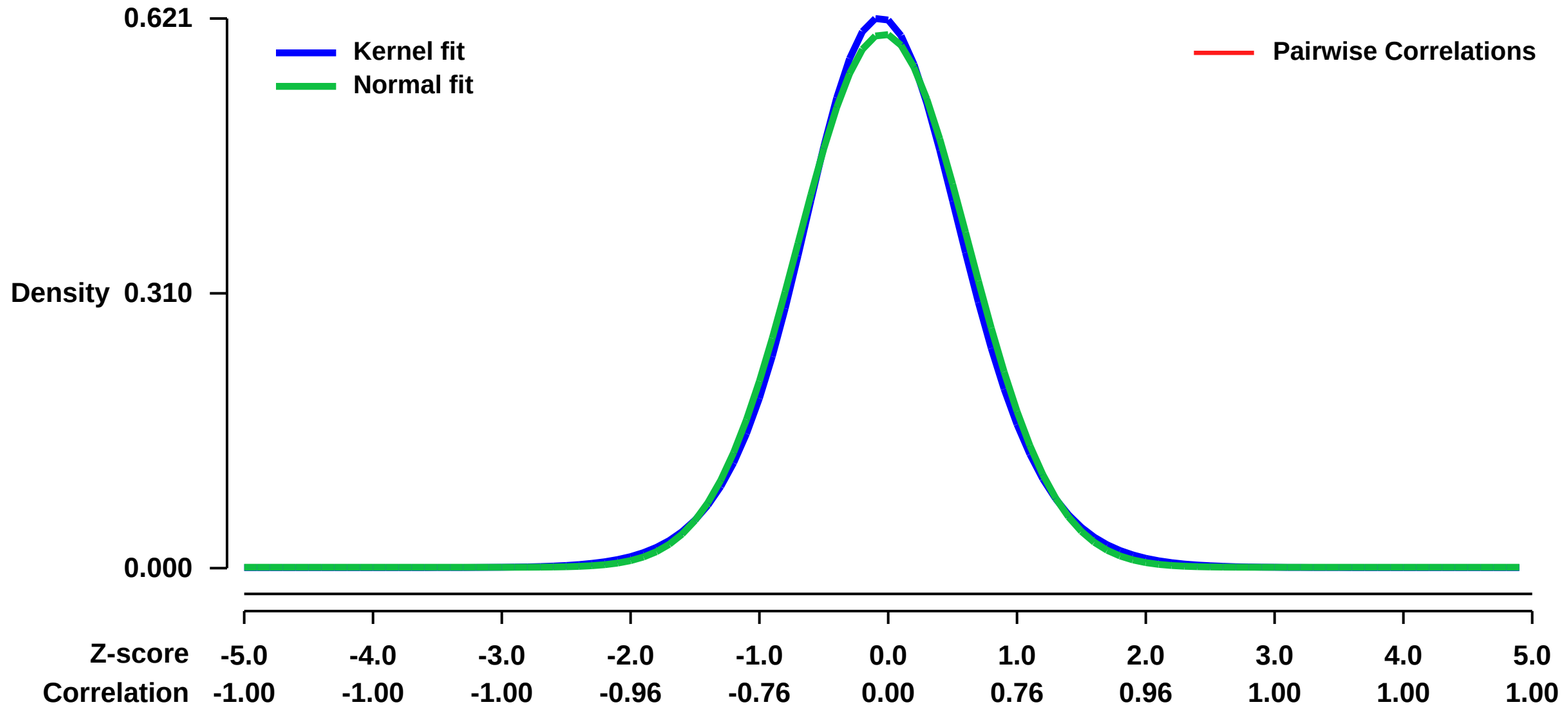

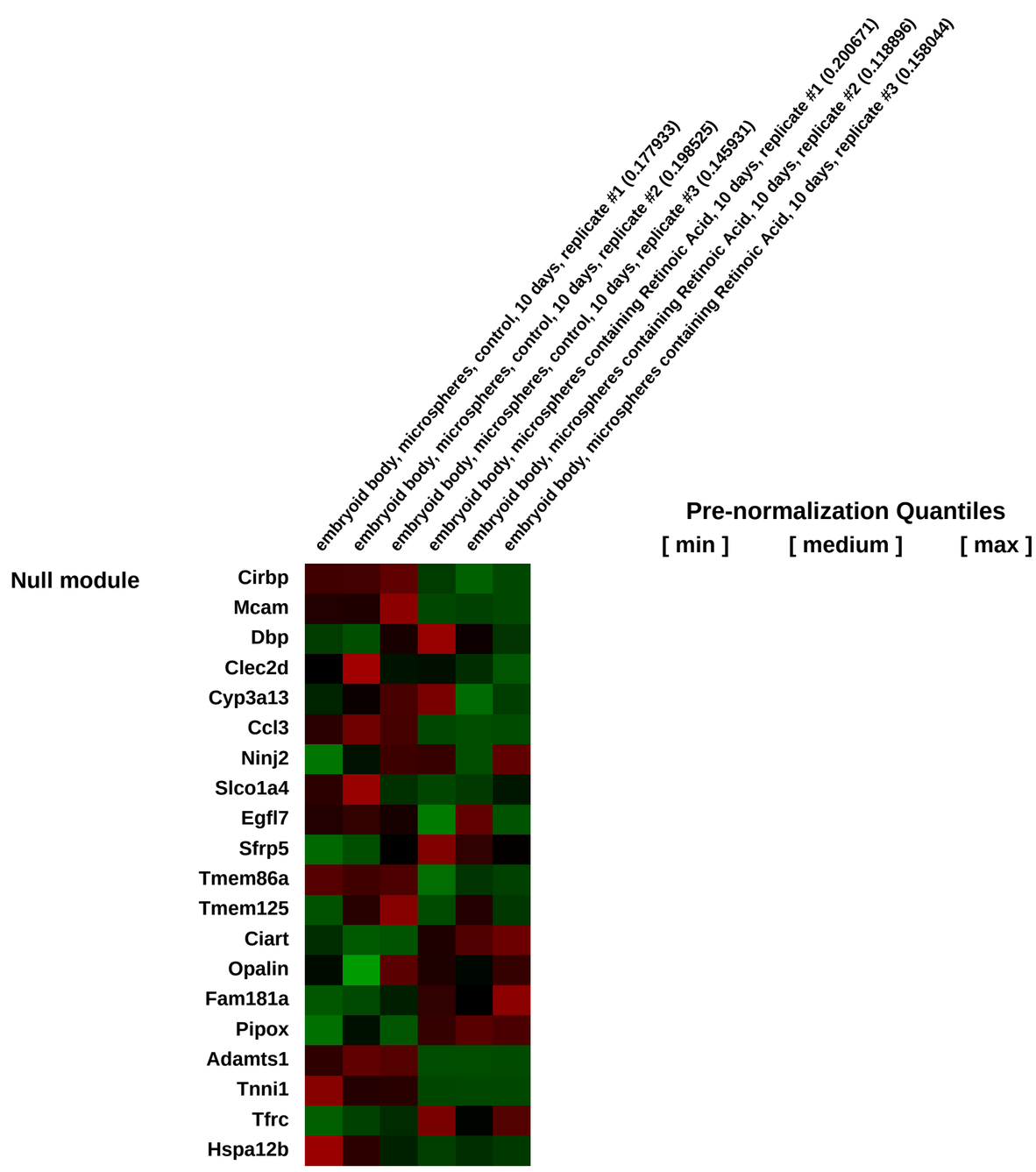

GEO Series "GSE12337" Expression Profiles

Num of samples in this series: 16

Scale of expression profile Z-scores

-3.0 -2.0 -1.0 0.0 1.0 2.0 3.0

GEO Link:	http://www.ncbi.nlm.nih.gov/geo/query/acc.cgi?acc=GSE12337
Status:	Public on Aug 06 2008
Title:	Transcriptomic analysis of PPARalpha-dependent alterations during cardiac hypertrophy
Organism:	Mus musculus
Experiment type:	Expression profiling by array
Platform:	GPL1261
Pubmed ID:	18812456
Summary & Design:	**Summary:** Findings suggest that PPARalpha plays a decisive role in the development of hypertrophy, affecting the functional outcome of the heart. Unfortunately, information on the nature of PPARalpha-dependent processes in cardiac hypertrophy is fragmentary and incomplete. The primary aim of this study was to identify the processes and signaling pathways regulated by PPARalpha in hearts challenged by a chronic pressure overload by means of whole genome transcriptomic analysis. Second, we wanted to gain insight how PPARalpha modulates the identified processes, e.g. by trans-activation or by trans-repression. Keywords: 28 days of TAC Overall design: Wild-type and PPARalpha-/- mice were sham-operated or subjected to TAC for 28 days. Left ventricular gene expression profile was determined using Affymetrix 430 2.0 arrays containing over 45,000 probe sets (covering over 34,000 mouse genes) to detect PPARalpha-related differences in cardiac gene expression under basal conditions and after imposition of a sustained hemodynamic stress.

Background corr dist: KL-Divergence = 0.2593, L1-Distance = 0.0606, L2-Distance = 0.0095, Normal std = 0.2974

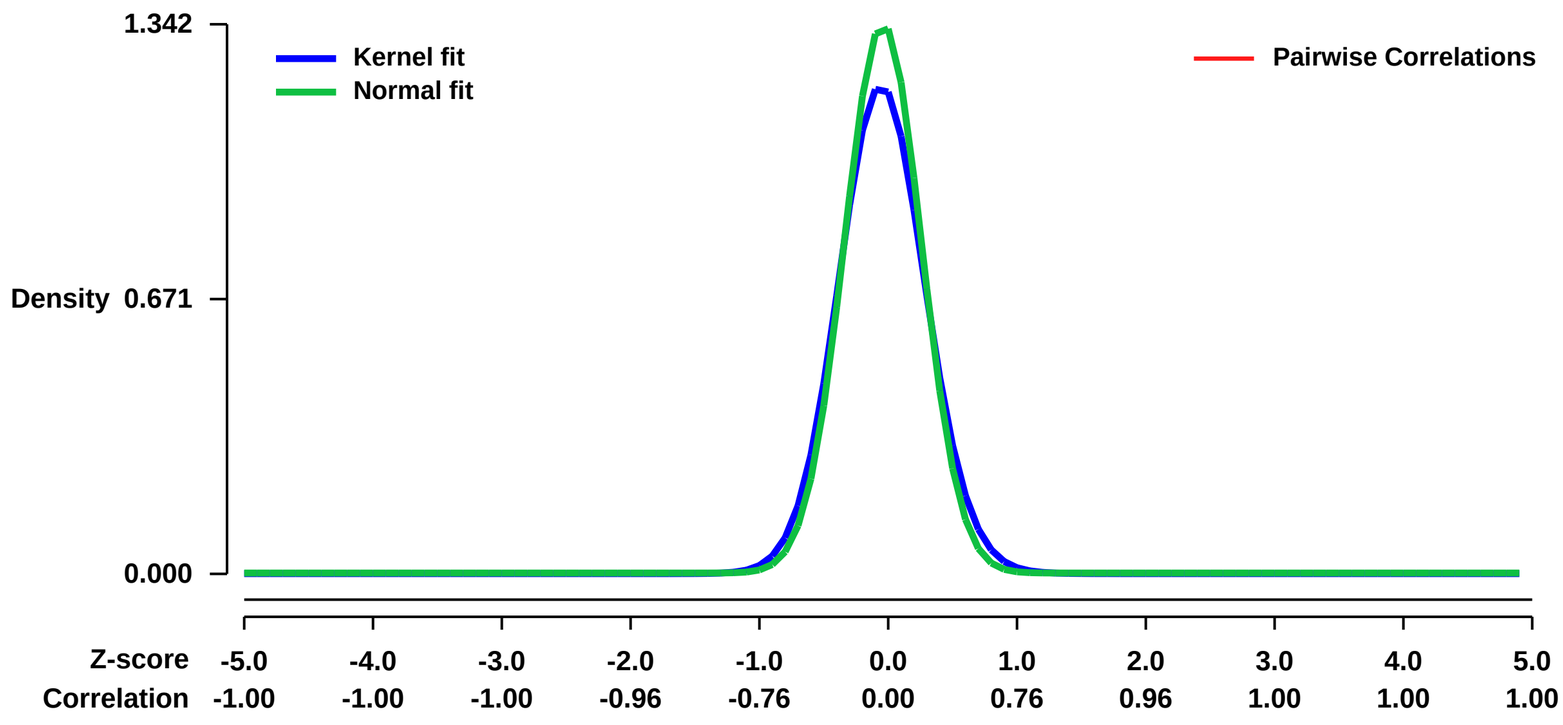

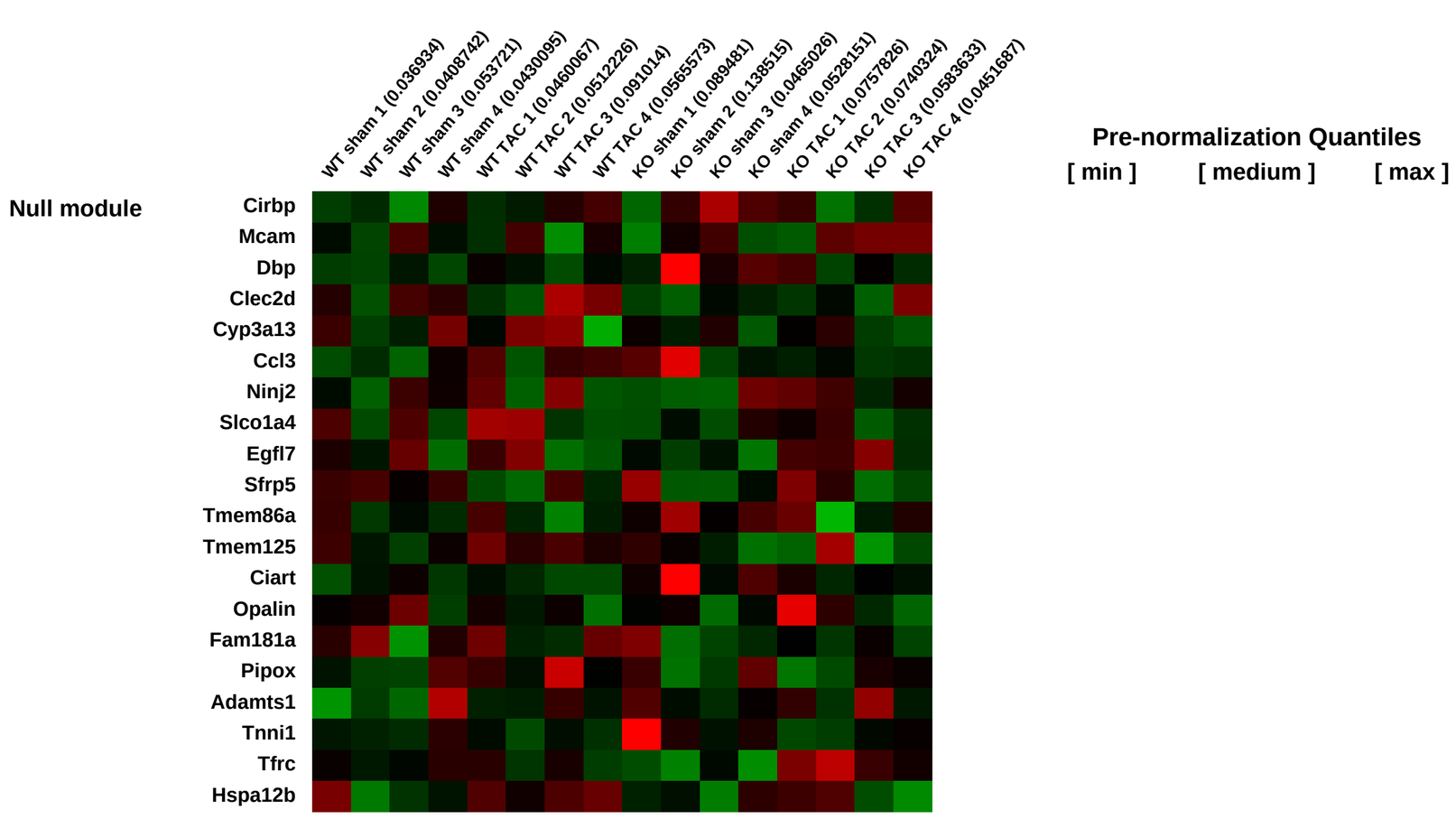

GEO Series "GSE12467" Expression Profiles

Num of samples in this series: 6

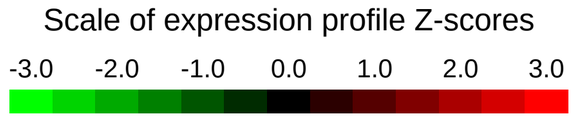

GEO Link:	**http://www.ncbi.nlm.nih.gov/geo/query/acc.cgi?acc=GSE12467**
Status:	**Public on Feb 20 2009**
Title:	**Differentially regulated genes in control and c-myc N-myc deficient LT-HSCs**
Organism:	**Mus musculus**
Experiment type:	**Expression profiling by array**
Platform:	**GPL1261**
Pubmed ID:	**19041778**
Summary & Design:	**Summary:** **Analysis of HSCs from control and c-myc N-myc deficient long-term hematopoietic stem cells. HSCs lacking both c-myc and N-myc display increased apoptosis rates. Data provide insight into the molecular changes occuring upon complete loss of Myc activity, clarifying the resulting apoptotic mechanism and the role of Myc family proteins in HSCs.** **Overall design:** **LT-HSC (Lin-Sca1+CD150+CD48-) cells were sorted from the BM of MxCre c-myc flox2 N-myc flox2 (experimental) and c-myc flox2 N-myc flox2 (control) mice 3 days after the last pI-pC injection. Each condition was analysed in triplicates, with each replicate consisting of a pool of 3 dKO mice or 2 control mice.**

Background corr dist: **KL-Divergence = 0.0377, L1-Distance = 0.0208, L2-Distance = 0.0005, Normal std = 0.6297**

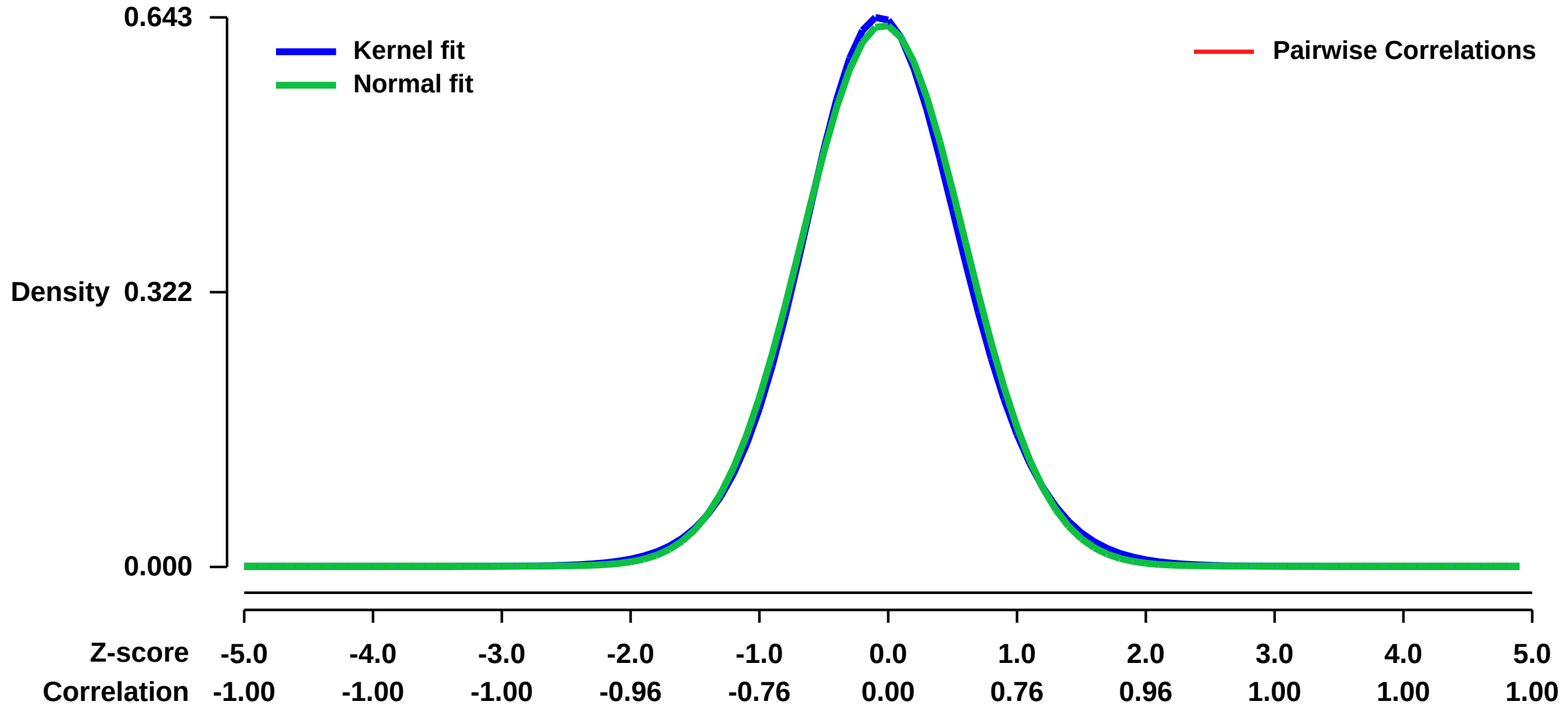

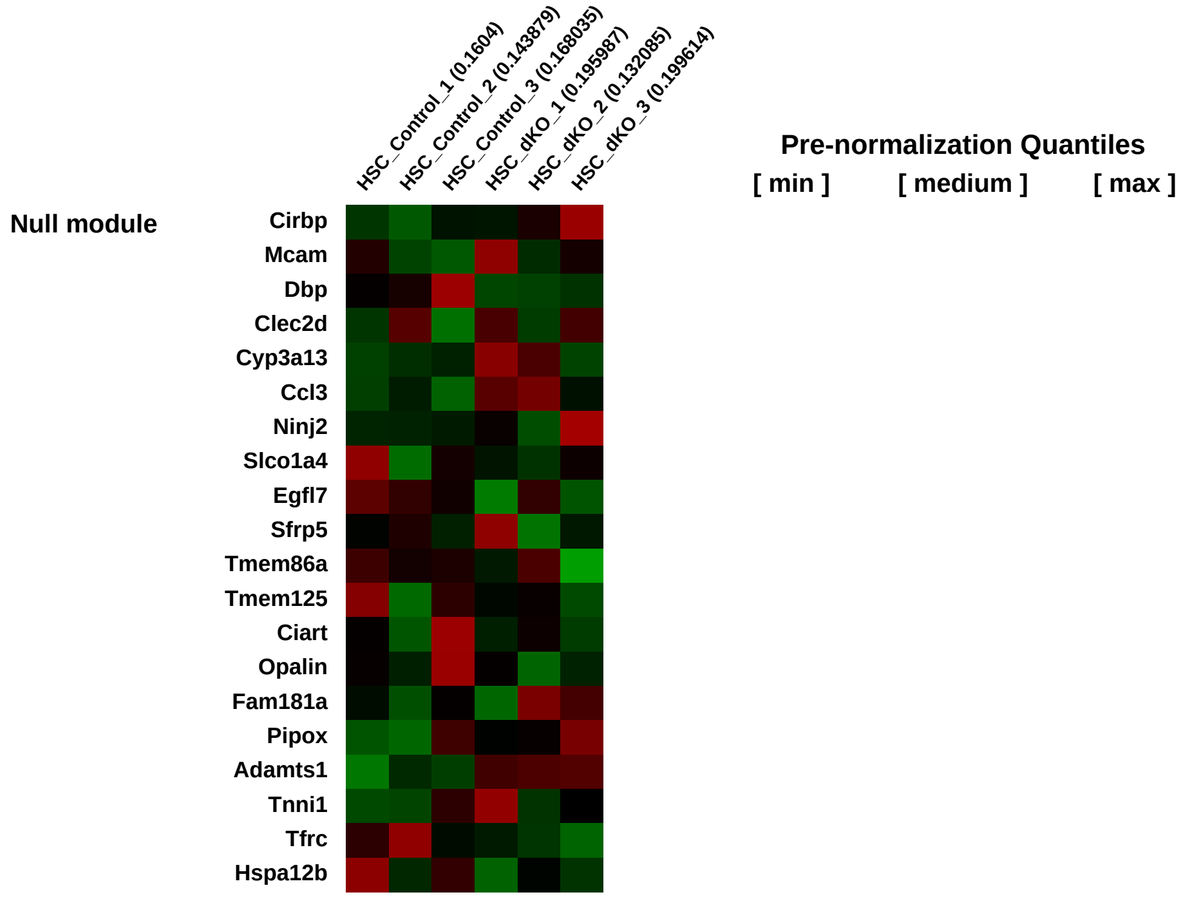

GEO Series "GSE12518" Expression Profiles

Num of samples in this series: 6

Scale of expression profile Z-scores

-3.0 -2.0 -1.0 0.0 1.0 2.0 3.0

GEO Link:	http://www.ncbi.nlm.nih.gov/geo/query/acc.cgi?acc=GSE12518
Status:	Public on Apr 15 2009
Title:	Differential expression profile between MNV-1 infected and mock-infected RAW 264.7 cells.
Organism:	Mus musculus
Experiment type:	Expression profiling by array
Platform:	GPL1261
Pubmed ID:	19211757
Summary & Design:	**Summary:** Noroviruses have been widely recognized for their importance as causative agents of non-bacterial gastroenteritis. Mouse norovirus is the only representative of the norovirus genus, family Caliciviridae, able to grow in cell culture. The aim of this study is to describe the differences in the expression profiles of MNV-1 and mock-infected macrophages (RAW 264.7 cells), in order to better understand the response of the host cell to norovirus infection. **Overall design:** This study compares two type of samples (MNV-infected and mock-infected RAW cells) in biological triplicates respectively. The MNV stock used for infection was obtained in the same cell line, and purified with a sucrose cushion in order to account for expression changes caused by virus infection only.

Background corr dist: KL-Divergence = 0.0217, L1-Distance = 0.0741, L2-Distance = 0.0057, Normal std = 0.9739

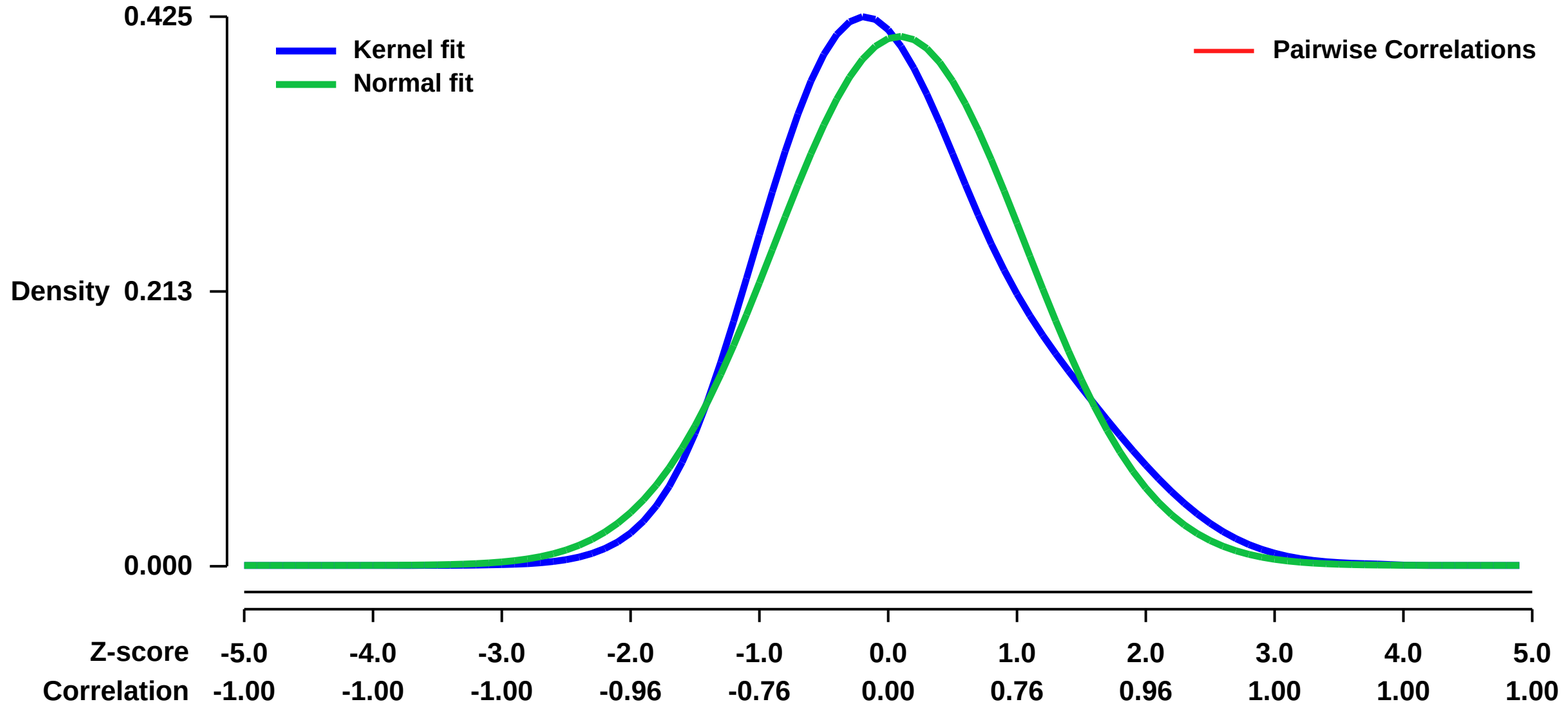

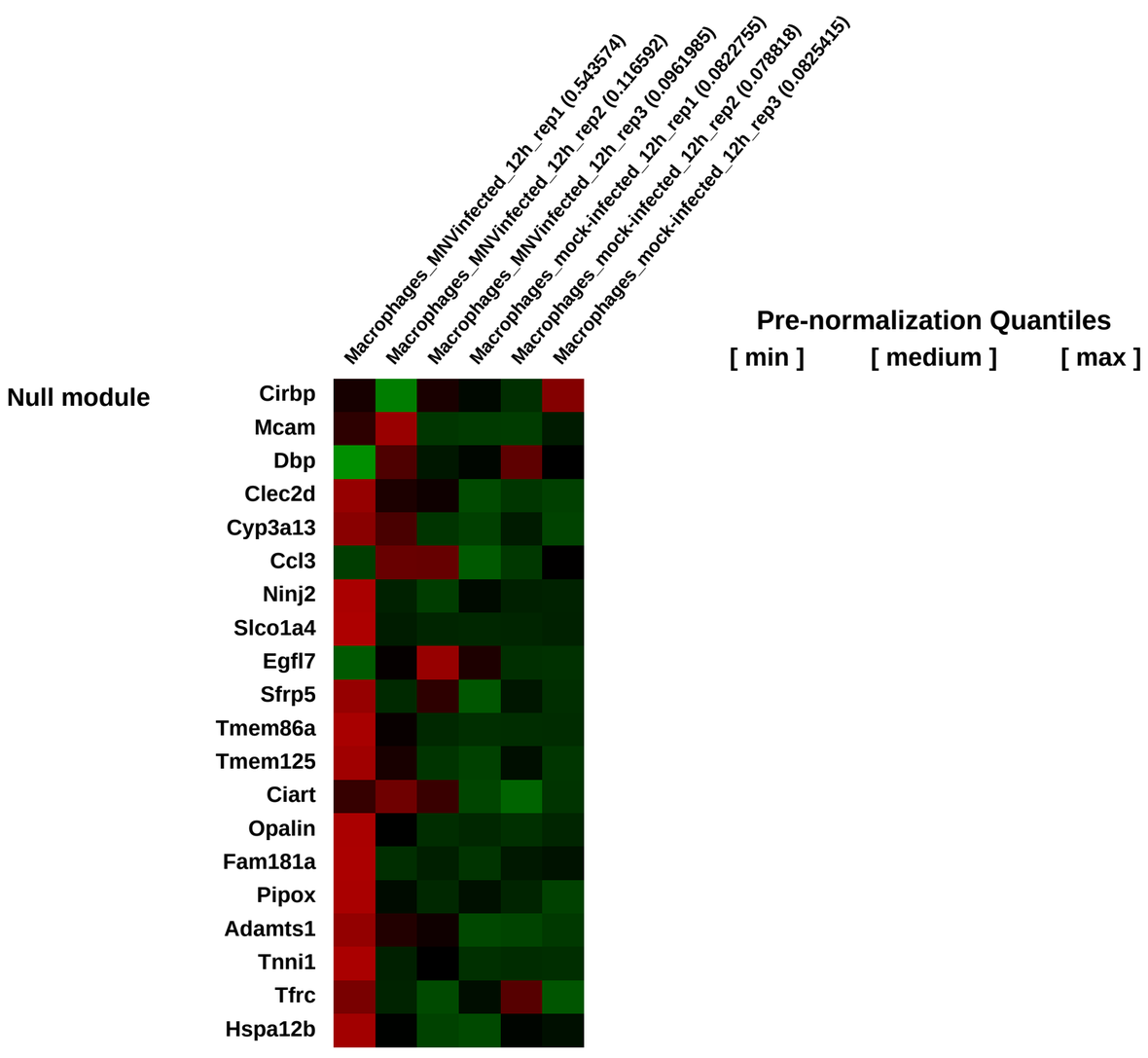

GEO Series "GSE12536" Expression Profiles

Num of samples in this series: 6

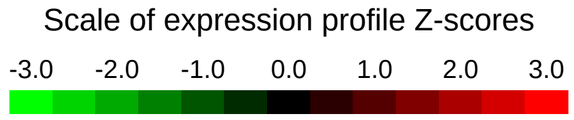

GEO Link:	http://www.ncbi.nlm.nih.gov/geo/query/acc.cgi?acc=GSE12536
Status:	Public on Feb 20 2009
Title:	Differentially regulated genes in control and c-myc N-myc deficient progenitors
Organism:	Mus musculus
Experiment type:	Expression profiling by array
Platform:	GPL1261
Pubmed ID:	19041778
Summary & Design:	**Summary:** Analysis of HSCs from control and c-myc N-myc deficient long-term hematopoietic stem cells. HSCs lacking both c-myc and N-myc display increased apoptosis rates. Data provide insight into the molecular changes occuring upon complete loss of Myc activity, clarifying the resulting apoptotic mechanism and the role of Myc family proteins in HSCs and commited progenitors. **Overall design:** Commited progenitors (Lin-Sca1+CD150+CD48+) cells were sorted from the BM of MxCre c-myc flox2 N-myc flox2 (experimental) and c-myc flox2 N-myc flox2 (control) mice 3 days after the last pI-pC injection. Each condition was analysed in triplicates, with each replicate consisting of a pool of 3 dKO mice or 2 control mice.

Background corr dist: KL-Divergence = 0.0340, L1-Distance = 0.0285, L2-Distance = 0.0011, Normal std = 0.6522

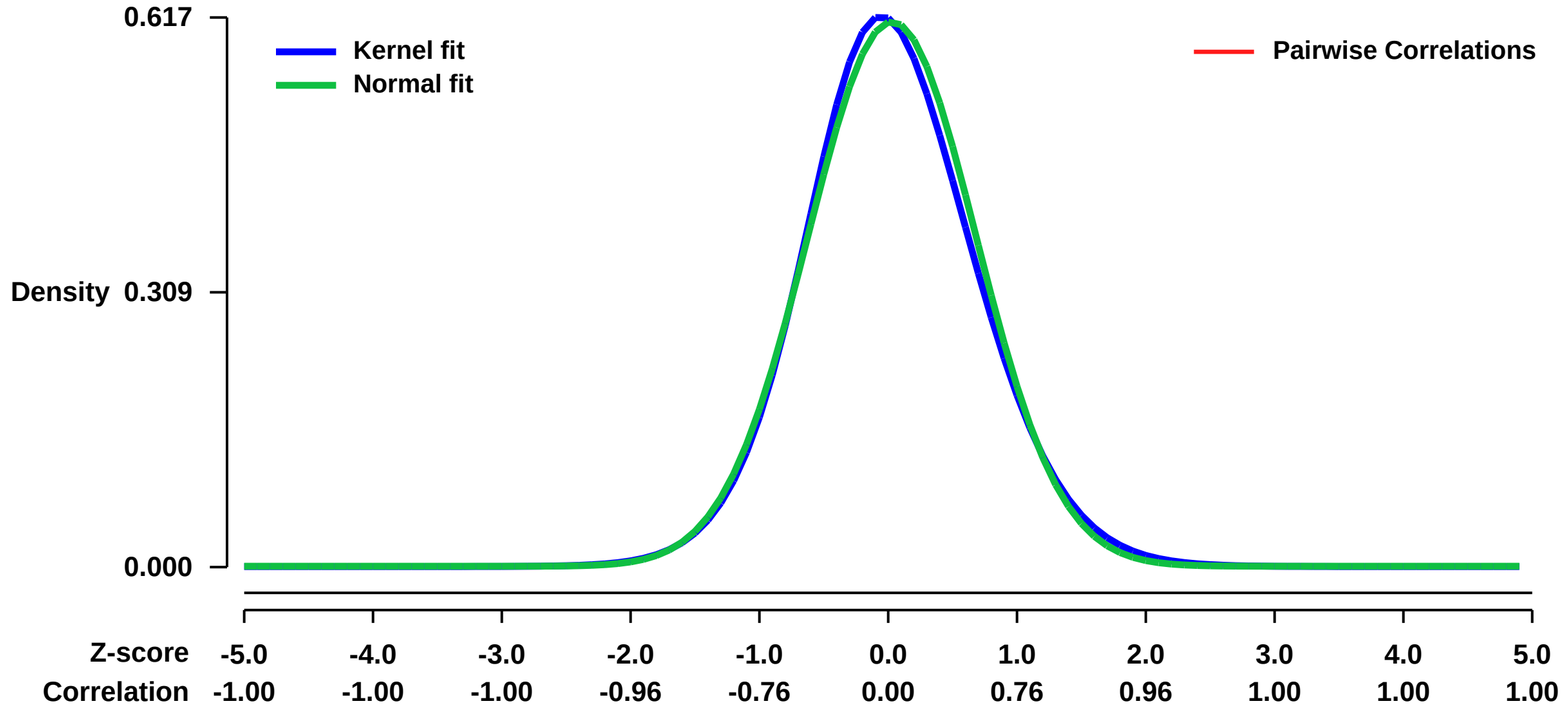

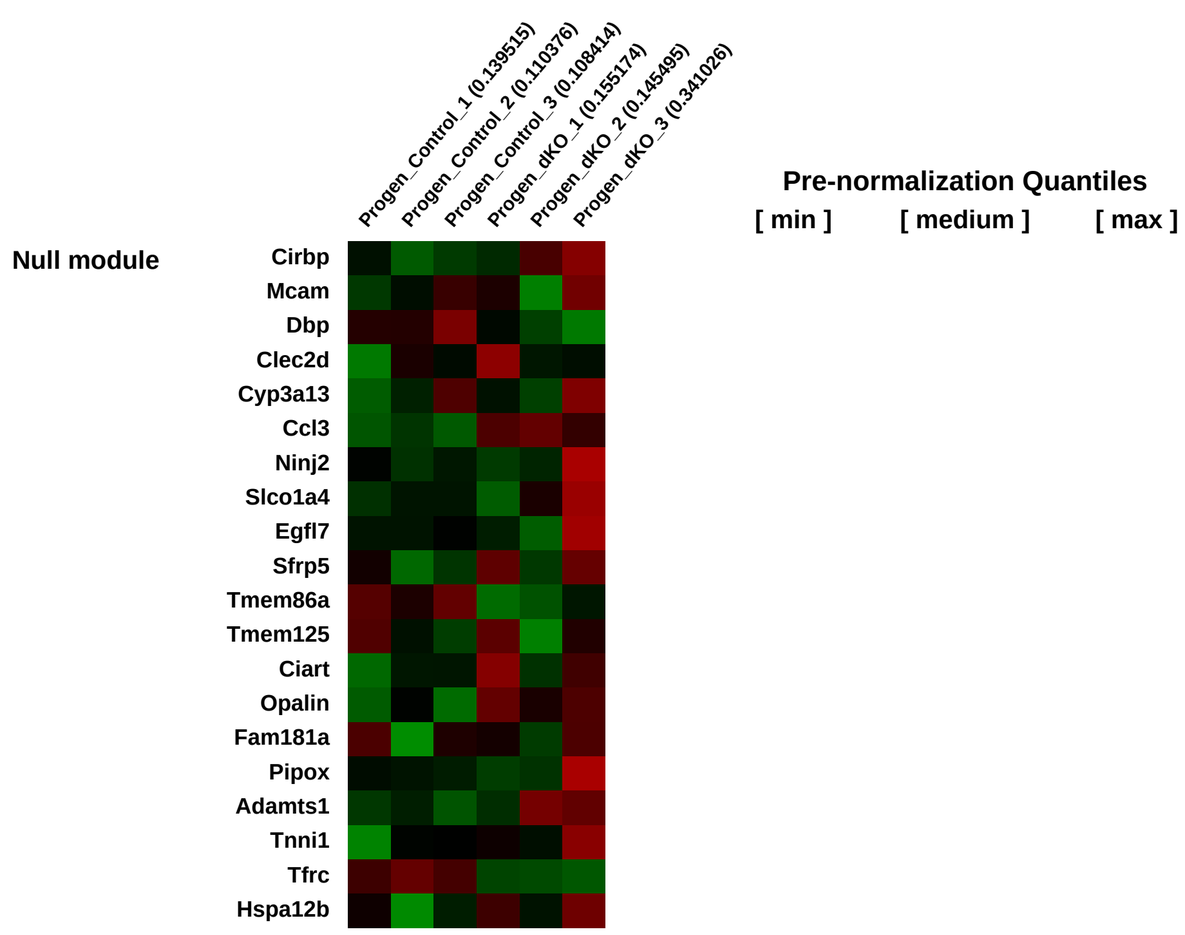

GEO Series "GSE12609" Expression Profiles

Num of samples in this series: 8

Scale of expression profile Z-scores

-3.0 -2.0 -1.0 0.0 1.0 2.0 3.0

GEO Link:	http://www.ncbi.nlm.nih.gov/geo/query/acc.cgi?acc=GSE12609
Status:	Public on Aug 30 2008
Title:	Transcription factor Arx null brains (fulp-affy-mouse-364520)
Organism:	Mus musculus
Experiment type:	Expression profiling by array
Platform:	GPL1261
Pubmed ID:	18799476
Summary & Design:	**Summary:** Arx is a paired-box homeodomain transcription factor and the vertebrate ortholog to the Drosophila aristaless (al) gene. Mutations in Arx are associated with a variety of human diseases, including X-linked infantile spasm syndrome (OMIM: 308350), X-linked myoclonic epilepsy with mental retardation and spasticity (OMIM: 300432), X-linked lissencephaly with ambiguous genitalia (OMIM: 300215), X-linked mental retardation 54 (OMIM: 300419), and agenesis of the corpus callosum with abnormal genitalia (OMIM: 300004). Arx-deficient mice exhibit a complex, pleiotrophic phenotype, including decreased proliferation of neuroepithelial cells of the cortex, dysgenesis of the thalamus and olfactory bulbs, and abnormal nonradial migration of GABAergic interneurons. It has been suggested that deficits in interneuron specification, migration, or function lead to loss of inhibitory neurotransmission, which then fails to control excitatory activity and leads to epilepsy or spasticities. Given that Arx mutations are associated with developmental disorders in which epilepsy and spasticity predominate and that Arx-deficient mice exhibit deficits in interneuron migration, understanding the function of Arx in interneuron migration will prove crucial to understanding the pathology underlying interneuronopathies. Yet, downstream transcriptional targets of Arx, to date, remain unidentified. The aim of this project is to identify bona fide transcriptional targets for the Arx, a transcription factor required for normal migration of interneurons from the ganglionic eminences to the cortex, and to investigate the functions of these genes in the Arx-dependent pathway regulating nonradial neuronal migration. We hypothesize that the genes regulated by the Arx transcription factor will play a critical role in the nonradial migration of interneurons and that the results of this study will provide novel insights into the molecular mechanisms of nonradial neuronal migration, in particular, and possibly the molecular and biochemical pathogenesis underlying epilepsy, mental retardation, infantile spasm syndromes, and other so-called interneuronopathies; We have recently generated a transgenic mouse with a floxed Arx allele (Arxflox). We have generated conditional knockouts in which Arx is removed specifically from the brain by mating Arxflox mice with transgenic mice expressing Cre behind the neural tube-specific transcriptional regulatory elements of the POU domain, class 3, transcription factor 4 promoter. Preliminary analyses of these mice suggest that conditional knockout mice recapitulate the nonradial migration defects associated with conventional knockout mice. We will compare the gene expression profiles of ganglion eminences (GEs; the anatomical source for nonradially migrating interneurons) from male Arxflox mice that express Pou3f-Cre to those from male mice without Arxflox allele. Animals will be prepared and sacrificed following our institutional protocol. Tissue will be rapidly dissected from E14.5 (the temporal peak of interneuron migration) GEs (MGE and LGE from both left and right hemispheres). Preliminary experiments suggest that the amounts of RNA that can be isolated from a pair of GEs is in the range of 2000-3500 ng, which should be sufficient for microarray analysis following linear amplification of RNA. The GEs from each animal will be combined, snap frozen in liquid nitrogen, and stored at -80 C until RNA is extracted. Total RNA will be extracted using Trizol followed by RNA purification with the RNeasy cleanup kit. We will be providing total RNA samples from four wildtype and four transgenic animals (true biological replicates) from three separate litters to mitigate any expression differences resulting from mouse to mouse or litter to litter variation. #!# **Overall design:**

Background corr dist: KL-Divergence = 0.0873, L1-Distance = 0.0223, L2-Distance = 0.0008, Normal std = 0.4610

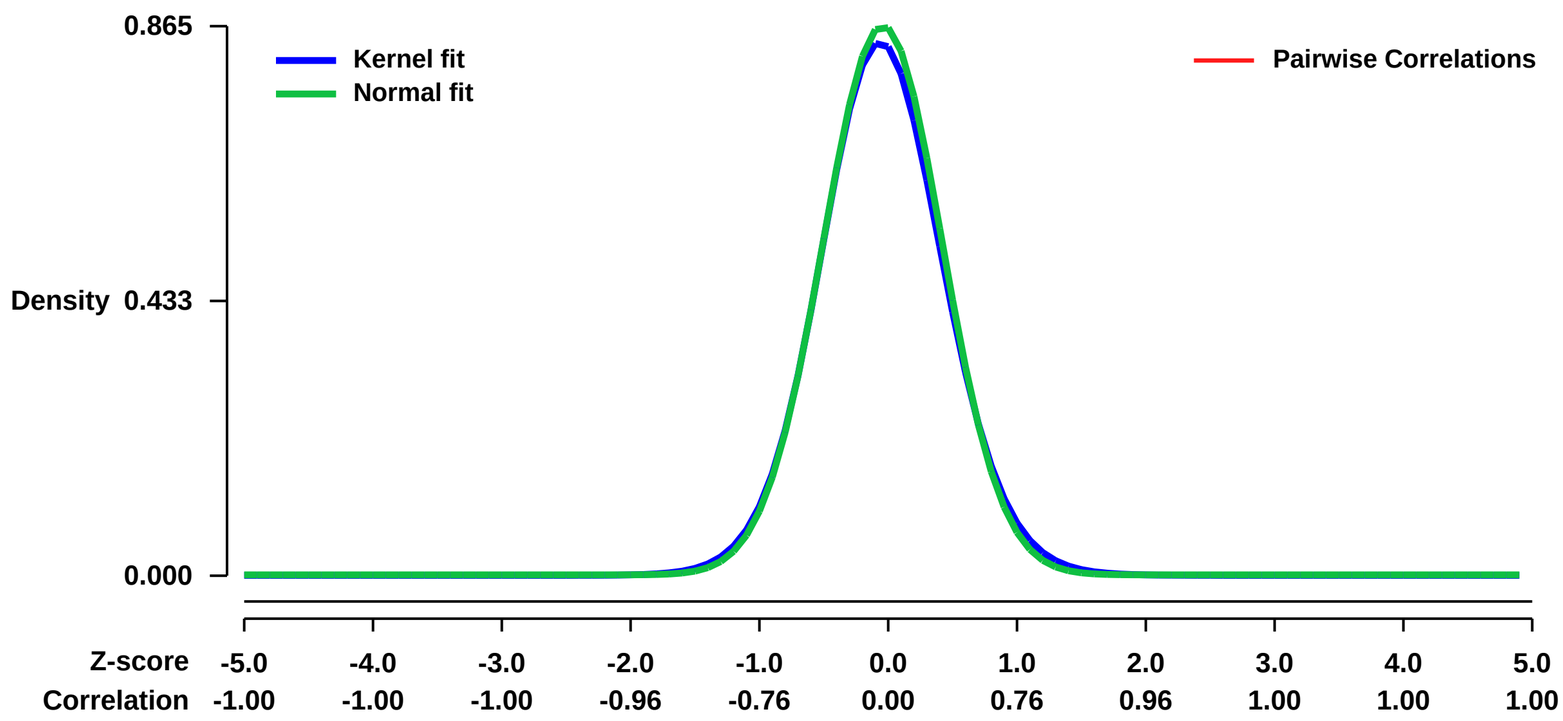

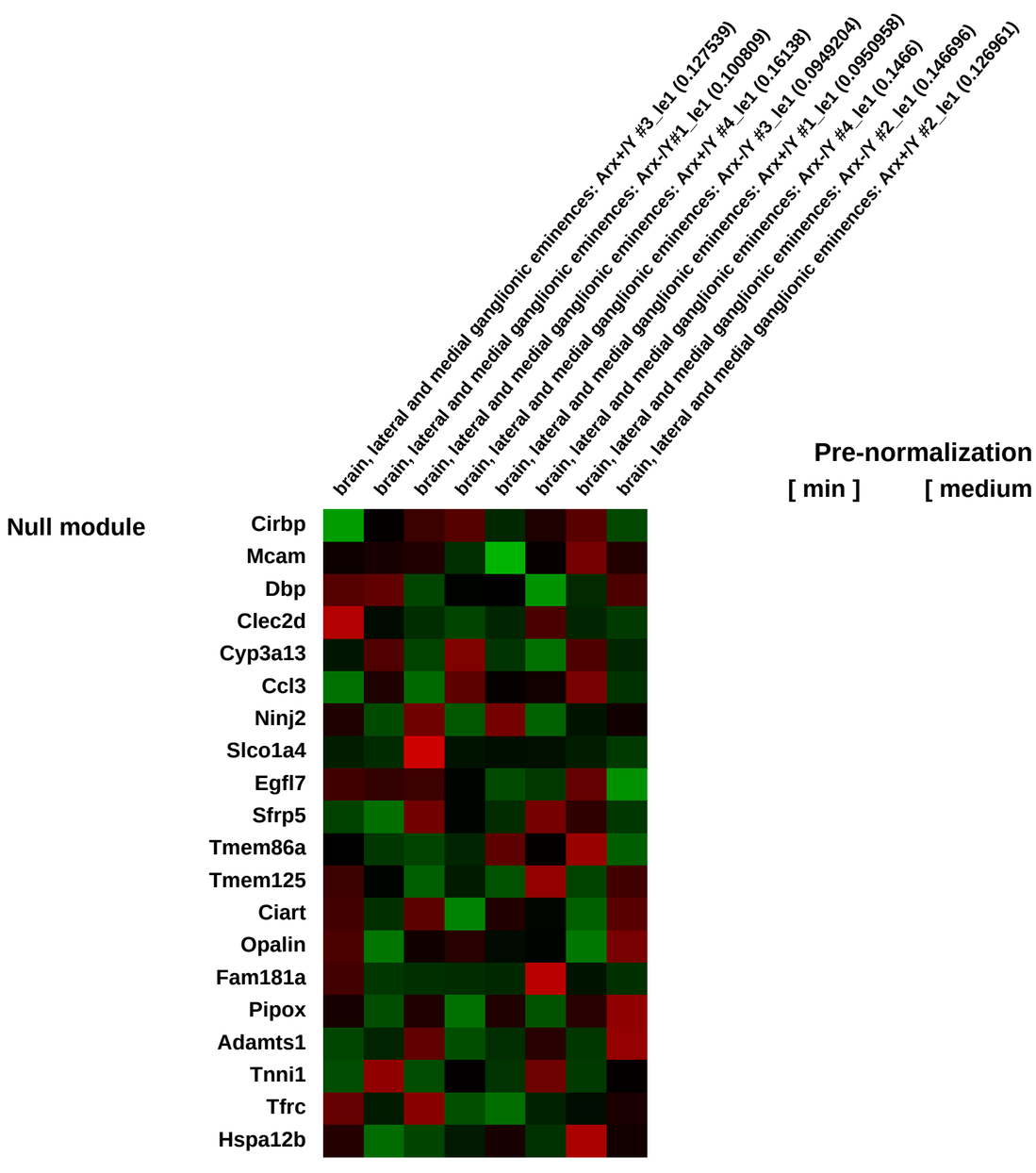

GEO Series "GSE12618" Expression Profiles

Num of samples in this series: 6

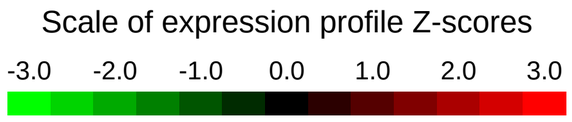

GEO Link:	**http://www.ncbi.nlm.nih.gov/geo/query/acc.cgi?acc=GSE12618**
Status:	**Public on Jan 16 2009**
Title:	**Gene expression profiles of E13 bladder compartments. (GUDMAP Series ID: 24)**
Organism:	**Mus musculus**
Experiment type:	**Expression profiling by array**
Platform:	**GPL1261**
Pubmed ID:	
Summary & Design:	**Summary:** **The long term objective is to create an encyclopedia of the expression levels of all genes in multiple components of the developing bladder. The central thesis is straightforward. The combination of microdissected tissues and FACS sorted cells plus microarray analysis offers a powerful, efficient and effective method for the creation of a global gene expression atlas of the developing urogenital system. Microarrays with essentially complete genome coverage can be used to quantitate expression levels of every gene. The ensuing rapid read-out provides an expression atlas that is more sensitive, more economical and more complete than would be possible by in situ hybridizations alone. The data submitted here delineates the gene expression profiles of the mesenchymal and epithelial compartments of the e13 mouse bladder.** **Keywords: Mouse embryonic day 13 bladder mesenchyme and epithelium.** **Overall design:** **FVB/N mice were time mated. At embryonic day 13 mice were euthanized by decapitation and the bladders were microdissected, cut just above the ureters, and treated with 20 ´µM EDTA for 20 minutes. Mesenchymal and epithelial compartments were then separated by rimming the bladder with a needle and harvested in RLT. Total RNA was isolated for gene expression analysis using the Affymetrix MOE430 microarray chip**

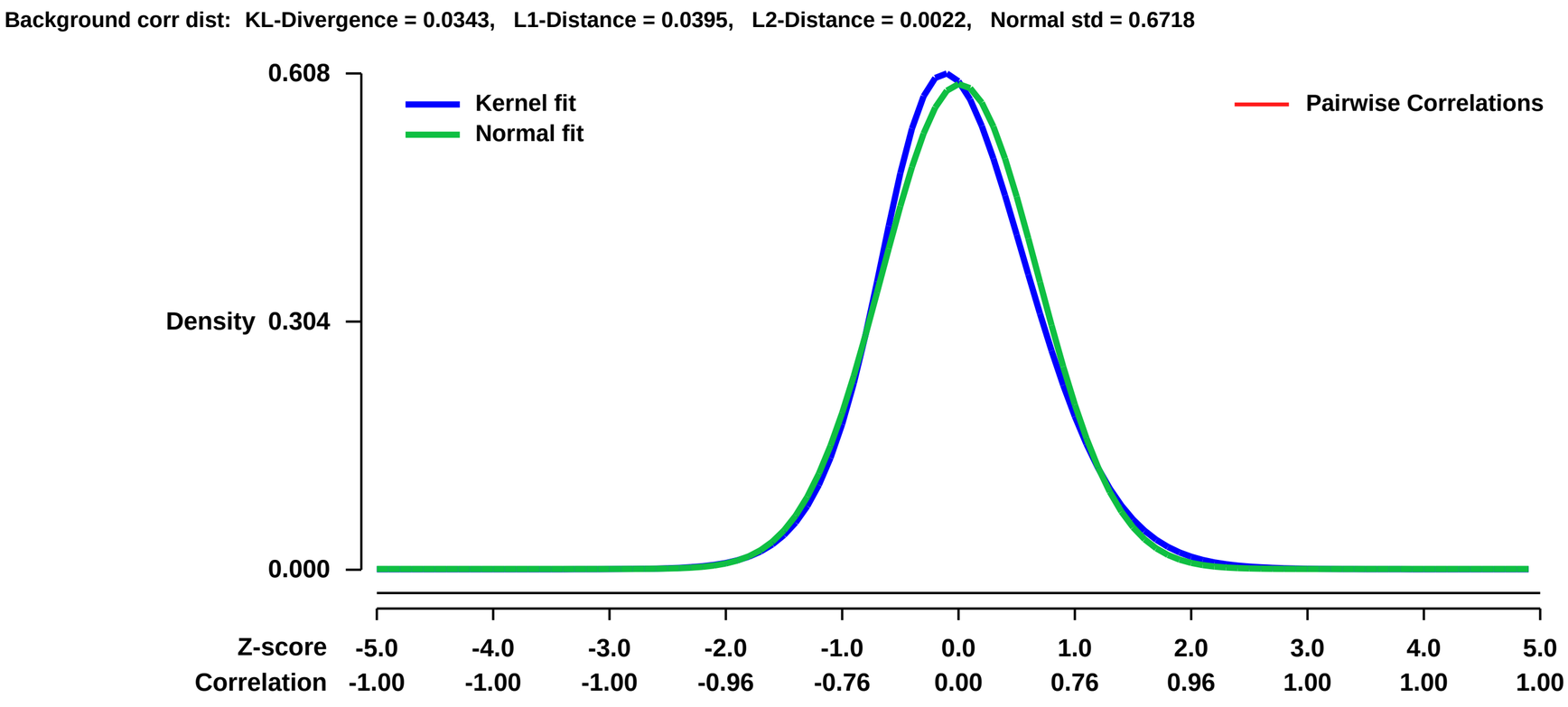

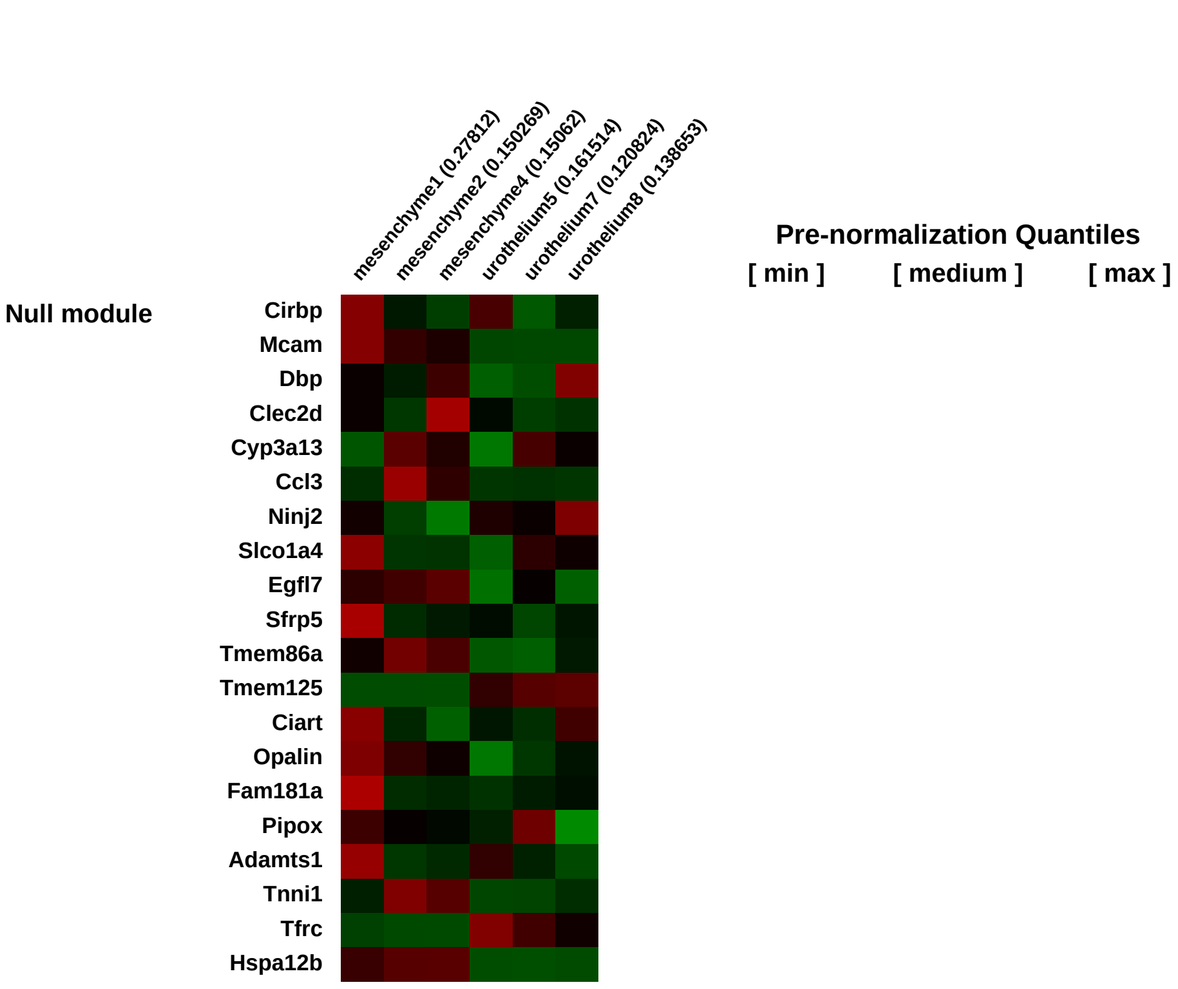

GEO Series "GSE12693" Expression Profiles

Num of samples in this series: 6

Scale of expression profile Z-scores

-3.0 -2.0 -1.0 0.0 1.0 2.0 3.0

GEO Link:	http://www.ncbi.nlm.nih.gov/geo/query/acc.cgi?acc=GSE12693
Status:	Public on Apr 09 2009
Title:	Hepatic gene expression profile of mice exposed to social stress
Organism:	Mus musculus
Experiment type:	Expression profiling by array
Platform:	GPL1261
Pubmed ID:	19106182
Summary & Design:	**Summary:** Social stress is well known to be involved in the occurrence and exacerbation of mental illness, and also various life-style related diseases such as hyperinsulinemia, hyperglycemia, cardiovascular diseases and cancer. However, there is little information on tissue-specific gene expression in response to social stress, which reflects our daily life. Liver is one of the most important organs, owing to its biological functions such as energy metabolic homeostasis, metabolization and detoxification of endo- and exogenous substances. In order to elucidate the mechanism underlying response to social stress in the liver, we investigated hepatic gene expression in mice exposed to isolation stress using DNA microarray. Male BALB/c mice (4 weeks old) were housed 5 per cage for 10 days acclimatization. Then mice were exposed to isolation stress for 30 days. After stress treatment, the mouse liver RNA was subjected to DNA microarray analysis. Taking the false discovery rate into account, isolation stress altered expression of 420 genes. Moreover, Gene Ontology analysis of these differentially expressed genes indicated that isolation stress remarkably down-regulated lipid metabolism-related pathway through peroxisome proliferator-activated receptor-alpha (PPARalpha), while lipid biosynthesis pathway regulated by sterol regulatory element binding factor-1 (SREBF-1), Golgi vesicle transport and secretory pathway-related genes were significantly up-regulated. These results suggested that isolation for 30 days, mild and consecutive social stress, not only regulate the systems for lipid metabolism but also cause the endoplasmic reticulum stress in mouse liver. **Overall design:** Male BALB/c mice (4 weeks old, Japan SLC, Shizuoka, Japan) weighing 14-18 g were housed 5 per cage. After acclimatization for 10 days, the mice were exposed to isolation (1 mouse per cage). All cages were placed in a foam plastic box in order to avoid social contact. To enhance the feeling of isolation, the bed volume in each cage for the isolated mice was reduced to one-tenth of that in the control group. The weight of bedding chips was about 2 g. All mice were housed in an air-conditioned room (room temperature: 23 ´– 1´℃, humidity: 55 ´– 5 %) under 12 h dark/12 h light cycles, with free access to tap water and MF diet (Oriental Yeast Co., Tokyo, Japan).

Background corr dist: KL-Divergence = 0.0484, L1-Distance = 0.0220, L2-Distance = 0.0006, Normal std = 0.5821

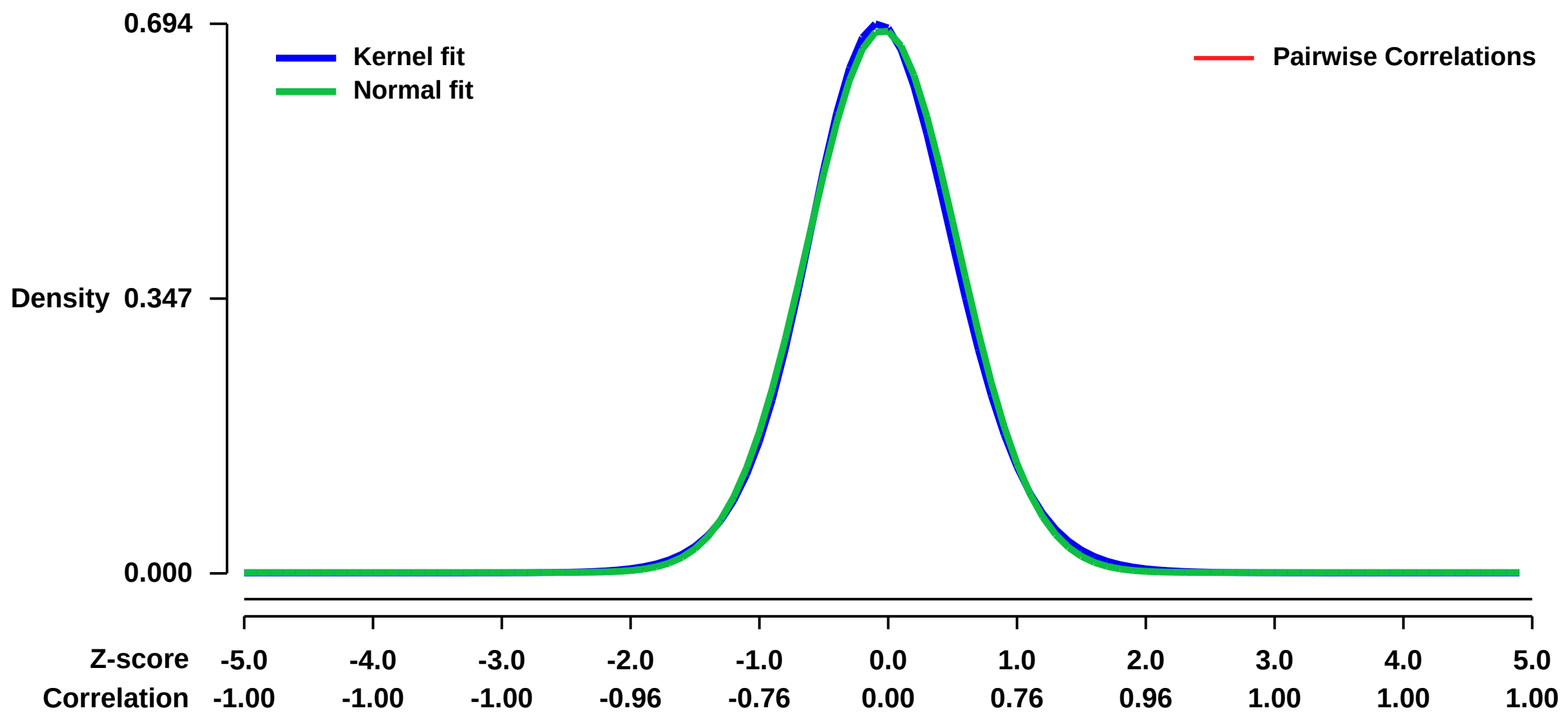

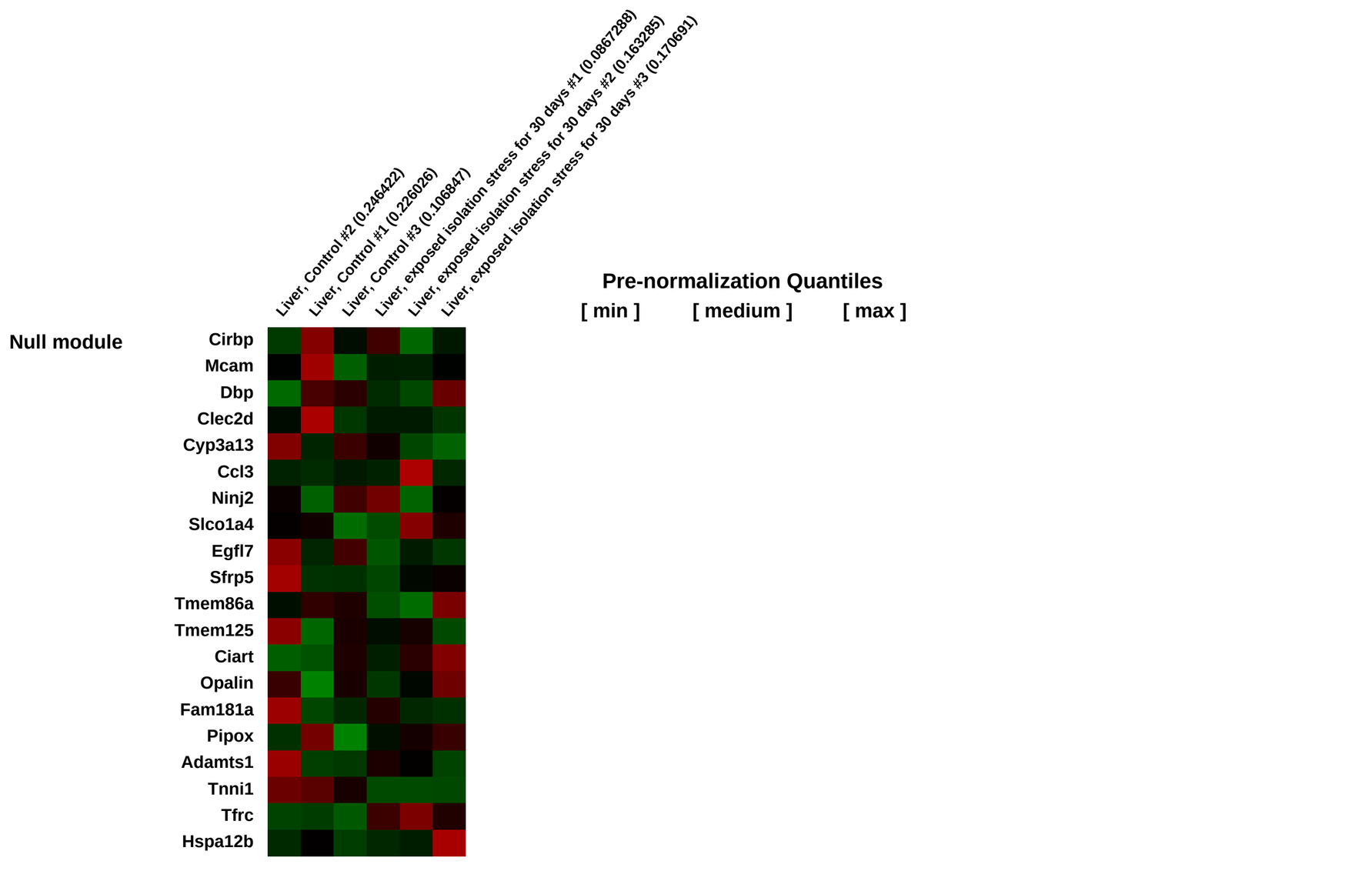

GEO Series "GSE12748" Expression Profiles

Num of samples in this series: 7

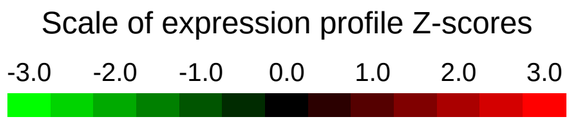

GEO Link:	http://www.ncbi.nlm.nih.gov/geo/query/acc.cgi?acc=GSE12748
Status:	Public on Sep 10 2009
Title:	Weighted Gene Coexpression Network Analysis Identifies Biomarkers in Glycerol Kinase Deficient Mice
Organism:	Mus musculus
Experiment type:	Expression profiling by array
Platform:	GPL1261
Pubmed ID:	19546021
Summary & Design:	**Summary:** Symptomatic glycerol kinase deficiency (GKD) is associated with episodic metabolic and central nervous system deterioration. We report here the first application of Weighted Gene Co-Expression Network Analysis (WGCNA) to investigate a knockout (KO) murine model of a human genetic disease. WGCNA identified networks and key hub transcripts from liver mRNA of glycerol kinase (Gyk) KO and wild type (WT) mice. Day of life 1 (dol1) samples from KO mice contained a network module enriched for organic acid metabolism before Gyk KO mice develop organic acidemia and die on dol3-4 and the module containing Gyk was enriched with apoptotic genes. Roles for the highly connected Acot, Psat and Plk3 transcripts were confirmed in cell cultures and subsequently validated by causality testing. We provide evidence that GK may have an apoptotic moonlighting role that is lost in GKD. This systems biology strategy has improved our understanding of GKD pathogenesis and suggests possible treatments. **Overall design:** Male WT and KO mouse pups were sacrificed on day of life (dol) 1 and each liver was harvested. Total RNA from 4 KO and 3 WT livers was isolated individually. Affymetrix mus 430 2.0 GeneChips were used to analyze differences in liver gene expression between KO and WT mice. Dol1 and 3 Gyk KO mice represent different disease states. Dol 1 was chosen because mice are phenotypically asymptomatic with respect to Glycerol Kinase Deficiency (GKD) and allowed us to look at alterations that occur before the overt disease state. Dol 3 mice are phenotypically symptomatic with respect to GKD.

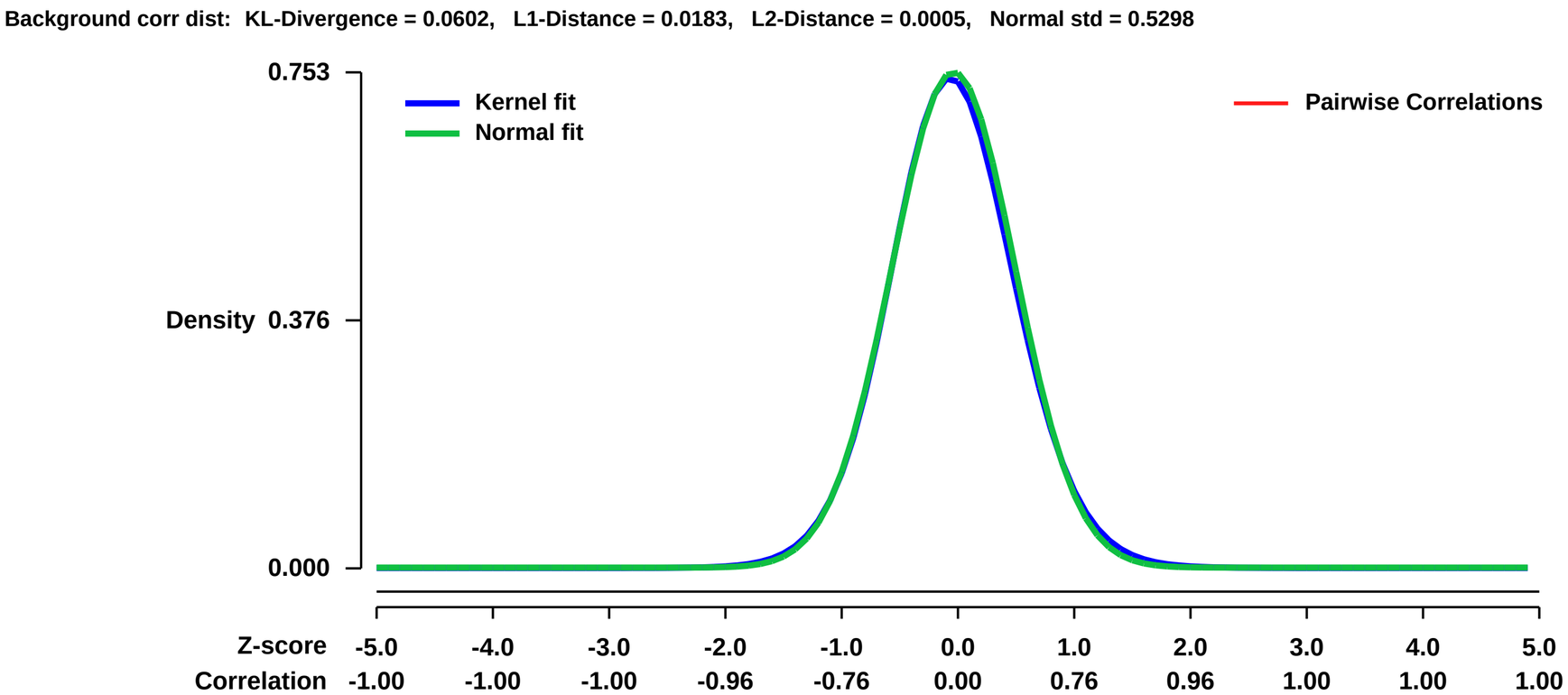

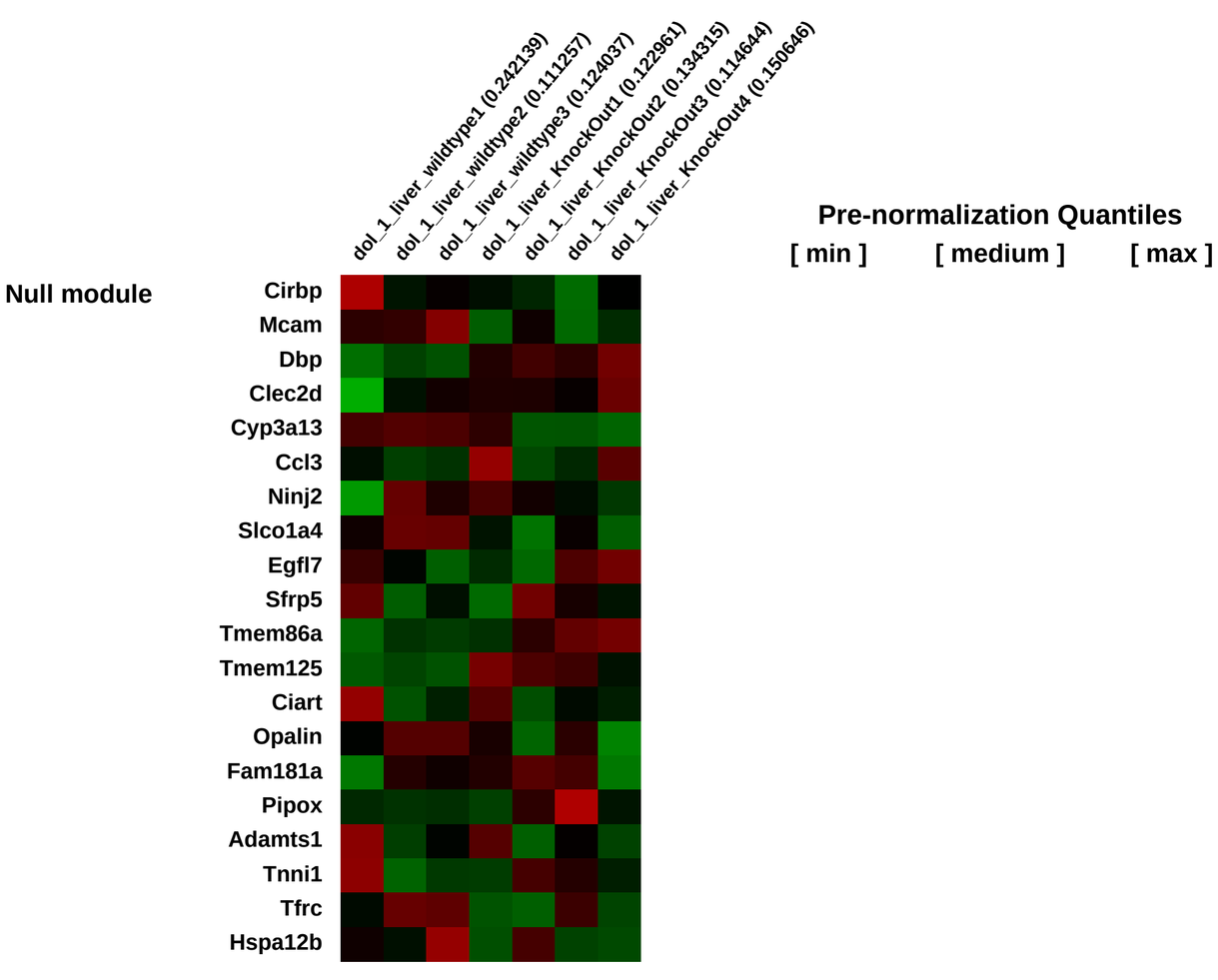

GEO Series "GSE12769" Expression Profiles

Num of samples in this series: 20

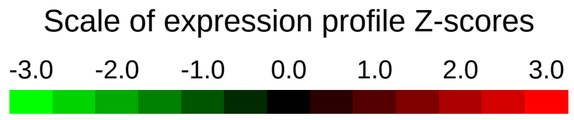

GEO Link:	**http://www.ncbi.nlm.nih.gov/geo/query/acc.cgi?acc=GSE12769**
Status:	**Public on Sep 18 2008**
Title:	**Murine postpartum testis developmental time course (0 to 35 day)**
Organism:	**Mus musculus**
Experiment type:	**Expression profiling by array**
Platform:	**GPL1261**
Pubmed ID:	
Summary & Design:	**Summary:** **Murine testis developmental time course created from tissue samples collected from birth through adulthood and hybridized to M430_2 chips in duplicate.** **Keywords: time-course** **Overall design:** **Time course of gene expression in the murine postpartum testis development (duplicates in day 0, 3, 6, 8, 10, 14, 18, 20, 30, 35). Total 20 samples.**
Background corr dist:	**KL-Divergence = 0.0289, L1-Distance = 0.0313, L2-Distance = 0.0017, Normal std = 0.6762**

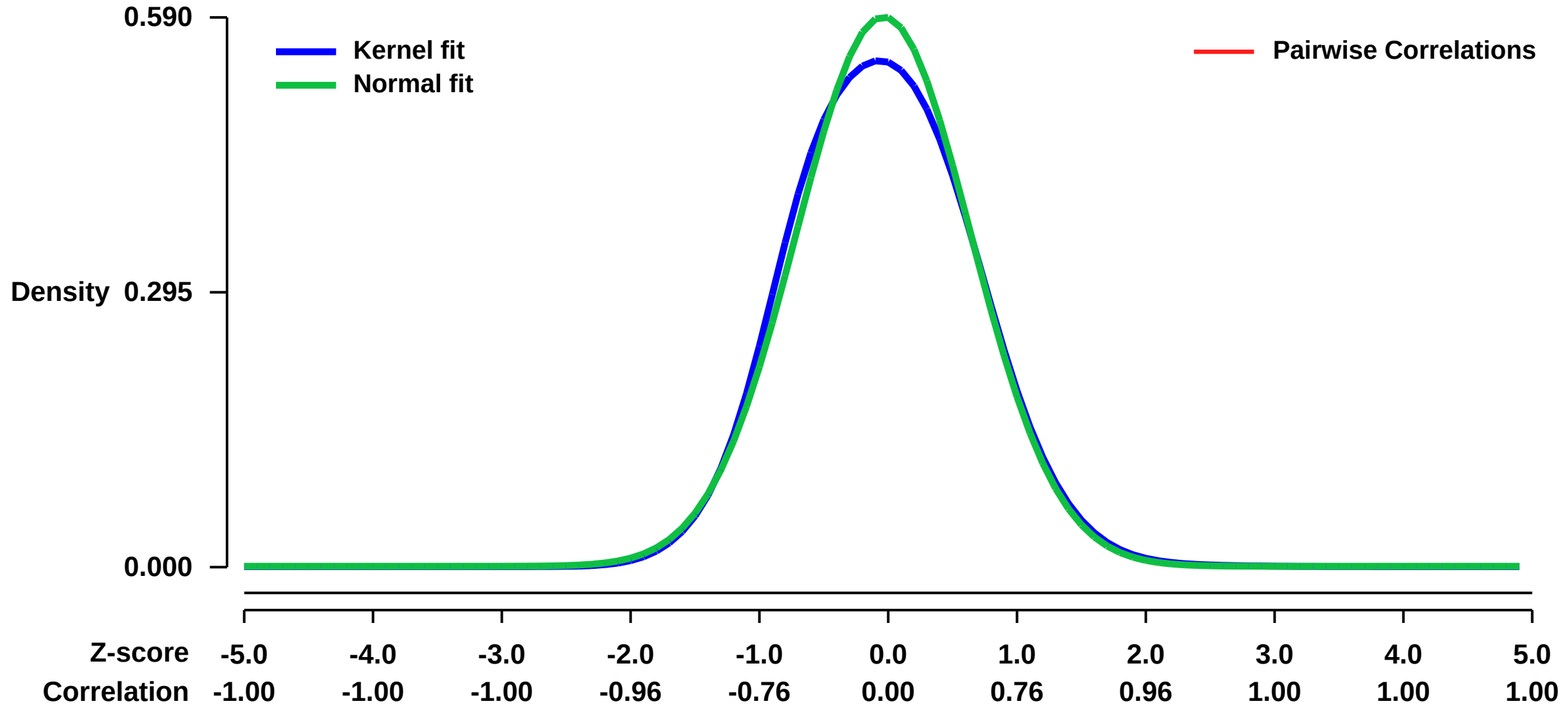

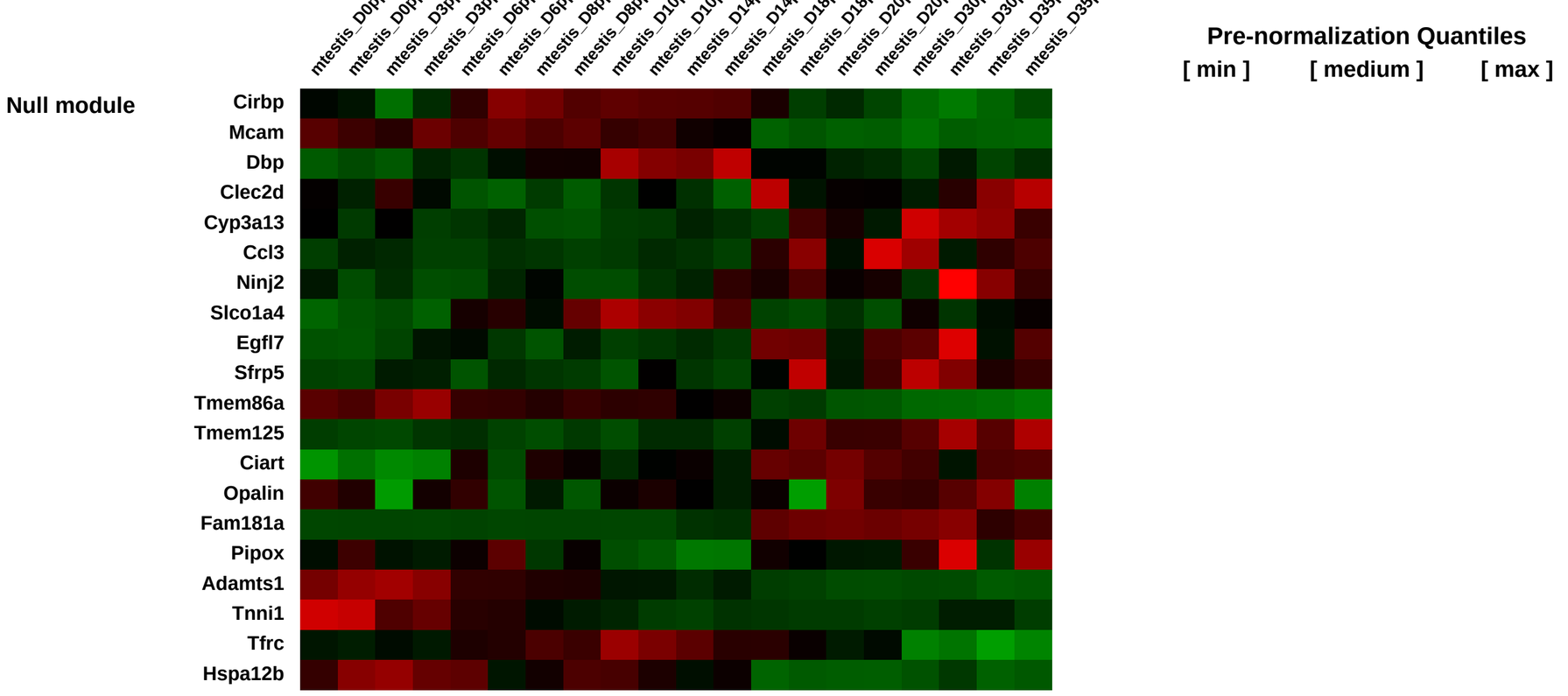

GEO Series "GSE12772" Expression Profiles

Num of samples in this series: 8

Scale of expression profile Z-scores

-3.0 -2.0 -1.0 0.0 1.0 2.0 3.0

GEO Link:	**http://www.ncbi.nlm.nih.gov/geo/query/acc.cgi?acc=GSE12772**
Status:	**Public on Dec 07 2008**
Title:	**Hematopoietic stem cell (HSC) expression alteration in an ADAR1 mouse model**
Organism:	**Mus musculus**
Experiment type:	**Expression profiling by array**
Platform:	**GPL1261**
Pubmed ID:	**19060901**
Summary & Design:	**Summary:** **Hematopoietic stem cells purified from +/+, +/- and -/- ADAR1 mice were compared with global gene expression analysis.** **Overall design:** **Each sample was purified from one mouse.**

Background corr dist: **KL-Divergence = 0.0542, L1-Distance = 0.0688, L2-Distance = 0.0083, Normal std = 0.5963**

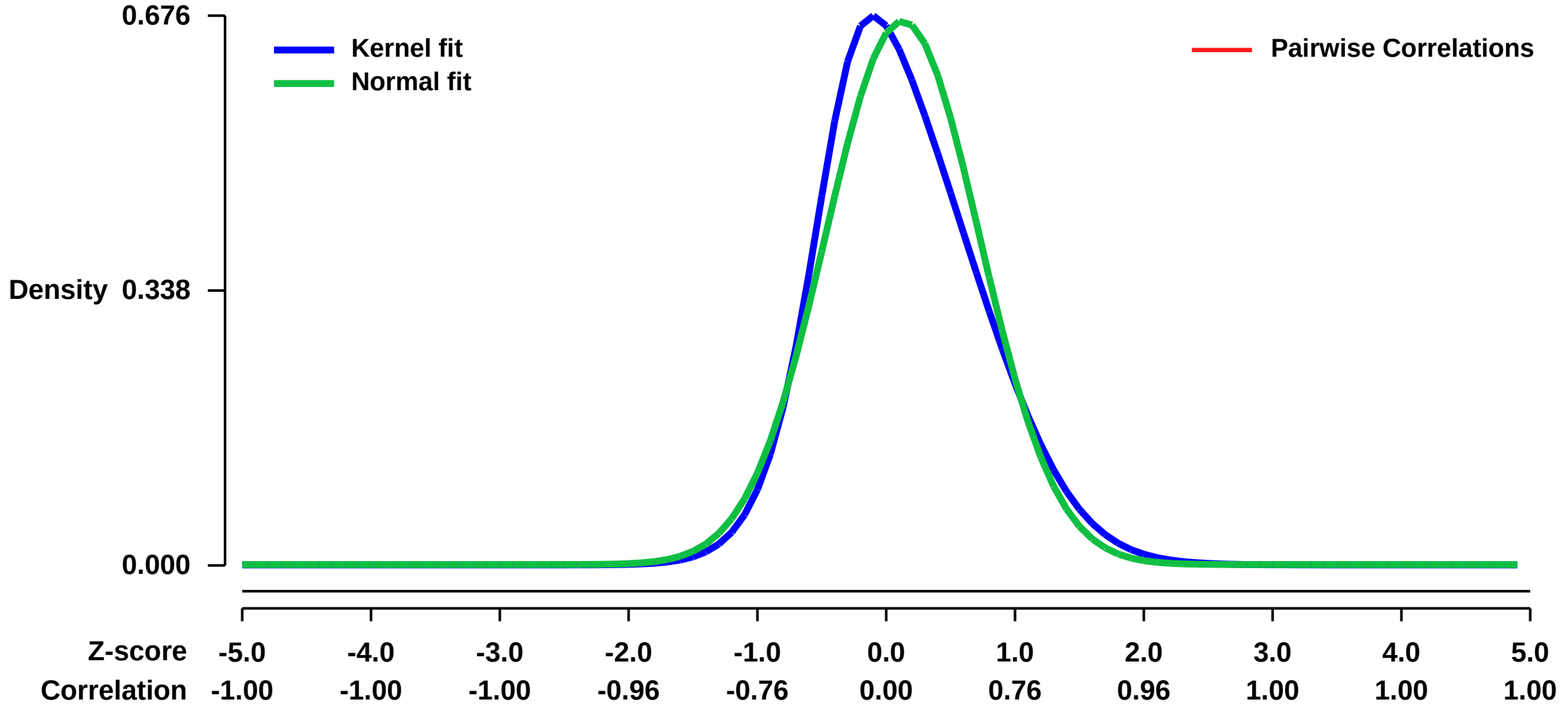

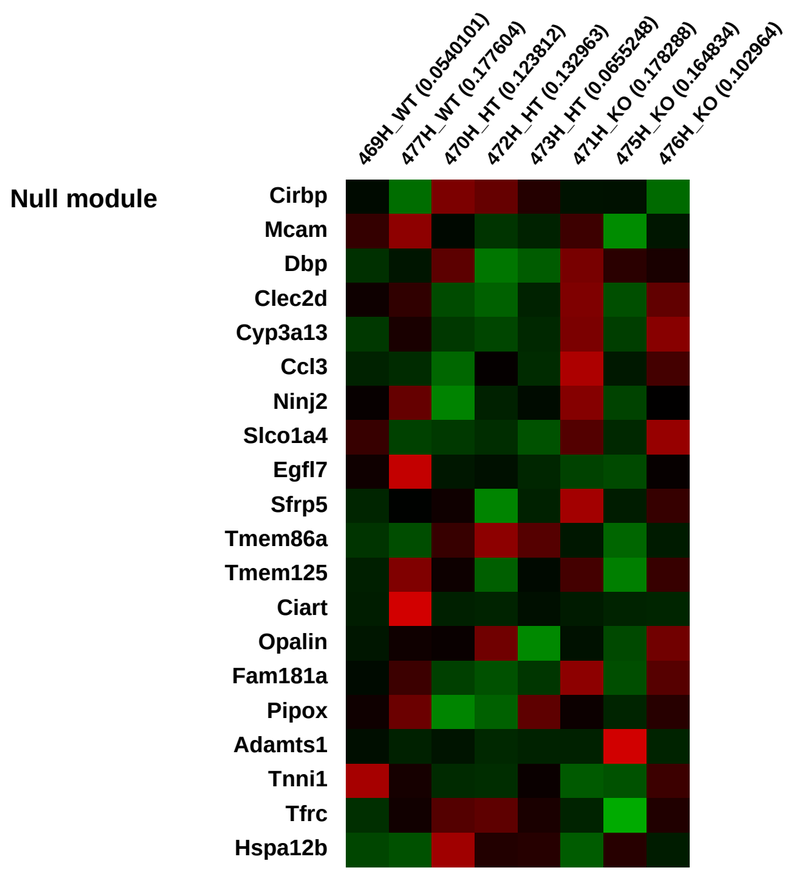

GEO Series "GSE12810" Expression Profiles

Num of samples in this series: 6

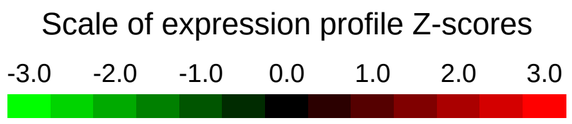

GEO Link:	http://www.ncbi.nlm.nih.gov/geo/query/acc.cgi?acc=GSE12810
Status:	Public on Sep 16 2009
Title:	Expression of Wnt Receptors in Adult Spiral Ganglion Neurons: Fzd 9 Located at Growth Cones of Regenerating Neurites
Organism:	Mus musculus
Experiment type:	Expression profiling by array
Platform:	GPL1261
Pubmed ID:	19716861
Summary & Design:	**Summary:** The fidelity of sound transmission by cochlear implants in patients with sensorineural hearing loss could be greatly improved by increasing the number of frequency channels. This could be achieved by stimulating and guiding neurite outgrowth to reduce the distance between the implant’s electrodes and the remnants of the spiral ganglion neurons. However, little is known about signaling pathways, besides those of neurotrophic factors, that are operational in the adult spiral ganglion. To systematically identify neuronal receptors for guidance cues in the adult cochlea, we conducted a genome-wide cDNA microarray screen with two-month-old CBA/CaJ mice. A meta-analysis of our data and those from older mice in two other studies revealed the presence of neuronal transmembrane receptors that represent all four established guidance pathwaysâ ephrin, netrin, semaphorin, and slitâ in the mature cochlea as late as 15 months. In addition, we observed the expression of all known receptors for the Wnt morphogens, whose neuronal guidance function has only recently been recognized. In situ hybridizations located the mRNAs of the Wnt receptors frizzled 1, 4, 6, 9, and 10 specifically in adult spiral ganglion neurons. Finally, frizzled 9 protein was found in the growth cones of adult spiral ganglion neurons that were regenerating neurites in culture. We conclude from our results that adult spiral ganglion neurons are poised to respond to neurite damage, owing to the constitutive expression of a large and diverse collection of guidance receptors. Wnt signaling, in particular, emerges as a candidate pathway for guiding neurite outgrowth towards a cochlear implant after sensorineural hearing loss. **Overall design:** GSE12810_Meta_GO_Eset_tTests.xls: Meta-analysis of neuronal transmembrane receptors in our study (GSE12810) and two previous studies by Someya and colleagues (GSE4786 & GSE4866) to estimate absolute expression levels in adult cochlea

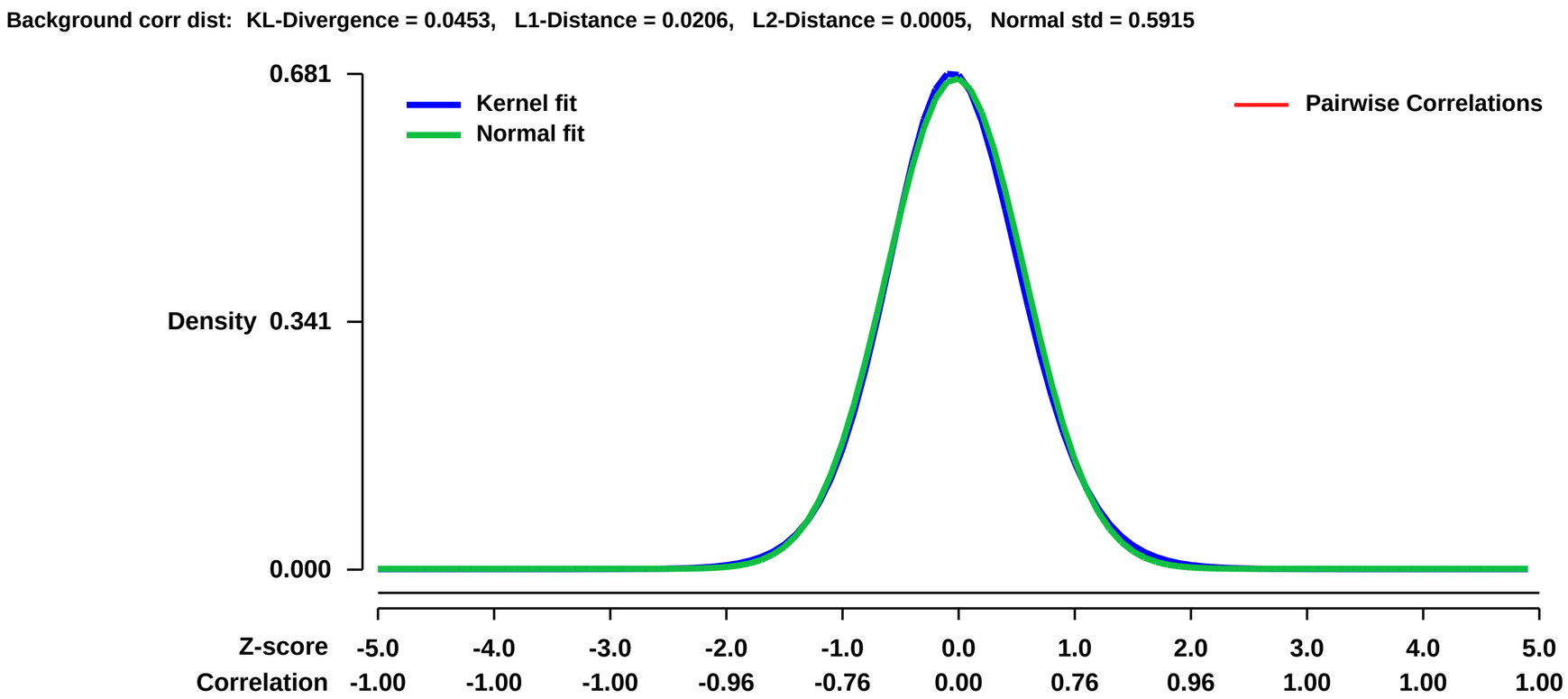

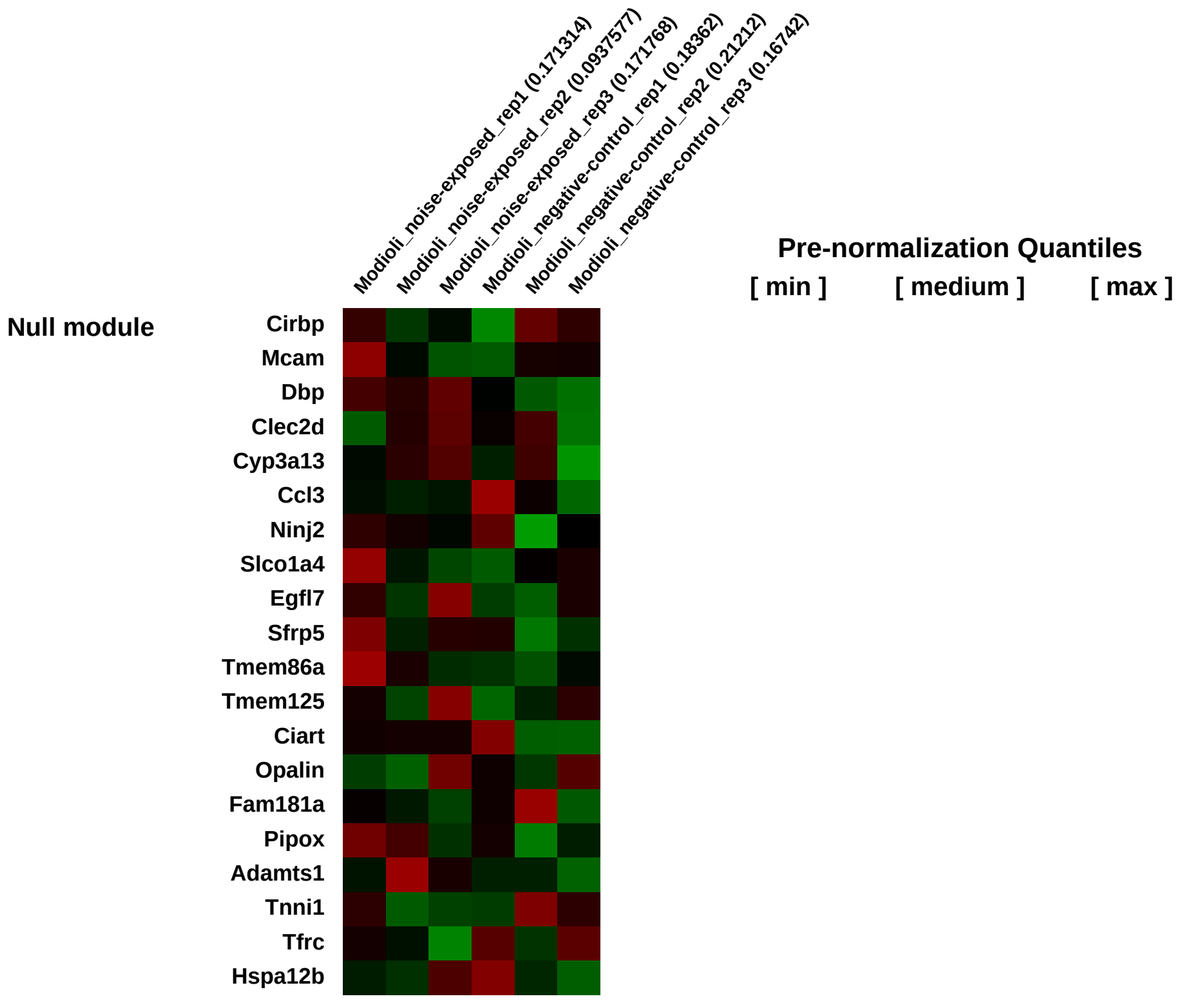

GEO Series "GSE12881" Expression Profiles

Num of samples in this series: 6

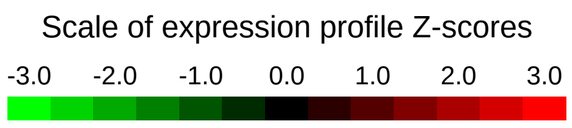

GEO Link:	http://www.ncbi.nlm.nih.gov/geo/query/acc.cgi?acc=GSE12881
Status:	Public on Jan 26 2009
Title:	Loss of Caveolin-3 Induces the Development of a Lactogenic Microenvironment
Organism:	Mus musculus
Experiment type:	Expression profiling by array
Platform:	GPL1261
Pubmed ID:	19164602
Summary & Design:	**Summary:** Here, we show that functional loss of a single gene is sufficient to confer constitutive milk protein production and protection against mammary tumor formation. Caveolin-3 (Cav-3), a muscle-specific caveolin-related gene, is highly expressed in striated and smooth muscle cells. We demonstrate that Cav-3 is also expressed in myoepithelial cells within the mammary gland. To determine if genetic ablation of Cav-3 expression affects adult mammary gland development, we next studied the phenotype(s) of Cav-3 (-/-) null mice. Interestingly, detailed analysis of Cav-3 (-/-) virgin mammary glands shows dramatic increases in ductal thickness, side-branching, and the development of extensive lobulo-alveolar hyperplasia, akin to the changes normally observed during pregnancy and lactation. Analysis by genome-wide expression profiling reveals the upregulation of gene transcripts associated with pregnancy/lactation, mammary stem cells, and human breast cancers, consistent with a constitutive lactogenic phenotype. The expression levels of three key transcriptional regulators of lactation, namely Elf5, Stat5a, and c-Myc are also significantly elevated. Experiments with pregnant mice directly show that Cav-3 (-/-) mice undergo precocious lactation. Finally, using orthotopic implantation of a transformed mammary cell line (known as Met-1), we demonstrate that virgin Cav-3 (-/-) mice are dramatically protected against mammary tumor formation. Interestingly, Cav-3 (+/-) mice also show similar protection, indicating that even reductions in Cav-3 levels are sufficient to render these mice resistant to tumorigenesis. Thus, Cav-3 (-/-) mice are a novel preclinical model to study the protective effects of a constitutive lactogenic microenviroment on mammary tumor onset and progression. Our current studies have broad implications for using the lactogenic micro-environment as a paradigm to discover new therapies for the prevention and/or treatment of human breast cancers. Most importantly, a lactation-based therapeutic strategy would provide a more natural and nontoxic approach to the development of novel anti-cancer therapies. **Overall design:** All WT and Cav-3 knockout (KO) mice used in this study were in the FVB/N genetic background. 4-month old virgin female mice were utilized in a micro array study between 3 wildtype and 3 Caveolin-3 knock-out mammary glands.

Background corr dist: KL-Divergence = 0.0260, L1-Distance = 0.0141, L2-Distance = 0.0002, Normal std = 0.6931

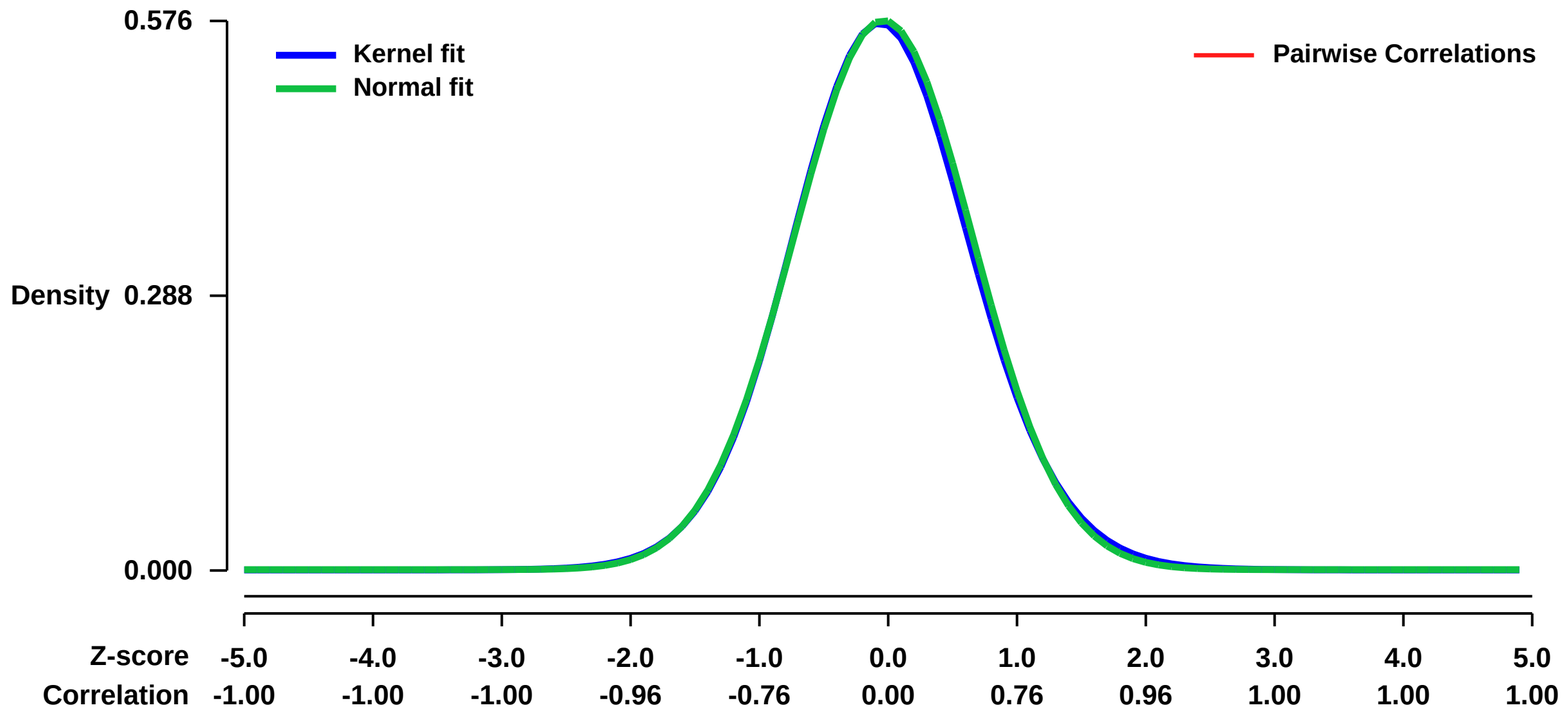

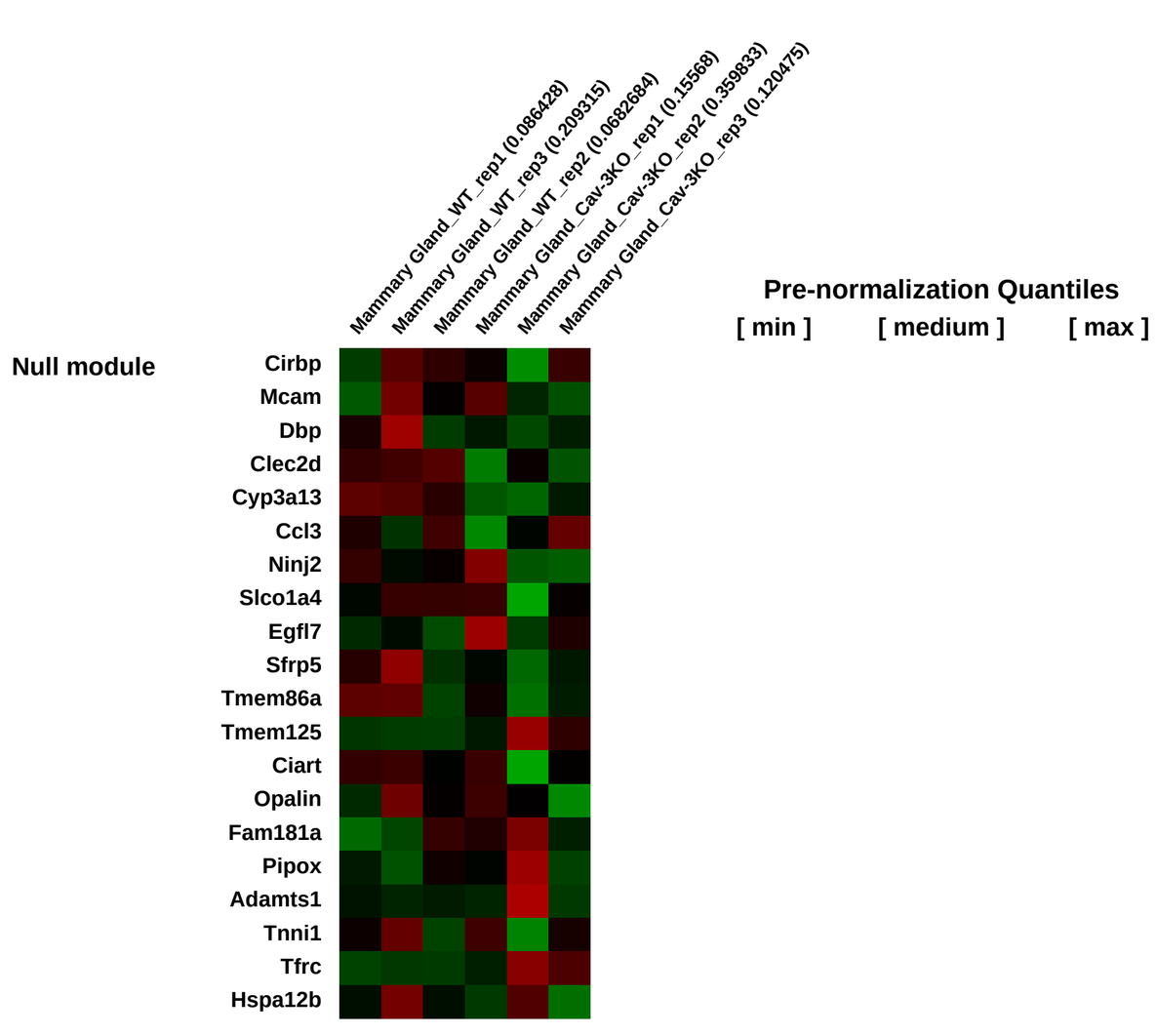

GEO Series "GSE12908" Expression Profiles

Num of samples in this series: 10

Scale of expression profile Z-scores

-3.0 -2.0 -1.0 0.0 1.0 2.0 3.0

GEO Link:	**http://www.ncbi.nlm.nih.gov/geo/query/acc.cgi?acc=GSE12908**
Status:	**Public on Dec 31 2008**
Title:	**Gene expression following miR-30a knockdown in bipotential mouse embryonic liver (BMEL) cells**
Organism:	**Mus musculus**
Experiment type:	**Expression profiling by array**
Platform:	**GPL1261**
Pubmed ID:	**19185580**
Summary & Design:	**Summary:** **The goal was to identify genes targeted by miR-30a.** **Keywords: Transfection of cultured cells with antisense oligonucleotide** **Overall design:** **RNA was isolated from BMELs tranfected with a locked nucleic acid (LNA) antisense oligonucleotide to miR-30a or with a scrambled control oligo.**

Background corr dist: **KL-Divergence = 0.1146, L1-Distance = 0.0300, L2-Distance = 0.0015, Normal std = 0.4135**

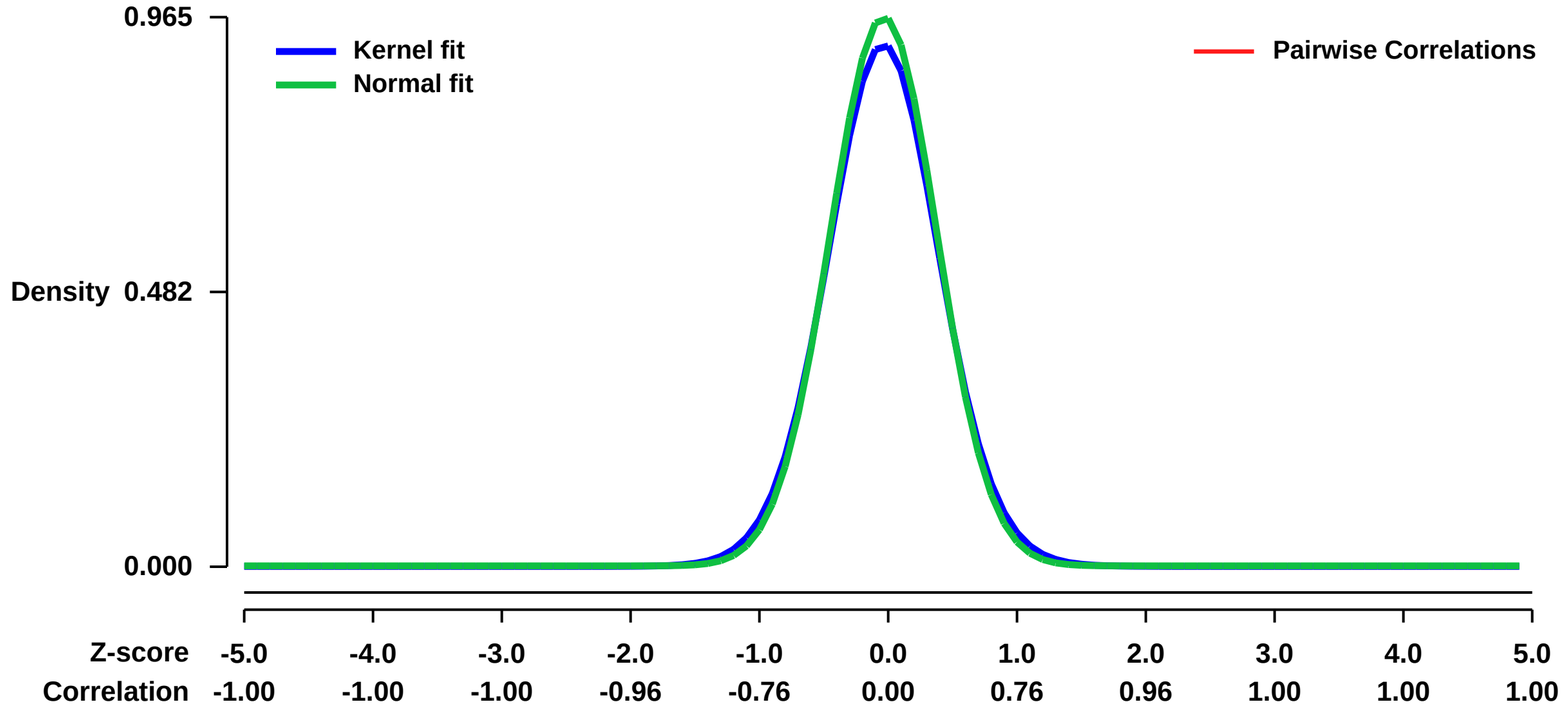

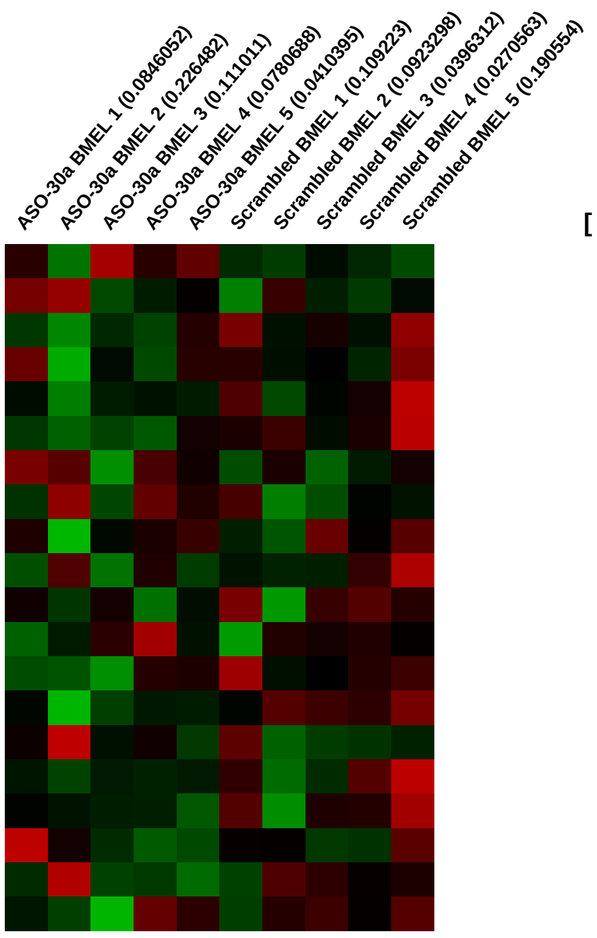

GEO Series "GSE12950" Expression Profiles

Num of samples in this series: 6

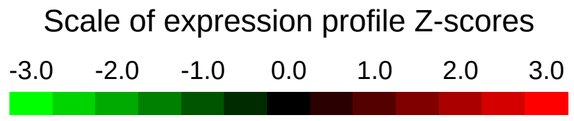

GEO Link:	**http://www.ncbi.nlm.nih.gov/geo/query/acc.cgi?acc=GSE12950**
Status:	**Public on Nov 01 2008**
Title:	**Gene expression profile of testes from three mouse strains, AKR/N, C57BL/6 and MRL/MpJ+/+**
Organism:	**Mus musculus**
Experiment type:	**Expression profiling by array**
Platform:	**GPL1261**
Pubmed ID:	
Summary & Design:	**Summary:** **Cryptorchidism and scrotal heating result in abnormal spermatogenesis but the mechanism(s) proscribing this temperature sensitivity are unknown. It was previously reported that the AKR/N or MRL/MpJ-+/+ mouse testis is more heat resistant than the testis from the C57BL/6 strain. We have attempted to probe into the mechanism(s) involved in heat sensitivity by examining global gene expression profiles of normal and heat-treated testes from C57BL/6, AKR/N and MRL/MpJ-+/+ mice by microarray analysis. In the normal C57BL/6 testis, 415 and 416 transcripts were differentially expressed (at least two-fold higher or lower) when compared to the normal AKR/N and MRL/MpJ-+/+ testis, respectively. The AKR/N and MRL/MpJ-+/+ strains revealed 268 differentially expressed transcripts between them. There were 231 transcripts differentially expressed between C57BL/6 and two purported heat-resistant strains, AKR/N and MRL/MpJ-+/+.** **Overall design:** **Total RNA of testes from 3 different strains of mice, C57BL/6, AKR/N and MRL/MpJ-+/+, were analyzed using microarray 430.20 chip. All mice were 8 weeks old, 2 mice/strain.**

Background corr dist: KL-Divergence = 0.0405, L1-Distance = 0.0184, L2-Distance = 0.0003, Normal std = 0.6139

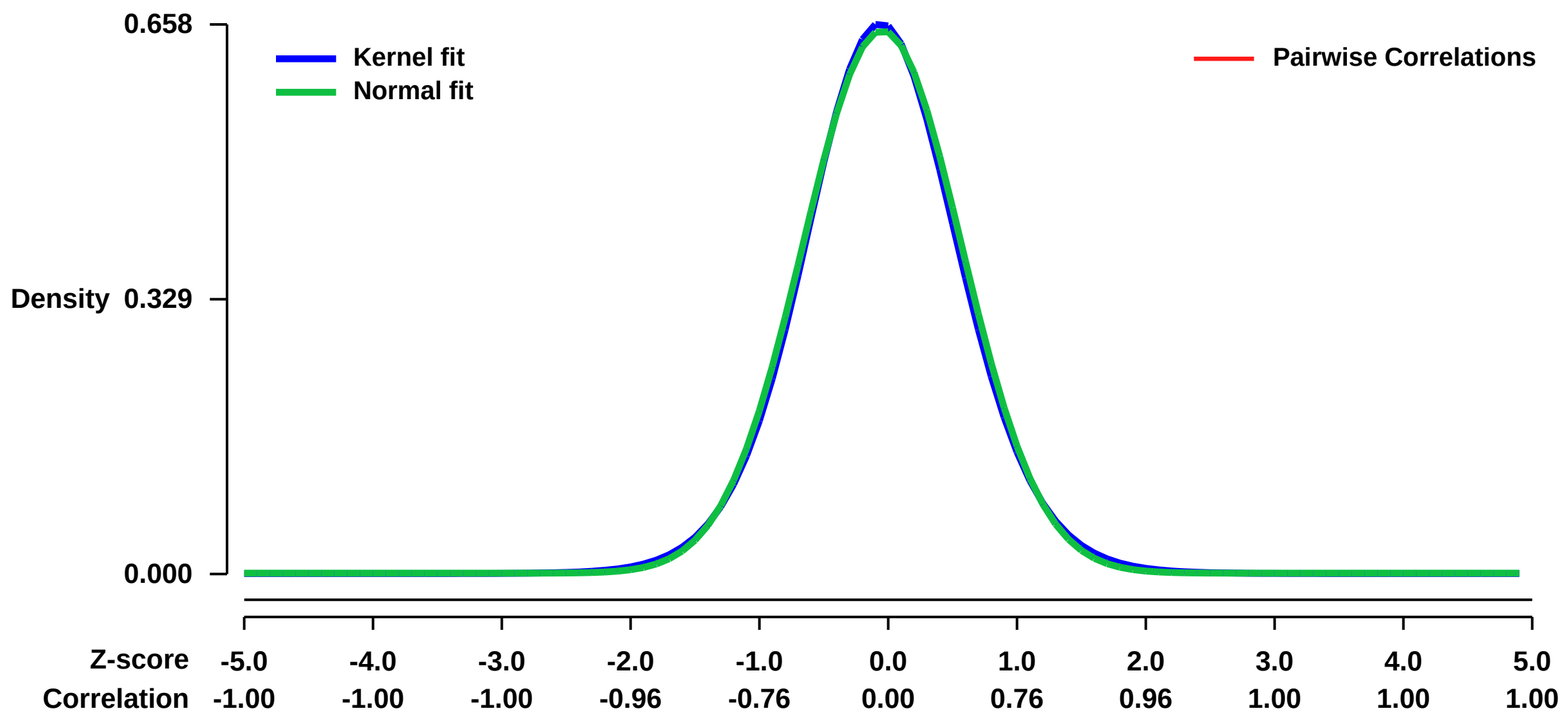

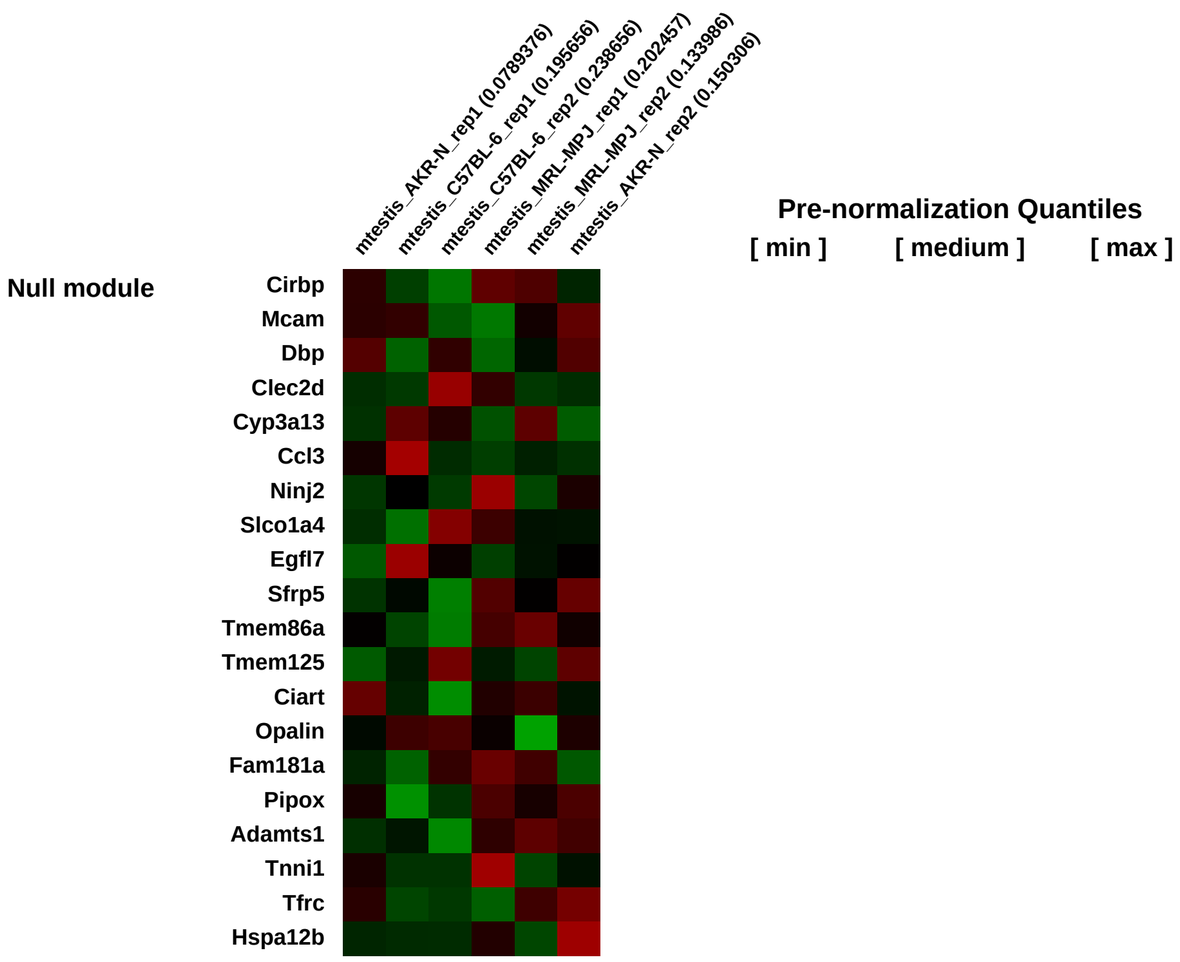

GEO Series "GSE12956" Expression Profiles

Num of samples in this series: 10

Scale of expression profile Z-scores

-3.0 -2.0 -1.0 0.0 1.0 2.0 3.0

GEO Link:	http://www.ncbi.nlm.nih.gov/geo/query/acc.cgi?acc=GSE12956
Status:	Public on Feb 26 2010
Title:	Arx acts as a key selector gene of the ventral telencephalon mainly through its repression transcriptional activity
Organism:	Mus musculus
Experiment type:	Expression profiling by array
Platform:	GPL1261
Pubmed ID:	23968833
Summary & Design:	**Summary:** The homeobox containing gene Arx is expressed during ventral telencephalon development and it is required for correct GABAergic interneuron tangential migration from the ganglionic eminences to the olfactory bulbs, cerebral cortex and striatum. Its human ortholog is associated with a variety of neurological clinical manifestations whose syntoms are compatible with a loss of cortical interneurons and altered basal ganglia related-activities in humans. Herein, we reported the identification by global expression profiling of a group of genes whose expression is consistently altered in Arx mutant ganglionic eminences. Following analysis revealed the striking ectopic expression in the ganglionic eminences of a number of genes normally not, or only marginally, expressed in the ventral telencephalon. Among them, we functionally analyzed Ebf3, whose ectopic expression in ventral telencephalon is preventingneuronal tangential migration. Further, we showed that Arx is sufficient to repress Ebf3 endogenous expression and that its silencing in Arx mutant tissue might marginally rescue tangential cell movements. Together, these data provide an initial analysis of the molecular pathways regulated by Arx and how their networking might regulate those specific cellular processes during telencephalon development strongly altered by loss of Arx. **Overall design:** Three timed-pregnant Arx heterozygous dams crossed with C57Bl/6 males were sacrificed at E14.5, the embryos harvested and placed into cold PBS. After brain isolarion, meninges and olfactory bulbs were removed, and the ventral telencephalon separated from the overlying cerebral cortex. The same procedure was repeated for 5 wt and 5 Arx mutant embryos.

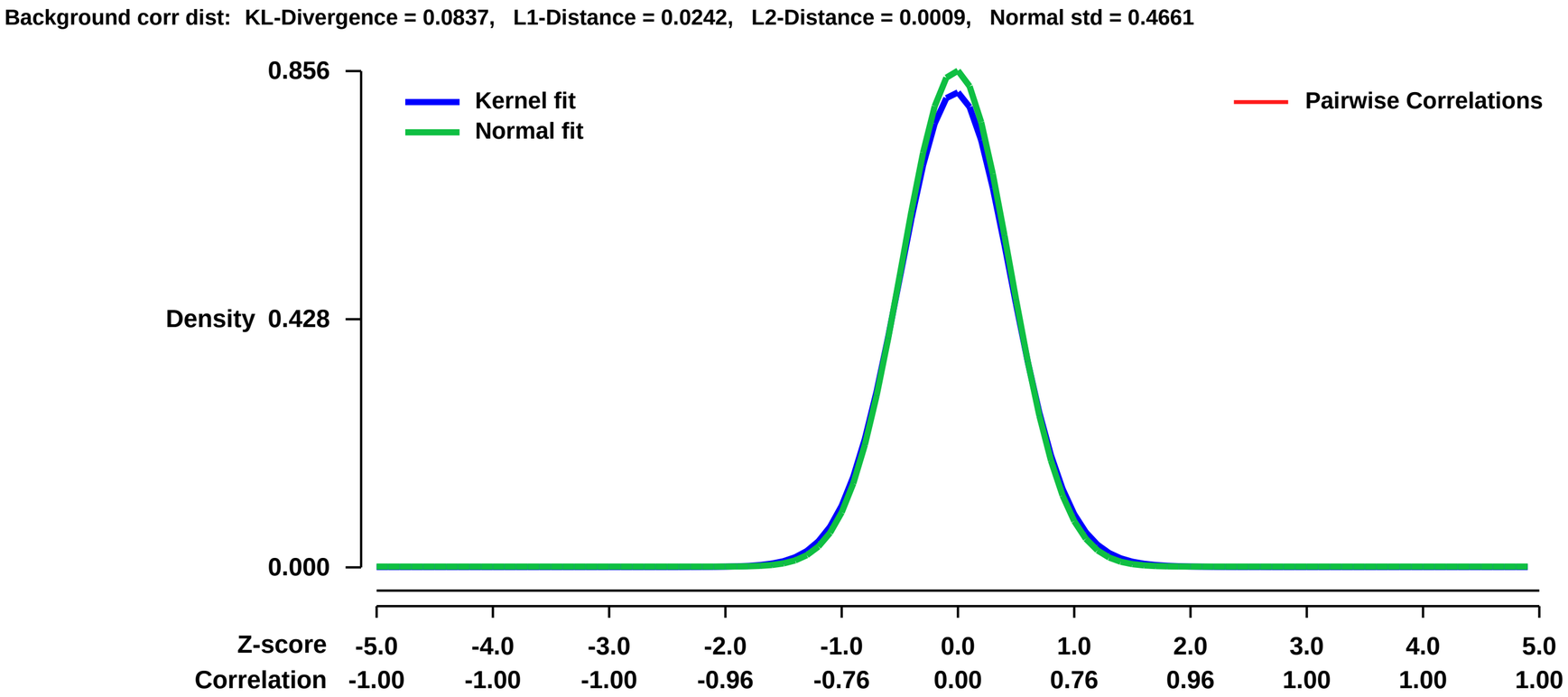

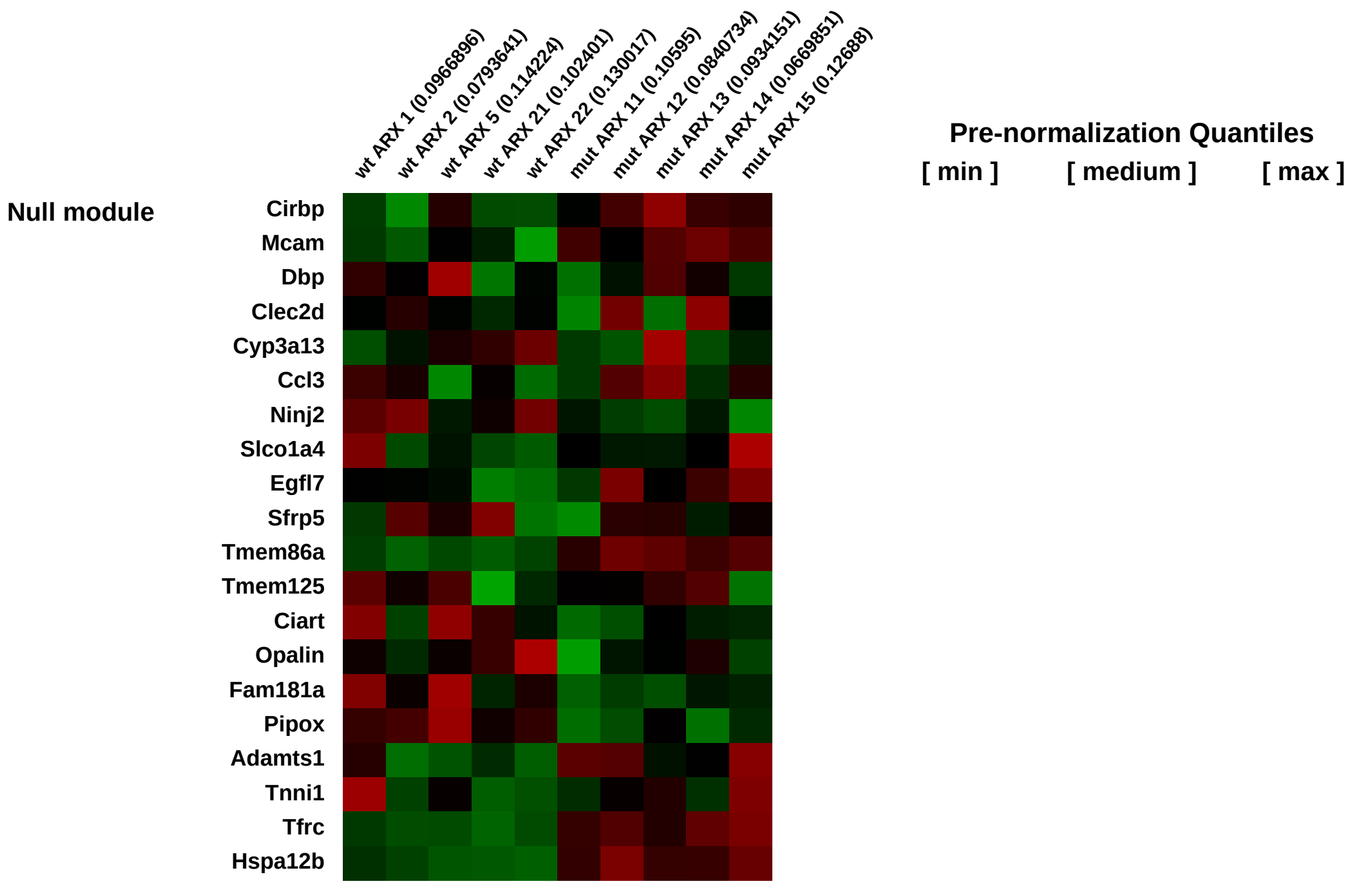

GEO Series "GSE12985" Expression Profiles

Num of samples in this series: 14

Scale of expression profile Z-scores

-3.0 -2.0 -1.0 0.0 1.0 2.0 3.0

GEO Link:	**http://www.ncbi.nlm.nih.gov/geo/query/acc.cgi?acc=GSE12985**
Status:	**Public on Feb 01 2010**
Title:	**Differentiation time course of trophoblast stem cells**
Organism:	**Mus musculus**
Experiment type:	**Expression profiling by array**
Platform:	**GPL1261**
Pubmed ID:	**20081188**
Summary & Design:	**Summary:** **To characterized the changes in gene expression during the differentiation of TS cells. TS cells can be derived from two time point during embryogenesis, cell lines tested were from each of these time points.** **Keywords: time course** **Overall design:** **TS cells derived from either E3.5 or E6.5 embryos were differentiated over 6 days by withdrawal of FGF4 and feeder conditioned medium. Cell were sampled every 24 hrs and assayed by microarray.**

Background corr dist: **KL-Divergence = 0.0675, L1-Distance = 0.0263, L2-Distance = 0.0011, Normal std = 0.5003**

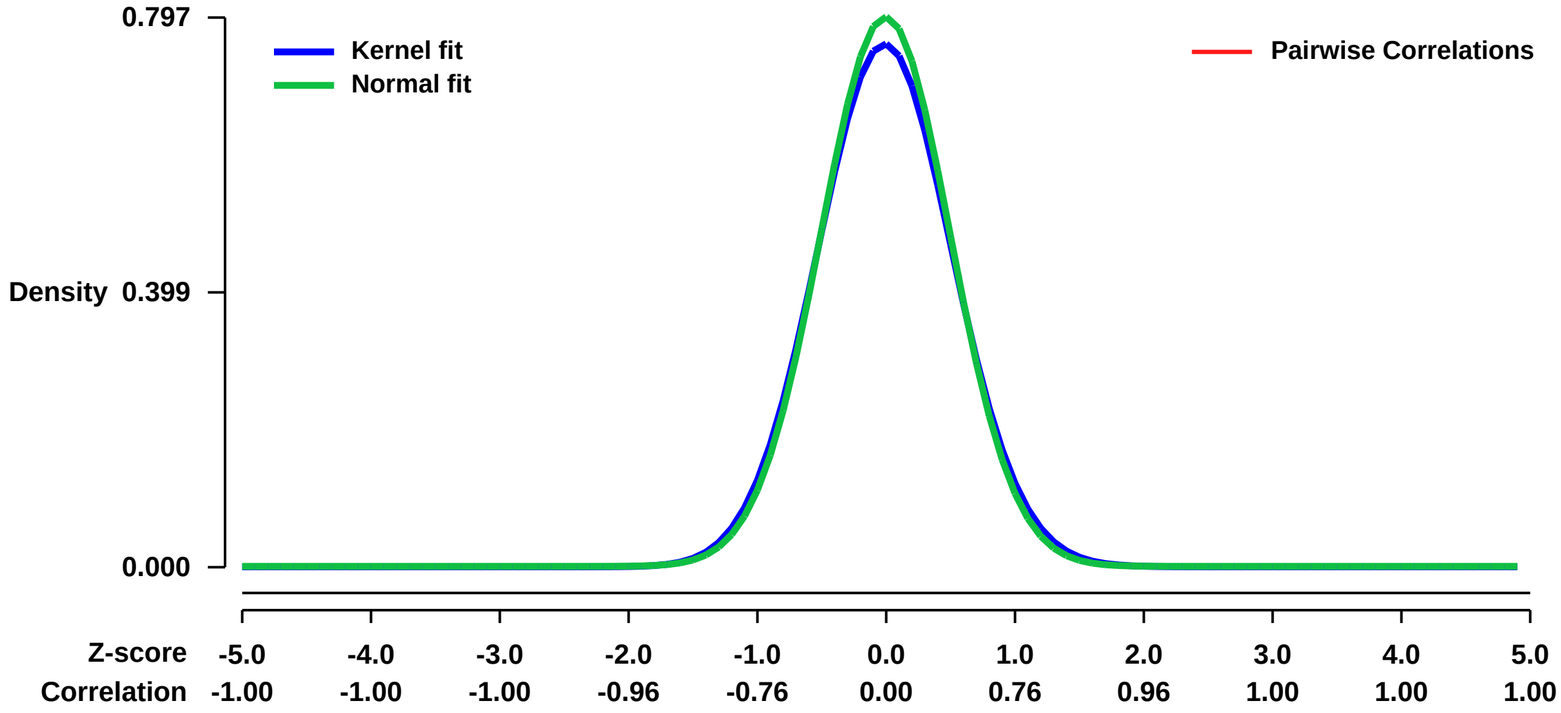

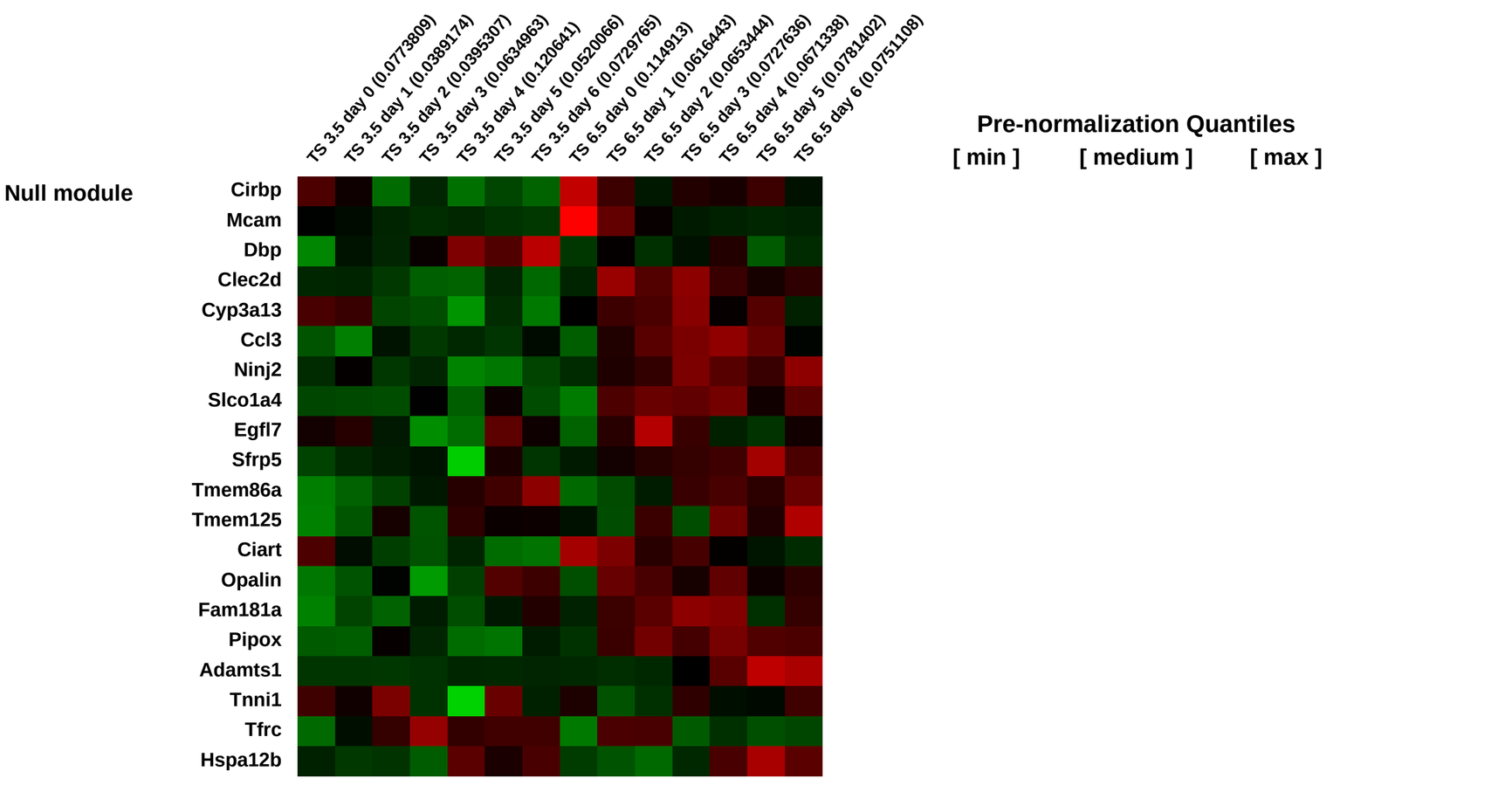

GEO Series "GSE12993" Expression Profiles

Num of samples in this series: 6

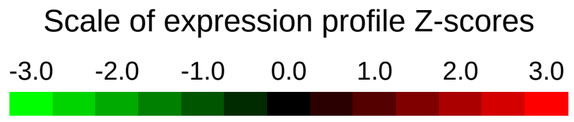

GEO Link:	**http://www.ncbi.nlm.nih.gov/geo/query/acc.cgi?acc=GSE12993**
Status:	**Public on Jul 31 2009**
Title:	**C2C12 culture: myogenesis timecourse and shRp58 treatment**
Organism:	**Mus musculus**
Experiment type:	**Expression profiling by array**
Platform:	**GPL1261**
Pubmed ID:	
Summary & Design:	**Summary:** **To predict Rp58-regulated gene involved in myogenesis, RNA profiling experiments were performed, comparing RNA derived from C2C12 with or without expressing shRNA for Rp58. As a result, 271 genes were upregulated in C2C12 stably expressing shRNA-Rp58 cells compared with control C2C12 cells. As Rp58 is repressor in C2C12, we hypothesized that Rp58 regulates gene cluster which expression is downregulated in accordance with Rp58 expression and myogenesis progression. In this regard, we also characterized dynamic gene expression patterns during myogenesis by microarray at 4 different stage (GM, day 0, 2, 4) of C2C12 myogenesis assays and found that 399 genes expression is characterized as downregulation pattern during myogenesis. Importantly, this down regulation gene set and upregulated genes by shRNA for Rp58 were highly overlapped.** **Keywords: time course, shRNA** **Overall design:** **MAPPFinder (www.genmapp.org) was used to integrate expression data with known pathways.**

Background corr dist: KL-Divergence = 0.0165, L1-Distance = 0.0127, L2-Distance = 0.0002, Normal std = 0.7749

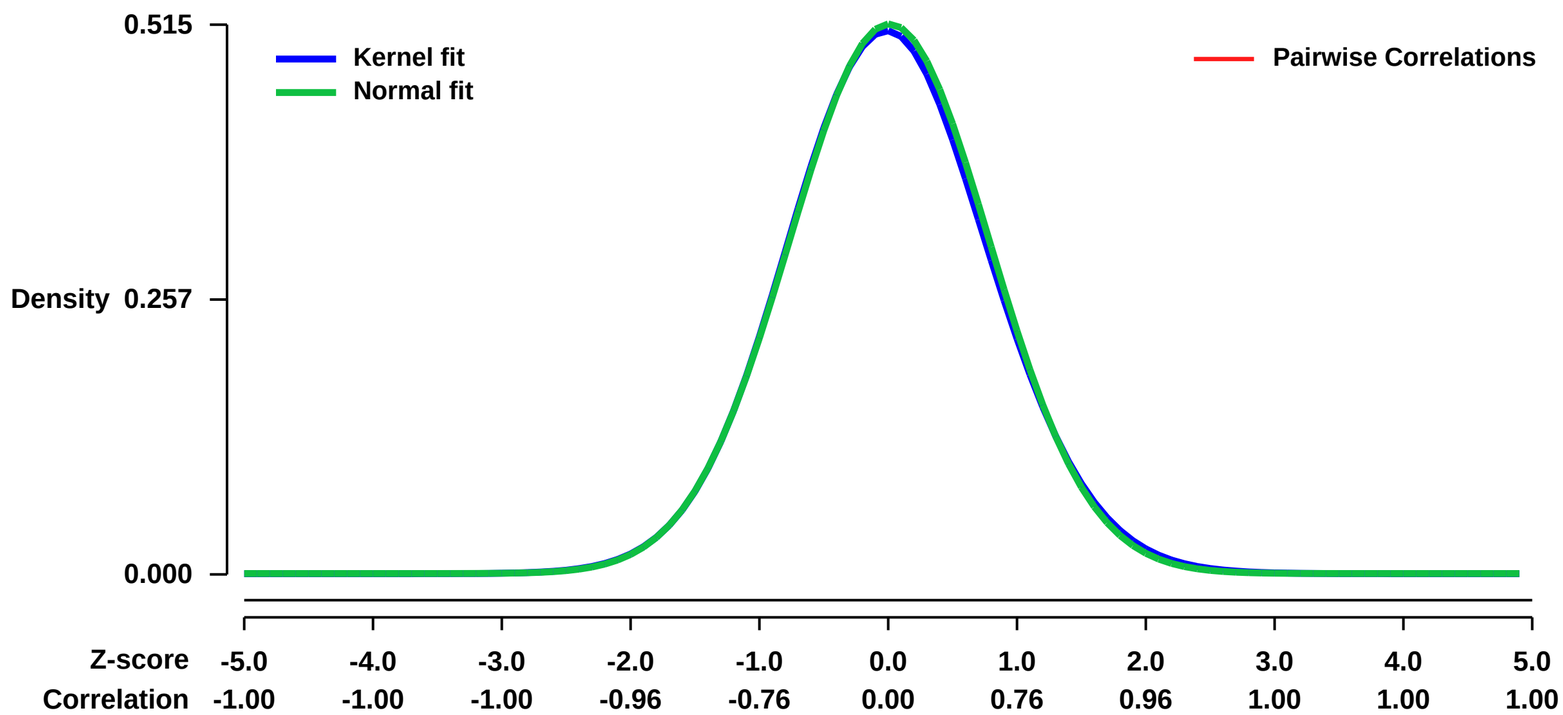

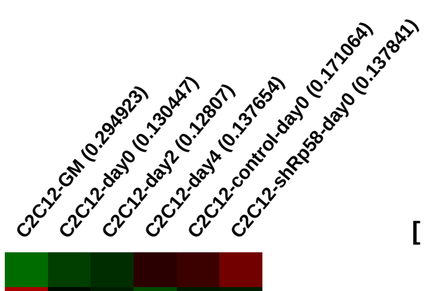

Pre-normalization Quantiles

[min] [medium] [max]

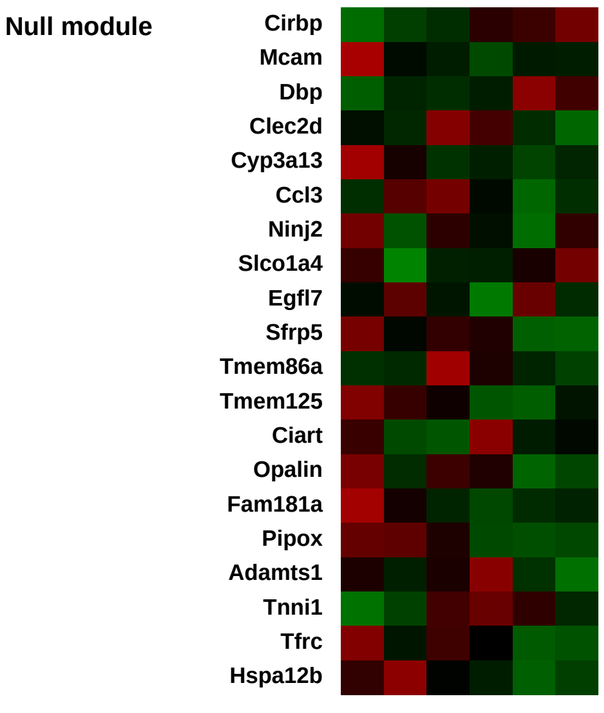

GEO Series "GSE13033" Expression Profiles

Num of samples in this series: 6

Scale of expression profile Z-scores

-3.0 -2.0 -1.0 0.0 1.0 2.0 3.0

GEO Link:	http://www.ncbi.nlm.nih.gov/geo/query/acc.cgi?acc=GSE13033
Status:	Public on Dec 01 2008
Title:	Differentially expressed genes in brain tissue from HtrA2 knockout mice
Organism:	Mus musculus
Experiment type:	Expression profiling by array
Platform:	GPL1261
Pubmed ID:	19023330
Summary & Design:	**Summary:** Cellular stress responses can be activated following functional defects in organelles such as mitochondria and the endoplasmic reticulum. Mitochondrial dysfunction caused by loss of the serine protease HtrA2 leads to a progressive movement disorder in mice and has been linked to parkinsonian neurodegeneration in humans. Here we demonstrate that loss of HtrA2 results in transcriptional up-regulation of nuclear genes characteristic of the integrated stress response, including the transcription factor CHOP, selectively in the brain. We also show that loss of HtrA2 results in the accumulation of unfolded proteins in the mitochondria, defective mitochondrial respiration and enhanced production of reactive oxygen species that contribute to the induction of CHOP expression and to neuronal cell death. CHOP expression is also significantly increased in Parkinsonâ s disease patientsâ brain tissue. We therefore propose that this brain-specific transcriptional response to stress may be important in the advance of neurodegenerative diseases. **Keywords:** genotype comparison **Overall design:** This experiment was set out to identify genes that are differentially expressed in brain tissue from the cortex of HtrA2 knockout (KO) mice compared to wild type (WT) littermates. We chose a cortical region since there is no evidence of neuronal loss in this region enabling us to compare mRNA transcripts in identical cellular populations. Brains of littermate WT and HtrA2 KO mice were dissected to obtain cortex tissue at post-natal day 29 (P29). RNA was isolated and samples were processed for hybridisation (6 samples in total, 3 replicates for each genotype).

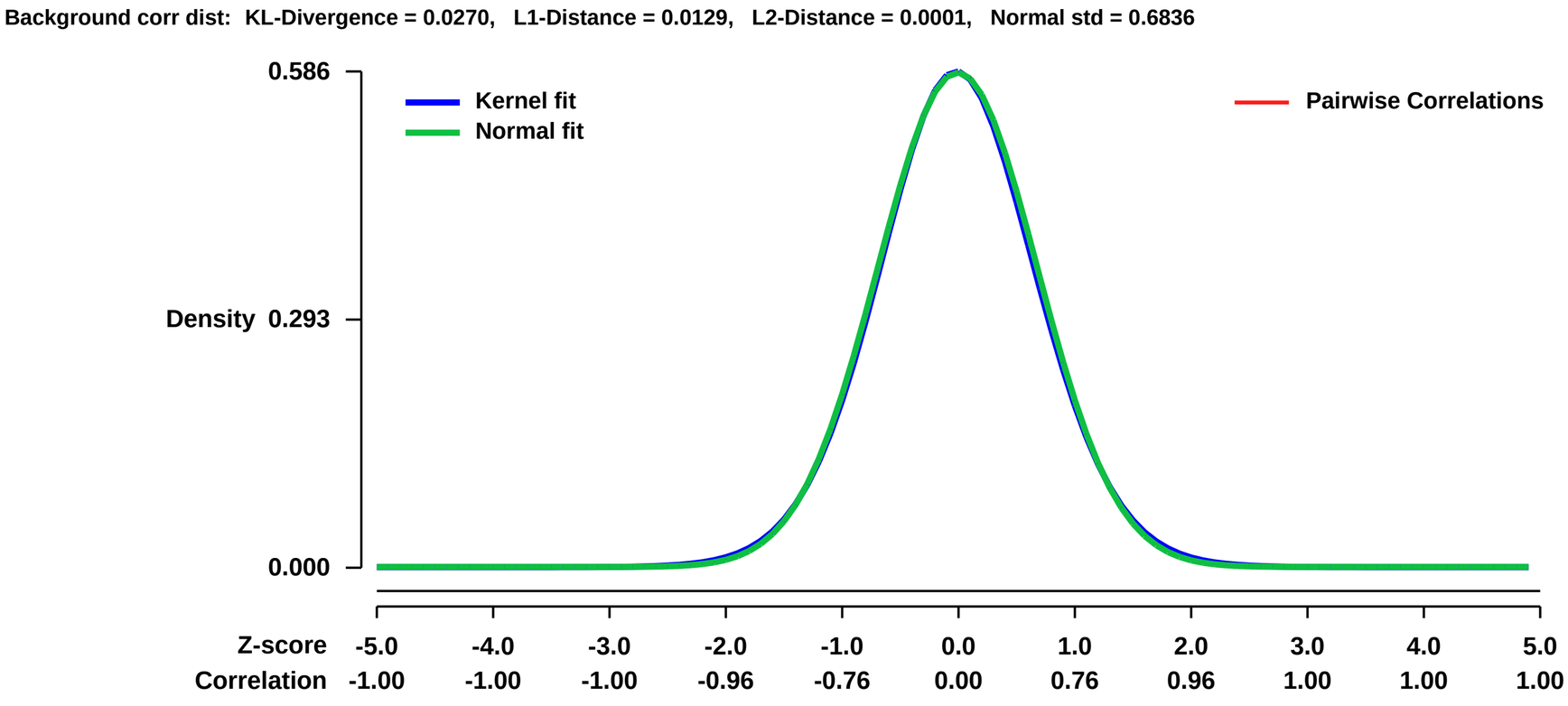

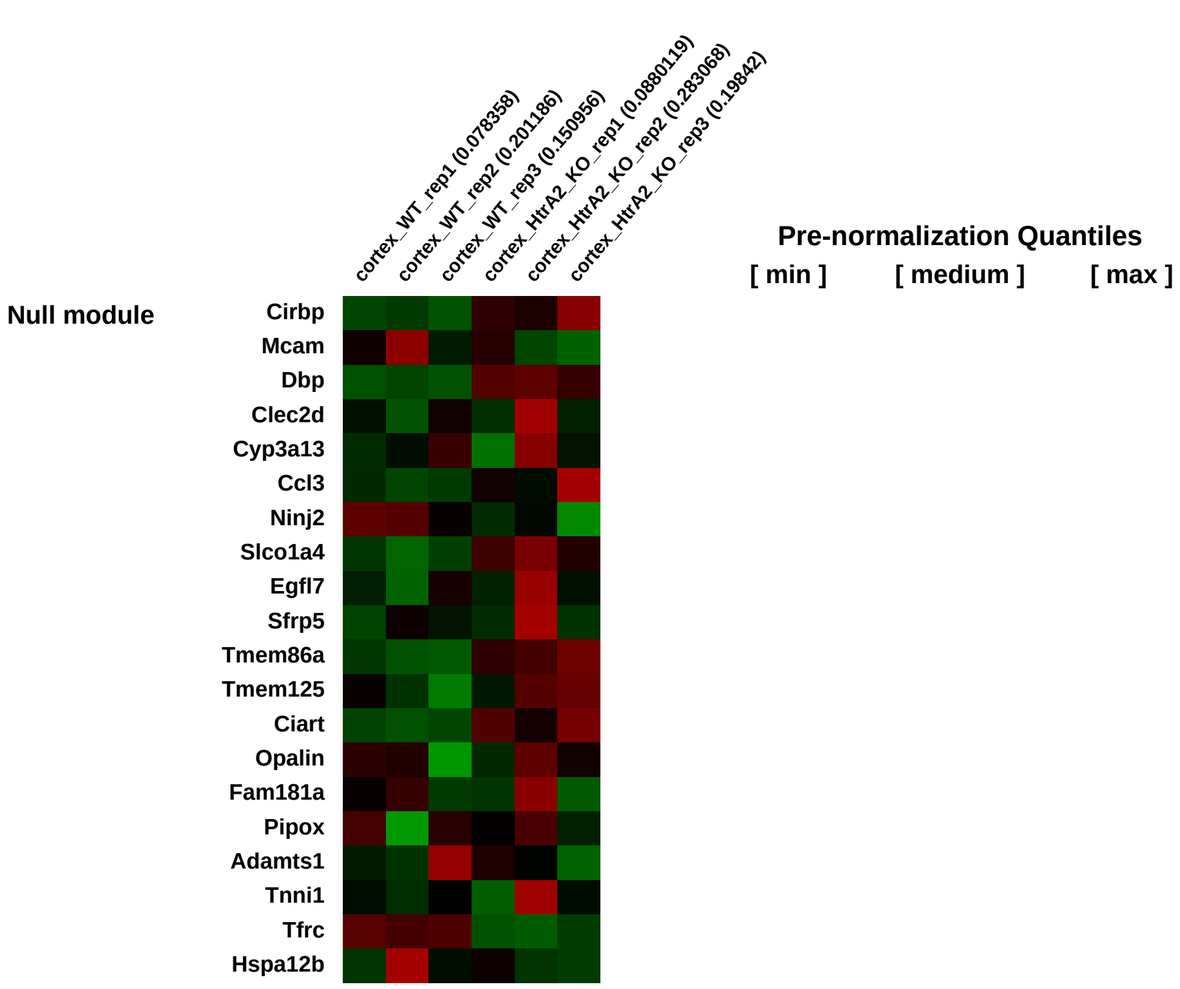

GEO Series "GSE13062" Expression Profiles

Num of samples in this series: 24

Scale of expression profile Z-scores

-3.0 -2.0 -1.0 0.0 1.0 2.0 3.0

GEO Link:	http://www.ncbi.nlm.nih.gov/geo/query/acc.cgi?acc=GSE13062
Status:	Public on Nov 23 2009
Title:	The effects of temporally restricted feeding on hepatic gene expression of Cry1, Cry2 double KO mice
Organism:	Mus musculus
Experiment type:	Expression profiling by array
Platform:	GPL1261
Pubmed ID:	19940241
Summary & Design:	**Summary:** Restricted feeding impacts the hepatic circadian clock of WT mice. Cry1, Cry2 double KO mice lack a circadian clock and are thus expected to show rhythmical gene expression in the liver. Imposing a temporally restricted feeding schedule on these mice shows how the hepatic circadian clock and rhythmic food intake regulate rhythmic transcription in parallel **Overall design:** Cry1, Cry2 double KO mice were entrained either to ad libitum or temporally restricted feeding (tRF) schedules. Food was made available to mice under the tRF regimen only between ZT(CT)1 and ZT(CT)9. Mice were then released into constant darkness while the respective feeding schedules were still maintained. Liver tissue was collected on the second day of constant darkness at the indicated timepoints. Total RNA was extracted and 5ug of RNA was used in the standard Affymetrix protocol for amplification, labeling and hybridization

Background corr dist: KL-Divergence = 0.1620, L1-Distance = 0.0794, L2-Distance = 0.0131, Normal std = 0.4340

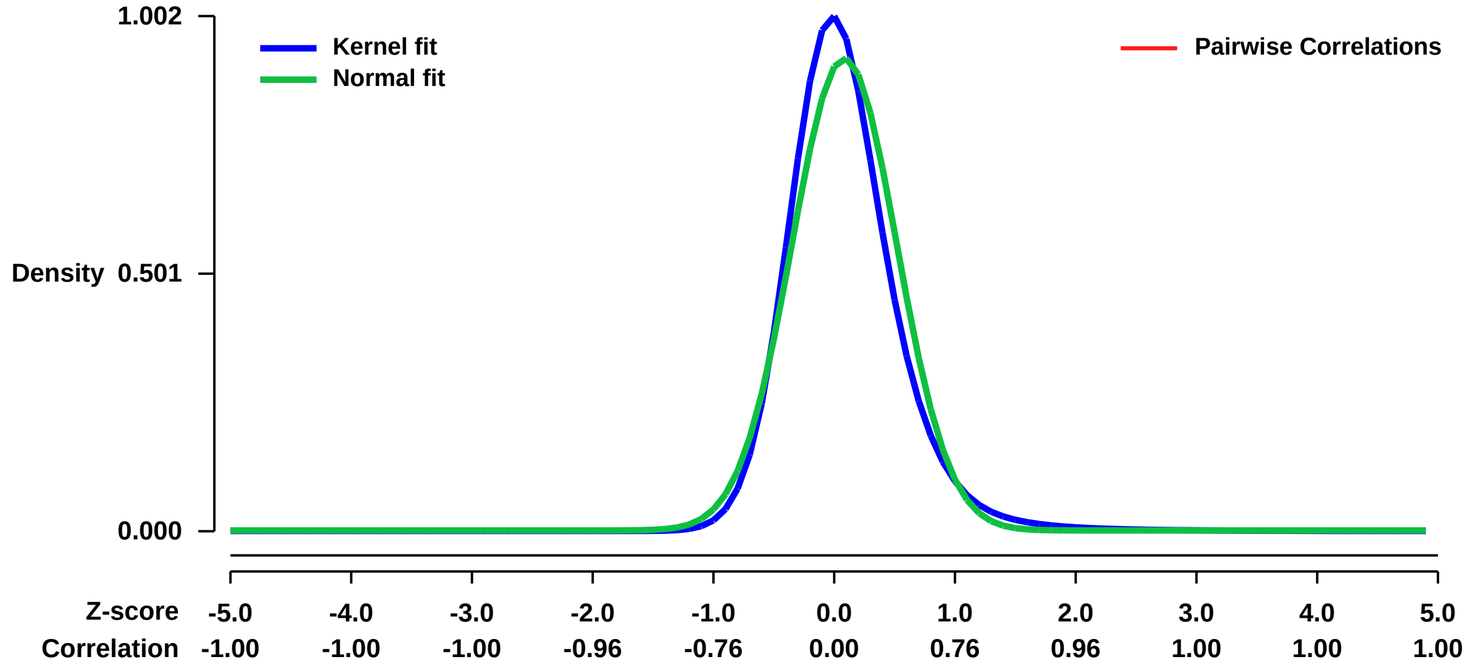

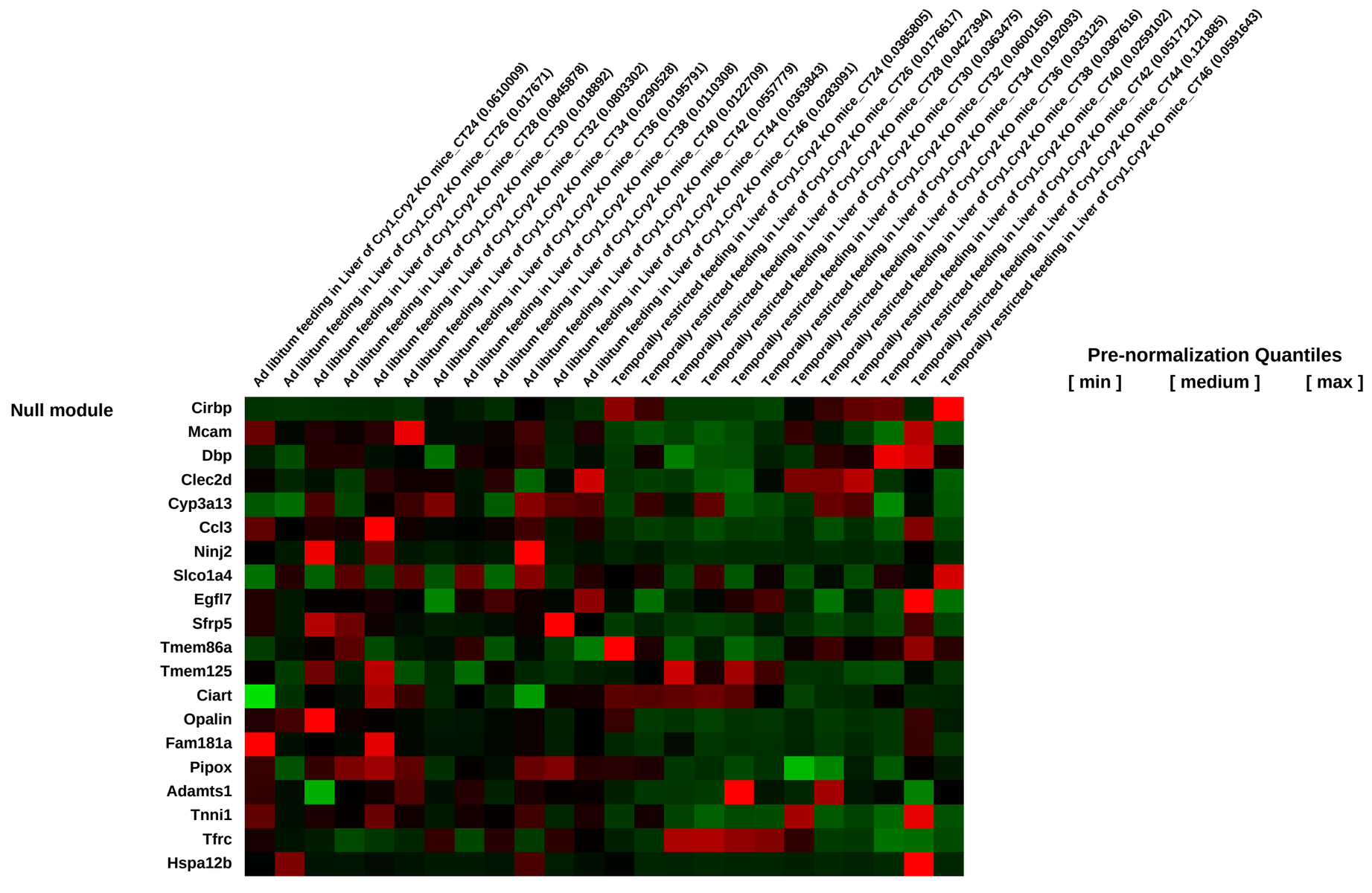

GEO Series "GSE13071" Expression Profiles

Num of samples in this series: 15

Scale of expression profile Z-scores

-3.0 -2.0 -1.0 0.0 1.0 2.0 3.0

GEO Link:	http://www.ncbi.nlm.nih.gov/geo/query/acc.cgi?acc=GSE13071
Status:	Public on Aug 26 2009
Title:	Knee joint synovium from different grades of inflammation in mouse collagen induced arthritis (CIA)
Organism:	Mus musculus
Experiment type:	Expression profiling by array
Platform:	GPL1261
Pubmed ID:	19690516
Summary & Design:	**Summary:** Knee joint synovium was used for gene expression analysis of mouse collagen induced arthritis (CIA). Synovium was prepared at day 30 after initial sensitization from: healthy controls, CIA animals with no, with mild, with moderate, or with severe joint inflammation. Each sample group is represented by three replicates, each consisting of tissue collected from three to four animals. **Keywords: disease severity analysis** **Overall design:** The data set consists of 15 samples: five groups with three replicates each. One sample group is from healthy controls, the other groups are from CIA animals with different degress of joint inflammation.

Background corr dist: KL-Divergence = 0.0611, L1-Distance = 0.0572, L2-Distance = 0.0049, Normal std = 0.5641

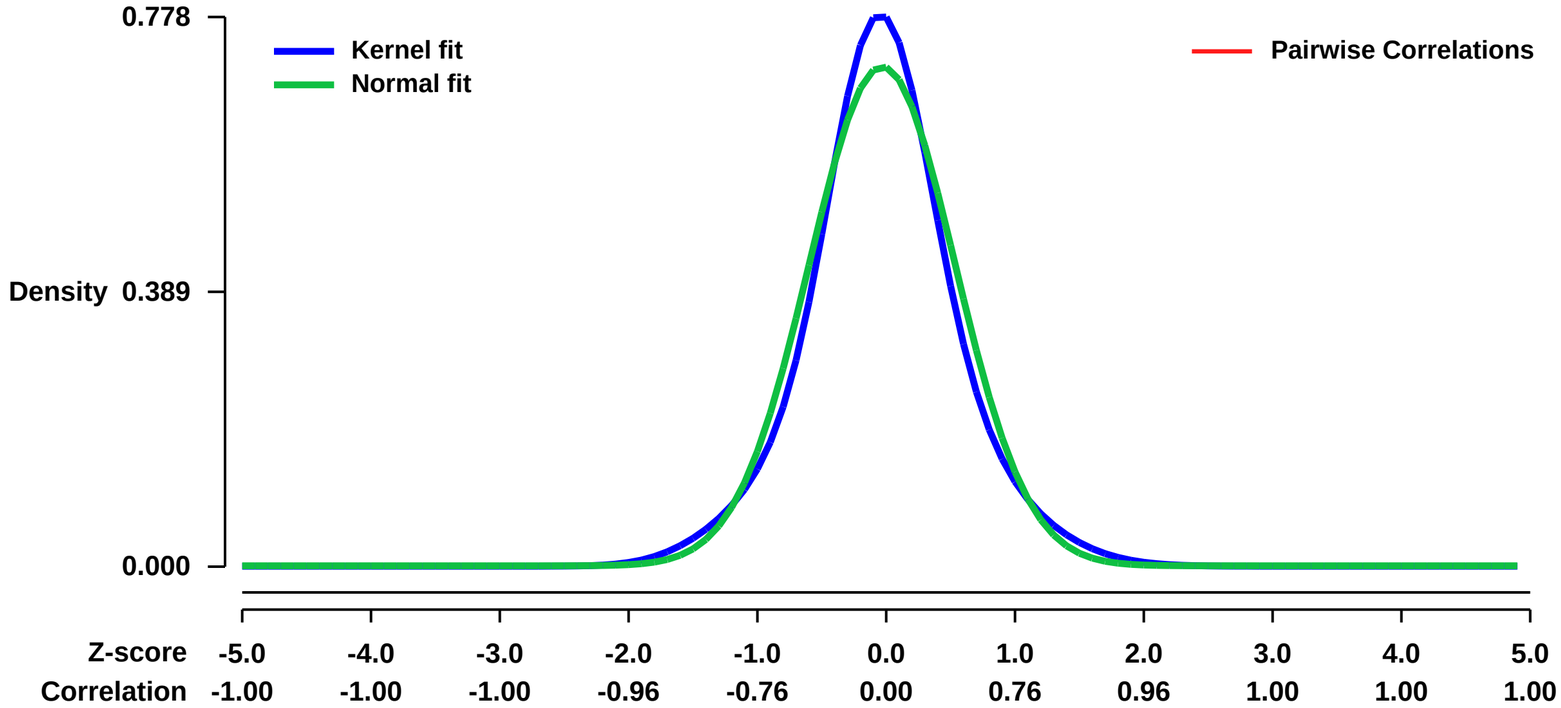

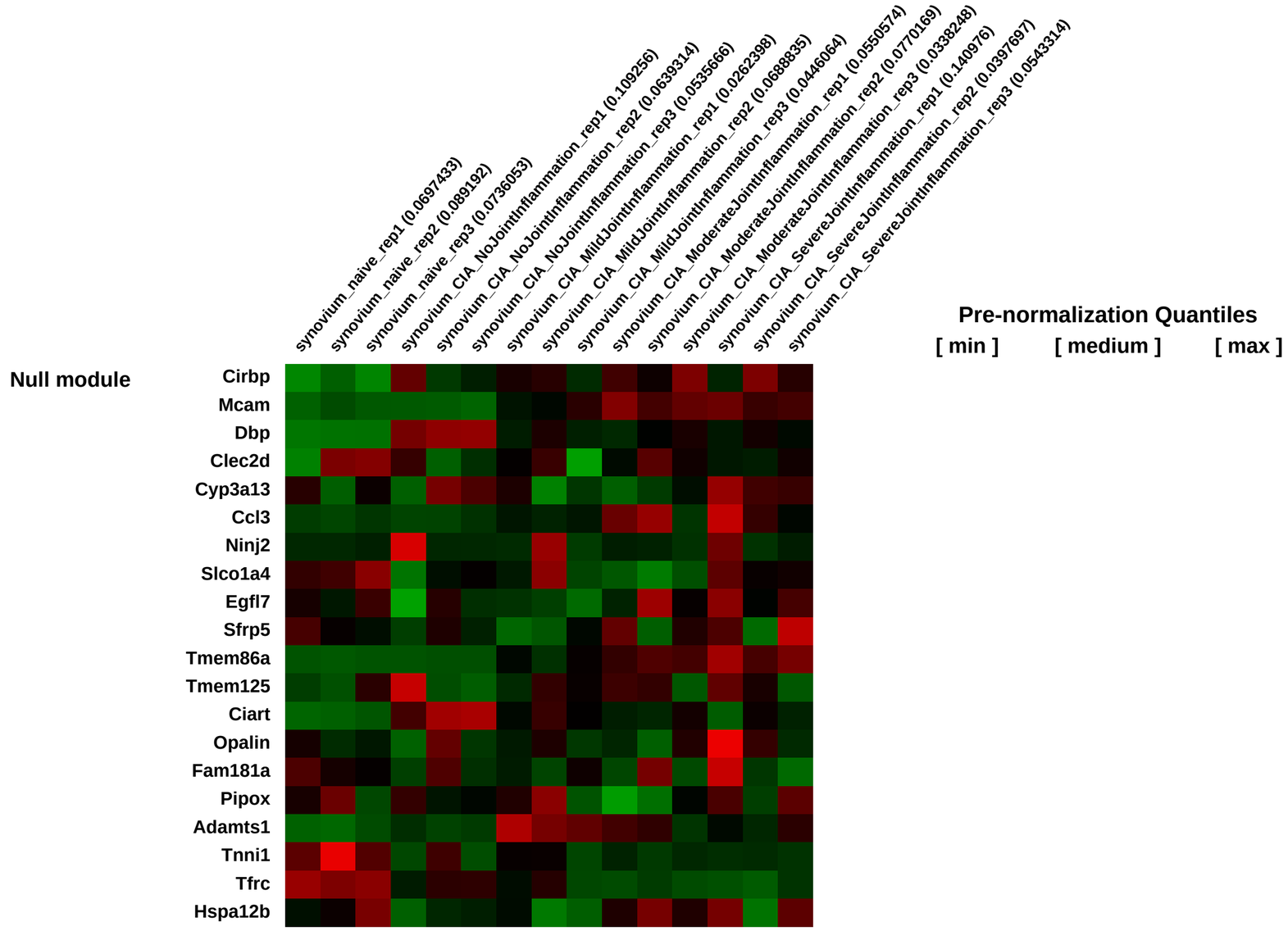

GEO Series "GSE13103" Expression Profiles

Num of samples in this series: 8

Scale of expression profile Z-scores

-3.0 -2.0 -1.0 0.0 1.0 2.0 3.0

GEO Link:	**http://www.ncbi.nlm.nih.gov/geo/query/acc.cgi?acc=GSE13103**
Status:	**Public on Oct 08 2008**
Title:	**Expression data from early mouse embryo eye development, specifically optic fissure.**
Organism:	**Mus musculus**
Experiment type:	**Expression profiling by array**
Platform:	**GPL1261**
Pubmed ID:	**19171890**
Summary & Design:	**Summary:** **The different stages of the optic fissure can be clearly visualized by making sagittal sections through the mouse eye during early development which represent the optic fissure at open (E10.5), closing (E11.5) and fused (E12.5) states. Laser capture microdissection (LCM) was employed to dissect tissue from the margins of the optic fissure consisting of the outer (presumptive RPE) and inner (presumptive neurosensory retina) layers of the retina.** **An approximately square-shaped block of optic fissure (50 x 50 mm) was dissected from each side of the fissure. Two rounds of linear amplification were performed on RNA isolated from each of the samples prior to microarray hybridization. Expression data were gathered in biological triplicate at E10.5, E11.5 and duplicate at E12.5, each array representing pooled optic fissure tissue from three embryos from a single litter. Expression signals were ascertained from 45,101 probe sets and normalized across arrays.** **Keywords: Time course** **Overall design:** **Differential gene expression over the course of three days in laser capture microdissected tissue from wild type mouse embryos.**

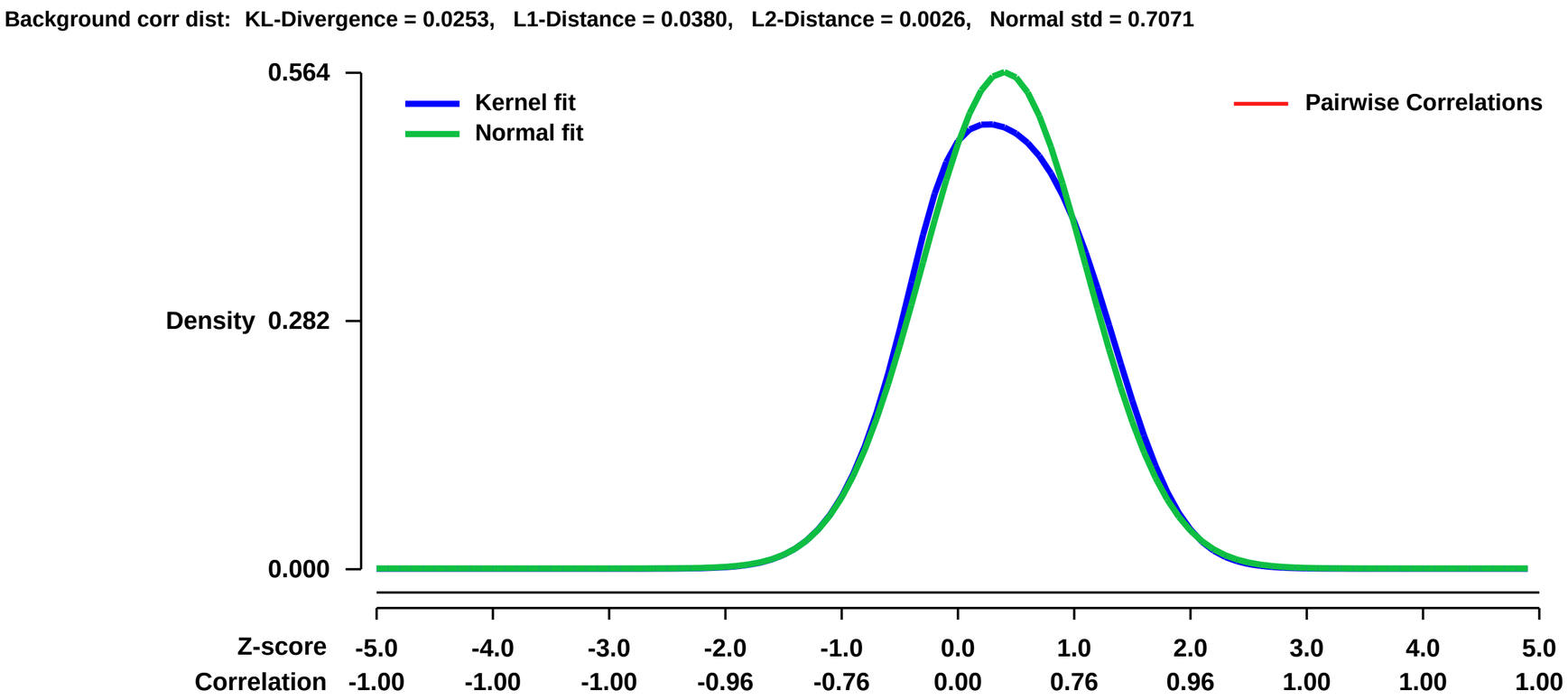

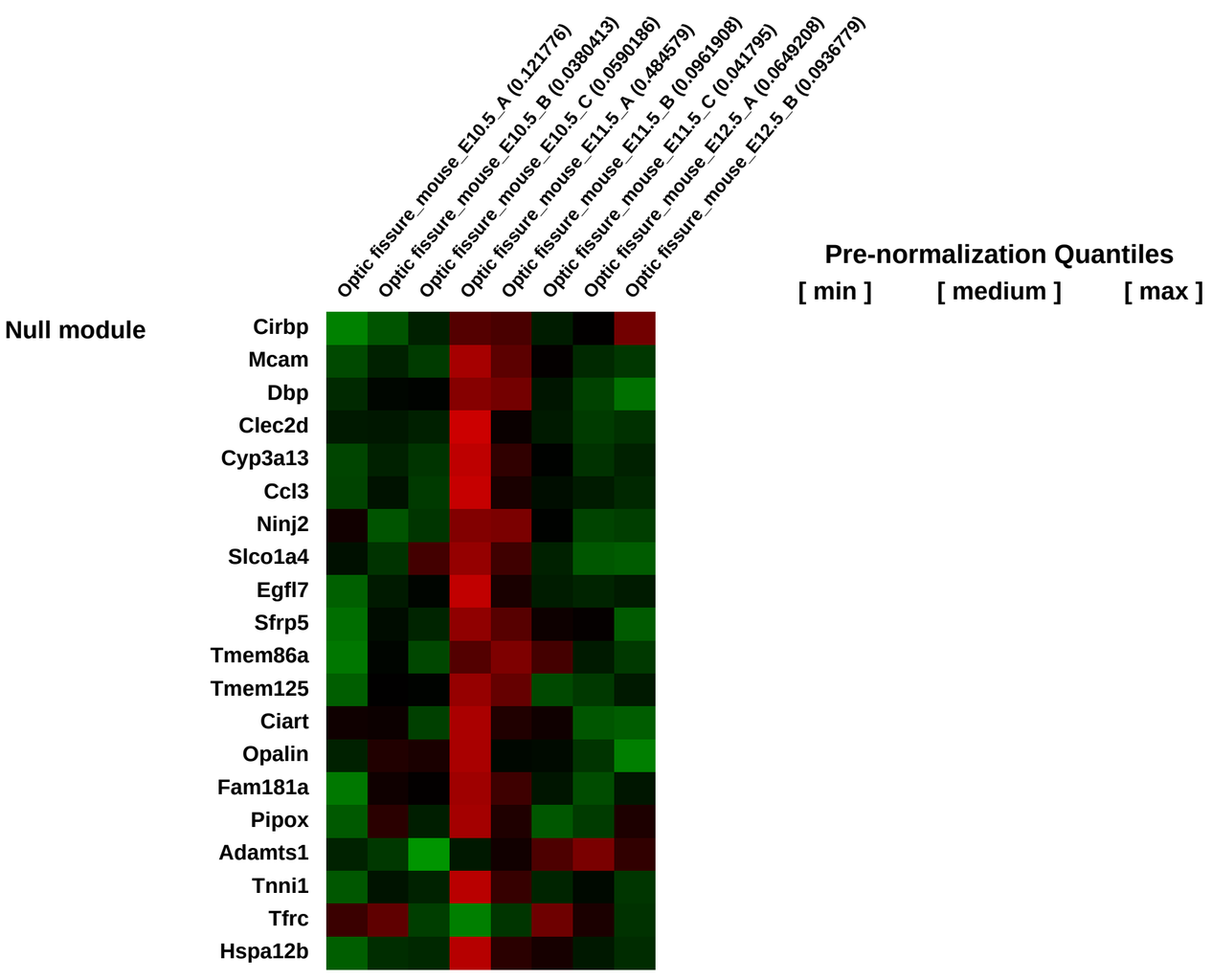

GEO Series "GSE13106" Expression Profiles

Num of samples in this series: 10

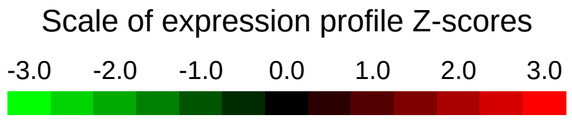

GEO Link:	http://www.ncbi.nlm.nih.gov/geo/query/acc.cgi?acc=GSE13106
Status:	Public on Sep 09 2009
Title:	Regulated SMAD signalling in development
Organism:	Mus musculus
Experiment type:	Expression profiling by array
Platform:	GPL1261
Pubmed ID:	19517569
Summary & Design:	**Summary:** Phosphorylation and subsequent nuclear translocation of SMAD proteins determine the cellular response to activin. Here we identify a novel means by which activin signalling is regulated to enable developmental stage-specific SMAD gene transcription. In response to activin A, immature proliferating mouse Sertoli cells exhibit nuclear accumulation of SMAD3, but not SMAD2, although both proteins are phosphorylated. In post-mitotic differentiating cells, both SMAD2 and SMAD3 accumulate in the nucleus. Furthermore, immature Sertoli cells are sensitive to activin dosage; at higher concentrations maximal SMAD3 nuclear accumulation is observed, accompanied by a small, but significant, increase in nuclear SMAD2. Microarray analysis confirmed that differential SMAD utilization correlated with altered transcriptional outcomes and identified new activin target genes, Gja1 and Serpina5, which are known to be required for Sertoli cell development and male fertility. In immature Sertoli cells, genetic or transient knockdown of SMAD3 enhanced SMAD2 nuclear accumulation in response to activin, with increased Serpina5 mRNA levels associated with nuclear localized SMAD2. In transgenic mice with altered activin bioactivity that display male fertility phenotypes, testicular Gja1 and Serpina5 mRNA levels reflected altered in vivo activin levels. We conclude that regulated nuclear accumulation of phosphorylated SMAD2 is a novel determinant of developmentally regulated activin signalling. **Overall design:** Murine 15dpp Sertoli Cell treated with 0ng, 5ng activin (duplicates). Total 10 samples.

Background corr dist: KL-Divergence = 0.0442, L1-Distance = 0.0746, L2-Distance = 0.0079, Normal std = 0.6871

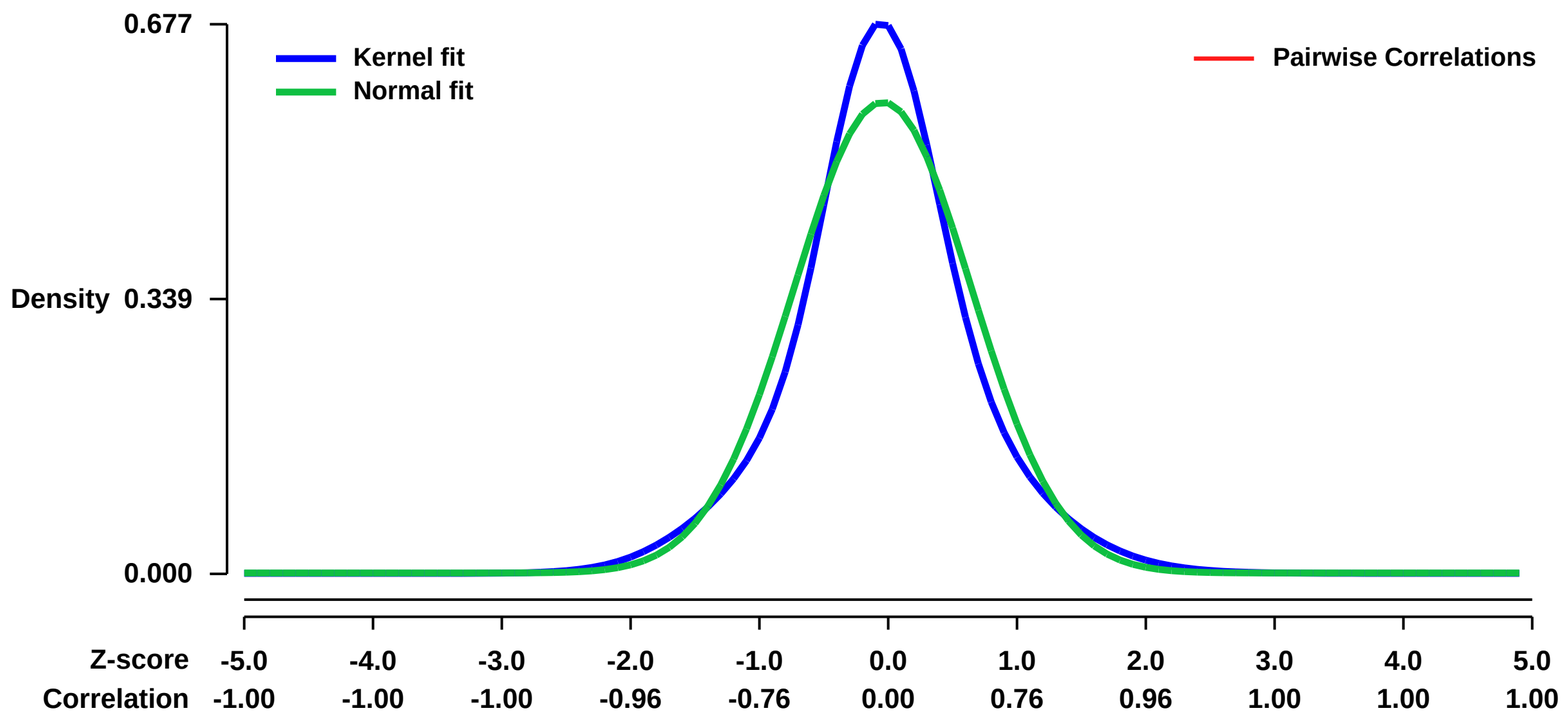

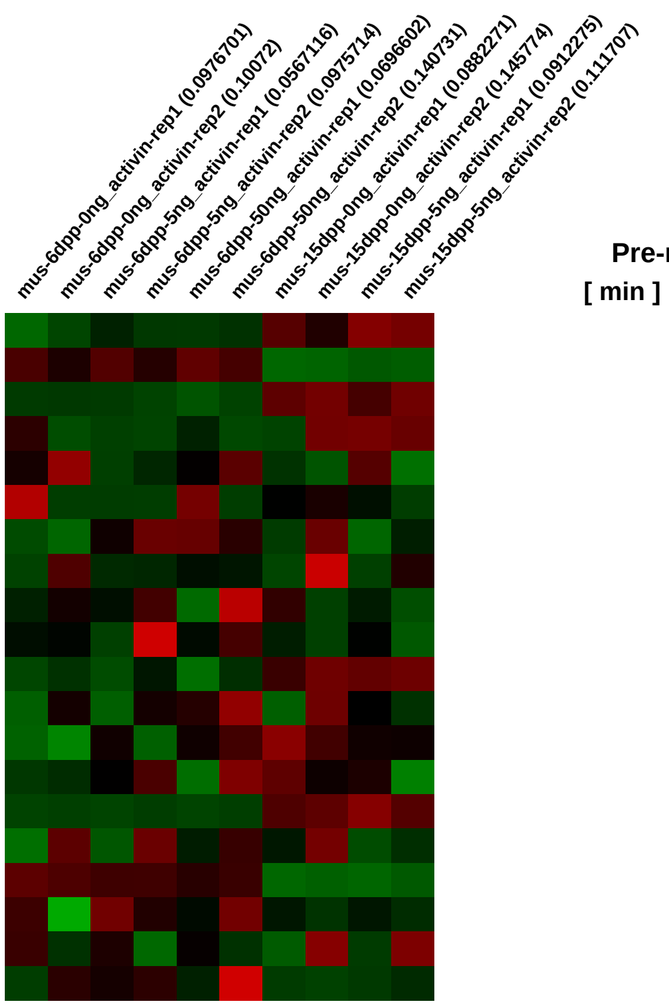

GEO Series "GSE13120" Expression Profiles

Num of samples in this series: 10

Scale of expression profile Z-scores

-3.0 -2.0 -1.0 0.0 1.0 2.0 3.0

GEO Link:	http://www.ncbi.nlm.nih.gov/geo/query/acc.cgi?acc=GSE13120
Status:	Public on Nov 26 2008
Title:	Age-related gene expression changes in mouse neocortex
Organism:	Mus musculus
Experiment type:	Expression profiling by array
Platform:	GPL1261
Pubmed ID:	19041753
Summary & Design:	**Summary:** Aging is associated with major nuclear changes affecting genomic integrity and gene expression. Here we compare the gene expression profiles in the neocortex of young (5 months old) and old (30 months old) B6xC3 F1 mice. In a related study, we compare genes that change expression with age to SIRT1 associated genes identified by ChIP on chip (NimbleGen) and find a significant overlap, indicating that SIRT1 target genes are preferentially deregulated with age. Keywords: gene expression comparison, age-comparison **Overall design:** Total neocortex RNA was hybridized on Affymetrix M430 2.0 arrays. RNA was isolated from five young (5 months) and 5 old (30 months) B6xC3 F1 mice, samples were hybridized individually.

Background corr dist: KL-Divergence = 0.0674, L1-Distance = 0.0204, L2-Distance = 0.0005, Normal std = 0.5033

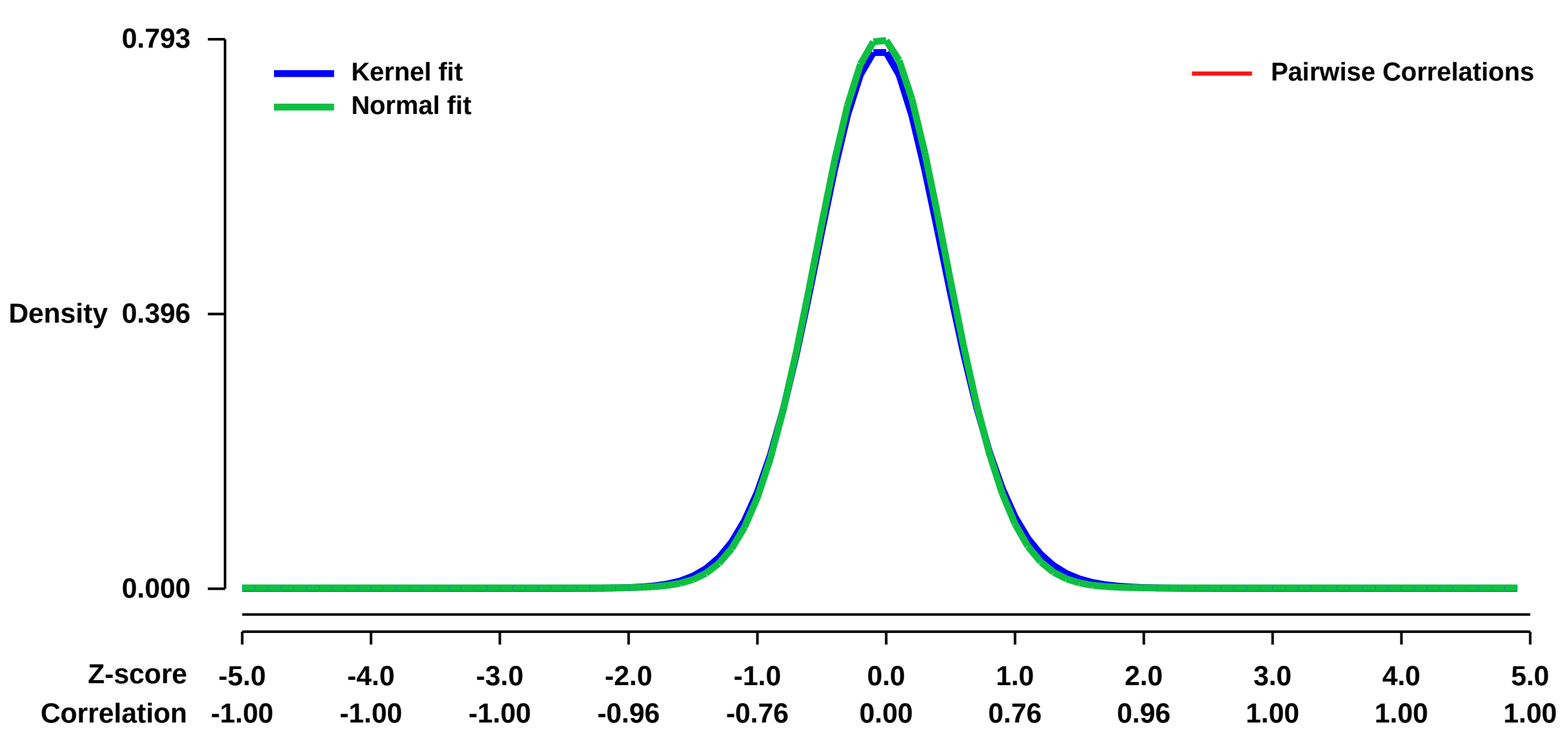

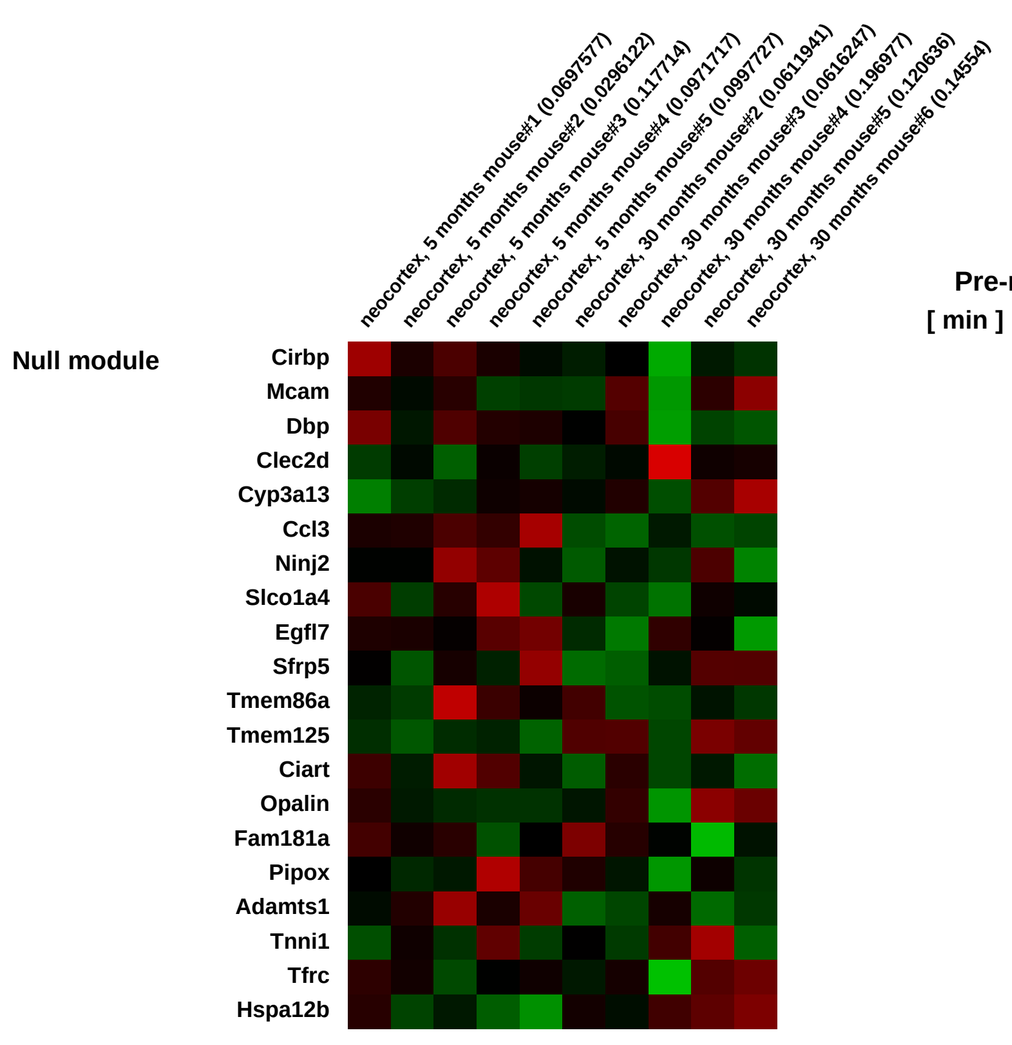

GEO Series "GSE13129" Expression Profiles

Num of samples in this series: 12

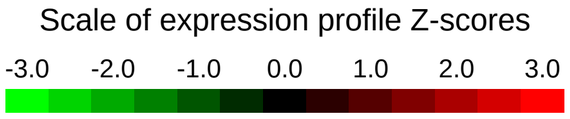

GEO Link:	**http://www.ncbi.nlm.nih.gov/geo/query/acc.cgi?acc=GSE13129**
Status:	**Public on Oct 15 2008**
Title:	**Analysis of genes regulated by FoxD3 in B16-F10 mouse melanoma cells**
Organism:	**Mus musculus**
Experiment type:	**Expression profiling by array**
Platform:	**GPL1261**
Pubmed ID:	
Summary & Design:	**Summary:** **We wished to examine the genes regulated by FoxD3 in pigment cells to gain understanding in how FoxD3 represses melanoblast specification in the neural crest. For technical reasons, we could not use neural crest cells, so we used melanoma cells, since they are derived from neural crest cells. To this end, we transfected B16-F10 mouse melanoma cells with constructs expressing FoxD3, or FoxD3-VP16, in which the C-terminal portion of FoxD3 (which contains the transcriptional repression domain) has been replaced by the VP16 transcriptional activation domain.** **Overall design:** **24 hours after transfection, EGFP-positive cells were collected by FACS and those cells were subjected to microarray analysis.**

Background corr dist: **KL-Divergence = 0.0752, L1-Distance = 0.0365, L2-Distance = 0.0027, Normal std = 0.4935**

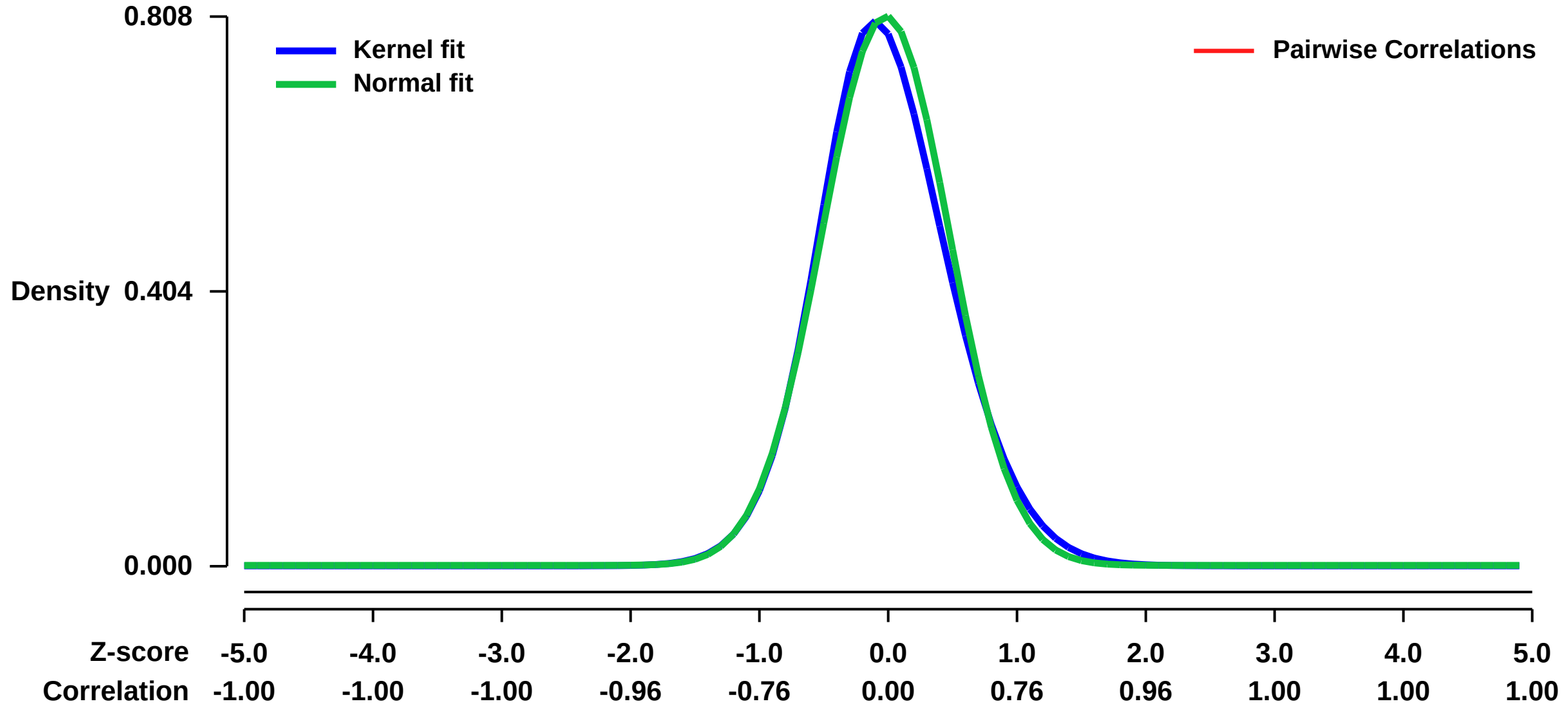

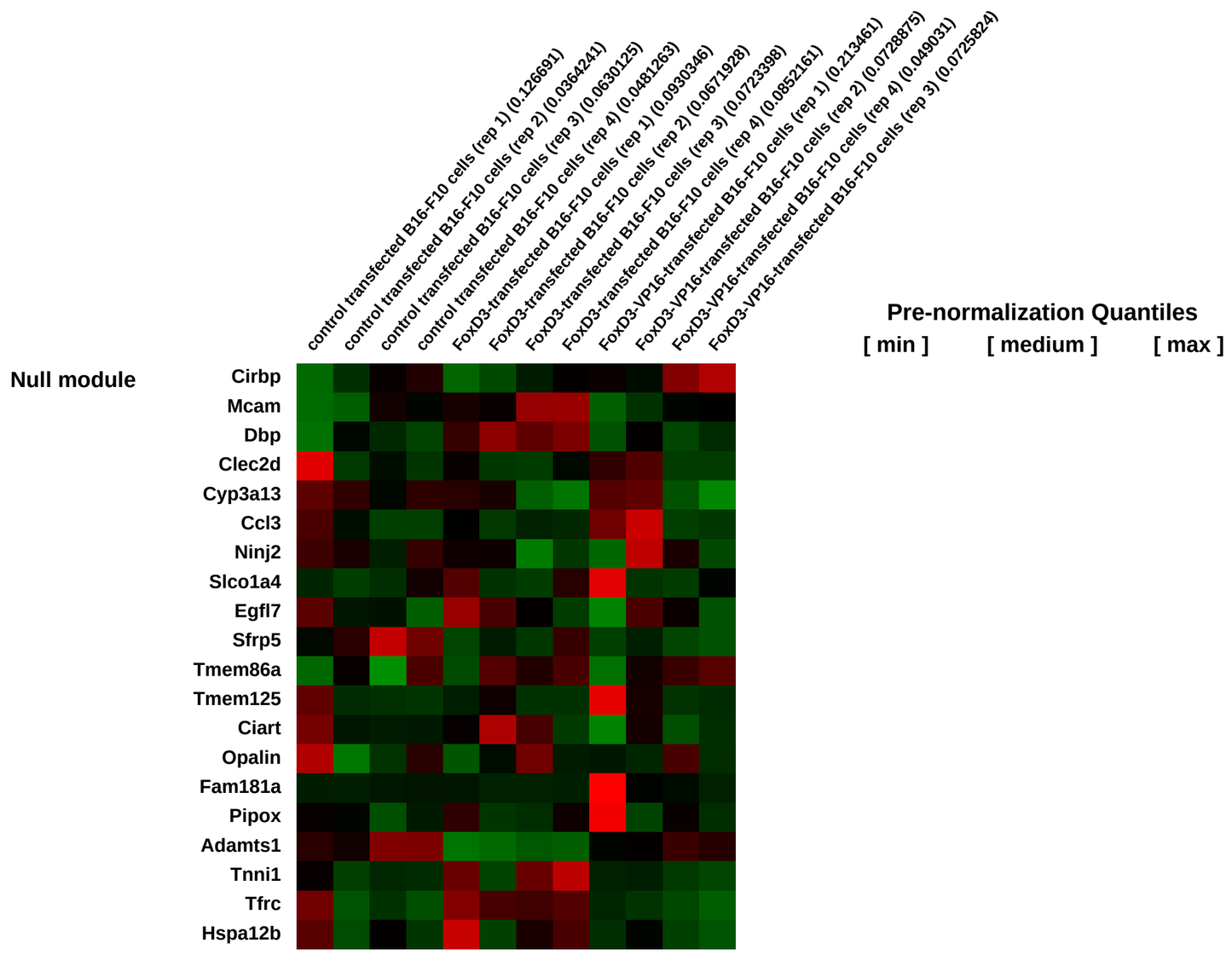

GEO Series "GSE13148" Expression Profiles

Num of samples in this series: 10

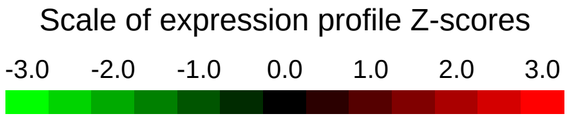

GEO Link:	**http://www.ncbi.nlm.nih.gov/geo/query/acc.cgi?acc=GSE13148**
Status:	**Public on Oct 09 2009**
Title:	**Effect of age on the arthritis susceptibility of BALB/c mice**
Organism:	**Mus musculus**
Experiment type:	**Expression profiling by array**
Platform:	**GPL1261**
Pubmed ID:	**19519881**
Summary & Design:	**Summary:** **Rheumatoid arthritis (RA) usually begins in females in their 4th-5th decade, suggesting that the aging of the immune system (immunosenescence) has a major impact on this disease.** **In the present microarray study, we set out to identify age- and arthritis-related gene expression pattern changes in proteoglycan (aggrecan)-induced arthritis (PGIA) model.** **Keywords: disease state analysis** **Overall design:** **We compared the gene expression profile of spleens from PG-immunized but non-arthritic old (older than 4 months) and young (1 month old) mice, and then made a comparison between non-arthritic and age-matched arthritic mice.**

Background corr dist: **KL-Divergence = 0.0719, L1-Distance = 0.0265, L2-Distance = 0.0011, Normal std = 0.4902**

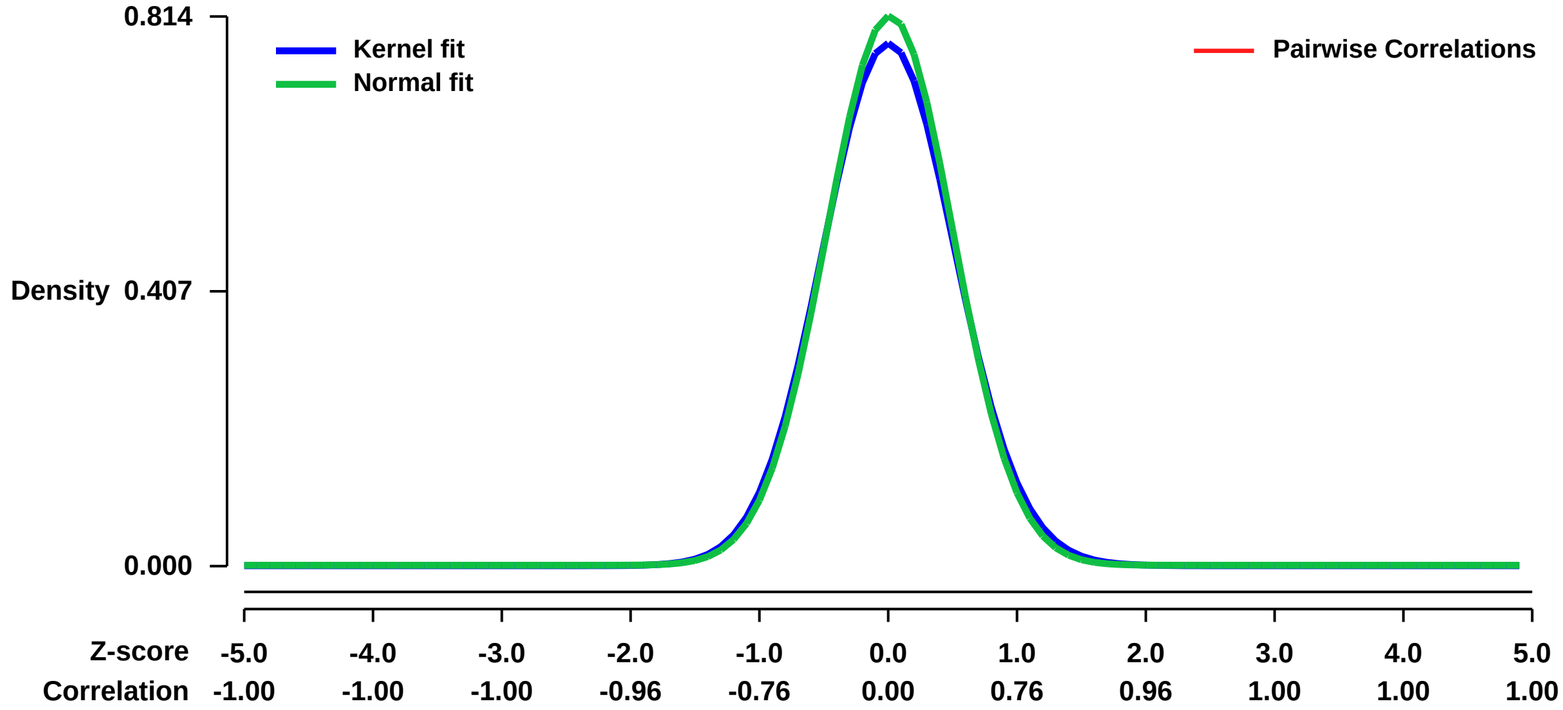

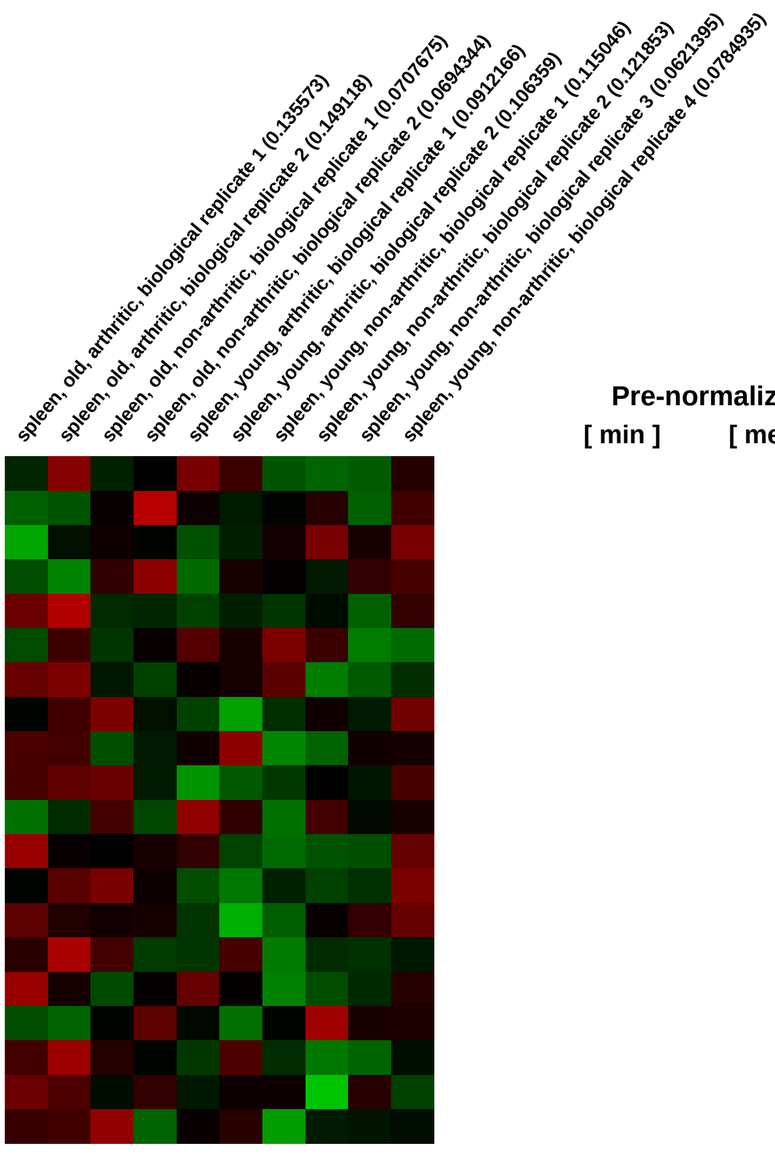

GEO Series "GSE13149" Expression Profiles

Num of samples in this series: 25

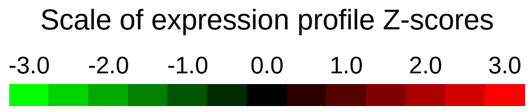

GEO Link:	http://www.ncbi.nlm.nih.gov/geo/query/acc.cgi?acc=GSE13149
Status:	Public on Oct 30 2008
Title:	Multi-stage analysis of gene expression in C57/B6 mouse liver development
Organism:	Mus musculus
Experiment type:	Expression profiling by array
Platform:	GPL1261
Pubmed ID:	19015022
Summary & Design:	**Summary:** The liver performs a number of essential functions for life. The development of such a complex organ relies on finely regulated gene expression profiles which change over time in the development and determine the phenotype and function of the liver. We used high-density oligonucleotide microarrays to study the gene expression and transcription regulation at 14 time points across the C57/B6 mouse liver development, which include E11.5 (embryonic day 11.5), E12.5, E13.5, E14.5, E15.5, E16.5, E17.5, E18.5, Day0 (the day of birth), Day3, Day7, Day14, Day21, and normal adult liver. With these data, we made a comprehensive analysis on gene expression patterns, functional preferences and transcriptional regulations during the liver development. **Keywords: time course** **Overall design:** Totally 25 microarrays have been used in this experiment, and 11 of the 14 time points have two technique repeat experiments.

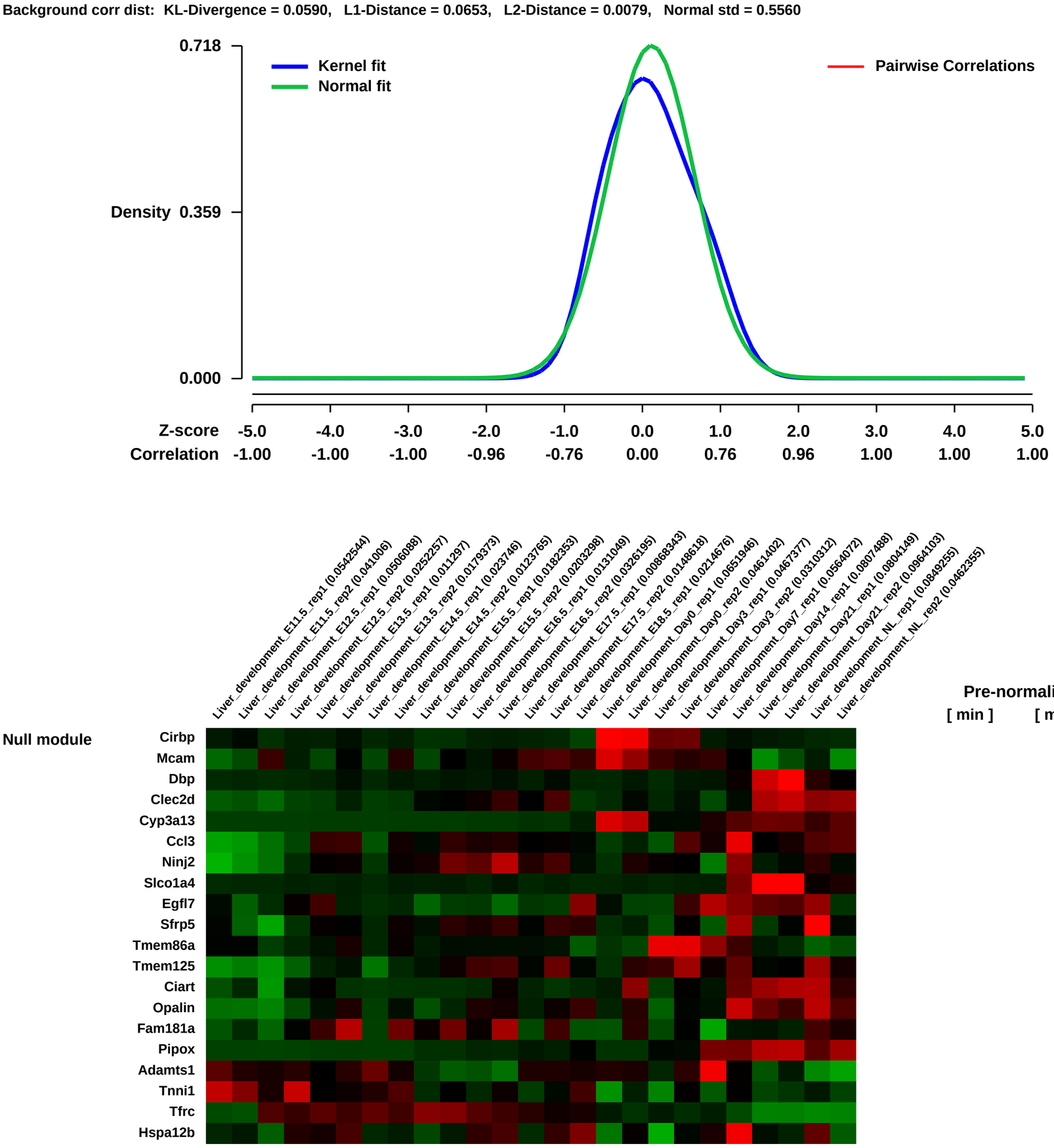

GEO Series "GSE13223" Expression Profiles

Num of samples in this series: 6

Scale of expression profile Z-scores

-3.0 -2.0 -1.0 0.0 1.0 2.0 3.0

GEO Link:	http://www.ncbi.nlm.nih.gov/geo/query/acc.cgi?acc=GSE13223
Status:	Public on Nov 30 2008
Title:	(AKR/J x FVB/NJ)F1 versus (DBA/2J x FVB)F1 bone marrow expression data
Organism:	Mus musculus
Experiment type:	Expression profiling by array
Platform:	GPL1261
Pubmed ID:	19118016
Summary & Design:	**Summary:** F1 hybrids from (AKR/J x FVB/NJ) and (DBA/2J x FVB/NJ) outcrosses display a 20-fold difference in mammary tumor metastatic capacity, due to differences in inherited polymorphisms. Expression studies were performed to determine whether polymorphism-driven gene expression signatures predictive of outcome could be generated from normal tissues **Keywords: Basal transcription profiles** **Overall design:** Bone Marrow from adult F1 animals from (AKR/J x FVB/NJ) and (DBA/2J x FVB/NJ) outcrosses was collected and arrayed on Affymetrics chip to identify basal differences in gene expression between the different genotypes

Background corr dist: KL-Divergence = 0.0268, L1-Distance = 0.0196, L2-Distance = 0.0004, Normal std = 0.6966

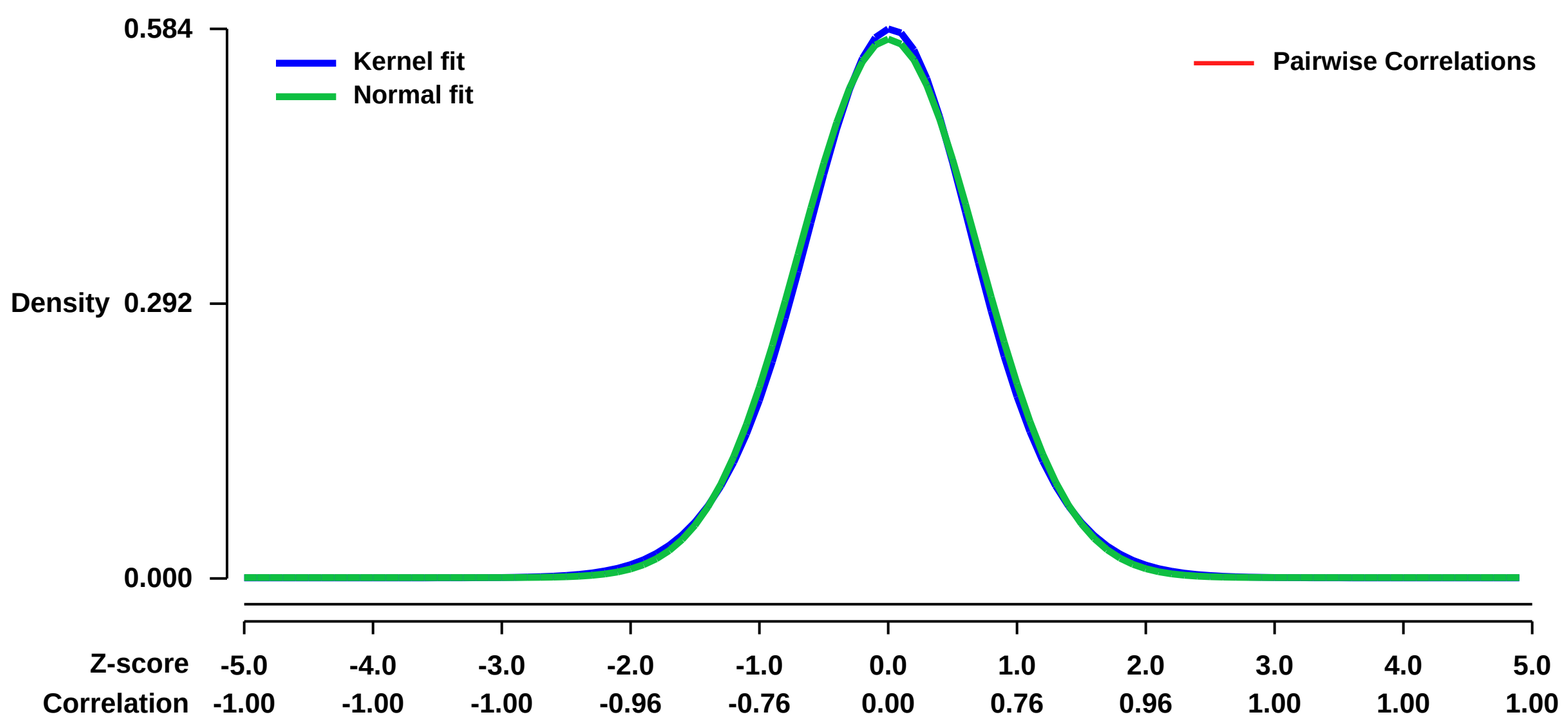

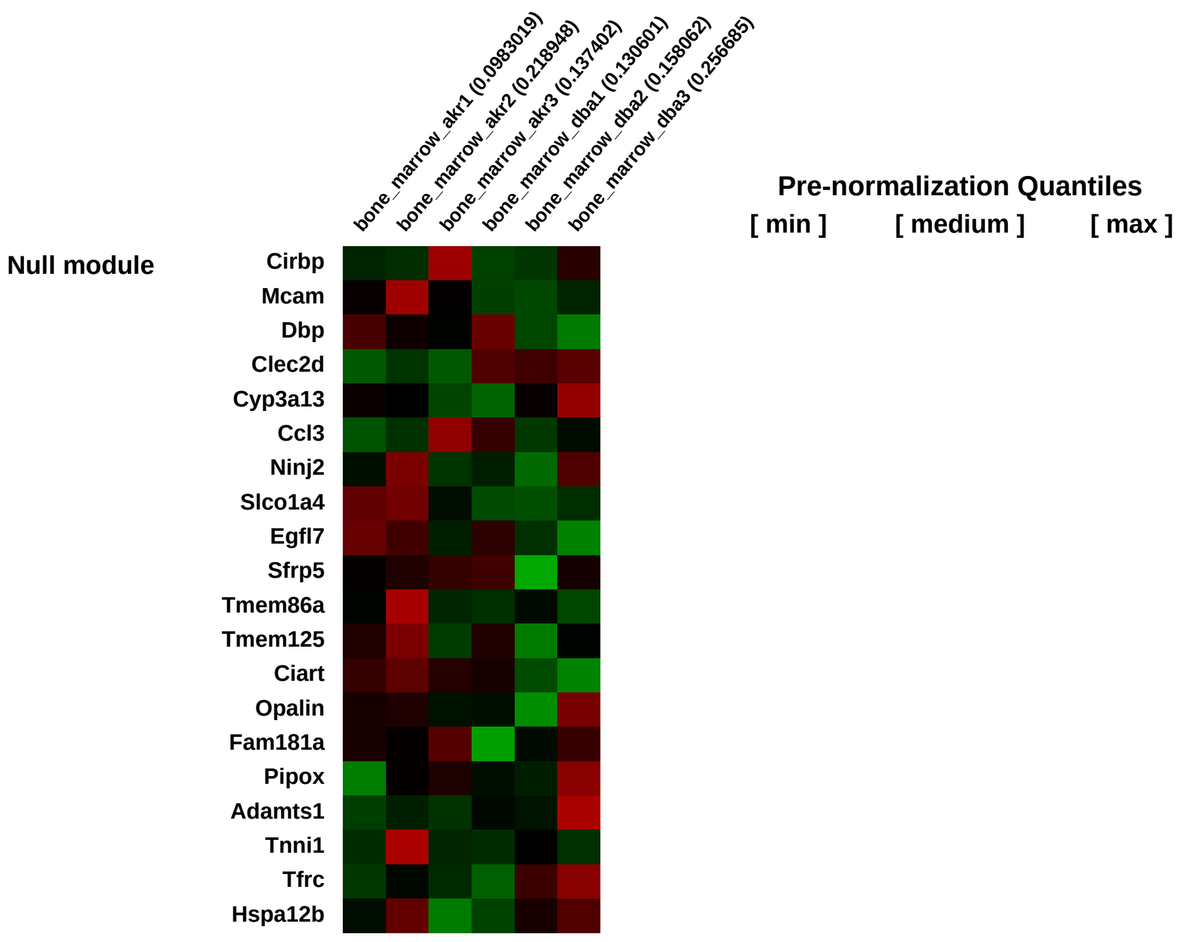

GEO Series "GSE13224" Expression Profiles

Num of samples in this series: 6

Scale of expression profile Z-scores

-3.0 -2.0 -1.0 0.0 1.0 2.0 3.0

GEO Link:	http://www.ncbi.nlm.nih.gov/geo/query/acc.cgi?acc=GSE13224
Status:	Public on Nov 30 2008
Title:	(AKR/J x FVB/NJ)F1 versus (DBA/2J x FVB)F1 lung expression data
Organism:	Mus musculus
Experiment type:	Expression profiling by array
Platform:	GPL1261
Pubmed ID:	19118016
Summary & Design:	**Summary:** F1 hybrids from (AKR/J x FVB/NJ) and (DBA/2J x FVB/NJ) outcrosses display a 20-fold difference in mammary tumor metastatic capacity, due to differences in inherited polymorphisms. Expression studies were performed to determine whether polymorphism-driven gene expression signatures predictive of outcome could be generated from normal tissues **Keywords: Basal transcription profiles** **Overall design:** Lung from adult F1 animals from (AKR/J x FVB/NJ) and (DBA/2J x FVB/NJ) outcrosses was collected and arrayed on Affymetrics chip to identify basal differences in gene expression between the different genotypes

Background corr dist: KL-Divergence = 0.0425, L1-Distance = 0.0175, L2-Distance = 0.0003, Normal std = 0.6020

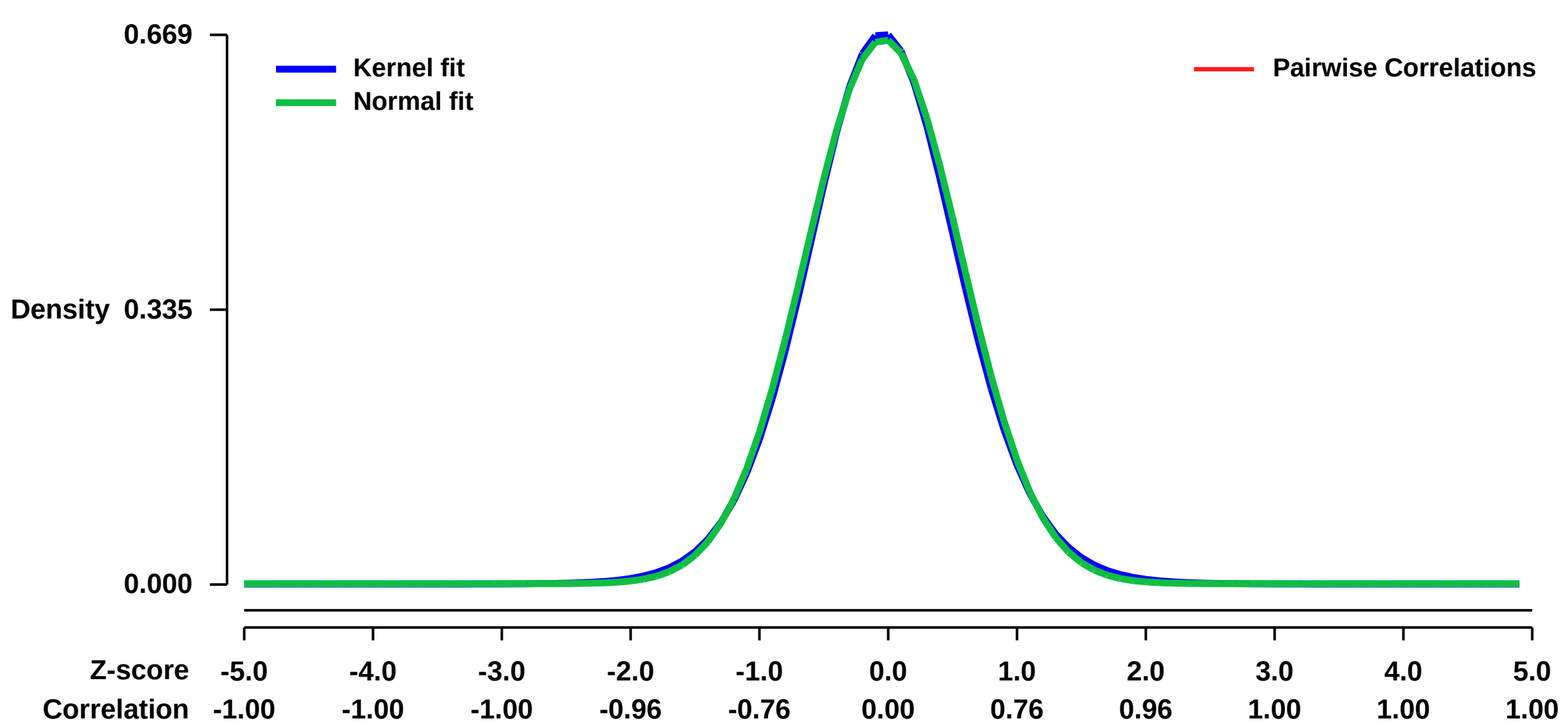

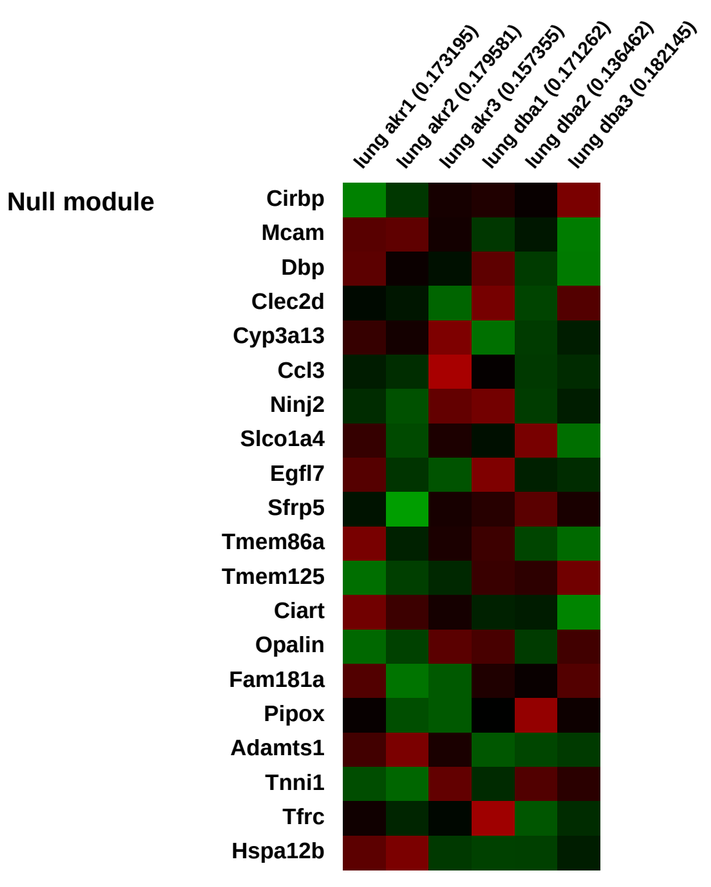

GEO Series "GSE13225" Expression Profiles

Num of samples in this series: 6

Scale of expression profile Z-scores

-3.0 -2.0 -1.0 0.0 1.0 2.0 3.0

GEO Link:	http://www.ncbi.nlm.nih.gov/geo/query/acc.cgi?acc=GSE13225
Status:	Public on Nov 30 2008
Title:	(AKR/J x FVB/NJ)F1 versus (DBA/2J x FVB)F1 spleen expression data
Organism:	Mus musculus
Experiment type:	Expression profiling by array
Platform:	GPL1261
Pubmed ID:	19118016
Summary & Design:	**Summary:** F1 hybrids from (AKR/J x FVB/NJ) and (DBA/2J x FVB/NJ) outcrosses display a 20-fold difference in mammary tumor metastatic capacity, due to differences in inherited polymorphisms. Expression studies were performed to determine whether polymorphism-driven gene expression signatures predictive of outcome could be generated from normal tissues **Keywords: Basal transcription profiles** **Overall design:** Spleen from adult F1 animals from (AKR/J x FVB/NJ) and (DBA/2J x FVB/NJ) outcrosses was collected and arrayed on Affymetrics chip to identify basal differences in gene expression between the different genotypes

Background corr dist: KL-Divergence = 0.0222, L1-Distance = 0.0130, L2-Distance = 0.0002, Normal std = 0.7145

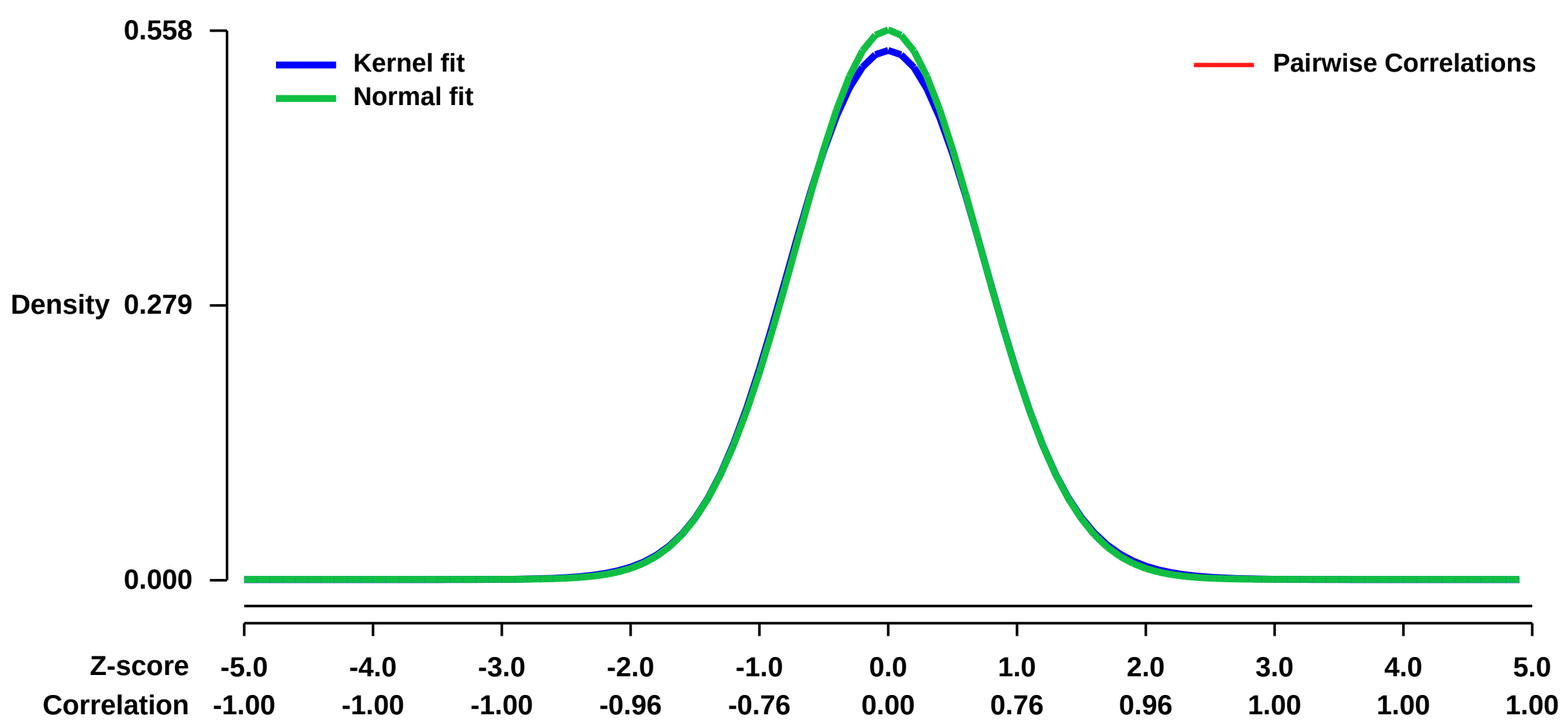

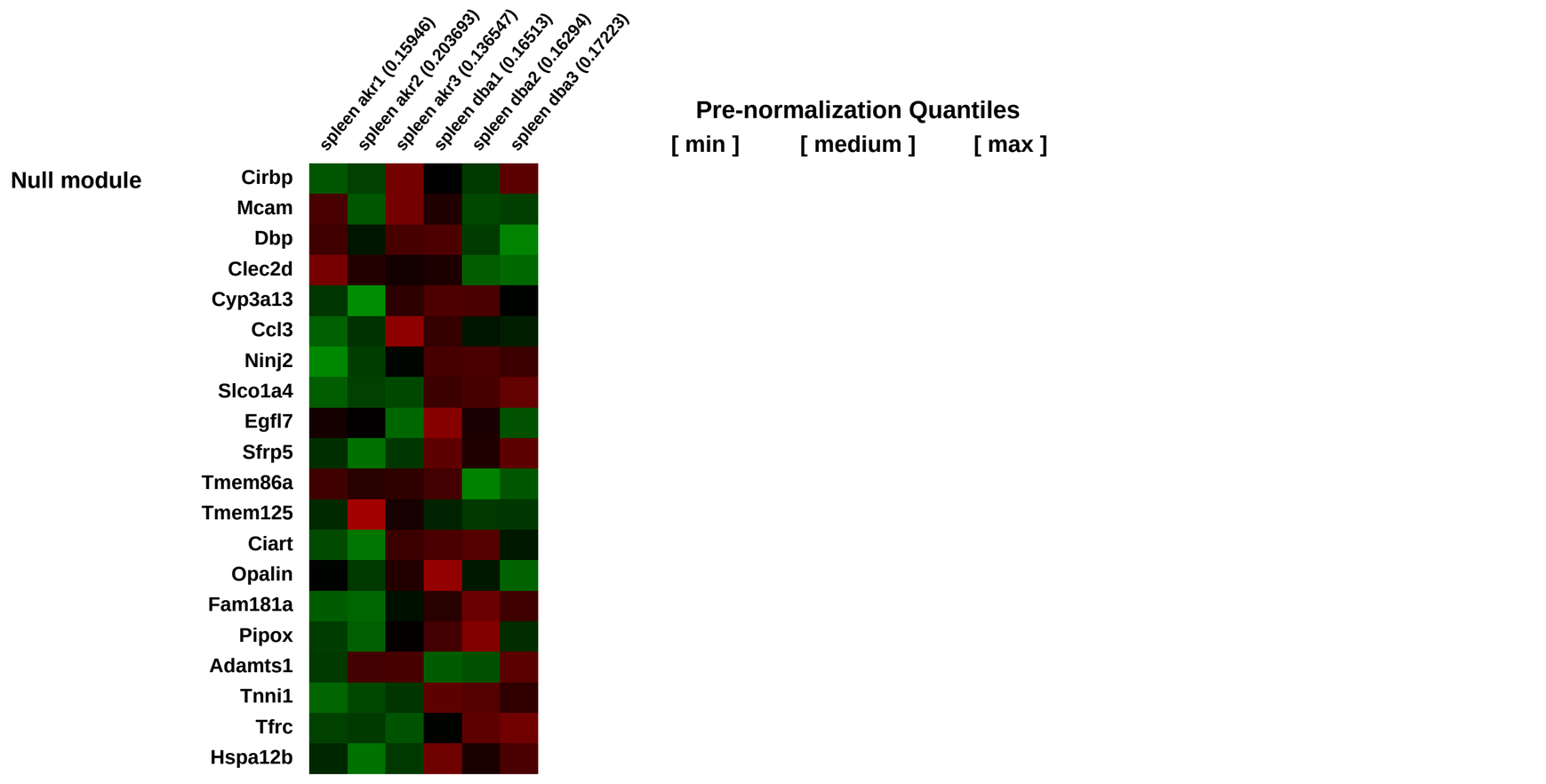

GEO Series "GSE13227" Expression Profiles

Num of samples in this series: 6

Scale of expression profile Z-scores

-3.0 -2.0 -1.0 0.0 1.0 2.0 3.0

GEO Link:	http://www.ncbi.nlm.nih.gov/geo/query/acc.cgi?acc=GSE13227
Status:	Public on Nov 30 2008
Title:	(AKR/J x FVB/NJ)F1 versus (DBA/2J x FVB)F1 Thymus expression data
Organism:	Mus musculus
Experiment type:	Expression profiling by array
Platform:	GPL1261
Pubmed ID:	19118016
Summary & Design:	**Summary:** F1 hybrids from (AKR/J x FVB/NJ) and (DBA/2J x FVB/NJ) outcrosses display a 20-fold difference in mammary tumor metastatic capacity, due to differences in inherited polymorphisms. Expression studies were performed to determine whether polymorphism-driven gene expression signatures predictive of outcome could be generated from normal tissues **Keywords: Basal transcription profiles** **Overall design:** Thymus from adult F1 animals from (AKR/J x FVB/NJ) and (DBA/2J x FVB/NJ) outcrosses was collected and arrayed on Affymetrics chip to identify basal differences in gene expression between the different genotypes

Background corr dist: KL-Divergence = 0.0229, L1-Distance = 0.0141, L2-Distance = 0.0002, Normal std = 0.7131

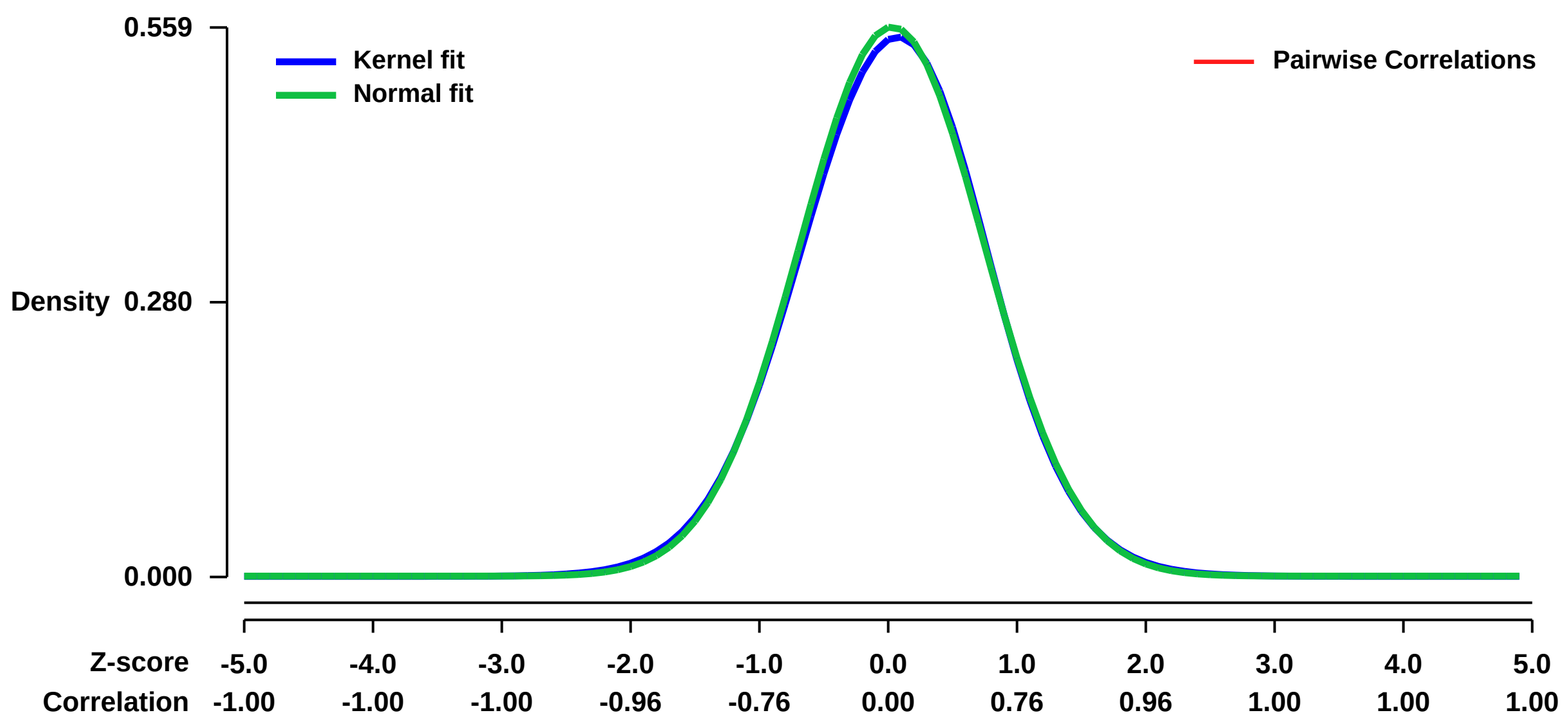

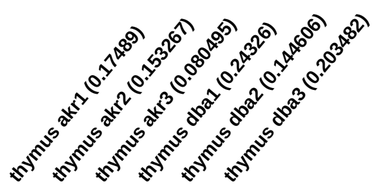

Pre-normalization Quantiles

[min] [medium] [max]

Null module

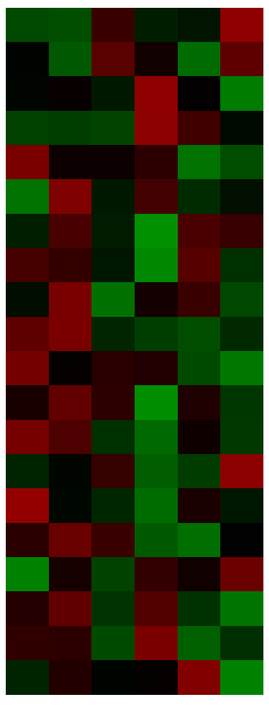

GEO Series "GSE13235" Expression Profiles

Num of samples in this series: 9

Scale of expression profile Z-scores

-3.0 -2.0 -1.0 0.0 1.0 2.0 3.0

GEO Link:	**http://www.ncbi.nlm.nih.gov/geo/query/acc.cgi?acc=GSE13235**
Status:	**Public on Oct 17 2008**
Title:	**Gene expression profile of mouse embryonic stem cells (D3-pOCT-mESC) grown in low concentrations of nitric oxide**
Organism:	**Mus musculus**
Experiment type:	**Expression profiling by array**
Platform:	**GPL1261**
Pubmed ID:	
Summary & Design:	**Summary:** **In order to identify the genes regulated in mouse embryonic stem cells (mESC) by the effect of low concentrations of nitric oxide (NO), we analysed the transcriptome of cells treated with NO and compared it to those of cells cultured in the absence of leukemia inhibitory factor (LIF), and in the presence of LIF. We used the cell line D3-pOct4, which carries the enhanced Green Fluorescence Protein gene (eGFP) under the control of the Oct-4 promotor. This line is continuously maintained in the undifferentiated state in the presence of LIF, in comparison with the wild type line .** **Overall design:** **D3-pOct4 cells cultured in the presence of 1000 U/ml of LIF, in the absence of LIF, and in the absence of LIF supplemented with 2uM of diethylenetriamine nitric oxide adduct (DETA)/NO (Sigma) used as donor of nitric oxide. Treatments were maintained for seven days. RNA was extracted and analyzed by Bioanalyzer of Agilent. The cDNA microarray chip used was Mouse Genome 430_2.0 (Affymetrix) and the data were analyzed with GeneChip Operating System v1.4.0.036 using global scaling as the normalization method.**

Background corr dist: **KL-Divergence = 0.0684, L1-Distance = 0.0302, L2-Distance = 0.0016, Normal std = 0.5120**

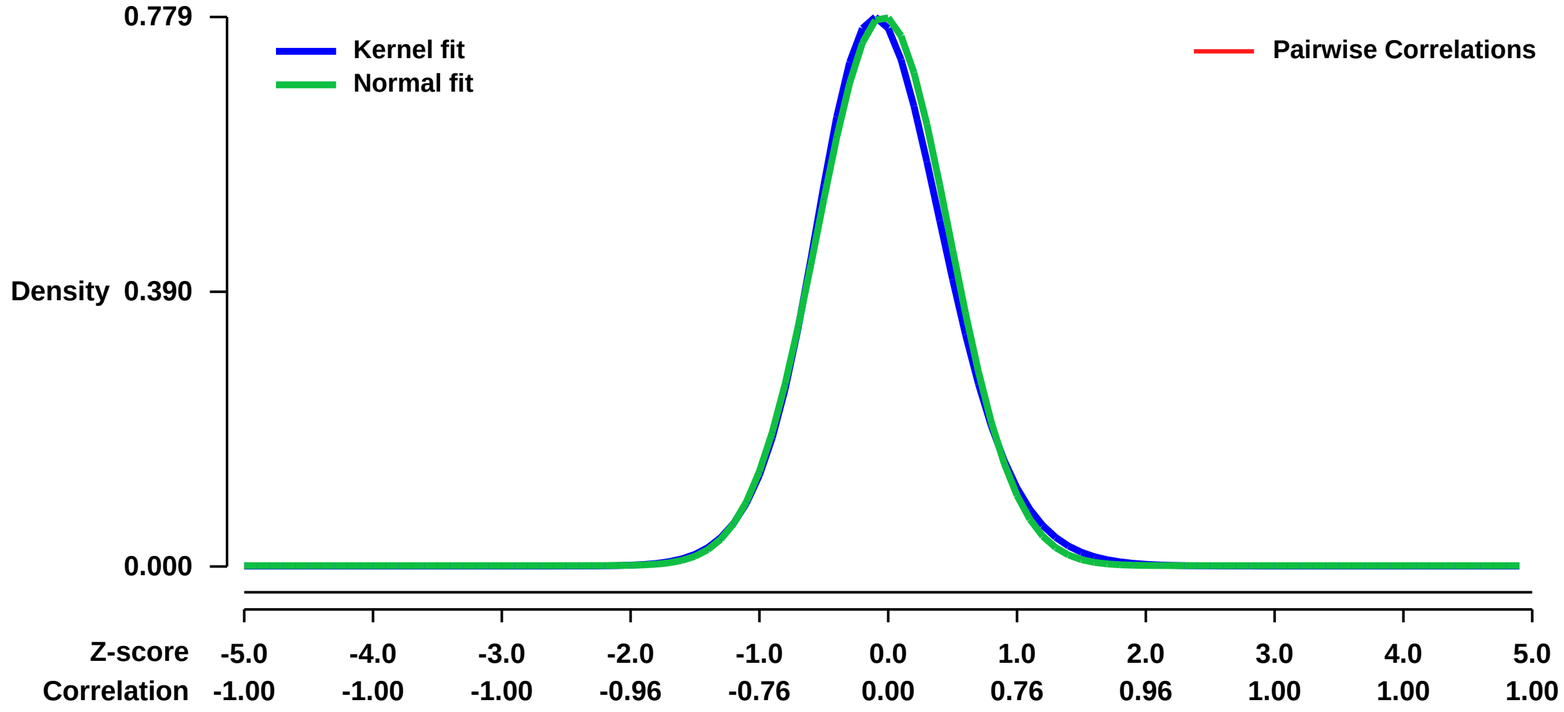

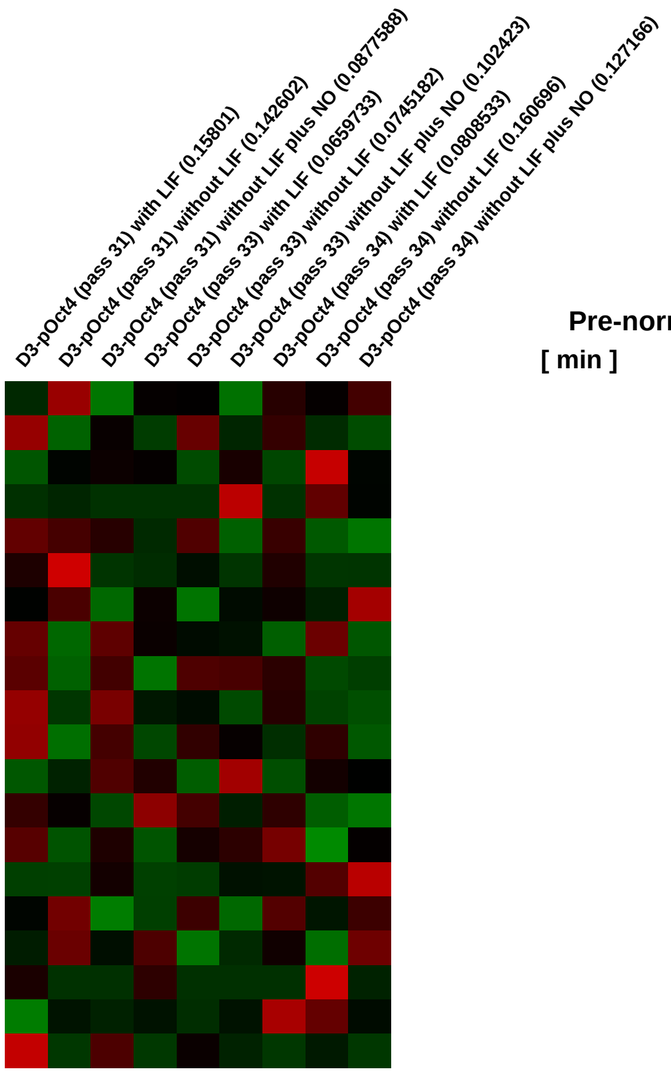

GEO Series "GSE13333" Expression Profiles

Num of samples in this series: 6

Scale of expression profile Z-scores

-3.0 -2.0 -1.0 0.0 1.0 2.0 3.0

GEO Link:	http://www.ncbi.nlm.nih.gov/geo/query/acc.cgi?acc=GSE13333
Status:	Public on Mar 01 2009
Title:	Srf conditional knockout in the mouse liver
Organism:	Mus musculus
Experiment type:	Expression profiling by array
Platform:	GPL1261
Pubmed ID:	19205030
Summary & Design:	**Summary:** Serum response factor (SRF) is a transcription factor that binds to the serum response element (SRE) of genes that are expressed in response to mitogens. SRF plays essential roles in muscle and nervous system development; however, little is known about the role of SRF during liver growth and function. To examine the function of SRF in the liver, we generated mice in which the Srf gene was specifically disrupted in hepatocytes. The survival of mice lacking hepatic SRF activity was lower than that of control mice; moreover, surviving mutant mice were smaller and had lower blood glucose and triglyceride levels compared with control mice. Srf-deficient livers were also smaller than control livers, hepatocyte morphology was abnormal, and liver-cell proliferation and viability was compromised. Gene array and quantitative RT-PCR analysis of SRF depleted livers revealed a reduction in mRNAs encoding components of the growth hormone/IGF1 pathway, cyclins, several metabolic regulators, and cytochrome p450 enzymes. Conclusion: SRF is essential for hepatocyte proliferation and survival, liver function, and control of postnatal body growth by regulating hepatocyte gene expression. **Overall design:**

Background corr dist: KL-Divergence = 0.0330, L1-Distance = 0.0376, L2-Distance = 0.0020, Normal std = 0.6811

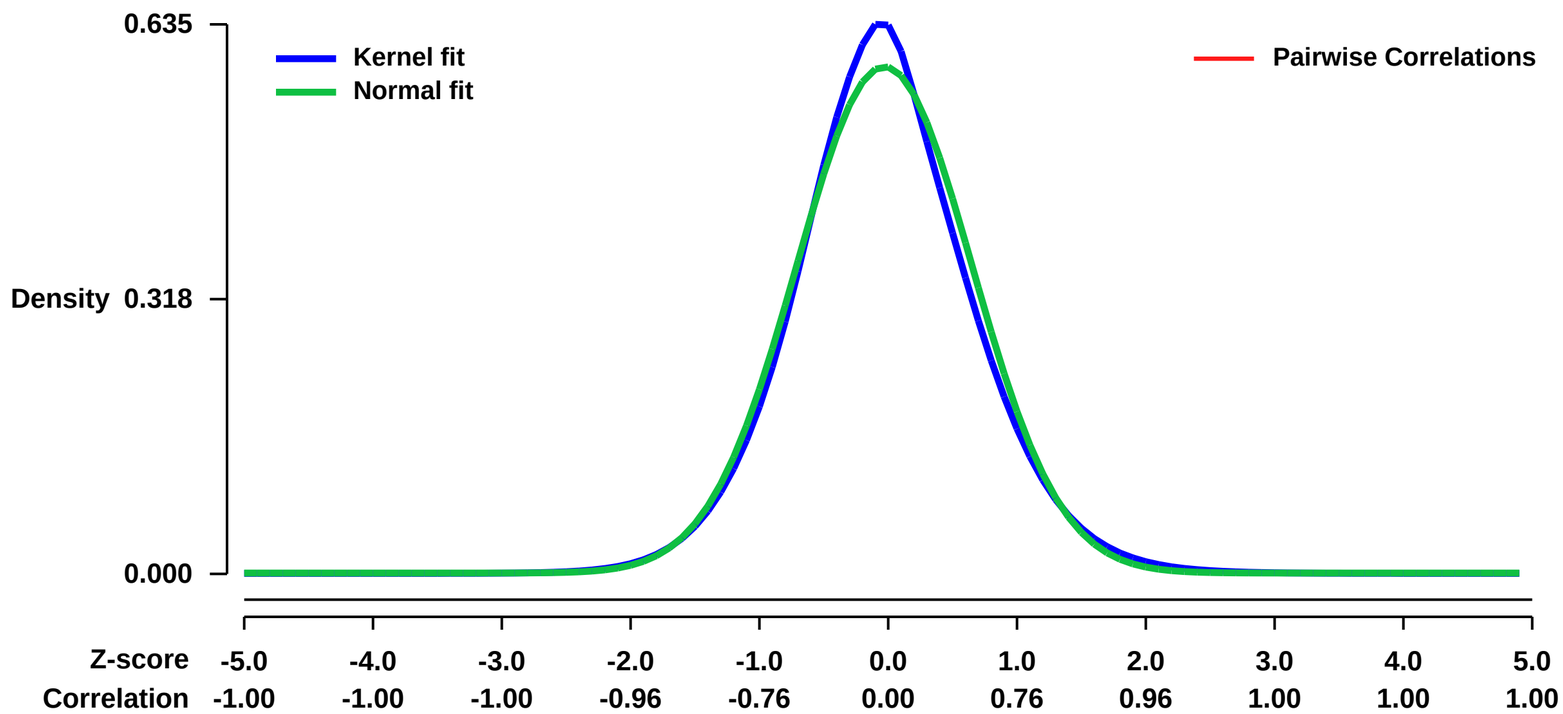

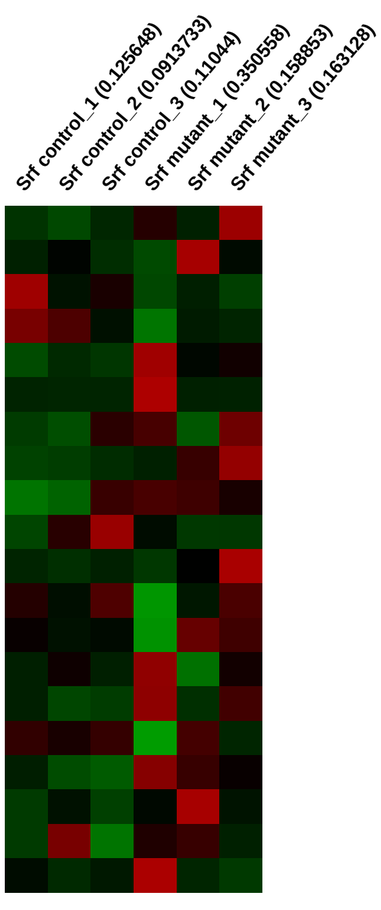

GEO Series "GSE13386" Expression Profiles

Num of samples in this series: 24

Scale of expression profile Z-scores

-3.0 -2.0 -1.0 0.0 1.0 2.0 3.0

GEO Link:	http://www.ncbi.nlm.nih.gov/geo/query/acc.cgi?acc=GSE13386
Status:	Public on Nov 14 2008
Title:	Comparative analysis of Drd1+ Medium Spiny Neurons, Drd2+ Medium Spiny Neurons, cocaine treatment
Organism:	Mus musculus
Experiment type:	Expression profiling by array
Platform:	GPL1261
Pubmed ID:	19013281
Summary & Design:	**Summary:** The cellular heterogeneity of the brain confounds efforts to elucidate the biological properties of distinct neuronal populations. Using Bacterial Artificial Chromosome (BAC) transgenic mice which express EGFP-tagged ribosomal protein L10a in defined cell populations, we have developed a methodology to affinity purify polysomal mRNAs from genetically defined cell populations in the brain. The utility of this approach is illustrated by the comparative analysis of four types of neurons, revealing hundreds of genes that distinguish these four cell populations. We find that even two morphologically indistinguishable, intermixed subclasses of medium spiny neuron display vastly different translational profiles and present examples of the physiological significance of such differences. This genetically targeted Translating Ribosome Affinity Purification (TRAP) methodology is a generalizable method useful for the identification of molecular changes in any genetically defined cell type in response to genetic alterations, disease, or pharmacological perturbations. **Keywords:** Cell Type Comparison **Overall design:** We recommend that only genes where more than one sample has a normalized intensity larger than 16 (4 in log2 scale) should be kept in the analysis.

Background corr dist: KL-Divergence = 0.1843, L1-Distance = 0.0598, L2-Distance = 0.0087, Normal std = 0.3672

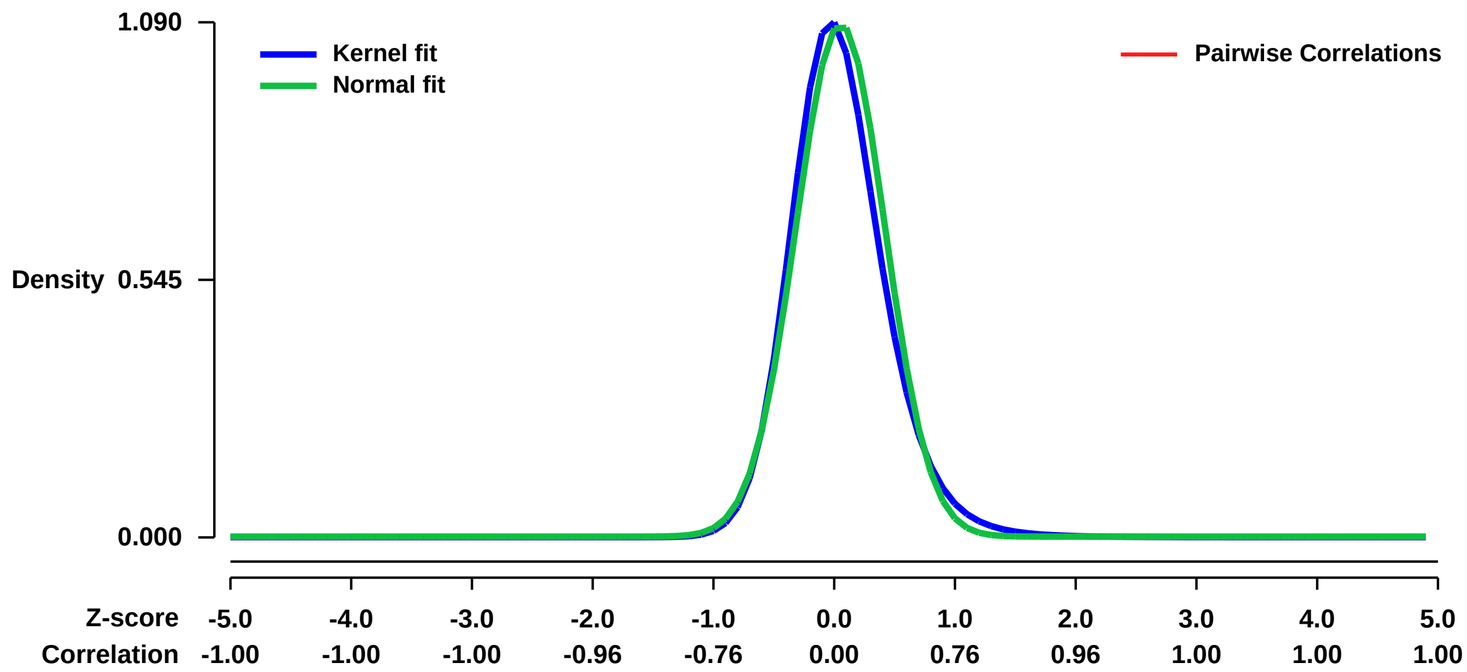

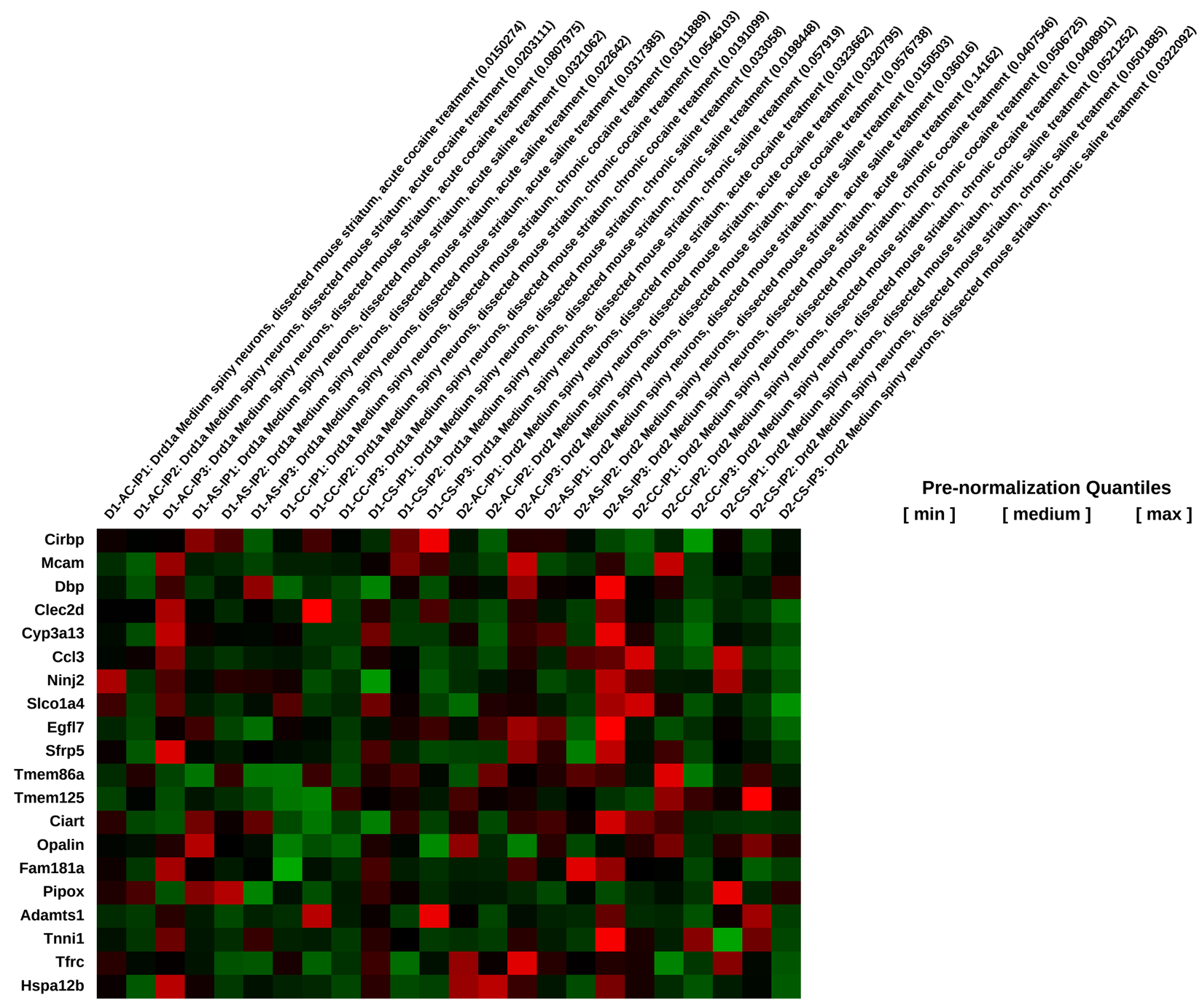

GEO Series "GSE13402" Expression Profiles

Num of samples in this series: 7

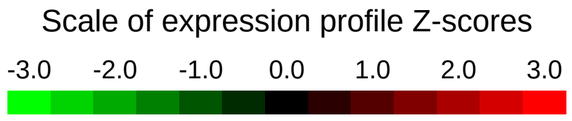

GEO Link:	http://www.ncbi.nlm.nih.gov/geo/query/acc.cgi?acc=GSE13402
Status:	Public on May 01 2009
Title:	SPARC-null vs. wild-type lens epithelium
Organism:	Mus musculus
Experiment type:	Expression profiling by array
Platform:	GPL1261
Pubmed ID:	19401199
Summary & Design:	**Summary:** SPARC is a matricellular glycoprotein involved in regulation of the extracellular matrix, growth factors, adhesion, and migration. SPARC-null mice have altered basement membranes and develop posterior sub-capsular cataracts with cell swelling and equatorial vacuoles. Exchange of fluid, nutrients, and waste products in the avascular lens is driven by a unique circulating ion current. Here we demonstrate that SPARC-null mouse lenses exhibit abnormal circulation of fluid, ion, and small molecules which leads to altered fluorescein distribution in vivo, loss of resting membrane polarization, and altered distribution of small molecules. Microarray analysis of SPARC-null lenses showed changes in gene expression of ion channels and receptors, matrix and adhesion genes, cytoskeleton, immune response genes, and cell signaling molecules. Our results demonstrate that the regulation of SPARC on cell-capsular matrix interactions can influence the circulation of fluid and ions in the lens, and the phenotype in the SPARC-null mouse lens is the result of multiple intersecting pathways. **Overall design:** Lens epithelial cells from 7 lenses of littermate mice were isolated by laser capture microdissection. 3 wild-type lenses from 3 different mice and 4 knock-out lenses from 3 different mice were used as biological replicates.

Background corr dist: KL-Divergence = 0.0641, L1-Distance = 0.0214, L2-Distance = 0.0007, Normal std = 0.5196

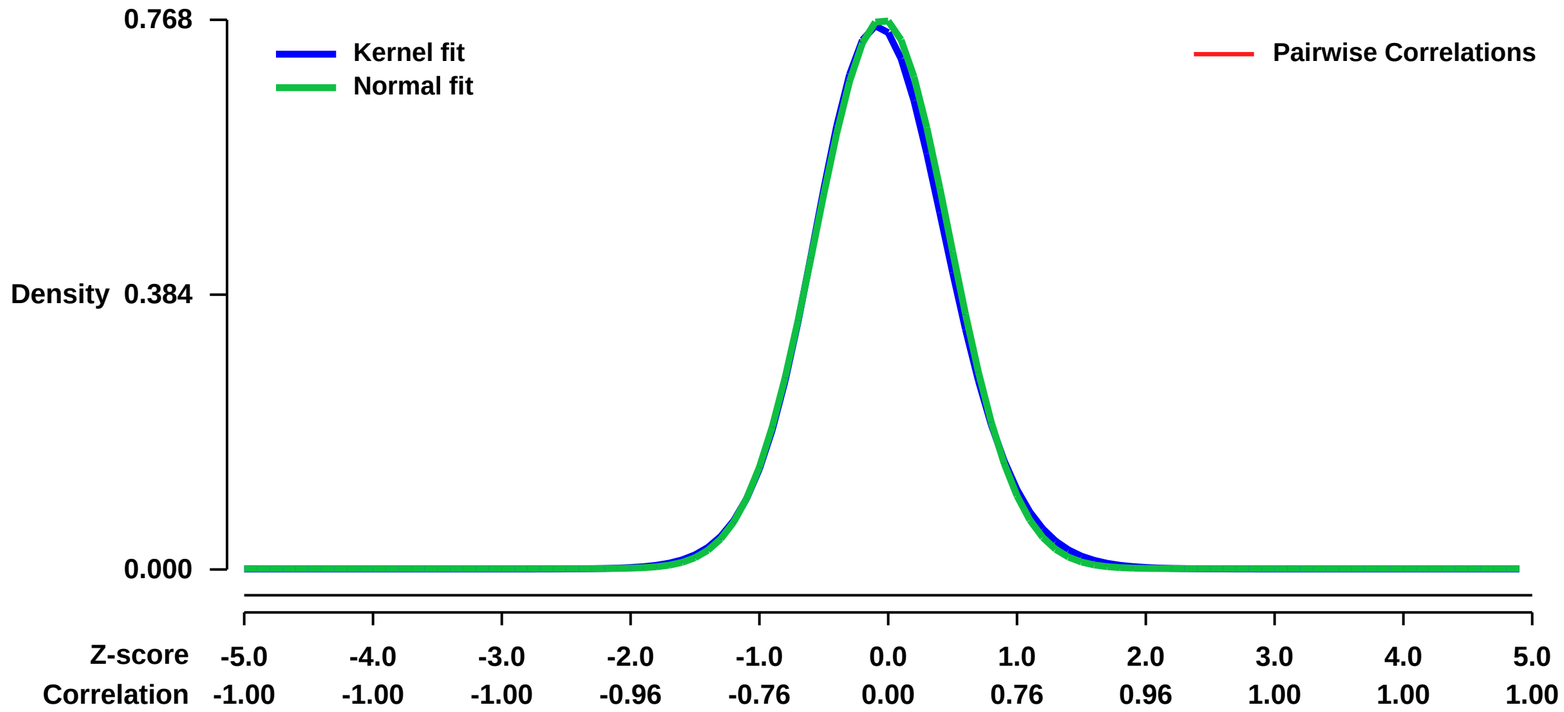

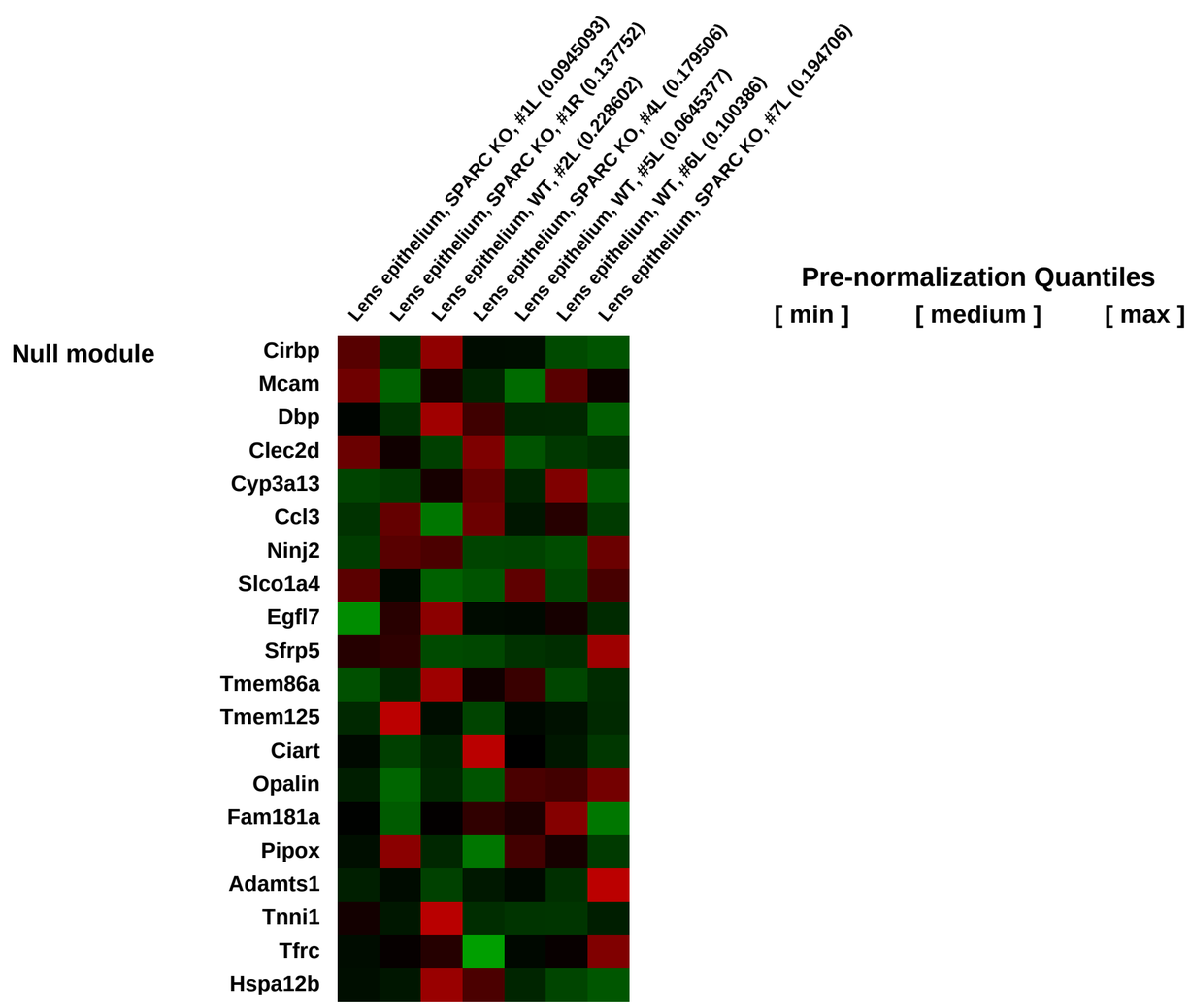

GEO Series "GSE13421" Expression Profiles

Num of samples in this series: 8

Scale of expression profile Z-scores

-3.0 -2.0 -1.0 0.0 1.0 2.0 3.0

GEO Link:	**http://www.ncbi.nlm.nih.gov/geo/query/acc.cgi?acc=GSE13421**
Status:	**Public on Nov 01 2008**
Title:	**CBA/CaJ mouse cochlea gene expression profile**
Organism:	**Mus musculus**
Experiment type:	**Expression profiling by array**
Platform:	**GPL1261**
Pubmed ID:	**19277783**
Summary & Design:	**Summary:** **This data set is intended as a public resource documenting the identity of roughly 10,000 genes that are abundantly expressed in the mouse cochlea. The data have many uses, including for making comparisons with proteomics studies, and for comparisons of expression profiles with other mouse strains and with other species. The CBA/CaJ strain was chosen because of its lack of known vulnerabilities to premature cochlear degeneration or to extreme reactions to cochlear stresses. It may therefore be considered a â normalâ mouse. No experimental manipulations were done on the mice of this study. Contamination of the results by genes expressed in the surrounding petrous bone and from those in blood cells was minimized.** **Keywords: normal controls** **Overall design:** **8 replicates, pooled ears from each of 8 mice**

Background corr dist: **KL-Divergence = 0.0701, L1-Distance = 0.0211, L2-Distance = 0.0007, Normal std = 0.5048**

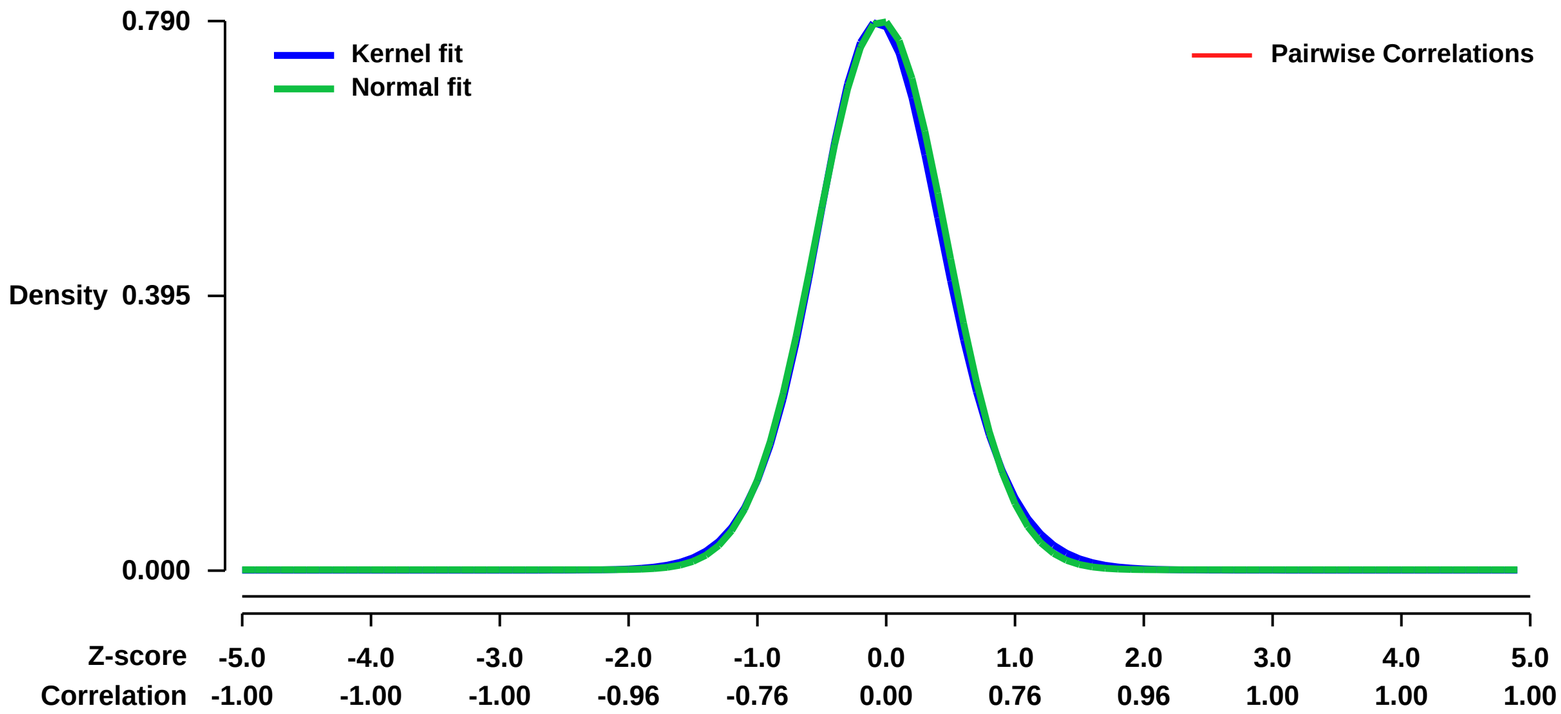

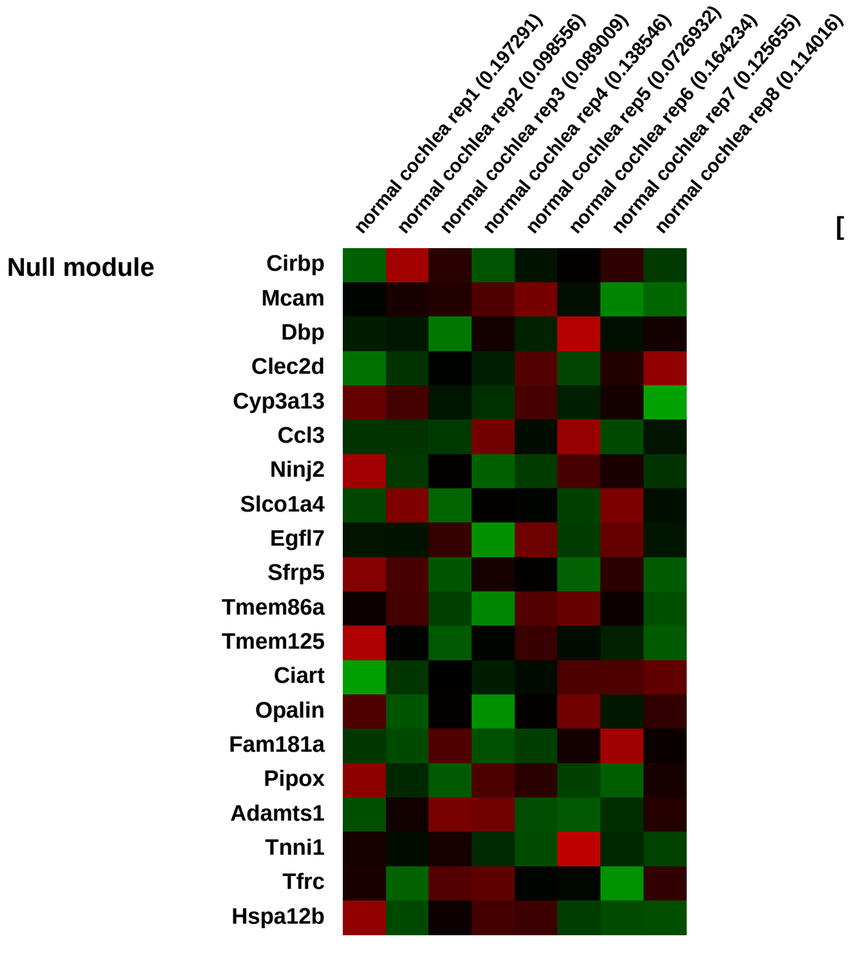

GEO Series "GSE13432" Expression Profiles

Num of samples in this series: 12

Scale of expression profile Z-scores

-3.0 -2.0 -1.0 0.0 1.0 2.0 3.0

GEO Link:	http://www.ncbi.nlm.nih.gov/geo/query/acc.cgi?acc=GSE13432
Status:	Public on Feb 01 2009
Title:	Adipose tissue exposed to cold
Organism:	Mus musculus
Experiment type:	Expression profiling by array
Platform:	GPL1261
Pubmed ID:	19117550
Summary & Design:	**Summary:** **Cold triggers VEGF dependent but hypoxia independent angiogenesis in adipose tissues and anti-VEGF agents modulate adipose metabolism** **The molecular mechanisms of angiogenesis in relation to adipose tissue metabolism remain poorly understood. Here we show that exposure of mice to cold led to conversion of white adipose tissue (WAT) to brown-like adipose tissue, accompanying the switch of an active angiogenic phenotype. Gene expression profile analysis showed VEGF was upregulated via most likely hypoxia-independent PGC-1 transcriptional activation. Intriguingly, VEGFR2 blockage abolished the cold-induced angiogenesis, significantly impaired nonshivering thermogenesis capacity, and markedly reduced adipose metabolism. Unexpectedly, VEGFR1 blockage resulted in opposite effects by increasing adipose vascularity and metabolism. These findings demonstrate that VEGFR2 and VEGFR1 mediate polarized activities in modulating adipose angiogenesis and metabolism. Taken together, our findings have conceptual implications in applying angiogenesis modulators for the treatment of obesity and metabolic disorders.** **Keywords: Time course** **Overall design:** **Mice were exposed to cold and white addipose tissue was collected at different time points**

Background corr dist: KL-Divergence = 0.0338, L1-Distance = 0.0273, L2-Distance = 0.0009, Normal std = 0.6614

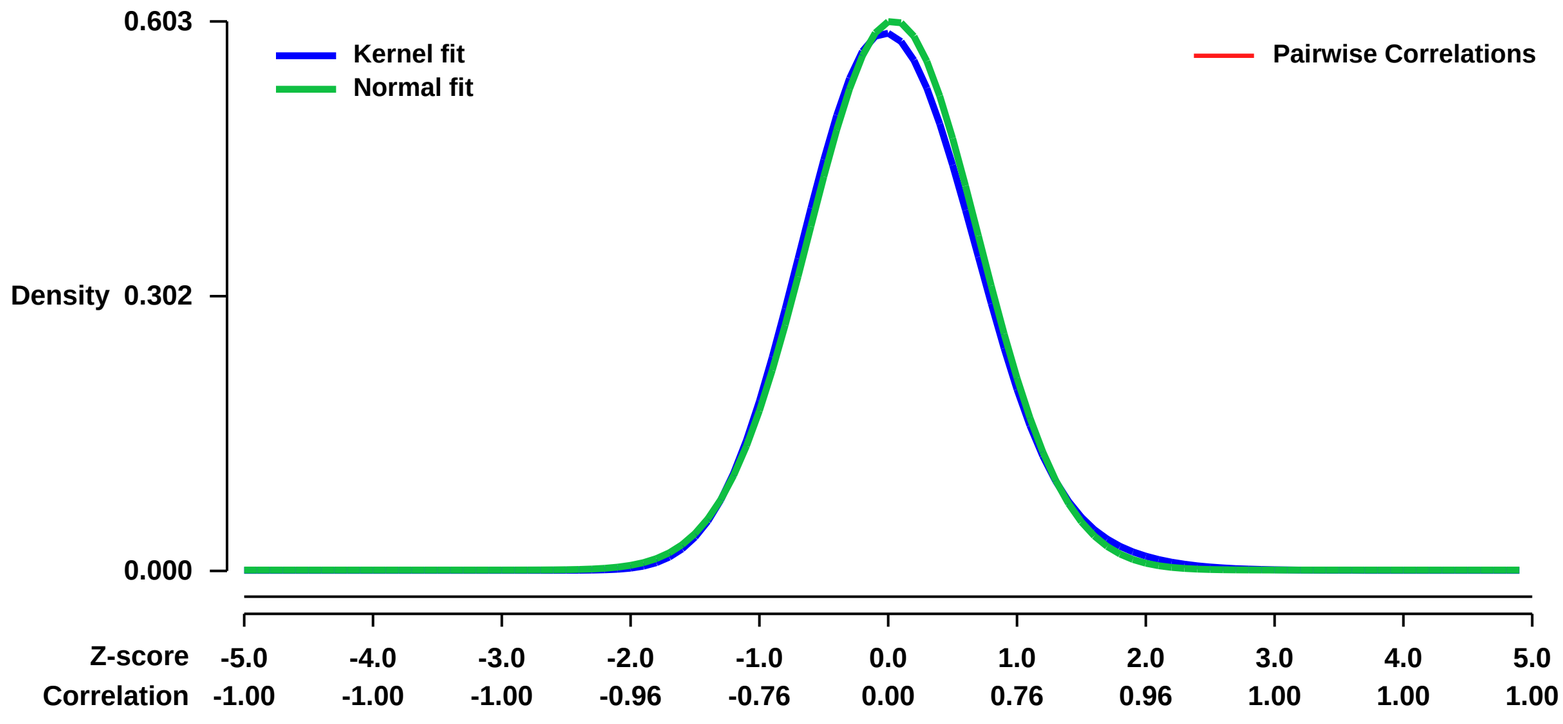

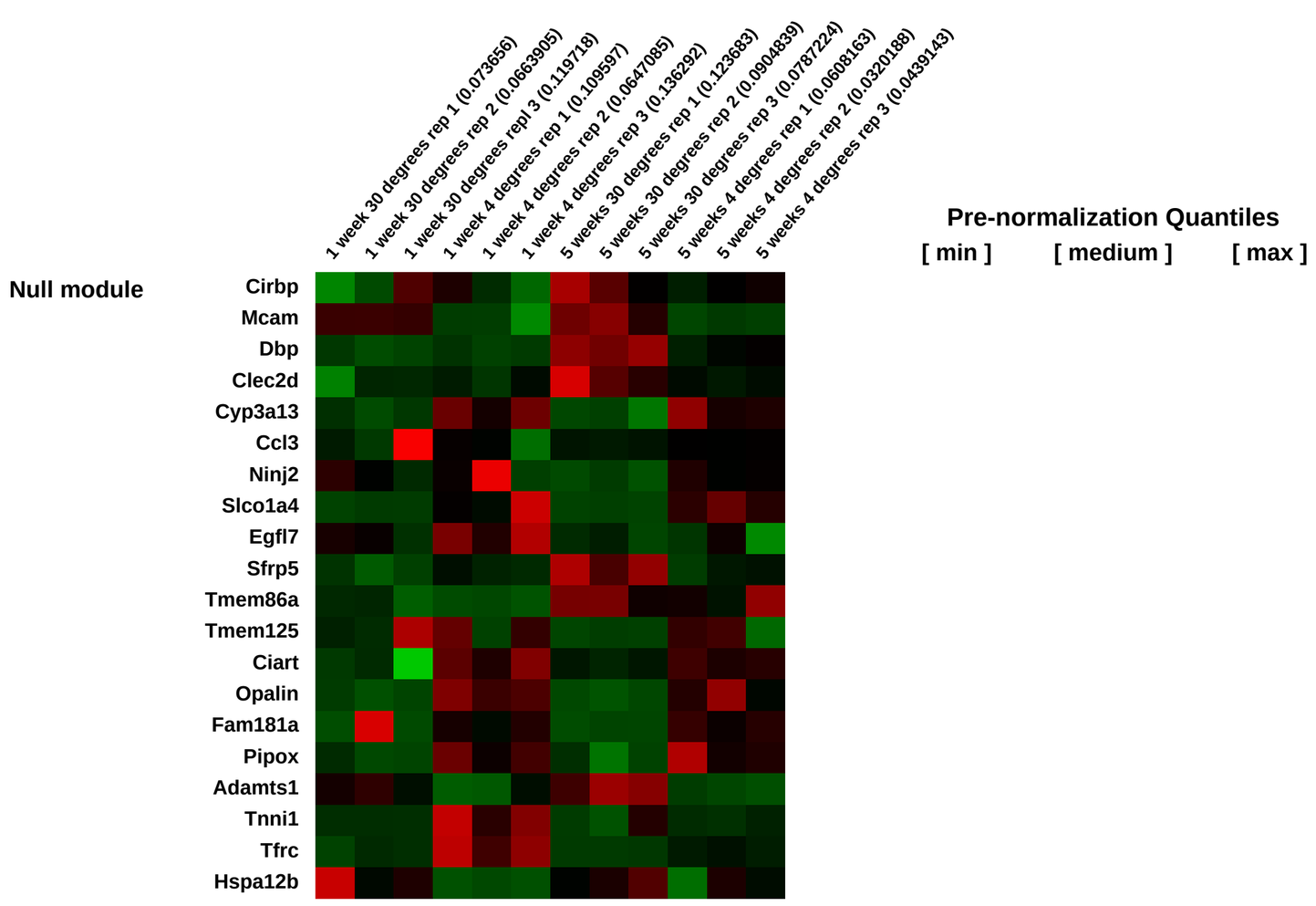

GEO Series "GSE13493" Expression Profiles

Num of samples in this series: 6

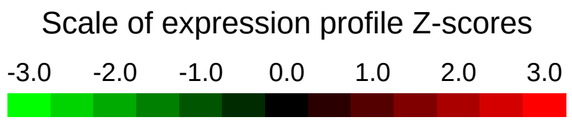

GEO Link:	http://www.ncbi.nlm.nih.gov/geo/query/acc.cgi?acc=GSE13493
Status:	Public on Mar 31 2009
Title:	Expression data from developing thymocytes of N15TCR transgenic Rag2 deficient mice
Organism:	Mus musculus
Experiment type:	Expression profiling by array
Platform:	GPL1261
Pubmed ID:	19027330
Summary & Design:	**Summary:** T cell development relies on the precise developmental control of various cellular functions for appropriate positive and negative selection. Previously, gene expression profiling of peptide-driven negative selection events in the N15 TCR class I MHC-restricted mouse and D011.10 TCR class II MHC-restricted mouse has offered insights into the coordinate engagement of biological processes affecting thymocyte development. However, there has been little comparable detailed in vivo global genome expression analysis reported for positive selection. We used microarrays to identify the genes differentially expressed during CD8 single positive T cell development in N15 TCR transgenic Rag2 deficient mice. **Overall design:** We have analyzed gene expression in the individual populations as development proceeds from DP, intermediate (Int), to SP subsets. To this end, we sorted the individual populations from six age and sex matched 5-6 week old N15 TCR tg+/+ RAG-2-/- H-2b mice for two independent experiments. For sorting subpopulations, cells were stained with anti-CD4 (L3T4) and anti-CD8 (Ly-2) antibodies (Pharmingen, San Diego, CA USA) and DP, Int and SP thymocytes were sorted on a MoFlo (Cytomation, Fort Collins, CO USA).

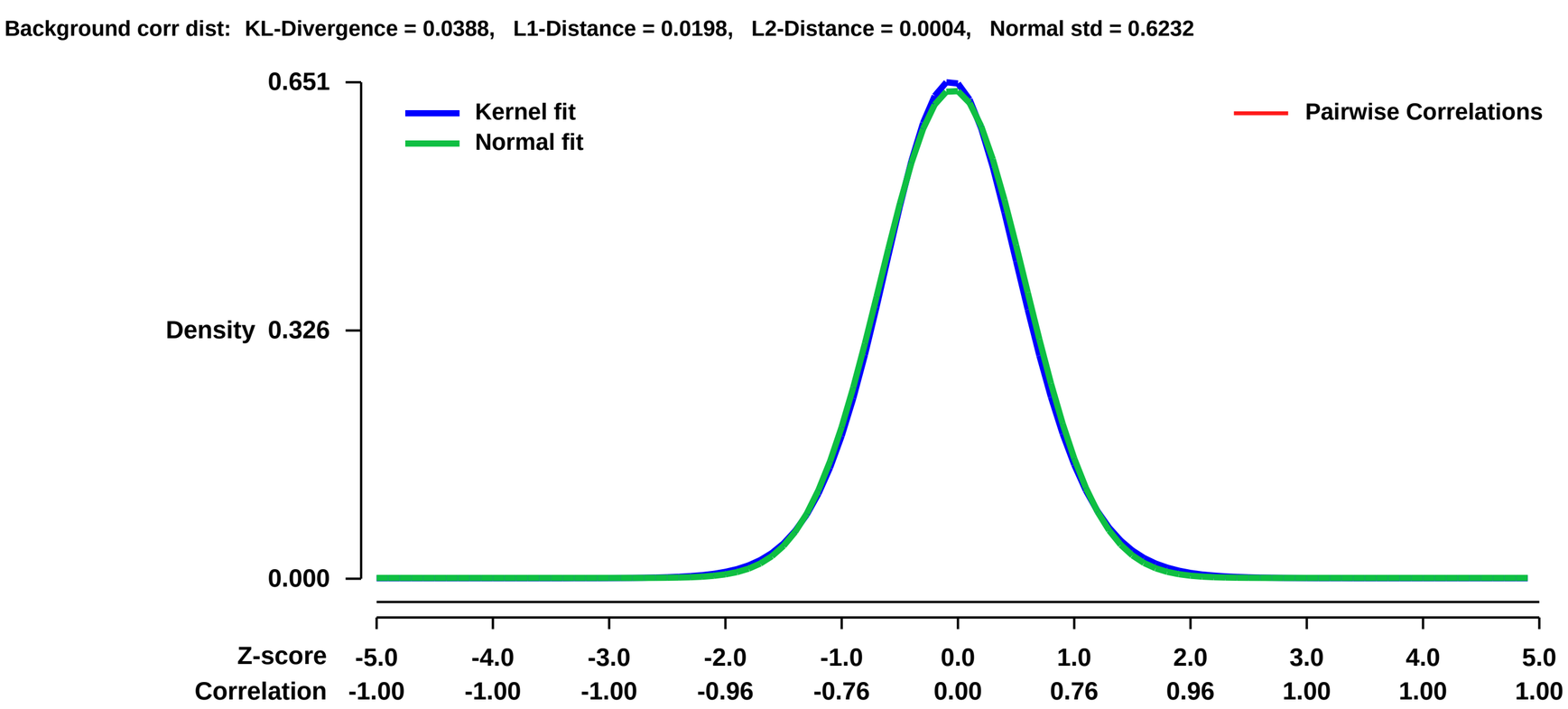

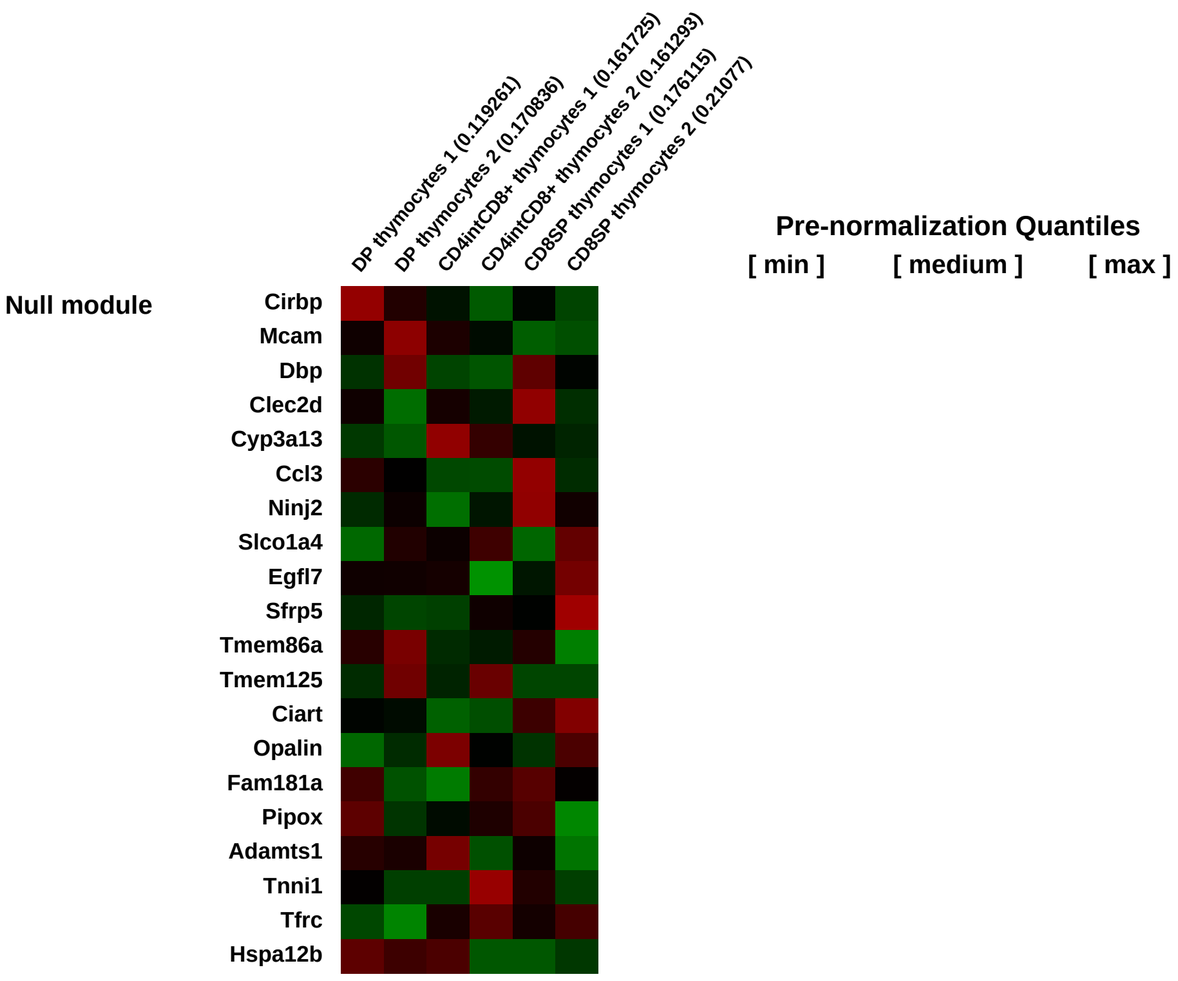

GEO Series "GSE13526" Expression Profiles

Num of samples in this series: 6

Scale of expression profile Z-scores

-3.0 -2.0 -1.0 0.0 1.0 2.0 3.0

GEO Link:	http://www.ncbi.nlm.nih.gov/geo/query/acc.cgi?acc=GSE13526
Status:	Public on Nov 05 2009
Title:	Transcript profiling of WT and Nxf2 KO post-natal day 21 testes
Organism:	Mus musculus
Experiment type:	Expression profiling by array
Platform:	GPL1261
Pubmed ID:	19345203
Summary & Design:	**Summary:** In euakryotes, mRNAs must be exported from the nucleus to the cytsoplasm. NXF2 is highly expressed in the mouse male germ cells. We are interested in its function in spermatogenesis, espically in the nuclear RNA export in the testis. To this end, we made Nxf2 mutant mice by gene targeting. In an attempt to identify the mRNA substrates of NXF2, we perform the microarray experiments on testes. We used microarrays to check the expression profiles of the Nxf2 WT and KO 21d testes on C57BL/6 background. **Overall design:** To examine the expression difference between WT and Nxf2 KO testes, we collected testes from juvenile mice of three ages (21d, 26d, 28d). Testis weight was similar between WT and KO mice at post-natal day 21. Three pairs of WT and KO 21d testes were chosen for microarray analysis.

Background corr dist: KL-Divergence = 0.0259, L1-Distance = 0.0249, L2-Distance = 0.0010, Normal std = 0.6980

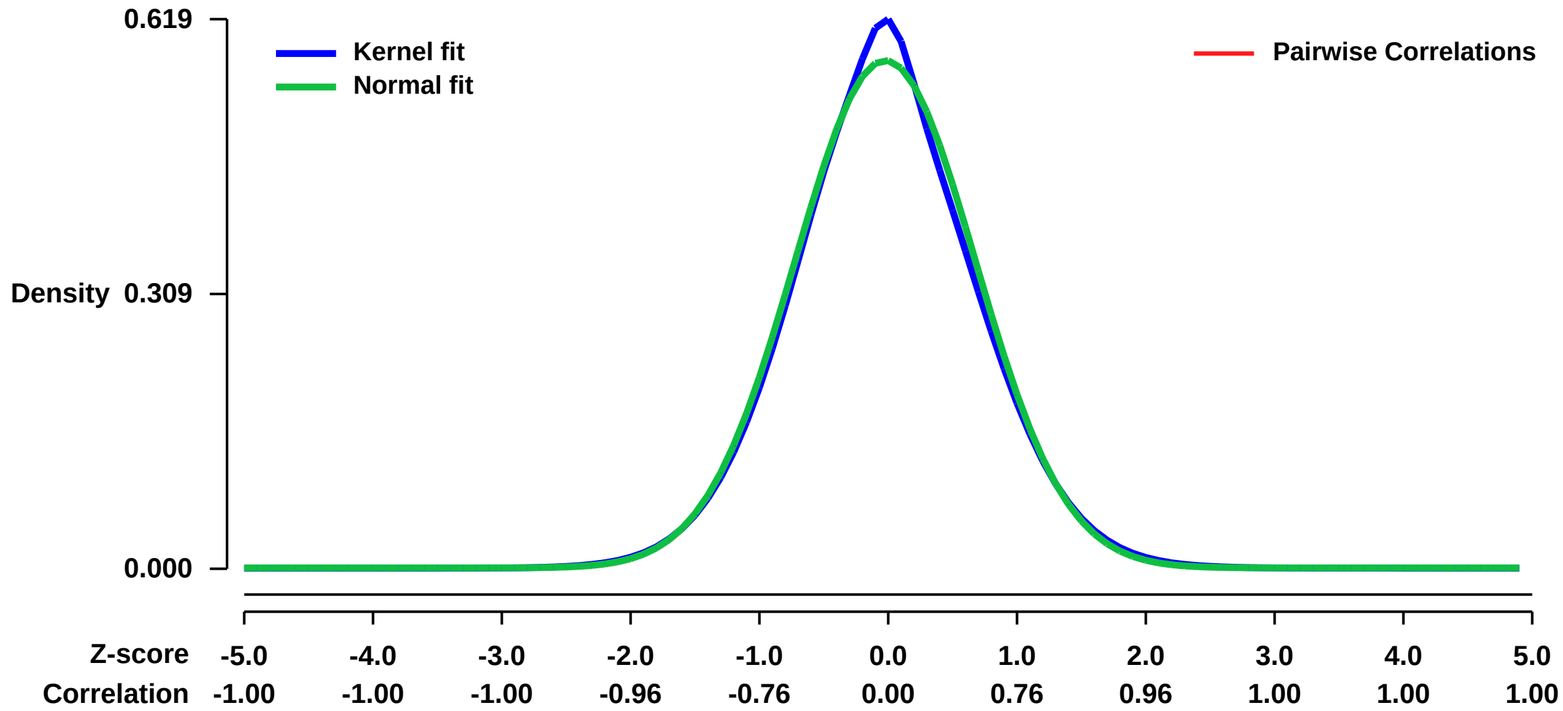

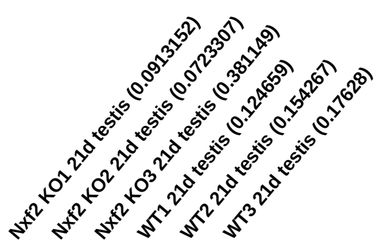

Pre-normalization Quantiles

[min] [medium] [max]

Null module

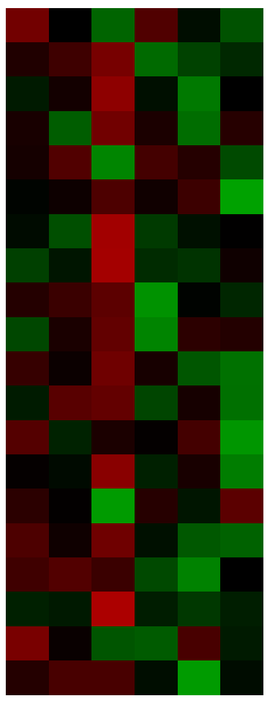

GEO Series "GSE13547" Expression Profiles

Num of samples in this series: 12

Scale of expression profile Z-scores

-3.0 -2.0 -1.0 0.0 1.0 2.0 3.0

GEO Link:	http://www.ncbi.nlm.nih.gov/geo/query/acc.cgi?acc=GSE13547
Status:	Public on Apr 17 2009
Title:	Zfx controls BCR-induced proliferation and survival of B lymphocytes
Organism:	Mus musculus
Experiment type:	Expression profiling by array
Platform:	GPL1261
Pubmed ID:	19329779
Summary & Design:	**Summary:** The development, homeostasis and function of B lymphocytes involve multiple rounds of B cell receptor (BCR)-controlled proliferation and prolonged maintenance. We analyzed the role of transcription factor Zfx, a recently identified regulator of stem cell maintenance, in B cell development and homeostasis. Conditional Zfx deletion in the bone marrow blocked B cell development at the pre-BCR selection checkpoint. Zfx deficiency in peripheral B cells caused impaired generation of the B-1 cell lineage, accelerated B cell turnover, depletion of mature recirculating cells, and delayed T-dependent antibody responses. Zfx-deficient B cells showed normal proximal BCR signaling, but impaired BCR-induced proliferation and survival. This was accompanied by aberrantly enhanced and prolonged integrated stress response, and delayed induction of Cyclin D2 and Bcl-xL proteins. Thus, Zfx restrains the stress response and couples antigen receptor signaling to B cell expansion and maintenance during development and peripheral homeostasis. **Keywords:** Expression profiling by array **Overall design:** For global gene expression analysis, 2.5 x 105 flow-sorted follicular B cells (B220+ AA4.1- CD23hi CD21int) were cultured in 200 ¸…L B cell media containing 10 ¸…g/mL ¸–-IgM for 0, 2, and 12 hrs. Cells were harvested in Trizol (Invitrogen). Total RNA was isolated using Trizol (Invitrogen), and 100 ng of each RNA sample were used for reverse transcription and two rounds of linear antisense RNA amplification/labeling (Ambion). The aRNA was amplified without labeling in the first round, and then labeled with Biotin-16-UTP(Roche Applied Sciences) and Biotin-11-CTP (PerkinElmer Life Sciences) in the second round. Labeled aRNA was fragmented in RNA Fragmentation Buffer (QIAGEN) prior to hybridization. Labeled RNA samples (10 ug/array) were hybridized in duplicate to Mouse Genome 430 2.0 arrays (Affymetrix) at the Columbia University Microarray Project core facility according to the manufacturer's instructions. Quality control and normalization were performed using positive and negative hybridization controls (Affymetrix) spiked into the RNA prior to labeling. Linear amplification of RNA was confirmed for every sample. Array scanning and raw data processing were done using GCOS 1.4 software (Affymetrix).

Background corr dist: KL-Divergence = 0.0888, L1-Distance = 0.0336, L2-Distance = 0.0016, Normal std = 0.4757

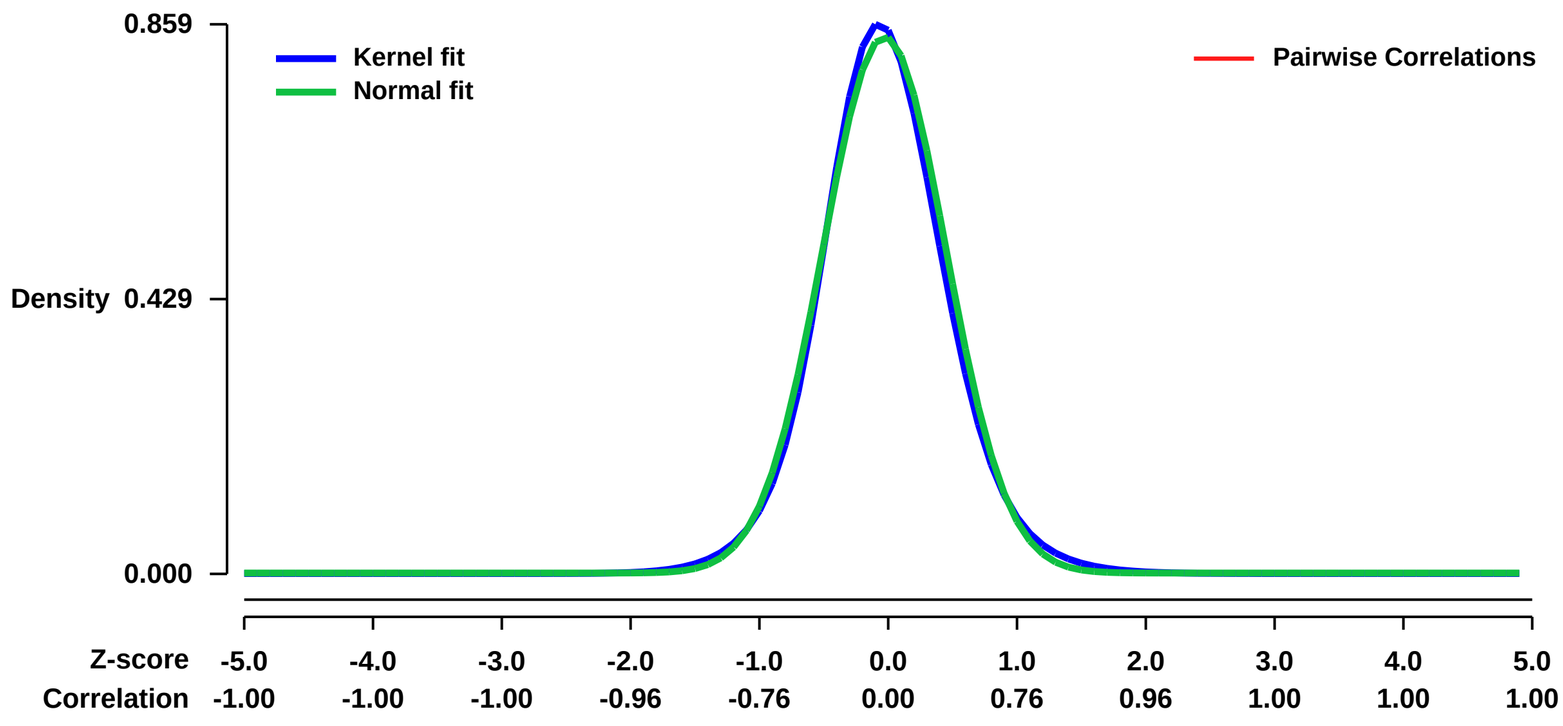

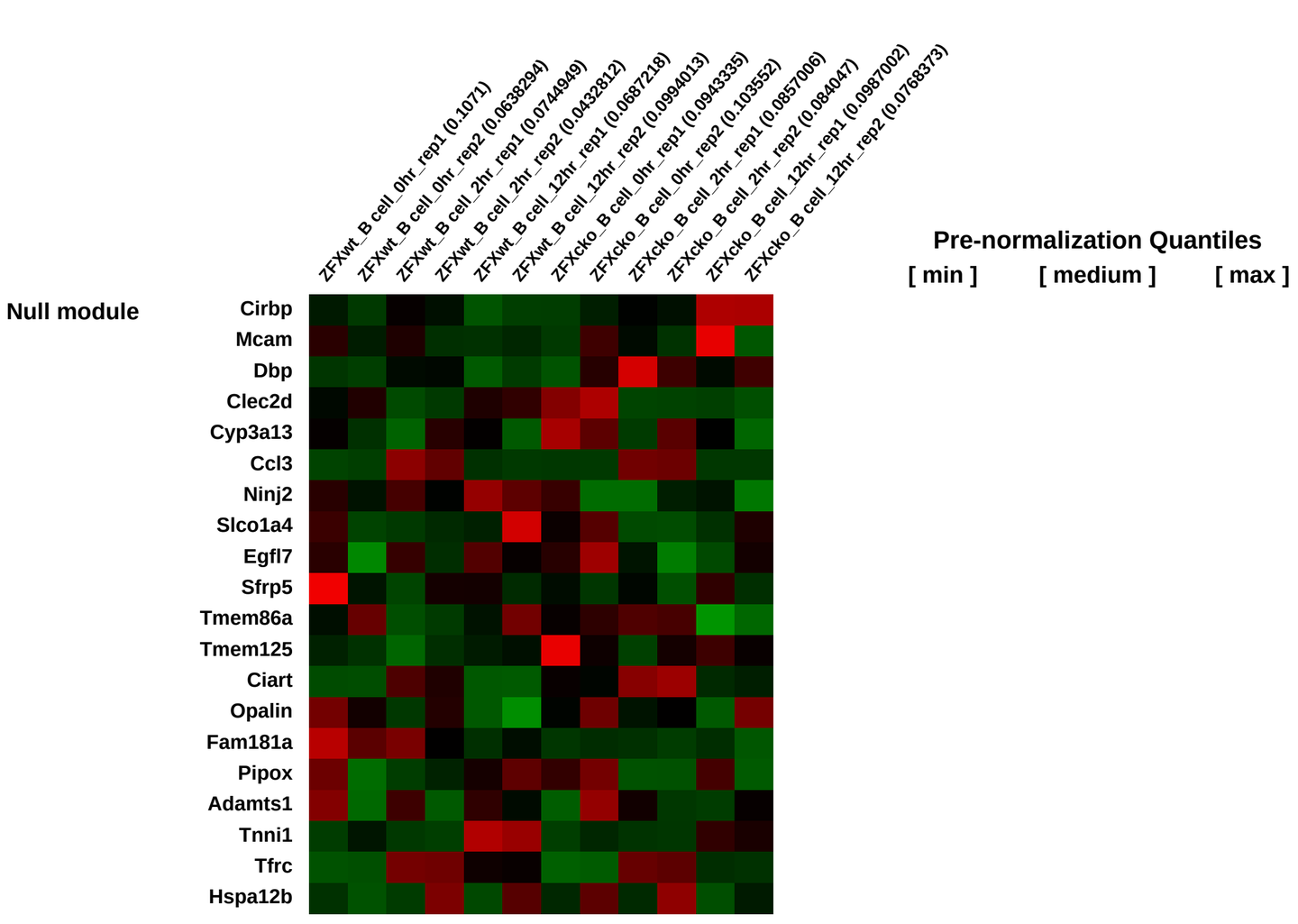

GEO Series "GSE13582" Expression Profiles

Num of samples in this series: 6

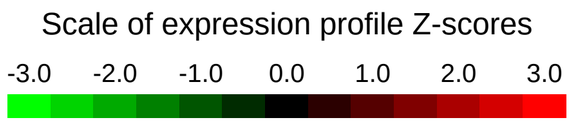

GEO Link:	http://www.ncbi.nlm.nih.gov/geo/query/acc.cgi?acc=GSE13582
Status:	Public on Jan 22 2009
Title:	Expression data from BAT of the KRAP deficient mice
Organism:	Mus musculus
Experiment type:	Expression profiling by array
Platform:	GPL1261
Pubmed ID:	19156225
Summary & Design:	**Summary:** KRAP (Ki-ras-induced actin-interacting protein) is a cytoskeleton-associated protein and a ubiquitous protein among tissues, originally identified as a cancer-related molecule. KRAP-deficient (KRAP-/-) mice show enhanced metabolic rate, decreased adiposity, improved glucose tolerance, hypoinsulinemia and hypoleptinemia. KRAP-/- mice are also protected against high-fat diet-induced obesity and insulin resistance despite of hyperphagia. **Overall design:** Total RNA was extracted from BAT of three pairs of littermates (KO1 vs. WT1, KO2 vs. WT2 and KO3 vs. WT3) fed normal chow.

Background corr dist: KL-Divergence = 0.0475, L1-Distance = 0.0257, L2-Distance = 0.0008, Normal std = 0.5908

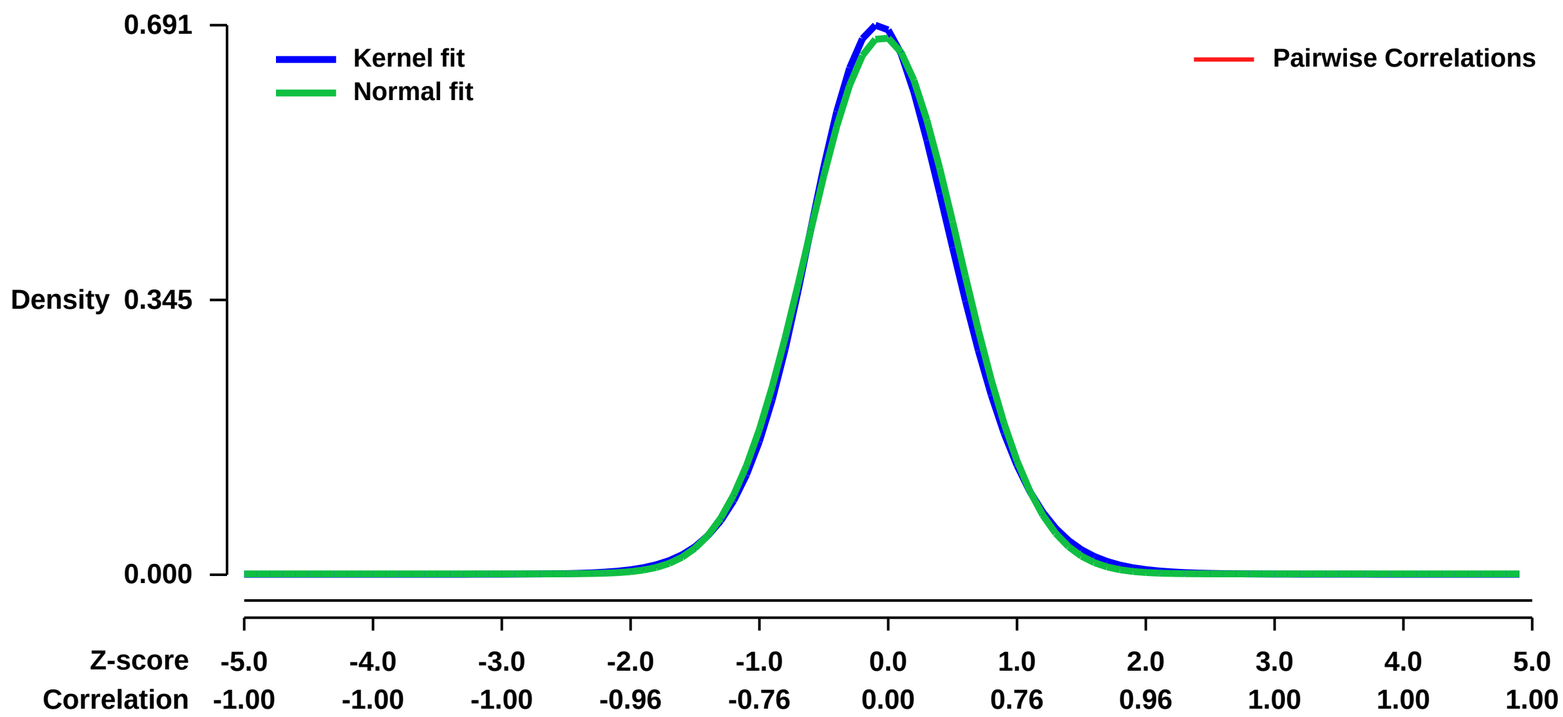

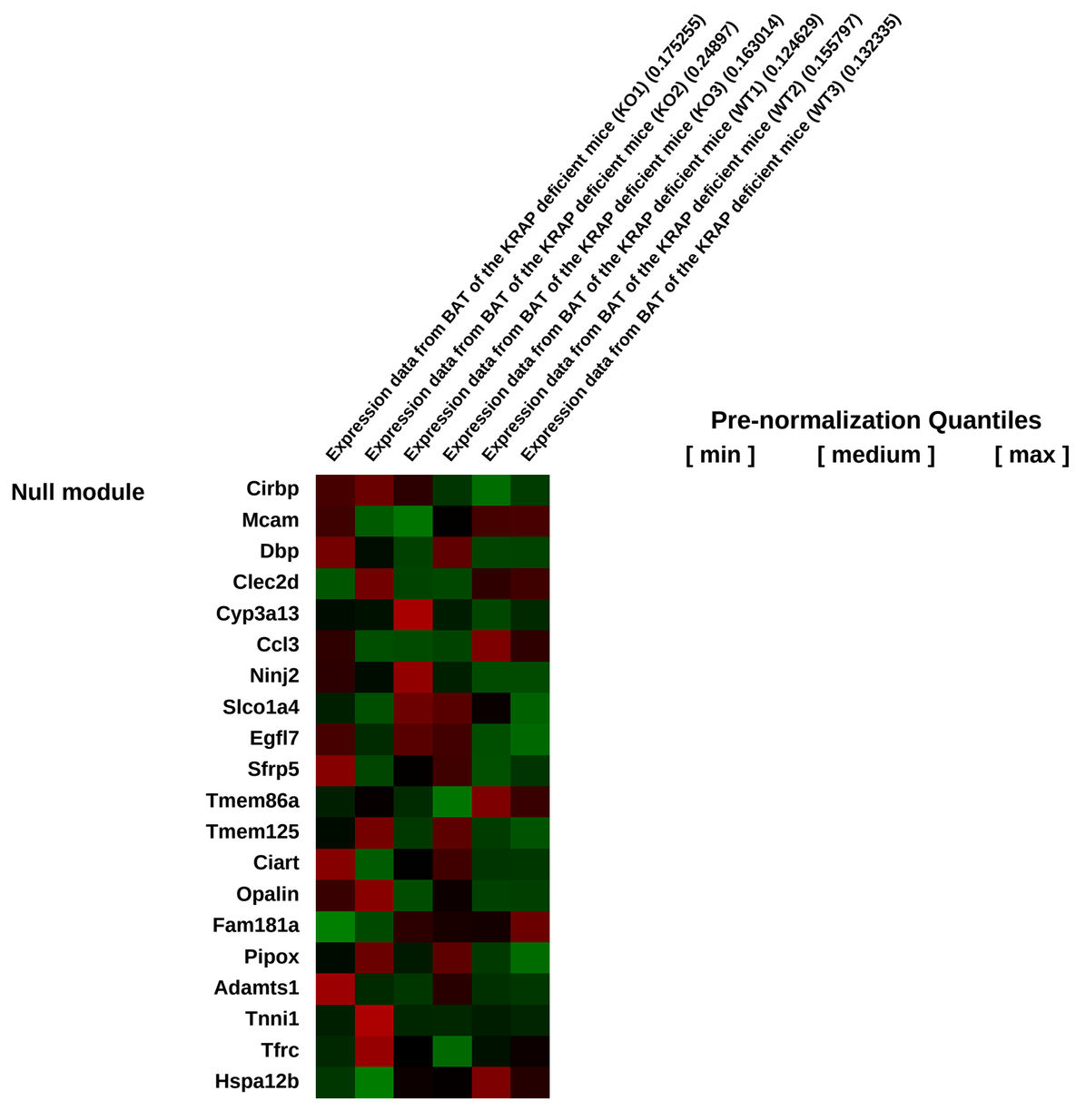

GEO Series "GSE13583" Expression Profiles

Num of samples in this series: 6

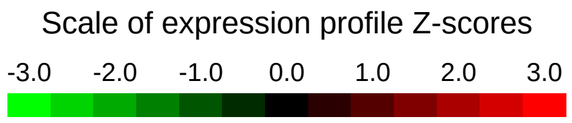

GEO Link:	http://www.ncbi.nlm.nih.gov/geo/query/acc.cgi?acc=GSE13583
Status:	Public on Jan 22 2009
Title:	Expression data from liver of the KRAP deficient mice
Organism:	Mus musculus
Experiment type:	Expression profiling by array
Platform:	GPL1261
Pubmed ID:	19156225
Summary & Design:	**Summary:** KRAP (Ki-ras-induced actin-interacting protein) is a cytoskeleton-associated protein and a ubiquitous protein among tissues, originally identified as a cancer-related molecule. KRAP-deficient (KRAP-/-) mice show enhanced metabolic rate, decreased adiposity, improved glucose tolerance, hypoinsulinemia and hypoleptinemia. KRAP-/- mice are also protected against high-fat diet-induced obesity and insulin resistance despite of hyperphagia. **Overall design:** Total RNA was extracted from livers of three pairs of littermates (KO1 vs. WT1, KO2 vs. WT2 and KO3 vs. WT3) fed normal chow.

Background corr dist: KL-Divergence = 0.0485, L1-Distance = 0.0224, L2-Distance = 0.0006, Normal std = 0.5811

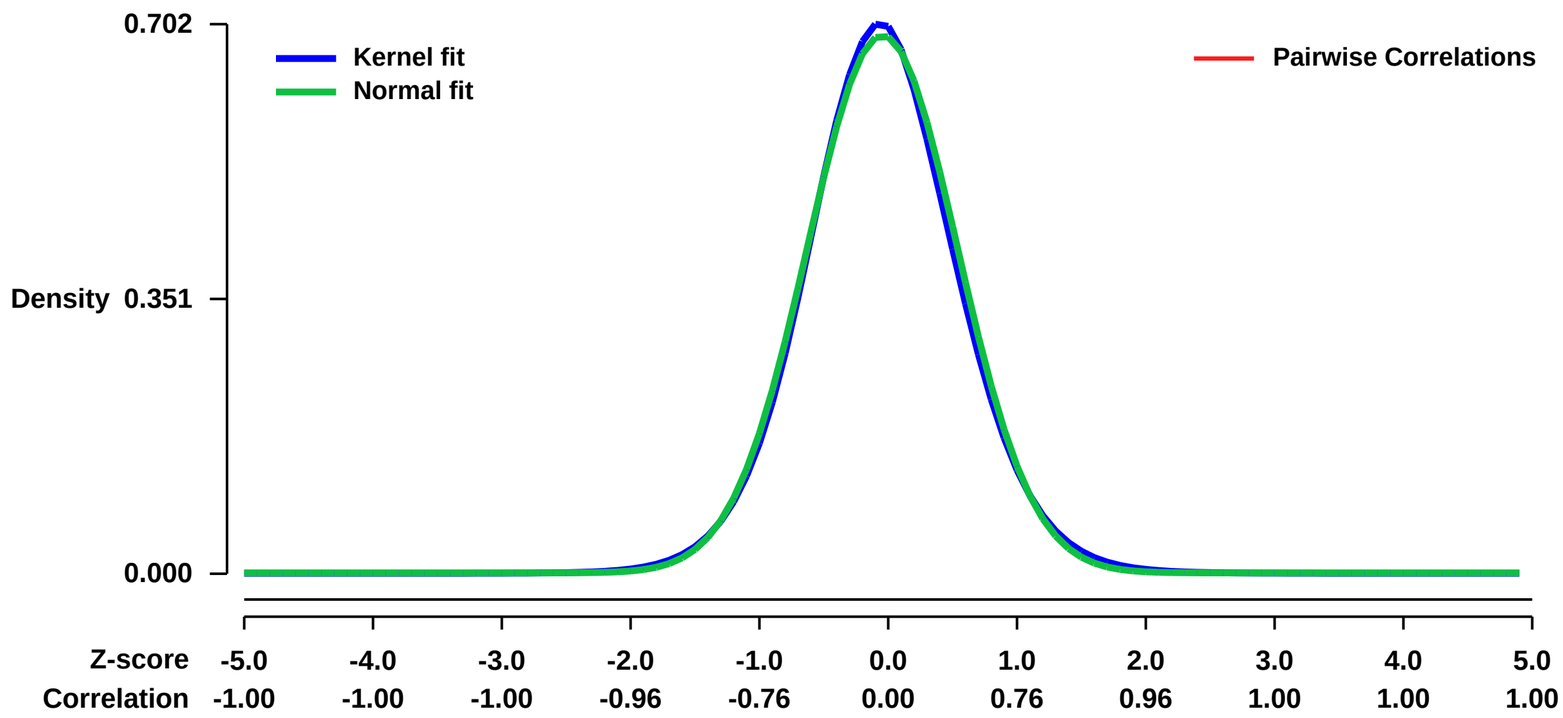

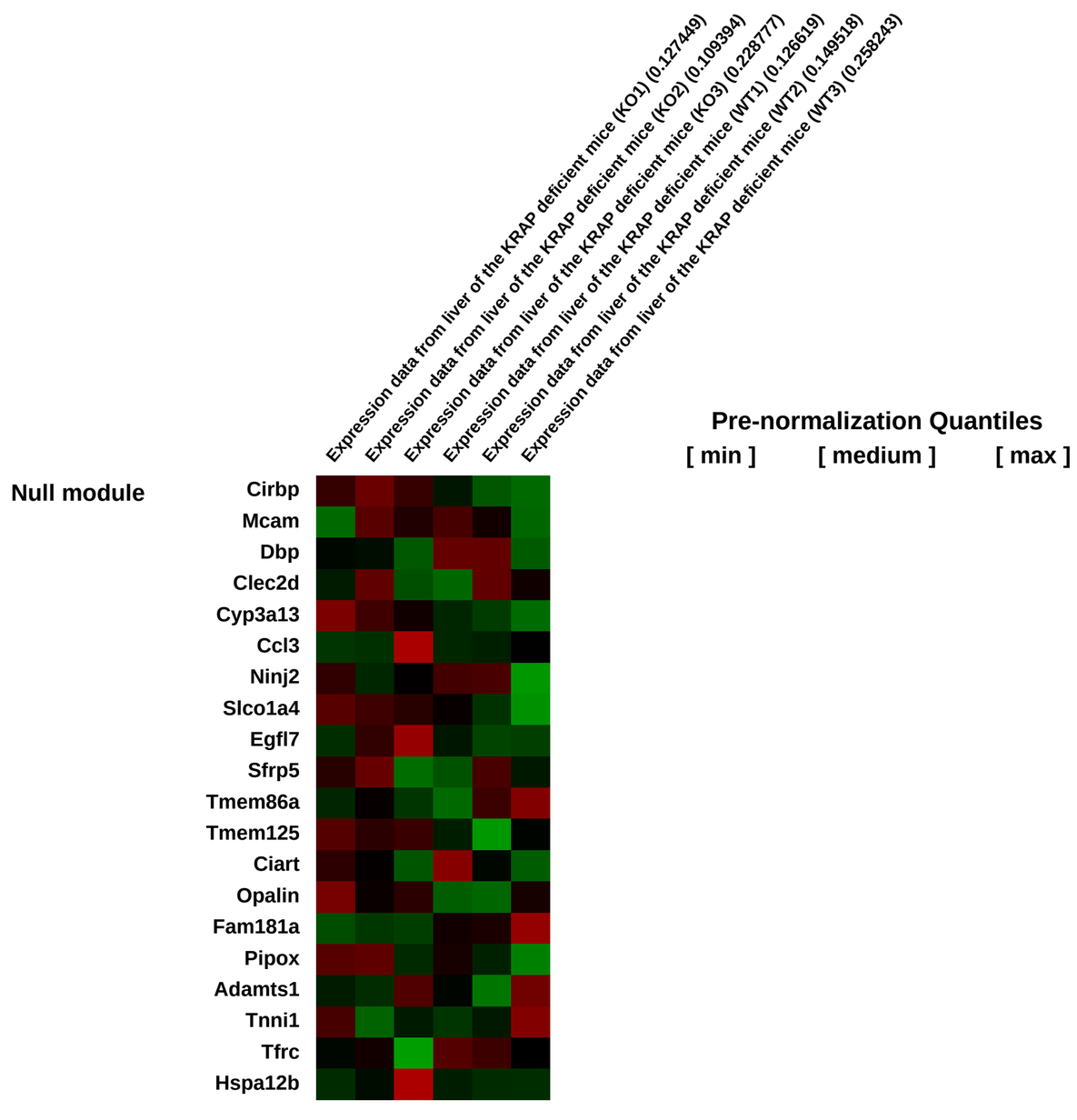

GEO Series "GSE13590" Expression Profiles

Num of samples in this series: 12

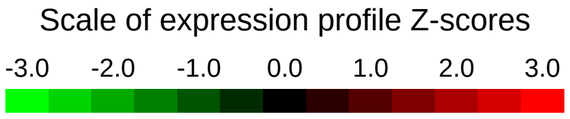

GEO Link:	http://www.ncbi.nlm.nih.gov/geo/query/acc.cgi?acc=GSE13590
Status:	Public on Nov 14 2008
Title:	Experimental identification of microRNA-140 targets by silencing and overexpressing miR-140
Organism:	Mus musculus
Experiment type:	Expression profiling by array
Platform:	GPL1261
Pubmed ID:	20071455
Summary & Design:	**Summary:** MicroRNAs (miRNAs) are short noncoding RNA molecules regulating the expression of mRNAs. Target identification of miRNAs is computationally difficult due to the relatively low homology between miRNAs and their targets. We present here an experimental approach to target identification where the cartilage-specific miR-140 was overexpressed and silenced in cells it is normally expressed in separate experiments. Expression of mRNAs was profiled in both experiments and the intersection of mRNAs repressed by miR-140 overexpression and derepressed by silencing of miR-140 was identified. The intersection contained only 49 genes, although both treatments affected the accumulation of hundreds of mRNAs. These 49 genes showed a very strong enrichment for the miR-140 seed sequence implying that the approach is efficient and specific. 21 of these 49 genes were predicted to be direct targets based on the presence of the seed sequence. Interestingly, none of these were predicted by the published target prediction methods we used. One of the potential target mRNAs, Cxcl12, was experimentally validated by Northern blot analysis and a luciferase reporter assay. **Overall design:** Each condition was profiled in triplicate. For over-expression experiment cells were transfected with siRNA-140 (miR-140 mimick) or siRNA-96 (as a control). For suppresion experiment cells were transfected with LNA-antimicroRNA-140 (suppressing endogenous miR-140) or LNA-antimicroRNA-449 (as a control).

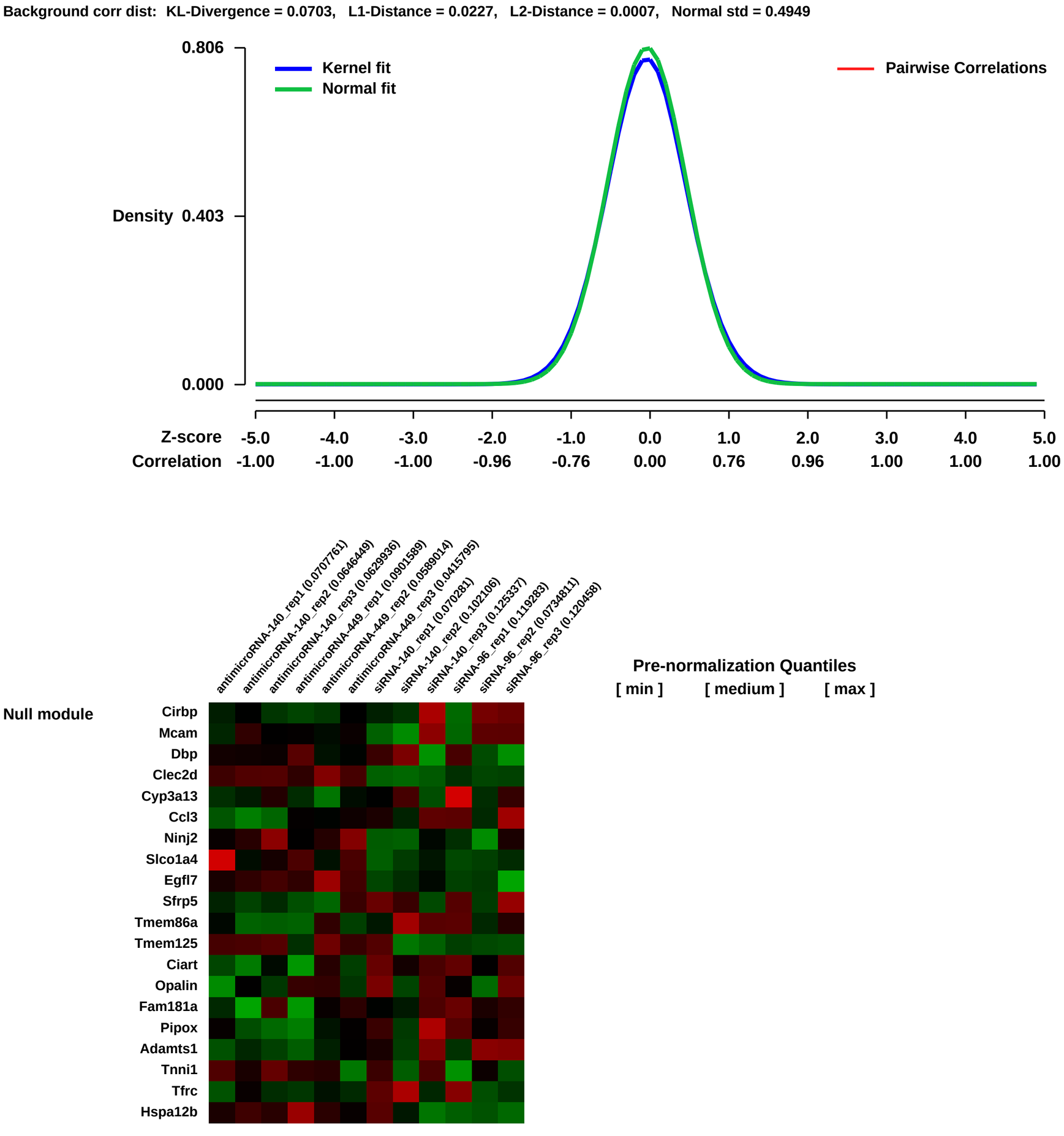

GEO Series "GSE13611" Expression Profiles

Num of samples in this series: 8

Scale of expression profile Z-scores

-3.0 -2.0 -1.0 0.0 1.0 2.0 3.0

GEO Link:	http://www.ncbi.nlm.nih.gov/geo/query/acc.cgi?acc=GSE13611
Status:	Public on Aug 15 2009
Title:	Affymetrix gene expression AID-GFP-positive vs AID-GFP-negative
Organism:	Mus musculus
Experiment type:	Expression profiling by array
Platform:	GPL1261
Pubmed ID:	19732723
Summary & Design:	Summary: Affymetrix gene expression AID-GFP-positive vs AID-GFP-negative Overall design: Affymetrix gene expression AID-GFP-positive vs AID-GFP-negative

Background corr dist: KL-Divergence = 0.0067, L1-Distance = 0.0275, L2-Distance = 0.0010, Normal std = 0.9603

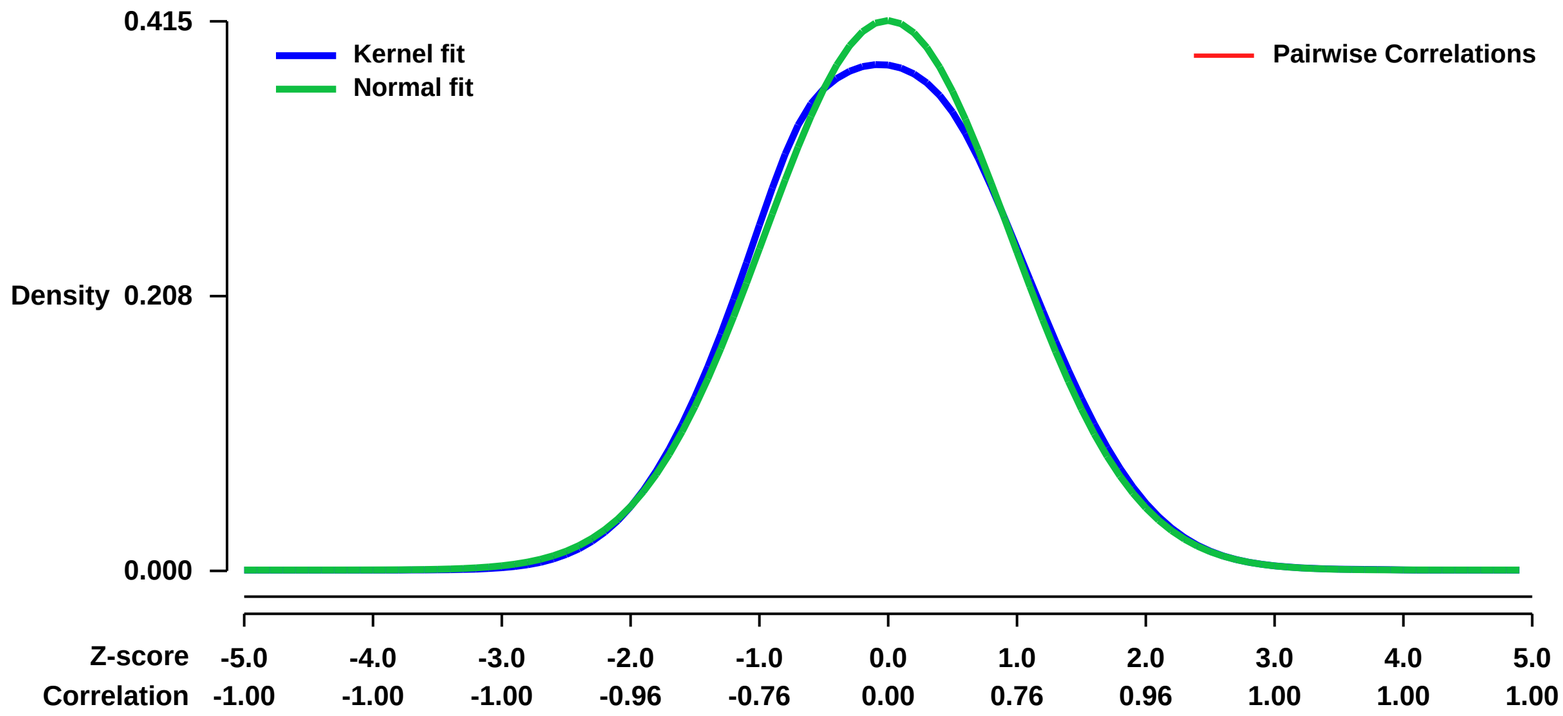

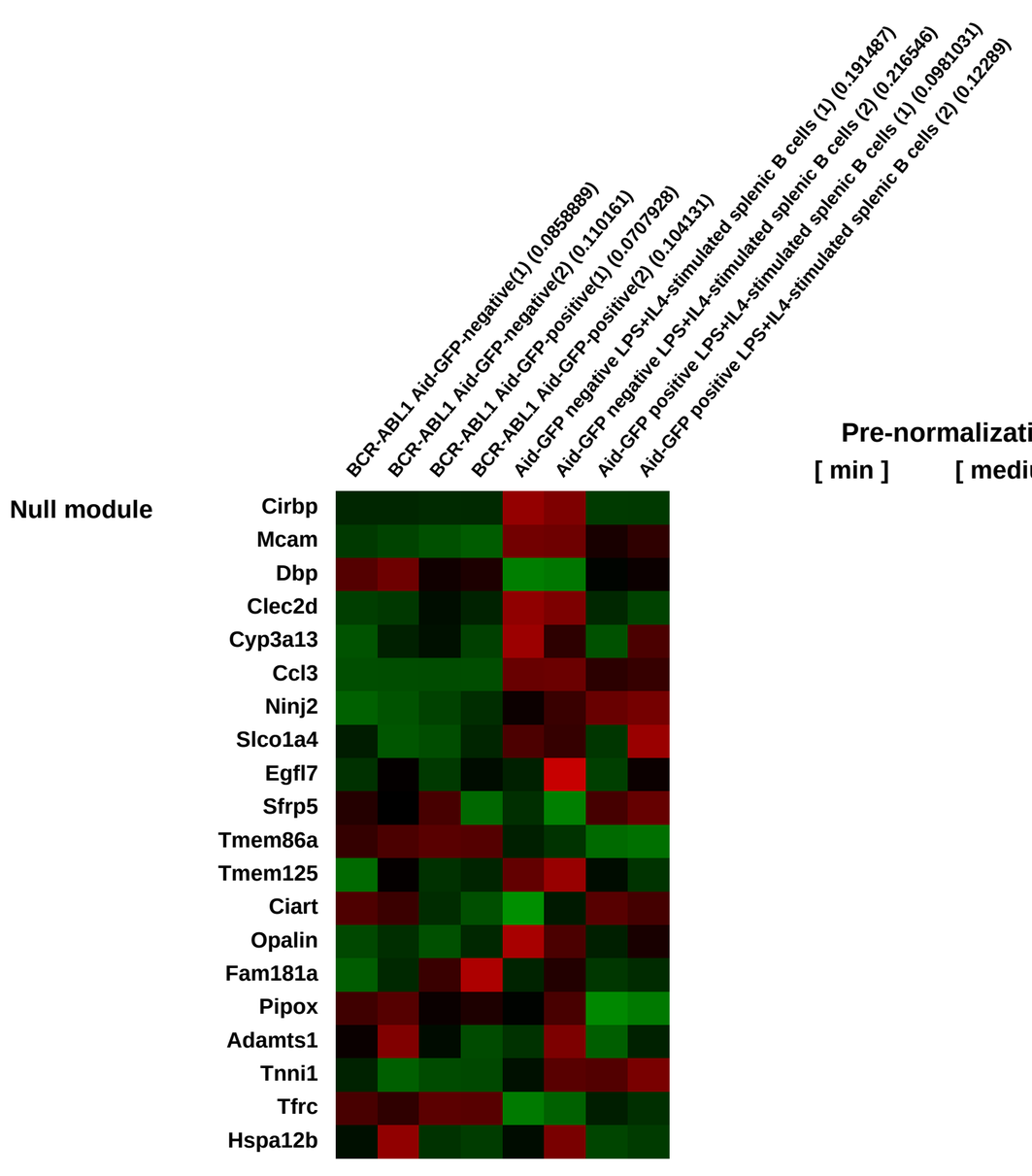

GEO Series "GSE13635" Expression Profiles

Num of samples in this series: 6

Scale of expression profile Z-scores

-3.0 -2.0 -1.0 0.0 1.0 2.0 3.0

GEO Link:	http://www.ncbi.nlm.nih.gov/geo/query/acc.cgi?acc=GSE13635
Status:	Public on Jan 29 2010
Title:	Gene expression change in cyclin D1 -/- retinas in comparison to wildtype.
Organism:	Mus musculus
Experiment type:	Expression profiling by array
Platform:	GPL1261
Pubmed ID:	20090754
Summary & Design:	**Summary:** Cyclin D1 belongs to the core cell cycle machinery1, and it is frequently overexpressed in human cancers2. The full repertoire of cyclin D1 functions in normal development and in cancer cells is currently unknown. To address this question, here we introduce a novel approach that allows one to determine the set of cyclin D1-interacting proteins (D1 â interactomeâ) and cyclin D1-bound genomic fragments (D1 â cistromeâ) in essentially any mouse organ, at any point of development or at any stage of cancer progression. Using this approach, we detected several novel tissue-specific interactors of cyclin D1. A significant number of these partners represent proteins involved in transcription. We show, using genome-wide location analysis3, that cyclin D1 occupies promoters of a very large number of genes in the developing mouse, where it binds in close proximity to transcription start sites. Bioinformatics analyses of cyclin D1-bound genomic segments in the developing embryo revealed DNA recognition sequences for several transcription factors. By querying SAGE libraries4, promoter CpG content5 and gene expression profiles of cyclin D1-null organs, we demonstrate that cyclin D1 binds promoters of highly expressed genes, and that it functions to activate or to repress gene expression in vivo. Analyses of cyclin D1 transcriptional targets reveal that cyclin D1 contributes to cell proliferation by upregulating genes required for S-phase entry and progression. Hence, cyclin D1 plays a broad transcriptional regulatory function in vivo during normal mouse development. **Overall design:** We wished to determine whether cyclin D1 functioned to positively or negatively regulate transcription of the target genes (identified by chip-on-chip) in vivo. To address this question, we asked how expression of cyclin D1-bound genes changes when cyclin D1 has been knocked-out. We dissected retinas from eyes of cyclin D1-/- or wild-type neonates, isolated RNA and hybridized it onto Affymetrix expression arrays.

Background corr dist: KL-Divergence = 0.0303, L1-Distance = 0.0162, L2-Distance = 0.0003, Normal std = 0.6631

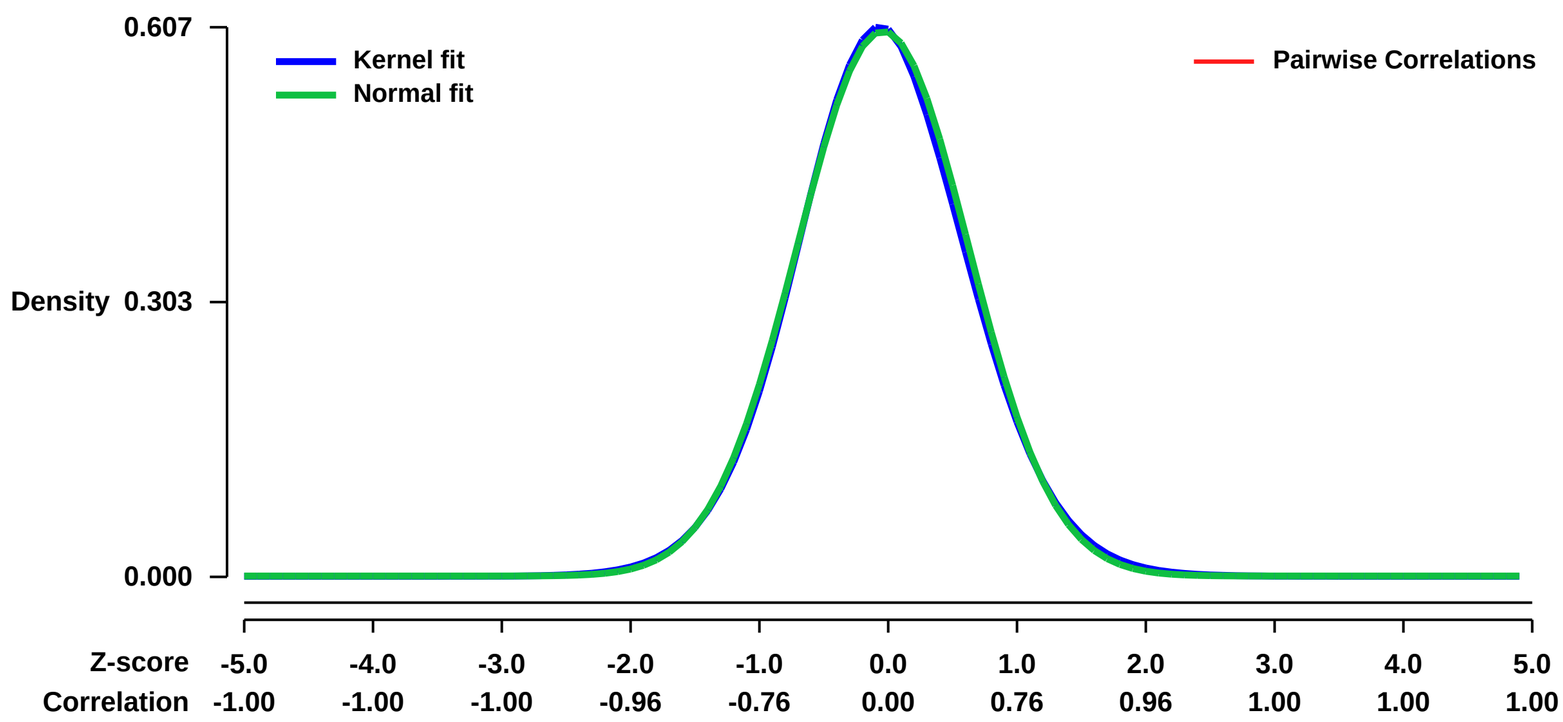

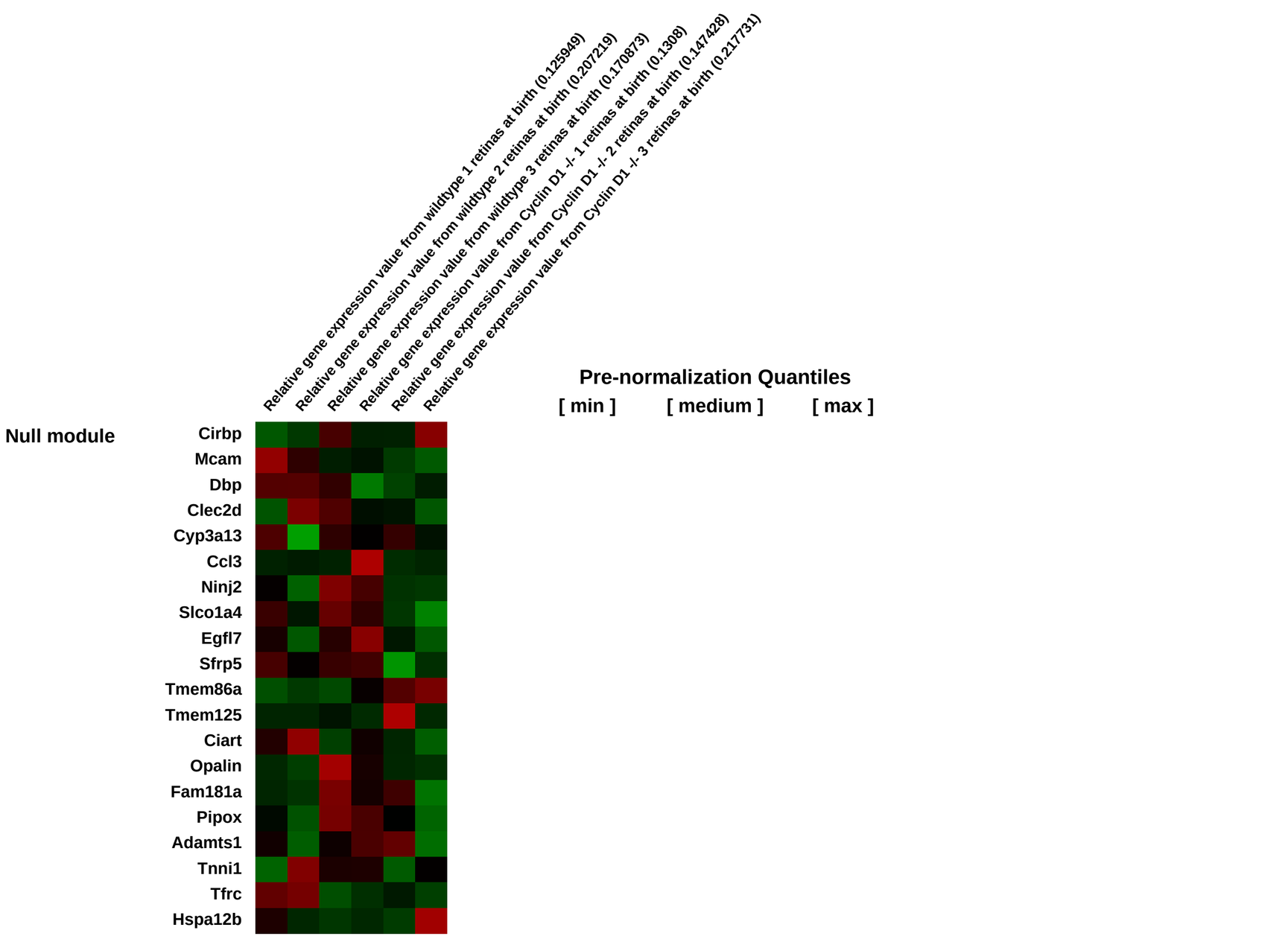

GEO Series "GSE13667" Expression Profiles

Num of samples in this series: 6

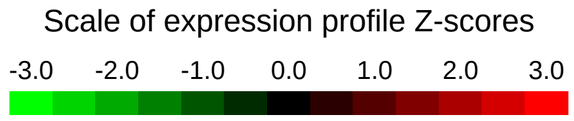

GEO Link:	http://www.ncbi.nlm.nih.gov/geo/query/acc.cgi?acc=GSE13667
Status:	Public on Jan 26 2009
Title:	mpkCCD_Cell_Clones
Organism:	Mus musculus
Experiment type:	Expression profiling by array
Platform:	GPL1261
Pubmed ID:	19190182
Summary & Design:	**Summary:** This series of microarray data contain transcript intensity of mpkCCD cells. **Overall design:** The mpkCCDc14 cells were cloned into colonies with varying aquaporin 2 (AQP2) expression levels in the presence of vasopressin analogy dDAVP. Transcript profiling was done for the original cells and cell clones 2, 3, 9, 10, and 11. By studying transcripts that correlate with AQP2 mRNA levels among cell clones, the objective was to identify transcripts responsible for cell-specific expression of AQP2.

Background corr dist: KL-Divergence = 0.0455, L1-Distance = 0.0247, L2-Distance = 0.0007, Normal std = 0.5960

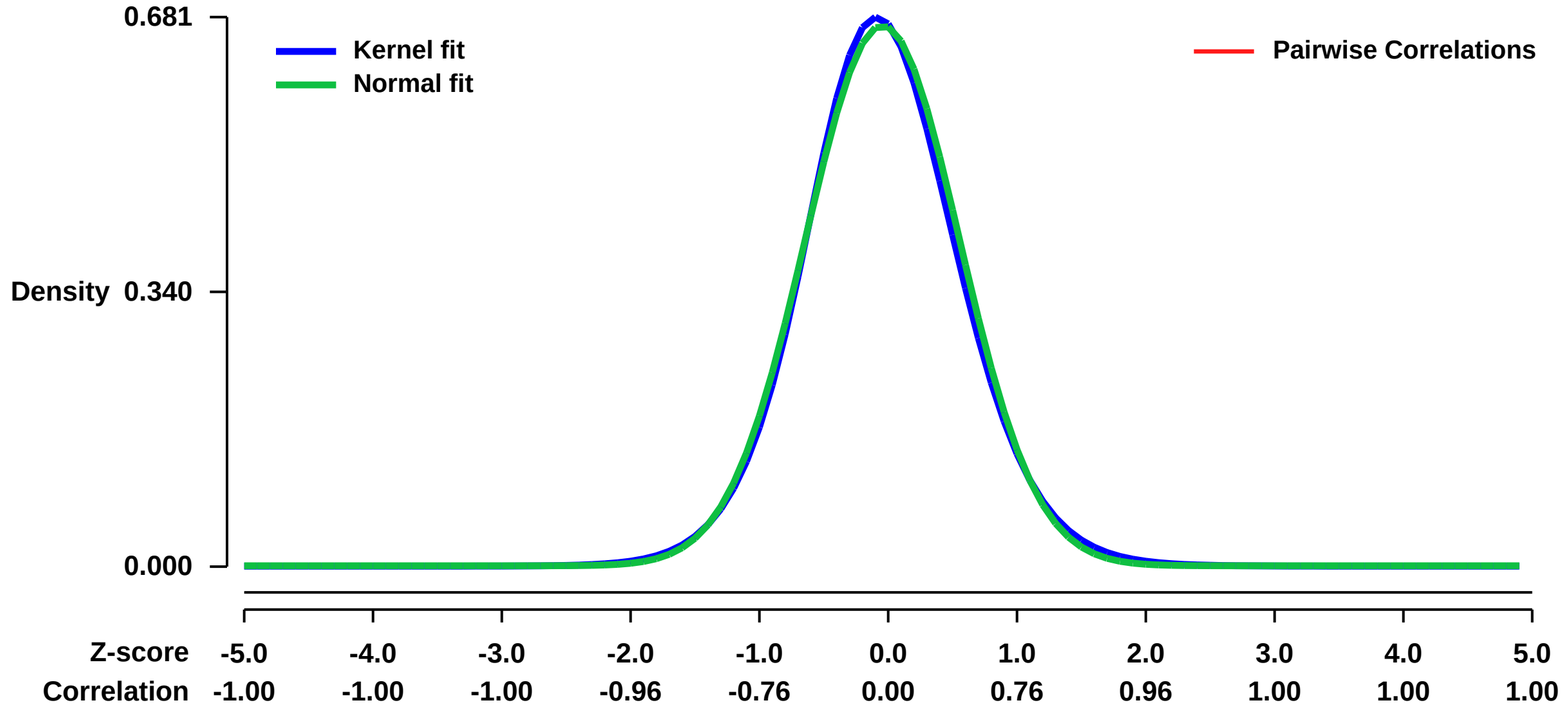

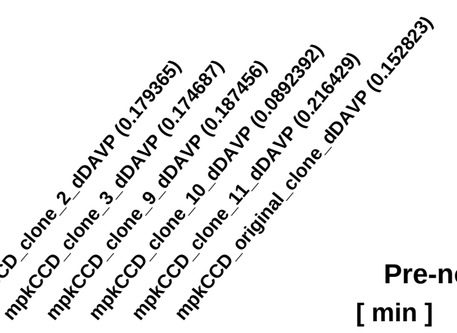

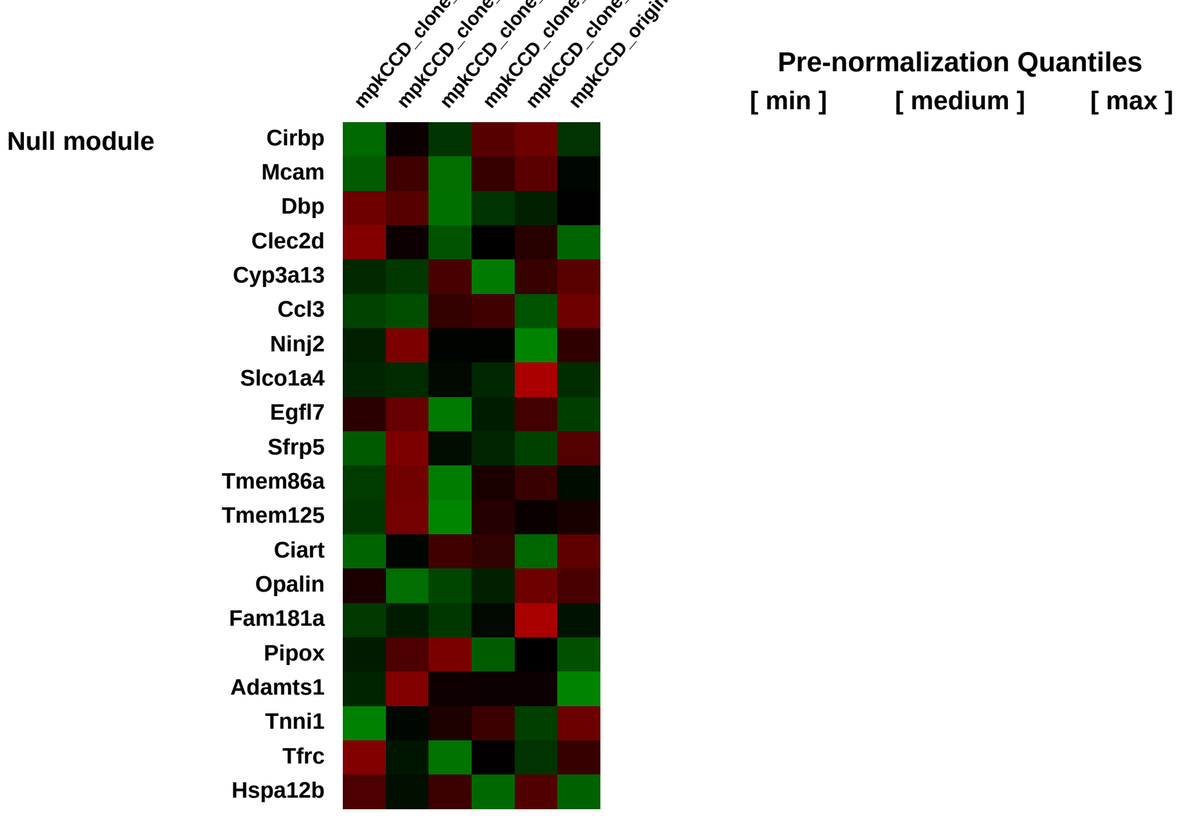

GEO Series "GSE13692" Expression Profiles

Num of samples in this series: 8

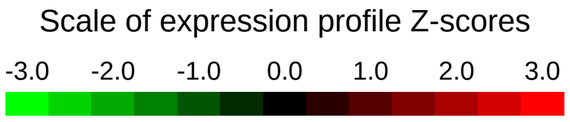

GEO Link:	http://www.ncbi.nlm.nih.gov/geo/query/acc.cgi?acc=GSE13692
Status:	Public on Feb 06 2009
Title:	Expression profiling of MLL-AF10 myeloid leukemia cellular subsets
Organism:	Mus musculus
Experiment type:	Expression profiling by array
Platform:	GPL1261
Pubmed ID:	19200802
Summary & Design:	**Summary:** Leukemia cells from mice with MLL-AF10 AML were fractionated into separate sub-populations on the basis of c-kit expression, which correlates with MLL LSC frequency (Somervaille and Cleary, 2006). The sorted AML sub-populations exhibited substantial differences in their frequencies of AML CFCs/LSCs (mean 14-fold) and morphologic features, consistent with a leukemia cell hierarchy with maturation through to terminally differentiated neutrophils. **Overall design:** Leukemic splenocytes from four mice with MLL-AF10 AML were sub-fractionated in to c-kit high and c-kit negative sub-populations by FACS.

Background corr dist: KL-Divergence = 0.0464, L1-Distance = 0.0346, L2-Distance = 0.0017, Normal std = 0.6099

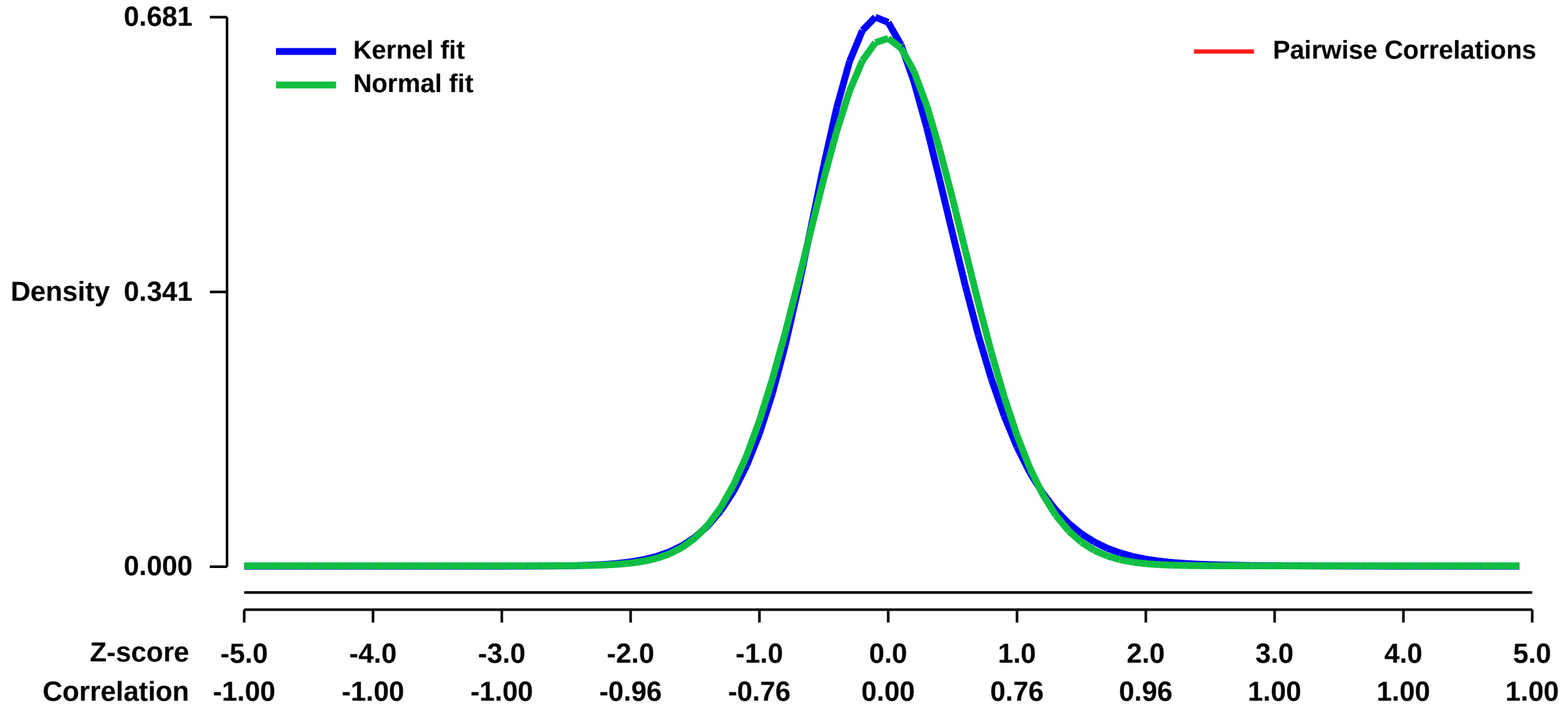

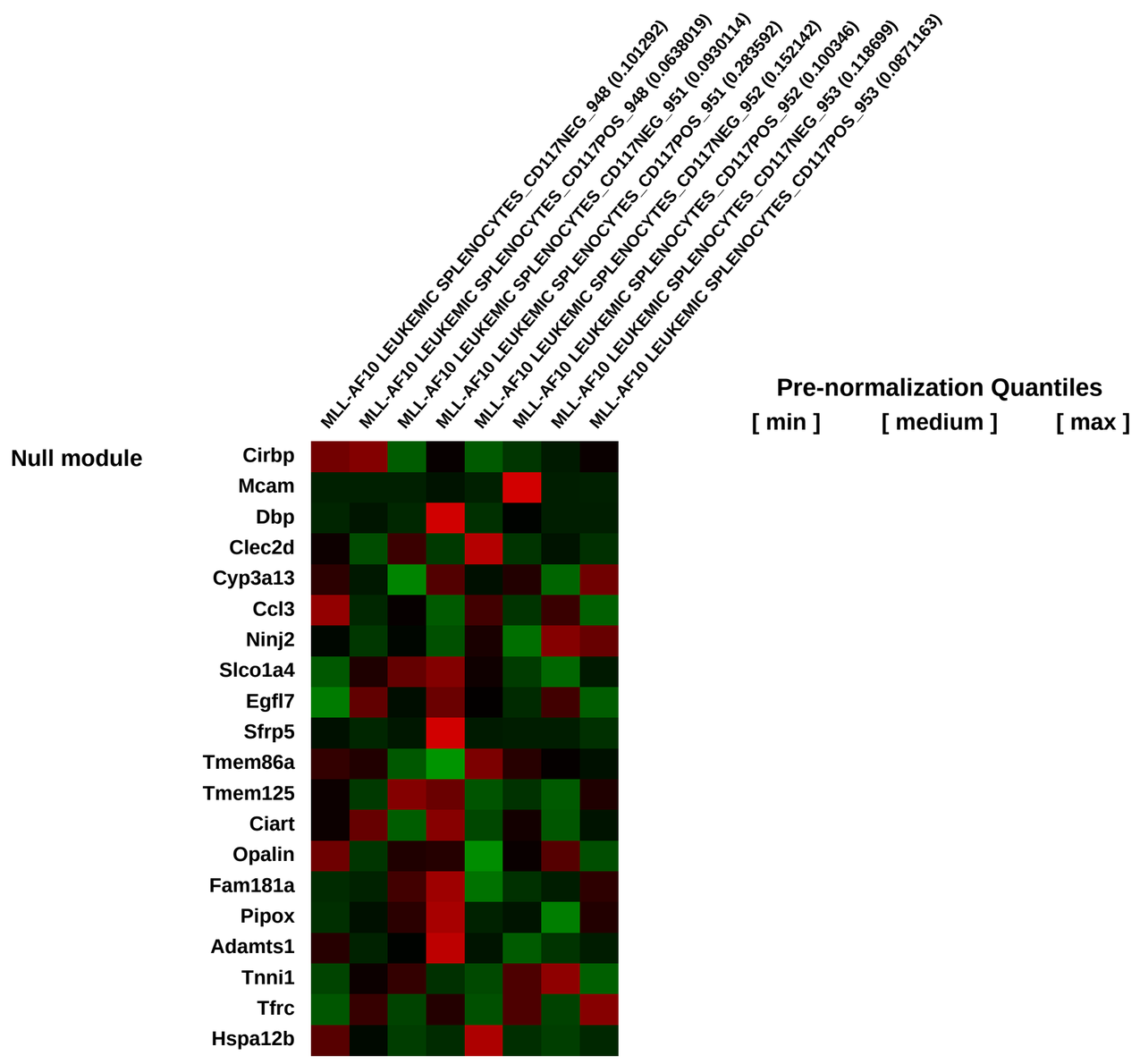

GEO Series "GSE13753" Expression Profiles

Num of samples in this series: 10

Scale of expression profile Z-scores

-3.0 -2.0 -1.0 0.0 1.0 2.0 3.0

GEO Link: http://www.ncbi.nlm.nih.gov/geo/query/acc.cgi?acc=GSE13753
Status: Public on Jun 08 2009
Title: E2F4 cooperates with pRB in the development of extra-embryonic, not embryonic, tissues
Organism: Mus musculus
Experiment type: Expression profiling by array
Platform: GPL1261
Pubmed ID:

Summary & Design:

Summary:
Homozygous mutation of the murine retinoblastoma tumor suppressor gene, Rb, results in embryonic lethality between E13.5 and E15.5 with defects in cellular proliferation, differentiation and apoptosis. Many of these defects are suppressed by mutation of an activating E2F, E2f1 or E2f3, indicating that they are key downstream targets of the retinoblastoma protein, pRB. In this study, we assess how E2F4 contributes to the developmental consequences of pRb-loss. In stark contrast to the activating E2Fs, the homozygous mutation of E2f4 shortened the lifespan of Rb-/- embryos. This resulted from an exacerbation of the placental defect of the Rb-/- mice indicating that E2F4 and pRB cooperate in the development of this tissue. Further analyses indicated that this defect reflects an increase in trophectoderm-like cells. Under conditions where the placenta was wild-type but the embryo mutant for E2f4 and pRb embryos survived to birth and exhibited all of the defects that were observed in the E2f4 and Rb single mutant embryos. Thus, while pRB and E2F4 cooperate in placental development, they play largely non-overlapping roles the development of many embryonic tissues.

Keywords: genetically modified tissue comparison

Overall design:
In one experiment, embryonic Day 13.5 placentas from wild-type and Rb -/- knock-out mice were compared. In the second experiment, embronic day 11.5 placentas from wild-type and Rb -/-;E2f4 -/- double knock-out mice were compared.

Background corr dist: KL-Divergence = 0.0302, L1-Distance = 0.0398, L2-Distance = 0.0027, Normal std = 0.6625

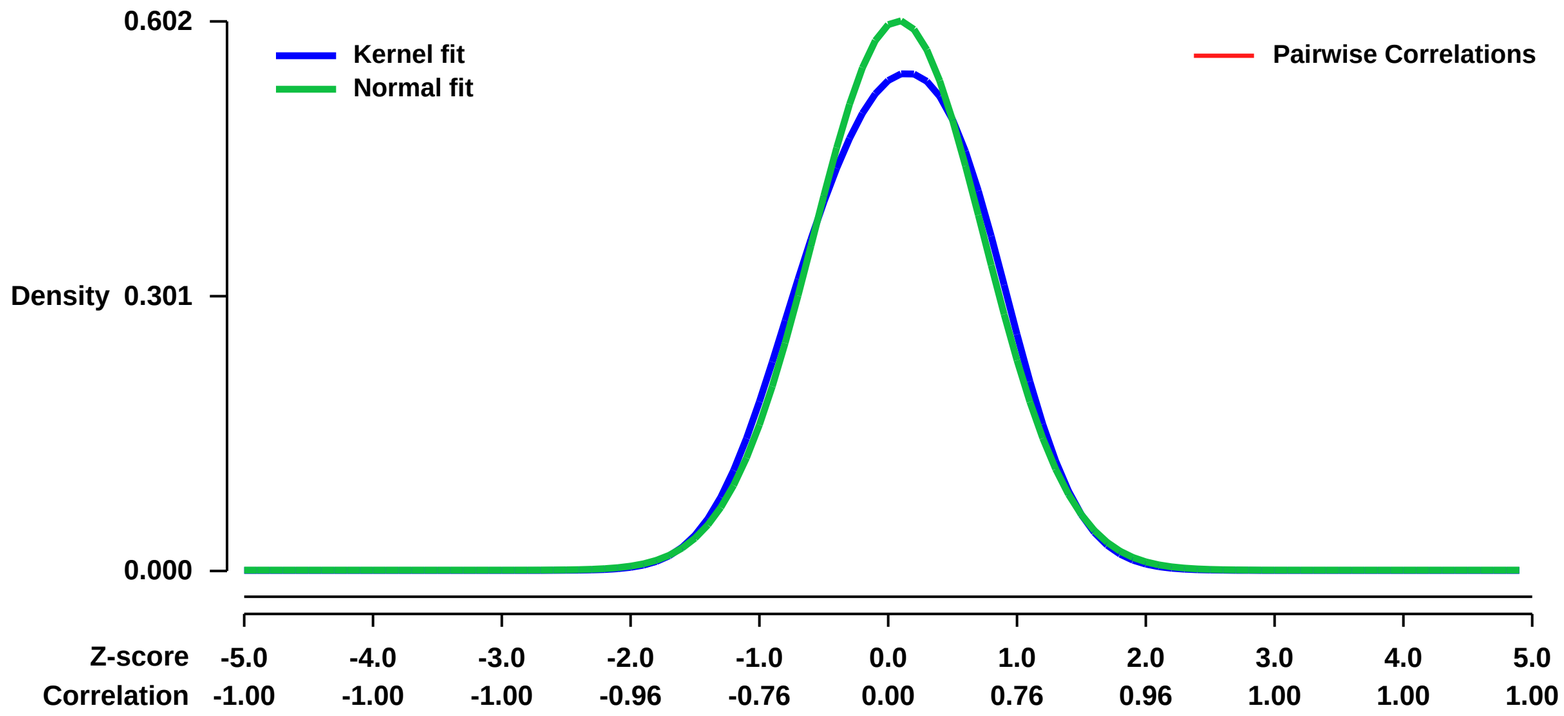

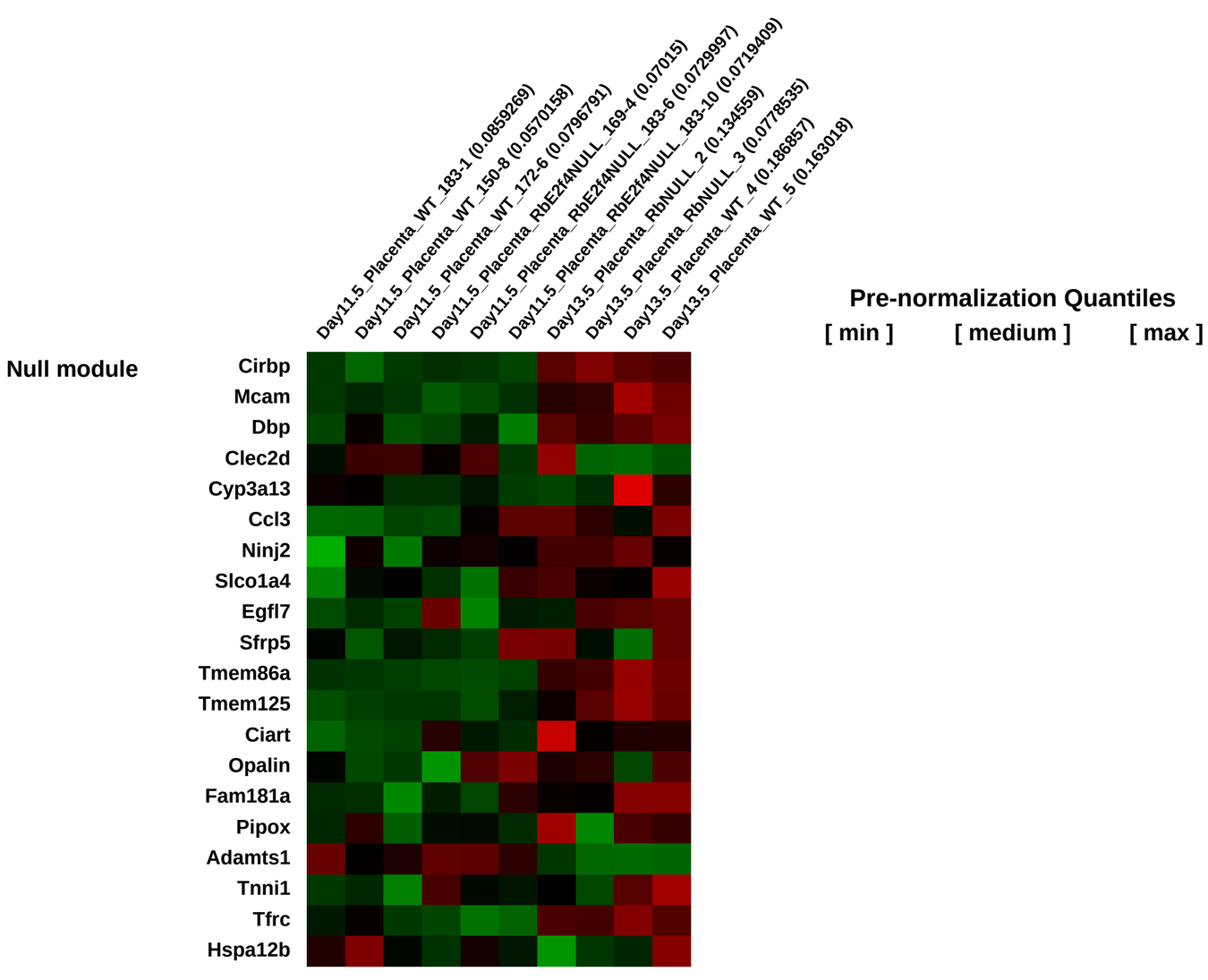

GEO Series "GSE13805" Expression Profiles

Num of samples in this series: 7

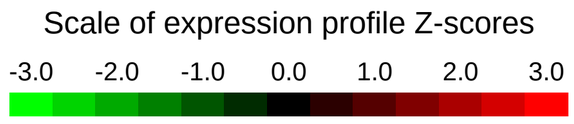

GEO Link:	http://www.ncbi.nlm.nih.gov/geo/query/acc.cgi?acc=GSE13805
Status:	Public on Dec 02 2009
Title:	Expression data from wild type and calreticulin deficient murine embryonic stem cells
Organism:	Mus musculus
Experiment type:	Expression profiling by array
Platform:	GPL1261
Pubmed ID:	20506533
Summary & Design:	**Summary:** Primordial genomic challenge compromises embryonic development and survival, and surveillance of deployed transcriptional programs may provide an early opportunity to forecast phenotype abnormalities. Here, comparisons between wild-type and calreticulin-ablated embryonic stem cells revealed transcriptome shifts precipitated by calreticulin loss. Bioinformatic analysis identified down and up-regulation in 1187 and 418 genes, respectively. Cardiovascular development precedes other organogenic programs, and examination of cardiogenic genes revealed a map of calreticulin-calibrated expression profiles that encompass the developmental regulators, Ccnd1, Ccnd2 and Notch1. Interrogation of primary function in the resolved network forecasted abnormalities during myocardial development. Whole embryo magnetic resonance imaging, verified by pathoanatomical analysis, diagnosed prominent ventricular septal defect. Correlation clustering and network resolution of probesets associated with protein folding/chaperoning and calcium handling demonstrated 14 and 19 genes, respectively, modulated by calreticulin deficiency. Calreticulin deletion provoked ontological re-prioritization of gene expression, molecular transport and protein trafficking that translated into multiple subcellular functional outcomes. Individual stem cell-derived cardiomyocytes lacking calreticulin demonstrated a disorganized contractile apparatus with mitochondrial paucity and architectural aberrations. Thus, bioinformatic deconvolution of primordial embryonic stem cell transcriptomes enables predictive phenotyping of defective developmental networks that coalesce from complex systems biology hierarchies. **Keywords:** Comparison of embryonic stem cell genomes between wild type and calreticulin knockouts **Overall design:** Stem cells cultured in triplicate (or more) were pooled to provide raw material per sample. Each sample represents material collected from three technical replicates or more. In this manner, two wild type samples, and five derived from calreticulin knockout samples, were obtained. Although sample content contains material from three or more technical replicates harvested contemporaneously, each sample is a distinct biological replicate. Total RNA was extracted from each of the samples and RNA pools were profiled on Affymetrix Mouse 430 2.0 Arrays to identify global gene expression changes invoked by genomic ablation of calreticulin.

Background corr dist: KL-Divergence = 0.0370, L1-Distance = 0.0281, L2-Distance = 0.0009, Normal std = 0.6423

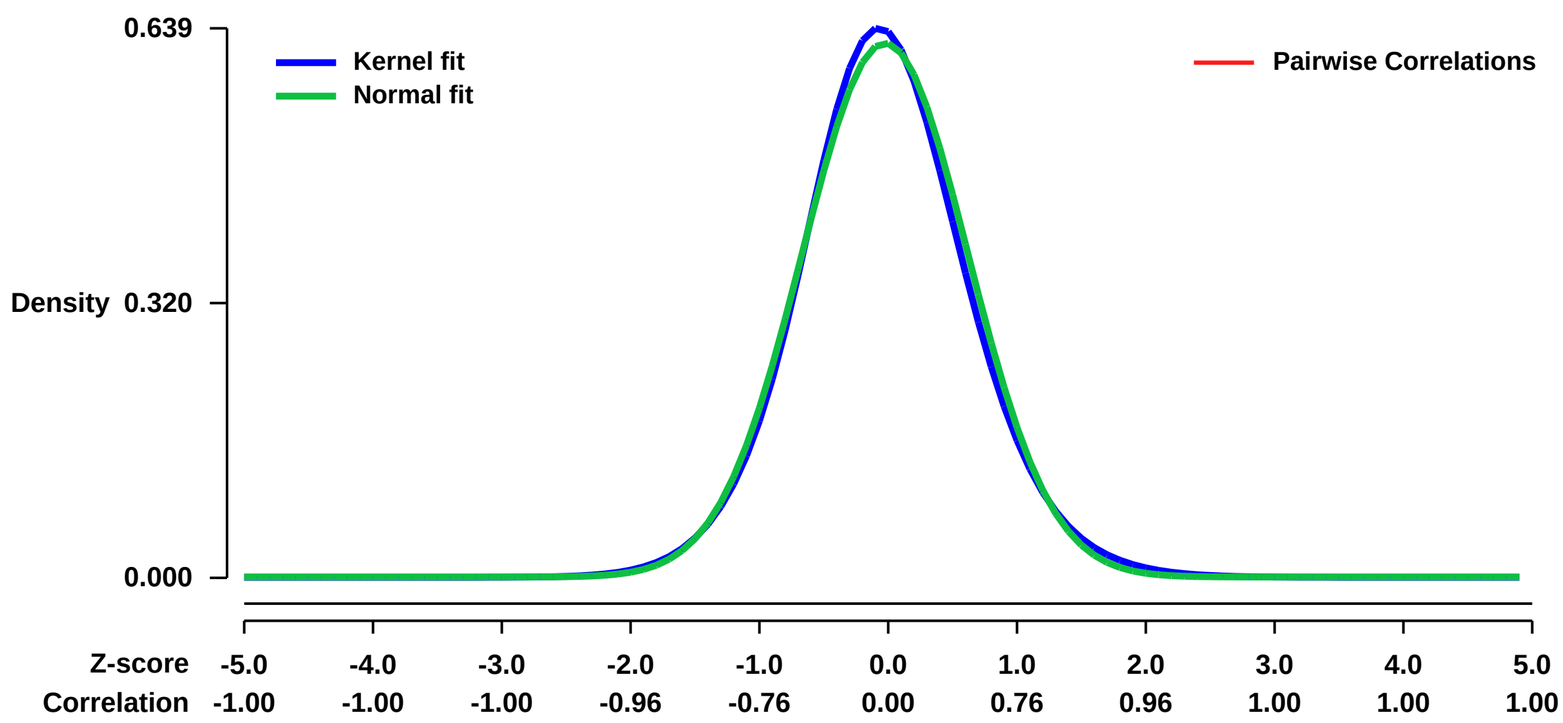

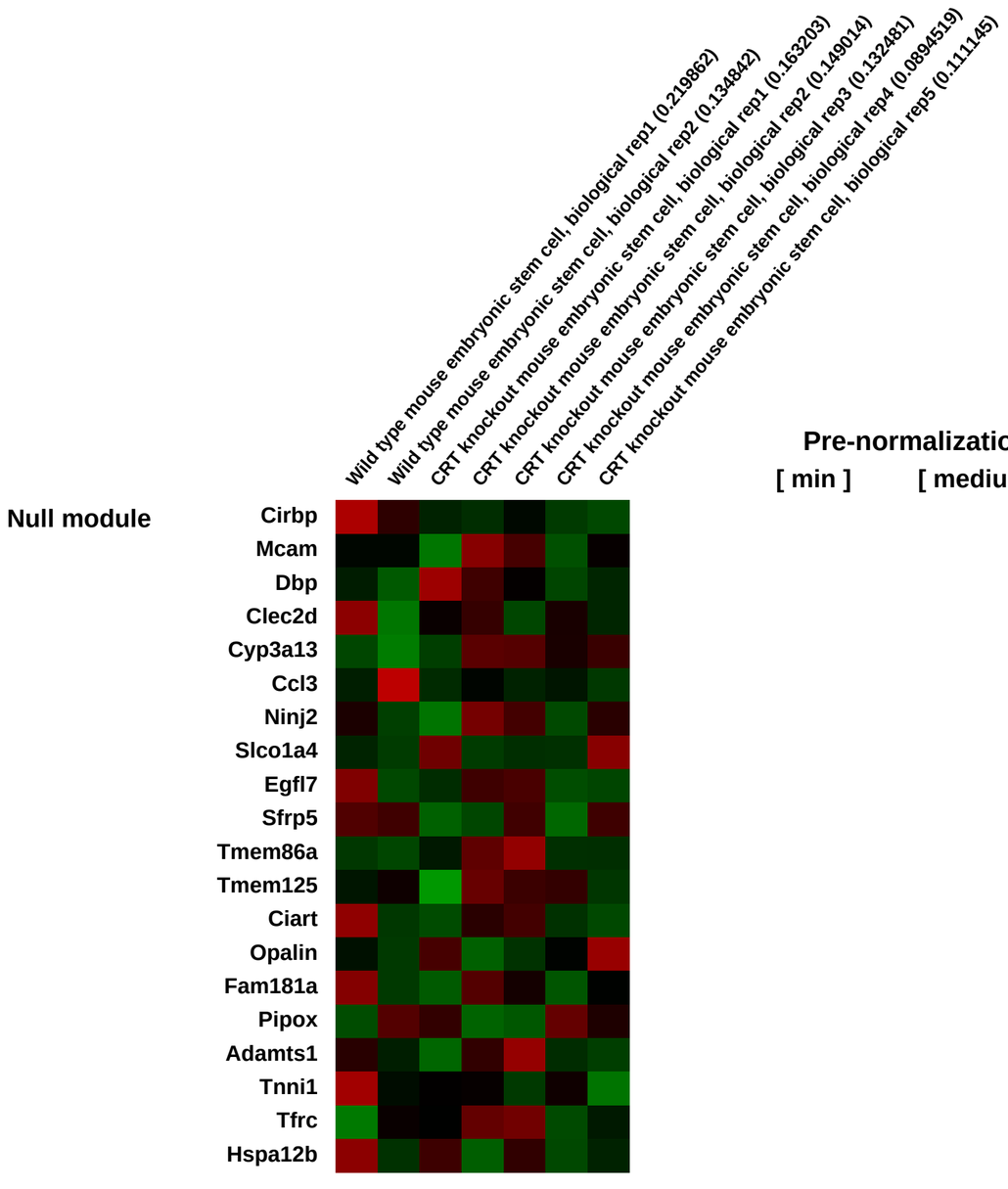

GEO Series "GSE13807" Expression Profiles

Num of samples in this series: 10

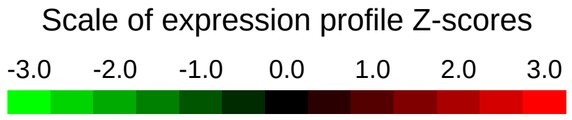

GEO Link:	**http://www.ncbi.nlm.nih.gov/geo/query/acc.cgi?acc=GSE13807**
Status:	**Public on Jan 31 2011**
Title:	**Identification and validation of gene expression changes upon removal of Dicer in the murine limb mesenchyme**
Organism:	**Mus musculus**
Experiment type:	**Expression profiling by array**
Platform:	**GPL1261**
Pubmed ID:	
Summary & Design:	**Summary:** **Wild type and Dicer null embryonic mouse limbs were analaysed using Affymetrix arrays to identify gene expression changes. Genes that were up-regulated in Dicer-null limbs were canidates for being miRNA targets.** **Potential miRNA target genes were validated using qRTPCR.** **Overall design:** **Mice carrying a heterozygous Dicer floxed allele and the prxcre driver allele were crossed to homozygous Dicer Floxed mice. Embryos were harvested from pregent moms and genotyped to determine heterozygous, Wild type and mutant limb buds. These limb buds were used to prepare RNA for array analysis.**

Background corr dist: **KL-Divergence = 0.0730, L1-Distance = 0.0212, L2-Distance = 0.0005, Normal std = 0.4901**

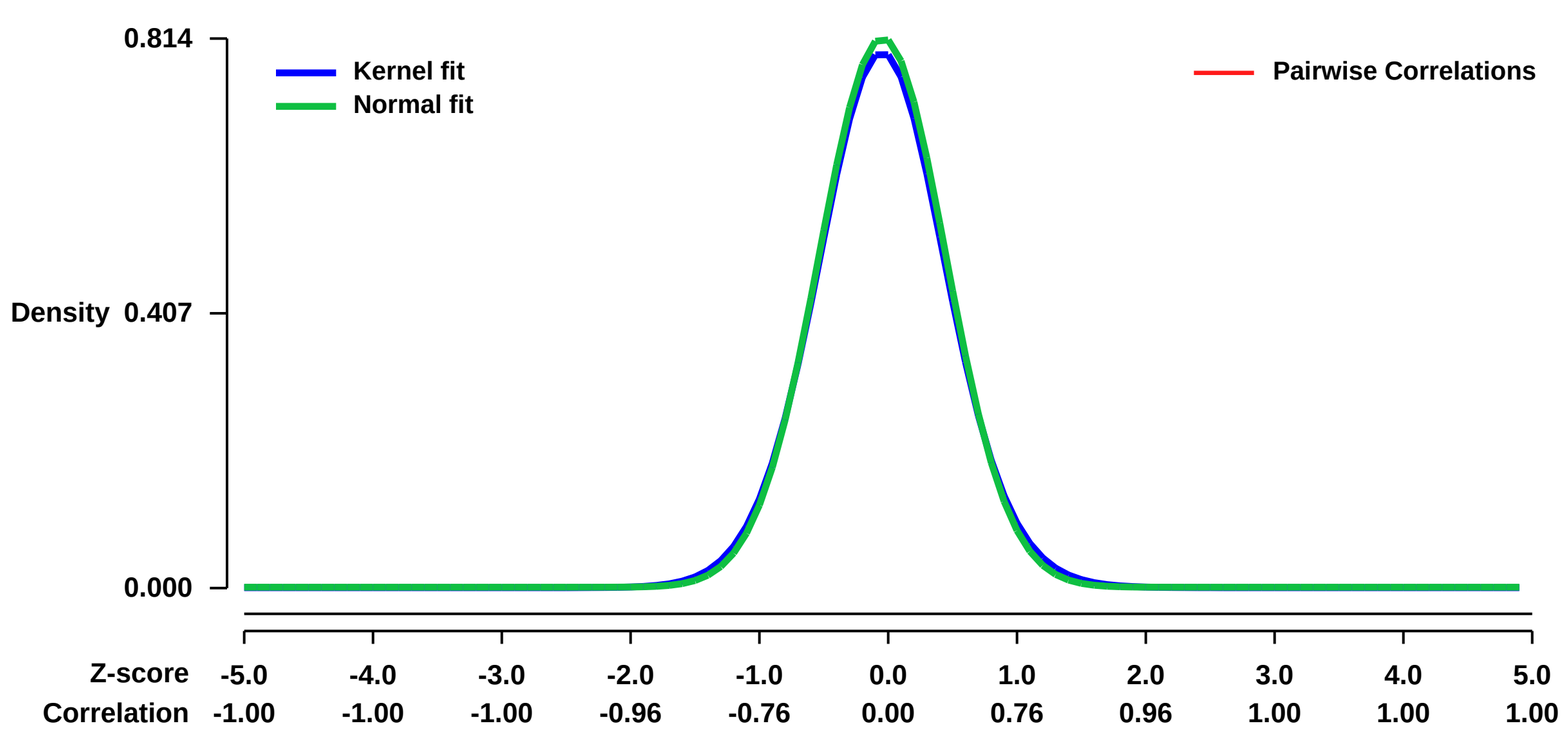

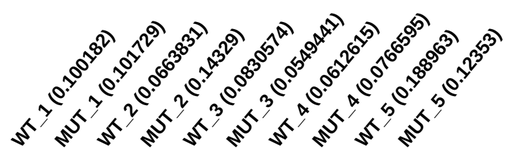

Pre-normalization Quantiles

[min] [medium] [max]

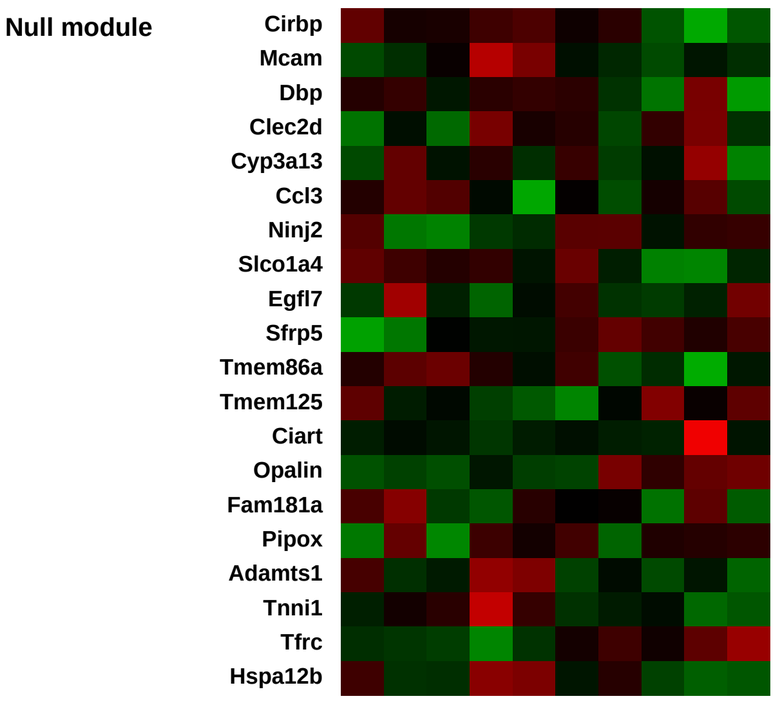

GEO Series "GSE13869" Expression Profiles

Num of samples in this series: 8

Scale of expression profile Z-scores

-3.0 -2.0 -1.0 0.0 1.0 2.0 3.0

GEO Link:	http://www.ncbi.nlm.nih.gov/geo/query/acc.cgi?acc=GSE13869
Status:	Public on Jan 24 2010
Title:	Transcriptome of the Nxnl1-/- mouse retina
Organism:	Mus musculus
Experiment type:	Expression profiling by array
Platform:	GPL1261
Pubmed ID:	20139892
Summary & Design:	**Summary:** Rod-derived Cone Viability Factor (RdCVF, alias nxnl1) is a retina-specific protein identified for its therapeutic potential in supporting cone survival during retinal degeneration. A nxnl1 knockout mouse model was created and the transcriptome used to demonstrate that the retina is compromised by the absence of nxnl1. Keywords: genetic modification, transcription-profile, retina **Overall design:** In total 9 samples were analyzed, they represent three different genotypes (wt/wt, ko/wt, ko/ko) that were tested in triplicate each.

Background corr dist: KL-Divergence = 0.0528, L1-Distance = 0.0188, L2-Distance = 0.0005, Normal std = 0.5499

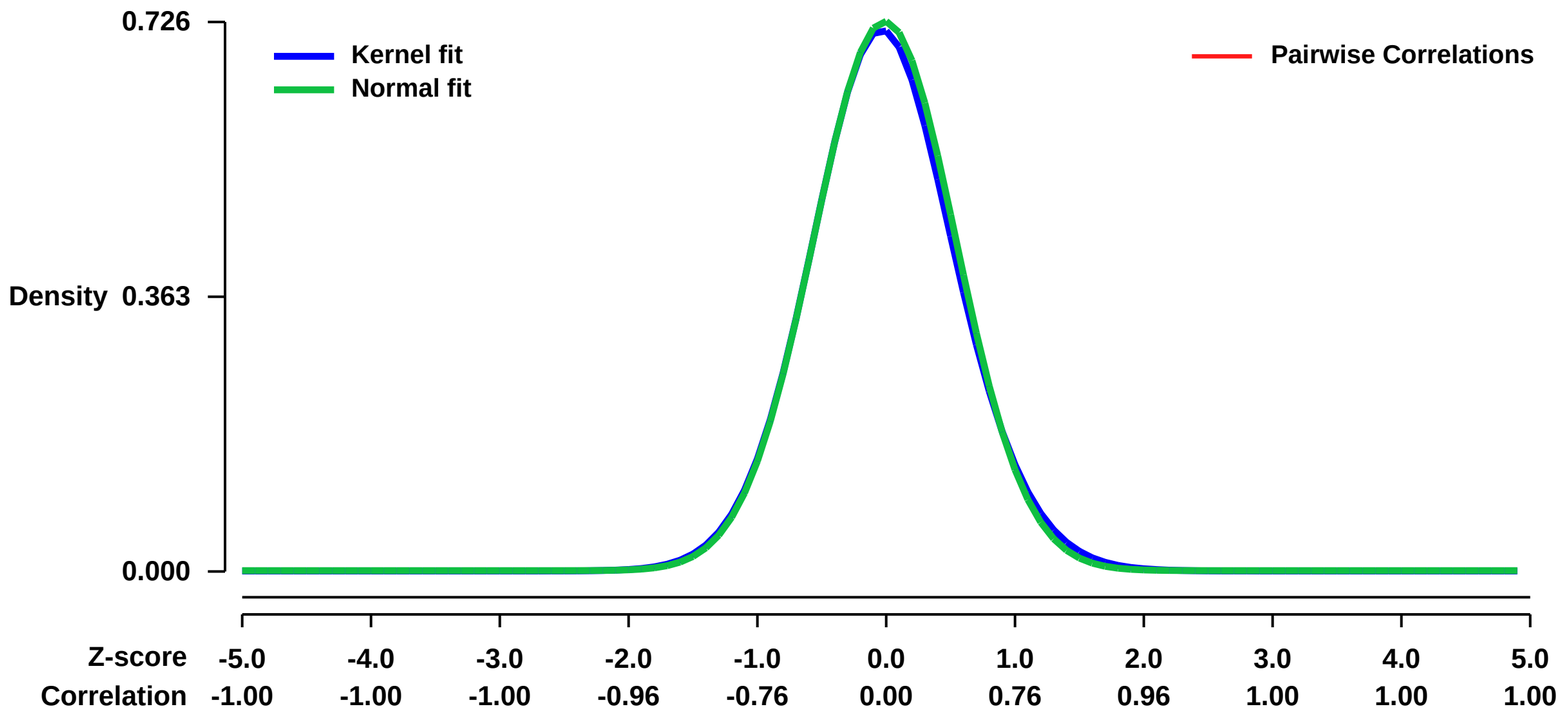

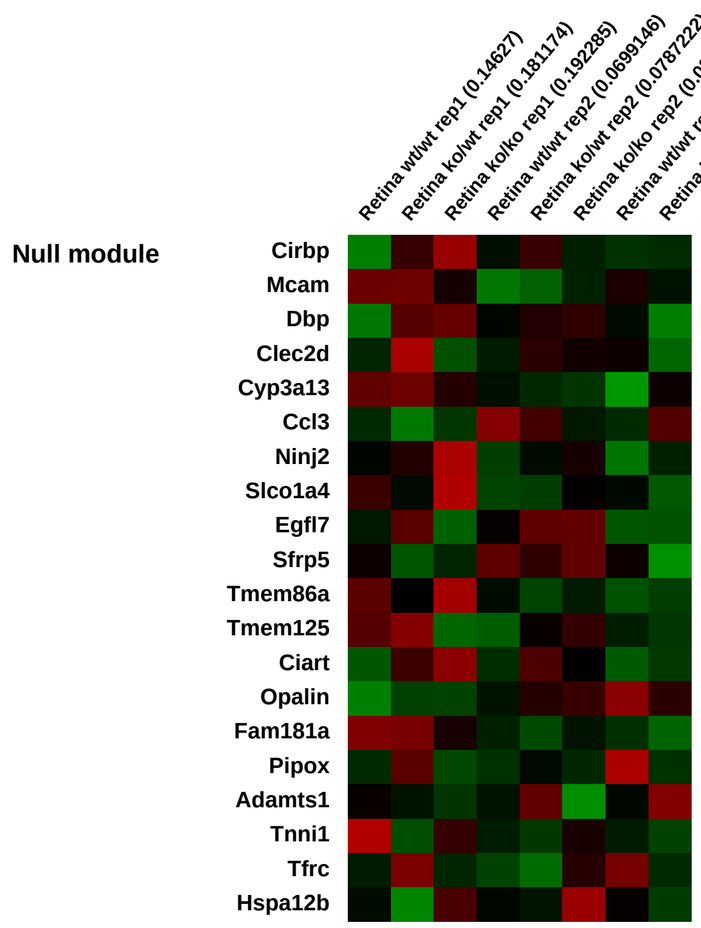

GEO Series "GSE13948" Expression Profiles

Num of samples in this series: 21

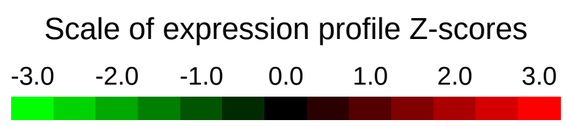

GEO Link:	http://www.ncbi.nlm.nih.gov/geo/query/acc.cgi?acc=GSE13948
Status:	Public on Dec 16 2008
Title:	Antagonism of microRNA-122 in mice by systemically administered LNA-antimiR
Organism:	Mus musculus
Experiment type:	Expression profiling by array
Platform:	GPL1261
Pubmed ID:	18158304
Summary & Design:	**Summary:** **Antagonism of microRNA-122 in mice by systemically administered LNA-antimiR leads to up-regulation of a large set of predicted target mRNAs in the liver** **MicroRNA-122 (miR-122) is an abundant liver-specific miRNA, implicated in fatty acid and cholesterol metabolism as well as hepatitis C viral replication. Here, we report that a systemically administered 16-nt, unconjugated LNA (locked nucleic acid)-antimiR oligonucleotide complementary to the 5' end of miR-122 leads to specific, dose-dependent silencing of miR-122 and shows no hepatotoxicity in mice. Antagonism of miR-122 is due to formation of stable heteroduplexes between the LNA-antimiR and miR-122 as detected by northern analysis. Fluorescence in situ hybridization demonstrated uptake of the LNA-antimiR in mouse liver cells, which was accompanied by markedly reduced hybridization signals for mature miR-122 in treated mice. Functional antagonism of miR-122 was inferred from a low cholesterol phenotype and de-repression within 24 h of 199 liver mRNAs showing significant enrichment for miR-122 seed matches in their 3' UTRs. Expression profiling extended to 3 weeks after the last LNA-antimiR dose revealed that most of the changes in liver gene expression were normalized to saline control levels coinciding with normalized miR-122 and plasma cholesterol levels. Combined, these data suggest that miRNA antagonists comprised of LNA are valuable tools for identifying miRNA targets in vivo and for studying the biological role of miRNAs and miRNA-associated gene-regulatory networks in a physiological context.** **Keywords: compound treatment** **Overall design:** **Female NMRI mice were treated at day 2 with either 25mg/kg antimiR-122 (SPC3372) or vehicle (saline). Mice were sacrificied at day 3, 9 and 23 and liver RNA assayed. Three biological replicates for each of the six groups.**

Background corr dist: KL-Divergence = 0.2960, L1-Distance = 0.0653, L2-Distance = 0.0117, Normal std = 0.2812

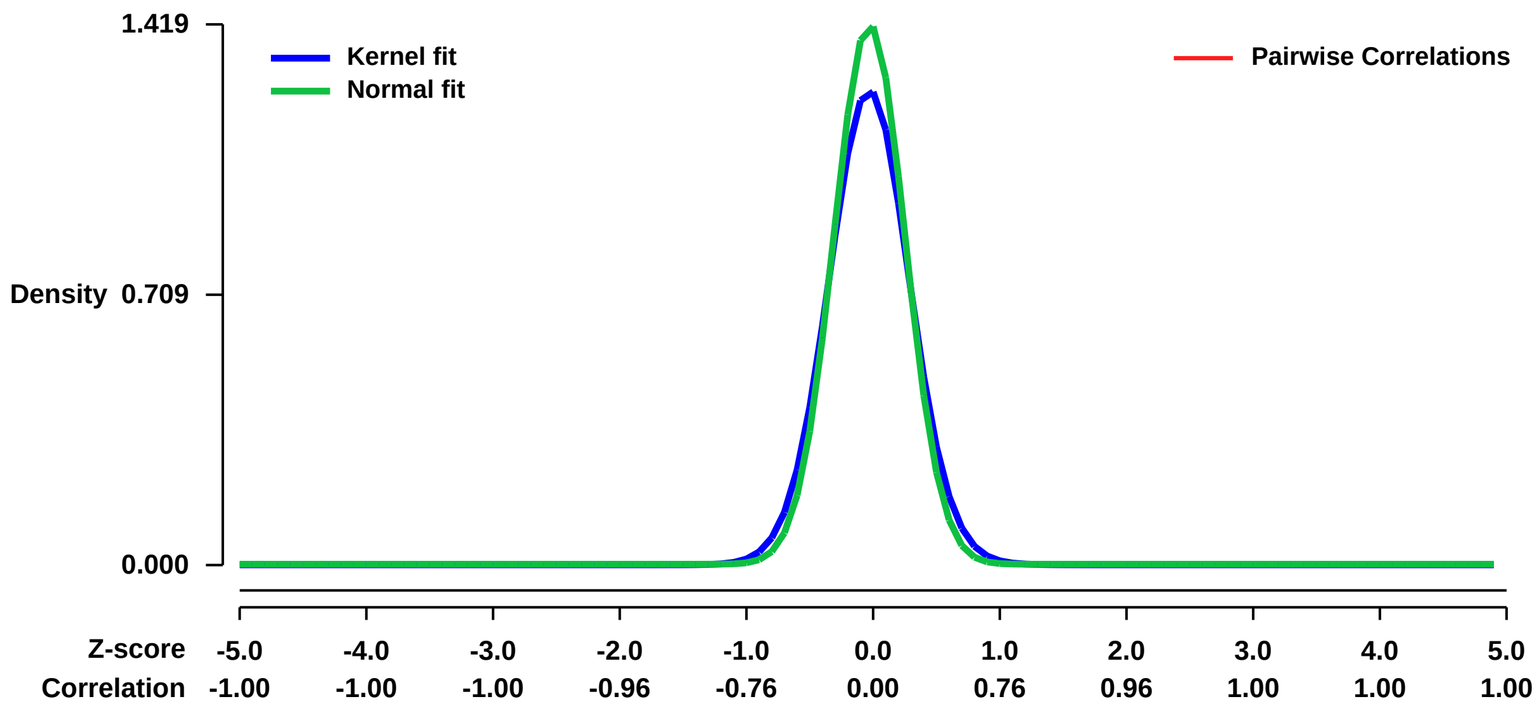

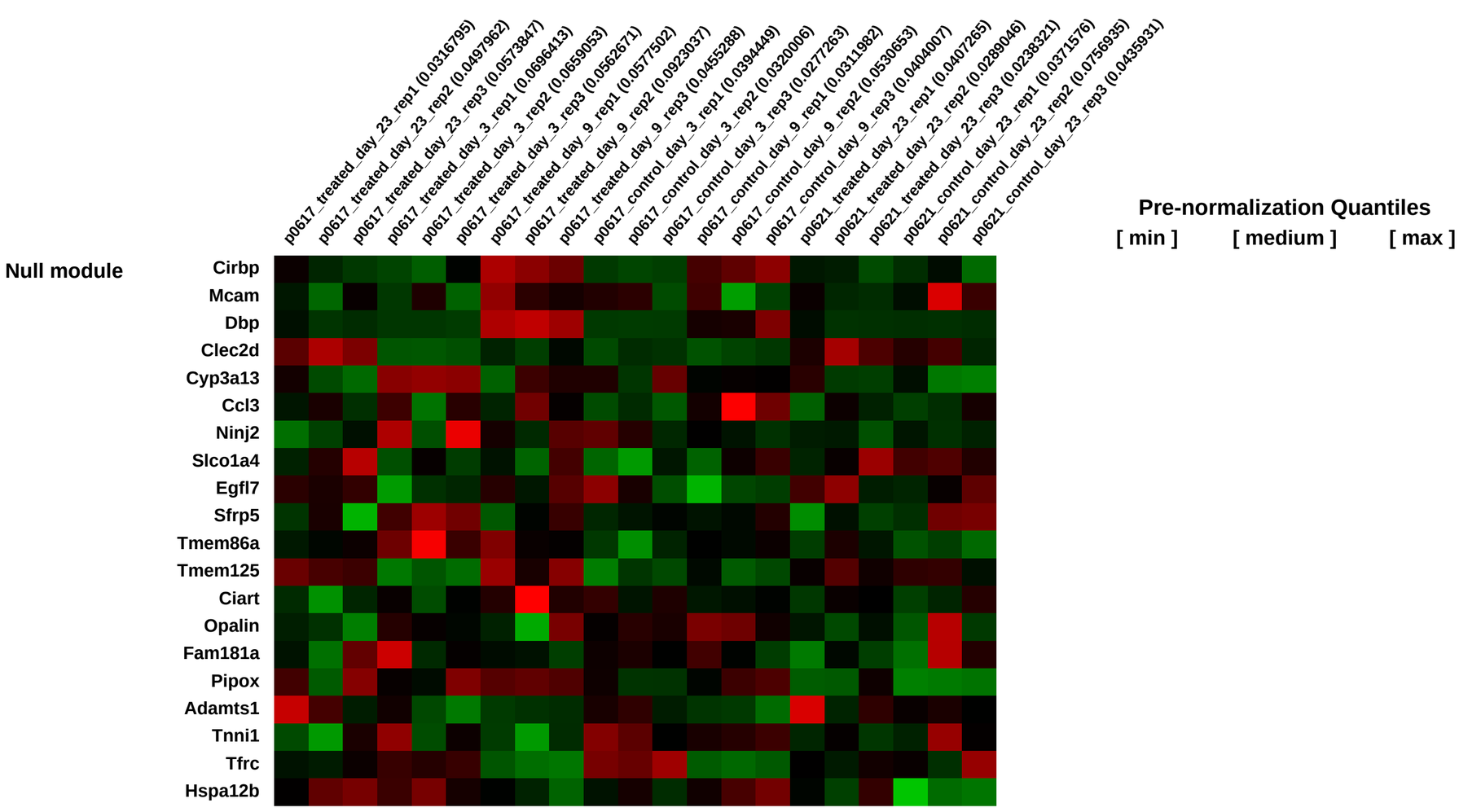

GEO Series "GSE14007" Expression Profiles

Num of samples in this series: 8

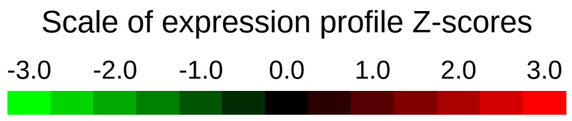

GEO Link:	**http://www.ncbi.nlm.nih.gov/geo/query/acc.cgi?acc=GSE14007**
Status:	**Public on Dec 23 2008**
Title:	**Gene expression of growth plate of mouse.**
Organism:	**Mus musculus**
Experiment type:	**Expression profiling by array**
Platform:	**GPL1261**
Pubmed ID:	
Summary & Design:	**Summary:** **The growth plate is histomorphologically classified into four zones {resting zone (RZ), proliferating zone (PZ), maturing zone (MZ) and hypertrophic zone (HZ)}. Gene expression profile analyses of 4 zones were performed using microarrays.** **Overall design:** **We performed global analysis of gene expression in tibias from nine-day-old mice. Chondrocytes layer was microdissected en-block from four anatomically distinct growth plate zones, and RNA expression was analyzed using microarrays.Chondrocytes from four anatomical zones were isolated from tibias of two mice. The eight samples were named after the mouse (1 or 2) and the growth plate zone, such as resting zone of 1st mouse (RZ01), 2nd mouse (RZ02), proliferation zone (PZ01, PZ02), maturing zone (MZ01, MZ02) and hypertrophic zone (HZ01, HZ02).**

Background corr dist: **KL-Divergence = 0.0621, L1-Distance = 0.0278, L2-Distance = 0.0013, Normal std = 0.5305**

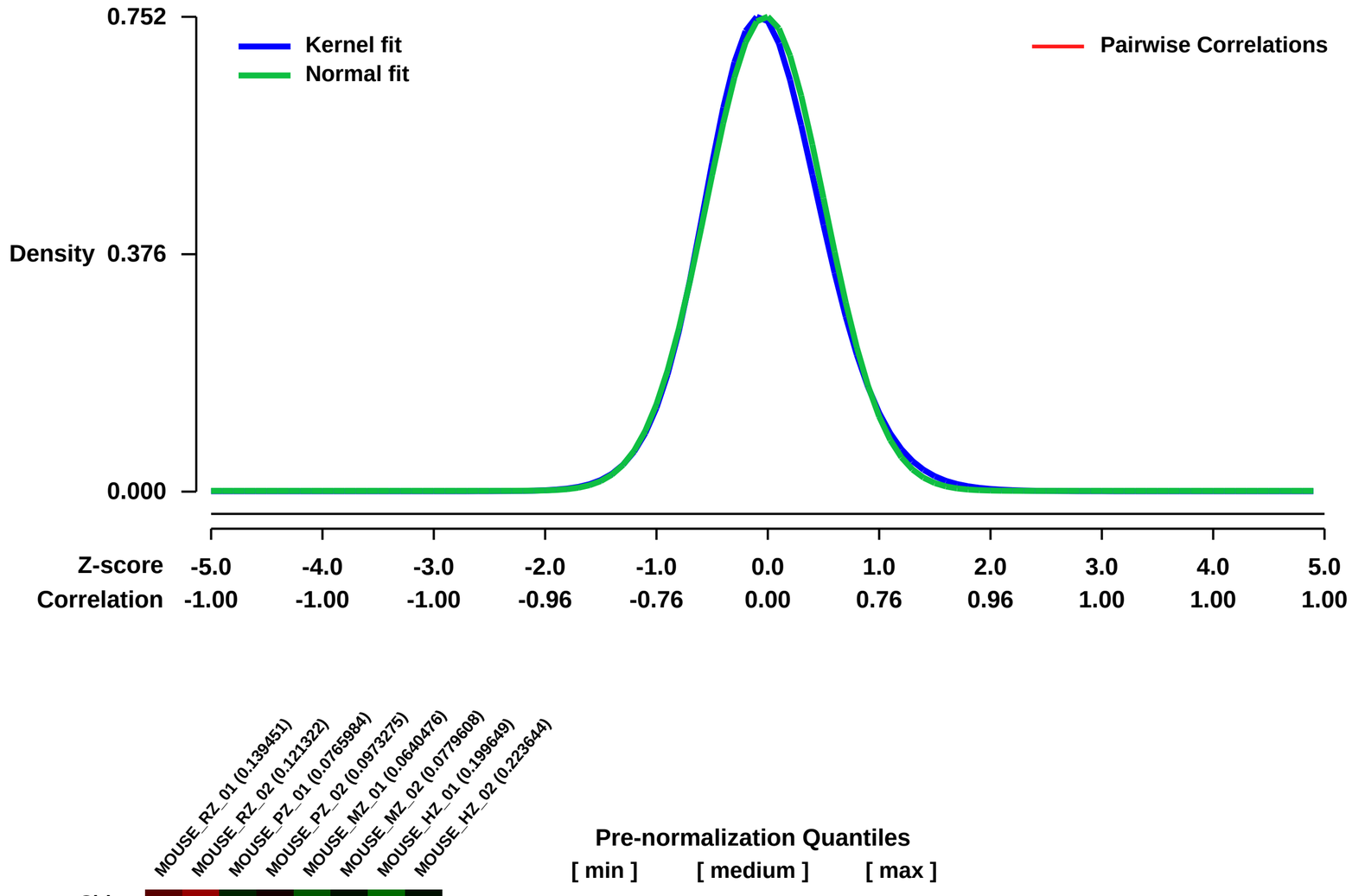

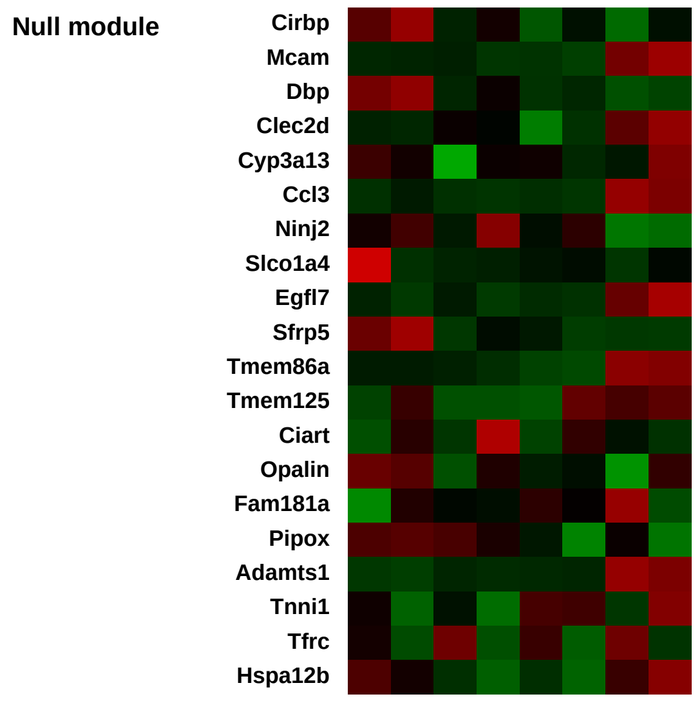

GEO Series "GSE14024" Expression Profiles

Num of samples in this series: 12

Scale of expression profile Z-scores

-3.0 -2.0 -1.0 0.0 1.0 2.0 3.0

GEO Link: http://www.ncbi.nlm.nih.gov/geo/query/acc.cgi?acc=GSE14024

Status: Public on May 27 2009

Title: Reversal of oncogene transformation and suppression of tumor growth by the novel IGF1R kinase inhibitor A-928605.

Organism: Mus musculus

Experiment type: Expression profiling by array

Platform: GPL1261

Pubmed ID: 19732452

Summary & Design:

Summary:
The insulin-like growth factor (IGF) axis is an important signaling pathway in the growth and survival of many cell types and has been implicated in multiple aspects of cancer progression from tumorigenesis to metastasis. The multiple roles of IGF signaling in cancer suggest that selective inhibition of the pathway might yield clinically effective therapeutics. Here we describe A-928605, a novel small molecule inhibitor of the receptor tyrosine kinase responsible for IGF signal transduction. This small molecule is able to abrogate activation of the pathway as shown by effects on the target and downstream effectors and is shown to be effective at inhibiting the proliferation of an oncogene addicted tumor model cell line (CD8-IGF1R 3T3) both in vitro and in vivo.

Keywords: Treatment Response

Overall design:
CD8-IGF1R 3T3 cells and 3T3 Vector control treated for 24 h with vehicle or IGF1R inhibitor A-928605, all with 3 replicates.

Background corr dist: KL-Divergence = 0.0597, L1-Distance = 0.0249, L2-Distance = 0.0008, Normal std = 0.5420

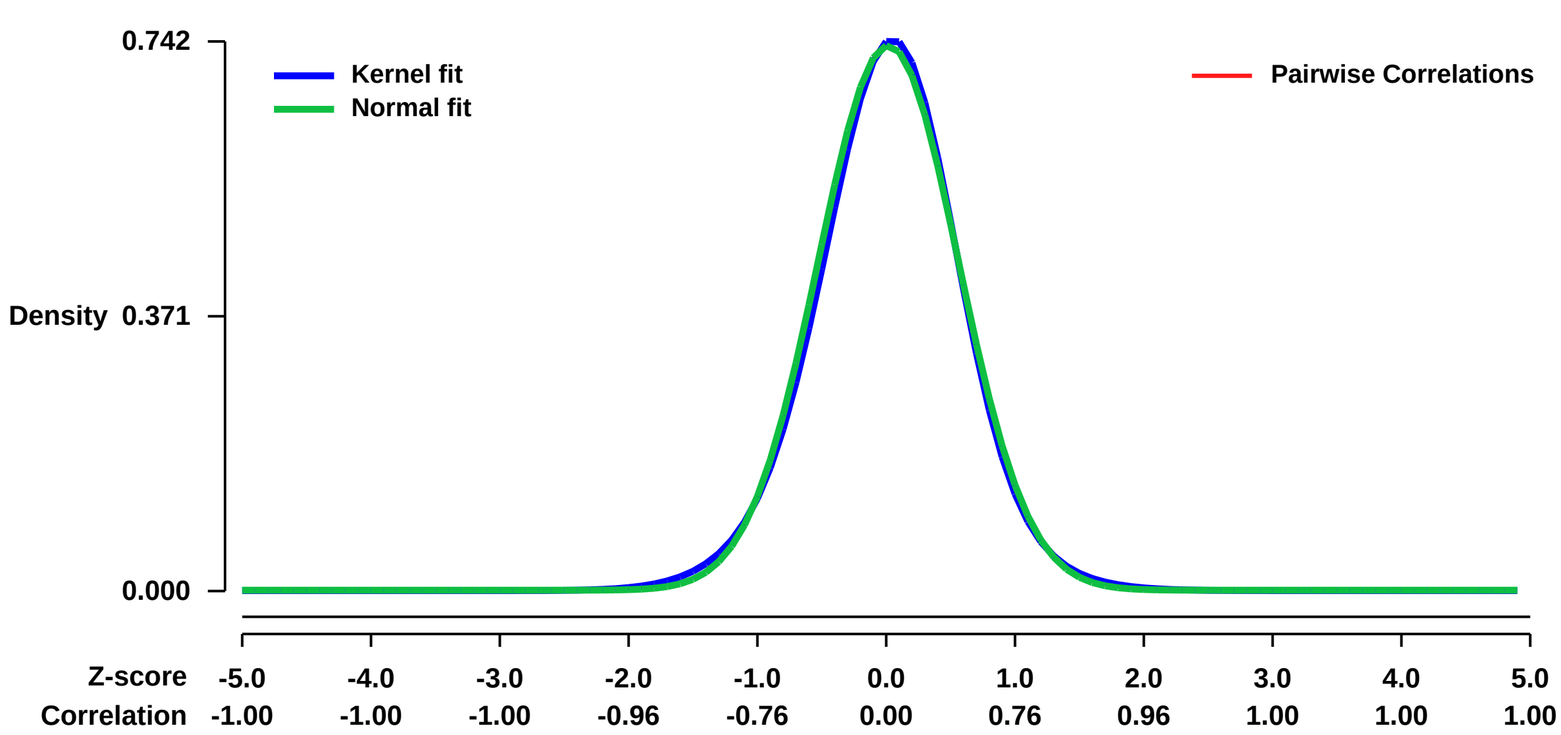

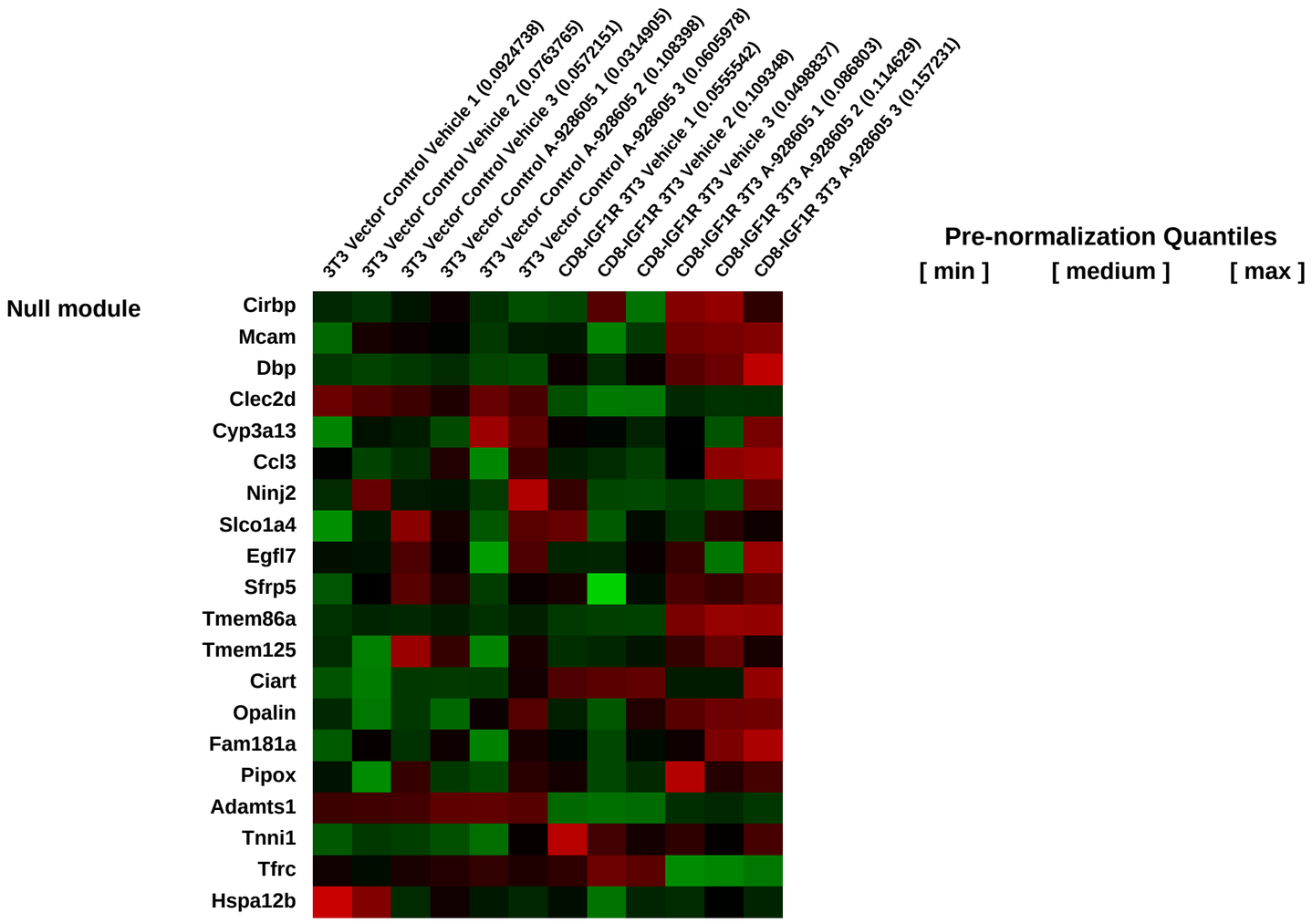

GEO Series "GSE14059" Expression Profiles

Num of samples in this series: 6

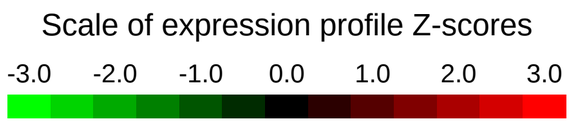

GEO Link:	**http://www.ncbi.nlm.nih.gov/geo/query/acc.cgi?acc=GSE14059**
Status:	**Public on Apr 01 2009**
Title:	**Gene expression profiles of heterozygous periphilin knockout mice compared to wt littermates**
Organism:	**Mus musculus**
Experiment type:	**Expression profiling by array**
Platform:	**GPL1261**
Pubmed ID:	
Summary & Design:	**Summary:** **Periphilin is a protein which is involved in multiple processes in vivo, including terminal differentiation of keratinozytes as well as cell-cycle and cancer related functions. Here we generated mice with a targeted disruption of the periphilin-1 gene to explore its physiological role from an organismic perspective. In accordance with a ubiquitous expression of periphilin in the murine embryo, the homozygous deficiency of periphilin is lethal in early embryogenesis. We therefore characterized mice with a disruption of only one periphilin allele. As heterozygous periphilin knockout mice show no obvious histological alterations and have no apparent behavioural phenotypes, we compared whole transcriptome RNA expression profiles of total brain tissue of periphilin+/- knockout mice and wild type littermates for an in-depth analysis of heterozygous animals. In periphilin+/- knockout mice, 3 probe sets were indicative of significant differential expression (p â∕0.05, SLR â¥ 1 which is equivalent to 2 fold). Two of these probe sets (1438864_at and 1439170_at) refer to unannotated or unclassifiable genes. According to the NetAffxâ¢ Analysis Center, the third probe set (1447831_s_at) is assigned to myotubularin related protein 7 (Mtmr7). The probe set, however, lies upstream of the Mtmr7 gene (Ensembl gene ENSMUSG00000039431), and its signal is therefore not representative for the Mtmr7 gene. Quantitative RT-PCR (qRT-PCR) analysis with a primer set specific for Mtmr7 confirmed that its expression is not altered in periphilin+/- knockout mice (relative expression compared to wild type: 0.924; p = 0.419). In summary, none of more than 45.000 covered transcripts is differentially expressed in periphilin+/- knockout mice in comparison to wild type littermates.** **Overall design:** **Whole brains of three male 2-months-old periphilin+/-knockout mice and three C57BL/6-wild type littermates**

Background corr dist: KL-Divergence = 0.0487, L1-Distance = 0.0187, L2-Distance = 0.0004, Normal std = 0.5774

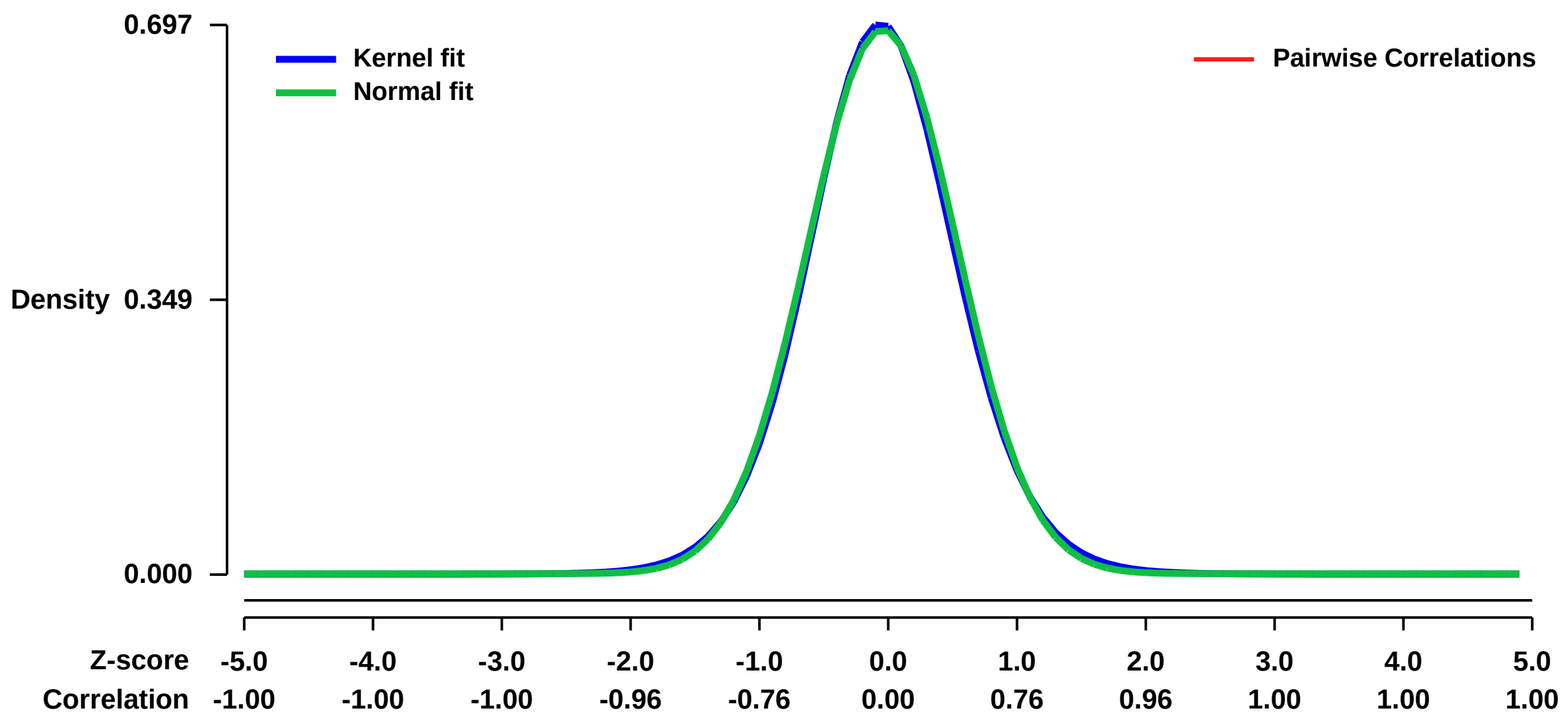

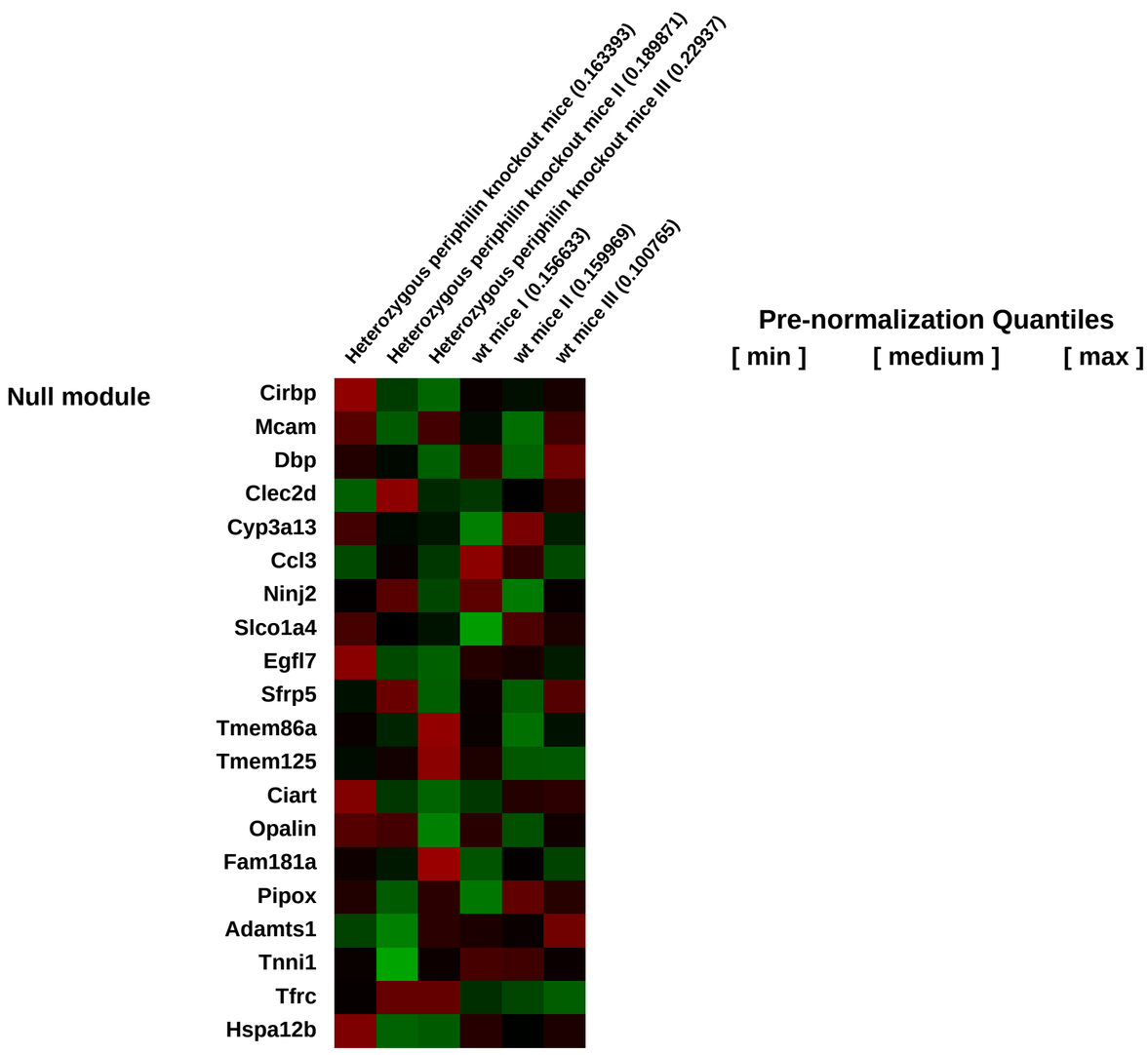

GEO Series "GSE14088" Expression Profiles

Num of samples in this series: 9

Scale of expression profile Z-scores

-3.0 -2.0 -1.0 0.0 1.0 2.0 3.0

GEO Link:	http://www.ncbi.nlm.nih.gov/geo/query/acc.cgi?acc=GSE14088
Status:	Public on Mar 24 2009
Title:	E2-RING expansion of the NEDD8 cascade confers specificity to cullin modification
Organism:	Mus musculus
Experiment type:	Expression profiling by array
Platform:	GPL1261
Pubmed ID:	19250909
Summary & Design:	**Summary:** Ubiquitin and ubiquitin-like proteins (UBLs) are directed to targets by cascades of E1, E2, and E3 enzymes. The largest ubiquitin E3 subclass consists of cullin-RING ligases (CRLs), which contain one each of several cullins (CUL1, -2, -3, -4, or -5) and RING proteins (RBX1 or -2). CRLs are activated by ligation of the UBL NEDD8 to a conserved cullin lysine. How is cullin NEDD8ylation specificity established? Here we report that, like UBE2M (also known as UBC12), the previously uncharacterized E2 UBE2F is a NEDD8-conjugating enzyme in vitro and in vivo. Biochemical and structural analyses indicate how plasticity of hydrophobic E1-E2 interactions and E1 conformational flexibility allow one E1 to charge multiple E2s. The E2s have distinct functions, with UBE2M/RBX1 and UBE2F/RBX2 displaying different target cullin specificities. Together, these studies reveal the molecular basis for and functional importance of hierarchical expansion of the NEDD8 conjugation system in establishing selective CRL activation. Mol Cell 33:483-495, 2009. Keywords: Comparison of gene expression profiles **Overall design:** NIH 3T3 cells were transduced with retroviral constructs containing shRNA directed against Ube2m or Ube2f. Three replicates of each condition were analyzed.

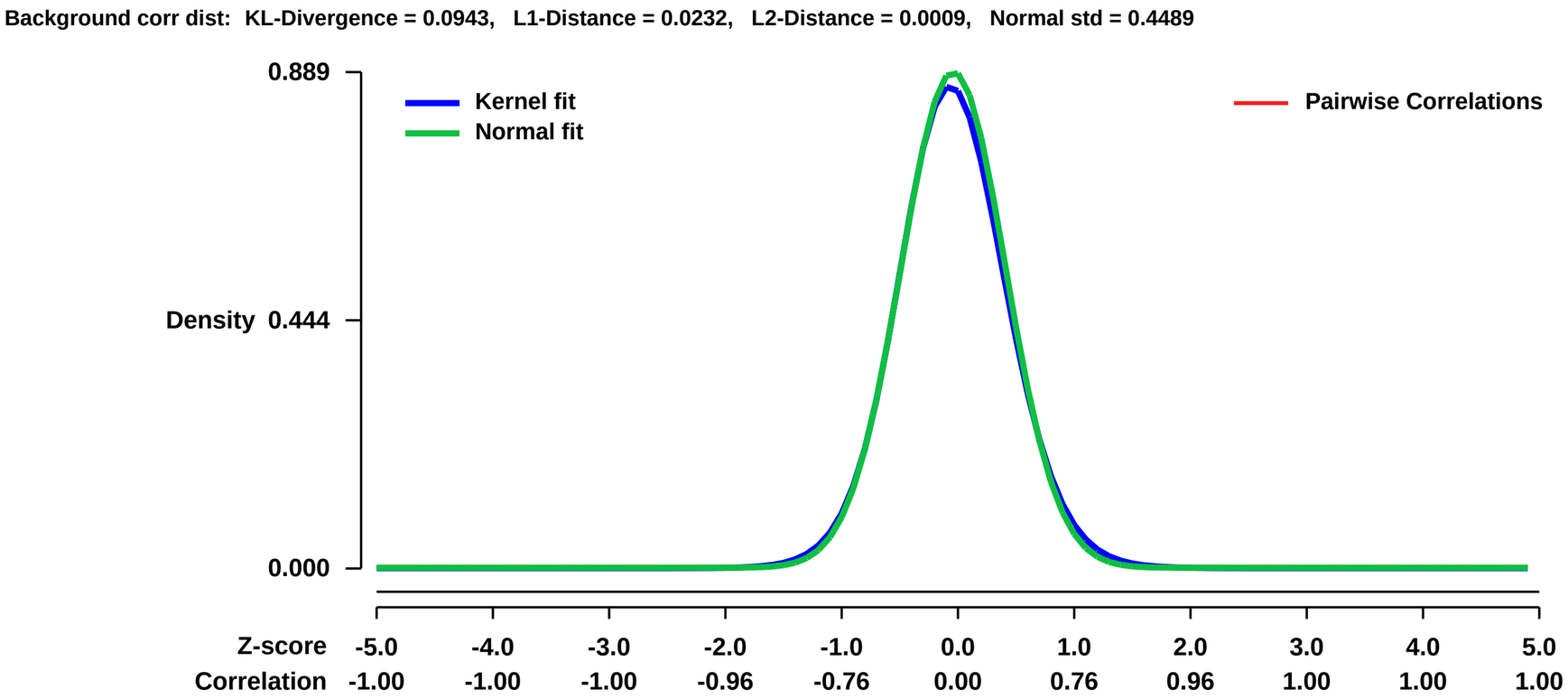

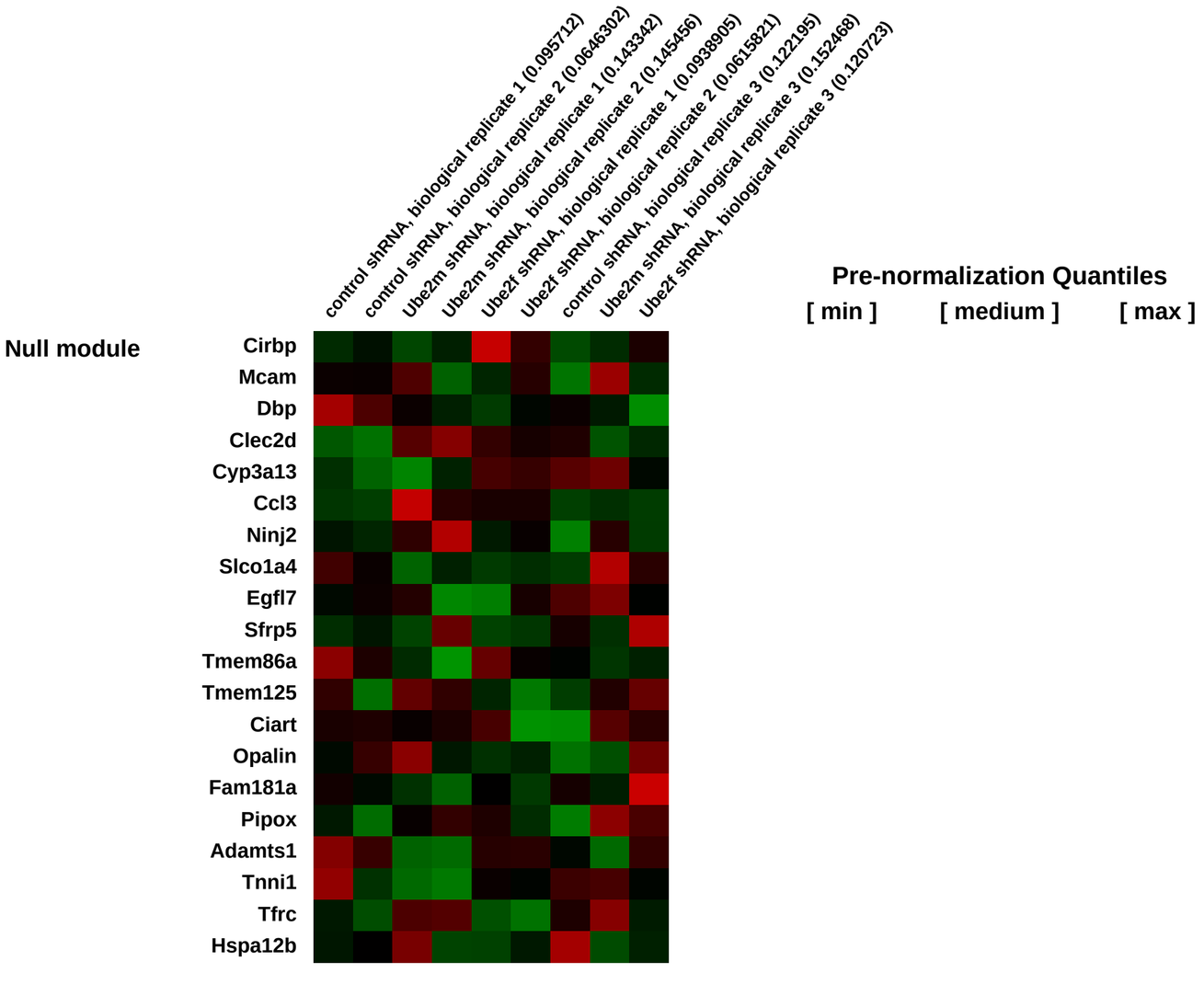

GEO Series "GSE14101" Expression Profiles

Num of samples in this series: 10

Scale of expression profile Z-scores

-3.0 -2.0 -1.0 0.0 1.0 2.0 3.0

GEO Link:	http://www.ncbi.nlm.nih.gov/geo/query/acc.cgi?acc=GSE14101
Status:	Public on Dec 23 2008
Title:	Genes regulated by Meis1 in murine Mll-AF9 leukemia cells
Organism:	Mus musculus
Experiment type:	Expression profiling by array
Platform:	GPL1261
Pubmed ID:	19109563
Summary & Design:	**Summary:** Leukemias with MLL-rearrangements are characterized by high expression of the homeo box gene MEIS1. In these studies, we knocked down Meis1 expression by shRNA lentivirus transduction in murine Mll-AF9 leukemia cells. Meis1 knockdown resulted in decreased proliferation and survival of murine Mll-AF9 leukemia cells. We also observed reduced clonogenic capacity and increased monocytic differentiation. The establishment of leukemia in transplant recipients was significantly delayed by Meis1 knockdown. Gene expression profiling of cells transduced with Meis1 shRNA showed reduced expression of genes associated with cell cycle entry and progression. shRNA mediated knockdown of MEIS1 in human MLL-fusion gene leukemia cell lines resulted in reduced cell growth. These results show that MEIS1 expression is important for MLL-rearranged leukemias and suggest that MEIS1 promotes cell cycle entry. Targeting MEIS1 may have therapeutic potential for treating leukemias expressing this transcription factor. **Keywords: Gene expression** **Overall design:** Murine Mll-AF9 leukemia (4166) cells were transduced with lentivirus expressing shRNA against Meis1 or control lentivirus (empty vector). Gene expression profiles were compared at 48 hours post transduction, using Puromycin as selection agent for transduced cells.

Background corr dist: KL-Divergence = 0.1103, L1-Distance = 0.0295, L2-Distance = 0.0014, Normal std = 0.4200

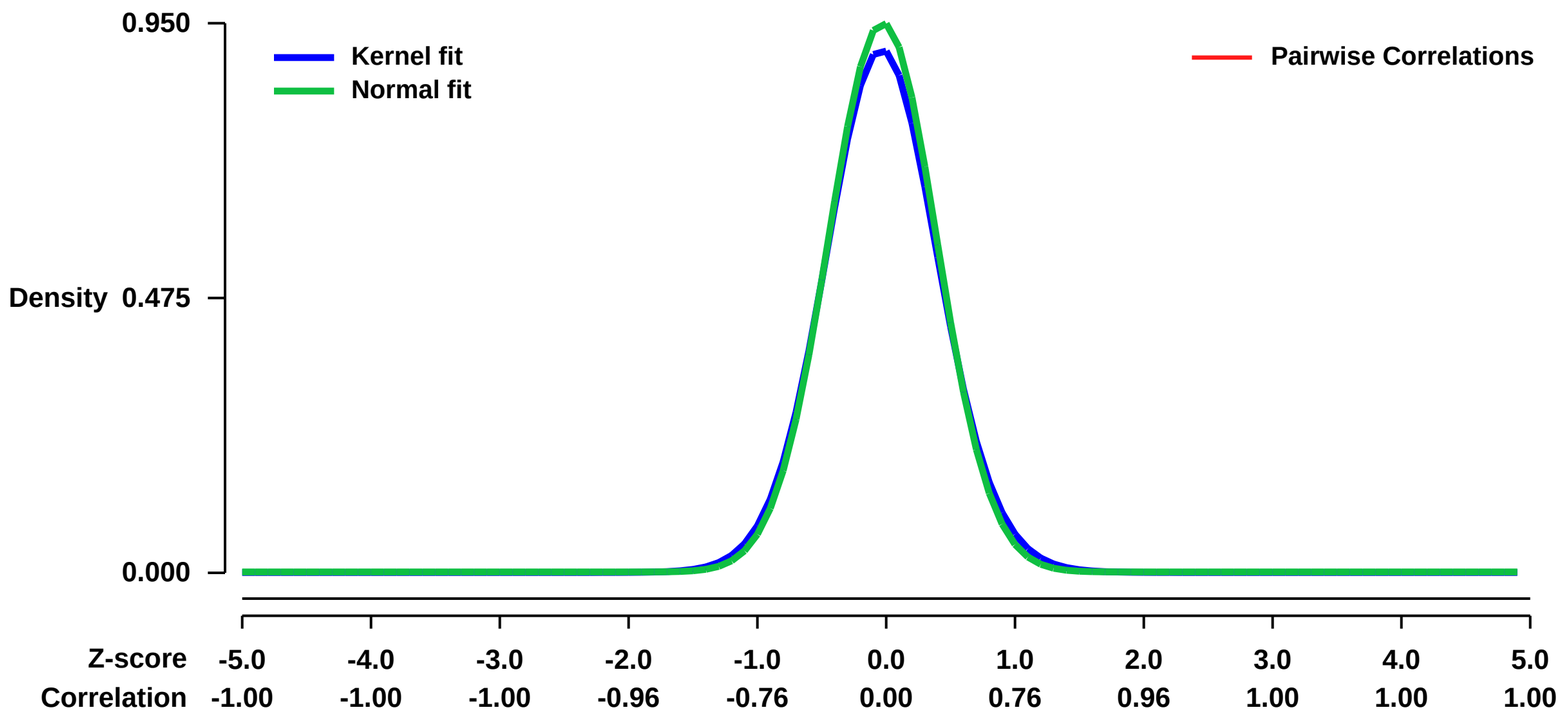

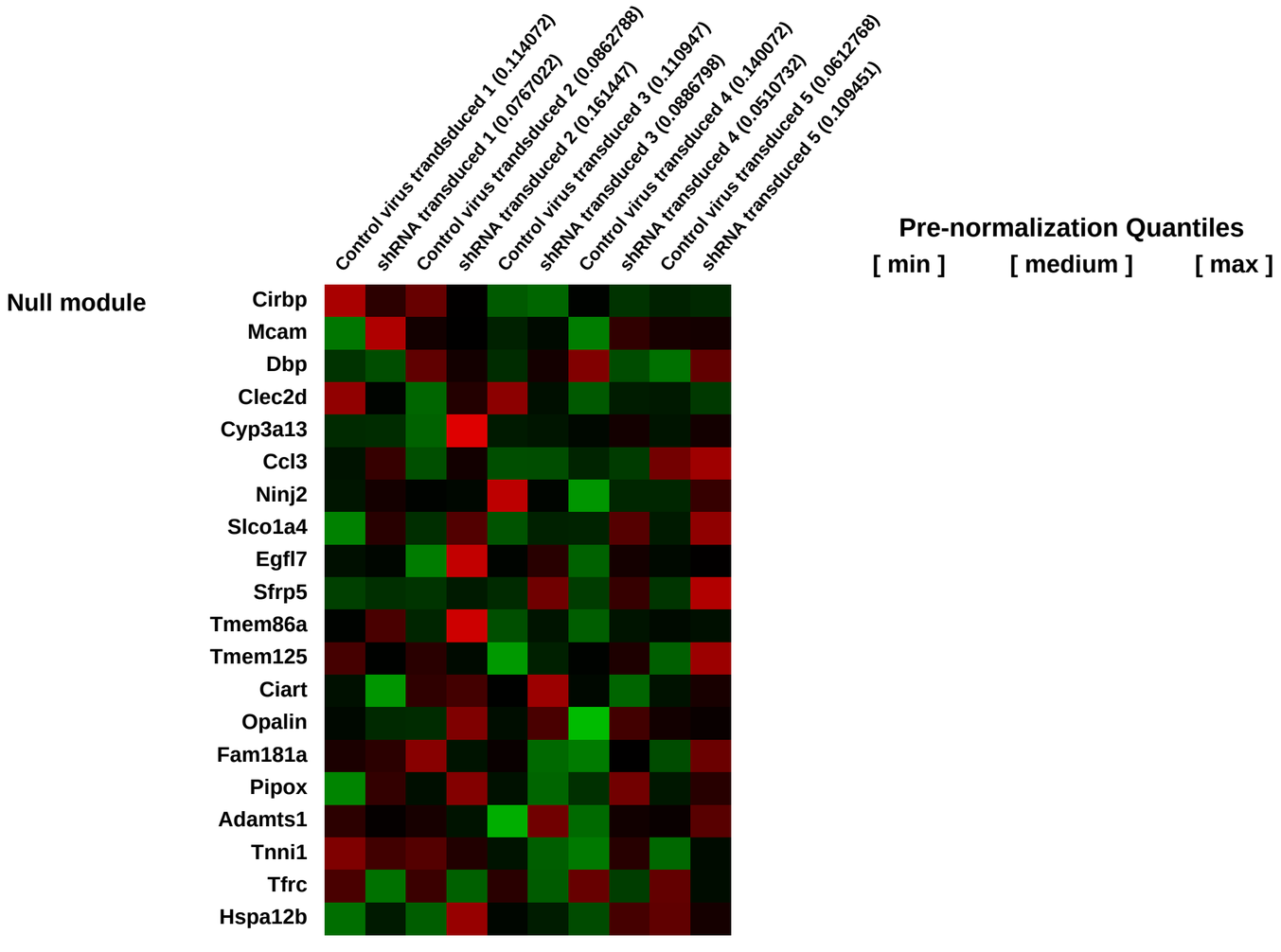

GEO Series "GSE14243" Expression Profiles

Num of samples in this series: 6

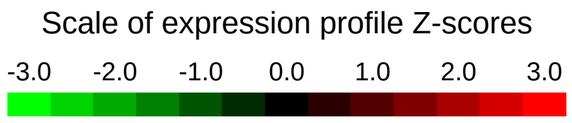

GEO Link:	http://www.ncbi.nlm.nih.gov/geo/query/acc.cgi?acc=GSE14243
Status:	Public on May 01 2009
Title:	Gene expression changes in As4.1 cells during treatment with interleukin (IL) or hydrogen peroxide (HP)
Organism:	Mus musculus
Experiment type:	Expression profiling by array
Platform:	GPL1261
Pubmed ID:	19433777
Summary & Design:	**Summary:** As4.1 cells are a renin-expressing cell line commonly used to study the molecular regulation of the mouse renin gene. In the present study, the global gene expression profile was assessed in these cells under control conditions (VEHICLE) and after treatment with interleukin (IL) or hydrogen peroxide (HP), both of which negatively regulate mouse renin gene expression. **Overall design:** For each experimental group, 2 separate cultures of As4.1 cells were used. Cells were treated with interleukin (IL), hydrogen peroxide (HP) or vehicle control (VEHICLE). Cellular RNA was prepared using conventional methods and quality was assessed using the Bioanalyzer 2100 (Agilent Technologies). All the microarray procedures were conducted at the University of Iowa DNA Core facility using standard Affymetrix protocols. In brief, approximately 5 ug of total RNA was used as input to a one-step amplification procedure to generate biotin-labeled RNA fragments for hybridization to the Affymetrix GeneChip Mouse Genome 430 2.0 array.

Background corr dist: KL-Divergence = 0.0412, L1-Distance = 0.0213, L2-Distance = 0.0005, Normal std = 0.6135

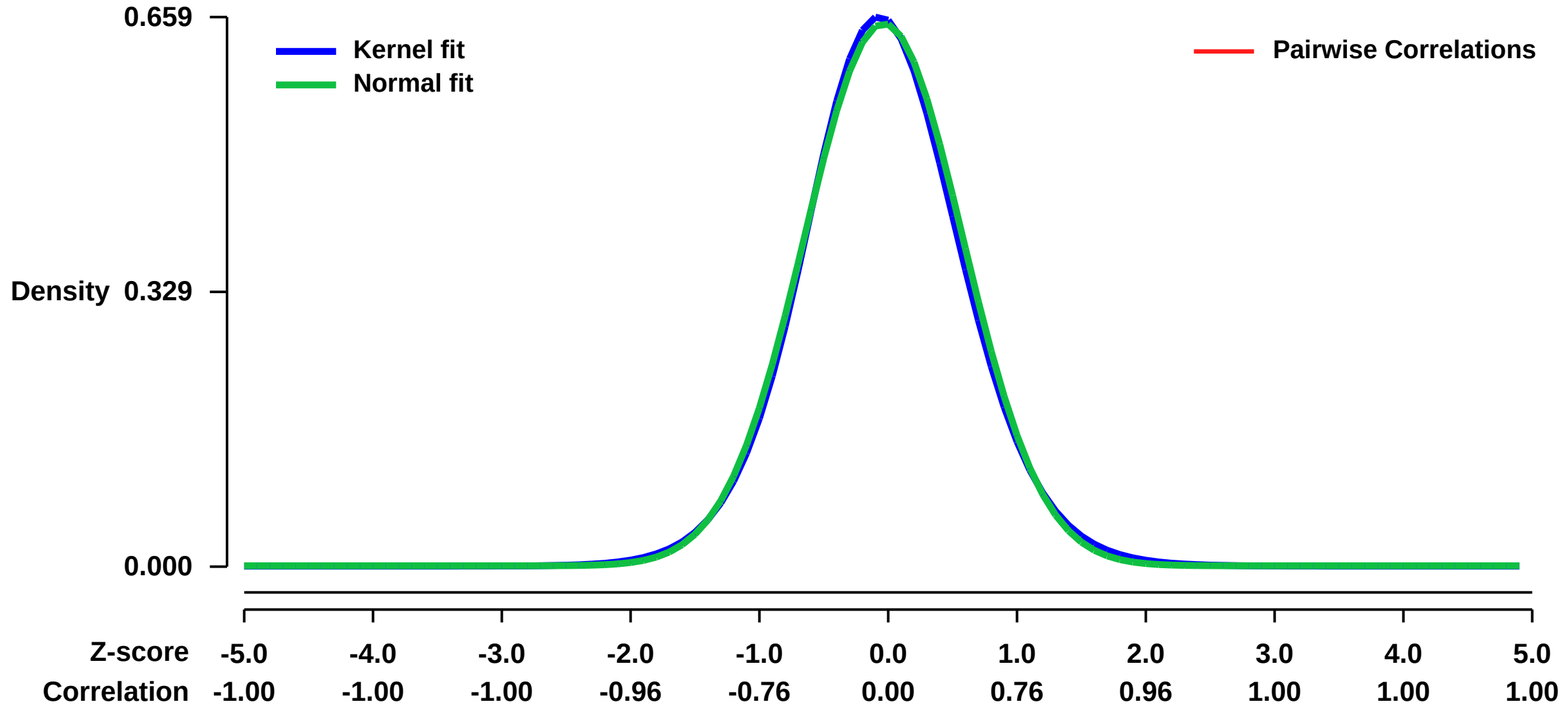

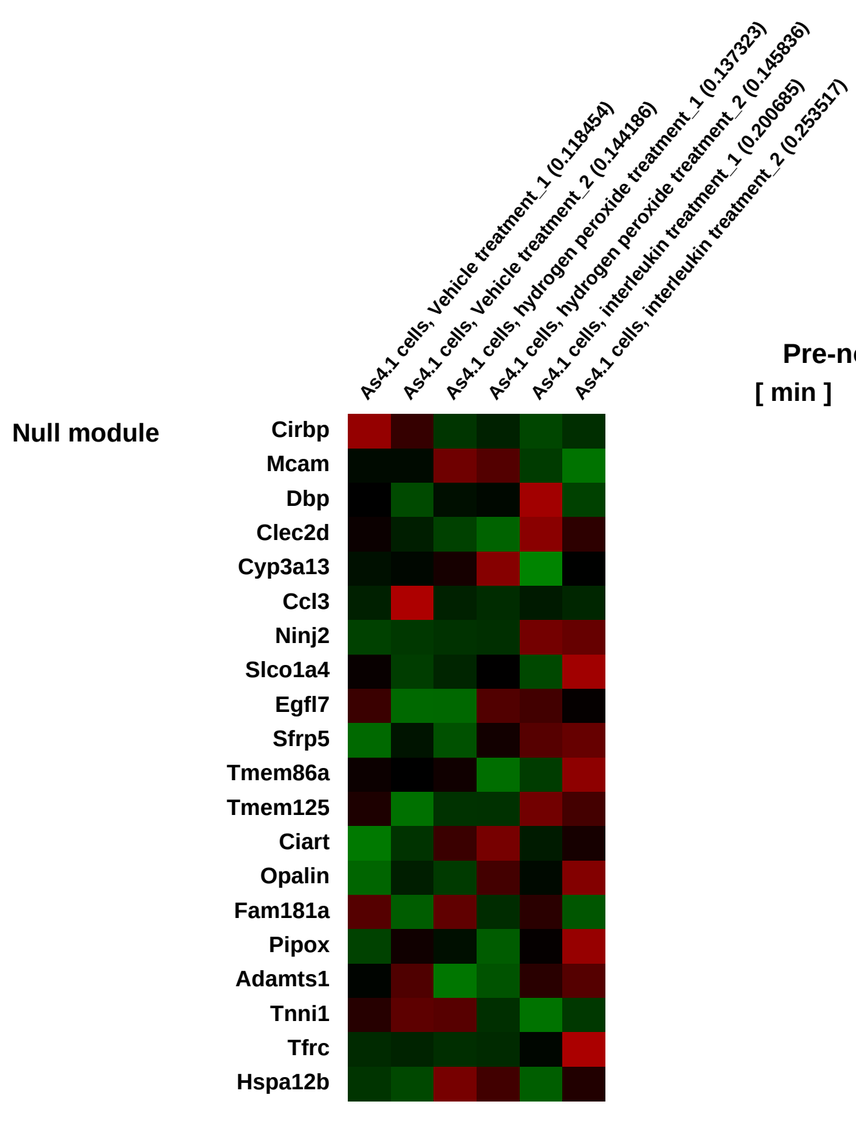

GEO Series "GSE14344" Expression Profiles

Num of samples in this series: 6

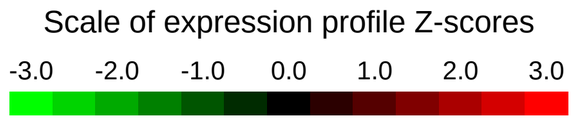

GEO Link:	http://www.ncbi.nlm.nih.gov/geo/query/acc.cgi?acc=GSE14344
Status:	Public on Jan 20 2009
Title:	esBAF is an essential component of the core pluripotency transcriptional network
Organism:	Mus musculus
Experiment type:	Genome binding/occupancy profiling by high throughput sequencing
Platform:	GPL1261
Pubmed ID:	19279218
Summary & Design:	**Summary:** Distinctive SWI/SNF-like ATP-dependent chromatin remodeling esBAF complexes are indispensable for the maintenance and pluripotency of mouse embryonic stem (ES) cells. To understand the mechanism underlying the roles of these complexes in ES cells, we performed high-resolution genome-wide mapping of the core ATPase subunit, Brg, using ChIP-Seq technology. We find that that esBAF, as represented by Brg, binds to genes encoding components of the core ES transcriptional circuitry, including Polycomb group proteins. esBAF colocalizes extensively with Oct4, Sox2 and Nanog genome-wide, and shows distinct functional interactions with Oct4 and Sox2 at its target genes. Surprisingly, no significant colocalization of esBAF with PRC2 complexes, represented by Suz12, is observed. Lastly, esBAF co-binds with Stat3 and Smad1 genome-wide, consistent with a direct and critical role in LIF and BMP signaling essential to maintain pluripotency. Taken together, our studies indicate that esBAF is both an essential component of the core pluripotency transcriptional network, and might also be a critical component of the LIF and BMP signaling pathways essential for maintenance of self-renewal and pluripotency. **Overall design:** Brg knockdown effect on expression, Brg ChIP-Seq

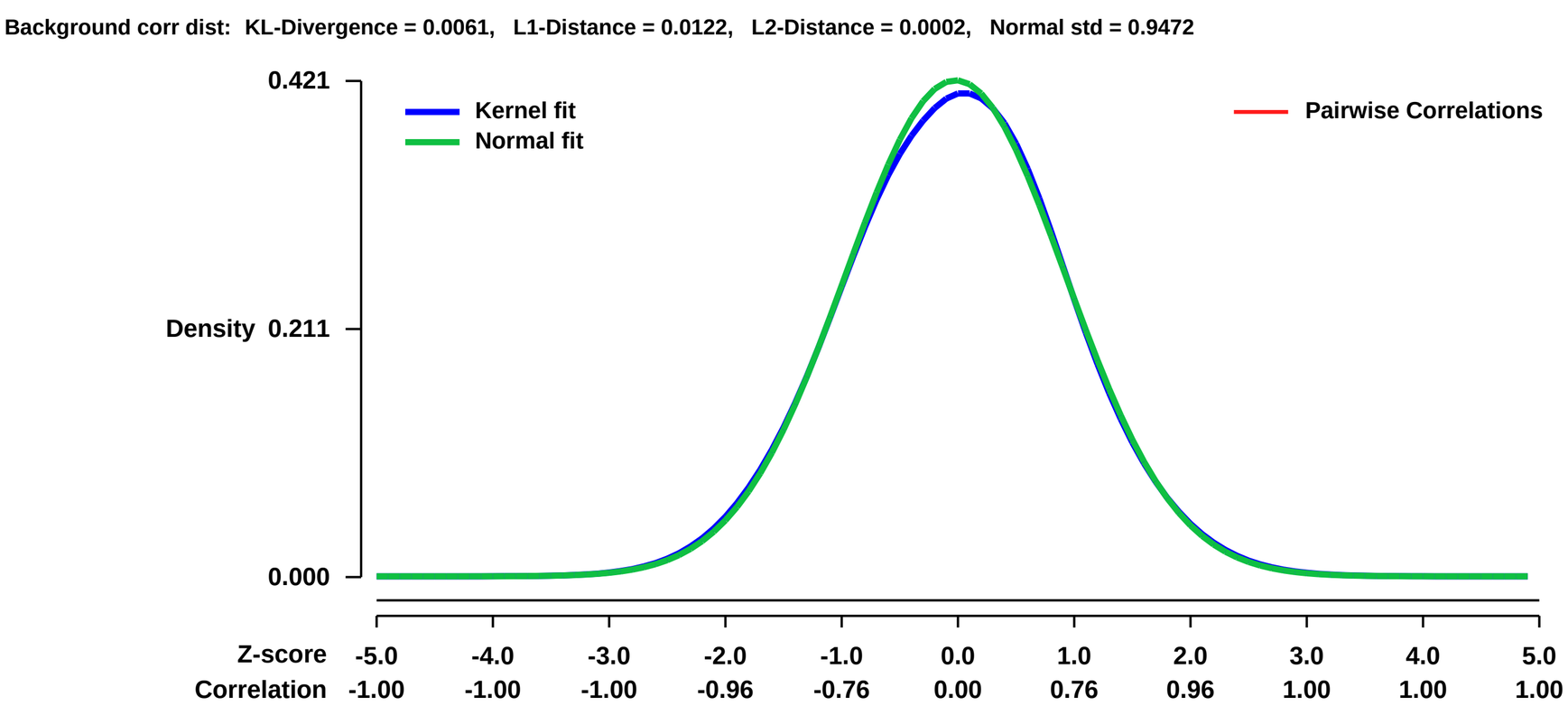

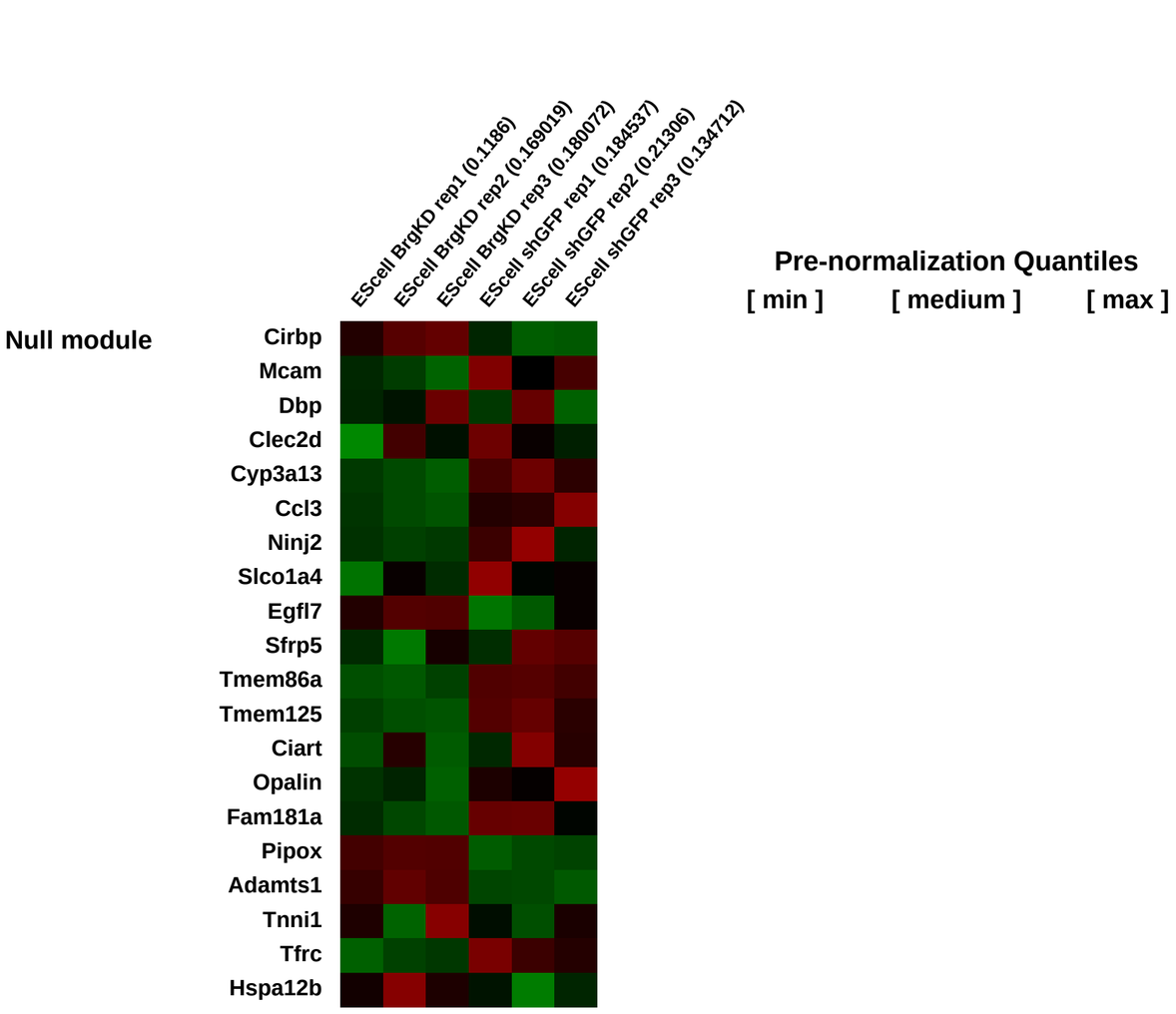

GEO Series "GSE14361" Expression Profiles

Num of samples in this series: 6

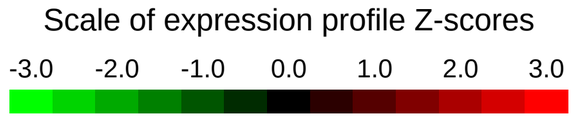

GEO Link:	http://www.ncbi.nlm.nih.gov/geo/query/acc.cgi?acc=GSE14361
Status:	Public on Jan 15 2009
Title:	IFNa activates dormant HSCs in vivo
Organism:	Mus musculus
Experiment type:	Expression profiling by array
Platform:	GPL1261
Pubmed ID:	19212321
Summary & Design:	**Summary:** Maintenance of the blood system is dependent on dormant haematopoietic stem cells (HSCs) with long-term self-renewal capacity. Upon injury these cells are induced to proliferate in order to quickly re-establish homeostasis. The signalling molecules promoting the exit of HSCs out of the dormant stage remain largely unknown. Here we show that in response to treatment of mice with interferon-alpha (IFN¸–), HSCs efficiently exit G0 and enter an active cell cycle. HSCs respond to IFN¸– treatment by increased phosphorylation of STAT1 and PKB/Akt, expression of IFN¸– target genes and up-regulation of stem cell antigen-1 (Sca-1). HSCs lacking either the interferon-¸–/¸† receptor (IFNAR), STAT1 or Sca-1 are insensitive to IFN¸– stimulation, demonstrating that STAT1 and Sca-1 mediate IFN¸– induced HSC proliferation. Although dormant HSCs are resistant to the anti-proliferative chemotherapeutic agent 5-FU1, HSCs pre-treated (primed) with IFN¸– and thus induced to proliferate are efficiently eliminated by 5-FU exposure in vivo. Conversely, HSCs chronically activated by IFN¸– are functionally compromised and are rapidly out competed by non-activatable IFNAR-/- cells in competitive repopulation assays. In summary, while chronic activation of the IFN¸– pathway in HSCs impairs their function, acute IFN¸– treatment promotes the proliferation of dormant HSCs in vivo. These data may help to clarify the so far unexplained clinical effects of IFN¸– on leukemic cells and raise the possibility for novel applications of type I interferons to target cancer stem cells. **Overall design:** cDNA microarray analysis was performed on sorted Lin neg, cKit+, CD150+, CD48neg HSCs from IFN¸– treated (16h after treatment) and untreated (littermate) mice. Per condition 3 independent biological replicates were analysed.

Background corr dist: KL-Divergence = 0.0491, L1-Distance = 0.0400, L2-Distance = 0.0025, Normal std = 0.5949

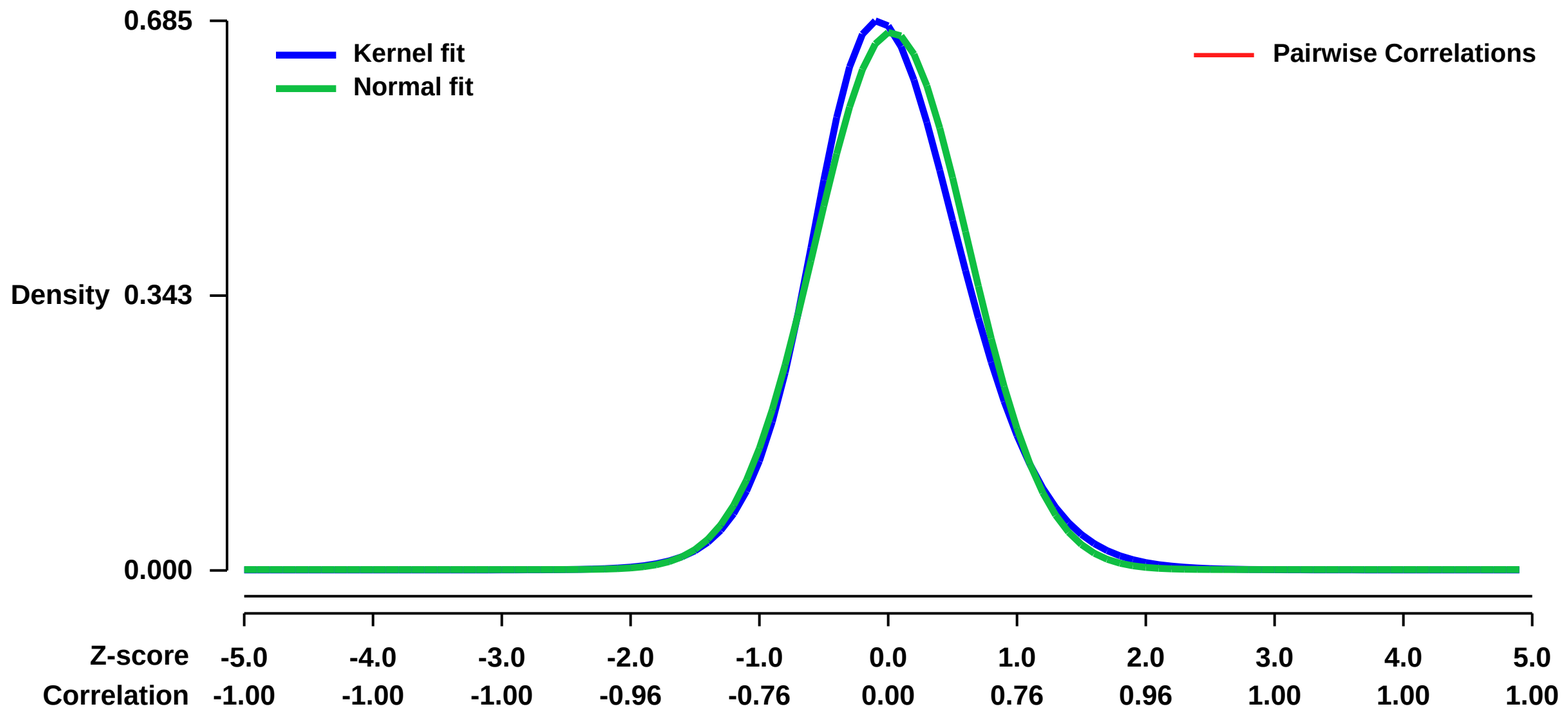

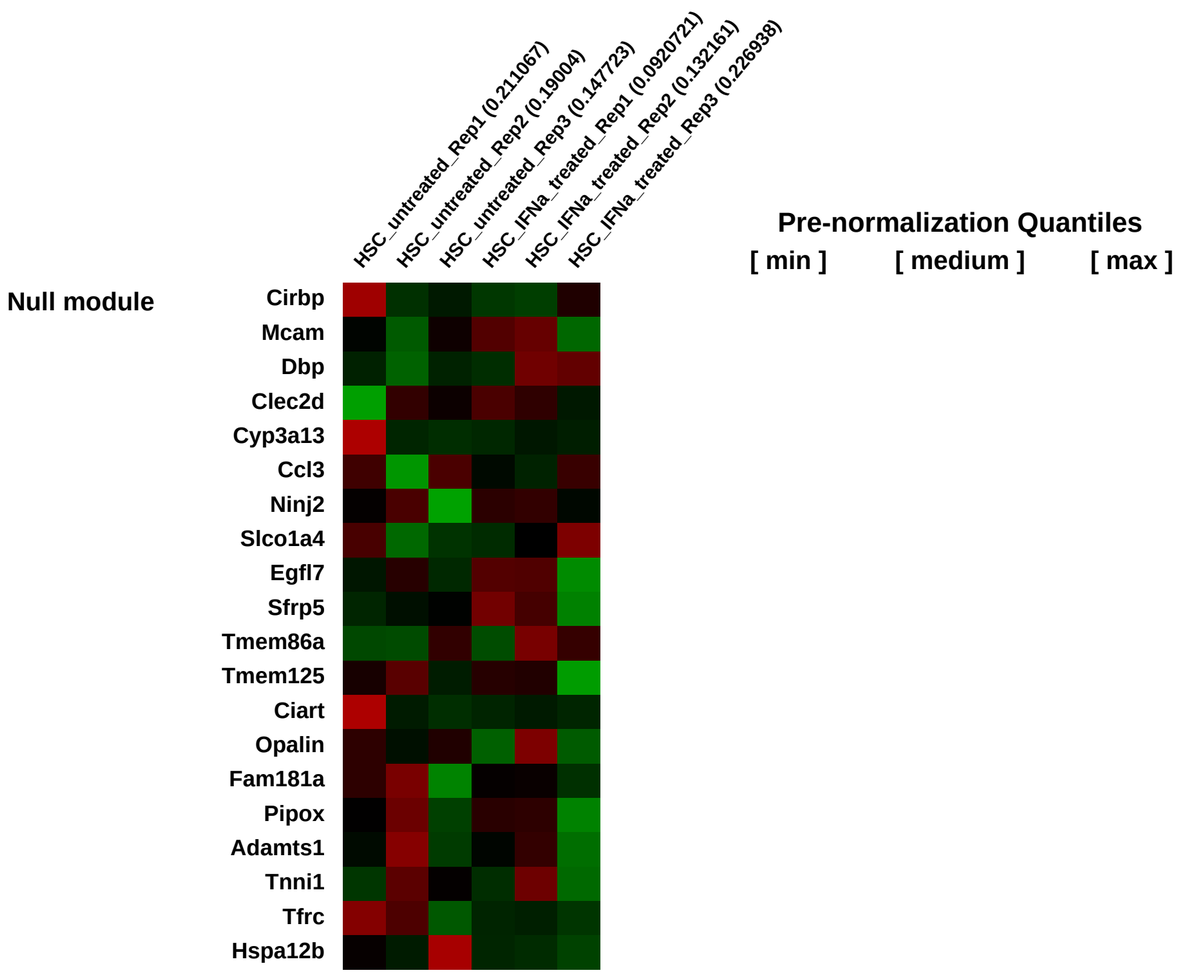

GEO Series "GSE14366" Expression Profiles

Num of samples in this series: 24

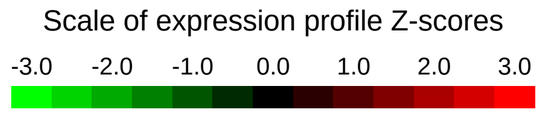

GEO Link:	http://www.ncbi.nlm.nih.gov/geo/query/acc.cgi?acc=GSE14366
Status:	Public on Jan 10 2009
Title:	Analysis of the retinal gene expression after hypoxic preconditioning identifies candidate genes for neuroprotection
Organism:	Mus musculus
Experiment type:	Expression profiling by array
Platform:	GPL1261
Pubmed ID:	18261226
Summary & Design:	**Summary:** Neuroprotective therapies for retinal degeneration may be used to rescue retinal cells and preserve vision. Hypoxic preconditioning stabilizes the transcription factor HIF-1¸ – in the retina and strongly protects photoreceptors in an animal model of light-induced retinal degeneration. Our data suggest that neuroprotection after hypoxic preconditioning of the retina is the result of the differential expression of a multitude of genes which may act in concert to protect visual cells against a toxic insult. Keywords: hypoxic preconditioning, neuroprotection, transcription-profile, retina **Overall design:** In total 24 samples were analyzed on Affymetrix mouse 430.2 arrays, the samples represent different durations of regeneration (none = 0 h, 2 h, 4 h and 16 h) from hypoxic or normoxic treatments, that were tested in triplicates.

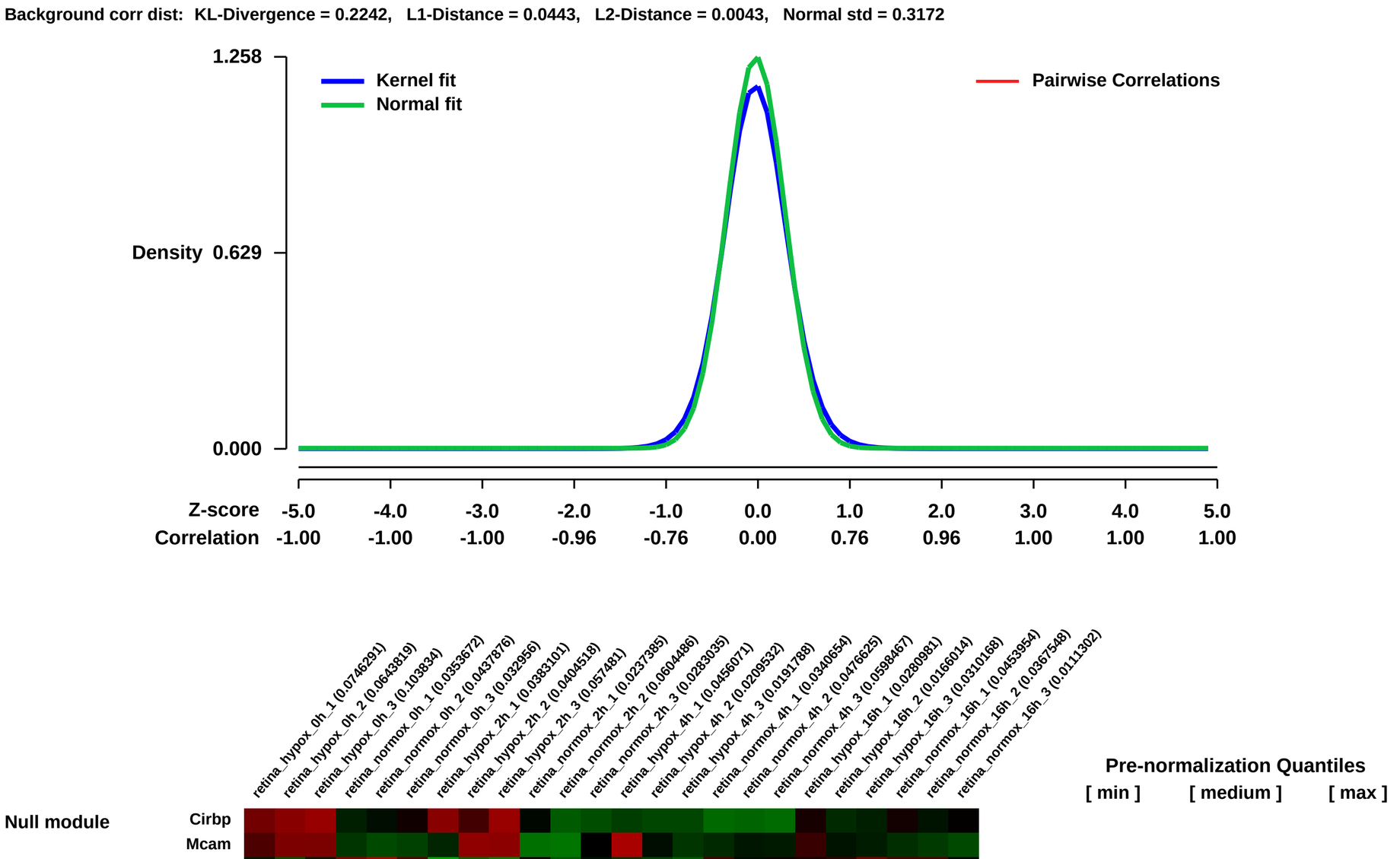

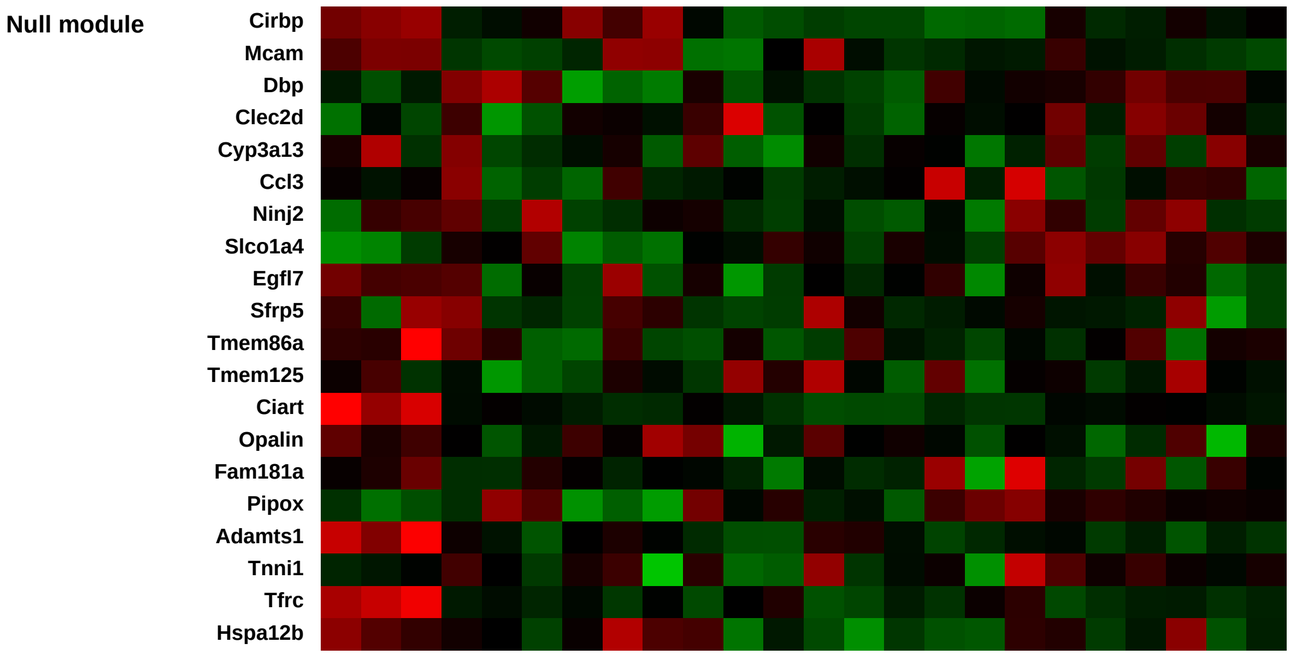

GEO Series "GSE14478" Expression Profiles

Num of samples in this series: 7

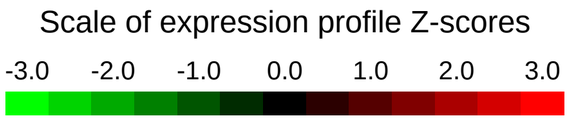

GEO Link:	http://www.ncbi.nlm.nih.gov/geo/query/acc.cgi?acc=GSE14478
Status:	Public on Jan 31 2009
Title:	SCL knockouts in mouse megakaryocytes
Organism:	Mus musculus
Experiment type:	Expression profiling by array
Platform:	GPL1261
Pubmed ID:	19211936
Summary & Design:	**Summary:** The bHLH transcription factor stem cell leukemia gene (Scl) is a master regulator for hematopoiesis essential for hematopoietic specification and proper differentiation of the erythroid and megakaryocyte lineages. However, the critical downstream targets of Scl remain undefined. Here, we identified a novel Scl target gene, transcription factor myocyte enhancer factor 2 C (Mef2C) from Sclfl/fl fetal liver progenitor cell lines. Analysis of Mef2C-/- embryos showed that Mef2C, in contrast to Scl, is not essential for specification into primitive or definitive hematopoietic lineages. However, adult VavCre+Mef2Cfl/fl mice exhibited platelet defects similar to those observed in Scl deficient mice. The platelet counts were reduced, while platelet size was increased and the platelet shape and granularity was altered. Furthermore, megakaryopoiesis was severely impaired in vitro. ChIP-on-chip analysis revealed that Mef2C is directly regulated by Scl in megakaryocytic cells, but not in erythroid cells. In addition, an Scl independent requirement for Mef2C in B-lymphoid homeostasis was observed in Mef2C-deficient mice, characterized as severe age-dependent reduction of specific B cell progenitor populations reminiscent of premature aging. In summary, this work identifies Mef2C as an integral member of hematopoietic transcription factors with distinct upstream regulatory mechanisms and functional requirements in megakaryocyte and B-lymphoid lineages. **Overall design:** ¸/¸ cell line, and the Scl ¸/¸ cell line was transduced with Scl retrovirus to re-introduce Scl expression (Scl ¸/¸ +Scl cell line). Megakaryocyte differentiation was enhanced by adding Tpo for 5 days before harvesting the cells. RNA was extracted with Trizol (Gibco BRL) and RNEasy (Qiagen) kits. Differential gene expression between Sclfl/fl, Scl ¸/¸ and Scl ¸/¸ +Scl cell lines was analyzed by Affymetrix MOE430_2 microarray in the microarray core facility at the Dana-Farber Cancer Institute.

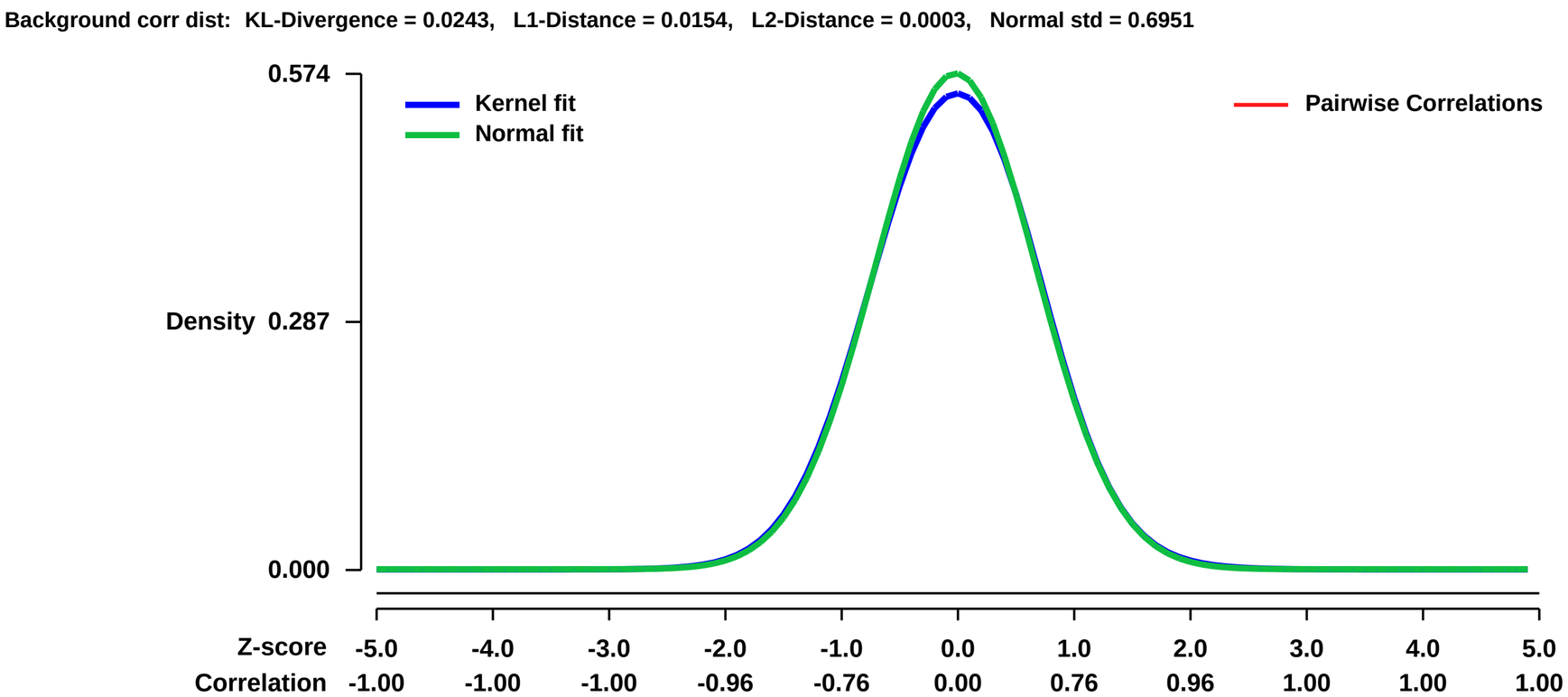

GEO Series "GSE14481" Expression Profiles

Num of samples in this series: 12

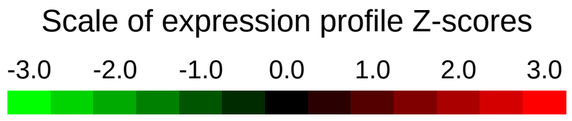

GEO Link:	**http://www.ncbi.nlm.nih.gov/geo/query/acc.cgi?acc=GSE14481**
Status:	**Public on Dec 31 2009**
Title:	**identification of TGCT genes involved in initiation and maintenance of transformed germ cells.**
Organism:	**Mus musculus**
Experiment type:	**Expression profiling by array**
Platform:	**GPL1261**
Pubmed ID:	
Summary & Design:	**Summary:** **Initially, we had compared gene expression differences in the embryonic gonads (E13.5) of the 129 and M19 strains by performing microarray analysis. These studies allowed us to identify downregulation of expression of the D19Bwg1357e, Zfp162 and Cox15 genes in the M19 strain.** **We next decided to examine gene expression profile changes in the embryonic gonads of 129 and M19 at additional stages so as to identify other TGCT genes from M19 that are also involved in initiation and maintenance of transformed germ cells. For this we isolated E13.5, E15.5 and E17.5 genital ridges from male embryos.** **Overall design:** **After data process and quality assessment, 38069 out of 45101 probe sets proceeded for further analysis to identify differentially expressed genes. Hierarchical cluster analysis shows that samples of two strains from the same stage were grouped together and separated from the other stages (Fig.8). The initial analysis indicates a number of trends in gene expression patterns. Moreover, downregulation of expression of D19Bwg1357e, Zfp162 and Cox15 genes in M19 was also verified in this analysis. These data are currently being analyzed with the help of Dr. Y. Ji and L. Xiao from the Department of Bioinformatics and Computational Biology and Department of Biostatistics at M.D. Anderson Cancer Center. The results are unpublished.**

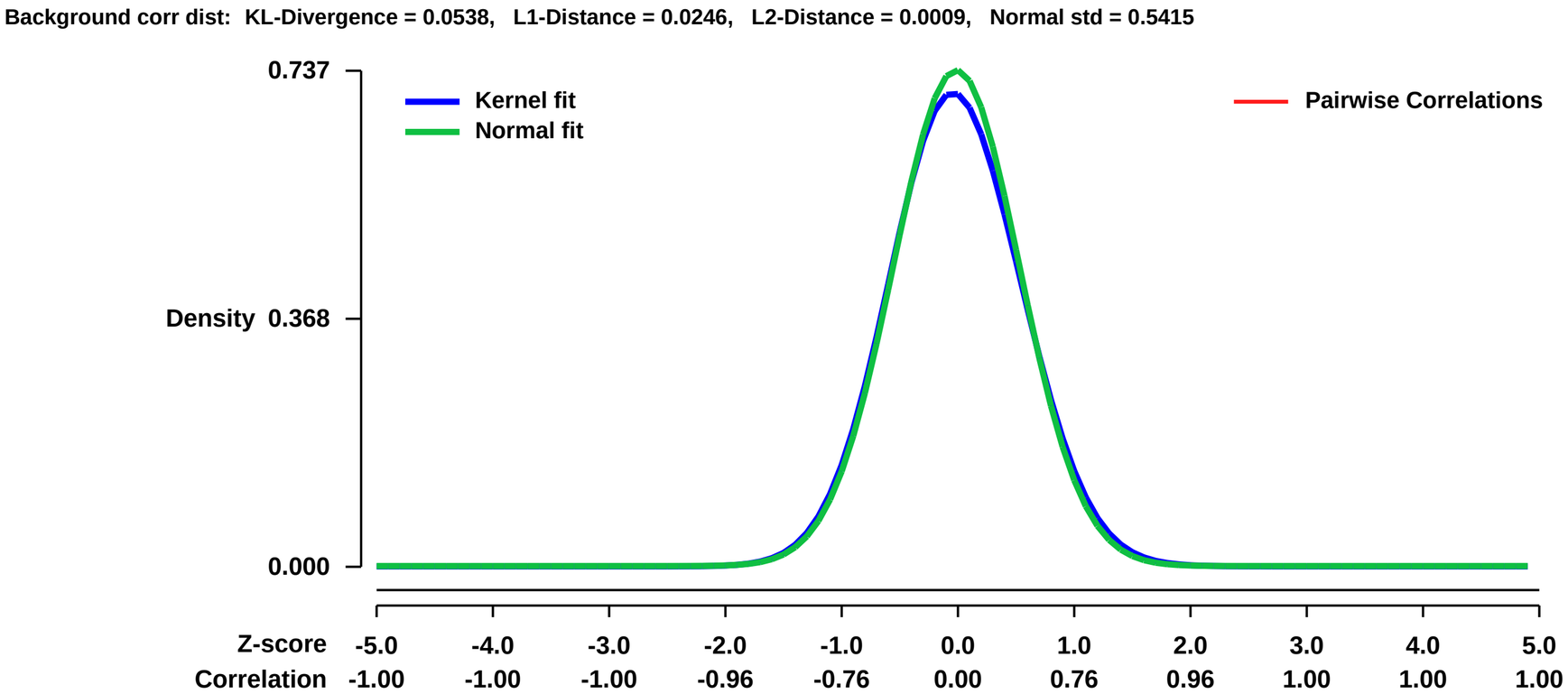

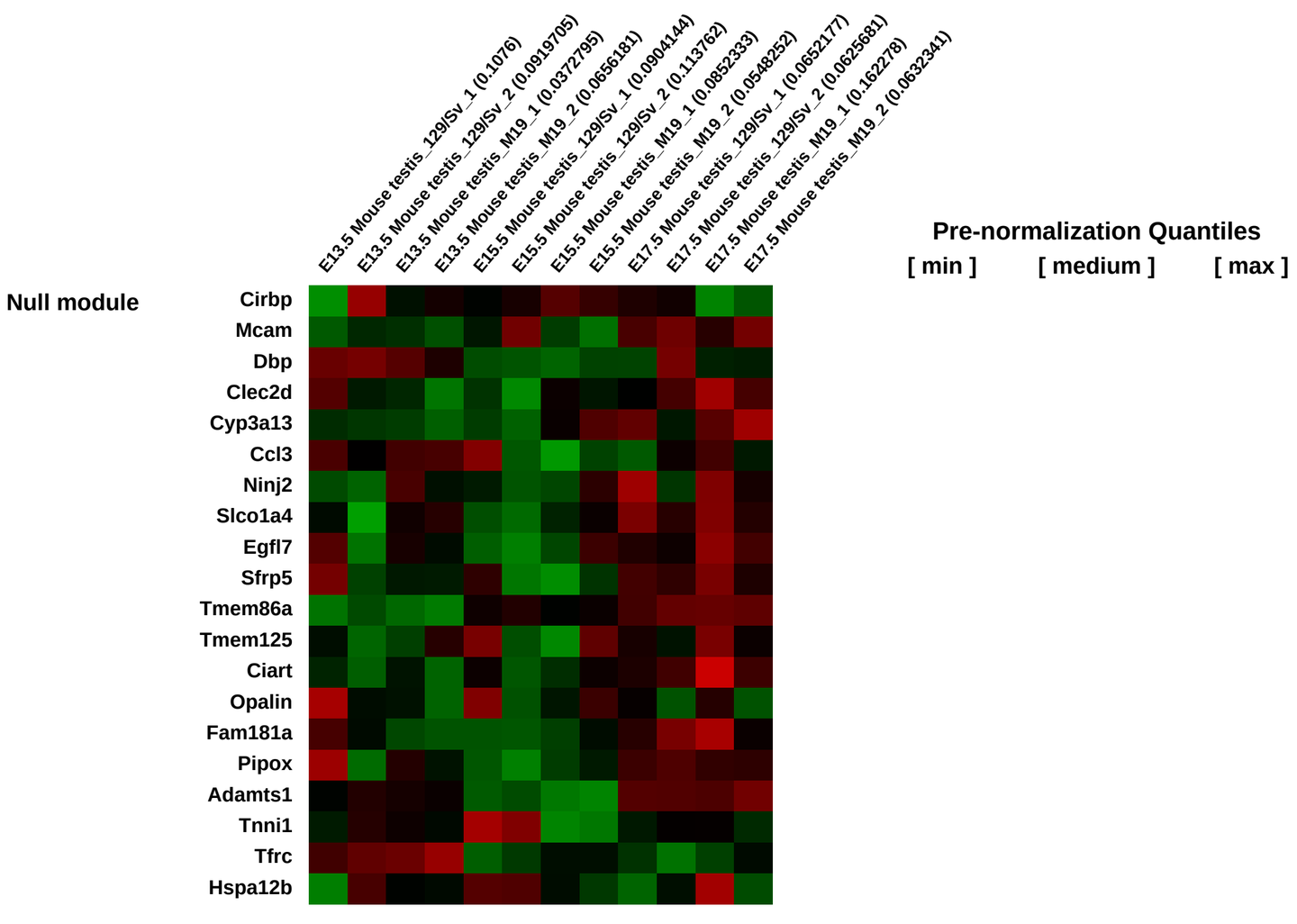

GEO Series "GSE14672" Expression Profiles

Num of samples in this series: 12

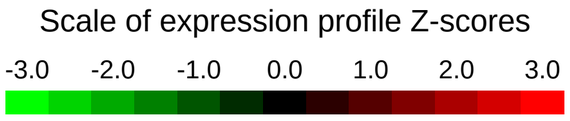

GEO Link:	http://www.ncbi.nlm.nih.gov/geo/query/acc.cgi?acc=GSE14672
Status:	Public on Sep 30 2009
Title:	GM-CSF-mediated granulopoiesis is regulated by the transcription factor STAT5A/B
Organism:	Mus musculus
Experiment type:	Expression profiling by array
Platform:	GPL1261
Pubmed ID:	19779039
Summary & Design:	**Summary:** GM-CSF controls the development of granulocytes but little is known about the contribution of the downstream mediating transcription factor STAT5A/B. To elucidate this pathway, we generated mice lacking the Stat5a and 5b genes in blood cells. Peripheral neutrophils were decreased and administration of 5-FU and GM-CSF failed to induce granulopoiesis in Stat5a/b-mutant mice. GMPs were isolated and cultured with GM-CSF. Both the number and size of STAT5A/B-null colonies were reduced and GM-CSF-induced survival of mature STAT5A/B-null neutrophils was impaired. Time-lapse cinematography and single cell tracking of GMPs revealed that STAT5A/B-null cells were characterized by a longer generation time and an increased cell death. Gene expression profiling experiments suggested that STAT5A/B directs GM-CSF signaling through the regulation of cell survival genes. #!# **Overall design:** Mice lacking or with the Stat5a and 5b genes in blood cells, which were treated w/o GMP

Background corr dist: KL-Divergence = 0.0805, L1-Distance = 0.0370, L2-Distance = 0.0028, Normal std = 0.4793

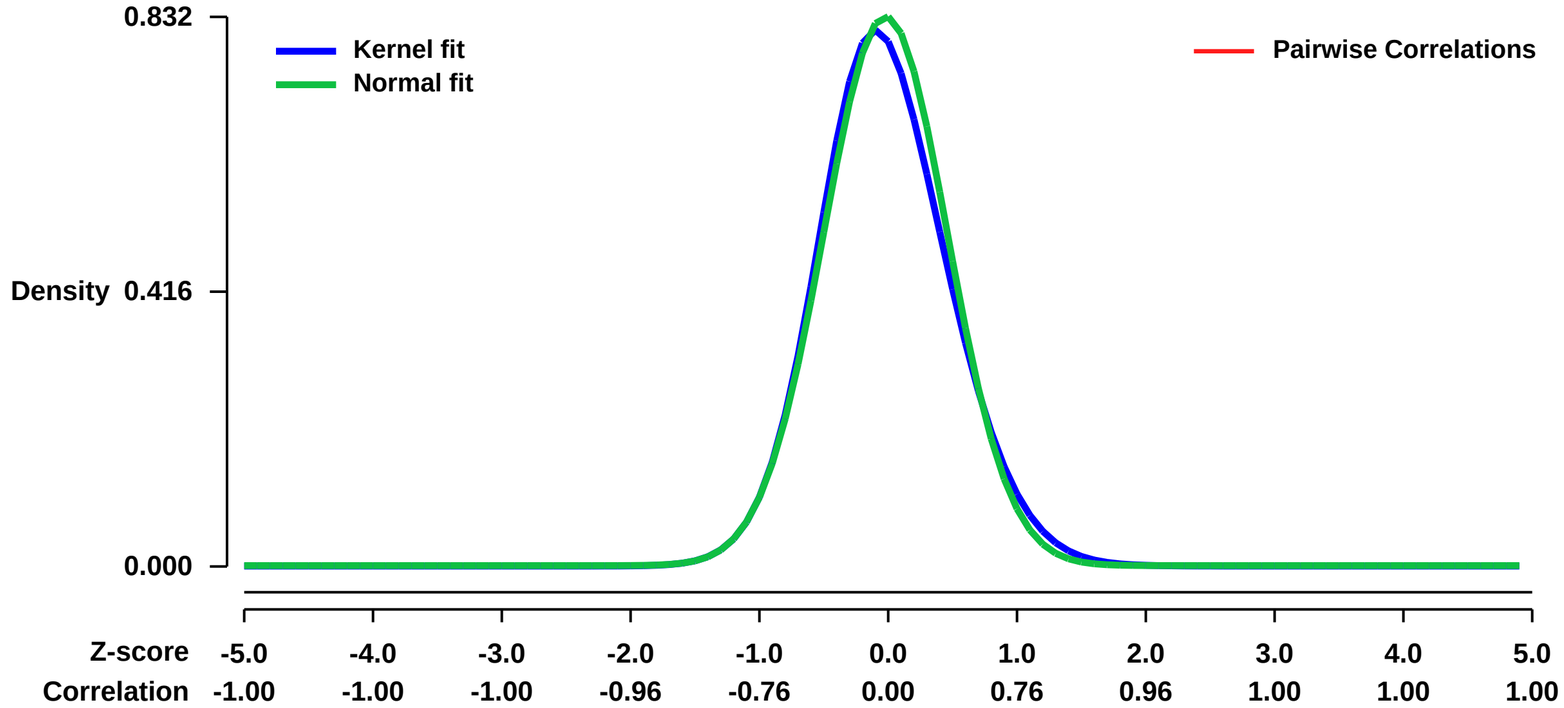

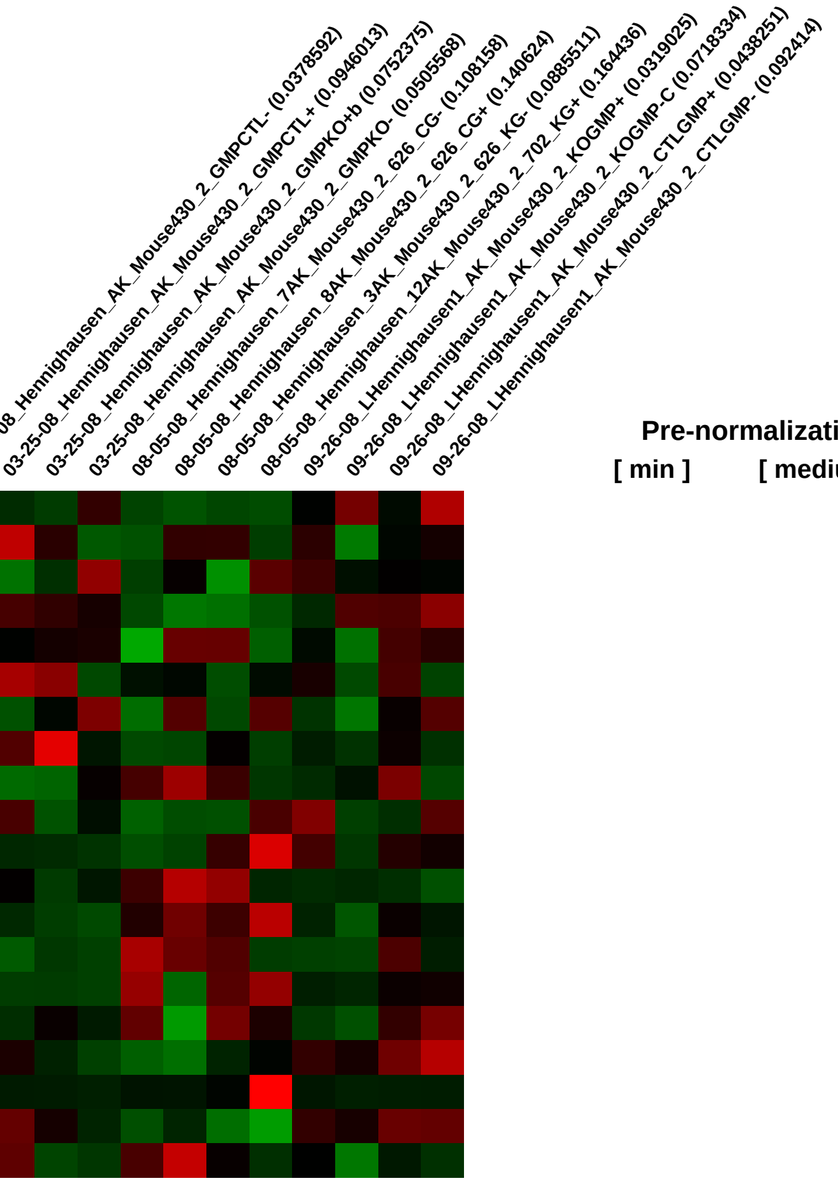

GEO Series "GSE14678" Expression Profiles

Num of samples in this series: 6

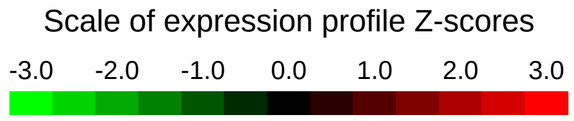

GEO Link:	**http://www.ncbi.nlm.nih.gov/geo/query/acc.cgi?acc=GSE14678**
Status:	**Public on Feb 26 2009**
Title:	**Expression Profile of Skeletal Muscle from Young and Aged C57B1/6 Mice**
Organism:	**Mus musculus**
Experiment type:	**Expression profiling by array**
Platform:	**GPL1261**
Pubmed ID:	
Summary & Design:	**Summary:** **Our laboratory wanted to define the transcription profile of aged skeletal muscle. For this reason, we performed a triplicate microarray study on young (3 weeks) and aged (24 months) gatrocnemius muscle from wild-type C57B16 Mice** **Keywords: other** **Overall design:** **this experiment include 2 samples and 6 replicates**

Background corr dist: **KL-Divergence = 0.0496, L1-Distance = 0.0330, L2-Distance = 0.0015, Normal std = 0.5866**

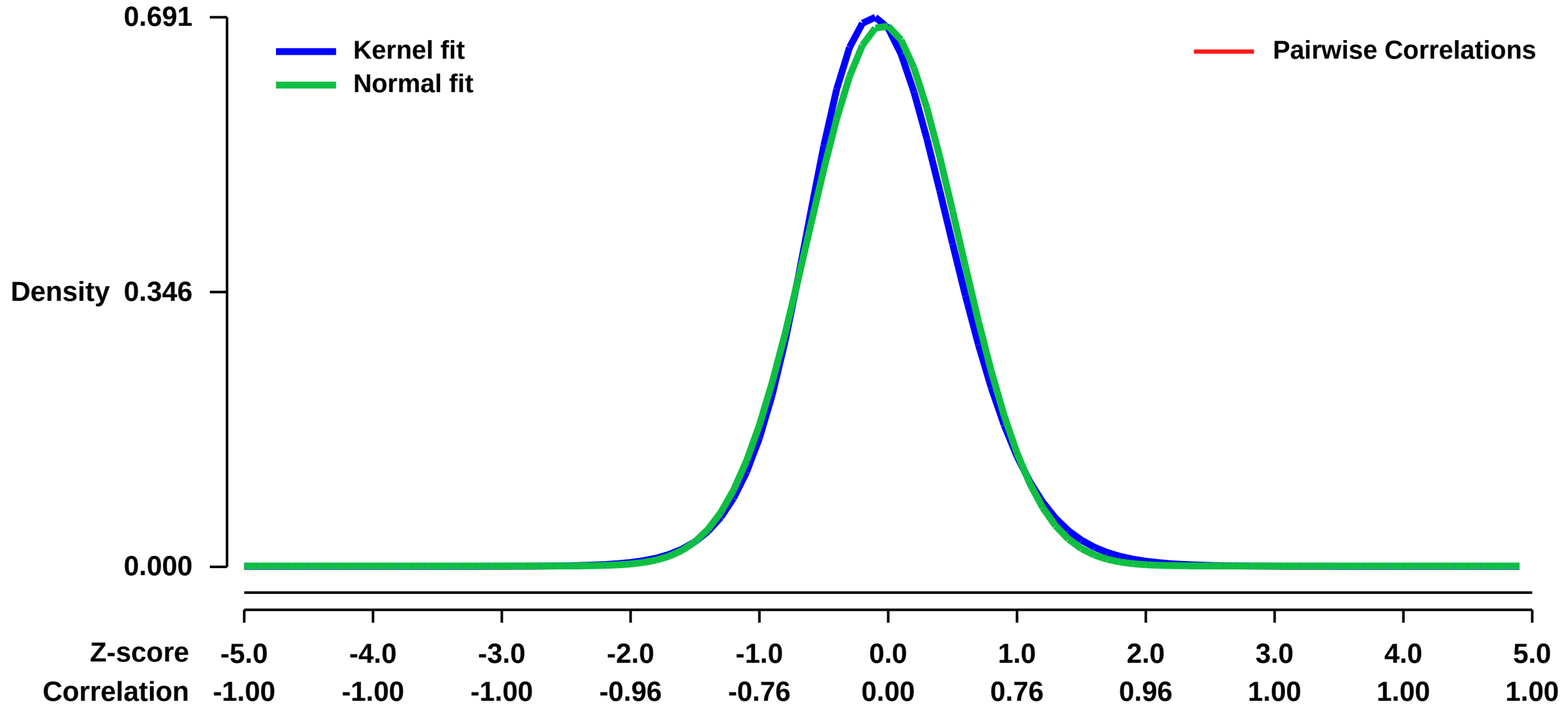

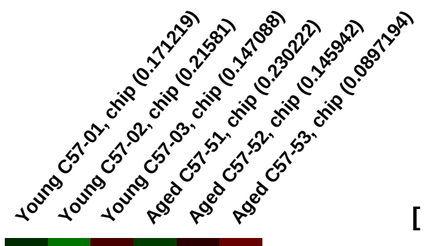

Pre-normalization Quantiles

[min] [medium] [max]

Null module

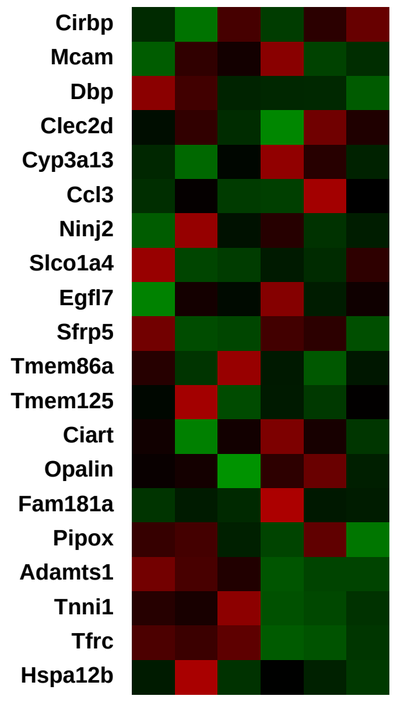

GEO Series "GSE14686" Expression Profiles

Num of samples in this series: 16

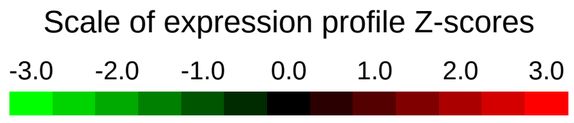

GEO Link:	http://www.ncbi.nlm.nih.gov/geo/query/acc.cgi?acc=GSE14686
Status:	Public on Mar 01 2009
Title:	Colonic transcriptional changes evoked by E. rectale-B. thetaiotaomicron co-colonization
Organism:	Mus musculus
Experiment type:	Expression profiling by array
Platform:	GPL1261
Pubmed ID:	19321416
Summary & Design:	**Summary:** The adult human gut microbial community is typically dominated by two bacterial phyla (divisions), the Firmicutes and the Bacteroidetes. Little is known about the factors that govern the interactions between their members. Here we examine the niches of representatives of both phyla in vivo. Finished genome sequences were generated from E. rectale and E. eligens, which belong to Clostridium Cluster XIVa, one of the most common gut Firmicute clades. Comparison of these and 25 other gut Firmicutes and Bacteroidetes indicated that the former possess smaller genomes and a disproportionately smaller number of glycan-degrading enzymes. Germ-free mice were then colonized with E. rectale and/or a prominent human gut Bacteroidetes, Bacteroides thetaiotaomicron, followed by whole genome transcriptional profiling of both organisms in their distal gut (cecal) habitat as well as host responses, high resolution proteomic analysis of cecal contents, and biochemical assays of carbohydrate metabolism. B. thetaiotaomicron adapts to E. rectale by upregulating expression of a variety of polysaccharide utilization loci (PULs) encoding numerous glycoside hydrolase gene families, and by signaling the host to produce mucosal glycans that it, but not E. rectale, can access. E. rectale adapts to B. thetaiotaomicron by decreasing production of its glycan-degrading enzymes, increasing expression of selected amino acid and sugar transporters, and facilitating glycolysis by reducing levels of NADH, in part via generation of butyrate from acetate, which in turn is utilized by the gut epithelium. This simplified model of the human gut microbiota illustrates niche specialization and functional redundancy within members of major gut bacterial phyla, and the importance of host glycans as a nutrient foundation that ensures ecosystem stability. **Overall design:** four biological replicates per group. NMRI mice, males (12-14 weeks old).

Background corr dist: KL-Divergence = 0.1134, L1-Distance = 0.0264, L2-Distance = 0.0010, Normal std = 0.4187

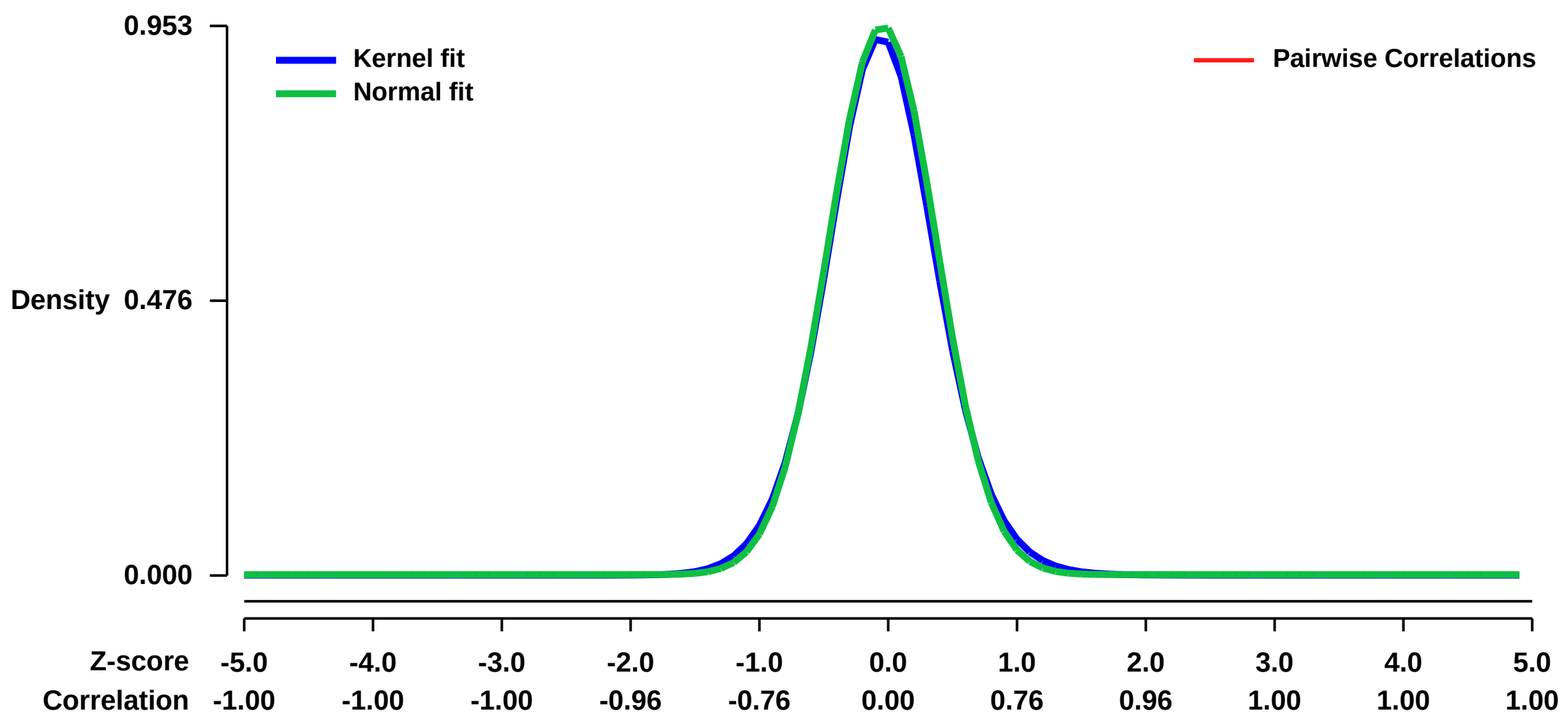

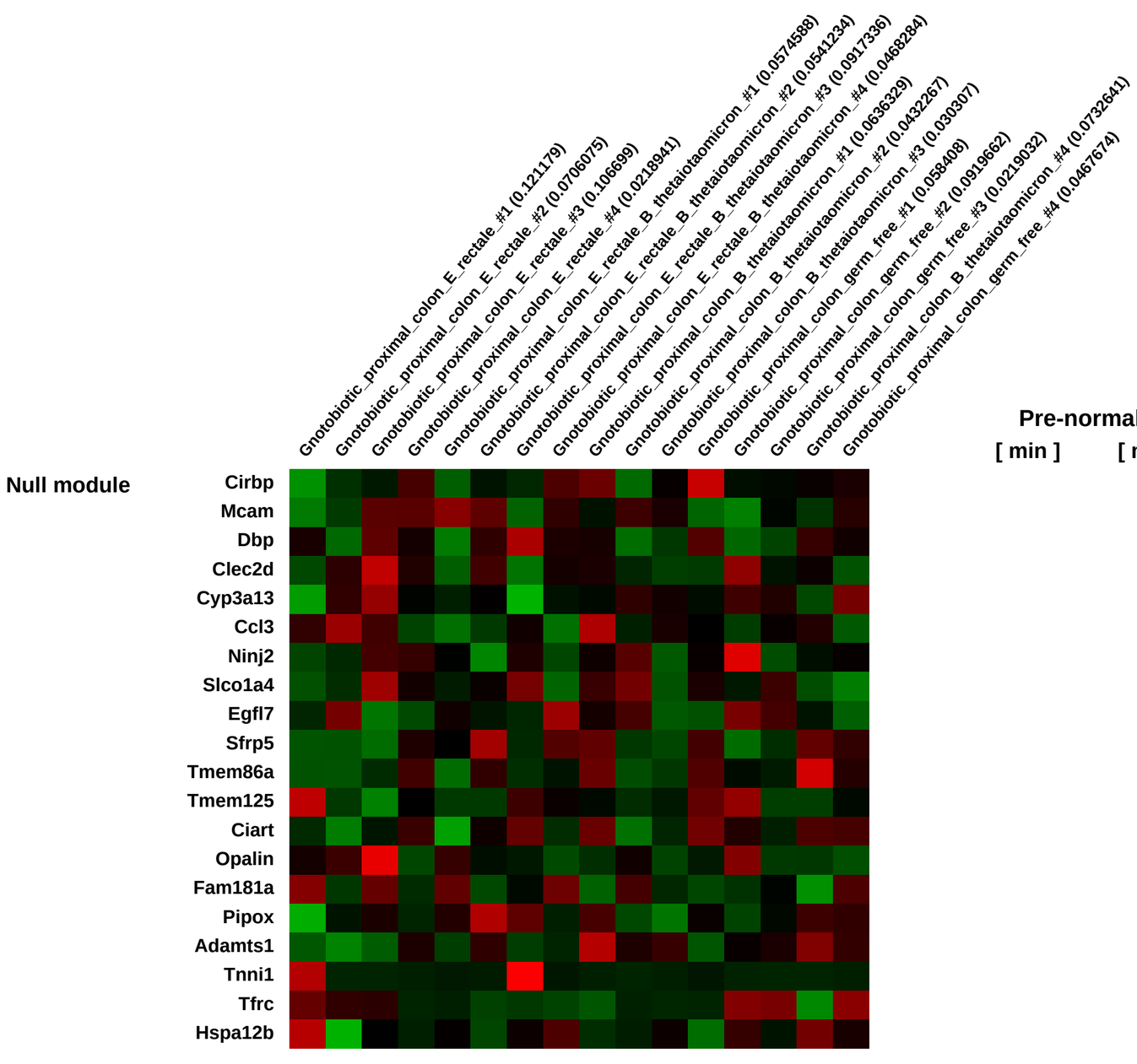

GEO Series "GSE14710" Expression Profiles

Num of samples in this series: 12

Scale of expression profile Z-scores

-3.0 -2.0 -1.0 0.0 1.0 2.0 3.0

GEO Link:	http://www.ncbi.nlm.nih.gov/geo/query/acc.cgi?acc=GSE14710
Status:	Public on Aug 18 2009
Title:	Skeletal muscle growth and fiber composition in mice are regulated through the transcription factors STAT5a/b
Organism:	Mus musculus
Experiment type:	Expression profiling by array
Platform:	GPL1261
Pubmed ID:	19417088
Summary & Design:	**Summary:** In skeletal muscle, STAT5a/b transcription factors are critical for normal postnatal growth, whole-animal glucose homeostasis, and local IGF-1 production. These observations have led us to hypothesize that STAT5a/b are critical for maintenance of normal muscle mass and function. To investigate this, mice with a skeletal muscle-specific deletion of the Stat5a/b genes (Stat5MKO) were used. Stat5MKO mice displayed reduced muscle mass, altered fiber-type distribution and reduced activity. On a molecular level, gene expression in skeletal muscle of Stat5MKO and control mice was analyzed by microarrays and real-time PCR, both in the presence and absence of growth hormone (GH) stimulation. Several genes involved in muscle growth, fiber-type and metabolism were significantly changed. Specifically in the quadriceps, a muscle almost exclusively composed of type II fibers, the absence of STAT5a/b led to increased expression of several genes associated with type I fibers and the de novo appearance of type I fibers. Additionally, it is shown here that expression of the androgen receptor gene (Ar) is controlled by GH through STAT5a/b. The link between STAT5a/b and Ar gene is likely through direct transcriptional regulation, as chromatin immunoprecipitaion of the Ar promoter region in C2C12 myoblasts was accomplished by antibodies against STAT5a. These experiments demonstrate an important role for STAT5a/b in skeletal muscle physiology and they provide a direct link to androgen signaling. **Keywords:** stat5 KO or WT treated or w/o GH **Overall design:** Total 6 WT controls and 6 stat5a/b KO mice, treated or w/o GH

Background corr dist: KL-Divergence = 0.1214, L1-Distance = 0.0271, L2-Distance = 0.0013, Normal std = 0.4073

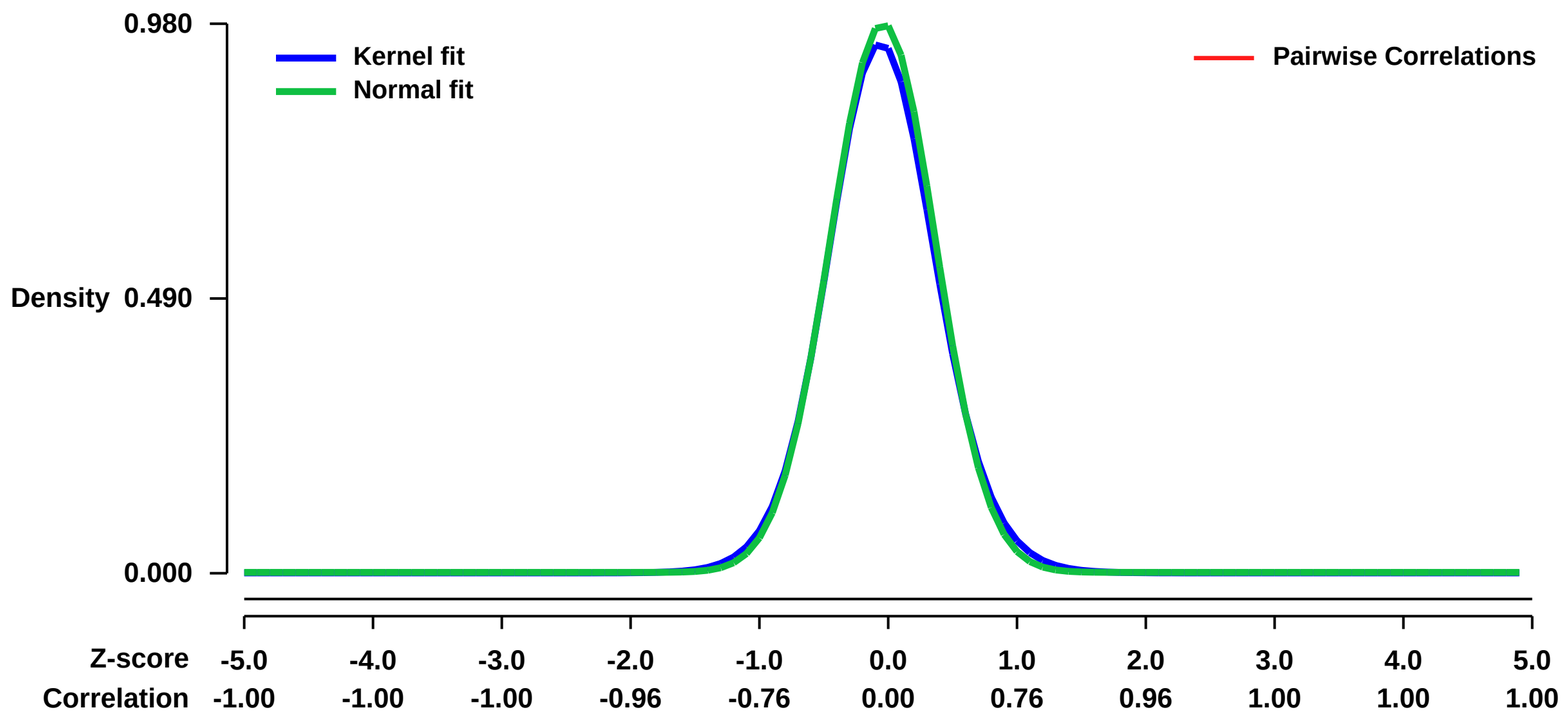

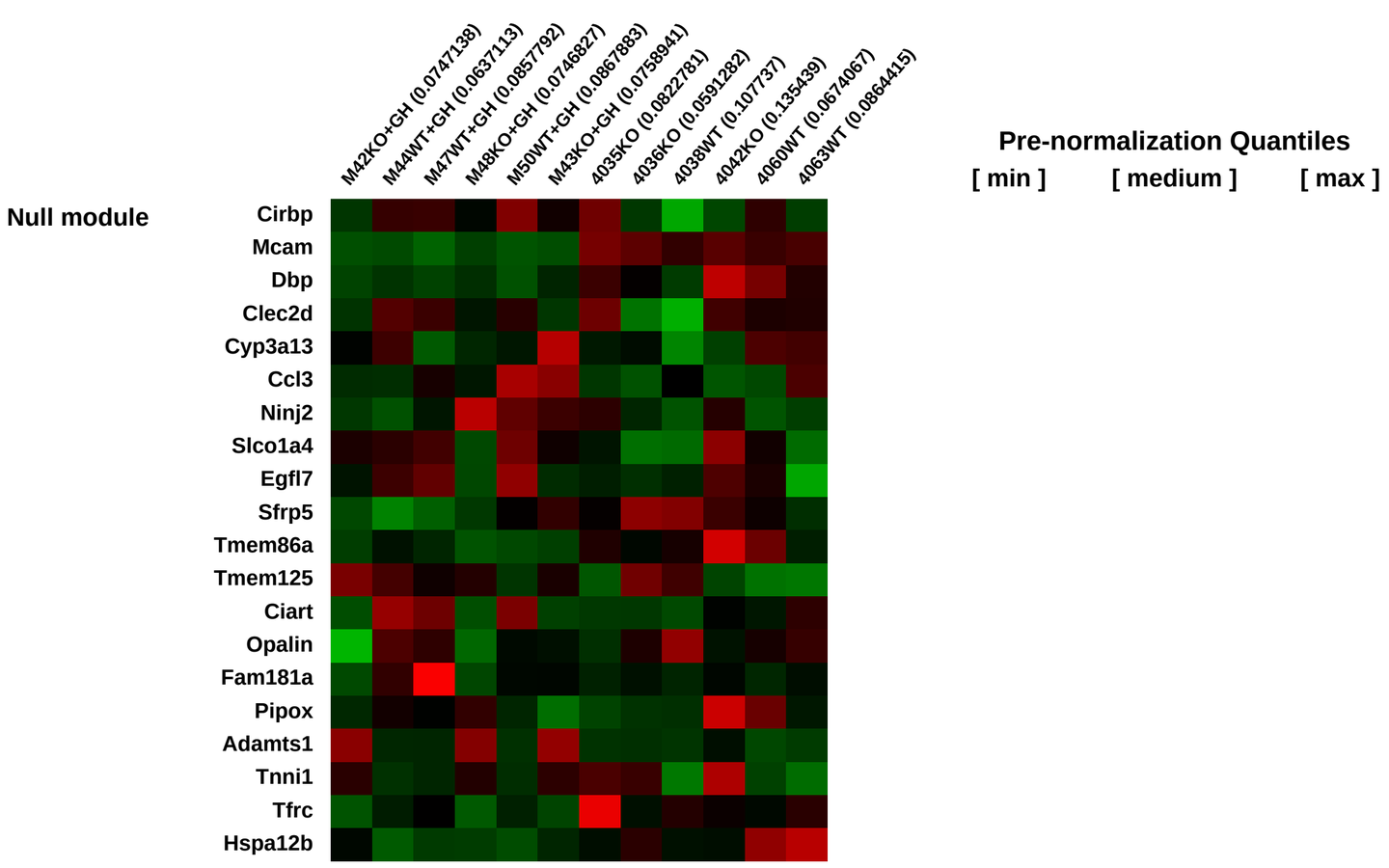

GEO Series "GSE1479" Expression Profiles

Num of samples in this series: 36

Scale of expression profile Z-scores

-3.0 -2.0 -1.0 0.0 1.0 2.0 3.0

GEO Link:	**http://www.ncbi.nlm.nih.gov/geo/query/acc.cgi?acc=GSE1479**
Status:	**Public on Jun 24 2004**
Title:	**C57BL/6 Benchmark Set for Early Cardiac Development**
Organism:	**Mus musculus**
Experiment type:	**Expression profiling by array**
Platform:	**GPL1261**
Pubmed ID:	
Summary & Design:	**Summary:** **Timed matings were performed using C57BL/6 mice and pregnant females sacrificed starting at embryonic day (E) 10.5, and then in daily intervals until E14.5. Gene expression was be further analyzed at E16.5 and E18.5, to monitor changes in gene expression related to maturation of the heart. At stage 10.5, the rostral and caudal parts of the embryo were removed and the middle part, which includes the heart, was subjected to expression analysis. From embryonic day 11.5 on, we isolated embryonic hearts and separated the ventricular from the atrial chambers.** **Keywords = heart** **Keywords = development** **Keywords = cardiac** **Keywords: time-course** **Overall design:**

Background corr dist: **KL-Divergence = 0.2433, L1-Distance = 0.0423, L2-Distance = 0.0035, Normal std = 0.3083**

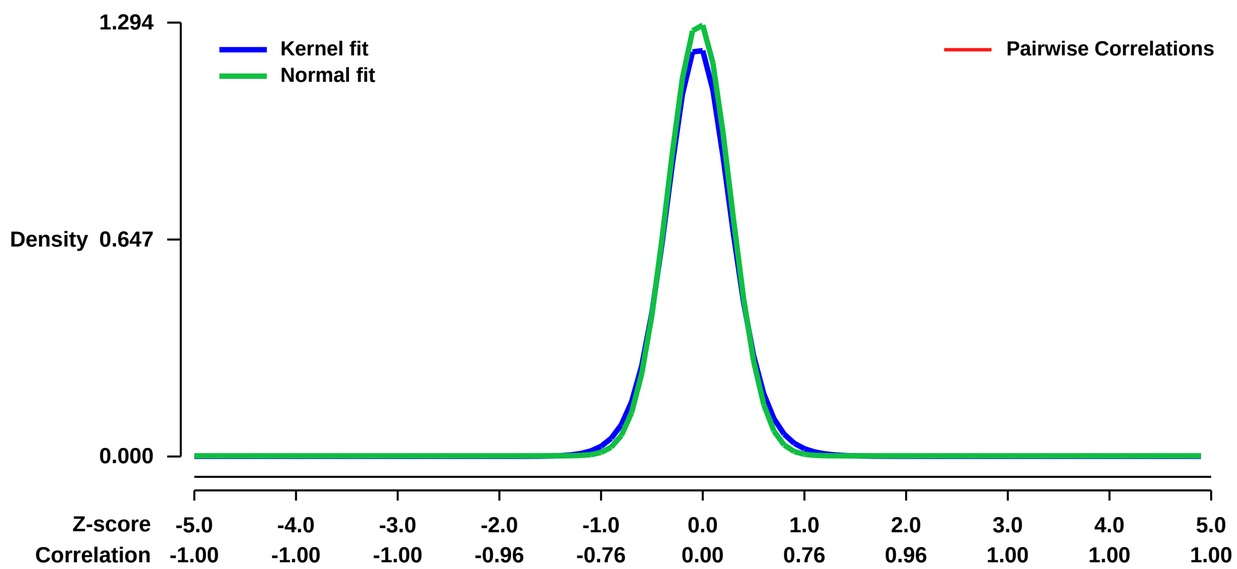

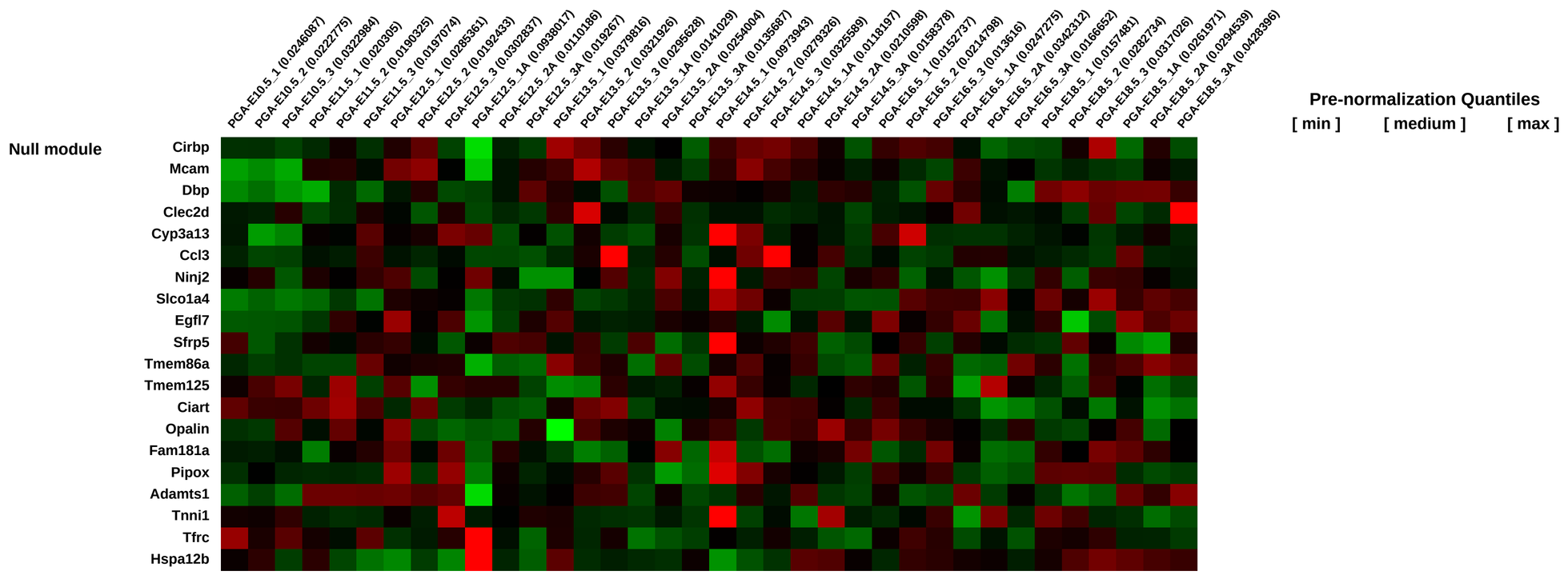

GEO Series "GSE14843" Expression Profiles

Num of samples in this series: 6

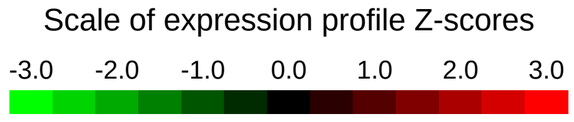

GEO Link:	http://www.ncbi.nlm.nih.gov/geo/query/acc.cgi?acc=GSE14843
Status:	Public on Nov 12 2009
Title:	Altered Hepatic Gene Expression Profiles Associated with Myocardial Ischemia
Organism:	Mus musculus
Experiment type:	Expression profiling by array
Platform:	GPL1261
Pubmed ID:	20160198

Summary & Design:

Summary:
Backgroundâ Acute coronary syndrome (ACS) is sometimes accompanied by accelerated coagulability, lipid metabolism, and inflammatory responses, which are not attributable to the cardiac events alone. We hypothesized that the liver plays a pivotal role in the pathophysiology of ACS. We simultaneously analyzed the gene expression profiles of the liver and heart during acute myocardial ischemia in mice.

Methods and Resultsâ Mice were divided into three treatment groups: sham-operation, ischemia-reperfusion (I/R), and myocardial infarction. Mice with liver I/R were included as additional controls. Marked changes in hepatic gene expression were observed after 24 hours, despite the lack of histological changes in the liver. Genes related to tissue remodeling, adhesion molecules, and morphogenesis were significantly upregulated in the livers of mice with myocardial I/R or infarction, but not in those with liver I/R. Myocardial ischemia, but not changes in the hemodynamic state, was postulated to significantly alter hepatic gene expression. Moreover, detailed analysis of the signaling pathway suggested the presence of humoral factors that intervened between the heart and liver. To address these points, we utilized isolated primary hepatocytes and showed that osteopontin released from the heart actually altered the signaling pathways of primary hepatocytes to those observed in the livers of mice under myocardial ischemia. Moreover, osteopontin stimulated primary hepatocytes to secrete vascular endothelial growth factor-A, which is important for tissue remodeling.

Conclusionsâ Hepatic gene expression is potentially regulated by cardiac humoral factors under myocardial ischemia. These results provide new insights into the pathophysiology of ACS.

Overall design:
C57BL/6J mice (n=46, BW 24.1´–1.42 g, 8â 10 weeks of age; Charles River Laboratories) were divided into the following treatment groups: sham-operated (n=11), I/R (n=10), myocardial infarction (n=10), liver I/R (n=10), and sham-operated plus hydralazine (n=5). In this study, we examined the response of hepatic gene expression to myocardial ischemia. Given the systemic inflammation that characterizes acute coronary syndromes, we postulated that regulation of hepatic genes occurs via inflammatory mediators and not via alterations in hemodynamics or hepatic perfusion. We therefore used whole genome transcriptional profiling to identify hepatic genes selectively regulated in the setting of myocardial ischemia. Moreover, detailed analysis of the signaling pathway suggested the presence of humoral factors that intervened between the heart and liver under myocardial ischemia. As a candidate humoral factors, osteopontin was further investigated. To evaluate whether the cardiac secreted protein affects hepatic gene expressions, we investigated primary hepatocytes treated with osteopontin by using microarray analysis. Affymetrix GeneChip Mouse Genome 430 2.0 Array was used to measure gene expression levels in primary hepatocytes at 8 hours after osteopontin stimulation (mock: n=3 and osteopontin: n=3).

Background corr dist: KL-Divergence = 0.0156, L1-Distance = 0.0483, L2-Distance = 0.0024, Normal std = 0.9256

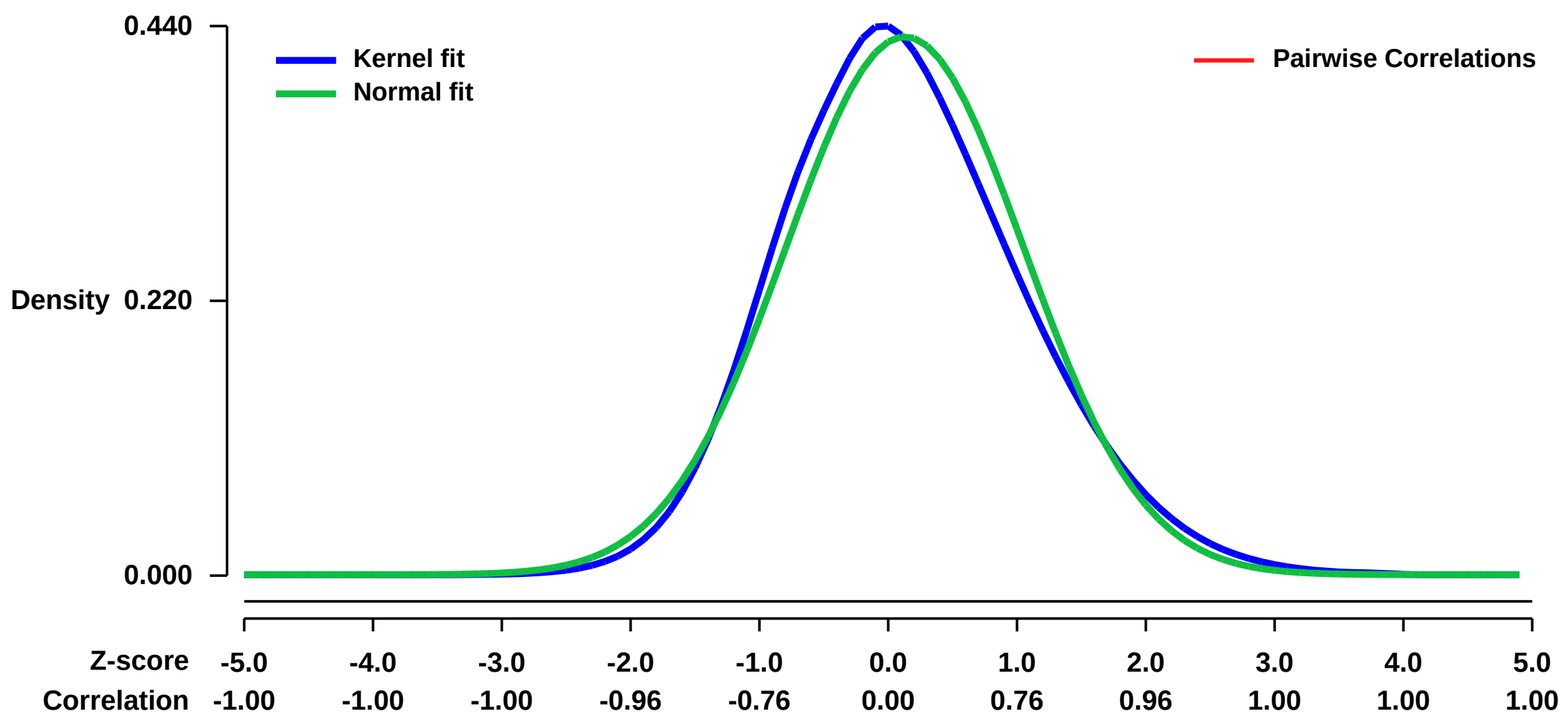

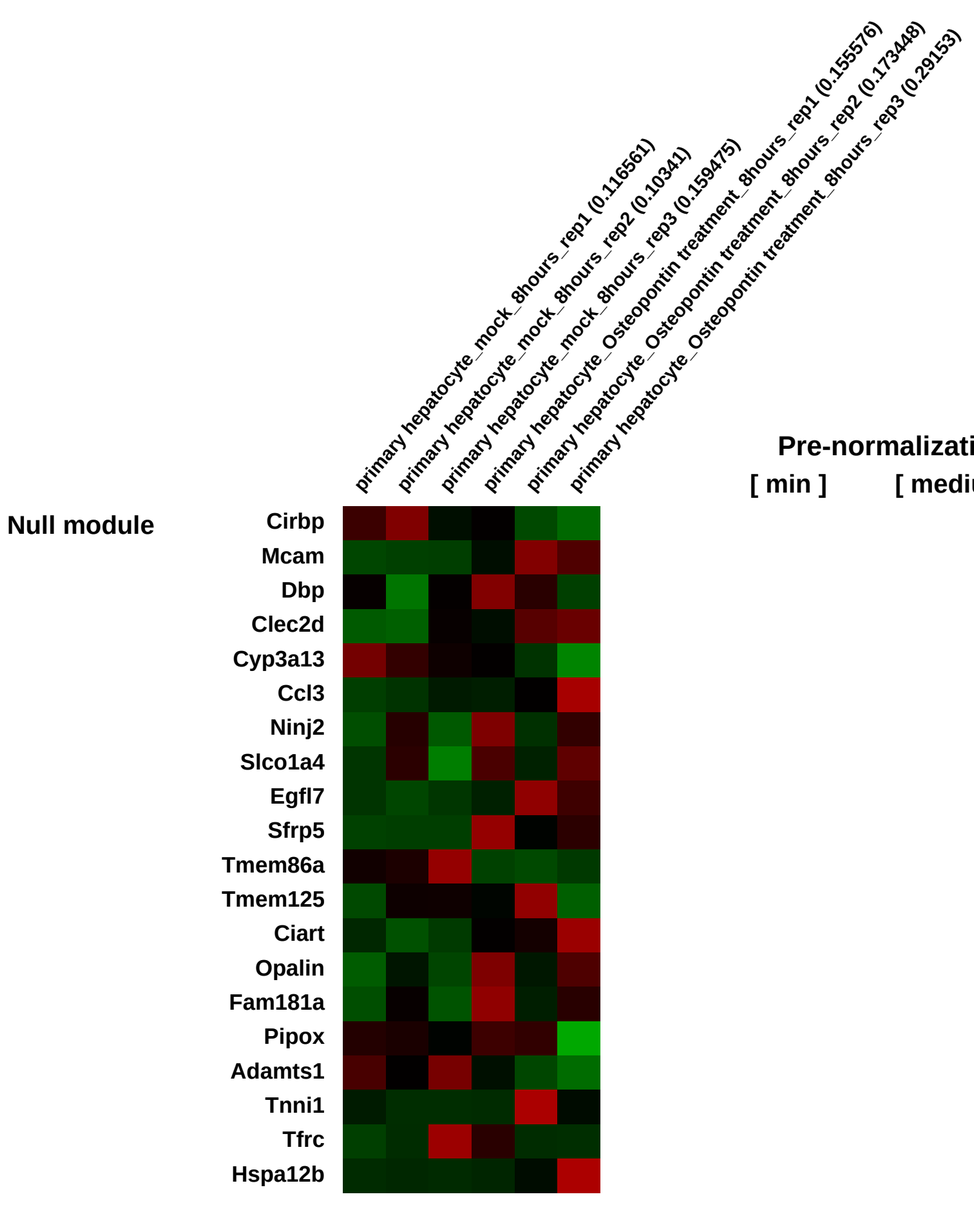

GEO Series "GSE14891" Expression Profiles

Num of samples in this series: 8

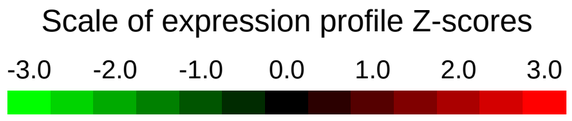

GEO Link:	http://www.ncbi.nlm.nih.gov/geo/query/acc.cgi?acc=GSE14891
Status:	Public on Feb 19 2009
Title:	Expression data of LPS-stimulated macrophages from wild-type and Zc3h12a-/- mice.
Organism:	Mus musculus
Experiment type:	Expression profiling by array
Platform:	GPL1261
Pubmed ID:	19322177
Summary & Design:	**Summary:** Lipopolysaccharide (LPS), a Toll-like receptor (TLR) 4 ligand, induces the expression of various genes including proinflammatory cytokines, and the expression is modified by the presence of Zc3h12a. We used microarrays to examine influence of Zc3h12a deficiency in LPS-inducible gene expression. Keywords: Time course after LPS (100 ng/ml) stimulation **Overall design:** Peritoneal macrophages from wild-type and Zc3h12a-/- mice were stimulated with LPS for 0, 1, 2 and 4 hours, followed by RNA extraction. Then hybridization on affymetrix microarrays was performed.

Background corr dist: KL-Divergence = 0.0555, L1-Distance = 0.0263, L2-Distance = 0.0011, Normal std = 0.5497

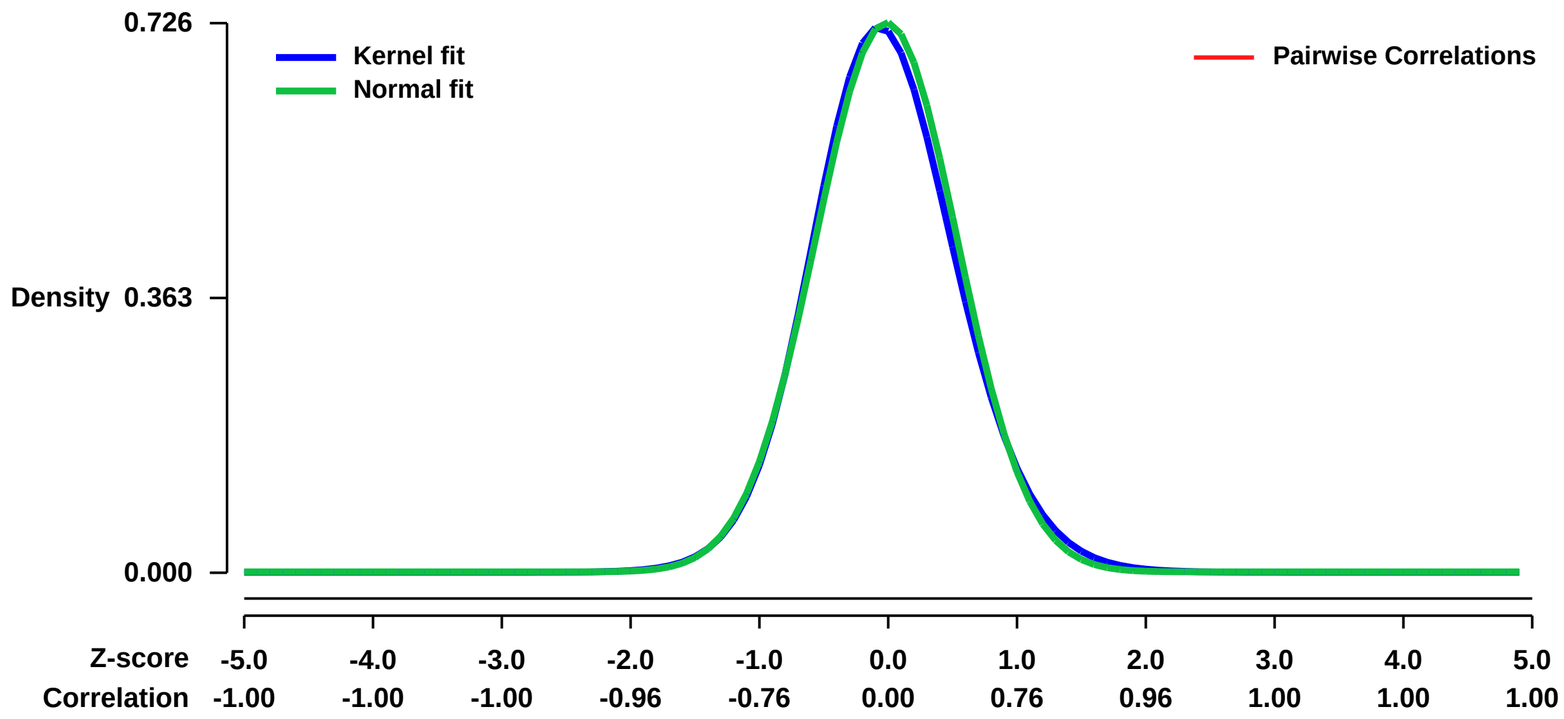

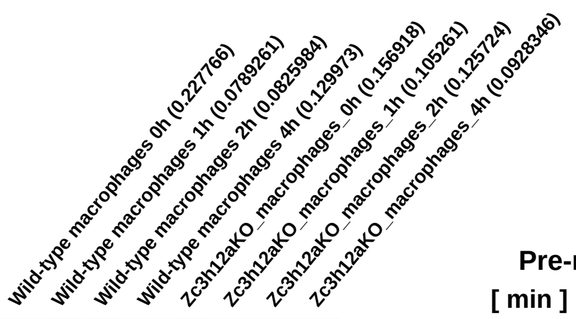

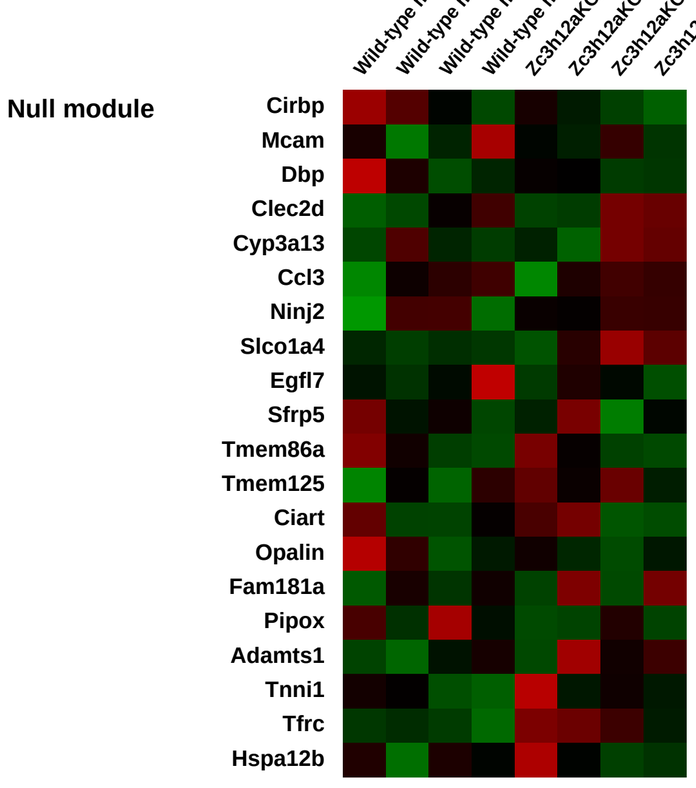

GEO Series "GSE14906" Expression Profiles

Num of samples in this series: 6

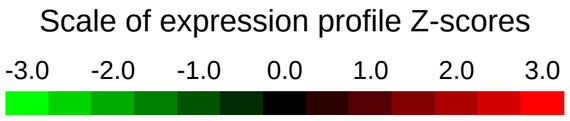

GEO Link:	http://www.ncbi.nlm.nih.gov/geo/query/acc.cgi?acc=GSE14906
Status:	Public on Feb 18 2010
Title:	The Gene Expression Analysis in E12.5 Mouse Hearts with GATA4-FOG2 Interaction Loss
Organism:	Mus musculus
Experiment type:	Expression profiling by array
Platform:	GPL1261
Pubmed ID:	19578715
Summary & Design:	**Summary:** In order to identify the targets of GATA4-FOG2 action in mammalian heart development we performed Affymetrix microarray comparisons of gene expression in normal and mutant at embryonic (E) day E12.5 hearts. We compared RNA samples from both Fog2-null and Gata4ki/ki mutant E12.5 hearts to the wild-type control E12.5 hearts. We reasoned that as the phenotypes of the Fog2 knockout and Gata4ki/ki mutation (a V217G mutation that specifically cripples the interaction between GATA4 and FOG proteins) are similar, we should expect to identify a similar set of differentially expressed genes in both experiments. As an additional control, we expected to find the Fog2 gene expression absent in the mutant (null) Fog2 cardiac sample, but not Gata4ki/ki sample. **Overall design:** We have analyzed 6 RNA samples total (3 from control hearts, 2 from FOG2 null hearts and 1 from GATA4ki hearts)

Background corr dist: KL-Divergence = 0.0388, L1-Distance = 0.0213, L2-Distance = 0.0005, Normal std = 0.6215

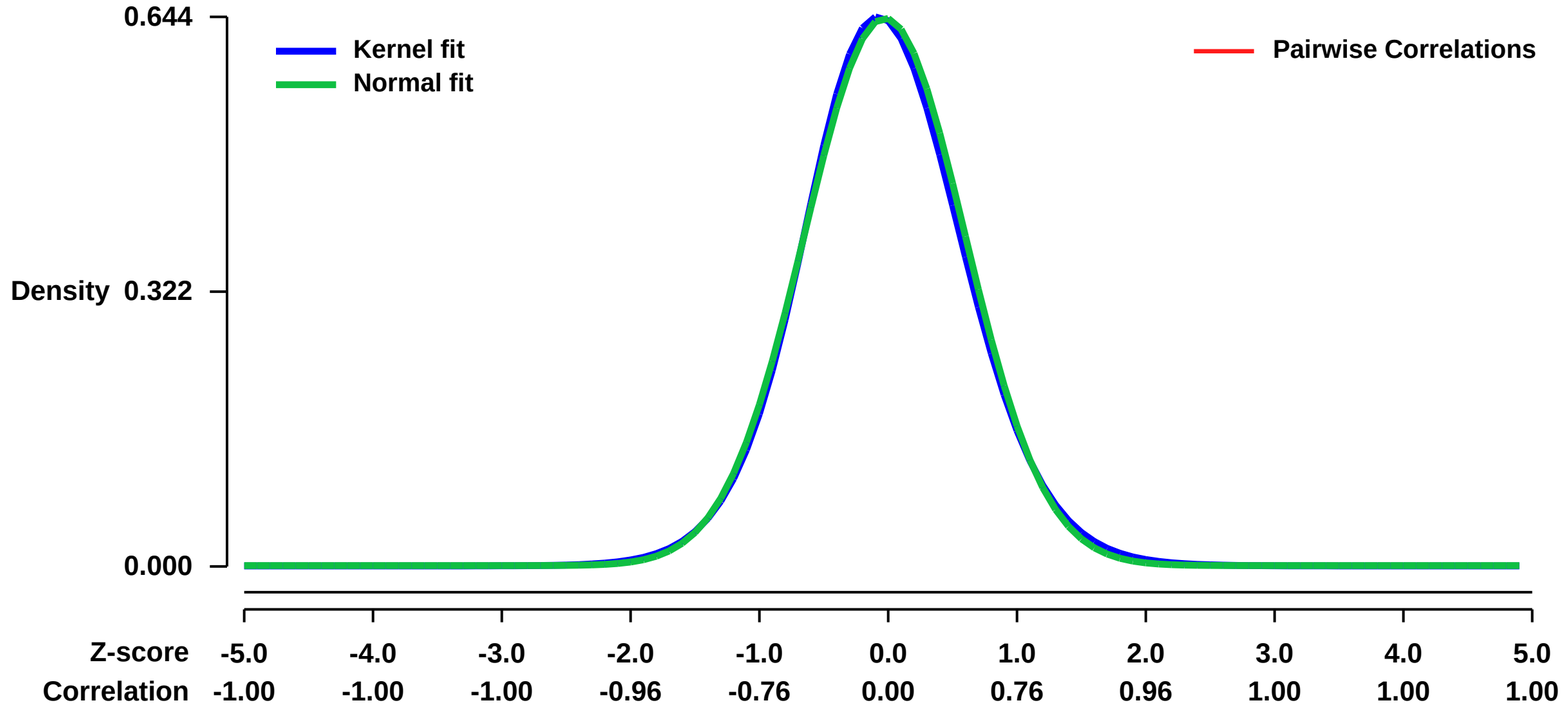

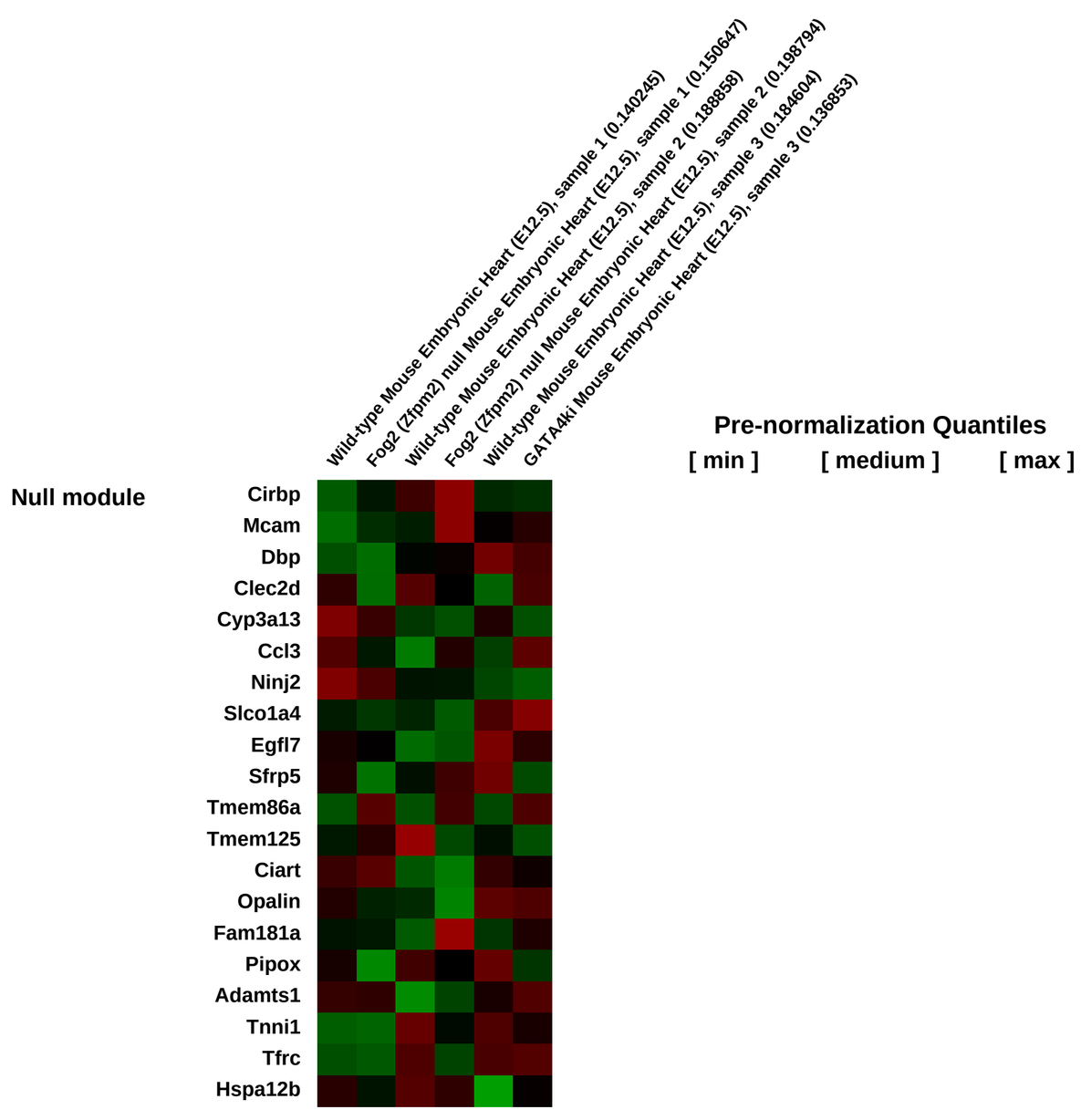

GEO Series "GSE14929" Expression Profiles

Num of samples in this series: 38

Scale of expression profile Z-scores

-3.0 -2.0 -1.0 0.0 1.0 2.0 3.0

GEO Link: http://www.ncbi.nlm.nih.gov/geo/query/acc.cgi?acc=GSE14929
Status: Public on Jun 23 2009
Title: Myocardial expression data from gnotobiotic wild-type and Ppara-/- mice
Organism: Mus musculus
Experiment type: Expression profiling by array
Platform: GPL1261
Pubmed ID: 20529848

Summary & Design:

Summary:
Germ free (GF) and conventionalized (CONV-D) wild-type C57Bl/6 male mice in the CARB-fed, 24h fasted, and 30d trained states; plus GF and CONV-D CARB-fed Ppara-/- mice. CARB-fed indicates a standard polysaccharide-rich mouse chow diet.

CONV-D mice are those that received a microbiota transplant from conventionally raised mice 2-3 weeks before experiment was initiated

Keywords: RNA Expression Array

Overall design:
Hearts from six to ten week-old GF and CONV-D mice, from the following eight treatment groups (GF, CONV-D) X (CARB-fed [wild-type], 24h fast [wild-type], 30d trained [wild-type], Ppara-/- [CARB-fed])

Background corr dist: KL-Divergence = 0.2177, L1-Distance = 0.0406, L2-Distance = 0.0032, Normal std = 0.3220

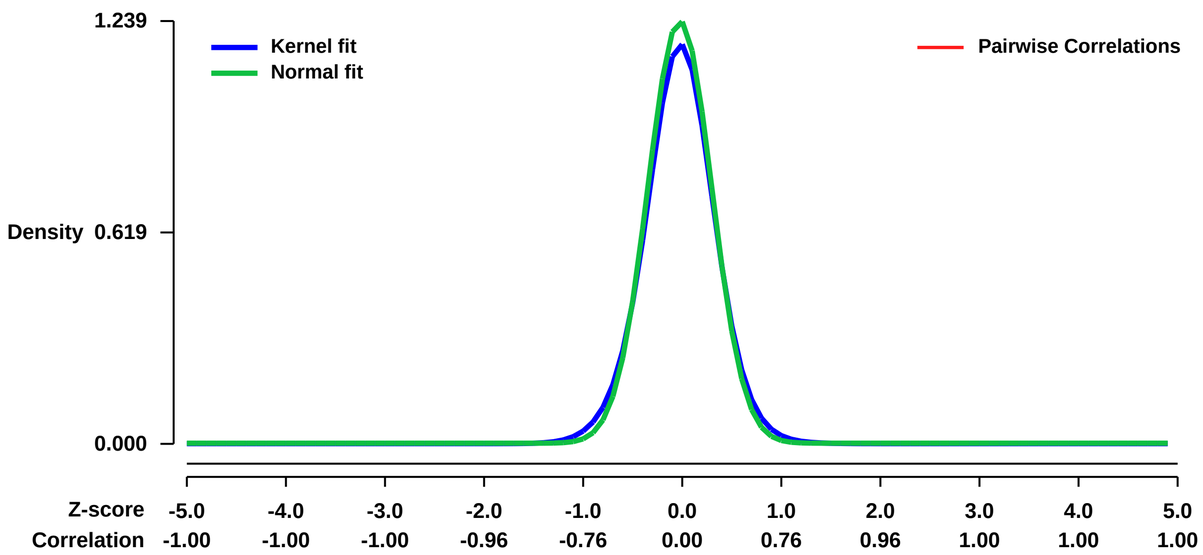

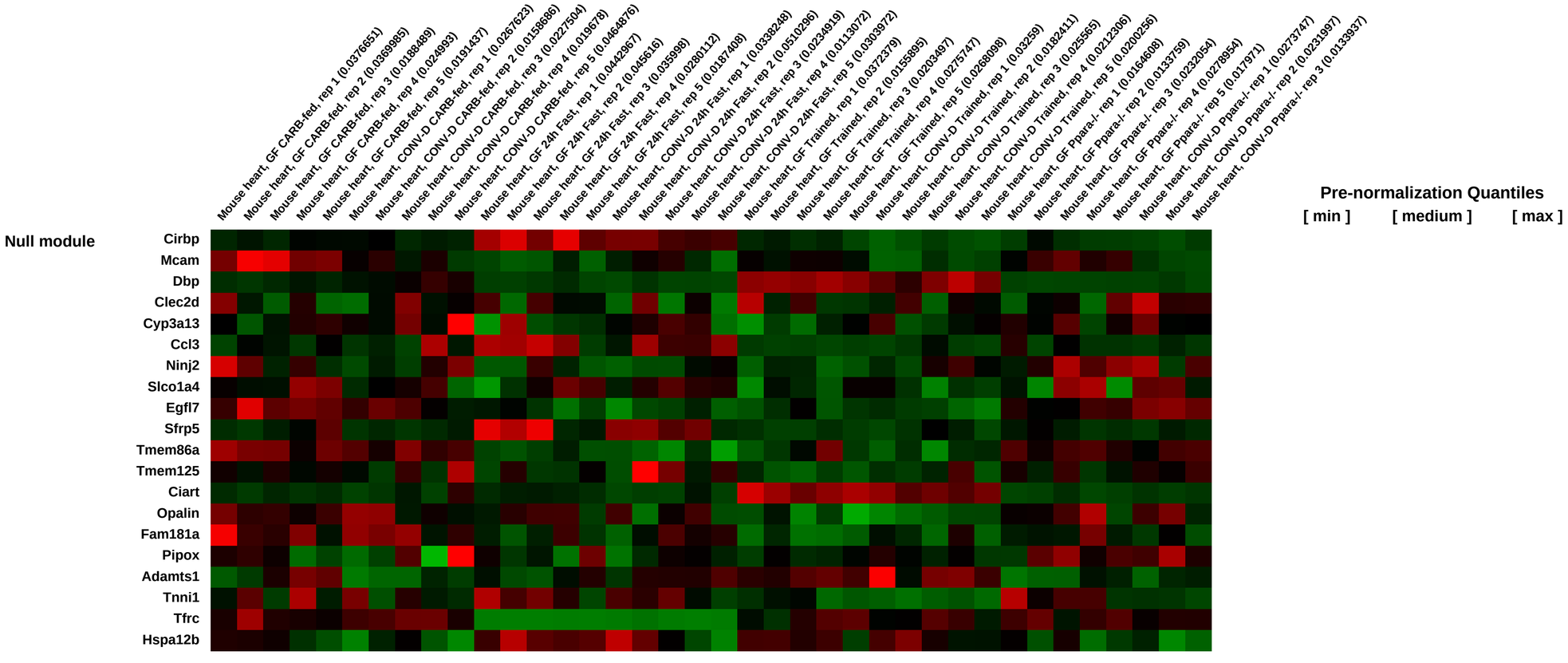

GEO Series "GSE15062" Expression Profiles

Num of samples in this series: 21

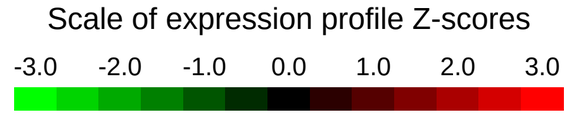

GEO Link:	http://www.ncbi.nlm.nih.gov/geo/query/acc.cgi?acc=GSE15062
Status:	Public on Nov 23 2009
Title:	Mouse aorta smooth muscle cells differentiate into lymphoid tissue organizers upon combined TNFR1/LTBR NF-kB signaling
Organism:	Mus musculus
Experiment type:	Expression profiling by array
Platform:	GPL1261
Pubmed ID:	20139359
Summary & Design:	**Summary:** Mouse aorta smooth muscle cells (SMCs) express TNF receptor superfamily member 1A (TNFR1) and lymphotoxin ˆ receptor (LTˆ R). Circumstantial evidence has linked the SMC LTˆ R to tertiary lymphoid organogenesis in diseased aortae of hyperlipidemic mice. Here, we explored potential roles of TNFR1 and LTˆ R activation in cultured SMCs. TNFR1 signaling by TNF activated the classical RelA NF-¸”B pathway, whereas LTˆ R signaling by agonistic anti LTˆ R antibody activated both the classical RelA and alternative RelB NF-¸”B pathways. Addition of both agonists synergized to enhance p100 inhibitor processing to the p52 subunit of NF-¸”B and promoted its nuclear translocation suggesting RelA-RelB cross-talk in transcription regulation. Correspondingly, microarrays showed that simultaneous TNFR1 and LTˆ R activation when compared to activation of single receptors was followed by markedly elevated levels of mRNAs encoding leukocyte homeostatic chemokines CCL2, CCL5, CXCL1, and CX3CL1. Furthermore, SMCs acquired prototypical features of mesenchymal cells known as lymphoid tissue organizers (LTOs), which control tertiary lymphoid organogenesis in autoimmune diseases, through hyperinduction of CCL7, CCL9, CXCL13, CCL19, CXCL16, VCAM-1, and ICAM-1. Experiments with ltbr-/- SMCs suggested that the LTˆ R-RelB activation component of NF-¸”B signaling was obligatory to generate the LTO phenotype. TNFR1-LTˆ R crosstalk also resulted in augmented synthesis and prolonged secretion of lymphorganogenic chemokine proteins into the culture medium. Thus, combined TNFR1-LTˆ R signaling triggers SMC transdifferentiation into a phenotype that strikingly resembles LTOs. LTO-like SMCs may adopt a thus far unrecognized role in diseased arteries, i.e. to coordinate tertiary lymphoid organogenesis in atherosclerosis, aortic aneurysm, and transplant vasculopathy. **Overall design:** Smooth muscle cells in tissue culture were stimulated with agonists and subsequently microarray, RT-PCR, and protein assays / analyses were performed

Background corr dist: KL-Divergence = 0.1735, L1-Distance = 0.0370, L2-Distance = 0.0025, Normal std = 0.3524

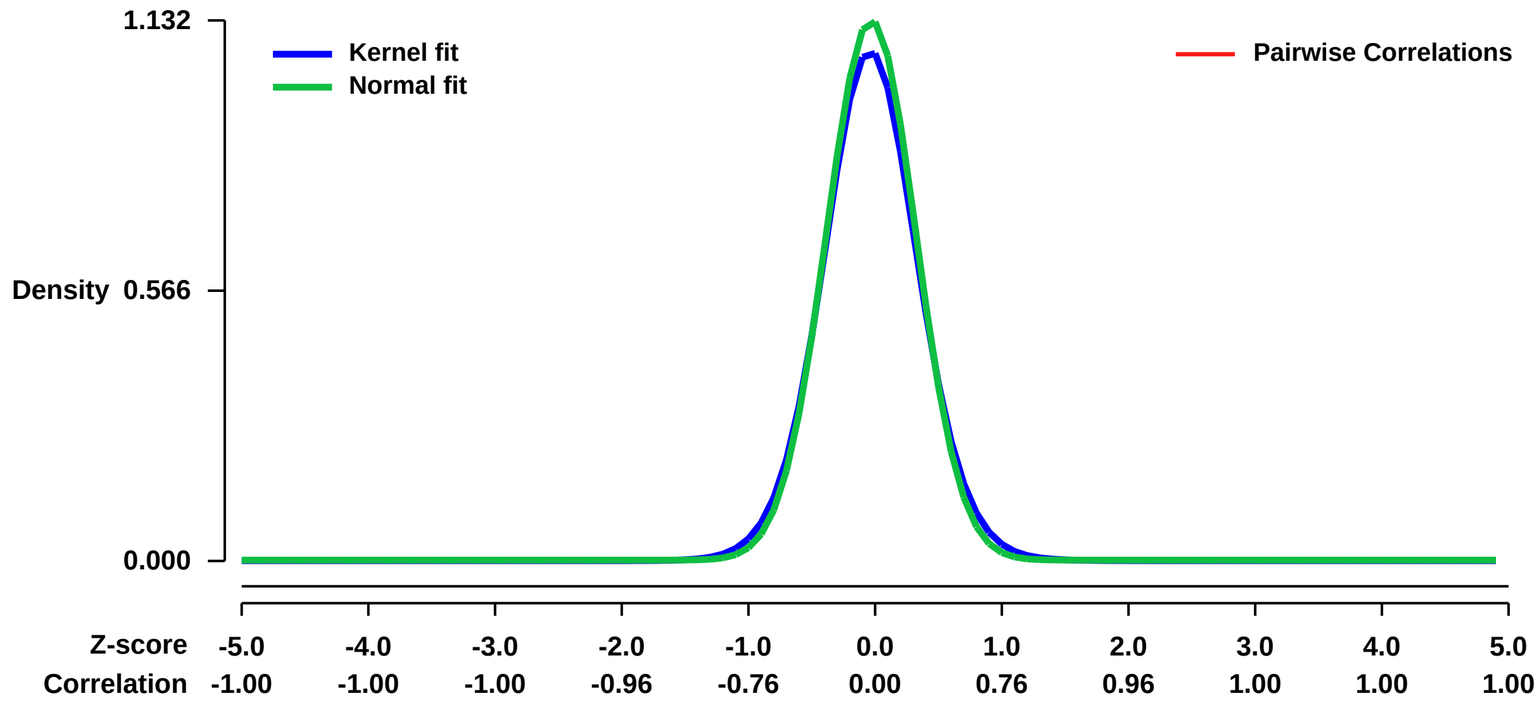

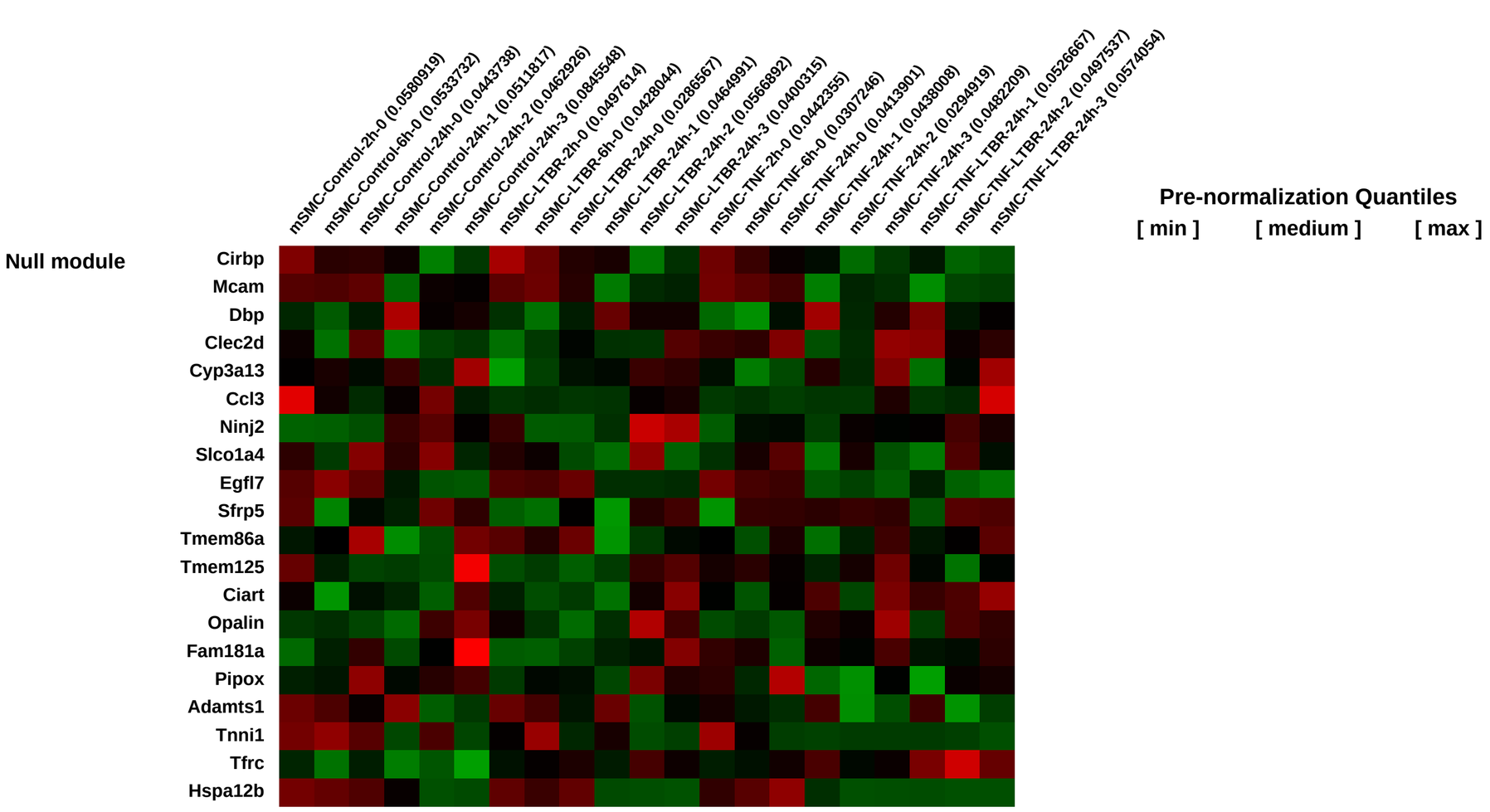

GEO Series "GSE15078" Expression Profiles

Num of samples in this series: 6

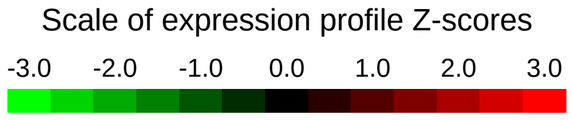

GEO Link:	**http://www.ncbi.nlm.nih.gov/geo/query/acc.cgi?acc=GSE15078**
Status:	**Public on Mar 05 2009**
Title:	**Fog2 regulation of gene expression in the adult heart**
Organism:	**Mus musculus**
Experiment type:	**Expression profiling by array**
Platform:	**GPL1261**
Pubmed ID:	**19411759**
Summary & Design:	**Summary:** **MHCaCre induced knockout of Fog2flox.** **Aberrant transcriptional regulation contributes to the pathogenesis of both congenital and adult forms of heart disease. While the transcriptional regulator FOG2 is known to be essential for heart morphogenesis and coronary development, its tissue specific function has not been previously investigated. Additionally, little is known about the role of FOG2 in the adult heart. Here we use spatiotemporally regulated inactivation of Fog2 to delineate its function both in embryo and adult heart. Early cardiomyocyte-restricted loss of Fog2 recapitulated the cardiac and coronary defects of the Fog2 germline knockouts. Later cardiomyocyte-restricted loss of Fog2 (Fog2MC) did not result in defects in cardiac structure or coronary vessel formation. However, Fog2MC adult mice had severely depressed ventricular function and died at 8-14 weeks. Fog2MC adult hearts displayed a paucity of coronary vessels. This was associated with myocardial hypoxia, increased cardiomyocyte apoptosis, and cardiac fibrosis. Induced inactivation of Fog2 in adult heart resulted in similar phenotype, as did ablation of FOG2 interaction with the transcription factor GATA4. Loss of FOG2 or FOG2-GATA4 interaction altered expression of a panel of angiogenesis-related genes. Collectively, our data indicated that FOG2 regulates adult heart function and coronary angiogenesis. #!#** **Overall design:** **Fog2flox/delta; MHCaCre (3) compared to Fog2flox/delta; no Cre (3). One heart per sample.**

Background corr dist: KL-Divergence = 0.0396, L1-Distance = 0.0184, L2-Distance = 0.0003, Normal std = 0.6169

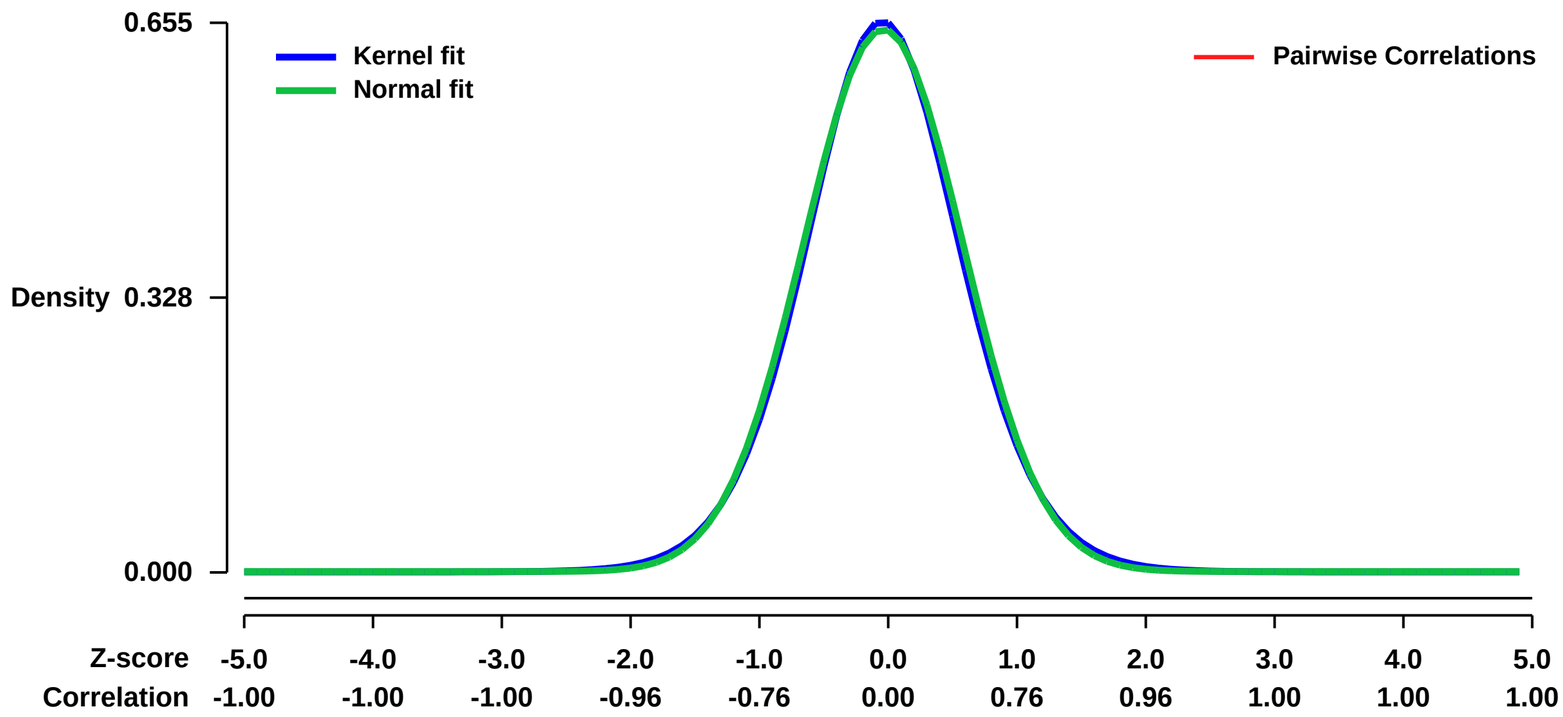

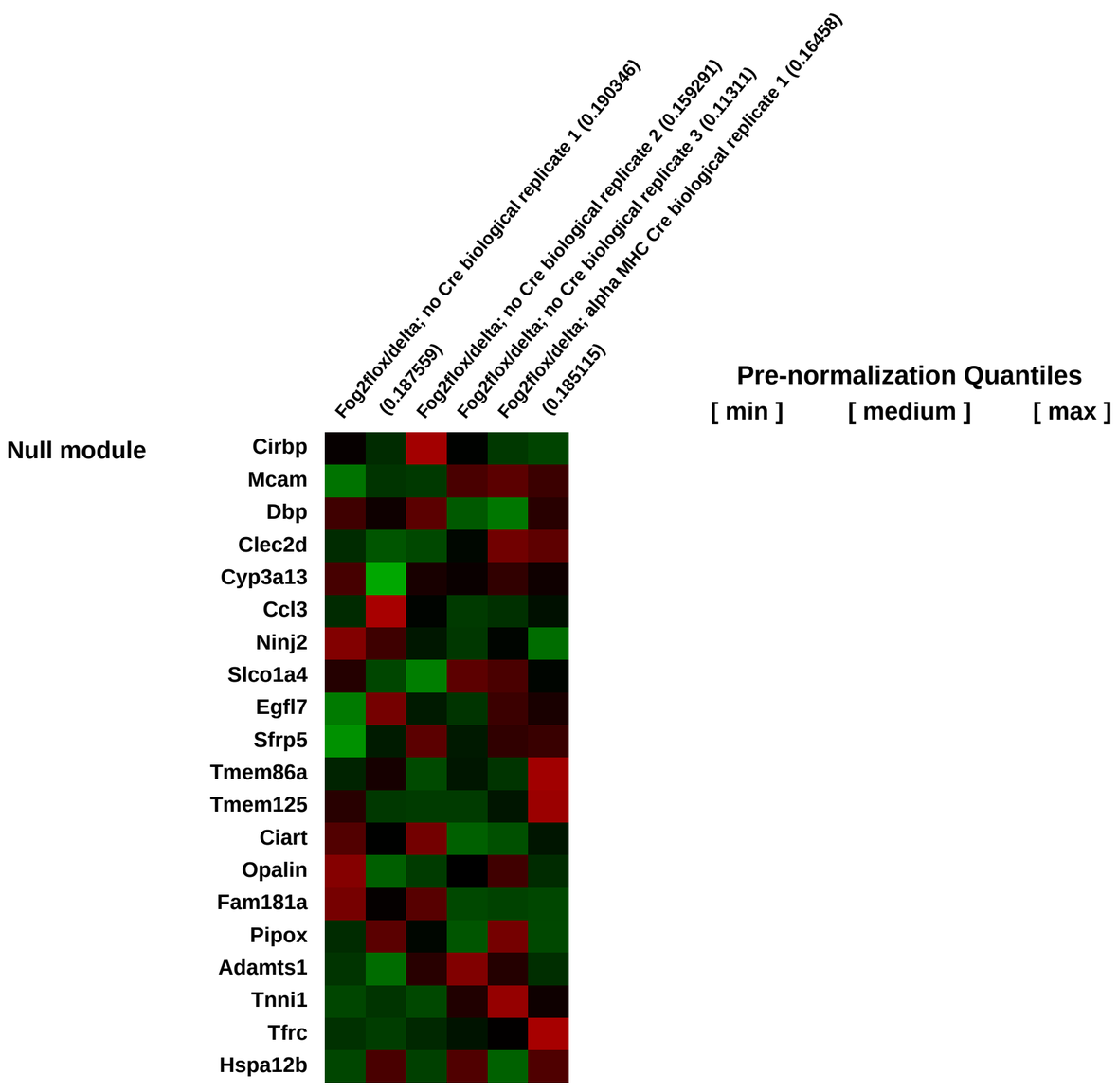

GEO Series "GSE15121" Expression Profiles

Num of samples in this series: 6

Scale of expression profile Z-scores

-3.0 -2.0 -1.0 0.0 1.0 2.0 3.0

GEO Link: http://www.ncbi.nlm.nih.gov/geo/query/acc.cgi?acc=GSE15121
Status: Public on Jan 01 2010
Title: Expression data from E10 cells with miR-129 over-expression
Organism: Mus musculus
Experiment type: Expression profiling by array
Platform: GPL1261
Pubmed ID:

Summary & Design:

Summary:
miRNAs are known to regulate gene expression by suppressing translation, but there is also a wealth of data showing that they can act as critical regulators of mRNA stability of their targets. In this experiment, we analyzed the mRNA expression profiles of E10 with high expression of miR-129 as compared to control cells to identify miR-129 targets.

E10 cells infected with miR-129 over-expressing lentivirus or the control lentivirus were cultured for 48 hours. More than 80% of cells were infected. Total RNA samples were isolated using Trizol (invitrogen), and subjected to labeling, fragmentation and hybridization, according to manufacturerâ s protocols. Mouse Genome 430 2.0 Array (Affymetrix) was used for mRNA expression profiling.

Overall design:
We compared the mRNA expression profiles between cells infected with miR-129 expressing lentivirus and the cells infected with control lentivirus

Background corr dist: KL-Divergence = 0.0330, L1-Distance = 0.0387, L2-Distance = 0.0017, Normal std = 0.6967

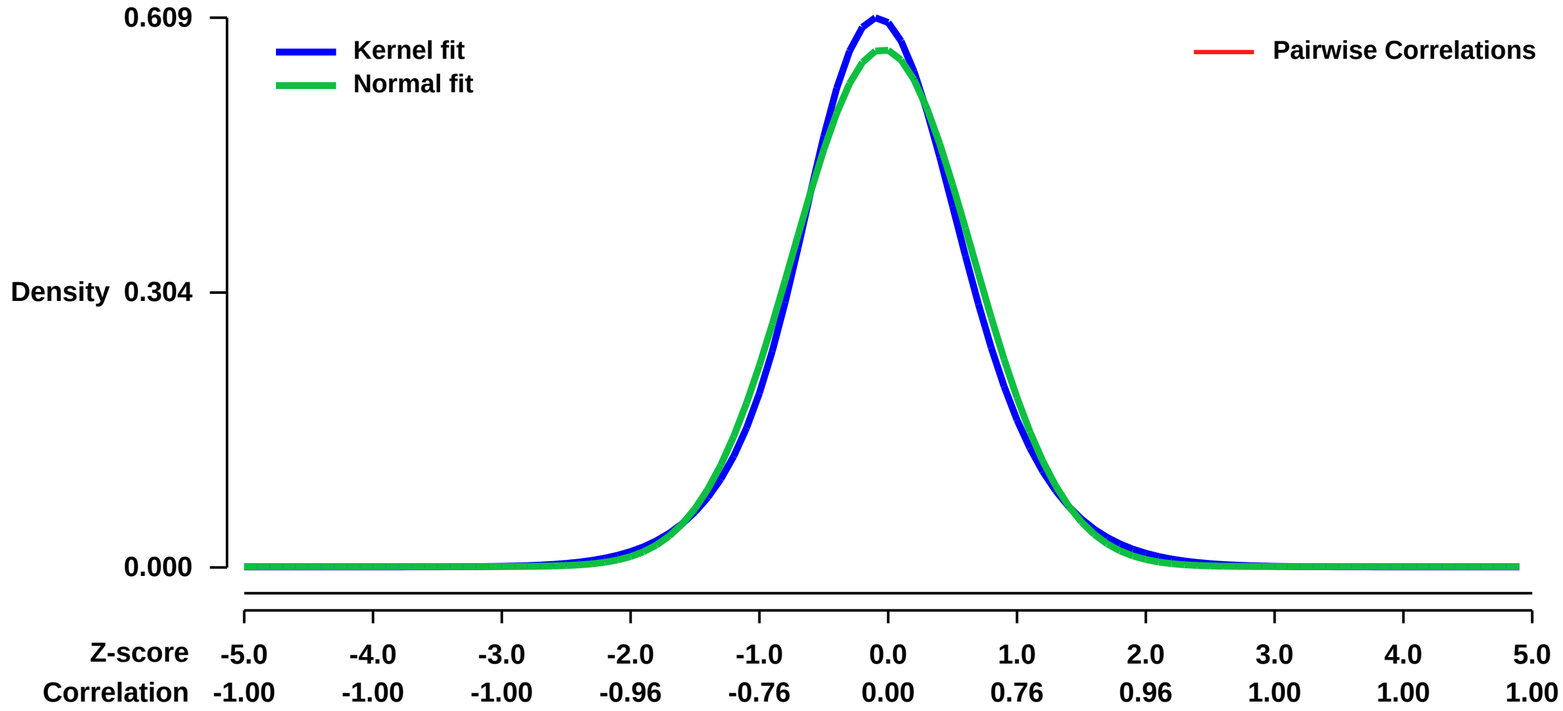

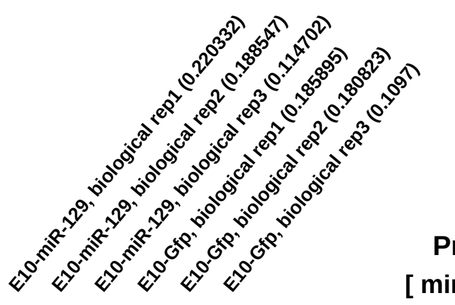

Pre-normalization Quantiles
[min] [medium] [max]

Null module

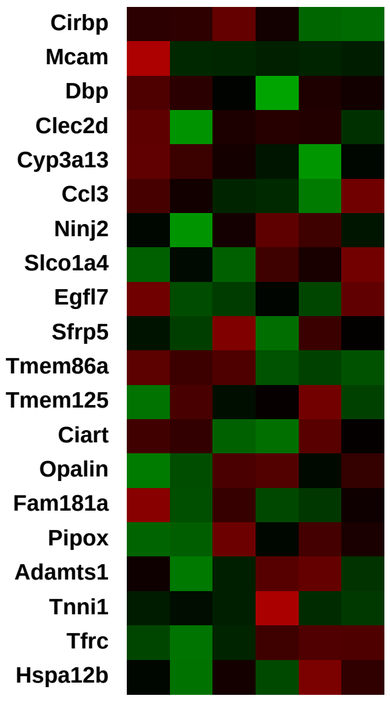

GEO Series "GSE15146" Expression Profiles

Num of samples in this series: 10

Scale of expression profile Z-scores

-3.0 -2.0 -1.0 0.0 1.0 2.0 3.0

GEO Link:	**http://www.ncbi.nlm.nih.gov/geo/query/acc.cgi?acc=GSE15146**
Status:	**Public on Aug 06 2009**
Title:	**mRNA expression in Zfp36L2 knockout E14.5 fetal liver**
Organism:	**Mus musculus**
Experiment type:	**Expression profiling by array**
Platform:	**GPL1261**
Pubmed ID:	**19633199**
Summary & Design:	**Summary:** **ZFP36L2, zinc finger protein 36, C3H type-like 2 (also known as Brf2, Erf2, Tis11D) is a member of the tristetraprolin (TTP; Zfp36) family of tandem CCCH zinc finger proteins that can bind to AU-rich elements (AREs) in the 3'-untranslated region of mRNAs, leading to their deadenylation and subsequent degradation. We have generated Zfp36l2 knockout mice. Knockout mice were born at the expected Mendelian frequency, but within several weeks of birth they died rather suddenly with pallor and frequent intestinal hemorrhage. These mice exhibited pancytopenia, decreased hematopoietic progenitor cells from fetal liver and yolk sac, and ineffective hematopoietic stem cells. Since ZFP26L2 is likely to function as an ARE-containing mRNA destabilizing protein, we were interested in identifying any abnormally stabilized transcripts in fetal livers from the Zfp36l2 knockout mice whose protein product may directly or indirectly affect hematopoietic stem cell function.** **Overall design:** **Total RNA was isolated from individual embryonic day 14.5 fetal livers. Five wild type and five knockout fetal livers were used to generate 5 wild type replicates and 5 knockout replicates. RNA expression from knockout fetal livers was compared to wild type fetal livers.**

Background corr dist: **KL-Divergence = 0.1379, L1-Distance = 0.0224, L2-Distance = 0.0011, Normal std = 0.3872**

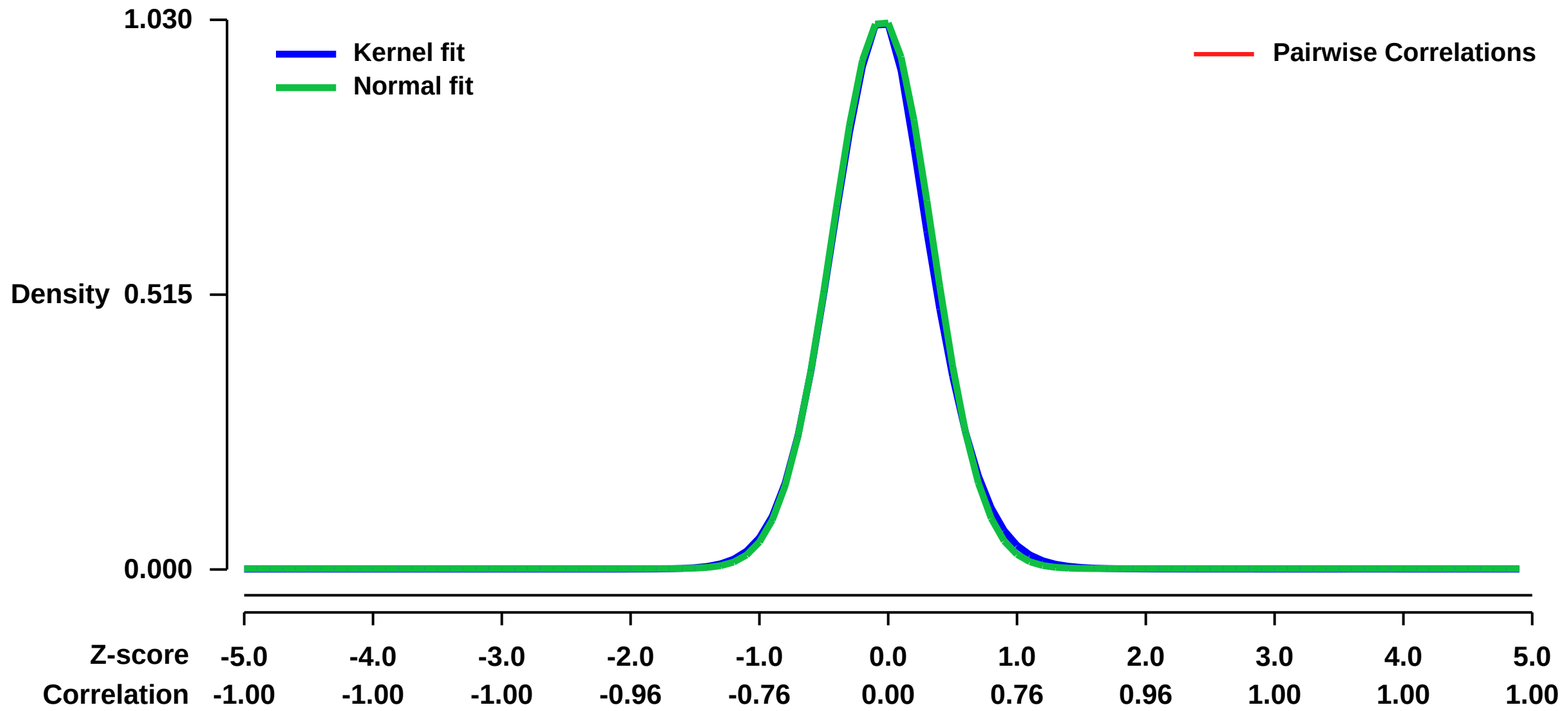

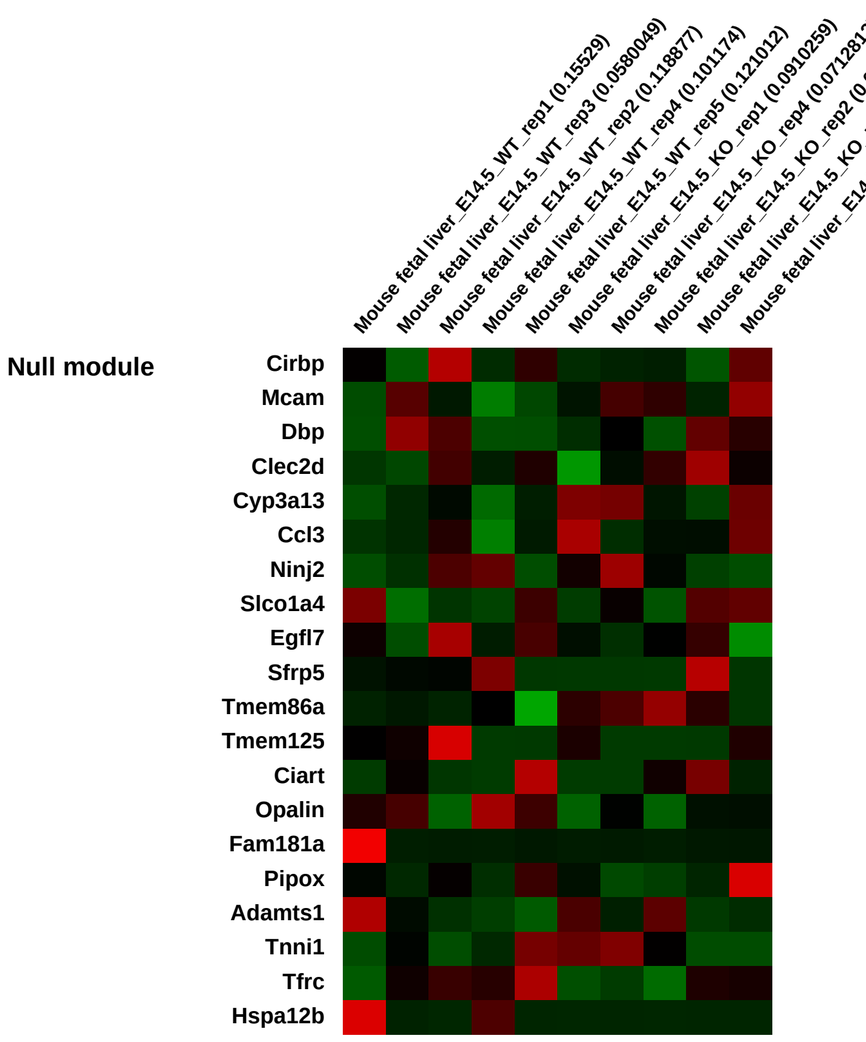

GEO Series "GSE15161" Expression Profiles

Num of samples in this series: 26

Scale of expression profile Z-scores

-3.0 -2.0 -1.0 0.0 1.0 2.0 3.0

GEO Link:	http://www.ncbi.nlm.nih.gov/geo/query/acc.cgi?acc=GSE15161
Status:	Public on Apr 10 2009
Title:	Expression data from retroviral vector-infected immortalized mouse embryonic fibroblasts (MEFs)
Organism:	Mus musculus
Experiment type:	Expression profiling by array
Platform:	GPL1261
Pubmed ID:	19483725
Summary & Design:	**Summary:** Cultured cancer cells exhibit substantial phenotypic heterogeneity when measured in a variety of ways such as sensitivity to drugs or the capacity to grow under various conditions. Among these, the ability to exhibit anchorage-independent cell growth (colony forming capacity in semisolid media) has been considered to be fundamental in cancer biology because it has been connected with tumor cell aggressiveness in vivo such as tumorigenic and metastatic potentials, and also utilized as a marker for in vitro transformation. Although multiple genetic factors for anchorage-independence have been identified, the molecular basis for this capacity is still largely unknown. To investigate the molecular mechanisms underlying anchorage-independent cell growth, we have used genome-wide DNA microarray studies to develop an expression signature associated with this phenotype. Using this signature, we identify a program of activated mitochondrial biogenesis associated with the phenotype of anchorage-independent growth and importantly, we demonstrate that this phenotype predicts potential for metastasis in primary breast and lung tumors. **Keywords:** c-Myc or v-Src retroviral vector-infected immortalized mouse embryonic fibroblasts. **Overall design:** Expression data of c-Myc and v-Src transformed MEFs was used to validate an expression signature generated from human cultured breast cancer cell lines with anchorage-independent growth ability.

Background corr dist: KL-Divergence = 0.2660, L1-Distance = 0.0442, L2-Distance = 0.0043, Normal std = 0.2972

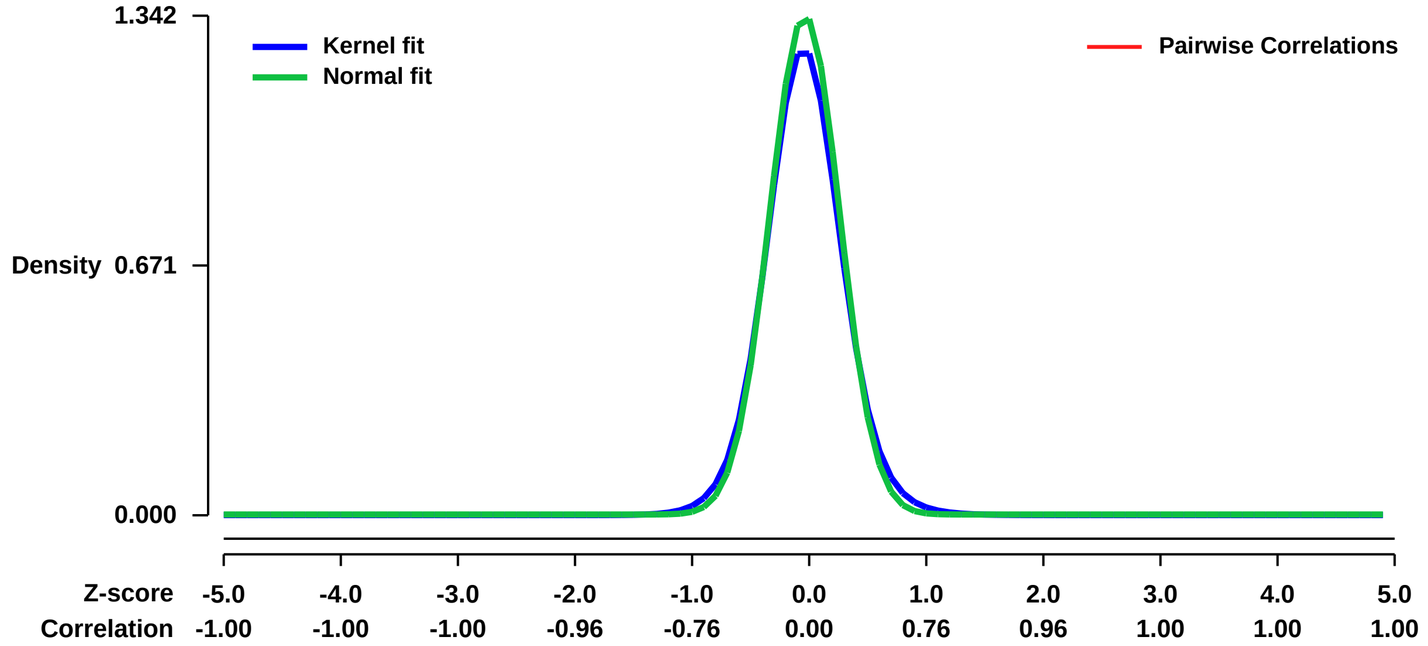

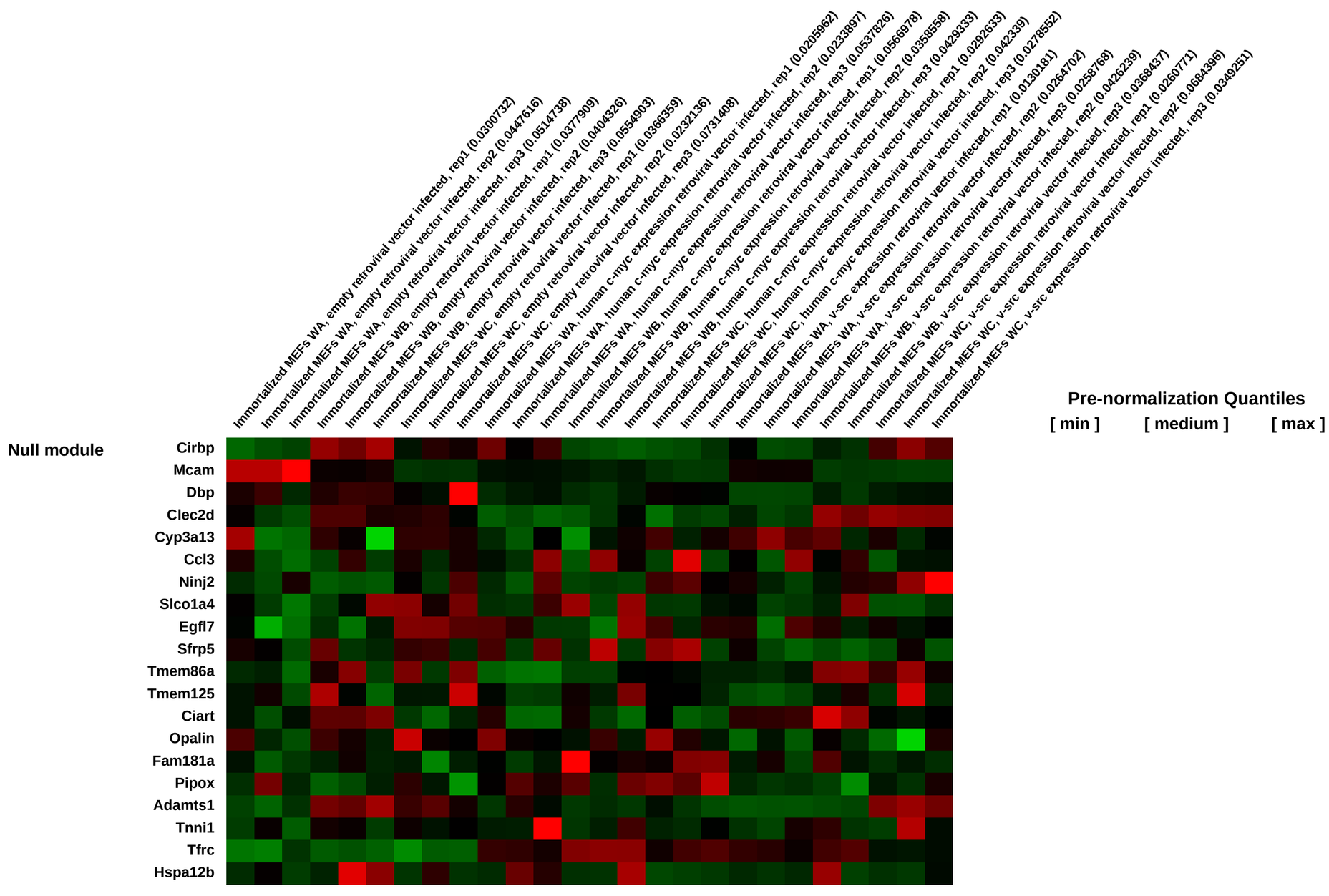

GEO Series "GSE15173" Expression Profiles

Num of samples in this series: 6

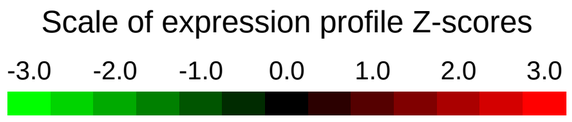

GEO Link:	http://www.ncbi.nlm.nih.gov/geo/query/acc.cgi?acc=GSE15173
Status:	Public on May 01 2009
Title:	Dppa4 is dispensable for embryonic stem cell identity and germ cell development, but essential for embryogenesis
Organism:	Mus musculus
Experiment type:	Expression profiling by array
Platform:	GPL1261
Pubmed ID:	19332562
Summary & Design:	**Summary:** Dppa4 (Developmental pluripotency-associated 4) has been identified in several highprofile screens as a gene that is expressed exclusively in pluripotent cells. It encodes a nuclear protein with a SAP-like domain and appears to be associated preferentially with transcriptionally active chromatin. Its exquisite expression pattern and results of RNA interference experiments have led to speculation that Dppa4, as well as its nearby homolog Dppa2, might play essential roles in embryonic stem cell function and/or germ cell development. To rigorously assess suggested roles, we have generated Dppa4-deficient and Dppa4/Dppa2 double-deficient ES cells, as well as mice lacking Dppa4. Contrary to predictions, we find that Dppa4 is completely dispensable for ES cell identity and germ cell development. Instead, loss of Dppa4 in mice results in late embryonic/peri-natal death and striking skeletal defects with partial penetrance. Thus, surprisingly, Dppa4-deficiency affects tissues, which never transcribed the gene, and at least some loss-of-function defects manifest phenotypically at an embryonic stage long after physiologic Dppa4 expression has ceased. Concomitant with targeted gene inactivation, we have introduced into the Dppa4 locus a red fluorescent marker (tandem-dimer RFP), which is compatible with GFP-based proteins and allows non-invasive visualization of pluripotent cells and reprogramming events. **Overall design:** Comparison of Dppa4 knockout ES cells (CI#243.12) against Dppa4 hemizygous parental ES cell line (CI#84.2). Both cell lines were grown in presence of mouse embrionic fibroblasts as feeder cells

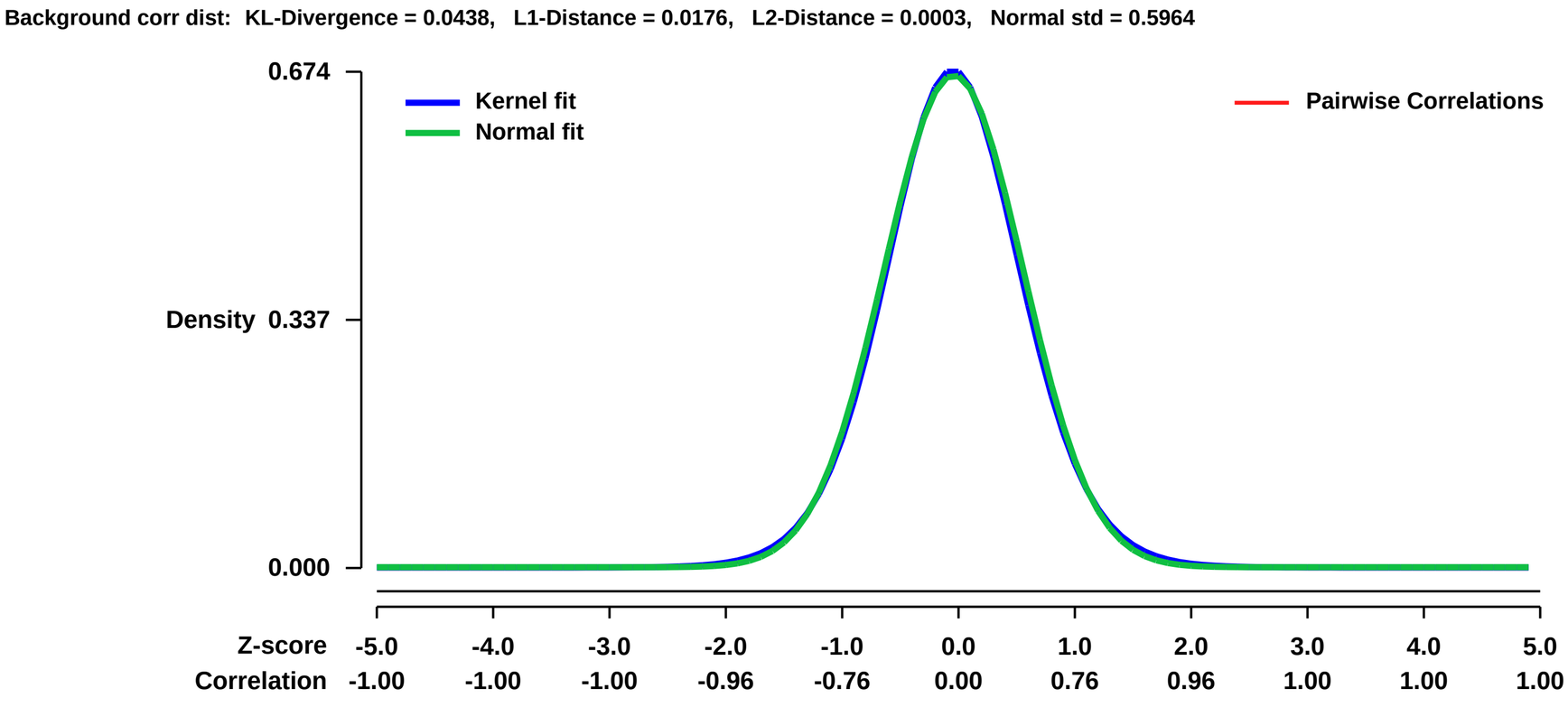

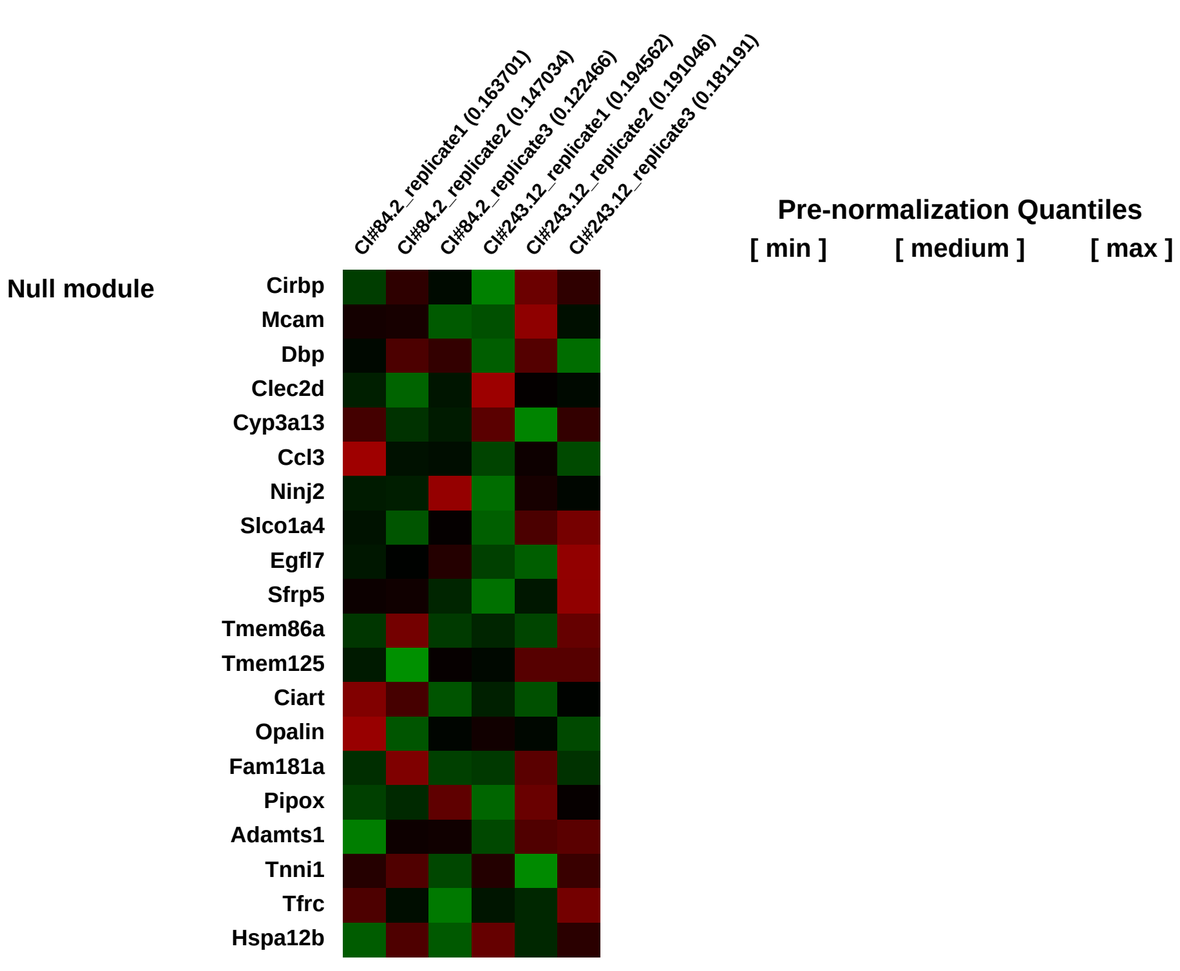

GEO Series "GSE15232" Expression Profiles

Num of samples in this series: 6

Scale of expression profile Z-scores

-3.0 -2.0 -1.0 0.0 1.0 2.0 3.0

GEO Link:	http://www.ncbi.nlm.nih.gov/geo/query/acc.cgi?acc=GSE15232
Status:	Public on May 13 2009
Title:	A Regulatory Pathway Involving Notch1/¸†-Catenin/Isl1 Determines Cardiac Progenitor Cell Fate
Organism:	Mus musculus
Experiment type:	Expression profiling by array
Platform:	GPL1261
Pubmed ID:	19620969
Summary & Design:	**Summary:** The regulation of multipotent cardiac progenitor cell (CPC) expansion and subsequent differentiation into cardiomyocytes, smooth muscle, or endothelial cells is a fundamental aspect of basic cardiovascular biology and cardiac regenerative medicine. However, the mechanisms governing these decisions remain unclear. Here, we show that Wnt/¸†-Catenin signaling, which promotes expansion of CPCs, is negatively regulated by Notch1-mediated control of phosphorylated ¸†-Catenin accumulation within CPCs, and that Notch1 activity in CPCs is required for their differentiation. Notch1 positively, and ¸†-Catenin negatively, regulated expression of the cardiac transcription factors, Isl1, Myocd and Smyd1. Surprisingly, disruption of Isl1, normally expressed transiently in CPCs prior to their differentiation, resulted in expansion of CPCs in vivo and in an embryonic stem (ES) cell system. Furthermore, Isl1 was required for CPC differentiation into cardiomyocyte and smooth muscle cells, but not endothelial cells. These findings reveal a regulatory network controlling CPC expansion and cell fate that involve unanticipated functions of ¸†-Catenin, Notch1 and Isl1 that may be leveraged for regenerative approaches involving CPCs. **Overall design:** YFP+ cells marking precardiac mesoderm (Isl1-cre domain) were FACS-sorted (w/wo stabilized Beta-catenin). Their total RNA was amplified with the WT-Ovation Pico RNA Amplification System, fragmented and labeled with the FL-Ovation cDNA Biotin Module V2 (Nugen). The hybridization, staining and scanning of the Affymetrix GeneChips were performed in the Gladstone Genomics Core Lab. Raw data generated from at least three independent experiments were further analyzed by the group of Dr. Ru-Fang Yeh at the Center for Informatics and Molecular Biostatistics, UCSF.

Background corr dist: KL-Divergence = 0.0450, L1-Distance = 0.0180, L2-Distance = 0.0003, Normal std = 0.5914

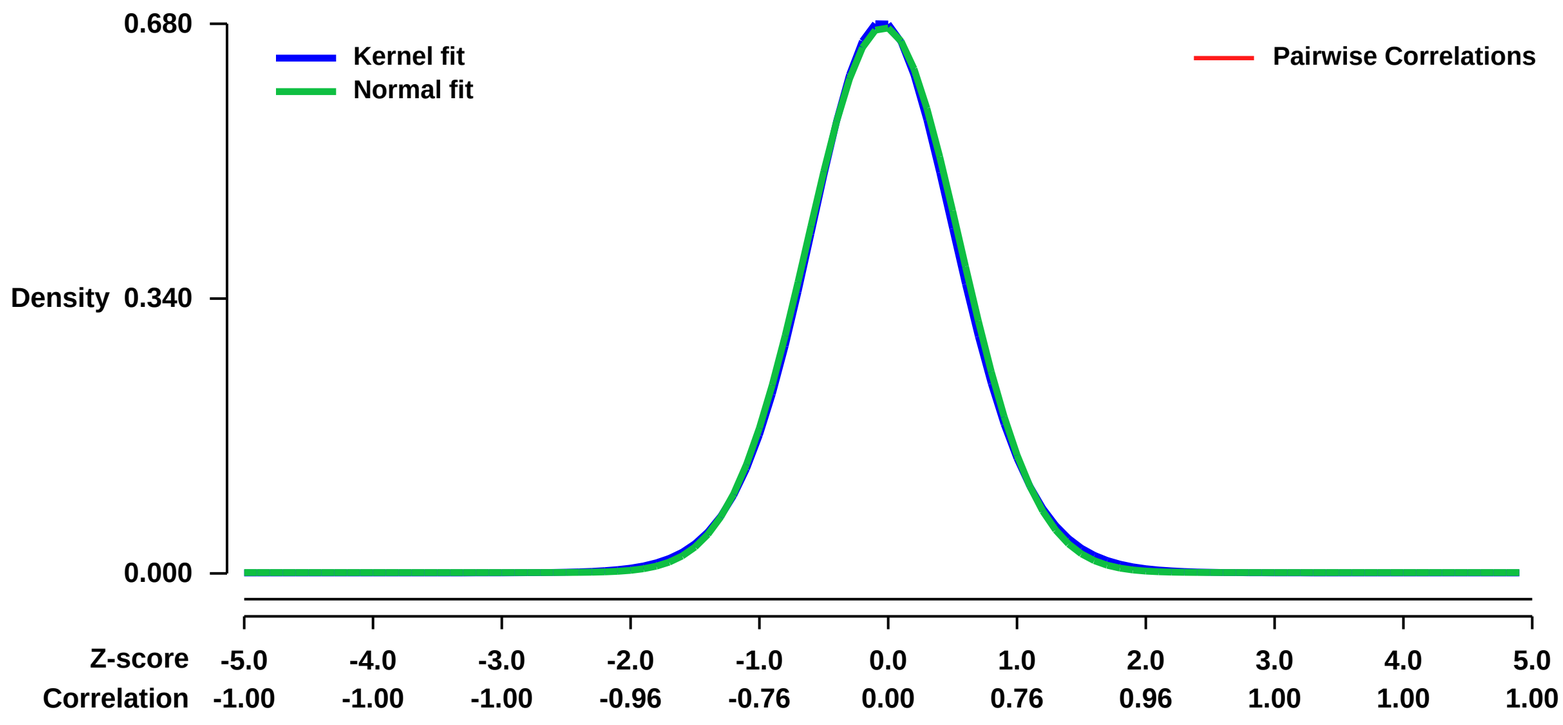

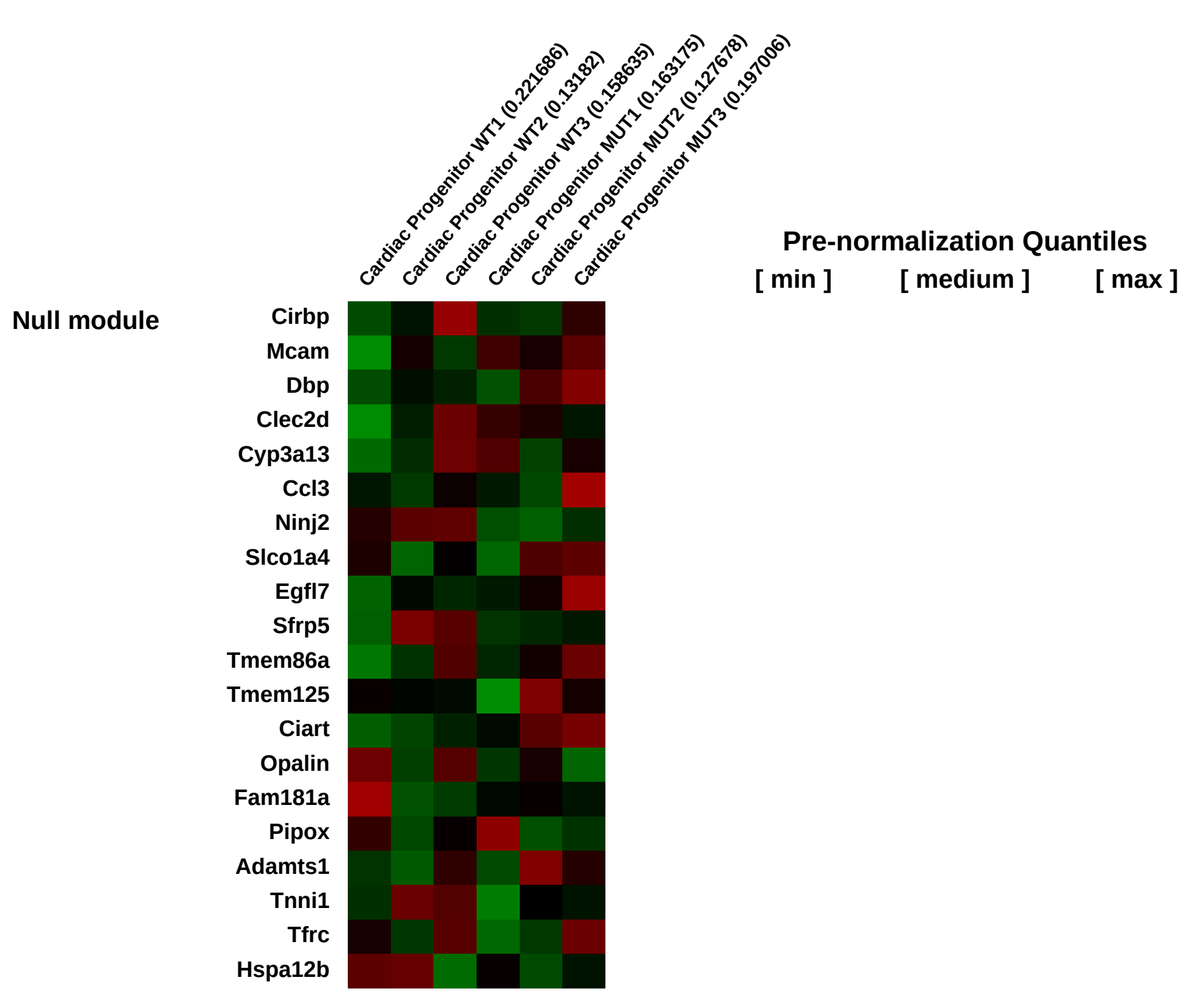

GEO Series "GSE15315" Expression Profiles

Num of samples in this series: 6

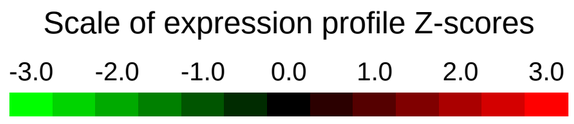

GEO Link:	http://www.ncbi.nlm.nih.gov/geo/query/acc.cgi?acc=GSE15315
Status:	Public on Mar 20 2009
Title:	ERK1/2 in Ovarian Granulosa Cells are Essential for Female Fertility
Organism:	Mus musculus
Experiment type:	Expression profiling by array
Platform:	GPL1261
Pubmed ID:	19443782
Summary & Design:	**Summary:** A surge of luteinizing hormone (LH) from the pituitary gland triggers ovulation, oocyte maturation, and luteinization for successful reproduction in mammals. Since the signaling molecules RAS and ERK1/2 are activated by a LH surge in granulosa cells of preovulatory follicles, we disrupted Erk1/2 in mouse granulosa cells and provide in vivo evidence that these kinases are necessary for LH-induced oocyte resumption of meiosis, ovulation, and luteinization. In addition, biochemical analyses and selected disruption of the Cebpb gene in granulosa cells demonstrate that C/EBP is a critical downstream mediator of ERK1/2 activation. These mouse models provide in vivo systems in which to define the context specific and molecular mechanisms by which granulosa cells respond to LH and these mechanisms are relevant to the regulation of human fertility and infertility. **Overall design:** Immature wild type or ERK1/2 conditonal knock-out mice were injected with 5IU equine chorionic gonadotropin (eCG)-48h followed by 5 IU hCG injection. The ovarian granulosa cells were collected at hCG 0h, 2.5h, or 4h and the gene expression pforiles were compared by microarray method.

Background corr dist: KL-Divergence = 0.0268, L1-Distance = 0.0170, L2-Distance = 0.0004, Normal std = 0.6851

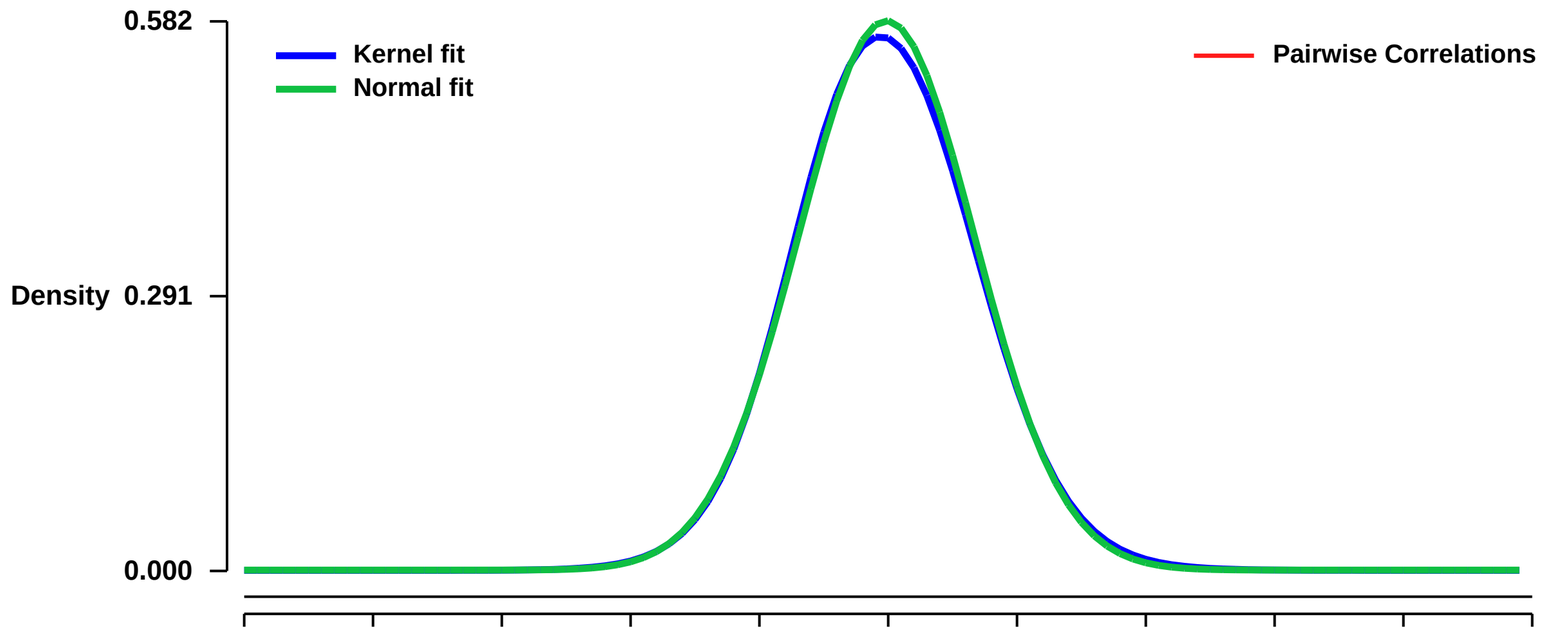

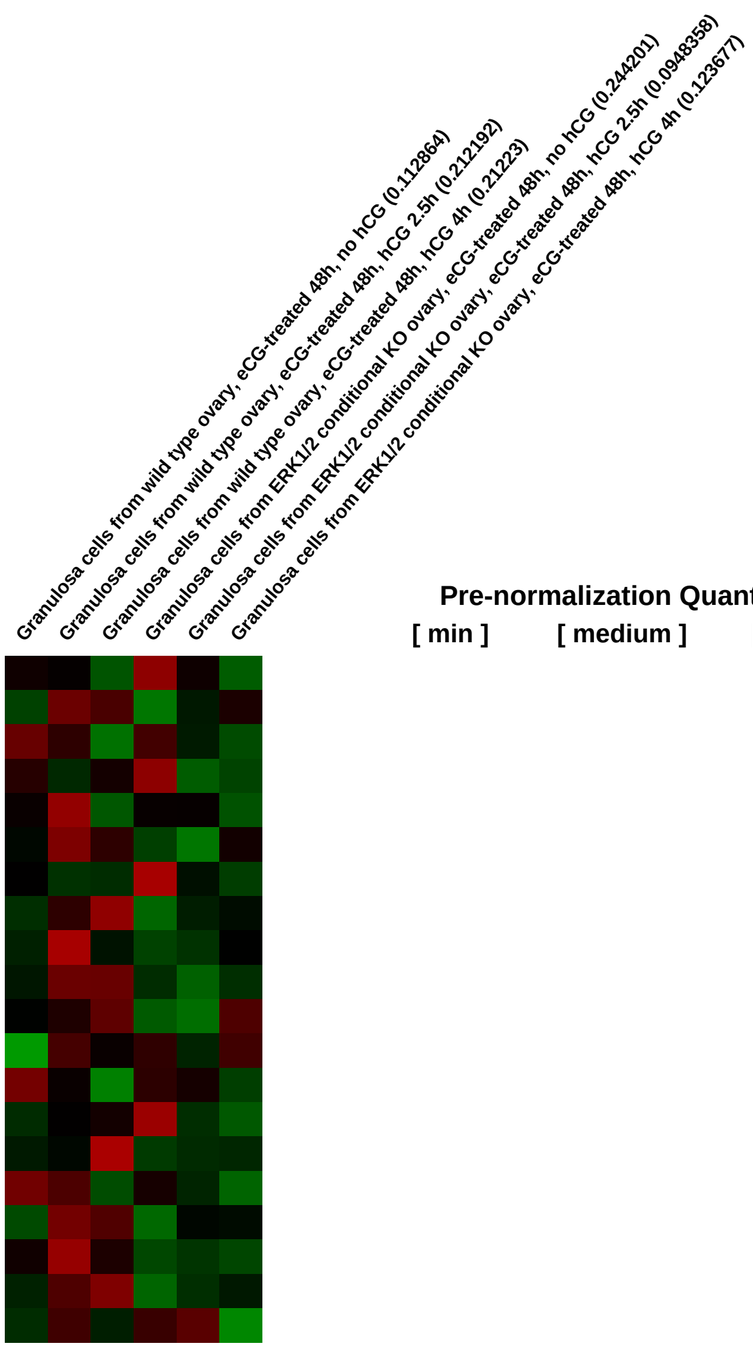

GEO Series "GSE15324" Expression Profiles

Num of samples in this series: 8

Scale of expression profile Z-scores

-3.0 -2.0 -1.0 0.0 1.0 2.0 3.0

GEO Link:	http://www.ncbi.nlm.nih.gov/geo/query/acc.cgi?acc=GSE15324
Status:	Public on Mar 24 2009
Title:	Control of CD8+ T cell proliferation by the transcription factor ELF4
Organism:	Mus musculus
Experiment type:	Expression profiling by array
Platform:	GPL1261
Pubmed ID:	19412182
Summary & Design:	**Summary:** Transcription factors that regulate quiescence, proliferation, and homing of lymphocytes are critical for effective immune system function. In the present study, we demonstrated that the transcription factor ELF4 directly activates the tumor suppressor KLF4 downstream of T cell receptor (TCR) signaling to induce cell cycle arrest in naˆflve CD8+ T cells. Elf4- and Klf4-deficient mice accumulated CD8+CD44hi T cells during steady-state conditions and generated more memory T cells after immunization. The homeostatic expansion of CD8+CD44hi T cells in Elf4-null mice resulted in a redistribution of cells to non-lymphoid tissue due to reduced expression of the transcription factor KLF2, and the surface proteins CCR7 and CD62L. This work describes the combinatorial role of lymphocyte-intrinsic factors in the control of T cell homeostasis, activation and homing. **Overall design:** RNAs isolated from wild type and Elf4 -/- CD8+ T cells were used in Affimetrix oligonucleotide arrays either untreated or after 3.5 days of activation.

Background corr dist: KL-Divergence = 0.0407, L1-Distance = 0.0476, L2-Distance = 0.0029, Normal std = 0.6550

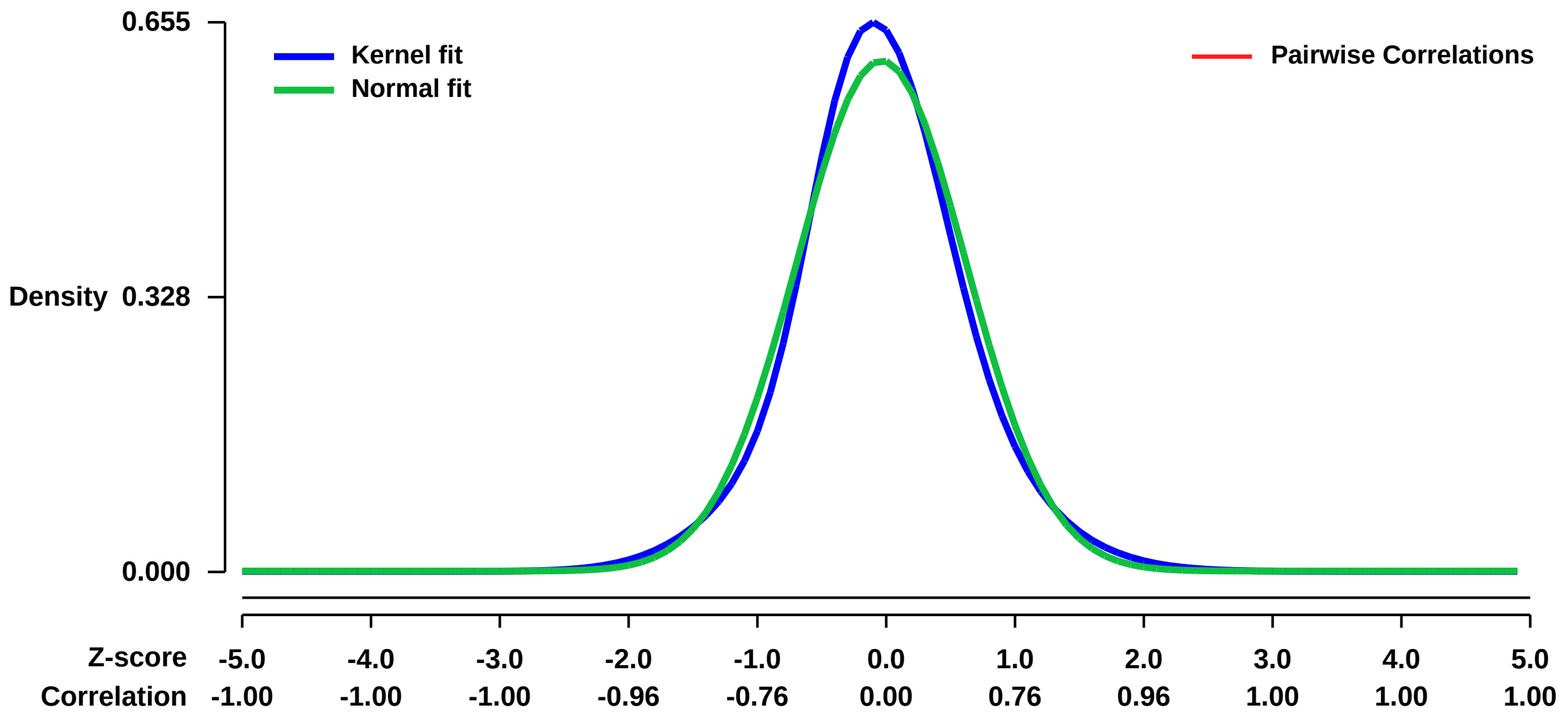

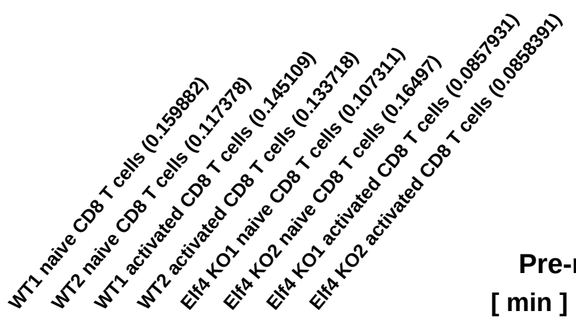

Pre-normalization Quantiles

[min] [medium] [max]

Null module

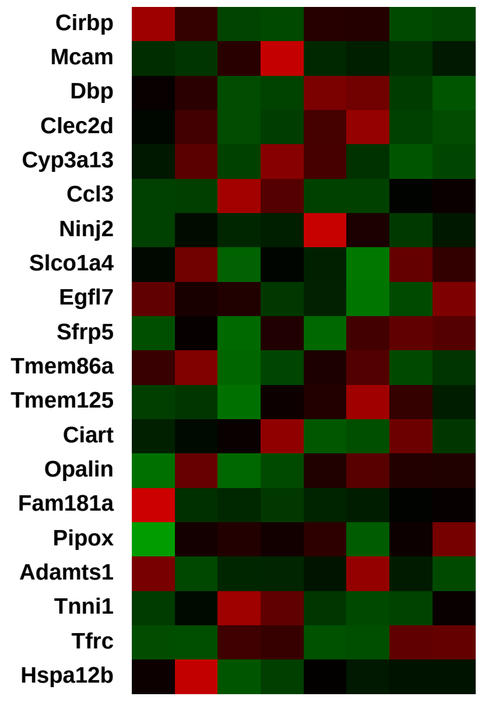

GEO Series "GSE15326" Expression Profiles

Num of samples in this series: 10

Scale of expression profile Z-scores

-3.0 -2.0 -1.0 0.0 1.0 2.0 3.0

GEO Link:	**http://www.ncbi.nlm.nih.gov/geo/query/acc.cgi?acc=GSE15326**
Status:	**Public on Mar 01 2010**
Title:	**LKR13-Kras-WT1-KO**
Organism:	**Mus musculus**
Experiment type:	**Expression profiling by array**
Platform:	**GPL1261**
Pubmed ID:	
Summary & Design:	**Summary:** **K-ras is one of the most frequently mutated human oncogenes. However, activation of K-ras can lead to either senescence or proliferation in primary cells. The precise mechanism governing these distinct outcomes remains unclear. Here we describe a novel loss-of-function screen to assess the role of specific genes identified as potential key regulators of K-ras driven oncogenesis. Using this approach, we identify the transcription factor Wt1 as an inhibitor of senescence in primary cells expressing oncogenic K-ras. Deletion or suppression of Wt1 expression leads to senescence of primary cells expressing oncogenic K-ras under the control of the native promotor and at physiological levels, but had no effect on cells expressing wild-type K-ras. Furthermore, loss of Wt1 in lung cancer cell lines that harbor mutant K-ras leads to apoptosis. Taken together, these observations reveal a novel role for Wt1 as a key regulator of the complex genetic network required for the oncogenic effect of the small GTPase K-ras.** **We compare the expression profiles of K-ras mutant mouse cell line (LKR13) upon shRNA knockdown of K-ras itself or Wt1. The study provides insights into the transcriptional role of Wt1 in the context of oncogenic K-ras.** **Overall design:** **LKR13 cells were infected with plko.1s vectors carrying one of two shRNAs against K-ras or Wt1. Control cells were infected with an shRNA against GFP. 48 hours after infection, cells were selected with puromycin for 3 days. RNA was isolated using Trizol 7 days after infection. RNA was further prepared by passage over an RNeasy column. cDNA synthesis, biotinylation of cRNA and hybridization to mouse Genechip 430A v2 containing 39,000 probes was performed according to the manufacturerâ s instructions (Affymetrix, Santa Clara). Microarray data was normalized with Expression Console software (Affymetrix, Santa Clara), using RMA algorithms.**

Background corr dist: KL-Divergence = 0.0699, L1-Distance = 0.0280, L2-Distance = 0.0013, Normal std = 0.4948

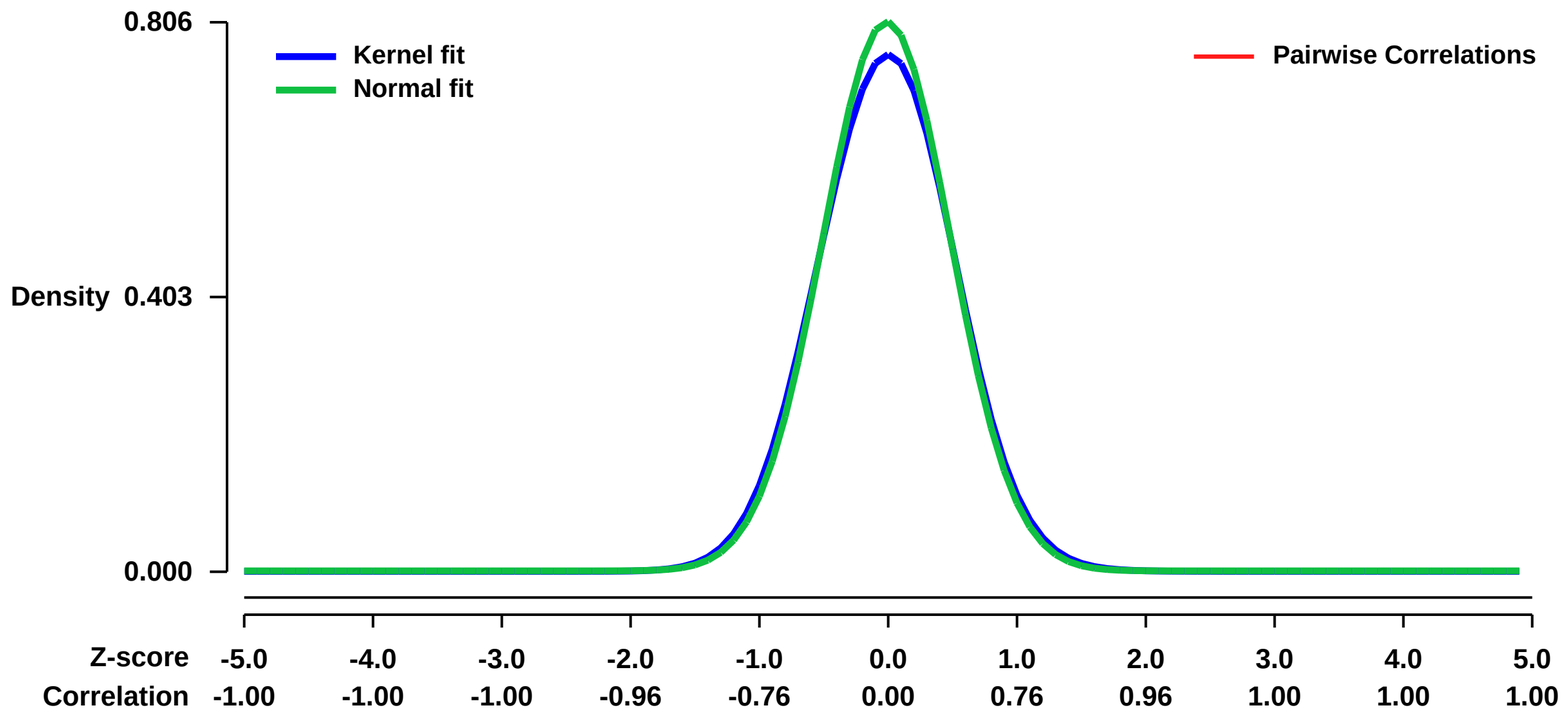

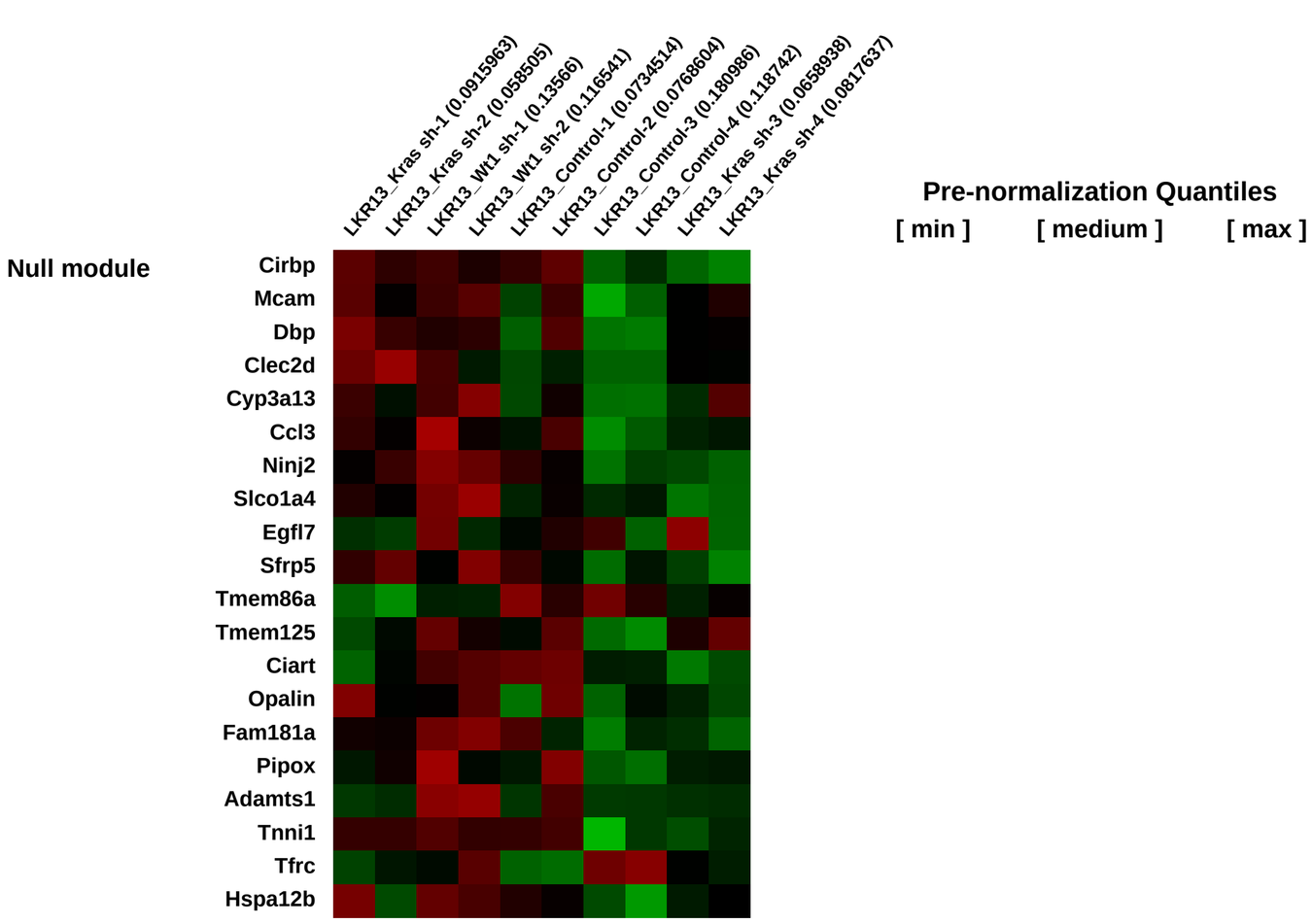

GEO Series "GSE15379" Expression Profiles

Num of samples in this series: 12

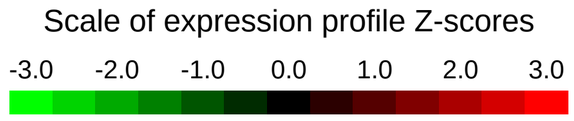

GEO Link:	**http://www.ncbi.nlm.nih.gov/geo/query/acc.cgi?acc=GSE15379**
Status:	**Public on Mar 04 2010**
Title:	**Expression data from lung of septic PPTA knockout mouse**
Organism:	**Mus musculus**
Experiment type:	**Expression profiling by array**
Platform:	**GPL1261**
Pubmed ID:	**20454520**
Summary & Design:	**Summary:** **In this study, we have explored microarray-based differential gene expression profile in mouse lung tissue 8 h after inducing polymicrobial sepsis and the effect of preprotachykinin-A (PPTA) gene deletion. A range of genes differentially expressed (> 2-fold) in microarray analysis was assessed, PPTA-knockout septic mice with their respective sham controls.** **Overall design:** **Lung samples from wild-type or PPTA-knockout mice were selected at 8 h after cecal ligation and puncture (CLP) or sham surgery for RNA extraction and hybridization to Affymetrix microarrays. Triplicates were performed for each condition.**

Background corr dist: **KL-Divergence = 0.1050, L1-Distance = 0.0235, L2-Distance = 0.0008, Normal std = 0.4333**

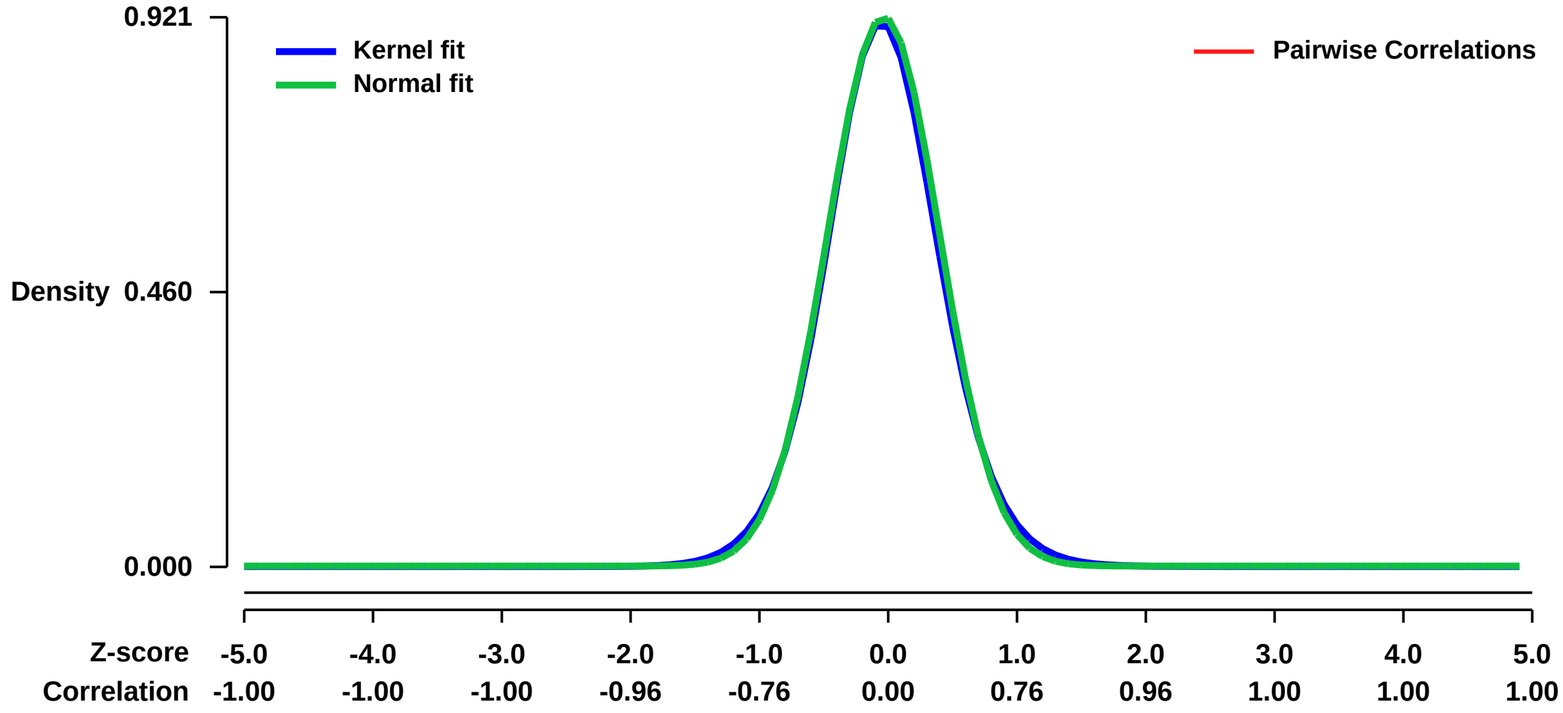

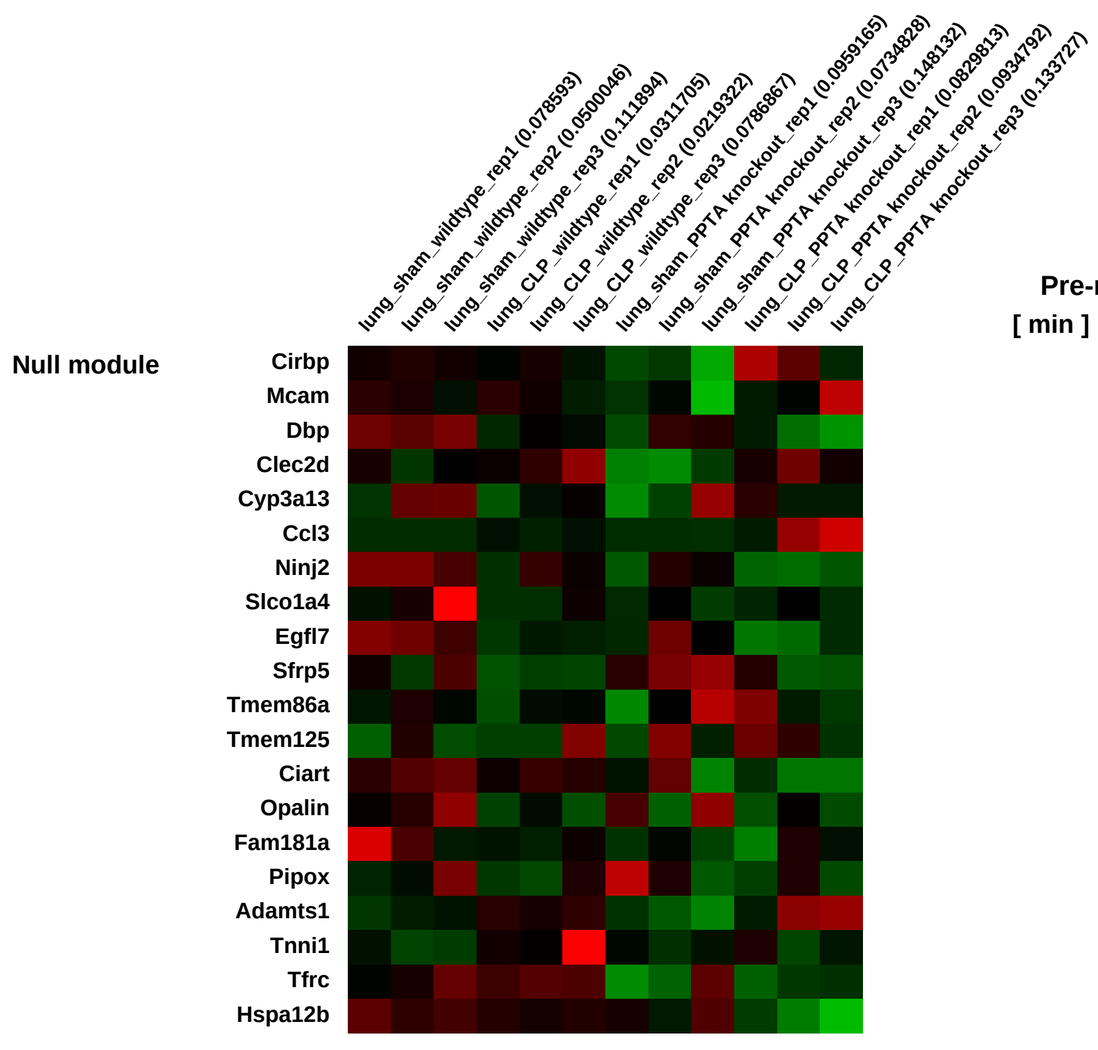

GEO Series "GSE15401" Expression Profiles

Num of samples in this series: 18

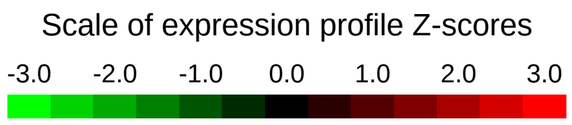

GEO Link:	**http://www.ncbi.nlm.nih.gov/geo/query/acc.cgi?acc=GSE15401**
Status:	**Public on Aug 09 2010**
Title:	**Expression data from mouse aorta during and following transient hyperglycaemia**
Organism:	**Mus musculus**
Experiment type:	**Expression profiling by array**
Platform:	**GPL1261**
Pubmed ID:	**20844862**
Summary & Design:	**Summary:** **Immediate and early effects of transient hyperglycaemia were examined using fully- reversible transgenic diabetic mice. Transient hyperglycaemia altered expression of 769 arterial genes, of which 200 did not reverse following recovery from hyperglycaemia. Many such genes are known to promote atherogenesis, including several implicated in arterial calcification and inflammation. This supports the view that hyperglycaemia causes not only very early deleterious changes in arterial gene expression but that to a large extent these persist for some time after restoration of normal blood glucose levels in vivo. Together, results support the contention that avoiding excess CVD risk in diabetes requires very early correction of hyperglycaemia.** **Overall design:** **As shown previously (Pelengaris et al., 2002 Cell), c-MycERTAM protein is activated in pancreatic beta cells of adult transgenic mice, by daily intraperitoneal (IP) administration of tamoxifen (TAM; Sigma-Aldrich, Dorset, UK) (1 mg/0.2 ml in peanut oil). Inactivation of c-MycERTAM protein was achieved through withdrawal of TAM. Adult female mice, 3-6 months of age, inbred into CBA-C57Bl/6 background and maintained under barrier conditions, were treated with TAM for up to 7 days (Myc â ONâ) and then monitored during recovery for more than 4 months (140 days) (Myc â OFFâ). Experimental timepoints were: Days 2, 4 and 7: c-Myc â ONâ ; days 0, 11, 26: c-Myc â OFFâ . Biological replicates: each timepoint included 3 biological replicates (n=3 mice).**

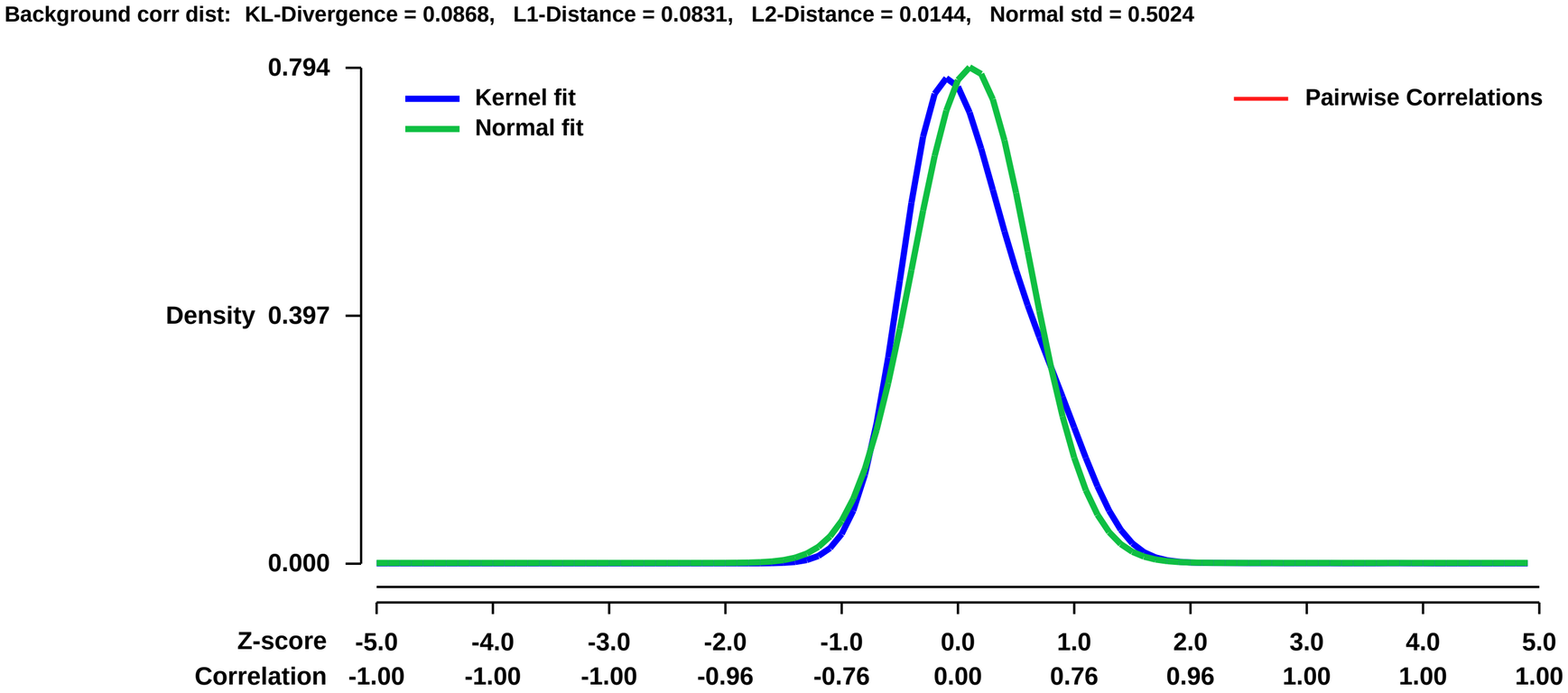

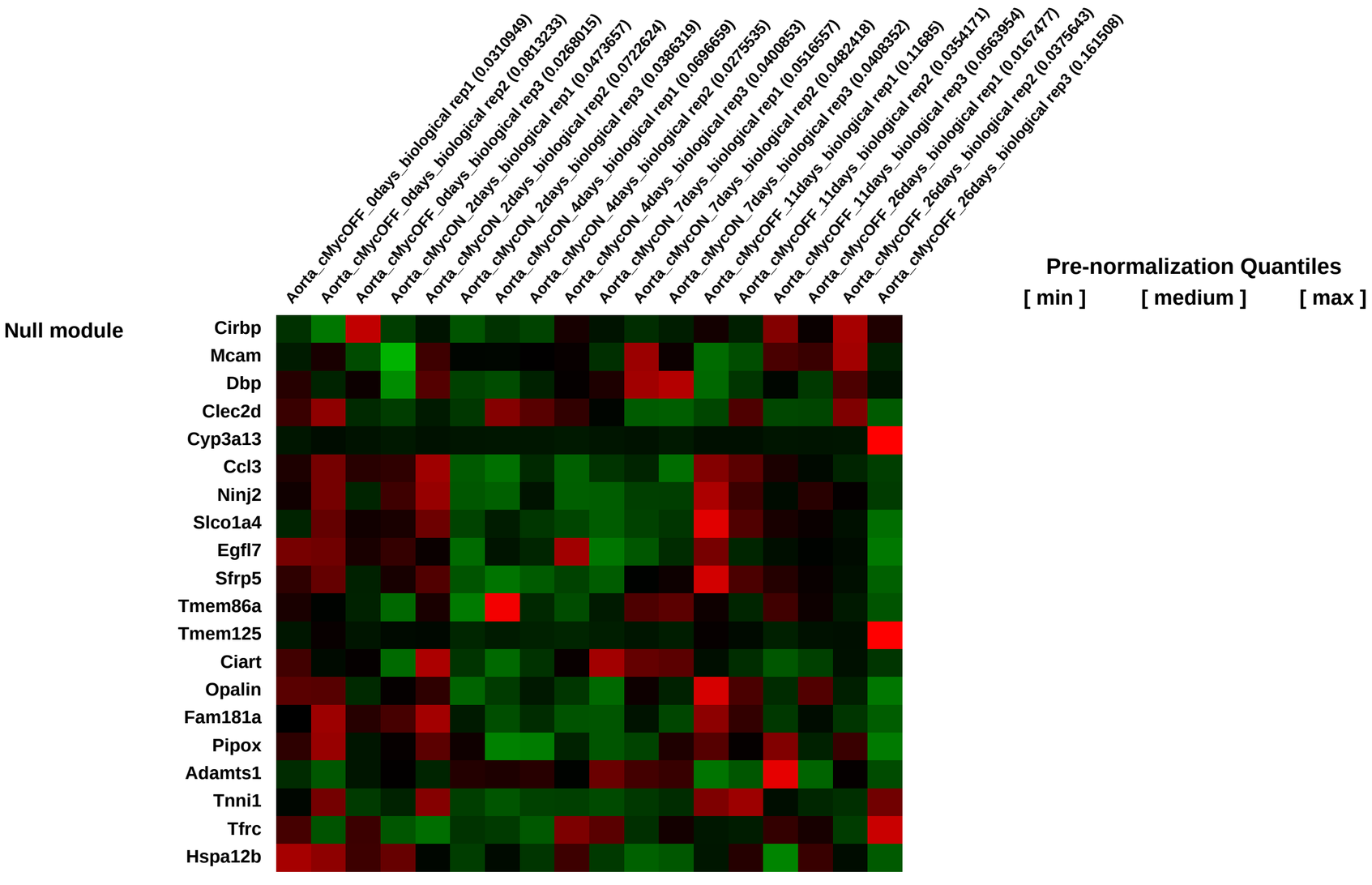

GEO Series "GSE15433" Expression Profiles

Num of samples in this series: 9

Scale of expression profile Z-scores

-3.0 -2.0 -1.0 0.0 1.0 2.0 3.0

GEO Link:	http://www.ncbi.nlm.nih.gov/geo/query/acc.cgi?acc=GSE15433
Status:	Public on Mar 27 2009
Title:	The PPARg2 A/B-domain plays a gene specific role in transactivation and co-factor recruitment
Organism:	Mus musculus
Experiment type:	Expression profiling by array
Platform:	GPL1261
Pubmed ID:	19282365
Summary & Design:	**Summary:** We have previously shown that adenoviral expression of peroxisome proliferator-activated receptors (PPARs) leads to rapid establishment of transcriptionally active complexes and activation of target gene expression within 5-8 h following transduction. Here we have used the adenoviral delivery system combined with expression array analysis to identify novel putative PPARgamma target genes in murine fibroblasts and to determine the role of the A/B-domain in PPARgamma mediated transactivation of genomic target genes. Of the 257 genes found to be induced by PPARgamma2 expression, only 25 displayed A/B-domain dependency, i.e. significantly reduced induction in the cells expressing the truncated PPARgamma lacking the A/B-domain (PPARgammaCDE). Nine of the 25 A/B-domain dependent genes were involved in lipid storage and in line with this, triglyceride accumulation was considerably decreased in the cells expressing PPARgammaCDE compared to cells expressing full length PPARgamma2. Using chromatin immunoprecipitation (ChIP) we demonstrate that PPARgamma binding to genomic target sites and recruitment of the mediator component TRAP220/MED1/PBP/DRIP205 is not affected by the deletion of the A/B-domain. By contrast, the PPARgamma-mediated CBP and p300 recruitment to A/B-domain dependent target genes is abolished by deletion of the A/B-domain. These results indicate that the A/B-domain of PPARgamma2 is specifically involved in the recruitment or stabilization of CBP and p300 containing co-factor complexes to a subset of target genes. **Overall design:** Total RNA samples were obtained from three individual experiments in which NIH-CAR (i.e. a clonal cell line of NIH-3T3 fibroblasts stably expressing the coxsackie-adenovirus receptor (CAR$_{\zeta}$ 1)) cells were transduced with adenovirus containing empty vector (AdEmpty) followed by addition of vehicle (DMSO) or transduced with adenovirus encoding either full length HA-tagged PPARg2 or A/B-domain deleted HA-PPARgCDE and treated with rosiglitazone.

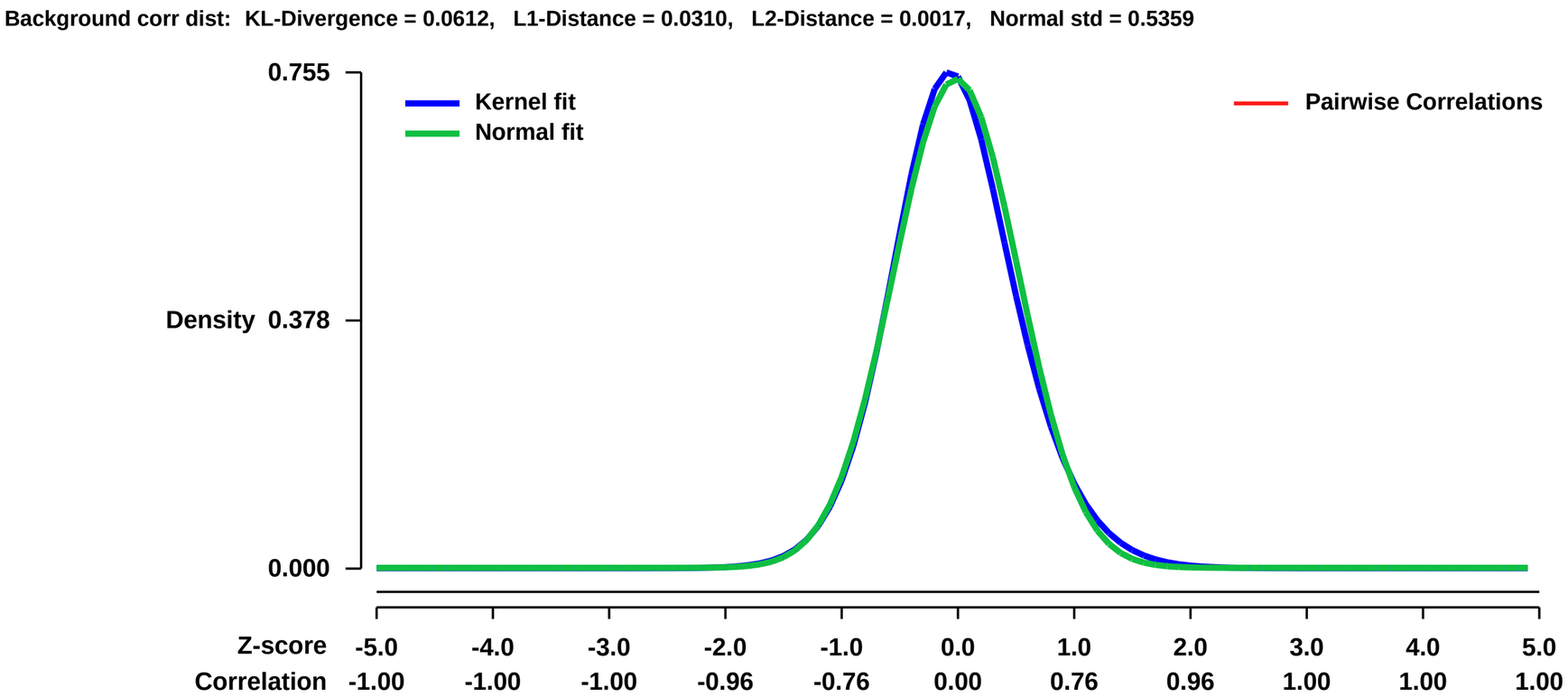

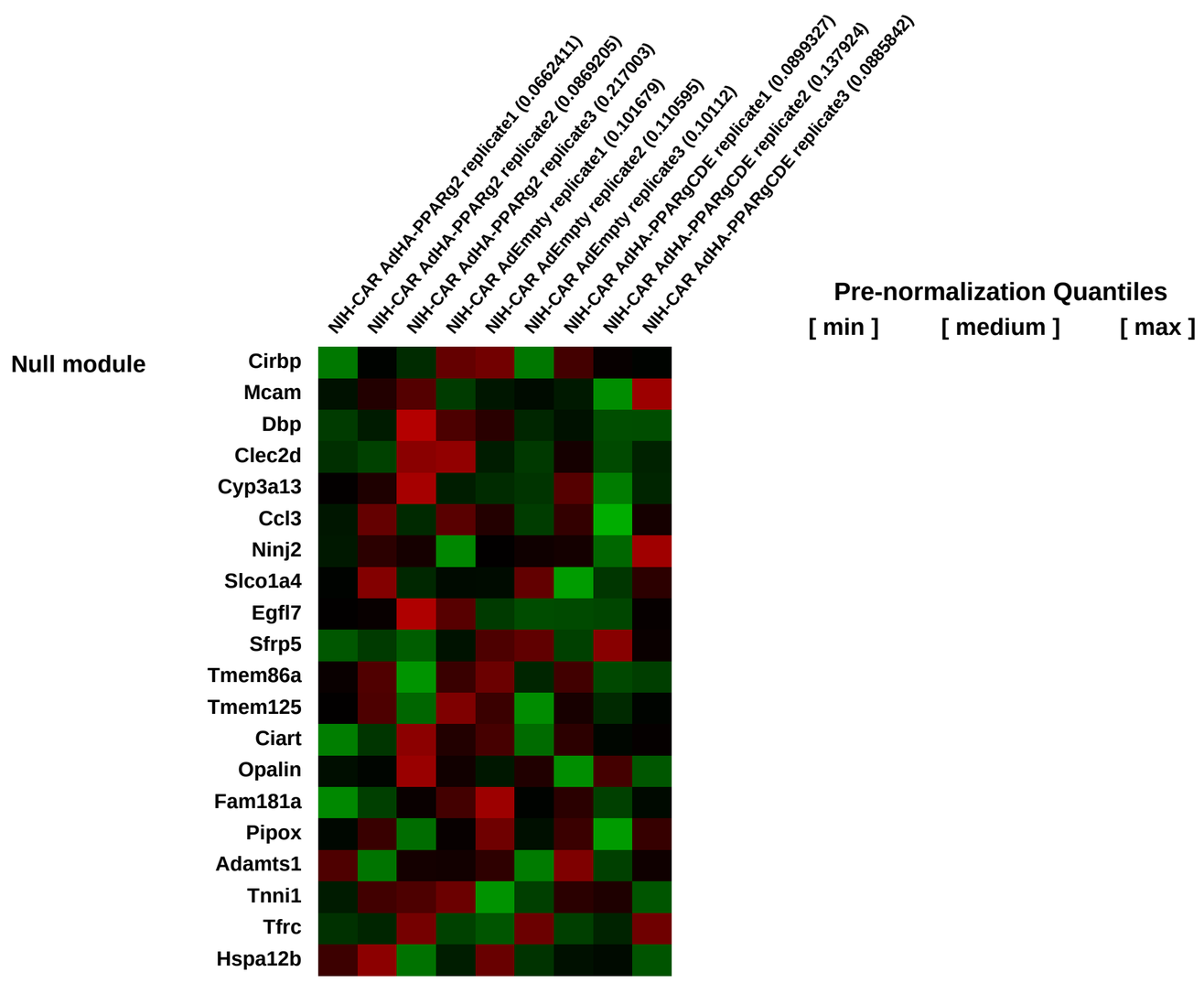

GEO Series "GSE15452" Expression Profiles

Num of samples in this series: 26

Scale of expression profile Z-scores

-3.0 -2.0 -1.0 0.0 1.0 2.0 3.0

GEO Link:	http://www.ncbi.nlm.nih.gov/geo/query/acc.cgi?acc=GSE15452
Status:	Public on Mar 31 2010
Title:	Expression data from lung of mice bearing mutations of FGFR3 and FGFR4
Organism:	Mus musculus
Experiment type:	Expression profiling by array
Platform:	GPL1261
Pubmed ID:	20093646
Summary & Design:	**Summary:** **Gene expression profiling of newborn lung tissue revealed few changes in compound FGFR3/FGFR4 deficient mice, consistent with their normal lung morphology at birth, suggesting the sequence of events leading to the phenotype initiates after birth in this model.** **Profiling of 4 week-old lung tissues revealed an induction of genes related to elastic fiber assembly in compound mutants.** **Overall design:** **Lung RNA isolated from three animals of each genotype-age group were pooled for each Affymetrix chip (n=3 chips for each, except n=2 for wild type at 4 weeks.**

Background corr dist: **KL-Divergence = 0.0340, L1-Distance = 0.0512, L2-Distance = 0.0041, Normal std = 0.6581**

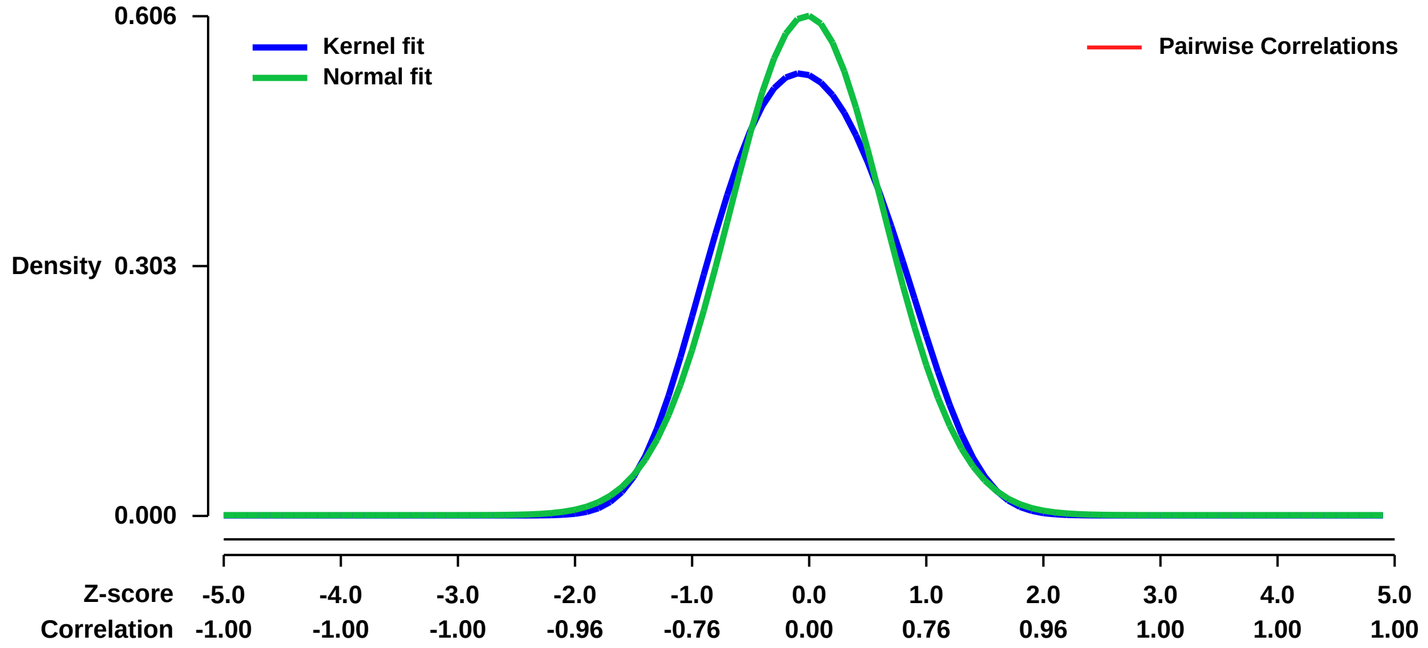

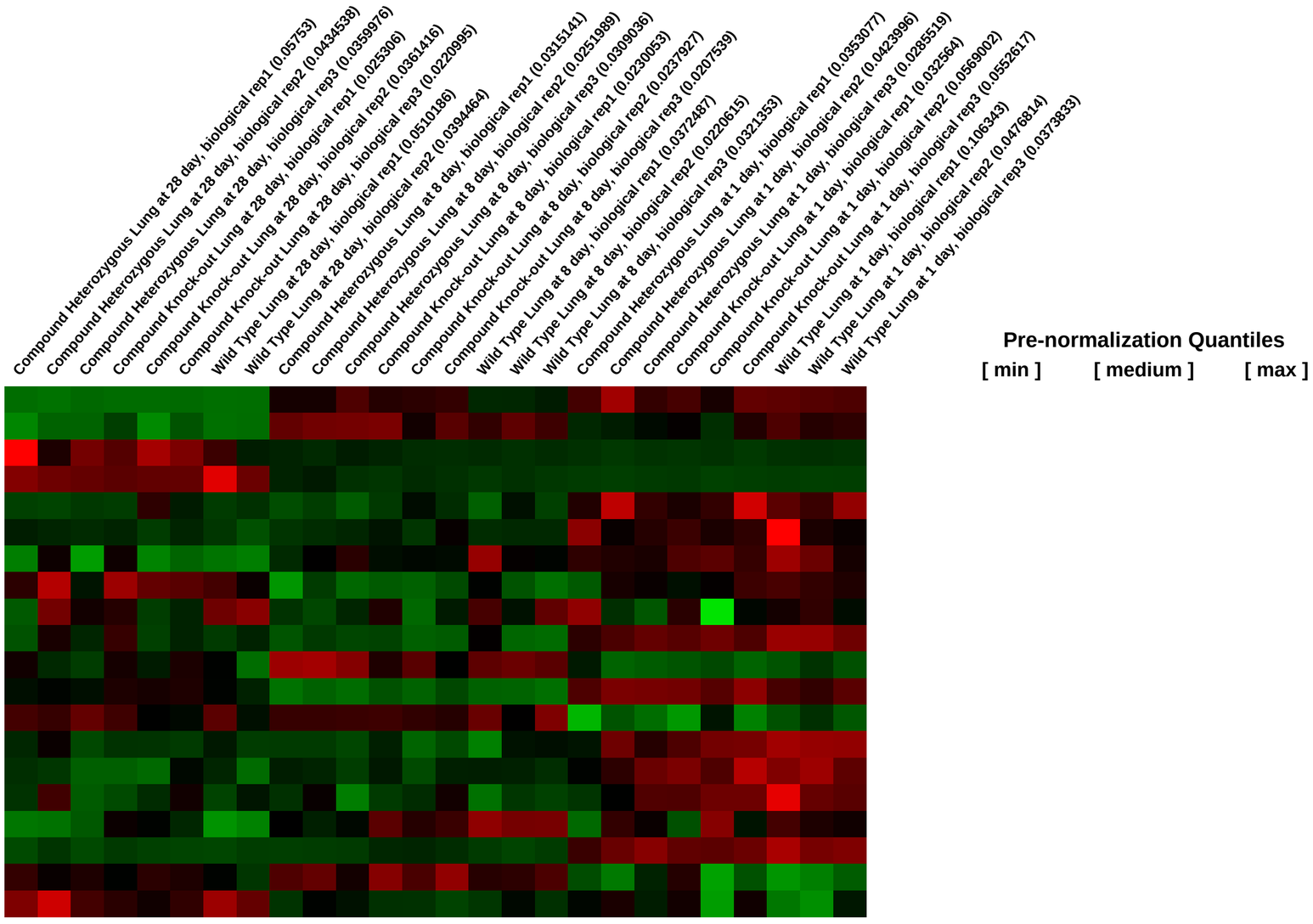

GEO Series "GSE15458" Expression Profiles

Num of samples in this series: 8

Scale of expression profile Z-scores

-3.0 -2.0 -1.0 0.0 1.0 2.0 3.0

GEO Link: http://www.ncbi.nlm.nih.gov/geo/query/acc.cgi?acc=GSE15458
Status: Public on Jun 30 2009
Title: Effect of v-erbA on T3-responsive genes in AML-12 hepatocytes
Organism: Mus musculus
Experiment type: Expression profiling by array
Platform: GPL1261
Pubmed ID:

Summary & Design:

Summary:
The v-erbA oncogene belongs to a superfamily of transcription factors called nuclear receptors, which includes the thyroid hormone receptors (TRs) responsible for mediating the effects of thyroid hormone (T3). Nuclear receptors bind to specific DNA sequences in the promoter region of target genes and v-erbA is known to exert a dominant negative effect on the activity of the TRs. The repressor activity of v-erbA has been linked to the development of hepatocellular carcinoma (HCC) in a mouse model. We have used microarray analysis to identify genes differentially expressed in hepatocytes in culture (AML12 cells) stably transfected with v-erbA and exposed to T3. We have found that v-erbA can negatively regulate expression of T3-responsive genes known to have a protective function against tumor development. We have also identified a number of v-erbA- (but not T3-) responsive genes that are known to be involved in carcinogenesis and which may play a role in the development of HCC.

Overall design:
AML12 control cells and v-erbA-transfected AML12 cells were exposed to 10 nM T3 for 3h or 24h. Using microarray analysis, we compared gene expression in the presence and absence of v-erbA and identified T3-regulated genes differentially expressed in the presence of v-erbA.

Background corr dist: KL-Divergence = 0.0342, L1-Distance = 0.0167, L2-Distance = 0.0003, Normal std = 0.6313

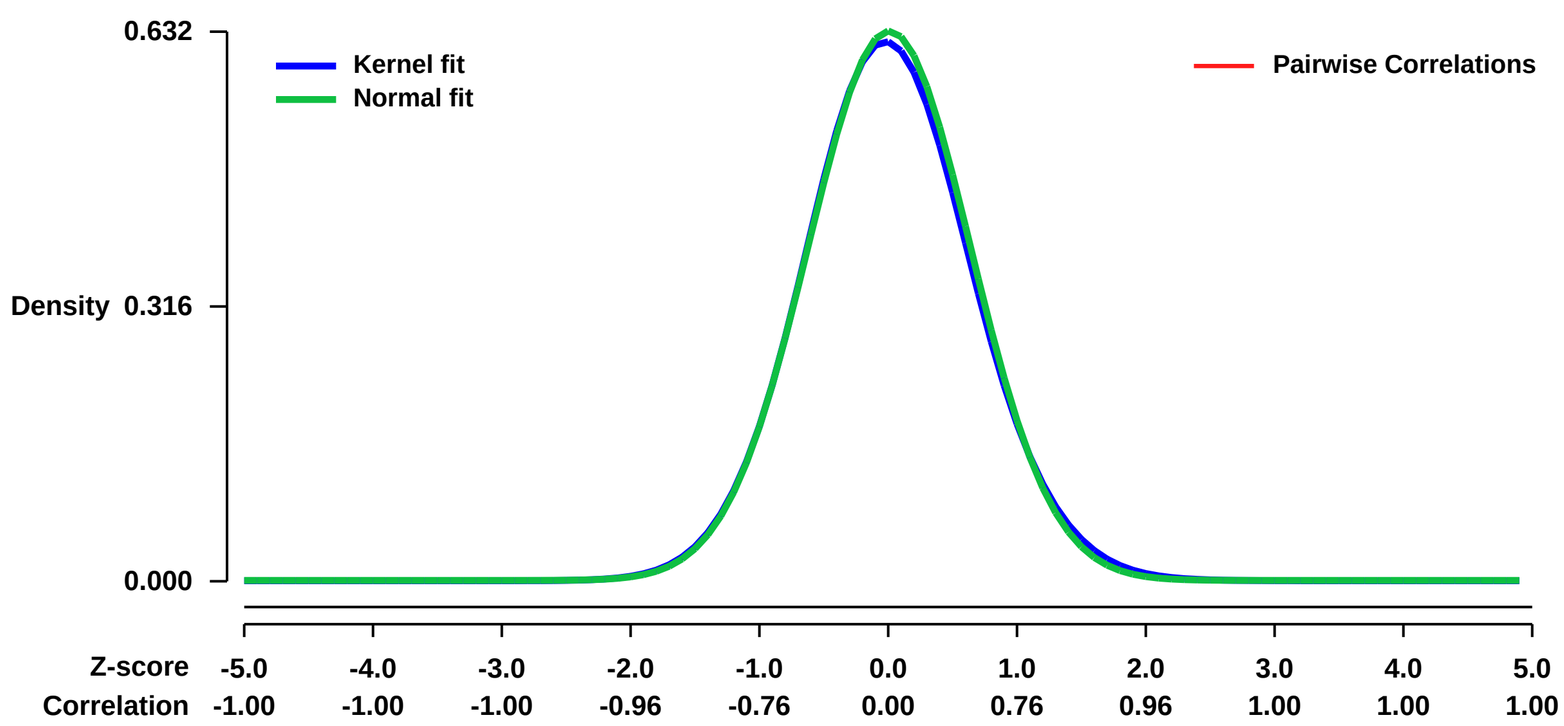

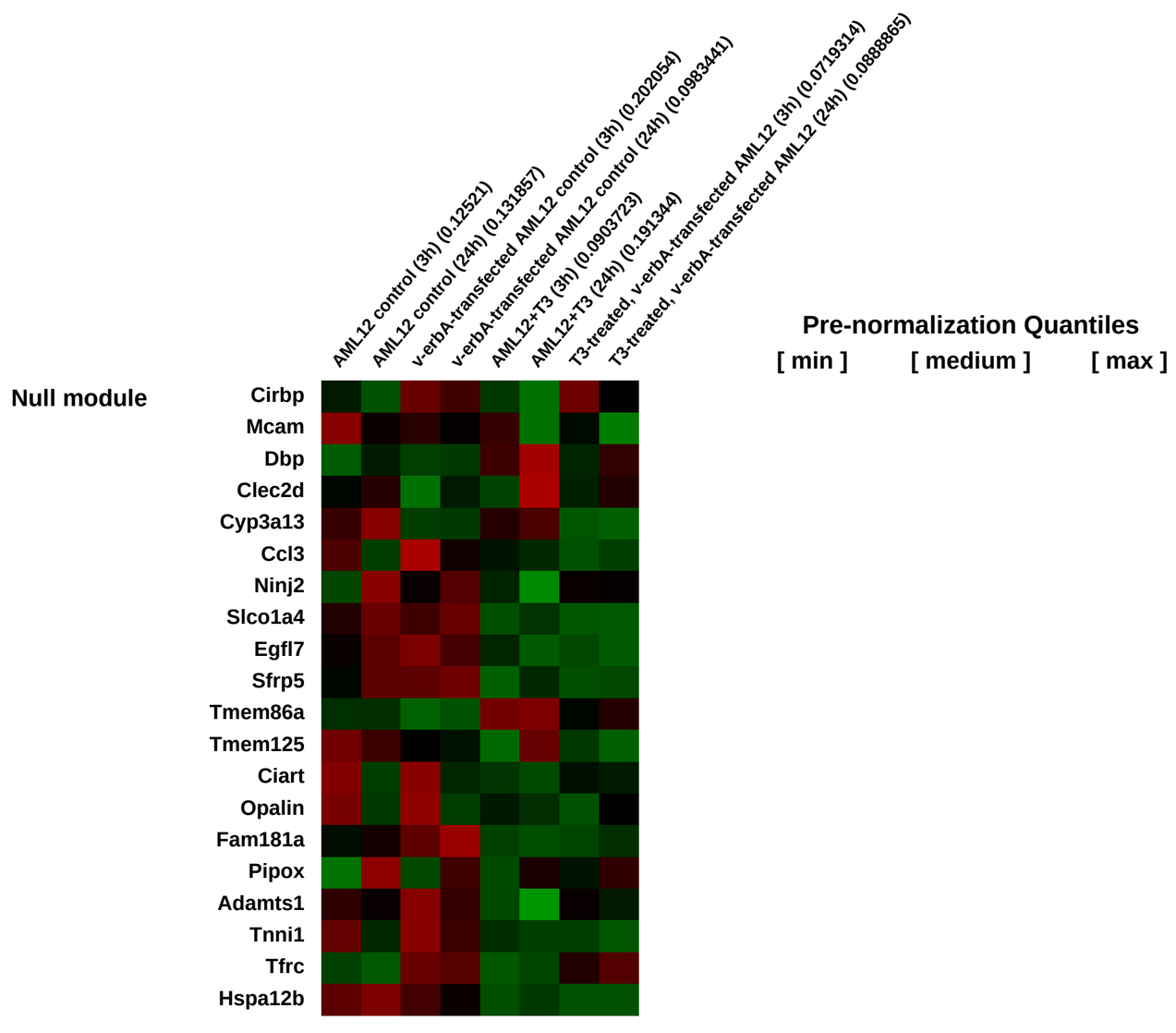

GEO Series "GSE15541" Expression Profiles

Num of samples in this series: 12

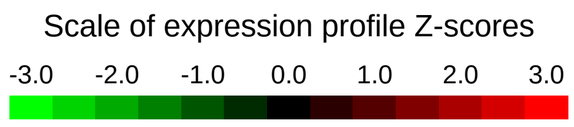

GEO Link:	http://www.ncbi.nlm.nih.gov/geo/query/acc.cgi?acc=GSE15541
Status:	Public on Apr 09 2009
Title:	Linkage of Meis1 leukemogenic activity to multiple downstream effectors including Trib2 and Ccl3
Organism:	Mus musculus
Experiment type:	Expression profiling by array
Platform:	GPL1261
Pubmed ID:	18375036
Summary & Design:	**Summary:** **OBJECTIVE: MEIS1, a HOX cofactor, collaborates with multiple HOX and NUP98-HOX fusion proteins to accelerate the onset of acute myeloid leukemia (AML) through largely unknown molecular mechanisms. MATERIALS AND METHODS: To further resolve these mechanisms, we conducted a structure-function analysis of MEIS1 and gene-expression profiling, in the context of NUP98-HOXD13 (ND13) leukemogenesis. RESULTS: We show, in a murine bone marrow transplantation model, that the PBX-interaction domain, the homeodomain, and the C-terminal domain of MEIS1, are all required for leukemogenic collaboration with ND13. In contrast, the N-terminal domain of MEIS1 is dispensable for collaboration with ND13, but is required for Flt3 upregulation, indicating additional roles for MEIS1 in induction of leukemia independent of alterations in Flt3 expression. Gene-expression profiling of a cloned ND13 preleukemic cell line transduced with wild-type or Meis1 mutant forms revealed deregulation of multiple genes, including a set not previously implicated as MEIS1 targets. Chromatin immunoprecipitation revealed the in vivo occupancy of MEIS1 on regulatory sequences of Trib2, Flt3, Dlk1, Ccl3, Ccl4, Pf4, and Rgs1. Furthermore, engineered overexpression of Trib2 complements ND13 to induce AML while Ccl3 potentiates the repopulating ability of ND13. CONCLUSION: This study shows that Meis1-induced leukemogenesis with ND13 can occur in the absence of Flt3 upregulation and reveals the existence of other pathways activated by MEIS1 to promote leukemia.** **Overall design:** **Establishment of pre-leukemic bone marrow cell lines following transduction with ND13 have been previously described (Pineault, Abramovich et al. 2005). In brief, lines were established from BM cells previously treated with 5-fluorouracil (5-FU) from (C57Bl/6Ly-Pep3b x C3H/HeJ) F1 (PepC3) (Ly5.1+/Ly5.2+) mice freshly transduced with the ND13-GFP or ND13pac virus and maintained in liquid culture. To generate ND13+Meis1 or ND13+Meis1 mutant BM cell lines, the ND13 BM cells were transduced by co-cultivation on irradiated (4,000 cGy) E86 producers for Meis1-YFP (or Meis1 mutant forms), respectively, for a period of 2 days in the presence of 5 ´µg/ml of protamine sulfate. Three independent experiments were performed for each of the four different conditions included in the study.**

Background corr dist: KL-Divergence = 0.0967, L1-Distance = 0.0283, L2-Distance = 0.0010, Normal std = 0.4561

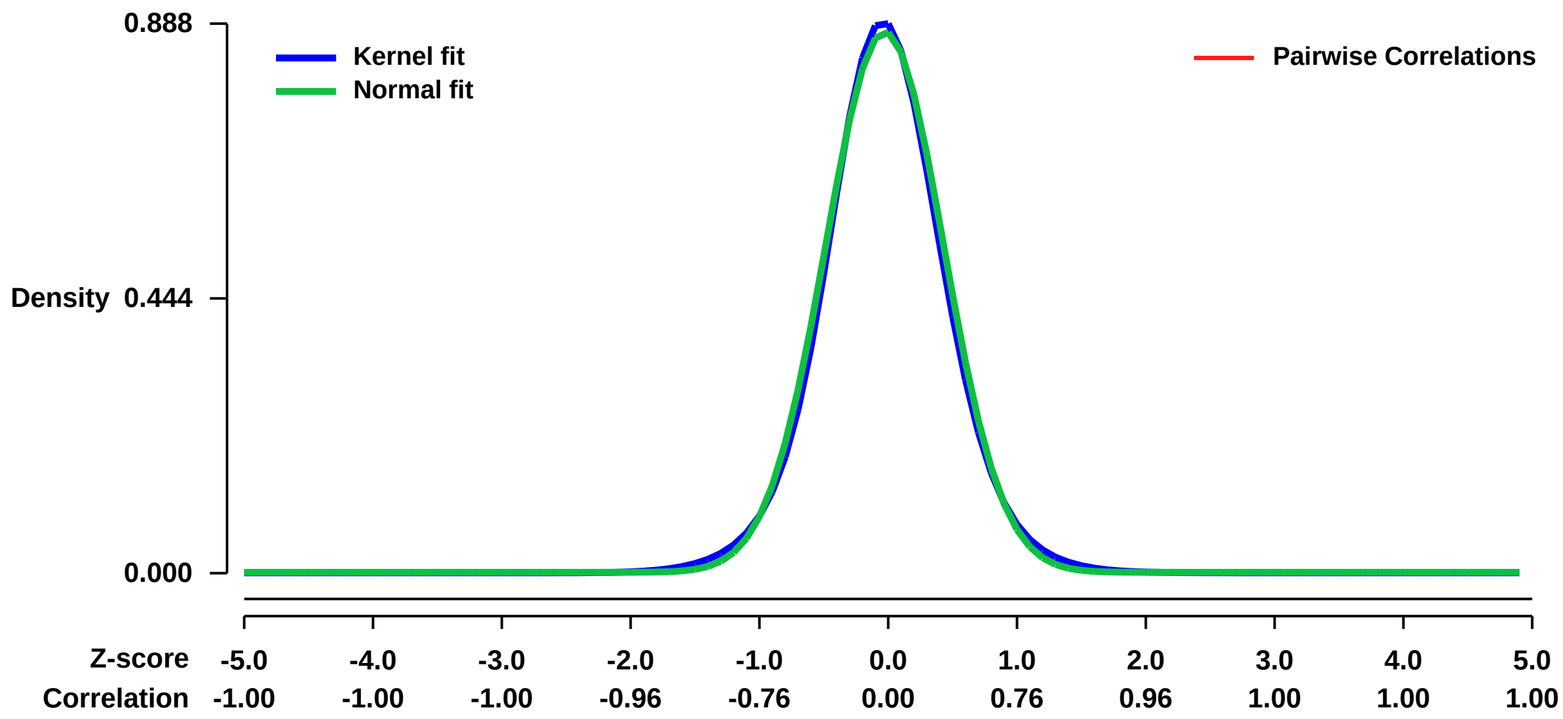

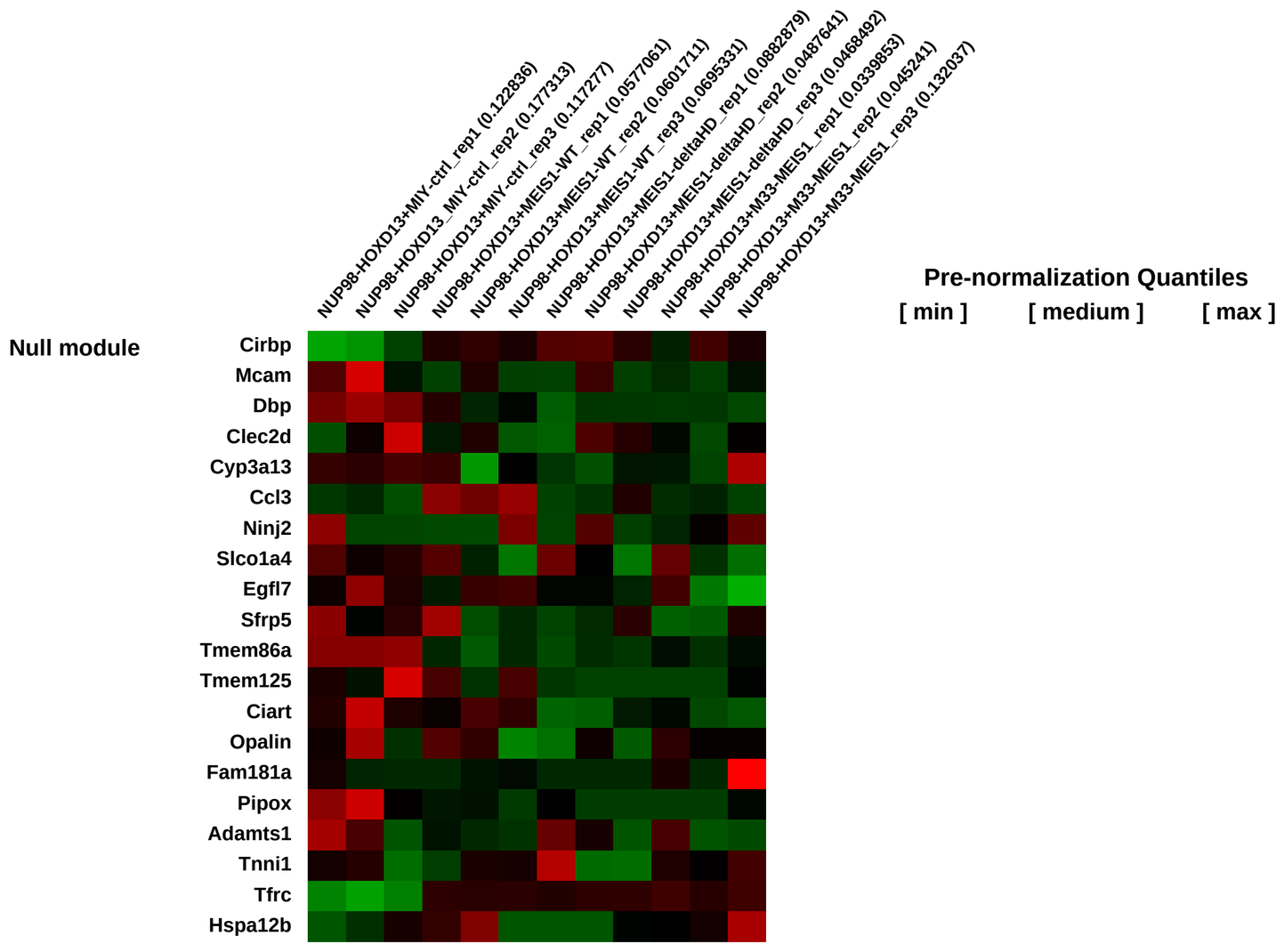

GEO Series "GSE15587" Expression Profiles

Num of samples in this series: 6

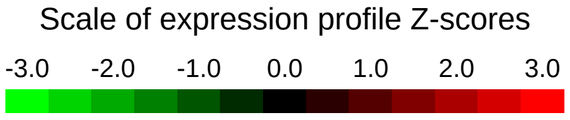

GEO Link:	http://www.ncbi.nlm.nih.gov/geo/query/acc.cgi?acc=GSE15587
Status:	Public on Feb 24 2011
Title:	Identification of Metastasis-prone Lung Adenocarcinoma Cell Population That Is Sensitive to Notch Inhibition
Organism:	Mus musculus
Experiment type:	Expression profiling by array
Platform:	GPL1261
Pubmed ID:	21403400
Summary & Design:	**Summary:** Tumor cells that give rise to metastatic disease are a primary cause of cancer-related death and have not been fully elucidated in patients with lung cancer. Here, we addressed this question by using tissues from a mouse that develops metastatic lung adenocarcinoma owing to expression of mutant K-ras and p53. We identified a metastasis-prone population of tumor cells that differed from those with low metastatic capacity on the basis of having sphere-forming capacity in Matrigel cultures, increased expression of CD133 and Notch ligands, and relatively low tumorigenicity in syngeneic mice. Knockdown of jagged1 or pharmacologic inhibition of its downstream mediator phosphatidylinositol 3-kinase abrogated the metastatic but not the tumorigenic activity of these cells. We conclude from these studies on a mouse model of lung adenocarcinoma that CD133 and Notch ligands mark a population of metastasis-prone tumor cells and that the efficacy of Notch inhibitors in metastasis prevention should be explored. **Keywords: two group comparison** **Overall design:** 344SQ subcutaneous tumors (from a lung adenocarcinoma cell line derived from a KrasLA1/+; p53R172HdelG/+ mouse that metastasizes widely following subcutaneous injection into syngeneic mice) were sorted by flow cytometry into CD133high and CD133low fractions. RNA samples from these fractions were processed and analyzed on Affymetrix Mouse Expression Array 430A 2.0 chips.

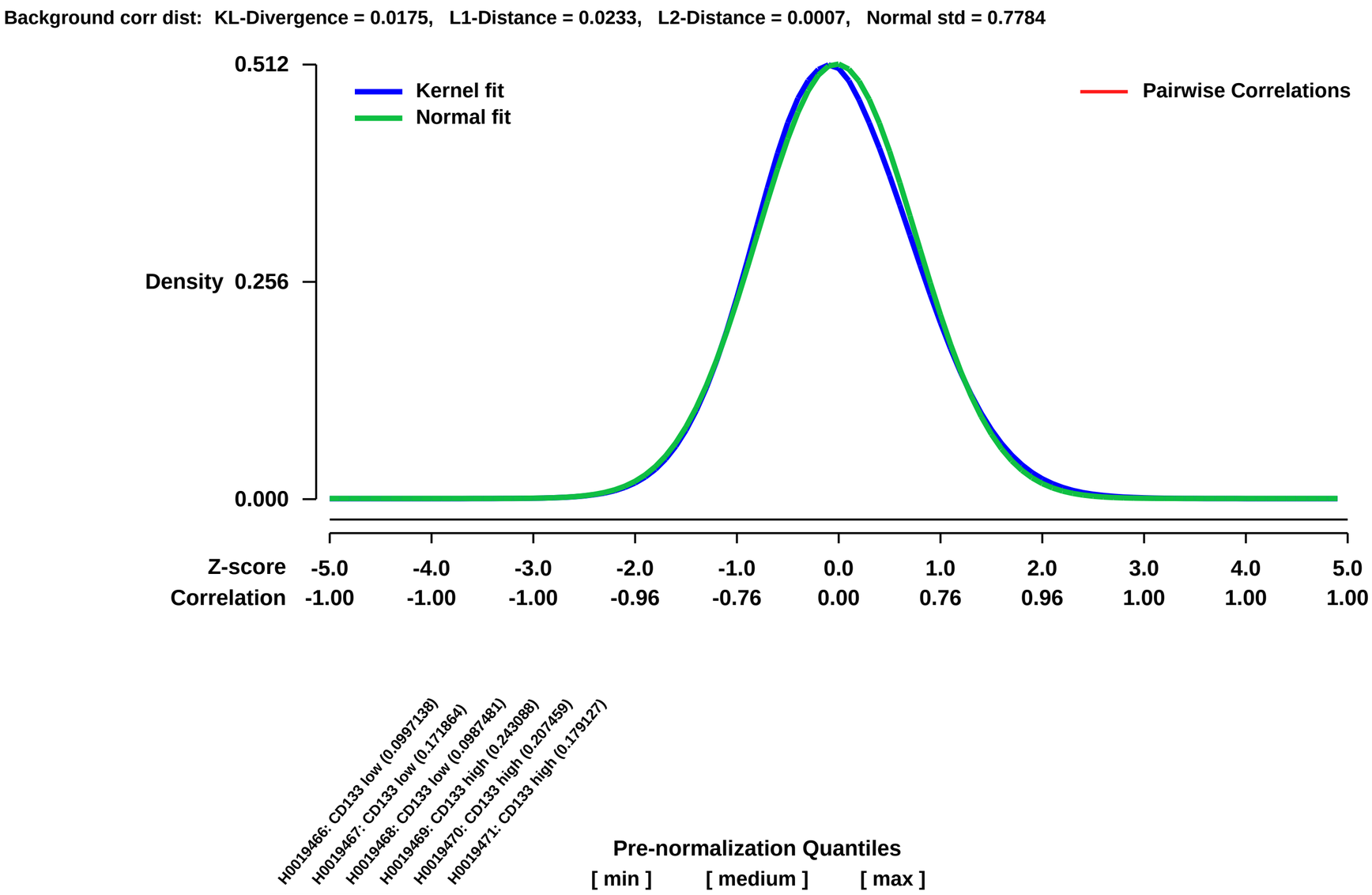

GEO Series "GSE15610" Expression Profiles

Num of samples in this series: 12

Scale of expression profile Z-scores

-3.0 -2.0 -1.0 0.0 1.0 2.0 3.0

GEO Link:	http://www.ncbi.nlm.nih.gov/geo/query/acc.cgi?acc=GSE15610
Status:	Public on Dec 22 2009
Title:	Knockout of the selenocysteine tRNA (Trsp) gene in mouse macrophage
Organism:	Mus musculus
Experiment type:	Expression profiling by array
Platform:	GPL1261
Pubmed ID:	19863805
Summary & Design:	**Summary:** **Comparative analysis of gene expression in bone marrow-derived macrophages (BMDM) from trsp knockout mice (Trspfl/fl-LysM-Cre+/-) and Control (Trspfl/fl-LysM-Cre-/-) mice.** **Selenium, a micronutrient whose deficiency in the diet causes immune dysfunction and inflammatory disorders, exerts its physiological effects partly in the form of selenium-containing proteins (selenoproteins). Incorporation of selenium into the amino acid selenocysteine (Sec), and subsequently into selenoproteins, is mediated by Sec tRNA[Ser]Sec. To identify macrophage-specific selenoprotein function, we generated mice with the Sec tRNA[Ser]Sec gene specifically deleted in myeloid cells. These mutant mice were devoid of the selenoproteome in macrophages, yet exhibited largely normal inflammatory responses. However, selenoprotein deficiency led to aberrant expression of extracellular matrix-related genes, and diminished migration of macrophages in a protein gel matrix. Therefore, selenium status may affect immune defense and tissue homeostasis through its effect on selenoprotein expression and the trafficking of tissue macrophages.** **Overall design:** **We have generated mice in which we have selectively removed the selenocysteine tRNA gene (trsp) in macrophages under the control of LysM-Cre promoter. Microarray analysis was performed on RNA samples taken from bone marrow-derived macrophages in knockout and control mice. 1. Control unstimulated 2. Knockout unstimulated 3. Control lipopolysaccharide (LPS) stimulated (4h) 4. Knockout LPS stimulated (4h). Three replicates for each condition. Thus, a total of 12 samples.**

Background corr dist: KL-Divergence = 0.0769, L1-Distance = 0.0376, L2-Distance = 0.0023, Normal std = 0.4963

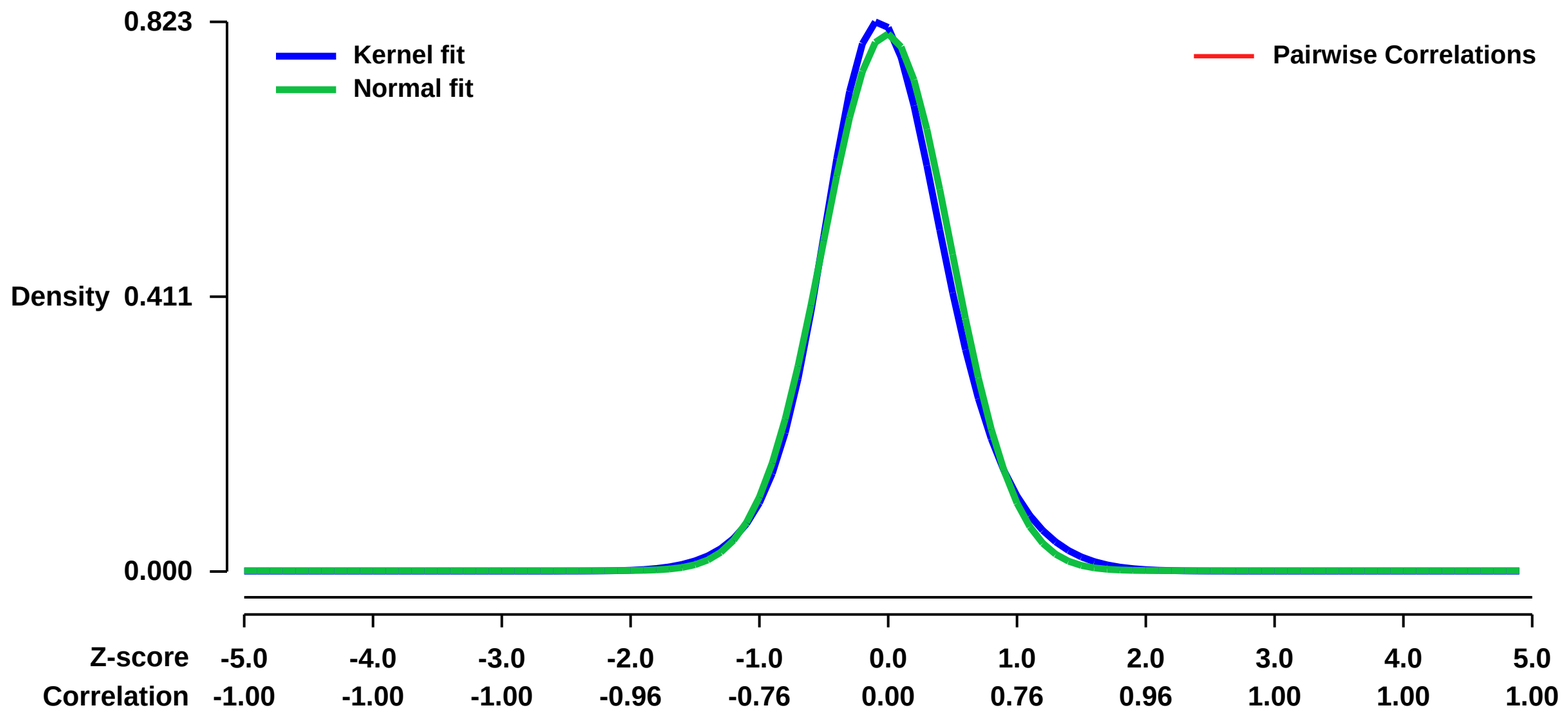

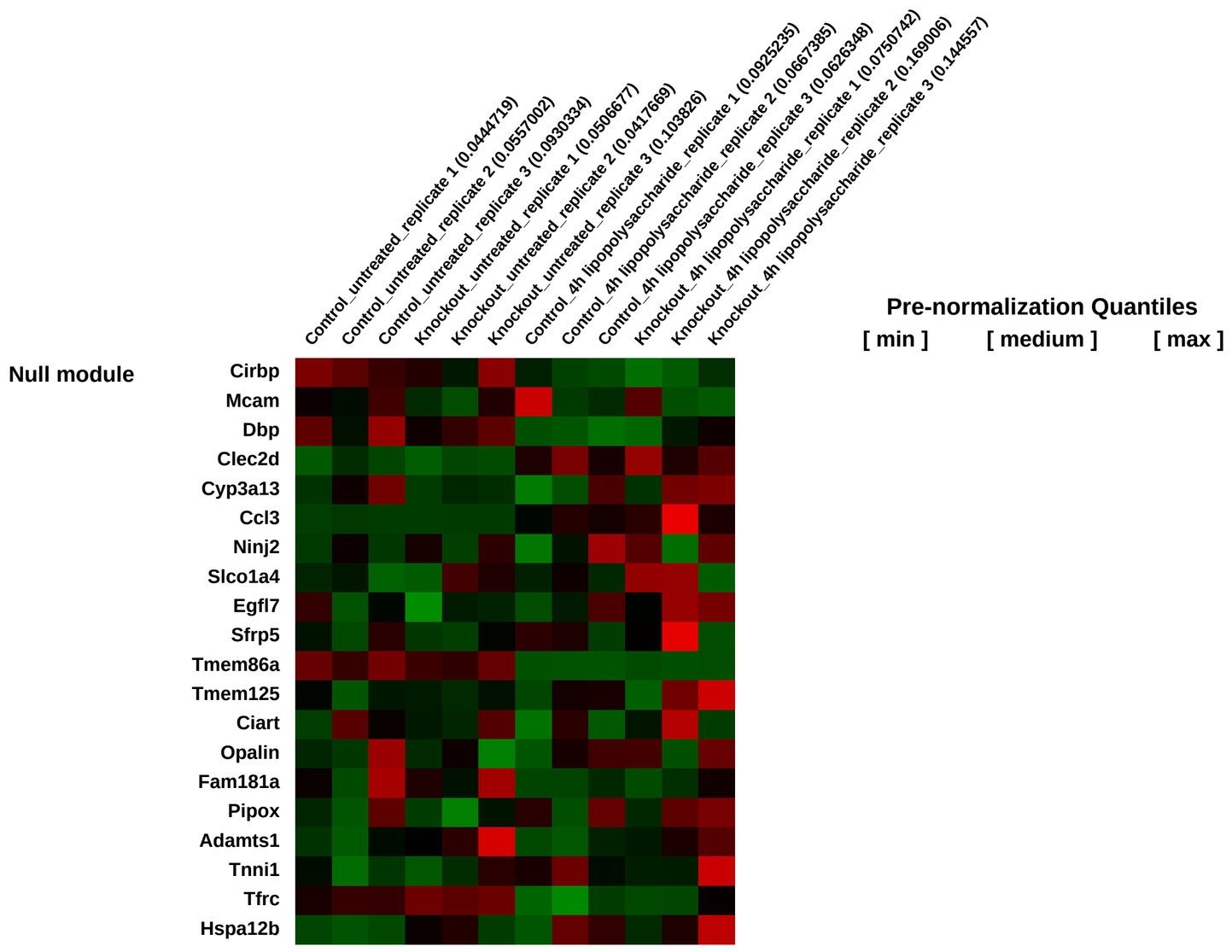

GEO Series "GSE15624" Expression Profiles

Num of samples in this series: 12

Scale of expression profile Z-scores

-3.0 -2.0 -1.0 0.0 1.0 2.0 3.0

GEO Link:	http://www.ncbi.nlm.nih.gov/geo/query/acc.cgi?acc=GSE15624
Status:	Public on Apr 10 2009
Title:	Regulation of T cell gene expression by Halofuginone (HF)
Organism:	Mus musculus
Experiment type:	Expression profiling by array
Platform:	GPL1261
Pubmed ID:	19498172
Summary & Design:	**Summary:** T cell differentiation to the Th17 effector subset requires stimulation through the T cell and co-stimulatory receptors, together with cytokine stimulation by TGFb and IL-6. The small molecule halofuginone (HF) inhibits Th17 cell development and induces a pattern of stress-regulated gene expression that mimics amino acid starvation. We used global transcript profiling to ask how halofuginone modulates gene expression induced during T cell activaiton and Th17 differentiation Keywords: T cell activation/ differentiation timecourse **Overall design:** Purified mouse CD4+ CD25- T cells were activated under Th17 polarizing cytokine conditions and treated with either halofuginone or its inactive derivative, MAZ1310, for 3- or 6-hours.

Background corr dist: KL-Divergence = 0.0801, L1-Distance = 0.0252, L2-Distance = 0.0011, Normal std = 0.4730

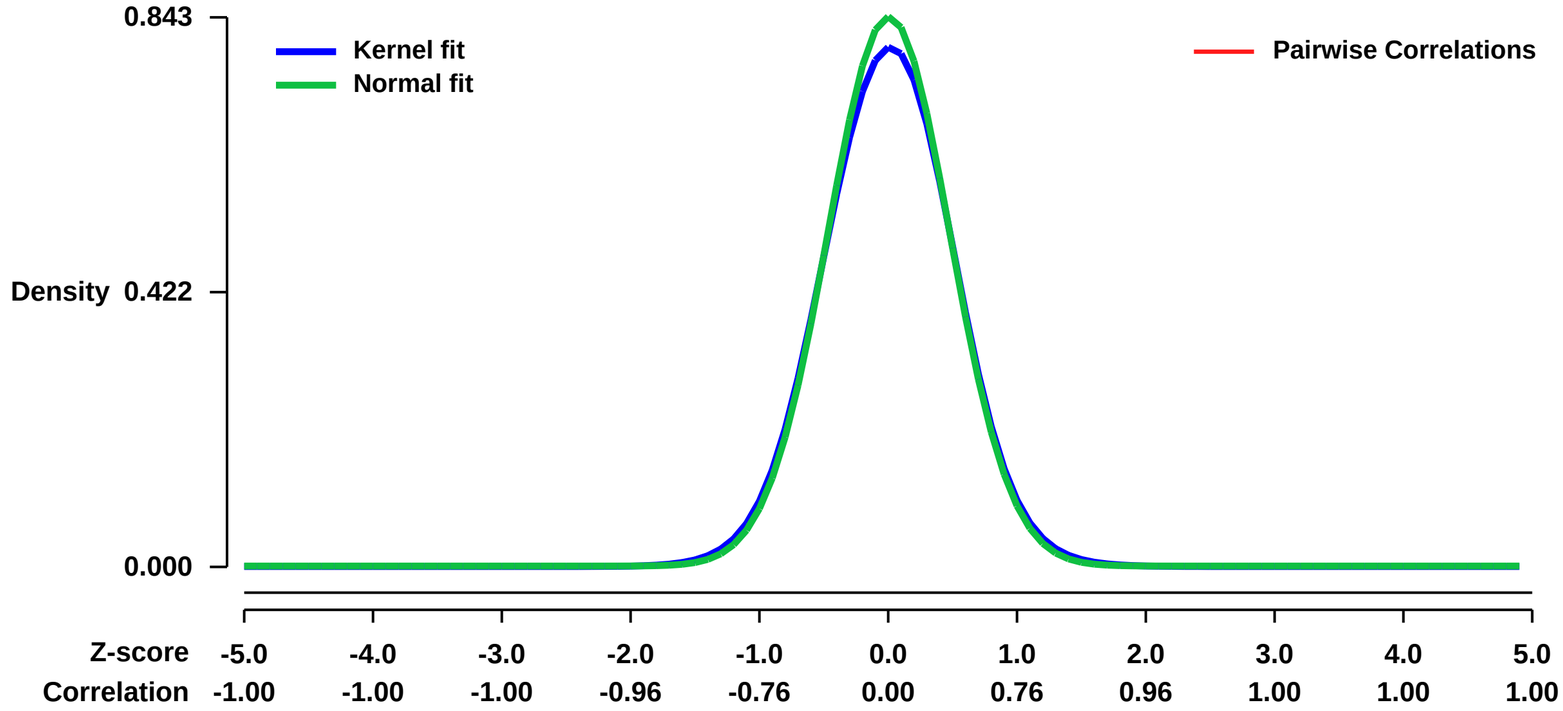

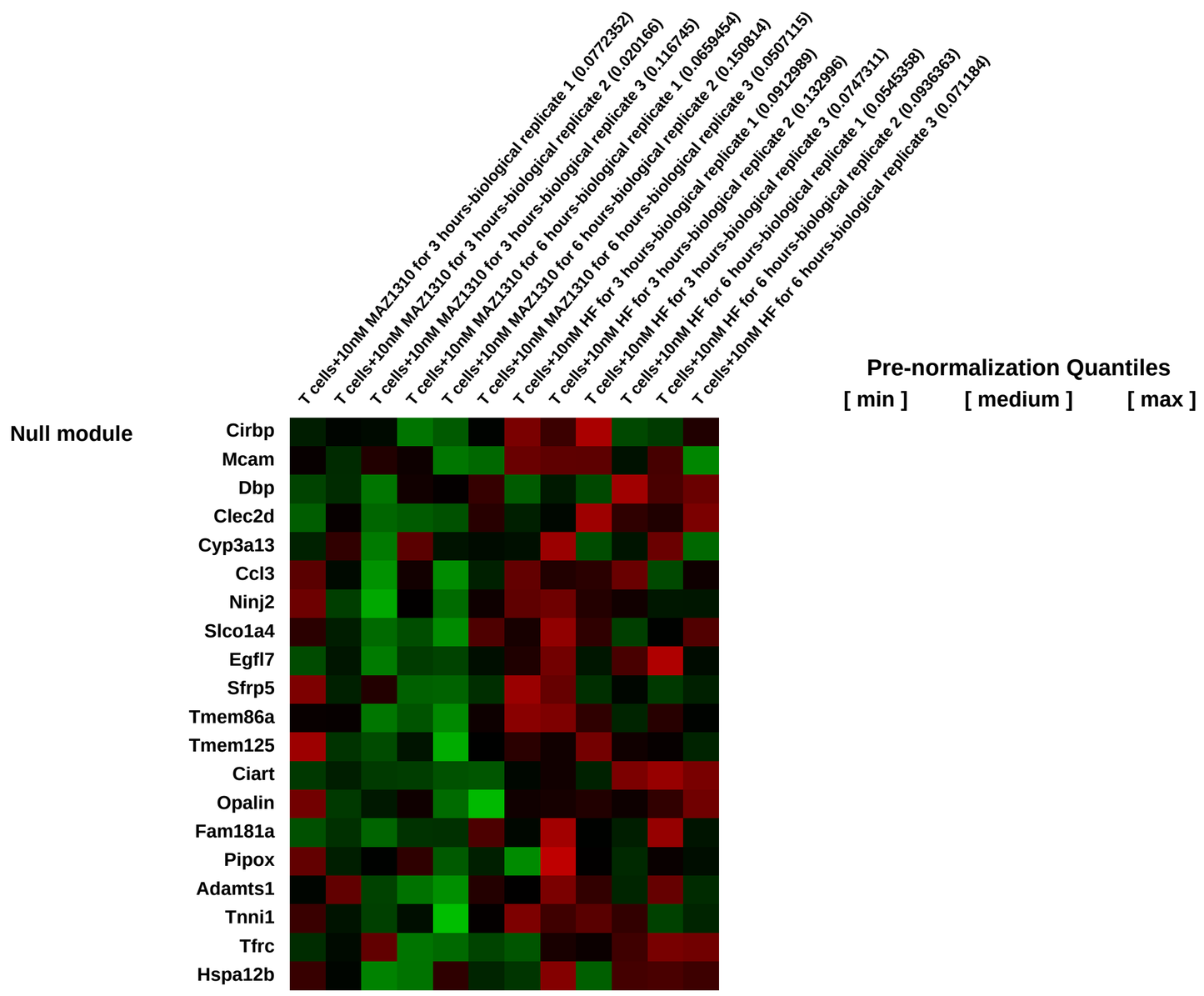

GEO Series "GSE1566" Expression Profiles

Num of samples in this series: 6

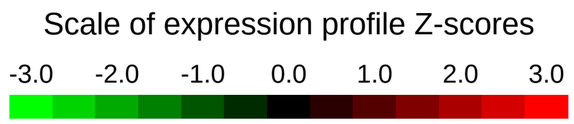

GEO Link:	**http://www.ncbi.nlm.nih.gov/geo/query/acc.cgi?acc=GSE1566**
Status:	**Public on Sep 01 2005**
Title:	**Ezh2 deficient T-cell**
Organism:	**Mus musculus**
Experiment type:	**Expression profiling by array**
Platform:	**GPL1261**
Pubmed ID:	**15882624**
Summary & Design:	**Summary:** **Lymph node T cells isolated from Ezh2fl/fl or Ezh2 deficient mice** **Keywords: repeat sample** **Overall design:**

Background corr dist: **KL-Divergence = 0.0471, L1-Distance = 0.0176, L2-Distance = 0.0003, Normal std = 0.5824**

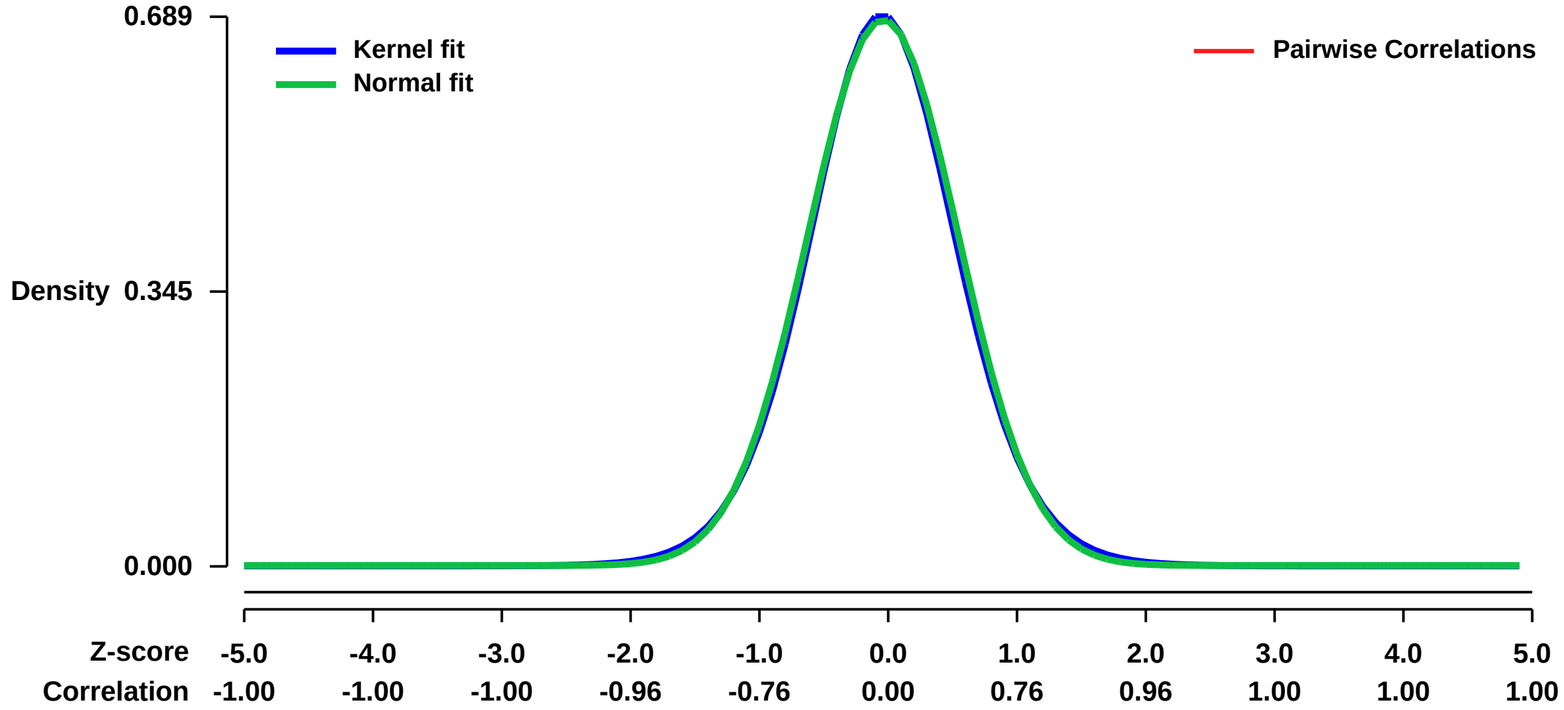

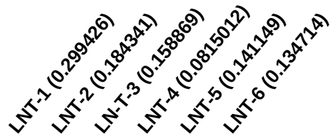

Pre-normalization Quantiles

[min] [medium] [max]

Null module

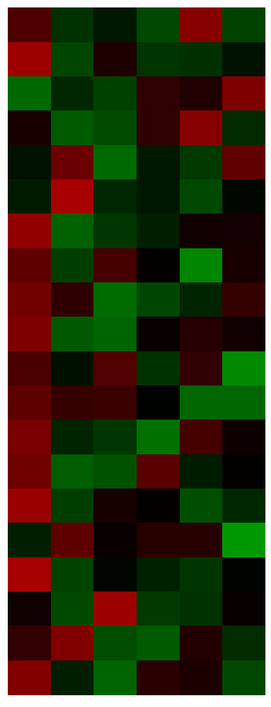

GEO Series "GSE15741" Expression Profiles

Num of samples in this series: 6

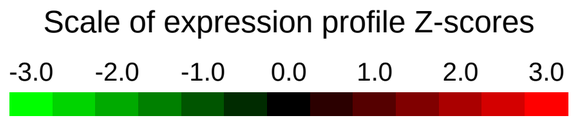

GEO Link:	http://www.ncbi.nlm.nih.gov/geo/query/acc.cgi?acc=GSE15741
Status:	Public on Nov 10 2009
Title:	Gene expression profiles of forced miR-200 expression in 344SQ lung adenocarcinoma cells with high metastatic potential
Organism:	Mus musculus
Experiment type:	Expression profiling by array
Platform:	GPL1261
Pubmed ID:	19759262
Summary & Design:	**Summary:** Metastatic disease is a primary cause of cancer-related death, and factors governing tumor cell metastasis have not been fully elucidated. Here we addressed this question by using tumor cell lines derived from mice that develop metastatic lung adenocarcinoma owing to expression of mutant K-ras and p53. A feature of metastasis-prone tumor cells that distinguished them from metastasis-incompetent tumor cells was plasticity in response to changes in their microenvironment. They transited reversibly between epithelial and mesenchymal states, forming highly polarized epithelial spheres in 3-dimensional culture that underwent epithelial-mesenchymal transition (EMT) following treatment with transforming growth factor-beta or injection into syngeneic mice. This plasticity was entirely dependent upon the microRNA-200 family, which decreased during EMT. Forced expression of miR-200 abrogated the capacity of these tumor cells to undergo EMT, invade, and metastasize and conferred transcriptional features of metastasis-incompetent tumor cells. We conclude that microenvironmental cues direct tumor metastasis by regulating miR-200 expression. **Overall design:** Cell lines from p53R172Hâ g/+ K-rasLA1/+ mice were derived from tumor tissues removed at autopsy from two different mice (#344 and #393). The tissues were minced, placed in culture, and passed serially in RPMI 1640 supplemented with 10% fetal bovine serum (FBS), which yielded mass populations of tumor cells derived from primary lung tumors (344P and 393P), mediastinal lymph nodes (344LN and 393LN), and a subcutaneous site (344SQ). Stable 344SQ cell lines expressing the miR-200b-200a-429 cluster or control vector were generated by transduction with lentivirus vectors. GFP positive transfectant pools were selected by growth in RPMI 1640 with 10% FBS and puromycin. RNA samples of miR-200b-200a-429 knockup versus control (from triplicate cultures of each) were processed and analyzed on Affymetrix Mouse Expression Array 430A 2.0 chips.

Background corr dist: KL-Divergence = 0.0327, L1-Distance = 0.0246, L2-Distance = 0.0007, Normal std = 0.6647

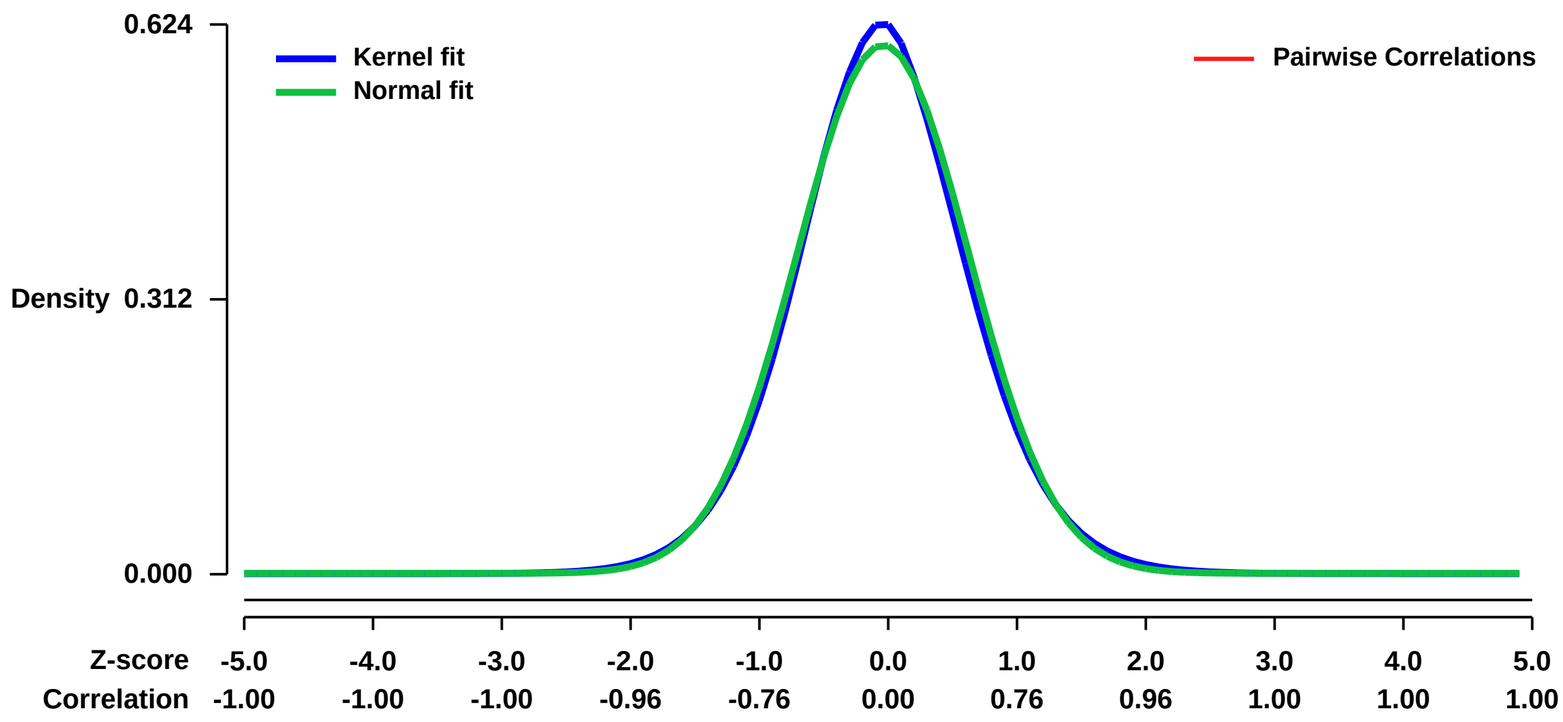

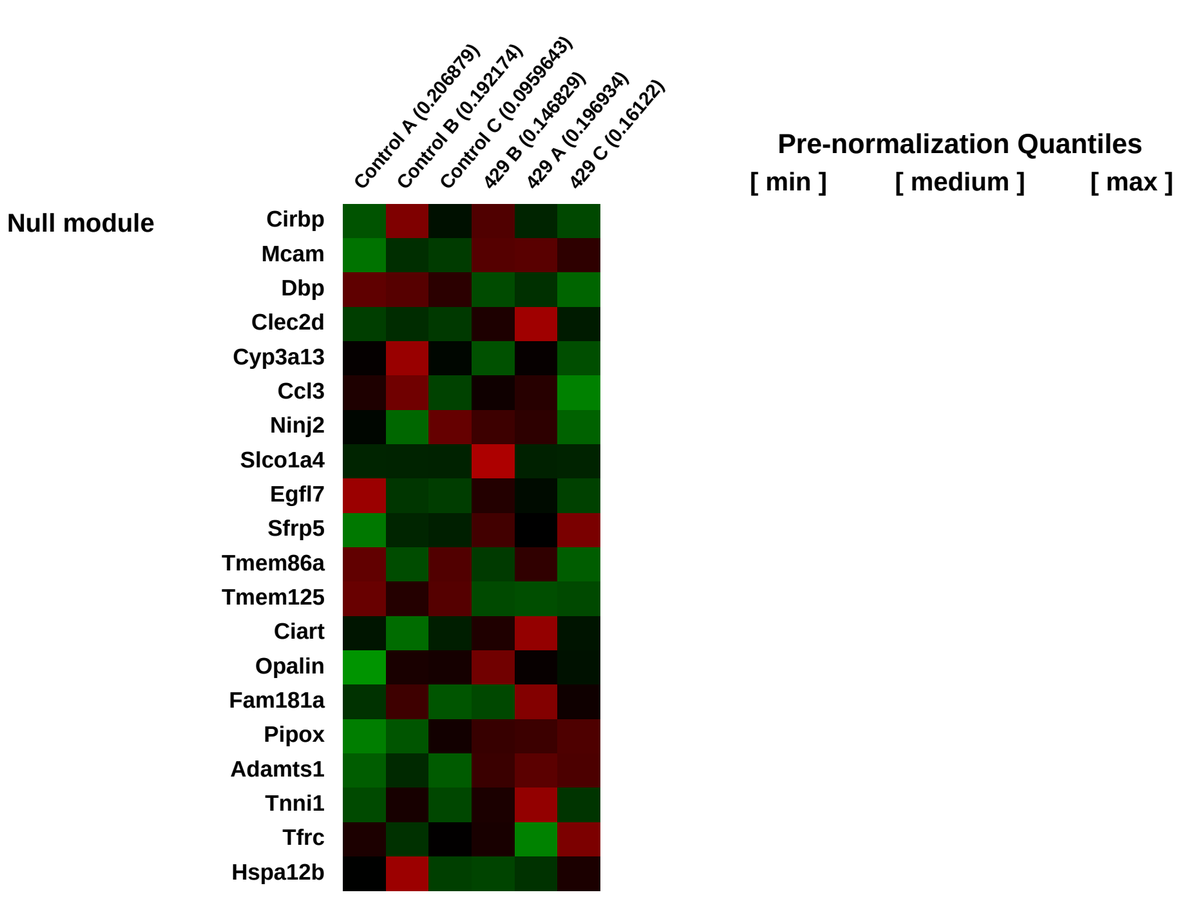

GEO Series "GSE15767" Expression Profiles

Num of samples in this series: 6

Scale of expression profile Z-scores

-3.0 -2.0 -1.0 0.0 1.0 2.0 3.0

GEO Link:	http://www.ncbi.nlm.nih.gov/geo/query/acc.cgi?acc=GSE15767
Status:	Public on Jun 05 2009
Title:	Heterogeneity of LN resident macrophage
Organism:	Mus musculus
Experiment type:	Expression profiling by array
Platform:	GPL1261
Pubmed ID:	19503106
Summary & Design:	**Summary:** **LN resident macrophages lining the lymphatic sinuses play critical roles in antigen capture and presentation as well as degradation.** **We used microarray to examine global gene expression profiles to compare SCS and med macrophages to determine the underlying molecular basis of their differential handling of antigens.** **Overall design:** **Primary SCS and med macrophages were isolated and purified from LNs by flourescence-activated cell sorting and RNA extracted, amplified and hybridized for Affymetrix analysis.**

Background corr dist: **KL-Divergence = 0.0309, L1-Distance = 0.0215, L2-Distance = 0.0005, Normal std = 0.6738**

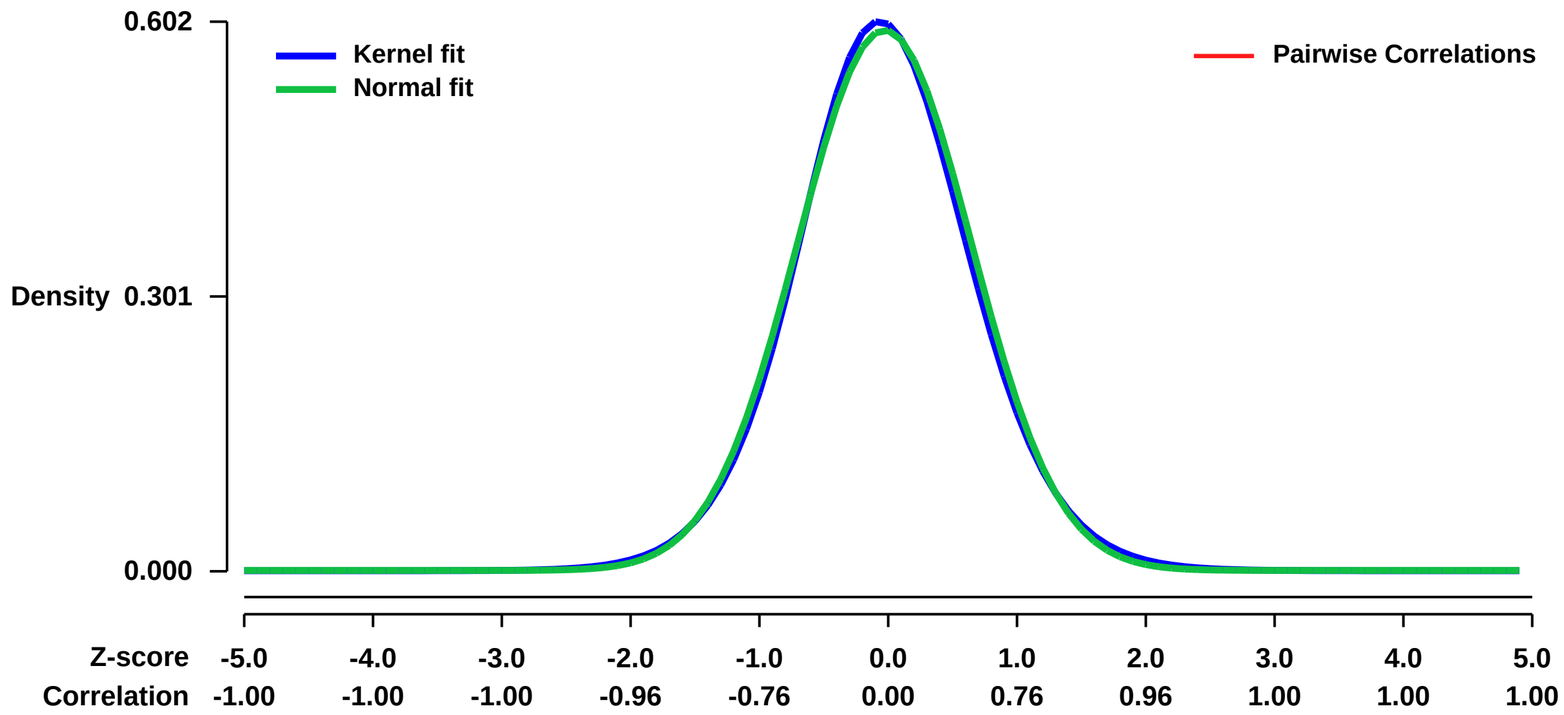

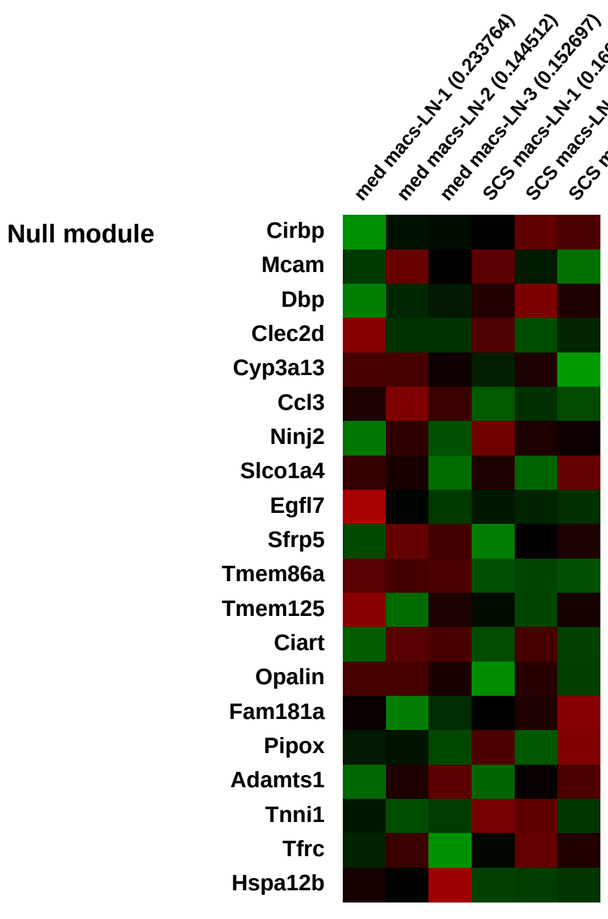

GEO Series "GSE15770" Expression Profiles

Num of samples in this series: 8

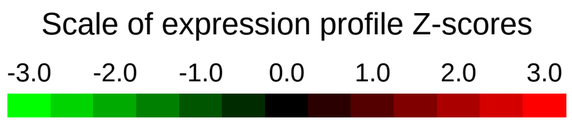

GEO Link:	http://www.ncbi.nlm.nih.gov/geo/query/acc.cgi?acc=GSE15770
Status:	Public on May 20 2009
Title:	WT and Get1 +/- Bladder Time Course
Organism:	Mus musculus
Experiment type:	Expression profiling by array
Platform:	GPL1261
Pubmed ID:	19494835
Summary & Design:	**Summary:** Skin and bladder epithelia form effective permeability barriers through the activation of distinct differentiation gene programs. Employing a genome-wide gene expression study, we identified transcription regulators whose expression correlates highly with that of differentiation markers both in bladder and skin, including the Grainyhead factor Get1/Grhl3, already known to be important for epidermal barrier formation. In the bladder, Get1 is most highly expressed in the differentiated umbrella cells and its mutation in mice leads to a defective bladder epithelial barrier formation due to failure of apical membrane specialization. Genes encoding components of the specialized urothelial membrane, the uroplakins, were downregulated in Get1-/- mice. At least one of these genes, Uroplakin II, is a direct target of Get1. The urothelial-specific activation of the Uroplakin II gene is due to selective binding of Get1 to the Uroplakin II promoter in urothelial cells, most likely regulated by histone modifications. These results demonstrate a key role for Get1 in urothelial differentiation and barrier formation. **Overall design:** To gain insights into common and unique transcriptional regulatory programs during bladder differentiation, we profiled global gene expression in whole mouse bladder at E14.5, E16.5, and E18.5.

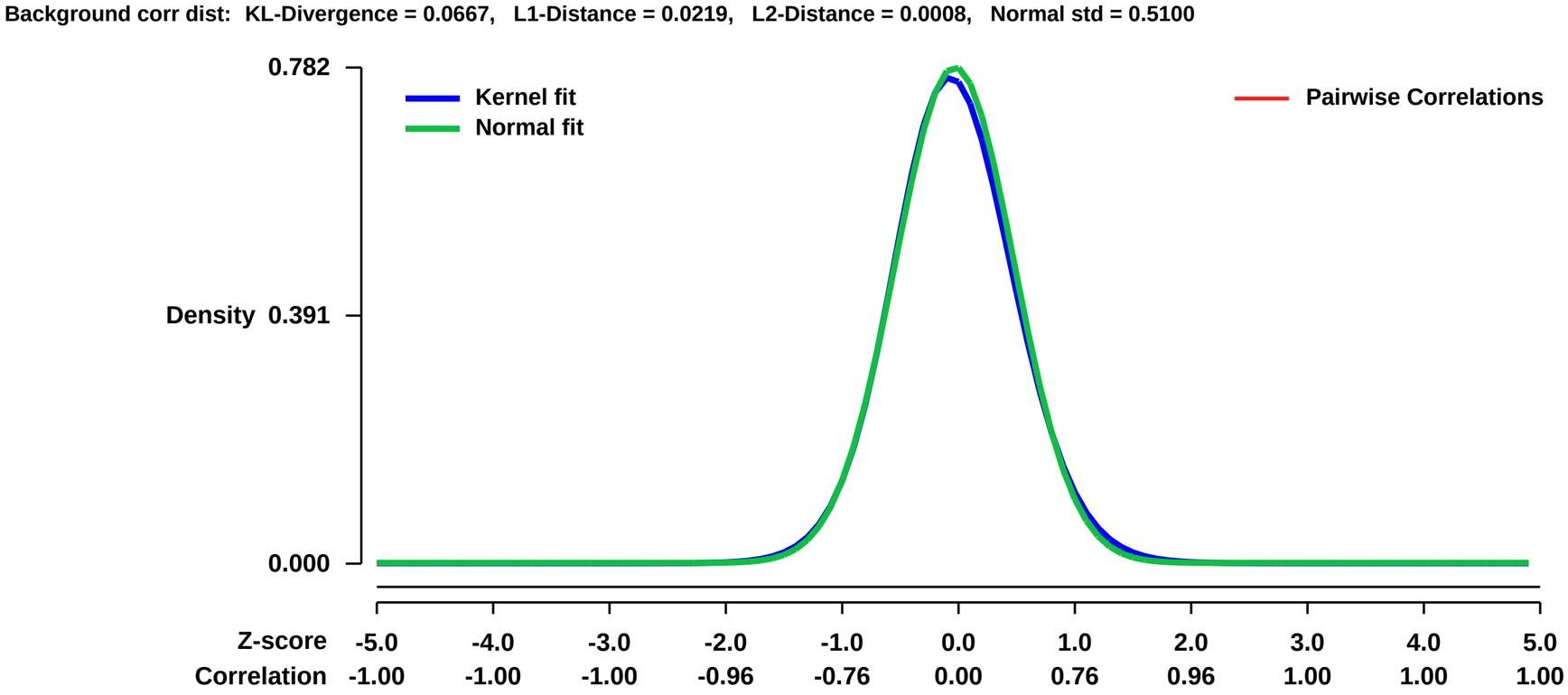

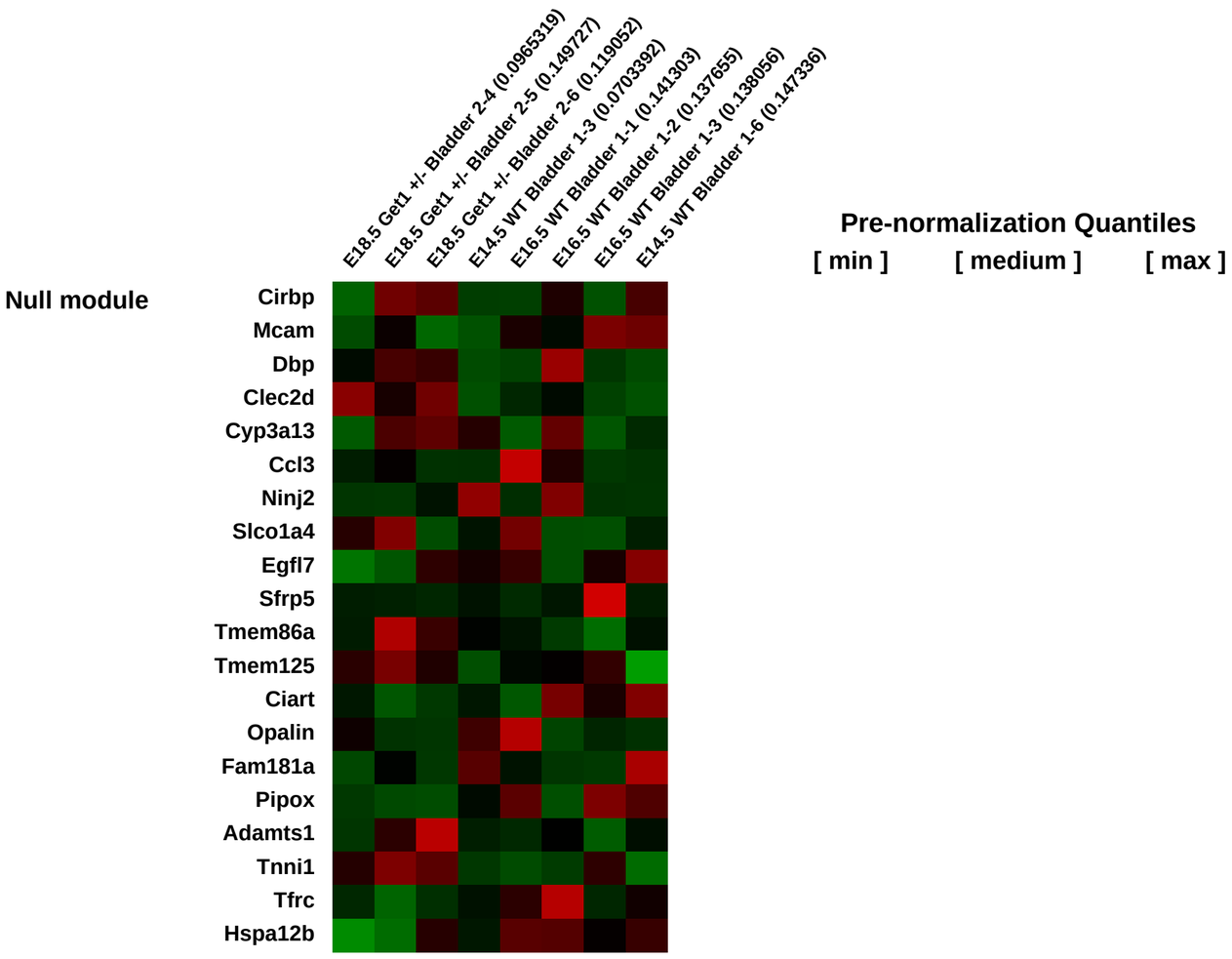

GEO Series "GSE15772" Expression Profiles

Num of samples in this series: 8

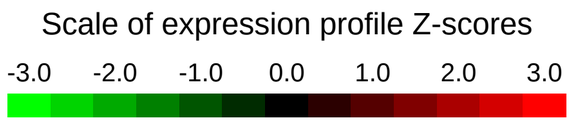

GEO Link:	http://www.ncbi.nlm.nih.gov/geo/query/acc.cgi?acc=GSE15772
Status:	Public on May 20 2009
Title:	WT Dorsal Skin Time Course
Organism:	Mus musculus
Experiment type:	Expression profiling by array
Platform:	GPL1261
Pubmed ID:	19494835
Summary & Design:	**Summary:** Skin and bladder epithelia form effective permeability barriers through the activation of distinct differentiation gene programs. Employing a genome-wide gene expression study, we identified transcription regulators whose expression correlates highly with that of differentiation markers both in bladder and skin, including the Grainyhead factor Get1/Grhl3, already known to be important for epidermal barrier formation. In the bladder, Get1 is most highly expressed in the differentiated umbrella cells and its mutation in mice leads to a defective bladder epithelial barrier formation due to failure of apical membrane specialization. Genes encoding components of the specialized urothelial membrane, the uroplakins, were downregulated in Get1-/- mice. At least one of these genes, Uroplakin II, is a direct target of Get1. The urothelial-specific activation of the Uroplakin II gene is due to selective binding of Get1 to the Uroplakin II promoter in urothelial cells, most likely regulated by histone modifications. These results demonstrate a key role for Get1 in urothelial differentiation and barrier formation. **Overall design:** To gain insights into common and unique transcriptional regulatory programs during epidermal differentiation, we profiled global gene expression in mouse dorsal skin at E14.5, E16.5, and E18.5.

Background corr dist: KL-Divergence = 0.0139, L1-Distance = 0.0232, L2-Distance = 0.0006, Normal std = 0.8175

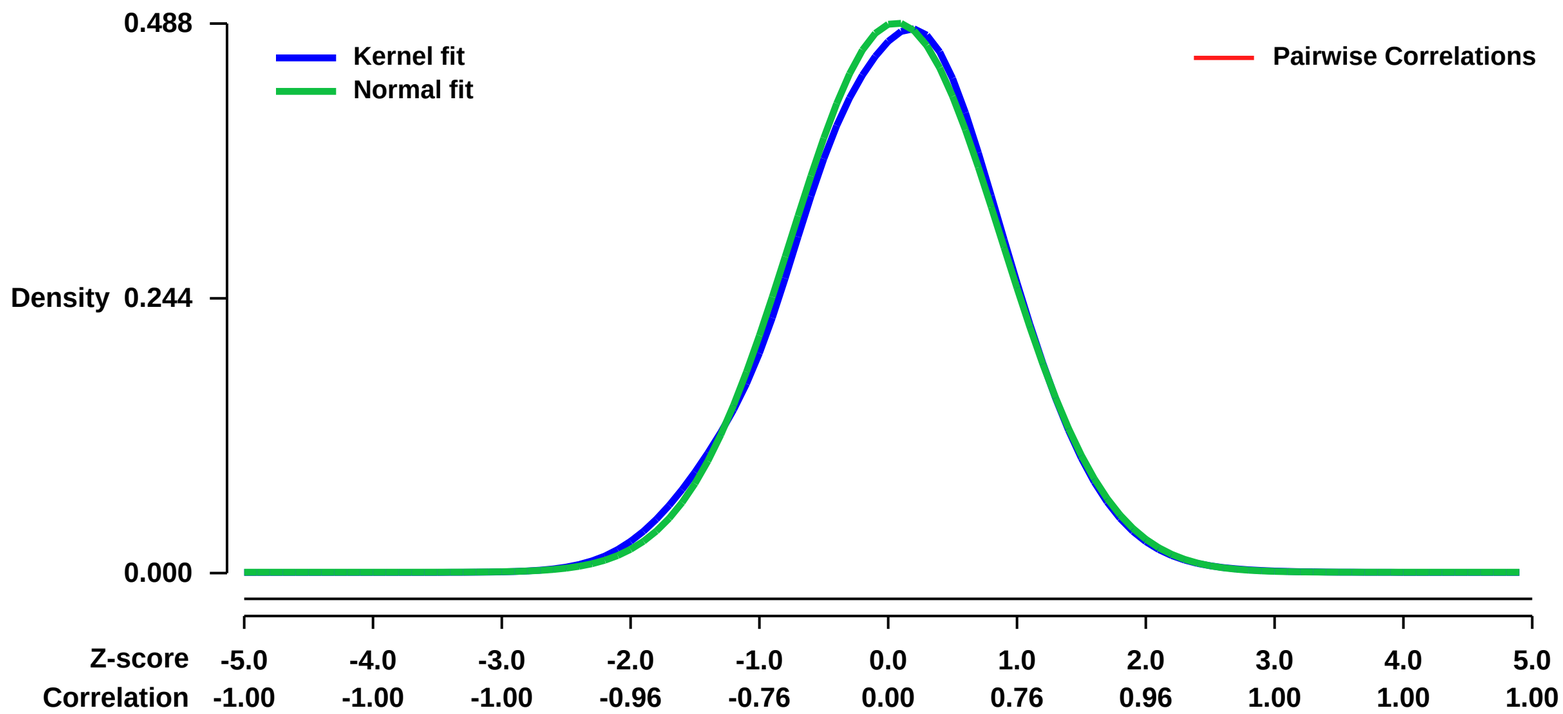

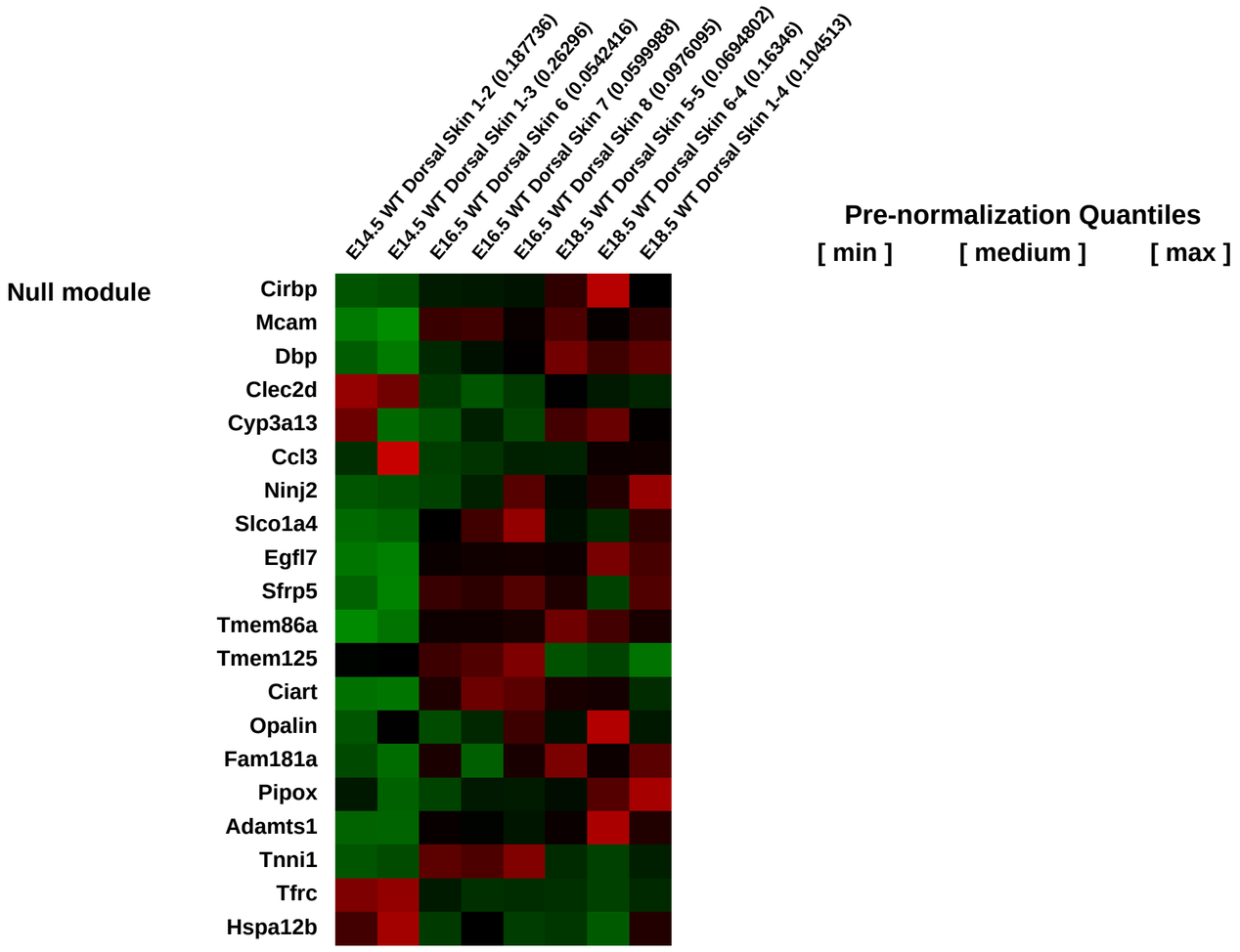

GEO Series "GSE15871" Expression Profiles

Num of samples in this series: 18

Scale of expression profile Z-scores

-3.0 -2.0 -1.0 0.0 1.0 2.0 3.0

GEO Link:	http://www.ncbi.nlm.nih.gov/geo/query/acc.cgi?acc=GSE15871
Status:	Public on Nov 05 2009
Title:	Expression data from NFI-C knock out embryonic fibroblasts
Organism:	Mus musculus
Experiment type:	Expression profiling by array
Platform:	GPL1261
Pubmed ID:	23402308
Summary & Design:	**Summary:** The Nuclear Factor I C (NFI-C) transcription factor has been implicated in TGF-¸† signaling, extracellular matrix deposition and skin appendage pathologies. We performed a global gene expression analysis in NFI-C-/- and wild-type embryonic primary murine fibroblasts. This indicated that NFI-C acts mostly to repress gene expression in response to TGF-¸†1. Misregulated genes featured a prominent over-representation of regulators of connective tissue inflammation and repair. **Overall design:** mRNAs were isolated from embryonic fibroblasts obtained from 3 wild-type and 3 NFI-C knock-out mice, and their levels were probed using microarrays. Prior to RNA extraction, fibroblast cultures were treated or not with TGF-¸†1 for 1 hour to examine the immediate response to the growth factor, or treated for 10 hours to assess the delayed response.

Background corr dist: KL-Divergence = 0.1186, L1-Distance = 0.0278, L2-Distance = 0.0011, Normal std = 0.4192

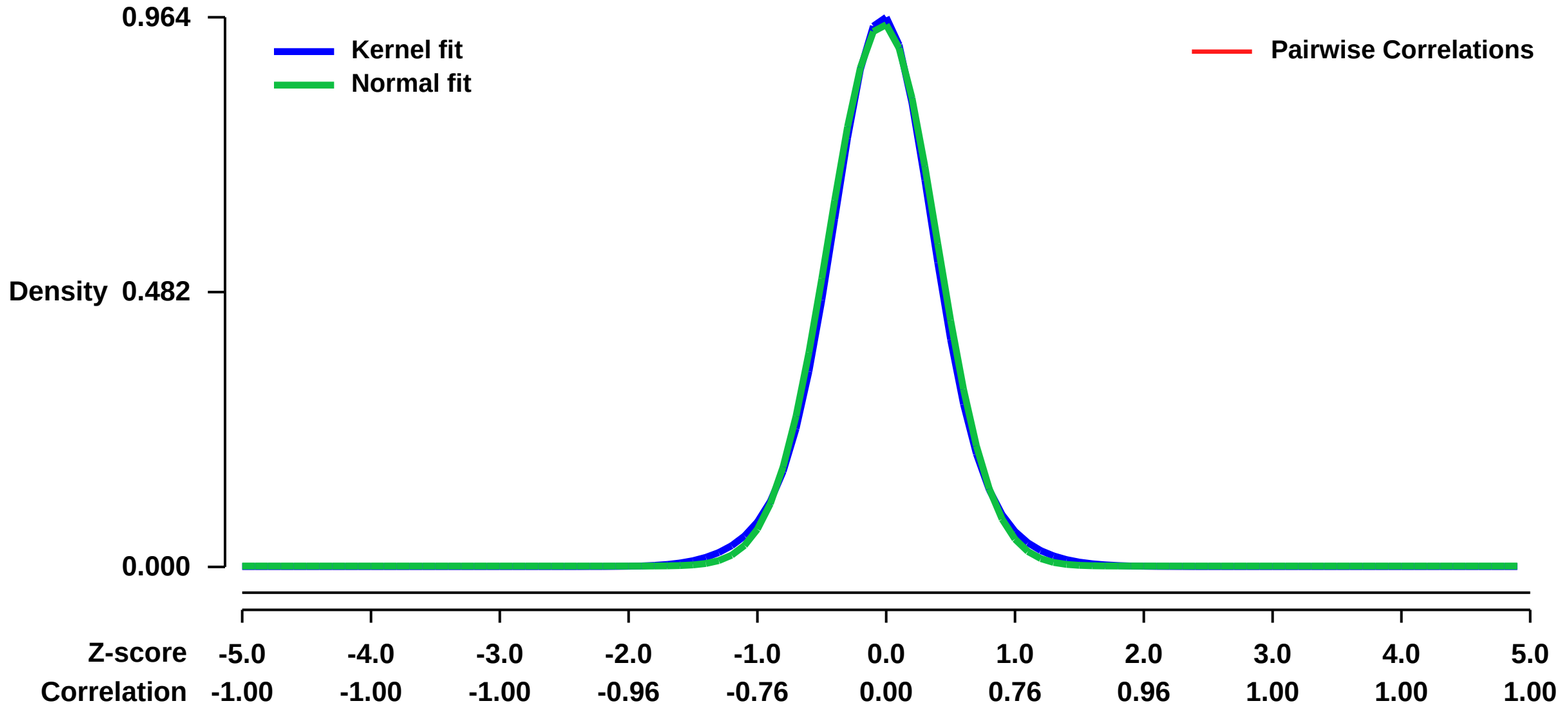

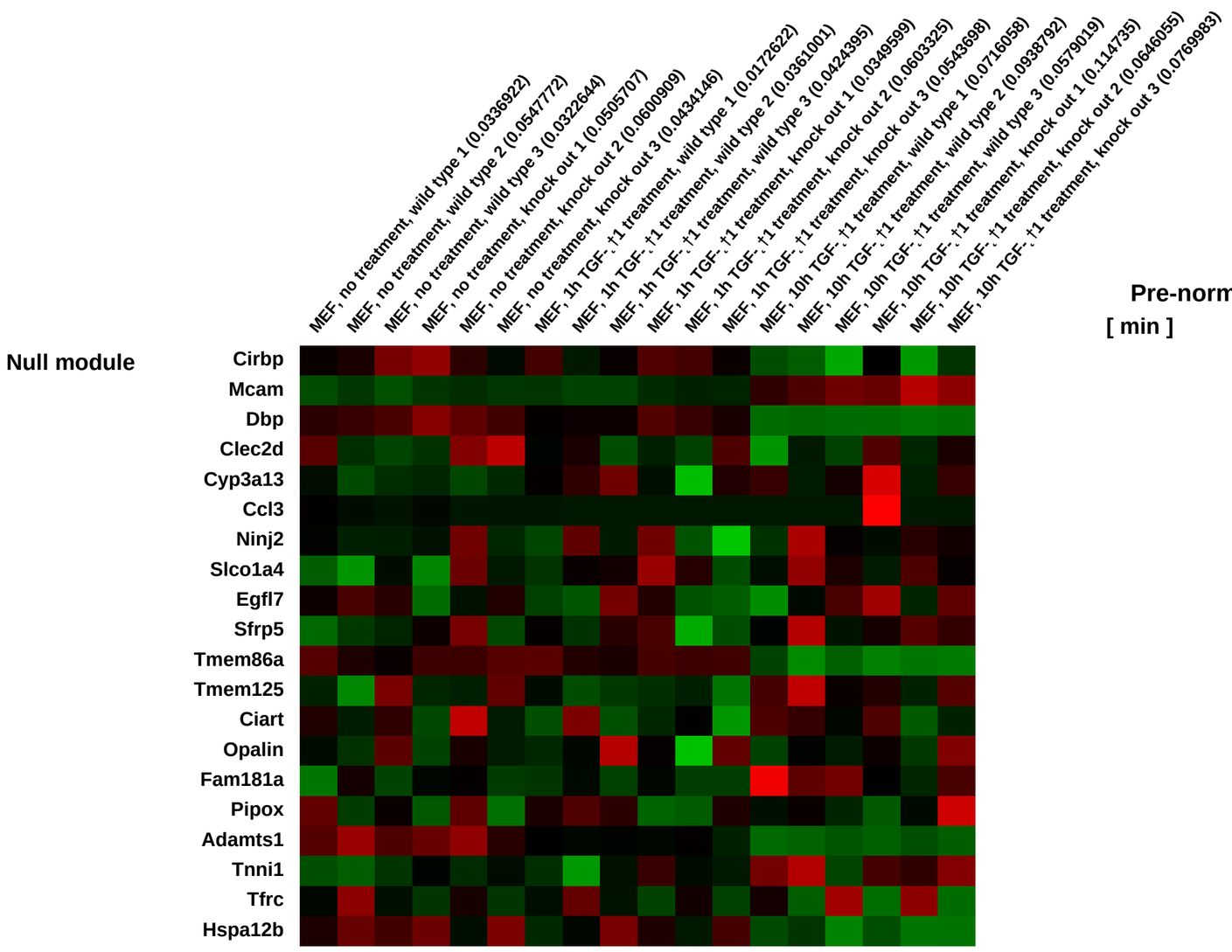

GEO Series "GSE15891" Expression Profiles

Num of samples in this series: 8

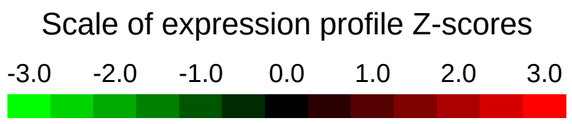

GEO Link:	http://www.ncbi.nlm.nih.gov/geo/query/acc.cgi?acc=GSE15891
Status:	Public on Apr 30 2009
Title:	Gene expression of Mus exposed to chronic hypoxia
Organism:	Mus musculus domesticus
Experiment type:	Expression profiling by array
Platform:	GPL1261
Pubmed ID:	20103700
Summary & Design:	**Summary:** **High altitude environments are characterized by the unique and unavoidable stress of chronic hypoxia. While much is known about gene expression responses to acute or in vitro hypoxia, less is known about the gene expression profiles of animals exposed to systemic chronic hypoxia, such as that experienced at high elevations. Here we simulated the hypoxic environment of two high altitude elevations,and a third chamber recieved ambient Reno air. Mice were housed in the hypoxic chambers for 32 days.** **We used microarrays to characterize the differential gene expression in the livers of mice housed in hypoxic environment of 4500 m versus 3000 and 1400 m. We used this data to draw hypotheses related to novel physiological responses to chronic systemic hypoxia** **Overall design:** **Mice were housed one of three chambers; the first received ambient Reno air (1400 m) and the other two received air mixed with nitrogen such that one chamber simulated the hypoxic environment of 3000 m and the third chamber simulated hypoxic environment of 4500 m. Twelve mice were housed in each chamber for 32 days. Liver were extracted, and RNA from livers of 4 mice were pooled such that each treatment was represented by 3 pooled samples.**

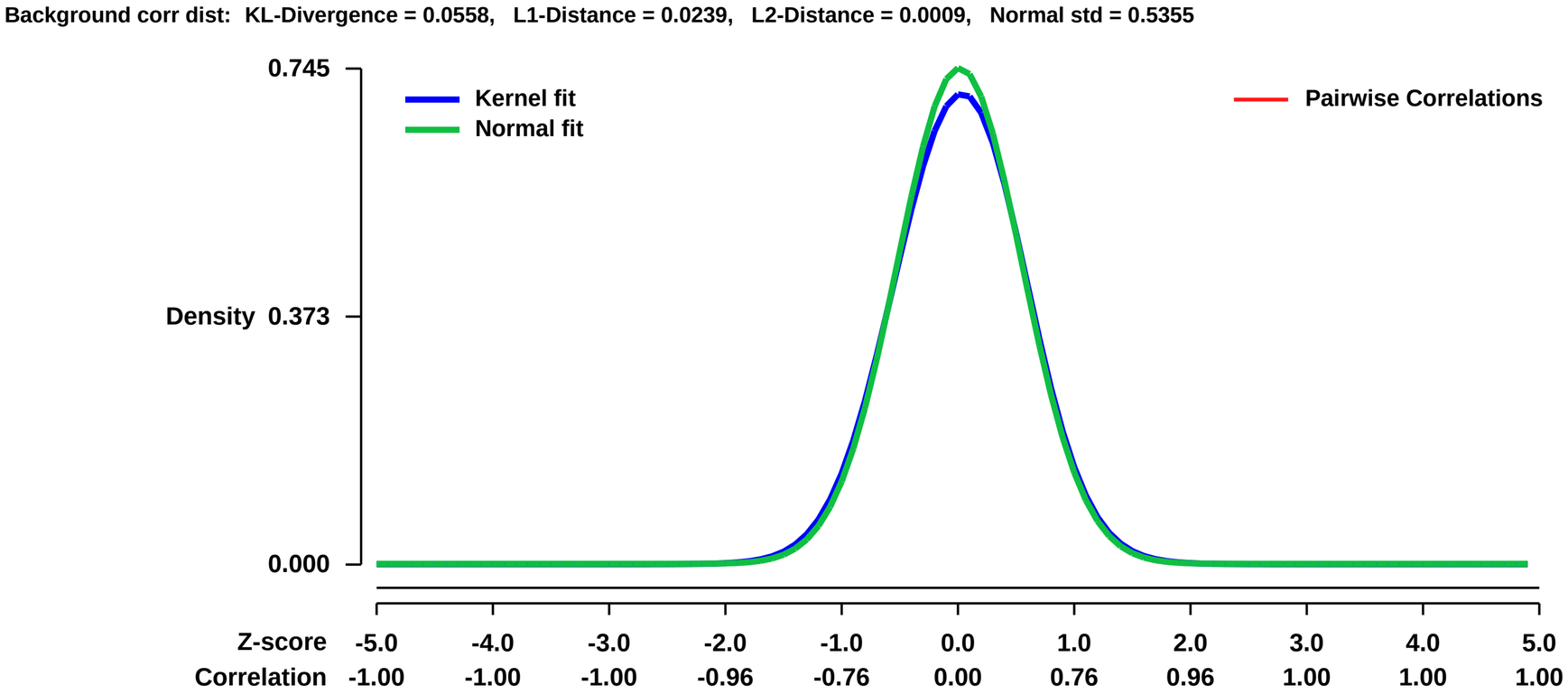

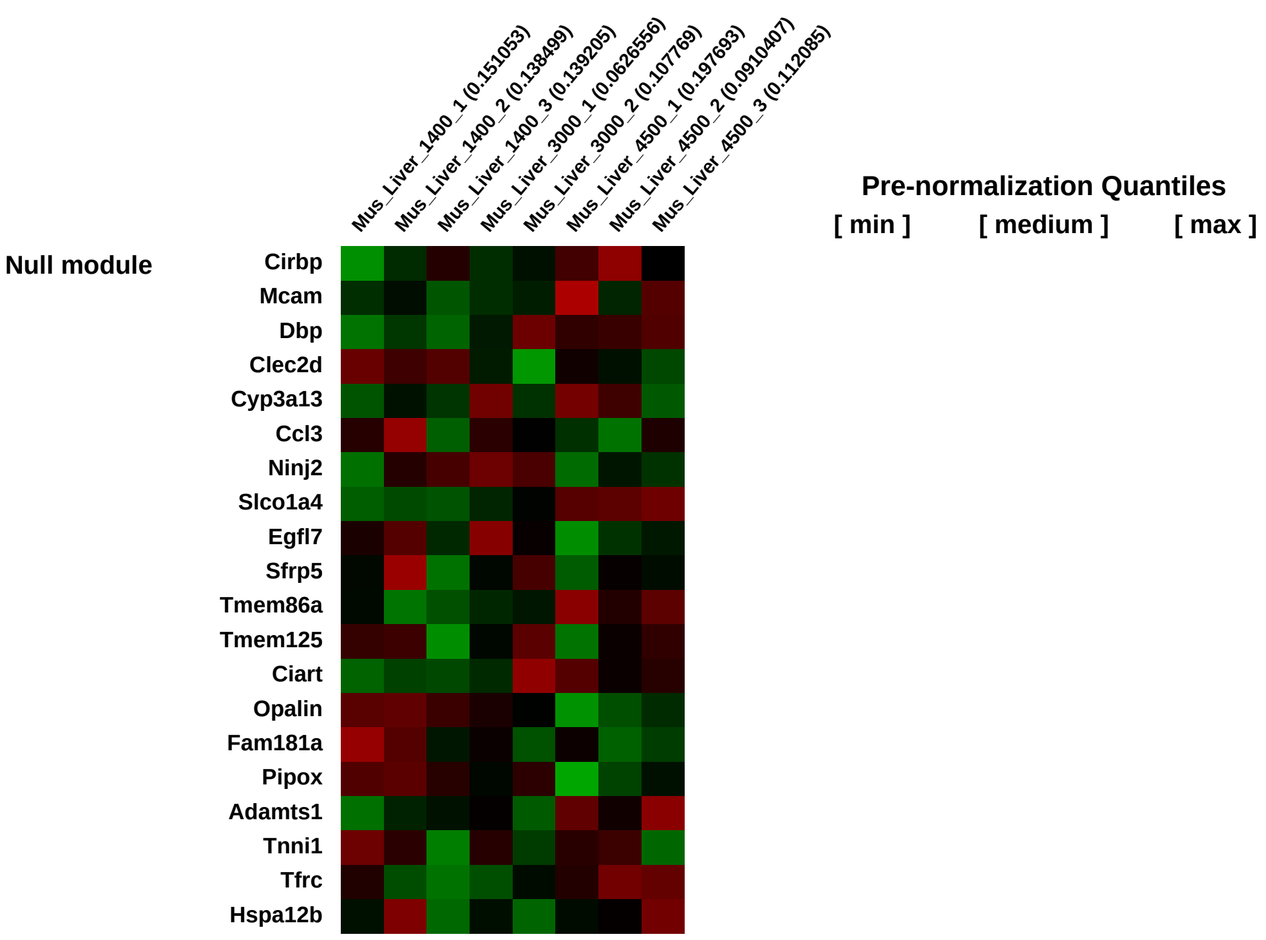

GEO Series "GSE15894" Expression Profiles

Num of samples in this series: 8

Scale of expression profile Z-scores

-3.0 -2.0 -1.0 0.0 1.0 2.0 3.0

GEO Link:	http://www.ncbi.nlm.nih.gov/geo/query/acc.cgi?acc=GSE15894
Status:	Public on Apr 25 2010
Title:	Comparison of gene expression in whole blood of mice subjected to normobaric hypoxia in vivo.
Organism:	Mus musculus
Experiment type:	Expression profiling by array
Platform:	GPL1261
Pubmed ID:	
Summary & Design:	**Summary:** To determine hypoxia mediated changes in whole blood, normal C57Bl/10 mice were gradually exposed to a chronic hypoxic environment, equivalent to an altitude of 6500m, for 2 weeks in vivo. Control, age-matched mice were maintained under normoxic, normobaric conditions by exposing them to ambient air in Philadelphia (c. 50 mts above sea level). #!# **Overall design:** Conclusion: Transcriptome level differences exist in the whole blood of animals subjected to normobaric hypoxia. Our definition of the normobaric hypoxia blood transcriptome provides insight into the functioning and response to hypoxia in whole blood.

Background corr dist: KL-Divergence = 0.0600, L1-Distance = 0.0331, L2-Distance = 0.0018, Normal std = 0.5385

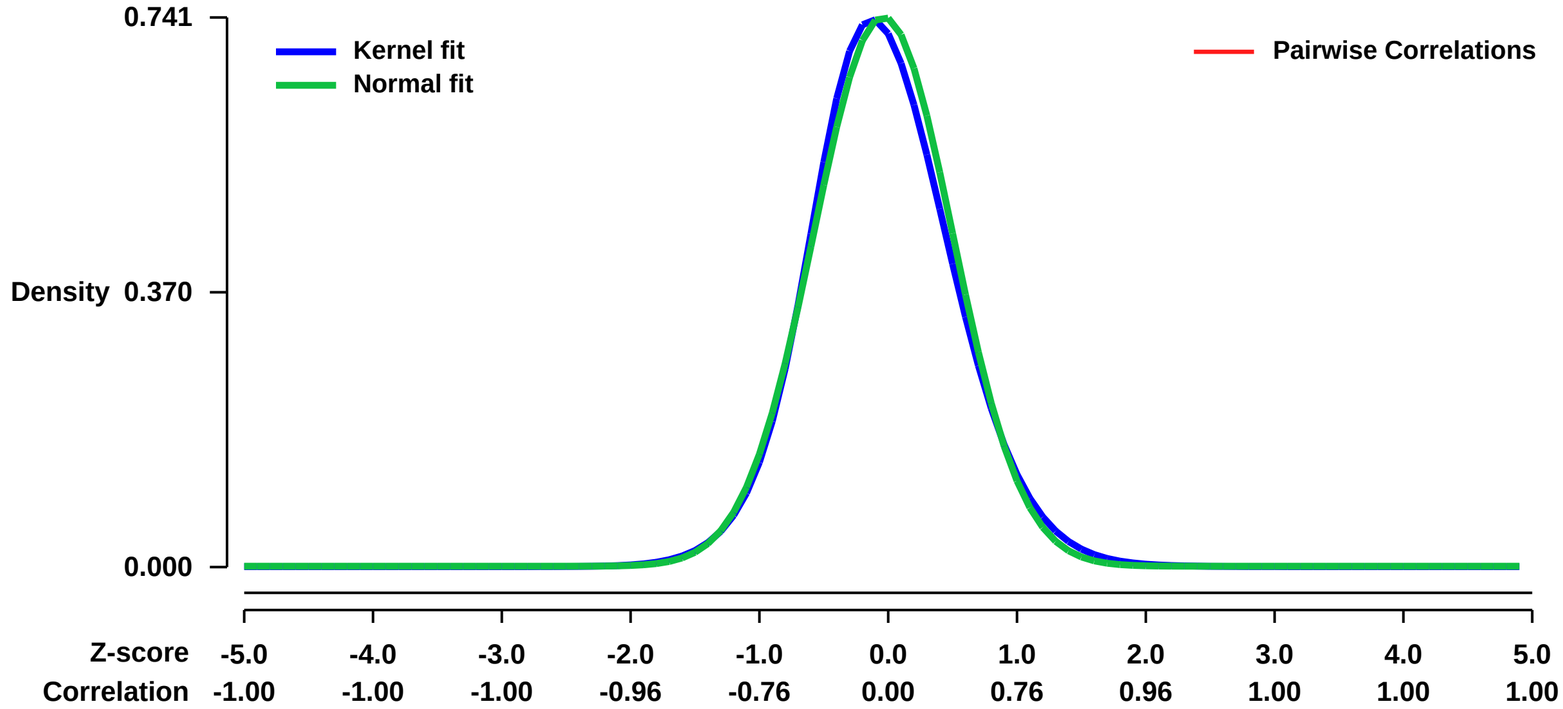

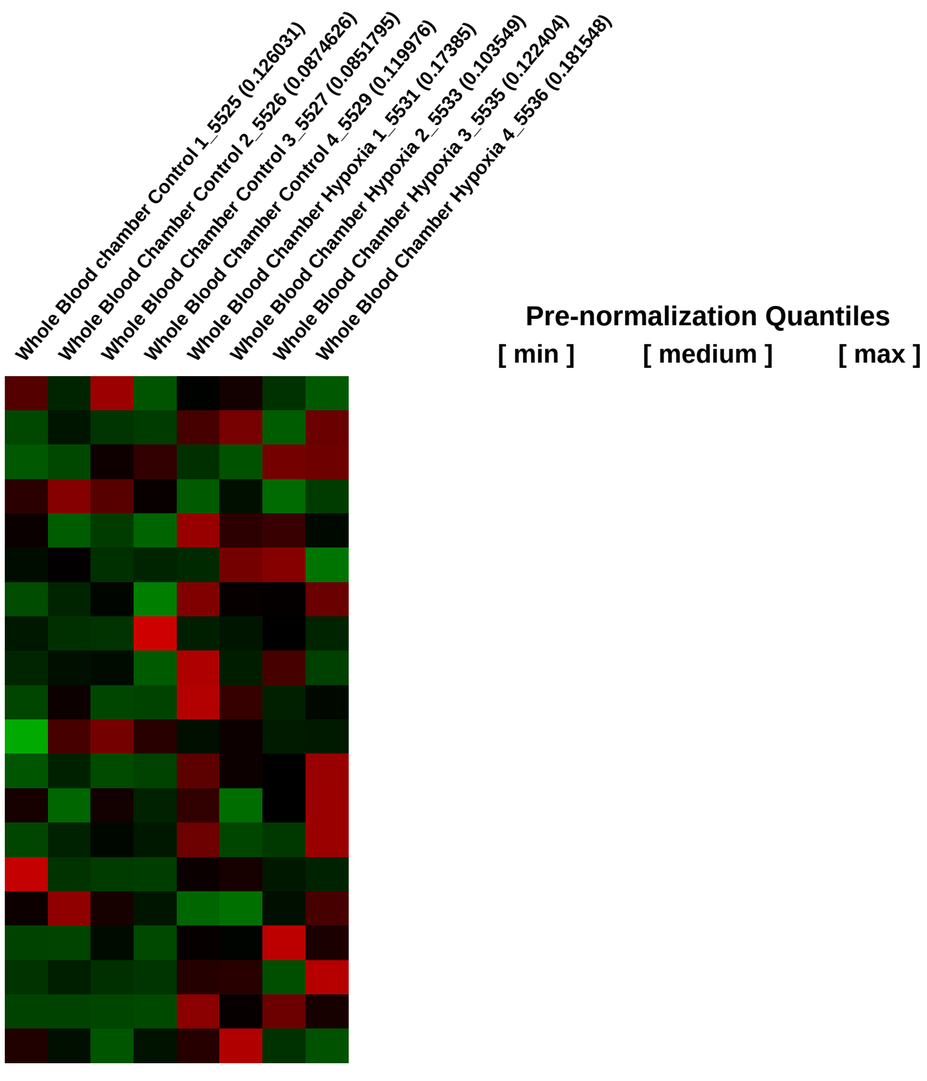

GEO Series "GSE15914" Expression Profiles

Num of samples in this series: 9

Scale of expression profile Z-scores

-3.0 -2.0 -1.0 0.0 1.0 2.0 3.0

GEO Link:	http://www.ncbi.nlm.nih.gov/geo/query/acc.cgi?acc=GSE15914
Status:	Public on Oct 01 2009
Title:	Interleukin-7 promotes monocyte/macrophage arrest on endothelial cells
Organism:	Mus musculus
Experiment type:	Expression profiling by array
Platform:	GPL1261
Pubmed ID:	21804111
Summary & Design:	**Summary:** **Background: It is recognized that atherosclerosis can regresses at least in animal models. However, little is known about the mechanisms. We induced regression of advanced atherosclerosis in apolipoprotein E deficient (APOE´›/´›) mice and studied underlying mechanisms. Unexpectedly, our study led to the role of interleukin-7 (IL-7) in atherogenesis.** **Methods and Results: We treated APOE´›/´› mice fed a high cholesterol diet for 30 weeks to induce advanced lesions with a helper-dependent adenoviral vector expressing human apoE3 (HDAd-gE3), and analyzed the regression of atherosclerosis after 41 weeks. Using microarray analysis, we identified IL-7 as one of most significantly affected genes by lowering cholesterol. To answer why IL-7 is downregulated by reduced cholesterol, we studied effects of IL-7 on endothelial cells (ECs). Our major findings were (1) long-term lowering cholesterol induced regression of advanced atherosclerosis. (2) Microarray analysis identified multiple signaling pathways affected by lowering cholesterol. (3) Correction for multiple testing revealed that IL-7 expression was downregulated, whereas gamma-sarcoglycan and ˆ´–-actin were upregulated. (4) Oxidized LDL upregulated IL-7 expression in macrophages but not in aorta ECs or smooth muscle cells. (5) IL-7 increased the expression of cell adhesion molecules and chemokine in ECs and promoted monocyte adhesion to ECs. (6) Systemic elevation of IL-7 induced inflammatory response and recruited monocyte/macrophage to the lesions without increasing plasma cholesterol.** **Conclusion: Our finding suggest that IL-7 inflames endothelium and triggers the adhesion/recruitment of monocyte/macrophages to the atherosclerotic lesions and thus plays a direct role in development of atherosclerosis.** **Key Words: arteriosclerosis, gene therapy, hypercholesterolemia, interleukins, cell adhesion molecules** **Overall design:** **12039: E3: vector control**

Background corr dist: KL-Divergence = 0.0908, L1-Distance = 0.0240, L2-Distance = 0.0008, Normal std = 0.4532

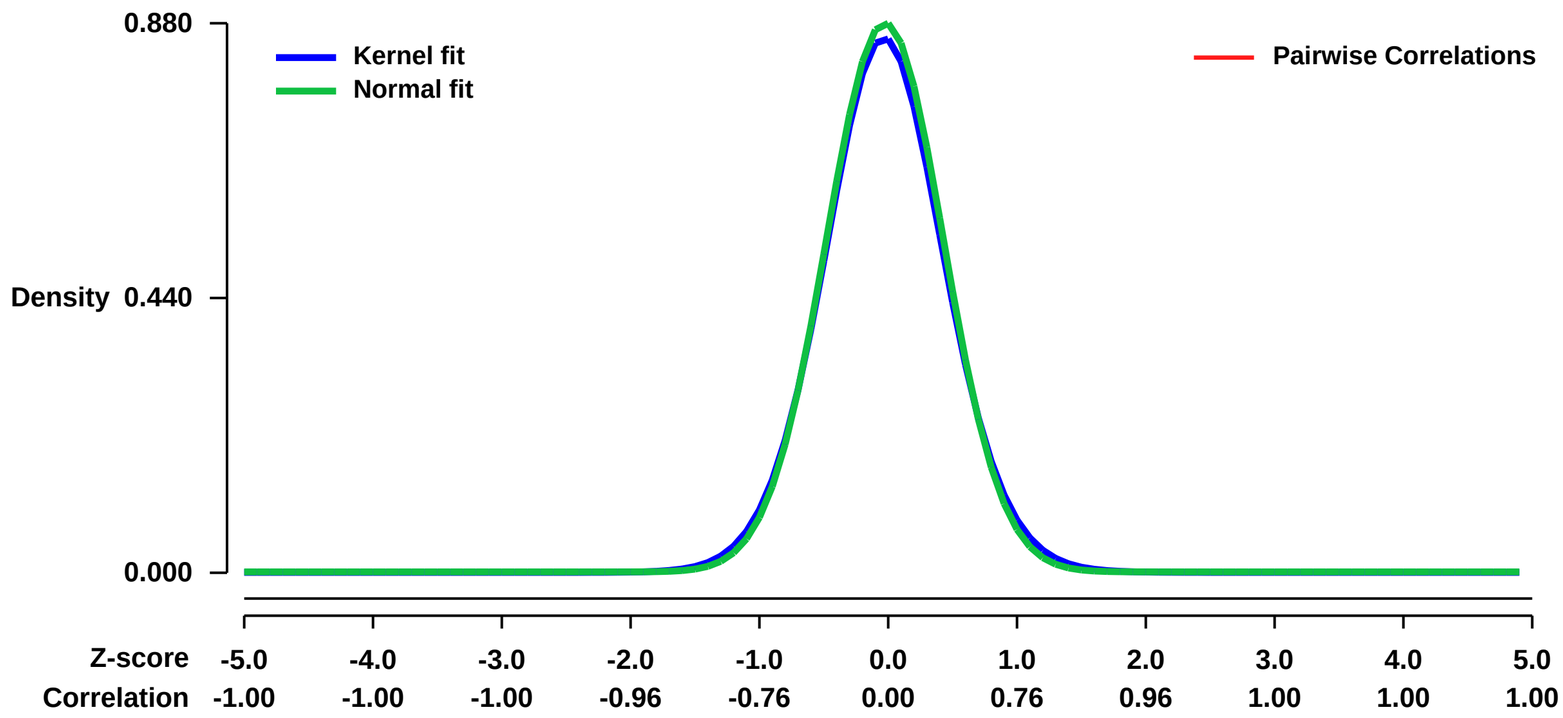

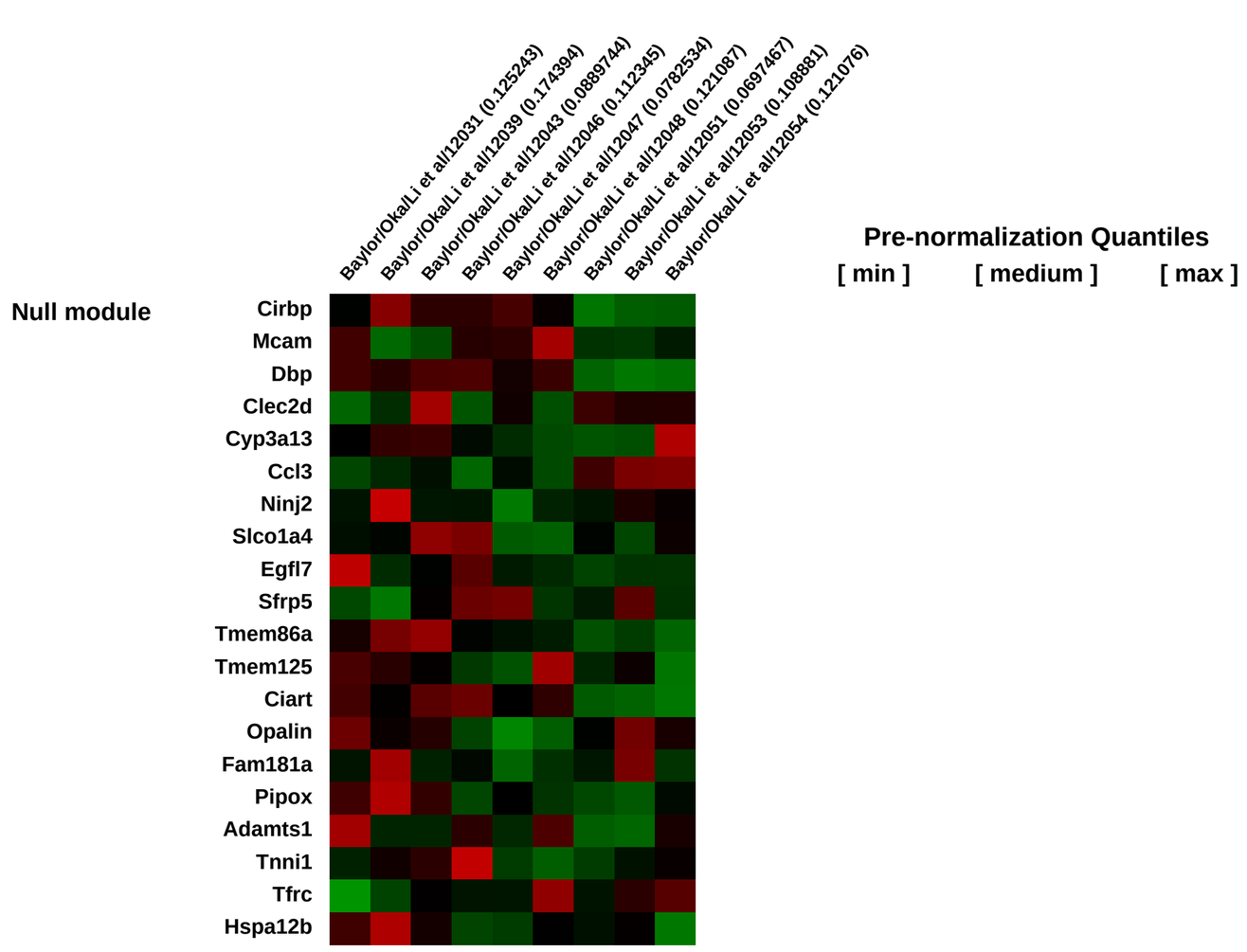

GEO Series "GSE15999" Expression Profiles

Num of samples in this series: 8

Scale of expression profile Z-scores

-3.0 -2.0 -1.0 0.0 1.0 2.0 3.0

GEO Link:	http://www.ncbi.nlm.nih.gov/geo/query/acc.cgi?acc=GSE15999
Status:	Public on May 08 2009
Title:	Mesenchymal signature of post-pneumonectomy lung regeneration in adult mice
Organism:	Mus musculus
Experiment type:	Expression profiling by array
Platform:	GPL1261
Pubmed ID:	19804646
Summary & Design:	**Summary:** The adult human lung has a very limited capacity to regenerate functional alveoli. In contrast, adult mice have a remarkable capacity for neoalveolarization following either lung resection or injury. The molecular basis for this unique capability to regenerate lung tissue in mice is largely unknown. We examined the transcriptomic responses to single lung pneumonectomy in adult mice in order to elucidate prospective molecular signaling used in this species during lung regeneration. Unilateral left pneumonectomy or sham thoracotomy was performed under general anesthesia (n = 8 mice per group for each of the four time points). Total RNA was isolated from the remaining lung tissue at four time points post-surgery (6 hours, 1 day, 3 days, 7 days) and analyzed using microarray technology. The observed transcriptomic patterns revealed mesenchymal cell signaling, including up-regulation of genes previously associated with activated fibroblasts (Tnfrsf12a, Tnc, Eln, Col3A1), as well as modulation of Igf1-mediated signaling. The data set also revealed early down-regulation of pro-inflammatory cytokine transcripts, up-regulation of genes involved in T cell development and function, but few similarities to transcriptomic patterns observed during embryonic or post-natal lung development. Immunohistochemical analysis suggests that early fibroblast but not myofibroblast proliferation is important during lung regeneration and may explain the preponderance of mesenchymal-associated genes that are over-expressed in this model. This appears to differ from embryonic alveologenesis. These data suggest that modulation of mesenchymal cell signaling and proliferation may act in concert with immunomodulation to control inflammation during post-pneumonectomy lung regeneration in adult mice. **Overall design:** For each of the four time points (6 hr, 1 day, 3 day, 7 day), the mice were divided into two groups: (1) pneumonectomy (PNY) and (2) sham operated (SHAM - thoracotomy without lung resection), with eight animals in each group. One microarray was performed on pooled lung tissue from these 8 animals for each time point. Analysis of expression in PNY vs SHAM animals was performed in two ways: using all four microarrays as replicates in a time-independent analysis, as well as analysis of each time point separately (time-dependent) without replicates.

Background corr dist: KL-Divergence = 0.0531, L1-Distance = 0.0180, L2-Distance = 0.0004, Normal std = 0.5463

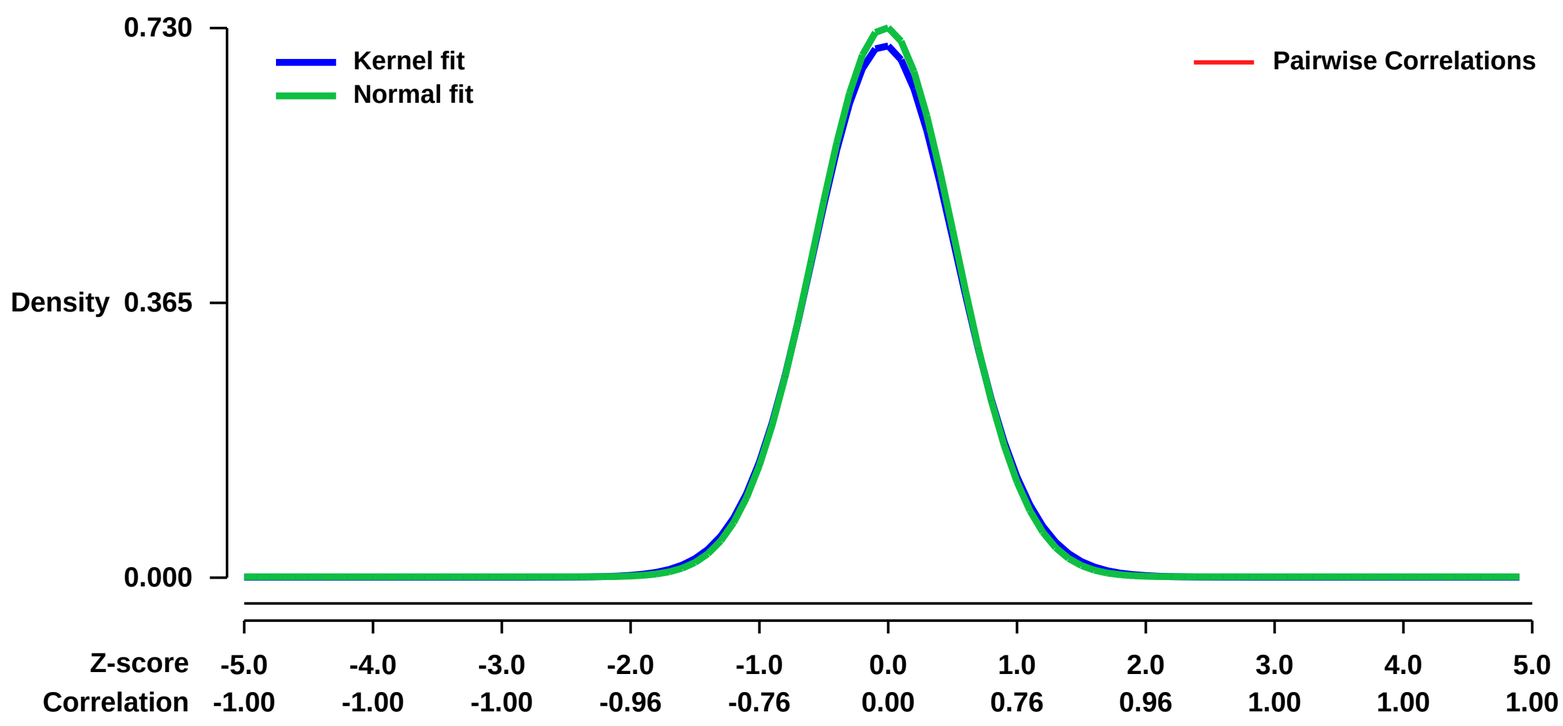

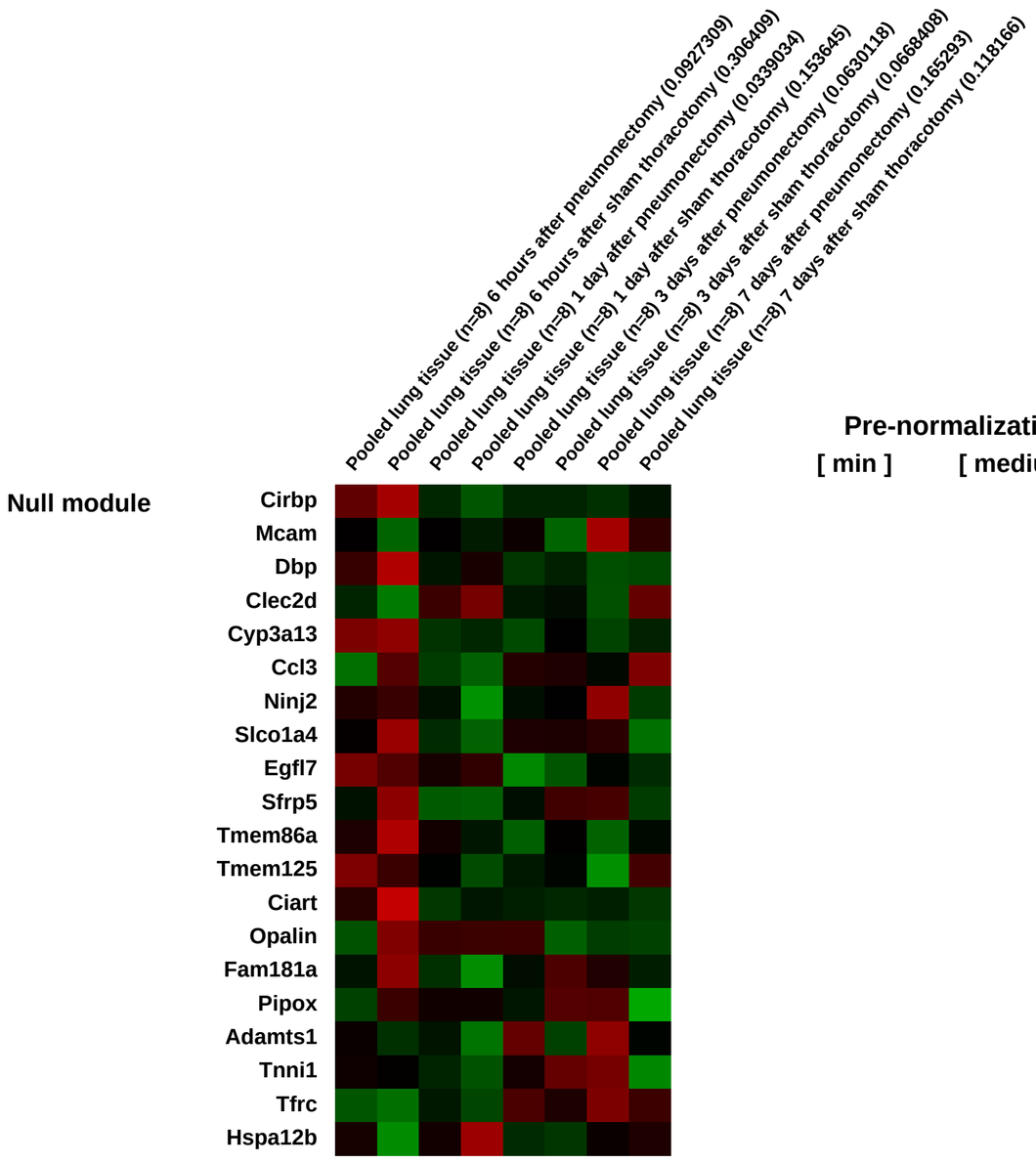

GEO Series "GSE16048" Expression Profiles

Num of samples in this series: 6

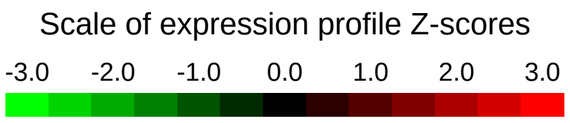

GEO Link:	http://www.ncbi.nlm.nih.gov/geo/query/acc.cgi?acc=GSE16048
Status:	Public on Aug 30 2012
Title:	Expression profiling of pancreatic beta-cells harboring a pancreatic-specific deletion of PPAR-beta
Organism:	Mus musculus
Experiment type:	Expression profiling by array
Platform:	GPL1261
Pubmed ID:	23093780
Summary & Design:	**Summary:** Peroxisome proliferator-activated receptor beta/delta protects against obesity by reducing dyslipidemia and insulin resistance via effects in various organs, including muscle, adipose tissue, liver, and heart. However, nothing is known about the function of PPAR-beta in pancreas, a prime organ in the control of glucose metabolism. To gain insight into so far hypothetical functions of this PPAR isotype in insulin production, we specifically ablated Ppar-beta in pancreas. The mutated mice developed a chronic hyperinsulinemia, due to an increase in both beta-cell mass and insulin secretion. Gene expression profiling indicated a broad repressive function of PPAR-beta impacting the vesicular compartment, actin cytoskeleton, and metabolism of glucose and fatty acids. Analyses of insulin release from the islets revealed an increased second-phase glucose-stimulated insulin secretion. Higher levels of PKD, PKC-delta and diacyglycerol in mutated animals lead to an enhanced formation of trans-Golgi network (TGN)-to-plasma-membrane transport carriers in concert with F-actin disassembly, which resulted in increased insulin secretion and its associated systemic effects. Taken together, these results provide evidence for PPAR-beta playing a repressive role on beta-cell growth and insulin exocytosis, which shed new light on its anti-obesity action. **Overall design:** Pancreas-specific knock-out animals were generated by breeding mice harbouring a floxed Ppar-beta (PPARbetafl/fl) to mice expressing the Cre transgene under the control of the Pdx1 promoter (Pdx1Cre). Islets from 3 different animals from the knock-out group Pdx1Cre;PPARbetafl/fl and the control littermates group PPARbetafl/fl were compared.

Background corr dist: KL-Divergence = 0.0416, L1-Distance = 0.0171, L2-Distance = 0.0003, Normal std = 0.6050

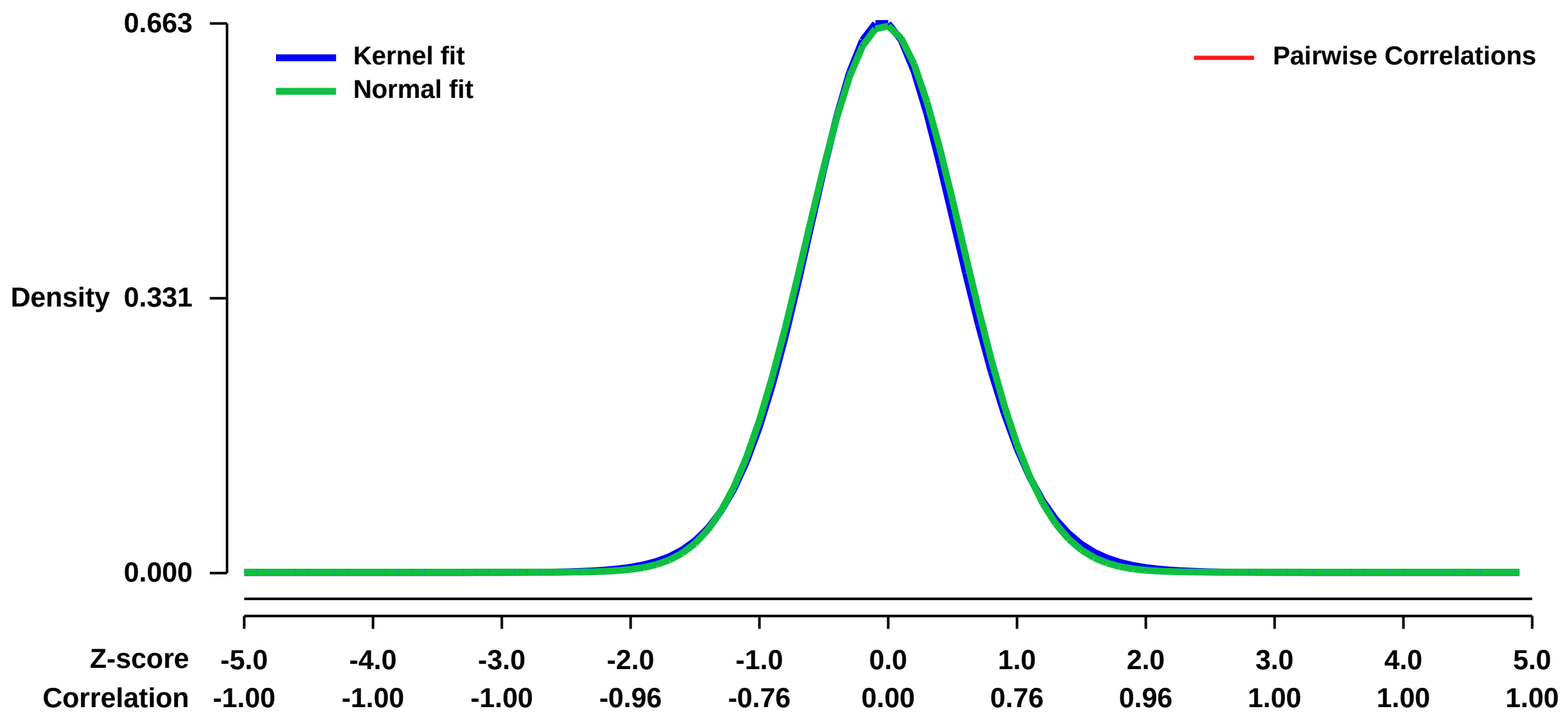

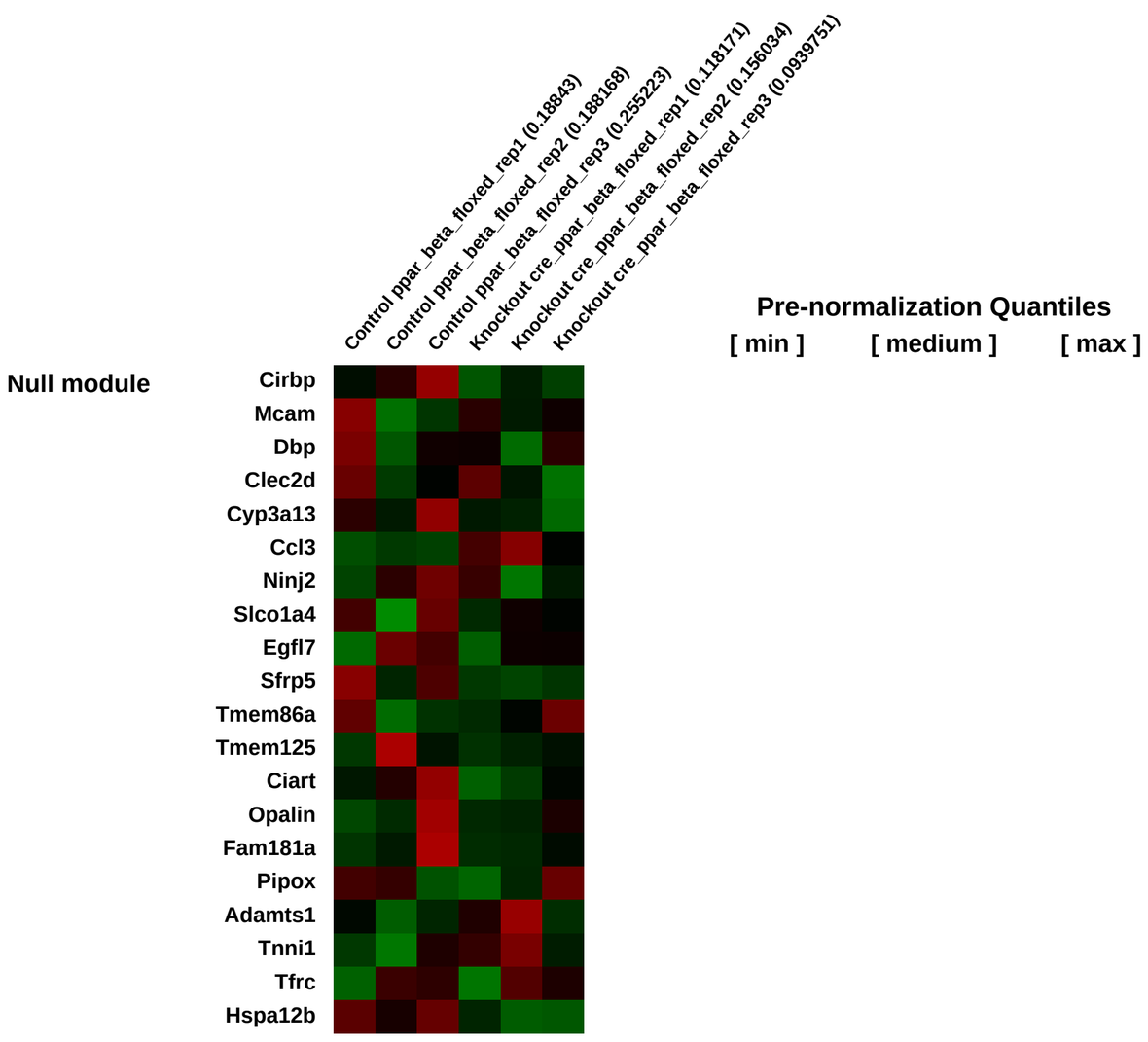

GEO Series "GSE16073" Expression Profiles

Num of samples in this series: 6

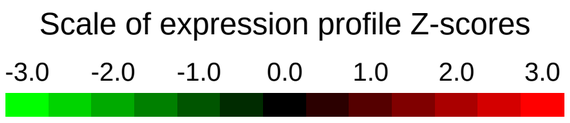

GEO Link:	http://www.ncbi.nlm.nih.gov/geo/query/acc.cgi?acc=GSE16073
Status:	Public on Oct 22 2009
Title:	Expression Data from Pten Null Fibroblasts
Organism:	Mus musculus
Experiment type:	Expression profiling by array
Platform:	GPL1261
Pubmed ID:	19847259
Summary & Design:	**Summary:** The tumor stroma is believed to contribute to some of the most malignant characteristics of epithelial tumors. However, signaling between stromal and tumor cells is complex and remains poorly understood. Here we show that genetic inactivation of Pten in stromal fibroblasts of mouse mammary glands accelerated the initiation, progression and malignant transformation of mammary epithelial tumors. Global gene expression profiling in mammary stromal cells identified a Pten-specific signature associated with massive extra-cellular matrix (ECM) remodeling, innate immune cell infiltraion and increased angiogenesis. Execution of this transcriptional program was mediated, in part, by the induction, phosphorylation and recruitment of Ets2 to target promoters. Remarkably, Ets2 inactivation in Pten stroma-deleted tumors was sufficient to decrease tumor growth and progression. These findings identify the Pten-Ets2 axis as a critical stroma-specific signaling pathway that suppresses mammary epithelial tumors. **Overall design:** Wild type and Pten null primary mammary fibroblasts isolated from 8 week old female mice were cultured, RNA was extracted and Affymetrix gene expression arrays were performed.

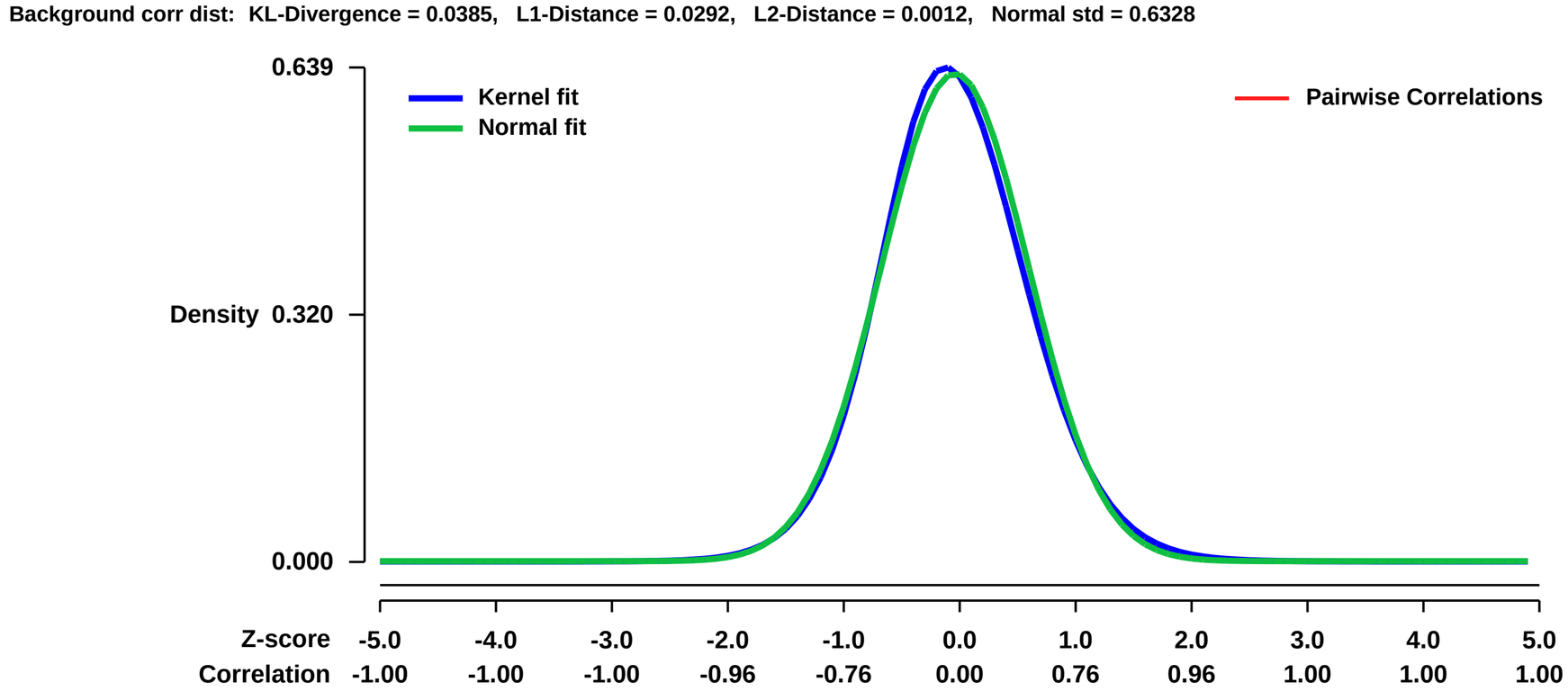

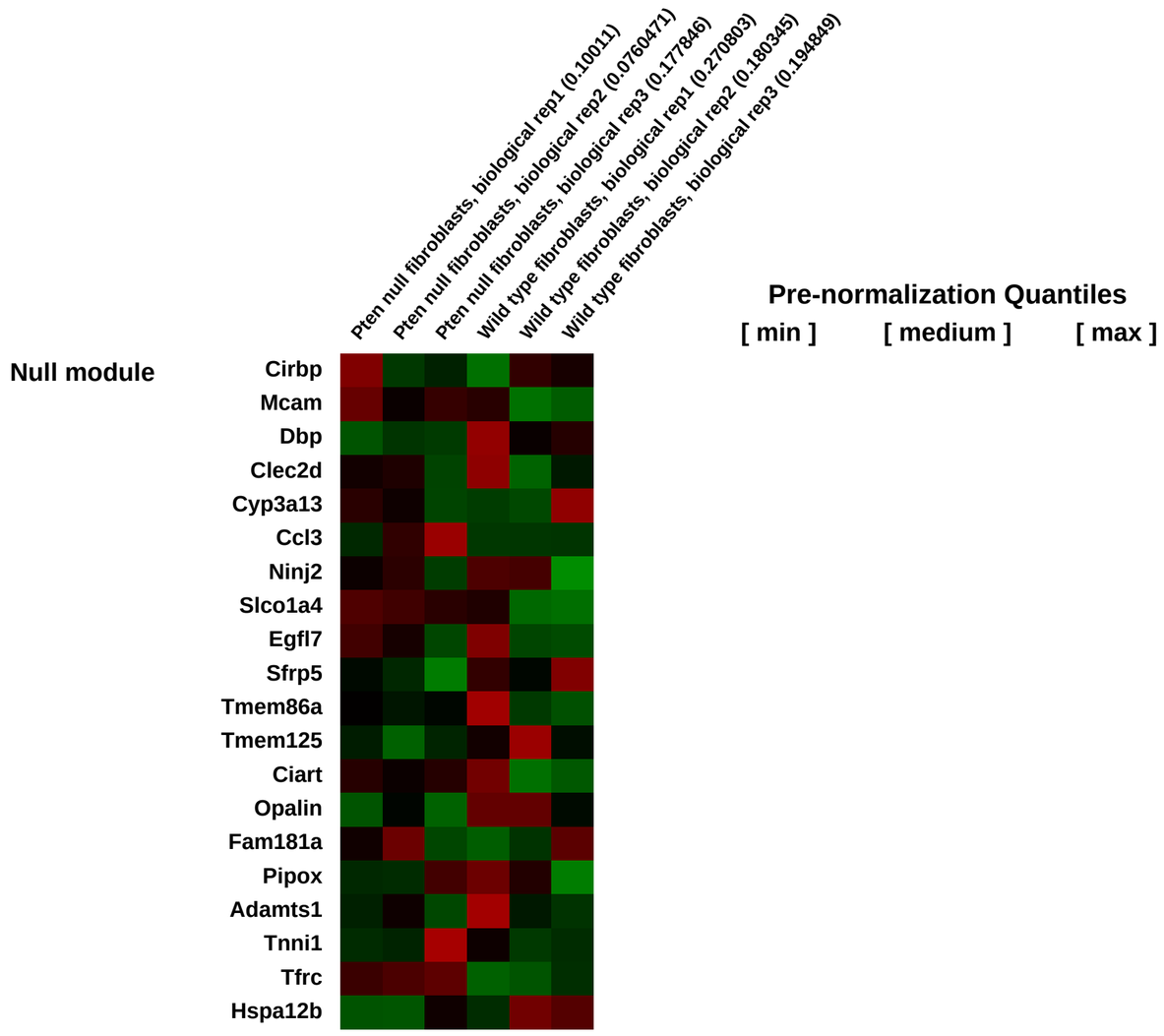

GEO Series "GSE16100" Expression Profiles

Num of samples in this series: 6

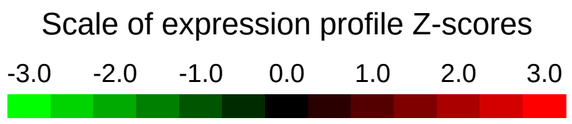

GEO Link:	http://www.ncbi.nlm.nih.gov/geo/query/acc.cgi?acc=GSE16100
Status:	Public on May 15 2009
Title:	Hematopoietic Stem Cells Reversibly Switch from Dormancy to Self-Renewal during Homeostasis and Repair
Organism:	Mus musculus
Experiment type:	Expression profiling by array
Platform:	GPL1261
Pubmed ID:	19062086
Summary & Design:	**Summary:** Bone marrow hematopoietic stem cells (HSCs) are crucial to maintain lifelong production of all blood cells. Although HSCs divide infrequently, it is thought that the entire HSC pool turns over every few weeks, suggesting that HSCs regularly enter and exit cell cycle. Here, we combine flow cytometry with label-retaining assays (BrdU and histone H2B-GFP) to identify a population of dormant mouse HSCs (d-HSCs) within the lin(-)Sca1+cKit+CD150+CD48(-)CD34(-) population. Computational modeling suggests that d-HSCs divide about every 145 days, or five times per lifetime. d-HSCs harbor the vast majority of multilineage long-term self-renewal activity. While they form a silent reservoir of the most potent HSCs during homeostasis, they are efficiently activated to self-renew in response to bone marrow injury or G-CSF stimulation. After re-establishment of homeostasis, activated HSCs return to dormancy, suggesting that HSCs are not stochastically entering the cell cycle but reversibly switch from dormancy to self-renewal under conditions of hematopoietic stress **Overall design:** cDNA microarray analysis was performed on sorted mouse bone marrow after 170 days of doxycycline treatment for CD34 Neg, Lin Neg, Sca1+, cKit+, CD150+, CD48 Neg, HSCs. HSCs were further sorted for GFP+ (LRC) and GFP neg (non-LRC) populations. Per condition, 3 independent biological replicates were analysed.

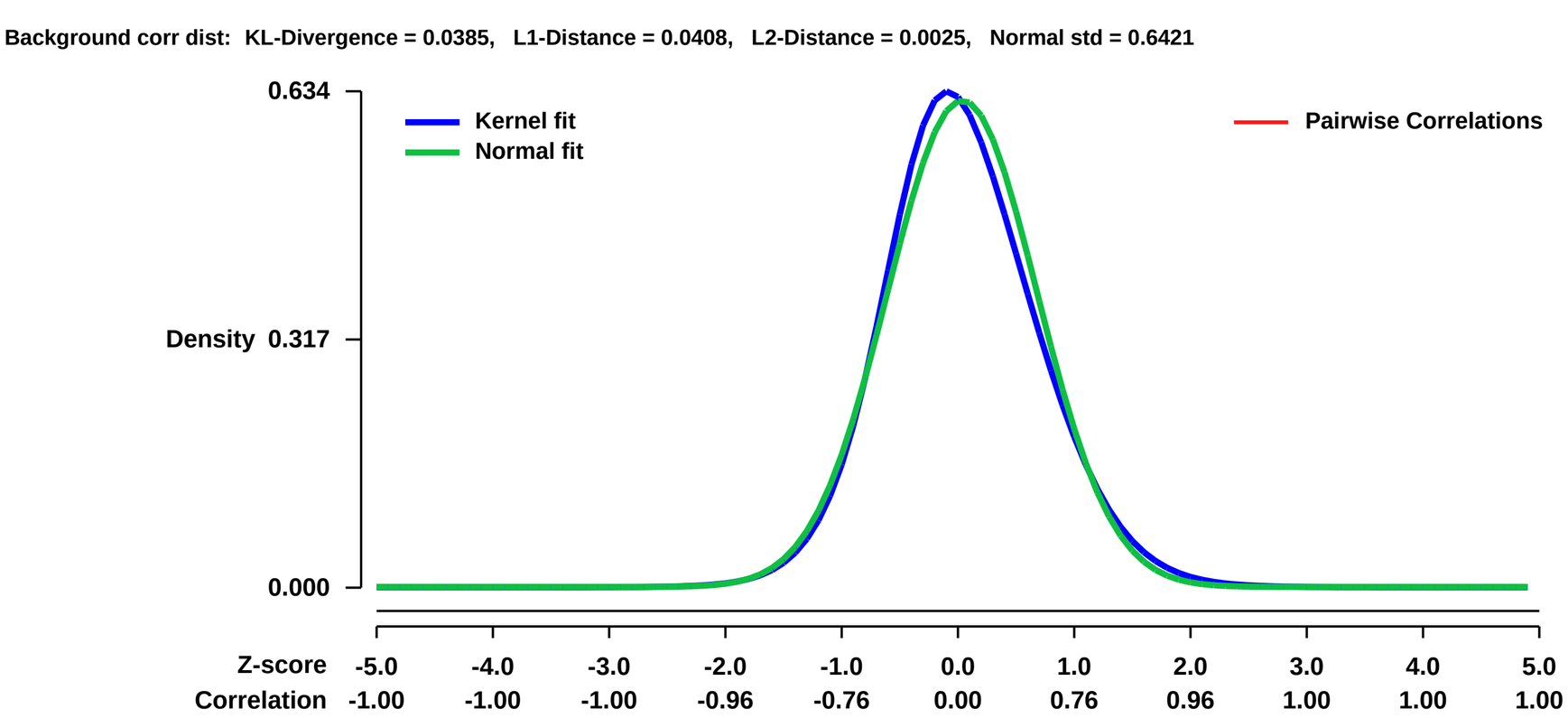

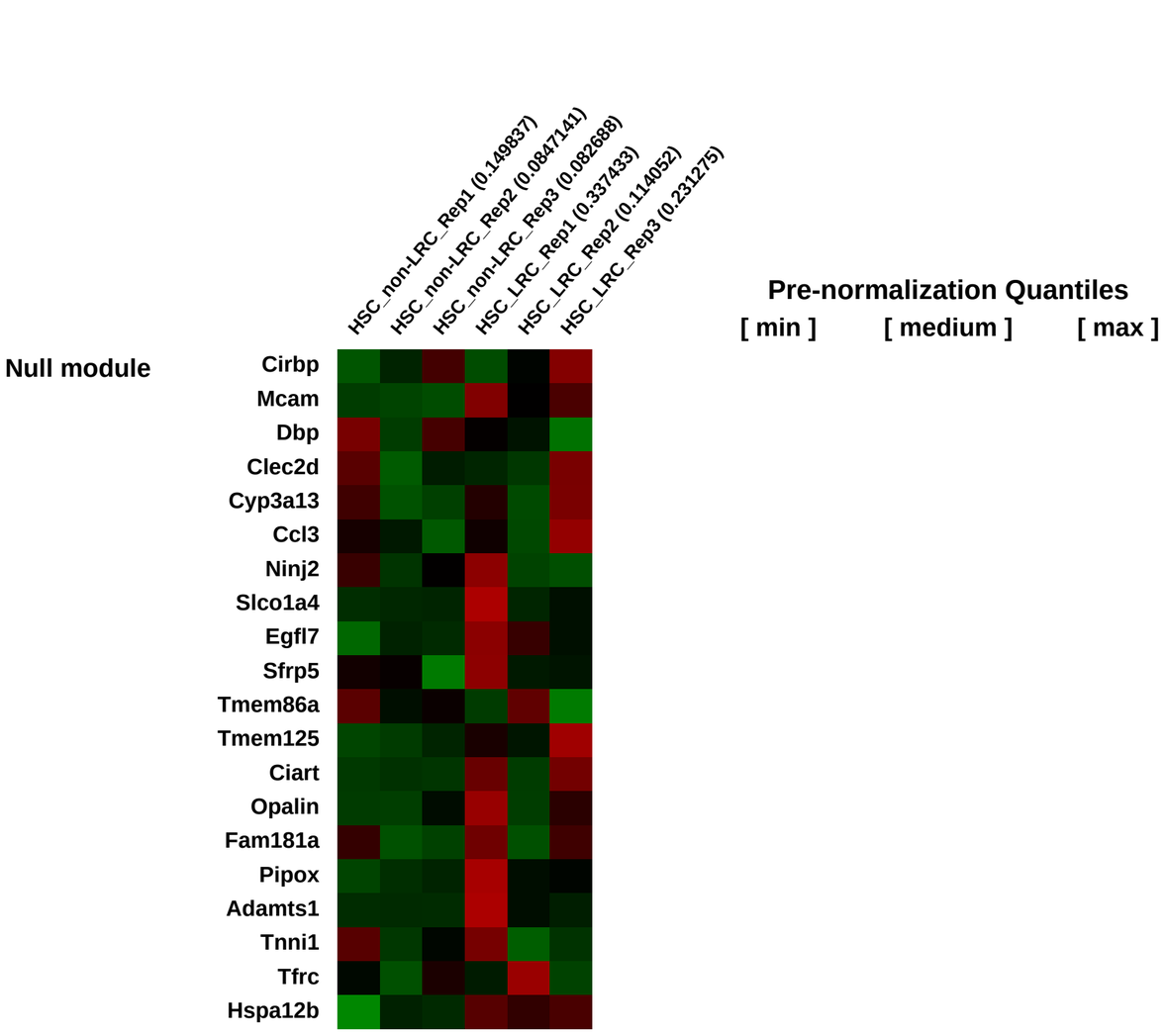

GEO Series "GSE16104" Expression Profiles

Num of samples in this series: 24

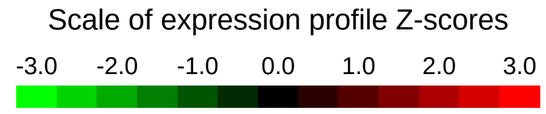

GEO Link:	**http://www.ncbi.nlm.nih.gov/geo/query/acc.cgi?acc=GSE16104**
Status:	**Public on Jul 01 2009**
Title:	**IL-1b responses in receptor-reconstituted AcP-deficient neurons**
Organism:	**Mus musculus**
Experiment type:	**Expression profiling by array**
Platform:	**GPL1261**
Pubmed ID:	**19481478**
Summary & Design:	**Summary:** **The purpose was to determine AcP- and AcPb-dependent gene responses to IL-1 by virally-reconstituting AcP-deficient mouse embryonic cortical neurons with CD25 (control), full length AcP, AcPb or the combination of both. A control population was transduced with a CD25-expressing virus. Half the samples were stimulated with IL-1-beta for four hours, RNA was analyzed by microarray.** **Overall design:** **Each in triplicate: CD25 cells, AcP cells, AcPb cells, AcP+AcPb cells. Cultures stimulated with IL-1b (10 ng/ml) for 4 hours then RNA was collected for processing and microarray analysis.**

Background corr dist: **KL-Divergence = 0.2710, L1-Distance = 0.0353, L2-Distance = 0.0030, Normal std = 0.2886**

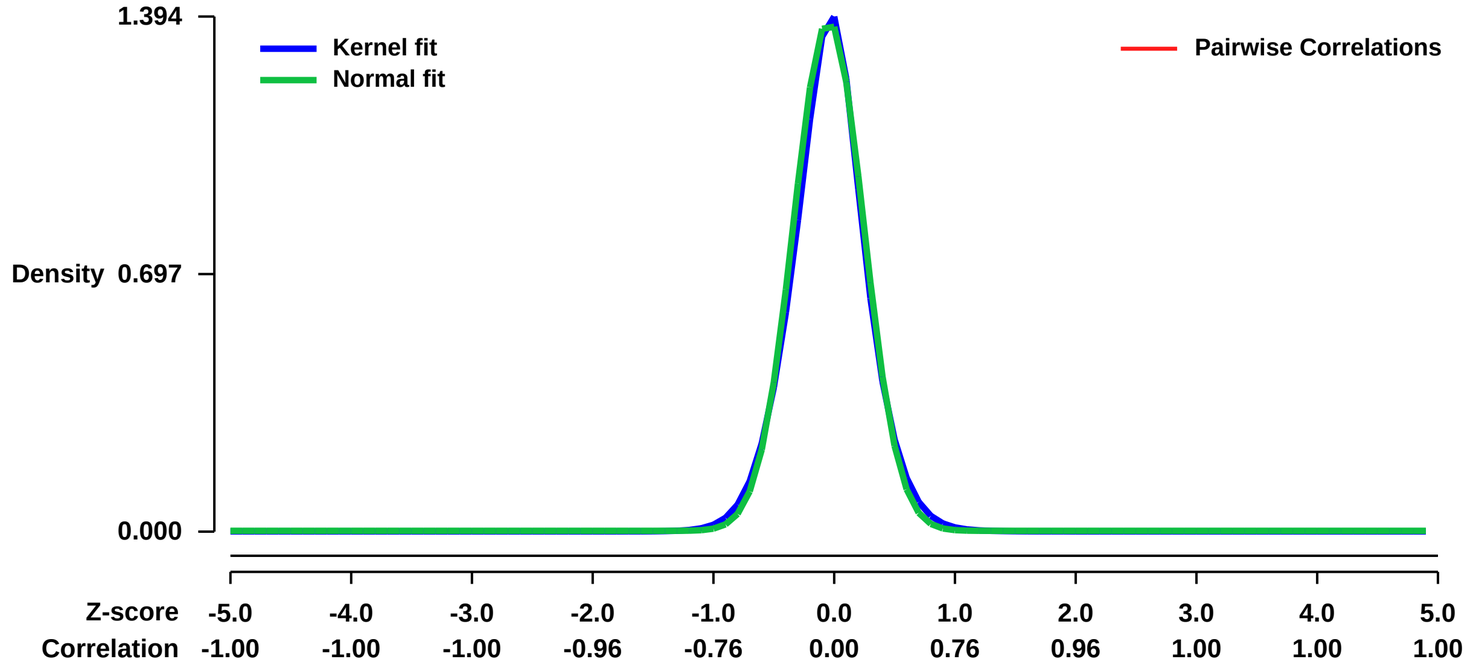

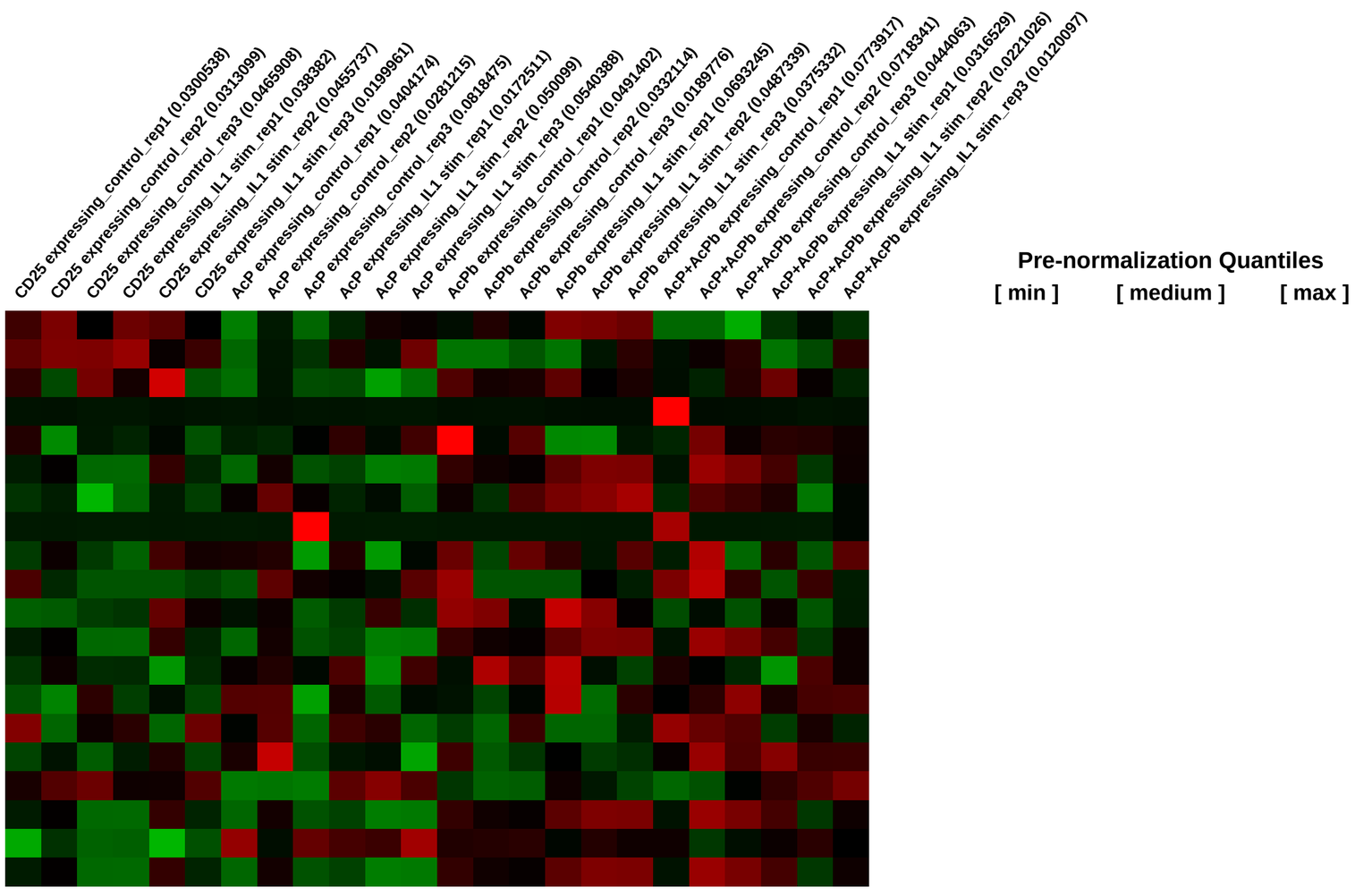

GEO Series "GSE16110" Expression Profiles

Num of samples in this series: 16

Scale of expression profile Z-scores

-3.0 -2.0 -1.0 0.0 1.0 2.0 3.0

GEO Link:	**http://www.ncbi.nlm.nih.gov/geo/query/acc.cgi?acc=GSE16110**
Status:	**Public on Jul 01 2009**
Title:	**Altered mouse mammary gland gene expression and tumor growth following chronic social isolation**
Organism:	**Mus musculus**
Experiment type:	**Expression profiling by array**
Platform:	**GPL1261**
Pubmed ID:	
Summary & Design:	**Summary:** **Clinical studies have revealed that social support improves the outcome of cancer patients while epidemiological studies suggest that social isolation increases the risk of death associated with several chronic diseases. However, the precise biological consequences of an unfavorable social environment have not been defined. To do so, robust, reproducible pre-clinical models are needed to study the mechanisms whereby an adverse environment impacts on gene expression and cancer biology. Because random assignment of inbred laboratory mice to well-defined social environments allows accurate and repeated measurements of behavioral and endocrine parameters, transgenic mice provide a pre-clinical framework with which to begin to determine gene-environment mechanisms. In this study, we found that female C3(1)/SV40 T-antigen mice deprived of social interaction from weaning exhibited increased expression of genes encoding key metabolic pathway enzymes in the pre-malignant mammary gland. Chronic social isolation was associated with upregulated fatty acid synthesis and glycolytic pathway gene expression - both pathways known to contribute to increased breast cancer growth. Consistent with the expression of metabolic genes, isolated mice subsequently developed significantly larger mammary gland tumors compared to group-housed mice. Endocrine evaluation confirmed that isolated mice developed a heightened corticosterone stress response compared to group-housed mice. Together, these transdisciplinary studies show for the first time that an adverse social environment is associated with altered mammary gland gene expression and tumor growth. Moreover, the identification of specific alterations in metabolic pathways favoring tumor growth suggests potential molecular biomarkers and/or targets (e.g. fatty acid synthesis) for preventive intervention in breast cancer.** **Overall design:** **SV40 Tag mice we isolated or grouped at weaning. Mouse mammary glands were rapidly excised at necropsy and immediatley flash frozen to detect difference in gene expression between thoraci MG from isolated versus group-housed female mice.**

Background corr dist: KL-Divergence = 0.0385, L1-Distance = 0.0261, L2-Distance = 0.0009, Normal std = 0.6020

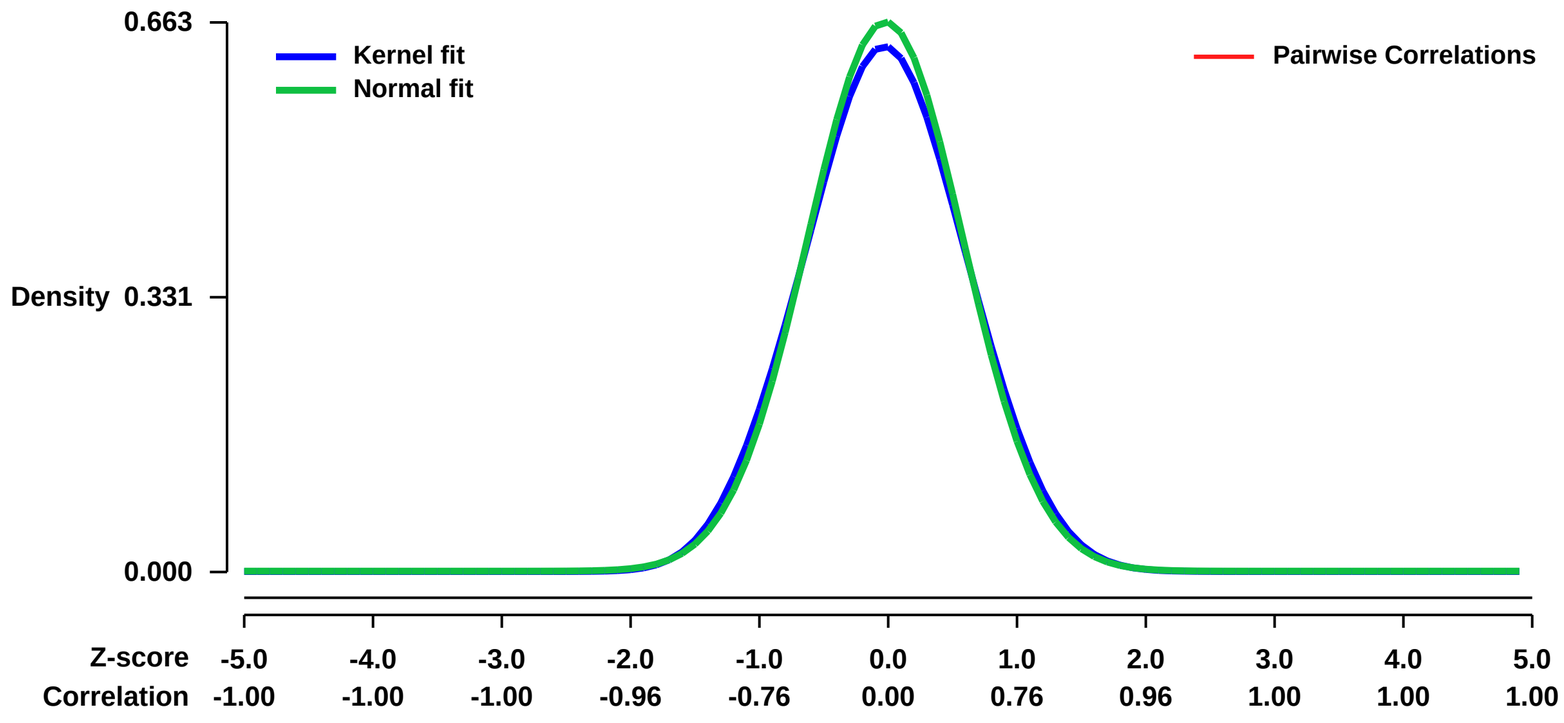

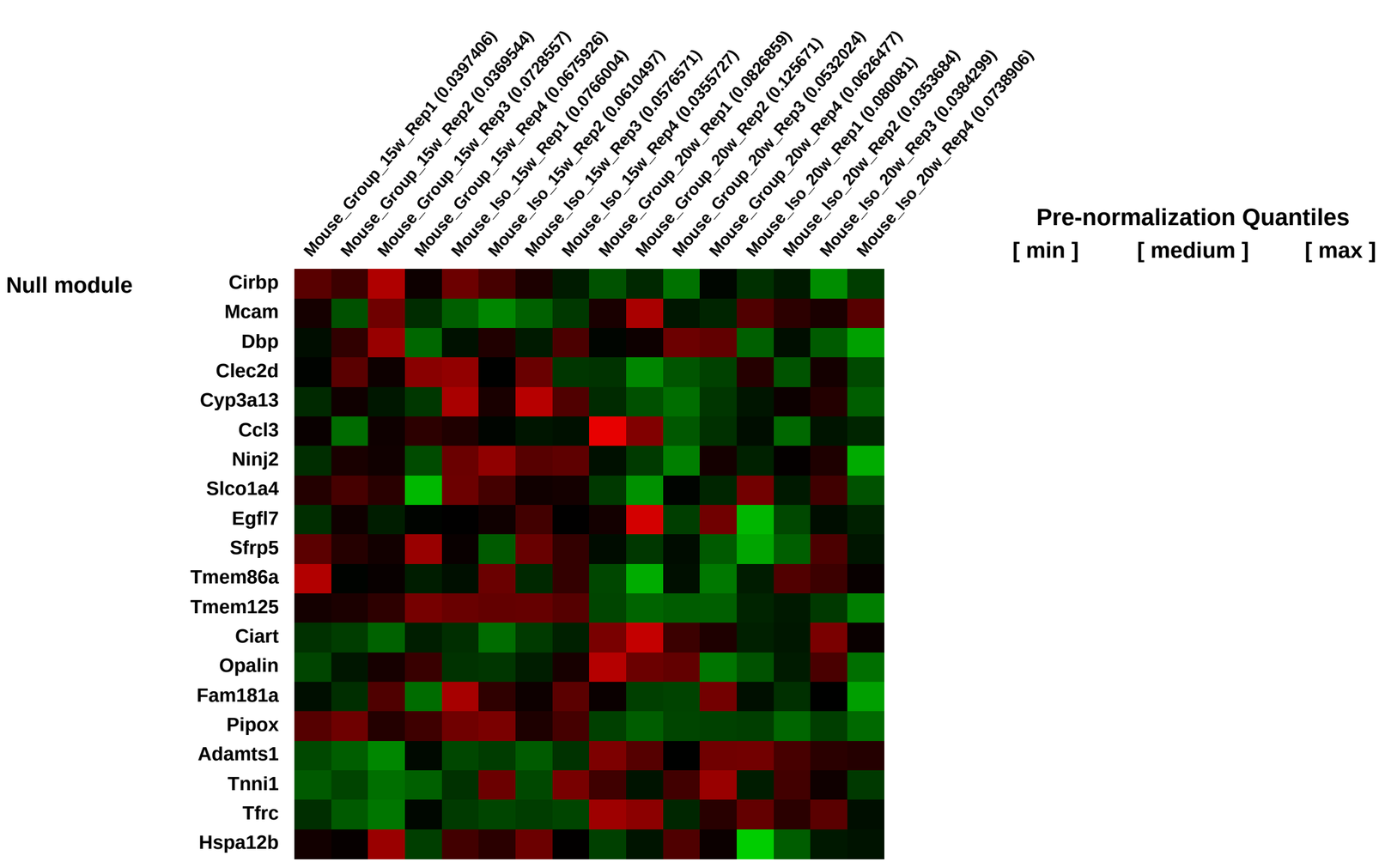

GEO Series "GSE16364" Expression Profiles

Num of samples in this series: 6

Scale of expression profile Z-scores

-3.0 -2.0 -1.0 0.0 1.0 2.0 3.0

GEO Link:	http://www.ncbi.nlm.nih.gov/geo/query/acc.cgi?acc=GSE16364
Status:	Public on Feb 05 2010
Title:	Polycomb-like 2 associates with PRC2 and is required for mouse embryonic stem cell
Organism:	Mus musculus
Experiment type:	Expression profiling by array
Platform:	GPL1261
Pubmed ID:	20144788
Summary & Design:	**Summary:** Polycomb group (PcG) proteins are highly conserved epigenetic transcriptional repressors important for the control of numerous developmental gene expression programs and have recently been implicated in the modulation of embryonic stem cell (ESC) identity. We identified the PcG protein PCL2 (polycomb-like 2) in a genome-wide screen for novel regulators of self-renewal and pluripotency and predicted that it would play an important role in mouse ESC fate determination. Using multiple biochemical strategies, we provide evidence that PCL2 is a novel Polycomb Repressive Complex 2 (PRC2)-associated protein in mouse ESCs. Knockdown of Pcl2 in ESCs resulted in heightened self-renewal characteristics, defects in differentiation and altered patterns of histone methylation. Through integration of global gene expression and promoter occupancy analyses of both PCL2 and PRC2 components EZH2 and SUZ12, we have predicted PCL2 target genes and formulated regulatory networks describing the role of PCL2 both in modulating transcription of ESC self-renewal genes in undifferentiated ESCs as well as developmental regulators during early commitment and differentiation. **Overall design:** Cells were stably expressing Pcl2 shRNA or shRNA mismatch control sequences. Hybridizations of three biological replicates for both the control and Pcl2 shRNA clone were performed.

Background corr dist: KL-Divergence = 0.0389, L1-Distance = 0.0217, L2-Distance = 0.0005, Normal std = 0.6242

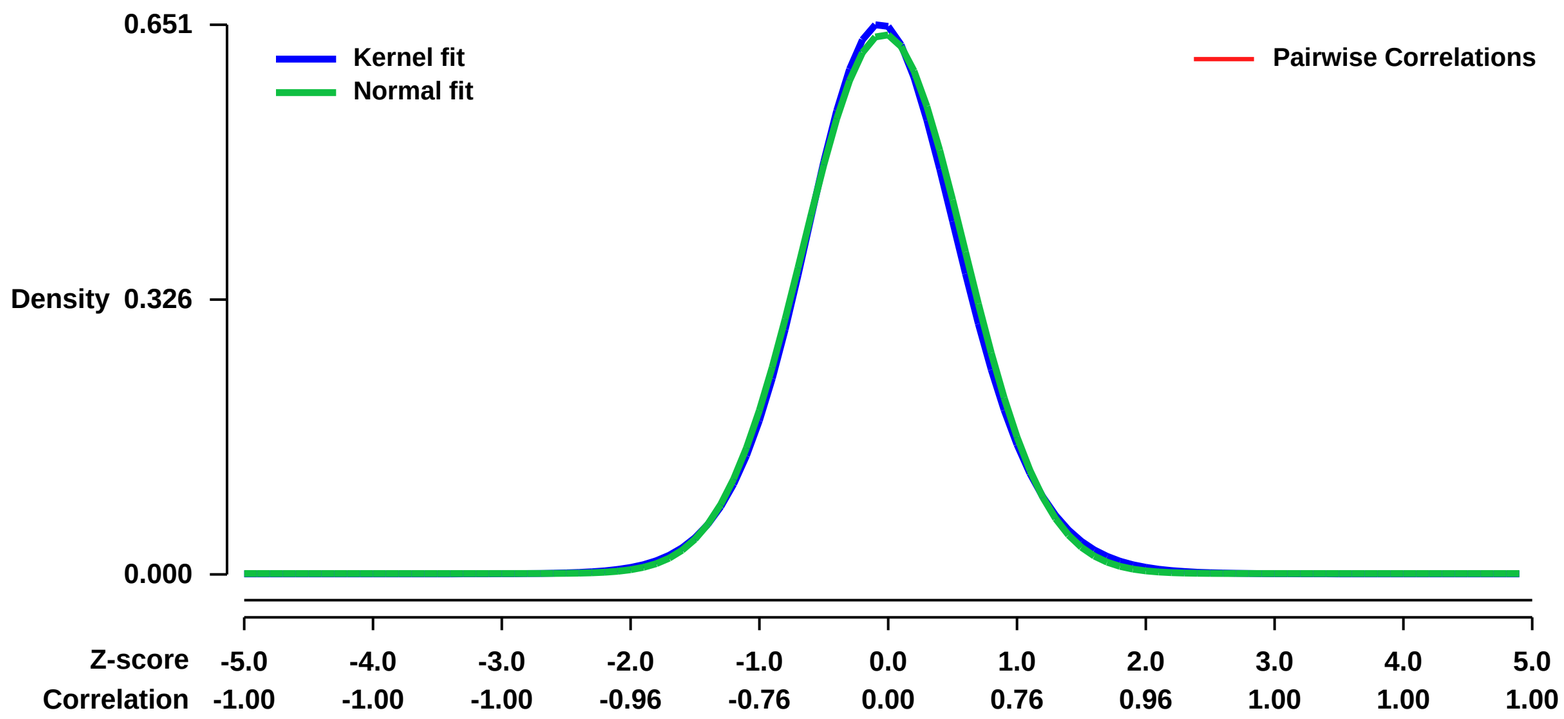

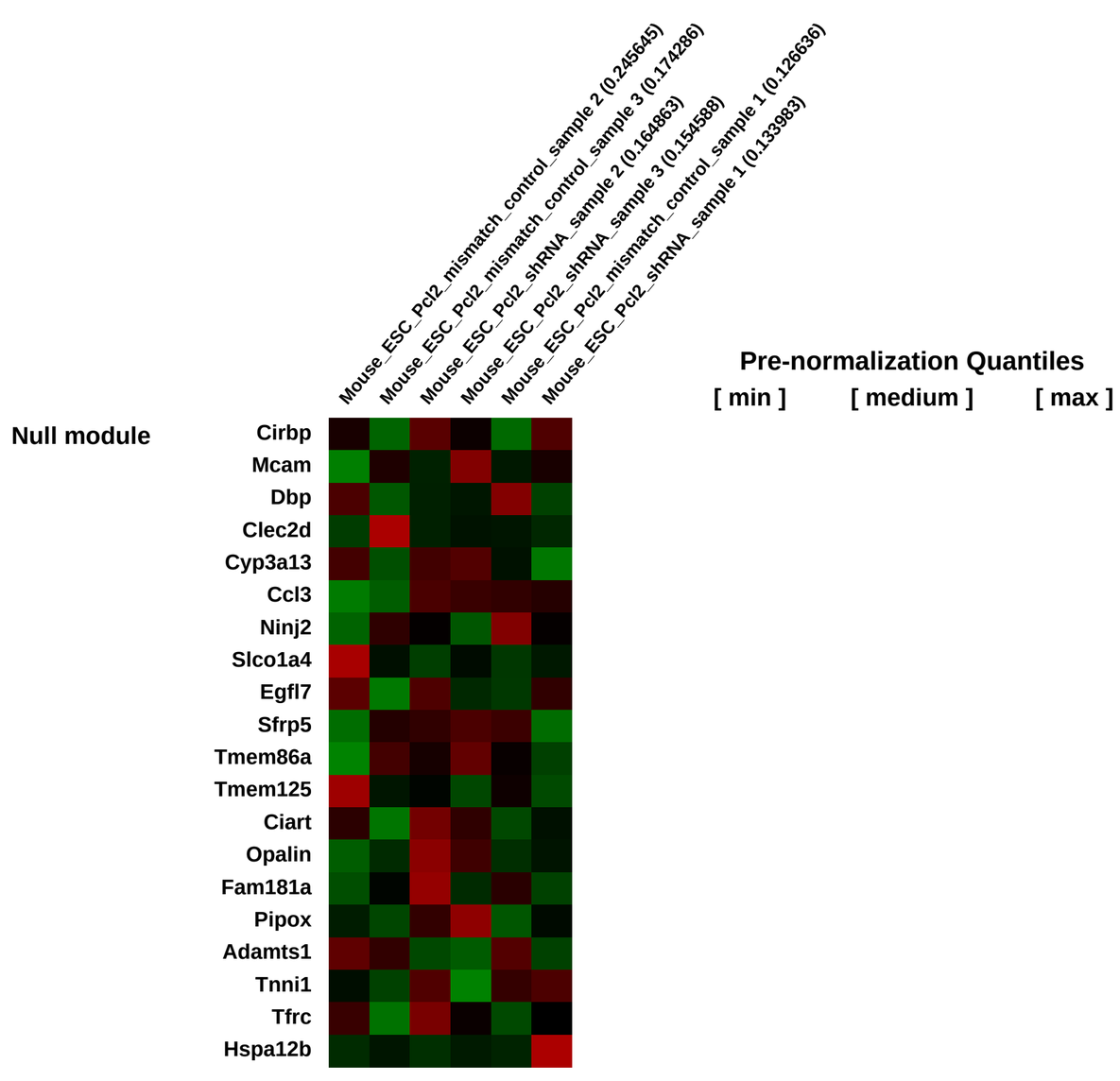

GEO Series "GSE16377" Expression Profiles

Num of samples in this series: 6

Scale of expression profile Z-scores

-3.0 -2.0 -1.0 0.0 1.0 2.0 3.0

GEO Link:	**http://www.ncbi.nlm.nih.gov/geo/query/acc.cgi?acc=GSE16377**
Status:	**Public on Jun 01 2010**
Title:	**wild type mouse lung control vs. high fat diet**
Organism:	**Mus musculus**
Experiment type:	**Expression profiling by array**
Platform:	**GPL1261**
Pubmed ID:	
Summary & Design:	**Summary:** **To study the effects of a high fat diet on the mouse lung transcrptional profile.** **Overall design:** **6 samples were analyzed. 3 wild type mice on a control diet (lung samples) vs. 3 wild type mice on a high fat diet (lung samples).**

Background corr dist: **KL-Divergence = 0.0411, L1-Distance = 0.0234, L2-Distance = 0.0007, Normal std = 0.6141**

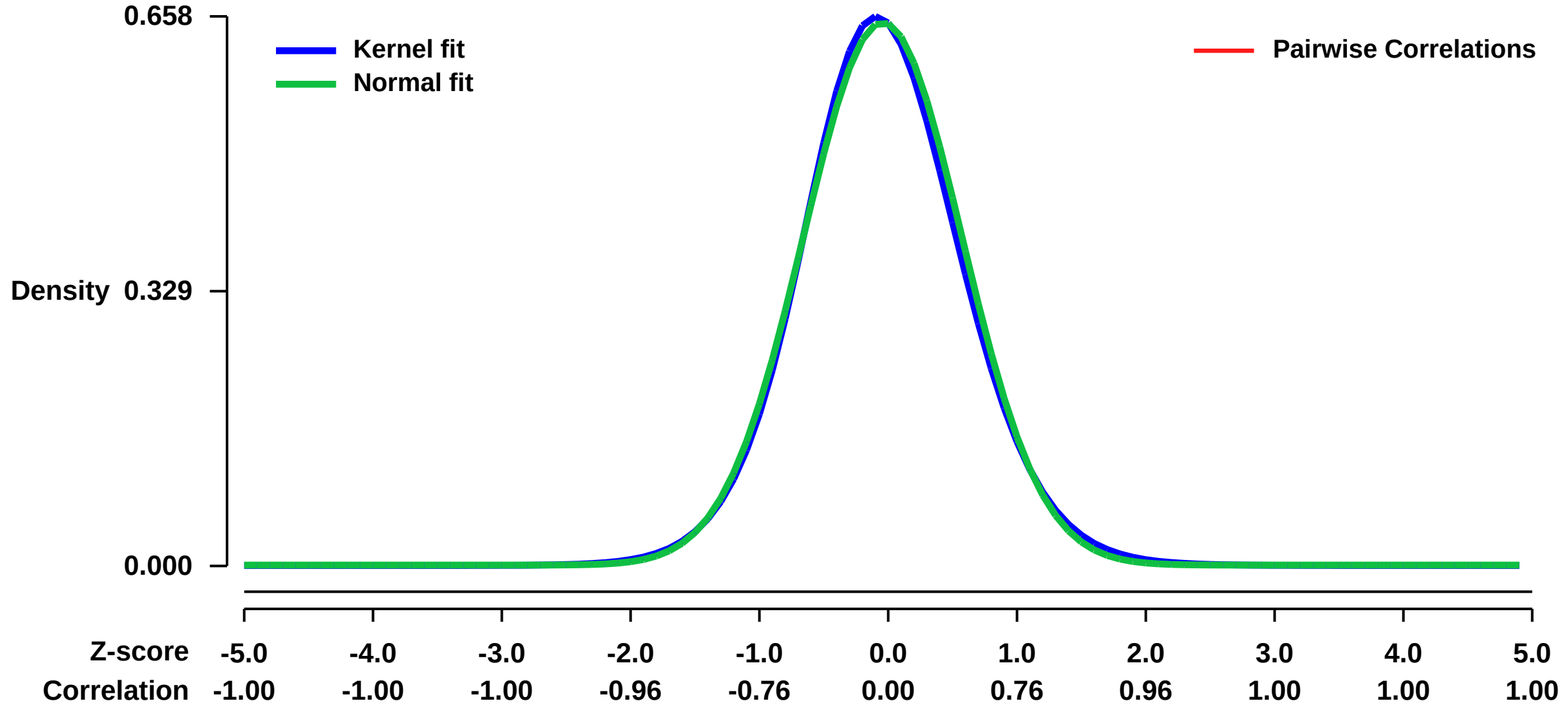

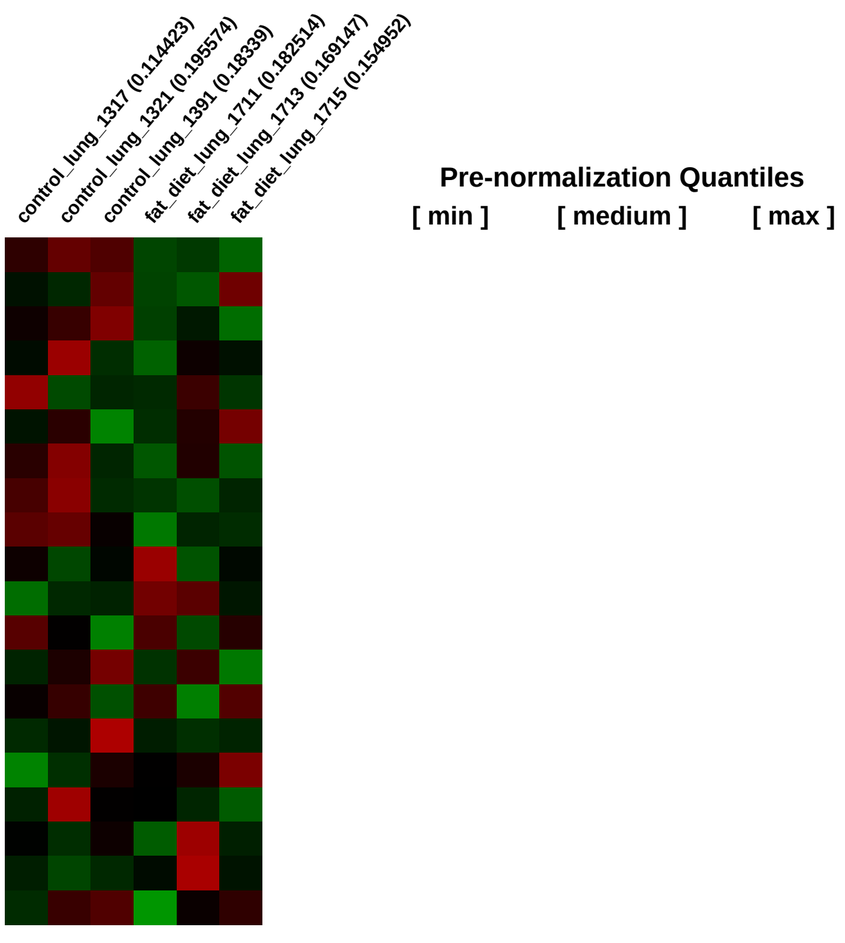

GEO Series "GSE16380" Expression Profiles

Num of samples in this series: 8

Scale of expression profile Z-scores

-3.0 -2.0 -1.0 0.0 1.0 2.0 3.0

GEO Link:	http://www.ncbi.nlm.nih.gov/geo/query/acc.cgi?acc=GSE16380
Status:	Public on Jan 28 2010
Title:	Gene expression analyses of C/EBPb knockout in stem/progenitor cell populations
Organism:	Mus musculus
Experiment type:	Expression profiling by array
Platform:	GPL1261
Pubmed ID:	20054865
Summary & Design:	**Summary:** CCAAT/enhancer binding protein beta (C/EBPb) is a member of a family of highly conserved transcription factors that regulates numerous genes involved in proliferation and differentiation in a variety of tissues. C/EBPb is deregulated in human breast cancer and germline deletion of this gene results in multiple defects in mammary gland development. We hypothesized that C/EBPb regulates mammary stem cell self-renewal, maintenance and/or differentiation through the regulation of multiple target genes that coordinate mammary gland development. Utilizing both a germline knockout mouse model and a conditional knockout strategy, we demonstrated that mammosphere formation was significantly decreased in C/EBPb-deficient mammary epithelial cells (MECs). The ability of C/EBPb-deleted MECs to regenerate the mammary gland in vivo was severely impaired when transplanted at limiting dilution. Furthermore, serial transplantation of C/EBPb-null mammary tissue resulted in decreased outgrowth potential when compared to wildtype, and an early senescence phenotype. Flow cytometric analysis revealed that C/EBPb-null MECs contain a lower frequency of repopulating stem cells accompanied by an increase in committed, differentiated luminal cells as compared to wildtype. Microarray analysis of stem/progenitor cell populations was performed and revealed an alteration in cell fate specification in C/EBPb-null glands, exemplified by the aberrant expression of basal markers in the luminal cell compartment. Collectively, our studies demonstrate that C/EBPb is a critical regulator of mammary stem cell differentiation, and an important determinant of luminal cell fate specification. **Keywords:** multiple group comparison **Overall design:** To identify potential signaling pathways regulated by C/EBPb in stem/progenitor cells, microarray analysis was performed on two stem/progenitor cell subpopulations. For this analysis, subpopulations defined by LIN-CD24+CD29hi and LIN-CD24hiCD29lo were FACS sorted from wildtype and germline C/EBPb-/- glands, and RNA was isolated from each group.

Background corr dist: KL-Divergence = 0.0627, L1-Distance = 0.0241, L2-Distance = 0.0009, Normal std = 0.5244

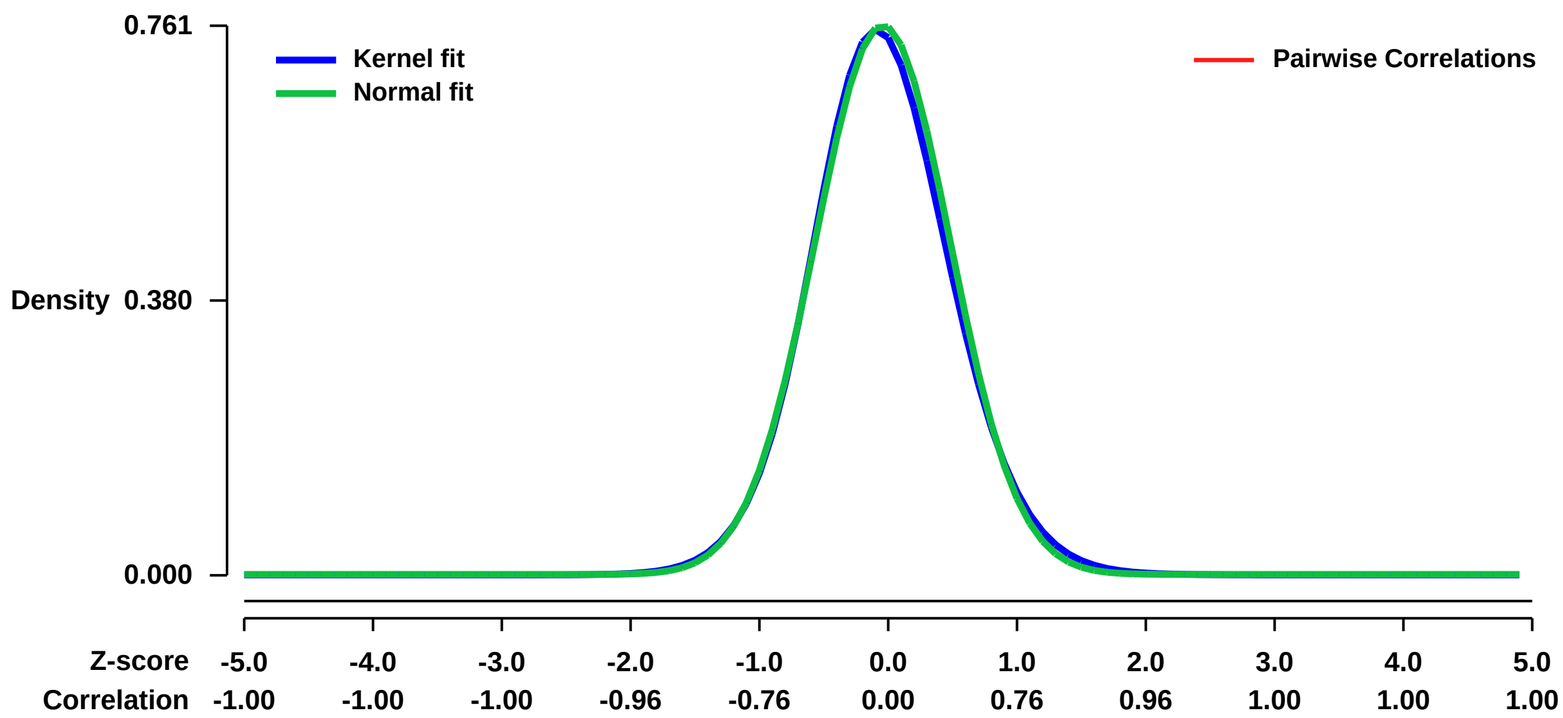

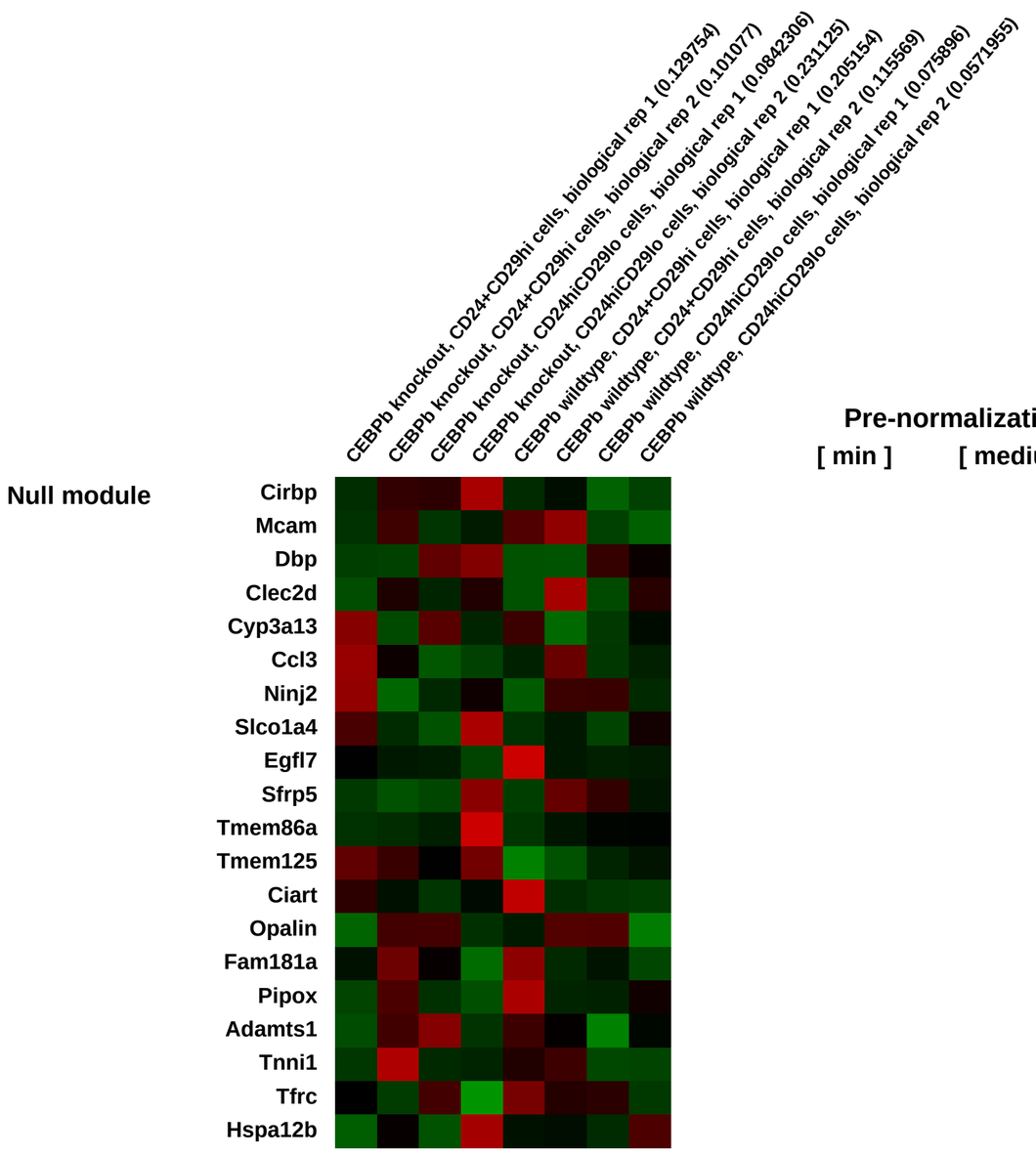

GEO Series "GSE16389" Expression Profiles

Num of samples in this series: 18

Scale of expression profile Z-scores

-3.0 -2.0 -1.0 0.0 1.0 2.0 3.0

GEO Link:	http://www.ncbi.nlm.nih.gov/geo/query/acc.cgi?acc=GSE16389
Status:	Public on Sep 01 2009
Title:	Global analysis of gene expression by SV40 T antigen in the mouse small intestine epithelium
Organism:	Mus musculus
Experiment type:	Expression profiling by array
Platform:	GPL1261
Pubmed ID:	19570859
Summary & Design:	**Summary:** SV40 large T antigen (TAg) contributes to cell transformation, in part, by targeting two well characterized tumor suppressors, pRb and p53. TAg expression affects the transcriptional circuits controlled by Rb and by p53. We have performed a microarray analysis to examine the global change in gene expression induced by wild-type TAg and TAg-mutants, in an effort to link changes in gene expression to specific transforming functions. For this analysis we have used enterocytes from the mouse small intestine expressing TAg. Expression of TAg in the mouse intestine results in hyperplasia and dysplasia. Our analysis indicates that practically all gene expression regulated by TAg in enterocytes is dependent upon its binding and inactivation of the Rb-family proteins. **Overall design:** Laser capture microdissection (LCM) was used to isolate villus enterocytes from three independent non-transgenic mice, four wild-type TAg transgenic mice, five N136 transgenic mice, three D44N transgenic mice and three 3213 transgenic mice. Total RNA was extracted from the enterocytes with the Pico Pure kit and amplified twice with the Ribo Amp kit (Arcturus). Amplified RNA was processed by the Genomics and Proteomics Core Laboratories at the University of Pittsburgh and hybridized to the Affymetrix GeneChip Mouse Genome 430 2.0 array. MAS 5.0 was used to obtain the present/absent calls and CEL files were normalized by RMA to obtain log2 expression values.

Background corr dist: KL-Divergence = 0.1739, L1-Distance = 0.0469, L2-Distance = 0.0050, Normal std = 0.3505

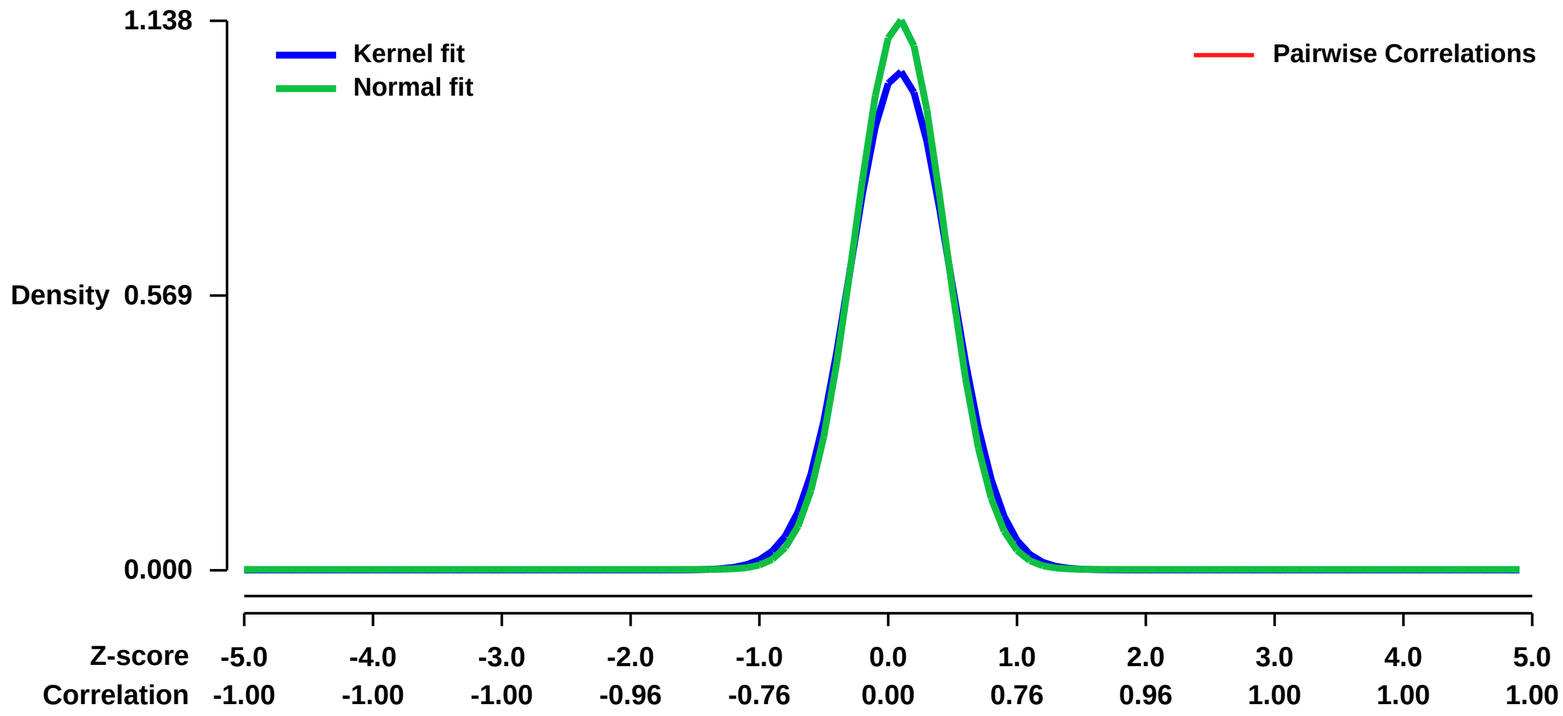

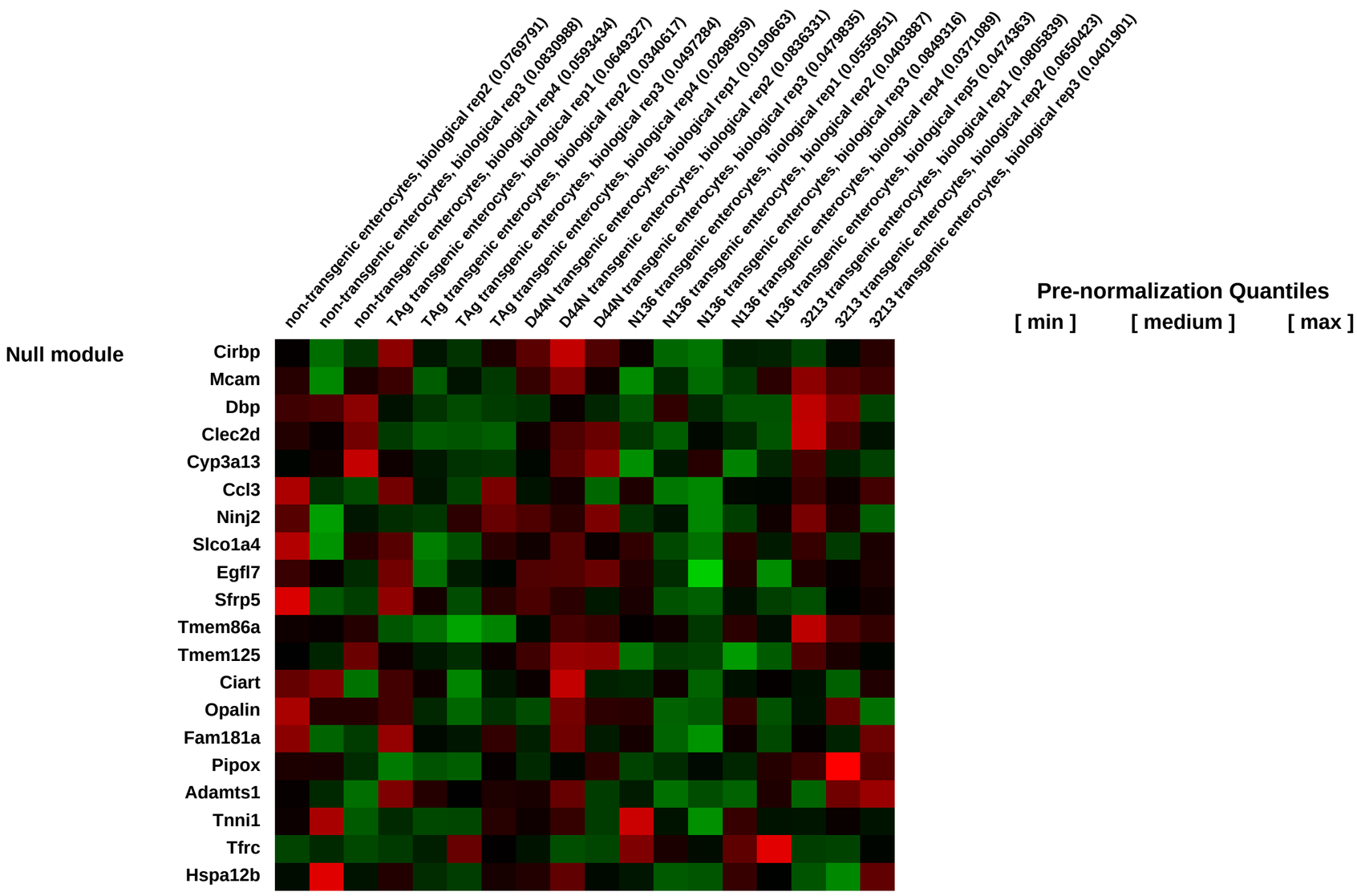

GEO Series "GSE16454" Expression Profiles

Num of samples in this series: 24

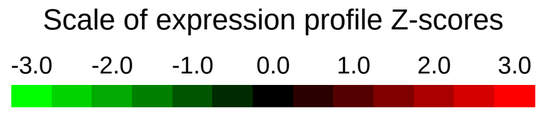

GEO Link:	**http://www.ncbi.nlm.nih.gov/geo/query/acc.cgi?acc=GSE16454**
Status:	**Public on Dec 17 2009**
Title:	**Gene expression data from small intestines**
Organism:	**Mus musculus**
Experiment type:	**Expression profiling by array**
Platform:	**GPL1261**
Pubmed ID:	**20016602**
Summary & Design:	**Summary:** **Rb and E2F are thought to play antagonistic roles in celll proliferation. However, this model is based mostly from in vitro cell culture systems. We used small intestines to test this model in vivo.** **We found that deletion of E2f1-3 in the small intestine of mice suppressed the ectopic expression of E2F targets and cell proliferation caused by Rb-deficiency. Surprisingly, E2f1-3 deletion failed to arrest the proliferation of intestinal cells containing an intact Rb gene, and instead led to E2F target derepression and apoptosis.** **Overall design:** **Total RNA of crypts and villi from wild-type, Rb-/-, E2f1-/-, E2f2-/-, E2f3-/-, E2f1-/-, E2f2-/-, and E2f3-/- small intestines. Small intestines were harvested 7 days after mice were injected intraperitoneally with beta-napthoflavone.**

Background corr dist: KL-Divergence = 0.1386, L1-Distance = 0.0283, L2-Distance = 0.0011, Normal std = 0.3877

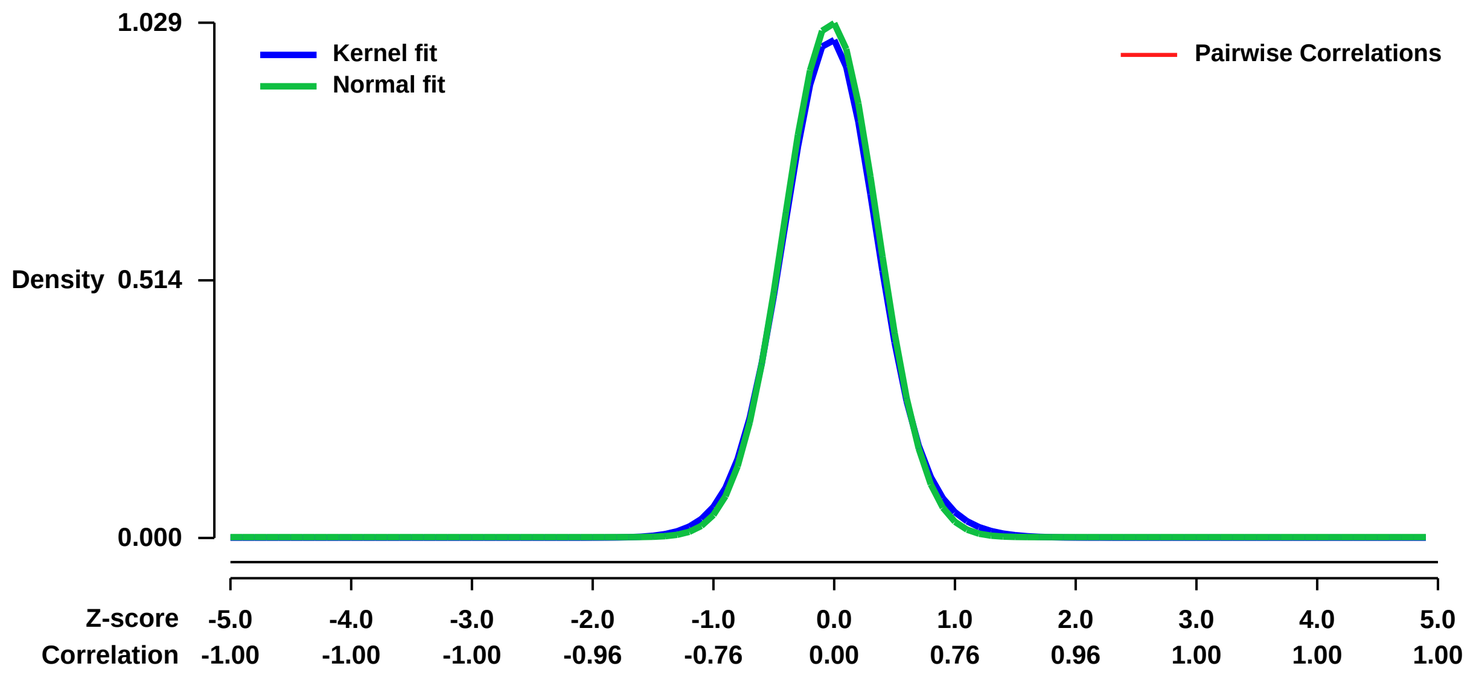

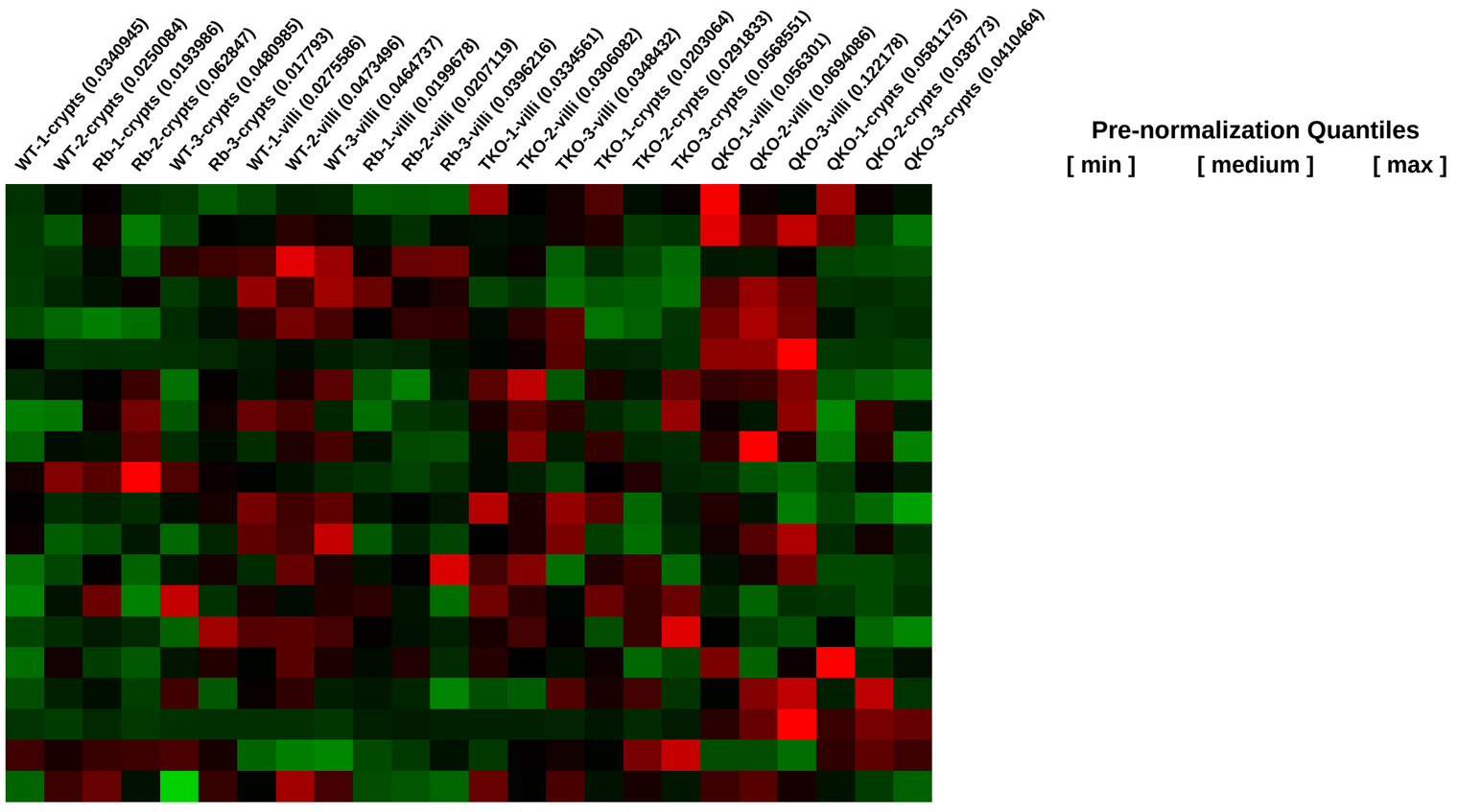

GEO Series "GSE16486" Expression Profiles

Num of samples in this series: 9

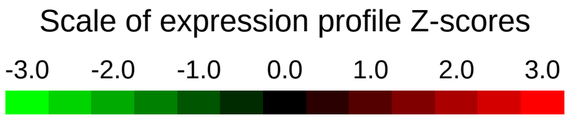

GEO Link:	http://www.ncbi.nlm.nih.gov/geo/query/acc.cgi?acc=GSE16486
Status:	Public on Jun 08 2009
Title:	Gene expression data from gastrocnemius muscle (m.Gas) in young adult mice
Organism:	Mus musculus
Experiment type:	Expression profiling by array
Platform:	GPL1261
Pubmed ID:	20403060
Summary & Design:	**Summary:** This study examined the effects of castration and testosterone replacement on global differential gene transcription in the gastrocnemius muscle (m.Gas) in young adult mice over 14-days. **Overall design:** Each of the 3 treatment groups was composed of 3 independent biological replicates, totaling 9 arrays. Equal amounts of the highest quality total RNA (4 ´µg) from three animals were pooled for each biological replicate, totaling the use of 27 animals in the 9-array experiment. The balanced design of this study enabled the use of a 1-way ANOVA, which was used to statistically determine which of the >34,000 genes (>45,000 probes) were differentially expressed between groups. The three pair-wise comparisons were: Castration vs. Sham (castration (C) effect); Testosterone vs. Castration (testosterone replacement (T) effect); and Testosterone vs. Sham (overall effects).

Background corr dist: KL-Divergence = 0.0262, L1-Distance = 0.0463, L2-Distance = 0.0036, Normal std = 0.7084

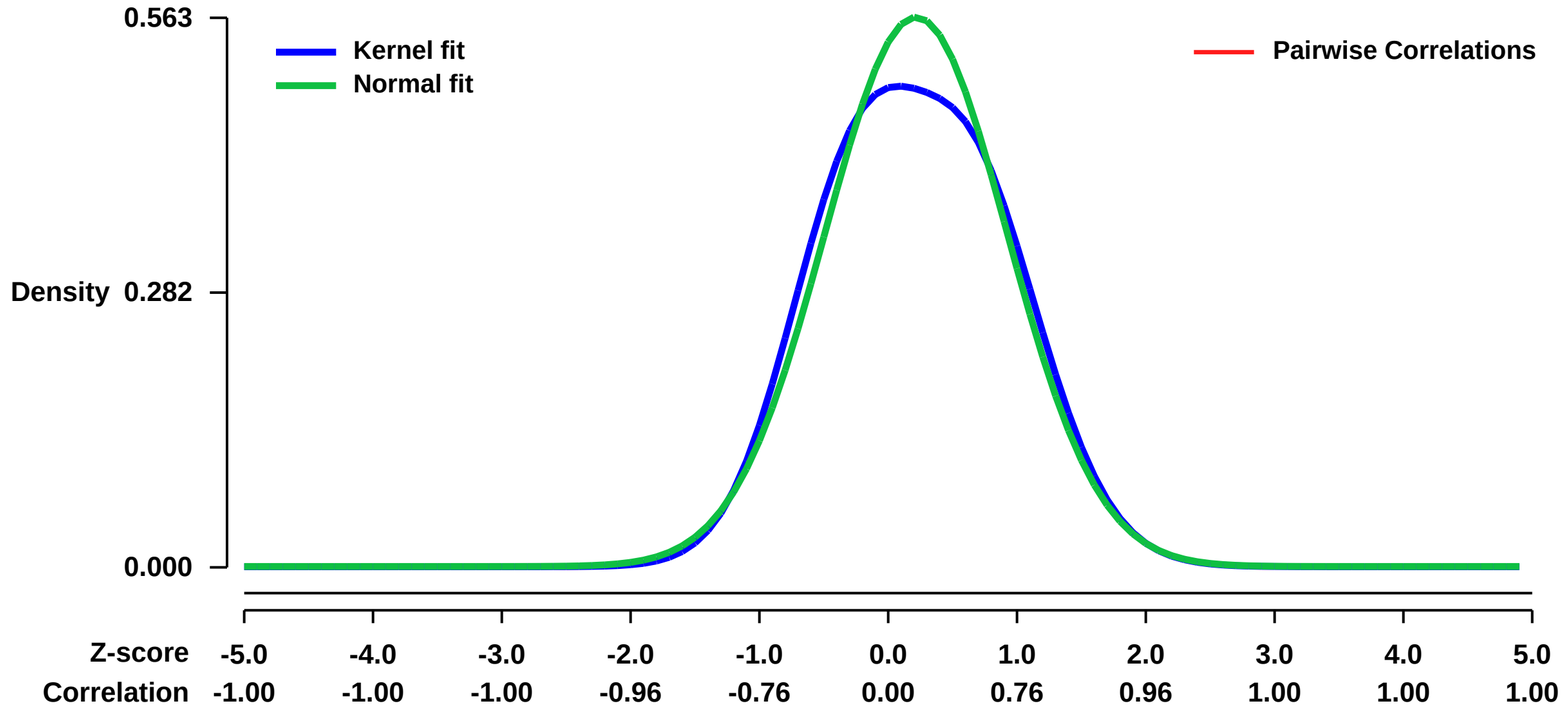

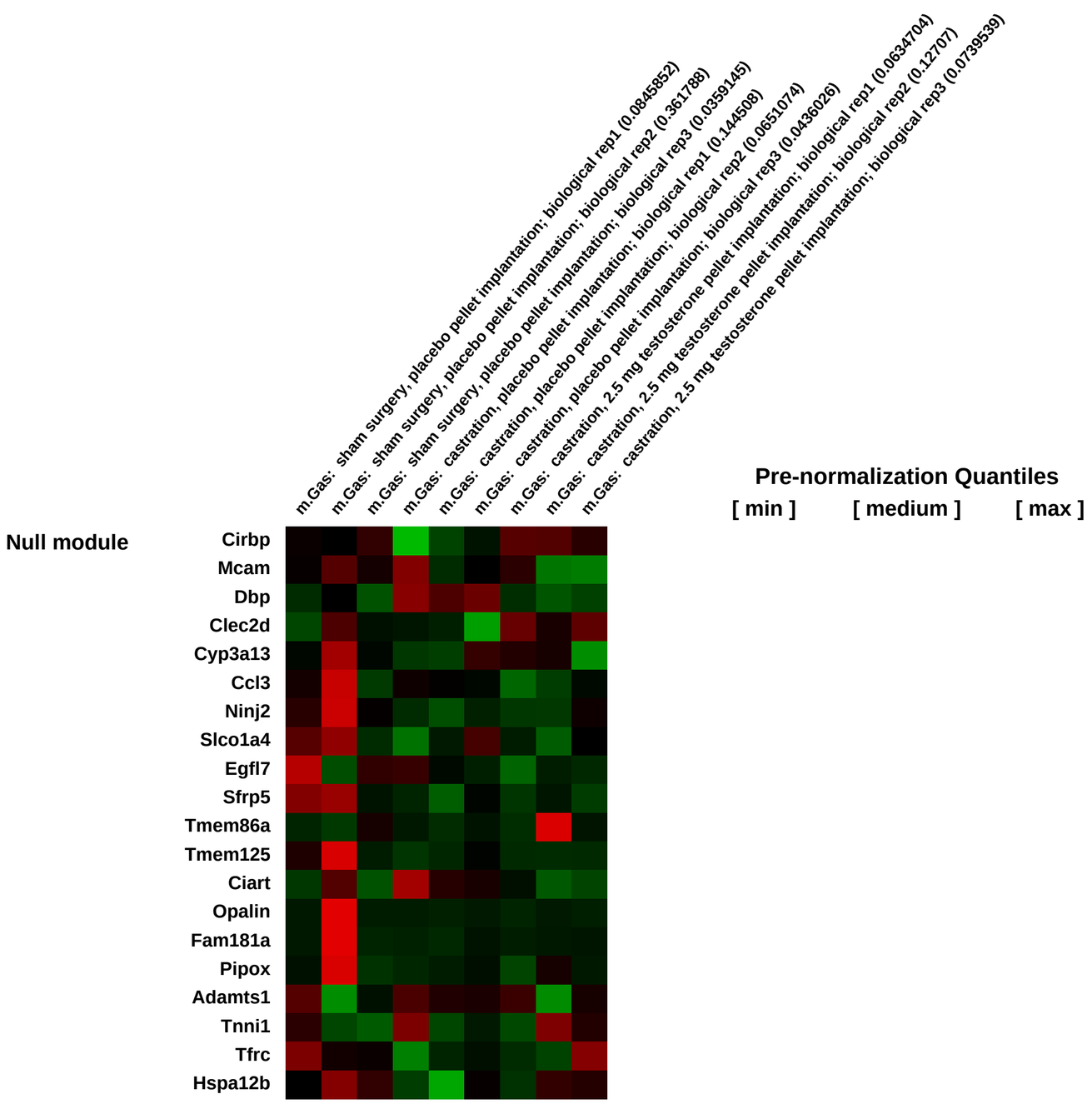

GEO Series "GSE16533" Expression Profiles

Num of samples in this series: 20

Scale of expression profile Z-scores

-3.0 -2.0 -1.0 0.0 1.0 2.0 3.0

GEO Link:	http://www.ncbi.nlm.nih.gov/geo/query/acc.cgi?acc=GSE16533
Status:	Public on Jun 10 2010
Title:	Expression data from lenses triply deficient for E2F1, E2F2, and E2F3 transcription factors
Organism:	Mus musculus
Experiment type:	Expression profiling by array
Platform:	GPL1261
Pubmed ID:	21185283
Summary & Design:	**Summary:** The E2F family consists of transcriptional repressors and activators that control cell proliferation. In the classic paradigm of cell cycle regulation, the three activators, E2F1, E2F2 and E2F3, are invariably depicted as the final components of a CDK/Rb signaling cascade that executes the transcriptional program necessary to commit cells to enter S phase. Unexpectedly, we find through analysis of Affymetrix expression array data that mature lens epithelial cells deficient for E2F1-3 fail to repress cell cycle-regulated genes (and other targets of E2F) and that this corresponds with subsequent apoptosis and cellular collapse in the lens. **Overall design:** Murine lenses were collected at two stages of development for RNA extraction and hybridization on Affymetrix microarrays. Our aim was to determine key events that lead to cellular collapse of lenses triply deficient for E2F1, E2F2, and E2F3 in neonates.

Background corr dist: KL-Divergence = 0.1098, L1-Distance = 0.0404, L2-Distance = 0.0035, Normal std = 0.4188

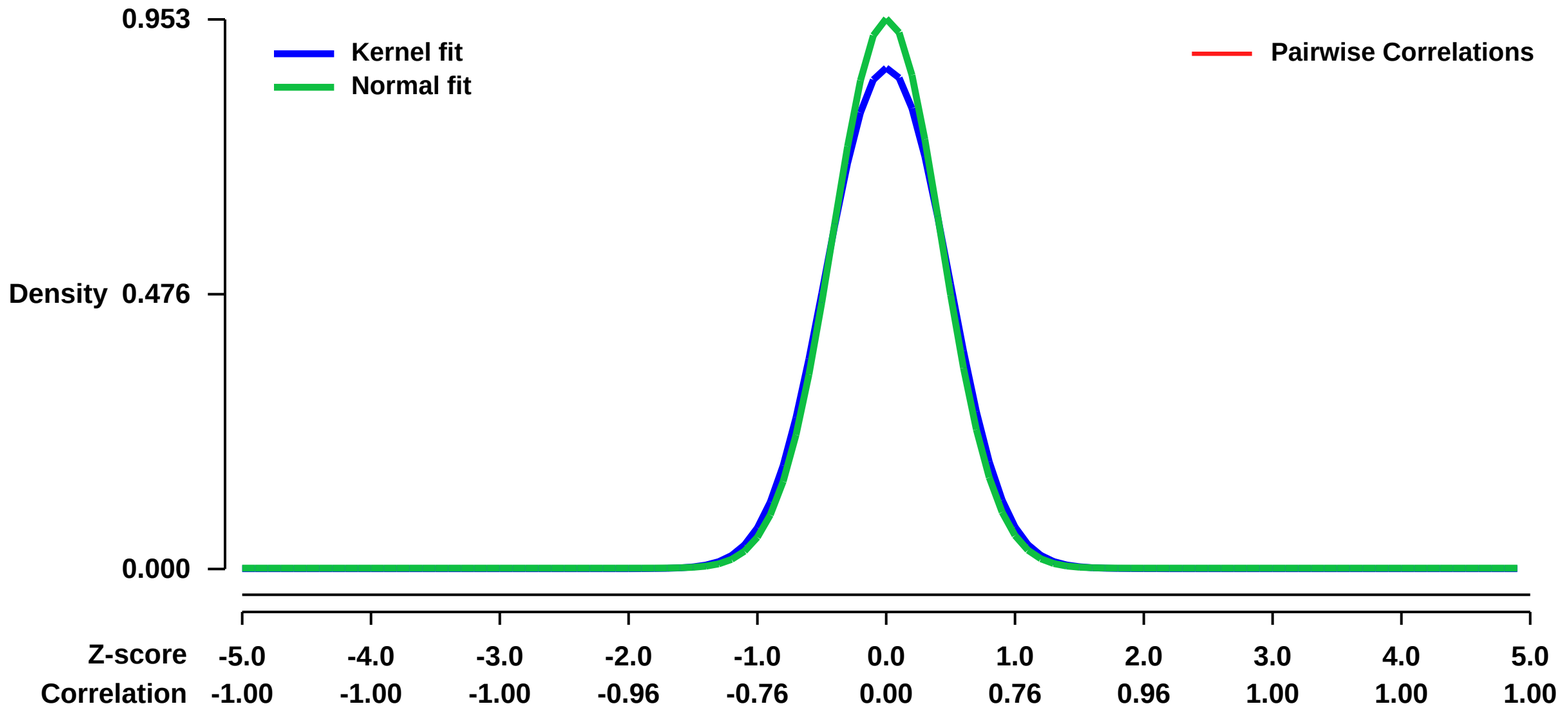

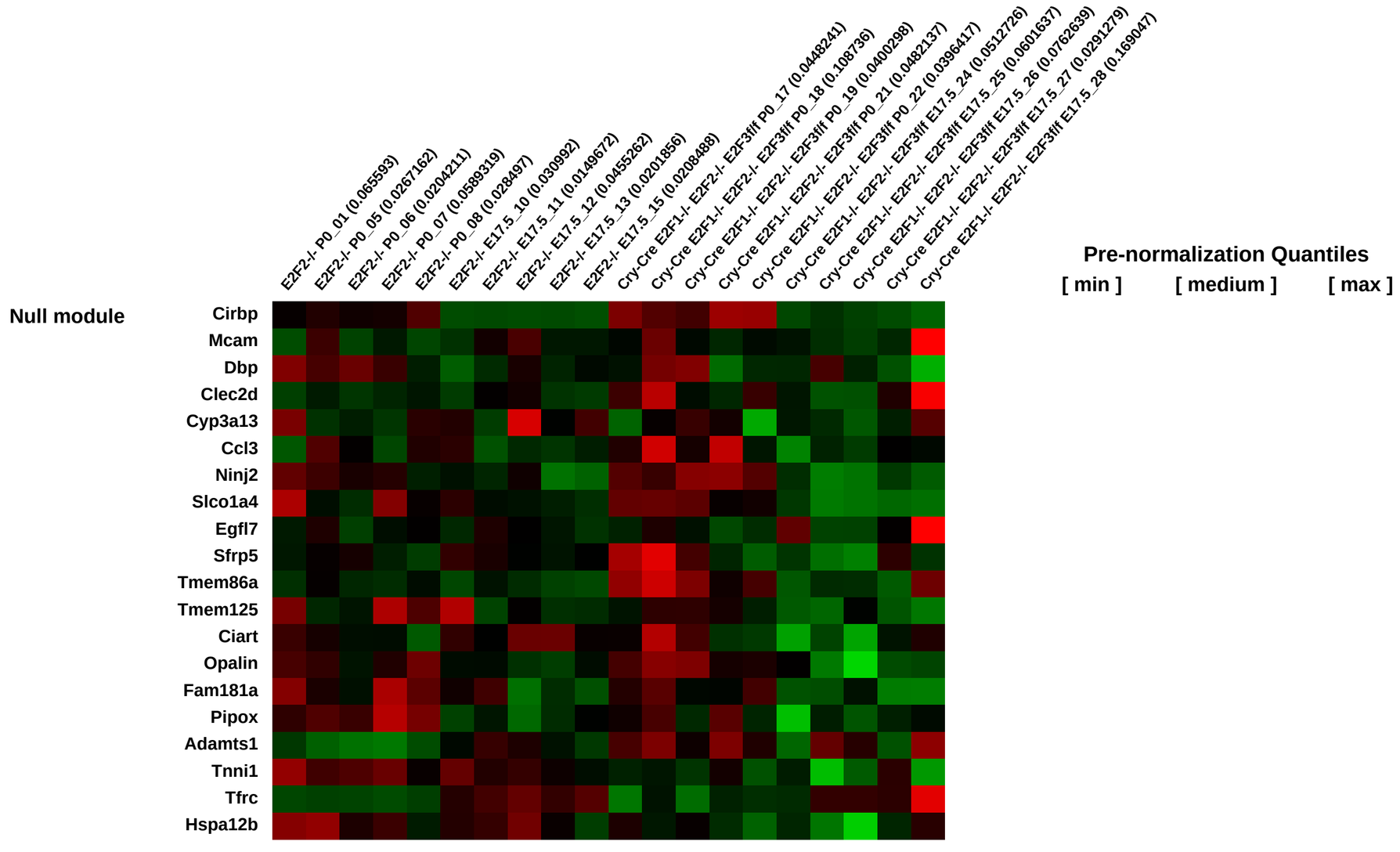

GEO Series "GSE16555" Expression Profiles

Num of samples in this series: 12

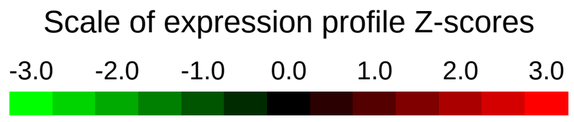

GEO Link:	http://www.ncbi.nlm.nih.gov/geo/query/acc.cgi?acc=GSE16555
Status:	Public on Jun 23 2010
Title:	Over-expression and knockdown of KLF5
Organism:	Mus musculus
Experiment type:	Expression profiling by array
Platform:	GPL1261
Pubmed ID:	20639455

Summary & Design:

Summary:
Activation of the Ras/Erk pathway upregulates expression of the Kruppel-like Factor 5 (KLF5) transcription factor, and KLF5 is a downstream mediator of Ras oncogenic signaling. Specifically, in bladder and colon cancer cell lines KLF5 upregulates the Ras-pathway target gene cyclin D1, and facilitates entry into the S phase of the cell cycle. Ras mutations are common in lung cancer, but a role for KLF5 in lung tumorigenesis has not been defined. To this end, we manipulated KLF5 expression in four Ras-mutant human lung adenocarcinoma cell lines to find that KLF5 significantly modulates anchorage-independent growth, a mutant Ras phenotype. However, in a mouse model of human lung adenocarcinoma, K-RasG12D does not critically require Klf5 to mediate oncogenesis or induce cyclin D1 expression.

Patients with lung tumors expressing high levels of KLF5 have significantly better prognosis than those with low or no KLF5 expression (opposite of mutant Ras prognosis). The latter may be explained by KLF5 transcriptional repression of the ATP-binding cassette, sub-family G (WHITE), member 2 (ABCG2), an anthracycline transporter. In agreement with this, KLF5 knockdown cells display significantly more Hoechst â side populationâ and resistance to doxorubicin. In summary, while KLF5 is not an obligate partner in Ras oncogenic signaling, KLF5 control of ABCG2 expression is significant to patient survival.

Overall design:
Total RNA was extracted from H441 cells transduced with KLF5-specific shRNA (KD), KLF5 over expression (OE) and MSCV empty vertor (NT) respectively. The cRNAs was then hybridized to Human Genome U133 Plus 2.0 Arrays (Affymetrix) according to manufacturerâ s protocol.

Background corr dist: KL-Divergence = 0.0806, L1-Distance = 0.0262, L2-Distance = 0.0010, Normal std = 0.4778

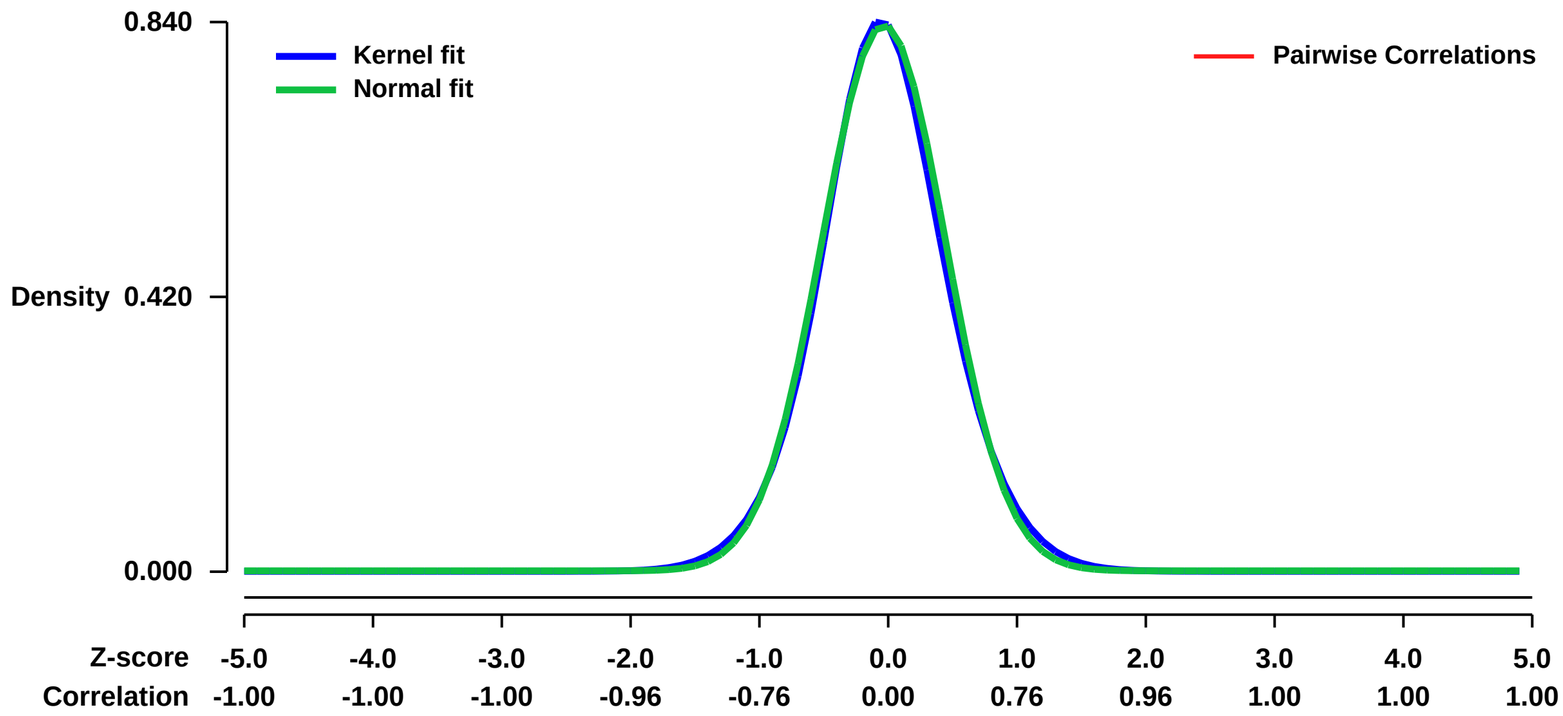

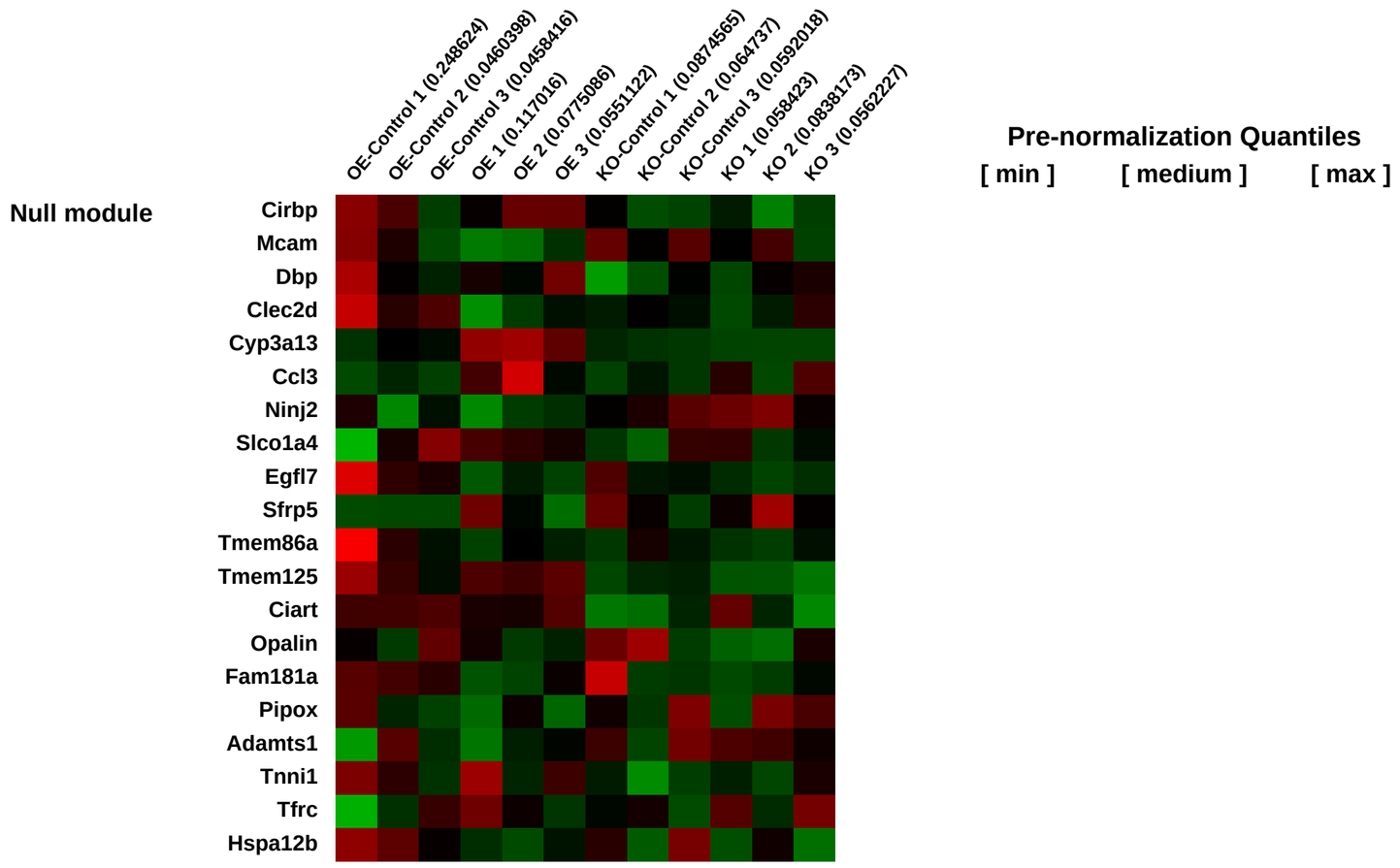

GEO Series "GSE16564" Expression Profiles

Num of samples in this series: 15

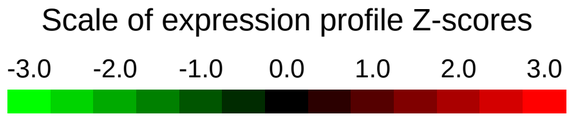

GEO Link:	http://www.ncbi.nlm.nih.gov/geo/query/acc.cgi?acc=GSE16564
Status:	Public on Jun 13 2009
Title:	Expression data from AtT20 mouse pituitary gland cells following overexpression or down regulation of NSBP1
Organism:	Mus musculus
Experiment type:	Expression profiling by array
Platform:	GPL1261
Pubmed ID:	19748358
Summary & Design:	**Summary:** Chromatin architectural protein NSBP1/HMGN5 belongs to the family of HMGN proteins which specifically interact with nucleosomes via Nucleosome Binding Domain, unfold chromatin and affect transcription. Mouse NSBP1 is a new and uncharacterized member of HMGN protein family. NSBP1 is a nuclear protein which is localized to euchromatin, binds to linker histone H1 and unfolds chromatin. We analyzed the effect of altered expression levels of mouse NSBP1 protein on global gene expression profile in AtT20 pituitary cells. We found that NSBP1 modulates the fidelity of cellular transcription in the nucleosome binding-dependent manner. **Overall design:** Stable clones overexpressing wild type mouse NSBP1 protein or mutated NSBP1SE protein which does not bind to nucleosomes were generated by retroviral infection of AtT20 cells. siRNA treatment was applied to down regulate NSBP1 in the cells. Total RNA was collected from biological triplicates and analyzed by Affymetrix expression arrays.

Background corr dist: KL-Divergence = 0.0509, L1-Distance = 0.0344, L2-Distance = 0.0022, Normal std = 0.5561

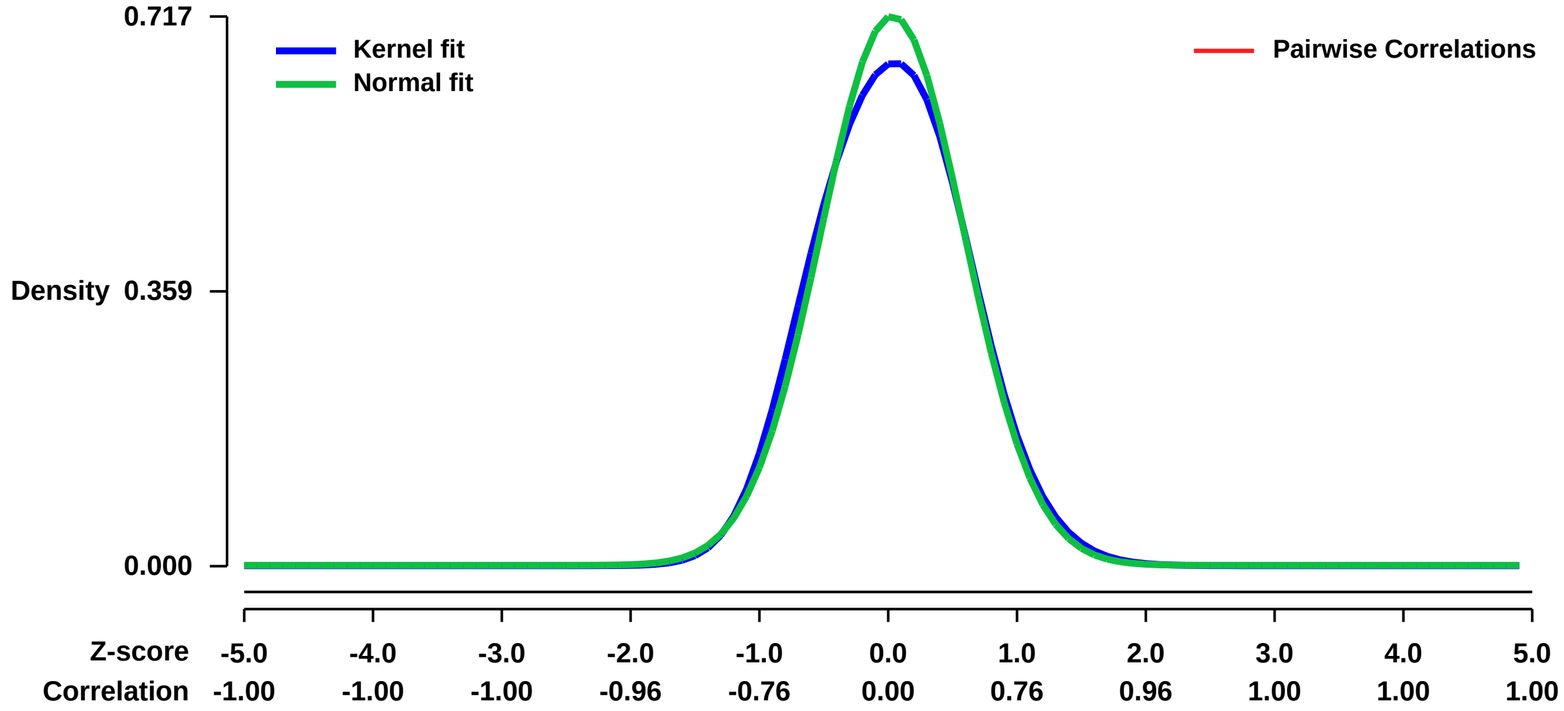

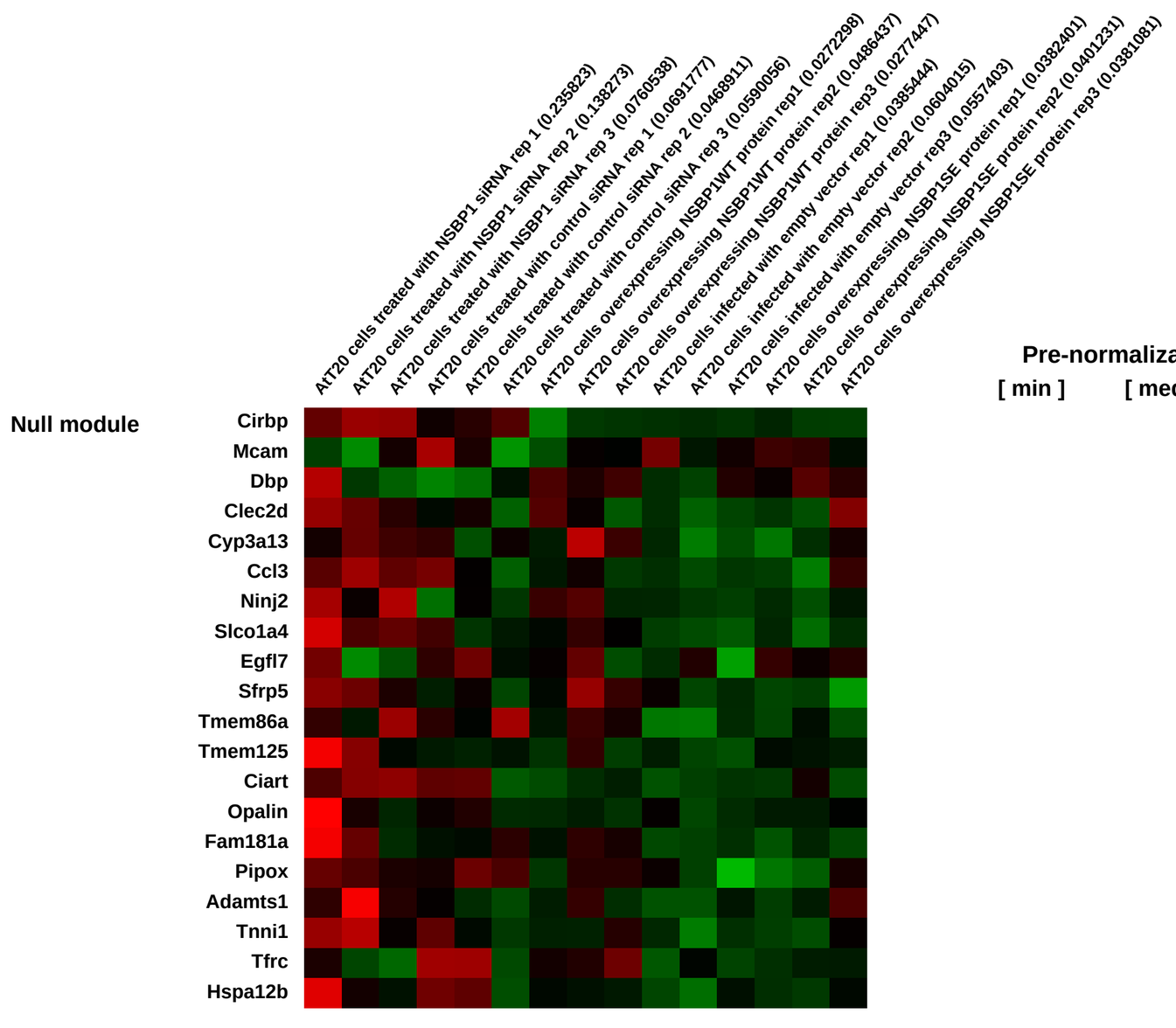

GEO Series "GSE16623" Expression Profiles

Num of samples in this series: 6

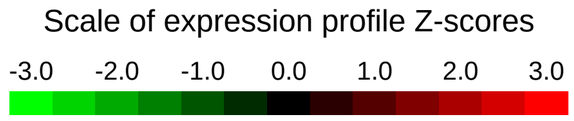

GEO Link:	http://www.ncbi.nlm.nih.gov/geo/query/acc.cgi?acc=GSE16623
Status:	Public on Apr 11 2010
Title:	Differential gene expression between ERRa KO and WT mouse kidneys
Organism:	Mus musculus
Experiment type:	Expression profiling by array
Platform:	GPL1261
Pubmed ID:	19901197
Summary & Design:	**Summary:** Estrogen-related receptor (ERR) alpha is an orphan nuclear receptor highly expressed in the kidneys. ERRalpha is implicated in renal sodium and potassium homeostasis and blood pressure regulation. We used microarray analysis to identify differentially expressed genes in ERR alpha knockout mice kidneys versus wild-type. The results provide insight on the roles of ERRalpha in the kidney. **Overall design:** Three biological replicates of WT and ERRaKO were performed, for a total of 6 samples. 2-3 month old males of each genotype were used.

Background corr dist: KL-Divergence = 0.0447, L1-Distance = 0.0165, L2-Distance = 0.0003, Normal std = 0.5914

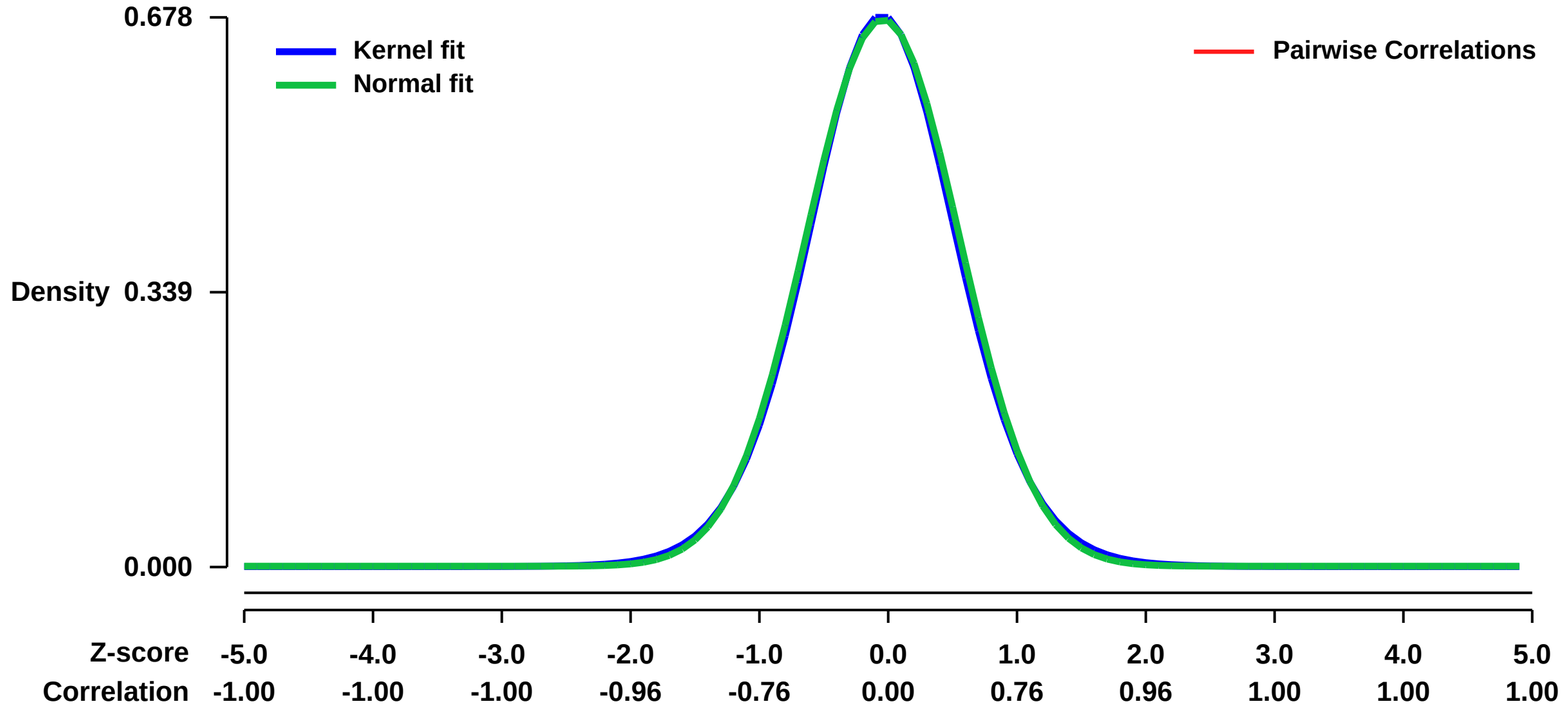

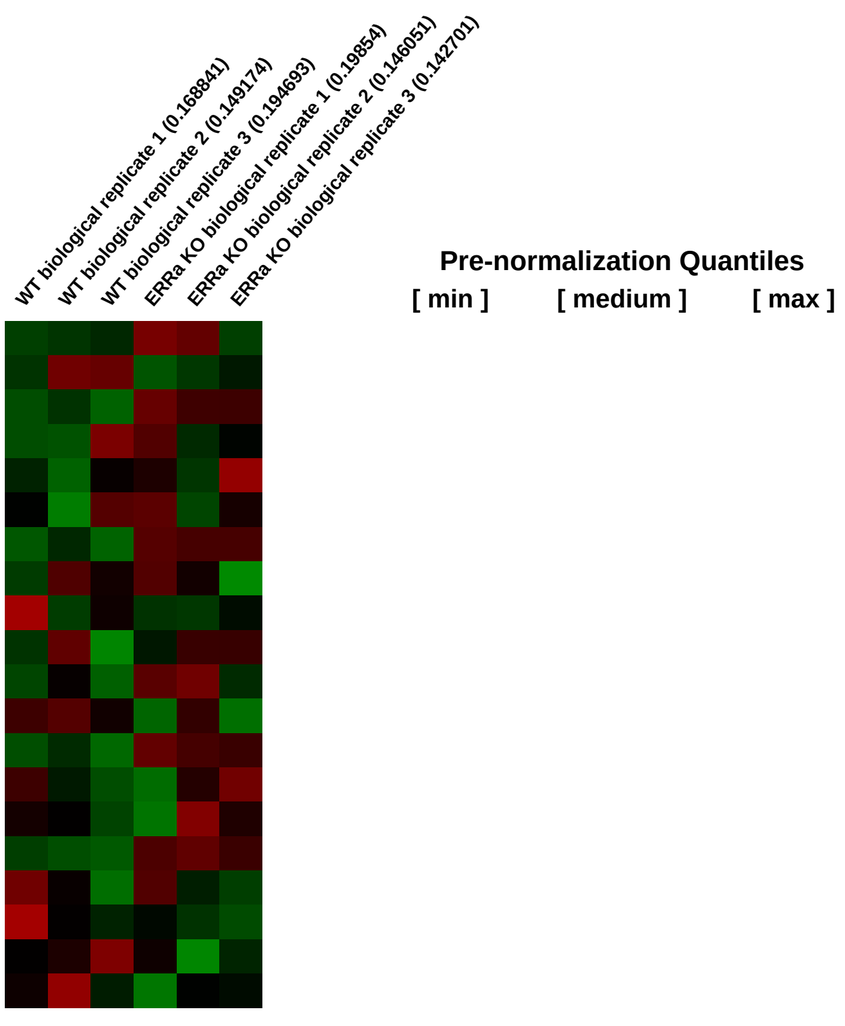

GEO Series "GSE16676" Expression Profiles

Num of samples in this series: 11

Scale of expression profile Z-scores

-3.0 -2.0 -1.0 0.0 1.0 2.0 3.0

GEO Link:	http://www.ncbi.nlm.nih.gov/geo/query/acc.cgi?acc=GSE16676
Status:	Public on Aug 01 2010
Title:	Rescue of murine Gata1s mutant M7 leukemic cells by full-length Gata1
Organism:	Mus musculus
Experiment type:	Expression profiling by array
Platform:	GPL1261
Pubmed ID:	20679399
Summary & Design:	**Summary:** In this project, we studied a mouse model of human Down Syndrome (DS) megakaryocytic leukemia involving mutations in the GATA1 transcription factor (called GATA1s mutation). The model was generated through retroviral insertional mutagenesis in Gata1s mutant fetal liver progenitors. In this study, we analyzed the dependency of these leukemic cells on the Gata1s mutant protein. Here we report Gata1s mutant leukemic cells were dependent on this mutant protein. Introduction of the full-length Gata1 protein to these cells led to their reduced proliferation and increased differentiation along the megakaryocytic lineage. **Overall design:** We transduced leukemic cells with Gata1/estrogen receptor fusion cDNA (Gata1-ER) and generated stable cell lines. Addition of beta-estradiol to culture medium led to activation of the full-length Gata1 protein in synchronized leukemic cells. Gene expression profiles were collected at multiple time points.

Background corr dist: KL-Divergence = 0.1370, L1-Distance = 0.0323, L2-Distance = 0.0018, Normal std = 0.3869

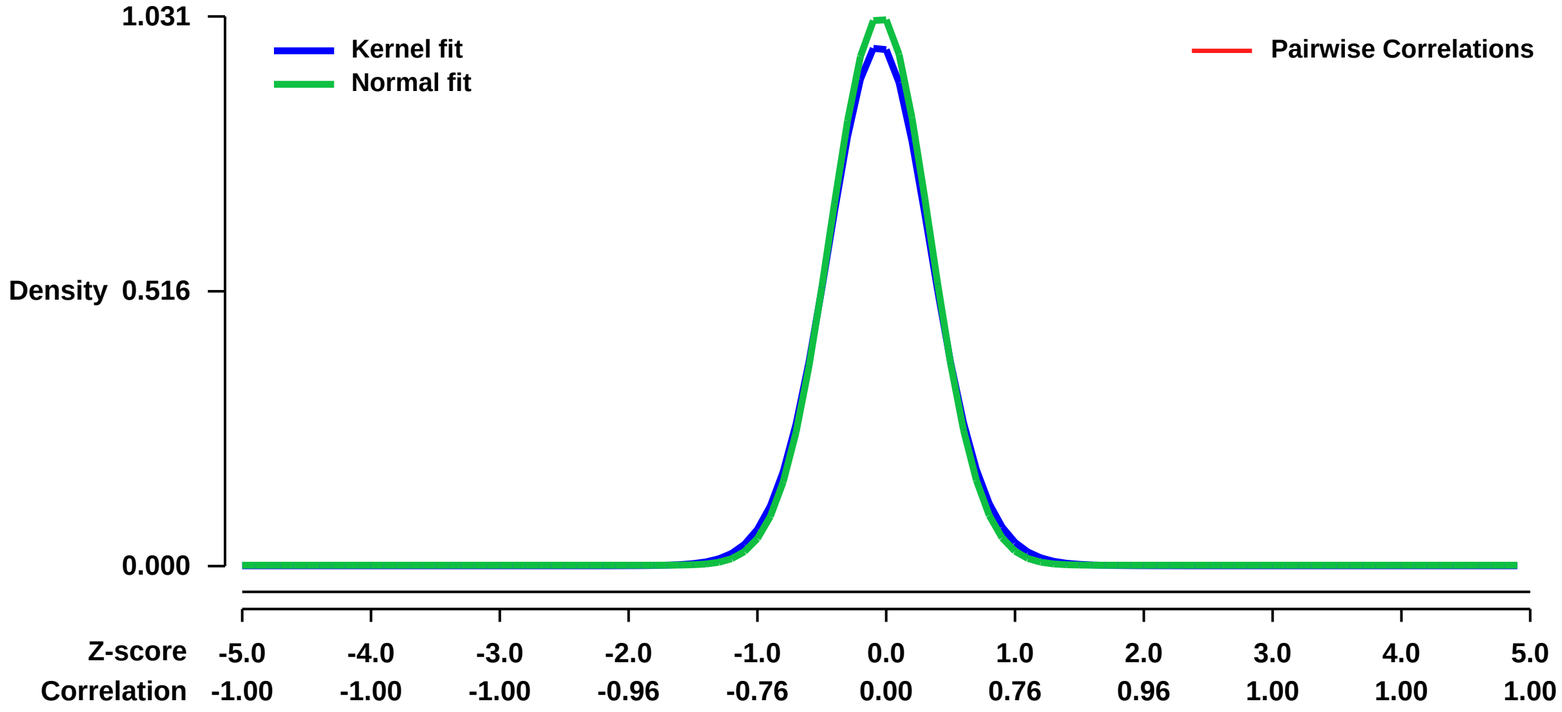

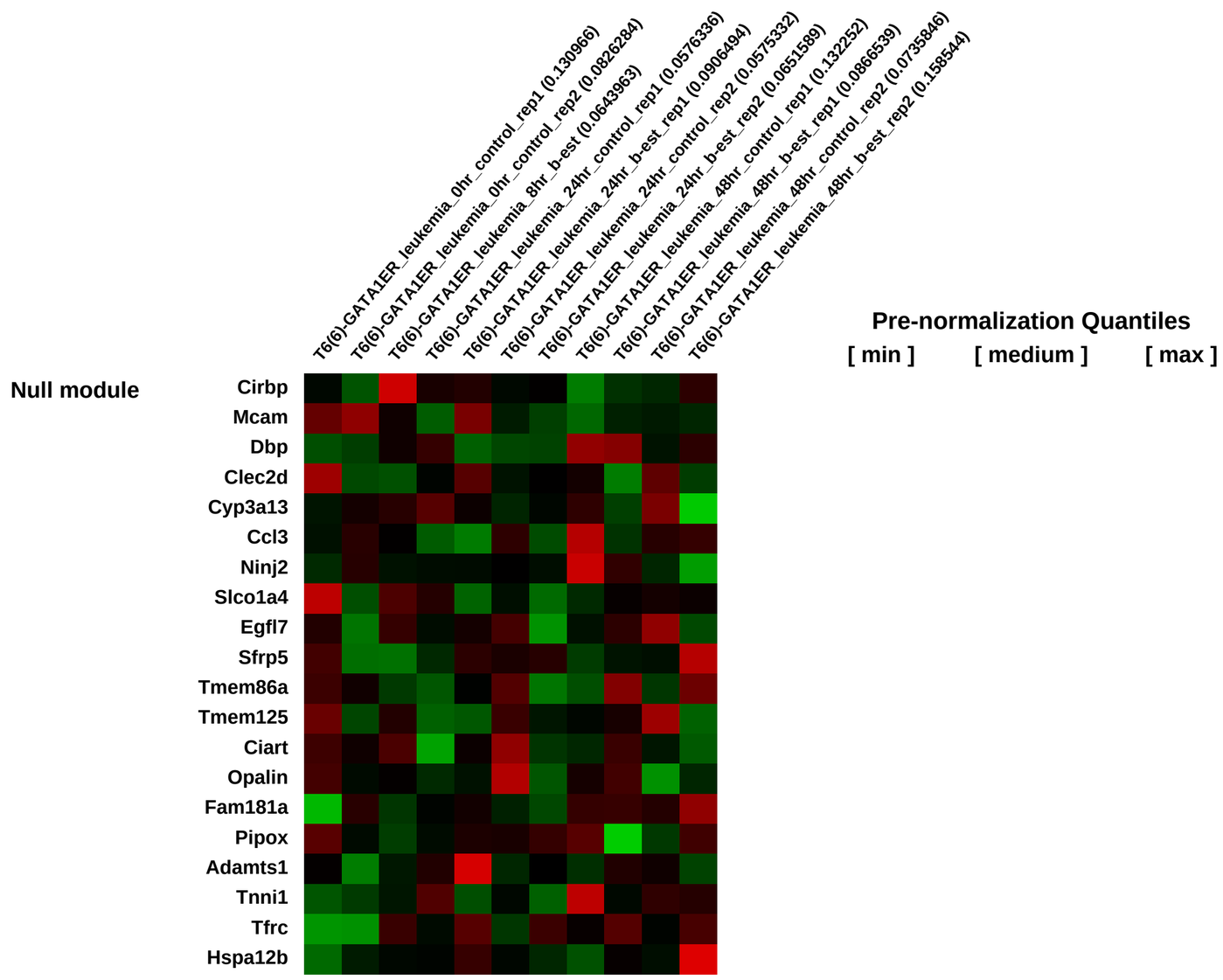

GEO Series "GSE16679" Expression Profiles

Num of samples in this series: 8

Scale of expression profile Z-scores

-3.0 -2.0 -1.0 0.0 1.0 2.0 3.0

GEO Link:	http://www.ncbi.nlm.nih.gov/geo/query/acc.cgi?acc=GSE16679
Status:	Public on Aug 01 2010
Title:	Plag1 overexpression cooperates with Evi1 overexpression and Gata1s mutation in leading to M7 leukemia
Organism:	Mus musculus
Experiment type:	Expression profiling by array
Platform:	GPL1261
Pubmed ID:	20679399
Summary & Design:	**Summary:** **The goal of this study is to develop a Plag1 signature and determine how its overexpression contributes to leukemogenesis.** **To study this, we transduced an immortalized (but not transformed) cell line (derived from Gata1s mutant fetal liver progenitor through insertional mutagenesis) by Plag1-expressing retrovirus. This turned a non-transformed cell line to a leukemogenic cell line. To study whether Plag1 overexpression led to deregulation of signaling pathways that may contribute to leukemic transformation, we generated microarray gene expression profiles of this cell line transduced with either Plag1 or the empty vector.** **Overall design:** **We generated gene expression profiles by microarray from stable cell lines transduced with either the empty vector or the Plag1-expressing vector.**

Background corr dist: **KL-Divergence = 0.0435, L1-Distance = 0.0264, L2-Distance = 0.0008, Normal std = 0.6089**

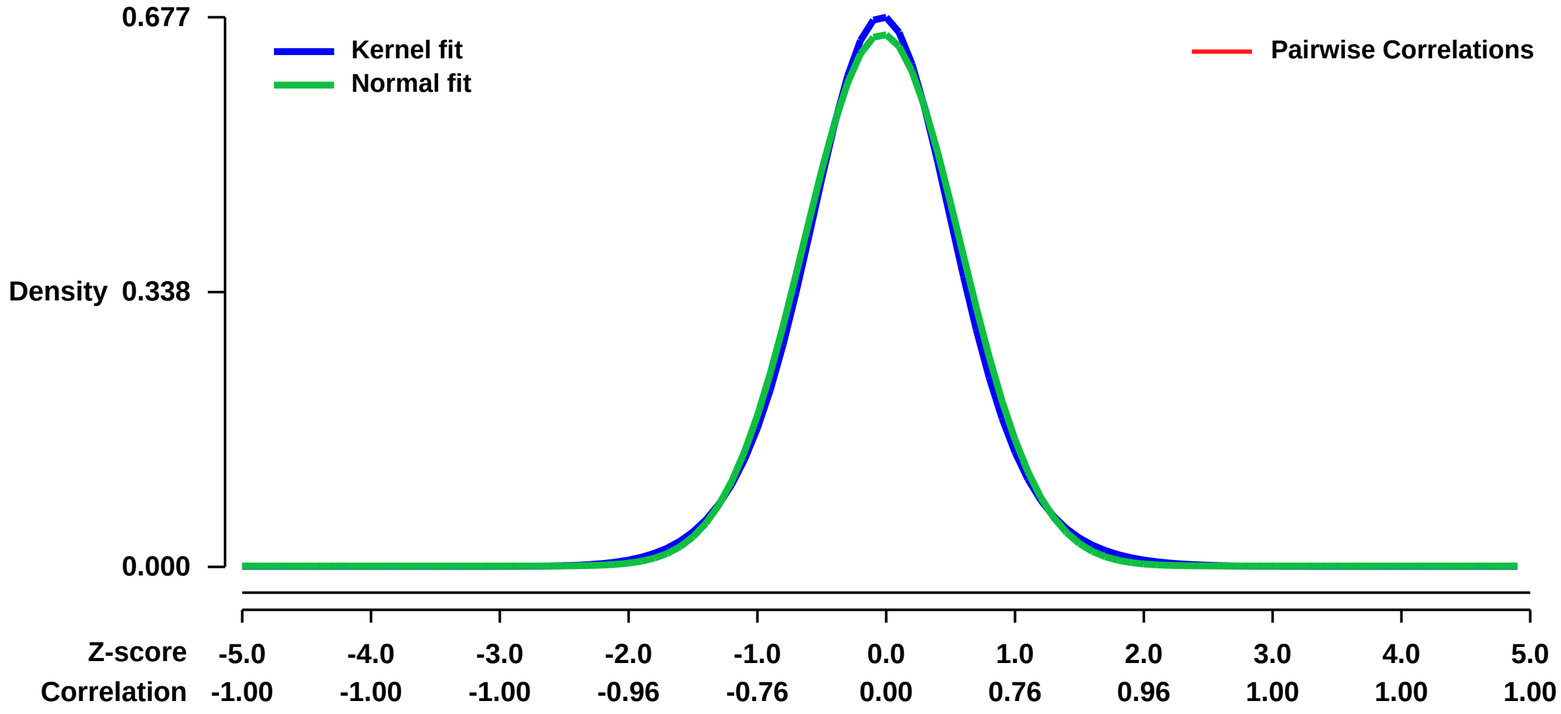

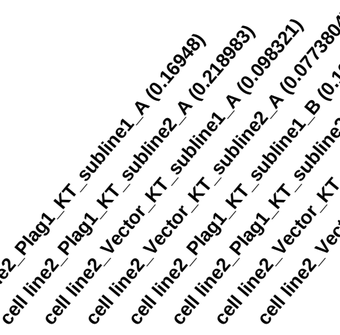

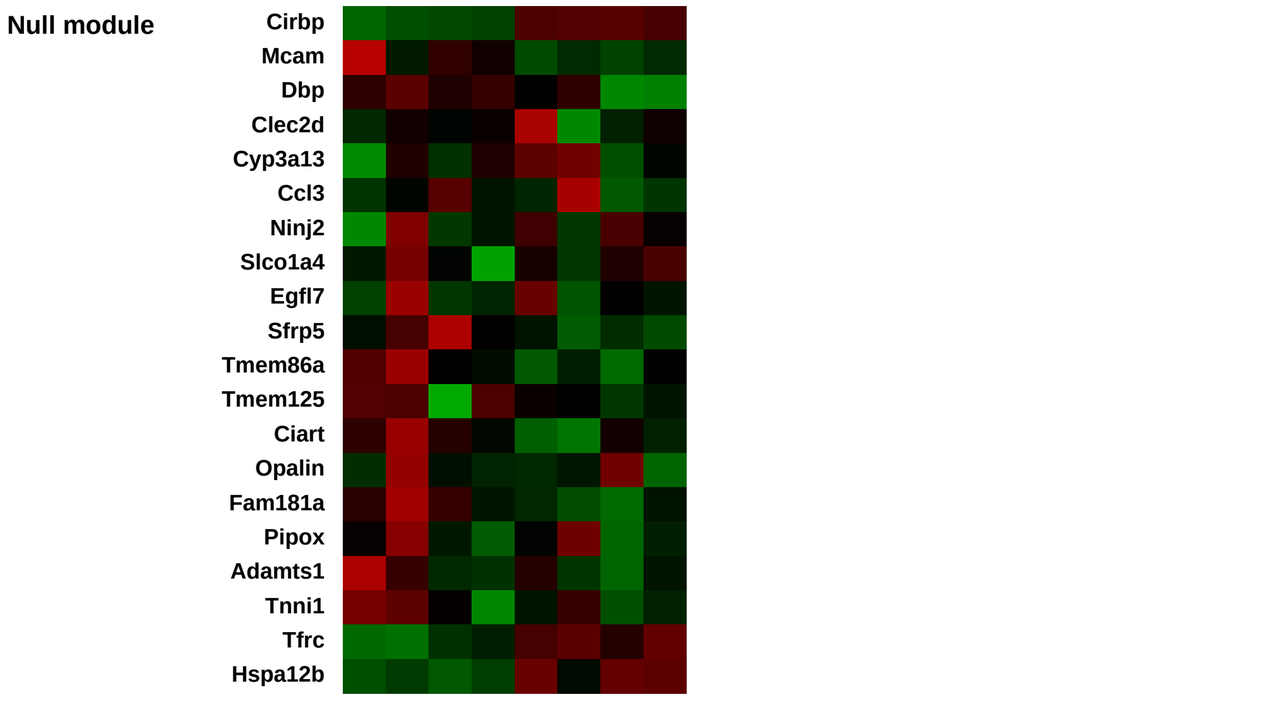

GEO Series "GSE16684" Expression Profiles

Num of samples in this series: 6

Scale of expression profile Z-scores

-3.0 -2.0 -1.0 0.0 1.0 2.0 3.0

GEO Link:	http://www.ncbi.nlm.nih.gov/geo/query/acc.cgi?acc=GSE16684
Status:	Public on Aug 01 2010
Title:	Murine M7 leukemia derived from retroviral insertional mutagenesis of Gata1s fetal progenitors depends on IGF signaling
Organism:	Mus musculus
Experiment type:	Expression profiling by array
Platform:	GPL1261
Pubmed ID:	20679399
Summary & Design:	**Summary:** The goal of this study is to derive a mouse model of human Down Syndrome (DS) megakaryocytic leukemia involving mutations in the hematopoietic transcription factor, GATA1 (called GATA1s mutation). We achieved this through transduction of Gata1s mutant fetal progenitors by MSCV-based retrovirus expressing a GFP marker, followed by in vitro selection (for immortalized cell lines), and then in vivo selection (for transformed cell lines) through transplantation. Here we report one such cell line [T6(6)] that gives rise to megakaryocytic leukemia (M7 leukemia) upon transplantation. We show knockdown of IGF1R in these cells leads to their reduced proliferation. **Overall design:** IGF1R was knocked down in these cells using a tet-regulatable shRNA-based lentiviral system. Cells infected with the empty vector or those infected with shRNA construct against IGF1R but in the absence of Doxycycline were used as controls. The latter cells in the presence of Doxycycline exhibited reduced IGF1R at the RNA level.

Background corr dist: KL-Divergence = 0.0413, L1-Distance = 0.0184, L2-Distance = 0.0003, Normal std = 0.6111

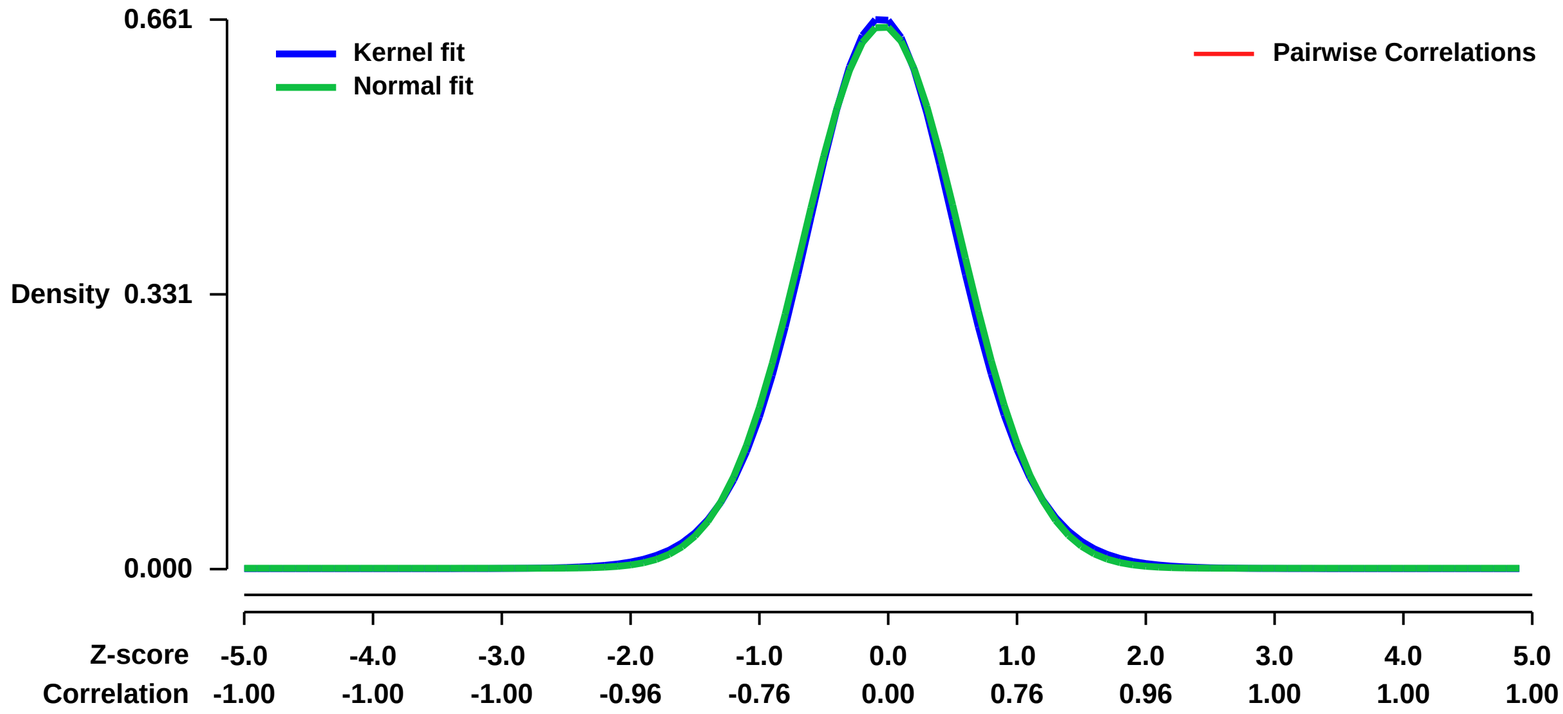

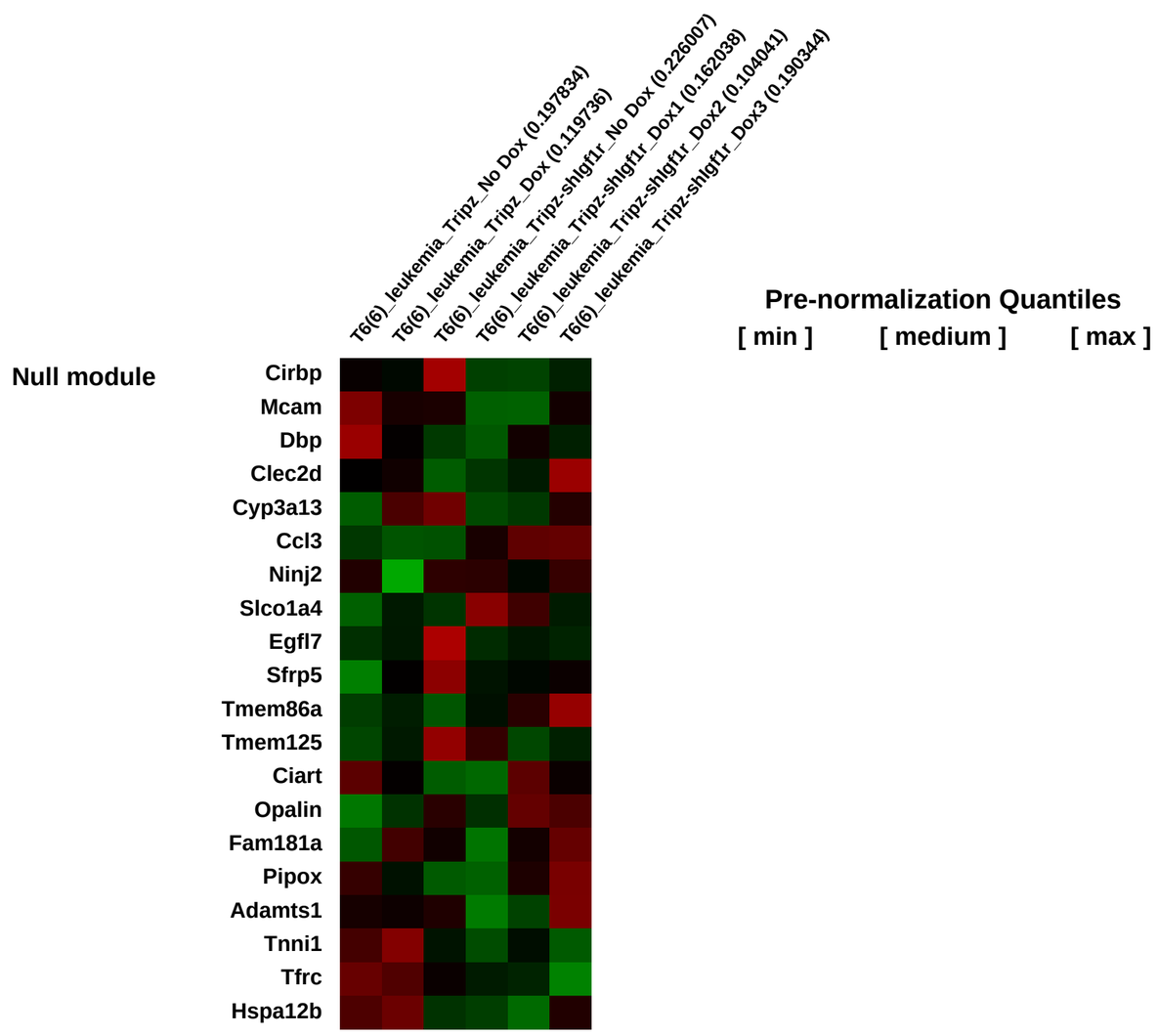

GEO Series "GSE16691" Expression Profiles

Num of samples in this series: 12

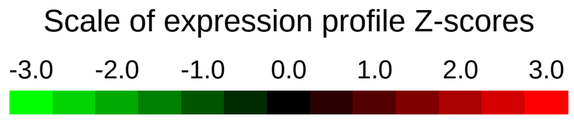

GEO Link:	http://www.ncbi.nlm.nih.gov/geo/query/acc.cgi?acc=GSE16691
Status:	Public on Oct 01 2009
Title:	Transcriptional regulation by Norrin-Frizzled4 signaling in the embryonic yolk sac
Organism:	Mus musculus
Experiment type:	Expression profiling by array
Platform:	GPL1261
Pubmed ID:	19837032
Summary & Design:	**Summary:** Transcriptional profiles of the embryonic yolk sac from embryos with ectopic Norrin expression were compared to their wild type littermate controls. The goal is to identify the transcriptional response to Norrin-Frizzled 4 signaling during embryonic angiogenesis. **Overall design:** Ectopic Norrin expression was achieved using a conditional over-expression strategy. Yolk sacs from 3-5 embryos were pooled for each sample and 3 replicates of both control and experimental groups were analyzed.

Background corr dist: KL-Divergence = 0.0423, L1-Distance = 0.0287, L2-Distance = 0.0014, Normal std = 0.5865

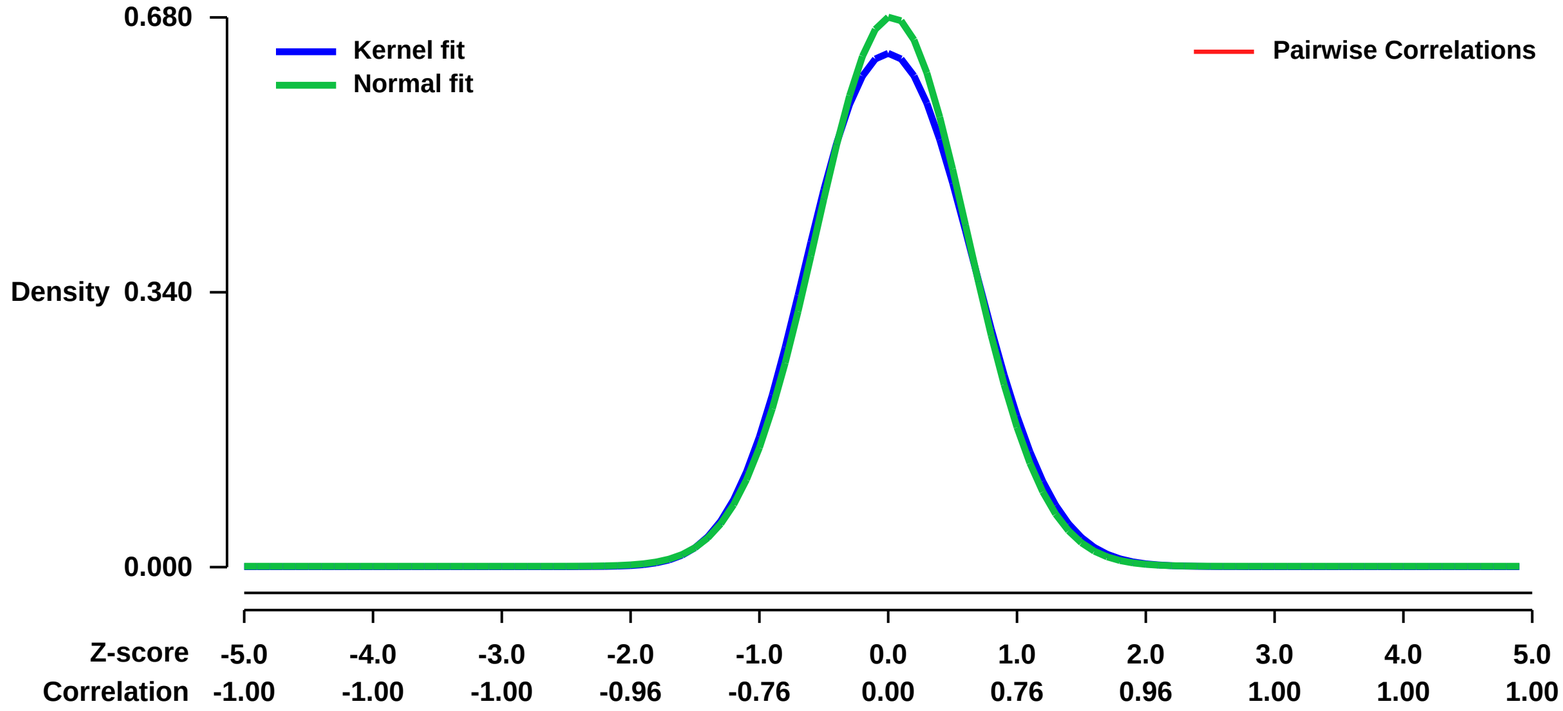

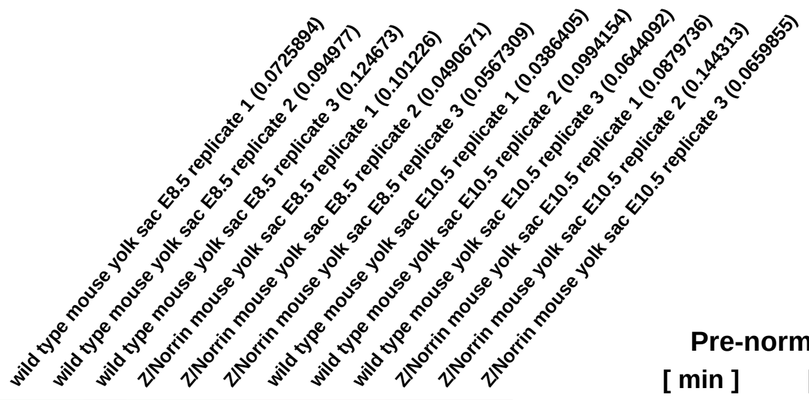

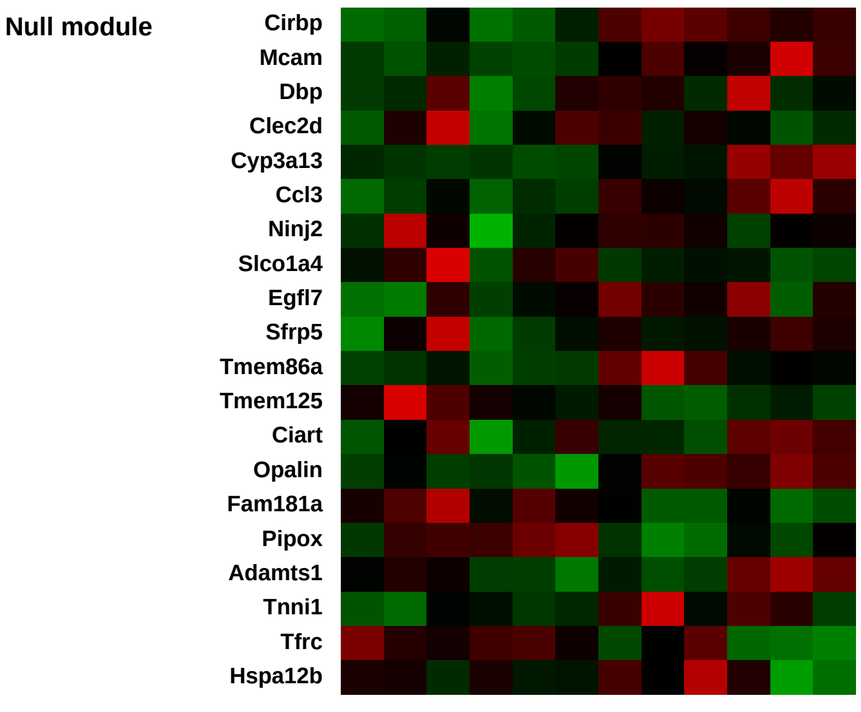

GEO Series "GSE16703" Expression Profiles

Num of samples in this series: 15

Scale of expression profile Z-scores

-3.0 -2.0 -1.0 0.0 1.0 2.0 3.0

GEO Link:	http://www.ncbi.nlm.nih.gov/geo/query/acc.cgi?acc=GSE16703
Status:	Public on Oct 01 2009
Title:	Long-term effect on the transcriptome of a decrement in Norrin/Frizzled4/Lrp signaling in retinal endothelial cells
Organism:	Mus musculus
Experiment type:	Expression profiling by array
Platform:	GPL1261
Pubmed ID:	19837032
Summary & Design:	**Summary:** To characterize the long-term effect on the transcriptome of a decrement in Norrin/Fz4/Lrp signaling, microarray hybridization was performed with RNA from acutely dissociated and anti-PECAM immunoaffinity-purified adult WT, Fz4-/-, Lrp5-/-, and Norrin- retinal vascular cells. **Overall design:** Retinal endothelial cells from 5-10 adult mice were pooled for each sample, the cell immuno-purification procedure follows that described by Matsubara et al. (2000) and Su et al. (2003). 3 replicates of each mutant and 6 replicates of control wild type animals were analyzed.

Background corr dist: KL-Divergence = 0.1043, L1-Distance = 0.0376, L2-Distance = 0.0029, Normal std = 0.4339

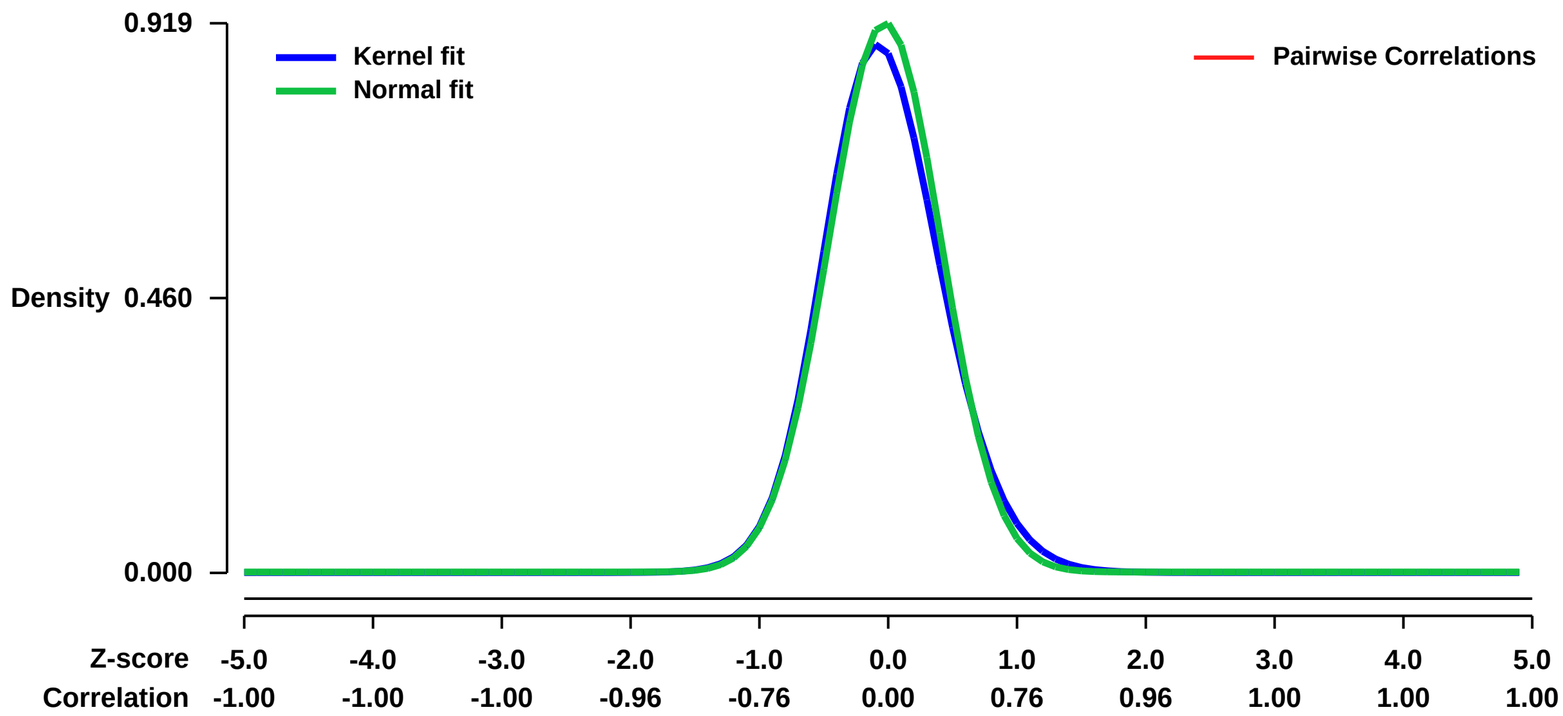

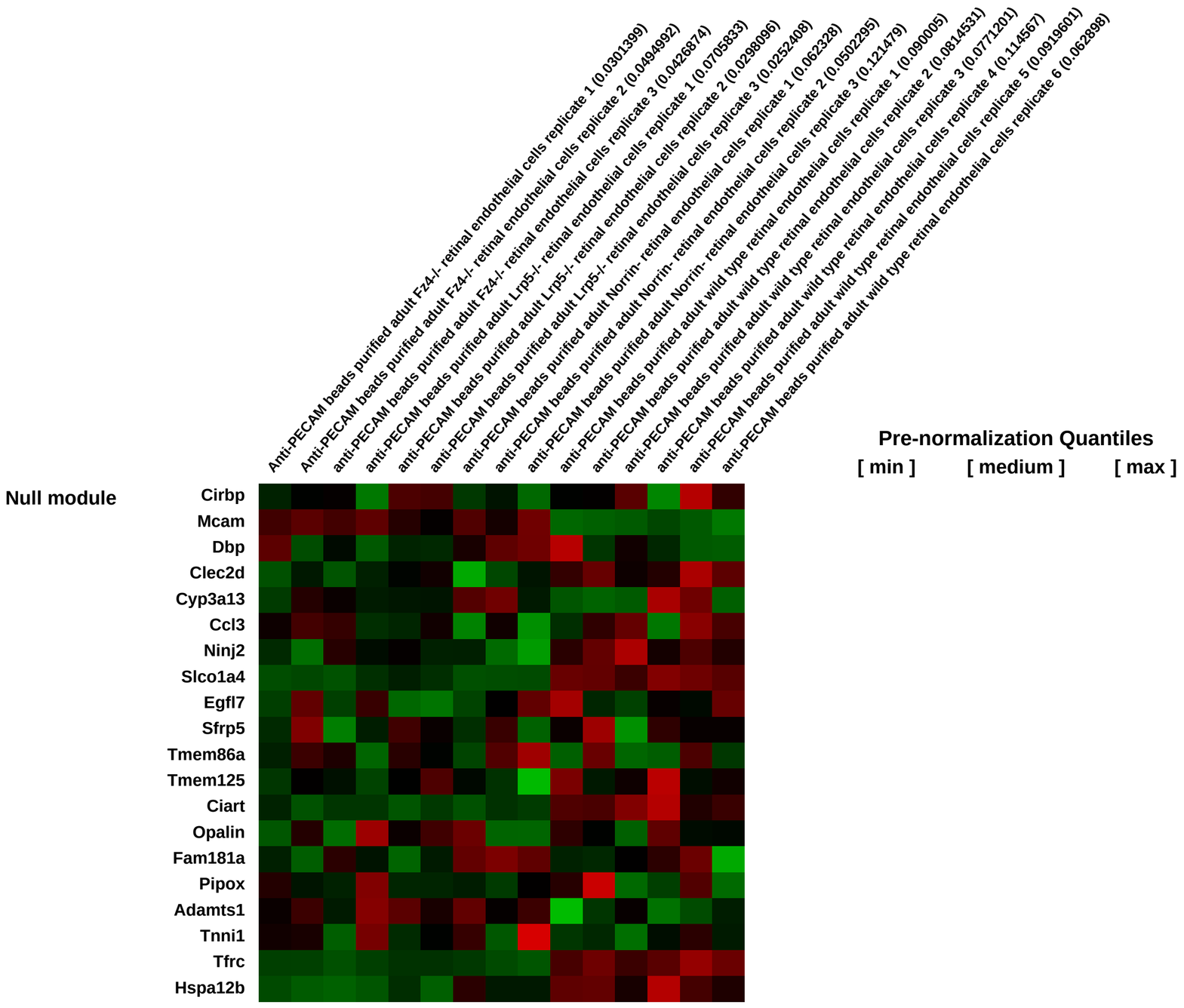

GEO Series "GSE16707" Expression Profiles

Num of samples in this series: 6

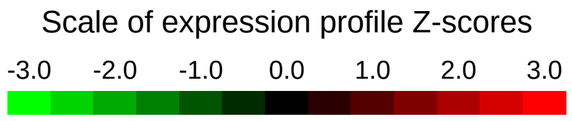

GEO Link:	http://www.ncbi.nlm.nih.gov/geo/query/acc.cgi?acc=GSE16707
Status:	Public on Oct 01 2009
Title:	Long-term effect on the transcriptome of loss of Frizzled4 signaling in cerebellar endothelial cells
Organism:	Mus musculus
Experiment type:	Expression profiling by array
Platform:	GPL1261
Pubmed ID:	19837032
Summary & Design:	**Summary:** Transcriptional profiles of the cerebellar endothelial cells from P16 Fz4-/- animals were compared to their wild type littermate controls. The goal is to characterize the long-term effect on the transcriptome of loss of Fz4 signaling in cerebellar endothelial cells. **Overall design:** Endothelial cells were immuno-purification from P16 cerebellum using anti-PECAM antibody coated dynabeads. The cell immuno-purification procedure follows that described by Matsubara et al. (2000) and Su et al. (2003). 3 replicates of both wild type and Fz4-/- cerebellar endothelial cells were analyzed.

Background corr dist: KL-Divergence = 0.0281, L1-Distance = 0.0235, L2-Distance = 0.0006, Normal std = 0.6913

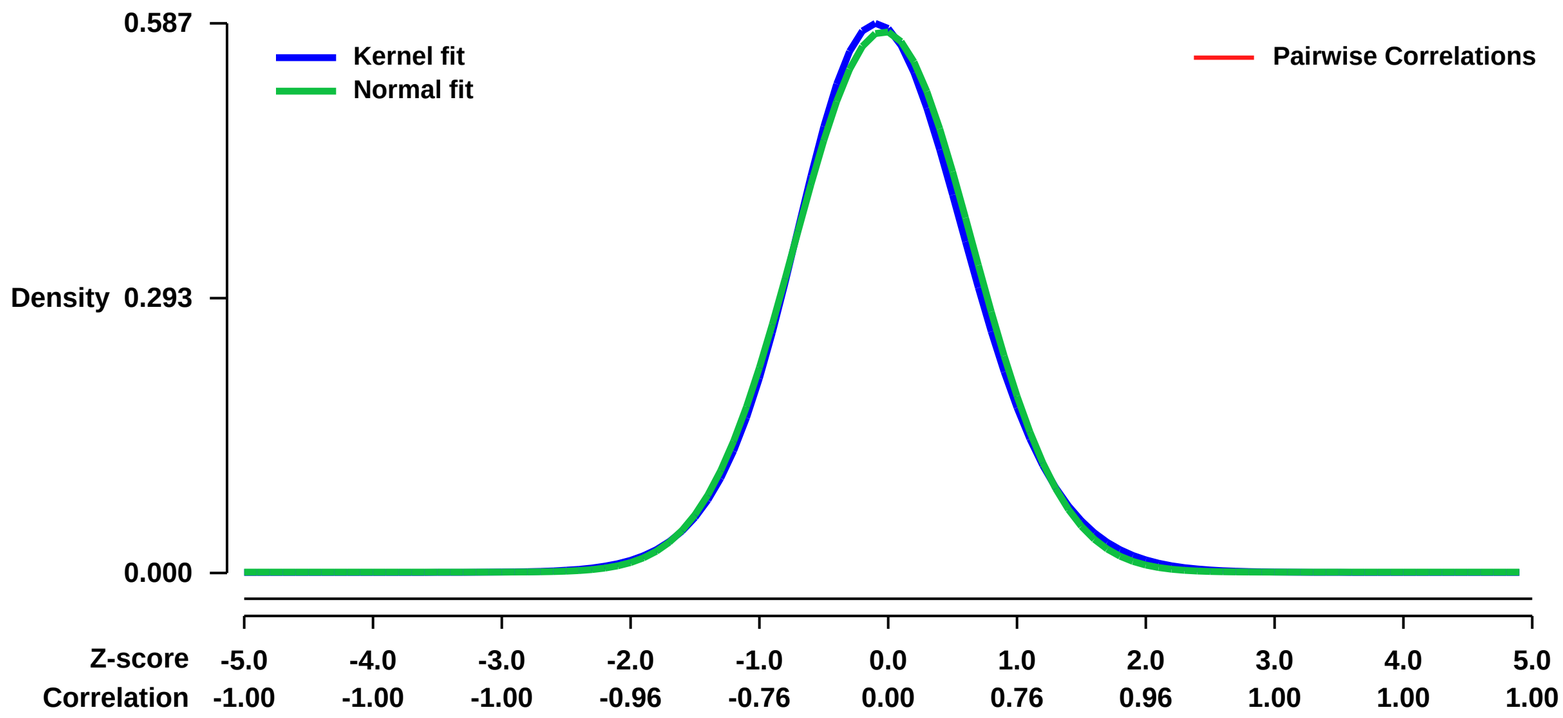

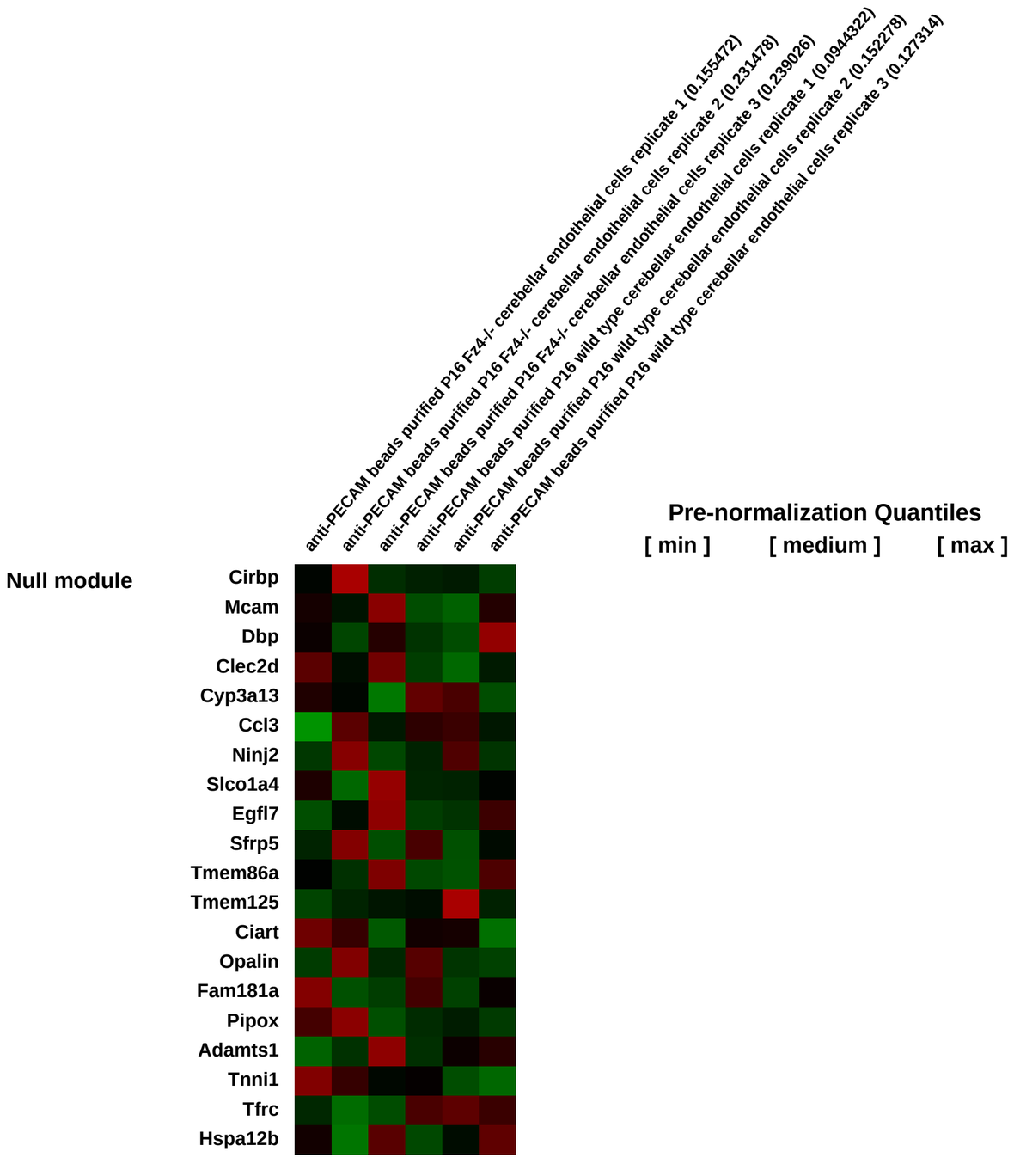

GEO Series "GSE16751" Expression Profiles

Num of samples in this series: 6

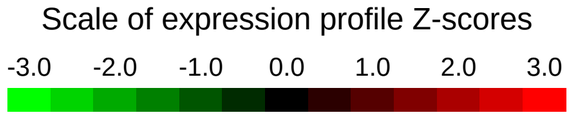

GEO Link:	http://www.ncbi.nlm.nih.gov/geo/query/acc.cgi?acc=GSE16751
Status:	Public on Jun 24 2009
Title:	Activation-induced cytidine deaminase accelerates clonal evolution in BCR-ABL1-driven acute lymphoblastic leukemia
Organism:	Mus musculus
Experiment type:	Expression profiling by array
Platform:	GPL1261
Pubmed ID:	
Summary & Design:	**Summary:** Activation-Induced Cytidine Deaminase (AID) is required for somatic hypermutation and immunoglobulin (Ig) class switch recombination in germinal center B lymphocytes. Occasionally, AID targets non-Ig genes, thereby contributing to B cell lymphomagenesis. We recently reported aberrant expression of AID in BCR-ABL1-driven acute lymphoblastic leukemia (ALL). To elucidate the biological significance of aberrant AID expression, we studied loss of AID function in a murine model of BCR-ABL1 ALL. Mice transplanted with BCR-ABL1-transduced AID-/- bone marrow had prolonged survival as compared to mice transplanted with leukemia cells generated from AID+/+ bone marrow. Consistent with a causative role of AID in genetic instability, AID-/- leukemia had a decreased frequency of amplifications, deletions and a lower frequency of mutations in non-Ig genes including Pax5 and Rhoh as compared to AID+/+ leukemias. AID-/- and AID+/+ ALL cells showed a markedly distinct gene expression pattern as determined by principle component analysis, with 2,365 genes differentially expressed. In contrast to AID+/+ leukemia, AID-/- ALL cells failed to downregulate a number of tumor suppressor genes such as Rhoh, Cdkn1a (p21), and Blnk (SLP65). We conclude that AID accelerates clonal evolution in BCR-ABL1 ALL by enhancing genetic instability, aberrant somatic hypermutation, and by transcriptional inactivation of tumor suppressor genes. **Overall design:** We used microarrays to detect differences in gene expression profiles between AID expressing leukemia and AID deficient leukemia

Background corr dist: KL-Divergence = 0.0295, L1-Distance = 0.0170, L2-Distance = 0.0003, Normal std = 0.6752

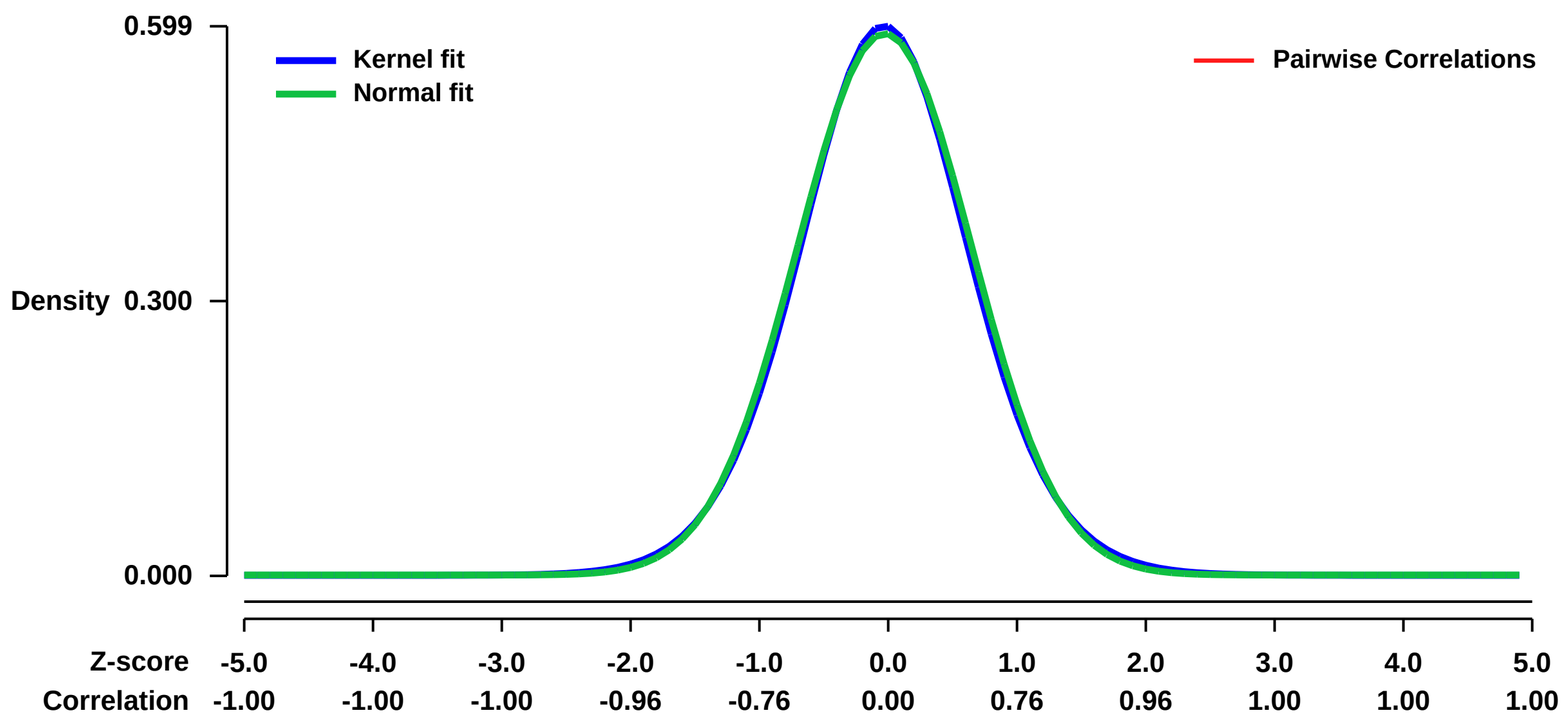

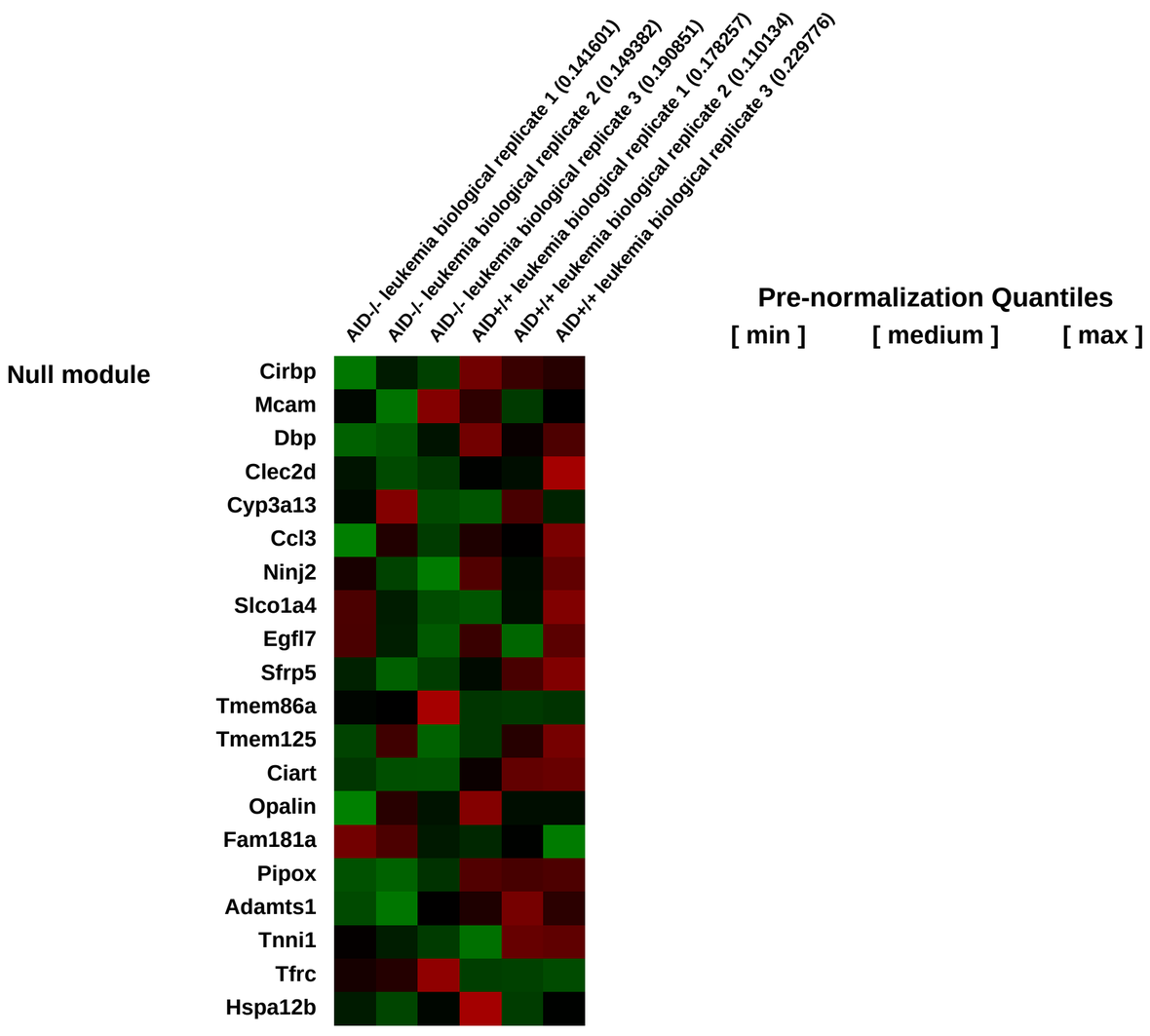

GEO Series "GSE16790" Expression Profiles

Num of samples in this series: 18

Scale of expression profile Z-scores

-3.0 -2.0 -1.0 0.0 1.0 2.0 3.0

GEO Link:	http://www.ncbi.nlm.nih.gov/geo/query/acc.cgi?acc=GSE16790
Status:	Public on Apr 29 2011
Title:	Caloric Restriction in Leptin Deficiency Worsens Myocardial Steatosis
Organism:	Mus musculus
Experiment type:	Expression profiling by array
Platform:	GPL1261
Pubmed ID:	21427359
Summary & Design:	**Summary:** **Caloric Restriction in Leptin Deficiency Worsens Myocardial Steatosis: Failure to Upregulate PPAR gamma and Thermogenic Glyecrolipid/Fatty Acid Cycling** **Growing evidence supports an anti-lipotoxic role for leptin in preventing inappropriate peripheral tissue lipid deposition. Obese, leptin deficient ob/ob mice develop left ventricular (LV) hypertrophy and myocardial steatosis with increased apoptosis and decreased longevity. Here we investigated the cardiac effects of caloric restriction in leptin deficiency. Echocardiography was performed on C57Bl/6 wild-type mice (WT) and 7-month-old ob/ob mice fed ad lib, leptin-repleted (LR-ob/ob), or calorie-restricted (CR-ob/ob) for four weeks. Ventricular tissue was examined by electron microscopy (EM), mitochondrial coupling assay, and microarray expression profiling. LR and CR-ob/ob mice showed decreased body weight, heart weight, and LV wall thickness compared to ad lib ob/ob mice. LV fractional shortening was decreased in ad lib ob/ob mice, but restored to WT levels in LR and CR groups. However, EM revealed severe cardiac steatosis in the CR-ob/ob group compared to only moderate steatosis in ad lib ob/ob . Despite marked cardiac steatosis, CR (like LR) restored mitochondrial coupling to WT levels. CR up-regulated genes associated with oxidative stress and cell death, changes suggestive of cardiac lipotoxicity. LR, but not CR was shown to induce core genes involved in glycerolipid/free fatty acid cycling, a highly thermogenic pathway that can reduce intracellular lipid stores. LR, but not CR up-regulated and restored PGC1-alpha and PPAR-alpha to wild type levels; CR paradoxically further suppressed cardiac PPAR-alpha. Thus, leptin is essential in protecting the heart from lipotoxicity, and the inability to up-regulate the thermogenic glycerolipid/free fatty acid cycling pathway may impair the response of leptin deficient animals to the lipotoxic stress of calorie restriction.** **Overall design:** **6 month aged ob/ob mice were either leptin repleted with osmotic mini-pumps, calorie restricted to match the caloric intake of the leptin repleted mice, or fed ad lib for one month. 6-8 month C57Bl/6J mice were aged to serve as controls.**

Background corr dist: KL-Divergence = 0.2714, L1-Distance = 0.0612, L2-Distance = 0.0098, Normal std = 0.2917

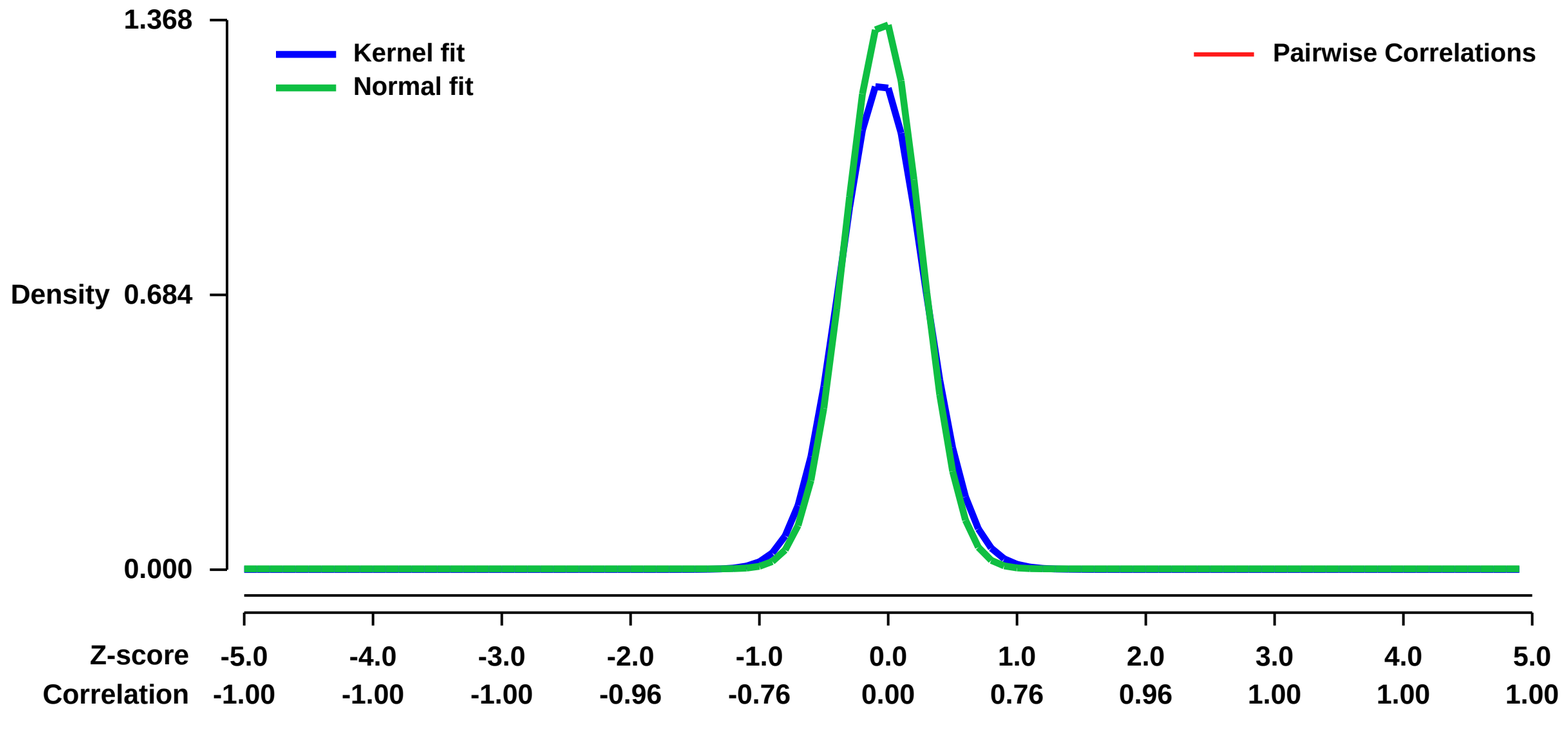

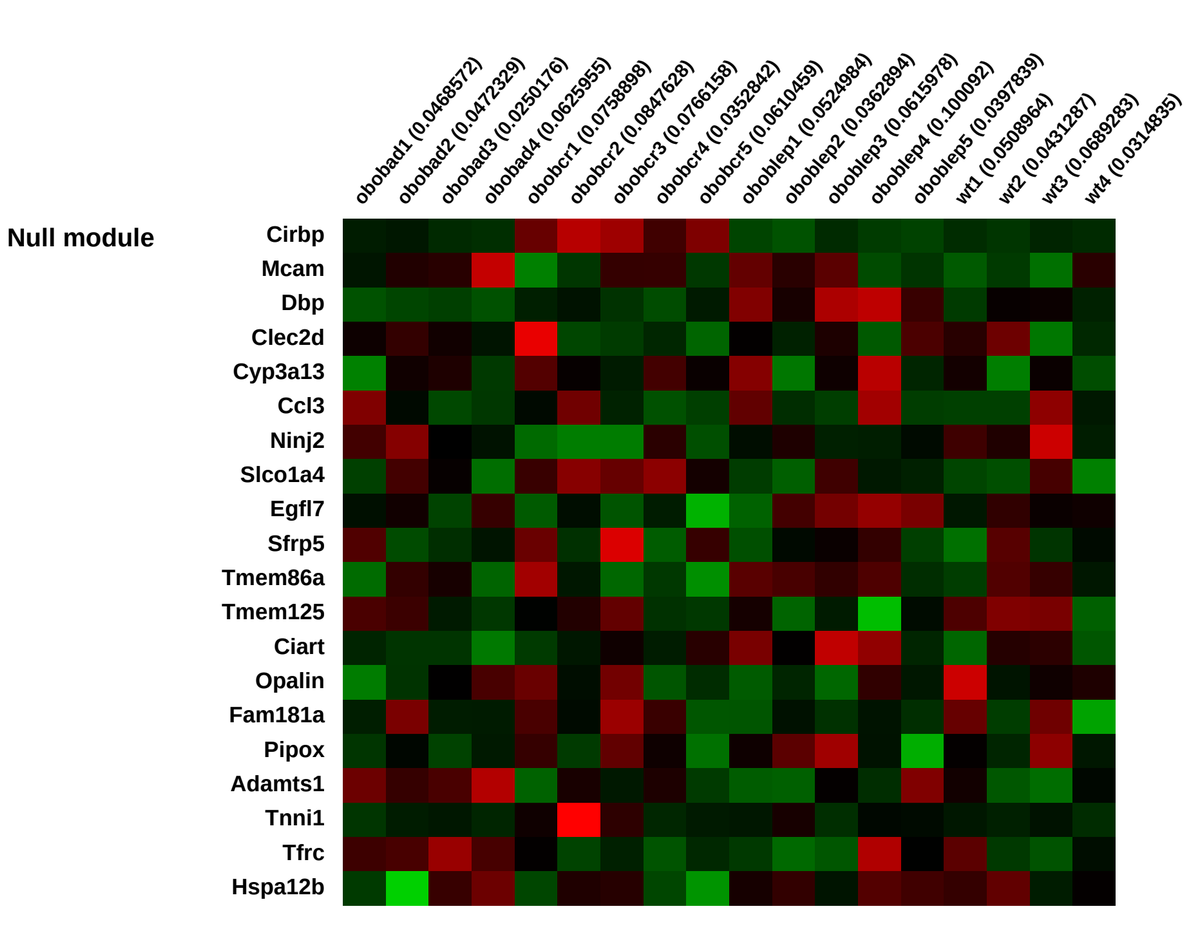

GEO Series "GSE16874" Expression Profiles

Num of samples in this series: 12

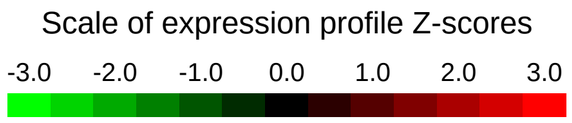

GEO Link:	http://www.ncbi.nlm.nih.gov/geo/query/acc.cgi?acc=GSE16874
Status:	Public on Dec 07 2010
Title:	Expression in wild type and TgDREAM mouse B cells unstimulated or 2 days after LPS+IL4 stimulation
Organism:	Mus musculus
Experiment type:	Expression profiling by array
Platform:	GPL1261
Pubmed ID:	21059893
Summary & Design:	**Summary:** DREAM/KChIP-3 is a calcium-dependent transcriptional repressor highly expressed in immune cells. Transgenic mice expressing a dominant active DREAM mutant show reduced serum immunoglobulin levels. In vitro assays show that reduced immunoglobulin secretion is an intrinsic defect of transgenic B cells that occurs without impairment in plasma cell differentiation but with an accelerated entry in cell division and an increase in class switch recombination. B cells from DREAM knockout mice did not show any phenotype, due to compensation by endogenous KChIP-2. Expression arrays revealed modified expression of Edem1 and Derlin3, two proteins related to the ER-associated degradation pathway and of Klf9, a cell-cycle regulator. Our results disclose a function of DREAM and KChIP-2 in Ig subclass production in B lymphocytes. **Overall design:** We used Affymetrix microarrays (GeneChip Mouse Genome 430 2.0) to compare global gene expression in wild type (WT) versus transgenic B cells (Tg), unstimulated and 2 days after LPS + IL4 stimulation. For ech type of sample three hybridizations were carried-out (independent biological replicates).

Background corr dist: KL-Divergence = 0.0300, L1-Distance = 0.0974, L2-Distance = 0.0115, Normal std = 0.9421

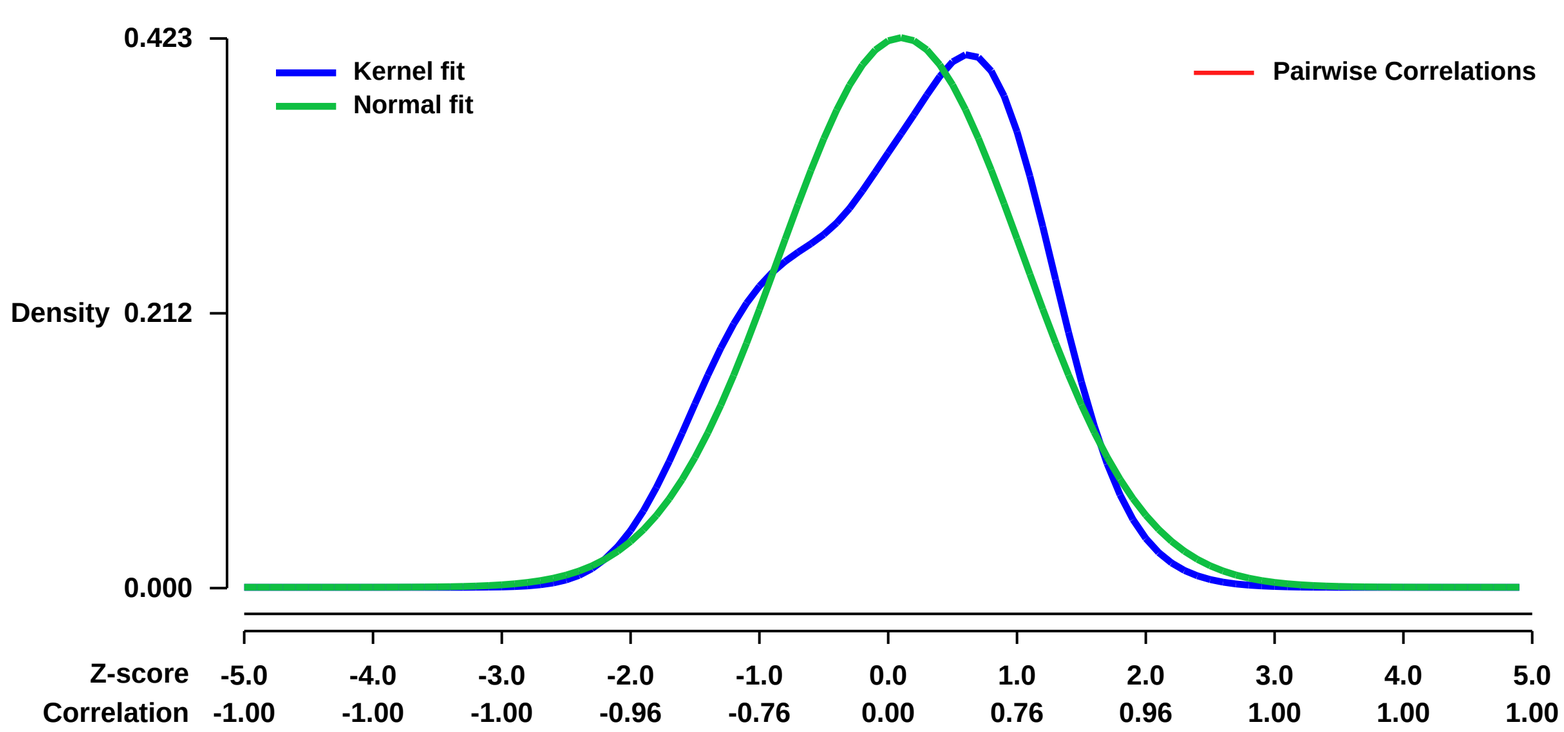

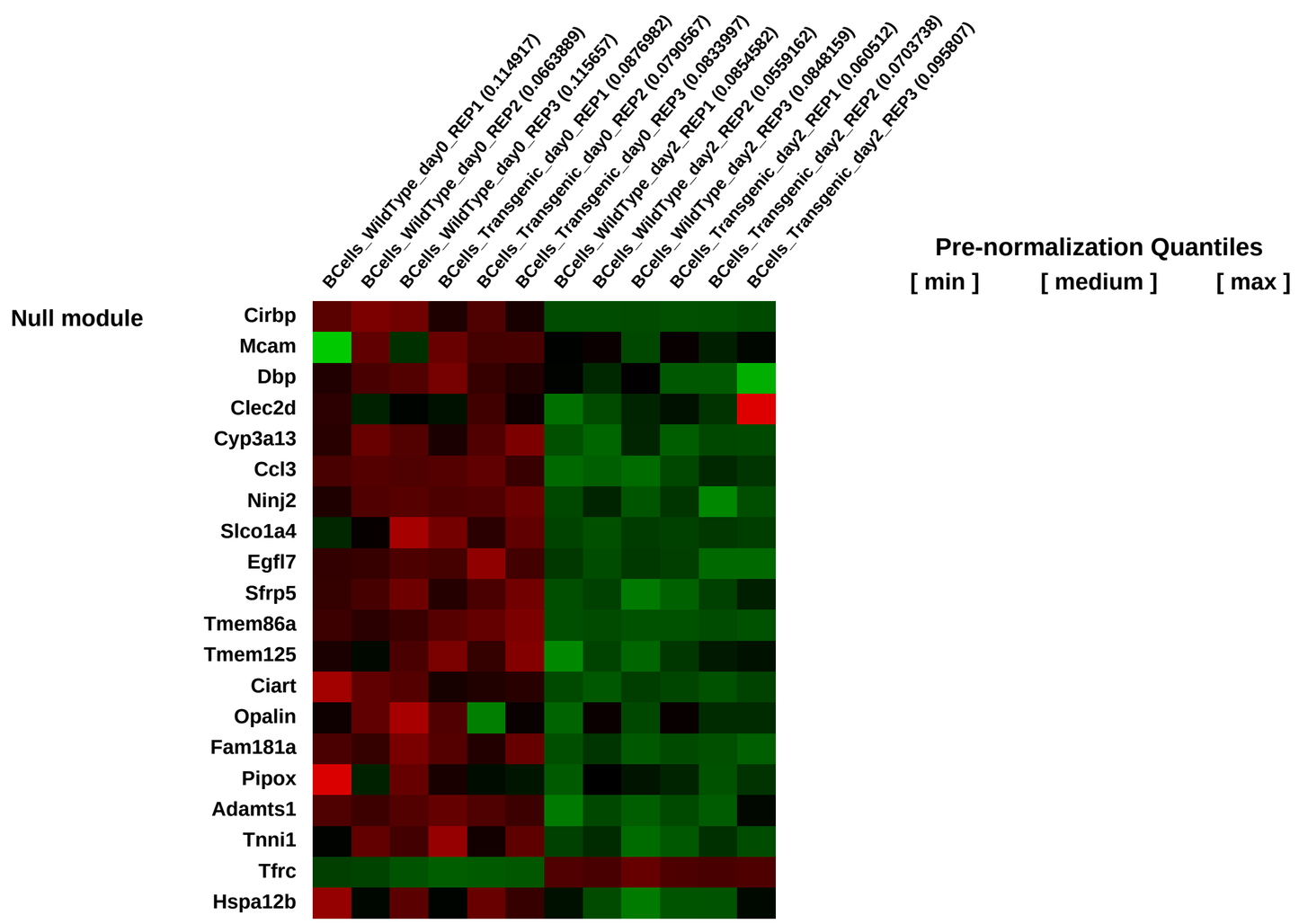

GEO Series "GSE16902" Expression Profiles

Num of samples in this series: 21

Scale of expression profile Z-scores

-3.0 -2.0 -1.0 0.0 1.0 2.0 3.0

GEO Link:	**http://www.ncbi.nlm.nih.gov/geo/query/acc.cgi?acc=GSE16902**
Status:	**Public on Jul 02 2009**
Title:	**Expression data from mouse gastric tumor models**
Organism:	**Mus musculus**
Experiment type:	**Expression profiling by array**
Platform:	**GPL1261**
Pubmed ID:	**20015407**
Summary & Design:	**Summary:** **Transgenic mice with prostaglandin E2 pathway in stomach develops gastric tumors. Simultaneous activation of both Wnt pathway and prostaglandin E2 pathway causes gastric adenocarcinoma. Combination of prostaglandin E2 pathway activation and suppression of BMP pathway leads to the development of gastric hamartomas.** **We used microarrays to find the mechanism of these tumor development and to evaluate whether these mouse models recapitulate human gastric tumors.** **Overall design:** **Glandular stomach from three C57BL/6 wild-type, five K19-Wnt1 transgenic, three K19-C2mE, five K19-Wnt1/C2mE, two K19-Nog, and three K19-Nog/C2mE transgenic mice were used. All mice were female at 18-65 weeks of age.**

Background corr dist: **KL-Divergence = 0.0934, L1-Distance = 0.0243, L2-Distance = 0.0010, Normal std = 0.4487**

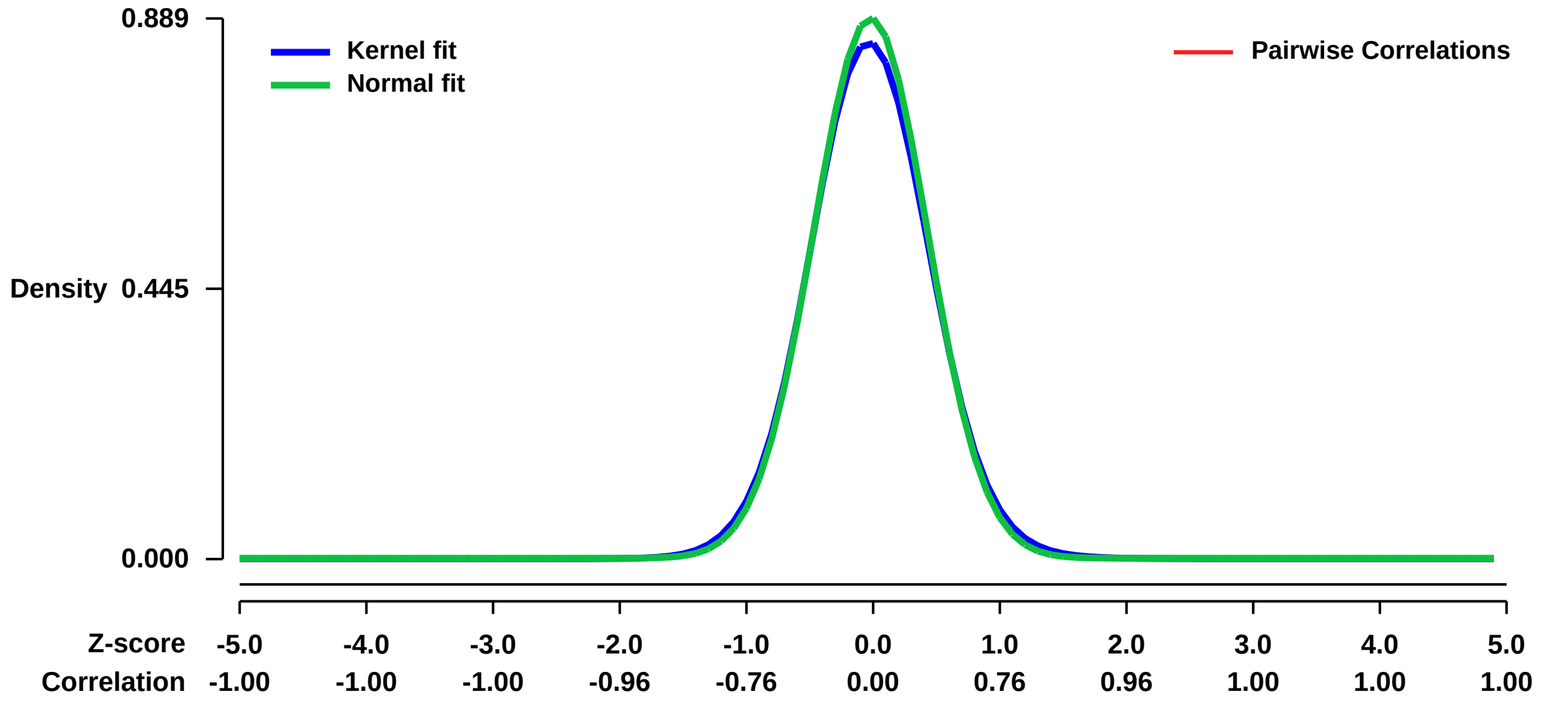

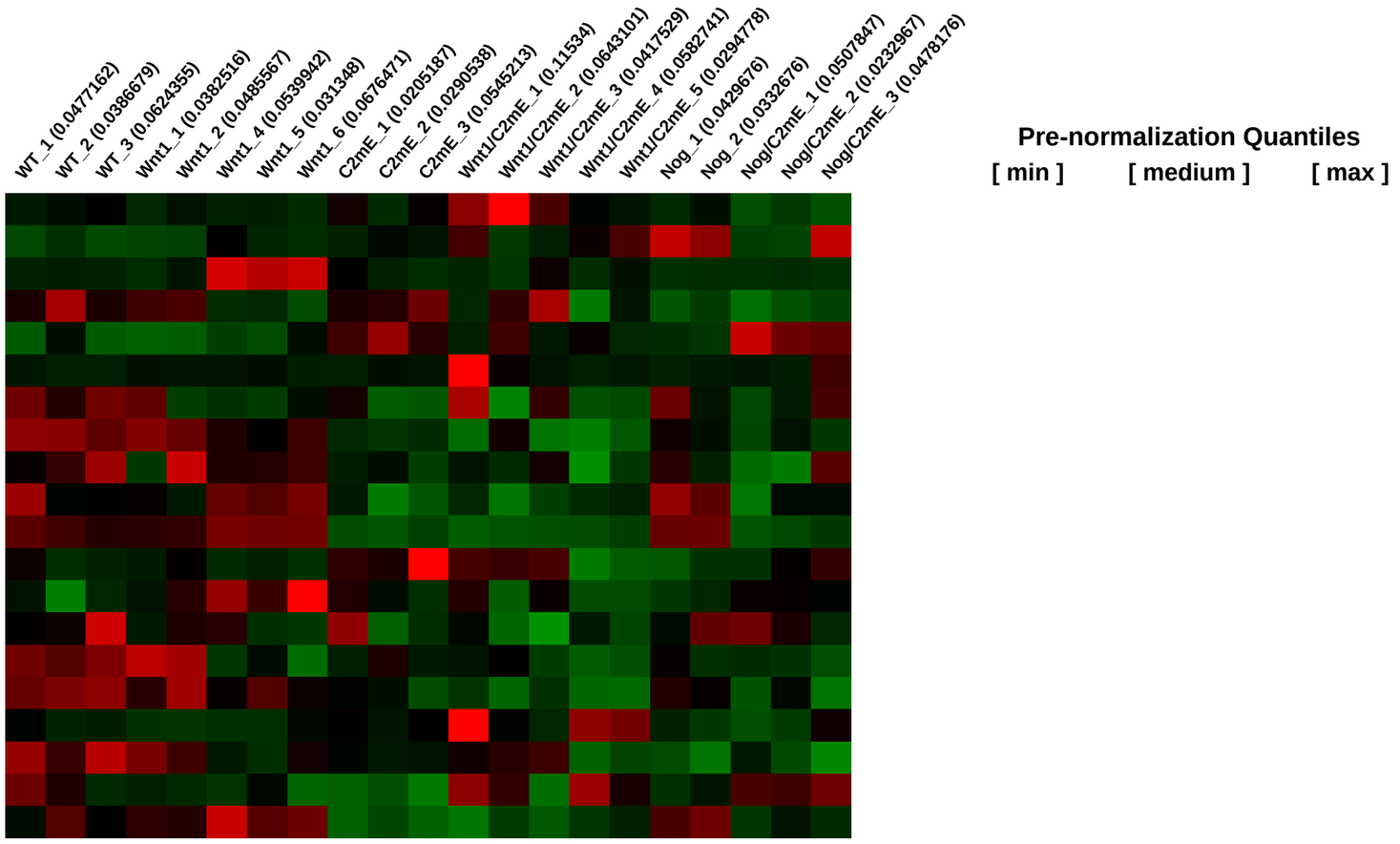

GEO Series "GSE16992" Expression Profiles

Num of samples in this series: 48

Scale of expression profile Z-scores

-3.0 -2.0 -1.0 0.0 1.0 2.0 3.0

GEO Link:	http://www.ncbi.nlm.nih.gov/geo/query/acc.cgi?acc=GSE16992
Status:	Public on Mar 21 2012
Title:	Expression Profiling of Early Myogenesis - Affymetrix Dataset
Organism:	Mus musculus
Experiment type:	Expression profiling by array
Platform:	GPL1261
Pubmed ID:	22147266
Summary & Design:	**Summary:** **Analysis of Early Myogenesis Reveals an Extensive Set of Transcriptional Regulators Whose Knock-down Can Inhibit Differentiation** **Myogenesis is a tightly controlled process involving the transcriptional activation and repression of thousands of genes. Although many components of the transcriptional network are known for the later phases of myogenesis, relatively little work has described the transcriptional landscape within the first 24 hours, when myoblasts commit to differentiate. Through dense temporal sampling of differentiating C2C12 myoblasts, we identify 266 transcriptional regulators (TRs) whose expression is altered within the first 12 hours of myogenesis. A high-content shRNA screen of 76 TRs involving 427 stable lines identified 48 genes whose knockdown significantly inhibits differentiation of C2C12 myoblasts. These include known regulators of myogenesis (Myod1, Myog and Myf5), as well as 26 regulators not previously associated with the process. Of the TRs differentially expressed within the first 24 hours, two-thirds inhibited differentiation when knocked down. Surprisingly, a similar proportion (67%) of shRNAs targeting TRs whose expression did not change during differentiation also inhibited myogenesis, suggesting that both stably and differentially expressed TRs are essential for this complex differentiation program. This implies that microarray-based approaches that concentrate functional validation studies on differentially-expressed genes will fail to identify many genes that are critically implicated in complex biological processes.** **Overall design:** **C2C12 myoblasts were differentiated into myotubes and sampled at various timepoints for gene expression measurement on MOE-430v2 chips. Cells grown in separate plates were harvested at 14 different timepoints: t_-24h, t_0h, t_0.5h, t_1h, t_1.5h, t_2h, t_3h, t_6h, t_9h, t_12h, t_24h, t_48h, t_96h, t_144h. Cells were also pre-treated with 50uM cycloheximide 1 hour prior to inducing differentiation and harvested at two timepoints: t_chx_1h, t_chx_3h. All harvests were performed in triplicate using growths from successive passages.**

Background corr dist: KL-Divergence = 0.1939, L1-Distance = 0.0505, L2-Distance = 0.0065, Normal std = 0.3363

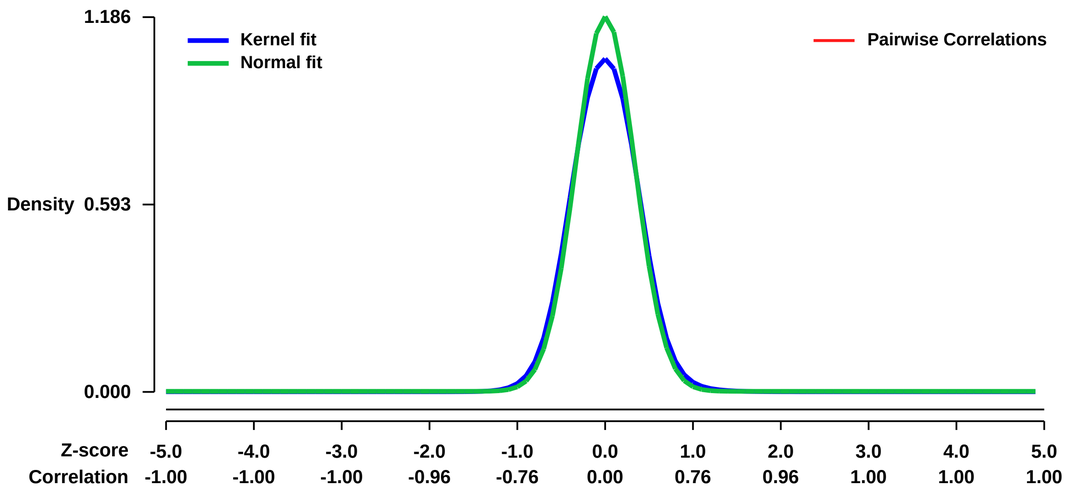

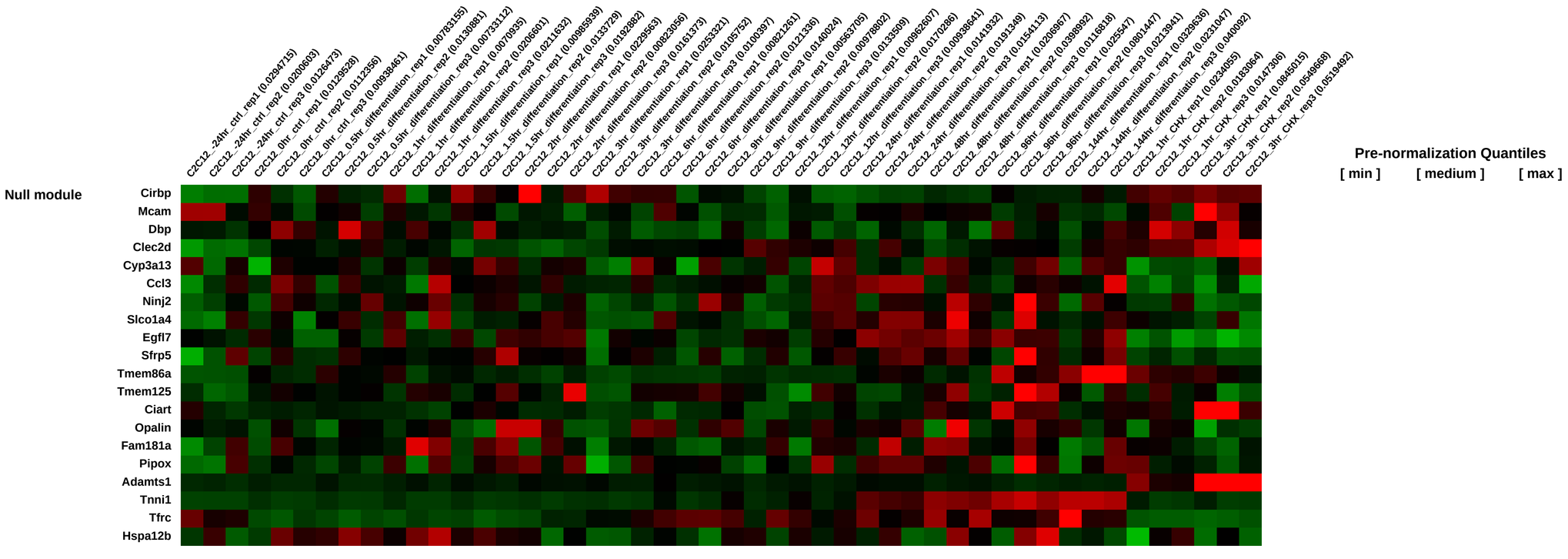

GEO Series "GSE17184" Expression Profiles

Num of samples in this series: 12

Scale of expression profile Z-scores

-3.0 -2.0 -1.0 0.0 1.0 2.0 3.0

GEO Link:	http://www.ncbi.nlm.nih.gov/geo/query/acc.cgi?acc=GSE17184
Status:	Public on Jul 21 2009
Title:	ConA-induced fulminant hepatitis in a mouse model
Organism:	Mus musculus
Experiment type:	Expression profiling by array
Platform:	GPL1261
Pubmed ID:	20398290
Summary & Design:	**Summary:** The goal of this experiment was to investigate the early mechanisms of human fulminant hepatitis through ConA-induced hepatitis model.Early diagnosis and interventions are important for patients with fulminant hepatitis and gene expression may be pivotal in the early diagnosis. Keyword :ConA-induced hepatitis model **Overall design:** ConA was injected through the mouse caudal vein at one of 4 time points (0 hr, 1 hr, 3 hr, 6 hr). The effects of ConA treatment on hepatic gene expression at these time points were analyzed .There are 3 replicates at each timepoint then 4*3=12 samples in all.

Background corr dist: KL-Divergence = 0.1011, L1-Distance = 0.0314, L2-Distance = 0.0014, Normal std = 0.4480

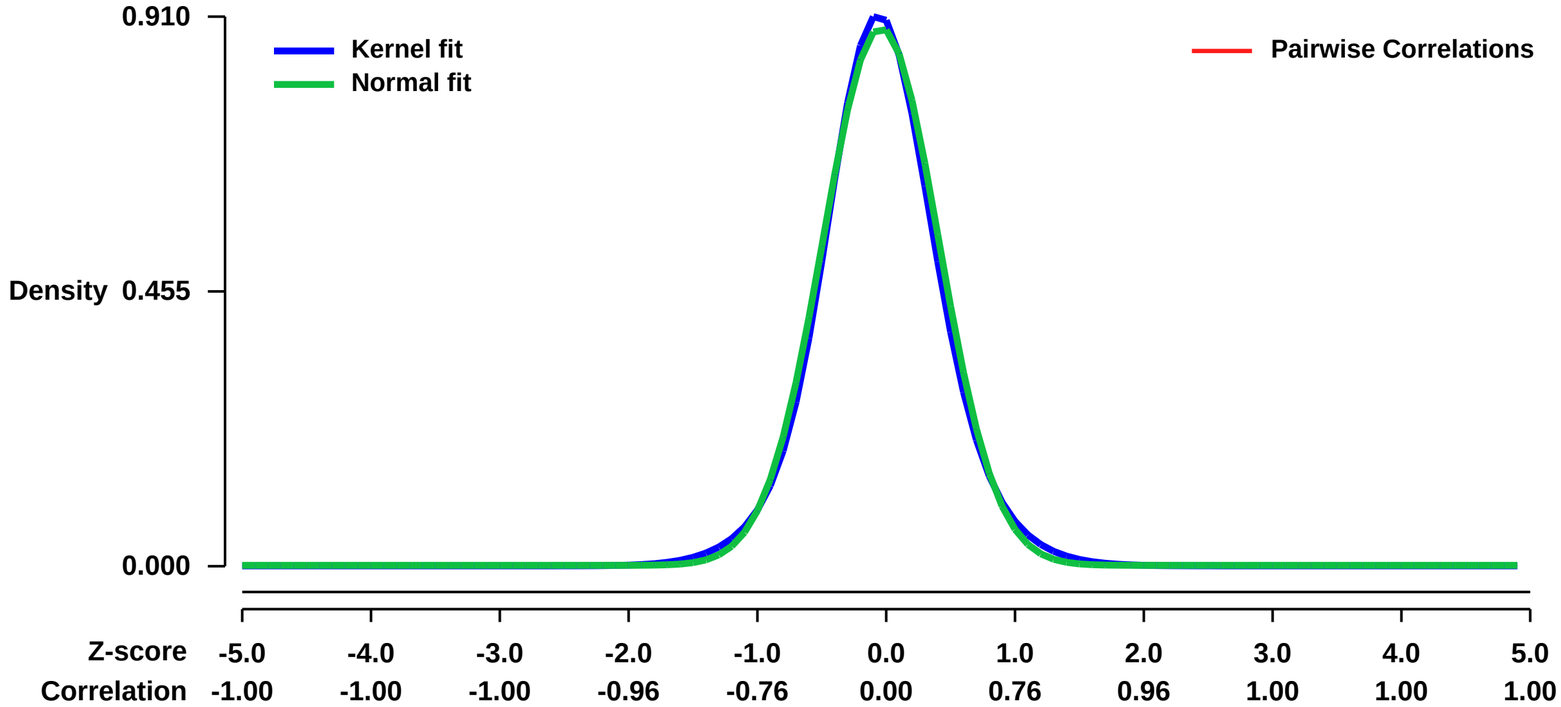

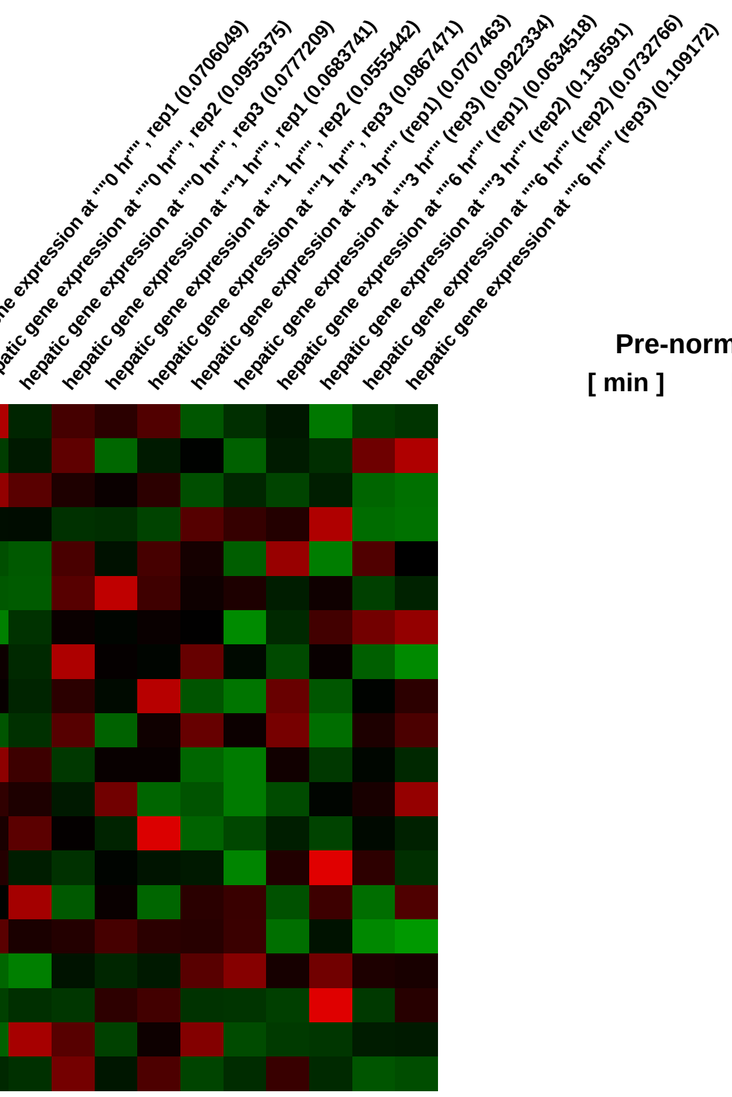

GEO Series "GSE17256" Expression Profiles

Num of samples in this series: 8

Scale of expression profile Z-scores

-3.0 -2.0 -1.0 0.0 1.0 2.0 3.0

GEO Link:	http://www.ncbi.nlm.nih.gov/geo/query/acc.cgi?acc=GSE17256
Status:	Public on Dec 04 2009
Title:	Comparison of gene expression profiles between human and mouse monocyte subsets [mouse data]
Organism:	Mus musculus
Experiment type:	Expression profiling by array
Platform:	GPL1261
Pubmed ID:	19965649
Summary & Design:	**Summary:** Human and mouse blood each contain two monocyte subsets. Here, we investigated the extent of their similarity using a microarray approach. Approximately 300 genes in human and 550 genes in mouse were differentially expressed between subsets. More than 130 of these gene expression differences were conserved between mouse and human monocyte subsets. We confirmed numerous differences at the cell surface protein level. Despite overall conservation, some molecules were conversely expressed between the two speciesâ subsets, including CD36, CD9, and TREM-1. Furthermore, other differences existed, including a prominent PPAR‹ signature in mouse monocytes absent in human. Overall, human and mouse monocyte subsets are far more broadly conserved than currently recognized. Thus, studies in mice may indeed yield relevant information regarding the biology of human monocyte subsets. However, differences between the species deserve consideration in models of human disease studied in the mouse. **Overall design:** The two major subsets of monocytes (Ly-6C+ and Ly-6Clo) from 12-week old C57Bl/6 mice were sorted and the RNA extracted and hybridized to Affymetrix GeneChip´fi 430 2.0 arrays. We pooled leukocytes from 5 mice for each sort and sorted 4 separate times for 4 biological replicates. The two major monocyte subsets (CD16- and CD16+) were isolated from venous heparinized blood from apparently healthy human volunteers using MACS technology with all reagents and tools from Miltenyi Biotec. Three separate donors were hybridized three different times to Affymetrix U133 Plus 2.0 array.

Background corr dist: KL-Divergence = 0.0564, L1-Distance = 0.0247, L2-Distance = 0.0007, Normal std = 0.5574

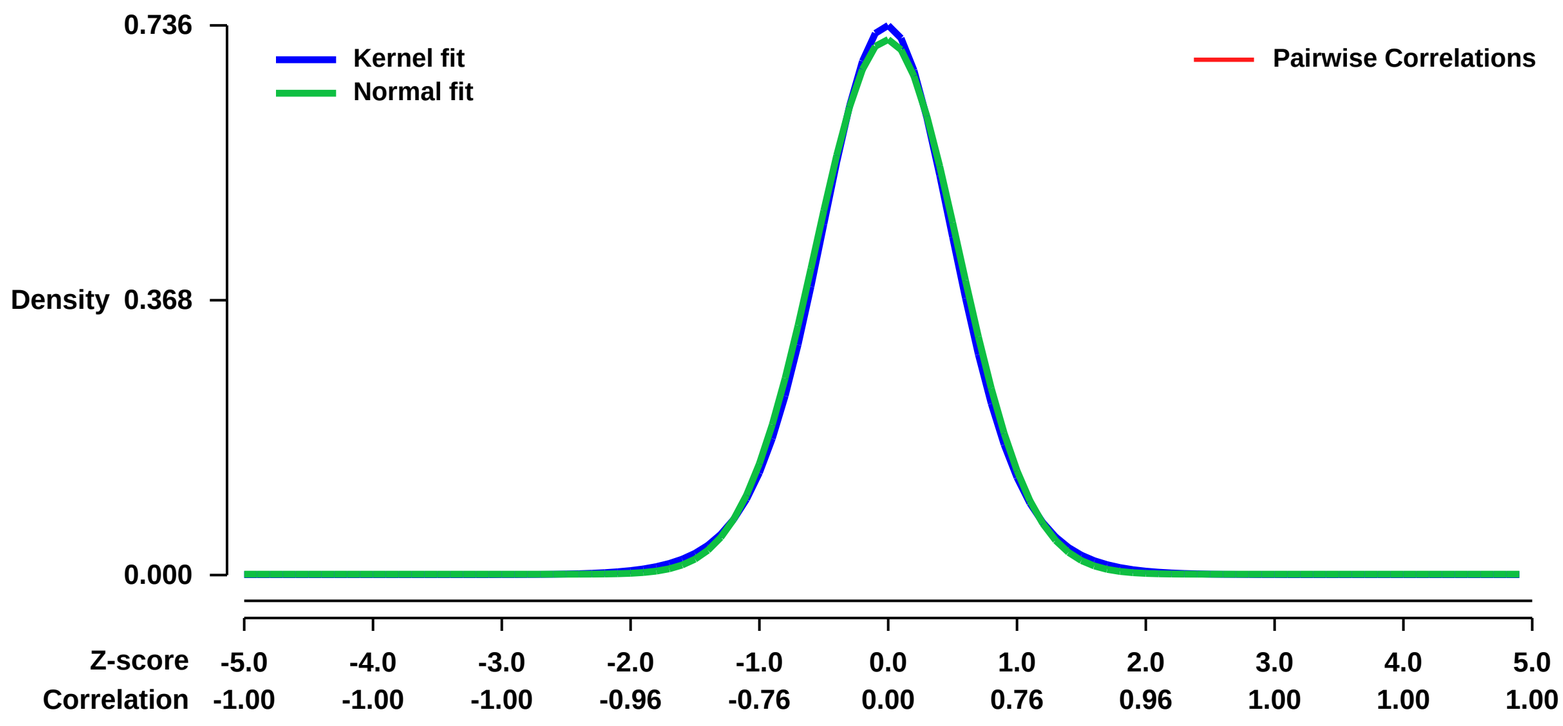

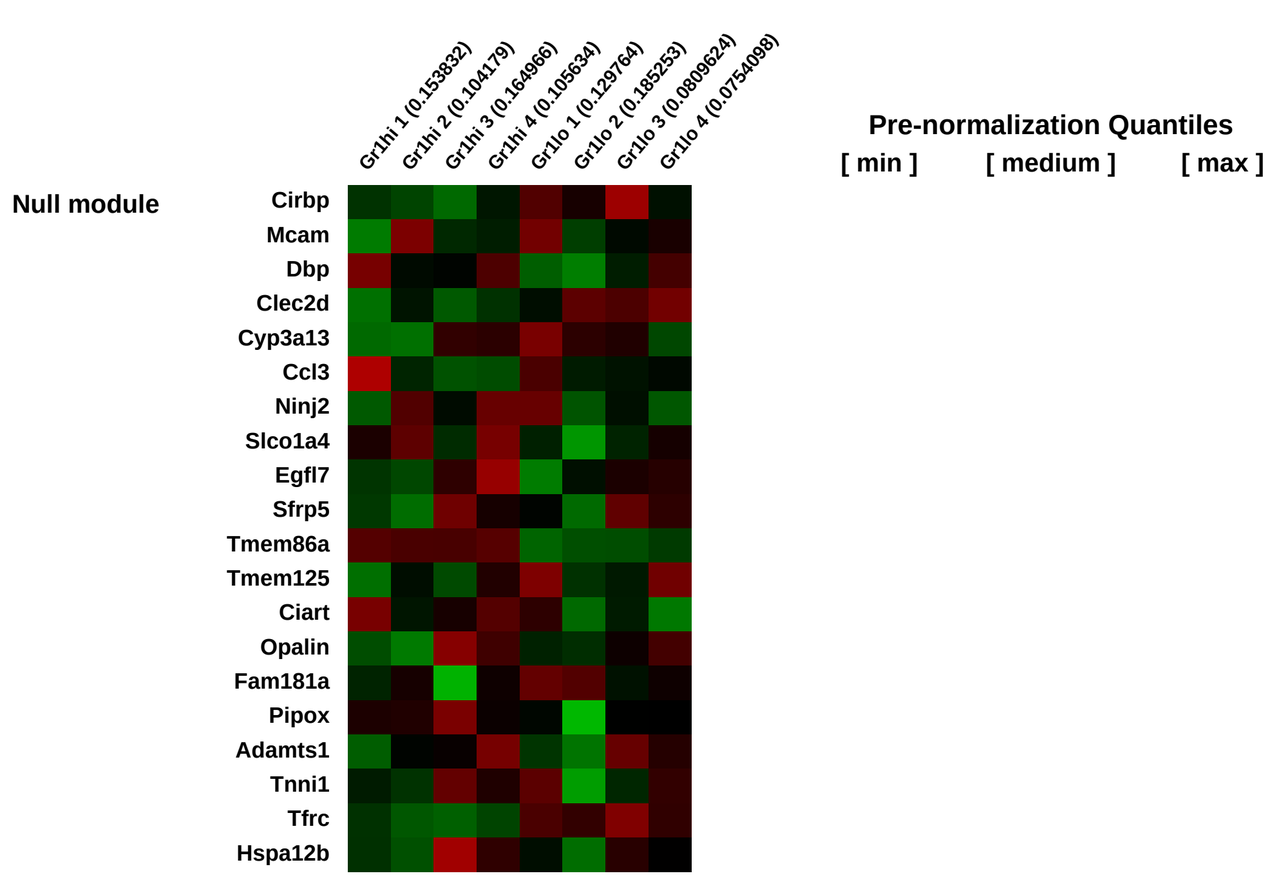

GEO Series "GSE17263" Expression Profiles

Num of samples in this series: 6

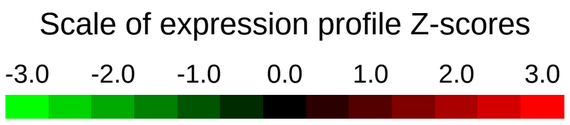

GEO Link:	http://www.ncbi.nlm.nih.gov/geo/query/acc.cgi?acc=GSE17263
Status:	Public on Apr 13 2010
Title:	Gene expression profiling of constitutive activation of Smoothened in the mouse uterus
Organism:	Mus musculus
Experiment type:	Expression profiling by array
Platform:	GPL1261
Pubmed ID:	20130264
Summary & Design:	**Summary:** In order to gain a better understanding of Ihh action during embryo implantation, we constitutively activated Smo in the murine uterus using the PRcre mouse model (PRcre/+SmoM2+; SmoM2). Female SmoM2 mice were infertile. They exhibited normal serum progesterone levels and normal ovulation, but ova failed to be fertilized in vivo and the uterus failed to undergo the artificially induced decidual response. SmoM2 mice exhibited uterine hypertrophy. The endometrium had a reduced number of uterine glands and the endometrial stroma lost its normal morphologic characteristics. Microarray analysis of 3 month old SmoM2 uteri demonstrated a chondrocytic signature and confirmed that constitutive activation of SmoM2 increased extracellular matrix production. Thus, constitutive activation of Smo in the mouse uterus alters the extracellular matrix which interferes with early pregnancy. **Keywords:** two group comparison **Overall design:** We constitutively activated Hh signaling in the uterus by the expression of a mutant SmoM2 allele. We crossed these mice to the PRcre mouse model to constitutively activate Smo in the murine uterus (PRcre/+SmoM2+; SmoM2). High density DNA microarray analysis was performed on 3 month old control and SmoM2 uteri.

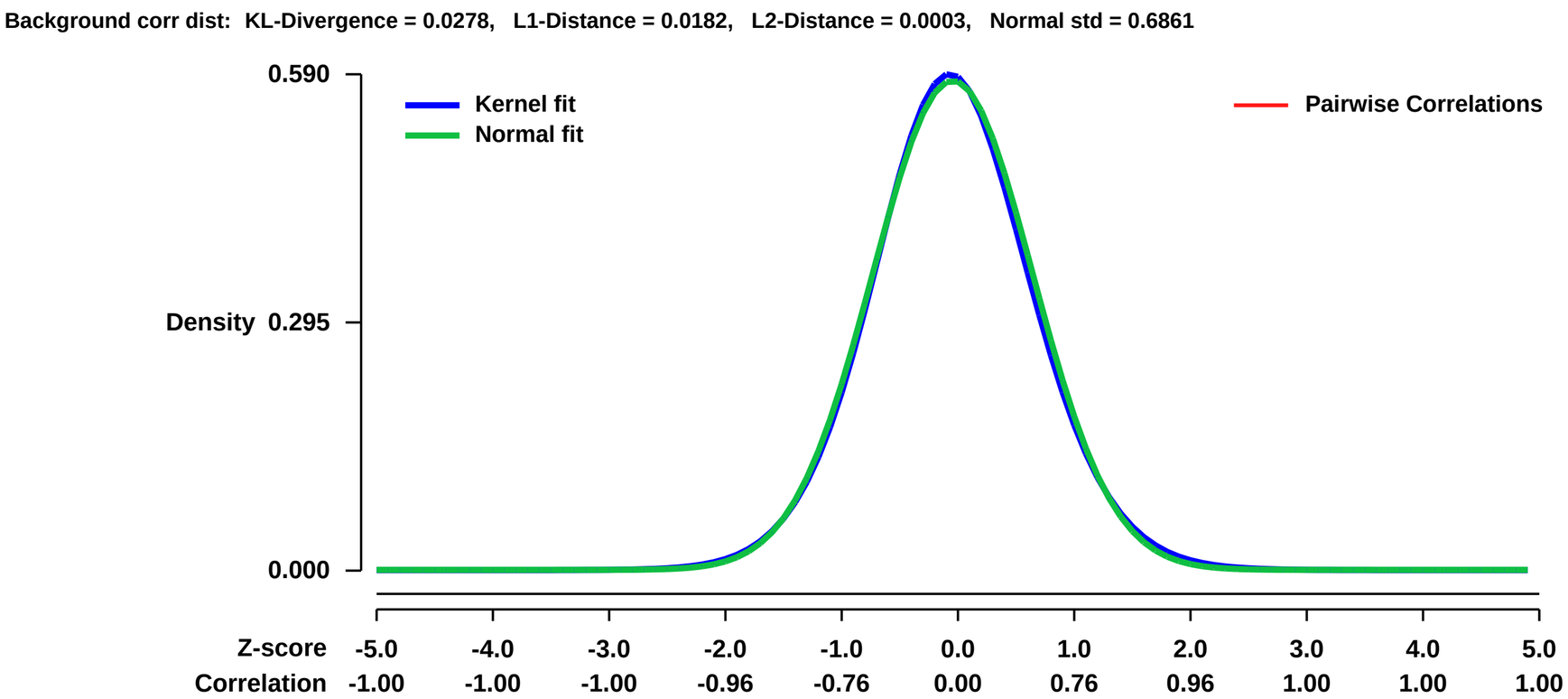

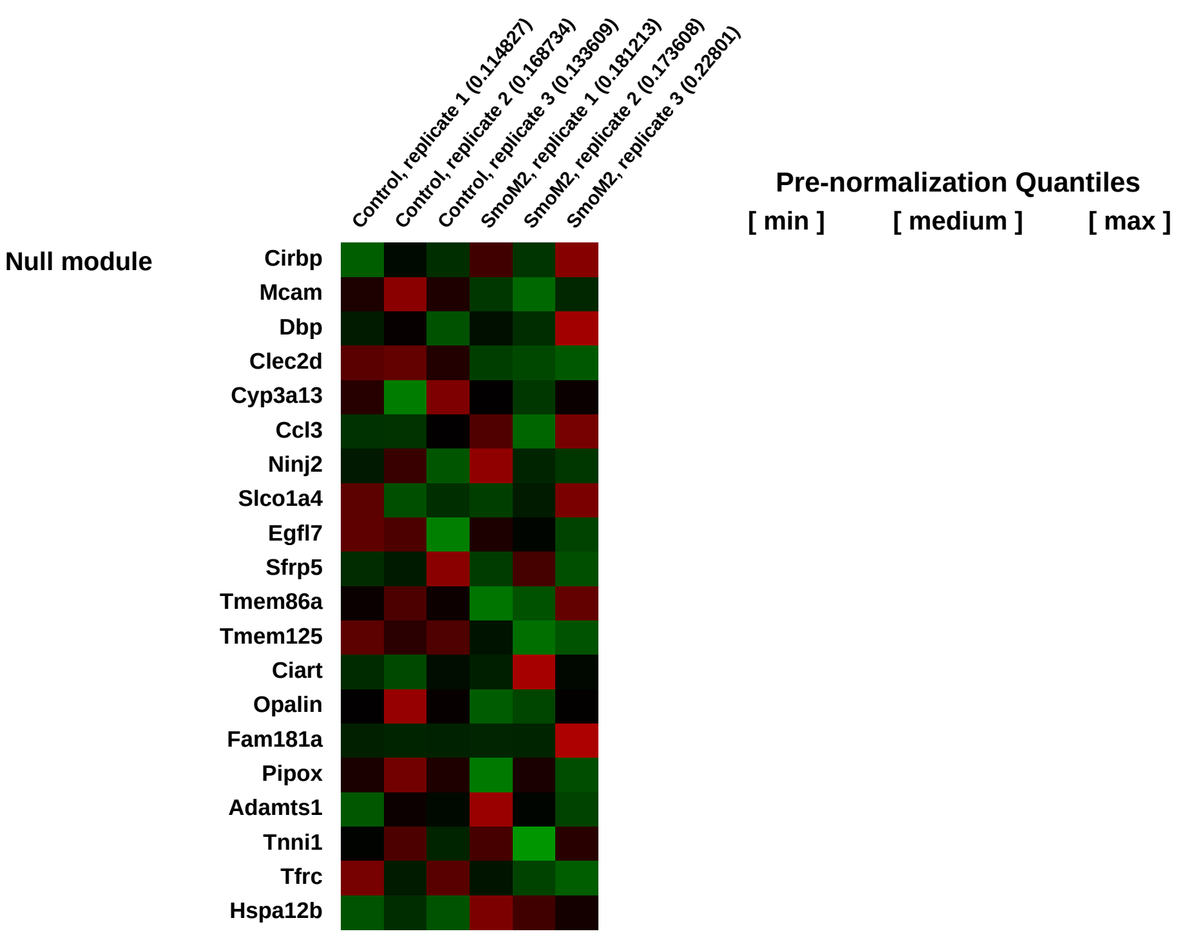

GEO Series "GSE17383" Expression Profiles

Num of samples in this series: 6

Scale of expression profile Z-scores

-3.0 -2.0 -1.0 0.0 1.0 2.0 3.0

GEO Link:	http://www.ncbi.nlm.nih.gov/geo/query/acc.cgi?acc=GSE17383
Status:	Public on Aug 05 2009
Title:	Toward a Better Understanding of Potential Roles of Astrocytes in HIV-1-associated Neurocognitive Disorders
Organism:	Mus musculus
Experiment type:	Expression profiling by array
Platform:	GPL1261
Pubmed ID:	19697136
Summary & Design:	**Summary:** We present a microarray analysis of primary mouse astrocytes exposed to HIV-1 in culture. Results are compared with previous genomic studies of HIV-1 effect in human astrocytes and human and macaque brains. **Overall design:** Day-two neonatal mouse astrocytes were exposed in triplicates to cell-free HIV-1/NL4-3 at m.o.i. of 1 and cultured for 24 hours. As control, cells were treated in triplicates with a mock virus concentrate at the same dilution (vol/vol) as the wild-type virus. As an example of large scale gene expression analysis we shall provide some details of the method; full description is in Kim et al. (S.-Y. Kim et al., 2004). Total RNA was prepared from cell cultures using the RNAeasy total RNA extraction kit (Qiagen, CA). RNA quality was assessed by electrophoresis and spectrophotometric analysis; between 1 and 10 ´µg of total RNA was used to generate a cDNA, and then 1 ´µg of cDNA product was used in an in vitro transcription reaction that contained biotinylated UTP and CTP. Twenty ´µg of full-length cRNA was fragmented and was subjected to gene expression analysis on the Affymetrix Mouse Genome 430 2.0 Array chip. Affymetrix software was used to generate CHP files. Significance analysis was performed using ArrayAssist software (Stratagene).

Background corr dist: KL-Divergence = 0.0419, L1-Distance = 0.0186, L2-Distance = 0.0004, Normal std = 0.6059

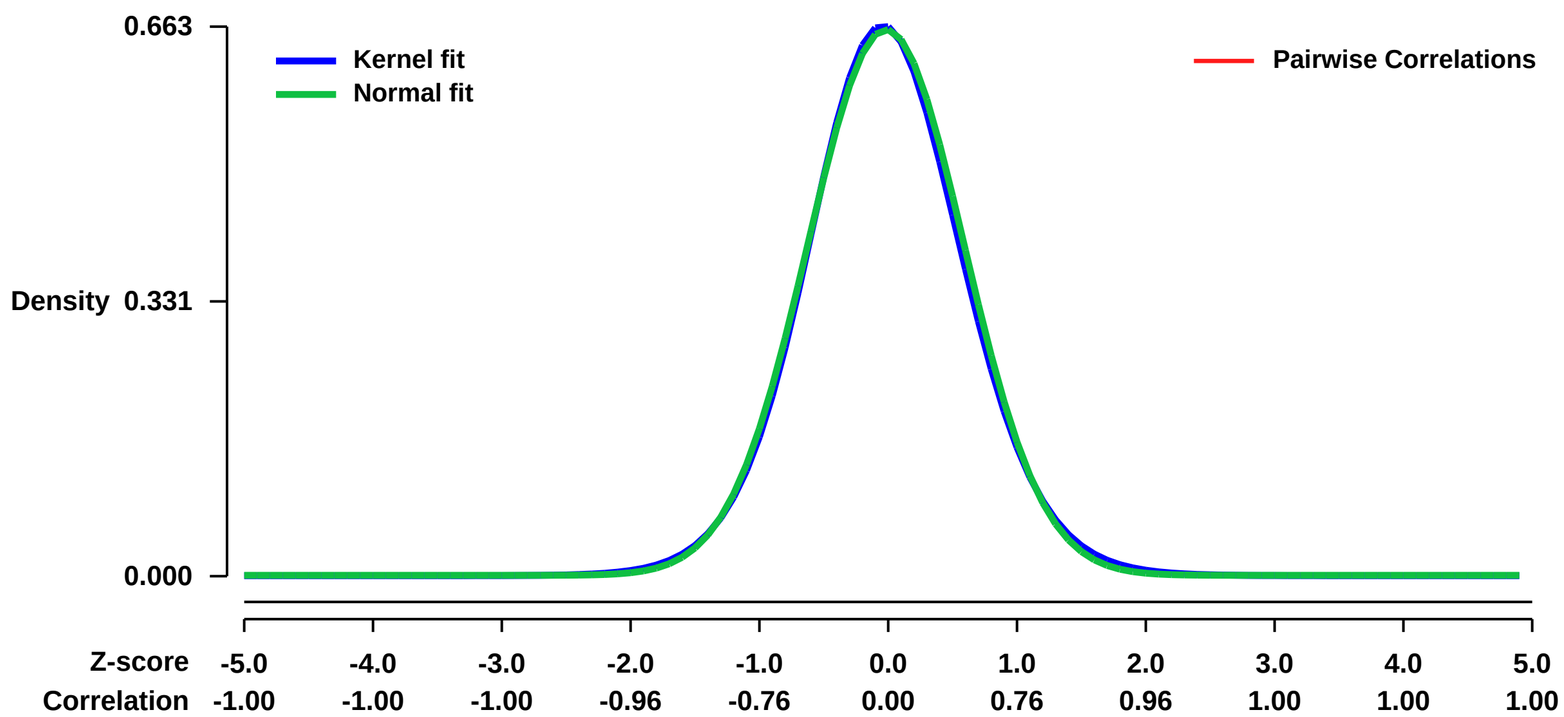

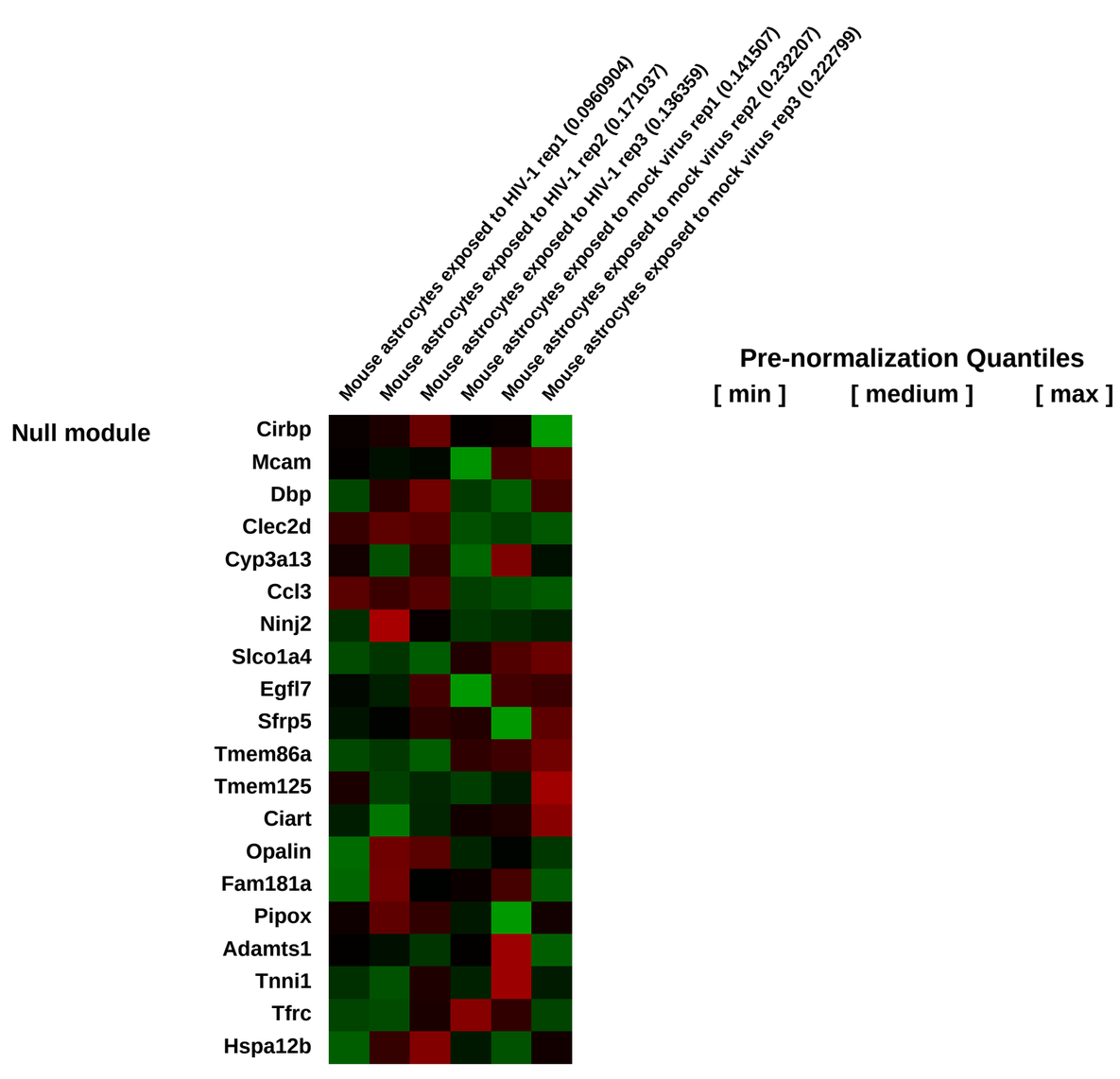

GEO Series "GSE17404" Expression Profiles

Num of samples in this series: 9

Scale of expression profile Z-scores

-3.0 -2.0 -1.0 0.0 1.0 2.0 3.0

GEO Link:	http://www.ncbi.nlm.nih.gov/geo/query/acc.cgi?acc=GSE17404
Status:	Public on Aug 10 2010
Title:	Activated AMPK and prostaglandins are involved in the response to conjugated linoleic acid and are sufficient to cause lipid reductions in adipocytes
Organism:	Mus musculus
Experiment type:	Expression profiling by array
Platform:	GPL1261
Pubmed ID:	20965713
Summary & Design:	**Summary:** Activated AMPK and prostaglandins are involved in the response to conjugated linoleic acid and are sufficient to cause lipid reductions in adipocytes. Trans-10, cis-12 conjugated linoleic acid (t10c12 CLA) reduces triglyceride levels in adipocytes. AMP-activated protein kinase (AMPK) was recently demonstrated to be involved in the emerging pathways regulating this response. This study investigated the role of AMPK and inflammation in lowering triglyceride levels by testing the following hypotheses: 1) A moderate activator of AMPK, such as metformin, and an inflammatory response are sufficient to reduce triglycerides, and 2) Strong activation of AMPK is also sufficient. These experiments were performed by adding compounds that affect these pathways and measuring their effects in 3T3-L1 adipocytes. Tumor necrosis factor ˛– (TNF-˛–), an inflammatory cytokine, increased the ability of metformin to reduce triglycerides, but TNF-˛– was observed to activate AMPK. A comparison of metformin, phenformin, TNF-˛–, and t10c12 CLA found a correlation between AMPK activity level and triglyceride reduction. Inhibitors of the prostaglandin (PG) biosynthetic pathway interfered with t10c12 CLA's ability to reduce triglycerides. Inhibitors of MAPK/ERK kinase or Jun N-terminal kinase interfered with the phosphorylation of phospholipase A2 and triglyceride reductions. **Keywords:** control/treatment **Overall design:** Limma data are available in the Supplementary files 'GSE17404_limma_CLAvsLA.txt', 'GSE17404_limma_PFMvsLA.txt', and 'GSE17404_limma_PFMvsCLA.txt'.

Background corr dist: KL-Divergence = 0.0361, L1-Distance = 0.0325, L2-Distance = 0.0019, Normal std = 0.6204

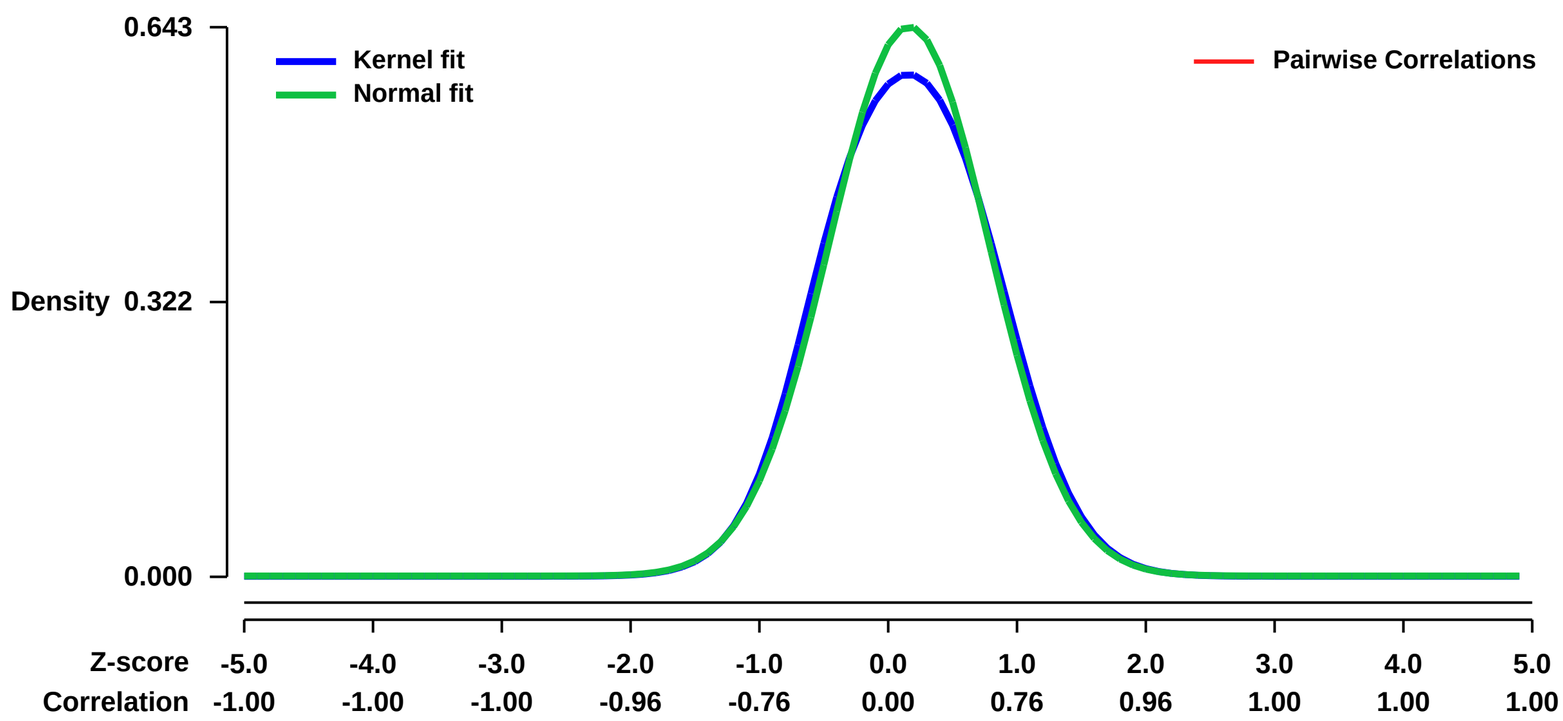

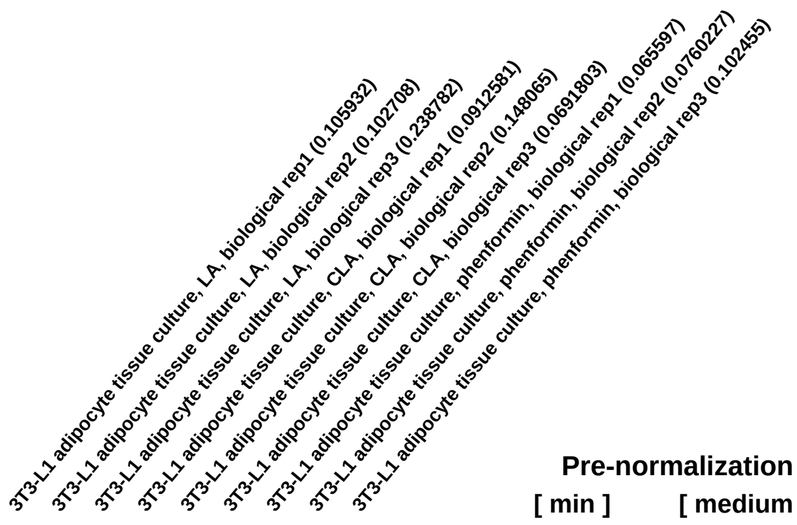

GEO Series "GSE17462" Expression Profiles

Num of samples in this series: 8

Scale of expression profile Z-scores

-3.0 -2.0 -1.0 0.0 1.0 2.0 3.0

GEO Link: http://www.ncbi.nlm.nih.gov/geo/query/acc.cgi?acc=GSE17462
Status: Public on Aug 01 2009
Title: Expression data from Bmi1-overexpressing Ink4a-Arf-null hepatoblasts
Organism: Mus musculus
Experiment type: Expression profiling by array
Platform: GPL1261
Pubmed ID:

Summary & Design:

Summary:
Forced expression of Bmi1 accelerated the self-renewal of hepatic stem/progenitor cells and eventually induced their transformation in an in vivo transplant model. The Ink4a/Arf locus, which encodes a cyclin-dependent kinase inhibitor, p16Ink4a, and a tumor suppressor, p19Arf, is a pivotal target of Bmi1. Therefore, it would be of importance to understand the contribution of the Ink4a/Arf locus to Bmi1 oncogenic functions in cancer and search for as-yet-unknown Bmi1 target genes other than Ink4a/Arf. We used microarrays to explore novel candidate downstream targets for Bmi1 in hepatic stem/progenitor cells

Overall design:
Purified Dlk-positive hepatoblasts at day 28 of culture were subjected to RNA extraction and hybridization on Affymetrix microarrays. Data were obtained for quadrant samples from four independent experiments.

Background corr dist: KL-Divergence = 0.0597, L1-Distance = 0.0375, L2-Distance = 0.0025, Normal std = 0.5470

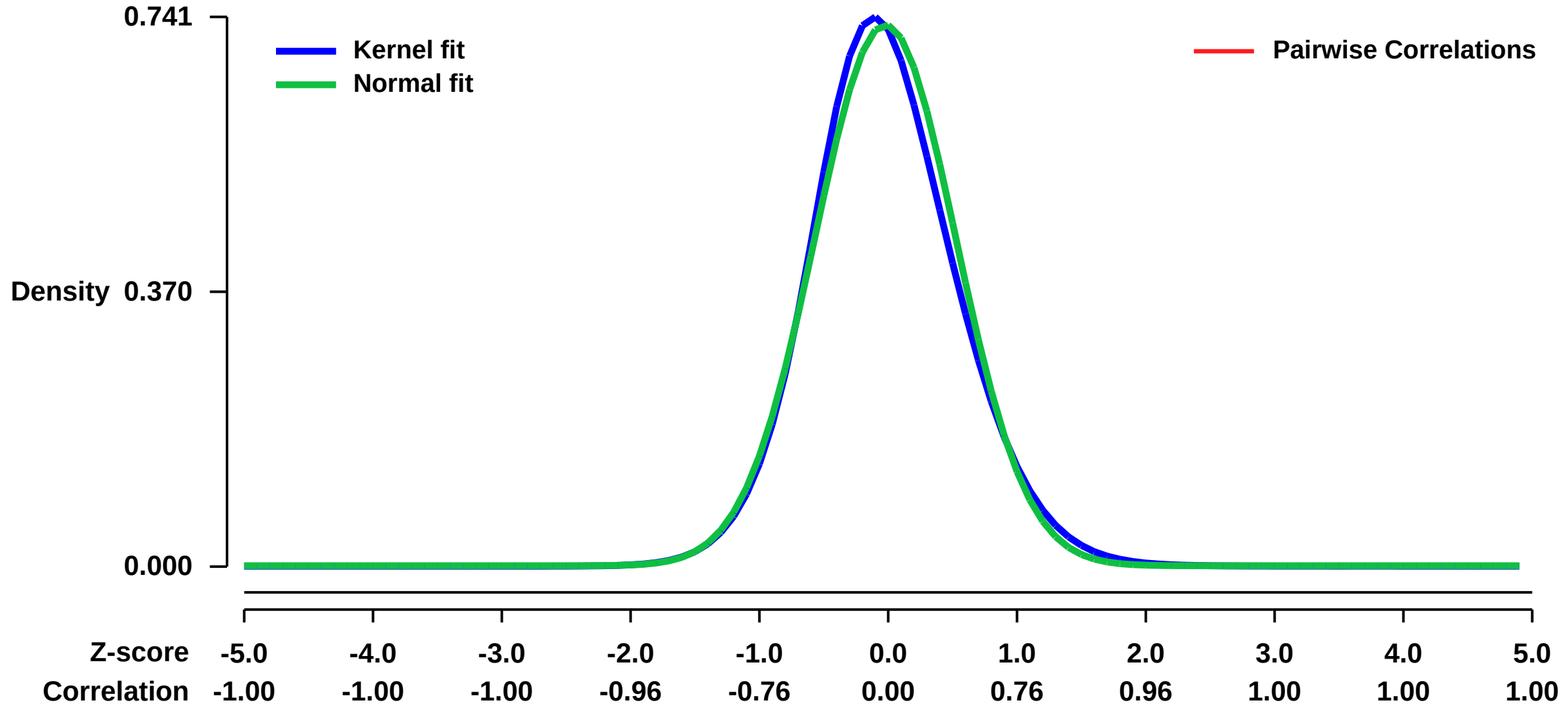

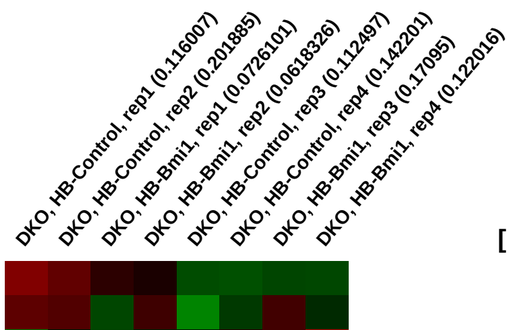

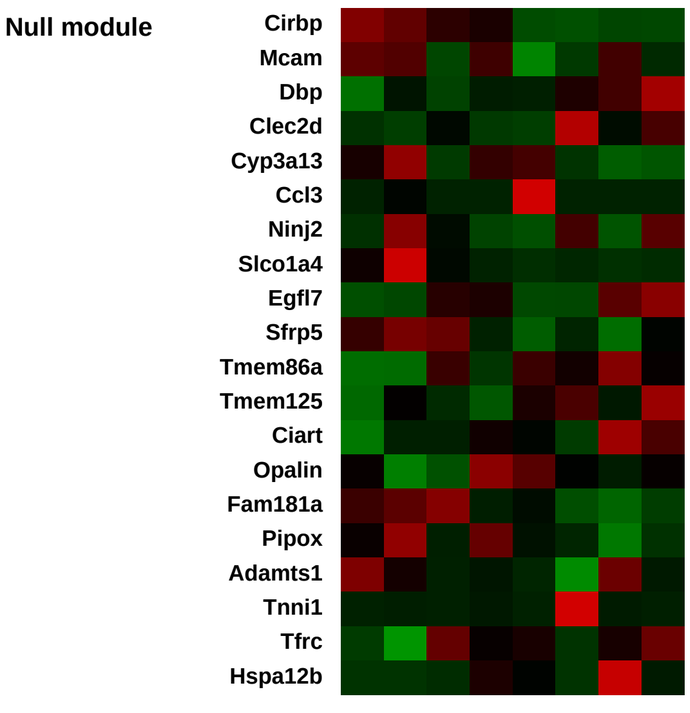

GEO Series "GSE17497" Expression Profiles

Num of samples in this series: 10

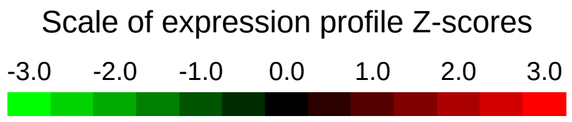

GEO Link:	http://www.ncbi.nlm.nih.gov/geo/query/acc.cgi?acc=GSE17497
Status:	Public on Aug 06 2009
Title:	Gene expression in murine acute lymphoblastic leukemia in vivo after allogeneic or syngeneic bone marrow transplantation
Organism:	Mus musculus
Experiment type:	Expression profiling by array
Platform:	GPL1261
Pubmed ID:	20602231
Summary & Design:	**Summary:** This study compared gene expression in murine bcr-abl positive acute lymphoblastic leukemia cells in vivo in allogeneic BMT recipients compared to syngneneic BMT recipients. **Overall design:** The goal of the experiment was to compare gene expression in leukemia cells that were in either an allogeneic transplant (5 samples) or syngeneic transplant (5 samples) immune environment in vivo. The bone marrow transplant model involved preparation of C57BL/6 recipients with total body irradiation and 5-fluoruracil. These recipients were then infused IV with either allogeneic C3.SW marrow and spleen cells or syngeneic C57BL/6 marrow and spleen cells. The leukemia cells were mixed in with the marrow and spleen cells. After a few weeks (2-3) the C57BL/6 leukemia cells were purified by flow cytometry and passed into other freshly transplanted animals. After three serial transplants the leukemia cells were flow purified and RNA prepared. Leukemia was C57BL/6 background (cells contain the human p210 bcr/abl oncogenic fusion gene and also have a deletion in the Ink4a/Arf locus, see: Biology of Blood and Marrow Transplantation. 14:622-630, 2008).

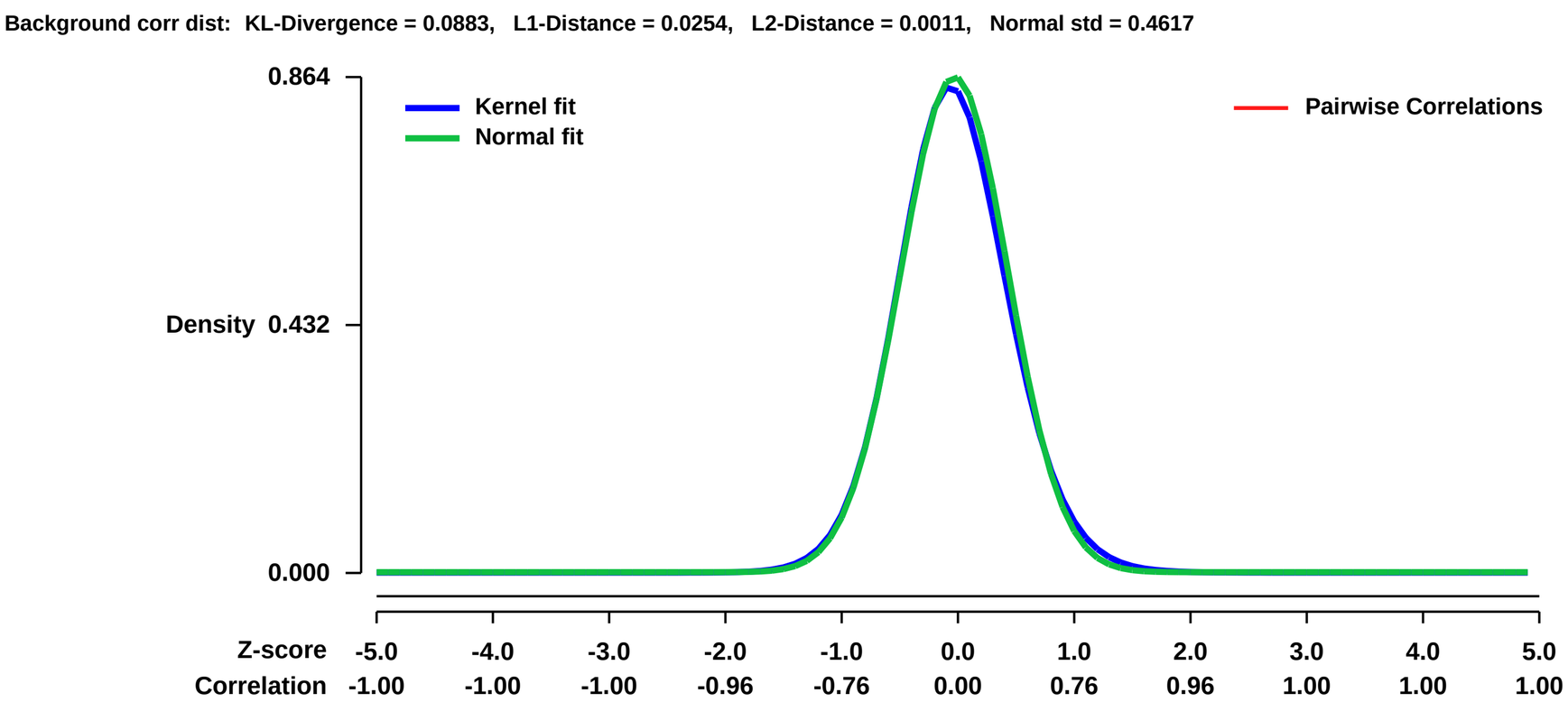

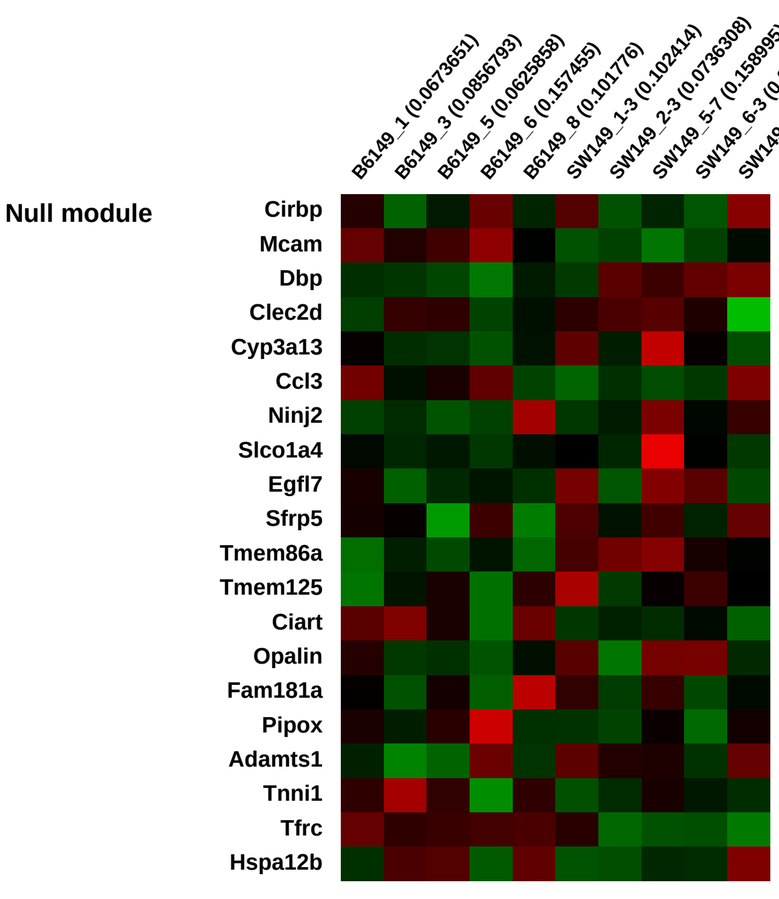

GEO Series "GSE17509" Expression Profiles

Num of samples in this series: 57

Scale of expression profile Z-scores

-3.0 -2.0 -1.0 0.0 1.0 2.0 3.0

GEO Link: http://www.ncbi.nlm.nih.gov/geo/query/acc.cgi?acc=GSE17509
Status: Public on Aug 20 2009
Title: Reduced levels of protein tyrosine phosphatase CD45 protect mice from the lethal effects of Ebola virus infection
Organism: Mus musculus
Experiment type: Expression profiling by array
Platform: GPL1261
Pubmed ID: 19683682

Summary & Design:

Summary:
To gain insight into the changes in gene expression pattern upon Ebola infection, CD45+/+ (100% protein level) and CD45+/- (62% protein level) mice were challenged with mouse adapted Ebola virus. At time-points day 0, 1, 3, 5, 7, 9, 11 and 13, spleen tissue was harvested and splenocytes isolated. Total RNA was isolated for mRNA expression analysis. The mouse genome 430 2.0 array (Affymetrix, Inc.), which consists of over 39,000 genes in a single array, was used. Based on gene expression patterns, the variable genes were grouped into sixteen clusters. Each cluster contained genes associated with cellular immune processes, signaling, cell-cycle, complement coagulation cascade, biosynthesis/metabolism, ubiquitous genes involved in several cascades, and genes of unknown function. Interestingly, gene expression in clusters 2 and 3 were significantly downregulated by day 1 following EBOV challenge in CD45100% mice. In contrast, at day 1 following EBOV infection, the CD45 62% mice maintained gene expression patterns similar to day 0. The differences in gene expression patterns between the CD45 100% and CD45 62% splenocytes were less apparent at day 3 following infection and by days 5 and 7 they became very similar. At day 9, when wild-type mice had succumbed to the disease, the pattern in CD45 62% mice remained similar to the day 7 patterns of CD45 100% and CD45 62% mice. The pattern at days 11 and 13 in the CD45 62% mice had returned to that of day 0 CD45 100% or CD45 62% mice. These results suggested that in CD45 100% mice, subversion of the cell transcriptional machinery during the early stages of EBOV infection (day 1) might represent a major factor leading to death of the mice. In CD45 62% mice, early control of gene regulation likely provided the appropriate antiviral responses leading to regulated inflammation, immune co-stimulation, and survival.

Overall design:
RNA expression in CD45 100% and 62% mice were compared at each time point: days 0, 1, 3, 5, and 7, using an empirical Bayes procedure. From 3 to 8 biological replicates were in each group. Samples for days 9, 11, and 13 (4 biological replicates each) were also available for only CD45 62%. Median expression values for highly variable genes within each group were clustered using agglomerative nesting over all available time points.

Background corr dist: KL-Divergence = 0.2878, L1-Distance = 0.0465, L2-Distance = 0.0049, Normal std = 0.2883

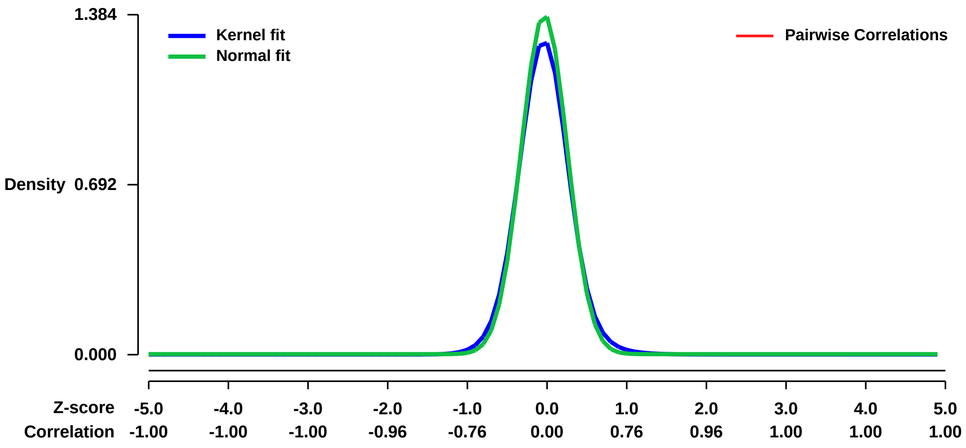

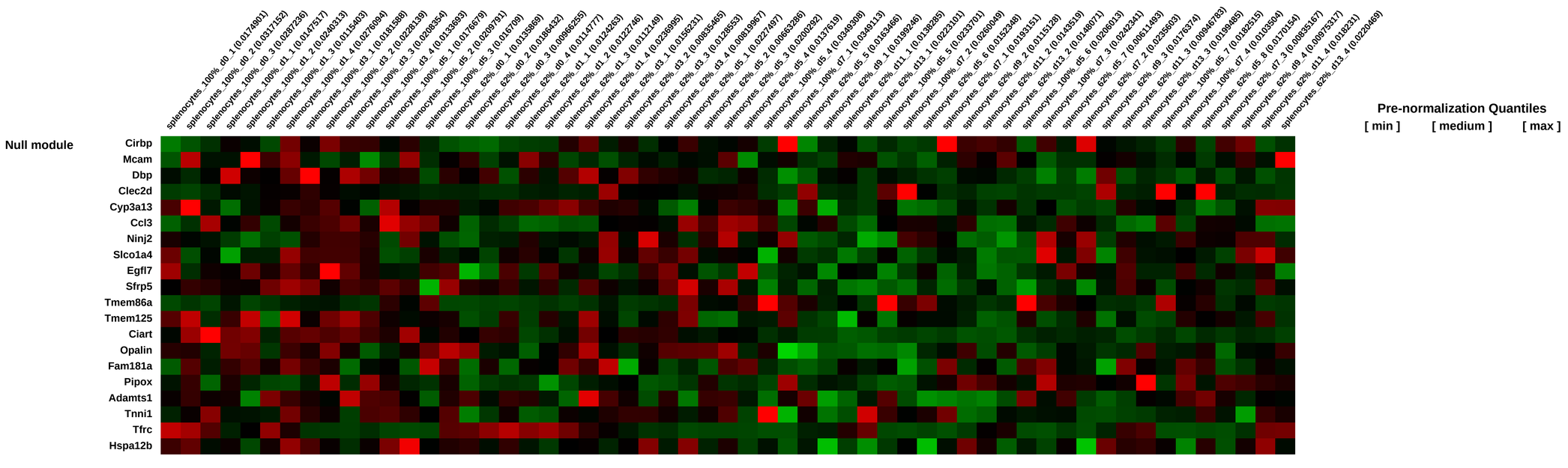

GEO Series "GSE17513" Expression Profiles

Num of samples in this series: 12

Scale of expression profile Z-scores

-3.0 -2.0 -1.0 0.0 1.0 2.0 3.0

GEO Link:	http://www.ncbi.nlm.nih.gov/geo/query/acc.cgi?acc=GSE17513
Status:	Public on Sep 01 2009
Title:	Expression data from murine embryonic stem cell derived cardiac progenitors
Organism:	Mus musculus
Experiment type:	Expression profiling by array
Platform:	GPL1261
Pubmed ID:	19833966
Summary & Design:	**Summary:** Mamamlian cardiogenesis occurs through the development of discreate populations of first and second heart field progenitors. We have used a dual transgenic color reproter system to isolate purified populations of these progenitors. We used microarrays to detail the global programme of gene expression underlying cardiac development in mouse All four populations of cells are derived from embryonic stem cells differentiating in vitro (day 6 of in vitro differentaition). The stem cell line has two transgenic reporters as follows: 1. The second heart field (SHF) specific reporter of the Mef2C gene (E. Dodou, S. M. Xu, B. L. Black, Mech Dev 120, 1021 (Sep, 2003)) driving the expression of dsRed 2. The cardiac specific enhancer (C. L. Lien et al., Development 126, 75 (Jan, 1999)) driving the expression of eGFP. Thus, the red cells are SHF specific, the green cells are cardiac specific, and the red/green are SHF and cardiac specific. These cells are compared to the double negative cells which serve as a control. **Overall design:** Embryonic stem cell derived progenitors were isolated into four distinct populations by FACS purifying these progenitors based on a two color reporter system. Four populations were then compared to each other by transcriptional profiling.

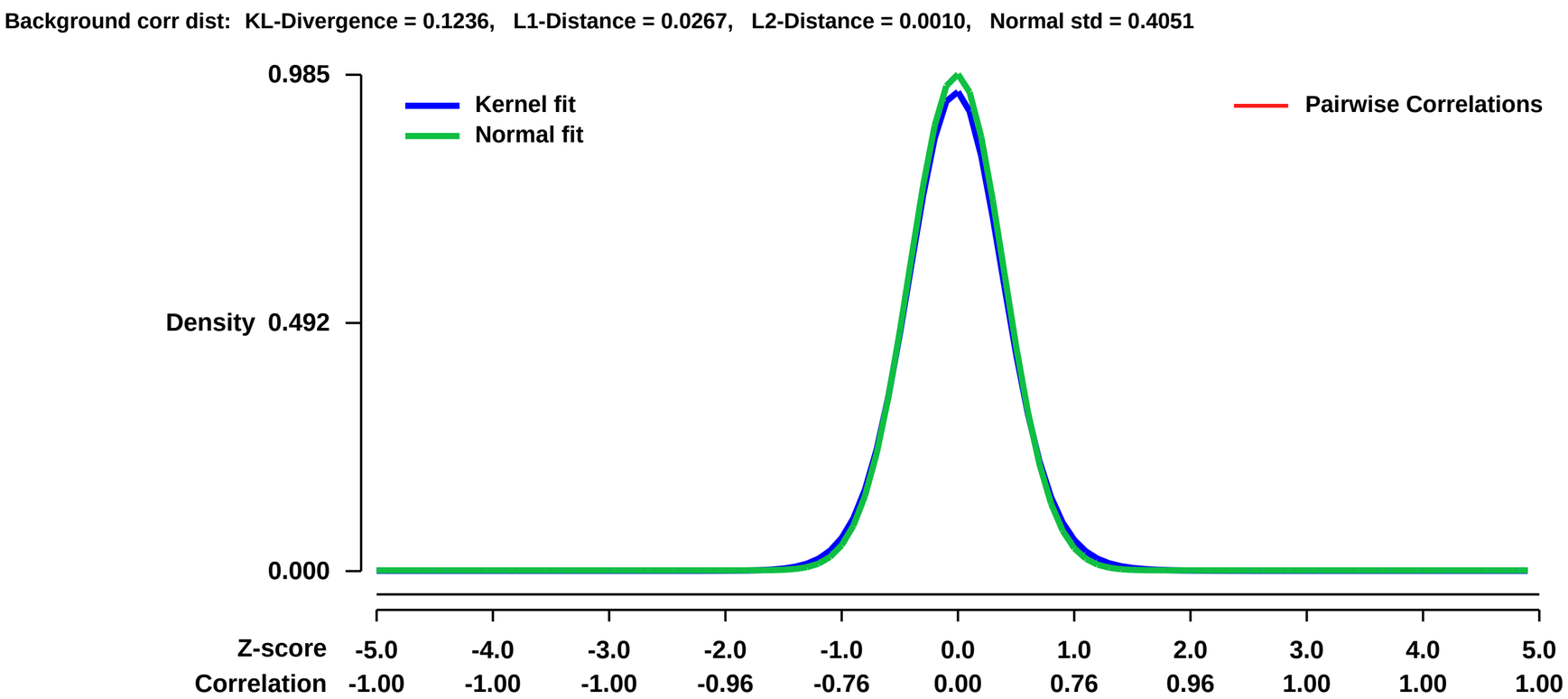

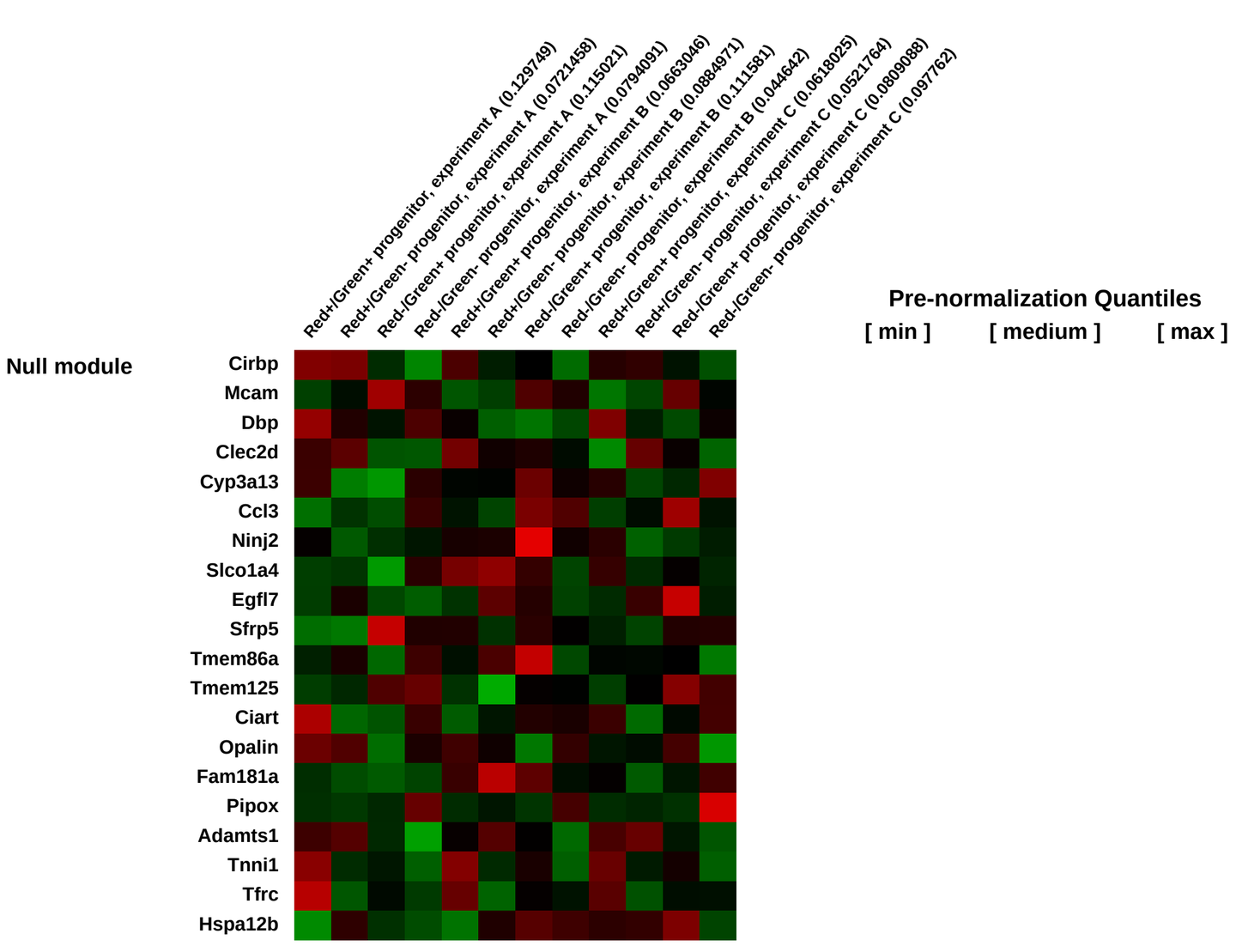

GEO Series "GSE17647" Expression Profiles

Num of samples in this series: 24

Scale of expression profile Z-scores

-3.0 -2.0 -1.0 0.0 1.0 2.0 3.0

GEO Link:	**http://www.ncbi.nlm.nih.gov/geo/query/acc.cgi?acc=GSE17647**
Status:	**Public on Aug 15 2009**
Title:	**Involvement of 4E-BP1 in the protection induced by HDLs on pancreatic beta cells**
Organism:	**Mus musculus**
Experiment type:	**Expression profiling by array**
Platform:	**GPL1261**
Pubmed ID:	**19574449**
Summary & Design:	**Summary:** **High-density lipoproteins (HDLs) protect pancreatic ¸† cells against apoptosis. This property might be related to the increased risk to develop diabetes in patients with low HDL blood levels. However, the mechanisms by which HDLs protect ¸† cells are poorly characterized. Here we use a transcriptomic approach to identify genes differentially modulated by HDLs in ¸† cells subjected to apoptotic stimuli.** **Overall design:** **Starvation medium + HDL (prep. HDL GSK3 or HDL GSK4) [HDL.S]**

Background corr dist: **KL-Divergence = 0.3267, L1-Distance = 0.0543, L2-Distance = 0.0075, Normal std = 0.2719**

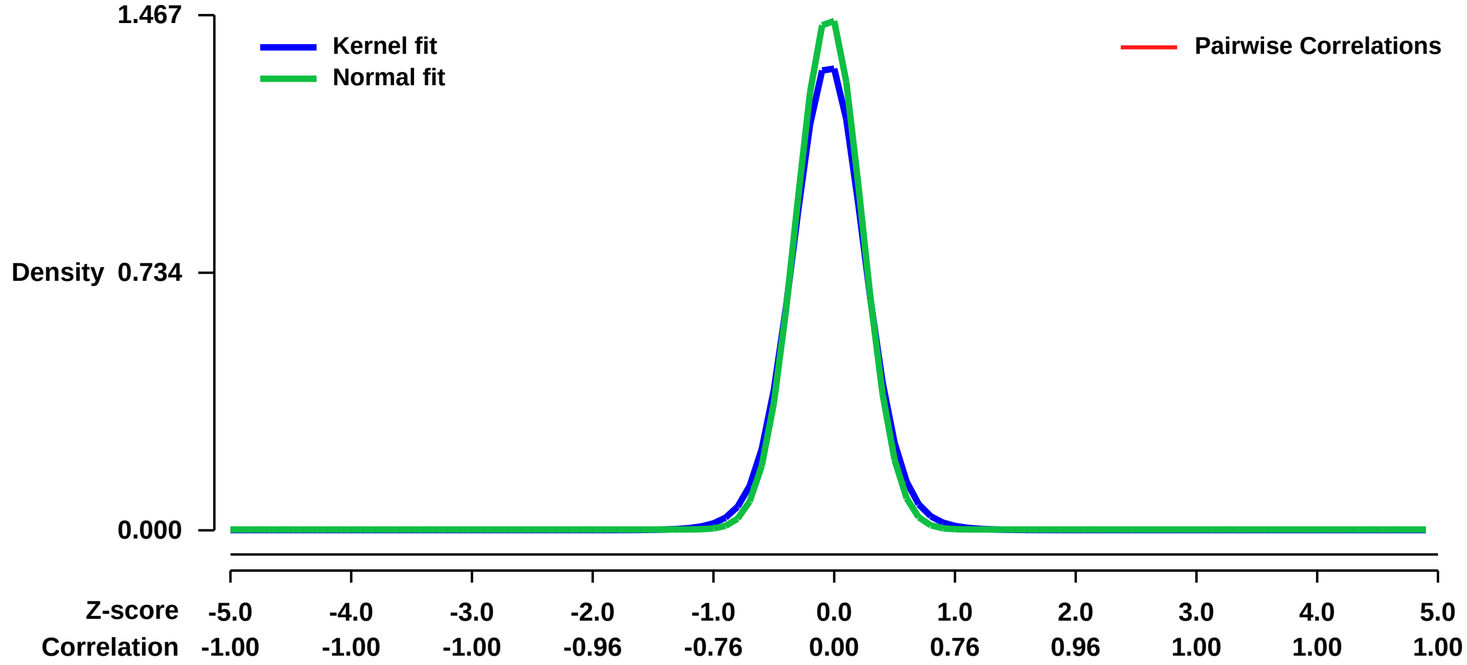

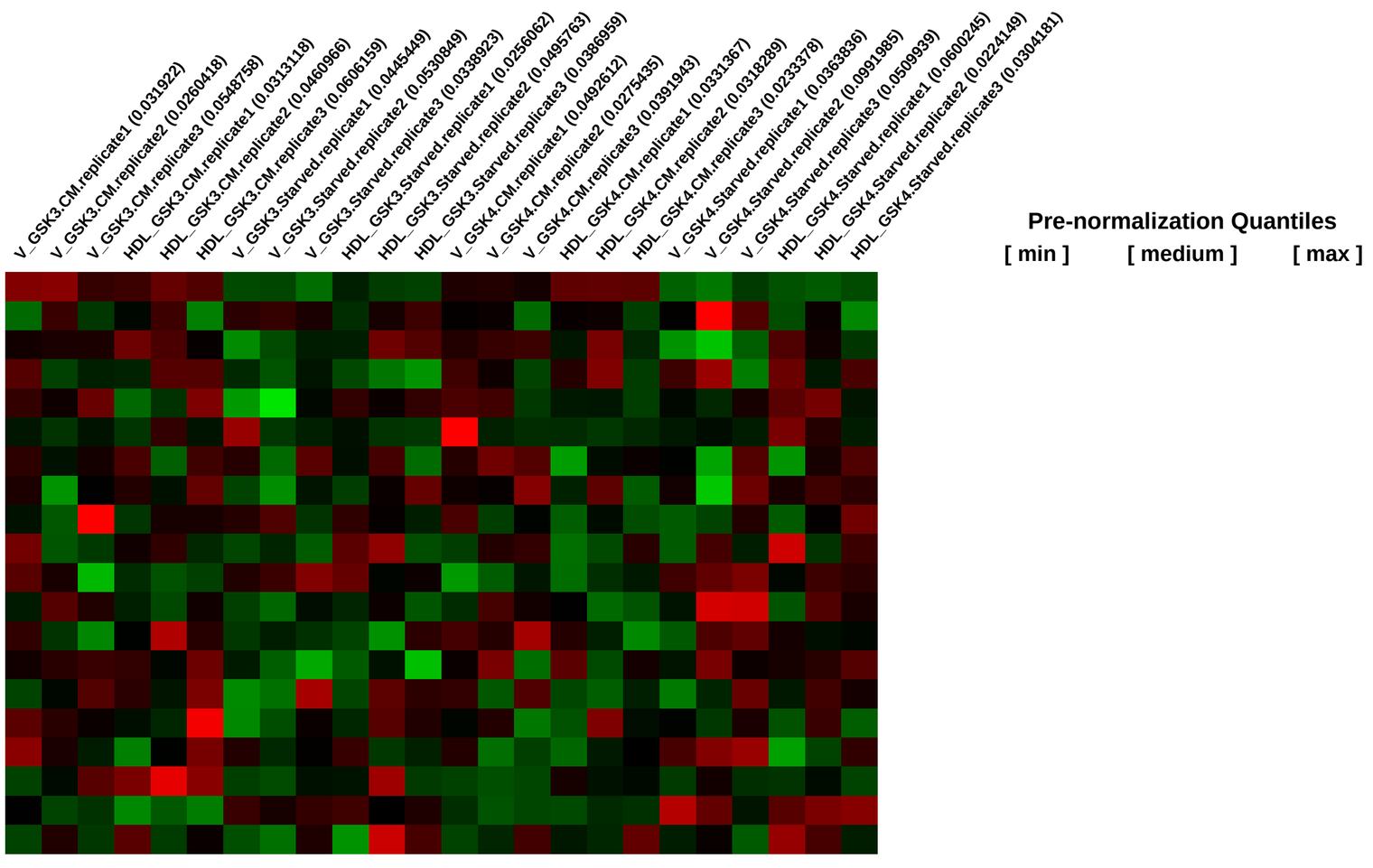

GEO Series "GSE17709" Expression Profiles

Num of samples in this series: 18

Scale of expression profile Z-scores

-3.0 -2.0 -1.0 0.0 1.0 2.0 3.0

GEO Link:	http://www.ncbi.nlm.nih.gov/geo/query/acc.cgi?acc=GSE17709
Status:	Public on Aug 19 2009
Title:	Gene expression analysis of a podocyte specific PTIP deletion in mouse glomerular preparations at 1 month of age
Organism:	Mus musculus
Experiment type:	Expression profiling by array
Platform:	GPL1261
Pubmed ID:	21060806
Summary & Design:	**Summary:** Glomerular RNA comparison between wild-type and podocyte specific deletion of the PTIP gene in 1 month old kidneys. The PTIP gene was deleted using a floxed allele and a Podocin-Cre driver strain. These mice develop protein urea by 3 months of age. This study was designed to find gene expression differences prior to the onset of the phenotype. **Overall design:** Kidneys were excised at 1 month of age. Glomeruli enriched fractions were generated by sieving of the tissue homogenates. RNA was prepared from glomerular enriched fractions.

Background corr dist: KL-Divergence = 0.0391, L1-Distance = 0.0385, L2-Distance = 0.0021, Normal std = 0.6195

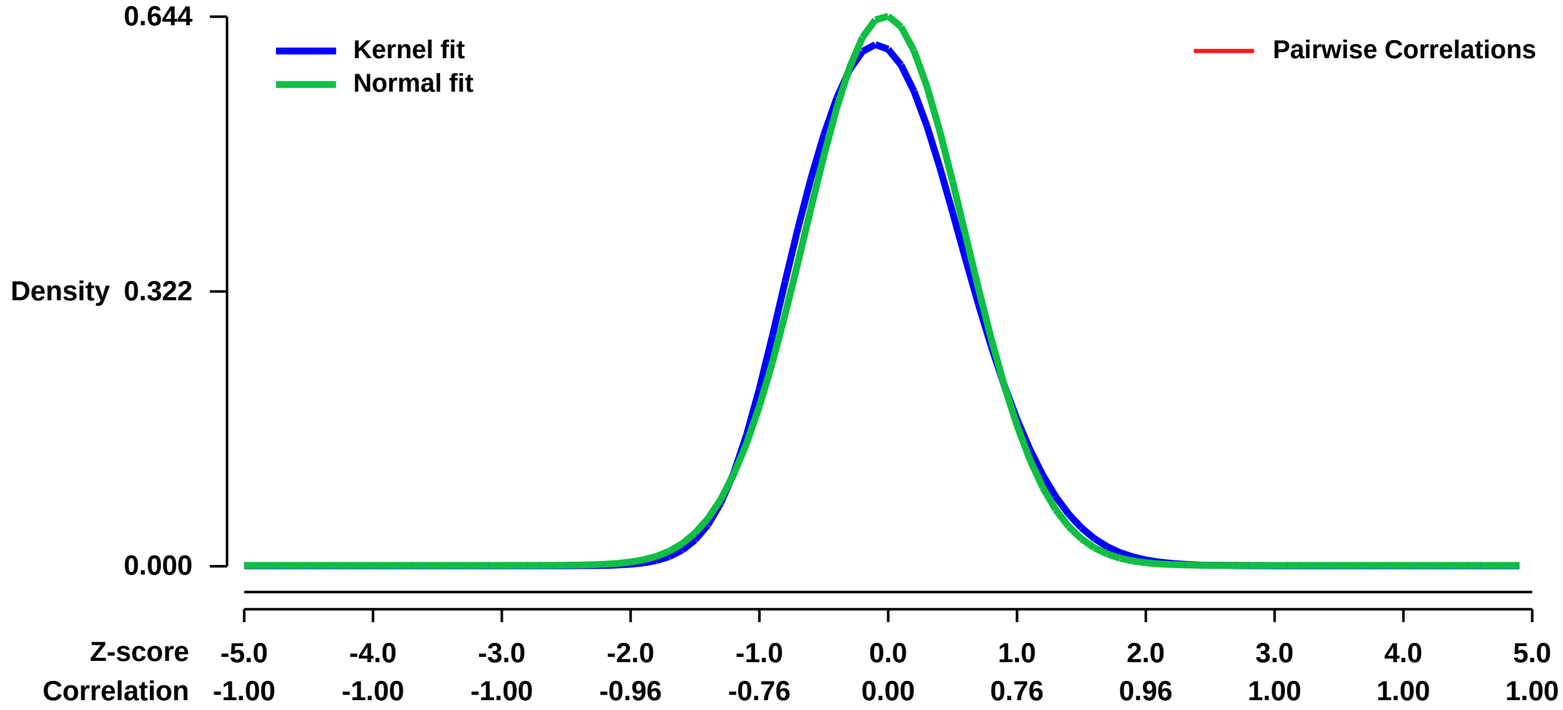

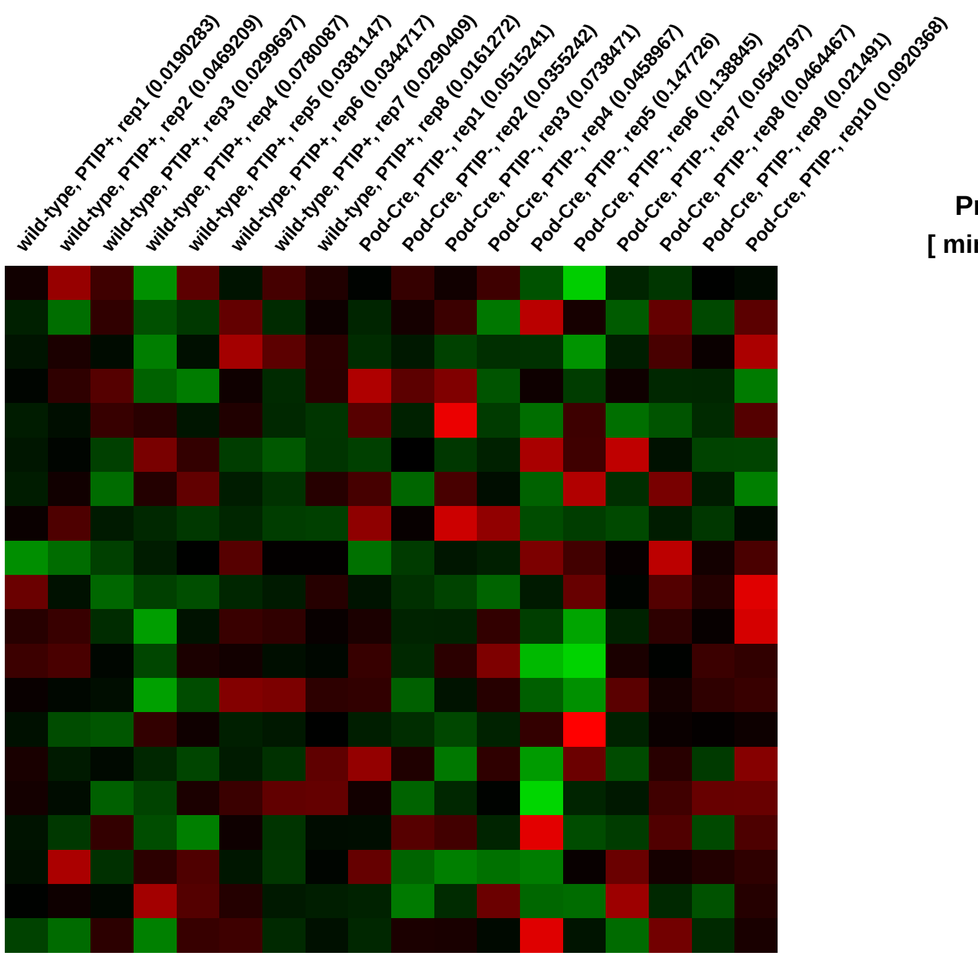

GEO Series "GSE17728" Expression Profiles

Num of samples in this series: 12

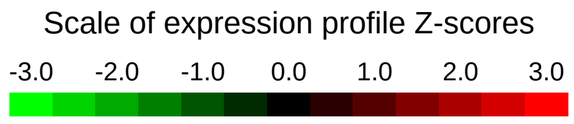

GEO Link:	http://www.ncbi.nlm.nih.gov/geo/query/acc.cgi?acc=GSE17728
Status:	Public on May 26 2012
Title:	Blood gene expression profile from mouse C57Bl/10 exposed to chronic hypoxia
Organism:	Mus musculus
Experiment type:	Expression profiling by array
Platform:	GPL1261
Pubmed ID:	22629407
Summary & Design:	**Summary:** In order to study the gene expression profile in C57Bl/10 mouse blood, we exposed three different groups of animals. First was exposed to PO2 21% or normoxia. The second was exposed to chronic hypoxia (from PO2 21% to PO2 8%) and the third was also exposed to the same chronic hypoxia (CH) protocol but followed by two weeks under normoxia, and called as recovery group. The blood was extracted from inferior vena cava, the RNA was extracted, amplified and hybridized to Affimetrix MOE 430 V2.o chip. The results were analyzed using Partek Genome suite software. Using two fold cuttoff and 0% FDR parameters, we observed genes 512 diferentially expressed, of which one gene was up-regulated in both hypoxic and recovery condition, 202 were up-regulated during CH and then down-regulated after the recovery, 18 genes were down-regulated afteh CH and the up-regulated after recovery, ans finally 9 genes were down-regulated in both CH and recovery conditions. **Overall design:** Each group of C57Bl/10 mouse had 4 individuals and they were divided into three different groups of animals. First was exposed to PO2 21% or normoxia for 14 days. The second was exposed to chronic hypoxia (from PO2 21% to PO2 8%) and the third was also exposed to the same chronic hypoxia (CH) protocol but followed by two weeks under normoxia, and called as recovery group. After the exposure period, the animals were anaesthetized with a mix of Ketamine (100 mg/mL) and xylasine (20 mg/mL) in a proportion of 1:1. A incison was made on abdominal area and from kidneis and liver area of inferior vena cava venus blood was collected The blood was extracted from inferior vena cava. Then, the RNA was extracted, amplified and hybridized to Affimetrix MOE 430 V2.o chip. The results were analyzed using Partek Genome suite software. Using two fold cuttoff and 0% FDR parameters, we observed genes 512 diferentially expressed, of which one gene was up-regulated in both hypoxic and recovery condition, 202 were up-regulated during CH and then down-regulated after the recovery, 18 genes were down-regulated afteh CH and the up-regulated after recovery, ans finally 9 genes were down-regulated in both CH and recovery conditions.

Background corr dist: KL-Divergence = 0.0545, L1-Distance = 0.0470, L2-Distance = 0.0038, Normal std = 0.5640

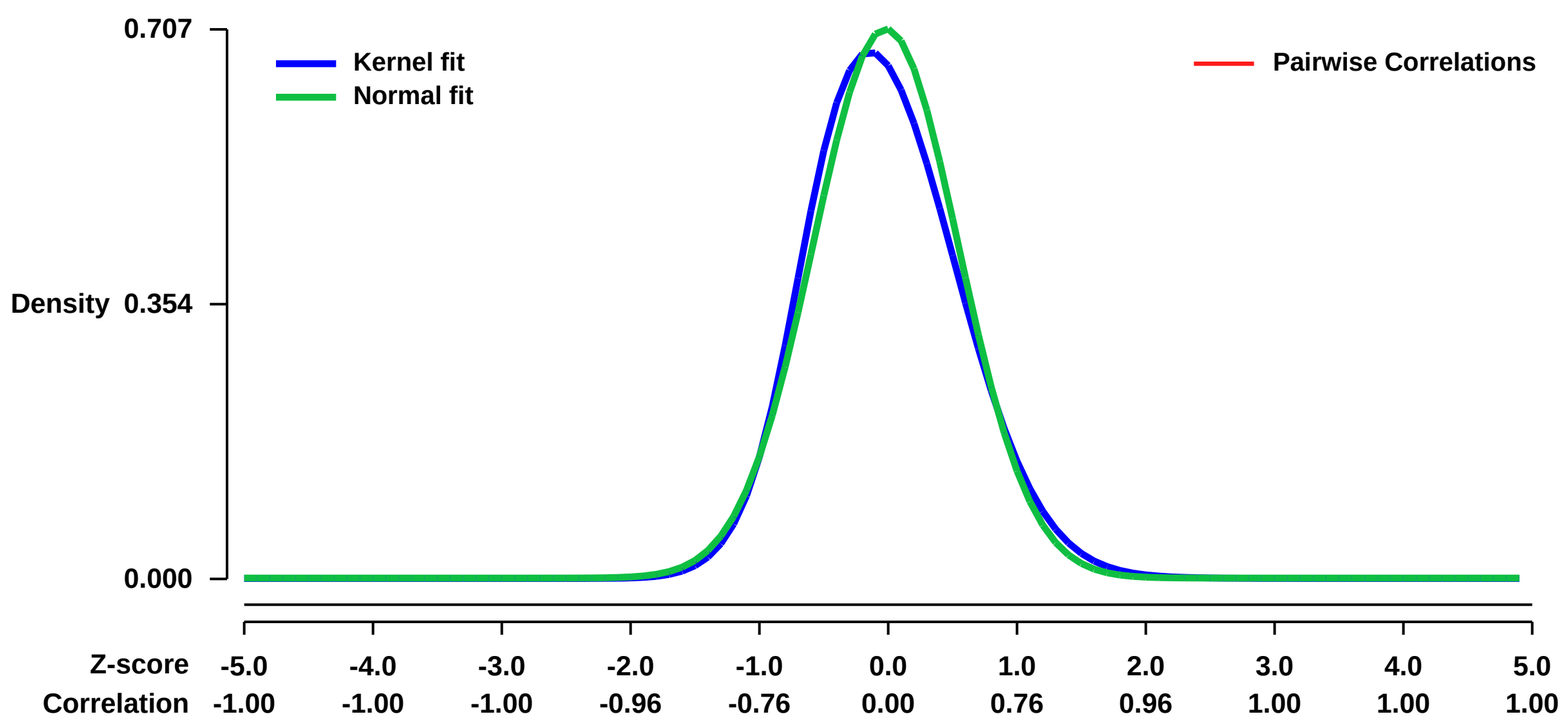

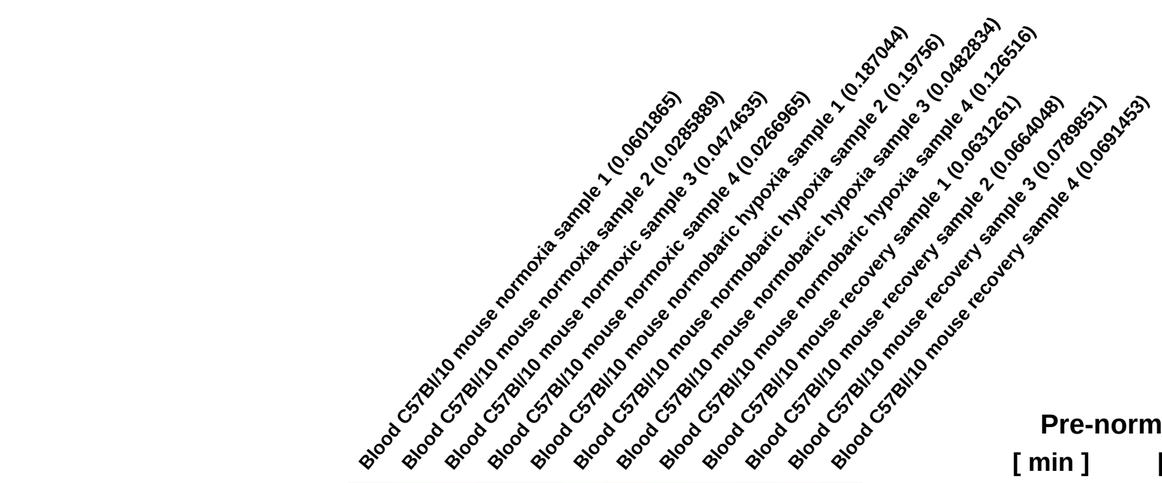

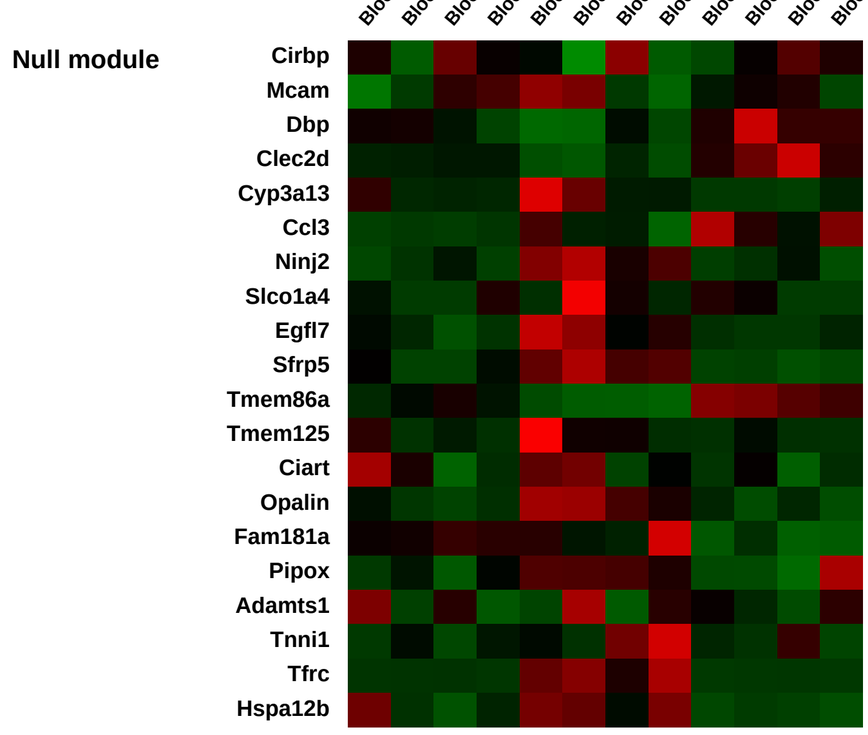

GEO Series "GSE17739" Expression Profiles

Num of samples in this series: 24

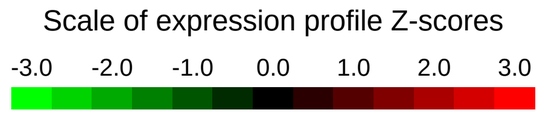

GEO Link:	**http://www.ncbi.nlm.nih.gov/geo/query/acc.cgi?acc=GSE17739**
Status:	**Public on Oct 22 2009**
Title:	**Circadian gene profiling in the distal nephron and collecting ducts**
Organism:	**Mus musculus**
Experiment type:	**Expression profiling by array**
Platform:	**GPL1261**
Pubmed ID:	**19805330**
Summary & Design:	**Summary:** **Renal excretion of water and major electrolytes exhibits a significant circadian rhythm. This functional periodicity is believed to result, at least in part, from circadian changes in secretion/reabsorption capacities of the distal nephron and collecting ducts. Here, we studied the molecular mechanisms underlying circadian rhythms in the distal nephron segments, i.e. distal convoluted tubule (DCT) and connecting tubule (CNT) and, the cortical collecting duct (CCD). Temporal expression analysis performed on microdissected mouse DCT/CNT or CCD revealed a marked circadian rhythmicity in the expression of a large number of genes crucially involved in various homeostatic functions of the kidney. This analysis also revealed that both DCT/CNT and CCD possess an intrinsic circadian timing system characterized by robust oscillations in the expression of circadian core clock genes (clock, bma11, npas2, per, cry, nr1d1) and clock-controlled Par bZip transcriptional factors dbp, hlf and tef. The clock knockout mice or mice devoid of dbp/hlf/tef (triple knockout) exhibit significant changes in renal expression of several key regulators of water or sodium balance (vasopressin V2 receptor, aquaporin-2, aquaporin-4, alphaENaC). Functionally, the loss of clock leads to a complex phenotype characterized by partial diabetes insipidus, dysregulation of sodium excretion rhythms and a significant decrease in blood pressure. Collectively, this study uncovers a major role of molecular clock in renal function.** **Keywords: time course** **Overall design:** **We examined the temporal profiles of gene expression in mouse distal nephron segments and collecting ducts. The RNA was extracted from microdissected distal convoluted tubules and connecting tubules (DCT/CNT samples) or, cortical collecting ducts (CCD samples). Animals were sacrificed for microdissection every 4 hours, i.e. at ZT0, ZT4, ZT8, ZT12, ZT16 and ZT20 (ZT â Zeitgeber (circadian) time, indicates time of light-on as ZT0 and time of light-off as ZT12). The microarray hybridization was performed in duplicates on two pools of RNA composed of equivalent amounts of RNA prepared from five animals at each ZT time-point.**

Background corr dist: KL-Divergence = 0.0374, L1-Distance = 0.0298, L2-Distance = 0.0014, Normal std = 0.6138

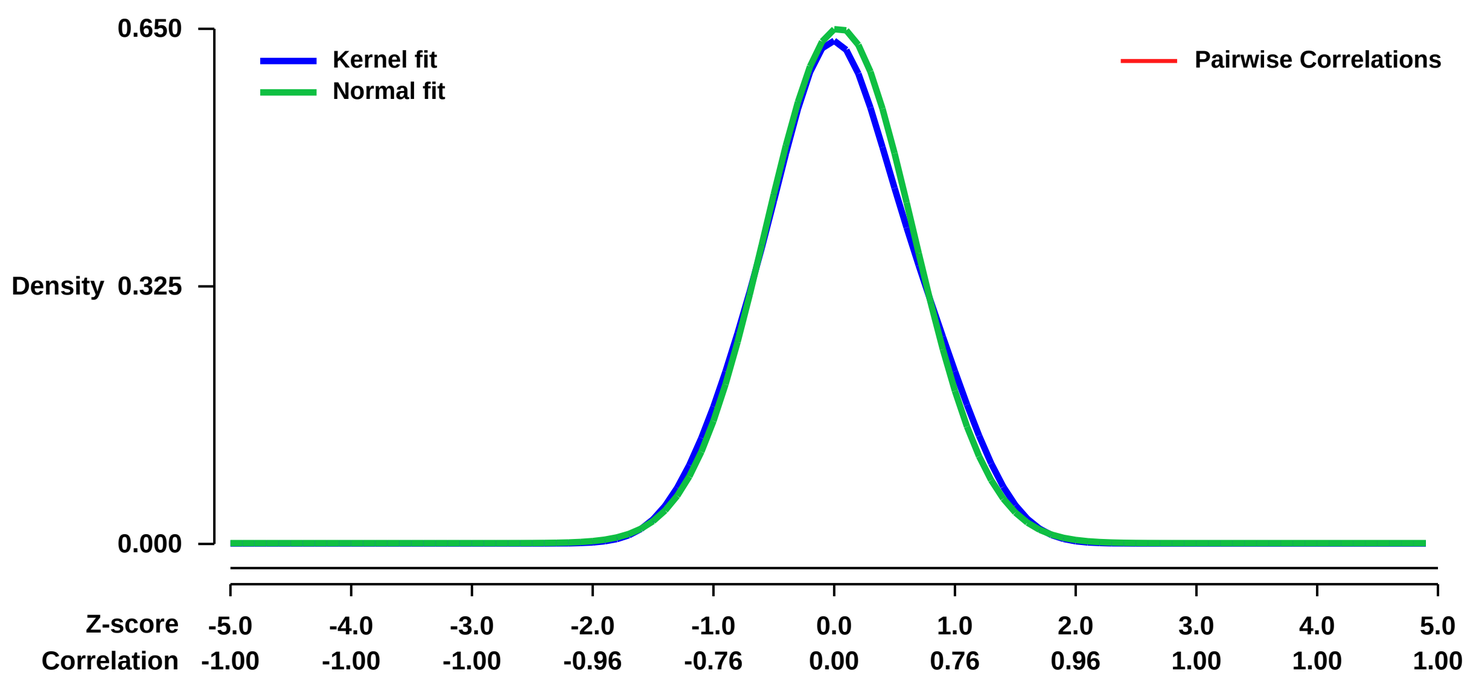

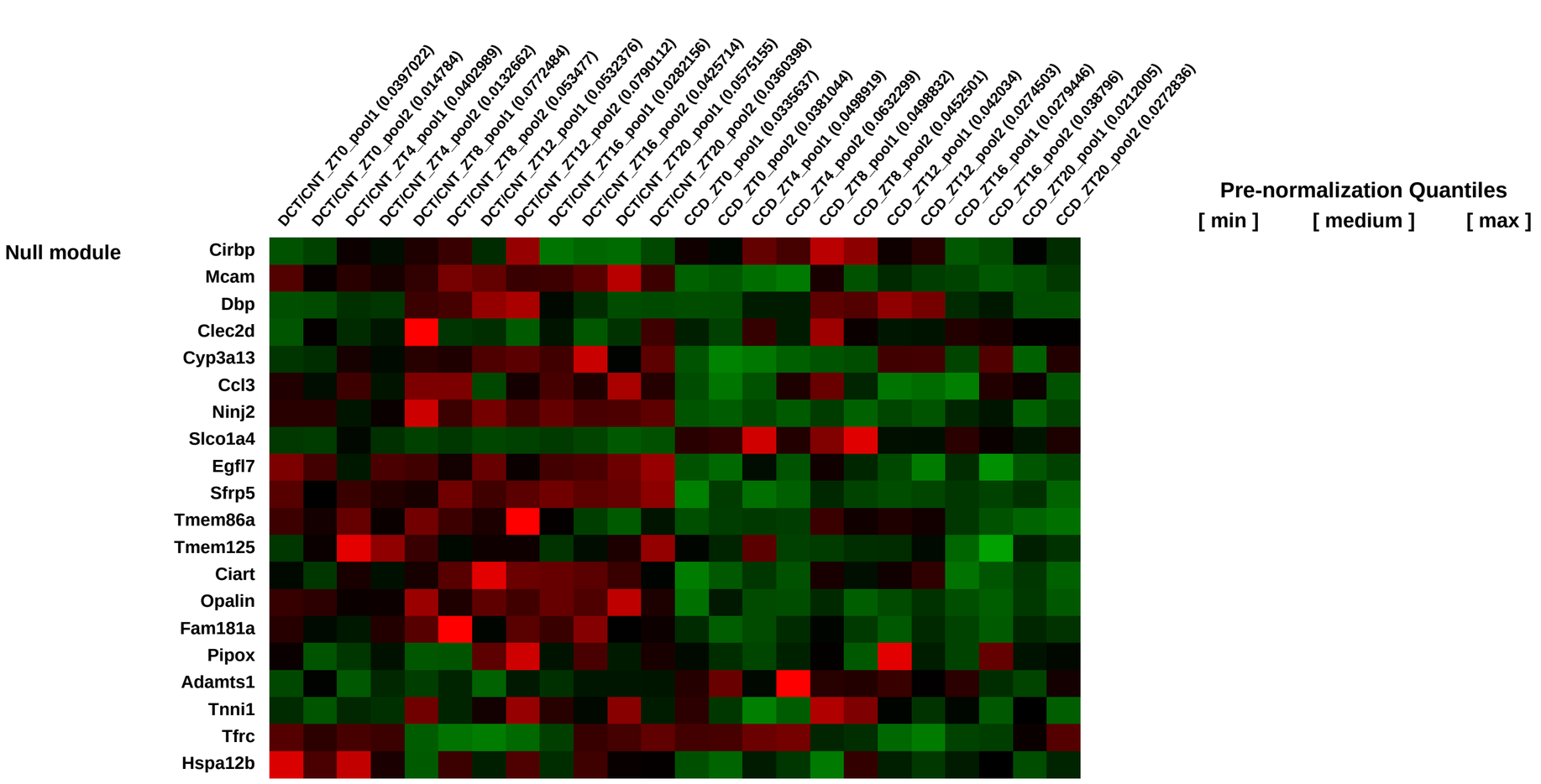

GEO Series "GSE17745" Expression Profiles

Num of samples in this series: 6

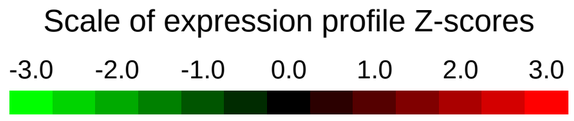

GEO Link:	**http://www.ncbi.nlm.nih.gov/geo/query/acc.cgi?acc=GSE17745**
Status:	**Public on Aug 20 2011**
Title:	**Identification of genes regulated by the RANK IVVY motif in macrophages**
Organism:	**Mus musculus**
Experiment type:	**Expression profiling by array**
Platform:	**GPL1261**
Pubmed ID:	
Summary & Design:	**Summary:** **Identification of genes regulated by RANK RVVY motif in macrophages by gene expression analysis of TNFR1-/-R2-/- BMMs expressing a chimeric receptor consisting of the external domain of mouse TNFR1 linked to the transmembrane and intracellular domain of mouse RANK (WT) and NFR1-/-R2-/- BMMs expressing a chimeric receptor consisting of the external domain of mouse TNFR1 linked to the transmembrane and intracellular domain of mouse RANK bearing inactivating mutations in the IVVY motif (Mu).** **Overall design:** **three replicates: rep1, rep2, and rep3**

Background corr dist: **KL-Divergence = 0.0309, L1-Distance = 0.0597, L2-Distance = 0.0044, Normal std = 0.7758**

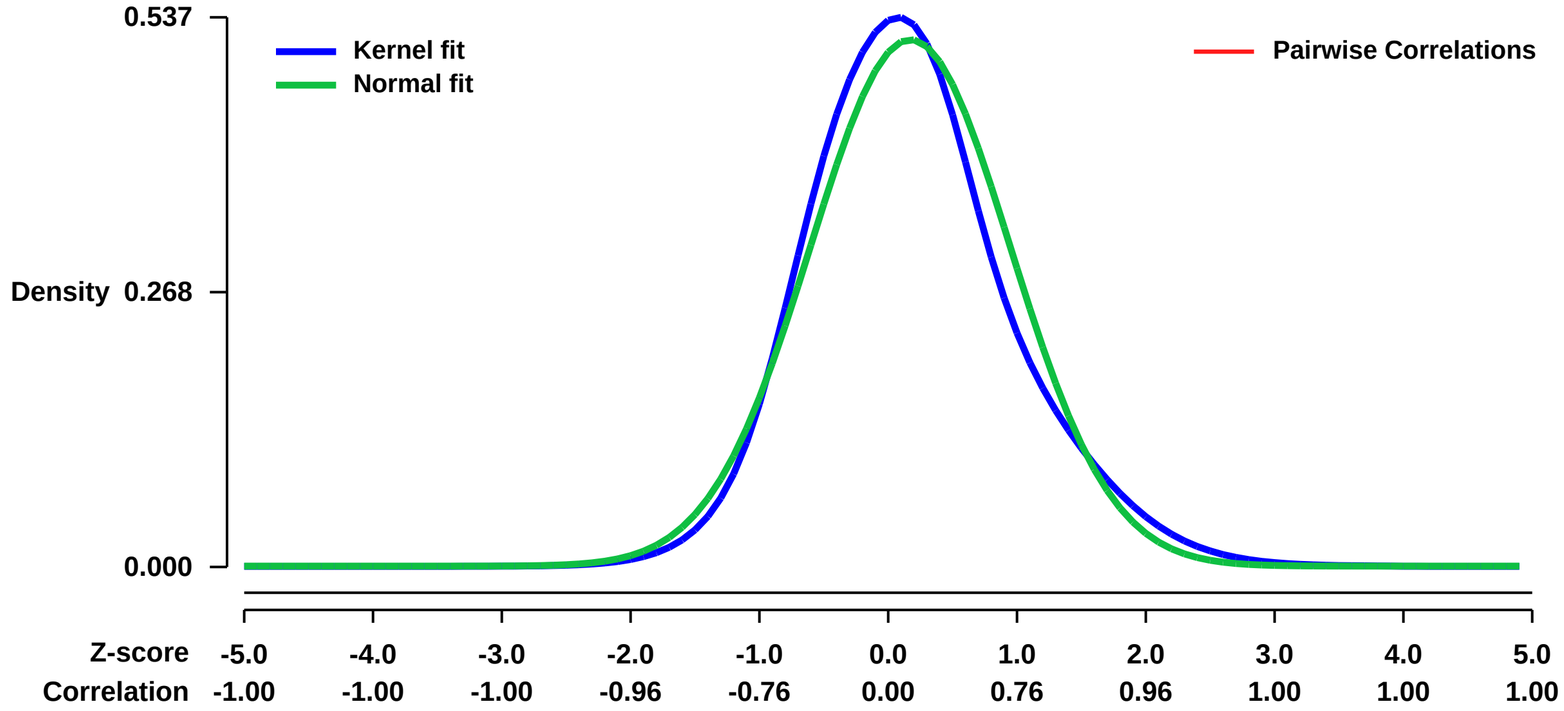

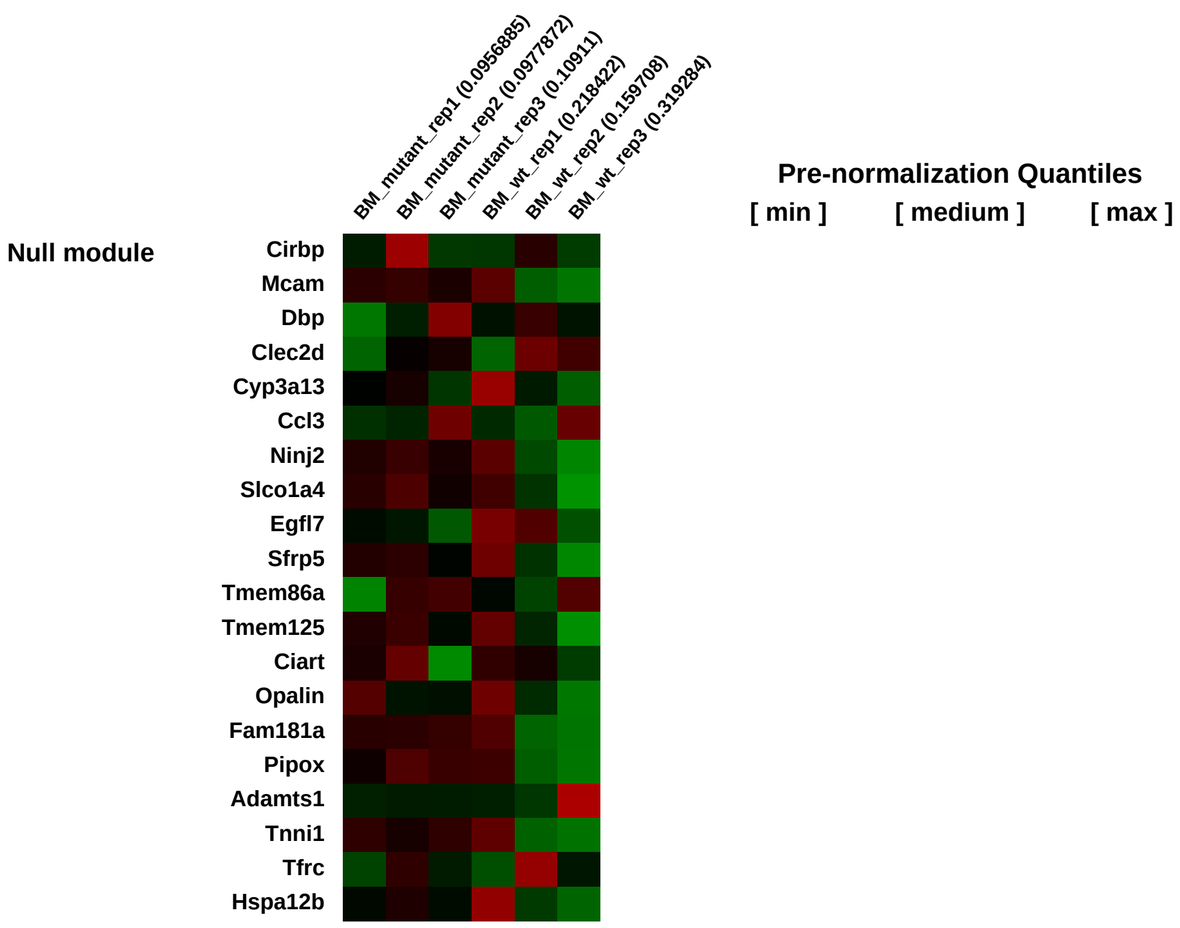

GEO Series "GSE17817" Expression Profiles

Num of samples in this series: 6

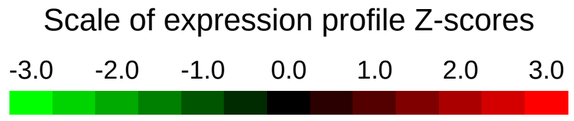

GEO Link:	http://www.ncbi.nlm.nih.gov/geo/query/acc.cgi?acc=GSE17817
Status:	Public on Sep 02 2009
Title:	CAFs are activated in incipient neoplasia to orchestrate tumor promoting inflammation in an NF-¸”B-dependent manner.
Organism:	Mus musculus
Experiment type:	Expression profiling by array
Platform:	GPL1261
Pubmed ID:	20138012
Summary & Design:	**Summary:** **Full title: Cancer Associated Fibroblasts are activated in incipient neoplasia to orchestrate tumor promoting inflammation in an NF-¸”B-dependent manner.** **Cancer Associated Fibroblasts (CAFs) support tumorigenesis by stimulating angiogenesis, cancer cell proliferation, and invasion. We demonstrate that CAFs also mediate tumor-enhancing inflammation. Using a mouse model of squamous skin cancer, we found a pro-inflammatory gene signature in CAFs isolated from dysplastic skin. This signature was also evident in CAFs from skin as well as mammary and pancreatic tumors in mice, and in human cancer. Surprisingly, the inflammatory signature was already activated in CAFs isolated from the incipient hyperplastic stage in multistep tumorigenesis. CAFs from this pathway functioned to promote macrophage recruitment, neovascularization and tumor growth in vivo, activities abolished when NF-¸”B signaling was inhibited. Additionally, we show that normal dermal fibroblasts can be â educatedâ by carcinoma cells to express pro-inflammatory genes.** **Overall design:** **We performed expression profiling analysis of dermal fibroblasts sorted from dysplastic skin tissue of K14-HPV16 mice, and from age matched non transgenic controls. This array analysis was repeated in triplicate. Amplified RNA was hybridized to the 430 2.0 Affymetrix mouse genome arrays.**

Background corr dist: KL-Divergence = 0.0273, L1-Distance = 0.0283, L2-Distance = 0.0010, Normal std = 0.7050

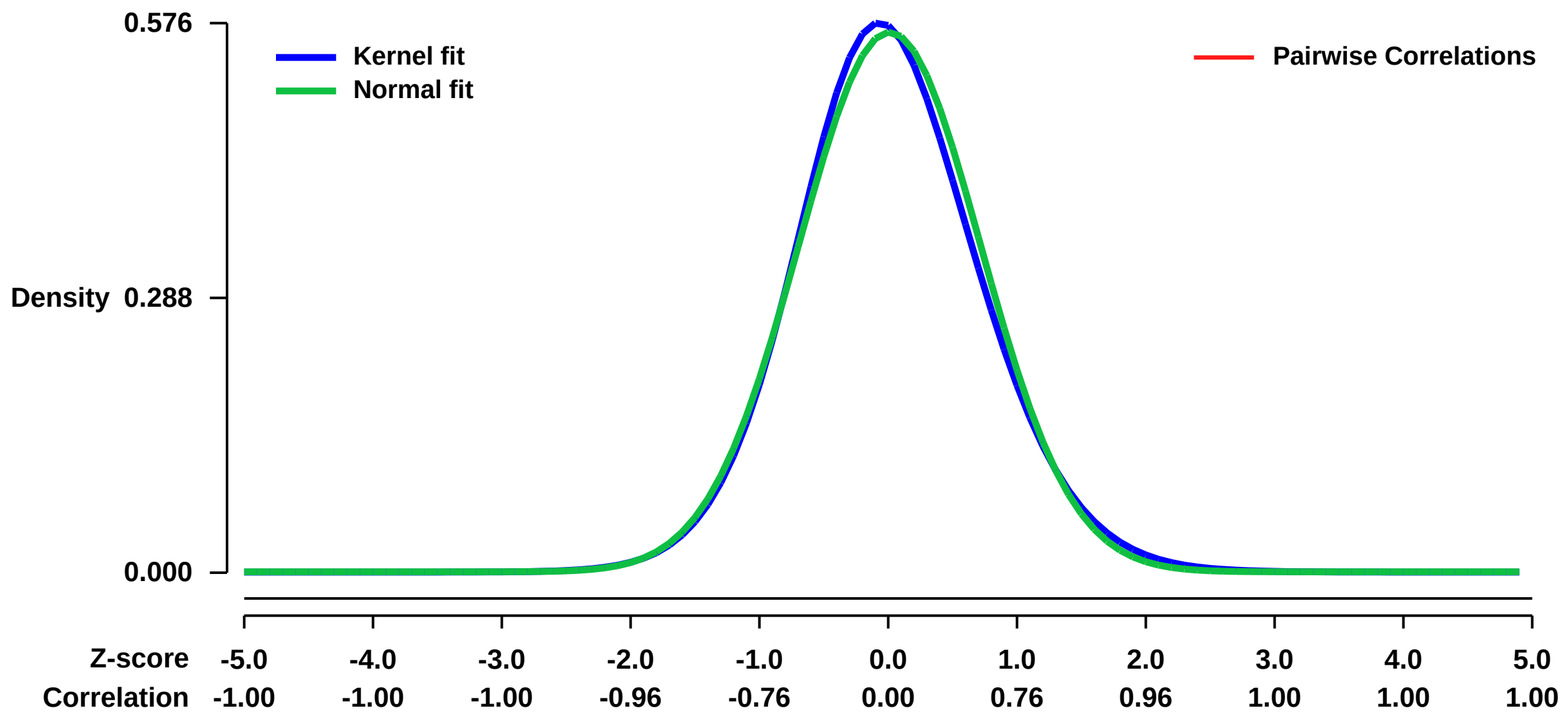

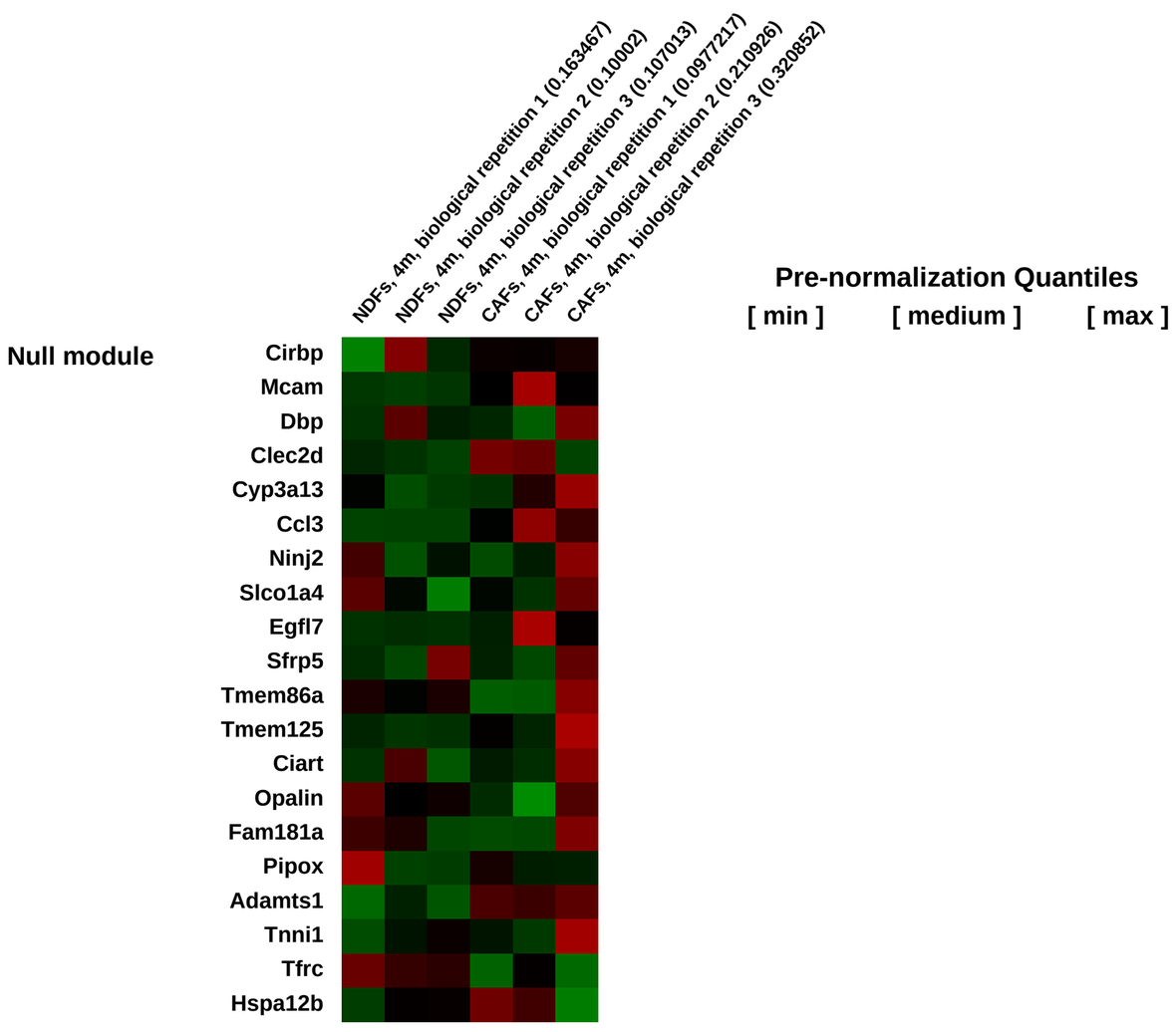

GEO Series "GSE17825" Expression Profiles

Num of samples in this series: 18

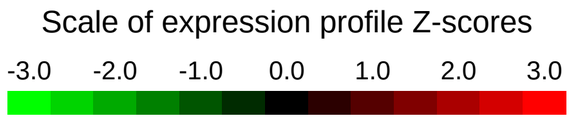

GEO Link:	http://www.ncbi.nlm.nih.gov/geo/query/acc.cgi?acc=GSE17825
Status:	Public on Sep 01 2009
Title:	Murine fracture healing
Organism:	Mus musculus
Experiment type:	Expression profiling by array
Platform:	GPL1261
Pubmed ID:	18752025
Summary & Design:	**Summary:** Time-point expression analysis of fractures calluses at 1, 3, and 5 days post-fracture in young and old BALB/c mice. **Overall design:** Femur fractures were generated on female c57Bl6 mice in triplicate: 8 month old retired breeders (old mice) and 6 week old mice (young mice) were used. 1, 3, and 5 days post-fracture, fracture calluses were dissected and total RNA isolated. Expression profiling was performed using Affymetrix's Mouse Genome 430 2.0 array.

Background corr dist: KL-Divergence = 0.0962, L1-Distance = 0.0386, L2-Distance = 0.0030, Normal std = 0.4412

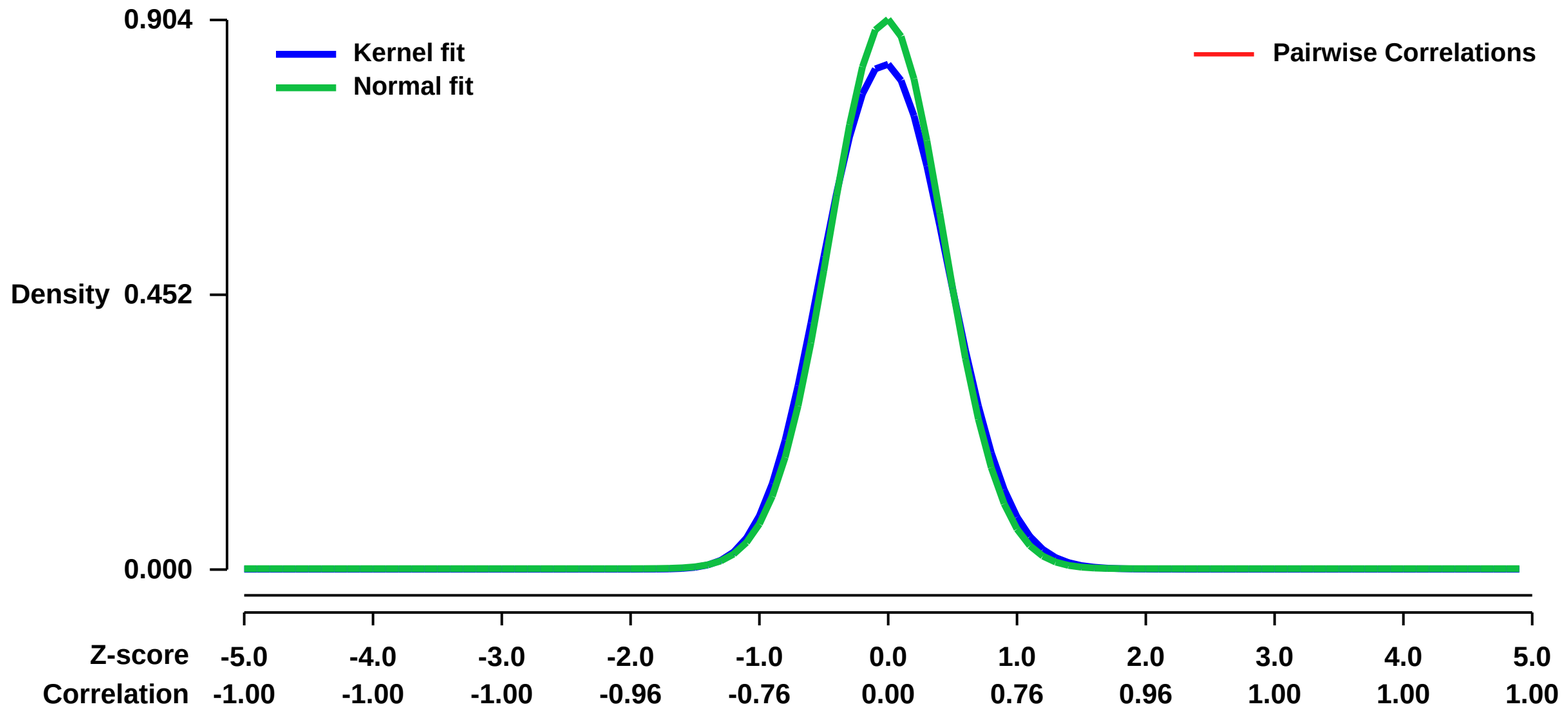

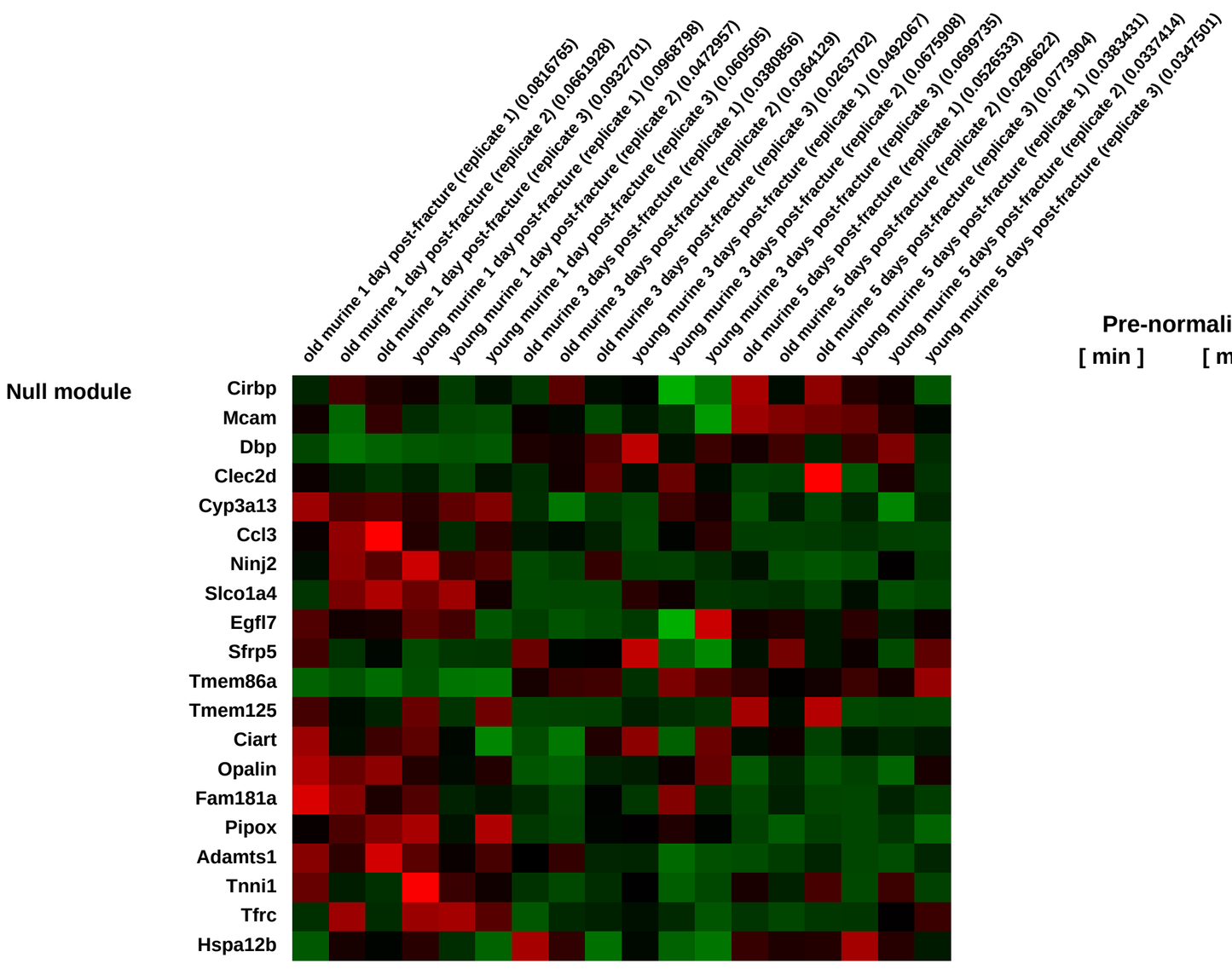

GEO Series "GSE17840" Expression Profiles

Num of samples in this series: 9

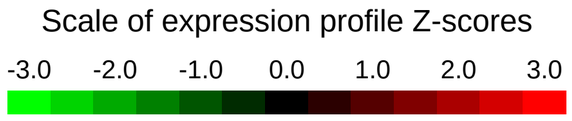

GEO Link:	http://www.ncbi.nlm.nih.gov/geo/query/acc.cgi?acc=GSE17840
Status:	Public on Oct 31 2009
Title:	Hedgehog is an anti-inflammatory epithelial signal for the intestinal lamina propria
Organism:	Mus musculus
Experiment type:	Expression profiling by array
Platform:	GPL1261
Pubmed ID:	20206176
Summary & Design:	**Summary:** Epithelial Hedgehog (Hh) ligands regulate several aspects of fetal intestinal organogenesis and emerging data implicate the Hh pathway in inflammatory signaling in adult colon. We investigated the effects of chronic Hh inhibition in vivo and profiled molecular pathways acutely modulated by Hh signaling in the intestinal mesenchyme. **Overall design:** E18.5 intestinal mesenchyme was isolated and cultured. Mesenchyme was treated with Sonic (Shh) or Indian (Ihh) hedgehog ligand or Vehicle (control) acutely to identify targets regulated by Hh signaling in intestinal mesenchyme.

Background corr dist: KL-Divergence = 0.0739, L1-Distance = 0.0254, L2-Distance = 0.0010, Normal std = 0.4855

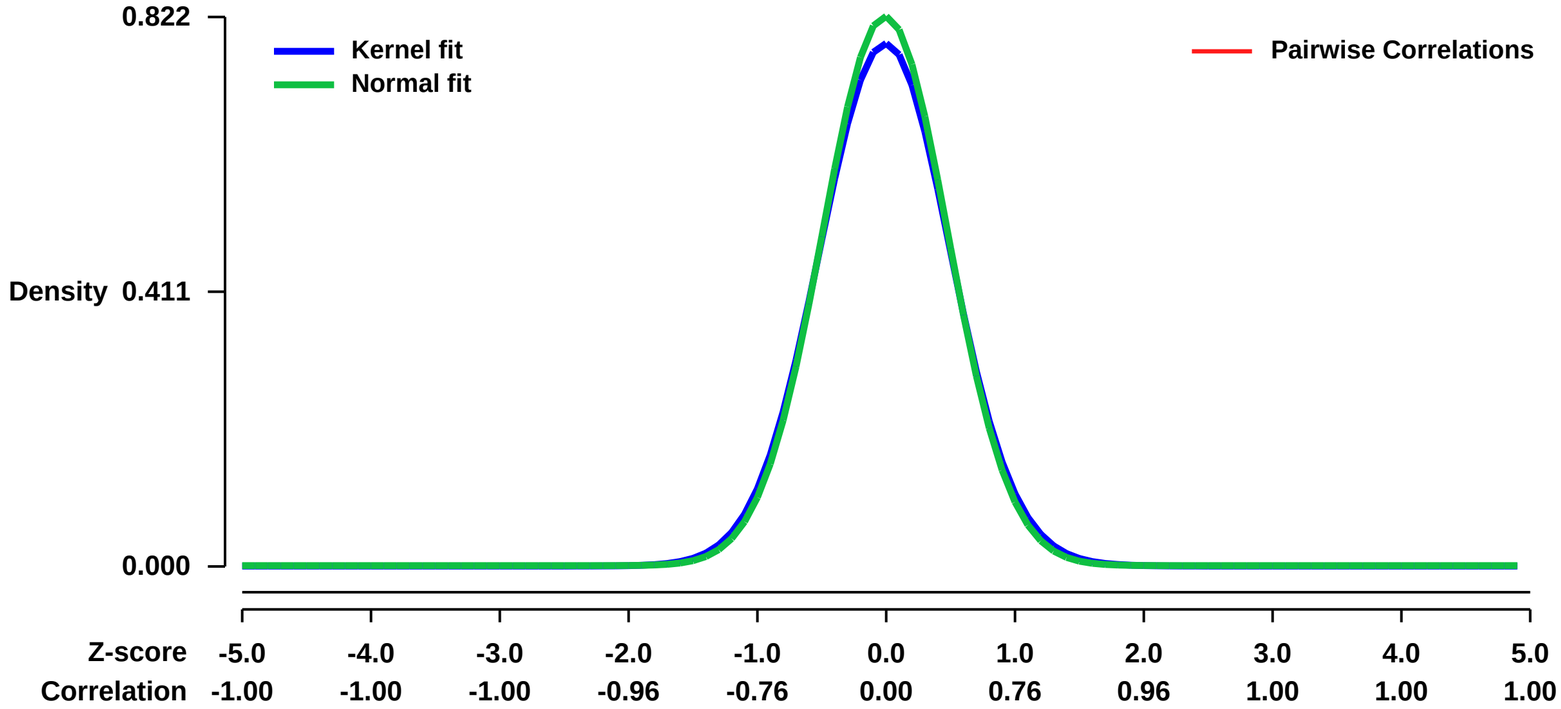

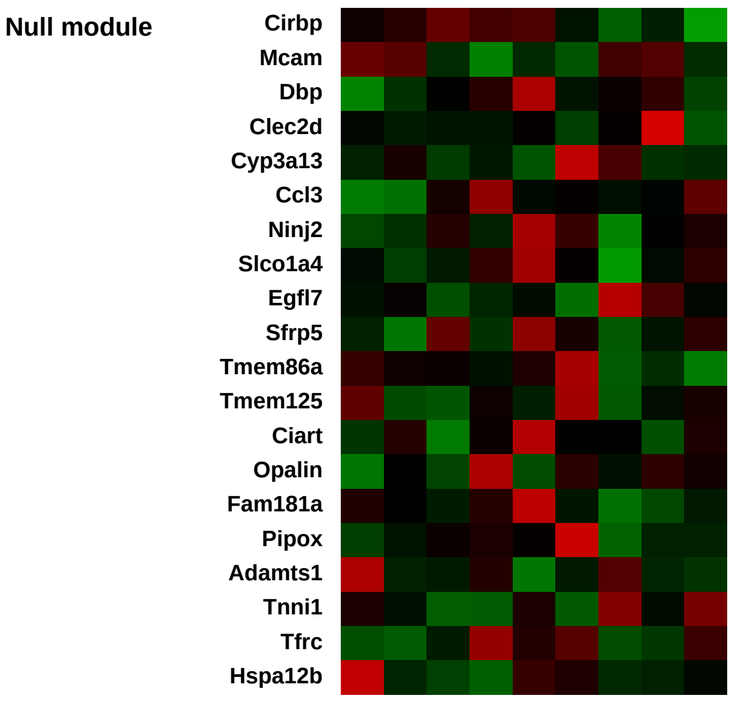

GEO Series "GSE17844" Expression Profiles

Num of samples in this series: 6

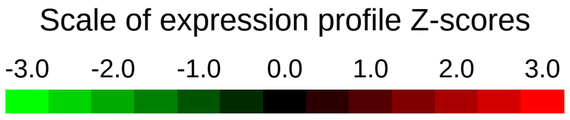

GEO Link:	**http://www.ncbi.nlm.nih.gov/geo/query/acc.cgi?acc=GSE17844**
Status:	**Public on Apr 25 2012**
Title:	**Basal expression in daDREAM transgenic mouse hippocampus**
Organism:	**Mus musculus**
Experiment type:	**Expression profiling by array**
Platform:	**GPL1261**
Pubmed ID:	
Summary & Design:	**Summary:** **Changes in nuclear Ca2+ homeostasis activate specific gene expression programs and are central to the acquisition and the plastic storage of memories. DREAM /KChIP proteins form heterotetramers that bind DNA and repress transcription in a Ca2+-dependent manner. Single ablation of one member of the DREAM/KChIP family may result in a mild or the absence of phenotype due to partial gene compensation. To study the function of DREAM/KChIP proteins in the brain, we used transgenic mice expressing a Ca2+-insensitive/CREB-independent dominant active mutant DREAM (daDREAM). We show that daDREAM controls the expression of several activity-dependent transcription factors including Npas4, Nr4a1, Mef2C, JunB and c-Fos, as well as the chromatin modifying enzyme Mbd4 and proteins related to actin polymerization like Arc and gelsolin. Thus, directly or through these targets, expression of daDREAM in the forebrain resulted in a complex phenotype characterized by i) impaired learning and memory, ii) loss of recurrent inhibition and enhanced LTP in the dentate gyrus without affecting Kv4-mediated potassium currents, and iii) modified spine density in DG granule neurons. Our results propose DREAM as a master-switch transcription factor regulating several activity-dependent gene expression programs to control synaptic plasticity, learning and memory.** **Overall design:** **We used Affymetrix microarrays (GeneChip Mouse Genome 430 2.0) to compare global gene expression in wild type (WT) versus transgenic hippocampi (L26 mice). For ech type of sample three hybridizations were carried-out (independent biological replicates).**

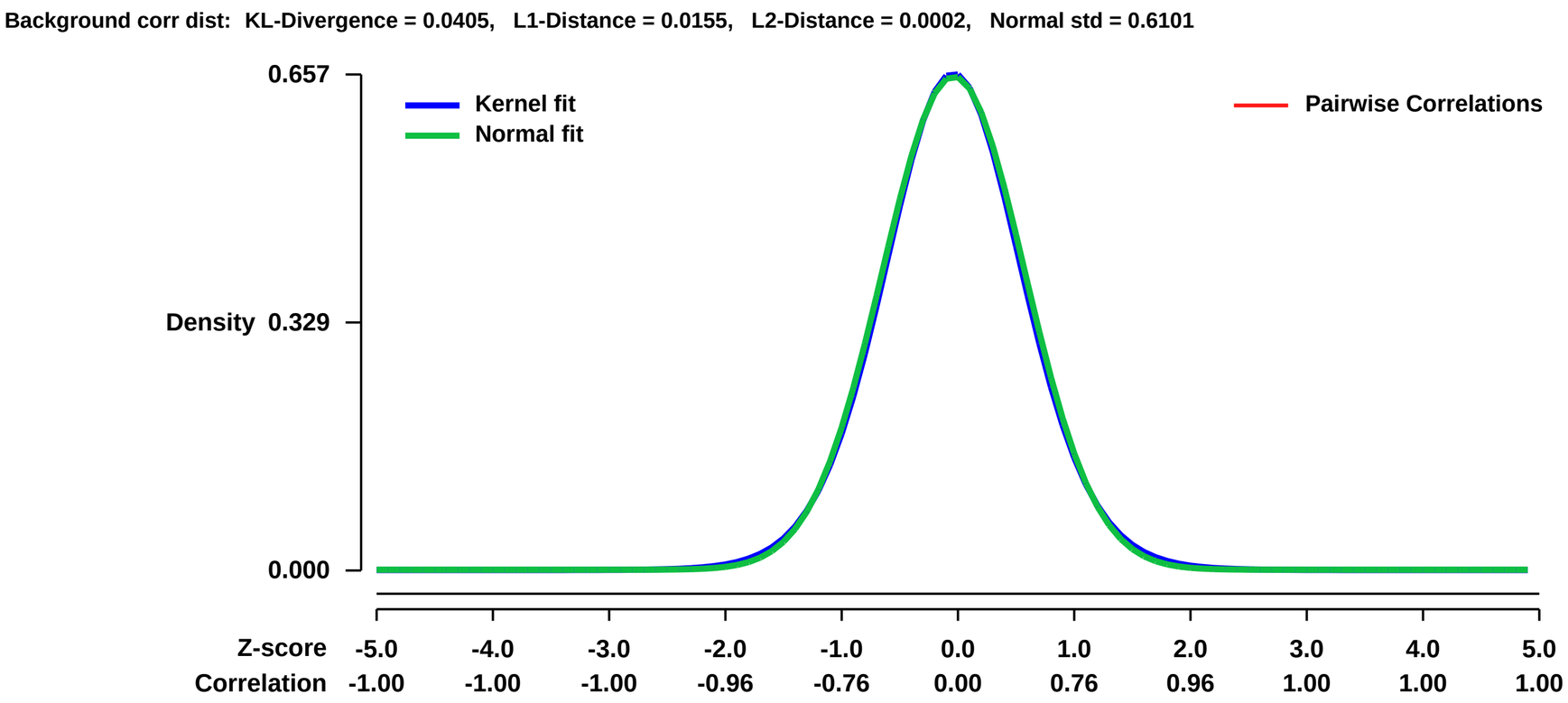

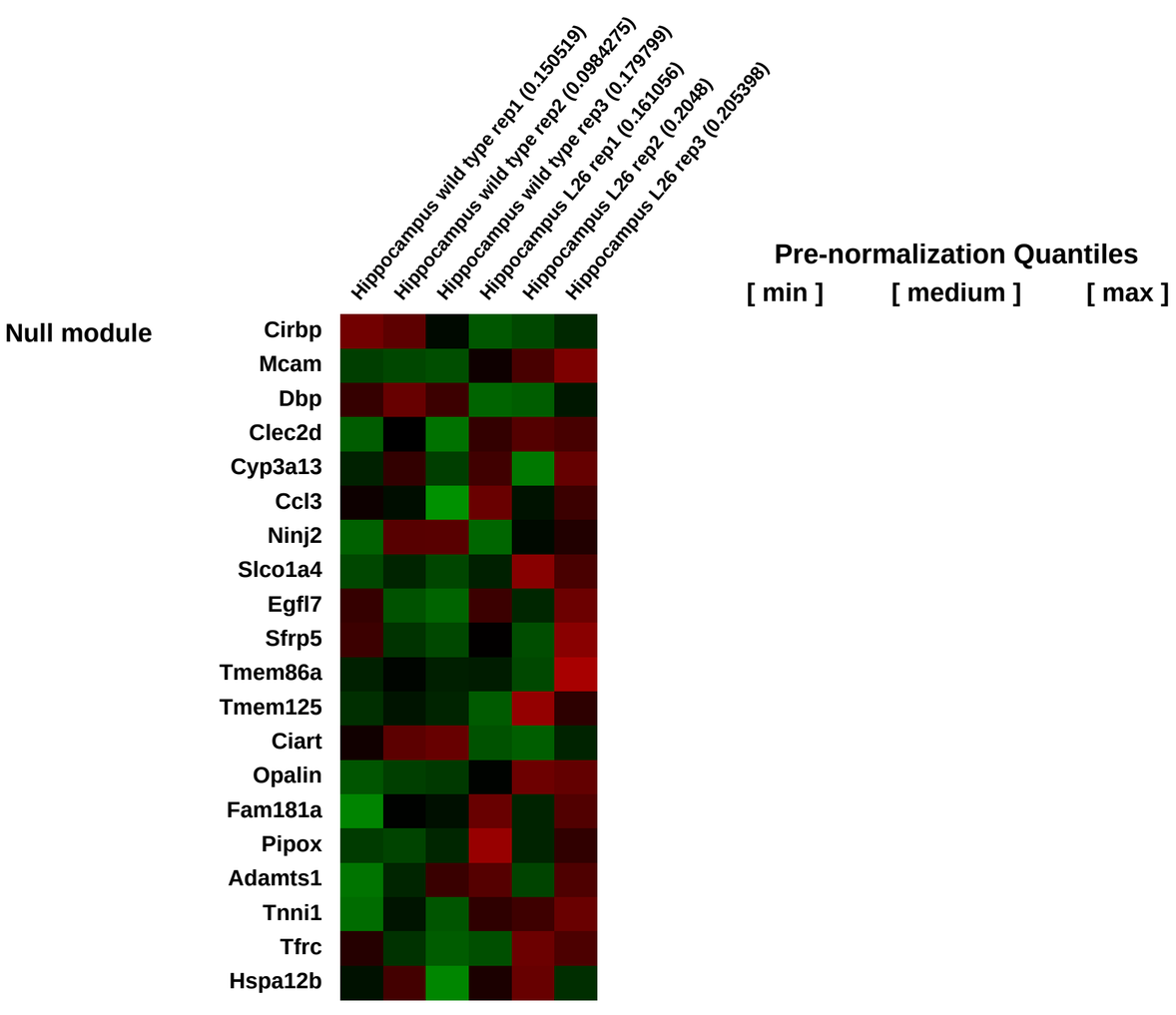

GEO Series "GSE17886" Expression Profiles

Num of samples in this series: 16

Scale of expression profile Z-scores

-3.0 -2.0 -1.0 0.0 1.0 2.0 3.0

GEO Link:	http://www.ncbi.nlm.nih.gov/geo/query/acc.cgi?acc=GSE17886
Status:	Public on Mar 22 2010
Title:	Gene expression data of BBB and BCB two-cell embryos
Organism:	Mus musculus
Experiment type:	Expression profiling by array
Platform:	GPL1261
Pubmed ID:	20107036
Summary & Design:	**Summary:** We constructed one-cell stage embryos by maternal pronuclear (mPN) transfer having B6 ooplasm, B6 paternal PN (pPN), and either B6 or C3H mPN (BBB and BCB, respectively). We collected embryos of each type that were either treated (BBB+a, BCB+a) or untreated with ¸–-amanitin (BBB, BCB) at the two-cell stage for microarray analysis. Comparison of the transcriptomes of these different kinds of embryos revealed genes for which expression differs according to maternal PN strain of origin, and the ¸–-amanitin data revealed which of these differences is due to gene transcription, as opposed to any transcription-independent differences attributable to ooplasm-derived maternal mRNA pools. **Overall design:** There are 4 replicates for each kind/treatment two-cell embryos (BBB, BCB, BBB+a, BCB+a).

Background corr dist: KL-Divergence = 0.0287, L1-Distance = 0.0723, L2-Distance = 0.0067, Normal std = 0.7860

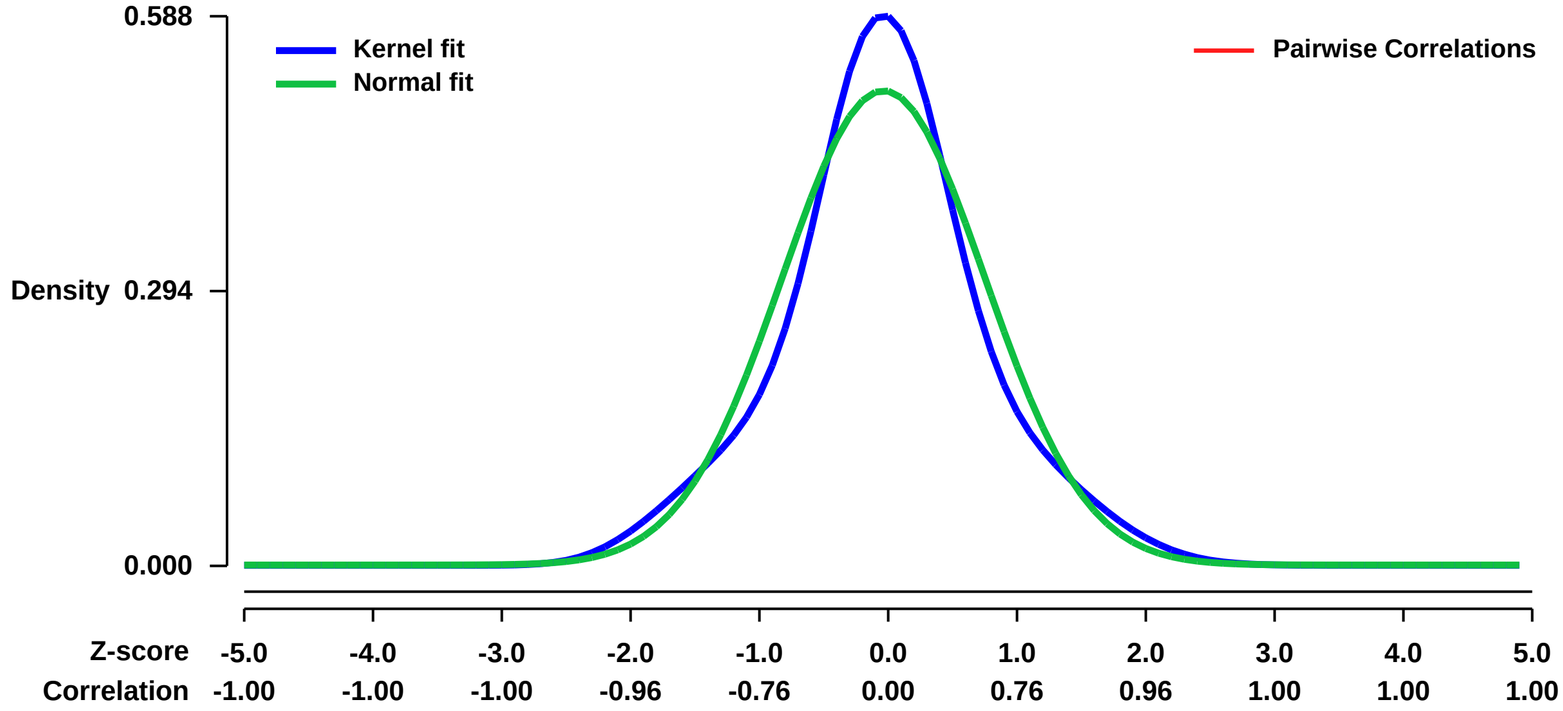

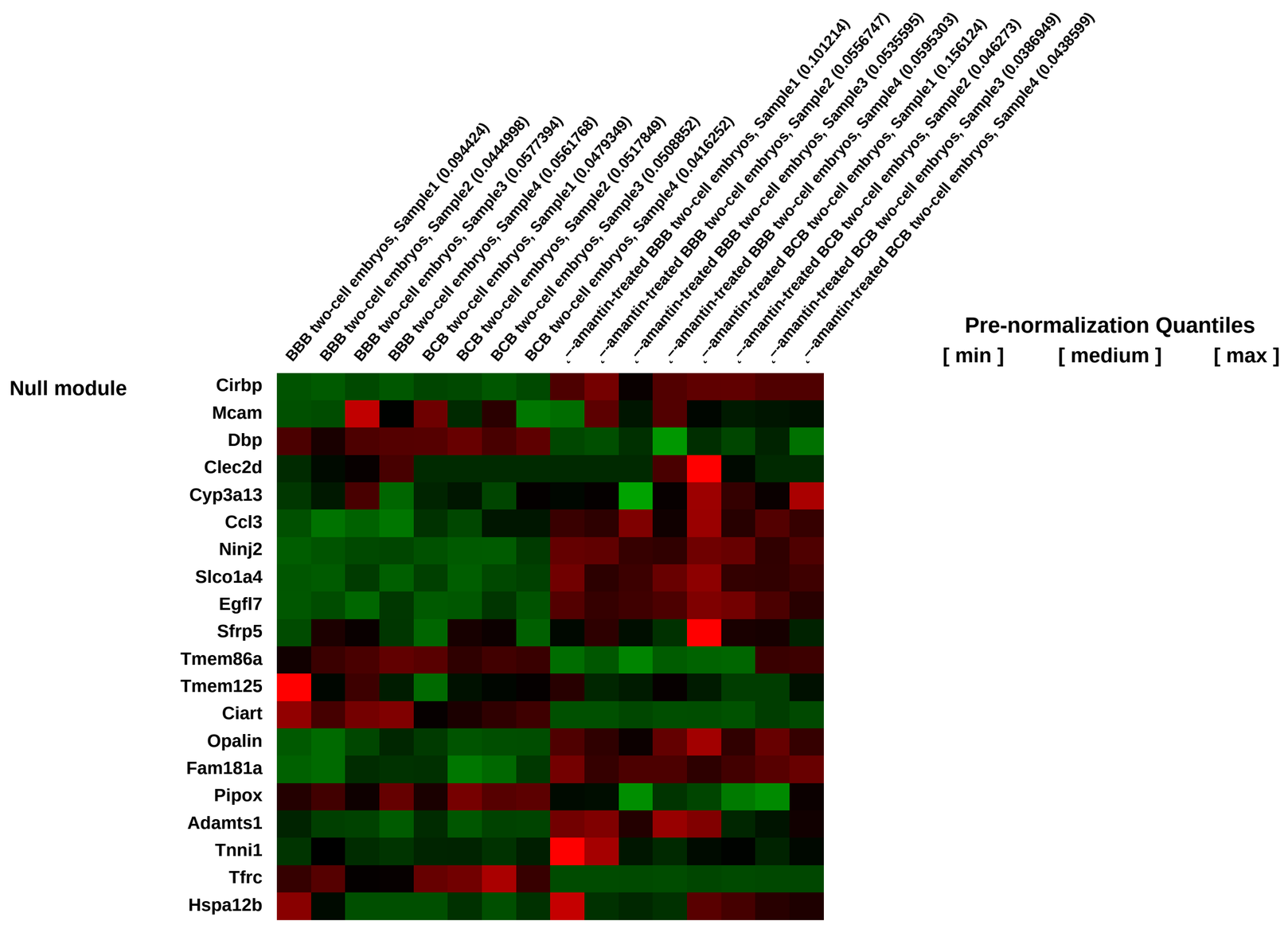

GEO Series "GSE17923" Expression Profiles

Num of samples in this series: 6

Scale of expression profile Z-scores

-3.0 -2.0 -1.0 0.0 1.0 2.0 3.0

GEO Link:	http://www.ncbi.nlm.nih.gov/geo/query/acc.cgi?acc=GSE17923
Status:	Public on Sep 03 2009
Title:	Gene Expression in White Adipose Tissue of KSR2-/- mice compared to wild type mice
Organism:	Mus musculus
Experiment type:	Expression profiling by array
Platform:	GPL1261
Pubmed ID:	19883615
Summary & Design:	**Summary:** The goal of this study was to define the gene expression changes that take place in the white adipose tissue of KSR2-/- mice at 6 months of age. **Overall design:** Three wild type mice and three KSR2-/- mice were used for total RNA extraction from white adipose tissue. The RNA from each mouse was analyzed on one Affymetrix gene chip and the differences were compared using Gene Set Enrichment Analysis.

Background corr dist: KL-Divergence = 0.0231, L1-Distance = 0.0257, L2-Distance = 0.0009, Normal std = 0.7211

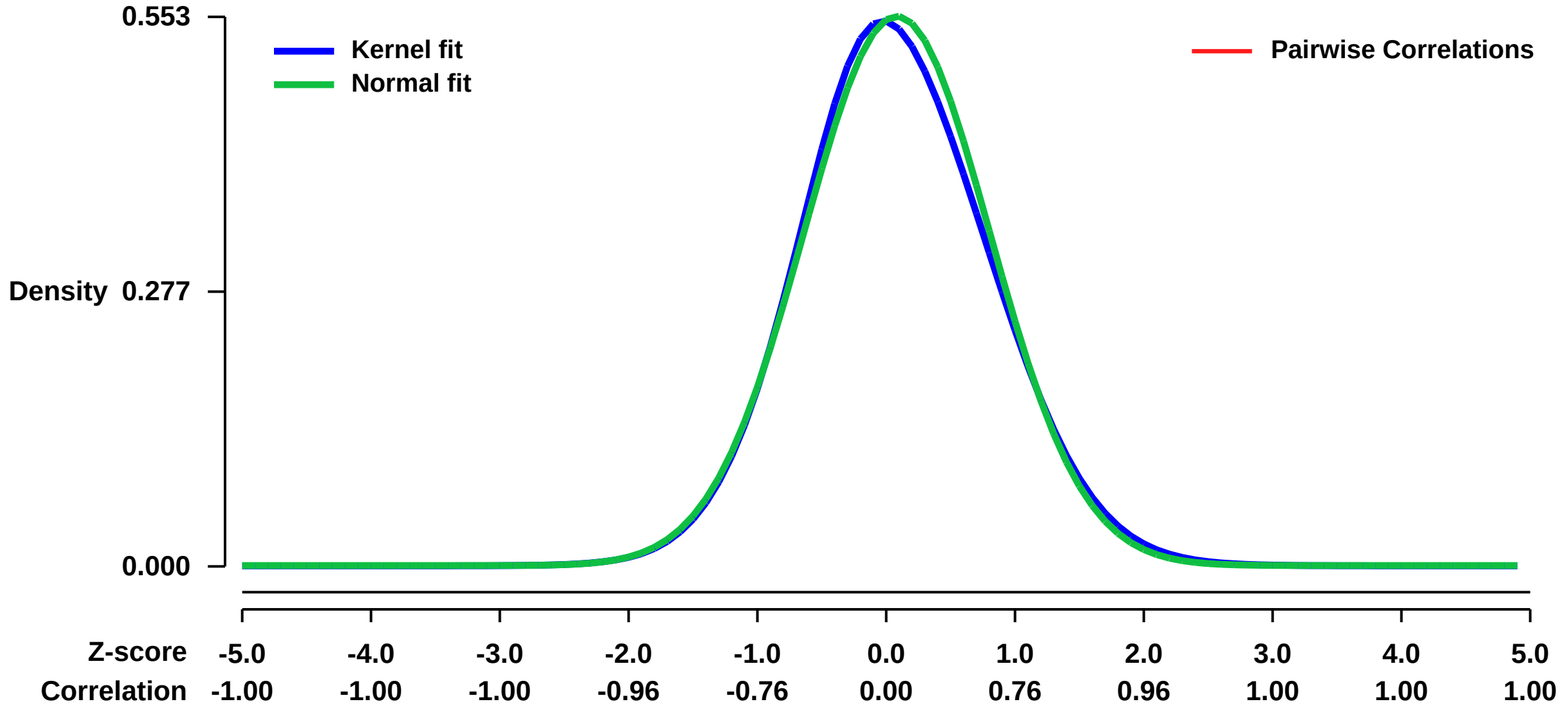

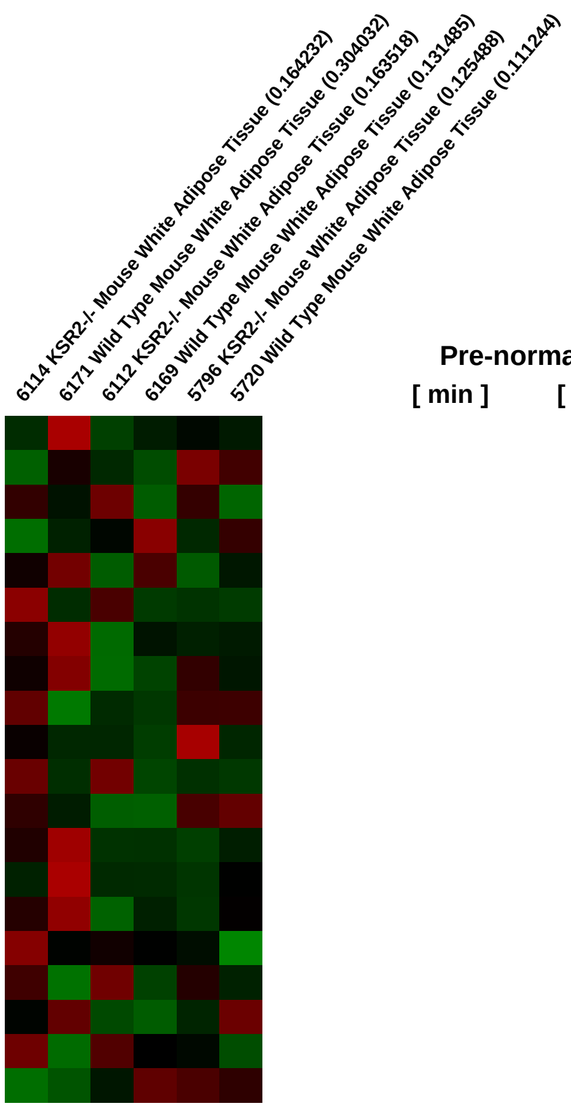

GEO Series "GSE17925" Expression Profiles

Num of samples in this series: 12

Scale of expression profile Z-scores

-3.0 -2.0 -1.0 0.0 1.0 2.0 3.0

GEO Link:	http://www.ncbi.nlm.nih.gov/geo/query/acc.cgi?acc=GSE17925
Status:	Public on Sep 03 2009
Title:	Gene expression from TCDD treated C57BL6/J and human Aryl hydrocarbon Receptor expressing primary mouse hepatocytes
Organism:	Mus musculus
Experiment type:	Expression profiling by array
Platform:	GPL1261
Pubmed ID:	20044593
Summary & Design:	**Summary:** The human and mouse aryl hydrocarbon receptor (hAHR and mAHRb) share limited (58%) transactivation domain sequence identity. Compared to the mAHRb allele, the hAHR displays 10-fold lower relative affinity for prototypical ligands such as 2,3,7,8 tetrachlorodibenzo-p-dioxin (TCDD). However, in previous studies we have demonstrated that the hAHR can display a higher relative ligand binding affinity than the mAHRb for specific AHR ligands such as indirubin. Each receptor has also been shown to differentially recruit LXXLL co-activator-motif proteins and to utilize different TAD subdomains in gene transactivation. Using hepatocytes isolated from C57BL6/J mice (Ahrb/b) and AHRTtr transgenic mice which express hAHR protein specifically in hepatocytes, we investigated whether the hAHR and mAHRb differentially regulate genes. Microarray and quantitative-PCR analysis of Ahrb/b and AHRTtr primary-mouse hepatocytes treated with 10 nM TCDD revealed that a number of established AHR target genes such as Cyp1a1 and Cyp1b1 are significantly induced by both receptors. Remarkably, of the 1752 genes induced by mAHRb and 1186 genes induced by hAHR, only 265 genes (<10%) were significantly activated by both receptors in response to TCDD. Conversely of the 1100 and 779 genes significantly repressed in mAHRb and hAHR hepatocytes respectively, only 462 (<25%) genes were significantly repressed by both receptors in response to TCDD treatment. Genes identified as differentially expressed are known to be involved in a number of biological pathways, including cell proliferation and inflammatory response which suggests that compared to the mAHRb, the hAHR may play contrasting roles in TCDD-induced toxicity and endogenous AHR-mediated gene regulation. **Overall design:** Isolated mouse hepatocytes from wild type and treated with 10nM TCDD for 6h were analyzed. 1 array per mouse (3 mice per treatment group) was used.GeneChip´fi Operating Software (Affymetrix) was utilized to preprocess CAB/CEL files generated from the 12 scanned microarrays which represented hepatocytes isolated from one mouse each. Data quality was initially assessed by checking the array image, B2 oligo performance, average background to noise ratios, poly-A controls, hybridization controls and the 3' to 5' probe-set ratios for control genes (e.g. ˆ-actin or GAPDH). Microarray data was normalized using Probe Logarithmic Intensity Error Approximation PLIER-MM algorithm (Affymetrix Expression Consoleâ¢ Software 1.1). Normalized microarray data outputs from TCDD and control treated Ahrb/band AHRTtr hepatocytes were compared for differential expression using Significance Analysis of Microarrays (SAM, version 2.23A (Pan 2002; Tusher et al. 2001)) with 100 permutations, KNN-10.

Background corr dist: KL-Divergence = 0.1387, L1-Distance = 0.0308, L2-Distance = 0.0018, Normal std = 0.3861

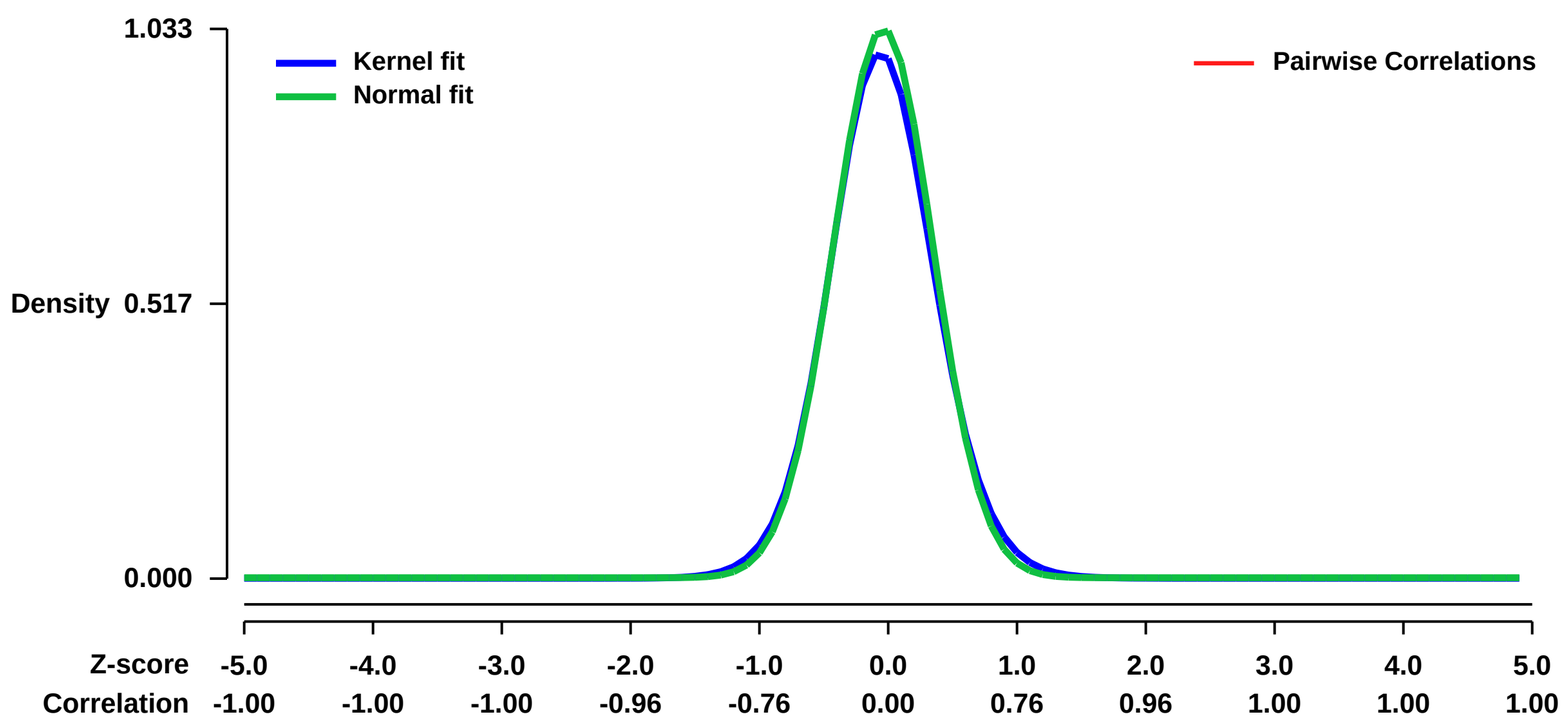

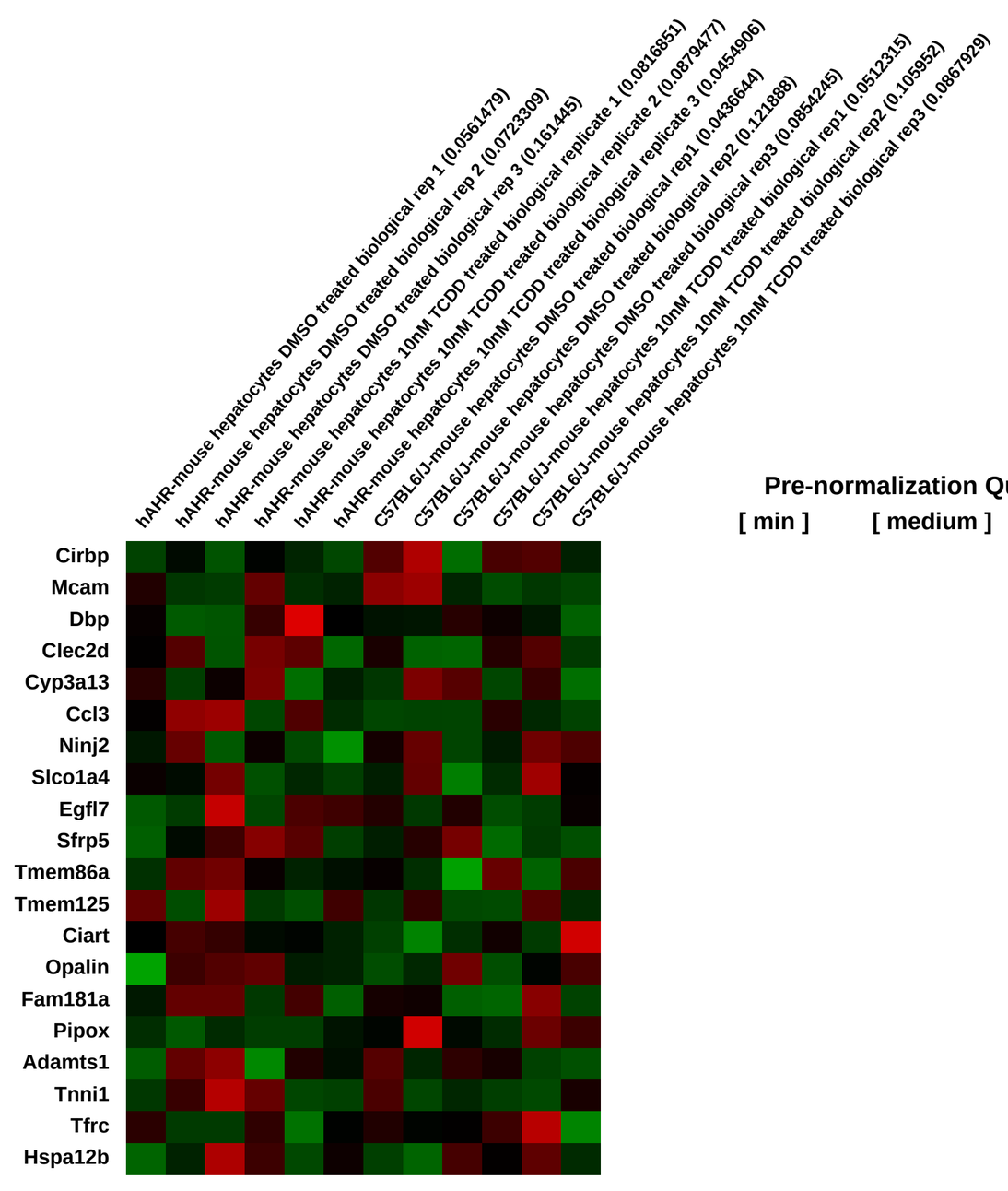

Null module

GEO Series "GSE17985" Expression Profiles

Num of samples in this series: 8

Scale of expression profile Z-scores

-3.0 -2.0 -1.0 0.0 1.0 2.0 3.0

GEO Link:	http://www.ncbi.nlm.nih.gov/geo/query/acc.cgi?acc=GSE17985
Status:	Public on Mar 05 2010
Title:	Gene expression profile of Dicer-deficient oocytes
Organism:	Mus musculus
Experiment type:	Expression profiling by array
Platform:	GPL1261
Pubmed ID:	20116252
Summary & Design:	**Summary:** Small RNAs, such as miRNAs and siRNAs, are involved in gene regulation in a variety of systems, including mouse oocytes. Dicer is a ribonuclease III enzyme essential for miRNA and siRNA biosynthesis. In an effort to uncover the function of small RNAs during oocyte growth, we specifically deleted Dicer in growing oocytes and analyzed the global pattern of gene expression in these Dicer-deficient oocytes. **Overall design:** Germinal vesicle-intact, fully grown oocytes were collected from eCG-primed wild-type or Dicer-deficient female mice and freed of attached cumulus cells by pipetting. Twenty oocytes per mouse were used for RNA extraction and hybridization on the MOE430 v2 Affymetrix microarray platform. Oocytes from four wild-type and four Dicer-knockout mice were analyzed.

Background corr dist: KL-Divergence = 0.0463, L1-Distance = 0.0174, L2-Distance = 0.0004, Normal std = 0.5715

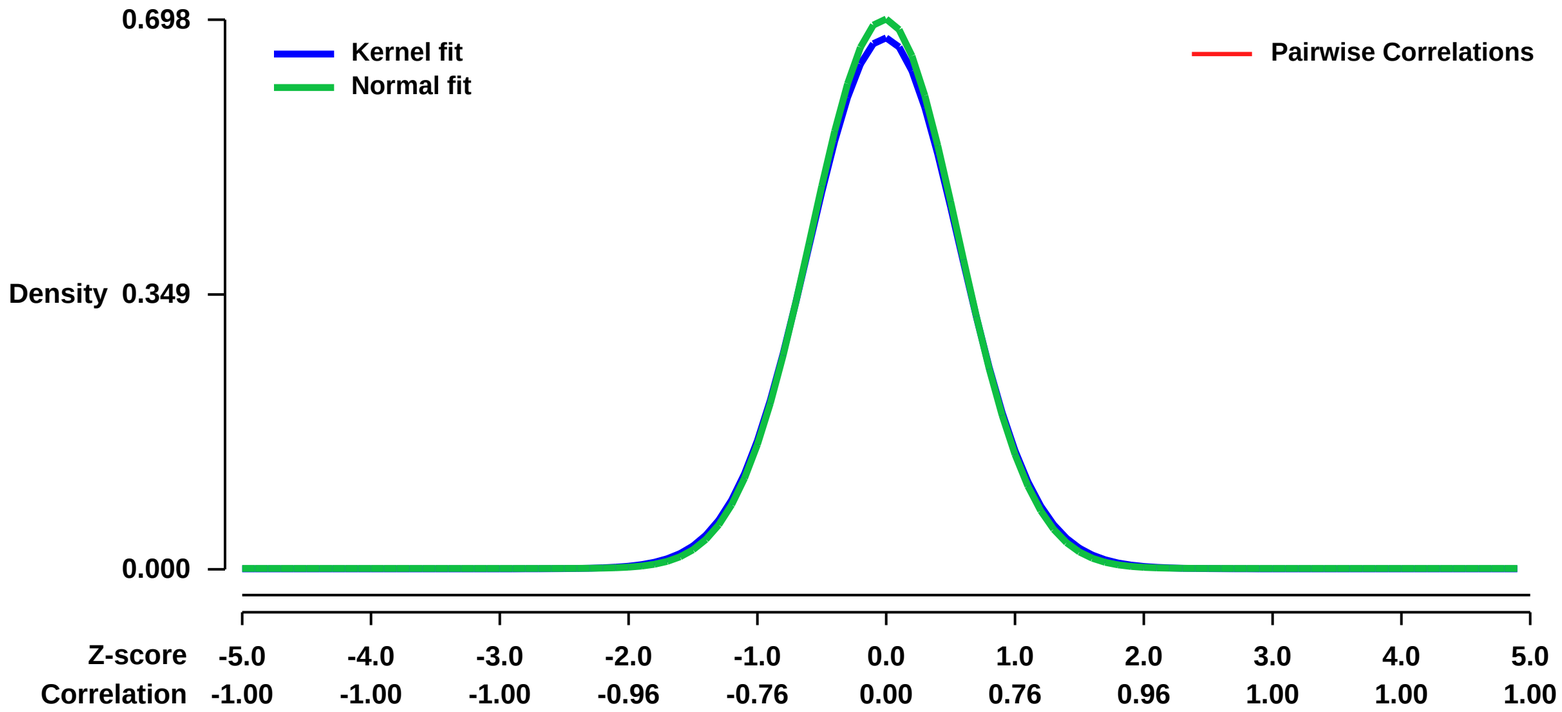

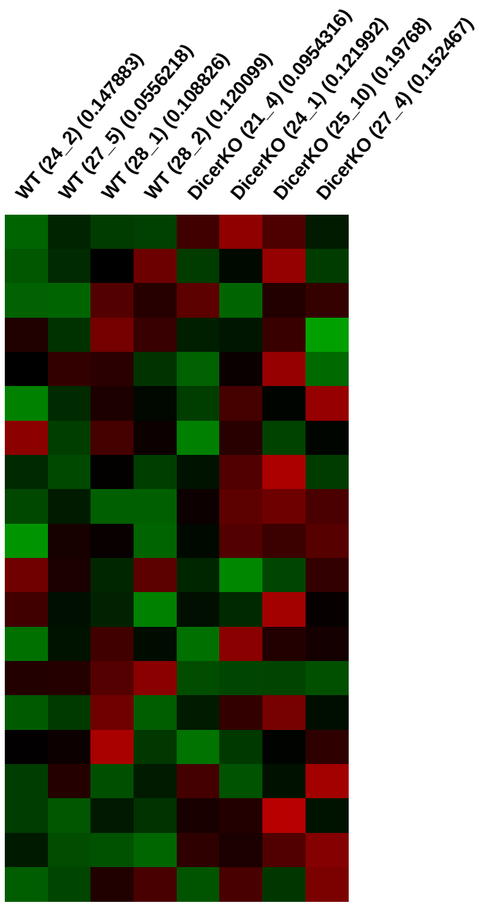

GEO Series "GSE18042" Expression Profiles

Num of samples in this series: 18

Scale of expression profile Z-scores

-3.0 -2.0 -1.0 0.0 1.0 2.0 3.0

GEO Link:	http://www.ncbi.nlm.nih.gov/geo/query/acc.cgi?acc=GSE18042
Status:	Public on Sep 10 2009
Title:	Erythroid differentiation: G1E model
Organism:	Mus musculus
Experiment type:	Expression profiling by array
Platform:	GPL1261
Pubmed ID:	19887574
Summary & Design:	**Summary:** Analysis of erythroid differentiation using Gata1 gene-disrupted G1E ER4 clone cells. Estradiol addition activates an ectopically expressed Gata-1-estrogen receptor fusion protein, triggering synchronous differentiation. 30 hour time course corresponds roughly to late burst-forming unit-erythroid stage (t=0 hrs) through orthochromatic erythroblast stage (t=30 hrs). **Overall design:** G1E ER4 cells cultured in G1E medium were treated at 6 time points with estradiol to initiate erythroid differentiation by activating Gata1 transcription factor and total RNAs from treated cells were extracted for microarray experiment. The erythroid differentiation status was confirmed by cell pellet color and expression of microRNA miR451. The design was similar to an earlier studies (Welch, J. J., Watts, J. A., Vakoc, C. R., Yao, Y., Wang, H., Hardison, R. C., Blobel, G. A., Chodosh, L. A., and Weiss, M. J. (2004)). Global regulation of erythroid gene expression by transcription factor GATA-1. Blood 104, 3136-3147), except that a more recent version of Affymetric chip was used to acheive greater transcriptome coverage.

Background corr dist: KL-Divergence = 0.0901, L1-Distance = 0.0663, L2-Distance = 0.0070, Normal std = 0.5071

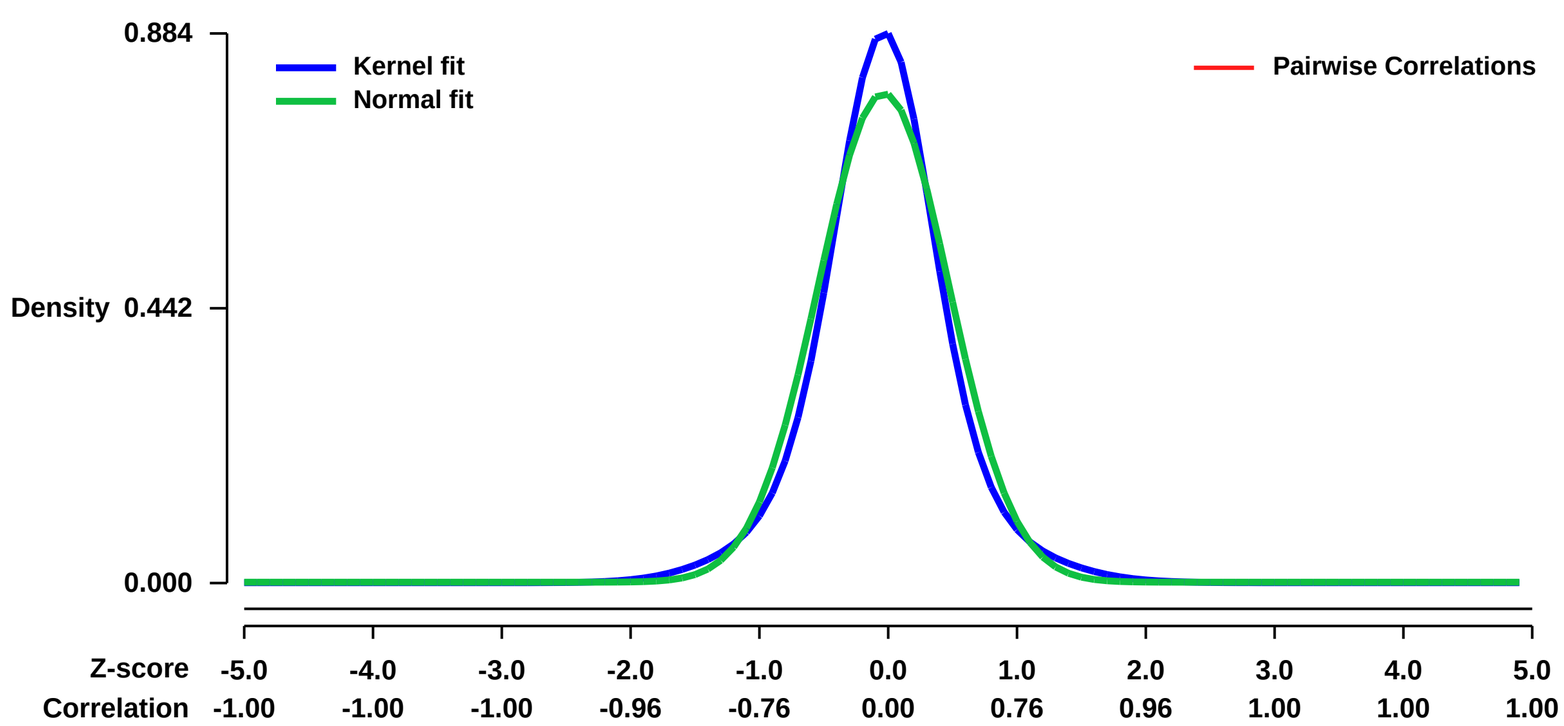

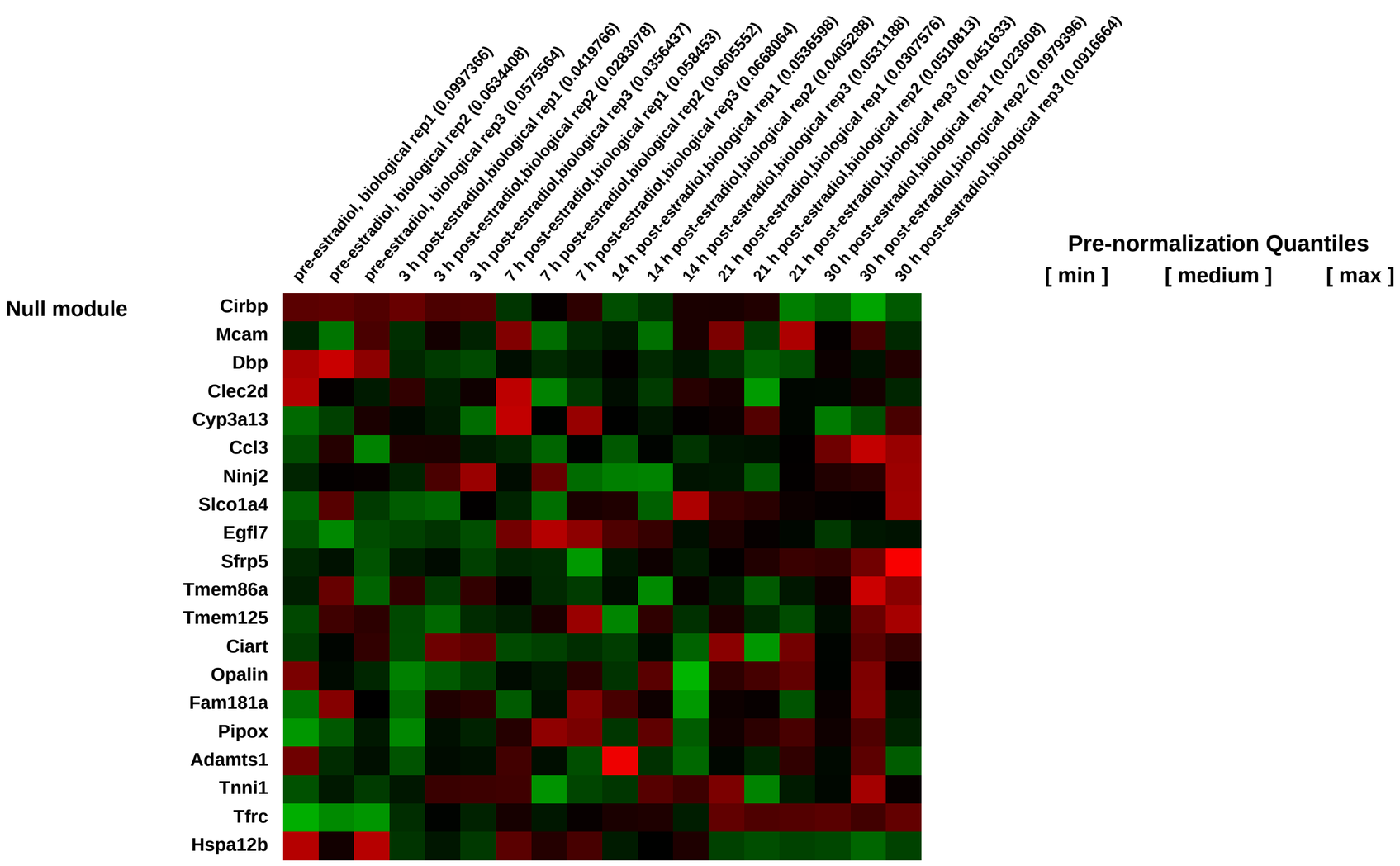

GEO Series "GSE18136" Expression Profiles

Num of samples in this series: 12

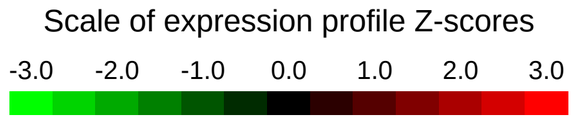

GEO Link:	**http://www.ncbi.nlm.nih.gov/geo/query/acc.cgi?acc=GSE18136**
Status:	**Public on Oct 15 2009**
Title:	**Punctual ablation of Foxp3+ T cells unleashes an autoimmune lesion**
Organism:	**Mus musculus**
Experiment type:	**Expression profiling by array**
Platform:	**GPL1261**
Pubmed ID:	
Summary & Design:	**Summary:** **How do Treg cells control an autoimmune lesion? We depleted Foxp3+ Treg cells in autoimmune prone TCR transgenic BDC2.5 mice on the NOD background** **Kinetic of gene-expression changes in CD4 T cells isolated for pancreas and pancreas draining lymph node (PLN) of Foxp3-DTR.BDC2.5/NOD mice after Treg cell ablation** **Keywords: T cell activation/ differentiation after Treg depletion timecourse** **Overall design:** **CD4 T cells were isolated from pancreas and PLN at 0, 15 and 24 hours after diphtheria toxin application into 4-6 week old female Foxp3-DTR.BDC2.5/NOD transgenic mice**

Background corr dist: KL-Divergence = 0.1270, L1-Distance = 0.0313, L2-Distance = 0.0017, Normal std = 0.3983

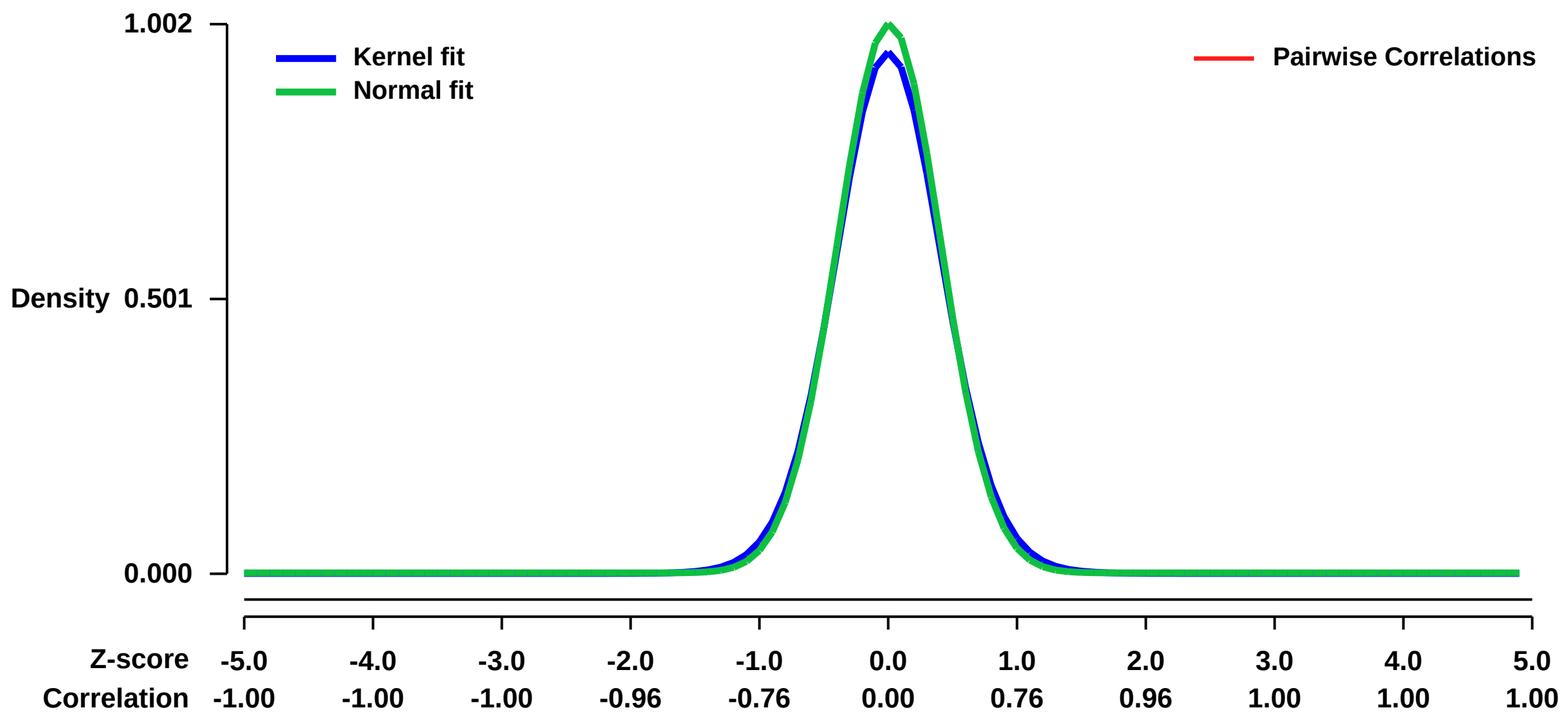

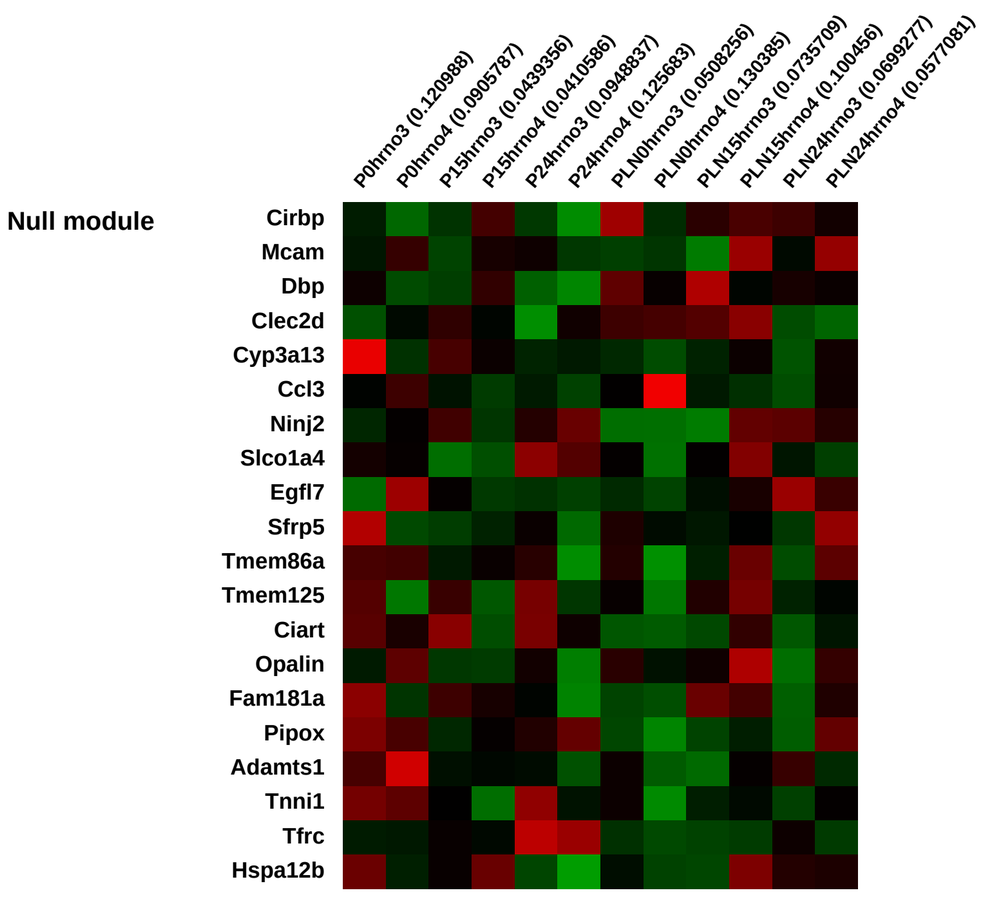

GEO Series "GSE18148" Expression Profiles

Num of samples in this series: 6

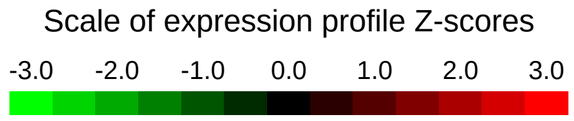

GEO Link:	http://www.ncbi.nlm.nih.gov/geo/query/acc.cgi?acc=GSE18148
Status:	Public on Sep 19 2009
Title:	Microarray analysis of Cbfb-deficient regulatory T cells
Organism:	Mus musculus
Experiment type:	Expression profiling by array
Platform:	GPL1261
Pubmed ID:	19800266
Summary & Design:	**Summary:** **Gene expression profiles of Cbfb-deficient and control Treg cells were compared.** **Abstract: Naturally arising regulatory T (Treg) cells express the transcription factor FoxP3, which critically controls the development and function of Treg cells. FoxP3 interacts with another transcription factor Runx1 (also known as AML1). Here we showed that Treg cell-specific deficiency of Cbf‚†, a cofactor for all Runx proteins, or that of Runx1, but not Runx3, induced lymphoproliferation, autoimmune disease, and hyper-production of IgE. Cbfb-deleted Treg cells exhibited impaired suppressive function in vitro and in vivo, with altered gene expression profiles including attenuated expression of FoxP3 and high expression of interleukin-4. The Runx complex bound to more than 3000 gene loci in Treg cells, including the Foxp3 regulatory regions and the Il4 silencer. In addition, knockdown of RUNX1 showed that RUNX1 is required for the optimal regulation of FoxP3 expression in human T cells. Taken together, our results indicate that the Runx1-Cbf‚† heterodimer is indispensable for in vivo Treg cell function, in particular, suppressive activity and optimal expression of FoxP3.** **Overall design:** **CD4+CD25hi cells, most of which were Foxp3+ Treg cells, were isolated from Cbfb-flox/flox: Foxp3-ires-Cre (n = 3) and control Cbfb-flox/wt: Foxp3-ires-Cre (n = 3) mice. Total RNA was extracted from those purified Cbfb-deficient or control Treg cells.**

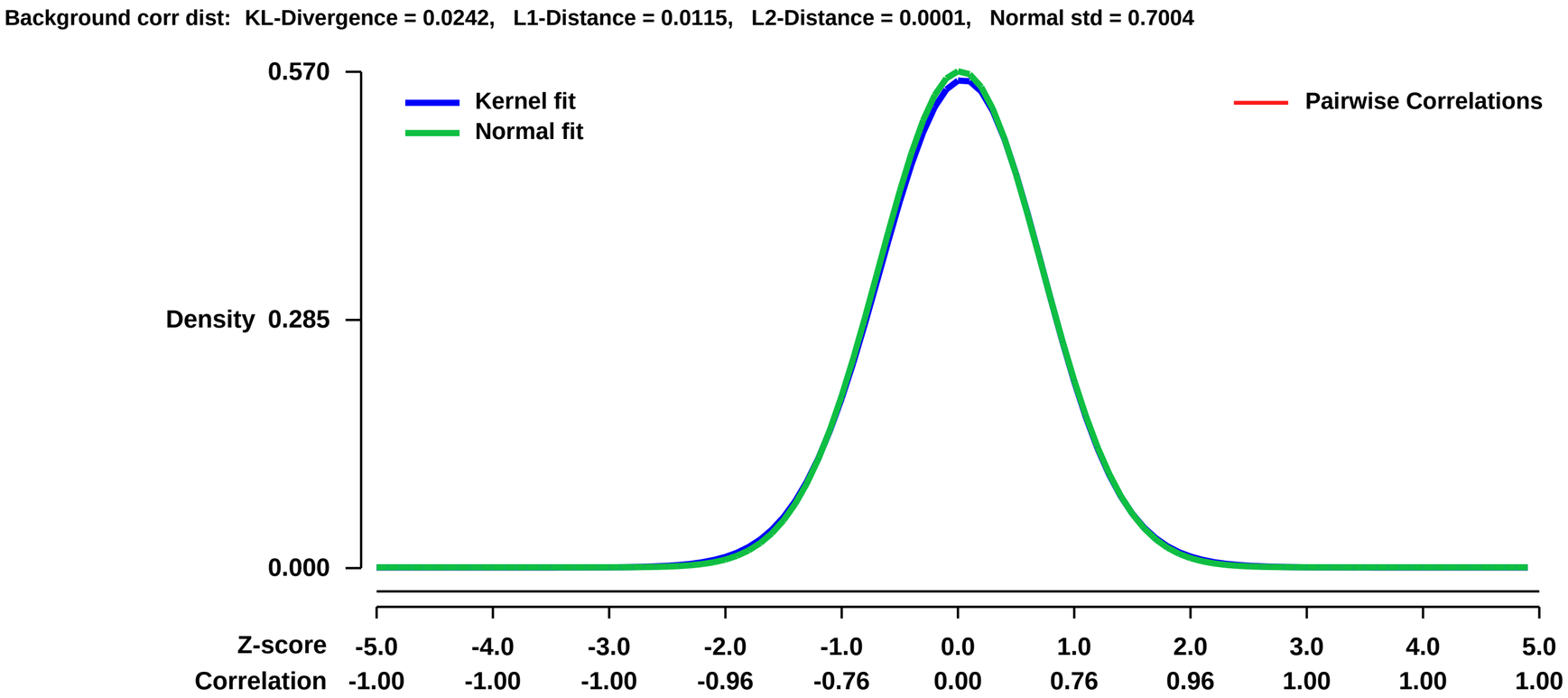

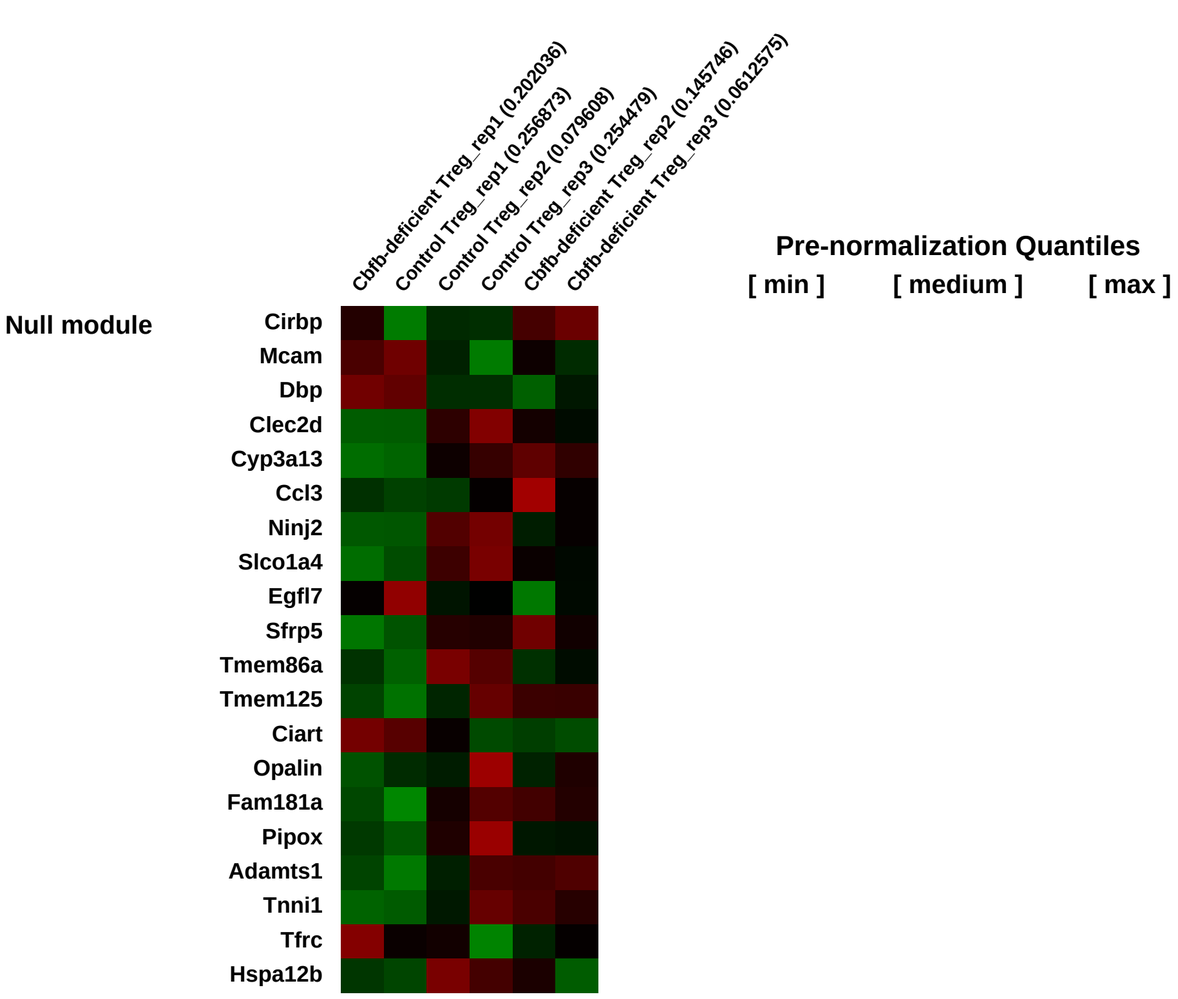

GEO Series "GSE18211" Expression Profiles

Num of samples in this series: 12

Scale of expression profile Z-scores

-3.0 -2.0 -1.0 0.0 1.0 2.0 3.0

GEO Link:	**http://www.ncbi.nlm.nih.gov/geo/query/acc.cgi?acc=GSE18211**
Status:	**Public on Nov 09 2009**
Title:	**New candidate gene identification for controlling mammalian gonadal sex determination**
Organism:	**Mus musculus**
Experiment type:	**Expression profiling by array**
Platform:	**GPL1261**
Pubmed ID:	**19864314**
Summary & Design:	**Summary:** **Mammalian gonadal sex determination is dependent on proper expression of sex determining genes in fetal gonadal somatic support cells (i.e., pre-granulosa and pre-Sertoli cells in XX and XY gonads, resp.). We used a unique transgenic mouse strain combined with microarray profiling to identify all the differentially expressed transcripts in XX and XY isolated somatic support cells during critical stages of gonadal development and differentiation.** **Overall design:** **XX and XY somatic support cells (SSC) were isolated by flow cytometry from embryonic day (E) 11.5 and E12.5 mouse gonads. Total RNA was isolated from pools of isolated cells; 3 pools per sex and each timepoint.**

Background corr dist: **KL-Divergence = 0.1005, L1-Distance = 0.0254, L2-Distance = 0.0015, Normal std = 0.4337**

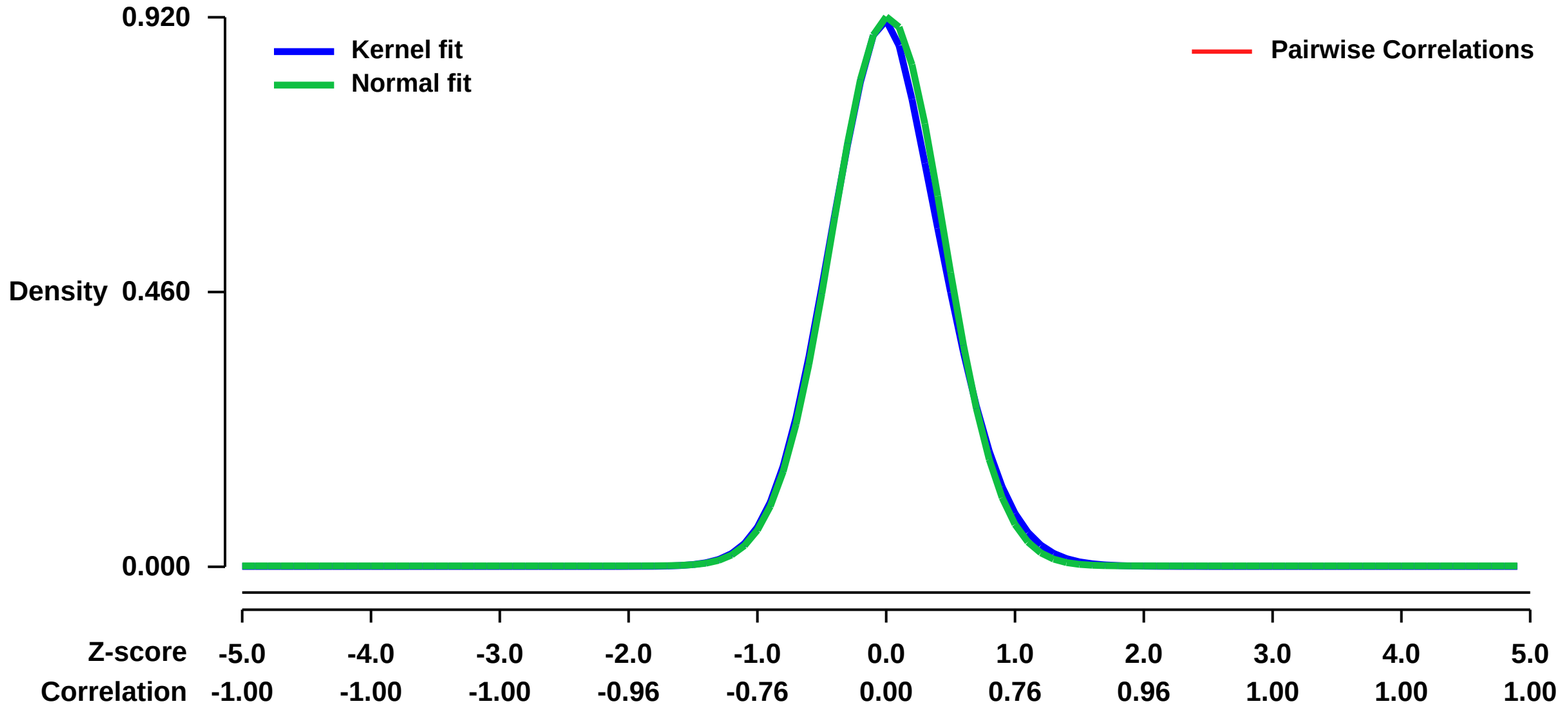

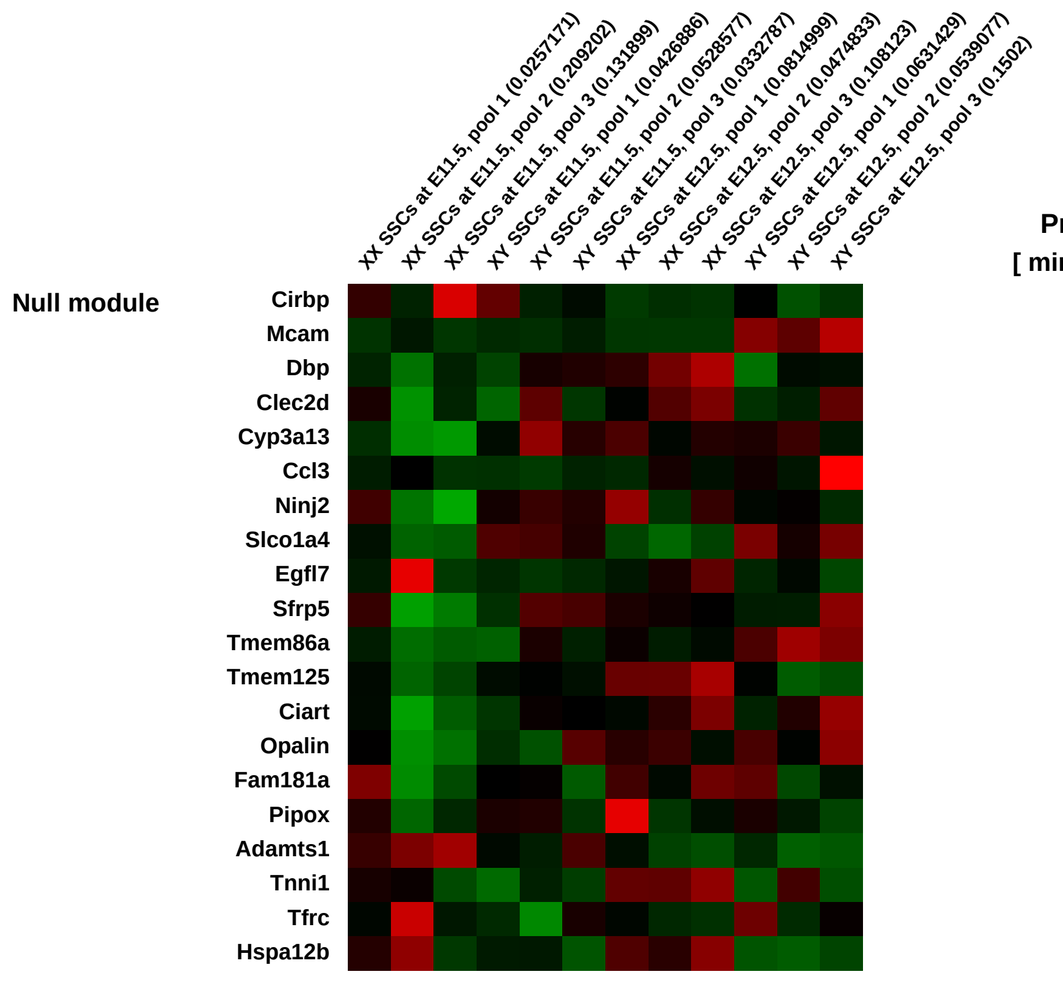

GEO Series "GSE18308" Expression Profiles

Num of samples in this series: 6

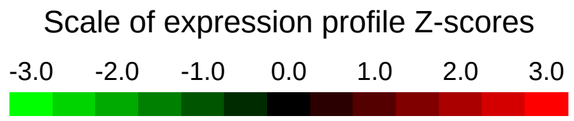

GEO Link:	**http://www.ncbi.nlm.nih.gov/geo/query/acc.cgi?acc=GSE18308**
Status:	**Public on Jan 01 2010**
Title:	**FoxOs cooperatively regulate diverse pathways governing neural stem cell homeostasis**
Organism:	**Mus musculus**
Experiment type:	**Expression profiling by array**
Platform:	**GPL1261**
Pubmed ID:	**19896444**
Summary & Design:	**Summary:** **FoxOs cooperatively regulate diverse pathways governing neural stem cell homeostasis** **Overall design:** **expression profile between six independant neural stem cell lines (three FoxO null and three wild type) were compared**

Background corr dist: **KL-Divergence = 0.0468, L1-Distance = 0.0219, L2-Distance = 0.0006, Normal std = 0.5893**

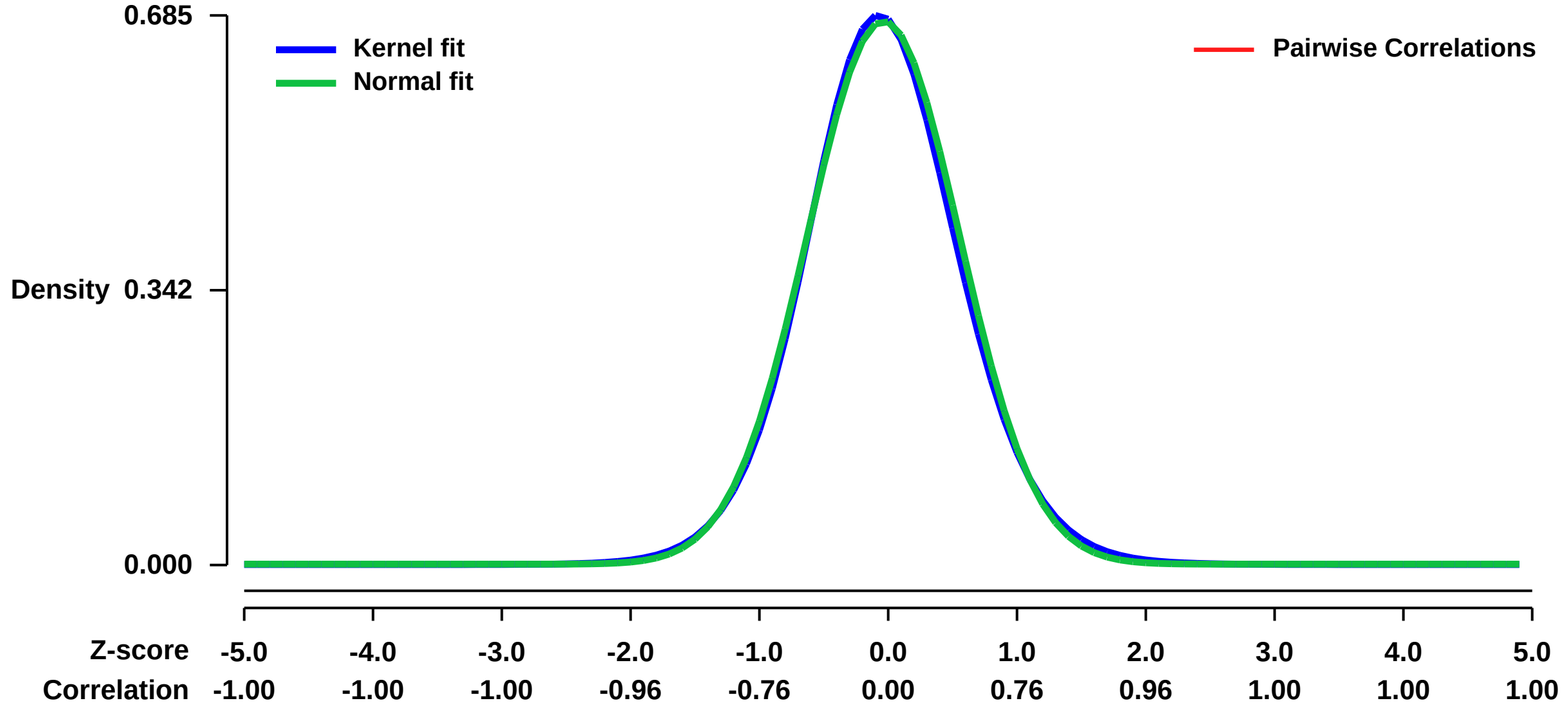

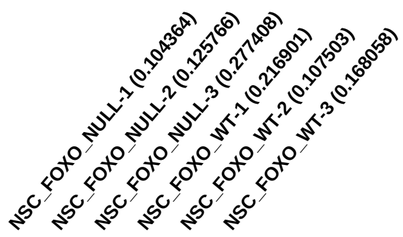

Pre-normalization Quantiles

[min] [medium] [max]

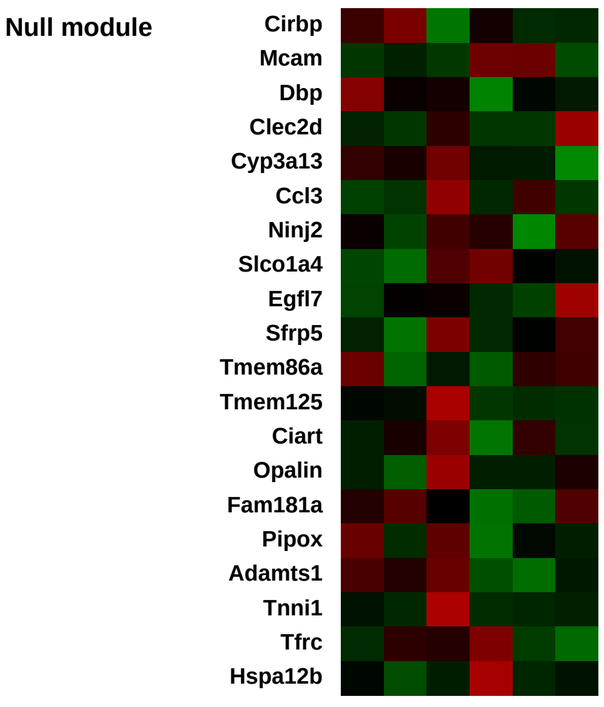

GEO Series "GSE18322" Expression Profiles

Num of samples in this series: 12

Scale of expression profile Z-scores

-3.0 -2.0 -1.0 0.0 1.0 2.0 3.0

GEO Link:	http://www.ncbi.nlm.nih.gov/geo/query/acc.cgi?acc=GSE18322
Status:	Public on Mar 01 2010
Title:	Gene Expression Analysis of Ara-C Resistance in AML
Organism:	Mus musculus
Experiment type:	Expression profiling by array
Platform:	GPL1261
Pubmed ID:	20508618
Summary & Design:	**Summary:** Using two independently derived murine BXH2 cell lines, Ara-C resistant derivatives were developed by exposure to increasing concentrations of Ara-C. Microarray analysis comparing the Ara-C resistant cells to their Ara-C sensitive parental cell lines identified potential genes involved in Ara-C resistance. **Overall design:** Two highly Ara-C-resistant cell lines, B117H and B140H, were derived from Ara-C-sensitive parental cell lines, B117P and B140P. Variations in gene expression between these Ara-C-resistant and -sensitive sets were studied. Three replicates per cell line.

Background corr dist: KL-Divergence = 0.0797, L1-Distance = 0.0246, L2-Distance = 0.0008, Normal std = 0.4839

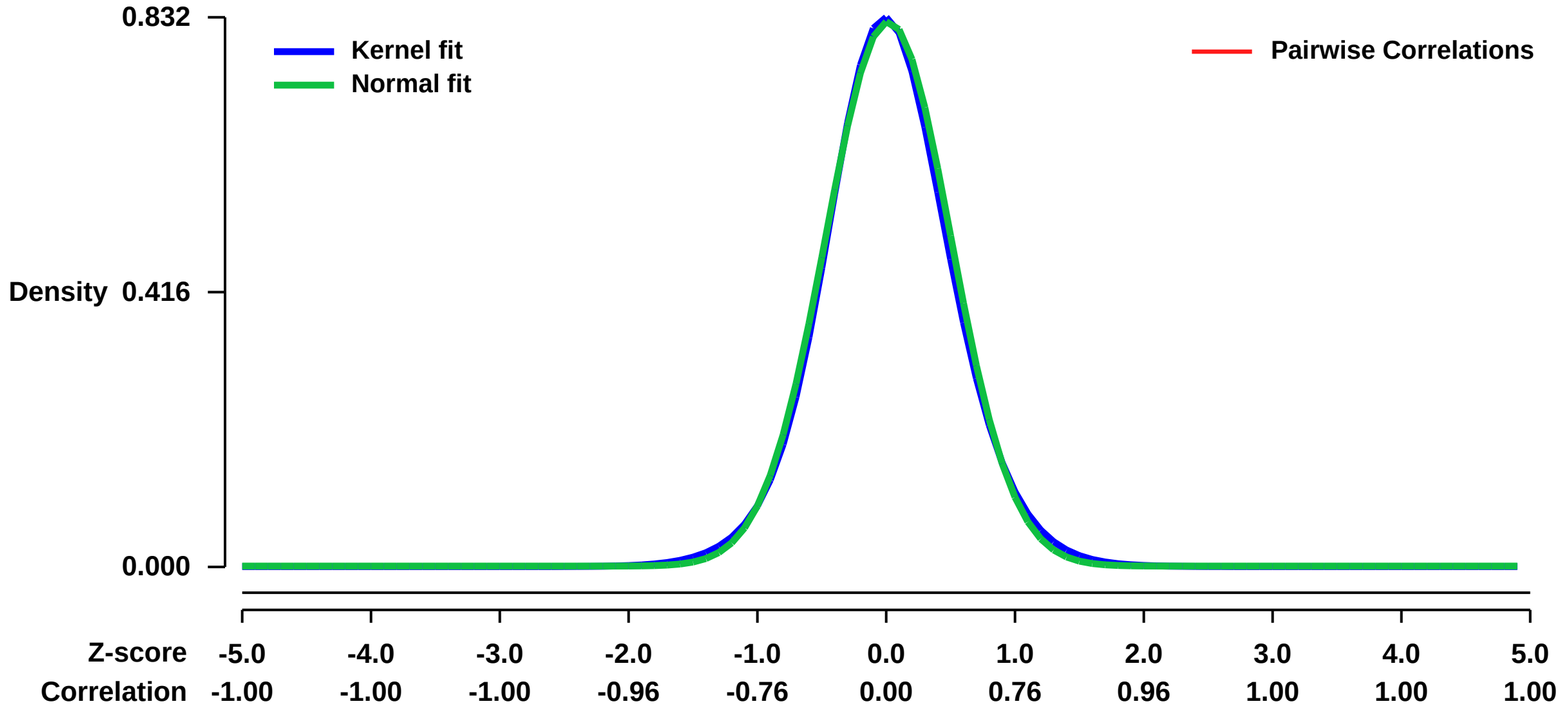

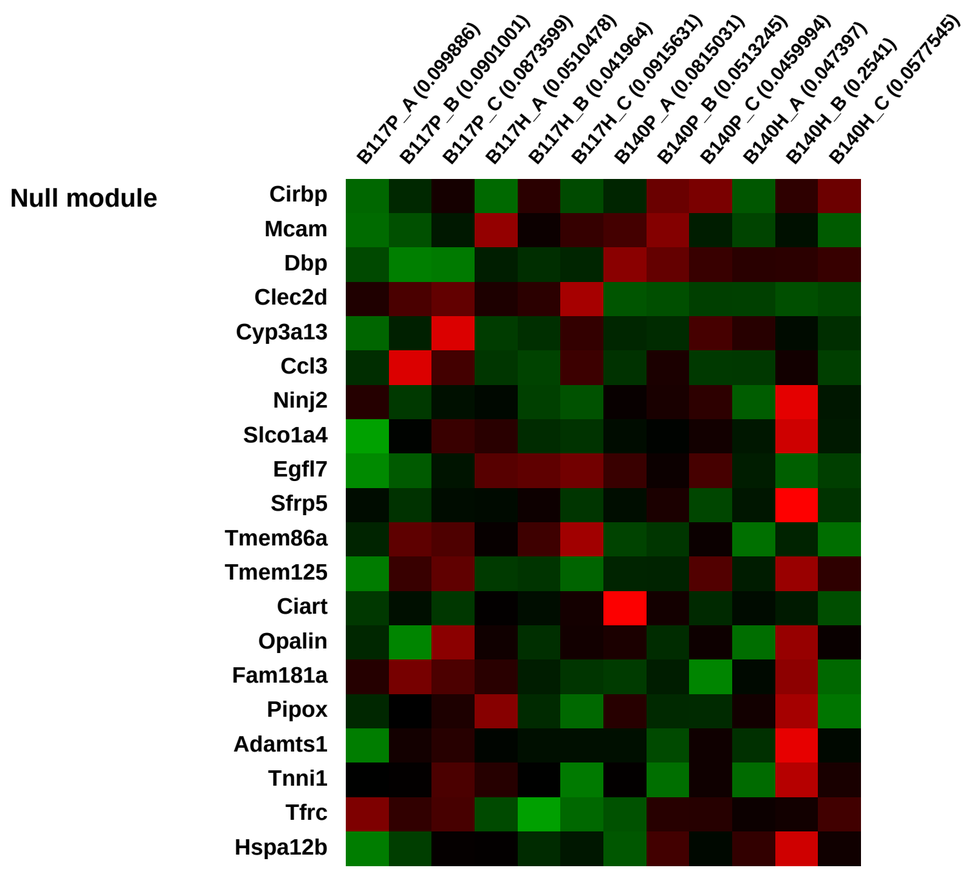

GEO Series "GSE18326" Expression Profiles

Num of samples in this series: 8

Scale of expression profile Z-scores

-3.0 -2.0 -1.0 0.0 1.0 2.0 3.0

GEO Link:	**http://www.ncbi.nlm.nih.gov/geo/query/acc.cgi?acc=GSE18326**
Status:	**Public on Nov 29 2009**
Title:	**Role of FoxO3 in adult neural stem cell maintenance in mice**
Organism:	**Mus musculus**
Experiment type:	**Expression profiling by array**
Platform:	**GPL1261**
Pubmed ID:	**19896443**
Summary & Design:	**Summary:** **In the nervous system, neural stem cells (NSC) are necessary for the generation of new neurons and for cognitive function. Here we show that FoxO3, a member of a transcription factor family known to extend lifespan in invertebrates, regulates the NSC pool. We find that adult FoxO3-/- mice have fewer NSC in vivo than wild type counterparts. NSC isolated from adult FoxO3-/- mice have decreased self-renewal and an impaired ability to generate different neural lineages. Identification of the FoxO3-dependent gene expression profile in NSC suggests that FoxO3 regulates the NSC pool by inducing a program of genes that preserves quiescence, prevents premature differentiation, and controls oxygen metabolism. The ability of FoxO3 to prevent the premature depletion of NSC might have important implications for counteracting brain aging in long-lived species.** **Overall design:** **mRNA expression from secondary neurospheres cultured from cells taken from mouse forebrains was compared between FoxO3+/+ (wildtype) and FoxO3-/- (null mutant) mice from the FVB/N background.**

Background corr dist: KL-Divergence = 0.0266, L1-Distance = 0.0225, L2-Distance = 0.0007, Normal std = 0.6723

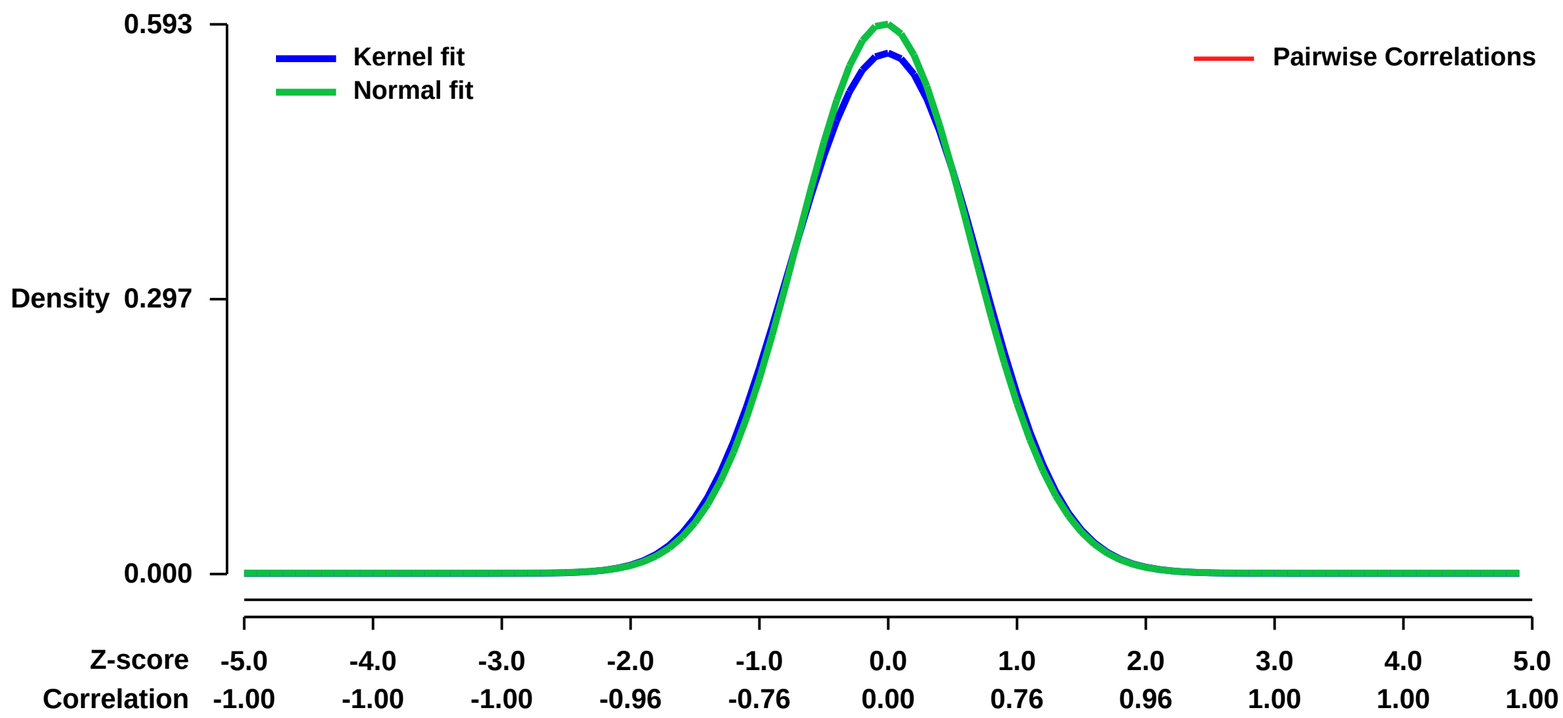

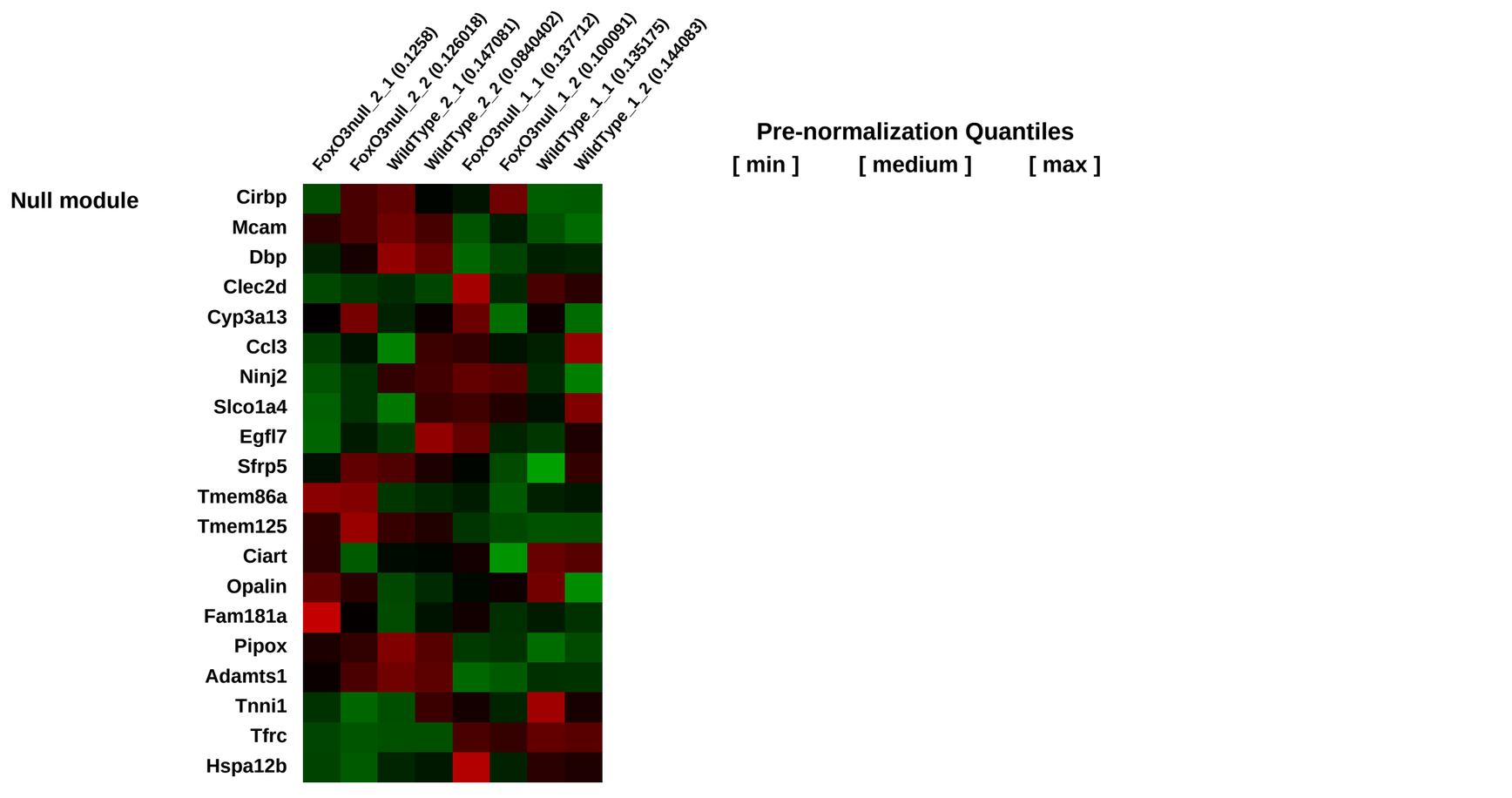

GEO Series "GSE18341" Expression Profiles

Num of samples in this series: 30

Scale of expression profile Z-scores

-3.0 -2.0 -1.0 0.0 1.0 2.0 3.0

GEO Link:	http://www.ncbi.nlm.nih.gov/geo/query/acc.cgi?acc=GSE18341
Status:	Public on Nov 23 2009
Title:	Age Dependent Gene Expression Responses to Inhaled Lipopolysaccharide Combined with Mechanical Ventilation
Organism:	Mus musculus
Experiment type:	Expression profiling by array
Platform:	GPL1261
Pubmed ID:	19901347
Summary & Design:	**Summary:** Children have a lower incidence and mortality from acute lung injury than adults, and infections are the most common event associated with acute lung injury (ALI). To study the effects of age on susceptibility to ALI, we investigated the responses to microbial products combined with mechanical ventilation in juvenile (21 day) and adult (16 week-old) mice. We hypothesized that the increased incidence and severity of lung injury associated with increasing age is due in large part to acquired changes in the way in which inflammatory responses are activated in the lungs in response to microbial products and mechanical ventilation. **Overall design:** Juvenile (21 day) and adult (16 week) C57BL/6 mice were treated with an aerosol of E. coli 0111:B4 lipopolysaccharide (LPS) (20 mL of 0.1 mg/mL) for 30 minutes in a sealed aerosol chamber, immediately followed by mechanical ventilation (LPS+MV) using tidal volume = 15 mL/kg, rate = 80 breaths/min, FiO2 = 30% and positive end expiratory pressure = 2 cm H2O for the duration of the study period time = 2 hours. Comparison groups included mice treated with LPS or mechanical ventilation (MV) alone, and untreated age-matched controls. There were N = 4 animals per group except the juvenile mice treated with MV alone and LPS+MV where there were N = 3. Each sample was an individual animal, therefore there were 30 samples. Mice treated with LPS alone were placed into a sealed aerosol chamber as stated above, and then allowed to breath spontaneously with free access to food and water for the duration of the study period time = 2 hours. Mice treated with MV alone were treated with the mechanical ventilation protocol stated above for the duration of the study period time = 2 hours. At the end of the study period, the mice were euthanized, and the lungs were immediately removed and placed into RNAlater (Ambion, Austin, TX) for at least 24 hr prior to isolation of total lung mRNA.

Background corr dist: KL-Divergence = 0.2657, L1-Distance = 0.0529, L2-Distance = 0.0068, Normal std = 0.2954

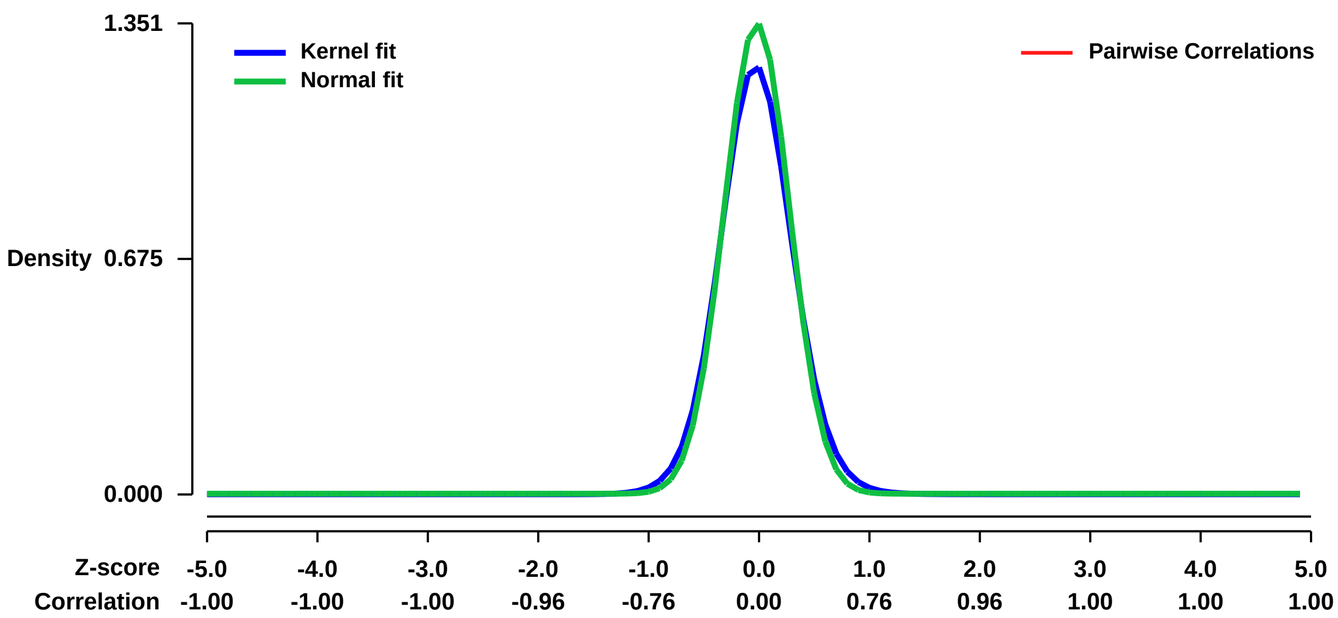

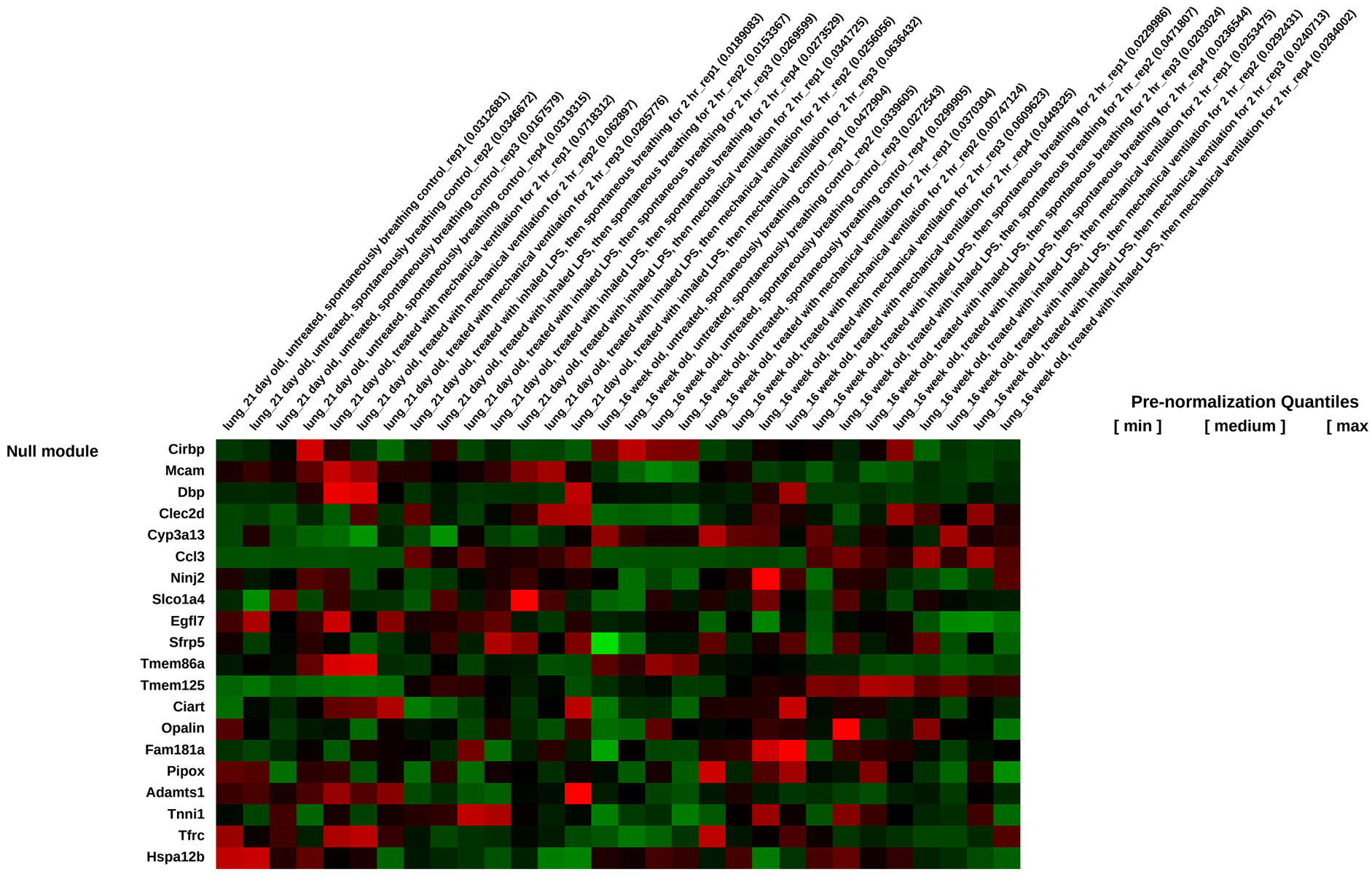

GEO Series "GSE18358" Expression Profiles

Num of samples in this series: 10

Scale of expression profile Z-scores

-3.0 -2.0 -1.0 0.0 1.0 2.0 3.0

GEO Link:	http://www.ncbi.nlm.nih.gov/geo/query/acc.cgi?acc=GSE18358
Status:	Public on Oct 02 2009
Title:	Gene Expression Profiling of Glomeruli from a mouse model of Denys-Drash Syndrome
Organism:	Mus musculus
Experiment type:	Expression profiling by array
Platform:	GPL1261
Pubmed ID:	19797313
Summary & Design:	**Summary:** The Wilms tumor-suppressor gene WT1, a key player in renal development, also has a crucial role in maintenance of the glomerulus in the mature kidney. However, molecular pathways orchestrated by WT1 in podocytes, where it is highly expressed, remain unknown. Their defects are thought to modify the cross-talk between podocytes and other glomerular cells and ultimately lead to glomerular sclerosis, as observed in diffuse mesangial sclerosis (DMS) a nephropathy associated with WT1 mutations. To identify podocyte WT1 targets, we generated a novel DMS mouse line, performed gene expression profiling in isolated glomeruli, and identified excellent candidates that may modify podocyte differentiation and growth factor signalling in glomeruli. Scel, encoding sciellin, a protein of the cornified envelope in the skin, and sulf1, encoding a 6-O endosulfatase, are shown to be expressed in wild type podocytes and to be strongly down-regulated in mutants. Co-expression of Wt1, Scel and Sulf1 was also found in a mesonephric cell line, and siRNA-mediated knockdown of WT1 decreased Scel and Sulf1 mRNAs and proteins. By ChIP we show that Scel and Sulf1 are direct WT1 targets. Cyp26a1, encoding an enzyme involved in the degradation of retinoic acid, is shown to be up-regulated in mutant podocytes. Cyp26a1 may play a role in the development of glomerular lesions but does not seem to be regulated by WT1. These results provide novel clues in our understanding of normal glomerular function and early events involved in glomerulosclerosis. **Overall design:** Isolation of glomeruli from mutant (FVB-N4 Wt1+/R394W) and wild-type (FVB-N4 Wt1+/+) was performed after cardiac Dynabead perfusion. GeneChip analysis of glomeruli from 5 Wt1+/R394W mice and 5 Wt1+/+ littermates (N4-FVB) were performed independently. Animals were unweaned 27-day-old males. The Wt1+/R394W mice used were showing little albuminuria (<3 ug/ul on Coomassie blue stained SDS-PAGE gel) and no evidence of mesangial lesions by light microscopy.

Background corr dist: KL-Divergence = 0.1193, L1-Distance = 0.0302, L2-Distance = 0.0016, Normal std = 0.4090

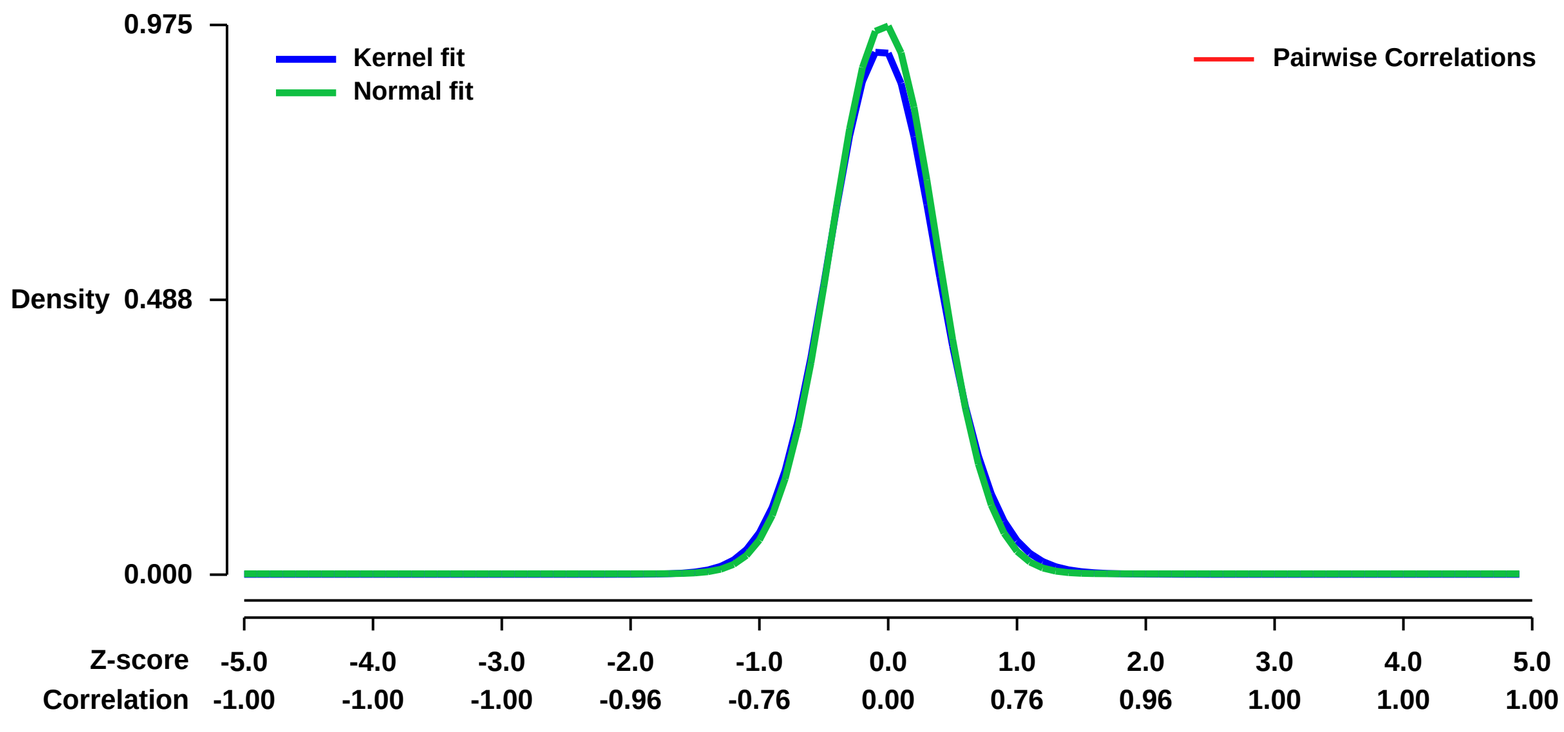

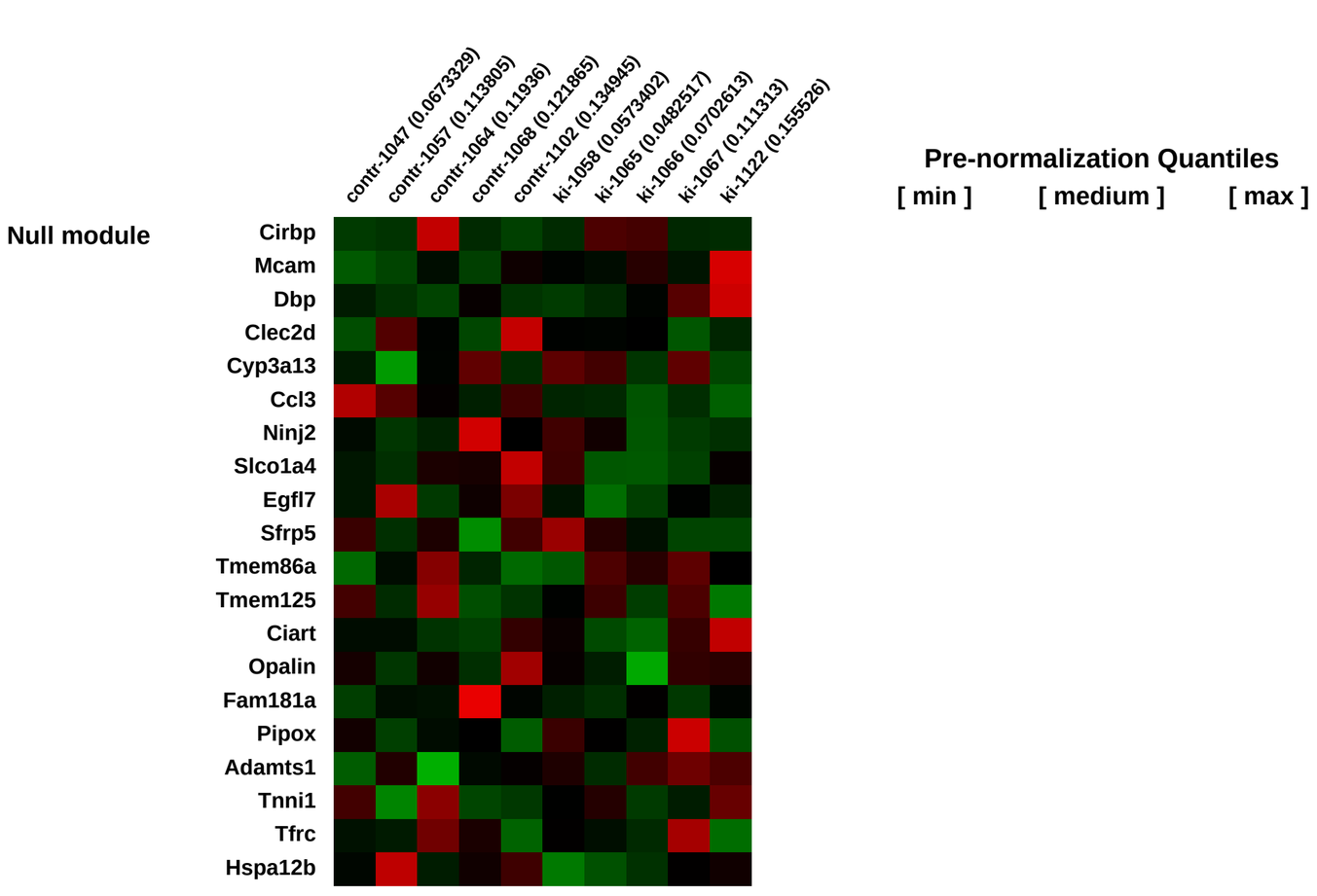

GEO Series "GSE18395" Expression Profiles

Num of samples in this series: 8

Scale of expression profile Z-scores

-3.0 -2.0 -1.0 0.0 1.0 2.0 3.0

GEO Link: http://www.ncbi.nlm.nih.gov/geo/query/acc.cgi?acc=GSE18395

Status: Public on Oct 01 2010

Title: Expression data from mouse adult fibroblasts with Rb deletion and/or p53DD expression exposed to cisplatin (CDDP)

Organism: Mus musculus

Experiment type: Expression profiling by array

Platform: GPL1261

Pubmed ID:

Summary & Design:

Summary:
The RB and p53 tumor suppressor pathways regulate the transcription of genes involved in cell cycle progression, DNA replication, DNA repair, and apoptosis. These tumor suppressors are critical modulators of the response to genotoxic damage and both pathways are frequently inactivated in human cancers.

We used microarrays to monitor gene expression patterns upon exposure to cisplatin treatment in fibroblasts harboring loss/inactivation of RB and/or p53.

Overall design:
We generated mouse adult fibroblasts harboring loss/inactivation of RB and/or p53 and subjected these cell populations to cisplatin treatment for 24 hours. Treated cell populations were allowed to recover from cisplatin exposure, generating a recurred cell popuation. Untreated and recurred cell populations were then subjected to RNA extraction and hybridization on Affymetrix microarrays.

Background corr dist: KL-Divergence = 0.0582, L1-Distance = 0.0193, L2-Distance = 0.0005, Normal std = 0.5297

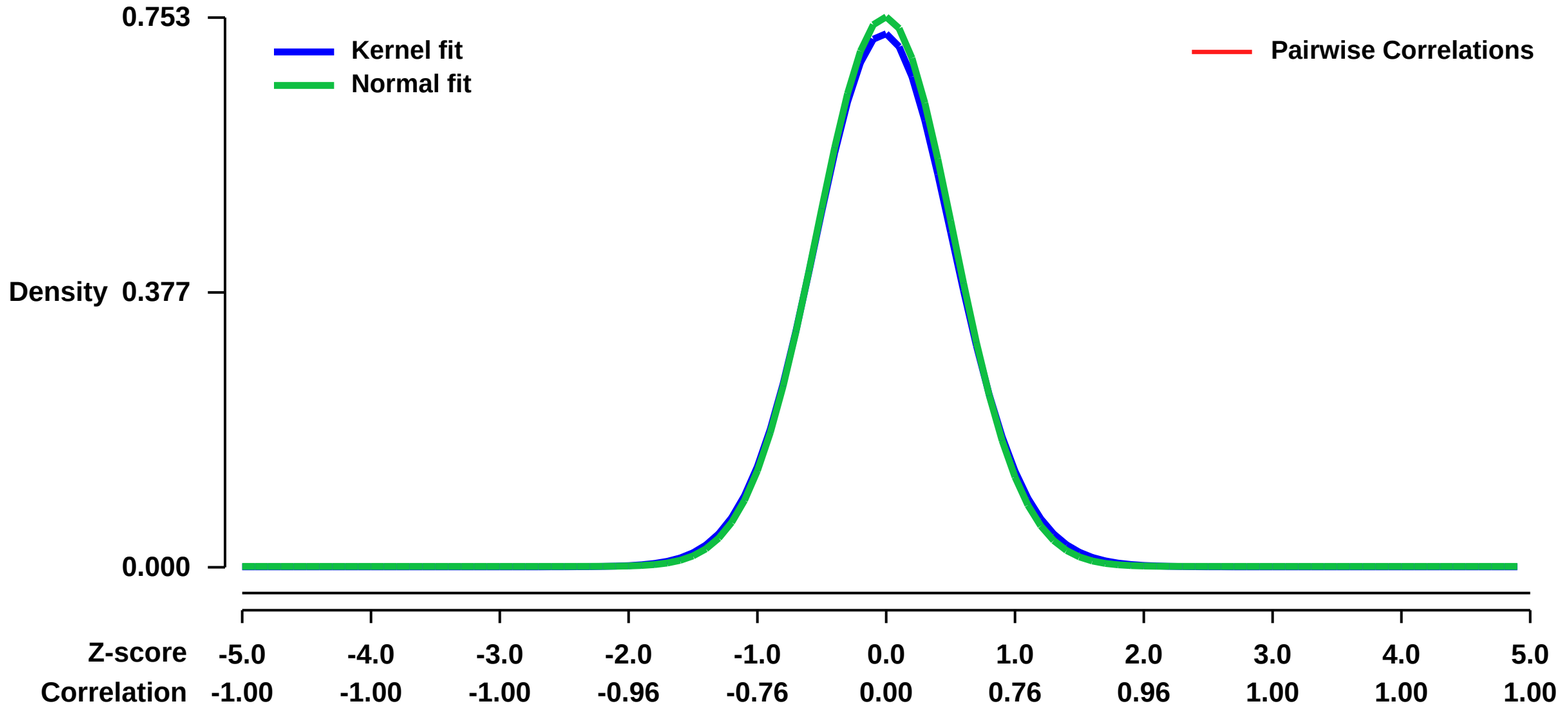

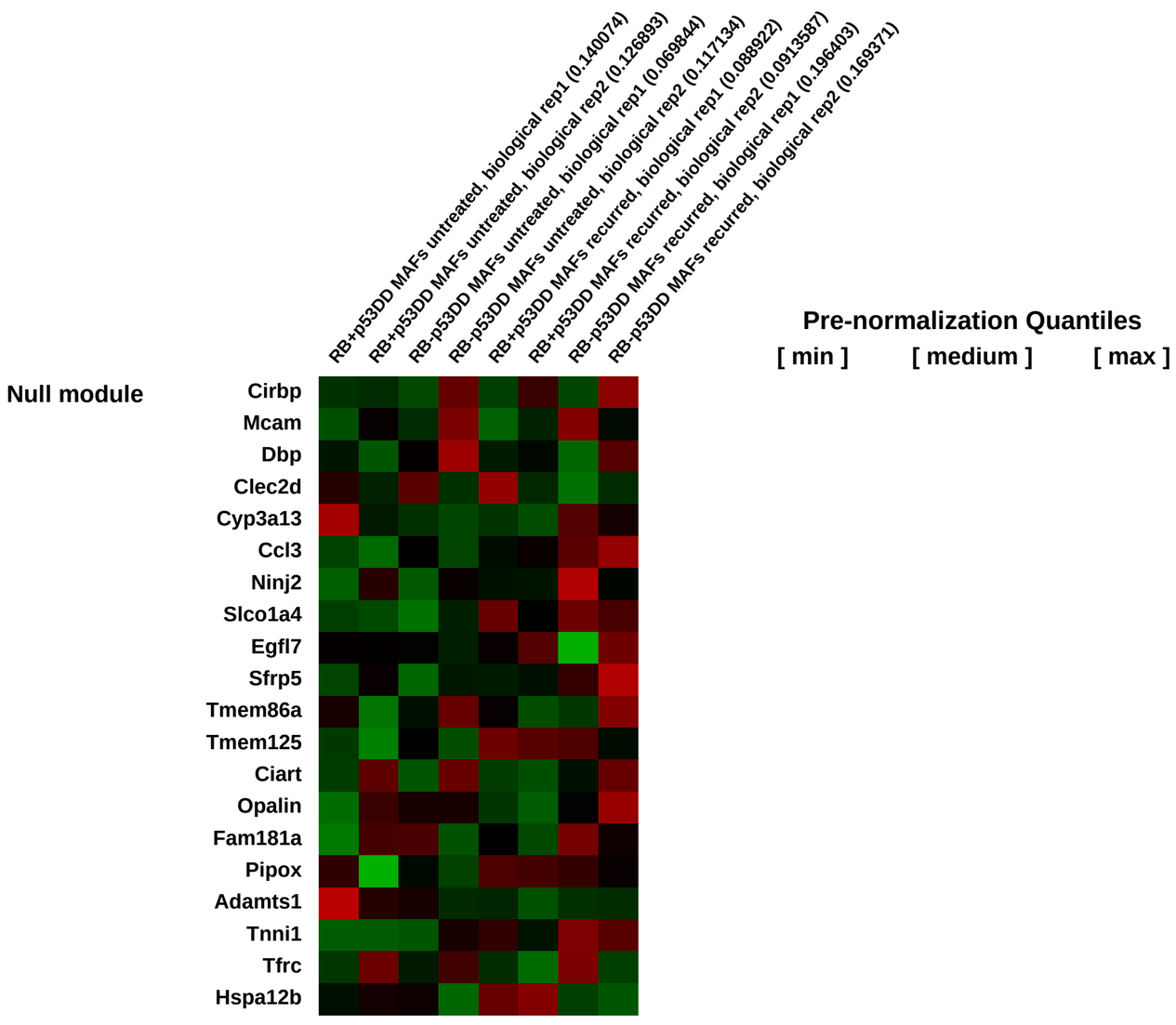

GEO Series "GSE18396" Expression Profiles

Num of samples in this series: 6

Scale of expression profile Z-scores

-3.0 -2.0 -1.0 0.0 1.0 2.0 3.0

GEO Link:	http://www.ncbi.nlm.nih.gov/geo/query/acc.cgi?acc=GSE18396
Status:	Public on Jun 30 2010
Title:	Dmrt1 (doublesex and mab-3 related transcription factor 1) knockout expression analyses in E13.5 testes in S6 background
Organism:	Mus musculus
Experiment type:	Expression profiling by array
Platform:	GPL1261
Pubmed ID:	20007774
Summary & Design:	**Summary:** Dmrt1 (doublesex and mab-3 related transcription factor 1) is a conserved transcriptional regulator of male differentiation required for testicular development in vertebrates. In mice of the 129Sv strain, loss of Dmrt1 causes a high incidence of teratomas. Mutant 129Sv germ cells undergo apparently normal differentiation up to embryonic day 13.5 (E13.5), but some cells fail to arrest mitosis and ectopically express pluripotency markers. Expression analysis and chromatin immunoprecipitation identified DMRT1 target genes whose misexpression may underly teratoma formation. **Overall design:** Comparison of E13.5 testes gene expression between Dmrt1(+/-) and Dmrt1(-,-) animals that show high incidence of teratoma formation.

Background corr dist: KL-Divergence = 0.0394, L1-Distance = 0.0172, L2-Distance = 0.0003, Normal std = 0.6150

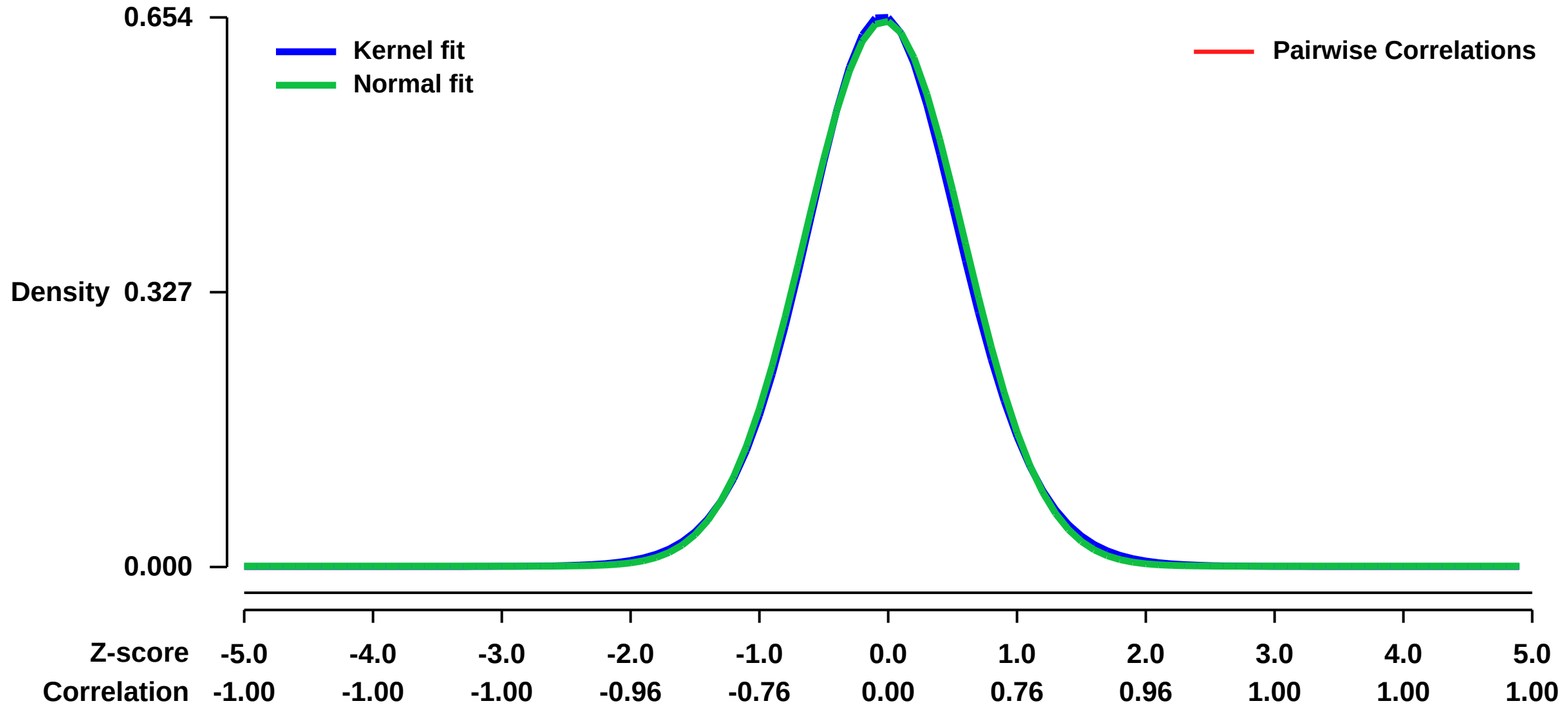

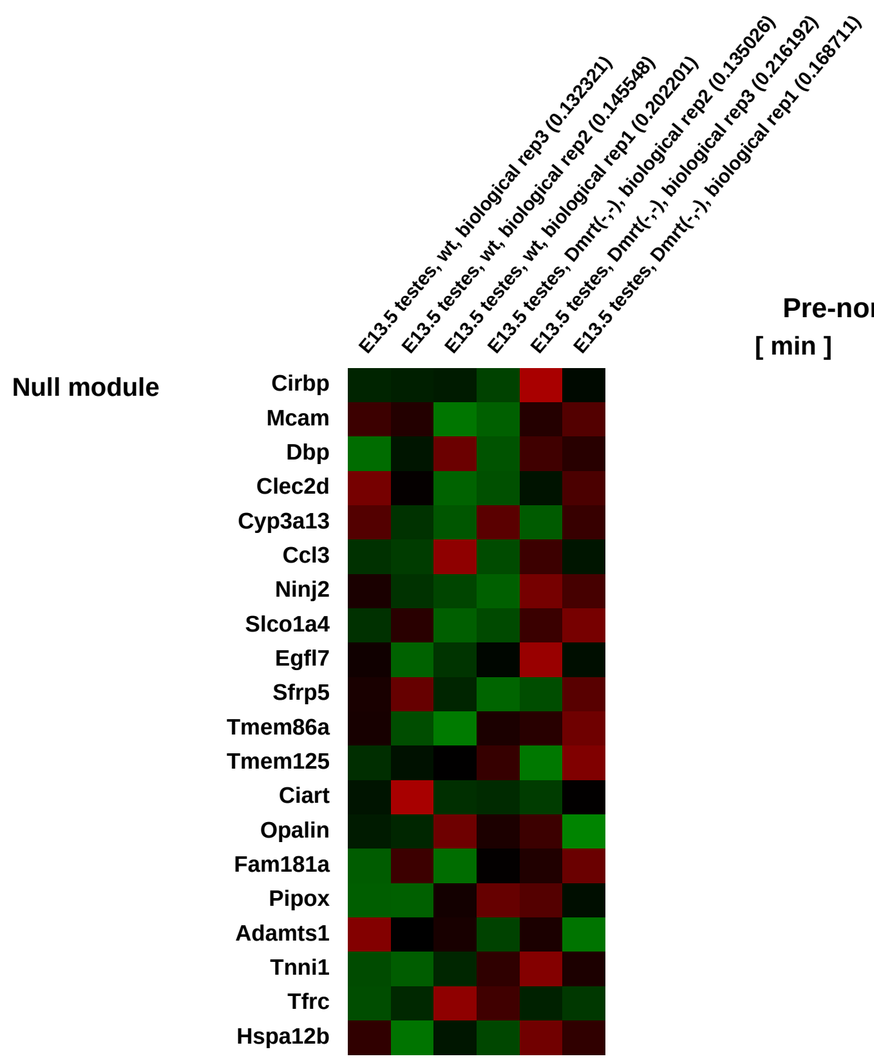

GEO Series "GSE18460" Expression Profiles

Num of samples in this series: 16

Scale of expression profile Z-scores

-3.0 -2.0 -1.0 0.0 1.0 2.0 3.0

GEO Link:	http://www.ncbi.nlm.nih.gov/geo/query/acc.cgi?acc=GSE18460
Status:	Public on Oct 08 2009
Title:	Lactobacillus acidophilus induces virus immune defense genes in murine dendritic cells by a TLR-2 dependent mechanism
Organism:	Mus musculus
Experiment type:	Expression profiling by array
Platform:	GPL1261
Pubmed ID:	20545783
Summary & Design:	**Summary:** Lactobacilli are probiotics that, among other health promoting effects, have been ascribed immunostimulating and virus preventive properties. Certain lactobacilli species have been shown to possess strong IL-12 inducing properties. As IL-12 production depends on the up-regulation of type I interferons, we hypothesized that the strong IL-12 inducing capacity of L. acidophilus NCFM in murine bone marrow derived DC is caused by an up-regulation of IFN-¿†, which subsequently stimulates the induction of IL-12 and the dsRNA binding toll like receptor (TLR)-3. The expression of the genes encoding IFN-¿†, IL-12, IL-10 and TLR-3 in DC upon stimulation with L. acidophilus NCFM was measured. L. acidophilus NCFM induced a much stronger expression of ifn-¿†, il-12 and il-10 compared to the synthetic dsRNA ligand Poly I:C, whereas the levels of expressed tlr-3 were similar. By the use of whole genome microarray gene expression, we investigated whether other genes related to the viral defence were up-regulated in DC upon stimulation with L. acidophilus NCFM and found that various virus defence related genes, both early and late, were among the strongest up-regulated genes. The IFN-¿† stimulating capability was also detected in another L. acidophilus strain, but was not a property of other probiotic bacteria tested (B. bifidum and E. coli nissle).The IFN-¿† inducing capacity was markedly reduced in TLR-2 -/- DCs, dependent on endocytosis and the major cause of the induction of il-12 and tlr-3 in L. acidophilus NCFM stimulated cells. Collectively, our results reveal that certain lactobacilli trigger the expression of viral defence genes in DC in a TLR-2 manner through induction of IFN- ¿†. **Overall design:** In the experiment Lactobacillus NCFM were added to murine dendritic cells and stimulated for 4, 10 or 18 hours. These were compared to control experiment at the same timepoints. Experiments were run in triplicates except for control 10h and control 18h which were only in duplicate, giving a total of 16 arrays.

Background corr dist: KL-Divergence = 0.0592, L1-Distance = 0.0699, L2-Distance = 0.0103, Normal std = 0.5549

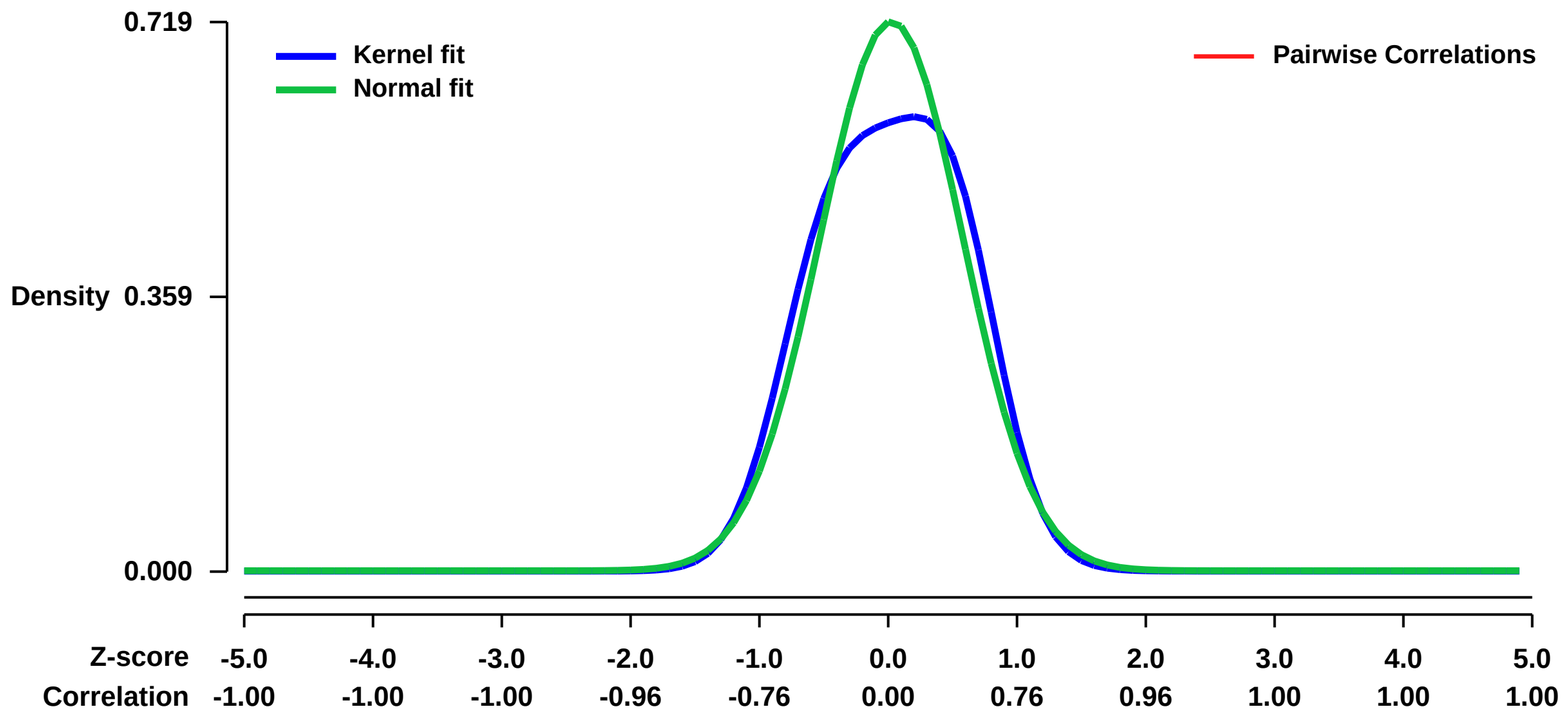

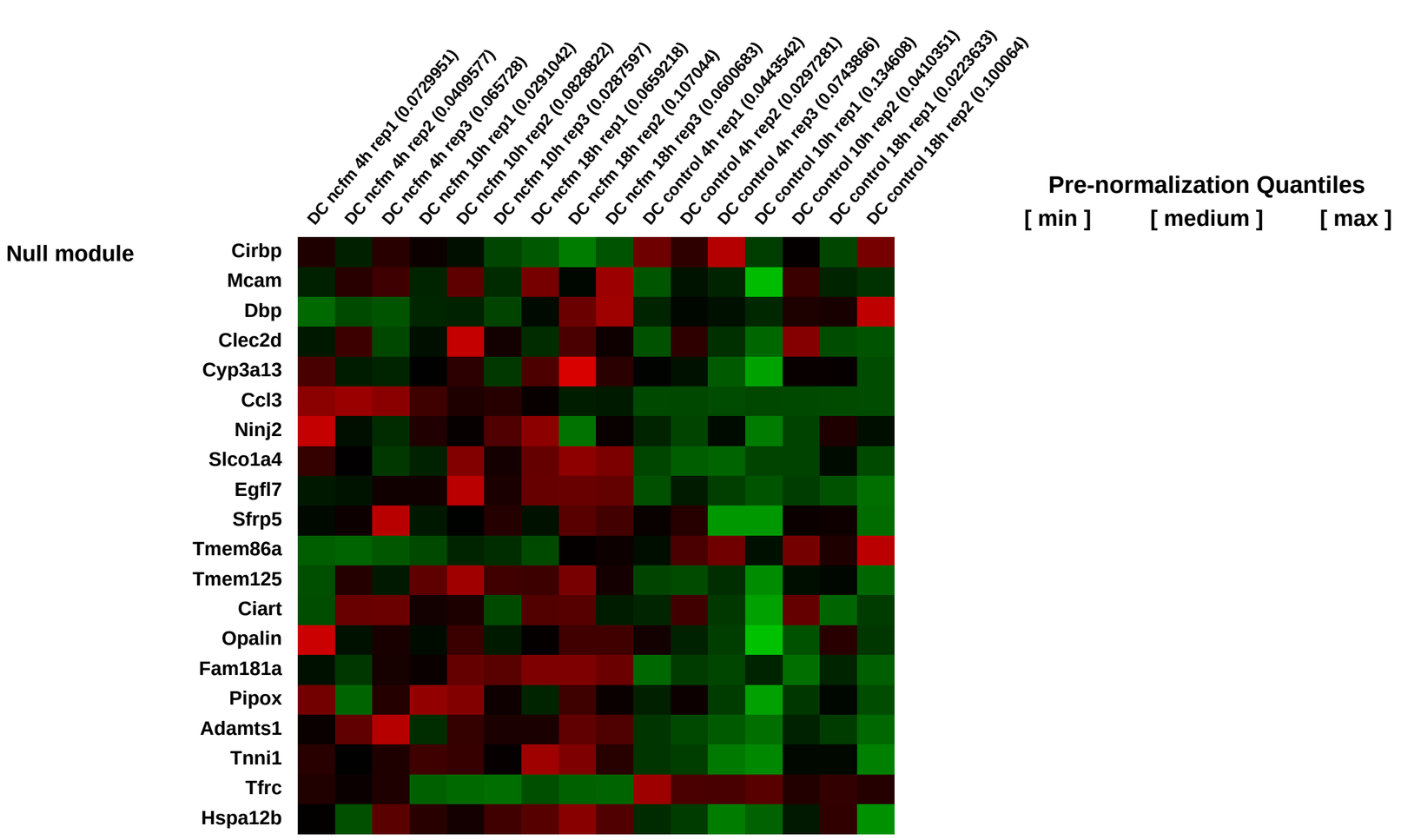

GEO Series "GSE18534" Expression Profiles

Num of samples in this series: 15

Scale of expression profile Z-scores

-3.0 -2.0 -1.0 0.0 1.0 2.0 3.0

GEO Link:	http://www.ncbi.nlm.nih.gov/geo/query/acc.cgi?acc=GSE18534
Status:	Public on Jun 01 2010
Title:	Mouse small cell lung cancer model
Organism:	Mus musculus
Experiment type:	Expression profiling by array
Platform:	GPL1261
Pubmed ID:	20406986
Summary & Design:	**Summary:** A mouse model for human small cell lung carcinoma (SCLC) has been developed based on evidence in human tumors that the tumor suppressor functions of RB and p53 are defective in more than 90% of SCLC cases. We also developed another mouse model also combines loss of p130 (Rbl2), an RB-related gene, with deletion of RB and p53. These two mouse tumors were shown to closely resemble human SCLC. **Overall design:** The goal of this array experiment is to assess genome-wide gene expression of those mouse tumors and determine the similarity of the mouse models to human SCLC. Gene expression from Mouse Rb/p53 (n=10) and Rb/p53/p130 primary tumors (n=3) as well as tumor-free adult mouse lungs (n=2) was measured using the Affymetrix GeneChip Mouse Genome 430-2.0 arrays.

Background corr dist: KL-Divergence = 0.0991, L1-Distance = 0.0337, L2-Distance = 0.0022, Normal std = 0.4651

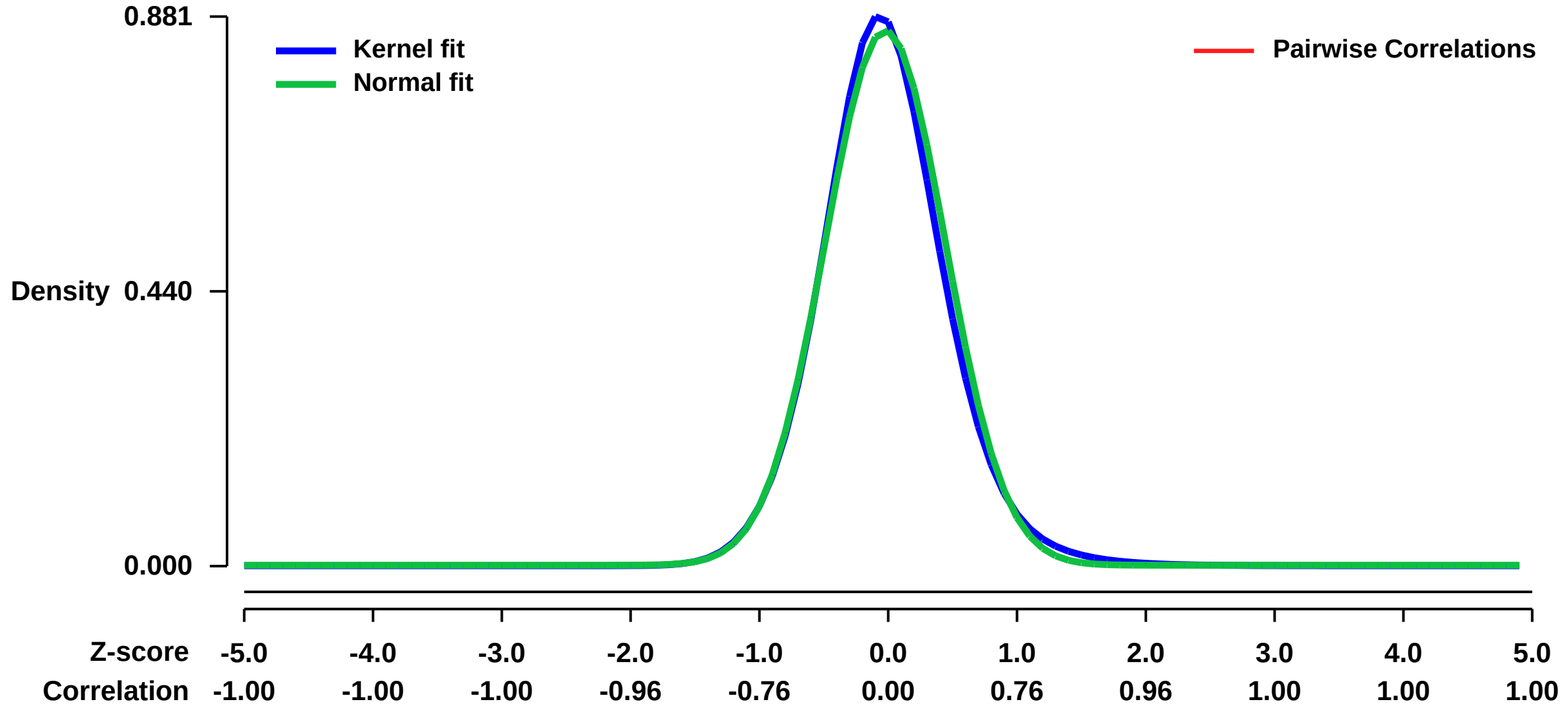

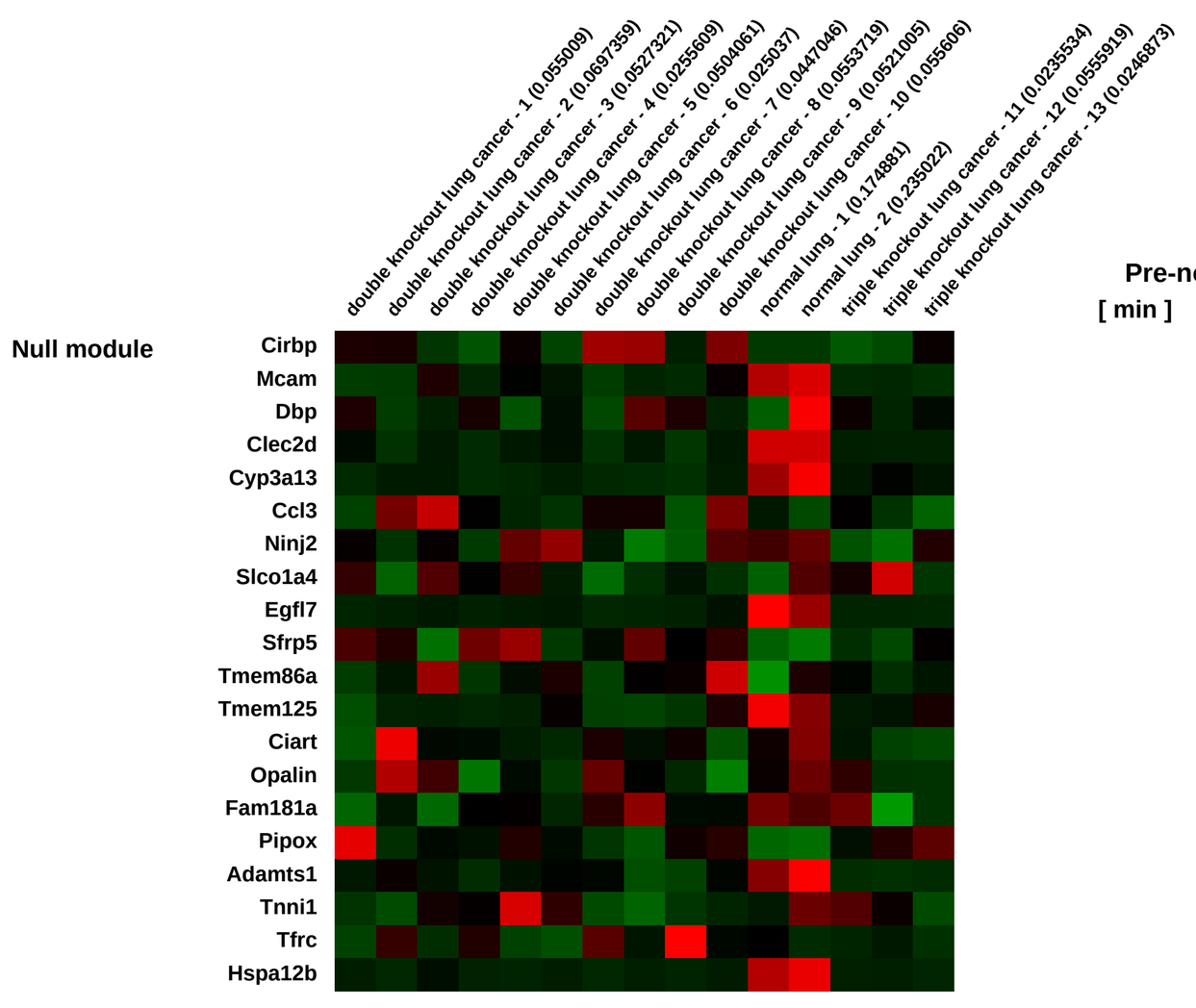

GEO Series "GSE18567" Expression Profiles

Num of samples in this series: 24

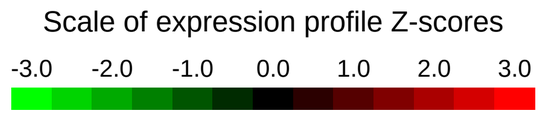

GEO Link:	http://www.ncbi.nlm.nih.gov/geo/query/acc.cgi?acc=GSE18567
Status:	Public on Mar 01 2010
Title:	Temporal profiling of gene expression in cochleae of wild type and alpha9 null mice
Organism:	Mus musculus
Experiment type:	Expression profiling by array
Platform:	GPL1261
Pubmed ID:	20140217
Summary & Design:	**Summary:** Efferent inhibition of cochlear outer hair cells is mediated by nicotinic cholinergic receptors containing alpha9 (a9) and alpha10 subunits. Mice lacking a9 nicotinic subunits fail to exhibit classic olivocochlear responses and are characterized by abnormal synaptic morphology at the base of outer hair cells. To detail molecular changes induced upon the loss of a9 subunit, we sampled cochlear RNA from wild type and a9 null mice at postnatal (P) days spanning periods of synapse formation and maturation (P3, P7, P13 and P60). Our findings point to a delay in cochlear maturation starting at the onset of hearing (P13), as well as an up-regulation of various GABA receptor subunits in adult mice lacking the a9 nicotinic subunit. **Overall design:** Cochleae were removed at postnatal ages P3, P7, P13 and P60. Cochlear tissues from 3-5 mice were pooled per replicate; biological triplicates were performed for each age and genotype.

Background corr dist: KL-Divergence = 0.1285, L1-Distance = 0.0372, L2-Distance = 0.0027, Normal std = 0.3964

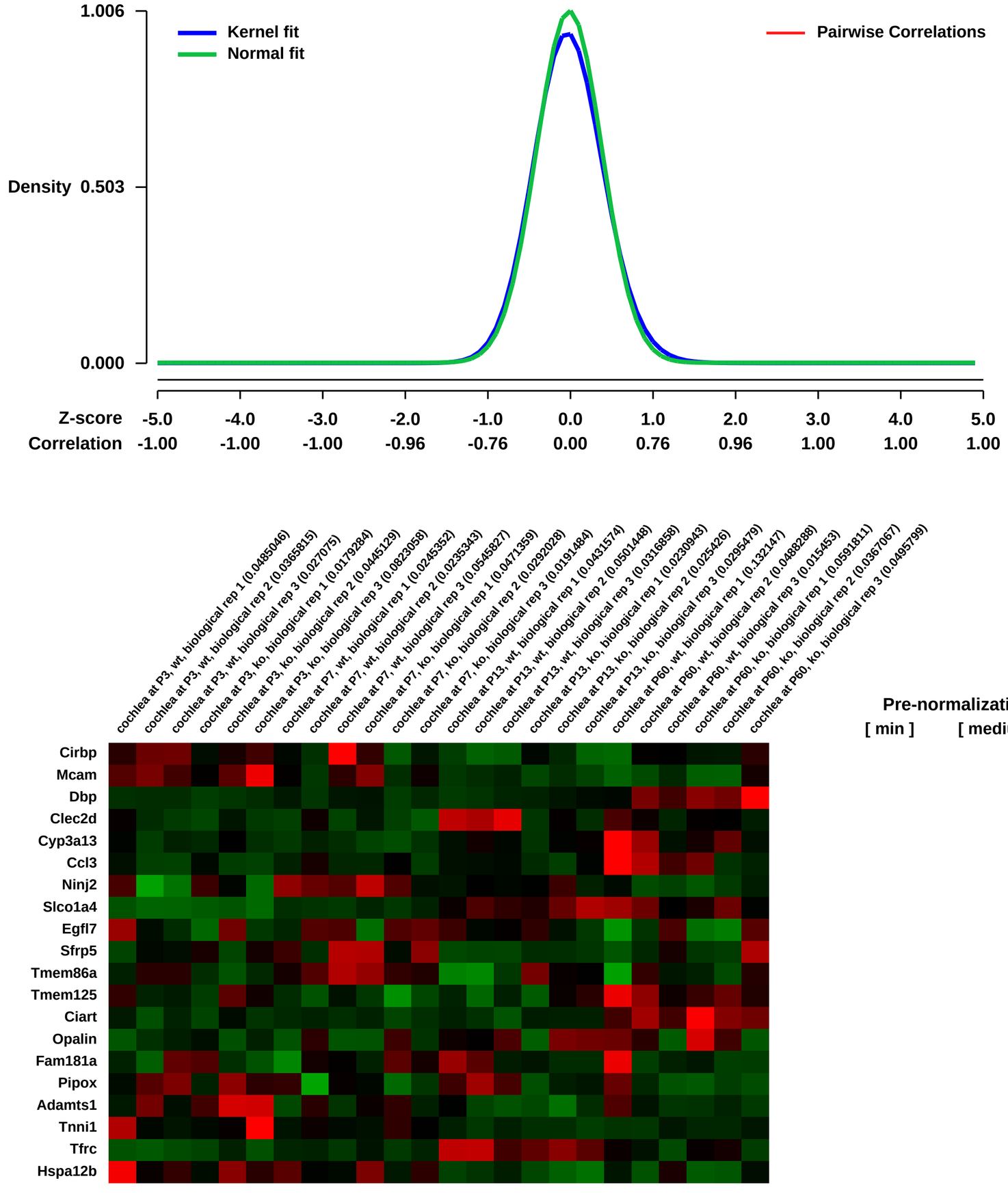

GEO Series "GSE18586" Expression Profiles

Num of samples in this series: 9

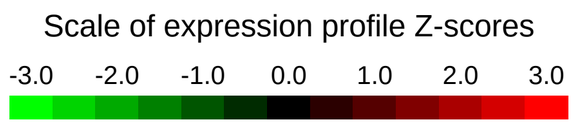

GEO Link:	http://www.ncbi.nlm.nih.gov/geo/query/acc.cgi?acc=GSE18586
Status:	Public on Jun 18 2012
Title:	Saturated fat stimulates obesity and hepatic steatosis and affects gut microbiota composition by an enhanced overflow of dietary fat to the distal intestine
Organism:	Mus musculus
Experiment type:	Expression profiling by array
Platform:	GPL1261
Pubmed ID:	22700822
Summary & Design:	**Summary:** We studied the effect of dietary fat type, varying in polyunsaturated/saturated fatty acid ratio's (P/S) on development of metabolic syndrome. C57Bl/6J mice were fed purified high-fat diets (45E% fat) containing palm oil (HF-PO; P/S 0.4), olive oil (HF-OO; P/S 1.1) or safflower oil (HF-SO; P/S 7.8) for 8 weeks. A low-fat palm oil diet (LF-PO; 10E% fat) was used as a reference. Additionally, we analyzed diet-induced changes in gut microbiota composition and mucosal gene expression. The HF-PO diet induced a higher body weight gain and liver triglyceride content compared to the HF-OO, HF-SO or LF-PO diet. In the intestine, the HF-PO diet reduced microbial diversity and increased the Firmicutes/Bacteroidetes ratio. Although this fits a typical obesity profile, our data clearly indicate that an overflow of the HF-PO diet to the distal intestine, rather than obesity itself, is the main trigger for these gut microbiota changes. A HF-PO diet-induced elevation of lipid metabolism-related genes in the distal small intestine confirmed the overflow of palm oil to the distal intestine. Some of these lipid metabolism-related genes were previously already associated with the metabolic syndrome. In conclusion, our data indicate that saturated fat (HF-PO) has a more stimulatory effect on weight gain and hepatic lipid accumulation than unsaturated fat (HF-OO and HF-SO). The overflow of fat to the distal intestine on the HF-PO diet induced changes in gut microbiota composition and mucosal gene expression. We speculate that both are directly or indirectly contributive to the saturated fat-induced development of obesity and hepatic steatosis. **Keywords:** Diet intervention study **Overall design:** Nine-week-old C57Bl/6J mice were fed a low-fat diet (LF-PO) and three different types of high-fat diet, based on palm oil (HF-PO; P/S1.0), olive oil (HF-OO; P/S4.6) and safflower oil (HF-SO; P/S10.1) for 8 weeks. Body weight was recorded weekly and after 7 weeks of diet intervention an oral glucose tolerance test was performed. After 2 weeks of diet intervention, 6 mice per high-fat diet group were anaesthetized with a mixture of isofluorane (1.5%), nitrous oxide (70%) and oxygen (30%) and the small intestines were excised. Adhering fat and pancreatic tissue were carefully removed. The small intestines were divided in three equal parts along the proximal to distal axis (SI 1, SI 2 and SI 3) and microarray analysis was performed on mucosal scrapings.

Background corr dist: KL-Divergence = 0.0644, L1-Distance = 0.0264, L2-Distance = 0.0008, Normal std = 0.5278

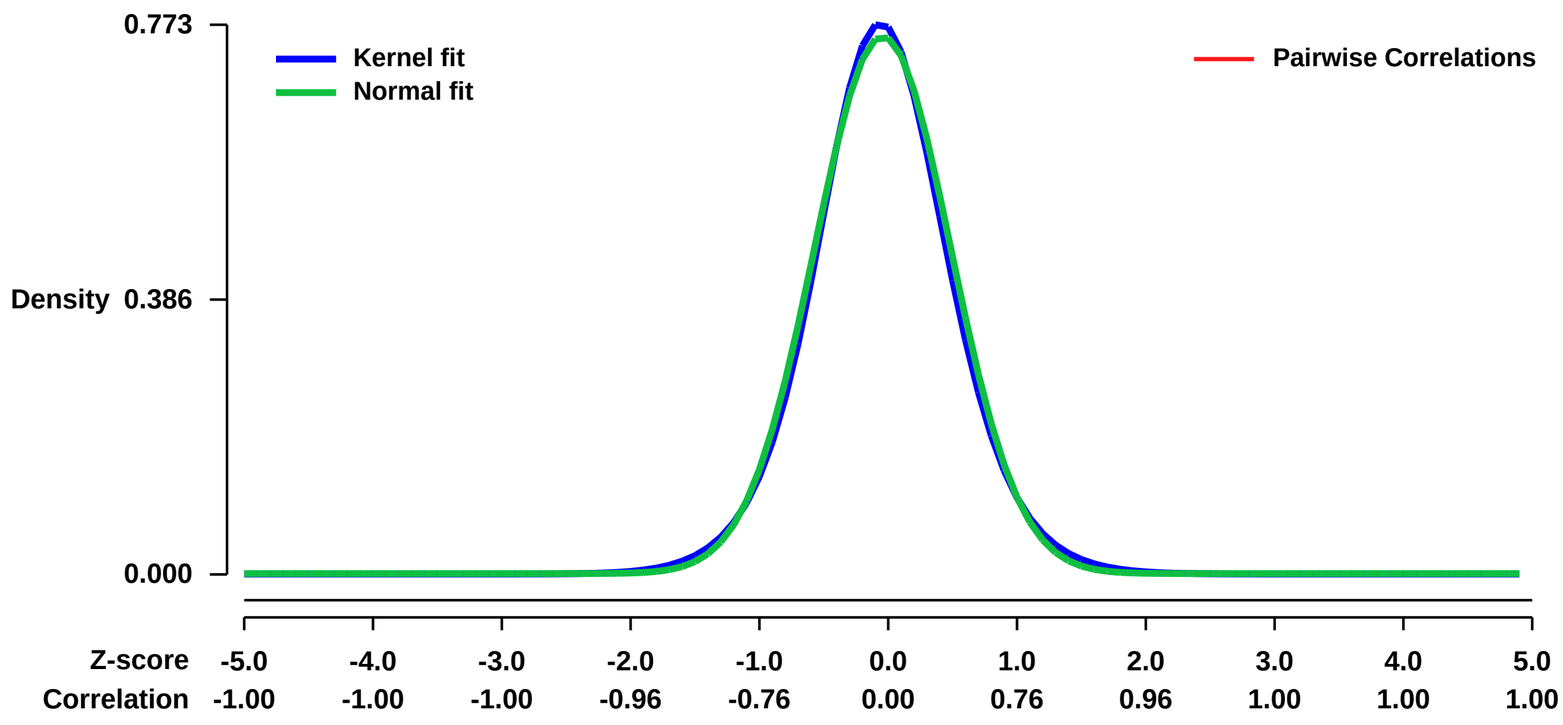

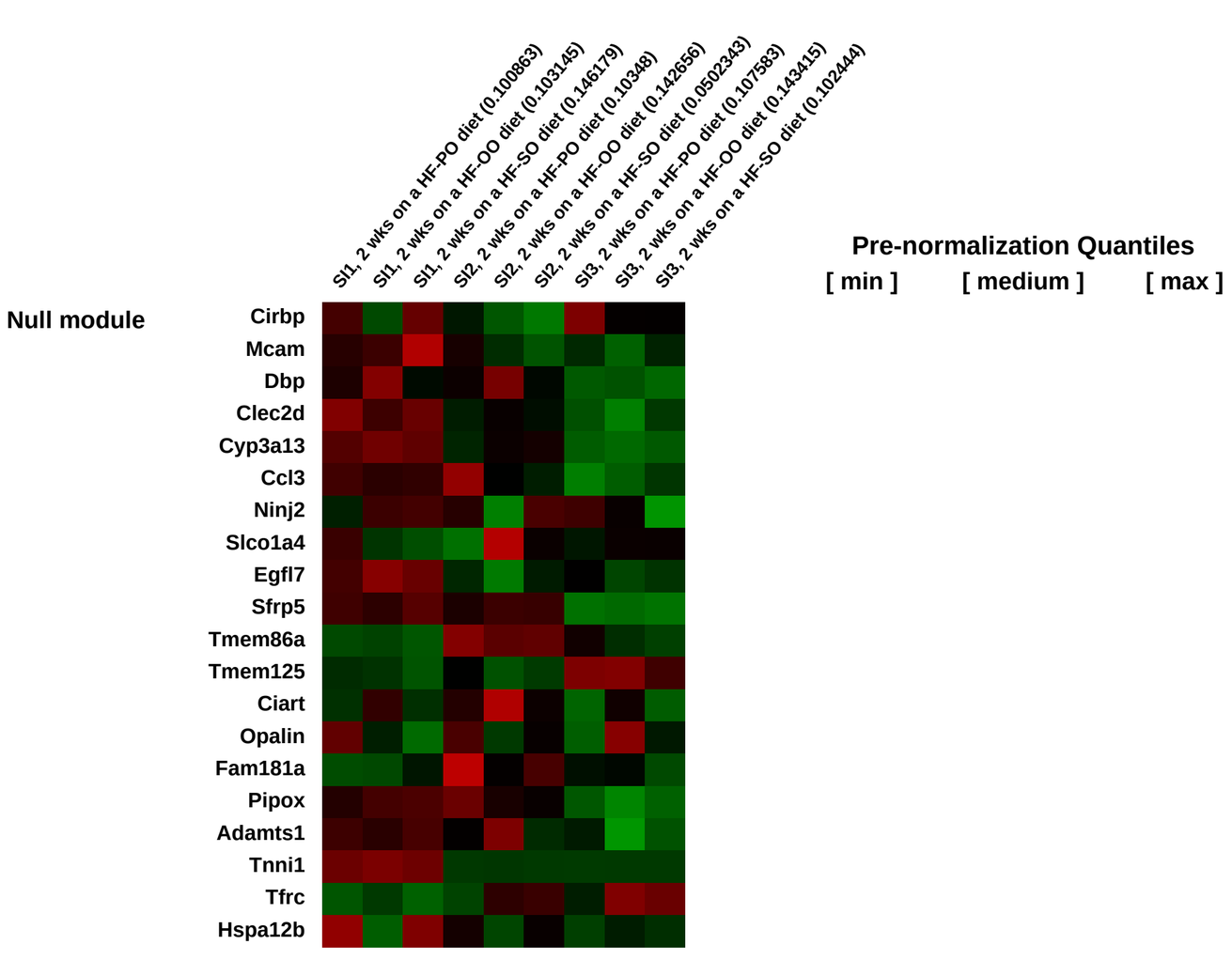

GEO Series "GSE18660" Expression Profiles

Num of samples in this series: 10

Scale of expression profile Z-scores

-3.0 -2.0 -1.0 0.0 1.0 2.0 3.0

GEO Link:	http://www.ncbi.nlm.nih.gov/geo/query/acc.cgi?acc=GSE18660
Status:	Public on Jan 03 2011
Title:	Modulation of calcium activated potassium channels induces cardiogenesis of pluripotent stem cells and enrichment of pacemaker- like cells
Organism:	Mus musculus
Experiment type:	Expression profiling by array
Platform:	GPL1261
Pubmed ID:	20956206
Summary & Design:	**Summary:** Background: Ion channels are key determinants for the function of excitable cells but little is known about their role and involvement during cardiac development. Earlier work identified Ca2+-activated potassium channels of small and intermediate conductance (SKCas) as important regulators of neural stem cell fate. Here, we have investigated their impact on the differentiation of pluripotent cells towards the cardiac lineage. Methods and Results: We have applied the SKCa-activator EBIO on embryonic stem cells and identified this particular ion channel family as a new critical target involved in the generation of cardiac pacemaker-like cells: SKCa-activation led to rapid remodeling of the actin cytoskeleton, inhibition of proliferation, induction of differentiation and diminished teratoma formation. Time-restricted SKCa-activation induced cardiac mesoderm and commitment to the cardiac lineage as shown by gene regulation, protein and functional electrophysiological studies. In addition, the differentiation into cardiomyocytes was modulated in a qualitative fashion, resulting in a strong enrichment of pacemaker-like cells. This was accompanied by induction of the sino-atrial gene program and in parallel by a loss of the chamber-specific myocardium. In addition, SKCa activity induced activation of the Ras-Mek-Erk signaling cascade, a signaling pathway involved in the EBIO-induced effects. Conclusions: SKCa-activation drives the fate of pluripotent cells towards the cardiac lineage and preferentially into pacemaker-like cardiomyocytes. This provides a novel strategy for the enrichment of cardiomyocytes and in particular, the generation of a specific subtype of cardiomyocytes, pacemaker-like cells, without genetic modification. **Overall design:** - EBIO-treated differentiated ES cells sample 2 (EBIO_day5+10_2)

Background corr dist: KL-Divergence = 0.0149, L1-Distance = 0.0633, L2-Distance = 0.0051, Normal std = 0.9657

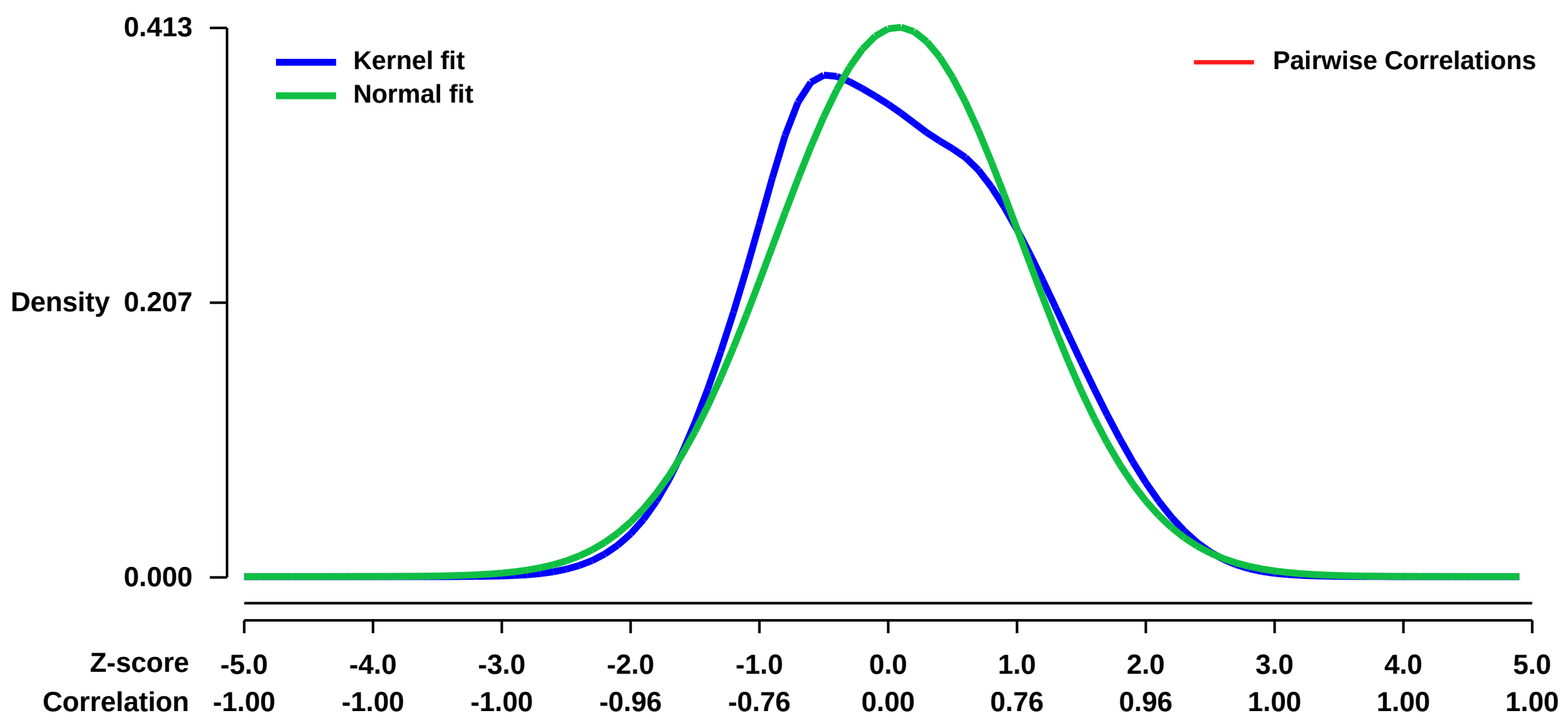

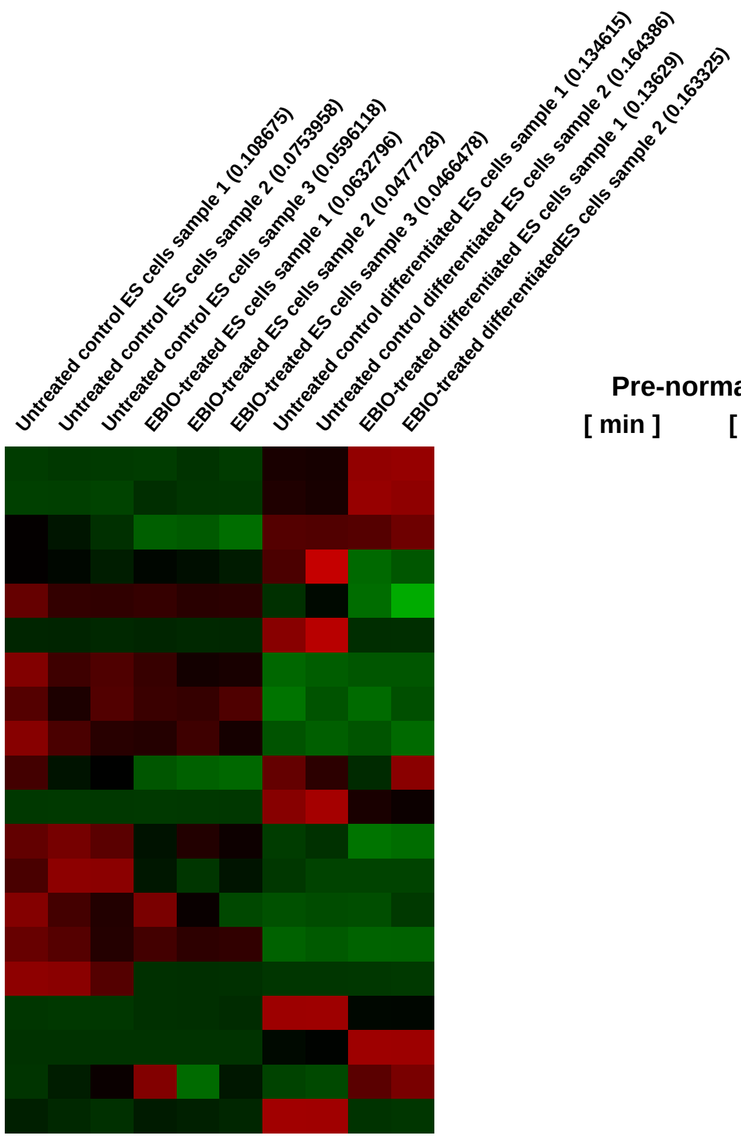

GEO Series "GSE18704" Expression Profiles

Num of samples in this series: 9

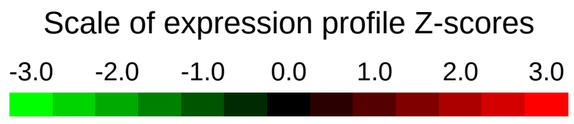

GEO Link:	http://www.ncbi.nlm.nih.gov/geo/query/acc.cgi?acc=GSE18704
Status:	Public on Oct 23 2009
Title:	WNT4 is required for ovarian follicle development and female fertility
Organism:	Mus musculus
Experiment type:	Expression profiling by array
Platform:	GPL1261
Pubmed ID:	20371632
Summary & Design:	**Summary:** To study the physiological role of WNT4 in the postnatal ovary, a mouse strain bearing a floxed Wnt4 allele was created and mated to the Amhr2tm3(cre)Bhr strain to target deletion of Wnt4 to granulosa cells. Wnt4flox/-;Amhr2tm3(cre)Bhr/+ mice had significantly reduced ovary weights and produced smaller litters (P<0.05). Serial follicle counting demonstrated that, while Wnt4flox/-;Amhr2tm3(cre)Bhr/+ mice were born with a normal ovarian reserve and maintained normal numbers of small follicles until puberty, they had only 25.2% of the normal number of healthy antral follicles. Some Wnt4flox/-;Amhr2tm3(cre)Bhr/+ mice had no antral follicles or corpora lutea and underwent premature follicle depletion. RTPCR analyses of Wnt4flox/-;Amhr2tm3(cre)Bhr/+ granulosa cells and cultured granulosa cells that overexpress WNT4 demonstrated that WNT4 regulates the expression of Star, Cyp11a1 and Cyp19, steroidogenic genes previously identified as downstream targets of the WNT signaling effector CTNNB1. WNT4- and CTNNB1-overexpressing cultured granulosa cells were analyzed by microarray for alterations in gene expression, which showed that WNT4 also regulates a series of genes involved in late follicle development and the cellular stress response via the WNT/CTNNB1 signaling pathway. Together, these data indicate that WNT4 is required for normal antral follicle development, and may act by regulating granulosa cell functions including steroidogenesis. **Overall design:** Granulosa cells were obtained from 20-26 day-old mice of various genotypes 48h after eCG treatment, using the needle puncture method as previously described. Cells were then infected with adenoviruses to express eGFP or Cre, or overexpress WNT4 in serum-free medium, and subsequently harvested for RNA extraction as described below. Preliminary experiments demonstrated that an infection efficiency of >80% could be obtained at an MOI of ~50 (as determined by analysis of fluorescent signal in Ad-eGFP-infected cells) and that the Ad-Cre and Ad-WNT4 viruses produced efficient recombination of the floxed Ctnnb1 alleles and robust WNT4 overexpression, respectively. Microarray analyses were done using triplicate RNA samples from each adenoviral treatment described above, and using mouse expression set 430 microarrays (Affymetrix, Santa Clara, CA).

Background corr dist: KL-Divergence = 0.0407, L1-Distance = 0.0344, L2-Distance = 0.0022, Normal std = 0.5970

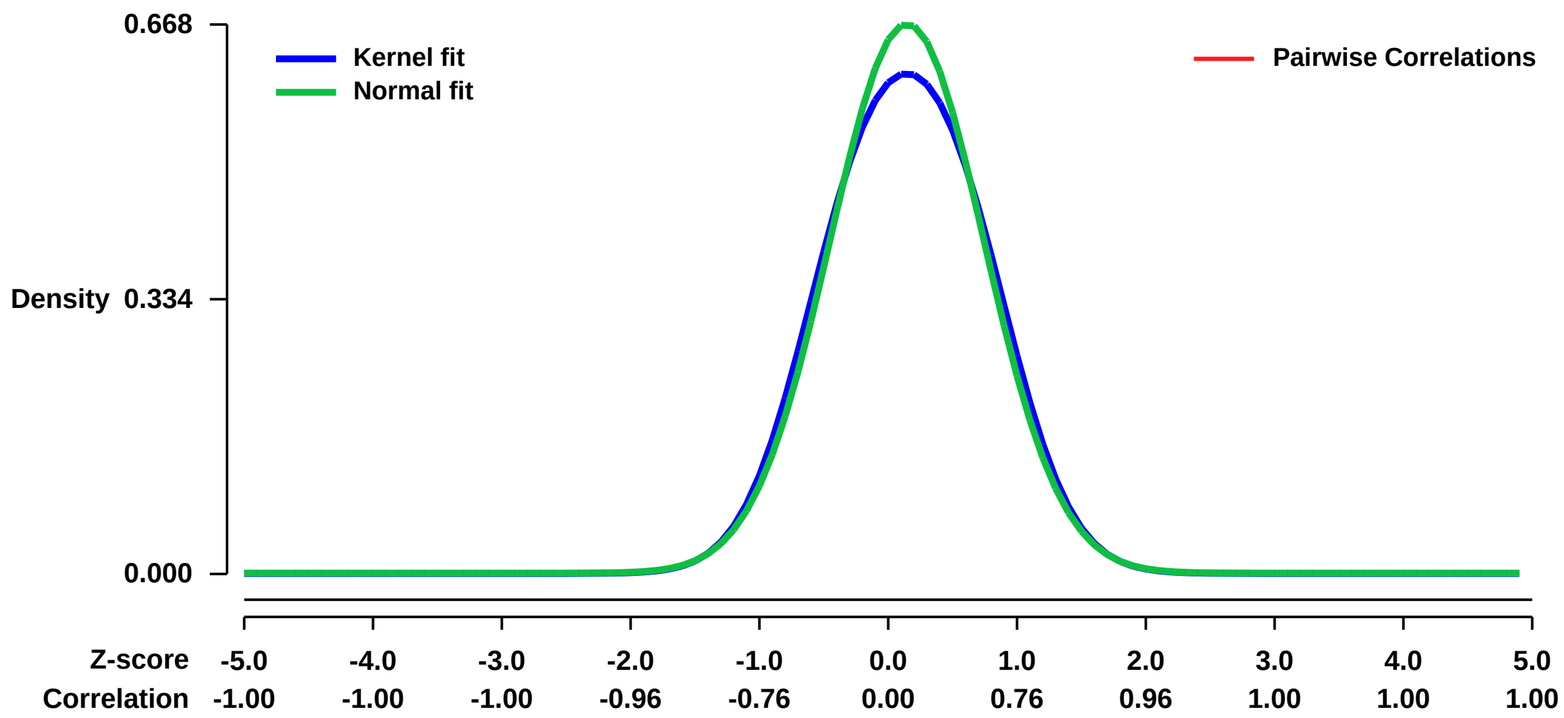

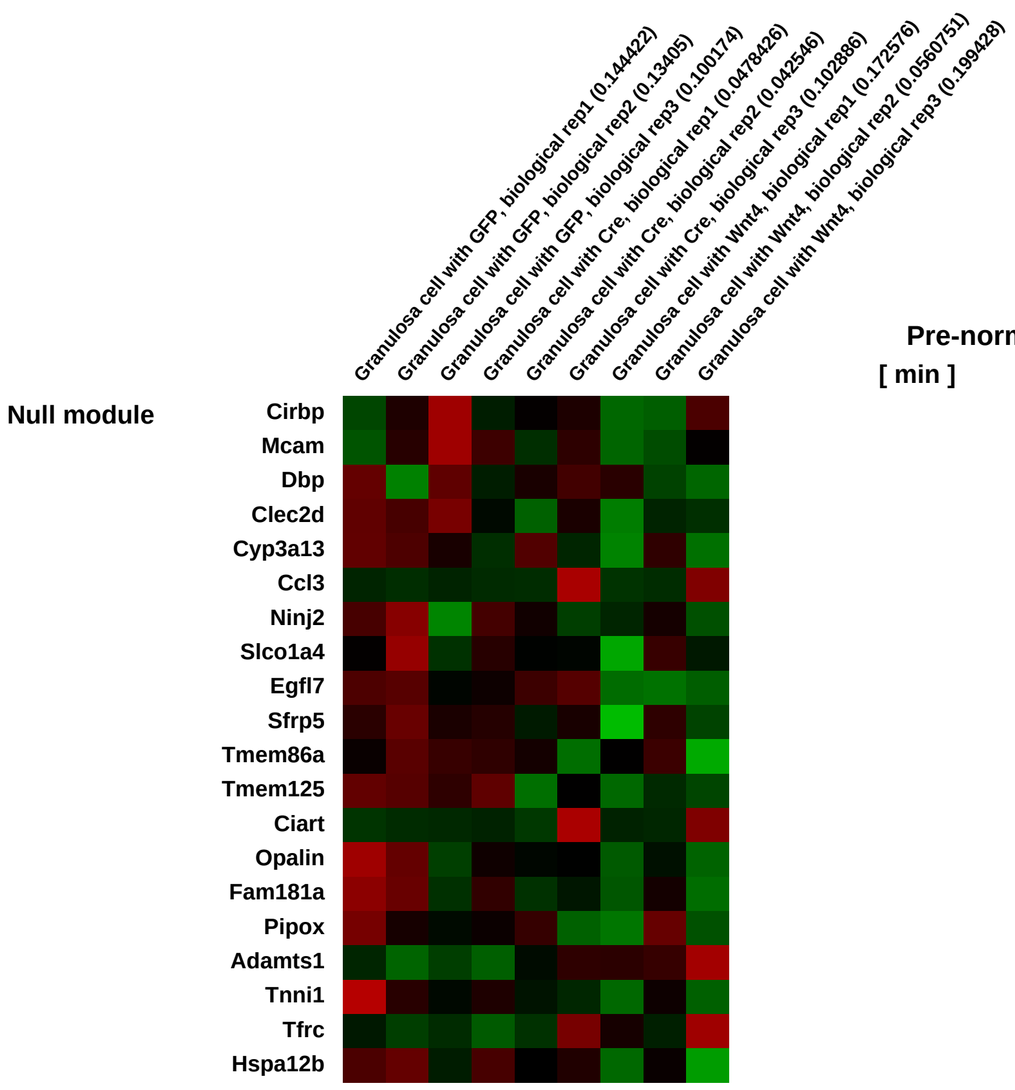

GEO Series "GSE1871" Expression Profiles

Num of samples in this series: 12

Scale of expression profile Z-scores

-3.0 -2.0 -1.0 0.0 1.0 2.0 3.0

GEO Link:	**http://www.ncbi.nlm.nih.gov/geo/query/acc.cgi?acc=GSE1871**
Status:	**Public on Oct 26 2004**
Title:	**SCCOR_MouseLung_Simva_LPS**
Organism:	**Mus musculus**
Experiment type:	**Expression profiling by array**
Platform:	**GPL1261**
Pubmed ID:	**15665042**
Summary & Design:	**Summary:** **This series contain mouse lung samples treated with Simvastatin and LPS and corresponded controls.** **Keywords: other** **Overall design:**

Background corr dist: **KL-Divergence = 0.0617, L1-Distance = 0.0228, L2-Distance = 0.0006, Normal std = 0.5246**

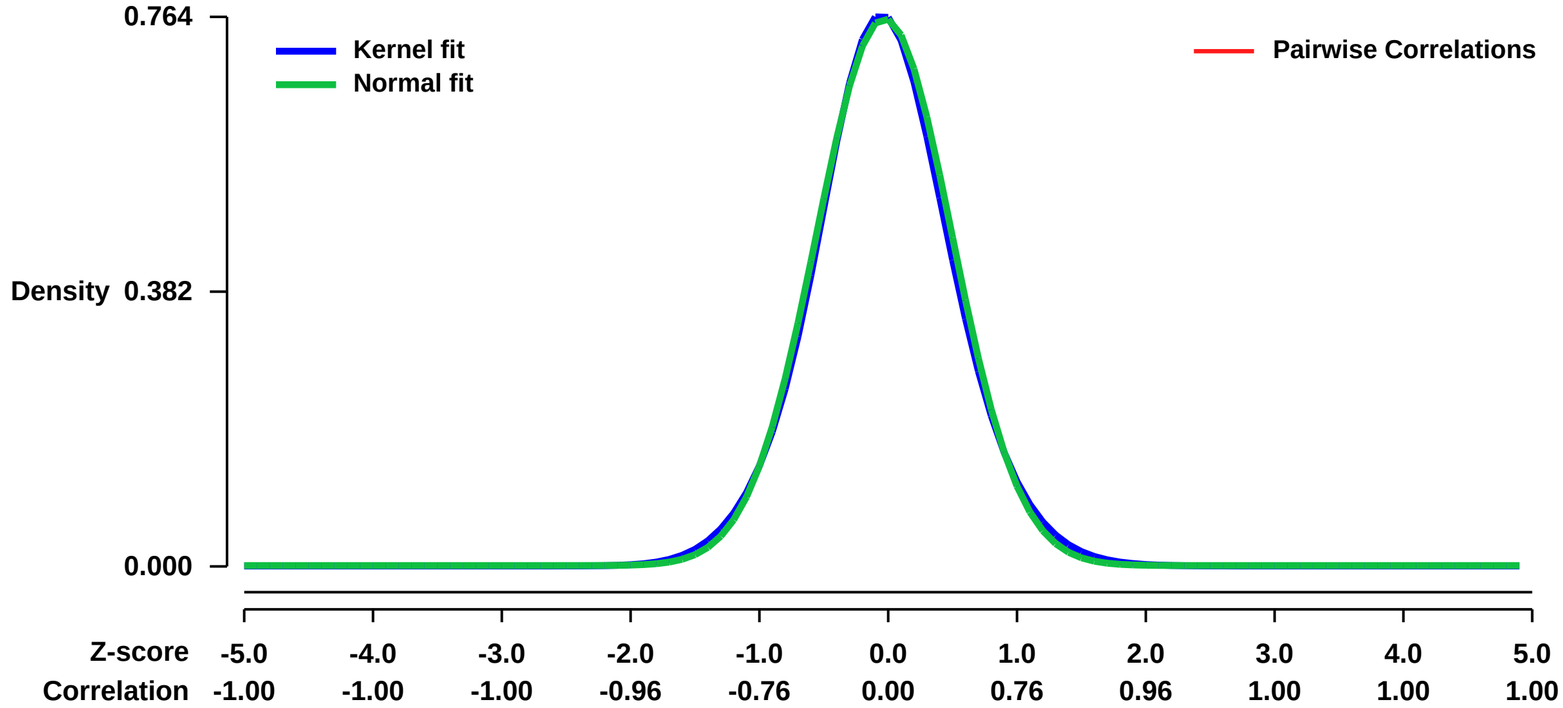

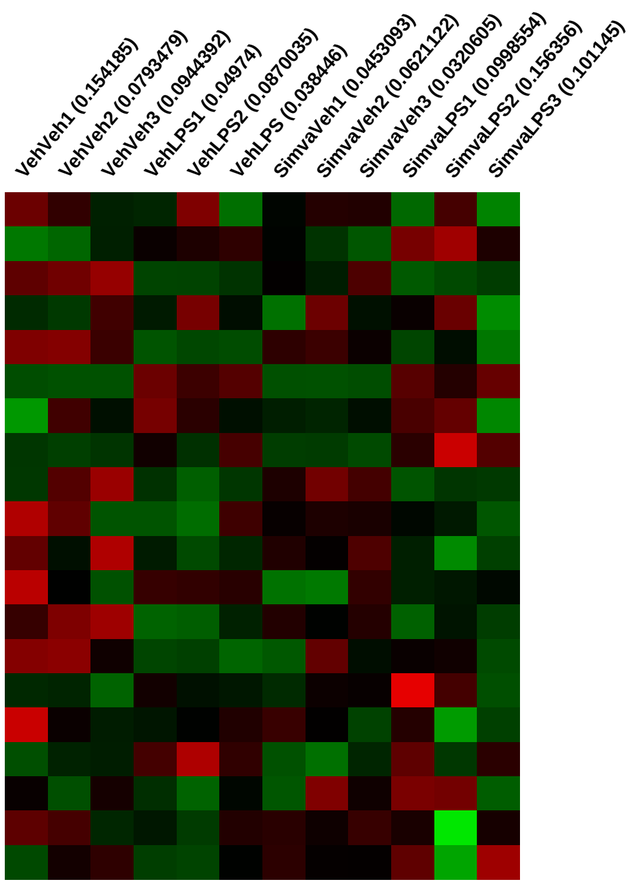

GEO Series "GSE18740" Expression Profiles

Num of samples in this series: 12

Scale of expression profile Z-scores

-3.0 -2.0 -1.0 0.0 1.0 2.0 3.0

GEO Link:	http://www.ncbi.nlm.nih.gov/geo/query/acc.cgi?acc=GSE18740
Status:	Public on Jan 19 2010
Title:	Luteolin has anti-inflammatory and neurotrophic effects on microglia
Organism:	Mus musculus
Experiment type:	Expression profiling by array
Platform:	GPL1261
Pubmed ID:	20074346
Summary & Design:	**Summary:** Our aim was to identify genes that were differentially expressed in microglia stimulated with Lipopolysaccharide, Luteolin, or both. Affymetrix microarrays were used to analyze RNA samples **Overall design:** RNA from control BV-2 cells, and cells treated for 24h with LPS, Luteolin, or LPS+Luteolin was analyzed with Affymetrix GeneChip Mouse Genome 430 2.0 Arrays. Biological triplicates were analyzed for each condition

Background corr dist: KL-Divergence = 0.1095, L1-Distance = 0.0333, L2-Distance = 0.0020, Normal std = 0.4207

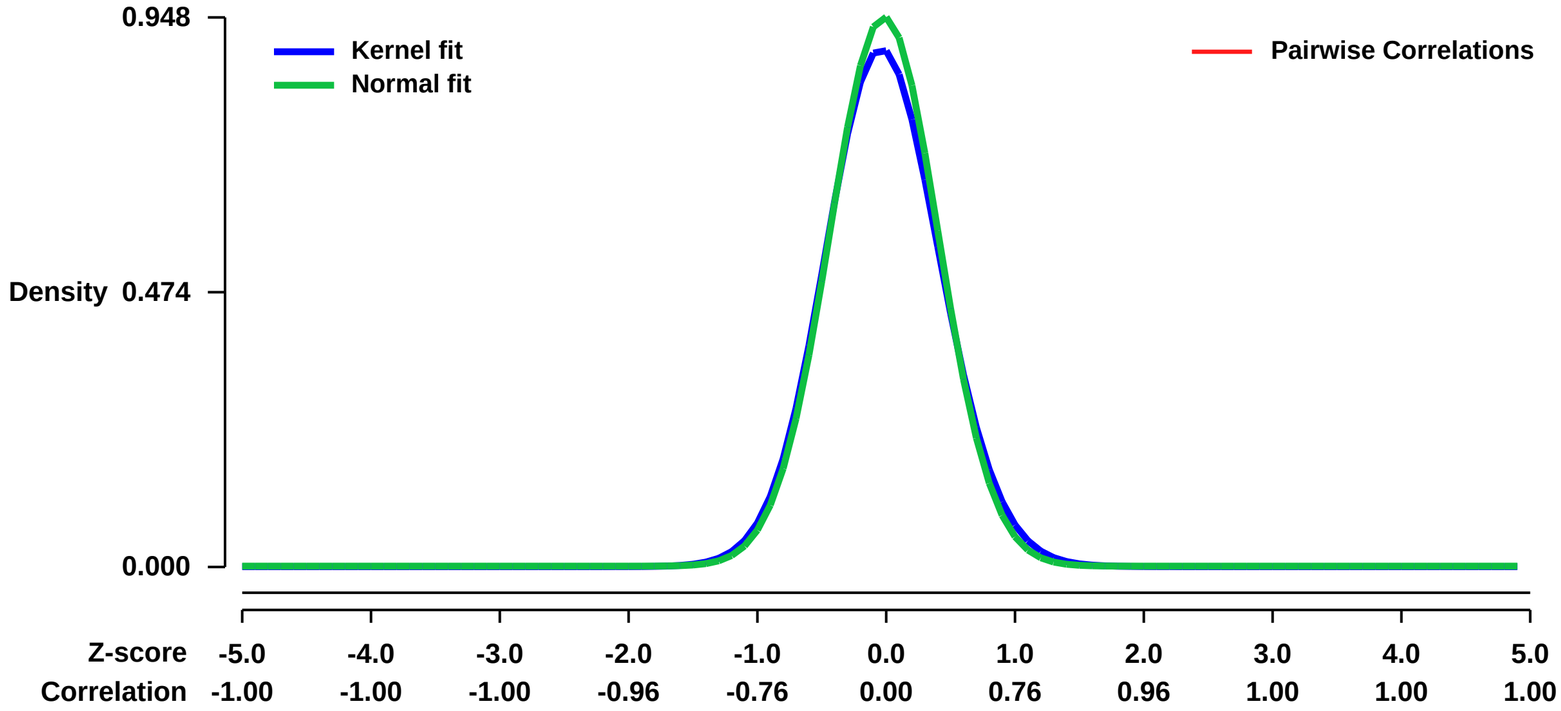

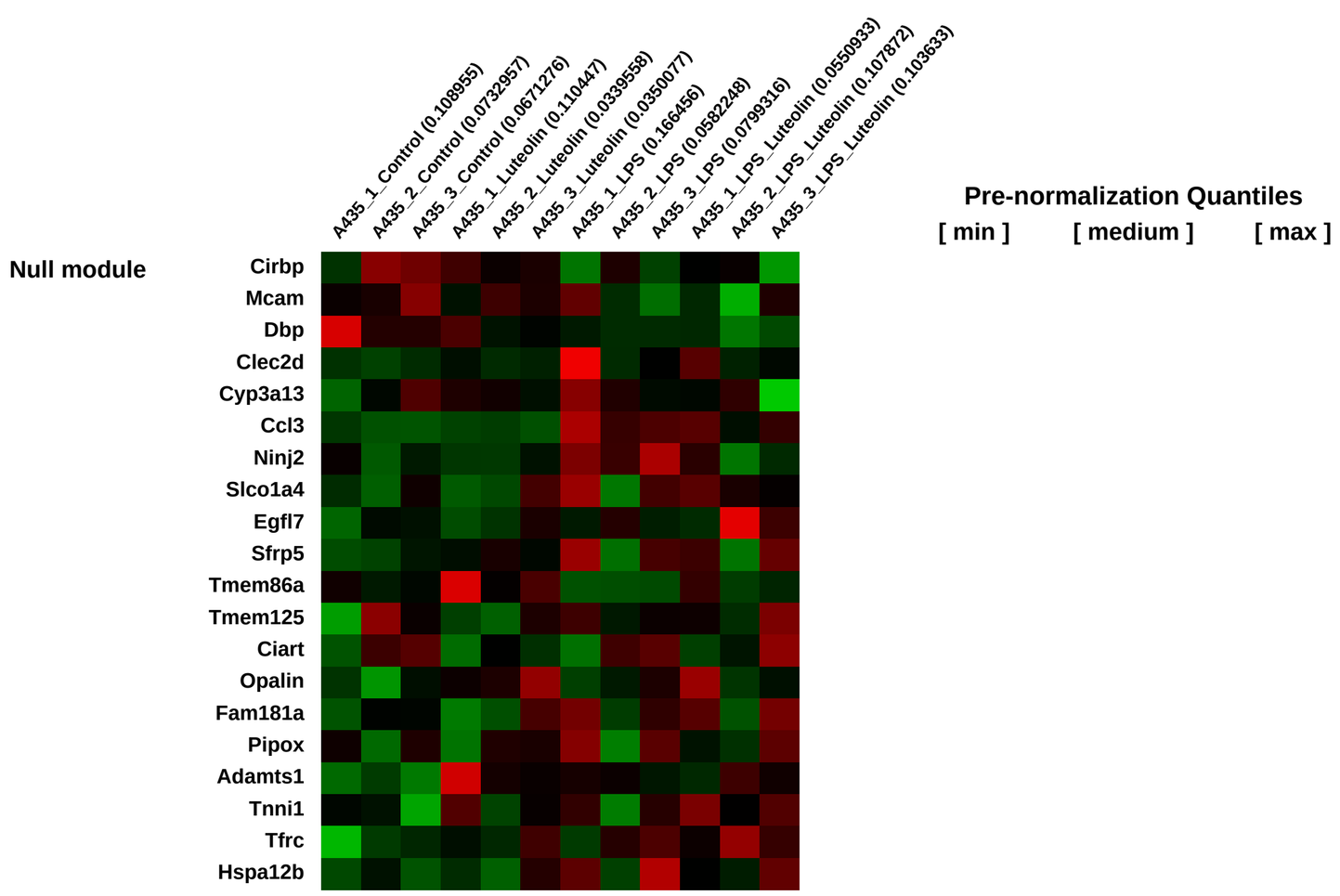

GEO Series "GSE18742" Expression Profiles

Num of samples in this series: 13

Scale of expression profile Z-scores

-3.0 -2.0 -1.0 0.0 1.0 2.0 3.0

GEO Link:	http://www.ncbi.nlm.nih.gov/geo/query/acc.cgi?acc=GSE18742
Status:	Public on Dec 17 2010
Title:	Increased Expression of Angiogenic Genes in the Brains of Mouse Meg3-null Embryos
Organism:	Mus musculus
Experiment type:	Expression profiling by array
Platform:	GPL1261
Pubmed ID:	20392836
Summary & Design:	**Summary:** MEG3 (Maternally Expressed Gene 3) is a non-coding RNA that is highly expressed in the normal human brain and pituitary. Expression of MEG3 is lost in gonadotroph-derived clinically non-functioning pituitary adenomas. Meg3 knock-out mice were generated to identify targets and potential functions of this gene in embryonic development and tumorigenesis. Gene expression profiles were compared in the brains of Meg3-null embryos and wild-type litter-mate controls using microarray analysis. Microarray data were analyzed with GeneSifter which uses Kyoto Encyclopedia of Genes and Genomes (KEGG) pathways and Gene Ontology (GO) classifications to identify signaling cascades and functional categories of interest within the data set. Differences were found in signaling pathways and ontologies related to angiogenesis between wild-type and knock-out embryos. Quantitative RT-PCR and histological staining showed increased expression of some VEGF pathway genes and increased cortical microvessel density in the knock-out embryos. These results are consistent with reported increases in VEGF signaling observed in human clinically non-functioning pituitary adenomas. In conclusion, Meg3 may play an important role in control of vascularization in the brain and may function as a tumor suppressor by preventing angiogenesis. **Overall design:** biological replicate: 148_15 KO, 219_12 KO, 238_1 KO, 238_5 KO, 250_1 KO, 250_3 KO, 262_1 KO

Background corr dist: KL-Divergence = 0.1145, L1-Distance = 0.0270, L2-Distance = 0.0012, Normal std = 0.4164

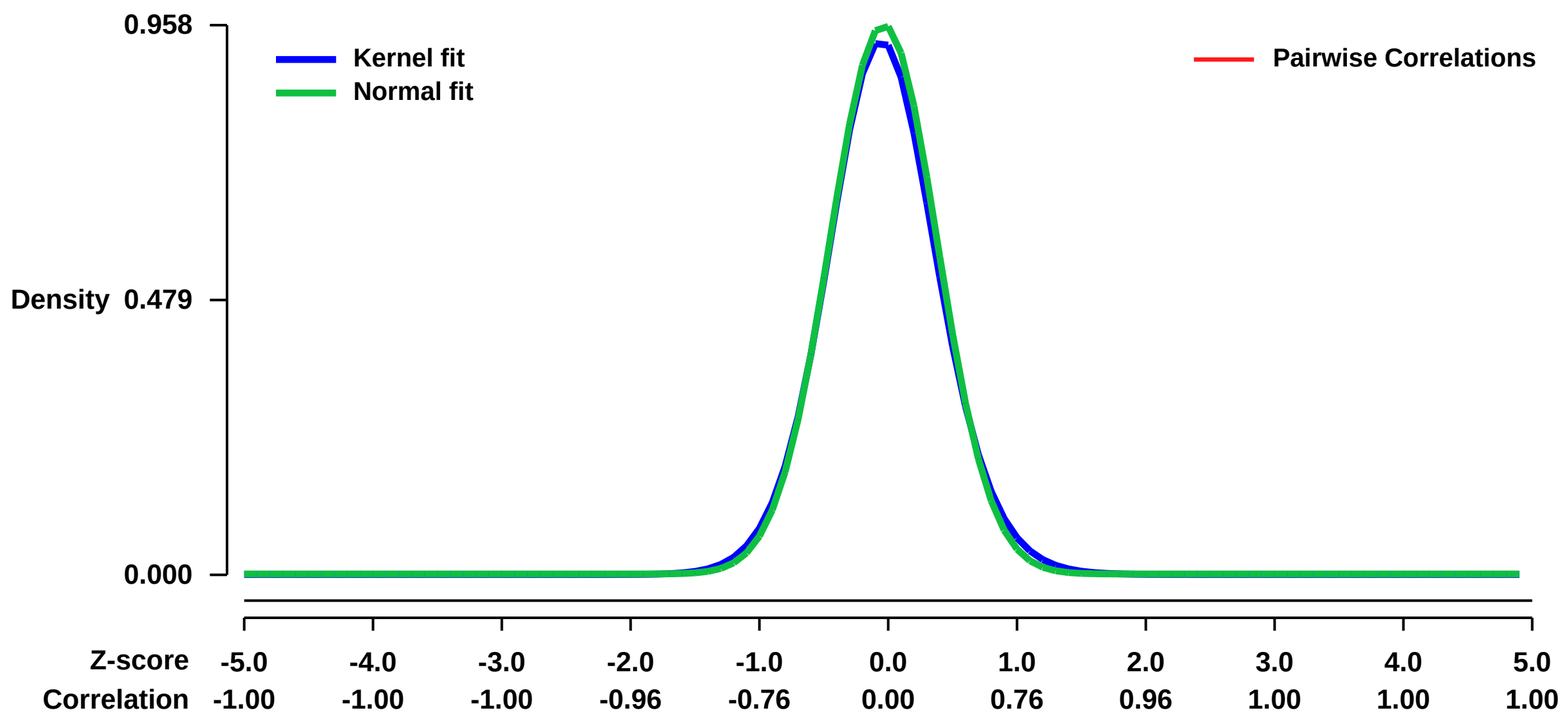

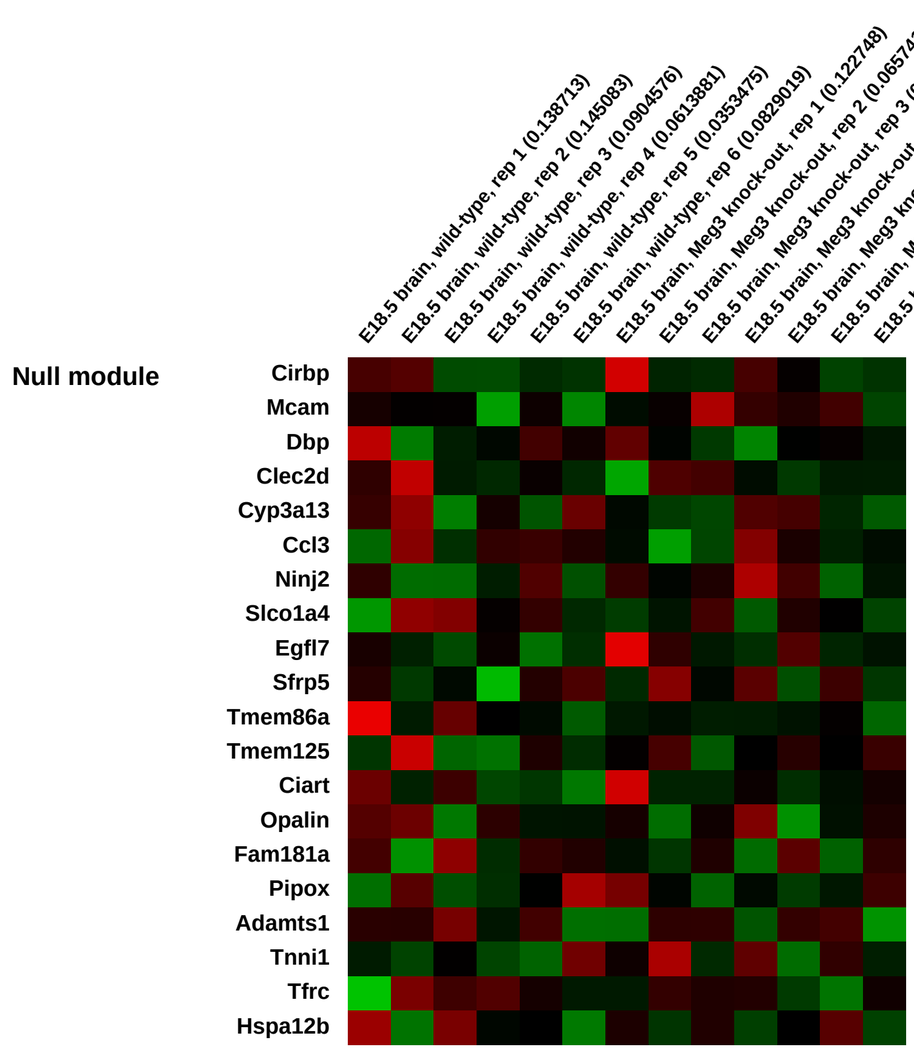

GEO Series "GSE18765" Expression Profiles

Num of samples in this series: 14

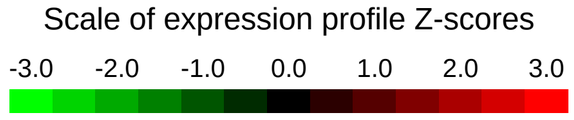

GEO Link:	http://www.ncbi.nlm.nih.gov/geo/query/acc.cgi?acc=GSE18765
Status:	Public on Nov 19 2010
Title:	The transcriptome of prospectively isolated adult neural stem cells
Organism:	Mus musculus
Experiment type:	Expression profiling by array
Platform:	GPL1261
Pubmed ID:	21112568
Summary & Design:	**Summary:** **Since the discovery of adult neural stem cells, their exact identity is still under discussion. Moreover, the lack of a reproducible procedure to purify neural stem cells prospectively rather than by growing them in vitro has so far precluded their study at the transcriptome level. Here we demonstrate a novel procedure to prospectively isolate neural stem cells from the adult mouse subependymal zone on the basis of their GFAP- and prominin1-expression by fluorescence-activated cell sorting. All self-renewing, multipotent stem cells are contained in this fraction at 70% purity. The stem cell identity of these double-positive cells is further demonstrated in vivo, by using a novel split-Cre-technology for fate mapping.** **Comparison of the transcriptome of these prospectively isolated neural stem cells to the transcriptomes of other astrocytes or ependymal cells revealed a distinct clustering of the stem cells, highlighting their unique features, as well as profound similarities to the astrocyte as well as ependyma transcriptome.** **Overall design:** **FACS-sorting was used to isolate prospective neural stem, astrocytes and ependymal cells from brain regions of hGFAP eGFP expressing mice. Total RNA from these cells was hybridised on Affymetrix MOE430 2.0 arrays and expression patterns were analysed.**

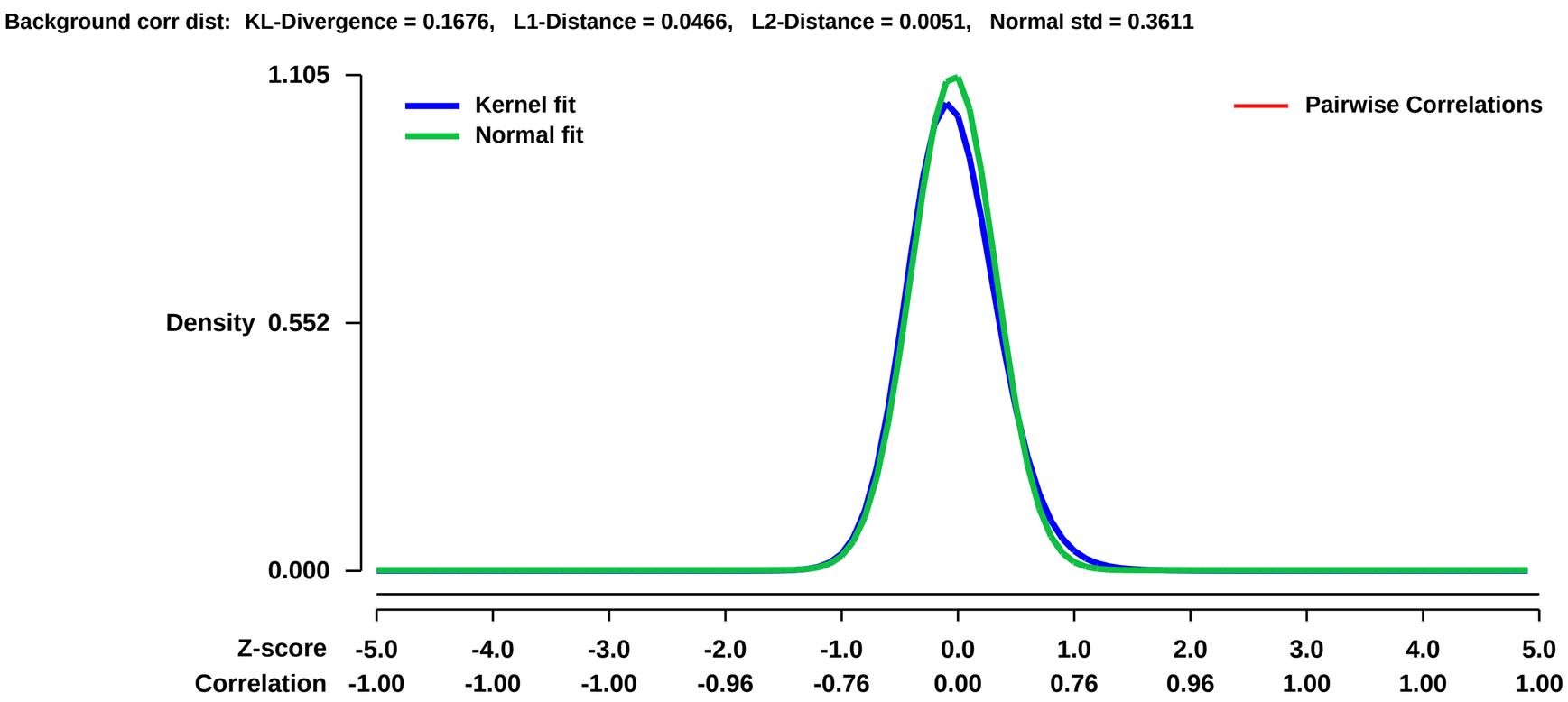

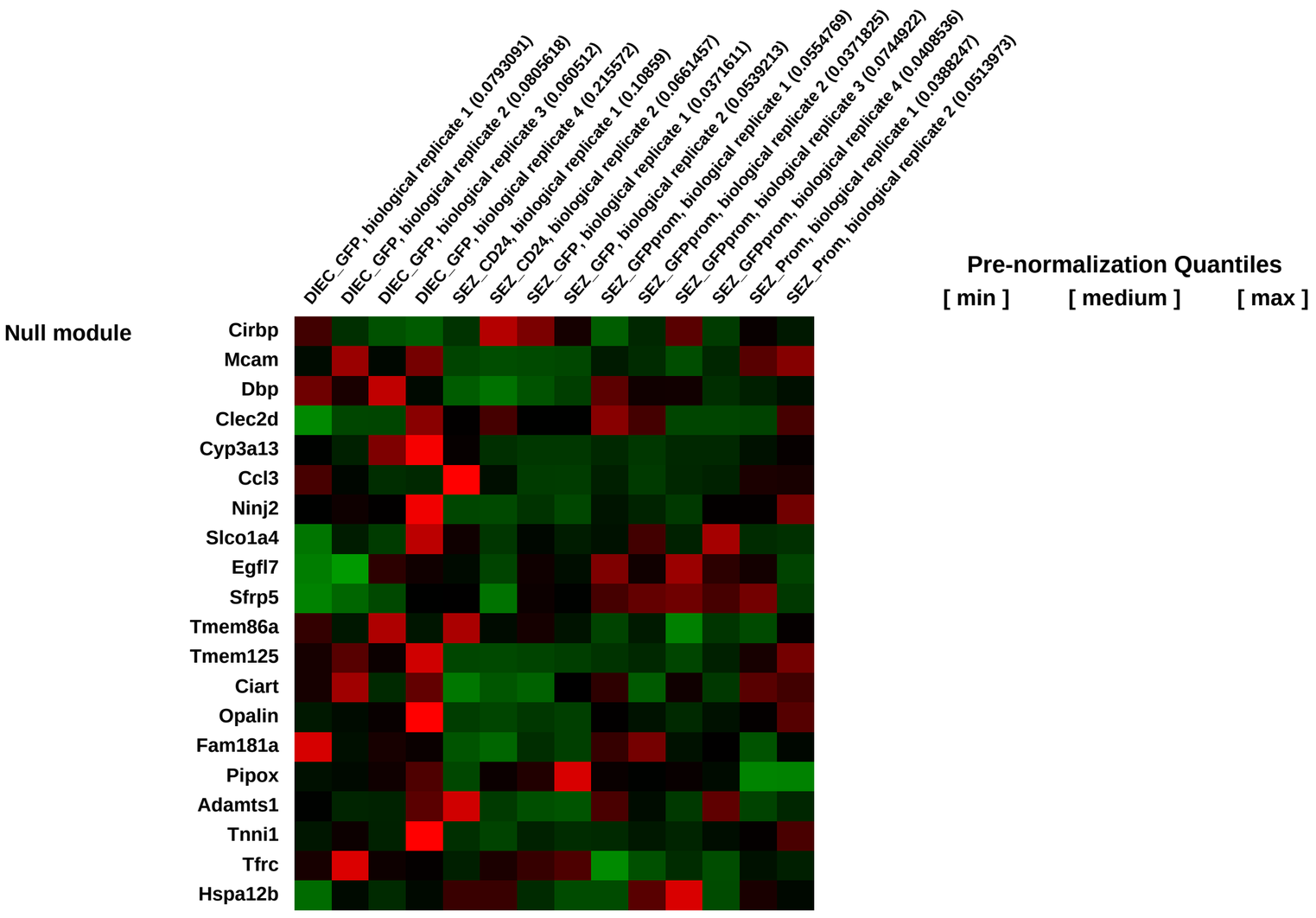

GEO Series "GSE18771" Expression Profiles

Num of samples in this series: 6

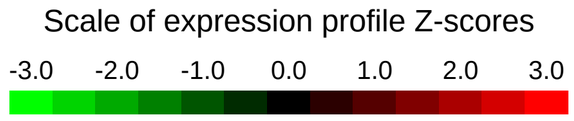

GEO Link:	**http://www.ncbi.nlm.nih.gov/geo/query/acc.cgi?acc=GSE18771**
Status:	**Public on Nov 04 2009**
Title:	**Mouse KIAA1718 knockdown ES cells**
Organism:	**Mus musculus**
Experiment type:	**Expression profiling by array**
Platform:	**GPL1261**
Pubmed ID:	
Summary & Design:	**Summary:** **Compare the gene expression profiles of ESCs stably expressing control and KIAA1718 short hairpin RNA, using Affymetrix microarray.** **Overall design:** **Mouse ES cells R1 were transformed with the respective lenti-virus expressing Luc shRNA or KIAA1718 shRNA1. The transformed ES cells were sorted for GFP. Total RNAs were extracted from cells using Trizol reagent (Invitrogen, Carlsbad, CA). For microarray experiments, RNA was processed and hybridized to Mouse Genome 430 2.0 arrays (Affymetrix) according to the manifactureâ s instruction.**

Background corr dist: **KL-Divergence = 0.0460, L1-Distance = 0.0328, L2-Distance = 0.0017, Normal std = 0.5977**

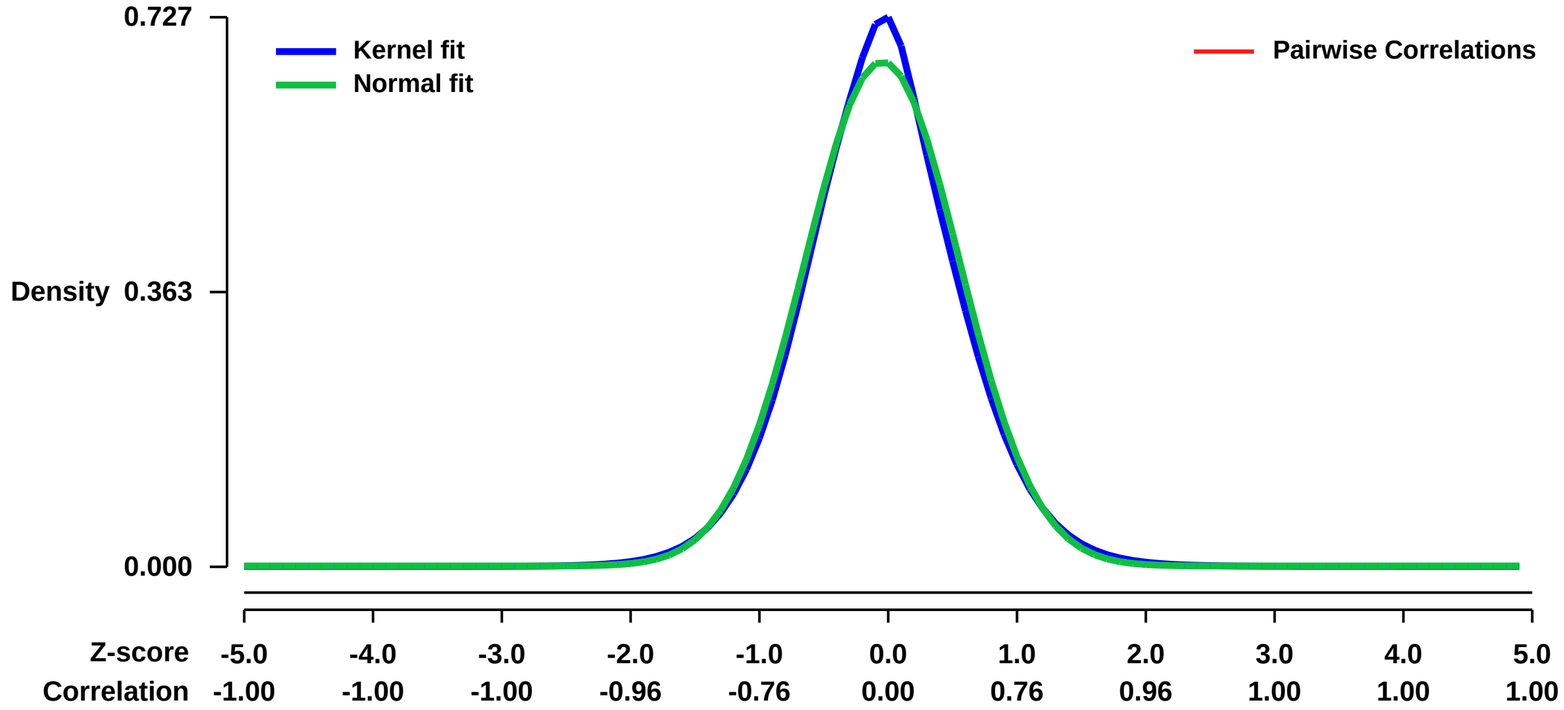

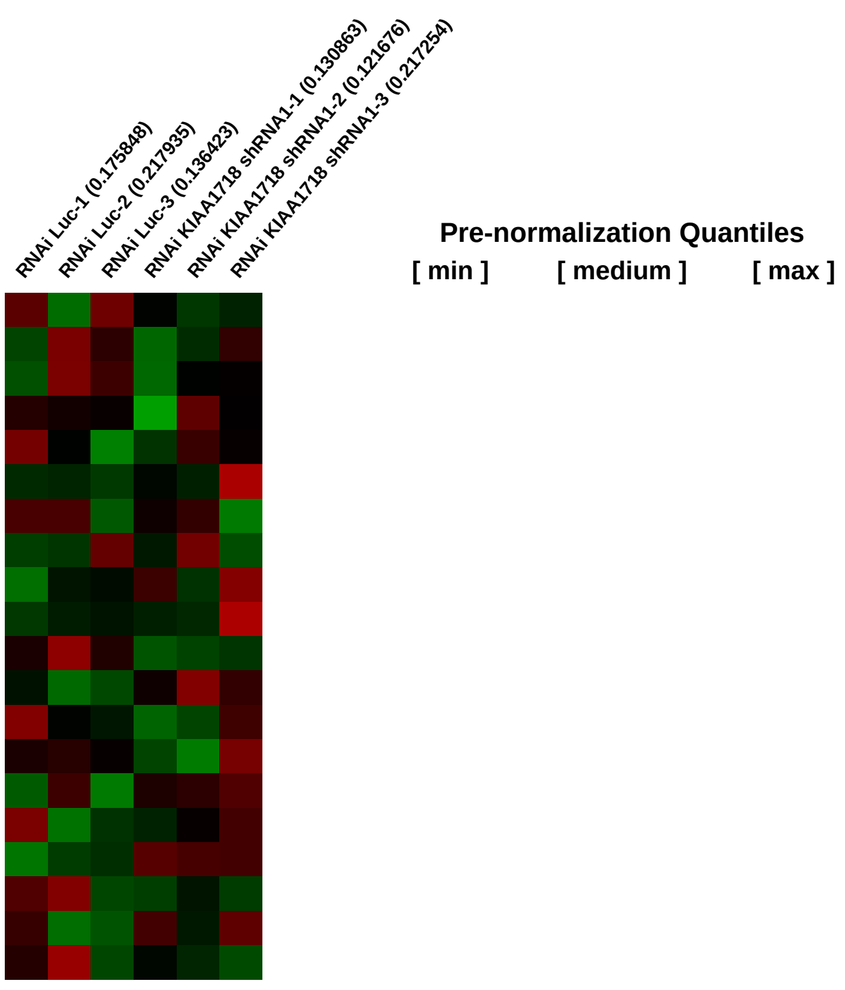

GEO Series "GSE18800" Expression Profiles

Num of samples in this series: 25

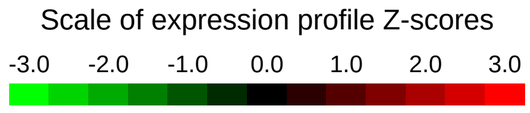

GEO Link:	**http://www.ncbi.nlm.nih.gov/geo/query/acc.cgi?acc=GSE18800**
Status:	**Public on Oct 30 2009**
Title:	**Effect of PGF receptor FP on bleomycin-induced pulmonary fibrosis in mice**
Organism:	**Mus musculus**
Experiment type:	**Expression profiling by array**
Platform:	**GPL1261**
Pubmed ID:	**19966781**
Summary & Design:	**Summary:** **We purposed to examine the effect of PGF receptor FP in development of bleomycin-induced pulmonary fibrosis in mice. We performed gene expression analysis in the lung of WT and FP-KO mice on Days 0, 7 and 14. We found out that fibrosis-related genes such as various isoforms of collagen, which were induced on Day 7 and continued to increase or remained unchanged on Day 14, were induced to less extent in FP-KO mice. In contrast, expression of inflammation-related genes peaked on Day 7 similarly in WT and FP-KO mice. These results suggest that FP functions in fibrosis-phase, not in peak inflammation phase, and facilitates fibrogenesis by enhancing expression of fibrosis-related genes.** **Overall design:** **compared with those in WT mice.**

Background corr dist: KL-Divergence = 0.2049, L1-Distance = 0.0359, L2-Distance = 0.0021, Normal std = 0.3323

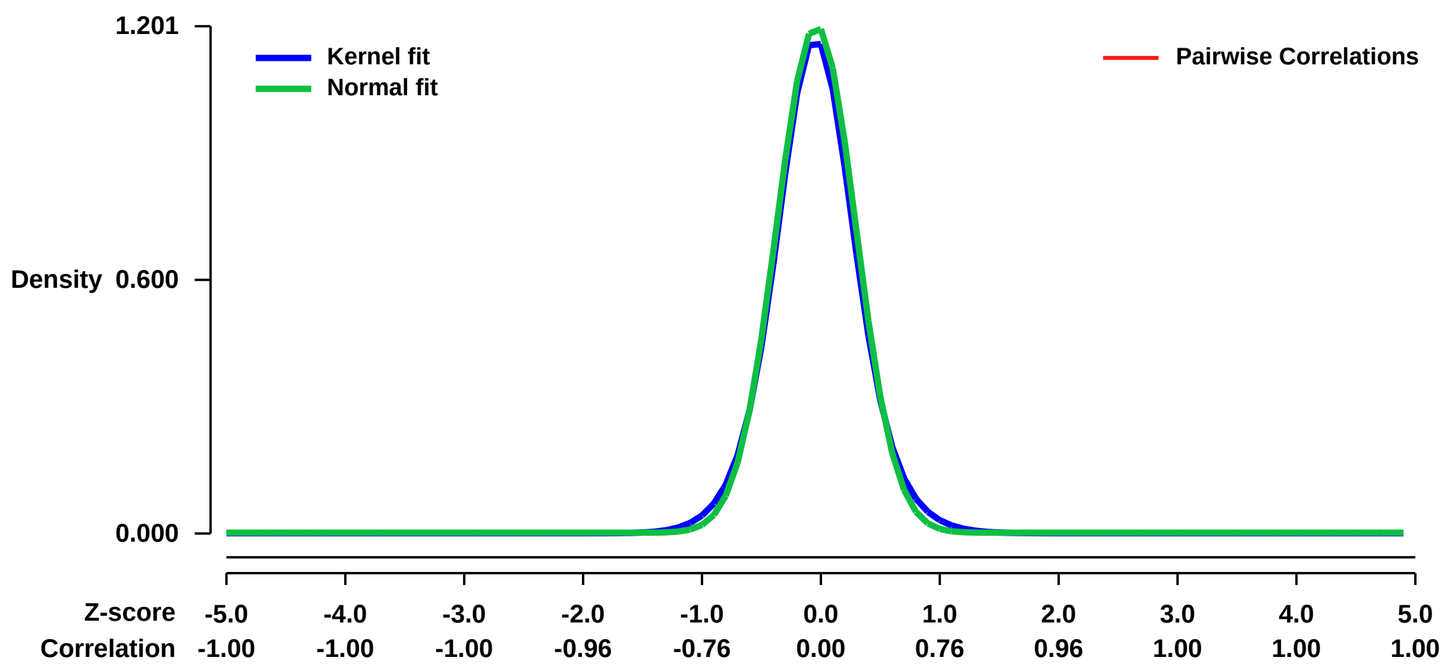

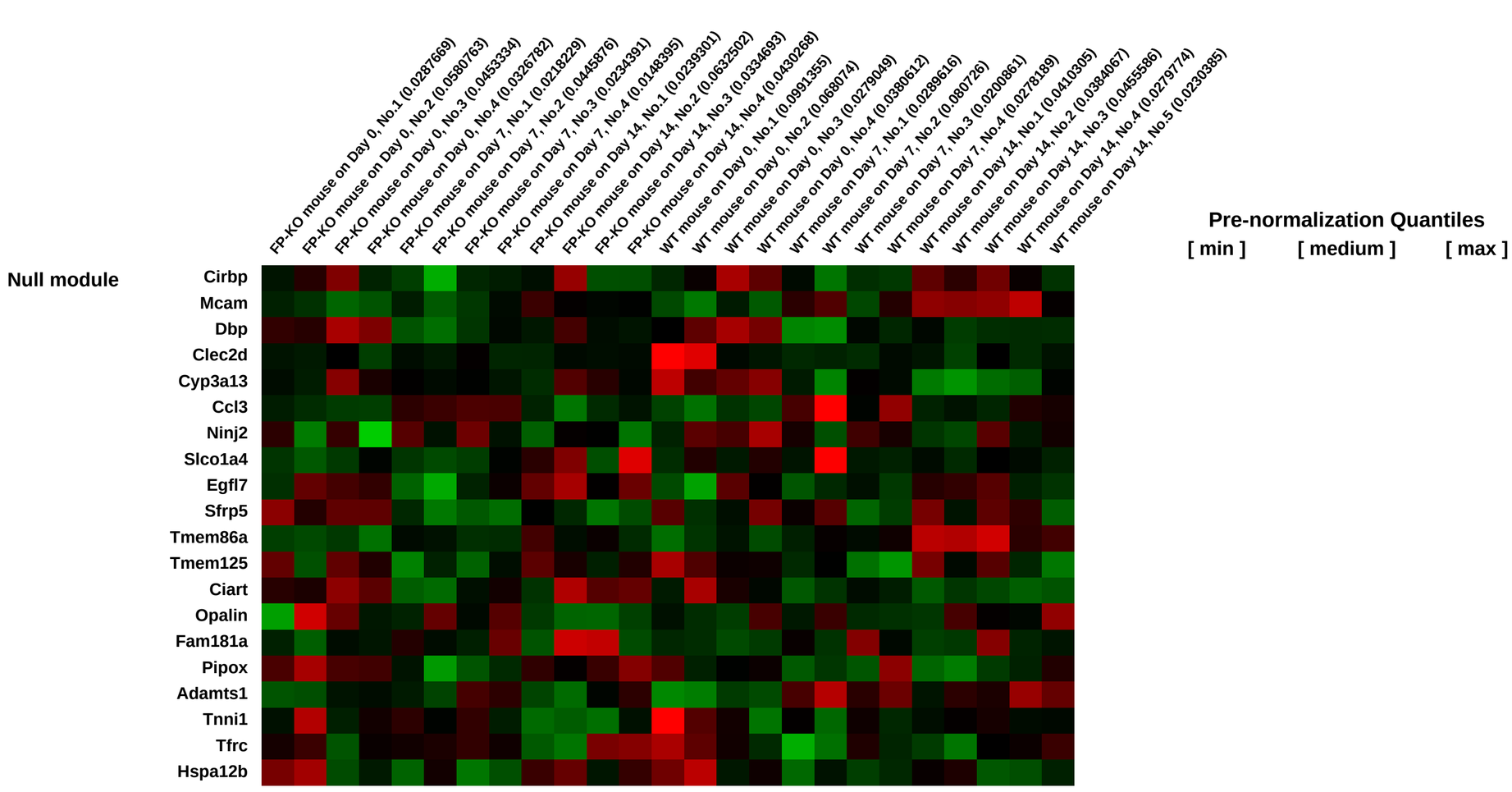

GEO Series "GSE18891" Expression Profiles

Num of samples in this series: 9

Scale of expression profile Z-scores

-3.0 -2.0 -1.0 0.0 1.0 2.0 3.0

GEO Link:	http://www.ncbi.nlm.nih.gov/geo/query/acc.cgi?acc=GSE18891
Status:	Public on Nov 05 2009
Title:	Foxl2 mediated expression data from KK1 granulosa cells
Organism:	Mus musculus
Experiment type:	Expression profiling by array
Platform:	GPL1261
Pubmed ID:	20167115
Summary & Design:	**Summary:** The Foxl2 transcription factor is required for ovarian function during follicular development. Our approach to begin to understand Foxl2 function is through the identification of Foxl2 regulated genes in the ovary. Transiently transfected KK1 mouse granulosa cells were used to identify genes that are potentially regulated by Foxl2. KK1 cells were transfected in three groups (mock, activated, and repressed) and twenty-four hours later RNA was isolated and submitted for Affymetrix microarray analysis. **Overall design:** To increase the potential of Foxl2 to alter gene expression levels of putative target genes, two fusions were constructed consisting of Foxl2 fused to the activation domain of the Herpes simplex virus VP16 transcription factor (Foxl2-VP16) and Foxl2 fused to the repression domain of the murine MAD transcription factor (Foxl2-MAD). Levels of gene expression were compared between mock transfected cells and those that were transfected with Foxl2-VP16 and Foxl2-MAD, respectively.

Background corr dist: KL-Divergence = 0.0983, L1-Distance = 0.0276, L2-Distance = 0.0014, Normal std = 0.4429

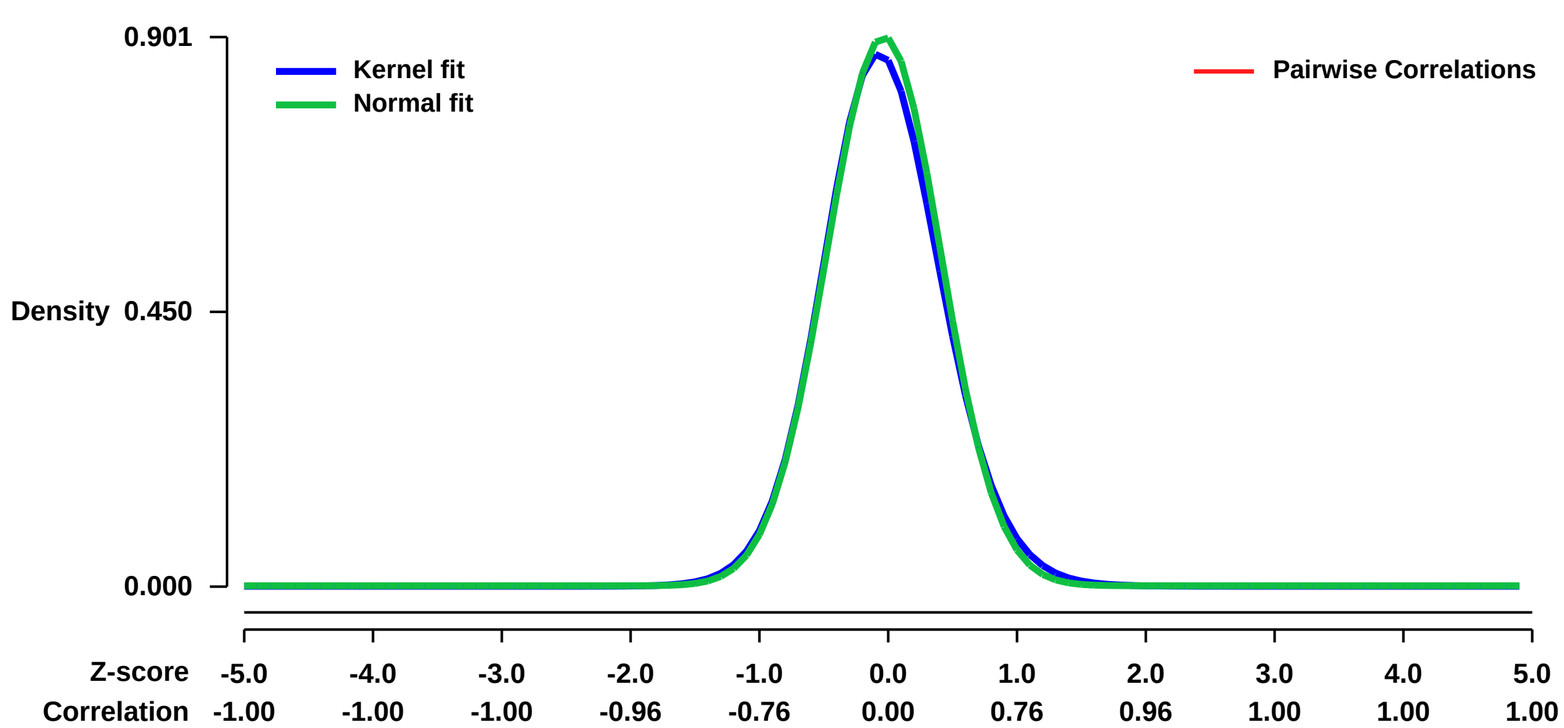

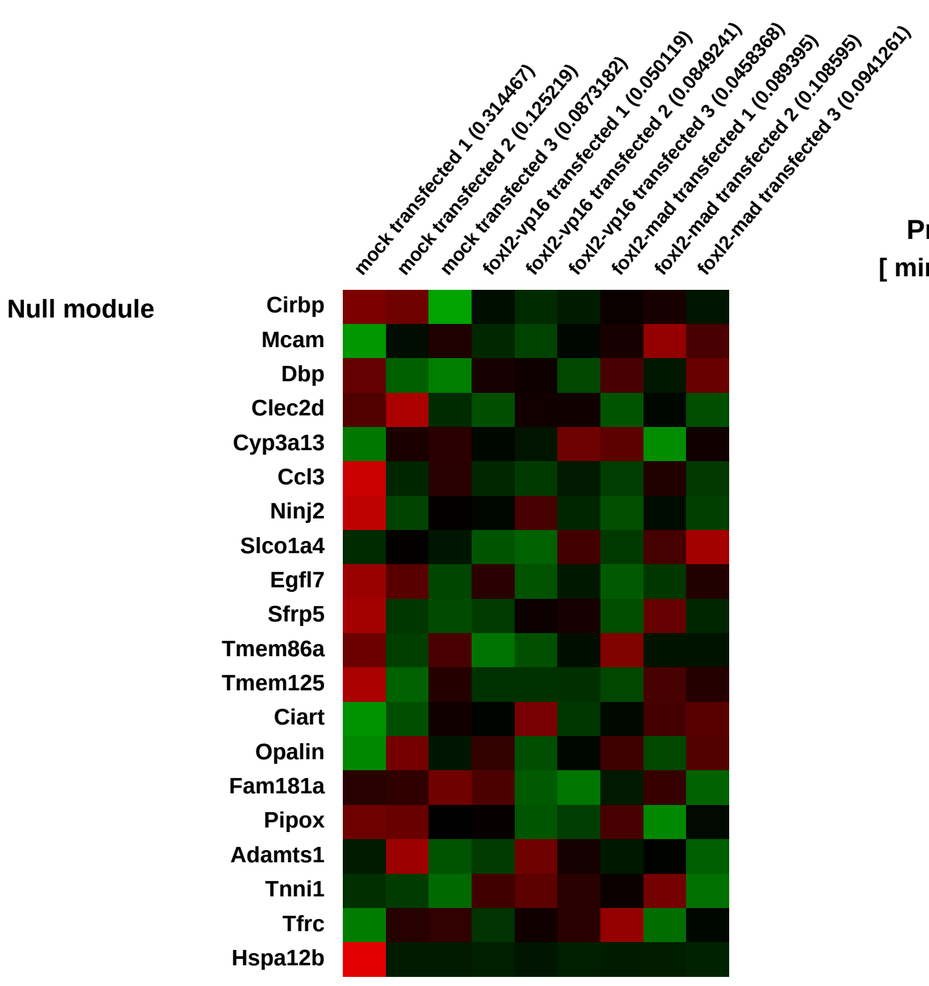

GEO Series "GSE18925" Expression Profiles

Num of samples in this series: 6

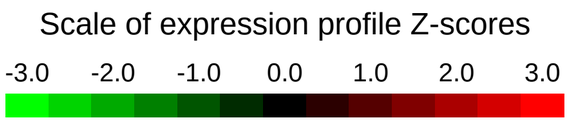

GEO Link:	http://www.ncbi.nlm.nih.gov/geo/query/acc.cgi?acc=GSE18925
Status:	Public on Dec 09 2011
Title:	Expression data from the liver of wild-type and Cnot3+/- mice: Fed vs Fasted
Organism:	Mus musculus
Experiment type:	Expression profiling by array
Platform:	GPL1261
Pubmed ID:	21897366
Summary & Design:	**Summary:** Decay of mRNAs initiates with shortening of the poly(A) tail. Although the CCR4-NOT complex participates in deadenylation, how it becomes activates remain obscure. We show that complete deficiency in CNOT3, subunit 3 of this complex, is lethal in mice, but that heterozygotes survive as lean mice with hepatic and adipose tissues containing reduced lipid levels. Cnot3+/- mice have enhanced metabolic rates and remain lean on high-fat diets. We further provide evidence suggesting that CNOT3, by changing its level in response to feeding conditions, affects the activity of the CCR4-NOT deadenylase against poly(A) tails of specific mRNAs coding for proteins involved in metabolism of carbohydrates and fats. Because the levels of CNOT3 protein were decreased under fasting conditions and increased upon refeeding and because CNOT3 could be a positive regulator of the CCR4-NOT deadenylase, we hypothesized that the levels of CCR4-NOT target mRNAs would be lower in fed mice than in fasted mice. We compared the gene expression profiles of fed and fasted wild-type mice. Microarray analysis revealed that approximately 1,200 mRNA transcripts were down-regulated in the livers of fed mice. Of these mRNAs, 68 corresponded to the genes up-regulated in the livers of Cnot3+/- mice and fasted wild-type mice. A large number of the 68 identified genes encoded proteins involved in metabolism, especially lipid metabolism and growth. **Overall design:** The livers were isolated from 8-week-old fed wild-type, fasted wild-type and fasted Cnot3+/- mice (n = 2 for each genotype).

Background corr dist: KL-Divergence = 0.0374, L1-Distance = 0.0187, L2-Distance = 0.0003, Normal std = 0.6293

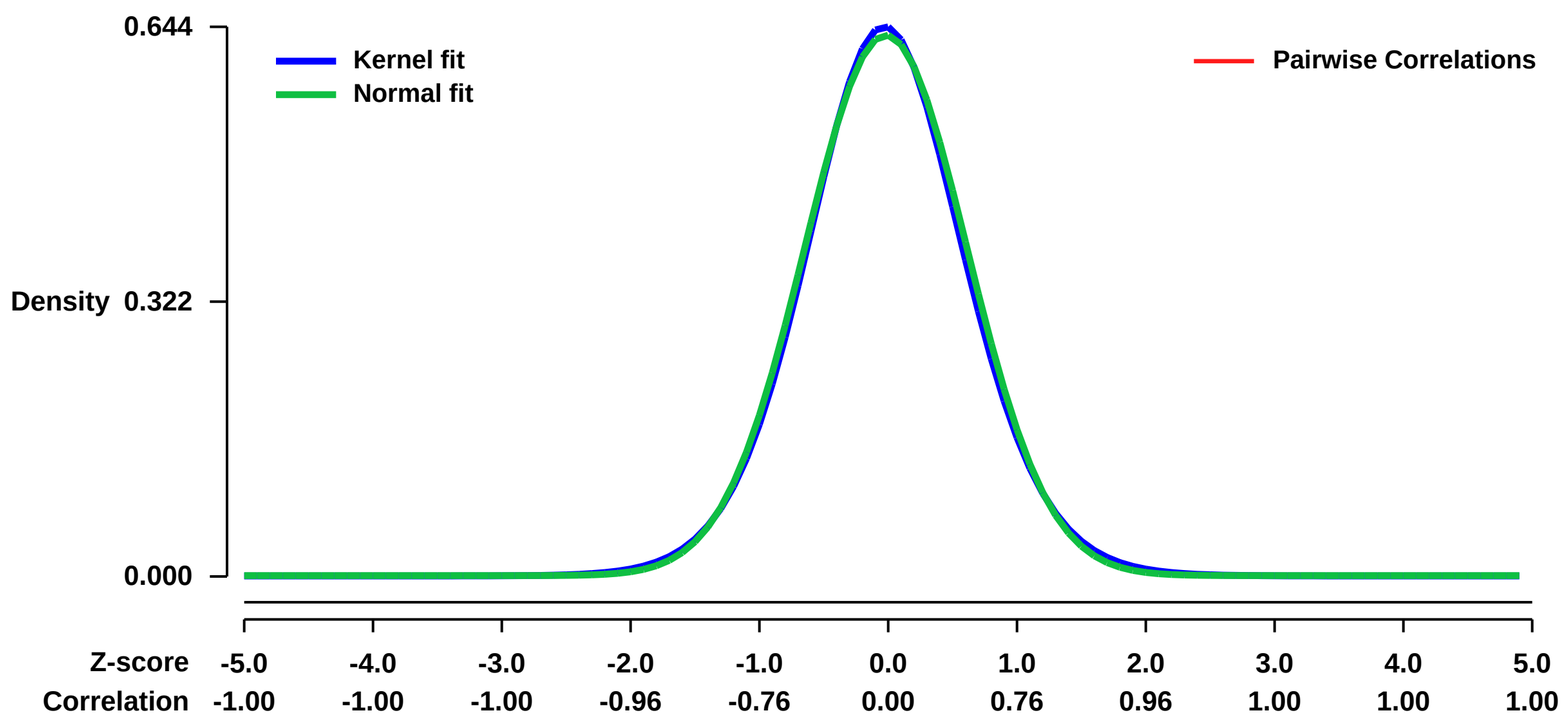

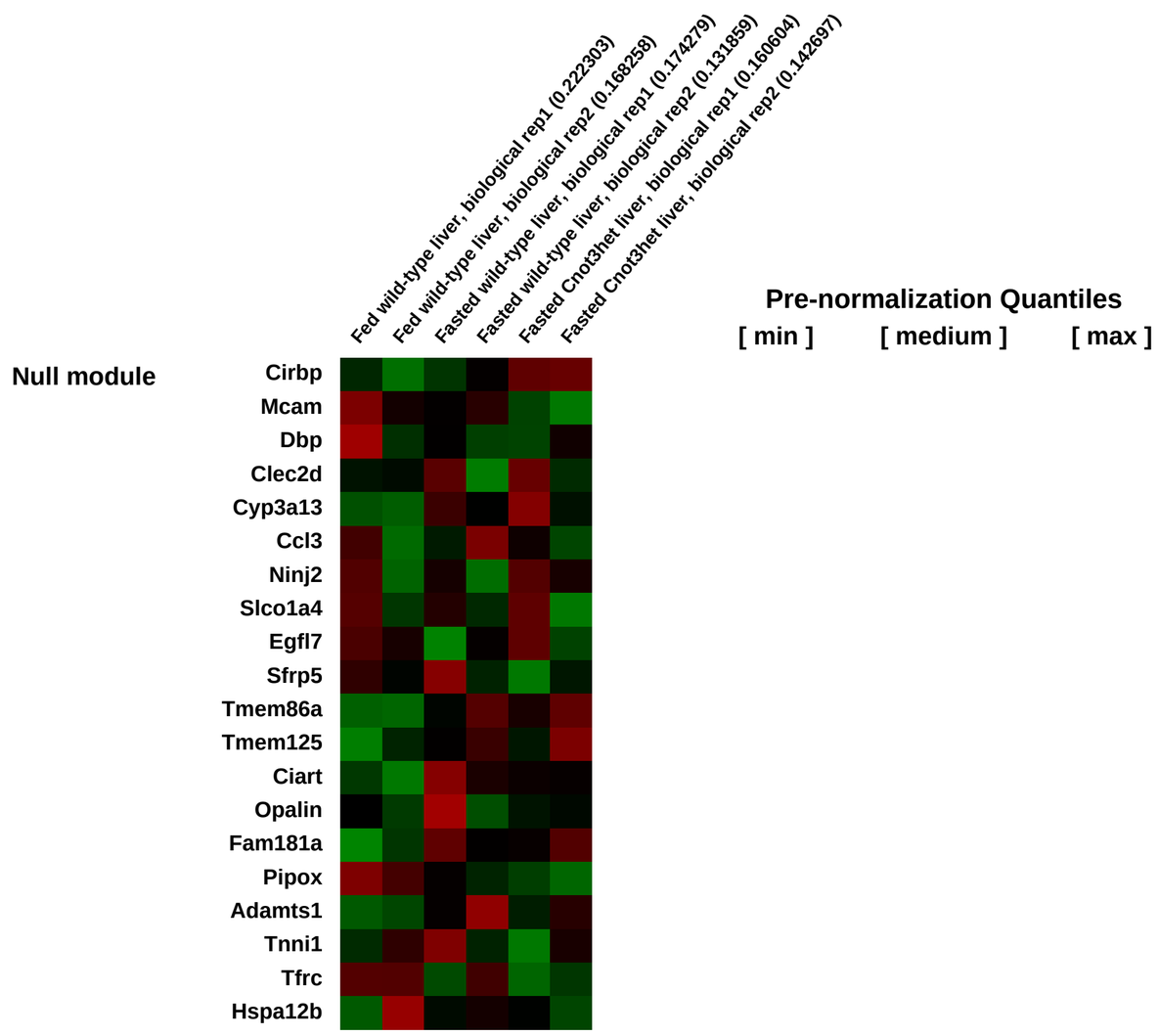

GEO Series "GSE18991" Expression Profiles

Num of samples in this series: 8

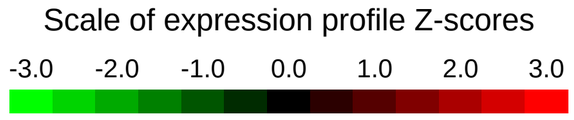

GEO Link:	**http://www.ncbi.nlm.nih.gov/geo/query/acc.cgi?acc=GSE18991**
Status:	**Public on Oct 15 2010**
Title:	**Overexpression of Hoxd4 transcription factor alters transcriptional profiles in mouse chondrocytes at E18.5**
Organism:	**Mus musculus**
Experiment type:	**Expression profiling by array**
Platform:	**GPL1261**
Pubmed ID:	
Summary & Design:	**Summary:** **Homeobox genes of the Hox class are required for proper patterning of skeletal elements and play a role in cartilage differentiation. In transgenic mice with overexpression of Hoxd4 during cartilage development, we observed severe defects, namely physical instability of cartilage, accumulation of immature chondrocytes, and decreased maturation to hypertrophy. To define the molecular basis underlying these defects, we performed gene expression profiling using the Affymetrix microarray platform.** **Overall design:** **Embryos were dissected from four different mouse litters at E18.5. Embryos from each litter were grouped according their genotype: TA=control; TR=transgenic.**

Background corr dist: **KL-Divergence = 0.0923, L1-Distance = 0.0235, L2-Distance = 0.0008, Normal std = 0.4509**

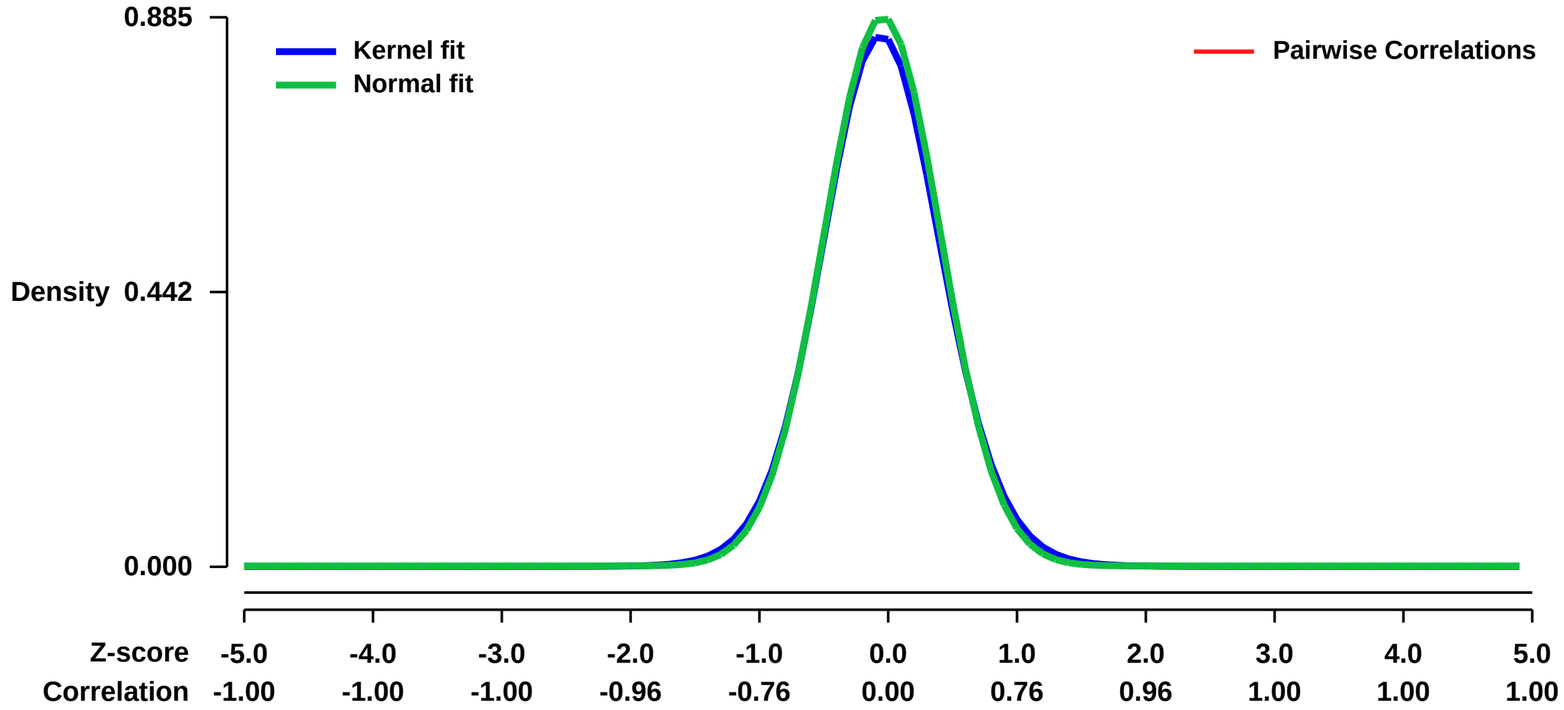

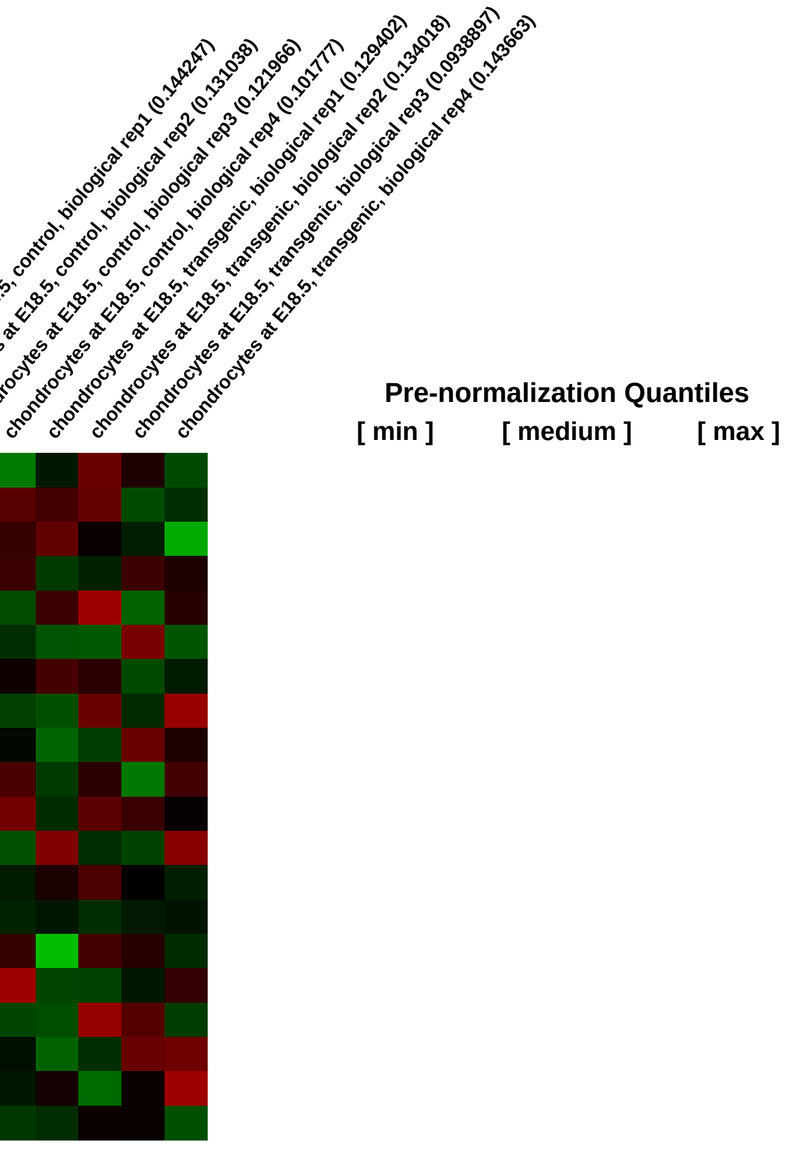

GEO Series "GSE18992" Expression Profiles

Num of samples in this series: 8

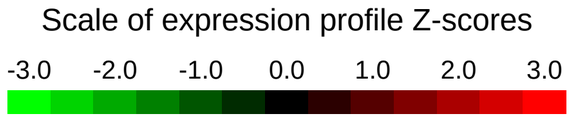

GEO Link:	**http://www.ncbi.nlm.nih.gov/geo/query/acc.cgi?acc=GSE18992**
Status:	**Public on Oct 15 2010**
Title:	**Overexpression of Hoxc8 transcription factor alters transcriptional profiles in mouse chondrocytes at E18.5**
Organism:	**Mus musculus**
Experiment type:	**Expression profiling by array**
Platform:	**GPL1261**
Pubmed ID:	
Summary & Design:	**Summary:** **Homeobox genes of the Hox class are required for proper patterning of skeletal elements and play a role in cartilage differentiation. In transgenic mice with overexpression of Hoxc8 during cartilage development, we observed severe defects, namely physical instability of cartilage, accumulation of immature chondrocytes, and decreased maturation to hypertrophy. To define the molecular basis underlying these defects, we performed gene expression profiling using the Affymetrix microarray platform.** **Overall design:** **Embryos were dissected from four different mouse litters at E18.5. Embryos from each litter were grouped according their genotype: TA=control; TR=transgenic.**

Background corr dist: **KL-Divergence = 0.0799, L1-Distance = 0.0208, L2-Distance = 0.0007, Normal std = 0.4762**

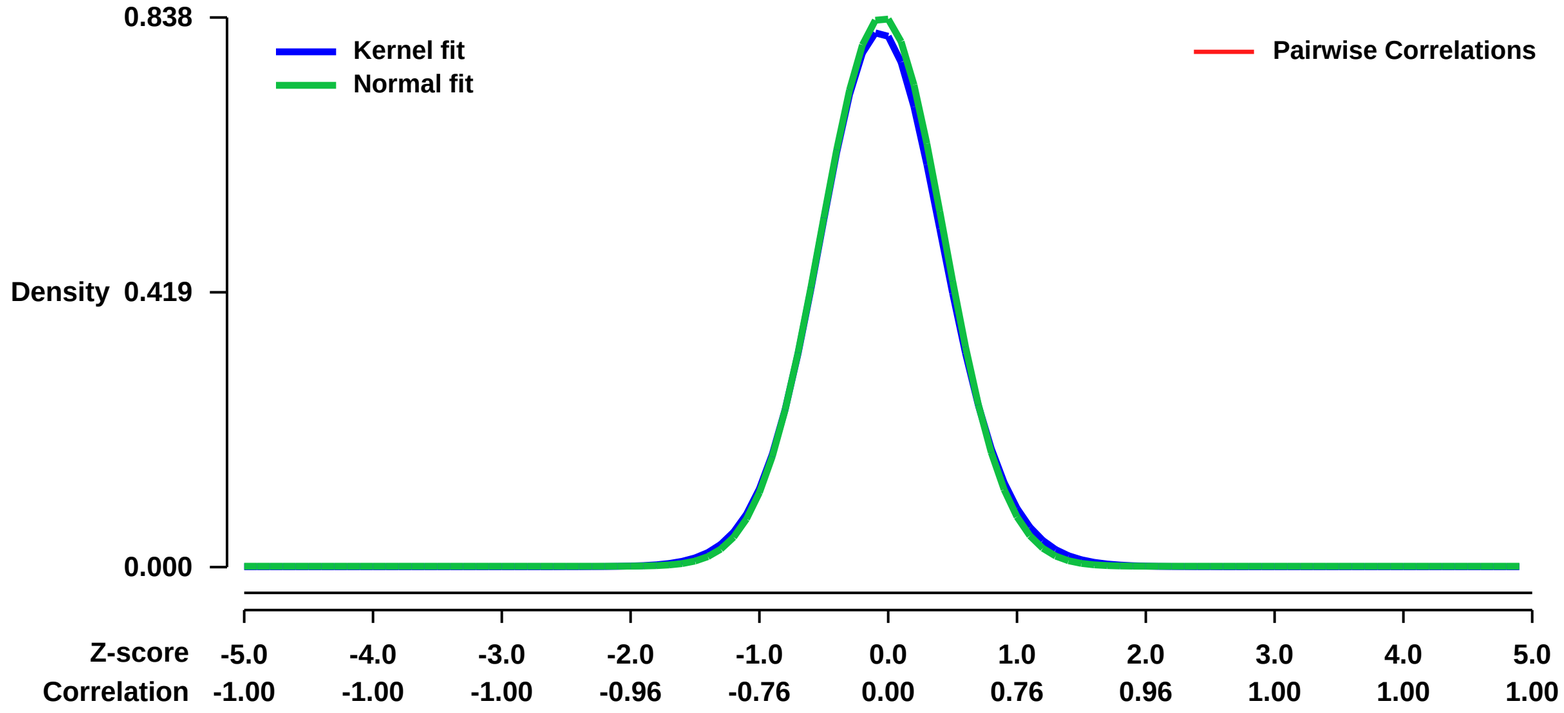

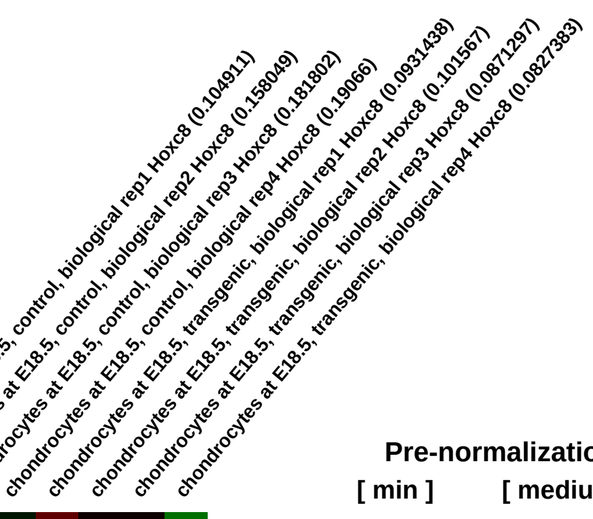

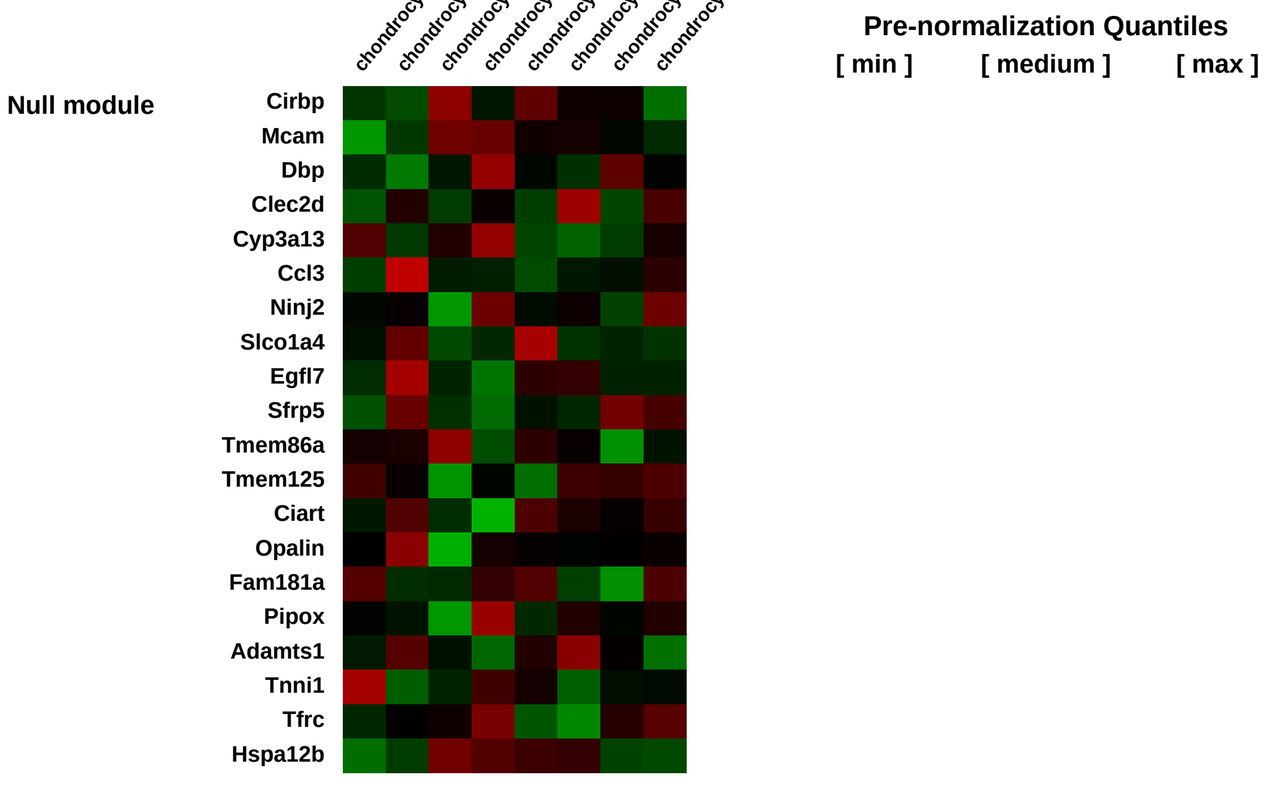

GEO Series "GSE18993" Expression Profiles

Num of samples in this series: 13

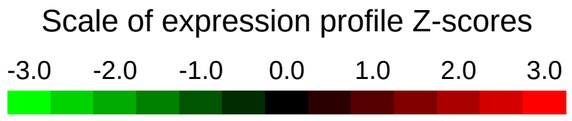

GEO Link:	http://www.ncbi.nlm.nih.gov/geo/query/acc.cgi?acc=GSE18993
Status:	Public on Jun 22 2011
Title:	Expression profiles from mouse prostate progenitor/stem cells treated with ethanol or 100nM 1,25 dihydroxyvitamin D3
Organism:	Mus musculus
Experiment type:	Expression profiling by array
Platform:	GPL1261
Pubmed ID:	21653679
Summary & Design:	**Summary:** A major goal in prostate stem cell biology is to identify genes, pathways, or networks that control self-renewal and multilineage differentiation. We hypothesize that 1,25 dihydroxyvitamin D3 can induce differentiation of prostatic progenitor/stem cells, thus serving as an in vitro model with which to study the molecular mechanisms of stem cell differentiation by 1,25 dihydroxyvitamin D3. 1,25 dihydroxyvitamin D3 elicits its effects primarily through transcriptional regulation of genes, so microarray studies were used to gain insight into the cellular response to 1,25 dihydroxyvitamin D3. We used microarrays to detail the global gene expression changes that occur upon 1,25 dihydroxyvitamin D3 treatment of prostatic progenitor/stem cells. **Overall design:** Adult mouse prostate progenitor/stem cells were plated at 1 x 10^5 cells per 10 cm culture dish and grown to 70% confluency before treatment with vehicle (0.1% ethanol) or 100 nM 1,25(OH)2D3 in cell culture media (n = 3 or 4). Cells were treated with control or experimental media for 6 hrs or 48 hrs before RNA isolation. The RNA from 6 hrs and 48 hrs was used to probe Affymetrix 430A oligonucleotide arrays (GPL339).

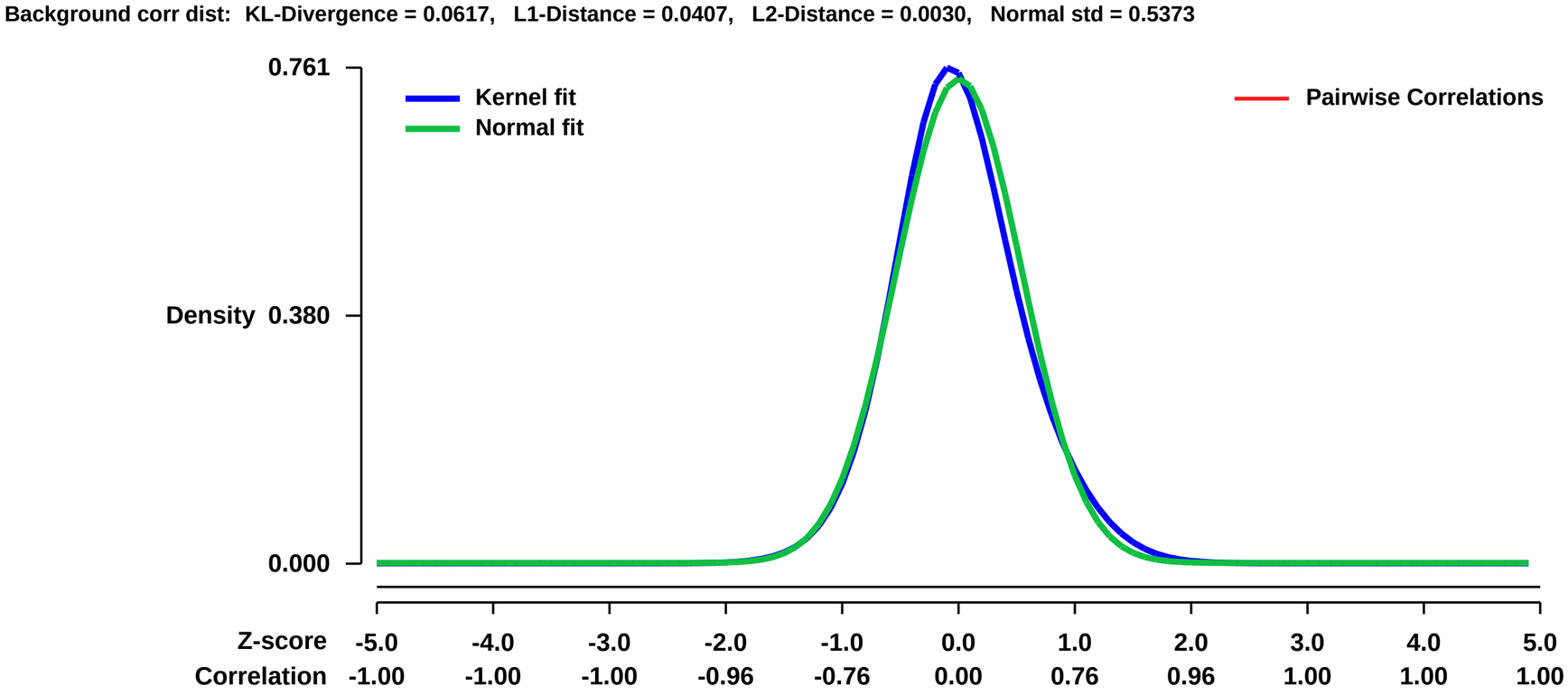

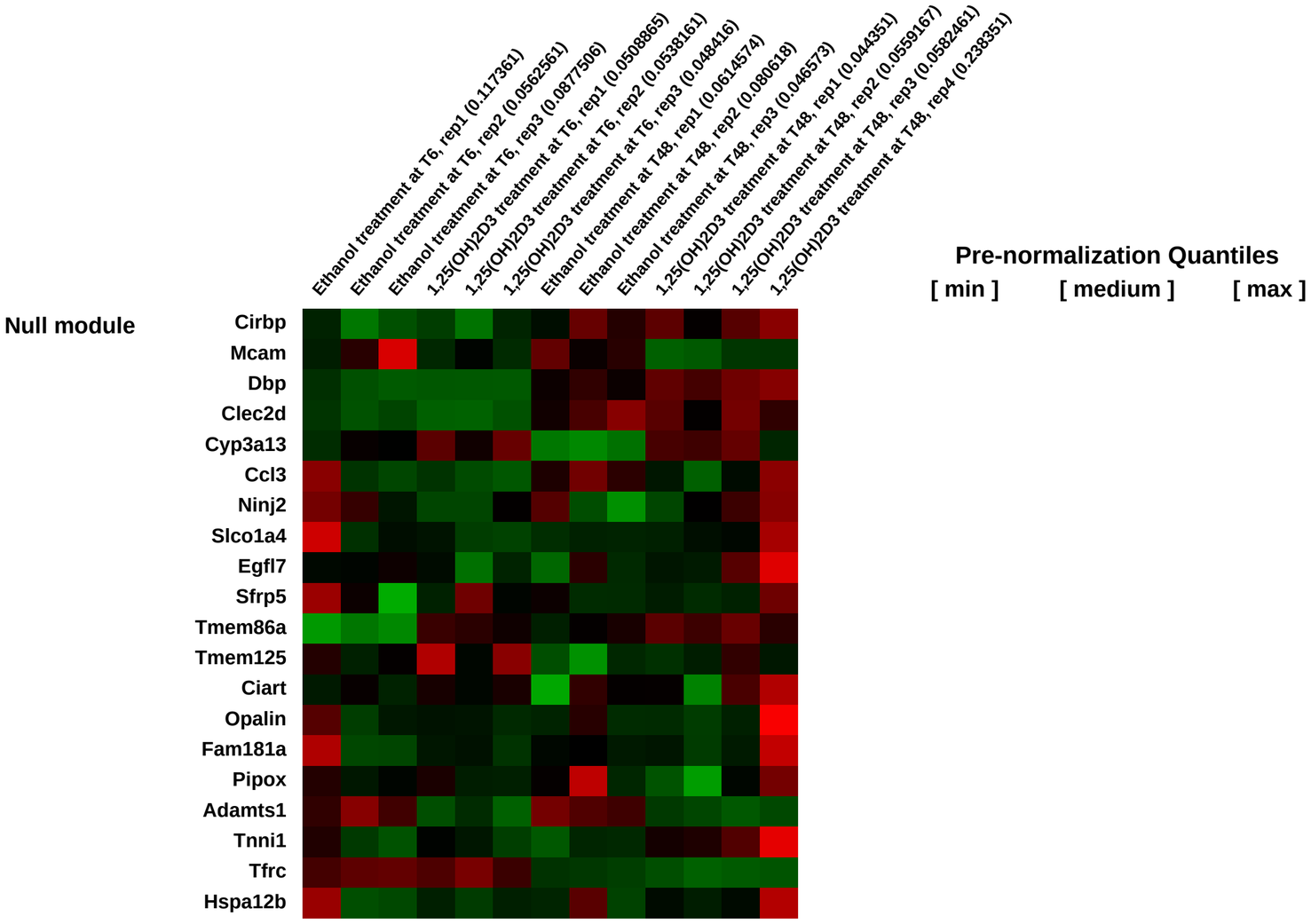

GEO Series "GSE19073" Expression Profiles

Num of samples in this series: 6

Scale of expression profile Z-scores

-3.0 -2.0 -1.0 0.0 1.0 2.0 3.0

GEO Link:	http://www.ncbi.nlm.nih.gov/geo/query/acc.cgi?acc=GSE19073
Status:	Public on Dec 01 2009
Title:	An Experimentally Derived Metastasis Gene Expression Profile Predicts Recurrence and Death in Colon Cancer Patients
Organism:	Mus musculus
Experiment type:	Expression profiling by array
Platform:	GPL1261
Pubmed ID:	22115830
Summary & Design:	**Summary:** **Functional genomics approach to metastatic colon cancer** **Mouse model translated to human colon cancer** **Overall design:** **Gene expression array differences between highly invasive mouse colon cancer cells and non-invasive colon cancer cells**

Background corr dist: **KL-Divergence = 0.0203, L1-Distance = 0.0183, L2-Distance = 0.0003, Normal std = 0.7524**

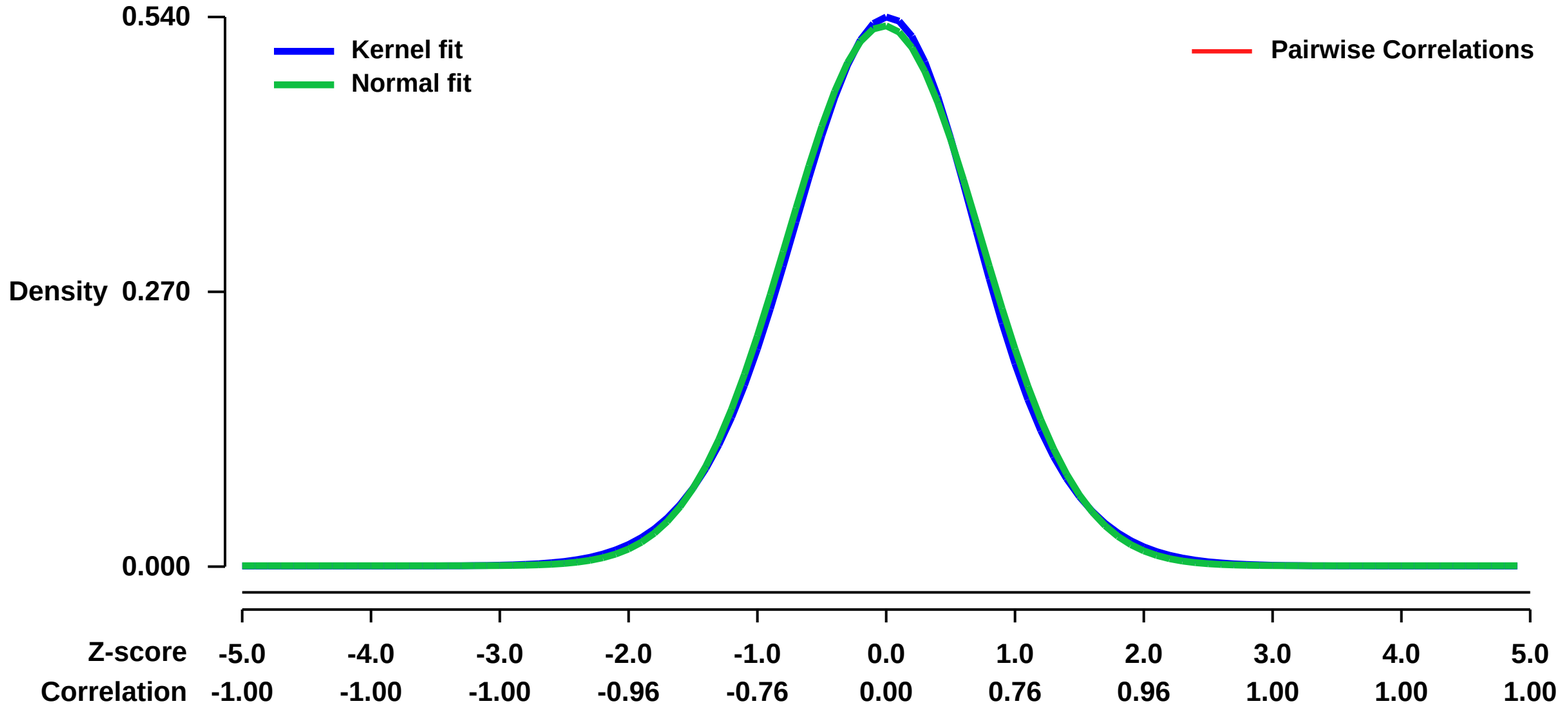

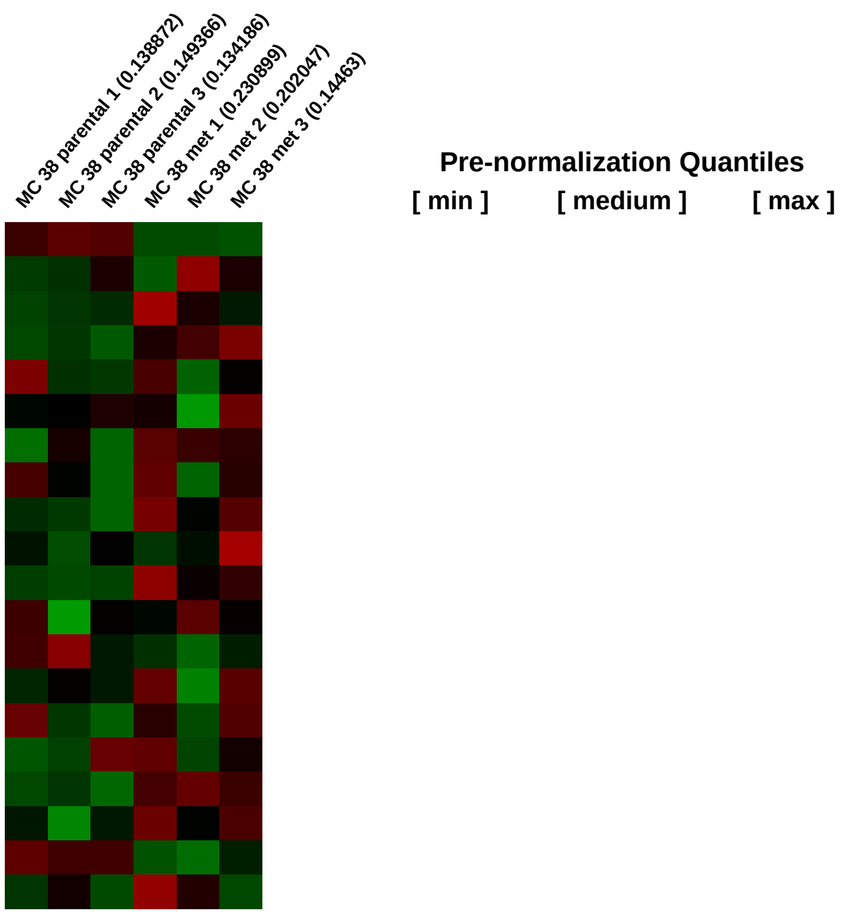

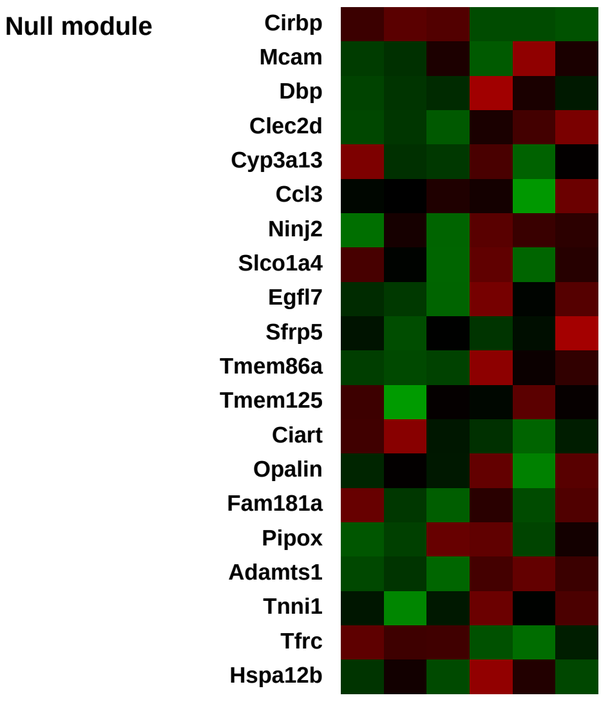

GEO Series "GSE19076" Expression Profiles

Num of samples in this series: 12

Scale of expression profile Z-scores

-3.0 -2.0 -1.0 0.0 1.0 2.0 3.0

GEO Link:	http://www.ncbi.nlm.nih.gov/geo/query/acc.cgi?acc=GSE19076
Status:	Public on Dec 01 2009
Title:	Expression data from wild type, Ring1B-/-, Eed-/-, and Ring1B/Eed double deficient mouse ES cells
Organism:	Mus musculus
Experiment type:	Expression profiling by array
Platform:	GPL1261
Pubmed ID:	20123906
Summary & Design:	**Summary:** Polycomb complexes establish chromatin modifications for maintaining gene repression and are essential for embryonic development in mice. Here we use pluripotent embryonic stem (ES) cells to demonstrate an unexpected redundancy between Polycomb repressive complex 1 (PRC1) and PRC2 during the formation of differentiated cells. ES cells lacking the function of either PRC1 or PRC2 can differentiate into cells of the three germ layers, whereas simultaneous loss of PRC1 and PRC2 abrogates differentiation. On the molecular level the differentiation defect is caused by the derepression of a set of genes that is redundantly repressed by PRC1 and PRC2 in ES cells. Furthermore, we find that genomic repeats are Polycomb targets and show that in the absence of Polycomb complexes endogenous MLV elements can mobilize. This indicates a contribution of the PcG system to the defense against parasitic DNA and a potential role of genomic repeats in Polycomb mediated gene regulation. **Overall design:** RNA from wt and PcG mutant ES cells was extracted using Trizol and hybridized to an Affymetrix Mouse 430_2.0 chip. Labeling, hybridization and primary data analysis were performed by a commercial provider (Atlas Biolabs, Berlin). Before RNA extraction, the undifferentiated ES cell state was confirmed by colony morphology. All genotypes were hybridized in biological triplicates.

Background corr dist: KL-Divergence = 0.1022, L1-Distance = 0.0263, L2-Distance = 0.0012, Normal std = 0.4327

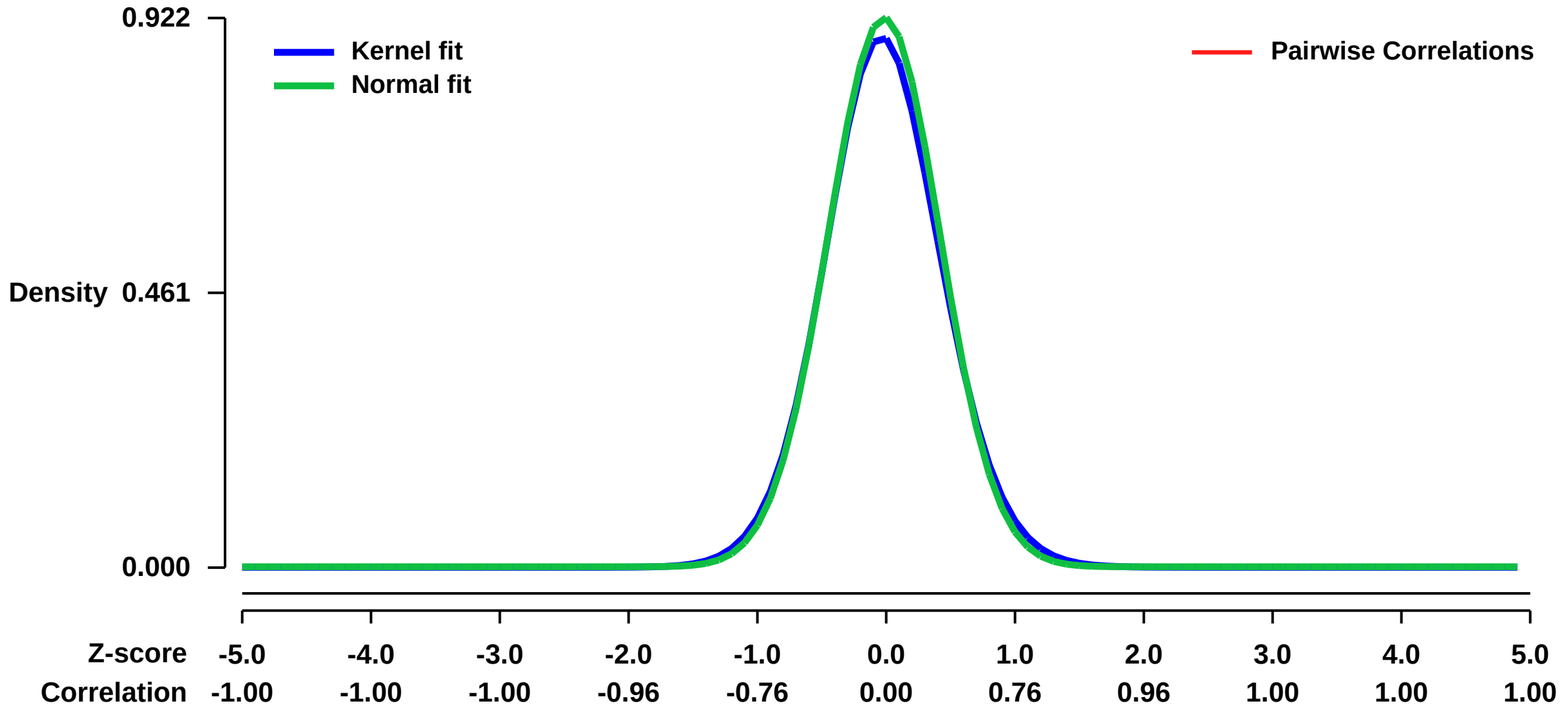

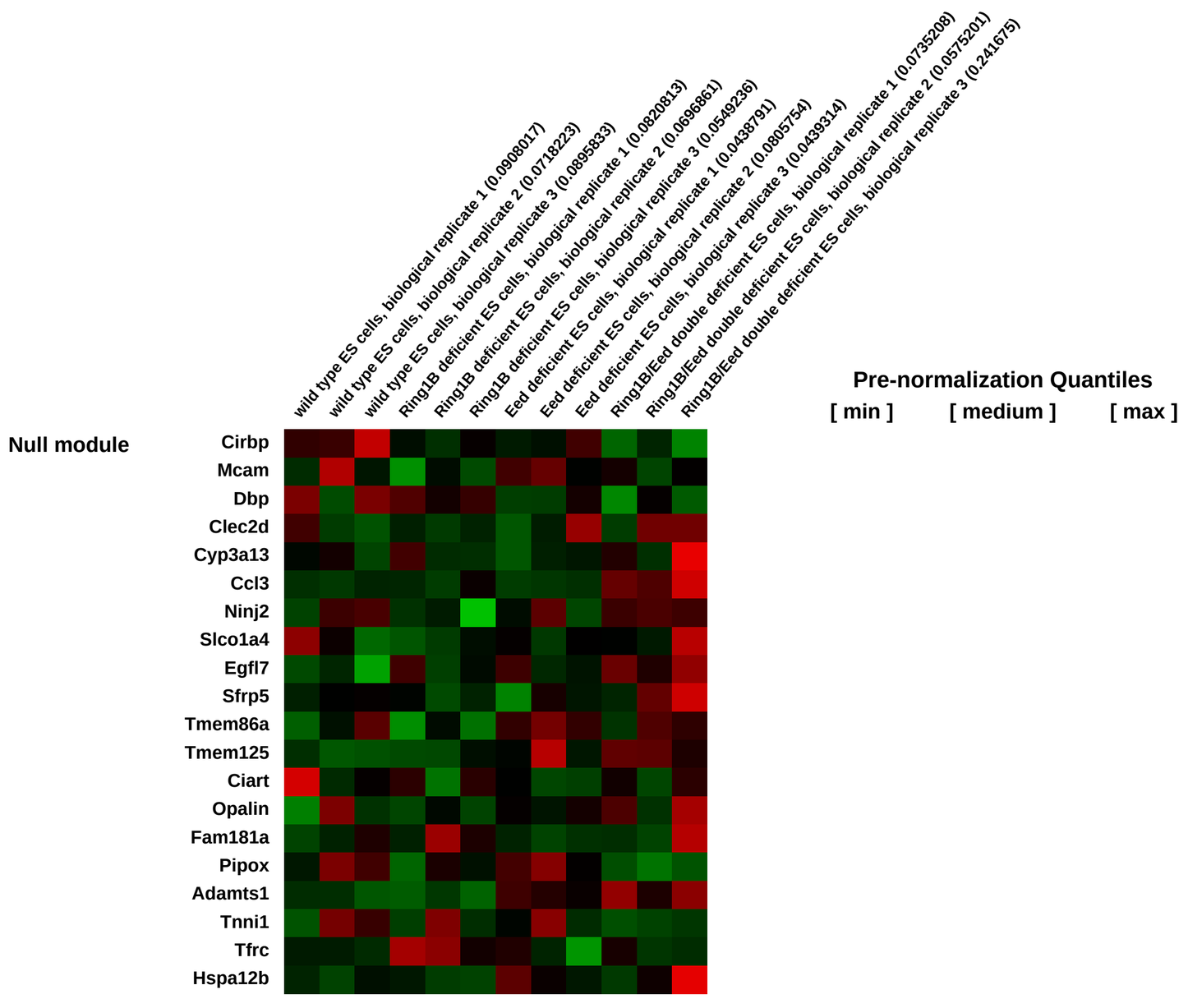

GEO Series "GSE19079" Expression Profiles

Num of samples in this series: 6

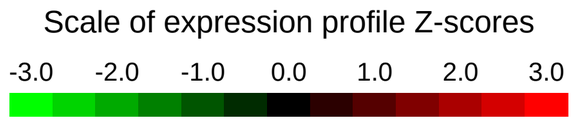

GEO Link:	**http://www.ncbi.nlm.nih.gov/geo/query/acc.cgi?acc=GSE19079**
Status:	**Public on Nov 19 2010**
Title:	**Myocardial expression data from wild-type and akt2-/- mice**
Organism:	**Mus musculus**
Experiment type:	**Expression profiling by array**
Platform:	**GPL1261**
Pubmed ID:	
Summary & Design:	**Summary:** **Wild-type (WT) C57Bl/6 and akt2-/- male mice.** **Keywords: RNA Expression Array** **Overall design:** **Left ventricles (LV) from 12-16 week-old male wild type mice and age-matched akt2-/- mice**

Background corr dist: **KL-Divergence = 0.0153, L1-Distance = 0.0204, L2-Distance = 0.0006, Normal std = 0.7977**

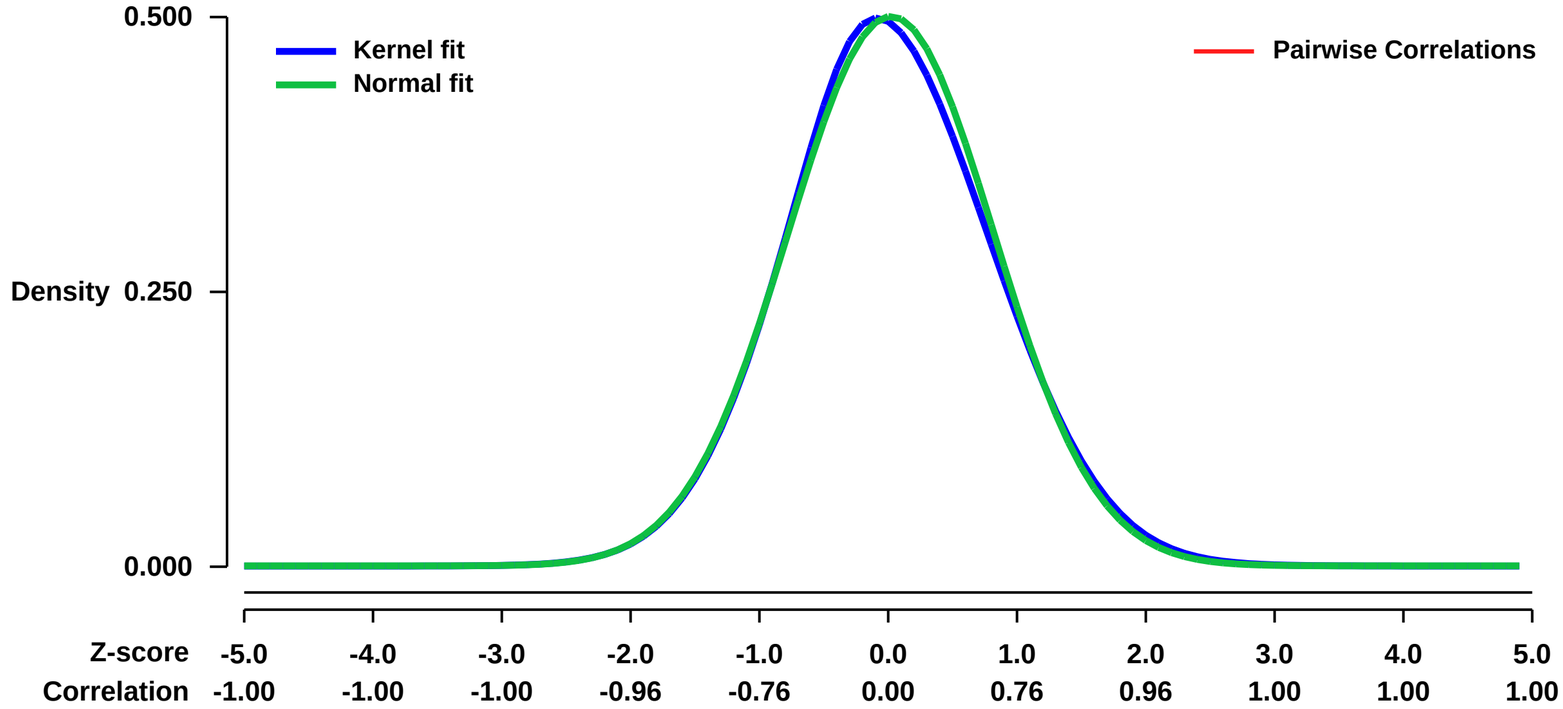

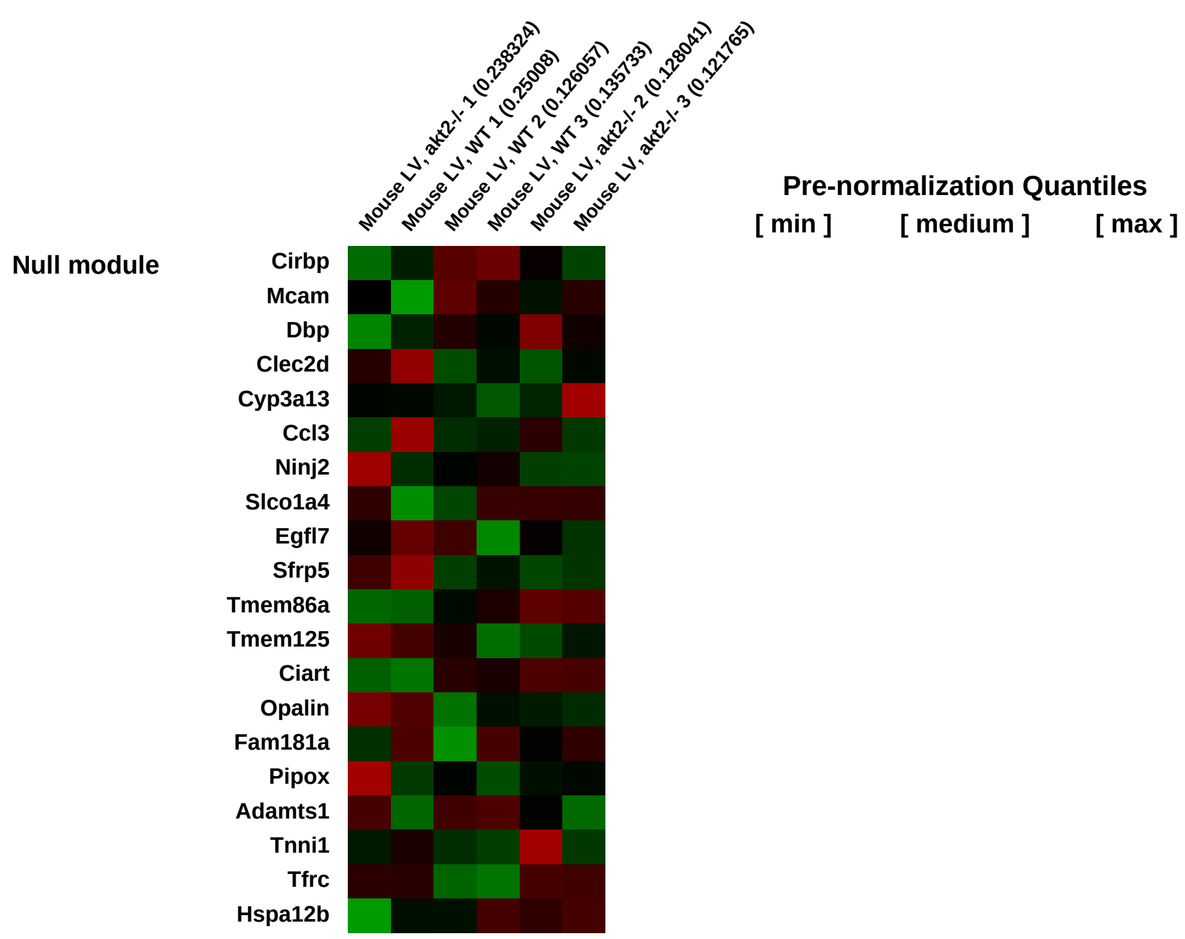

GEO Series "GSE19091" Expression Profiles

Num of samples in this series: 6

Scale of expression profile Z-scores

-3.0 -2.0 -1.0 0.0 1.0 2.0 3.0

GEO Link:	http://www.ncbi.nlm.nih.gov/geo/query/acc.cgi?acc=GSE19091
Status:	Public on Oct 01 2011
Title:	Transcriptional profiling of MKK4-depleted cells
Organism:	Mus musculus
Experiment type:	Expression profiling by array
Platform:	GPL1261
Pubmed ID:	21896780
Summary & Design:	**Summary:** Mitogen-activated protein kinase kinase 4 (MKK4) is a dual-specificity kinase activated by environmental stress, cytokines, and peptide growth factors that reportedly can promote or inhibit tumor cell growth and metastasis. Somatic mutations in the gene encoding MKK4 (MAP2K4) have been identified in various human cancers, but the consequences of these mutations on MKK4 function and the biology of tumor cells that have them have not been elucidated. Here we report that, of the eleven mutations within the MAP2K kinase domain described thus far, one had gain-of-function (Q142L) and six had loss-of-function. Three of the loss-of-function mutations are nonsense mutations that produced C-terminally-truncated proteins (I295fs*23, R304*, and W310*) that were highly ubiqitinated and rapidly degraded when introduced into cells, and three are missense mutations in the ATP-binding pocket (N234I), activation loop (S251N), or C-lobe (P326L). We modeled the consequences of MAP2K4 loss-of-function mutations on cells by introducing MKK4 short-hairpin RNA constructs and found that MKK4 depletion enhanced the ability of a weakly tumorigenic murine cancer cell to metastasize when injected into syngeneic mice but had no effect on primary tumor formation. MKK4-depleted cells exhibited an increased capacity to migrate across PET filters and to invade through matrigel but no change in anchorage-dependent or -independent proliferation. Transcriptional profiling of these cells revealed gene expression changes that promote epithelial-to-mesenchymal transition and angiogenesis. We conclude that MKK4 inactivation promoted metastasis but not primary tumor formation. Collectively, these findings implicate loss-of-function MAP2K4 somatic mutations in tumor metastasis and provide one of the few examples of a somatic mutation in cancer cells that exerts a metastasis-specific effect. **Keywords:** Two-group comparison. **Overall design:** 393P cells were infected with retroviruses expressing a MKK4-specific shRNA construct (shZ) or scrambled control (scr). 393P-shZ and 393P-scr were transcriptionally profiled in triplicate cultures.

Background corr dist: KL-Divergence = 0.0393, L1-Distance = 0.0240, L2-Distance = 0.0006, Normal std = 0.6276

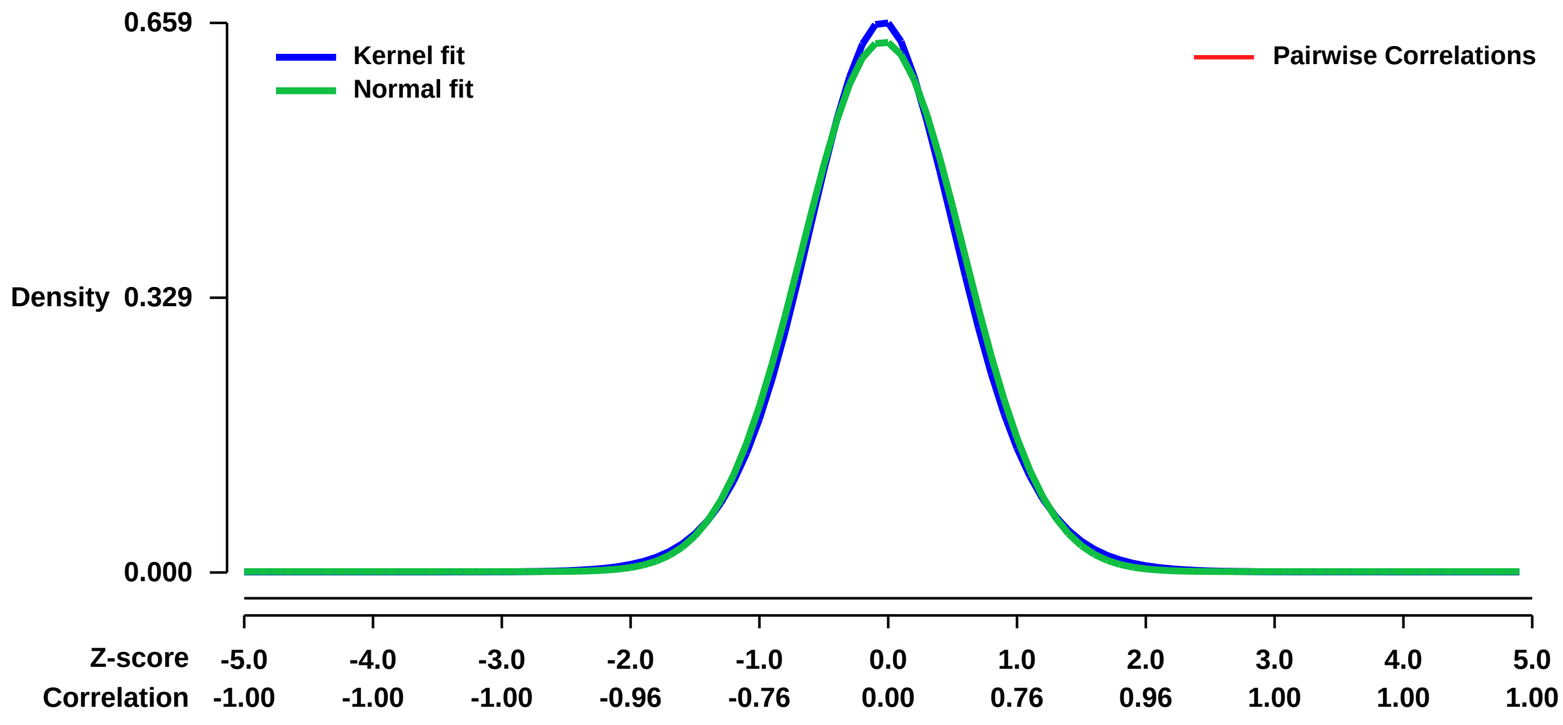

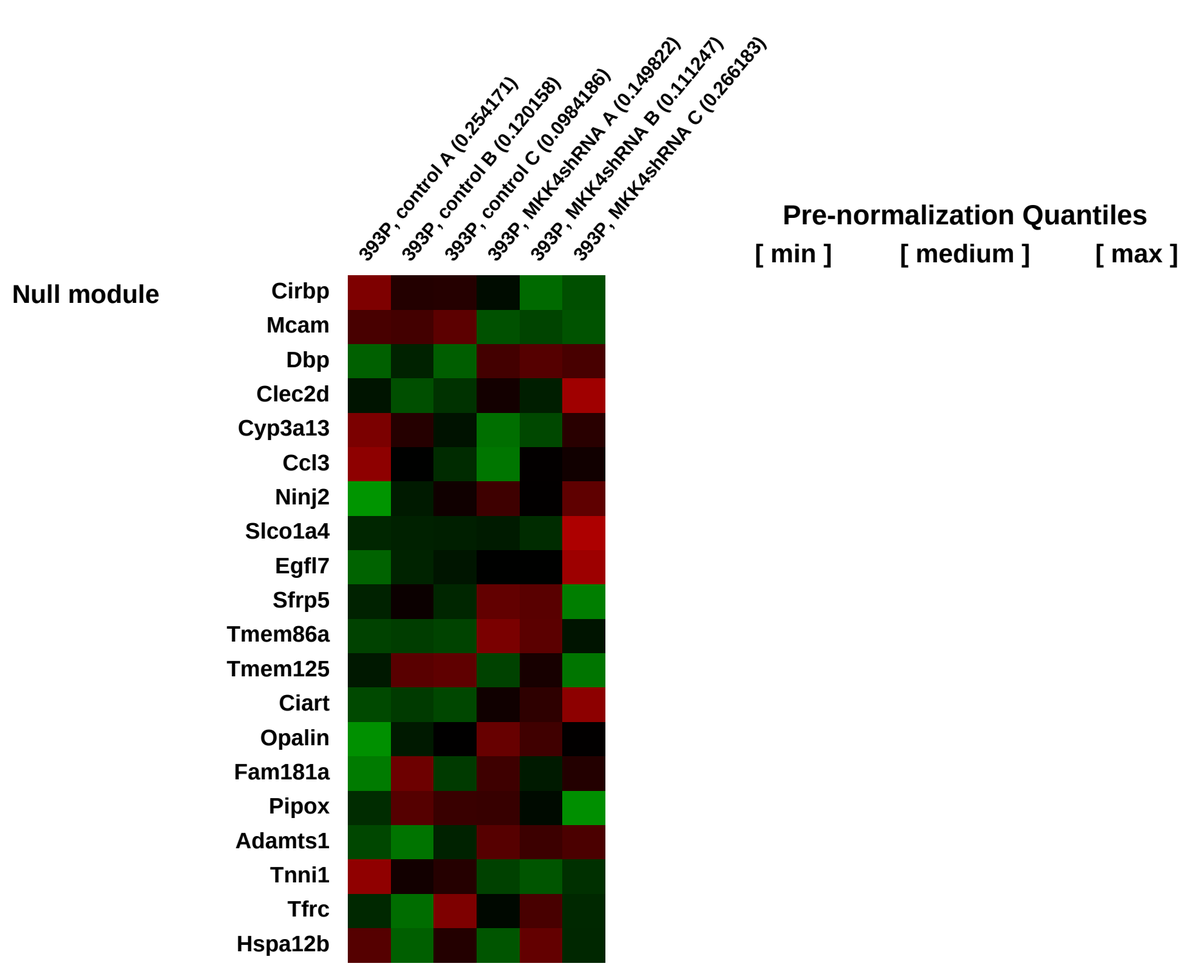

GEO Series "GSE19181" Expression Profiles

Num of samples in this series: 6

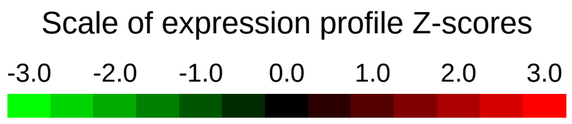

GEO Link:	http://www.ncbi.nlm.nih.gov/geo/query/acc.cgi?acc=GSE19181
Status:	Public on Dec 23 2010
Title:	Expression data from macroH2A shRNA lines
Organism:	Mus musculus
Experiment type:	Expression profiling by array
Platform:	GPL1261
Pubmed ID:	21179167
Summary & Design:	**Summary:** Cancer is a disease of both genetic and epigenetic changes. While increasing evidence demonstrates that oncogenic progression entails chromatin-mediated changes such as DNA methylation, the role of histone variants in cancer initiation and progression currently remains unexplored. Here, we report that the histone variant macroH2A (mH2A) suppresses tumour progression of malignant melanoma. We hypothesized that loss of mH2A could contribute to melanoma progression by relieving repression of cell cycle- and metastasis-related genes. To gain insight into the transcriptional state of mH2A1 and mH2A2-deficient cells, we examined their gene expression profiles using Affymetrix microarrays. **Overall design:** Murine B16-F1 cells with lentiviral shRNAs against mH2A1 and mH2A2 were generated along with control shRNA (against GFP) and used for the microarray analysis. Two independent biological replicates were used.

Background corr dist: KL-Divergence = 0.0449, L1-Distance = 0.0241, L2-Distance = 0.0007, Normal std = 0.5998

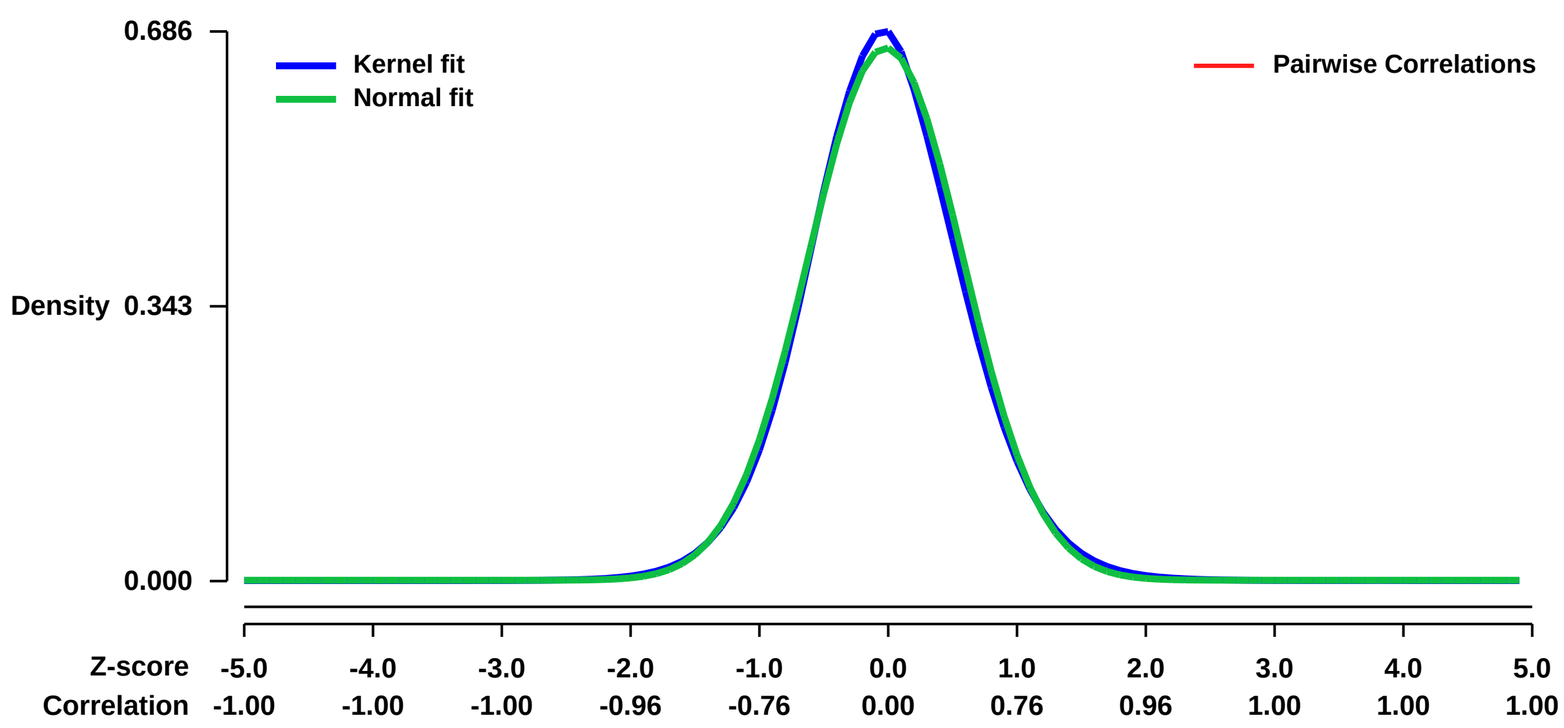

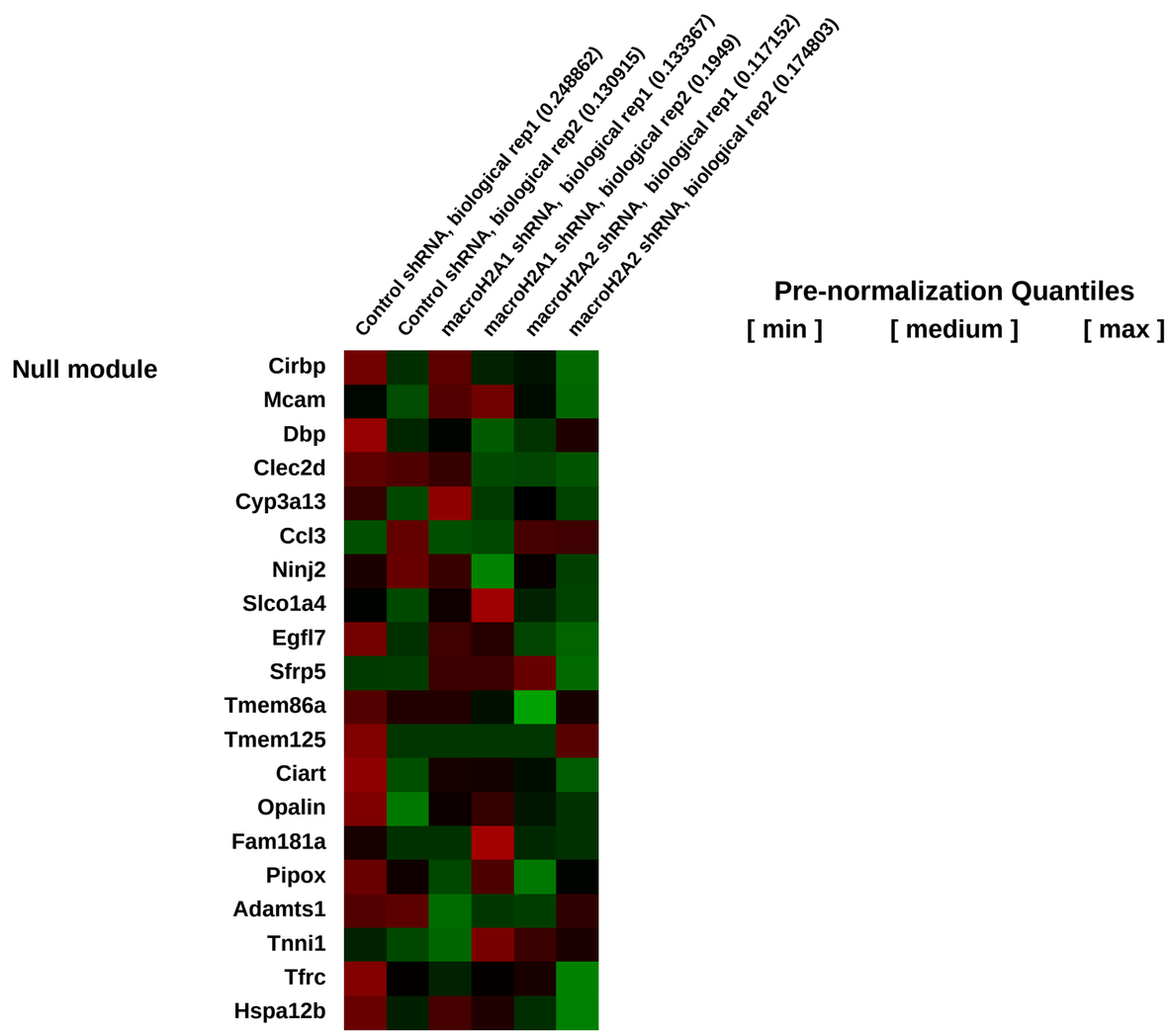

GEO Series "GSE19194" Expression Profiles

Num of samples in this series: 14

Scale of expression profile Z-scores

-3.0 -2.0 -1.0 0.0 1.0 2.0 3.0

GEO Link:	http://www.ncbi.nlm.nih.gov/geo/query/acc.cgi?acc=GSE19194
Status:	Public on Mar 31 2010
Title:	Cbfb/Runx1-repression independent blockage of differentiation and accumulation of Csf2rb expressing cells by Cbfb-MYH11
Organism:	Mus musculus
Experiment type:	Expression profiling by array
Platform:	GPL1261
Pubmed ID:	20007544
Summary & Design:	**Summary:** It is known that CBFB-MYH11, the fusion gene generated by inversion of chromosome 16 in human acute myeloid leukemia, is causative for oncogenic transformation. However, the mechanism by which CBFB-MYH11 initiates leukemogenesis is not clear. Previously published reports showed that CBFB-MYH11 dominantly inhibits RUNX1 and CBFB, and such inhibition has been suggested as the mechanism for leukemogenesis. However, knockin mice expressing Cbfb-MYH11 (Cbfb+/MYH11) showed defects in primitive hematopoiesis not seen in Cbfb null (Cbfb-/-) embryos indicating that Cbfb-MYH11 has repression independent activities as well. To identify gene expression changes associated with this novel activity, we compared the gene expression profile in the blood cells of Cbfb+/MYH11 and Cbfb-/- embryonic day 12.5 (E12.5) embryos with that of their wildtype littermates. **Overall design:** Cbfb-MYH11 chimeras were mated to C57/Bl6 females to generate Cbfb+/MYH11 (Cbfb+/MYH11) and Cbfb+/+ (WT) embryos. Cbfb+/- x Cbfb+/- matings were used to generate Cbfb+/+ (Cbfb+/+) and Cbfb-/- (Cbfb-/-) embryos. Blood from 8-10 E12.5 embryos of the same genotype was pooled, and RNA was isolated, labeled, and hybridized to Affymetrix Genechip mouse microarray (430 2.0) chips. 4 chips were used for both the Cbfb+/MYH11 and littermate control samples. 3 chips were used for the Cbfb-/- samples and littermate control samples.

Background corr dist: KL-Divergence = 0.0464, L1-Distance = 0.0796, L2-Distance = 0.0113, Normal std = 0.6373

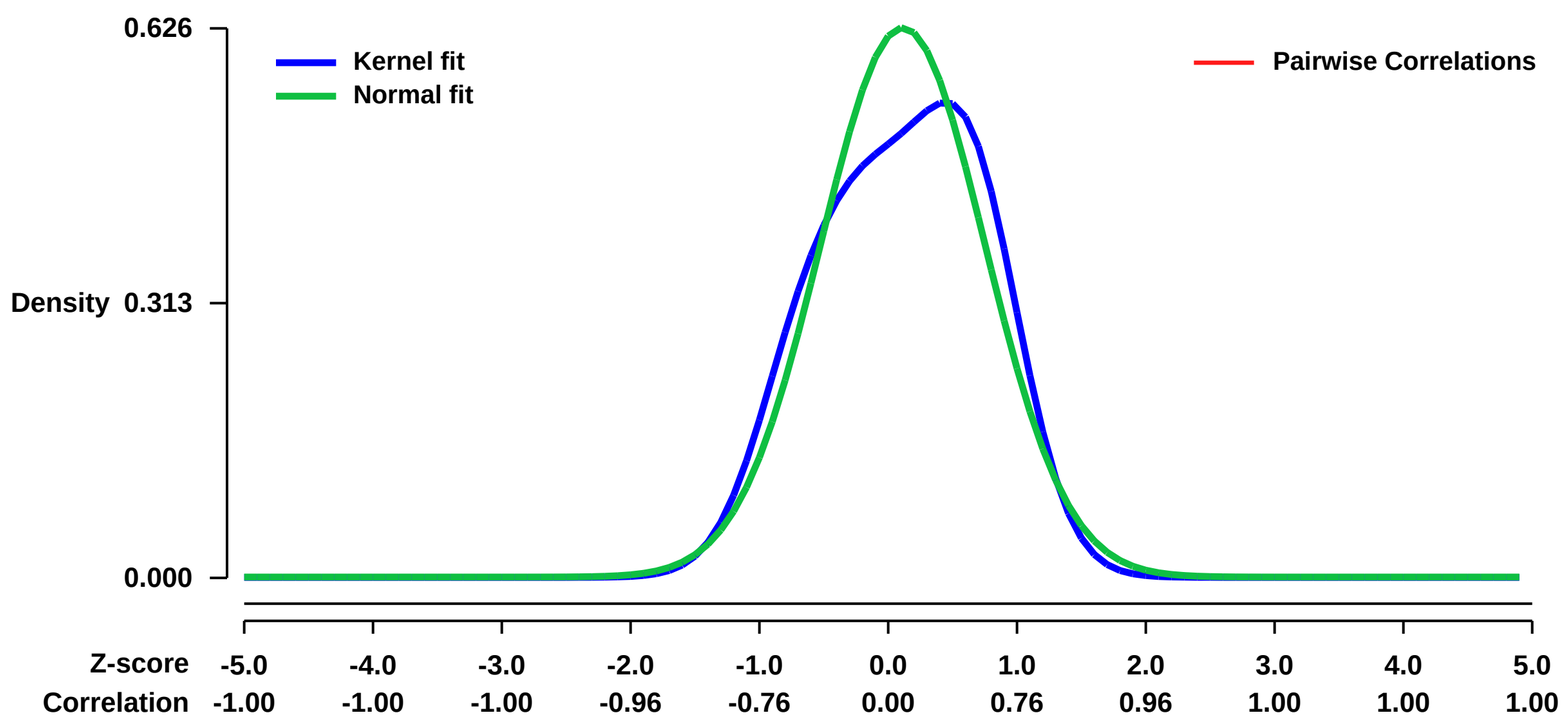

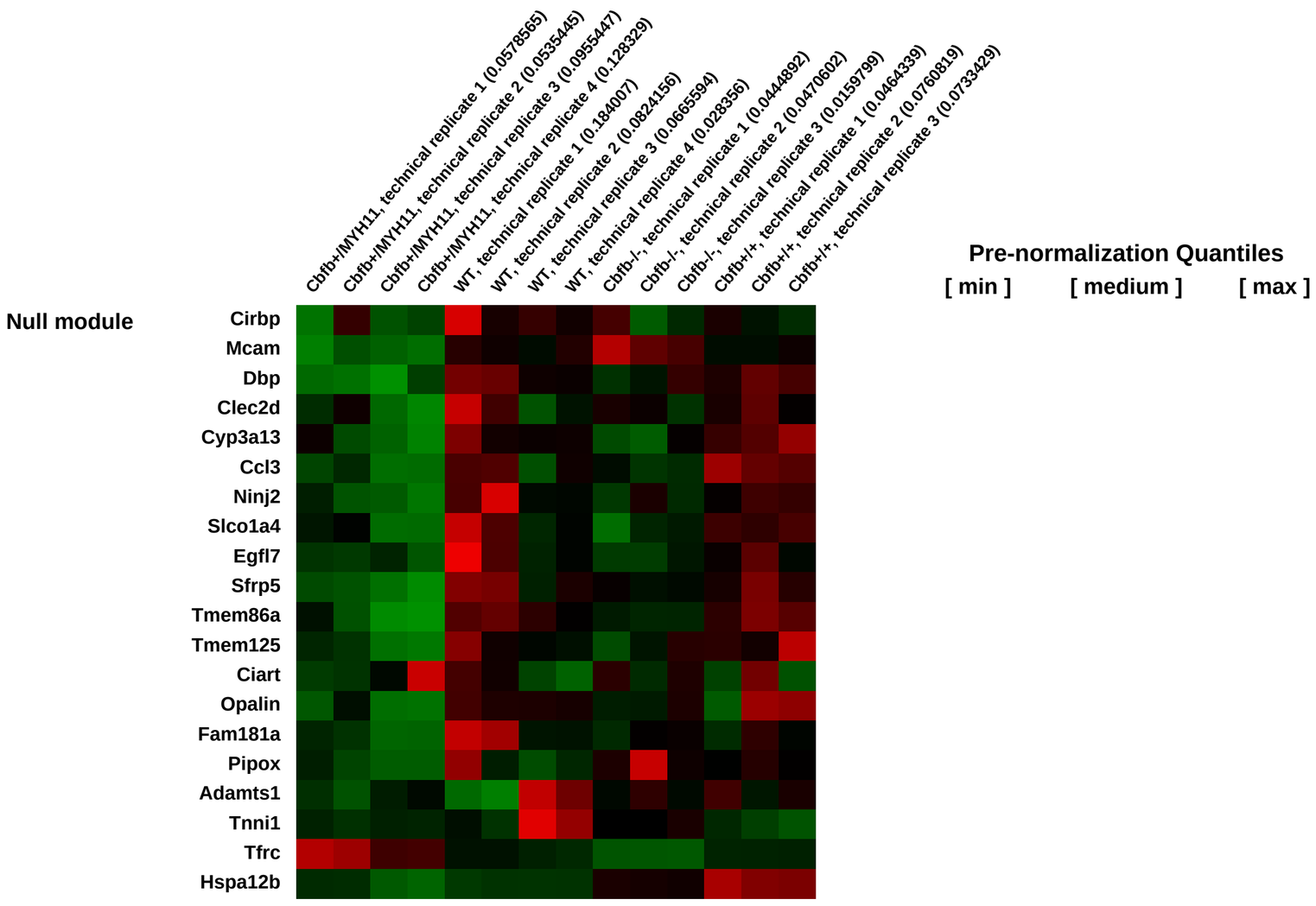

GEO Series "GSE19204" Expression Profiles

Num of samples in this series: 6

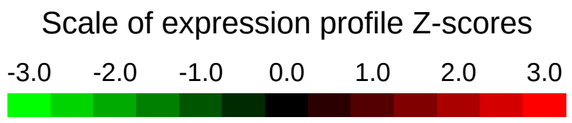

GEO Link:	http://www.ncbi.nlm.nih.gov/geo/query/acc.cgi?acc=GSE19204
Status:	Public on Feb 25 2010
Title:	Foxa2 programs Th2-cell mediated innate immunity in the developing lung.
Organism:	Mus musculus
Experiment type:	Expression profiling by array
Platform:	GPL1261
Pubmed ID:	20483781
Summary & Design:	**Summary:** Deletion of the gene encoding Foxa2, a winged helix transcription factor selectively expressed in respiratory epithelial cells, caused spontaneous pulmonary eosinophilic inflammation and goblet cell metaplasia. Loss of Foxa2 induced the recruitment and activation of myeloid dendritic cells (mDCs) and Th2 cells in the lung, and was associated with the increased production of T helper 2 (Th2) cytokines and chemokines. mRNA microarray analysis demonstrated that deletion of Foxa2 induced the expression of a number of mRNAs regulating pulmonary dendritic cell activation, Th2 mediated inflammation, and goblet cell differentiation. The spontaneous pulmonary inflammation and goblet cell metaplasia caused by loss of Foxa2 was inhibited by treatment of newborn Foxa2â /â mice with monoclonal IL-4Ralpha antibody. Expression of Foxa2 in non-ciliated secretory cells (Clara cells) in vivo inhibited goblet cell differentiation induced by pulmonary allergen exposure. The respiratory epithelium plays a central role in the regulation of Th2-mediated inflammation and innate immunity in the developing lung in a process regulated by Foxa2. **Overall design:** To investigate the role of Foxa2 and its downstream targets associated with the Th2 inflammation and goblet cell hyperplasia, RNAs were isolated from the lungs of Foxa2-/- and control littermates at PN15. Lung cRNA was hybridized to the murine genome MOE430 V2 chips.

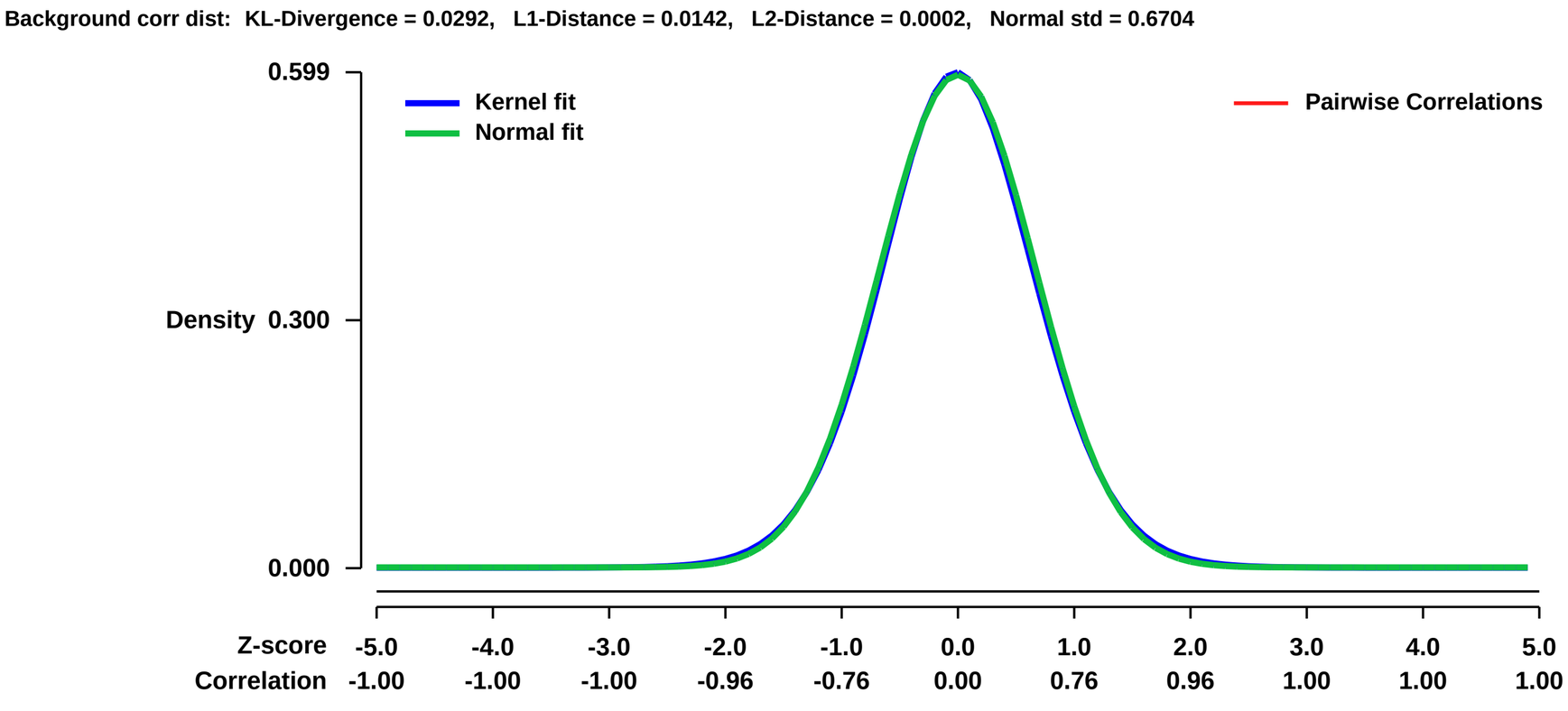

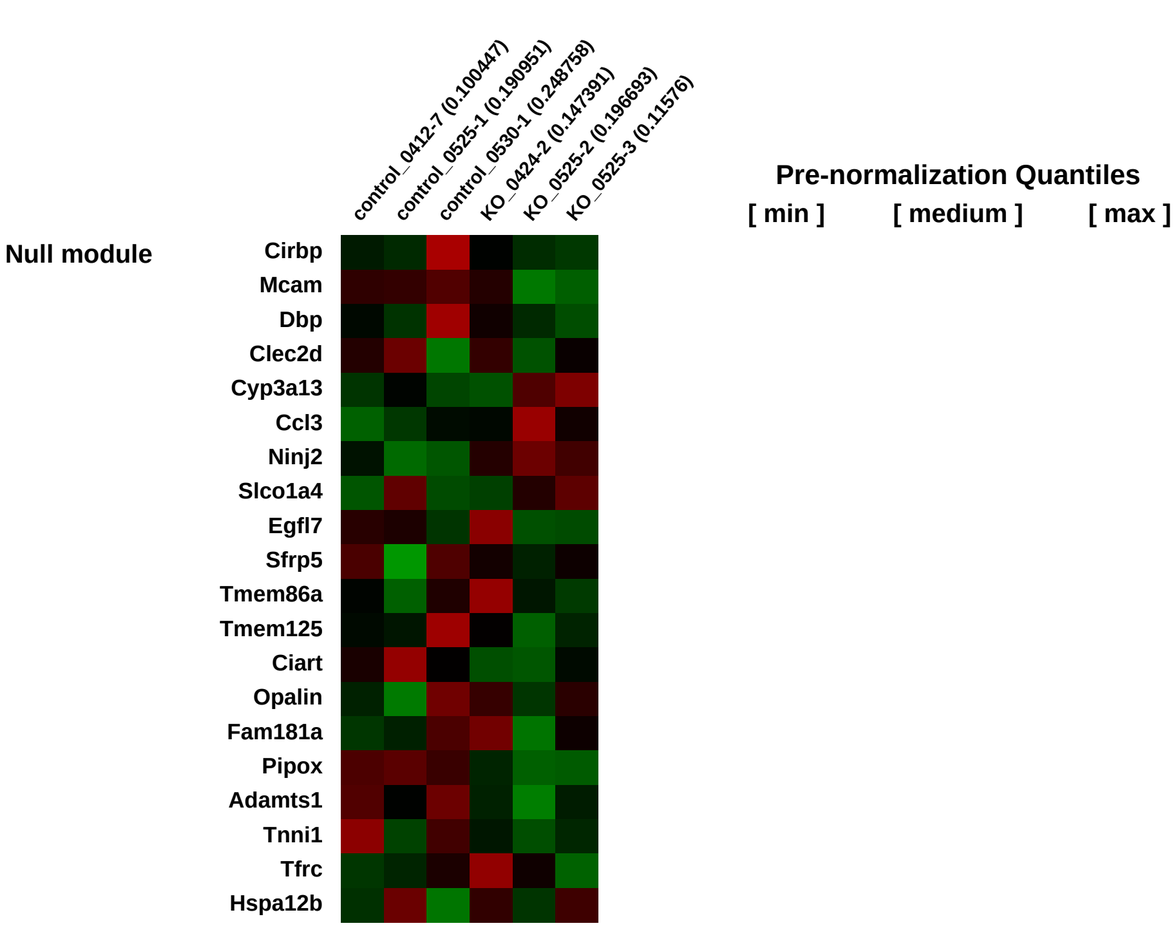

GEO Series "GSE19299" Expression Profiles

Num of samples in this series: 6

Scale of expression profile Z-scores

-3.0 -2.0 -1.0 0.0 1.0 2.0 3.0

GEO Link:	http://www.ncbi.nlm.nih.gov/geo/query/acc.cgi?acc=GSE19299
Status:	Public on Dec 04 2009
Title:	Expression data with mouse osteoblast cell from wild-type and retinoblastoma tumor suppressor(Rb) knock-out.
Organism:	Mus musculus
Experiment type:	Expression profiling by array
Platform:	GPL1261
Pubmed ID:	21085651
Summary & Design:	**Summary:** Here we report the characterization of a novel role for the retinoblastoma protein (pRb) as a regulator of osteoblast adhesion. Abrogation of pRb in osteoblasts resulted in aberrant cadherin expression and loss of adherens junctions. This produced defects suggestive of a transformed phenotype such as impaired cell-to-cell adhesion, loss of contact-dependent growth arrest, and the capacity to evade anoikis. This also resulted in profound abnormalities in bone structure. Consistent with this, microarray analyses showed that pRb regulates a wide repertoire of osteoblast cell adhesion genes. In addition, pRb loss also resulted in altered expression and function of several known regulators of cellular adhesion and adherens junction assembly, such as the Rho GTPase Rac1 and the merlin tumor suppressor. Taken together, our results show that pRb controls cell adhesion by regulating the expression and adherens junction components and by regulating the function of molecules involved in adherens junction assembly and stability. Microarray results helped us to portrait the overall influence on cell adhesion via both individual genes and pathway analysis. **Overall design:** MC3T3 cells were obtained from immortalizing primary cultured mouse osteoblast cells by using 3T3 protocol. There are 3 biological replicates for each group, 6 samples in total were analyzed.

Background corr dist: KL-Divergence = 0.0176, L1-Distance = 0.0417, L2-Distance = 0.0018, Normal std = 0.8480

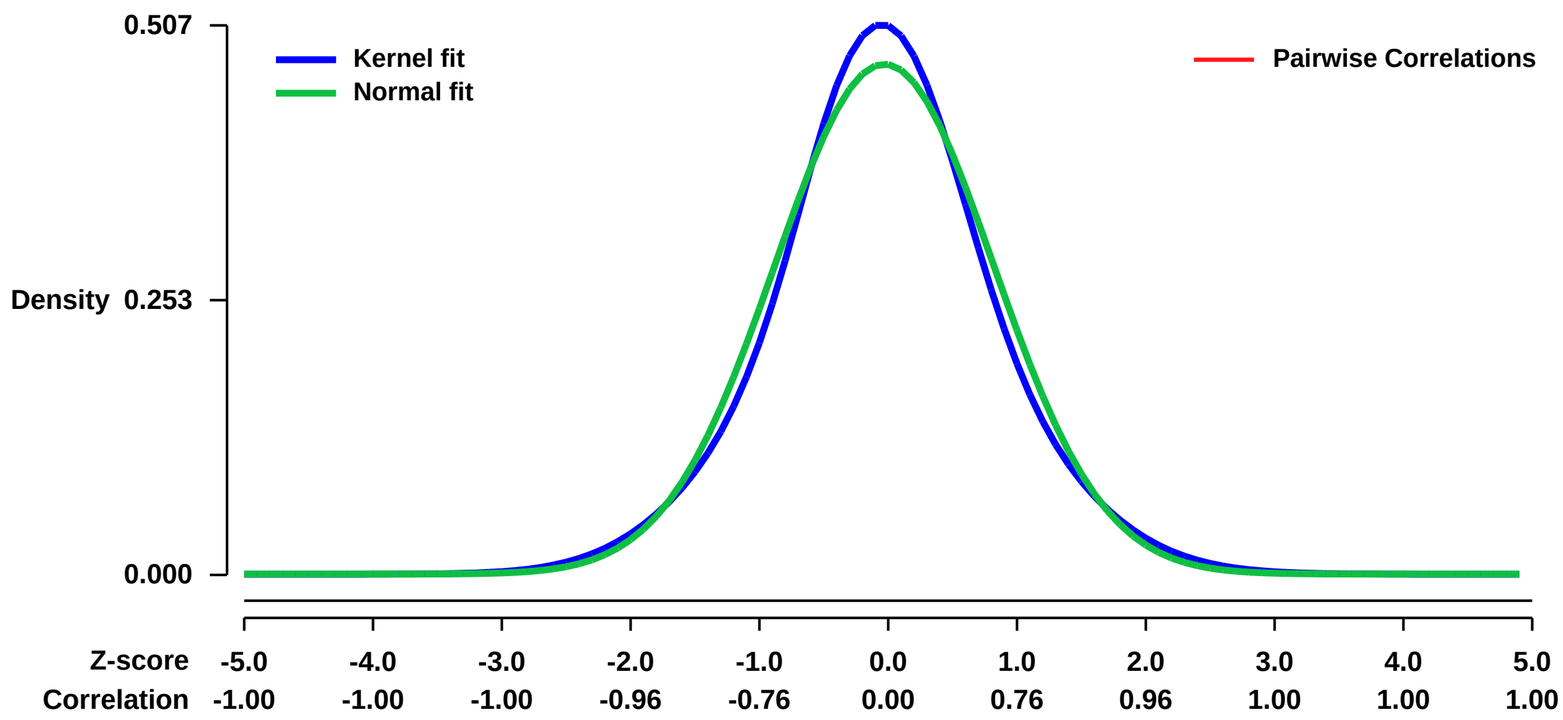

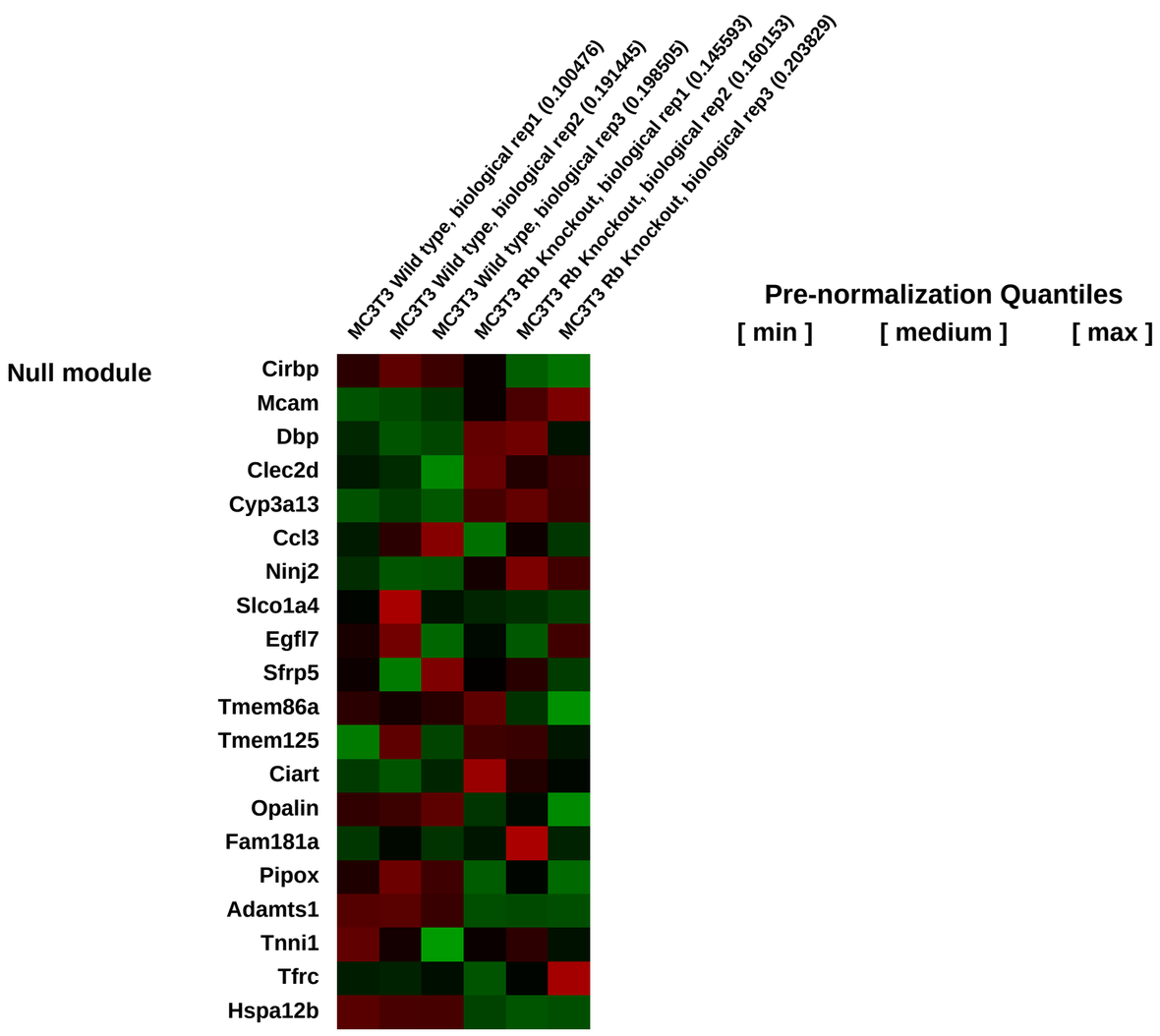

GEO Series "GSE19355" Expression Profiles

Num of samples in this series: 6

Scale of expression profile Z-scores

-3.0 -2.0 -1.0 0.0 1.0 2.0 3.0

GEO Link:	http://www.ncbi.nlm.nih.gov/geo/query/acc.cgi?acc=GSE19355
Status:	Public on May 03 2010
Title:	Silencing of mrhl non coding RNA in mouse spermatoginial cells GC1-Spg
Organism:	Mus musculus
Experiment type:	Expression profiling by array
Platform:	GPL1261
Pubmed ID:	22665494
Summary & Design:	**Summary:** Mrhl is a non coding RNA identified from mouse chromosome 8. It is a 2.4kb poly adenylated, nuclear restricted RNA expressed in multiple tissues. The 2.4 kb RNA also undergoes a nuclear processing event mediated through Drosha that generates an 80nt intermediate RNA. This study was aimed at understanding the functiion of mrhl by silencing the mrhl RNA in the mouse spermatogonial cells using a pool of siRNAs targeted against the mrhl and analyse the global gene expression change using Affymetrix mouse expression array. The mRNAs that showed significant change in expression in mrhl siRNA treated cells against control were studied further for their biological significance with respect to mrhl silencing. **Overall design:** The mouse spermatogonial cells that were either mock silenced using scrambled siRNA or silenced using siRNAs against mrhl were harvested at 44hrs post transfection. The silencing efficiency was checked by realtime quantitative PCR and was found be almost 80% in all three independent experiments.The total RNA was extracted using Trizol and was taken further for microarray expriment. All the subsequent steps were according to the Affymetrix protocol. Gene expression was profiled for control and mrhl silenced cells.

Background corr dist: KL-Divergence = 0.0351, L1-Distance = 0.0184, L2-Distance = 0.0003, Normal std = 0.6402

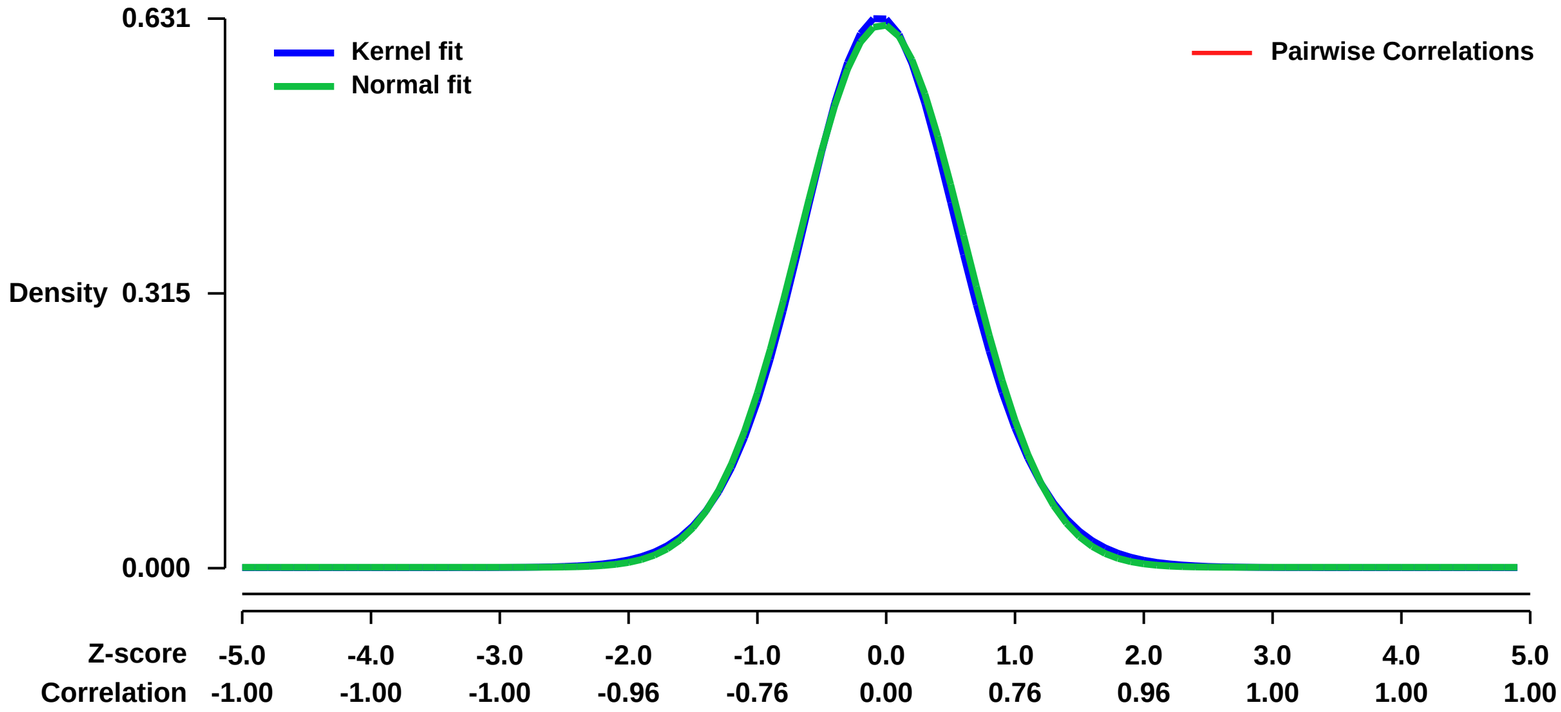

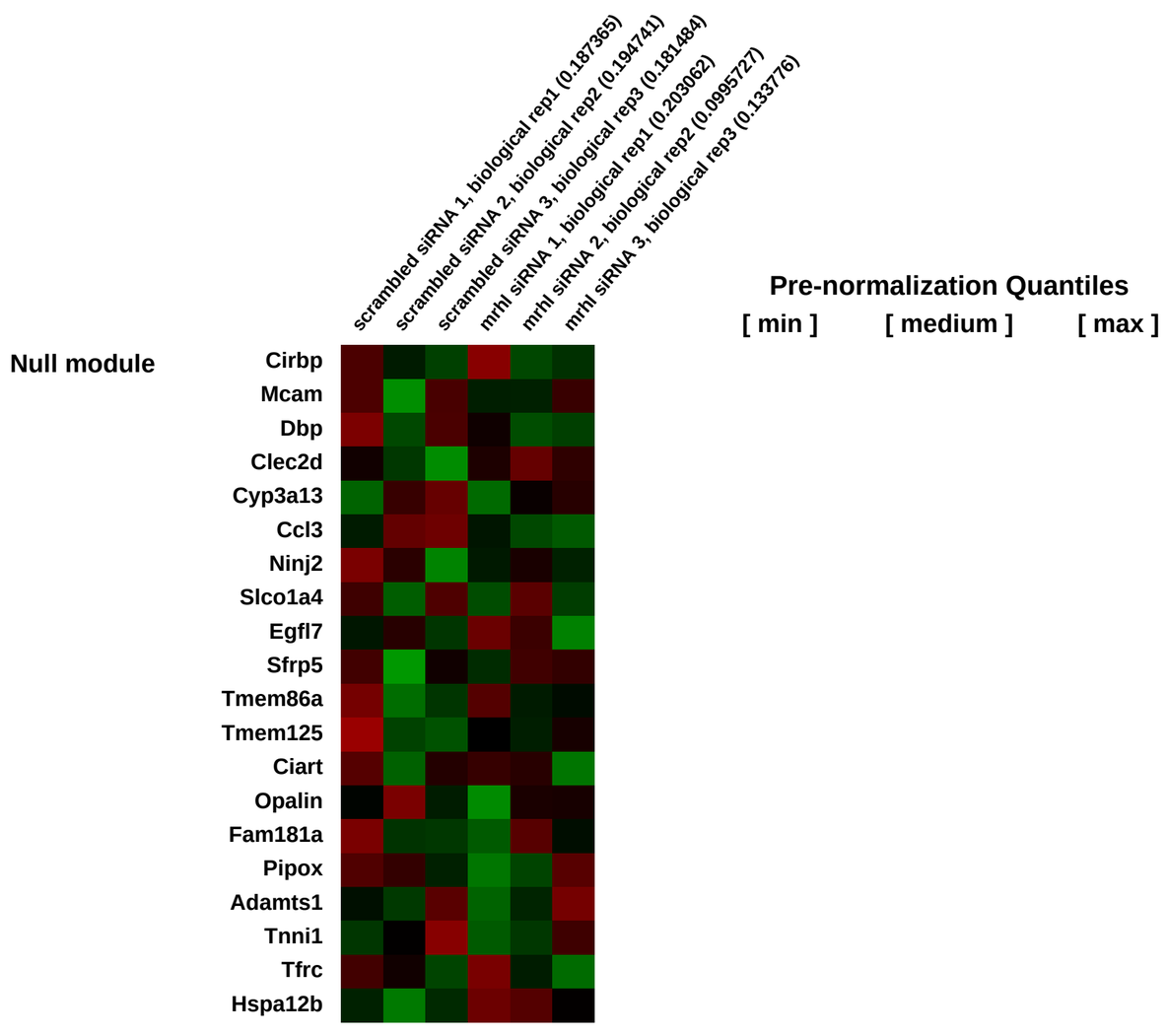

GEO Series "GSE19369" Expression Profiles

Num of samples in this series: 8

Scale of expression profile Z-scores

-3.0 -2.0 -1.0 0.0 1.0 2.0 3.0

GEO Link: http://www.ncbi.nlm.nih.gov/geo/query/acc.cgi?acc=GSE19369

Status: Public on Sep 13 2010

Title: Stimulatory effect of Echinacea purpurea extract on trafficking activity in mouse dendritic cells

Organism: Mus musculus

Experiment type: Expression profiling by array

Platform: GPL1261

Pubmed ID:

Summary & Design:

Summary:
To seek scientific evidence supporting therapeutic use of Echinacea, the transcriptomic effects of Echinacea purpurea extract on mouse bone marrow-derived dendritic cells (BMDCs) were analyzed using primary cultures. Affymetrix DNA microarray and bioinformatics analyses of genes differentially expressed in DCs treated with [BF/S+L/Ep] for 4 or 12 h revealed that the majority of responsive genes were related to cell adhesion or motility (Cdh10, Itga6, Cdh1, Gja1 and Mmp8), or were chemokines (Cxcl2, Cxcl7) or signaling molecules (Nrxn1, Pkce and Acss1).

Overall design:
BMDCs from mice were treated with [BF/S+L/Ep] or DMSO for 4 h or 12 h in duplicates.

Background corr dist: KL-Divergence = 0.0782, L1-Distance = 0.0197, L2-Distance = 0.0006, Normal std = 0.4830

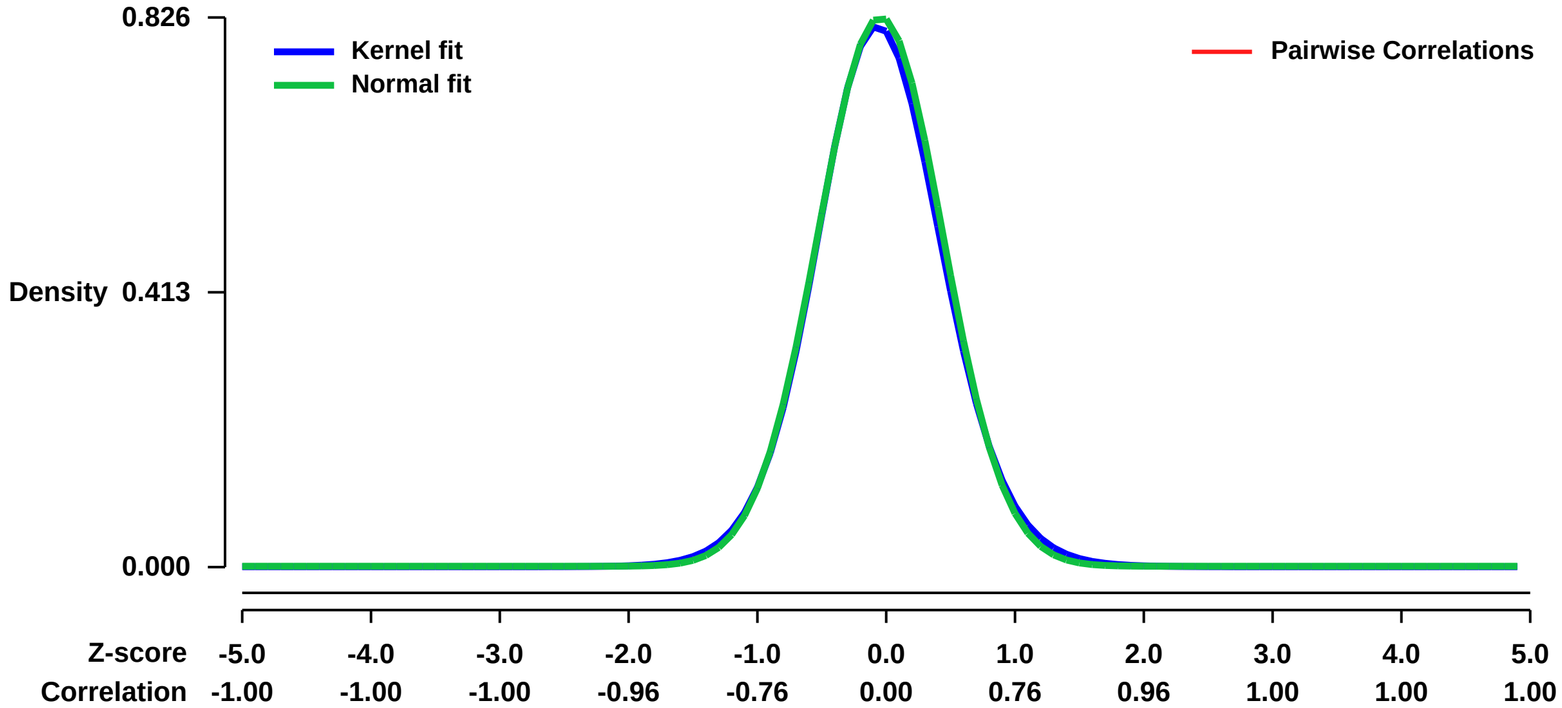

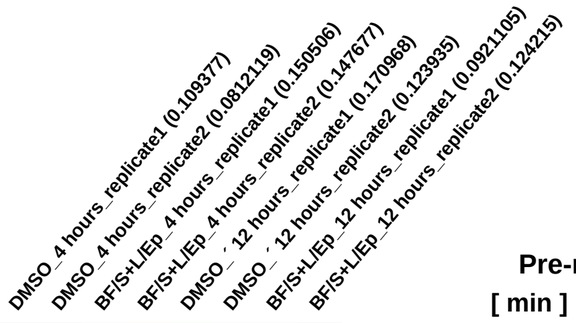

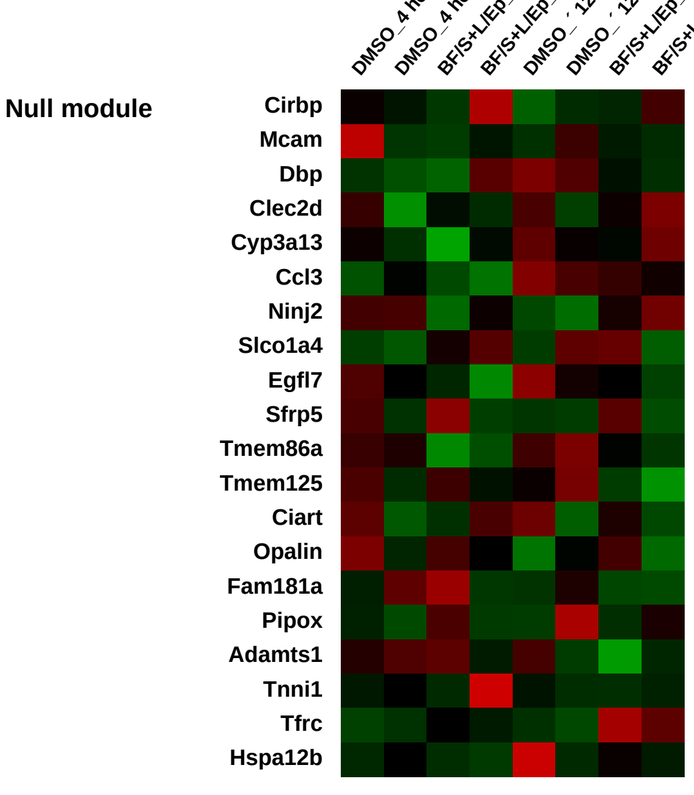

GEO Series "GSE19403" Expression Profiles

Num of samples in this series: 12

Scale of expression profile Z-scores

-3.0 -2.0 -1.0 0.0 1.0 2.0 3.0

GEO Link:	http://www.ncbi.nlm.nih.gov/geo/query/acc.cgi?acc=GSE19403
Status:	Public on Dec 10 2009
Title:	Dysregulation of the Wnt pathway inhibits timely myelination and remyelination in the mammalian CNS
Organism:	Mus musculus
Experiment type:	Expression profiling by array
Platform:	GPL1261
Pubmed ID:	21706018
Summary & Design:	**Summary:** The progressive loss of CNS myelin in patients with multiple sclerosis (MS) has been proposed to result from the combined effects of damage to oligodendrocytes and failure of remyelination. A common feature of demyelinated lesions is the presence of oligodendrocyte precursors (OLPs) blocked at a premyelinating stage. However, the mechanistic basis for inhibition of myelin repair is incompletely understood. To identify novel regulators of OLP differentiation, potentially dysregulated during repair, we performed a genome-wide screen of 1040 transcription factor-encoding genes expressed in remyelinating rodent lesions. We report that â…50 transcription factor-encoding genes show dynamic expression during repair and that expression of the Wnt pathway mediator Tcf4 (aka Tcf7l2) within OLPs is specific to lesionedâ but not normalâ adult white matter. We report that ¸†-catenin signaling is active during oligodendrocyte development and remyelination in vivo. Moreover, we observed similar regulation of Tcf4 in the developing human CNS and lesions of MS. Data mining revealed elevated levels of Wnt pathway mRNA transcripts and proteins within MS lesions, indicating activation of the pathway in this pathological context. We show that dysregulation of Wntâ¸†-catenin signaling in OLPs results in profound delay of both developmental myelination and remyelination, based on (1) conditional activation of ¸†-catenin in the oligodendrocyte lineage in vivo and (2) findings from APCMin mice, which lack one functional copy of the endogenous Wnt pathway inhibitor APC. Together, our findings indicate that dysregulated Wntâ¸†-catenin signaling inhibits myelination/remyelination in the mammalian CNS. Evidence of Wnt pathway activity in human MS lesions suggests that its dysregulation might contribute to inefficient myelin repair in human neurological disorders. **Overall design:** 12 samples total. Two variables in the experiment: genotype (wild type or Olig2cre/DA-Cat) and Developmental stage (Day 4 or Day 15). 4 phenotypes in total with 3 biological replicates for each phenotype.

Background corr dist: KL-Divergence = 0.0423, L1-Distance = 0.0614, L2-Distance = 0.0055, Normal std = 0.6512

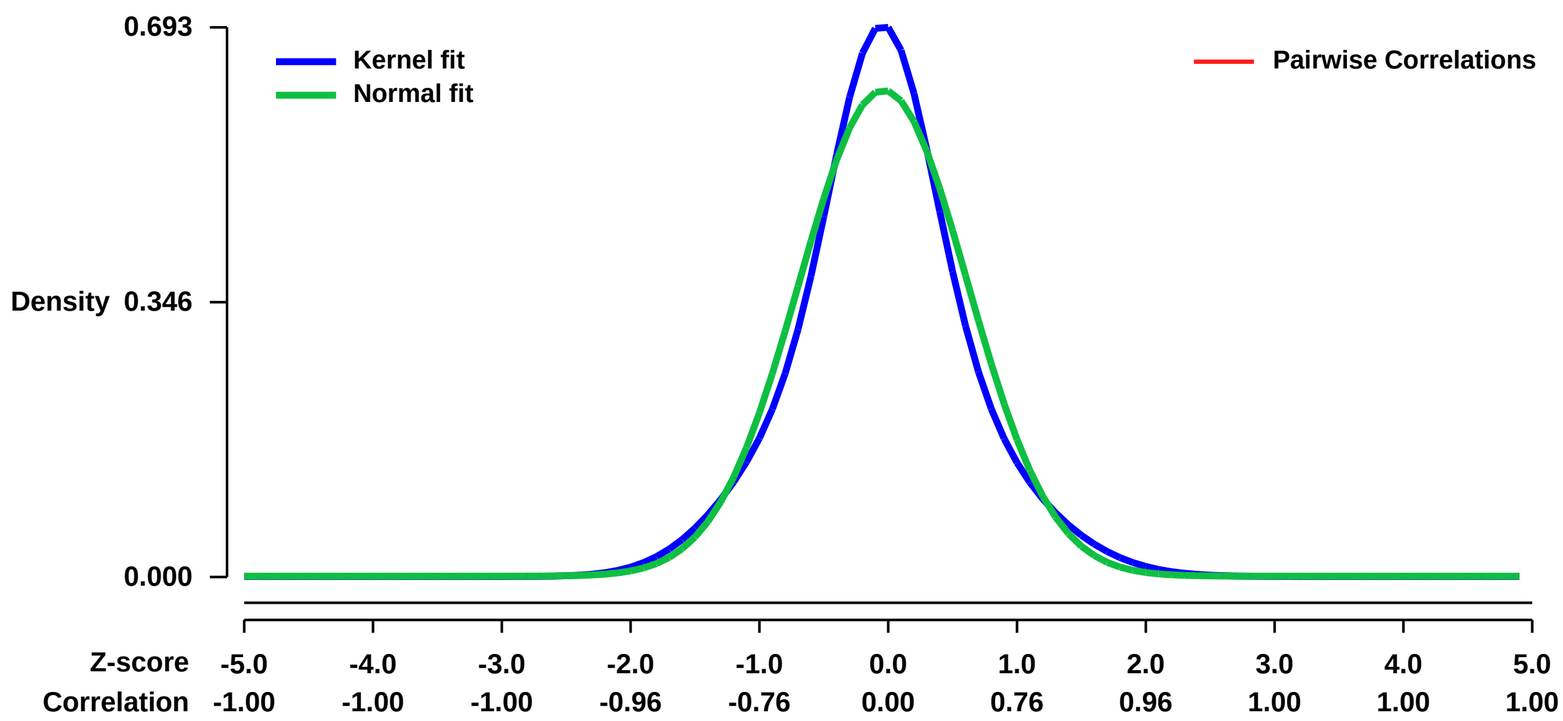

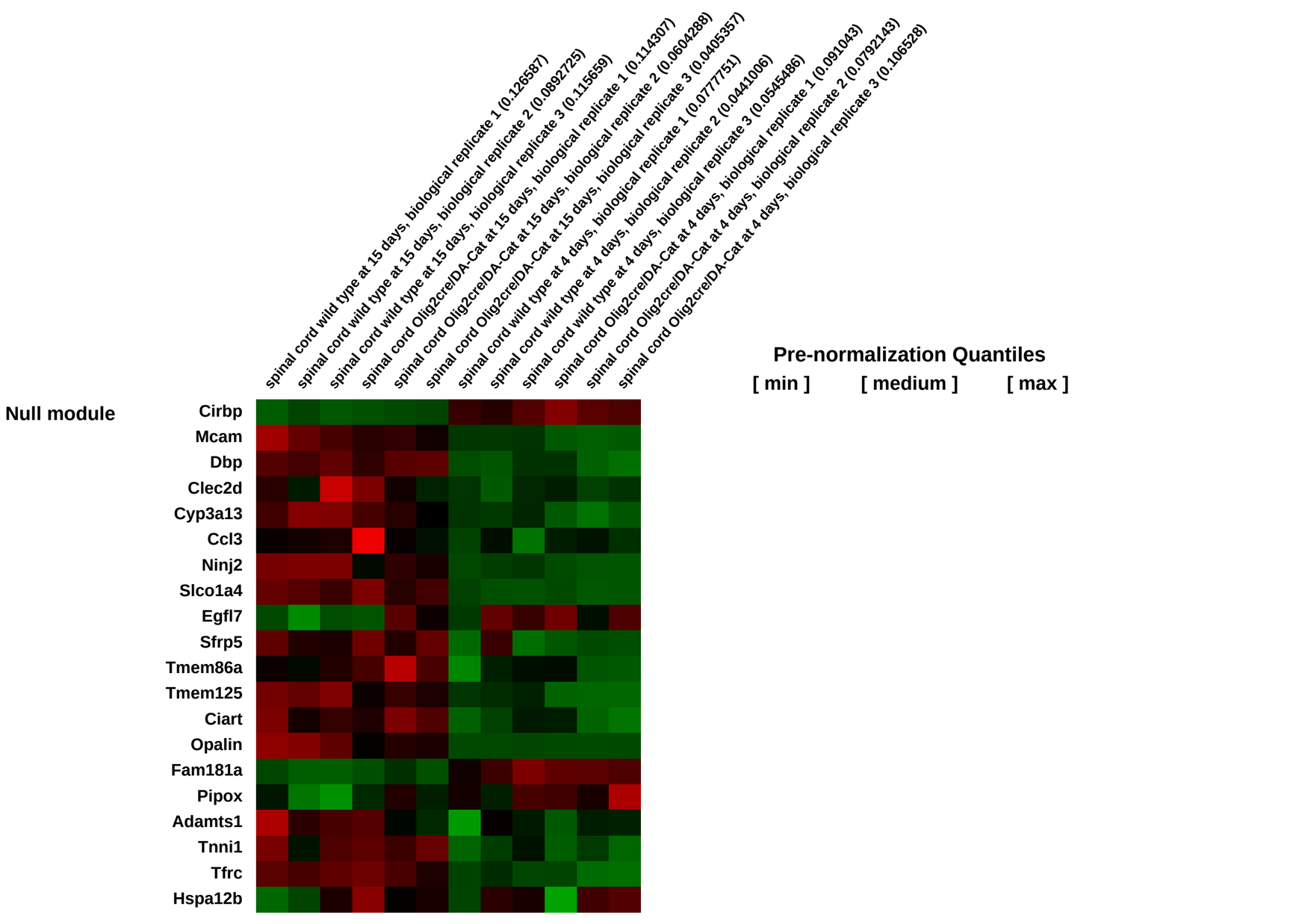

GEO Series "GSE19436" Expression Profiles

Num of samples in this series: 8

Scale of expression profile Z-scores

-3.0 -2.0 -1.0 0.0 1.0 2.0 3.0

GEO Link:	http://www.ncbi.nlm.nih.gov/geo/query/acc.cgi?acc=GSE19436
Status:	Public on Apr 01 2010
Title:	Transcriptional alterations in cycling neural stem cells underlying alcohol use disorders
Organism:	Mus musculus
Experiment type:	Expression profiling by array
Platform:	GPL1261
Pubmed ID:	23095216
Summary & Design:	**Summary:** Ethanol inhibits the proliferation of neural stem cells in the fetal, adolescent, and adult brain. The consequences are cognitive deficits associated with fetal alcohol spectrum disorder and alcohol use disorder. We tested the hypothesis that ethanol affects progression through cell cycle checkpoints by differentially modifying transcriptional processes. Monolayer cultures of NS-5 neural stem cells were treated for 48 hr with the mitogenic agent FGF2 or the anti-mitogenic TGF¸†1 in the absence or presence of ethanol. Cell cycle elongation was induced by a global down-regulation of genes involved in cell cycle progression, including the cyclin E system. Checkpoint regulation occurred downstream of p21 and Jun-oncogene signaling cascades. Thus, ethanol can affect cell cycle progression by altering transcript expression of strategic genes downstream of the G1/S checkpoint. **Overall design:** NS5 neural stem cells were grown in Euromed Media supplemented with N2 and glutamine. Cells were plated on poly-ornathine and laminin in the presence of FGF2 (10 ng/ul) and EGF (10 ng/ul) for 24 hrs. Media was removed, cells were rinsed, and placed in growth factor free conditions for 4 hrs. NS5 cells were then exposed to one of four treatment for 48 hrs: FGF2 (10 ng/ul) only, FGF2 (10 ng/ul) and ethanol (400 mg/dl), TGF-beta1 (10 ng/ul) only, or TGF-beta1 (10 ng/ul) and ethanol (400 mg/dl). Total RNA was collected immediately following treatment.

Background corr dist: KL-Divergence = 0.0738, L1-Distance = 0.0276, L2-Distance = 0.0013, Normal std = 0.4934

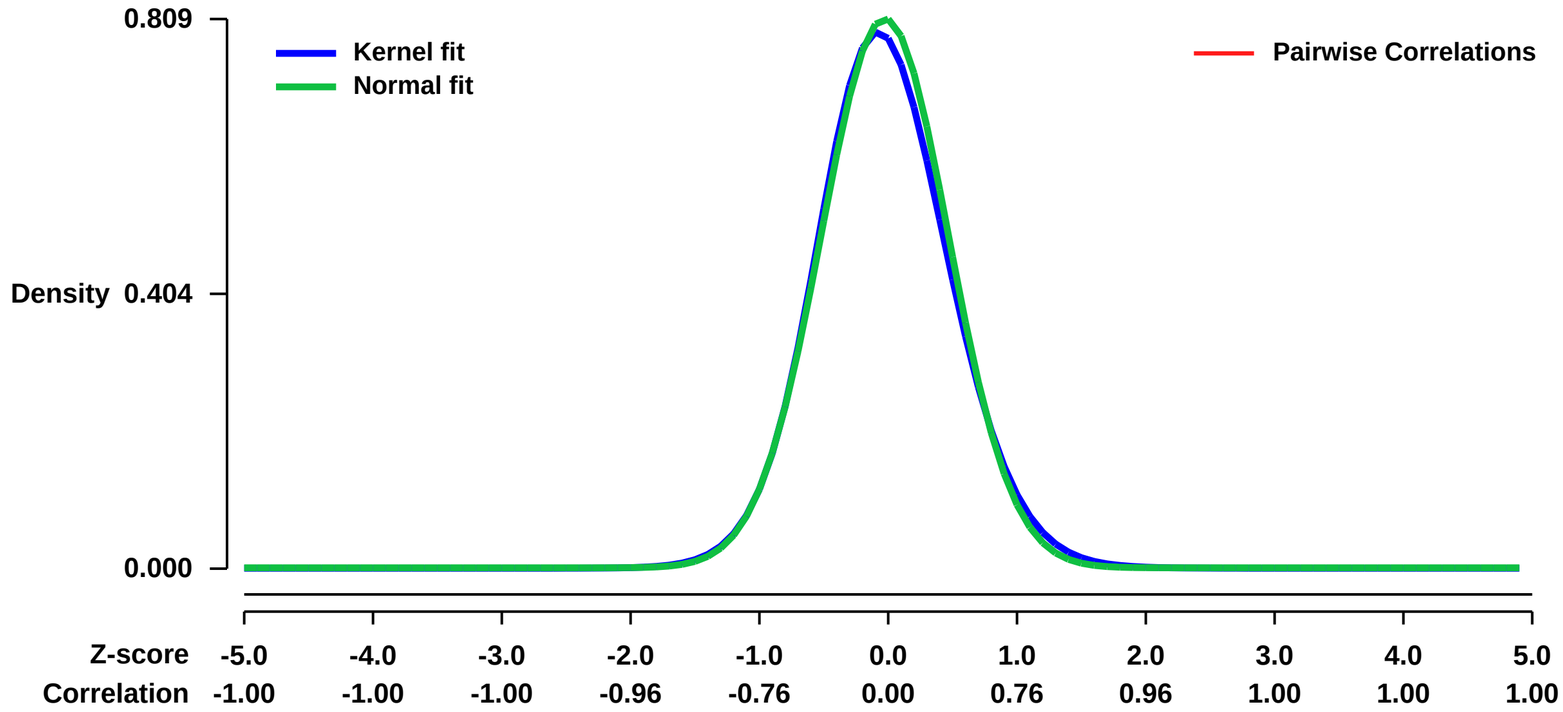

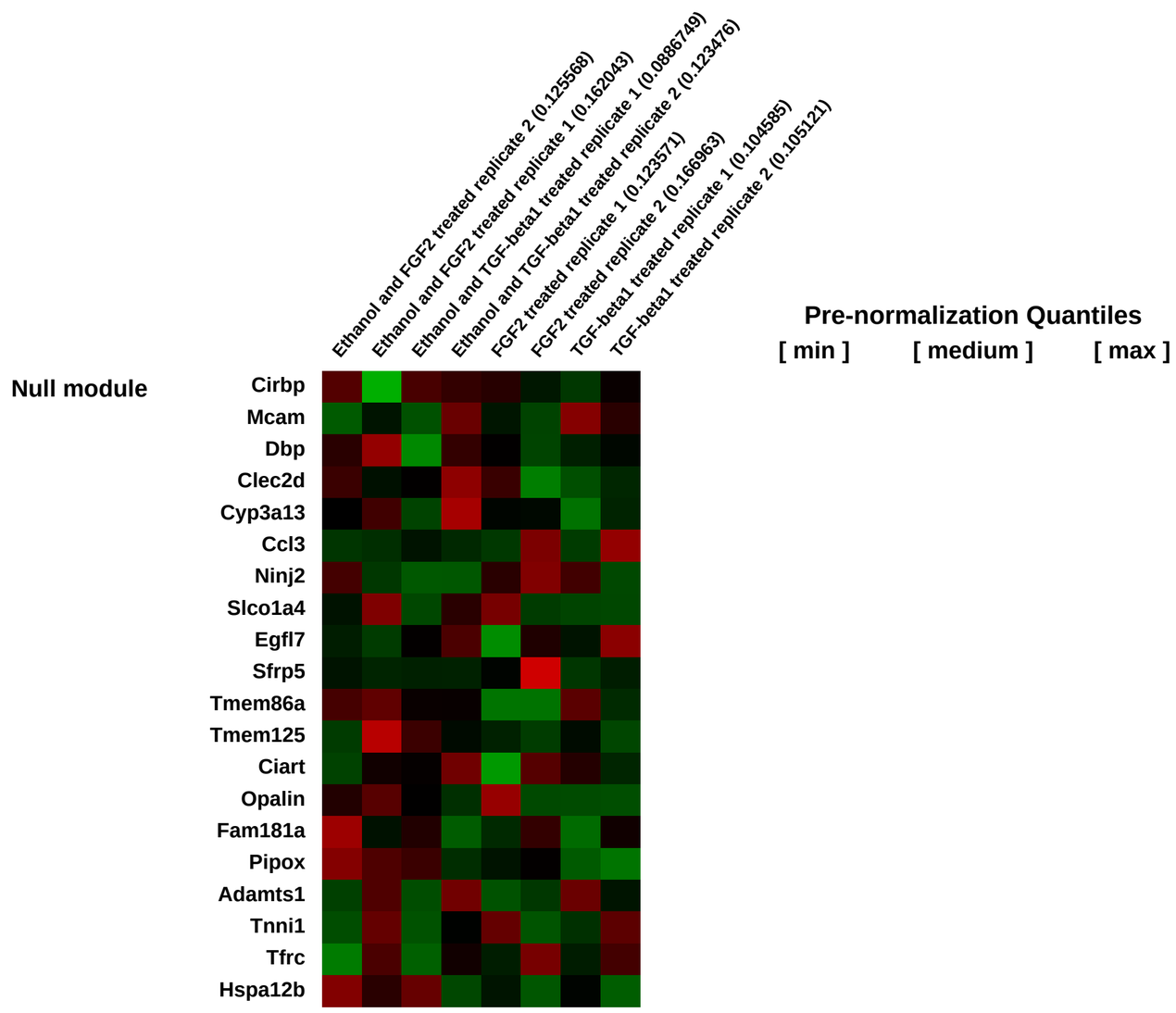

GEO Series "GSE19474" Expression Profiles

Num of samples in this series: 12

Scale of expression profile Z-scores

-3.0 -2.0 -1.0 0.0 1.0 2.0 3.0

GEO Link:	http://www.ncbi.nlm.nih.gov/geo/query/acc.cgi?acc=GSE19474
Status:	Public on Dec 16 2009
Title:	Expression data from E12.5 ePet-EYFP rostral and caudal serotonin (5HT) neurons purified by flow cytometry
Organism:	Mus musculus
Experiment type:	Expression profiling by array
Platform:	GPL1261
Pubmed ID:	20071532
Summary & Design:	**Summary:** The 5HT system is organized into rostral and caudal populations with discrete anatomical locations and opposite axonal trajectories in the developing hindbrain. 5HT neuron cell bodies in the rostral subdivision migrate to the midbrain and pons and extend ascending projections throughout the forebrain. 5HT cell bodies in the caudal subdivision migrate to the ventral medulla and caudal half of the pons and provide descending projections to the brainstem and spinal cord. **Overall design:** We used microarrays to determine genes expressed by both rostral and caudal 5HT neurons as well as genes that are differentially expressed between rostral and caudal 5HT neurons at E12.5 when axon pathfinding and cell migration are underway. E12.5 neural tubes were isolated from ePet-EYFP embryos and dissected into a rostral domain (mesecephalic flexure to pontine flexure) and a caudal domain (pontine flexure to spinal cord). After cell dissociation (details under growth protocol), cells were subjected to fluorescent activated cell sorting (FACS) to obtain 4 cell populations. R+ = rostral ePetEYFP positive 5HT neurons; R- = YFP negative non-serotonergic cells in the rostral neural tube; C+ = caudal ePetEYFP positive 5HT neurons; C- = YFP negative non-serotonergic cells in the caudal neural tube. 200,000 cells for each of the 4 cell types (R+, R-, C+, C-) were collected for RNA extraction and hybridization to Affymetrix Mouse 430 2.0 arrays.

Background corr dist: KL-Divergence = 0.1218, L1-Distance = 0.0274, L2-Distance = 0.0013, Normal std = 0.4067

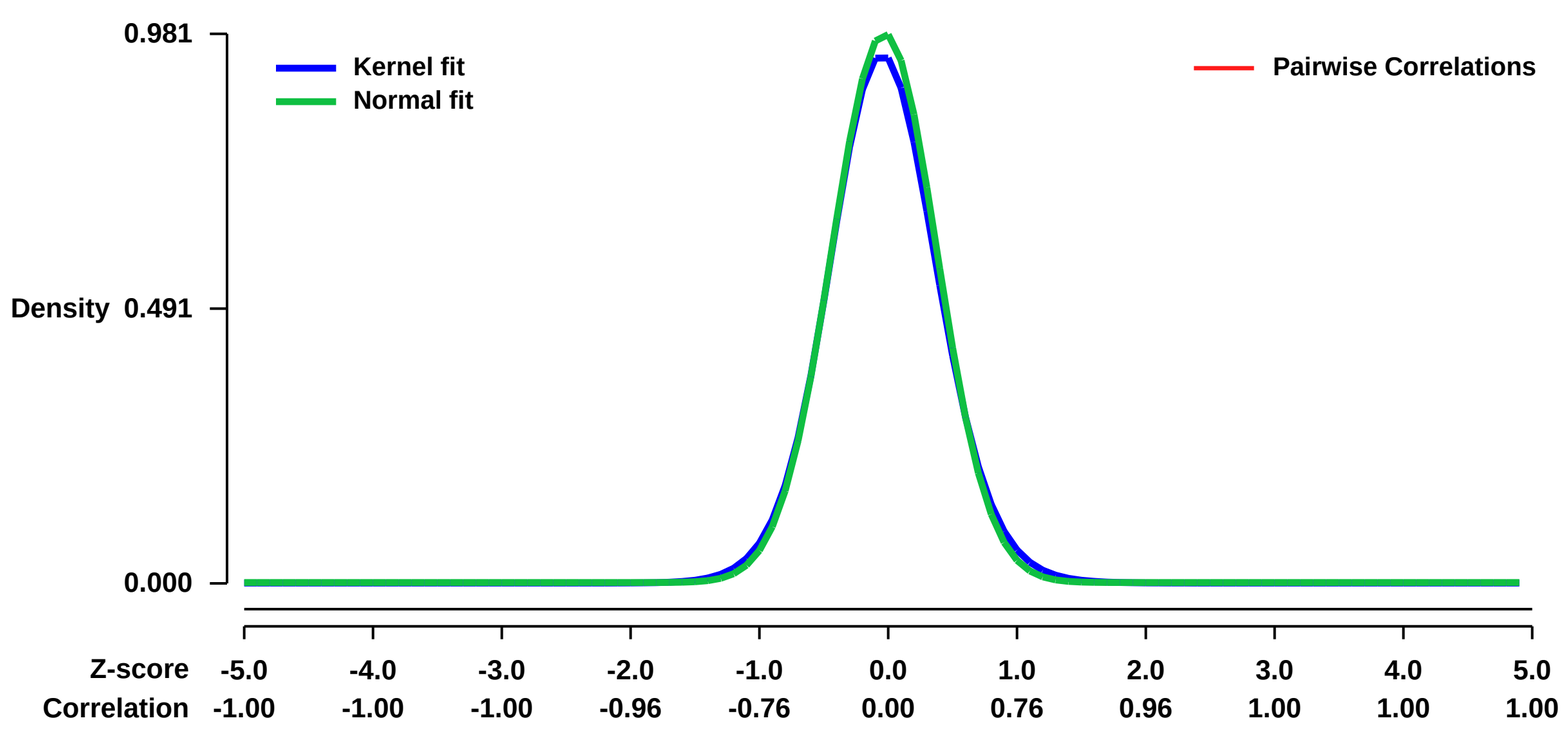

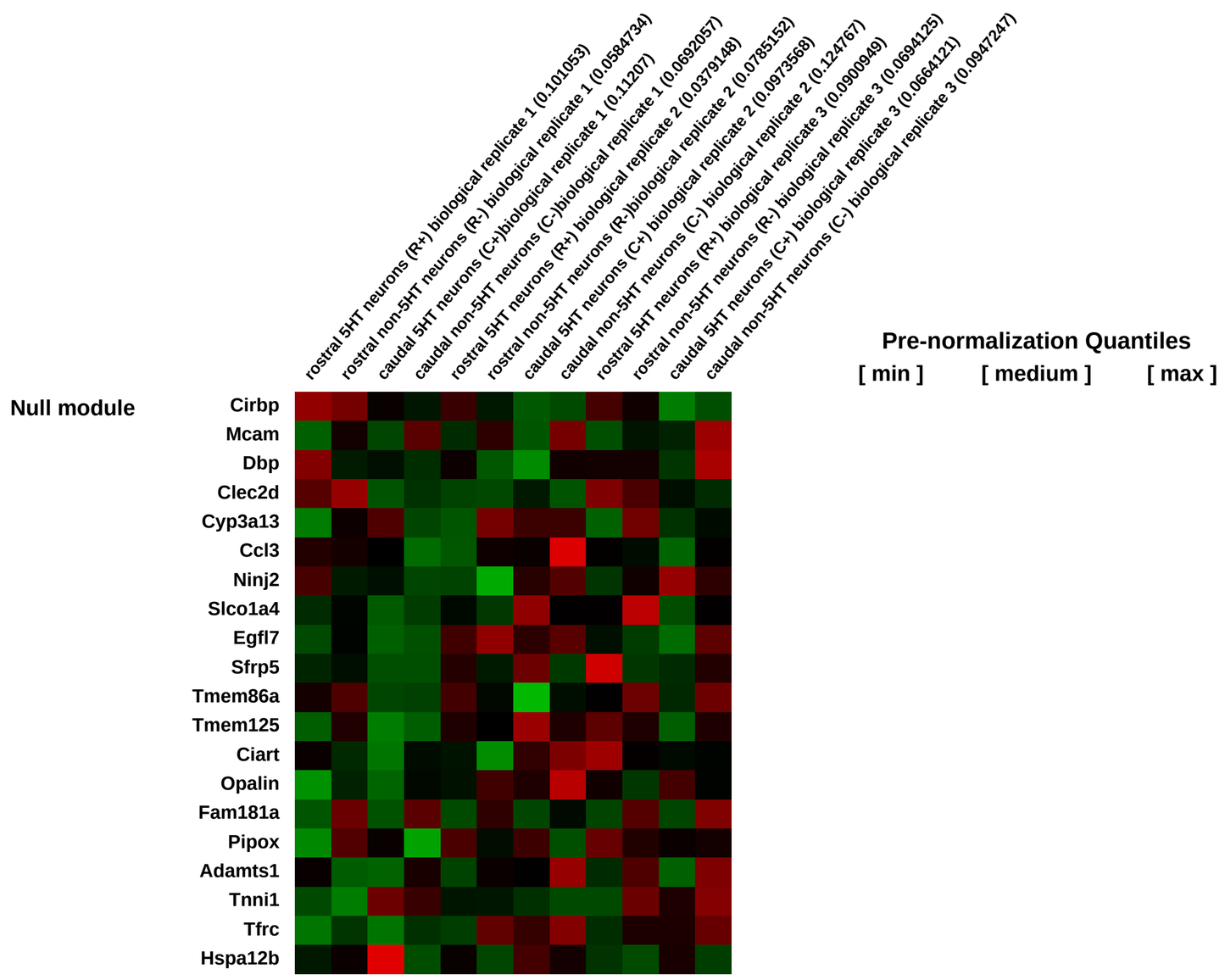

GEO Series "GSE19512" Expression Profiles

Num of samples in this series: 6

Scale of expression profile Z-scores

-3.0 -2.0 -1.0 0.0 1.0 2.0 3.0

GEO Link:	http://www.ncbi.nlm.nih.gov/geo/query/acc.cgi?acc=GSE19512
Status:	Public on Jun 30 2011
Title:	Gene expression profiling of in vivo derived induced and natural FOXP3+ regulatory T cells in the mouse
Organism:	Mus musculus
Experiment type:	Expression profiling by array
Platform:	GPL1261
Pubmed ID:	21723159
Summary & Design:	**Summary:** The relative contribution of induced and natural Foxp3+ regulatory T cells (iTreg and nTreg cells, respectively) to the maintenance of tolerance is unknown. We examined their respective roles by in vivo adoptive transfer immunotherapy of newborn Foxp3-deficient BALB/c mice. Survival, weight gain, tissue infiltration, T cell activation, and the concentration of proinflammatory cytokines were used as outcome measurements. Treatment with iTreg cells alone was not successful. While effective in preventing death, treatment with nTreg cells alone was associated with chronic inflammation and autoimmunity. Outcomes markedly improved when conventional T (Tconv) cells were transferred together with the nTreg cells, where 10% of the peripheral Treg cell pool was derived by in-situ conversion. This enhancement depended upon the capacity of Tconv cells to express Foxp3. The gene expression profile of in vivo derived iTreg cells was similar to the established nTreg cell genetic signature. These results identify iTreg cells as an essential regulatory subset that supplements tolerance maintained by nTreg cells. **Overall design:** In vitro derived iTreg cells 72 hours after Foxp3 induction: GSM360147 - GSM360151

Background corr dist: KL-Divergence = 0.0200, L1-Distance = 0.0212, L2-Distance = 0.0007, Normal std = 0.7342

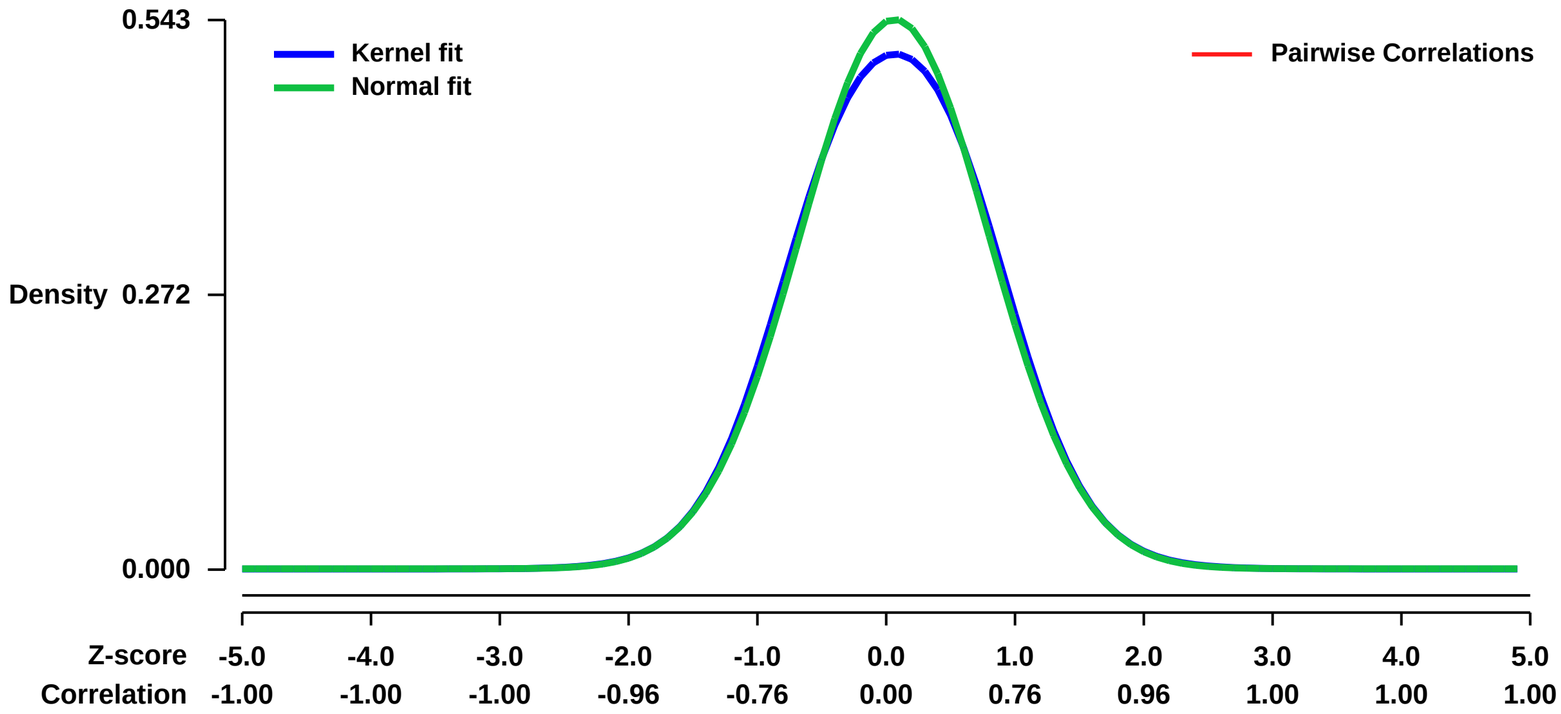

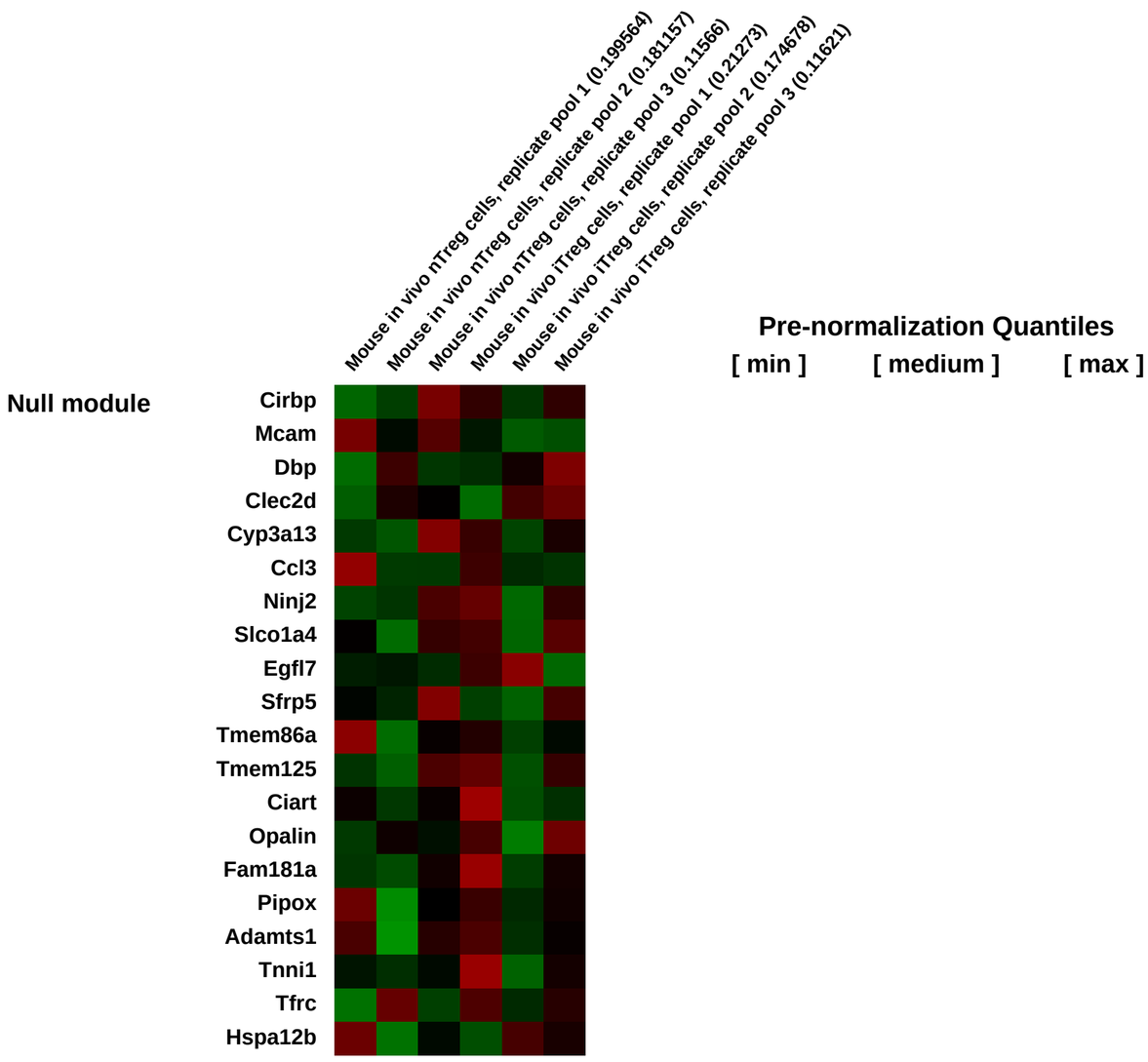

GEO Series "GSE19517" Expression Profiles

Num of samples in this series: 6

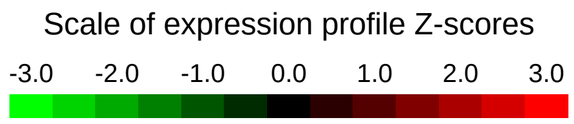

GEO Link:	http://www.ncbi.nlm.nih.gov/geo/query/acc.cgi?acc=GSE19517
Status:	Public on Mar 01 2010
Title:	Gene expression profiling of conditional ablation of Indian hedgehog in the mouse uterus
Organism:	Mus musculus
Experiment type:	Expression profiling by array
Platform:	GPL1261
Pubmed ID:	20056671
Summary & Design:	**Summary:** Conditional ablation of Indian hedgehog (Ihh) in the murine uterus results in mice that are sterile due to defects in embryo implantation. We performed microarray analysis on these mice at the time point at which the Ihh target genes are induced by the administration of exogenous hormone to mimic day 3.5 of pregnancy. This analysis identified 863 genes altered by the conditional ablation of Ihh. Of these, genes that regulated the cell cycle were overrepresented. In addition, genes involved in epidermal growth factor (EGF) and estrogen (E2) signaling were found to be deregulated upon Ihh ablation. Furthermore, upon conditional ablation of Ihh, 15 month old mice exhibited hallmarks of estrogenized uteri such as cystically dilated glands and hyalinized stroma. Thus, Ihh regulates embryo implantation by impacting the cell cycle, EGF signaling, and E2 signaling. **Keywords:** two group comparison **Overall design:** We conditionally ablated Indian hedgehog in the mouse uterus using the PRcre mouse model (PRcre/+Ihhf/f; Ihhd/d). High density DNA microarray analysis was performed on Day -1 of the artificial decidual response on Ihhf/f and Ihhd/d uteri.

Background corr dist: KL-Divergence = 0.0158, L1-Distance = 0.0218, L2-Distance = 0.0006, Normal std = 0.7834

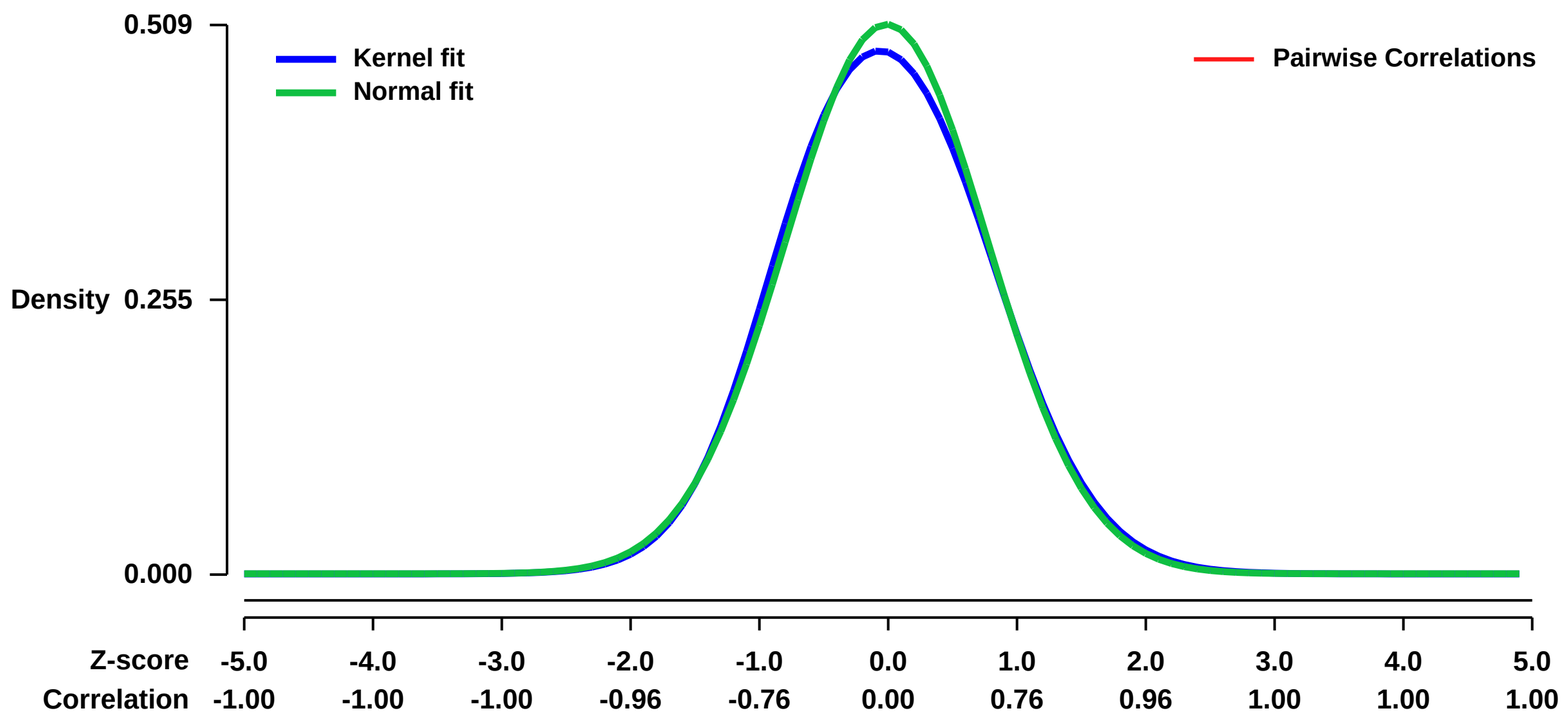

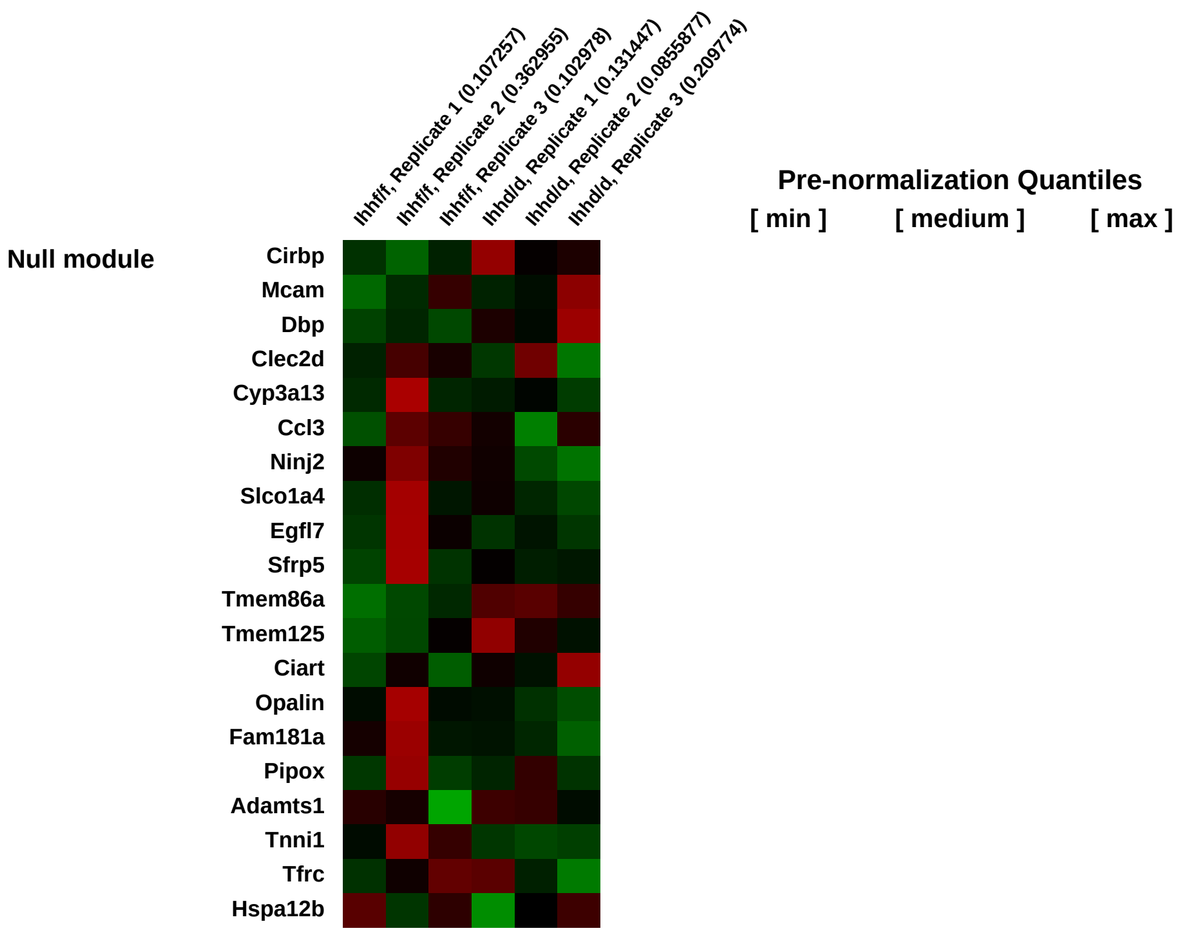

GEO Series "GSE19528" Expression Profiles

Num of samples in this series: 8

Scale of expression profile Z-scores

-3.0 -2.0 -1.0 0.0 1.0 2.0 3.0

GEO Link:	http://www.ncbi.nlm.nih.gov/geo/query/acc.cgi?acc=GSE19528
Status:	Public on Jan 22 2010
Title:	Effect of c-Myb deficiency on pre-selection DP thymocytes
Organism:	Mus musculus
Experiment type:	Expression profiling by array
Platform:	GPL1261
Pubmed ID:	20142358
Summary & Design:	**Summary:** Comparing the mRNA expression profiles of c-Myb deficient and c-Myb sufficient Tcra-/- DP thymocytes. Results provide insight into the role of c-Myb in the regulation of survival and differentiation during the pre-selection DP stage where c-Myb expression is abundant during T cell development. **Overall design:** DP thymocytes were purified from four c-Myb deficient and four c-Myb sufficient mice over magnetic columns. RNA from each biological replicate was individually hybridized onto a total of eight MOE430 2.0 Chips.

Background corr dist: KL-Divergence = 0.0791, L1-Distance = 0.0206, L2-Distance = 0.0007, Normal std = 0.4804

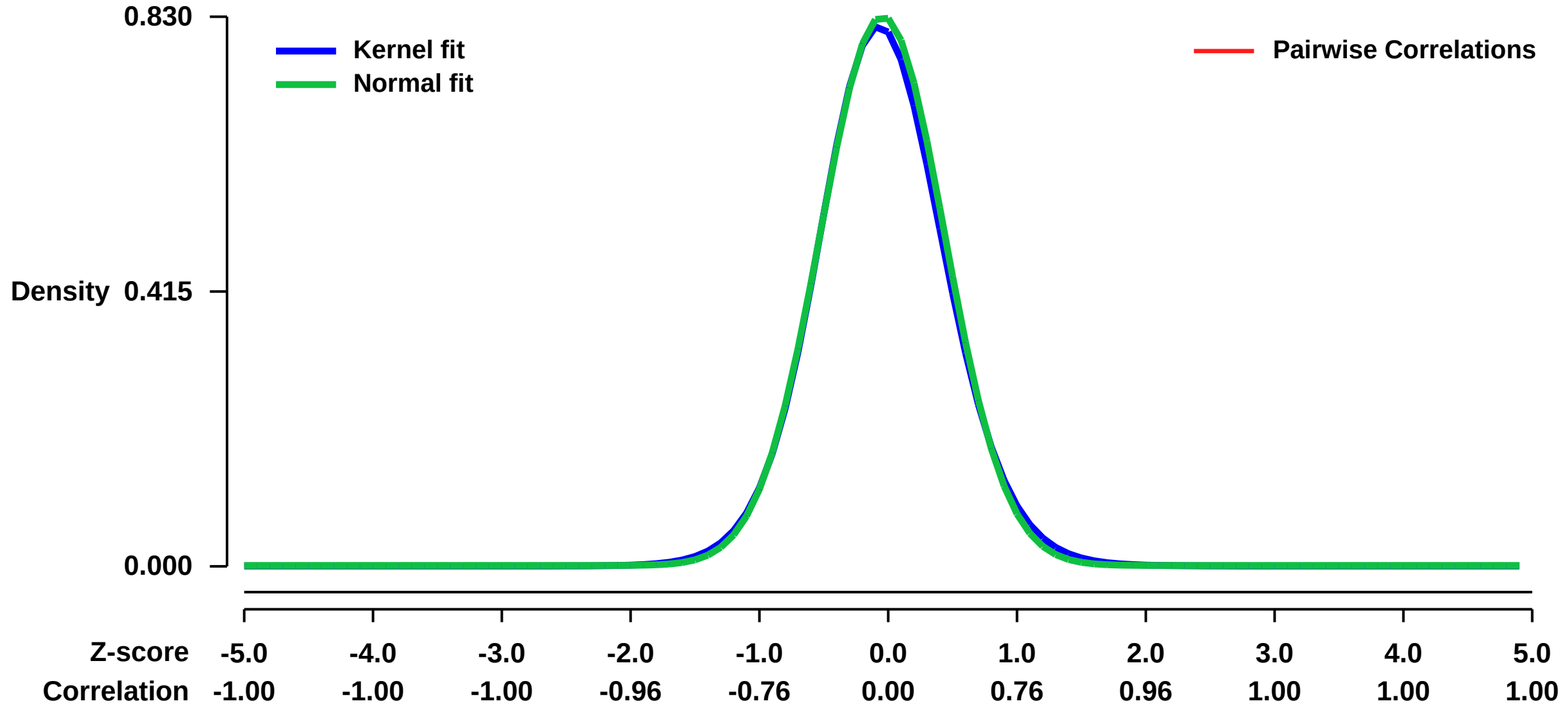

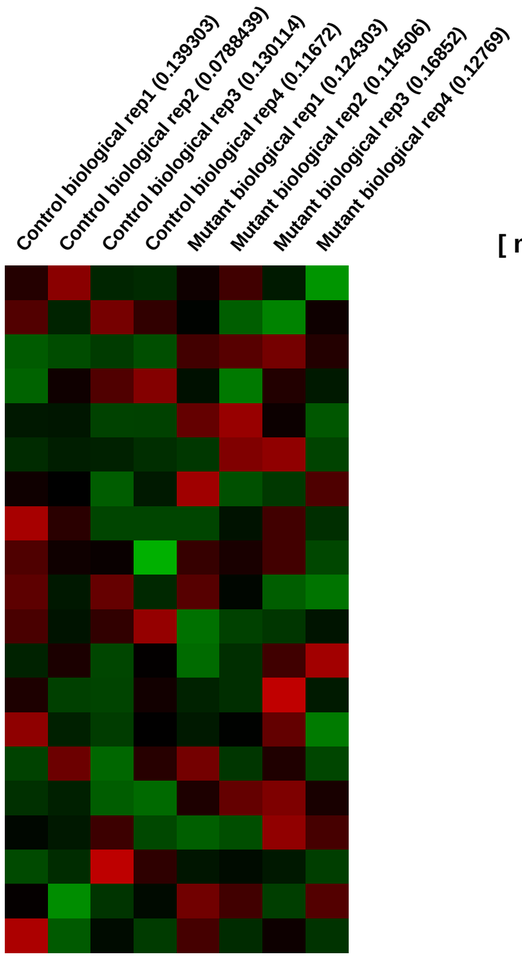

GEO Series "GSE19616" Expression Profiles

Num of samples in this series: 16

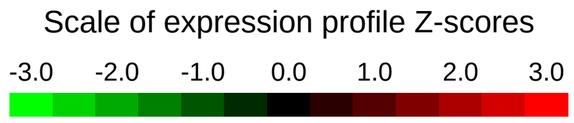

GEO Link:	http://www.ncbi.nlm.nih.gov/geo/query/acc.cgi?acc=GSE19616
Status:	Public on Jul 20 2010
Title:	Gene expression profiling of mouse p53-deficient epidermal carcinoma defines molecular determinants of human cancer malignancy (testing dataset)
Organism:	Mus musculus
Experiment type:	Expression profiling by array
Platform:	GPL1261
Pubmed ID:	20630075
Summary & Design:	**Summary:** The epidermal specific ablation of Trp53 gene leads to the spontaneous development of aggressive tumors in mice through a process that is accelerated by the simultaneous ablation of Rb gene. Since alterations of p53-dependent pathway are common hallmarks of aggressive, poor prognostic human cancers, these mouse models can recapitulate the molecular features of some of these human malignancies. To evaluate this possibility, gene expression microarray analysis was performed in mouse samples. The mouse tumors display increased expression of cell cycle and chromosomal instability associated genes. Remarkably, they are also enriched in human embryonic stem cell gene signatures, a characteristic feature of human aggressive tumors. Using cross-species comparison and meta-analytical approaches, we also observed that spontaneous mouse tumors display robust similarities with gene expression profiles of human tumors bearing mutated TP53, or displaying poor prognostic outcome, from multiple body tissues. We have obtained a 20-gene signature whose genes are overexpressed in mouse tumors and can identify human tumors with poor outcome from breast cancer, astrocytoma and multiple myeloma. This signature was consistently overexpressed in additional mouse tumors using microarray analysis. Two of the genes of this signature, AURKA and UBE2C, were validated in human breast and cervical cancer as potential biomarkers of malignancy. Our analyses demonstrate that these mouse models are promising preclinical tools aimed to search for malignancy biomarkers and to test targeted therapies of prospective use in human aggressive tumors and/or with p53 mutation or inactivation. **Overall design:** Control skin was compared with skin tumors arising in k14Cre;p53loxP/loxP and k14Cre;p53loxP/loxP;pRbloxP/loxP animals, giving a mouse p53-tumor signature

Background corr dist: KL-Divergence = 0.1802, L1-Distance = 0.0477, L2-Distance = 0.0056, Normal std = 0.3576

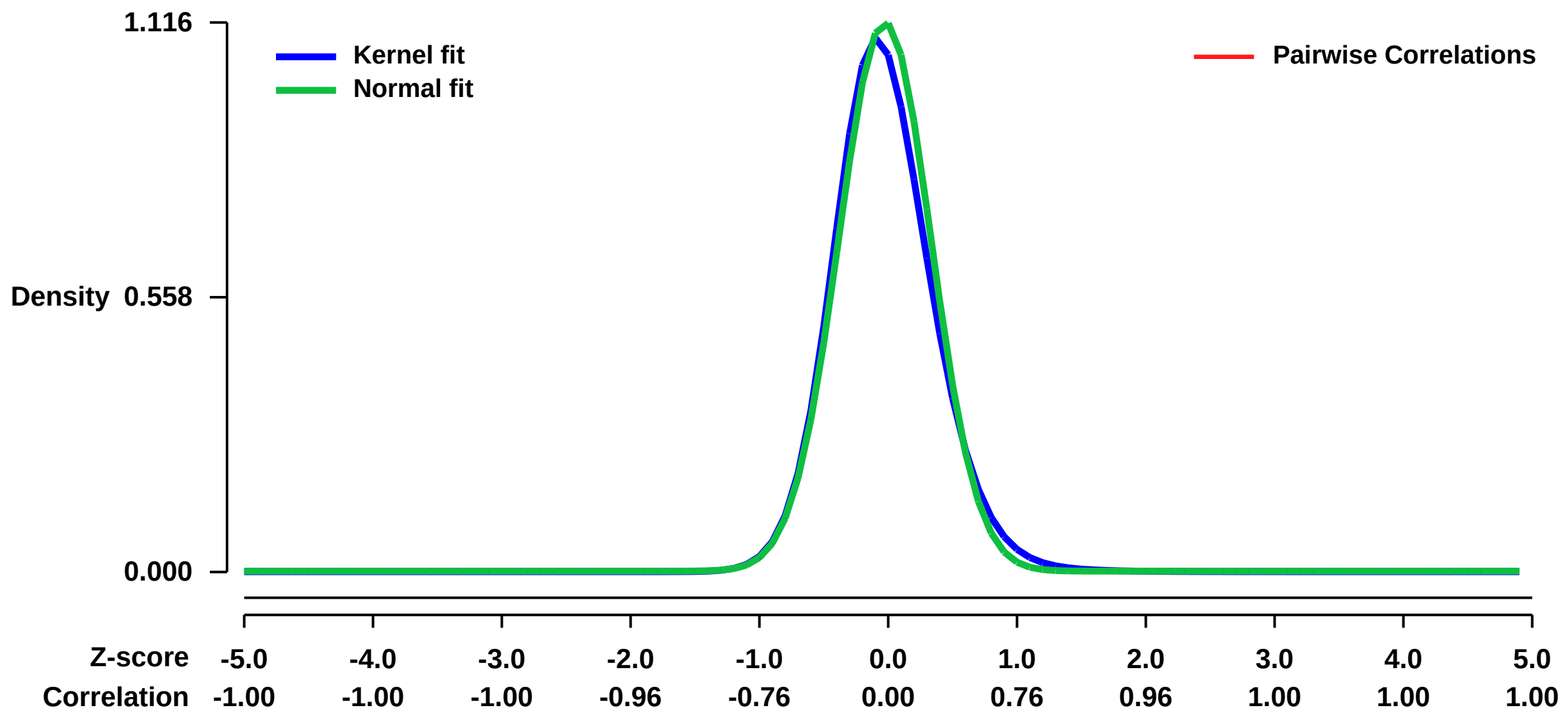

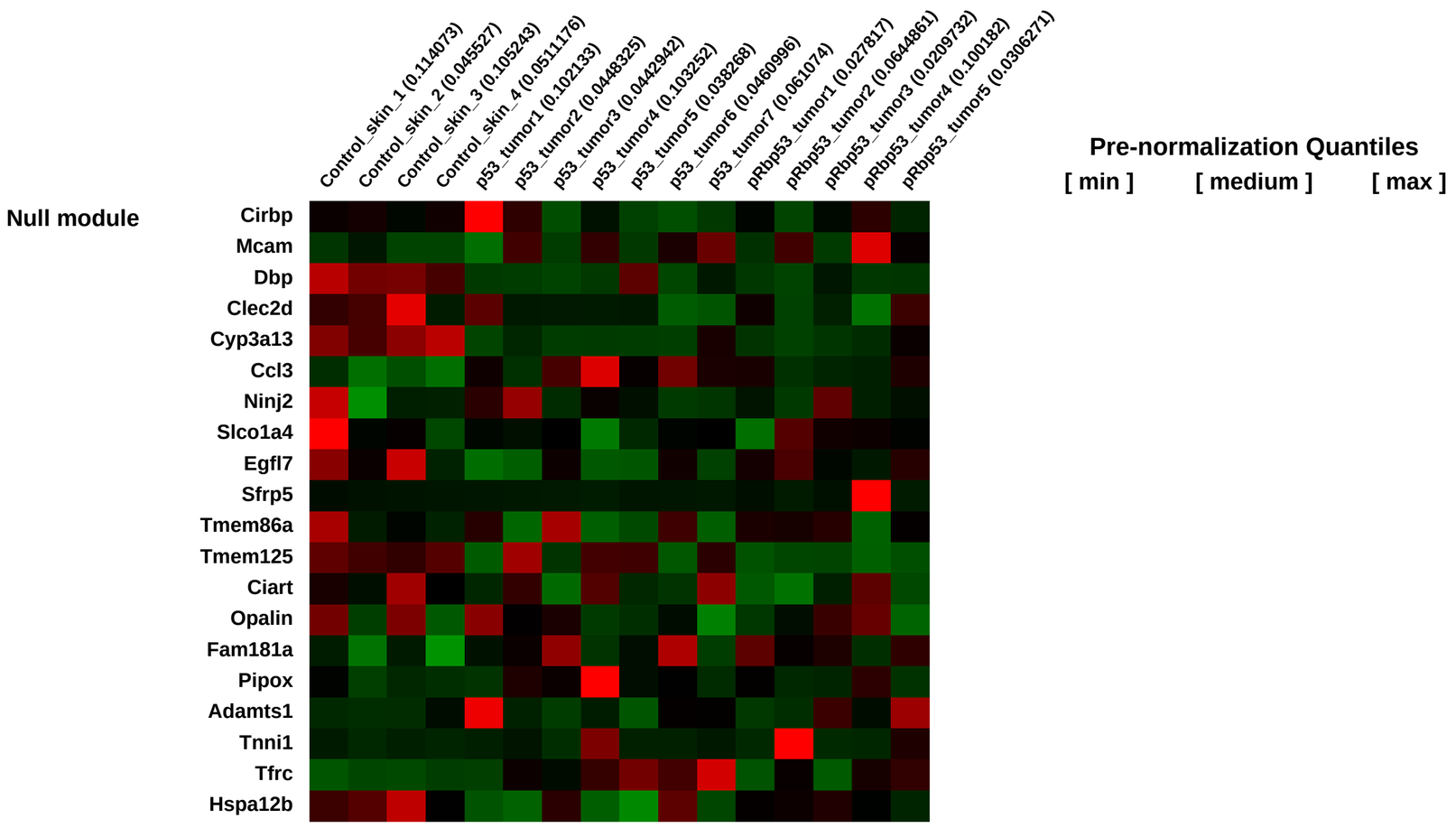

GEO Series "GSE19657" Expression Profiles

Num of samples in this series: 21

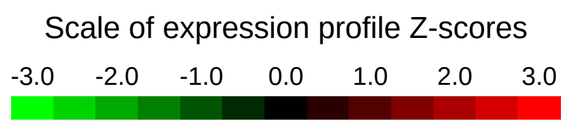

GEO Link:	http://www.ncbi.nlm.nih.gov/geo/query/acc.cgi?acc=GSE19657
Status:	Public on Sep 29 2010
Title:	Targeting resistance to Smoothened antagonists by inhibiting the PI3K pathway
Organism:	Mus musculus
Experiment type:	Genome variation profiling by genome tiling array
Platform:	GPL1261
Pubmed ID:	20881279
Summary & Design:	**Summary:** Mutations in Hedgehog (Hh) pathway genes, leading to constitutive activation of Smoothened (Smo), occur in sporadic medulloblastoma, the most common brain cancer in children. Antagonists of Smo induce tumor regression in mouse models of medulloblastoma and hold great promise for targeted therapy for this tumor. However, acquired resistance has emerged as one of the major challenges of targeted cancer therapy. Here, we describe novel mechanisms of acquired resistance to Smo antagonists in medulloblastoma. NVP-LDE225, a potent and selective Smo antagonist, inhibits Hh signaling and induces tumor regressions in allograft models of medulloblastoma that are driven by mutations of Patched (Ptch), a tumor suppressor in the Hh pathway. However, after long-term treatment, evidence of acquired resistance was observed. Genome-wide profiling of resistant tumors revealed distinct mechanisms to evade the inhibitory effects of Smo antagonists. Chromosomal amplification of Gli2, a downstream effector of Hh signaling, reactivated Hh signaling and restored tumor growth. Analysis of pathway gene-expression signatures selectively deregulated in resistant tumors identified increased phosphoinositide-3-kinase (PI3K) signaling as another potential resistance mechanism. Probing the functional relevance of increased PI3K signaling, we showed that the combination of NVP-LDE225 with the dual PI3K/mTOR inhibitor NVP-BEZ235 markedly delayed the development of resistance. Our findings have important clinical implications for future treatment strategies in medulloblastoma. **Overall design:** aCGH: DNA was prepared from tumors from vehicle or NVP-LDE225 treated nude mice allografted with medulloblastoma tumors derived from Ptch+/-p53-/- transgenic mouse and hybridized on Agilent mouse CGH 244K Array.

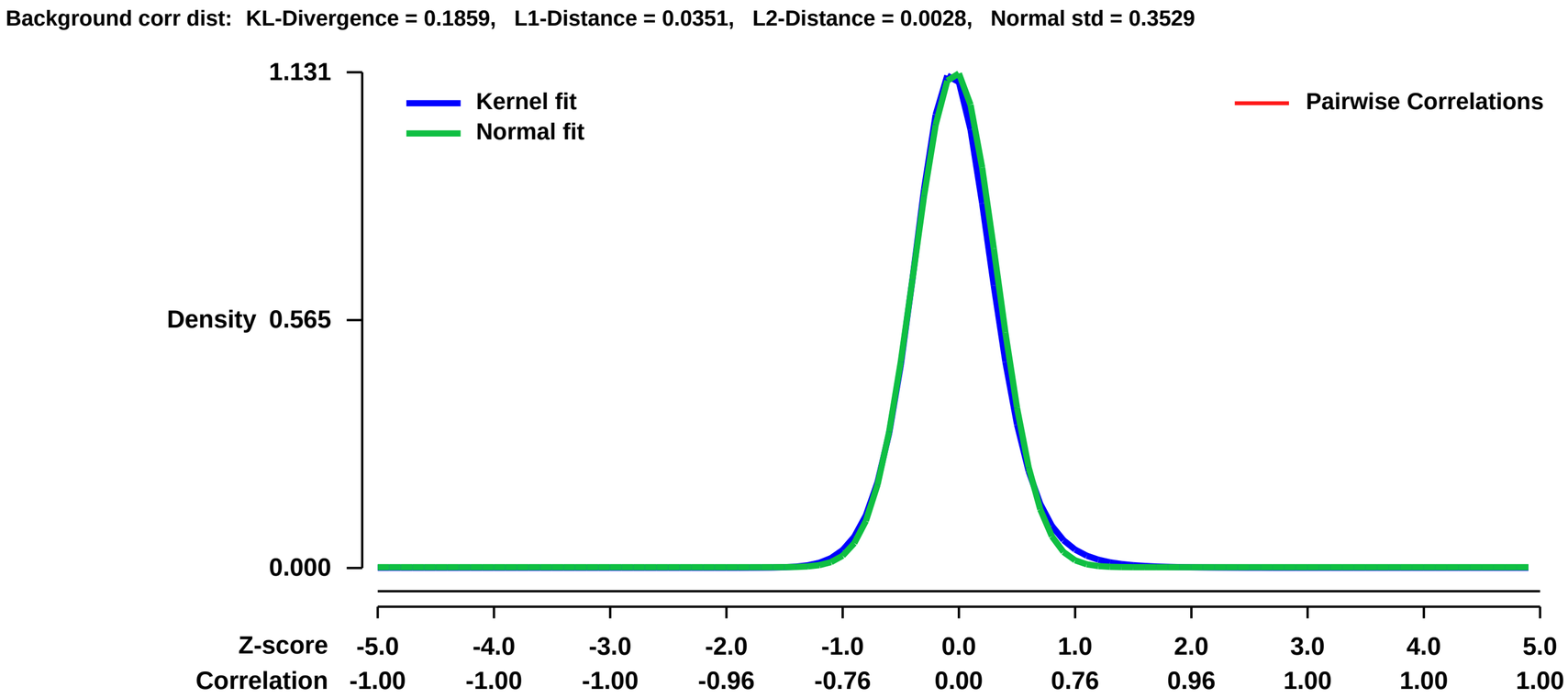

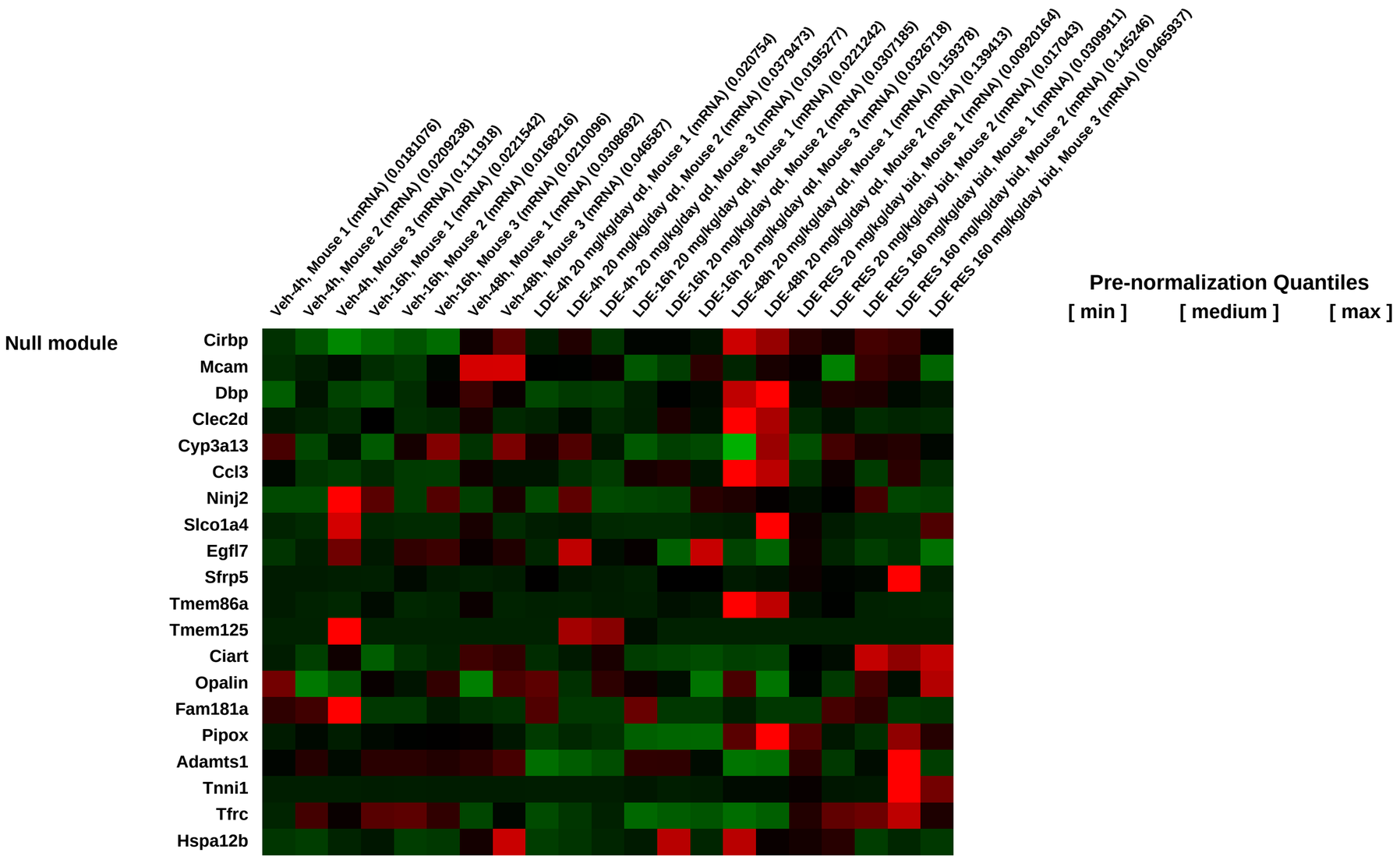

GEO Series "GSE19668" Expression Profiles

Num of samples in this series: 50

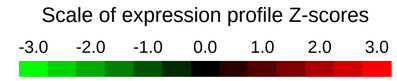

GEO Link:	http://www.ncbi.nlm.nih.gov/geo/query/acc.cgi?acc=GSE19668
Status:	Public on Aug 01 2010
Title:	Genetic Determinants for Susceptibility to Staphylococcus aureus Infection in A/J and C57BL/6J
Organism:	Mus musculus
Experiment type:	Expression profiling by array
Platform:	GPL1261
Pubmed ID:	20824097
Summary & Design:	**Summary:** Although it has recently been shown that A/J mice are highly susceptible to Staphylococcus aureus sepsis as compared to C57BL/6J, the specific genes responsible for this differential phenotype are unknown. Using chromosome substitution strains (CSS), we found that factors on chromosomes (chr) 8, 11, and 18 are responsible for susceptibility to S. aureus sepsis in A/J mice. F1 mice from C57BL/6J X CSS8 cross (C8A) and C57BL/6J X CSS18 (C18A) were also susceptible to S. aureus (median survival < 48 h), whereas F1 mice from C57BL/6J X CSS11 cross (C11A) were resistant (median survival > 120 h) to S. aureus. Bacterial loads in the kidney were consistent with F1 median survivals, with higher bacterial counts in susceptible mice. No sexlinked associations with susceptibility were noted in F1 intercrosses. Using whole genome transcription profiling, we identified a total of 192 genes on chromosomes 8, 11, and 18 which are differentially expressed between A/J and C57BL/6J in the setting of S. aureus infection. Of these, 28 genes had Gene Ontology annotations indicating a potential immune response function. These 28 genes are associated with susceptibility to S. aureus in A/J mice, and are potential determinants of susceptibility to S. aureus infection in humans. **Overall design:** To identify genes for which differential expression between A/J and C57BL/6J mice could contribute to host susceptibility to S. aureus infection, we compared the gene expression profiles between uninfected A/J and C57BL/6J mice and between infected A/J and C57BL/6J mice at 2, 4, 6, and 12 hours after infection.

Background corr dist: KL-Divergence = 0.1340, L1-Distance = 0.0649, L2-Distance = 0.0110, Normal std = 0.3963

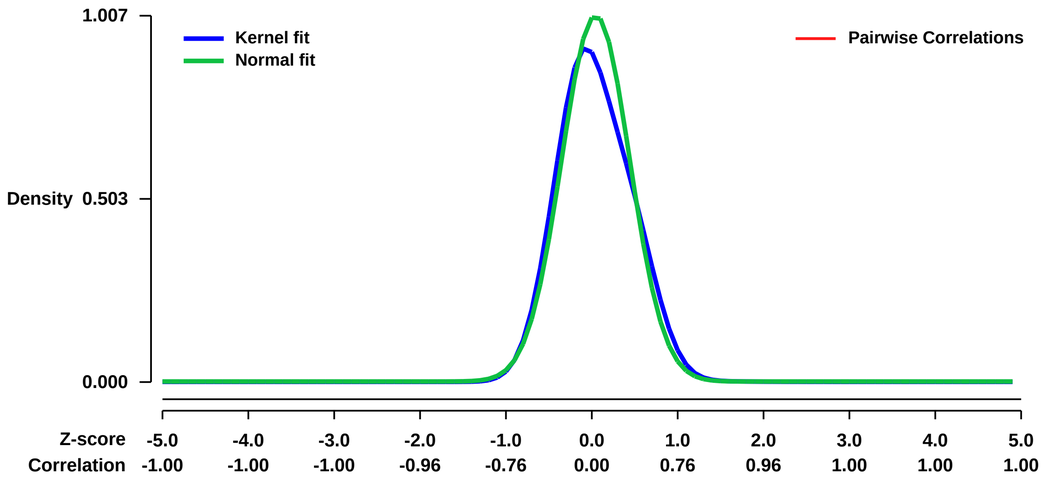

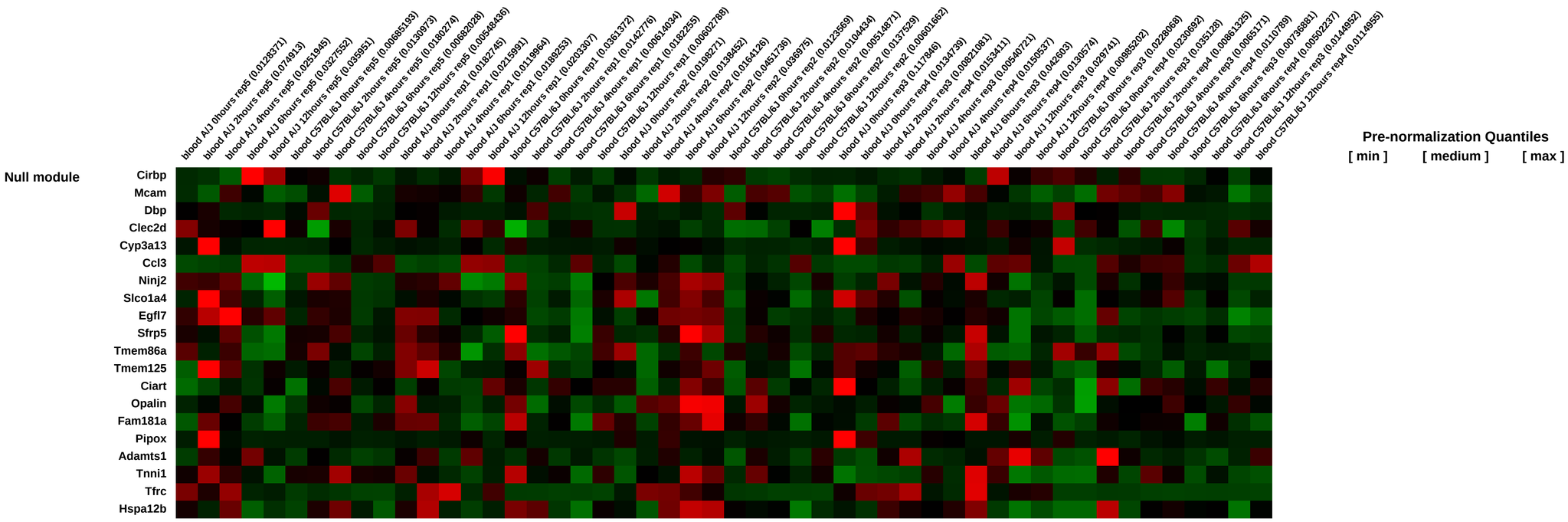

GEO Series "GSE19675" Expression Profiles

Num of samples in this series: 22

Scale of expression profile Z-scores

-3.0 -2.0 -1.0 0.0 1.0 2.0 3.0

GEO Link:	http://www.ncbi.nlm.nih.gov/geo/query/acc.cgi?acc=GSE19675
Status:	Public on Aug 02 2011
Title:	Negative regulation of the IFN/STAT signaling pathway by the Trim24 tumor suppressor protein through Rara inhibition
Organism:	Mus musculus
Experiment type:	Expression profiling by array
Platform:	GPL1261
Pubmed ID:	21768647
Summary & Design:	**Summary:** Recent genetic studies in mice have established a key role for the nuclear receptor coregulator Trim24 in liver tumor suppression and provided evidence that Trim24 suppresses hepatocarcinogenesis by inhibiting retinoic acid receptor alpha (Rara)-dependent transcription and cell proliferation. However, it is unknown which downstream targets of Rara regulated by Trim24 are critical for tumorigenesis. We report here that loss of Trim24 results in the overexpression of interferon (IFN)/STAT pathway genes in the liver, a process that occurs early in tumorigenesis and is more pronounced in tumors, despite the enhanced expression, late in the disease, of negative regulators such as Usp18, Socs1 and Socs2. Remarkably, Rara haplodeficiency, which was previously shown to suppress tumor development in Trim24-/- mice, also suppresses overexpression of the IFN/STAT pathway, thus providing evidence for a cross-pathway control that may be relevant to the transformation process. Biochemical studies revealed that Trim24 binds to the retinoic acid (RA)-responsive element in the Stat1 promoter in a RA-dependent manner and represses RA-induced transcription from this promoter. Together, these results identify Trim24 as a novel regulator of the IFN/STAT pathway and indicate that Trim24-mediated repression of the IFN/STAT signaling through Rara inhibition may play a critical role in preventing liver cancer. **Overall design:** Transcriptional profiling of mice at 5-weeks and 14-weeks of age.

Background corr dist: KL-Divergence = 0.1693, L1-Distance = 0.0423, L2-Distance = 0.0038, Normal std = 0.3544

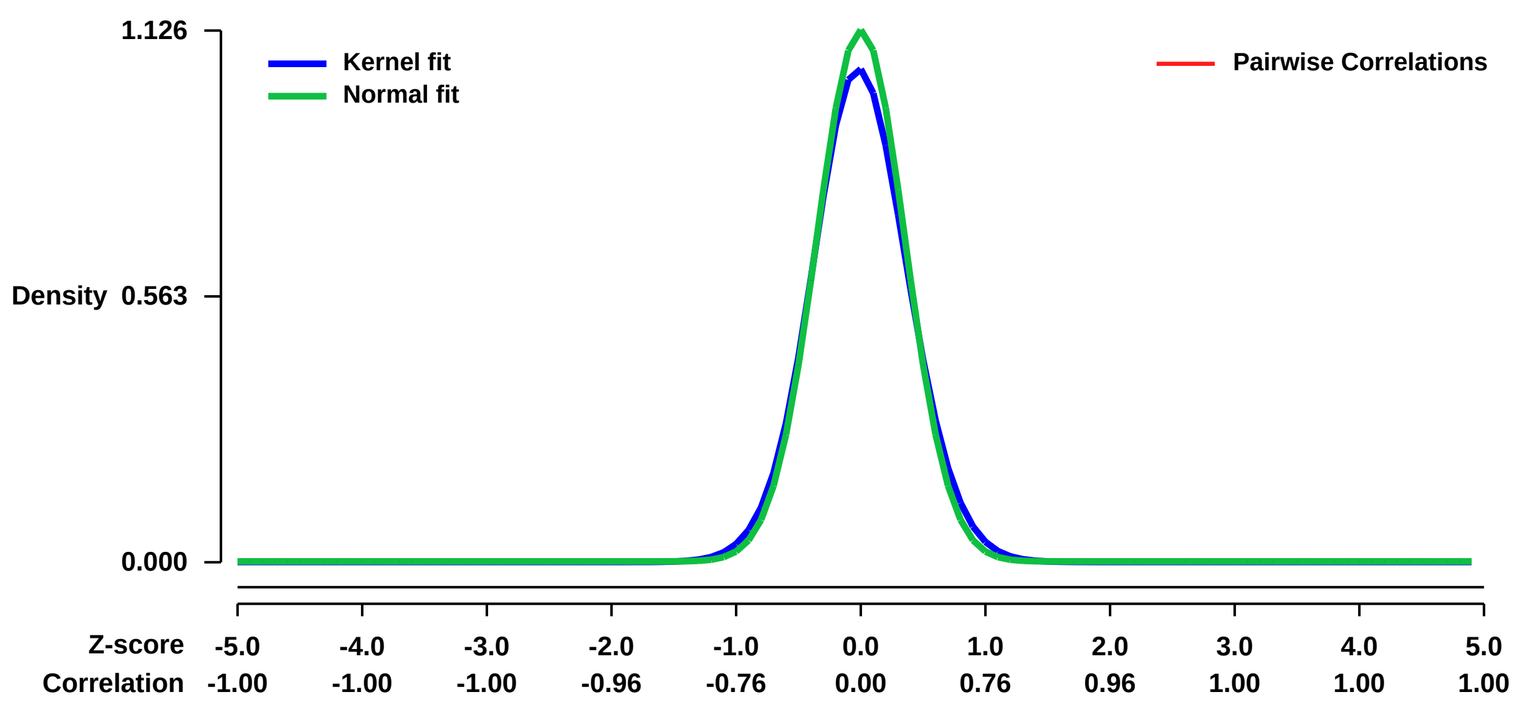

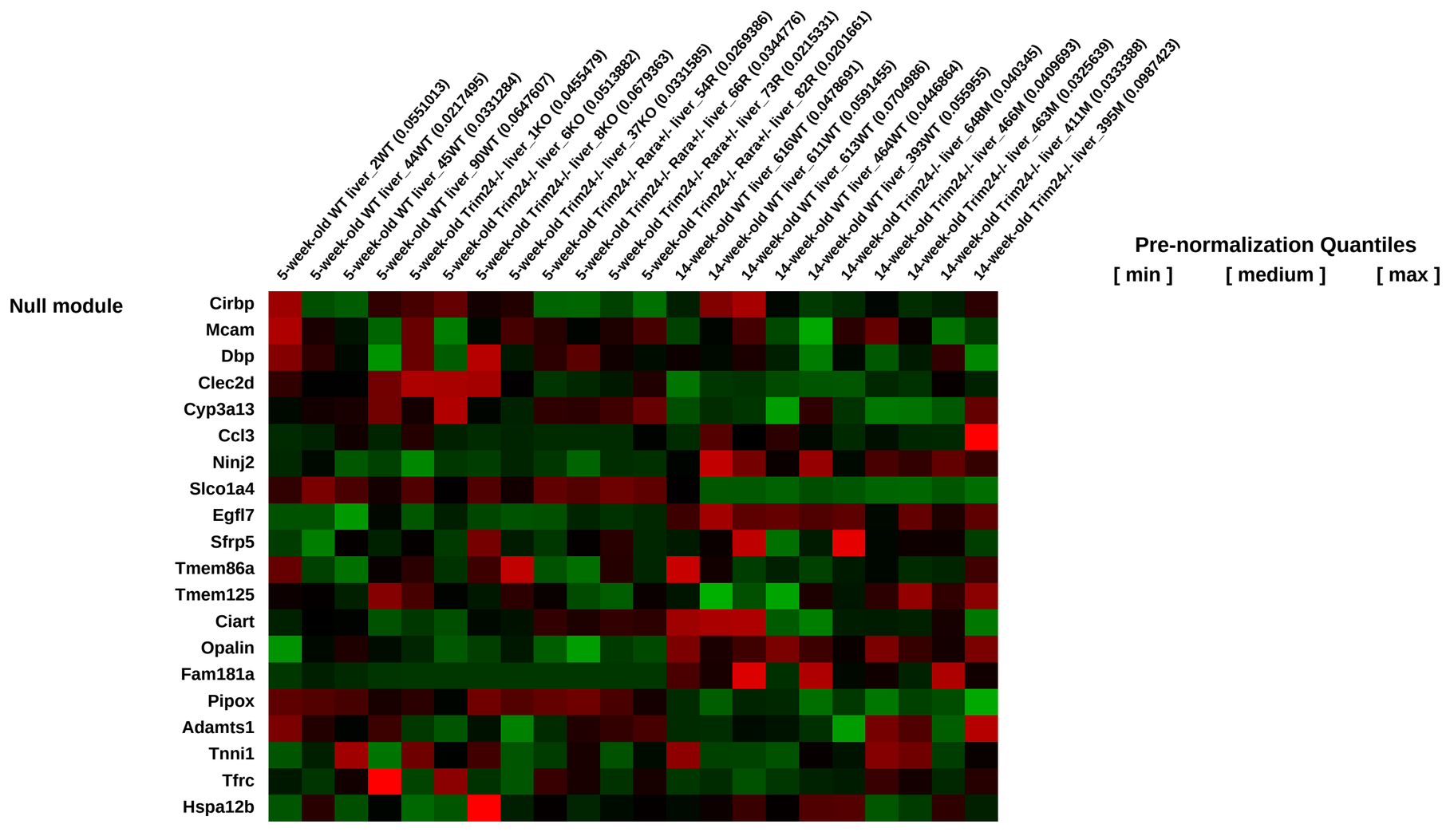

GEO Series "GSE19687" Expression Profiles

Num of samples in this series: 9

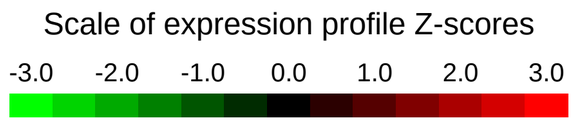

GEO Link:	**http://www.ncbi.nlm.nih.gov/geo/query/acc.cgi?acc=GSE19687**
Status:	**Public on Dec 30 2009**
Title:	**shGFP- and shQk-transduced Ink4a/Arf-/- Pten-/- primary mouse astrocytes**
Organism:	**Mus musculus**
Experiment type:	**Expression profiling by array**
Platform:	**GPL1261**
Pubmed ID:	
Summary & Design:	**Summary:** **Identify potential QK-regulated mRNAs and linked pathways by comparing the transcriptional profiles of shGFP- and shQK-transduced Ink4a/Arf-/- Pten-/- primary mouse astrocytes** **Overall design:** **Ink4a/Arf-/- Pten-/- primary mouse astrocytes infected with shQk-1, shQk-2 and infected with shGFP as control**

Background corr dist: **KL-Divergence = 0.1127, L1-Distance = 0.0284, L2-Distance = 0.0014, Normal std = 0.4172**

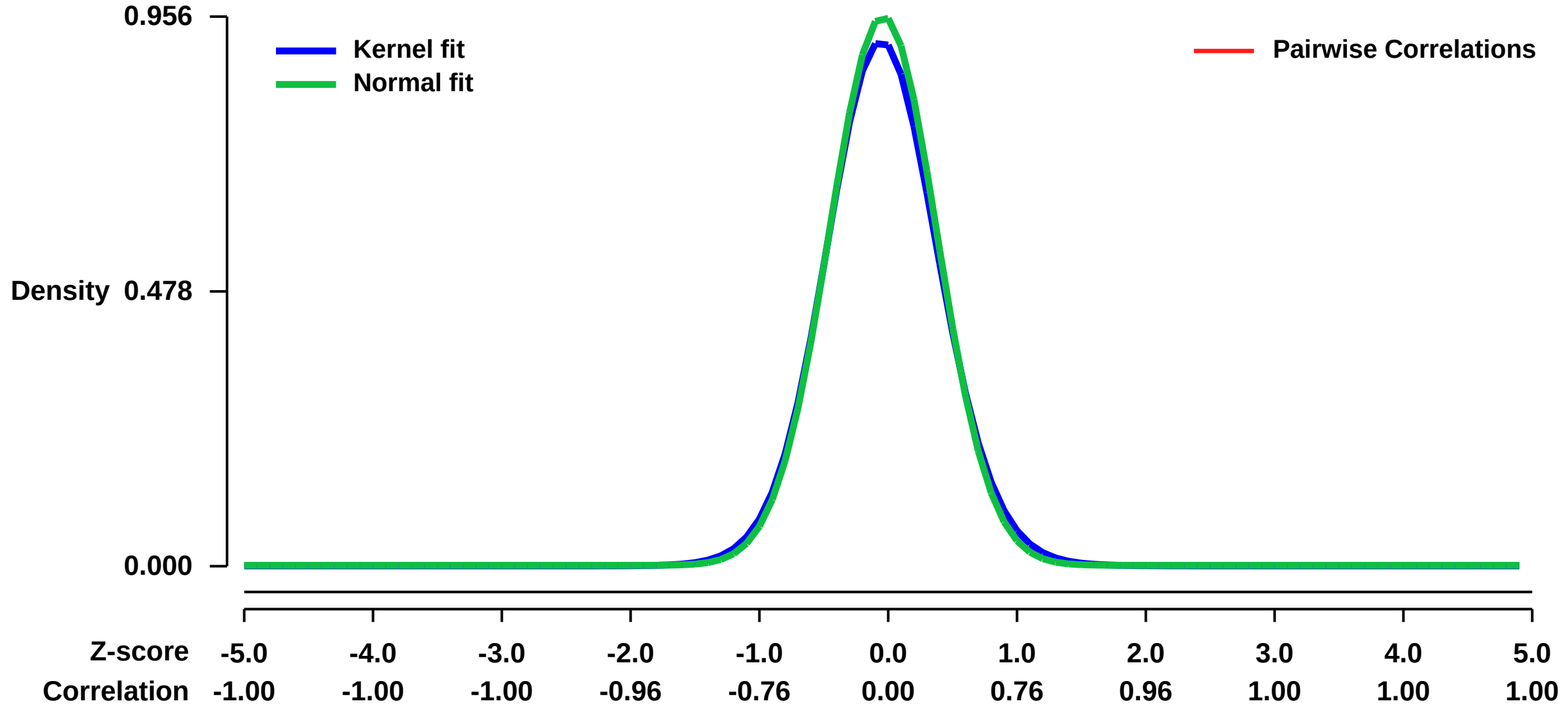

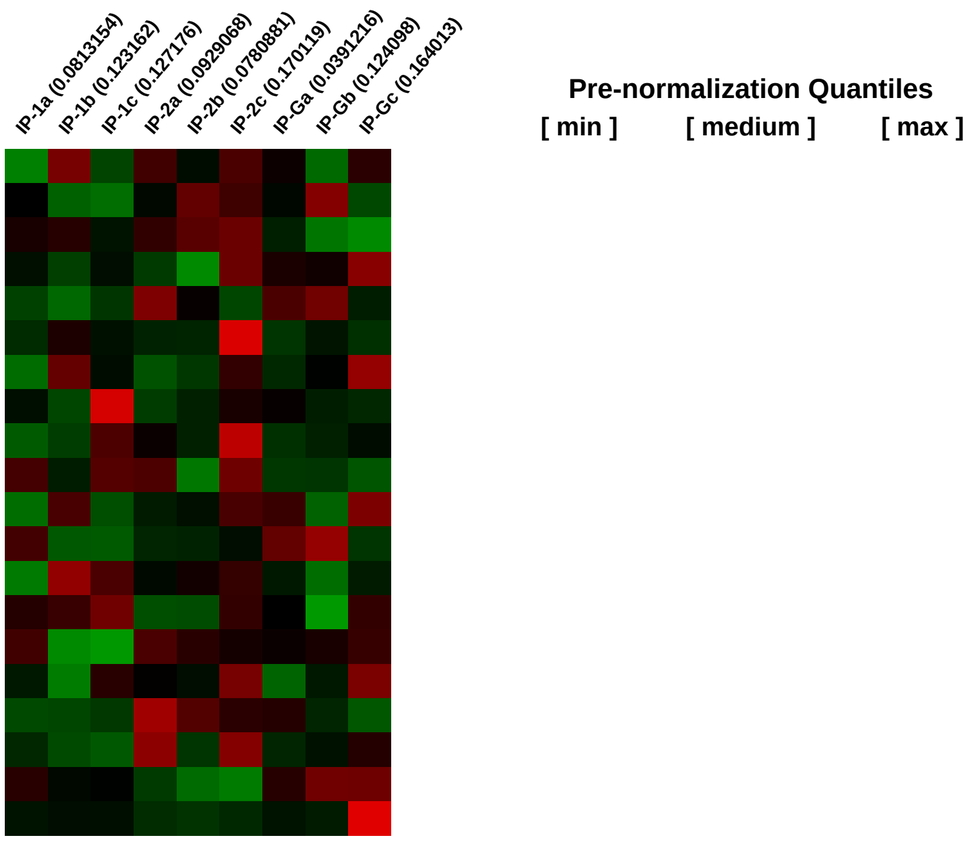

GEO Series "GSE19732" Expression Profiles

Num of samples in this series: 20

Scale of expression profile Z-scores

-3.0 -2.0 -1.0 0.0 1.0 2.0 3.0

GEO Link:	http://www.ncbi.nlm.nih.gov/geo/query/acc.cgi?acc=GSE19732
Status:	Public on Feb 01 2010
Title:	Identification of genes characteristic of committed preadipocyte fibroblasts
Organism:	Mus musculus
Experiment type:	Expression profiling by array
Platform:	GPL1261
Pubmed ID:	20200519
Summary & Design:	**Summary:** In order to identify the molecular mechanisms controlling preadipocyte commitment we derived new sublines of Swiss 3T3 fibroblasts with varying potential for adipogenesis. Swiss 2, Swiss 8, Swiss 9, and Swiss 19 differentiate into fat cells while Swiss 3, Swiss 5, and Swiss 22 have a lower propensity to differentiate into fat cells. The overall goal was to identify genes whose expression in the fibroblast state correlates with the ultimate potential of the cells to undergo adipogenesis **Overall design:** 4 preadipose fibroblast cell lines (Swiss 2, Swiss 8, Swiss 9, and Swiss 19 in triplicate or duplicate) were compared to 3 non-adipogenic fibroblast cell lines (Swiss 3, Swiss 5, Swiss 22 in triplicate)

Background corr dist: KL-Divergence = 0.2375, L1-Distance = 0.0460, L2-Distance = 0.0048, Normal std = 0.3101

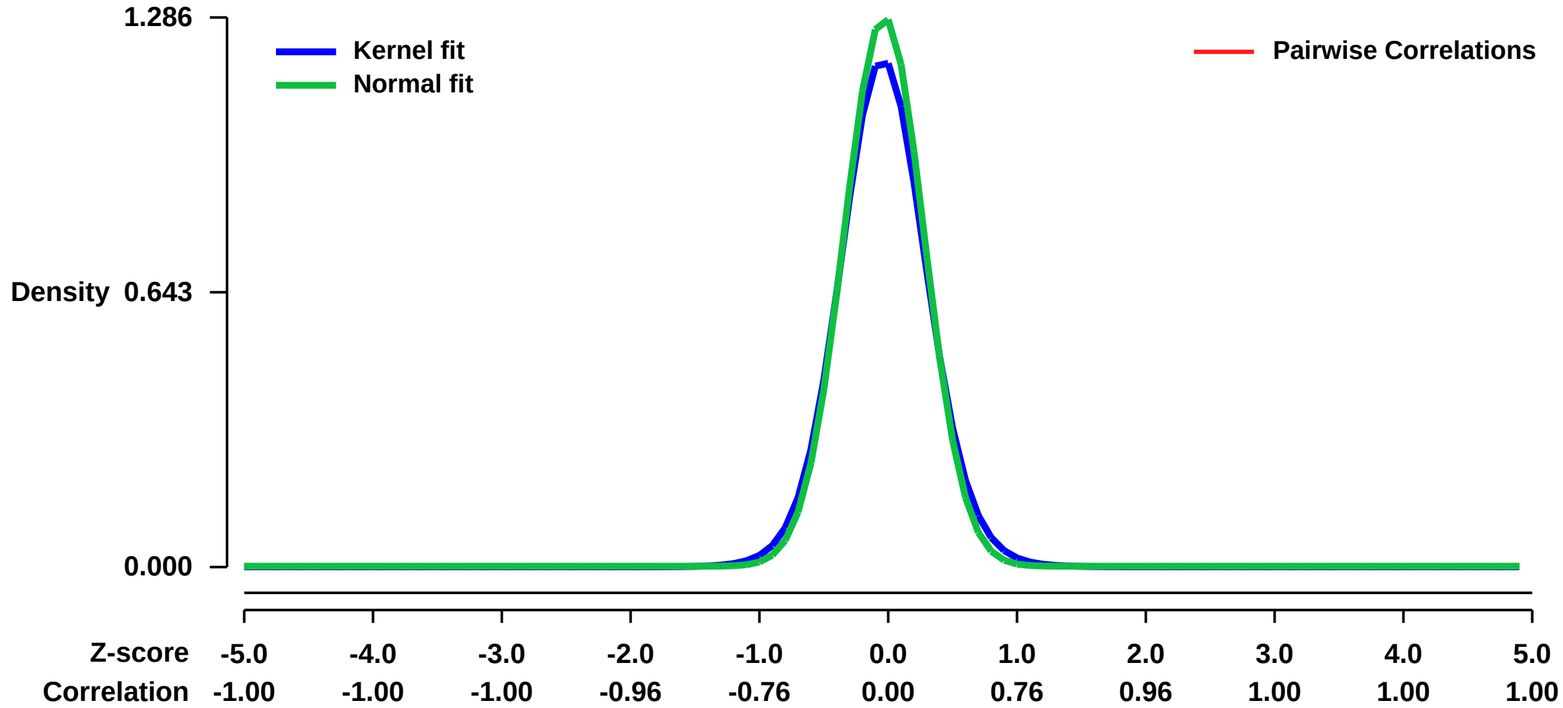

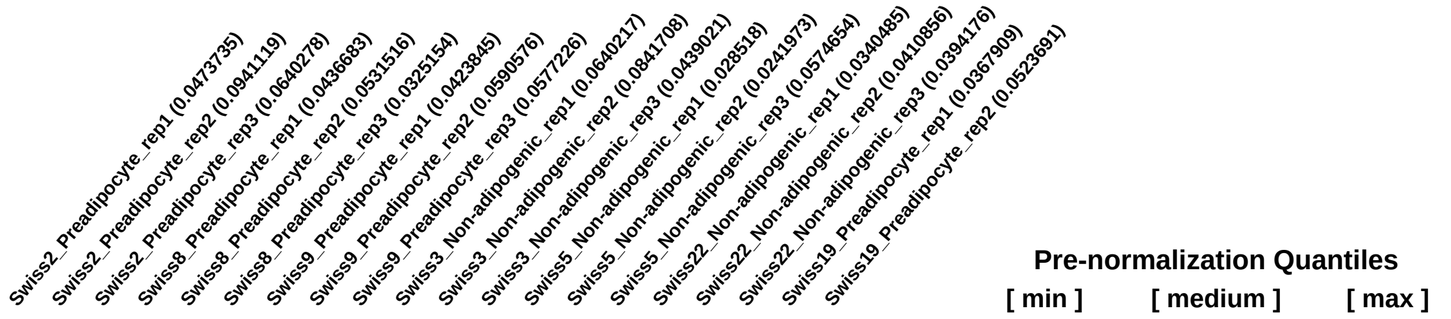

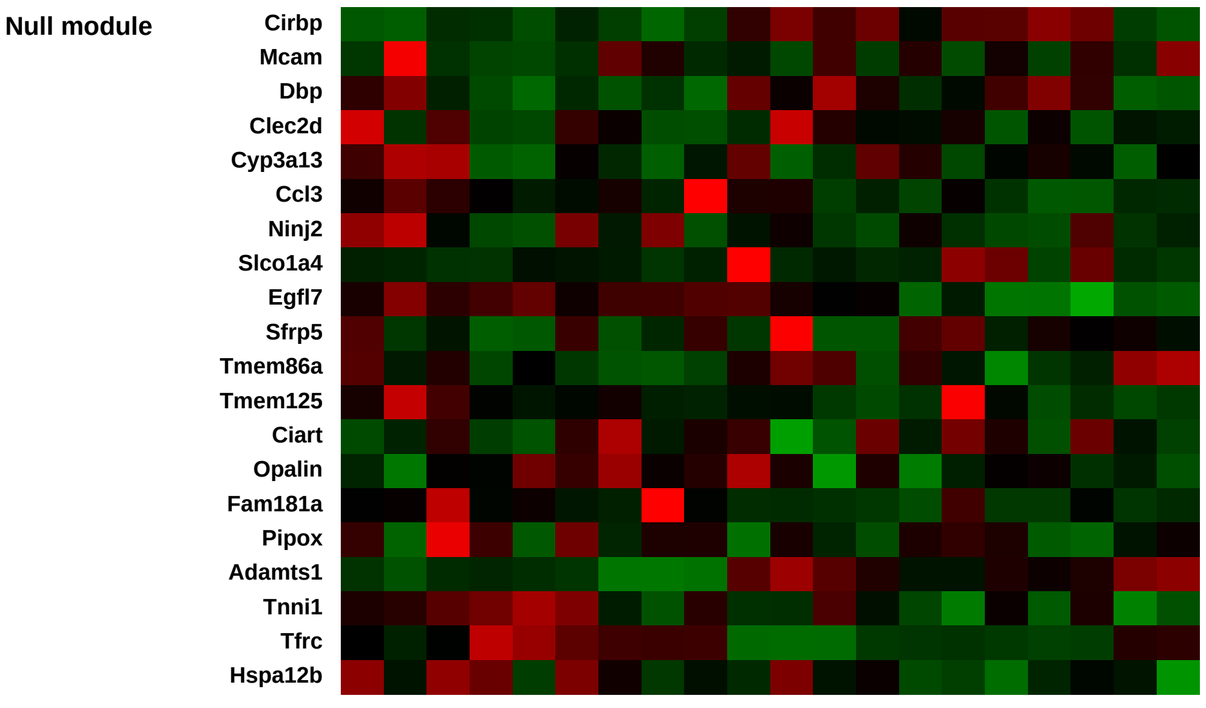

GEO Series "GSE19753" Expression Profiles

Num of samples in this series: 29

Scale of expression profile Z-scores

-3.0 -2.0 -1.0 0.0 1.0 2.0 3.0

GEO Link:	http://www.ncbi.nlm.nih.gov/geo/query/acc.cgi?acc=GSE19753
Status:	Public on Jan 15 2010
Title:	Mad2-induced chromosome instability leads to lung tumor relapse after oncogene withdrawal
Organism:	Mus musculus
Experiment type:	Expression profiling by array
Platform:	GPL1261
Pubmed ID:	20173739
Summary & Design:	**Summary:** Inhibition of an initiating oncogene often leads to extensive tumor cell death, a phenomenon known as oncogene addiction. This has led to the search for compounds that specifically target and inhibit oncogenes as anti-cancer agents. Whether chromosomal instability (CIN) generated as a result of deregulation of the mitotic checkpoint pathway, a frequent characteristic of solid tumors, has any effect on oncogene addiction, however, has not been explored systematically. We show here that induction of chromosome instability by overexpression of the mitotic checkpoint gene Mad2 does not affect the regression of Kras driven lung tumors upon Kras inhibition. However, tumors that experience transient Mad2 overexpression and consequent chromosome instability recur at dramatically elevated rates. The recurrent tumors are highly aneuploid and have varied activation of pro-proliferative pathways. Thus, early CIN may be responsible for tumor relapse after seemingly effective anti-cancer treatments. **Overall design:** Lung tumor tissue from TI-K (CCSP-rtTA;TRE-KrasV12), TI-KM (CCSP-rtTA; TRE-KrasV12; TRE-Mad2), recurrence (TI-KM) or normal lung tissue (CCSP-rtTA) was subjected to RNA extraction and individual samples hybridized to array platform MOE430A 2.0 Affymetrix.

Background corr dist: KL-Divergence = 0.1767, L1-Distance = 0.0485, L2-Distance = 0.0056, Normal std = 0.3528

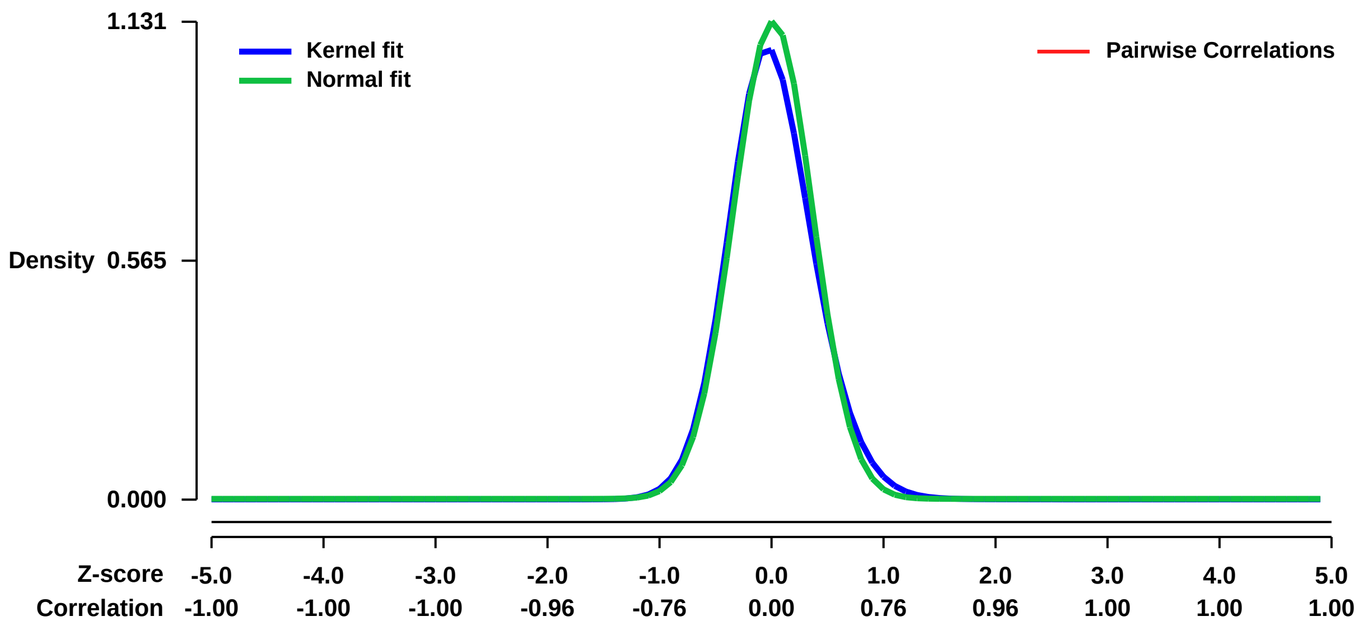

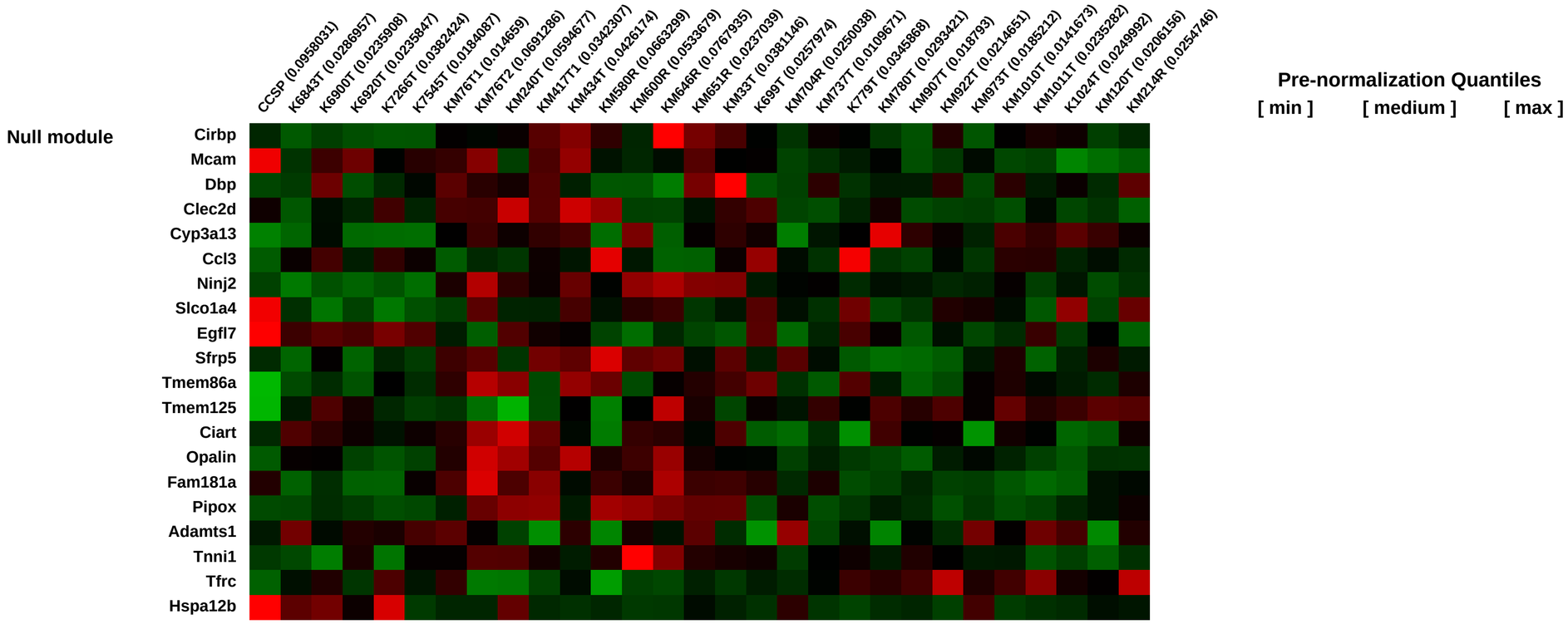

GEO Series "GSE19778" Expression Profiles

Num of samples in this series: 6

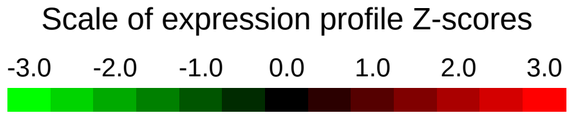

GEO Link:	http://www.ncbi.nlm.nih.gov/geo/query/acc.cgi?acc=GSE19778
Status:	Public on Jan 01 2011
Title:	The soluble intracellular domain of megalin does not affect renal proximal tubular function in vivo
Organism:	Mus musculus
Experiment type:	Expression profiling by array
Platform:	GPL1261
Pubmed ID:	20531455
Summary & Design:	**Summary:** The endocytic receptor megalin constitutes the main pathway for clearance of plasma proteins from the glomerular filtrate in the proximal tubules. However, little is know about the mechanisms that control receptor activity. A widely discussed hypothesis states that the intracellular domain (ICD) of megalin, released upon ligand binding, acts as a transcription regulator to suppress receptor expression - a mechanism proposed to safeguard the proximal tubules from protein overload. Here, we have put this hypothesis to the test by generating a mouse model co-expressing the soluble ICD and the full-length receptor. Despite pronounced expression in the proximal tubules, the ICD failed to exert any effects on renal proximal tubular function such as megalin expression, protein retrieval, or renal gene transcription. Thus, our data argue that the ICD does not play a role in regulation of megalin activity in vivo in the proximal tubules. We used microarrays to compare gene expression profile in adult kidney from a new mouse model expressing the intracellular domain of megalin with wildtype. **Overall design:** 10 week old mice were collected for RNA extraction and hybridization on Affymetrix microarrays. Three individuals for each genotype were analyzed comparing heterozygous animals for the intracellular domain of megalin with littermates controls.

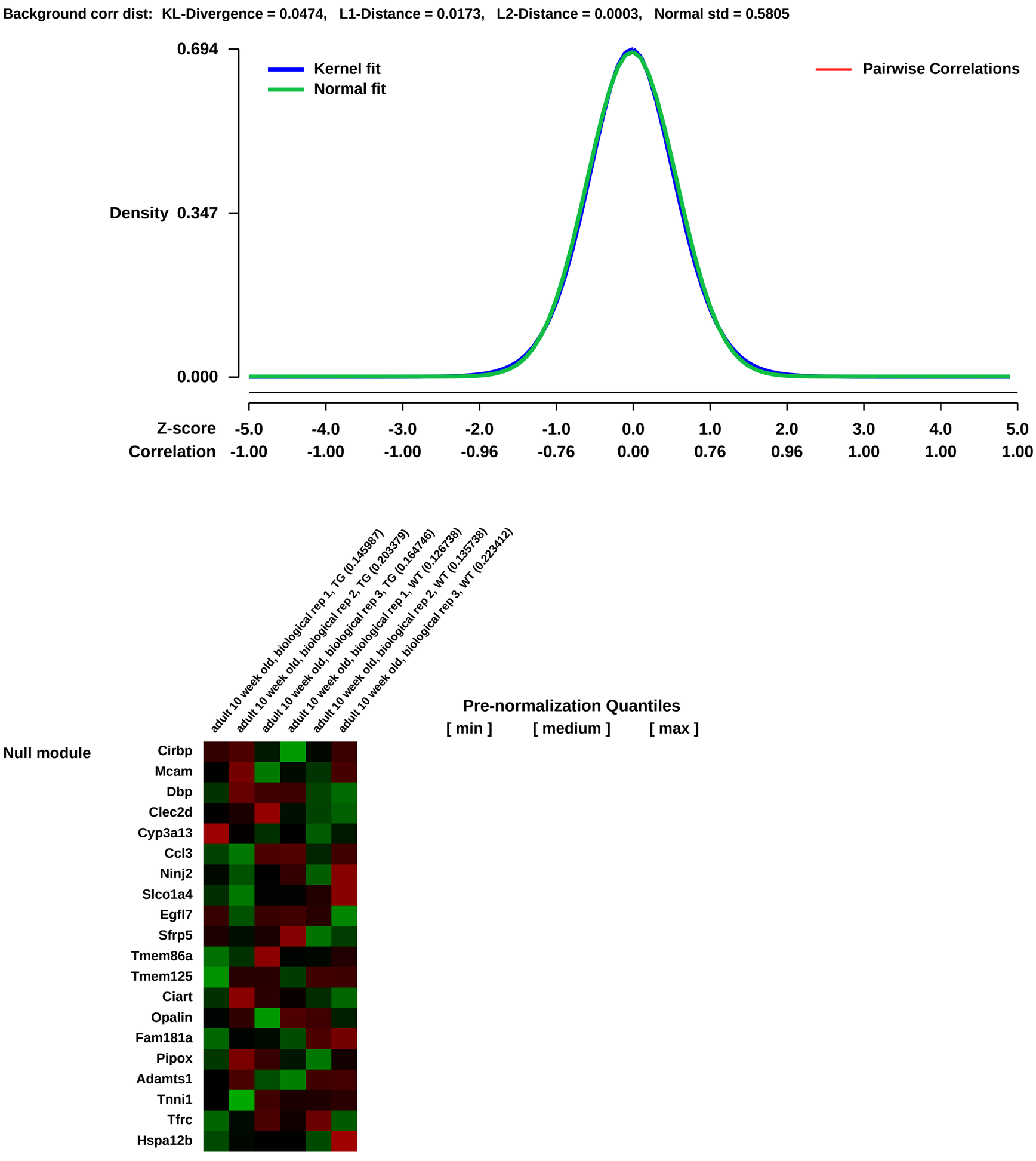

GEO Series "GSE19793" Expression Profiles

Num of samples in this series: 32

Scale of expression profile Z-scores

-3.0 -2.0 -1.0 0.0 1.0 2.0 3.0

GEO Link:	http://www.ncbi.nlm.nih.gov/geo/query/acc.cgi?acc=GSE19793
Status:	Public on Jun 24 2010
Title:	MyD88-mediated signaling prevents development of adenocarcinomas of the colon via interleukin-18
Organism:	Mus musculus
Experiment type:	Expression profiling by array
Platform:	GPL1261
Pubmed ID:	
Summary & Design:	**Summary:** Inflammation has pleiotropic effects on carcinogenesis and tumor progression. Signaling through the adaptor protein MyD88 promotes carcinogenesis in several chemically induced cancer models. Interestingly, we observed a protective role for MyD88 in the development of AOM/DSS colitis-associated cancer. The inability of Myd88-/- mice to heal ulcers generated upon injury creates an inflammatory environment that increases the frequency of mutations and results in a dramatic increase in adenoma formation and cancer progression. Susceptibility to colitis development and enhanced polyp formation were also observed in Il18-/- mice upon AOM/DSS treatment, suggesting that the phenotype of MyD88 knockouts is in part due to their inability to signal through the IL-18 receptor. This study revealed a previously unknown level of complexity surrounding MyD88 activities downstream of different receptors that differentially impact tissue homeostasis and carcinogenesis. **Overall design:** The Myd88 knockout mice were backcrossed to obtain at least 98% congenicity to B6NCr background. As control groups, wild type mice of identical background were used. Ten biological repeats were performed for the treated wild type and Myd88 samples. Six biological repeats were performed for the untreated wild type and Myd88 samples.

Background corr dist: KL-Divergence = 0.3306, L1-Distance = 0.0446, L2-Distance = 0.0044, Normal std = 0.2690

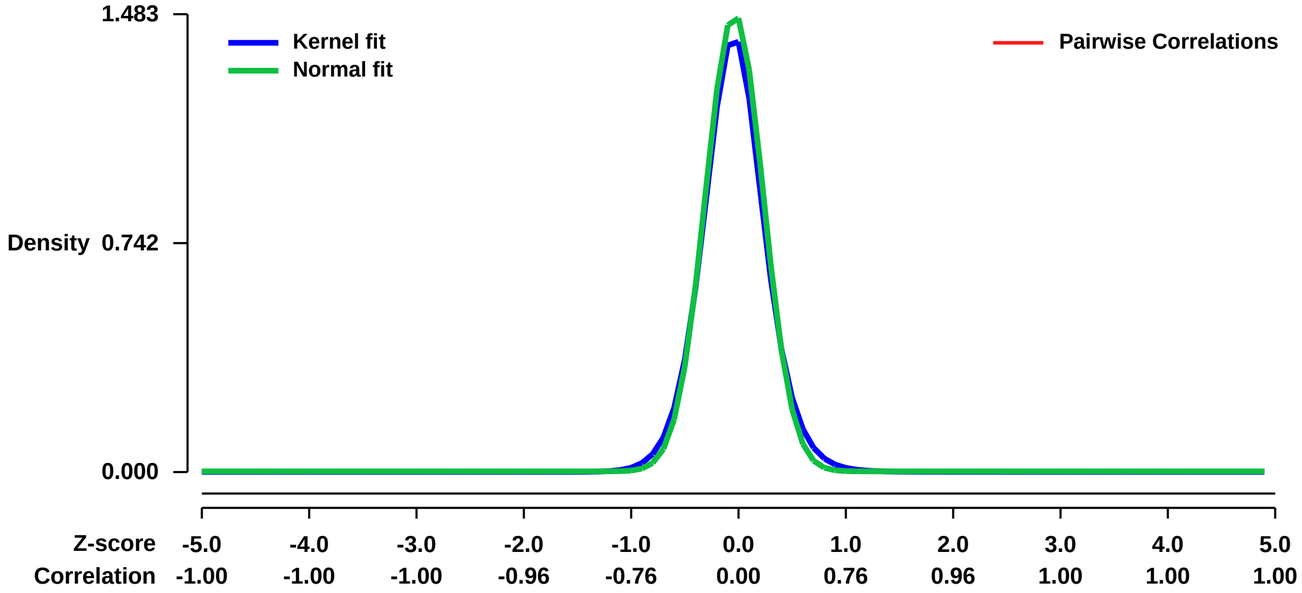

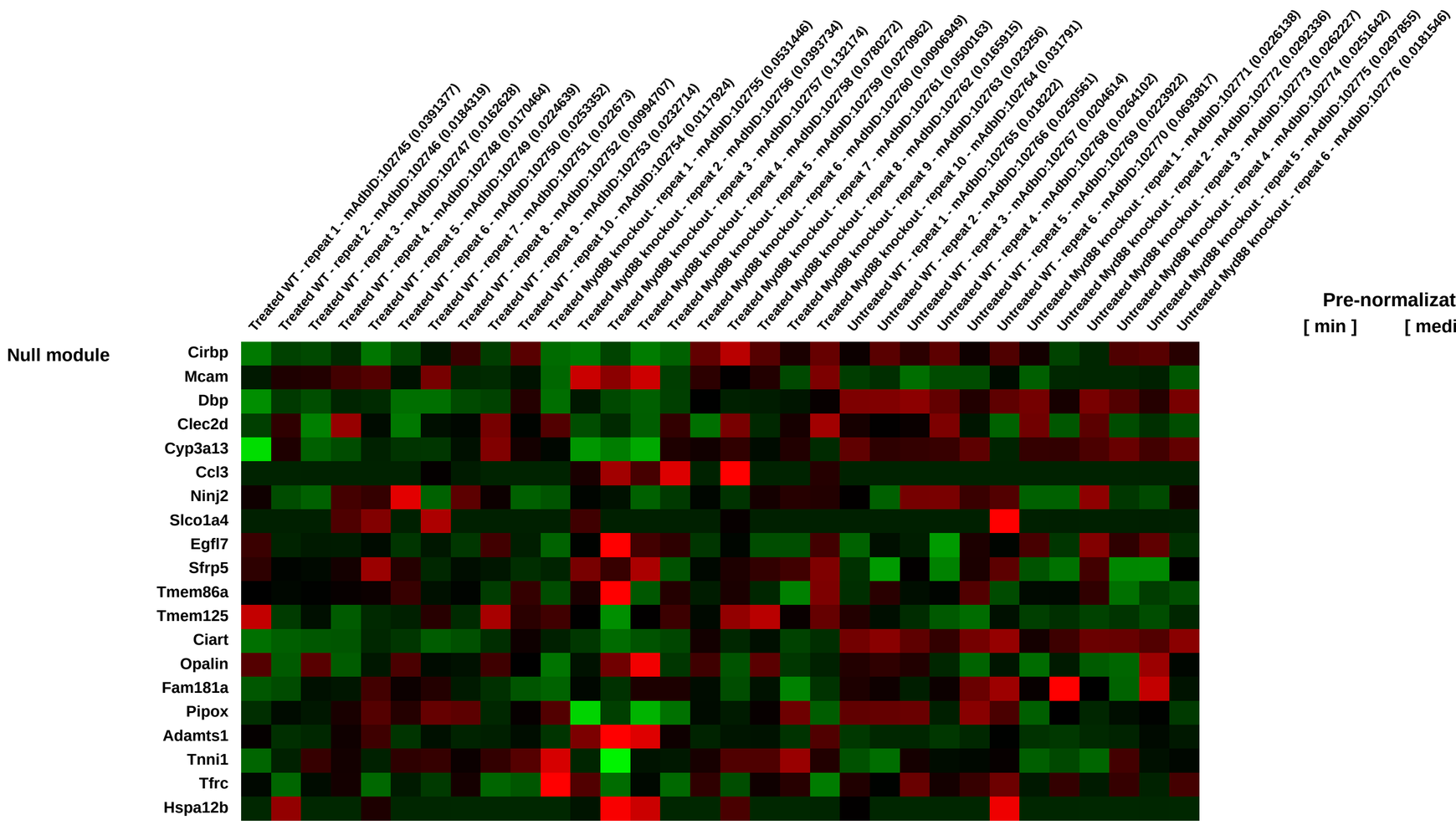

GEO Series "GSE19875" Expression Profiles

Num of samples in this series: 12

Scale of expression profile Z-scores

-3.0 -2.0 -1.0 0.0 1.0 2.0 3.0

GEO Link:	http://www.ncbi.nlm.nih.gov/geo/query/acc.cgi?acc=GSE19875
Status:	Public on Jan 14 2010
Title:	Expression data from murine hearts exposed to ischemic preconditioning comparing A2BAR null and wildtype BL6/C57 mice
Organism:	Mus musculus
Experiment type:	Expression profiling by array
Platform:	GPL1261
Pubmed ID:	22504483
Summary & Design:	**Summary:** Genetically targeted mice with deficiency for the A2BAR show increased susceptibility to acute myocardial ischemia and are not protected by IP, a powerful strategy for cardioprotection, where short and repeated episodes of ischemia and reperfusion prior to myocardial infarction result in attenuation of infarct size. The purpose of this study was to identify genes that are potentially under the control of the cardiac A2B adenosine receptor **Overall design:** Untreated wildtype and A2BAR-/- mice were compared to wildtype and A2BAR-/- mice with IP treatment following a 2 hours reperfusion period

Background corr dist: KL-Divergence = 0.1380, L1-Distance = 0.0290, L2-Distance = 0.0015, Normal std = 0.3889

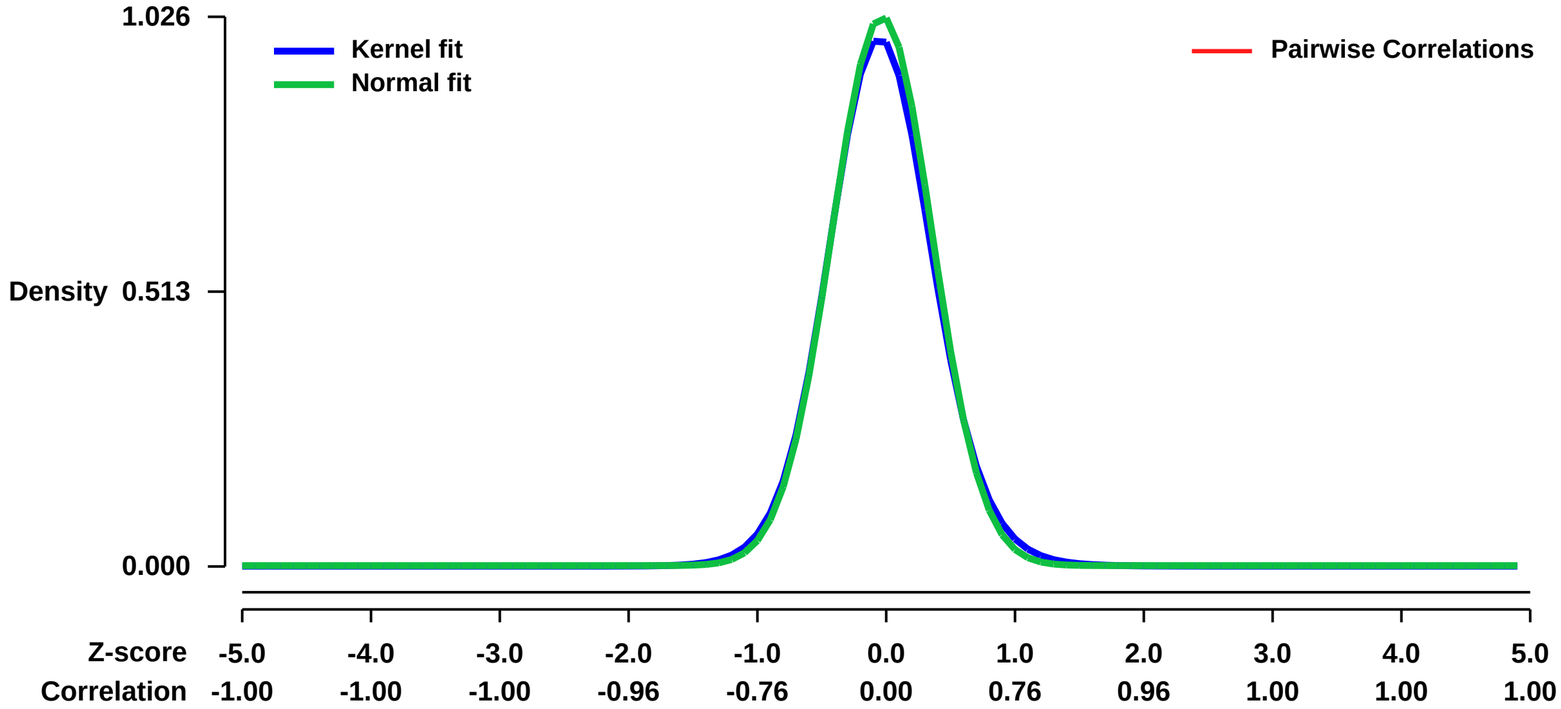

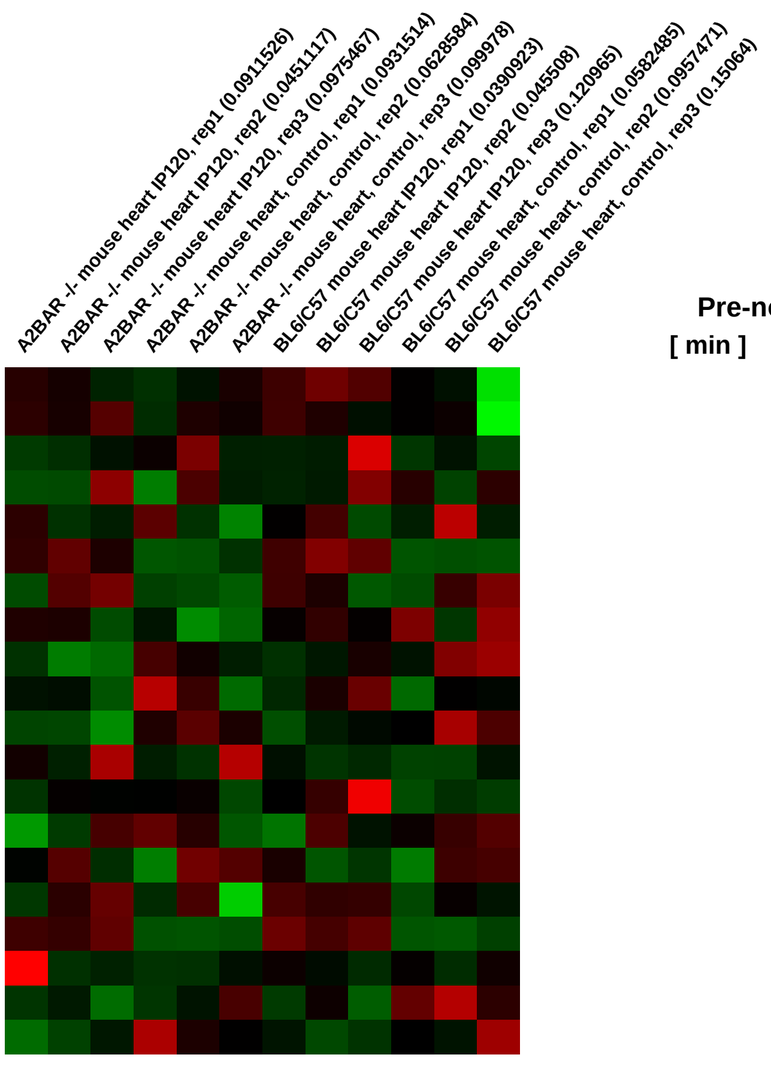

GEO Series "GSE19885" Expression Profiles

Num of samples in this series: 9

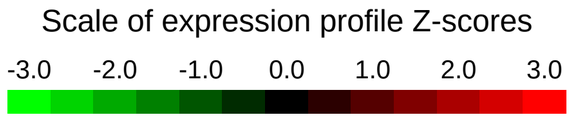

GEO Link:	http://www.ncbi.nlm.nih.gov/geo/query/acc.cgi?acc=GSE19885
Status:	Public on Feb 08 2013
Title:	Gene expression data from rapamycin resistant and sensitive cell lines
Organism:	Mus musculus
Experiment type:	Expression profiling by array
Platform:	GPL1261
Pubmed ID:	23300087
Summary & Design:	**Summary:** The mammalian target of rapamycin (mTOR) is a central regulator of cell proliferation. Inhibitors of mTOR are being evaluated as anti-tumor agents. Given the emerging role of microRNAs (miRNAs) in tumorgenesis we hypothesized that miRNAs could play important roles in the response of tumors to mTOR inhibitors. Rapamycin resistant myogenic cells developed by long-term rapamycin treatment showed extensive reprogramming of miRNAs expression, characterized by up-regulation of the mir-17~92 and related clusters and down-regulation of tumor-suppressor miRNAs. Antagonists of oncogenic miRNA families and mimics of tumor suppressor miRNAs (let-7) restored rapamycin sensitivity in resistant tumor cells. This study identified miRNAs as new downstream components of the mTOR-signaling pathway, which may determine the response of tumors to mTOR inhibitors. **Overall design:** Total RNA extraction and hybridization on Affymetrix microarrays of rapamycin sensitive (RS) cells (BC3H1, mouse brain tumor cell line with myogenic properties, ATCC) cultured in Dulbeccoâ s modified essential medium (DMEM) media supplemented with 20% fetal bovine serum (FBS), penicillin (100 U/ml) and streptomycin (100 mg/ml). Rapamycin resistant cells (RR1) were developed by culturing BC3H1 cells in the presence of 1 uM rapamycin for 6 months. Three samples in triplicates: 1) Rapamycin sensitive cells treated with DMSO for 24 h(BC3H1, reference), 2) Rapamycin sensitive cells treated for 24 h with 100 nM rapamycin (BC3H1+R), 3) Rapamycin resistant cells constantly treated with 1uM Rapamycion (RR1+R).

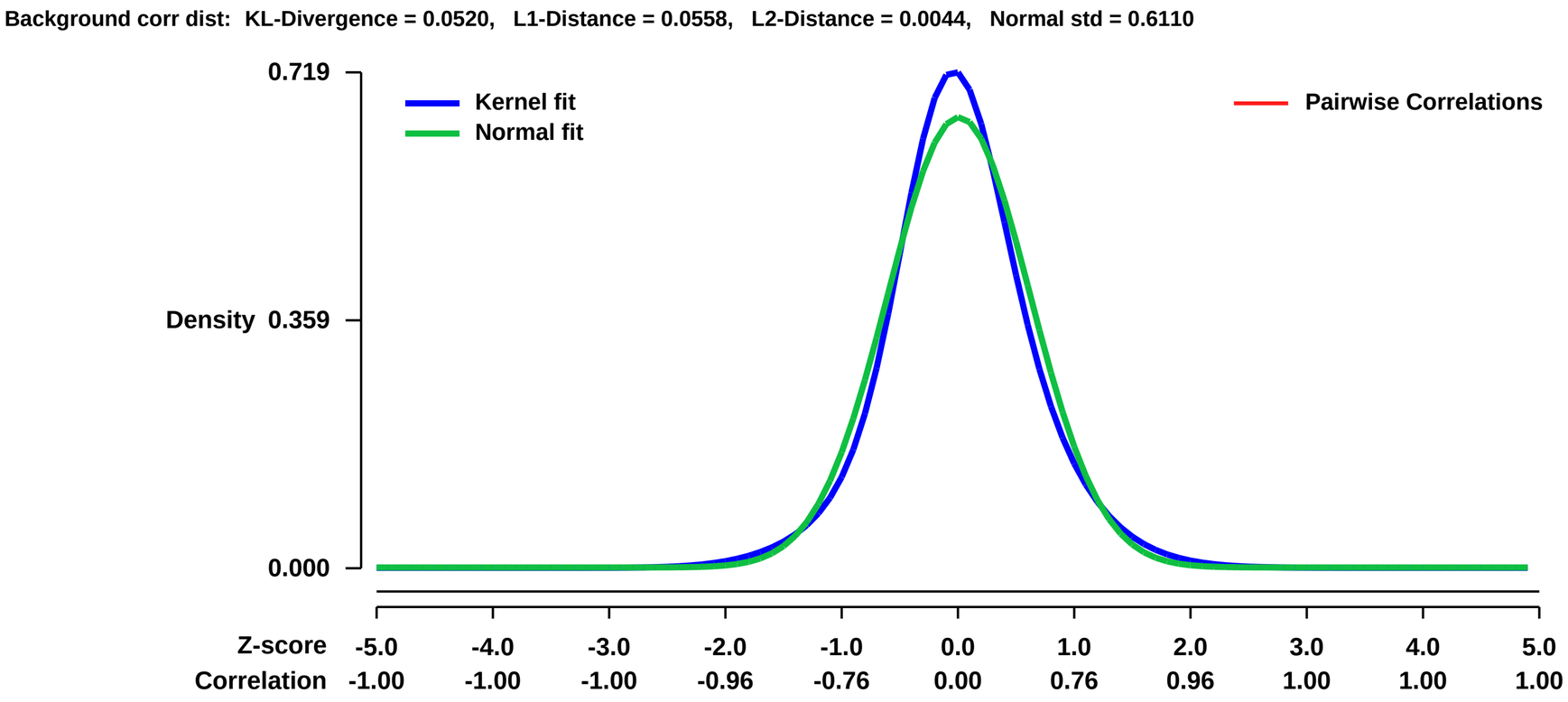

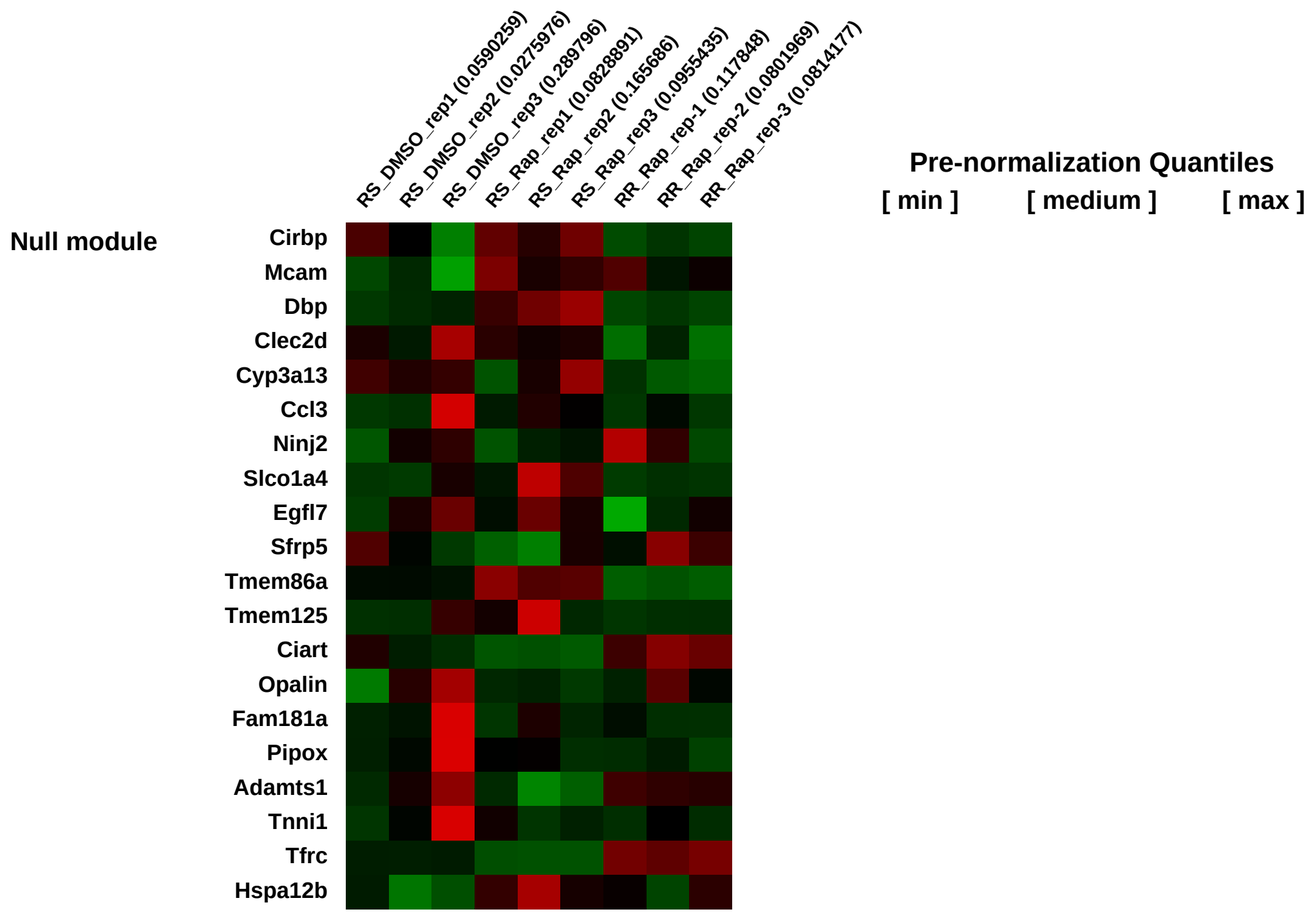

GEO Series "GSE19925" Expression Profiles

Num of samples in this series: 6

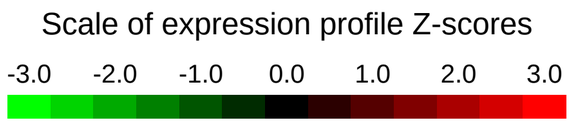

GEO Link:	http://www.ncbi.nlm.nih.gov/geo/query/acc.cgi?acc=GSE19925
Status:	Public on Dec 18 2010
Title:	Gene expression profile of the mammary stroma in Rarb -/- mice compared to their wild type littermates
Organism:	Mus musculus
Experiment type:	Expression profiling by array
Platform:	GPL1261
Pubmed ID:	21187396
Summary & Design:	**Summary:** Inactivation of RAR-b, which has been reported as a tumor suppressing gene by numerous studies, results in protective effect against the tumorigenesis induced by activated ErbB2. Moreover, tissue recombination indicates that the RAR-b deficient-microenvironment, rather than the RAR-b status of mammary epithelial cells, plays a key-determining role in the initiation and progression of the mammary carcinoma. Ablation of RAR-b extensively modulates the remodeling of stroma during tumor progression through suppressing the activation and transdifferetiation of myofibroblasts. RNA microarray has been employed to identify the gene expression signature in the mammary stroma of our RAR-b null animals. We want to find out the underlining mechanism of the protective effects resulted from Rarb abliton. **Overall design:** A global gene expression profile of mouse mammary stroma was obtained on total RNA from the cleared mammary fat pads (stroma) of both RAR-b KO (n=3) and their wild type (n=3) littermates at the age of four weeks.

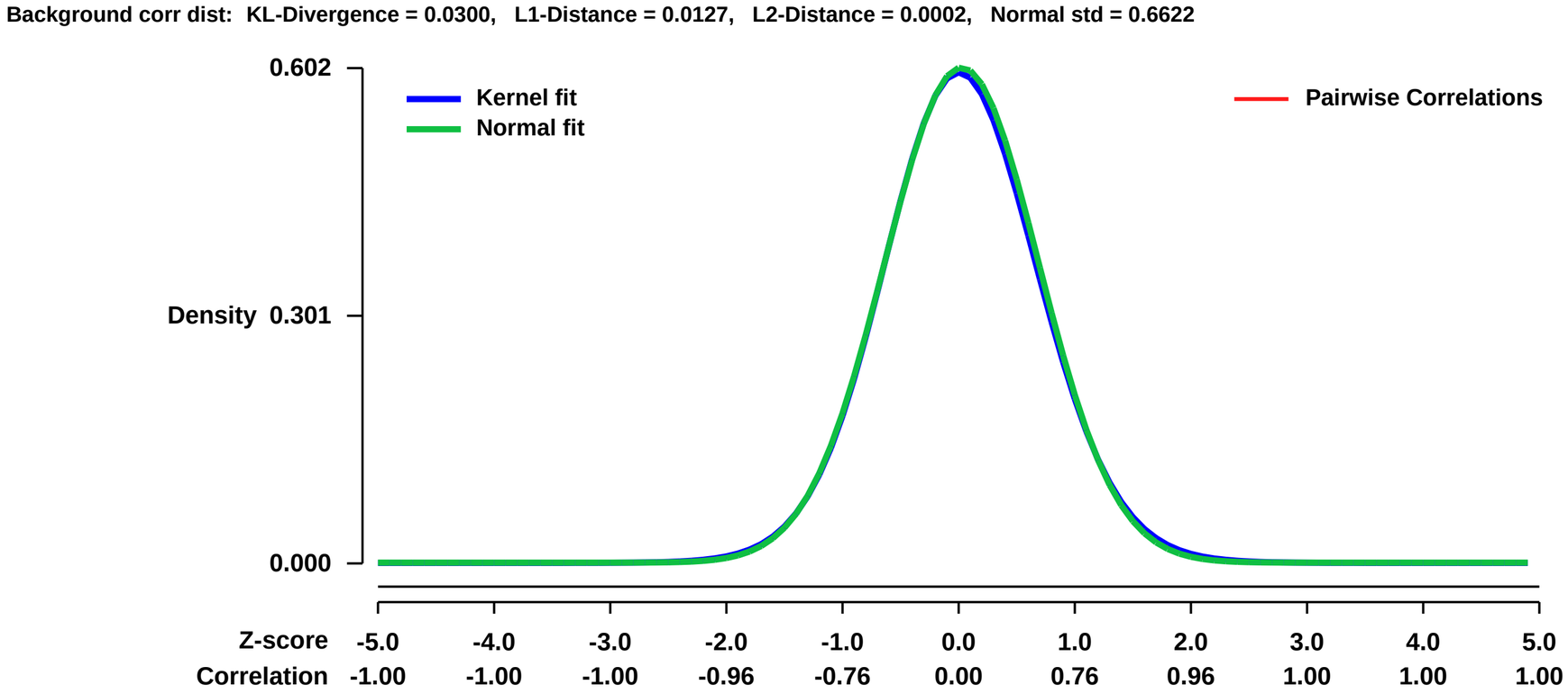

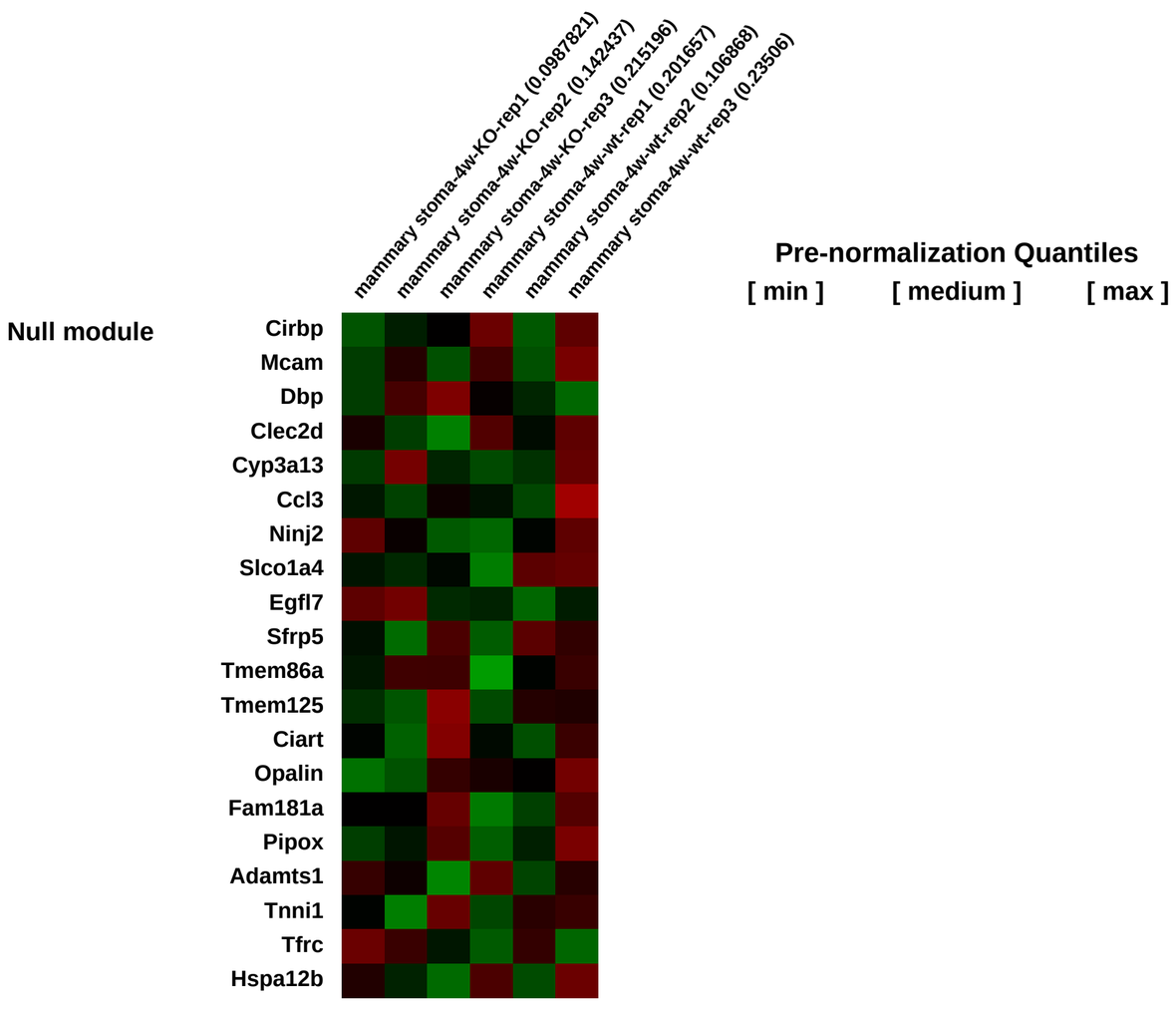

GEO Series "GSE19979" Expression Profiles

Num of samples in this series: 6

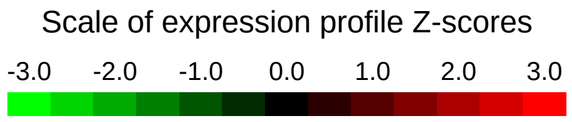

GEO Link:	http://www.ncbi.nlm.nih.gov/geo/query/acc.cgi?acc=GSE19979
Status:	Public on Jan 22 2010
Title:	Gene expression profiles of P7 bladder epithelium compartments isolated from Upk1b mice. (GUDMAP Series ID: 34)
Organism:	Mus musculus
Experiment type:	Expression profiling by array
Platform:	GPL1261
Pubmed ID:	
Summary & Design:	**Summary:** The long term objective is to create an encyclopedia of the expression levels of all genes in multiple components of the developing genitourinary tract The central thesis is straightforward. The combination of microdissected tissues and FACS sorted cells plus microarray analysis offers a powerful, efficient and effective method for the creation of a global gene expression atlas of the developing urogenital system. Microarrays with essentially complete genome coverage can be used to quantitate expression levels of every gene. The ensuing rapid read-out provides an expression atlas that is more sensitive, more economical and more complete than would be possible by in situ hybridizations alone. The data submitted here delineates the gene expression profiles of the epithelial compartments of the P7 mouse bladder. **Overall design:** At postnatal day 7 mice were euthanized by CO2 asphyxiation and the bladders were removed and cut at the bladder neck. The bladder was cut into rings and treated with 1 mg/ml trypsin in Tyrode's solution for 30 minutes at 37 ´°C. The layers were separated by gentle microdissection and the epithelial layer was further digested in a mixture of Blendzymes 1 & 4 at 37 ´°C until a single cell suspension was obtained. The samples were placed in RLT and stored at -80 ´°C.RNA was prepared and the Epicentre 2-round amplification scheme described under the Lessard Group Protocols on the GUDMAP pages were performed. The Affymetrix GeneChip Mouse Genome 430 2.0 Array was used to interrogate the amplified RNA.

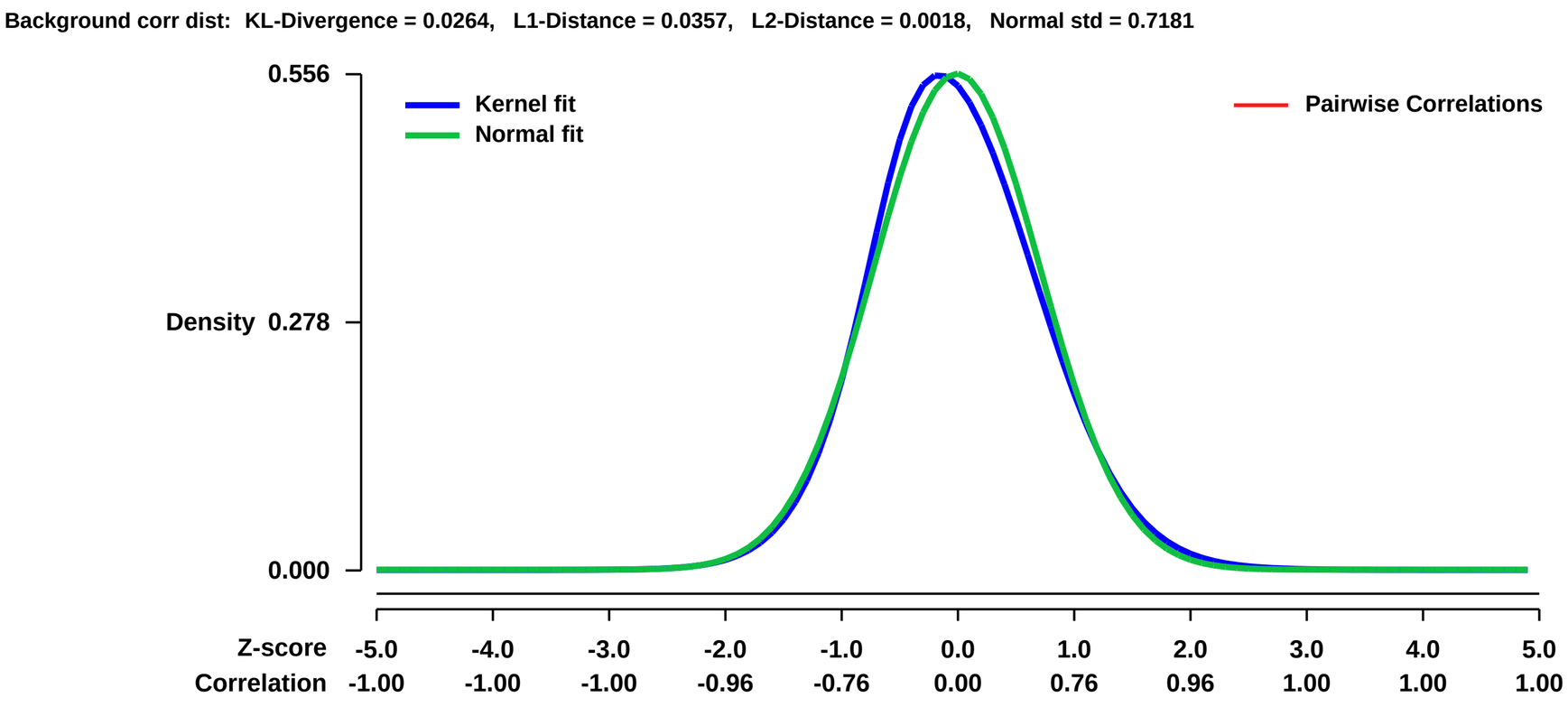

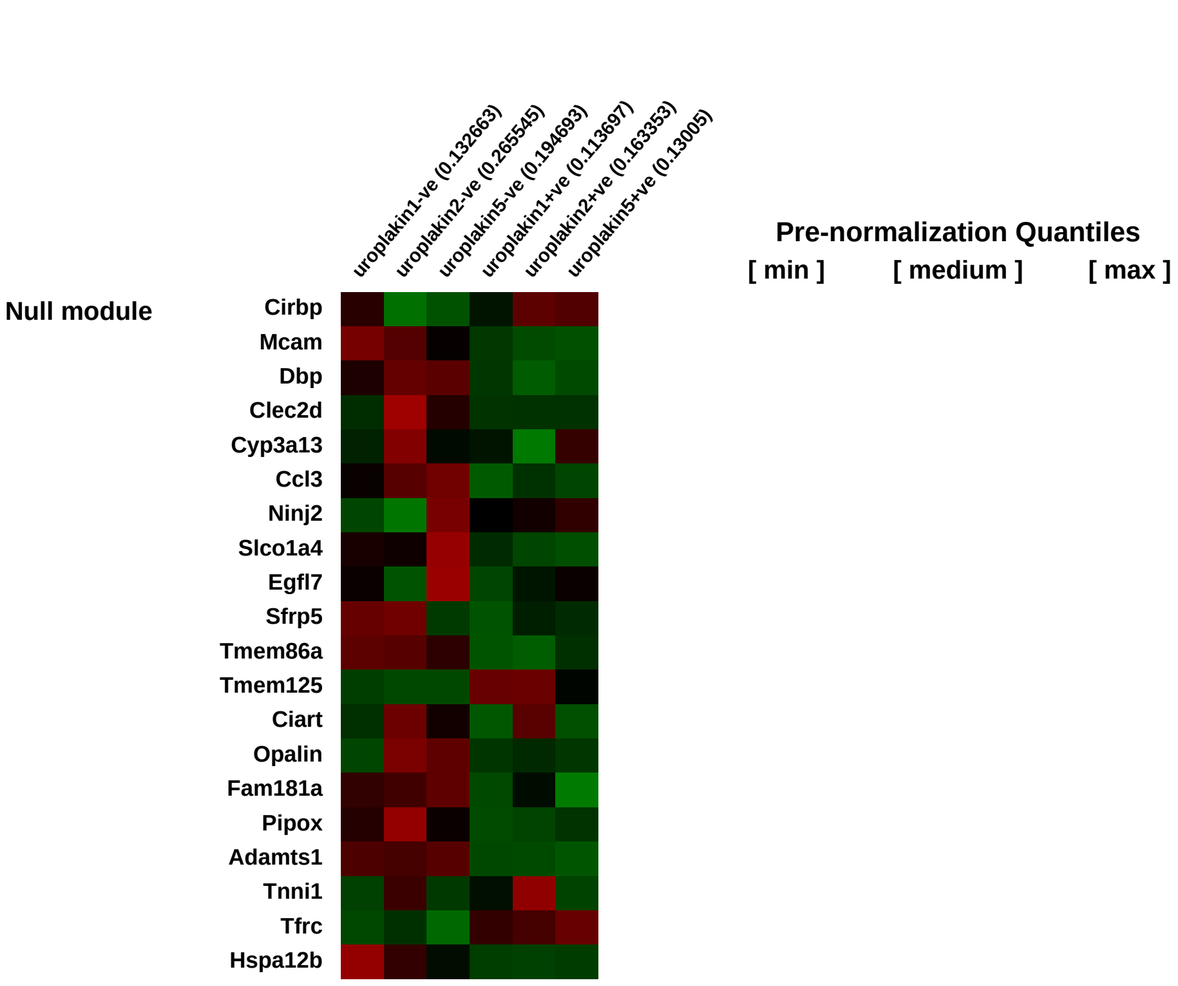

GEO Series "GSE1999" Expression Profiles

Num of samples in this series: 15

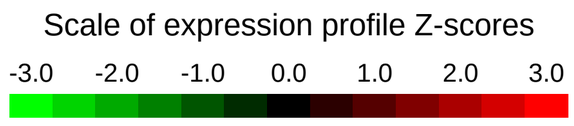

GEO Link:	**http://www.ncbi.nlm.nih.gov/geo/query/acc.cgi?acc=GSE1999**
Status:	**Public on Nov 24 2004**
Title:	**Neuroprotective effects of erythropoietin. Wilson-5R01NS028208-15**
Organism:	**Mus musculus**
Experiment type:	**Expression profiling by array**
Platform:	**GPL1261**
Pubmed ID:	

Summary & Design:

Summary:
Hypoxic-ischemic (HI) injury in the developing brain is a common cause of disability in children, and there are no effective treatments at this time. Erythropoietin (EPO) has recently gained interest as a neuroprotective drug, and EPO and its receptor are expressed within the central nervous system. We have recently shown that pretreatment with EPO markedly reduced brain injury caused by unilateral hypoxic-ischemic insult in 7 day old mice. EPO did not reduce early signs of neuronal injury at 6 hours, but significantly protected the neonatal brain when assessed 24 hours and 7 days after HI. The mechanism of this delayed protection is unclear, but is thought to involve transcription of neuroprotective genes, possibly subsequent to activation of NFkB. By comparing gene expression in EPO- and vehicle-(VEH) treated mice after HI, we should gain insight into the mechanisms underlying the neuroprotective effects of EPO and may identify additional targets for therapeutic interventions.

We will compare gene expression patterns in 7-day old mouse forebrain after 1) VEH pretreatment plus sham surgery, 2) VEH pretreatment plus HI, and 3) EPO pretreatment plus HI. We will thus identify genes induced by HI in the developing brain and characterize changes in gene expression caused by EPO pretreatment. We will use the model of neonatal hypoxic-ischemic injury and EPO treatment parameters that were used in our prior studies demonstrating neuroprotection. Based on the time-course of neuroprotection defined in our prior study and the pharmacokinetic profile of EPO, we will examine gene expression 18 hours after HI.

We hypothesize that changes in gene expression after EPO pretreatment underlie the neuroprotective effects of this cytokine after neonatal hypoxic ischemic injury.

We will examine gene expression in 3 groups: 1) 1) VEH pretreatment + sham surgery, 2) VEH pretreatment + HI, and 3) EPO pretreatment + HI. EPO (5U/g, i.p.) or VEH was injected in 7 day old mice, drawn from 4 litters, with 3 to 4 pups per treatment group in each litter. One hour later, the right common carotid artery was ligated under isoflurane anesthesia, animals were allowed to recover for 90 min and were then placed in hypoxic chambers (10% oxygen, balance nitrogen) for 50 min. The animals subjected to sham surgery received isoflurane anesthesia for a comparable period, incision and dissection to visualize the common carotid artery, but no ligation and no hypoxia. Eighteen hrs later, animals were anesthetized with isoflurane and the right hemisphere was rapidly dissected and placed in RNA Later (Qiagen) at 4C. Total RNA was isolated using an RNeasy lipid tissue mini kit (QIAzol lysis and RNeasy purification, Qiagen). RNA concentrations were determined spectrophotometrically and an aliquot of each sample was examined by gel electrophoresis to screen for degradation. Samples were stored at -80C. After quality control screening, we selected 5 male and 5 female samples per treatment group (extra samples were reserved). We plan to pool 1 male and 1 female for each microarray sample and we plan to run 5 microarrays from each treatment group, for a total of 15 microarrays. We would like to have Agilent Bioanalyzer quality control assays on the individual samples carried out by the consortium before pooling. We will send 10 micrograms of each sample for Agilent QC and subsequent pooling of equimolar amounts. We would like to use Affymetrix mouse gene chips (please advise which specific chips are available; are you using the GeneChip Mouse Expression array 430A or the GeneChip Mouse Genome 430 2.0 Array?).

Keywords: dose response

Overall design:

Background corr dist: KL-Divergence = 0.1184, L1-Distance = 0.0326, L2-Distance = 0.0019, Normal std = 0.4083

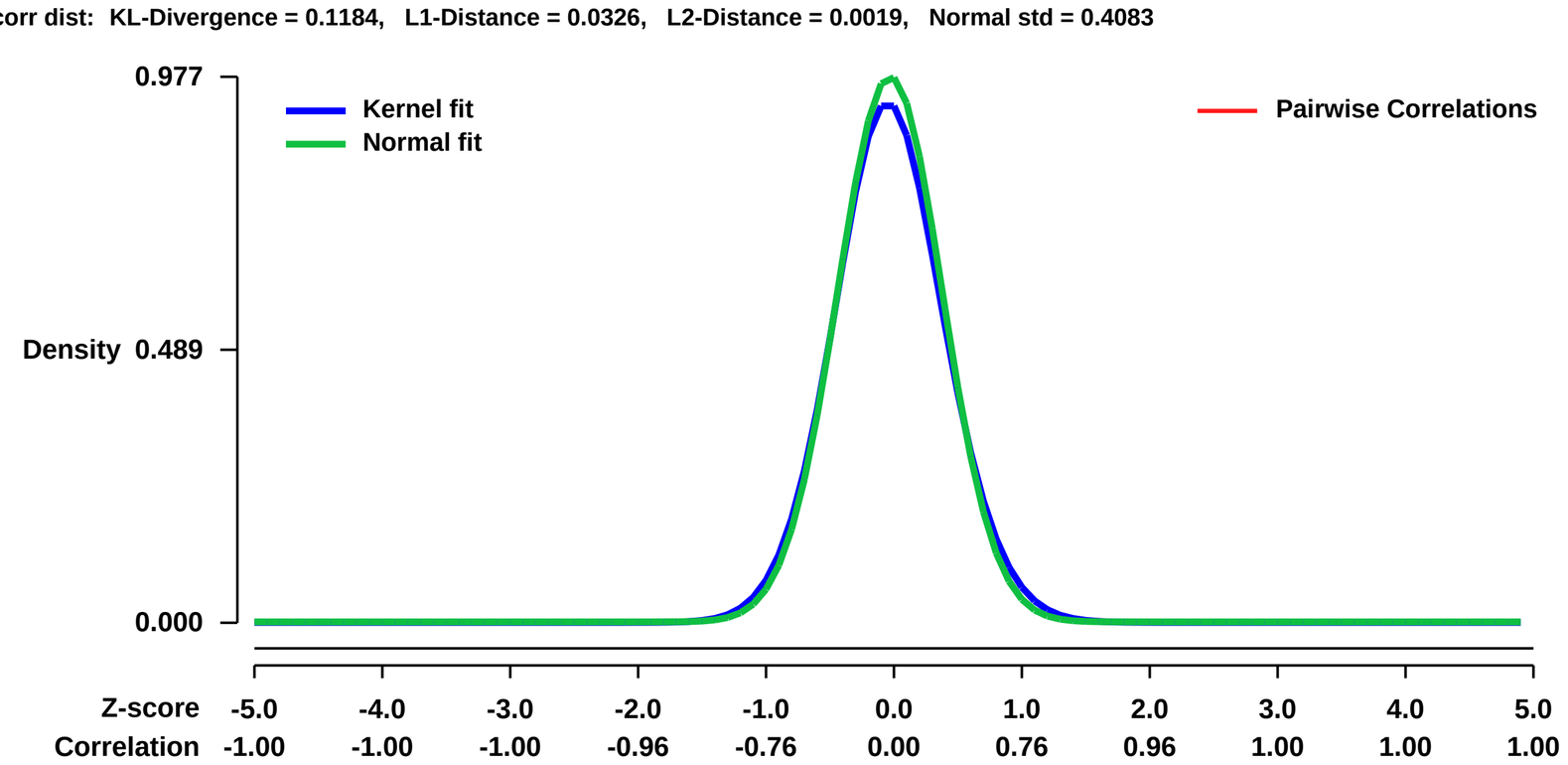

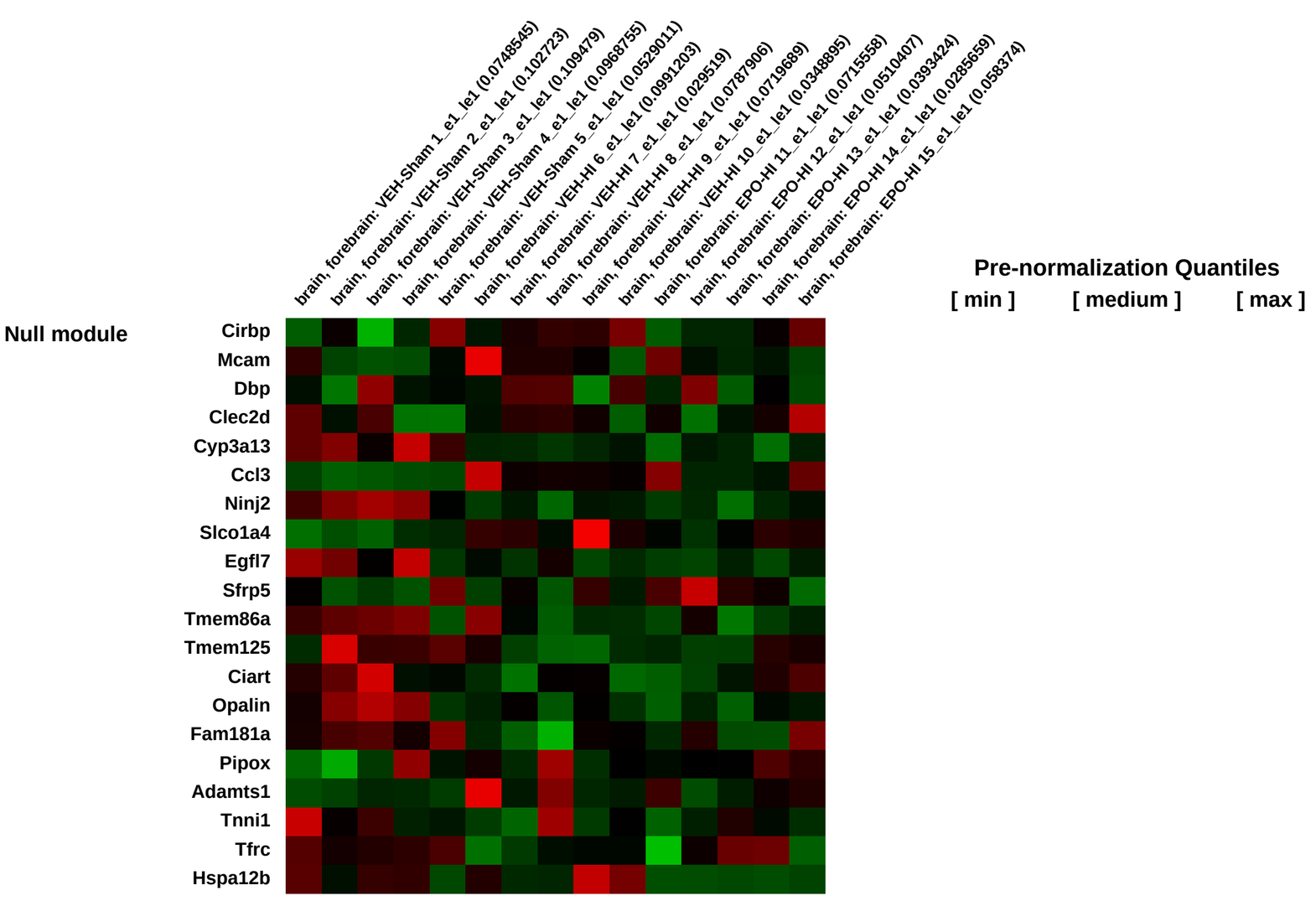

GEO Series "GSE19997" Expression Profiles

Num of samples in this series: 9

Scale of expression profile Z-scores

-3.0 -2.0 -1.0 0.0 1.0 2.0 3.0

GEO Link:	http://www.ncbi.nlm.nih.gov/geo/query/acc.cgi?acc=GSE19997
Status:	Public on Apr 09 2010
Title:	POU4F1 is associated with t(8;21) AML and contributes directly to its unique transcriptional signature
Organism:	Mus musculus
Experiment type:	Expression profiling by array
Platform:	GPL1261
Pubmed ID:	20376082
Summary & Design:	**Summary:** POU4F1 is associated with t(8;21) acute myeloid leukemia (AML) and contributes directly to its unique transcriptional signature **Overall design:** To identify targets of POU4F1, we performed gene expression profiling, comparing Pou4f1+/+ or Pou4f1-/- fetal liver cells to cells overexpressing POU4F1 and identified 140 differentially expressed genes.

Background corr dist: KL-Divergence = 0.0360, L1-Distance = 0.0369, L2-Distance = 0.0026, Normal std = 0.6235

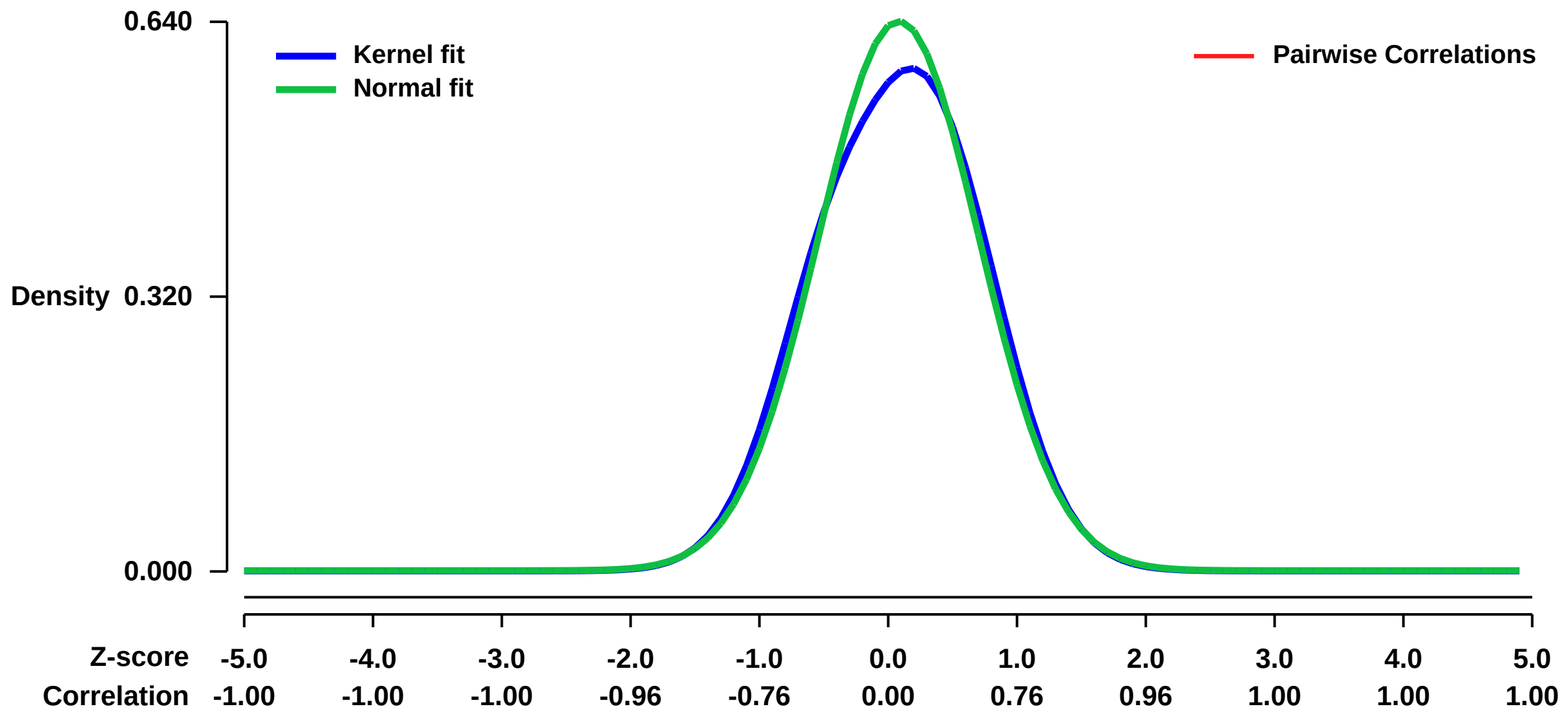

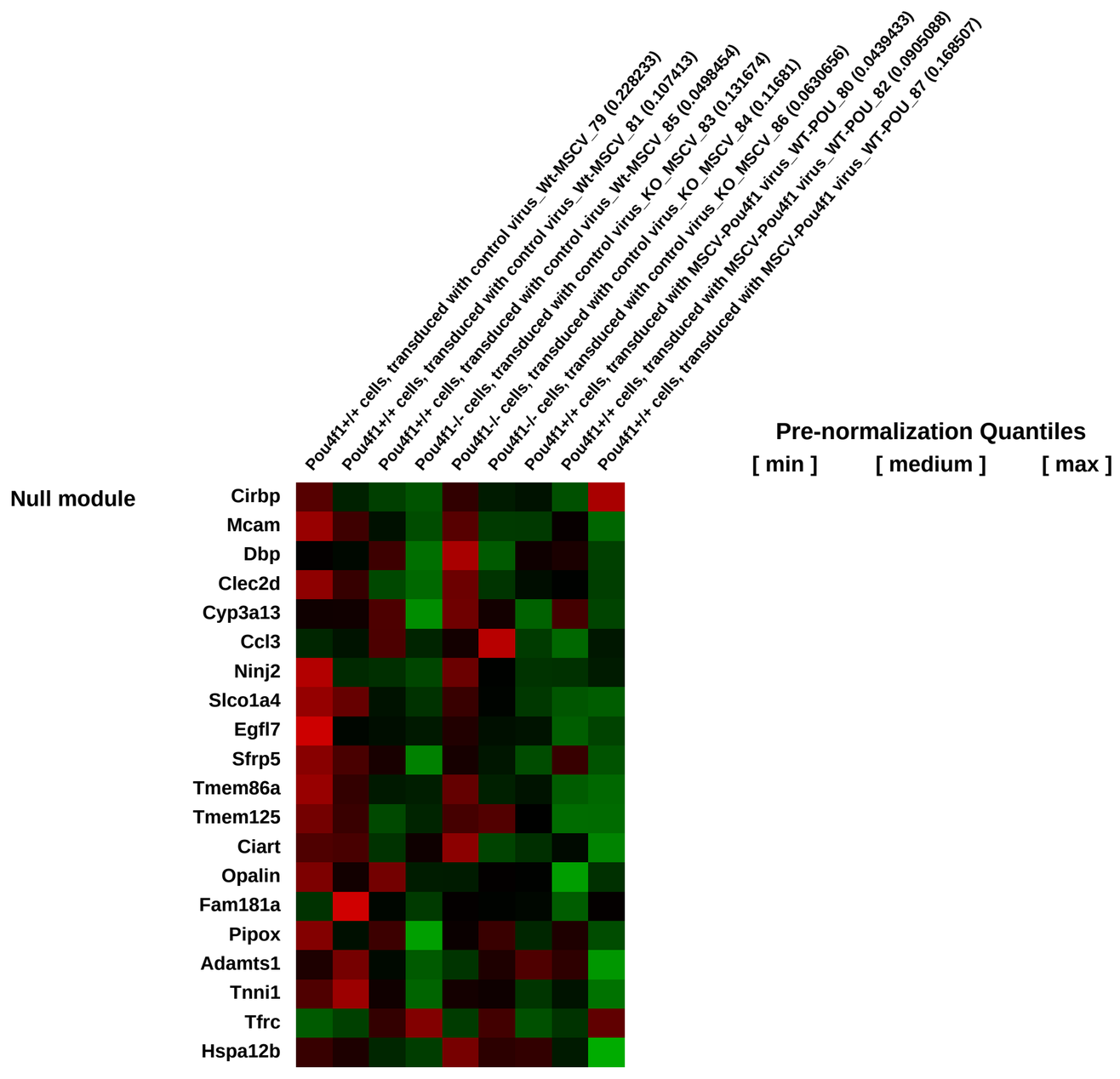

GEO Series "GSE20008" Expression Profiles

Num of samples in this series: 6

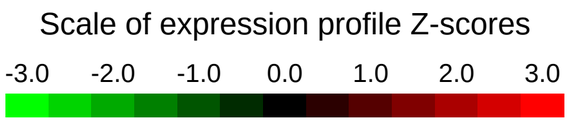

GEO Link:	**http://www.ncbi.nlm.nih.gov/geo/query/acc.cgi?acc=GSE20008**
Status:	**Public on Dec 31 2013**
Title:	**PCAF/GCN5-regulated genes in MEFs**
Organism:	**Mus musculus**
Experiment type:	**Expression profiling by array**
Platform:	**GPL1261**
Pubmed ID:	
Summary & Design:	**Summary:** **Histone acetyltransferases (HATs) GCN5/PCAF and CBP/p300 are transcription coactivators. However, how these HATs regulate ligand-induced nuclear receptor target gene expression remains unclear. Here we show in mouse embryonic fibroblasts (MEFs), deletion of GCN5/PCAF specifically eliminates acetylation on H3K9 (H3K9Ac) while deletion of CBP/p300 selectively reduces acetylation on H3K18 and H3K27 (H3K18/27Ac). Treating MEFs with a specific ligand for nuclear receptor PPARdelta induces sequential increases of H3K18/27Ac and H3K9Ac on the promoter of PPARdelta target gene Angptl4, which correlates with a robust ligand-induced Angptl4 expression. Inhibiting transcription elongation blocks ligand-induced H3K9Ac but not H3K18/27Ac on Angptl4 promoter. Finally, we show CBP/p300 and their HAT activities are required, while GCN5/PCAF and H3K9Ac are dispensable, for ligand-induced PPARdelta target gene expression in MEFs. These results highlight the substrate and site specificities of HATs in cells, and suggest that GCN5/PCAF- and CBP/p300-mediated histone acetylations play distinct roles in regulating ligand-induced nuclear receptor target gene expression.** **Overall design:** **PCAF and GCN5 have some redundant function. To identify PCAF/GCN5-regulated genes, immortalized MEFs with PCAF knockout and GCN5 conditional knockout were infected with retroviruses expressing either Cre recombinase or vector alone. We prepared duplicated RNAs from either vector or Cre infected cells (PCAF-/-;GCN5+/- or PCAF-/-;GCN5+/-) and RNAs from either Vector or Cre infected the other independently immortalized cells for 6 affymetrix microarray.**

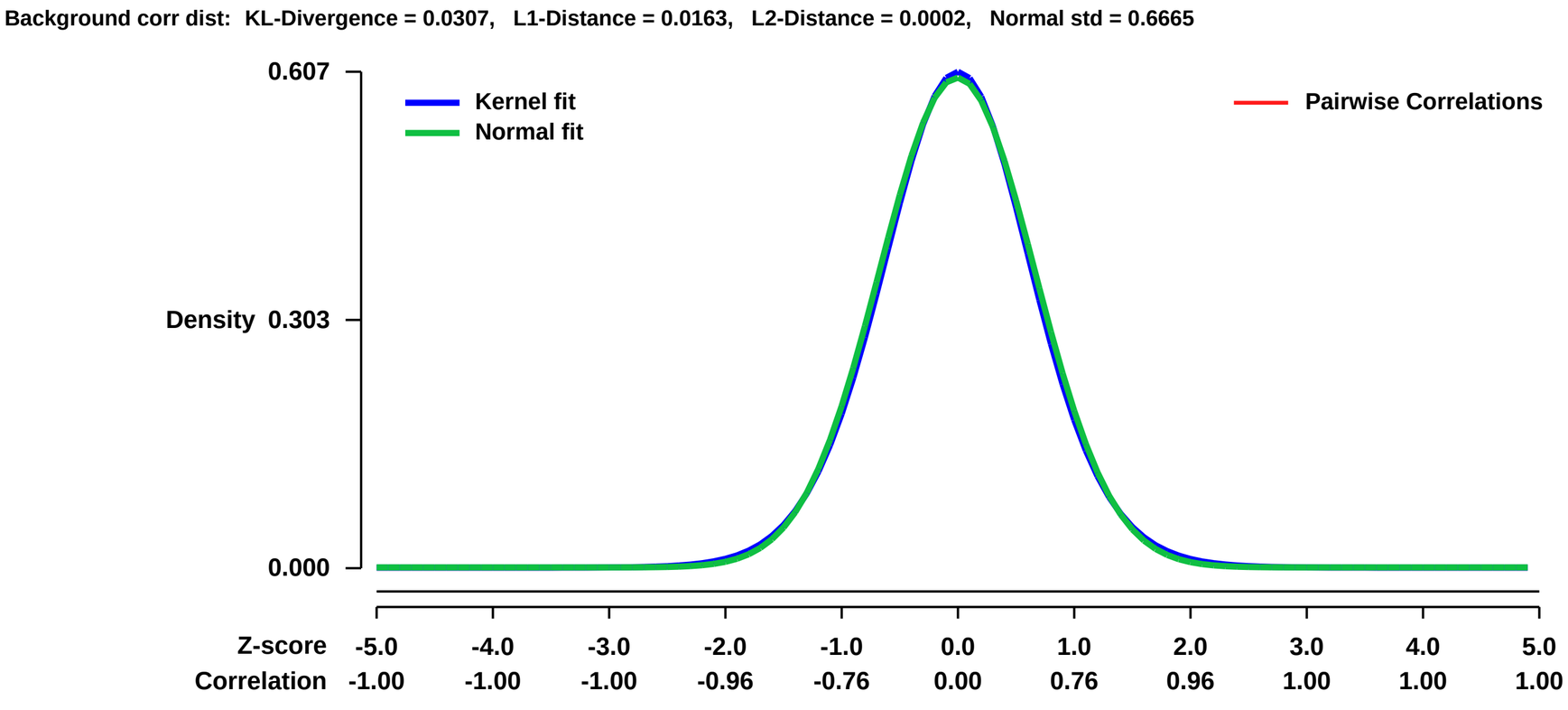

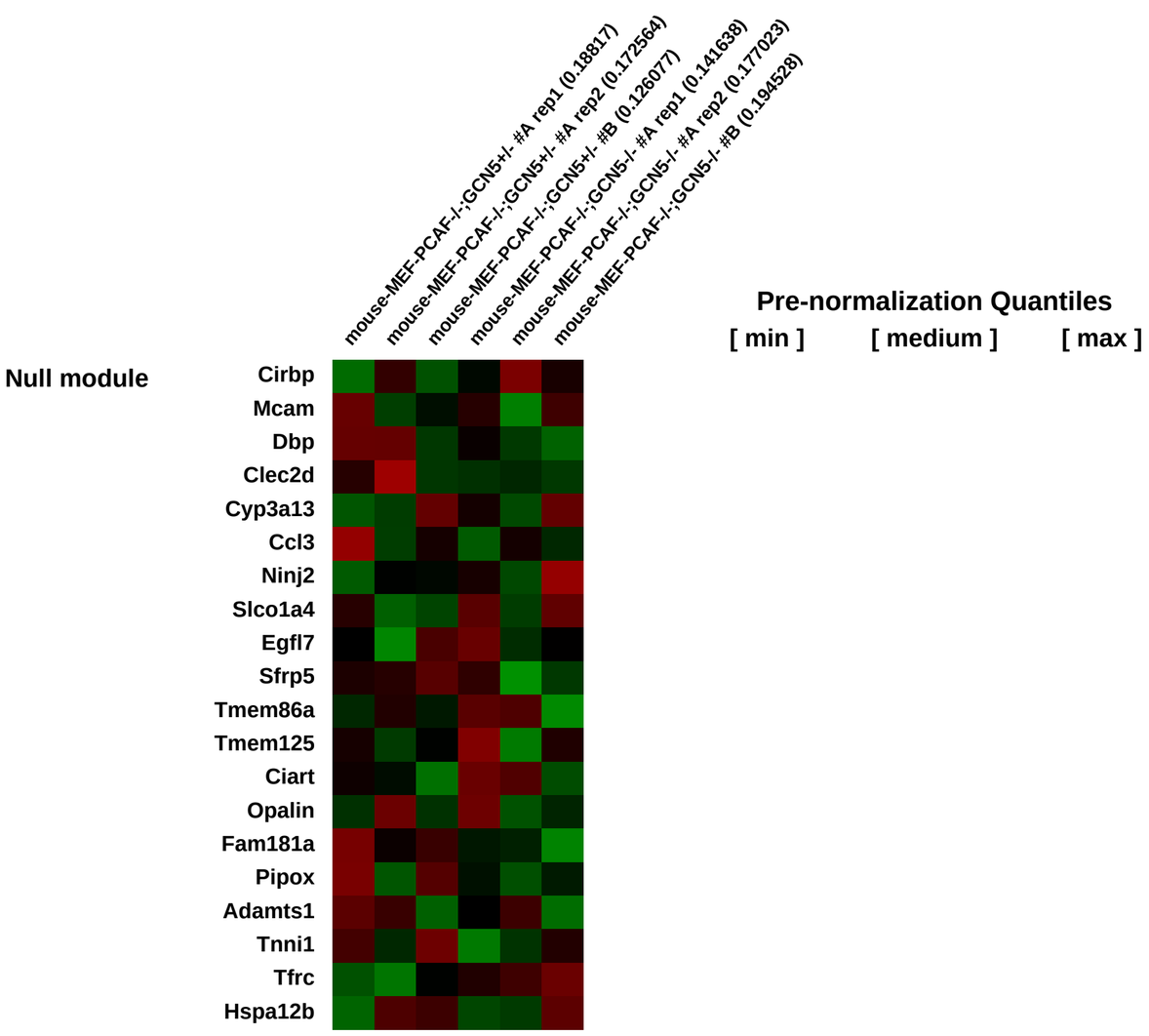

GEO Series "GSE20100" Expression Profiles

Num of samples in this series: 15

Scale of expression profile Z-scores

-3.0 -2.0 -1.0 0.0 1.0 2.0 3.0

GEO Link:	http://www.ncbi.nlm.nih.gov/geo/query/acc.cgi?acc=GSE20100
Status:	Public on Jul 01 2010
Title:	Expression data from primary MEF lacking either HDAC1, HDAC2 or both
Organism:	Mus musculus
Experiment type:	Expression profiling by array
Platform:	GPL1261
Pubmed ID:	20194438
Summary & Design:	**Summary:** Previously published data suggested some redundant functions between HDAC1 and HDAC2 in mouse. To test this hypothesis, we used microarrays to have a genome wide analysis at the transcription level of primary MEFs lacking HDAC1, HDAC2. **Overall design:** MEF HDAC1 F/F were were transduced with two different retroviruses: one virus expresses the Tamoxifen-inducible cre recombinase Cre-ERT2 and the second virus expresses either a small hairpin micro-RNA against HDAC2 or a scrambled version. HDAC1F/F MEFs expressing either a scrambled micro-RNA or a micro-RNA against HDAC2 can be induced by addition of Tamoxifen to delete HDAC1, thereby generating four different genotypes: WT, HDAC1 KO, HDAC2 knockdown (Kd) and HDAC1/2 KO/Kd.

Background corr dist: KL-Divergence = 0.0906, L1-Distance = 0.0823, L2-Distance = 0.0115, Normal std = 0.5232

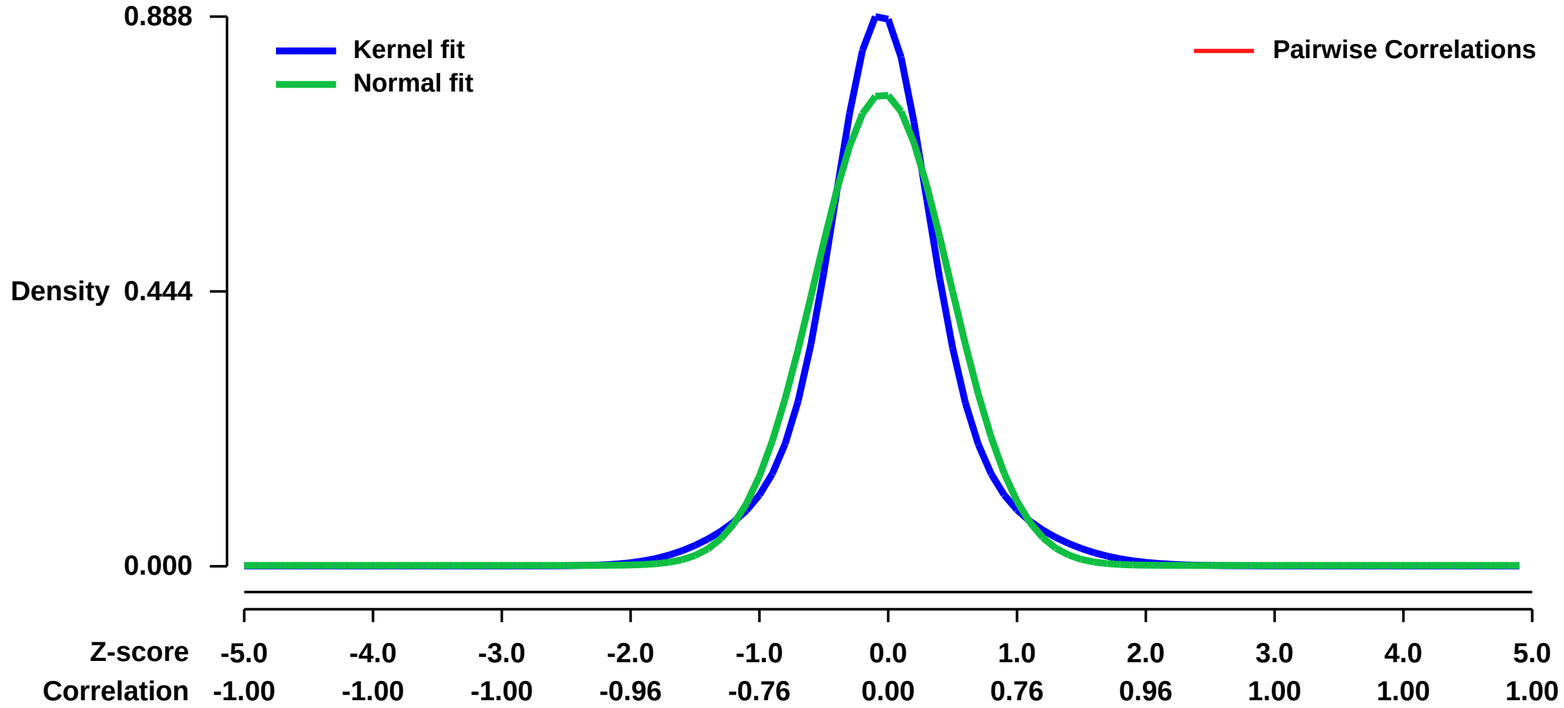

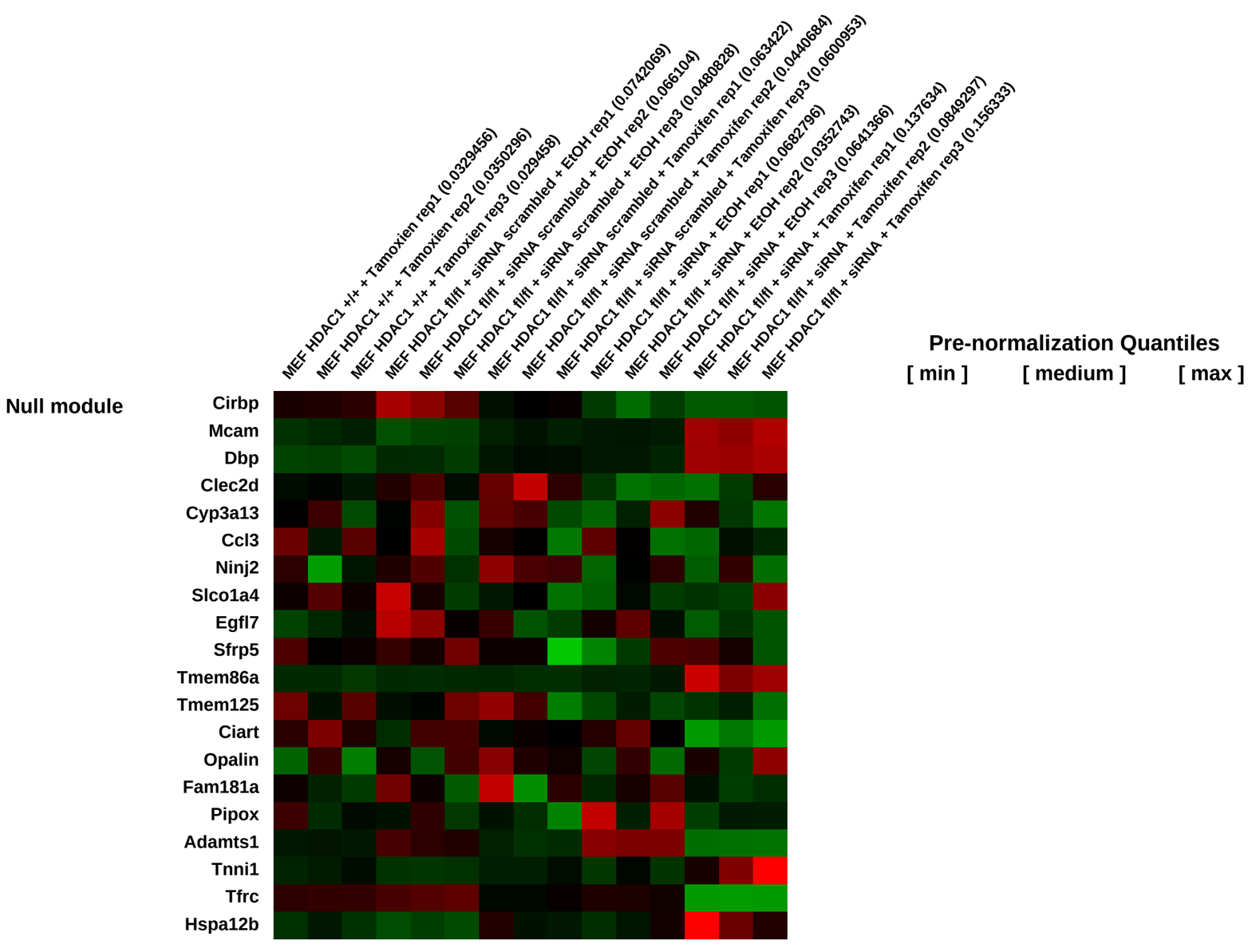

GEO Series "GSE20152" Expression Profiles

Num of samples in this series: 8

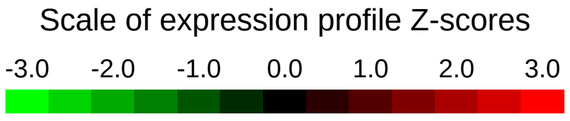

GEO Link:	http://www.ncbi.nlm.nih.gov/geo/query/acc.cgi?acc=GSE20152
Status:	Public on Jan 15 2011
Title:	The role of SphK1 in hTNF$_{\epsilon}$– induced inflammation
Organism:	Mus musculus
Experiment type:	Expression profiling by array
Platform:	GPL1261
Pubmed ID:	20644167
Summary & Design:	**Summary:** The study analyzes analyzes gene expression changes in the ankle joint in mouse TNFa overexpression models with or without sphingosine kinase 1 activity. SphK1 is a sphingolipid enzyme that converts sphingosine to bioactive sphingosine-1-phosphate (S1P). Recent data suggest a potential relationship between SphK1 and TNF$_{\epsilon}$– and have implicated SphK1/S1P in the development and progression of inflammation. Here we further study the relationship of TNF$_{\epsilon}$– and SphK1 using an in vivo model. Transgenic hTNF$_{\epsilon}$– mice, which develop a spontaneous arthritis (limited to paws) at 20 weeks, were crossed with SphK1 activity null mice (SphK1-/-) to study the development of inflammatory arthritis in the functional absence of SphK1. Results show that hTNF/SphK1-/- have significantly less severity and progression of arthritis and bone erosions as measured through micro-CT images. Additionally, less COX-2 protein, mTNF$_{\epsilon}$– transcript levels and fewer Th 17 cells were detected in the joints of hTNF/SphK1-/- compared to hTNF/SphK1+/+ mice. Microarray analysis of the ankle joint showed that hTNF/SphK1-/- mice have increased transcript levels of IL-6 and SOCS3 compared to hTNF/SphK1+/+ mice. Finally, fewer mature osteoclasts were detected in the ankle joints of hTNF/SphK1-/- mice compared to hTNF/SphK1+/+ mice. These data show that SphK1 plays a role in hTNF$_{\epsilon}$– induced inflammatory arthritis, potentially through a novel pathway involving IL-6 and SOCS3. **Overall design:** Two wild-type replicates; three replicates of human TNFa transgene overexpression and normal sphingosine kinase 1; three replicates of human TNFa transgene overexpression and sphingosine kinase 1 null.

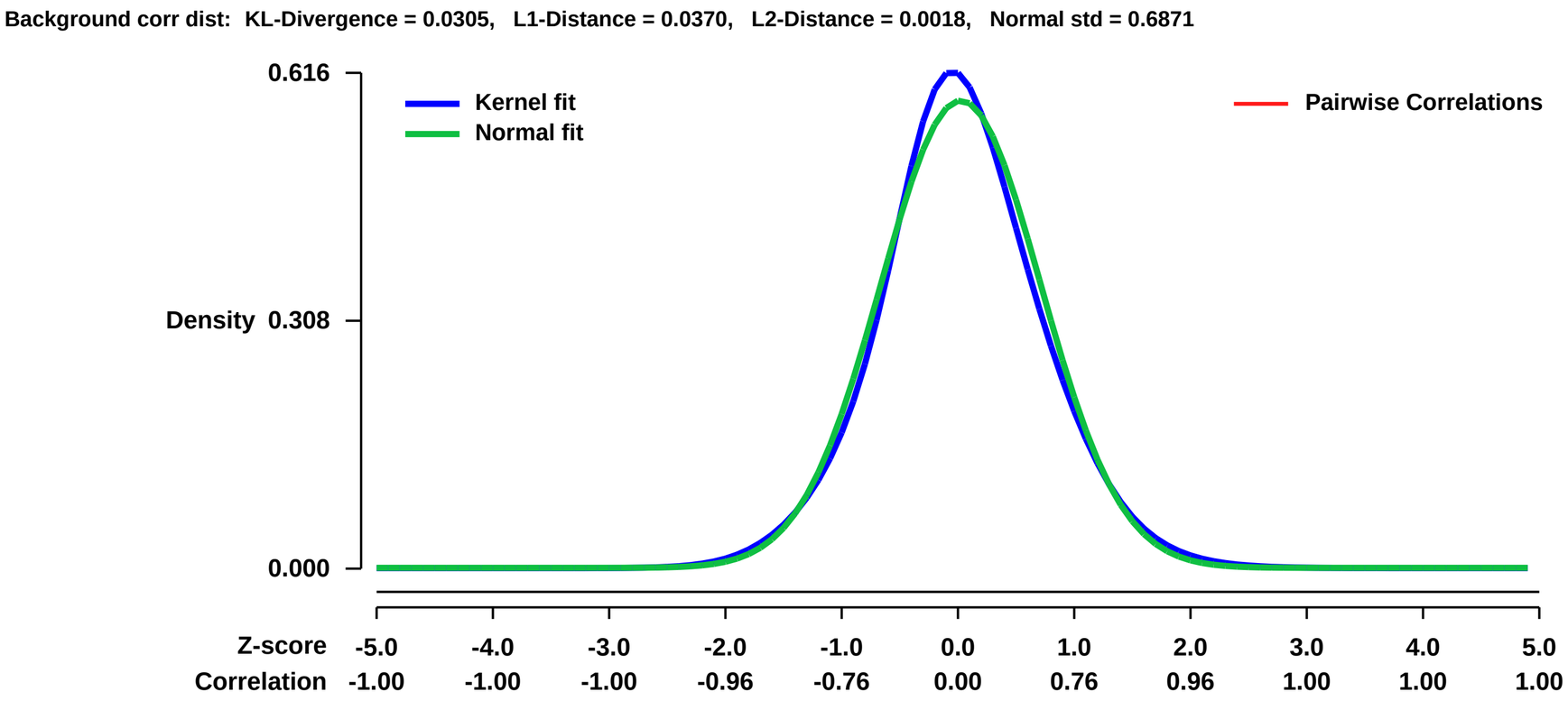

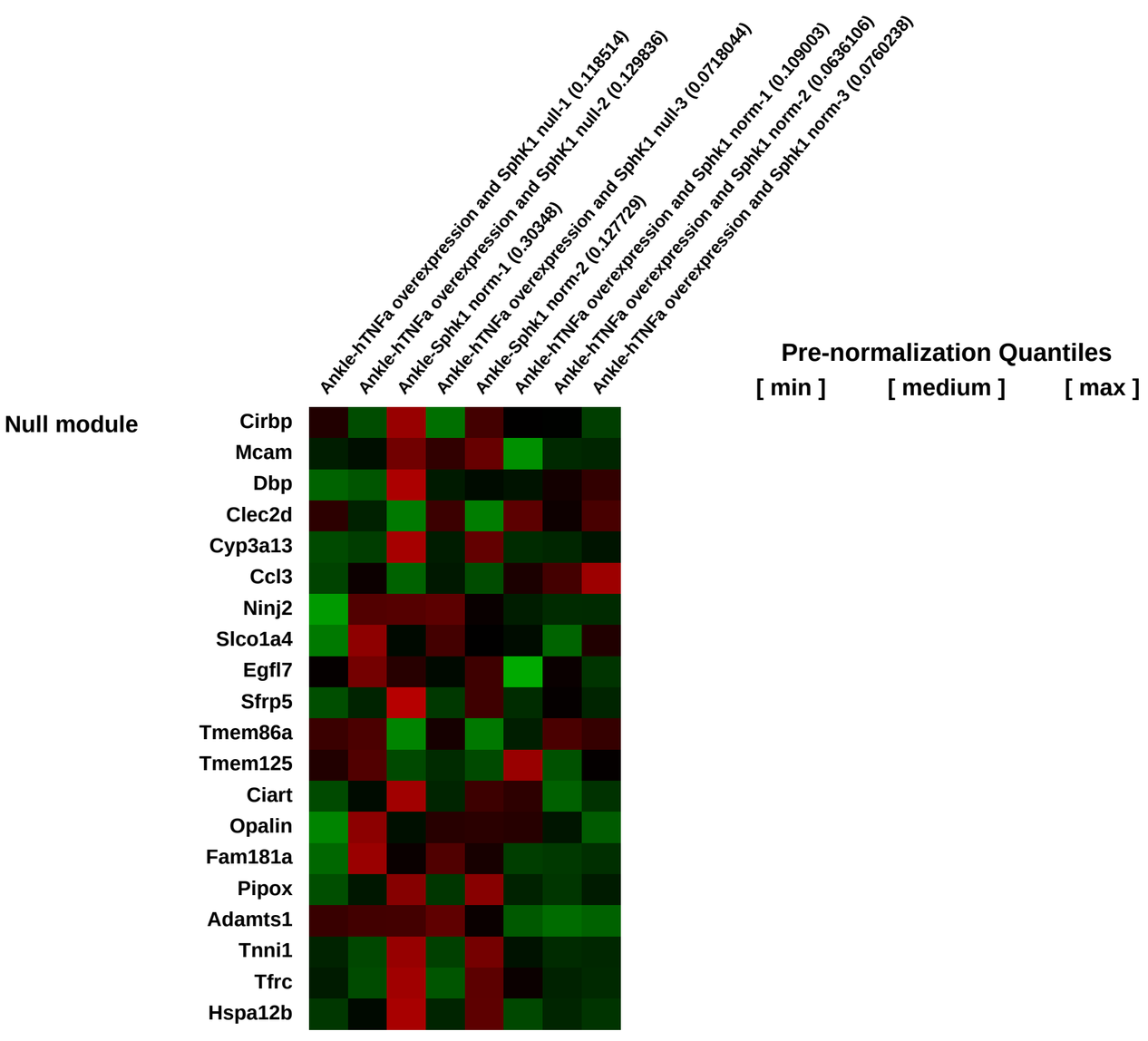

GEO Series "GSE20235" Expression Profiles

Num of samples in this series: 6

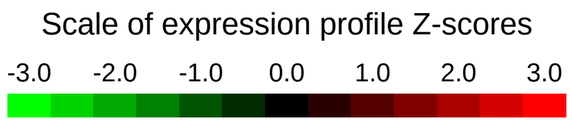

GEO Link:	http://www.ncbi.nlm.nih.gov/geo/query/acc.cgi?acc=GSE20235
Status:	Public on Aug 03 2010
Title:	RNA expression data from glomeruli lacking von Hippel-Lindau protein in podocytes
Organism:	Mus musculus
Experiment type:	Expression profiling by array
Platform:	GPL1261
Pubmed ID:	20522651
Summary & Design:	**Summary:** We and others have previously shown that glomerular endothelial cells and podocytes express hypoxia-inducible transcription factors (HIFs). HIFs bind to hypoxia response elements in target genes, such as vascular endothelial growth factor, which is continually produced by podocytes throughout life. To further assess function of HIFs in podocyte biology, podocin-Cre mice were mated with floxed von Hippel-Lindau (VHL) mice to selectively delete VHL, a component of an E3 ligase complex responsible for degradation of HIFs in normoxia. We reasoned that cells lacking VHL would overexpress stable HIFs and upregulate hypoxia-responsive genes. Progeny from these crosses displayed two phenotypes, non-proteinuric with glomerular basement membrane (GBM) defects and proteinuric with GBM defects and end-stage renal failure at ~6 months of age. Gene changes associated with the mild, non-proteinuric phenotype were studied using isolated glomeruli from wildtype and Pod-Cre fVHL mice. **Overall design:** At 4 weeks of age, urine was collected and urinary albumin was quantified by Albuwell elisa from Pod-Cre fVHL litters. At 6 weeks of age, glomeruli from 3 wildtype littermate controls and 3 non-proteinuric Pod-Cre fVHL mice were collected using the magnetic bead method. RNA was extracted and hybridized to Affymetrix microarrays.

Background corr dist: KL-Divergence = 0.0402, L1-Distance = 0.0228, L2-Distance = 0.0006, Normal std = 0.6194

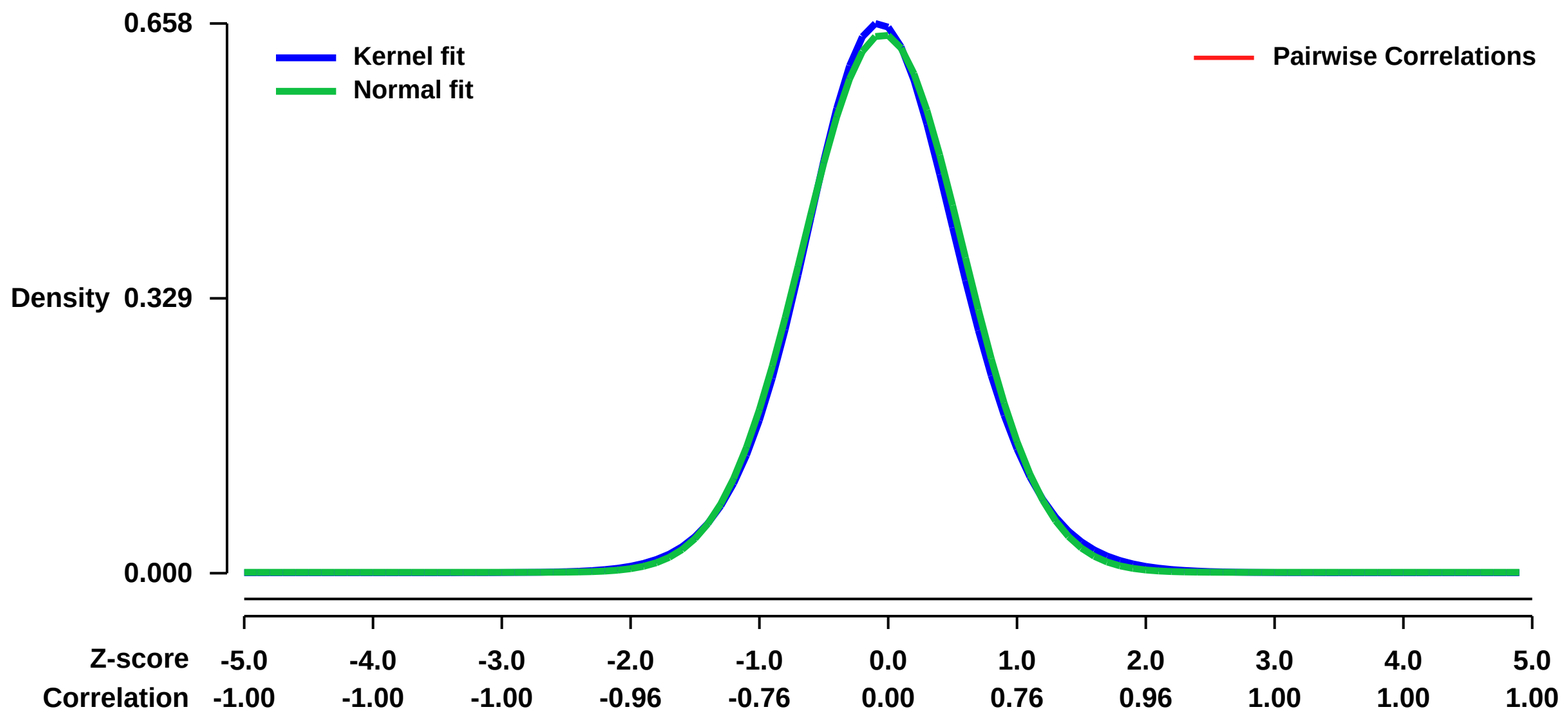

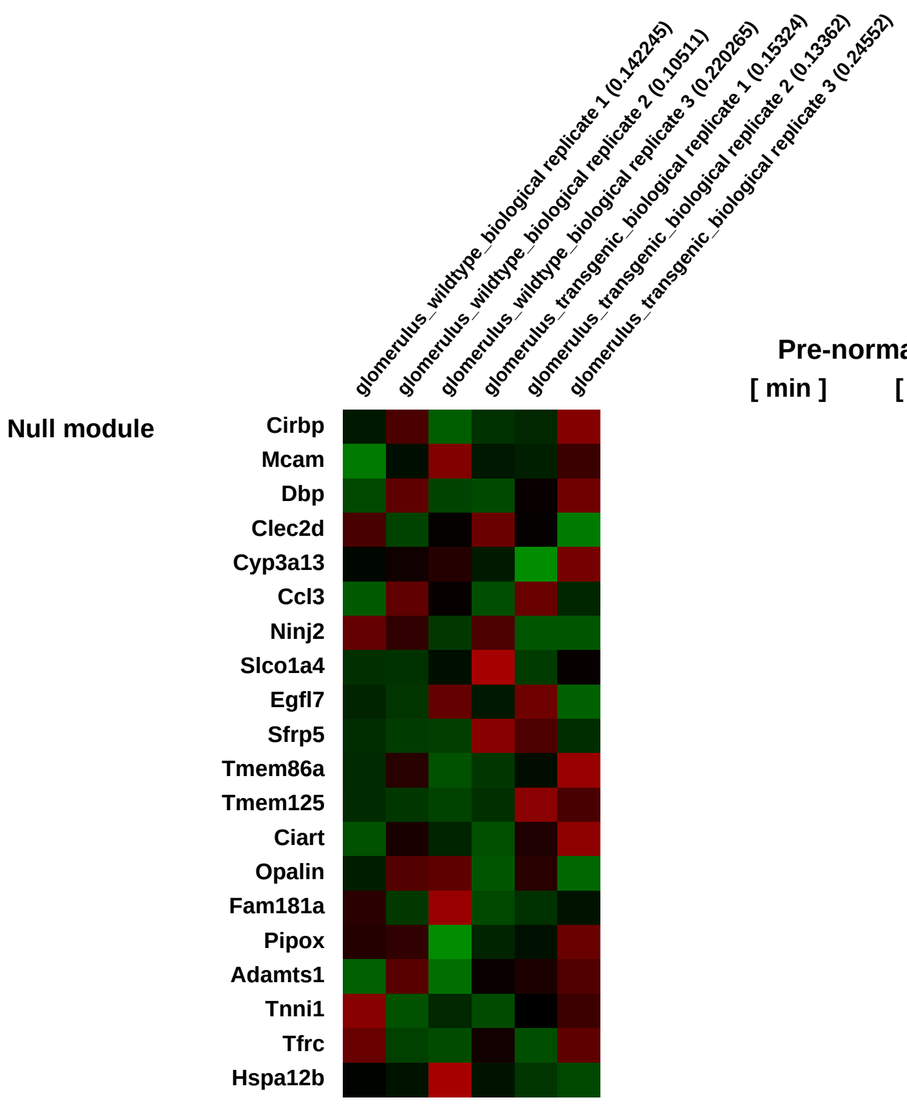

GEO Series "GSE20260" Expression Profiles

Num of samples in this series: 48

Scale of expression profile Z-scores

-3.0 -2.0 -1.0 0.0 1.0 2.0 3.0

GEO Link:	http://www.ncbi.nlm.nih.gov/geo/query/acc.cgi?acc=GSE20260
Status:	Public on Dec 19 2012
Title:	Consequences of exchanging carbohydrates for proteins in the cholesterol metabolism of mice fed a high-fat diet
Organism:	Mus musculus
Experiment type:	Expression profiling by array
Platform:	GPL1261
Pubmed ID:	23139832
Summary & Design:	**Summary:** Dietary proteins have profound effects on lipid metabolism but the mechanism remains to be elucidated. In the present study, we examined the temporal impact of dietary proteins in isoenergetic high fat diets on lipid metabolism of C57BL/6J mice. **Overall design:** Mice were first fed a low protein (P) to carbohydrate (C) ratio high-fat diet (L-P/C-HF) for 10 weeks and then a half of mice were changed to a high protein to carbohydrate ratio high-fat diet (H-P/C-HF) for additional 4 weeks whereas the remaining mice continued eating the L-P/C-HF diet.

Background corr dist: KL-Divergence = 0.1358, L1-Distance = 0.0700, L2-Distance = 0.0128, Normal std = 0.3939

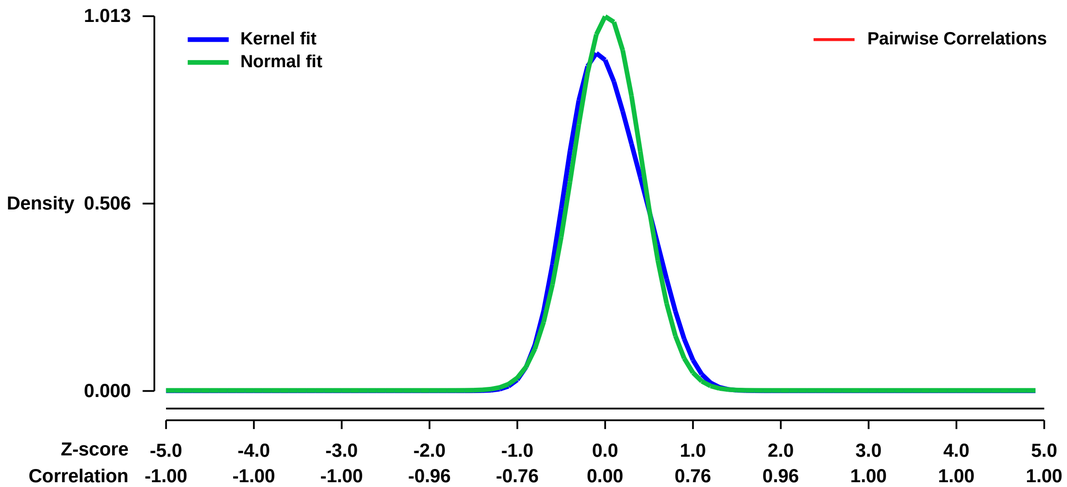

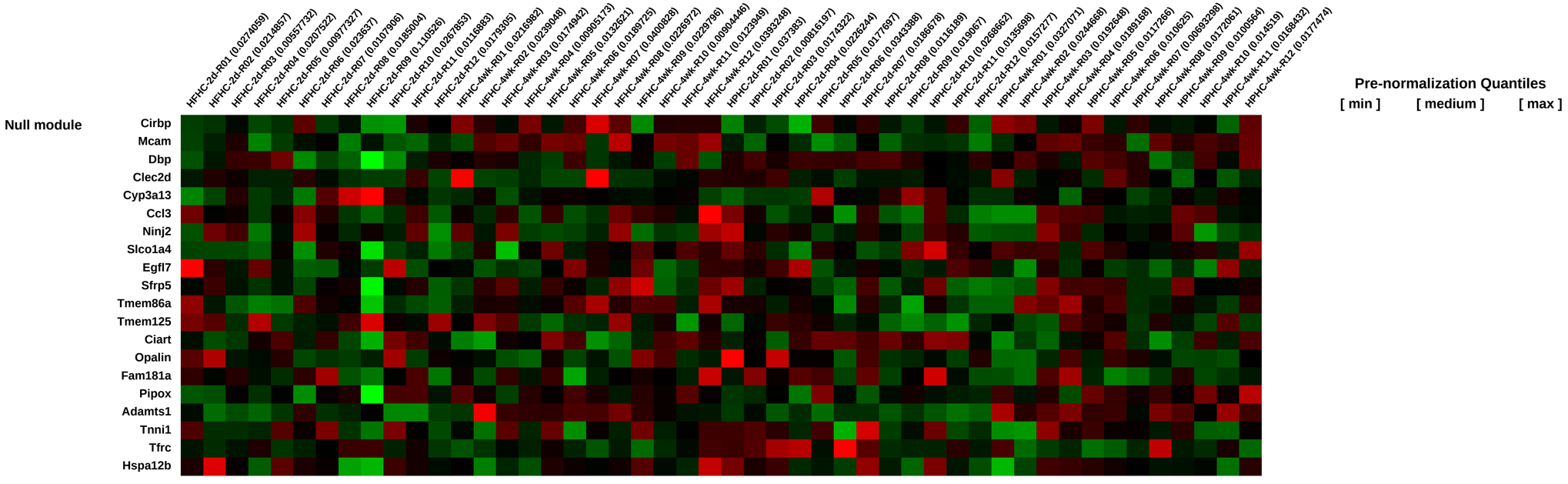

GEO Series "GSE20325" Expression Profiles

Num of samples in this series: 6

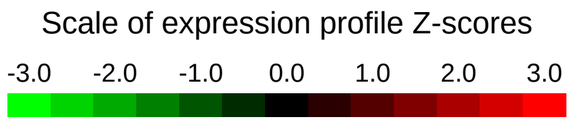

GEO Link:	http://www.ncbi.nlm.nih.gov/geo/query/acc.cgi?acc=GSE20325
Status:	Public on Mar 28 2011
Title:	Stabilization of ^ -catenin during murine Kidney Development
Organism:	Mus musculus
Experiment type:	Expression profiling by array
Platform:	GPL1261
Pubmed ID:	21436291
Summary & Design:	**Summary:** We define a pathogenic role for a ^ -catenin-activated genetic pathway in murine renal dysplasia. Cre-mediated stabilization of ^ -catenin in the ureteric cell lineage prior to the onset of kidney development increased ^ -catenin levels and caused renal aplasia or severe hypodysplasia. A genome-wide analysis of mRNA expression in dysplastic tissue identified down-regulation of genes required for ureteric branching and up regulation of Tgf^ 2 and Dkk1. **Overall design:** Hoxb7-Cre:EGFP mice (Zhao, et al. (2004) Dev Biol 276:403-415) were crossed with mice containing loxP sites flanking exon 3 of the ^ -catenin allele (^ -catdelta3/delta3) (Harada,et al. (2002) Cancer Res 62:1971-1977) to generate ^ -catenin gain-of-function mutant mice specific to the uteric bud, termed ^ -catGOF-UB .Eighteen ^ -catGOF-UB mutant kidneys and 9 WT kidneys were micro-dissected at E12.5. Mutant kidneys were divided into three random pools (n=3) consisting of 6 kidneys each and mRNA expression assessed by microarray.

Background corr dist: KL-Divergence = 0.0416, L1-Distance = 0.0228, L2-Distance = 0.0006, Normal std = 0.6103

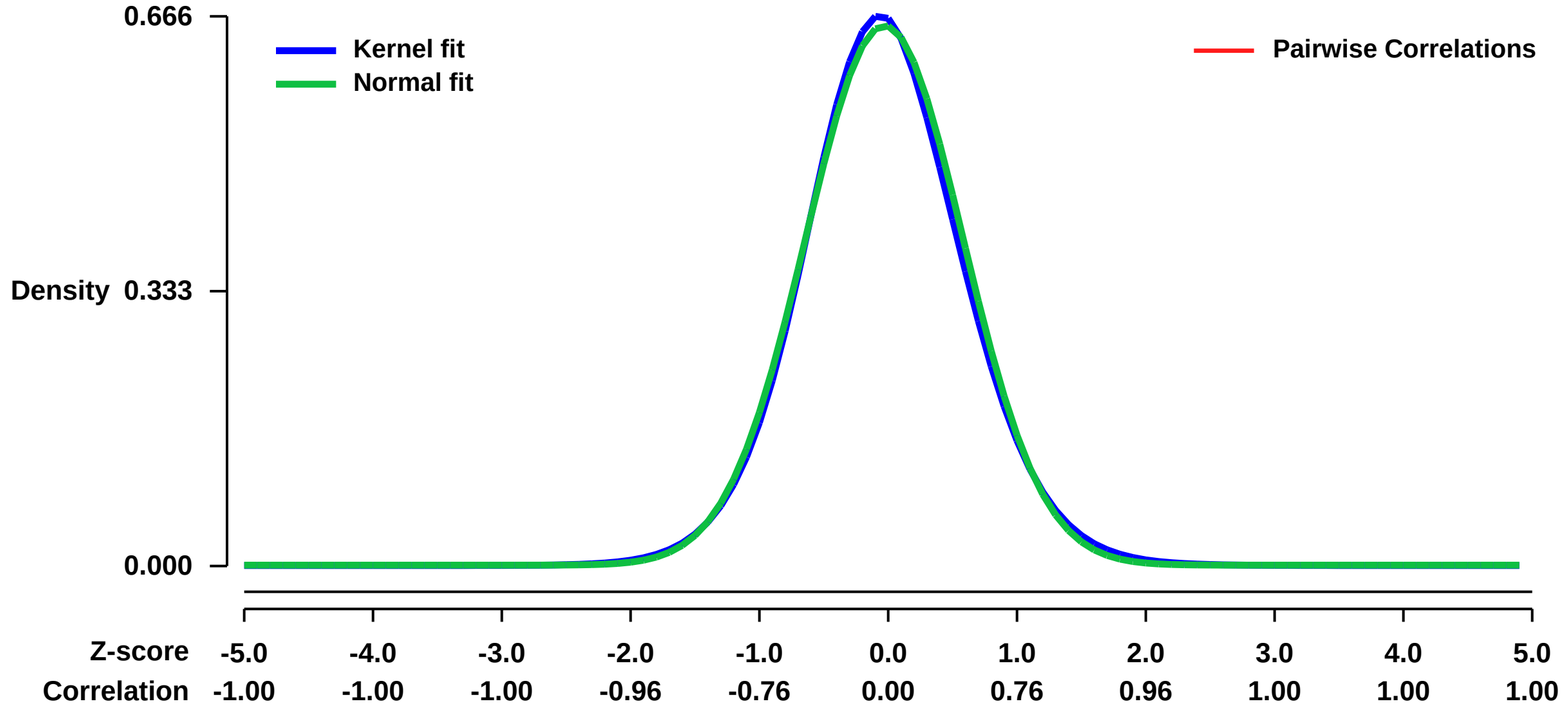

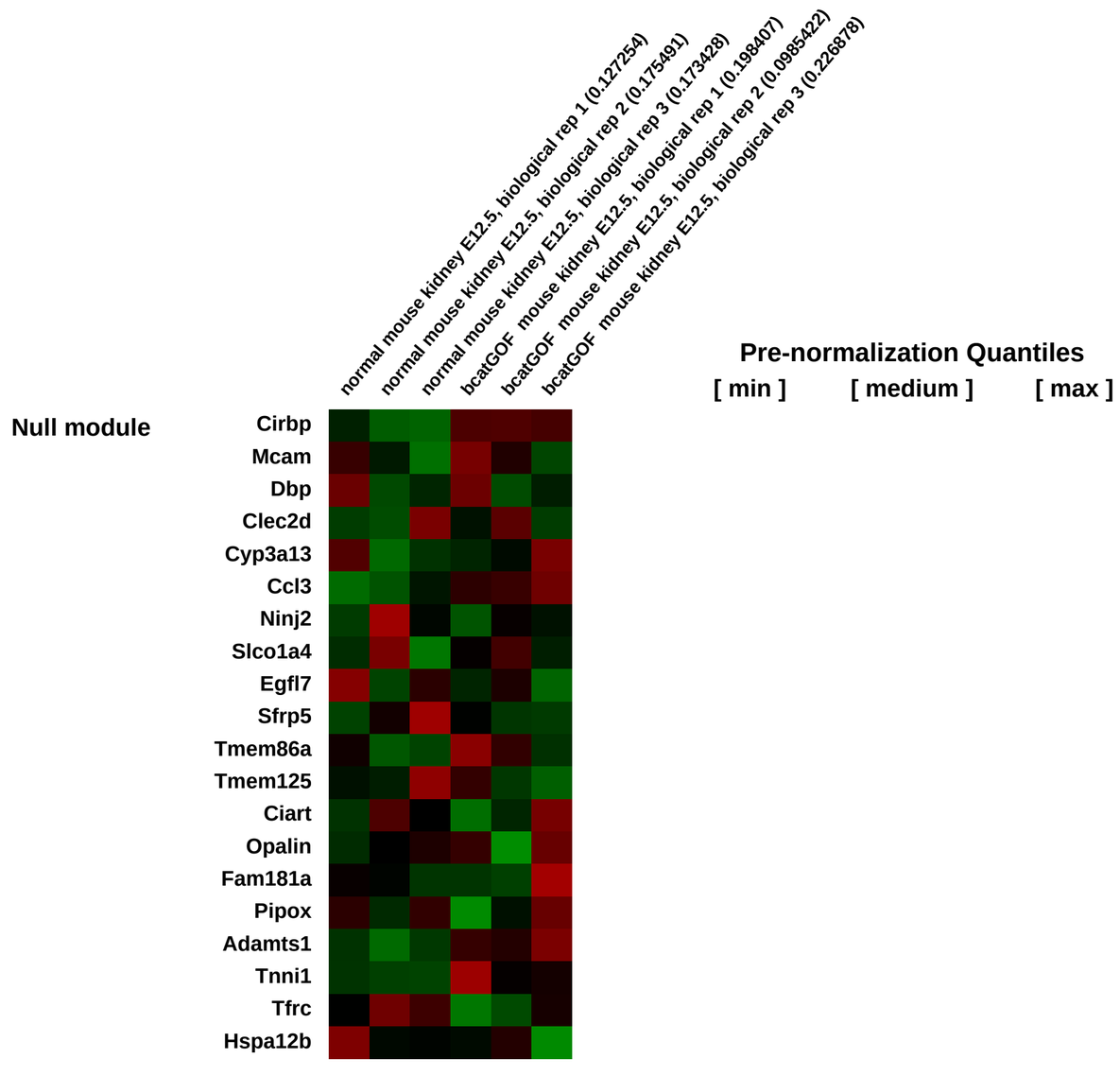

GEO Series "GSE20335" Expression Profiles

Num of samples in this series: 8

Scale of expression profile Z-scores

-3.0 -2.0 -1.0 0.0 1.0 2.0 3.0

GEO Link:	http://www.ncbi.nlm.nih.gov/geo/query/acc.cgi?acc=GSE20335
Status:	Public on Apr 17 2010
Title:	Expression analysis data from large T antigen-immortalized murine embryonic fibroblasts (MEFs)
Organism:	Mus musculus
Experiment type:	Expression profiling by array
Platform:	GPL1261
Pubmed ID:	20399150
Summary & Design:	**Summary:** Microarrays were used to examine the genome-wide expression in FIH null, VHL null and VHL/FIH double null MEFs. We used these data to analyze how deletion of FIH or VHL alone affects gene expression and if VHL and FIH have synergistic effects and differential selectivity on regulating gene expression. **Overall design:** To assess how deletion of FIH, VHL or both VHL and FIH affect gene expression genome-wide, we generated FIH null, VHL null and VHL/FIH double null MEFs after adeno-cre virus infection on large T-immortalized FIHdf, VHLdf, and VHLdf/FIHdf MEFs. These MEFs were cultured under normoxia (21% O2) with complete culture medium before RNA extraction. Total RNA were isolated by using the Qiagen RNeasy kit and treated with on-column DNase digestion. Affymetrix GeneChip Mouse Genome 430 2.0 Array was used.

Background corr dist: KL-Divergence = 0.0547, L1-Distance = 0.0269, L2-Distance = 0.0009, Normal std = 0.5587

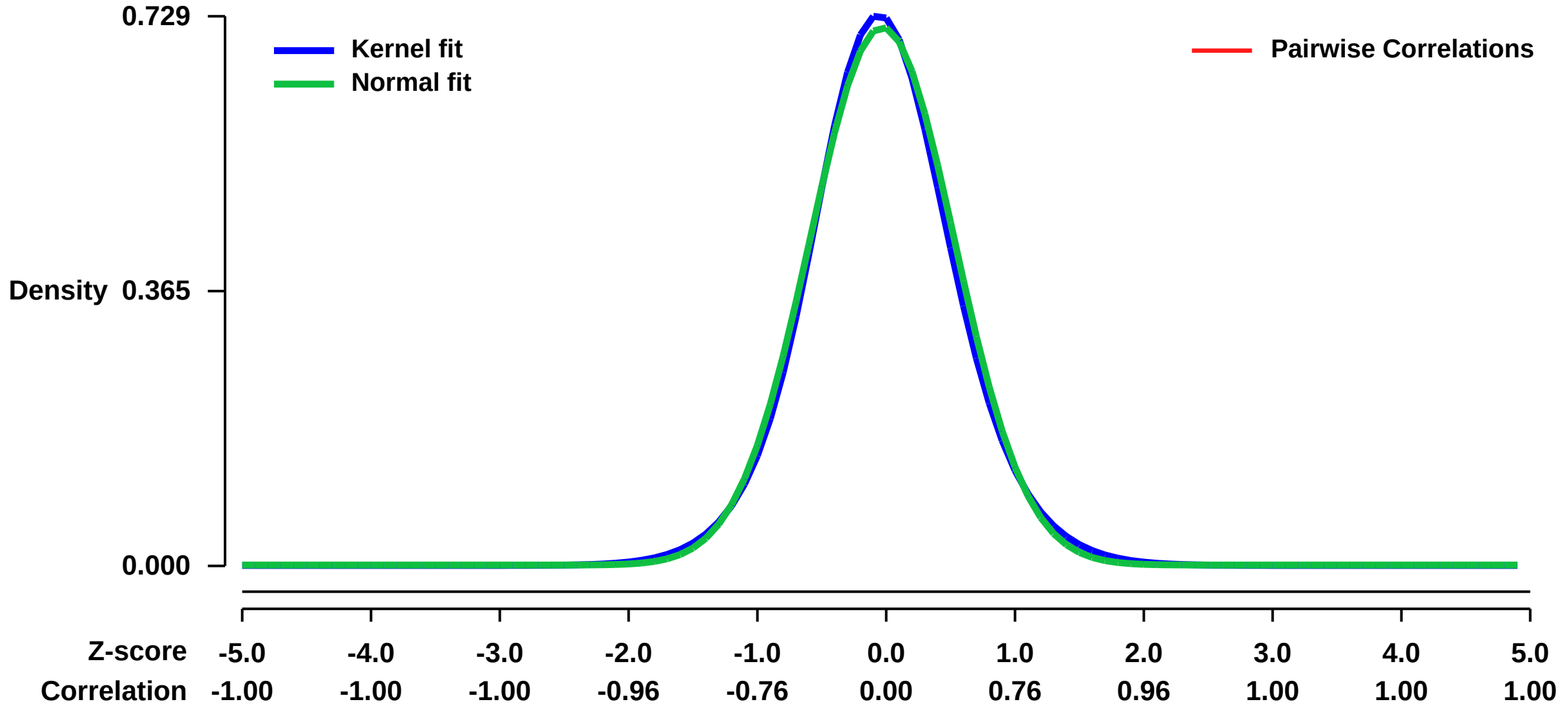

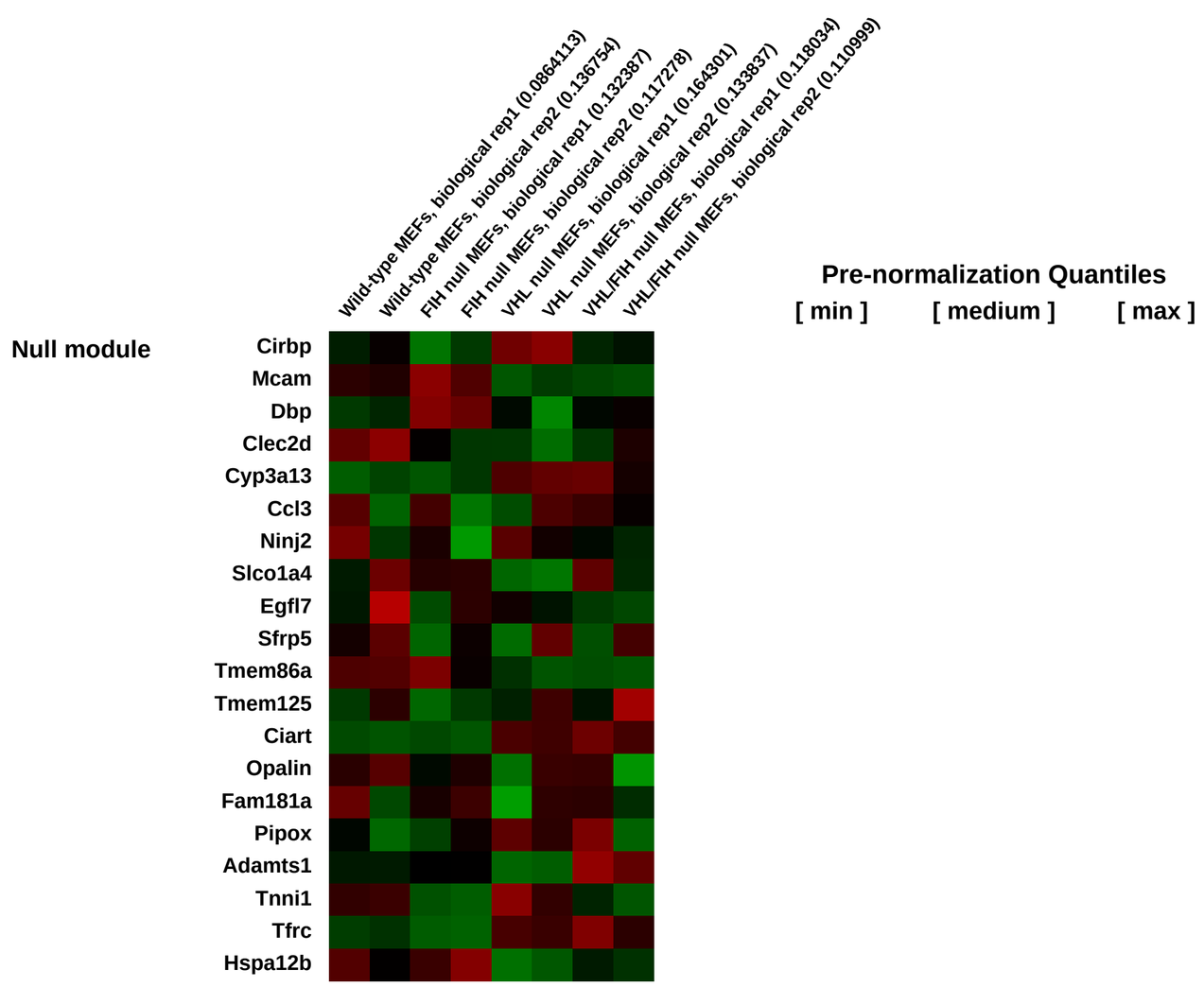

GEO Series "GSE20352" Expression Profiles

Num of samples in this series: 6

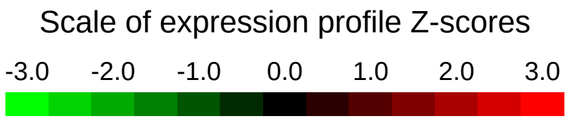

GEO Link:	http://www.ncbi.nlm.nih.gov/geo/query/acc.cgi?acc=GSE20352
Status:	Public on Feb 16 2010
Title:	The Apcmin mouse has altered hematopoietic stem cell function and provides a model for MPD/MDS
Organism:	Mus musculus
Experiment type:	Expression profiling by array
Platform:	GPL1261
Pubmed ID:	20197553
Summary & Design:	**Summary:** Apc, a negative regulator of the canonical Wnt signaling pathway, is a bona-fide tumor suppressor whose loss of function results in intestinal polyposis. APC is located in a commonly deleted region on human chromosome 5q, associated with myelodysplastic syndrome (MDS) suggesting that haploinsufficiency of APC contributes to the MDS phenotype. Analysis of the hematopoietic system of mice with the Apcmin allele that results in a premature stop codon and loss of function, showed no abnormality in steady state hematopoiesis. Bone marrow derived from Apcmin mice showed enhanced repopulation potential, indicating of a cell intrinsic gain of function in the long-term hematopoietic stem cell (HSC) population. However, Apcmin bone marrow was unable to repopulate secondary recipients due to loss of the quiescent HSC population. Apcmin mice developed a myelodysplastic/ myeloproliferative phenotype. Our data indicate that Wnt activation through haploinsufficiency of Apc causes insidious loss of HSC function that is only evident in serial transplantation strategies. These data provide a cautionary note for HSC expansion strategies through Wnt pathway activation, provide evidence that cell extrinsic factors can contribute to the development of myeloid disease and indicate that loss of function of APC may contribute to the phenotype observed in patients with MDS and del(5q). **Overall design:** LKS+ cells were isolated from Apcmin or WT mice using high-speed multiparameter flow cytometry. At least 2x104 cells per mouse were isolated with confirmed purity in excess of 90%. The cells were treated with RLT lysis buffer (Qiagen) containing beta-mercaptoethanol to stabilize RNA. RNA was extracted using Qiagen RNeasy Micro Kit according to manufacturers instruction. The RNA was amplified using a linear amplification protocol (Nugen Ovation V2 amplification system). cDNA was fragmented and biotinylated before hybridization onto Affymetrix mouse genome 430 2.0 Array chips

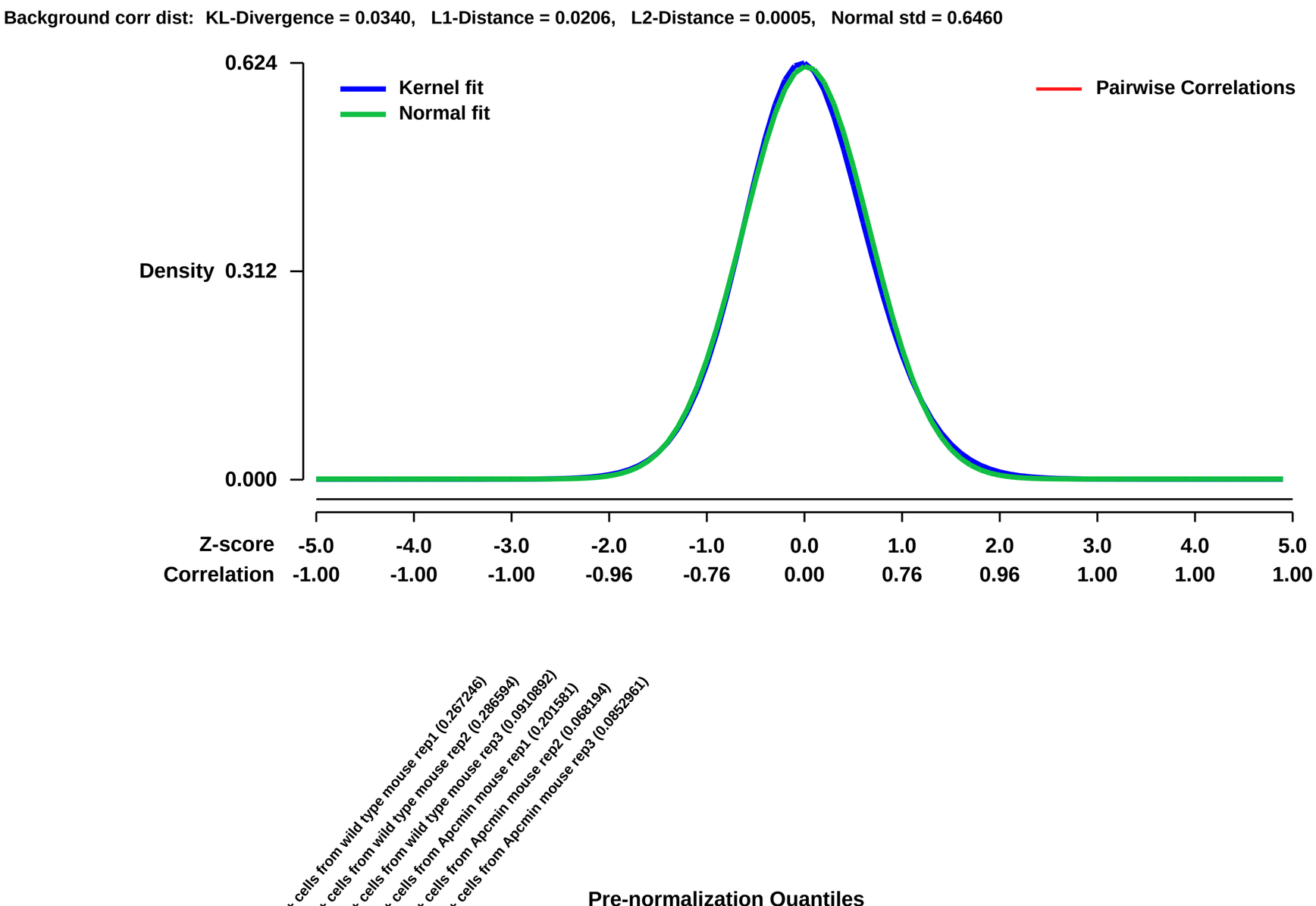

GEO Series "GSE20371" Expression Profiles

Num of samples in this series: 12

Scale of expression profile Z-scores

-3.0 -2.0 -1.0 0.0 1.0 2.0 3.0

GEO Link:	**http://www.ncbi.nlm.nih.gov/geo/query/acc.cgi?acc=GSE20371**
Status:	**Public on Dec 31 2013**
Title:	**PPARd target genes in MEFs**
Organism:	**Mus musculus**
Experiment type:	**Expression profiling by array**
Platform:	**GPL1261**
Pubmed ID:	
Summary & Design:	**Summary:** **The PPAR (Peroxisome proliferator-activated receptor) family of nuclear receptors has three members: PPARg, PPARa and PPARd. Although they share similar structures, their biological functions are distinct. PPARg controls lipid storage and adipogenesis, while PPARd is associated with fat burning. The highly specific synthetic ligand for PPARd, GW501516, is a promising drug candidate for obesity and diabetes. Here we use Affymetrix microarray to analyze gene expression profile in mouse embryo fibroblasts treated with 100 nM GW501516 for 0, 2, 8 and 24 hours. These data may provide new clues into the molecular mechanism by which GW501516 ameliorates obesity and diabetes.** **Overall design:** **Wild type mouse embryonic fibroblasts (MEFs) stably infected with retroviruses MSCVpuro expressing PPARd were plated at 0.5 million per 10 cm dish. After overnight incubation, cells were treated with 100nM GW501516 for 0h, 2h, 8h and 48h. Cells were collected at subconfluent condition. Total RNAs were sequentially purified with Trizol (Invitrogen) and RNeasy kit (Qiagen) and analyzed in triplicate on Mouse Genome 430 2.0 Array (Affymetrix) at NIDDK Microarray Core Facility following standard protocols.**

Background corr dist: **KL-Divergence = 0.1745, L1-Distance = 0.0430, L2-Distance = 0.0040, Normal std = 0.3502**

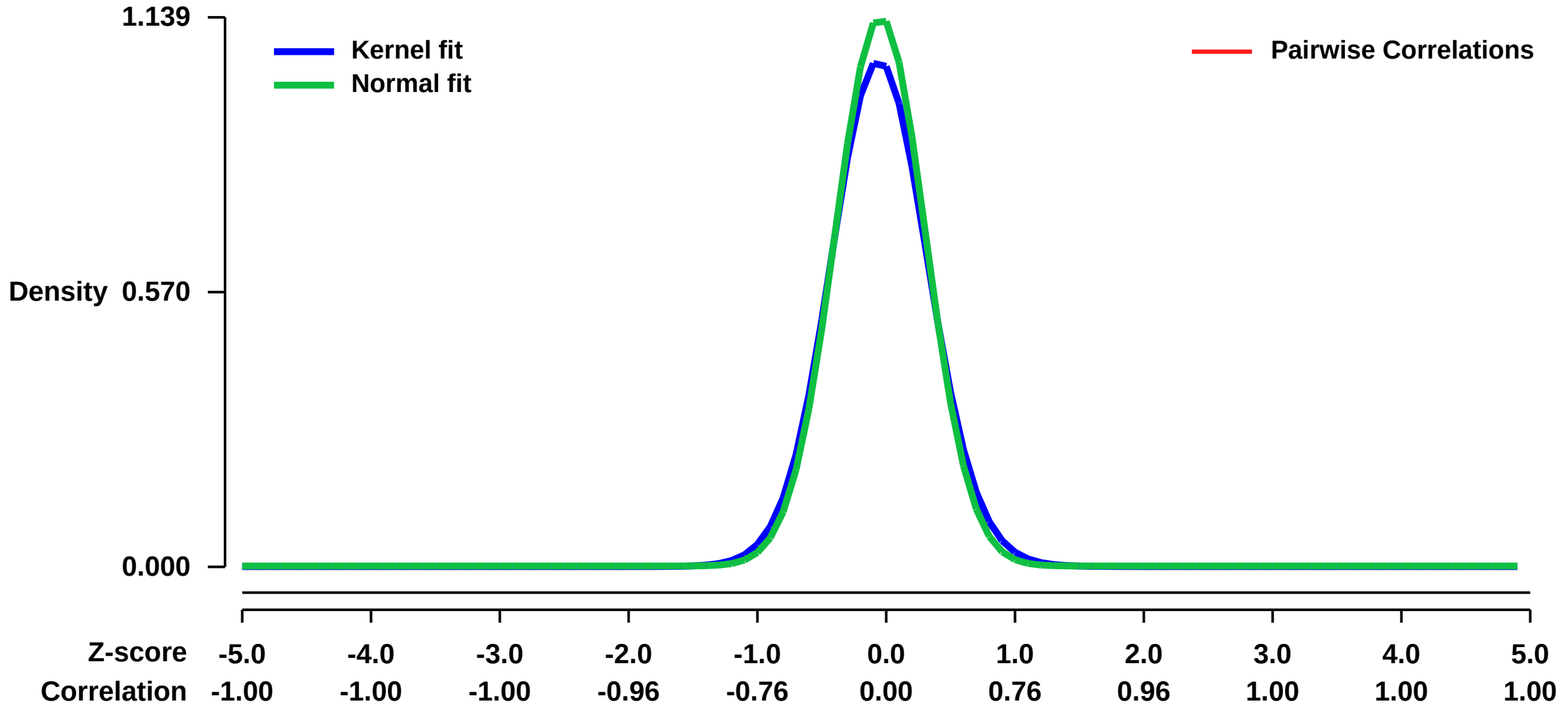

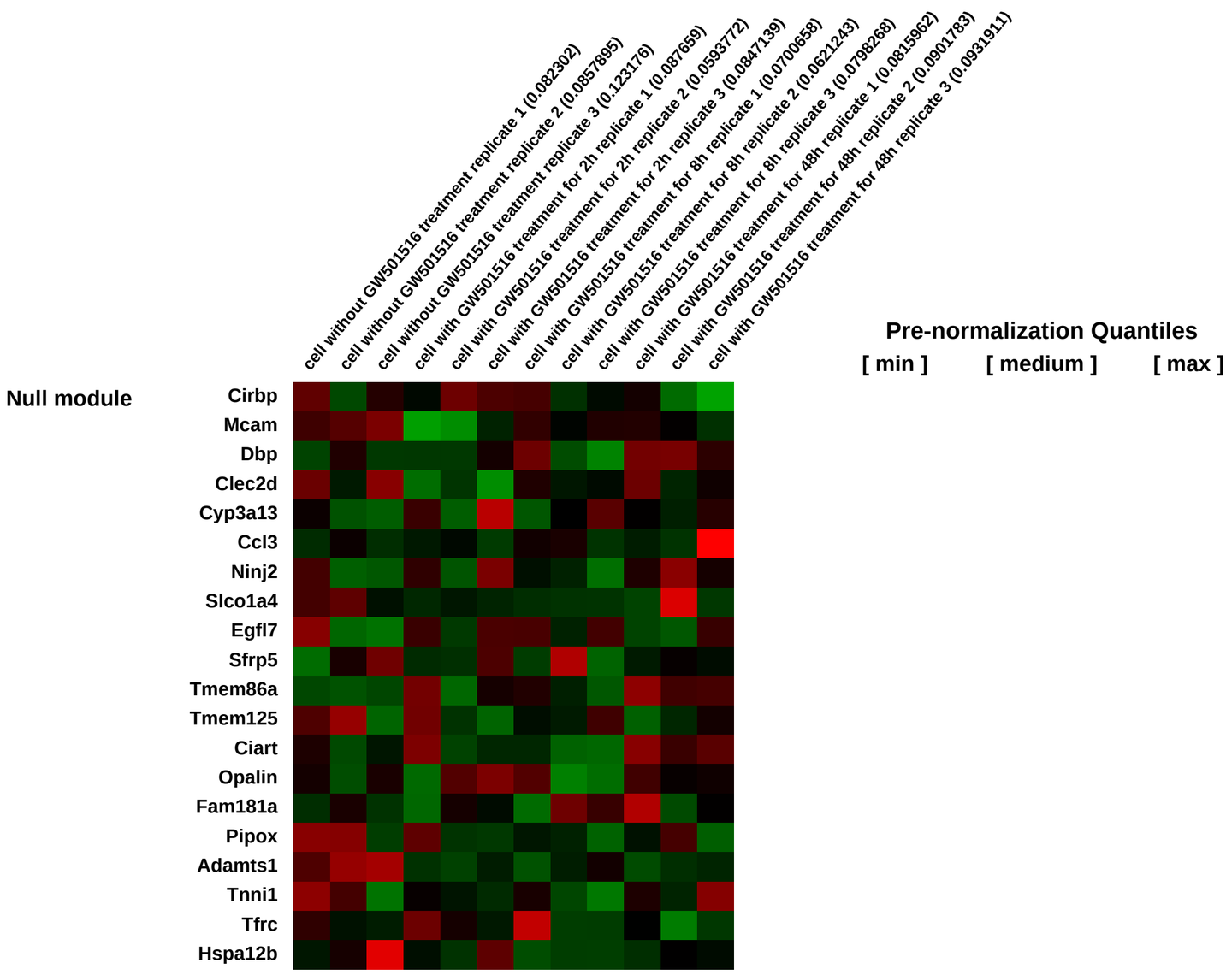

GEO Series "GSE20372" Expression Profiles

Num of samples in this series: 6

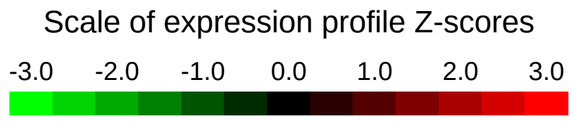

GEO Link:	**http://www.ncbi.nlm.nih.gov/geo/query/acc.cgi?acc=GSE20372**
Status:	**Public on Feb 15 2011**
Title:	**Gene expression in E14 TG2a cells grown with or without LIF and sorted for 5T4 expression**
Organism:	**Mus musculus**
Experiment type:	**Expression profiling by array**
Platform:	**GPL1261**
Pubmed ID:	**20376365**
Summary & Design:	**Summary:** **E14 TG2a cells grown with LIF were disaggregated and FACS sorted for cell surface 5T4 negativity versus E14 TG2a cells grown without LIF for 3 days and sorted for 5T4 positivity.** **Overall design:** **Two samples in triplicate. 5T4- vs. 5T4+**
Background corr dist:	**KL-Divergence = 0.0286, L1-Distance = 0.0298, L2-Distance = 0.0012, Normal std = 0.6906**

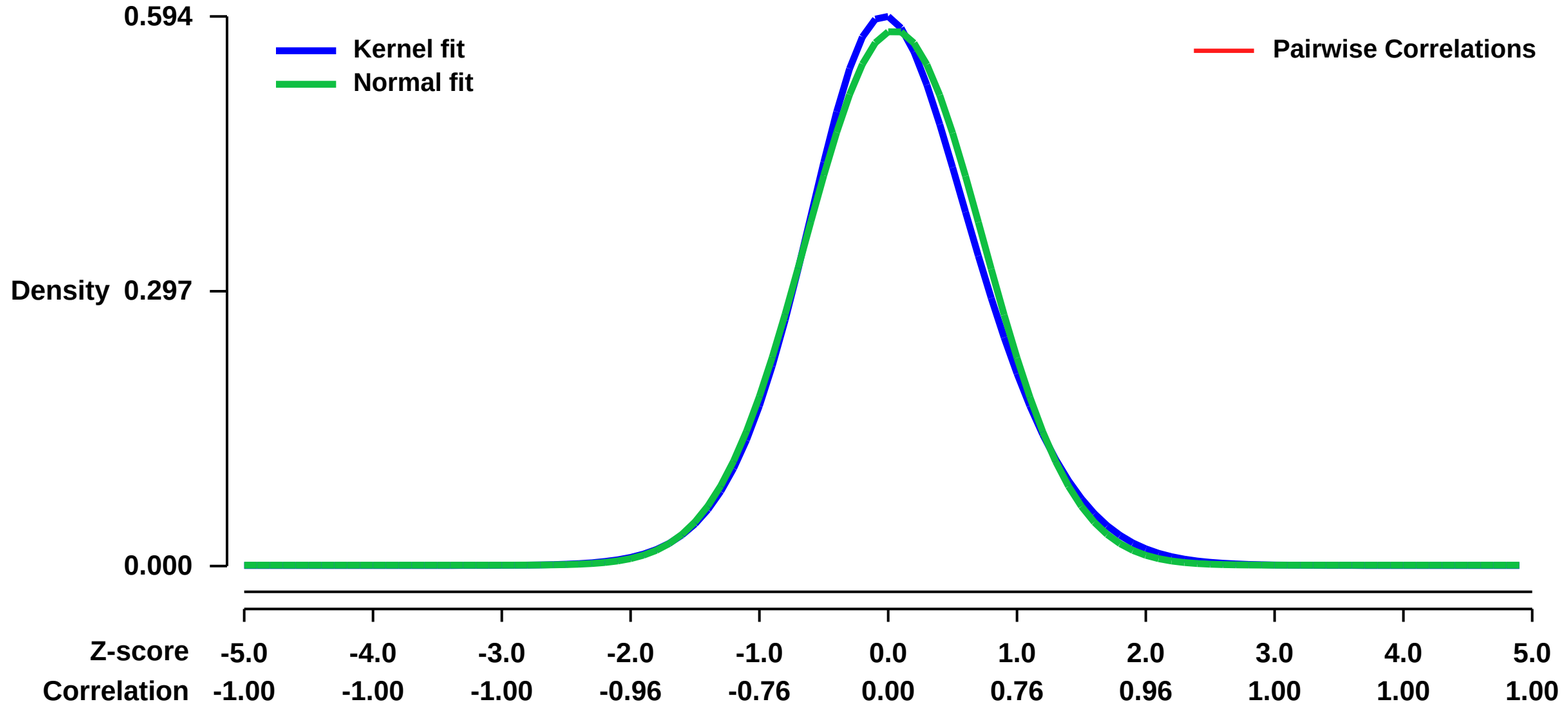

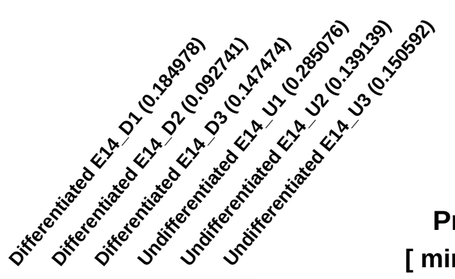

Pre-normalization Quantiles

[min] [medium] [max]

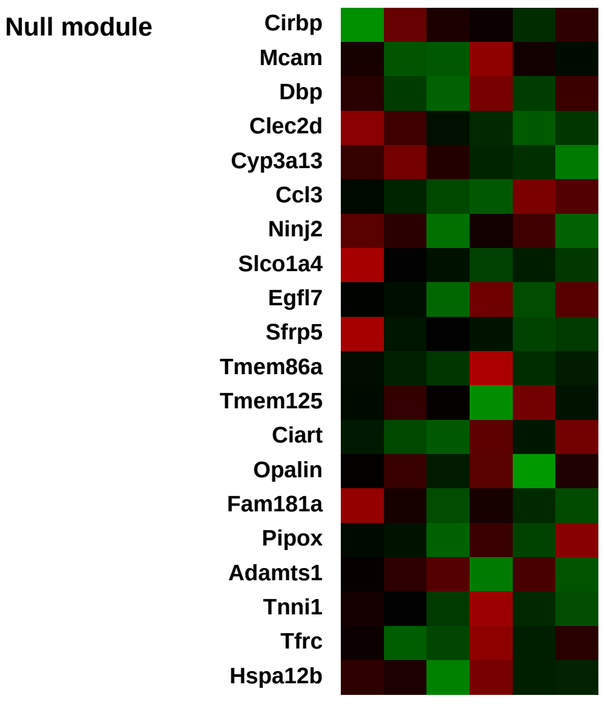

GEO Series "GSE20390" Expression Profiles

Num of samples in this series: 6

Scale of expression profile Z-scores

-3.0 -2.0 -1.0 0.0 1.0 2.0 3.0

GEO Link:	http://www.ncbi.nlm.nih.gov/geo/query/acc.cgi?acc=GSE20390
Status:	Public on Jul 07 2010
Title:	Deficiency in the 15 kDa Selenoprotein Inhibits Tumorigenicity and Metastasis of Colon Cancer Cells
Organism:	Mus musculus
Experiment type:	Expression profiling by array
Platform:	GPL1261
Pubmed ID:	20388823
Summary & Design:	**Summary:** Selenium has cancer preventive activity that is mediated, in part, through selenoproteins. The role of the 15 kDa selenoprotein (Sep15) in colon cancer was assessed by preparing and using mouse colon CT26 cells stably transfected with shRNA constructs targeting Sep15. Metabolic 75Se-labeling and Northern and Western blot analyses revealed that more than 90% of Sep15 was knocked down. Growth of the resulting Sep15-deficient CT26 cells was reduced (p<0.01) and cells formed significantly (p<0.001) fewer colonies in soft agar compared to control CT26 cells. Whereas most (14/15) BALB/c mice injected with control cells developed tumors, few (3/30) mice injected with Sep15 knockdown cells developed tumors (p<0.0001). The ability to form pulmonary metastases had similar results. Mice injected with the plasmid-transfected control cells had >250 lung metastases/mouse; however, mice injected with the Sep15 knockdown cells only had 7.8 +/- 5.4 metastases. To investigate molecular targets affected by Sep15 status, gene expression patterns between control and knockdown CT26 cells were compared. Ingenuity Pathways Analysis was used to analyze the 1045 genes that were significantly (p<0.001) affected by Sep15 deficiency. The highest scored biological functions were cancer and cellular growth and proliferation. Consistent with these observations, subsequent analyses revealed a G2/M cell cycle arrest in Sep15 CT26 knockdown cells. In contrast, to CT26 cells Sep15 knockdown in Lewis Lung Carcinoma (LLC1) cells did not affect anchorage-dependent or â independent cell growth. These data suggest tissue specificity in the cancer protective effects of Sep15 knockdown, which are mediated, at least in part, by influencing the cell cycle. **Overall design:** mRNA was isolated from plasmid-transfected control and shSep15 knockdown CT26 cells (three replicates of each). Microarray analysis was performed on Affymetrix Mouse 430_2 gene chips. Three arrays were analyzed from different mRNA samples for each construct.

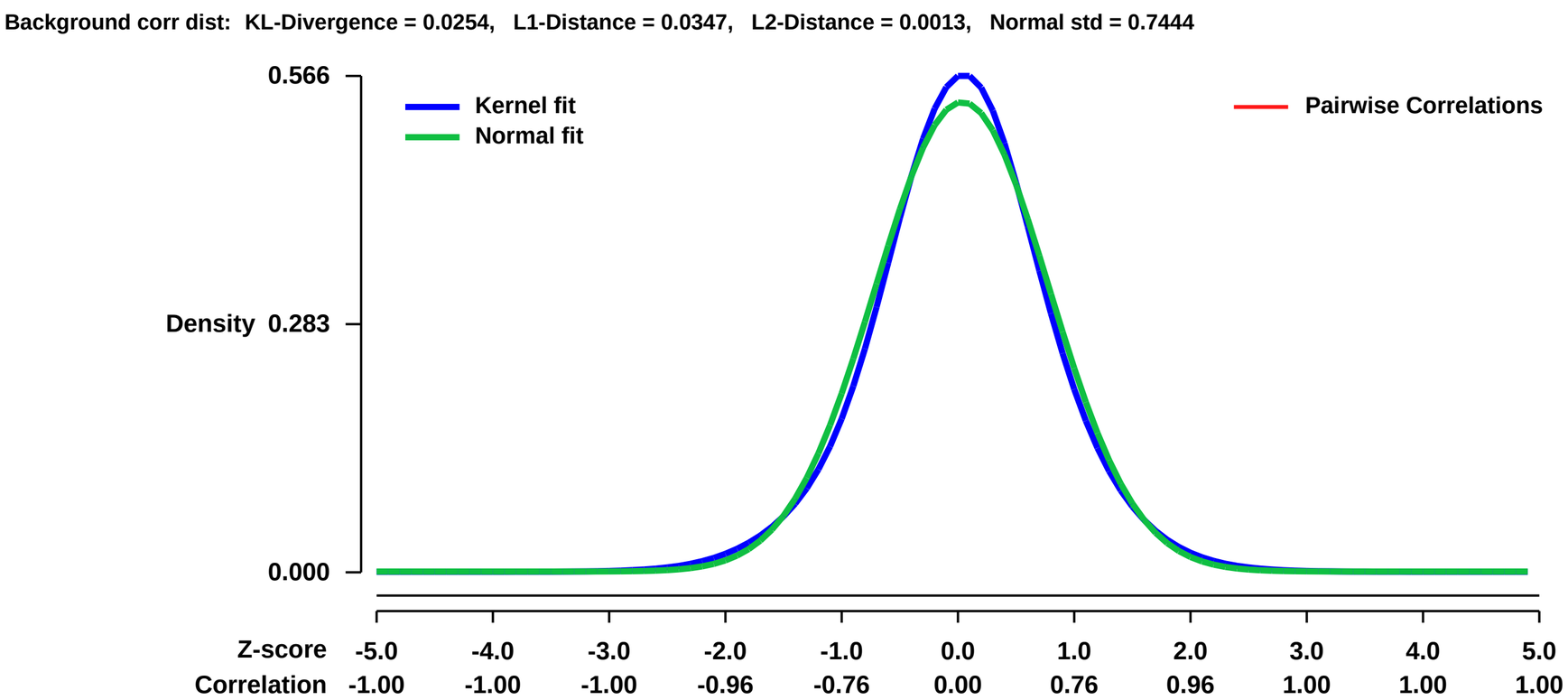

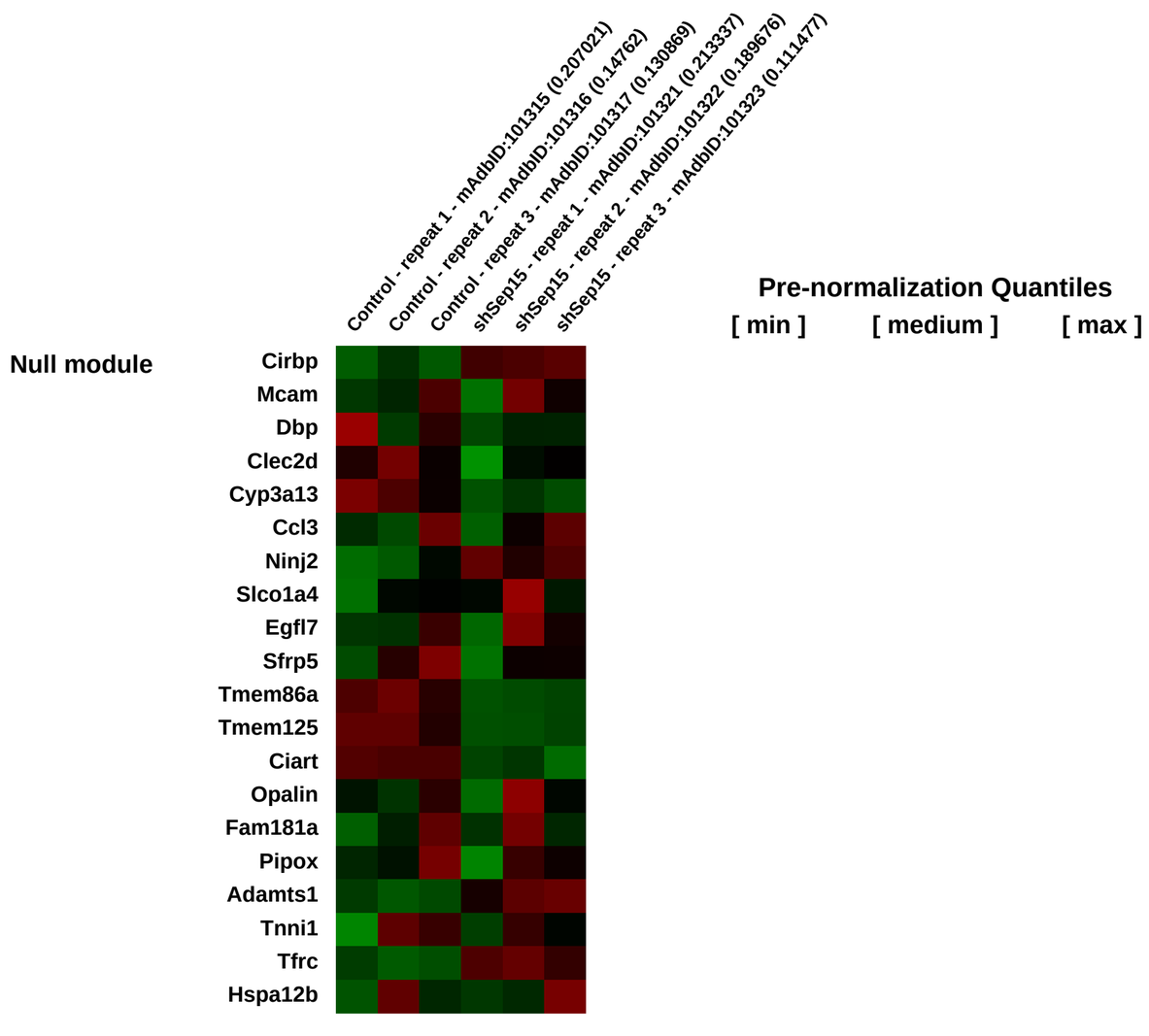

GEO Series "GSE20391" Expression Profiles

Num of samples in this series: 11

Scale of expression profile Z-scores

-3.0 -2.0 -1.0 0.0 1.0 2.0 3.0

GEO Link:	http://www.ncbi.nlm.nih.gov/geo/query/acc.cgi?acc=GSE20391
Status:	Public on Jun 16 2010
Title:	Comprehensive expression profiling across primary fetal liver terminal erythroid differentiation
Organism:	Mus musculus
Experiment type:	Expression profiling by array
Platform:	GPL1261
Pubmed ID:	20231426
Summary & Design:	**Summary:** Primary murine fetal liver cells were freshly isolated from day e14.5 livers and then sorted for successive differentiation stages by Ter119 and CD71 surface expression (ranging from double-negative CFU-Es to Ter-119 positive enucleated erythrocytes) [Zhang, et al. Blood. 2003 Dec 1; 102(12):3938-46]. RNA isolated from each freshly isolated, stage-sorted population was reverse-transcribed, labelled, and then hybridized onto 3' oligo Affymetrix arrays. Important erythroid specific genes as well as the proteins that regulate them were elucidated through this profiling based on coexpression and differential expression patterns as well as by extracting specific GO categories of genes (such as DNA-binding proteins). **Overall design:** Gene-targeting experiments report that the homeodomain-interacting protein kinases 1 and 2, Hipk1 and Hipk2, are essential but redundant in hematopoietic developmentâ because Hipk1/Hipk2 double-deficient animals exhibit severe defects in hematopoiesis and vasculogenesis while the single knockouts do not. These serine-threonine kinases phosphorylate, and consequently modify the functions of, several important hematopoietic transcription factors and cofactors. Here we show that Hipk2 knockdown alone plays a significant role in terminal fetal liver erythroid differentiation. Hipk1 and Hipk2 are highly induced during primary mouse fetal liver erythropoiesis. Specific knockdown of Hipk2 inhibits terminal erythroid cell proliferationâ explained in part by impaired cell cycle progression as well as increased apoptosisâ and terminal enucleation as well as the accumulation of hemoglobin. Hipk2 knockdown also reduces the transcription of many genes involved in proliferation and apoptosis as well as important, erythroid-specific genes involved in hemoglobin biosynthesisâ such as alpha-globin and mitoferrin 1â demonstrating that Hipk2 plays an important role in some but not all aspects of normal terminal erythroid differentiation.

Background corr dist: KL-Divergence = 0.0629, L1-Distance = 0.0458, L2-Distance = 0.0040, Normal std = 0.5380

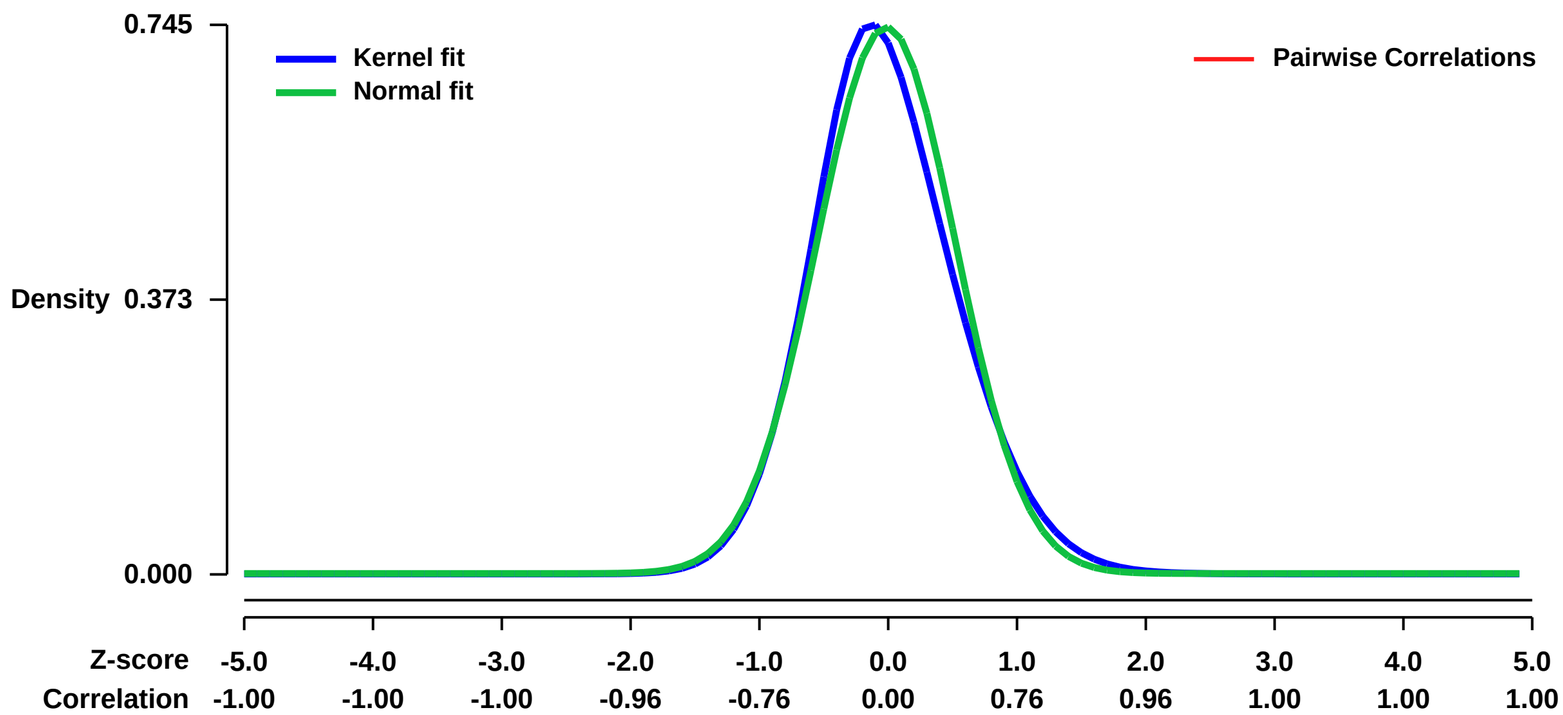

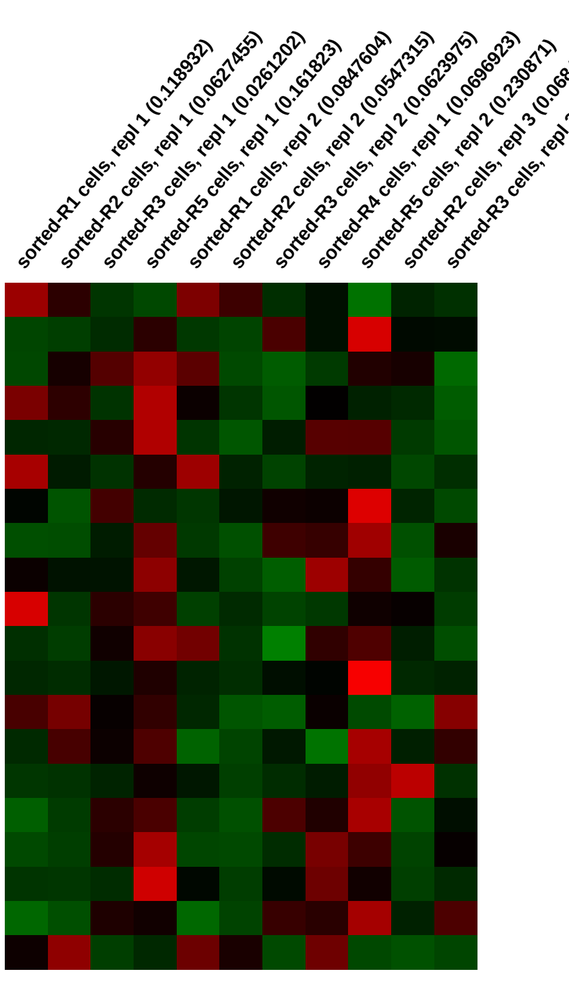

GEO Series "GSE20398" Expression Profiles

Num of samples in this series: 30

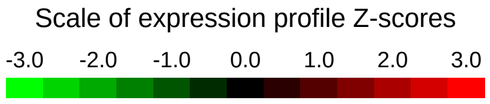

GEO Link:	http://www.ncbi.nlm.nih.gov/geo/query/acc.cgi?acc=GSE20398
Status:	Public on Apr 01 2010
Title:	Regulation of chondrogenesis in early murine limb mesenchyme by BMP signals
Organism:	Mus musculus
Experiment type:	Expression profiling by array
Platform:	GPL1261
Pubmed ID:	20501701
Summary & Design:	**Summary:** Numerous studies have established a critical role for BMP signaling in skeletal development. In the developing axial skeleton, sequential SHH and BMP signals are required for specification of a chondrogenic fate in somitic tissue. A similar paradigm is thought to operate in the limb, but the signals involved are unclear. To investigate the nature of these signals we examined BMP action in mesenchymal populations derived from the early murine limb bud (~ E10.5). These populations exhibited a graded response to BMPs, in which early limb mesenchymal (EL) cells (from the distal hind limb) displayed an anti-chondrogenic response, whereas BMPs promoted chondrogenesis in older cell populations. To better understand the molecular basis of disparate BMP action in these various populations, gene expression profiling with Affymetrix microarrays was employed to identify BMP-regulated genes. These analyses showed that BMPs induced a distinct gene expression pattern in the EL cultures versus later mesenchymal limb populations (IM and LT). **Overall design:** Mouse embryos at gestational age E10.5 were collected and various portions of the limb were micro-dissected. These led to the generation of three populations of cells, early (EL) limb mesenchymal cells from the distal half of the hind limb, an intermediate (IM) population derived from the distal 1/3 of the fore limb, and a later (LT) population from the proximal 2/3 of the fore limb. Mesenchymal cells were isolated and cultured with and without BMP4 treatment. RNA was extracted from cultures at either Day 0,1 or 2, labelled and hybridized to Affymetrix 430 2.0 microarrays. For each time point, RNA was collected from two biological replicates for each treatment condition.

Background corr dist: KL-Divergence = 0.2351, L1-Distance = 0.0379, L2-Distance = 0.0024, Normal std = 0.3143

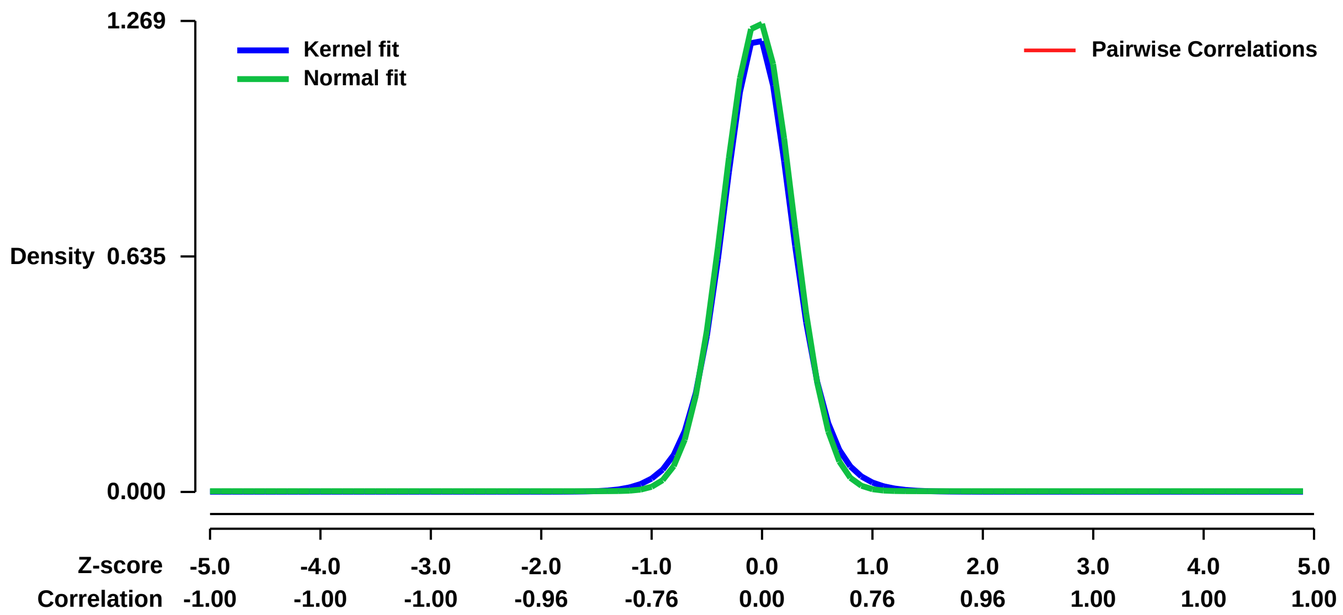

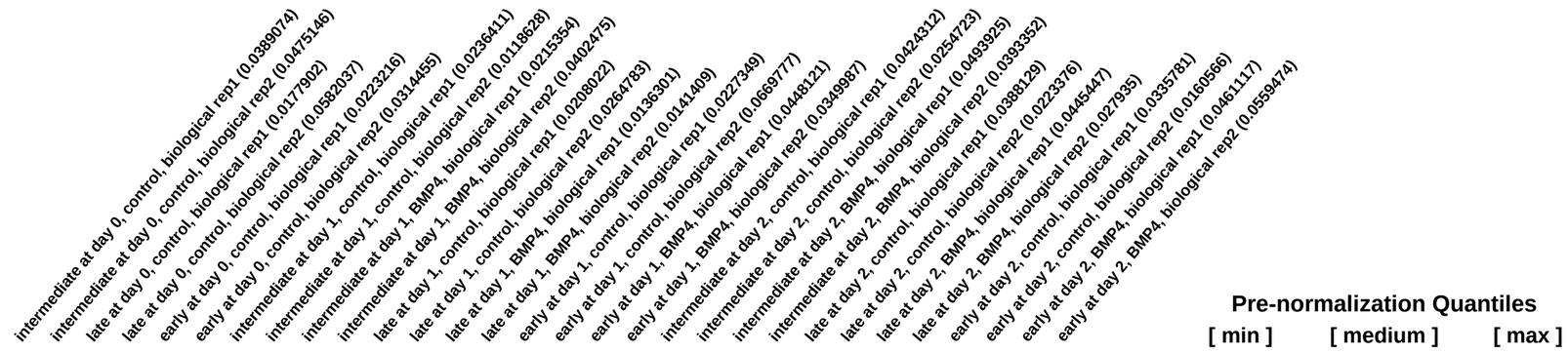

Null module

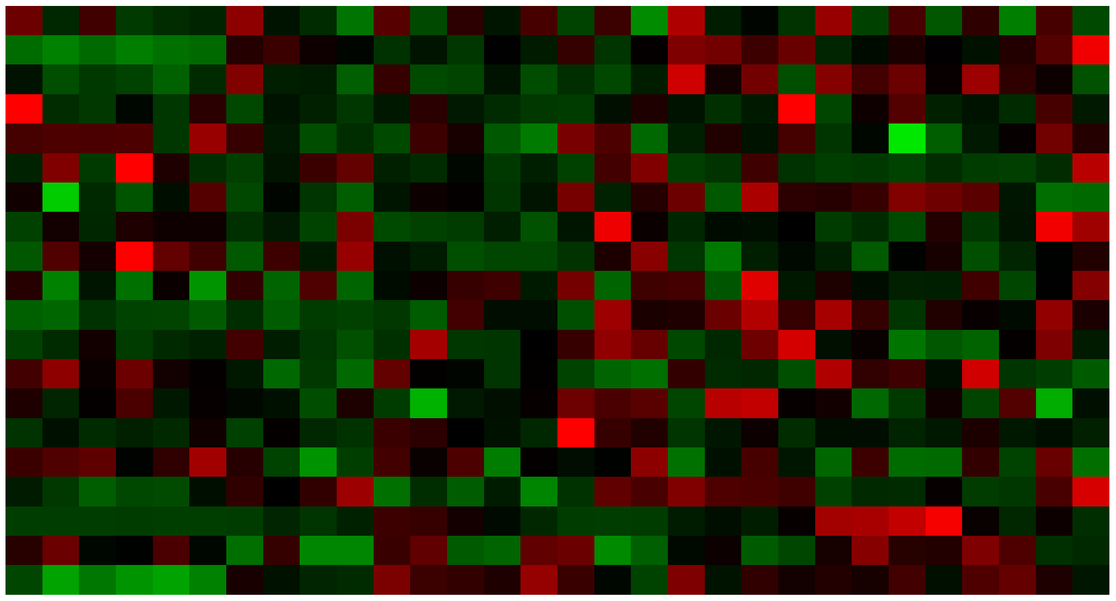

GEO Series "GSE20411" Expression Profiles

Num of samples in this series: 20

Scale of expression profile Z-scores

-3.0 -2.0 -1.0 0.0 1.0 2.0 3.0

GEO Link:	http://www.ncbi.nlm.nih.gov/geo/query/acc.cgi?acc=GSE20411
Status:	Public on Jan 01 2011
Title:	The effects of aging vs. alpha7 nAChR subunit deficiency on the mouse brain transcriptome
Organism:	Mus musculus
Experiment type:	Expression profiling by array
Platform:	GPL1261
Pubmed ID:	20526689
Summary & Design:	**Summary:** Aging is accompanied by expression changes in multiple genes and the brain is one of the tissues most vulnerable to aging. Since the alpha7 nicotinic acetylcholine receptor (nAChR) subunit has been associated with neurodevelopmental disorders and cognitive decline during aging, we hypothesized that its absence might affect gene expression profiles in aged brains. To study whether transcriptional changes occur due to aging, alpha7 deficiency or both, we analyzed whole brain transcriptomes of young (8 week) and aged (2 year) alpha7 deficient and wild-type control mice, using Mouse Genome 430 2.0 microarray. Highly significant expression changes were detected in 47 and 1543 genes (after Bonferroni and FDR correction) in the brains of aged mice compared to young mice, regardless of their genotype. These included genes involved in immune system function and ribosome structure, as well as genes that were previously demonstrated as differentially expressed in aging human brains. Genotype-dependent changes were detected in only 3 genes, Chrna7 which encodes the alpha7 nAChR subunit, and two closely linked genes, likely due to a mouse background effect. Expression changes dependent on age-genotype interaction were detected in 207 genes (with a low significance threshold). Age-dependent differential expression levels were approved in all nine genes that were chosen for validation by real-time RT-PCR. Our results suggest that the robust effect of aging on brain transcription clearly overcomes the almost negligible effect of alpha7 nAChR subunit deletion, and that germline deficiency of this subunit has a minor effect on brain expression profile in aged mice. **Overall design:** Total of 20 samples. 10 from young adult mice (8 weeks) and 10 from aged mice (2 years). In each age group, 5 were wild-type control mice and 5 alpha7 nAChR subunit defecient mice

Background corr dist: KL-Divergence = 0.2632, L1-Distance = 0.0538, L2-Distance = 0.0070, Normal std = 0.2961

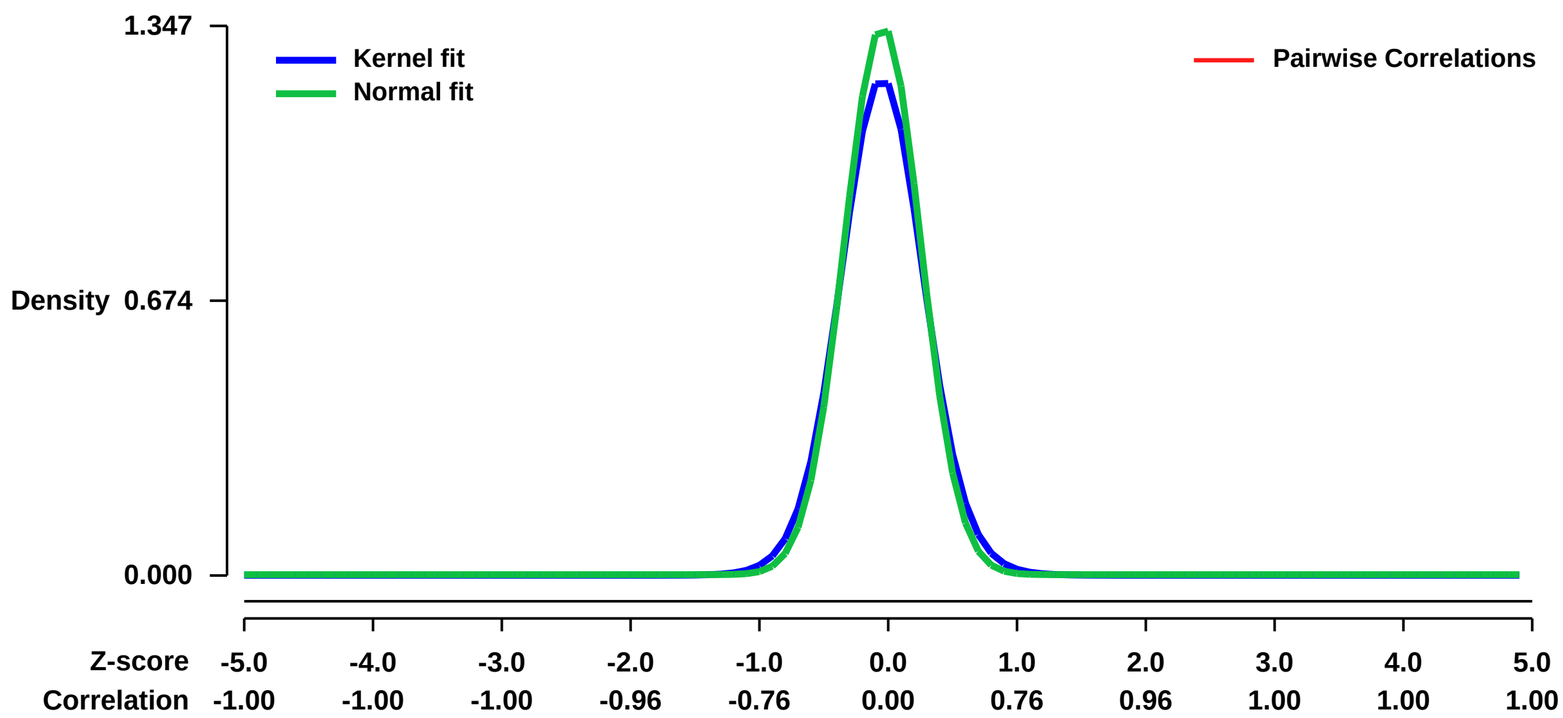

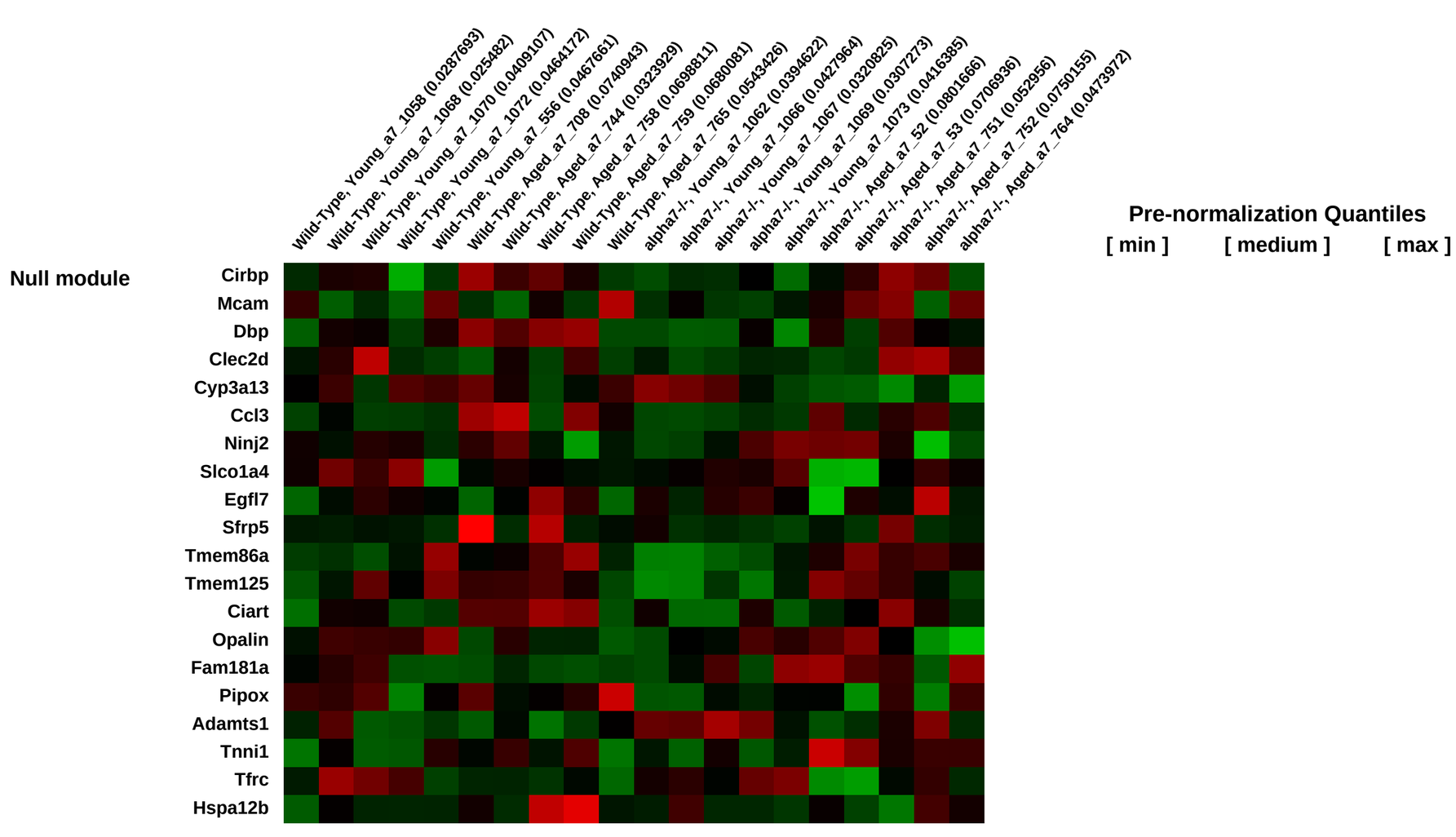

GEO Series "GSE20426" Expression Profiles

Num of samples in this series: 35

Scale of expression profile Z-scores

-3.0 -2.0 -1.0 0.0 1.0 2.0 3.0

GEO Link:	http://www.ncbi.nlm.nih.gov/geo/query/acc.cgi?acc=GSE20426
Status:	Public on Feb 16 2011
Title:	Hepatic gene expression during liver regeneration in response to partial hepatectomy: late time points (24h, 38h, 48h)
Organism:	Mus musculus
Experiment type:	Expression profiling by array
Platform:	GPL1261
Pubmed ID:	21719609
Summary & Design:	**Summary:** The process of liver regeneration can be divided into a series of stages that include initial inductive or priming events through cellular mitosis. Following two-thirds liver resection, the liver undergoes the â primingâ phase, in which cytokines TNF-a and IL-6 activate their respective receptors in hepatocytes. This leads to the activation of several key transcription factors: NF-kB, AP-1, Stat 3, Stat 1, and C/EBP-b and -d . These transcription factors induce the expression of immediate early genes. HGF is also expressed at this time and involved in the transition of quiescent hepatocytes into the G1 phase of the cell cycle. During the G1 phase, delayed early genes are expressed followed by induction of cell cycleâ related genes, both of which require new protein synthesis for their production. Increased expression of FoxM1B and TGF-a occurs at the G1/S transition and is correlated with increased expression of cyclinD1 and decreased expression of cdk inhibitors. During the G2/M phase of the cell cycle, FoxM1B directly elevates cyclinB1, cyclinB2, and cdc25B expression. Additionally, FoxM1B is associated with increased cyclinF and p55cdc, which are involved in completion of the cell cycle following partial hepatectomy. In mice, two-thirds partial hepatectomy promotes proliferation of liver cells and rapid growth of the remaining liver tissue, resulting in complete restoration of organ mass in approximately 7 days (Mackey S. et al. Hepatology 2003 Dec;38(6):1349-52). **Overall design:** Liver tissue was collected 0h, 24h, 38h, and 48h after partial hepatectomy or sham surgery from both young (5-6 months) and old (25-27 months) CB6F1 mice. All control and partial hepatectomy samples were assayed in triplicate. Relative gene expression levels were determined using Affymetrix moe430_2 oligo arrays.

Background corr dist: KL-Divergence = 0.1371, L1-Distance = 0.0498, L2-Distance = 0.0059, Normal std = 0.3856

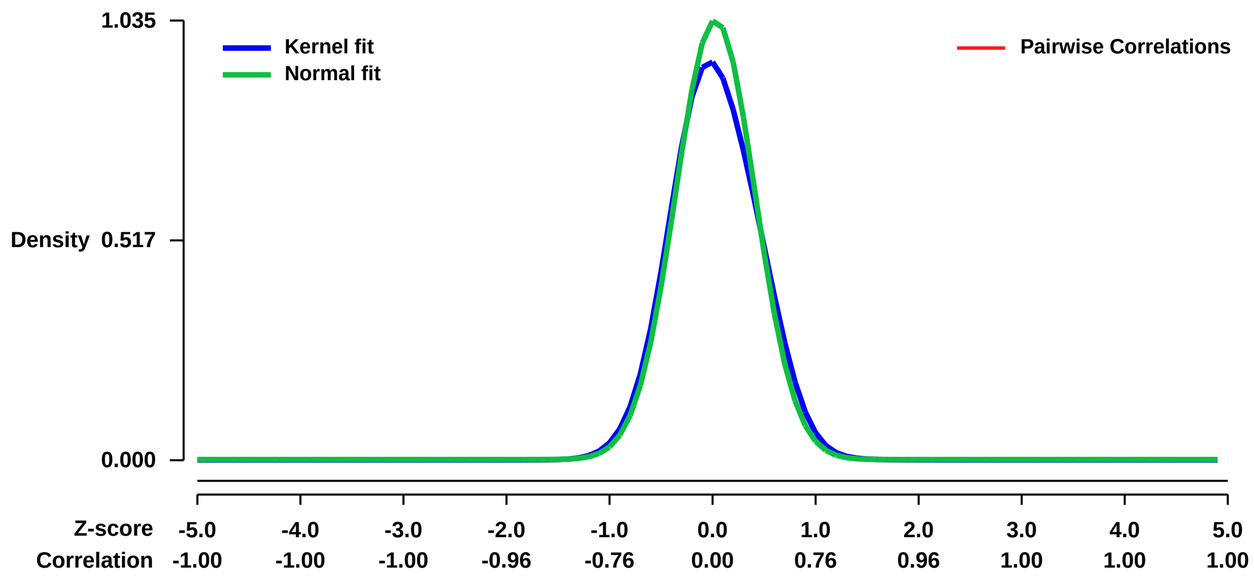

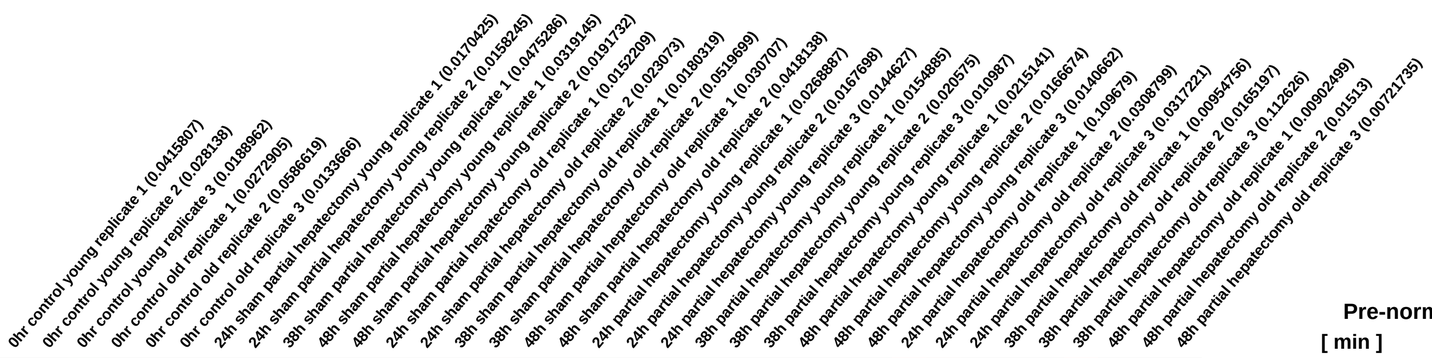

GEO Series "GSE20500" Expression Profiles

Num of samples in this series: 6

Scale of expression profile Z-scores

-3.0 -2.0 -1.0 0.0 1.0 2.0 3.0

GEO Link:	http://www.ncbi.nlm.nih.gov/geo/query/acc.cgi?acc=GSE20500
Status:	Public on Feb 14 2011
Title:	T cell genes regulated by retinoic acid
Organism:	Mus musculus
Experiment type:	Expression profiling by array
Platform:	GPL1261
Pubmed ID:	20664575
Summary & Design:	**Summary:** This is to determine the T cell genes regulated by retinoic acid. **Overall design:** 2 arrays were used for each group

Background corr dist: KL-Divergence = 0.0330, L1-Distance = 0.0460, L2-Distance = 0.0029, Normal std = 0.7128

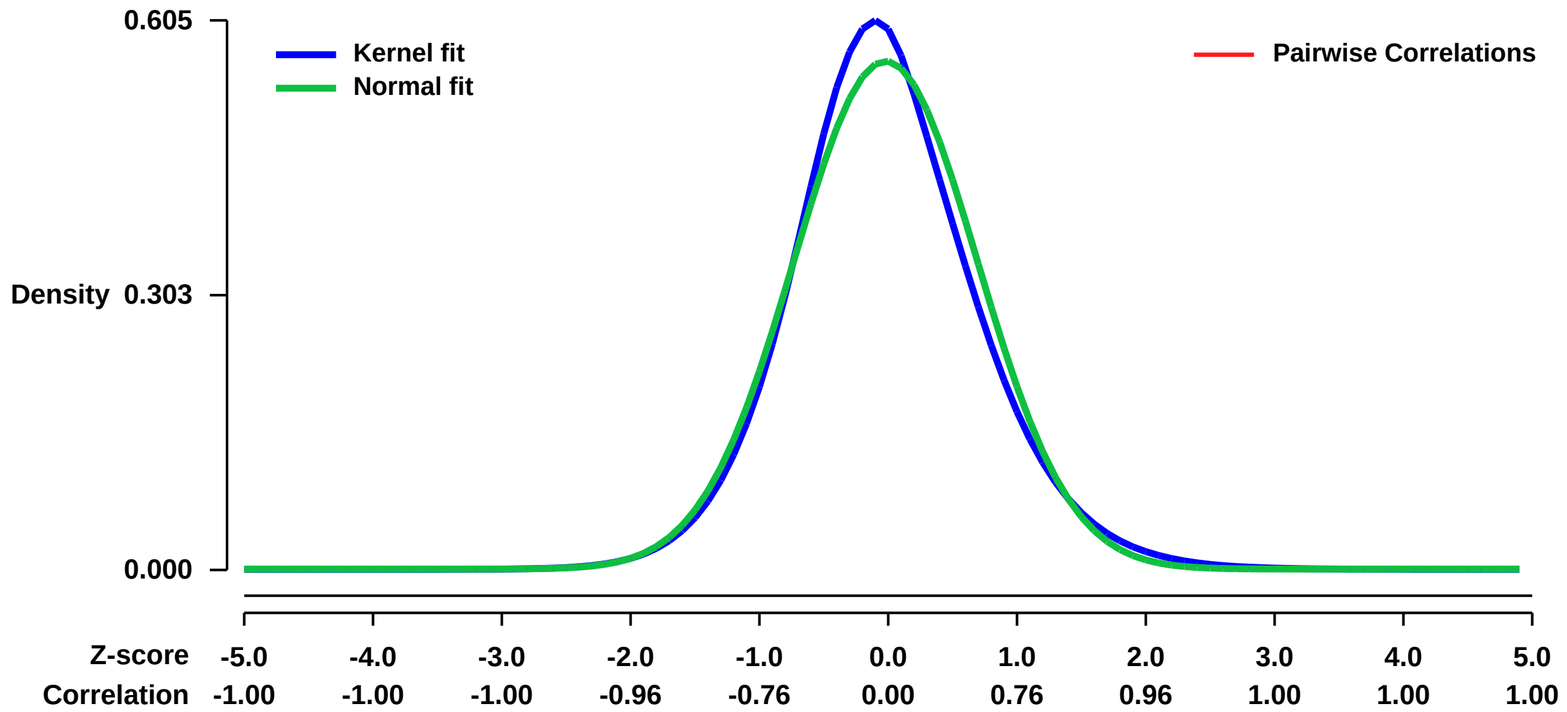

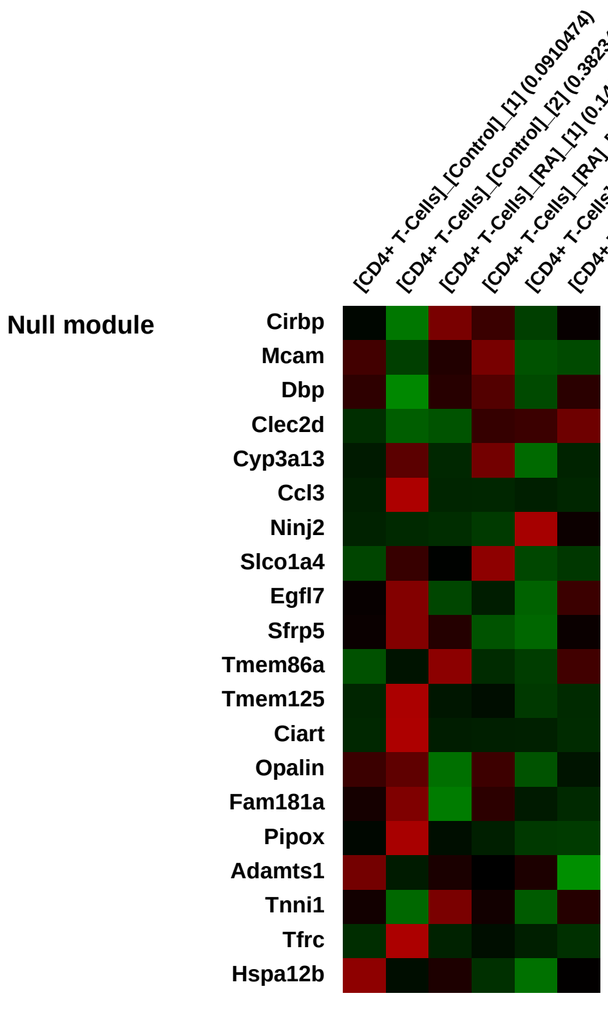

GEO Series "GSE20513" Expression Profiles

Num of samples in this series: 12

Scale of expression profile Z-scores

-3.0 -2.0 -1.0 0.0 1.0 2.0 3.0

GEO Link:	http://www.ncbi.nlm.nih.gov/geo/query/acc.cgi?acc=GSE20513
Status:	Public on Jun 15 2010
Title:	Expression data from (bezafibrate treated-wild type, Clock mutant, and PPARalpha-null) mouse liver
Organism:	Mus musculus
Experiment type:	Expression profiling by array
Platform:	GPL1261
Pubmed ID:	20400680
Summary & Design:	**Summary:** A functional interaction between peroxisome proliferator-activated receptor alpha (PPARalpha) and components of the circadian clock has been suggested; however, it remains to be clarified whether those transcriptional factors interact with each other to regulate the expression of their target genes. In this study, we used a ligand of PPARalpha, bezafibrate, to search the PPARalpha-regulated genes that express in a CLOCK-dependent circadian manner. Microarrays analyses using hepatic RNA isolated from bezafibrate treated-wild type, Clock mutant (Clk/Clk), and PPARalpha-null mice revealed that 136 genes are transcriptionally regulated by PPARalpha in a CLOCK-dependent manner. **Overall design:** To examine the PPARalpha-regulated genes that express in a CLOCK-dependent manner in mice, we performed oligonucleotide microarray analysis at ZT14, when CLOCK/BMAL1 transcriptional activity is maximal, using RNA isolated from wild-type (n = 3), Clock mutant (n = 3), and PPARalpha-null mice (n = 3) treated with bezafibrate for 5 days, and control wild-type mice (n = 3). Livers were collected and frozen in liquid nitrogen. Total RNA (250 ng) was extracted using RNAiso.

Background corr dist: KL-Divergence = 0.0812, L1-Distance = 0.0202, L2-Distance = 0.0004, Normal std = 0.4749

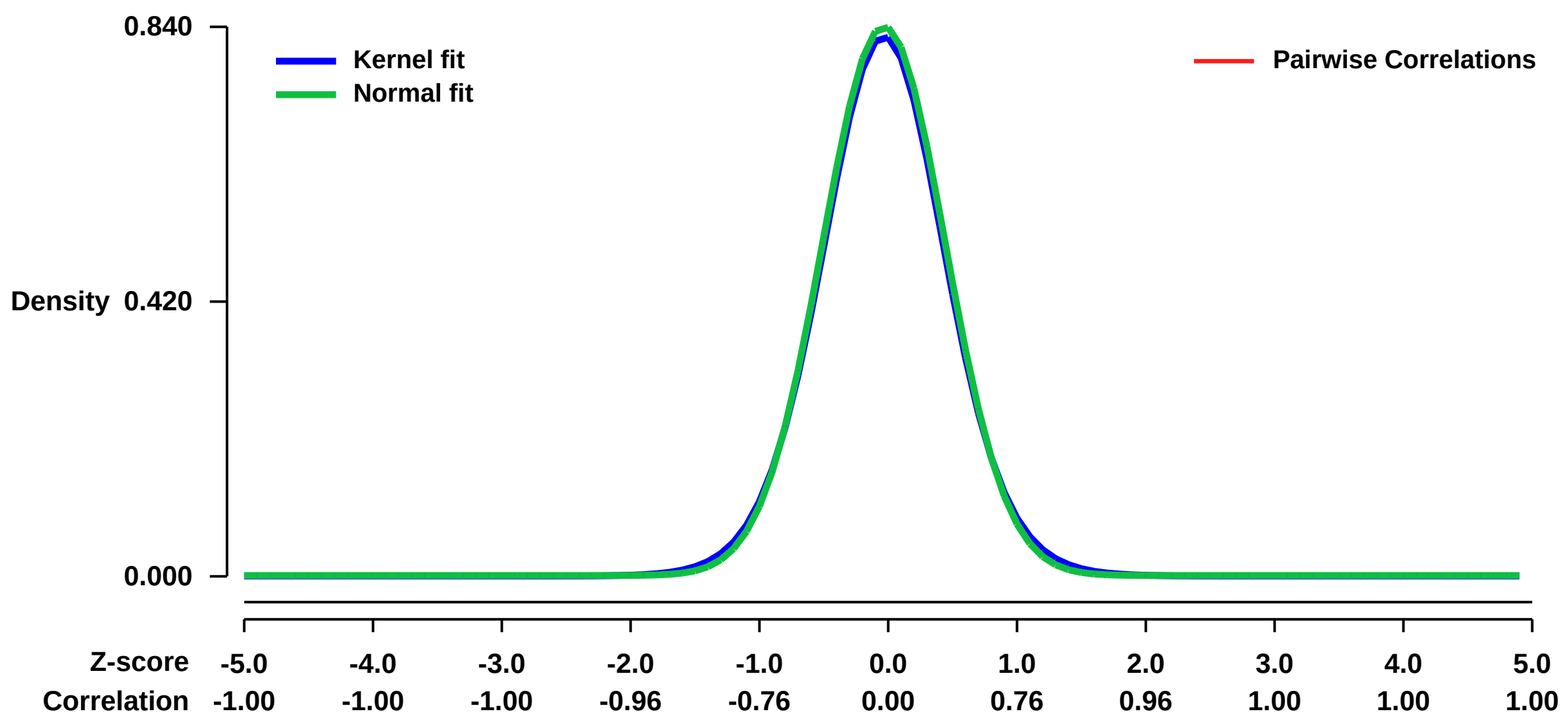

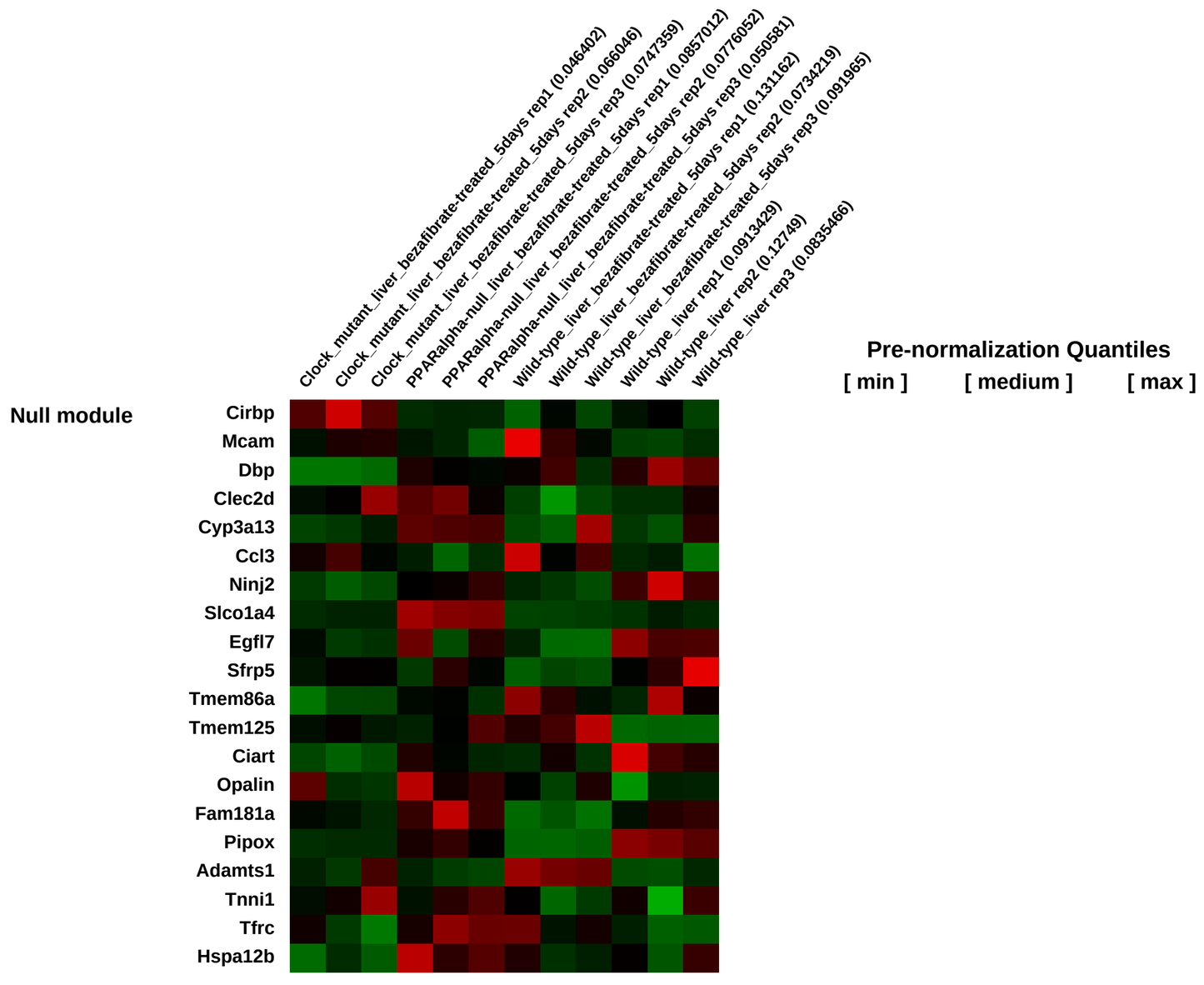

GEO Series "GSE20523" Expression Profiles

Num of samples in this series: 17

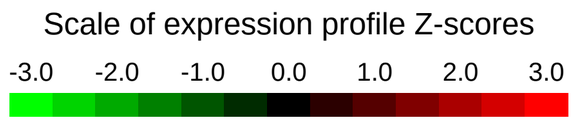

GEO Link:	http://www.ncbi.nlm.nih.gov/geo/query/acc.cgi?acc=GSE20523
Status:	Public on Jun 21 2010
Title:	Immunoregulatory actions of T cell PPAR g at the colonic mucosa
Organism:	Mus musculus
Experiment type:	Expression profiling by array
Platform:	GPL1261
Pubmed ID:	20537136
Summary & Design:	**Summary:** **BACKGROUND: Peroxisome proliferator-activated receptor g (PPAR g) is a nuclear receptor whose activation has been shown to modulate macrophage and epithelial cell-mediated inflammation. The objective of this study was to use a systems approach for investigating the mechanism by which the deletion of PPAR g in T cells modulates the severity of dextran-sodium sulfate (DSS)-induced colitis, immune cell distribution and global gene expression.** **METHODS: Wild-type (WT) or PPAR g flfl; CD4 Cre+ (CD4cre) mice in a C57BL/6 background were challenged with 2.5% DSS in their drinking water for 0, 2, or 7 days. Mice were scored on disease severity both clinically and histopathologically. Flow cytometry was used to assess lymphocyte and macrophage populations in the blood, spleen, and mesenteric lymph nodes (MLN). Global gene expression in colonic mucosa was profiled using Affymetrix microarrays.** **RESULTS: Both disease severity and inflammation-related body weight loss were accelerated by the deficiency of PPAR g in T cells. Examination of colon histopathology revealed significantly greater epithelial erosion, leukocyte infiltration, and mucosal thickening in the CD4cre mice on day 7. CD4cre mice had more CD8+ T cells than wt mice and fewer CD4+FoxP3+ regulatory T cells (Treg) and IL10+CD4+ T cells in blood and MLN, respectively. Transcriptomic profiling revealed around 3000 genes being transcriptionally altered as a result of DSS challenge in CD4cre mice. These included up-regulated adhesion molecules on day 7 and proinflammatory cytokines interleukin-6 (IL-6) and IL-1b, and suppressor of cytokine signaling 3 (SOCS-3) mRNA expression.** **CONCLUSIONS: These findings suggest that T cell PPAR g down-regulates inflammation during DSS colitis by inhibiting colonic expression of inflammatory mediators and increasing MLN Treg.** **Overall design:** **Colonic mucosa from wt and CD4cre mice were sampled at 0 (no DSS), 2, and 7 days of DSS-induced experimental colitis**

Background corr dist: KL-Divergence = 0.1498, L1-Distance = 0.0988, L2-Distance = 0.0202, Normal std = 0.4522

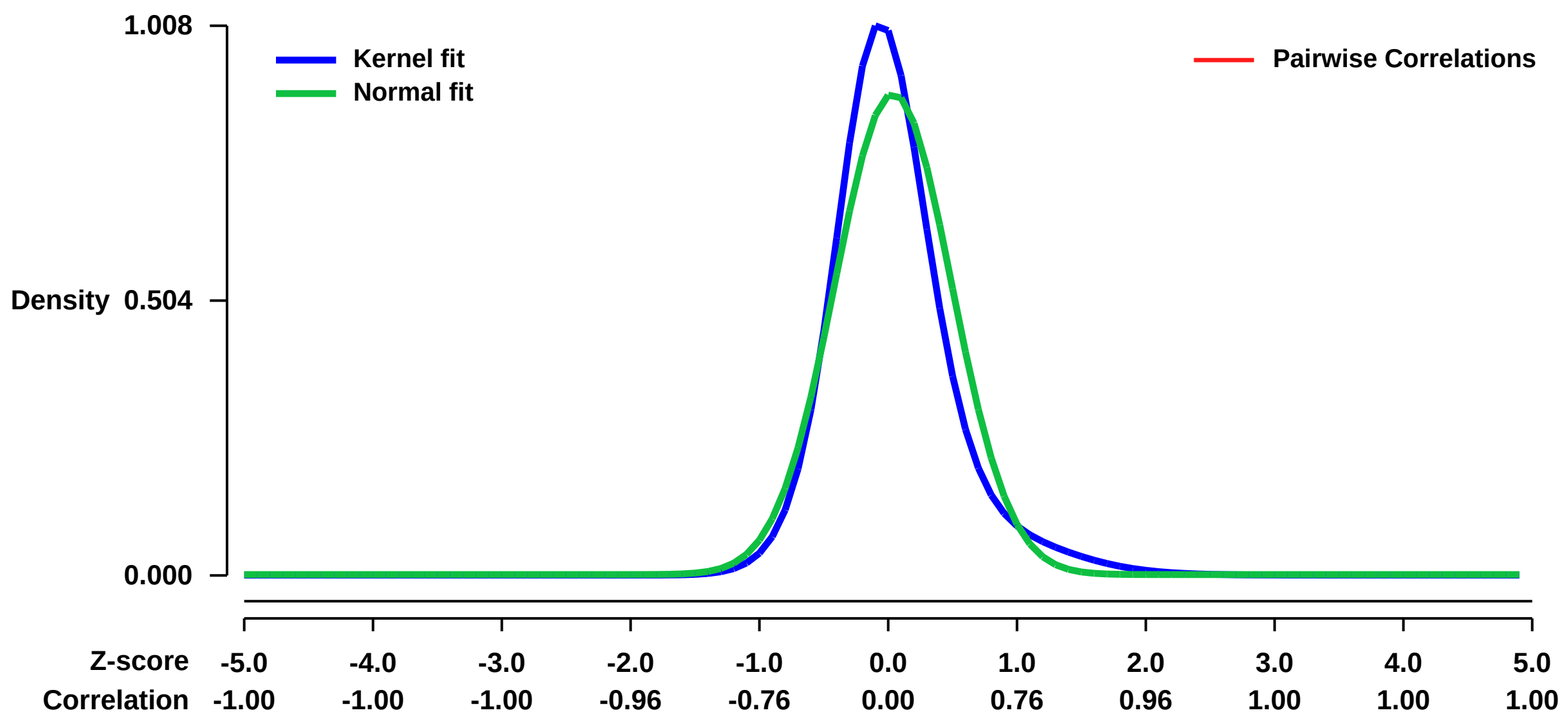

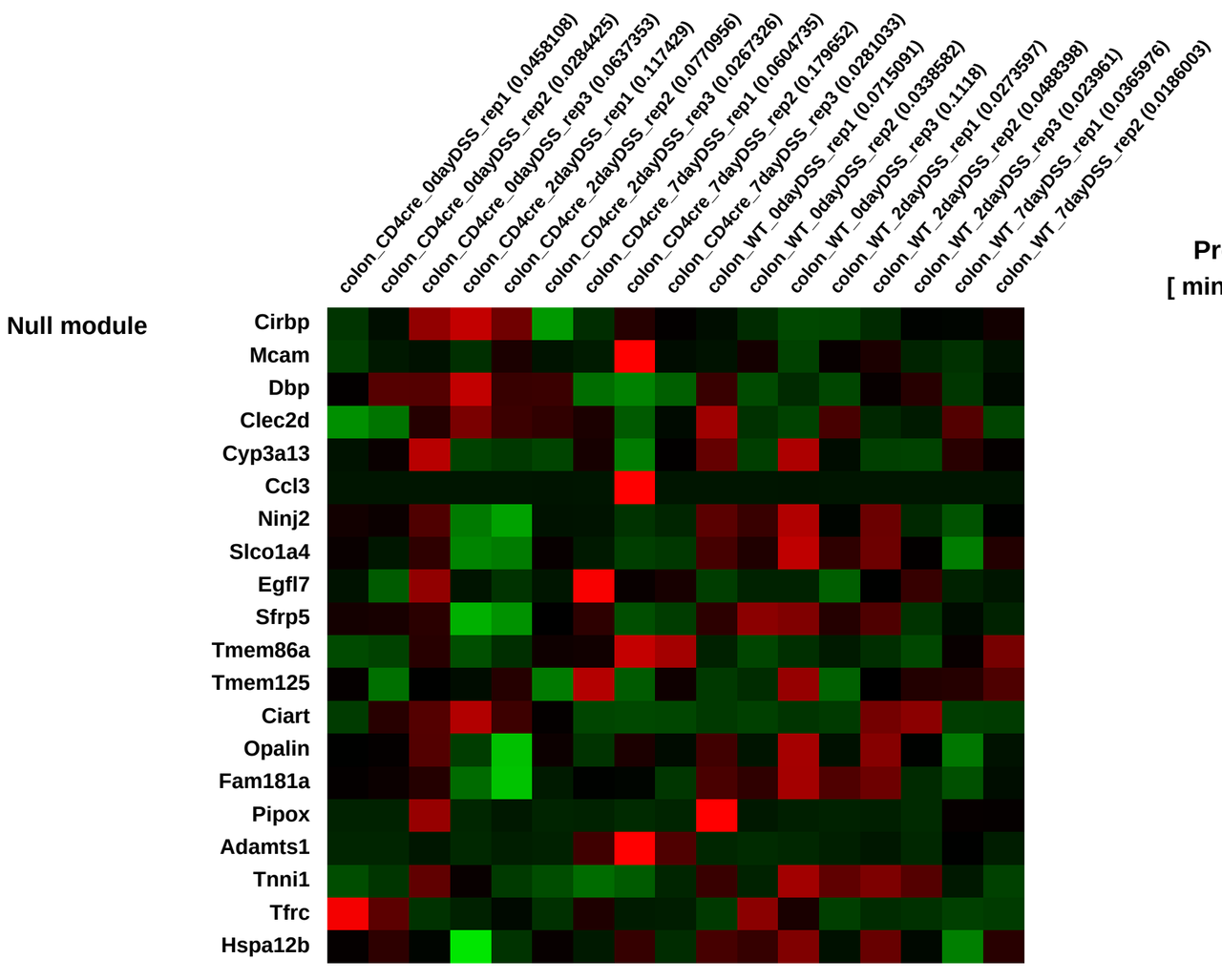

GEO Series "GSE20570" Expression Profiles

Num of samples in this series: 6

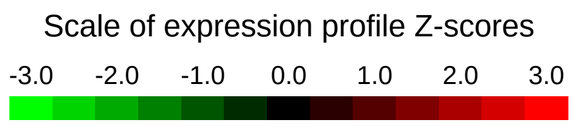

GEO Link:	**http://www.ncbi.nlm.nih.gov/geo/query/acc.cgi?acc=GSE20570**
Status:	**Public on Mar 02 2010**
Title:	**Gene profile of PTIP deletion in adult murine cardiac tissue**
Organism:	**Mus musculus**
Experiment type:	**Expression profiling by array**
Platform:	**GPL1261**
Pubmed ID:	

Summary & Design:

Summary:
Methylation of histone H3 lysine 4 (H3K4me) at actively expressed, cell type-specific genes is established during development by the Trithorax group of epigenetic regulators. In mammals, the Trithorax family includes KMT2A-D (MLL1-4), a family of SET domain proteins that function in large complexes to impart mono-, di-, and trimethylation at H3K4. Individual KMT2s and their co-factors are essential for embryonic development and the establishment of correct gene expression patterns, presumably by demarcating the active and accessible regions of the genome in a cell specific and heritable manner. Despite the importance of H3K4me marks in development, little is known about the importance of histone methylation in maintaining gene expression patterns in fully differentiated and non-dividing cell types. In this report, we utilized an inducible cardiac-specific Cre driver to delete the PTIP protein, a key component of a H3K4me complex, and ask whether this activity is still required to maintain the phenotype of terminally differentiated cardiomyocytes. Our results demonstrate that reducing the H3K4me3 marks is sufficient to alter gene expression patterns and significantly augment systolic heart function. These results clearly show that maintenance of H3K4me3 marks is necessary for the stability of the transcriptional program in differentiated cells. The array we performed allowed us to identify genes that are regulated by PTIP and histone methylation.

Overall design:
8-week-old littermate mice on a mixed C57B6 and B6129 background were utilized. Three mice were on a background with a PTIP floxed allele and a wild type PTIP allele (PTIP+1, PTIP+2, PTIP+3). Three mice had a transgene that expresses a modified estrogen receptor -Cre recombinase fusion protein under the control of a cardiac-specific driver (alpha myosin heavy chain, Jackson Lab stock #005650) and a floxed PTIP allele and a null PTIP (PTIPKO1, PTIPKO2, PTIPKO3). Both groups of mice were injected with tamoxifen at 8 weeks of age. Tamoxifen deletes the floxed PTIP allele in the PTIPKO mice. 5 days after tamoxifen injection, RNA was harvested from left ventricle (LV) apices in both groups. RNA was then sent to the University of Michigan microarray facility core for analysis.

Background corr dist: KL-Divergence = 0.0394, L1-Distance = 0.0187, L2-Distance = 0.0004, Normal std = 0.6171

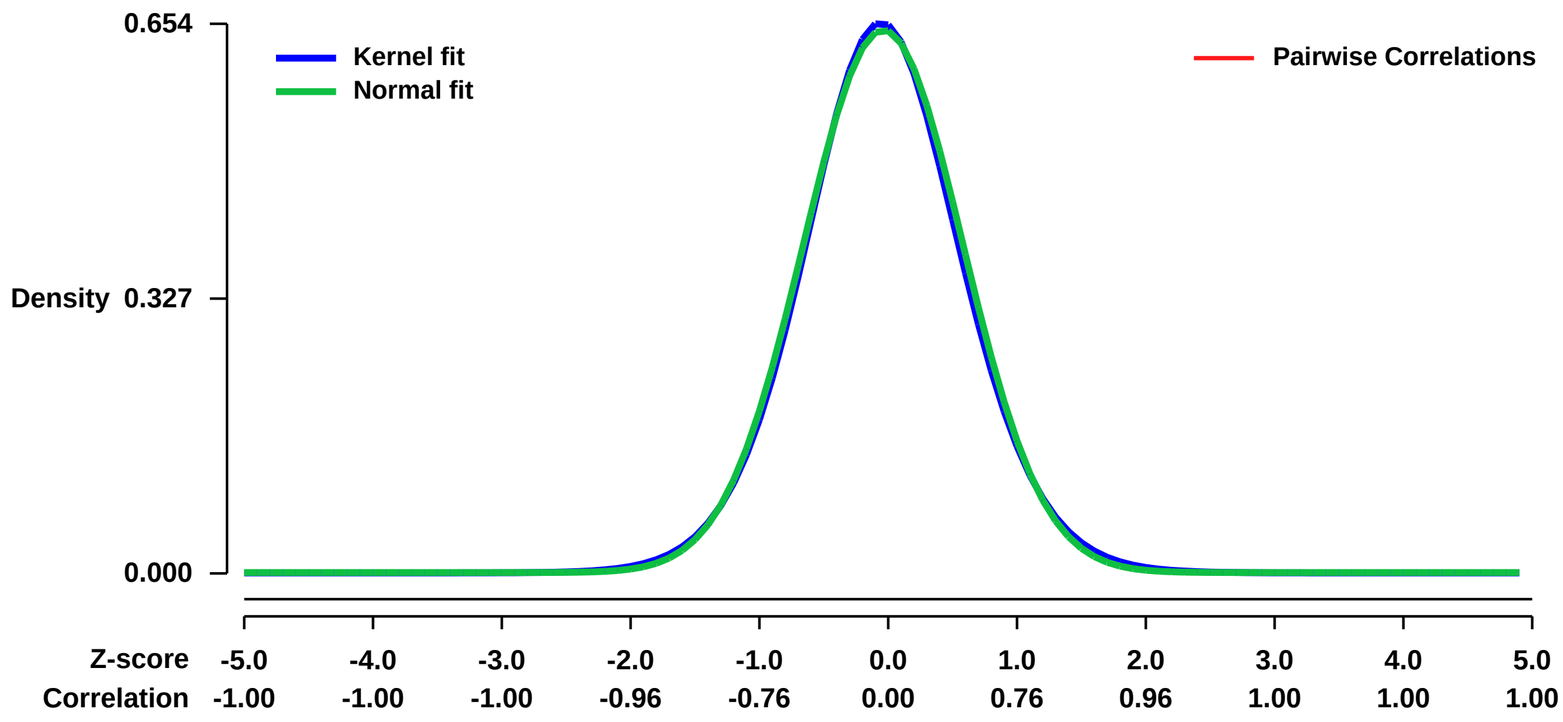

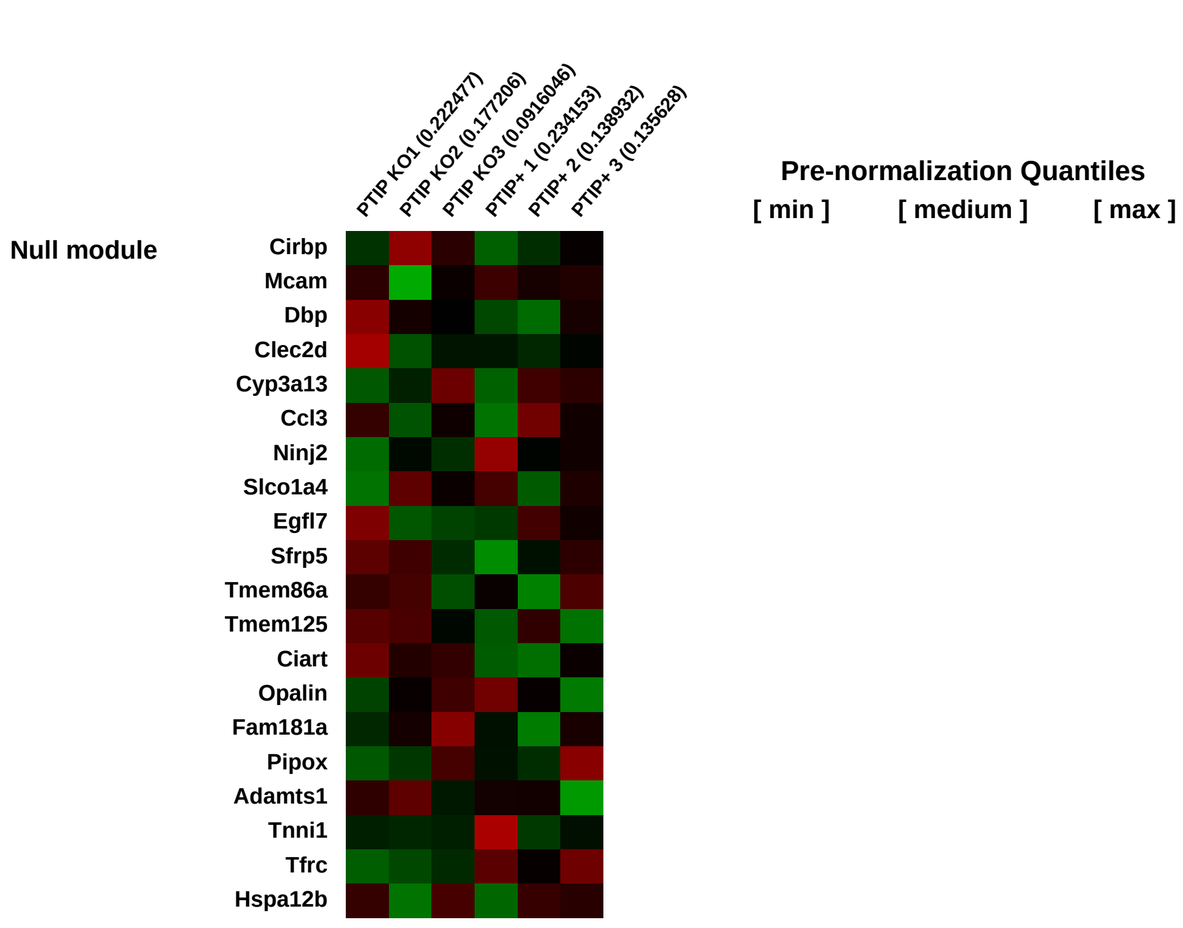

GEO Series "GSE20604" Expression Profiles

Num of samples in this series: 6

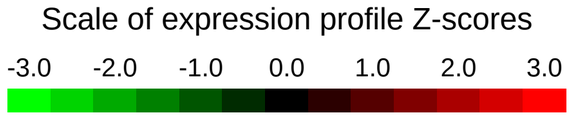

GEO Link:	http://www.ncbi.nlm.nih.gov/geo/query/acc.cgi?acc=GSE20604
Status:	Public on Apr 20 2010
Title:	Downstream Targets of HOXB4 in the primitive hematopoietic progenitor EML Cell line
Organism:	Mus musculus
Experiment type:	Genome binding/occupancy profiling by genome tiling array
Platform:	GPL1261
Pubmed ID:	20404135
Summary & Design:	**Summary:** Enforced expression of the homeobox transcription factor HOXB4 has been shown to enhance hematopoietic stem cell (HSC) self-renewal and expansion ex vivo and in vivo. In order to investigate the largely unknown downstream targets of HOXB4 in hematopoietic progenitor cells, HOXB4 was constitutively overexpressed in the primitive hematopoietic progenitor cell line, EML. Gene expression differences were compared between KLS (c-Kit+, Lin-, Sca-1+)-EML cells that overexpressed HOXB4 (KLS-EML-HOXB4) to control KLS-EML cells that were transduced with vector alone. ChIP-chip was used to identify promoter regions bound by HOXB4. **Overall design:** We overexpressed HOXB4 in EML cells. We isolated 3 separate single cell clones as assessed by Southern Blot Analysis (3 clones for EML-HOXB4 and 3 clones for control EML-GFP cells). RNA was isolated from the KLS (c-Kit+, Lin-, Sca-1+) fraction of each single cell clone population and processed for hybridization to array chips using established lab protocols. Chip-Chip analysis of the three HOXB4 overexpressing clones was performed to identify HOXB4 bound promoters.

Background corr dist: KL-Divergence = 0.0195, L1-Distance = 0.0316, L2-Distance = 0.0018, Normal std = 0.7515

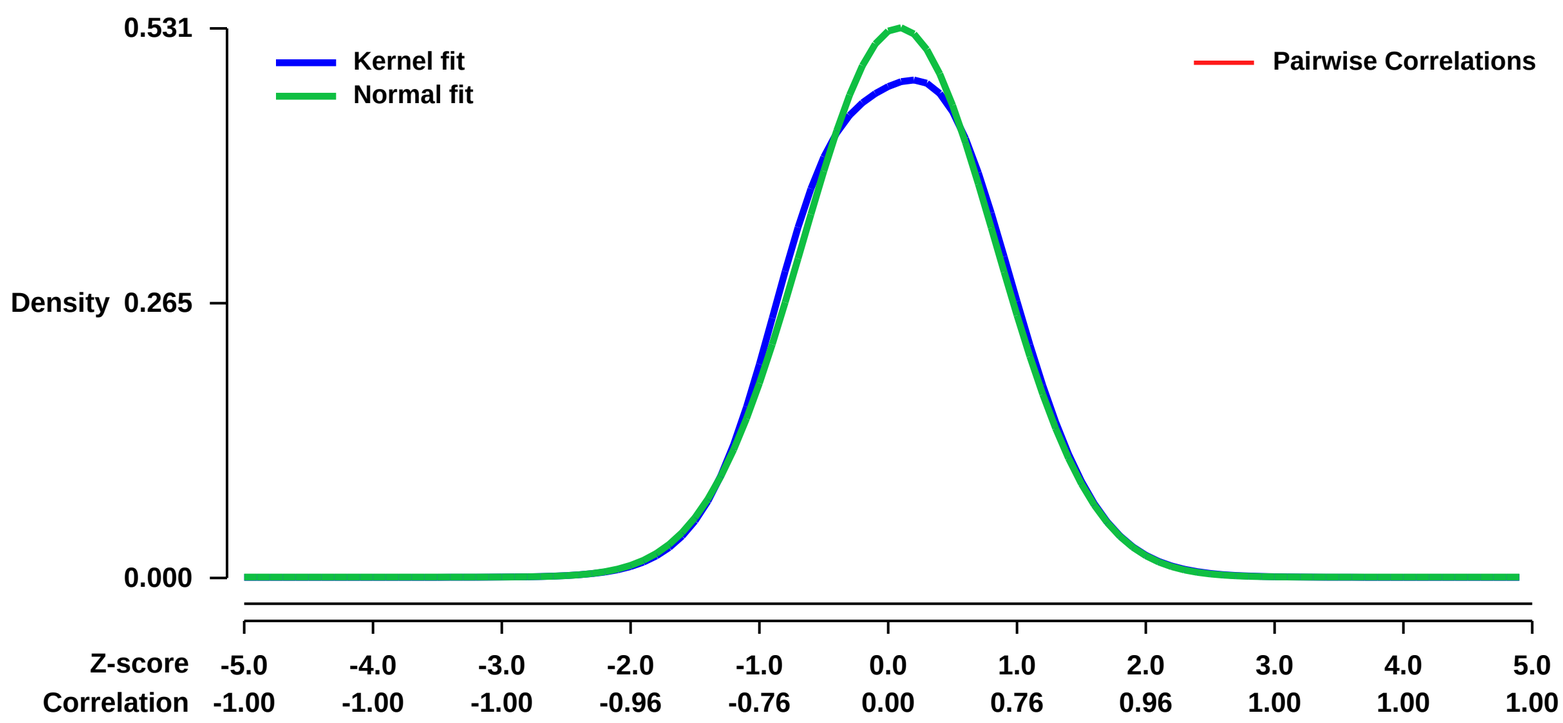

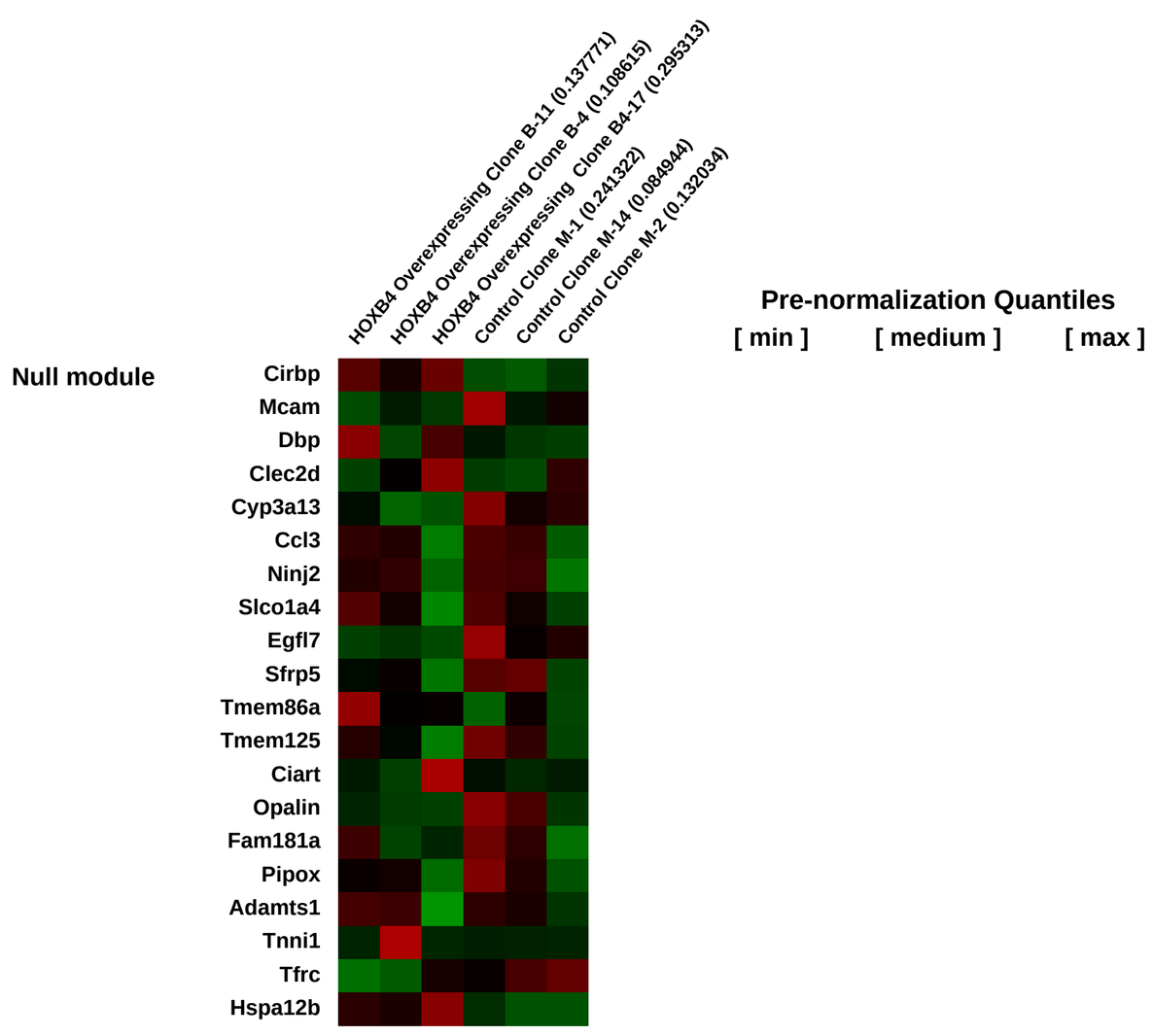

GEO Series "GSE20620" Expression Profiles

Num of samples in this series: 22

Scale of expression profile Z-scores

-3.0 -2.0 -1.0 0.0 1.0 2.0 3.0

GEO Link:	http://www.ncbi.nlm.nih.gov/geo/query/acc.cgi?acc=GSE20620
Status:	Public on Aug 31 2010
Title:	Global analysis of gene expression by SV40 T antigen in mouse embryo fibroblasts
Organism:	Mus musculus
Experiment type:	Expression profiling by array
Platform:	GPL1261
Pubmed ID:	20692676
Summary & Design:	**Summary:** SV40 large T antigen (TAg) contributes to cell transformation, in part, by targeting two well characterized tumor suppressors, pRb and p53. TAg expression affects the transcriptional circuits controlled by Rb and by p53. We have performed a microarray analysis to examine the global change in gene expression induced by wild-type TAg and TAg-mutants, in an effort to link changes in gene expression to specific transforming functions. For this analysis we have used MEFs expressing TAg or infected by SV40. Our analysis indicates that TAg can induce interferon-stimulated genes in MEFs and that this induction depends upon the LXCXE motif and p53 binding. **Overall design:** Two independent wild-type MEFs and three independent MEF cell lines expressing TAg and the mutants were used. Additionally, three independent mock and SV40 infections were conduted in MEFs. Total RNA was isolated from with the RNeasy kit. Total RNA was processed by the Genomics and Proteomics Core Laboratories at the University of Pittsburgh and hybridized to the Affymetrix GeneChip Mouse Genome 430 2.0 array. MAS 5.0 was used to obtain the present/absent calls and CEL files were normalized by RMA to obtain log2 expression values.

Background corr dist: KL-Divergence = 0.1241, L1-Distance = 0.0433, L2-Distance = 0.0041, Normal std = 0.4128

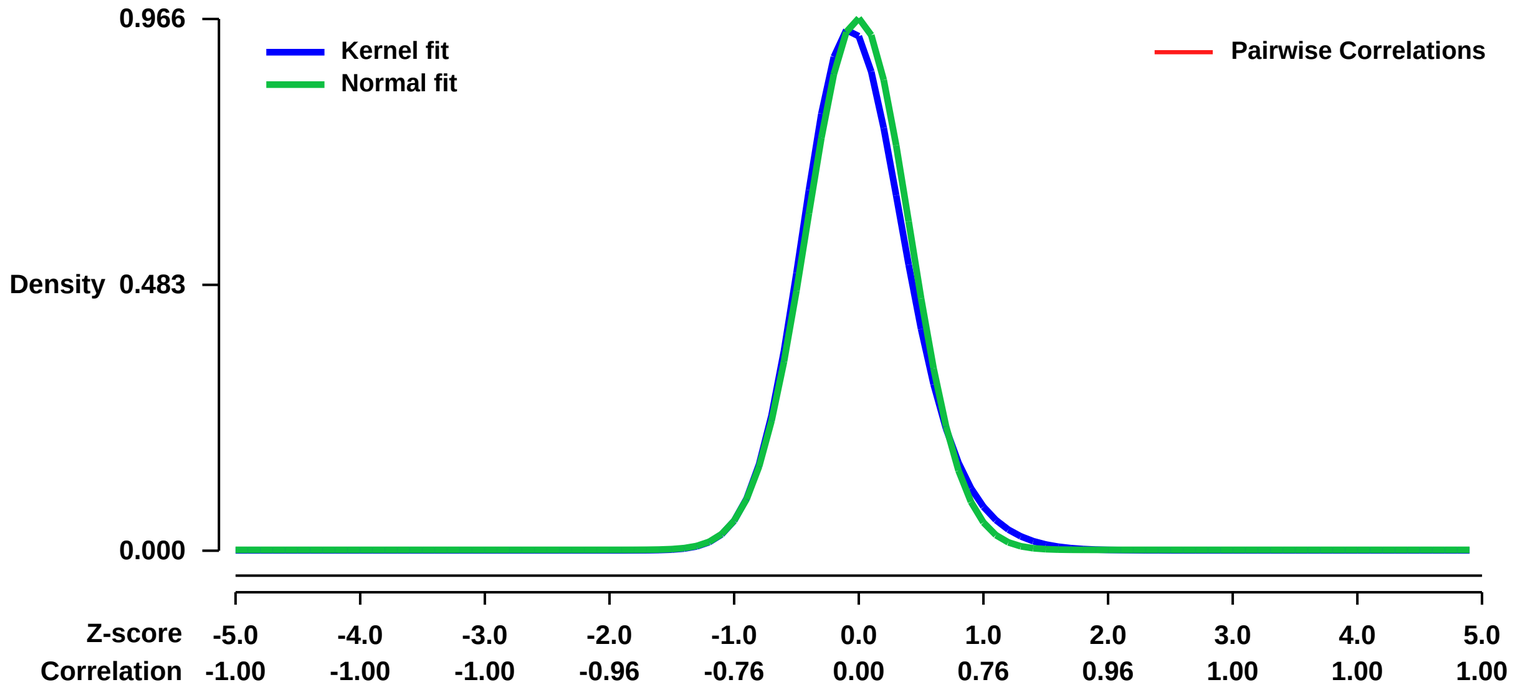

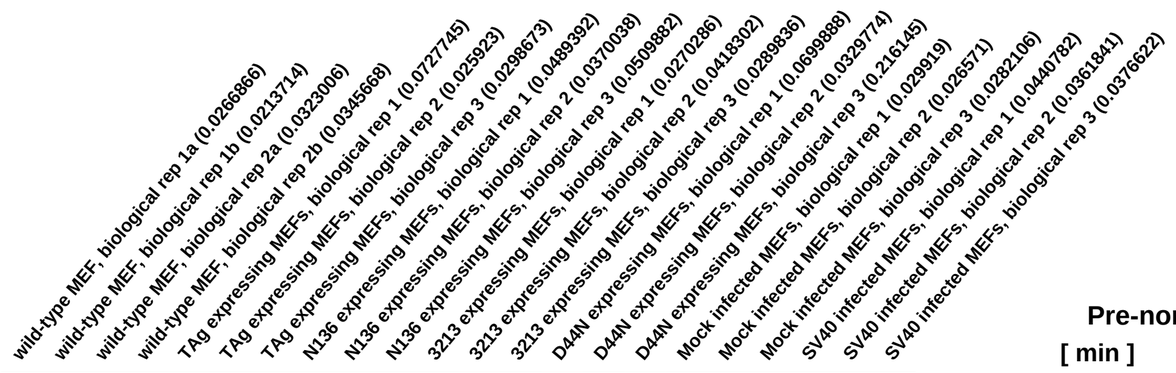

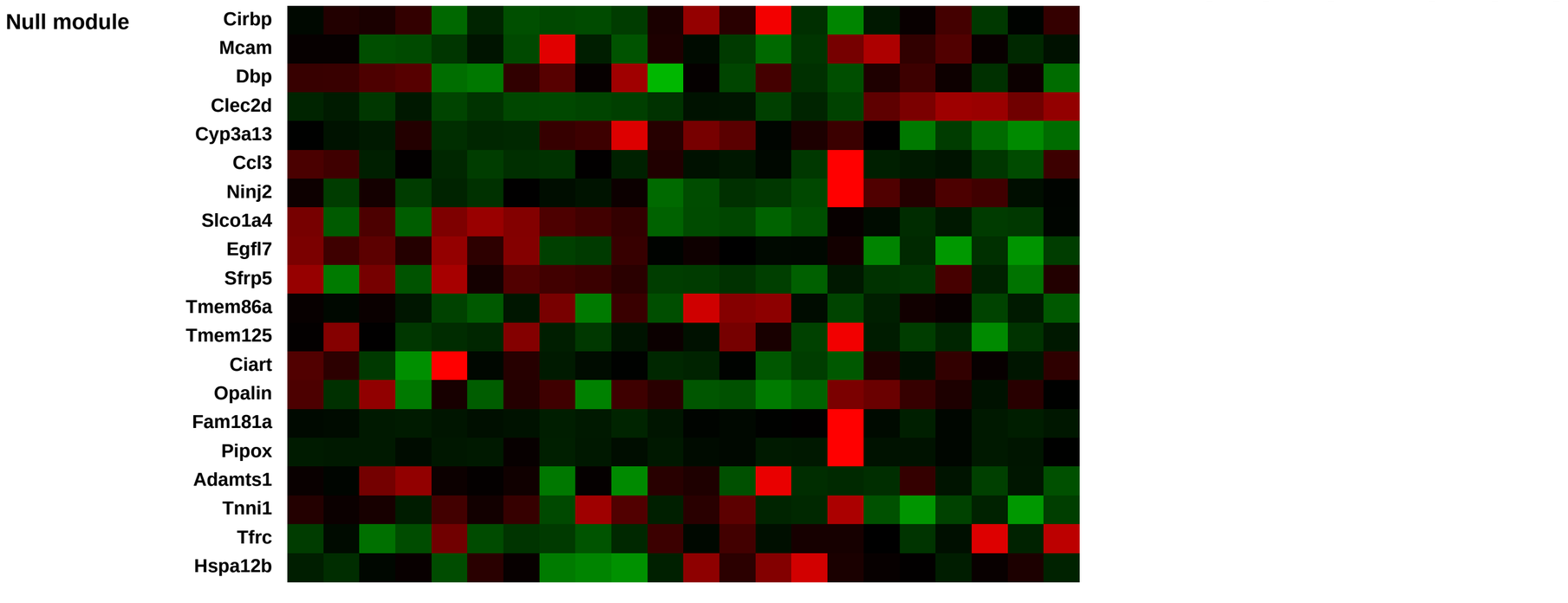

GEO Series "GSE20636" Expression Profiles

Num of samples in this series: 35

Scale of expression profile Z-scores

-3.0 -2.0 -1.0 0.0 1.0 2.0 3.0

GEO Link:	http://www.ncbi.nlm.nih.gov/geo/query/acc.cgi?acc=GSE20636
Status:	Public on Mar 06 2010
Title:	Expression data from OVE26 diabetic mouse kidney
Organism:	Mus musculus
Experiment type:	Expression profiling by array
Platform:	GPL1261
Pubmed ID:	
Summary & Design:	**Summary:** OVE26 mouse was chosen to study the progressive changes in renal gene expression because it displays the most advanced albuminuria mouse models that assembles advanced human diabetic nephropathy. OVE26 mice induce inflammatory gene expression changes consistent with advanced renal disease, associated with severe albuminuria and not reported in any other diabetic models. They provide the first opportunity in a model of diabetic nephropathy to assess the effect of induction of inflammatory proteins that have been implicated in renal injury. **Overall design:** Microarray expression was performed on whole kidney from control and diabetic mice at 2, 4 and 8 months of age and validated by rtPCR, in situ hybridization or immunohistochemistry.

Background corr dist: KL-Divergence = 0.0571, L1-Distance = 0.0288, L2-Distance = 0.0013, Normal std = 0.5364

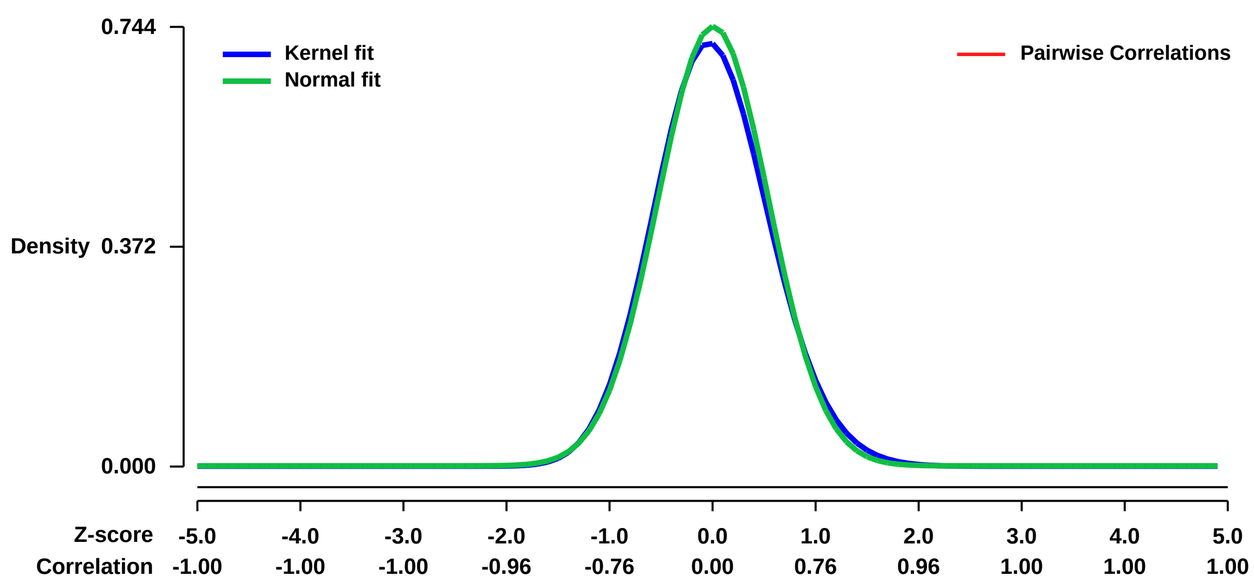

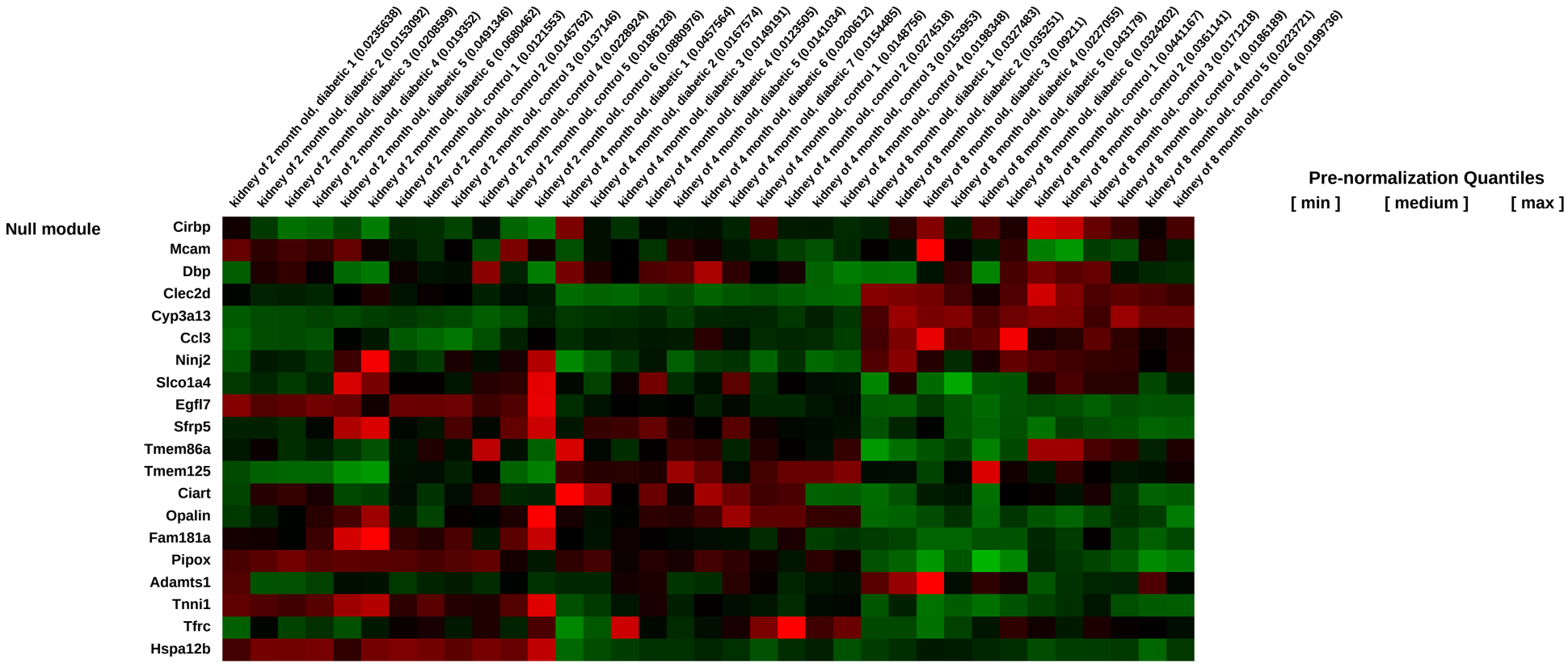

GEO Series "GSE20645" Expression Profiles

Num of samples in this series: 8

Scale of expression profile Z-scores

-3.0 -2.0 -1.0 0.0 1.0 2.0 3.0

GEO Link:	**http://www.ncbi.nlm.nih.gov/geo/query/acc.cgi?acc=GSE20645**
Status:	**Public on Mar 06 2010**
Title:	**The difference of gene expression in mouse OPCs in normothermic and hypothermic culture**
Organism:	**Mus musculus**
Experiment type:	**Expression profiling by array**
Platform:	**GPL1261**
Pubmed ID:	**20936704**
Summary & Design:	**Summary:** **We have found that the cell yield of oligodendrocyte precursor cells (OPCs) are higher in 31.5 â than in 37 â not by suppression of apoptosis but by enhancement of proliferation.** **Here, we performed transcriptome analysis using Affymetrix GeneChip on the primary cultured oligodendrocyte precursor cells prepared from the brain of ICR mice.** **Overall design:** **Oligodendrocyte precursor cells were prepared from primary mixed cell cultures of embryonic mouse cerebral hemispheres. The cerebral hemispheres from 15-day-old mouse embryos were enzymatically dissociated, seeded and cultured for 5 days in D-MEM containing 10% FBS. The cells were passaged to serum-free basal medium and cultured for further 48 hr at 37 â and 31.5 â .**

Background corr dist: **KL-Divergence = 0.0653, L1-Distance = 0.0185, L2-Distance = 0.0005, Normal std = 0.5114**

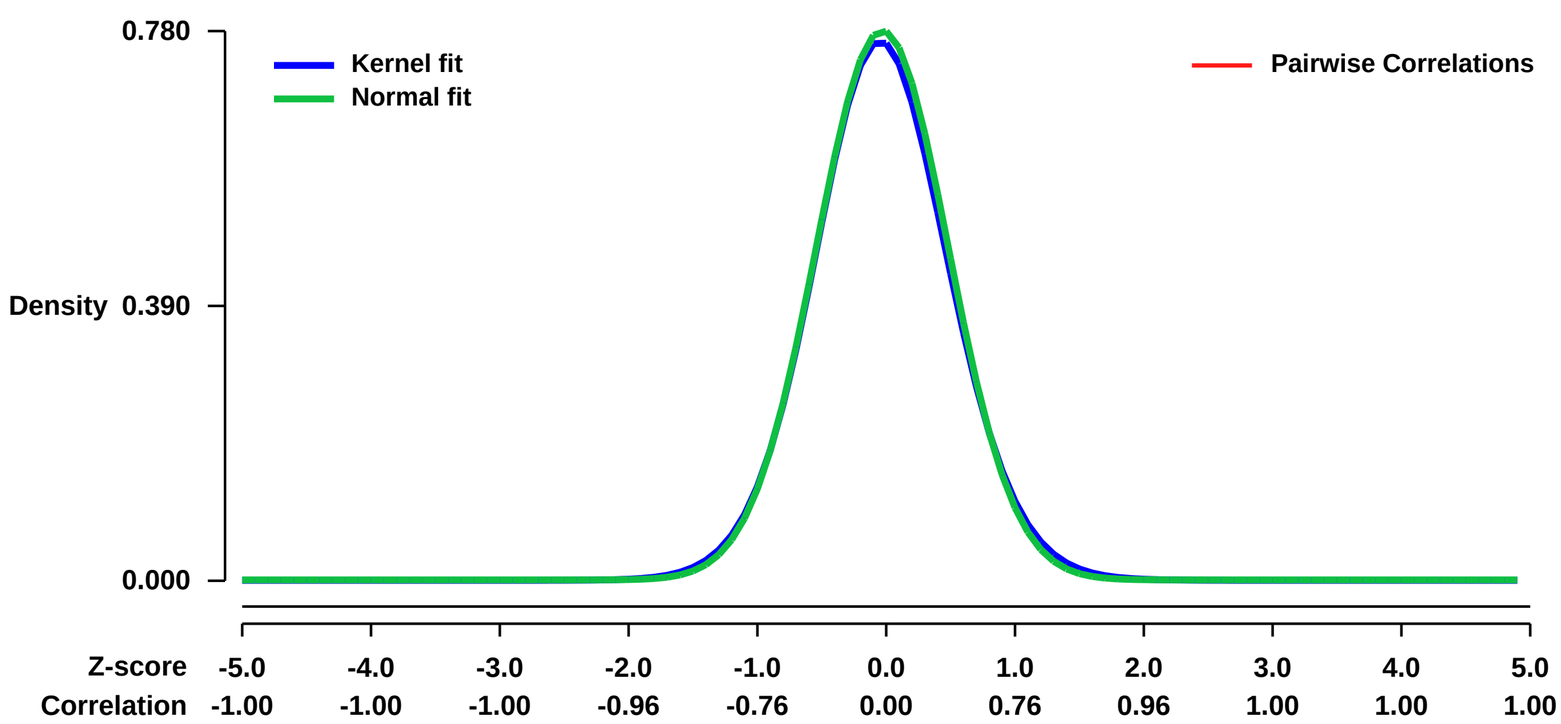

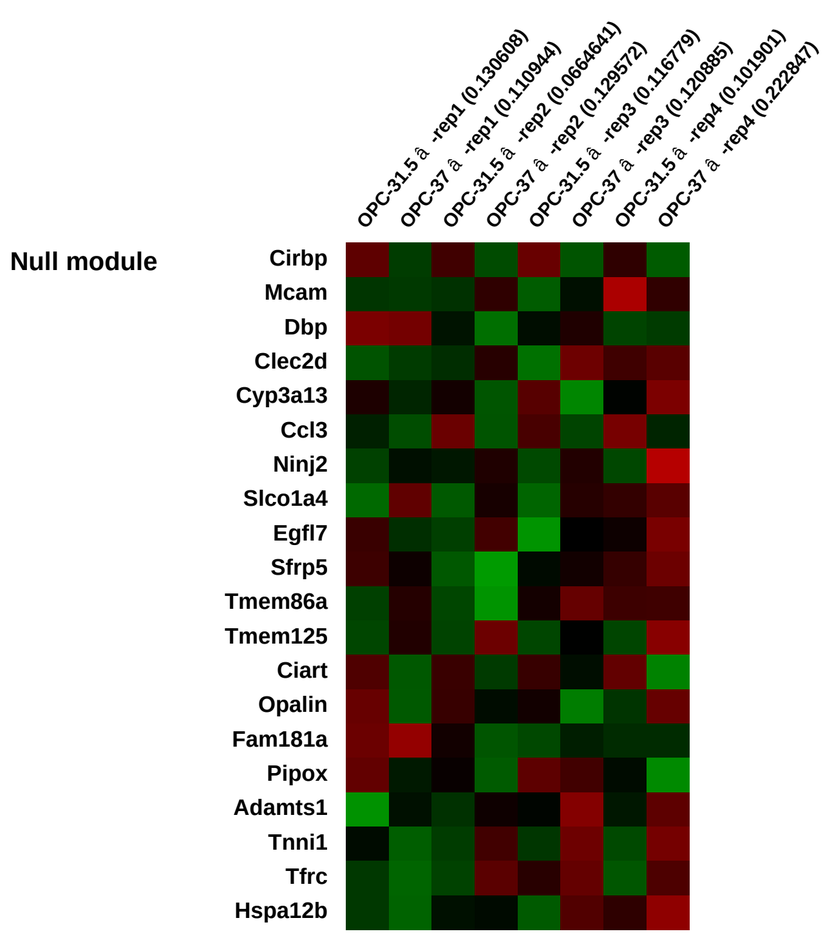

GEO Series "GSE20684" Expression Profiles

Num of samples in this series: 12

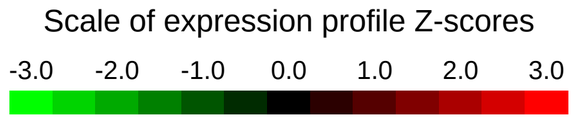

GEO Link:	http://www.ncbi.nlm.nih.gov/geo/query/acc.cgi?acc=GSE20684
Status:	Public on Aug 25 2010
Title:	The gene encoding the hematopoietic stem cell regulator CCN3 (NOV) is under direct cytokine control through the transcription factors STAT5a/b.
Organism:	Mus musculus
Experiment type:	Expression profiling by array
Platform:	GPL1261
Pubmed ID:	20720003
Summary & Design:	**Summary:** Cytokines control the biology of hematopoietic stem and progenitor cells in part through the transcription factors STAT5a/b. CCN3/NOV has been reported as a positive regulator of hematopoietic stem and progenitor cells. We report microarray analyses of Lineage- Sca-1+ c-Kit+ (KSL) cells in the presence and absence of STAT5a/b. Expression of the ccn3 gene was induced over 100-fold in control, but not STAT5a/b-null cells, upon stimulation with a cocktail containing IL-3, IL-6, SCF, TPO and Flt3 ligand. Among the cytokines, IL-3 elevated ccn3 mRNA level in Lineage- c-Kit+ (KL) cells and 32D cells. ChIP assays using 32D cells revealed IL-3-induced binding of STAT5a/b to a GAS site in the ccn3 gene promoter. This is the first report to link two molecules with importance in the regulation of HSCs, CCN3 and STAT5a/b. We report that the regulation and expression of the ccn3 gene is directly controlled by IL-3 through the transcription factors STAT5a/b. **Overall design:** Six Control and Six Stat5a/b-null KSL cells, including three biological replications, were unstimulated or stimulated with a cocktail containing IL-3, IL-6, SCF, TPO and FL.

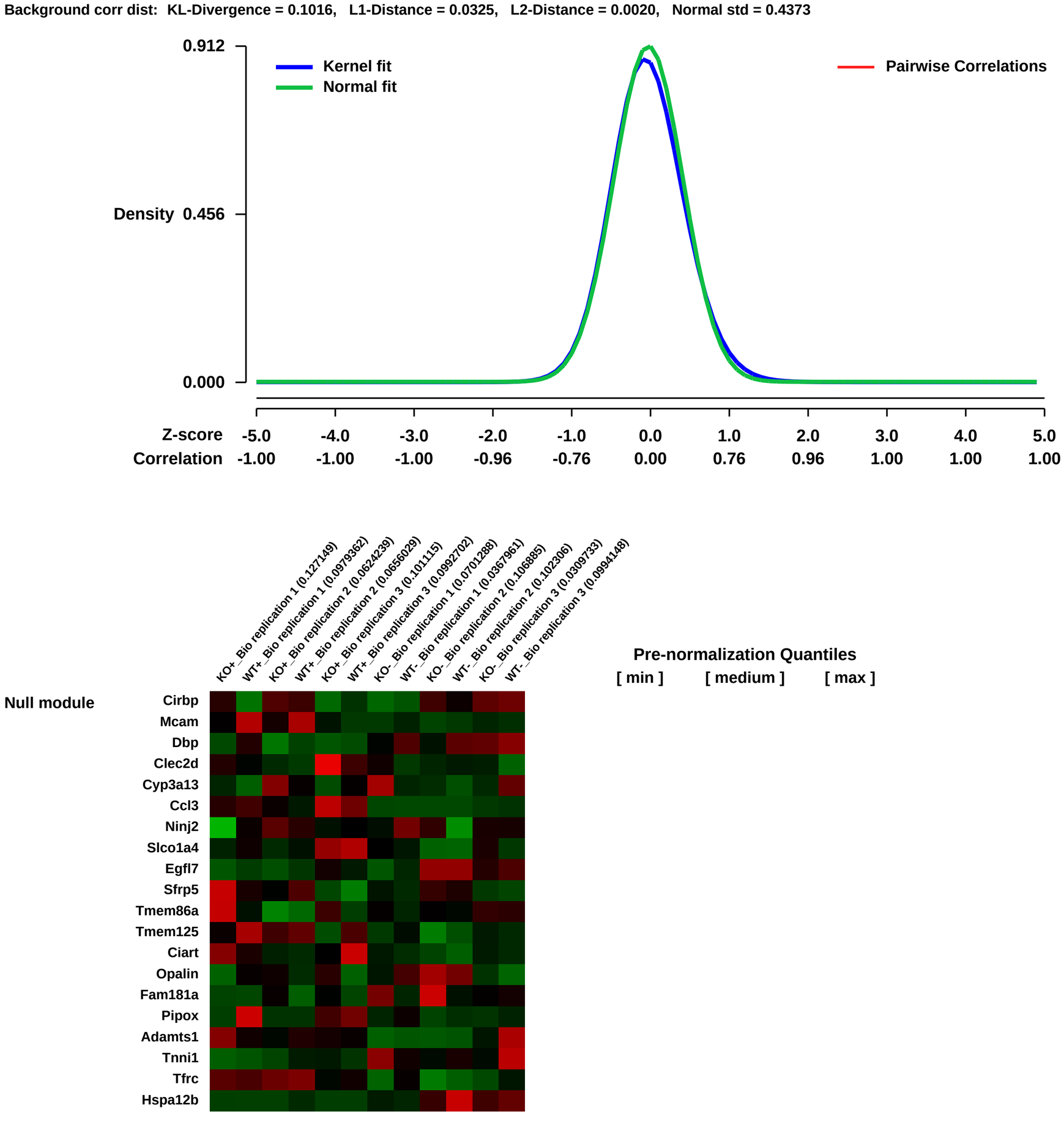

GEO Series "GSE20696" Expression Profiles

Num of samples in this series: 8

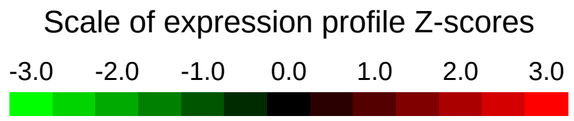

GEO Link:	**http://www.ncbi.nlm.nih.gov/geo/query/acc.cgi?acc=GSE20696**
Status:	**Public on Sep 30 2010**
Title:	**Expression profiling of 3T3-L1 adipogenesis**
Organism:	**Mus musculus**
Experiment type:	**Expression profiling by array**
Platform:	**GPL1261**
Pubmed ID:	**20887899**
Summary & Design:	**Summary:** **3T3-L1 pre-adipocyte cells were grown to confluence and induced to differentiate in adipogeneic media.** **Overall design:** **Two technical replicates from four time points relative to induction of adipogenesis (day 0)**

Background corr dist: **KL-Divergence = 0.0408, L1-Distance = 0.0317, L2-Distance = 0.0012, Normal std = 0.6378**

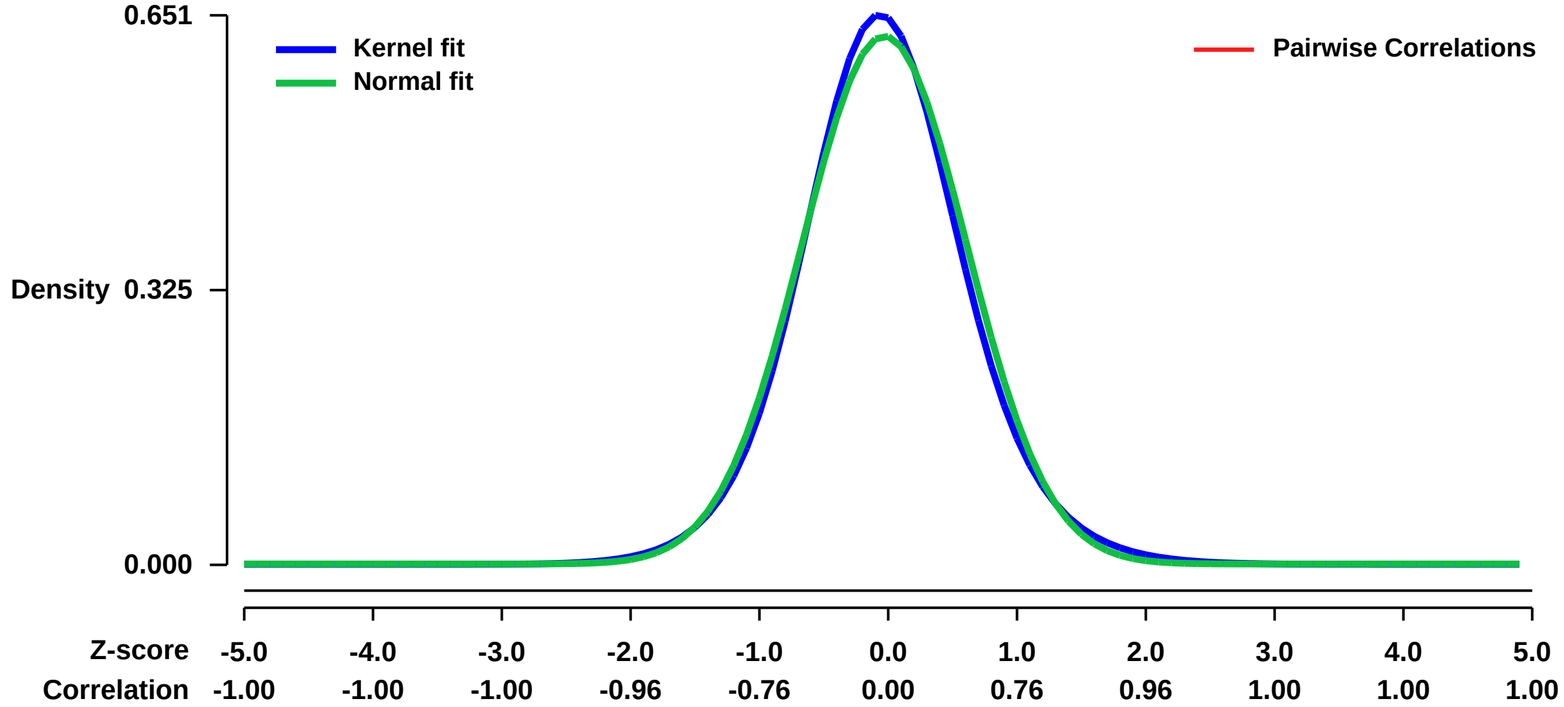

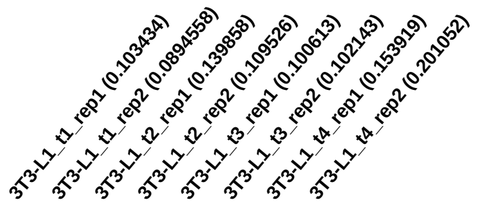

Pre-normalization Quantiles

[min] [medium] [max]

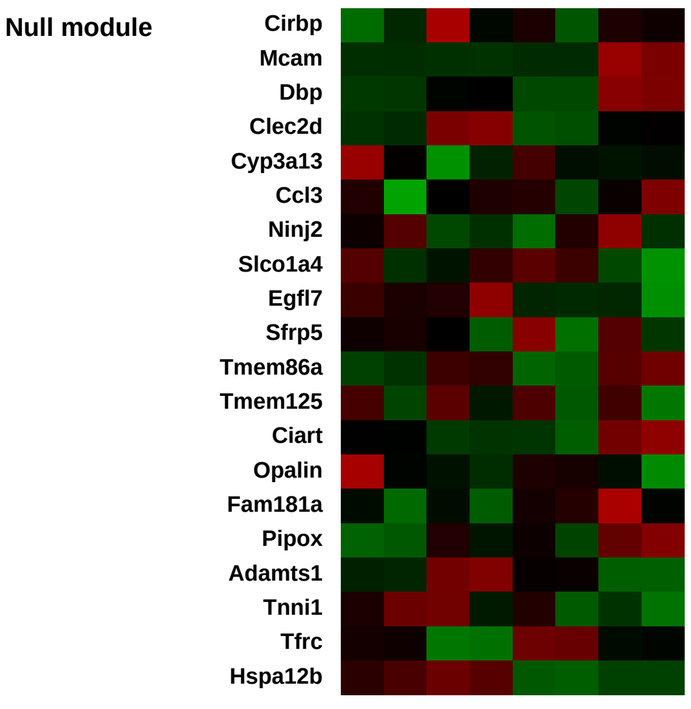

GEO Series "GSE20726" Expression Profiles

Num of samples in this series: 9

Scale of expression profile Z-scores

-3.0 -2.0 -1.0 0.0 1.0 2.0 3.0

GEO Link:	http://www.ncbi.nlm.nih.gov/geo/query/acc.cgi?acc=GSE20726
Status:	Public on Mar 10 2011
Title:	Gene expression analysis of mouse ear samples treated with chemical allergen
Organism:	Mus musculus
Experiment type:	Expression profiling by array
Platform:	GPL1261
Pubmed ID:	22974541
Summary & Design:	**Summary:** **Identification of chemical allergen inducible genes in mouse skin.** **Ear samples were isolated from CL57BL/6 mice 6 hours after topical application of a prototypic chemical allergen, a skin irritant or vehicle alone.** **Overall design:** **Total RNA were extracted from ear skin samples treated with a chemical allergen, a skin irritant, or vehicle alone for 6 hours.**

Background corr dist: **KL-Divergence = 0.0921, L1-Distance = 0.0243, L2-Distance = 0.0009, Normal std = 0.4511**

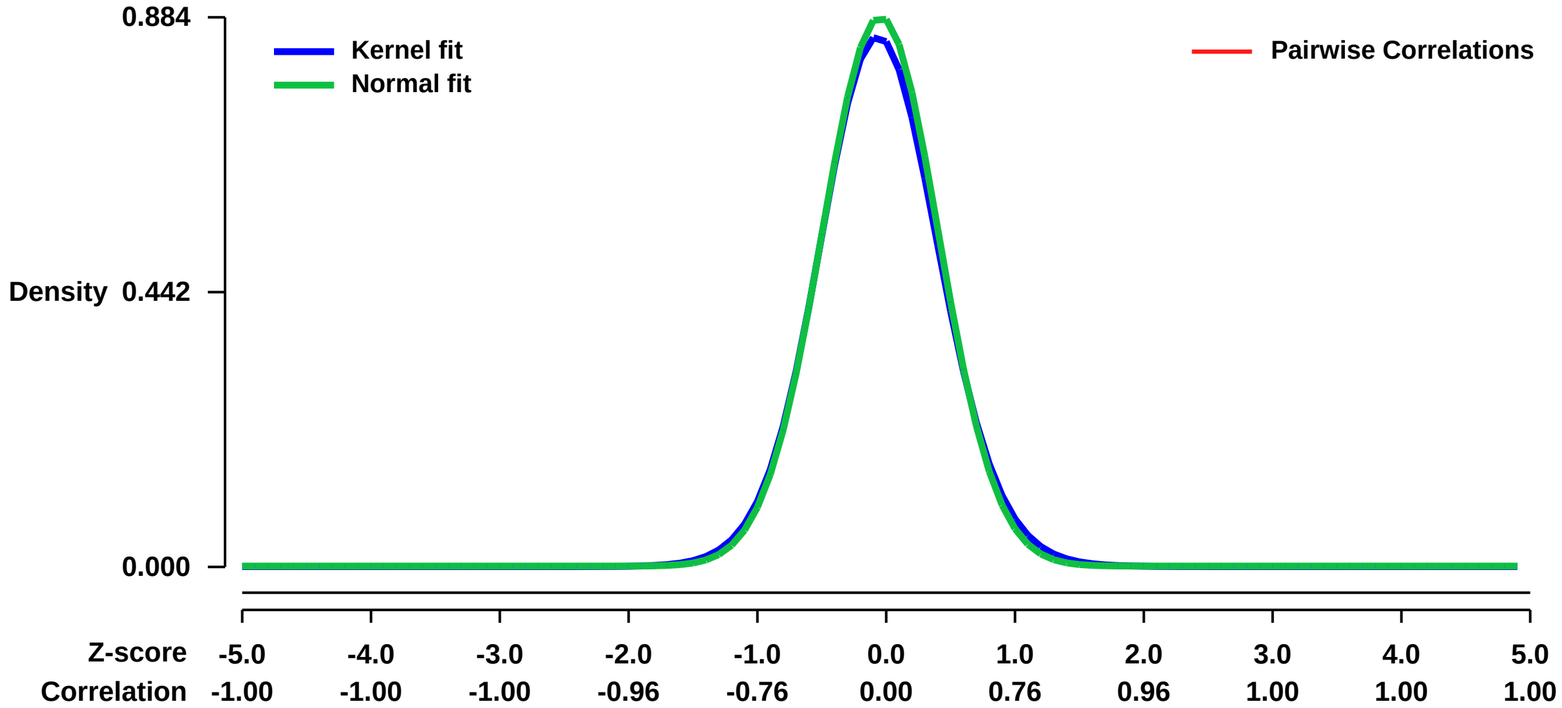

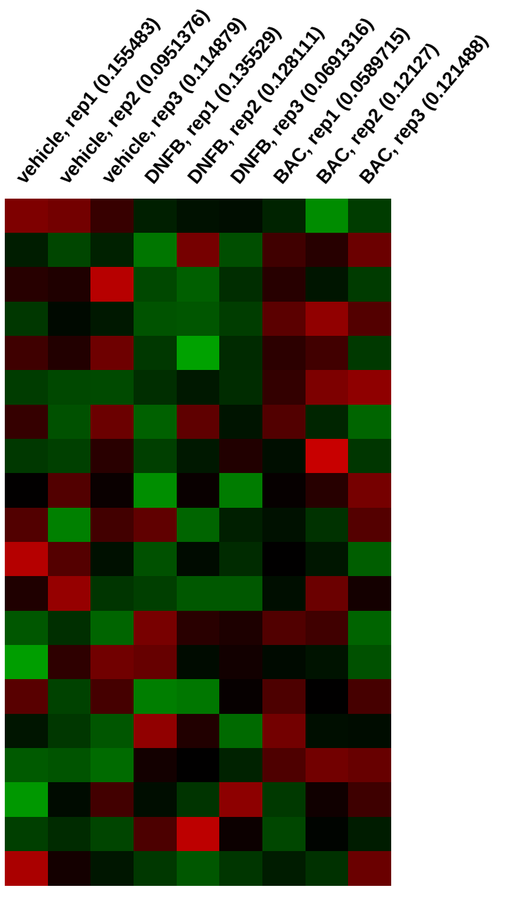

GEO Series "GSE20918" Expression Profiles

Num of samples in this series: 6

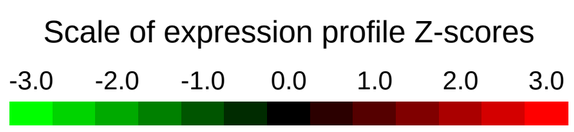

GEO Link:	http://www.ncbi.nlm.nih.gov/geo/query/acc.cgi?acc=GSE20918
Status:	Public on Sep 06 2010
Title:	GENE EXPRESSION ALTERATIONS IN ADULT UTP14b (jsd) MICE BY CONDITIONAL KNOCKOUT OF ANDROGEN RECEPTOR IN SERTOLI CELLS
Organism:	Mus musculus
Experiment type:	Expression profiling by array
Platform:	GPL1261
Pubmed ID:	20650881

Summary & Design:

Summary:
Spermatogenesis is dependent primarily on testosterone action on the Sertoli cells. Although the identification of testosterone-regulated target genes in Sertoli cells has been approached using microarray analysis to compare gene expression in mice with androgen receptor (AR) elimination in the Sertoli cells (SCARKO) and wild type mice, the analysis has been complicated by alteration of germ cell composition of the testis when pubertal or adult mice were used and differences in Sertoli-cell gene expression from those in adult when prepubertal mice were used. Since the testicular cell components of adult jsd (Utp14bjsd ,juvenile spermatogonial depletion) mice and SCARKO-jsd mice are essentially identical, consisting of only type A spermatogonia and somatic cells, comparisons of gene expression profiles between jsd and SCARKO-jsd testes would identify AR regulated genes in adult Sertoli cells, with minimum effects of cell number changes. Microarray analysis identified 161 genes as downregulated and 202 genes as upregulated in the SCARKO-jsd mice compared to jsd mice. Some of the genes identified in the previous studies, including Rhox5, Drd4, and Fhod3, were also AR-regulated in the jsd testes but others, such as proteases and components of junctional complexes, were not androgen regulated in our model. Surprisingly, a set of germ-cell-specific genes preferentially expressed in differentiated spermatogonia and meiotic cells, including Meig1, Sycp3, and Ddx4, were all upregulated about 2-fold in SCARKO-jsd testes, demonstrating that, although there was no significant differentiation to spermatocytes in SCARKO-jsd mice, AR-regulated genes in Sertoli cells are involved in the regulation of spermatogonial differentiation. Further gene ontogeny analysis revealed possible sets of genes whose expression changes may be involved in the disruption of Sertoli cell organization in SCARKO-jsd testes.

Overall design:
Comparisons of gene expression profiles between the testis of jsd mice (n=3) and SCARKO-jsd mice (n=3).

Background corr dist: KL-Divergence = 0.0295, L1-Distance = 0.0137, L2-Distance = 0.0002, Normal std = 0.6682

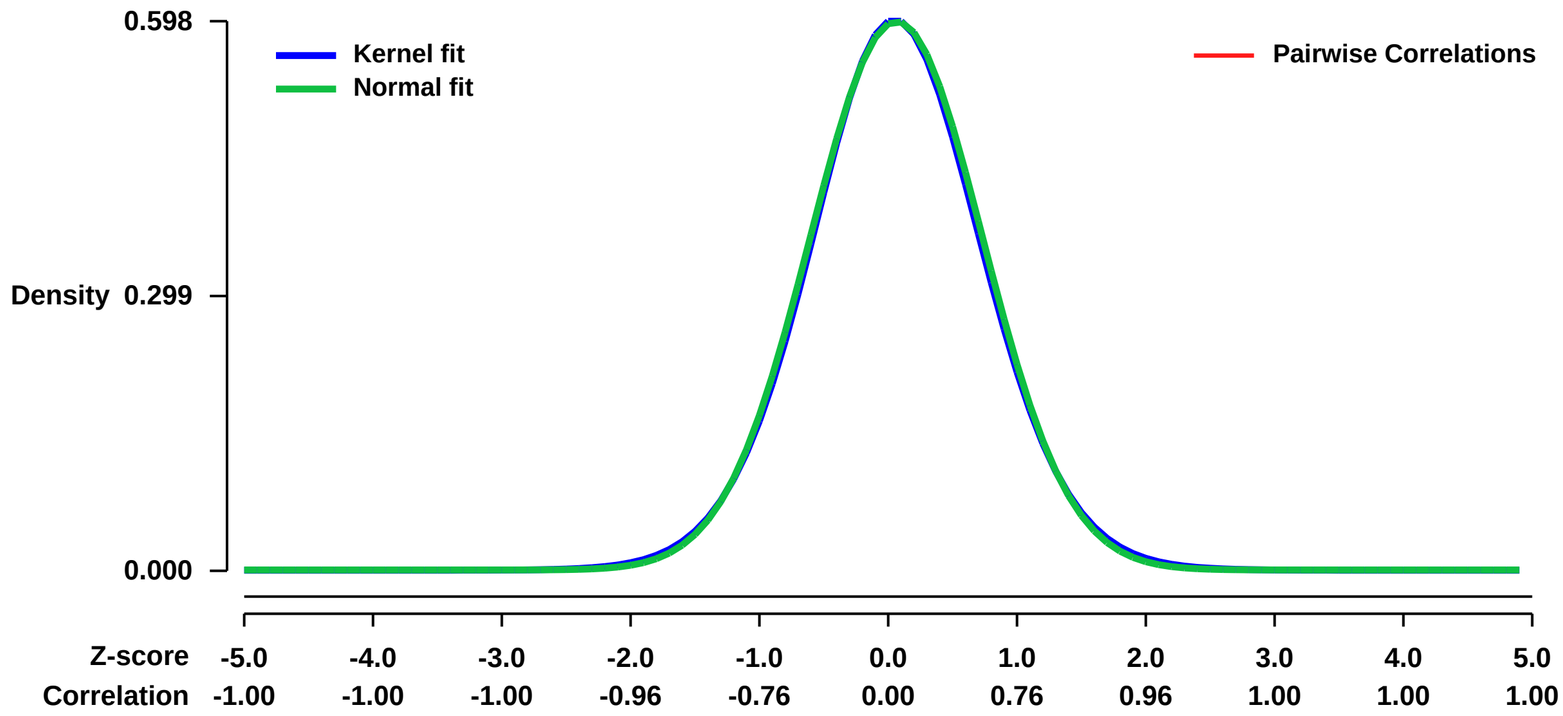

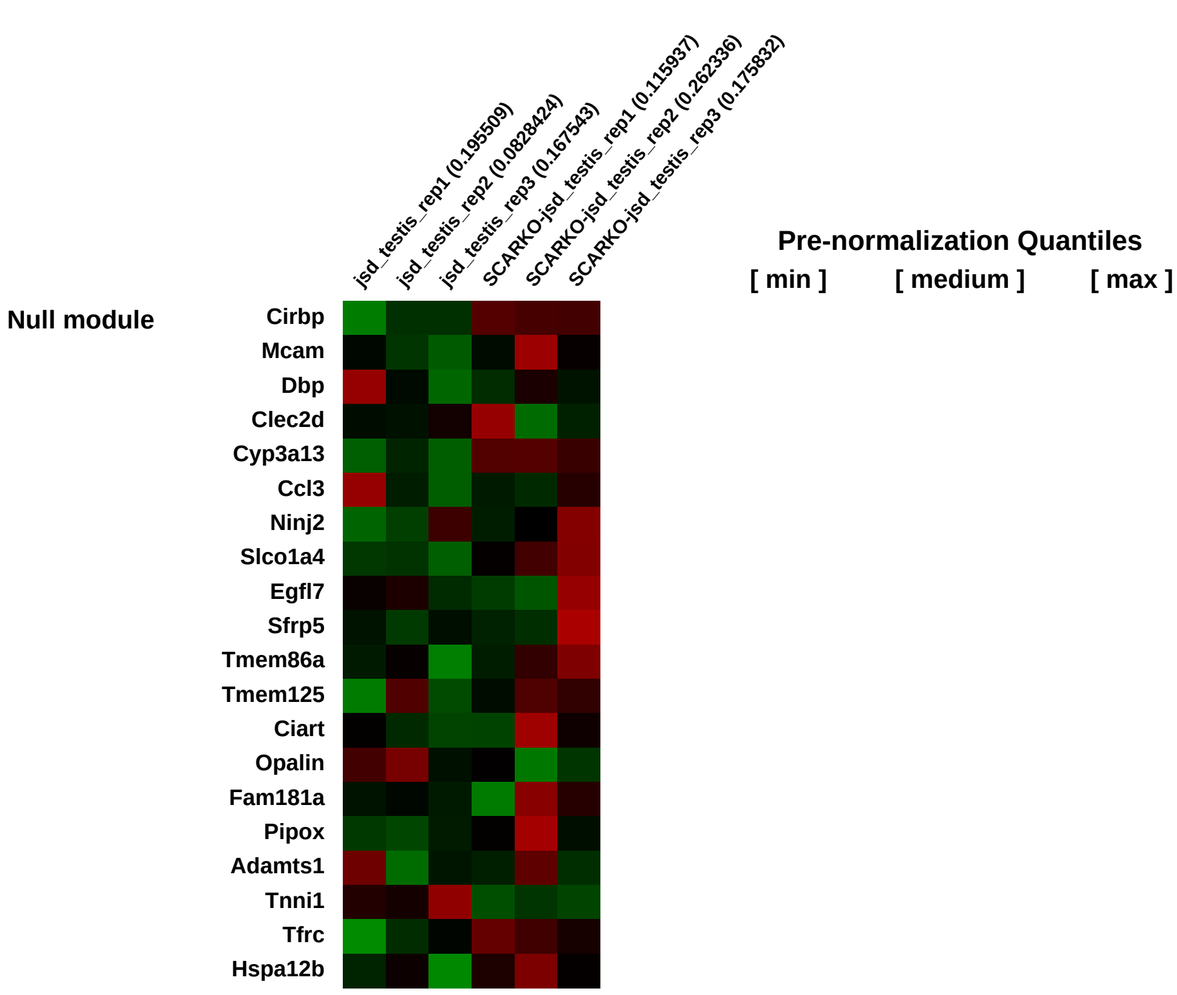

GEO Series "GSE20944" Expression Profiles

Num of samples in this series: 18

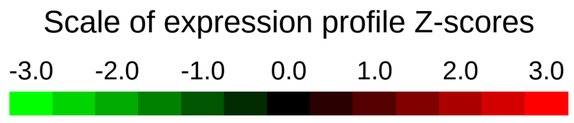

GEO Link:	http://www.ncbi.nlm.nih.gov/geo/query/acc.cgi?acc=GSE20944
Status:	Public on Oct 09 2010
Title:	Impact of dietary fatty acids on gene expression of liver-specific knockout of cytochrome P450 reductase
Organism:	Mus musculus
Experiment type:	Expression profiling by array
Platform:	GPL1261
Pubmed ID:	21098682

Summary & Design:

Summary:
In the present study, we explored the hypothesis that the fatty liver phenotype and associated gene expression changes associated with the specific deletion of the POR gene in adult mouse liver could be abrogated by supplementation of the mouse diet with the very long chain highly unsaturated fatty acids, arachidonic acid (C20:4ˇ 6), eicosapentaenoic acid (C20:5ˇ 3) and docosahexaenoic acid (C22:6ˇ 3). We expected the fatty liver phenotype would not be reduced by the polyunsaturated fatty acids linoleic (C18:2ˇ 6) or linolenic acid (C18:3ˇ 3), since these accumulated in the fatty livers of LivPORKO animals. This proved to be the case. However, we also made two surprising observations. First, control animals fed a diet enriched in PUFA had fatty livers and gene expression profiles similar to animals fed a lard diet, which was deficient in both PUFA and HUFA. Second, while a diet enriched in HUFA did result in reduced steatosis in livers of the LivPOKO animals, fat accumulation was still elevated relative to controls. Array analyses indicated most differences in gene expression were related to fatty acid metabolism and could explain differences in fat accumulation in LivPORKO livers with dietary treatment.

Overall design:
Generation of the founder line with hepatic ablation of POR is described in Wu, et al. ((2003) Genesis 36, 177-181). Male test animals used in this study had the genotype Alb-Cre+/-/POR-lox+/+ and were called LivPORKOs. For each series of experiments, mice were placed on one of three synthetic diets upon weaning. Siblings of the same genotype were randomized between dietary groups. Upon weaning (four weeks after birth) male mice of each genotype were placed on one of the test diets for eight weeks. Synthetic diets used base diet AIN-93G and contained 18.7% protein, 64.7% carbohydrate, 5% fiber, 6% fat, 0.025% cholesterol, 0.008% sodium cholate, and 3.97 kcal per gram. The added fats were as follows: 6% lard (lard diet); 6% canola oil (canola diet); or 3.27% ARASCO oil (Martek Biosciences Corp.) and 2.73% menhadin oil (fish/fungal diet). After 8 weeks on the test diets (12 weeks of age) the animals were fasted for four hours prior to sacrifice. Liver samples were placed in mRNAlater´fi for mRNA analysis and immediately frozen and stored at -80´℃. To reduce variability between arrays, three RNA samples from individual mice of the same genotype/diet group were pooled using equivalent RNA amounts for each animal. Three microarrays on three pools were done per genotype/diet. The quality of RNA was analyzed using an Agilent 2100 Bioanalyzer. Three micrograms of RNA was reverse transcribed to make cDNA. Hybridization of cDNA, washing, and scanning of the Affymetrix GeneChip Mouse Genome 430 2.0 (containing 45,101 probe sets representing over 34,000 mouse genes) was performed according to standard Affymetrix protocol.

Background corr dist: KL-Divergence = 0.2208, L1-Distance = 0.0574, L2-Distance = 0.0081, Normal std = 0.3174

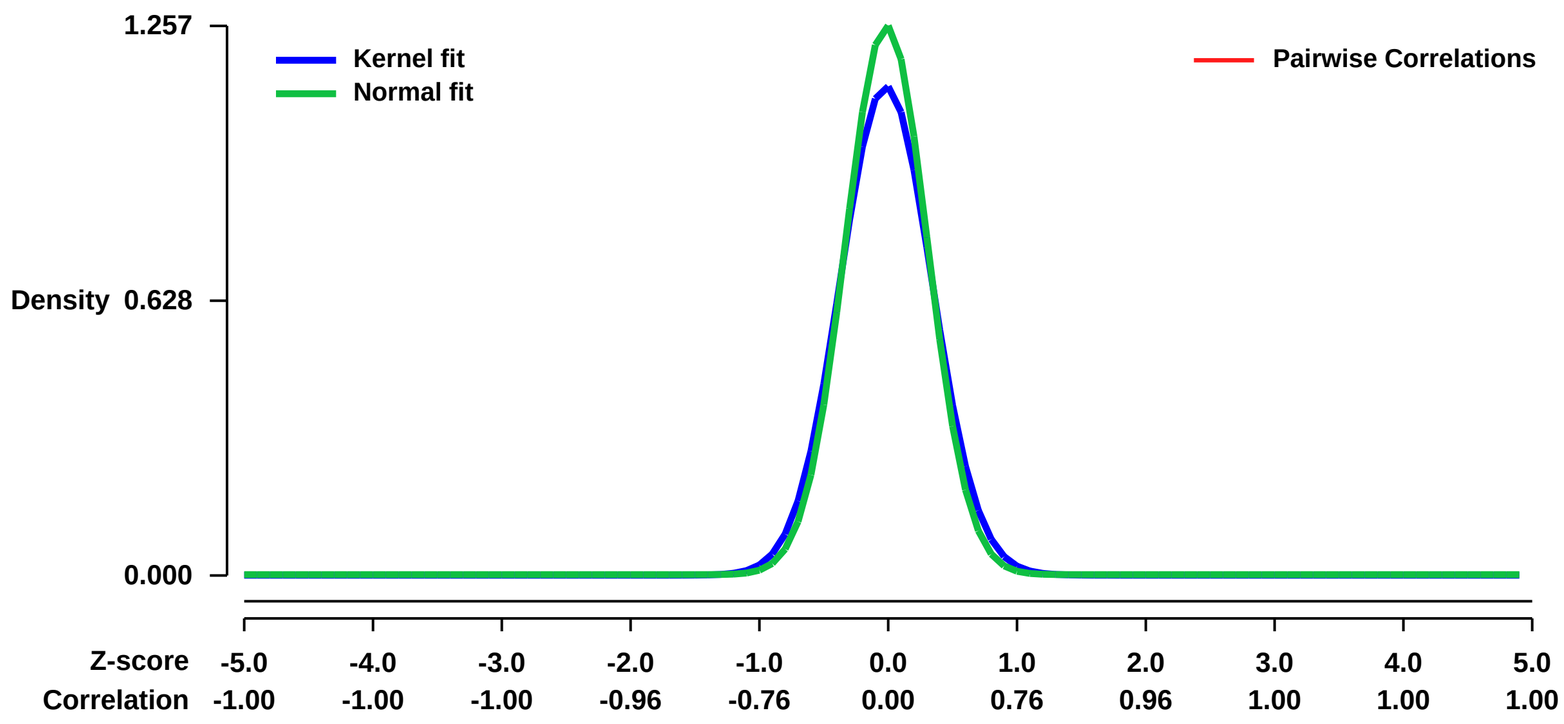

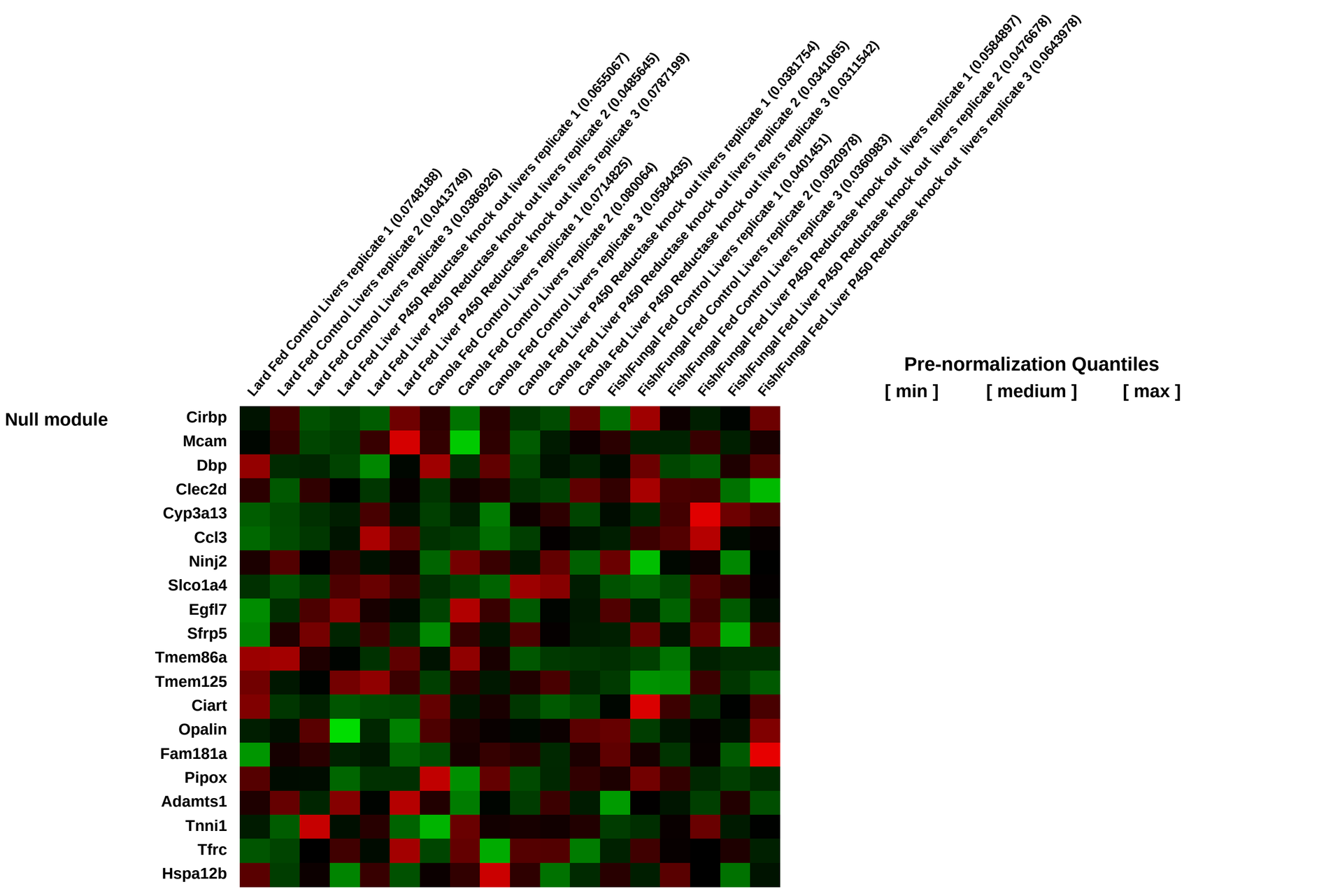

GEO Series "GSE20954" Expression Profiles

Num of samples in this series: 14

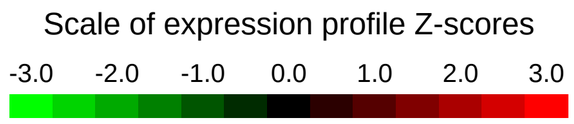

GEO Link:	**http://www.ncbi.nlm.nih.gov/geo/query/acc.cgi?acc=GSE20954**
Status:	**Public on Aug 17 2010**
Title:	**mRNA expression profile in mouse lung development**
Organism:	**Mus musculus**
Experiment type:	**Expression profiling by array**
Platform:	**GPL1261**
Pubmed ID:	**20520778**
Summary & Design:	**Summary:** **We performed miRNA and mRNA profiling over a 7-point time course, encompassing all recognized stages of lung development and explore dynamically regulated miRNAs and potential miRNA-mRNA interaction networks specific to mouse lung development** **Overall design:** **replicated time course of mouse lung development in 7 time points**

Background corr dist: **KL-Divergence = 0.0229, L1-Distance = 0.0372, L2-Distance = 0.0026, Normal std = 0.7245**

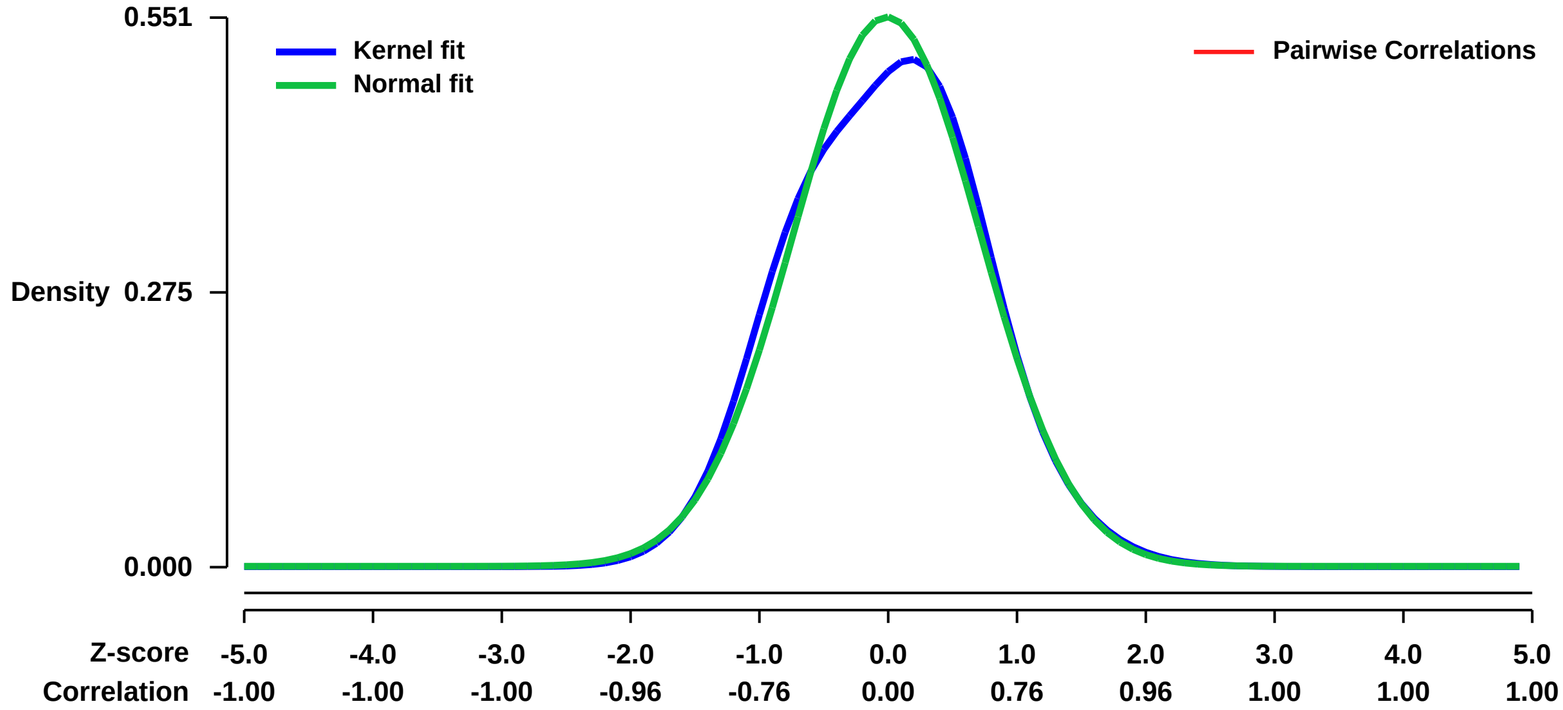

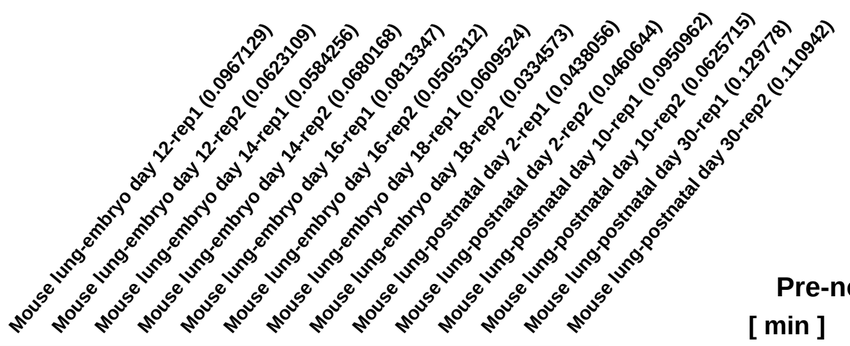

Pre-normalization Quantiles

[min] [medium] [max]

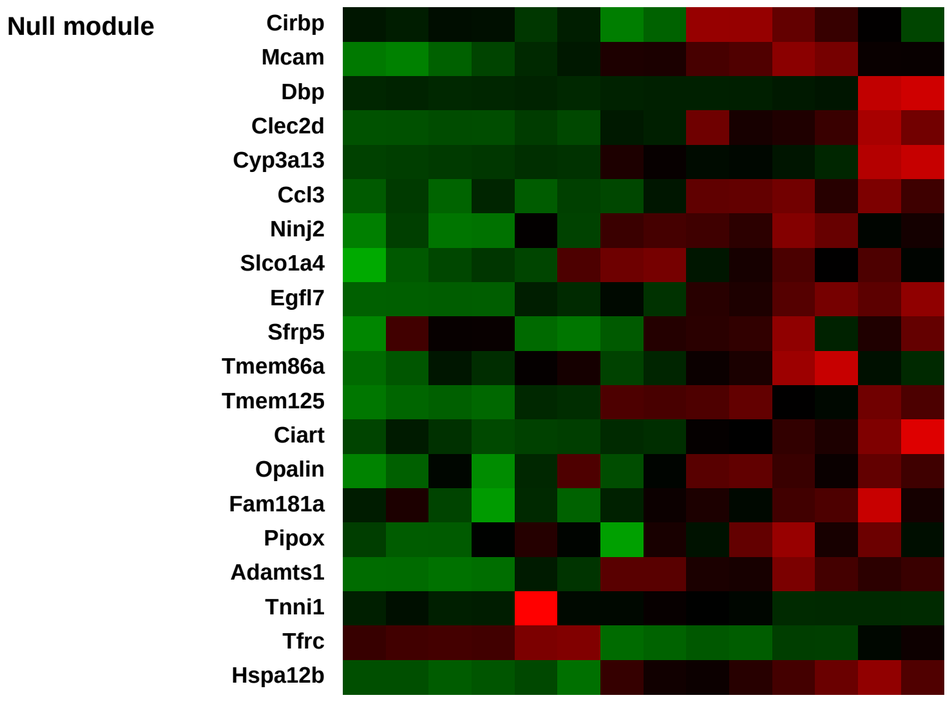

GEO Series "GSE20968" Expression Profiles

Num of samples in this series: 6

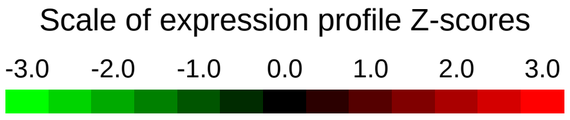

GEO Link:	http://www.ncbi.nlm.nih.gov/geo/query/acc.cgi?acc=GSE20968
Status:	Public on Jan 01 2011
Title:	Hepatocyte-nuclear-factor-4a promotes gut neoplasia in mice and protects against the production of reactive oxygen species
Organism:	Mus musculus
Experiment type:	Expression profiling by array
Platform:	GPL1261
Pubmed ID:	21062980
Summary & Design:	**Summary:** Hepatocyte-nuclear-factor-4¿– (Hnf4¿–) is a transcription factor that controls epithelial cell polarity and maturation during embryogenesis. Hnf4¿– conditional deletion during post-natal development results in minor consequences on intestinal epithelium integrity but promotes activation of the Wnt/¿†-catenin pathway. Here we show that Hnf4¿– does not act as a tumor suppressor gene but is crucial to promote gut tumorigenesis in mice. Polyp multiplicity in ApcMin mice that lacks Hnf4¿– is suppressed in comparison to littermate ApcMin controls. Analysis of microarray gene expression profiles from mice lacking Hnf4¿– in the intestinal epithelium identifies its novel function in regulating the expression of reactive oxygen species (ROS) detoxifying genes. This role is supported with the demonstration that HNF4¿– is functionally involved in the protection against spontaneous and 5-fluorouracil chemotherapy-induced production of intracellular ROS in colorectal cancer cell lines. The analysis of a colorectal cancer patient cohort establishes that HNF4¿– is significantly up-regulated at both gene transcript and protein levels in tumors relative to adjacent benign epithelial resections. Several genes involved in ROS neutralization are also up-regulated in correlation with HNF4¿– expression. All together, the findings point to the nuclear receptor HNF4¿– as a potential therapeutic target to eradicate aberrant epithelial cell resistance to ROS production during intestinal tumorigenesis. **Overall design:** HNF4alpha was conditionally knockout in the mouse epithelial intestine with the 12.4-kb VillinCRE. A total of 3 control and 3 mutant littermates individuals were sacrificed at 7 months of age. The distal jejunum was harvested and Total RNA was isolated from each individuals. Each RNA sample was independently used to generate probes to screen affymetrix chips.

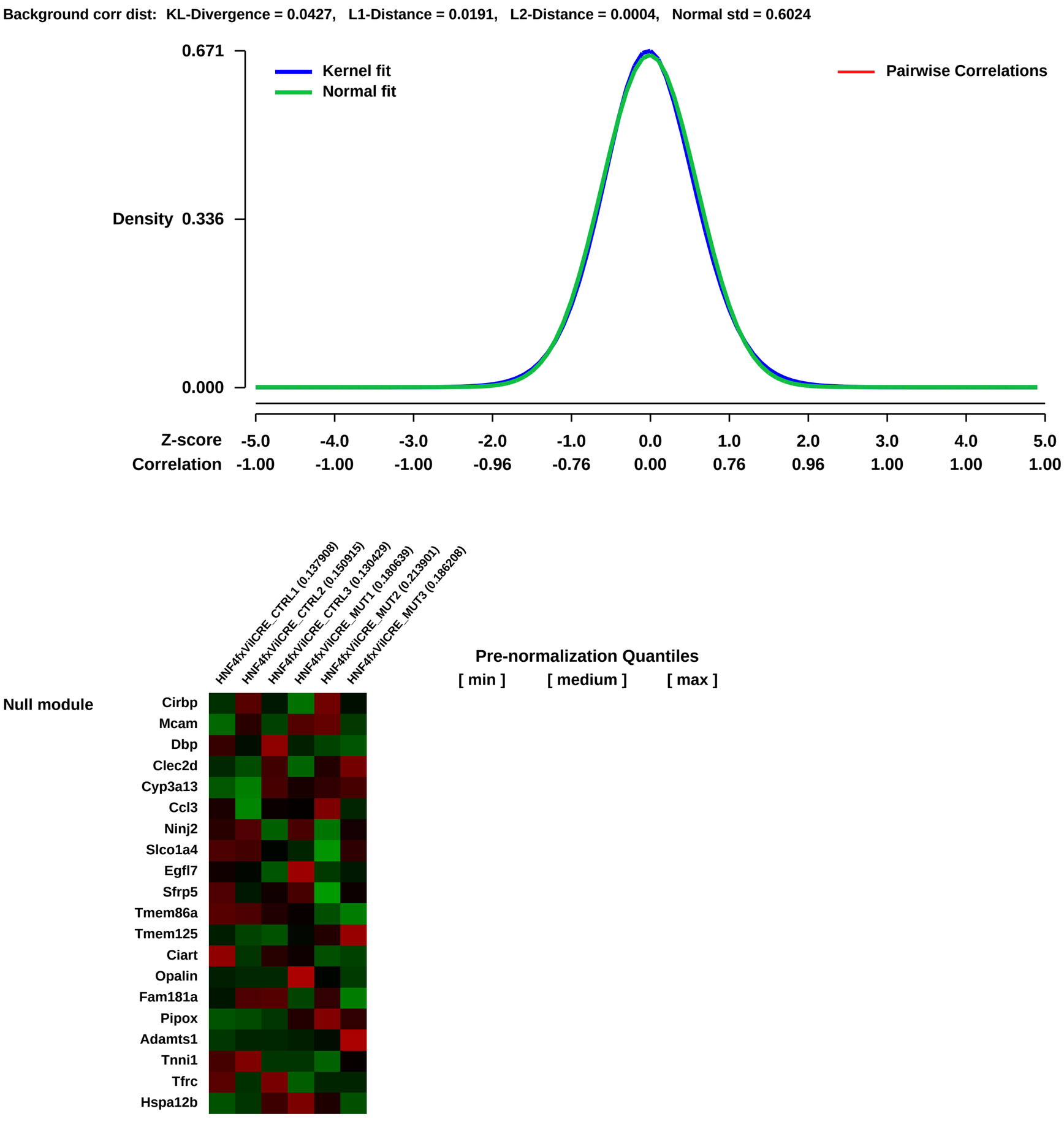

GEO Series "GSE20987" Expression Profiles

Num of samples in this series: 12

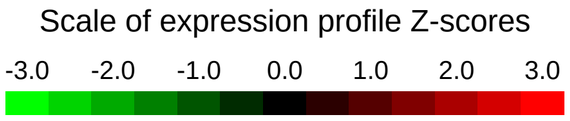

GEO Link:	http://www.ncbi.nlm.nih.gov/geo/query/acc.cgi?acc=GSE20987
Status:	Public on May 10 2010
Title:	Gene expression data of BCR-ABL1 transformed B cell precursors from BCL6 wild-type and BCL6 knockout mice
Organism:	Mus musculus
Experiment type:	Expression profiling by array
Platform:	GPL1261
Pubmed ID:	21911423
Summary & Design:	**Summary:** To elucidate the mechanism of BCL6-mediated pre-B cell survival signaling, we investigated the gene expression pattern in BCR-ABL1-transformed BCL6+/+ and BCL6-/- B cell precursors. Pharmacological inhibition of BCR-ABL1 was performed with the BCR-ABL1 kinase inhibitor STI571 (Imatinib). **Overall design:** BCR-ABL1 transformed B cell precursors of BCL6 wildtype and BCL6 knockout mice were either treated with 10´µM STI571 (Imatinib) for 16 hours or cultured in absence of STI571. Three samples for each condition were processed.

Background corr dist: KL-Divergence = 0.0587, L1-Distance = 0.0336, L2-Distance = 0.0015, Normal std = 0.5553

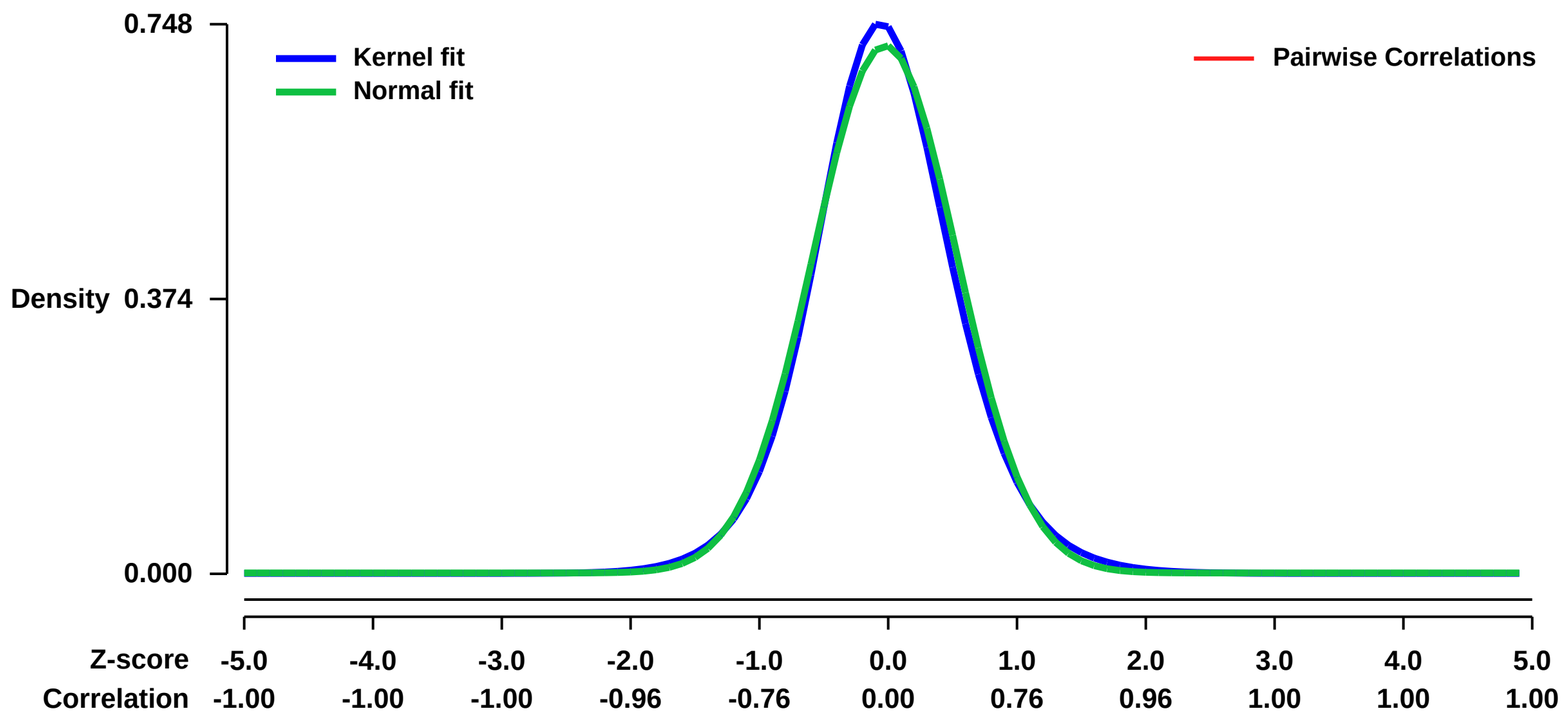

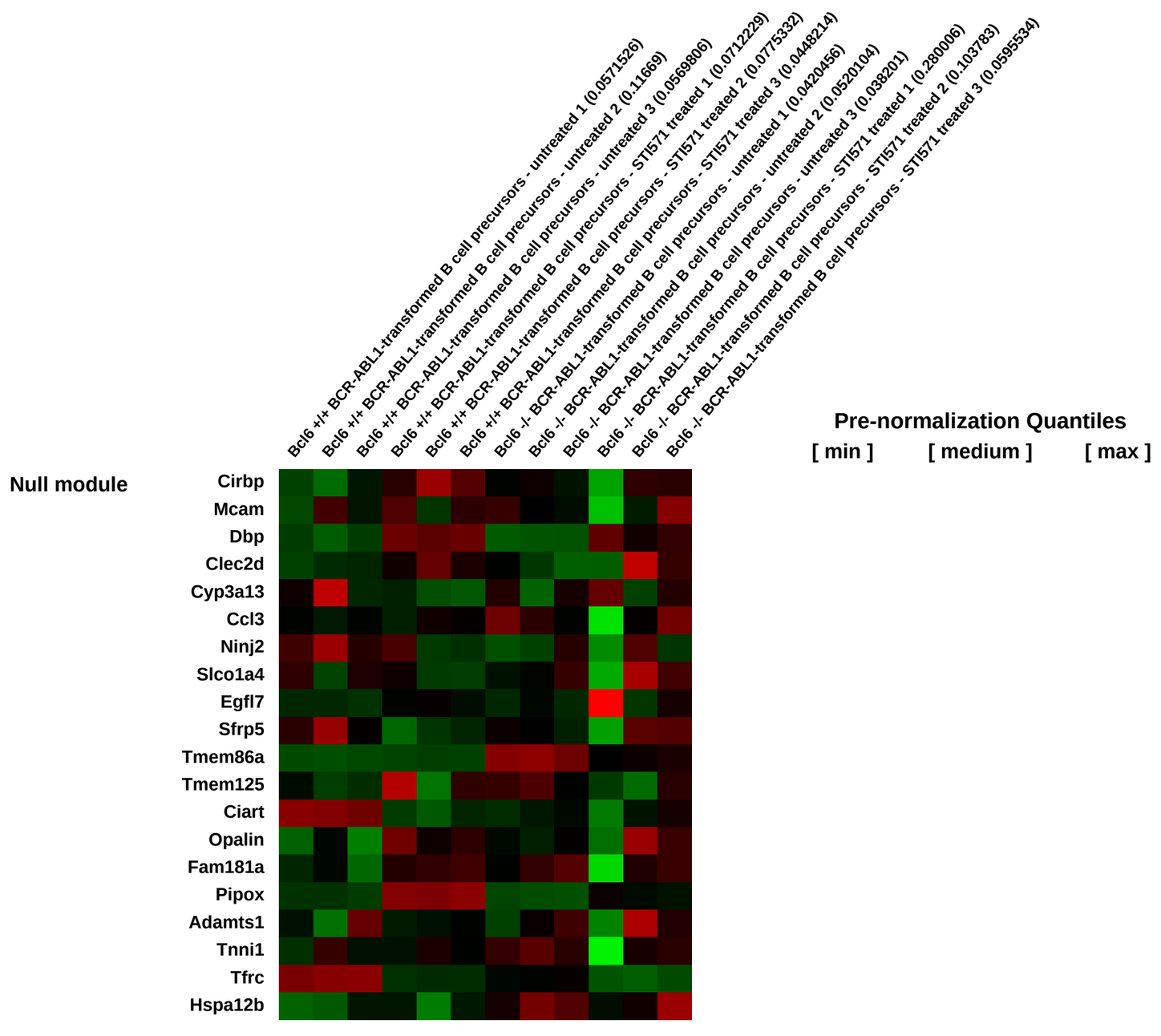

GEO Series "GSE21018" Expression Profiles

Num of samples in this series: 6

Scale of expression profile Z-scores

-3.0 -2.0 -1.0 0.0 1.0 2.0 3.0

GEO Link:	**http://www.ncbi.nlm.nih.gov/geo/query/acc.cgi?acc=GSE21018**
Status:	**Public on Aug 22 2010**
Title:	**Cooperation of IRF-4 and IRF-8 deficiencies in the development of hematological malignancies**
Organism:	**Mus musculus**
Experiment type:	**Expression profiling by array**
Platform:	**GPL1261**
Pubmed ID:	
Summary & Design:	**Summary:** **We found that mice deficient in both IRF-4 and IRF-8 develop from a very early age a more aggressive CML-like disease than mice deficient in IRF-8 alone. IRF-4 deficiency dramatically enhanced the effect of IRF-8 deficiency on expansion of granulocyte-monocyte progenitors (GMPs). All mice deficient in both IRF-4 and IRF-8 eventually develop and succumb to a B-lymphoblastic leukemia/lymphoma at approximately 25 weeks of age. The results demonstrate that IRF-4 and IRF-8 deficiencies can cooperate in the development of both myeloid and lymphoid tumors.** **To gain insights into how loss of IRF-4 affects the transcriptional program underlying leukemogenesis, we analyzed the genome-wide transcription profiles of GMPs from WT, IRF-8 KO and IRF-4/8 DKO mice. Microarray analysis revealed genes differentially expressed in IRF-4/8 DKO and IRF-8 KO GMPs, including genes that are involved in cell growth regulation and/or tumorigenesis.** **Overall design:** **Total RNA was extracted from GMPs (Lin-/IL-7R-/Sca1-/Kit+/CD34+/FcRII/IIIhi) of wild type, IRF8 KO and IRF4/8 DKO mice (two samples each group) using the Qiagen RNAeasy Micro kit. Affymetrix Mouse Genome 430 2.0 microarray with 45,000 probe sets was used at the BIDMC Genomics Center. Hybridization data were normalized and expression values were determined using the PM/MM difference model by dChip 1.3 (DNA-Chip analyzer).**

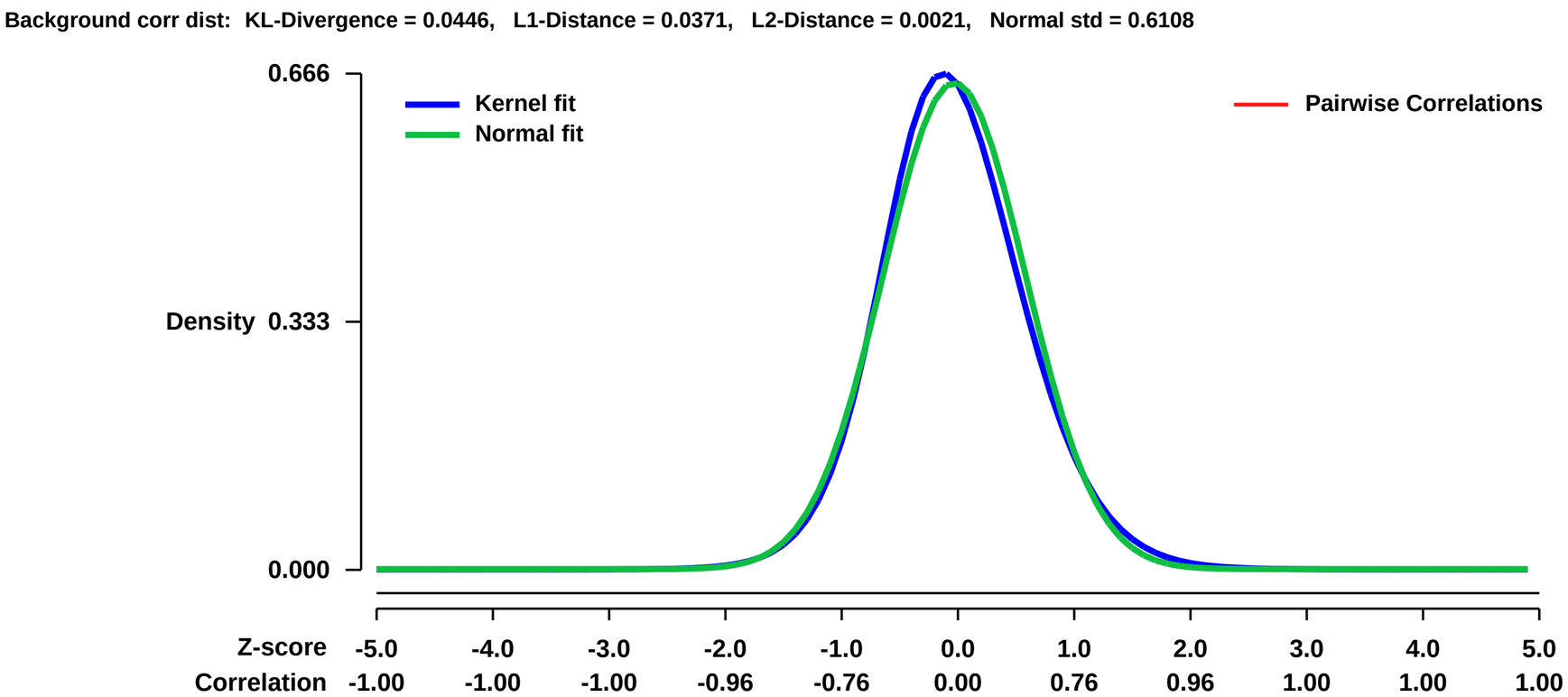

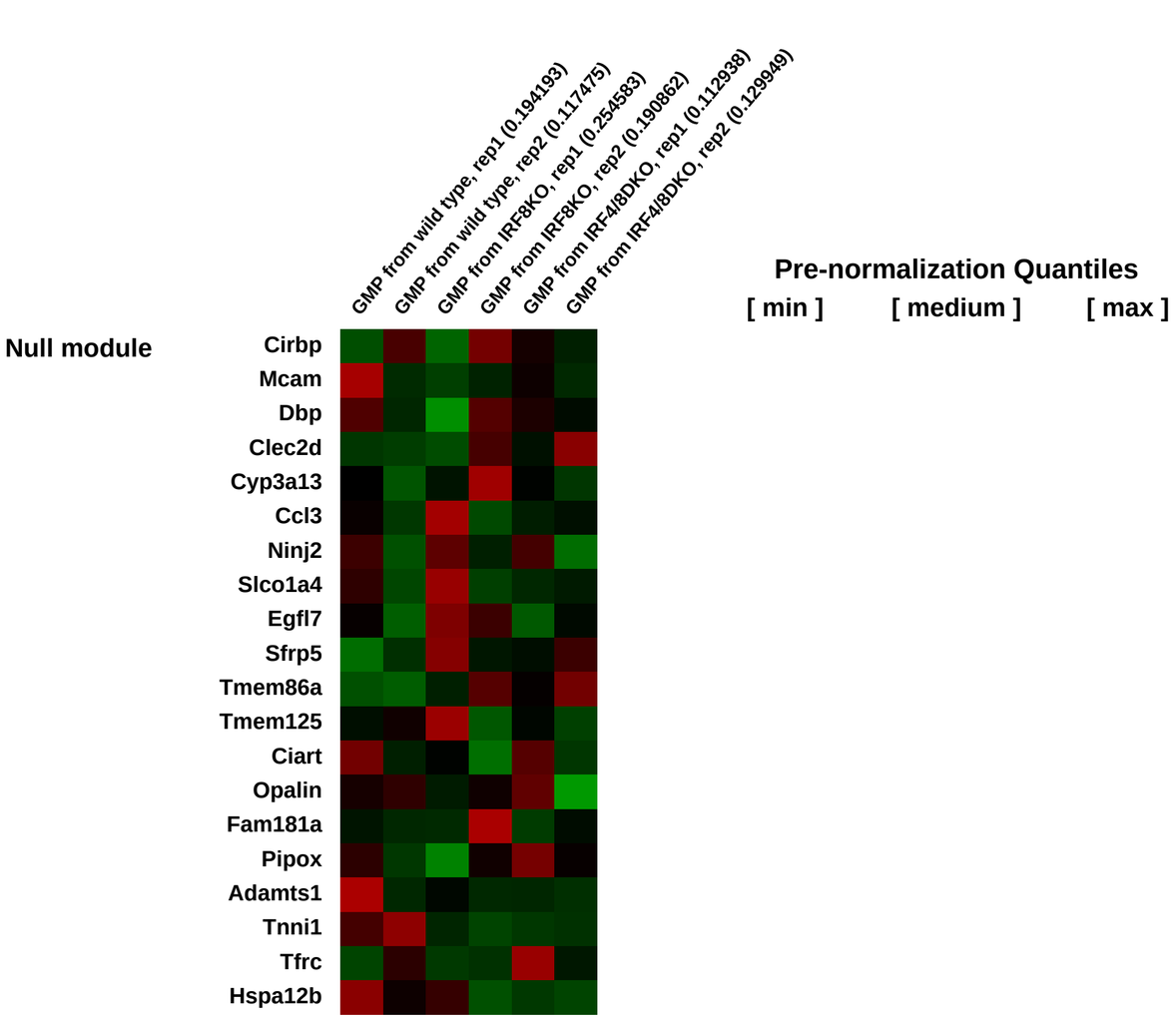

GEO Series "GSE21031" Expression Profiles

Num of samples in this series: 12

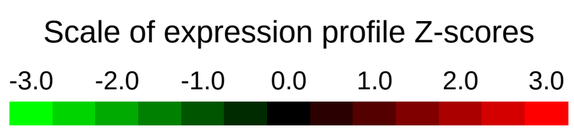

GEO Link:	http://www.ncbi.nlm.nih.gov/geo/query/acc.cgi?acc=GSE21031
Status:	Public on Mar 24 2010
Title:	Time-series of IL-6 stimulated primary mouse hepatocytes
Organism:	Mus musculus
Experiment type:	Expression profiling by array
Platform:	GPL1261
Pubmed ID:	21118515
Summary & Design:	**Summary:** External stimulations of cells by hormones, growth factors or cytokines activate signal transduction pathways that subsequently induce a rearrangement of cellular gene expression. The representation and analysis of changes in the gene response is complicated, and essentially consists of multiple layered temporal responses. In such situations, matrix factorization techniques may provide efficient tools for the detailed temporal analysis. Related methods applied in bioinformatics intentionally do not take prior knowledge into account. In signal processing, factorization techniques incorporating data properties like second-order spatial and temporal structures have shown a robust performance. However, large-scale biological data rarely imply a natural order that allows the definition of an autocorrelation function. We therefore develop the concept of graph-autocorrelation. We encode prior knowledge like transcriptional regulation, protein interactions or metabolic pathways as a weighted directed graph. By linking features along this underlying graph, we introduce a partial ordering of the samples to define an autocorrelation function. Using this framework as constraint to the matrix factorization task allows us to set up the fast and robust graph decorrelation (GraDe) algorithm. To analyze the alterations in the gene response in IL-6 stimulated primary mouse hepatocytes by GraDe, a time-course microarray experiment was performed. Extracted gene expression profiles show that IL-6 activates genes involved in cell cycle progression and cell division in a time-resolved manner. On the contrary, genes linked to metabolic and apoptotic processes are down-regulated indicating that IL-6 mediated priming rendered hepatocytes more responsive towards cell proliferation and reduces expenses for the energy household. **Overall design:** Primary mouse hepatocytes were used in the analysis comprising stimulations with 1 nM IL-6 for 1 h, 2 h, 4 h and an unstimulated control (0 h), each performed in triplicate.

Background corr dist: KL-Divergence = 0.1375, L1-Distance = 0.0314, L2-Distance = 0.0016, Normal std = 0.3866

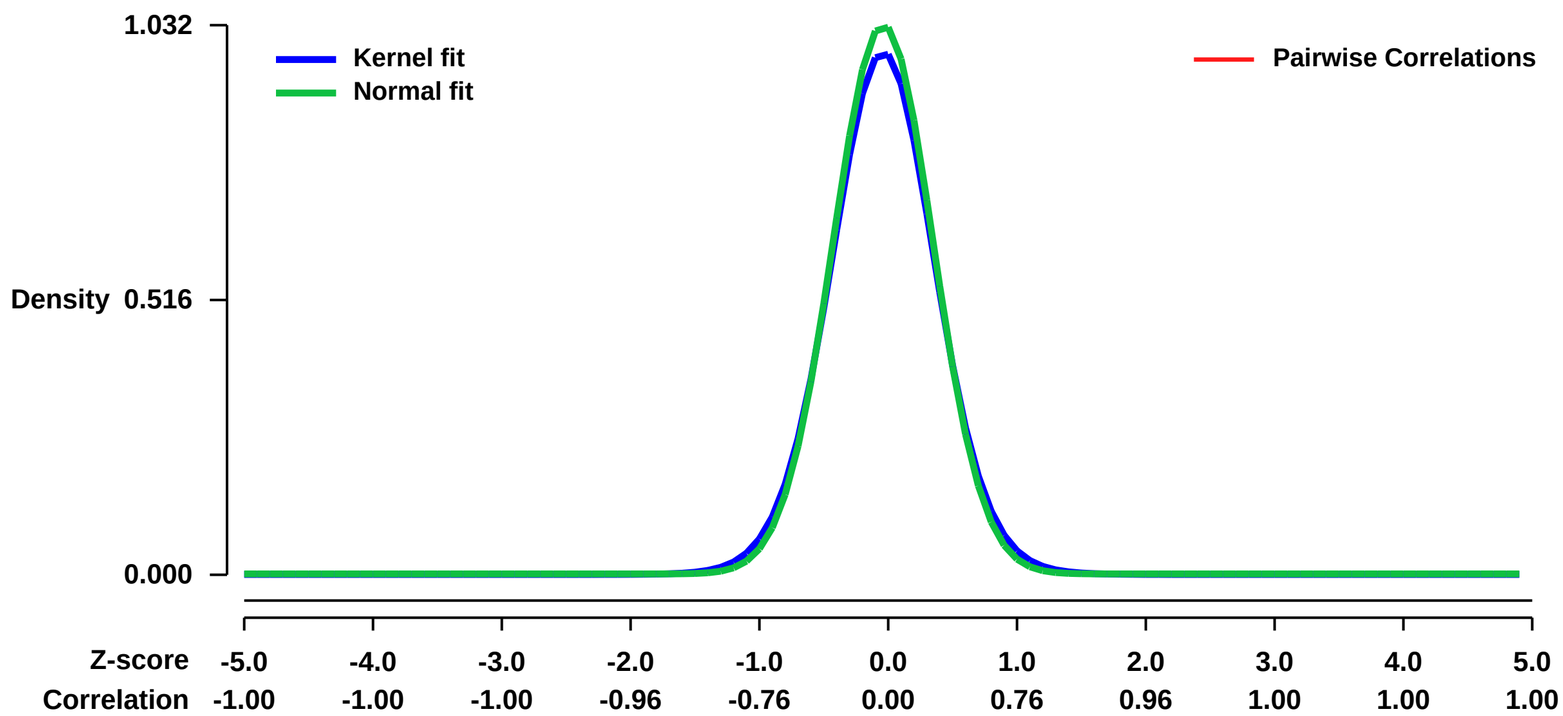

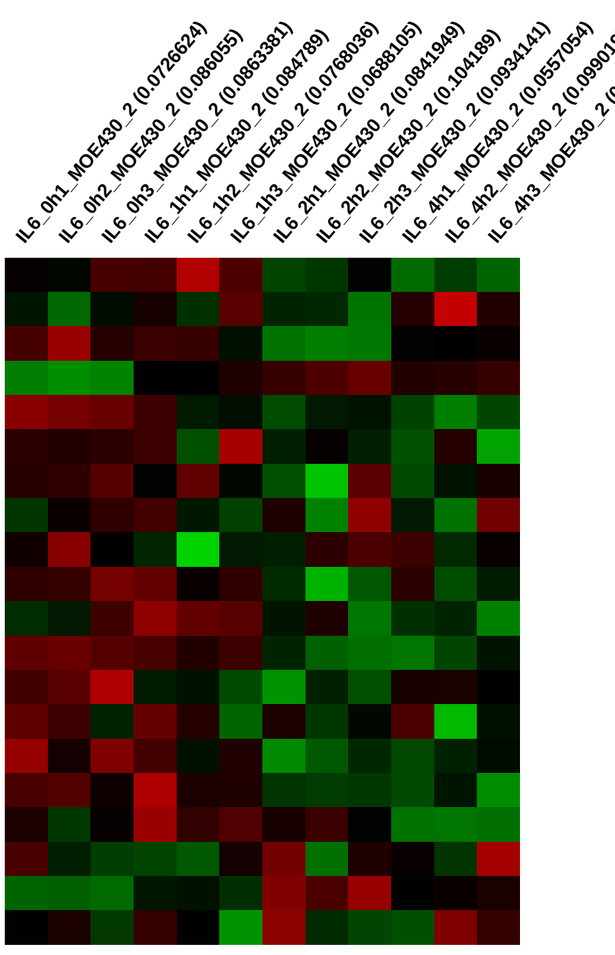

GEO Series "GSE21033" Expression Profiles

Num of samples in this series: 12

Scale of expression profile Z-scores

-3.0 -2.0 -1.0 0.0 1.0 2.0 3.0

GEO Link:	http://www.ncbi.nlm.nih.gov/geo/query/acc.cgi?acc=GSE21033
Status:	Public on Aug 26 2010
Title:	Timecourse analysis of gene expression by murine bone marrow-generated dendritic cells following treatment with Poly I:C
Organism:	Mus musculus
Experiment type:	Expression profiling by array
Platform:	GPL1261
Pubmed ID:	20682054
Summary & Design:	**Summary:** **BACKGROUND: Dendritic cells (DC) play a central role in primary immune responses and become potent stimulators of the adaptive immune response after undergoing the critical process of maturation. Understanding the dynamics of DC maturation would provide key insights into this important process. Time course microarray experiments can provide unique insights into DC maturation dynamics. Replicate experiments are necessary to address the issues of experimental and biological variability. Statistical methods and averaging are often used to identify significant signals. Here a novel strategy for filtering of replicate time course microarray data, which identifies consistent signals between the replicates, is presented and applied to a DC time course microarray experiment.** **RESULTS: The temporal dynamics of DC maturation were studied by stimulating DC with poly(I:C) and following gene expression at 5 time points from 1 to 24 hours. The novel filtering strategy uses standard statistical and fold change techniques, along with the consistency of replicate temporal profiles, to identify those differentially expressed genes that were consistent in two biological replicate experiments. To address the issue of cluster reproducibility a consensus clustering method, which identifies clusters of genes whose expression varies consistently between replicates, was also developed and applied. Analysis of the resulting clusters revealed many known and novel characteristics of DC maturation, such as the up-regulation of specific immune response pathways. Intriguingly, more genes were down-regulated than up-regulated. Results identify a more comprehensive program of down-regulation, including many genes involved in protein synthesis, metabolism, and housekeeping needed for maintenance of cellular integrity and metabolism.** **CONCLUSIONS: The new filtering strategy emphasizes the importance of consistent and reproducible results when analyzing microarray data and utilizes consistency between replicate experiments as a criterion in both feature selection and clustering, without averaging or otherwise combining replicate data. Observation of a significant down-regulation program during DC maturation indicates that DC are preparing for cell death and provides a path to better understand the process. This new filtering strategy can be adapted for use in analyzing other large-scale time course data sets with replicates. #!#** **Overall design:** **DC were generated from the bone marrow of C57BL/6 mice using GM-CSF, Treated with poly I:C, and RNA was isolated at 0, 1, 3, 6, 12 and 24 hours, and subjected to microarray analysis. Two independent replicate experiments were performed.**

Background corr dist: **KL-Divergence = 0.1114, L1-Distance = 0.0281, L2-Distance = 0.0014, Normal std = 0.4266**

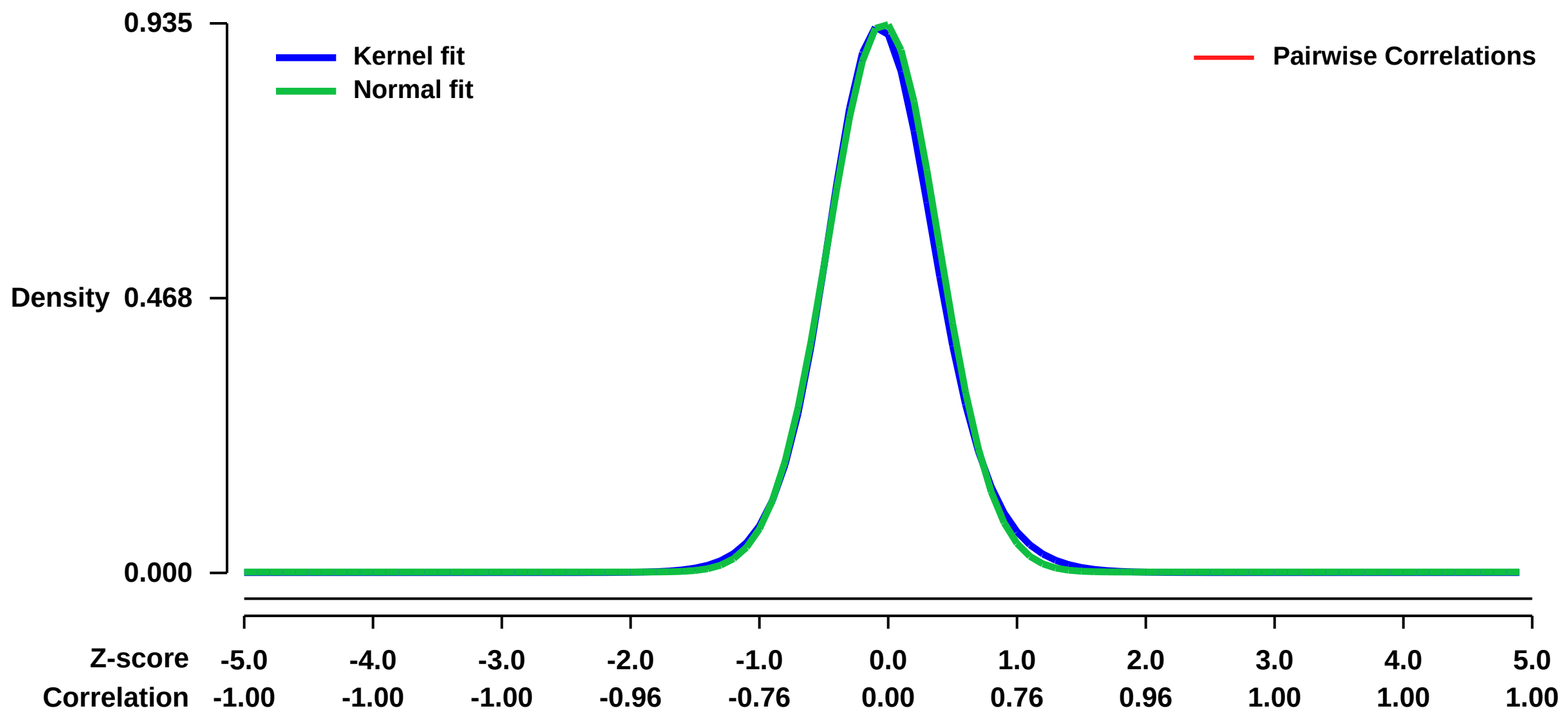

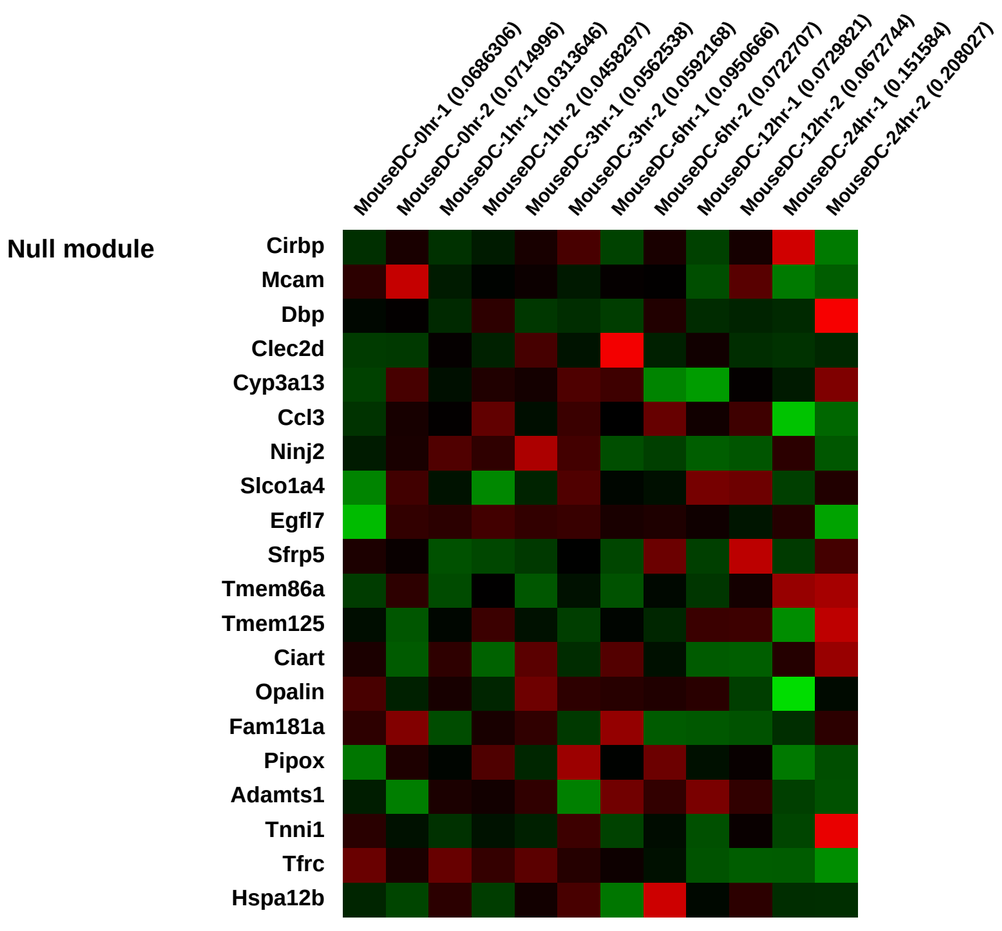

GEO Series "GSE21041" Expression Profiles

Num of samples in this series: 6

Scale of expression profile Z-scores

-3.0 -2.0 -1.0 0.0 1.0 2.0 3.0

GEO Link:	**http://www.ncbi.nlm.nih.gov/geo/query/acc.cgi?acc=GSE21041**
Status:	**Public on Jul 15 2010**
Title:	**Transcriptome analysis of miR-144/451-null bone marrow erythroid cells**
Organism:	**Mus musculus**
Experiment type:	**Expression profiling by array**
Platform:	**GPL1261**
Pubmed ID:	**20679398**
Summary & Design:	**Summary:** **microRNA miR-144/451 is highly expressed during erythropoiesis. We deleted the miR-144/451 gene locus in mice and compared the transcriptomes of miR-144/451-null bone marrow erythroid precursors to stage-matched wild-type control cells.** **Overall design:** **Ter119+/CD71+/FSC-high bone marrow erythroblasts were sorted directly into Trizol LS reagent. Total RNAs extracted from three miR-144/451 knock-out and three wide type mice were analyzed using Affymetrix Mouse Genome 430 2.0 Arrays.**

Background corr dist: **KL-Divergence = 0.0360, L1-Distance = 0.0159, L2-Distance = 0.0003, Normal std = 0.6337**

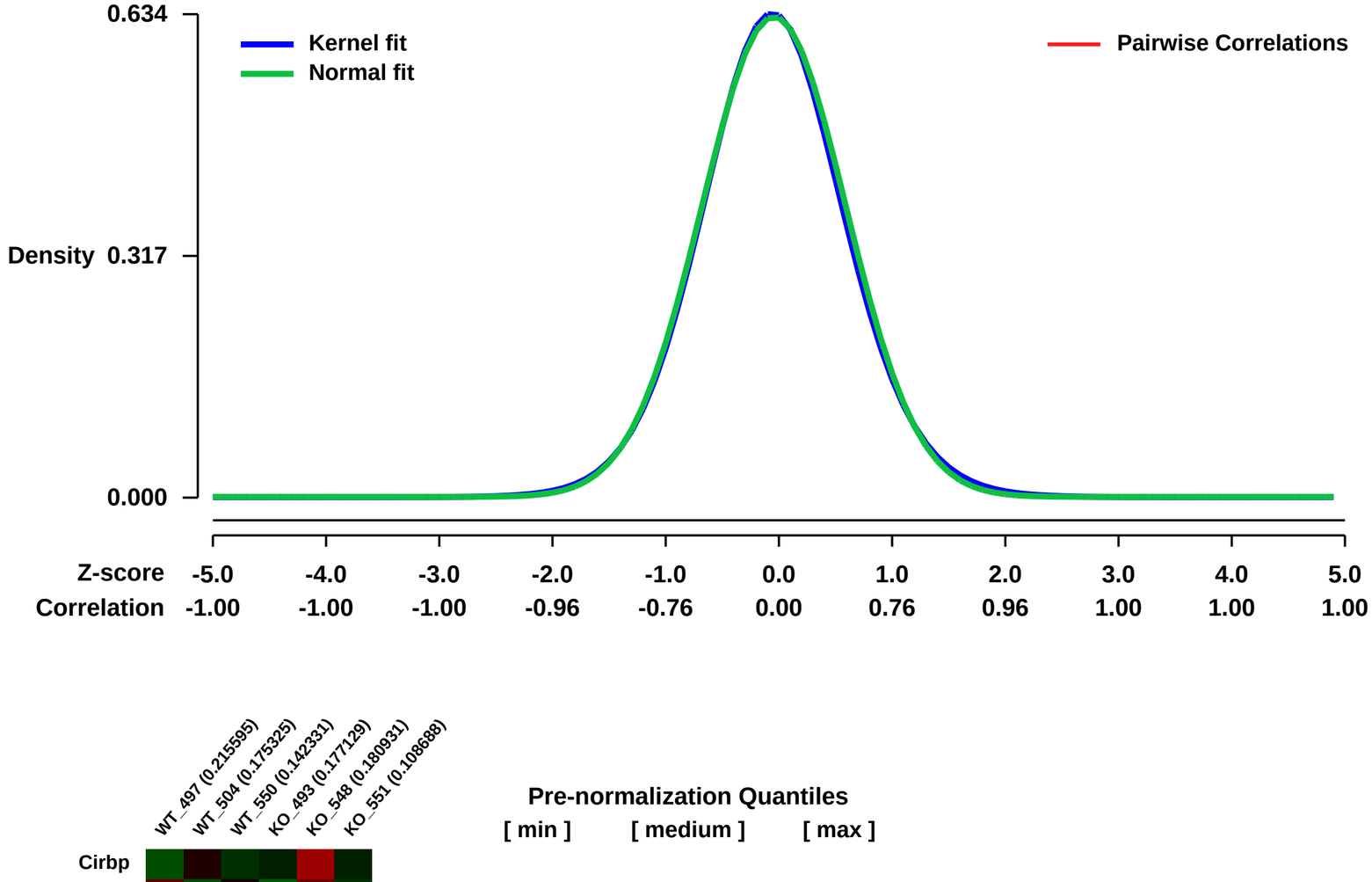

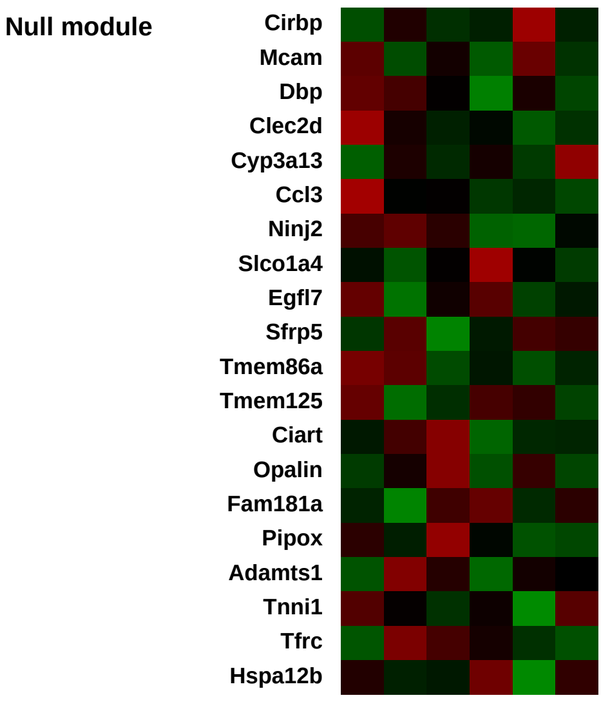

GEO Series "GSE21054" Expression Profiles

Num of samples in this series: 8

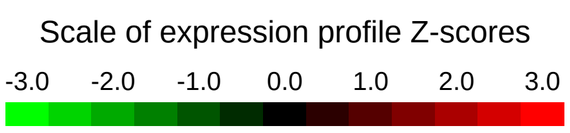

GEO Link:	http://www.ncbi.nlm.nih.gov/geo/query/acc.cgi?acc=GSE21054
Status:	Public on Sep 13 2010
Title:	Differential roles of Sall4 isoforms in ES cell pluripotency: expression
Organism:	Mus musculus
Experiment type:	Expression profiling by array
Platform:	GPL1261
Pubmed ID:	20837710
Summary & Design:	**Summary:** Murine embryonic stem cells (ESCs) are defined by continuous self-renewal and pluripotency. A diverse repertoire of protein isoforms arising from alternative splicing are expressed in ES cells without defined biological roles. Sall4, a transcription factor essential for pluripotency, exists as two isoforms (Sall4a and Sall4b). By genome-wide location analysis, we have determined that Sall4b, and not Sall4a, binds preferentially to highly expressed loci in ES cells. Sall4a and Sall4b binding sites are distinguished by both epigenetic marks at target loci and their clustering with binding sites of other pluripotency factors. When ESCs expressing a single isoform of Sall4 are generated, Sall4b alone could maintain the pluripotent state, although it could not completely suppress all differentiation markers. Sall4a and Sall4b collaborate in maintenance of the pluripotent state, but play distinct roles. Our work is novel in establishing such isoform-specific differences in ES cells. **Overall design:** Cells infected with an empty lentivirus (Wt) are compared with cells missing both isoforms of Sall4 (WT+shRNA) or a single isoform (Sall4aIMM+shRNA or Sall4bIMM+shRNA). ES cells expressing a single isoform of Sall4 (either Sall4a or Sall4b) were generated by using a lentivirally based shRNA (Open Biosystems TRC0000097821) that depleted both endogenous isoforms and then adding back a single isoform cDNA that was immune to the shRNA. Transcriptome analysis was performed 48 hrs after infection to identify changes in gene expression at various loci when only a single isoform of Sall4 was present.

Background corr dist: KL-Divergence = 0.0685, L1-Distance = 0.0207, L2-Distance = 0.0006, Normal std = 0.5015

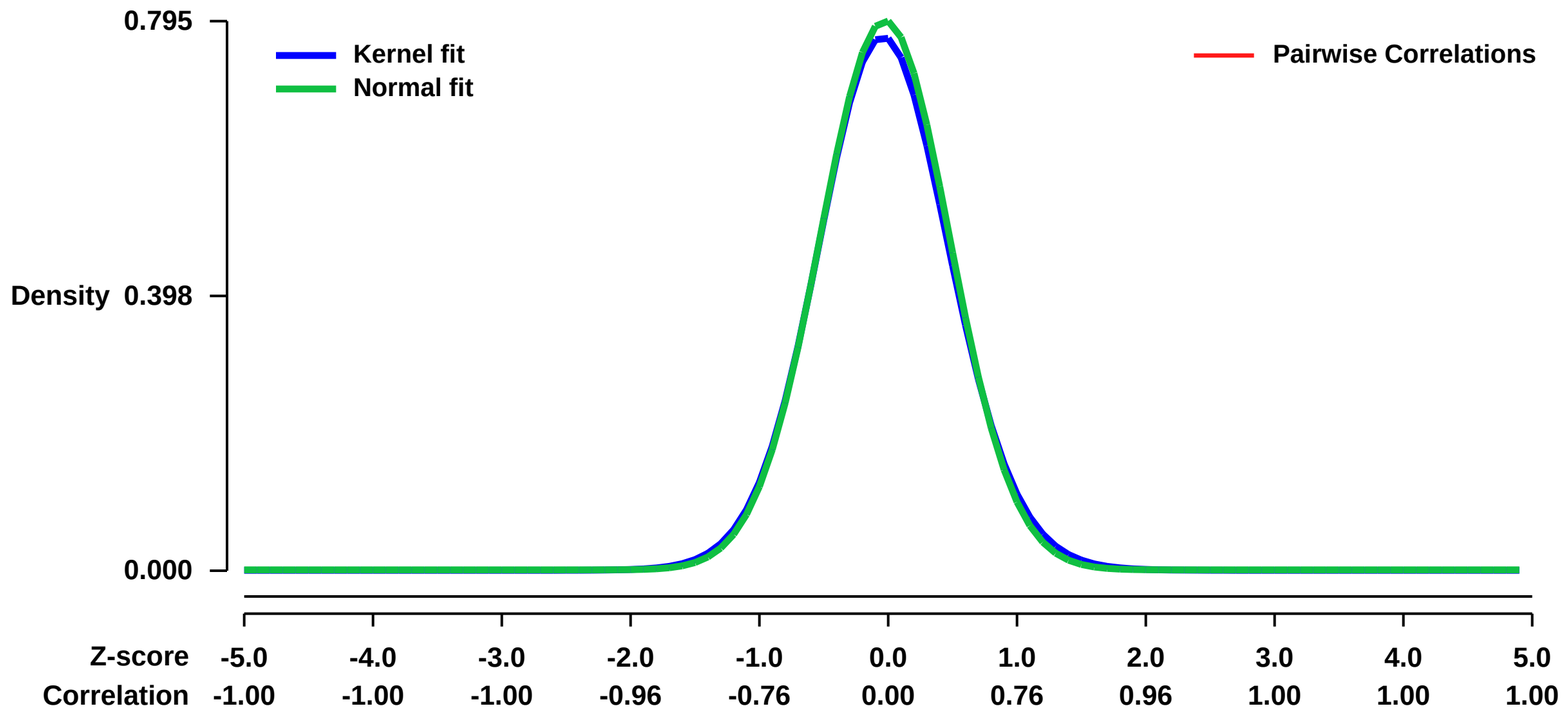

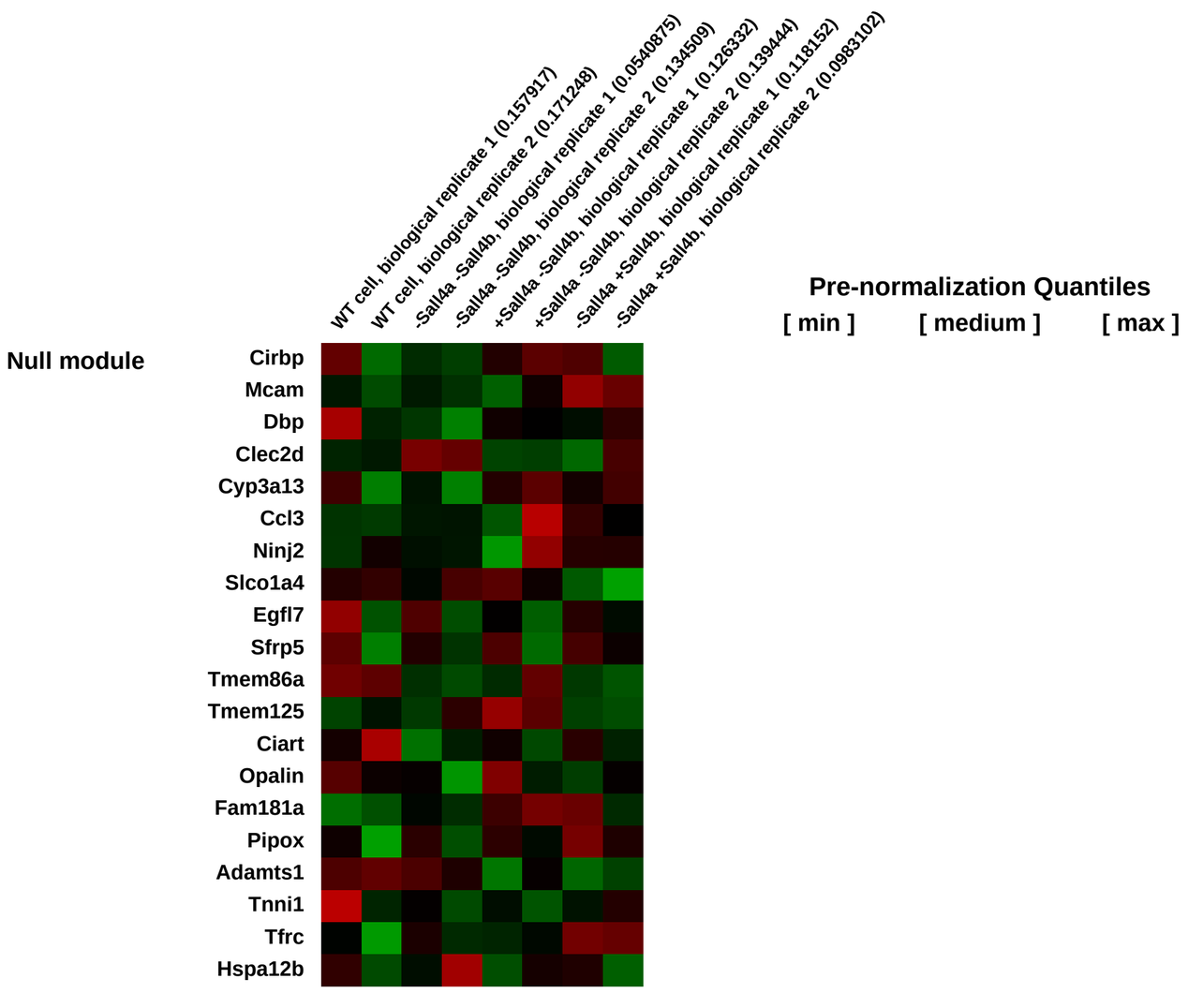

GEO Series "GSE21063" Expression Profiles

Num of samples in this series: 24

Scale of expression profile Z-scores

-3.0 -2.0 -1.0 0.0 1.0 2.0 3.0

GEO Link:	http://www.ncbi.nlm.nih.gov/geo/query/acc.cgi?acc=GSE21063
Status:	Public on Mar 24 2011
Title:	NFATc1 controls the survival, function and suppressive capacity of B lymphocytes upon B cell receptor stimulation
Organism:	Mus musculus
Experiment type:	Expression profiling by array
Platform:	GPL1261
Pubmed ID:	21464221
Summary & Design:	**Summary:** Triggering of B cell receptors (BCR) induces a massive synthesis of NFATc1 in splenic B cells. By inactivating the Nfatc1 gene and re-expressing NFATc1 we show that NFATc1 levels are critical for the survival of splenic B cells upon BCR stimulation. NFATc1 ablation led to decreased BCR-induced Ca++ flux and proliferation of splenic B cells, increased apoptosis and suppressed germinal centre formation and immunoglobulin class switch by T cell-independent antigens. By controlling IL-10 synthesis in B cells, NFATc1 supported the proliferation and IL-2 synthesis of T cells in vitro and appeared to contribute to the mild clinical course of Experimental Autoimmune Encephalomyelitis in mice bearing NFATc1-/- B cells. These data indicate NFATc1 as a key factor controlling B cell function. **Overall design:** Splenic mice cells were isolated from mice bearing NFATc1 deficient B-cells and from control mice, stimulated with anti-IgM for 0h, 3h, 8h and 16h, respectively and isolated using Milteny beads to enrich the B cell population. This experiment was performed in 3 biological replicates.

Background corr dist: KL-Divergence = 0.1823, L1-Distance = 0.0423, L2-Distance = 0.0030, Normal std = 0.3613

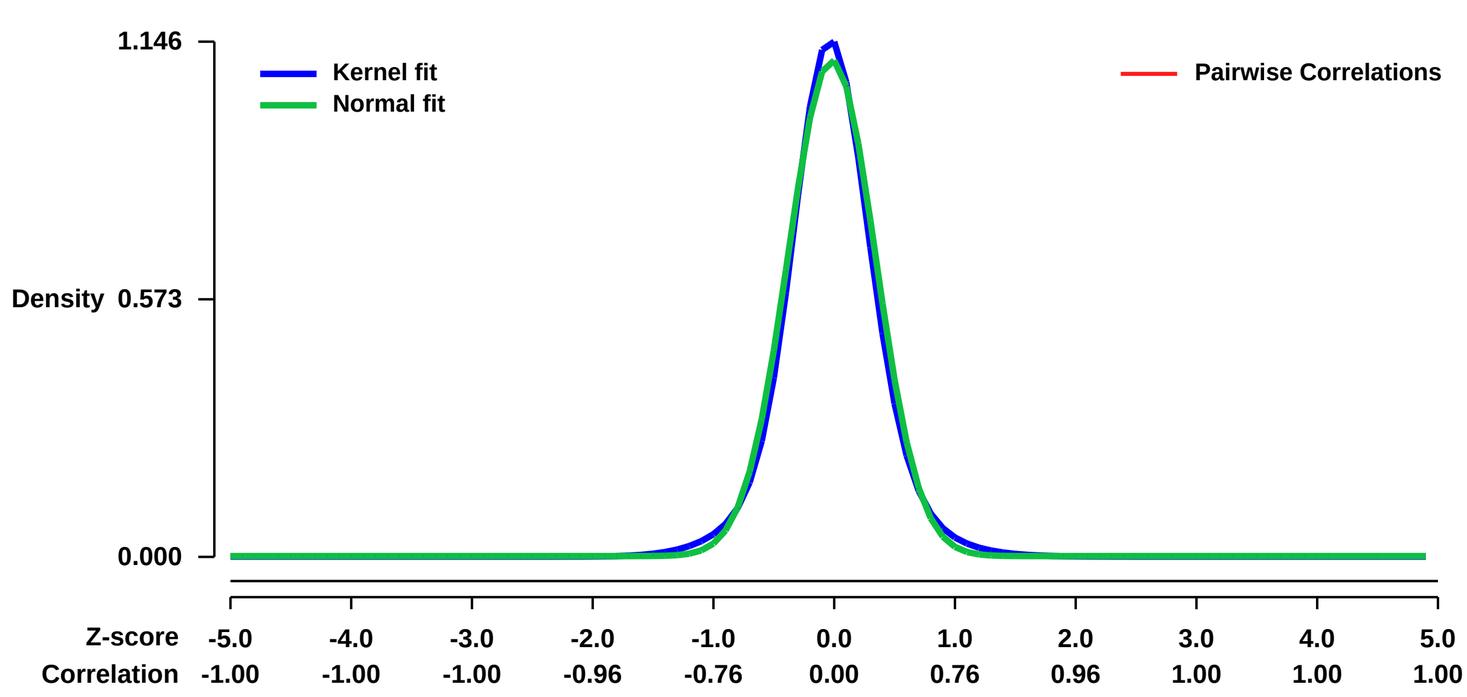

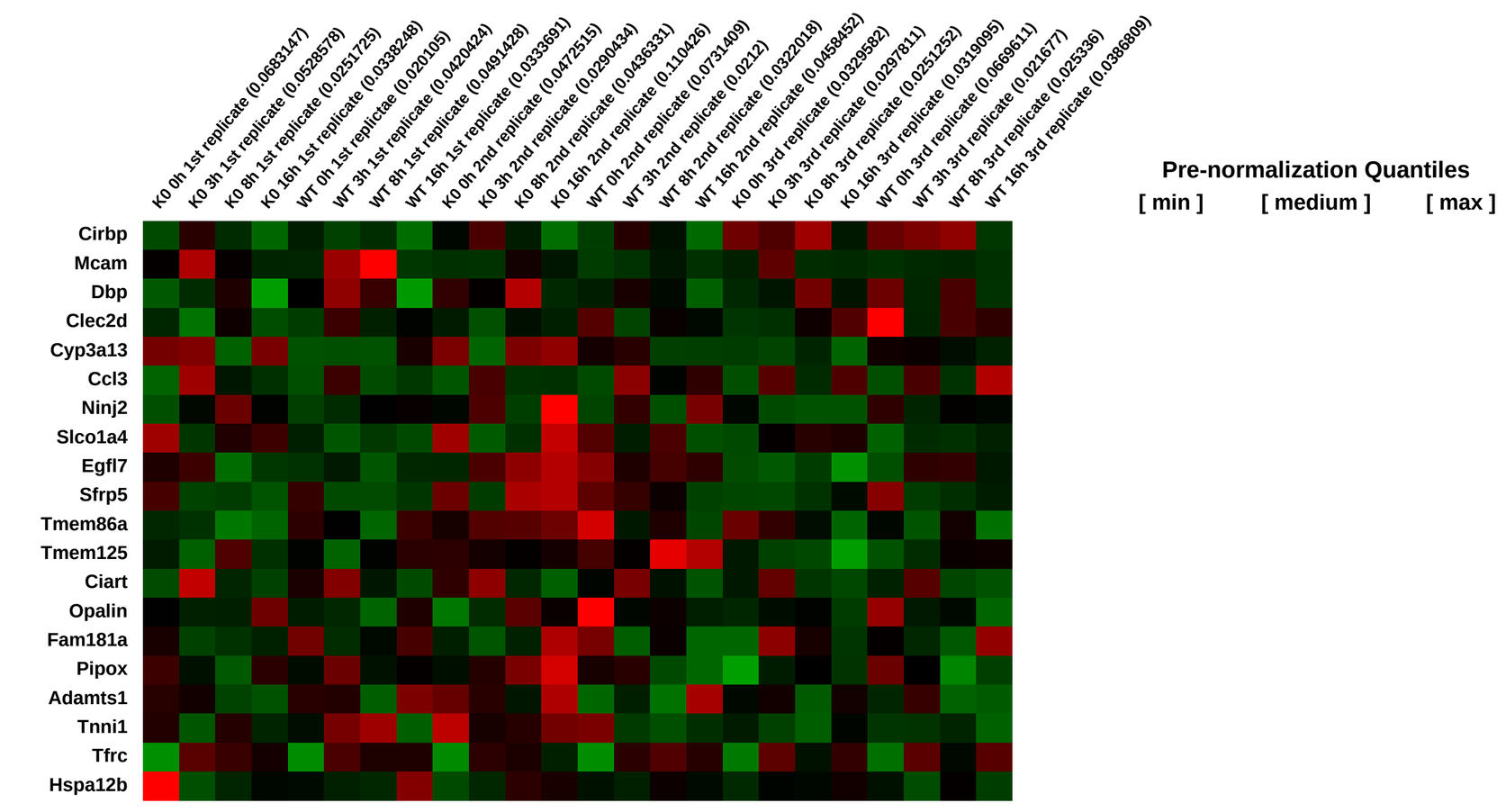

GEO Series "GSE21117" Expression Profiles

Num of samples in this series: 42

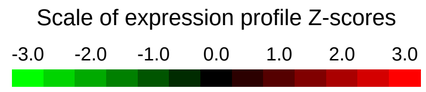

GEO Link:	http://www.ncbi.nlm.nih.gov/geo/query/acc.cgi?acc=GSE21117
Status:	Public on Jun 24 2011
Title:	Microarrays of macrophages infected with smooth or rough Brucella suis
Organism:	Mus musculus
Experiment type:	Expression profiling by array
Platform:	GPL1261
Pubmed ID:	21464087
Summary & Design:	**Summary:** The macrophage-Brucella interaction is critical for the establishment of a chronic Brucella infection. Smooth virulent B. suis strain 1330 (S1330) prevents macrophage cell death. However, rough attenuated B. suis strain VTRS1 induces strong macrophage cell death. To further investigate the mechanism of VTRS1-induced macrophage cell death, microarrays were used to analyze temporal transcriptional responses of murine macrophage-like J774. A1 cells infected with S1330 or VTRS1. **Overall design:** Murine J774.A1 macrophages were plated in T75 at 8 x 10^6 cells per flask one day prior to infection, and then infected with B. suis S1330 or VTRS1 at a MOI of 200:1. Total RNAs were isolated by TRIzol and further purified using Qiagen RNeasy Mini Kit (Qiagen, Valencia, CA) at 0, 1, 2, 4, 8, 24, and 48 h post infection. The RNA samples were stored at -80 ´”C until an Agilent 2100 BioAnalyzer (Agilent Technologies, Palo Alto, CA) was used to assess the concentrations and quality of RNA samples. Total RNA (20 ´µg) per sample was used for hybridization with Affymetrix mouse GeneChip 430 2.0 array. Preparation of cDNA, hybridization, quality controls and scanning of the GeneChip 430 2.0 arrays were performed according to the manufacturer’s protocol (Affymetrix, Santa Clara, CA) .

Background corr dist: KL-Divergence = 0.2179, L1-Distance = 0.0528, L2-Distance = 0.0072, Normal std = 0.3211

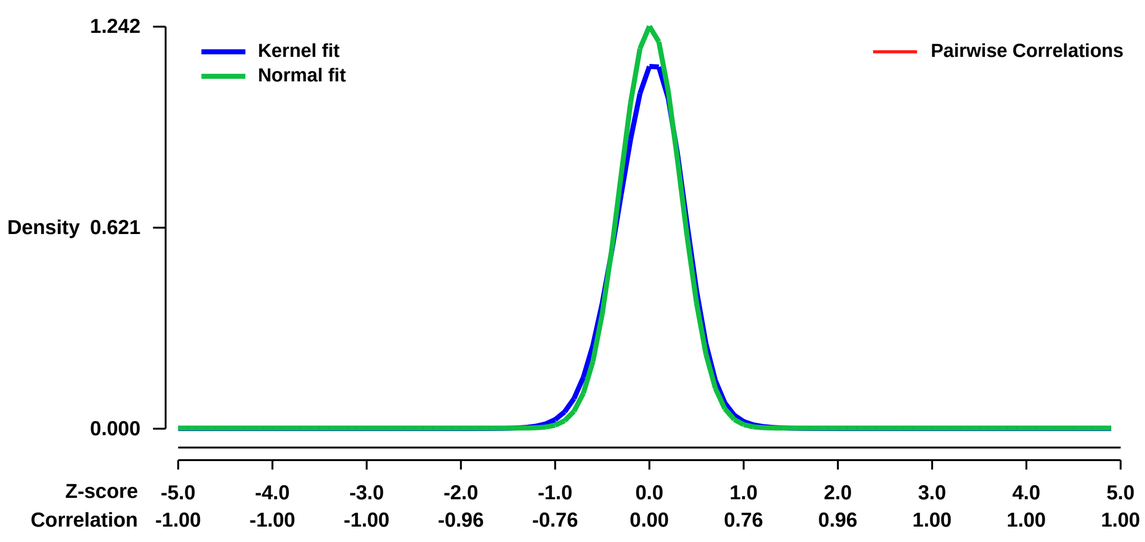

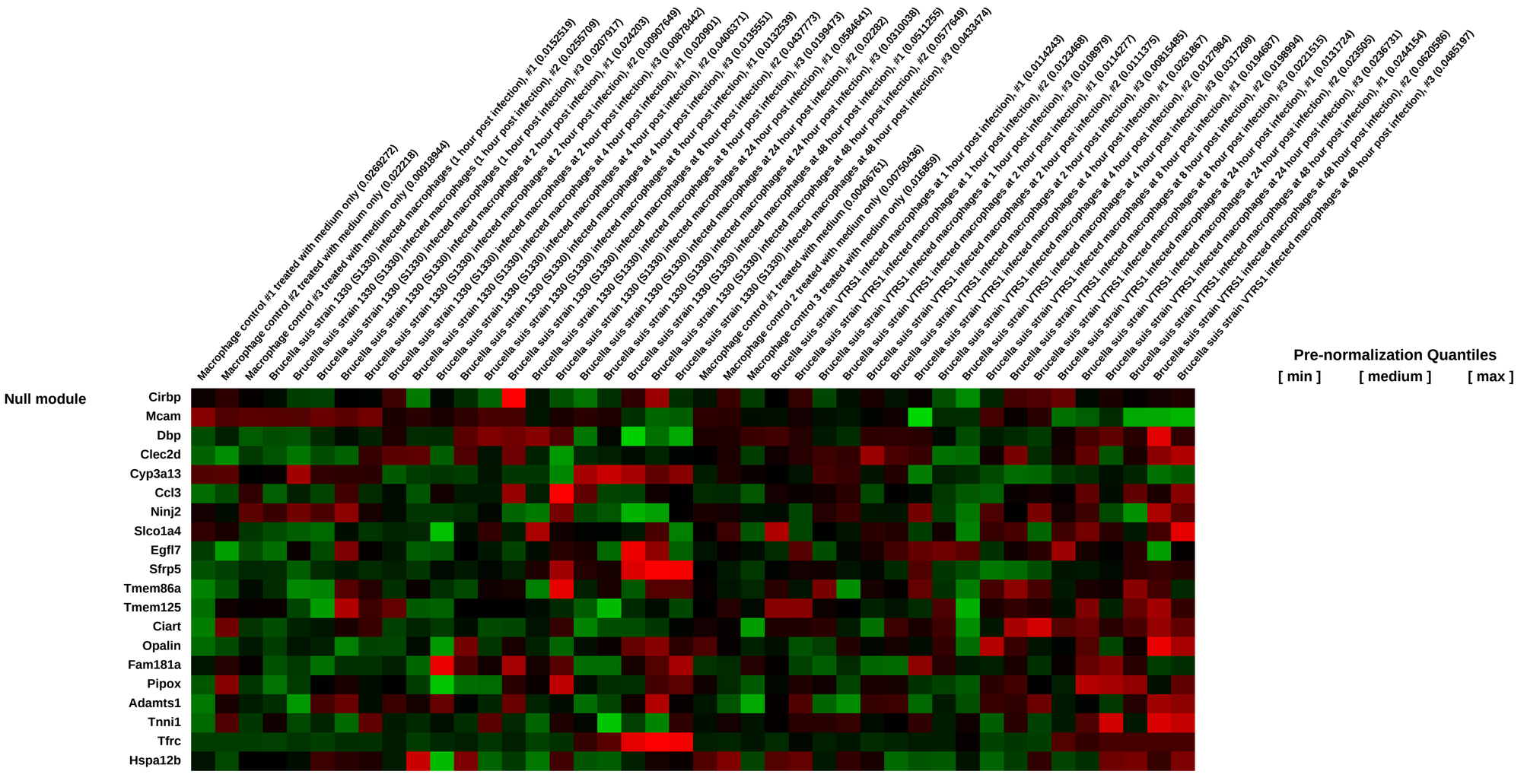

GEO Series "GSE21143" Expression Profiles

Num of samples in this series: 6

Scale of expression profile Z-scores

-3.0 -2.0 -1.0 0.0 1.0 2.0 3.0

GEO Link:	http://www.ncbi.nlm.nih.gov/geo/query/acc.cgi?acc=GSE21143
Status:	Public on Jun 14 2010
Title:	PLAGL2 regulates Wnt signaling to impede differentiation in neural stem cells and glioma
Organism:	Mus musculus
Experiment type:	Expression profiling by array
Platform:	GPL1261
Pubmed ID:	20478531
Summary & Design:	**Summary:** A hallmark feature of glioblastoma (GBM) cells is its strong self-renewal potential and immature differentiation state -- stem cell-like properties which may contribute to the plasticity and intense therapeutic resistance of GBM. The molecular basis of the immature differentiation profile remains an area of active investigation. Here, integrated genomic and biological analyses identified PLAGL2 as a potent proto-oncogene targeted for amplification/gain in malignant gliomas as well as in colorectal cancers. High level of PLAGL2 expression strongly suppresses neural stem cell (NSC) and glioma-initiating cell (GIC) differentiation while promoting their proliferation and self-renewal capacity under differentiation induction conditions. On the mechanistic level, the PLAGL2 transcriptome analysis revealed that these differentiation suppressive activities are attributable in part to PLAGL2 modulation of Wnt/beta-catenin signaling via up-regulation of Wnt6 ligand as well as Fzd9 and Fzd2 receptor expression. Correspondingly, inhibition of Wnt signaling in PLAGL2-expressing NSC partially restores their differentiation capacity. The identification of PLAGL2 as a glioma oncogene highlights the importance of a growing class of cancer genes functioning to impart stem cell-like characteristics on malignant cells. **Overall design:** p53-null mouse NSCs are infected with retrovirus expressing either control vector or PlagL2. Total RNA were collected upon differentiation in 1% FBS for 24 hr. 3 replicates each.

Background corr dist: KL-Divergence = 0.0436, L1-Distance = 0.0242, L2-Distance = 0.0007, Normal std = 0.6035

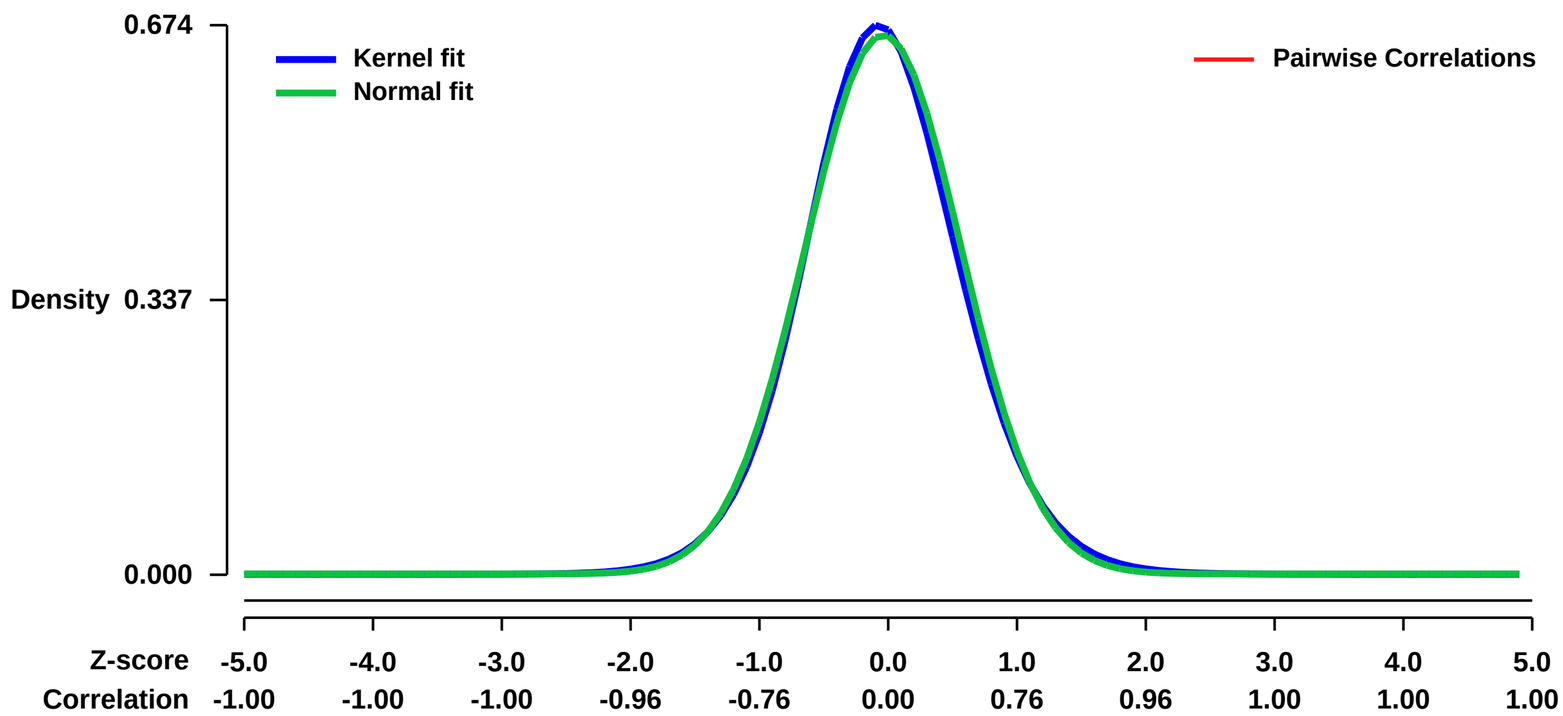

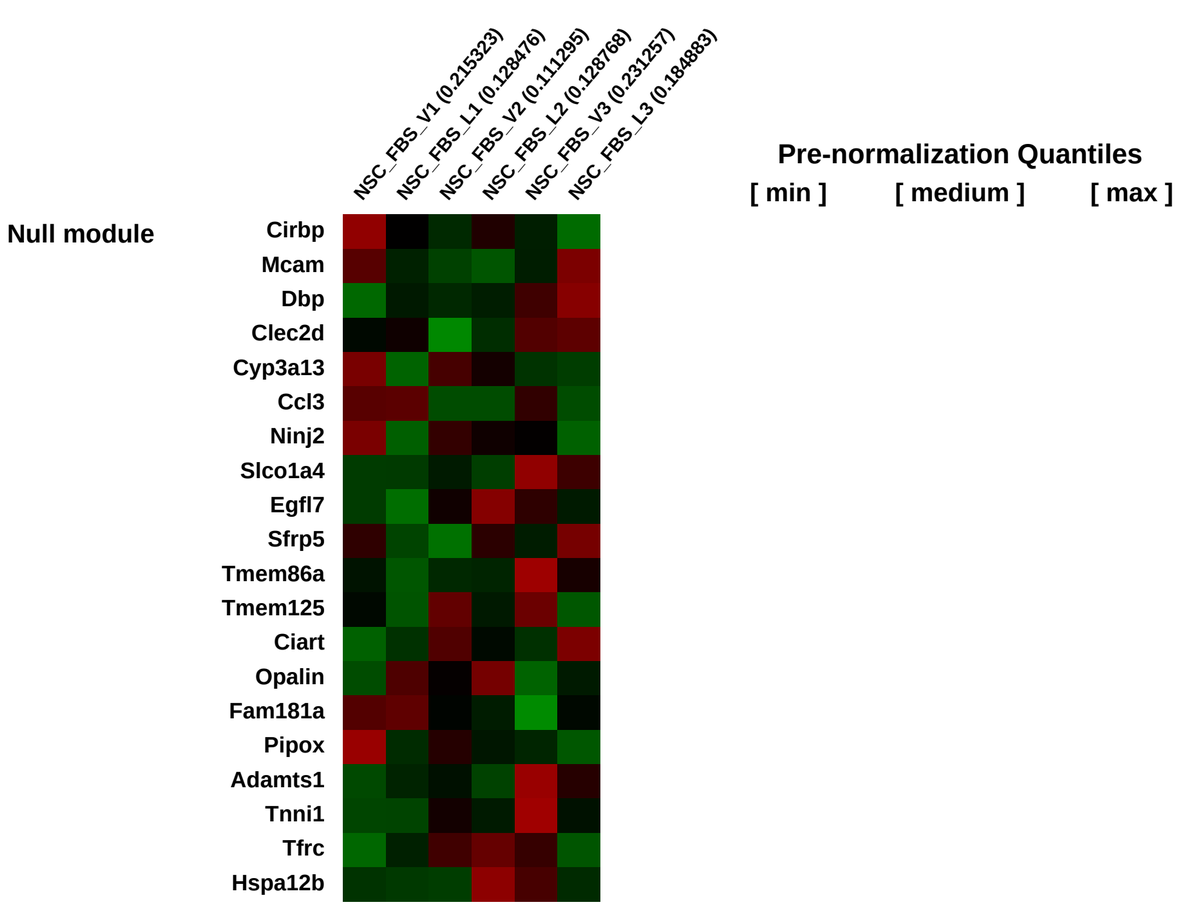

GEO Series "GSE21155" Expression Profiles

Num of samples in this series: 8

Scale of expression profile Z-scores

-3.0 -2.0 -1.0 0.0 1.0 2.0 3.0

GEO Link:	http://www.ncbi.nlm.nih.gov/geo/query/acc.cgi?acc=GSE21155
Status:	Public on Mar 29 2011
Title:	Accelerated leukemogenesis by truncated CBFb-SMMHC defective in high-affinity binding with RUNX1
Organism:	Mus musculus
Experiment type:	Expression profiling by array
Platform:	GPL1261
Pubmed ID:	20478528
Summary & Design:	**Summary:** Dominant RUNX1 inhibition has been proposed as a common pathway for CBF-leukemia. CBFb-SMMHC, a fusion protein in human acute myeloid leukemia (AML), dominantly inhibits RUNX1 largely through its RUNX1 high-affinity binding domain (HABD). We generated knock-in mice expressing CBFb-SMMHC with a HABD deletion, CBFb-SMMHCd179-221. These mice developed leukemia highly efficiently, even though hematopoietic defects associated with Runx1-inhibition were partially rescued. To identify changes in gene expression with the deletion of the HABD, we compared the gene expression profile in leukemia samples from mice expressing CBFb-SMMHCd179-221 with those from mice expressing full length CBFb-SMMHC. **Overall design:** Spleen cells were isolated from leukemic knock-in mice with full length CBFb-SMMHC at 2 months after ENU treatment and 2 leukemic CBFb-SMMHCd179-221 expressing chimeric mice at 3 weeks after birth. For each genotype, we performed two independent experiments with 4 Affymetrix GeneChip 430 chips.

Background corr dist: KL-Divergence = 0.0542, L1-Distance = 0.0201, L2-Distance = 0.0005, Normal std = 0.5550

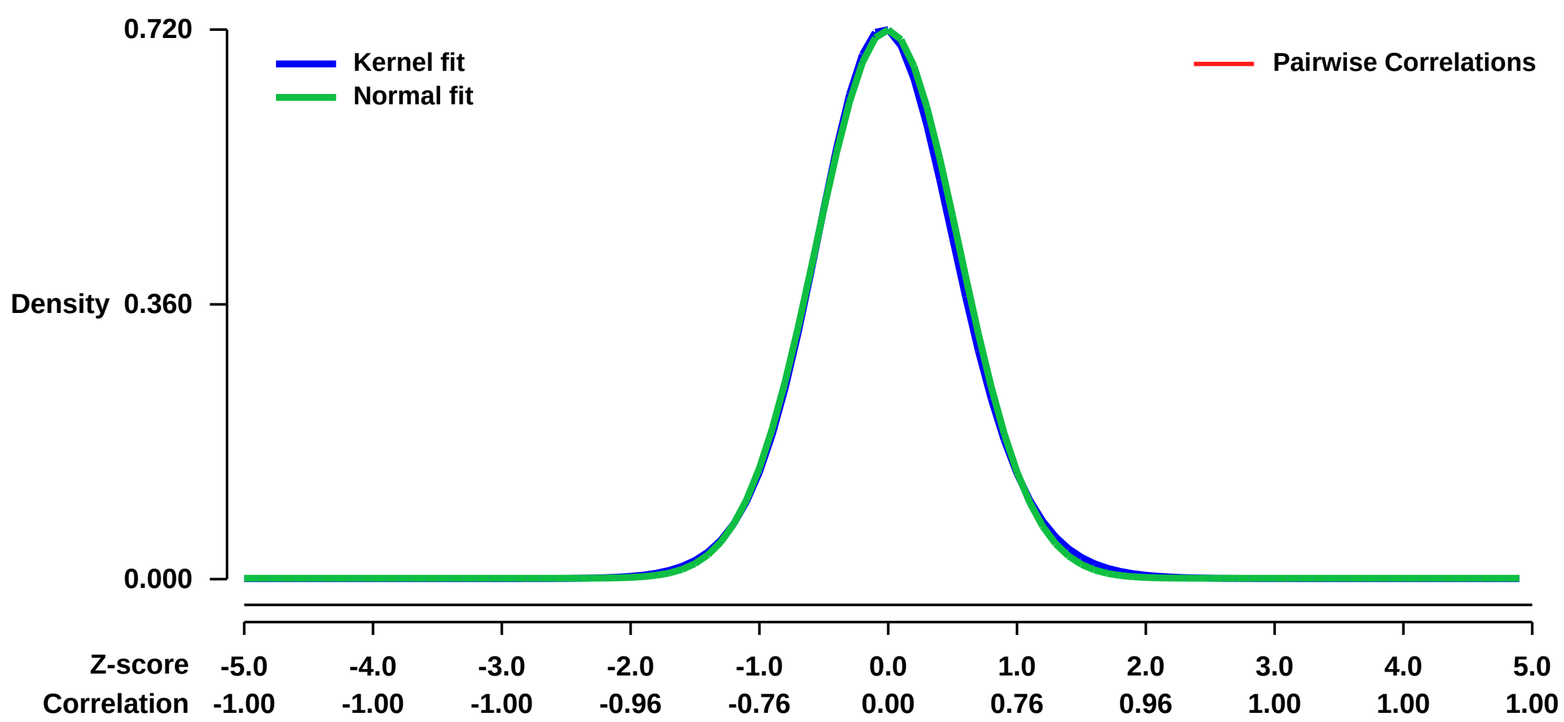

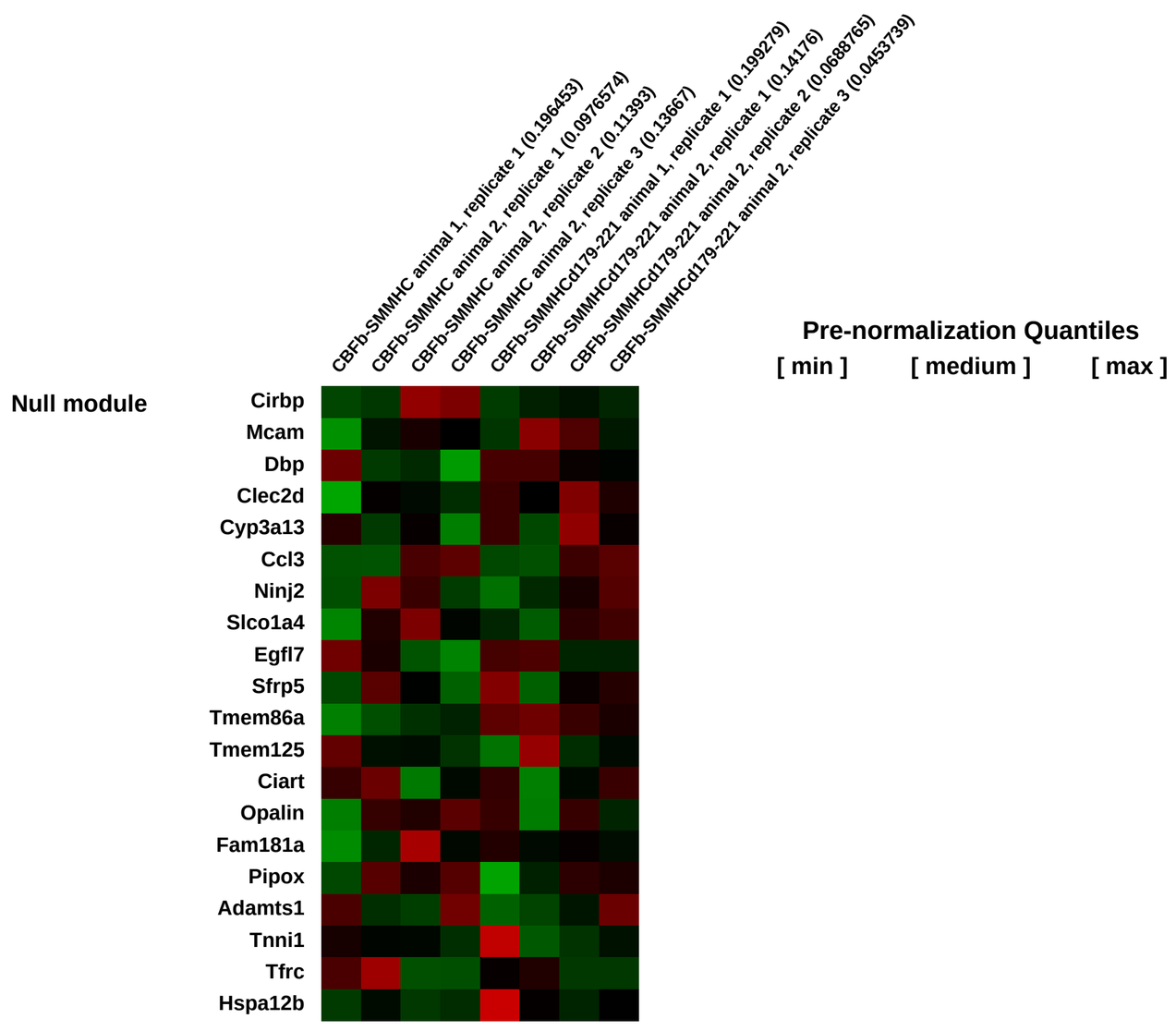

GEO Series "GSE21156" Expression Profiles

Num of samples in this series: 6

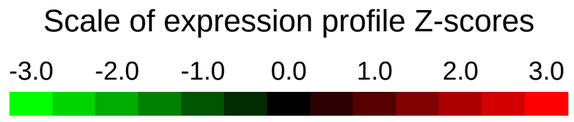

GEO Link:	http://www.ncbi.nlm.nih.gov/geo/query/acc.cgi?acc=GSE21156
Status:	Public on Apr 02 2010
Title:	Expression data from rostral forebrains of wild-type and Fezf1-/- Fezf2-/- mice
Organism:	Mus musculus
Experiment type:	Expression profiling by array
Platform:	GPL1261
Pubmed ID:	20431123
Summary & Design:	**Summary:** Zinc-finger genes Fezf1 and Fezf2 encode transcriptional repressors. Fezf1 and Fezf2 are expressed in the early neural stem/progenitor cells and control neuronal differentiation in mouse dorsal telencephalon. We compared gene expression profiles of rostral forebrains, which contain the telencephalon and the rostral part of the diencephalon, from embryonic day (E) 9.5, E10.5, and E12.5 wild-type control and Fezf1-/- Fezf2 -/- mouse embryos. **Overall design:** The forebrain rostral to the caudal limit of the lateral ventricles was isolated manually from E9.5, E10.5, and E12.5 wild-type and Fezf1-/- Fezf2-/- mice. Total RNAs were isolated by Separsol-RNA I and were used for microarray analyses.

Background corr dist: KL-Divergence = 0.0250, L1-Distance = 0.0333, L2-Distance = 0.0012, Normal std = 0.7381

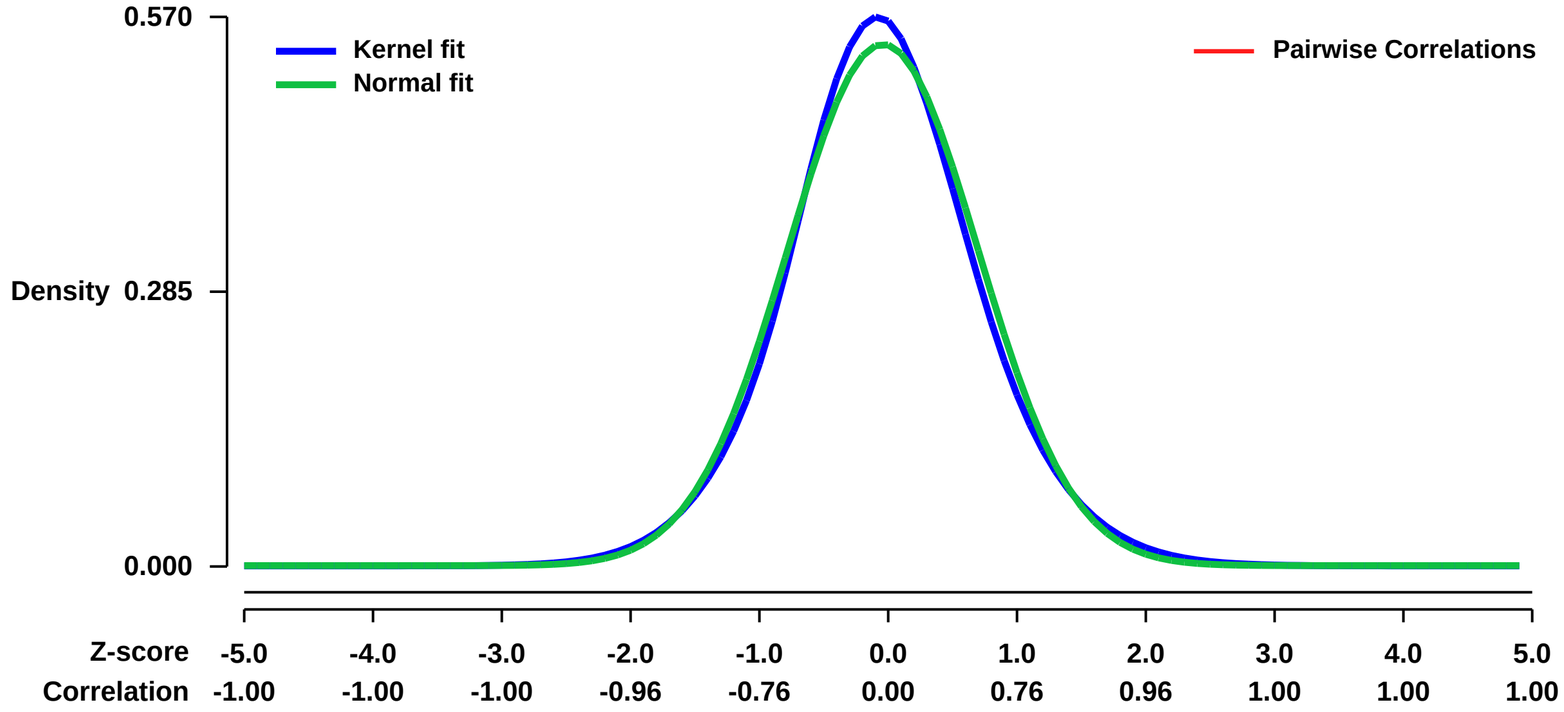

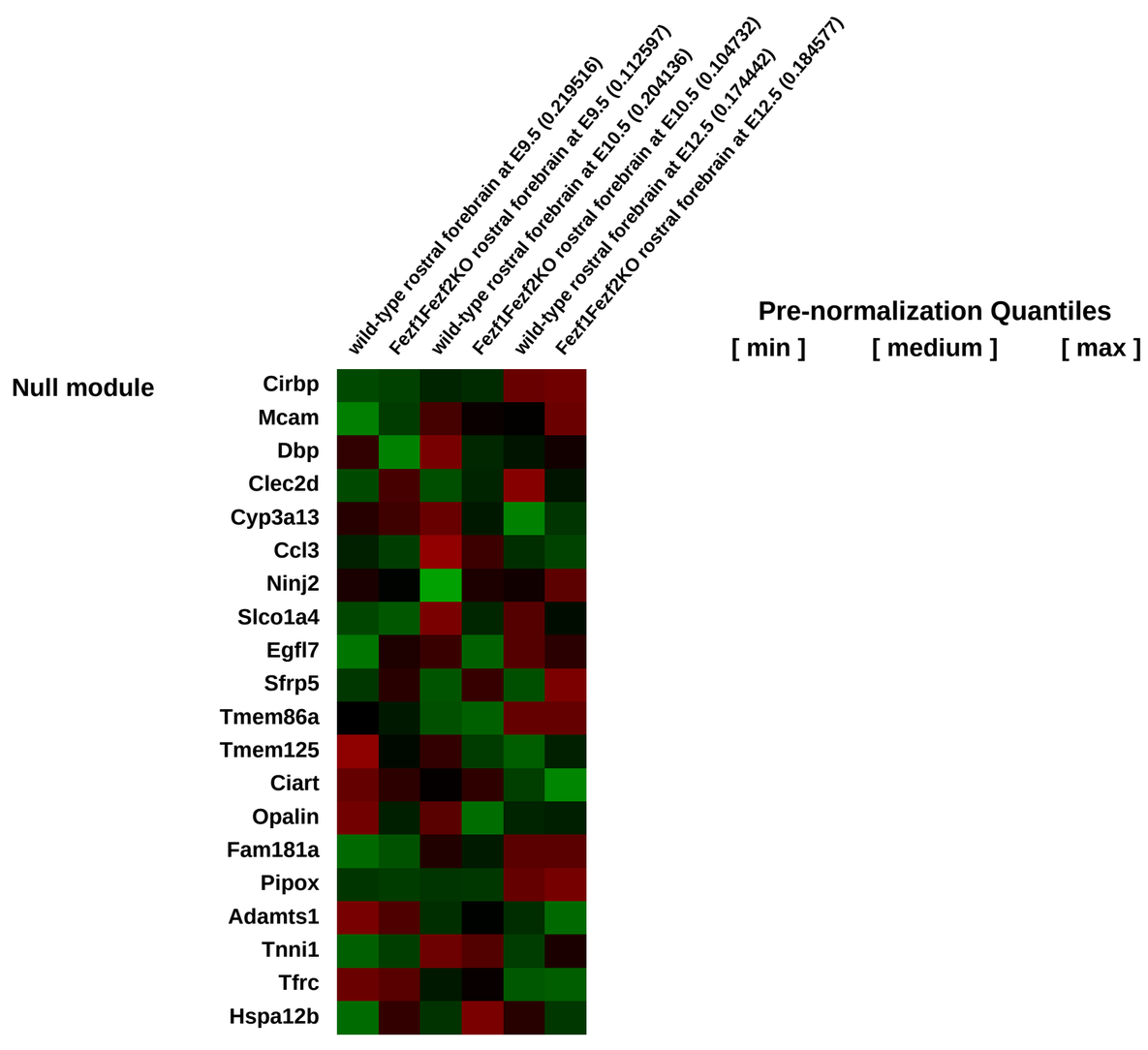

GEO Series "GSE21189" Expression Profiles

Num of samples in this series: 10

Scale of expression profile Z-scores

-3.0 -2.0 -1.0 0.0 1.0 2.0 3.0

GEO Link:	http://www.ncbi.nlm.nih.gov/geo/query/acc.cgi?acc=GSE21189
Status:	Public on May 01 2010
Title:	Mitochondrial DNA mutations induce supression of nuclear encoded mitochondrial Genes in skeletal muscle
Organism:	Mus musculus
Experiment type:	Expression profiling by array
Platform:	GPL1261
Pubmed ID:	20628647
Summary & Design:	**Summary:** To identify and analyze mtDNA mutation-responsive genes, a comparison of gastrocnemius muscle tissues from WT (control) and D257A mice was conducted. We examined changes in gene expression in the muscle associated with mtDNA mutations. **Overall design:** 5) Quality control measures were not used. No replicates were done. Dye swap was not used.

Background corr dist: KL-Divergence = 0.1134, L1-Distance = 0.0276, L2-Distance = 0.0014, Normal std = 0.4173

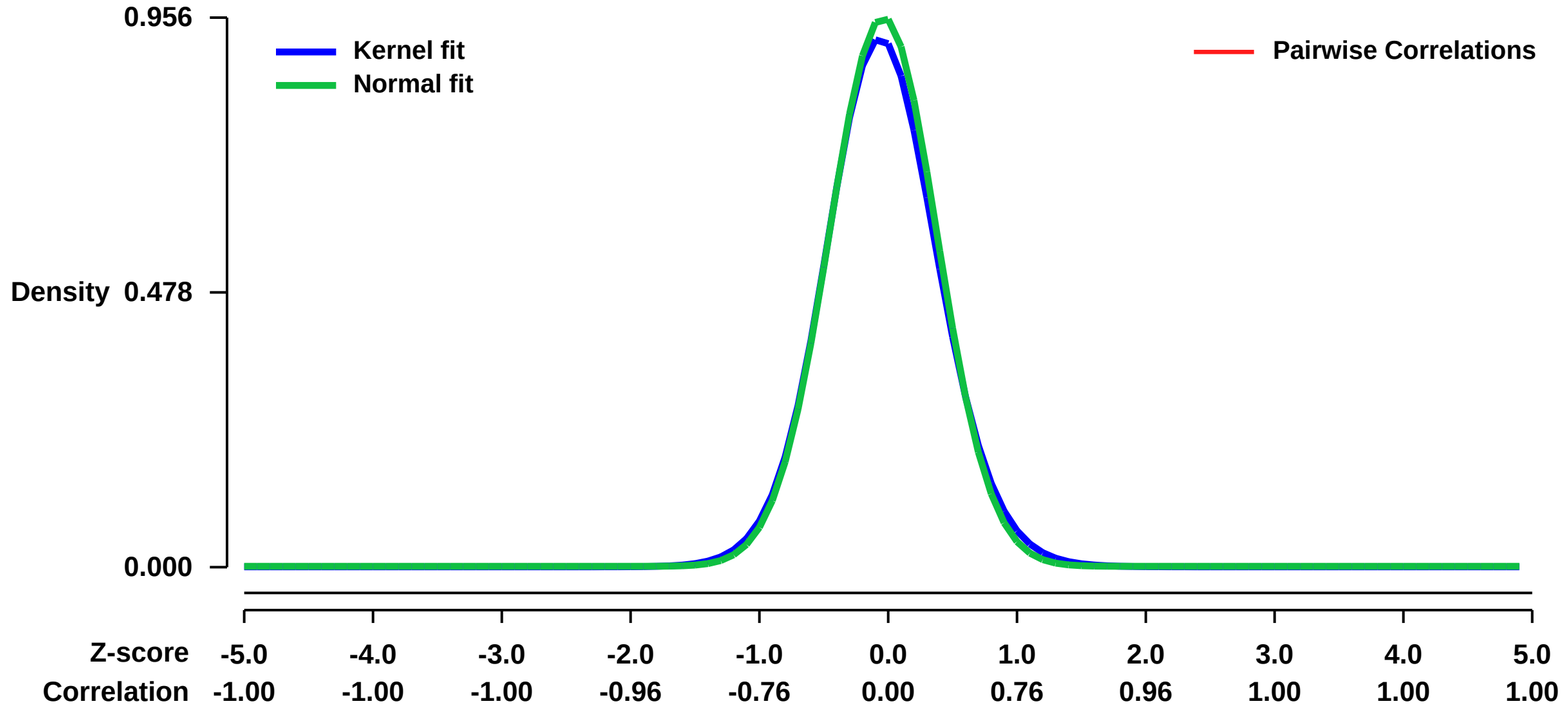

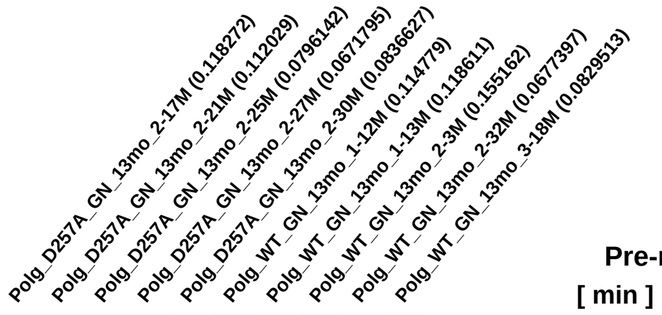

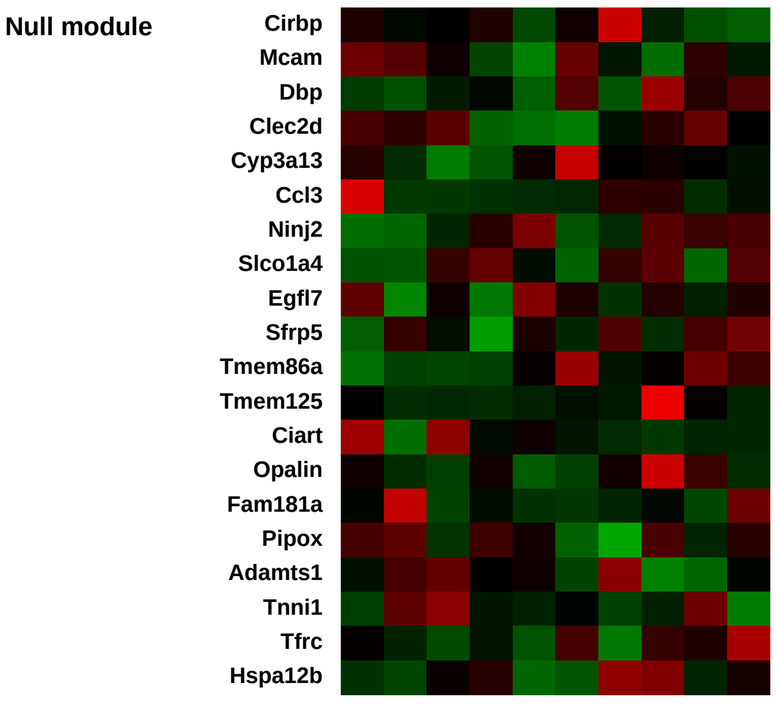

GEO Series "GSE21193" Expression Profiles

Num of samples in this series: 10

Scale of expression profile Z-scores

-3.0 -2.0 -1.0 0.0 1.0 2.0 3.0

GEO Link:	http://www.ncbi.nlm.nih.gov/geo/query/acc.cgi?acc=GSE21193
Status:	Public on Jul 22 2010
Title:	The effects of subchronic arsenate exposure on gene expression in the mouse lung
Organism:	Mus musculus
Experiment type:	Expression profiling by array
Platform:	GPL1261
Pubmed ID:	20667999
Summary & Design:	**Summary:** Eight week old female C57BL/6 mice were exposed to arsenate in drinking water (50 ppm) for a period of twelve weeks (n = 5). Control animals received distilled deionized water (n = 5). Lung tissue was dissected and used for RNA isolation and gene expression microarray analysis. **Overall design:** Eight week old female C57BL/6 mice were exposed to arsenate in drinking water (50 ppm) for a period of twelve weeks (n = 5). Control animals received distilled deionized water (n = 5). Lung tissue was dissected and used for RNA isolation and gene expression microarray analysis.

Background corr dist: KL-Divergence = 0.0535, L1-Distance = 0.0371, L2-Distance = 0.0023, Normal std = 0.5581

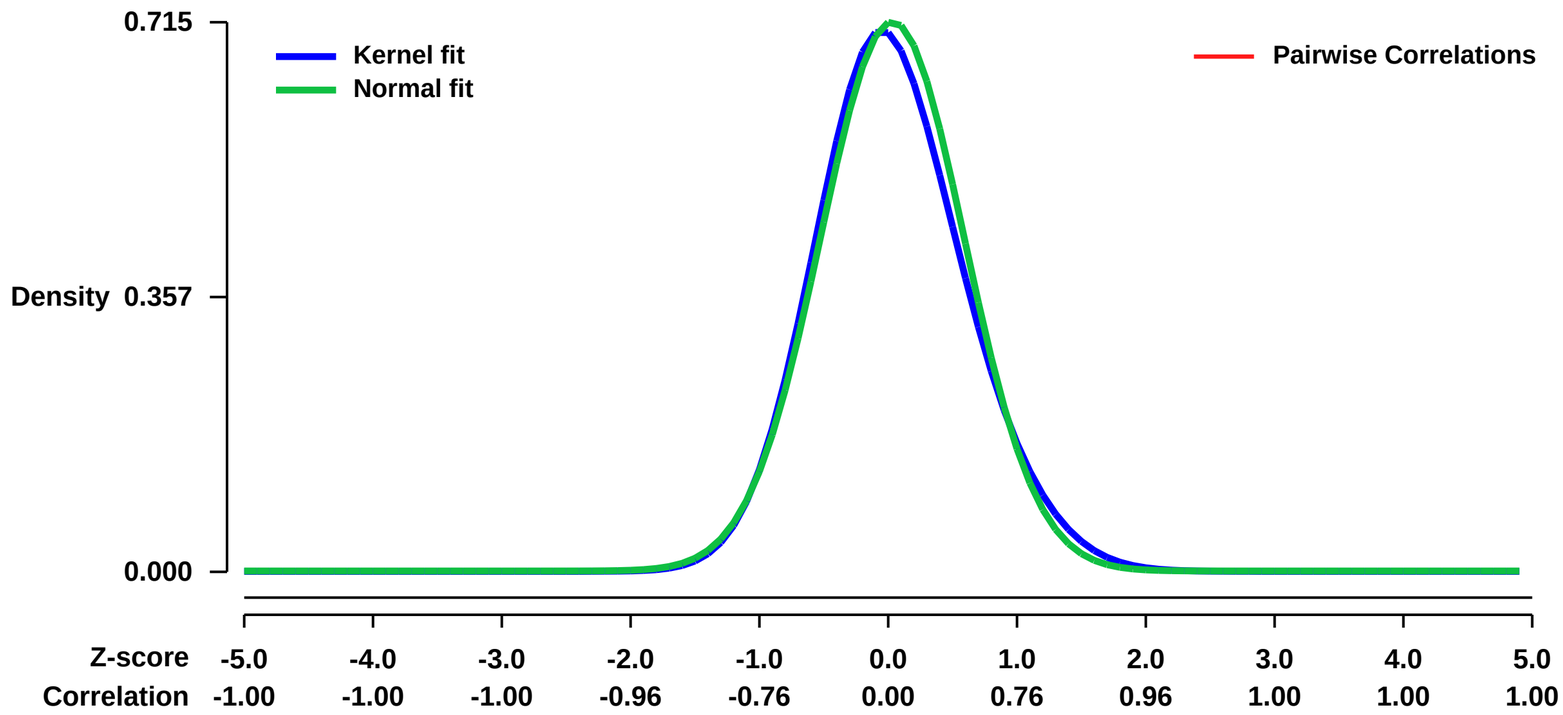

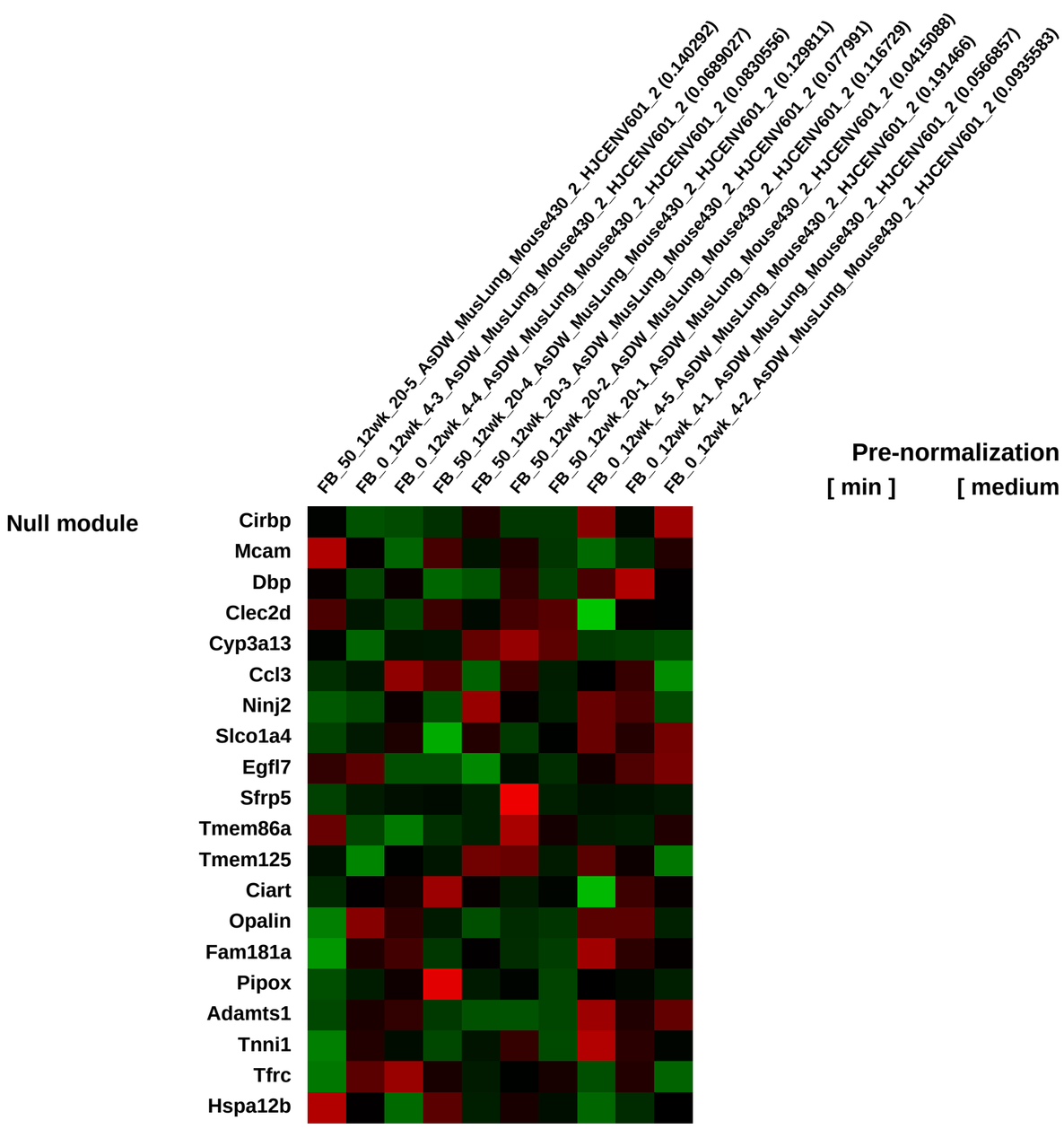

GEO Series "GSE21224" Expression Profiles

Num of samples in this series: 16

Scale of expression profile Z-scores

-3.0 -2.0 -1.0 0.0 1.0 2.0 3.0

GEO Link:	http://www.ncbi.nlm.nih.gov/geo/query/acc.cgi?acc=GSE21224
Status:	Public on Oct 01 2010
Title:	Transcriptional ontogeny of the developing liver
Organism:	Mus musculus
Experiment type:	Expression profiling by array
Platform:	GPL1261
Pubmed ID:	22260730
Summary & Design:	**Summary:** We characterized gene expression changes in the developing mouse liver at gestational days (GD) 11.5, 12.5, 13.5, 14.5, 16.5, and 19.5 and in the neonate (postnatal day (PND) 7 and 30) using full-genome microarrays and compared these changes to that in the adult liver. The fetal liver, and to a lesser extent the neonatal liver, exhibited dramatic differences in gene expression compared to adults. Canonical pathway analysis of the fetal liver signature demonstrated increases in functions important in cell replication and DNA fidelity whereas most metabolic pathways of intermediary metabolism were suppressed. Comparison of the dataset to a number of previously published datasets revealed 1) a striking similarity between the fetal liver and that of the pancreas in both mice and humans, 2) a nucleated erythrocyte signature in the fetus and 3) suppression of most xenobiotic metabolism genes throughout development, except a number of transporters associated with expression in hematopoietic cells. **Keywords:** gene expression/microarray **Overall design:** We characterized gene expression changes in the developing mouse liver at gestational days (GD) 19 and in the neonate (postnatal day (PND) 7 and 30) using full-genome microarrays and compared these changes to that in the adult liver. Total RNA was isolated from liver samples and gene expression analyzed using Affymetrix Mouse 430 2.0 GeneChips. Data from 16 samples, with four mice in each of the four age groups, were analyzed.

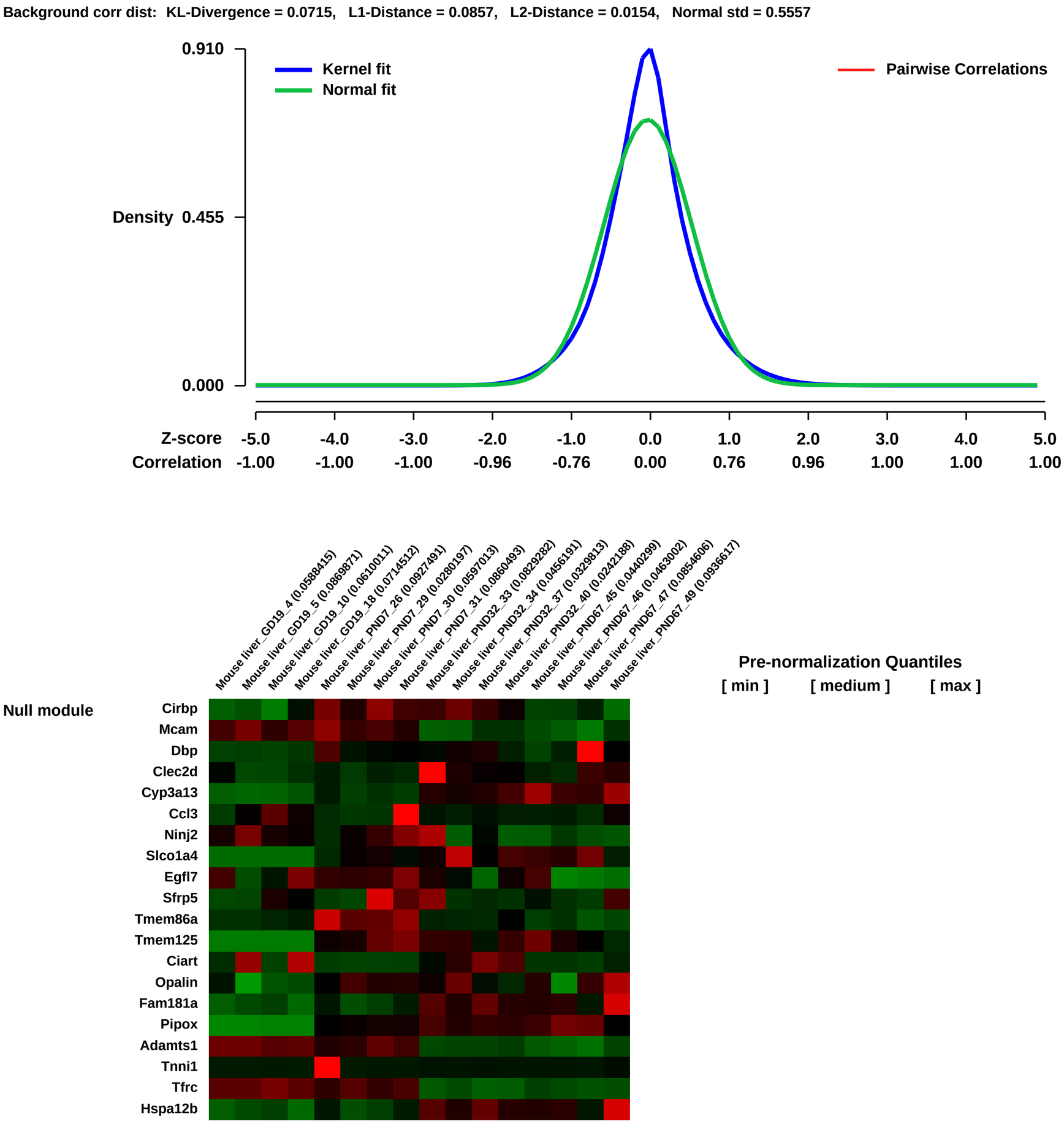

GEO Series "GSE21247" Expression Profiles

Num of samples in this series: 60

Scale of expression profile Z-scores

-3.0 -2.0 -1.0 0.0 1.0 2.0 3.0

GEO Link: http://www.ncbi.nlm.nih.gov/geo/query/acc.cgi?acc=GSE21247
Status: Public on Dec 22 2010
Title: Network Analysis of Skin Tumor Progression Identifies a Rewired Genetic Architecture Affecting Inflammation and Tumor Susceptibility (carcinomas)
Organism: Mus musculus
Experiment type: Expression profiling by array
Platform: GPL1261
Pubmed ID: 21244661

Summary & Design:

Summary:
Germline polymorphisms influence gene expression networks in normal mammalian tissues. Analysis of this genetic architecture can identify single genes and whole pathways that influence to complex traits including inflammation and cancer susceptibility. Changes in the genetic architecture during the development of benign and malignant tumours have not been investigated. Here, we document major changes in germline control of gene expression during skin tumour development as a consequence of cell selection, somatic genetic events, and changes in tumour microenvironment. Immune response genes such as Interleukin 18 and Granzyme E are under germline control in tumours but not in normal skin. Gene expression networks linked to tumour susceptibility and hair follicle stem cell markers in normal skin undergo significant reorganization during tumour progression. Our data highlight opposing roles of Interleukin-1 signaling networks in tumour susceptibility and tumour progression and have implications for the development of chemopreventive strategies to reduce cancer incidence.

Overall design:
Skin tumors were induced on dorsal back skin from a Mus spretus / Mus musculus backcross ([SPRET/Ei X FVB/N] X FVB/N) mice by treatment of dorsal back skin with dimethyl benzanthracene (DMBA) and tetradecanoyl-phorbol acetate (TPA). This treatment induced multiple benign papillomas as well as malignant squamous cell carcinomas (SCC) and spindle cell carcinomas. 60 carcinomas were harvested from 55 mice; five mice provided two carcinomas each.

Background corr dist: KL-Divergence = 0.5541, L1-Distance = 0.0998, L2-Distance = 0.0338, Normal std = 0.2152

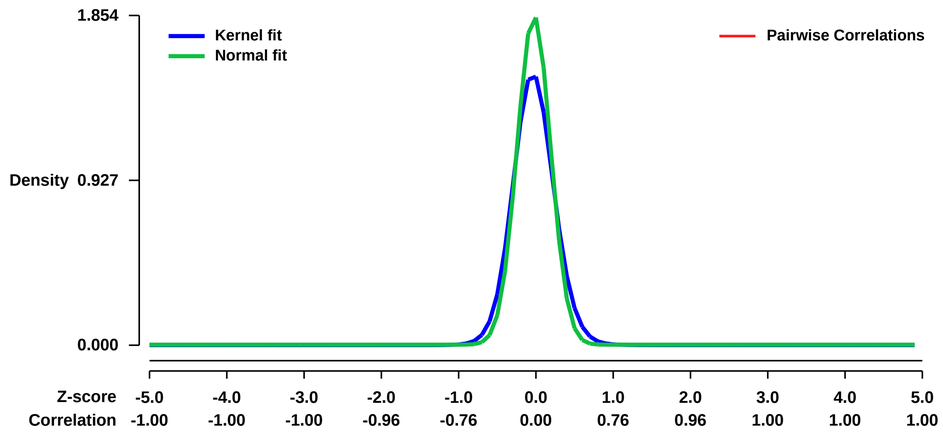

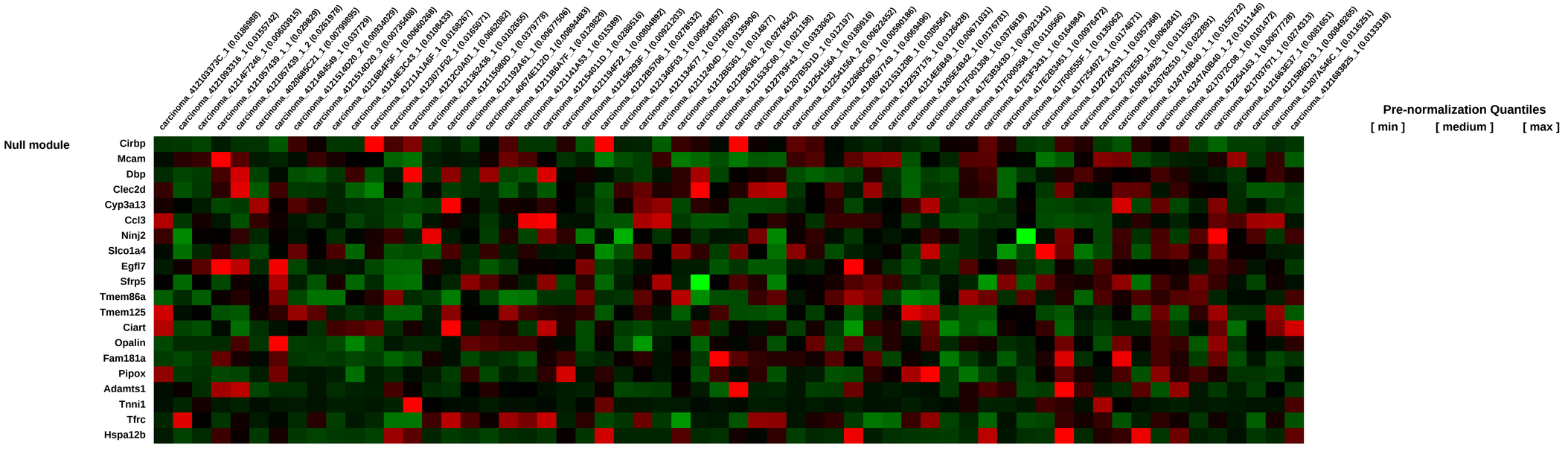

GEO Series "GSE21263" Expression Profiles

Num of samples in this series: 68

Scale of expression profile Z-scores

-3.0 -2.0 -1.0 0.0 1.0 2.0 3.0

GEO Link: http://www.ncbi.nlm.nih.gov/geo/query/acc.cgi?acc=GSE21263

Status: Public on Dec 22 2010

Title: Network Analysis of Skin Tumor Progression Identifies a Rewired Genetic Architecture Affecting Inflammation and Tumor Susceptibility (papillomas)

Organism: Mus musculus

Experiment type: Expression profiling by array

Platform: GPL1261

Pubmed ID: 21244661

Summary & Design:

Summary:
Germline polymorphisms influence gene expression networks in normal mammalian tissues. Analysis of this genetic architecture can identify single genes and whole pathways that influence to complex traits including inflammation and cancer susceptibility. Changes in the genetic architecture during the development of benign and malignant tumours have not been investigated. Here, we document major changes in germline control of gene expression during skin tumour development as a consequence of cell selection, somatic genetic events, and changes in tumour microenvironment. Immune response genes such as Interleukin 18 and Granzyme E are under germline control in tumours but not in normal skin. Gene expression networks linked to tumour susceptibility and hair follicle stem cell markers in normal skin undergo significant reorganization during tumour progression. Our data highlight opposing roles of Interleukin-1 signaling networks in tumour susceptibility and tumour progression and have implications for the development of chemopreventive strategies to reduce cancer incidence.

Overall design:
Skin tumors were induced on dorsal back skin from a Mus spretus / Mus musculus backcross ([SPRET/Ei X FVB/N] X FVB/N) mice by treatment of dorsal back skin with dimethyl benzanthracene (DMBA) and tetradecanoyl-phorbol acetate (TPA). This treatment induced multiple benign papillomas as well as malignant squamous cell carcinomas (SCC) and spindle cell carcinomas. Gene expression analysis was performed on mRNA extracted from 68 papillomas: two papillomas from each of 31 FVBBX mice and a single papilloma from six additional FVBBX mice. Papillomas were harvested when mice were sacrificed due to presence of a carcinoma or termination of the experiment.

Background corr dist: KL-Divergence = 0.4519, L1-Distance = 0.0925, L2-Distance = 0.0279, Normal std = 0.2347

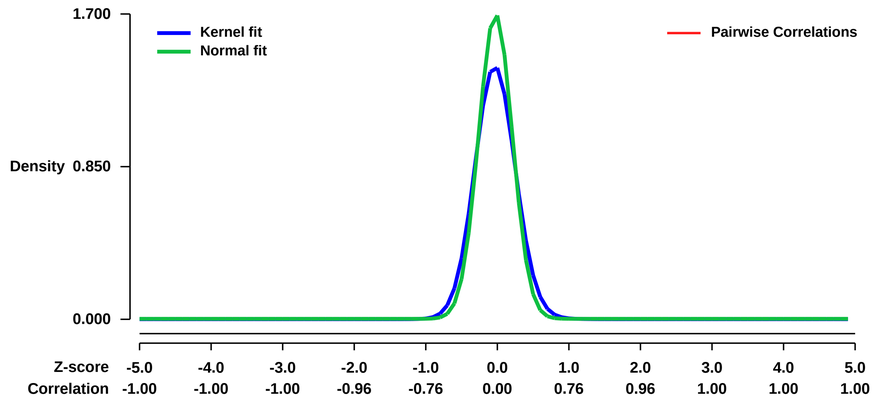

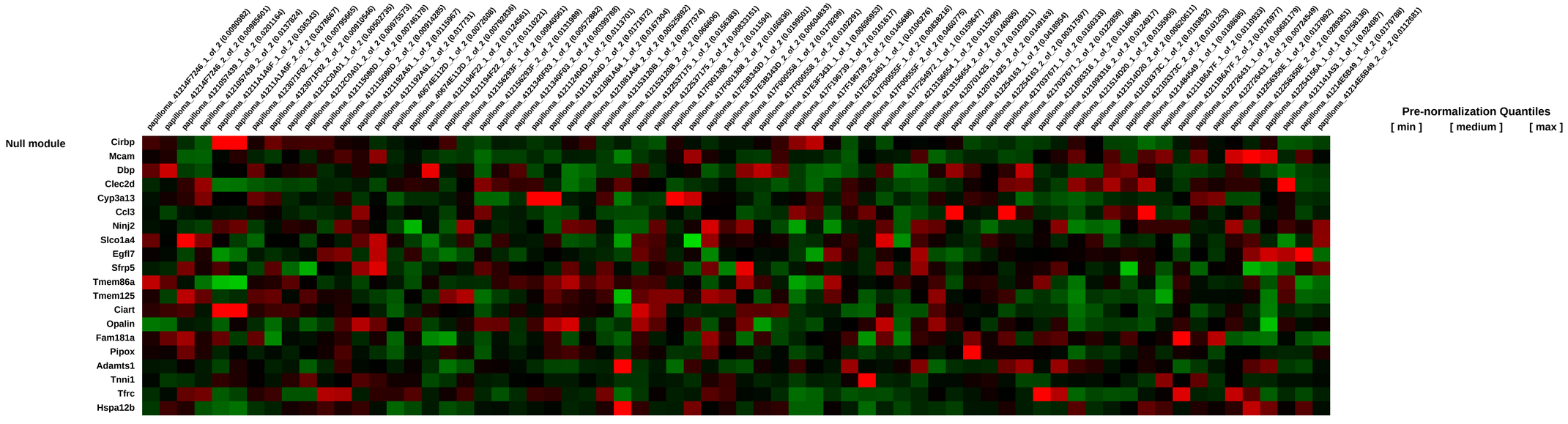

GEO Series "GSE21272" Expression Profiles

Num of samples in this series: 44

Scale of expression profile Z-scores

-3.0 -2.0 -1.0 0.0 1.0 2.0 3.0

GEO Link:	http://www.ncbi.nlm.nih.gov/geo/query/acc.cgi?acc=GSE21272
Status:	Public on Oct 21 2010
Title:	Time Course Gene Expression Microarray Analysis of a Mouse B-cell Line (CH12.LX) Activated with Lipopolysaccharide and Treated with 2,3,7,8-Tetrachlorodibenzo-p-dioxin
Organism:	Mus musculus
Experiment type:	Expression profiling by array
Platform:	GPL1261
Pubmed ID:	20819909
Summary & Design:	**Summary:** The objective of the study was to characterize gene expression cascade involved in the suppression of B-cell activation and differentiation by 2,3,7,8-tetrachlorodibenzo-p-dixoxin (TCDD). The underlying hypothesis was that multiple nodes in the B-cell differentiation network are directly or indirectly regulated by TCDD through its receptor, the AHR. **Overall design:** The mouse B-cell line (CH12.LX) was plated at 1X10^5 cells/ml at time 0 and activated with lipopolysaccharide (LPS, Salmonella typhosa). The cells were then treated with either dimethyl sulfoxide (DMSO, 0.01%) or 10 nM 2,3,7,8-tetrachlorodibenzo-p-dixoxin (TCDD). The cells were harvested at 0, 8, 12, 24, 36, and 48 hrs post-treatment. At the 0 hr time point, cells were untreated. A total of 4 experimental replicates per time point per treatment group were included with the cells for each replicate treated and harvested on separate days. Single color Affymetrix Mouse 430 2.0 arrays were used.

Background corr dist: KL-Divergence = 0.2971, L1-Distance = 0.0472, L2-Distance = 0.0048, Normal std = 0.2838

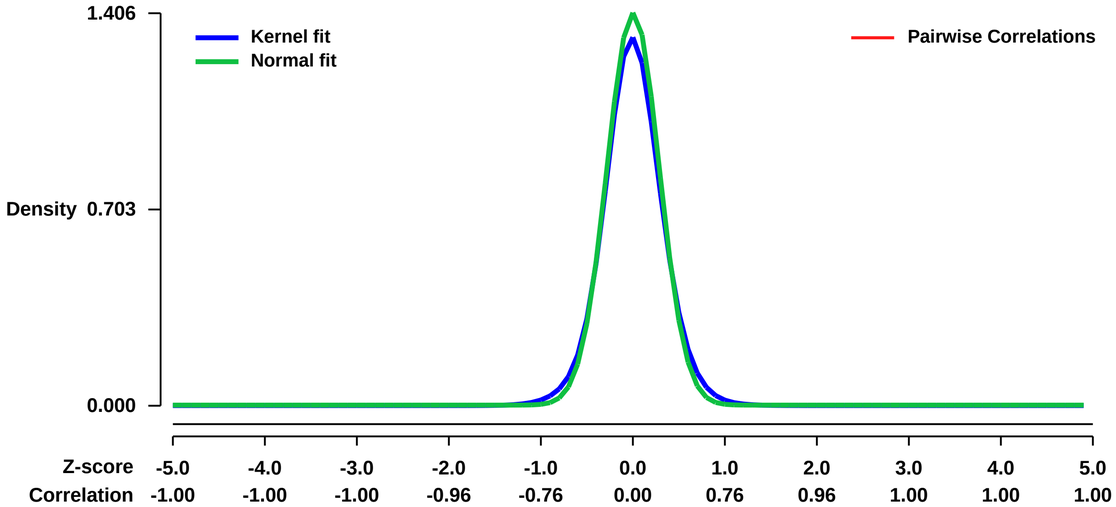

Z-score	-5.0	-4.0	-3.0	-2.0	-1.0	0.0	1.0	2.0	3.0	4.0	5.0
Correlation	-1.00	-1.00	-1.00	-0.96	-0.76	0.00	0.76	0.96	1.00	1.00	1.00

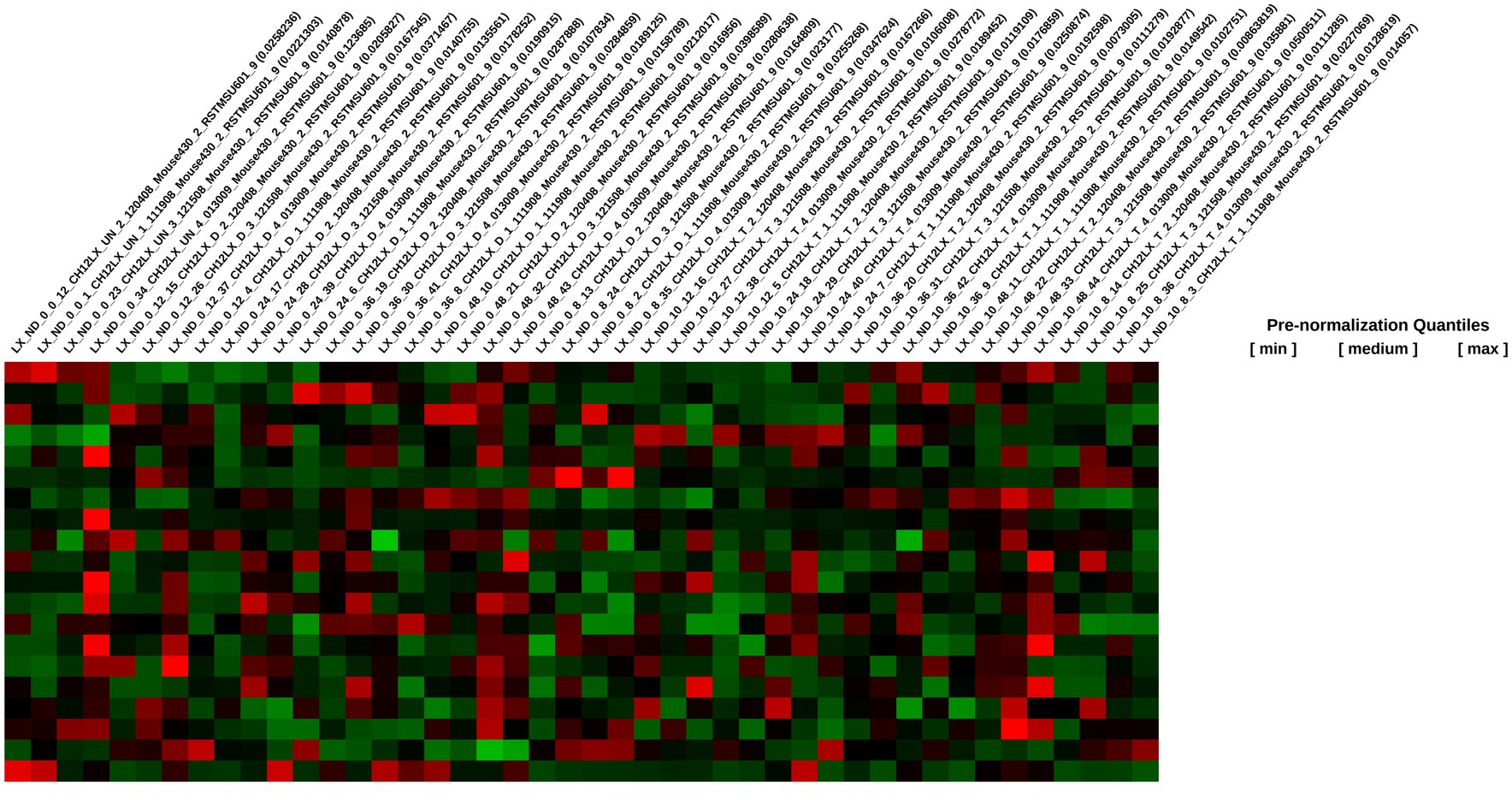

GEO Series "GSE21299" Expression Profiles

Num of samples in this series: 12

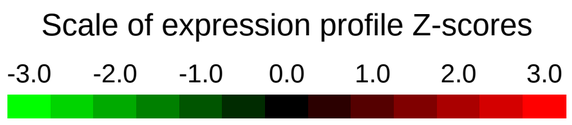

GEO Link:	http://www.ncbi.nlm.nih.gov/geo/query/acc.cgi?acc=GSE21299
Status:	Public on Feb 01 2011
Title:	Expression data from murine cell line transduced with epitope tagged forms of Hoxa9
Organism:	Mus musculus
Experiment type:	Expression profiling by array
Platform:	GPL1261
Pubmed ID:	20541477
Summary & Design:	**Summary:** **Importantly increasing evidence shows that Hox genes such as Hoxa9 are key regulators of stem cell self-renewal and hematopoiesis. Hoxa9 is expressed in early hematopoietic progenitor cells and promotes stem cell expansion. In contrast Hoxa9 down regulation is associated with hematopoietic differentiation. In addition to its role in development, HOXA9 has been intensively studied because of its central role in human acute leukemias. Despite their obvious biomedical importance, the mechanisms through which Hoxa9 and its partner proteins exert their downstream functions are poorly understood.** **Using whole-genome gene expression profiling, we identified direct targets of Hoxa9 in murine MHPs after 4-OHT withdraw, resulting in cell differentiation.** **Overall design:** **Bone marrow cells were harvested from 5-Fluorouracil treated female 6-8 week old C57BL/6 mice and transduced with an MSCV-based retrovirus expressing Hoxa9 fused to a modified estrogen receptor ligand binding domain (Hoxa9-ER). Hoxa9-ER cells were washed 3x and resuspended in IL-3+ media with/without 100 nM 4-OHT (Sigma). At selected intervals, cells were removed for flow cytometric analysis using anti-Gr1 and anti-Mac1 antibodies (BD biosciences), morphologic assessment by cytocentrifugation and staining with Diff-Quick reagents (Intl. Med. Equip.), and RNA collection. For RNA, Pellets were lysed in Trizol reagent (Invitrogen) and RNA was extracted following manufacturer's instructions until phase separation, after which RNeasy columns (Qiagen) were employed for further purification. cRNA probes were synthesized at the University of Michigan microarray core. Probes were hybridized to Affymetrix Mouse 430 2.0 array.**

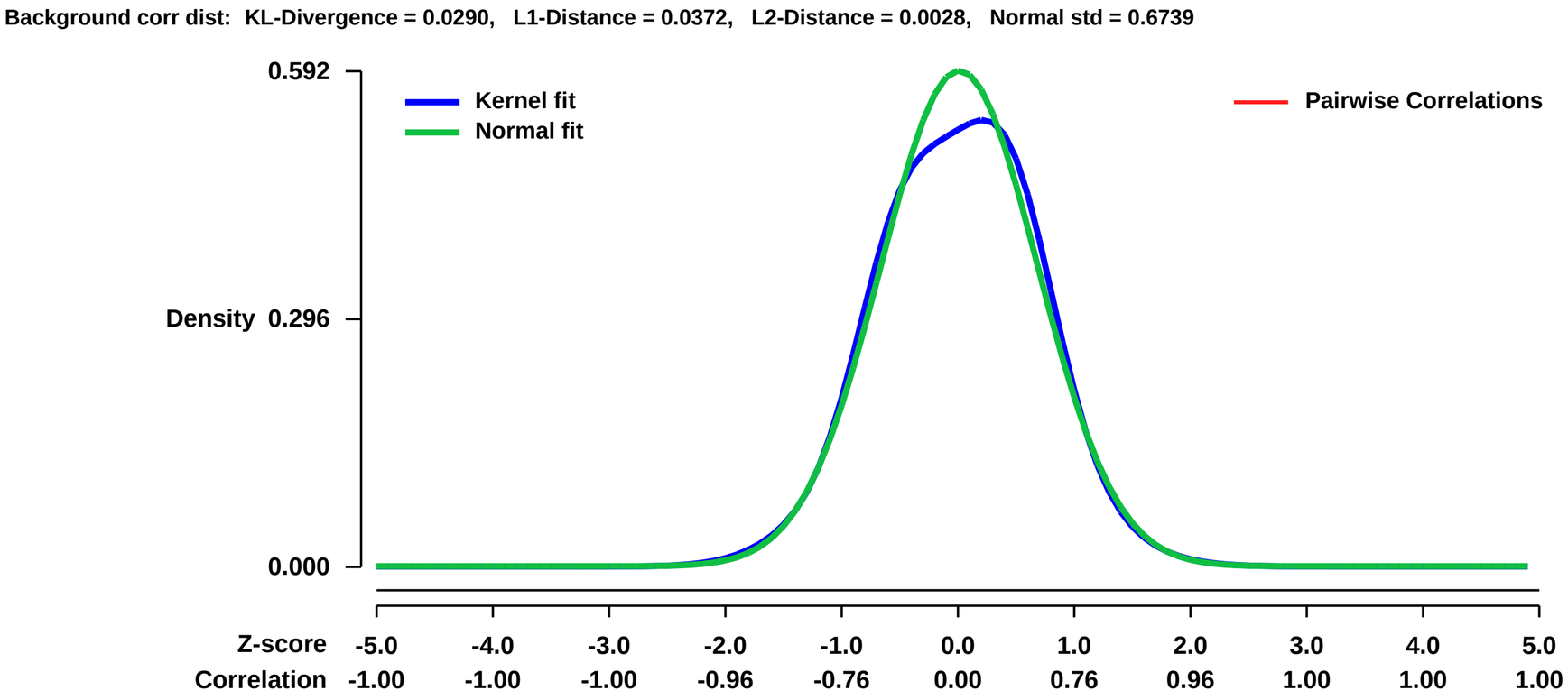

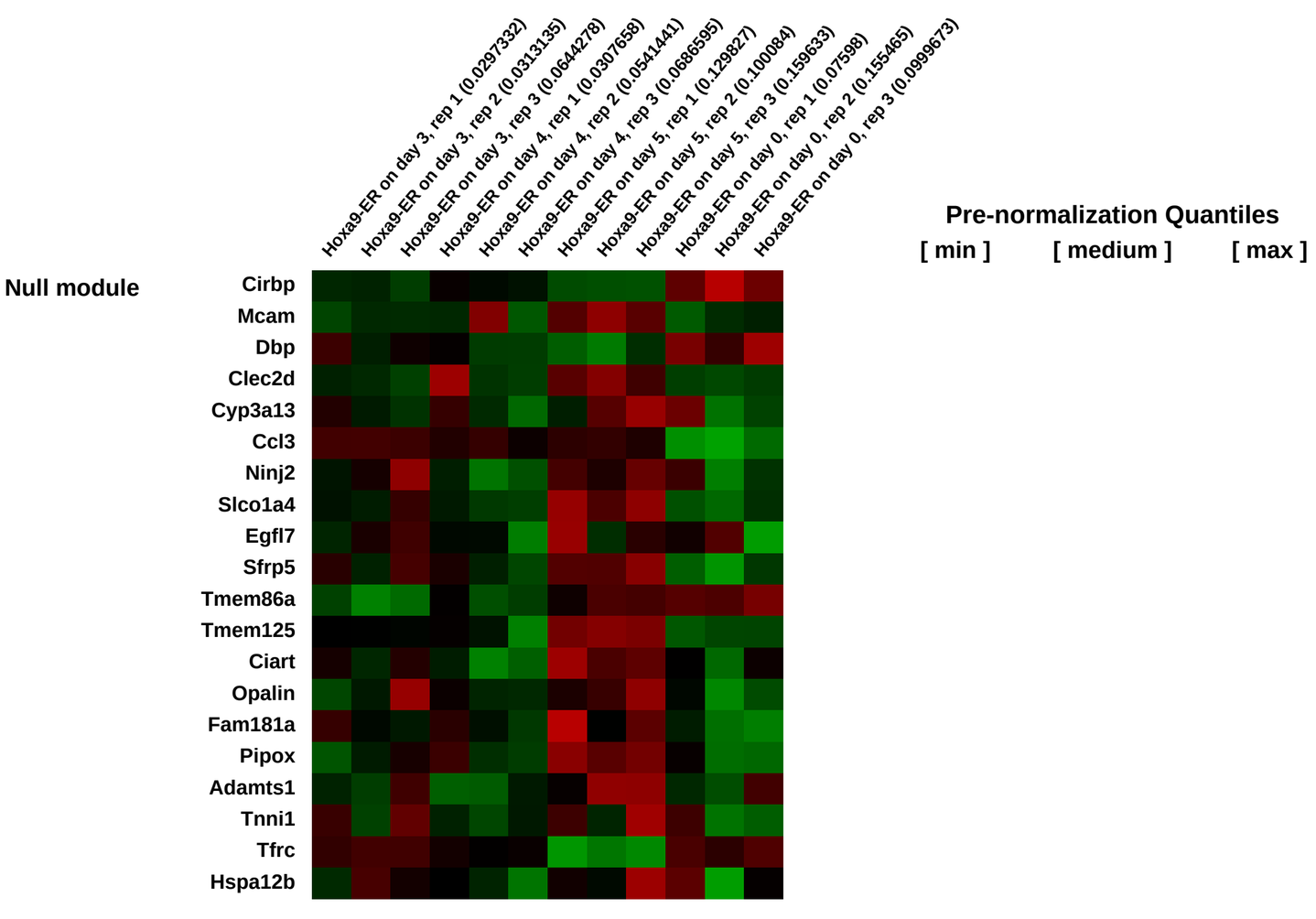

GEO Series "GSE21379" Expression Profiles

Num of samples in this series: 10

Scale of expression profile Z-scores

-3.0 -2.0 -1.0 0.0 1.0 2.0 3.0

GEO Link:	http://www.ncbi.nlm.nih.gov/geo/query/acc.cgi?acc=GSE21379
Status:	Public on Apr 20 2010
Title:	Expression Data from WT and Sh2d1a-/- in vivo follicular helper CD4 T cells (TFH) versus non follicular helper CD4 T cells (non-TFH)
Organism:	Mus musculus
Experiment type:	Expression profiling by array
Platform:	GPL1261
Pubmed ID:	20525889
Summary & Design:	**Summary:** CD4 T cell help is critical for both the generation and maintenance of germinal centers, and T follicular helper (TFH) cells are the CD4 T cell subset required for this process. SAP (SH2D1A) expression in CD4 T cells is essential for germinal center development. However, SAP-deficient mice have only a moderate defect in TFH differentiation as defined by common TFH surface markers. CXCR5+ TFH cells are found within the germinal center as well as along the boundary regions of T/B cell zones. Here we show that germinal center associated T cells (GC TFH) can be identified by their co-expression of CXCR5 and the GL7 epitope, allowing for phenotypic and functional analysis of TFH and GC TFH populations. Here we show GC TFH are a functionally discrete subset of further polarized TFH cells, with enhanced B cell help capacity and a specialized ability to produce IL-4 in a TH2-independent manner. Strikingly, SAP-deficient mice have an absence of the GC TFH subset and SAP- TFH are defective in IL-4 and IL-21 production. We further demonstrate that SLAM (Slamf1, CD150), a surface receptor that utilizes SAP signaling, is specifically required for IL-4 production by GC TFH. GC TFH cells require IL-4 and IL-21 production for optimal help to B cells. These data illustrate complexities of SAP-dependent SLAM family receptor signaling, revealing a prominent role for SLAM receptor ligation in IL-4 production by germinal center CD4 T cells but not in TFH and GC TFH differentiation. **Overall design:** Analysis of in vivo antigen-specific (LCMV-specific, SMARTA TCR transgenic) WT and Sh2d1a-/- follicular helper CD4 T cells (CXCR5high),versus non-follicular helper CD4 T cells (CXCR5low), eight days after viral infection.

Background corr dist: KL-Divergence = 0.0691, L1-Distance = 0.0416, L2-Distance = 0.0025, Normal std = 0.5262

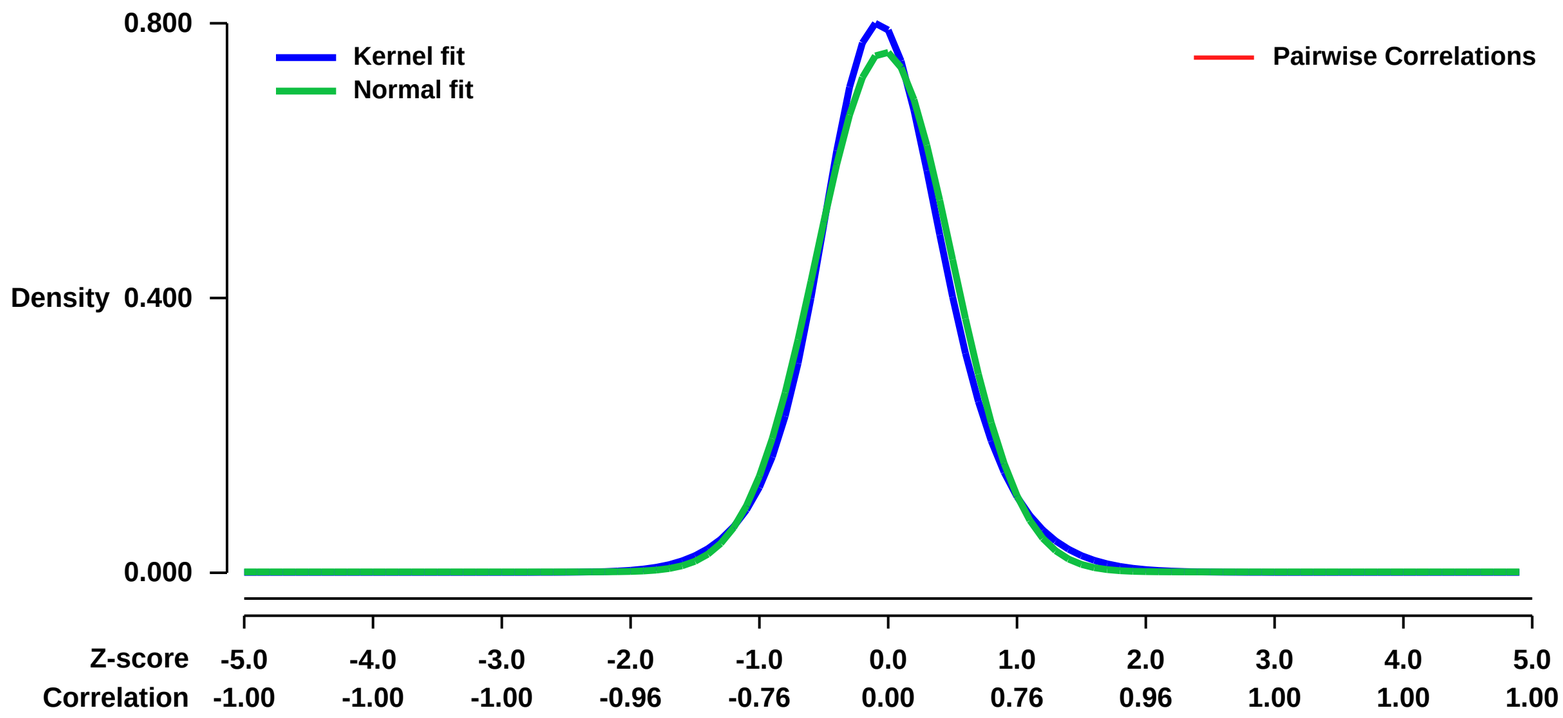

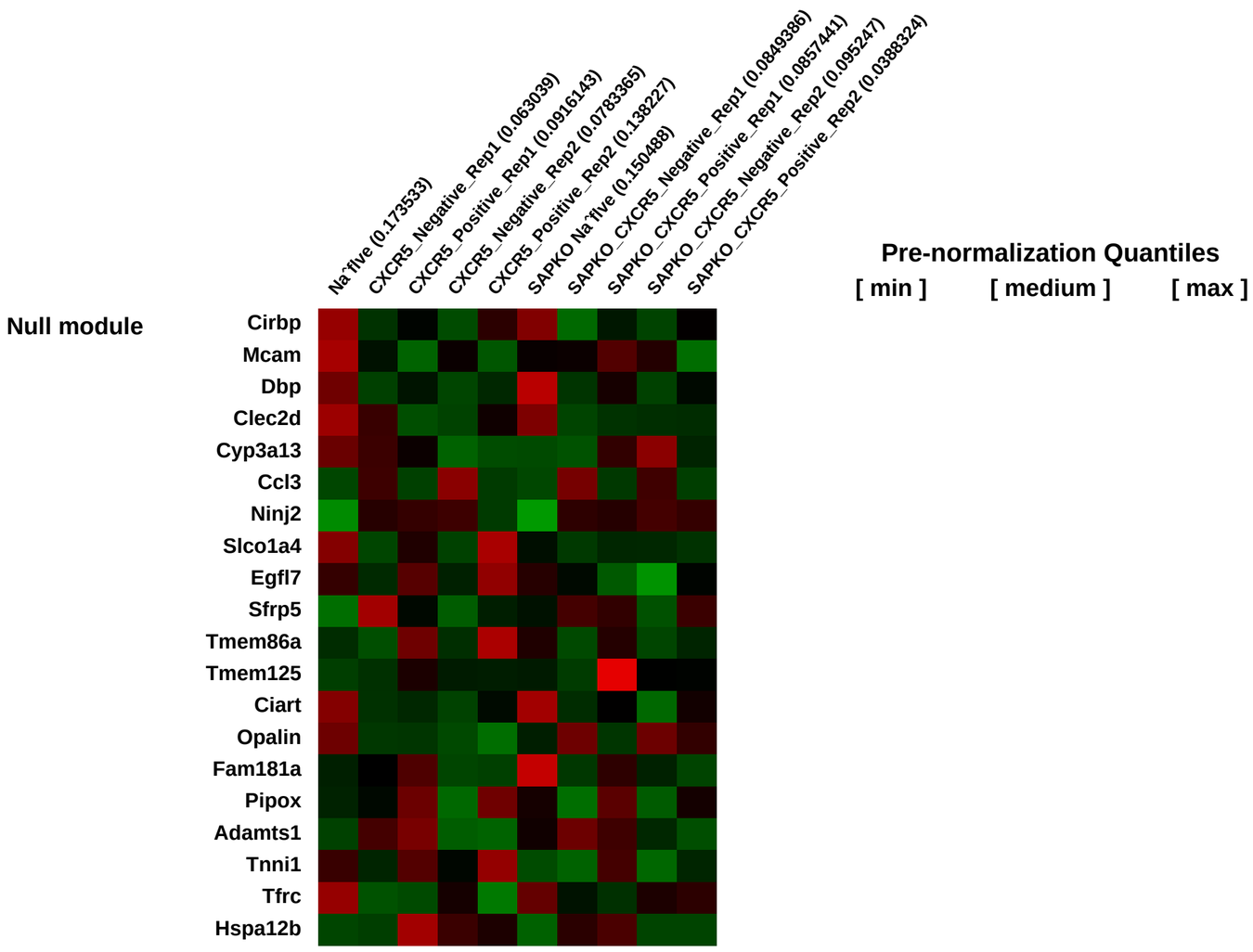

GEO Series "GSE21380" Expression Profiles

Num of samples in this series: 7

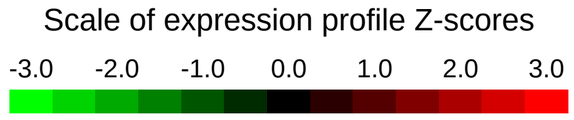

GEO Link:	http://www.ncbi.nlm.nih.gov/geo/query/acc.cgi?acc=GSE21380
Status:	Public on Apr 20 2010
Title:	Expression Data from in vivo Tfh vs GC Tfh vs non-Tfh
Organism:	Mus musculus
Experiment type:	Expression profiling by array
Platform:	GPL1261
Pubmed ID:	20525889
Summary & Design:	**Summary:** CD4 T cell help is critical for both the generation and maintenance of germinal centers, and T follicular helper (TFH) cells are the CD4 T cell subset required for this process. SAP (SH2D1A) expression in CD4 T cells is essential for germinal center development. However, SAP-deficient mice have only a moderate defect in TFH differentiation as defined by common TFH surface markers. CXCR5+ TFH cells are found within the germinal center as well as along the boundary regions of T/B cell zones. Here we show that germinal center associated T cells (GC TFH) can be identified by their co-expression of CXCR5 and the GL7 epitope, allowing for phenotypic and functional analysis of TFH and GC TFH populations. Here we show GC TFH are a functionally discrete subset of further polarized TFH cells, with enhanced B cell help capacity and a specialized ability to produce IL-4 in a TH2-independent manner. Strikingly, SAP-deficient mice have an absence of the GC TFH subset and SAP- TFH are defective in IL-4 and IL-21 production. We further demonstrate that SLAM (Slamf1, CD150), a surface receptor that utilizes SAP signaling, is specifically required for IL-4 production by GC TFH. GC TFH cells require IL-4 and IL-21 production for optimal help to B cells. These data illustrate complexities of SAP-dependent SLAM family receptor signaling, revealing a prominent role for SLAM receptor ligation in IL-4 production by germinal center CD4 T cells but not in TFH and GC TFH differentiation. **Overall design:** Analysis of in vivo follicular helper CD4 T cells (CXCR5high GL7low), versus germinal center follicular helper CD4 T cells (CXCR5hi GL7hi), versus non-follicular helper CD4 T cells (CXCR5low) eight days after viral infection.

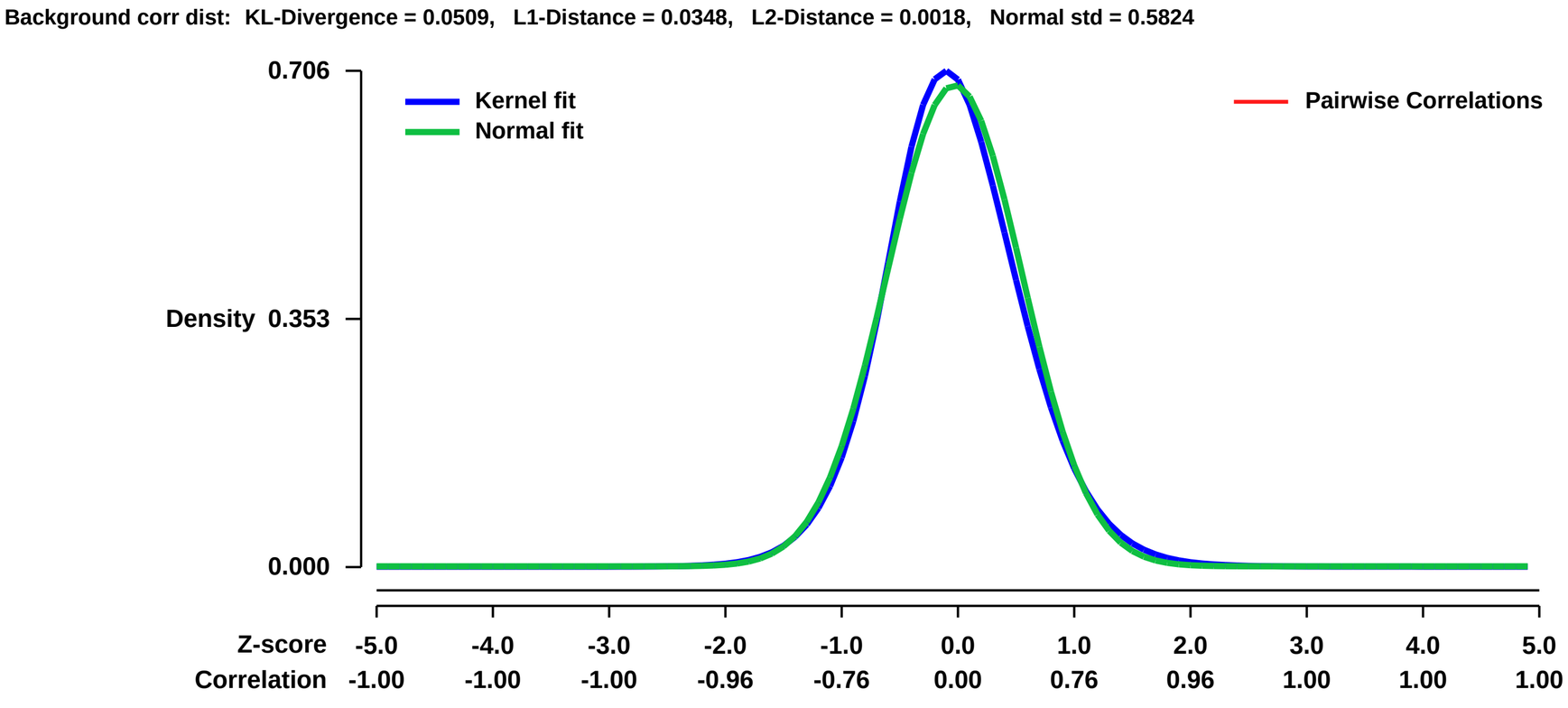

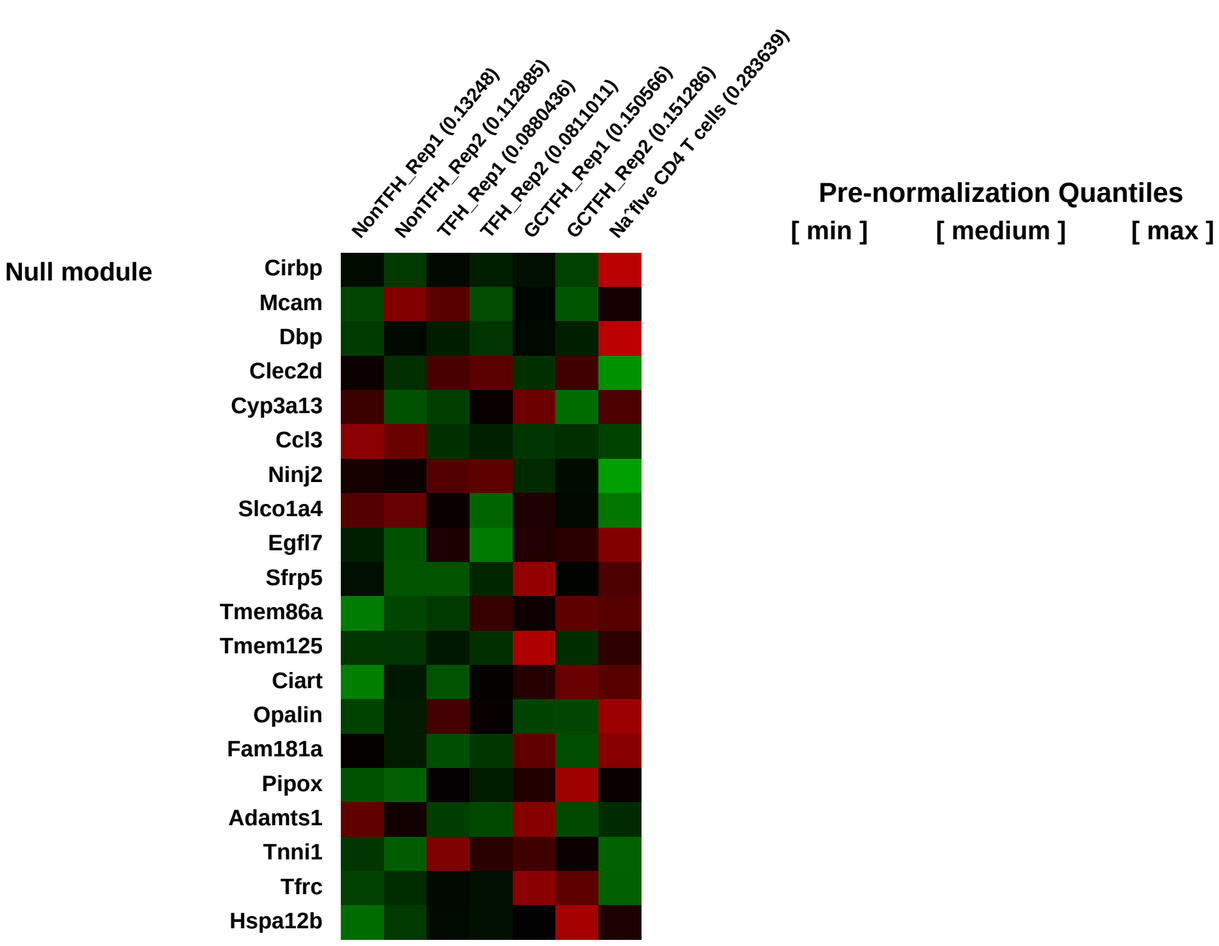

GEO Series "GSE21515" Expression Profiles

Num of samples in this series: 18

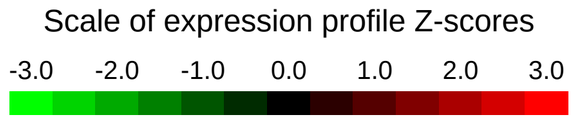

GEO Link:	http://www.ncbi.nlm.nih.gov/geo/query/acc.cgi?acc=GSE21515
Status:	Public on May 13 2010
Title:	Expression data from mouse ES and iPS cells
Organism:	Mus musculus
Experiment type:	Expression profiling by array
Platform:	GPL1261
Pubmed ID:	20382743
Summary & Design:	**Summary:** Induced pluripotent stem (iPS) cells were produced from reprogramming of somatic cells, and they are shown to possess pluripotent properties similar to embryonic stem (ES) cells. Here we used microarrays to detail the global expression pattern among the ES cells and iPS cells, as well as the original mouse embryo fibroblast (MEF), to identify important players involved in the reprogramming process. **Overall design:** Mouse ES cell cultures, as well as selected iPS cell lines and the original MEF cells they were derived from, were used for RNA extraction and hybridization on Affymetrix microarrays. Three biological replicates for each sample were processed. GeneChips were processed and data were analyzed using the RMA package of Bioconductor.

Background corr dist: KL-Divergence = 0.0662, L1-Distance = 0.0310, L2-Distance = 0.0018, Normal std = 0.5048

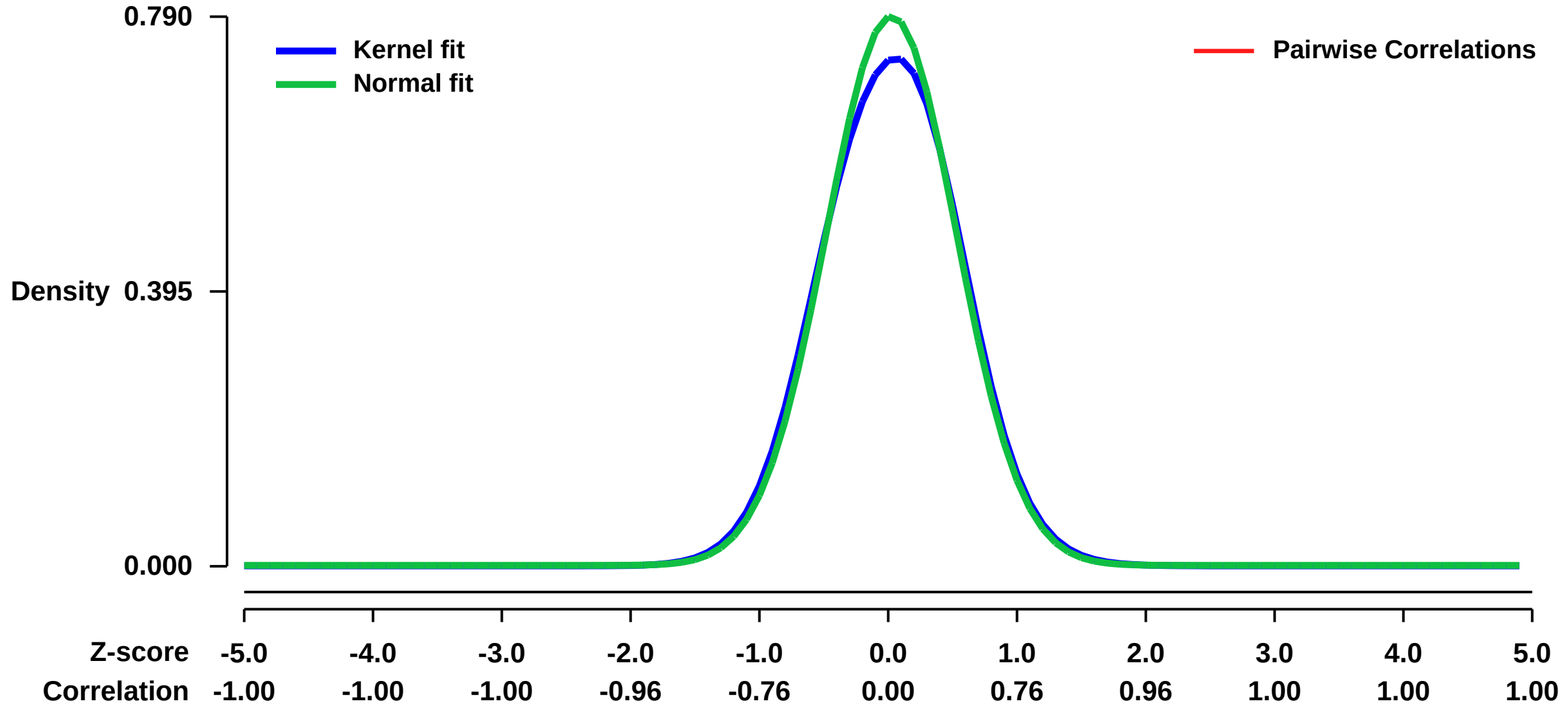

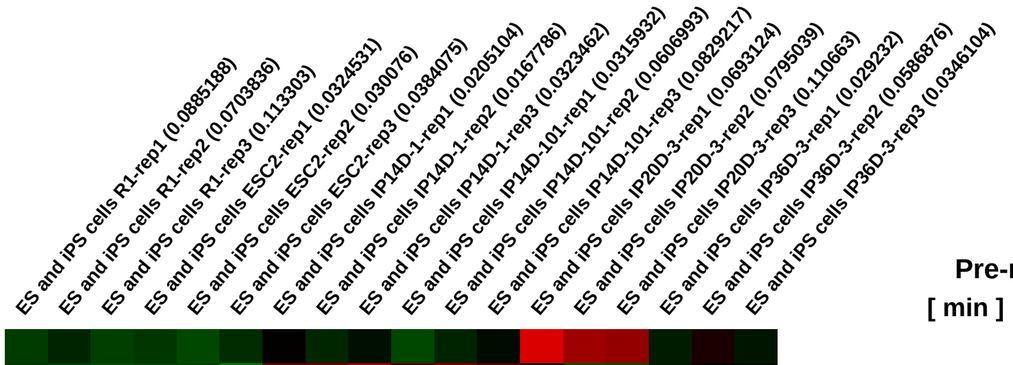

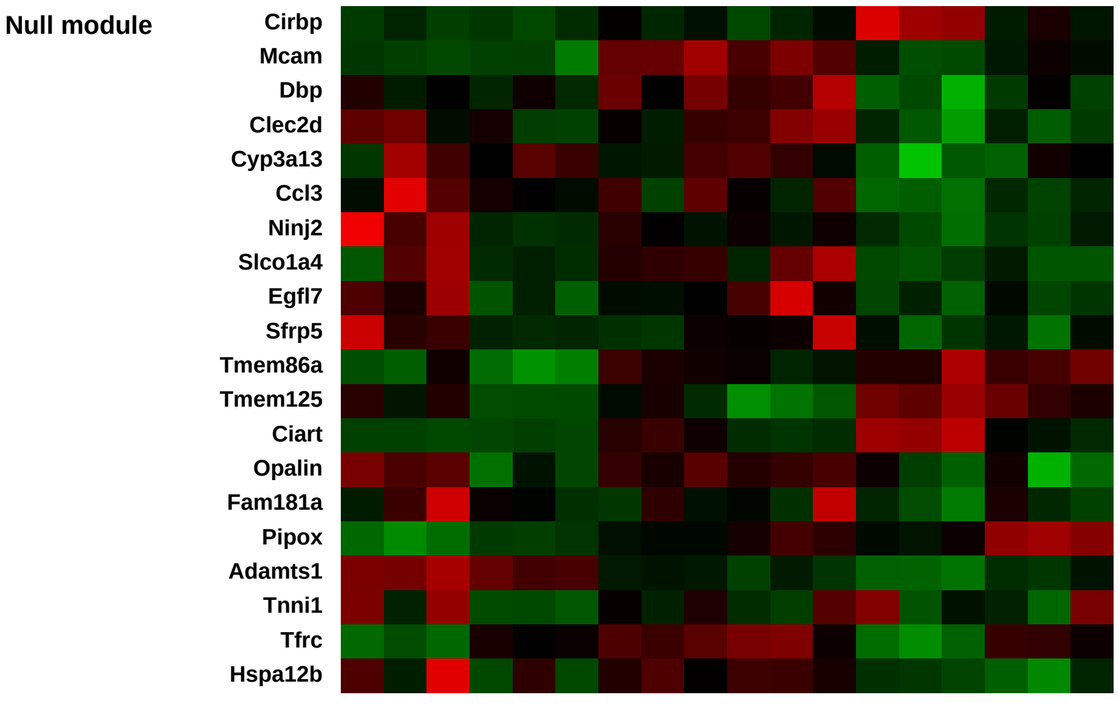

GEO Series "GSE21525" Expression Profiles

Num of samples in this series: 12

Scale of expression profile Z-scores

-3.0 -2.0 -1.0 0.0 1.0 2.0 3.0

GEO Link:	http://www.ncbi.nlm.nih.gov/geo/query/acc.cgi?acc=GSE21525
Status:	Public on Apr 27 2010
Title:	Expression data from testis of day-7 Sohlh1 knock-out mice
Organism:	Mus musculus
Experiment type:	Expression profiling by array
Platform:	GPL1261
Pubmed ID:	16564520
Summary & Design:	**Summary:** Sohlh1 and Sohlh2 encode a germ cell-specific basic helix-loop-helix transcriptional regulator critical in spermatogonial differentiation. Seven-day-old Sohlh1 or Sohlh2 knockout and wild-type testes were arrayed on the Affy 430 2.0 platform. **Overall design:** The following mice were analyzed at postnatal day 7: wild-type, Sohlh1-/-, and Sphlh2-/-. 4 samples/group.

Background corr dist: KL-Divergence = 0.1447, L1-Distance = 0.0339, L2-Distance = 0.0021, Normal std = 0.3785

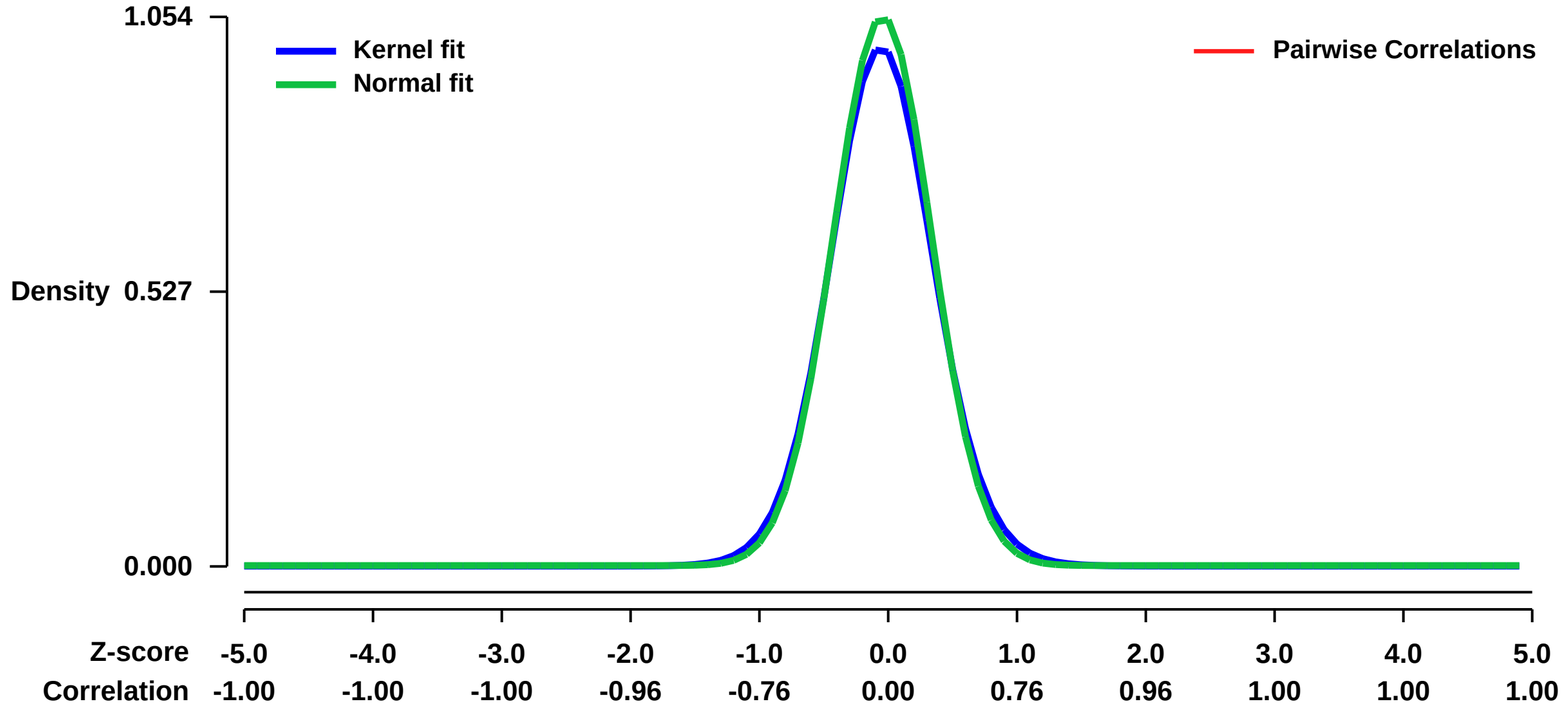

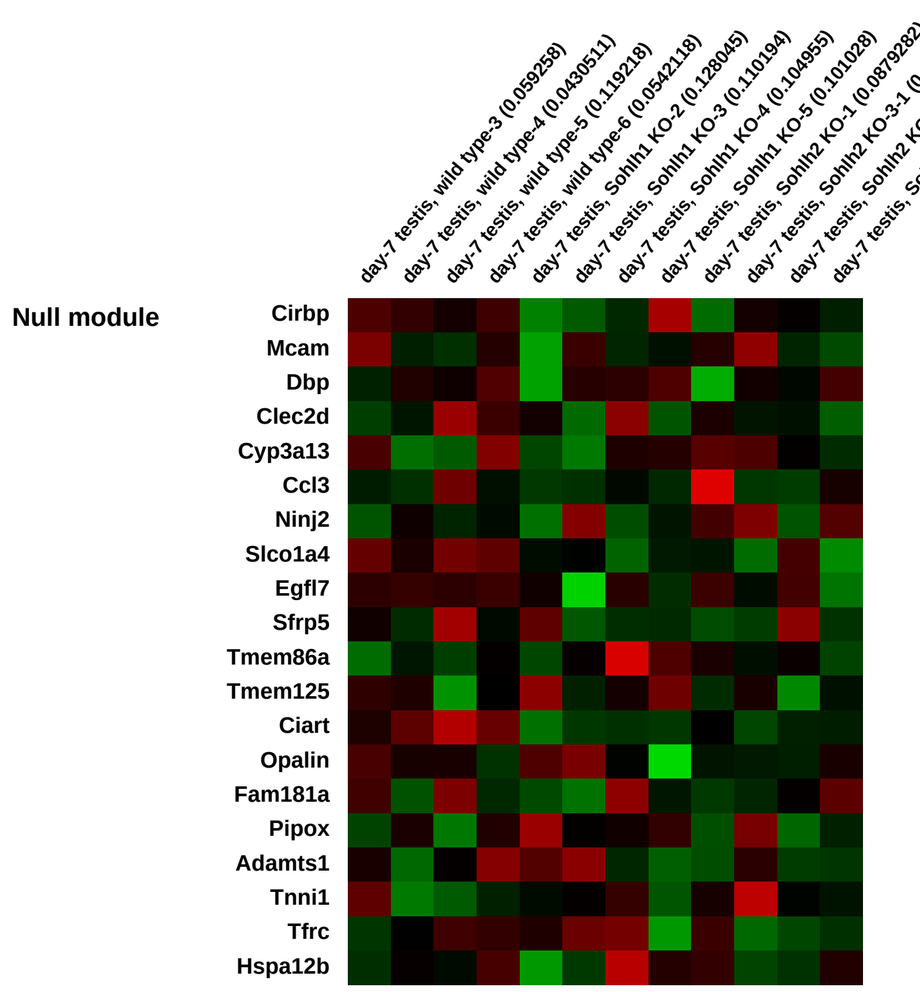

Pre-normalization Quantiles

[min] [medium] [max]

GEO Series "GSE21549" Expression Profiles

Num of samples in this series: 6

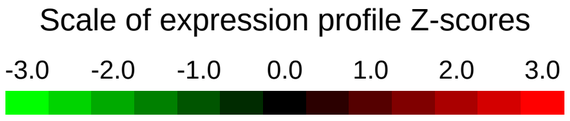

GEO Link:	http://www.ncbi.nlm.nih.gov/geo/query/acc.cgi?acc=GSE21549
Status:	Public on Sep 01 2010
Title:	Expression profiles of EDTA-dissociated colon epithelial cells of wild-type mice and vil-Cre-Bcl9-/-/Bcl9l-/- mice.
Organism:	Mus musculus
Experiment type:	Expression profiling by array
Platform:	GPL1261
Pubmed ID:	20682801
Summary & Design:	**Summary:** To assess potential changes in Wnt signaling more comprehensively, EDTA-dissociated colon epithelial cells from three pools of wild-type and Bcl9/Bcl9l-mutant mice were subjected to an exploratory comparative gene expression profiling. **Overall design:** Total RNA of three samples of EDTA-dissociated colon epithelial cells of wild-type mice and three samples of vil-Cre-Bcl9-/-/Bcl9l-/- mice, each sample consisting of material of two or three different mice, was collected and resulting amplified cDNA hybridized to Affymetrix Mouse Genome 430 2.0 arrays. Samples are labeled as follows: Genotype_PoolID _UniqueID_NumberOfMice.

Background corr dist: KL-Divergence = 0.0455, L1-Distance = 0.0200, L2-Distance = 0.0005, Normal std = 0.5924

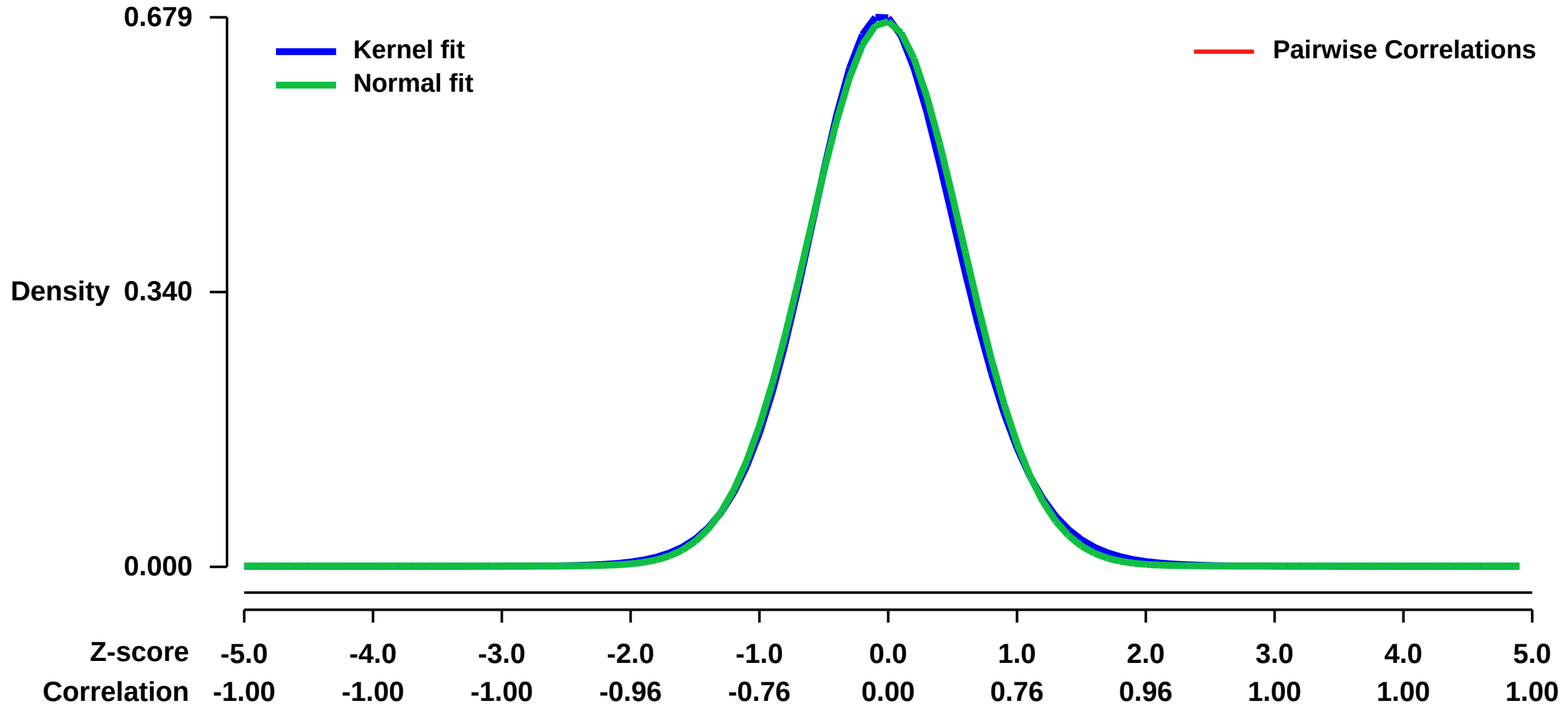

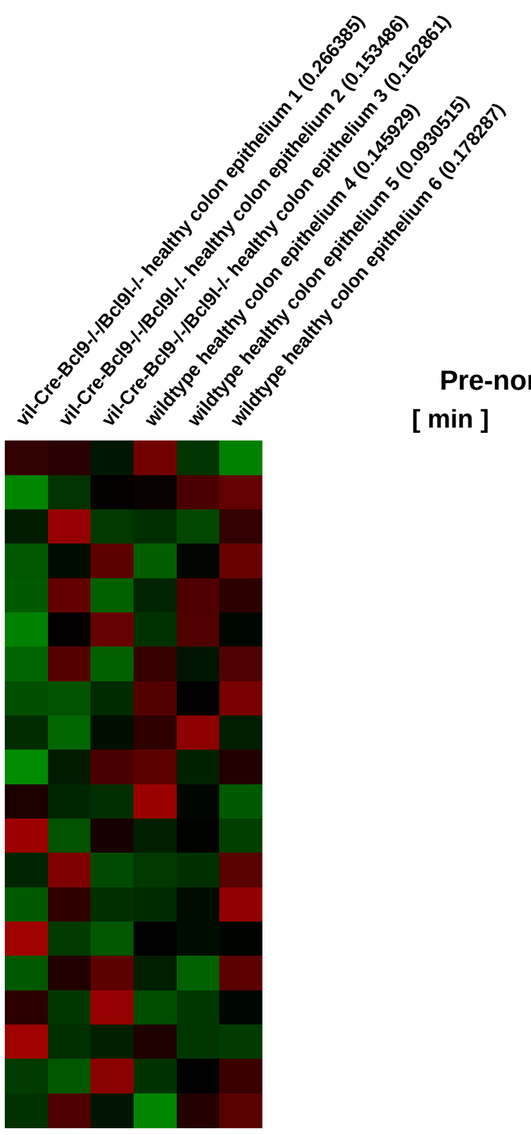

GEO Series "GSE21568" Expression Profiles

Num of samples in this series: 12

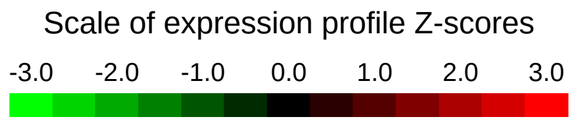

GEO Link:	http://www.ncbi.nlm.nih.gov/geo/query/acc.cgi?acc=GSE21568
Status:	Public on Jan 12 2011
Title:	Mouse bulge (CD34+CD200+CD49+) versus secondary hair germ (CD34-CD200+CD49+) versus interfollicular epidermis (CD34-CD200-CD49+)
Organism:	Mus musculus
Experiment type:	Expression profiling by array
Platform:	GPL1261
Pubmed ID:	21206086
Summary & Design:	**Summary:** Mouse back skin was disassociated to single cells, sorted by cell surface markers and tested by microarrray To compare the gene expression of mouse bulge (CD34+CD200+CD49+) versus secondary hair germ (CD34-CD200+CD49+) versus interfollicular epidermis (CD34-CD200-CD49+) xx Bald scalp retains hair follicle stem cells but lacks CD200-rich and CD34-positive hair follicle progenitor cells Androgenetic alopecia (AGA) or common baldness results from a marked decrease in hair follicle size. This miniaturization may be related to loss of hair follicle stem or progenitor cells. To test this hypothesis, we analyzed bald and non-bald scalp from the same individuals for the presence of hair follicle stem and progenitor cells using flow cytometry to quantitate cells expressing CYTOKERATIN 15 (KRT15), CD200, CD34 and ALPHA-6-INTEGRIN (ITGA6). High levels of KRT15 expression correlated with stem cell properties of small cell size and quiescence. Cells with the highest level of KRT15 expression were maintained in bald scalp; however, distinct populations of CD200high ITGA6high cells and CD34-positive cells were markedly diminished. Consistent with a progenitor cell phenotype, the diminished populations localized closely to the stem-cell rich bulge area but were larger and more proliferative than the bulge stem cells. In functional assays, analogous CD200 high /Itga6 high cells from murine hair follicles were multipotent and generated new hair follicles in skin reconstitution assays. These findings suggest that a defect in stem cell activation plays a role in the pathogenesis of AGA. **Overall design:** 4 independent biologic replicates (each pooled from 3 distinct mice) were sorted for Mouse bulge (CD34+CD200+CD49+) versus secondary hair germ (CD34-CD200+CD49+) versus interfollicular epidermis (CD34-CD200-CD49+)

Background corr dist: KL-Divergence = 0.0683, L1-Distance = 0.0257, L2-Distance = 0.0012, Normal std = 0.5061

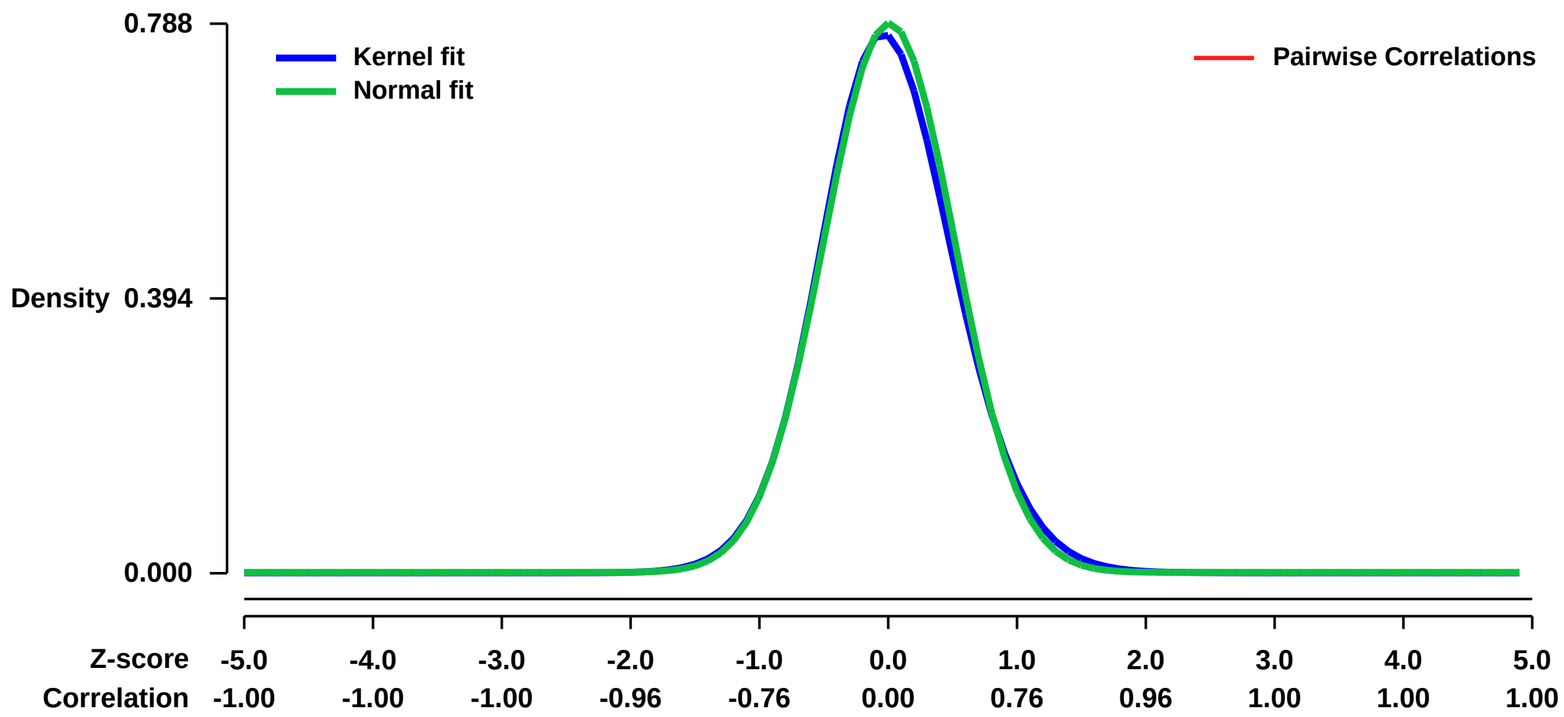

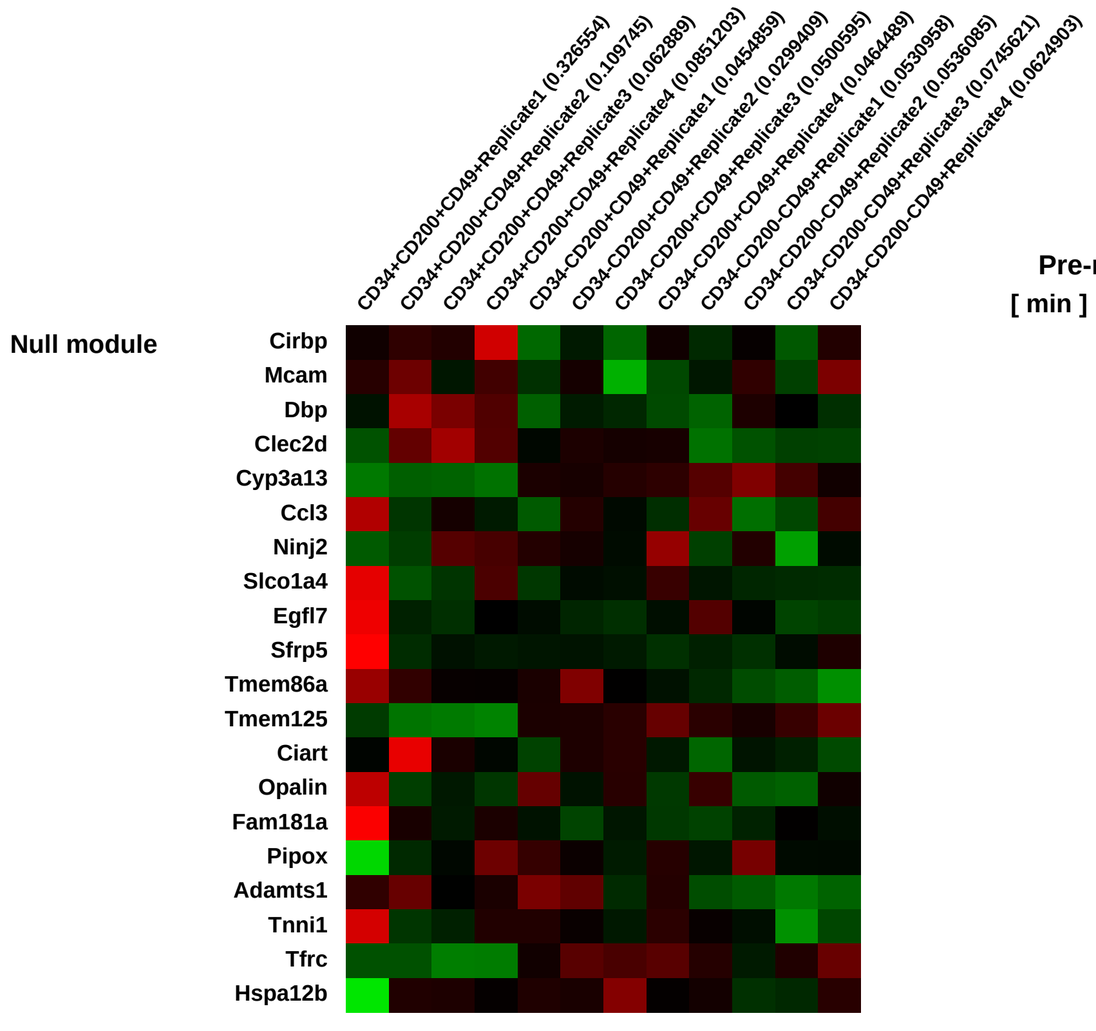

GEO Series "GSE21576" Expression Profiles

Num of samples in this series: 10

Scale of expression profile Z-scores

-3.0 -2.0 -1.0 0.0 1.0 2.0 3.0

GEO Link:	http://www.ncbi.nlm.nih.gov/geo/query/acc.cgi?acc=GSE21576
Status:	Public on Sep 01 2010
Title:	Expression profiles of laser dissected colon tumor samples of wild-type mice and vil-Cre-Bcl9-/-/Bcl9l-/- mice
Organism:	Mus musculus
Experiment type:	Expression profiling by array
Platform:	GPL1261
Pubmed ID:	20682801
Summary & Design:	**Summary:** To investigate the impact of ablating Bcl9/Bcl9l on tumorigenesis, 6-8- week-old mice were exposed first to a single dose dimethylhydrazine (DMH, 44 mg/kg body weight), which is metabolized in the liver to carcinogenic azoxymethane (AOM), followed by 7 days oral administration of 2 % dextrane sulfate sodium (DSS) in the drinking water. This regimen results in the emergence of dysplastic adenomas, which progress to differentiated adenocarcinomas that are morphologically similar to human colorectal adenocarcinomas and typically harbor ¸†-catenin stabilizing mutations of GSK3ˆ phosphorylation sites. Accordingly, these tumors present hallmarks of active Wnt signaling such as accumulation of nuclear ¸†-catenin and expression of Wnt target genes. **Overall design:** Total RNA of laser dissected samples from five different tumors each of two wild-type mice and three vil-Cre-Bcl9-/-/Bcl9l-/- mice was collected and resulting amplified cDNA hybridized to Affymetrix Mouse Genome 430 2.0 arrays. Samples are labeled as follows: Genotype_TumorID_MouseID_UniqueID.

Background corr dist: KL-Divergence = 0.1042, L1-Distance = 0.0294, L2-Distance = 0.0015, Normal std = 0.4299

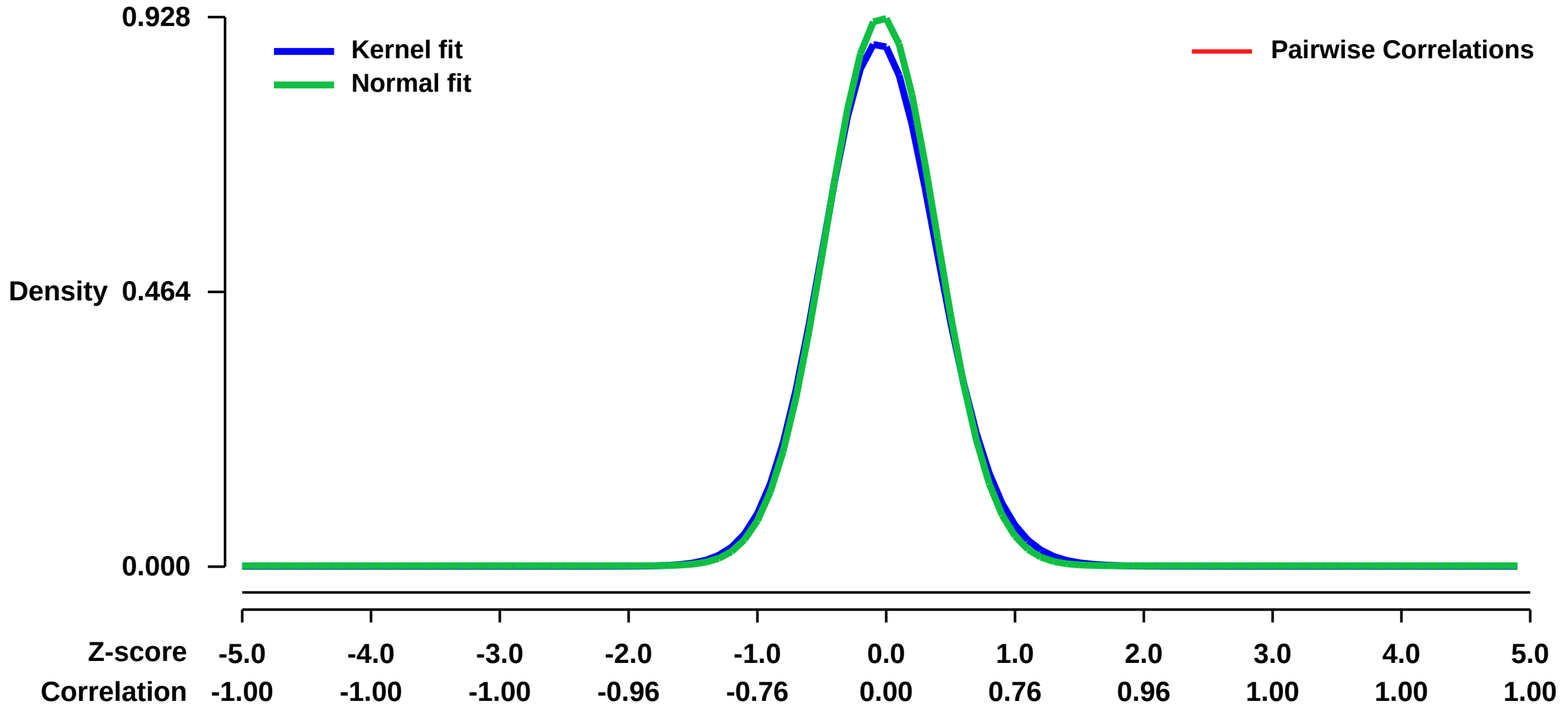

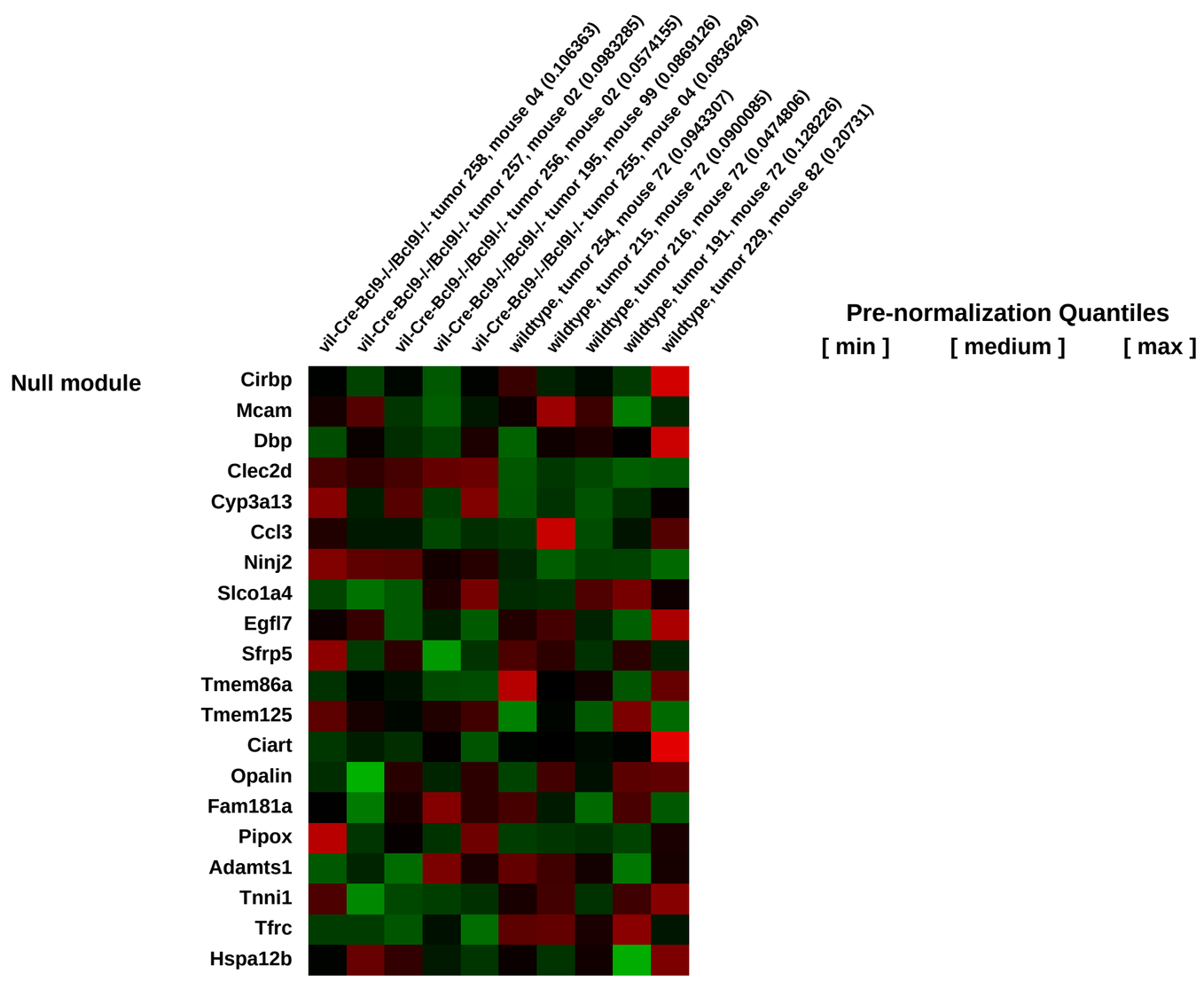

GEO Series "GSE21583" Expression Profiles

Num of samples in this series: 8

Scale of expression profile Z-scores

-3.0 -2.0 -1.0 0.0 1.0 2.0 3.0

GEO Link:	http://www.ncbi.nlm.nih.gov/geo/query/acc.cgi?acc=GSE21583
Status:	Public on Aug 25 2010
Title:	Effects of ACE2 on BMPR2 mutation-mediated defects in gene expression
Organism:	Mus musculus
Experiment type:	Expression profiling by array
Platform:	GPL1261
Pubmed ID:	22180660
Summary & Design:	**Summary:** BMPR2 mutation causes pulmonary arterial hypertension (PAH); ACE2 treatment can resolve established BMPR2-mediated PAH. The purpose of this study was to uncover the molecular mechanism behind this. **Overall design:** Four groups: +/- ACE2 and +/- BMPR2 transgene, two arrays each, each array a pool of three animals.

Background corr dist: KL-Divergence = 0.0925, L1-Distance = 0.0232, L2-Distance = 0.0007, Normal std = 0.4506

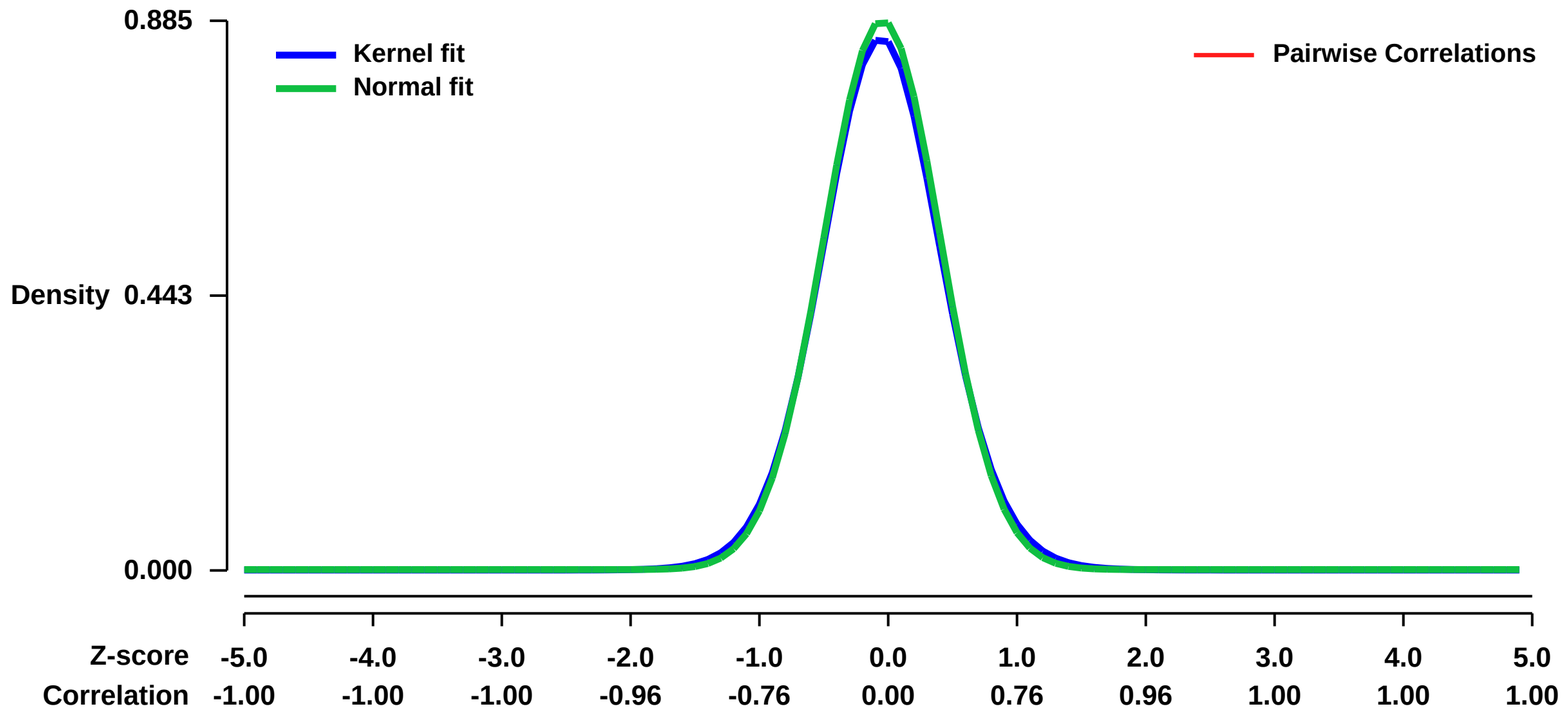

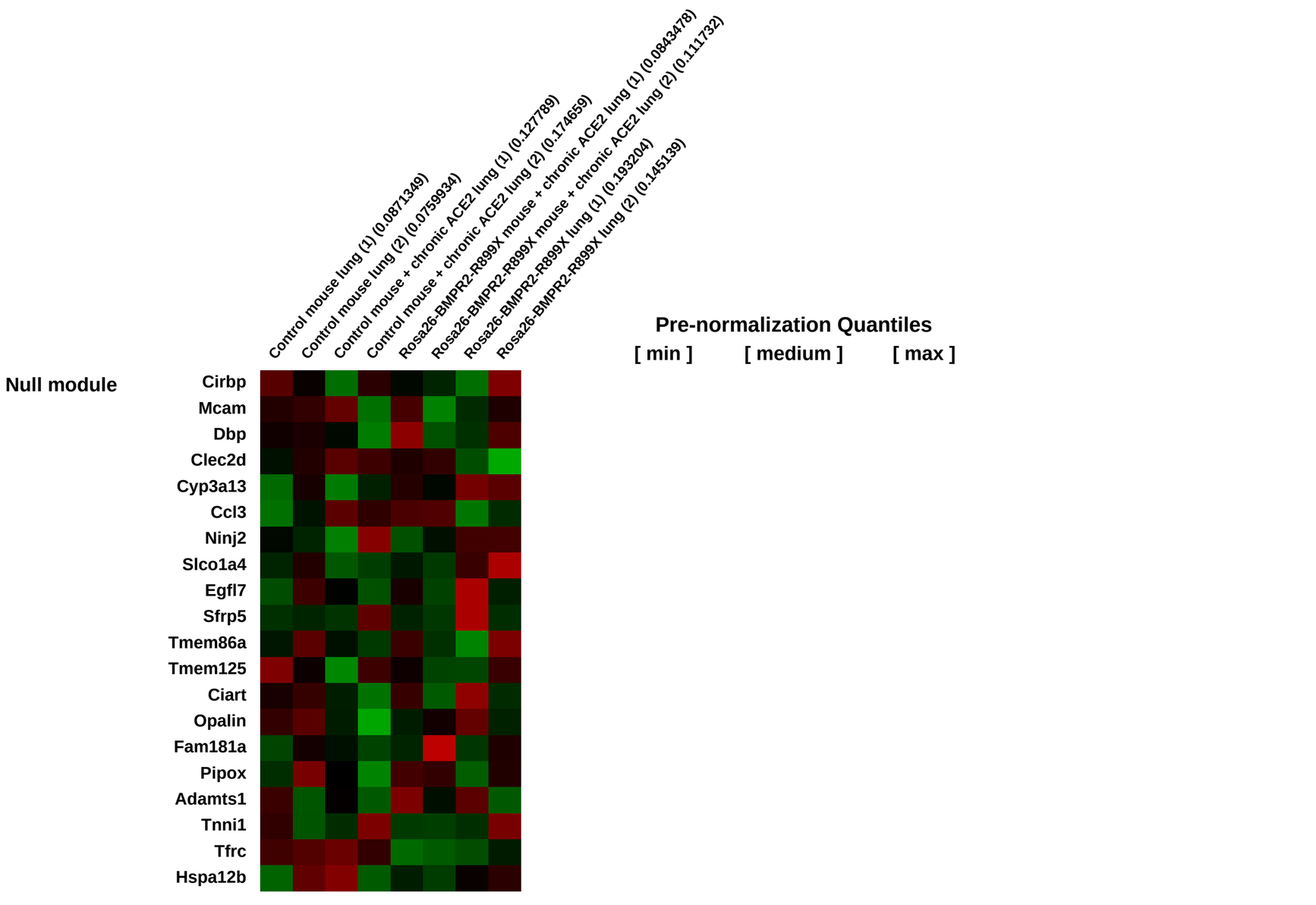

GEO Series "GSE21594" Expression Profiles

Num of samples in this series: 12

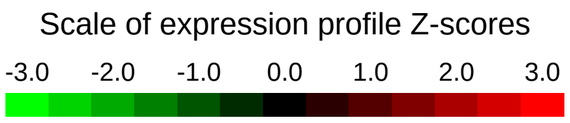

GEO Link:	http://www.ncbi.nlm.nih.gov/geo/query/acc.cgi?acc=GSE21594
Status:	Public on May 07 2013
Title:	Multiple Roles for Steroid Receptor RNA Activator (SRA) in Regulation of Adipogenesis and Insulin Sensitivity
Organism:	Mus musculus
Experiment type:	Expression profiling by array
Platform:	GPL1261
Pubmed ID:	21152033
Summary & Design:	**Summary:** PPARγ‡ is a master transcriptional regulator of adipogenesis. Hence, the identification of PPARγ‡ coactivators should help reveal mechanisms controlling gene expression in adipose tissue development and physiology. We show that the non-coding RNA Steroid receptor RNA Activator, SRA, associates with PPARγ‡ and coactivates PPARγ‡-dependent reporter gene expression. Overexpression of SRA in ST2 adipocyte precursor cells promotes their differentiation into adipocytes. Conversely, knockdown of endogenous SRA inhibits 3T3-L1 preadipocyte differentiation. Microarray analysis reveals hundreds of SRA-responsive genes in adipocytes, including genes in cell cycle, insulin and TNFγ– signaling pathways. Some functions of SRA may involve mechanisms other than coactivation of PPARγ‡. SRA increases insulin-stimulated glucose uptake in adipocytes. SRA promotes S-phase entry during mitotic clonal expansion, decreases expression of cyclin-dependent kinase inhibiters p21Cip1 and p27Kip1, and increases phosphorylation of Cdk1/Cdc2. SRA also inhibits the TNFγ–-induced phosphorylation of c-Jun NH2-terminal kinase. In conclusion, SRA enhances adipogenesis and adipocyte function through multiple pathways. **Overall design:** Total RNA was isolated from fully differentiated (MDIT day 4) SRA overexpressing (pMSCV-SRA) and control (pMSCV empty vector) ST2 adipocytes, or fully differentiated (MDIT day 8) shSRA knockdown (pSuperior-shSRA) or shControl (pSuperior-shcontrol) 3T3-L1 adipocytes. Genome wide gene expression analysis was performed using Affymetrix mouse genome 430 2.0 arrays. Triplicate samples were analyzed.

Background corr dist: KL-Divergence = 0.0309, L1-Distance = 0.0263, L2-Distance = 0.0009, Normal std = 0.6494

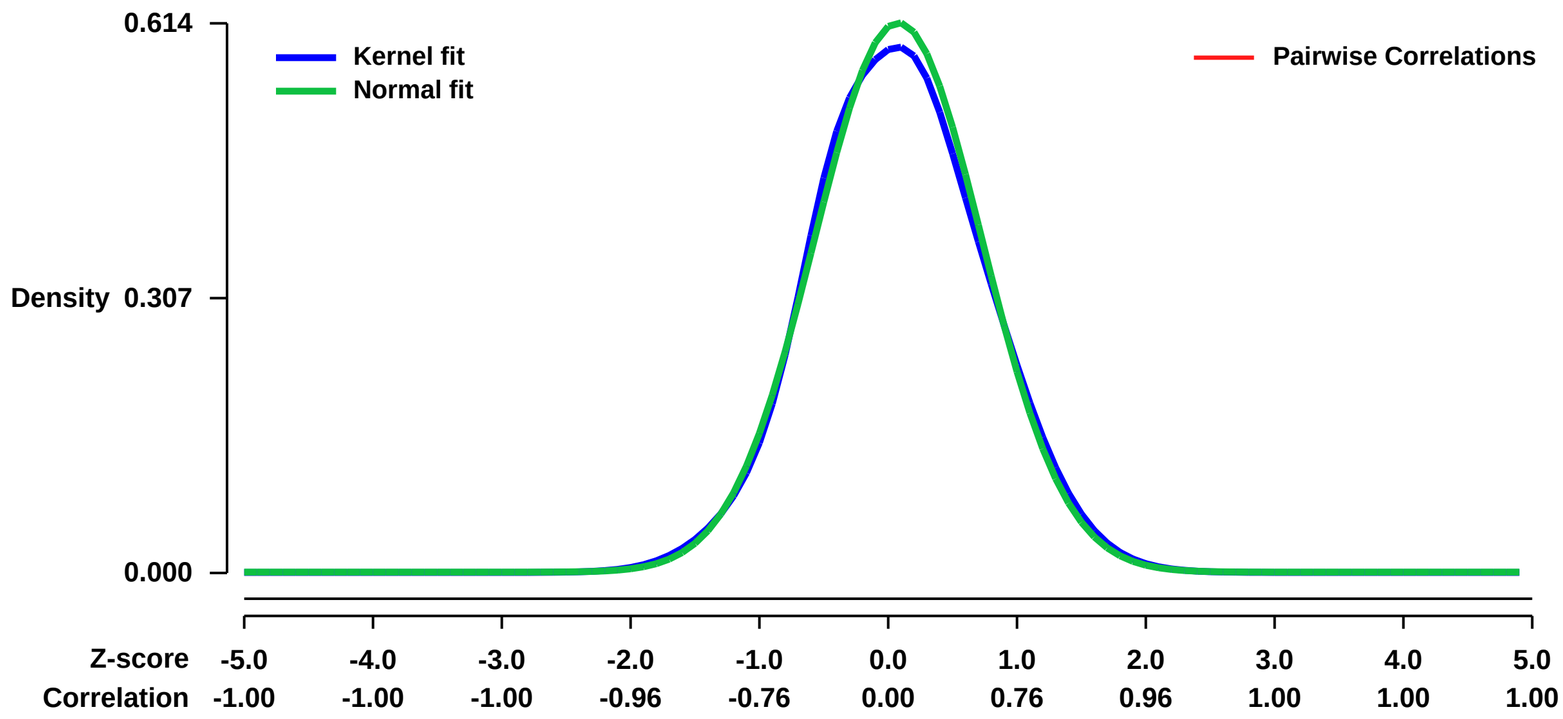

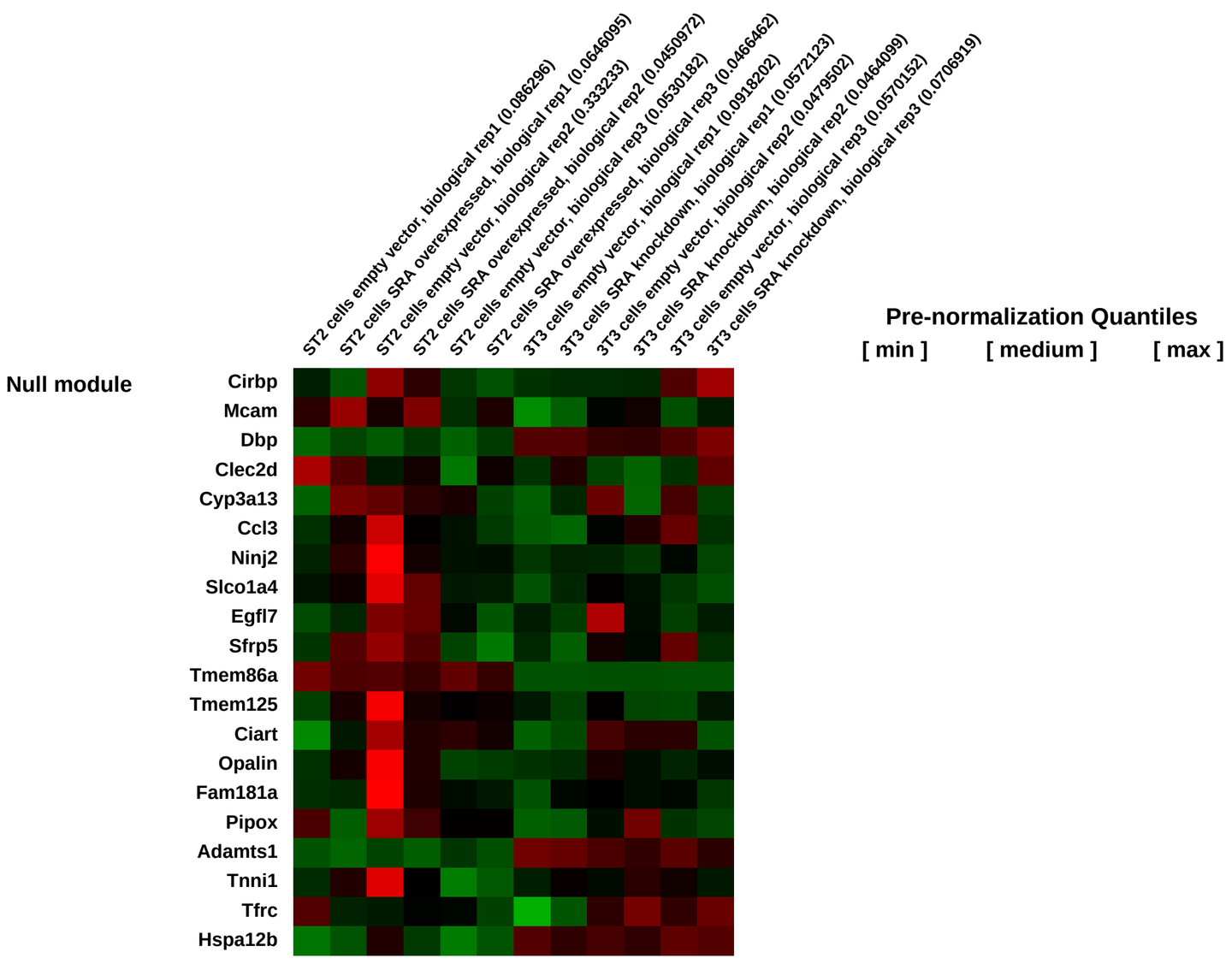

GEO Series "GSE21606" Expression Profiles

Num of samples in this series: 6

Scale of expression profile Z-scores

-3.0 -2.0 -1.0 0.0 1.0 2.0 3.0

GEO Link:	http://www.ncbi.nlm.nih.gov/geo/query/acc.cgi?acc=GSE21606
Status:	Public on Jul 07 2010
Title:	Expression profiling of murine neonatal lung tissue from Carm1 knockouts and wild type controls
Organism:	Mus musculus
Experiment type:	Expression profiling by array
Platform:	GPL1261
Pubmed ID:	20530543
Summary & Design:	**Summary:** Coactivator associated arginine methyltransferase I (CARM1, also known as Protein aRginine MethylTransferase 4, or PRMT4) regulates gene expression by multiple mechanisms including methylation of histones and coactivation of steroid receptor transcription. Mice lacking CARM1 are smaller than their littermates, fail to breath, and die shortly after birth, demonstrating the critical role of CARM1 in development.We performed gene expression analysis to identify genes that are responsible for hyperproliferaion in CARM1 knockout lung. **Overall design:** RNA extracted from murine lung at E18.5 with carm1 knockouts and wild type controls was hybridised to Affymetrix mouse430.2 GeneChips to identify differentially expressed genes in the disease state.

Background corr dist: KL-Divergence = 0.0455, L1-Distance = 0.0209, L2-Distance = 0.0005, Normal std = 0.5932

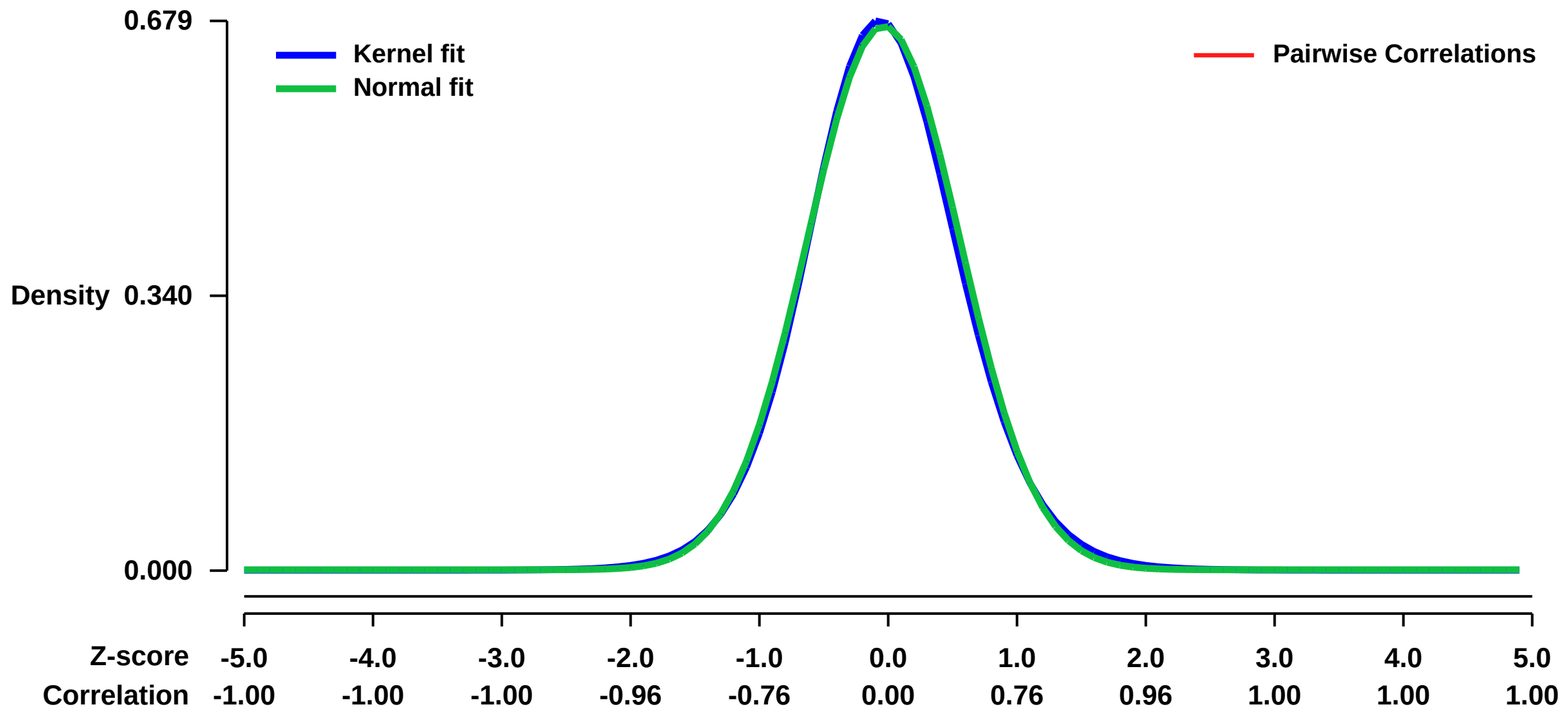

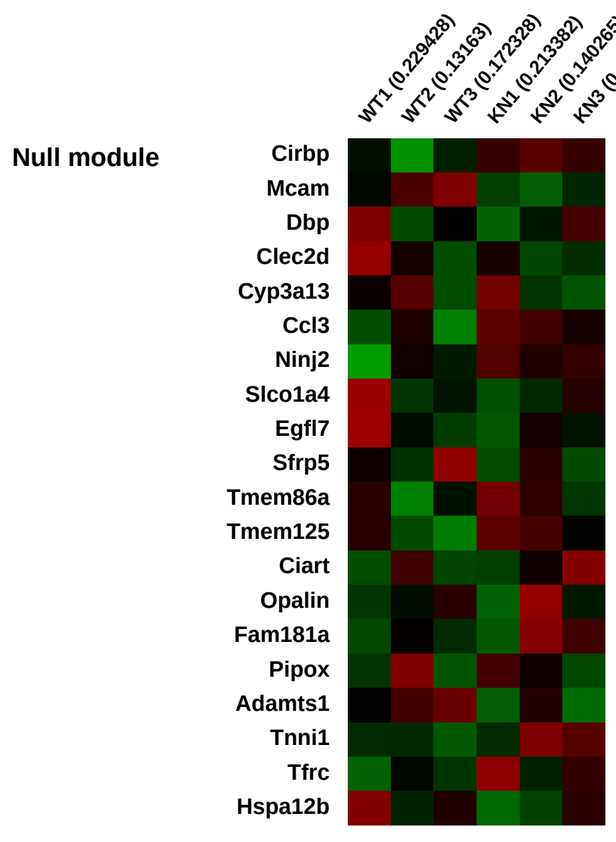

GEO Series "GSE2161" Expression Profiles

Num of samples in this series: 8

Scale of expression profile Z-scores

-3.0 -2.0 -1.0 0.0 1.0 2.0 3.0

GEO Link:	http://www.ncbi.nlm.nih.gov/geo/query/acc.cgi?acc=GSE2161
Status:	Public on Feb 02 2005
Title:	Identification of genes that are dysregulated in the telencephalon of Dlx1/2 mutants. Rubenstein-2R01MH049428-11
Organism:	Mus musculus
Experiment type:	Expression profiling by array
Platform:	GPL1261
Pubmed ID:	
Summary & Design:	**Summary:** **The Dlx homeodomain transcription factors are implicated in regulating the function of inhibitory neurons; therefore understanding their functions will provide insights into disorders such as epilepsy, mental retardation, autism and cerebral palsy.** **Identify genes that are dysregulated in the telencephalon of Dlx1/2 mutants. I am sending separate samples of the Basal Ganglia (BG) and cortex (Ctx).** **Comparing gene expression in the embryonic basal ganglia and cortex in wild type and dlx1/2 mutant mice will provide information regarding the types of genes that are downstream of Dlx1/2 function.** **Perform gene array analyses in duplicate or triplicate; compare expression profile of total RNA from wild type and dlx1/2 telencephalons. I am sending separate samples of the Basal Ganglia (BG) and cortex. I want to perform gene expression comparison between: 1) wild type and dlx1/2 basal ganglia (BG) 2) wild typee and dlx1/2 cortex (ctx) Age of all mice has been indicated as 14 days to satisfy system requirements, however all mice are embryonic day 14.5.** **Keywords: other** **Overall design:**

Background corr dist: **KL-Divergence = 0.0460, L1-Distance = 0.0154, L2-Distance = 0.0002, Normal std = 0.5784**

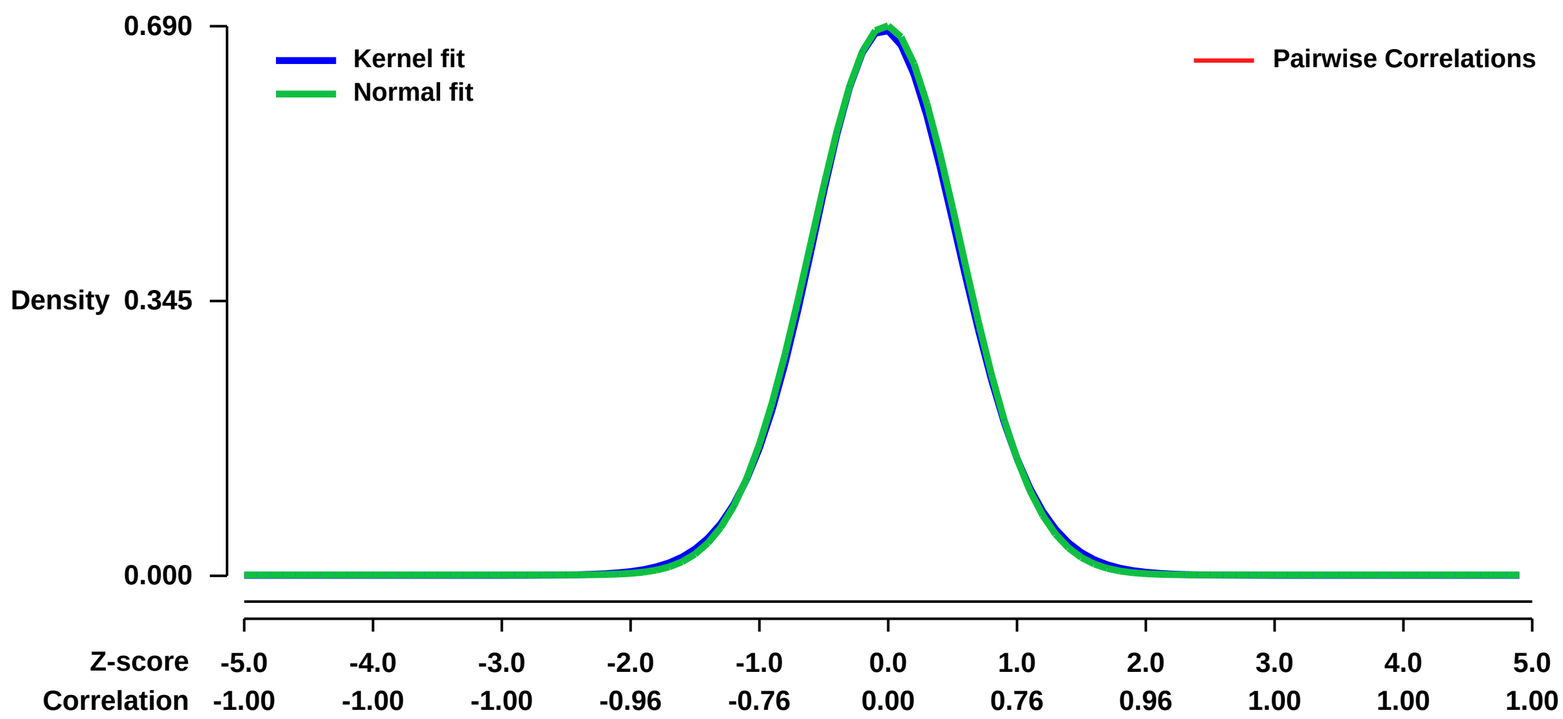

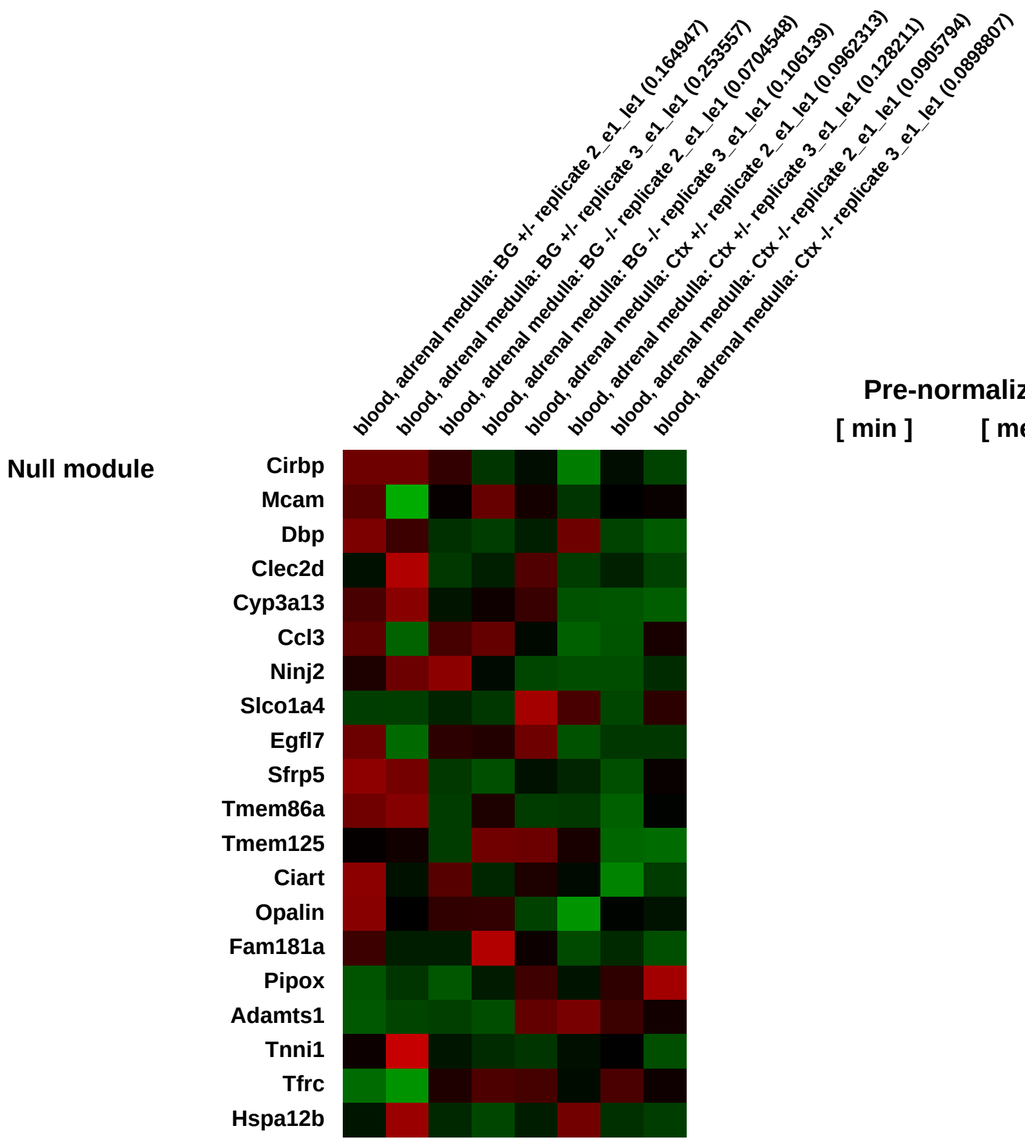

GEO Series "GSE21670" Expression Profiles

Num of samples in this series: 16

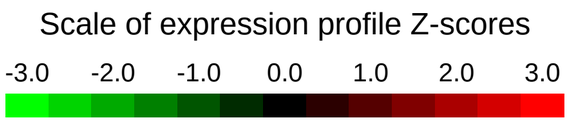

GEO Link:	http://www.ncbi.nlm.nih.gov/geo/query/acc.cgi?acc=GSE21670
Status:	Public on May 30 2010
Title:	Diverse Targets of the Transcription Factor STAT3 Contribute to T Cell Pathogenicity and Homeostasis [Affymetrix Expression]
Organism:	Mus musculus
Experiment type:	Expression profiling by array
Platform:	GPL1261
Pubmed ID:	20493732
Summary & Design:	**Summary:** STAT3, an essential transcription factor with pleiotropic functions, plays critical roles in the pathogenesis of autoimmunity. Despite recent data linking STAT3 with inflammatory bowel disease, exactly how it contributes to chronic intestinal inflammation is not known. Using a T cell transfer model of colitis we found that STAT3 expression in T cells was essential for the induction of both colitis and systemic inflammation. STAT3 was critical in modulating the balance of T helper 17 (Th17) and regulatory T (Treg) cells, as well as in promoting CD4+ T cell proliferation. We used chromatin immunoprecipitation and massive parallel sequencing (ChIP-Seq) to define the genome-wide targets of STAT3 in CD4+ T cells. We found that STAT3 bound to multiple genes involved in Th17 cell differentiation, cell activation, proliferation and survival, regulating both expression and epigenetic modifications. Thus, STAT3 orchestrates multiple critical aspects of T cell function in inflammation and homeostasis. **Overall design:** WT and STAT3-deficient CD4+ T cells were activated with anti-CD3 and anti-CD28, in the presence of cytokines (interleukin (IL)-6 and TGFb) or medium alone for three days. RNA was extracted and hybridized to Affymetrix microarray chips.

Background corr dist: KL-Divergence = 0.1042, L1-Distance = 0.0408, L2-Distance = 0.0034, Normal std = 0.4302

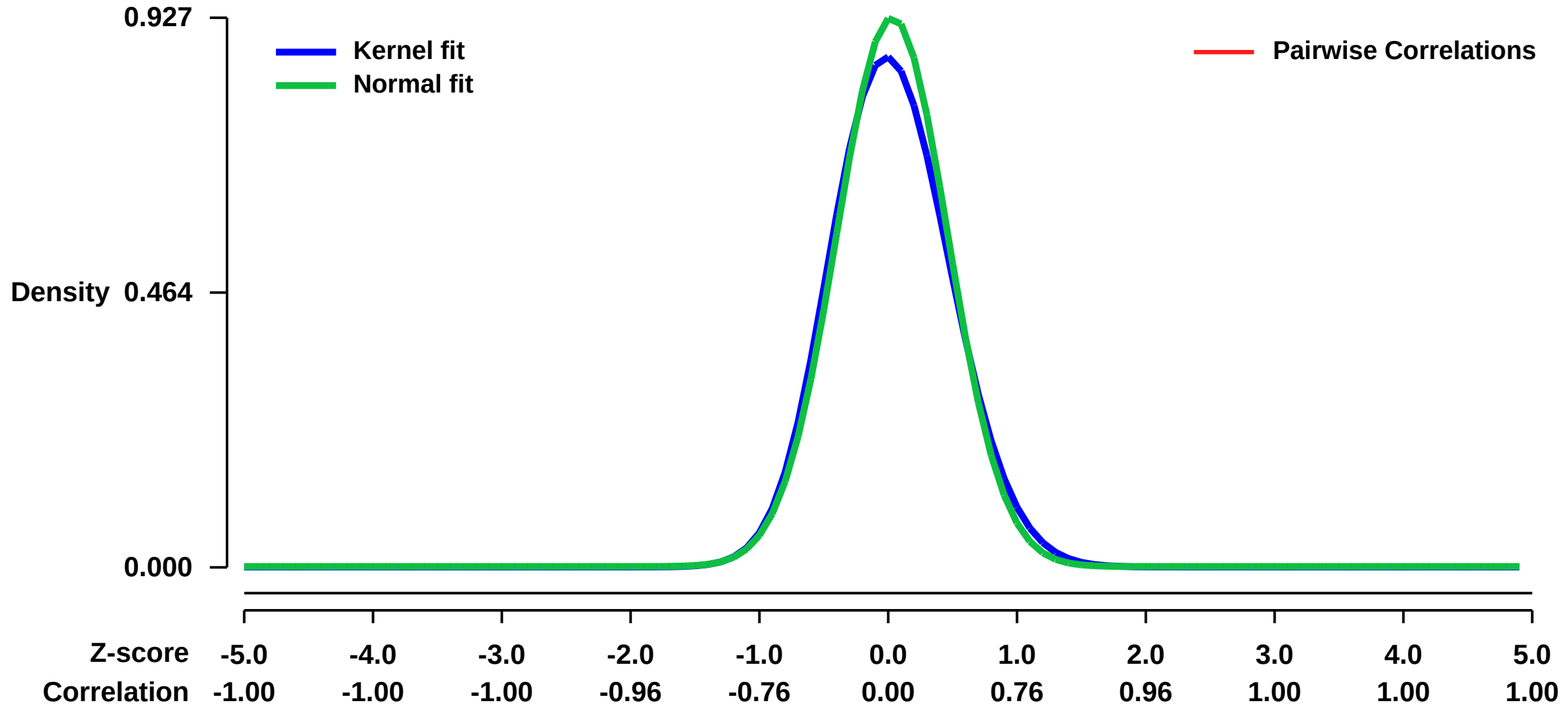

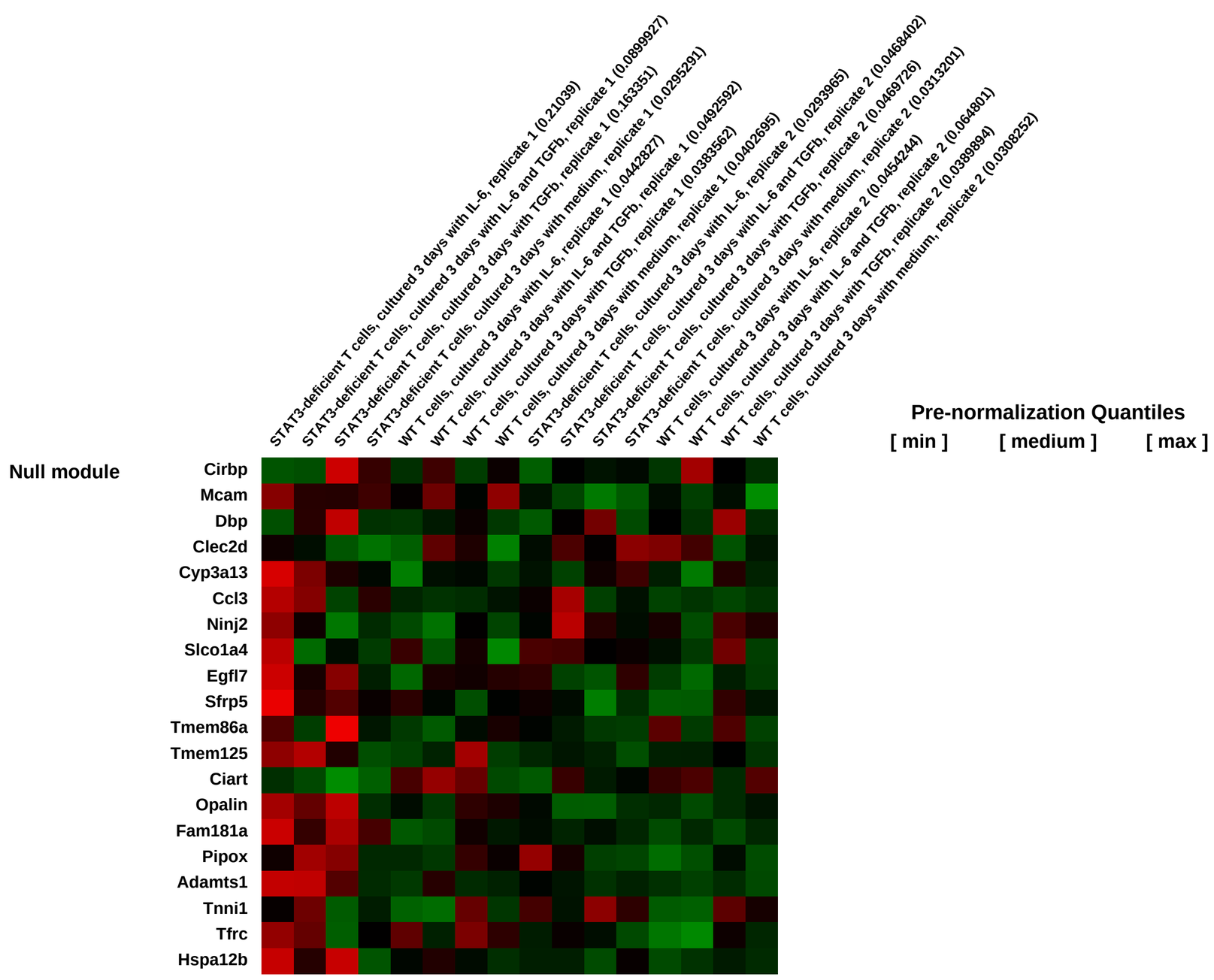

GEO Series "GSE21716" Expression Profiles

Num of samples in this series: 28

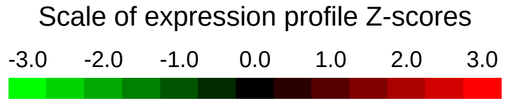

GEO Link:	http://www.ncbi.nlm.nih.gov/geo/query/acc.cgi?acc=GSE21716
Status:	Public on Oct 01 2010
Title:	Hepatic xenobiotic metabolizing enzyme gene expression through the life stages of the mouse
Organism:	Mus musculus
Experiment type:	Expression profiling by array
Platform:	GPL1261
Pubmed ID:	
Summary & Design:	**Summary:** **Using full-genome arrays, the expression of all XMEs was examined during fetal (gestation day (GD) 19), neonatal (postnatal day (PND) 7), prepubescent (PND30), middle age (12 mon), and old age (18 and 24 mon) in the C57Bl6/J mouse liver and compared to young adults. Fetal and neonatal life stages had a dramatic effect on XME expression compared to the relatively minor effects of old age. At all life stages except PND30 down-regulated genes outnumbered up-regulated genes. The altered XMEs included those in all of the major metabolic phases including phase I (alcohol and aldehyde dehydrogenase and Cyp genes), phase II (aldo-keto reductase, glutathione-S-transferases, sulfotransferases and UDP-glucuronosyl transferases) and phase III (transporters). We have generated a comprehensive catalog of XME hepatic gene changes through the life stages of the mouse that can be used to predict chemicals and chemical classes different life stages are more sensitive to. Some CEL files used in this study have been submitted through GSE21224.** **Keywords: gene expression/microarray** **Overall design:** **We characterized gene expression changes in the developing mouse liver at gestational days (GD) 19), neonatal (postnatal day (PND) 7), prepubescent (PND30), middle age (12 mon), and old age (18 and 24 mon) in the C57Bl6/J mouse liver using full-genome microarrays and compared these changes to that in the adult liver.. We also compared results to GD19, PND32, and PND67 C3H mice. Total RNA was isolated from liver samples and gene expression analyzed using Affymetrix Mouse 430 2.0 GeneChips. Data from 28 samples, four mice in each of the age groups for C57BL/6 and C3H, were analyzed.**

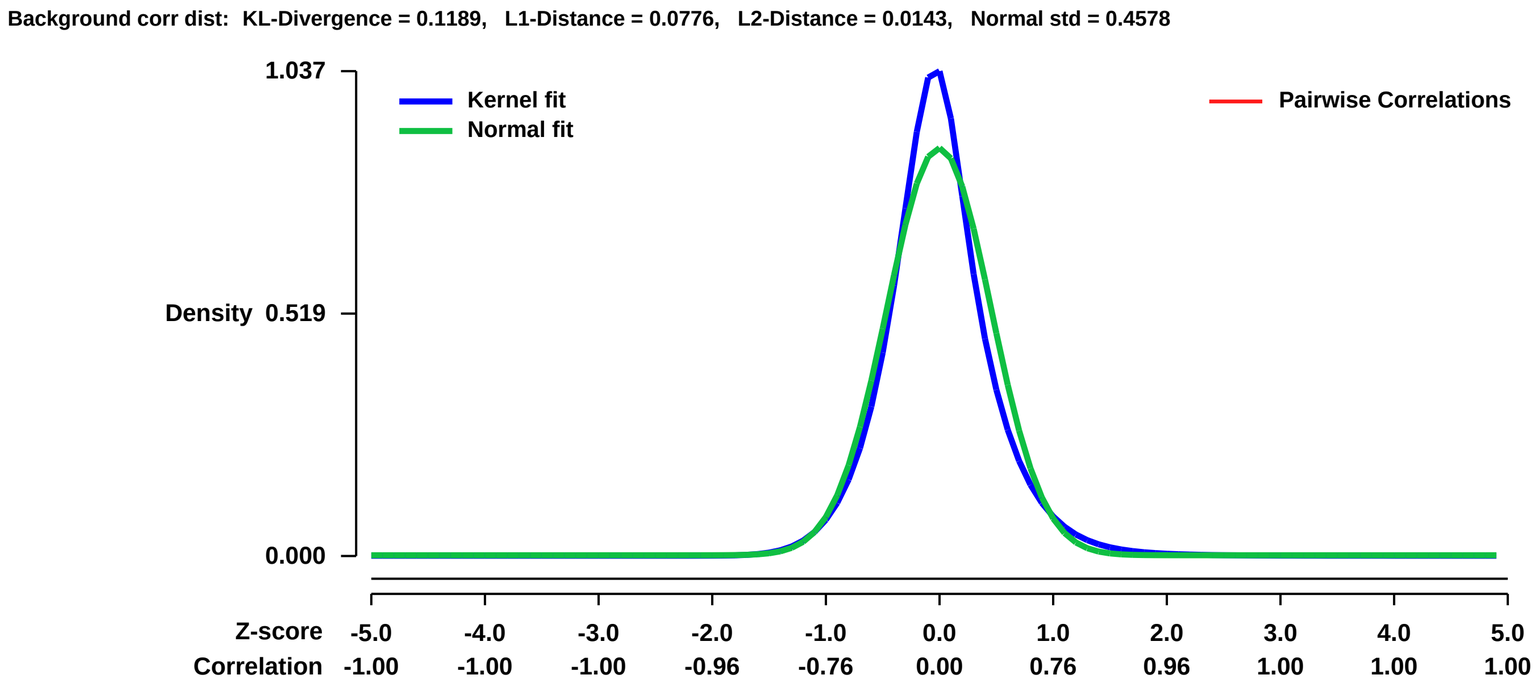

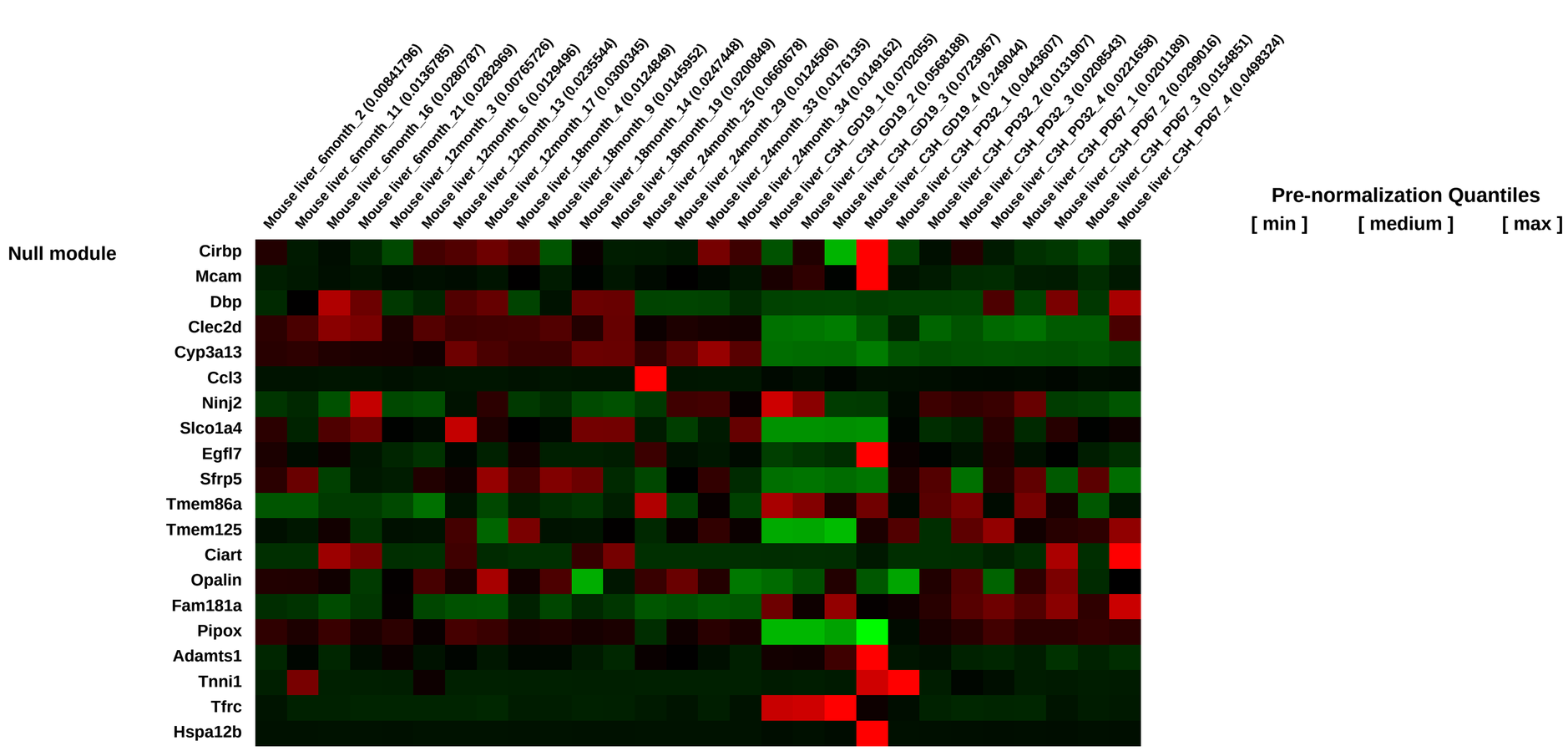

GEO Series "GSE21755" Expression Profiles

Num of samples in this series: 25

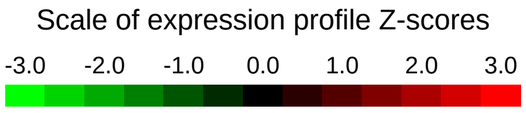

GEO Link:	http://www.ncbi.nlm.nih.gov/geo/query/acc.cgi?acc=GSE21755
Status:	Public on Jul 30 2010
Title:	Rapamycin effect on Wild Type and TSC deficient Mouse Embryonic Fibroblasts : Time Course
Organism:	Mus musculus
Experiment type:	Expression profiling by array
Platform:	GPL1261
Pubmed ID:	20670887
Summary & Design:	**Summary:** Aberrant activation of the mammalian target of rapamycin (mTOR) complex 1 (mTORC1) is a common molecular event in a large variety of pathological settings, including genetic tumor syndromes, cancer, and obesity. However, the cell intrinsic consequences of mTORC1 activation remain poorly defined. Here, we identify global trancriptional changes in TSC1 and TSC2 null MEFs, which exhibit constitutive activation of mTORC1, compared to wild-type littermate control lines. A rapamycin time course is included to determine those changes that are dependent on mTORC1 signaling, revealing mTORC1 induced and repressed transcripts. In order to identify mTORC1-dependent transcriptional changes, we compared wild-type MEFs to both Tsc1-/- and Tsc2-/- MEFs following serum starvation, where mTORC1 signaling is off in wild-type cells and fully active in TSC-deficient cells. All cell lines were serum-starved for 24 h, and the Tsc1-/- and Tsc2-/- cells were treated with a time course of rapamycin prior to the isolation of mRNA for microarray analysis. **Overall design:** Immortalized wild-type (Tsc2+/+ p53-/-), Tsc1-/- (p53+/+, 3T3-immortalized), and Tsc2-/- (p53-/-, derived from a littermate of the wild-type cell line) MEFs are the three cell lines used in this study and were derived in the laboratory of David J. Kwiatkowski (Brigham and Women's Hospital, Harvard Medical School, Boston, MA). Wild-type and null MEFs were grown to 70% confluence in 10 cm plates and were serum starved for 24 h in the presence of vehicle (DMSO) for 24 h or rapamycin (20 nM) for 2, 6, 12, or 24 h. All vehicle-treated samples (0 h time points) were plated in triplicate and all rapamycin time course samples were plated in duplicate. For each replicate, expression analysis was performed by hybridization to an Affymetrix Mouse 430_2 oligonucleotide microarray chip.

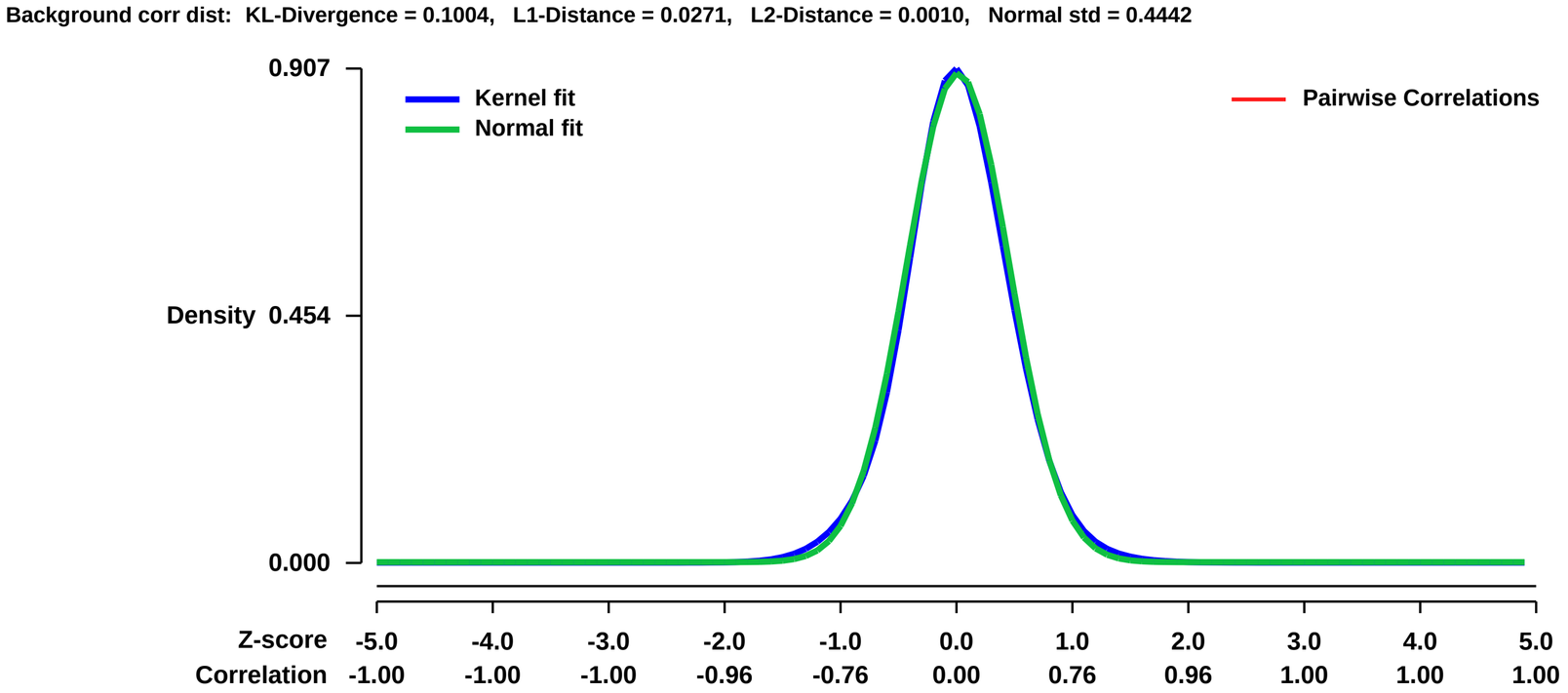

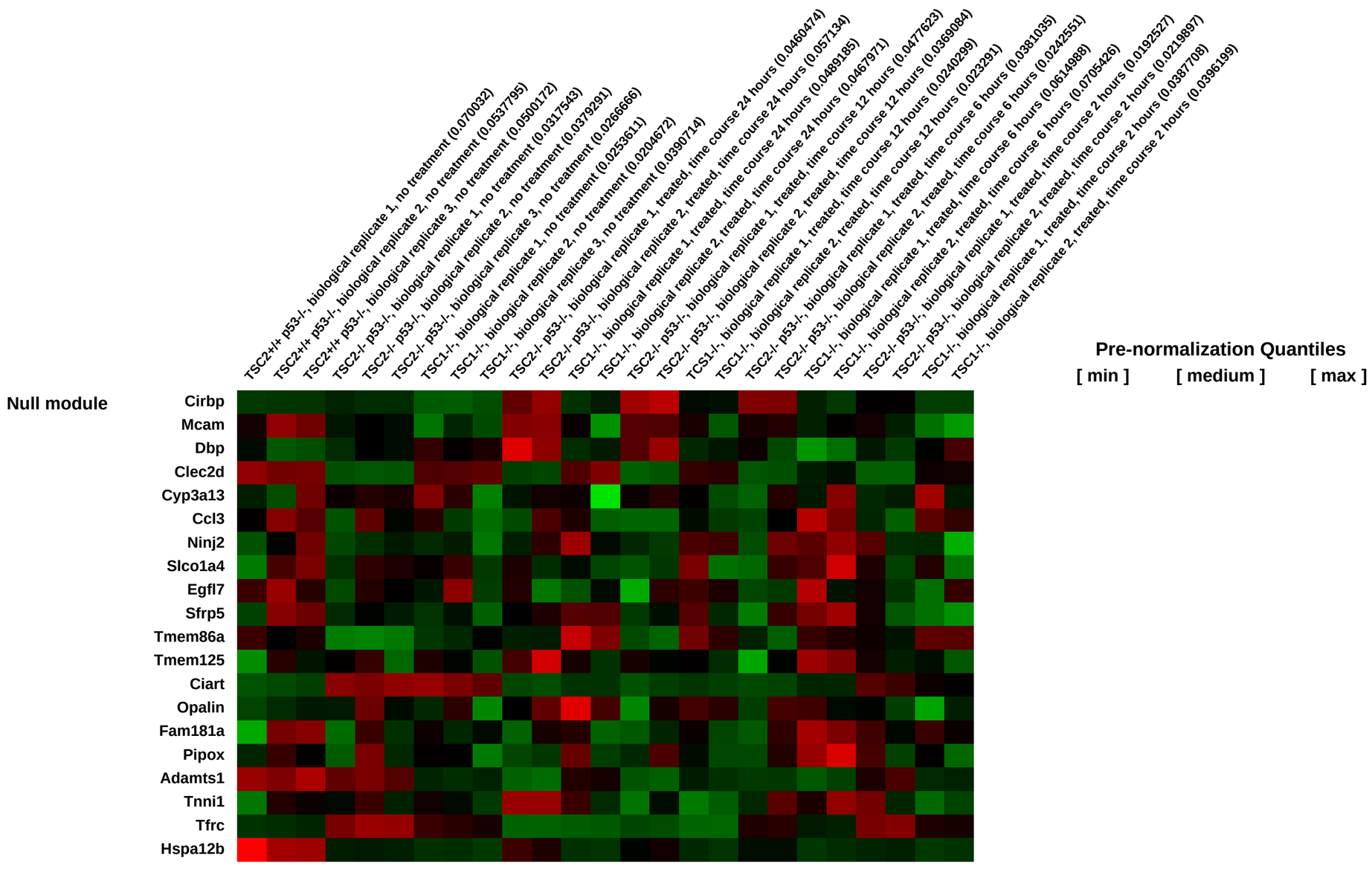

GEO Series "GSE21822" Expression Profiles

Num of samples in this series: 12

Scale of expression profile Z-scores

-3.0 -2.0 -1.0 0.0 1.0 2.0 3.0

GEO Link:	http://www.ncbi.nlm.nih.gov/geo/query/acc.cgi?acc=GSE21822
Status:	Public on Oct 02 2010
Title:	Role of sex chromosome complement in autosomal gene expression
Organism:	Mus musculus
Experiment type:	Expression profiling by array
Platform:	GPL1261
Pubmed ID:	20833369
Summary & Design:	**Summary:** It has generally been assumed that most differences between males and females are due to developmental and hormonal differences between the sexes. Here we investigate the contribution of sex chromosomal complement to such sexual dimorphisms. These genome-wide transcription profiling showed that the expression of hundreds of autosomal genes was sensitive to sex chromosome complement, rather than gender. The existence of such differences between males and females holds important implications for understanding sexual dimorphisms in physiology and disease hitherto attributed solely to gender or hormonal effects. **Overall design:** Thymic total RNA was isolated from 7-8 week old mice, with 3 biological replicates for each of four genotypes with different sex chromosome complements

Background corr dist: KL-Divergence = 0.1577, L1-Distance = 0.0398, L2-Distance = 0.0032, Normal std = 0.3646

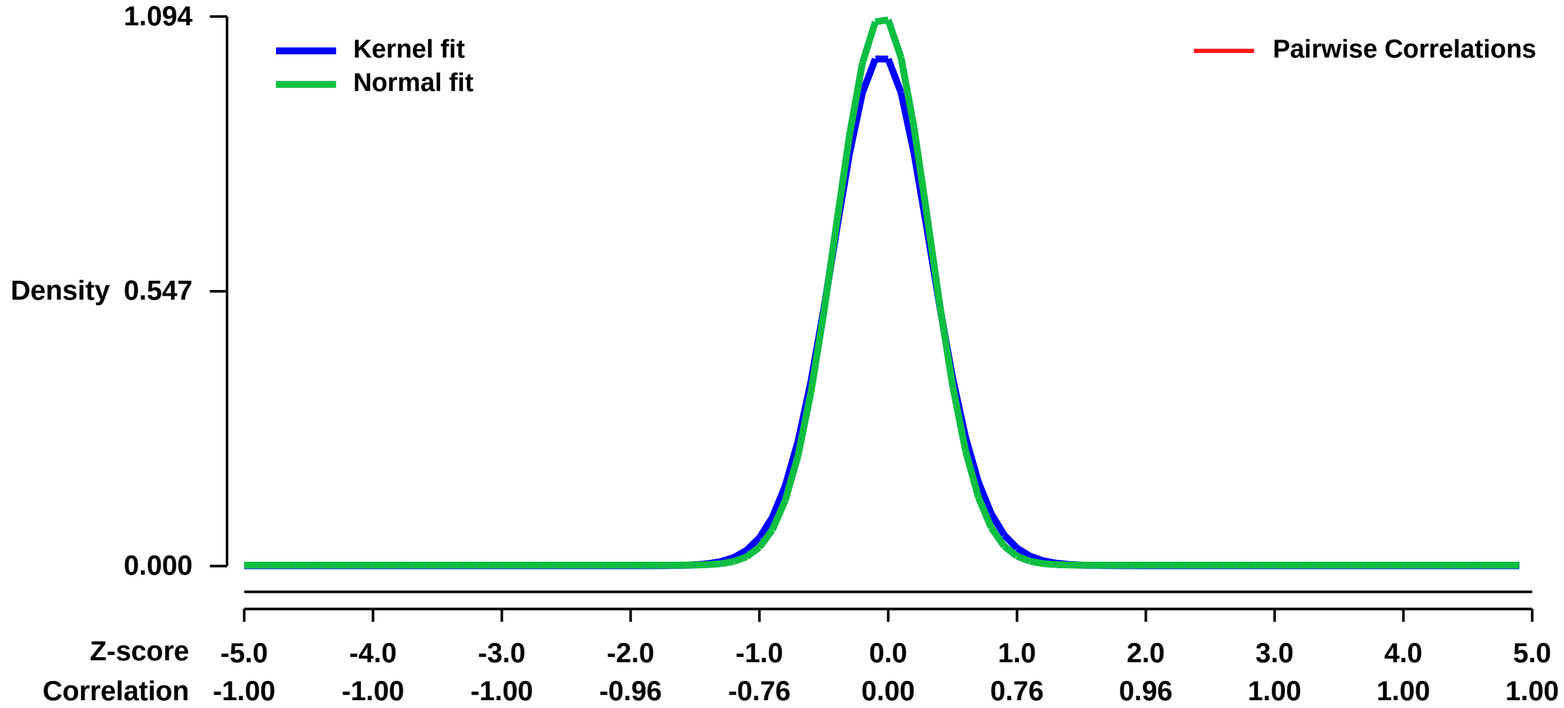

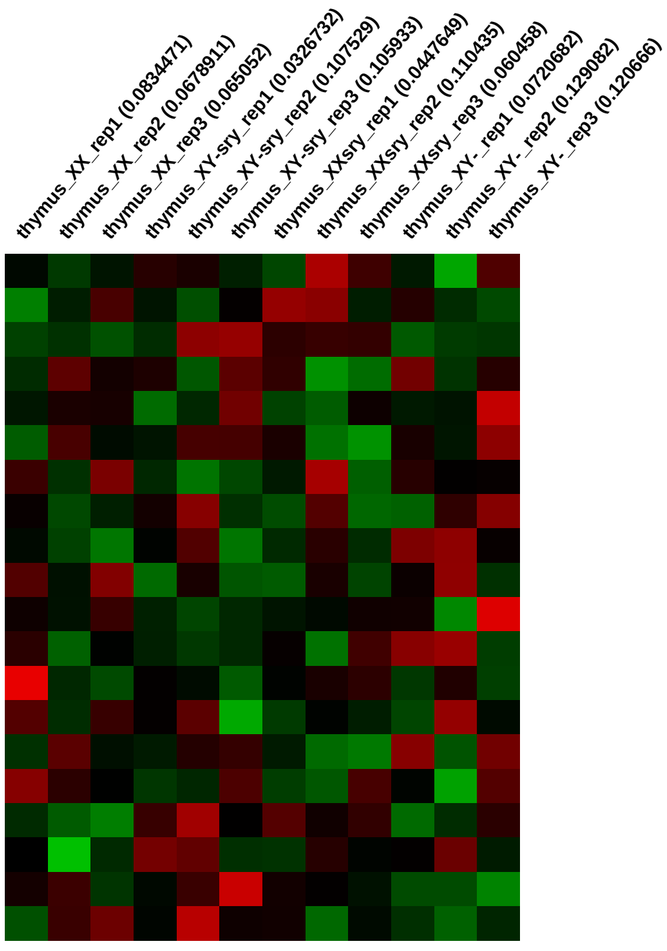

GEO Series "GSE21836" Expression Profiles

Num of samples in this series: 8

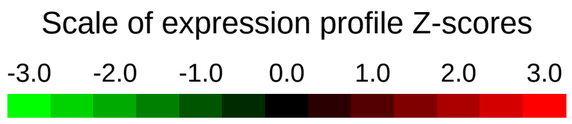

GEO Link:	http://www.ncbi.nlm.nih.gov/geo/query/acc.cgi?acc=GSE21836
Status:	Public on May 15 2010
Title:	Tob1 is a Constitutively Expressed Repressor of Liver Regeneration
Organism:	Mus musculus
Experiment type:	Expression profiling by array
Platform:	GPL1261
Pubmed ID:	20513747
Summary & Design:	**Summary:** How proliferative and inhibitory cell signals integrate to control liver regeneration remains poorly understood. A screen for antiproliferative factors repressed after liver injury identified Tob1, a member of the PC3/BTG1 family of mitoinhibitory molecules as a target for further evaluation. Tob1 protein decreases after 2/3 hepatectomy in mice secondary to post-transcriptional mechanisms. Deletion of Tob1 increases hepatocyte proliferation and accelerates restoration of liver mass after hepatectomy. Down-regulation of Tob1 is required for normal liver regeneration and Tob1 controls hepatocyte proliferation in a dose-dependent fashion. Tob1 associates directly with both Caf1 and the Cyclin/cdk complex to modulate kinase activity. In addition, Tob1 has significant effects on the transcription of critical cell cycle components, including E2F targets and genes involved in p53 signaling. These studies provide direct evidence that levels of an inhibitory factor control the rate of liver regeneration. Our data identify Tob1 as a crucial check-point molecule that acts by by modulating levels and activity of cell cycle proteins. **Overall design:** Samples from wild type and Tob1 null mice as normal adults and 24 hours after 2/3 hepatectomy are used. Each experimental point used data from two chips, each having a different set of three pooled animals. In summary we had 8 chips: 2 for WT time 0, 2 for WT time 24, 2 for KO time 0, 2 for KO time 24.

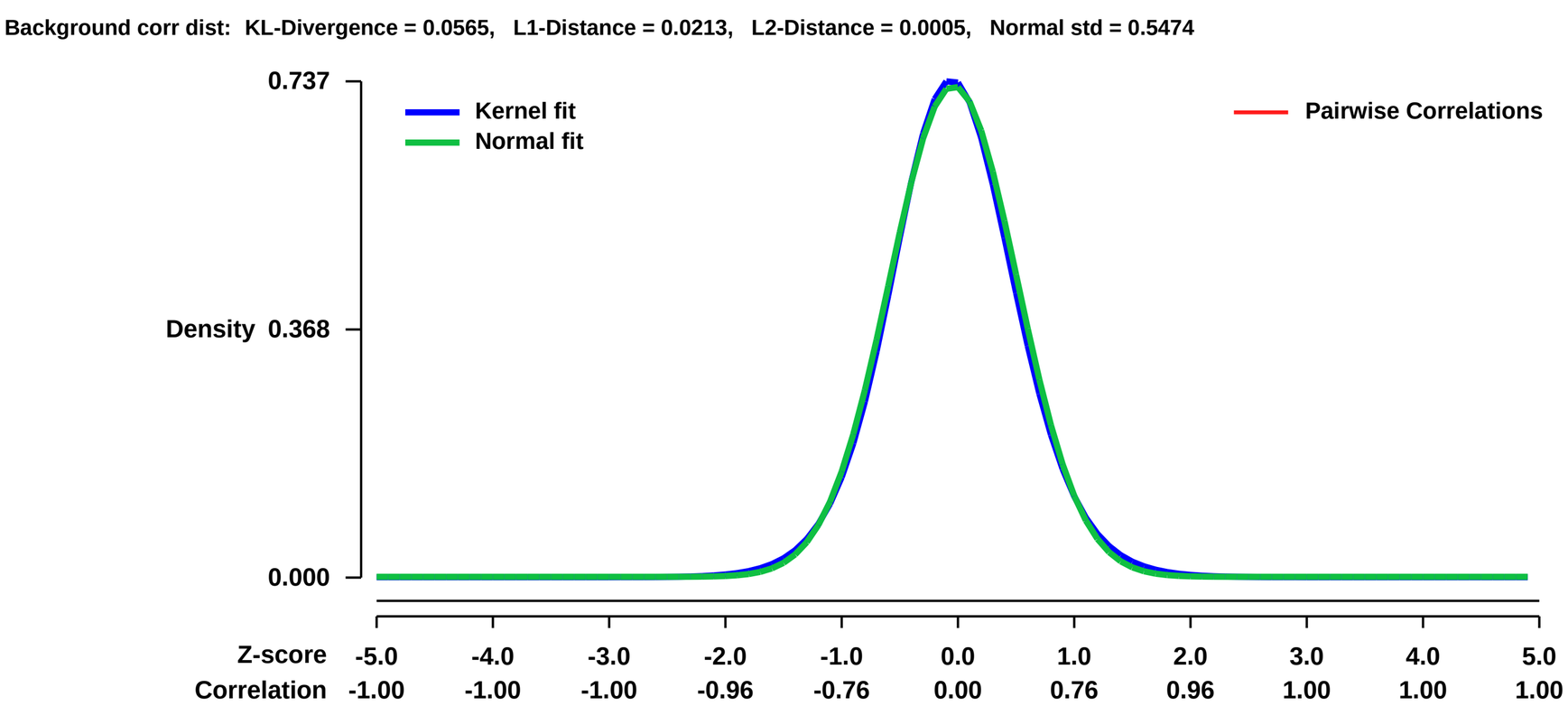

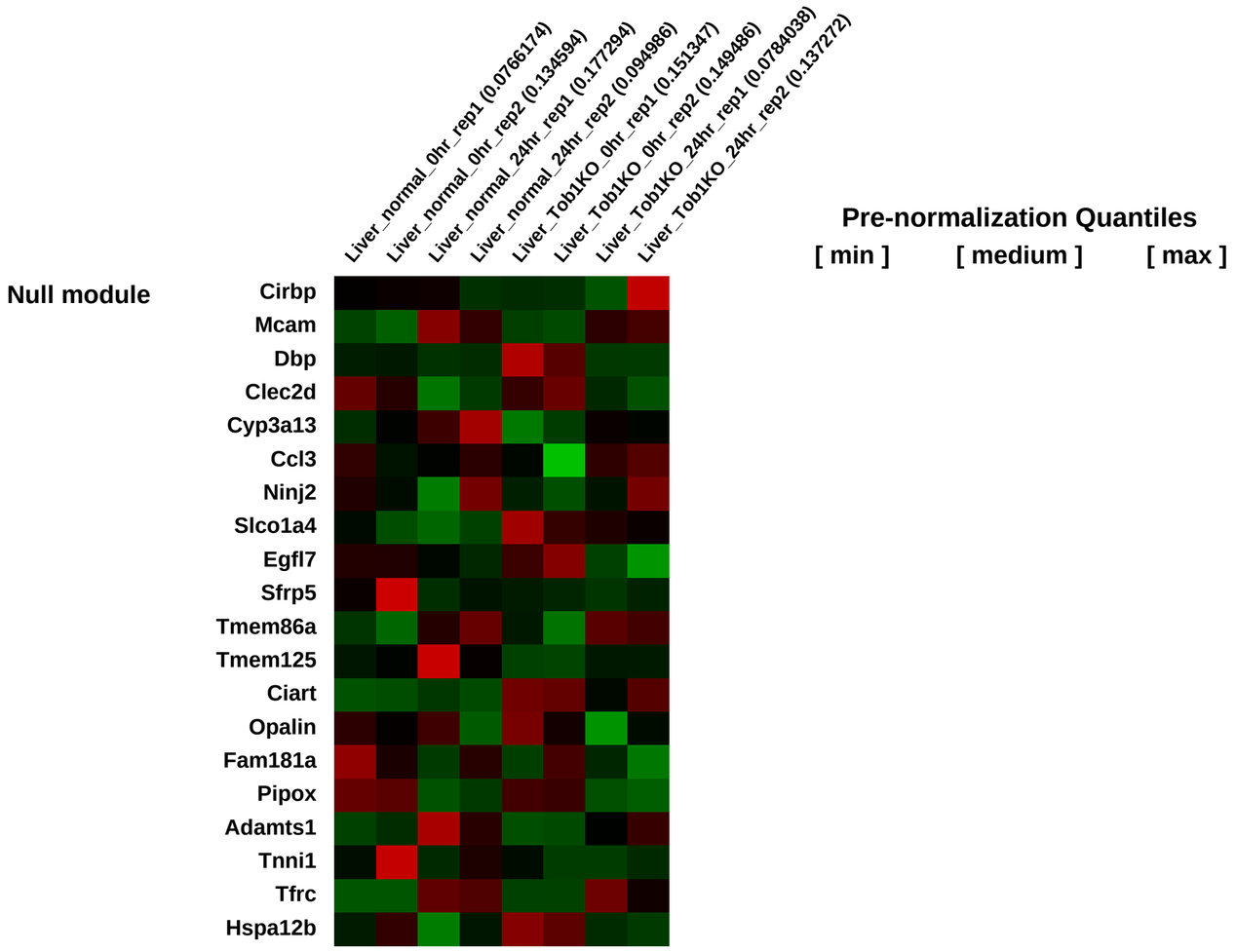

GEO Series "GSE21842" Expression Profiles

Num of samples in this series: 8

Scale of expression profile Z-scores

-3.0 -2.0 -1.0 0.0 1.0 2.0 3.0

GEO Link:	http://www.ncbi.nlm.nih.gov/geo/query/acc.cgi?acc=GSE21842
Status:	Public on May 15 2010
Title:	Physiological Jak2V617F expression causes a lethal myeloproliferative neoplasm with differential effects on hematopoietic stem and progenitor cells
Organism:	Mus musculus
Experiment type:	Expression profiling by array
Platform:	GPL1261
Pubmed ID:	20541703
Summary & Design:	**Summary:** We report a Jak2V617F knock-in mouse myeloproliferative neoplasm (MPN) model resembling human polycythemia vera (PV). The MPN is serially transplantable and we demonstrate that the hematopoietic stem cell (HSC) compartment has the unique capacity for disease initiation but does not have a selective competitive advantage over wild type HSCs. In contrast, myeloid progenitor populations are expanded and skewed towards the erythroid lineage, but cannot transplant the disease. Treatment with a JAK2 kinase inhibitor ameliorated the MPN phenotype, but did not eliminate the disease-initiating population. These findings provide insights into the consequences of JAK2 activation on HSC differentiation and function and have the potential to inform therapeutic approaches to JAK2V617F positive MPN. **Overall design:** LKS cells were isolated from wild type (n=4) and JAK2V617F mutant mice (n=4). RNA was extracted using Qiagen RNeasy Micro Kit according to manufacturers instruction and amplified using NUGEN amplification kit. cDNA was fragmented and biotinylated before hybridization onto Affymetrix Mouse Expression Array 430 2.0.

Background corr dist: KL-Divergence = 0.0704, L1-Distance = 0.0212, L2-Distance = 0.0006, Normal std = 0.4959

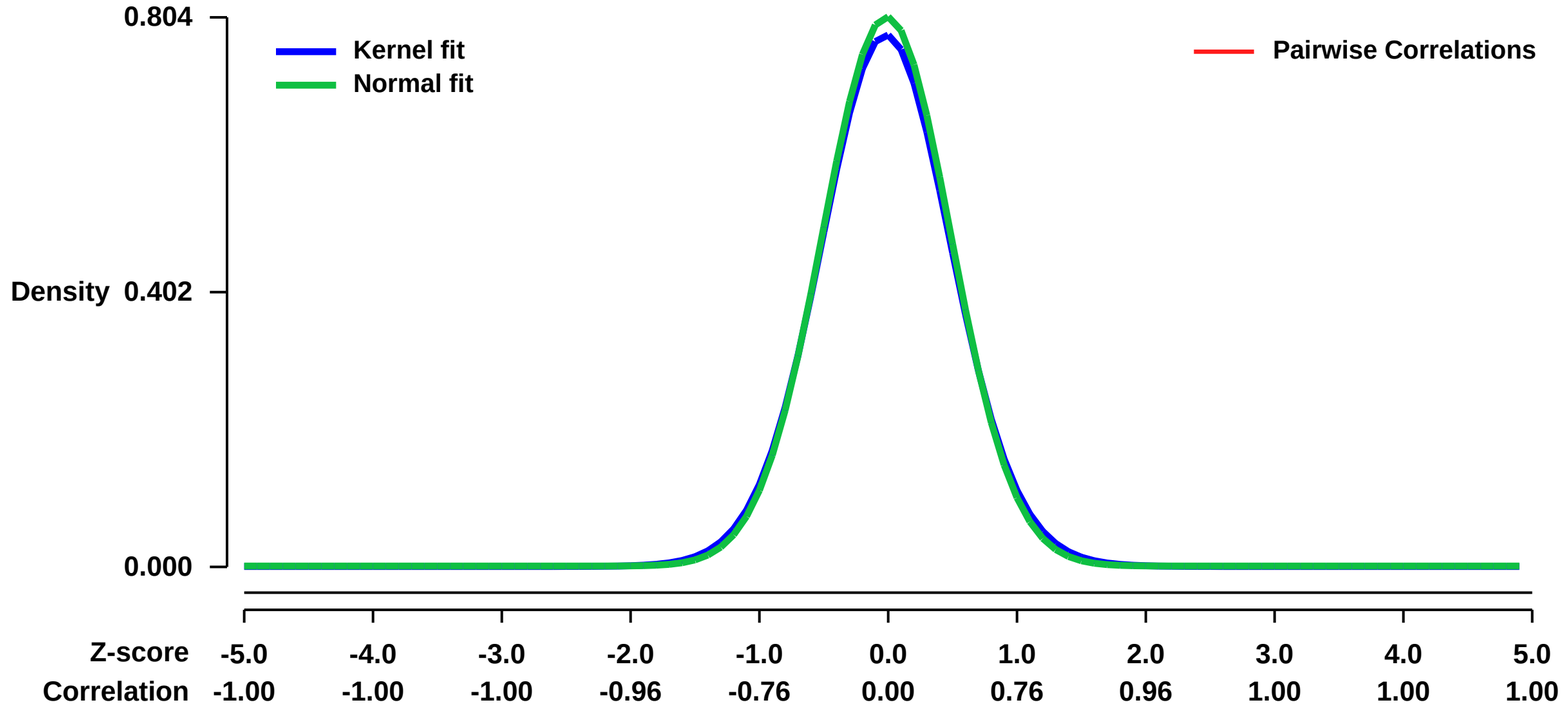

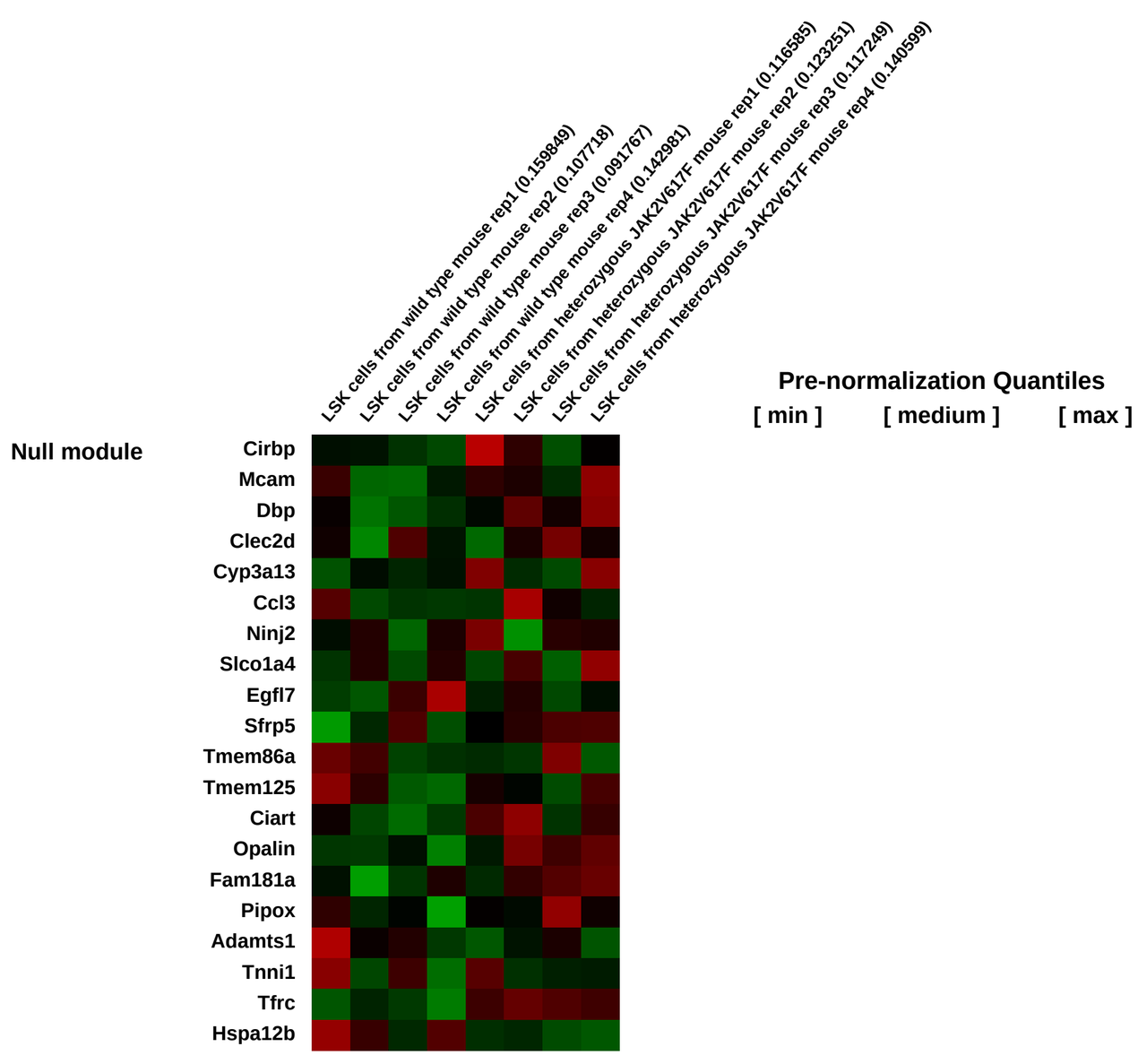

GEO Series "GSE21900" Expression Profiles

Num of samples in this series: 12

Scale of expression profile Z-scores

-3.0 -2.0 -1.0 0.0 1.0 2.0 3.0

GEO Link:	http://www.ncbi.nlm.nih.gov/geo/query/acc.cgi?acc=GSE21900
Status:	Public on May 18 2011
Title:	Expression profiling of the Otx2 CKO retina
Organism:	Mus musculus
Experiment type:	Expression profiling by array
Platform:	GPL1261
Pubmed ID:	21602925
Summary & Design:	**Summary:** In the vertebrate retina, the Otx2 transcription factor plays a crucial role in the cell fate determination of both rod and cone photoreceptors. Otx2 conditional knockout (CKO) mice exhibited a total absence of rods and cones in the retina due to their cell fate conversion to amacrine-like cells. In order to investigate the entire transcriptome regulated by Otx2 in the developing retina, we performed microarray analysis on the Otx2 CKO retina. **Overall design:** In order to clarify the molecular role of Otx2 in transcriptional regulation during development, we investigated the expression profile of the Otx2 CKO retina compared with that of the control retina with the genotype Otx2flox/flox;Crx-cre- using microarrays at two time points, P1 and P12.

Background corr dist: KL-Divergence = 0.0680, L1-Distance = 0.0265, L2-Distance = 0.0012, Normal std = 0.5091

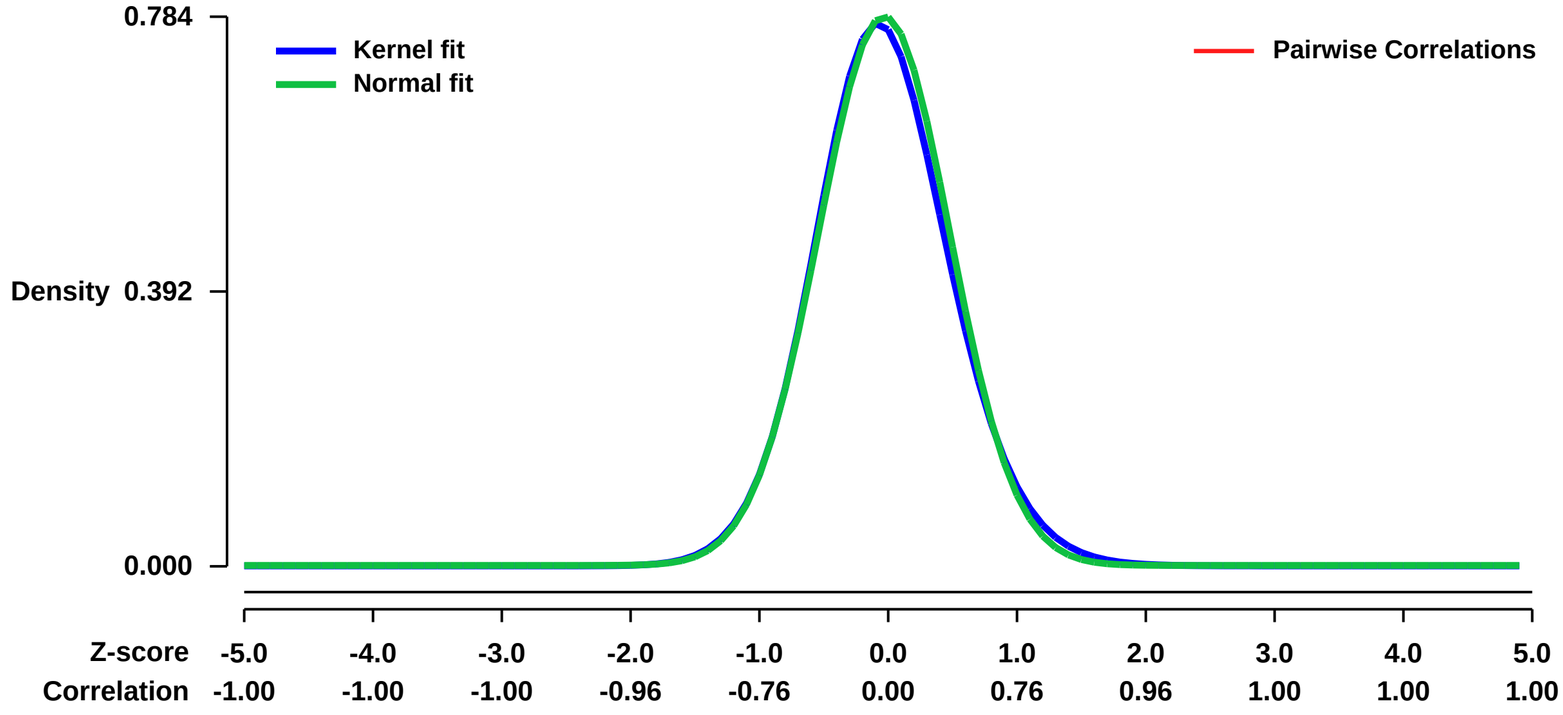

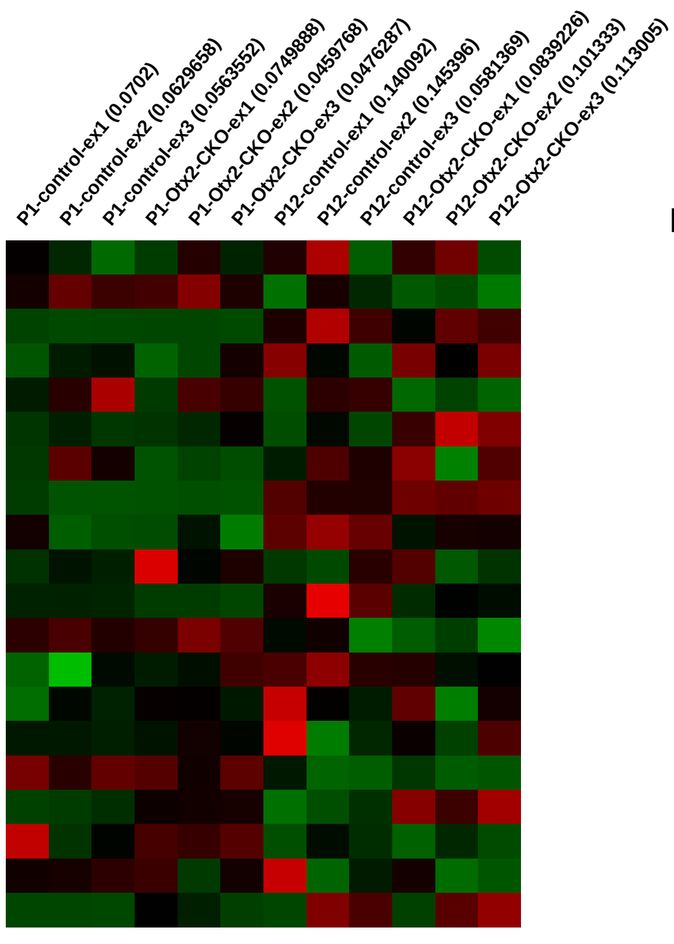

GEO Series "GSE21905" Expression Profiles

Num of samples in this series: 6

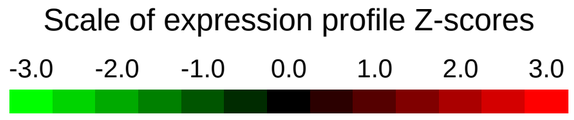

GEO Link:	**http://www.ncbi.nlm.nih.gov/geo/query/acc.cgi?acc=GSE21905**
Status:	**Public on May 21 2010**
Title:	**Gene expression in Lineage negative bone marrow cells of C57B/L6 and B.D(Chr5) mice**
Organism:	**Mus musculus**
Experiment type:	**Expression profiling by array**
Platform:	**GPL1261**
Pubmed ID:	
Summary & Design:	**Summary:** **These mouse strains differ in absolute numbers of hematopoietic stem cells but differ genetically only at the Chr 5 congenic locus.** **We used microarray analysis to identify candidate regulators of hematopoietic stem cells based on differential gene expression patterns.** **Overall design:** **Triplicate RNA samples were isolated from 500,00-800,000 Lineage negative bone marrow cells from each strain. Each of the six samples were analyzed on 6 separate MG 430 2.0 Affymetrix Microarray Chips.**

Background corr dist: **KL-Divergence = 0.0472, L1-Distance = 0.0190, L2-Distance = 0.0004, Normal std = 0.5846**

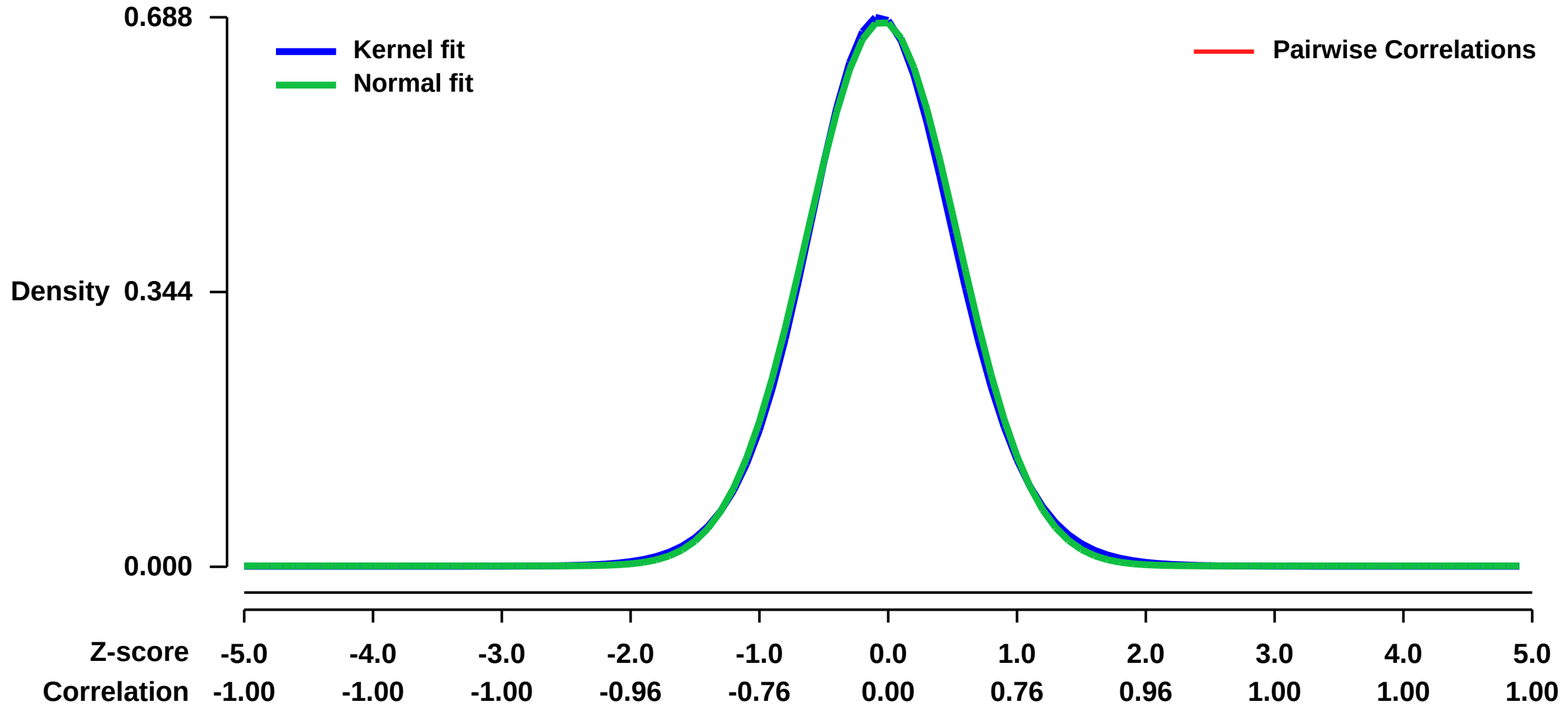

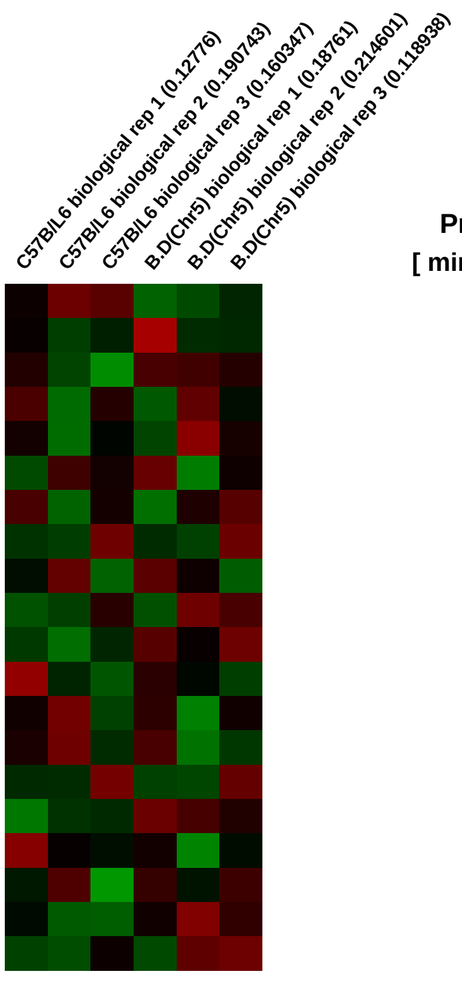

GEO Series "GSE21944" Expression Profiles

Num of samples in this series: 6

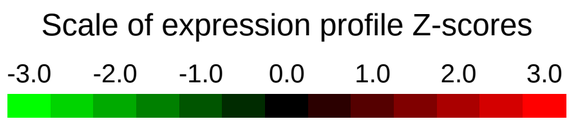

GEO Link:	http://www.ncbi.nlm.nih.gov/geo/query/acc.cgi?acc=GSE21944
Status:	Public on Jul 02 2010
Title:	The orphan nuclear hormone receptor ERR‚† controls rod photoreceptor survival.
Organism:	Mus musculus
Experiment type:	Expression profiling by array
Platform:	GPL1261
Pubmed ID:	20534447
Summary & Design:	**Summary:** Mutation of rod photoreceptor-enriched transcription factors is a major cause of inherited blindness. We identified the orphan nuclear hormone receptor ERR‚† as selectively expressed in rod photoreceptors. Overexpression of ERR‚† induces expression of rod-specific genes in retinas of both wildtype and in Nrl-/- mice, which lack rod photoreceptors. Mutation of ERR‚† results in dysfunction and degeneration of rods, while inverse agonists of ERR‚† trigger rapid rod degeneration, which is rescued by constitutively active mutants of ERR‚†. ERR‚† coordinates expression of multiple genes that are rate-limiting regulators of ATP generation and consumption in photoreceptors. Furthermore, enhancing ERR‚† activity rescues photoreceptor defects that result from loss of the photoreceptor-specific transcription factor Crx. Our findings demonstrate that ERR‚† is a critical regulator of rod photoreceptor function and survival, and suggest that ERR‚† agonists may be useful in the treatment of certain retinal dystrophies. **Overall design:** Affymetrix MOE430 microarrays were used to analyze the expression patterns of P21 mouse retinal tissues. The results were compared across the variable of Genotype, specifically ERR‚† knockout versus wildtype.

Background corr dist: KL-Divergence = 0.0113, L1-Distance = 0.0143, L2-Distance = 0.0002, Normal std = 0.8473

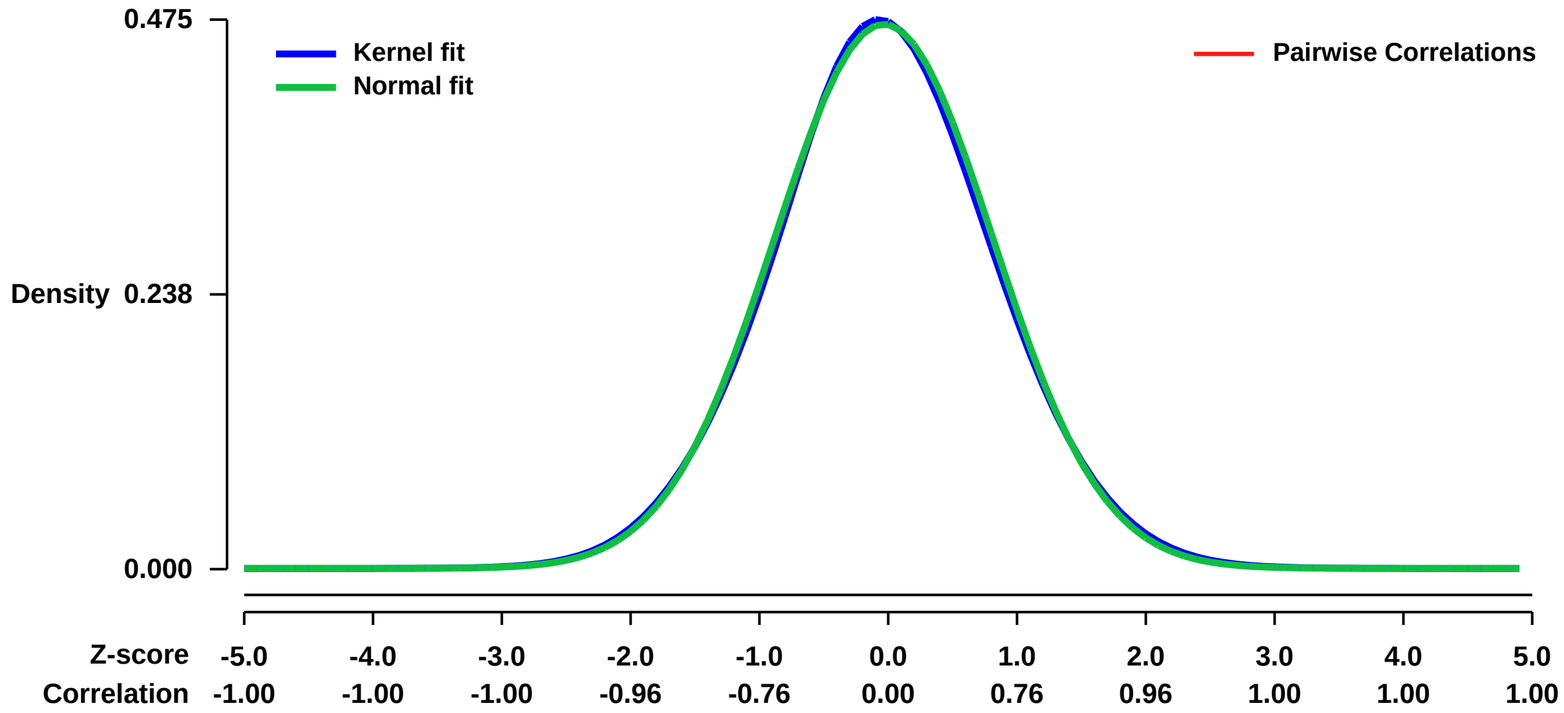

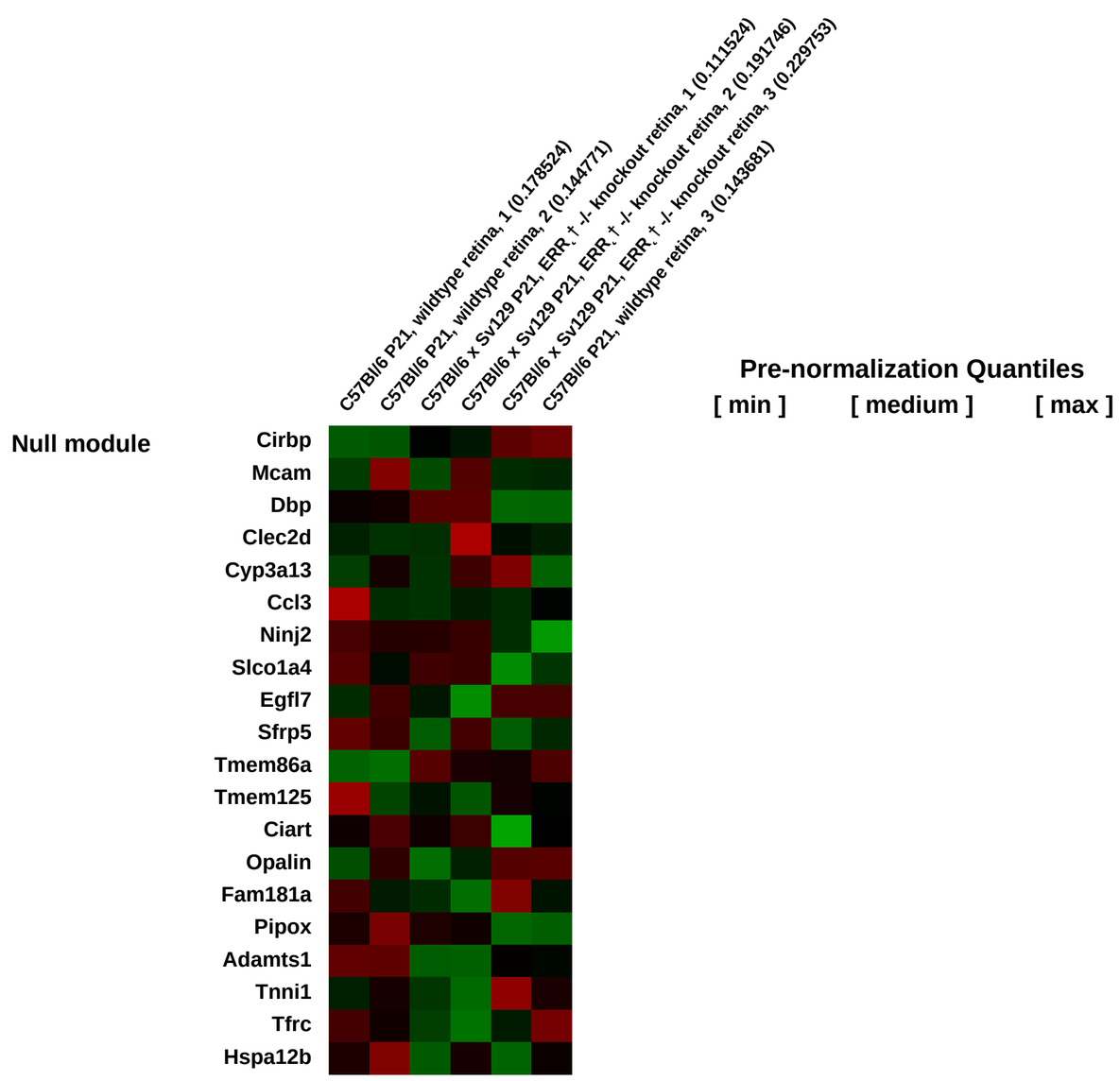

GEO Series "GSE22005" Expression Profiles

Num of samples in this series: 23

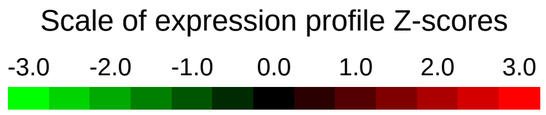

GEO Link:	**http://www.ncbi.nlm.nih.gov/geo/query/acc.cgi?acc=GSE22005**
Status:	**Public on Sep 29 2010**
Title:	**Medulloblastoma tumors derived from Ptch+/-HIC+/- transgenic mouse allografted in nude mice**
Organism:	**Mus musculus**
Experiment type:	**Expression profiling by array**
Platform:	**GPL1261**
Pubmed ID:	
Summary & Design:	**Summary:** **Nude mice were allografted with medulloblastoma tumors derived from Ptch+/-HIC+/- transgenic mouse and treated with vehicle or NVP-LDE225.** **Overall design:** **RNA was prepared from tumours from vehicle or NVP-LDE225 treated nude mice allografted with medulloblastoma tumors derived from Ptch+/-HIC+/- transgenic mouse and hybridized on the Affymetrix Mouse Genome 430A 2.0 RNA expression microarray.**

Background corr dist: **KL-Divergence = 0.1856, L1-Distance = 0.0392, L2-Distance = 0.0027, Normal std = 0.3550**

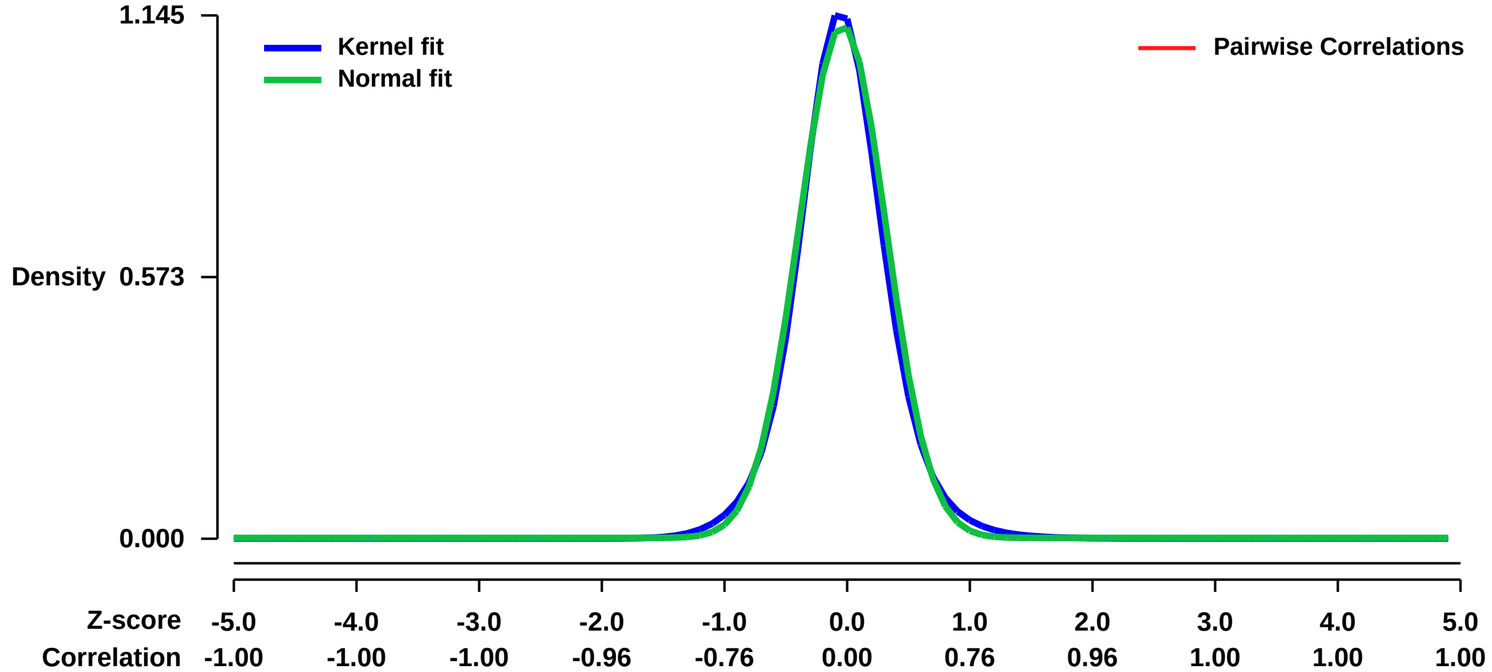

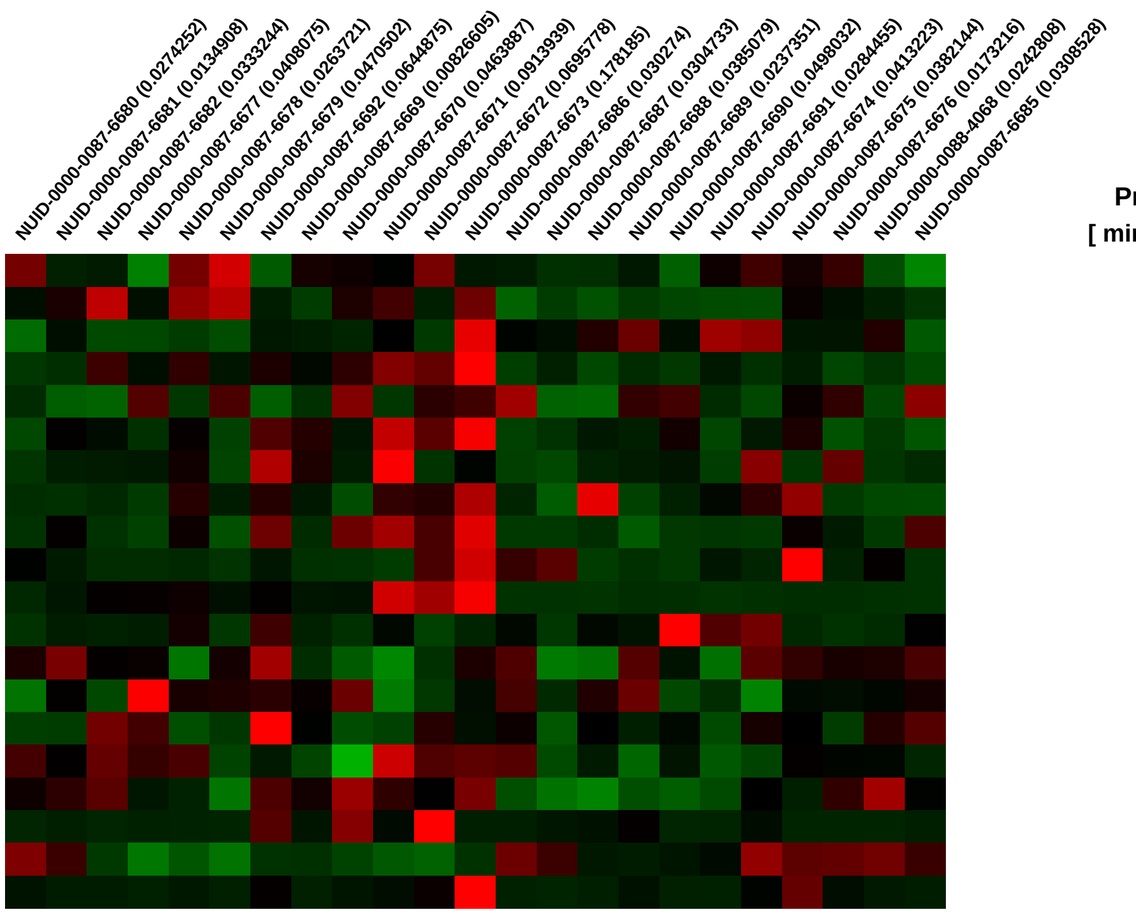

GEO Series "GSE22006" Expression Profiles

Num of samples in this series: 19

Scale of expression profile Z-scores

-3.0 -2.0 -1.0 0.0 1.0 2.0 3.0

GEO Link:	**http://www.ncbi.nlm.nih.gov/geo/query/acc.cgi?acc=GSE22006**
Status:	**Public on Sep 29 2010**
Title:	**Medulloblastoma tumors derived from Ptch+/-p53-/- transgenic mouse allografted in nude mice**
Organism:	**Mus musculus**
Experiment type:	**Expression profiling by array**
Platform:	**GPL1261**
Pubmed ID:	
Summary & Design:	**Summary:** **Nude mice were allografted with medulloblastoma tumors derived from Ptch+/-p53-/- transgenic mouse and treated with vehicle or NVP-LDE225.** **Overall design:** **RNA was prepared from tumours from vehicle or NVP-LDE225 treated nude mice allografted with medulloblastoma tumors derived from Ptch+/-p53-/- transgenic mouse and hybridized on the Affymetrix Mouse Genome 430A 2.0 RNA expression microarray.**

Background corr dist: **KL-Divergence = 0.2745, L1-Distance = 0.0620, L2-Distance = 0.0103, Normal std = 0.2907**

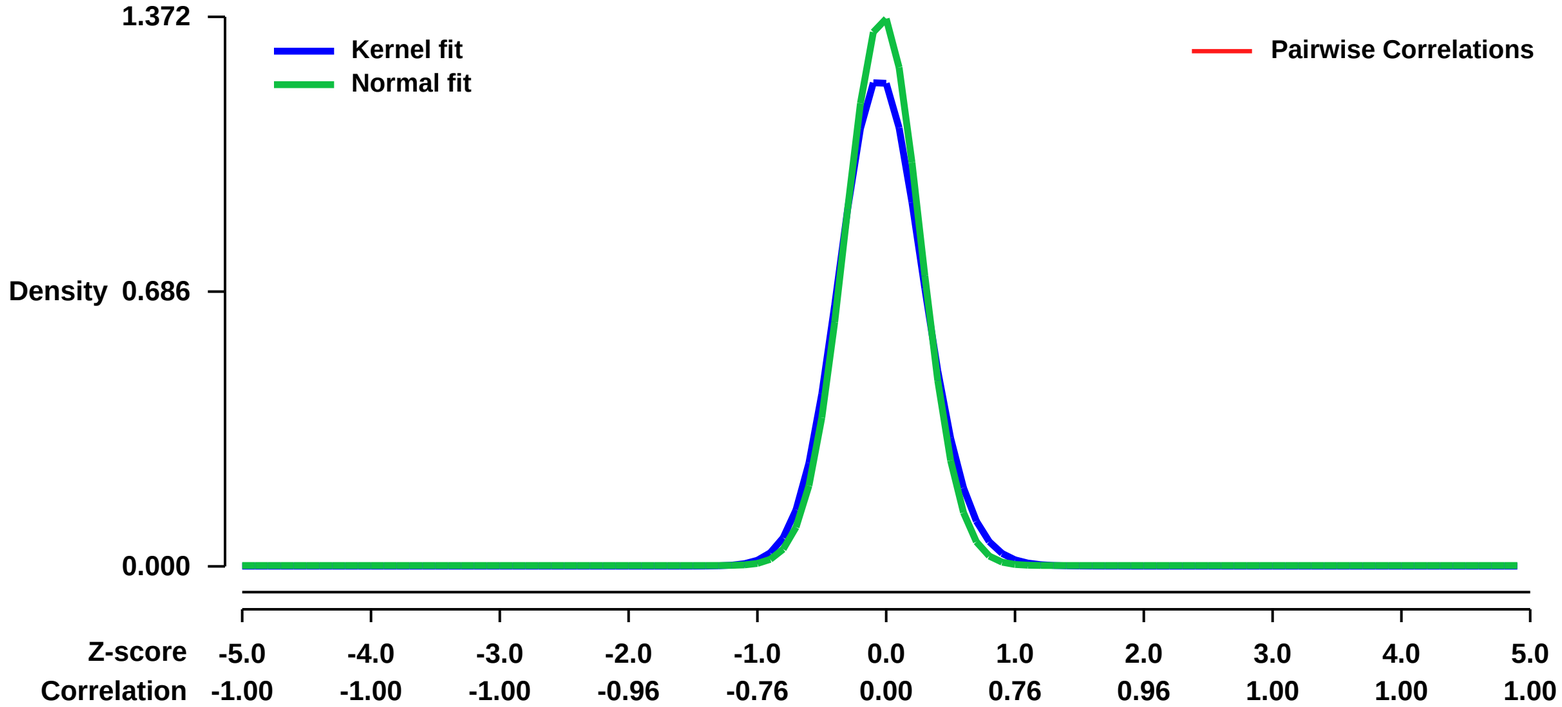

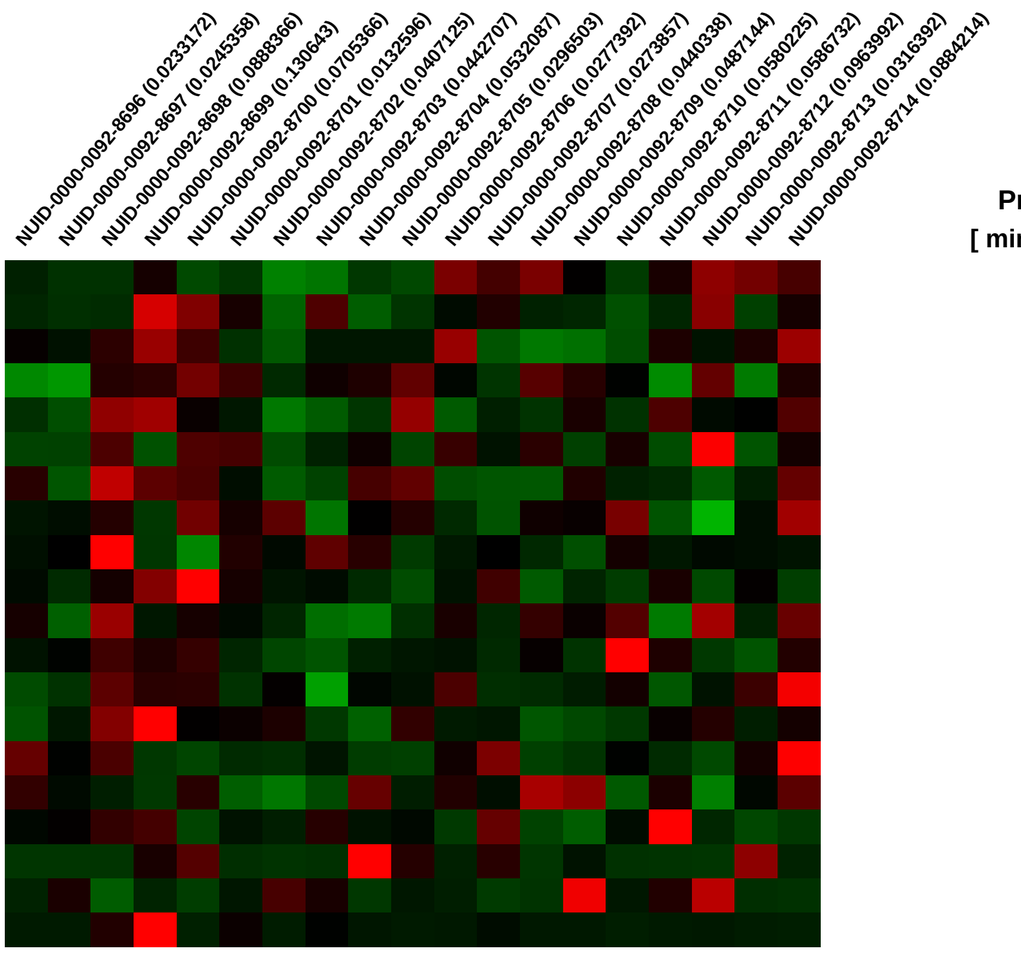

GEO Series "GSE22034" Expression Profiles

Num of samples in this series: 8

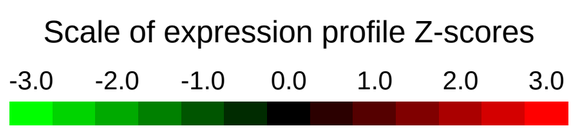

GEO Link:	http://www.ncbi.nlm.nih.gov/geo/query/acc.cgi?acc=GSE22034
Status:	Public on Jun 16 2012
Title:	Transcriptional profiling of ex vivo isolated mouse blood vascular and lymphatic endothelial cells
Organism:	Mus musculus
Experiment type:	Expression profiling by array
Platform:	GPL1261
Pubmed ID:	22723300
Summary & Design:	**Summary:** The lymphatic vascular system plays important roles in the maintenance of interstitial fluid pressure, the afferent immune response and the absorption of dietary lipids. However, the molecular mechanisms that control lymphatic vessel network maturation and function remain largely unknown. To identify novel players in lymphatic vessel function, we isolated pure populations of lymphatic and blood vascular endothelial cells from mouse intestine using fluorescence-activated high-speed cell sorting and performed transcriptional profiling. We found that the axonal guidance molecules semaphorin 3A (Sema3A) and Sema3D were specifically expressed by lymphatic vessels. Quantitative PCR of ex vivo isolated cells and immunohistochemical analysis confirmed these results. Importantly, we found that the semaphorin receptor neuropilin-1 (Nrp-1) is expressed on the valves of collecting lymphatic vessels. Treatment of mice in utero (E12.5-E16.5) with an antibody that blocks Sema3A binding to Nrp-1, but not with an antibody that blocks VEGFA binding to Nrp-1, resulted in abnormal development of collecting lymphatic vessels and valves, and aberrant smooth muscle cell coverage. Conversely, Sema3A-deficient mice displayed branching defects of collecting lymphatic vessels as well as impaired valve development. Together, these results reveal an unanticipated role of Sema3A/Nrp-1 signaling in the maturation of the lymphatic vascular network. **Overall design:** Colon single-cell suspensions were prepared by a fast protocol that minimizes the RNA degradation. Fluorescence-activated cell sorting (FACS) was used to sort blood vascular endothelial cells (BEC) and lymphatic endothelial cells (LEC). 4 animal-matched pairs of LEC and BEC were chosen based on the quality of extracted and amplified material to provide homogenous groups of biological replicates. This gave 8 samples to analyze. Samples present LEC and BEC isolated from 4 healthy normal mice. The 4 mice used present the 4 biological replicates.

Background corr dist: KL-Divergence = 0.1053, L1-Distance = 0.0915, L2-Distance = 0.0169, Normal std = 0.4951

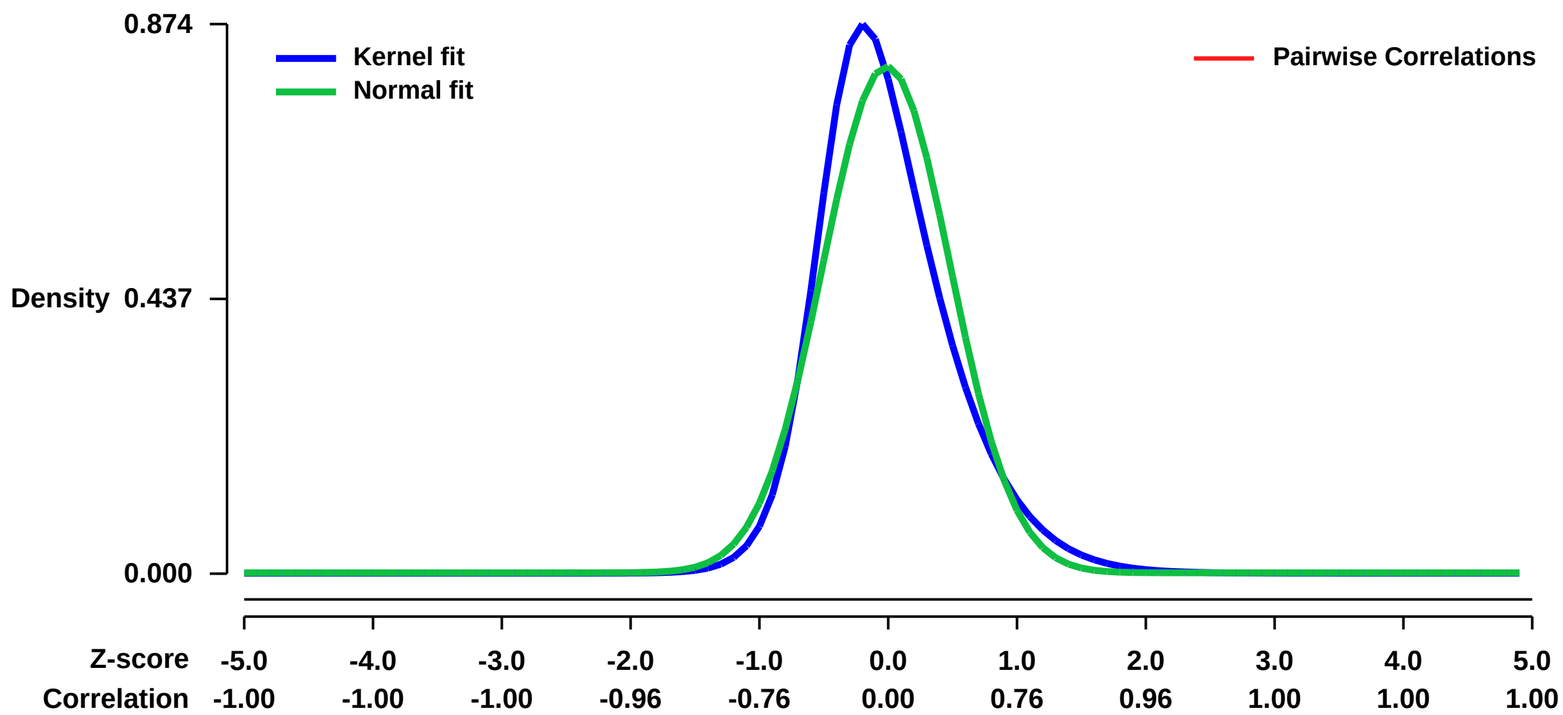

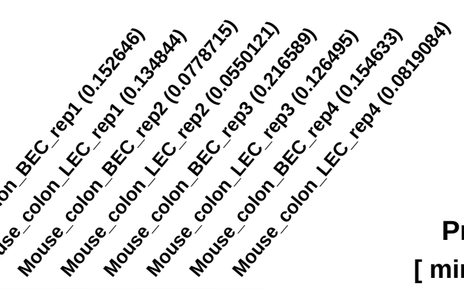

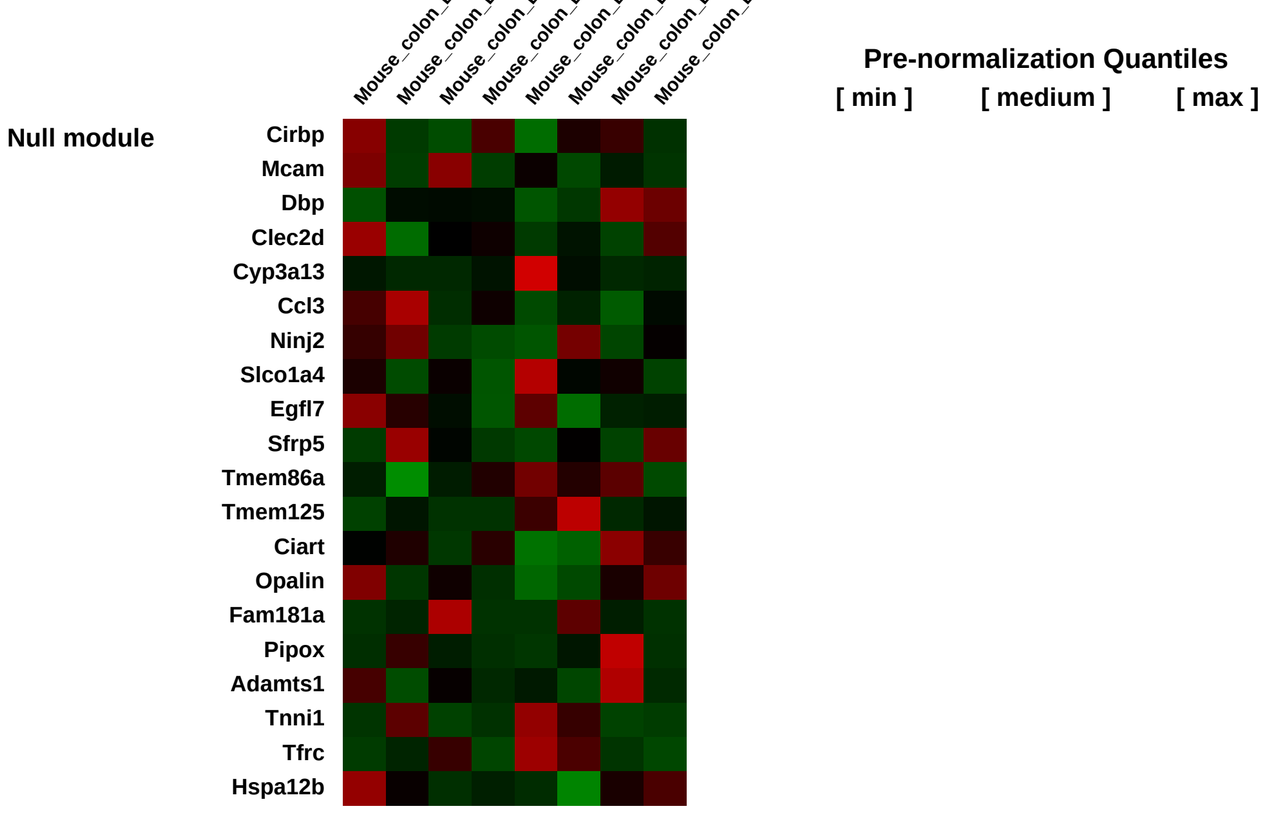

GEO Series "GSE22039" Expression Profiles

Num of samples in this series: 9

Scale of expression profile Z-scores

-3.0 -2.0 -1.0 0.0 1.0 2.0 3.0

GEO Link:	**http://www.ncbi.nlm.nih.gov/geo/query/acc.cgi?acc=GSE22039**
Status:	**Public on Dec 01 2010**
Title:	**Gene expression data from forelimb buds of E10.5 mouse embryos**
Organism:	**Mus musculus**
Experiment type:	**Expression profiling by array**
Platform:	**GPL1261**
Pubmed ID:	
Summary & Design:	**Summary:** **We used microarrays to identify Pax3 targets during myogenesis in the mouse embryo** **Overall design:** **Mouse embryos were genotyped Pax3GFP/+ or Pax3PAX3-FKHR/GFP and dissected at E10.5 under a fluorescent binocular. The forelimb buds were dissected and dissociated and GFP positive cells were then sorted by flow cytometry before RNA extraction and hybridization on Affymetrix microarrays. We also sorted GFP negative cells.**

Background corr dist: **KL-Divergence = 0.0643, L1-Distance = 0.0217, L2-Distance = 0.0007, Normal std = 0.5113**

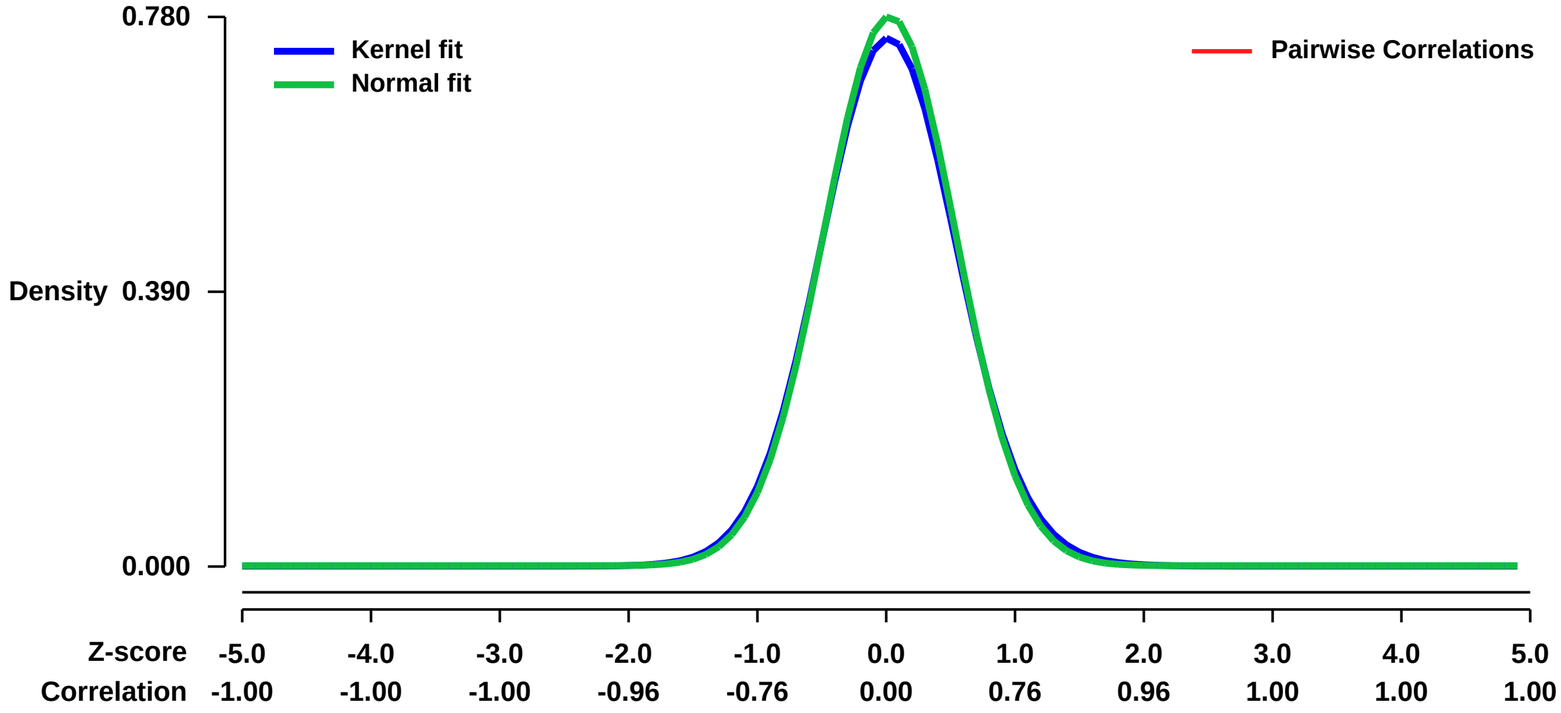

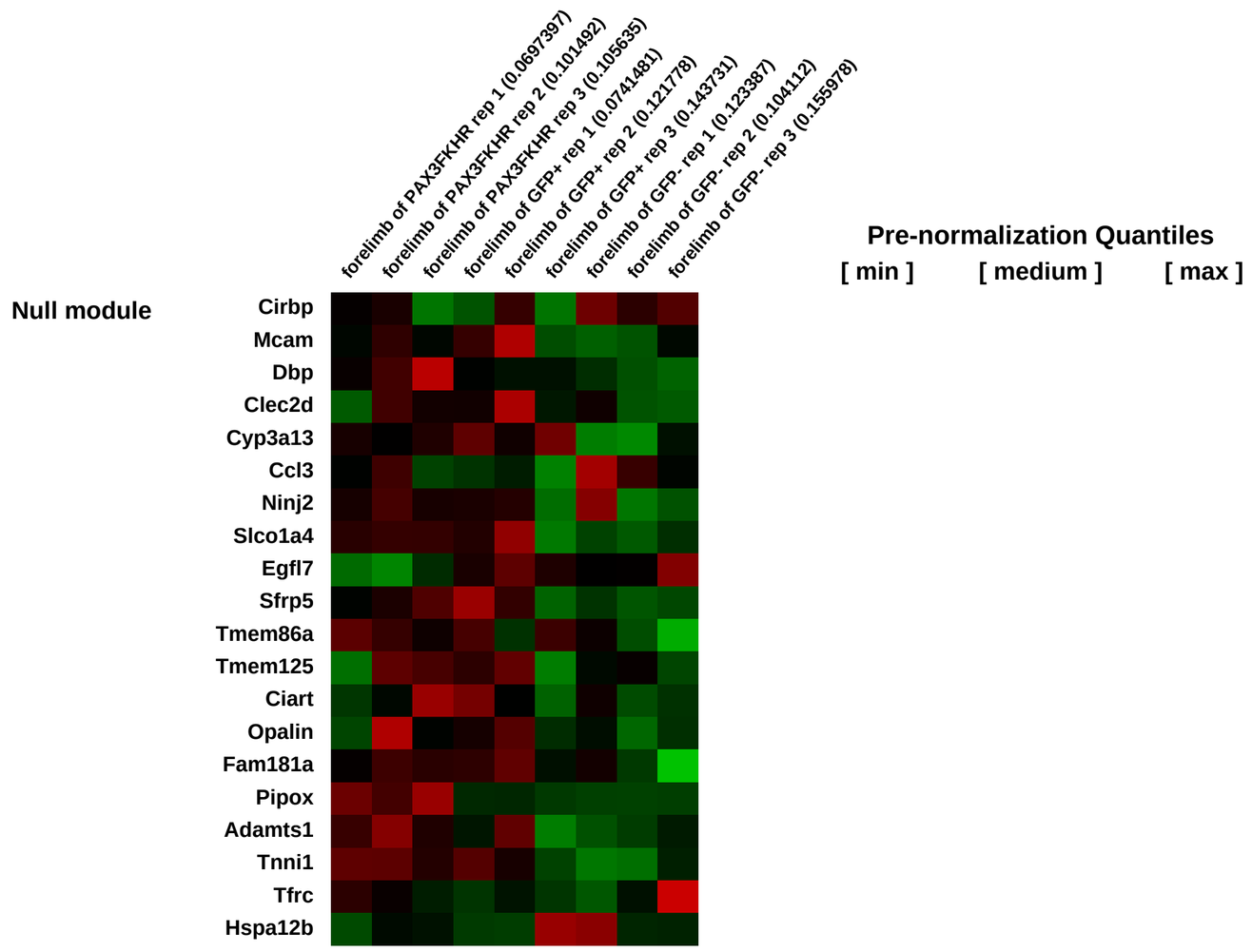

GEO Series "GSE22040" Expression Profiles

Num of samples in this series: 9

Scale of expression profile Z-scores

-3.0 -2.0 -1.0 0.0 1.0 2.0 3.0

GEO Link: http://www.ncbi.nlm.nih.gov/geo/query/acc.cgi?acc=GSE22040
Status: Public on Dec 01 2010
Title: Gene expression data from somites of E9.5 mouse embryos
Organism: Mus musculus
Experiment type: Expression profiling by array
Platform: GPL1261
Pubmed ID:
Summary & Design:

Summary:
We used microarrays to identify Pax3 targets during myogenesis in the mouse embryo

Overall design:
Mouse embryos were genotyped Pax3GFP/+ or Pax3PAX3-FKHR/GFP and dissected at E9.5 under a fluorescent binocular. Somites were dissected from the interlimb region and the more hypaxial domain separated from the neural tube and the epaxial extremity of the somites. GFP positive cells were then sorted by flow cytometry before RNA extraction and hybridization on Affymetrix microarrays. We also sorted GFP negative cells.

Background corr dist: KL-Divergence = 0.0785, L1-Distance = 0.0184, L2-Distance = 0.0003, Normal std = 0.4841

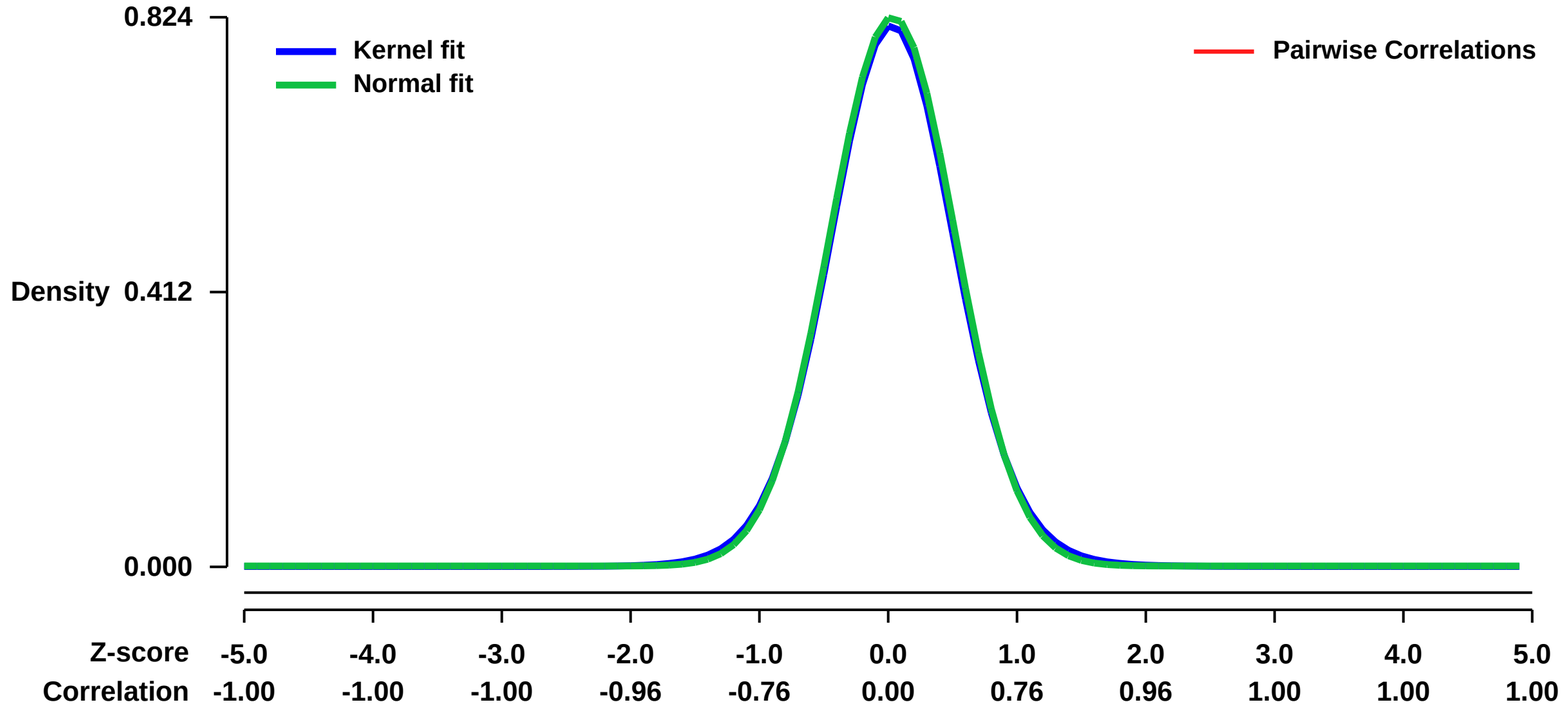

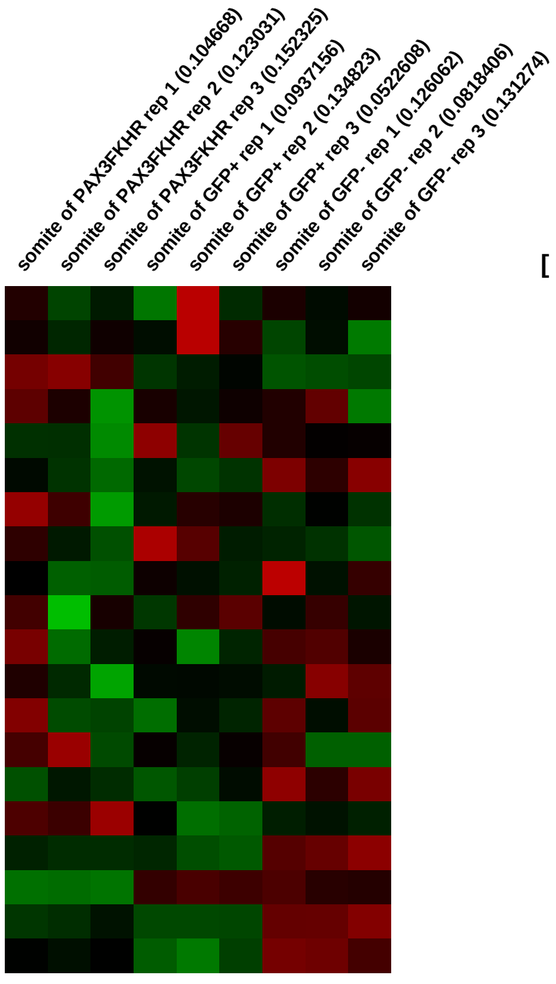

Null module

GEO Series "GSE22073" Expression Profiles

Num of samples in this series: 6

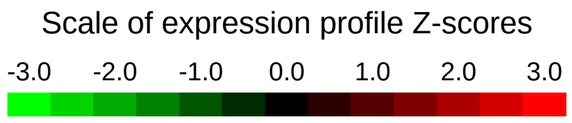

GEO Link:	http://www.ncbi.nlm.nih.gov/geo/query/acc.cgi?acc=GSE22073
Status:	Public on Jun 02 2010
Title:	Testis samples from Alkbh1 wild-type and KO mice
Organism:	Mus musculus
Experiment type:	Expression profiling by array
Platform:	GPL1261
Pubmed ID:	21072209
Summary & Design:	**Summary:** The aim of the study was to elucidate the role of Alkbh1 by targeted deletion in C57/BL6 mice. Alkb deficiency results in sex-ratio distortion of offspring and apoptosis in adult testes, most likely caused by defects in the pachytene stage during spermatogenesis. Due to the pivotal role of Alkbh1 in mouse survival and potentially in germ cells, we searched for Alkbh1-regulated genes in adult testes. **Overall design:** Testes from 12 week old mice were selected for RNA extraction and hybridization on Affymetrix microarrays. We used testes from 3 wild type mice and 3 KO mice

Background corr dist: KL-Divergence = 0.0352, L1-Distance = 0.0146, L2-Distance = 0.0002, Normal std = 0.6347

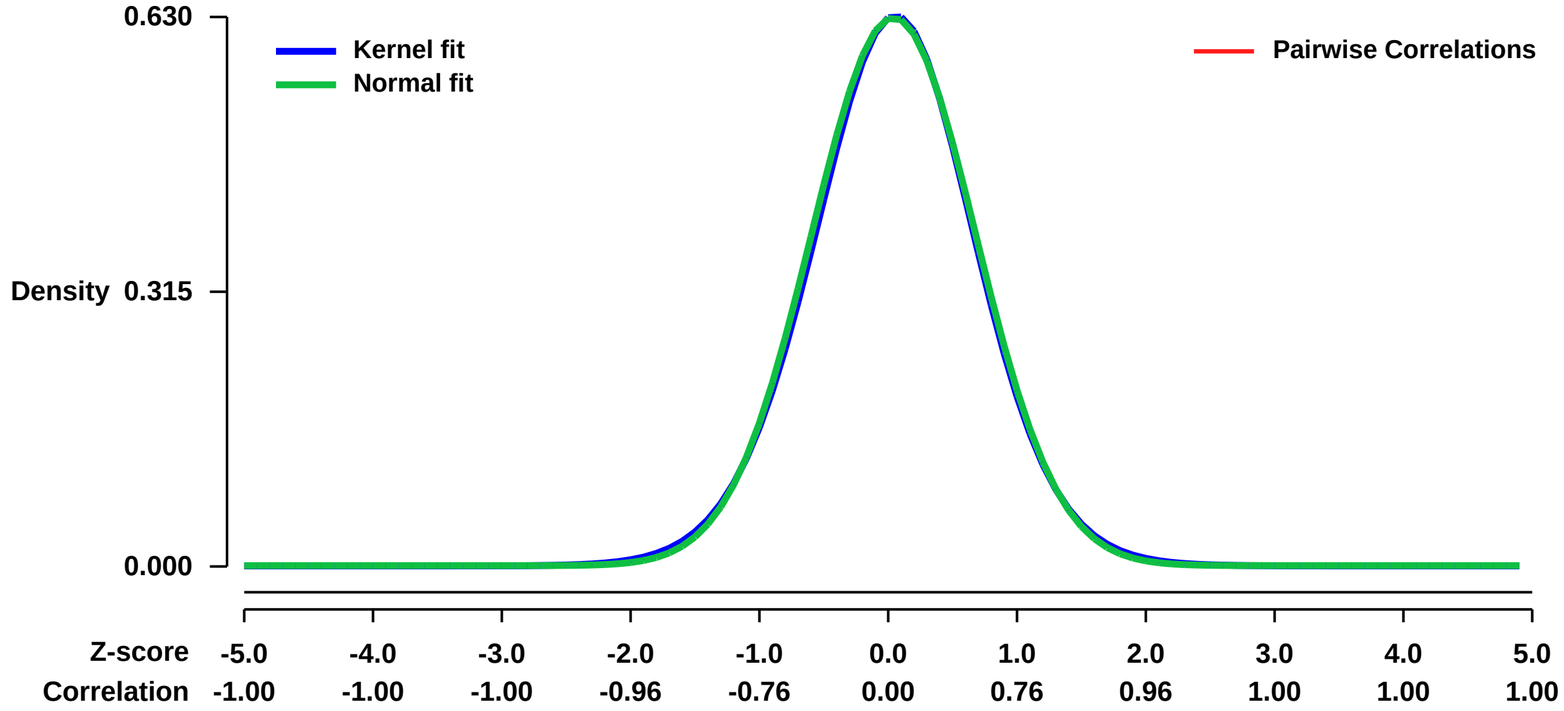

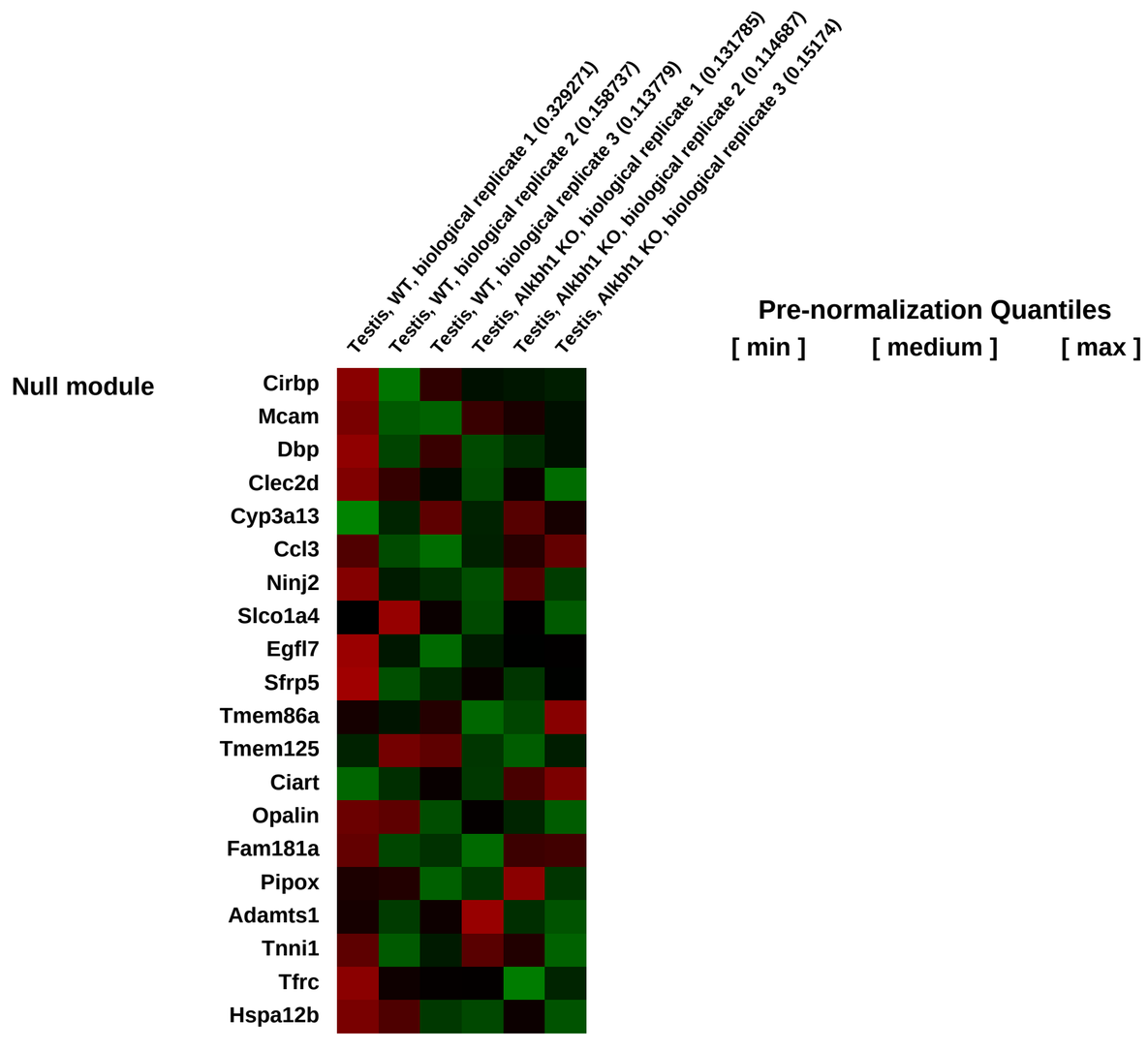

GEO Series "GSE22086" Expression Profiles

Num of samples in this series: 6

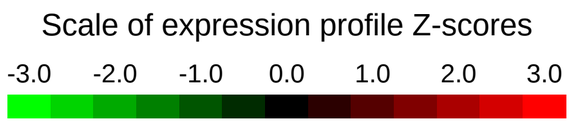

GEO Link:	**http://www.ncbi.nlm.nih.gov/geo/query/acc.cgi?acc=GSE22086**
Status:	**Public on Sep 19 2011**
Title:	**Expression data from quadriceps muscle of WT and ERRgamma transgenic mice**
Organism:	**Mus musculus**
Experiment type:	**Expression profiling by array**
Platform:	**GPL1261**
Pubmed ID:	**21356518**
Summary & Design:	**Summary:** **We show that the orphan nuclear receptor ERRg is expressed at high levels in type I muscle and when transgenically expressed in anaerobic type II muscles (ERRGO mice) or cultured cells, powerfully regulates VEGF expression, angiogenesis and vascular supply in absence of exercise. ERRGO mice show increased expression of genes promoting fat metabolism, mitochondrial respiration and type I fiber specification. In parallel, the type II muscle in ERRGO mice display an activated angiogenic program marked by myofibrillar induction and secretion of pro-angiogenic factors, frank neo-vascularization and a 100% increase in running endurance. Surprisingly, the induction of VEGF and type I muscle properties by ERRg does not involve the transcriptional co-activator PGC1a. Instead, ERRg genetically activates the energy sensor AMPK which is typically inactive in absence of exercise. Therefore, ERRg and AMPK, known regulators of mitochondrial function and metabolism, together control a novel angiogenic pathway that anatomically synchronizes vascular arborization to oxidative metabolism revealing an exercise-independent mechanism for matching supply and demand.** **Keywords: ERRgamma overexpression compared to wild-type** **Overall design:** **Comparison of gene expression from quadriceps muscles isolated from wild type and alpha-skeletal actin-ERRgamma-transgenic mice.**

Background corr dist: KL-Divergence = 0.0412, L1-Distance = 0.0214, L2-Distance = 0.0005, Normal std = 0.6143

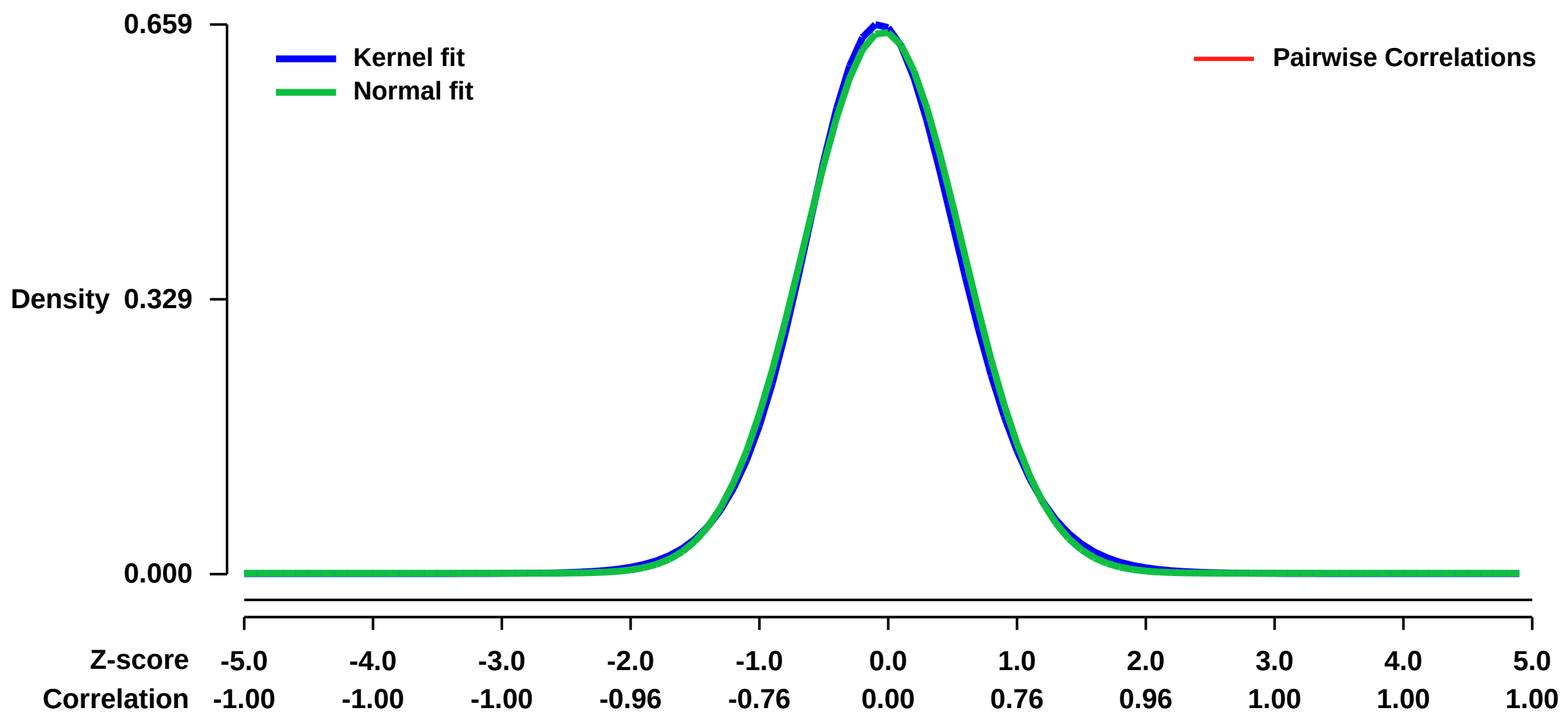

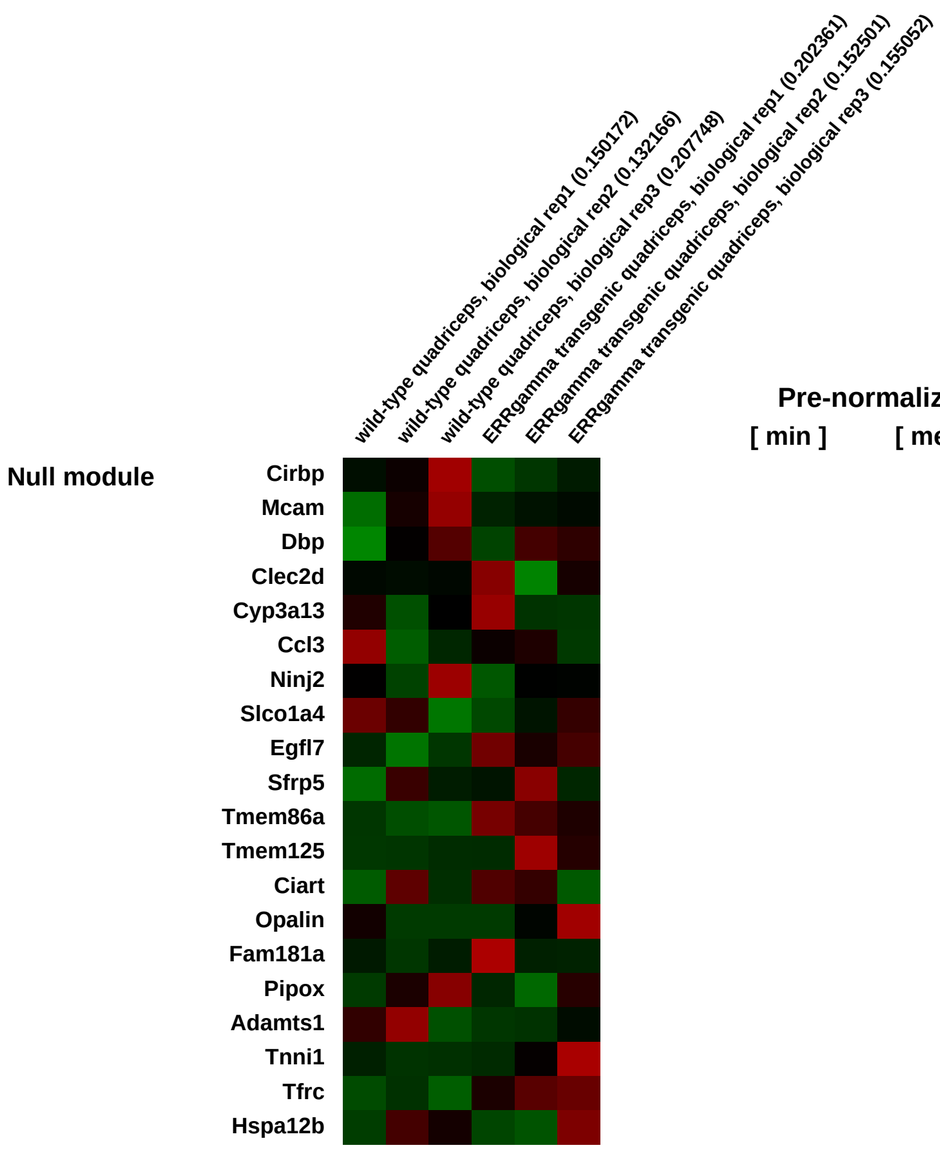

GEO Series "GSE22094" Expression Profiles

Num of samples in this series: 12

Scale of expression profile Z-scores

-3.0 -2.0 -1.0 0.0 1.0 2.0 3.0

GEO Link:	http://www.ncbi.nlm.nih.gov/geo/query/acc.cgi?acc=GSE22094
Status:	Public on Jul 01 2010
Title:	Bone marrow transcriptomal differences between wild type, Fancc-deficient, Fancg-deficient, and doubly deficient (Fancc/Fancg) mice.
Organism:	Mus musculus
Experiment type:	Expression profiling by array
Platform:	GPL1261
Pubmed ID:	20606166
Summary & Design:	**Summary:** Seeking to challenge the current dogma that the nuclear core-complex proteins function in an entirely epistatic manner, Dr. Clapp's group developed a new double-knockout mouse nullizygous for Fancc and Fancg. Because the hematopoietic phenotype was more severe than single knockout mice, we reasoned that transcriptomal differences would exist and lead to the identification of molecular defects unique to each FA gene. **Overall design:** RNA was purified from unfractionated and uncultured bone marrow cells from three types of Fanconi anemia gene knockout mice: nullizygous for Fancc, Fancg, or both Fancc and Fancg.. Three wild type C57Bl/6 mice served as controls. Each of three marrow samples provided one RNA sample (the RNA samples were not pooled).

Background corr dist: KL-Divergence = 0.1250, L1-Distance = 0.0337, L2-Distance = 0.0021, Normal std = 0.3997

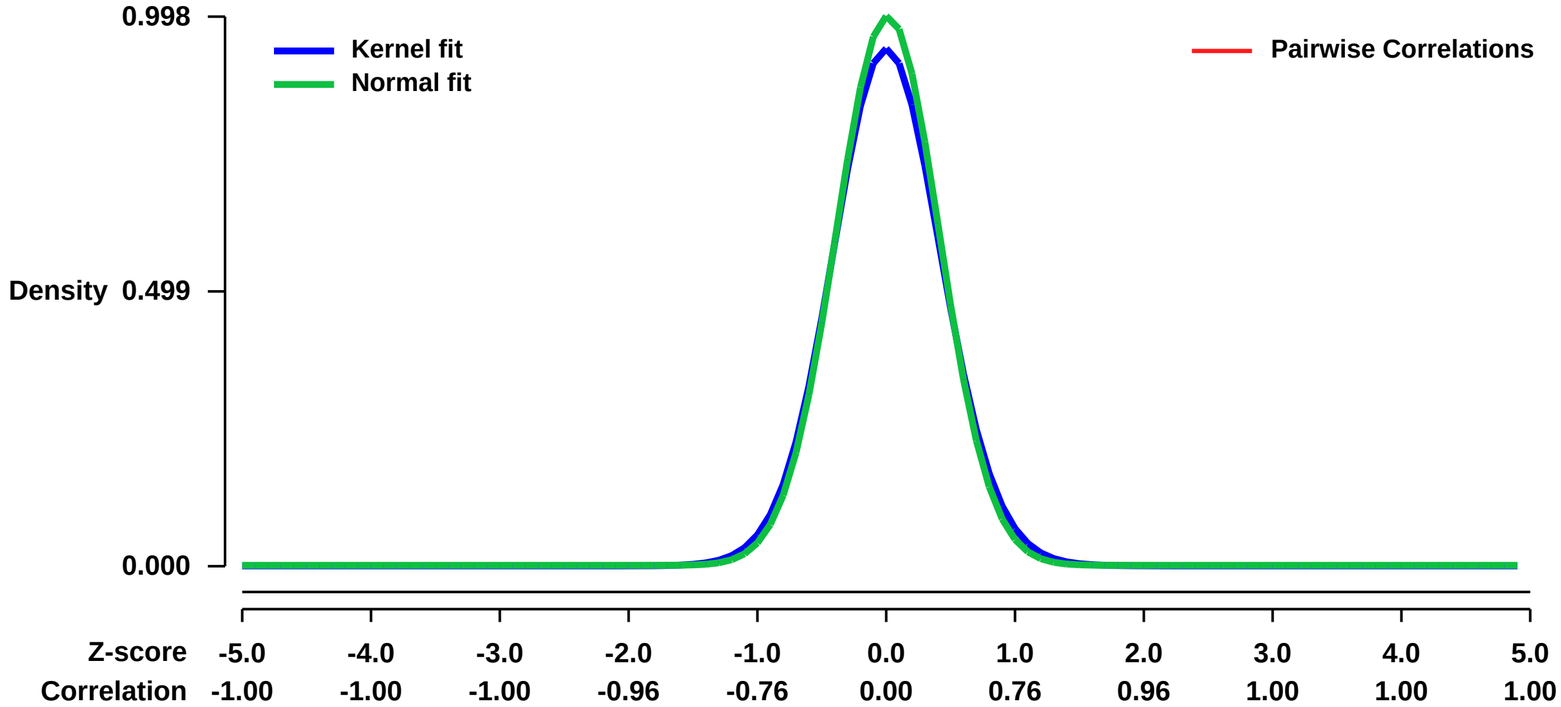

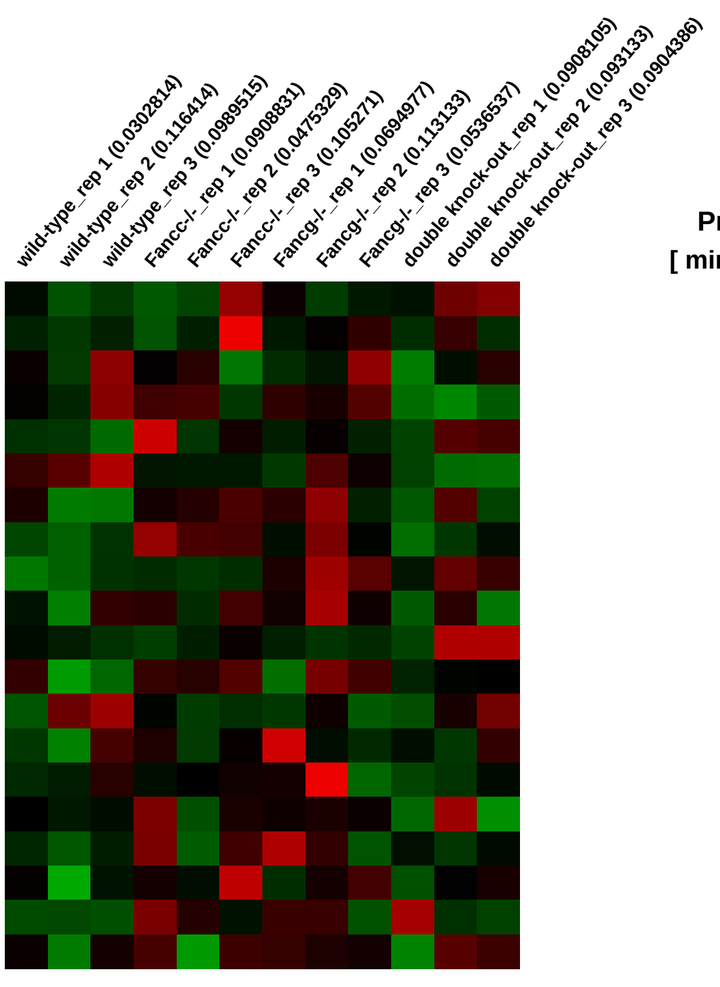

GEO Series "GSE22125" Expression Profiles

Num of samples in this series: 6

Scale of expression profile Z-scores

-3.0 -2.0 -1.0 0.0 1.0 2.0 3.0

GEO Link:	http://www.ncbi.nlm.nih.gov/geo/query/acc.cgi?acc=GSE22125
Status:	Public on Jun 04 2010
Title:	Mouse pancreatic islets during pregnancy
Organism:	Mus musculus
Experiment type:	Expression profiling by array
Platform:	GPL1261
Pubmed ID:	20581837
Summary & Design:	**Summary:** During pregnancy, pancreatic islets undergo structural and functional changes that lead to enhance insulin release in response to increased insulin demand, which is rapidly reversed at parturition. One of the most important changes is expansion of pancreatic ¸†-cell mass mainly by increased proliferation of ¸† cells. We used microarrays to detail the global programme of gene expression and identified distinct up- or down-regulated genes during pregnancy. **Overall design:** Maternal islet were isolated from mice at dpc 0 and 12.5 dpc of pregnancy for RNA extraction and hybridization on Affymetrix microarrays. We sought to identify the responsible factors for the proliferation of islets during pregnancy.

Background corr dist: KL-Divergence = 0.0435, L1-Distance = 0.0196, L2-Distance = 0.0004, Normal std = 0.6024

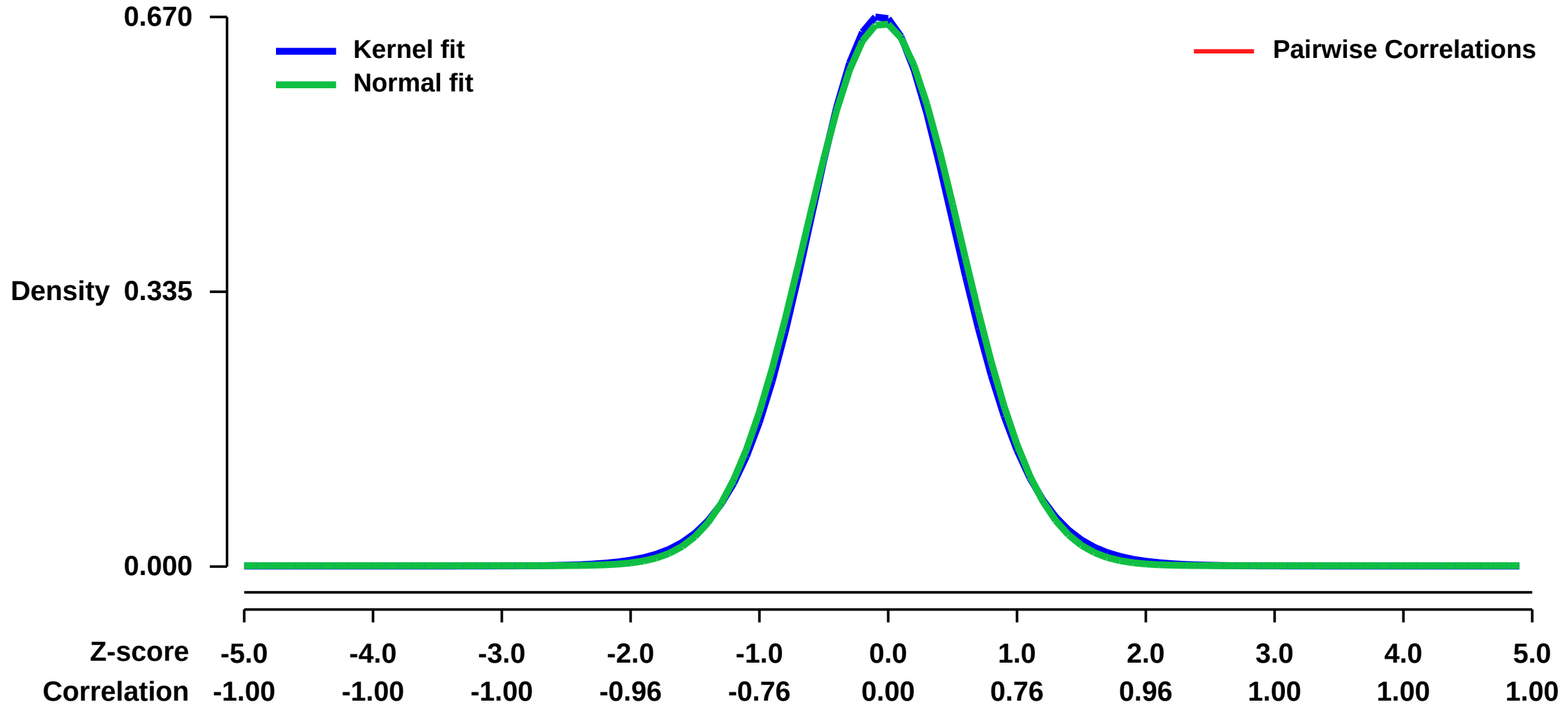

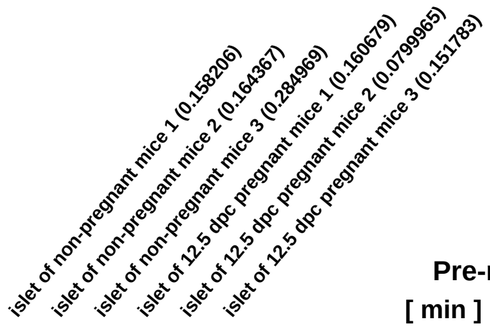

Pre-normalization Quantiles

[min] [medium] [max]

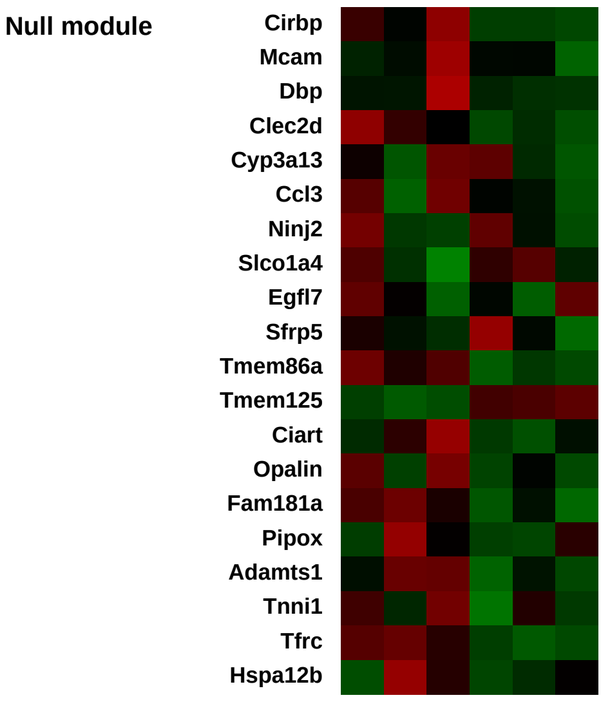

GEO Series "GSE22140" Expression Profiles

Num of samples in this series: 13

Scale of expression profile Z-scores

-3.0 -2.0 -1.0 0.0 1.0 2.0 3.0

GEO Link:	http://www.ncbi.nlm.nih.gov/geo/query/acc.cgi?acc=GSE22140
Status:	Public on Jun 05 2010
Title:	Arthritic KRN T cells and wild type T cells from germ free and specific pathogen free mice
Organism:	Mus musculus
Experiment type:	Expression profiling by array
Platform:	GPL1261
Pubmed ID:	20620945
Summary & Design:	**Summary:** A general defect of GF K/BxN T cell proliferation response toward antigen motivated us to look for the impairment in GF K/BxN T cells that might leads to the low Ab production and reduced disease phenotype seen in GF K/BxN mice. To find the difference between GF and SPF K/BxN T cells in a broad and non-biased fashion, we performed gene-expression profiling of these cells using microarrays. **Overall design:** All gene expression profiles were obtained from highly purified T cell populations sorted by flow cytometry. To reduce variability, cells from multiple mice were pooled for sorting, and triplicates or quadruplates were generated for all groups. Raw data were preprocessed with the RMA algorithm in GenePattern, and averaged expression values were used for analysis.

Background corr dist: KL-Divergence = 0.0478, L1-Distance = 0.0480, L2-Distance = 0.0044, Normal std = 0.5756

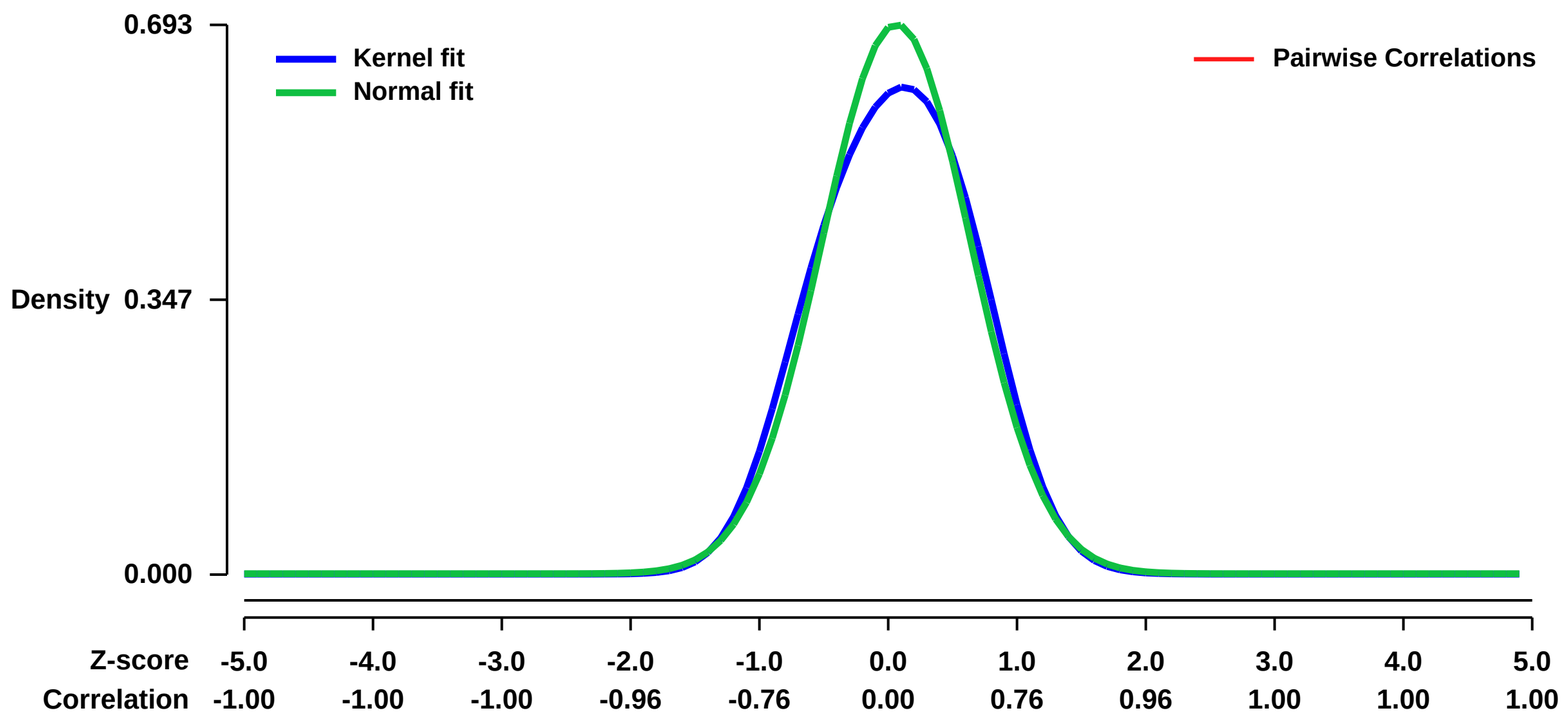

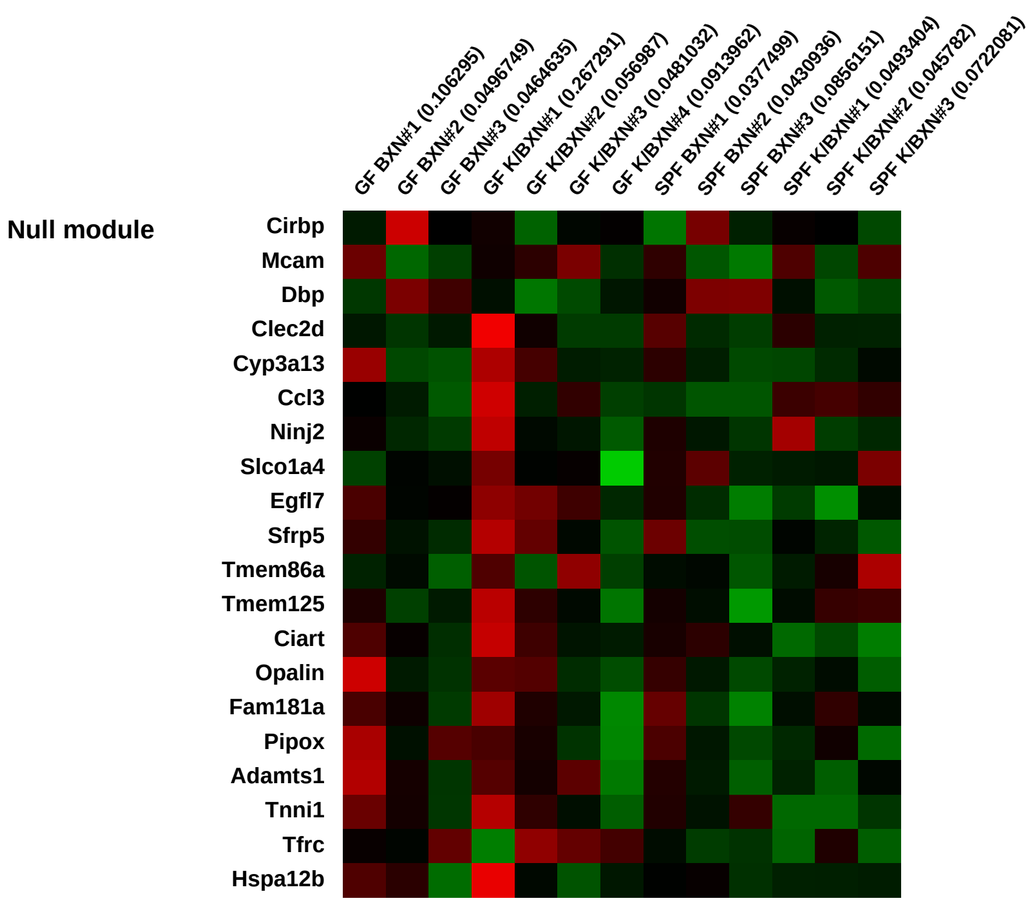

GEO Series "GSE22251" Expression Profiles

Num of samples in this series: 9

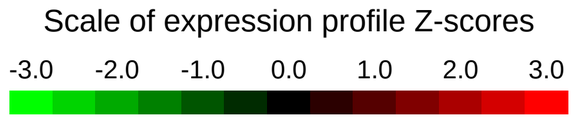

GEO Link:	http://www.ncbi.nlm.nih.gov/geo/query/acc.cgi?acc=GSE22251
Status:	Public on Sep 09 2011
Title:	Necdin, a Negative Growth Regulator, is a Novel STAT3 Target Gene Down-Regulated in Human Cancer
Organism:	Mus musculus
Experiment type:	Expression profiling by array
Platform:	GPL1261
Pubmed ID:	22046235
Summary & Design:	**Summary:** We took a broad approach to identify novel STAT3 regulated genes by examining changes in the genome-wide gene expression profile by microarray, using cells expressing constitutively-activated STAT3. Using computational analysis, we were able to define the gene expression profiles of cells containing activated STAT3 and identify candidate target genes with a wide range of biological functions. We demonstrated that STAT3 has an important role in regulating, both positively and negatively, a diverse array of cellular processes, including cell adhesion, cytoskeletal remodeling, nucleotide, lipid and protein metabolism, as well as signal transduction. This suggest that STAT3 coordinates expression of genes involved in multiple metabolic and biosynthetic pathways, integrating signals that lead to global transcriptional changes and oncogenesis. **Overall design:** Balb/c-3T3 mouse fibroblasts, v-Src 3T3 cells and STAT3-C 3T3 cells were grown in DMEM/10% bovine calf serum supplemented with 1% penicillin and streptomycin. At each of 3 passages, cells from the five dishes were pooled and total RNA was extracted.

Background corr dist: KL-Divergence = 0.0448, L1-Distance = 0.0153, L2-Distance = 0.0002, Normal std = 0.5807

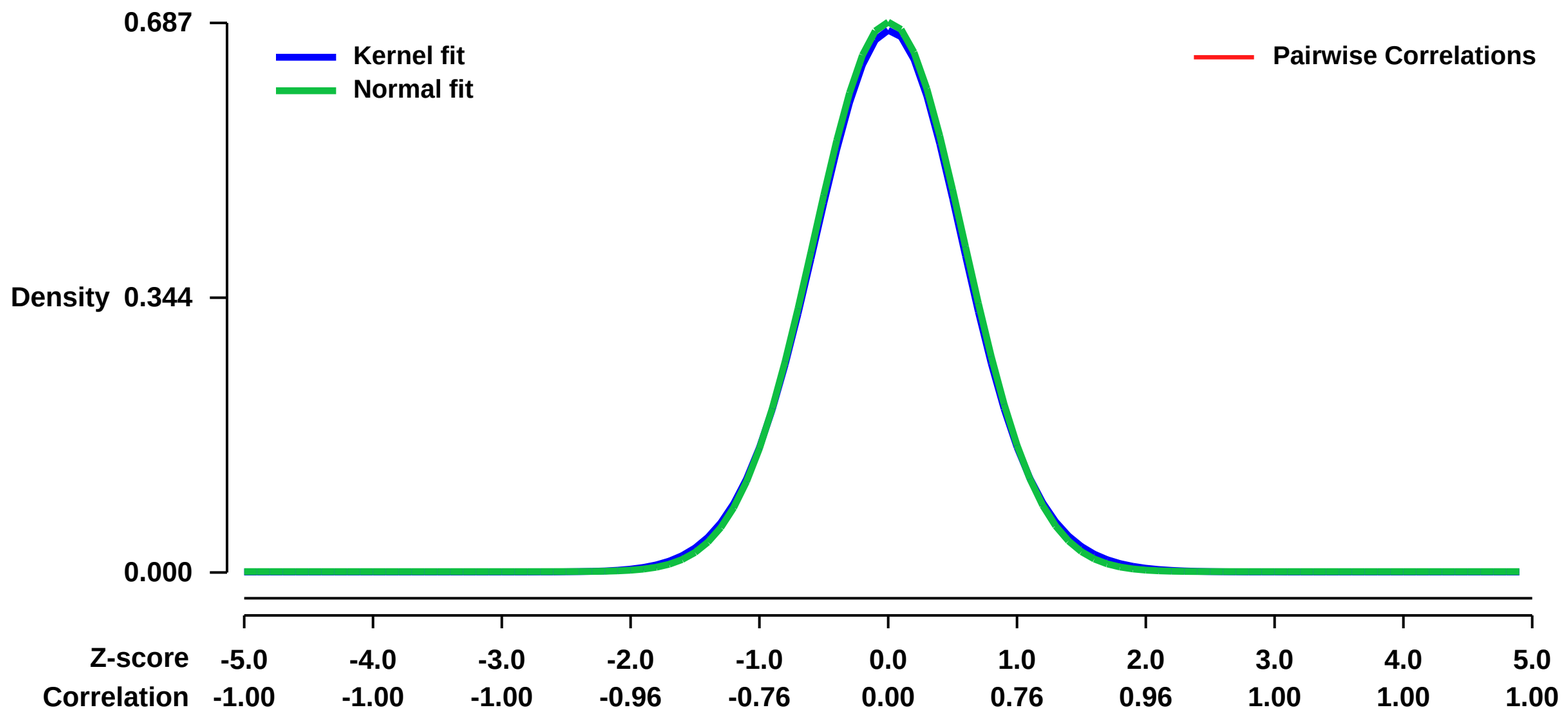

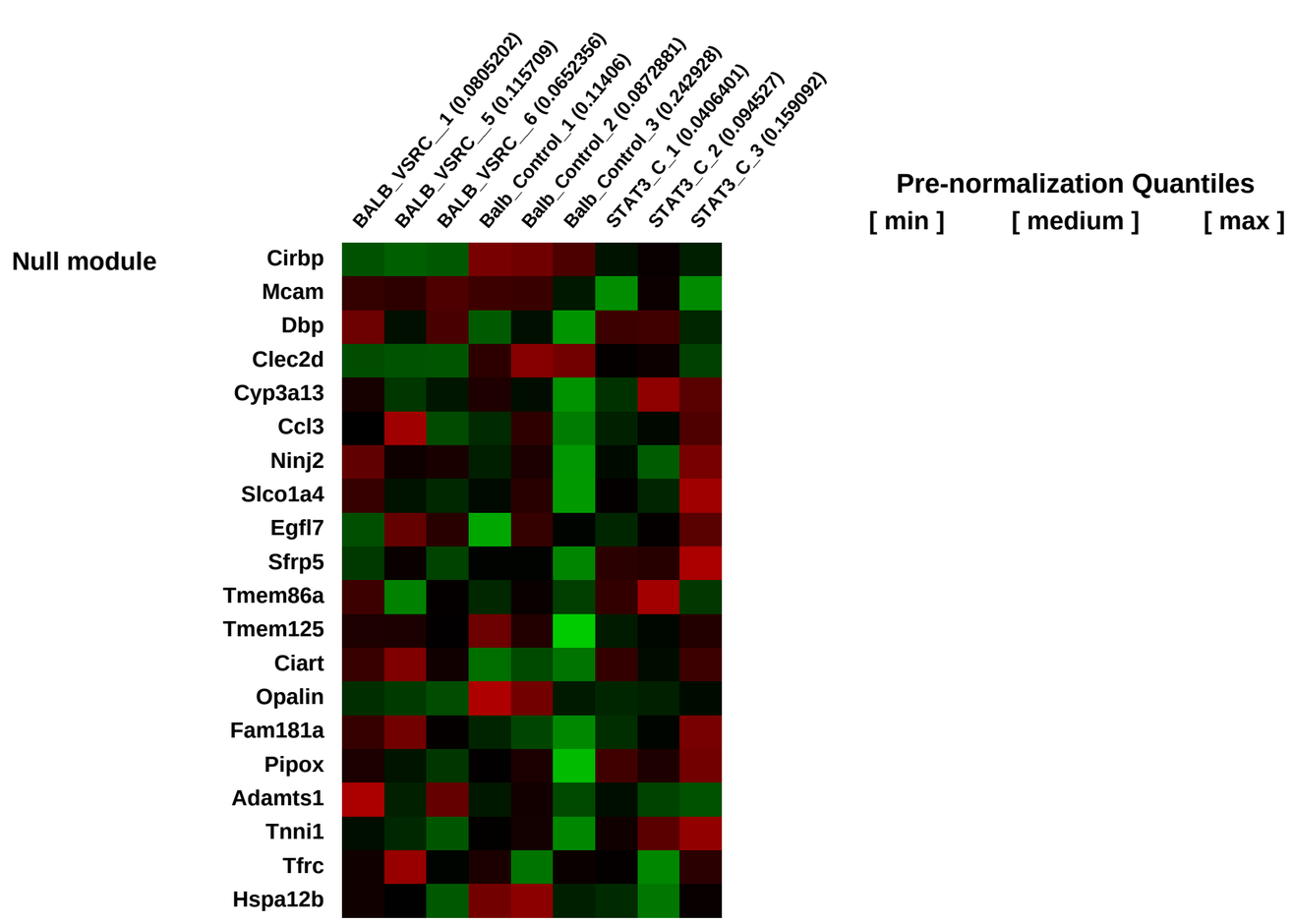

GEO Series "GSE22283" Expression Profiles

Num of samples in this series: 8

Scale of expression profile Z-scores

-3.0 -2.0 -1.0 0.0 1.0 2.0 3.0

GEO Link:	http://www.ncbi.nlm.nih.gov/geo/query/acc.cgi?acc=GSE22283
Status:	Public on Jul 06 2011
Title:	expression data in lung of mice bearing inducible FGF18 transgene
Organism:	Mus musculus
Experiment type:	Expression profiling by array
Platform:	GPL1261
Pubmed ID:	21878612
Summary & Design:	**Summary:** Better understanding alveolarization mechanisms could help improving prevention and treatment of diseases characterized by reduced alveolar number, especially bronchopulmonary dysplasia (BPD). Although signaling through fibroblast growth factor (FGF) receptors is essential for alveolarization, involved ligands are unidentified. FGF18 whose expression peaks during alveolar septation is likely to be involved. Herein, a mouse model of inducible, lung-targeted FGF18-transgene was used to advance the onset of FGF18 expression, and genome-wide expression changes were determined. keywords: transgenic mice, alveolarization, angiogenesis, fibrosis, epithelial-mesenchymal transition. **Overall design:** Four pairs of simple and double transgenic pups issued from 4 different litters were selected on the basis of FGF18 transgene induction. RNA from the mice lung were extracted and hybridized on Affymetrix microarrays.

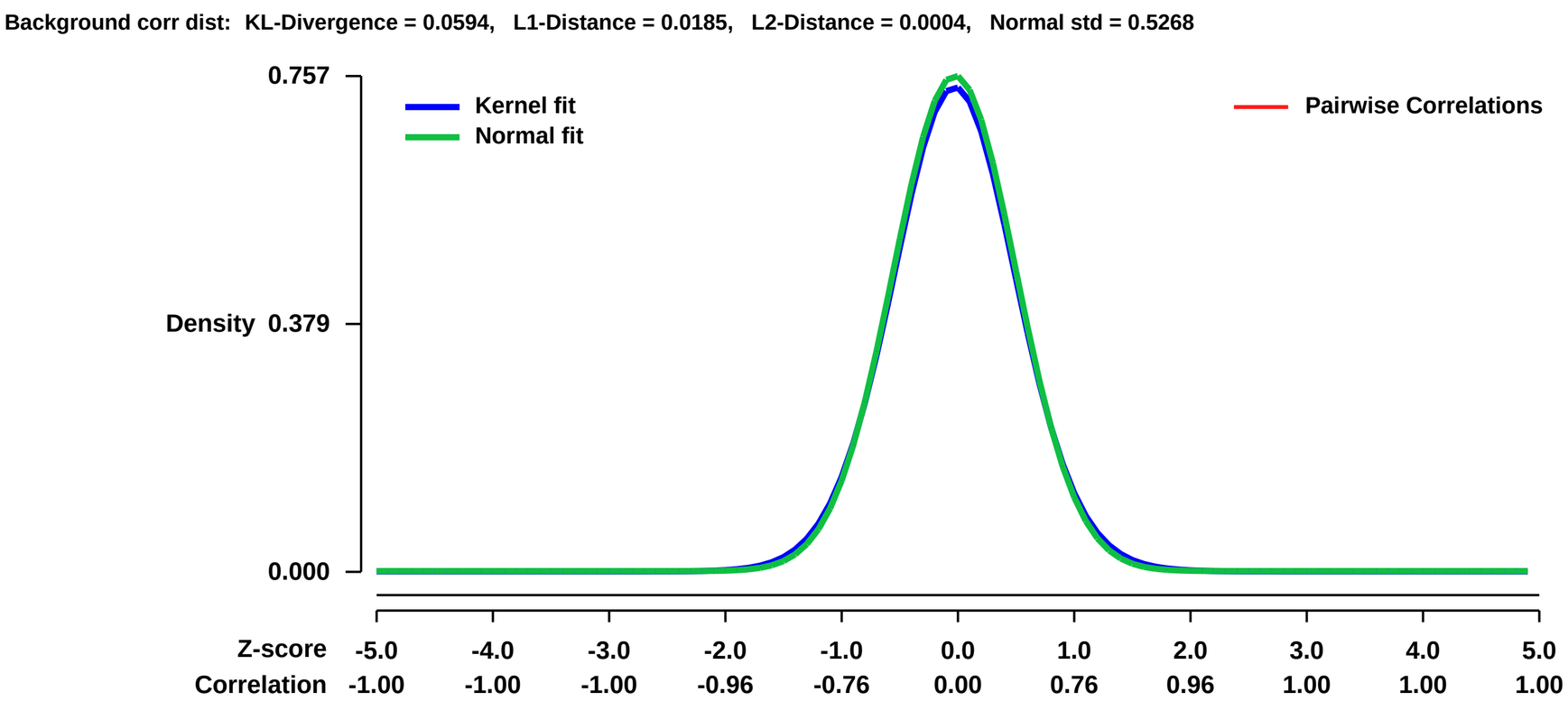

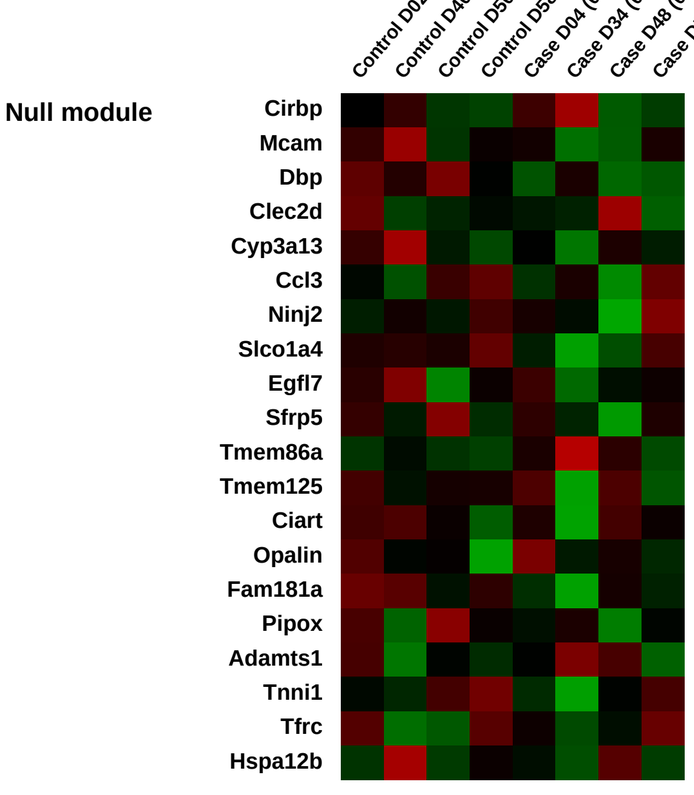

GEO Series "GSE2229" Expression Profiles

Num of samples in this series: 8

Scale of expression profile Z-scores

-3.0 -2.0 -1.0 0.0 1.0 2.0 3.0

GEO Link:	http://www.ncbi.nlm.nih.gov/geo/query/acc.cgi?acc=GSE2229
Status:	Public on Apr 01 2005
Title:	Mouse preimplantation development
Organism:	Mus musculus
Experiment type:	Expression profiling by array
Platform:	GPL1261
Pubmed ID:	15772134
Summary & Design:	**Summary:** We examined expression profiles of genes that could be regulated by the MAPK pathways during mouse preimplantation development. We used Affymetrix GeneChips for microarray analysis, and three independent experiments were carried out. 8-cell stage embryos were treated or untreated with MAPK inhibitors, and blastocyst stage embryos were recruited for the study. Hybridization was carried out with the GeneChip Mouse Expression Set 430 or GeneChip Mouse Genome 430 2.0 Array following Affymetrix instructions. The array was then washed and stained using the GeneChip fluidics station according to the manufacture's instructions. Hybridized arrays were scanned using an Affymetrix GeneChip Scanner. Expression analysis was performed using GeneChip Operating Software 1.0 (Affymetrix) and scaled to an average probe set intensity of 500. **Keywords:** other **Overall design:**

Background corr dist: KL-Divergence = 0.0853, L1-Distance = 0.0251, L2-Distance = 0.0011, Normal std = 0.4660

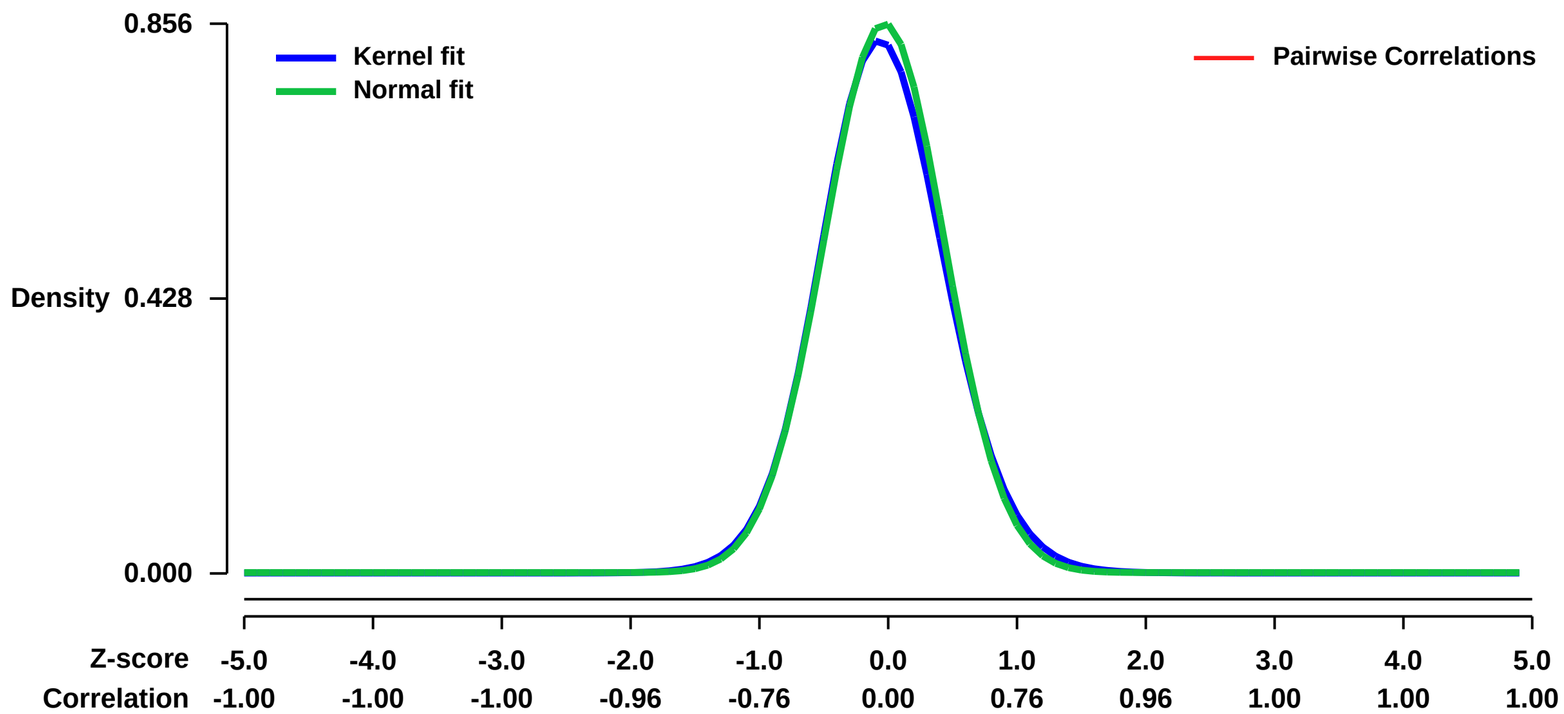

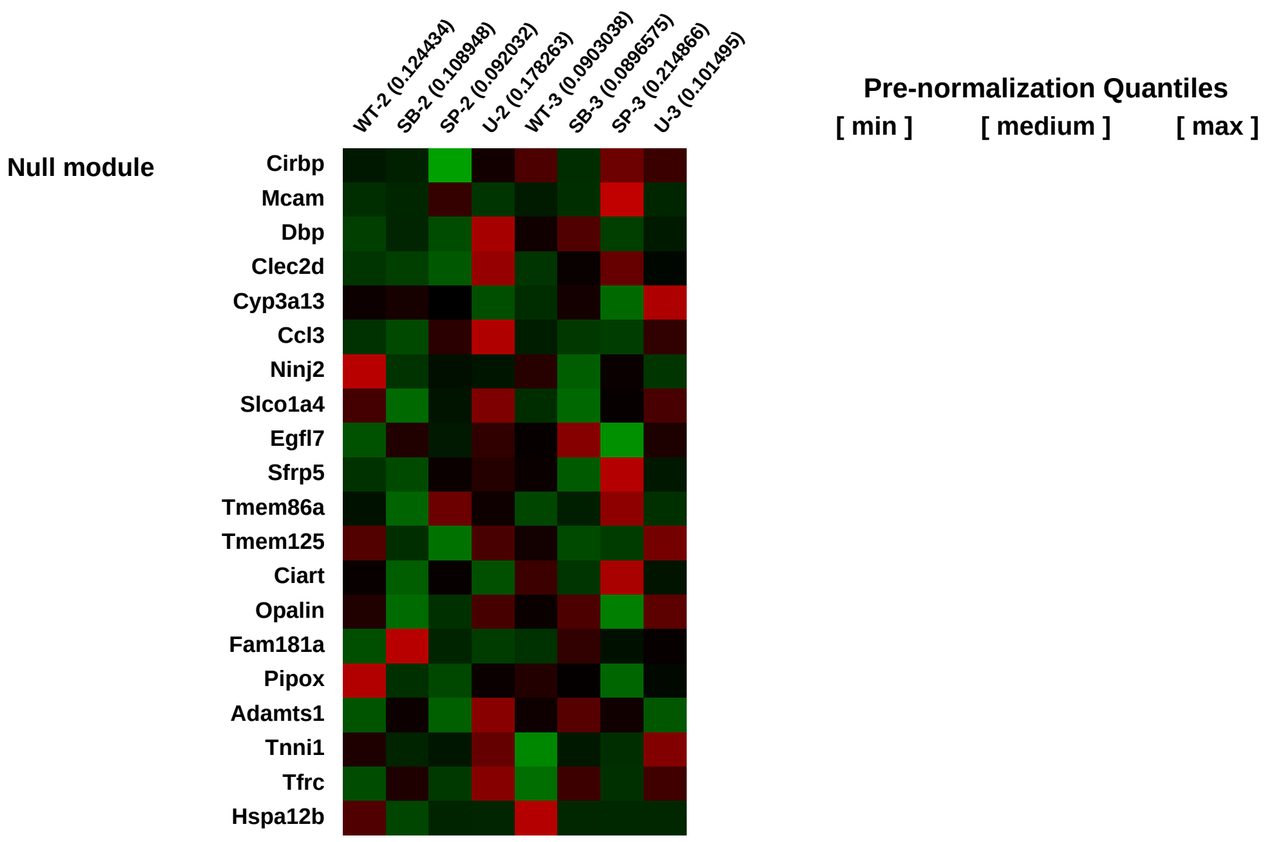

GEO Series "GSE22307" Expression Profiles

Num of samples in this series: 23

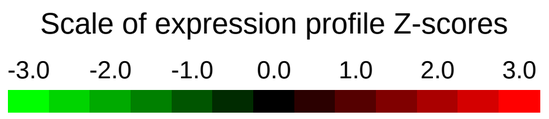

GEO Link:	http://www.ncbi.nlm.nih.gov/geo/query/acc.cgi?acc=GSE22307
Status:	Public on Oct 13 2010
Title:	Expression data from mouse colon tissue response to DSS induction at day 0, 2, 4 and 6
Organism:	Mus musculus
Experiment type:	Expression profiling by array
Platform:	GPL1261
Pubmed ID:	20923862
Summary & Design:	**Summary:** **Temporal genome profiling of DSS colitis** **The DSS induced mouse colitis model is often used to emulate Ulcerative Colitis (UC) in order understand pathophysiological mechanism of inflammatory bowel disease (IBD). Given the progressive nature of IBD, colon tissue gene expression changes during the evolution of disease, and knowing the changes in gene expression profiles could indentify potential diagnostic markers or additional therapeutic targets for colitis. Therefore, we performed temporal genome expression profiling analysis using the Affymetrix genome wide microarray system to identify broad scale changes in gene expression associated with the development of colitis.** **Keywords: Expression time course of mouse colon tissue induced by 3% DSS.** **Overall design:** **C57BL/6J mice were given 3% DSS in the drinking water and tissues from individual cohorts were collected at days 0, 2, 4 and 6. Total RNA were extracted from the colon tissue and detected by Affymerix GeneChip Mouse Genome 430 2.0 Array.**

Background corr dist: **KL-Divergence = 0.2821, L1-Distance = 0.0519, L2-Distance = 0.0064, Normal std = 0.2889**

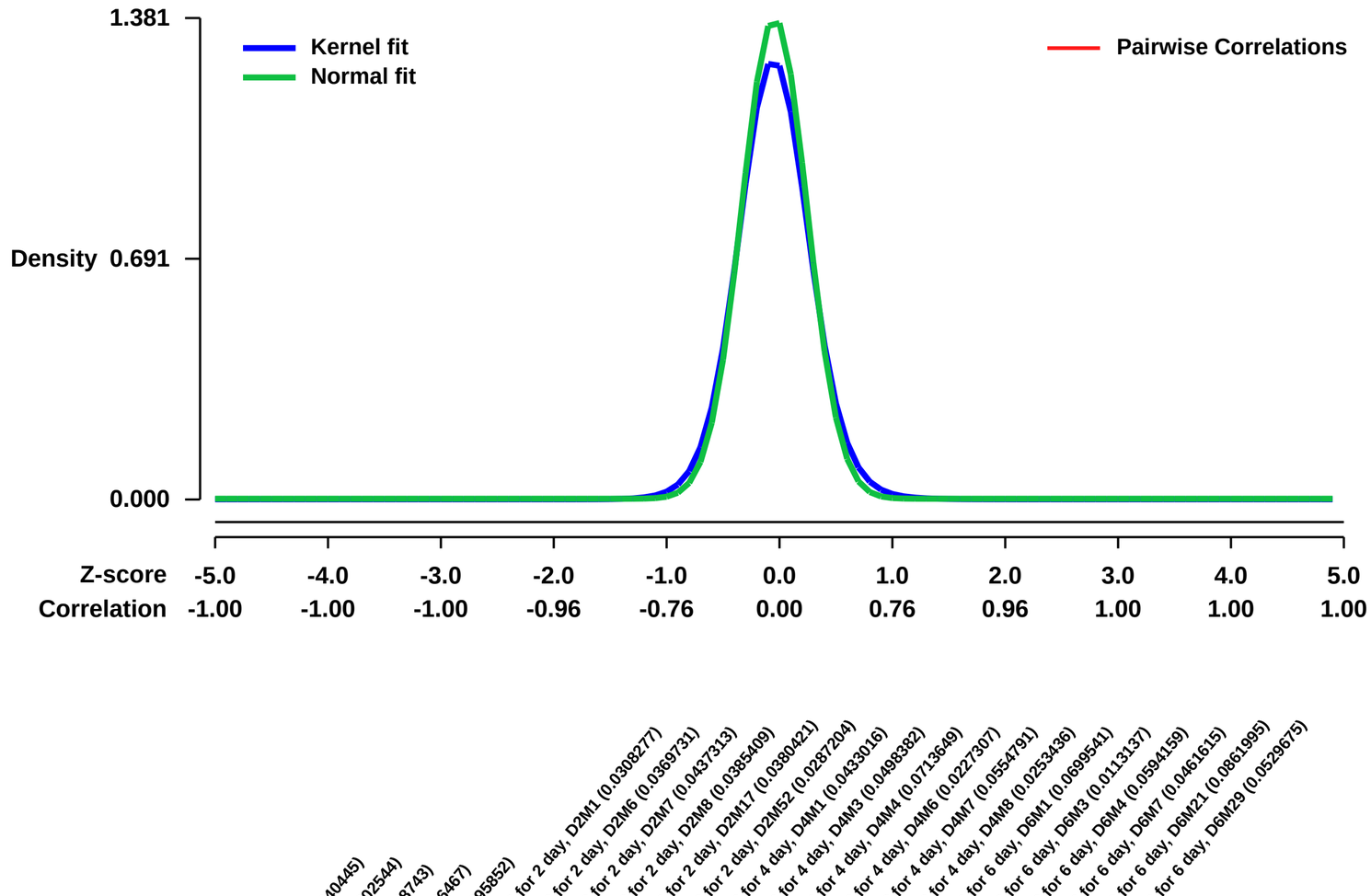

GEO Series "GSE22371" Expression Profiles

Num of samples in this series: 6

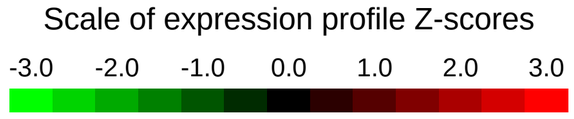

GEO Link:	http://www.ncbi.nlm.nih.gov/geo/query/acc.cgi?acc=GSE22371
Status:	Public on Jul 27 2010
Title:	Tbr1 regulates regional and laminar identity of postmitotic neurons in developing neocortex
Organism:	Mus musculus
Experiment type:	Expression profiling by array
Platform:	GPL1261
Pubmed ID:	20615956
Summary & Design:	**Summary:** Areas and layers of the cerebral cortex are specified by genetic programs that are initiated in progenitor cells and then, implemented in postmitotic neurons. Here, we report that Tbr1, a transcription factor expressed in postmitotic projection neurons, exerts positive and negative control over both regional (areal) and laminar identity. Tbr1 null mice exhibited profound defects of frontal cortex and layer 6 differentiation, as indicated by down-regulation of gene-expression markers such as Bcl6 and Cdh9. Conversely, genes that implement caudal cortex and layer 5 identity, such as Bhlhb5 and Fezf2, were up-regulated in Tbr1 mutants. Tbr1 implements frontal identity in part by direct promoter binding and activation of Auts2, a frontal cortex gene implicated in autism. Tbr1 regulates laminar identity in part by downstream activation or maintenance of Sox5, an important transcription factor controlling neuronal migration and corticofugal axon projections. Similar to Sox5 mutants, Tbr1 mutants exhibit ectopic axon projections to the hypothalamus and cerebral peduncle. Together, our findings show that Tbr1 coordinately regulates regional and laminar identity of postmitotic cortical neurons. **Overall design:** Mouse E14.5 neocortices and Postnatal day (P) 0.5 brains: E14.5 neocortices KO, 3; E14.5 neocortices WT, 3; Postnatal day (P) 0.5 brains frontal WT, 4; Postnatal day (P) 0.5 brains frontal KO, 4; Postnatal day (P) 0.5 brains parietal WT, 4; Postnatal day (P) 0.5 brains parietal KO, 4; Postnatal day (P) 0.5 brains occipital WT, 4; Postnatal day (P) 0.5 brains occipital KO, 4.

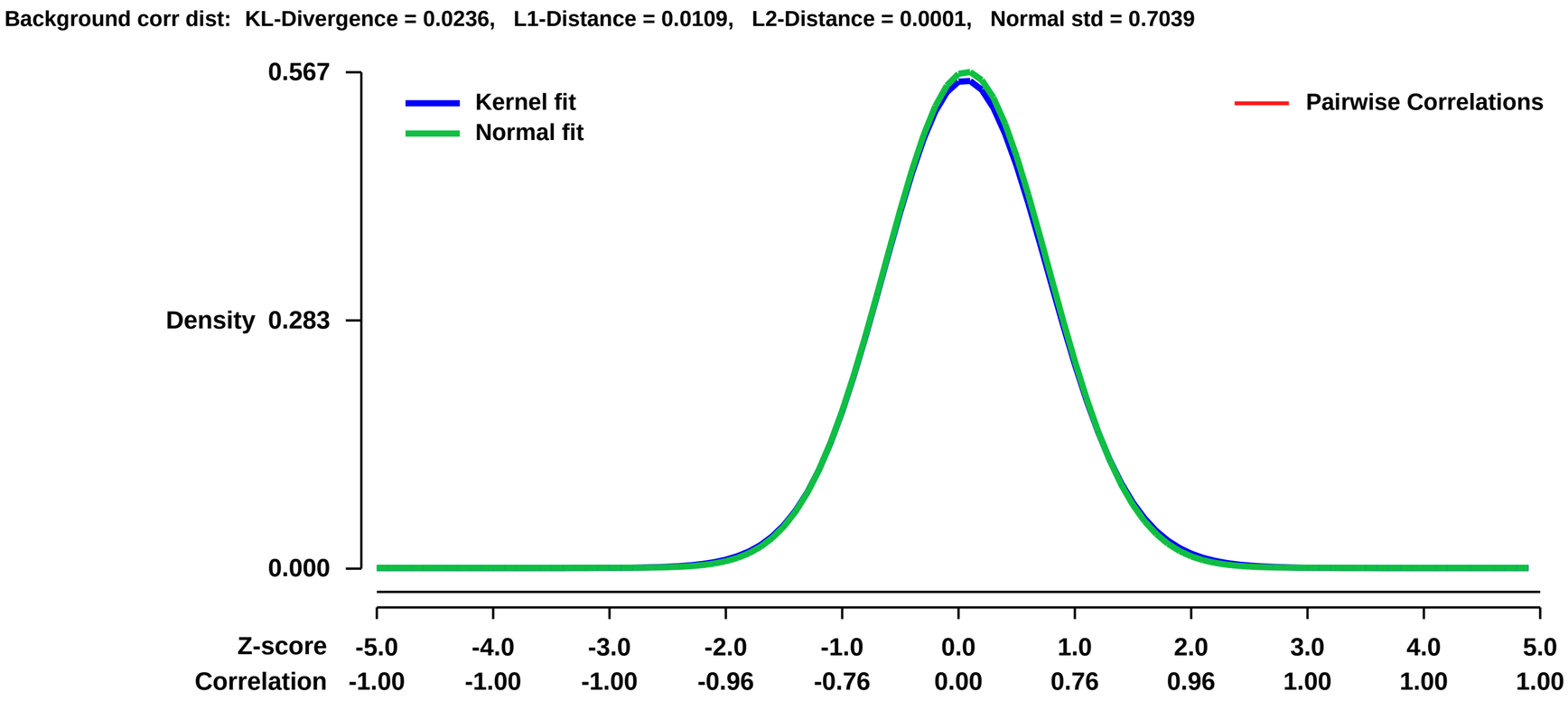

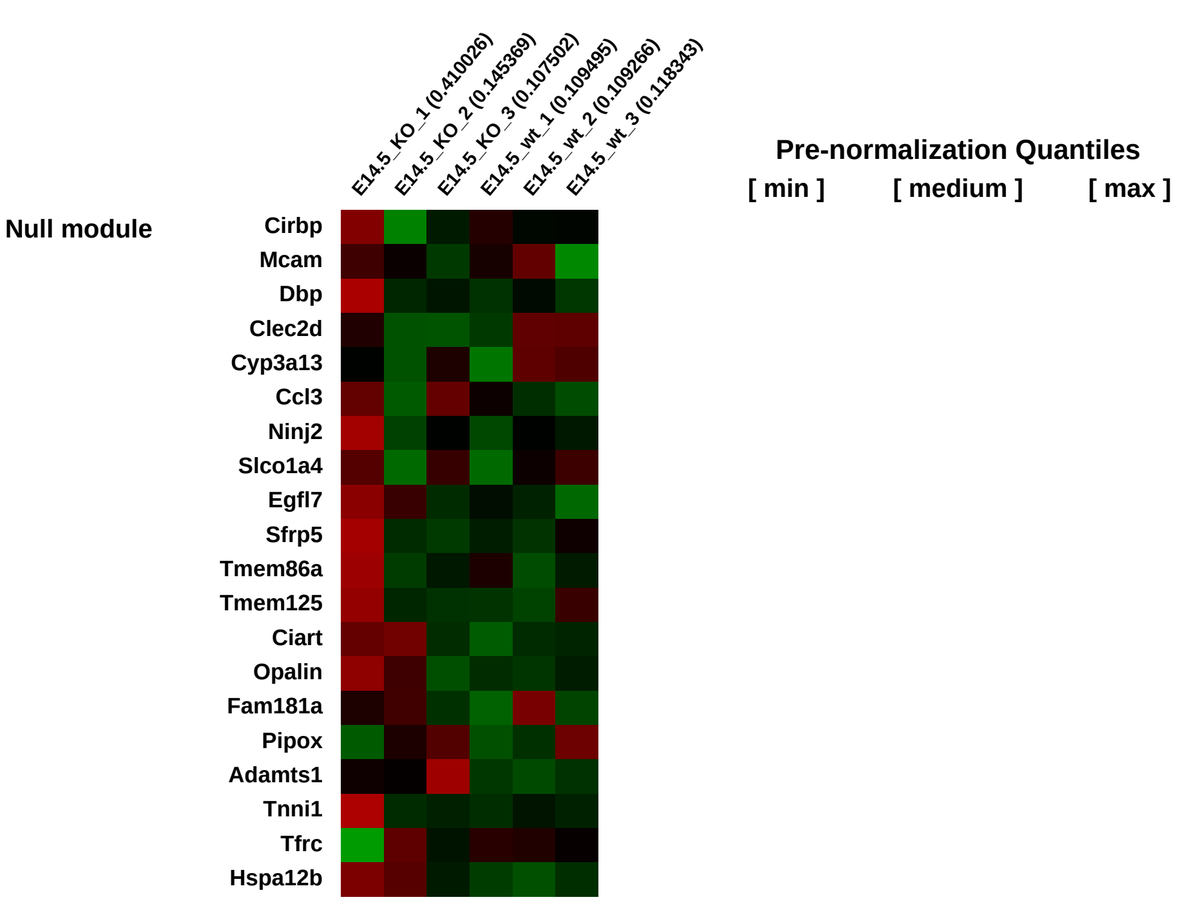

GEO Series "GSE22418" Expression Profiles

Num of samples in this series: 8

Scale of expression profile Z-scores

-3.0 -2.0 -1.0 0.0 1.0 2.0 3.0

GEO Link:	http://www.ncbi.nlm.nih.gov/geo/query/acc.cgi?acc=GSE22418
Status:	Public on Jun 18 2010
Title:	Comparison of gene expression between wild type, Notch1-activated, and RBPJ loss-of-function embryonic mouse yolk sac tissue at E9.5
Organism:	Mus musculus
Experiment type:	Expression profiling by array
Platform:	GPL1261
Pubmed ID:	21352545
Summary & Design:	**Summary:** The signaling cascades that direct the morphological differentiation of the vascular system during early embryogenesis are not well defined. To further understand the role of Notch signaling during endothelial differentiation, this study uses both an in vivo gain-of-function and an in vivo loss-of-function approach. At embryonic day 9.5, embryos with activated Notch1 signaling in the endothelia display a variety of growth and cardiovascular defects, and die soon after E10.5. Most notably, the extra-embryonic vasculature of the yolk sac displays remodeling differentiation defects. In the wild-type yolk sac, the primary vascular network has begun to reorganize, forming the large primary vessels and the smaller capillaries. In the activated Notch1 embryos, remodeling is defective; the vasculature have an enlarged surface with decreased inter-vessel space. Embryos with ablated Notch signaling also display growth and vascular defects at E9.5 similar to the activated Notch1 embryos, however they exhibit a lack of vascular remodeling in the yolk sac, retaining the simple vascular plexus seen at E8.5. These results indicate that Notch signaling plays a critical role in the remodeling of the vasculature in the early embryo, particularly in the extra-embryonic region. **Overall design:** A conditional transgenic system was used in this study to activate Notch signaling. The ubiquitous ROSA26Notch transgene with a Neo/stop cassette flanked by loxP sites, followed by the N1-ICD cDNA, was recombined with a Tie2-CRE mouse, resulting in the removal of the STOP cassette and the subsequent activation of the Notch1 intracellular domain. This allowed for the overexpression and expansion of Notch signaling in all endothelial cells. Male Tie2-Cre mice were mated with female ROSA26Notch mice and the resulting embryos were dissected at embryonic day 9.5. To ablate Notch signaling, Tie2-Cre mice were used in a two-generation cross to obtain Tie2-Cre; Rbpj flox/flox embryos. These embryos lack RBPJ binding activity in the endothelia. In both instances, embryos were used for genotyping and the yolk sac were separated and used to isolate total RNA with an RNeasy mini kit. The RNA was analyzed with the Mouse Genome 430A Array from Affymetrix. Samples were performed in duplicate, and RNA from wild type yolk sac tissues was compared to activated Notch and RBPJ loss-of-function yolk sac tissues.

Background corr dist: KL-Divergence = 0.0384, L1-Distance = 0.0242, L2-Distance = 0.0010, Normal std = 0.6041

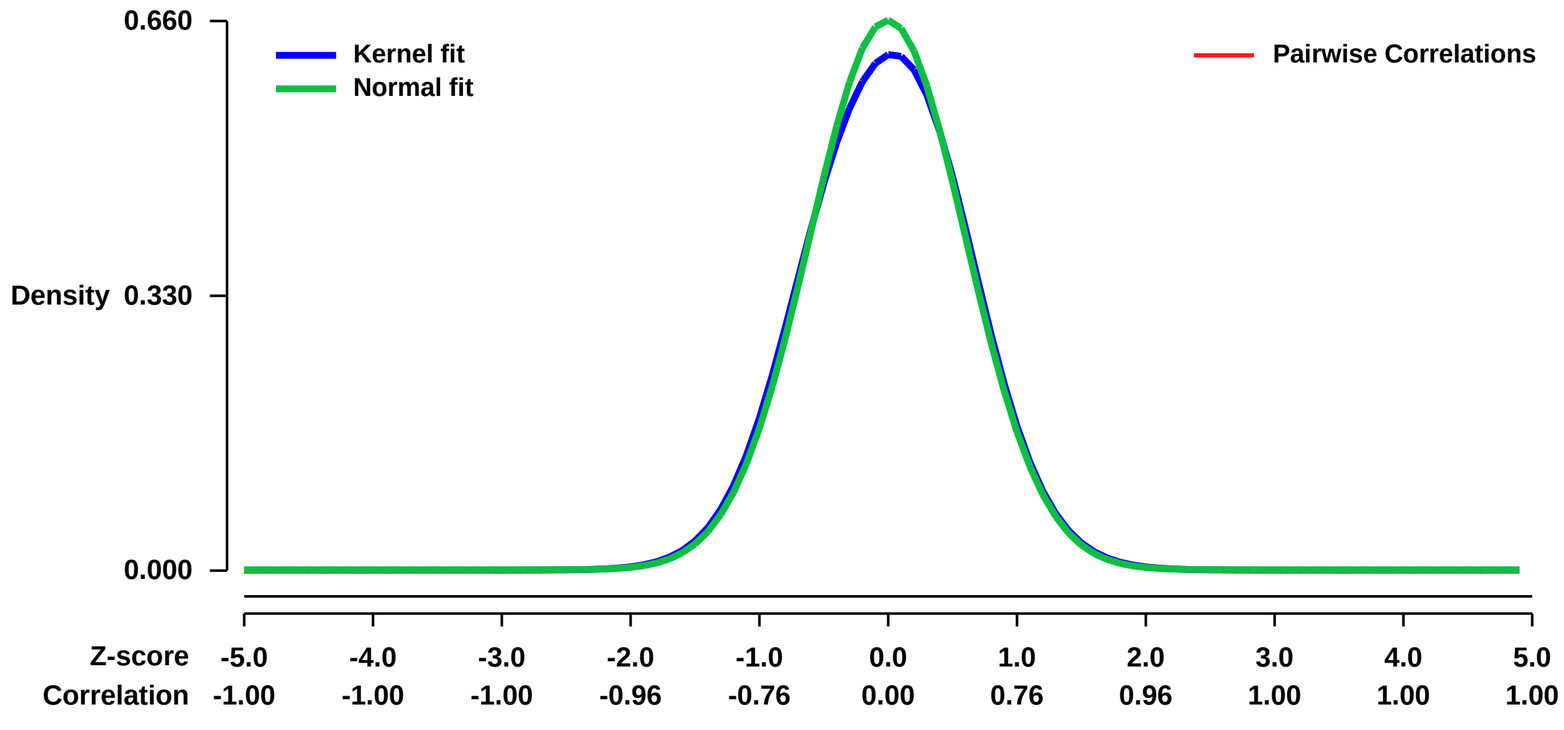

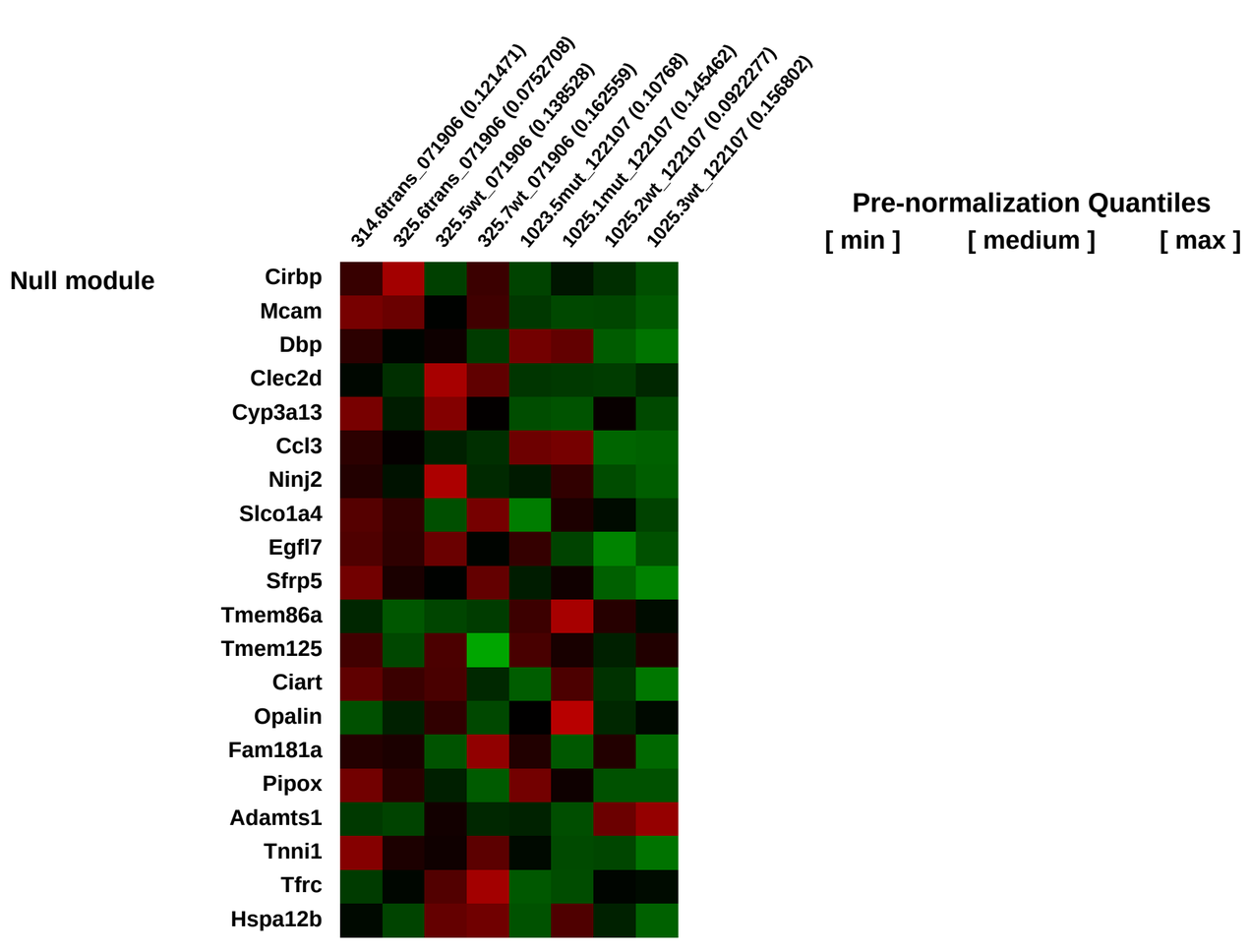

GEO Series "GSE22434" Expression Profiles

Num of samples in this series: 8

Scale of expression profile Z-scores

-3.0 -2.0 -1.0 0.0 1.0 2.0 3.0

GEO Link:	http://www.ncbi.nlm.nih.gov/geo/query/acc.cgi?acc=GSE22434
Status:	Public on Jun 18 2010
Title:	Expression data from Evi1-transduced primary bone marrow cells
Organism:	Mus musculus
Experiment type:	Expression profiling by array
Platform:	GPL1261
Pubmed ID:	21289308
Summary & Design:	**Summary:** Evi1 is essential for proliferation of hematopoietic stem cells and implicated in the development of myeloid disorders. Particularly, high Evi1 expression defines one of the largest clusters in acute myeloid leukemia and is significantly associated with extremely poor prognosis. Improvement of the therapeutic outcome of leukemia with activated Evi1 is one of the most challenging issues. However, mechanistic basis of Evi1-mediated leukemogenesis has not been fully elucidated. Here we show that Evi1 directly represses PTEN transcription in the murine bone marrow, which leads to activation of AKT/mTOR signaling. In a murine bone marrow transplantation model, Evi1 leukemia showed remarkable sensitivity to an mTOR inihibitor rapamycin. Furthermore, we found that Evi1 binds to several polycomb group proteins and recruits polycomb repressive complexes for PTEN downregulation, which reveals a novel epigenetic mechanism of AKT/mTOR activation in leukemia. Expression analyses and chromatin immunoprecipitation assays using human samples indicate that our findings in mice models are recapitulated in human leukemic cells. Dependence of Evi1-expressing leukemic cells on AKT/mTOR signaling provides the first example of targeted therapeutic modalities that suppress the leukemogenic activity of Evi1. The PTEN/AKT/mTOR signaling pathway and the Evi1-polycomb interaction can be promising therapeutic targets for leukemia with activated Evi1. **Overall design:** 5-FU-primed mononuclear bone marrow cells harvested from C57/B6 mice were retrovirally transduced with Evi1-GFP or GFP. GFP positive cells were sorted and analyzed by Affymetrix´fi Mouse Genome 430 2.0 Array´fi for gene expression. Four independent experiments were performed.

Background corr dist: KL-Divergence = 0.0778, L1-Distance = 0.0209, L2-Distance = 0.0006, Normal std = 0.4805

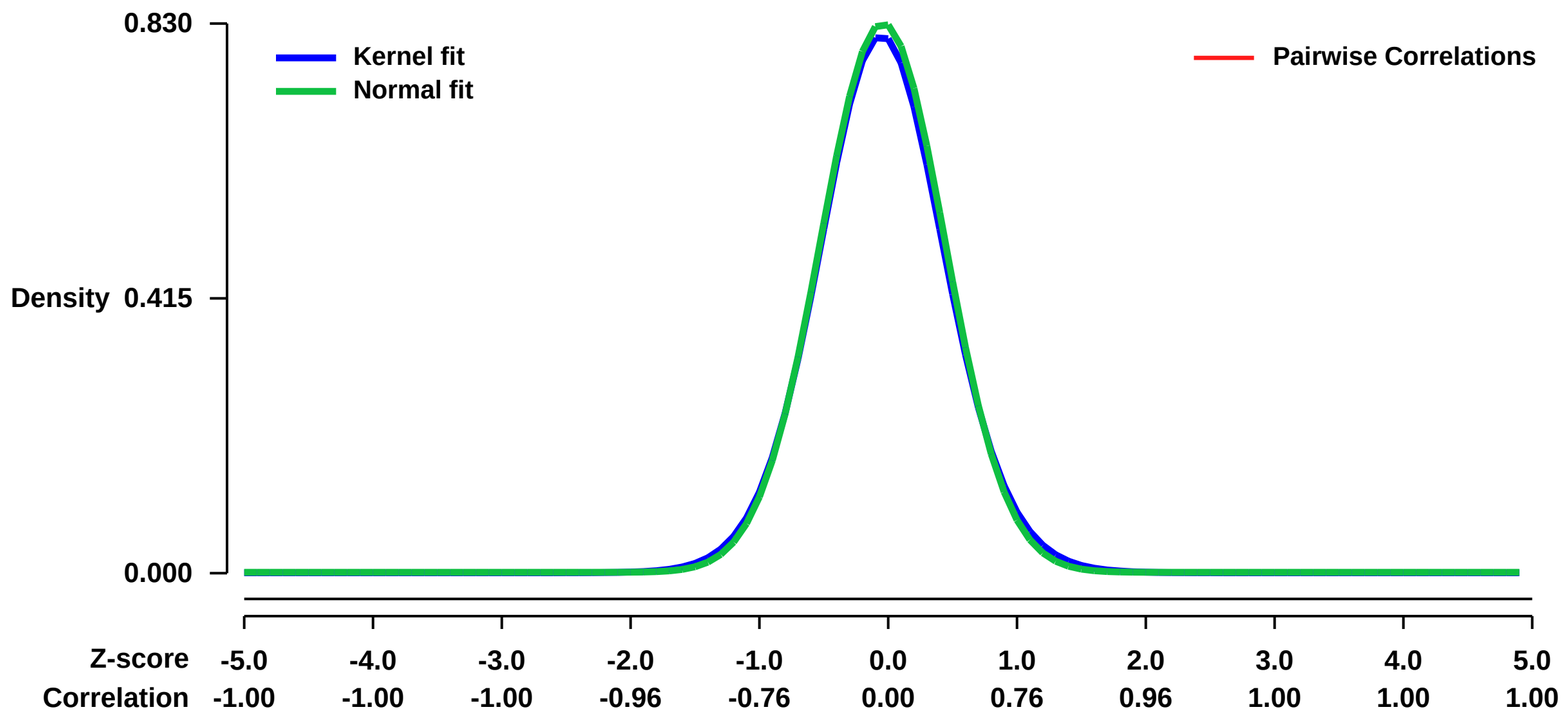

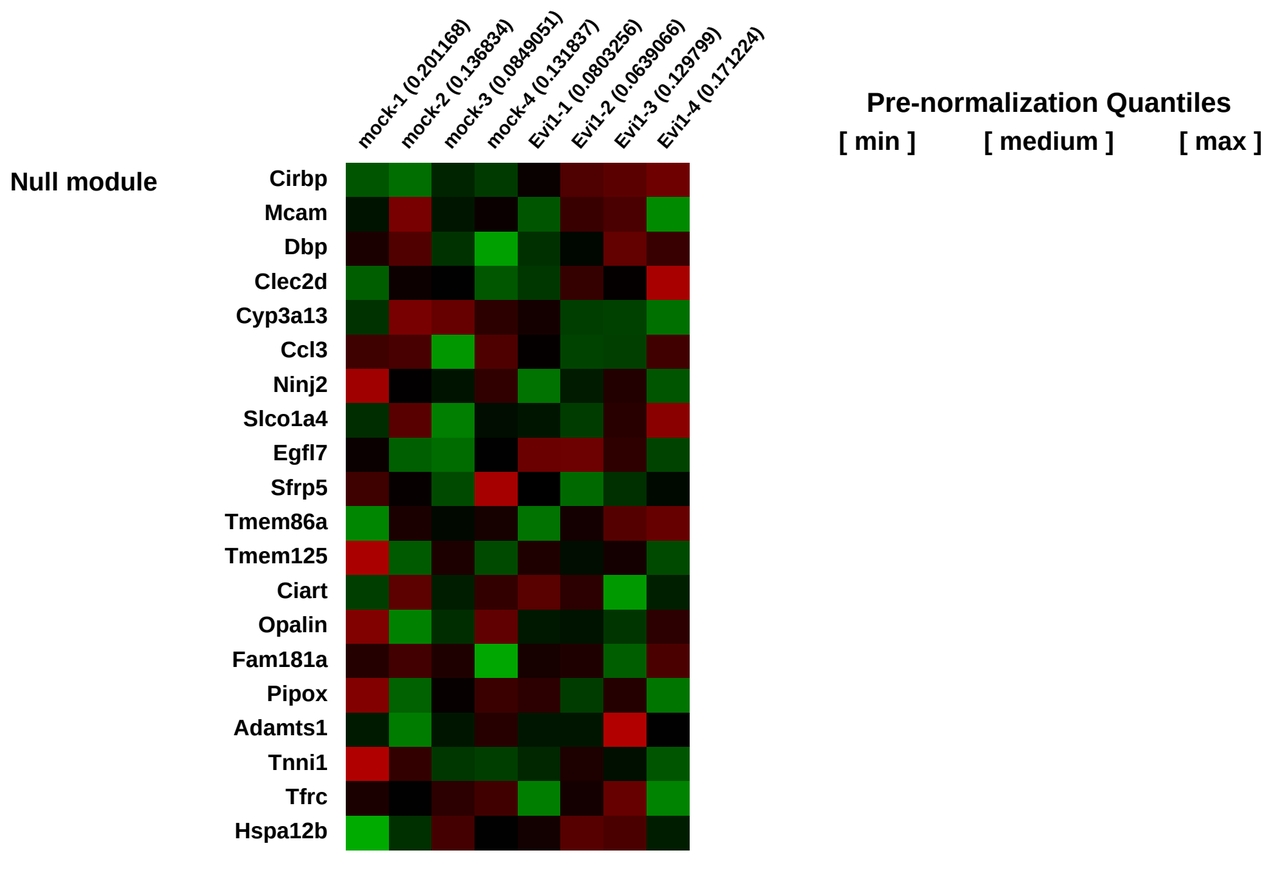

GEO Series "GSE22448" Expression Profiles

Num of samples in this series: 6

Scale of expression profile Z-scores

-3.0 -2.0 -1.0 0.0 1.0 2.0 3.0

GEO Link:	http://www.ncbi.nlm.nih.gov/geo/query/acc.cgi?acc=GSE22448
Status:	Public on Dec 22 2010
Title:	Gene expression data from wild-type and Nlrc5 knockout GM-CSF induced bone marrow dendritic cells infected with Newcastle Disease virus.
Organism:	Mus musculus
Experiment type:	Expression profiling by array
Platform:	GPL1261
Pubmed ID:	21148033
Summary & Design:	**Summary:** Nlrc5 is encoding a Nod-like receptor protein NLRC5/NOD27. To check the involvement of Nlrc5 in antiviral response, we examined gene expression profile in wild-type and Nlrc5 knockout GM-CSF bone marrow macrophage with using microarrays. **Overall design:** Bone marrow cells were cultured with GM-CSF and harvested on day 6. The induced dendritic cells were then stimulated with NDV at moi 1, collected at 0, 2, and 4 hours after infection. Total RNA was extracted and subjected to microarray experiment according to manufactures' instructions.

Background corr dist: KL-Divergence = 0.0228, L1-Distance = 0.0249, L2-Distance = 0.0011, Normal std = 0.7158

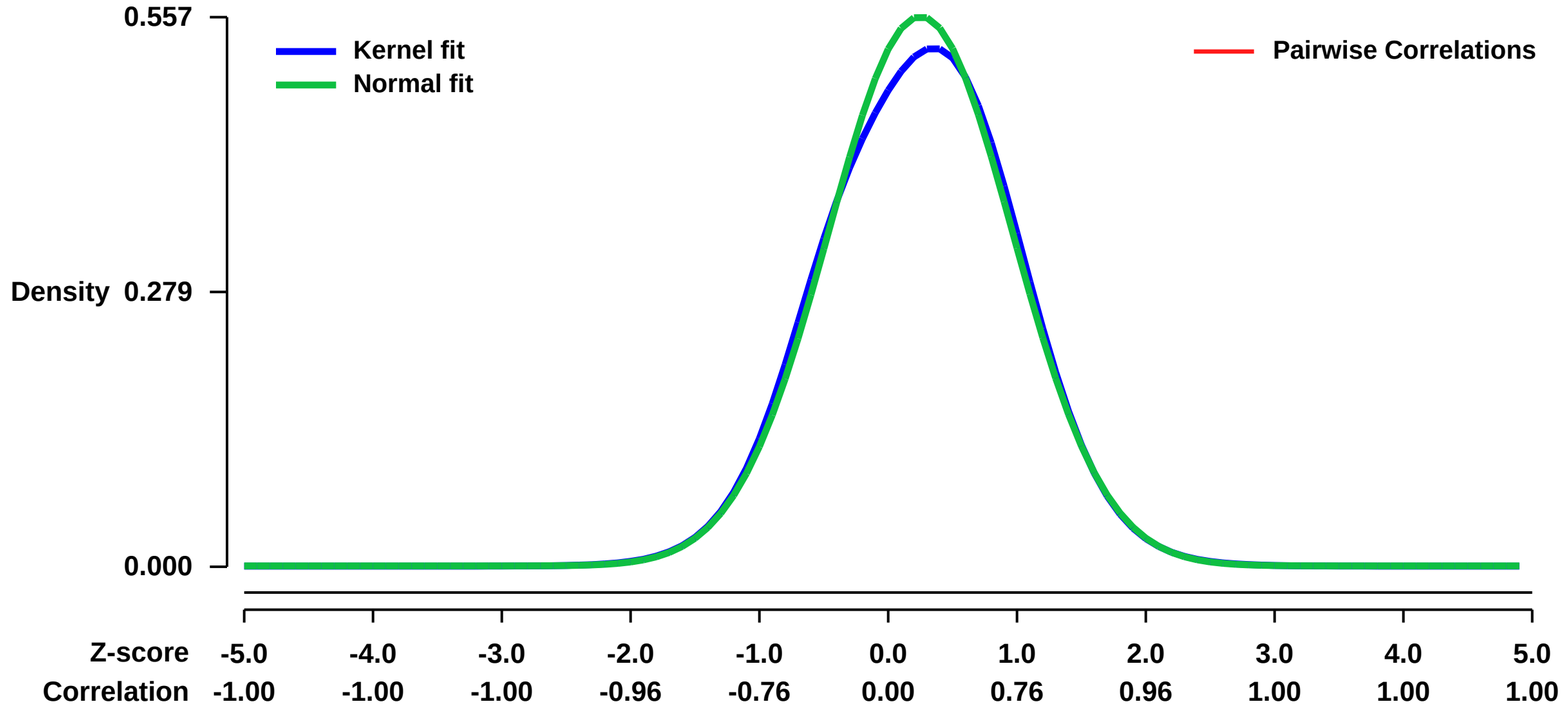

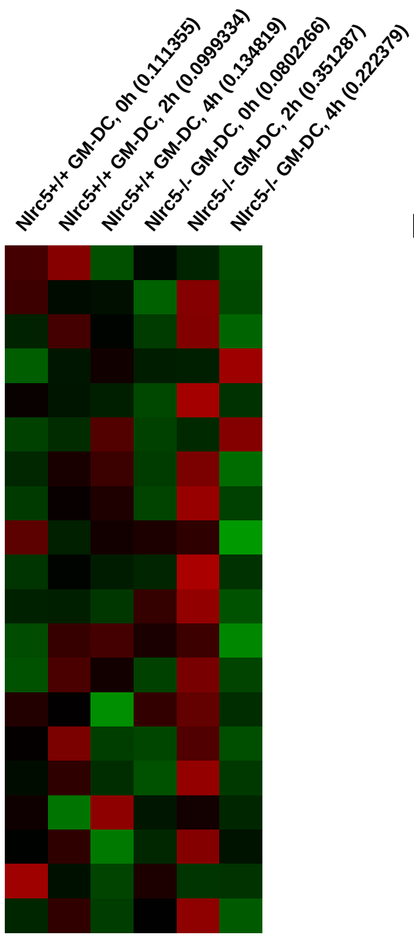

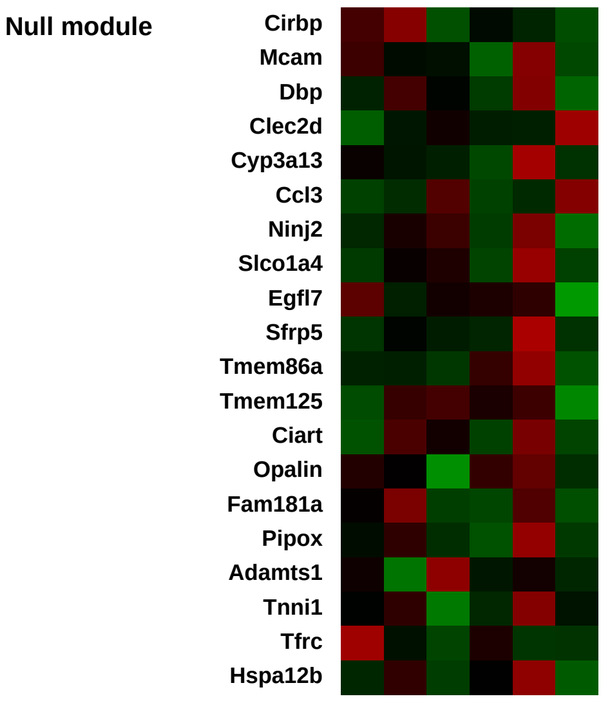

GEO Series "GSE2250" Expression Profiles

Num of samples in this series: 18

Scale of expression profile Z-scores

-3.0 -2.0 -1.0 0.0 1.0 2.0 3.0

GEO Link: http://www.ncbi.nlm.nih.gov/geo/query/acc.cgi?acc=GSE2250
Status: Public on Sep 11 2009
Title: Effects of irradiation on mouse lung
Organism: Mus musculus
Experiment type: Expression profiling by array
Platform: GPL1261
Pubmed ID:

Summary & Design:

Summary:
Total lung RNA from 3 mouse strains after 18Gy thoracic irradiation.

Thoracic cavity radiotherapy is limited by the development of alveolitis and fibrosis in susceptible patients. To define the response to 18 Gy pulmonary irradiation in mice, at the expression level, and to identify pathways which may influence the alveolitis and fibrosis phenotypes expression profiling was completed. Male mice of three strains, A/J (late alveolitis response), C3H/HeJ (C3H, early alveolitis response) and C57BL/6J (B6, fibrosis response) were exposed to thoracic radiation, euthanised when moribund and lung tissue gene expression was assessed with microarrays.

Overall design:
treated vs. control in 3 strains

Background corr dist: KL-Divergence = 0.2095, L1-Distance = 0.0449, L2-Distance = 0.0045, Normal std = 0.3259

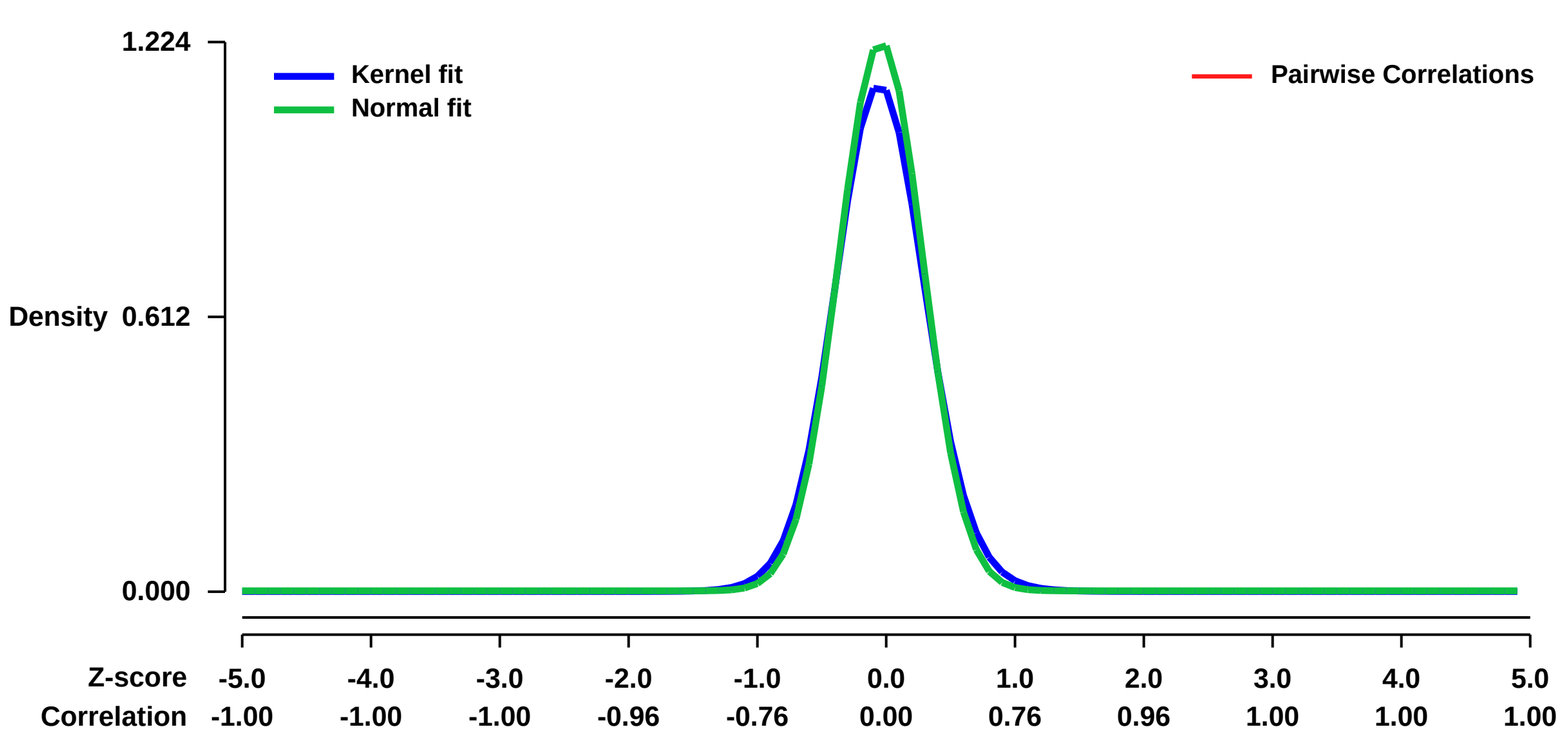

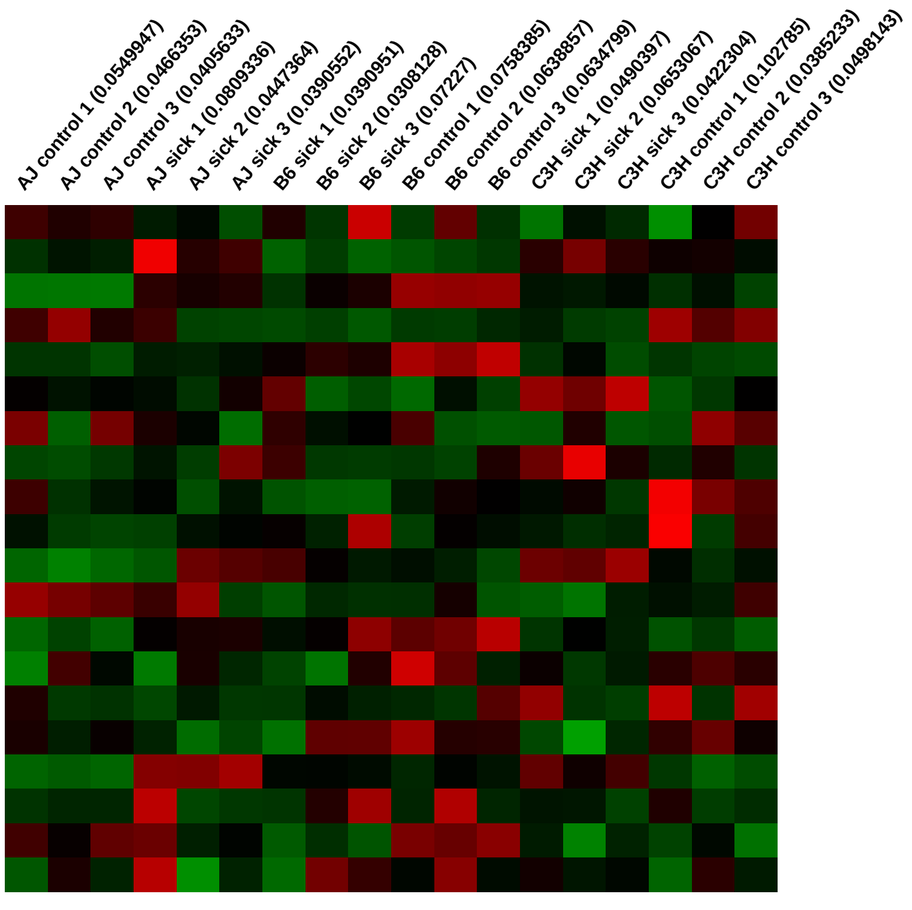

GEO Series "GSE22527" Expression Profiles

Num of samples in this series: 6

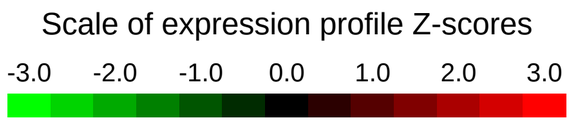

GEO Link:	http://www.ncbi.nlm.nih.gov/geo/query/acc.cgi?acc=GSE22527
Status:	Public on Jun 23 2010
Title:	Anti-CD3 therapy permits regulatory T cells to surmount T cell receptor-specified peripheral niche constraints
Organism:	Mus musculus
Experiment type:	Expression profiling by array
Platform:	GPL1261
Pubmed ID:	20679403
Summary & Design:	**Summary:** Treatment with anti-CD3 is a promising therapeutic approach for autoimmune diabetes, but its mechanism of action remains unclear. Foxp3+ regulatory T (Treg) cells may be involved, but the evidence has been conflicting, and there is great uncertainty as to possible mechanistic connections. We investigated this issue in mice derived from the NOD model, which were engineered mice in which Treg populations were perturbed, or could be manipulated by acute ablation or transfer. The data highlighted the involvement of Foxp3+ cells in anti-CD3 action. Rather than a generic influence on all Treg cells, the therapeutic effect seemed to involve an striking expansion of previously constrained Treg cell populations; this expansion occurred not through conversion from Foxp3- Tconv cells but from a dramatic proliferative expansion. We found that Treg cells are normally constrained by TCR-specific niches in secondary lymphoid organs, and that intraclonal competition restrains their possibility for conversion and expansion in the spleen and lymph nodes, much as niche competition limits their selection in the thymus. The strong perturbations induced by anti-CD3 overcame these niche limitations, in a process dependent on receptors for trophic cytokines, interleukin-2 receptor (IL-2R) and IL-7R. **Keywords:** Treatment response **Overall design:** All gene expression profiles were obtained from highly purified T cell populations sorted by flow cytometry. RNA from 5 - 50 x 104 cells was amplified, labeled, and hybridized to Affymetrix M430v2. Raw data were preprocessed with the RMA algorithm in GenePattern, and averaged expression values were used for analysis.

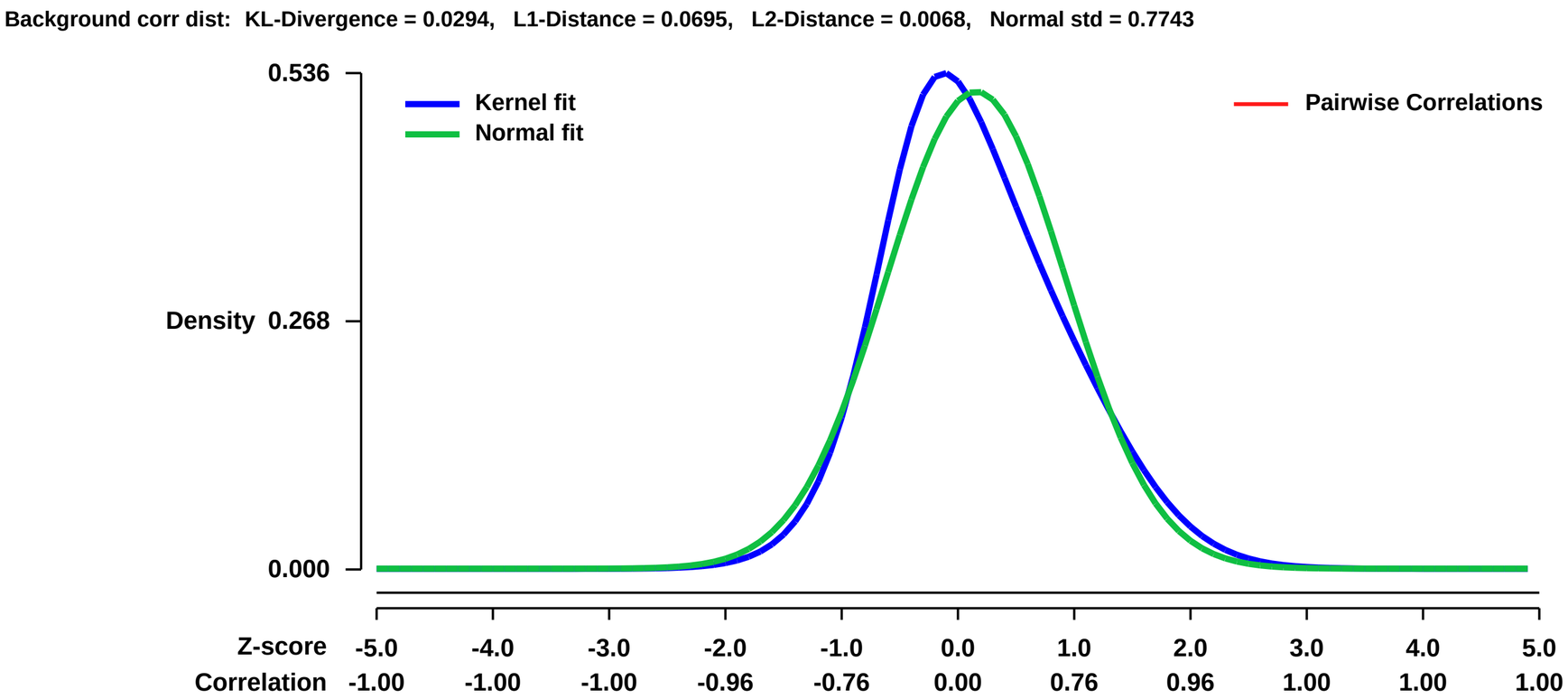

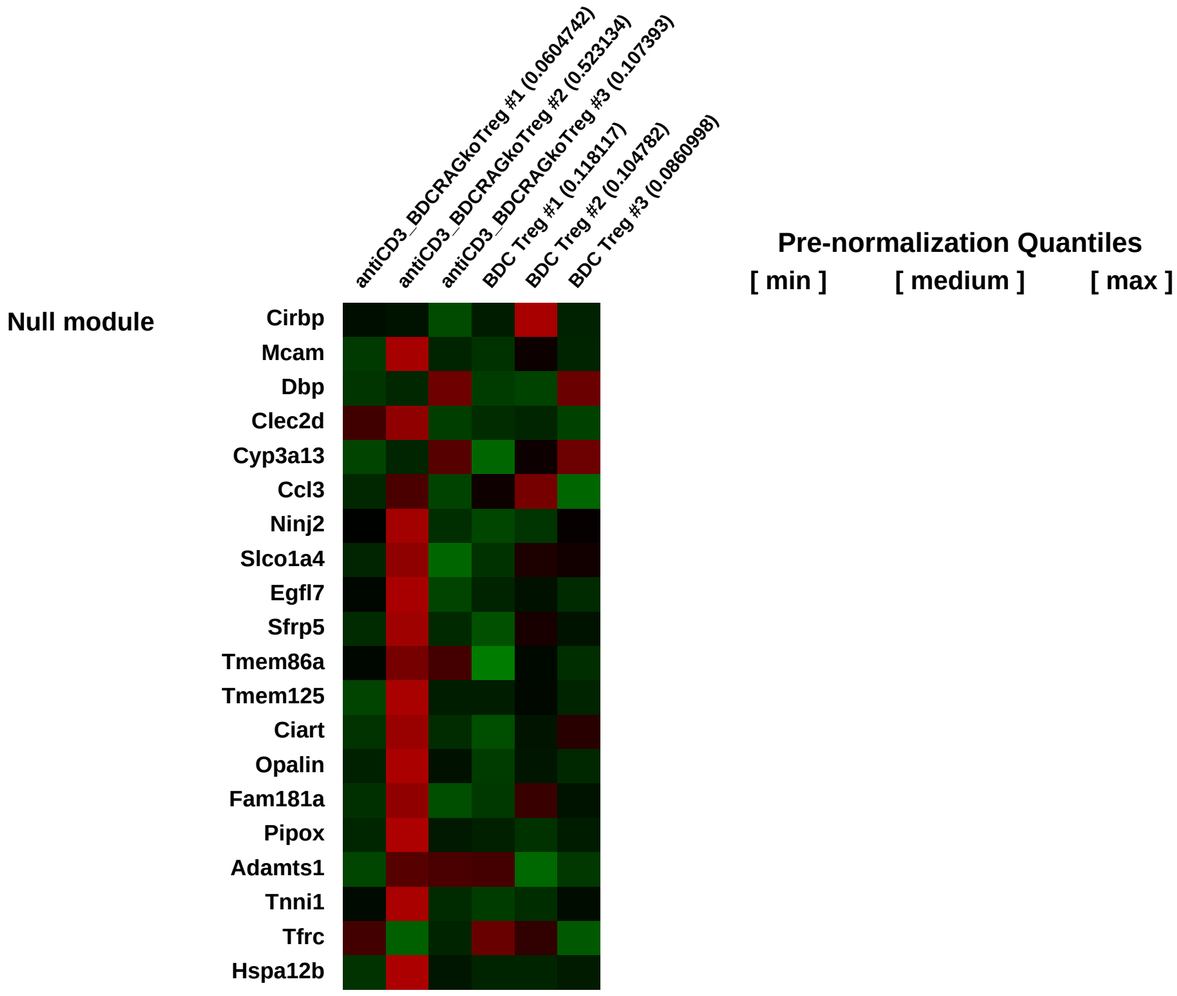

GEO Series "GSE22841" Expression Profiles

Num of samples in this series: 12

Scale of expression profile Z-scores

-3.0 -2.0 -1.0 0.0 1.0 2.0 3.0

GEO Link:	http://www.ncbi.nlm.nih.gov/geo/query/acc.cgi?acc=GSE22841
Status:	Public on Nov 10 2011
Title:	Discrete subsets of myogenic and mesenchymal precursors give rise to soft tissue sarcomas of distinct lineage differentiation
Organism:	Mus musculus
Experiment type:	Expression profiling by array
Platform:	GPL1261
Pubmed ID:	22135462
Summary & Design:	**Summary:** This work examines sarcoma formation within discrete subsets of KRAS(G12V)-expressing p16p19null myogenic and mesenchymal cells found normally in skeletal muscle. We show that prospectively isolated skeletal muscle precursor cells (SMPs) within the satellite cell pool can serve as cancer cells-of-origin for mouse rhabdomyosarcomas (soft tissue sarcomas with features of myogenic differentiation). Alternatively, non-myogenic progenitors (ScaPCs) induce sarcomas lacking myogenic differentiation markers. **Overall design:** We used Affymetrix whole mouse genome 430 2.0 microarrays to gain deeper insights into the molecular underpinnings of the three types of KRAS; p16p19null mouse soft-tissue sarcomas (originating from SMPs, ScaPCs and CD45-MAC1-TER119-Sca1-CXCR4- cells). Four replicates of each type.

Background corr dist: KL-Divergence = 0.1135, L1-Distance = 0.0242, L2-Distance = 0.0008, Normal std = 0.4203

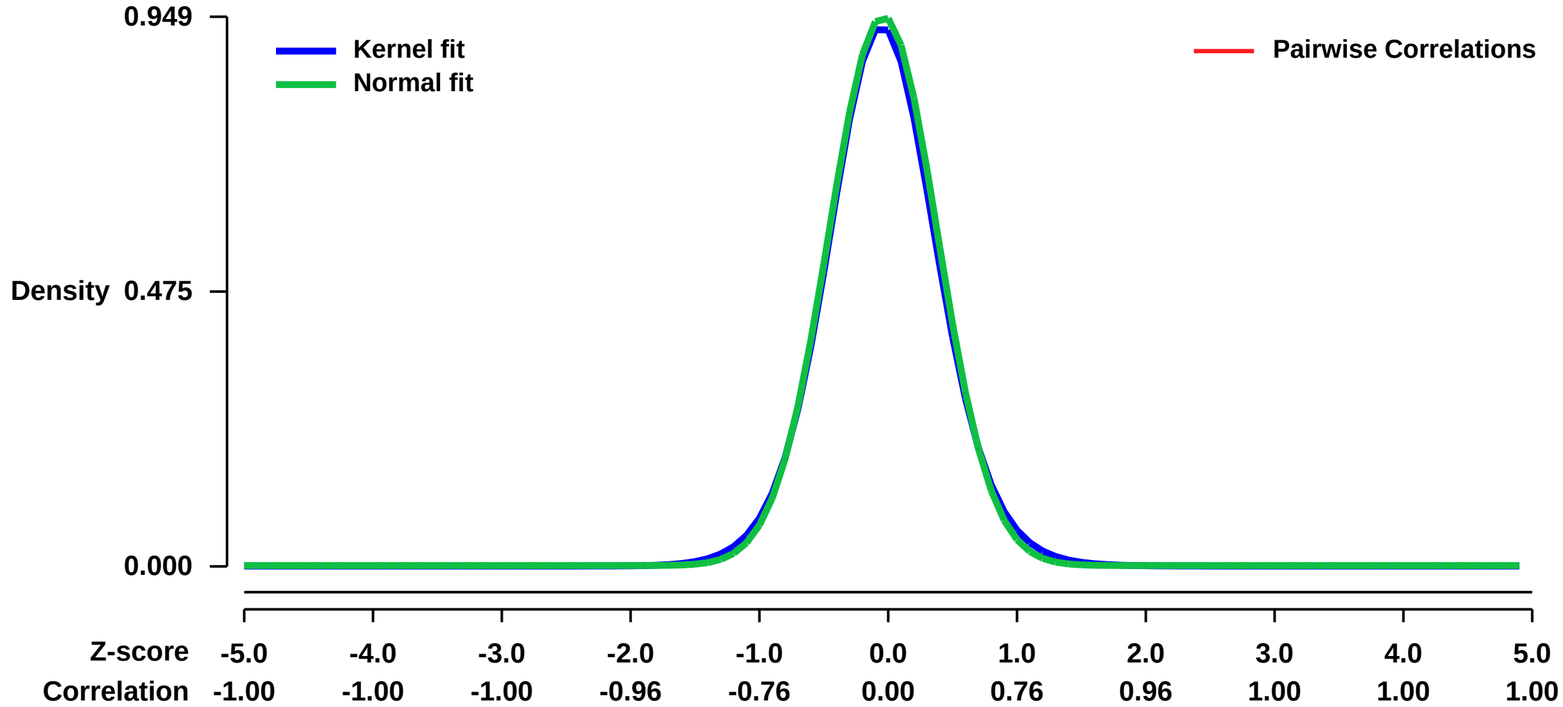

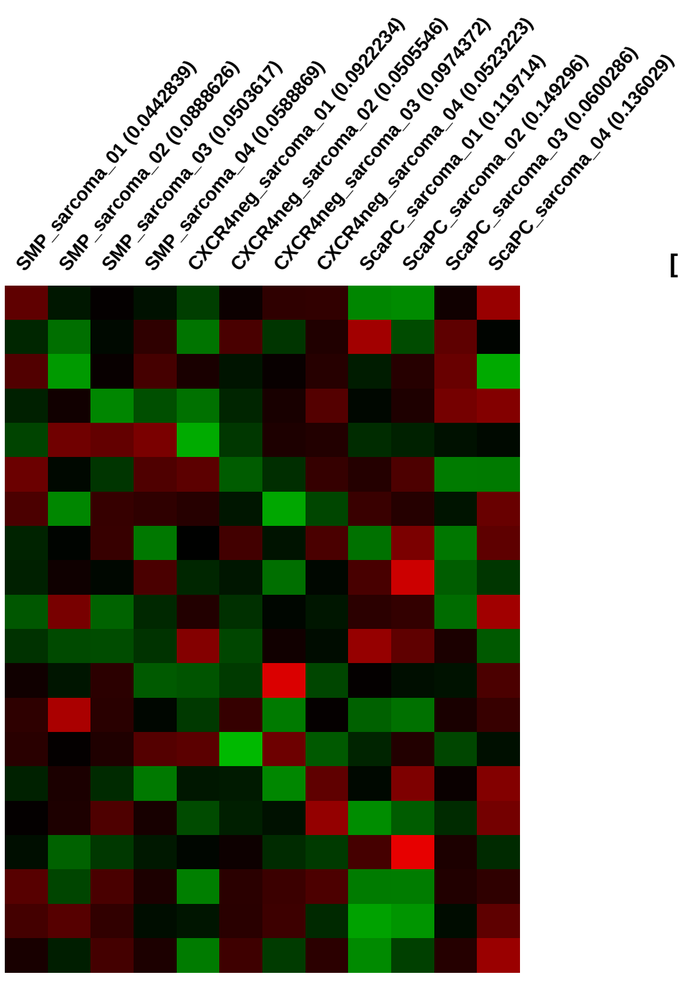

GEO Series "GSE22871" Expression Profiles

Num of samples in this series: 30

Scale of expression profile Z-scores

-3.0 -2.0 -1.0 0.0 1.0 2.0 3.0

GEO Link:	http://www.ncbi.nlm.nih.gov/geo/query/acc.cgi?acc=GSE22871
Status:	Public on Oct 01 2010
Title:	Expression data from wild-type and PPARalpha-null mice exposed to perfluorooctane sulfonate (PFOS)
Organism:	Mus musculus
Experiment type:	Expression profiling by array
Platform:	GPL1261
Pubmed ID:	20936131
Summary & Design:	**Summary:** Perfluorooctane sulfonate (PFOS) is a perfluoroalkyl acid (PFAA) and a persistent environmental contaminant found in the tissues of humans and wildlife. Although blood levels of PFOS have begun to decline, health concerns remain because of the long half-life of PFOS in humans. Like other PFAAs, such as perfluorooctanoic acid (PFOA), PFOS is an activator of peroxisome proliferator-activated receptor-alpha (PPARˌ–) and exhibits hepatocarcinogenic potential in rodents. PFOS is also a developmental toxicant in rodents where, unlike PFOA, itâ s mode of action is independent of PPARˌ–. Wild-type (WT) and PPARˌ–-null (Null) mice were dosed with 0, 3, or 10 mg/kg/day PFOS for 7 days. Animals were euthanized, livers weighed, and liver samples collected for histology and preparation of total RNA. Gene profiling was conducted using Affymetrix 430_2 microarrays. In WT mice, PFOS induced changes that were characteristic of PPARˌ– transactivation including regulation of genes associated with lipid metabolism, peroxisome biogenesis, proteasome activation, and inflammation. PPARˌ–-independent changes were indicated in both WT and Null mice by altered expression of genes related to lipid metabolism, inflammation, and xenobiotic metabolism. Such results are similar to prior studies done with PFOA and are consistent with modest activation of the constitutive androstane receptor (CAR) and possibly PPARˌ‡ and/or PPARˌ†/ˌ·. Unique treatment-related effects were also found in Null mice including altered expression of genes associated with ribosome biogenesis, oxidative phosphorylation and cholesterol biosynthesis. Of interest was up-regulation of Cyp7a1, a gene which is under the control of various transcription regulators. Hence, in addition to its ability to modestly activate PPARˌ–, PFOS induces a variety of â off-targetâ effects as well. **Overall design:** PPARalpha-null and wild-type male mice at 6-9 months of age were dosed by gavage for 7 consecutive days with either 0, 3, or 10 mg/kg PFOS (potassium salt) in 0.5% Tween 20. Five biological replicates consisting of individual animals were included in each dosage group. Data were compared to results previously published by our group for PFOA and Wy-14,643, a commonly used agonist of PPARalpha (Rosen et al., Toxicol Pathol. 36:592-607, 2008; GSE9796)

Background corr dist: KL-Divergence = 0.2576, L1-Distance = 0.0583, L2-Distance = 0.0086, Normal std = 0.2982

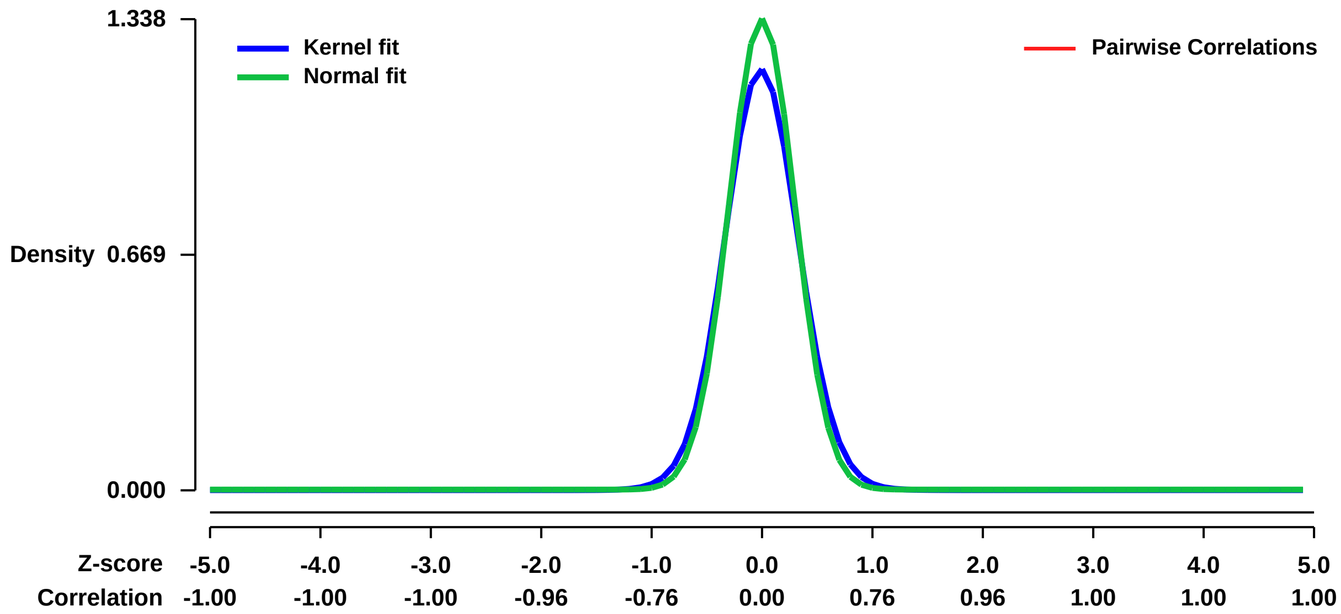

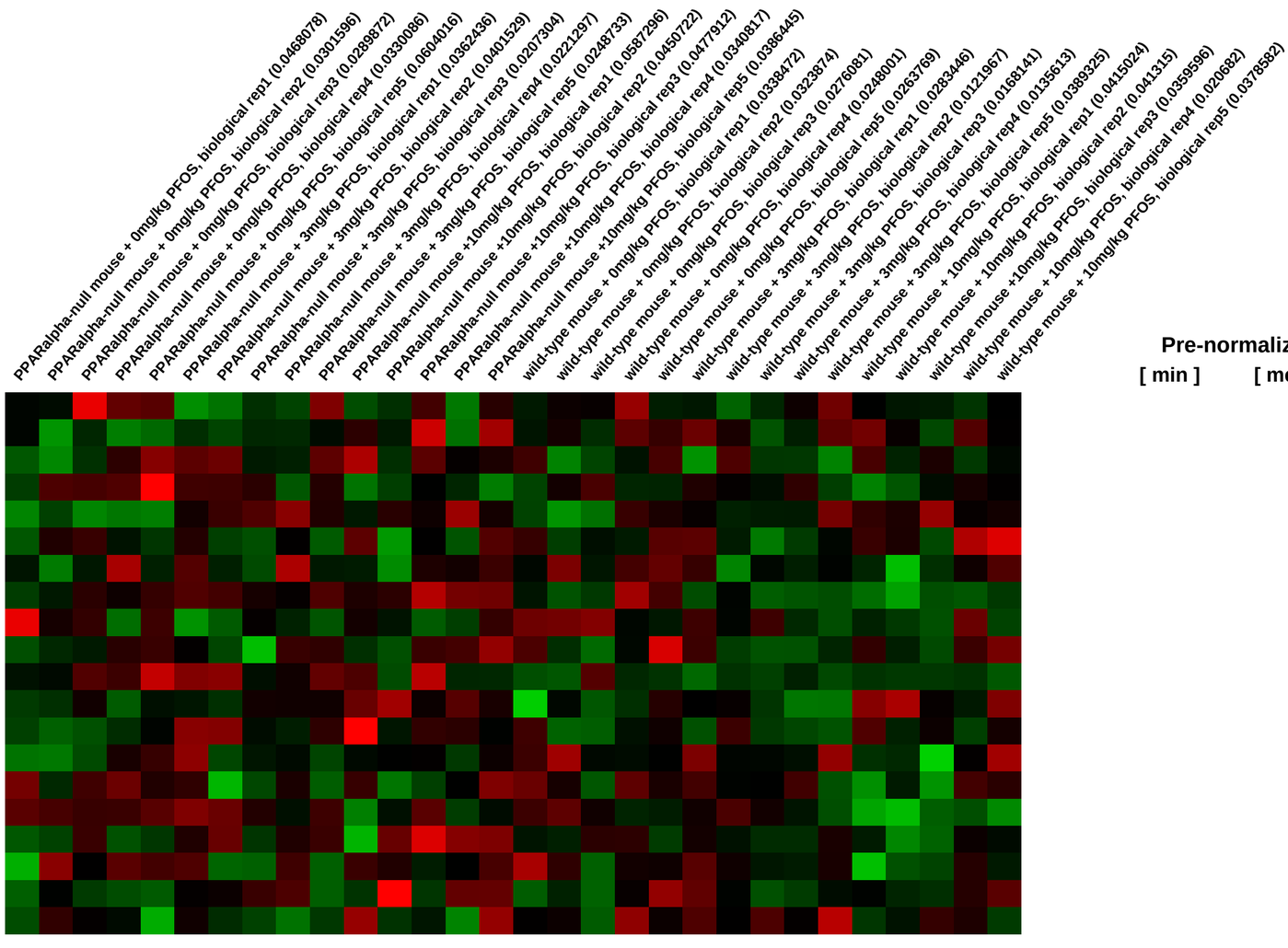

GEO Series "GSE22873" Expression Profiles

Num of samples in this series: 19

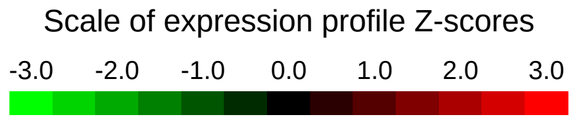

GEO Link:	**http://www.ncbi.nlm.nih.gov/geo/query/acc.cgi?acc=GSE22873**
Status:	**Public on Jun 26 2012**
Title:	**Ager (Rage) and Myd88 deletion in resected mouse livers**
Organism:	**Mus musculus**
Experiment type:	**Expression profiling by array**
Platform:	**GPL1261**
Pubmed ID:	**22075646**
Summary & Design:	**Summary:** **The effect of resection of mouse livers on survival serve as a model for the effect of resection of human livers, which are performed for both the purposes of removing sick tissue and for transplanting healthy tissue. When less than 70% of a mouse liver is resected, the mouse usually lives. However, when more than 70% is resected, there is an increased probability that the mouse will die. We have found that deletion of Ager (Advanced Glycation End products receptor) (Rage) increases the chance of mouse survival relavtive to WT. Conversely, the deletion of Myd88 decreases the chances of survival, as does the simultaneous deletion of both Ager and Myd88. To understand these genotype/phenotype relations, we performed gene expression measurements.** **Overall design:** **Gene expression of livers of WT C57BL/6 mice, Ager-null C57BL/6 mice, Myd88-null C57BL/6 mice, and Ager-null/Myd88-null C57BL/6 mice, all 10-12 weeks-old and sacrificed 2 hours after 85% liver resection, were compared. 4-6 replicates each group.**

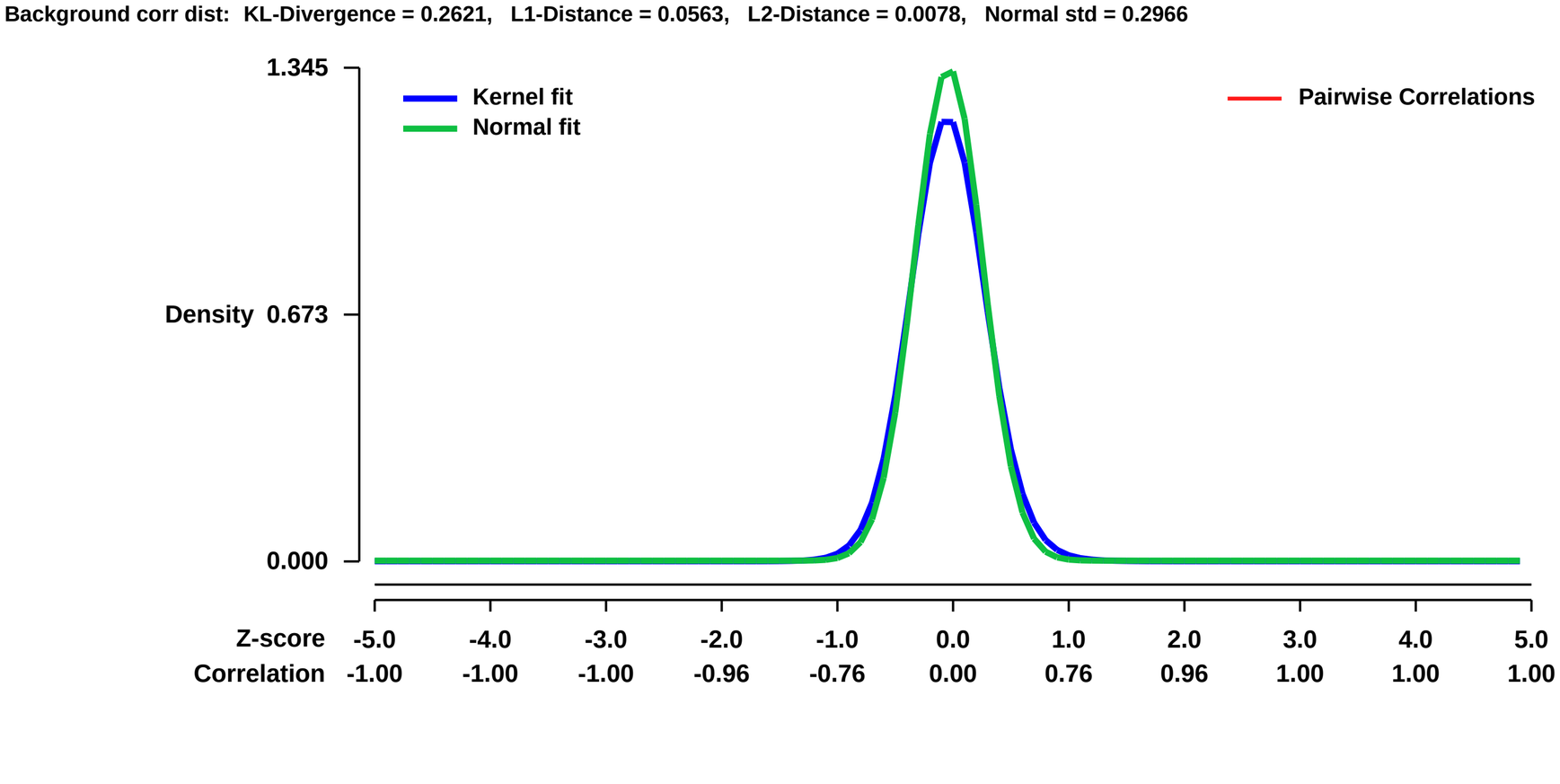

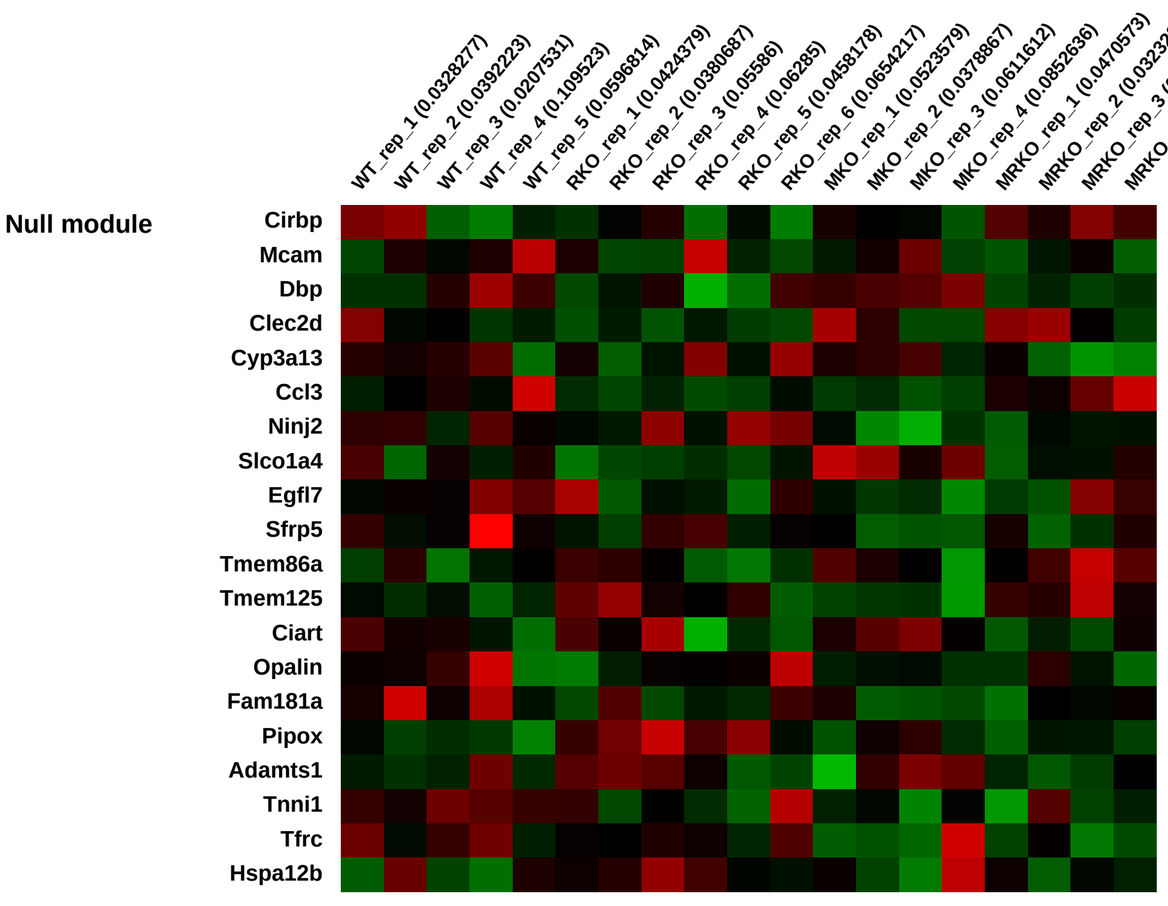

GEO Series "GSE22903" Expression Profiles

Num of samples in this series: 24

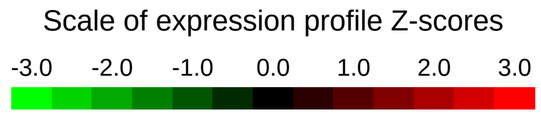

GEO Link:	http://www.ncbi.nlm.nih.gov/geo/query/acc.cgi?acc=GSE22903
Status:	Public on Nov 14 2011
Title:	Ribosomal deficiencies in Diamond-Blackfan anemia impair translation of transcripts essential for differentiation of murine and human erythroblasts
Organism:	Mus musculus
Experiment type:	Expression profiling by array
Platform:	GPL1261
Pubmed ID:	22058113
Summary & Design:	Summary: Diamond Blackfan Anemia (DBA) is associated with developmental defects and profound anemia. Mutations in genes encoding a ribosomal protein of the small (e.g. Rps19) or large (e.g. Rpl11) ribosomal subunit are found in over half of these patients. The mutations cause ribosomal haploinsufficiency, which reduces overall translation efficiency of cellular mRNAs. We reduced expression of *Rps19* or *Rpl11* in mouse erythroblasts and investigated mRNA polyribosome association, which revealed deregulated translation initiation of specific transcripts. Among these were *Bag1*, encoding a Hsp70 co-chaperone, and *Csde1*, encoding an RNA binding protein, both expressed at increased levels in erythroblasts. Their translation initiation is cap-independent and starts from an internal ribosomal entry site (IRES), which appeared sensitive to knock down of Rps19 or Rpl11. Mouse embryos lacking Bag1 die at embryonic day E13.5 with reduced erythroid colony forming cells in the fetal liver, and low Bag1 expression impairs erythroid differentiation in vitro. Reduced expression of Csde1 impairs proliferation and differentiation of erythroid blasts. Protein but not mRNA expression of *BAG1* and *CSDE1* was reduced in erythroblasts cultured from DBA patients. Our data suggest that impaired IRES-mediated translation of mRNAs expressed at increased levels in erythroblasts contributes to the erythroid phenotype of DBA. Overall design: 3 biological replicates of erythroblasts treated with different shRNA were used for polyribosomal sucrose gradients; RNA was extracted from gradients in 2 samples - mRNA associated with polyribosomes (poly) and the rest (sub).

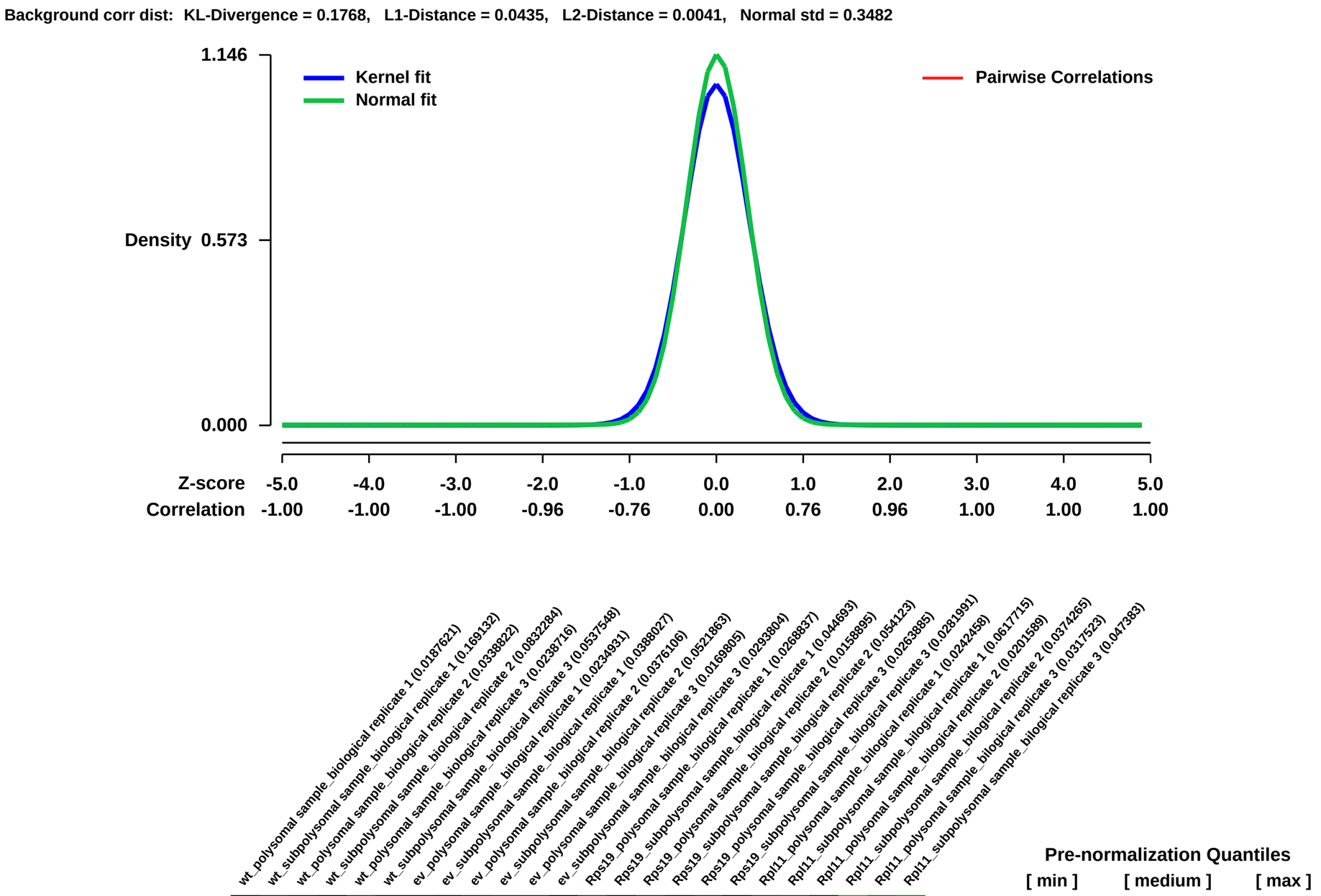

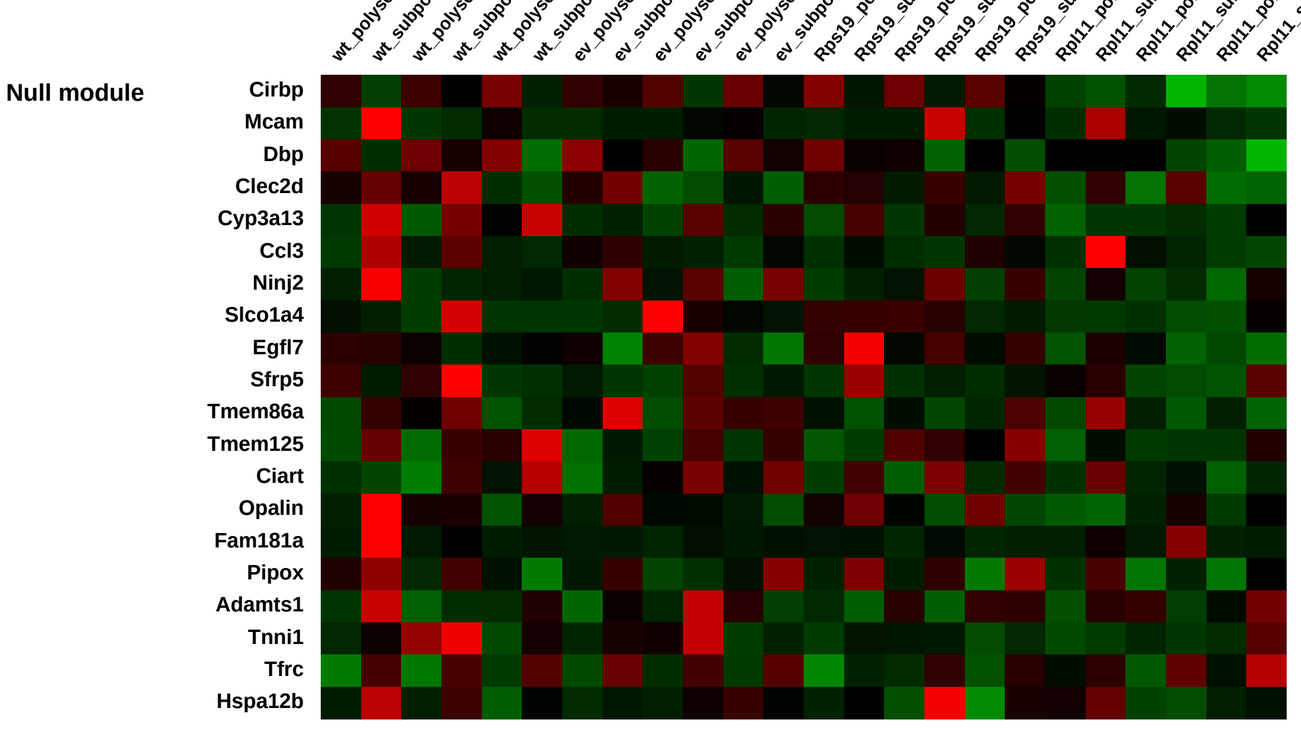

GEO Series "GSE22922" Expression Profiles

Num of samples in this series: 8

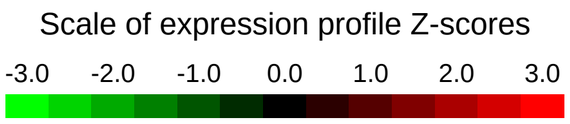

GEO Link: http://www.ncbi.nlm.nih.gov/geo/query/acc.cgi?acc=GSE22922

Status: Public on Jan 30 2013

Title: The Molecular Signature Induced by HMGA1 During Lymphoid Tumorigenesis

Organism: Mus musculus

Experiment type: Expression profiling by array

Platform: GPL1261

Pubmed ID:

Summary & Design:

Summary:
We are exploring the molecular pathways activated during lymphoid transformation with the long term goal of developing better therapies. Our focus is the HMGA1a oncogene because our studies indicate that it plays an important role in aggressive human lymphoid leukemia and lymphoma. We have developed the transgenic mouse over-expressing HMGA1a in lymphoid cells that develop aggressive lymphoid tumors by 8-10 months with histopathologic findings resembling human T-cell acute lymphocytic leukemia. By analyzing the gene expression profiles of our HMGA1a mouse model we plan to identify molecular pathways activated by HMGA1a in lymphoid transformation. Results from these studies will enhance our understanding of the pathogenesis of lymphoid malignancies and should lead to the development of better therapies.

Overall design:
A total of 20,669 genes represented on the Affymetrix Mouse 430 2.0 GeneChipTM array were screened with cRNA prepared from lymphoid cells of HMGA1a transgenic mice at different stages in tumorigenesis. These mice develop lymphoid tumors with complete penetrance at 8-12 months of age. We isolated RNA from splenocytes at 2 months (before tumors develop) and at 12 months (after tumors are well-established). These results were compared to splenocytes from control littermates. We used two statistical approaches to define differentially expressed genes, including a parametric (Partek genomics suite analysis) and nonparametric (CAM) approach.

Background corr dist: KL-Divergence = 0.0637, L1-Distance = 0.0182, L2-Distance = 0.0004, Normal std = 0.5171

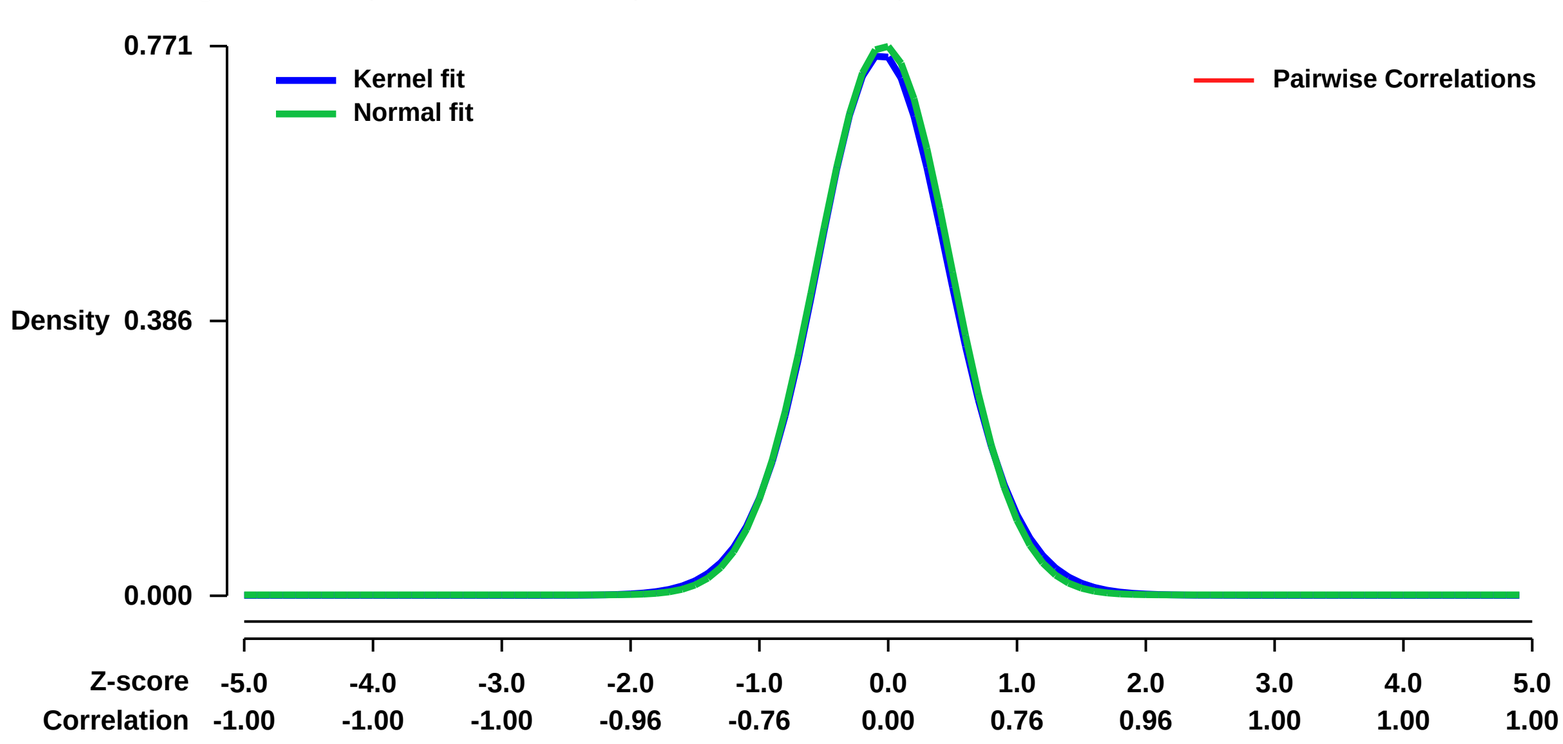

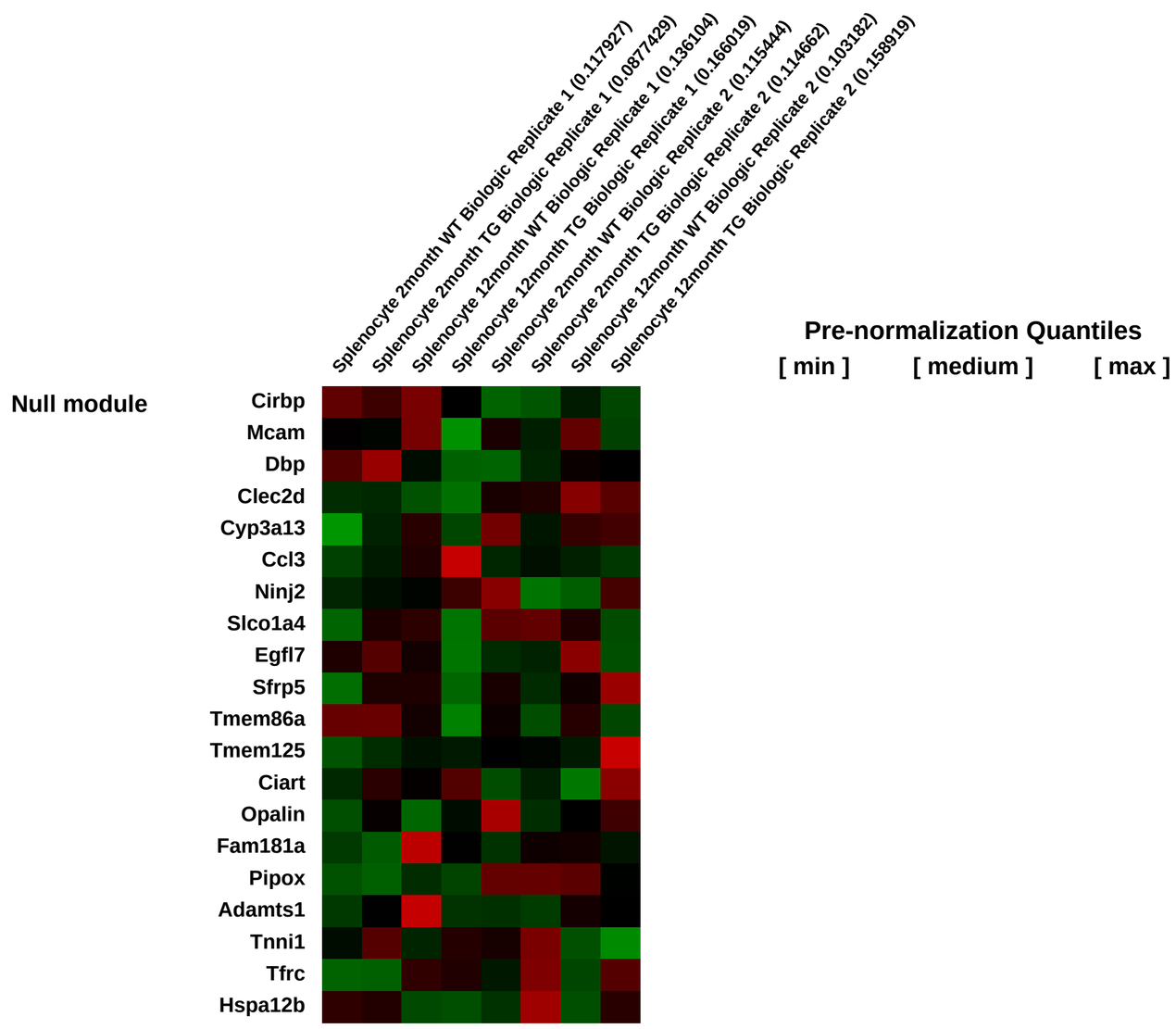

GEO Series "GSE22927" Expression Profiles

Num of samples in this series: 38

Scale of expression profile Z-scores

-3.0 -2.0 -1.0 0.0 1.0 2.0 3.0

GEO Link:	http://www.ncbi.nlm.nih.gov/geo/query/acc.cgi?acc=GSE22927
Status:	Public on Mar 23 2011
Title:	Hierarchical synergy of Pten, p53 and Rb pathways in high-grade astrocytoma induced in adult brain
Organism:	Mus musculus
Experiment type:	Genome variation profiling by genome tiling array
Platform:	GPL1261
Pubmed ID:	21397855
Summary & Design:	**Summary:** Mutations in the PTEN, TP53 and RB1 pathways are obligate events in the pathogenesis of human glioblastomas, the highest grade of astrocytoma. To investigate synergy between these tumor suppressors in mice, we induced various combinations of compound deletions conditionally in astrocytes and neural precursors in the mature brain. The resulting highly penetrant astrocytomas showed a spectrum of histopathological variation reminiscent of human tumors, and ranged from grade III to grade IV (glioblastoma). Secondary somatic mutations varied depending on the combination of initiating deletions and were relevant to human disease. Receptor tyrosine kinase amplifications were frequent in tumors initiated by combined conditional deletion of Pten and Tp53, but not when Rb, Pten and Tp53 were simultaneously deleted. Multiple mutations within PI3K and Rb pathways were acquired, however, Mapk activation was not consistently detected in astrocytomas. Gene expression profiling revealed striking similarities to previously described human astrocytoma subclasses. A subset of astrocytomas initiated outside of proliferative niches in the adult brain. **Overall design:** Gene expression of 8 human brain samples including 2 normal brainstem and 6 brainstem low-grade gliomas were profiled using HG-U133 plus 2 arrays. Gene expression of 38 mouse tumor samples, including 24 Pten;p53 double knockout and 14 Pten;p53;Rb1 triple knockout, were profiled using Affymetrix Mouse Genome 430 v2 arrays. Copy number changes of 51 double knockout tumor samples were analysed using Roswell Park Cancer Institute 6.5k BAC arrays. Copy number changes of 21 triple knockout tumor samples were analysed using Agilent mouse genome CGH mocirarray 244A.

Background corr dist: KL-Divergence = 0.4712, L1-Distance = 0.0871, L2-Distance = 0.0244, Normal std = 0.2319

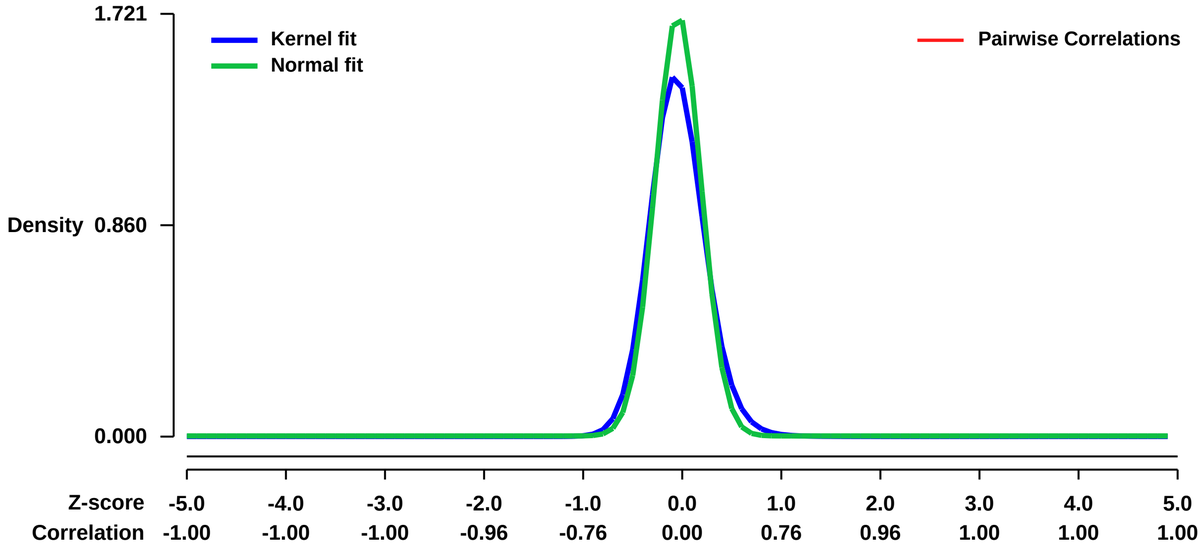

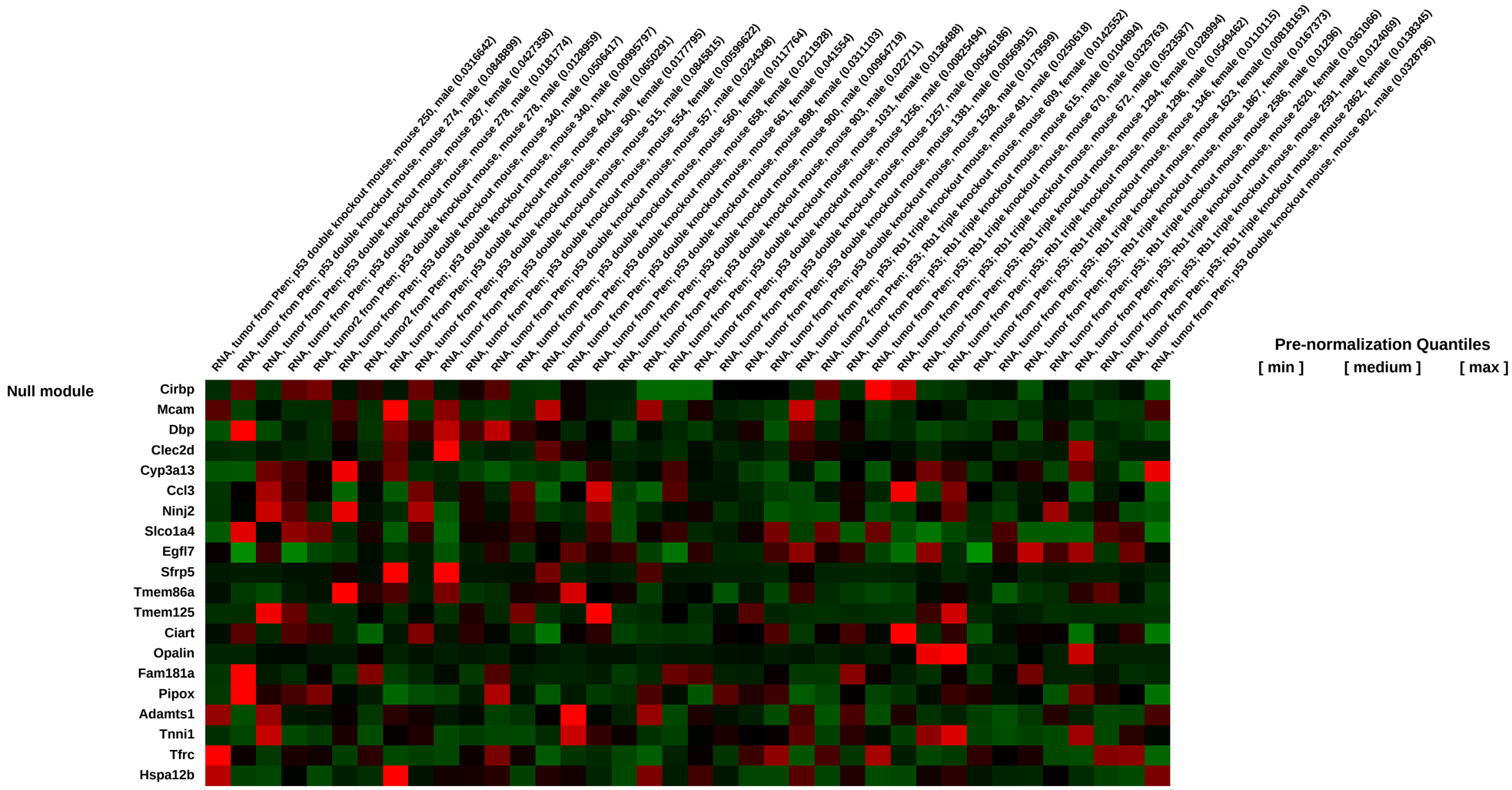

GEO Series "GSE22935" Expression Profiles

Num of samples in this series: 24

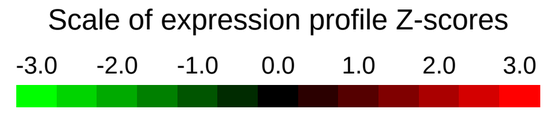

GEO Link:	http://www.ncbi.nlm.nih.gov/geo/query/acc.cgi?acc=GSE22935
Status:	Public on Jul 14 2010
Title:	Arginine utilization following mycobacteria infection in macrophages is dependent on autocrine-paracrine signaling
Organism:	Mus musculus
Experiment type:	Expression profiling by array
Platform:	GPL1261
Pubmed ID:	20716764
Summary & Design:	**Summary:** Nitric oxide (NO) produced by macrophages (Mˆ s) is toxic to both host tissues and invading pathogens and its regulation is therefore essential to suppress host cytotoxicity. Mˆ arginase 1 (Arg1) inhibits NO production by competing with NO synthases for arginine, the common substrate of NO synthases and arginases. Two signal transduction pathways control Arg1 expression in Mˆ s. First, a MyD88-dependent pathway induces Arg1 in intracellular infections, while a second Stat6-dependent pathway is required for Arg1 expression in alternativelyactivated Mˆ s. We found that mycobacteria-infected Mˆ s produce soluble factors that induce Arg1 in an autocrine-paracrine manner via Stat3. We identify these factors as IL-6, IL-10 and GCSF. We further establish that Arg1 expression is controlled by the MyD88-dependent production of IL-6, IL-10 and G-CSF rather than cell intrinsic MyD88 signaling to Arg1. Our data reveal the MyD88-dependent pathway of Arg1induction following BCG infection requires Stat3 activation and may result in the development of an immunosuppressive niche in granulomas due to the induced Arg1 production in surrounding uninfected Mˆ s **Overall design:** We used microarrays to perform genome wide expression analysis in mycobacteria-infected macrophages from C57Bl/6 WT and MyD88-knockout mice.

Background corr dist: KL-Divergence = 0.2765, L1-Distance = 0.0406, L2-Distance = 0.0034, Normal std = 0.2944

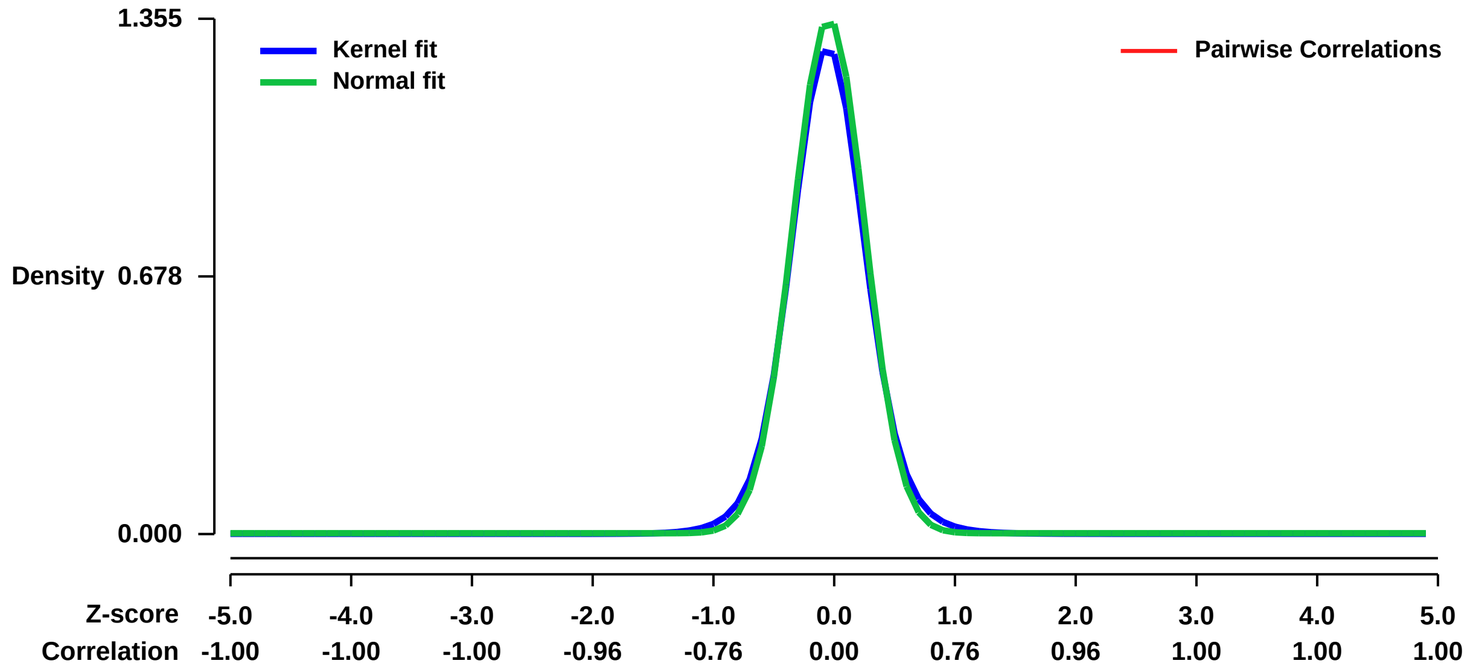

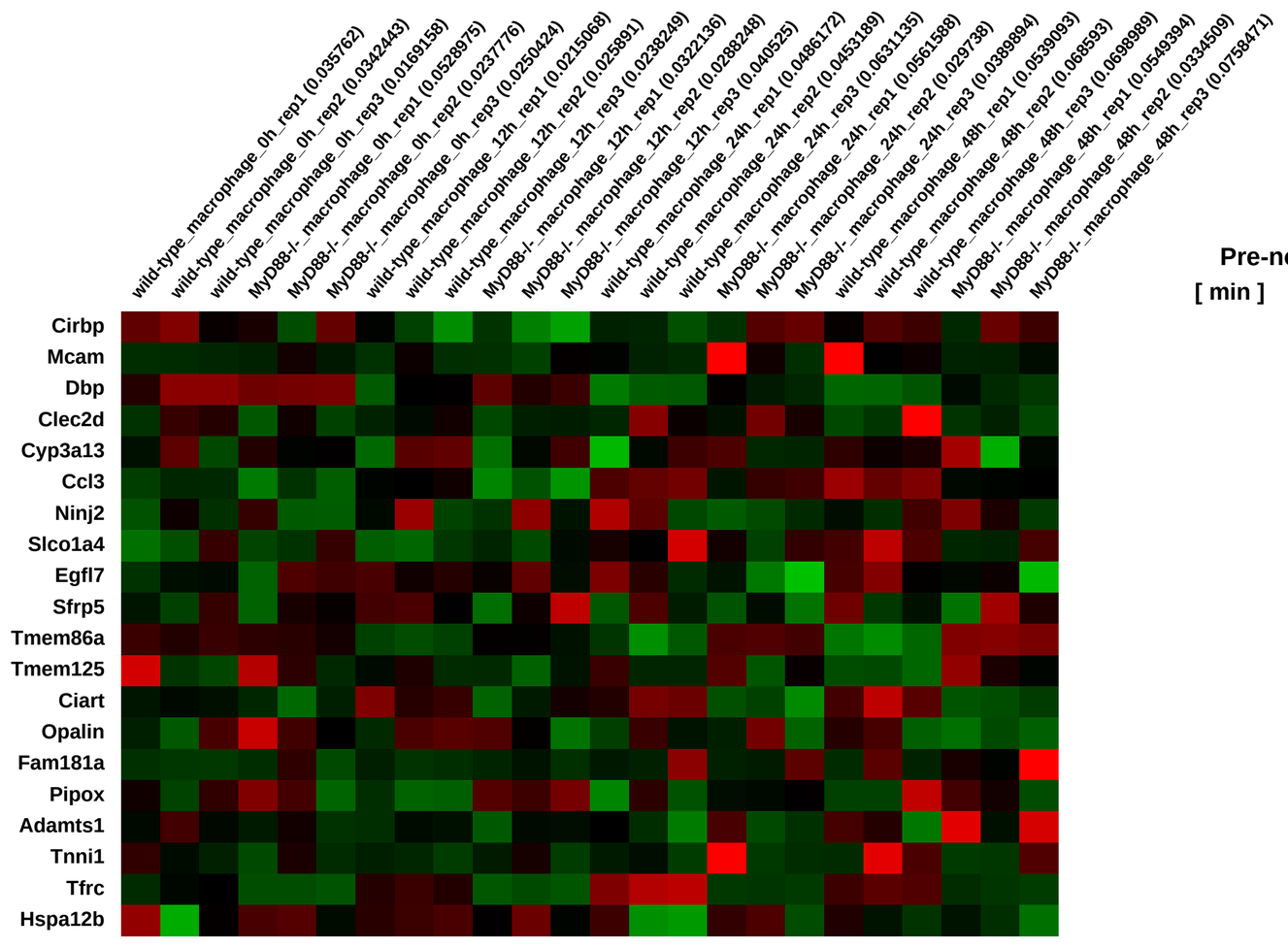

GEO Series "GSE22989" Expression Profiles

Num of samples in this series: 10

Scale of expression profile Z-scores

-3.0 -2.0 -1.0 0.0 1.0 2.0 3.0

GEO Link:	http://www.ncbi.nlm.nih.gov/geo/query/acc.cgi?acc=GSE22989
Status:	Public on Nov 29 2011
Title:	Gene expression profiling of Tgfbr2 mutant mouse models of cleft palate
Organism:	Mus musculus
Experiment type:	Expression profiling by array
Platform:	GPL1261
Pubmed ID:	22123828
Summary & Design:	**Summary:** The overall goal of this project is to investigate the role of TGF-beta signaling in palate development in order to discover candidate therapeutics for preventing and treating congenital birth defects. Here, we conducted gene expression profiling of embryonic palatal tissue from wild type mice as well as those with a neural crest specific conditional inactivation of the Tgfbr2 gene. The latter mice provide a model of cleft palate formation. **Overall design:** To investigate the mechanism of cleft palate resulting from mutations in TGFBR2, we analyzed neural crest specific conditional inactivation of Tgfbr2 in mice (Tgfbr2fl/fl;Wnt1-Cre). We performed microarray analyses using the palatal tissue of Tgfbr2fl/fl;Wnt1-Cre mice at embryonic day E13.5 (prior to palatal fusion, n=6 per genotype) and E14.5 (during palatal fusion, n=5 per genotype) to examine the genes regulated by Tgf-beta during palate formation.

Background corr dist: KL-Divergence = 0.0820, L1-Distance = 0.0225, L2-Distance = 0.0007, Normal std = 0.4701

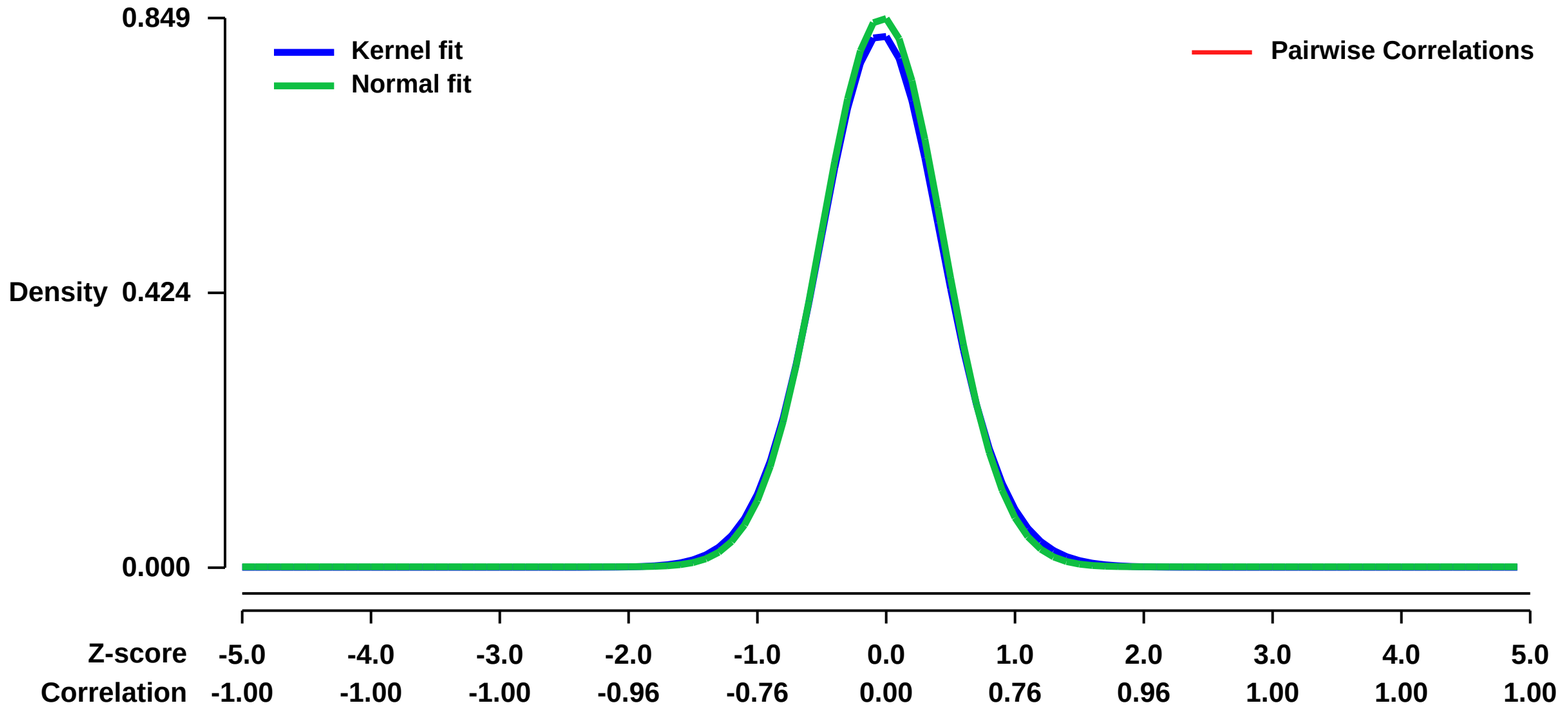

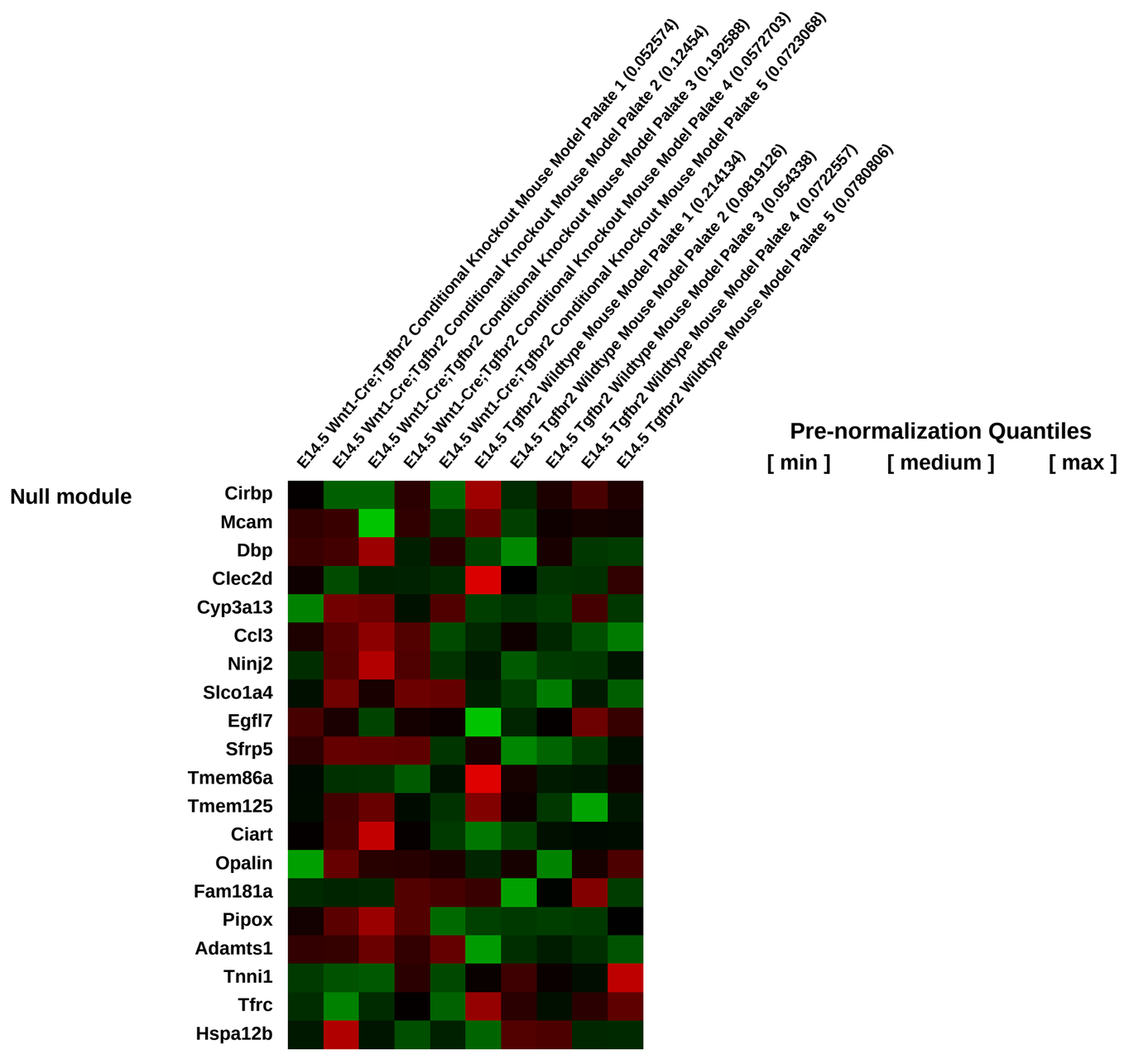

GEO Series "GSE23002" Expression Profiles

Num of samples in this series: 8

Scale of expression profile Z-scores

-3.0 -2.0 -1.0 0.0 1.0 2.0 3.0

GEO Link:	http://www.ncbi.nlm.nih.gov/geo/query/acc.cgi?acc=GSE23002
Status:	Public on Jul 20 2010
Title:	Transcriptional and Phenotypic Reprogramming of Tumors by Host Stroma Deficient in TNF¸– Signaling
Organism:	Mus musculus
Experiment type:	Expression profiling by array
Platform:	GPL1261
Pubmed ID:	
Summary & Design:	**Summary:** **Background: We previously demonstrated that B16F1 melanoma tumors growing in syngeneic germline-deleted TNFR1,2 -/- mice were more sensitive to ionizing radiation (IR) compared to tumors growing in C57BL/6 wild-type mice; however, the mechanisms linked to this difference in radiosensitivity are not fully understood.** **Methodology/ Principal Findings: We used DNA microarrays to identify alterations in the expression of functional gene clusters associated with the radiosensitization of B16F1 tumors growing in TNFR1,2 -/- mice. At the basal level, disruption of host stromal TNF¸– signaling resulted in the over-expression of tumor genes involved in extracellular matrix remodeling and angiogenesis. Phenotypically, these tumors exhibited a reduced vascular density, which induced the expression of oxidative stress signaling pathways and increased levels of tissue hypoxia and necrosis. These alterations were paralleled by the suppression of genes involved in chromosomal stability and key effectors of the ATM-dependent/ non-homologous end-joining pathways including phosphorylated-ATM, BRCA1, and RAD51, which resulted in greater DNA double-strand breaks and caspase 3 activation following IR treatment.** **Conclusions/ Significance: Taken together, these results demonstrate that disruption of TNF¸– signaling in the host stroma mediates transcriptional and phenotypic changes in tumors which may alter tumor radiosensitivity. These results suggest a critical role for TNF¸– in the maintenance of tumor-associated vasculature and radioresistance. They also indicate that TNF¸– signaling blockade in stromal cells may represent a strategy for tumor radiosensitization.** **Overall design:** **To investigate the genes associated with the radiosensitization of B16F1 melanoma tumors in the context of disrupted stromal TNF¸– signaling, we performed expression profiling of B16F1 tumors grown in syngeneic TNFR 1, 2 -/- and wild-type C57BL/6 mice. Tumors were lysed to collect total RNA, pooled by treatment group according to total RNA level, and analyzed in duplicates with Affymetrix GeneChip´fi Mouse Genome 430 2.0 Arrays.**

Background corr dist: KL-Divergence = 0.0476, L1-Distance = 0.0310, L2-Distance = 0.0011, Normal std = 0.5957

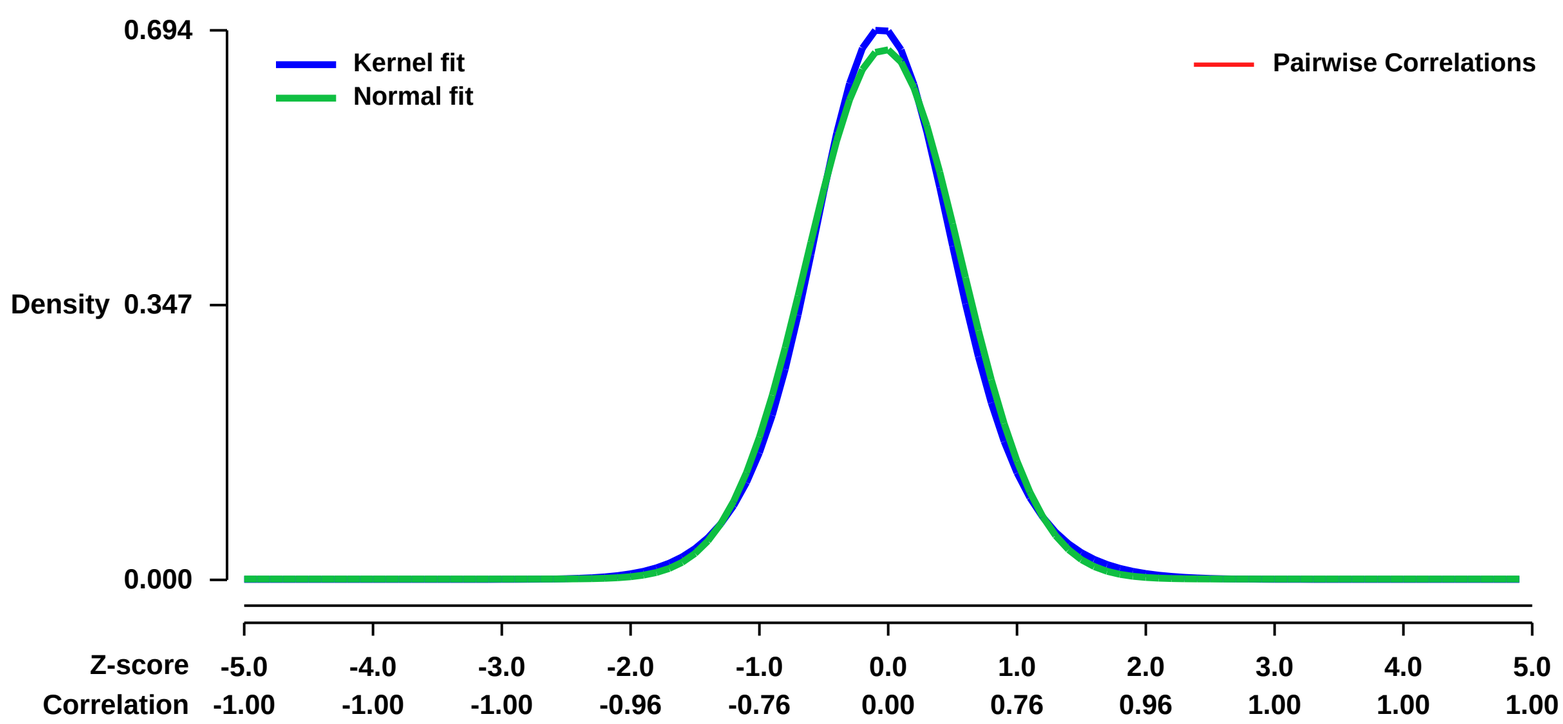

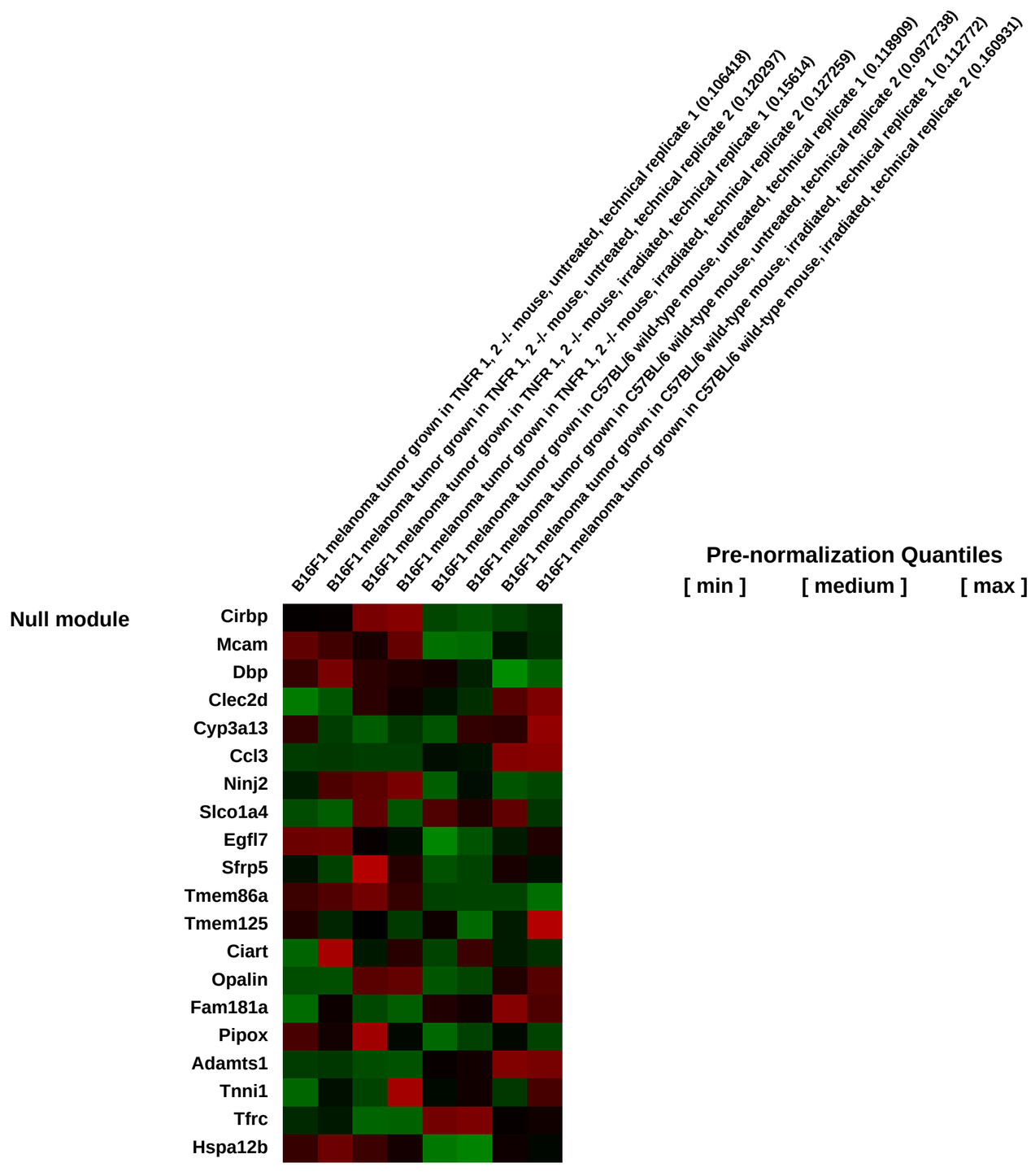

GEO Series "GSE23016" Expression Profiles

Num of samples in this series: 9

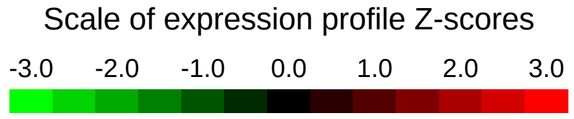

GEO Link:	**http://www.ncbi.nlm.nih.gov/geo/query/acc.cgi?acc=GSE23016**
Status:	**Public on Mar 07 2011**
Title:	**Alternatively Spliced Variants of Interleukin-4 Promote Inflammation Differentially**
Organism:	**Mus musculus**
Experiment type:	**Expression profiling by array**
Platform:	**GPL1261**
Pubmed ID:	**21285395**
Summary & Design:	**Summary:** **IL-4d2 is a natural splice variant of IL-4 which lacks the region encoded by the second exon. Numerous recent reports suggested that the expression levels of IL-4d2 change in various diseases, especially those with pulmonary involvement, but the effects of IL-4d2 on the lungs in vivo have never been studied. Replication-deficient adenovirus-mediated gene delivery of mouse IL-4d2 to mouse lungs in vivo was used, and the effects compared with similar adenoviral delivery of mouse IL-4 or with infection with a NULL viral construct.** **The objective was to determine whether full-length wild-type Interleukin-4 encoded by exons 1-4 (IL-4) and alternatively spliced variant econded by exons 1,3, and 4 (IL-4d2) differentially affect gene expression in the lungs in vivo. The results show that IL-4d2 and IL-4 affected global gene expression differentially.** **Keywords: Comparative analysis of gene delivery of alternative splice variants in vivo** **Overall design:** **There were three mice overexpressing mouse IL-4 in their lungs, three mice overexpressing mouse IL-4d2 in their lungs, and three mice similarly infected with control AdV-NULL virus not encoding a cytokine.**

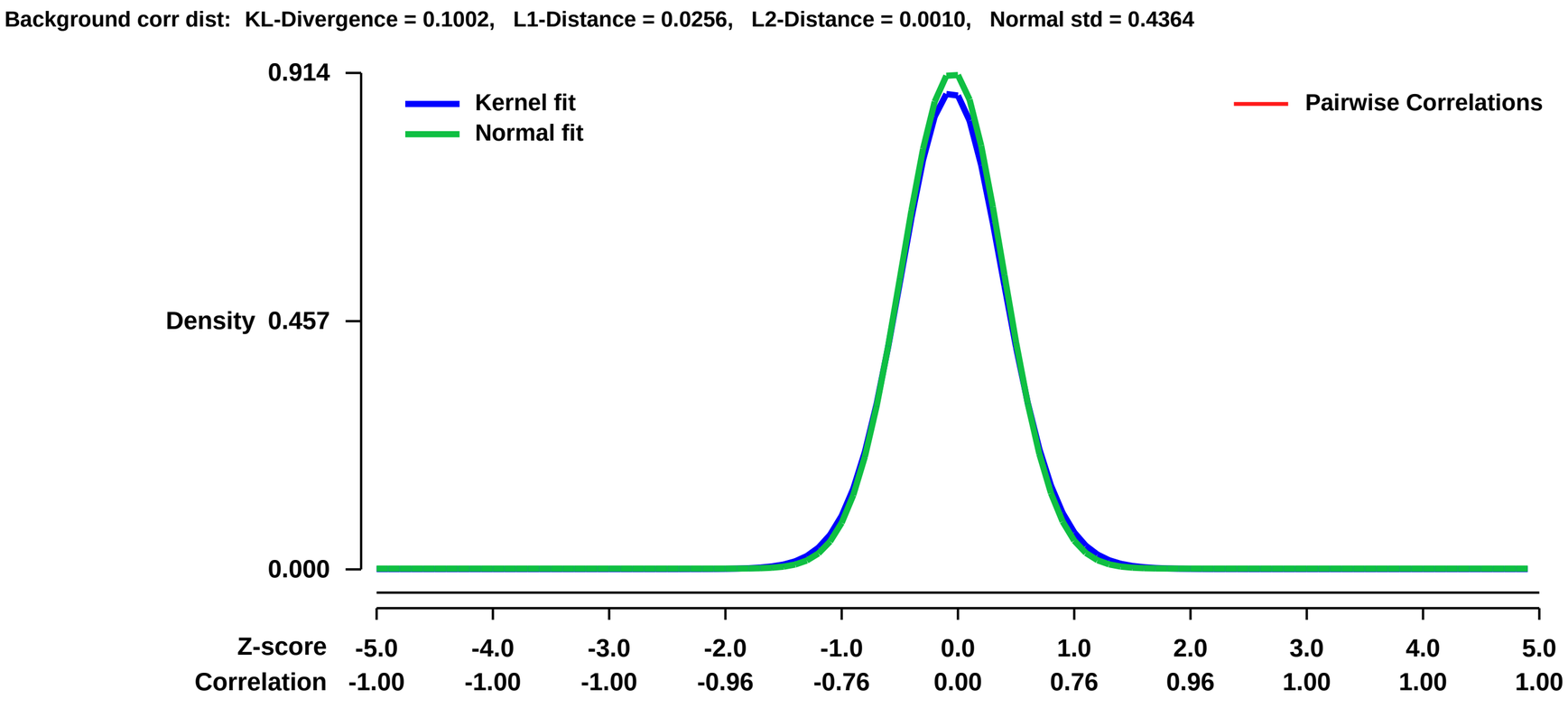

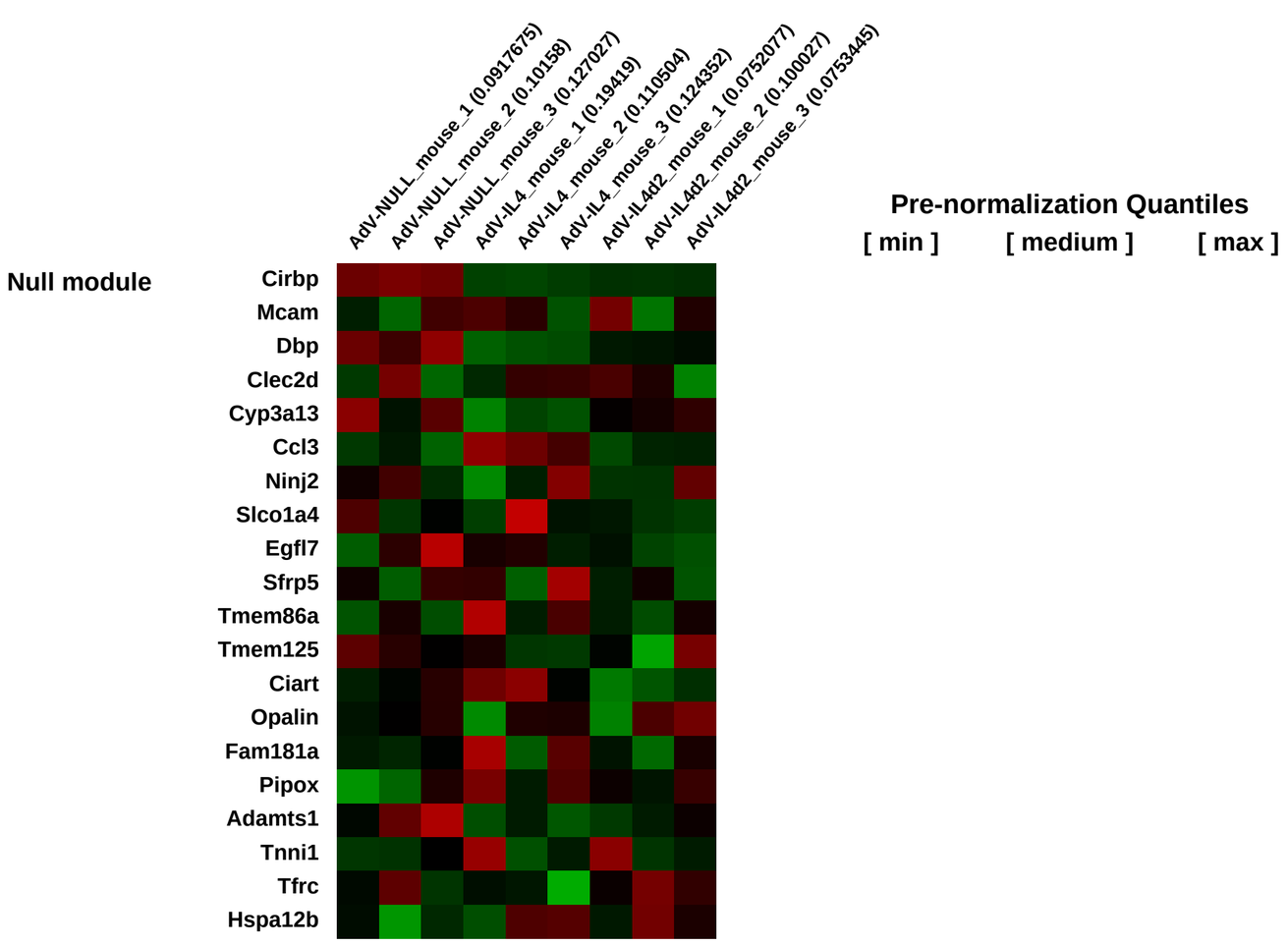

GEO Series "GSE23040" Expression Profiles

Num of samples in this series: 6

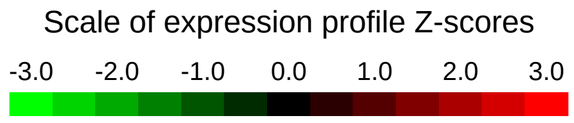

GEO Link:	http://www.ncbi.nlm.nih.gov/geo/query/acc.cgi?acc=GSE23040
Status:	Public on Jan 01 2011
Title:	Loss of Hepatocyte-Nuclear-Factor-1$_{\alpha}$– Impacts on Adult Mouse Intestinal Epithelial Cell Growth and Cell Lineages Differentiation
Organism:	Mus musculus
Experiment type:	Expression profiling by array
Platform:	GPL1261
Pubmed ID:	20808783
Summary & Design:	**Summary:** Although hepatocyte-nuclear-factor-1$_{\alpha}$– (Hnf1$_{\alpha}$–) is crucial for pancreas and liver functions, it is believed to play a limited functional role for intestinal epithelial functions. The aim of this study was to assess the consequences of abrogating Hnf1$_{\alpha}$– on the maintenance of adult small intestinal epithelial functions. Methodology/Principal Findings An Hnf1$_{\alpha}$– knockout mouse model was used. Assessment of histological abnormalities, crypt epithelial cell proliferation, epithelial barrier, glucose transport and signalling pathways were measured in these animals. Changes in global gene expression were also analyzed. Mice lacking Hnf1$_{\alpha}$– displayed increased crypt proliferation and intestinalomegaly as well as a disturbance of intestinal epithelial cell lineages production during adult life. This phenotype was associated with a decrease of the mucosal barrier function and lumen-to-blood glucose delivery. The mammalian target of rapamycin (mTOR) signalling pathway was found to be overly activated in the small intestine of adult Hnf1$_{\alpha}$– mutant mice. The intestinal epithelium of Hnf1$_{\alpha}$– null mice displayed a reduction of the enteroendocrine cell population. An impact was also observed on proper Paneth cell differentiation with abnormalities in the granule exocytosis pathway. Conclusions/Significance Together, these results unravel a functional role for Hnf1$_{\alpha}$– in regulating adult intestinal growth and sustaining the functions of intestinal epithelial cell lineages. **Overall design:** HNF1alpha was knocked out. A total of 3 control and 3 mutant littermate individuals were sacrificed at 4 months of age. The jejunum was harvested and total RNA was isolated from each individual. Each RNA sample was independently used to generate probes to screen Affymetrix chips.

Background corr dist: KL-Divergence = 0.0372, L1-Distance = 0.0151, L2-Distance = 0.0002, Normal std = 0.6258

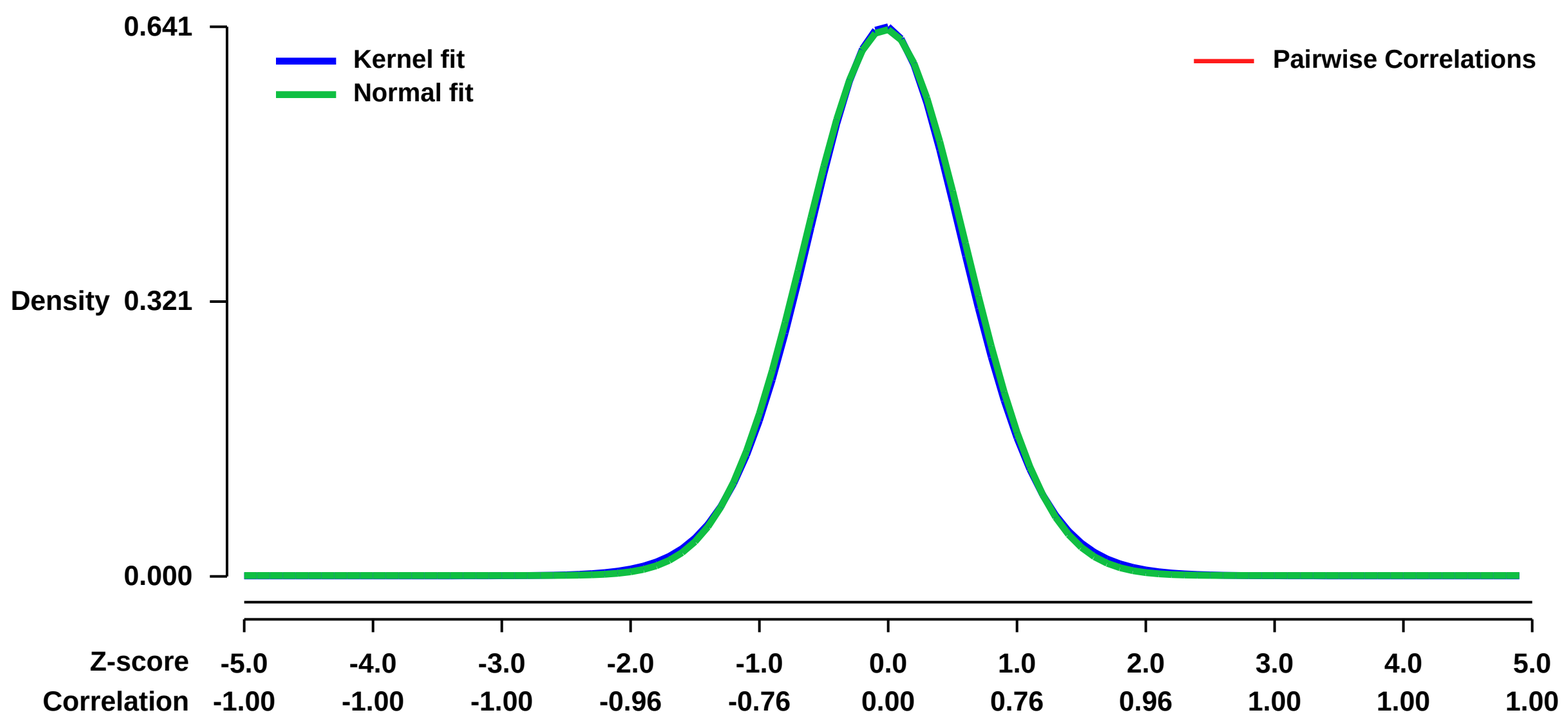

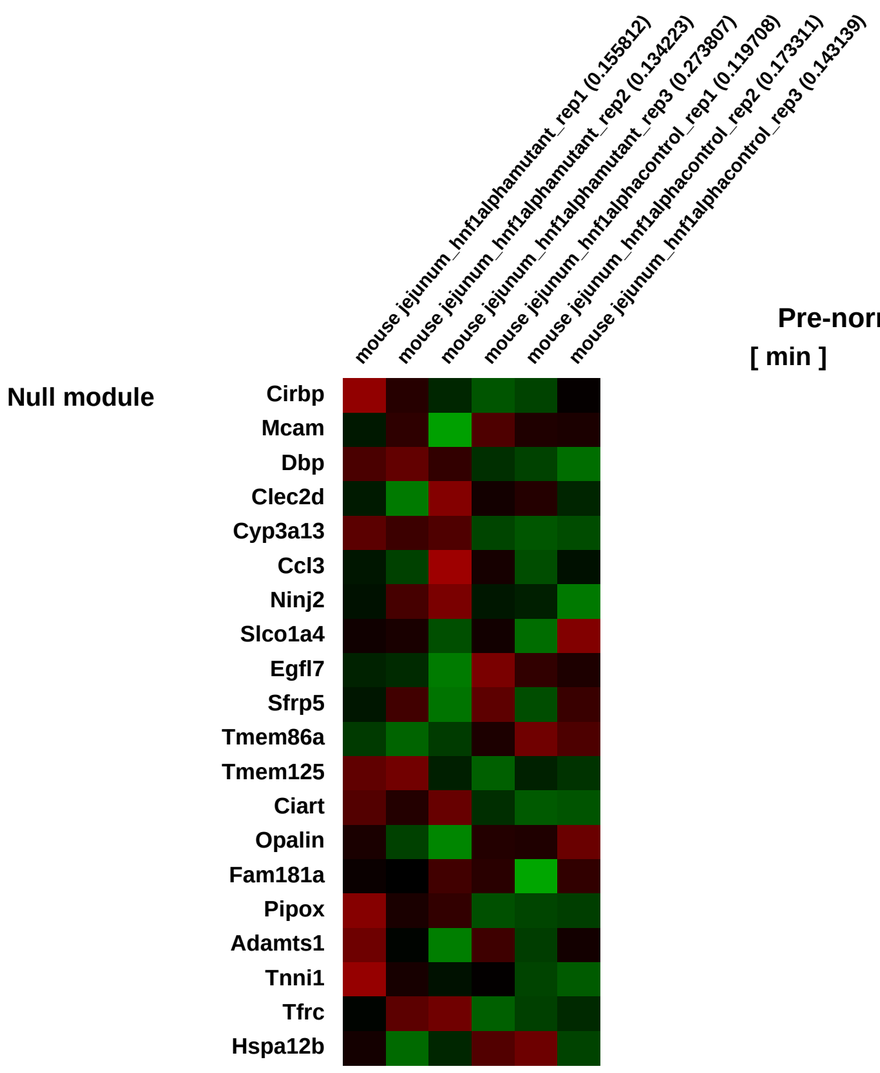

GEO Series "GSE23081" Expression Profiles

Num of samples in this series: 6

Scale of expression profile Z-scores

-3.0 -2.0 -1.0 0.0 1.0 2.0 3.0

GEO Link:	http://www.ncbi.nlm.nih.gov/geo/query/acc.cgi?acc=GSE23081
Status:	Public on Apr 20 2011
Title:	Identification of microRNA targets in the mammalian inner ear using a comprehensive transcriptome and proteome integrated approach
Organism:	Mus musculus
Experiment type:	Expression profiling by array
Platform:	GPL1261
Pubmed ID:	21483685
Summary & Design:	**Summary:** We have employed a novel approach for the identification of functionally important microRNA (miRNA)-target interactions using integrated miRNA, transcriptome and proteome profiles with advanced in silico analysis. By looking at both the transcript and protein levels of expression, a thorough coverage of miRNA regulation was obtained. Microdissected auditory and vestibular sensory epithelia were used as the model system, thus being the first time such a comparison was carried out in a neuroepithelial system. Moreover, this is one of only a few studies employing proteome screening for the identification of miRNA targets. Notably, this approach can be employed for the study of other tissues and organs. We detected the expression of 157 miRNAs in the inner ear sensory epithelia, with 53 miRNAs differentially expressed between the cochlea and vestibule. By searching for enrichment and depletion of miRNA targets in the transcript and protein datasets with a reciprocal or similar expression, respectively, as the regulatory miRNA, we identified functionally important miRNAs. Finally, the interaction between miR-135b and PSIP1-P75, a transcriptional coacitvator previously unknown in the inner ear, was identified and validated experimentally. We suggest that miR-135b may serve as a cellular effector, involved in regulating some of the differences between the cochlear and vestibular hair cells. **Overall design:** We investigated the mRNA expression profile of the cochlear and vestibular sensory epithelia from inner ears of postnatal day 2 mice using the Affymetrix GeneChip´fi 430 2Mouse Genome array. Cochlear and vestibular sensory epithelia were dissected from wild type C3H mice and collected separately. The vestibular epithelia consisted of the saccule, utricle and the lateral and anterior cristae. Both the cochlear and vestibular sensory epithelia were dissected with their underlying mesenchyma. Altogether three pools, three biological replicates, of each tissue type were collected consisting of cochlear or vestibular sensory epithelia dissected from 10 to 12 inner ears.

Background corr dist: KL-Divergence = 0.0241, L1-Distance = 0.0102, L2-Distance = 0.0001, Normal std = 0.7062

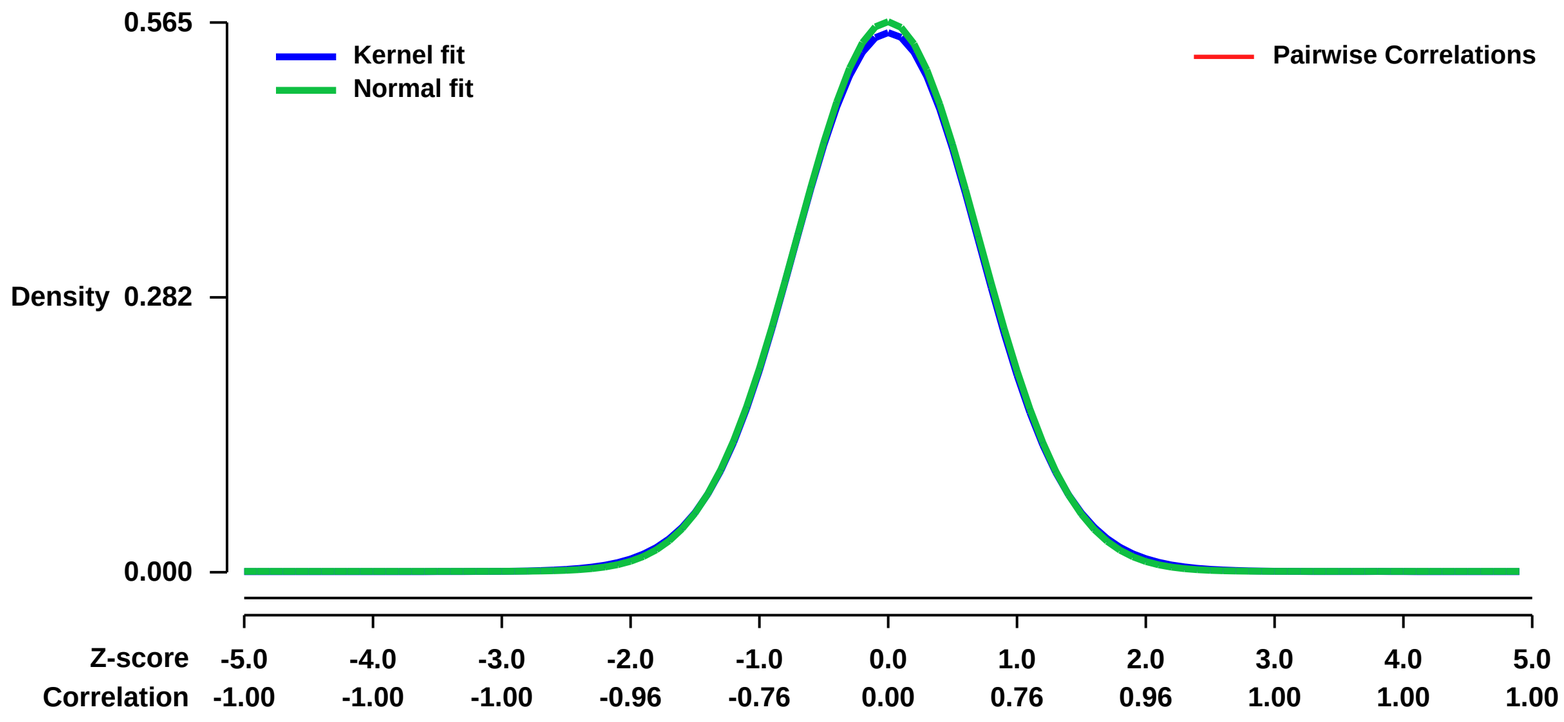

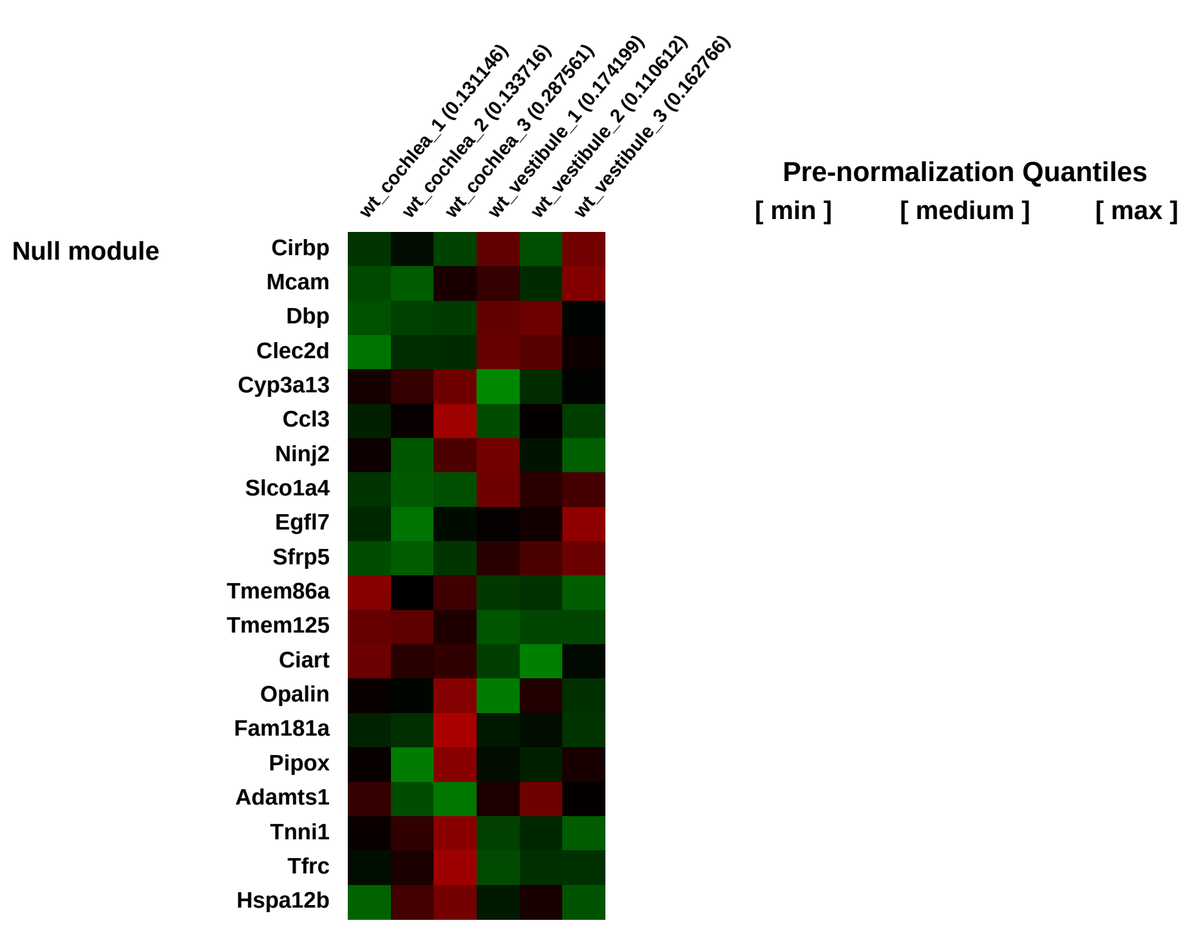

GEO Series "GSE23101" Expression Profiles

Num of samples in this series: 20

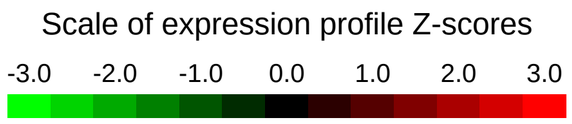

GEO Link:	**http://www.ncbi.nlm.nih.gov/geo/query/acc.cgi?acc=GSE23101**
Status:	**Public on Mar 31 2013**
Title:	**Comparative Effects of Statins on Murine Cardiac Gene Expression Profiles in Normal Mice**
Organism:	**Mus musculus**
Experiment type:	**Expression profiling by array**
Platform:	**GPL1261**
Pubmed ID:	**23524094**
Summary & Design:	**Summary:** **Recent clinical data suggest that the efficacy of statin treatment in patients with heart failure varies depending on the drugs administered. Therefore, the present study was undertaken to compare murine cardiac gene expression following treatment with four different statins.** **Statins directly regulated cardiac gene expression in a drug-specific manner in mice. The influence of each statin on the cardiac mRNA expression of various genes, including several genes that might be involved in the development of cardiac disease, was not a general effect of this class of drugs.** **Overall design:** **Male C57BL/6J mice (n = 20) were treated with or without a statin (pitavastatin calcium, pravastatin sodium, rosuvastatin calcium, or atorvastatin calcium hydrate) (n = 4 in each group) for four weeks. Total RNA was isolated from the left ventricle of each animal. The fragmented and labeled amplified cDNA was hybridized to a GeneChip Mouse Genome 430 2.0 Array (Affymetrix). Data and statistical analysis were performed with GeneSpring GX version 11.0 software (Agilent Technologies).**

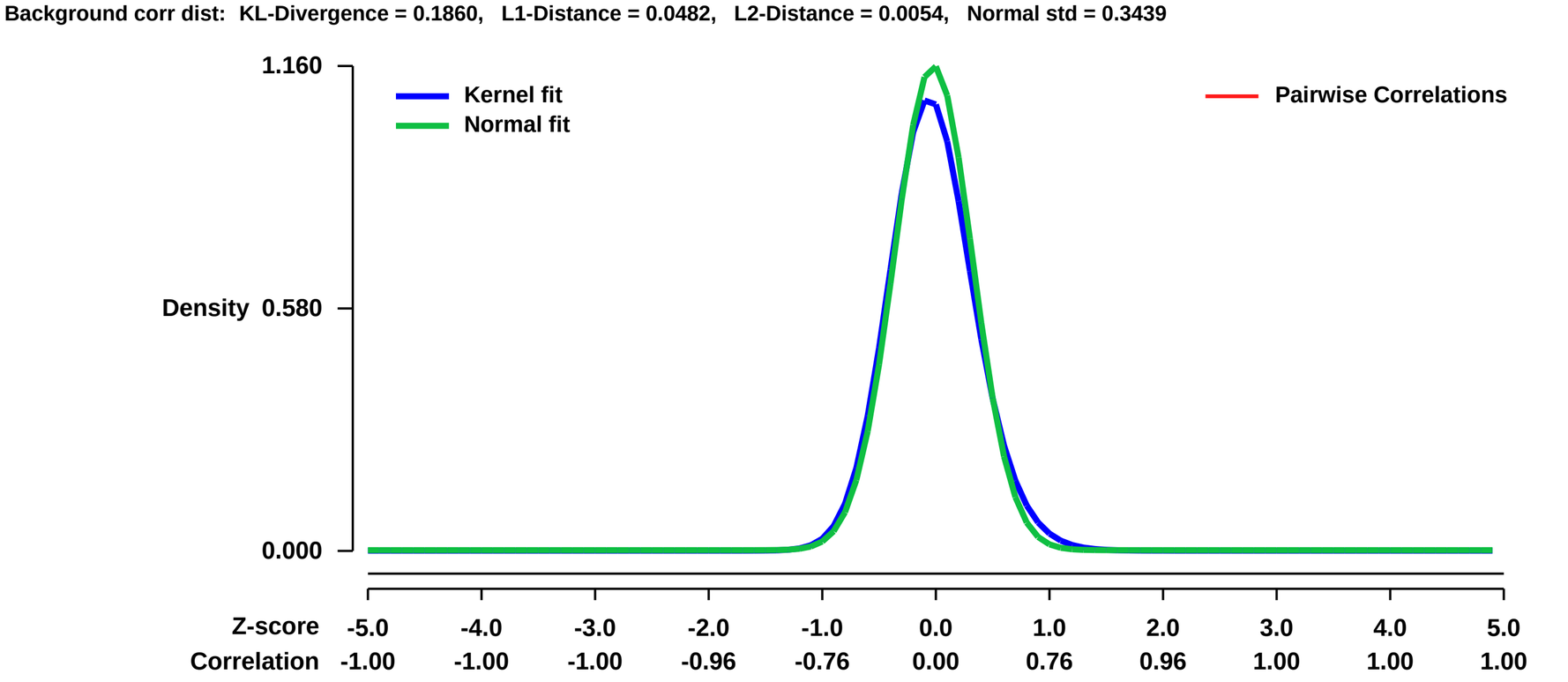

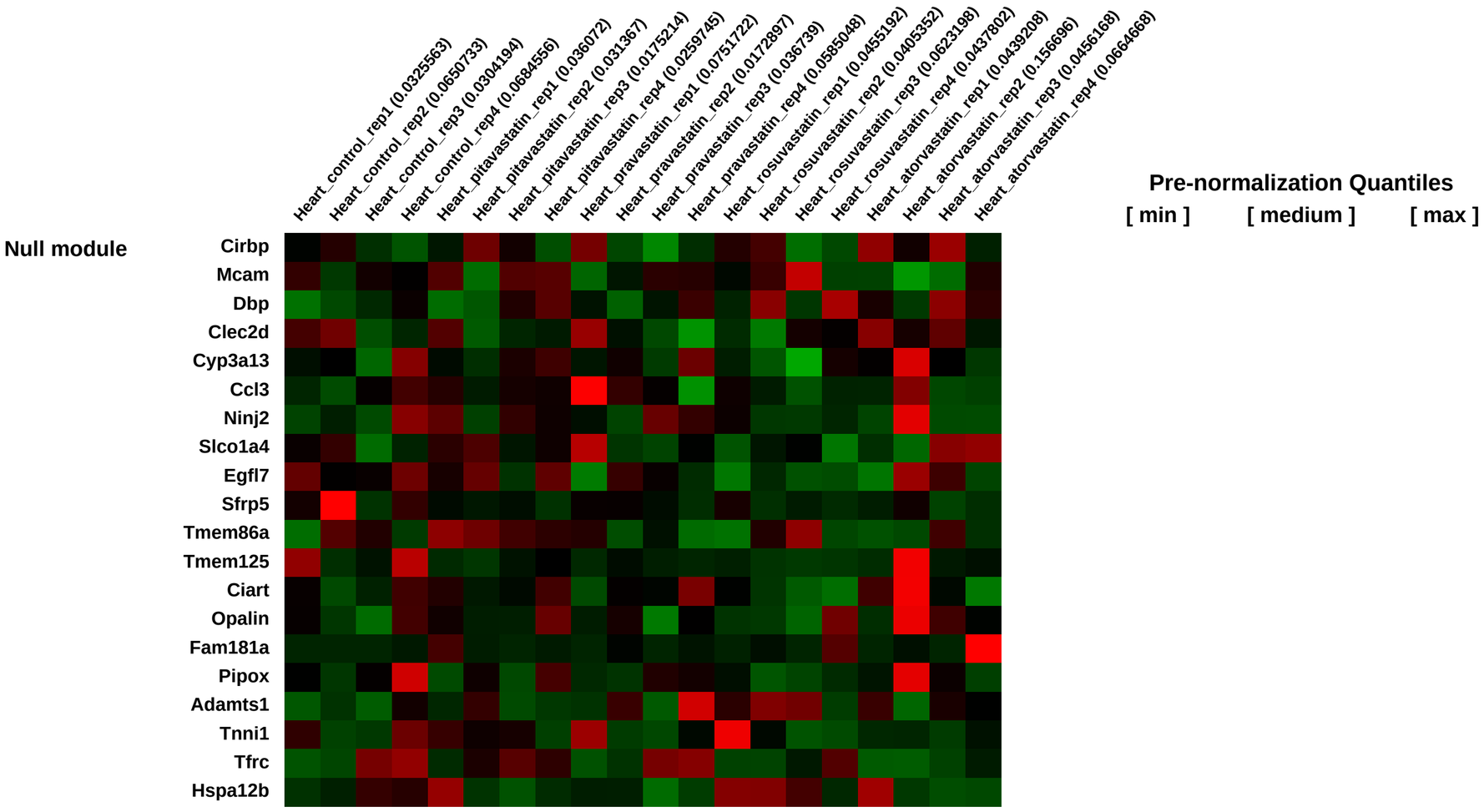

GEO Series "GSE23119" Expression Profiles

Num of samples in this series: 9

Scale of expression profile Z-scores

-3.0 -2.0 -1.0 0.0 1.0 2.0 3.0

GEO Link:	http://www.ncbi.nlm.nih.gov/geo/query/acc.cgi?acc=GSE23119
Status:	Public on Aug 03 2010
Title:	Effect of vitamin A deficiency (VAD) on mouse spermatogonial transcriptome profiles
Organism:	Mus musculus
Experiment type:	Expression profiling by array
Platform:	GPL1261
Pubmed ID:	23253600
Summary & Design:	**Summary:** The objective of this study was to understand the genetic mechanisms of Vitamin-A-Deficiency (VAD)-induced arrest of spermatogonial stem-cell differentiation. Vitamin A and its derivatives (the retinoids) participate in many physiological processes including vision, cellular differentiation and reproduction. VAD affects spermatogenesis, the subject of our present study. Spermatogenesis is a highly regulated process of differentiation and complex morphologic alterations that, in the postnatal testis, leads to the formation of sperm in the seminiferous epithelium. VAD causes early cessation of spermatogenesis, characterized by degeneration of meiotic germ cells, leading to seminiferous tubules containing mostly type A spermatogonia and Sertoli cells. In this study, we investigated the molecular basis of VAD on spermatogenesis in mice. We used adult Balb/C mice fed with a Control or VAD diet for an extended period of time (8-28 weeks) and selected two time points (18 and 25 weeks) for microarray analysis. To understand the effect of VAD on the spermatogonial stem cell transcriptome, we studied isolated pure populations of spermatogonia from control and vitamin-A-deficient mice from two representative time points (18 and 25 weeks) using Affymetrix GeneChip microarrays. We identified target genes involved in the arrest of spermatogonial differentiation and spermatogenesis. Our results establish a better understanding of the chronology and magnitude of the consequences of VAD on mouse testes and add to the current knowledge of the molecular regulatory mechanisms of germ cell development. **Overall design:** Spermatogonia were isolated by the STATPUT procedure with minor modifications. VAD mice were sacrificed at 18 and 25 weeks of VAD treatment for spermatogonia isolation. Decapsulated testes from 2 mice were suspended in RPMI medium containing collagenase (0.6 mg/ml), Hyaluronidase (0.12 mg/ml) and DNAse I (1.25 mg/ml) and incubated at 37´”C for 30 minutes in a shaking water bath. The tissues were then allowed to come down the tube and the supernatant (containing interstitial cells) was removed. The pellet was incubated with 3 ml of 0.25% Trypsin /EDTA (GIBCO, Invitrogen, USA), in the presence of DNAse I (0.2 mg/ml) at 37´”C for 15 minutes in a shaking water bath. The dispersed cells were washed twice with RPMI medium containing 10% heat inactivated FBS to neutralize the protease activity, and filtered through a sterile 0.22 nylon to remove any undigested fragments. Cells of the dissociated seminiferous epithelium were then plated overnight in a 34´”C 3% CO2 incubator. The following day, germ cells, in suspension, were separated by sedimentation with use of a 2-4% BSA gradient. The cells were allowed to sediment for a standard period of 2.5 h, and fractions of 2-ml volume were collected. The cells of each fraction were examined under a phase contrast microscope, and fractions containing cells of similar size and morphology were pooled and spun down by low-speed centrifugation. Purity of spermatogonia was estimated and was routinely higher than 90%. Total RNA was extracted from the isolated germ cells using TRIzol ´fi Reagent, and cleaned with RNeasy minicolumns. RNA content was determined by measurement of optical density at 260 nm. Only the RNA samples showing an OD 260/280 ratio higher than 1.8 were used for microarray hybridization. Raw expression values in Affymetrix CEL file format were generated by GeneChip Operating Software.

Background corr dist: KL-Divergence = 0.0289, L1-Distance = 0.0374, L2-Distance = 0.0019, Normal std = 0.6920

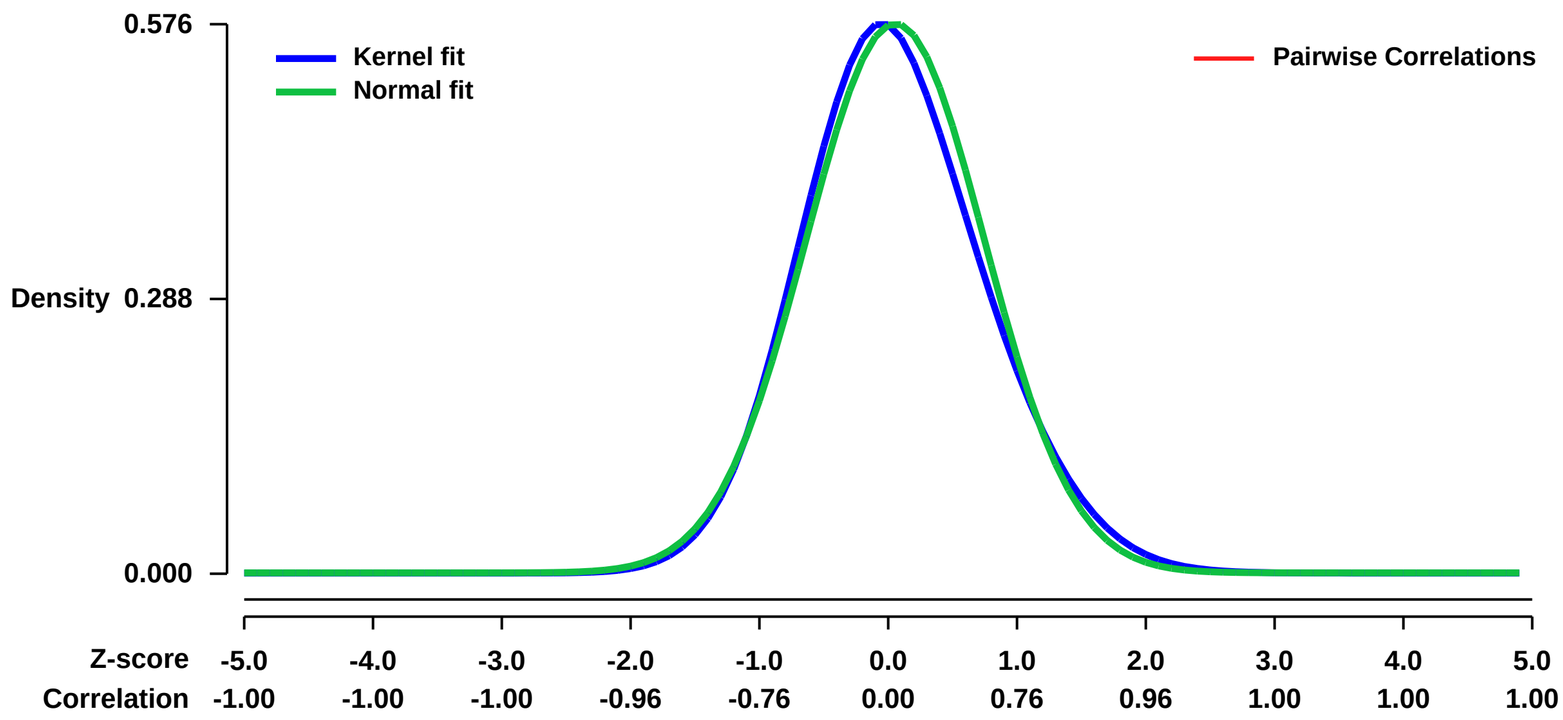

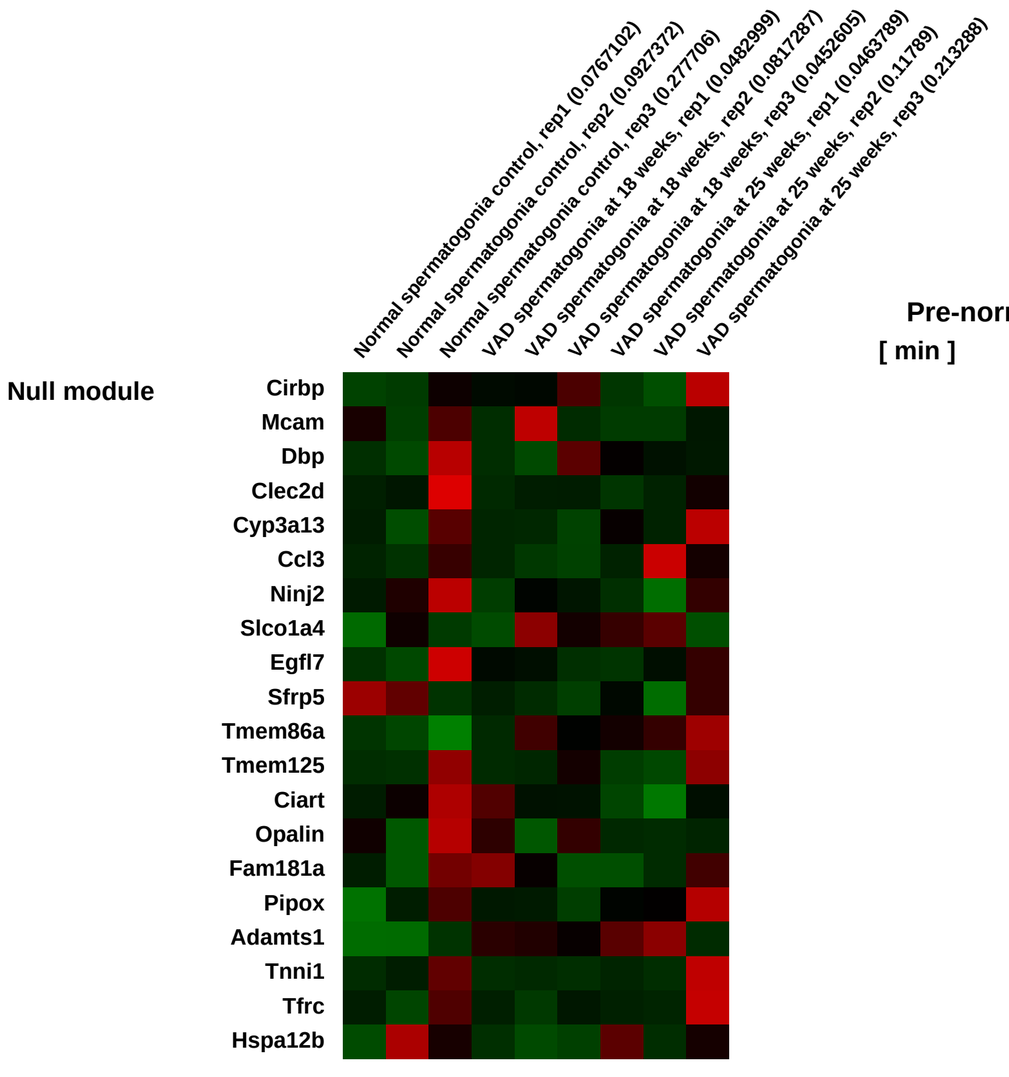

GEO Series "GSE23161" Expression Profiles

Num of samples in this series: 8

Scale of expression profile Z-scores

-3.0 -2.0 -1.0 0.0 1.0 2.0 3.0

GEO Link:	http://www.ncbi.nlm.nih.gov/geo/query/acc.cgi?acc=GSE23161
Status:	Public on Jun 30 2011
Title:	Beta cell overexpression of HSD11B1 in high fat fed mice
Organism:	Mus musculus
Experiment type:	Expression profiling by array
Platform:	GPL1261
Pubmed ID:	22315313
Summary & Design:	**Summary:** To model the potential diabetogenic effects of higher level of HSD11B1 in b-cells of the pancreas in vivo, we created a transgenic model overexpressing HSD11B1 under the mouse insulin I promoter (MIP-HSD1) in diabetes-prone C57Bl/KsJ mice. KsJ wild type and MIP-HSD1 heterozygous mice have been high fat fed for 12 weeks. Pancreata have been perfused with collagenase and islets isolated by hand picking. Isolated islets (around 500) coming from at least 3 mice (around 200/mice) have been directly lysed in Trizol. Total RNA have been extracted by Trizol plus RNA Purification Kit (invitrogen). **Overall design:** Four biological replicates per group: Wild type KsJ mice on High Fat diet (KsJ1, KsJ2, KsJ3, KsJ4) and MIP-HSD1 transgenic mice on High Fat diet (MIP1, MIP2, MIP3, MIP4) were used to prepare RNA for microarray analysis.

Background corr dist: KL-Divergence = 0.0157, L1-Distance = 0.0347, L2-Distance = 0.0013, Normal std = 0.8338

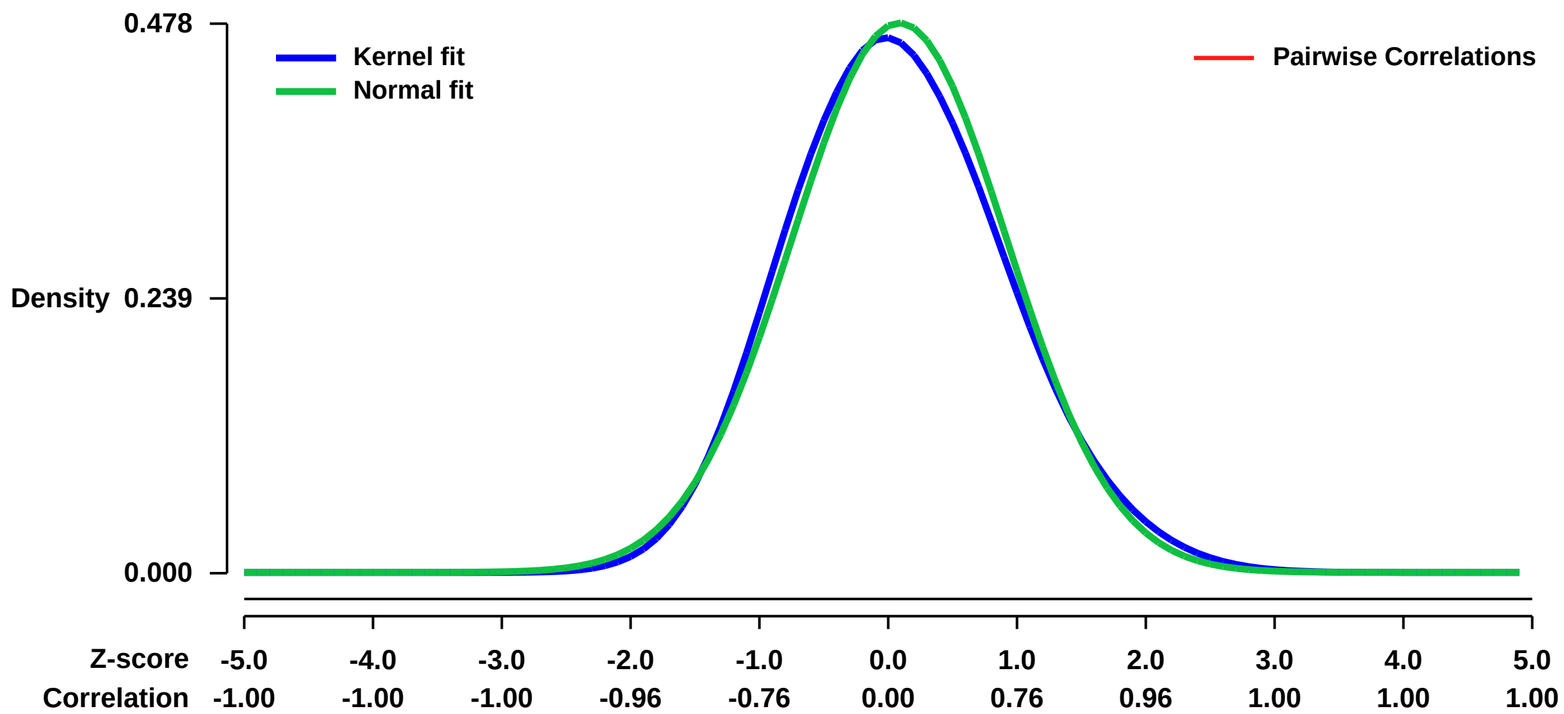

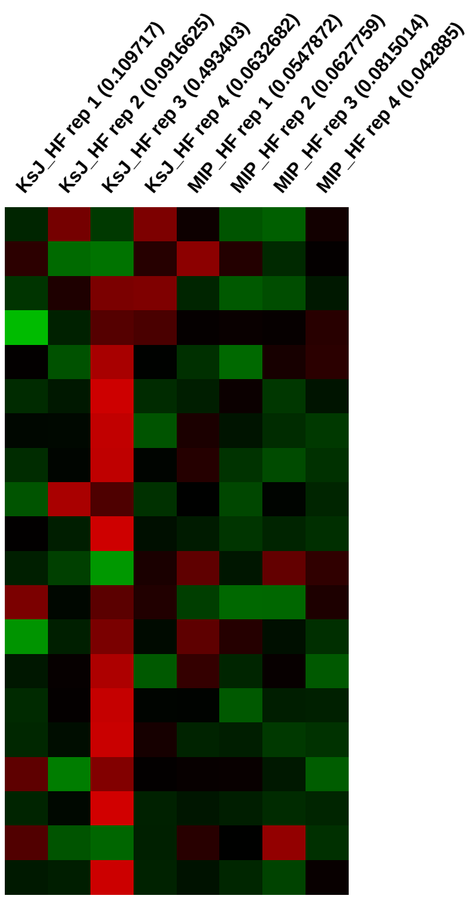

GEO Series "GSE23178" Expression Profiles

Num of samples in this series: 6

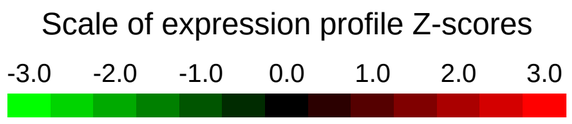

GEO Link:	http://www.ncbi.nlm.nih.gov/geo/query/acc.cgi?acc=GSE23178
Status:	Public on Jul 29 2010
Title:	Expression data analysis in lungs from mice induced for pulmonary arterial hypertension (PAH) by inhalation of Stachybotrys chartarum spores
Organism:	Mus musculus
Experiment type:	Expression profiling by array
Platform:	GPL1261
Pubmed ID:	23157700
Summary & Design:	**Summary:** It has been reported that repeated intra-tracheal instillation of S. chartarum spores induced significant pulmonary arterial remodeling in mice, which resulted in pathological changes like human pulmonary arterial hypertension (PAH) and elevation right ventricle systolic pressure. Then, we used microarrays to know the complex molecular mechanisms that underlie pathogenesis of PAH. **Overall design:** Isolates of Stachybotrys chartarum were used. Ddy mice were anesthetized and the spore suspension was intratracheally injected 12 times, i.e. 1^ 104 spores into each mouse at 4-5 day intervals for 8 weeks. Mice were sacrificed one week after the final injection and then examined. Lung tissue specimens from mice model of PAH (n=3) and normal controls (n=3) were obtained. RNA targets preparation were performed according to the manufacturer's protocol using GeneChip(R) 3' IVT Express Kit (Affymetrix). One hundred nanograms of total RNA was converted into double-stranded cDNA template for transcription. In vitro transcription synthesized amplified RNA (aRNA) and incorporated a biotin-conjugated nucleotide. After purification and fragmentation of aRNA, 12.5 ug of them was hybridized to GeneChip(R) Mouse Genome 430 2.0 Array (Affymetrix).The Probe Array was scanned using a GeneChip(R) Scanner 3000 7G.

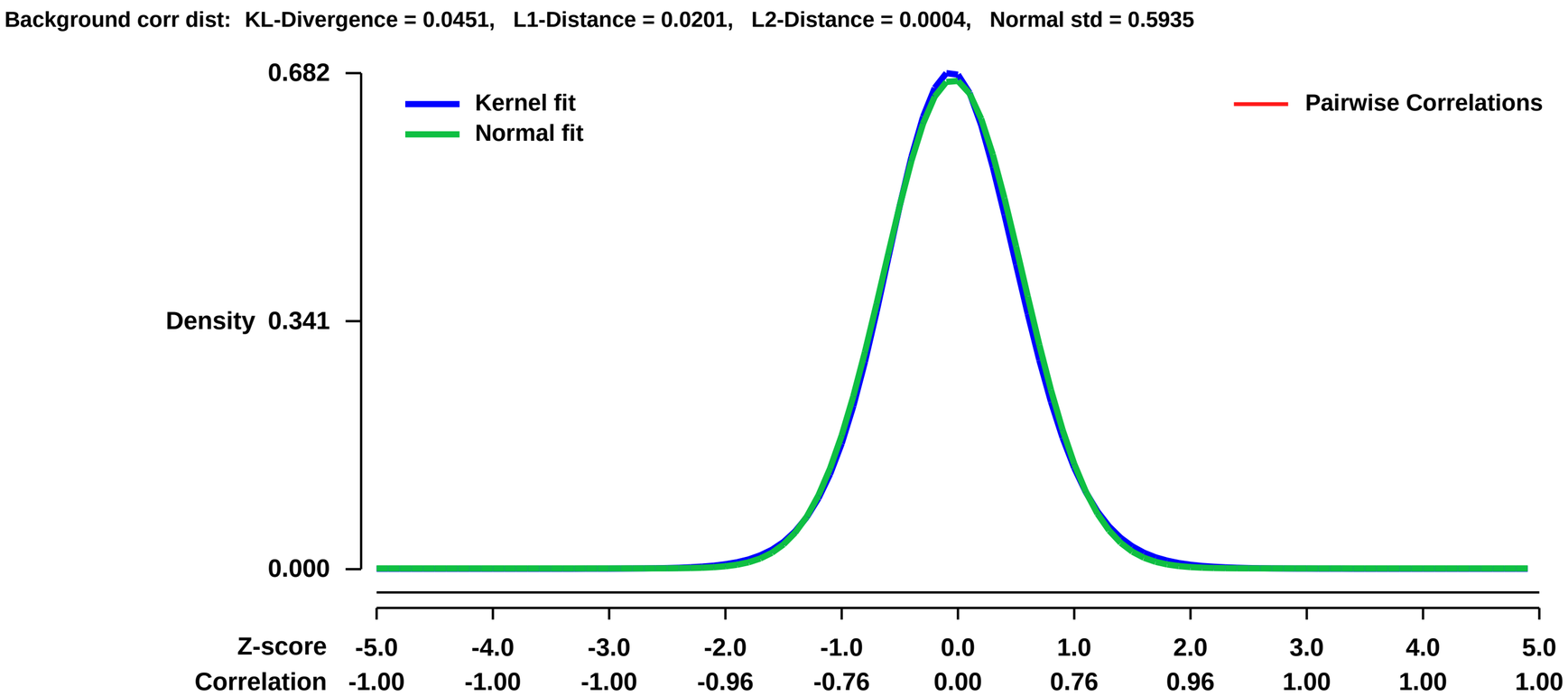

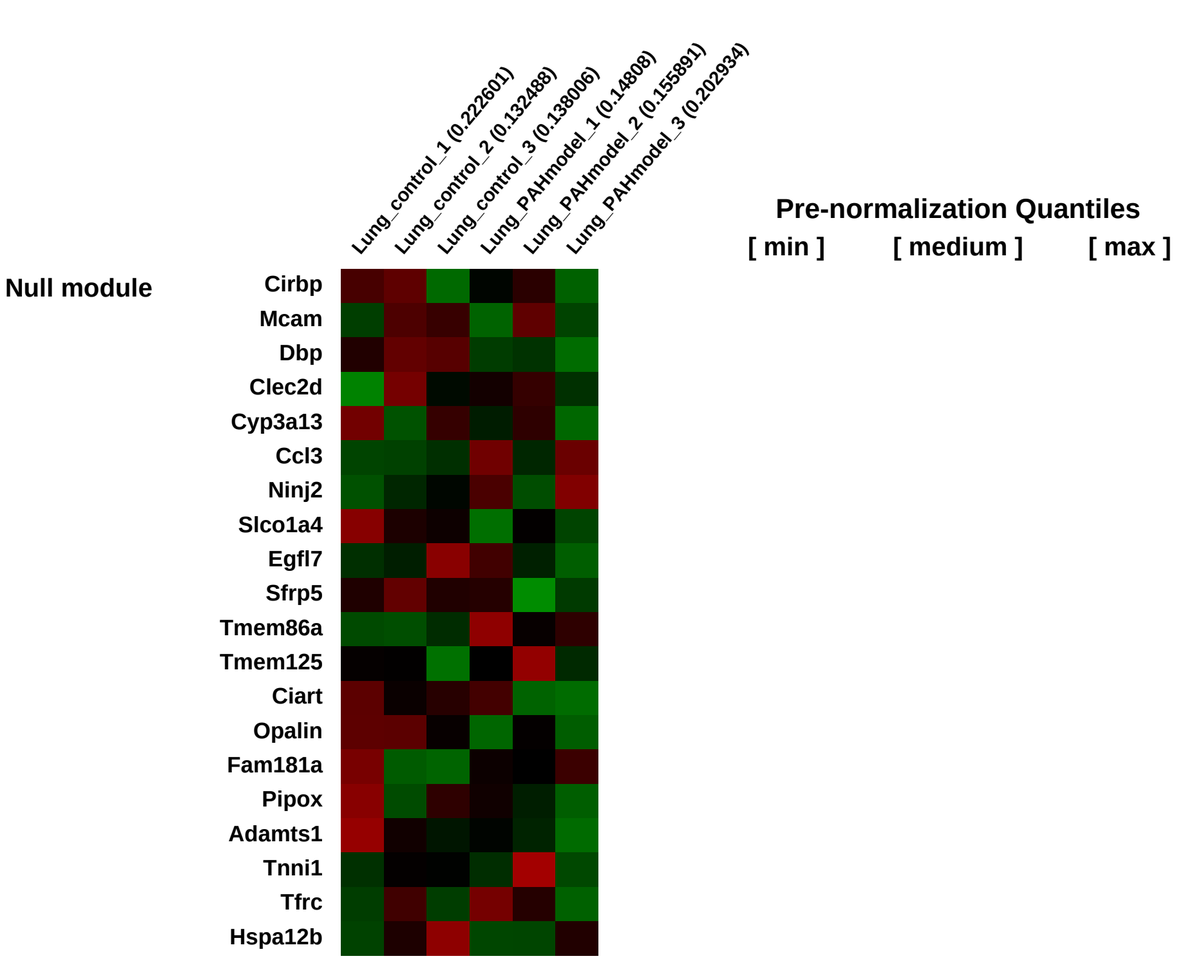

GEO Series "GSE23182" Expression Profiles

Num of samples in this series: 12

Scale of expression profile Z-scores

-3.0 -2.0 -1.0 0.0 1.0 2.0 3.0

GEO Link:	http://www.ncbi.nlm.nih.gov/geo/query/acc.cgi?acc=GSE23182
Status:	Public on Jul 28 2010
Title:	Systemic inflammation modulates Fc receptor expression on microglia in chronic neurodegeneration
Organism:	Mus musculus
Experiment type:	Expression profiling by array
Platform:	GPL1261
Pubmed ID:	21572034
Summary & Design:	**Summary:** To investigate the inflammatory response in neurodegenerative disease during an episode of systemic inflammation using the ME7 prion model. Comparison of ME7-infected mice with mice innoculated with Normal brain homogenate (NBH). 18 weeks post-innoculation mice were administered 500ug/kg LPS or an equivalent volume of saline as a control. **Overall design:** Total RNA was extracted from the hippocampus, amplified and reverse transcribed to cDNA using WT ovation kit and hybridised to mouse 430_2.0 Affymetrix Arrays. There were three biological replicates (individual mice) per group.

Background corr dist: KL-Divergence = 0.1371, L1-Distance = 0.0285, L2-Distance = 0.0013, Normal std = 0.3892

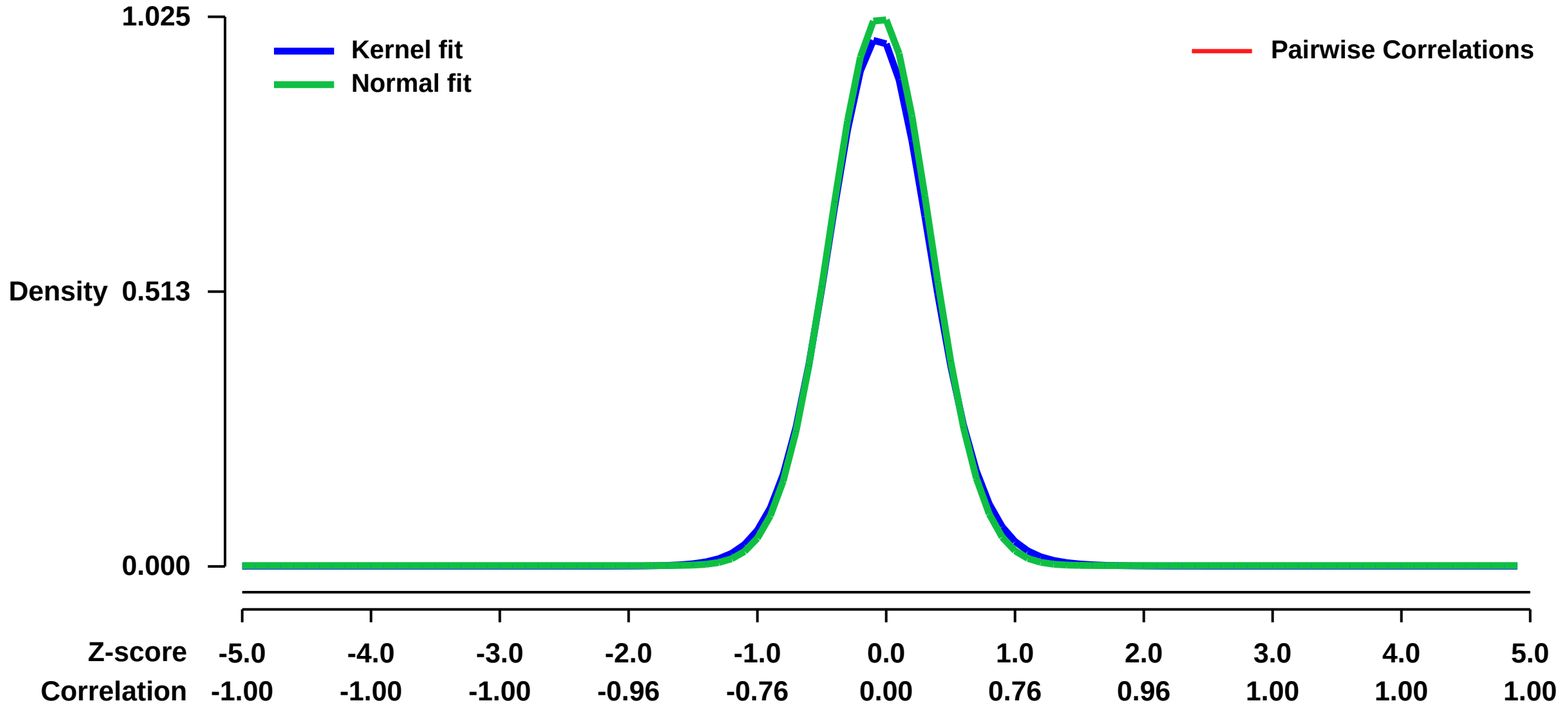

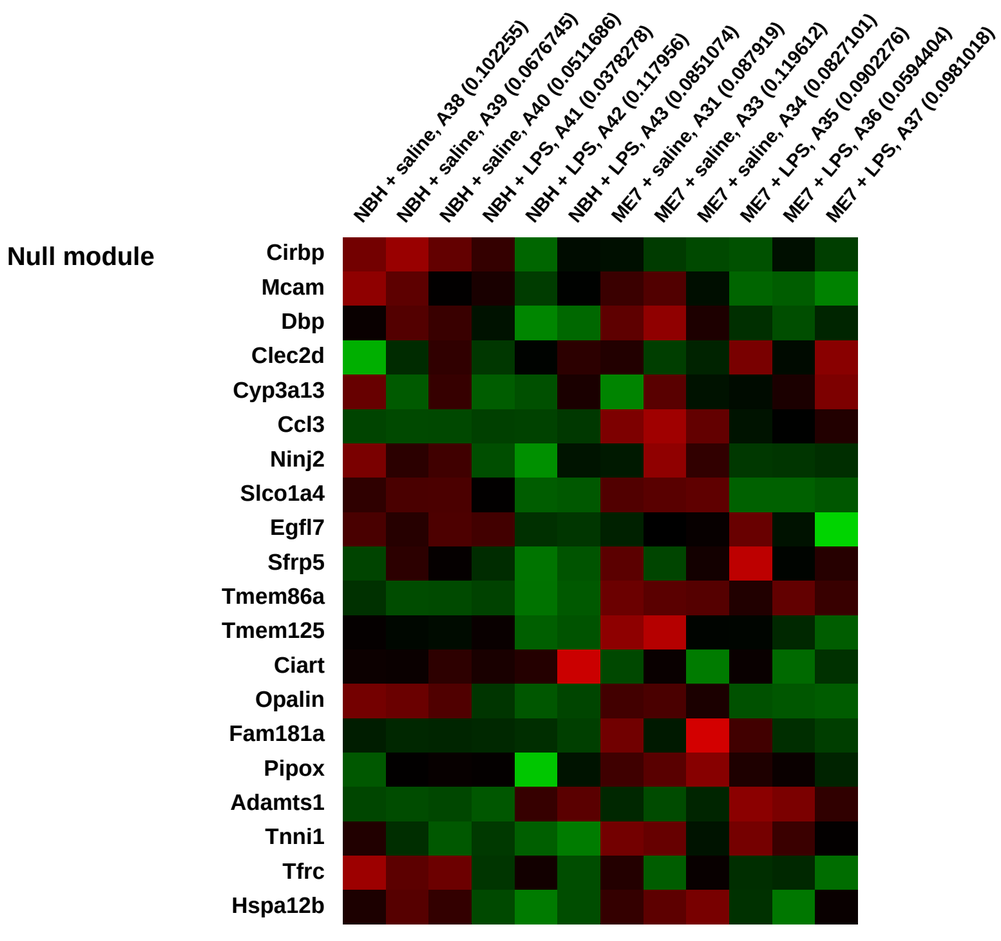

GEO Series "GSE23200" Expression Profiles

Num of samples in this series: 6

Scale of expression profile Z-scores

-3.0 -2.0 -1.0 0.0 1.0 2.0 3.0

GEO Link:	http://www.ncbi.nlm.nih.gov/geo/query/acc.cgi?acc=GSE23200
Status:	Public on Jun 23 2011
Title:	Immunoprotective properties of sertoli cells: potential genes and pathways that confer immune privilege for sertoli cell transplantation and in the testis
Organism:	Mus musculus
Experiment type:	Expression profiling by array
Platform:	GPL1261
Pubmed ID:	21900683
Summary & Design:	**Summary:** Immune privileged Sertoli cells (SC) survive when transplanted across immunological barriers and prolong the survival of co-transplanted allogeneic and xenogeneic cells in rodent models. However, the mechanism for this survival and protection remains unresolved. We have recently identified a mouse Sertoli cell line (MSC-1) that lacks some of the immunoprotective abilities associated with primary SC. The objective of this study was to compare the survival and gene expression profiles of primary SC and MSC-1 cells to identify factors or immune-related pathways potentially important for SC immune privilege. Primary SC or MSC-1 cells were transplanted as allografts to the renal subcapsular area of naˆflve BALB/c mice and cell survival was analyzed by immunohistochemistry. Additionally, transcriptome differences were investigated by microarray and pathway analyses. While primary SC were detected within the grafts with 100% graft survival throughout the 20-day study, MSC-1 cells w ere rejected between 11 and 14 days with 0% graft survival at 20 days post-transplantation. Microarray analysis identified 3198 genes that were differentially expressed with a ´– 4-fold or higher level in primary SC. Cluster and pathway analyses indicate that the mechanism of SC immune privilege is likely complex with multiple immune modulators being involved such as immunosuppressive cytokines and complement inhibitors, lipid mediators for controlling inflammation, and junctional molecules that control leukocyte movement in and out of the immune privileged space. Further study of these immune modulators will increase our understanding of SC immune privilege and in the long-term lead to improvements in transplantation success. **Overall design:** Aggregated 19 to 20-day mice primary Sertoli cells and MSC-1 cell line were used to determine the global transcriptome differences important for the survival and protection of transplanted cells.

Background corr dist: KL-Divergence = 0.0095, L1-Distance = 0.0345, L2-Distance = 0.0013, Normal std = 0.9520

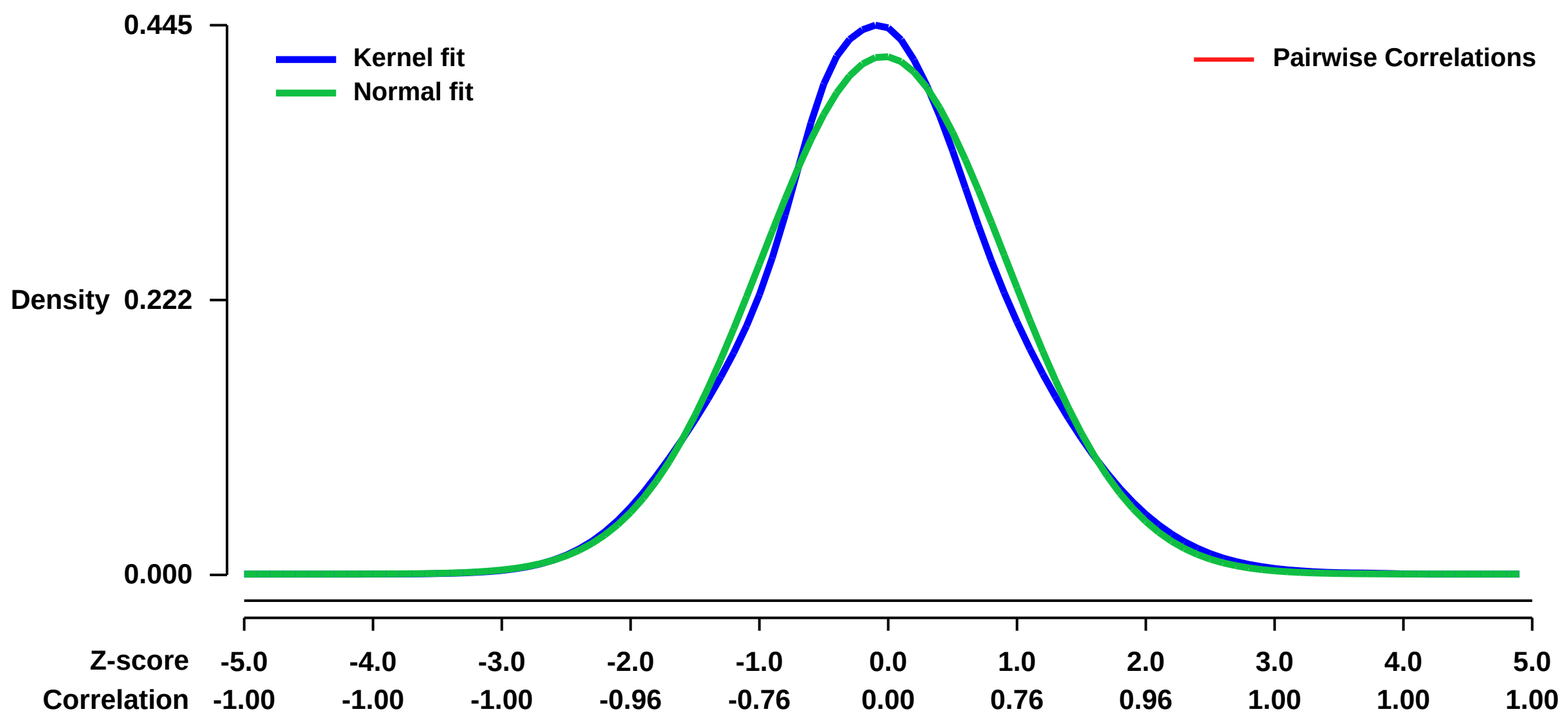

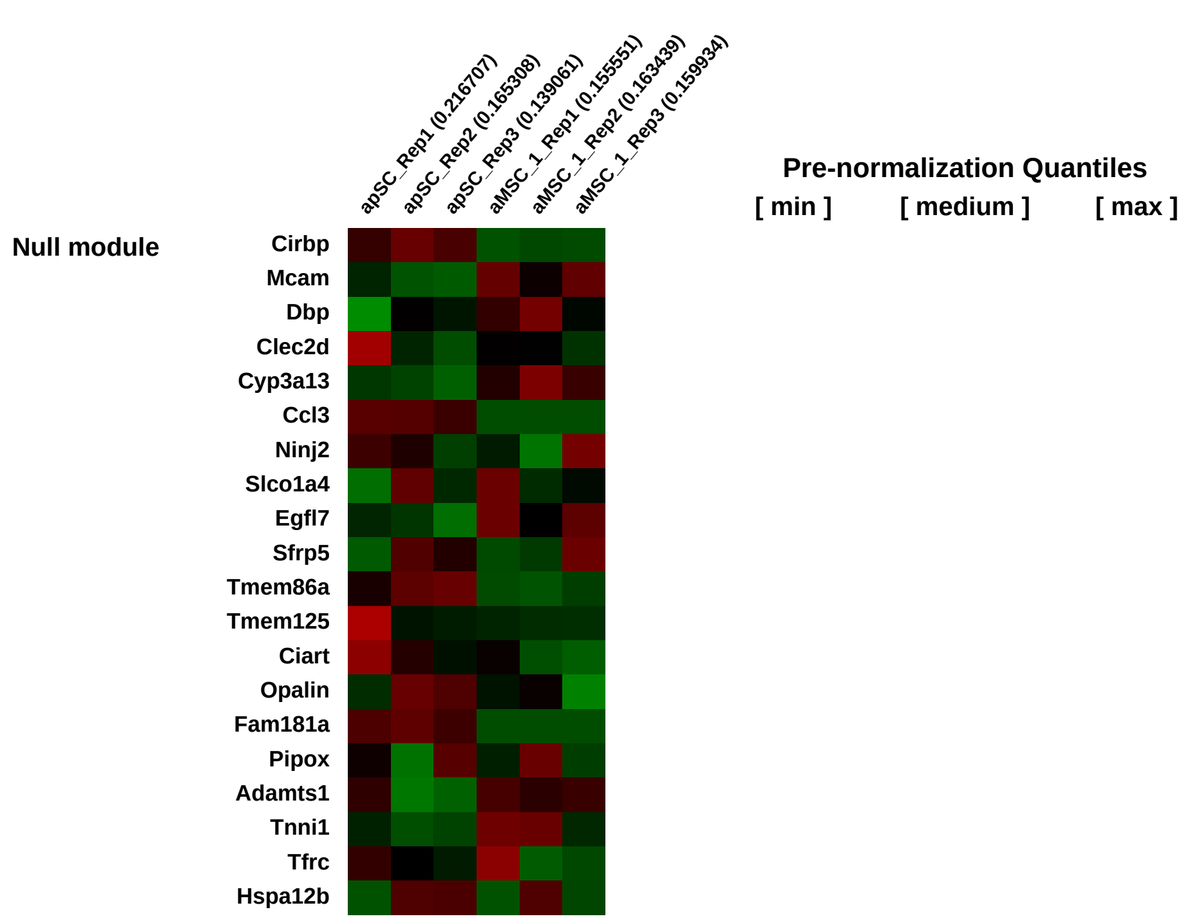

GEO Series "GSE23398" Expression Profiles

Num of samples in this series: 7

Scale of expression profile Z-scores

-3.0 -2.0 -1.0 0.0 1.0 2.0 3.0

GEO Link:	http://www.ncbi.nlm.nih.gov/geo/query/acc.cgi?acc=GSE23398
Status:	Public on Sep 18 2012
Title:	IL-2 regulated genes in scurfy CD4+ T-cells
Organism:	Mus musculus
Experiment type:	Expression profiling by array
Platform:	GPL1261
Pubmed ID:	21169543
Summary & Design:	**Summary:** The goal of the study was to identify the genes which are regulated by Interleukin-2 in the CD4+ T cells of the scurfy mice during regulatory T-cell deficiency. Scurfy (Sf) mice bear a mutation in the forkhead box P3 (Foxp3) transcription factor, lack regulatory T-cells (Treg), develop multi-organ inflammation, and die prematurely. The major target organs affected are skin, lungs, and liver. Sf mice lacking the Il2 gene (Sf.Il2-/-), despite devoid of Treg, did not develop skin and lung inflammation, but the inflammation in liver, pancreas, submandibular gland and colon remained. Genome-wide microarray analysis revealed hundreds of genes were differentially regulated among Sf, Sf.Il2-/-, and B6 CD4+ T-cells but the most changes were those encoding receptors for trafficking/chemotaxis/retention and lymphokines. Our study suggests that IL-2 controls the skin and lung inflammation in Sf mice in an apparent ""organ-specific"" manner through two novel mechanisms: by regulating the expression of genes encoding receptors for T-cell trafficking/chemotaxis/retention and by regulating Th2 cell expansion and lymphokine production. Thus, IL-2 is a master regulator for multi-organ inflammation and an underlying etiological factor for various diseases associated with skin and lung inflammation. Methods: CD4+ T cells were purified by Fluorescence Assisted Cell Sorting from the peripheral lymph nodes of (A) three individual Scurfy (Sf; B6.Cg-Foxp3sf/J) male mice, (B) three individual Sf.Il2-/- male mice (Scurfy mice carrying a null Interleukin (IL)-2 gene (B6.129P2-Il2tm1Hor/J)) and (C) a pooled sample of lymph nodes from two B6 (C57BL/6J) mice. All the mice were 3 weeks old. Total RNA was prepared using RNeasy mini kit (Qiagen). RNA samples were converted to cRNA, labeled and hybridized to Affymetrix Mouse 430_2 chips (Mouse Genome 430 2.0 Array, Affymetrix, Santa Clara, CA) at the University of Virginia DNA Sciences Core Facility. **Overall design:** 3. RNA from CD4+ T cells purified from peripheral lymph nodes of Sf.Il2-/- mice - 3 biological replicates.

Background corr dist: KL-Divergence = 0.0394, L1-Distance = 0.0267, L2-Distance = 0.0011, Normal std = 0.6124

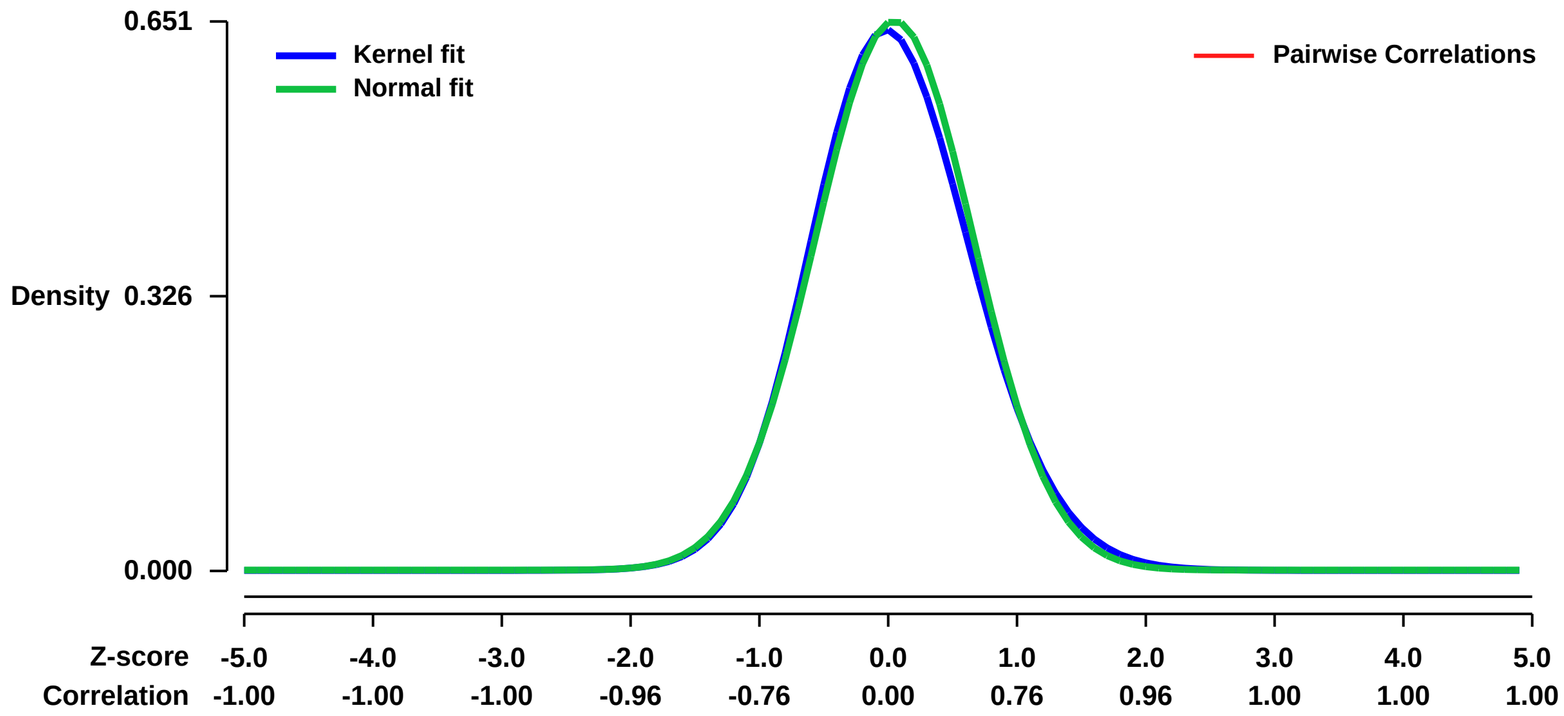

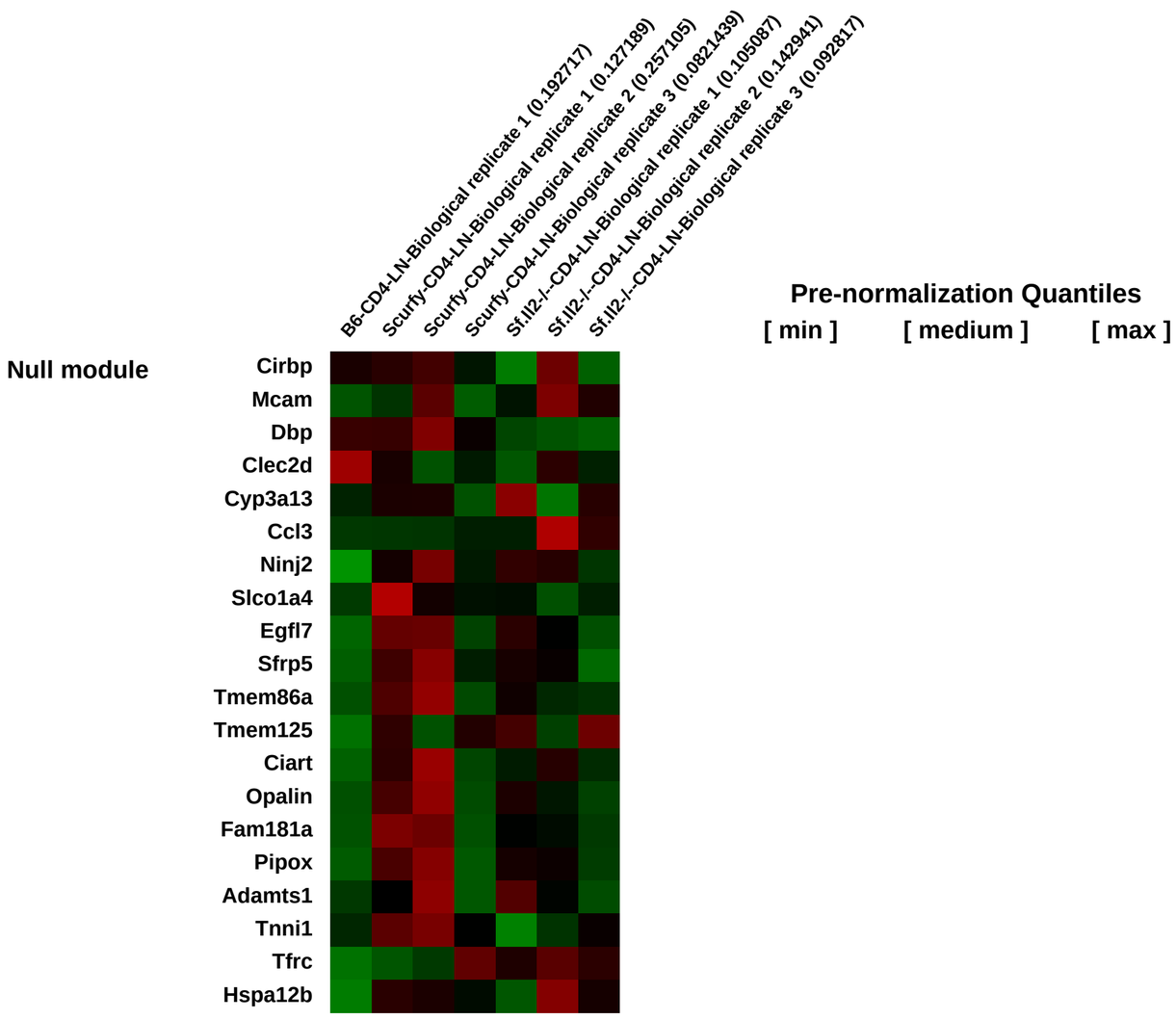

GEO Series "GSE23495" Expression Profiles

Num of samples in this series: 6

Scale of expression profile Z-scores

-3.0 -2.0 -1.0 0.0 1.0 2.0 3.0

GEO Link:	**http://www.ncbi.nlm.nih.gov/geo/query/acc.cgi?acc=GSE23495**
Status:	**Public on Aug 09 2010**
Title:	**Lmnadelta9 mouse gene expression study**
Organism:	**Mus musculus**
Experiment type:	**Expression profiling by array**
Platform:	**GPL1261**
Pubmed ID:	**20833363**
Summary & Design:	**Summary:** **Lmnadelta9 mice derived in the C57bl6X129S3/J background have been identified as exhibiting a progeric phenotype. Using this mouse model we show that a truncated variant of Lamin A (Lmnaâ 9) causes the proliferative arrest of post-natal fibroblasts. Arrest is due to the cells inability to produce a functional extracellular matrix (ECM).** **We used microarrays to compare gene expression of adult primary fibroblasts from wildtype and Lmnadelta9 mice in order to understand whether the Lmnadelta9 adult MEF defective proliferation is due to alterations of specific signaling associated with ECM functions.** **Overall design:** **Three independent replicate samples of sibling-derived wild-type and Lmnaâ 9 post-natal fibroblast lines at passage 3 were serum-starved for 72 hours and used as the source of mRNA for microarray analysis. RNA was extracted with Trizol, and hybridized to Affymetrix microarrays.**

Background corr dist: KL-Divergence = 0.0360, L1-Distance = 0.0186, L2-Distance = 0.0004, Normal std = 0.6348

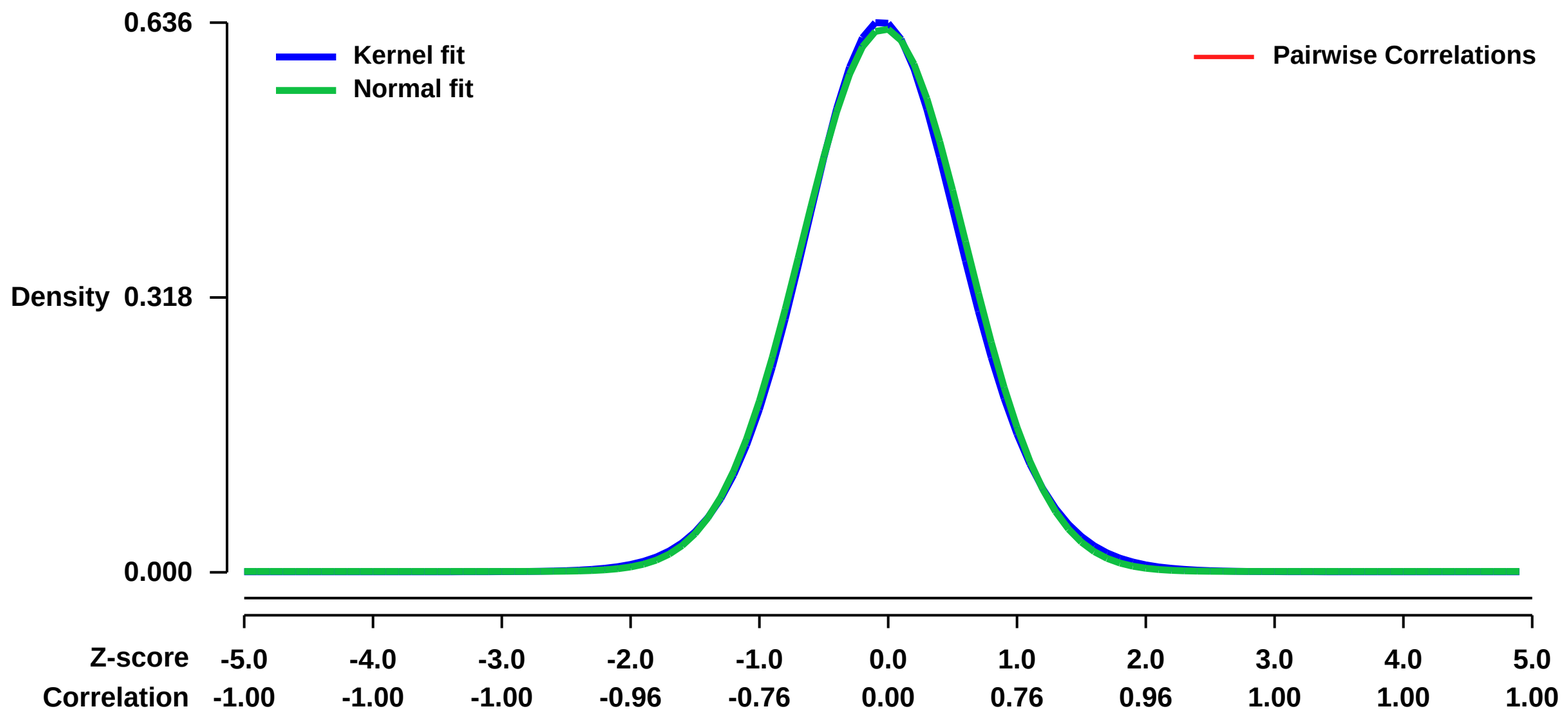

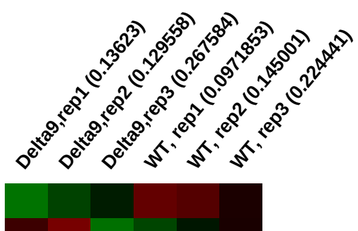

Pre-normalization Quantiles

[min] [medium] [max]

Null module

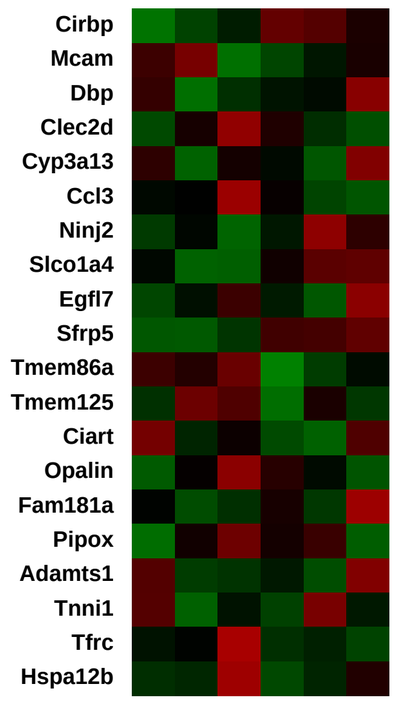

GEO Series "GSE23496" Expression Profiles

Num of samples in this series: 9

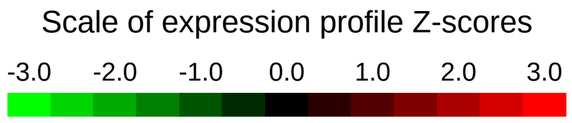

GEO Link:	http://www.ncbi.nlm.nih.gov/geo/query/acc.cgi?acc=GSE23496
Status:	Public on Dec 31 2011
Title:	Expression data from osteocytes in virgin,lactating and post lactation mice
Organism:	Mus musculus
Experiment type:	Expression profiling by array
Platform:	GPL1261
Pubmed ID:	22308018
Summary & Design:	**Summary:** We have previously shown that during lactation, osteocytes directly remodel their perilacunar and pericanalicular matrix, thereby mobilizing calcium and contributing to maternal bone loss. To identify genes potentially responsible for perilacunar remodeling, microarray analysis was performed on osteocytes from CD-1 virgin and lactating mice and mice sacrificed on day 7 post weaning. By comparing how gene expression changes in osteocytes among virgin, lactation and post lactation, the goal is to identify the genes osteocytes use to remodel their perilacunar matrix **Overall design:** To identify genes responsible for perilacunar remodeling, microarray analysis was performed on tibiae from CD-1 virgin and lactating mice and mice sacrificed on day 7 post weaning. Periosteum and bone marrow were removed from the tibiae and the bone fragments underwent sequential collagenase/trypsin digestion and were examined histologically to ensure removal of all surface cells and confirm osteocyte enrichment prior to RNA extraction. Microarray Affy M430 arrays, n=3 per group were performed and Genepattern and Bioconductor were used to analyse the microdata.

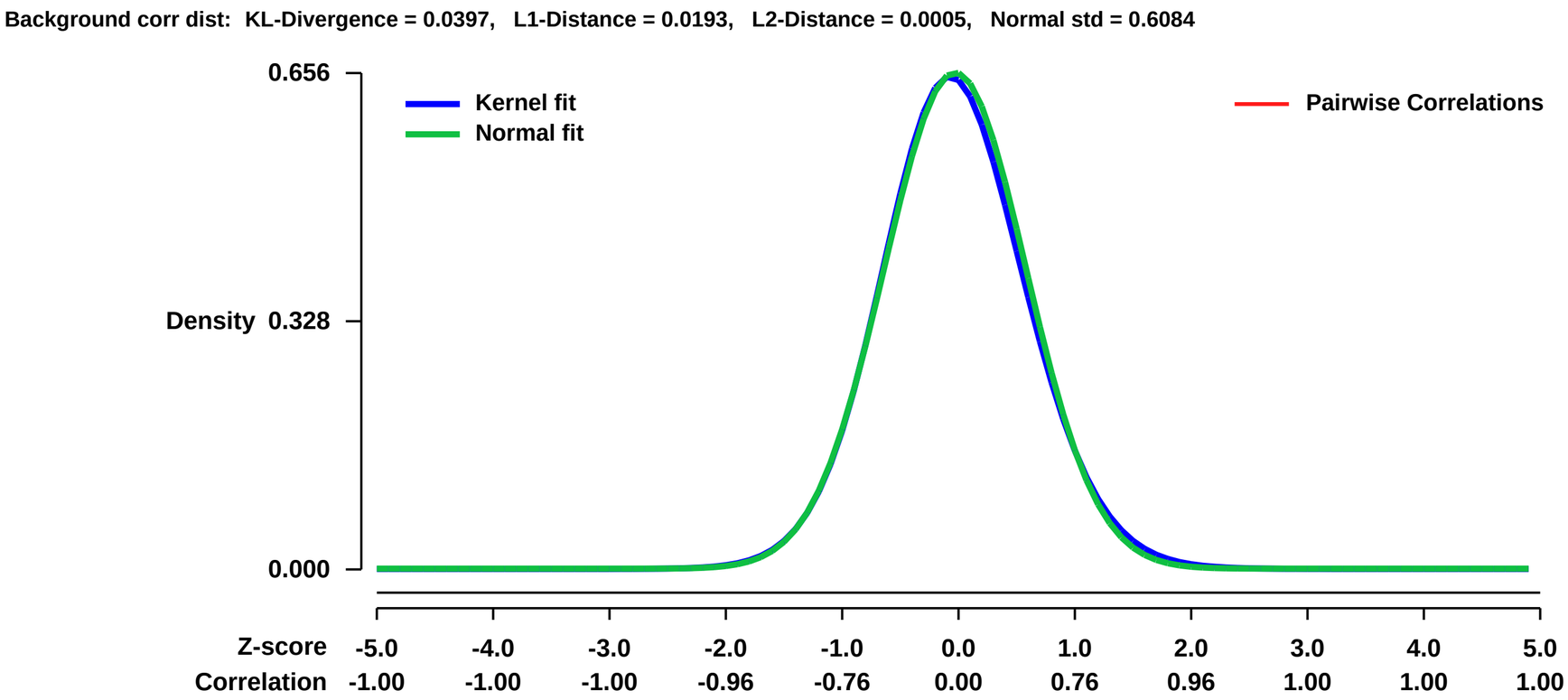

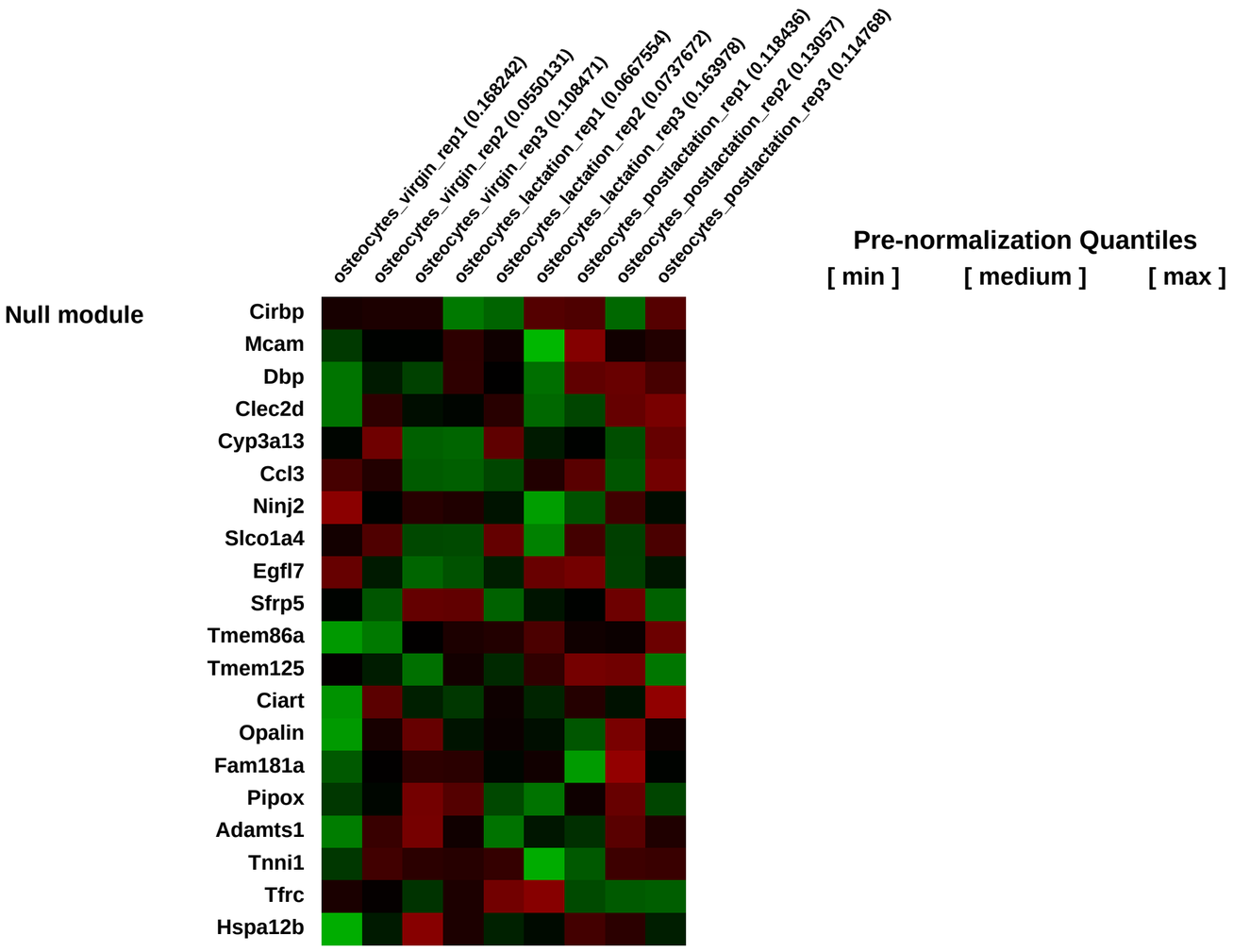

GEO Series "GSE23502" Expression Profiles

Num of samples in this series: 8

Scale of expression profile Z-scores

-3.0 -2.0 -1.0 0.0 1.0 2.0 3.0

GEO Link:	http://www.ncbi.nlm.nih.gov/geo/query/acc.cgi?acc=GSE23502
Status:	Public on Dec 15 2010
Title:	Differentially expressed genes of CD11b+Gr-1+ myeloid cells
Organism:	Mus musculus
Experiment type:	Expression profiling by array
Platform:	GPL1261
Pubmed ID:	21170045
Summary & Design:	**Summary:** Differentially expressed genes of CD11b+Gr-1+ immature myeloid cells (IMCs) in the bone marrow and colonic tumor setting of histidine decarboxylase (HDC)-KO mice were examined by microarray (Affymetrix Mouse 430.2 array). Myeloid differentiation-related candidate genes were sought to be isolated and functionally studied. **Overall design:** Four sets of comparisons were performed to screen for upregulated or downregulated genes in the HDC-KO CD11b+Gr-1+ IMCs or MDSCs (experiment group) compared to the WT group: (1) HDC-expressing CD11b+Gr-1+ IMCs of bone marrow of HDC KO mice compared to bone marrow IMCs of WT mice; (2) CD11b+Gr-1+ MDSCs in tumors of HDC-KO mice compared to WT mice; (3) CD11b+Gr-1+ MDSCs of WT colon tumors compared to IMCs in the WT bone marrow; and (4) CD11b+Gr-1+ MDSCs of colon tumors of HDC-KO mice compared to IMCs in the bone marrow of HDC-KO mice.

Background corr dist: KL-Divergence = 0.0311, L1-Distance = 0.0412, L2-Distance = 0.0020, Normal std = 0.7230

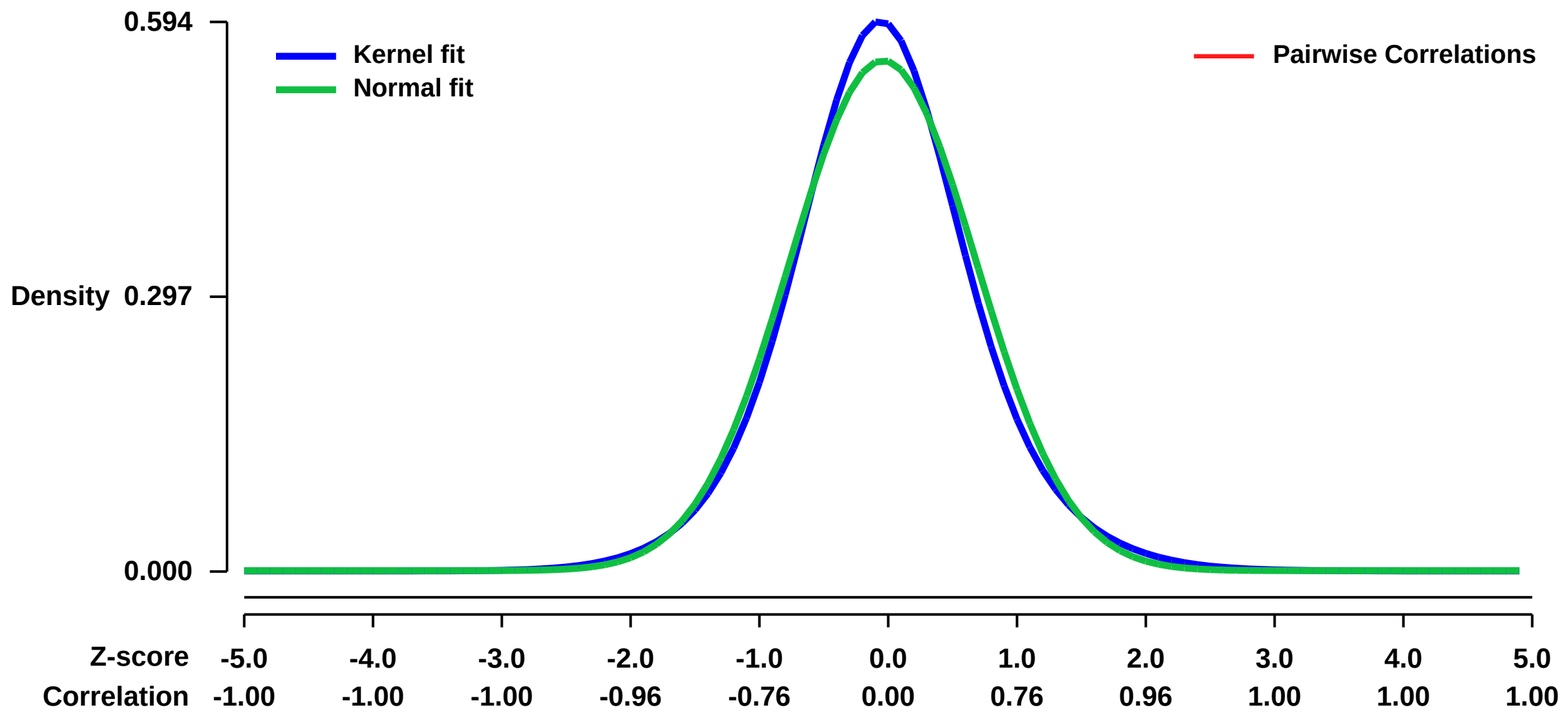

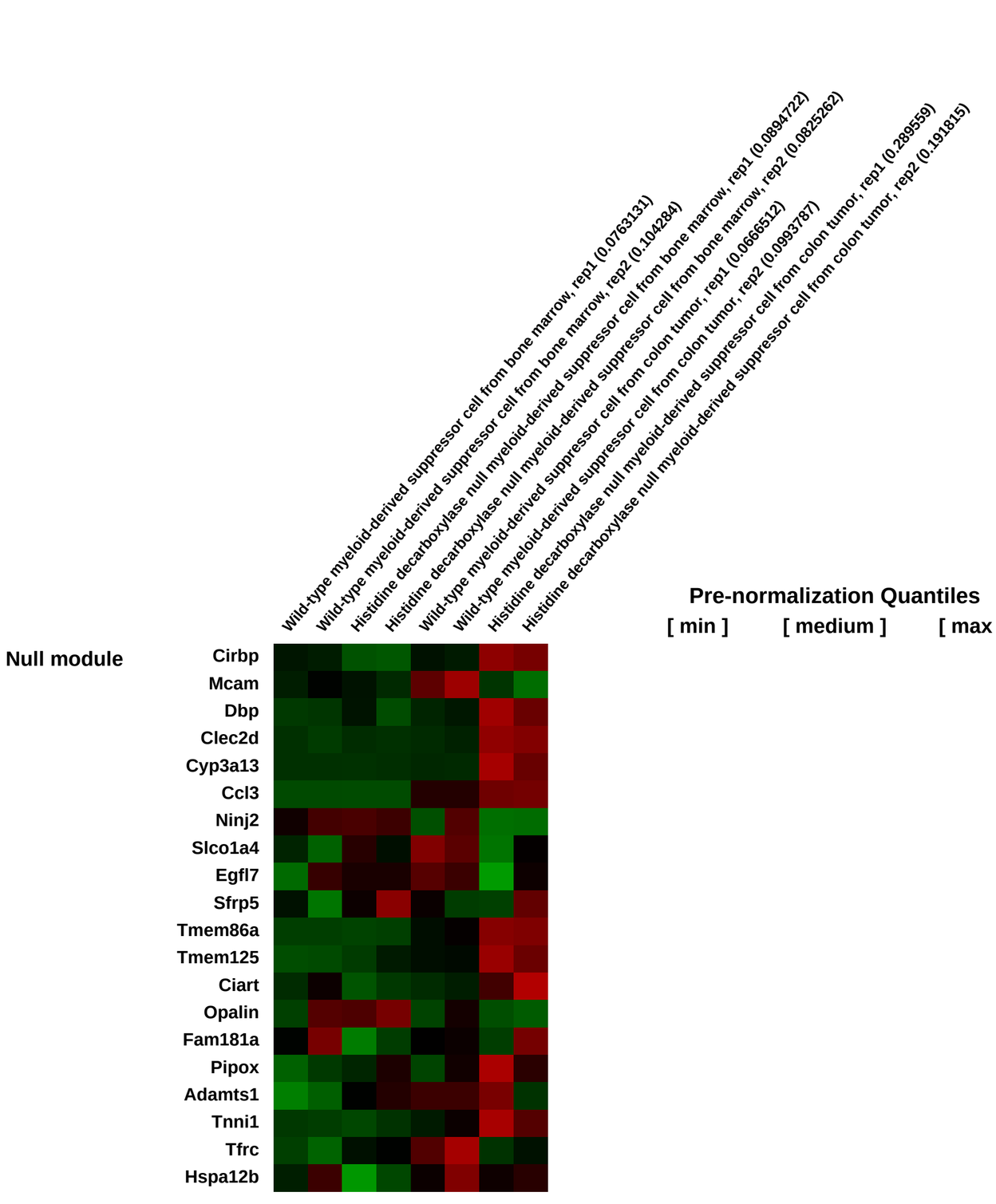

GEO Series "GSE23505" Expression Profiles

Num of samples in this series: 10

Scale of expression profile Z-scores

-3.0 -2.0 -1.0 0.0 1.0 2.0 3.0

GEO Link:	http://www.ncbi.nlm.nih.gov/geo/query/acc.cgi?acc=GSE23505
Status:	Public on Aug 31 2010
Title:	Enhanced Pathogenicity of Th17 cells Generated in the Absence of Transforming Growth Factor-¸† Signaling
Organism:	Mus musculus
Experiment type:	Expression profiling by array
Platform:	GPL1261
Pubmed ID:	20962846
Summary & Design:	**Summary:** CD4+ T cells that selectively produce interleukin (IL)-17, are critical for host defense and autoimmunity1-4. Crucial for T helper17 (Th17) cells in vivo5,6, IL-23 has been thought to be incapable of driving initial differentiation. Rather, IL-6 and transforming growth factor (TGF)-¸†1 have been argued to be the factors responsible for initiating specification7-10. Herein, we show that Th17 differentiation occurs in the absence of TGF-¸† signaling. Neither IL-6 nor IL-23 alone efficiently generated Th17 cells; however, these cytokines in combination with IL-1¸† effectively induced IL-17 production in naˆflve precursors, independently of TGF-¸†. Epigenetic modification of the Il17a/Il17f and Rorc promoters proceeded without TGF-¸†1, allowing the generation of cells that co-expressed Ror¸‡t and T-bet. T-bet+Ror¸‡t+ Th17 cells are generated in vivo during experimental allergic encephalomyelitis (EAE), and adoptively transferred Th17 cells generated with IL-23 in the absence of TGF-¸†1 were more pathogenic in this experimental disease. These data suggest a new model for Th17 differentiation. Consistent with genetic data linking the IL23R with autoimmunity, our findings re-emphasize the role of IL-23 and therefore have important implications for the development of new therapies. **Overall design:** Mouse T helper 17 cell differentiation with or without TGFB

Background corr dist: KL-Divergence = 0.0691, L1-Distance = 0.0488, L2-Distance = 0.0040, Normal std = 0.5469

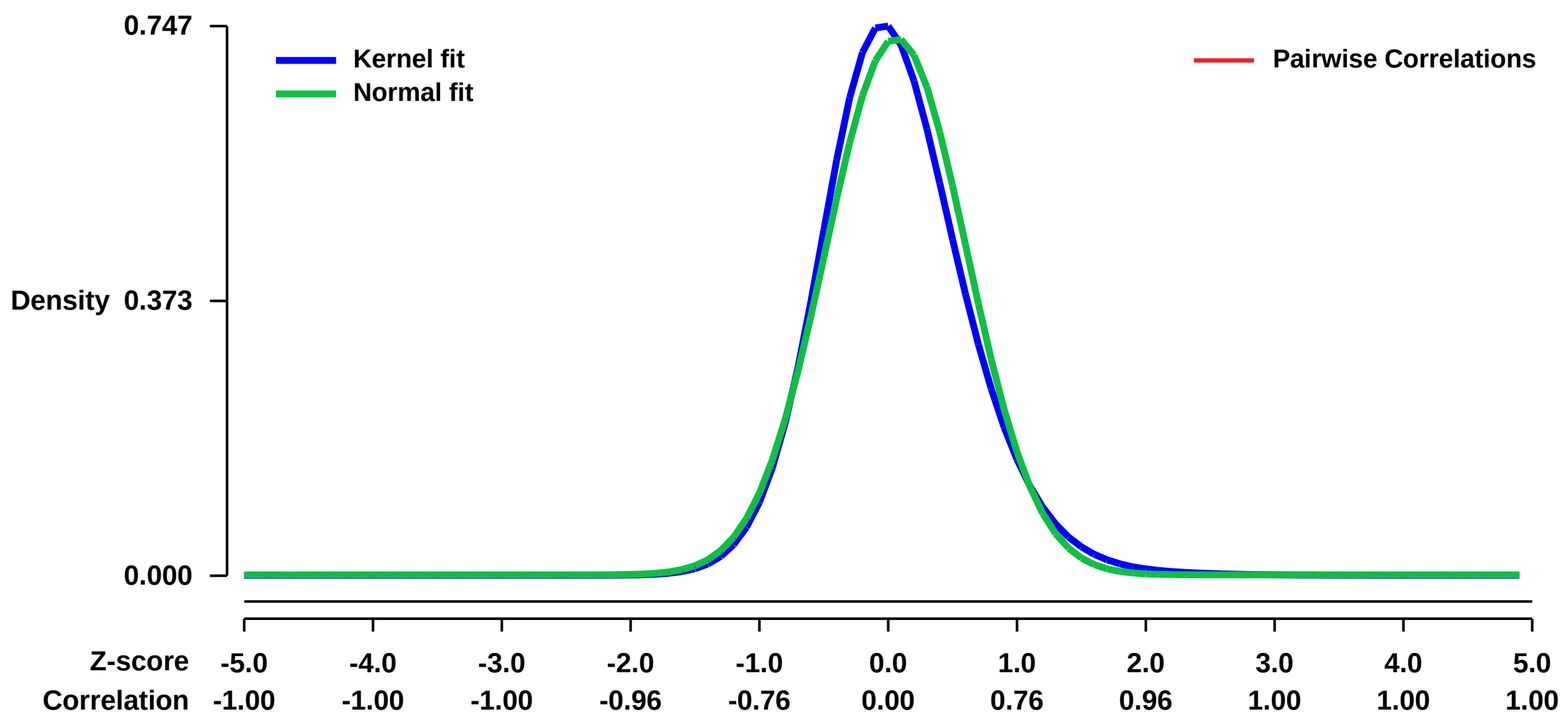

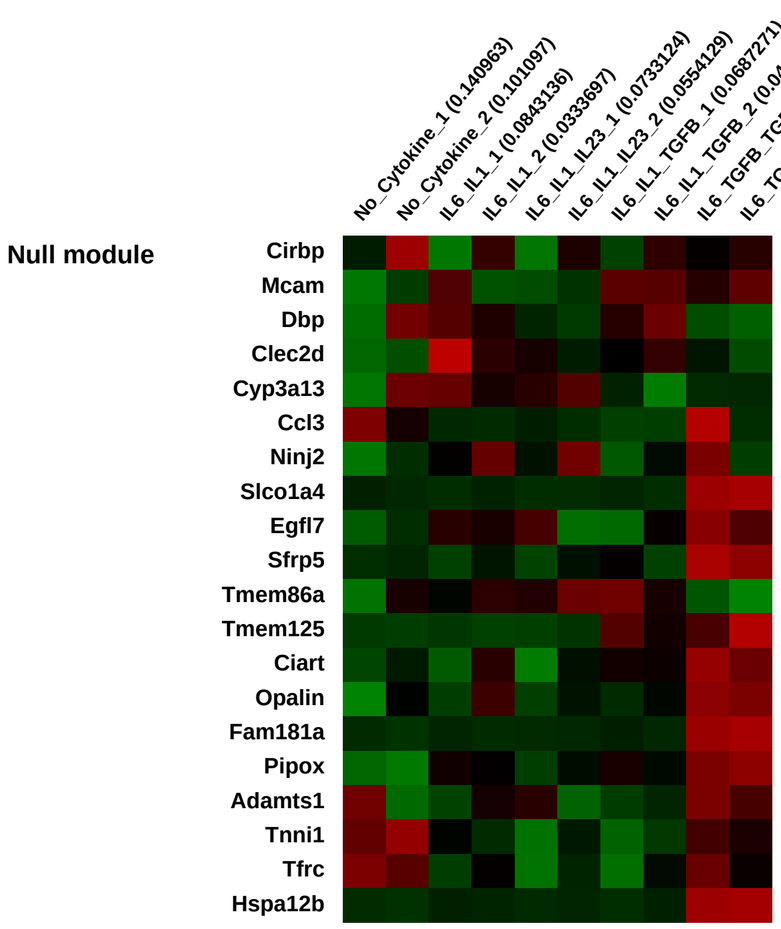

GEO Series "GSE23584" Expression Profiles

Num of samples in this series: 36

Scale of expression profile Z-scores

-3.0 -2.0 -1.0 0.0 1.0 2.0 3.0

GEO Link:	http://www.ncbi.nlm.nih.gov/geo/query/acc.cgi?acc=GSE23584
Status:	Public on Dec 31 2011
Title:	The Identification of Genetic Factors Influencing Susceptibility to Staphylococcus aureus Infection in mice susceptible and resistant to S. aureus infection
Organism:	Mus musculus
Experiment type:	Expression profiling by array
Platform:	GPL1261
Pubmed ID:	22690378
Summary & Design:	**Summary:** It has been shown that inbred strains of mice exhibit variable susceptibility to S. aureus infection, but the specific genes responsible for this differential phenotype are unknown. Using ISHM to identify genomic regions associated with the phenotypes, we considered genes within those interval to be candidate genes and used the gene expression patterns of the genes contained in the region to determine whether the genes are differentially expressed between the 2 phenotypically different groups of mice. **Overall design:** To identify genes differentially expressed between mice susceptible and resistant to S. aureus infection that could contribute to host susceptibility to S. aureus infection, we compared the gene expression profiles between 2 groups of mice where 3 were susceptible (A/J, BALBcBy/J, AKR/J) and resistant (C57BL/J, C3H/HeJ, NOD/ShiLtJ) to S. aureus. The susceptible group had high bacterial count values in the kidney while the resistant group had low values.

Background corr dist: KL-Divergence = 0.0904, L1-Distance = 0.0952, L2-Distance = 0.0201, Normal std = 0.4948

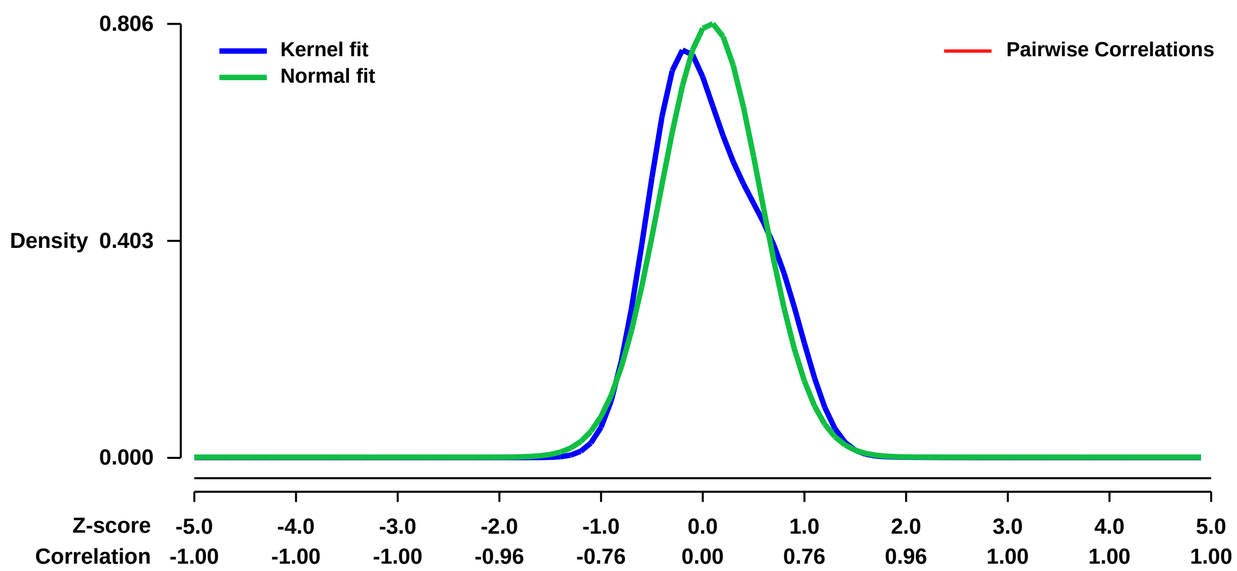

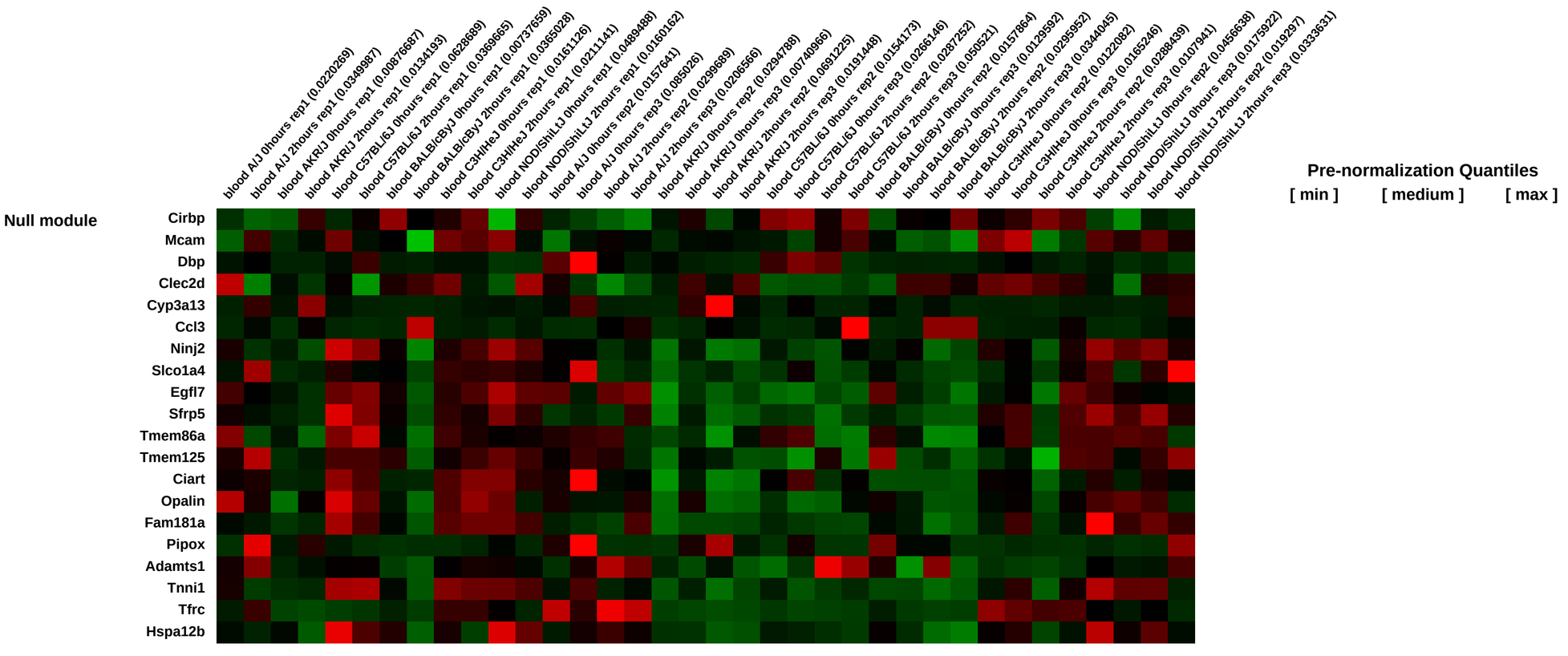

GEO Series "GSE23598" Expression Profiles

Num of samples in this series: 8

Scale of expression profile Z-scores

-3.0 -2.0 -1.0 0.0 1.0 2.0 3.0

GEO Link: http://www.ncbi.nlm.nih.gov/geo/query/acc.cgi?acc=GSE23598

Status: Public on Aug 10 2013

Title: Global gene expression profiles of MT knockout and wild-type mice in the condition of doxorubicin-induced cardiomyopathy

Organism: Mus musculus

Experiment type: Expression profiling by array

Platform: GPL1261

Pubmed ID:

Summary & Design:

Summary:
The present study was designed using MT knockout mice in concert with genomic approaches to explore the possible molecular and cellular mechanisms involved in the protective effects of MT against DOX cardiotoxicity. MT-â /â¡ null (MT-/-) mice and corresponding wild-type mice (MT+/+) were administrated with a single dose of DOX (15 mg/kg, i.p.) or an equal volume of saline. Animals were sacrificed on the 4th day after DOX administration and samples were collected for further analyses. Global gene expression profiles of cardiac mRNA from two genotype mice revealed that 381 characteristically MT-responsive genes were identified between MT+/+ mice and MT-/- mice in response to DOX, including fos, ucp3, car3, atf3, map3k6, etc.. Functional analysis implied MAPK signaling pathway, p53 signaling pathway, Jak-STAT signaling pathway, PPAR signaling pathway, Wnt signaling pathway, etc. might be involved to mediate the protection of DOX cardiomyopathy by MT. Results from the present study not only validated the previously reported possible mechanisms of MT protection against DOX toxicity, but also provided new clues into the molecular mechanisms involved in this process.

Overall design:
Male MT+/+ & MT-/- mice (6-8 weeks old) were randomly assigned to treatment or control groups and administrated with a single dose of DOX (15 mg/kg, i.p.) or an equal volume of normal saline solution (NS) respectively. Animals were sacrificed on the 4th day after DOX injection, and samples were collected for further microarray analyses.

Background corr dist: KL-Divergence = 0.0554, L1-Distance = 0.0180, L2-Distance = 0.0004, Normal std = 0.5396

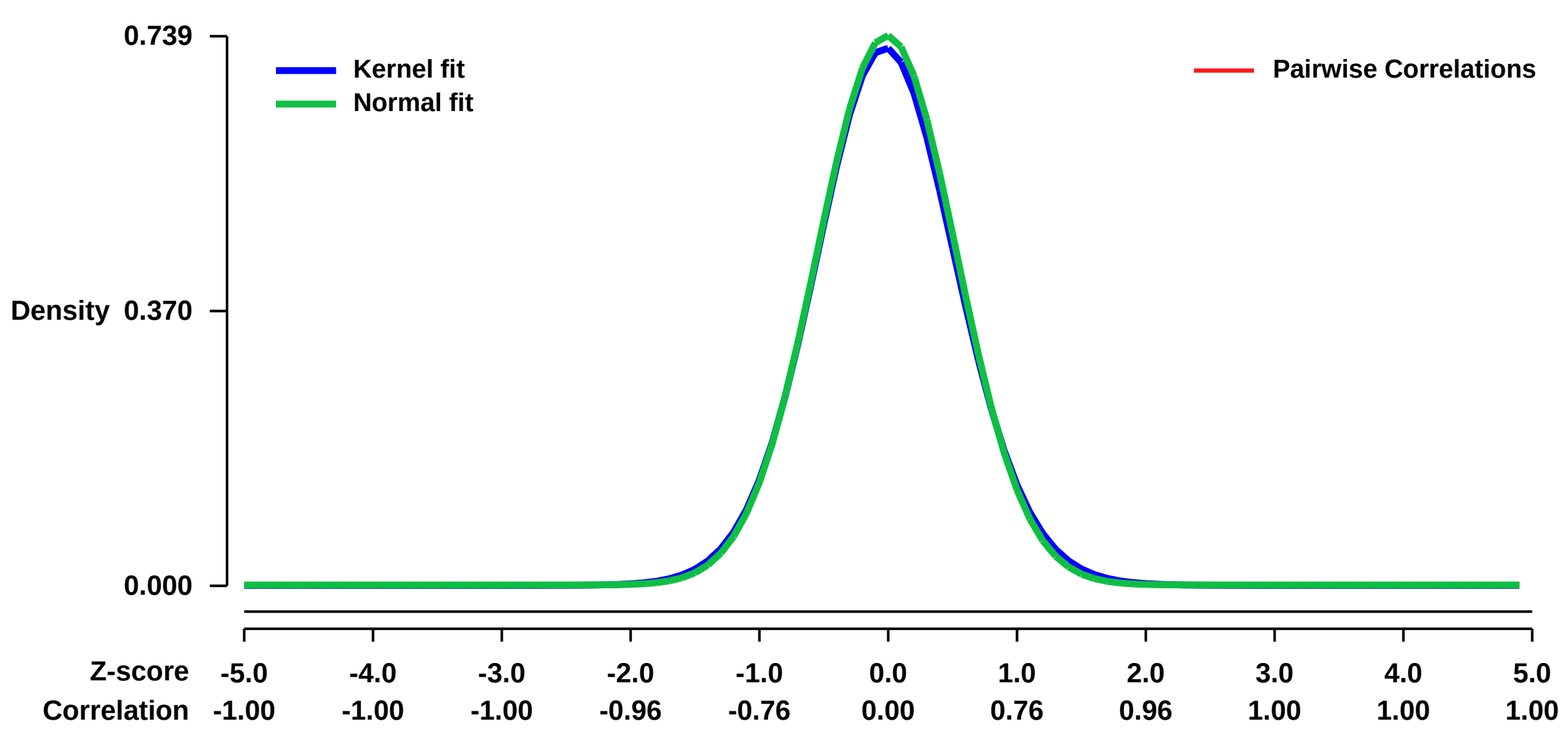

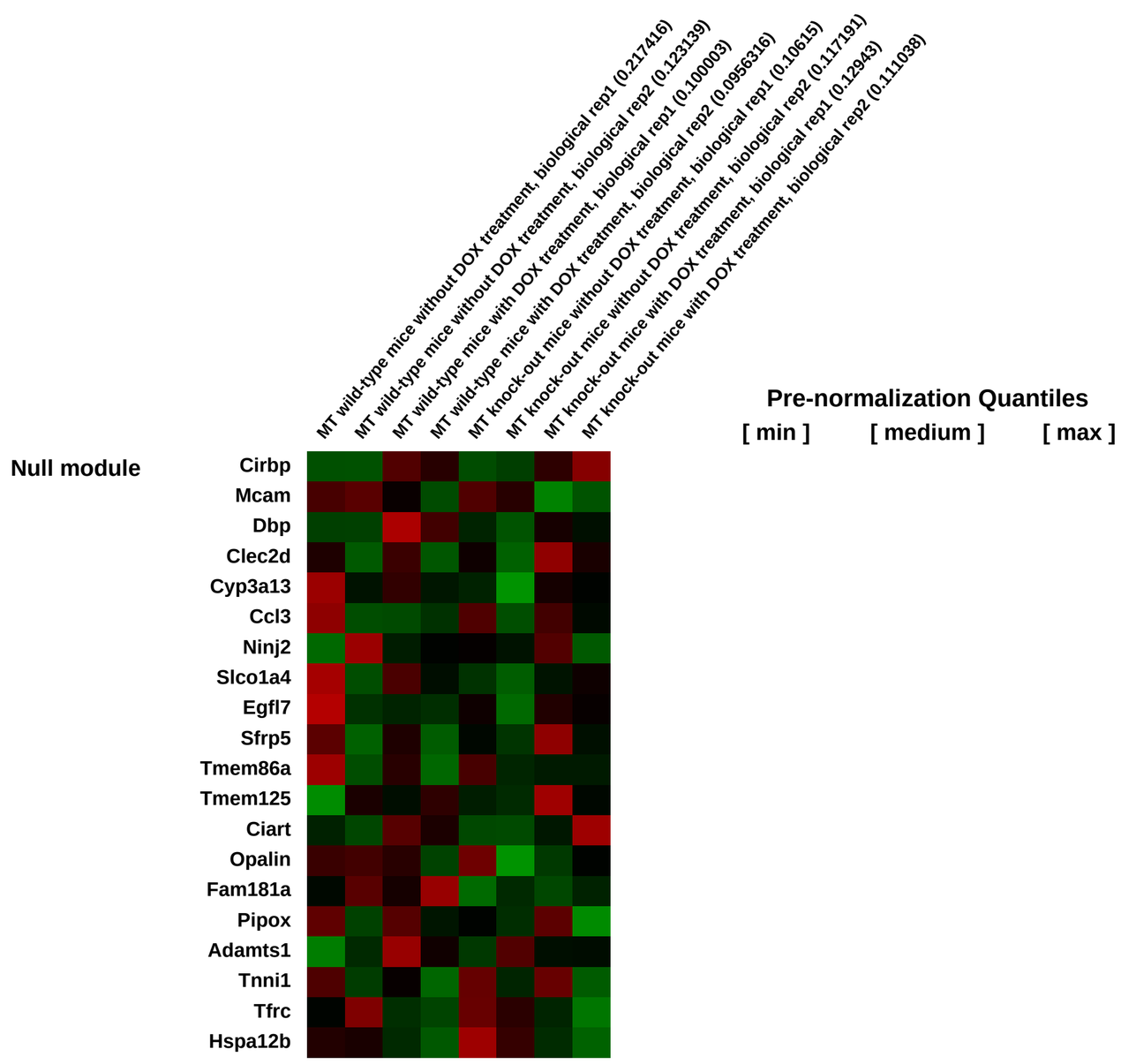

GEO Series "GSE23600" Expression Profiles

Num of samples in this series: 10

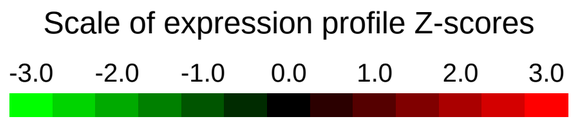

GEO Link:	http://www.ncbi.nlm.nih.gov/geo/query/acc.cgi?acc=GSE23600
Status:	Public on Aug 13 2010
Title:	Expression data from sorted Treg cells from WT or motheaten mice
Organism:	Mus musculus
Experiment type:	Expression profiling by array
Platform:	GPL1261
Pubmed ID:	20952680
Summary & Design:	**Summary:** **The importance of regulatory T cells (Treg) for immune tolerance is well recognized, yet the signaling molecules influencing their suppressive activity are relatively poorly understood. We identified the cytoplasmic tyrosine phosphatase SHP-1 as a novel â endogenous brakeâ and modifier of the suppressive ability of Treg cells; consistent with this notion, loss of SHP-1 expression strongly augments the ability of Treg cells to suppress inflammation in a mouse model. Specific harmacological inhibition of SHP-1 enzymatic activity via the cancer drug sodium stibogluconate (SSG) potently augmented Treg cell suppressor activity both in vivo and ex vivo.** **We evaluated the gene expression profiles of sorted T reg cells (CD4+CD25+) from wild type (wt) mice and mice that were heterozygous (he) or homozygous (me) for SHP-1 knockout (motheaten phenotype).** **Overall design:** **T reg (CD4+CD25+) cells were isolated form wild type (WT) mice and that were heterozygous (he) or homozygous (me) for SHP-1 knockout (motheaten phenotype); totalRNA was isolated using Arcturus reagents; aRNA was generated and amplified using Arcturus reagents; and labeled product was hybridized to Affymetrix chips to asses gene expression patterns.**

Background corr dist: KL-Divergence = 0.0252, L1-Distance = 0.0859, L2-Distance = 0.0097, Normal std = 0.9258

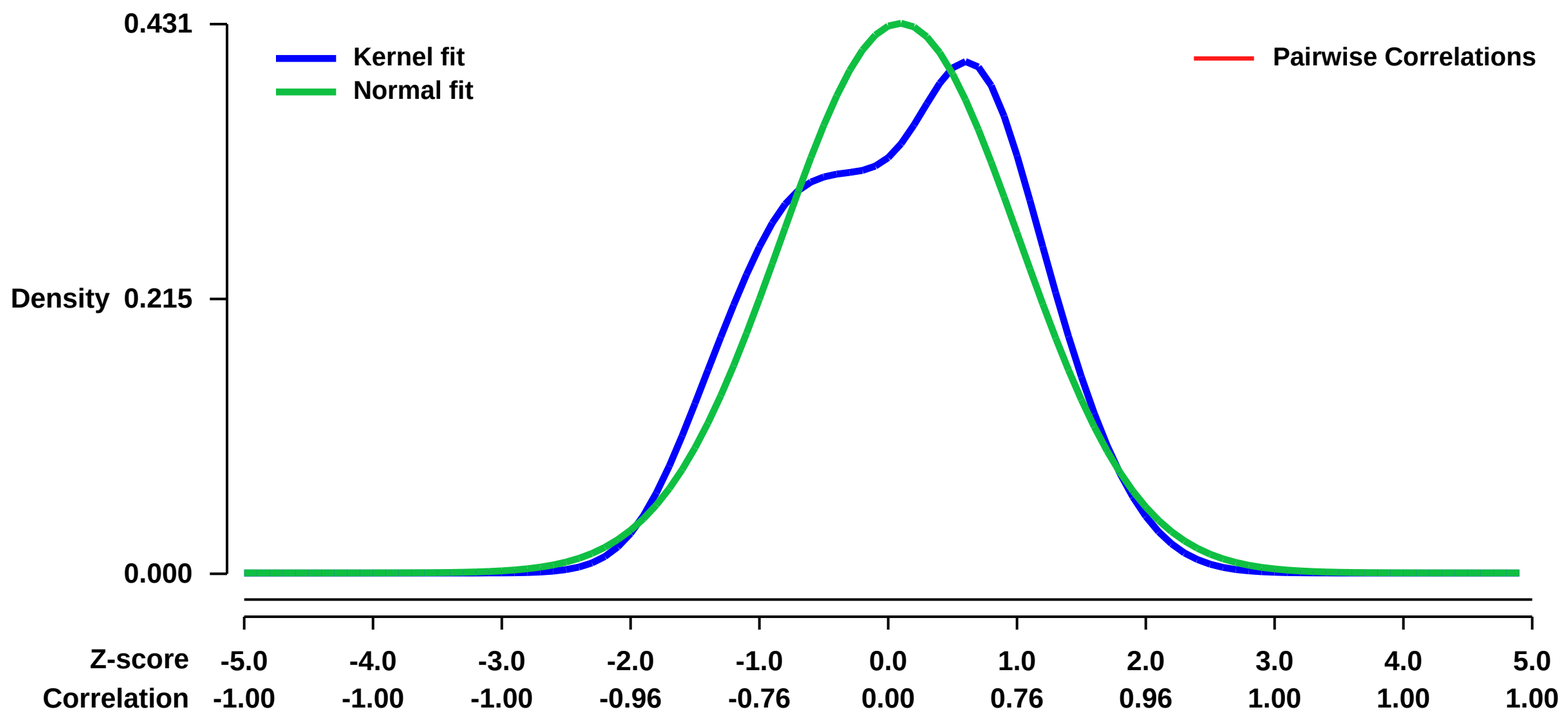

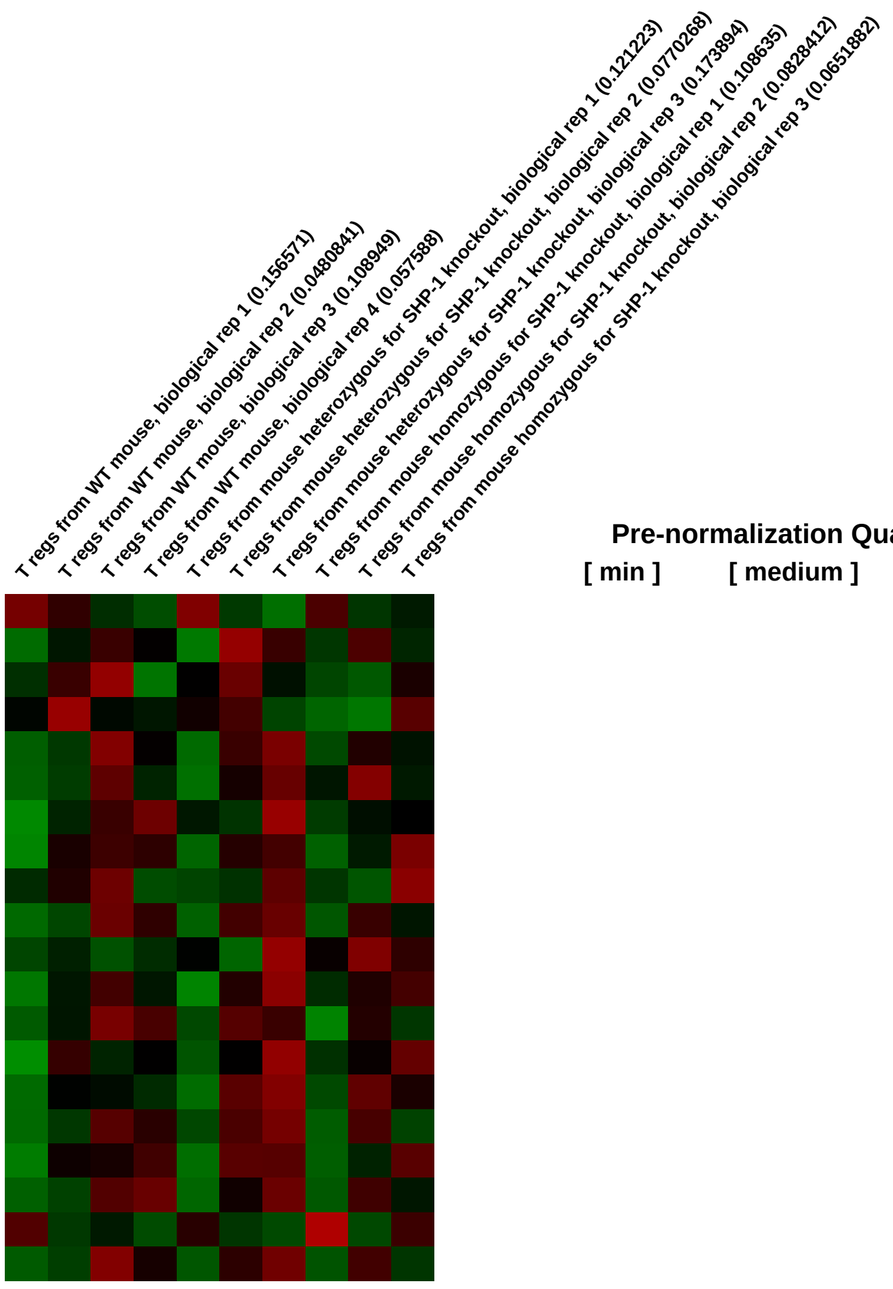

GEO Series "GSE23724" Expression Profiles

Num of samples in this series: 8

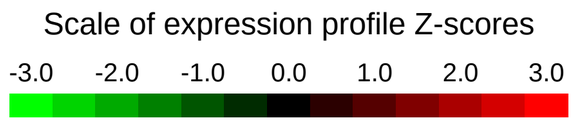

GEO Link:	http://www.ncbi.nlm.nih.gov/geo/query/acc.cgi?acc=GSE23724
Status:	Public on Aug 21 2010
Title:	Genes differentially regulated by the glucocorticoid receptor in developing skin of the GR knock out and wt embryos.
Organism:	Mus musculus
Experiment type:	Expression profiling by array
Platform:	GPL1261
Pubmed ID:	20880987
Summary & Design:	**Summary:** To understand the transcriptional program by which GR regulates skin development, we performed a microarray analysis using the skin of E18.5 GR-/- and GR+/+ mouse embryos. **Overall design:** RNA from four dorsal skin samples from GR-/- and GR+/+ E18.5 mouse embryos was collected and analyzed using Affymetrix Mouse Genome 430 2.0 GeneChips.
Background corr dist:	KL-Divergence = 0.0611, L1-Distance = 0.0186, L2-Distance = 0.0004, Normal std = 0.5230

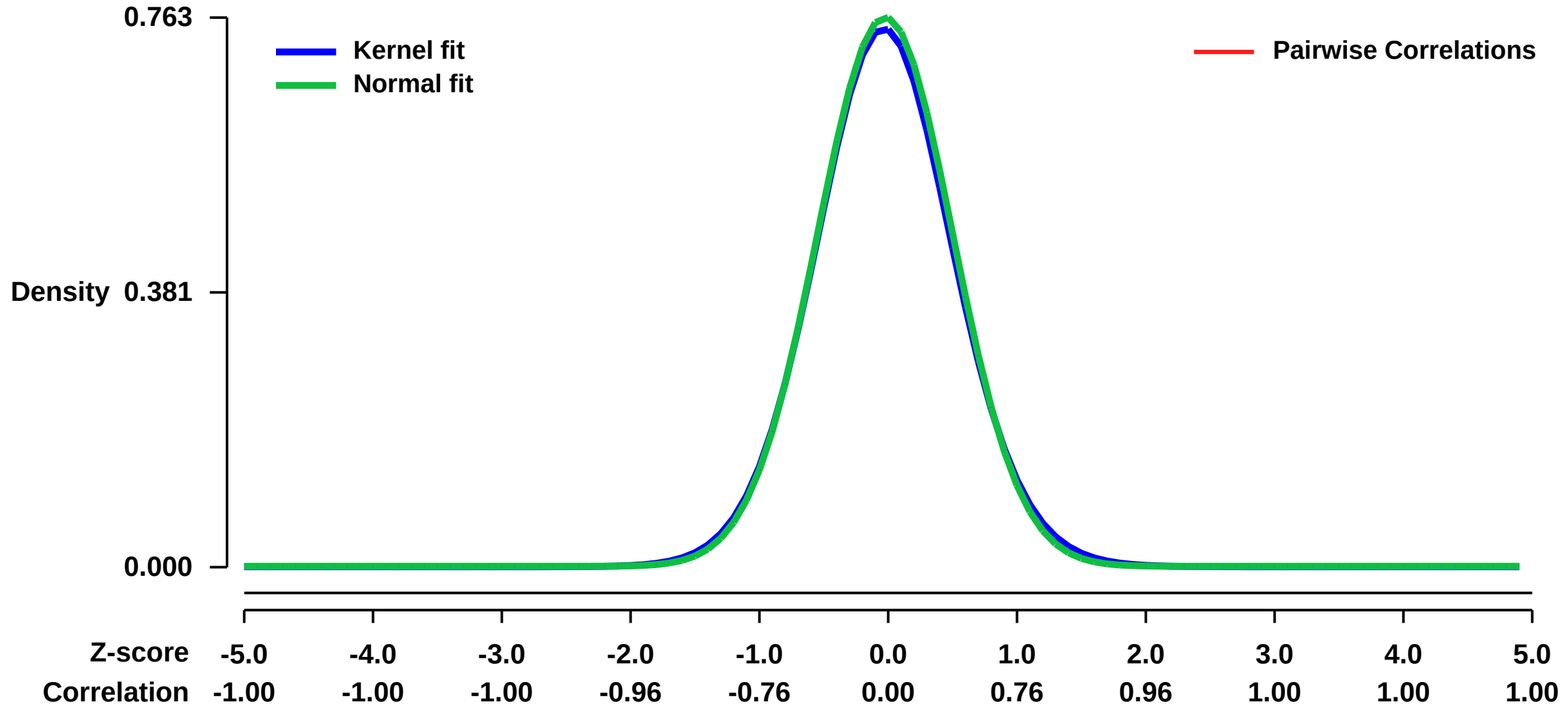

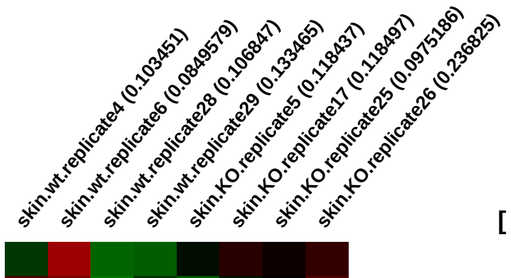

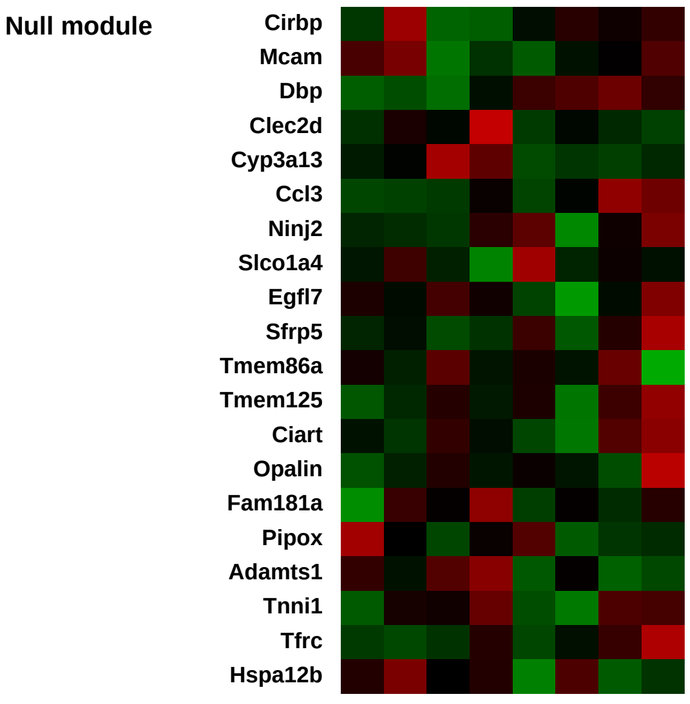

GEO Series "GSE23725" Expression Profiles

Num of samples in this series: 12

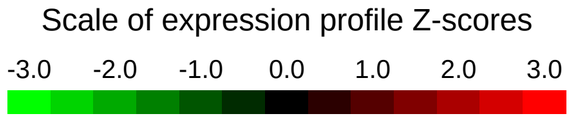

GEO Link:	http://www.ncbi.nlm.nih.gov/geo/query/acc.cgi?acc=GSE23725
Status:	Public on Aug 21 2010
Title:	Expression data from mouse neonatal ovarian xenobiotic culture experiments
Organism:	Mus musculus
Experiment type:	Expression profiling by array
Platform:	GPL1261
Pubmed ID:	20829426
Summary & Design:	**Summary:** Mammalian females are born with a finite number of non-renewing primordial follicles, the majority of which remain in a quiescent state for many years. Due to their non-renewing nature, these â restingâ oocytes are particularly vulnerable to xenobiotic insult, resulting in premature ovarian senescence and the formation of dysfunctional oocytes. In this study we characterised the mechanisms of ovotoxicity for three ovotoxic agents, 4-Vinylcyclohexene Diepoxide (VCD), Methoxychlor (MXC), and Menadione (MEN), all of which target immature follicles. Neonatal mouse ovaries (PND3-4) were cultured in the presence of 4-Vinylcyclohexene Diepoxide (50uM), Methoxychlor (50uM), and Menadione (5uM) for 96 hours to observe their effects on the ovarian transcriptome. This was done in the hopes of gaining a better understanding of the mechanisms underpinning xenobiotic induced pre-antral ovotoxicity. **Overall design:** Ovaries from day 3-4 Swiss neonatal mice were cultured in xenobiotic containing media for 96 hours. The ovaries were then collected for RNA extraction and hybridization on Affymetrix microarrays (Mouse 430 version 2.0 GeneChip).

Background corr dist: KL-Divergence = 0.0684, L1-Distance = 0.0239, L2-Distance = 0.0011, Normal std = 0.5027

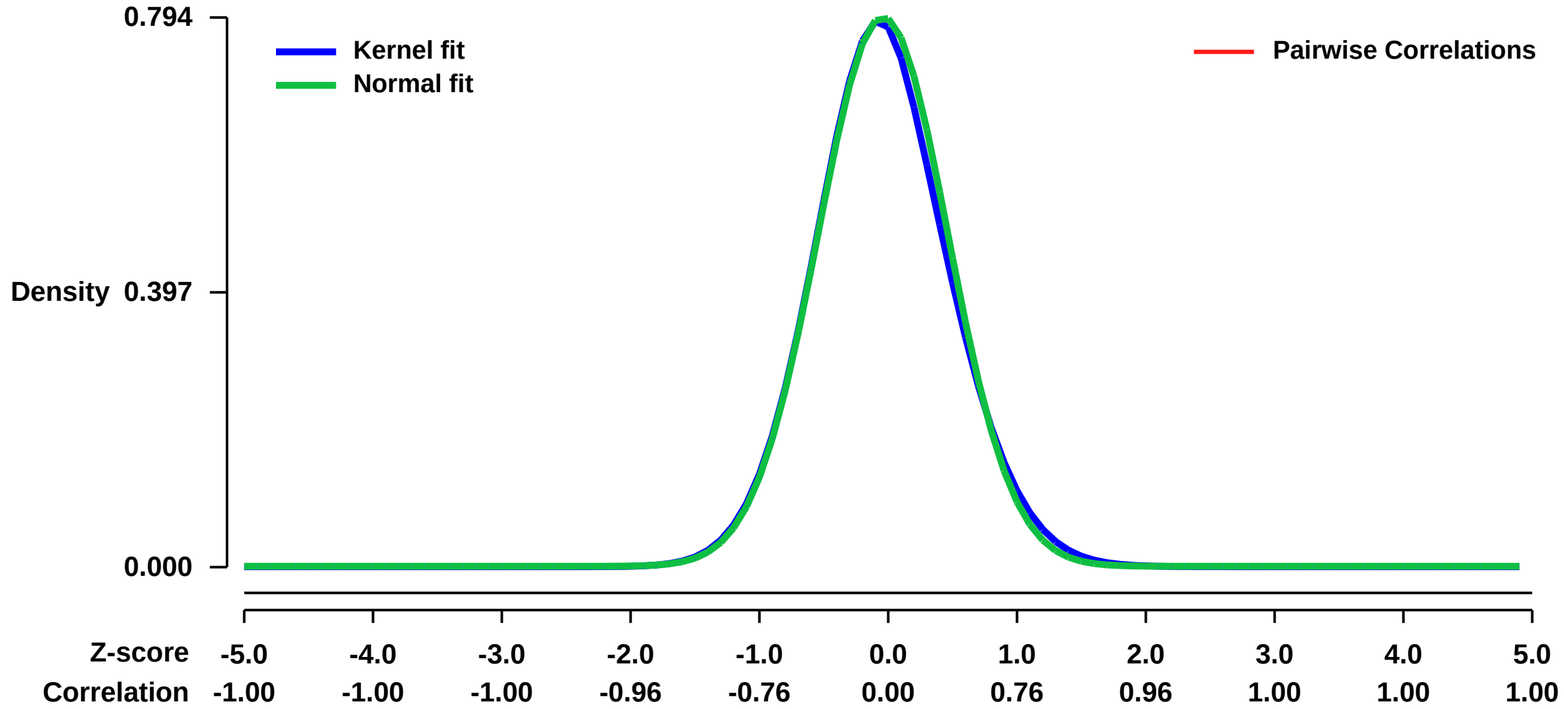

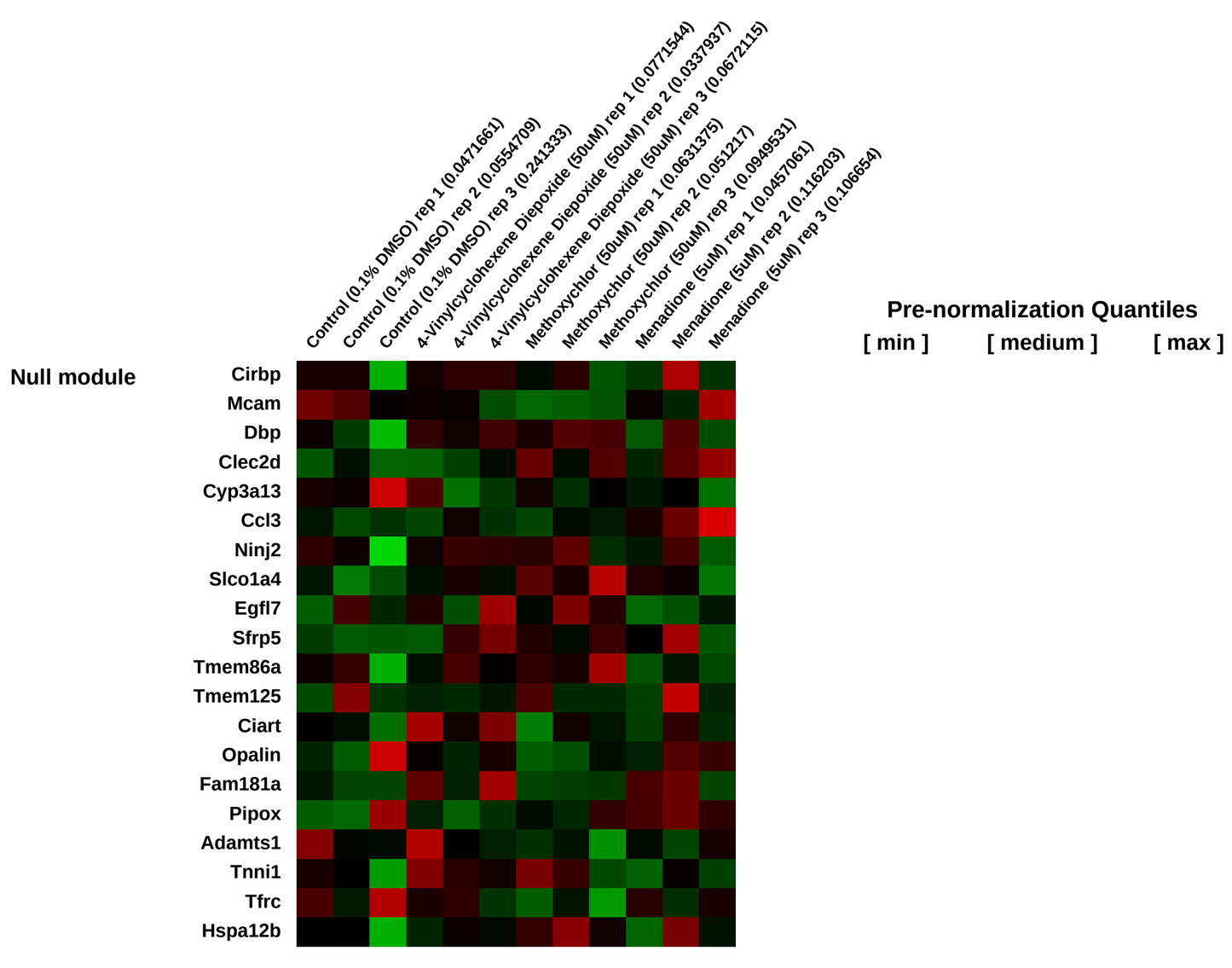

GEO Series "GSE23738" Expression Profiles

Num of samples in this series: 17

Scale of expression profile Z-scores

-3.0 -2.0 -1.0 0.0 1.0 2.0 3.0

GEO Link:	http://www.ncbi.nlm.nih.gov/geo/query/acc.cgi?acc=GSE23738
Status:	Public on Aug 22 2010
Title:	Global changes of expression patterns of vaccinia virus infected lungs of C57BL/6 mice.
Organism:	Mus musculus
Experiment type:	Expression profiling by array
Platform:	GPL1261
Pubmed ID:	20943971
Summary & Design:	**Summary:** Vaccinia virus infection of mouse lungs produces a focal infection within the lung remaining at the large bronchi throughout the course of infection. Animals die of respiratory failure with little edema and few infiltrating immune cells. It is well established that poxviruses control the host immune system by encoding multiple host defense pathway antagonists. The goal of this study was to examine the local response to infection within the lung given that the virus controls the host immune response. **Overall design:** The global changes exhibited over the course of a lung infection with vaccinia virus were analyzed by arrays of lungs harvested from 1 to 5 day post infection using Affymetrix Mouse 430A 2.0 arrays.

Background corr dist: KL-Divergence = 0.2052, L1-Distance = 0.0397, L2-Distance = 0.0033, Normal std = 0.3305

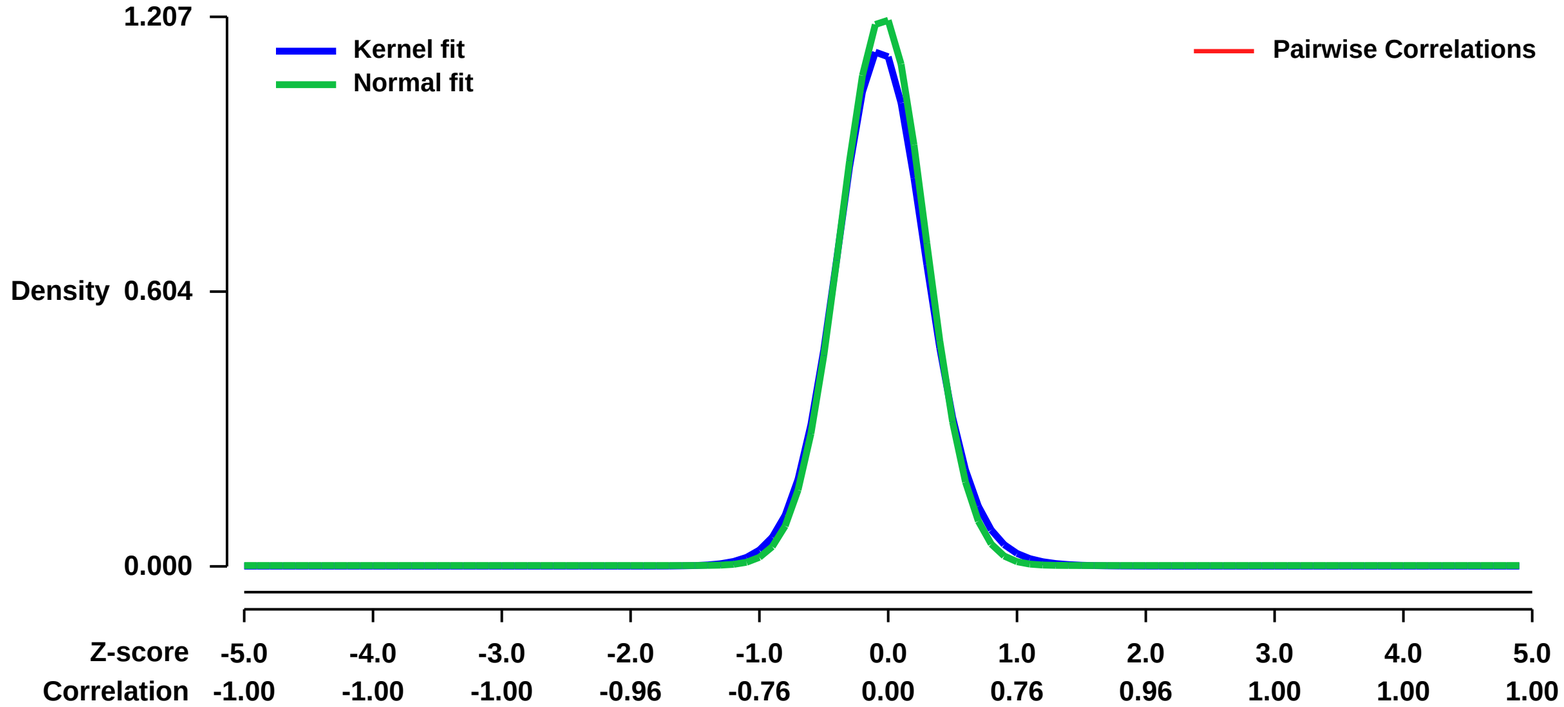

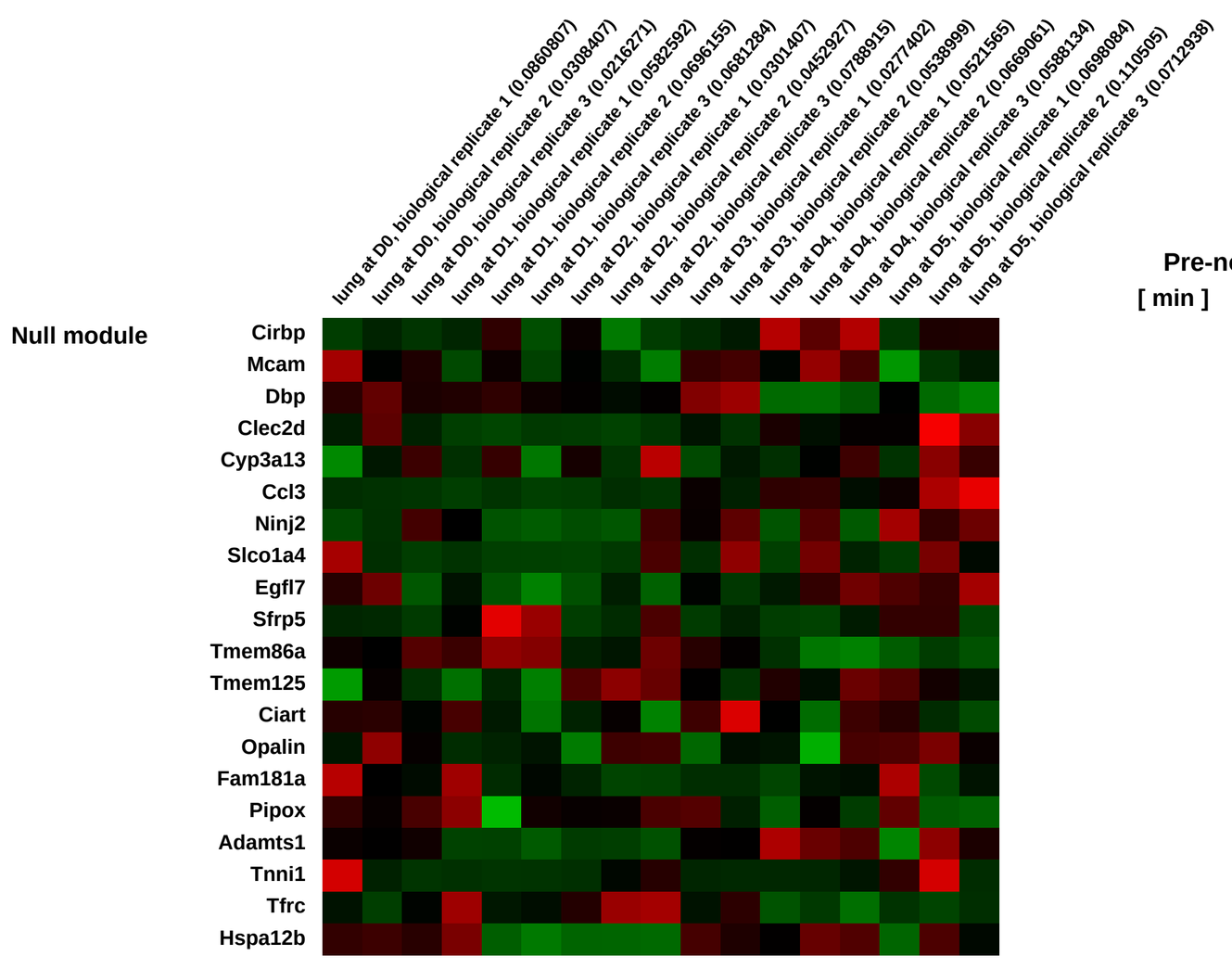

GEO Series "GSE23781" Expression Profiles

Num of samples in this series: 6

Scale of expression profile Z-scores

-3.0 -2.0 -1.0 0.0 1.0 2.0 3.0

GEO Link:	http://www.ncbi.nlm.nih.gov/geo/query/acc.cgi?acc=GSE23781
Status:	Public on Mar 23 2011
Title:	Expression data from E13.5 Fz4-/- and Fz4+/+ kidneys
Organism:	Mus musculus
Experiment type:	Expression profiling by array
Platform:	GPL1261
Pubmed ID:	21343368
Summary & Design:	**Summary:** Fz4 and Fz8 cooperate in regulating the branching morhpogenesis of the developing kidney during mouse embryonic development, hence determines the eventual kidney size. We used microarrays to study the global gene expression profiles regulated by Fz4 and Fz8 signaling during early kidney development, and to understand the collaboration between the signaling events mediated by Fz4 and Fz8 **Overall design:** Kidney rudiments were dissected from E13.5 mouse embryos for RNA extraction and hybridization on Affymetrix MOE430.2 arrays. Three biological replicates of each genotype were analyzed.

Background corr dist: KL-Divergence = 0.0214, L1-Distance = 0.0173, L2-Distance = 0.0004, Normal std = 0.7180

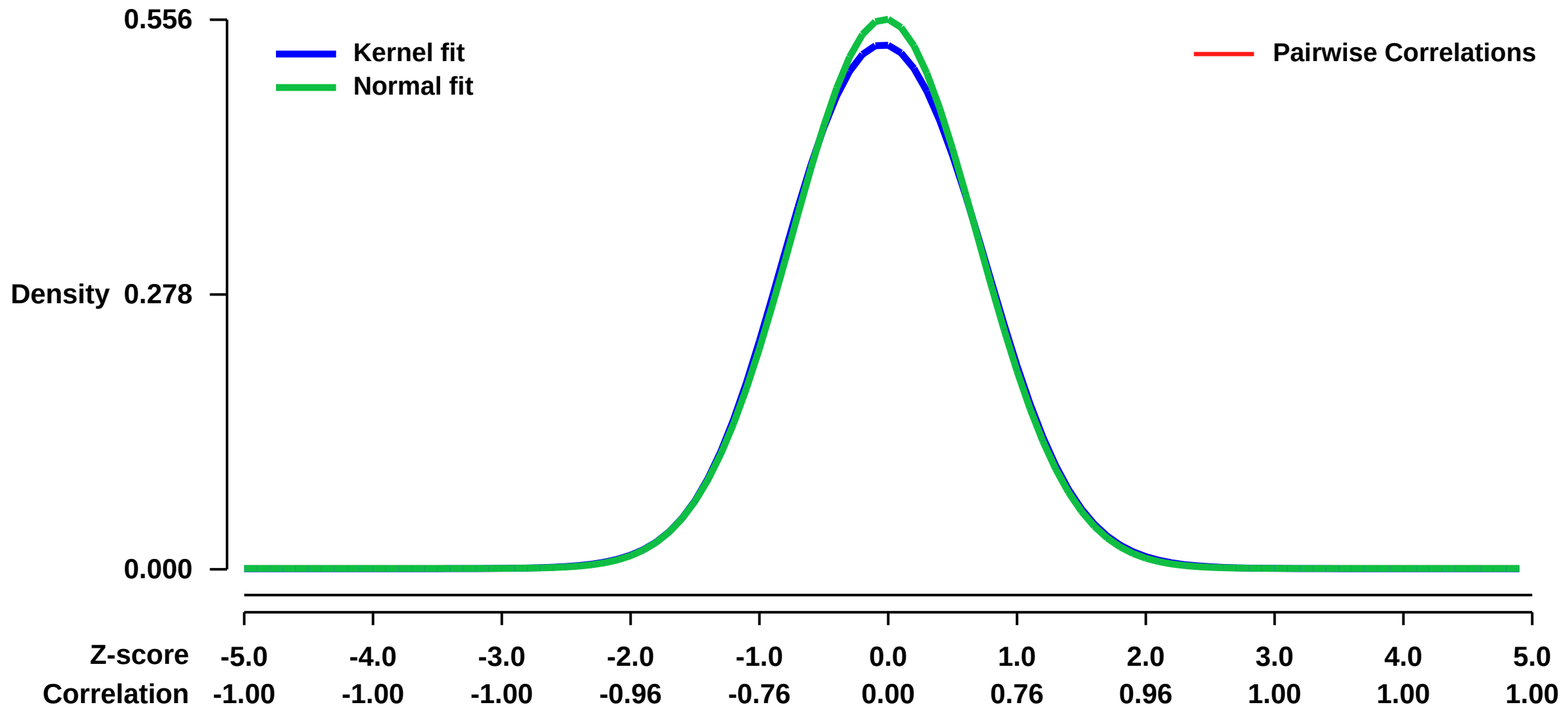

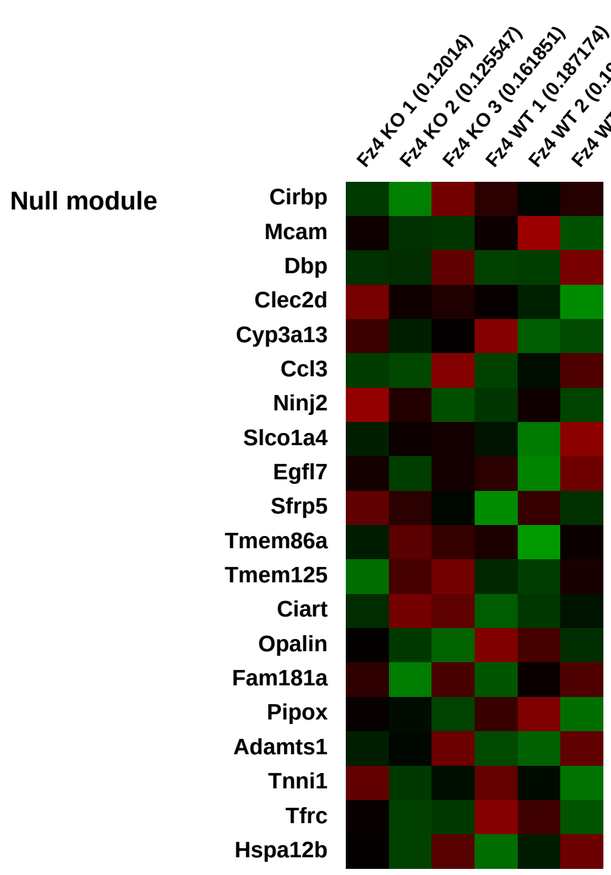

GEO Series "GSE23845" Expression Profiles

Num of samples in this series: 15

Scale of expression profile Z-scores

-3.0 -2.0 -1.0 0.0 1.0 2.0 3.0

GEO Link:	http://www.ncbi.nlm.nih.gov/geo/query/acc.cgi?acc=GSE23845
Status:	Public on Aug 28 2010
Title:	Time course for bladder UCC development in UPII-SV40Tag mice
Organism:	Mus musculus
Experiment type:	Expression profiling by array
Platform:	GPL1261
Pubmed ID:	20501863
Summary & Design:	**Summary:** We have identified genes that are differentially expressed between the bladders of UPII-SV40Tag mice and their age-matched wild-type littermates at 3, 6, 20, and 30 weeks of age. These are ages that correspond to premalignant, carcinoma in situ, and early-stage and later stage invasive UCC, respectively Analysis of the microarray data sets has revealed â…1,900 unique genes differentially expressed (â¥3-fold difference at one or more time points) between wild-type and UPII-SV40Tag urothelium during the time course of tumor development. **Overall design:** RNA from the urothelium of duplicate UPII-SV40Tag hemizygous and age-matched wild type littermate mice was isolated at 3, 6, 20, and 30 weeks of age and gene expression profiles were obtained.

Background corr dist: KL-Divergence = 0.1356, L1-Distance = 0.0293, L2-Distance = 0.0013, Normal std = 0.3985

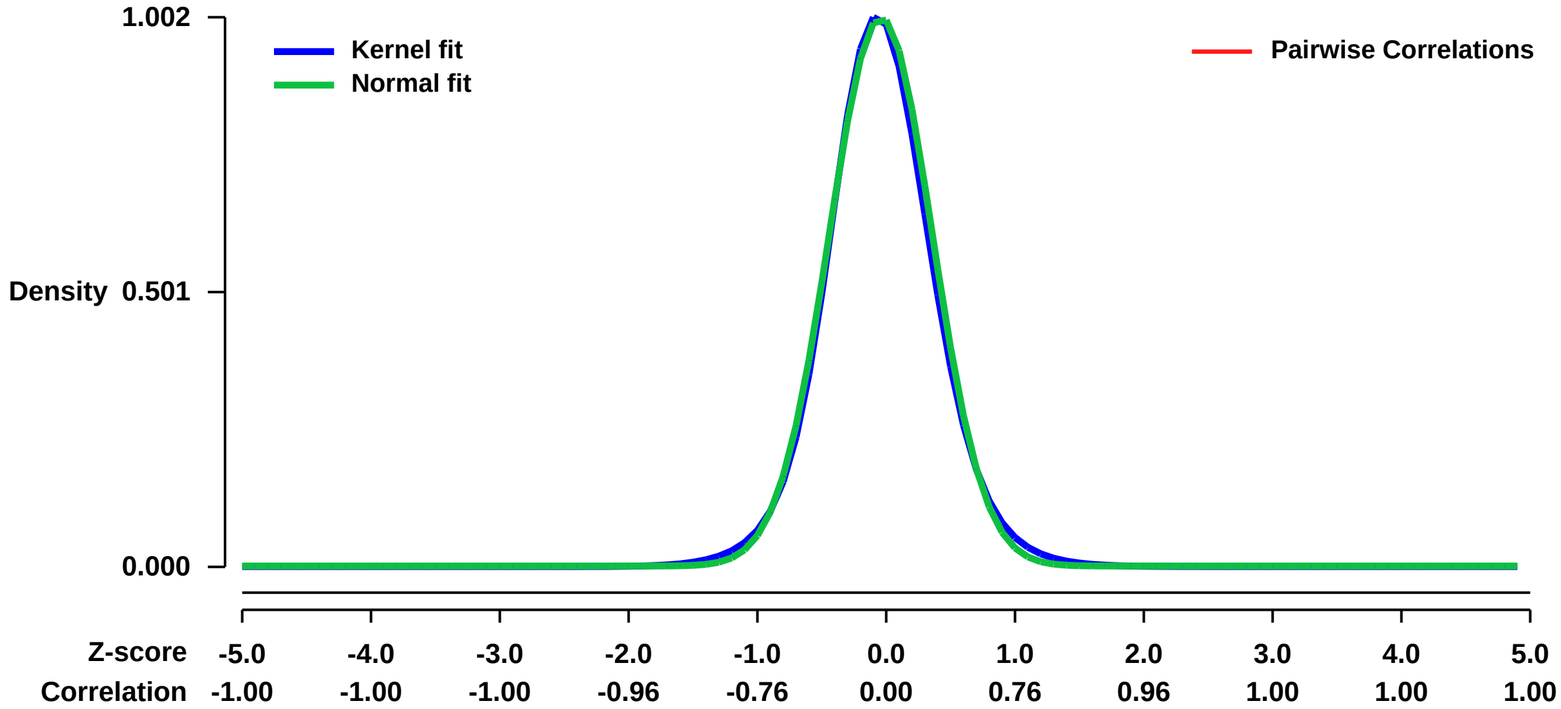

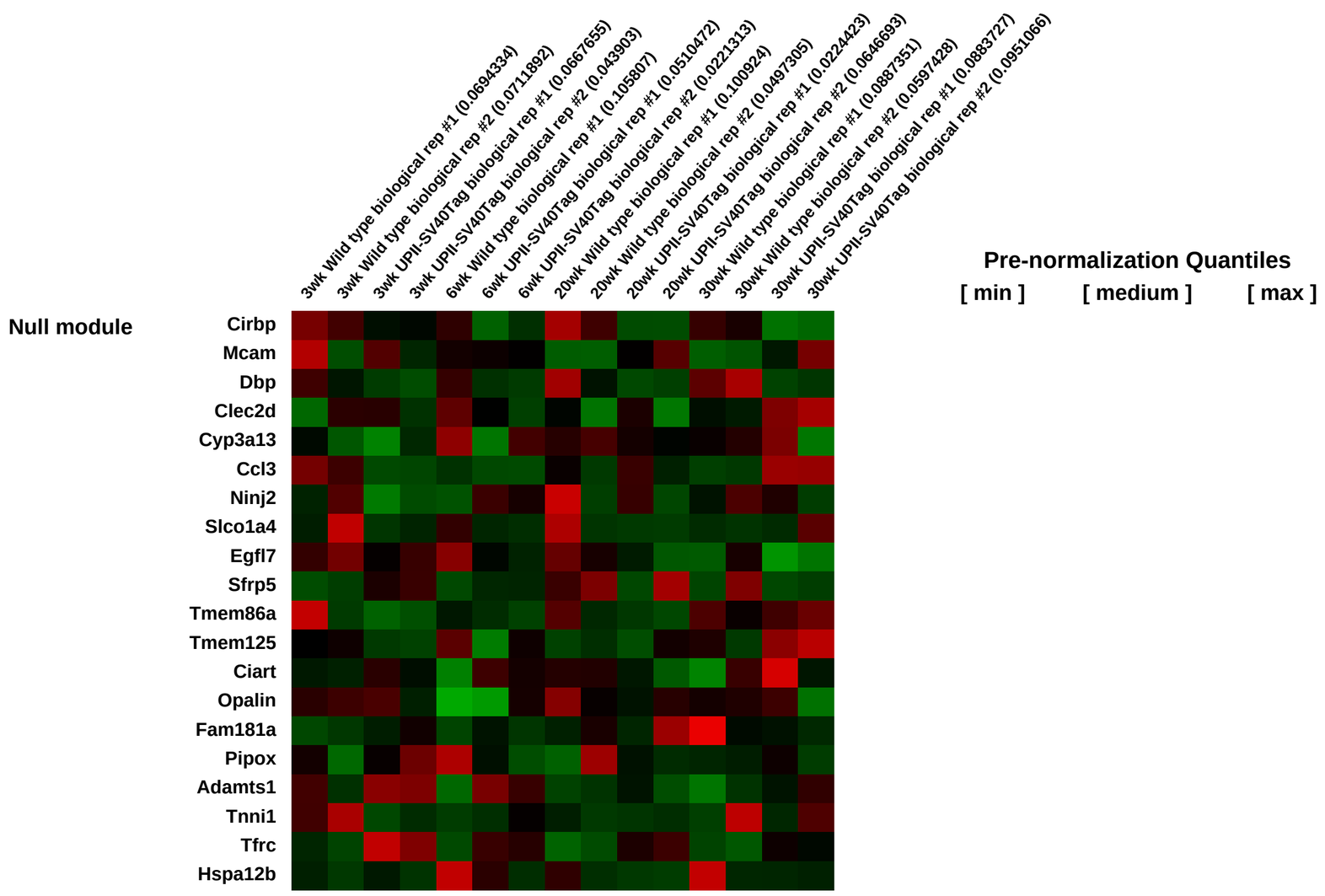

GEO Series "GSE23923" Expression Profiles

Num of samples in this series: 8

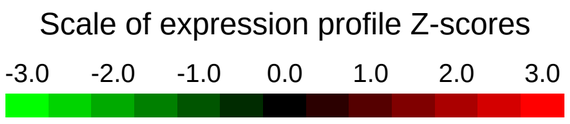

GEO Link:	http://www.ncbi.nlm.nih.gov/geo/query/acc.cgi?acc=GSE23923
Status:	Public on May 19 2011
Title:	Expression data from Rad21 knock-down in ES cells
Organism:	Mus musculus
Experiment type:	Expression profiling by array
Platform:	GPL1261
Pubmed ID:	21589869
Summary & Design:	**Summary:** The Cohesin complex has recently been described to regulate gene expression. We wanted to determine the gene expression profile specific in mouse ES cells after depletion of the Cohesin subunit Rad21. We used microarrays to detail the global programme of gene expression underlying depletion of Rad21 and identified distinct early development related genes up-regulated and many pluripotency related genes downregulated. **Overall design:** Rad21 was depleted in R1/E ES cells for 48h using esiRNAs against Rad21. An esiRNA against non-targeting Luciferase was used as a negative control

Background corr dist: KL-Divergence = 0.0270, L1-Distance = 0.0288, L2-Distance = 0.0015, Normal std = 0.6782

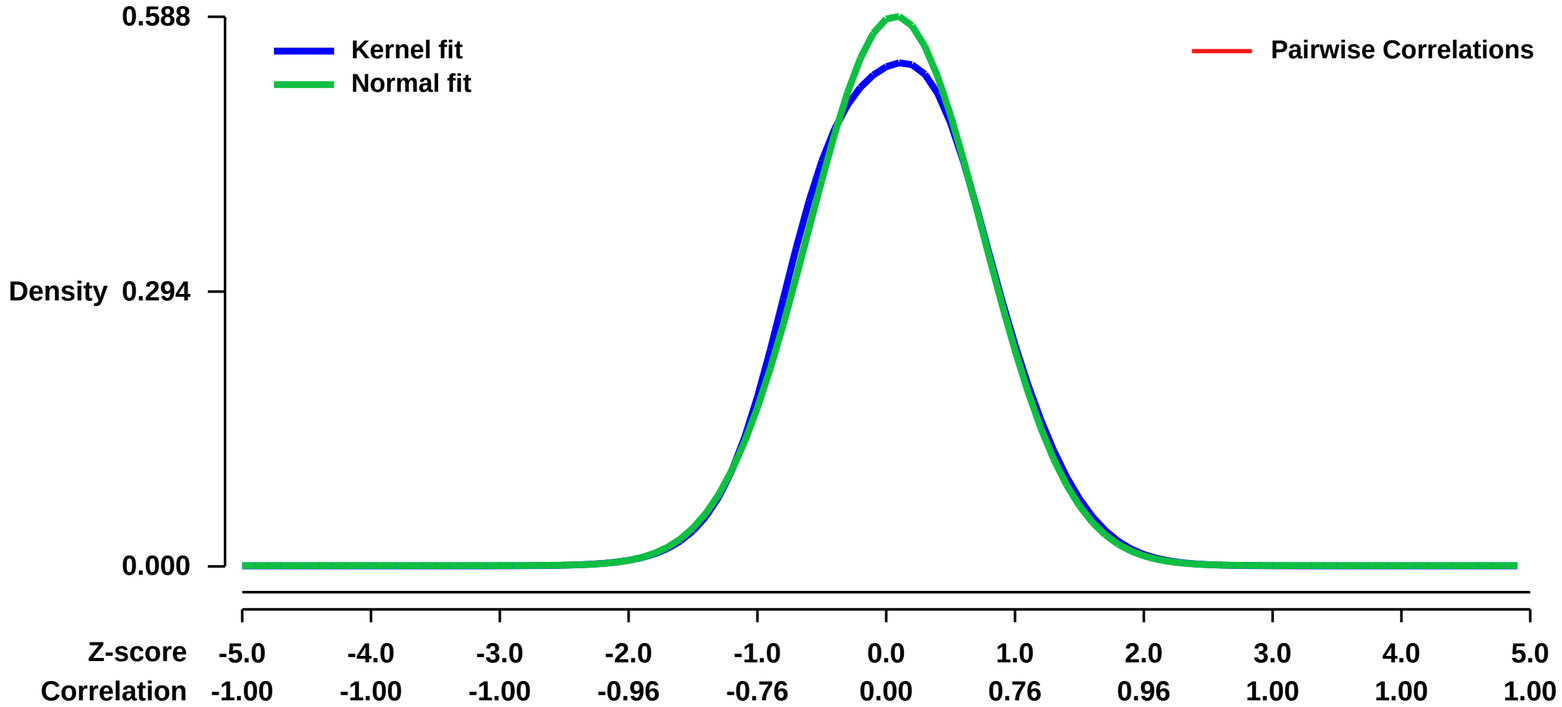

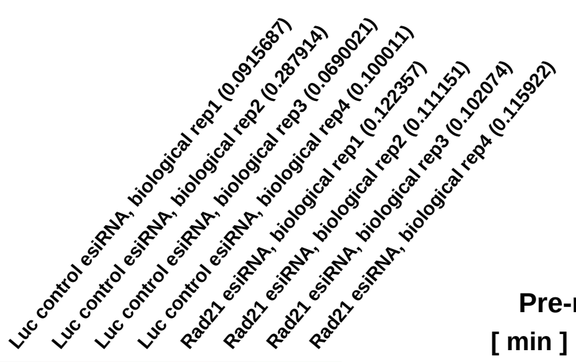

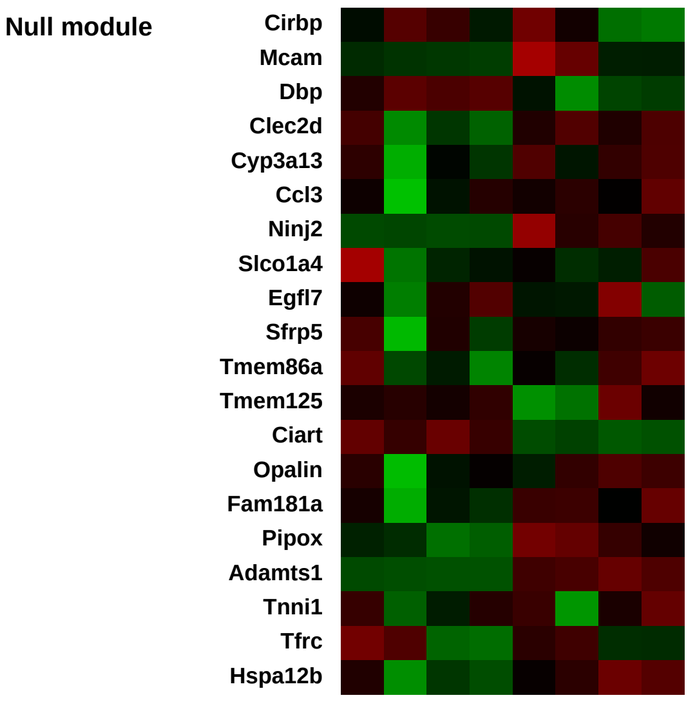

GEO Series "GSE23972" Expression Profiles

Num of samples in this series: 6

Scale of expression profile Z-scores

-3.0 -2.0 -1.0 0.0 1.0 2.0 3.0

GEO Link:	http://www.ncbi.nlm.nih.gov/geo/query/acc.cgi?acc=GSE23972
Status:	Public on Sep 03 2010
Title:	Ikaros deficient mouse thymic lymphomas
Organism:	Mus musculus
Experiment type:	Expression profiling by array
Platform:	GPL1261
Pubmed ID:	20829372
Summary & Design:	**Summary:** This dataset comprises expression profiles from 3 thymic lymphomas from Ikaros deficient mice (IkL/L model, see Dumortier et al, Mol. Cell. Biol. 26, 209-220, 2006 for a description of the tumor model) and 3 thymic lymphomas from IkL/L mice that harbor a mutation of the Notch1 gene (deletion of floxed sequences comprising the promoter and exon 1 with the CD4-Cre transgene). The results from this experimpent is that the expression of Notch target genes was unexpectedly not altered in the tumors with the Notch1 deletion. This result is explained by the activation of a cryptic 3' Notch1 promoter in the deleted tumors, which leads to constitutive Notch1 activation. These results are described in the following publication: R Jeannet, J Mastio, B Macias-Garcia, A Oravecz, T Ashworth, AS Geimer-Lelay, B Jost, S Le Gras, J Ghysdael, T Gridley, T Honjo, F Radtke, J Aster, S Chan and P Kastner. Oncogenic activation of the Notch1 gene in mouse T-cell leukemia by deletion of its promoter. Blood, in press (2010) **Overall design:** Primary thymic tumors from 3 IkL/L Notch1+/+ CD4-Cre+ mice (aged 18-20 weeks) were compared to similar tumors from 3 IkL/L Notch1f/f CD4-Cre+ mice (aged 8-10 weeks).

Background corr dist: KL-Divergence = 0.0466, L1-Distance = 0.0348, L2-Distance = 0.0017, Normal std = 0.6050

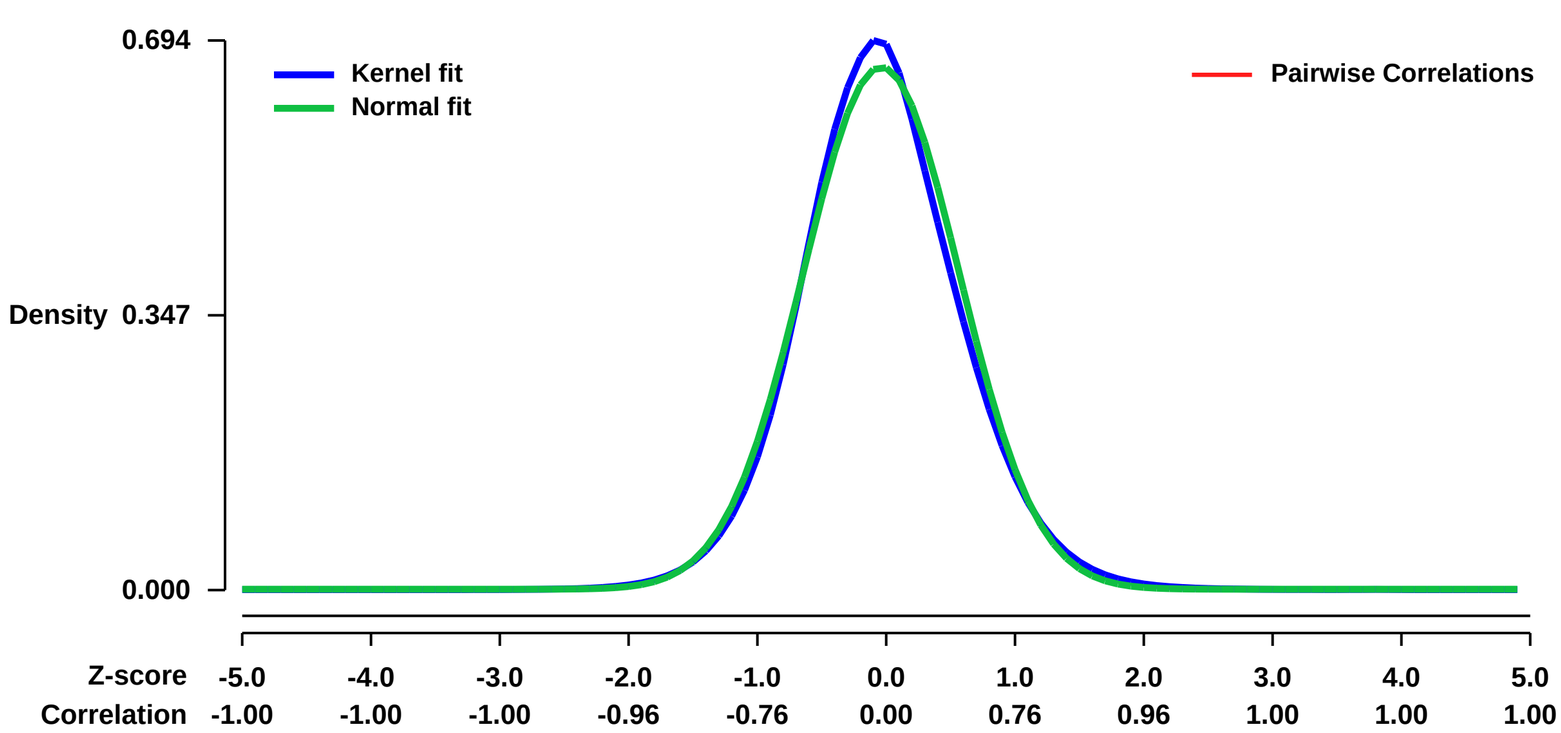

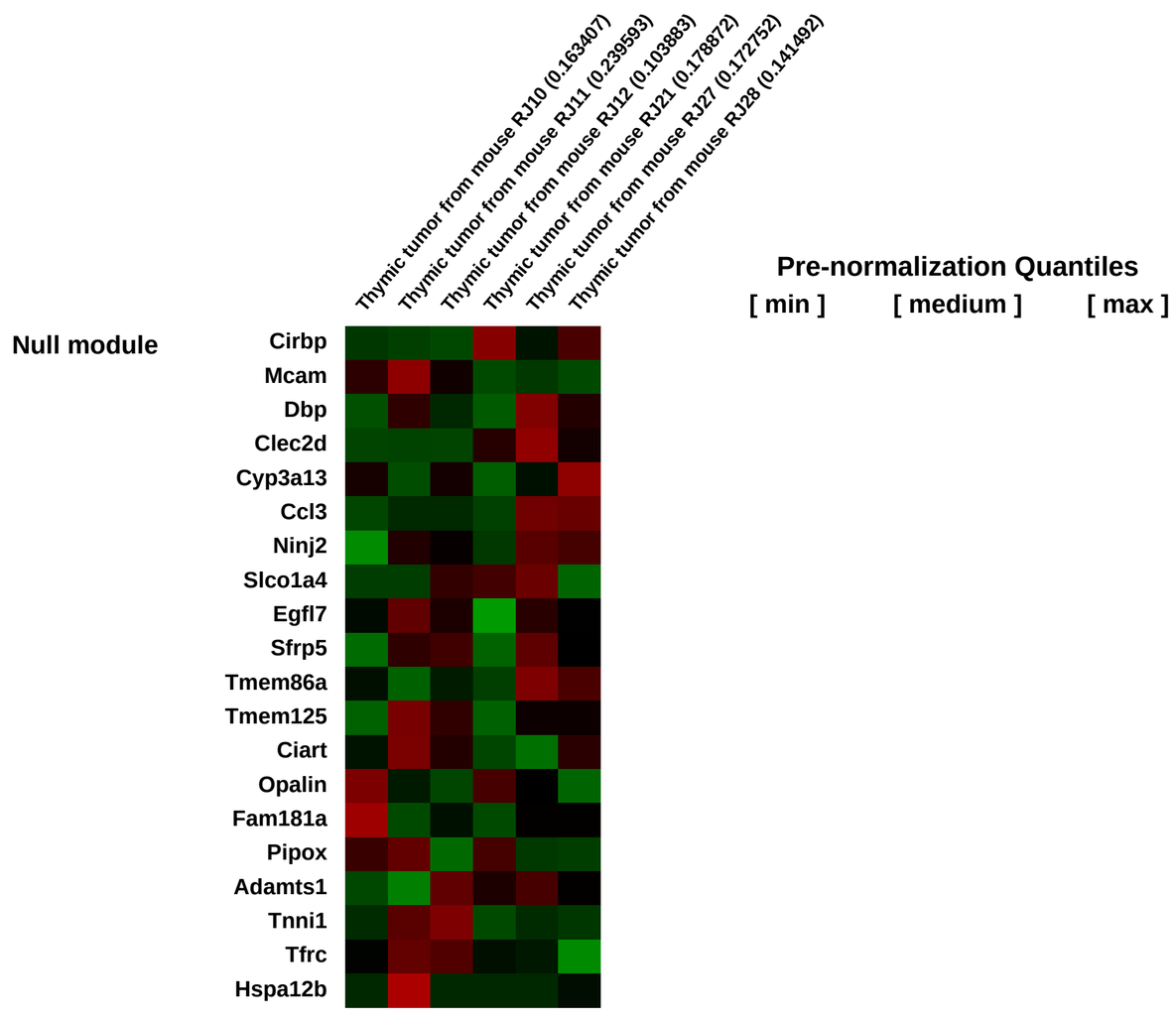

GEO Series "GSE24031" Expression Profiles

Num of samples in this series: 18

Scale of expression profile Z-scores

-3.0 -2.0 -1.0 0.0 1.0 2.0 3.0

GEO Link:	http://www.ncbi.nlm.nih.gov/geo/query/acc.cgi?acc=GSE24031
Status:	Public on Sep 09 2010
Title:	Adipose tissue dysfunction signals progression of hepatic steatosis towards nonalcoholic steatohepatitis in C57Bl/6 mice
Organism:	Mus musculus
Experiment type:	Expression profiling by array
Platform:	GPL1261
Pubmed ID:	20858684
Summary & Design:	**Summary:** **Objective: Nonalcoholic fatty liver disease (NAFLD) is linked to obesity and diabetes, suggesting an important role of adipose tissue in the pathogenesis of NAFLD. Here we aim to investigate the interaction between adipose tissue and liver in NAFLD, and identify potential early plasma markers that predict NASH. Research Design and Methods: C57Bl/6 mice were chronically fed a high fat diet to induce NAFLD and compared with mice fed low fat diet. Extensive histological and phenotypical analyses coupled with a time-course study of plasma proteins using multiplex assay was performed. Results: Mice exhibited pronounced heterogeneity in liver histological scoring, leading to classification into 4 subgroups: LF-low (LFL) responders displaying normal liver morphology, LF-high (LFH) responders showing benign hepatic steatosis, HF-low (HFL) responders displaying pre-NASH with macrovesicular lipid droplets, and HF-high (HFH) responders exhibiting overt NASH characterized by ballooning of hepatocytes, presence of Mallory bodies, and activated inflammatory cells. Compared to HFL responders, HFH mice gained weight more rapidly and exhibited adipose tissue dysfunction characterized by decreased final fat mass, enhanced macrophage infiltration and inflammation, and adipose tissue remodelling. Plasma haptoglobin, IL-1¸†, TIMP-1, adiponectin and leptin were significantly changed in HFH mice. Multivariate analysis indicated that in addition to leptin, plasma CRP, haptoglobin, eotaxin and MIP-1¸– early in the intervention were positively associated with liver triglycerides. Intermediate prognostic markers of liver triglycerides included IL-18, IL-1¸†, MIP-1¸‡ and MIP-2, whereas insulin, TIMP-1, GCP-2 and MPO emerged as late markers. Conclusions: Our data support the existence of a tight relationship between adipose tissue dysfunction and NASH pathogenesis and point to several novel potential predictive biomarkers for NASH.** **Keywords: Expression profiling by array** **Overall design:** **Male wildtype C57Bl/6 mice were fed LFD or HFD for 21 weeks. Mice were divided into 4 groups based on liver histology.**

Background corr dist: KL-Divergence = 0.2859, L1-Distance = 0.0624, L2-Distance = 0.0104, Normal std = 0.2854

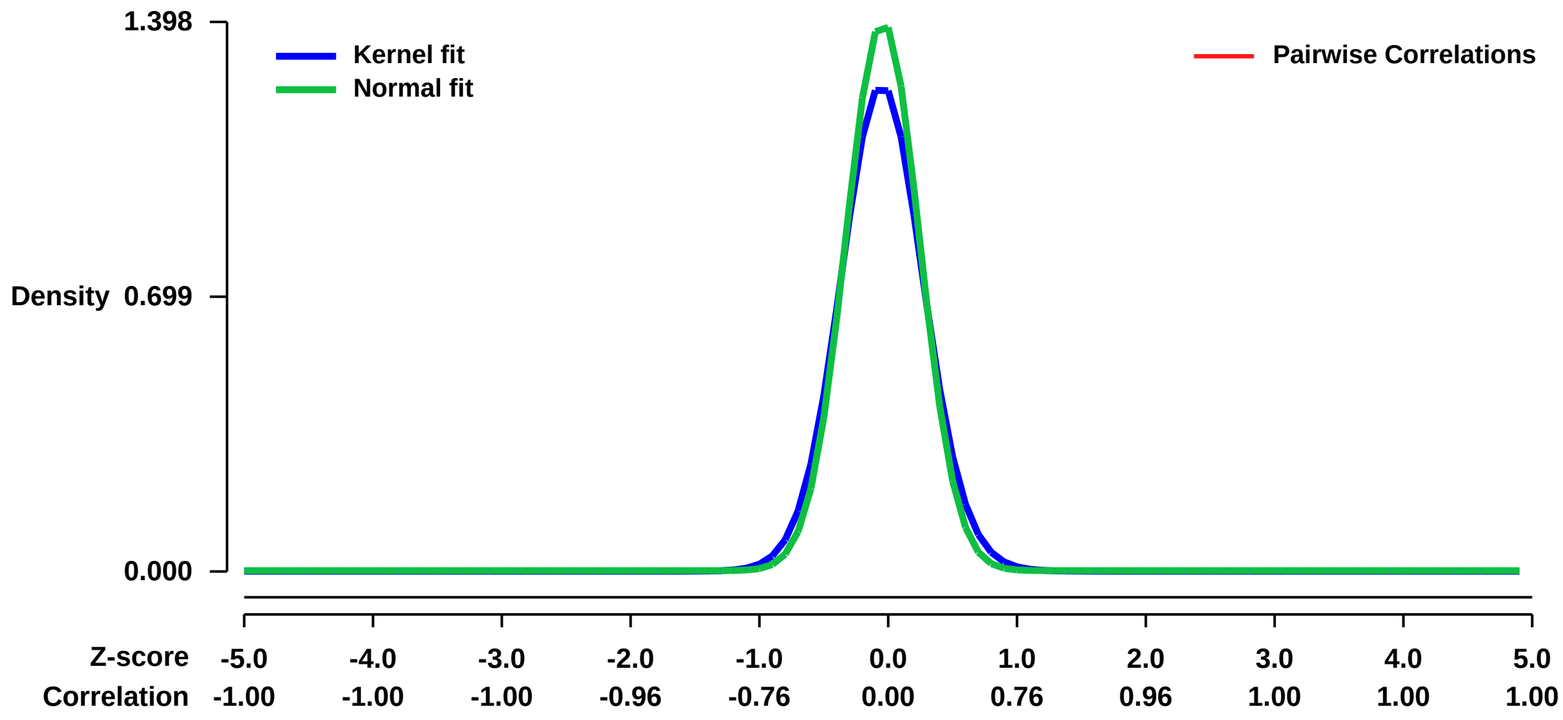

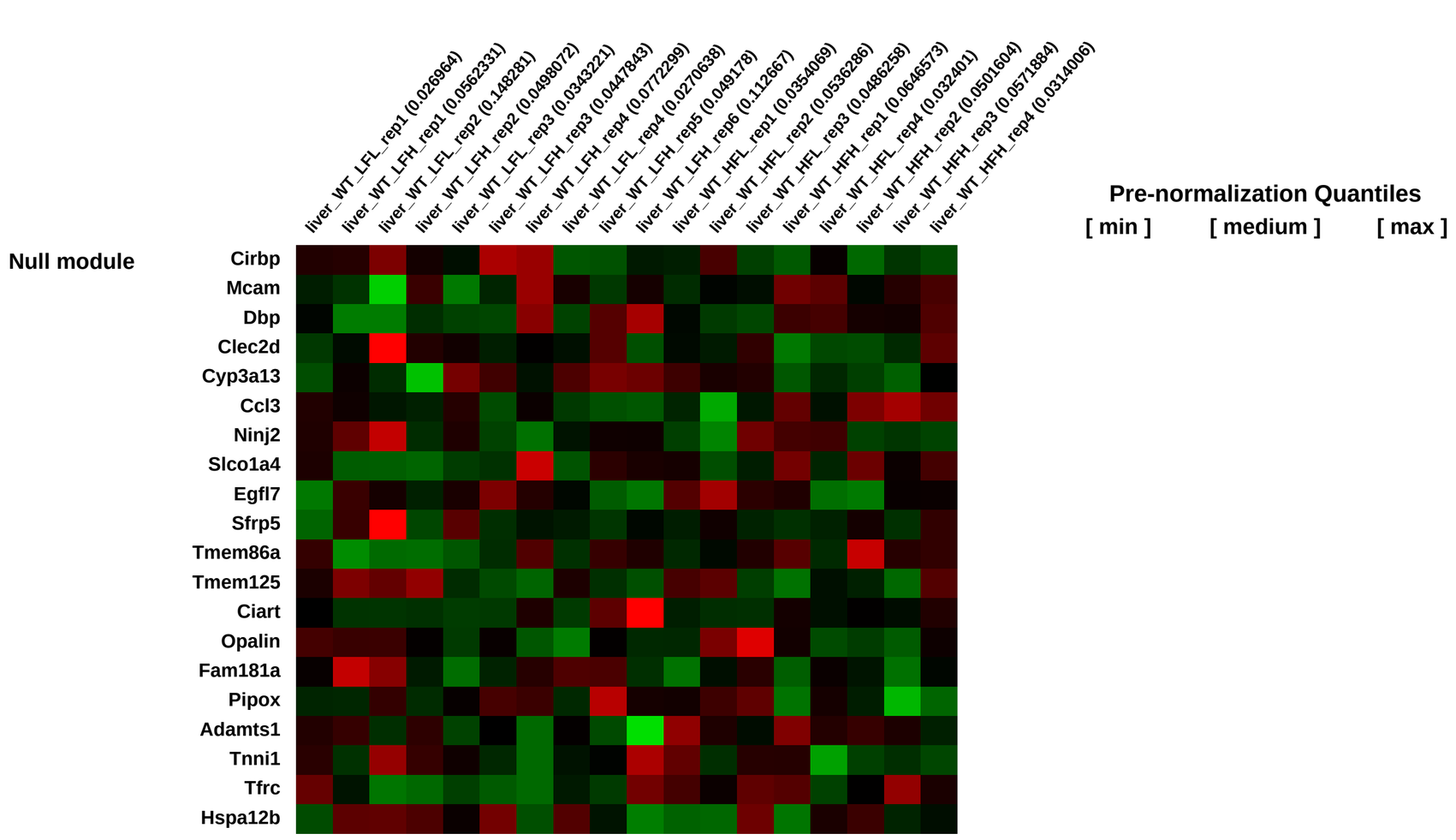

GEO Series "GSE24061" Expression Profiles

Num of samples in this series: 88

Scale of expression profile Z-scores

-3.0 -2.0 -1.0 0.0 1.0 2.0 3.0

GEO Link:	http://www.ncbi.nlm.nih.gov/geo/query/acc.cgi?acc=GSE24061
Status:	Public on Sep 10 2010
Title:	MAQC-II Project: Hamner data set
Organism:	Mus musculus
Experiment type:	Expression profiling by array
Platform:	GPL1261
Pubmed ID:	20676074
Summary & Design:	**Summary:** The Hamner data set (endpoint A) was provided by The Hamner Institutes for Health Sciences (Research Triangle Park, NC, USA). The study objective was to apply microarray gene expression data from the lung of female B6C3F1 mice exposed to a 13-week treatment of chemicals to predict increased lung tumor incidence in the 2-year rodent cancer bioassays of the National Toxicology Program. If successful, the results may form the basis of a more efficient and economical approach for evaluating the carcinogenic activity of chemicals. Microarray analysis was performed using Affymetrix Mouse Genome 430 2.0 arrays on three to four mice per treatment group, and a total of 70 mice were analyzed and used as the MAQC-II's training set (GEO Series GSE6116). Additional data from another set of 88 mice were collected later and provided as the MAQC-II's external validation set (this Series). The training dataset had already been deposited in GEO by its provider and its accession number is GSE6116. **Overall design:** 88 Samples

Background corr dist: KL-Divergence = 0.2466, L1-Distance = 0.0659, L2-Distance = 0.0092, Normal std = 0.3191

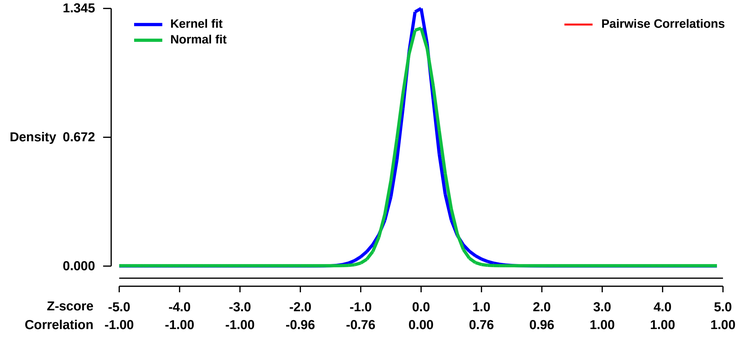

Z-score	-5.0	-4.0	-3.0	-2.0	-1.0	0.0	1.0	2.0	3.0	4.0	5.0
Correlation	-1.00	-1.00	-1.00	-0.96	-0.76	0.00	0.76	0.96	1.00	1.00	1.00

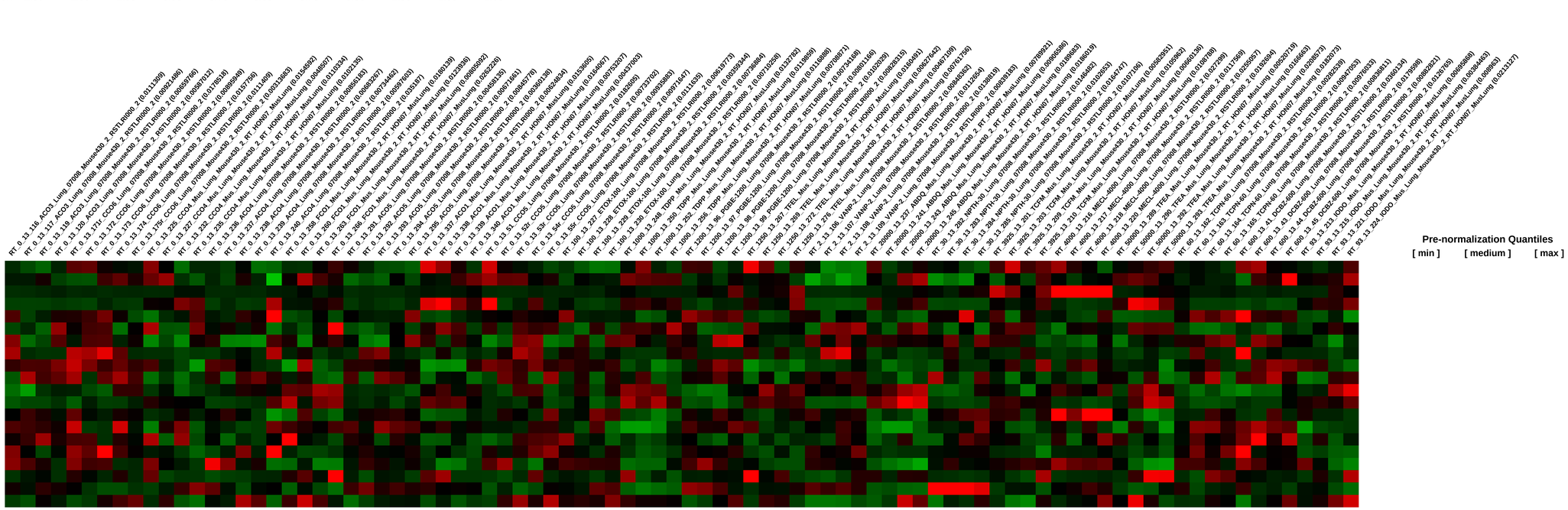

GEO Series "GSE24078" Expression Profiles

Num of samples in this series: 6

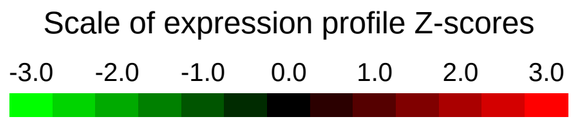

GEO Link:	**http://www.ncbi.nlm.nih.gov/geo/query/acc.cgi?acc=GSE24078**
Status:	**Public on Sep 11 2010**
Title:	**Expression data from SSEA1+ differentiated murine embryonic stem cells**
Organism:	**Mus musculus**
Experiment type:	**Expression profiling by array**
Platform:	**GPL1261**
Pubmed ID:	
Summary & Design:	**Summary:** **SSEA1+ cells sorted from mouse embryonic stem cells differentiated for 4 days in 10uM Retinoic acid do not form teratomas when transplated into SCID mice while Pten-/- cells do.** **We used microarrays to identify genes and pathways besides Pten that could explain this difference in tumorigenicity.** **Keywords: wild type vs Pten-/-** **Overall design:** **Wild type and Pten mutant SSEA1 positive differentiated cells were compared as the wild type cells were non-tumorigenic upon transplant to SCID mice and the Pten-/- cells were tumorigenic.**

Background corr dist: **KL-Divergence = 0.0388, L1-Distance = 0.0202, L2-Distance = 0.0005, Normal std = 0.6194**

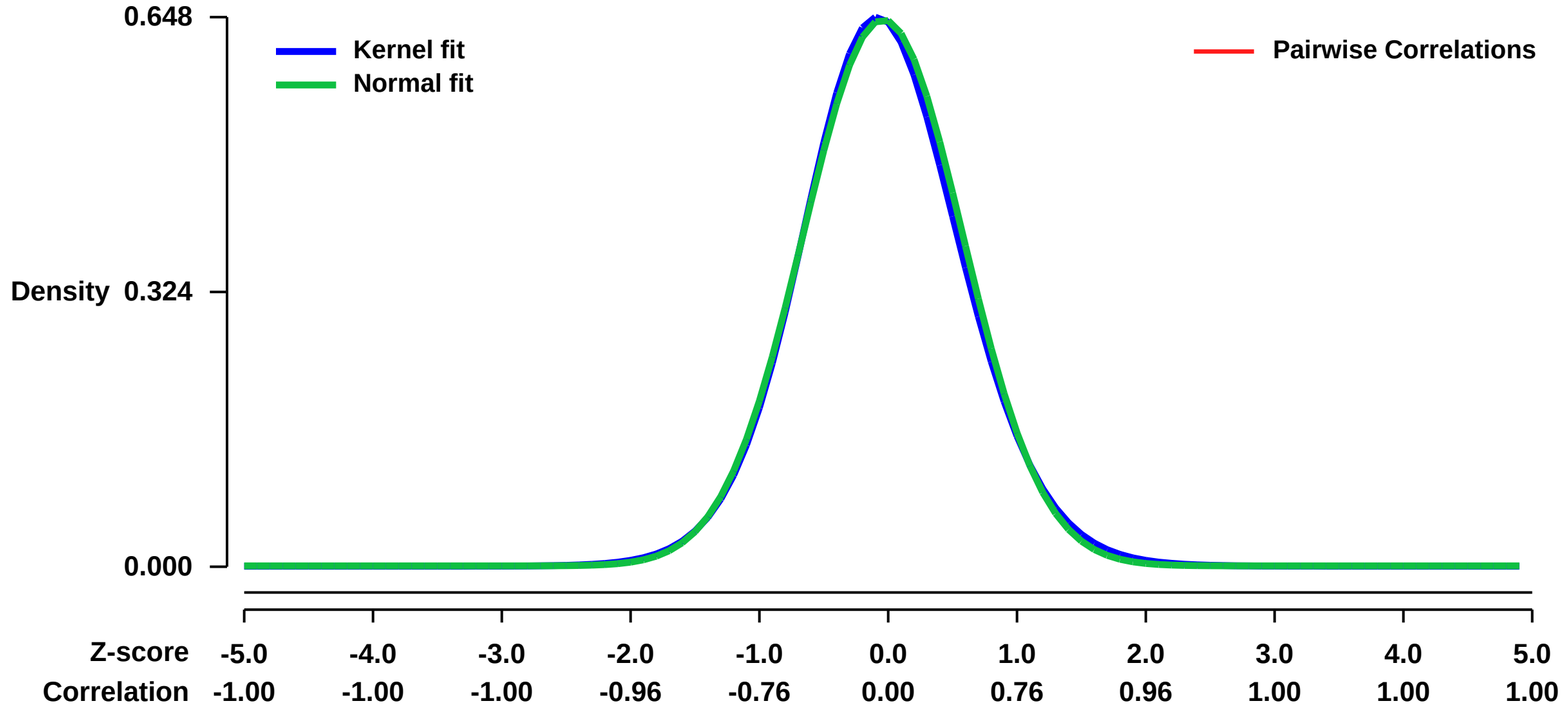

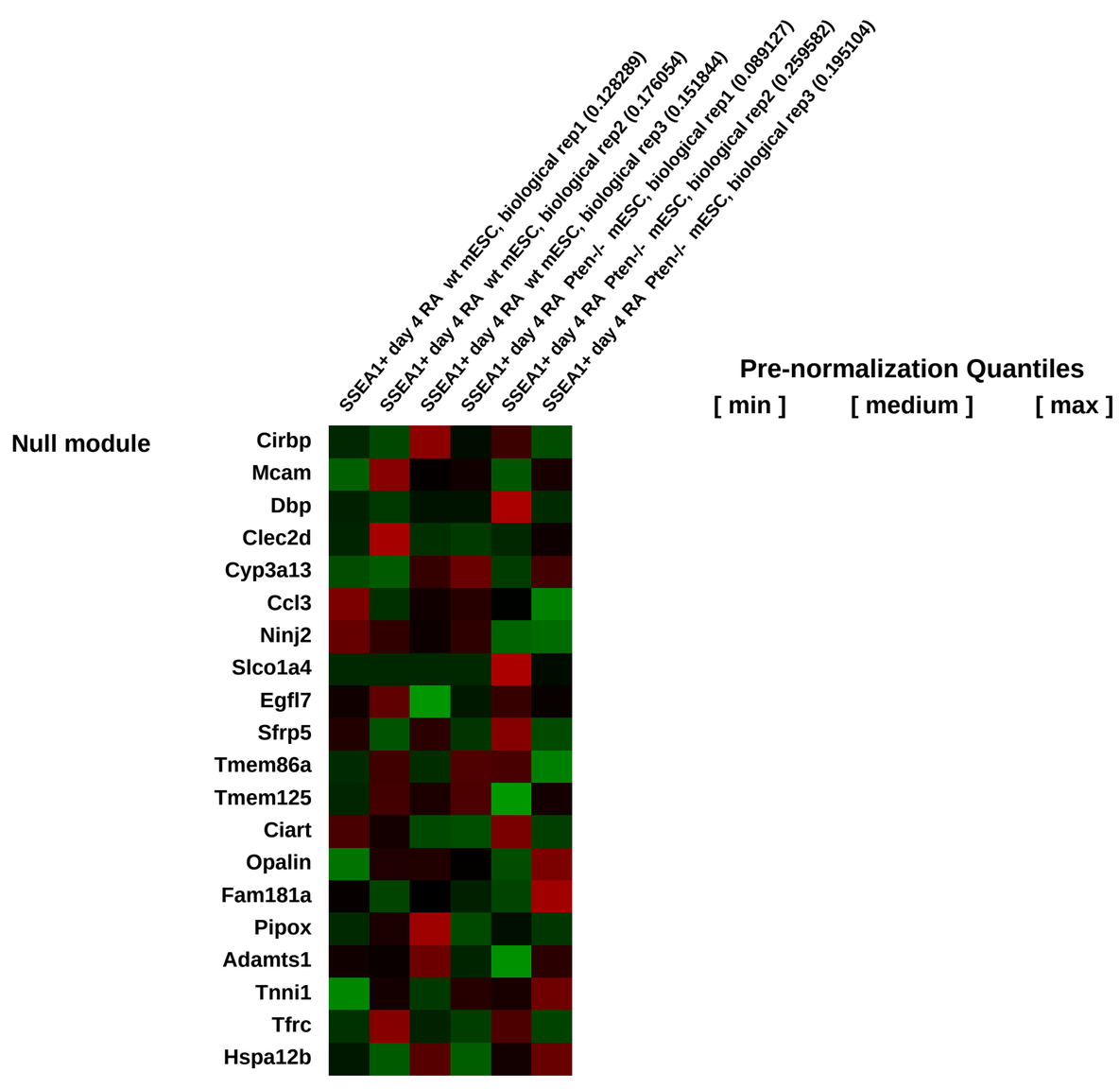

GEO Series "GSE24121" Expression Profiles

Num of samples in this series: 9

Scale of expression profile Z-scores

-3.0 -2.0 -1.0 0.0 1.0 2.0 3.0

GEO Link:	**http://www.ncbi.nlm.nih.gov/geo/query/acc.cgi?acc=GSE24121**
Status:	**Public on Oct 20 2010**
Title:	**Oligoarray analysis of mRNA species from DCs treated with C. parvum for 24 h.**
Organism:	**Mus musculus**
Experiment type:	**Expression profiling by array**
Platform:	**GPL1261**
Pubmed ID:	
Summary & Design:	**Summary:** **To investigate whether C. parvum treatment of DCs regulates other inflammatory genes, mouse BMDCs (CD11c and CD11b positive) were treated with C. parvum for 24 hr. Control groups included untreated BMDCs and DCs treated with E. cuniculi. We noticed that a significant upregulation of the expression of interferon-related genes, which may correlation the critical role of interferon in host defense against C. parvum infection.** **Overall design:** **DCs were treated with C. parvum for 24 hr. Control groups included untreated BMDCs and DCs treated with E. cuniculi. Group comparison was performed using the data of 3 replicate arrays from each time point.**

Background corr dist: **KL-Divergence = 0.0664, L1-Distance = 0.0336, L2-Distance = 0.0016, Normal std = 0.5257**

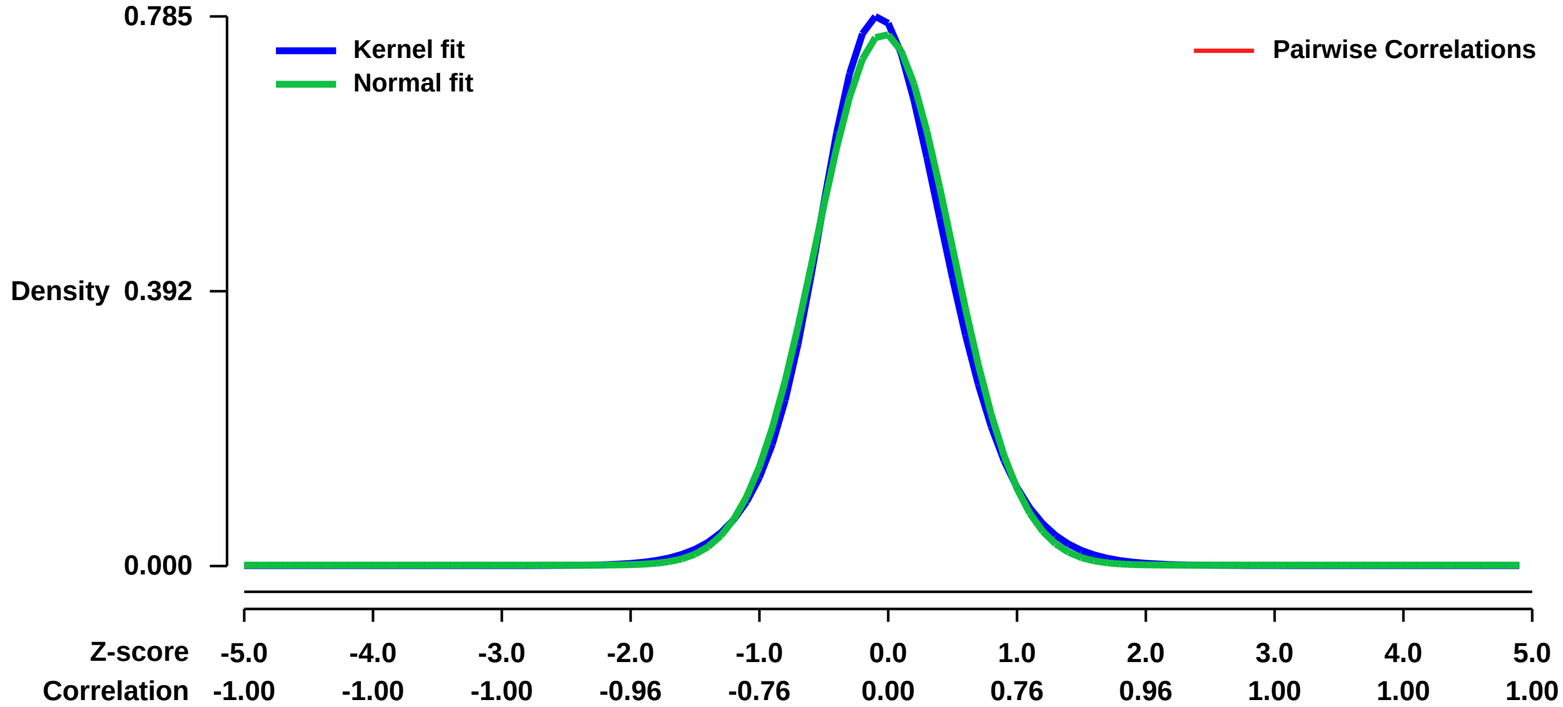

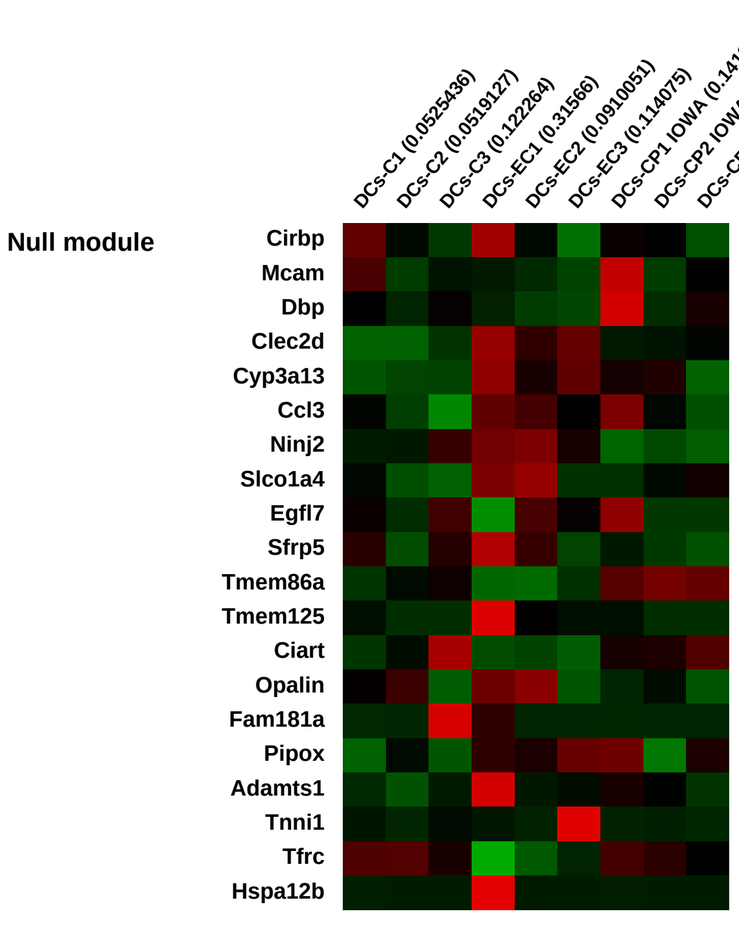

GEO Series "GSE24203" Expression Profiles

Num of samples in this series: 8

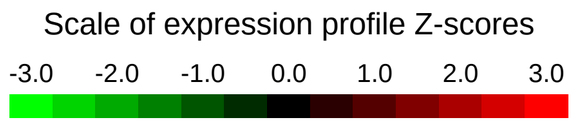

GEO Link:	**http://www.ncbi.nlm.nih.gov/geo/query/acc.cgi?acc=GSE24203**
Status:	**Public on Sep 18 2010**
Title:	**A20 Role in Liver regeneration**
Organism:	**Mus musculus**
Experiment type:	**Expression profiling by array**
Platform:	**GPL1261**
Pubmed ID:	
Summary & Design:	**Summary:** **Genome wide transcriptional profiling on liver mRNA retrieved from recombinant adenovirus A20 (rAd.A20) and rAd.bgalactosidase transduced livers, before and 24 hours after 78% extended liver resection. Overexpression of the NF-kB inhibitory protein A20 improves recovery of liver function and mass following extended liver resection and severe liver ischemia reperfusion injury in mice. In this project, we explored effects of A20 using transcriptional profiling on liver mRNA retrieved from recombinant adenovirus A20 (rAd.A20) and rAd.bgalactosidase transduced livers, before and 24 hours after 78% extended liver resection.** **Overall design:** **A20 or beta-galactosidase gene expression in the mouse liver was achieved by penile vein injection of 1x109 pfu of rAd. in 100uL of normal saline, which results in optimal transgene expression 5 days after injection in 30% to 40% of hepatocytes (Longo et al, 2005). Extended (78%) LR, consisting of resection of the lateral, medial, left, and right lobes, was performed 5 days following rAd. administration in 8-week old BALB/c mice weighing 25 to 30 grams (Taconic, Germantown, NY), as described (Longo et al, 2005). RNA was extracted from the resected portion of the liver (before samples) and from the remnant liver 24 hours after resection (after samples). RNA from three animals was pooled per microarray and 2 microarrays per group were performed.**

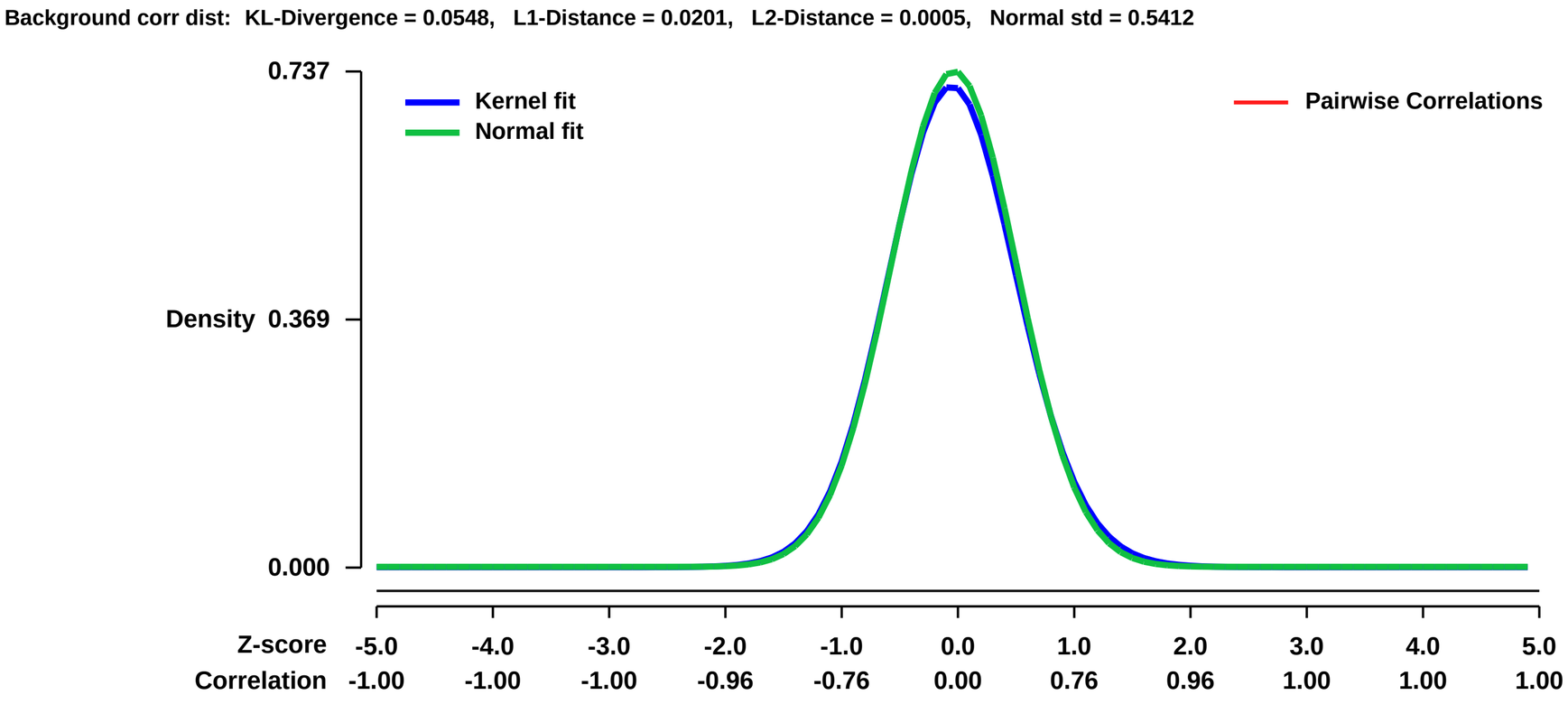

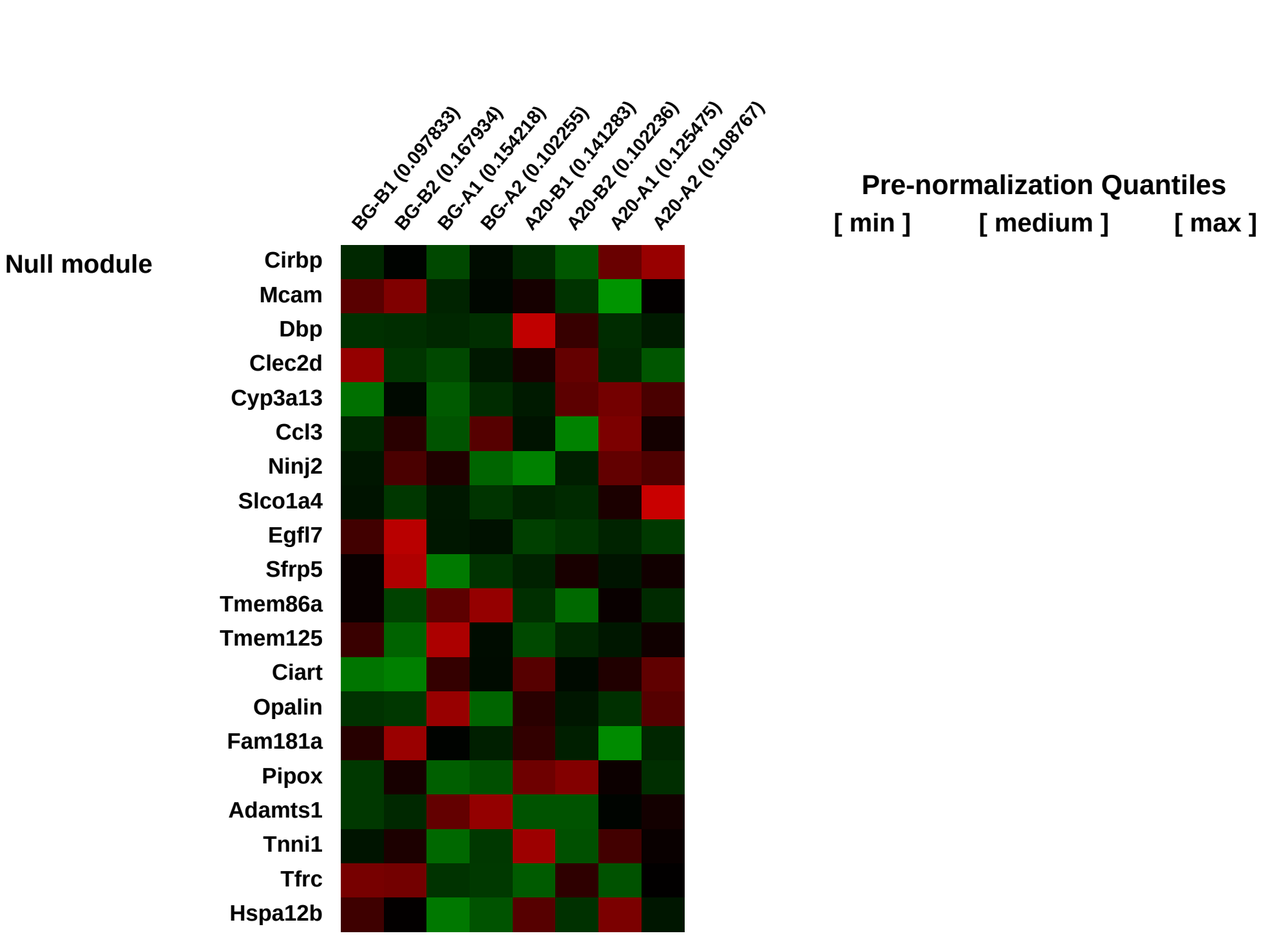

GEO Series "GSE24243" Expression Profiles

Num of samples in this series: 6

Scale of expression profile Z-scores

-3.0 -2.0 -1.0 0.0 1.0 2.0 3.0

GEO Link:	http://www.ncbi.nlm.nih.gov/geo/query/acc.cgi?acc=GSE24243
Status:	Public on May 09 2011
Title:	Murine skin gene expression analysis of skin-specific Scd1-deficient and control mice
Organism:	Mus musculus
Experiment type:	Expression profiling by array
Platform:	GPL1261
Pubmed ID:	21573029
Summary & Design:	**Summary:** **To help elucidate the metabolic changes in the skin that contribute to the obesity resistance and skin pathology in mice lacking Scd1, we performed microarray analysis of skin gene expression in male skin Scd1 knockout (SKO) and Scd1 flox/flox control (Lox) mice fed a standard rodent diet.** **We identified an extraordinary number of differentially expressed genes that support the previously documented histological observations of sebocyte atrophy, inflammation and epidermal hyperplasia in SKO mice. Additionally, transcript levels were reduced in skin of SKO mice for genes involved in fatty acid synthesis, elongation and desaturation, which may be attributed to decreased abundance of key transcription factors including SREBP1c, ChREBP and LXR$_c$–. Conversely, genes involved in cholesterol synthesis were increased, suggesting an imbalance between skin fatty acid and cholesterol synthesis. Unexpectedly, we observed a robust elevation in skin retinol, retinoic acid and retinoic acid-induced genes in SKO mice. These results highlight the importance of monounsaturated fatty acid synthesis for maintaining retinol homeostasis and point to disturbed retinol metabolism as a novel contributor to the Scd1 deficiency-induced skin pathology.** **Overall design:** **We analyzed dorsal skin gene expression in non-fasted 8-9 week old male skin Scd1 knockout (SKO) mice (n=3) and Scd1flox/flox (Lox) control mice (n=3)on a C57BL/6J background using Affymetrix 430 2.0 microarrays.**

Background corr dist: KL-Divergence = 0.0198, L1-Distance = 0.0107, L2-Distance = 0.0001, Normal std = 0.7416

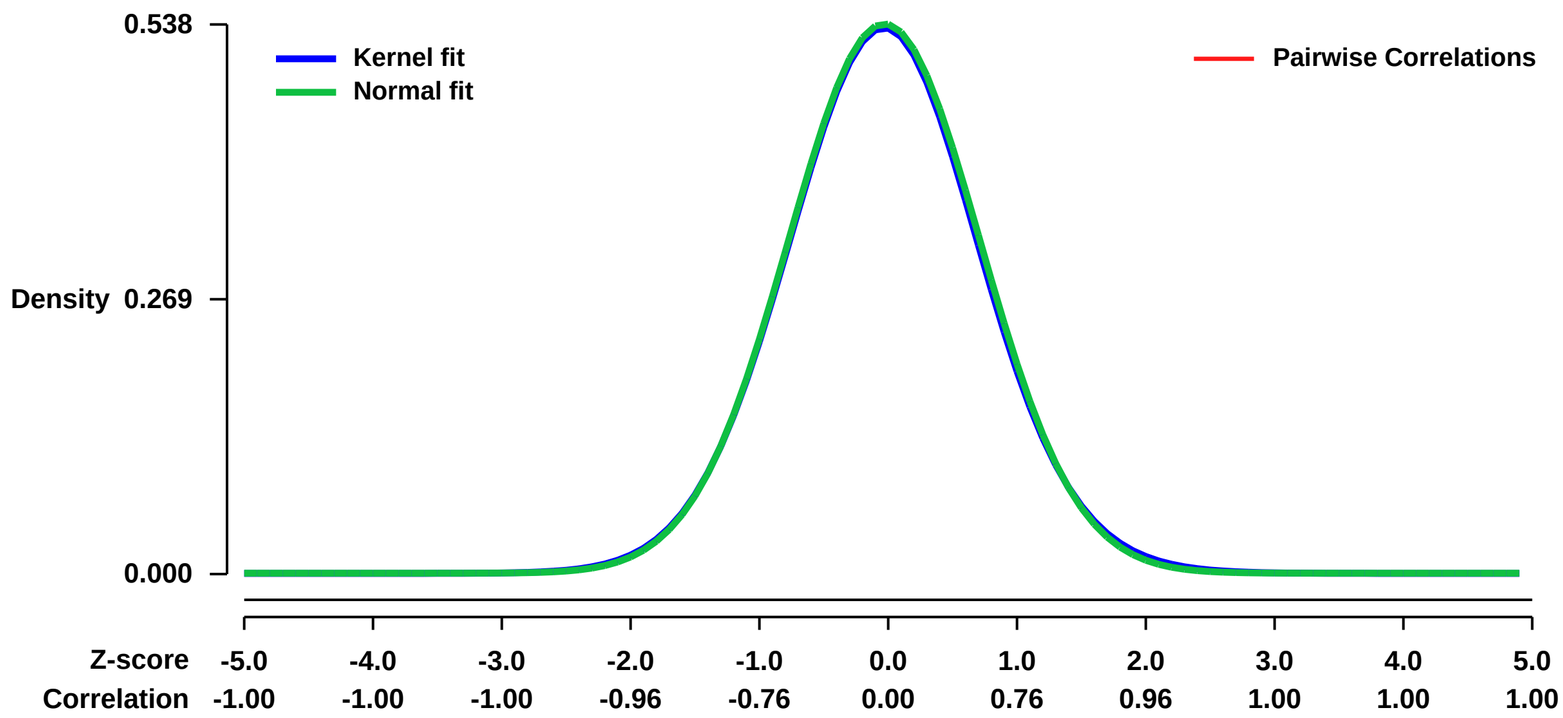

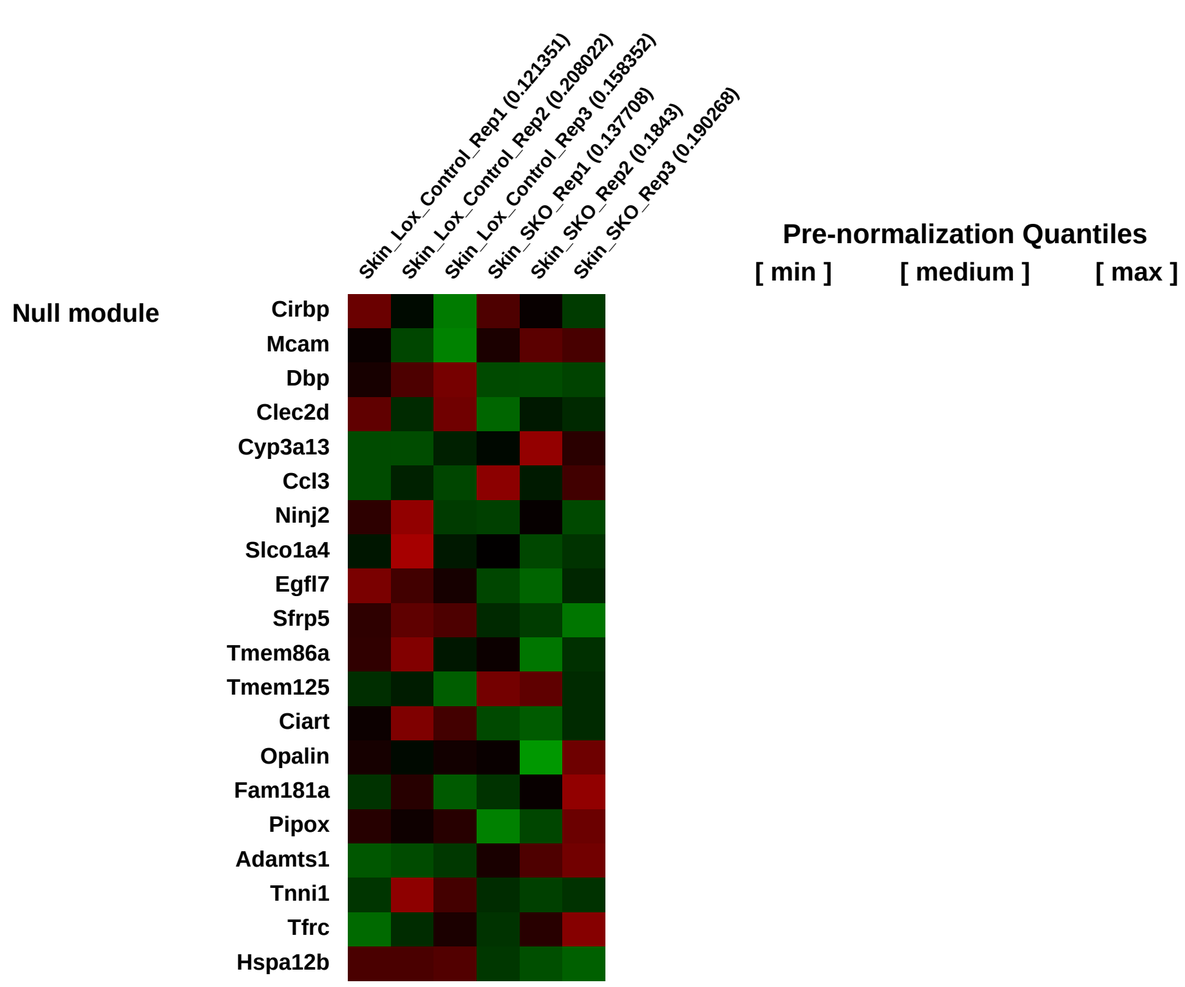

GEO Series "GSE24276" Expression Profiles

Num of samples in this series: 6

Scale of expression profile Z-scores

-3.0 -2.0 -1.0 0.0 1.0 2.0 3.0

GEO Link:	http://www.ncbi.nlm.nih.gov/geo/query/acc.cgi?acc=GSE24276
Status:	Public on Sep 22 2010
Title:	Fz1Fz2 double knock out mouse palate microarray (E13.5)
Organism:	Mus musculus
Experiment type:	Expression profiling by array
Platform:	GPL1261
Pubmed ID:	20940229
Summary & Design:	**Summary:** The closure of an open anatomical structure by the directed growth and fusion of two tissue masses is a recurrent theme in mammalian embryology, and this process plays an integral role in the development of the palate, ventricular septum, neural tube, urethra, diaphragm, and eye. In mice, targeted mutations of the genes encoding frizzled1 (Fz1) and frizzled2 (Fz2) show that these highly homologous integral membrane receptors play an essential and partially redundant role in closure of the palate and ventricular septum, and in the correct positioning of the cardiac outflow tract. When combined with a mutant allele of the planar cell polarity (PCP) gene Vangl2 (Vangl2Lp), Fz1 and/or Fz2 mutations also cause defects in neural tube closure and mis-orientation of inner ear sensory hair cells. These observations indicate that frizzled signaling is involved in diverse tissue closure processes, defects in which account for some of the most common congenital anomalies in humans. **Overall design:** Supplementary file below reports fold change data.

Background corr dist: KL-Divergence = 0.0240, L1-Distance = 0.0129, L2-Distance = 0.0002, Normal std = 0.7002

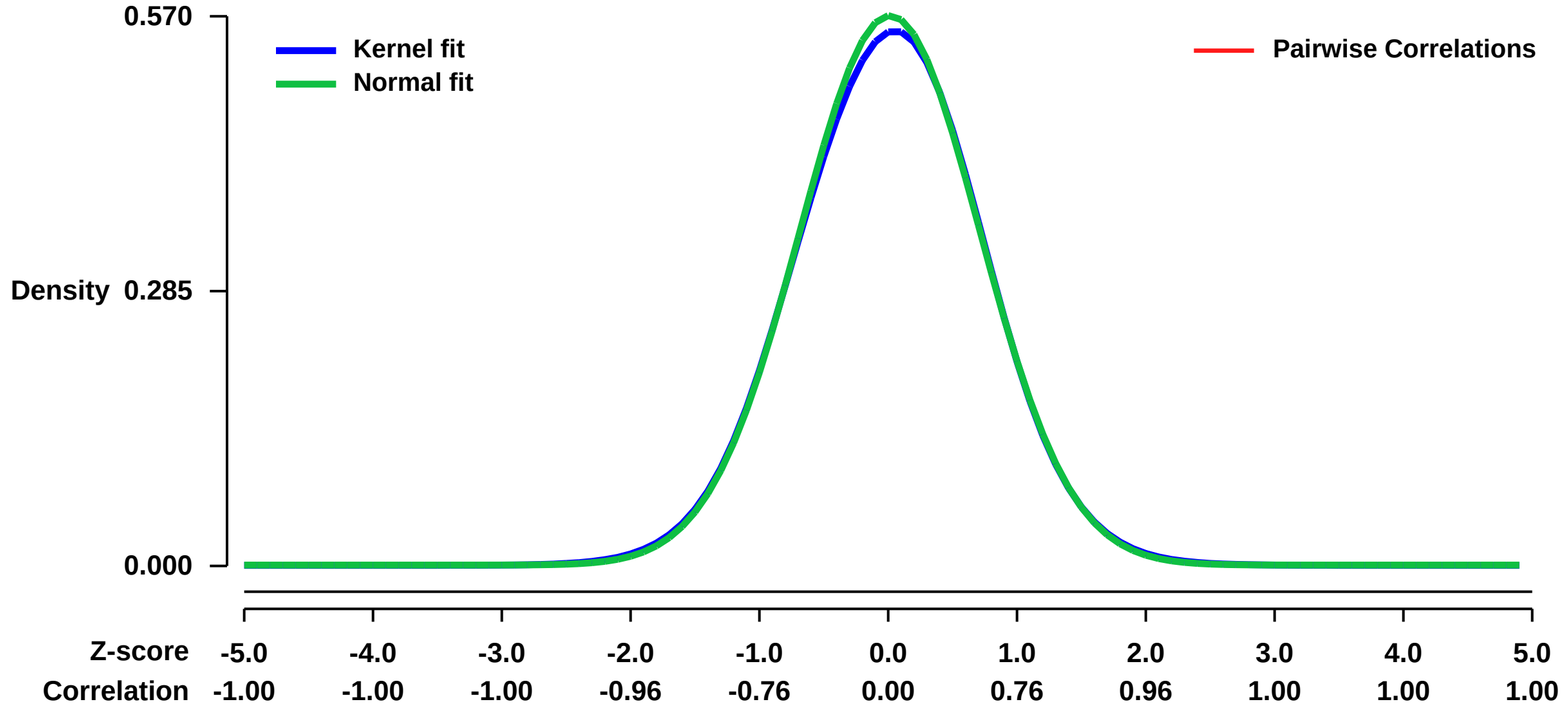

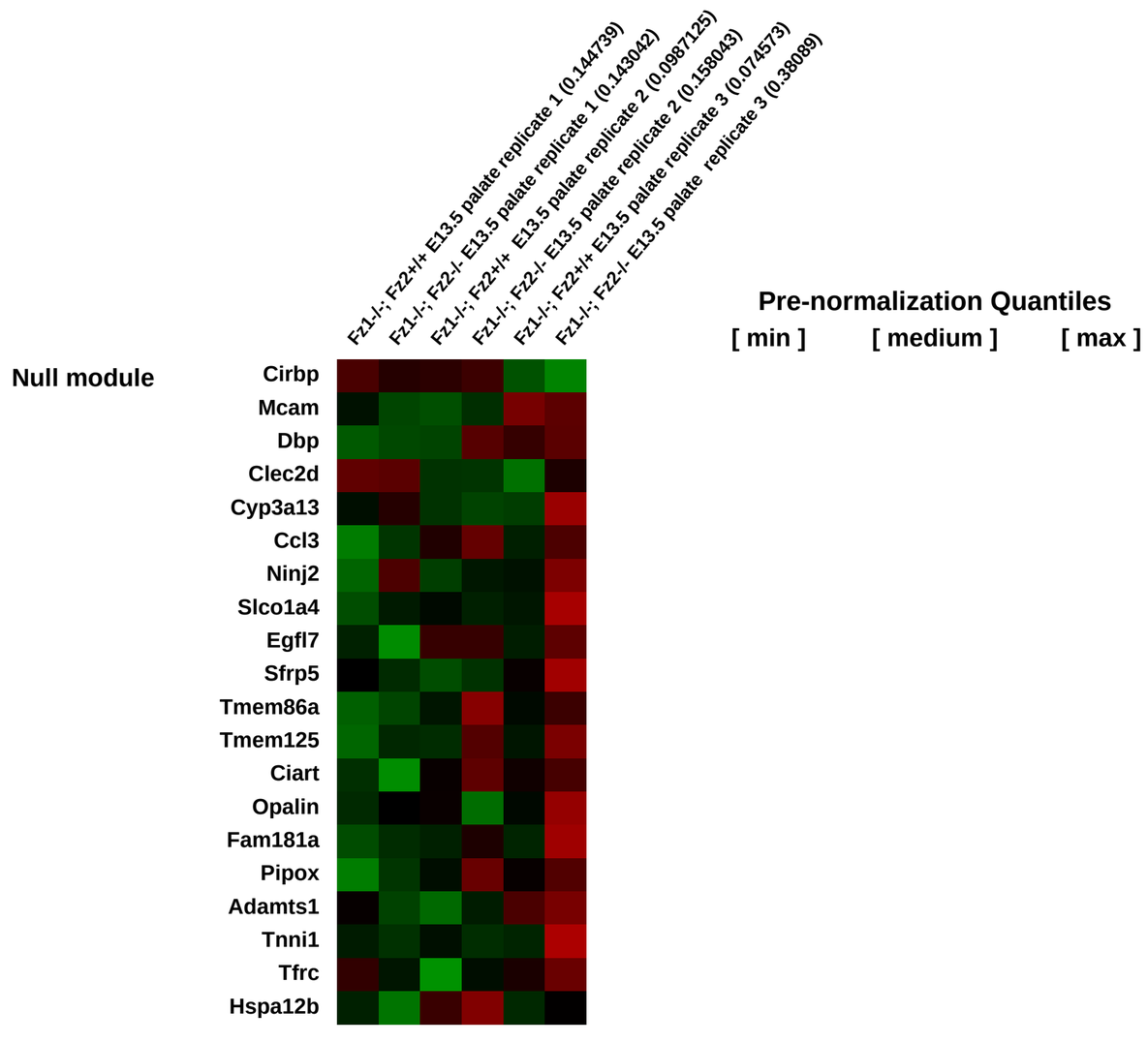

GEO Series "GSE24289" Expression Profiles

Num of samples in this series: 6

Scale of expression profile Z-scores

-3.0 -2.0 -1.0 0.0 1.0 2.0 3.0

GEO Link:	http://www.ncbi.nlm.nih.gov/geo/query/acc.cgi?acc=GSE24289
Status:	Public on Sep 22 2011
Title:	Expression data from differentiating ES cells expressing miR-200c and miR-141
Organism:	Mus musculus
Experiment type:	Expression profiling by array
Platform:	GPL1261
Pubmed ID:	
Summary & Design:	**Summary:** ES cells express the miR-200 family which becomes down-regulated during the course of differentiation in serum. We generated an ES cell line which expresses miR-200c and miR-141 upon addition of doxycycline. Microarrays were used to gain a global picture of differentiation when miR-200c and miR-141 expression were maintained throughout differentiation through the addition of doxycycline. **Overall design:** A2.miR200c ES cells, which express miR-200c/miR-141 upon addition of doxycycline, were differentiated as embryoid bodies in six petri dishes. Half of the samples were treated with doxycycline on both days 2 and 4 of differentiation, and RNA was collected from all samples on days 3, 4, and 5.

Background corr dist: KL-Divergence = 0.0303, L1-Distance = 0.0253, L2-Distance = 0.0007, Normal std = 0.6791

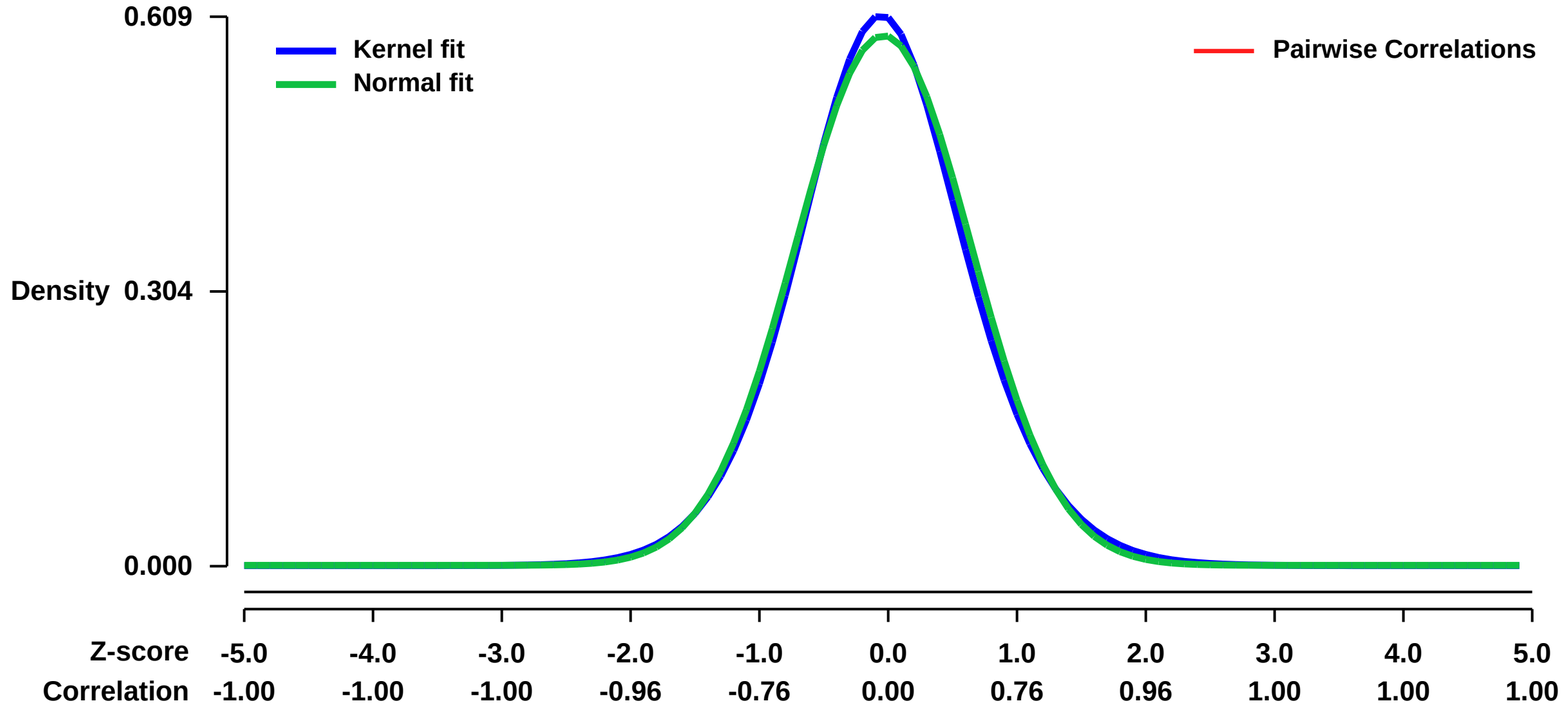

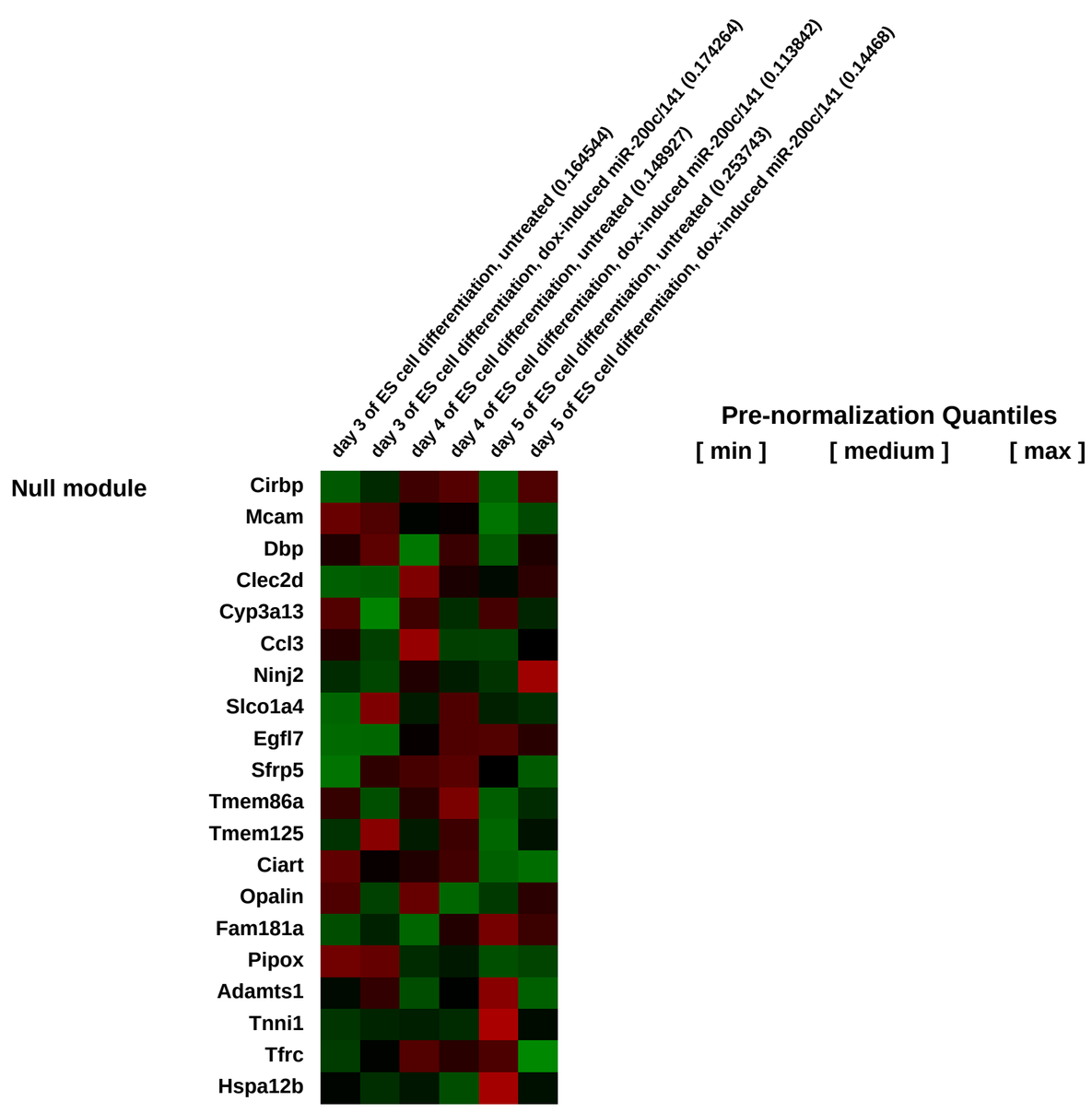

GEO Series "GSE24291" Expression Profiles

Num of samples in this series: 6

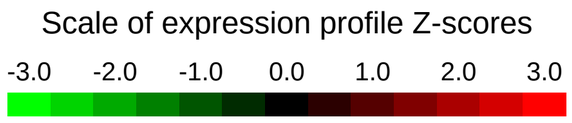

GEO Link:	http://www.ncbi.nlm.nih.gov/geo/query/acc.cgi?acc=GSE24291
Status:	Public on Sep 22 2011
Title:	Expression data from differentiating ES cells expressing Snail during Wnt inhibition
Organism:	Mus musculus
Experiment type:	Expression profiling by array
Platform:	GPL1261
Pubmed ID:	21394833
Summary & Design:	**Summary:** ES cells differentiated in the presence of the Wnt inhibitor DKK1 fail to express the transcription factor Snail and undergo EMT. We generated an ES cell line, A2.snail, that induced Snail expression upon addition of doxycycline addition. Microarrays were used to gain a global picture of ES cell differentiation at early timepoints after Snail was expressed during Wnt inhibition. **Overall design:** A2.snail ES cells, which express Snail upon addition of doxycycline, were differentiated as embryoid bodies in differentiation media and DKK1. Total RNA was harvested from control (no doxycycline) and Snail-induced (doxycycline at day 2) cultures at 6, 12, and 24 hours after doxycycline addition (corresponding to days 2.25, 2.5, and 3 of differentiation).

Background corr dist: KL-Divergence = 0.0278, L1-Distance = 0.0167, L2-Distance = 0.0003, Normal std = 0.6839

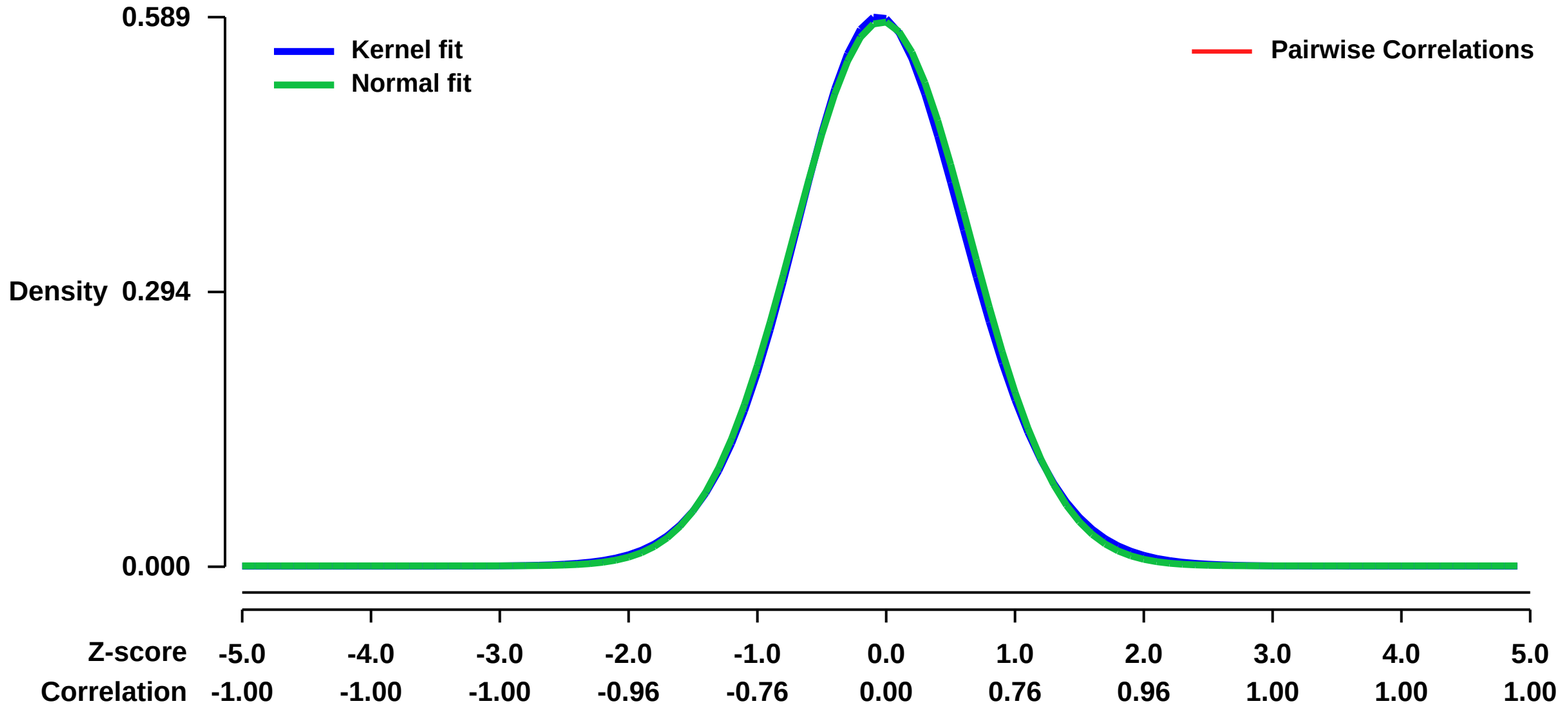

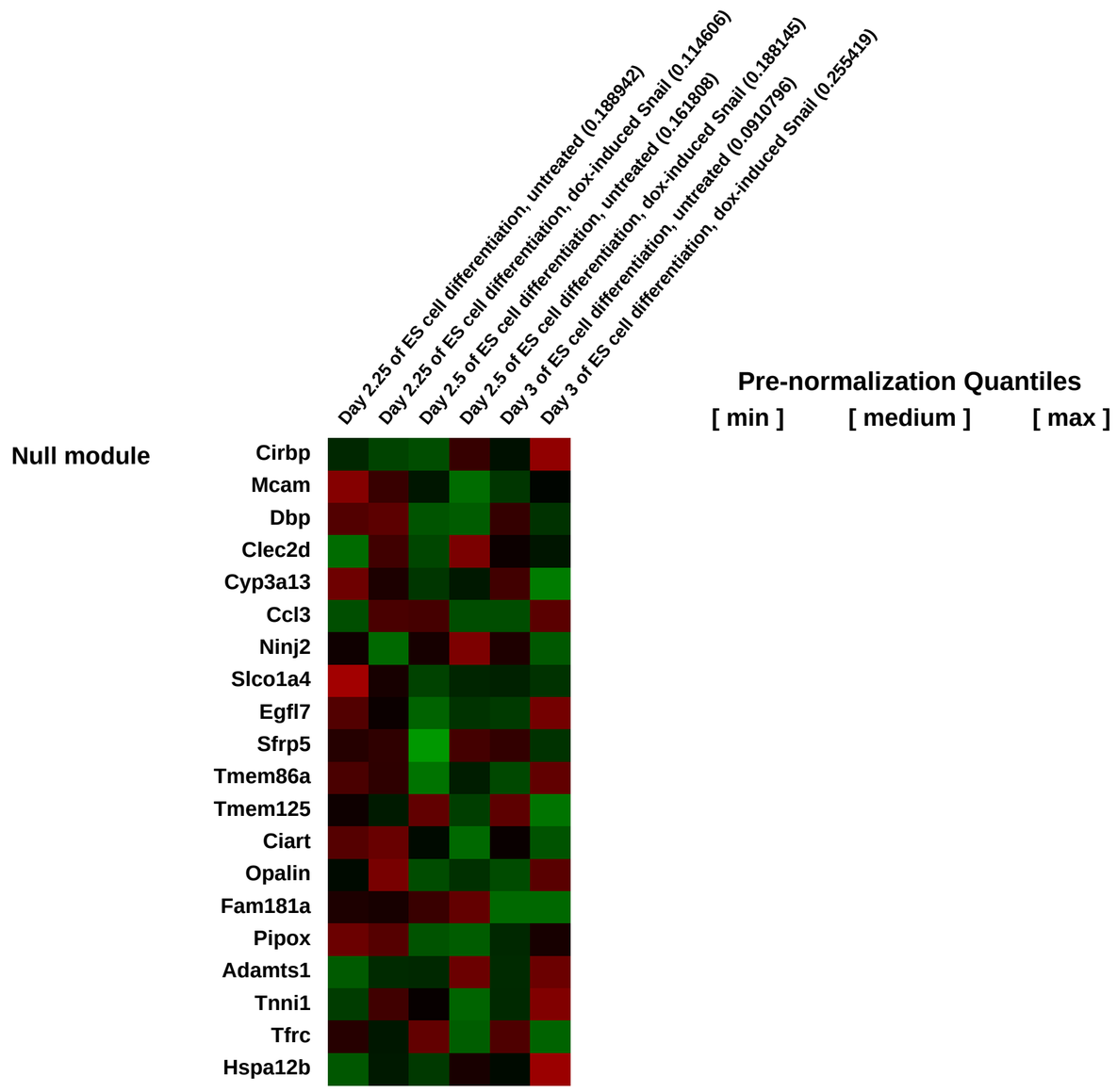

GEO Series "GSE2433" Expression Profiles

Num of samples in this series: 10

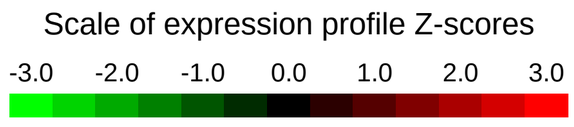

GEO Link:	**http://www.ncbi.nlm.nih.gov/geo/query/acc.cgi?acc=GSE2433**
Status:	**Public on May 14 2005**
Title:	**Expression profiling of GATA-1 wild type and mutant fetal megakaryocytes**
Organism:	**Mus musculus**
Experiment type:	**Expression profiling by array**
Platform:	**GPL1261**
Pubmed ID:	**15895080**
Summary & Design:	**Summary:**

Background:

Children with Down syndrome (DS) are predisposed to acute megakaryoblastic leukemia (AMKL, or AML M7) and a related myeloid disorder, referred to as transient myeloproliferative disorder (TMD), or transient leukemia (TL). Recently, acquired mutations in the erythroid/megakaryocytic lineage-specific transcription factor GATA-1 have been identified in megakaryoblasts from virtually all DS patients with AMKL (DS-AMKL), as well as in nearly all DS neonates with TMD. These mutations prevent synthesis of full-length GATA-1, but lead to synthesis of a truncated GATA-1 protein (GATA-1s) that lacks the N-terminal transactivation domain.

To determine the in vivo requirement of GATA-1 N-terminal domain in hematopoiesis and to model DS megakaryocytic leukemia initiated by GATA-1 mutation, we generated a GATA-1 knockin allele with a truncation at this domain (GATA-1deltaN). ES cells bearing this mutant allele generated a unique type of large Thrombopoietin (Tpo)-dependent megakaryocytes-containing colonies, when differentiated in vitro. Fetal livers from mice carrying this mutant allele contained elevated numbers of CD41+ cells throughout embryonic development, especially during mid-gestation. In in vitro hematopoietic colony assays, mutant cells from yolk sacs and mid-gestation fetal livers gave rise to a large number of macroscopic hyperproliferative megakaryocytic colonies (CFU-MKs). Consistent with that, when mutant fetal liver progenitors were cultured in liquid medium in the presence of Tpo, the derived megakaryocytes displayed marked hyperproliferation and grew for longer period of time than WTs.

Specific aims:

To understand the molecular basis for the megakaryocytic hyperproliferation phenotype of the GATA-1deltaN mutants, we plan to profile gene expression patterns of fetal liver-derived primary megakaryocytes and megakaryocytic progenitors from the GATA-1deltaN mutants and compare them with WTs, as well as GATA-1deltaNeodeltaHS mutants (GATA-1â megakaryocytes).

Experimental design:

E12.5 fetal livers were harvested from either GATA-1 WT and mutant embryos. Single cell suspensions were made from these livers and the cells were cultured in liquid medium in the presence of Tpo for 3 days. On day 3, primary megakaryocytes were enriched by a BSA gradient, and further enriched by anti-CD41 antibody and magnetic microbeads. Megakaryocytic progenitors were collected by FACS sorting for small cells in the same culture that express low level of CD41. Total RNAs were then prepared from these two populations and submitted for microarray profiling.

Conclusions:

When examining genes that are normally upregulated upon megakaryocyte differentiation (many of this class are megakaryocyte-specific genes), we found in GATA-1deltaN megakaryocytes, the majority of these genes are upregulated, although not to the full extent as seen in WTs. In contrast, this class of genes is largely not upregulated in GATA-1deltaNeodeltaHS megakaryocytes, which are blocked at an immature stage of differentiation. Genes that are downregulated during megakaryocyte differentiation include those that are normally repressed by GATA-1. Among genes that are not properly downregulated in GATA-1deltaN megakaryocytes, five transcription factors (Myc, Myb, GATA-2, PU.1, Ikaros) are of particular interest. Inadequate GATA-1s-mediated repression of transcription factors required for proliferation of hematopoietic progenitors (Myc, Myb and GATA-2) and for specifying lineage choices other than megakaryocyte/erythrocyte (PU.1 and Ikaros) may contribute to hyperproliferation of GATA-1deltaN megakaryocytes.

Keywords = GATA-1

Keywords = megakaryocyte

Keywords = mouse model

Keywords: other

Overall design:

Background corr dist: KL-Divergence = 0.0391, L1-Distance = 0.0161, L2-Distance = 0.0003, Normal std = 0.6072

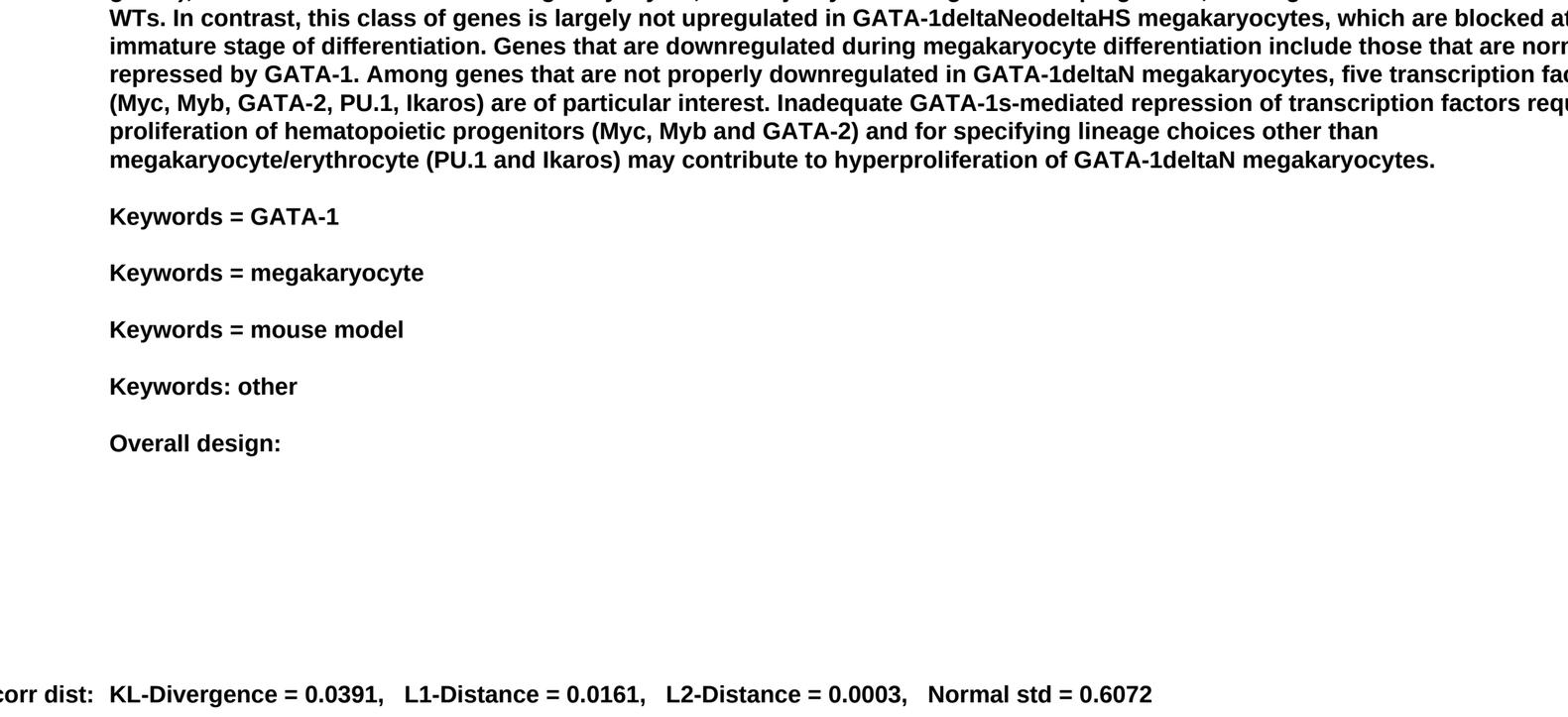

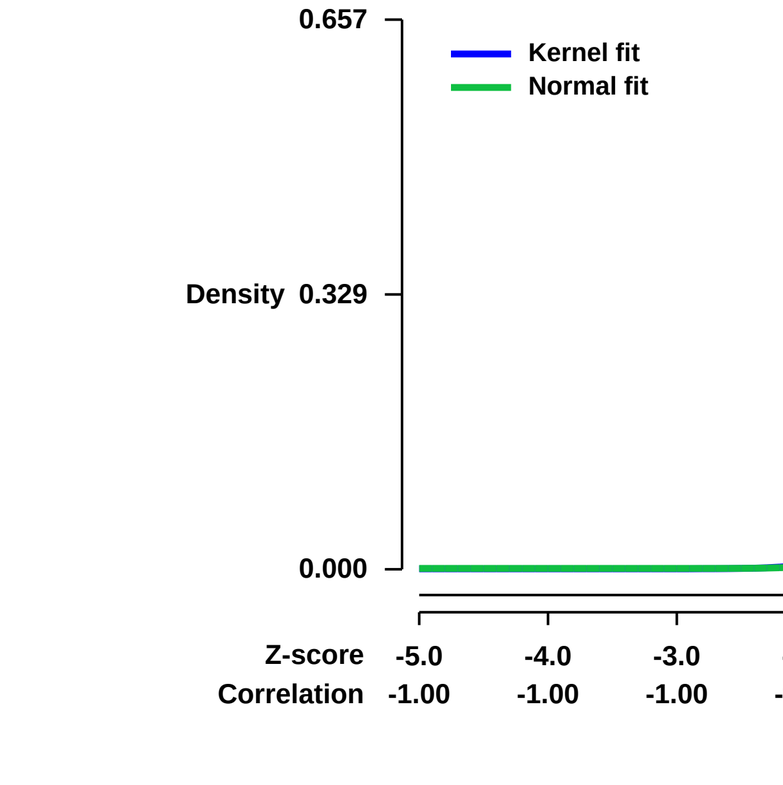

GEO Series "GSE24350" Expression Profiles

Num of samples in this series: 8

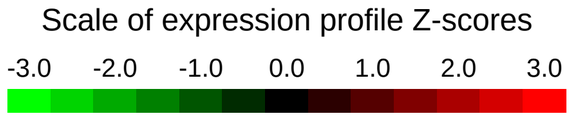

GEO Link:	**http://www.ncbi.nlm.nih.gov/geo/query/acc.cgi?acc=GSE24350**
Status:	**Public on Sep 28 2010**
Title:	**Expression data from peptidoglycan stimulated CD11b+ cells from NOD and NOD.Idd3**
Organism:	**Mus musculus**
Experiment type:	**Expression profiling by array**
Platform:	**GPL1261**
Pubmed ID:	
Summary & Design:	**Summary:** **CD11b+ CD11c- cells were isolated by cell sorting from the spleens of NOD and NOD.Idd3 mice. Cells were then either unstimulated or stimulated with peptidoglycan (5ug/ml) for 4 hours at 37 degrees prior to RNA extraction. Peptidoglycan was chosen as a stimulus due to its know ability to stimulate CD11b+ cells through Toll-like receptor 2 and our previous data showing biological differences between NOD and NOD.Idd3-derived CD11b+CD11c- cells after stimulation with peptidoglycan.** **Overall design:** **CD11b+ cells from NOD and NOD.Idd3 were either unstimulated or stimulated with peptidoglycan(PGN) for 4 hours at 37 degerees prior to RNA extraction.**

Background corr dist: **KL-Divergence = 0.0550, L1-Distance = 0.0253, L2-Distance = 0.0010, Normal std = 0.5461**

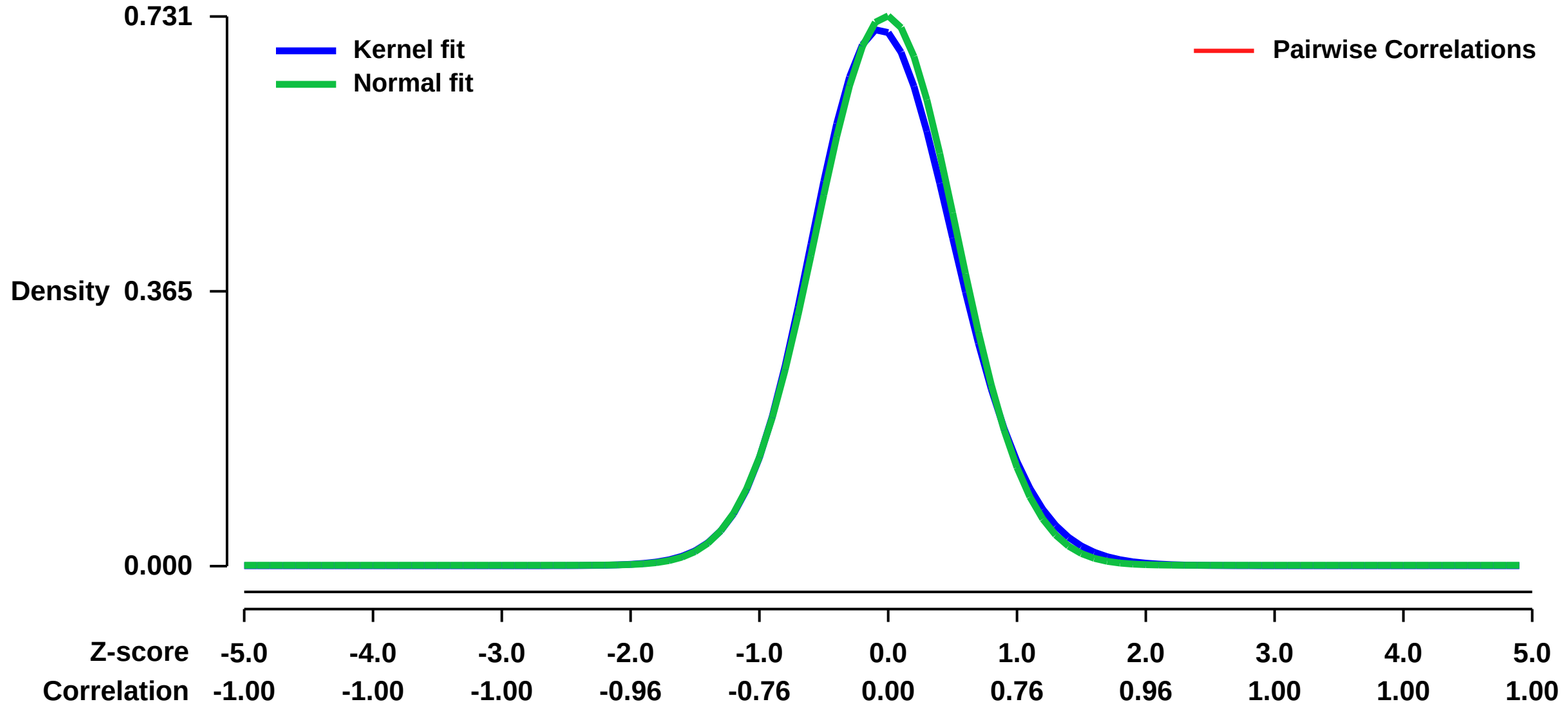

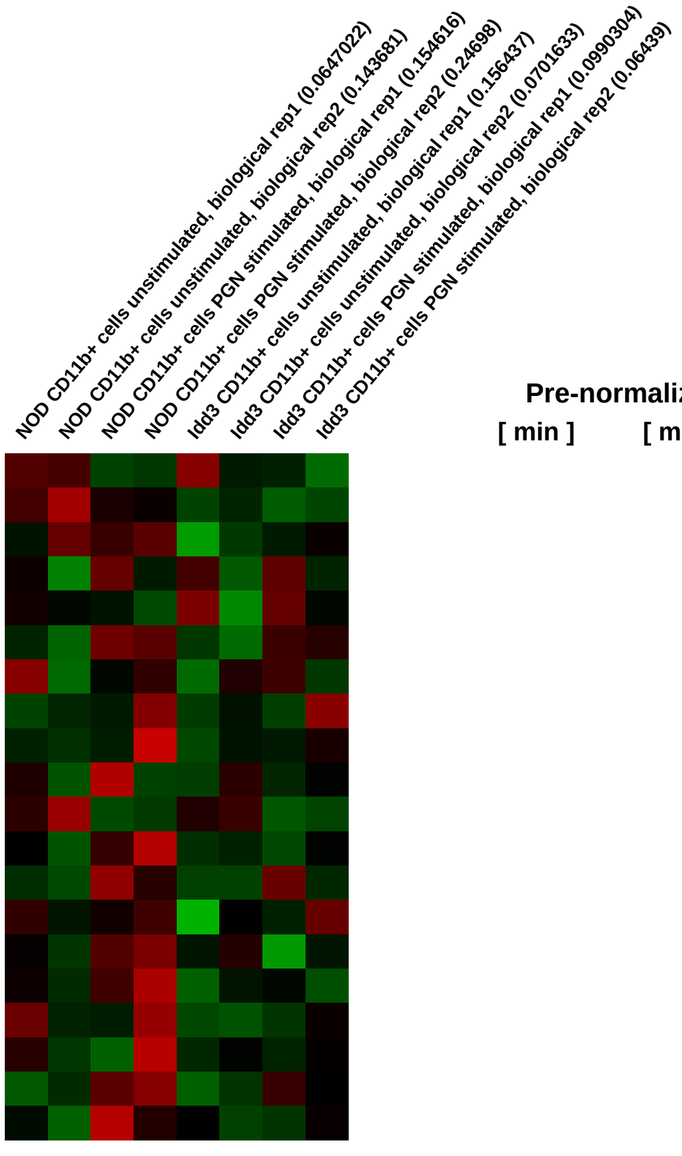

GEO Series "GSE24437" Expression Profiles

Num of samples in this series: 6

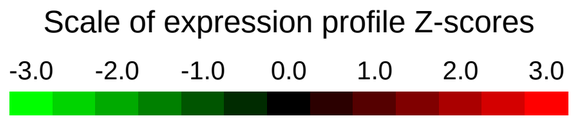

GEO Link:	http://www.ncbi.nlm.nih.gov/geo/query/acc.cgi?acc=GSE24437
Status:	Public on Sep 30 2010
Title:	Persistence of effector memory Th1 cells is regulated by the homeobox only protein Group1 Hopx-/-, Group2 Hopx+/-, Group3 Hopx+/+
Organism:	Mus musculus
Experiment type:	Expression profiling by array
Platform:	GPL1261
Pubmed ID:	19265543
Summary & Design:	**Summary:** Hopx appears to be needed for persistence of Th1 effector memory cells. IFN-gamma-producing Th cells are significantly reduced in Hopx-deficient mice compared to Hopx-expressing littermates and Hopx-deficient Th1 cells show a defective persistence upon adoptive transfer. Moreover, Hopx protects Th1 cells from Fas-mediated cell death in vitro. To further dissect the role of Hopx and to identify target genes of Hopx, we have performed transcriptome analysis to compare gene expression in Hopx-deficient versus Hopx-competent Th1 cells. In agreement with the role of Hopx in supporting survival of Th1 effector memory cells, anti-apoptotic cells were up-regulated and pro-apoptotic genes were down-regulated in Hopx-competent compared to Hopx-deficient Th1 cells. **Overall design:** Gene expression profiles of Hopx-/- versus Hopx+/- and Hopx+/+ Th1 cells, respectively. Naˆflve Th cells were isolated from Hopx+/+, Hopx+/- and Hopx-/- OT2 mice and activated in vitro with their cognate antigen (OVA) under Th1 polarizing conditions. On day 6, viable cells were repeatedly activated. On day 12, viable cells were harvested and compared using Affymetrix 430A Version 2 GeneChip arrays. After total RNA extraction, reverse transcription, cDNA extraction, the biotinylated cRNA was transcribed, fragmented, and 15 ´µg cRNA hybridized in duplicates for each of the three groups to the GeneChip arrays. Group1: Hopx-/-, Group2: Hopx+/-, Group3: Hopx+/+. Lists of differentially regulated genes were created using High Performance Chip Data Analysis (HPCDA) with Bioretis database (http://www.bioretis-analysis.de). Worldwide data sharing is possible via Bioretis, please ask the authors.

Background corr dist: KL-Divergence = 0.0490, L1-Distance = 0.0373, L2-Distance = 0.0024, Normal std = 0.5962

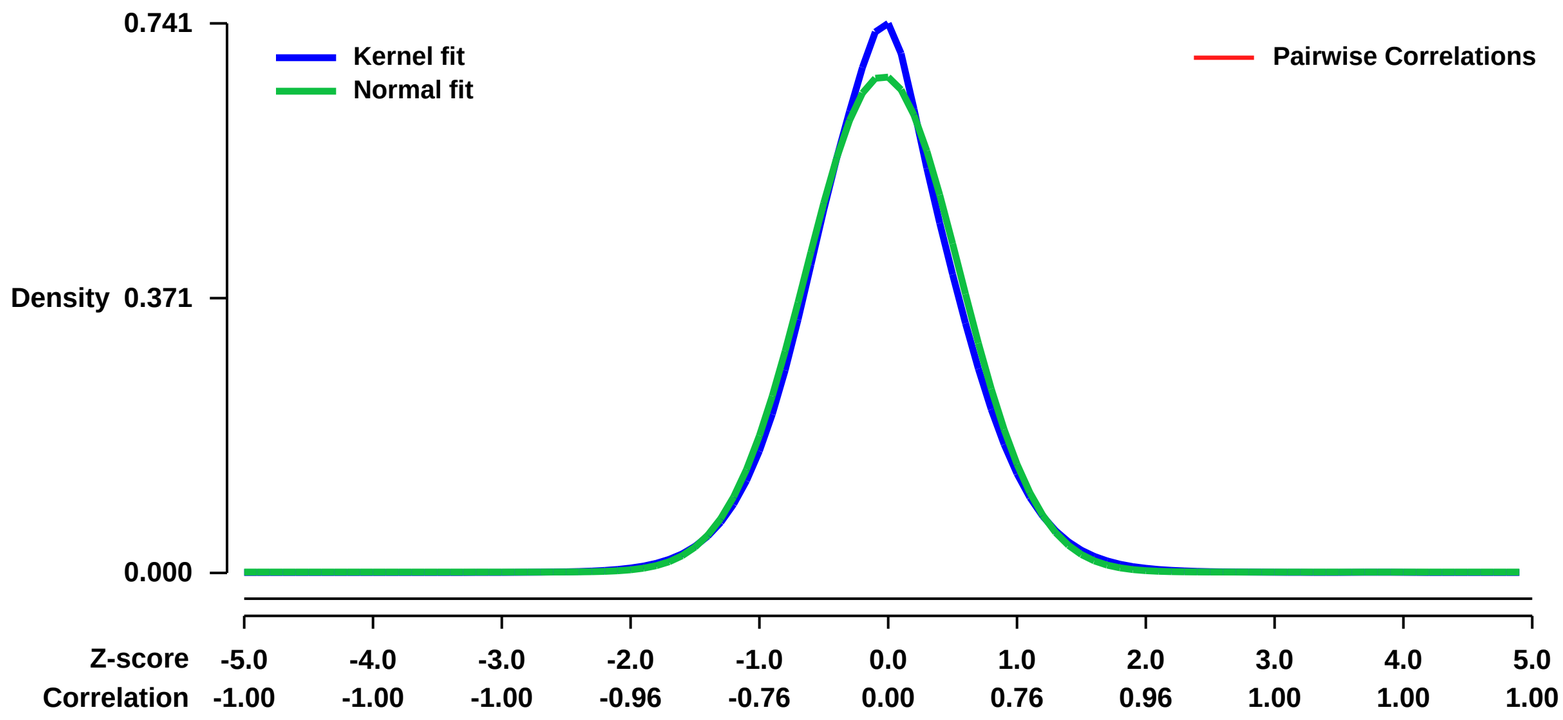

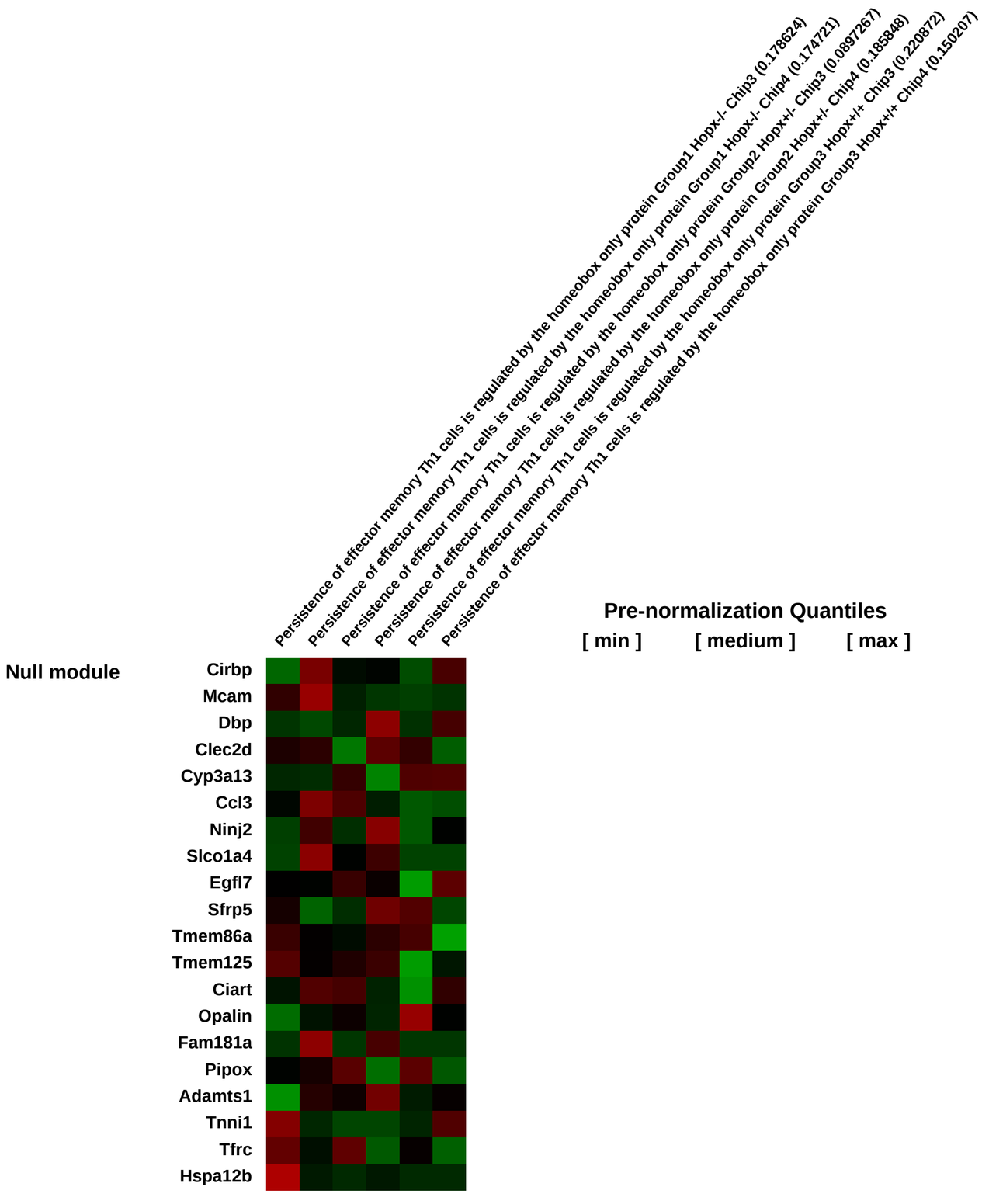

GEO Series "GSE24451" Expression Profiles

Num of samples in this series: 6

Scale of expression profile Z-scores

-3.0 -2.0 -1.0 0.0 1.0 2.0 3.0

GEO Link:	http://www.ncbi.nlm.nih.gov/geo/query/acc.cgi?acc=GSE24451
Status:	Public on Nov 26 2010
Title:	Knockout of the Acyl CoA binding protein (ACBP) in mice - expression profile from the liver of 21 days old ACBP-/- and +/+ mice.
Organism:	Mus musculus
Experiment type:	Expression profiling by array
Platform:	GPL1261
Pubmed ID:	21106527
Summary & Design:	**Summary:** The ACBP knockout were created by targeted disruption of the gene in mice. The expression profiling was performed on liver tissue from ACBP-/- (KO) and +/+ (WT) mice at the age of 21 days, which in our study is the time immediately before weaning. The mice used for this experiment were taken directly away from their mother. Thus, having free access to chow and breast milk until sacrificed at 8-11am **Overall design:** 15 ACBP-/- and 15 +/+ control mice divided into 6 groups (KO1, KO2, KO3, WT1, WT2 and WT3) with 5 individuals in each group were used for this study.

Background corr dist: KL-Divergence = 0.0405, L1-Distance = 0.0171, L2-Distance = 0.0003, Normal std = 0.6111

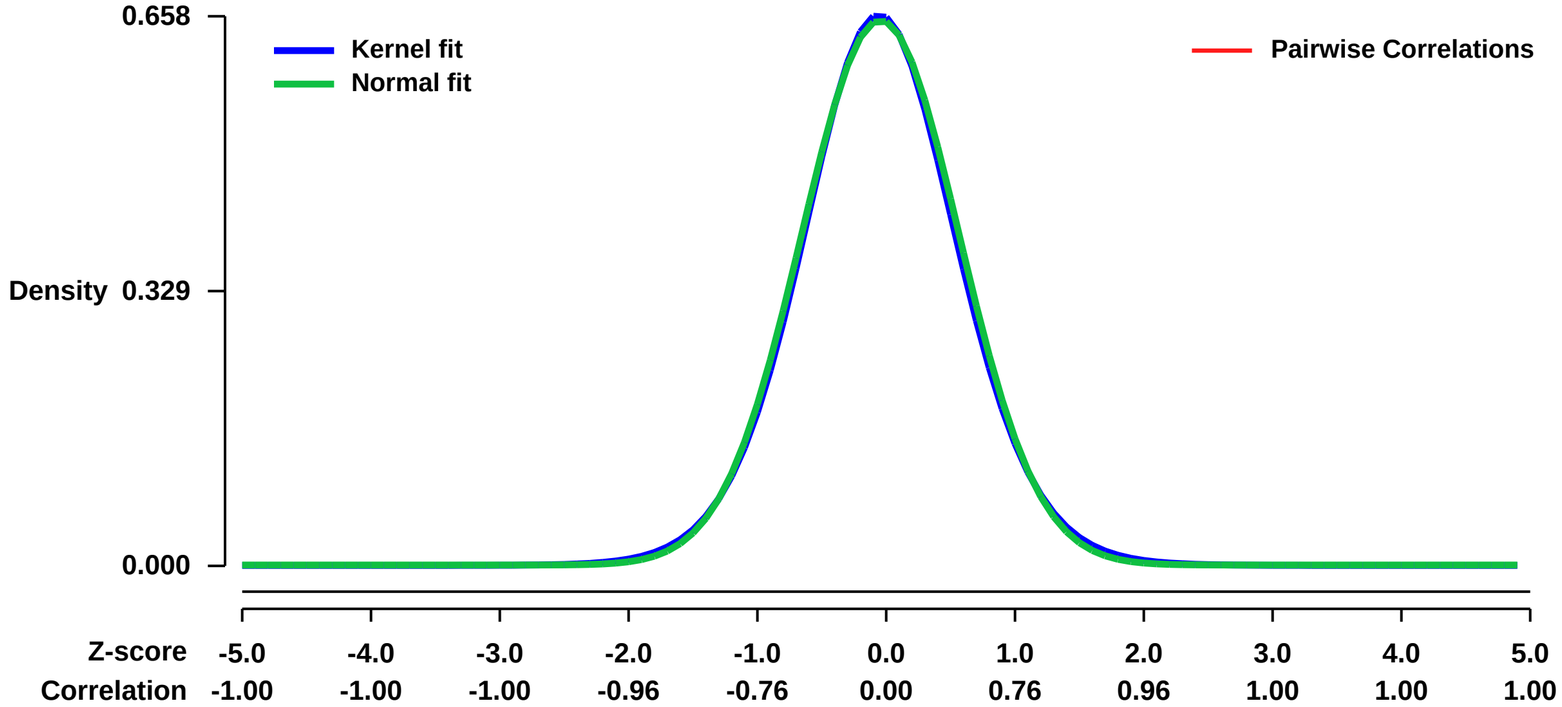

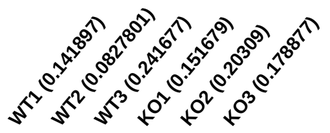

Pre-normalization Quantiles

[min] [medium] [max]

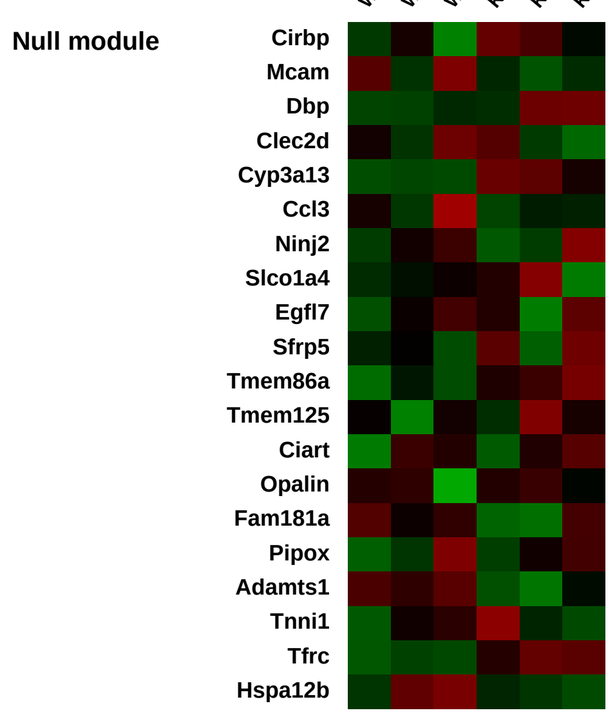

GEO Series "GSE24465" Expression Profiles

Num of samples in this series: 6

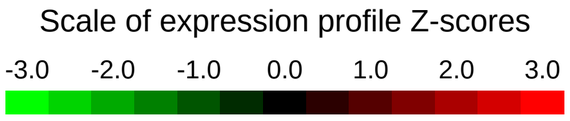

GEO Link:	http://www.ncbi.nlm.nih.gov/geo/query/acc.cgi?acc=GSE24465
Status:	Public on Sep 29 2011
Title:	Mesenchymal Nuclear factor I B regulates cell proliferation and epithelial differentiation during lung maturation
Organism:	Mus musculus
Experiment type:	Expression profiling by array
Platform:	GPL1261
Pubmed ID:	
Summary & Design:	**Summary:** We generated Nfibf/f mice and then cross with Dermo1-Cre mice to obtain Nfibf/f, Dermo1-Cre mice. In these Nfibf/f, Dermo1-Cre mice, there are defects in sacculation and epithelial cell differentiation. We performed micoarray analysis to find the genes which are possibley regulated by NFI-B and related to lung maturation during lung development. **Overall design:** We used microarrays to performing transcriptional profiling of Nfibf/f, Dermo1-Cre and Nfibf/f lungs at E18.5

Background corr dist: KL-Divergence = 0.0391, L1-Distance = 0.0205, L2-Distance = 0.0004, Normal std = 0.6225

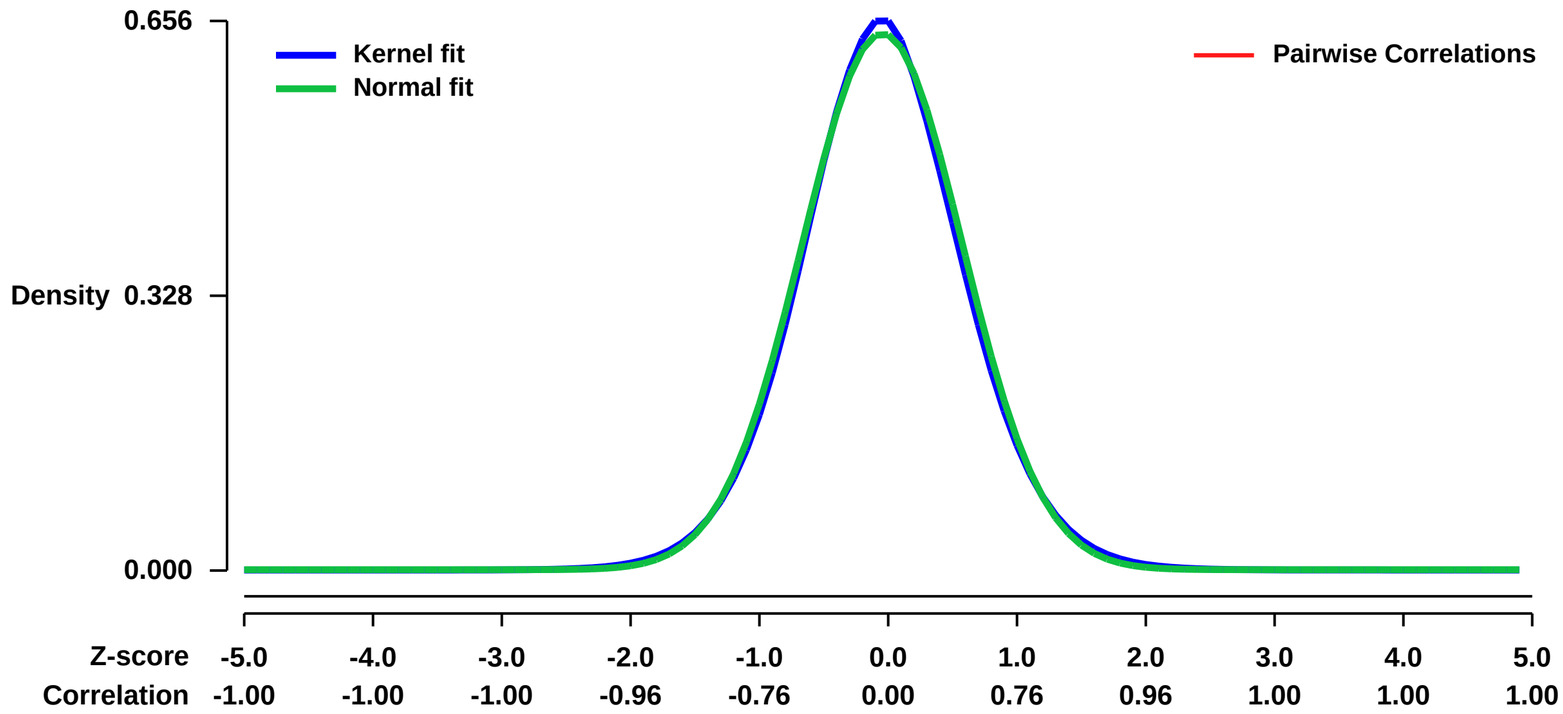

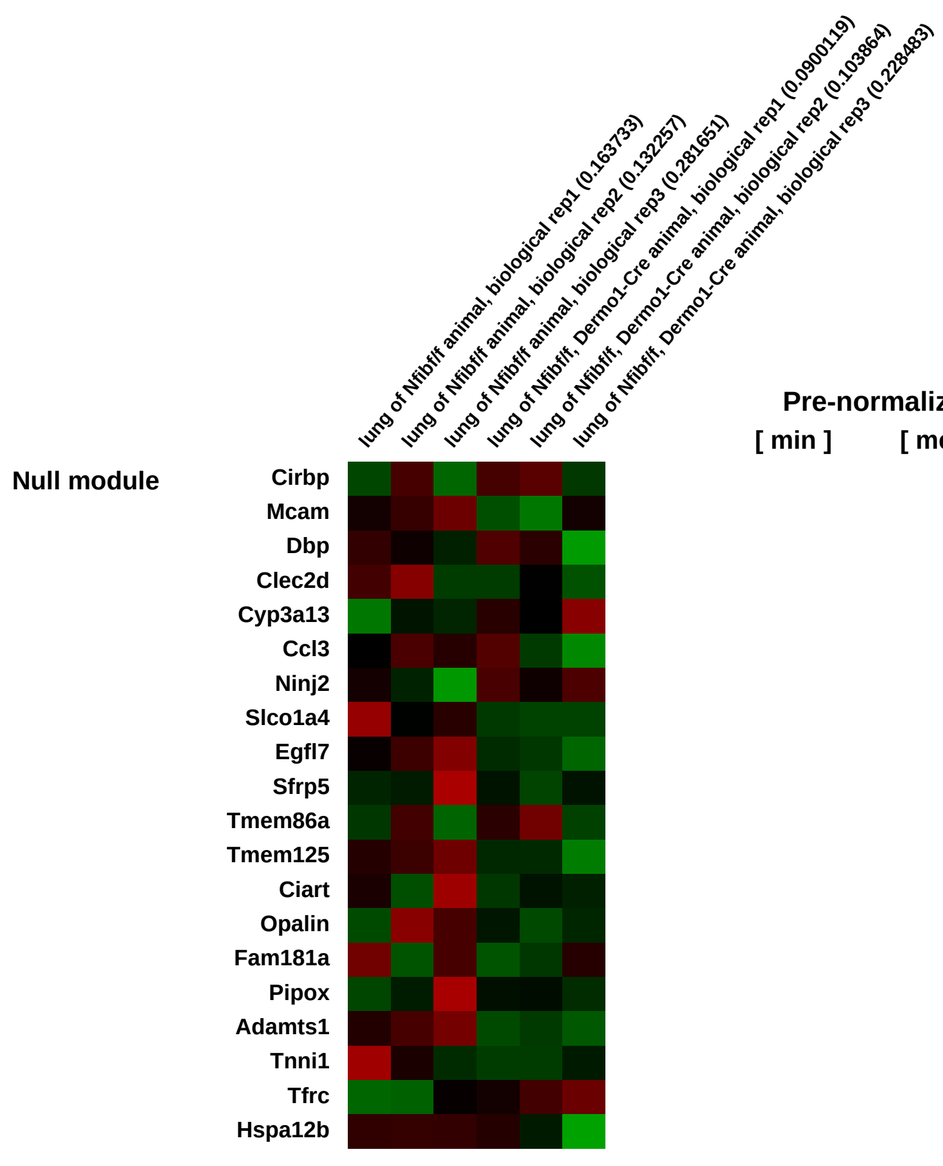

GEO Series "GSE24489" Expression Profiles

Num of samples in this series: 14

Scale of expression profile Z-scores

-3.0 -2.0 -1.0 0.0 1.0 2.0 3.0

GEO Link:	http://www.ncbi.nlm.nih.gov/geo/query/acc.cgi?acc=GSE24489
Status:	Public on Dec 31 2010
Title:	Effect of H11 Kinase/Hsp22 deletion in response to cardiac stress
Organism:	Mus musculus
Experiment type:	Expression profiling by array
Platform:	GPL1261
Pubmed ID:	21747053
Summary & Design:	**Summary:** The expression of the small molecular weight heat shock protein (Hsp) H11 kinase/Hsp22 (Hsp22) is restricted to a limited number of tissues, including the heart and skeletal muscle, both in rodents and in humans. We generated a mouse knockout (KO) model, and investigated the role of Hsp22 in regulating cardiac hypertrophy in response to pressure overload. We compared gene expression profiles between WT and KO mice in basal condition and three days pressure overload after transverse aortic constriction (TAC). These data illustrated a novel mechanism of Hsp22-related gene expression in response to cardiac stress. **Overall design:** We used microarray to examine differential gene expression by Hsp22 deletion at baseline and 3-day pressure overload. Left ventricles from wild type and Hsp22 knockout mice were selected from basal condition (each, n=3) and TAC surgery (each, n=4).

Background corr dist: KL-Divergence = 0.0453, L1-Distance = 0.0832, L2-Distance = 0.0130, Normal std = 0.6502

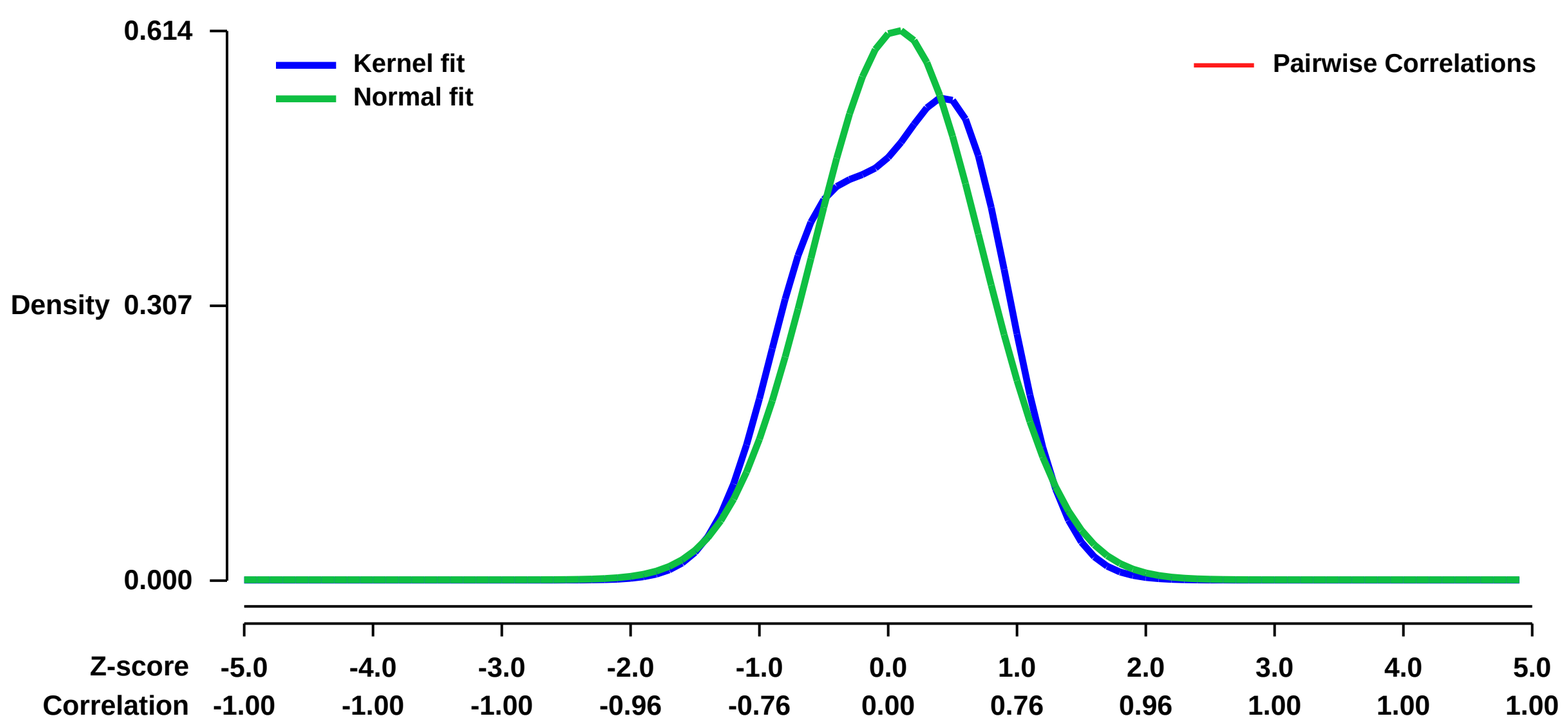

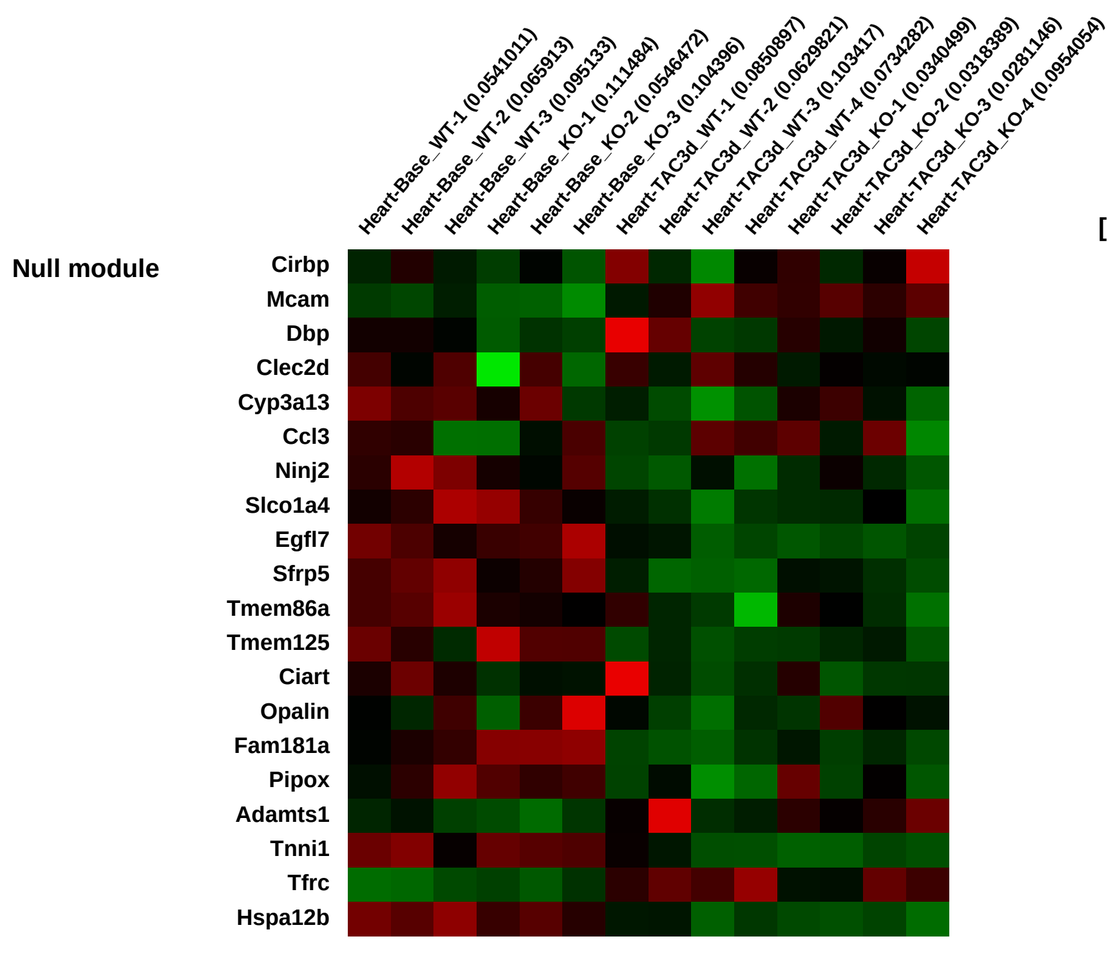

GEO Series "GSE24614" Expression Profiles

Num of samples in this series: 6

GEO Link:	**http://www.ncbi.nlm.nih.gov/geo/query/acc.cgi?acc=GSE24614**
Status:	**Public on Jun 15 2011**
Title:	**Variegated gene expression caused by cell-specific long-range DNA interactions**
Organism:	**Mus musculus**
Experiment type:	**Other**
Platform:	**GPL1261**
Pubmed ID:	**21706023**
Summary & Design:	**Summary:** **Mammalian genomes contain numerous DNA elements with potential transcription regulatory function but unknown target genes. We used transgenic, gain-of-function mice with an ectopic copy of the beta-globin locus control region (LCR) to better understand how regulatory elements dynamically search the genome for target genes. We find that the LCR samples a restricted nuclear sub-volume in which it forms preferential contacts with genes controlled by shared transcription factors. One contacted gene, betah1, located on another chromosome, is upregulated, providing genetic demonstration that mammalian enhancers can function between chromosomes. Upregulation is not pan-cellular but confined to selected â jackpotâ cells significantly enriched for inter-chromosomal LCR-betah1 interactions. This implies that long-range DNA contacts are relatively stable and cell-specific and, when functional, cause variegated expression. We refer to this as spatial effect variegation (SEV). The data provide a dynamic and mechanistic framework for enhancer action, important for assigning function to the one- and three-dimensional structure of DNA.** **Overall design:** **At the RNA level these mice were characterized with Affymetrix expression arrays. We analyzed three biological replicates for the WT and the knock-in.**

Background corr dist: **KL-Divergence = 0.0272, L1-Distance = 0.0584, L2-Distance = 0.0041, Normal std = 0.8832**

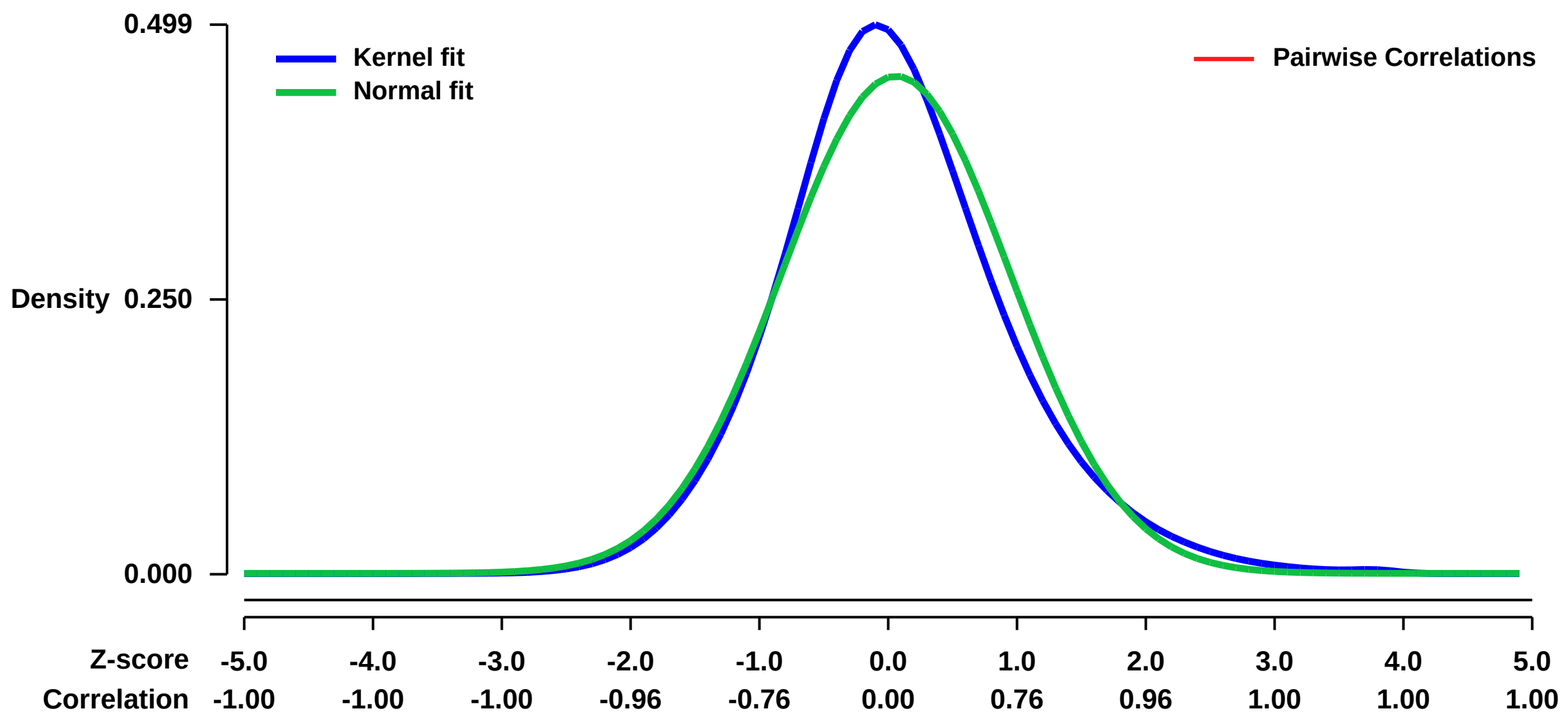

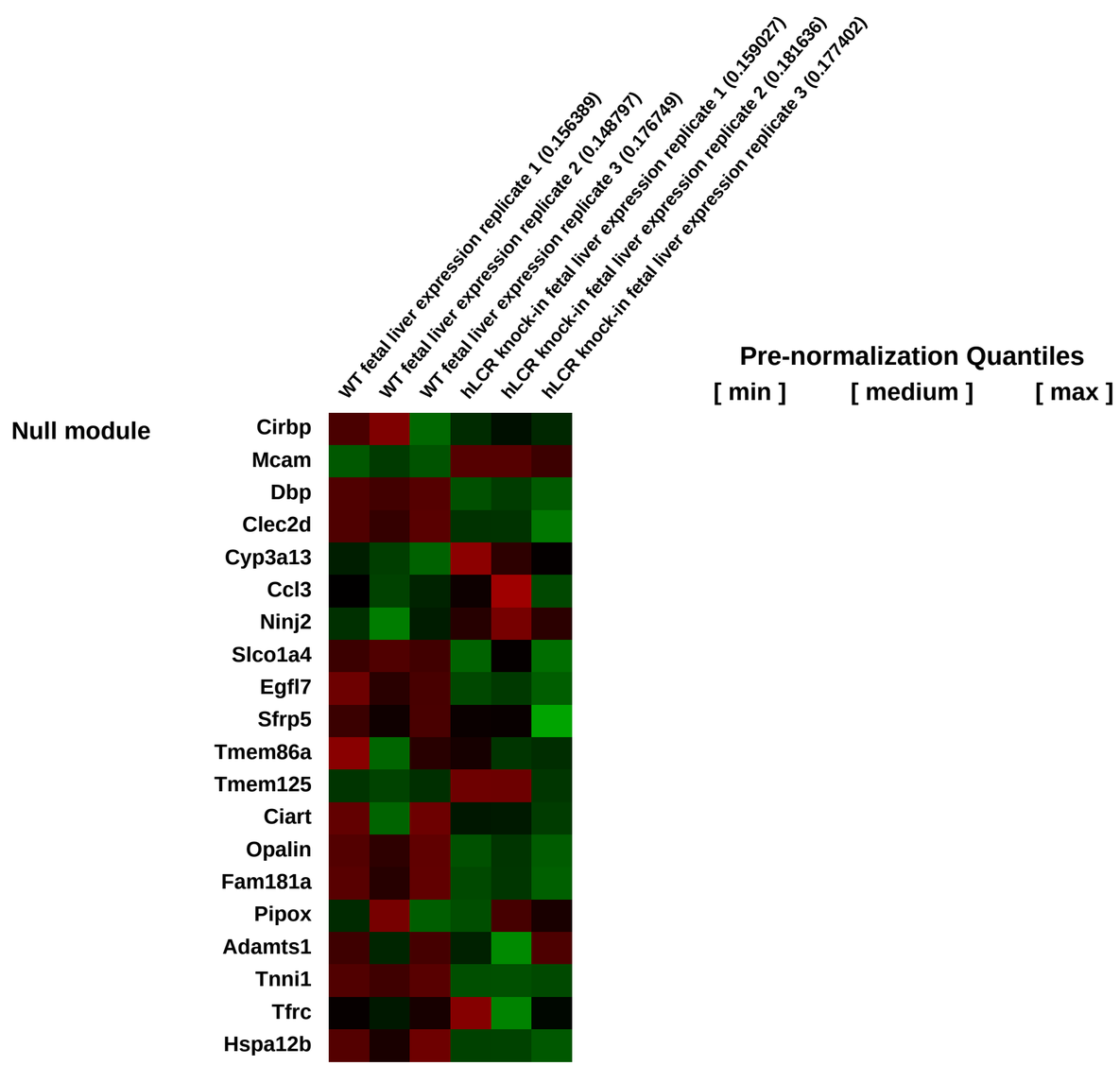

GEO Series "GSE24625" Expression Profiles

Num of samples in this series: 12

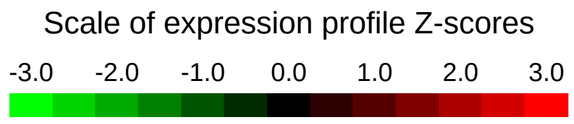

GEO Link:	http://www.ncbi.nlm.nih.gov/geo/query/acc.cgi?acc=GSE24625
Status:	Public on Jan 01 2012
Title:	Transcriptome in 129sv and Crx-/- pineal gland at ZT (Zeitgeber time) 6 and ZT20
Organism:	Mus musculus
Experiment type:	Expression profiling by array
Platform:	GPL1261
Pubmed ID:	21797868
Summary & Design:	**Summary:** The cone-rod homeobox gene (Crx) encodes Crx, a transcription factor selectively expressed in two cell types, retinal photoreceptors and the melatonin secreting pinealocytes of the pineal gland. In this report the role of Crx in regulating gene expression in the mammalian pineal gland was extended using Affymetrix GeneChip technology. Deletion of Crx results in broad modulation of the mouse pineal transcriptome, including a >2-fold downregulation of 543 genes and a >2-fold upregulation of 745 genes. In addition to Crx, there was a >10-fold downregulation of 13 other genes. Of special interest was the discovery of a link between Crx and the homeobox gene Hoxc4, which was upregulated ~20-fold in the Crx-/- pineal gland. Analysis of night and day expression of genes indicated that a set of 51 genes exhibited differential expression in control animals. Of these genes, only eight were also differentially expressed in Crx-/- animals. This group included Aanat, which encodes the enzyme that controls the daily rhythm in melatonin synthesis in the vertebrate pineal gland. Accordingly, Crx appears to be essential for the 24-hour rhythmic component of expression of some genes in the pineal gland. In the Crx-/- mouse pineal gland, 41 genes exhibited differential night/day expression that was not seen in control animals, suggesting that Crx may function to modulate rhythmic expression of these genes as well. Together, the results of this investigation indicate that Crx broadly modulates the pineal transcriptome, perhaps in part through suppressive effects on expression of the homeobox gene Hoxc4. **Overall design:** Log(2) fold change independently of time of day. Up regulated genes: genes which are up regulated in Crx-/- compared to the control; down regulated genes: genes which are down regulated in Crx-/- compared to the control.

Background corr dist: KL-Divergence = 0.0827, L1-Distance = 0.0236, L2-Distance = 0.0009, Normal std = 0.4734

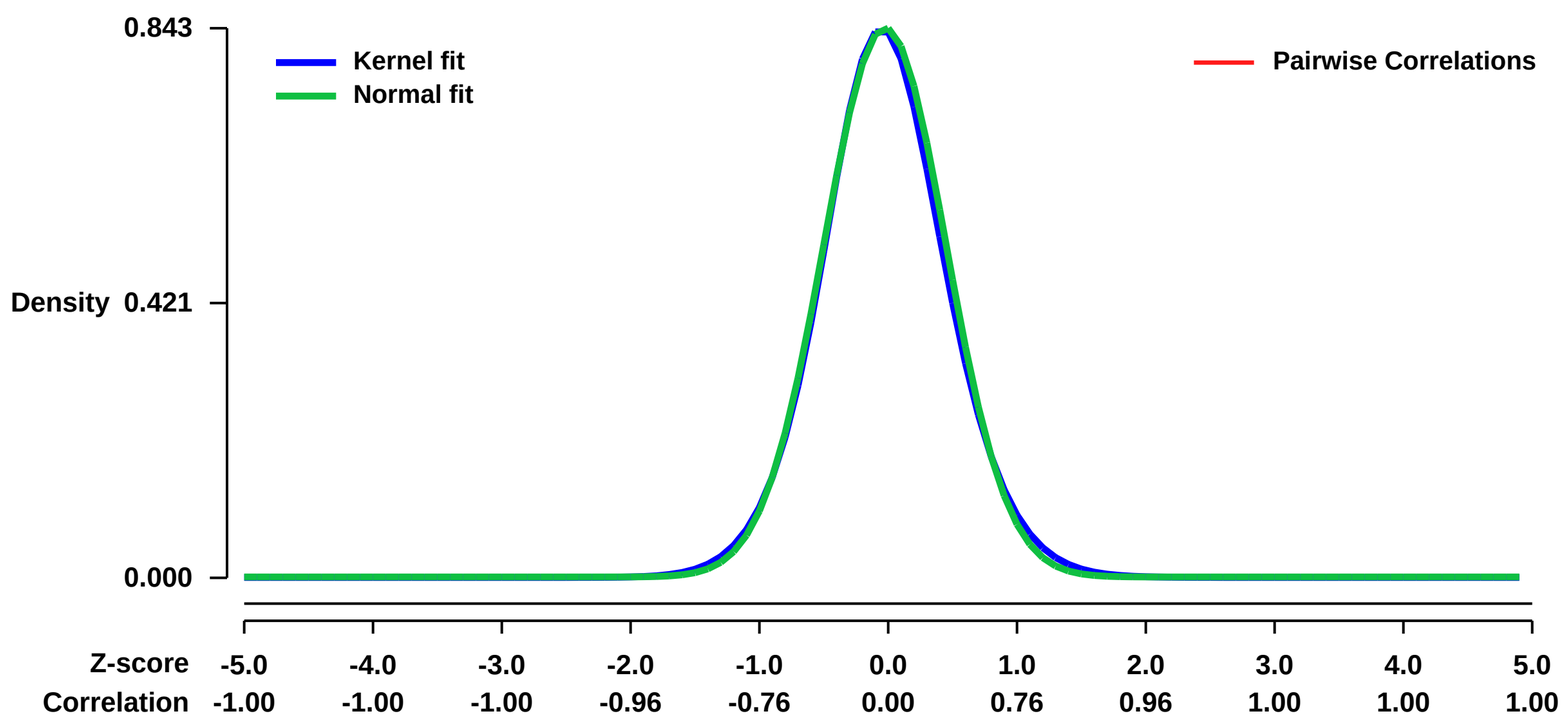

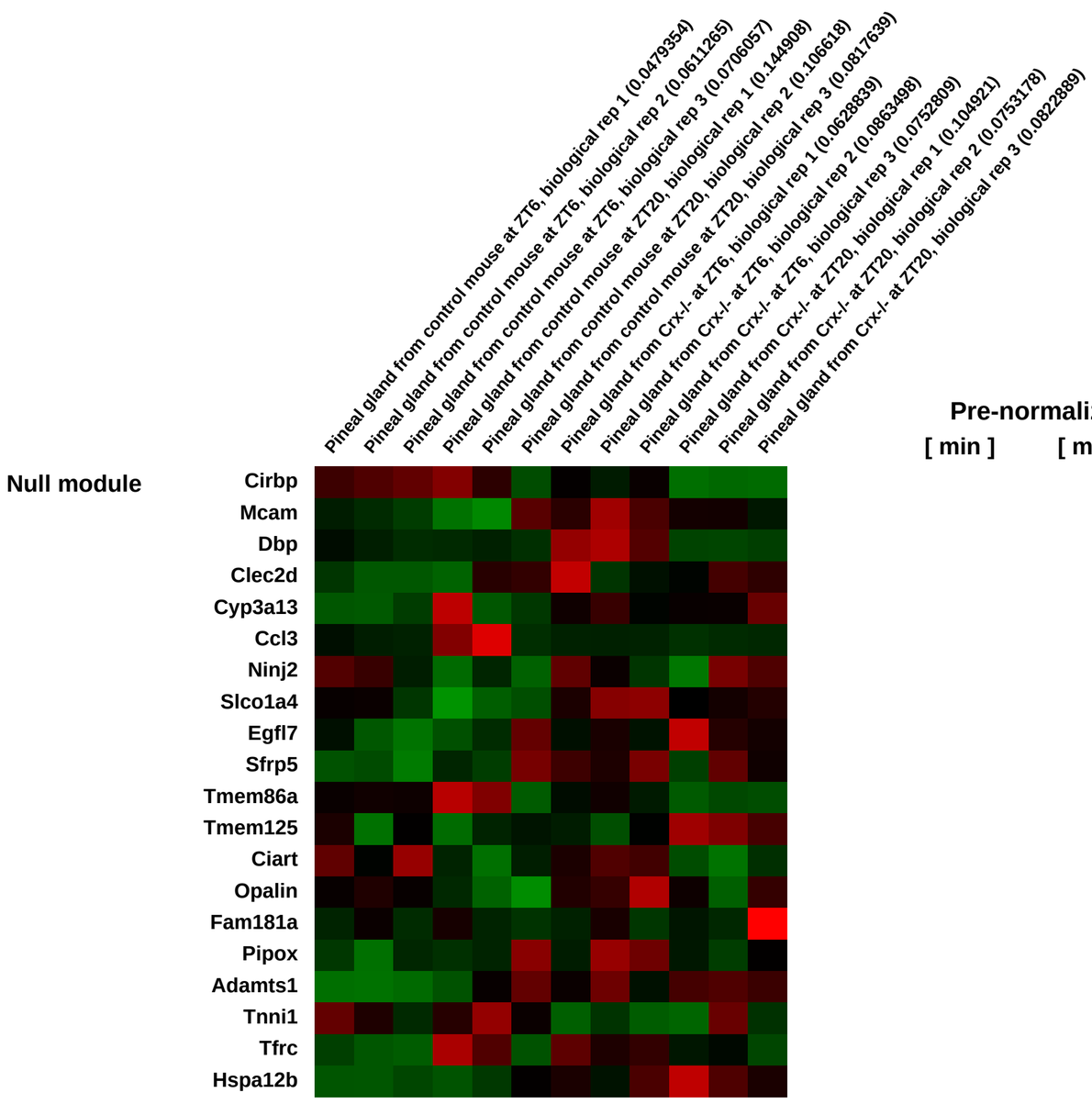

GEO Series "GSE24628" Expression Profiles

Num of samples in this series: 16

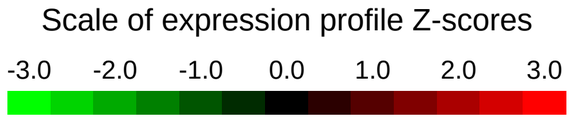

GEO Link:	http://www.ncbi.nlm.nih.gov/geo/query/acc.cgi?acc=GSE24628
Status:	Public on Nov 01 2010
Title:	Subtypes of medulloblastoma have distinct developmental origins
Organism:	Mus musculus
Experiment type:	Expression profiling by array
Platform:	GPL1261
Pubmed ID:	21150899
Summary & Design:	**Summary:** Medulloblastoma encompasses a collection of clinically and molecularly diverse tumor subtypes that together comprise the most common malignant childhood brain tumor. These tumors are thought to arise within the cerebellum, with approximately 25% originating from granule neuron precursor cells (GNPCs) following aberrant activation of the Sonic Hedgehog pathway (hereafter, SHH-subtype). The pathological processes that drive heterogeneity among the other medulloblastoma subtypes are not known, hindering the development of much needed new therapies. Here, we provide evidence that a discrete subtype of medulloblastoma that contains activating mutations in the WNT pathway effector CTNNB1 (hereafter, WNT-subtype), arises outside the cerebellum from cells of the dorsal brainstem. We found that genes marking human WNT-subtype medulloblastomas are more frequently expressed in the lower rhombic lip (LRL) and embryonic dorsal brainstem than in the upper rhombic lip (URL) and developing cerebellum. Magnetic resonance imaging (MRI) and intra-operative reports showed that human WNT-subtype tumors infiltrate the dorsal brainstem, while SHH-subtype tumors are located within the cerebellar hemispheres. Activating mutations in Ctnnb1 had little impact on progenitor cell populations in the cerebellum, but caused the abnormal accumulation of cells on the embryonic dorsal brainstem that included aberrantly proliferating Zic1+ precursor cells. These lesions persisted in all mutant adult mice and in 15% of cases in which Tp53 was concurrently deleted, progressed to form medulloblastomas that recapitulated the anatomy and gene expression profiles of human WNT-subtype medulloblastoma. We provide the first evidence that subtypes of medulloblastoma have distinct cellular origins. Our data provide an explanation for the marked molecular and clinical differences between SHH and WNT-subtype medulloblastomas and have profound implications for future research and treatment of this important childhood cancer. **Overall design:** A total of 16 samples are analyzed, repsresenting 4 experimental groups: Ctnnb1 medulloblastoma (3 samples); Ptch1 medulloblastoma (6 samples); embryonic dorsal brainstem (4 samples); and postnatal granule neuron precursor cells (3 samples). Every sample was prepared from a different mouse.

Background corr dist: KL-Divergence = 0.1173, L1-Distance = 0.0431, L2-Distance = 0.0036, Normal std = 0.4305

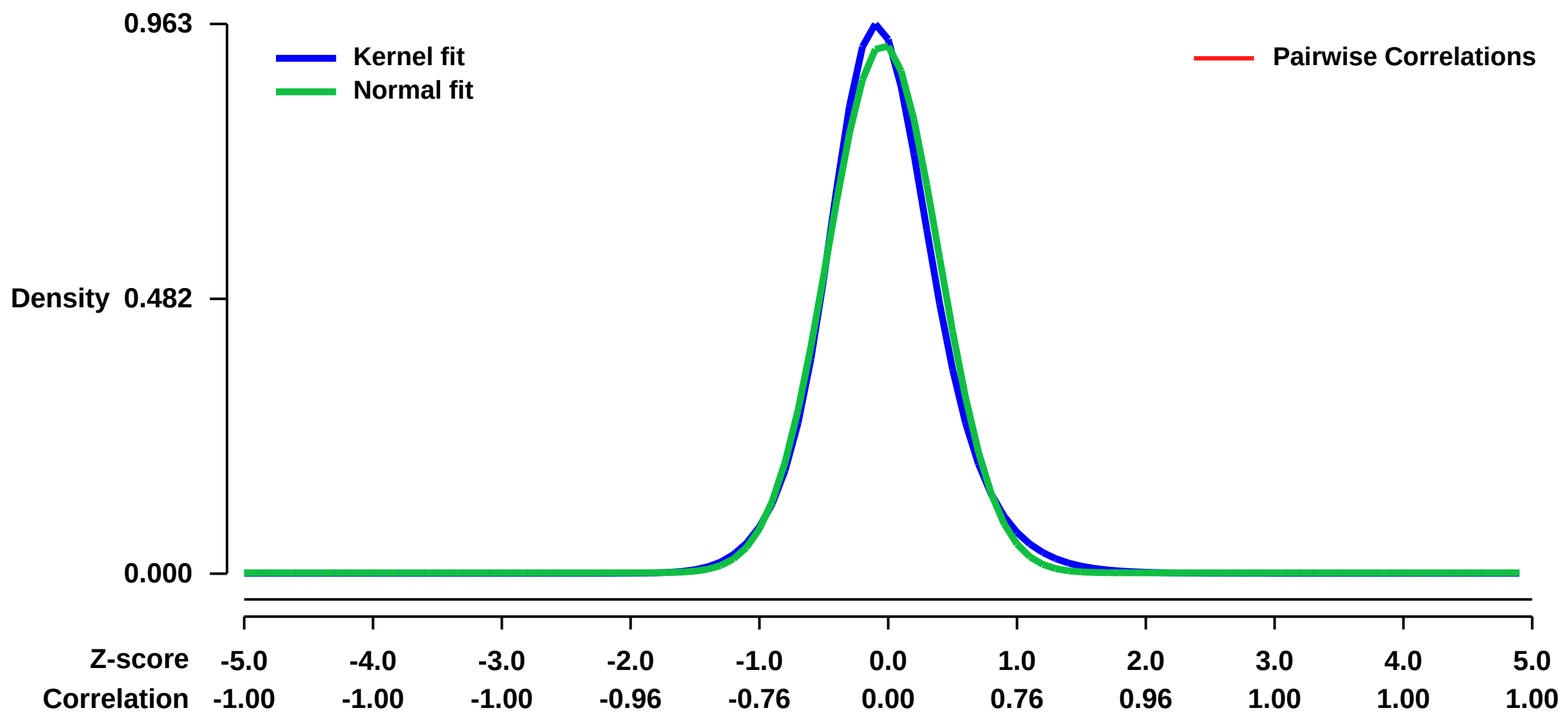

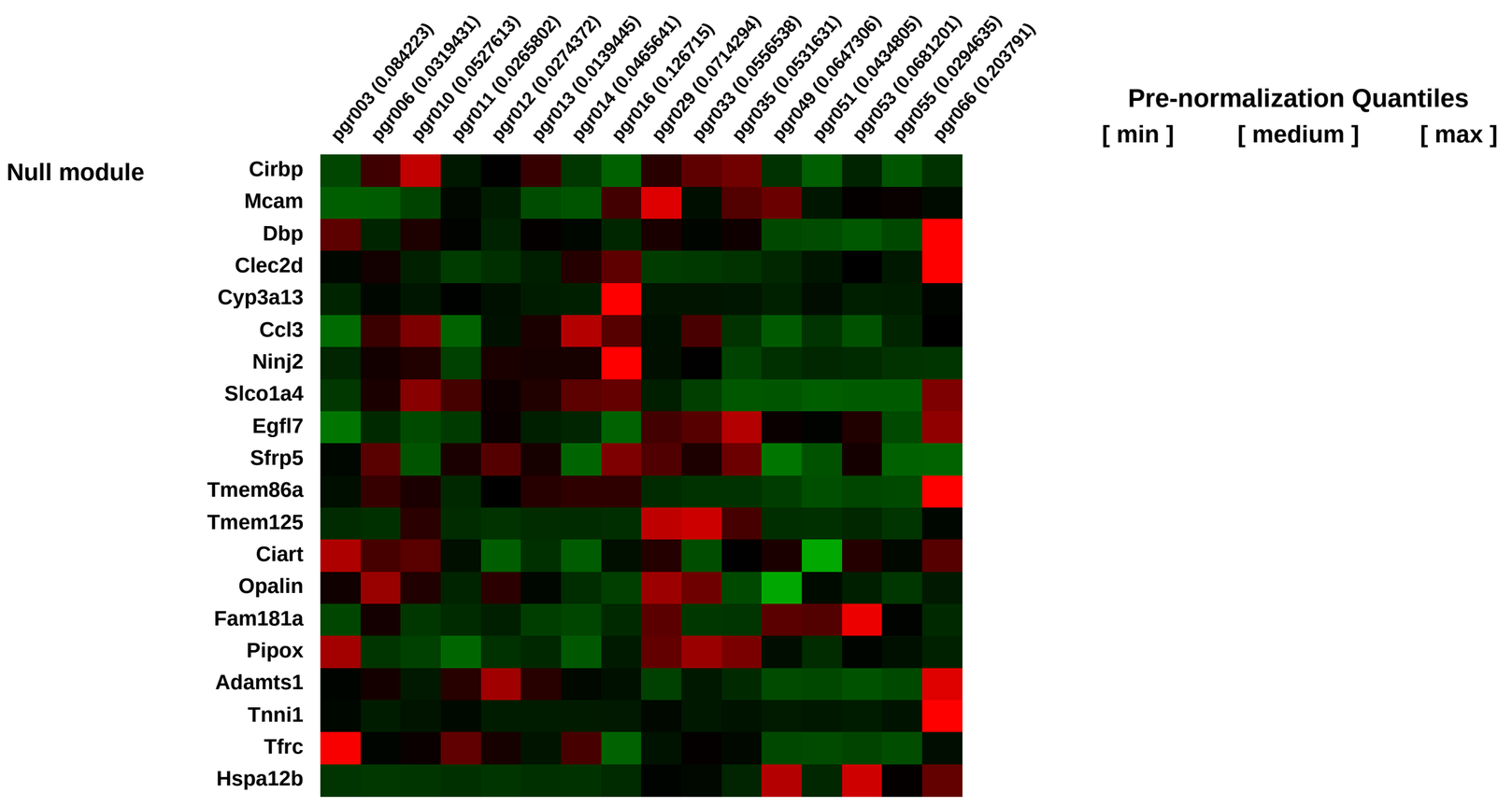

GEO Series "GSE24683" Expression Profiles

Num of samples in this series: 8

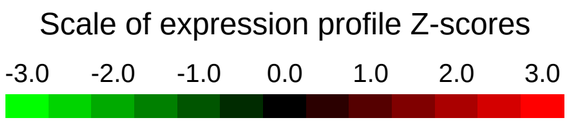

GEO Link:	**http://www.ncbi.nlm.nih.gov/geo/query/acc.cgi?acc=GSE24683**
Status:	**Public on Mar 31 2012**
Title:	**Dicer knockout mouse subcutaneous preadipocytes**
Organism:	**Mus musculus**
Experiment type:	**Expression profiling by array**
Platform:	**GPL1261**
Pubmed ID:	**22958919**
Summary & Design:	**Summary:** **Dicer is required for miRNA processing and RNA interference. Here we knocked out Dicer in SV40 T antigen immortalized subcutaneous preadipocytes isolated from Dicer flox mice by transducing these cells with adenoviruses harboring Cre recombinase. Control cells were transduced with adenovirus harboring GFP.** **We used microarrays to detail the gene expression profile of Dicer knockout preadipocytes.** **Overall design:** **Four days after adenovirus infection, cells were harvested for RNA isolation and hybridization on Affymetrix microarrays. At this point, Dicer knockout was confirmed by several methods.**

Background corr dist: **KL-Divergence = 0.0810, L1-Distance = 0.0212, L2-Distance = 0.0006, Normal std = 0.4734**

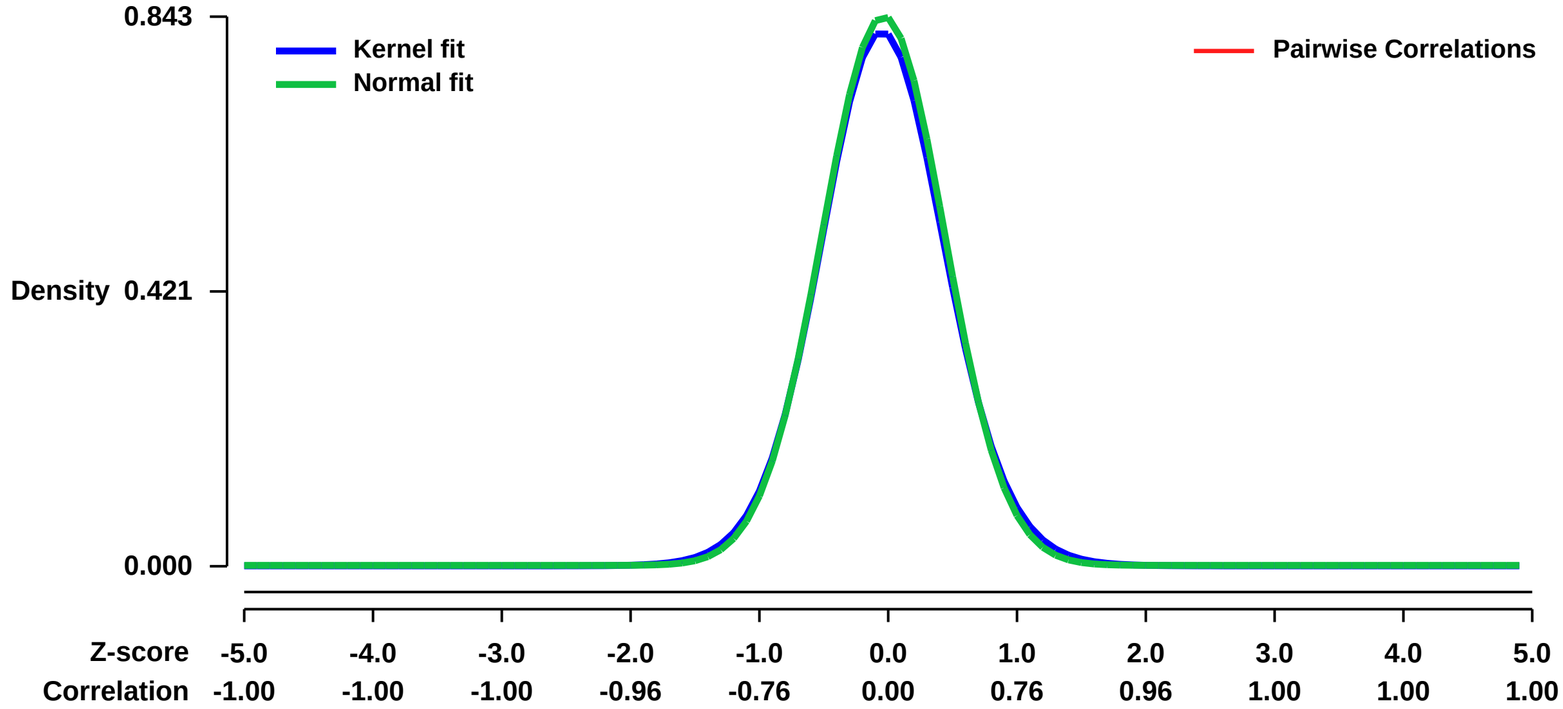

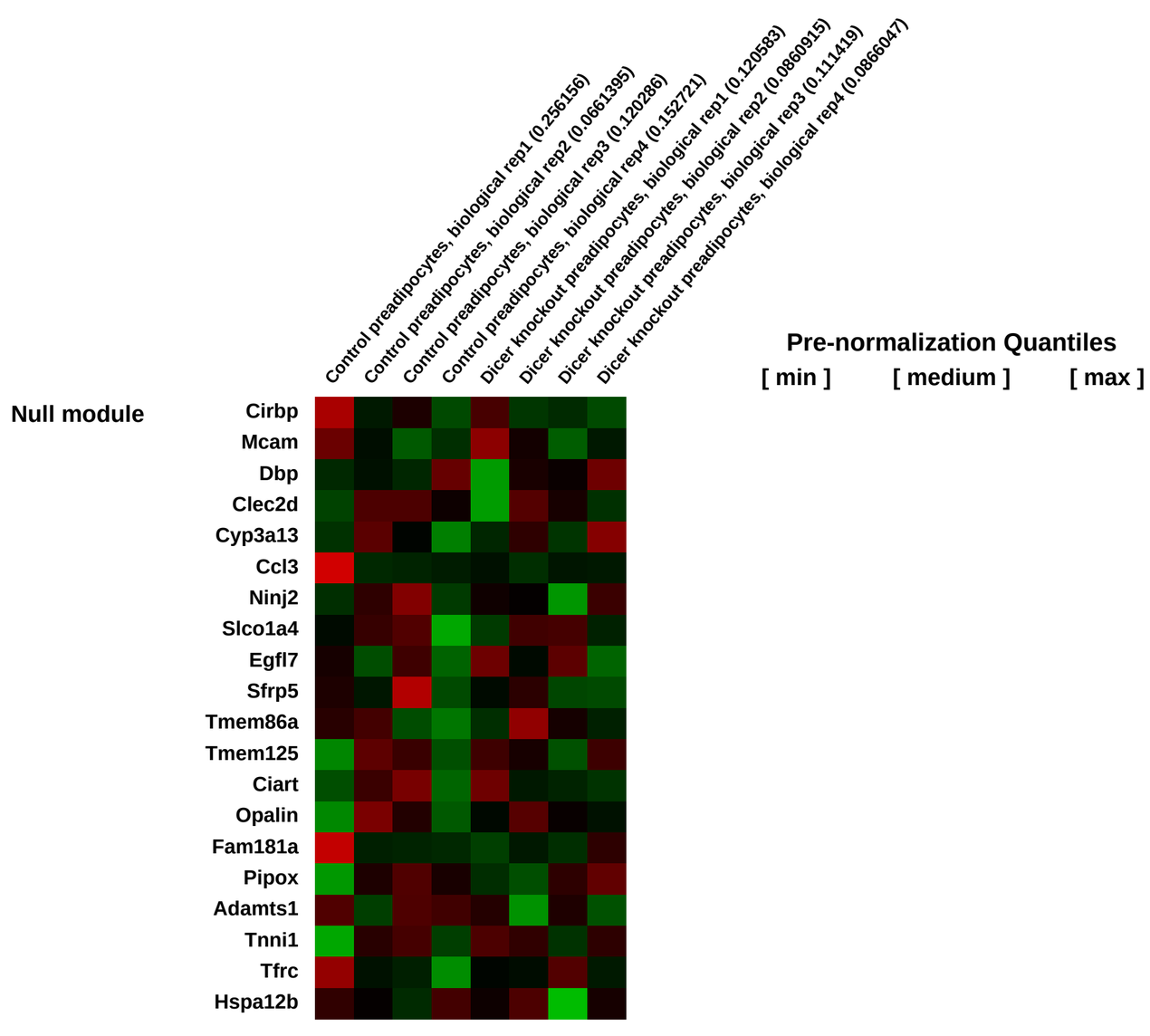

GEO Series "GSE24695" Expression Profiles

Num of samples in this series: 9

Scale of expression profile Z-scores

-3.0 -2.0 -1.0 0.0 1.0 2.0 3.0

GEO Link:	http://www.ncbi.nlm.nih.gov/geo/query/acc.cgi?acc=GSE24695
Status:	Public on Oct 15 2010
Title:	Transcription Factor Redundancy Ensures Induction of the Antiviral State
Organism:	Mus musculus
Experiment type:	Expression profiling by array
Platform:	GPL1261
Pubmed ID:	20943654
Summary & Design:	**Summary:** **Transcriptional response to virus infection in mice lacking type I and type III signaling** **The transcriptional response to virus infection is thought to be predominantly induced by interferon (IFN) signaling. Here we demonstrate that, in the absence of IFN signaling, an IFN-like transcriptome is still maintained. This transcriptional activity is mediated from IFN-stimulated response elements (ISREs) that bind to both the IFN stimulated gene factor 3 (ISGF3) as well as to IFN response factor 7 (IRF7). Through a combination of both in vitro biochemistry and in vivo transcriptional profiling, we have dissected what constitutes IRF-specific, ISGF3-specific, or universal ISREs. Taken together, the data presented here suggests that IRF7 can induce an IFN-like transcriptome in the absence of type-I or -III signaling and therefore provides a level of redundancy to cells to ensure the induction of the antiviral state.** **Overall design:** **Human: Analysis of IRF7 transcriptome in U3A cell line was performed in duplicates.**

Background corr dist: **KL-Divergence = 0.0750, L1-Distance = 0.0207, L2-Distance = 0.0006, Normal std = 0.4869**

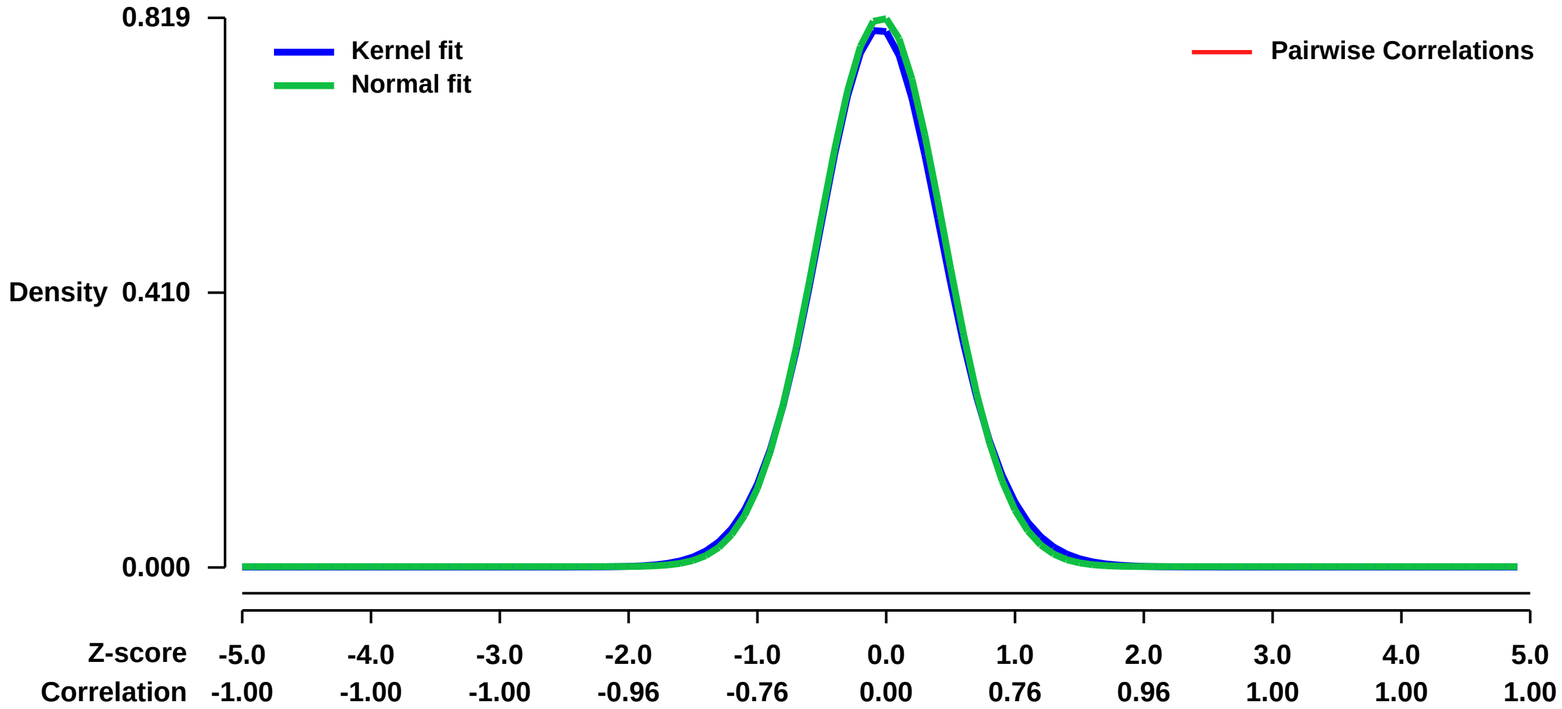

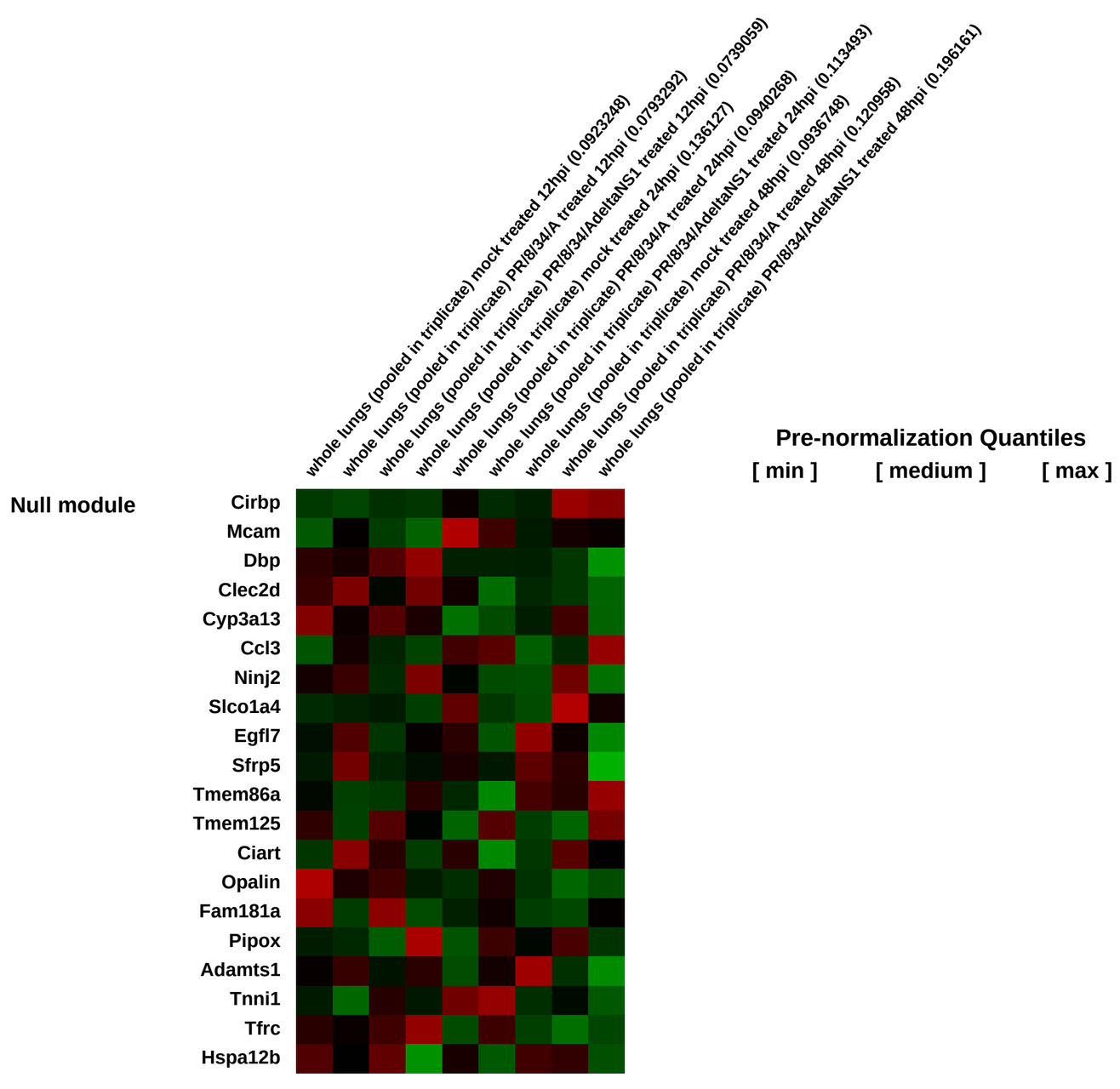

GEO Series "GSE24726" Expression Profiles

Num of samples in this series: 8

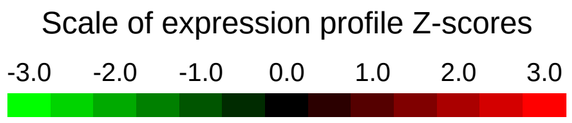

GEO Link:	http://www.ncbi.nlm.nih.gov/geo/query/acc.cgi?acc=GSE24726
Status:	Public on Dec 21 2010
Title:	Gene expression profile of mature plasmacytoid dendritic cells (PDC) after the deletion of transcription factor E2-2
Organism:	Mus musculus
Experiment type:	Expression profiling by array
Platform:	GPL1261
Pubmed ID:	21145760
Summary & Design:	**Summary:** The interferon-producing plasmacytoid dendritic cells (PDC) share common progenitors with antigen-presenting classical dendritic cells (cDC), yet they possess distinct morphology and molecular features resembling those of lymphocytes. It is unclear whether the unique cell fate of PDC is actively maintained in the steady state. We report that the deletion of transcription factor E2-2 from mature peripheral PDC caused their spontaneous differentiation into cells with cDC properties. This included the loss of PDC markers, increase in MHC class II expression and T cell priming capacity, acquisition of dendritic morphology and induction of cDC signature genes. Genome-wide chromatin immunoprecipitation revealed direct binding of E2-2 to key PDC-specific and lymphoid genes, as well as to certain genes enriched in cDC. Thus, E2-2 actively maintains the cell fate of mature PDC and opposes the â defaultâ cDC fate, in part through direct regulation of lineage-specific gene expression programs. **Overall design:** Inducible deletion of E2-2 (Tcf4) has been performed by administering tamoxifen to conditional E2-2flox/flox Rosa26-CreER+ mice or to E2-2flox/flox Rosa26-CreER- control littermates. Four or six days later total splenocytes were isolated, pooled from 2-3 mice and PDC (CD11b- B220+ CD11clow Bst2+) were isolated by sorting. Global gene expression profiles of E2-2-deficient (null) and control (Ctrl) PDC were compared using Affymetrix microarrays (GPL1261).

Background corr dist: KL-Divergence = 0.0689, L1-Distance = 0.0375, L2-Distance = 0.0025, Normal std = 0.5200

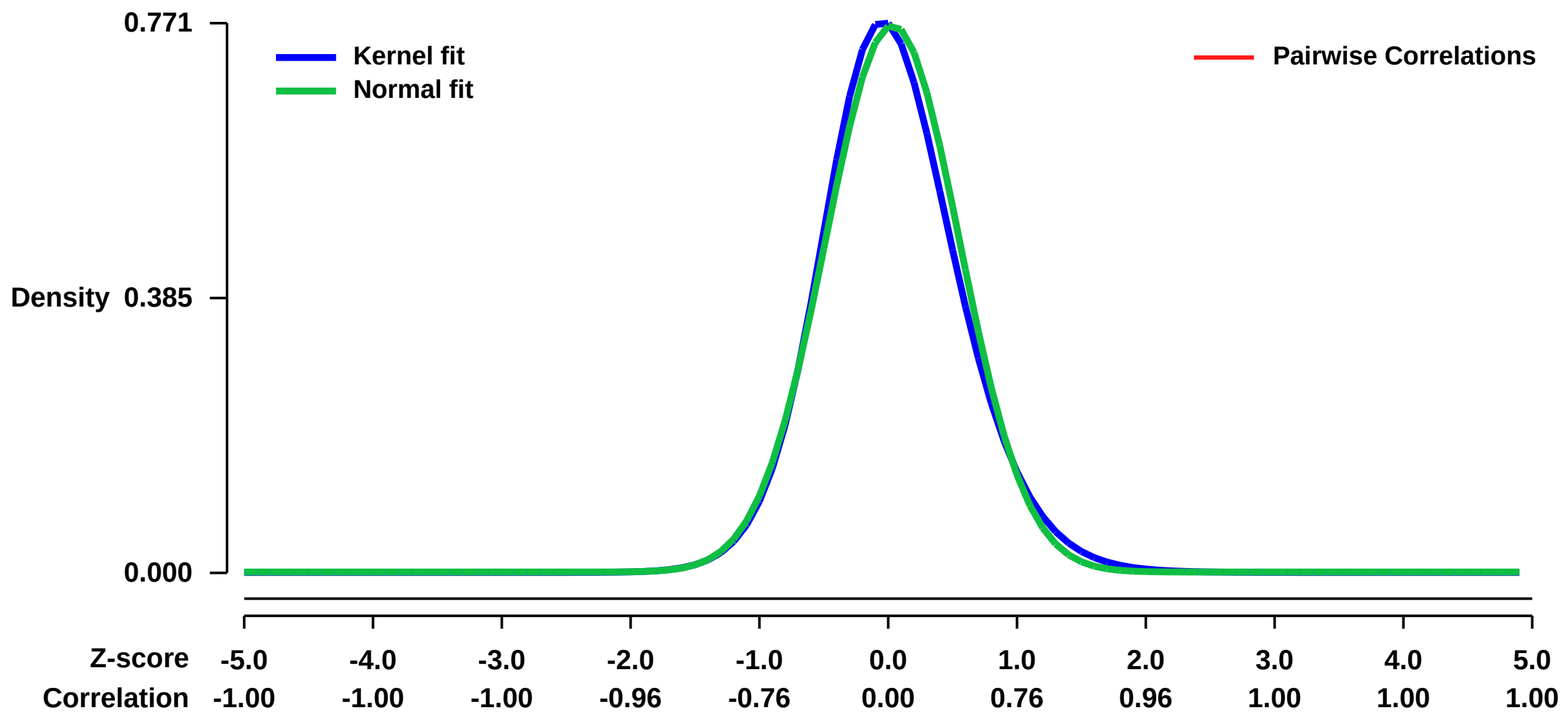

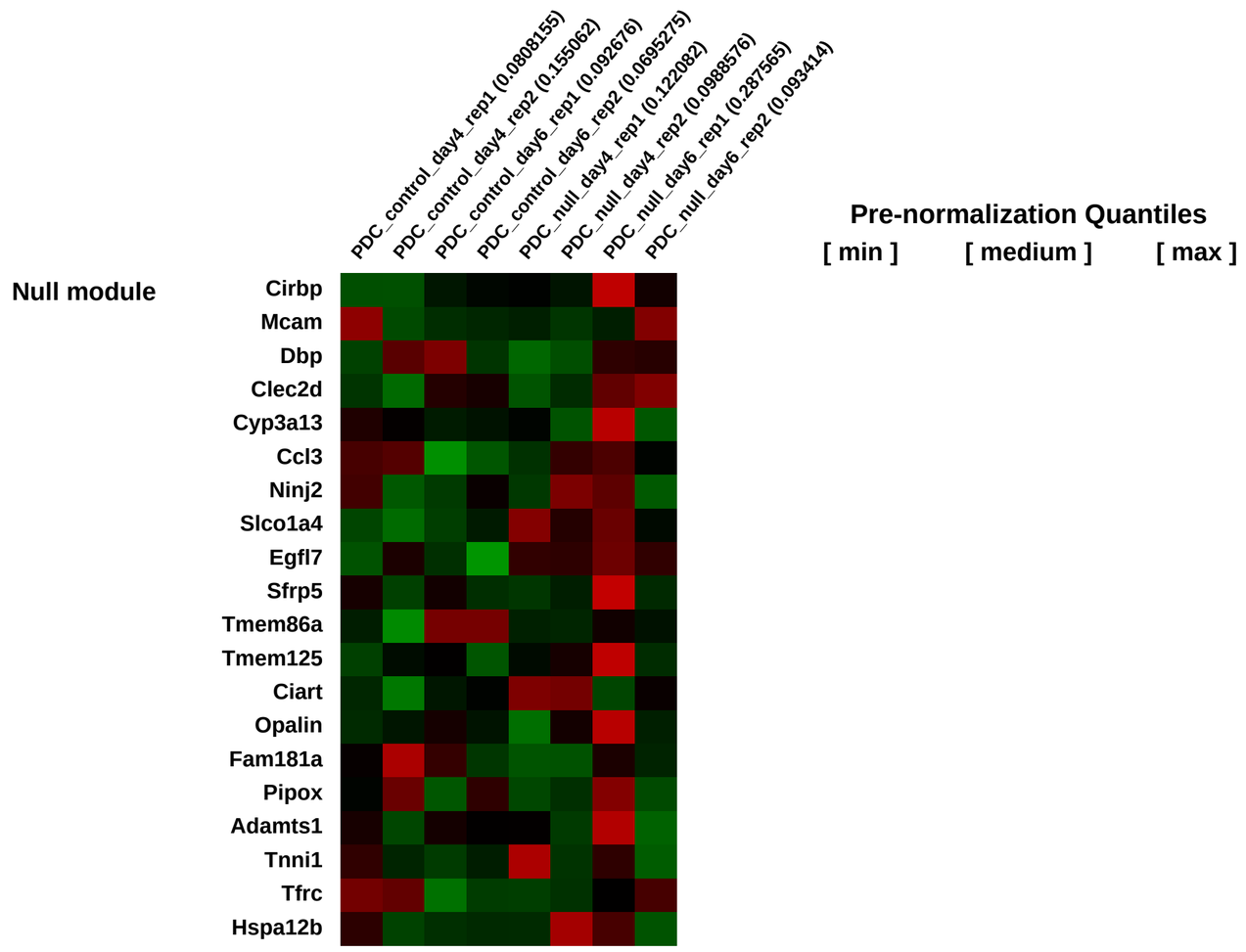

GEO Series "GSE24775" Expression Profiles

Num of samples in this series: 48

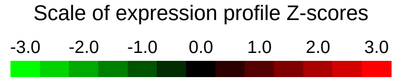

GEO Link:	http://www.ncbi.nlm.nih.gov/geo/query/acc.cgi?acc=GSE24775
Status:	Public on Dec 02 2010
Title:	Genome-wide expression analysis of the mouse pars tuberalis (PT) under chronic short-day and long-day conditions
Organism:	Mus musculus
Experiment type:	Expression profiling by array
Platform:	GPL1261
Pubmed ID:	21129973
Summary & Design:	**Summary:** Living organisms detect seasonal changes in day length (photoperiod), and alter their physiological functions accordingly, to fit seasonal environmental changes. This photoperiodic system is implicated in seasonal affective disorders and the season-associated symptoms observed in bipolar disease and schizophrenia. Thyroid-stimulating hormone beta subunit (Tshb), induced in the pars tuberalis (PT), plays a key role in the pathway that regulates animal photoperiodism. However, the upstream inducers of Tshb expression remain unknown. Here we show that late-night light stimulation acutely triggers the Eya3-Six1 pathway, which directly induces Tshb expression. Using melatonin-proficient CBA/N mice, which preserve the photoperiodic Tshb-expression response, we performed a genome-wide expression analysis of the PT under chronic short-day and long-day conditions. These data comprehensively identified long-day and short-day genes, and indicated that late-night light stimulation induces long-day genes. We verified this by advancing and extending the light period by 8 hours, which acutely induced Tshb expression, within one day. In a genome-wide expression analysis under this condition, we searched for candidate upstream genes by looking for expression that preceded Tshbâ s, and identified Eya3 gene. These results elucidate the comprehensive transcriptional photoperiodic response in the PT, revealing the complex regulation of Tshb expression and unexpectedly rapid response to light changes in the mammalian photoperiodic system. **Overall design:** Mice were separated into 2 groups. One group was maintained under the short-day conditions (light: dark = 8 h:16 h, ZT0 = lights on, ZT8 = lights off, 400 lux) and the other was housed under long-day conditions (light:dark = 16 h:8 h, ZT0 = lights on, ZT16 = lights off, 400 lux) for 2 weeks. The PTs of both groups were retrieved every 4 h for 1 day (6 time points for each group), starting at ZT0. For the experiments performed during the first day of the long-day conditions, we applied two different conditions, following 3 weeks under short-day conditions. In one, the light-onset was advanced by 8 hours (advance condition), and in the other, the dark period was delayed by 8 hours (delay condition). PTs from both groups were obtained every 4 h for 1 day, starting at the lights-on time. (Lights on for the advance condition was ZT16 as defined by the short-day condition. Lights on for the delay condition was ZT0). We sampled 25 mice at each time point. This whole procedure was repeated twice (n = 2) to obtain experimental replicates.

Background corr dist: KL-Divergence = 0.1963, L1-Distance = 0.0481, L2-Distance = 0.0054, Normal std = 0.3344

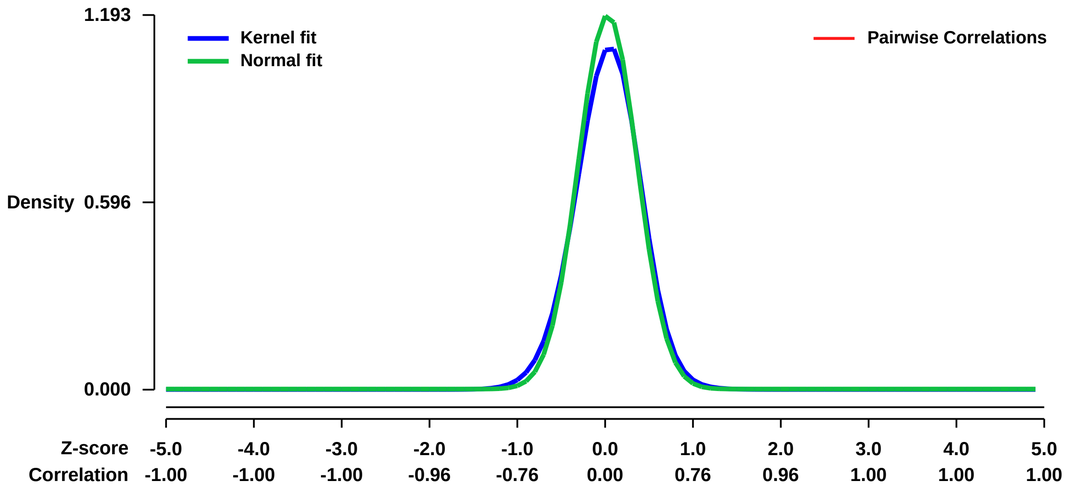

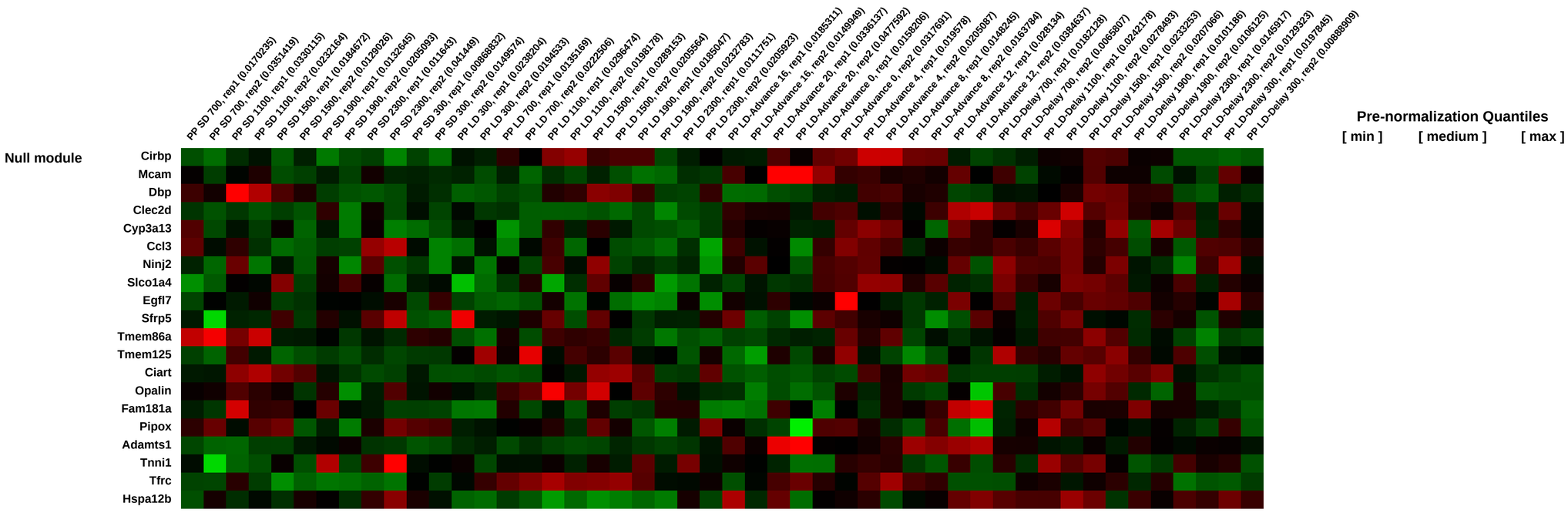

GEO Series "GSE24793" Expression Profiles

Num of samples in this series: 8

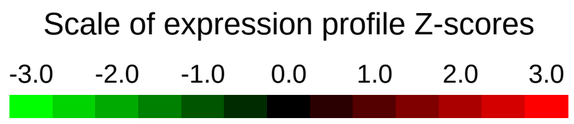

GEO Link:	http://www.ncbi.nlm.nih.gov/geo/query/acc.cgi?acc=GSE24793
Status:	Public on Mar 30 2012
Title:	Target genes of thyroid hormone in cerebellum neurons
Organism:	Mus musculus
Experiment type:	Expression profiling by array
Platform:	GPL1261
Pubmed ID:	22586439
Summary & Design:	**Summary:** Cerebellar post-natal development is particularly sensitive to thyroid hormone and low levels of thyroid hormone (hypothyroidism) result in permanent defects in cerebellar architecture and function. All cell types of the cerebellum are affected, but the main sign of hypothyroidism in mice is the persistence of the external granular layer, composed of mitotic neuronal precursors at P21. To make the genetic link between thyroid hormone and cerebellar development, we sought to identify new thyroid hormone target genes, in particular in granule cells which represent the vast majority of cerebellar cells. **Overall design:** Primary cultures of cerebellar neurons were made by dissociation of cerebella from newborn wild-type mice. These cells were plated 48 hours in serum-free medium to avoid invasion of the culture by glial cells. In order to include a kinetic and a maximum number of target genes, several cultures were either treated or left untreated as controls for 6 hours (T1), 16 hours (T2), 24 hours (T3) or 48 hours (T4) and results were pairwise compared for each time point.

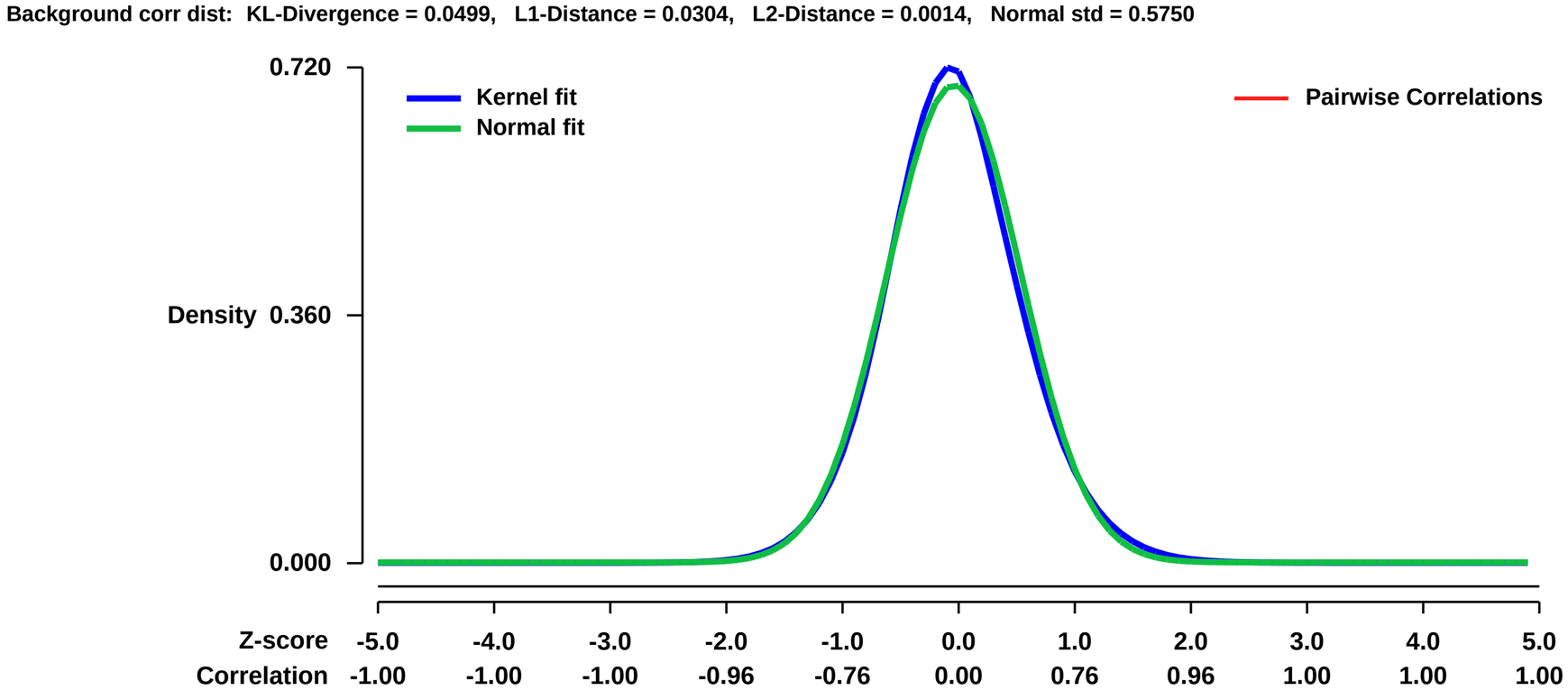

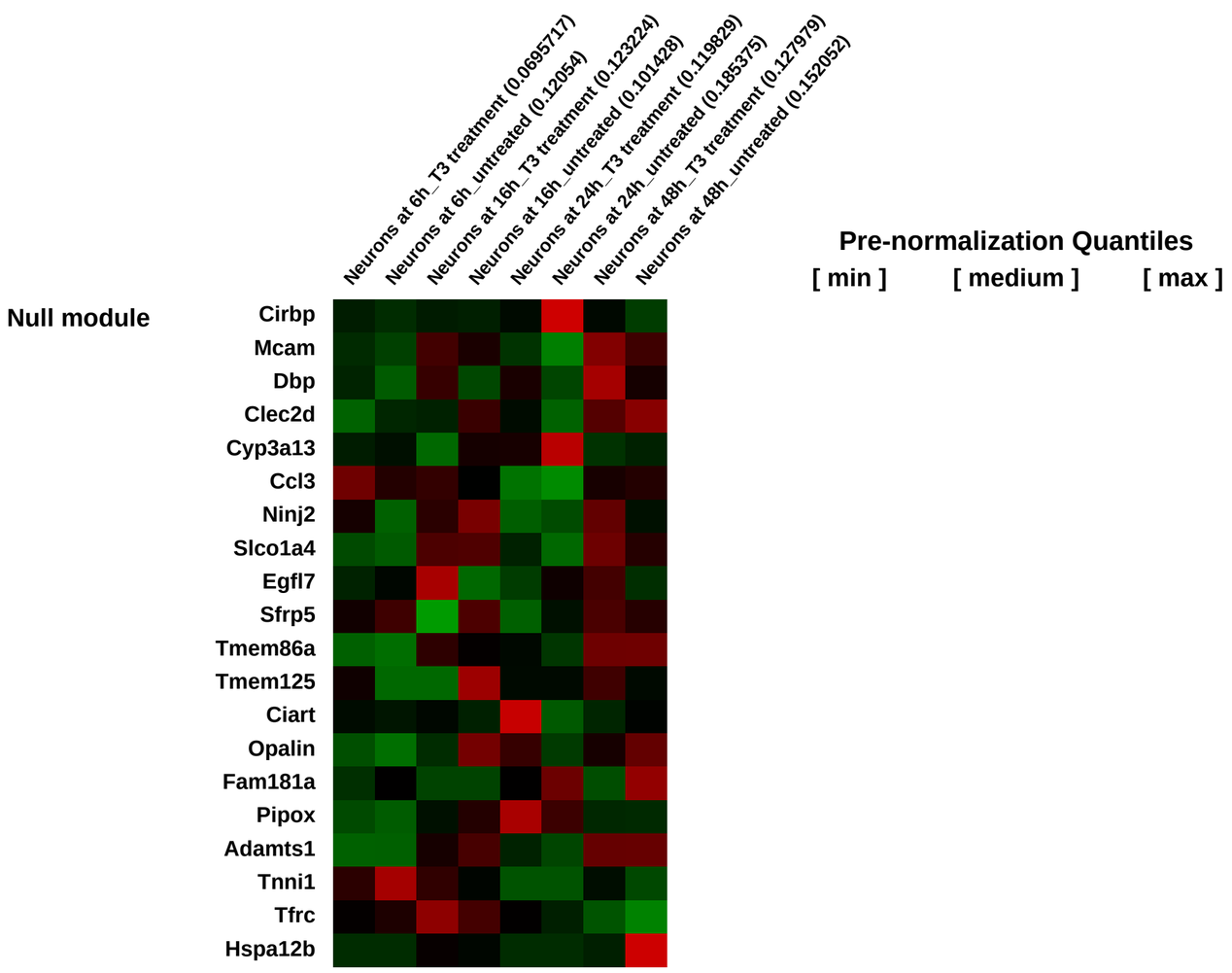

GEO Series "GSE24813" Expression Profiles

Num of samples in this series: 10

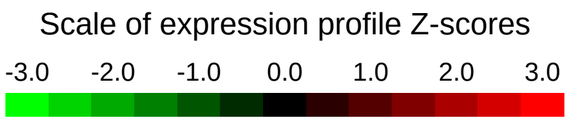

GEO Link:	http://www.ncbi.nlm.nih.gov/geo/query/acc.cgi?acc=GSE24813
Status:	Public on Aug 24 2011
Title:	Gene expression data of BCR-ABL1 transformed myeloid cells from BCL6 wild-type and BCL6 knockout mice treated with and without Imatinib and RI-BPI
Organism:	Mus musculus
Experiment type:	Expression profiling by array
Platform:	GPL1261
Pubmed ID:	21911423
Summary & Design:	**Summary:** To identify differences in the gene regulation between BCL6+/+ and BCL6-/- CML cells a gene expression analysis has been performed. We investigated the gene expression pattern in BCL6+/+ cells in the presence or absence of Imatinib and a combination of Imatinib and RI-BPI (a novel retro-inverso BCL6 peptide inhibitor). In BCL6-/- CML cells, we investigated the gene expression pattern in the presence or absence of Imatinib. **Overall design:** BCR-ABL1 transformed myeloid cells from BCL6+/+ mice were cultured in the presence or absence of 10´µM Imatinib or 10´µM Imatinib and 20´µM RI-BPI for 16 hours. BCR-ABL1 transformed myeloid cells from BCL6-/- mice were cultured in the presence or absence of 10´µM Imatinib. Two samples for each condition were processed.

Background corr dist: KL-Divergence = 0.0654, L1-Distance = 0.0414, L2-Distance = 0.0023, Normal std = 0.5423

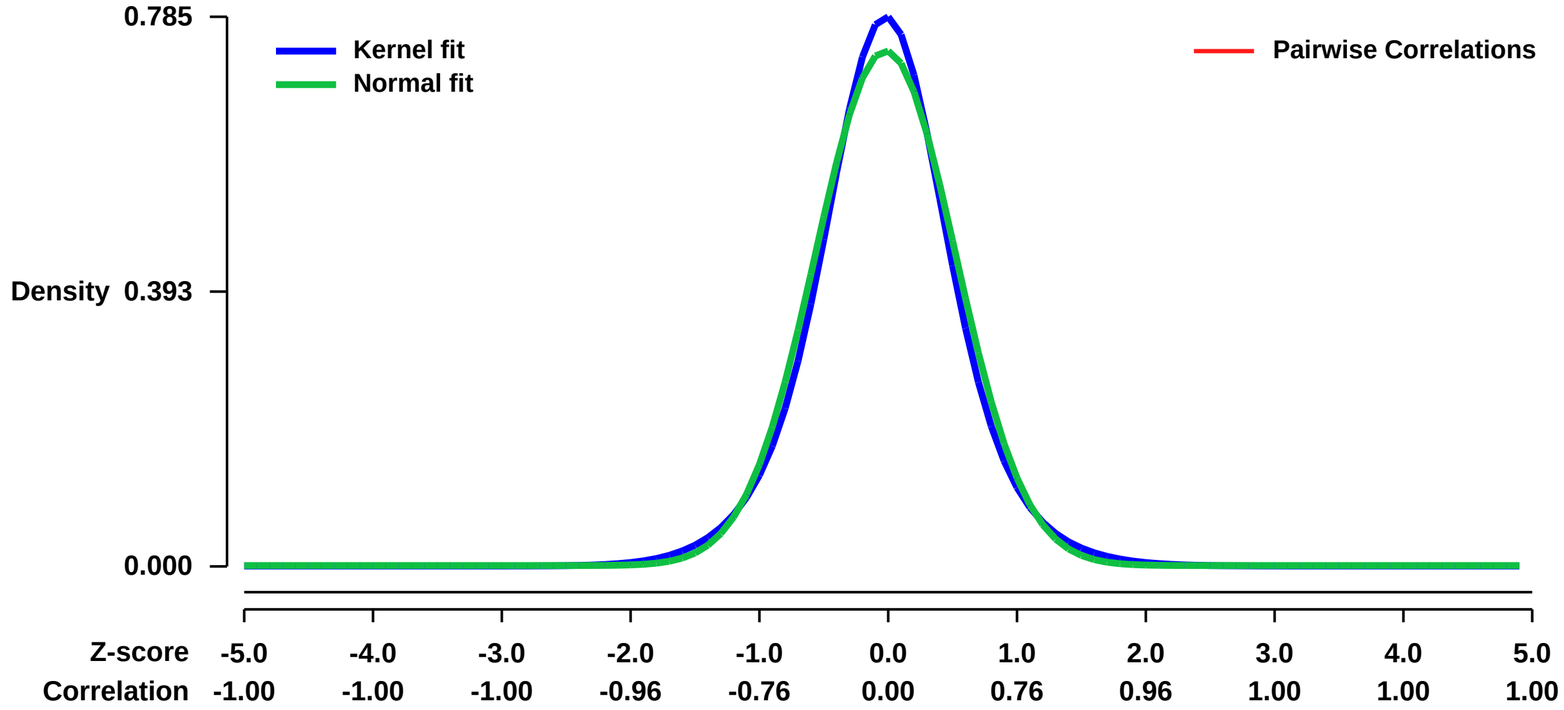

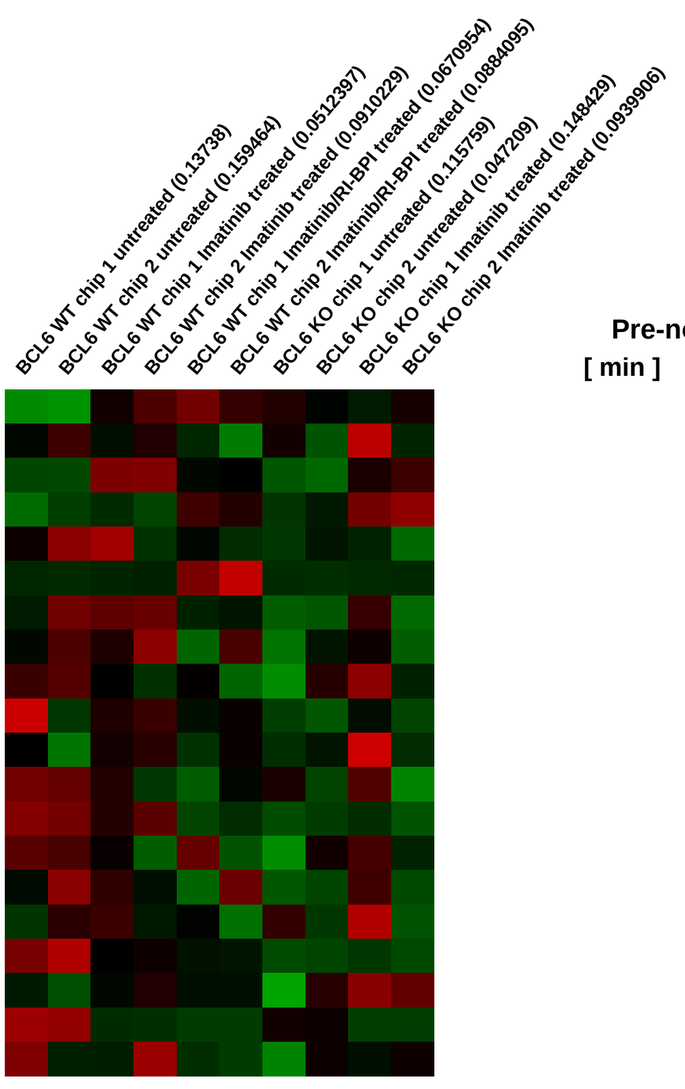

GEO Series "GSE24873" Expression Profiles

Num of samples in this series: 48

Scale of expression profile Z-scores

-3.0 -2.0 -1.0 0.0 1.0 2.0 3.0

GEO Link:	http://www.ncbi.nlm.nih.gov/geo/query/acc.cgi?acc=GSE24873
Status:	Public on Oct 19 2011
Title:	IL-17-induced NF-kB activation via CIKS/Act1: Physiologic significance and signaling mechanisms
Organism:	Mus musculus
Experiment type:	Expression profiling by array
Platform:	GPL1261
Pubmed ID:	21335551
Summary & Design:	**Summary:** Interleukin-17 (IL-17) is essential in host defense against extracellular bacteria and fungi, especially at mucosal sites, but it also contributes significantly to inflammatory and autoimmune disease pathologies. Binding of IL-17 to its receptor leads to recruitment of the adaptor protein CIKS/Act1 via heterotypic association of their respective SEFIR domains and to activation of the transcription factor NF-kB; it is not known whether CIKS and/or NF-kB are required for all gene induction events. Here we report that CIKS is essential for all IL-17 induced immediate-early genes in primary mouse embryo fibroblasts, while NF-kB is profoundly involved.´ We also identify a novel sub-domain in the N-terminus of CIKS that is essential for IL-17-mediated NF-kB activation. This domain is both necessary and sufficient for the interaction between CIKS and TRAF6, an adaptor required for NF-kB activation.´ The ability of decoy peptides to block this interaction may provide a new therapeutic strategy for intervention in IL-17-driven autoimmune and inflammatory diseases. **Keywords:** strain comparisons **Overall design:** strain comparisons

Background corr dist: KL-Divergence = 0.5409, L1-Distance = 0.0905, L2-Distance = 0.0273, Normal std = 0.2178

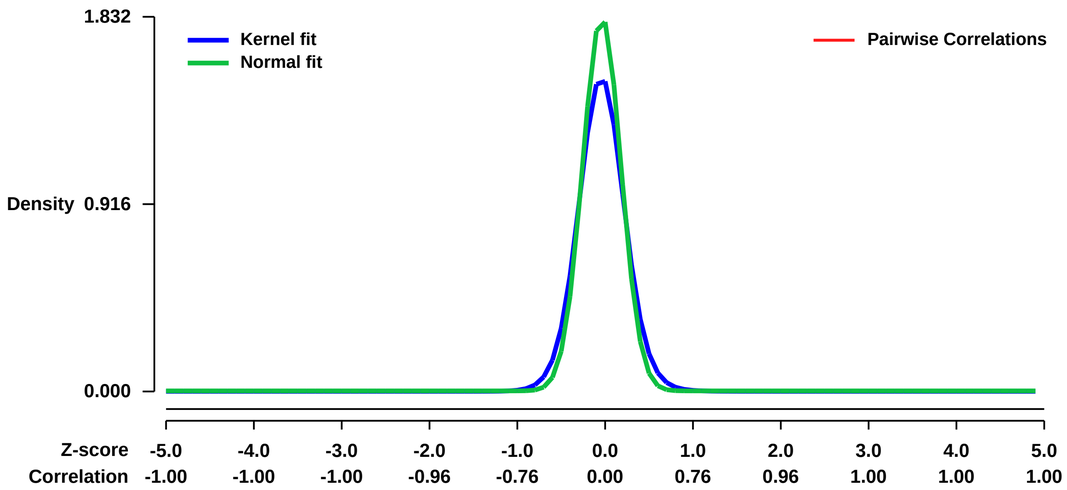

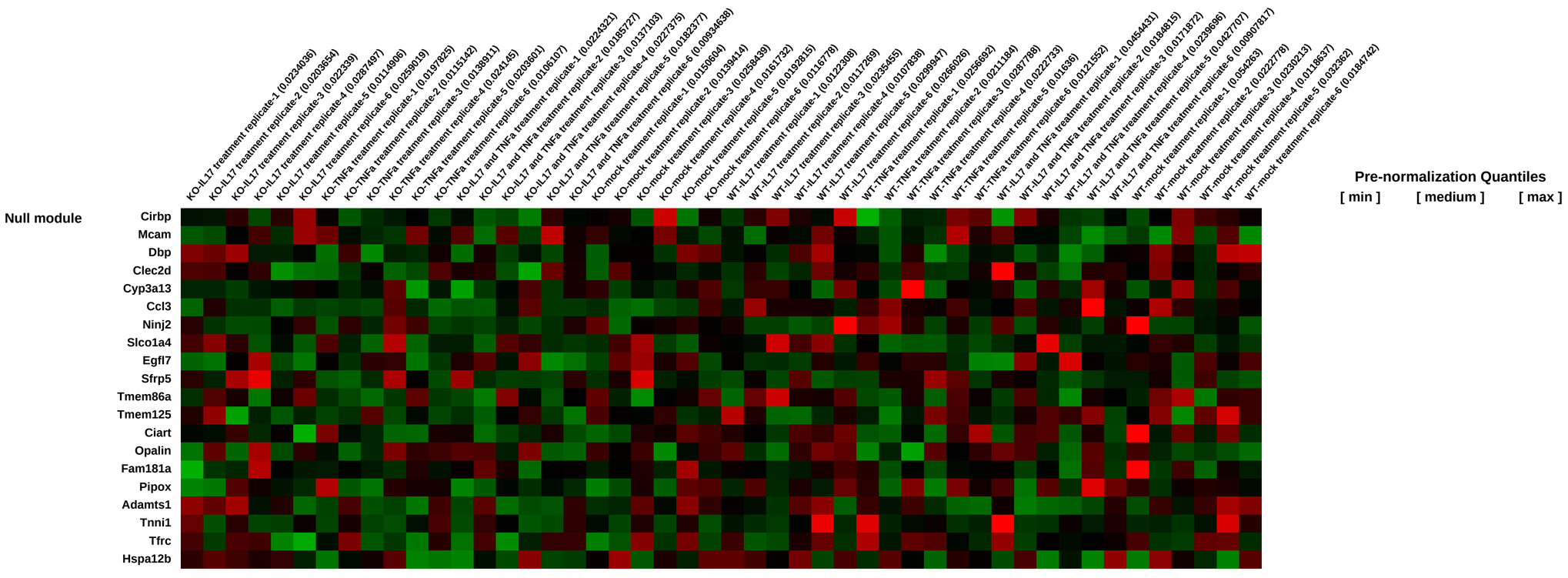

GEO Series "GSE24920" Expression Profiles

Num of samples in this series: 19

Scale of expression profile Z-scores

-3.0 -2.0 -1.0 0.0 1.0 2.0 3.0

GEO Link: http://www.ncbi.nlm.nih.gov/geo/query/acc.cgi?acc=GSE24920
Status: Public on Oct 21 2012
Title: Gene Expression in Myotonic Dystrophy
Organism: Mus musculus
Experiment type: Expression profiling by array
Platform: GPL1261
Pubmed ID:

Summary & Design:

Summary:
In order to examine the changes in gene expression between normal and myotonic dystrophic animals, gene expression array studies were done with extensor digitorum longus (EDL) of transgenic HSALR line 20b mice using Affymetrix MOE430 2.0 microarrays.

We used EDL muscle from transgenic HSALR line 20b mice, maintained as homozygotes in an FVB inbred background and wild-type FVB mice purchased from Taconic.

Overall design:
Affymetrix gene expression arrays were performed on HSALR and wild type EDL muscle

Background corr dist: KL-Divergence = 0.2353, L1-Distance = 0.0438, L2-Distance = 0.0042, Normal std = 0.3125

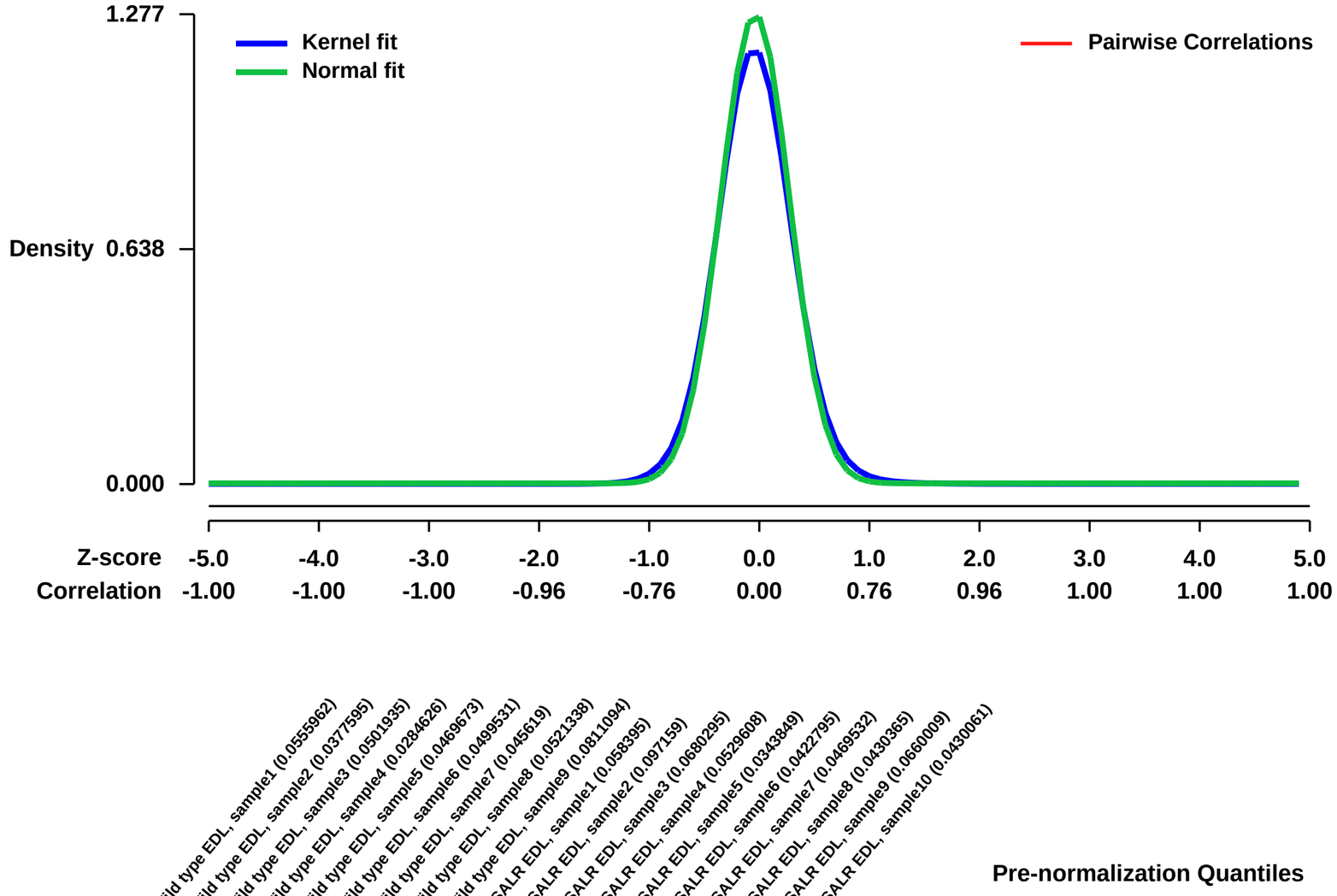

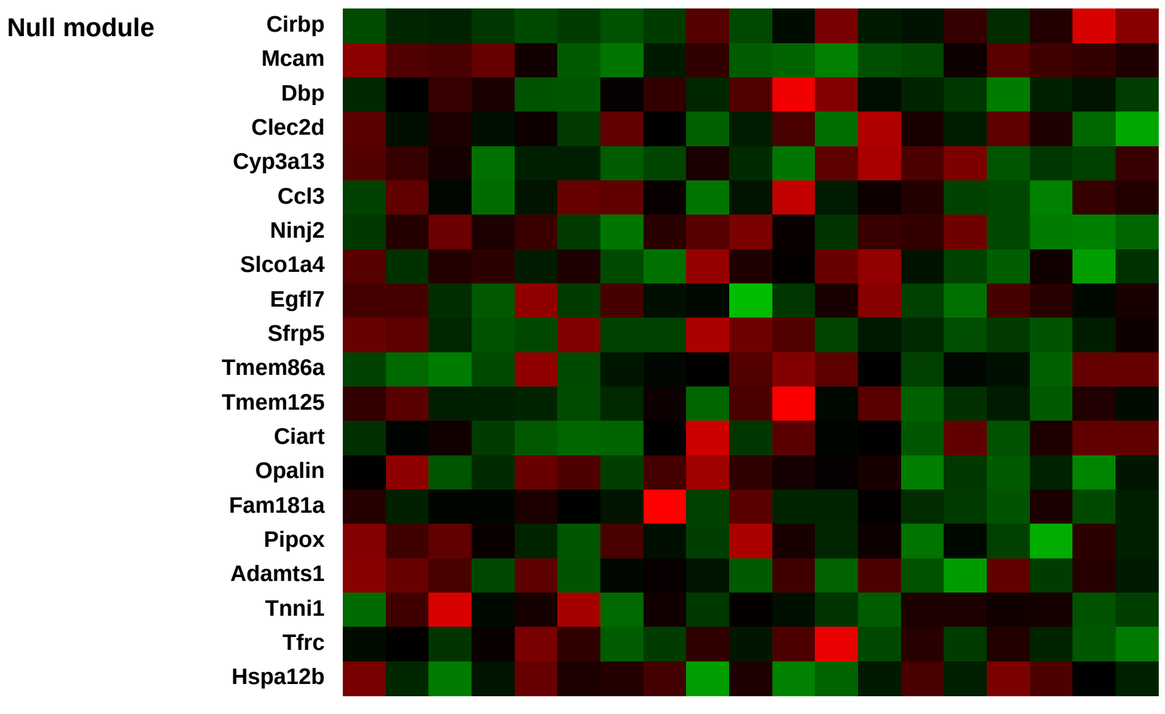

GEO Series "GSE24928" Expression Profiles

Num of samples in this series: 9

Scale of expression profile Z-scores

-3.0 -2.0 -1.0 0.0 1.0 2.0 3.0

GEO Link:	http://www.ncbi.nlm.nih.gov/geo/query/acc.cgi?acc=GSE24928
Status:	Public on Dec 06 2010
Title:	Gene expression change induced by bisphenol A in mouse urogenital sinus
Organism:	Mus musculus
Experiment type:	Expression profiling by array
Platform:	GPL1261
Pubmed ID:	21123812
Summary & Design:	**Summary:** **Bisphenol A (BPA), an endocrine-disrupting chemical (EDC), is a well-known, ubiquitous estrogenic chemical. To investigate the effects of fetal exposure to low-dose BPA on the development of the prostate, we first examined the alterations of in situ sex steroid hormonal environment in the mouse urogenital sinus (UGS).** **Next, to investigate the BPA-specific gene alterations related to increases of the E2 levels and aromatase activity, we performed comprehensive gene expression analysis using Affymetrix GeneChip in the BPA-treated or DES-treated male UGS at embryonic day 17th and postnatal day 1st.** **Overall design:** **Pregnant female C57BL/6 mice were exposed to BPA (20 ¸…g/kg/day) or synthetic estrogen Diethylstilbestrol (DES: 0.2 ¸…g/kg/day), which were dissolved in tocopherol-stripped corn oil, on embryonic day 13 (E13) to E16. Between E17 and postnatal day 1 (P1), all animals were terminated by an overdose of isoflurane followed by cervical dislocation. Fetuses were collected at E17, E18, P0, and P1. The bladder and urethra were removed and dissected to isolate UGS and collected in RNA later. To isolate pure UGS, other tissues such as the bladder, urethra, Wolffian duct (WD), seminal vesicle (SV), and Mullerian duct (MD) were removed from both the male and female urogenital tracts. The histopathology of the mouse UGS was then examined by hematoxylin and eosin staining. Total RNA was extracted using the Qiagen mini RNA Easy kit. Each RNAs were linearly amplified and hybridized to Affymetrix GeneChip.**

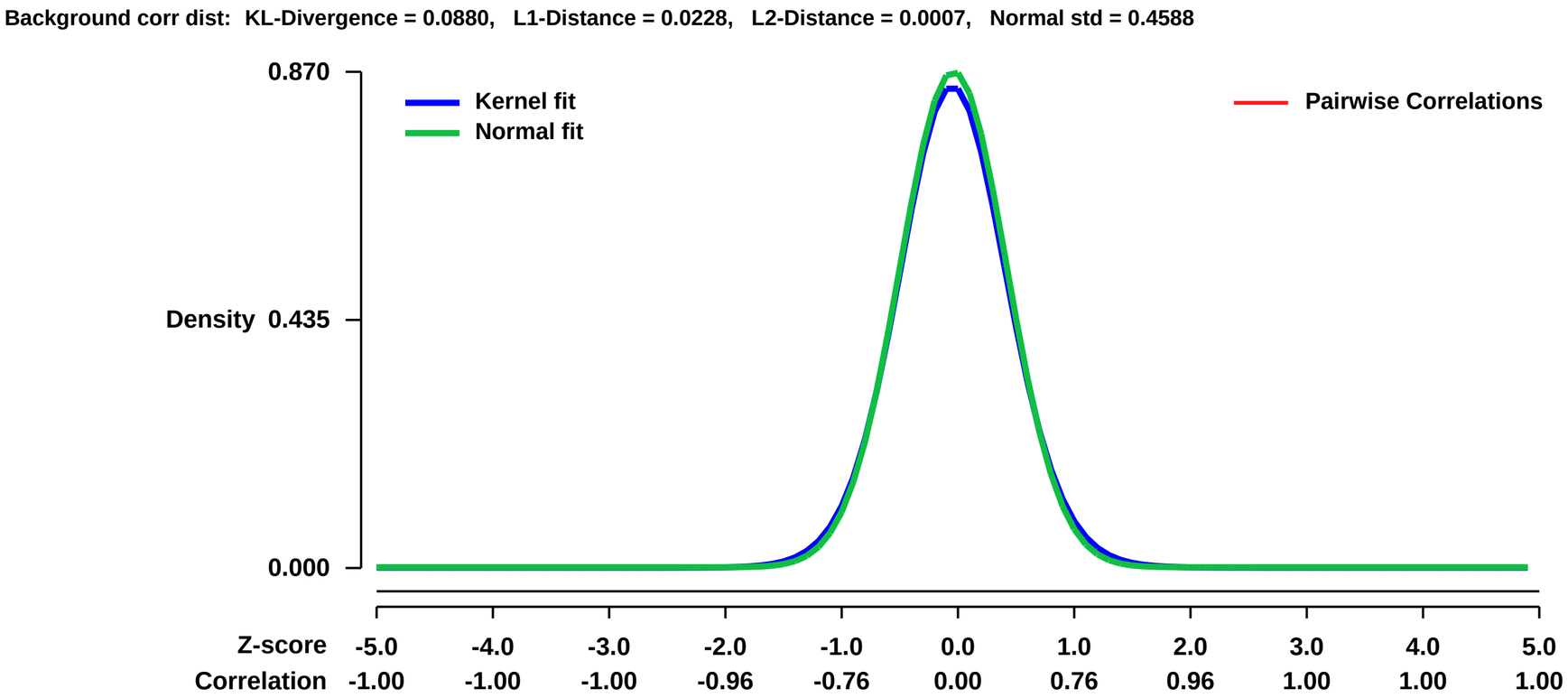

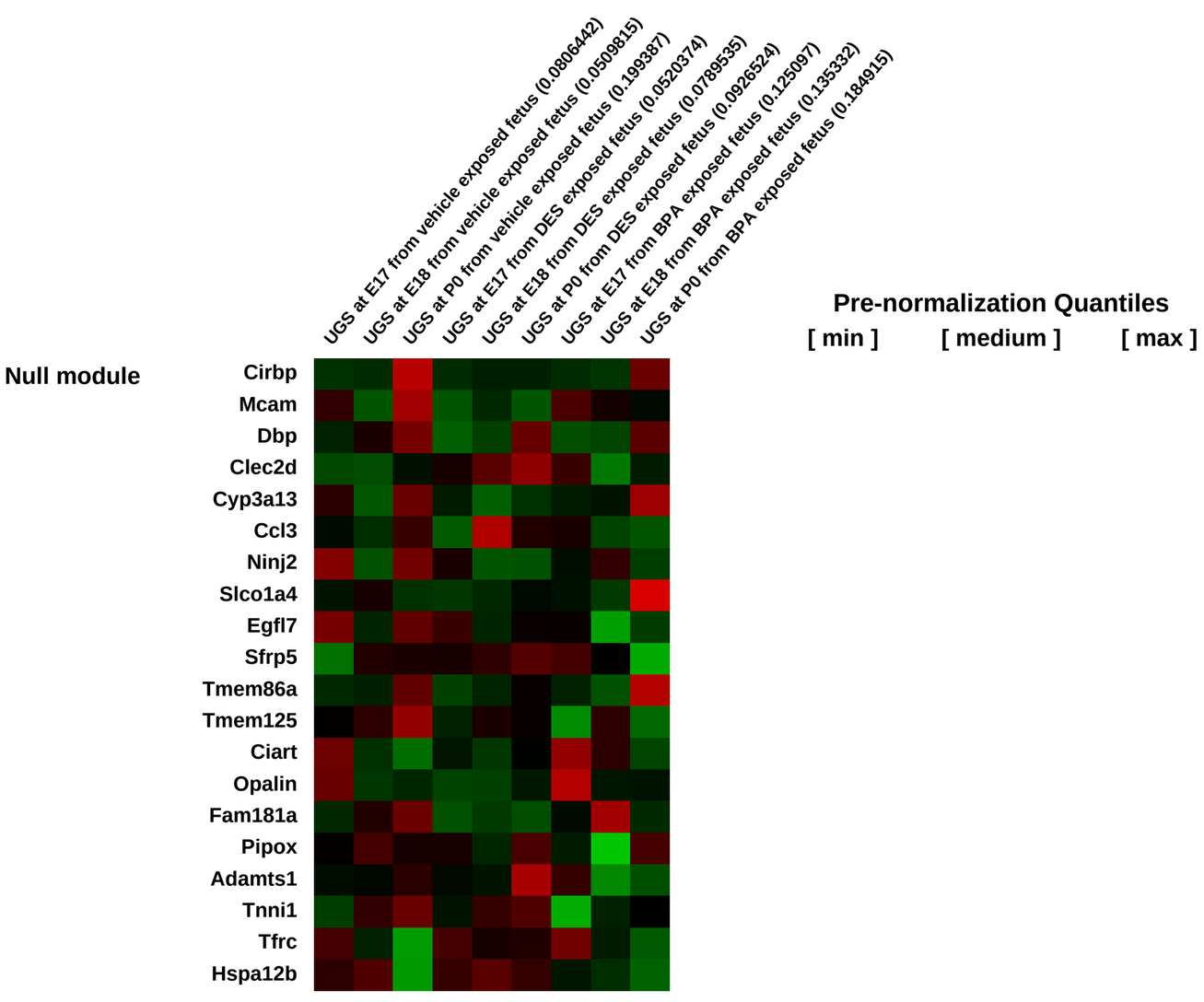

GEO Series "GSE25029" Expression Profiles

Num of samples in this series: 56

Scale of expression profile Z-scores

-3.0 -2.0 -1.0 0.0 1.0 2.0 3.0

GEO Link:	http://www.ncbi.nlm.nih.gov/geo/query/acc.cgi?acc=GSE25029
Status:	Public on Jul 01 2011
Title:	Ionizing radiation in GI tract of Tweak KO mice
Organism:	Mus musculus
Experiment type:	Expression profiling by array
Platform:	GPL1261
Pubmed ID:	21893119
Summary & Design:	**Summary:** TWEAK/Fn14 signaling may regulate the expression of genes involved in epithelial repair and mucosal inflammation. Comparing the gene signatures in WT and TWEAK KO mice will inform the biology of TWEAK/Fn14 pathway in the GI tract. **Overall design:** Mice were treated with 3 Gy of ionizing radiation. After 6h and 24h mice were sacrificed, and whole colon and jejunum were harvested, and RNA was isolated from these tissues. Each CEL file represents a different mouse.

Background corr dist: KL-Divergence = 0.0433, L1-Distance = 0.0713, L2-Distance = 0.0046, Normal std = 0.9679

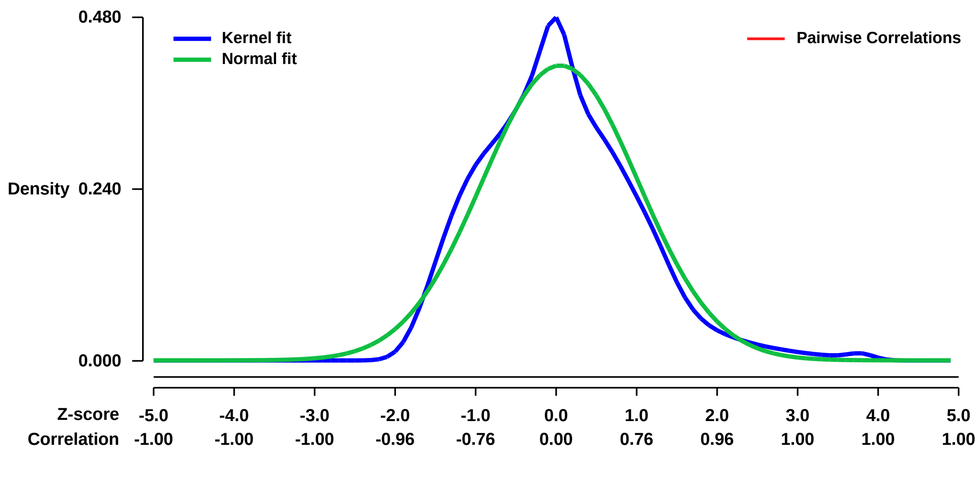

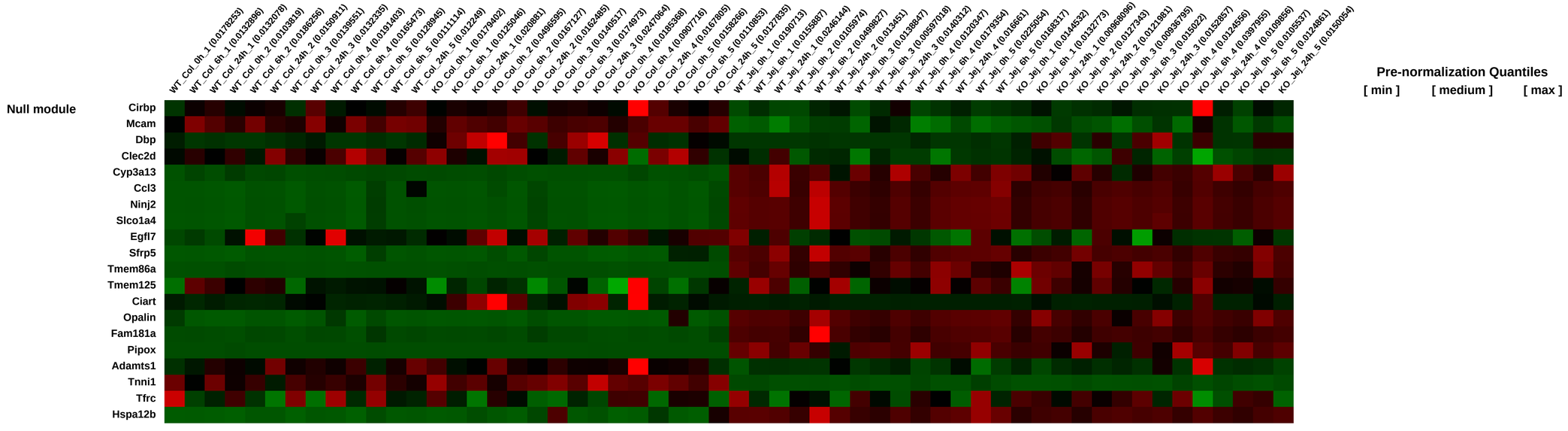

GEO Series "GSE25088" Expression Profiles

Num of samples in this series: 24

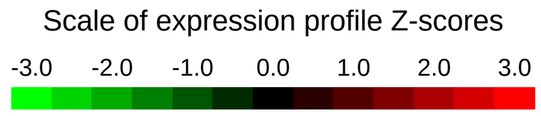

GEO Link:	http://www.ncbi.nlm.nih.gov/geo/query/acc.cgi?acc=GSE25088
Status:	Public on Nov 18 2010
Title:	PPARg and IL-4-induced gene expression data from wild-type and STAT6 knockout mouse bone marrow-derived macrophages
Organism:	Mus musculus
Experiment type:	Expression profiling by array
Platform:	GPL1261
Pubmed ID:	21093321
Summary & Design:	**Summary:** C57Bl/6 wild-type and STAT6 KO mice were used to study PPARg and IL-4 signaling. Bone marrow of 3 mice per group was isolated and differentiated to macrophages with M-CSF (20 ng/ml). 20 ng/ml IL-4 was used to induce alternative macrophage activation and 1 uM Rosiglitazone (RSG) was used to activate PPARg. From each mouse 4 samples were generated: 1. M-CSF, 2. M-CSF+RSG, 3. IL-4 and 4. IL-4+RSG. All compounds were added throughout the whole differentiation process, and frech media was added every other day. Control cells were treated with vehicle (DMSO:ethanol). After 10 days, RNA was isolated and gene expression profiles were analyzed using Mouse Genome 430 2.0 microarrays from Affymetrix. **Overall design:** 3 C57Bl/6 wild-type and 3 STAT6 KO mice were used to isolate bone marrow and from each macrophages were differentiated with or without IL-4 and simultaneously treated with vehicle or RSG. Altogether we analyzed 24 samples with 3 biological replicates as below.

Background corr dist: KL-Divergence = 0.2287, L1-Distance = 0.0913, L2-Distance = 0.0220, Normal std = 0.3531

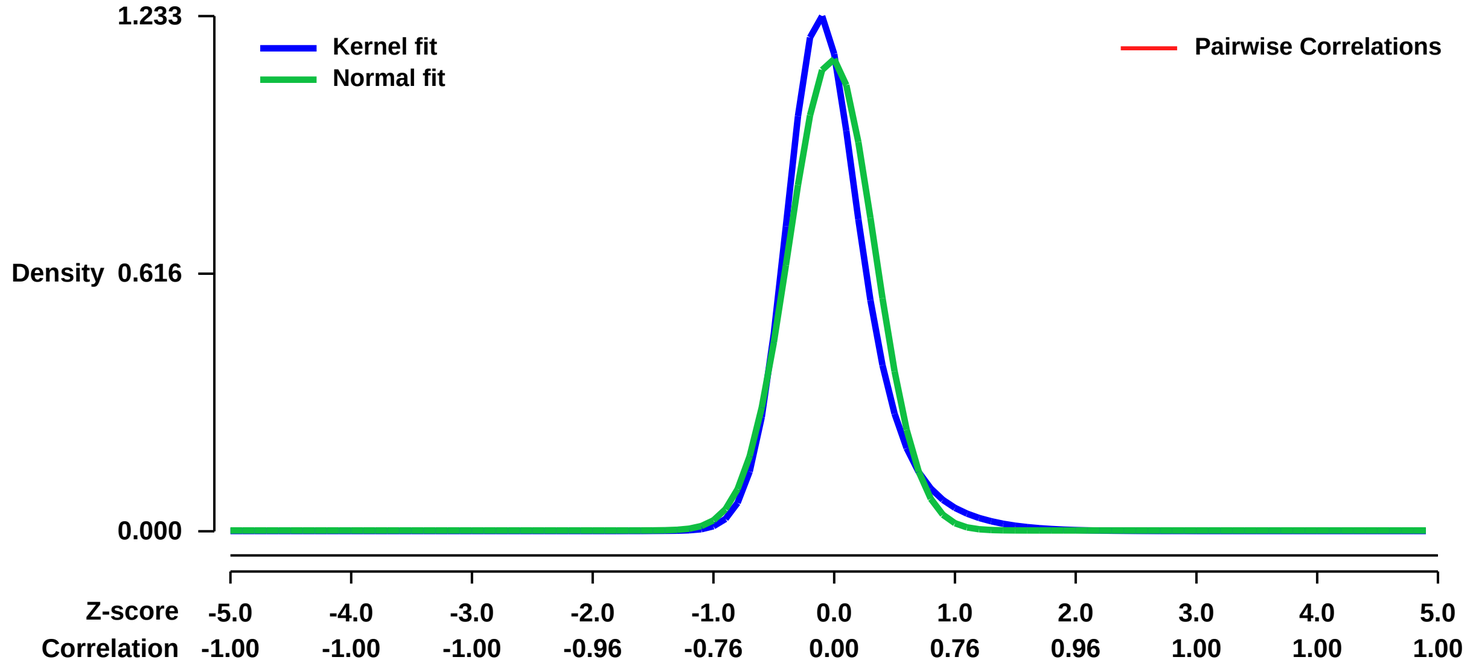

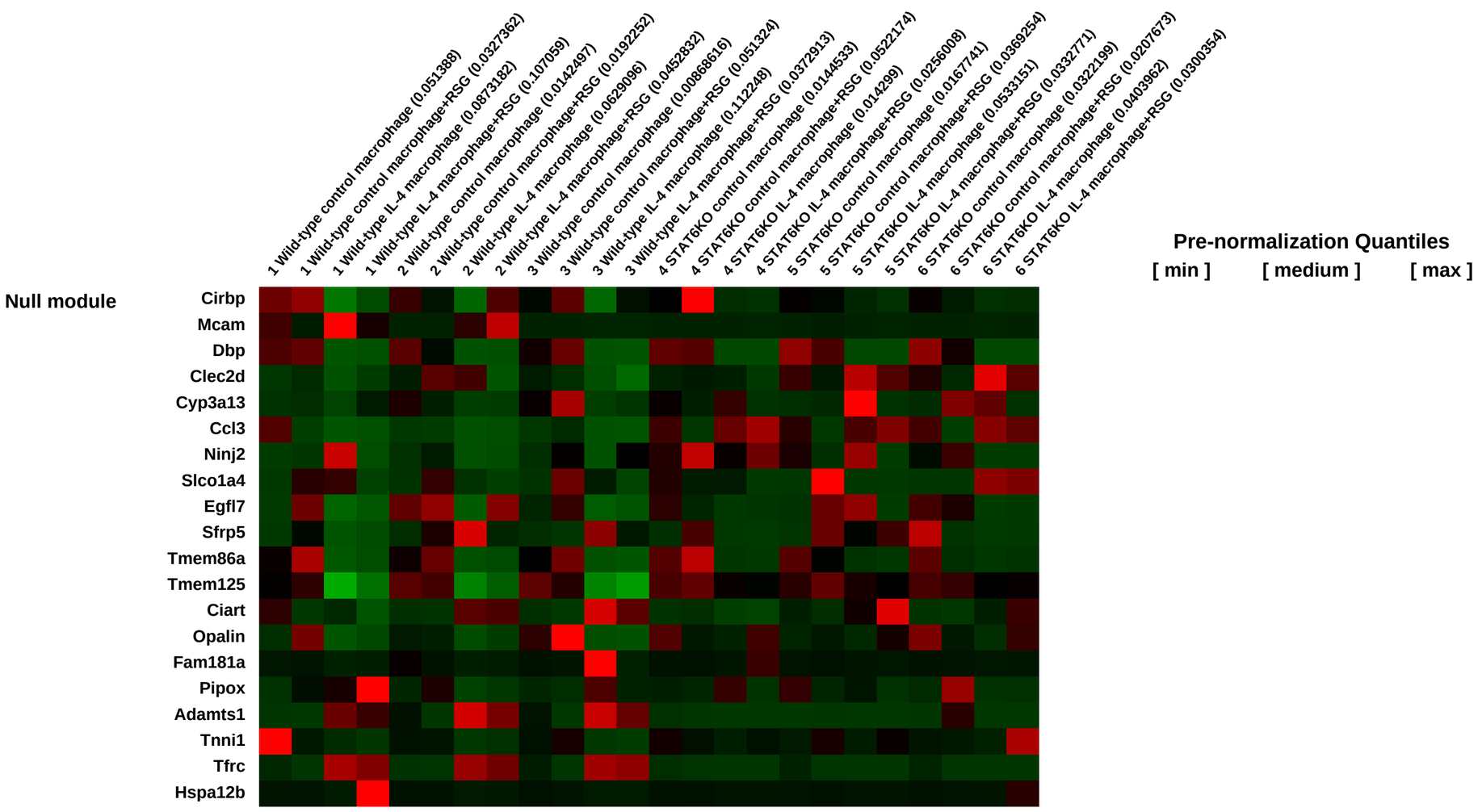

GEO Series "GSE25100" Expression Profiles

Num of samples in this series: 6

Scale of expression profile Z-scores

-3.0 -2.0 -1.0 0.0 1.0 2.0 3.0

GEO Link:	http://www.ncbi.nlm.nih.gov/geo/query/acc.cgi?acc=GSE25100
Status:	Public on Nov 04 2010
Title:	Expression data from CD19-positive splenic B cells isolated from 1-month old ID4+/-TCL1-tg and ID4+/+TCL1-tg mice
Organism:	Mus musculus
Experiment type:	Expression profiling by array
Platform:	GPL1261
Pubmed ID:	21098398
Summary & Design:	**Summary:** The function of ID4 in CLL development was studied in vivo using TCL1 transgenic mouse model that develop leukemia similar to human CLL. TCL1 mice with ID4 single knockout gene have accelerated CLL progression. Results from the animal study suggest ID4 as a tumor suppressor gene that might regulate cell proliferation and apoptosis in B lymphocytes. **Overall design:** Gene expression in CD19-positive splenic B cells collected from 1-month old ID4+/-TCL1-tg and ID4+/+TCL1-tg mice was compared by microarray, the goal is to find ID4-regulated genes involved in CLL development.

Background corr dist: KL-Divergence = 0.0420, L1-Distance = 0.0183, L2-Distance = 0.0003, Normal std = 0.6059

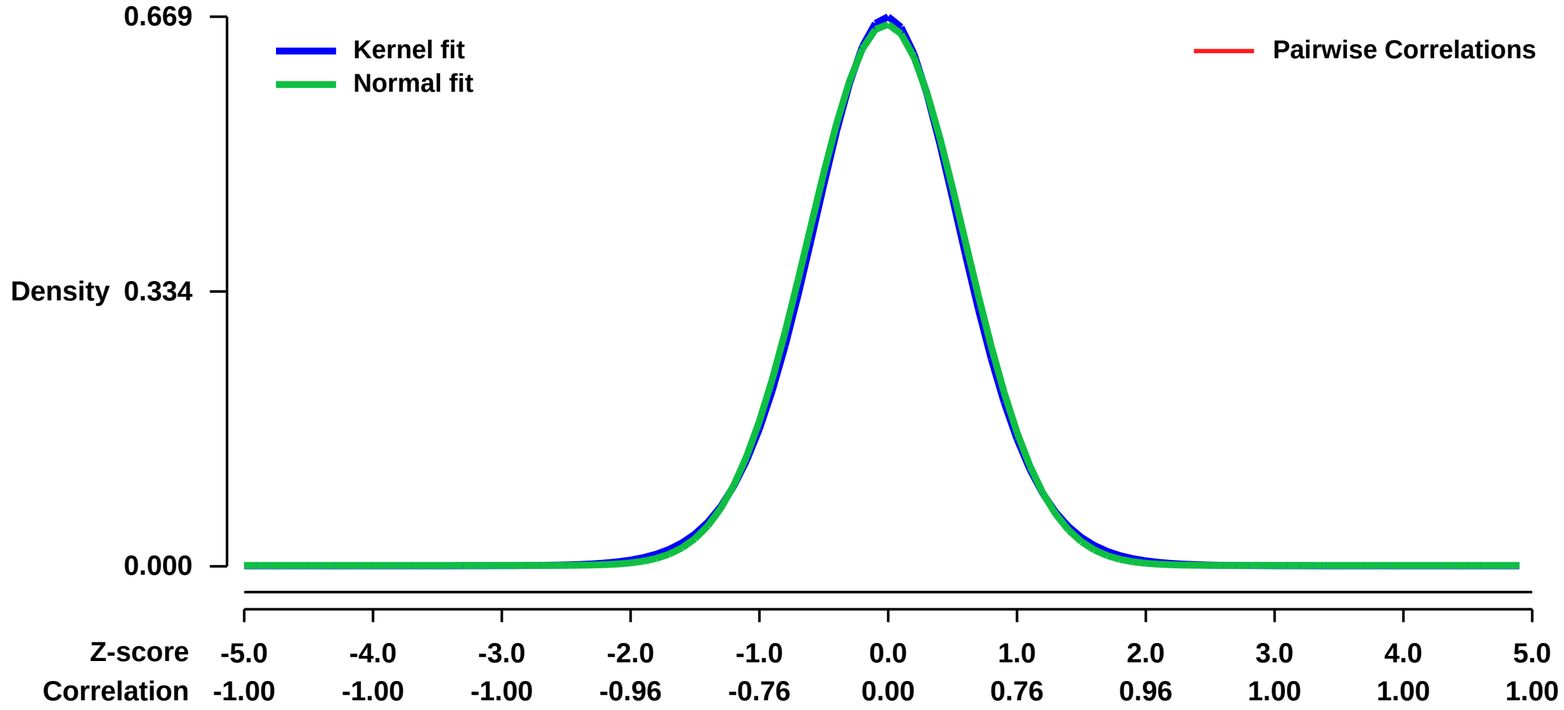

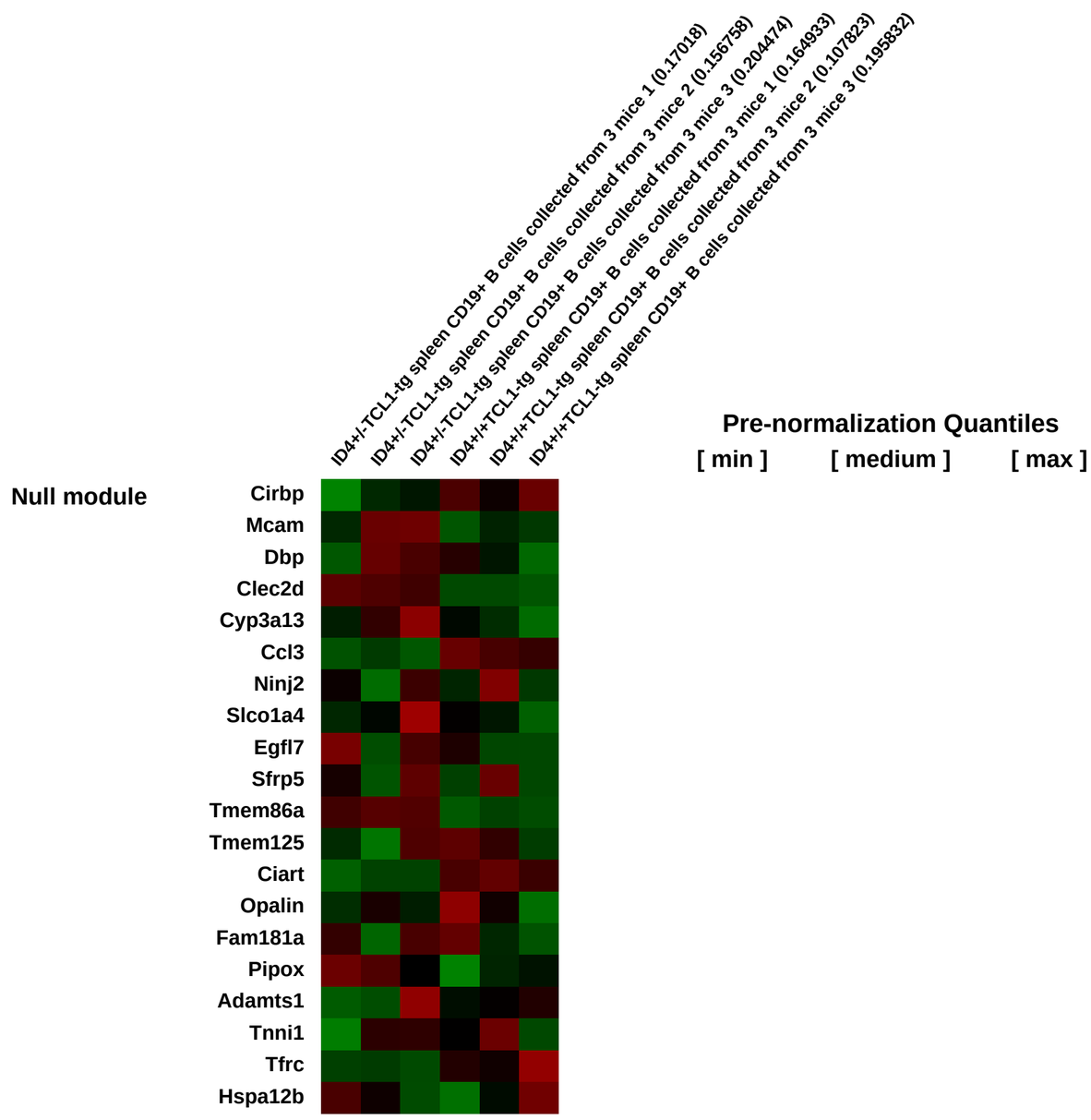

GEO Series "GSE25244" Expression Profiles

Num of samples in this series: 9

Scale of expression profile Z-scores

-3.0 -2.0 -1.0 0.0 1.0 2.0 3.0

GEO Link:	http://www.ncbi.nlm.nih.gov/geo/query/acc.cgi?acc=GSE25244
Status:	Public on Aug 03 2011
Title:	Patterns of gene expression associated with temporal phases of S. aureus infection
Organism:	Mus musculus
Experiment type:	Expression profiling by array
Platform:	GPL1261
Pubmed ID:	21887823
Summary & Design:	**Summary:** To acquire more information regarding the local immune events during the different phases of S. aureus infection, gene profiling using microarray technology was used to identify host genes whose expression is substantively altered in the kidneys during the acute (T2) and persistent phase of infection (T28). Genes associated with the distinct transcript profiles were identified by comparing the relative abundance of transcripts at 2 days (acute) and 28 days (persistent) of infection to their abundance in the kidneys of uninfected control animals (CTL). **Keywords: gene expression** **Overall design:** identification of host genes whose expression is substantively altered in the kidneys during the acute (T2) and persistent phase of infection (T28) compared to uninfected control (CTL).

Background corr dist: KL-Divergence = 0.0707, L1-Distance = 0.0248, L2-Distance = 0.0011, Normal std = 0.5021

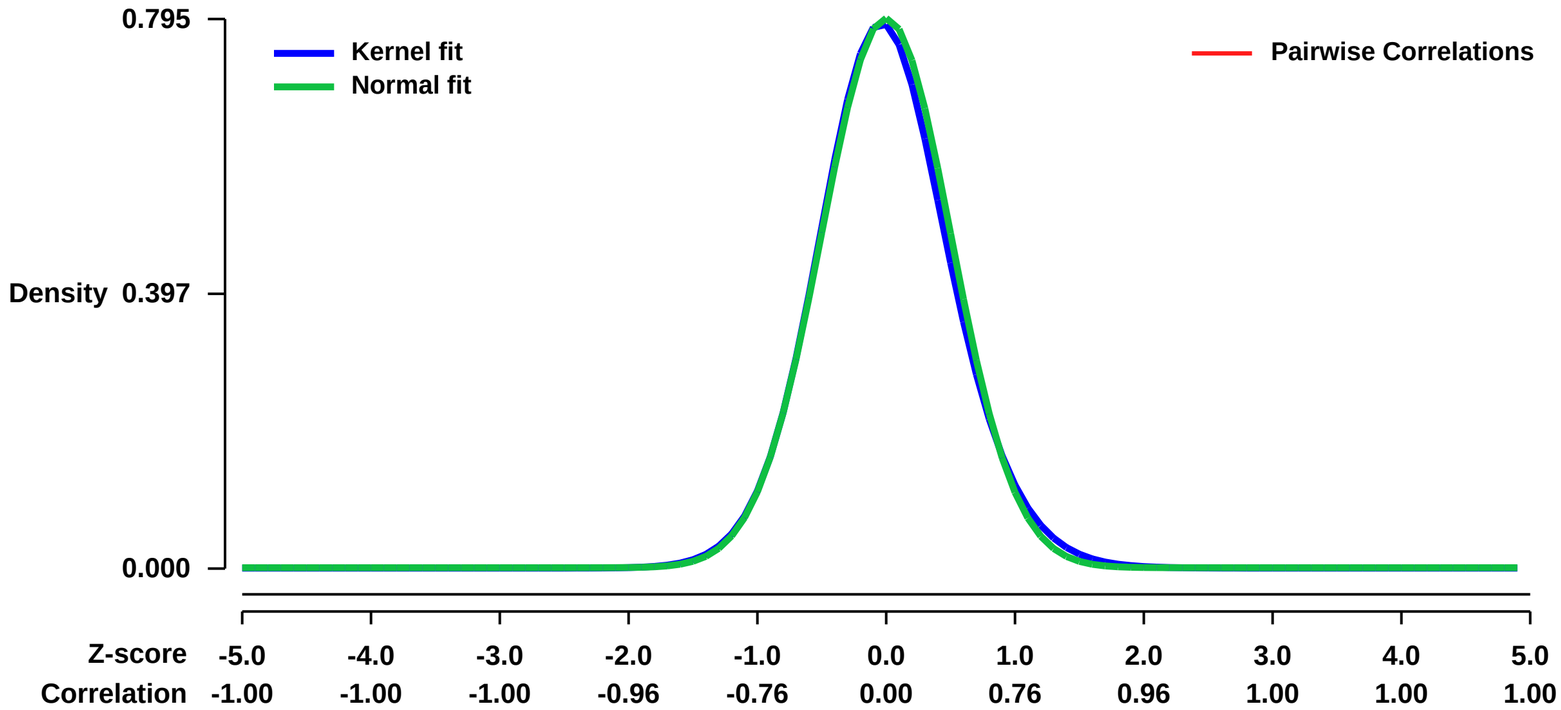

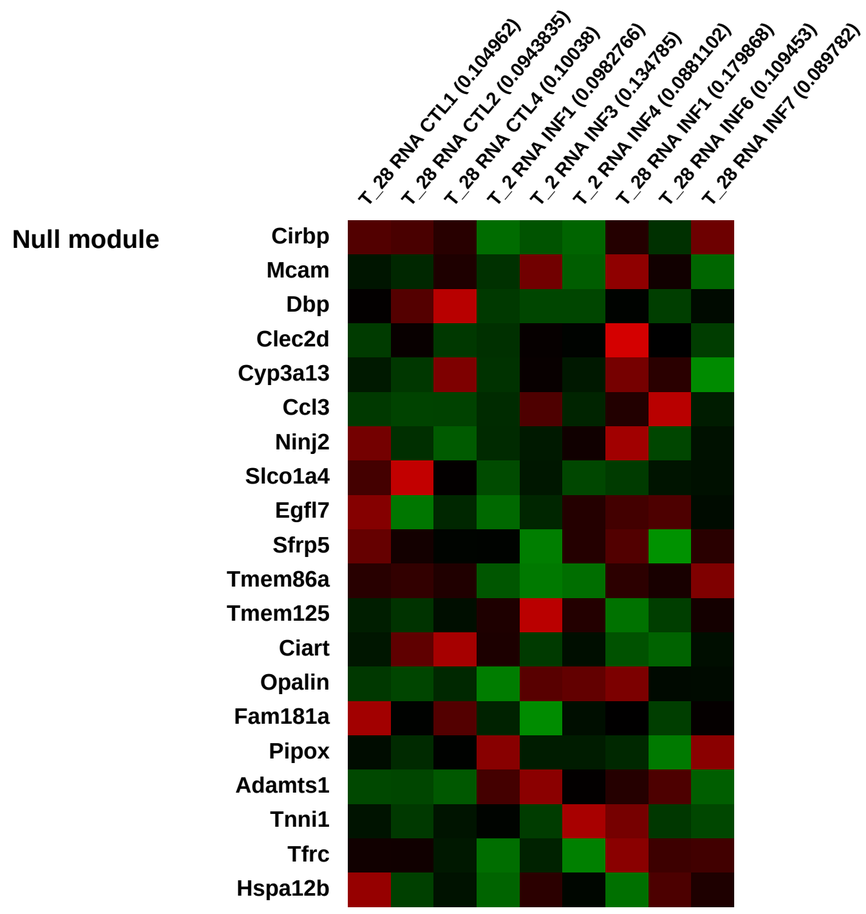

GEO Series "GSE25257" Expression Profiles

Num of samples in this series: 6

Scale of expression profile Z-scores

-3.0 -2.0 -1.0 0.0 1.0 2.0 3.0

GEO Link:	**http://www.ncbi.nlm.nih.gov/geo/query/acc.cgi?acc=GSE25257**
Status:	**Public on Nov 11 2010**
Title:	**Expression data from wild-type and Zmpste24-/- mouse embryonic fibroblasts (MEFs) at an early passage (passage 3, P3)**
Organism:	**Mus musculus**
Experiment type:	**Expression profiling by array**
Platform:	**GPL1261**
Pubmed ID:	
Summary & Design:	**Summary:** **Zmpste24 is a metalloproteinase processing prelamin A into mature lamin A, a nuclear structure protein. Zmpste24-/- mice which accumulate prelamin A in cells recapitulate accelerated aging phenotypes observed in human premature aging disorder, Hutchinson Gilford progeria sydrome (HGPS). Zmpste24-/- mouse embryonic fibroblasts (MEFs) exhibited genomic instabiliy and accelerated aging at cellular level, which is premature senescence.** **We performed microarray analysis on Zmpste24-/- MEFs, compared to wild-type littermates' MEFs, at an early passage (P3), which is a pre-symptom stage before cellular senescence occurs in the mutant MEFs, in order to examine gene expression profile and figure out the underneath mechanism triggering the premature aging process.** **Overall design:** **Early passage wild-type and Zmpste24-/- MEFs were collected for RNA extraction, the quality of RNAs were determinded by Electrophoresis Assay (2100 Bioanalyzer, Agilent) and RNA extractions were used for hybridization on Affymetrix microarrays.**

Background corr dist: KL-Divergence = 0.0217, L1-Distance = 0.0450, L2-Distance = 0.0023, Normal std = 0.8008

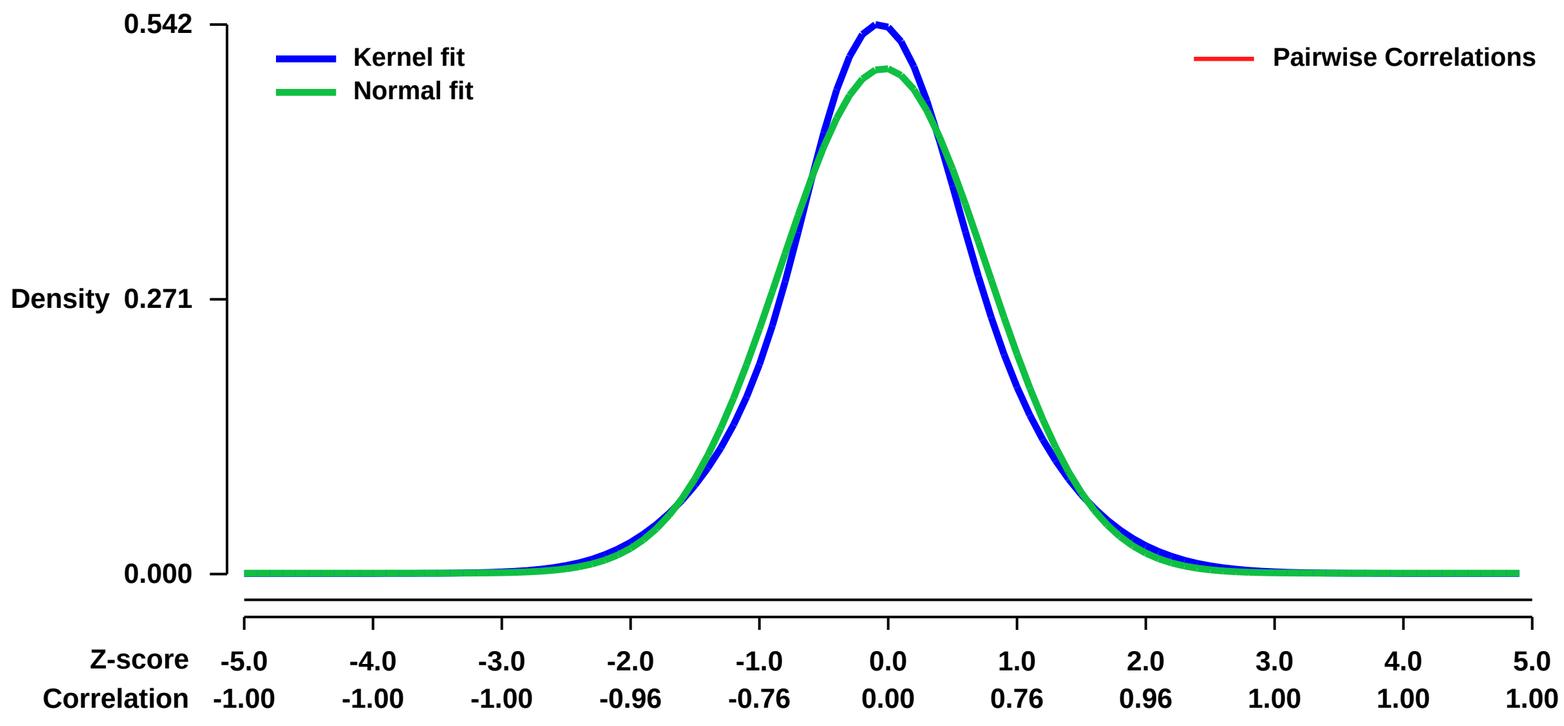

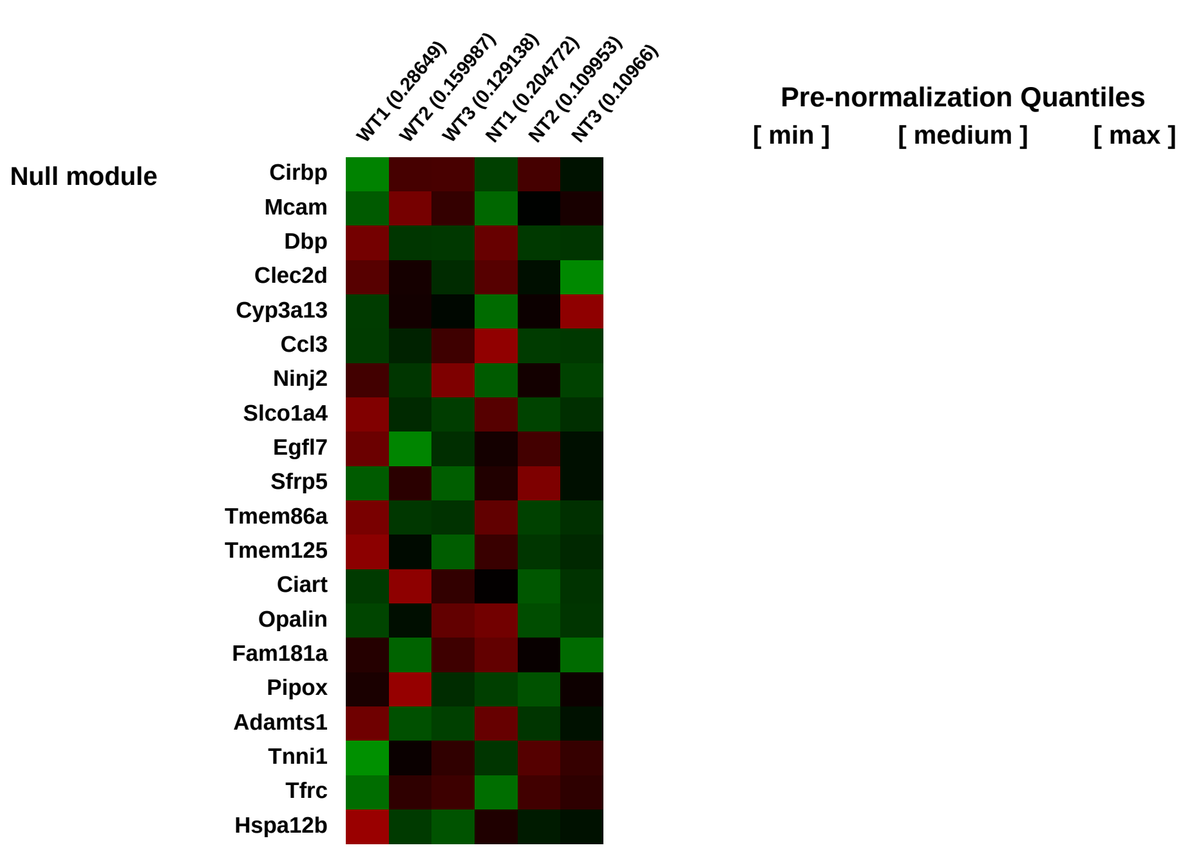

GEO Series "GSE2527" Expression Profiles

Num of samples in this series: 6

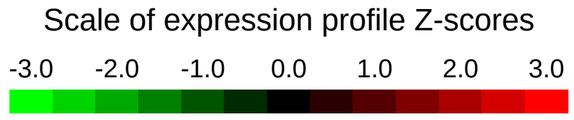

GEO Link:	http://www.ncbi.nlm.nih.gov/geo/query/acc.cgi?acc=GSE2527
Status:	Public on May 06 2005
Title:	Gata-1 Knock Down - Wild Type Megakaryocyte Gene Expression
Organism:	Mus musculus
Experiment type:	Expression profiling by array
Platform:	GPL1261
Pubmed ID:	15860665
Summary & Design:	**Summary:** Hematopoietic progenitor cells were isolated from 13.5 day mouse fetal livers by lineage depletion and expanded for three days. Fetal livers were isolated from both wild type and Gata-1 knock embryos. Gata-1 knock embryos contain a deletion of the Gata-1 promoter sequence that results in undetectable levels of Gata-1 protein specifically in the megakaryocyte lineage. Following progenitor outgrowth megakaryocytes were enriched in a differentiation media for three days and isolated on a discontinuous BSA gradient. The resulting megakaryocytes were >90% pure as determined by acetylcholinesterase staining. These cells were lysed in Trizol and the resulting RNA was used for hybridization. **Keywords = Gata-1** **Keywords = Megakaryocytes** **Keywords: other** **Overall design:**

Background corr dist: KL-Divergence = 0.0240, L1-Distance = 0.0329, L2-Distance = 0.0011, Normal std = 0.7666

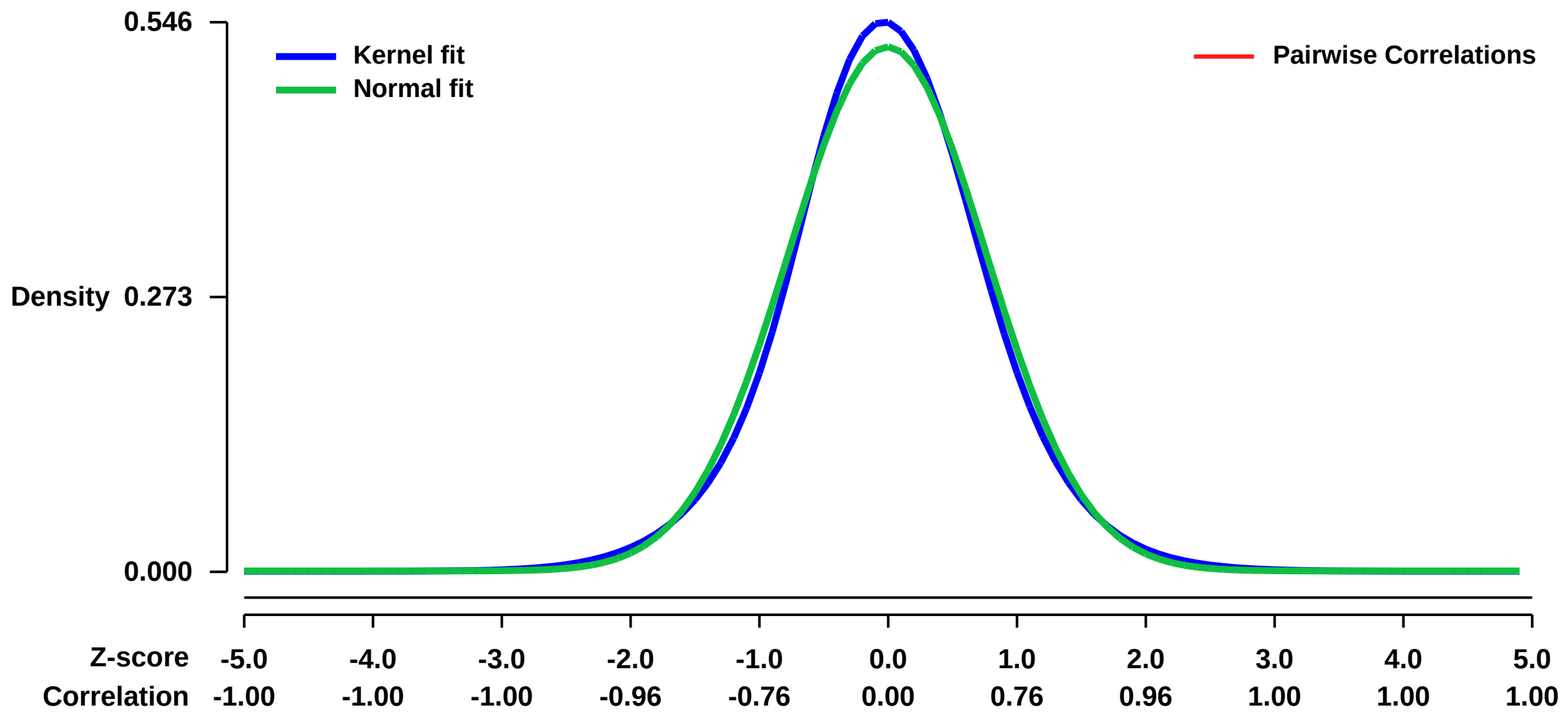

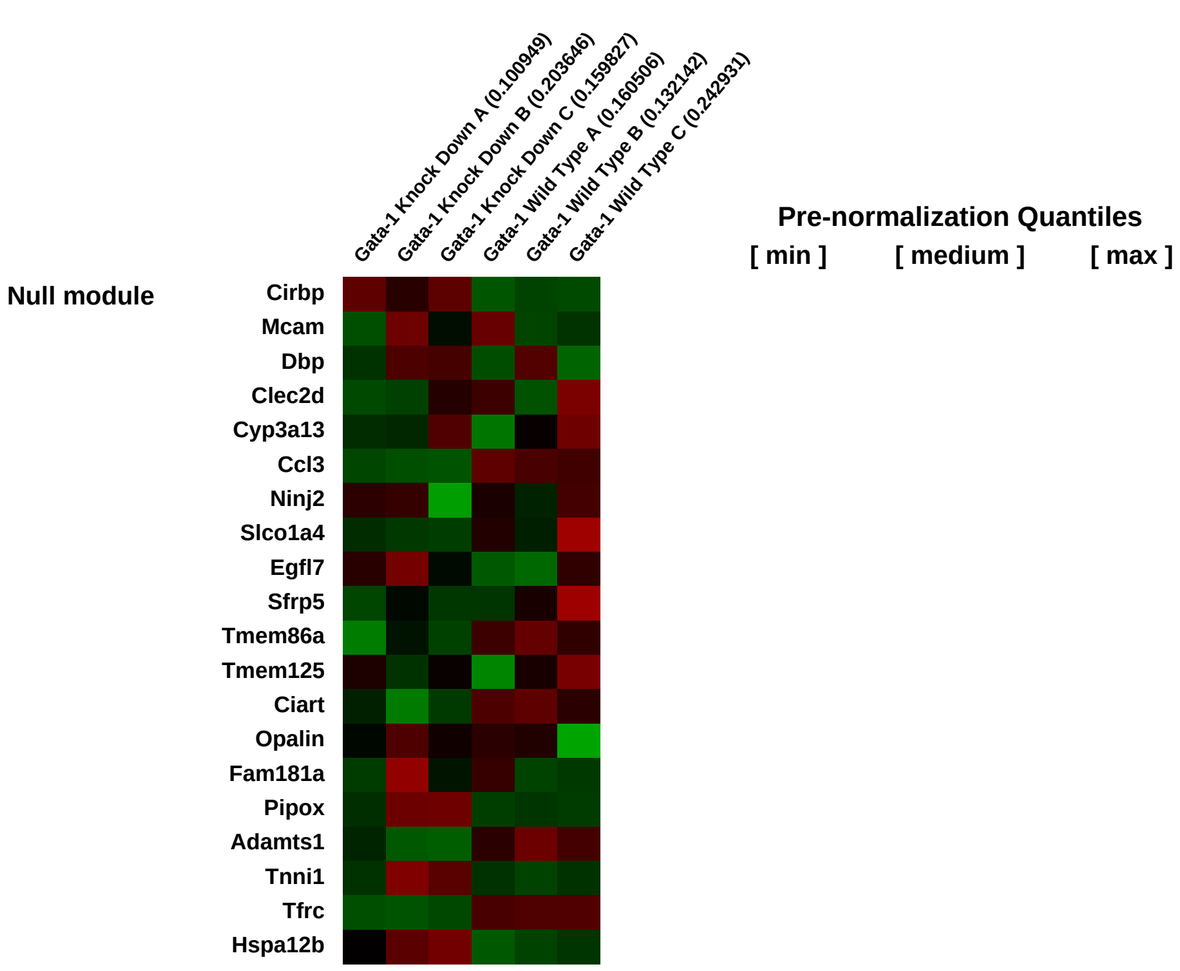

GEO Series "GSE25286" Expression Profiles

Num of samples in this series: 10

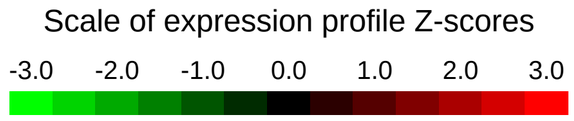

GEO Link:	**http://www.ncbi.nlm.nih.gov/geo/query/acc.cgi?acc=GSE25286**
Status:	**Public on May 01 2012**
Title:	**mRNA expression profile in a murine model of hyperoxia-induced bronchopulmonary dysplasia**
Organism:	**Mus musculus**
Experiment type:	**Expression profiling by array**
Platform:	**GPL1261**
Pubmed ID:	
Summary & Design:	**Summary:** **We performed miRNA and mRNA profiling at postnatal day 14 and day 29 to compare hyperoxia-induced bronchopulmonary dysplasia and wild type. We built potential miRNA-mRNA interaction networks specific to brochopulmonary dysplasia.** **Overall design:** **Replicated time course of mouse lung development at 2 time points (P14, P29). Three replicates per time point for bronchopulmonary dysplasia induced by hyperoxia mouse lung, and two replicates per time point for wild type mouse lung. This dataset represents the mRNA expression profiling component of the study.**

Background corr dist: **KL-Divergence = 0.0273, L1-Distance = 0.0359, L2-Distance = 0.0021, Normal std = 0.6782**

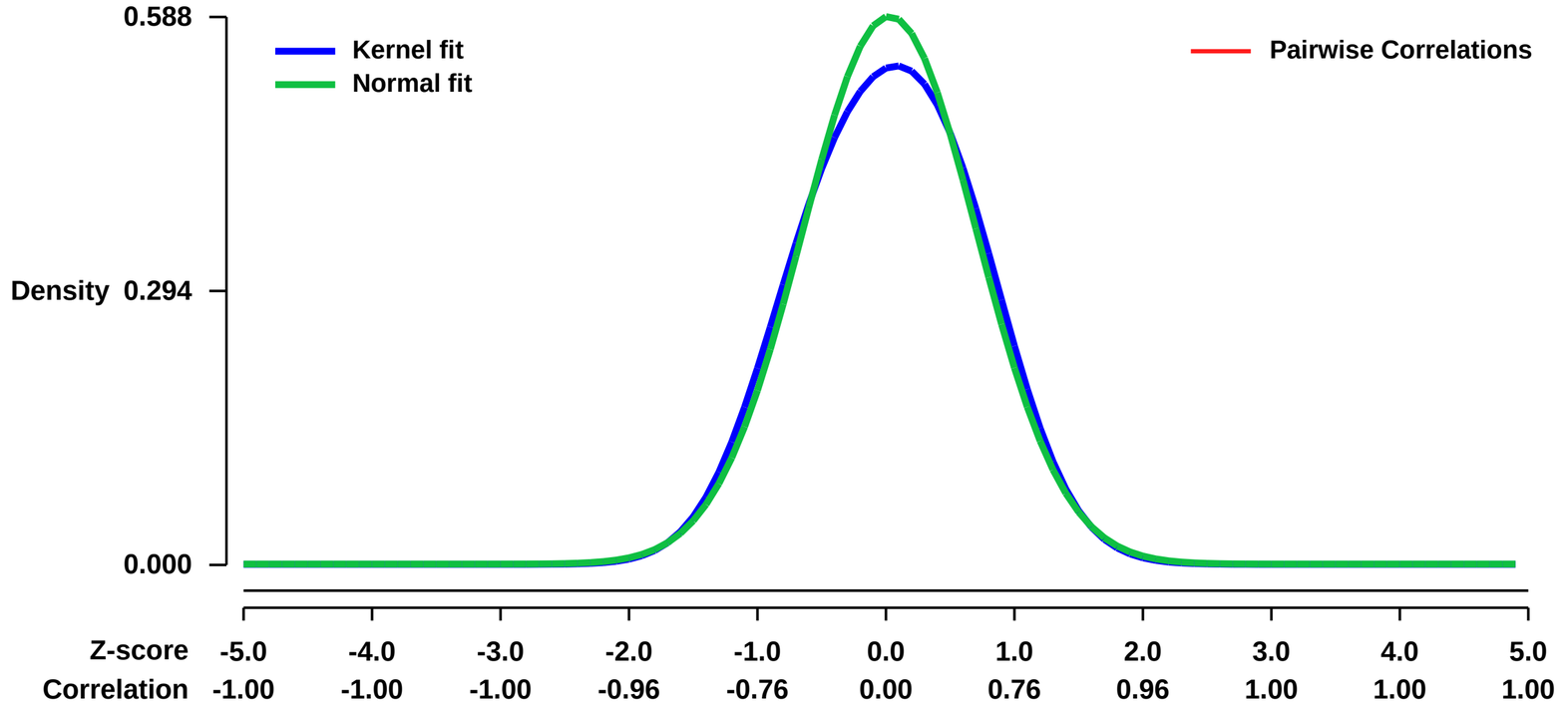

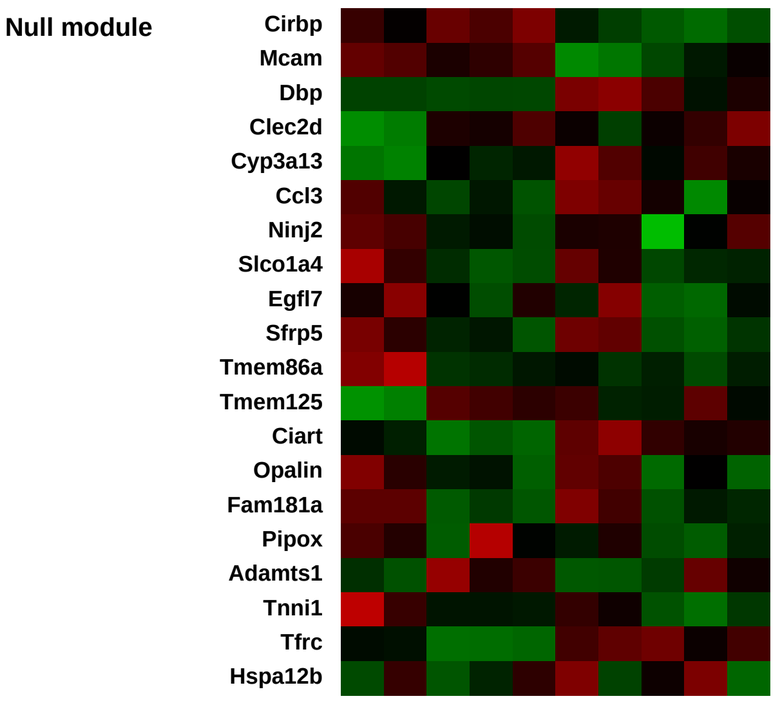

GEO Series "GSE25423" Expression Profiles

Num of samples in this series: 10

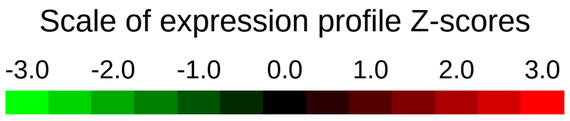

GEO Link:	http://www.ncbi.nlm.nih.gov/geo/query/acc.cgi?acc=GSE25423
Status:	Public on Dec 31 2013
Title:	LSD1 knockdown in 3T3-L1 preadipocytes
Organism:	Mus musculus
Experiment type:	Expression profiling by array
Platform:	GPL1261
Pubmed ID:	23595969
Summary & Design:	**Summary:** Obesity is often associated with a low-grade systemic inflammation state that contributes to the development of insulin resistance and atherosclerotic complications. This is usually coupled with increased macrophage infiltration in the adipose tissue and a defect in adipocyte differentiation that results in accumulation of hypertrophic fat cells characterized by a deregulated pattern of adipokine expression. Here we show that knockdown of histone demethylase lsd1 in 3T3-L1 preadipocytes results in defective adipogenesis and derepression of an inflammatory program in these cells. **Overall design:** The 24h sample groups (siC.24h and siLsd1.24h) consist of two biological replicate samples; the 48h sample groups (siC.48h and siLsd1.48h) consist of three biological replicate samples. Each sample was hybridized to a separate array, for a total of ten arrays.

Background corr dist: KL-Divergence = 0.0685, L1-Distance = 0.0356, L2-Distance = 0.0017, Normal std = 0.5250

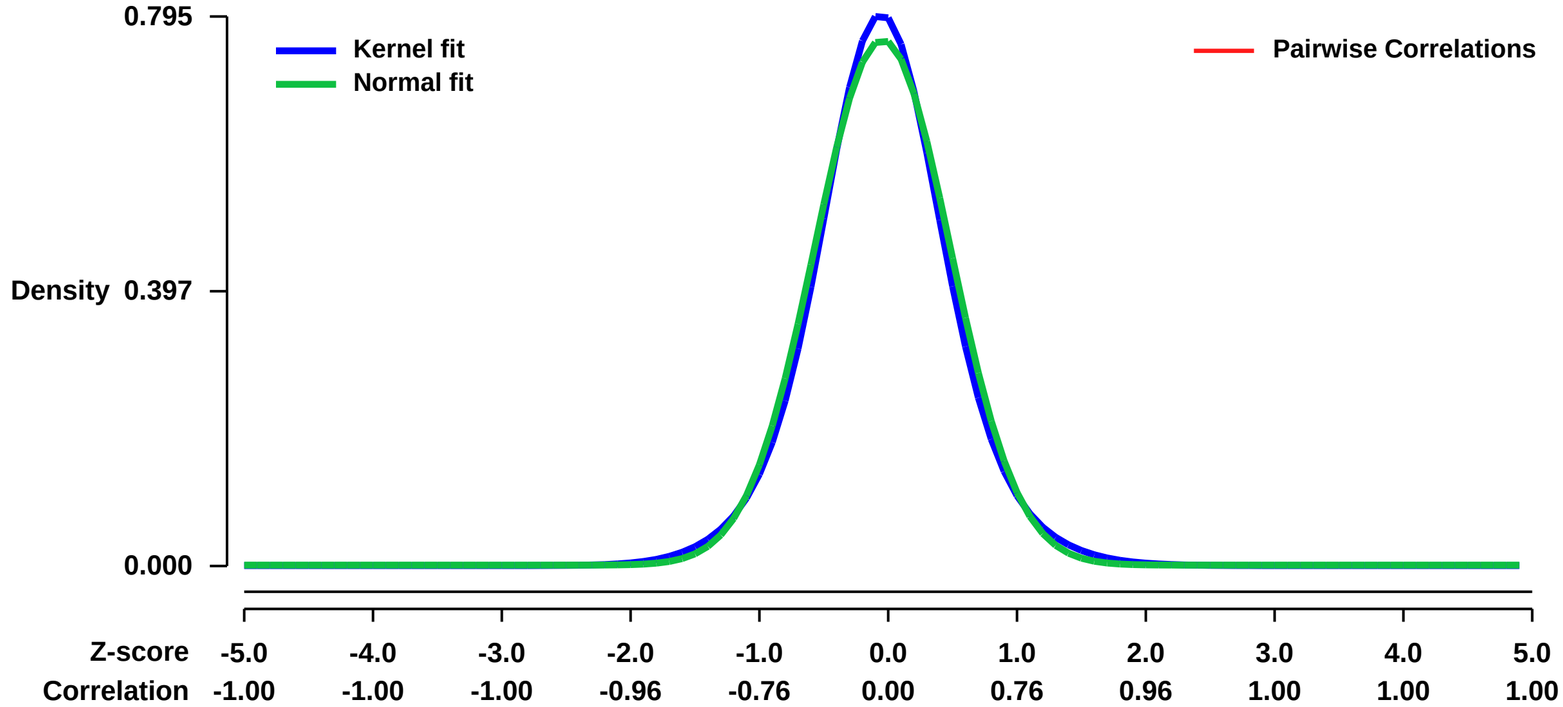

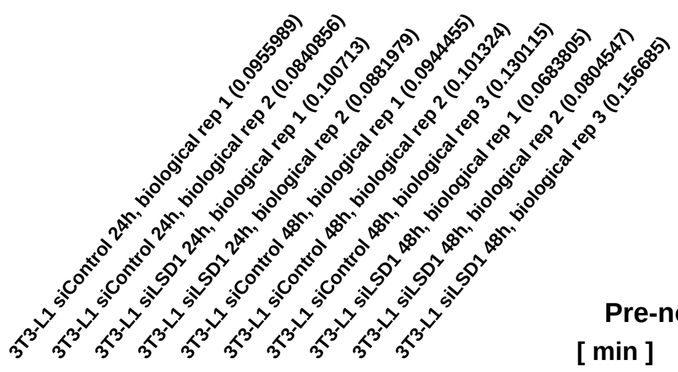

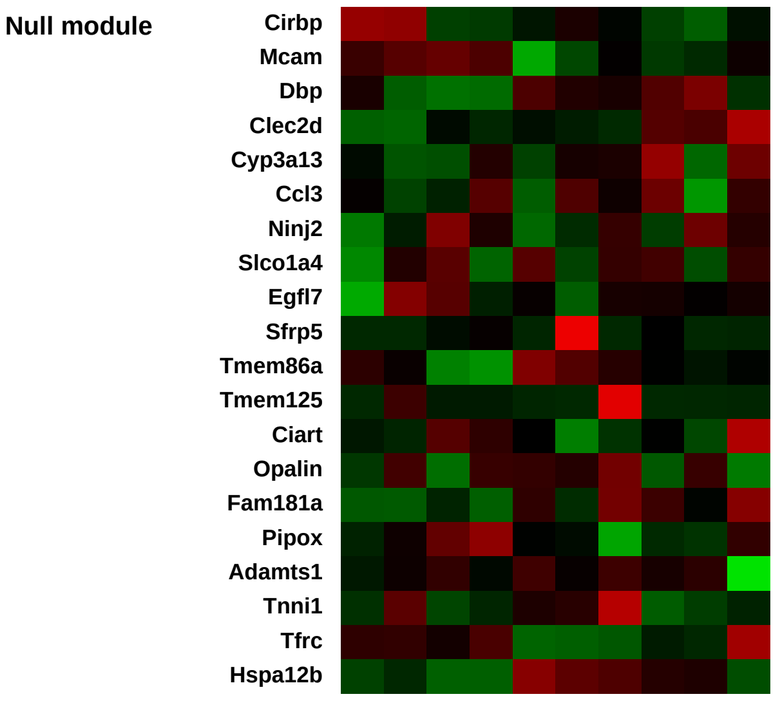

GEO Series "GSE25515" Expression Profiles

Num of samples in this series: 6

Scale of expression profile Z-scores

-3.0 -2.0 -1.0 0.0 1.0 2.0 3.0

GEO Link: http://www.ncbi.nlm.nih.gov/geo/query/acc.cgi?acc=GSE25515

Status: Public on Dec 25 2012

Title: Effect of Lira treatment on heart in obese mice

Organism: Mus musculus

Experiment type: Expression profiling by array

Platform: GPL1261

Pubmed ID:

Summary & Design:

Summary:
C57BL/6 Male mice were treated with high fat diet at the age of 8 weeks and continue the diet for 16 weeks(4 mo) and then injected them with placebo/drug for 1 week before scarifice. Their were sacrifised at the age of 6 months.

Drug: Lira is used to reduce morbidity and mortality due to obesity and its effect on heart.

Overall design:
10 C57BL/6 Male mice under high fat diet for 16 weeks treated with eithe Placebo/drug were chosen for the microarray analysis. Heart from each mouse was disected and the left ventricle was used for TRNA extraction.

Background corr dist: KL-Divergence = 0.0493, L1-Distance = 0.0195, L2-Distance = 0.0004, Normal std = 0.5757

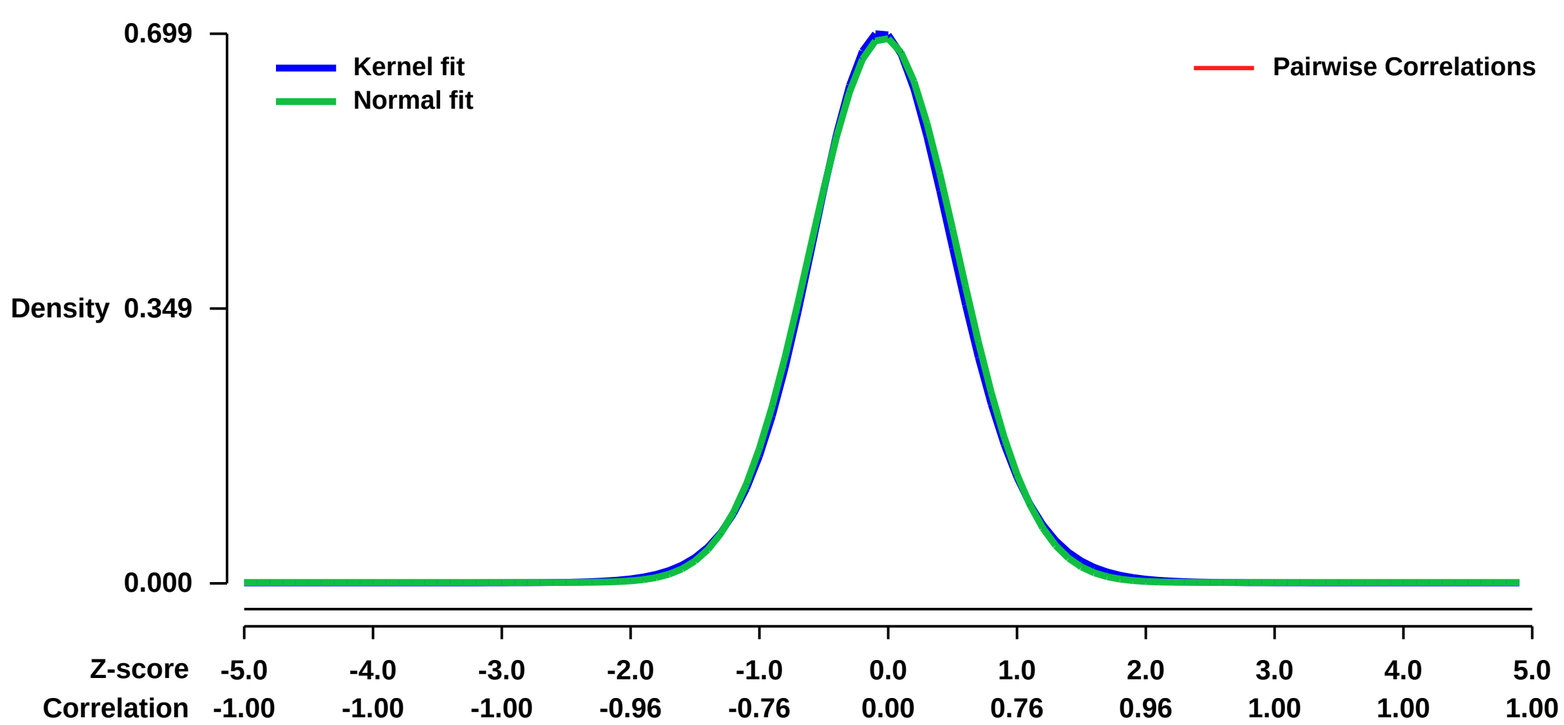

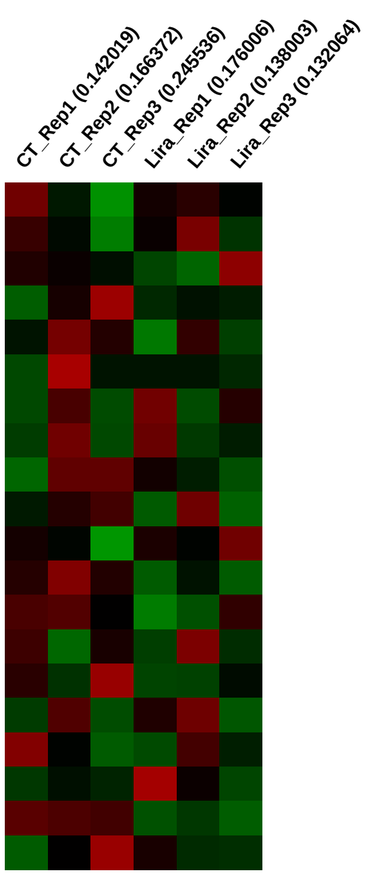

GEO Series "GSE2557" Expression Profiles

Num of samples in this series: 6

Scale of expression profile Z-scores

-3.0 -2.0 -1.0 0.0 1.0 2.0 3.0

GEO Link:	http://www.ncbi.nlm.nih.gov/geo/query/acc.cgi?acc=GSE2557
Status:	Public on Jan 01 2006
Title:	Transcriptome Profiling of High Glucose and Glucosamine-Induced Mouse Mesangial Cells
Organism:	Mus musculus
Experiment type:	Expression profiling by array
Platform:	GPL1261
Pubmed ID:	17178593

Summary & Design:

Summary:
The renal mesangial cells play an important role in the development of diabetic glomerulosclerosis and renal failure. We have previously demonstrated some of the effects of high glucose are mediated via the hexosamine biosynthesis pathway (HBP) in which fructose-6-phosphate is converted to glucosamine-6-phosphate by the rate-limiting enzyme glutamine:fructose-6-phosphate amidotransferase (GFAT). Using Affymetrix murine expression U430 2.0 chips, we examined the global effects of high glucose (HG) and glucosamine (GlcN) on the transcriptomes of a mouse mesangial cell line (MES-13). Of the 34,000 genes on the chip, ~55-60% genes are detected in MES-13 cells. HG induces the expression of ~369 genes at >2-fold where 263 genes are up and 106 genes down regulated. Similarly, GlcN increases the expression of 120 genes and decreases 94 genes. Seventy-two genes are commonly regulated by HG and GlcN, in which 33 genes are up and 39 genes are down. The differential expressions of several genes found in the microarray are also confirmed by quantitative PCR. Significant pathways co-modulated by HG and GlcN are the thioredoxin system (a 20-fold increase in thioredoxin interacting protein expression), endoplasmic reticulum (ER) stress, extracellular matrix and interferon-inducible genes. Furthermore, HG and GlcN target various intracellular pathways including the mitogen-activated protein kinase, TOLL-like receptor, fructose and mannose metabolism, and the biosynthesis of steroids and N-glycans. We conclude from this microarray data and other experimental results that the HBP mediates several effects of high glucose on mesangial cell metabolism, which promotes ER stress, oxidative stress and the interferon-inducible gene expression to cause cell cycle arrest, ECM gene expression and apoptosis.

Cell culture: Stable murine mesangial (MES-13) cells transformed with non-capsid-forming SV-40 virus were obtained from the ATCC, Manassas, VA. These cells display a differentiated mesangial cell phenotype including the typical spindle-like appearance, positive staining for vimentin and desmin, and contraction in response to ANG II and expression of AT1 receptor. The cells were maintained in DMEM and F-12 Nutrient Mixture (Ham's) (4:1 ratio) (GIBCO BRL, Gaithersburg, MD) containing a normal D-glucose concentration of 5.5 mmol/L, 2% FCS, 100 ´µg/ml streptomycin, 100 U/ml penicillin, and 2 mmol/L glutamine (26). The cells were incubated in a humidified incubator of 5% CO2 at 37 ´°C and routinely passaged at confluence every 3 days by trypsinization using 10-cm culture dishes. Approximately 50% confluent monolayers were starved in the above medium without FCS for 1 day and then incubated in the starvation medium with the desired concentrations of glucose and GlcN for 48h (LG, 5.5 mM; HG, 25 mM and GlcN, 1.5 mM + LG).

Total RNA isolation, cDNA and cRNA synthesis and genechip hybridization: Total RNA was isolated using Trizol reagent (Life Technologies, Inc., Massachusetts). cDNA and cRNA synthesis, genechip hybridization, and scanning of the Affymetrix murine expression U430 2.0 chips (the Affymetrix U430 2.0 chip contains 39,000 transcripts targeted at 34,000 well characterized genes) were performed according to the manufacturer's protocol (Affymetrix, Santa Clara, CA). Briefly, 5 mg of RNA (from LG, HG and GlcN treated MES-13 cells) was converted into double-stranded cDNA by reverse transcription using a cDNA synthesis kit (SuperScript Choice, Life Technologies, Inc., MA) with an oligo(dT) 24 primer containing a T7 RNA polymerase promoter site added 3' of the poly(T) (Genset, La Jolla, CA). After second-strand synthesis, labeled cRNA was generated from the cDNA sample by an in vitro transcription reaction supplemented with biotin-11-CTP and biotin-16-UTP (Enzo, Farmingdale, NY). The labeled-cRNAs were purified in RNeasy spin columns (Qiagen, Valencia, CA). Fifteen mg of each cRNA was fragmented at 94 ´°C for 35 min in a fragmentation buffer (40 mM Tris acetate, pH 8.1, 100 mM potassium acetate, 30 mM magnesium acetate). These cRNA fragments were then used to prepare 300 ml of hybridization mixture (100 mM MES, 0.1 mg/ml herring sperm DNA (Promega), 1M sodium chloride, 10 mM Tris, pH 7.6, 0.005% Triton X-100). The solution was equilibrated at 45 ´°C for 5 min and clarified by centrifugation (14,000 x g) at room temperature for 5 min. Aliquots of each sample (10 mg of cRNA in 200 ml of the mater mix) were hybridized to GeneChip Mouse Genome U430 2.0 Array at 45 ´°C for 16 h in a rotisserie oven set at 60 rpm. After the overnight hybridization, the chips were washed with a non-stringent wash buffer (6x saline/sodium phosphate/EDTA) at 25 ´°C, followed by a stringent wash buffer (100 mM MES (pH 6.7), 0.1 M NaCl, 0.01% Tween-20) at 50 ´°C. The GeneChips were then stained with streptavidin-phycoerythrin (Molecular Probe), washed with 6x saline/sodium phosphate/EDTA, incubated with biotinylated anti-streptavidin IgG, followed by a second staining with streptavidin-phycoerythrin. Finally, a third wash with 6x saline/sodium phosphate/EDTA was performed using the GeneChip Fluidics Station 450. The arrays were then scanned in a GeneChip Scanner 3000 (Affymetrix). Each experiment was repeated twice.

Microarray Data analysis: The chips were read with Affymetrix GCOS v1.2, and the probe intensity files were modeled with DChip 1.3 (Harvard School of Public Health) in both PM-only and PM-MM modes. Consensus differentially regulated genes were initially derived from repeat experiments on the bases of a 90% CI of greater than 2-fold change in expression and with p<0.05 of error in paired t-test across repeats. This was further validated through modeling of variance between sample groups (one-way ANOVA) conducted in GeneSpring 6 (Silicon Genetix). The consensus gene-set was clustered in DChip and GeneSpring 6.0, with OntoExpress (Wayne State University) to explore ontological associations. Further ontological and pathway analyses were conducted with the GeneGo software and NIH's DAVID bioinformatics programs (http://appls.niaid.nih.gov/david).

Keywords = glucose

Keywords = glucosamine

Keywords = mesangial cells

Keywords = hexosamine

Keywords: repeat sample

Overall design:

Background corr dist: KL-Divergence = 0.0110, L1-Distance = 0.0200, L2-Distance = 0.0005, Normal std = 0.8500

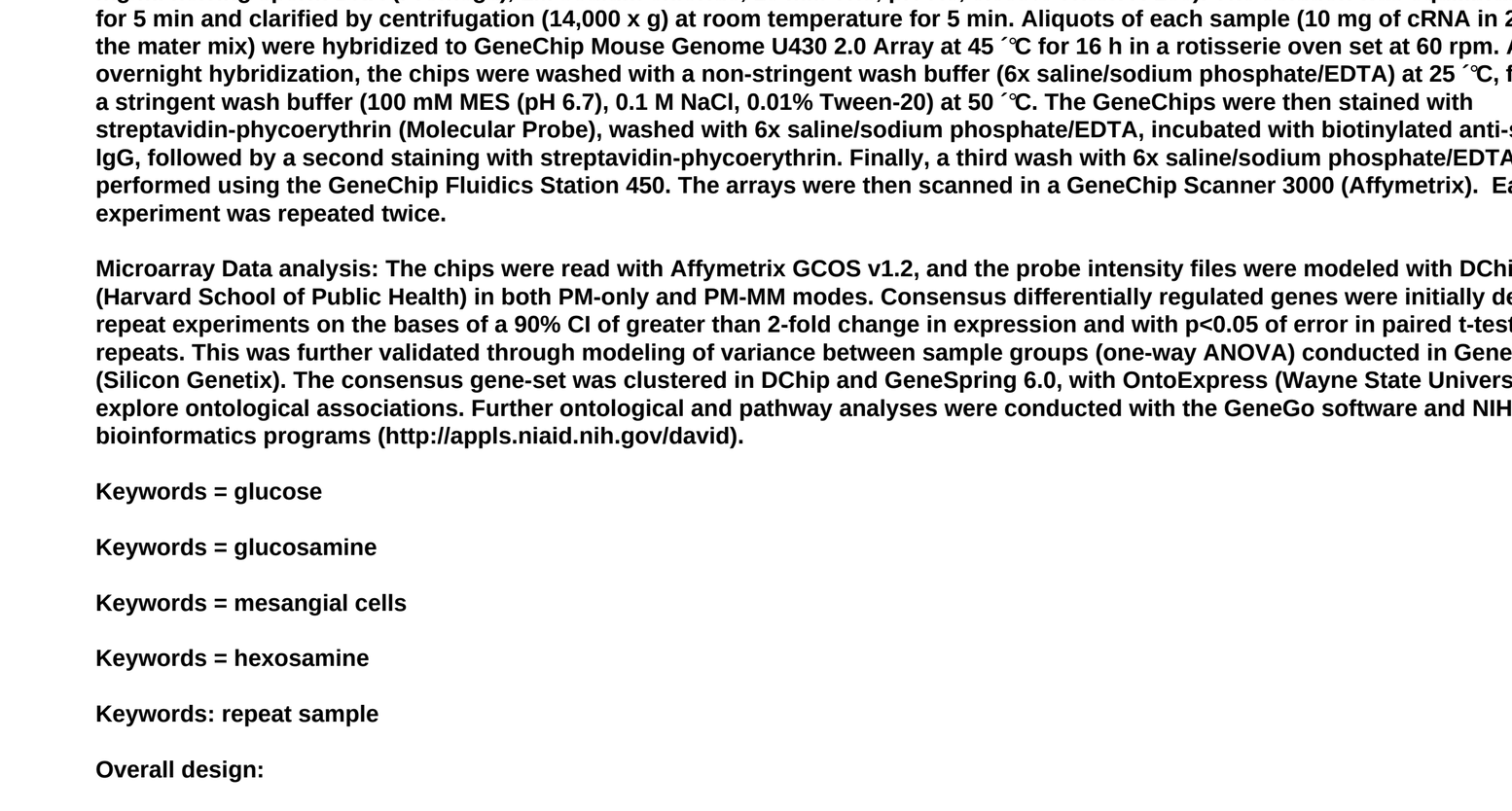

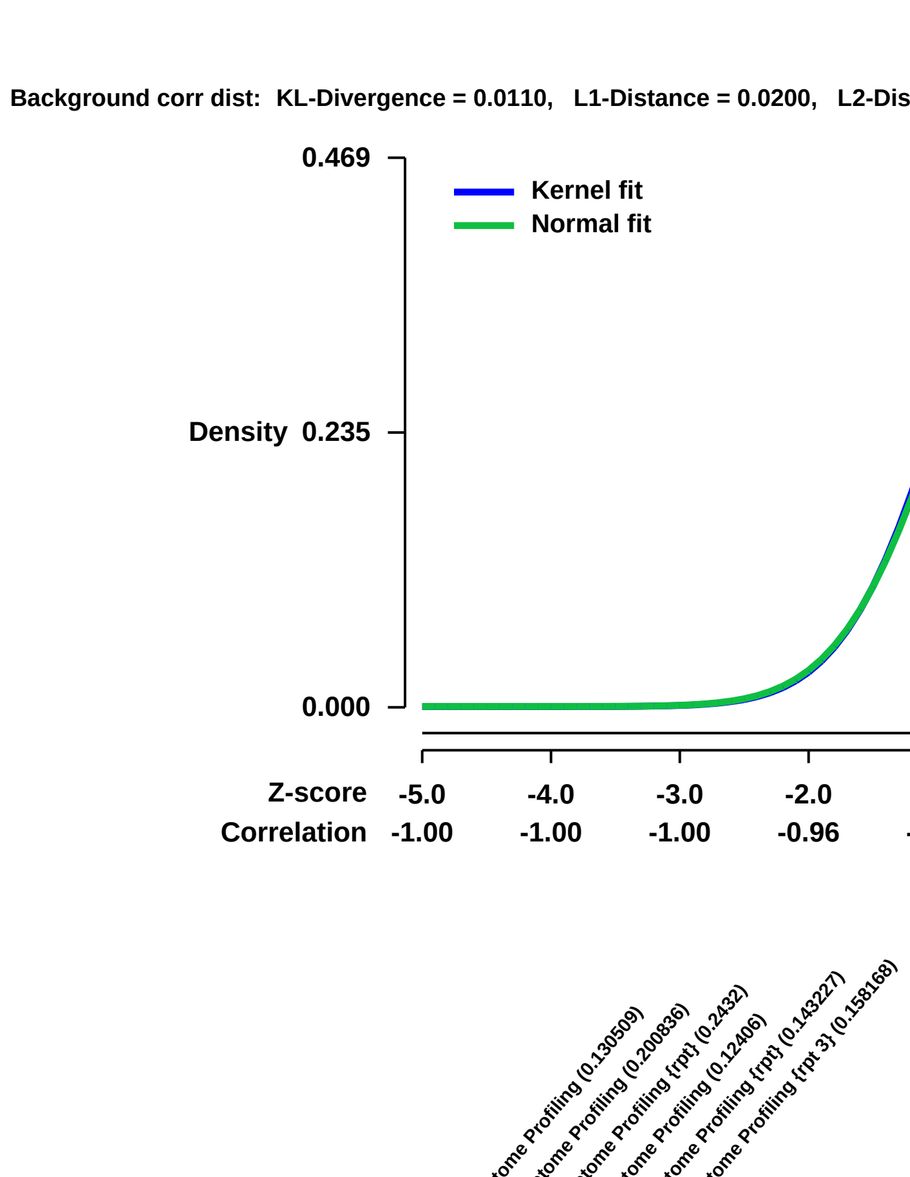

GEO Series "GSE25574" Expression Profiles

Num of samples in this series: 8

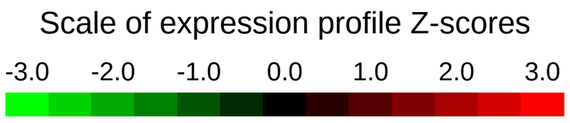

GEO Link:	http://www.ncbi.nlm.nih.gov/geo/query/acc.cgi?acc=GSE25574
Status:	Public on Nov 29 2010
Title:	Hypothalamic transcriptome plasticity in two rodent species reveals divergent differential gene expression but conserved pathways
Organism:	Mus musculus
Experiment type:	Expression profiling by array
Platform:	GPL1261
Pubmed ID:	21070396
Summary & Design:	**Summary:** We have addressed the question of how different rodent species cope with the life-threatening homeostatic challenge of dehydration at the level of transcriptome modulation in the supraoptic nucleus (SON), a specialised hypothalamic neurosecretory apparatus responsible for the production of the antidiuretic peptide hormone arginine vasopressin (AVP). AVP maintains water balance by promoting water conservation at the level of the kidney. Dehydration evokes a massive increase in the regulated release of AVP from SON axon terminals located in the posterior pituitary, and this is accompanied by a plethora of changes in the morphology, electrophysiological properties, biosynthetic and secretory activity of this structure. Microarray analysis was used to generate a definitive catalogue of the genes expressed in the mouse SON, and to describe how the gene expression profile changes in response to dehydration. Comparison of the genes differentially expressed in the mouse SON as a consequence of dehydration with those of the rat has revealed many similarities, pointing to common processes underlying the function-related plasticity in this nucleus. In addition we have identified many genes that are differentially expressed in a species-specific manner. However, in many cases, we have found that the hyperosmotic cue can induce species-specific alterations in the expression of different genes in the same pathway. The same functional end can be served by different means, via differential modulation, in different species, of different molecules in the same pathway. We suggest that pathways, rather than specific genes, should be the focus of integrative physiological studies based on transcriptome data. **Overall design:** Microarray analysis. Separate microarrays (n=4) were probed using independently generated target. For each completely independent replicate, tissue from 1 mouse was used for RNA extraction.

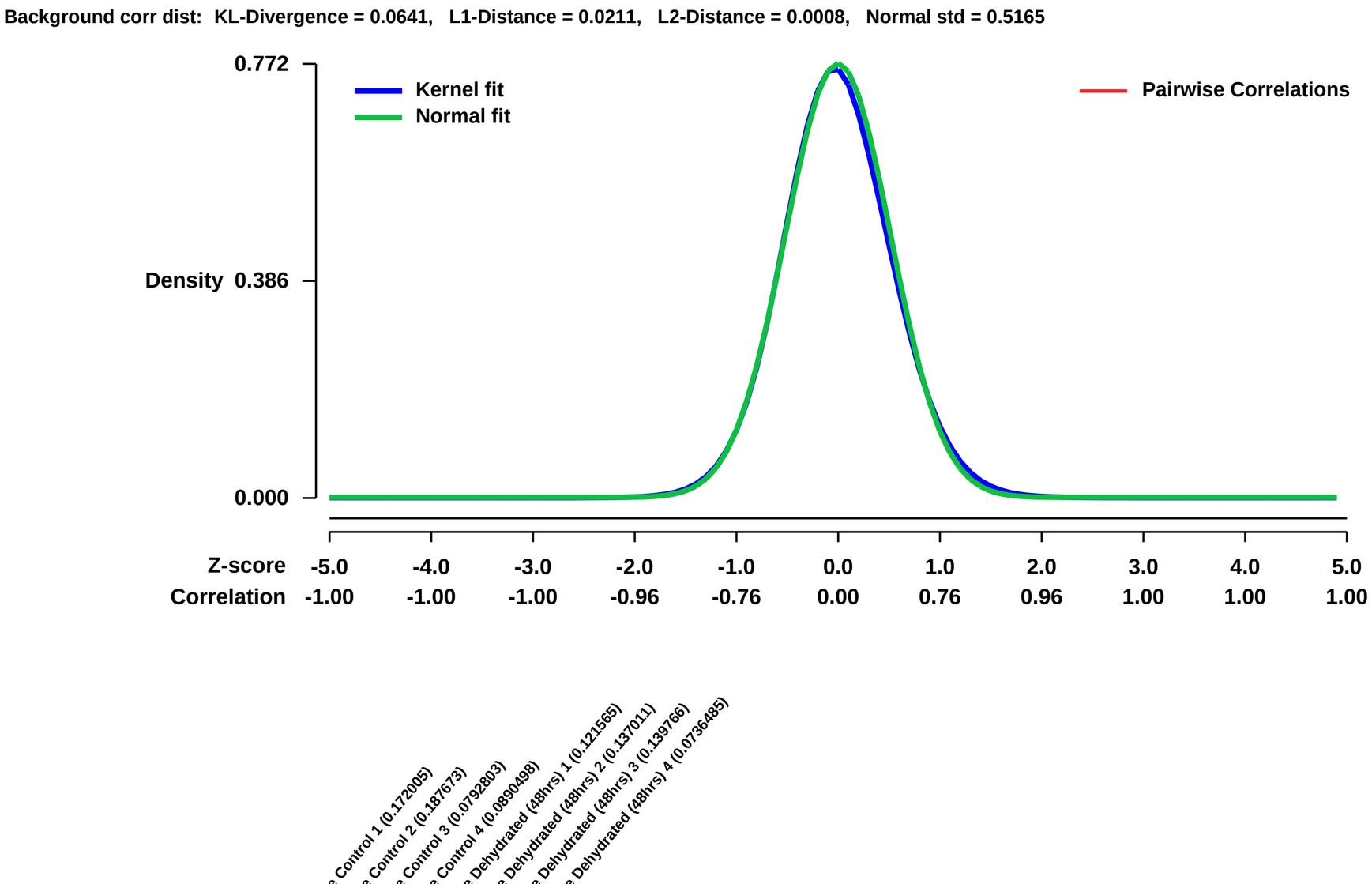

GEO Series "GSE25616" Expression Profiles

Num of samples in this series: 10

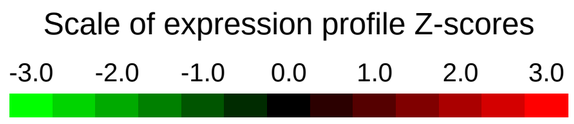

GEO Link:	**http://www.ncbi.nlm.nih.gov/geo/query/acc.cgi?acc=GSE25616**
Status:	**Public on Jun 21 2011**
Title:	**Liver expression data from lactating QSi5 mice**
Organism:	**Mus musculus**
Experiment type:	**Expression profiling by array**
Platform:	**GPL1261**
Pubmed ID:	
Summary & Design:	**Summary:** **The liver plays a crucial role in energy partitioning and is particularly important for the increased demand from the mammary gland during lactation. The present study identifies genes associated with negative energy balance in lactating mice.** **We used microarrays to detail the gene expression underlying negative energy balance and identified distinct classes of up-regulated genes.** **Overall design:** **The pregnant mice was fed a high GI diet during and throughout pregnancy until peak lactation (HGI group; n = 5). The second group was fed a low GI diet over the same period (LGI group; n = 5). The HGI diet included 51.4% (W/W basis) of glucose and a gross energy of 15.6MJ/Kg and the LGI diet contained 51.4% (W/W basis) of high amylase starch (Hi-Maze) and a gross energy of 16.3MJ/Kg. At the end of this period, mice were euthanazed and livers were removed and microarray was performed.**

Background corr dist: KL-Divergence = 0.0978, L1-Distance = 0.0327, L2-Distance = 0.0020, Normal std = 0.4415

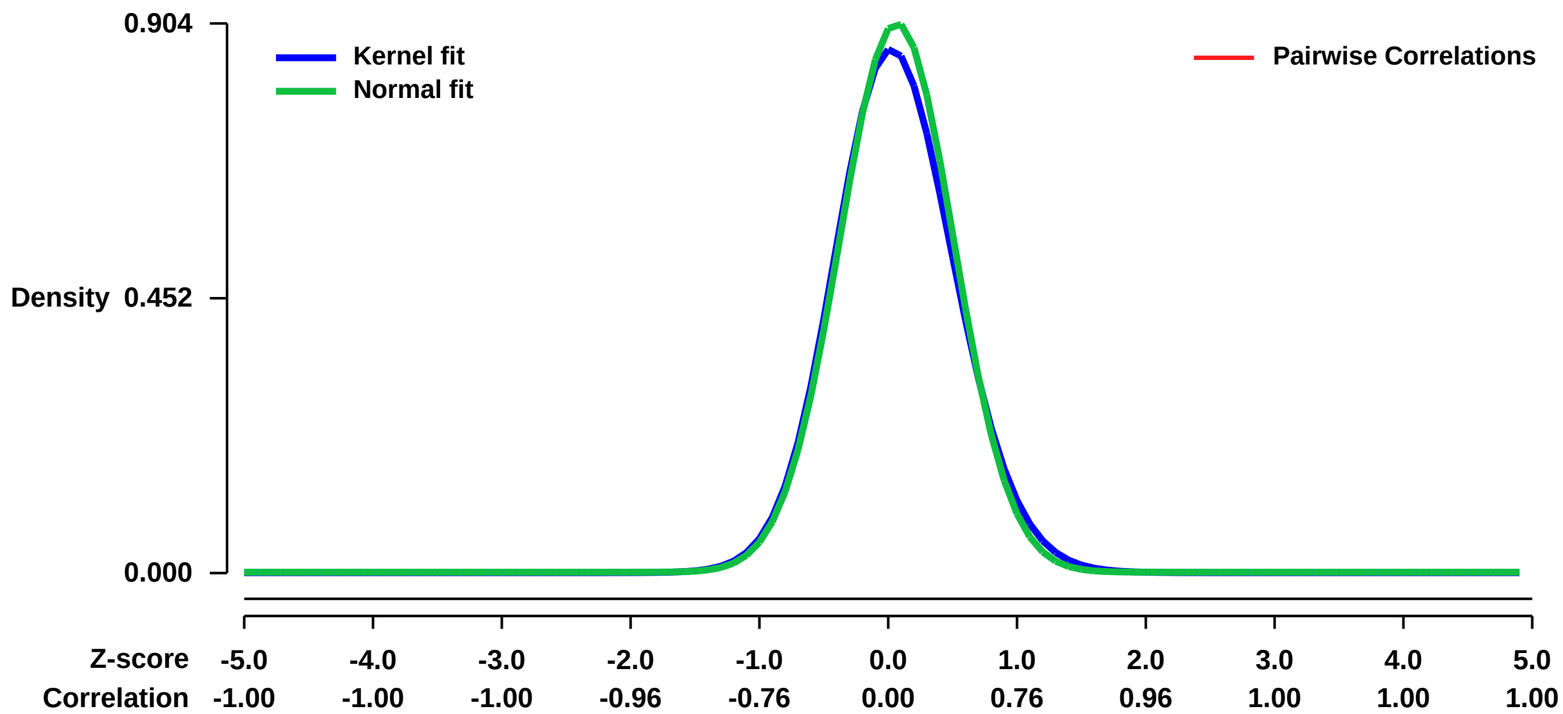

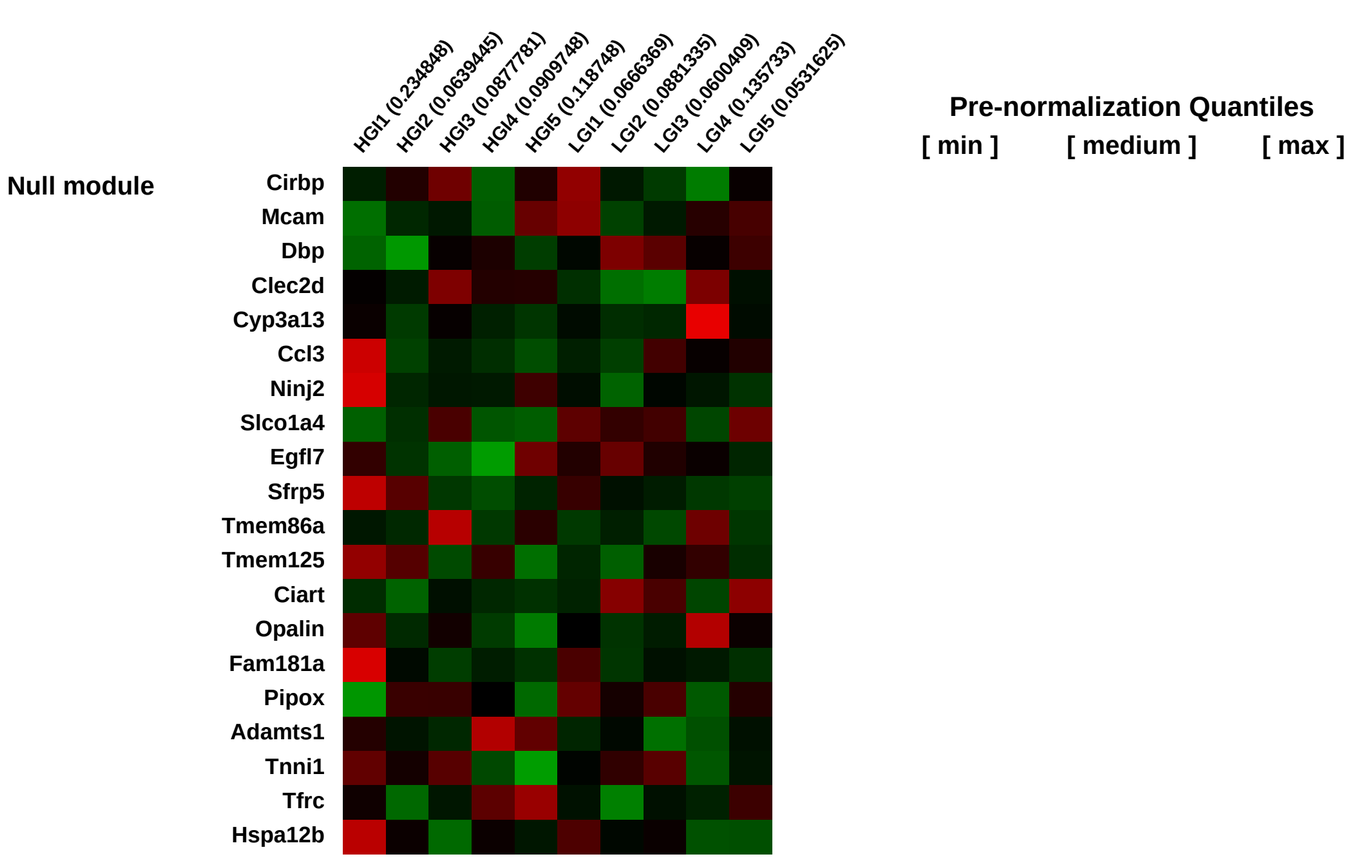

GEO Series "GSE25636" Expression Profiles

Num of samples in this series: 8

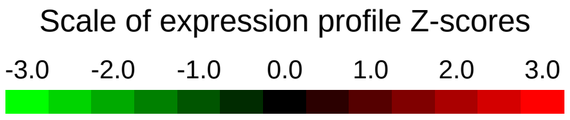

GEO Link:	http://www.ncbi.nlm.nih.gov/geo/query/acc.cgi?acc=GSE25636
Status:	Public on Jul 10 2012
Title:	A mouse model of deregulation of the malt1 oncogene recapitulates the pathogenesis of human malt lymphoma [MouseSca1 dataset]
Organism:	Mus musculus
Experiment type:	Expression profiling by array
Platform:	GPL1261
Pubmed ID:	22689981
Summary & Design:	**Summary:** Attempts at modeling chromosomal translocations involving MALT1 gene, hallmarks of human mucosa-associated lymphoid tissue (MALT) lymphoma, have failed to reproduce the disease in mice. Here we describe a transgenic model in which MALT1 expression was targeted to mouse hematopoietic stem/progenitor cells. In Sca1-MALT1 mice, MALT1 deregulation activated the NF-kappaB pathway in Sca1+ cells, promoting selective B-cell differentiation and mature lymphocyte accumulation in extranodal tissues, progressively leading to the development of clonal B-cell lymphomas. These tumors recapitulated the histopathological features of human MALT lymphomas, presenting typical lymphoepithelial lesions and plasmacytic differentiation. Transcriptional profiling of Sca1-MALT1 murine lymphomas revealed overlapping molecular signatures with human MALT lymphomas, including MALT1-mediated NFkappaB activation, pro-inflammatory signaling and XBP1-induced plasmacytic differentiation. Moreover, murine Malt1 showed proteolytic activity by cleaving Bcl10 in Sca1-MALT1 lymphomas. Our novel technological approach has allowed modeling human MALT lymphoma in mice, which represent unique tools study MALT lymphoma biology and evaluate anti-MALT1 therapies. **Keywords:** Genetic modification, wt vs. transgenic, MALT1 expression **Overall design:** 8 sorting purified Sca1+Lin- samples were analized of which 5 were from Sca1-MALT1 transgenic mice and 3 were from WT mice.

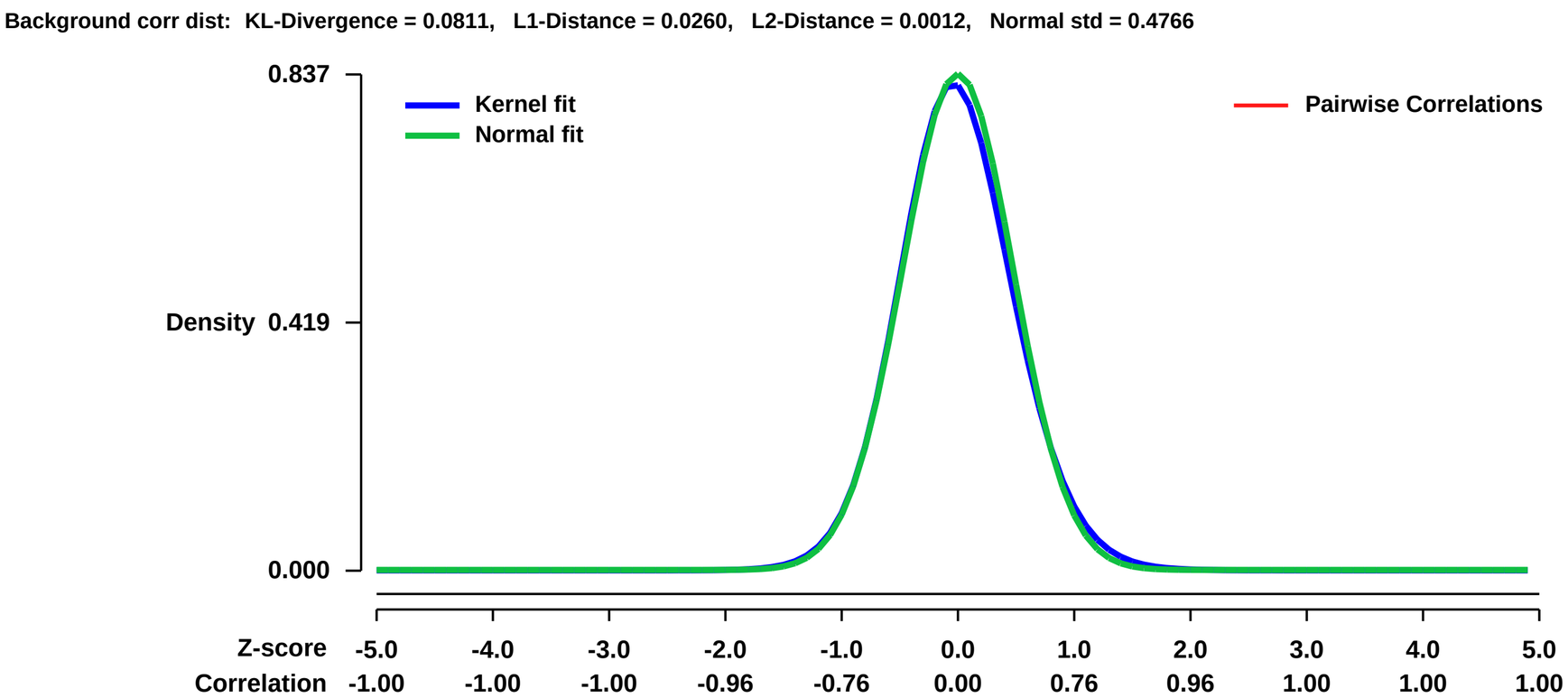

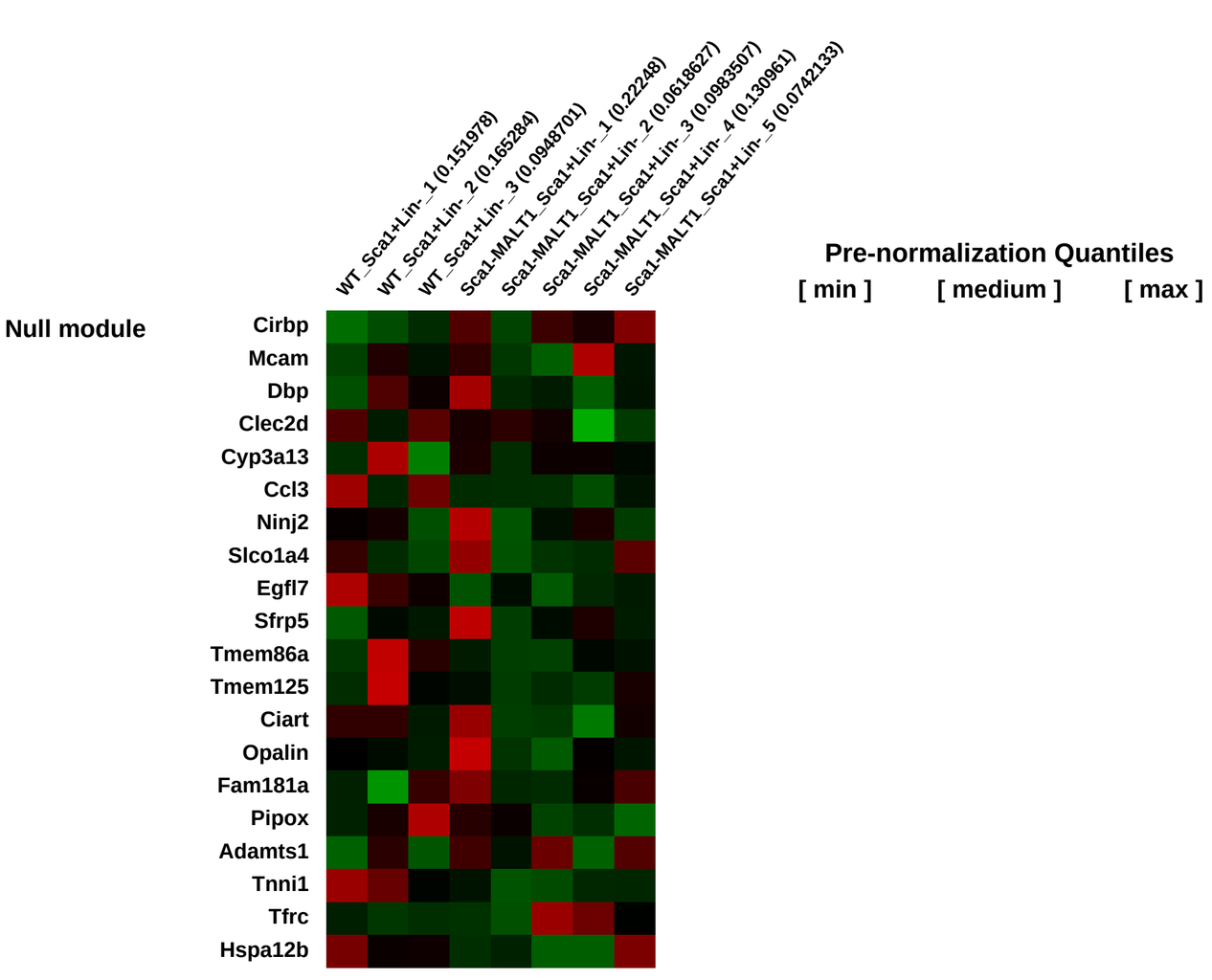

GEO Series "GSE25637" Expression Profiles

Num of samples in this series: 9

Scale of expression profile Z-scores

-3.0 -2.0 -1.0 0.0 1.0 2.0 3.0

GEO Link:	http://www.ncbi.nlm.nih.gov/geo/query/acc.cgi?acc=GSE25637
Status:	Public on Jul 10 2012
Title:	A mouse model of deregulation of the malt1 oncogene recapitulates the pathogenesis of human malt lymphoma [Spleen dataset]
Organism:	Mus musculus
Experiment type:	Expression profiling by array
Platform:	GPL1261
Pubmed ID:	22689981
Summary & Design:	**Summary:** Attempts at modeling chromosomal translocations involving MALT1 gene, hallmarks of human mucosa-associated lymphoid tissue (MALT) lymphoma, have failed to reproduce the disease in mice. Here we describe a transgenic model in which MALT1 expression was targeted to mouse hematopoietic stem/progenitor cells. In Sca1-MALT1 mice, MALT1 deregulation activated the NF-kappaB pathway in Sca1+ cells, promoting selective B-cell differentiation and mature lymphocyte accumulation in extranodal tissues, progressively leading to the development of clonal B-cell lymphomas. These tumors recapitulated the histopathological features of human MALT lymphomas, presenting typical lymphoepithelial lesions and plasmacytic differentiation. Transcriptional profiling of Sca1-MALT1 murine lymphomas revealed overlapping molecular signatures with human MALT lymphomas, including MALT1-mediated NFkappaB activation, pro-inflammatory signaling and XBP1-induced plasmacytic differentiation. Moreover, murine Malt1 showed proteolytic activity by cleaving Bcl10 in Sca1-MALT1 lymphomas. Our novel technological approach has allowed modeling human MALT lymphoma in mice, which represent unique tools study MALT lymphoma biology and evaluate anti-MALT1 therapies. **Keywords: Genetic modification, wt vs. transgenic, disease analysis, MALT lymphoma** **Overall design:** 9 samples were analized of which 5 were splenic lymphomas from Sca1-MALT1 transgenic mice and 4 were spleens from WT mice.

Background corr dist: KL-Divergence = 0.0723, L1-Distance = 0.0185, L2-Distance = 0.0004, Normal std = 0.4976

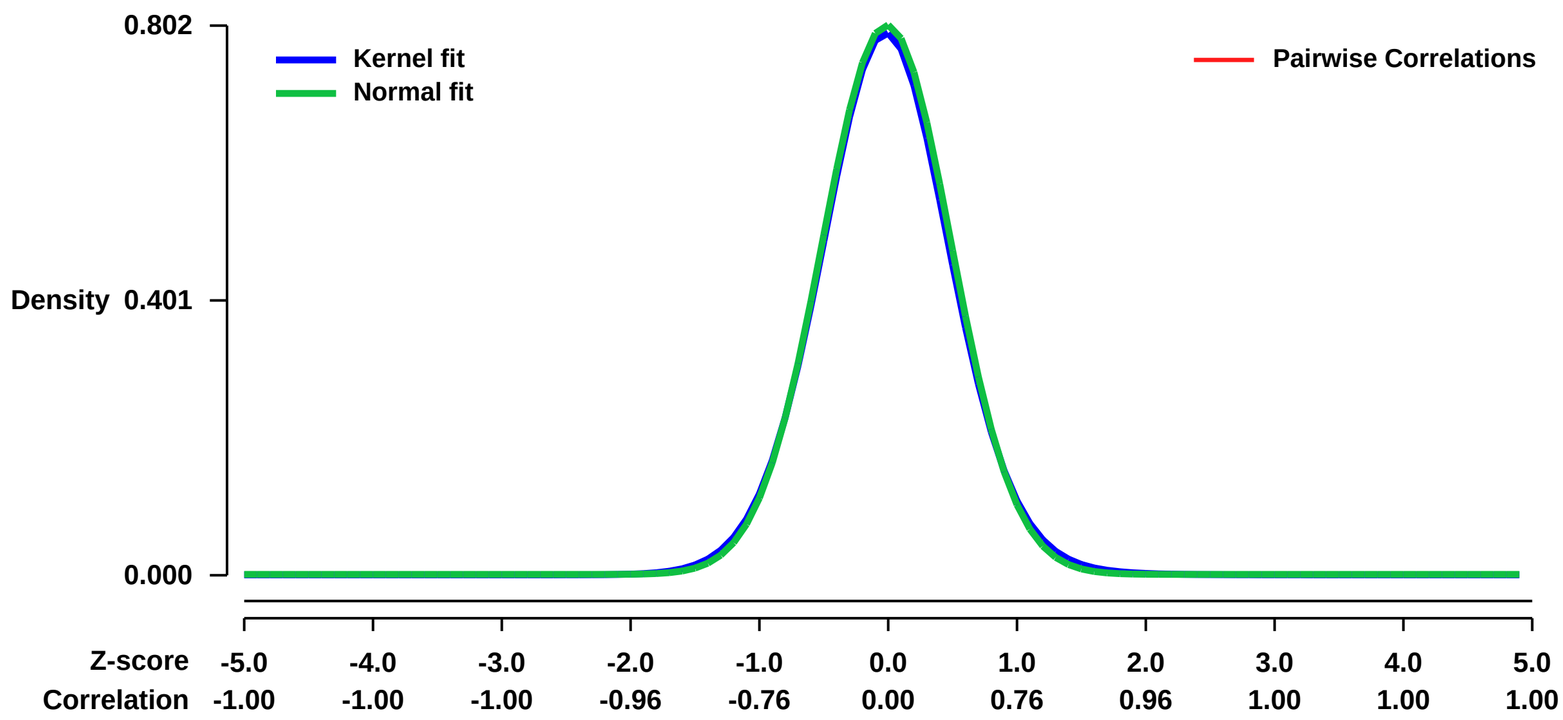

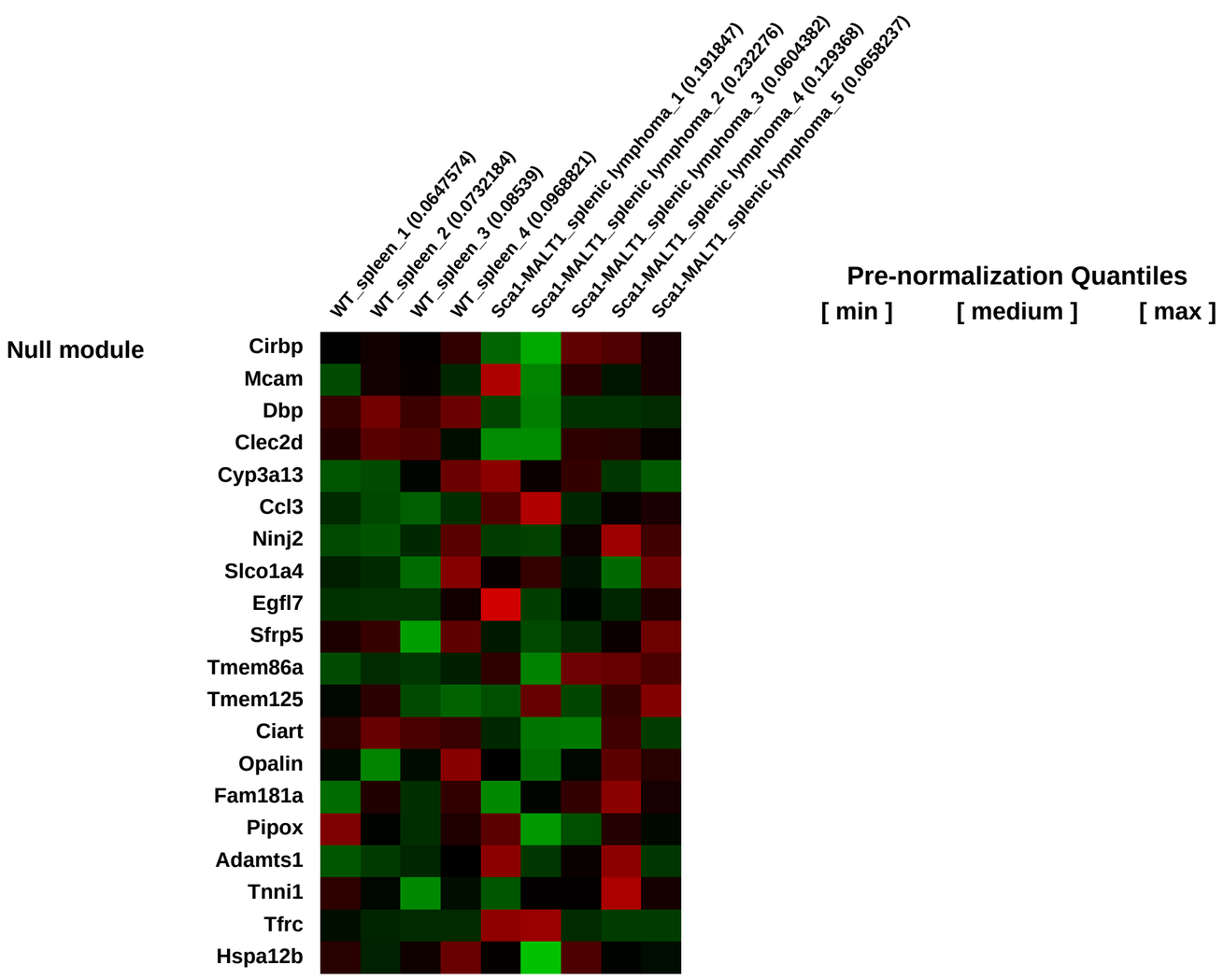

GEO Series "GSE25640" Expression Profiles

Num of samples in this series: 12

Scale of expression profile Z-scores

-3.0 -2.0 -1.0 0.0 1.0 2.0 3.0

GEO Link:	http://www.ncbi.nlm.nih.gov/geo/query/acc.cgi?acc=GSE25640
Status:	Public on Nov 29 2010
Title:	Expression data from wild type or FIZZ2 knockout murine lungs
Organism:	Mus musculus
Experiment type:	Expression profiling by array
Platform:	GPL1261
Pubmed ID:	21602491
Summary & Design:	**Summary:** To study the possible fibrotic role of FIZZ2, bleomycin was used to induce pulmonary fibrosis in wild type and FIZZZ2 knockout mice, lungs were then harvested and processed for RNA isolation. We used microarrays to detail the global gene expression regulated by FIZZ2 during fibrotic process. **Overall design:** Bleomycin/saline treated wild type or FIZZ2 knockout lungs at day 21 post injection were harvested for RNA isolation and hybridization on Affymetrix microarrays

Background corr dist: KL-Divergence = 0.0807, L1-Distance = 0.0207, L2-Distance = 0.0005, Normal std = 0.4759

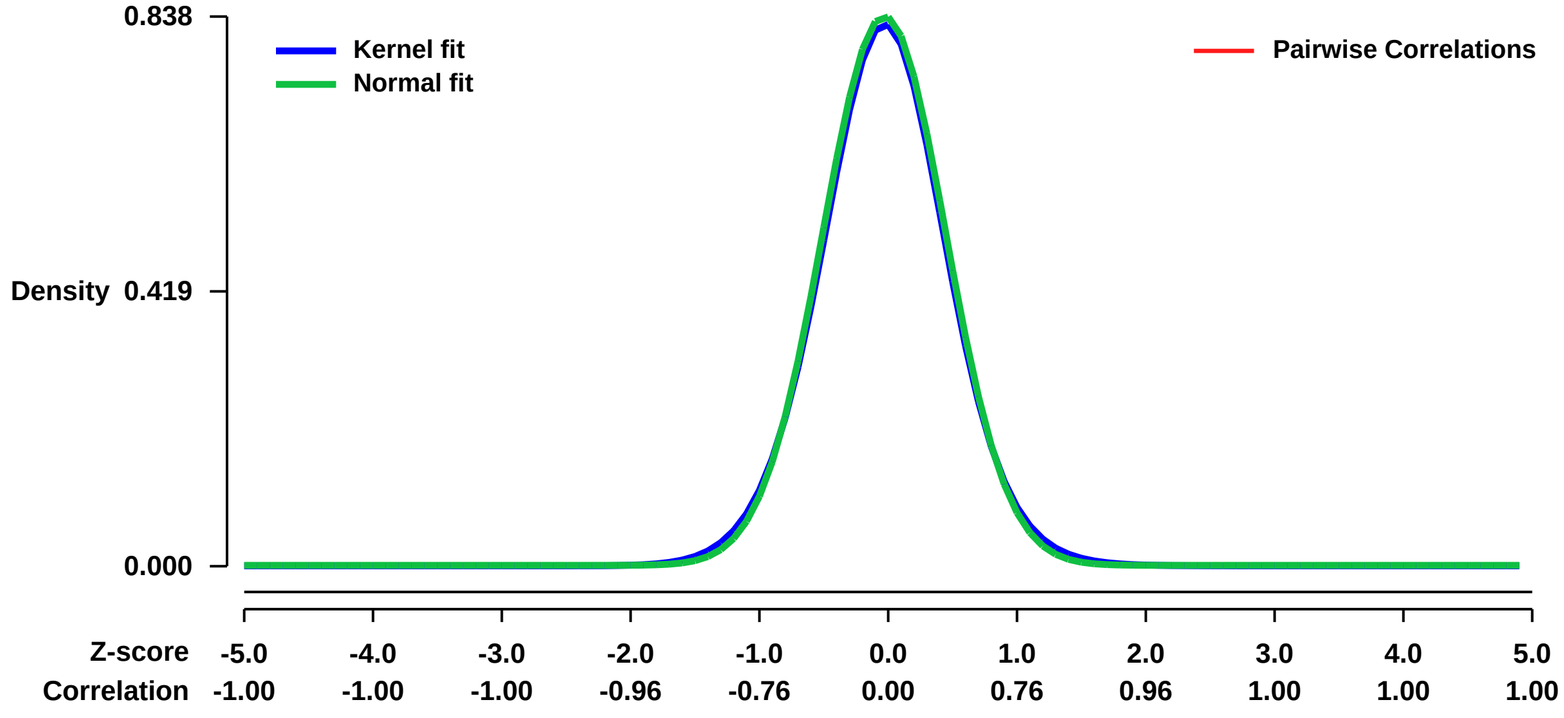

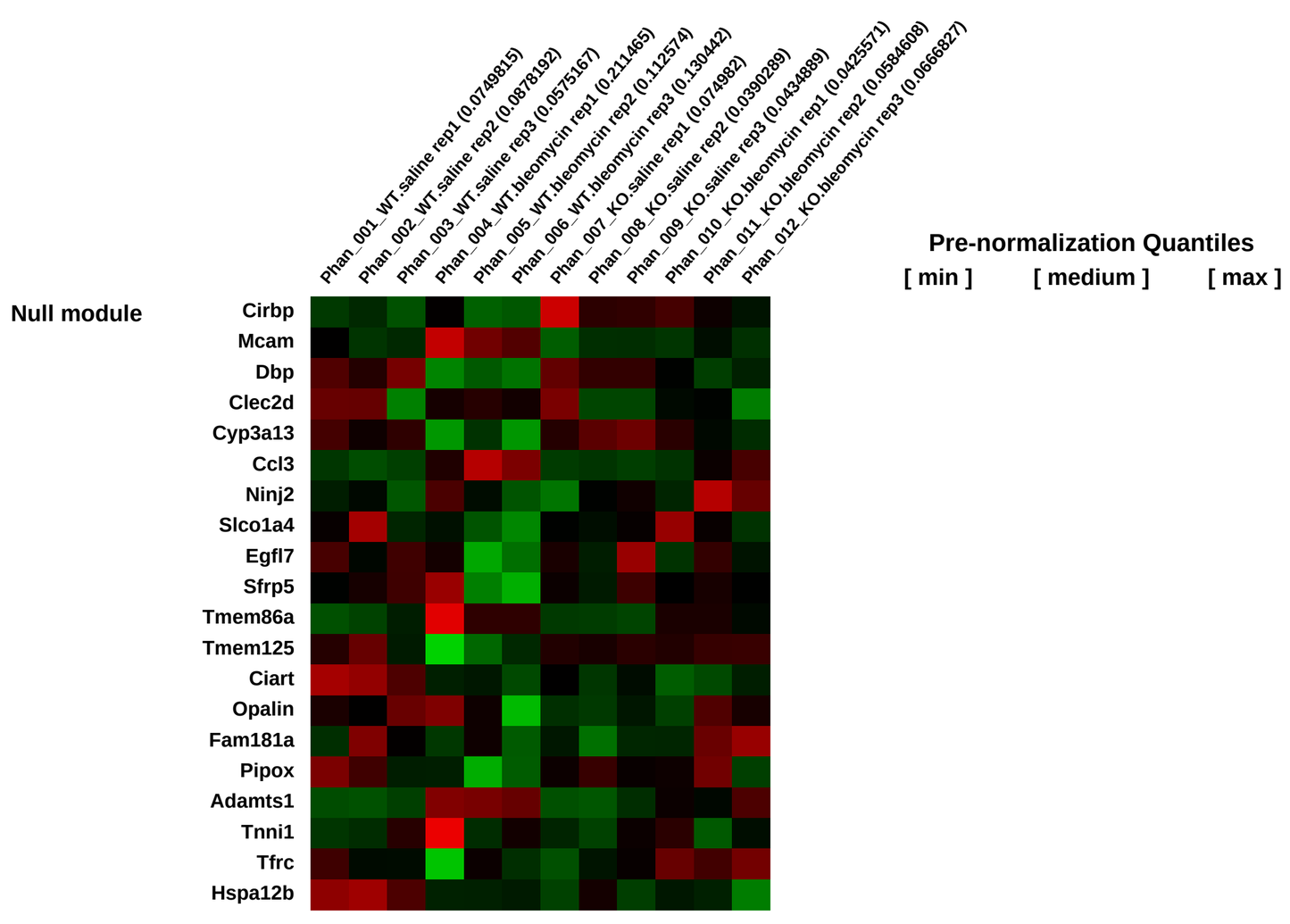

Pre-normalization Quantiles

[min] [medium] [max]

GEO Series "GSE25645" Expression Profiles

Num of samples in this series: 17

Scale of expression profile Z-scores

-3.0 -2.0 -1.0 0.0 1.0 2.0 3.0

GEO Link:	http://www.ncbi.nlm.nih.gov/geo/query/acc.cgi?acc=GSE25645
Status:	Public on May 09 2011
Title:	Ebf1 or Pax5 Haploinsufficiency Synergizes with STAT5 Activation to Initiate Acute Lymphoblastic Leukemia
Organism:	Mus musculus
Experiment type:	Expression profiling by array
Platform:	GPL1261
Pubmed ID:	21606506
Summary & Design:	**Summary:** STAT5 is critical for differentiation, proliferation and survival of progenitor B cells suggesting a possible role in Acute Lymphoblastic Leukemia (ALL). Herein, we show increased expression of activated STAT5 in ALL patients, which correlates with treatment outcome. Mutations in Ebf1 and Pax5, genes critical for B cell development have also been identified in human ALL. To determine whether mutations in Ebf1 or Pax5 synergize with STAT5 activation to induce ALL we crossed mice expressing a constitutively active form of STAT5 (Stat5b-CA) with mice heterozygous for Ebf1 or Pax5. Haploinsufficiency of either Pax5 or Ebf1 synergized with Stat5b-CA to rapidly induce ALL in 100% of the mice. The leukemic cells displayed reduced expression of both Pax5 and Ebf1 but this had little affect on most EBF1 or PAX5 target genes. However, a subset of these genes was deregulated and included a large percentage of potential tumor suppressor genes and oncogenes. Further, most of these genes appear to be jointly regulated by both EBF1 and PAX5. Our findings suggest a model whereby small perturbations in a self-reinforcing network of transcription factors critical for B cell development, specifically PAX5 and EBF1, cooperate with STAT5 activation to initiate ALL. **Overall design:** Gene expression profiling was performed on cells isolated from lymph nodes of Stat5b-CA x Ebf1+/- and Stat5b-CA x Rag2-/- leukemic mice and pre B cells sorted from bone marrow of C57BL/6 mice and Stat5b-CA transgenic mice. 17 Samples.

Background corr dist: KL-Divergence = 0.0897, L1-Distance = 0.0378, L2-Distance = 0.0030, Normal std = 0.4540

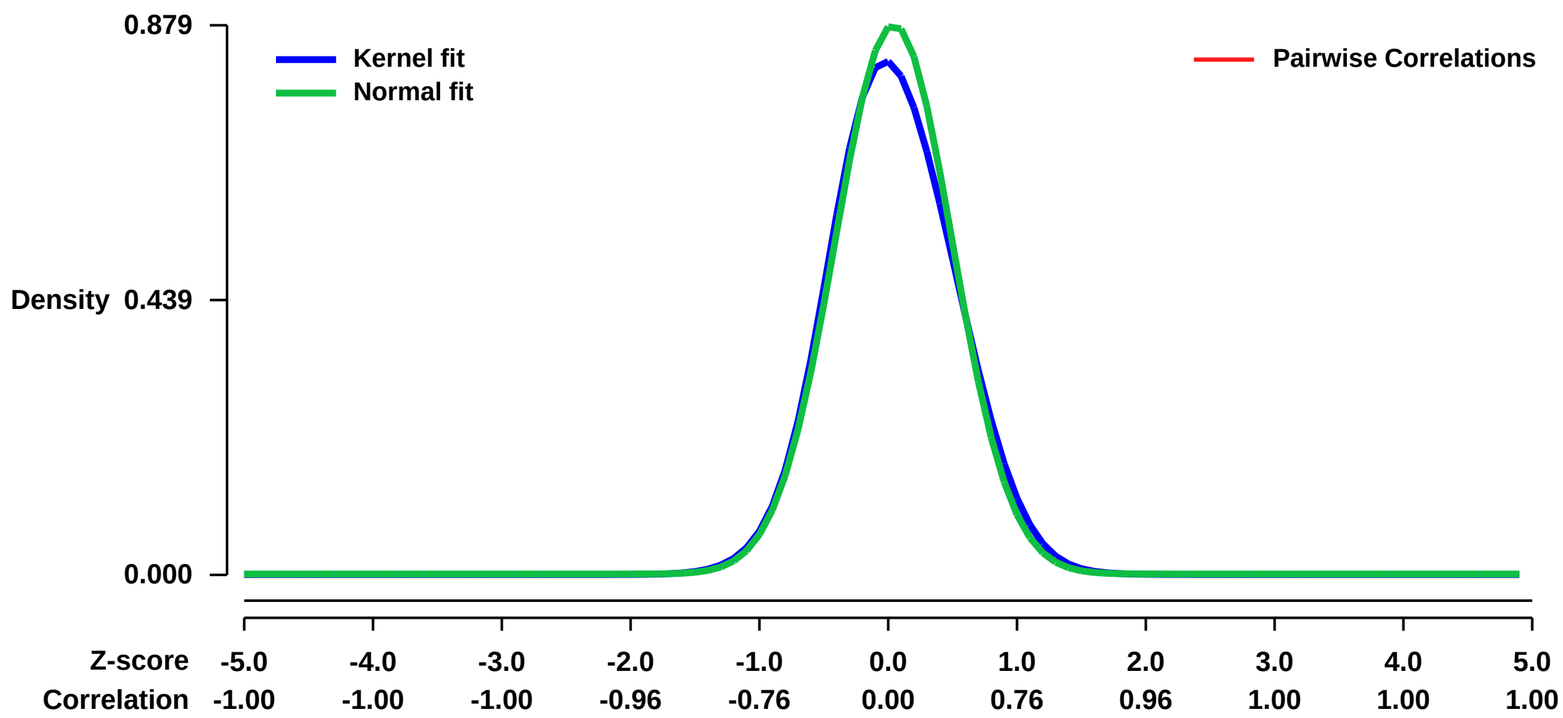

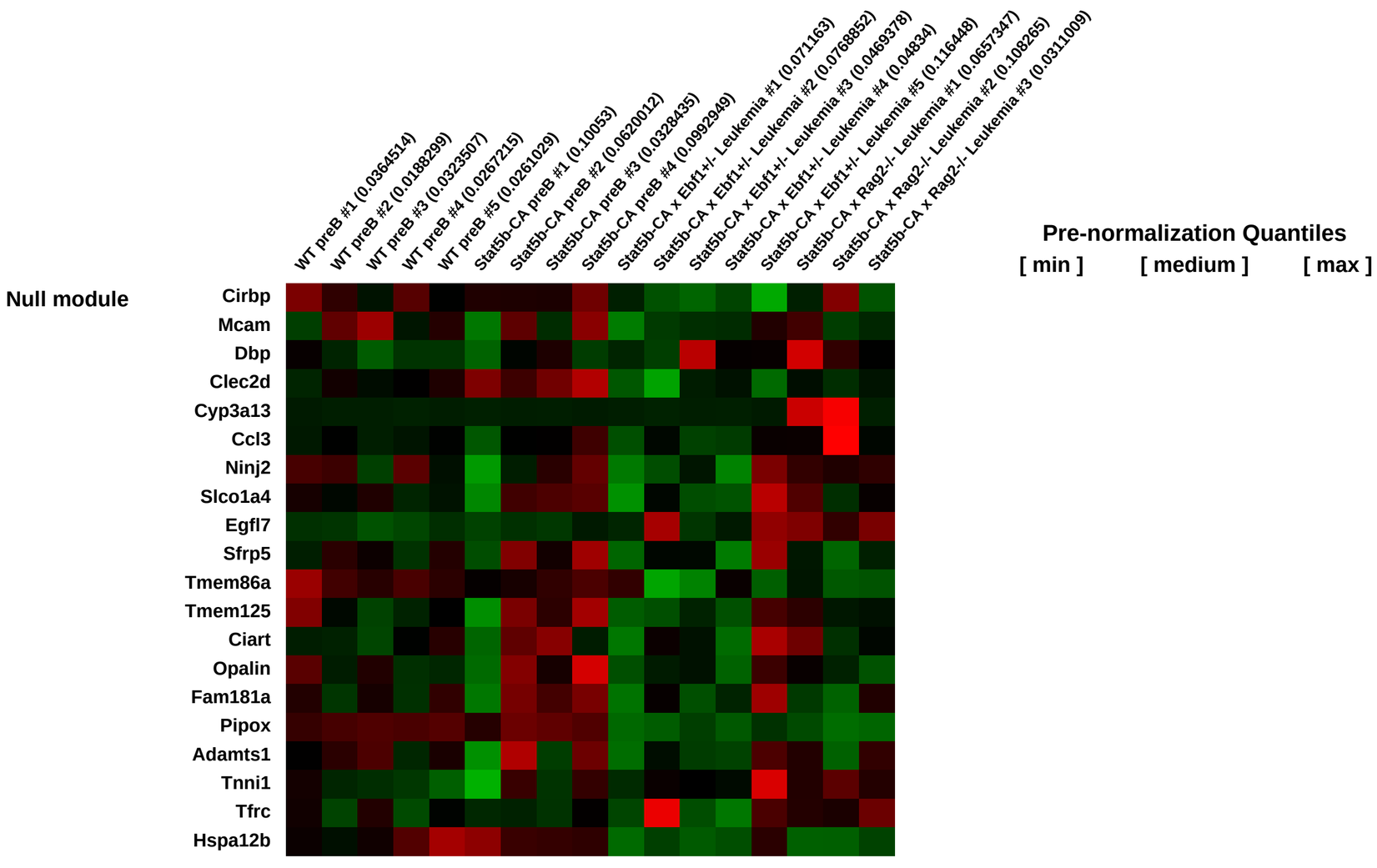

GEO Series "GSE25729" Expression Profiles

Num of samples in this series: 12

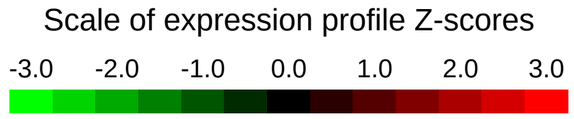

GEO Link:	**http://www.ncbi.nlm.nih.gov/geo/query/acc.cgi?acc=GSE25729**
Status:	**Public on Dec 25 2012**
Title:	**Role of ILK in cardiac regeneration**
Organism:	**Mus musculus**
Experiment type:	**Expression profiling by array**
Platform:	**GPL1261**
Pubmed ID:	
Summary & Design:	**Summary:** **Two different mouse models of cardiac-specific ILK expression (ILKS343D and ILKR211A) were used to investigate the role of ILK in cardiac regeneration** **Overall design:** **4 groups with 3 mice (biological replicates) in each group with the total of 12 heart samples were used in this microarray experiment**

Background corr dist: **KL-Divergence = 0.1828, L1-Distance = 0.0456, L2-Distance = 0.0046, Normal std = 0.3433**

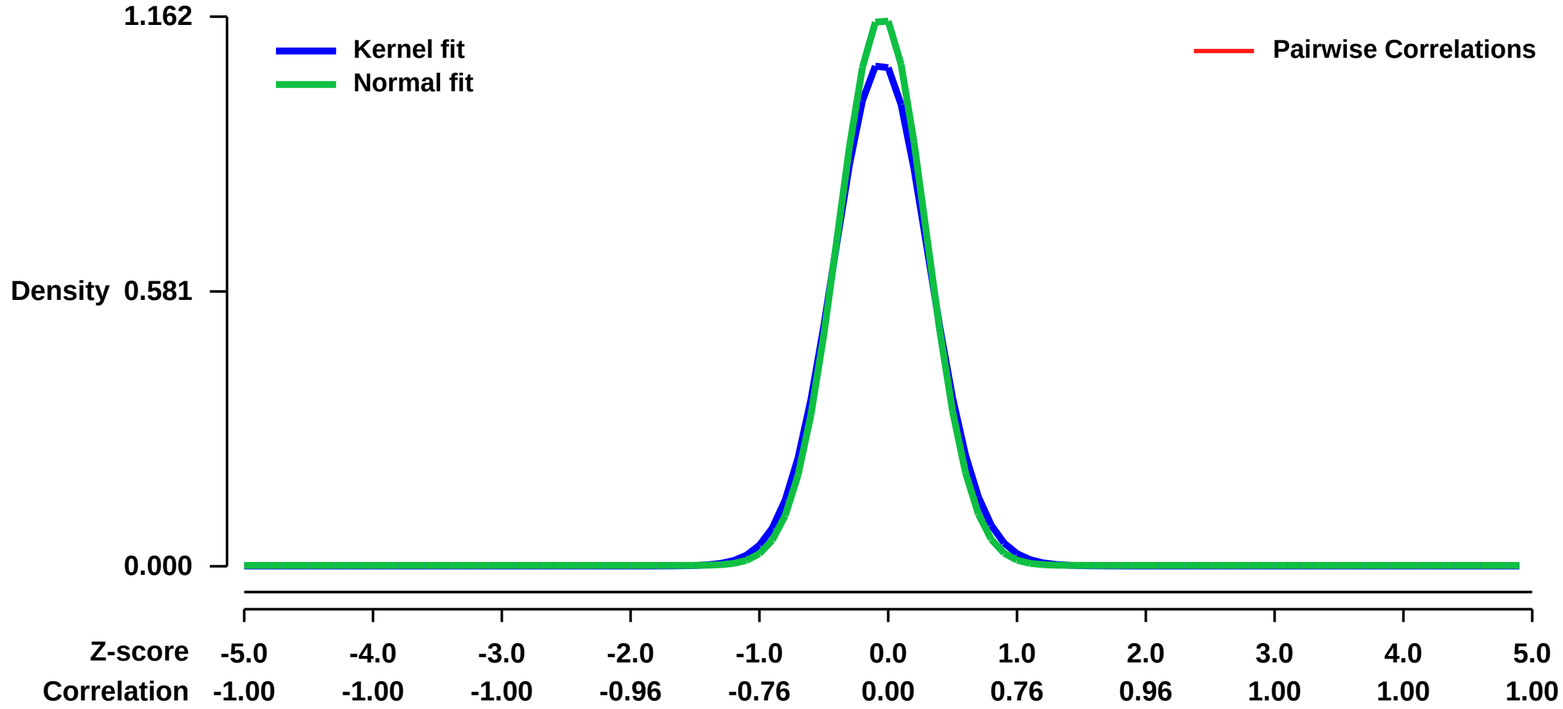

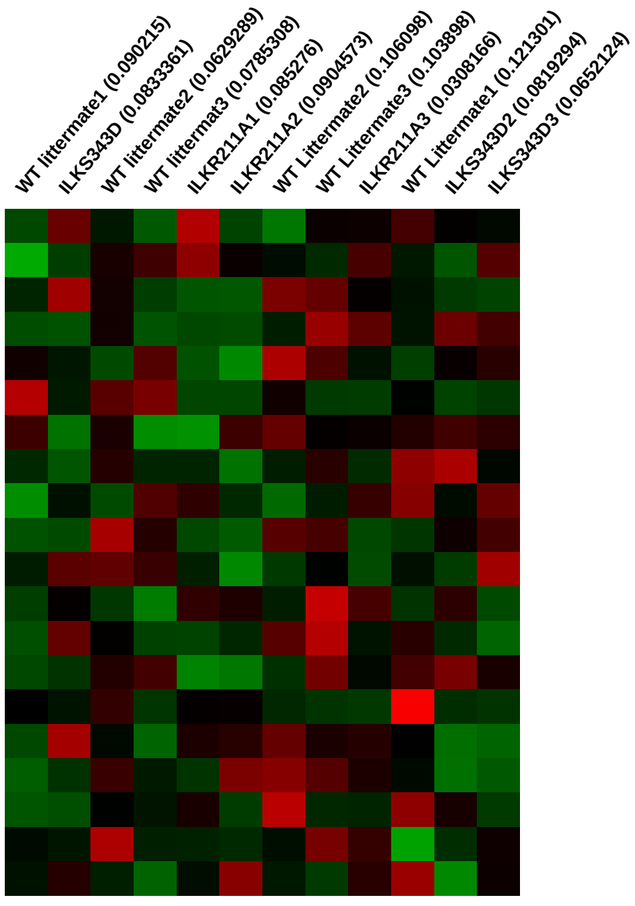

GEO Series "GSE25737" Expression Profiles

Num of samples in this series: 6

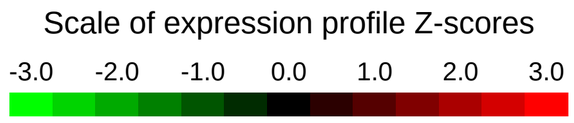

GEO Link:	http://www.ncbi.nlm.nih.gov/geo/query/acc.cgi?acc=GSE25737
Status:	Public on Mar 18 2011
Title:	Geminin-regulated genes during neural fate acquisition of mouse embryonic stem cells
Organism:	Mus musculus
Experiment type:	Expression profiling by array
Platform:	GPL1261
Pubmed ID:	21300881
Summary & Design:	**Summary:** Formation of the complex vertebrate nervous system begins when pluripotent cells of the early embryo are directed to acquire a neural fate. Although cell intrinsic controls play an important role in this process, the molecular nature of this regulation is not well defined. Here we assessed the role for Geminin, a nuclear protein expressed in embryonic cells, in neural fate acquisition from mouse embryonic stem (ES) cells. While Geminin knockdown does not affect the ability of ES cells to maintain or exit pluripotency, we found that it significantly impairs their ability to acquire a neural fate. Conversely, Geminin overexpression promotes neural gene expression, even in the presence of growth factor signaling that antagonizes neural transcriptional responses. These data demonstrate that Gemininá s activity contributes to mammalian neural cell fate acquisition. We investigated the mechanistic basis of this phenomenon and found that Geminin maintains a hyperacetylated and open chromatin conformation at neural genes. Interestingly, recombinant Geminin protein also rapidly alters chromatin acetylation and accessibility even when Geminin is combined with nuclear extract and chromatin in vitro. These findings define a novel activity for Geminin in regulation of chromatin structure. Together, these data support a role for Geminin as a cell intrinsic regulator of neural fate acquisition that promotes expression of neural genes by regulating chromatin accessibility and histone acetylation. #!# **Overall design:** Mouse embryonic stem cells were differentiated for two days in N2B27 medium, with or without Doxycycline-inducible shRNAmir knockdown of Geminin and compared by microarray. Three independent experiments were conducted, using two different mouse embryonic stem cell lines for Doxycycline-inducible knockdown of Geminin. The two ES lines express unique shRNAmir sequences targeting Geminin (shRNAmir #9 and #11) to control for off-target effects.

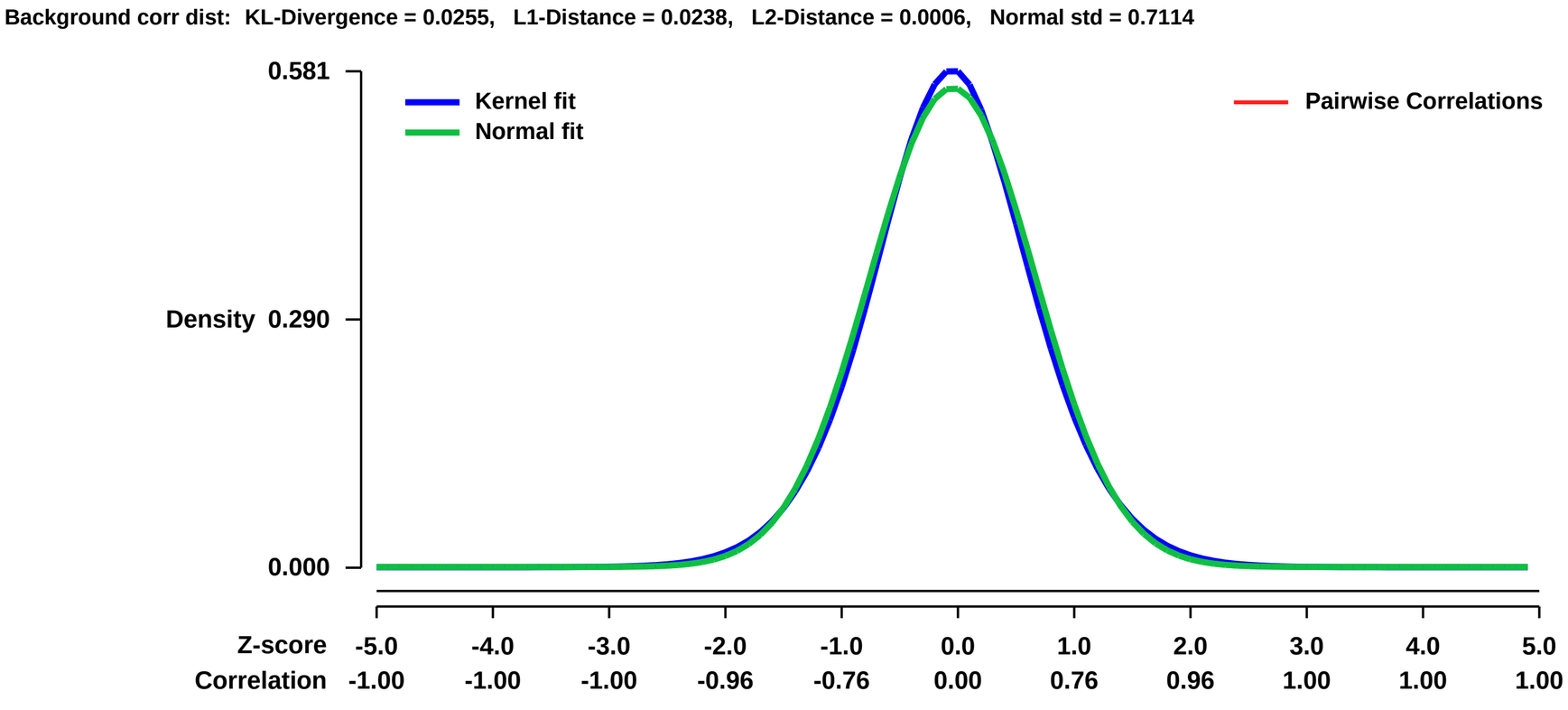

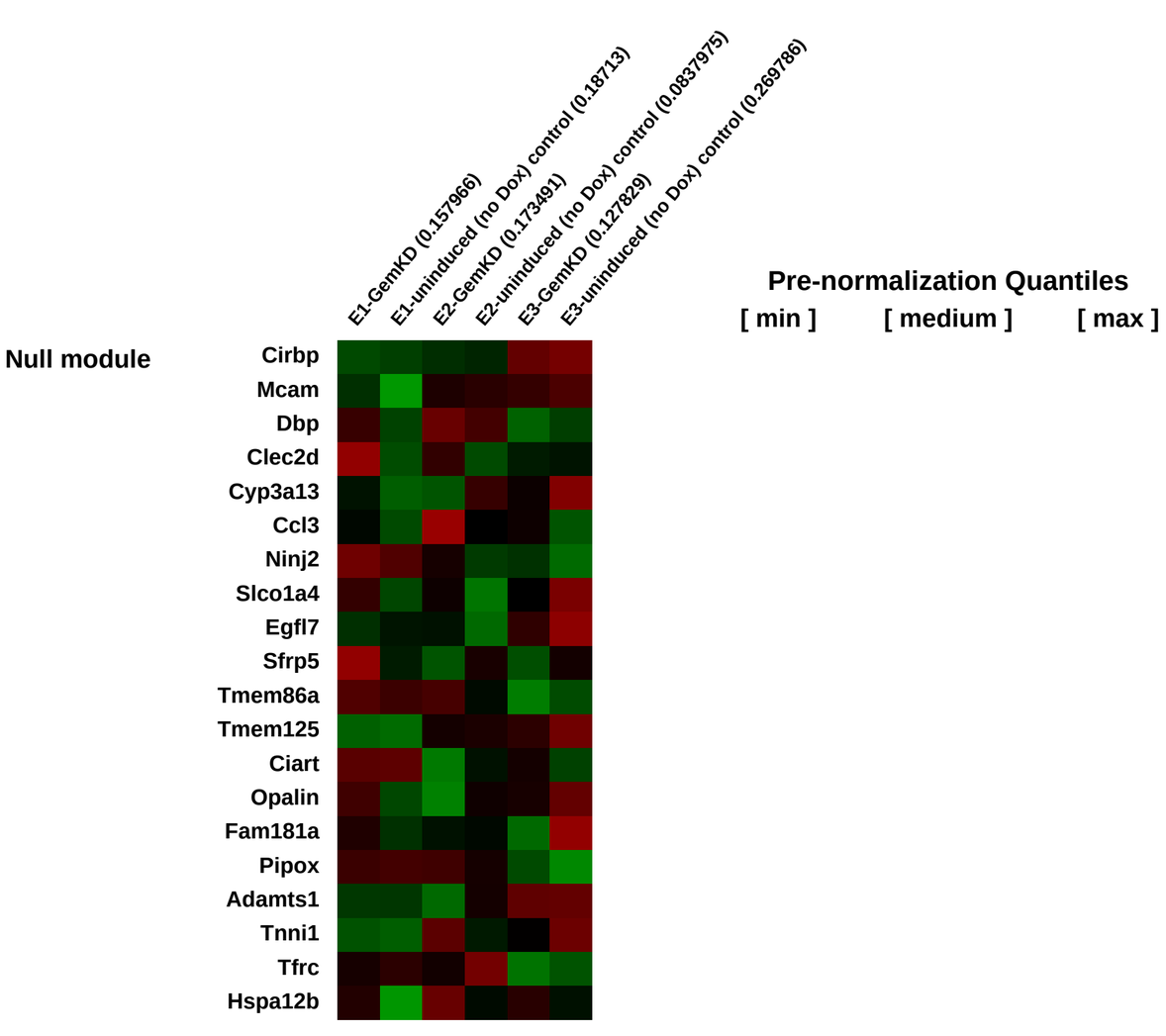

GEO Series "GSE25766" Expression Profiles

Num of samples in this series: 6

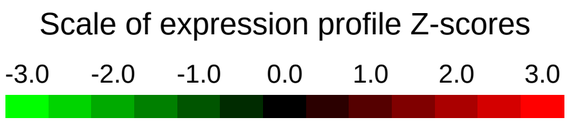

GEO Link:	http://www.ncbi.nlm.nih.gov/geo/query/acc.cgi?acc=GSE25766
Status:	Public on Dec 03 2010
Title:	Cardiac gene expression profiling of heart failure treatment with the anti-ischemic drug ranolazine
Organism:	Mus musculus
Experiment type:	Expression profiling by array
Platform:	GPL1261
Pubmed ID:	21711241
Summary & Design:	**Summary:** Heart failure is a leading cause of cardiovascular mortality with limited options for treatment. We analyzed whether the anti-ischemic drug ranolazine could retard the progression of heart failure in an experimental model of heart failure induced by 6 months of chronic pressure overload. The study showed that 2 months of ranolazine treatment improved cardiac function of aortic constricted C57BL/6J (B6) mice with symptoms of heart failure as assessed by echocardiography. The microarray gene expression study of heart tissue from failing hearts relative to ranolazine-treated and healthy control hearts identified heart failure-specific genes that were normalized during treatment with the anti-ischemic drug ranolazine. **Overall design:** Microarray gene expression profiling was performed with heart tissue isolated from three study groups: (i) untreated 10 month-old C57BL/6J (B6) mice with heart failure induced by 6 months of abdominal aortic constriction (AAC), (ii) 10 month-old B6 mice with 6 months of AAC and two months of treatment with the anti-ischemic drug ranolazine (200 mg/kg), and (iii) age-matched, untreated, sham-operated B6 control mice.

Background corr dist: KL-Divergence = 0.0360, L1-Distance = 0.0242, L2-Distance = 0.0006, Normal std = 0.6490

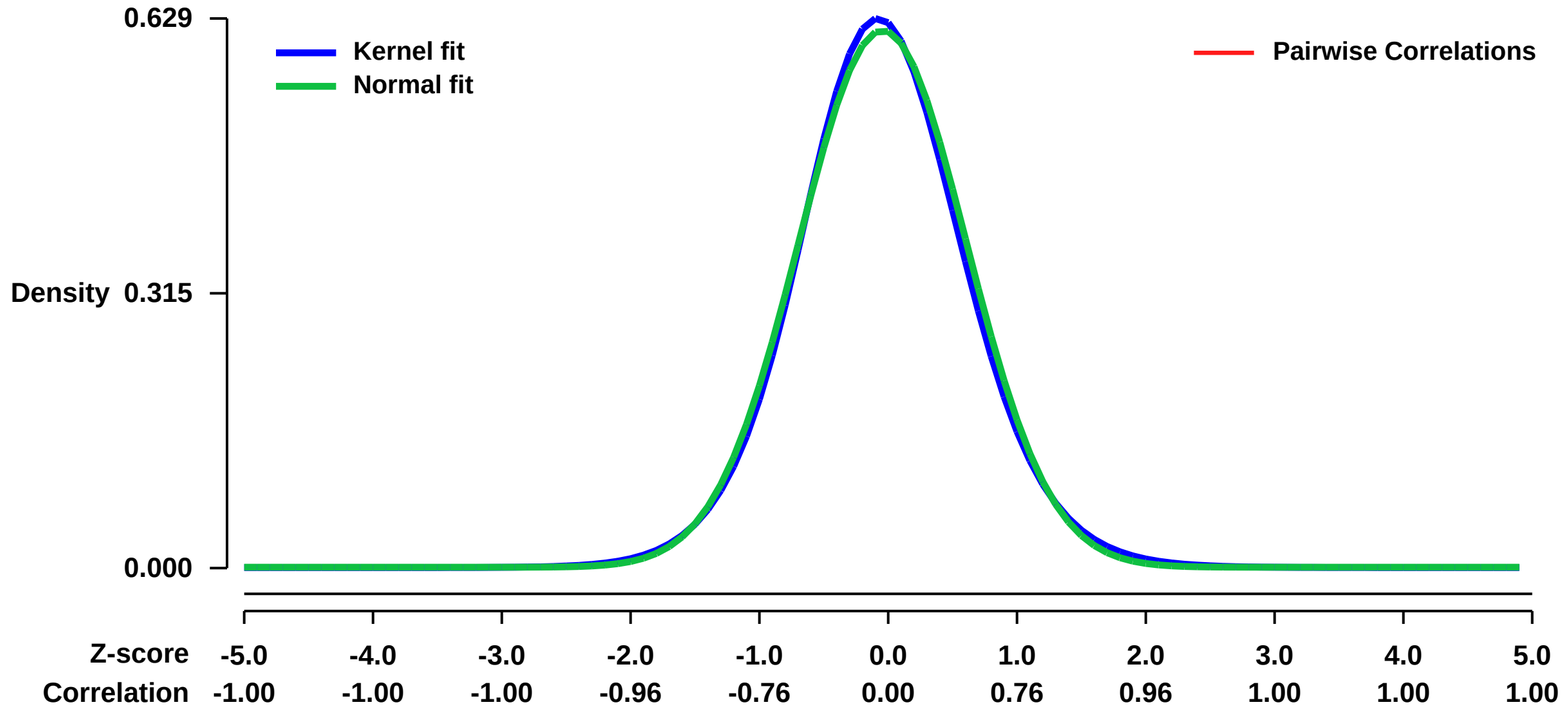

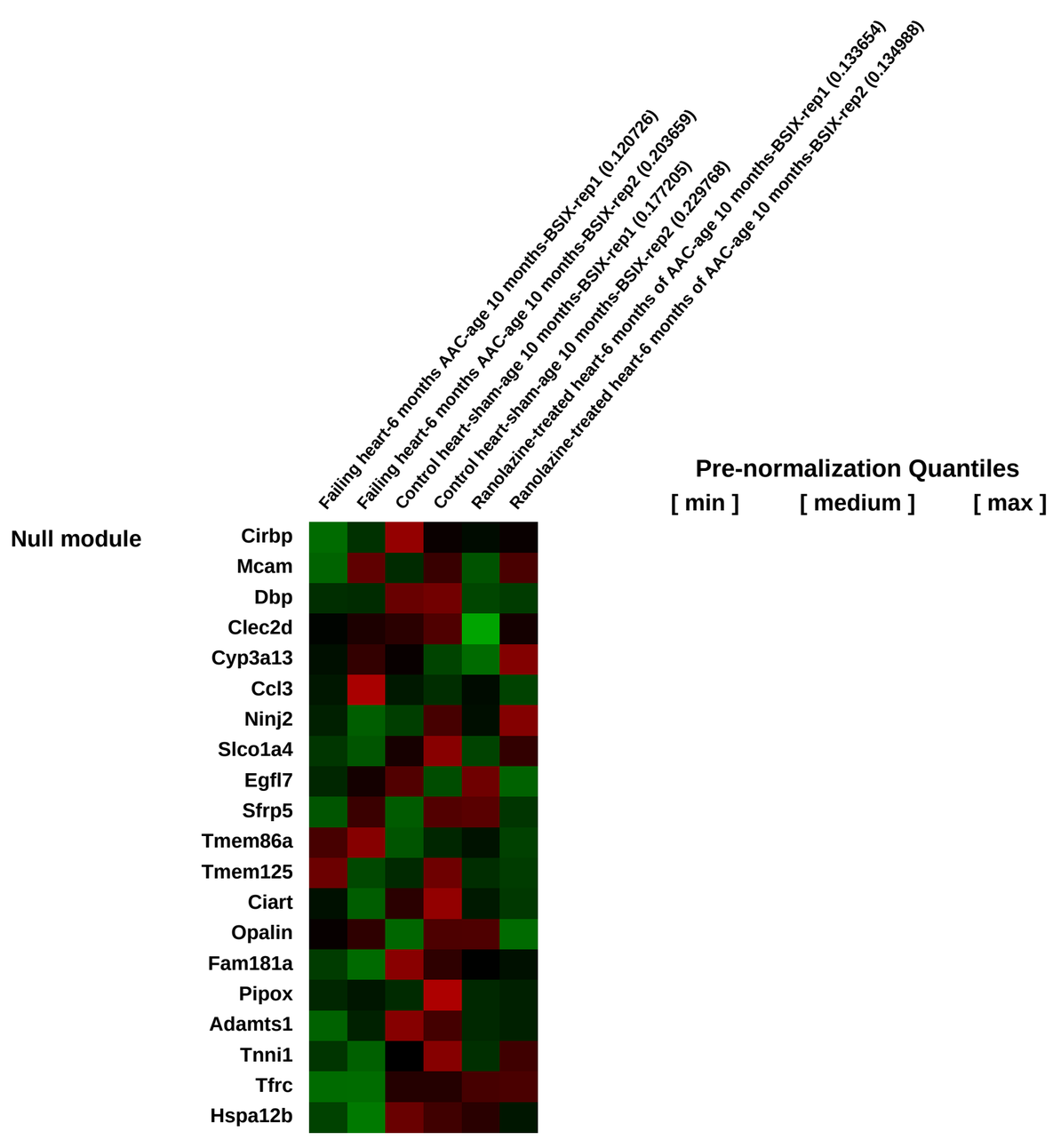

GEO Series "GSE25767" Expression Profiles

Num of samples in this series: 6

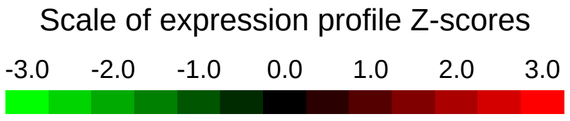

GEO Link:	http://www.ncbi.nlm.nih.gov/geo/query/acc.cgi?acc=GSE25767
Status:	Public on Dec 03 2010
Title:	Cardiac gene expression profiling of apoE-deficient mice receiving heart failure treatment with the anti-ischemic drug ranolazine
Organism:	Mus musculus
Experiment type:	Expression profiling by array
Platform:	GPL1261
Pubmed ID:	21711241
Summary & Design:	**Summary:** Heart failure is a leading cause of cardiovascular mortality with limited options for treatment. We used 18 month-old apolipoprotein E (apoE)- deficient mice as a model of atherosclerosis-induced heart failure to analyze whether the anti-ischemic drug ranolazine could retard the progression of heart failure. The study showed that 2 months of ranolazine treatment improved cardiac function of 18 month-old apoE-deficient mice with symptoms of heart failure as assessed by echocardiography. To identify changes in cardiac gene expression induced by treatment with ranolazine a microarray study was performed with heart tissue from failing hearts relative to ranolazine-treated and healthy control hearts. The microarray approach identified heart failure-specific genes that were normalized during treatment with the anti-ischemic drug ranolazine. **Overall design:** Microarray gene expression profiling was performed with heart tissue isolated from (i) untreated 18 month-old apoE-deficient mice with heart failure relative to (ii) 18 month-old apoE-deficient mice treated for two months with the anti-ischemic drug ranolazine (200 mg/kg), and (iii) age-matched non-transgenic C57BL/6J (B6) control mice.

Background corr dist: KL-Divergence = 0.0357, L1-Distance = 0.0287, L2-Distance = 0.0009, Normal std = 0.6630

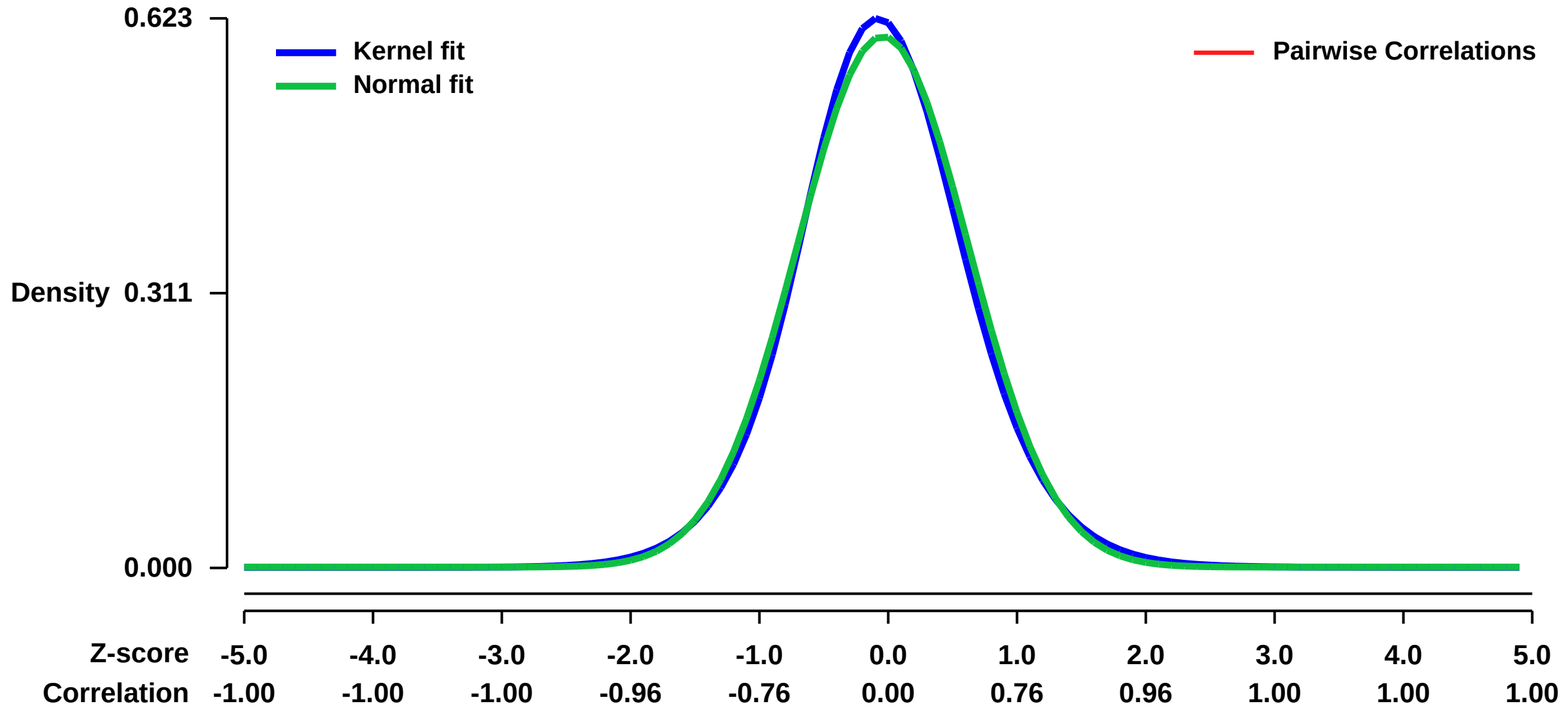

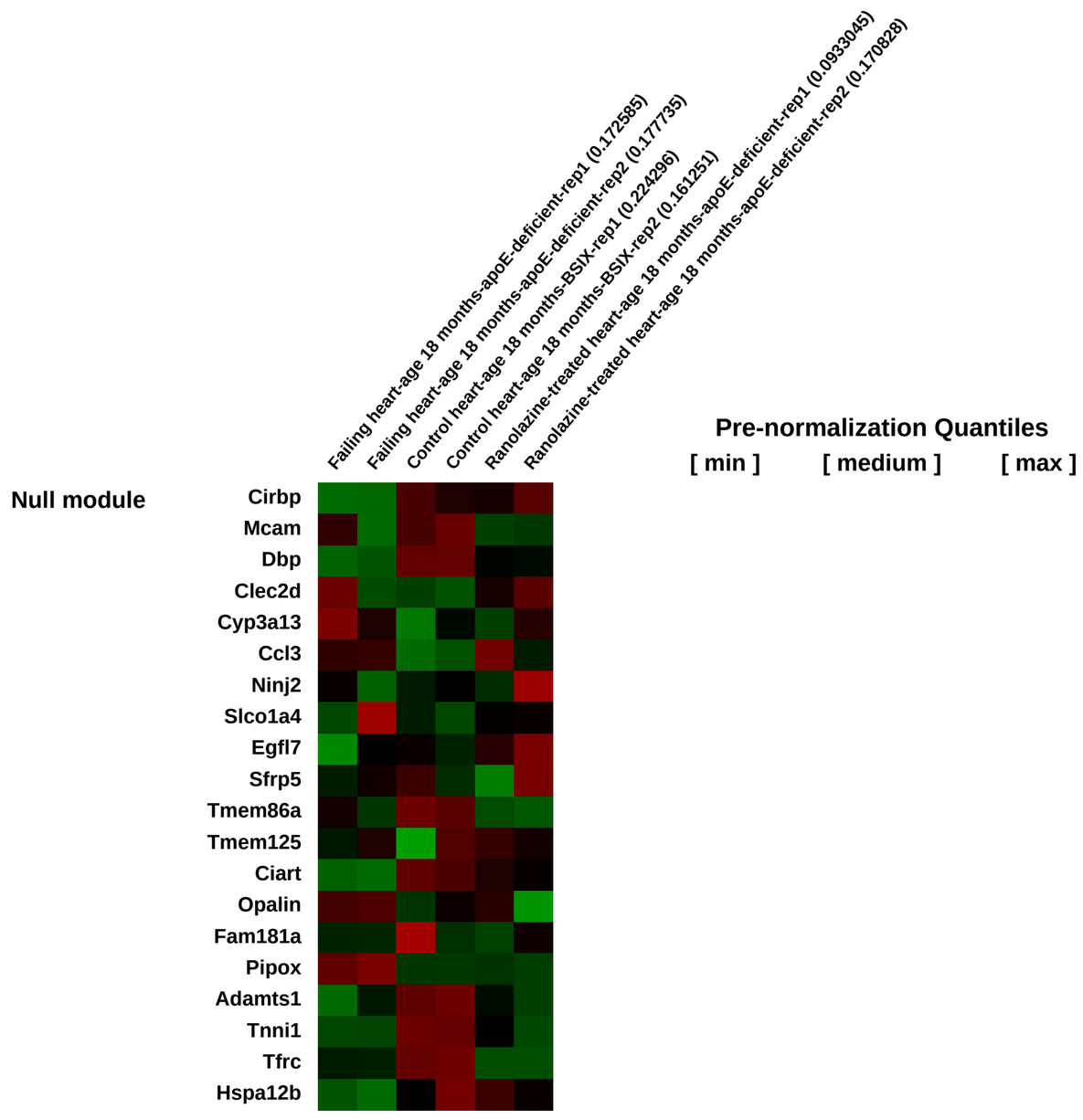

GEO Series "GSE25768" Expression Profiles

Num of samples in this series: 6

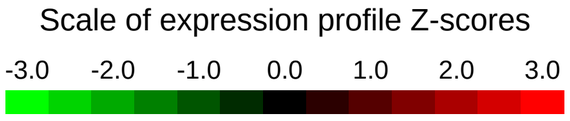

GEO Link:	http://www.ncbi.nlm.nih.gov/geo/query/acc.cgi?acc=GSE25768
Status:	Public on Dec 03 2010
Title:	Model of heart failure induced by mild thiol-blocking with cystamine
Organism:	Mus musculus
Experiment type:	Expression profiling by array
Platform:	GPL1261
Pubmed ID:	21711241
Summary & Design:	**Summary:** Depletion of cardiac ATP content is a characteristic feature of heart failure in patients and experimental animal models. To analyze the impact of insufficient ATP supply on heart function we inhibited cellular respiration by disulfide poisoning with the mild thiol-blocking agent, cystamine. We chose 4 month-old apolipoprotein E (apoE)-deficient mice, which are highly vulnerable to increased oxygen and ATP demands. After 4 weeks of cystamine treatment (300 mg/kg in drinking water), echocardiography and histology analyses demonstrated that apoE-deficient mice had developed heart failure with cardiac dilation. The microarray gene expression study of heart tissue from cystamine-treated apoE-deficient mice relative to untreated mice confirmed the development of heart failure showing up-regulation heart failure-specific genes by mild thiol-blocking with cystamine. **Overall design:** Microarray gene expression profiling was performed with heart tissue isolated from three study groups: (i) cystamine-treated 5 month-old apolipoprotein- (apoE)- deficient mice with symptoms of heart failure, (ii) untreated 5 month-old apoE- deficient mice, and (iii) age-matched, untreated, non-transgenic B6 control mice.

Background corr dist: KL-Divergence = 0.0389, L1-Distance = 0.0232, L2-Distance = 0.0006, Normal std = 0.6303

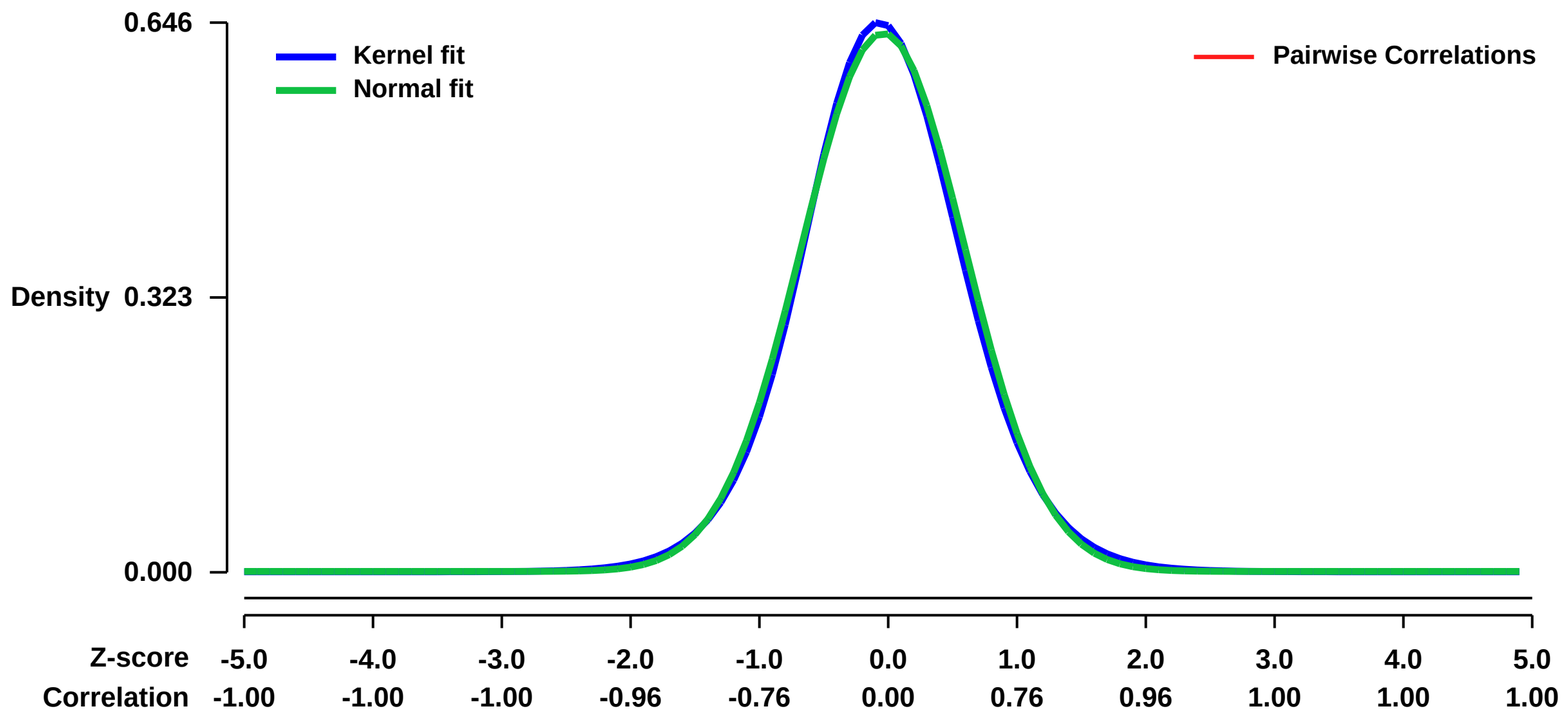

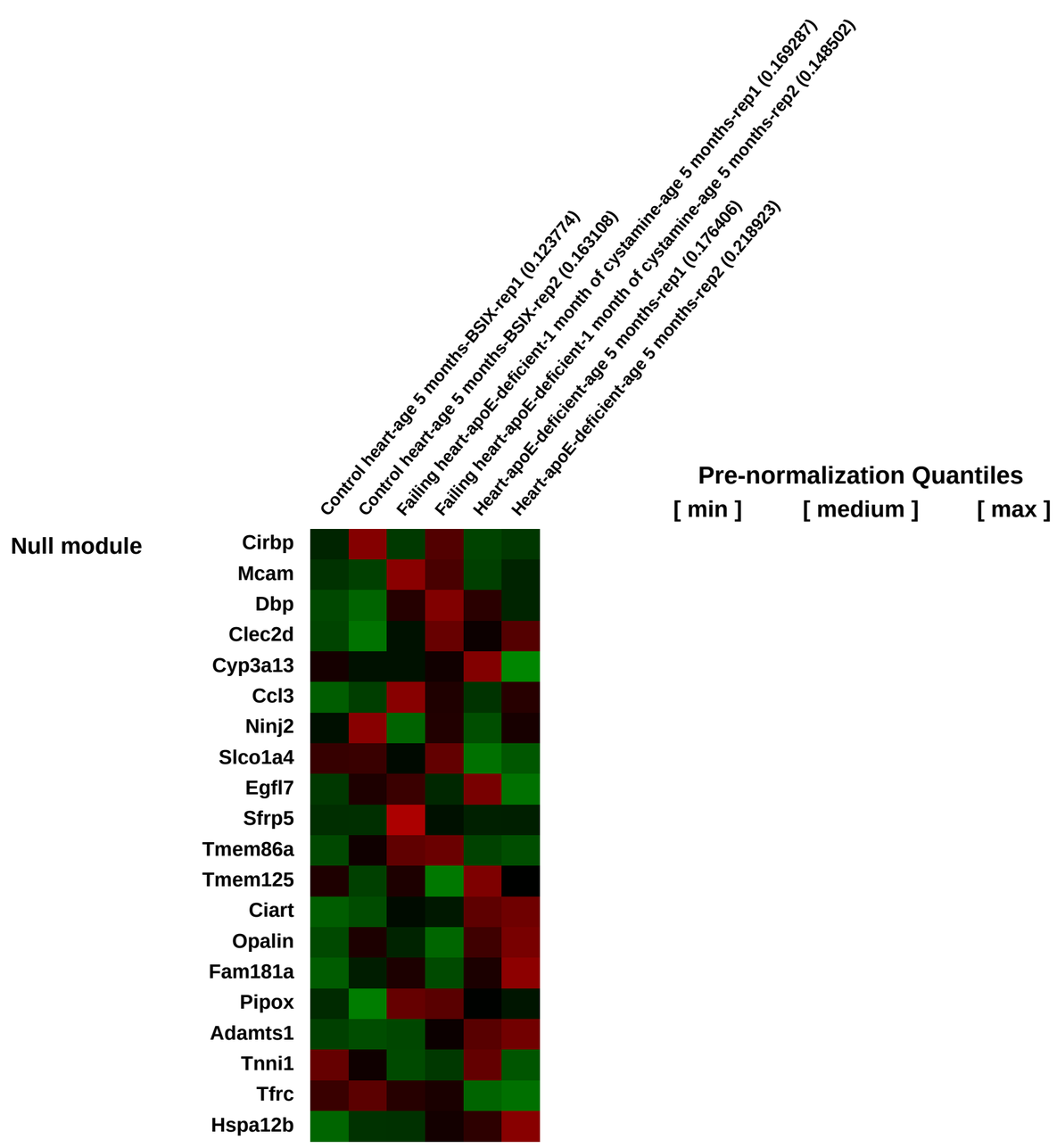

GEO Series "GSE25778" Expression Profiles

Num of samples in this series: 6

Scale of expression profile Z-scores

-3.0 -2.0 -1.0 0.0 1.0 2.0 3.0

GEO Link:	http://www.ncbi.nlm.nih.gov/geo/query/acc.cgi?acc=GSE25778
Status:	Public on Dec 03 2010
Title:	Genome profiling of mouse pulmonary epithelial type II cells
Organism:	Mus musculus
Experiment type:	Expression profiling by array
Platform:	GPL1261
Pubmed ID:	
Summary & Design:	**Summary:** Pulmonary alveoli contain two distinct populations of epithelial cells. Type II cells produce pulmonary surfactant lipids and surfactant-associated proteins (SP) required for maintaining alveolar surface tension at the air-liquid interface and host defense against respiratory pathogens. Type II cells are also progenitors for epithelial type I cells, a terminally differentiated elongated cell that covers microvascular endothelial cells and participates in gas exchange. Despite some indirect evidence, it is unknown whether subpopulations of type II cells exist. We created a line of transgenic mice expressing enhanced green fluorescent protein (EGFP) under control of the human SP-C promoter. Expression of EGFP may define a subpopulation of type II cells because it is 1) expressed in approximately 10% of type II cells, 2) appears much later in embryonic development than SP-C, and 3) selectively proliferates in mice infected with influenza A virus. To determine whether EGFP defines a unique subpopulation of type II cells, RNA was isolated from EGFP-positive and negative type II cells and hybridized to affymetrix arrays. Of the genes detected in EGFP-positive cells, most were equally detected in EGFP-negative cells. However, approximately 350 genes were selectively elevated â¥5-fold in EGFP-positive cells and 1500 genes selectively expressed by EGFP-negative cells. These findings suggest EGFP defines a subpopulation of type II epithelial cells in this line of transgenic mice. **Overall design:** Type II cells were harvested from approximately 10 young adult (8-week) mice and sorted into EGFP-positive (sample EGFP-1) and EGFP-negative (sample nonEGFP-1) populations using a B-D FACSVantage SE cell sorter. RNA was prepared from approximately two million cells and hybridized to Affymetrix M430 2.0 array as a one by one comparison. The isolation and gene expression analysis of EGFP-positive and EGFP-negative type II cells was repeated a second (using EGFP-2 and nonEGFP-2 samples) and third (using EGFP-3 and nonEGFP-3 samples) time.

Background corr dist: KL-Divergence = 0.0244, L1-Distance = 0.0296, L2-Distance = 0.0011, Normal std = 0.7429

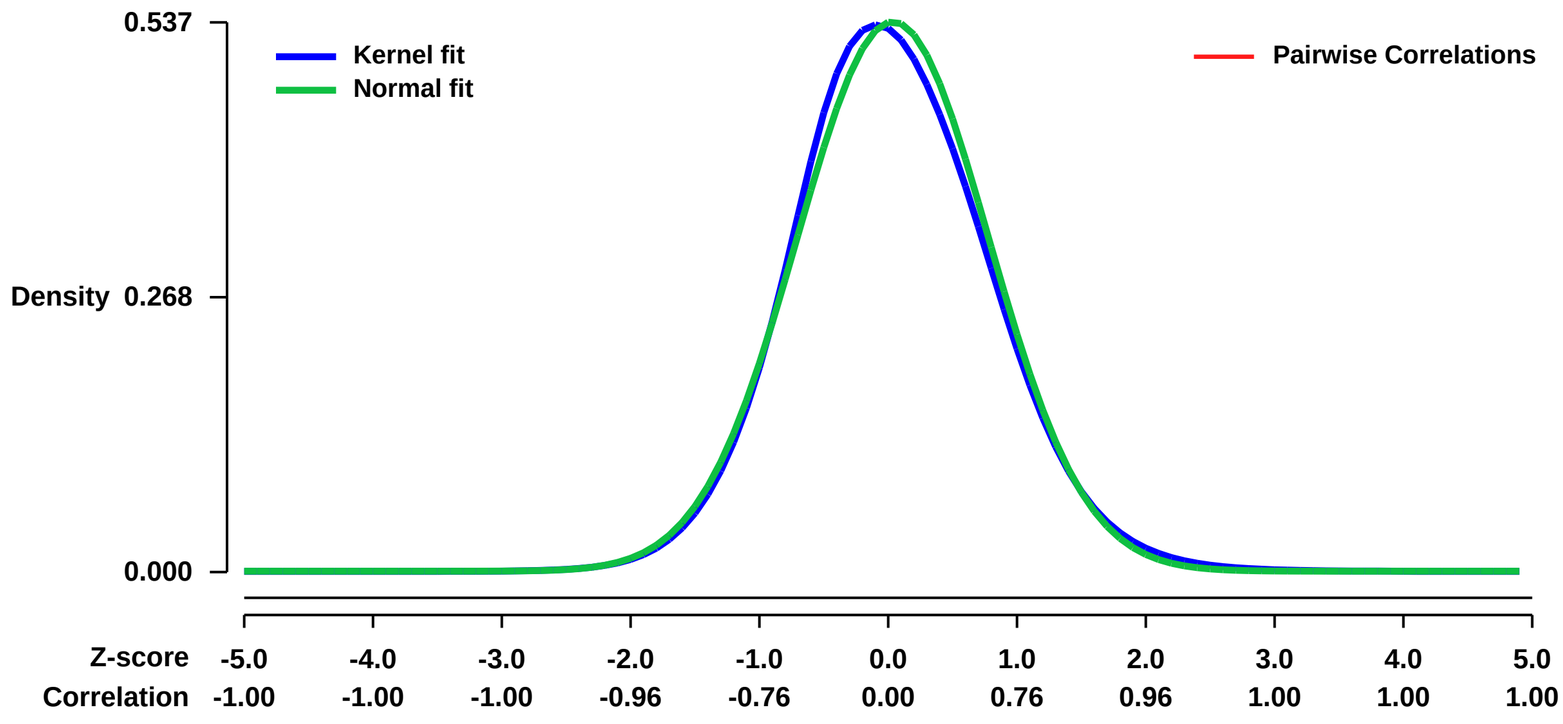

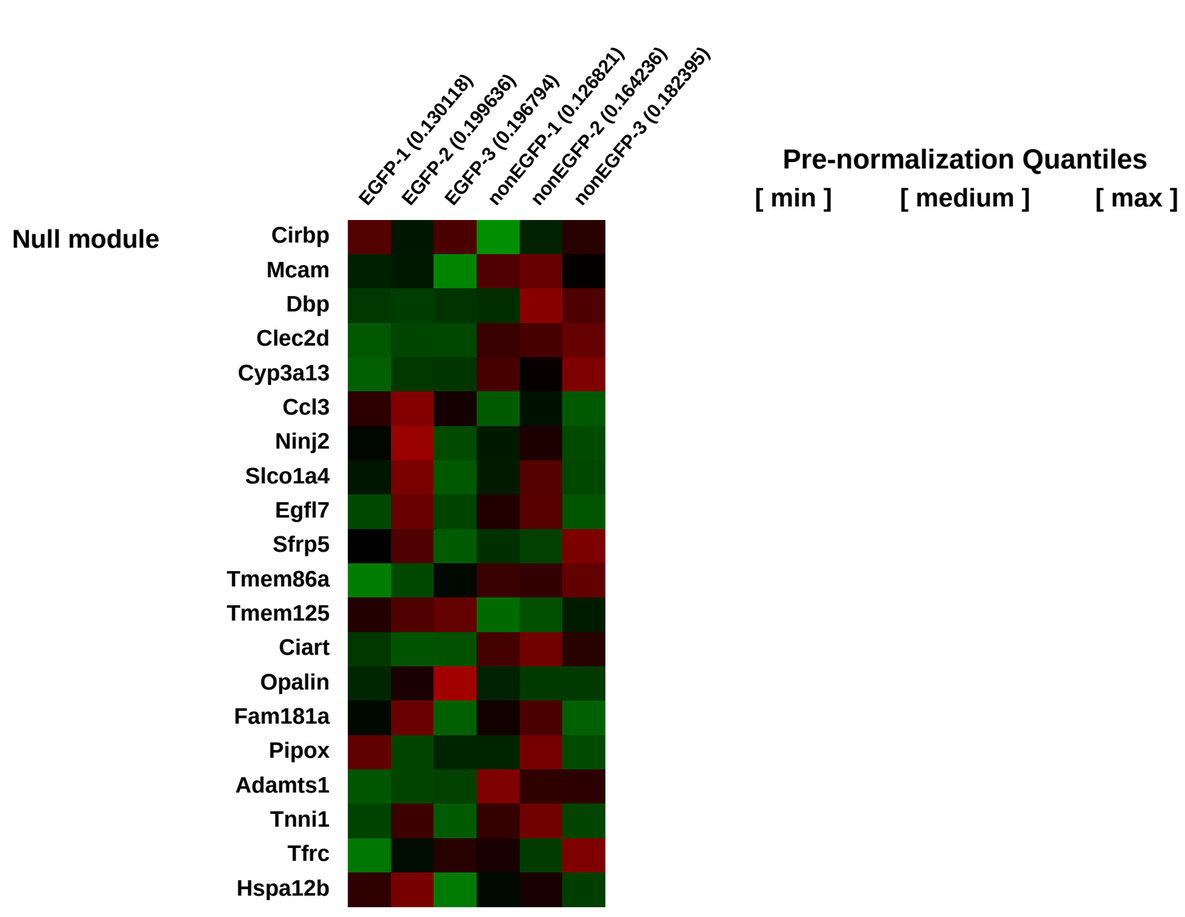

GEO Series "GSE25911" Expression Profiles

Num of samples in this series: 26

Scale of expression profile Z-scores

-3.0 -2.0 -1.0 0.0 1.0 2.0 3.0

GEO Link:	http://www.ncbi.nlm.nih.gov/geo/query/acc.cgi?acc=GSE25911
Status:	Public on Sep 13 2011
Title:	Expression changes after loss of Dot1l in murine MLL-AF9 leukemia cells
Organism:	Mus musculus
Experiment type:	Expression profiling by array
Platform:	GPL1261
Pubmed ID:	21741597
Summary & Design:	**Summary:** MLL-fusions may induce leukemogenic gene expression programs by recruiting the histone H3K79 methyltransferase to MLL-target promoters. We evaluated gene expression changes after cre-mediated loss of Dot1l in leukemia cells obtained from mice injected with MLL-9 transformed lineage negative bone marrow cells. **Overall design:** MLL-AF9 murine leukemia cells carrying two conditional Dot1l alleles were retrovirally transduced with Cre or empty control vector, and gene expression changes were monitored on day 3, 5, and 7 after transduction.

Background corr dist: KL-Divergence = 0.0792, L1-Distance = 0.0746, L2-Distance = 0.0111, Normal std = 0.5107

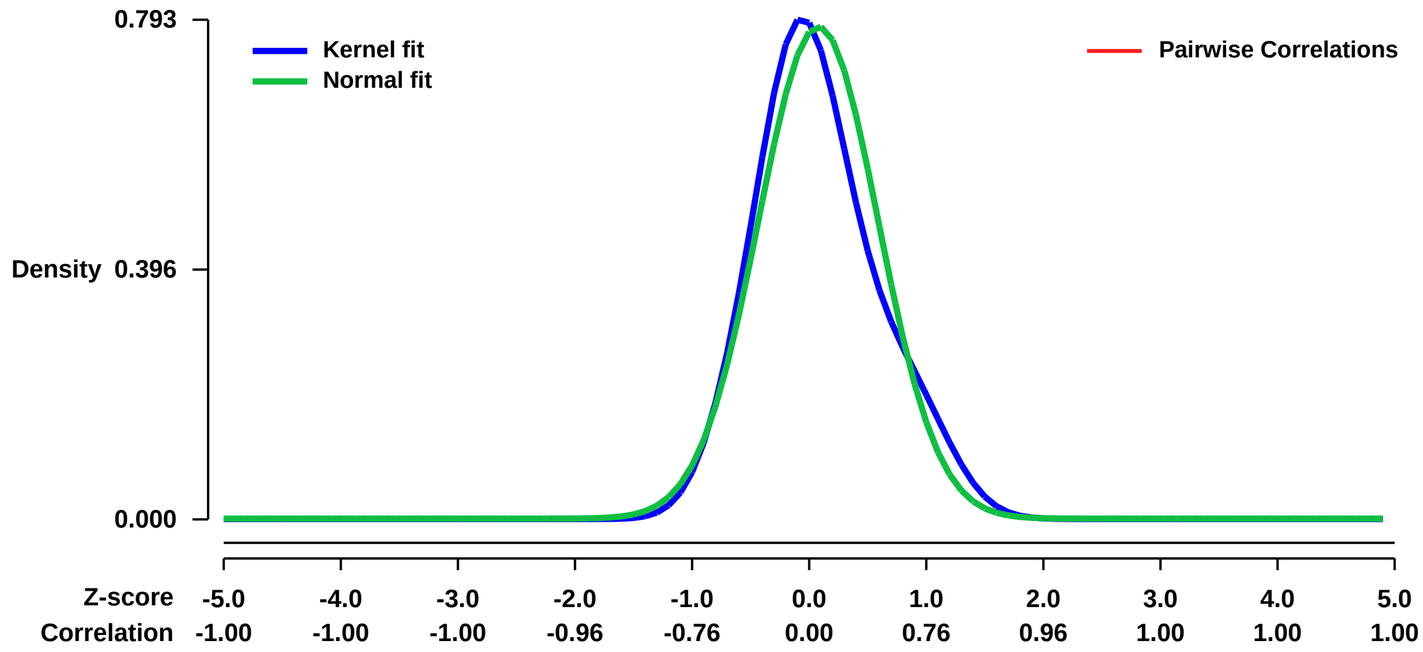

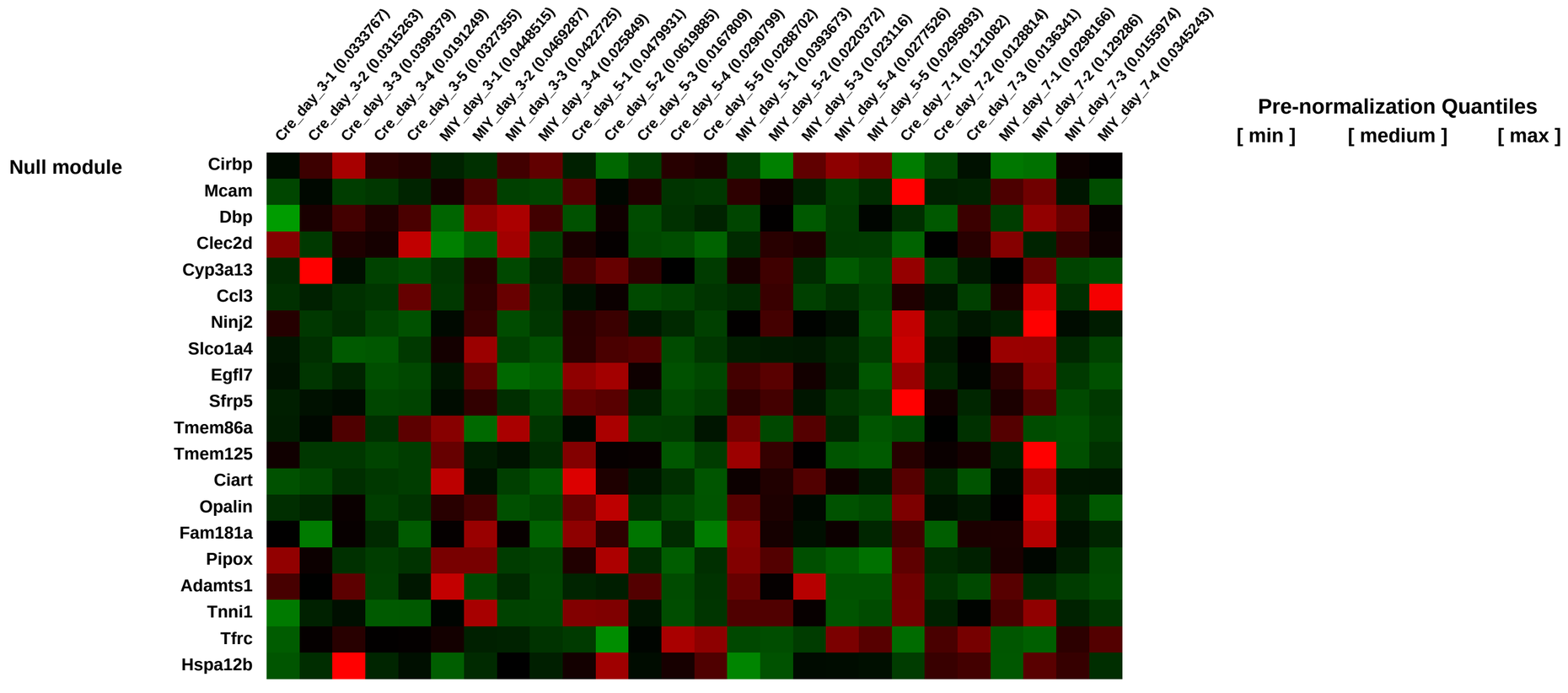

GEO Series "GSE25926" Expression Profiles

Num of samples in this series: 15

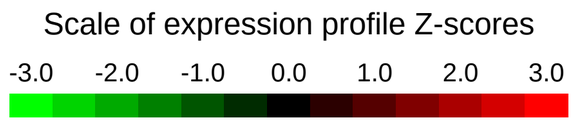

GEO Link:	http://www.ncbi.nlm.nih.gov/geo/query/acc.cgi?acc=GSE25926
Status:	Public on Mar 18 2011
Title:	Comparative transcriptome profiling of Amyloid Precursor Protein APP family members in the adult cortex
Organism:	Mus musculus
Experiment type:	Expression profiling by array
Platform:	GPL1261
Pubmed ID:	21435241
Summary & Design:	**Summary:** **The ˛†-amyloid precursor protein APP and the related APLPs, undergo complex proteolytic processing giving rise to several fragments. Whereas it is well established that A˛† accumulation is a central trigger for Alzheimer disease (AD), the physiological role of APP family members and their diverse proteolytic products is still largely unknown. The secreted APPs˛– ectodomain has been shown to be involved in neuroprotection and synaptic plasticity. The ˛‡-secretase generated APP intracellular domain AICD, functions as a transciptional regulator in heterologous reporter assays, although its role for endogenous gene regulation has remained controversial. To gain further insight into the molecular changes associated with knockout phenotypes and to elucidate the physiological functions of APP family members including their proposed role as transcriptional regulators we performed a DNA microarray transcriptome profiling of the frontal cortex of adult wild type, APP-/-, APLP2-/- and APPs˛– knockin (KI) mice, APP˛–/˛–, expressing solely the secreted APPs˛– ectodomain. Biological pathways affected by the lack of APP family members included regulation of neurogenesis, regulation of transcription and regulation of neuron projection development. Comparative analysis of transcriptome changes and qPCR validation identified co-regulated gene sets. Interestingly, these included heat shock proteins and plasticity related genes that were down-regulated in knock-out cortices. In contrast, we failed to detect significant differences in expression of previously proposed AICD target genes including Bace1, Kai1, Gsk3b, p53, Tip60 and Vglut2. Only Egfr was slightly up-regulated in APLP2-/- mice. Comparison of APP-/- and APP˛–/˛– with wild-type mice revealed a high proportion of co-regulated genes indicating an important role of the C-terminus for cellular signaling. Finally, comparison of APLP2-/- on different genetic backgrounds revealed that background related transcriptome changes may dominate over changes due to the knockout of a single gene. Shared transcriptome profiles corroborated closely related physiological functions of APP family members in the adult central nervous system. As expression of proposed AICD target genes was not altered in adult cortex, this may indicate that these genes are not affected by lack of APP under resting conditions or only in a small subset of cells.** **Overall design:** **Prefrontal cortices of adult male mice (24 - 28 weeks) of the following genotypes were analyzed: WT (n=3), APP-/- (n=3), APP˛–/˛– (n=3), APLP2-/- (n=3), APLP2(R1)-/- (n=3). WT, APP-/-, APP˛–/˛–, APLP2-/- had been backcrossed for six generations to C57BL/6 mice. APLP2(R1)-/- harbors the identical knockout allele as APLP2-/- but was back-crossed only once.**

Background corr dist: KL-Divergence = 0.1865, L1-Distance = 0.0462, L2-Distance = 0.0047, Normal std = 0.3406

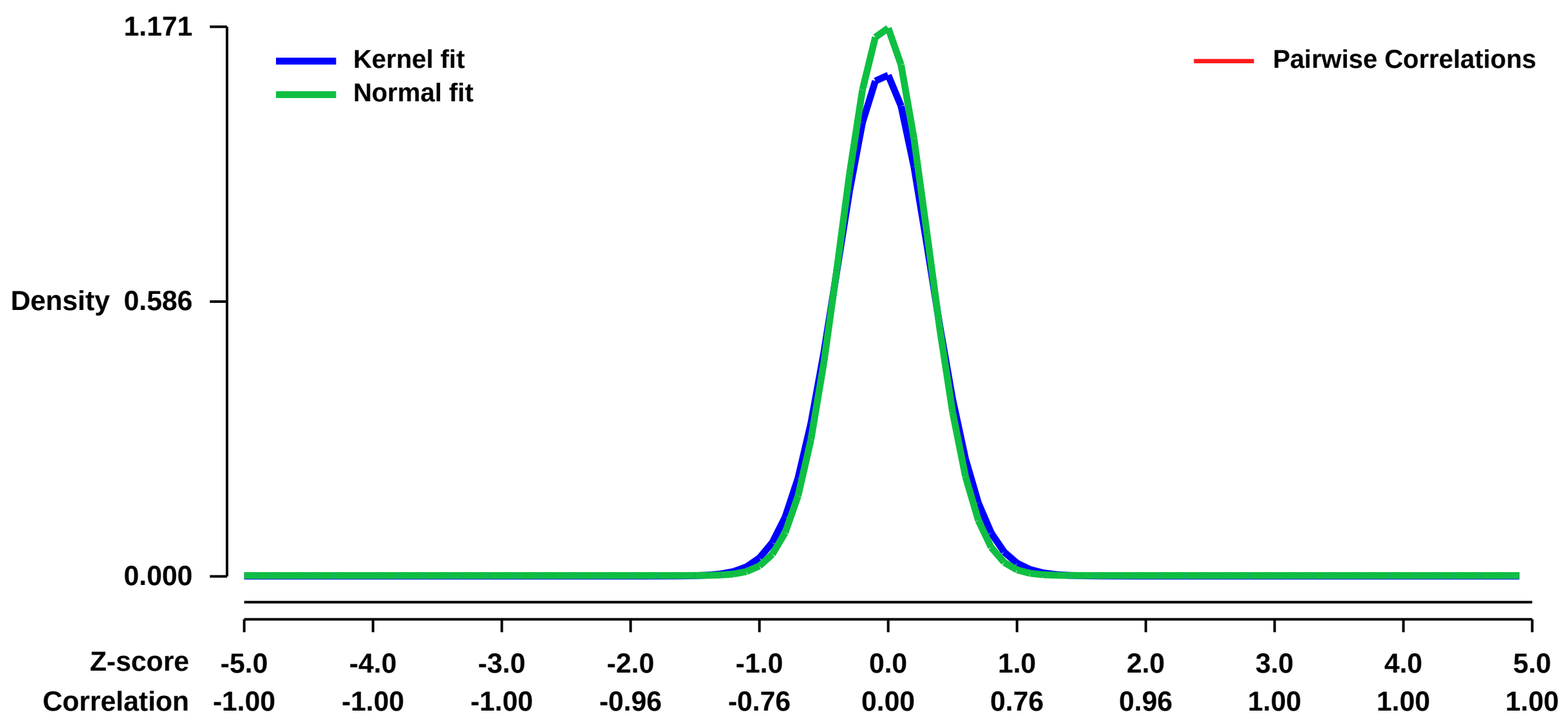

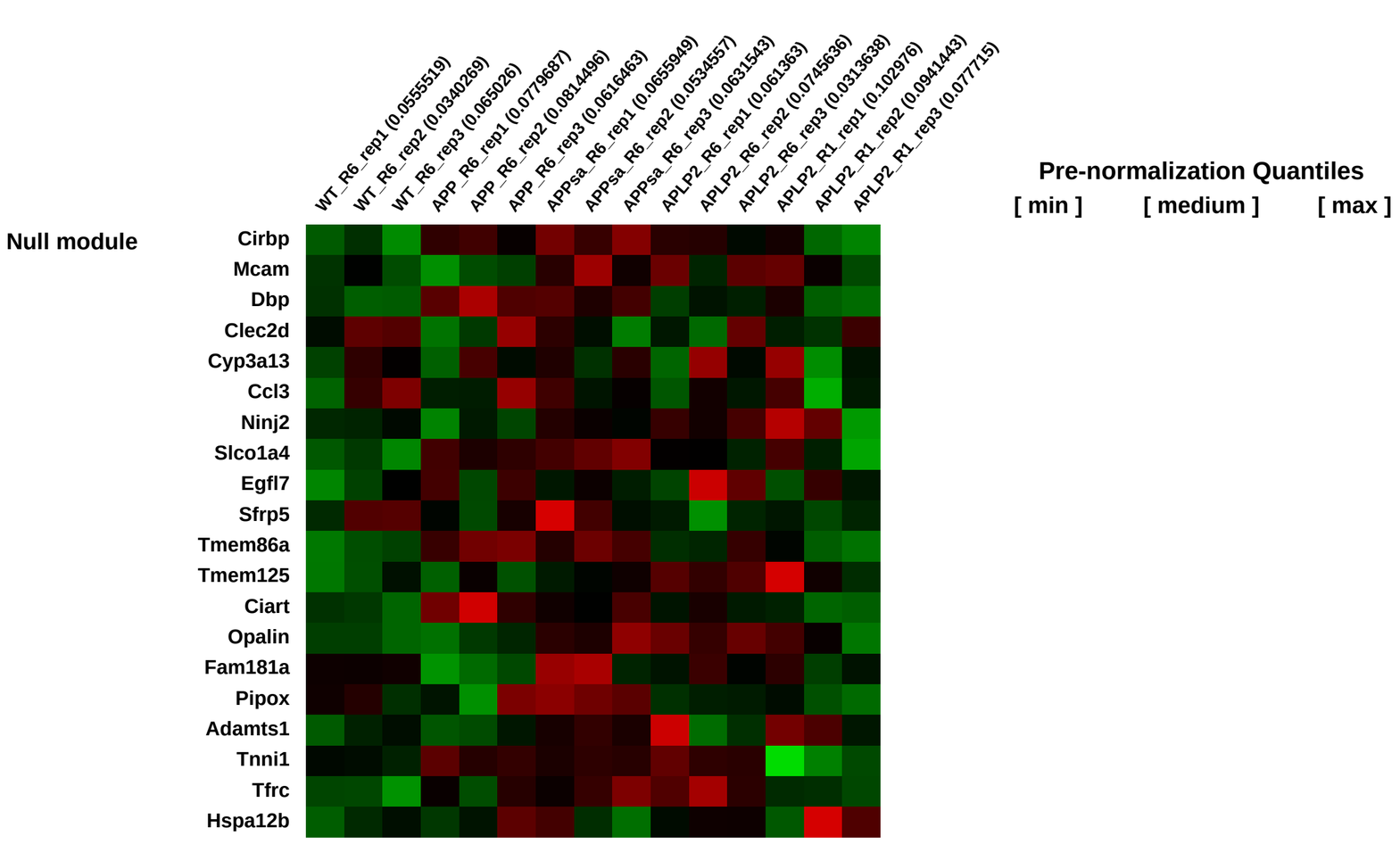

GEO Series "GSE26023" Expression Profiles

Num of samples in this series: 6

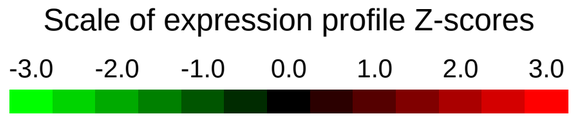

GEO Link:	http://www.ncbi.nlm.nih.gov/geo/query/acc.cgi?acc=GSE26023
Status:	Public on Feb 08 2011
Title:	Prolyl hydroxylase PHD3 is essential for hypoxic regulation of neutrophilic inflammation in humans and mice
Organism:	Mus musculus
Experiment type:	Expression profiling by array
Platform:	GPL1261
Pubmed ID:	21317538
Summary & Design:	**Summary:** Neutrophils were isolated form peripheral blood of wildtype and Phd3 null mice, cultured for 4 hours in hypoxia (3% O2) and micro array analysis performed The aim of the present study is to identify the mechanism by which phd3 is required for the hypoxia mediated survival of neutrophils **Overall design:** Murine peripheral blood neutrophils were isolated from wildtype and phd3 null mice, cultured for 4 hours in hypoxia (3% O2) and micro array analysis performed

Background corr dist: KL-Divergence = 0.0468, L1-Distance = 0.0286, L2-Distance = 0.0011, Normal std = 0.5961

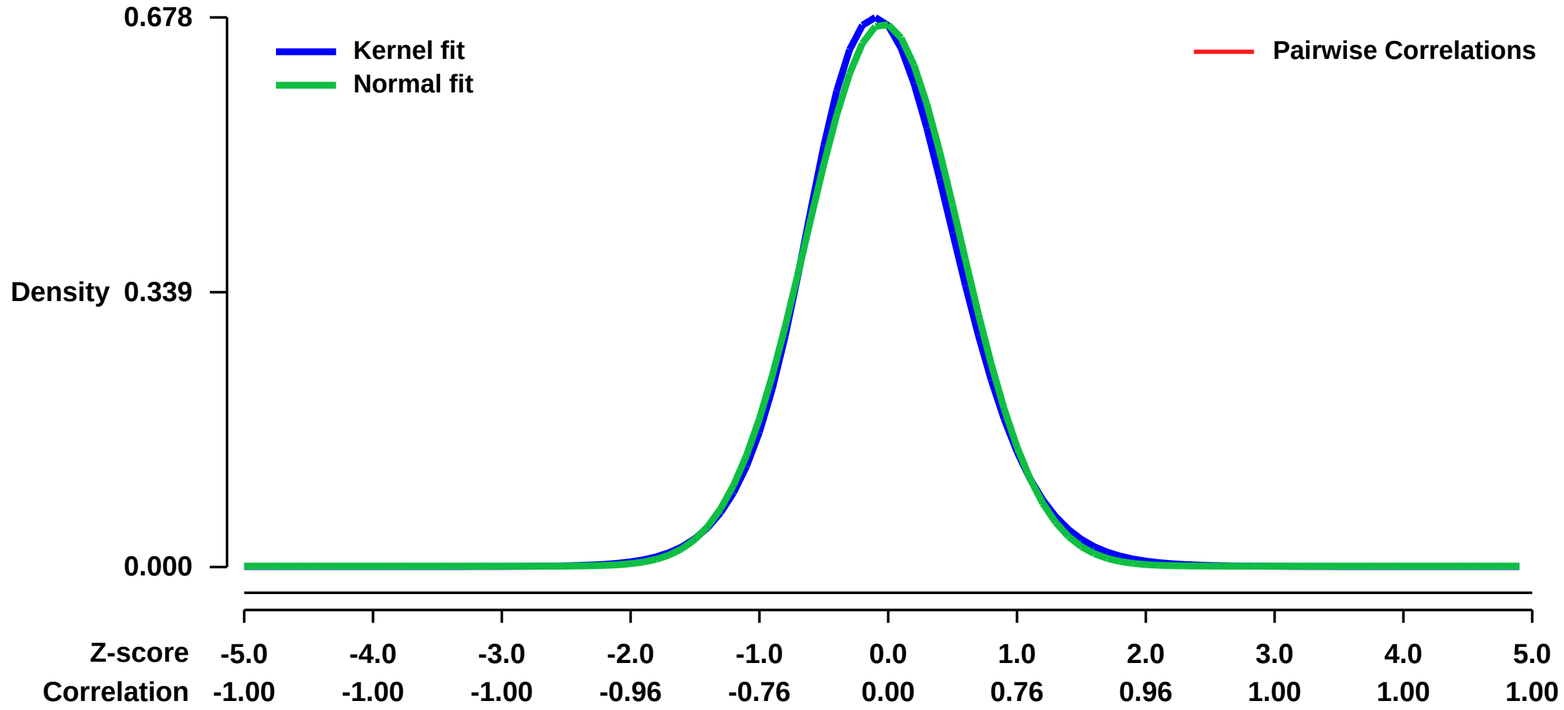

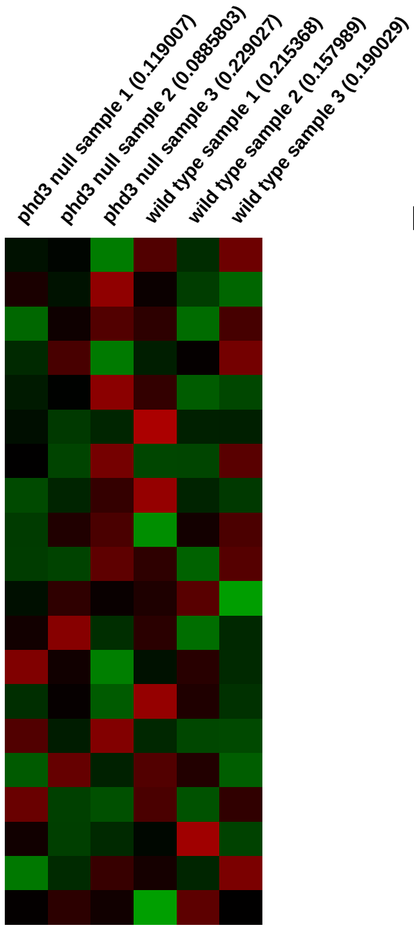

GEO Series "GSE26025" Expression Profiles

Num of samples in this series: 12

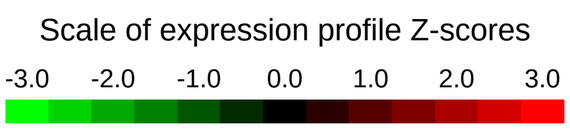

GEO Link:	http://www.ncbi.nlm.nih.gov/geo/query/acc.cgi?acc=GSE26025
Status:	Public on Dec 12 2011
Title:	Sex-specific effects of prenatal stress in 5-Htt deficient mice: towards molecular mechanisms of gene x environment interactions
Organism:	Mus musculus
Experiment type:	Expression profiling by array
Platform:	GPL1261
Pubmed ID:	21857948
Summary & Design:	**Summary:** **prenatal stress response, genetic modification** **Background: Prenatal stress (PS) exposure has been shown to increase the risk for emotional disorders in later life. Furthermore, the serotonin transporter (5-HTT) genotype is suggested to exert a modulating effect on the association between early life stress and the risk for depression. In the present study, we use a 5-HTT x PS paradigm to investigate whether the effects of PS are dependent upon the 5-HTT genotype. Methods: The effects of PS on cognition, anxiety- and depression-related behaviour were examined using a maternal restraint stress paradigm of PS in C57BL6 wild-type (WT) and heterozygous (+/-) 5-HTT knockout mice. Additionally, in the female offspring, a genome-wide hippocampal gene expression screening was performed. Results: 5-HTT +/- offspring showed enhanced memory performance and signs of reduced anxiety as compared to WT offspring. Conversely, exposure of 5-HTT +/- mice to PS was associated with altered stress-responsivity and increased depressive-like behaviour, particularly in female offspring. Further, 5-HTT genotype, PS and their interaction differentially affected the expression of numerous genes and related pathways within the female hippocampus. Specifically, MAPK and neurotrophin signalling were regulated by both the 5-HTT +/- genotype and PS exposure, whereas cytokine and Wnt signalling were affected in a 5-HTT genotype x PS manner, indicating a gene x environment interaction at the molecular level. Conclusions: The long-term behavioural effects of PS in C57BL6 mice are partly dependent on the 5-HTT genotype. Further, hippocampal gene expression profiles suggest that distinct molecular mechanisms mediate the behavioural effects of the 5-HTT genotype, PS exposure, and their interaction.** **Overall design:** **total samples analysed are 12**

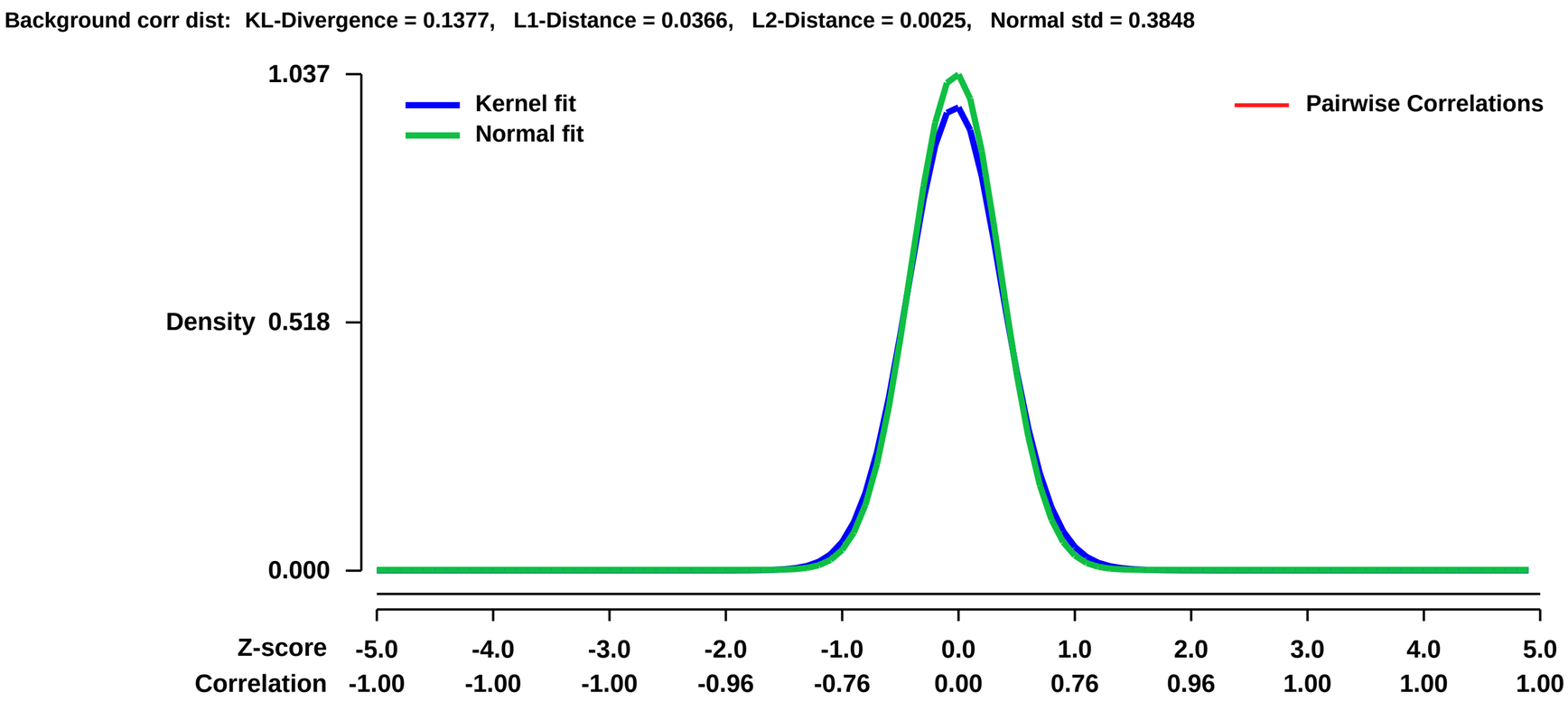

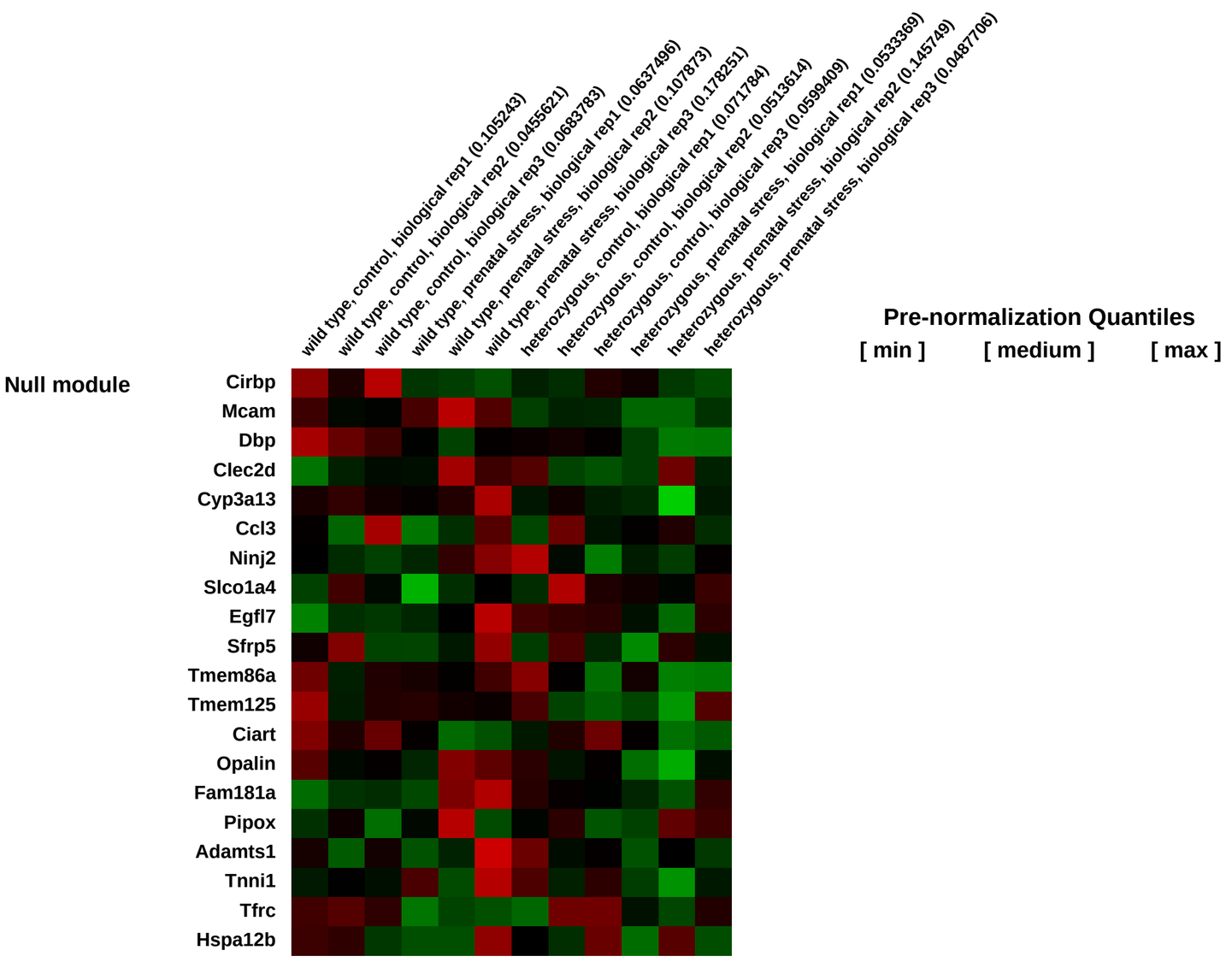

GEO Series "GSE26037" Expression Profiles

Num of samples in this series: 7

Scale of expression profile Z-scores

-3.0 -2.0 -1.0 0.0 1.0 2.0 3.0

GEO Link:	http://www.ncbi.nlm.nih.gov/geo/query/acc.cgi?acc=GSE26037
Status:	Public on Dec 14 2010
Title:	Gene expression analysis in the absence of Creb in Pomc-expressing neurons of the hypothalamus
Organism:	Mus musculus
Experiment type:	Expression profiling by array
Platform:	GPL1261
Pubmed ID:	21187319
Summary & Design:	**Summary:** Brain-derived serotonin favors appetite in mice following its binding to the Htr1a and Htr2b receptors in arcuate neurons of the hypothalamus. In this study, we identified that CREB is the transcriptional effector of brain-derived serotonin control of appetite in arcuate nuclei. **Overall design:** We isolated hypothalami of wild type and Creb-pomcCre-/- (deleted for Creb selectively in arcuate neurons of the hypothalamus) mice and performed microarray experiments.

Background corr dist: KL-Divergence = 0.0609, L1-Distance = 0.0175, L2-Distance = 0.0003, Normal std = 0.5248

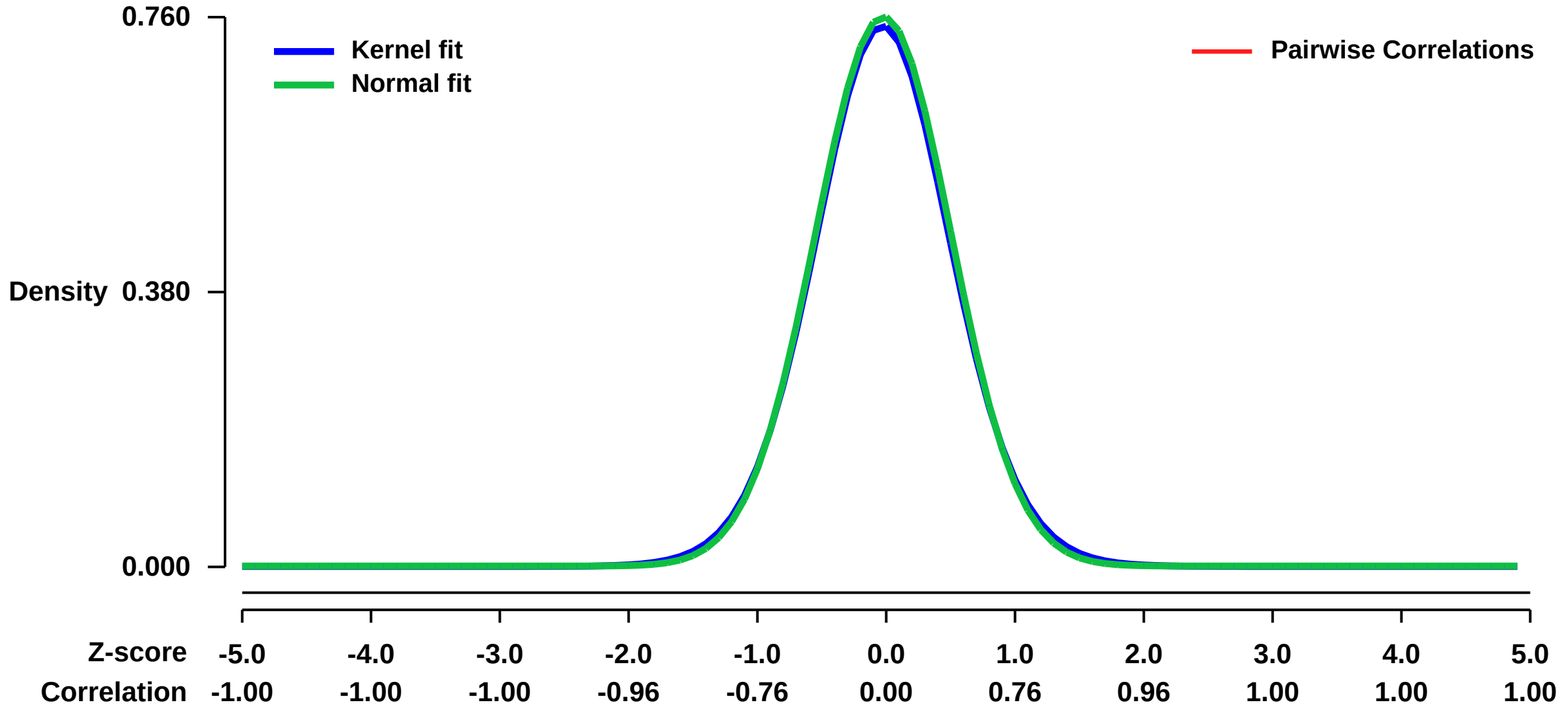

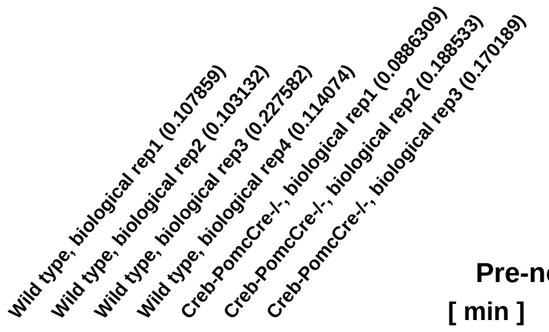

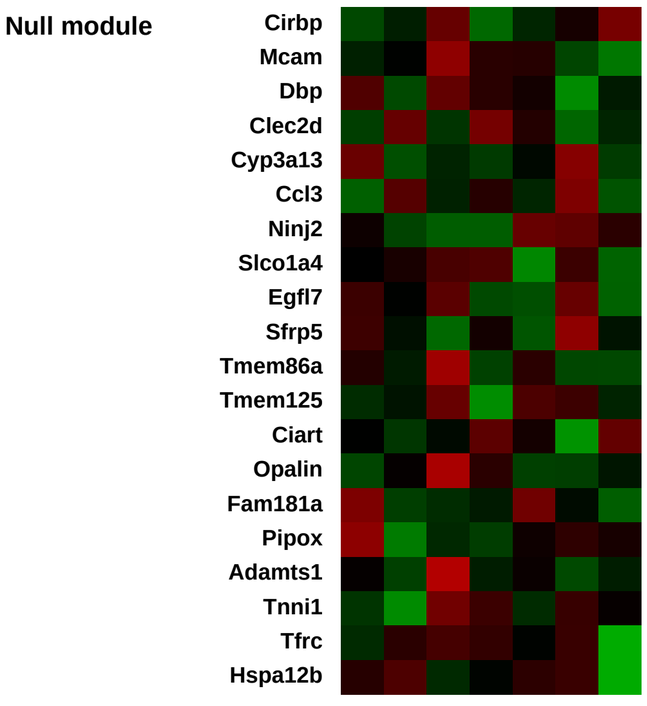

GEO Series "GSE26076" Expression Profiles

Num of samples in this series: 12

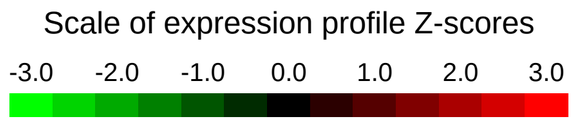

GEO Link:	http://www.ncbi.nlm.nih.gov/geo/query/acc.cgi?acc=GSE26076
Status:	Public on Jun 15 2011
Title:	Mouse conjunctival forniceal gene expression during postnatal development and its regulation by Kruppel-like factor 4
Organism:	Mus musculus
Experiment type:	Expression profiling by array
Platform:	GPL1261
Pubmed ID:	21398290
Summary & Design:	**Summary:** **Purpose: To identify the changes in postnatal mouse conjunctival forniceal gene expression and their regulation by Klf4 around eye opening stage when the goblet cells first appear.** **Methods: Laser-capture-microdissection was used to collect conjunctival forniceal epithelial cells from postnatal-day (PN) 9, PN14 and PN20 wild-type (WT), and PN14 Klf4-conditional null (Klf4CN) mice, where goblet cells are absent, developing, present, and missing, respectively. Microarrays were used to compare gene expression among these four groups. Expression of selected genes was validated by Q-RT-PCR, and spatiotemporal expression assessed by in situ hybridization. Results: We identified 668, 251, 1160 and 139 genes that were upregulated and 492, 377, 1419 and 57 genes that were downregulated between PN9 and PN14, PN14 and PN20, PN9 and PN20, and PN14 WT and Klf4CN conjunctiva, respectively. Transcription factors Spdef, FoxA1 and FoxA3 that regulate goblet cell development in other mucosal epithelia, and epithelial specific Ets (ESE) transcription factor family members were upregulated during conjunctival development. Mesenchymal-epithelial transition (MET) was favored and diverse pathways related to glycoprotein biosynthesis, mucosal immunity, signaling, endocytic and neural regulation were affected during conjunctival development. Conjunctival Klf4-target genes differed significantly from the previously identified corneal Klf4-target genes, implying tissue-dependant regulatory targets for Klf4.** **Conclusions: We have identified the changes in gene expression accompanying mouse conjunctival development and the role of Klf4 in this process. These studies provide new probes to study conjunctival epithelial development and function, and reveal that the gene regulatory network required for goblet cell development is conserved across different mucosal epithelia.** **Overall design:** **Three independent samples in each of four developmental groups**

Background corr dist: KL-Divergence = 0.1081, L1-Distance = 0.0315, L2-Distance = 0.0019, Normal std = 0.4256

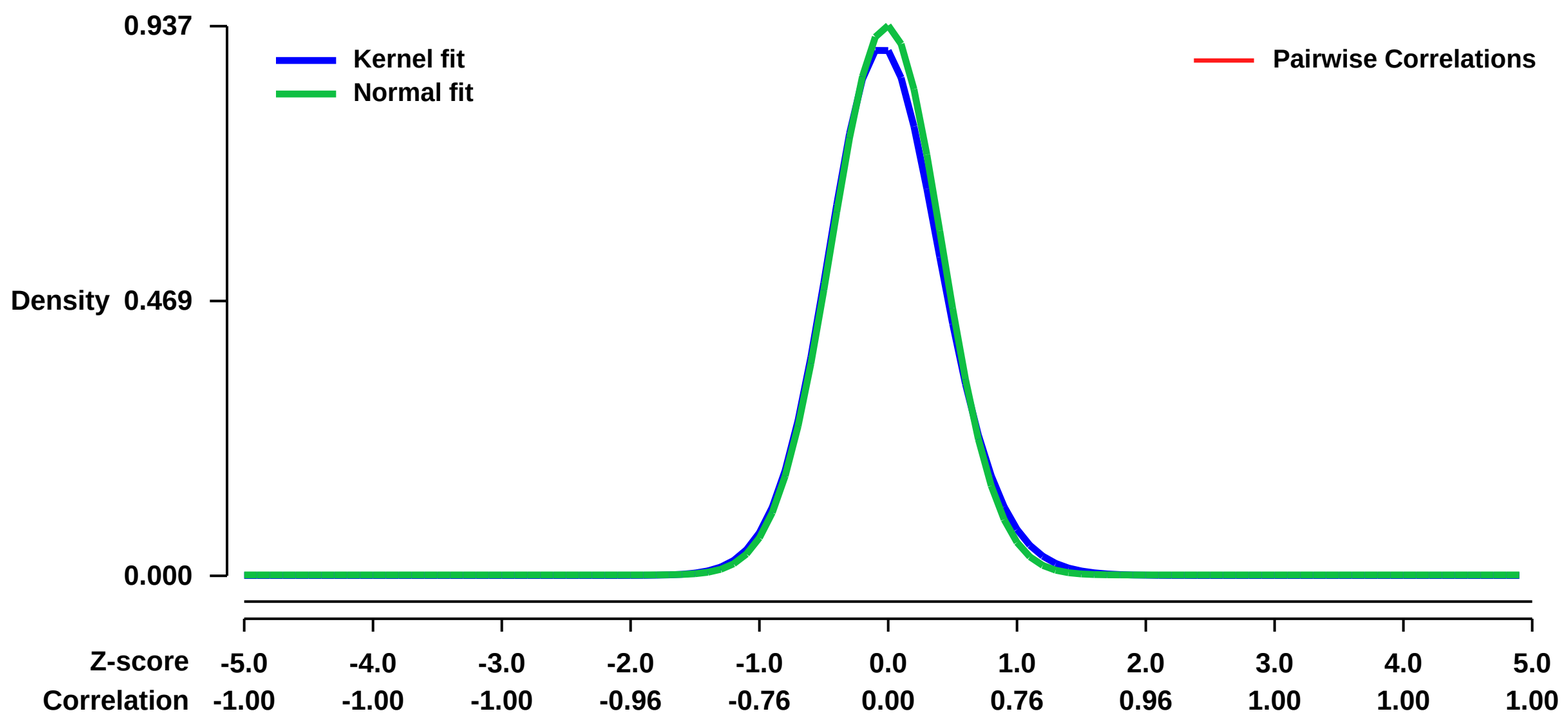

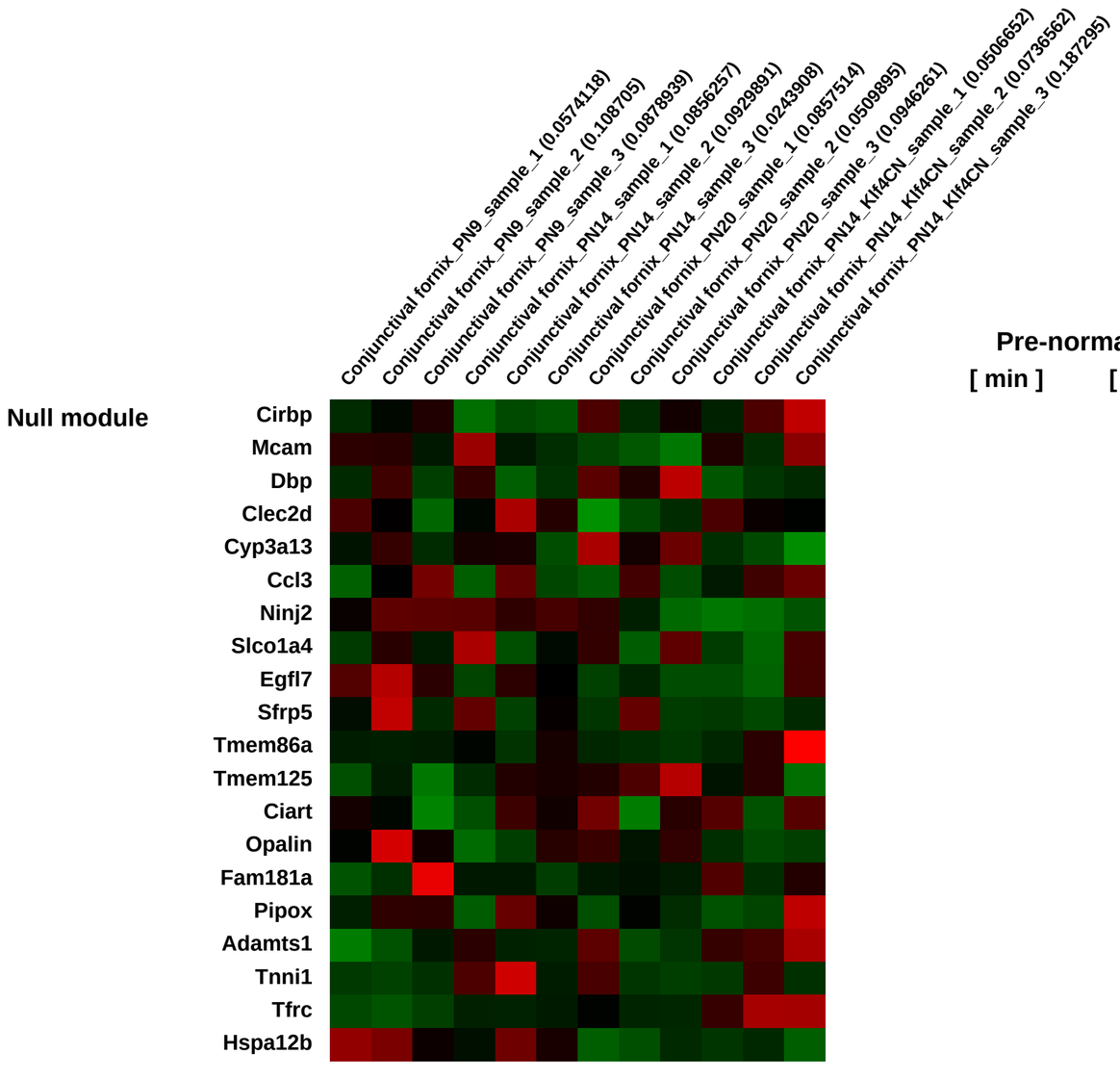

GEO Series "GSE26096" Expression Profiles

Num of samples in this series: 10

Scale of expression profile Z-scores

-3.0 -2.0 -1.0 0.0 1.0 2.0 3.0

GEO Link:	http://www.ncbi.nlm.nih.gov/geo/query/acc.cgi?acc=GSE26096
Status:	Public on Jan 03 2011
Title:	Widespread targeted chromatin remodeling during the initial phase of somatic cell reprogramming [expression]
Organism:	Mus musculus
Experiment type:	Expression profiling by array
Platform:	GPL1261
Pubmed ID:	21211784
Summary & Design:	**Summary:** Despite rapid progress in characterizing transcription factor-driven reprogramming of somatic cells to an induced pluripotent stem (iPS) cell state, many mechanistic questions still remain. To gain insight into the earliest events in the reprogramming process, we systematically analyzed the transcriptional and epigenetic changes that occur during early factor induction after discrete numbers of divisions. We observed rapid, genome-wide changes in the euchromatic histone modification, H3K4me2, at more than a thousand loci including large subsets of pluripotency or developmentally related gene promoters and enhancers. In contrast, patterns of the repressive H3K27me3 modification remained largely unchanged except for focused depletion specifically at positions where H3K4 methylation is gained. These chromatin regulatory events precede transcriptional changes within the corresponding loci. Our data provide evidence for an early, organized, and population-wide epigenetic response to ectopic reprogramming factors that clarify the temporal order through which somatic identity is reset during reprogramming. **Overall design:** Gene expression was measured by Affymetric microarrays during the initial phase of the reprogramming of mouse embryonic fibroblasts.

Background corr dist: KL-Divergence = 0.0618, L1-Distance = 0.0293, L2-Distance = 0.0012, Normal std = 0.5376

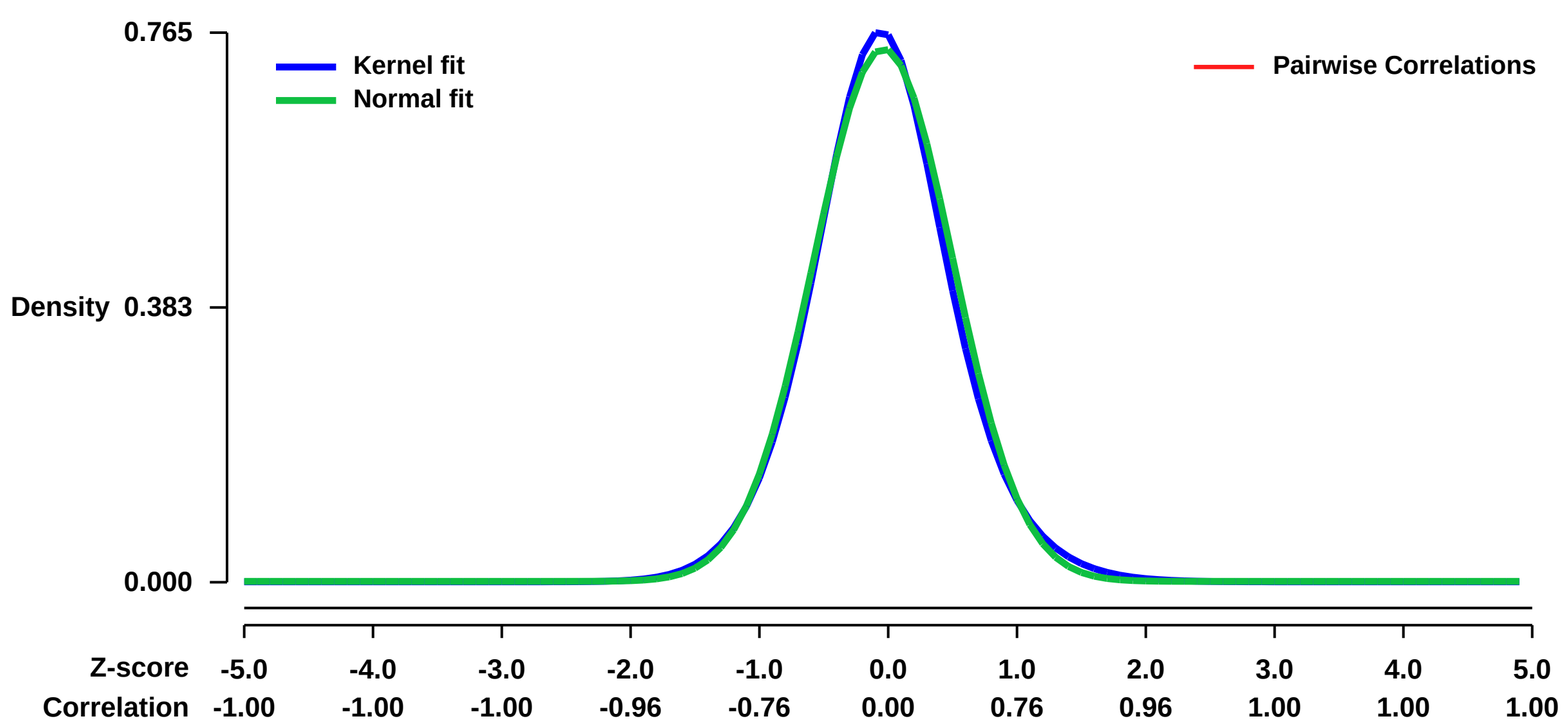

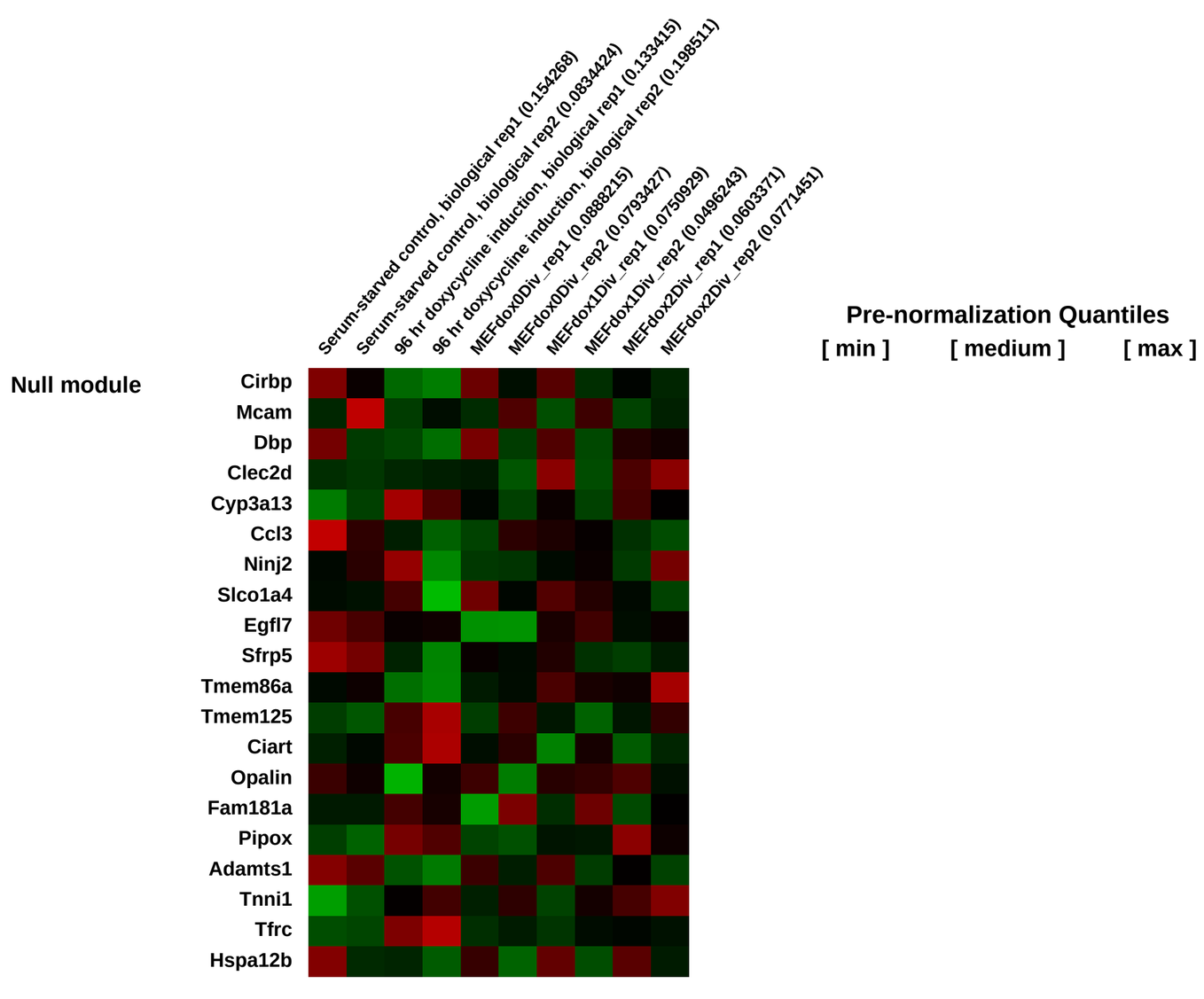

GEO Series "GSE26151" Expression Profiles

Num of samples in this series: 20

Scale of expression profile Z-scores

-3.0 -2.0 -1.0 0.0 1.0 2.0 3.0

GEO Link:	http://www.ncbi.nlm.nih.gov/geo/query/acc.cgi?acc=GSE26151
Status:	Public on Jun 30 2011
Title:	Splitting Function enables Dual Feedback Regulation to Control JAK2/STAT5 Signaling for a Wide Ligand Range
Organism:	Mus musculus
Experiment type:	Expression profiling by array
Platform:	GPL1261
Pubmed ID:	21772264
Summary & Design:	**Summary:** **Cellular signal transduction is governed by multiple feedback mechanisms to elicit robust cellular decisions. We combined mathematical modeling and extensive time-resolved data sets in primary erythroid progenitor cells and dissected the roles of the two transcriptional feedback regulators of the SOCS family, CIS and SOCS3 in JAK2/STAT5 signaling. Our model revealed that both feedbacks are most effective at different ligand concentration ranges.** **To identify the relevant transcriptional feedback regulators that are involved in attenuation of Epo-induced JAK2-STAT5 signaling in addition to CIS, we performed a time-resolved genome-wide expression profiling of murine erythroid progenitor cells at the colony forming unit erythroid (CFU-E) stage up to 24 and 7 hours after EPO stimulation and in control, repectively. The analysis identified SOCS3 as the only further de novo regulated gene upon Epo-induced JAK2-STAT5 signaling. From subsequent mathematical modeling, we calculated the STAT5 response in previously unobserved Epo concentrations, which provided a quantitative link between cell survival and the integrated response of STAT5 in the nucleus. In conclusion, our combined modeling approach revealed novel insights into the orchestrated action of feedback control to regulate STAT5-mediated survival decisions over a broad range of ligand concentrations.** **Overall design:** **Freshly sorted CFU-E cells were starved for 1 h in Panserin 401 supplemented with BSA and 50 ´µM ¸†-Mercaptoethanol. Subsequently, cells were stimulated with 0.5 U/ml Epo or left untreated and RNA was extracted at different time points (0,1,2,3,4,5,6,7,8,14,19,24 hrs after Epo stimulation and at 0,1,2,3,4,5,6,7 hrs without Epo treatment) using the RNeasy Mini Plus Kit (Qiagen, Hilden, Germany).**

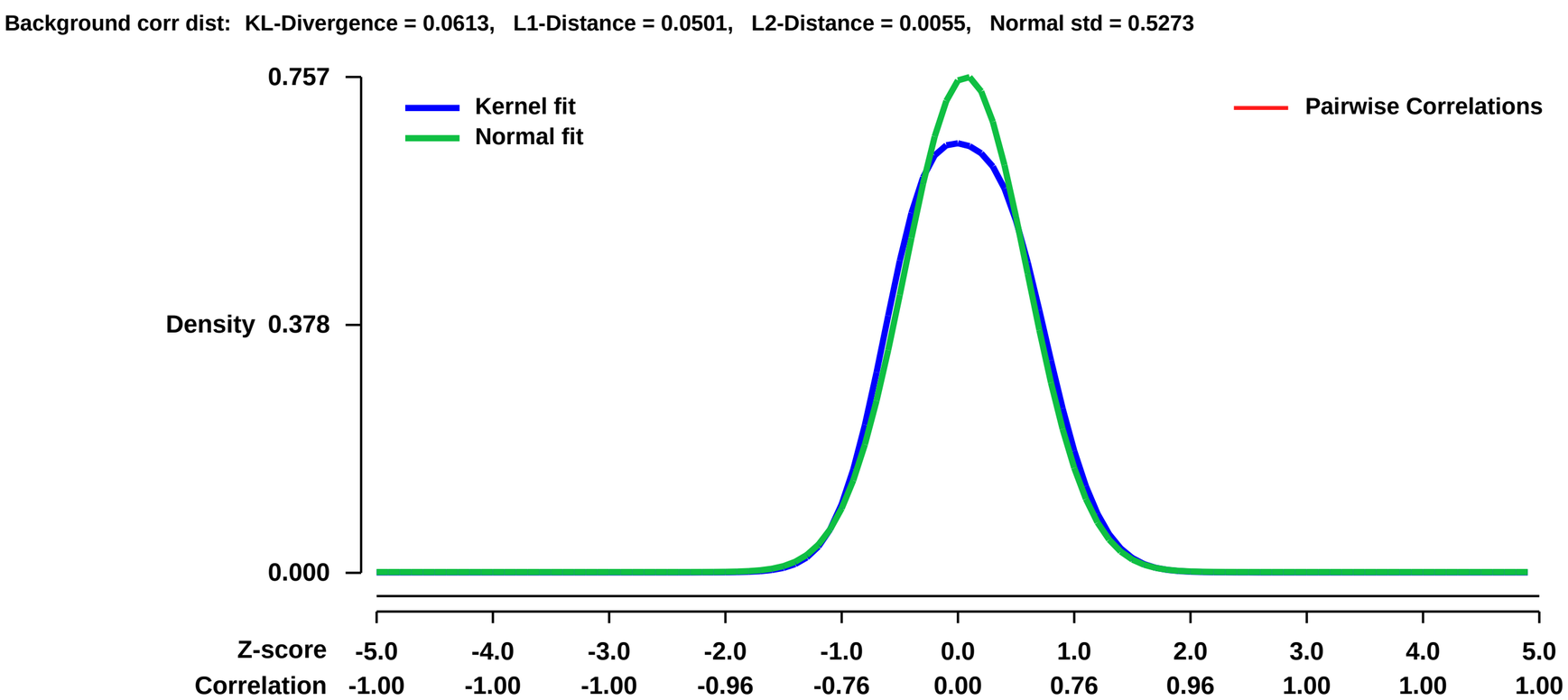

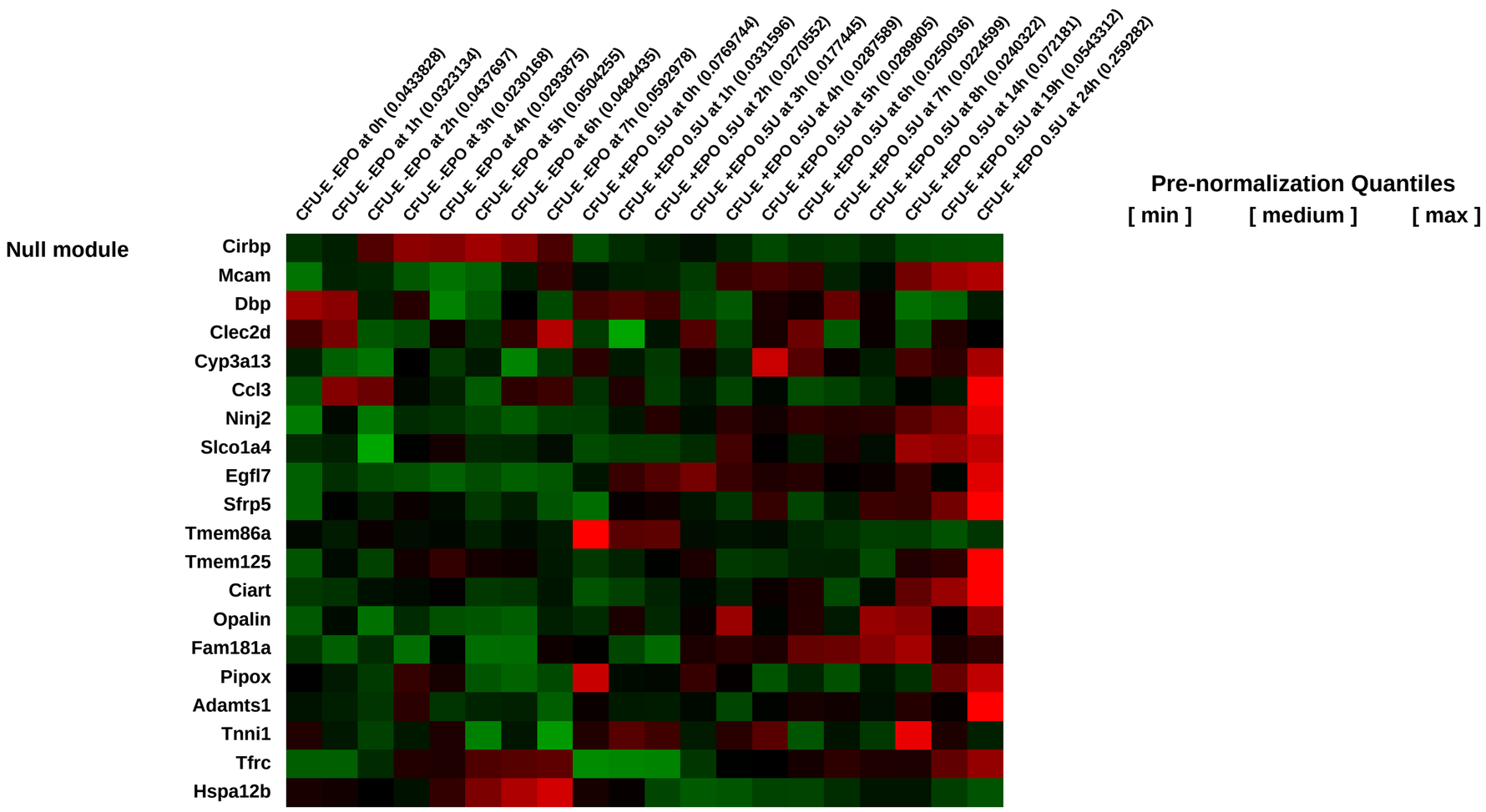

GEO Series "GSE26229" Expression Profiles

Num of samples in this series: 8

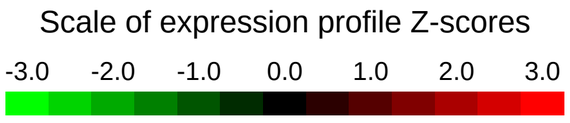

GEO Link:	http://www.ncbi.nlm.nih.gov/geo/query/acc.cgi?acc=GSE26229
Status:	Public on May 20 2011
Title:	Transcriptional profiling of ex vivo isolated inflammed mouse lymphatic endothelial cells
Organism:	Mus musculus
Experiment type:	Expression profiling by array
Platform:	GPL1261
Pubmed ID:	21596851
Summary & Design:	**Summary:** Chemokines and adhesion molecules upregulated in lymphatic endothelial cells (LECs) during tissue inflammation are believed to enhance dendritic cell (DC) migration to draining lymph nodes (dLNs), but the in vivo control of this process is not well understood. By performing transcriptional profiling of LECs isolated from murine skin, we found that inflammation induced by a contact hypersensitivity (CHS) response upregulated the adhesion molecules ICAM-1 and VCAM-1 and inflammatory chemokines in LECs. Furthermore, lymphatic lineage markers like Prox-1, VEGFR3 and LYVE-1 were significantly downregulated during CHS. By contrast, skin inflammation induced by Complete Freundâ s adjuvant (CFA) induced a different pattern of chemokine and lymphatic marker gene expression and almost no ICAM-1 up-regulation in LECs. In FITC painting experiments, DC migration to dLNs was more strongly increased in CFA- as compared to CHS-induced inflammation. Interestingly, DC migration did not correlate with the induction of CCL21 and ICAM-1 in LECs. However, the requirement for CCR7 signaling became further pronounced during inflammation, whereas CCR7-independent signals only had a minor role in enhancing DC migration. Collectively, these findings indicate that inflammation-induced DC migration is stimulus-dependent and only moderately enhanced by LEC-induced genes other than CCL21. **Overall design:** Mouse ear skin single-cell suspensions were prepared by a fast protocol that minimizes the RNA degradation. Fluorescence-activated cell sorting (FACS) was used to sort lymphatic endothelial cells (LEC) from CHS inflammed and control skin. 4 pairs (each with one control and one CHS inflammed sample, sorted and extracted on the same day) of LECs were chosen based on the quality of extracted and amplified material. This gave 8 samples to analyze (4 biological replicates in each condition). Each sample was sorted from 3 mice.

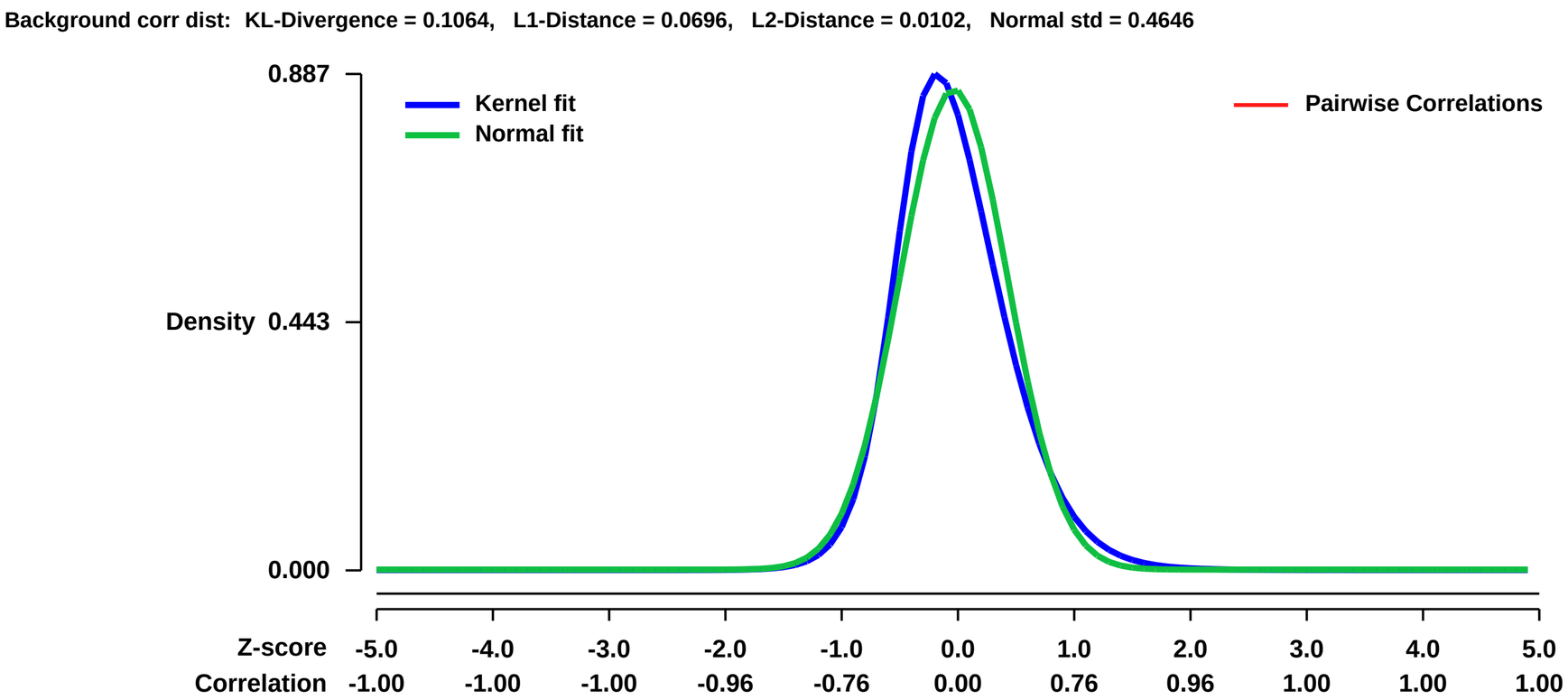

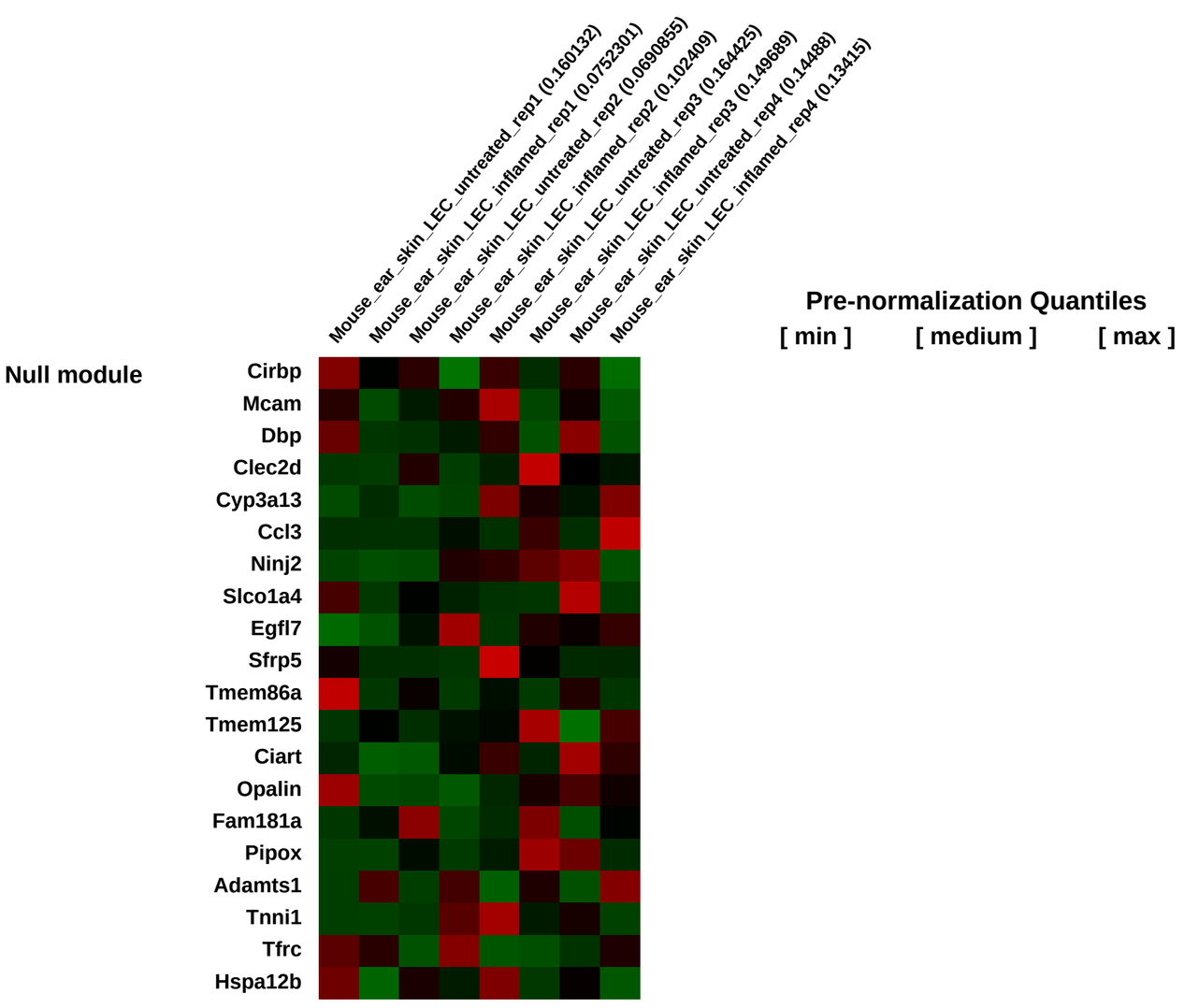

GEO Series "GSE26355" Expression Profiles

Num of samples in this series: 6

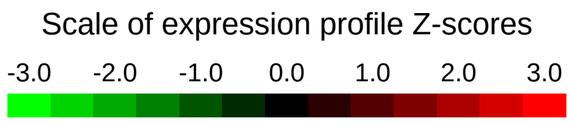

GEO Link:	http://www.ncbi.nlm.nih.gov/geo/query/acc.cgi?acc=GSE26355
Status:	Public on Jan 01 2011
Title:	Expression data from early and late born Atoh1 lineages within the E14.5 rhombomere 1 and isthmus
Organism:	Mus musculus
Experiment type:	Expression profiling by array
Platform:	GPL1261
Pubmed ID:	21440680
Summary & Design:	**Summary:** Following neural tube closure at around E9.5, the rhombic lip within the rhombomere 1/isthmus region (""upper rhombic lip"") produces a sequence of neuronal lineages that populate the brainstem and cerebellum. The transcription factor Atoh1 (Math1) is required for this specialized neurogenesis, although the genetic programs that delineate the temporal cell fate changes downstream of Atoh1 are not well characterized. We examined the gene expresion changes that take place within Atoh1 lineages **Overall design:** We purified early (E10.5) and late (E13.5) born Atoh1 expressing cells from E14.5 embryos using a transgenic labeling strategy, and analyzed differences in gene expression across the two populations using the microarray data shown below.

Background corr dist: KL-Divergence = 0.0310, L1-Distance = 0.0295, L2-Distance = 0.0010, Normal std = 0.6844

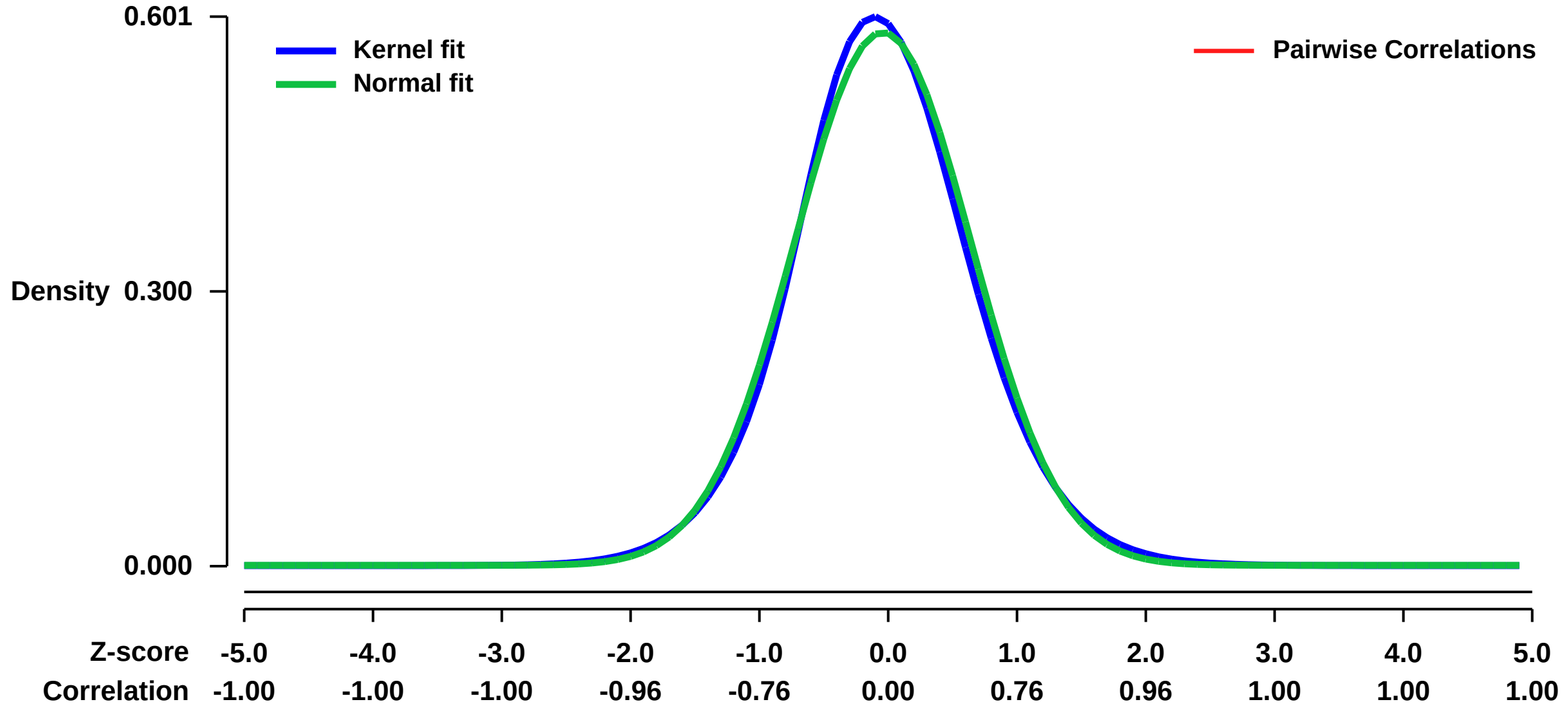

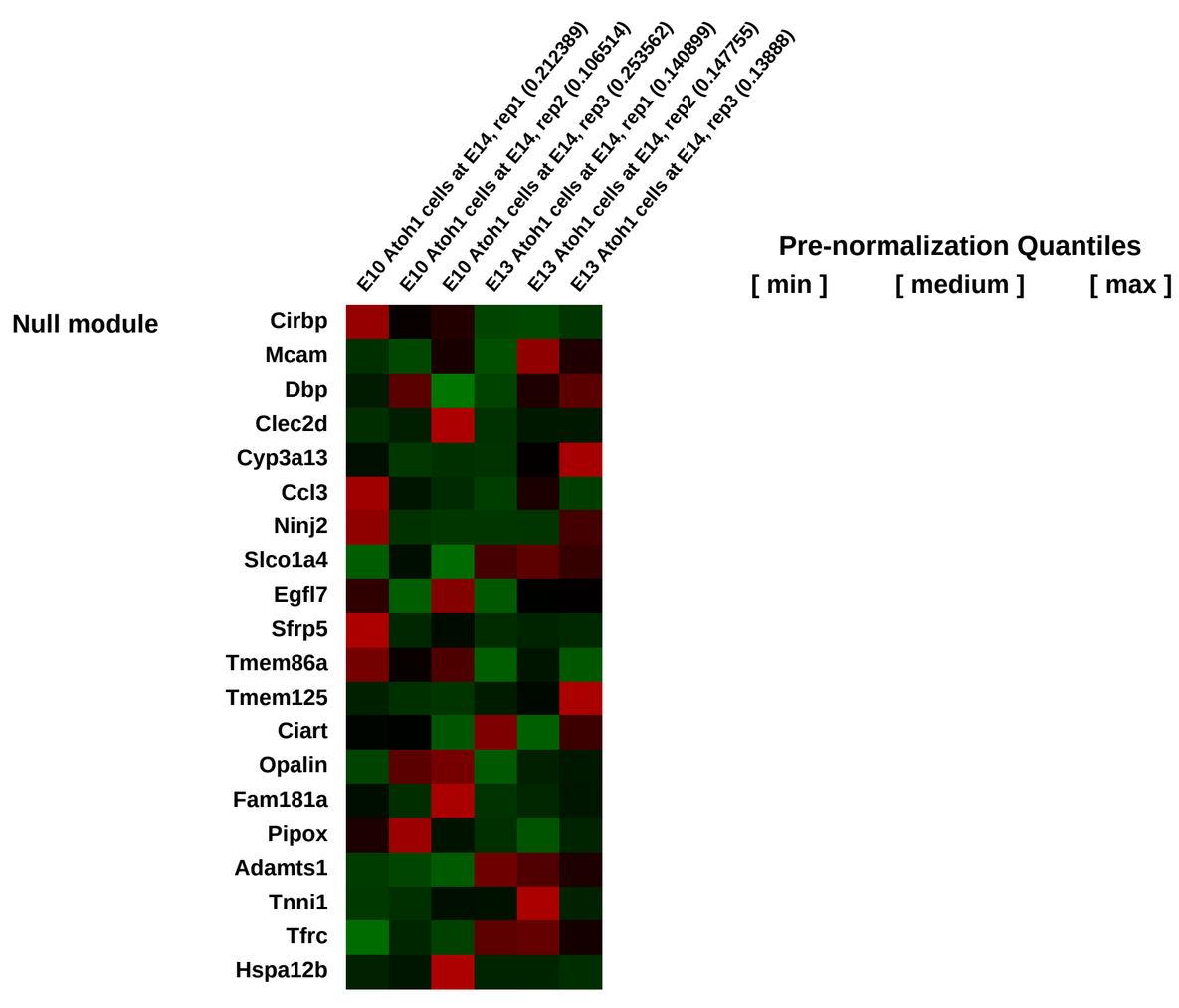

GEO Series "GSE26403" Expression Profiles

Num of samples in this series: 6

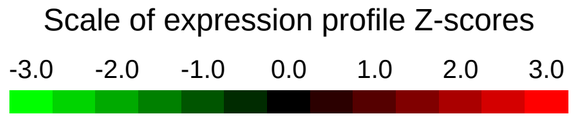

GEO Link:	http://www.ncbi.nlm.nih.gov/geo/query/acc.cgi?acc=GSE26403
Status:	Public on Jan 03 2011
Title:	Gene therapy of Mpl -/- mouse LSK cells
Organism:	Mus musculus
Experiment type:	Expression profiling by array
Platform:	GPL1261
Pubmed ID:	21289307
Summary & Design:	**Summary:** Comparison of Mpl-/- mouse LSK cells, either treated with control (GFP) or Mpl lentivirus. Lineage negative bone marrow cells were isolated and transduced and transplanted into Mpl-/- recipient mice. After transplantation and follow up mice were sacrificed and LSK (lineage negative, Sca-1 positive, cKit positive) cells were isolated by FACS. RNA was isolated using RNeasy Micro Kit (Qiagen GmbH, Hilden, Germany) and RNA was amplified for microarray hybridization using the Nugen Ovation system (Nugen Technologies, AC Bemmel, Netherlands). The resulting material was hybridized to Affymetrix Mouse 430 2.0 arrays. RMA normalization and summarization was performed in R 2.10 using Bioconductor packages. The aim was to show the normalization of Mpl associated gene expression. **Overall design:** 3 control (GFP transduced) samples of Mpl -/- mouse LSK cells and 3 treatment (Mpl transduced) samples of Mpl -/- mouse LSK cells.

Background corr dist: KL-Divergence = 0.0346, L1-Distance = 0.0714, L2-Distance = 0.0073, Normal std = 0.7501

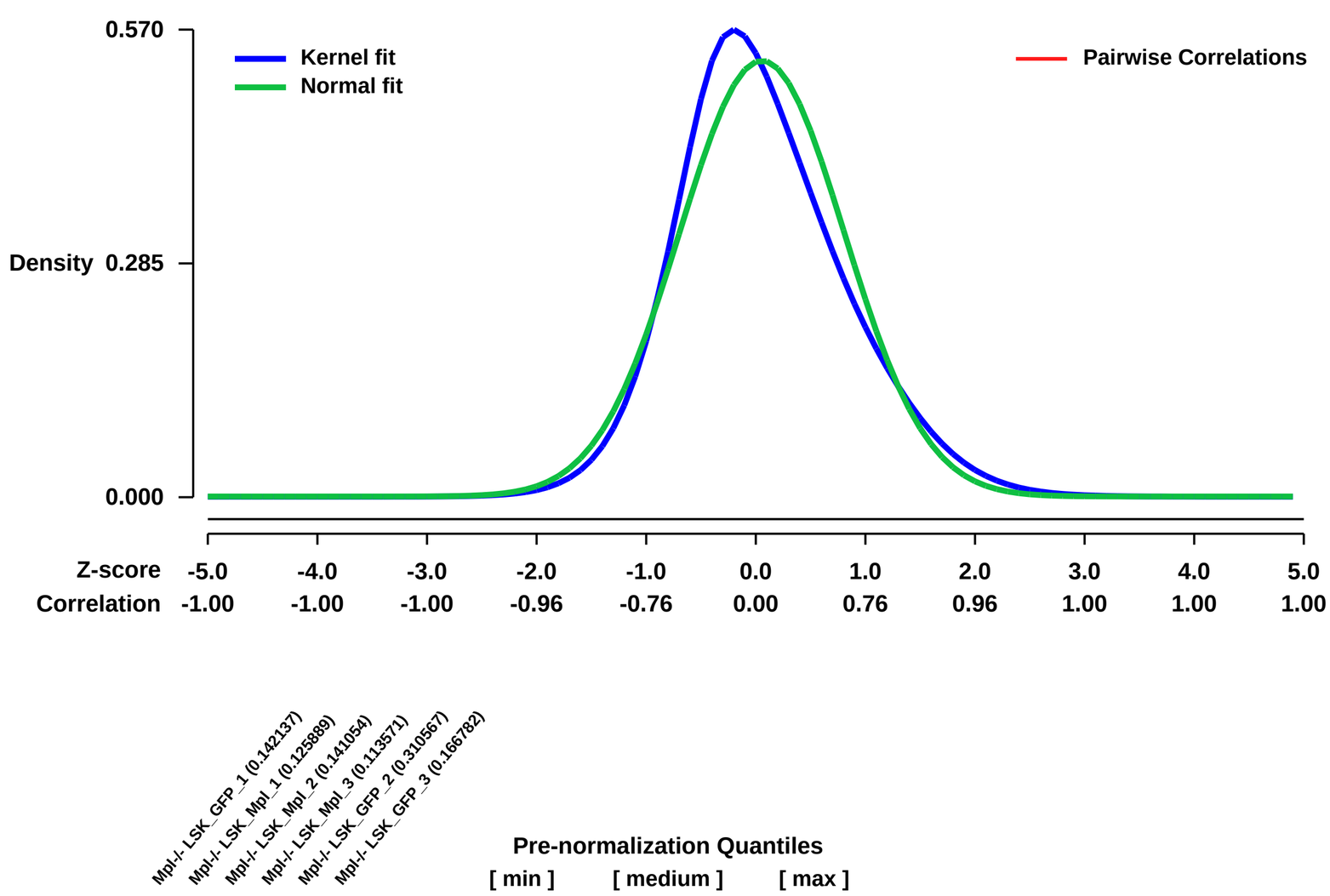

Pre-normalization Quantiles

[min] **[medium]** **[max]**

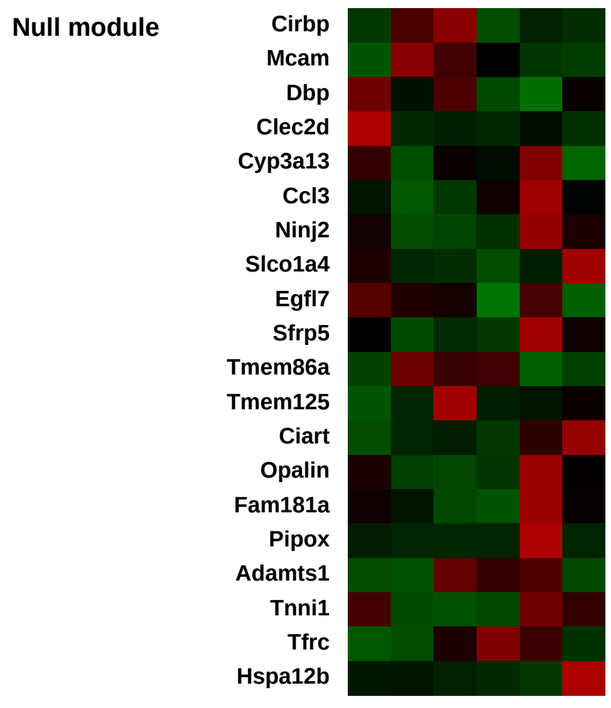

GEO Series "GSE26446" Expression Profiles

Num of samples in this series: 8

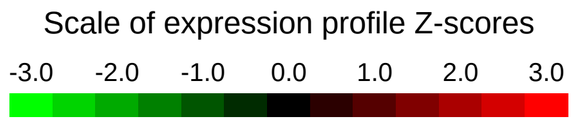

GEO Link:	http://www.ncbi.nlm.nih.gov/geo/query/acc.cgi?acc=GSE26446
Status:	Public on Jul 20 2011
Title:	Expression data from Rbp2f/f and Rbp2-/- ES cells before and after differentiation
Organism:	Mus musculus
Experiment type:	Expression profiling by array
Platform:	GPL1261
Pubmed ID:	21788502
Summary & Design:	**Summary:** Aberrations in epigenetic processes, such as histone methylation, can lead to cancer. Retinoblastoma Binding Protein 2 (RBP2)(also called JARID1A or KDM5A) can demethylate tri- and di-methylated lysine 4 in histone H3, which are epigenetic marks for transcriptionally active chromatin, whereas the MEN1 tumor suppressor promotes H3K4 methylation. Previous studies suggested that inhibition of RBP2 contributed to tumor suppression by pRB. Here we show RBP2 loss promotes cellular differentiation in vitro. We use mouse expression array 430 2.0 array to profile gene expression patterns of Rbp2f/f and Rbp2-/- ES cells in ES cell medium and after 6 days in ES cell medium without LIF. **Overall design:** Subconfluent Rbp2f/f and Rbp2-/- ES cells in ES cell medium and after 6 days in ES cell medium without LIF were harvested for RNA isolation using RNeasy mini kit with on-column DNase digestion (Qiagen). Gene expression profiling was performed using Affymetrix GeneChip mouse genome 430 2.0 arrays. Duplicate samples were used

Background corr dist: KL-Divergence = 0.0611, L1-Distance = 0.0239, L2-Distance = 0.0008, Normal std = 0.5304

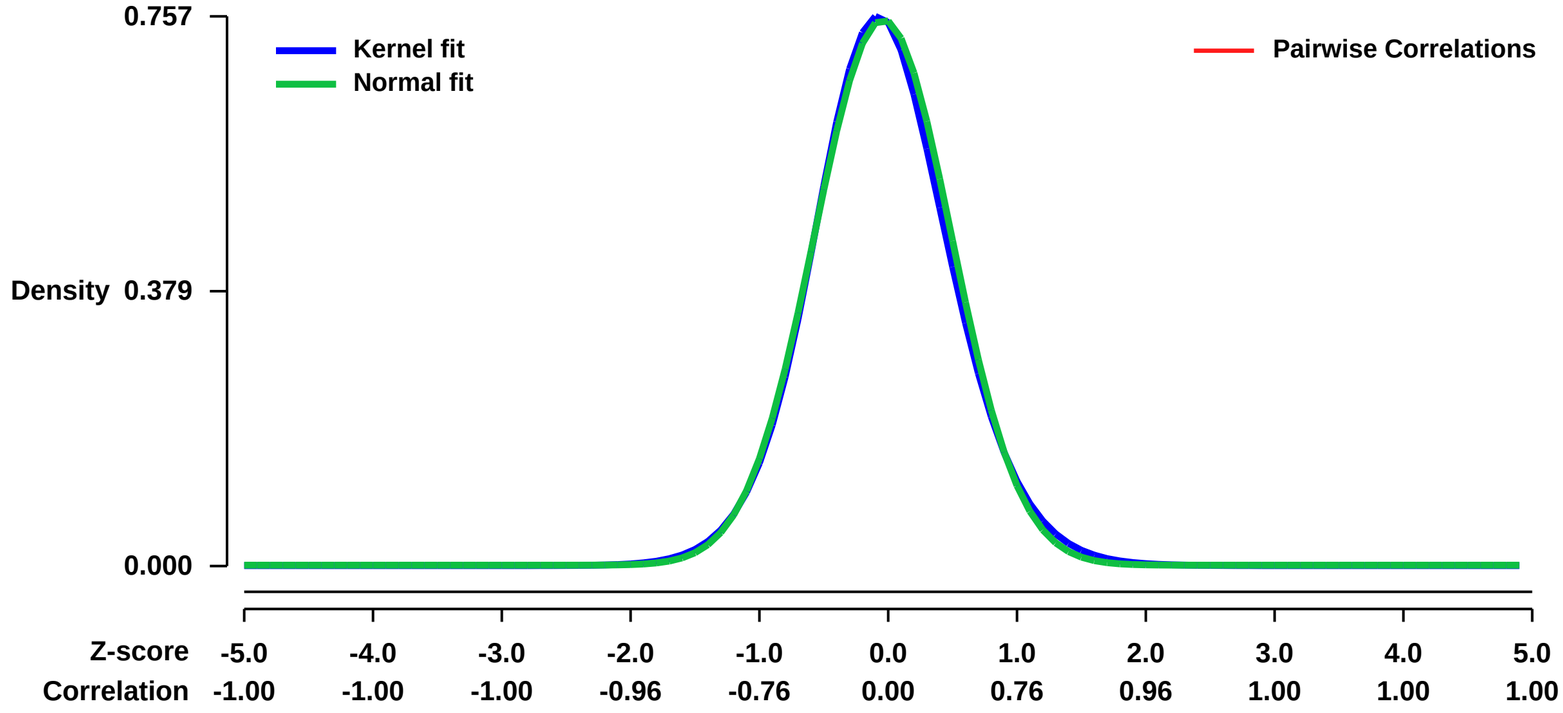

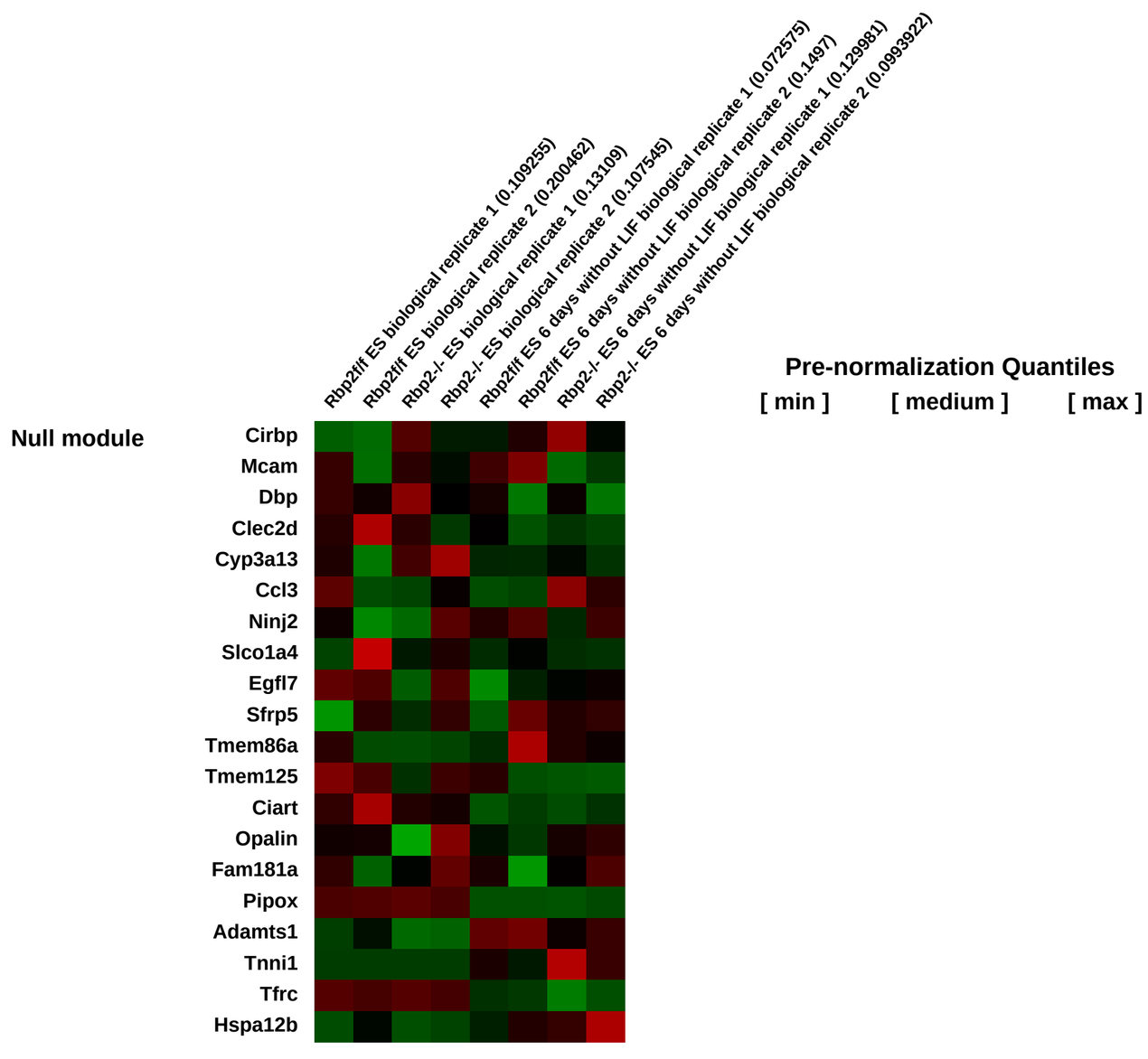

GEO Series "GSE26461" Expression Profiles

Num of samples in this series: 6

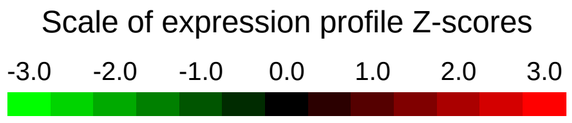

GEO Link:	http://www.ncbi.nlm.nih.gov/geo/query/acc.cgi?acc=GSE26461
Status:	Public on Dec 01 2012
Title:	Epigenetic regulation of type 1 diabetes in nonobese diabetic mice
Organism:	Mus musculus
Experiment type:	Expression profiling by array
Platform:	GPL1261
Pubmed ID:	23383062
Summary & Design:	**Summary:** **Background: Epigenetic alteration of the genome has been shown to provide palliative effects in mouse models of certain human autoimmune disorders. We have investigated whether chromatin remodeling could provide protection against autoimmune diabetes in nonobese diabetic (NOD) mice. Treatment of female mice during the transition from prediabetic to diabetic stage (18-24 weeks of age) with the well-characterized histone deacetylase inhibitor, Trichostatin A (TSA) effectively reduced the incidence of diabetes and abrogated the ability of splenocytes to adoptively transfer the disease into immunodeficient NOD.scid mice. Protection against diabetes was accompanied by histone hyperacetylation in pancreas and spleen, increased frequency of CD4+ CD62L+ cells in the spleen, reduction in cellular infiltration of islets, restoration of normoglycemia and glucose-induced insulin release by beta cells. In vitro activation of splenic T lymphocytes derived from protected mice resulted in enhanced expression of IFN-gamma mRNA and protein without altering the expression of Il4, Il17, Il18, Inos, and Tnfa genes nor the secretion of IL-2, IL-4, IL-17 and TNF-alpha proteins. Consistently, expression of the transcription factor involved in Ifng transcription, Tbet/Tbx21 but not Gata3 and Rorgt, respectively required for the transcription of Il4 and Il17, was upregulated in activated splenocytes of protected mice. These data indicate that abrogation of autoimmune diabetes is associated with the selective upregulation of certain inducible genes in T lymphocytes.** **Microarray analysis was performed to determine the changes in global gene expression underlying abrogation of autoimmune diabetes by TSA-mediated epigenetic modulation and identified a distinct group of genes down-regulated during this process.** **Overall design:** **Female NOD mice were treated with Trichostatin A (500 ´¡g/Kg body weight) between 18-24 weeks of age or left untreated.**

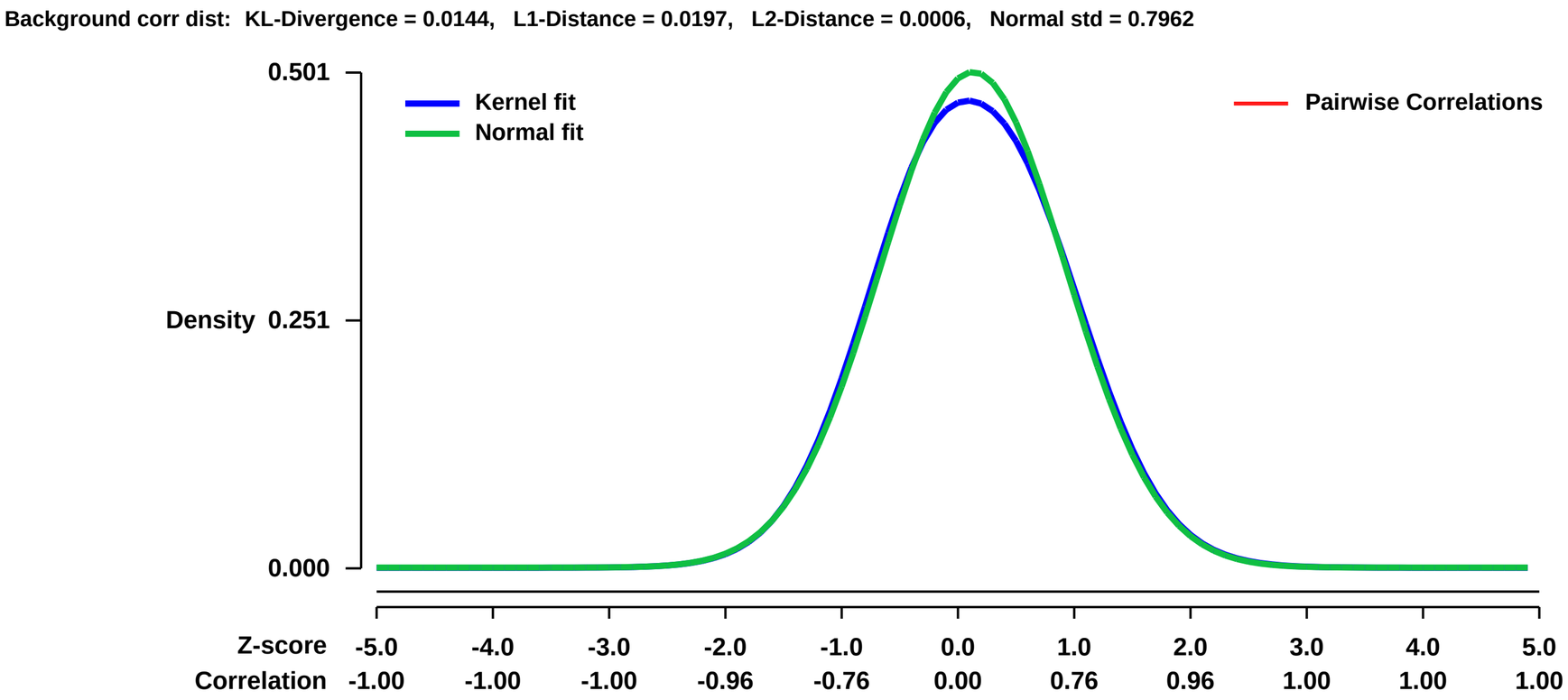

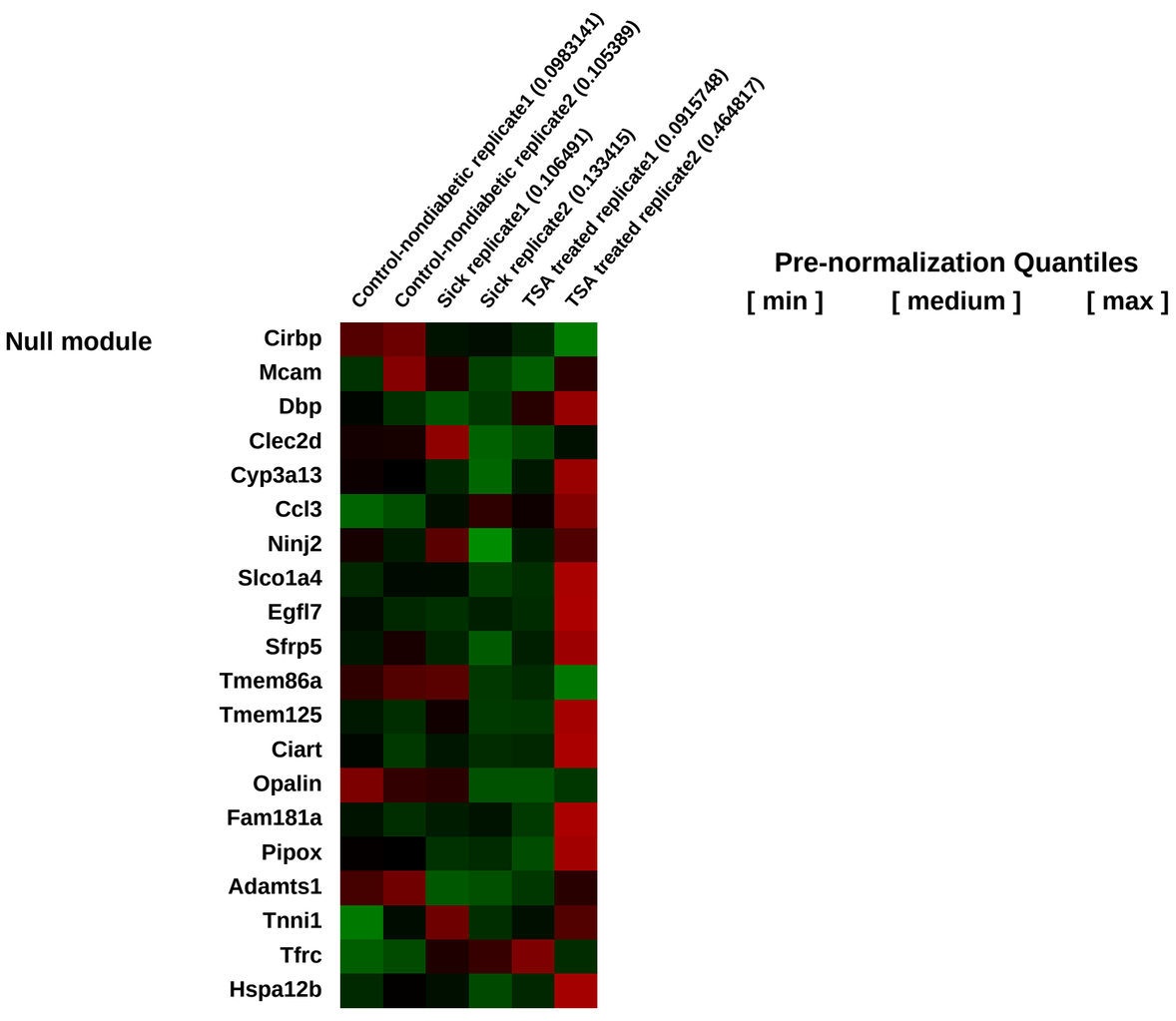

GEO Series "GSE26476" Expression Profiles

Num of samples in this series: 6

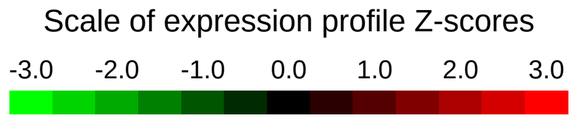

GEO Link:	http://www.ncbi.nlm.nih.gov/geo/query/acc.cgi?acc=GSE26476
Status:	Public on Jan 07 2011
Title:	Smooth muscle IL-4 receptor activation induces airway hyper-responsiveness
Organism:	Mus musculus
Experiment type:	Expression profiling by array
Platform:	GPL1261
Pubmed ID:	21464224
Summary & Design:	**Summary:** **Selective stimulation of IL-4 receptor on smooth muscle induces airway hyper-responsiveness in mice.** **Abstract: Production of the cytokines IL-4 and IL-13 is increased in both human asthma and mouse asthma models and Stat6 activation by the common IL-4/IL-13R drives most mouse model pathophysiology, including airway hyperresponsiveness (AHR). However, the precise cellular mechanisms through which IL-4R$_{\alpha}$– induces AHR remain unclear. Overzealous bronchial smooth muscle constriction is thought to underlie AHR in human asthma, but the smooth muscle contribution to AHR has never been directly assessed. Furthermore, differences in mouse vs. human airway anatomy and observations that selective IL-13 stimulation of Stat6 in airway epithelium induces murine AHR raise questions about the importance of direct IL-4R effects on smooth muscle in murine asthma models and relevance of these models to human asthma. Using transgenic mice in which smooth muscle is the only cell type that expresses or fails to express IL-4R$_{\alpha}$–, we demonstrate that direct smooth muscle activation by IL-4, IL-13, or allergen is sufficient, but not necessary, to induce AHR and show that 5 genes known to promote smooth muscle migration, proliferation and contractility are activated by IL-13 in smooth muscle in vivo. These observations demonstrate that IL-4R$_{\alpha}$– promotes AHR through multiple mechanisms and provide a model for testing smooth muscle-directed asthma therapeutics.** **Overall design:** **Gene transcripts were identified that differed in their relative expression as a function of IL4R expression on the smooth muscle cells.**

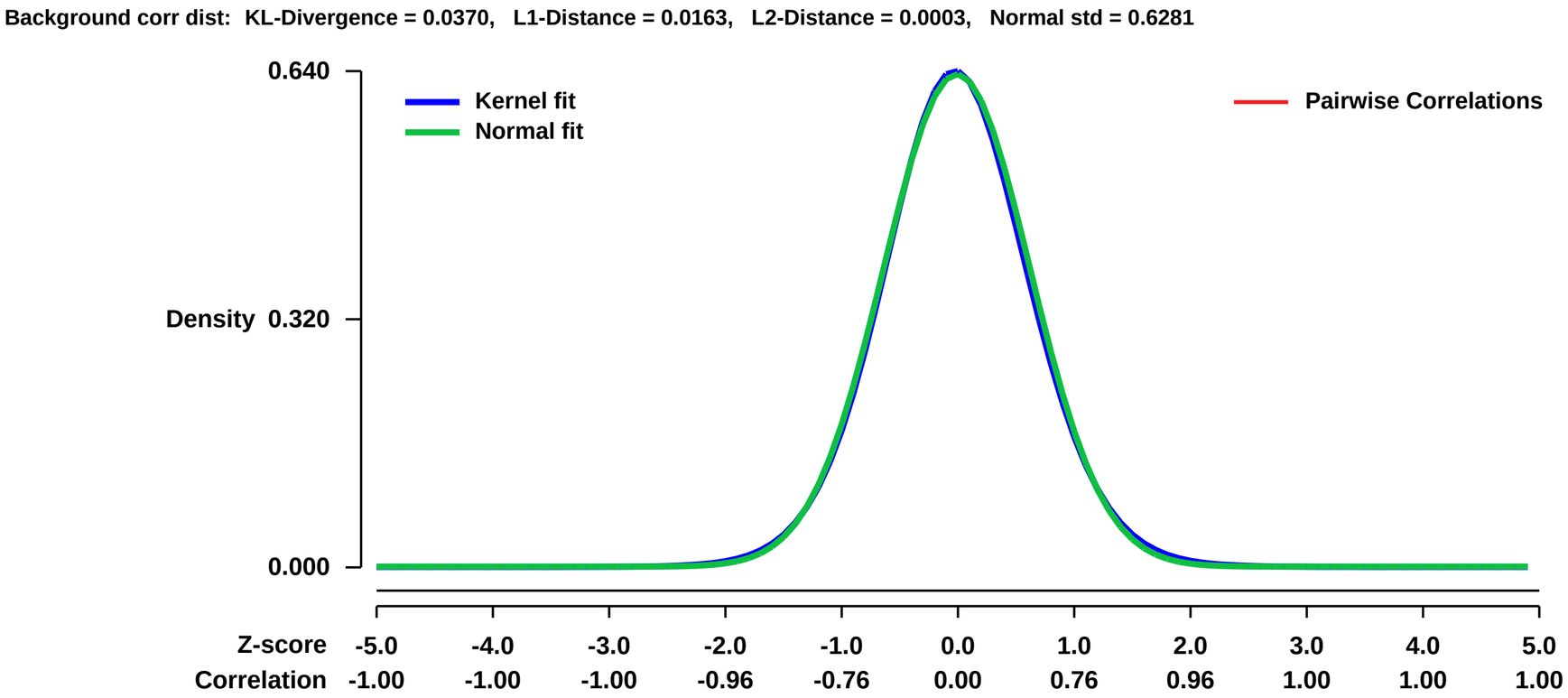

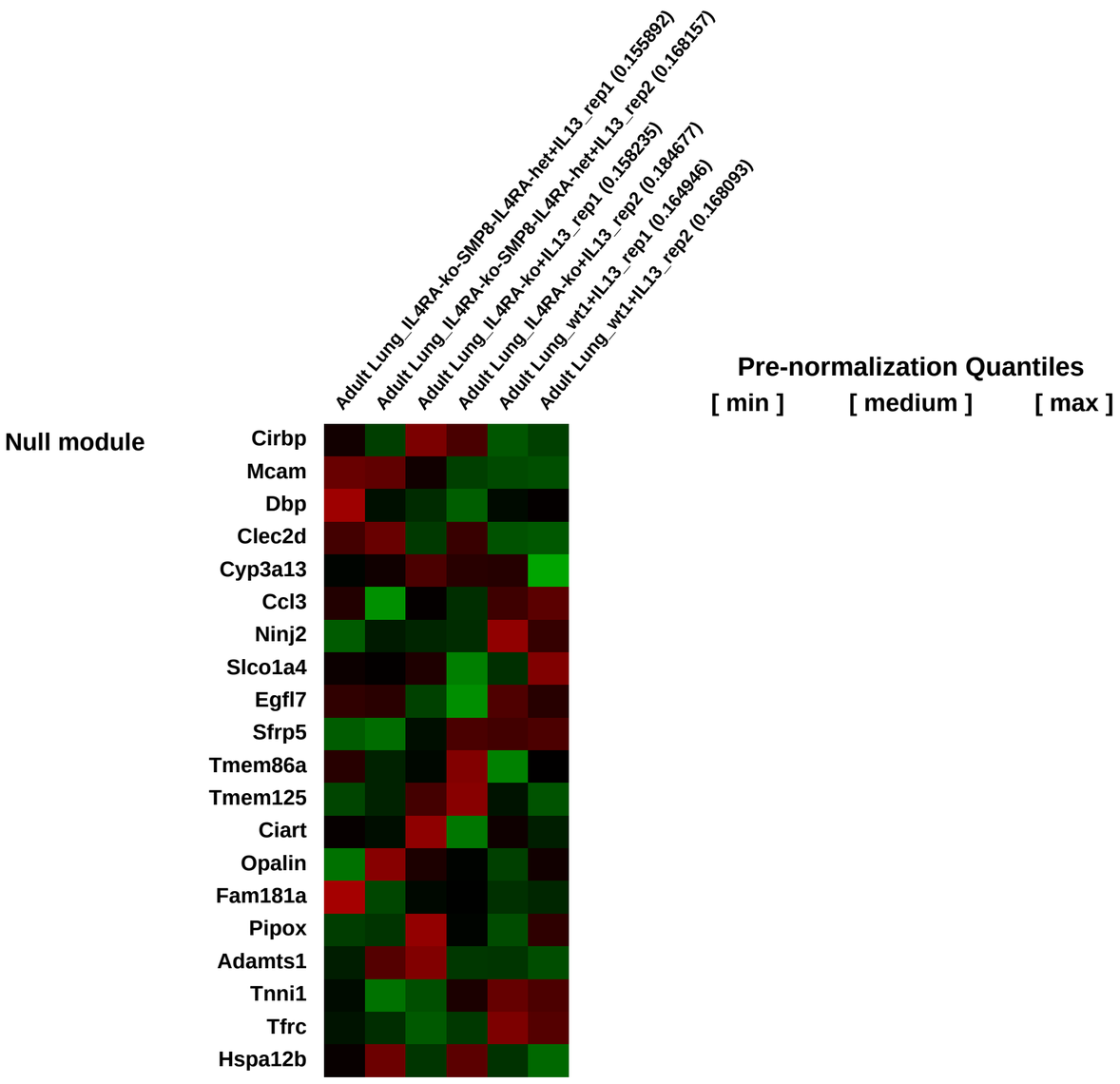

GEO Series "GSE26496" Expression Profiles

Num of samples in this series: 6

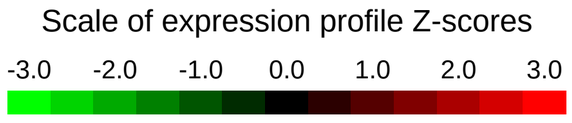

GEO Link:	**http://www.ncbi.nlm.nih.gov/geo/query/acc.cgi?acc=GSE26496**
Status:	**Public on Jan 08 2011**
Title:	**Deletion of Scap in Alveolar Type II Cells Influences Lung Lipid Homeostasis and Identifies a Compensatory Role for Pulmonary Lipofibroblasts**
Organism:	**Mus musculus**
Experiment type:	**Expression profiling by array**
Platform:	**GPL1261**
Pubmed ID:	
Summary & Design:	**Summary:** **Pulmonary function after birth is dependent upon surfactant lipids that reduce surface tension in the alveoli. The sterol-responsive element-binding proteins (SREBPs) are transcription factors regulating expression of genes controlling lipid homeostasis in many tissues. To identify the role of SREBPs in the lung, we conditionally deleted the SREBP cleavage-activating protein gene, Scap, in respiratory epithelial cells (Scapâ /â) in vivo. Prior to birth (E18.5), deletion of Scap decreased the expression of both SREBPs and a number of genes regulating fatty acid and cholesterol metabolism. Nevertheless, Scapâ /â mice survived postnatally, surfactant and lung tissue lipids being substantially normalized in adult Scapâ /â mice. Although phospholipid synthesis was decreased in type II cells from adult Scapâ /â mice, lipid storage, synthesis, and transfer by lung lipofibroblasts were increased. mRNA microarray data indicated that SCAP influenced two major gene networks, one regulating lipid metabolism and the other stress-related responses. Deletion of the SCAP/SREBP pathway in respiratory epithelial cells altered lung lipid homeostasis and induced compensatory lipid accumulation and synthesis in lung lipofibroblasts.** **Overall design:** **To identify the role of SREBPs in the lung, we conditionally deleted the SREBP cleavage-activating protein gene, Scap, in respiratory epithelial cells (Scapâ /â) in vivo.Lung cRNA was hybridized to the murine genome MOE430 V2 chips.**

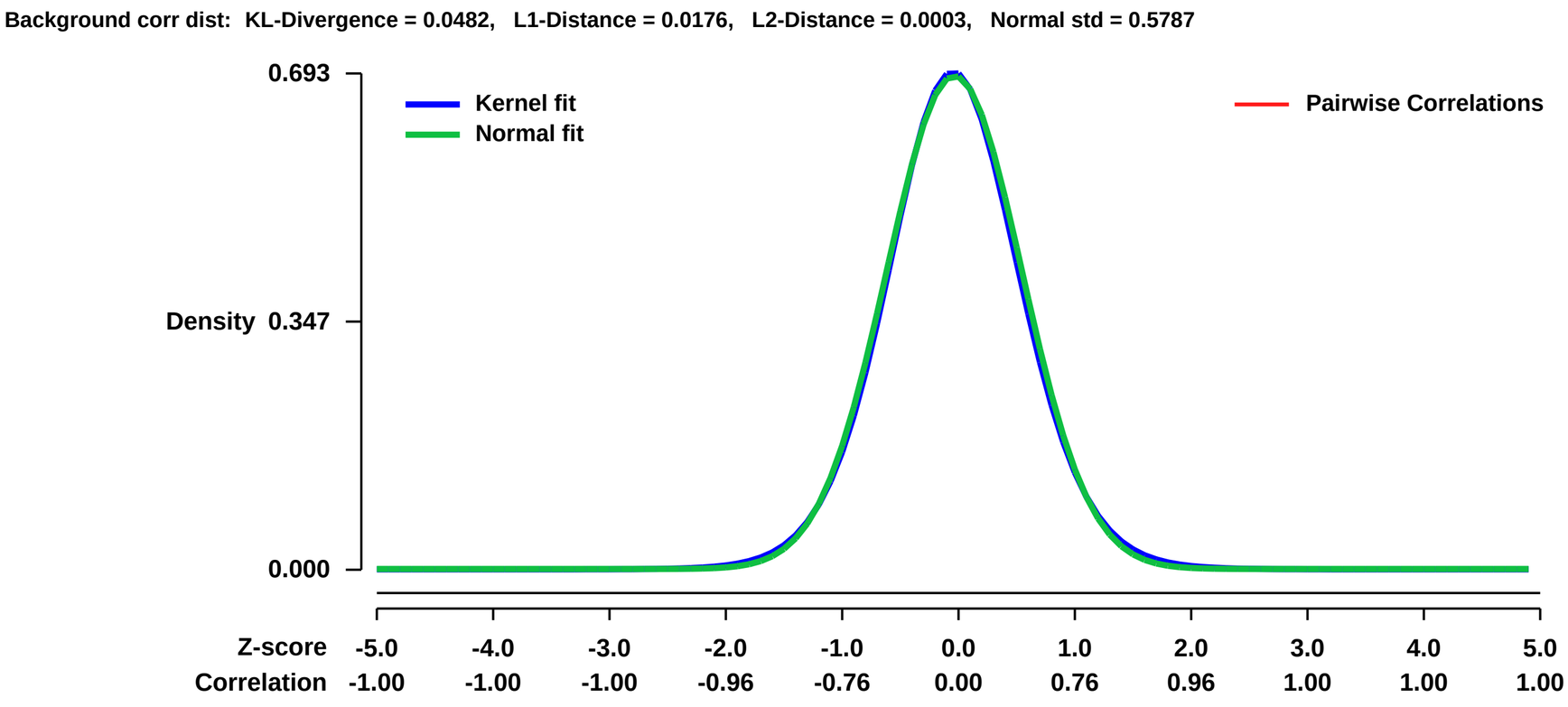

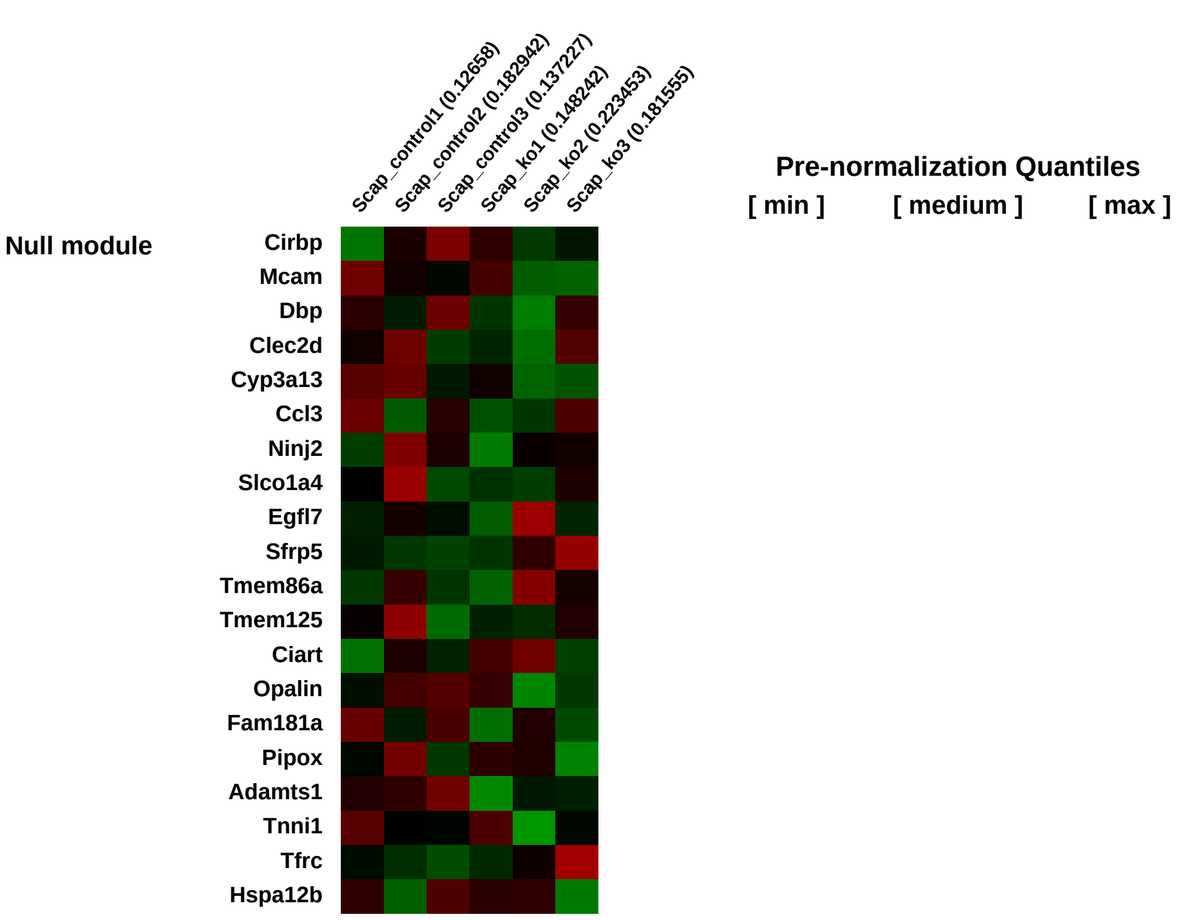

GEO Series "GSE26568" Expression Profiles

Num of samples in this series: 6

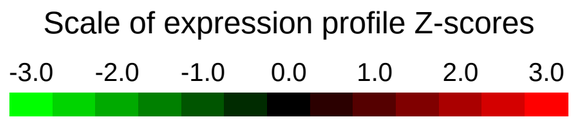

GEO Link:	**http://www.ncbi.nlm.nih.gov/geo/query/acc.cgi?acc=GSE26568**
Status:	**Public on May 31 2013**
Title:	**Impact of KLF2 expression on T cell genetic program**
Organism:	**Mus musculus**
Experiment type:	**Expression profiling by array**
Platform:	**GPL1261**
Pubmed ID:	**24155966**
Summary & Design:	**Summary:** **On triggering of the T cell receptor CD8 T lymphocytes downregulate expression of the transcription factor KLF2. KLF2 expression remains low as these cells differentiate to Cytotoxic T lymphocytes (CTL) but may be re-expressed depending on the local environmental signals.** **We used retroviral transduction to enforce KLF2 expression in CTL to determine the impact of it re-expression on the CTL genetic program.** **Overall design:** **T lymphocytes with a transgenic T cell receptor (P14 LCMV) isolated from murine spleens were activated with gp33-41 peptide for 2 days and transduced with empty vector (evGFP) or GFP-KLF2. After differentiation to CTL in culture with Interleukin-2 for 2 further days, cells positive for GFP were isolated by Fluorescence Activated Cell Sorting and the RNA extracted for microarray analysis.**

Background corr dist: **KL-Divergence = 0.0293, L1-Distance = 0.0215, L2-Distance = 0.0005, Normal std = 0.6816**

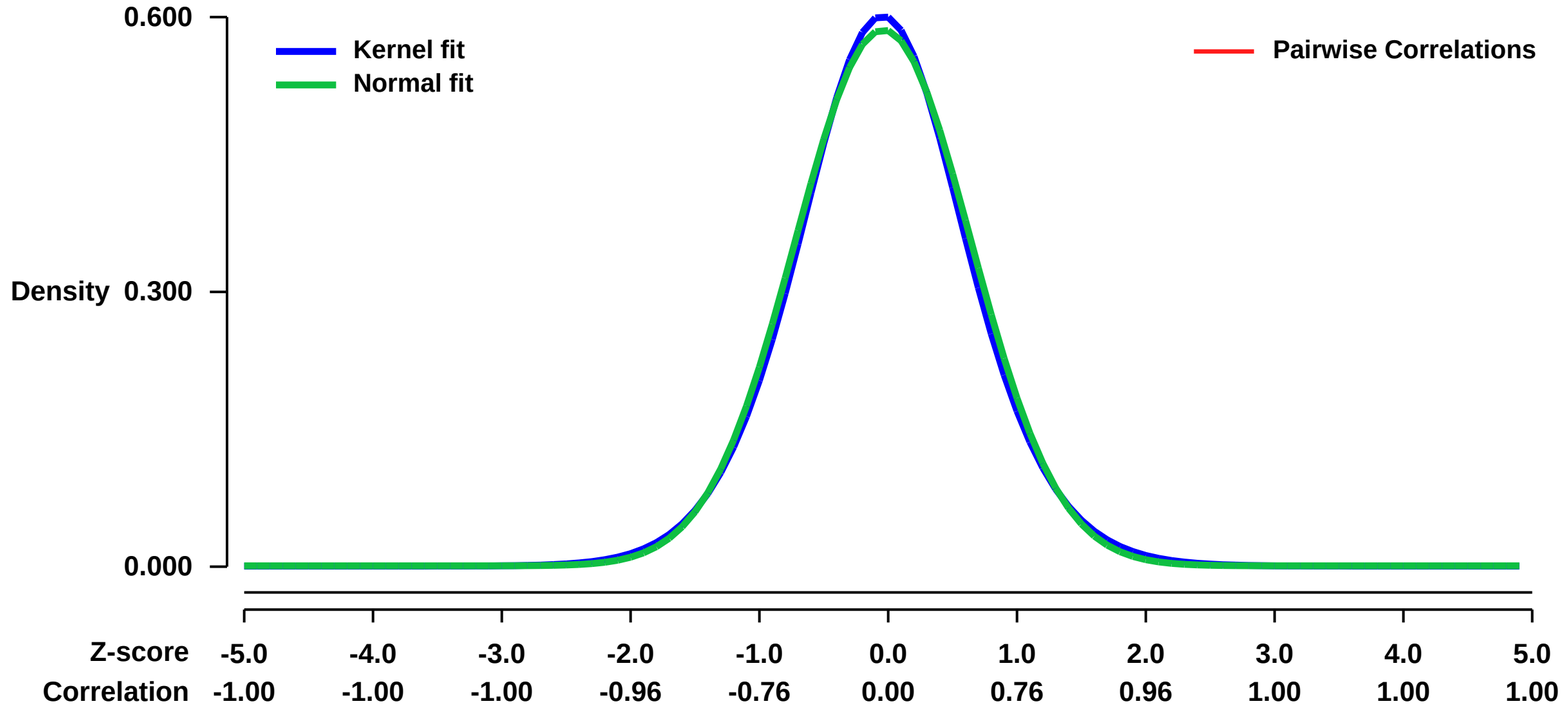

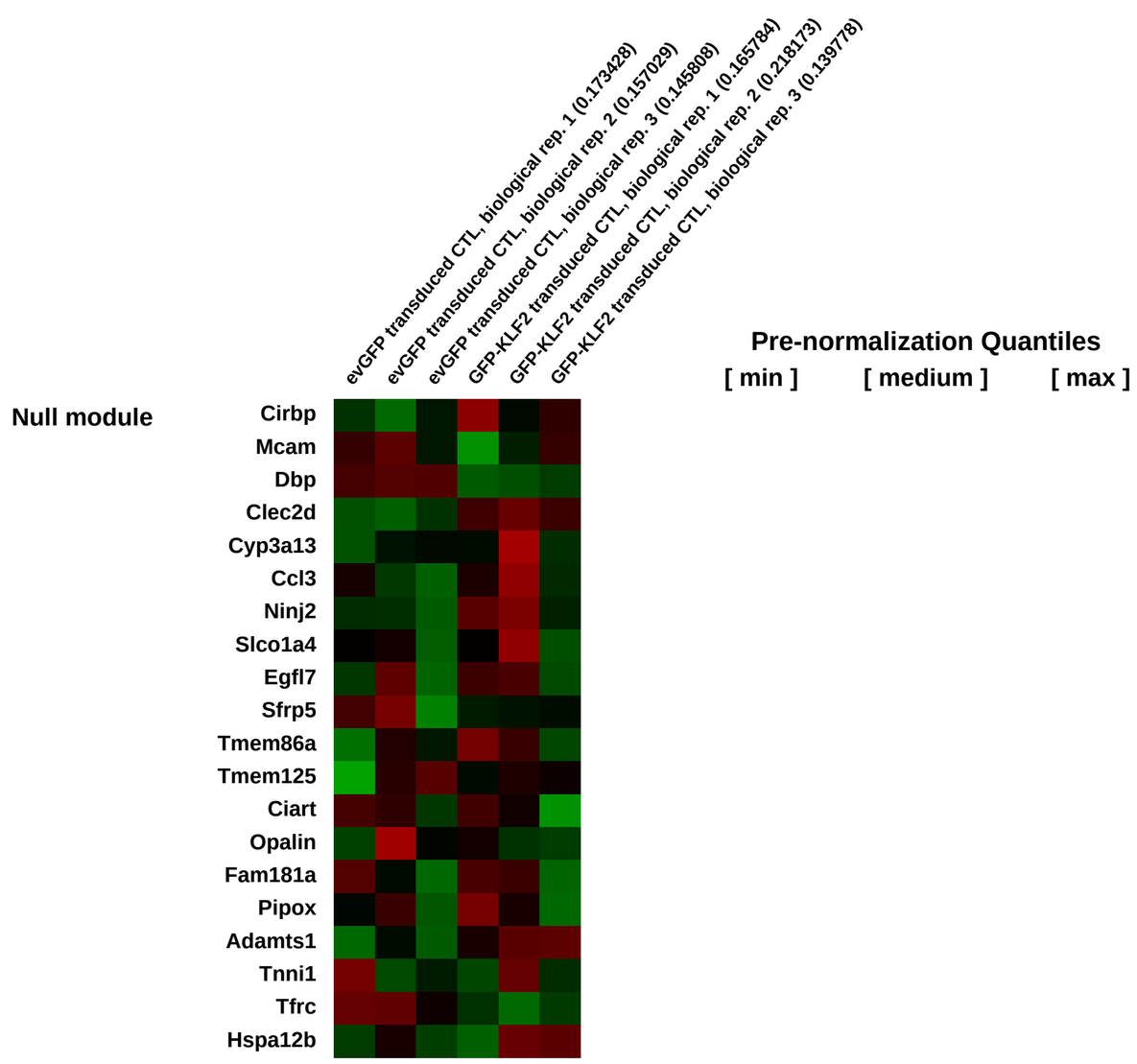

GEO Series "GSE26668" Expression Profiles

Num of samples in this series: 6

Scale of expression profile Z-scores

-3.0 -2.0 -1.0 0.0 1.0 2.0 3.0

GEO Link:	http://www.ncbi.nlm.nih.gov/geo/query/acc.cgi?acc=GSE26668
Status:	Public on Mar 23 2011
Title:	Expression data from E13.5 Fz4-/-Fz8-/- and Fz4+/+Fz8-/- kidneys
Organism:	Mus musculus
Experiment type:	Expression profiling by array
Platform:	GPL1261
Pubmed ID:	21343368
Summary & Design:	**Summary:** Fz4 and Fz8 cooperate in regulating the branching morhpogenesis of the developing kidney during mouse embryonic development, hence determines the eventual kidney size. We used microarrays to study the global gene expression profiles regulated by Fz4 and Fz8 signaling during early kidney development, and to understand the collaboration between the signaling events mediated by Fz4 and Fz8 **Overall design:** Kidney rudiments were dissected from E13.5 mouse embryos for RNA extraction and hybridization on Affymetrix MOE430.2 arrays. Three biological replicates of each genotype were analyzed.

Background corr dist: KL-Divergence = 0.0193, L1-Distance = 0.0128, L2-Distance = 0.0002, Normal std = 0.7424

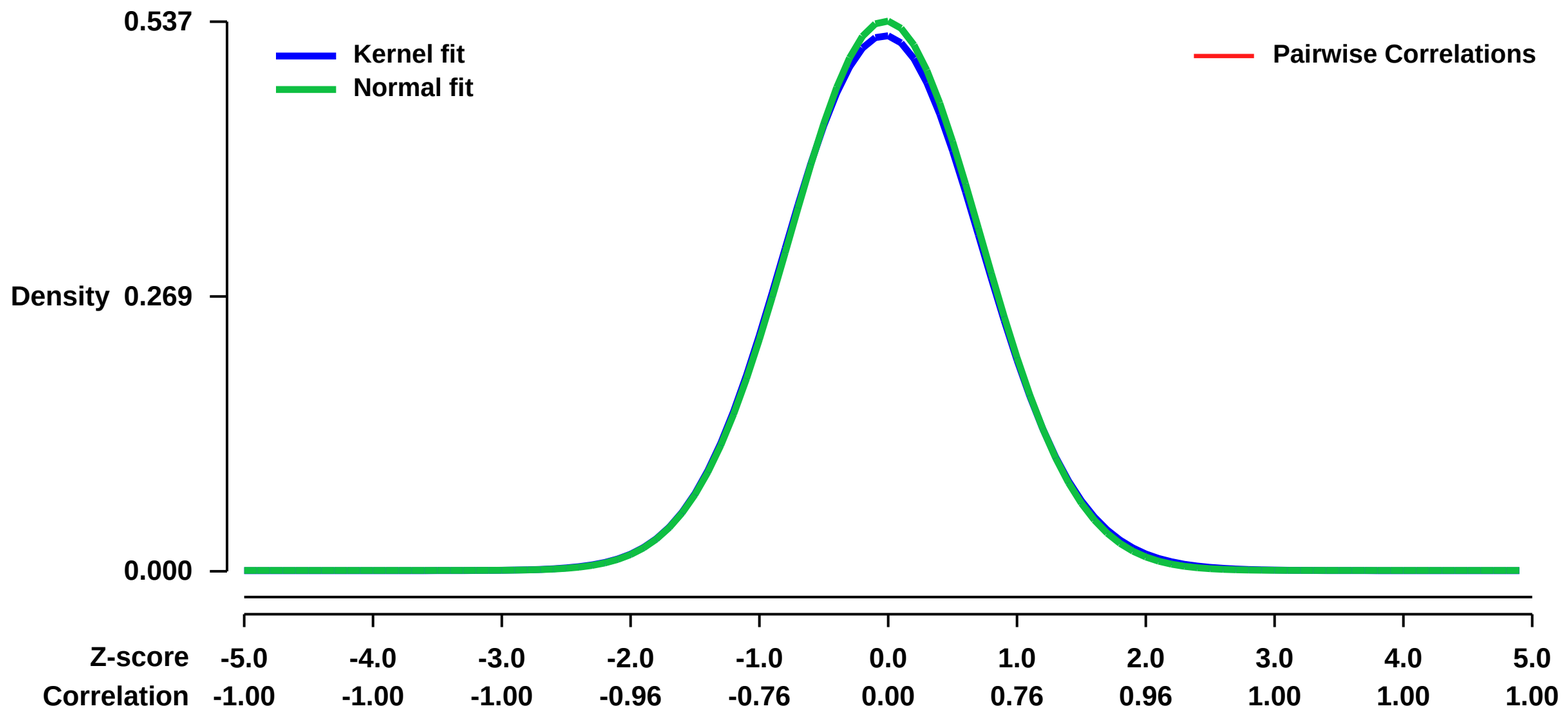

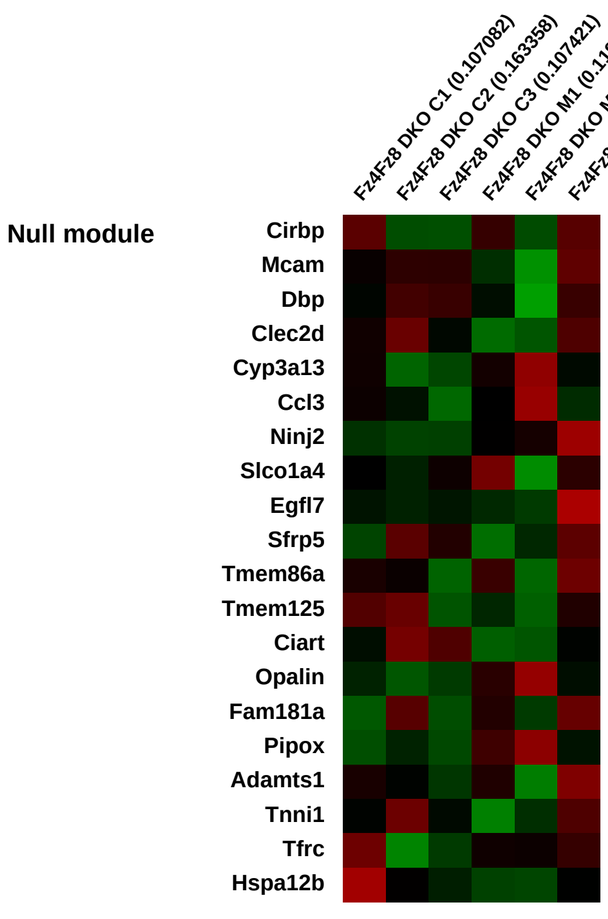

GEO Series "GSE26695" Expression Profiles

Num of samples in this series: 20

Scale of expression profile Z-scores

-3.0 -2.0 -1.0 0.0 1.0 2.0 3.0

GEO Link:	http://www.ncbi.nlm.nih.gov/geo/query/acc.cgi?acc=GSE26695
Status:	Public on Jan 24 2011
Title:	Transcriptomic response of murine liver to severe injury and hemorrhagic shock: Affymetrix portion of dual platform
Organism:	Mus musculus
Experiment type:	Expression profiling by array
Platform:	GPL1261
Pubmed ID:	21828244
Summary & Design:	**Summary:** A dual platform microarray analysis was used to characterize the temporal transcriptomic response in the mouse liver following trauma and hemmorhagic shock **Overall design:** Mice were divided into five groups, anesthetized and surgically treated to simulate a time course and trauma severity model: non-manipulated animals (C), minor trauma (MT), 1.5 hour of hemorrhagic shock and severe trauma (HS/T), 1.5 hour HS/T followed by 1 hour resuscitation (HS/T+1.0R), 1.5 hour HS/T followed by 4.5 hours resuscitation (HS/T+4.5R)

Background corr dist: KL-Divergence = 0.2191, L1-Distance = 0.0407, L2-Distance = 0.0035, Normal std = 0.3217

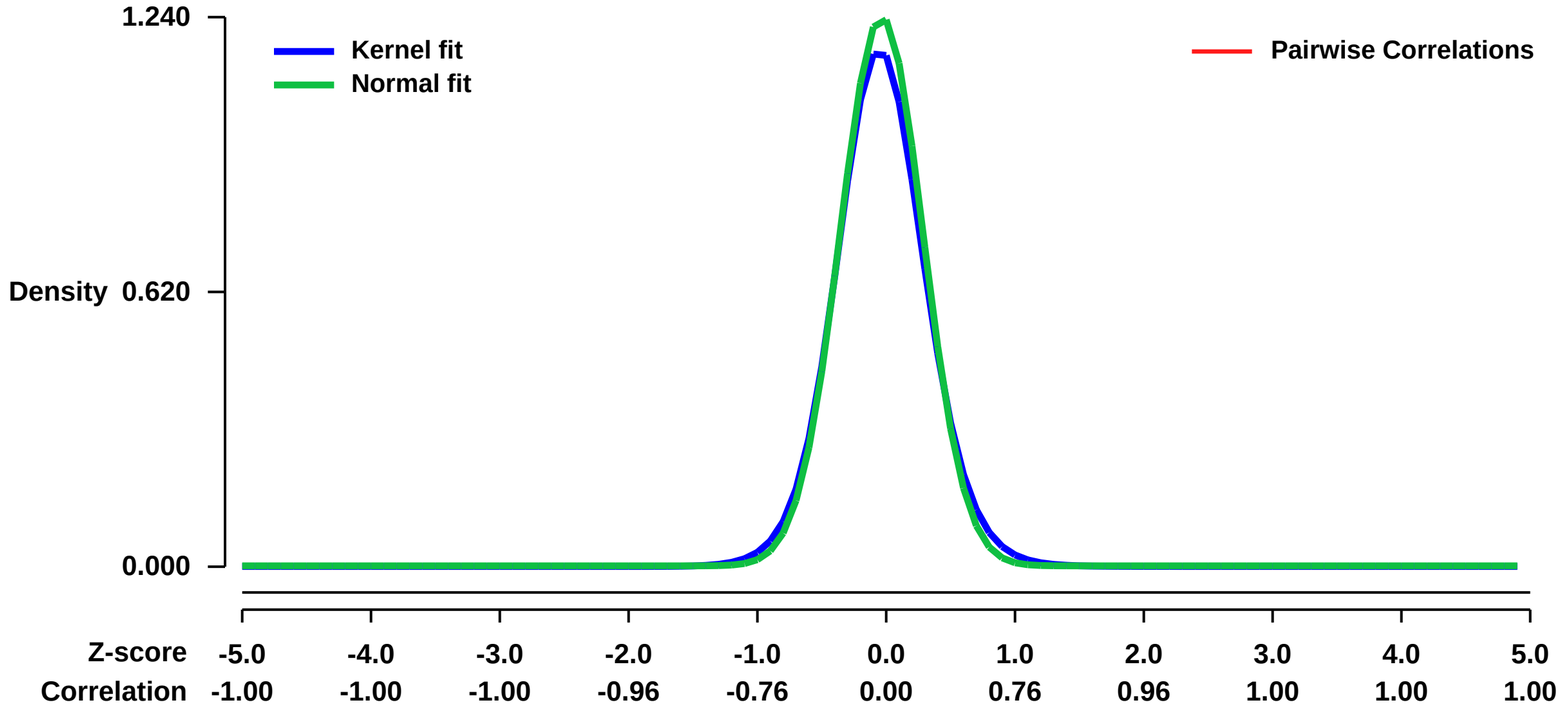

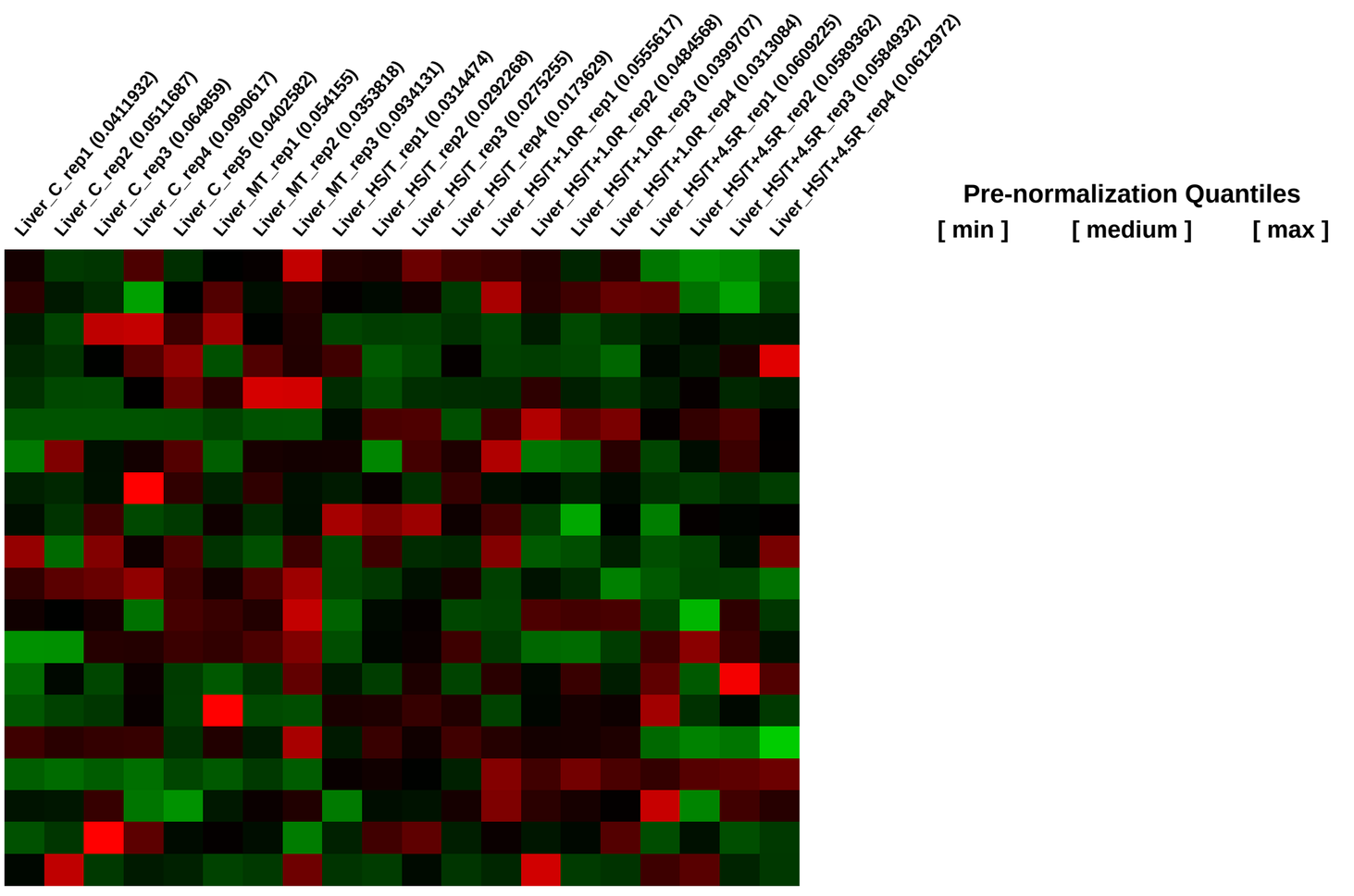

GEO Series "GSE26745" Expression Profiles

Num of samples in this series: 24

Scale of expression profile Z-scores

-3.0 -2.0 -1.0 0.0 1.0 2.0 3.0

GEO Link:	http://www.ncbi.nlm.nih.gov/geo/query/acc.cgi?acc=GSE26745
Status:	Public on Jul 21 2011
Title:	Comparison of total and polyribosome-associated mRNA levels in male Fmr1 KO mice and male WT littermates
Organism:	Mus musculus
Experiment type:	Expression profiling by array
Platform:	GPL1261
Pubmed ID:	21784246
Summary & Design:	**Summary:** The Fragile X Mental Retardation Protein, FMRP, is thought to regulate the translation of a specific set of neuronal mRNAs on polyribosomes. Therefore, we prepared polyribosomes on sucrose gradients and purified mRNA specifically from these fractions, as well as the total mRNA levels, to determine whether a set of mRNAs might be changed in its % association with polyribosomes in the absence of FMRP in the KO mouse model. No significant differences were found, other than the Fmr1 transcript itself, in total mRNA levels or % polyribosome association that withstood multiple test correction, in P7 Fmr1 KO mouse cerebral cortex compared with WT littermates.. **Overall design:** We prepared polyribosomes on sucrose gradients from 6 littermate pairs of Fmr1 KO and WT littermates (FVB background, P7 males, cerebral cortex) and purified RNA from both polyribosomal fractions and input to the gradient, reflecting total mRNA levels for comparison.

Background corr dist: KL-Divergence = 0.1111, L1-Distance = 0.0459, L2-Distance = 0.0033, Normal std = 0.4392

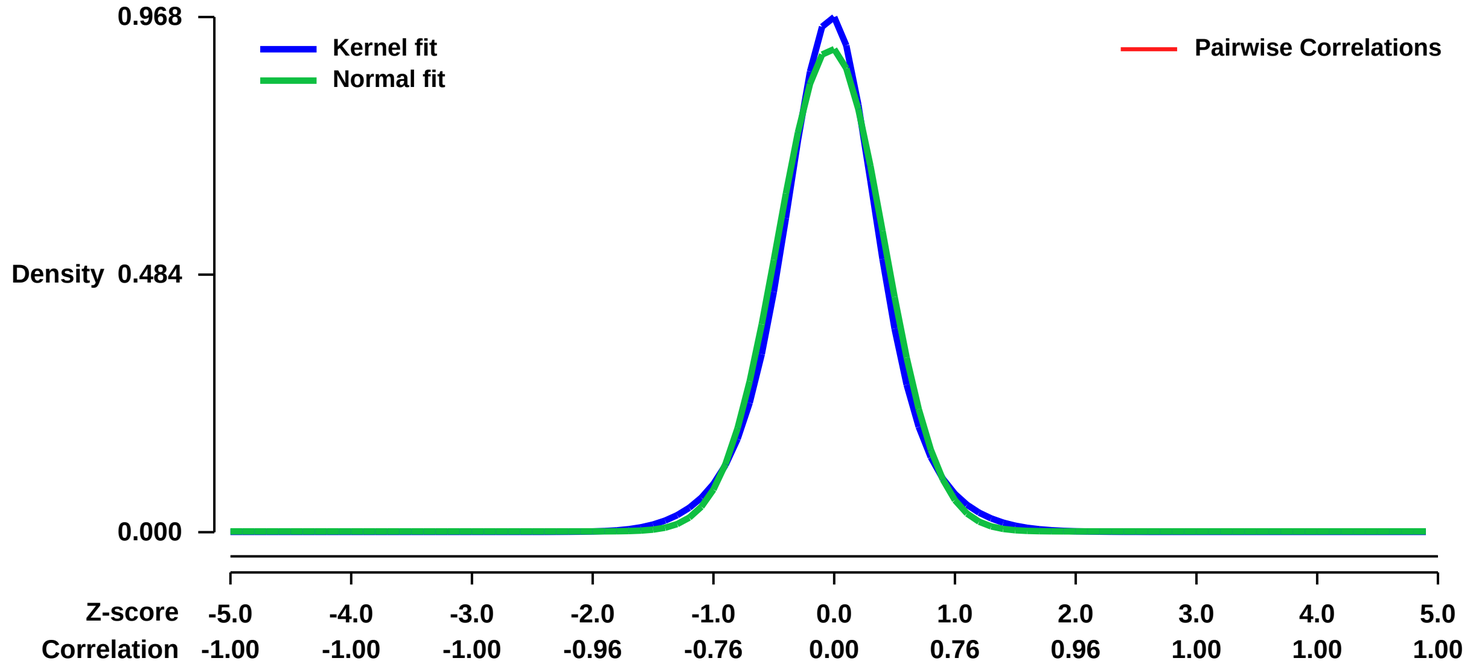

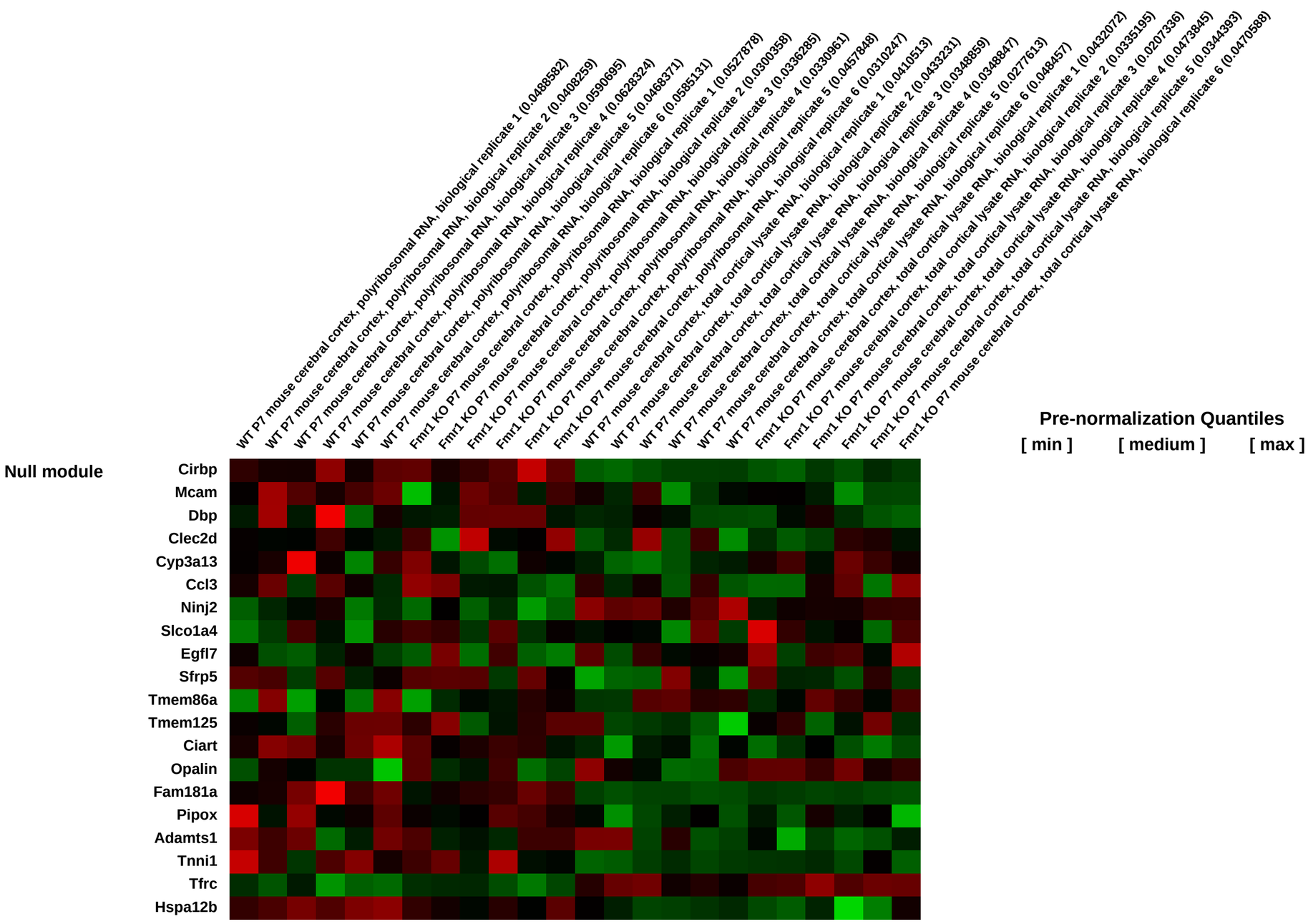

GEO Series "GSE26771" Expression Profiles

Num of samples in this series: 12

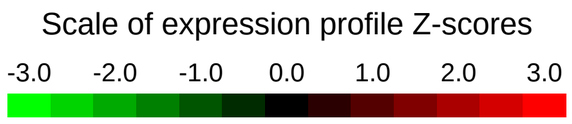

GEO Link:	**http://www.ncbi.nlm.nih.gov/geo/query/acc.cgi?acc=GSE26771**
Status:	**Public on Jan 22 2011**
Title:	**Expression data from primary mammary epithelial cells expressing ectopic p190B RhoGAP**
Organism:	**Mus musculus**
Experiment type:	**Expression profiling by array**
Platform:	**GPL1261**
Pubmed ID:	
Summary & Design:	**Summary:** **P190B RhoGAP is required for mammary gland development, and its overexpression disrupts mammary gland branching morphogenesis. To better understand the mechanisms by which p190B regulates mammary gland development we performed gene expression microarray analysis on mammary epithelial cells isolated from p190B overexpressing transgenic mice compared to control mice.** **Overall design:** **The mice used in this study were previously developed to inducibly overexpress p190B selectively in the mammary gland (Vargo-Gogola 2006). FVB/N mice carrying the MMTV-rtTA and TetO-p190B-IRES-luciferase transgenes or the MMTV-rtTA transgene only (Gunther EJ, FASEB) were fed doxycycline (Dox) chow (2 g/kg) for 7 d prior to removal of mammary glands and isolation of primary mammary epithelial cells at 6 weeks of age.**

Background corr dist: **KL-Divergence = 0.1492, L1-Distance = 0.0372, L2-Distance = 0.0027, Normal std = 0.3734**

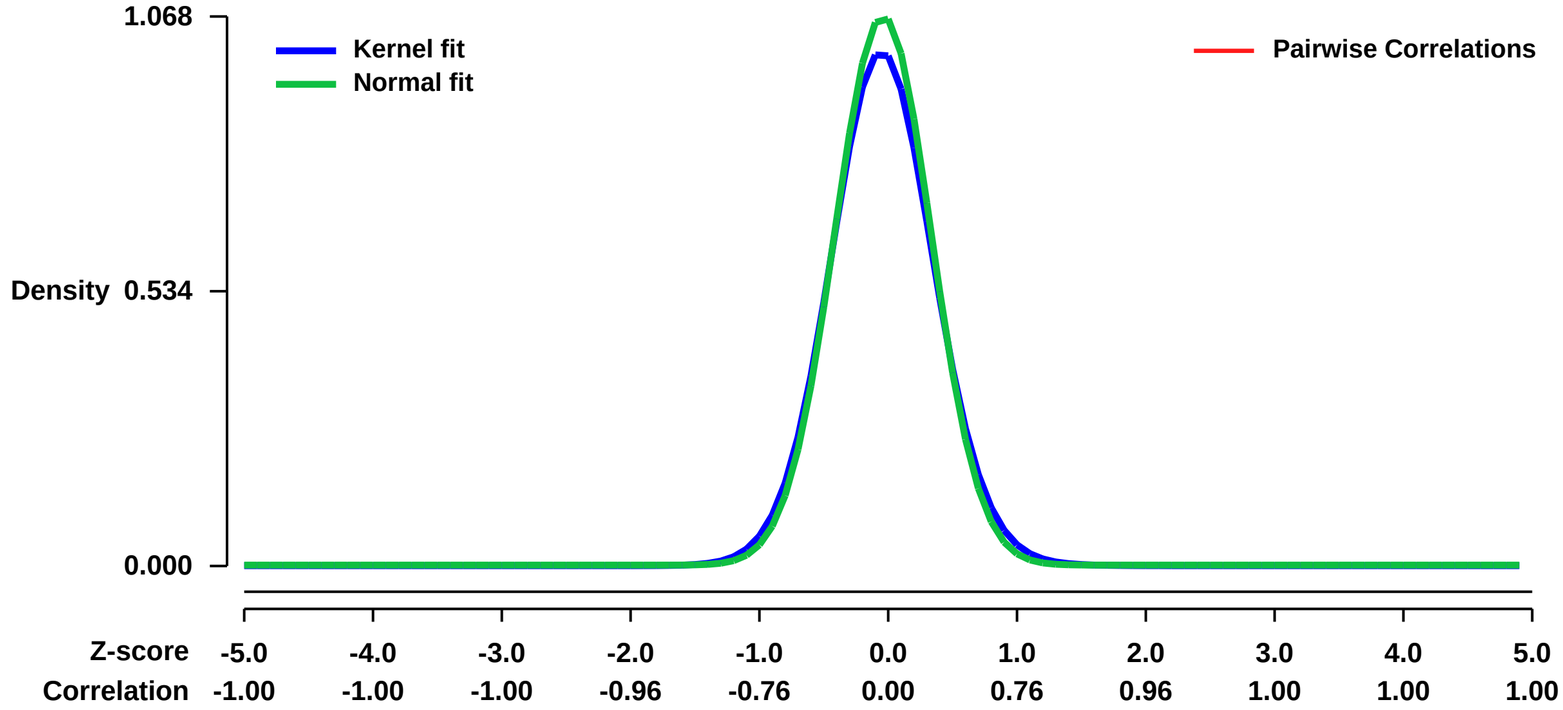

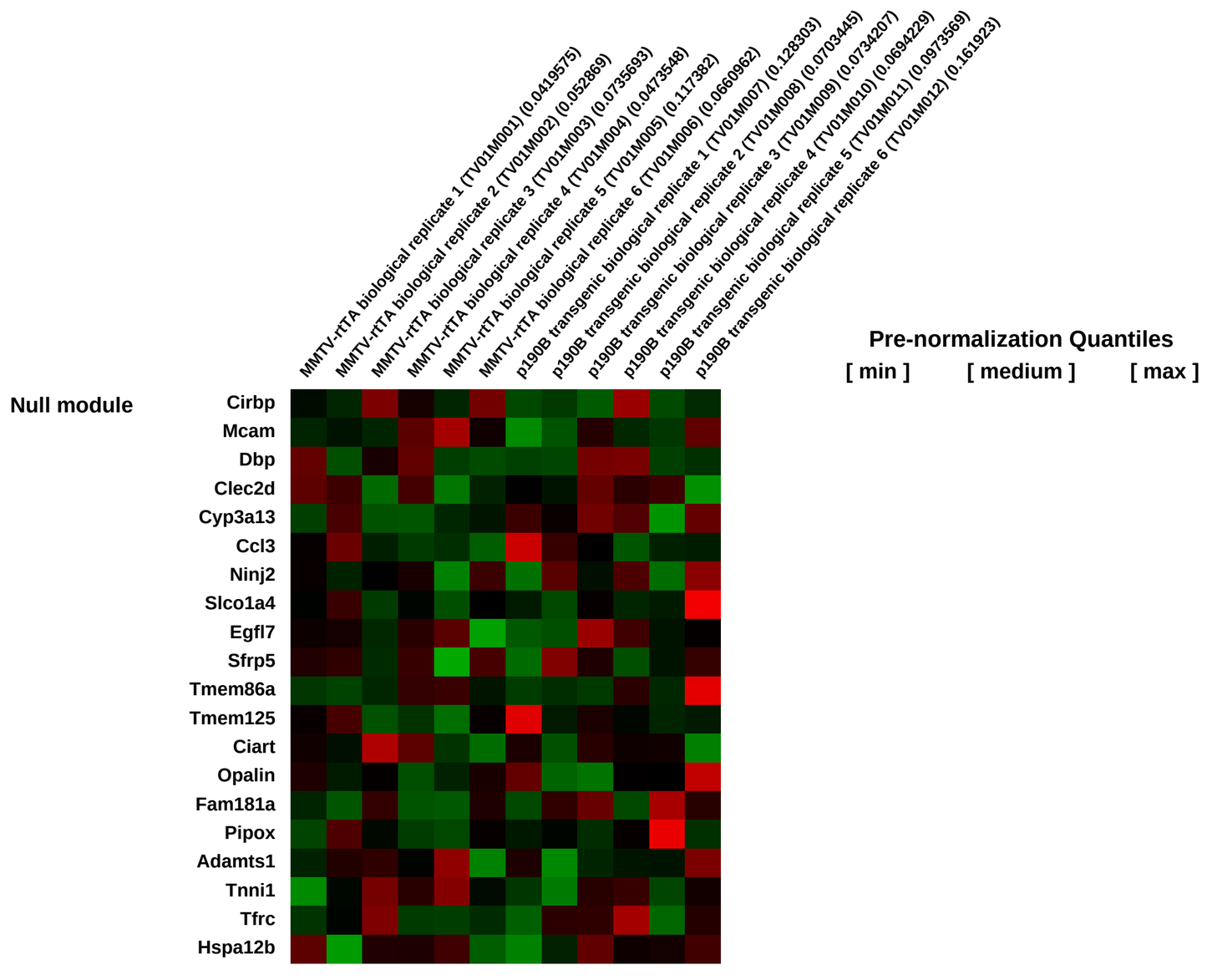

GEO Series "GSE26822" Expression Profiles

Num of samples in this series: 8

Scale of expression profile Z-scores

-3.0 -2.0 -1.0 0.0 1.0 2.0 3.0

GEO Link:	http://www.ncbi.nlm.nih.gov/geo/query/acc.cgi?acc=GSE26822
Status:	Public on Jan 01 2012
Title:	Expression data from postnatal mouse apical and basal organ of Corti from Dicer1 conditional knockout and littermate control cochleae.
Organism:	Mus musculus
Experiment type:	Expression profiling by array
Platform:	GPL1261
Pubmed ID:	21360794
Summary & Design:	**Summary:** Cre recombinase-mediated conditional knockout of floxed Dicer1 alleles causes depletion of small RNAs including microRNAs, which function to repress target mRNA expression by inhibiting translation and/or stimulating mRNA degradation. We used microarrays to examine gene expression in apical versus basal organ of Corti from the cochleae of control and mutant mice in which Dicer1 was deleted and microRNAs were depleted specifically in sensory hair cells by Atoh1 promoter-driven Cre recombinase expression. **Overall design:** Each biological replicate represents the combined apical or combined basal segments of organ of Corti from both cochleae of a single mouse. Two biological replicates for apical and basal organ of Corti from Dicer1 conditonal knockout and littermate controls were collected for RNA extraction and microarray analysis.

Background corr dist: KL-Divergence = 0.0736, L1-Distance = 0.0220, L2-Distance = 0.0008, Normal std = 0.4919

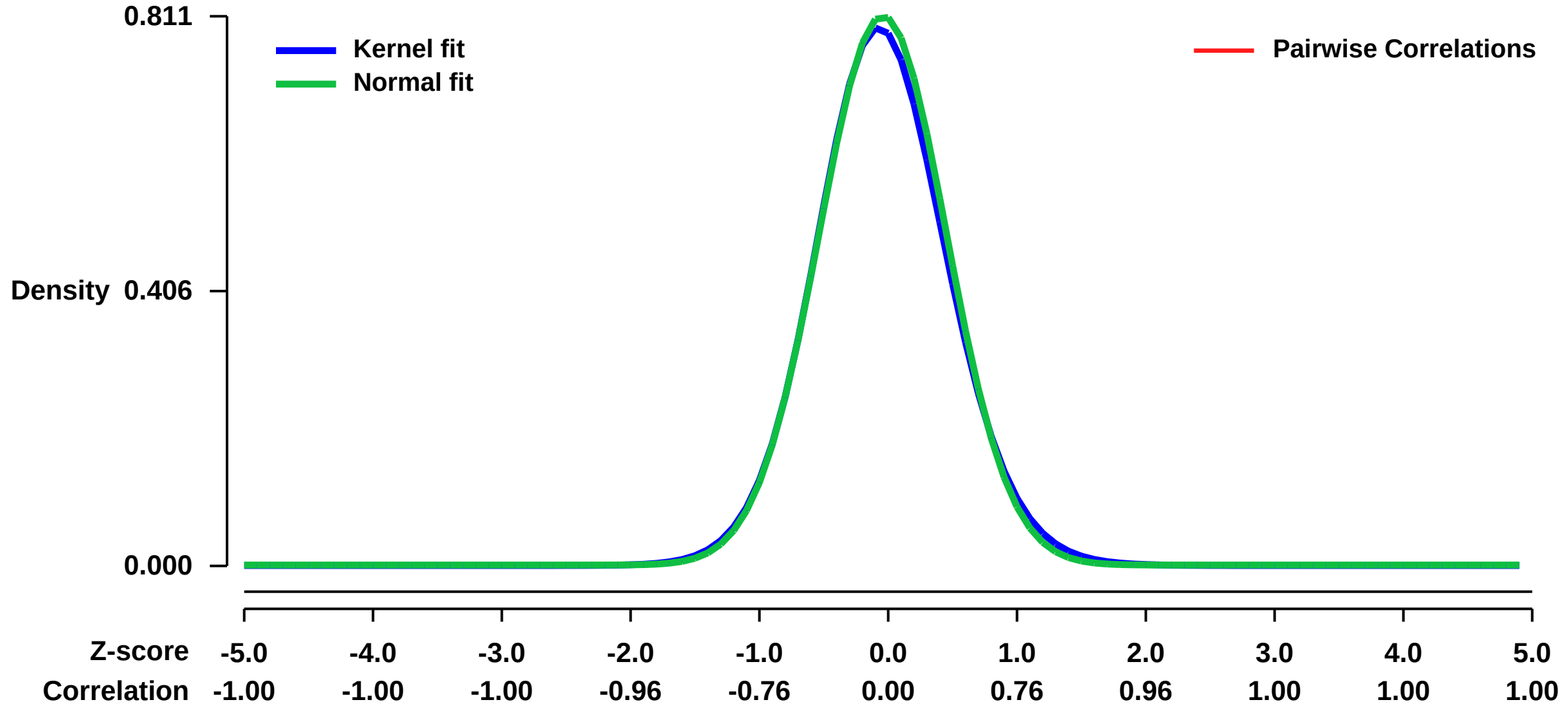

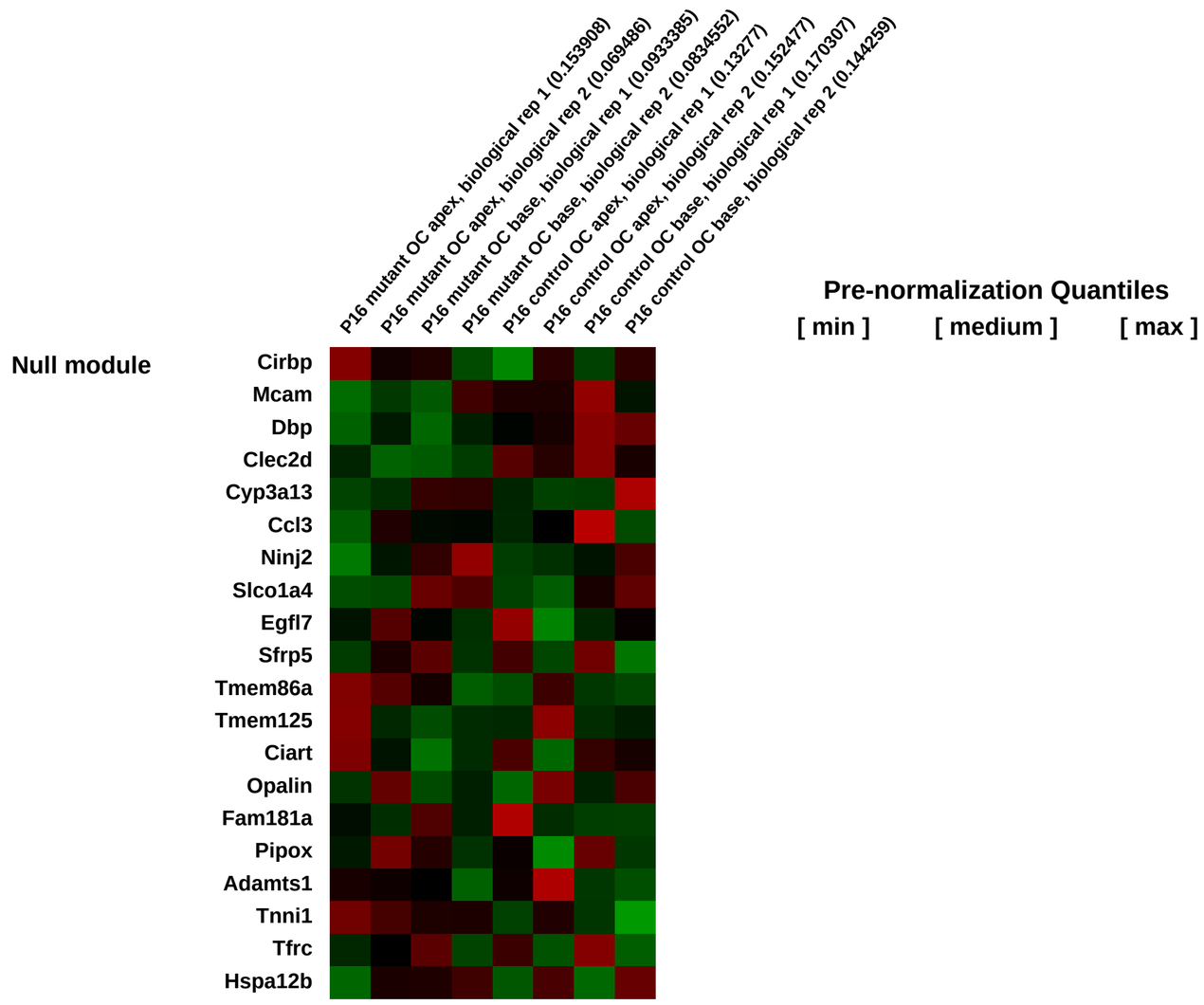

GEO Series "GSE26830" Expression Profiles

Num of samples in this series: 12

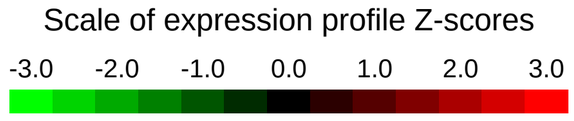

GEO Link:	http://www.ncbi.nlm.nih.gov/geo/query/acc.cgi?acc=GSE26830
Status:	Public on Mar 30 2011
Title:	Dual functions of Tet1 in transcriptional regulation in mouse embryonic stem cells (mRNA)
Organism:	Mus musculus
Experiment type:	Expression profiling by array
Platform:	GPL1261
Pubmed ID:	21460036
Summary & Design:	**Summary:** Epigenetic modification of the mammalian genome by DNA methylation (5-methylcytosine) has a profound impact on chromatin structure, gene expression and maintenance of cellular identity. Recent demonstration that members of the Ten-eleven translocation (Tet) family proteins can convert 5-methylcytosine (5mC) to 5-hydroxymethylcytosine (5hmC) raised the possibility that Tet proteins are capable of establishing a distinct epigenetic state. We have recently demonstrated that Tet1 is specifically expressed in murine embryonic stem (ES) cells and is required for ES cell self-renewal and maintenance. Using chromatin immunoprecipitation coupled with high-throughput DNA sequencing (ChIP-seq), here we show that Tet1 is preferentially bound to CpG-rich sequences at promoters of both transcriptionally active and Polycomb-repressed genes. Despite a general increase in levels of DNA methylation at Tet1 binding-sites, Tet1 depletion does not lead to down-regulation of all the Tet1 targets. Interestingly, while Tet1-mediated promoter hypomethylation is required for maintaining the expression of a group of transcriptionally active genes, it is also required for repression of Polycomb-targeted developmental regulators. Tet1 contributes to silencing of this group of genes by facilitating recruitment of PRC2 to CpG-rich gene promoters. Thus, our study not only establishes a role for Tet1 in modulating DNA methylation levels at CpG-rich promoters, but also reveals a dual function of Tet1 in promoting transcription of pluripotency factors as well as participating in the repression of Polycomb-targeted developmental regulators. **Overall design:** Mouse ES cells infected with control knockdown (KD) or Tet1 KD lentiviruses were FACS-sorted for RNA extraction and hybridization on Affymetrix microarrays. We also investigated the effect of Nanog overexpression (OE) in Tet1 KD mouse ES cells on dys-regulated Tet1 targets. We have collected four biologically independent replicates for each treatment.

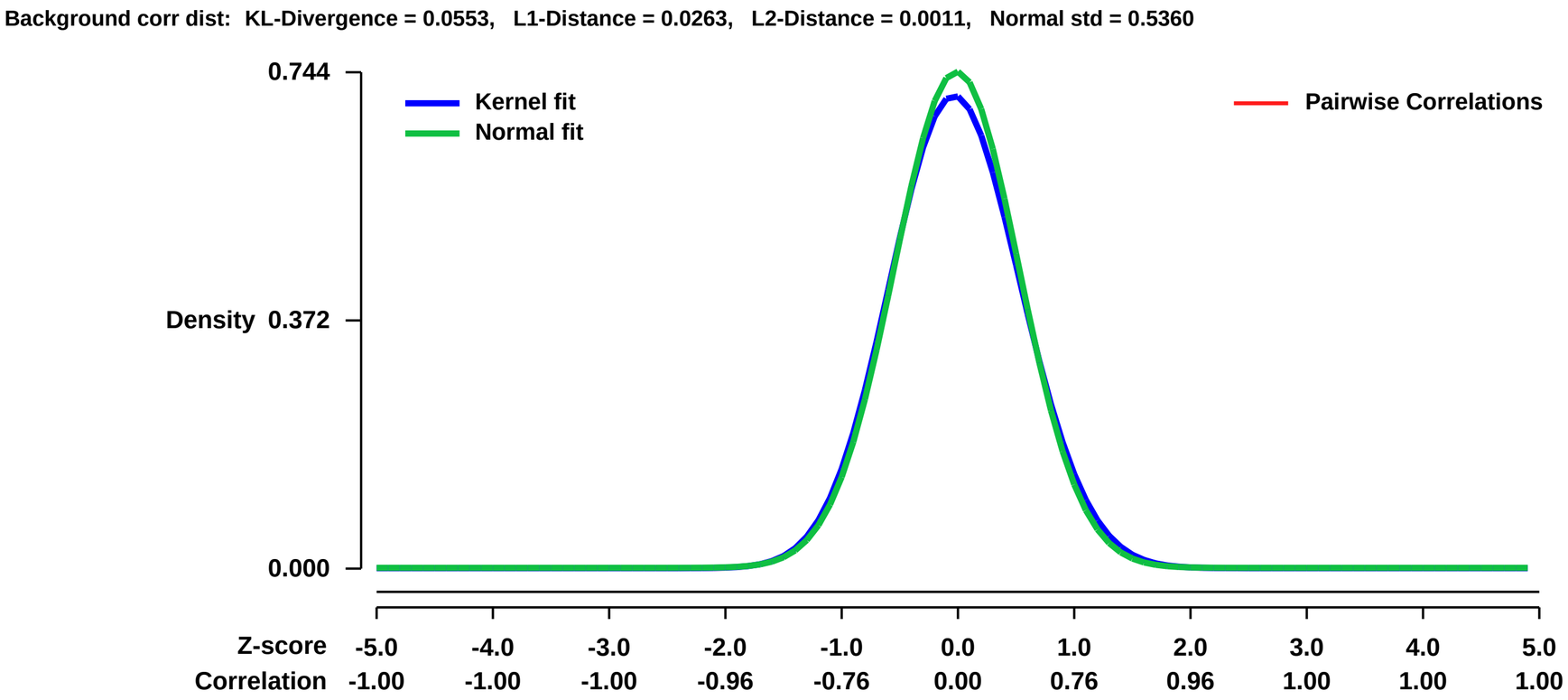

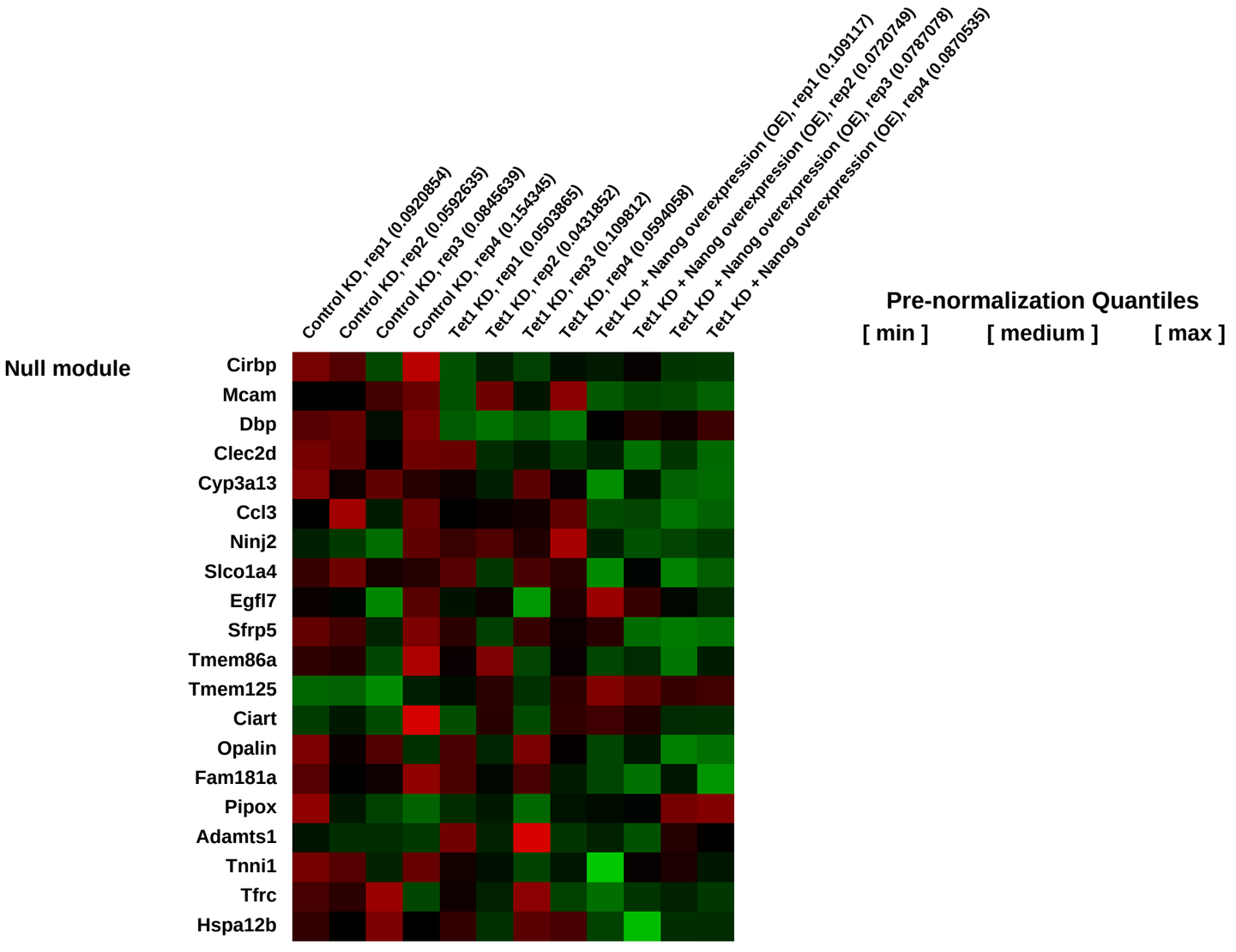

GEO Series "GSE27019" Expression Profiles

Num of samples in this series: 6

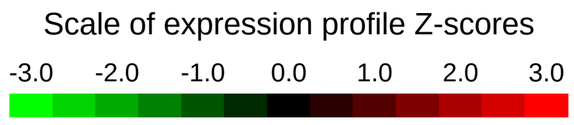

GEO Link:	**http://www.ncbi.nlm.nih.gov/geo/query/acc.cgi?acc=GSE27019**
Status:	**Public on Aug 01 2012**
Title:	**Role of transcriptional regulators IFRD1 and IFRD2 in intestinal lipid absorption and obesity**
Organism:	**Mus musculus**
Experiment type:	**Expression profiling by array**
Platform:	**GPL1261**
Pubmed ID:	
Summary & Design:	**Summary:** **Because of the epidemic rise of obesity worldwide, the identification of novel target genes for pharmacological treatment of obesity and related disorders is becoming of high importance. IFRD1 and IFRD2 are members of a novel transcriptional regulators family. Intestinal over-expression of mouse homologue of IFRD1 promoted intestinal triglyceride uptake and induced whole body adiposity in mice. To further elucidate the role of IFRD1 and IFRD2 in vivo, we generated mice lacking both mouse homologues of IFRD1 (TIS7) and IFRD2 (SKMc15) genes. Here, we report that mice deficient in TIS7 and SKMc15 genes, despite normal calorie intake had severely reduced amount of adipose tissue, were resistant to diet-induced obesity and displayed high glucose tolerance. Lower dietary fat entry into the circulation suggested that this phenotype resulted from impaired intestinal lipid transport. We identified down-regulation of CD36, a fatty acid transporter, both on RNA and protein levels. Reporter assays indicated that TIS7 and SKMc15 transcriptionally regulated CD36 expression and CD36 overexpression partially restored fatty acid uptake in vitro. Hence, our study suggested that TIS7 and SKMc15 play an important role in the regulation of the lipid metabolism and might represent a novel strategy for treatment of disorders caused by excess fat intake.** **To determine whether decreased intestinal lipid absorption might be caused by changes in expression of lipid processing and transport molecules, we performed Affymetrix microarray analyses of total RNA samples isolated from the jejunum of HFD-fed WT type and dKO animals. The moderated t-test was used to calculate p-values for significance of differential gene expression between 3 dKO and 3 wild type mice. These raw p-values were adjusted for multiple hypothesis testing using the method from Benjamini and Hochberg for a strong control of the false discovery rate (FDR) and genes with thus adjusted p-values < 0.05 were considered significant.** **Overall design:** **Age-matched (7-10 week old) male wild type and TIS7 (Ifrd1) SKMc15 (Ifrd2) double knock out mice (C57Bl6 background) were caged individually and maintained from 3 weeks up to 8 weeks on a synthetic high saturated fat (HFD) diet (Ssniff). Small intestines (jejunum) were harvested for total RNA isolation. RNAs from 3 WT and 3 dKO mice were subjected to Affymetrix based whole genome gene expression analysis (Mouse 430.2 GeneChip).**

Background corr dist: KL-Divergence = 0.0401, L1-Distance = 0.0172, L2-Distance = 0.0003, Normal std = 0.6130

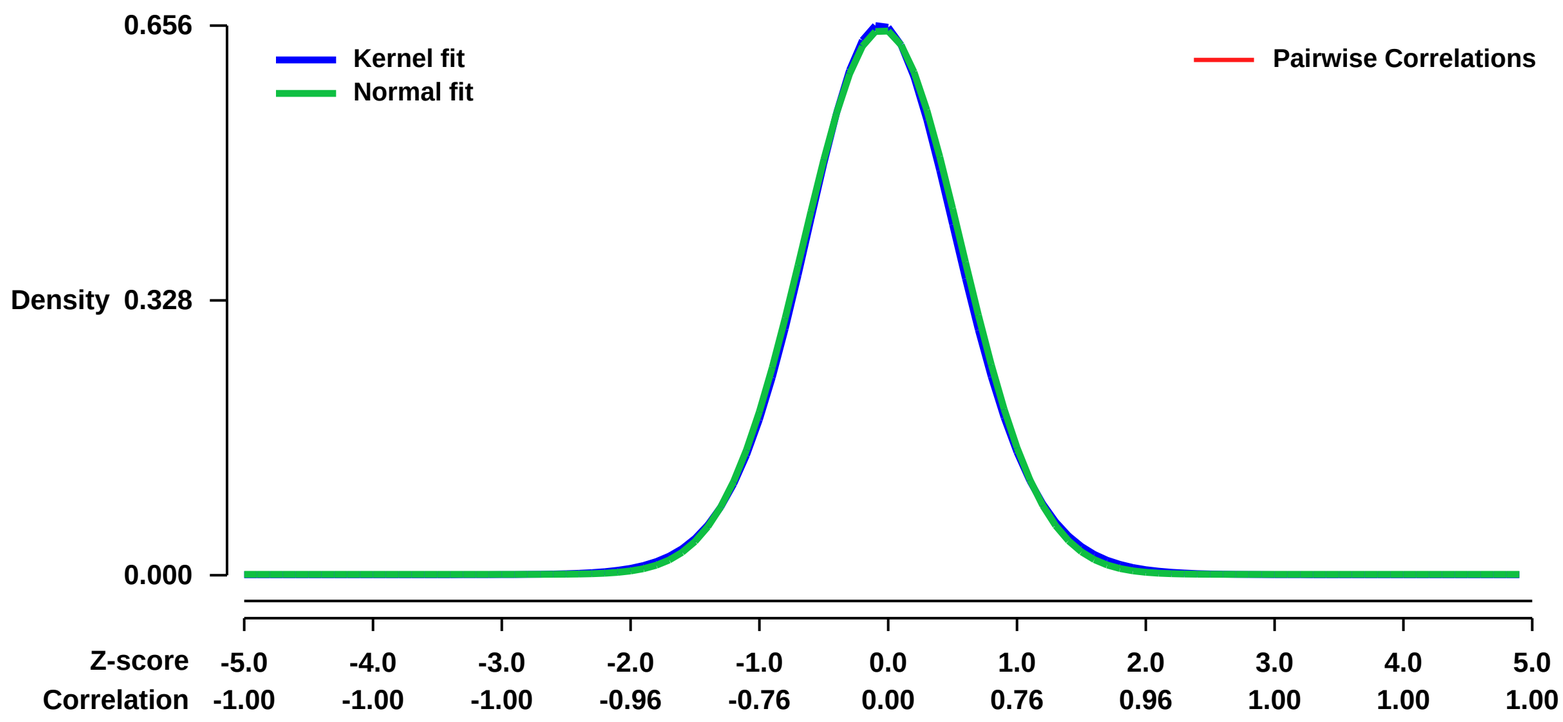

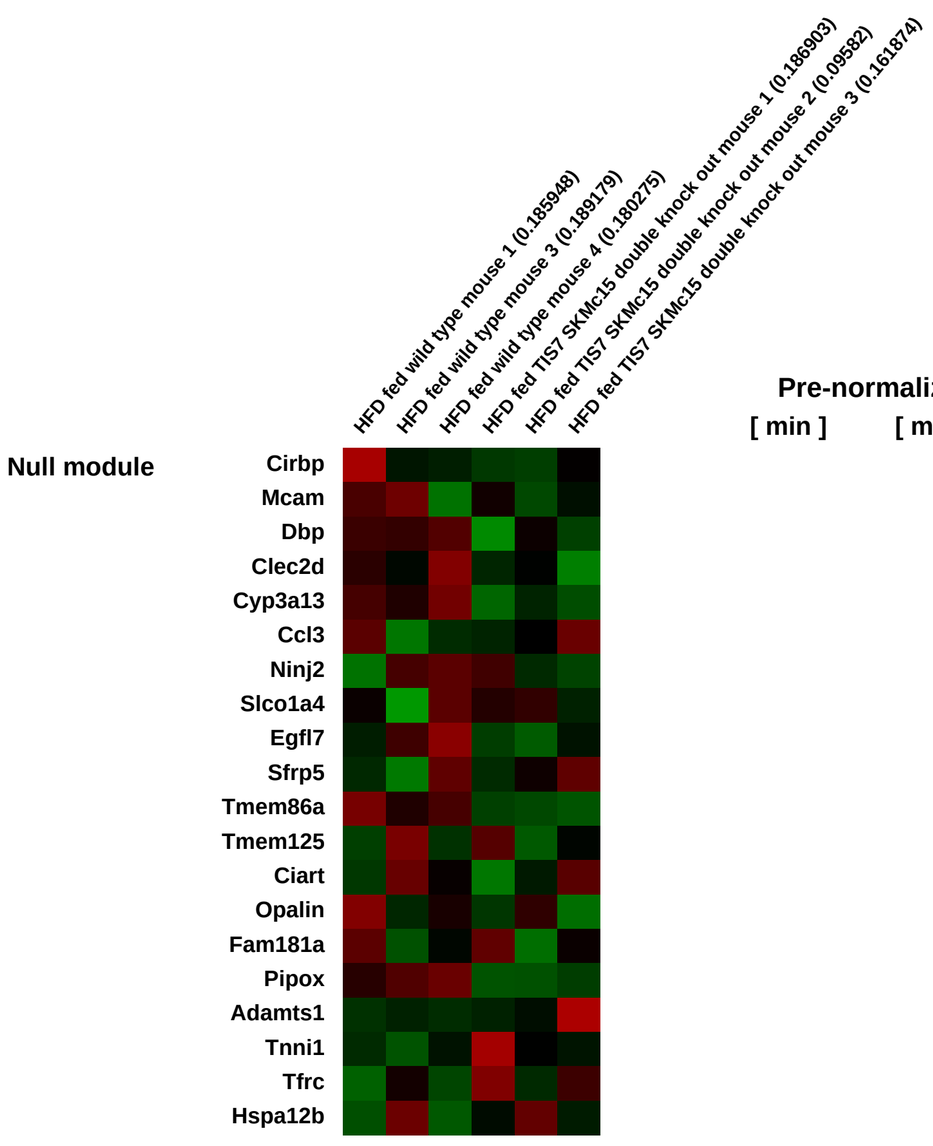

GEO Series "GSE27038" Expression Profiles

Num of samples in this series: 12

Scale of expression profile Z-scores

-3.0 -2.0 -1.0 0.0 1.0 2.0 3.0

GEO Link:	http://www.ncbi.nlm.nih.gov/geo/query/acc.cgi?acc=GSE27038
Status:	Public on Feb 03 2011
Title:	Expression data from the Ire1$_{c}$– null and control murine livers in the absence or presence of ER stress
Organism:	Mus musculus
Experiment type:	Expression profiling by array
Platform:	GPL1261
Pubmed ID:	21407177
Summary & Design:	**Summary:** Ire1$_{c}$– conditional null or control mice of 3-months old were injected intraperitoneally with TM or vehicle. At 8 hours after the injection, total RNA was isolated from murine liver tissue and subjected to Affymetrix microarray analysis. **Overall design:** We used microarrays to profile the global programme of gene expression in the livers of Ire1$_{c}$– null and control mice in the absence or presence of ER stress.

Background corr dist: KL-Divergence = 0.1000, L1-Distance = 0.0233, L2-Distance = 0.0009, Normal std = 0.4442

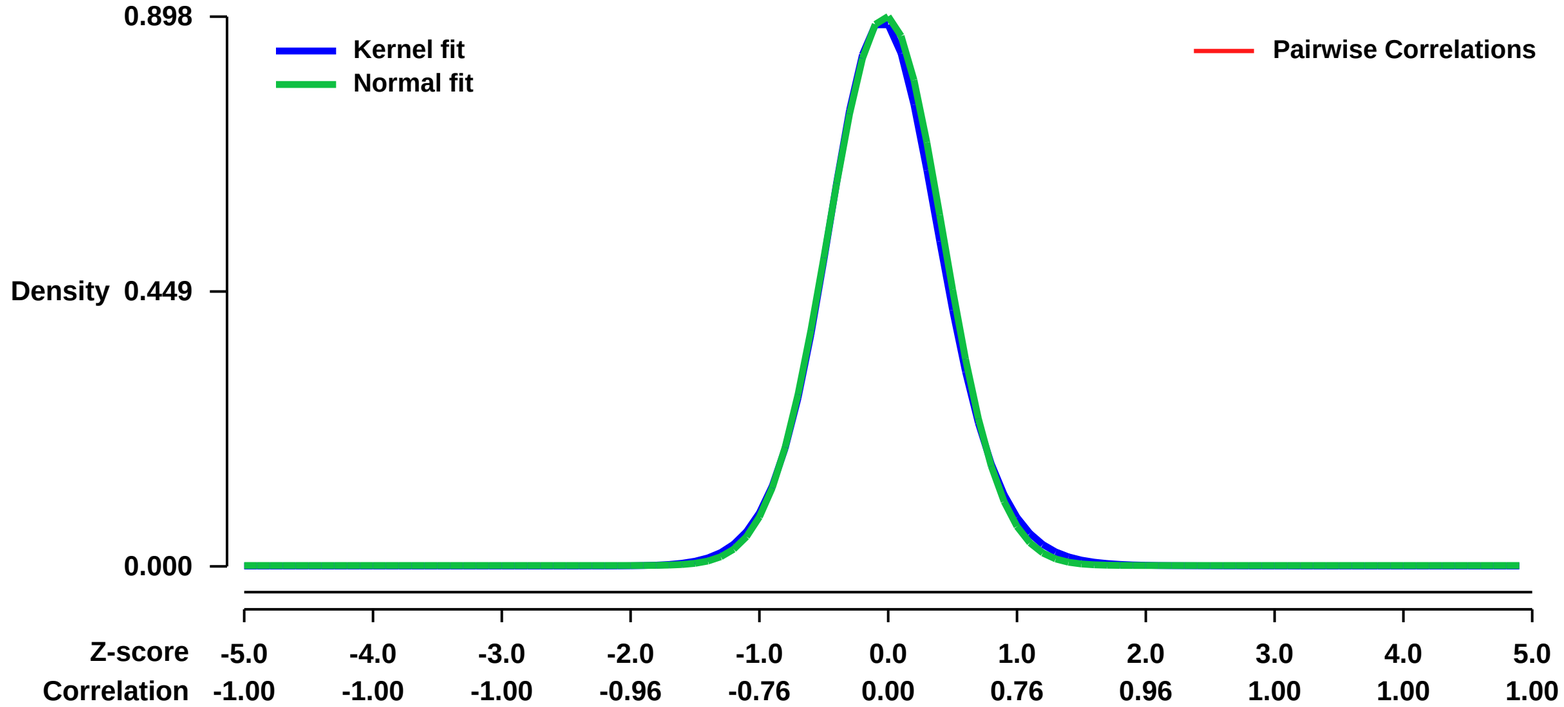

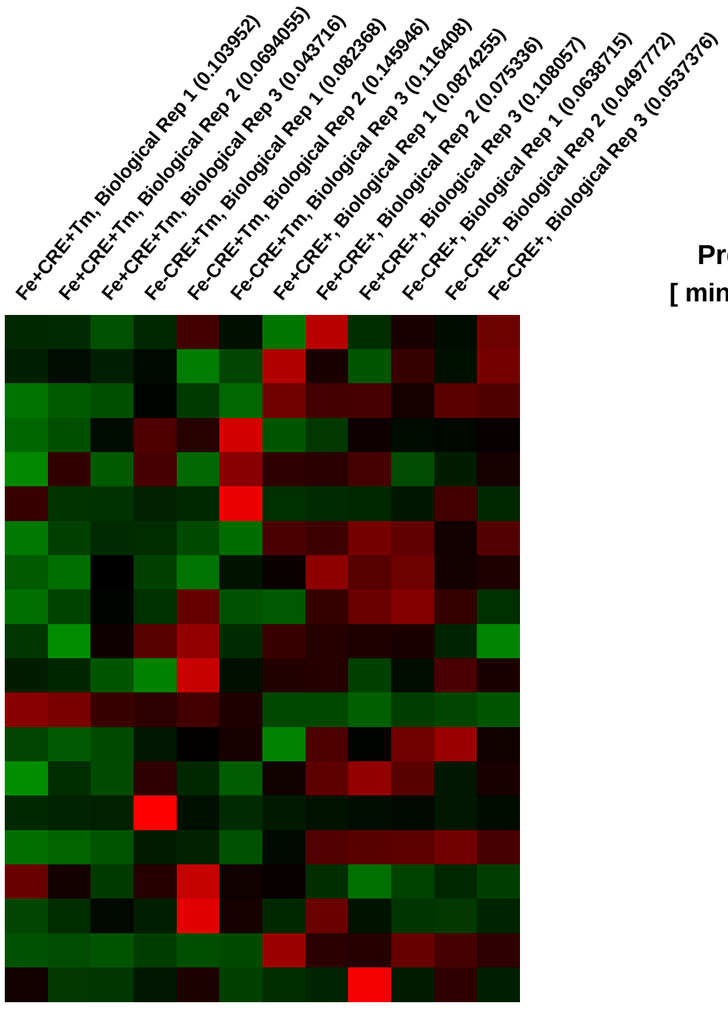

GEO Series "GSE27092" Expression Profiles

Num of samples in this series: 6

Scale of expression profile Z-scores

-3.0 -2.0 -1.0 0.0 1.0 2.0 3.0

GEO Link:	http://www.ncbi.nlm.nih.gov/geo/query/acc.cgi?acc=GSE27092
Status:	Public on Mar 13 2011
Title:	Expression data from P14 TCR cytotoxic T cells overexpressing HDAC7 phosphorylation deficient mutant
Organism:	Mus musculus
Experiment type:	Expression profiling by array
Platform:	GPL1261
Pubmed ID:	21399638
Summary & Design:	**Summary:** The present study reports an unbiased analysis of the cytotoxic T cell serine-threonine phosphoproteome using high resolution mass spectrometry. Approximately 2,000 phosphorylations were identified in CTLs of which approximately 450 were controlled by TCR signaling. A significantly overrepresented group of molecules identified in the phosphoproteomic screen were transcription activators, co-repressors and chromatin regulators. A focus on the chromatin regulators revealed that CTLs have high expression of the histone deacetylase HDAC7 but continually phosphorylate and export this transcriptional repressor from the nucleus. HDAC7 dephosphorylation results in its nuclear accumulation and suppressed expression of genes encoding key cytokines, cytokine receptors and adhesion molecules that determine CTL function. The screening of the CTL phosphoproteome thus reveals intrinsic pathways of serine-threonine phosphorylation that target chromatin regulators in CTLs and determine the CTL functional program. We used Affymetrix microarray analysis to explore the molecular basis for the role of HDAC7 in CTLs and the impact of GFP-HDAC7 phosphorylation deficient mutant expression on the CTL transcriptional profile. **Overall design:** In vitro generated P14 TCR cytotoxic T cells were retrovirally infected with a construct encoding GFP-HDAC7 phosphorylation deficient mutant, sorted in base of GFP expression (GFP positive and GFP negative) and processed for microarray analysis in three biological replicas.

Background corr dist: KL-Divergence = 0.0166, L1-Distance = 0.0217, L2-Distance = 0.0007, Normal std = 0.7816

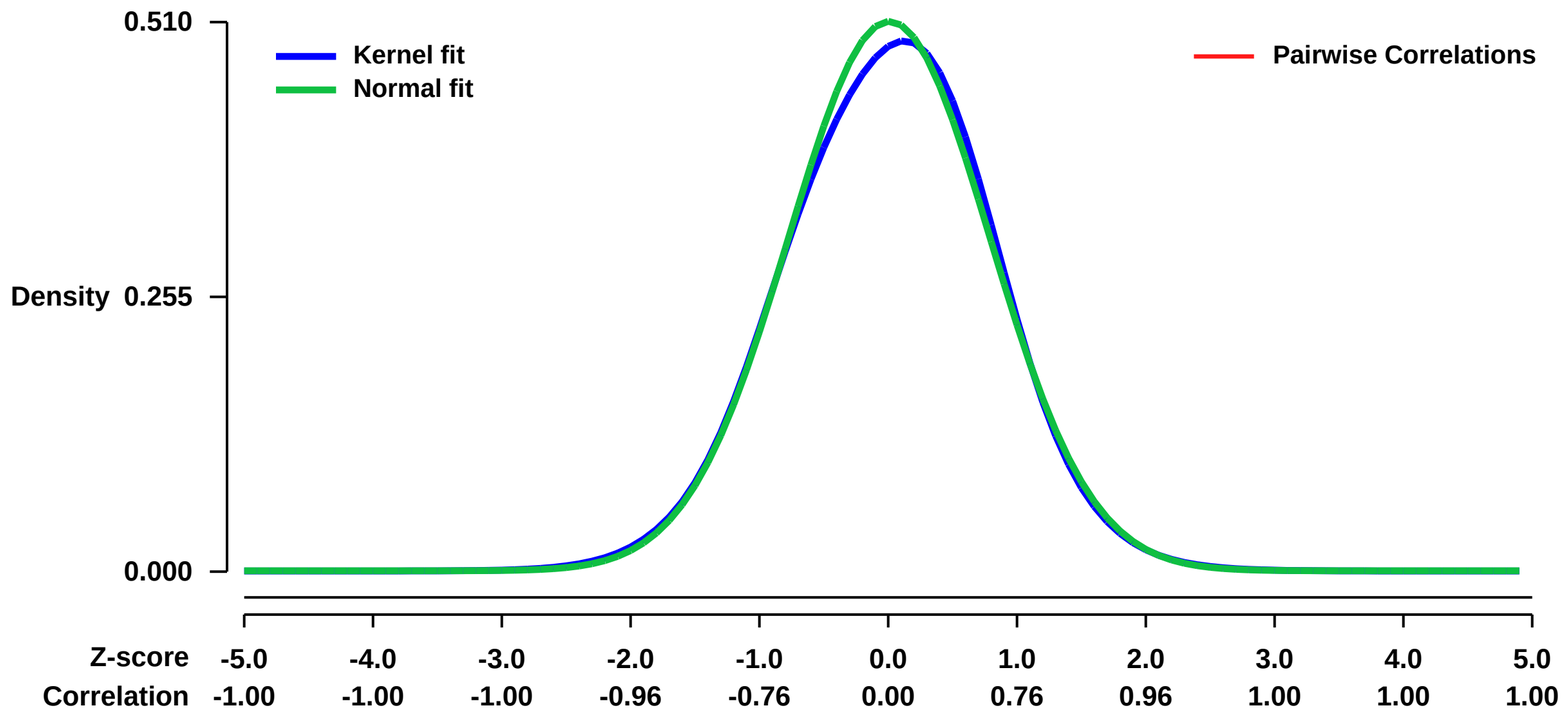

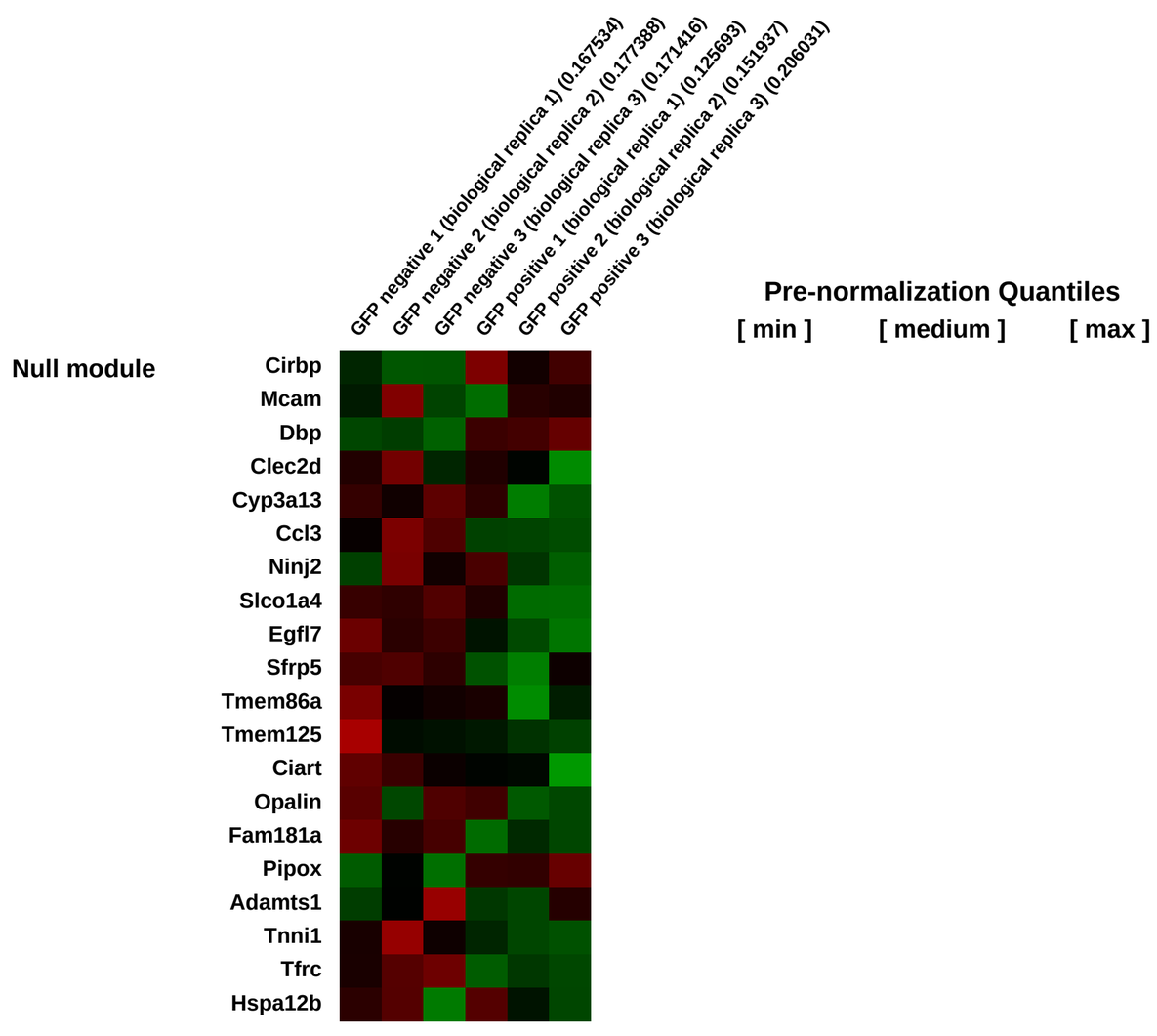

GEO Series "GSE27114" Expression Profiles

Num of samples in this series: 6

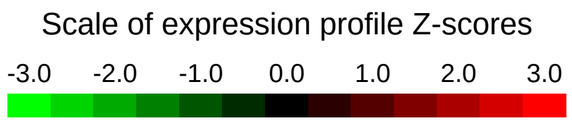

GEO Link:	http://www.ncbi.nlm.nih.gov/geo/query/acc.cgi?acc=GSE27114
Status:	Public on Sep 04 2012
Title:	Expression data from REST knock-out versus REST wild type cells during in vitro neurogenesis
Organism:	Mus musculus
Experiment type:	Expression profiling by array
Platform:	GPL1261
Pubmed ID:	22964890
Summary & Design:	**Summary:** While changes in chromatin are integral to transcriptional reprogramming during cellular differentiation, it is currently unclear how chromatin modifications are targeted to specific loci. We developed a computational model on the premise that transcription factors (TFs) direct dynamic chromatin changes during cell fate decisions. When applied to a neurogenesis paradigm, this approach predicted the TF REST as a determinant of gain of Polycomb-mediated H3K27me3 in neuronal progenitor cells. We prove this prediction experimentally by showing that the absence of REST causes loss of H3K27me3 at target promoters in trans at the same cellular state. Moreover, promoter fragments containing a REST binding site are sufficient to recruit H3K27me3 in cis, while deletion of their REST site results in loss of H3K27me3. These findings illustrate that computational modeling can systematically identify TFs that regulate chromatin dynamics genome-wide. Local determination of Polycomb activity by REST exemplifies such TF based regulation of chromatin. **Overall design:** Expression profiling of REST knock-out (RESTko) versus REST wildtype (RESTwt) or REST heterozygous knock-out (RESThet) cells at three stages of in vitro neuronal differentiation. RESTko and RESTwt/RESThet embryonic stem (ES) cells were differentiated to terminal neurons (TN) via a defined neuronal progenitor (NP) state. Three biological replicates (suffixes a to c).

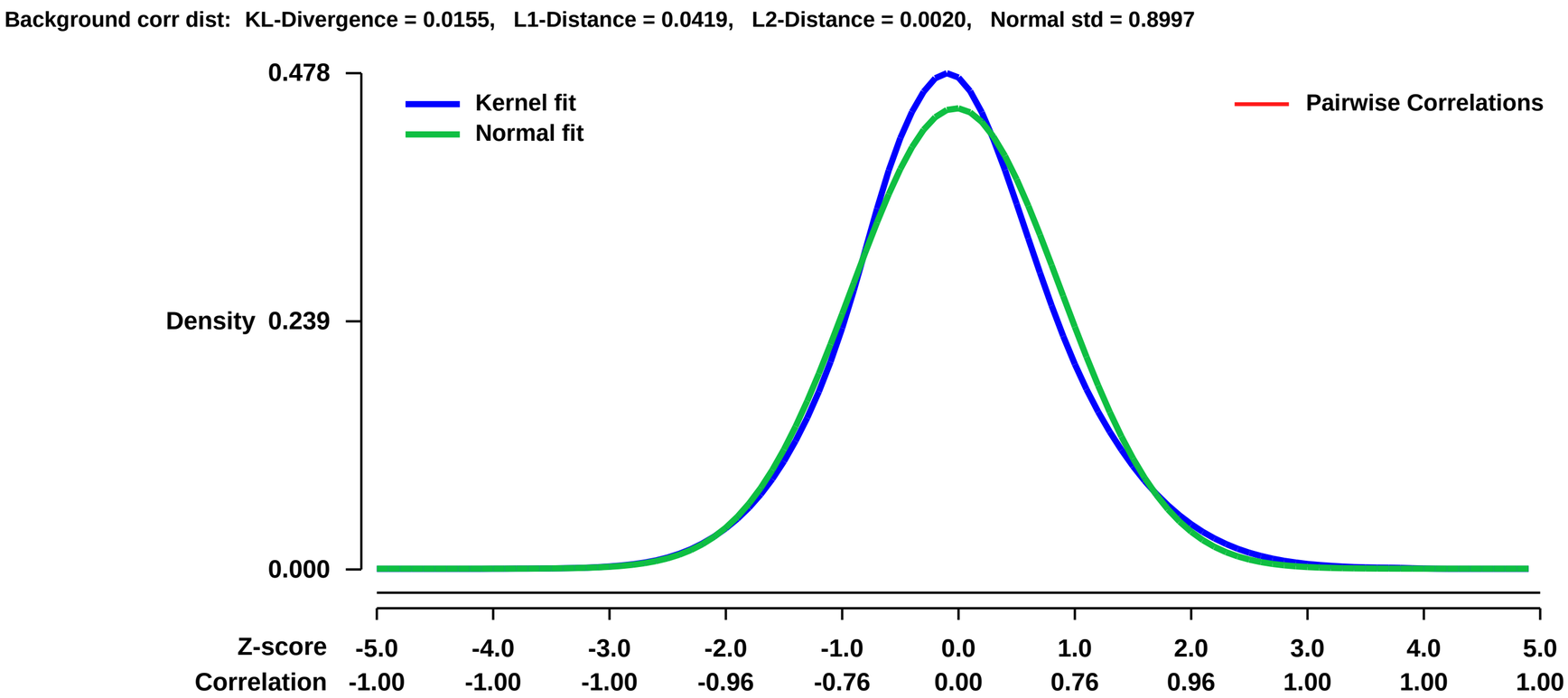

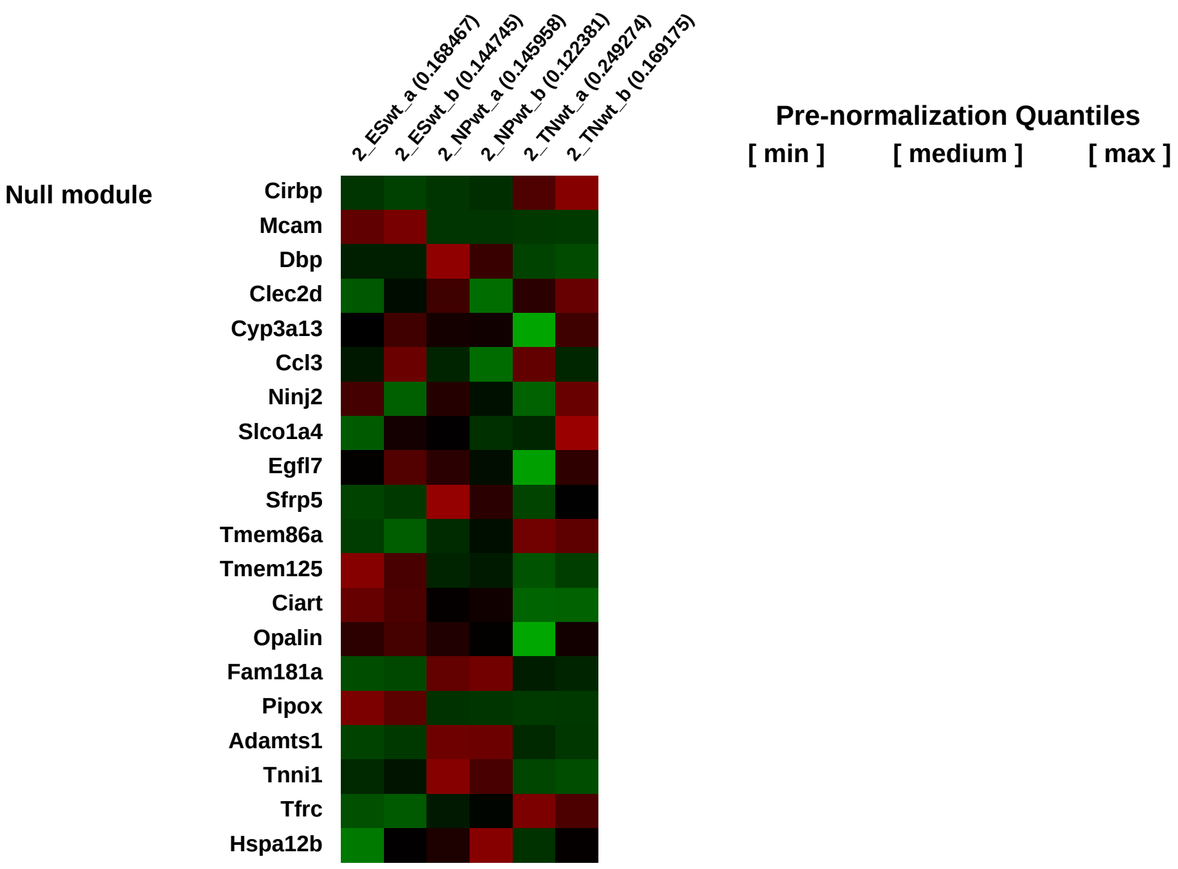

GEO Series "GSE27159" Expression Profiles

Num of samples in this series: 8

Scale of expression profile Z-scores

-3.0 -2.0 -1.0 0.0 1.0 2.0 3.0

GEO Link:	**http://www.ncbi.nlm.nih.gov/geo/query/acc.cgi?acc=GSE27159**
Status:	**Public on Apr 30 2012**
Title:	**Expression profiling of the murine neural crest precursor cell line, JoMa1**
Organism:	**Mus musculus**
Experiment type:	**Expression profiling by array**
Platform:	**GPL1261**
Pubmed ID:	
Summary & Design:	**Summary:** **JoMa1 cells are pluripotent precursor cells, derived from the neural crest of mice transgenic for tamoxifen-inducible c-Myc. Following transfection with a cDNA encoding for MYCN, cells become immortlized even in the absence of tamoxifen.** **Overall design:** **The expression profile of JoMa1 cells was compared to cell lines derived from tumors induced by JoMa1 transfected with MYCN.**

Background corr dist: **KL-Divergence = 0.0379, L1-Distance = 0.0219, L2-Distance = 0.0005, Normal std = 0.6256**

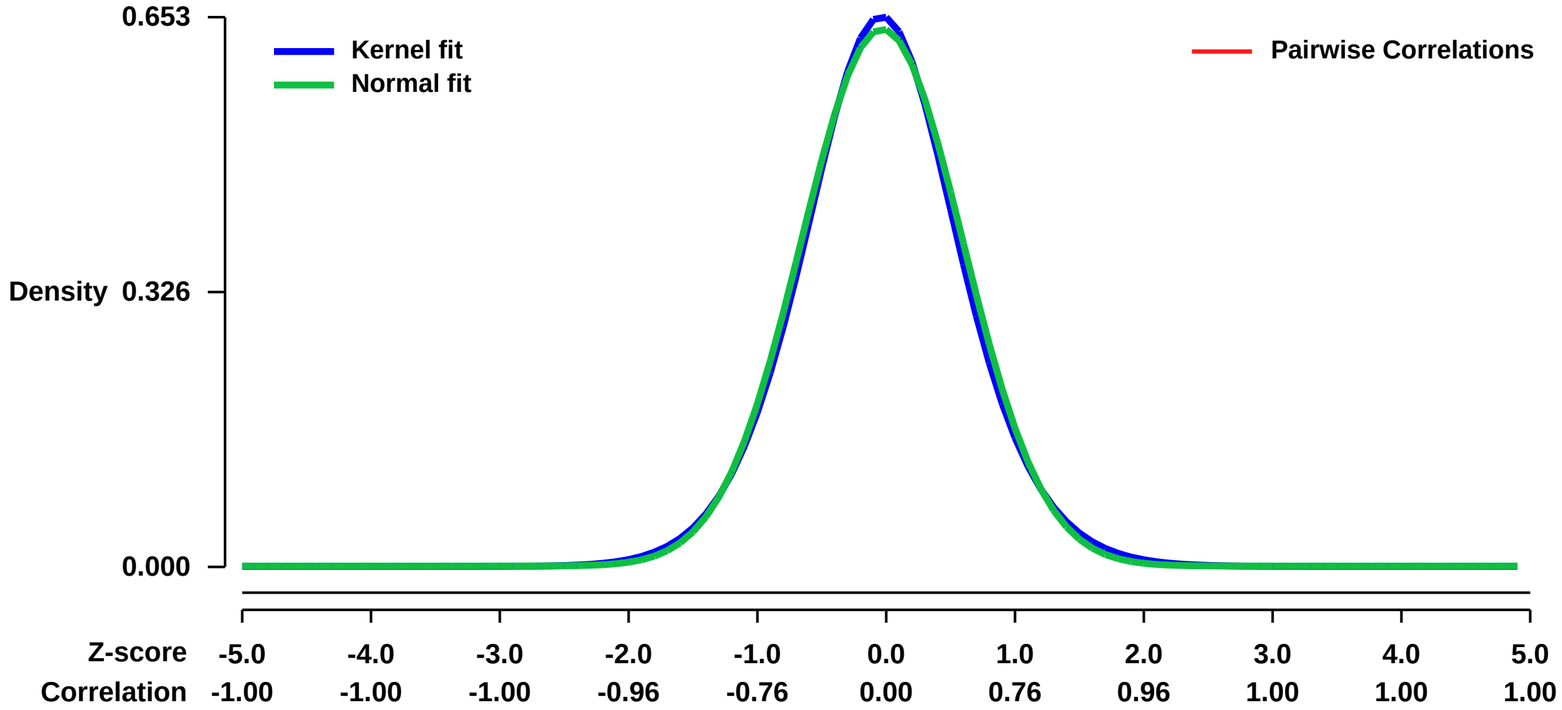

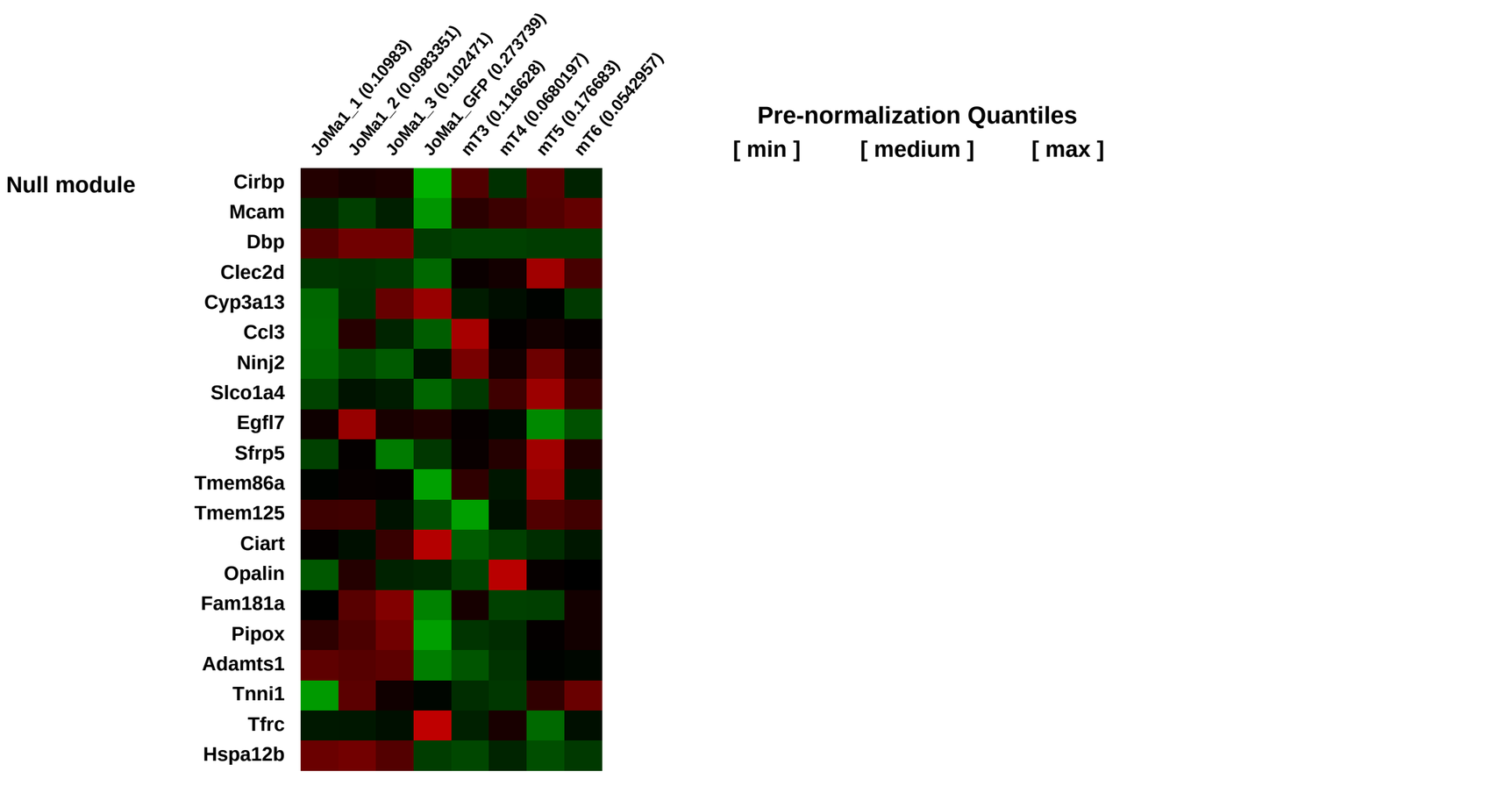

GEO Series "GSE27195" Expression Profiles

Num of samples in this series: 6

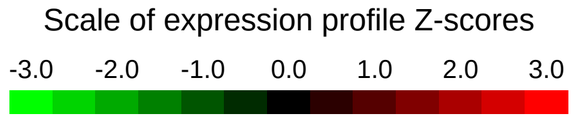

GEO Link:	**http://www.ncbi.nlm.nih.gov/geo/query/acc.cgi?acc=GSE27195**
Status:	**Public on Sep 01 2011**
Title:	**Ciliary neurotrophic factor induces genes associated with inflammatory response and gliosis in the retina: A gene profiling study of flow-sorted, Muller (glial) cells**
Organism:	**Mus musculus**
Experiment type:	**Expression profiling by array**
Platform:	**GPL1261**
Pubmed ID:	**21637858**
Summary & Design:	**Summary:** **Our data suggest that CNTF remodels the transcription profile of Mˆ…ller (glial) cells leading to induction of networks associated with transcription, cell cycle regulation and inflammatory response. CNTF also appears to function as an inducer of gliosis in the retina. These studies provide new insights into the biological functions of cytokines in the retina.** **Overall design:** **Muller glial cells treated with CNTF for 1 and 3 days**

Background corr dist: **KL-Divergence = 0.0457, L1-Distance = 0.0255, L2-Distance = 0.0008, Normal std = 0.5956**

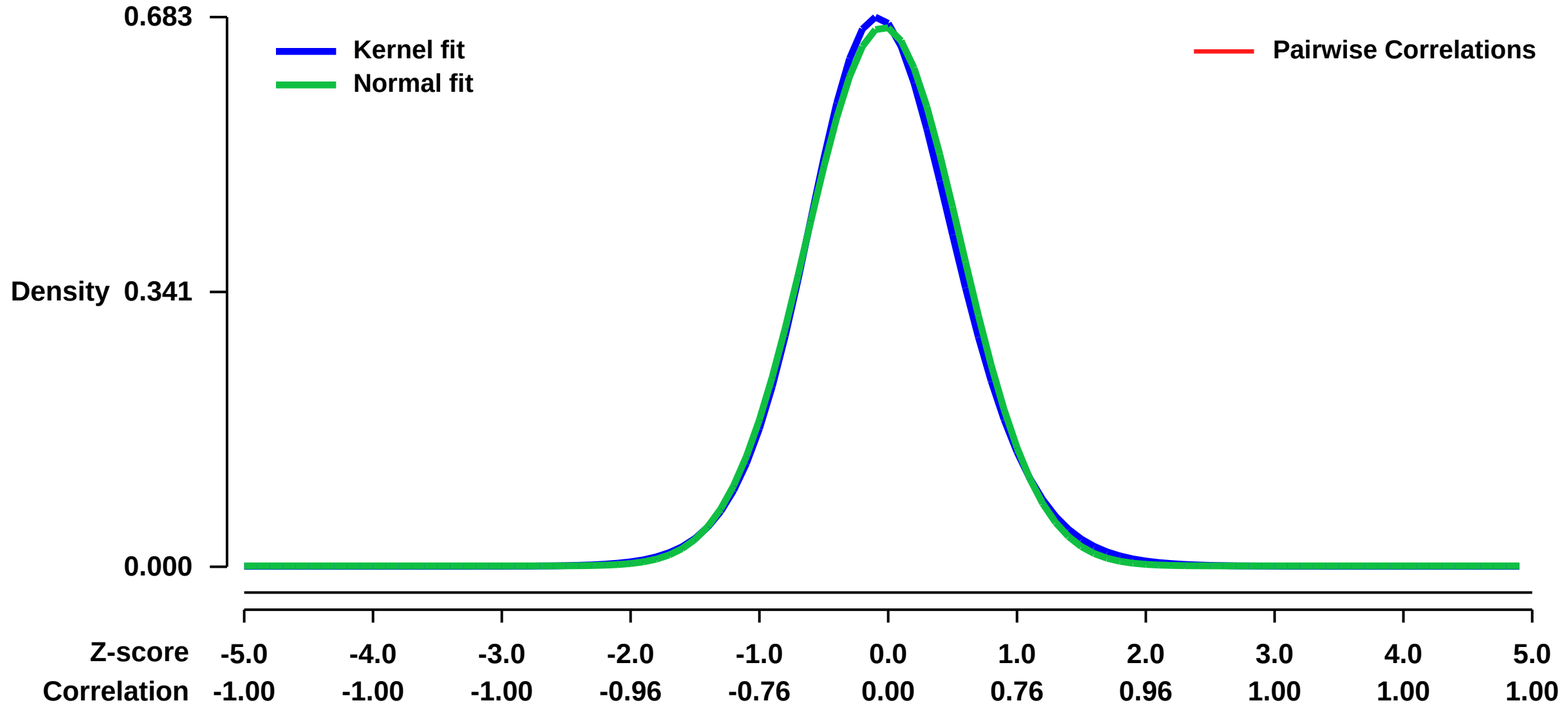

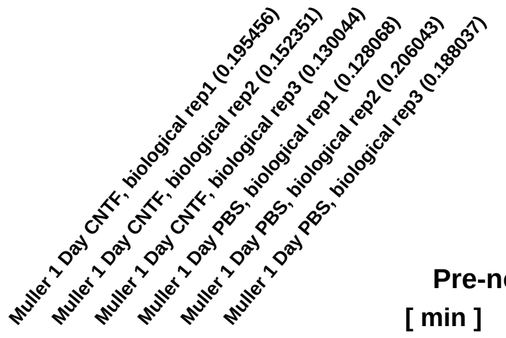

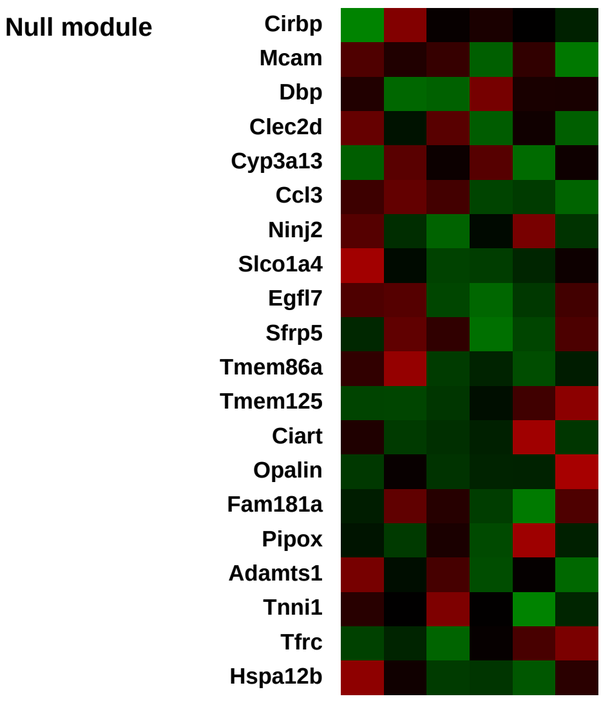

GEO Series "GSE27302" Expression Profiles

Num of samples in this series: 16

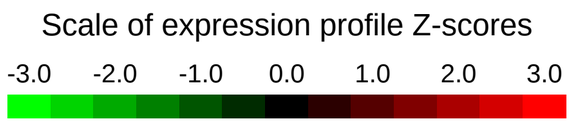

GEO Link:	**http://www.ncbi.nlm.nih.gov/geo/query/acc.cgi?acc=GSE27302**
Status:	**Public on Jan 11 2013**
Title:	**Expression data from mouse colon tissue response to T cell transfer at week 0, 2, 4 and 6**
Organism:	**Mus musculus**
Experiment type:	**Expression profiling by array**
Platform:	**GPL1261**
Pubmed ID:	**22179924**
Summary & Design:	**Summary:** **Temporal geneome profiling of T cell transfer colitis model** **T cells critically regulate clinical inflammatory bowel diseases and T cell dependent experimental colitis models have gained prominent favor as useful models to identify potential pathogenic mechanisms. The naˆflve CD4+CD45Rbhigh cell transfer model into recombinase activating gene-1 deficient (RAG-/-) mice induces both colitis and small bowel inflammation reflecting Crohn's disease with unclear pathogenic mechanisms. Given the pathological similarities between the T cell transfer model of colitis and clinical disease, we sought to identify changes in whole genome expression profiles over time during the delelopment of colitis.** **Overall design:** **Male RAG-1-/- C57BL/6 mice were injected with a half million CD4+CD45RBhigh T cells from healthy wild type C57BL/6 male mice. The colon tissue from individual cohorts were collected at weeks 0, 2, 4 and 6. Total RNA were extracted from the colon tissue and detected by Affymetrix GeneChip Mouse Genome 430 2.0 Array.**

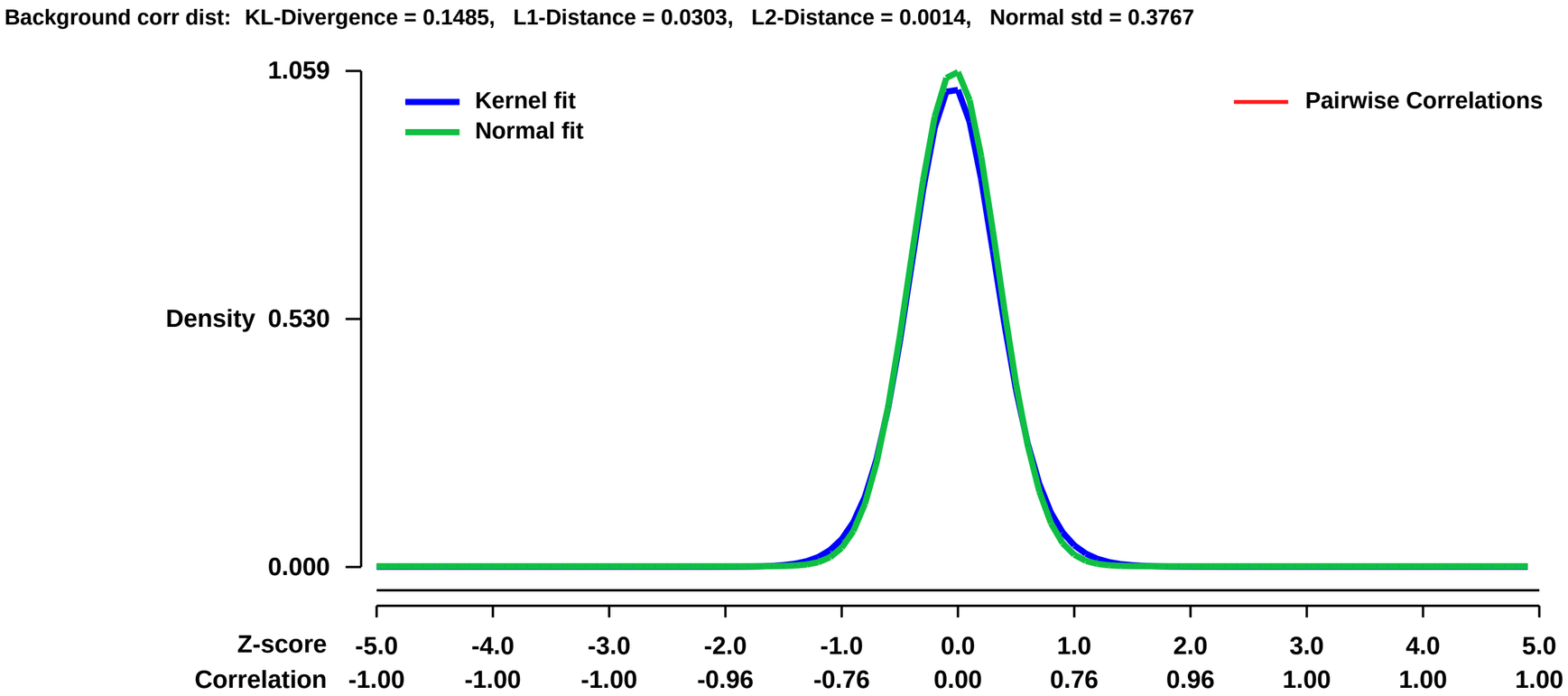

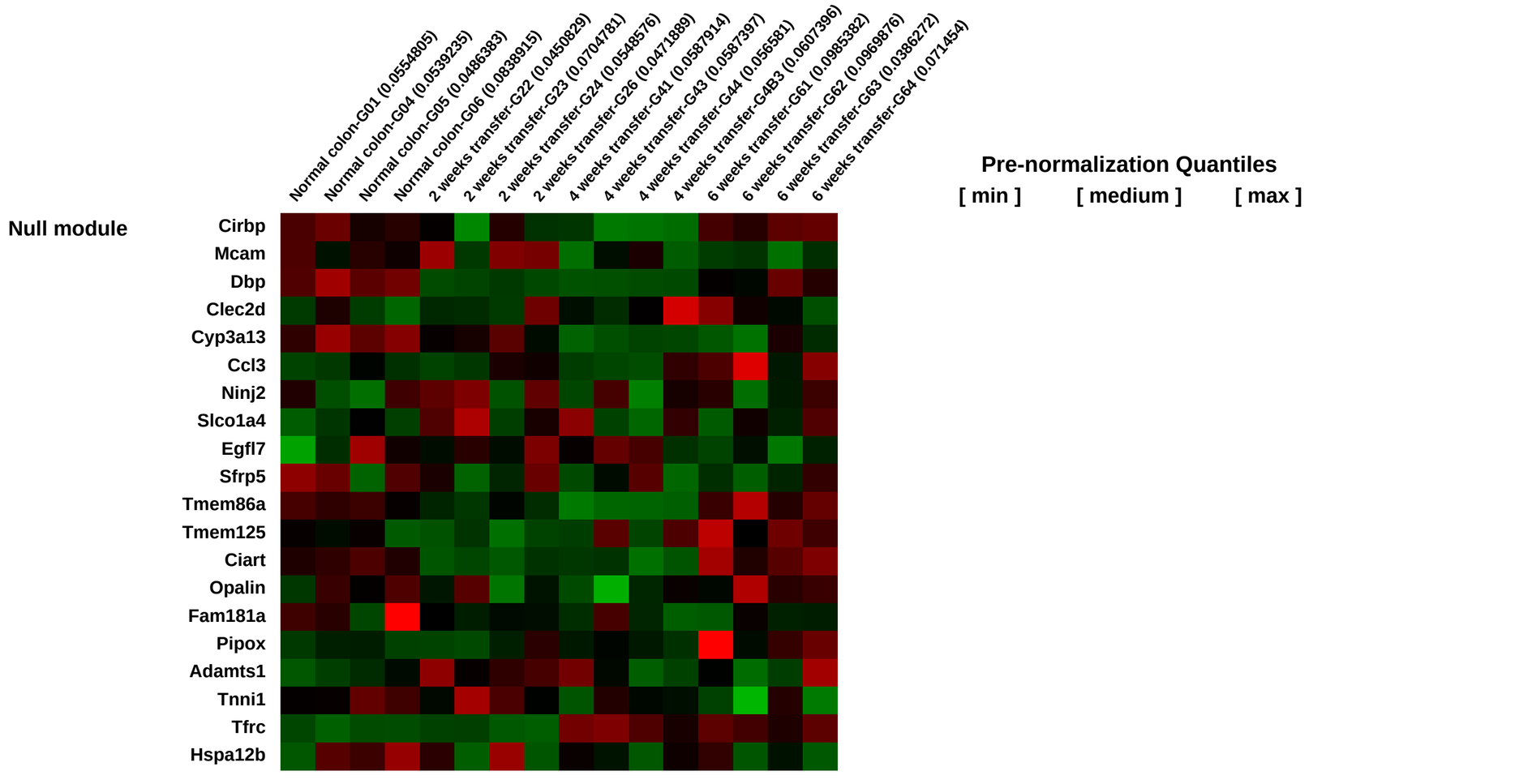

GEO Series "GSE27309" Expression Profiles

Num of samples in this series: 10

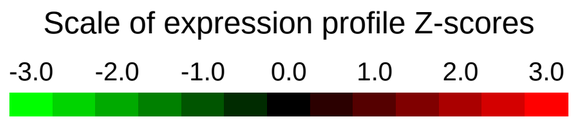

GEO Link:	http://www.ncbi.nlm.nih.gov/geo/query/acc.cgi?acc=GSE27309
Status:	Public on Mar 15 2011
Title:	SIRT3 opposes metabolic reprogramming of cancer cells through HIF1a destabilization
Organism:	Mus musculus
Experiment type:	Expression profiling by array
Platform:	GPL1261
Pubmed ID:	21397863
Summary & Design:	**Summary:** Tumor cells exhibit aberrant metabolism characterized by high glycolysis even in the presence of oxygen. This metabolic reprogramming, known as the Warburg effect, provides tumor cells with the substrates and redox potential required for the generation of biomass. Here, we show that the mitochondrial NAD-dependent deacetylase SIRT3 is a crucial regulator of the Warburg effect. SIRT3 loss promotes a metabolic profile consistent with high glycolysis required for anabolic processes in vivo and in vitro. Mechanistically, SIRT3 mediates metabolic reprogramming independently of mitochondrial oxidative metabolism and through HIF1a, a transcription factor that controls expression of key glycolytic enzymes. SIRT3 loss increases reactive oxygen species production, resulting in enhanced HIF1a stabilization. Strikingly, SIRT3 is deleted in 40% of human breast cancers, and its loss correlates with the upregulation of HIF1a target genes. Finally, we find that SIRT3 overexpression directly represses the Warburg effect in breast cancer cells. In sum, we identify SIRT3 as a regulator of HIF1a and a suppressor of the Warburg effect. **Overall design:** RNA isolated from brown adipose tissue of SIRT3 WT and KO mice. 5 wild-type samples and 5 SIRT3 KO samples

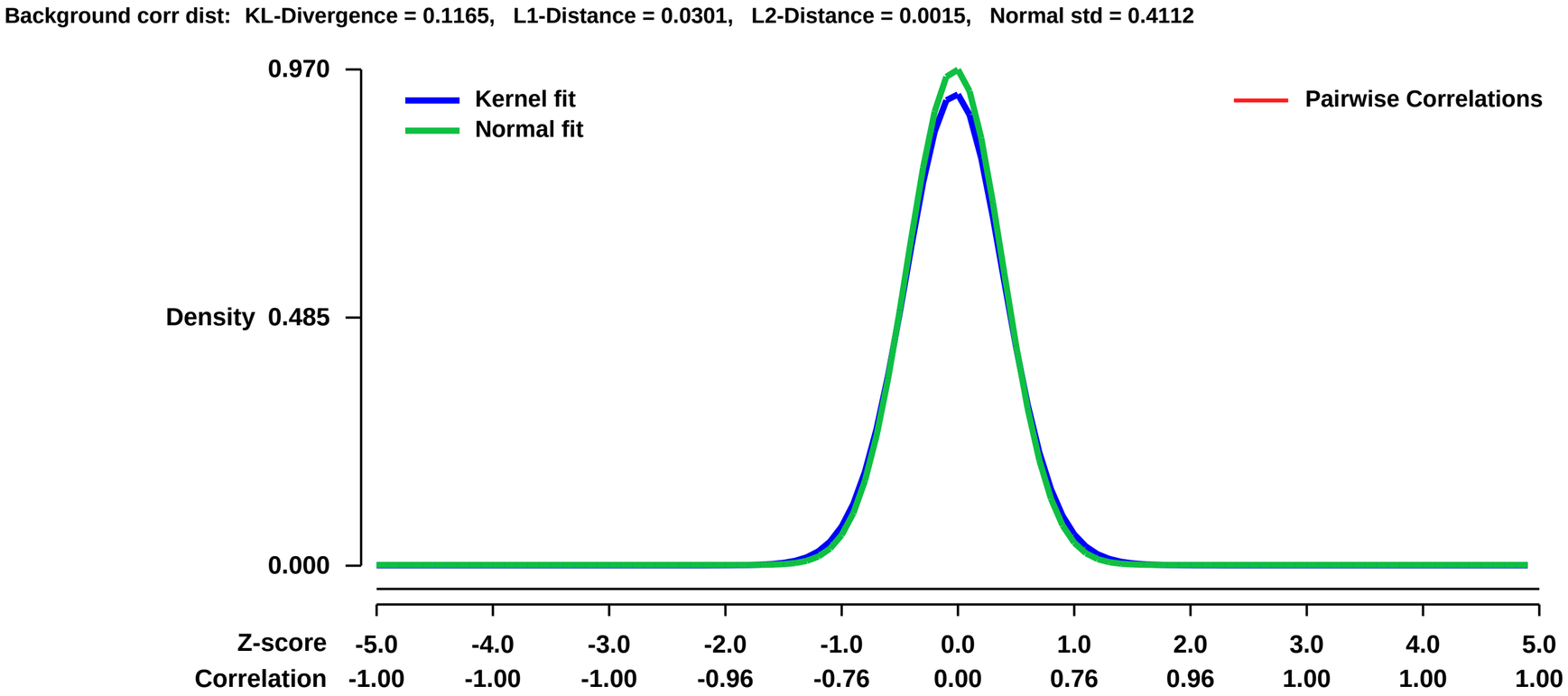

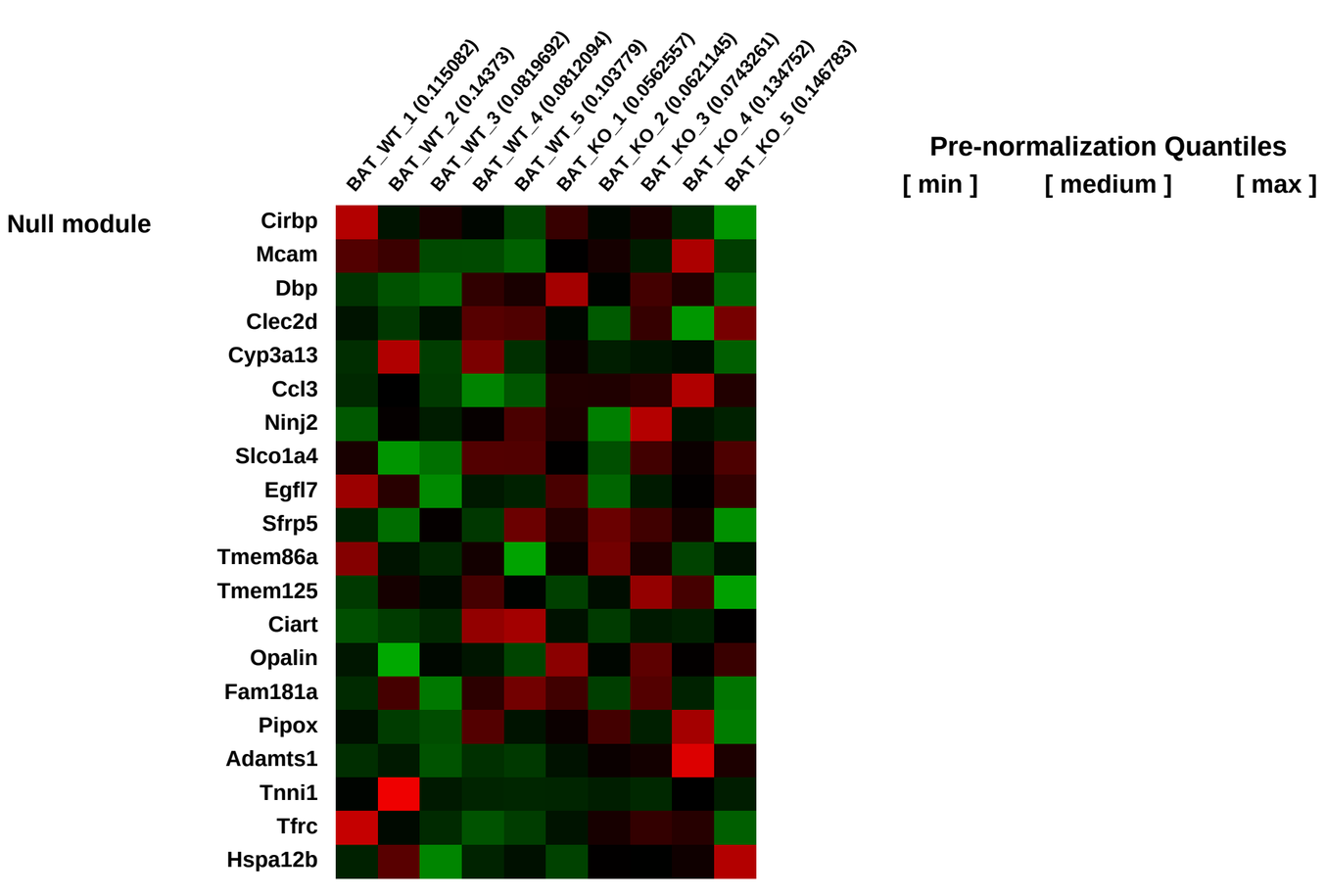

GEO Series "GSE27329" Expression Profiles

Num of samples in this series: 24

Scale of expression profile Z-scores

-3.0 -2.0 -1.0 0.0 1.0 2.0 3.0

GEO Link:	http://www.ncbi.nlm.nih.gov/geo/query/acc.cgi?acc=GSE27329
Status:	Public on Nov 30 2012
Title:	Genome-Wide Analysis of Gene Program Activation by Defined Cardiac Transcription Factor Tbx5, Gata4 and Myocardin
Organism:	Mus musculus
Experiment type:	Expression profiling by array
Platform:	GPL1261
Pubmed ID:	23144723
Summary & Design:	**Summary:** **Background: Cardiac transcription factors are master regulators during heart development. Recently, some were shown to transdifferentiate noncardiac mesoderm cells and cardiac fibroblasts into cardiomyocytes. However, the individual roles of each transcription factors in activating cardiac gene program have not been elucidated. We examined cardiac-specific and genome-wide gene expression in fibroblasts induced with cardiac transcription factors Nkx2.5 (N), Tbx5 (T), Gata4 (G), Myocardin (M) alone or different combinations.** **Methodology/Principal Findings: We applied different combinations of human Nkx2.5 (N), Tbx5 (T), Gata4 (G) and Myocardin (M) lentiviruses into 10T1/2 fibroblasts. Immunostaining and quantitative reverse transcription polymerase chain reaction (qRT-PCR) showed that N, T, G or M alone did not induce expression of cardiac marker genes ¸–-myosin heavy chain (¸–MHC) and cardiac troponin T (cTnT). Only T+M and T+G+M combinations induced ¸–MHC and cTnT expression. Microarray-based gene ontology analysis revealed that T alone inhibited most genes involved in cardiac-related processes and activated genes involved in Wnt receptor signaling pathway and in aberrant processes. M alone inhibited genes involved in Wnt receptor signaling pathway and activated genes involved in cardiac-related processes and in aberrant processes. G alone inhibited genes involved in ectoderm development. T+G+M combination was the most effective activator of genes associated with cardiac-related processes including muscle cell differentiation, sarcomere, striated muscle contraction, regulation of heart contraction, and glucose metabolism and fatty acid oxidation (two significant forms of cardiomyocyte energy metabolism). And unlike T, M, G alone or T+M, T+G+M did not activate genes associated with aberrant processes.** **Conclusions: Tbx5, Gata4 and Myocardin play different roles in activating cardiac gene program and in avoiding aberrant gene program activation. The combination of T+G+M activated cardiac gene program and avoided aberrant gene program activation.** **Overall design:** **Two weeks after doxycline induction, total RNA was isolated from 10T1/2-tTA cells infected with different combinations of Tbx5, Gata4, and Myocardin lentiviruses. Biological triplicated.**

Background corr dist: KL-Divergence = 0.1953, L1-Distance = 0.0380, L2-Distance = 0.0026, Normal std = 0.3365

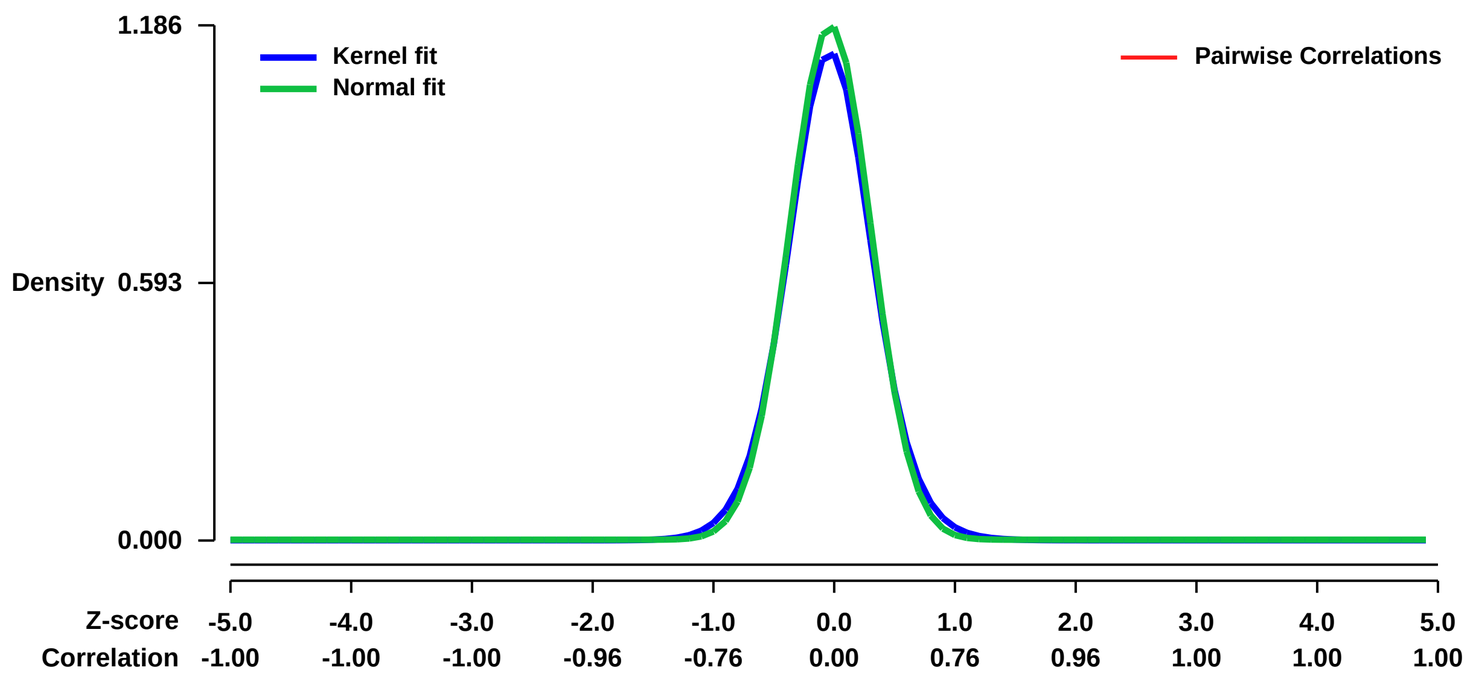

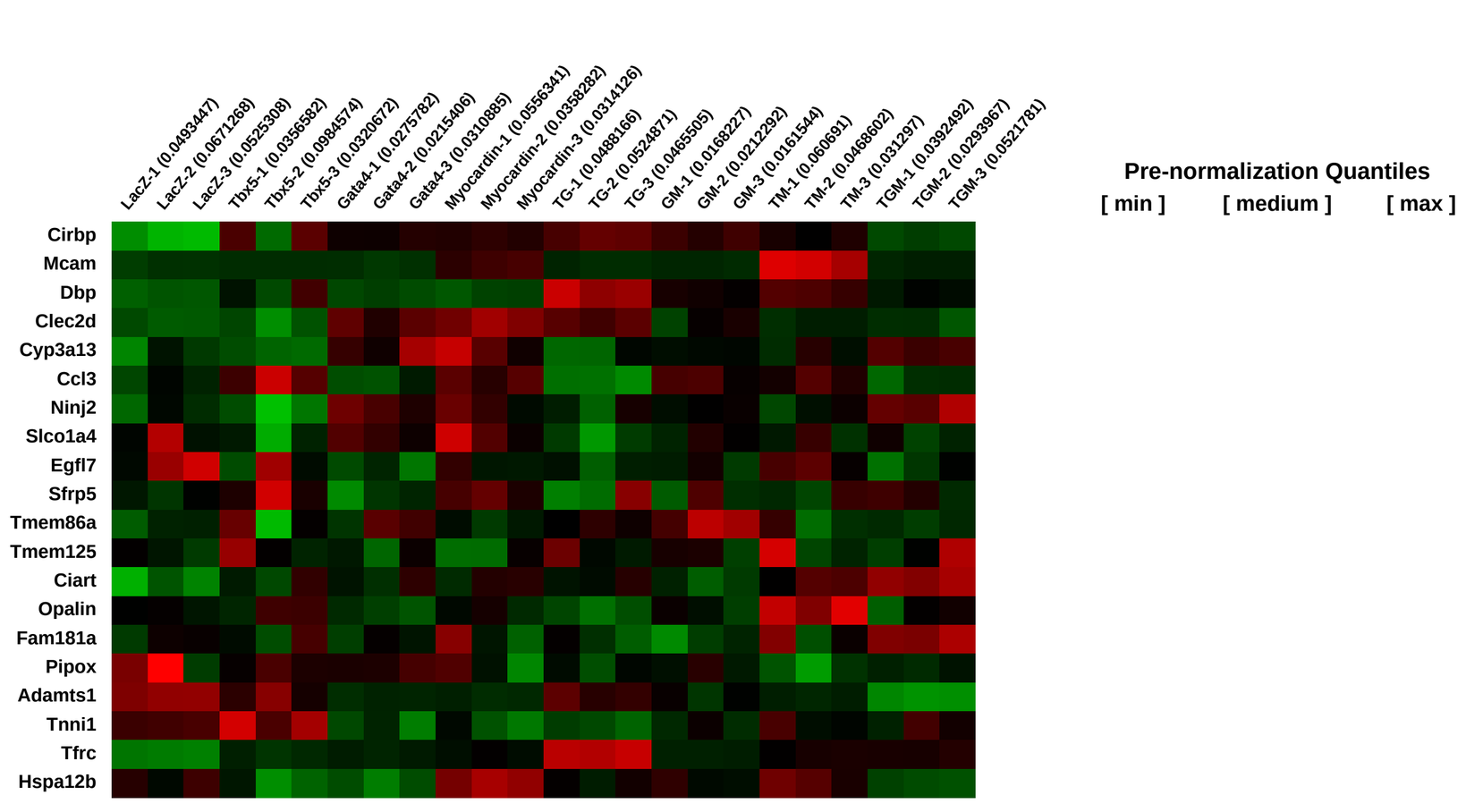

GEO Series "GSE27378" Expression Profiles

Num of samples in this series: 8

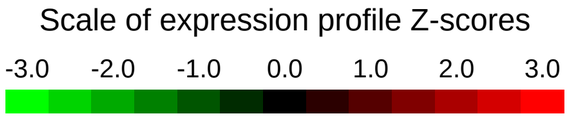

GEO Link:	http://www.ncbi.nlm.nih.gov/geo/query/acc.cgi?acc=GSE27378
Status:	Public on Dec 01 2011
Title:	Differential effects of inhibition of bone morphogenic protein (BMP) signalling on T-cell activation and differentiation
Organism:	Mus musculus
Experiment type:	Expression profiling by array
Platform:	GPL1261
Pubmed ID:	22144105
Summary & Design:	**Summary:** Dorsomorphin is a small molecule inhibitor of type I bone morphogenic protein receptors (BMPRs). We have found that dorsomorphin affects a wide range of T cell function. In order to obtain the bigger picture of the effects of DM in T cell activation. transcriptomic analysis was performed using mouse primary CD25-CD4+ T cells with either DM (4 ¸…M) or vehicle in the presence or absence of stimulation by anti-CD3 and -CD28 antibodies. **Overall design:** Mouse CD4+ T cells were prepared and cultured with or without stimulation by plate bound anti-CD3 mAb and soluble anti-CD28 mAb for 1 hour. Subsequently, 4 ¸…M DM or DMSO was added and cells were incubated for 6 hours. Total RNA was isolated using Qiagen RNeasy mini kits.

Background corr dist: KL-Divergence = 0.0595, L1-Distance = 0.0472, L2-Distance = 0.0033, Normal std = 0.5727

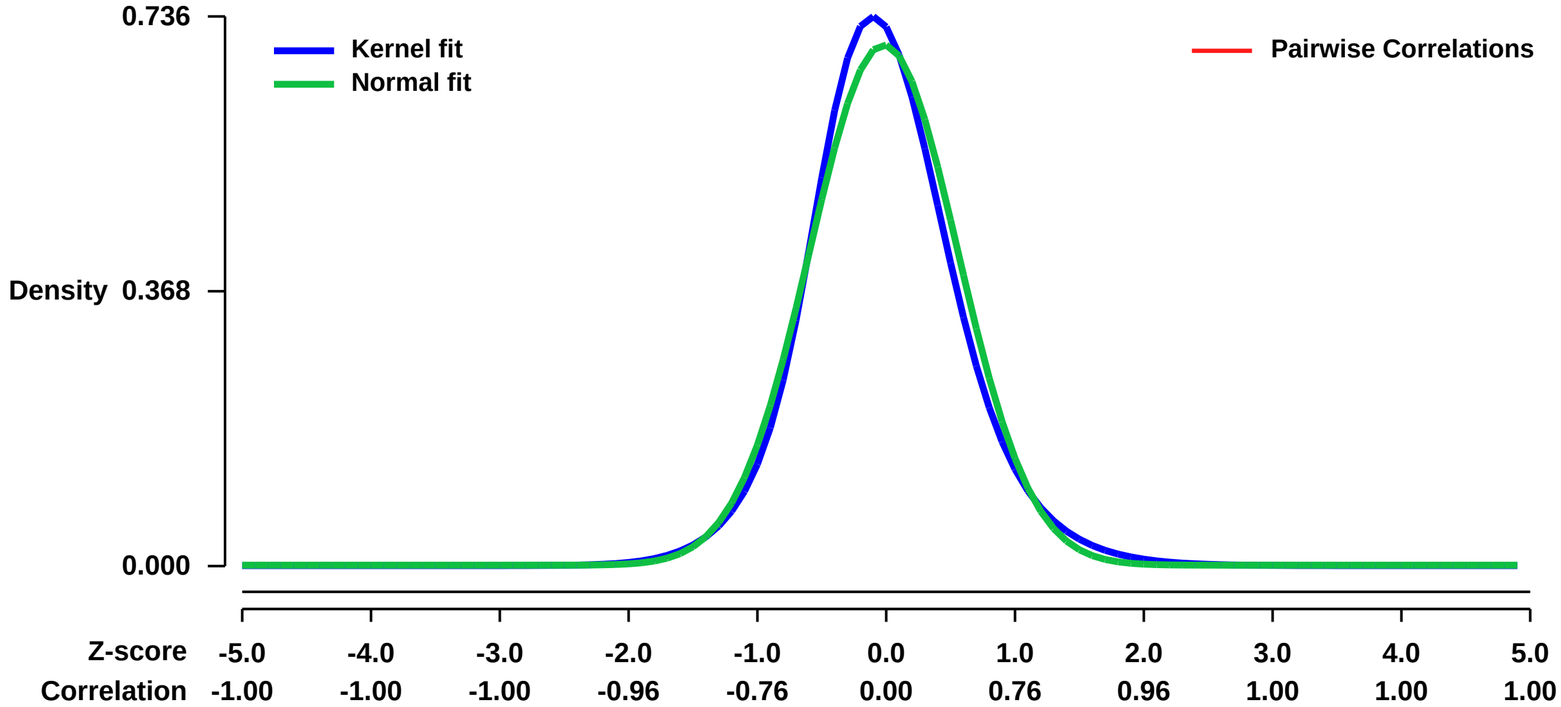

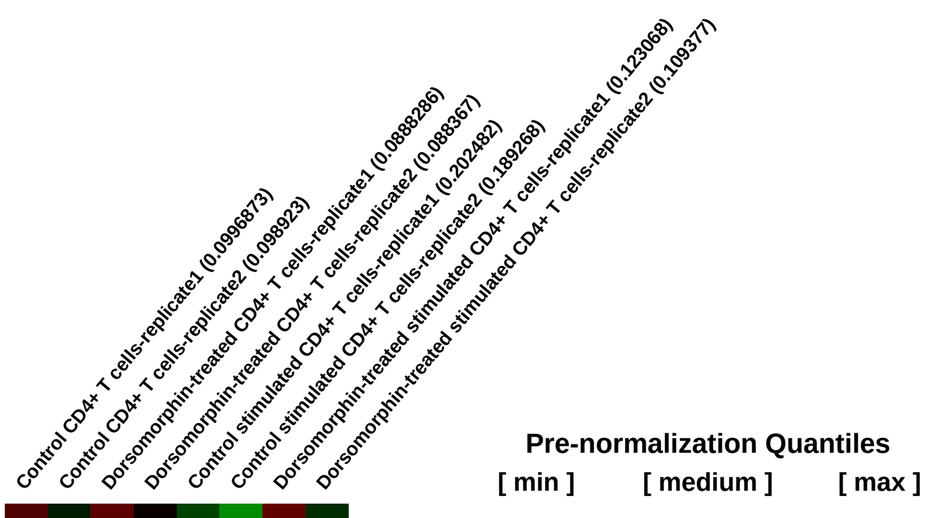

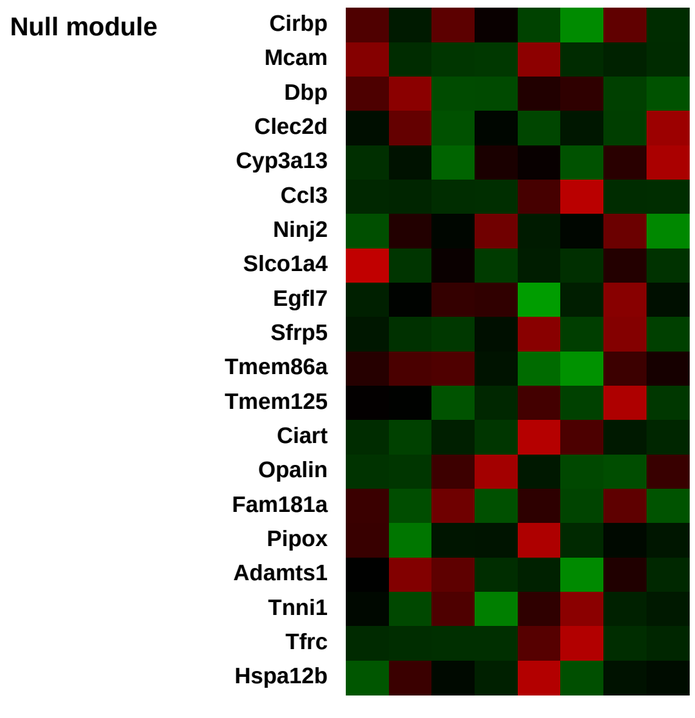

GEO Series "GSE27395" Expression Profiles

Num of samples in this series: 12

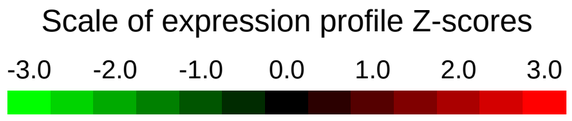

GEO Link:	**http://www.ncbi.nlm.nih.gov/geo/query/acc.cgi?acc=GSE27395**
Status:	**Public on Sep 15 2011**
Title:	**Analysis of Gsk-3-Deficient Embryonic Stem Cells Reveals Large-Scale Alterations in Gene Expression**
Organism:	**Mus musculus**
Experiment type:	**Expression profiling by array**
Platform:	**GPL1261**
Pubmed ID:	
Summary & Design:	**Summary:** **The two vertebrate Gsk-3 isoforms, Gsk-3a and Gsk-3b, are encoded by distinct genetic loci and exhibit mostly redundant function in murine embryonic stem cells (ESCs). Here we report that deletion of both Gsk-3a and Gsk-3b in mouse ESCs results in significant changes in gene expression. In contrast, deletion of either Gsk-3a or Gsk-3b individually had little effect on gene expression. These data support the notion that Gsk-3 isoforms are functionally redundant in embryonic stem cells. In addition, we did not find the expected upregulation of known Wnt target genes. Our data suggests that Gsk-3-meidated regulation of gene expression in embryonic stem cells is complex, and likely involves affects on numerous signaling pathways.** **Overall design:** **The study was designed to examine the changes in gene expression between wild-type, Gsk-3a-/-, Gsk-3b-/-, and Gsk-3a-/-;Gsk-3b-/- mouse embryonic stem cells.**

Background corr dist: **KL-Divergence = 0.1042, L1-Distance = 0.0230, L2-Distance = 0.0009, Normal std = 0.4460**

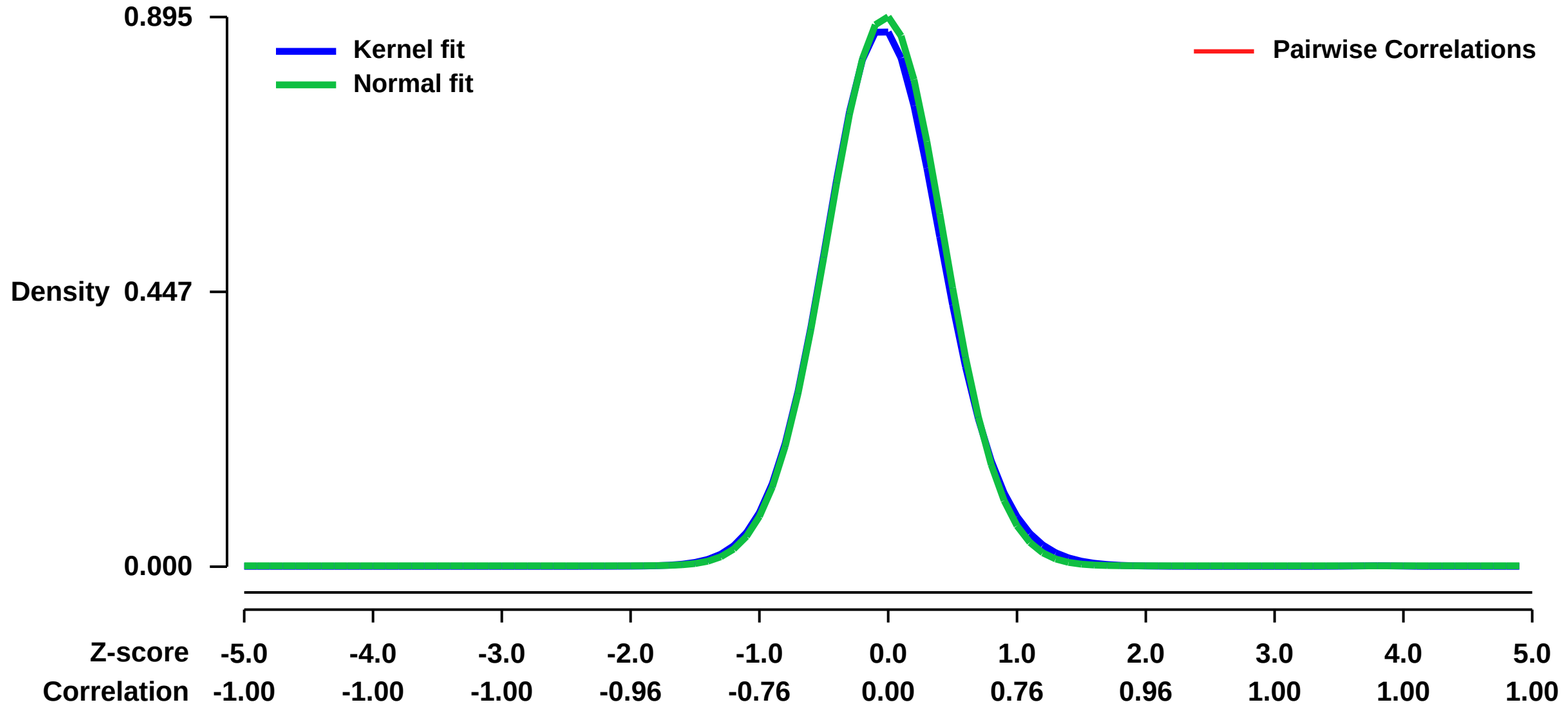

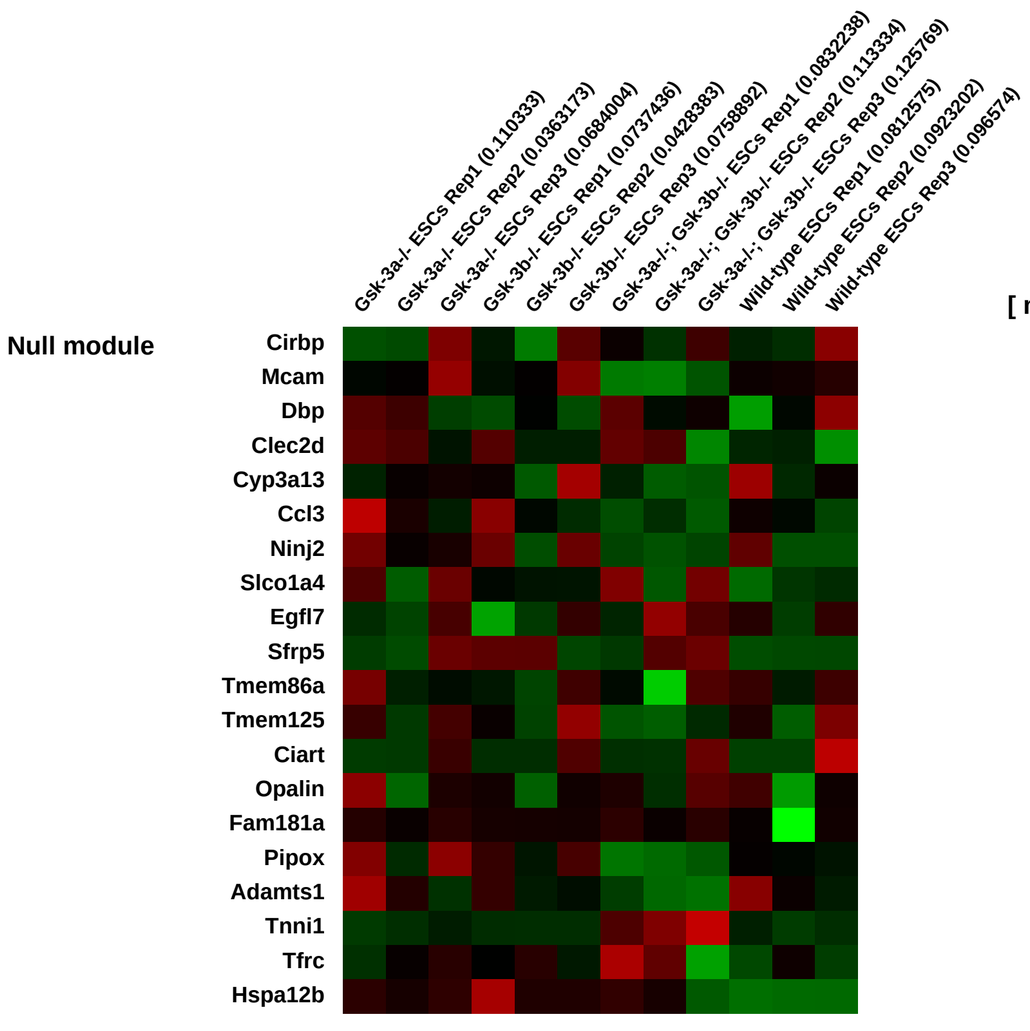

GEO Series "GSE27402" Expression Profiles

Num of samples in this series: 8

Scale of expression profile Z-scores

-3.0 -2.0 -1.0 0.0 1.0 2.0 3.0

GEO Link:	http://www.ncbi.nlm.nih.gov/geo/query/acc.cgi?acc=GSE27402
Status:	Public on Nov 22 2011
Title:	Expression data from WT, HEB-KO and E2A-KO LY6D- CLP cells
Organism:	Mus musculus
Experiment type:	Expression profiling by array
Platform:	GPL1261
Pubmed ID:	21972416
Summary & Design:	**Summary:** The E-protein transcription factors E2A and HEB play important roles at several stages of hematopoiesis. However, the exact mechanism for theire action and the main targets in the LY6D negative common lymphoid progentior (CLP) compartment remains unknown. By adressing this question, we will gain important infromation regarding the early events leading to B-cell specification. **Overall design:** FACS sorted LY6D negative common lymphoid progenitors from WT, HEB-KO and E2A-KO mice were subjected to RNA extraction and hybridization on Affymetrix microarrays. At least two independent sorts were performed per genotype. During each sort, cells were pooled from several bone marrows.

Background corr dist: KL-Divergence = 0.0437, L1-Distance = 0.0309, L2-Distance = 0.0016, Normal std = 0.5853

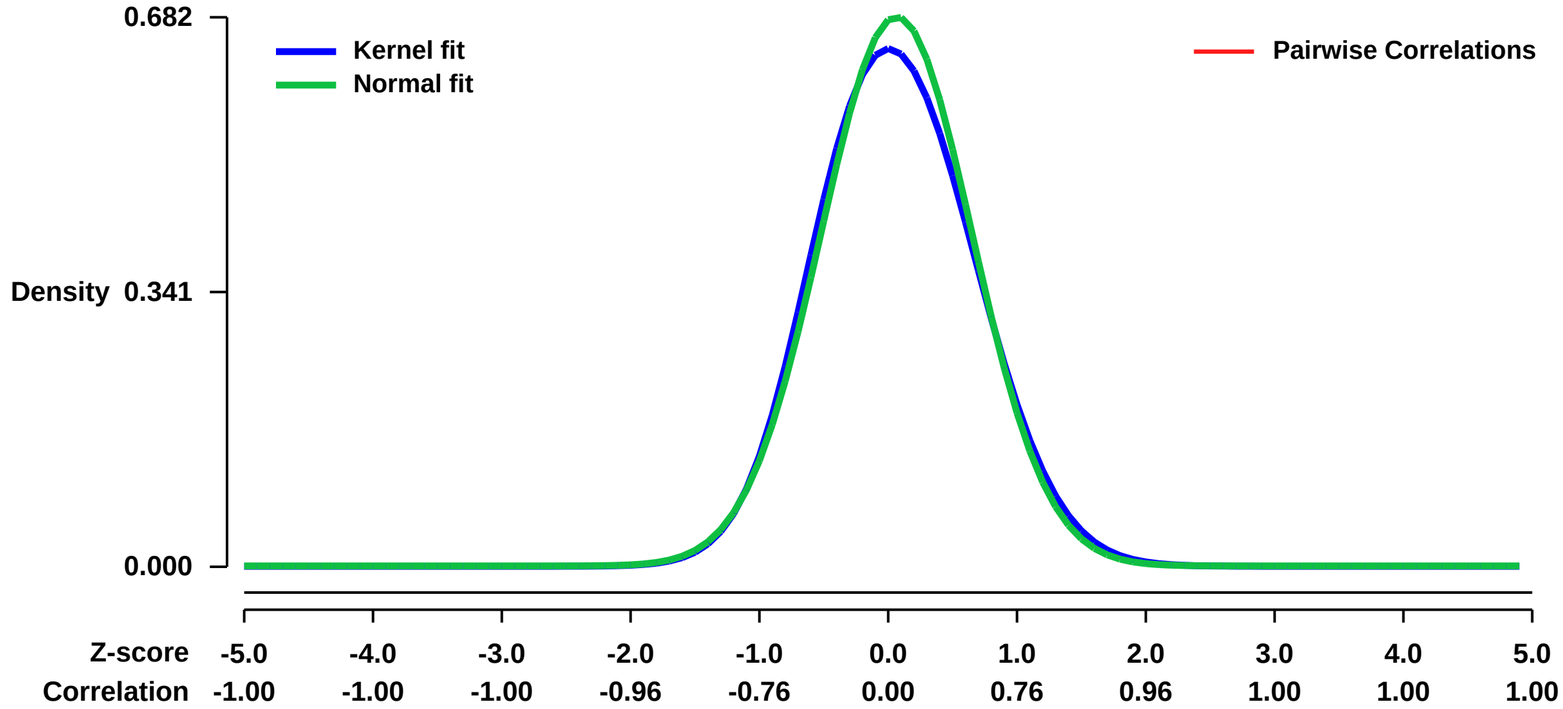

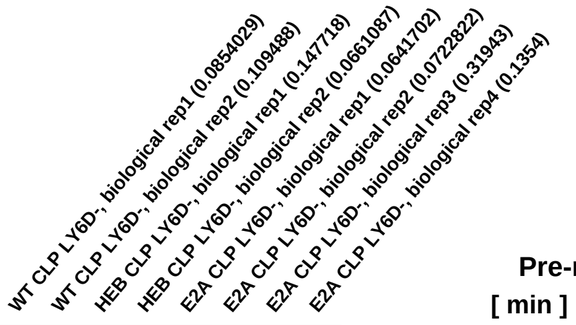

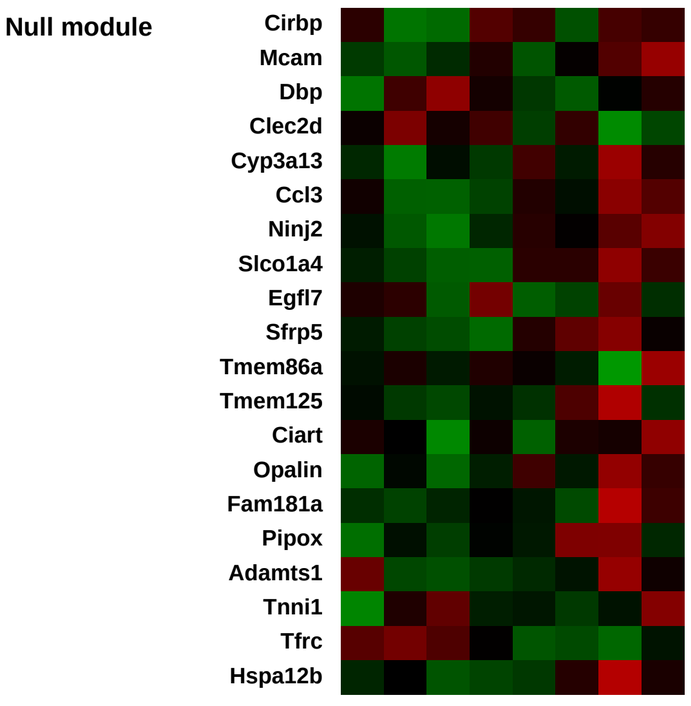

GEO Series "GSE27429" Expression Profiles

Num of samples in this series: 8

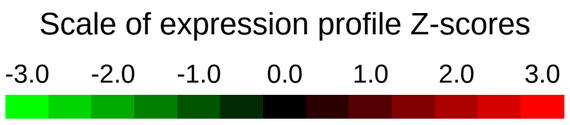

GEO Link:	http://www.ncbi.nlm.nih.gov/geo/query/acc.cgi?acc=GSE27429
Status:	Public on Feb 22 2011
Title:	Expression data at 24 hours after the blocking of Shh signaling in tooth germs at embryonic day 14
Organism:	Mus musculus
Experiment type:	Expression profiling by array
Platform:	GPL1261
Pubmed ID:	21447550
Summary & Design:	**Summary:** The genetic mechanism governing the spatial patterning of teeth still remains to be elucidated. Sonic hedgehog (Shh) is one of key signaling molecules involved in the spatial patterning of teeth. By utilizing maternal transfer of 5E1 (an IgG1 monoclonal antibody against Shh protein) through the placenta to block Shh signaling, we investigated the changes in tooth patterning and in gene expression. We used microarrays to detect specific genes related with Shh signaling in tooth germs and identified some specific genes up- or down-regulated after blocking of Shh signaling activity. **Overall design:** Gene-chip expression analysis was performed with RNA from mandibular tooth germs from embryos of pregnant mice at one´ day after injection of 5E1 (an IgG1 monoclonal antibody against Shh protein; number of replicates =2), 40-1a (an IgG1 monoclonal antibody against ¸†-galactosidase; number of replicates=2), cyclopamine (a specific Smo antagonist; number of replicates=2) or PBS (Phosphate buffered saline; number of replicates=2), using a Affymetrix mouse gene microarray.

Background corr dist: KL-Divergence = 0.0607, L1-Distance = 0.0181, L2-Distance = 0.0004, Normal std = 0.5258

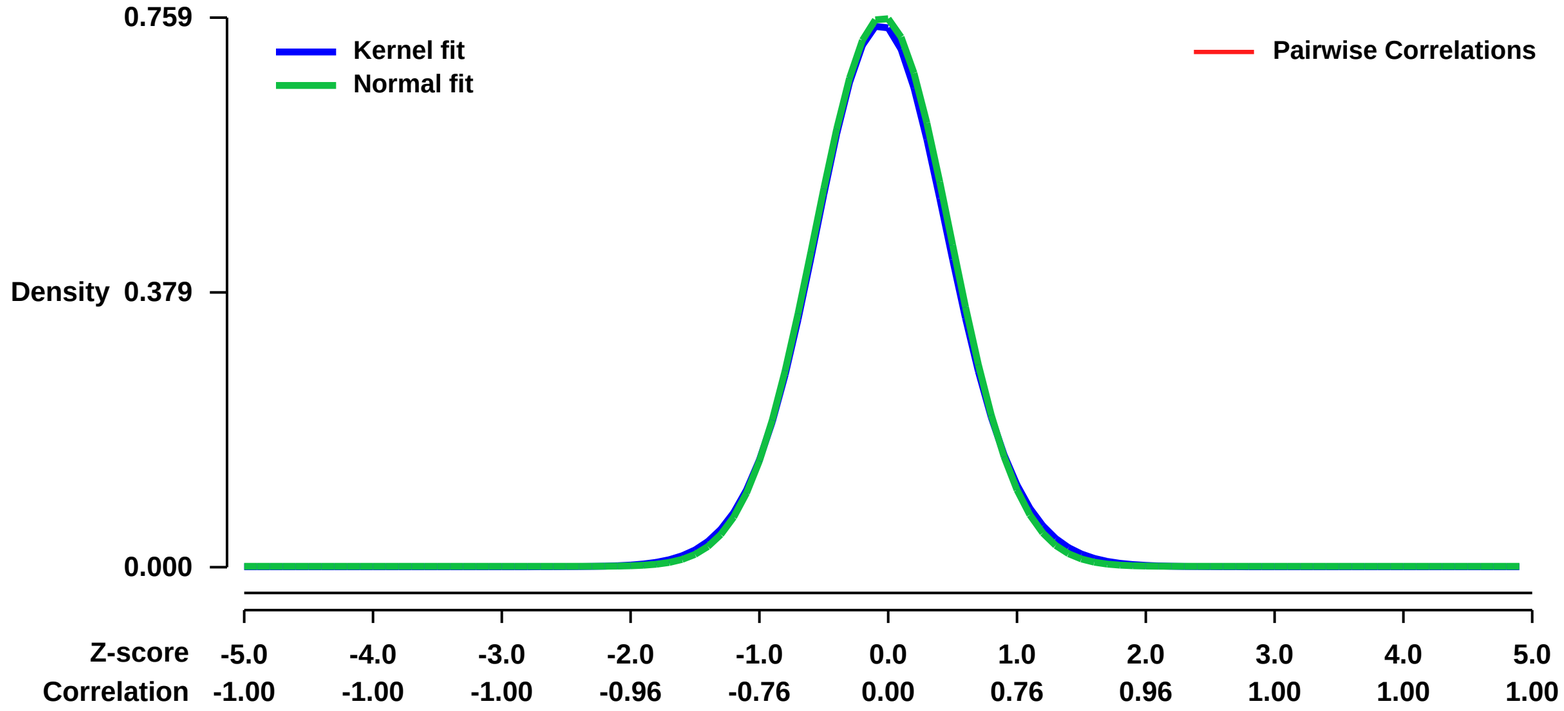

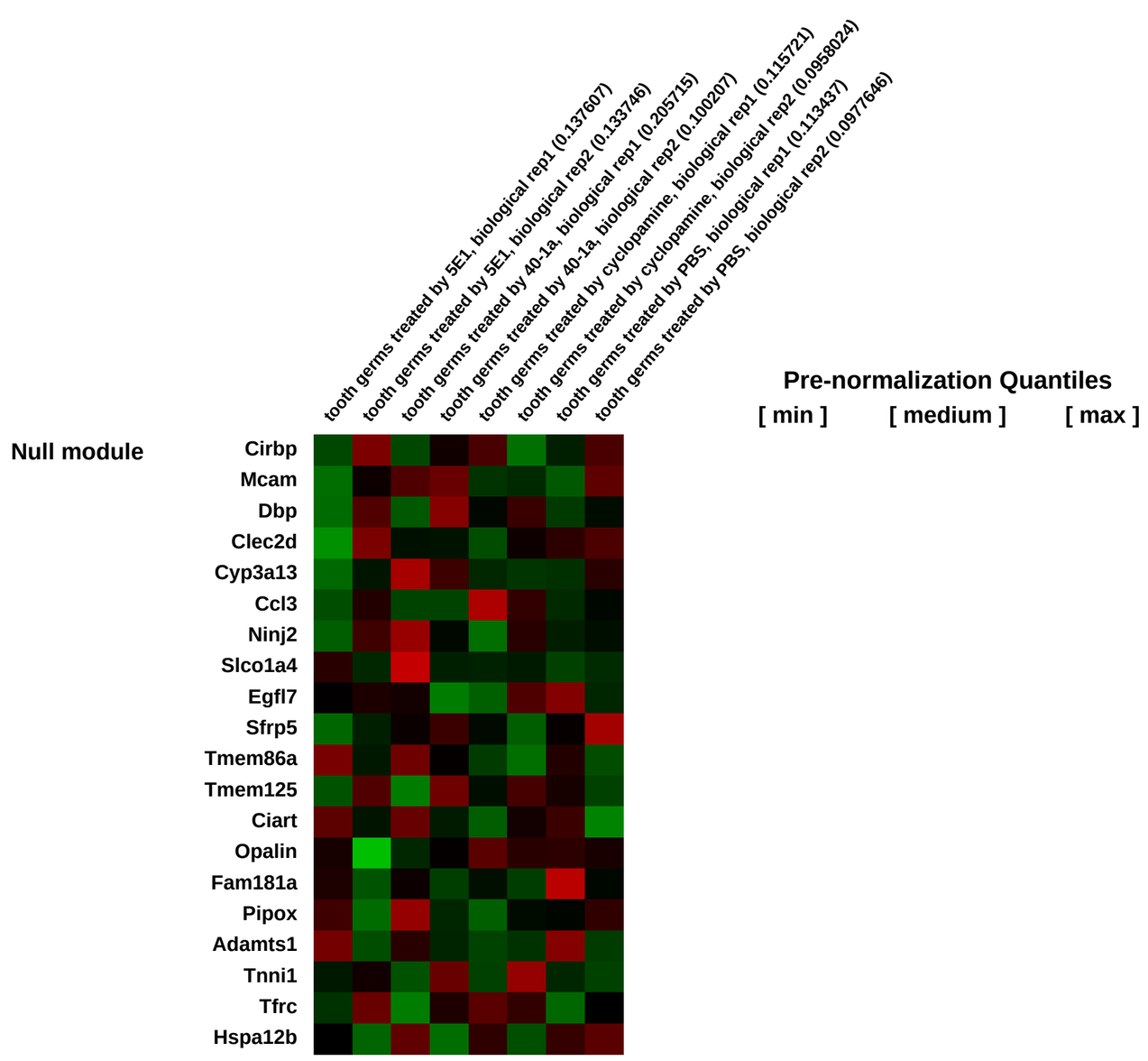

GEO Series "GSE27451" Expression Profiles

Num of samples in this series: 6

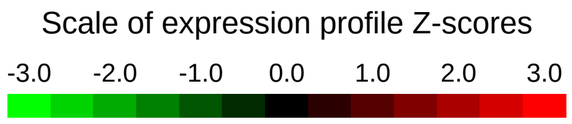

GEO Link:	http://www.ncbi.nlm.nih.gov/geo/query/acc.cgi?acc=GSE27451
Status:	Public on Feb 25 2011
Title:	Functions of HDAC1 and HDAC2 in Schwann cells during postnatal
Organism:	Mus musculus
Experiment type:	Expression profiling by array
Platform:	GPL1261
Pubmed ID:	21423190
Summary & Design:	**Summary:** The aim of our study is to determine the functions of histone deacetylases (HDACs) 1 and 2 in Schwann cells during postnatal development of the peripheral nervous system (PNS). Schwann cells are the myelinating glial cells of the PNS. At birth, mouse sciatic nerves mature in 2 subsequent phases: 1/ big caliber axons get sorted into a 1 to 1 relationship with Schwann cells, 2/ Schwann cells build a myelin sheath around sorted axons. In mice where both HDAC1 & HDAC2 have been specifically knocked out in Schwann cells, both phases are impaired. HDACs are chromatin remodeling enzymes, they can thus alter gene expression directly. We want to identify which genes controlled by HDAC1 and HDAC2 in Schwann cells are necessary for the maturation of sciatic nerves. Because HDAC1 and HDAC2 can compensate for each other loss to some extend, we will first analyze changes of gene expression in HDAC1/HDAC2 double KO animals. We expect to gain critical insights into the molecular mechanisms controlling Schwann cell differentiation and myelination. This knowledge is of key importance for the success of regenerative medicine in peripheral neuropathies, nerve tumors, and transplantation paradigms in non-regenerative CNS lesions and in large PNS injuries. **Overall design:** 3 double knockout mutants for HDAC1 and HDAC2 and 3 control littermates were analyzed. Tissues analyzed: sciatic nerves of 2 day-old mouse pups

Background corr dist: KL-Divergence = 0.0264, L1-Distance = 0.0155, L2-Distance = 0.0002, Normal std = 0.6935

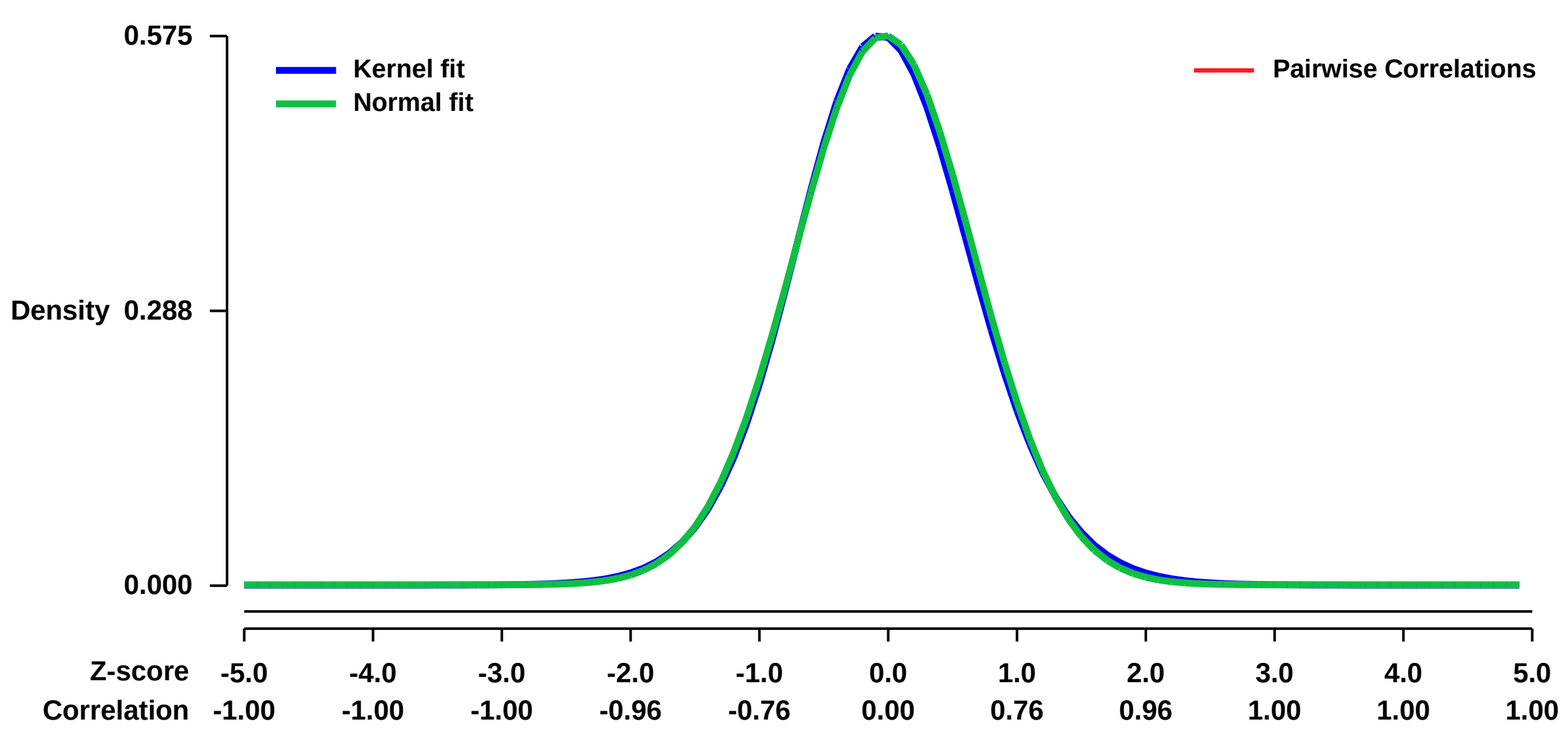

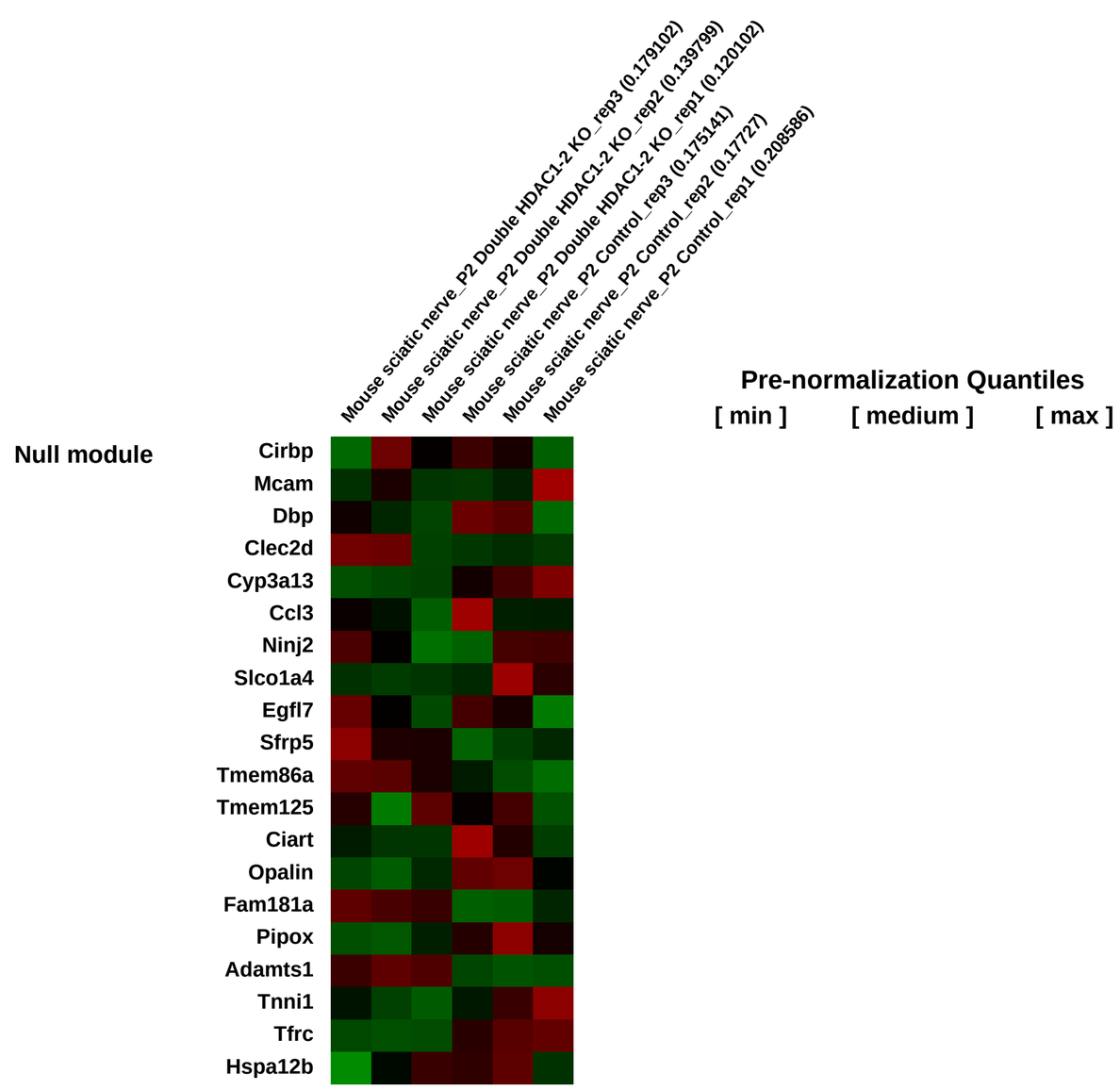

GEO Series "GSE27455" Expression Profiles

Num of samples in this series: 12

Scale of expression profile Z-scores

-3.0 -2.0 -1.0 0.0 1.0 2.0 3.0

GEO Link:	http://www.ncbi.nlm.nih.gov/geo/query/acc.cgi?acc=GSE27455
Status:	Public on Feb 24 2011
Title:	Wnt and Tcf3-mediated regulation of gene expression in mouse embryonic stem cells
Organism:	Mus musculus
Experiment type:	Expression profiling by array
Platform:	GPL1261
Pubmed ID:	21685894
Summary & Design:	**Summary:** The observation that Tcf3 (MGI name: Tcf7l1) bound the same genes as core stem cell transcription factors, Oct4 (MGI name:Pou5f1), Sox2 and Nanog, revealed a potentially important aspect of the poorly understood mechanism whereby Wnts stimulate self renewal of pluripotent mouse embryonic stem (ES) cells. Although the conventional view of Tcf proteins as the ¸†-catenin-binding effectors of Wnt signaling suggested Tcf3 should activate target genes in response to Wnts, here we show that Wnt3a and Tcf3 effectively antagonize each otherâ s effects on gene expression. Genetic ablation of Tcf3 caused similar effects as treating cells with recombinant Wnt3a. Moreover, Tcf3 was not necessary for Wnt3a-stimulation of gene expression as the majority of Wnt3a-stimulated genes exhibited a greater increase in Tcf3-/- ES cells than in Tcf3+/+ ES cells. These expression data, together with genetic experiments, show that Wnt3a stimulates ES cell self renewal by inhibiting Tcf3. **Overall design:** Tcf3+/+ and Tcf3-/- mouse embryonic stem cells were cultured in self renewal conditions containing recombinant Wnt3a for RNA extraction and hybridization on Affymetrix microarrays.

Background corr dist: KL-Divergence = 0.0555, L1-Distance = 0.0185, L2-Distance = 0.0004, Normal std = 0.5419

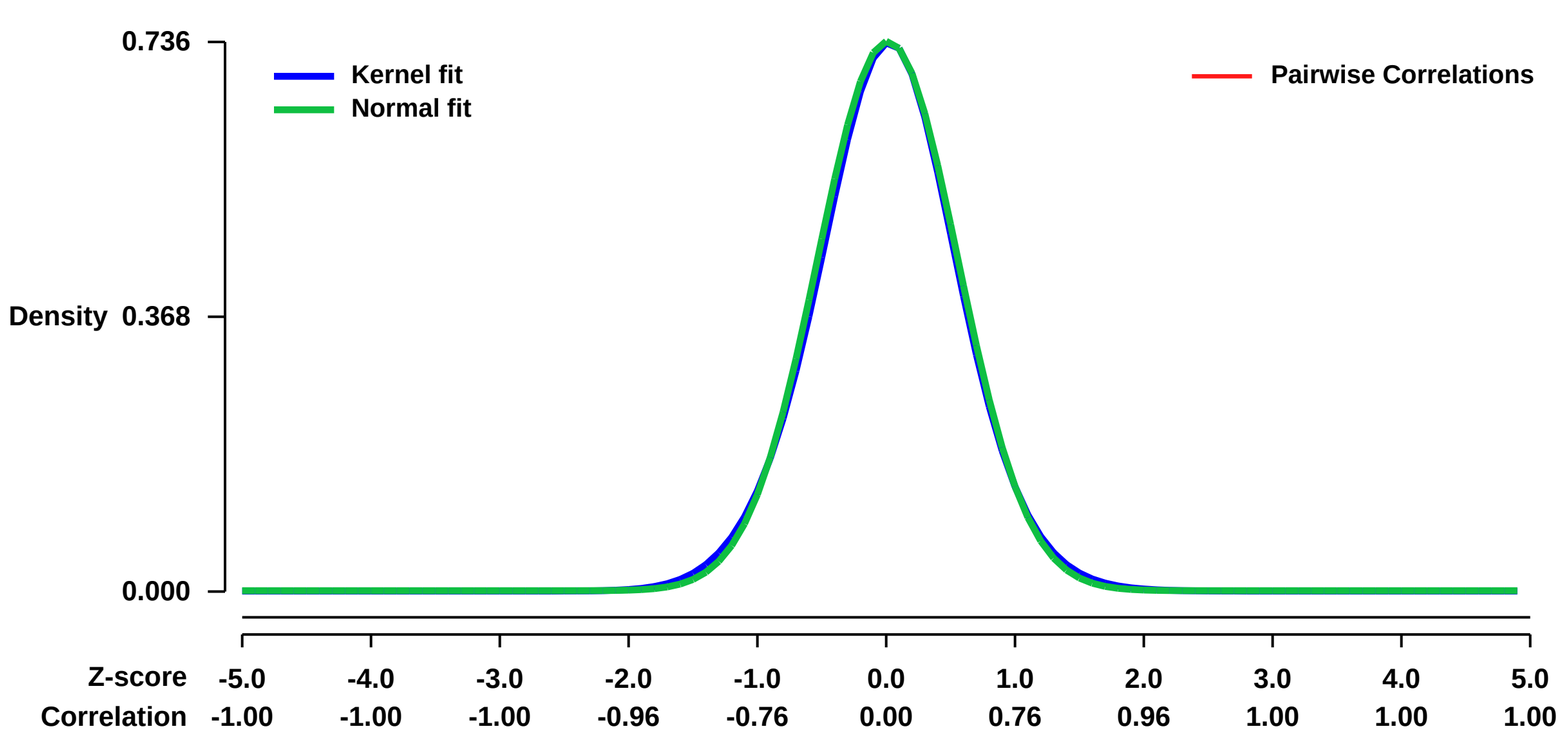

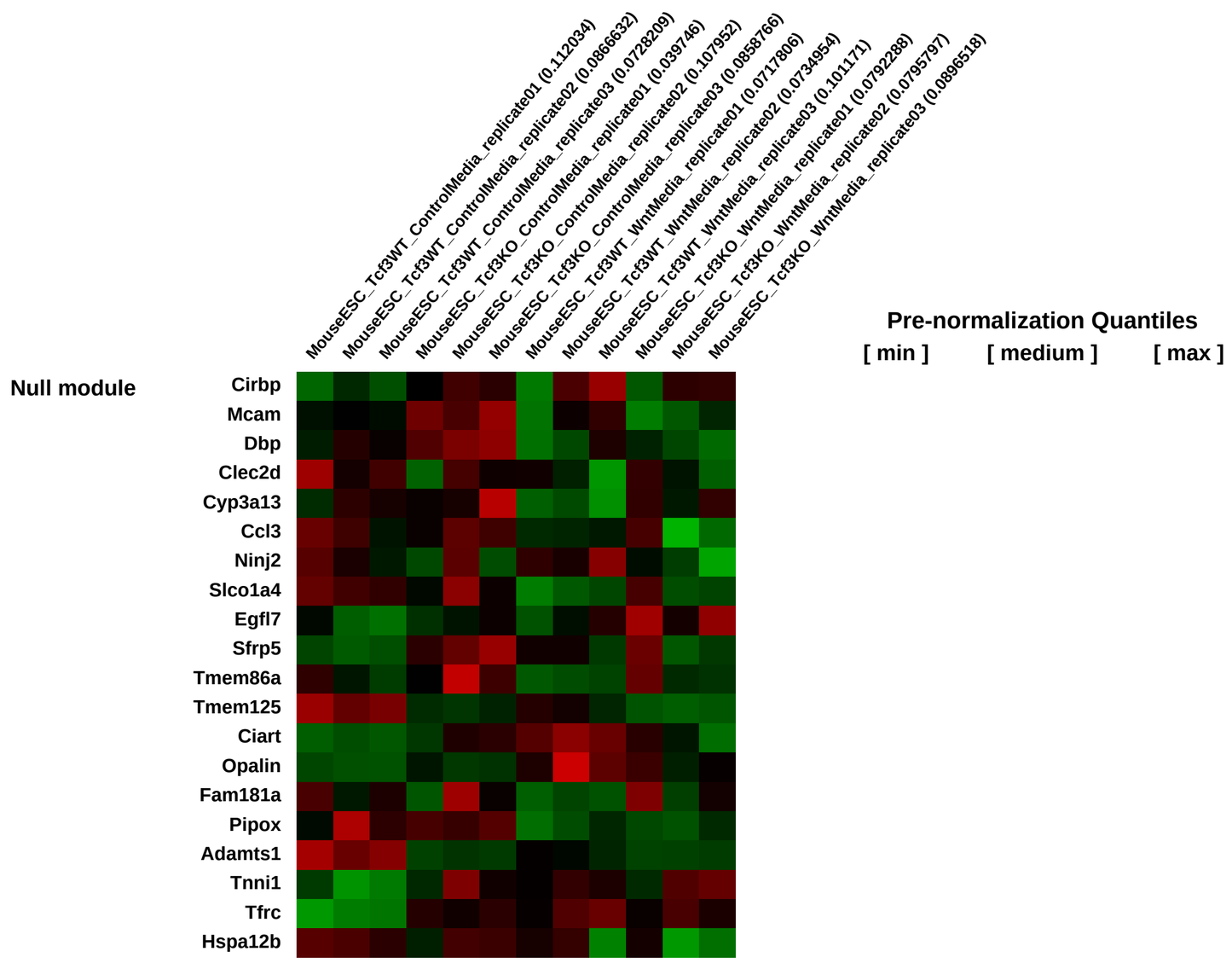

GEO Series "GSE27516" Expression Profiles

Num of samples in this series: 17

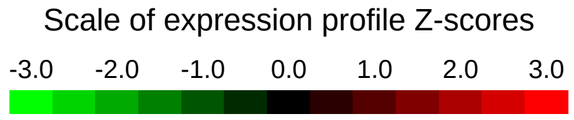

GEO Link:	**http://www.ncbi.nlm.nih.gov/geo/query/acc.cgi?acc=GSE27516**
Status:	**Public on Mar 17 2011**
Title:	**Preclinical Models for Neuroblastoma: Establishing a Baseline for Treatment**
Organism:	**Mus musculus**
Experiment type:	**Expression profiling by array**
Platform:	**GPL1261**
Pubmed ID:	**21559450**
Summary & Design:	**Summary:** **Here we characterize and optimize both systems to increase their utility for preclinical studies. We show that TH-MYCN mice develop tumors in the paraspinal ganglia, but not in the adrenal, with cellular and gene expression patterns similar to human NB. In addition, we present a new ultrasound guided, non-invasive orthotopic xenograft method. This injection technique is rapid, provides accurate targeting of the injected cells and leads to efficient engraftment. We also demonstrate that tumors can be detected, monitored and quantified prior to visualization using ultrasound, MRI and bioluminescence. Finally we develop and test a â standard of careâ chemotherapy regimen. This protocol, which is based on current treatments for neuroblastoma, provides a baseline for comparison of new therapeutic agents.** **Overall design:** **A total of 17 samples are provided reprsenting TH-MYCN tumors derived from mice**

Background corr dist: **KL-Divergence = 0.2494, L1-Distance = 0.0536, L2-Distance = 0.0071, Normal std = 0.3045**

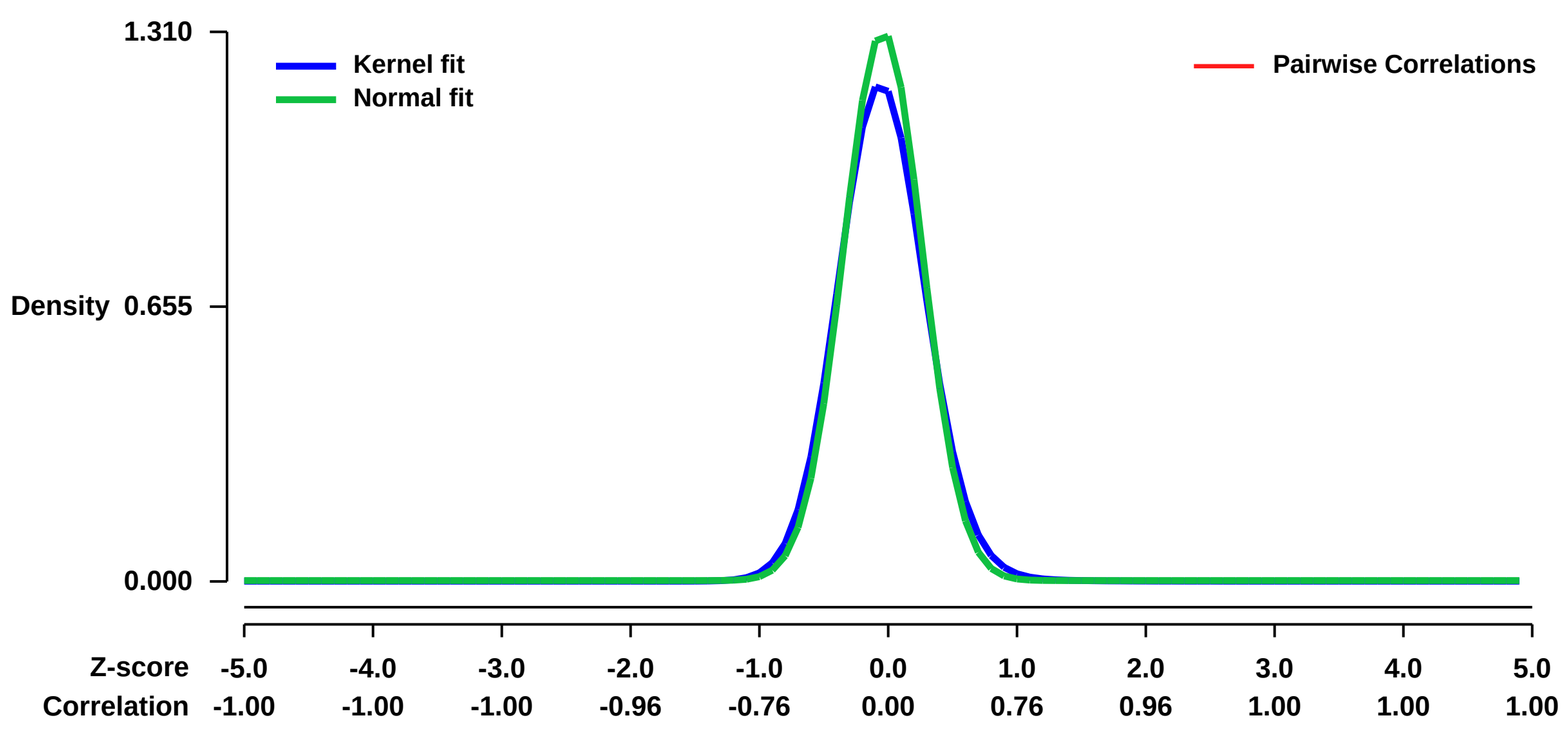

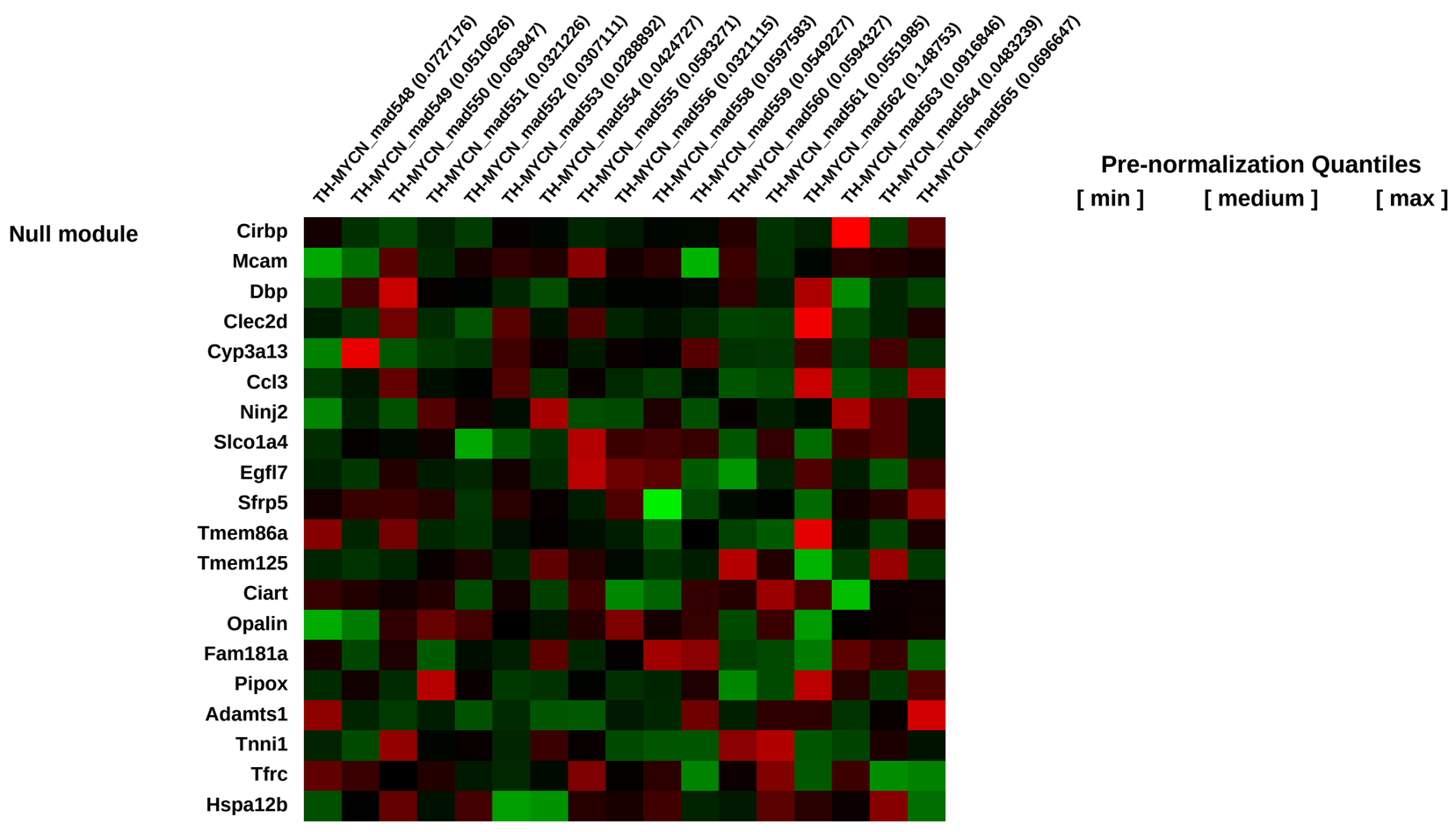

Pre-normalization Quantiles

[min] [medium] [max]

GEO Series "GSE27547" Expression Profiles

Num of samples in this series: 17

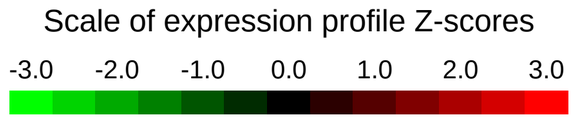

GEO Link:	http://www.ncbi.nlm.nih.gov/geo/query/acc.cgi?acc=GSE27547
Status:	Public on Feb 28 2011
Title:	Gene expression differences in mouse islets after isolation at different time points (0-48hr)
Organism:	Mus musculus
Experiment type:	Expression profiling by array
Platform:	GPL1261
Pubmed ID:	21471441
Summary & Design:	**Summary:** TGFbi (transforming growth factor-beta-induced) is a secreted protein and is capable of binding to both extracellular matrix (ECM) and cells. It thus acts as a bifunctional molecule enhancing ECM and cell interactions, a lack of which results in dysfunction of many cell types. In this study, we investigated the role of TGFbi in the function and survival of islets. Based on DNA microarray analysis followed by qPCR confirmation, the TGFbi gene showed drastic increases in expression in islets after culture. We demonstrated that recombinant TGFbi could preserve the integrity and enhance the function of cultured islets. Such a beneficial effect was mediated via signalling through FAK. Exogenous TGFbi was capable of sustaining high-level FAK phosphorylation in isolated islets, and FAK knockdown by siRNA in islets resulted in compromised islet function. TGFbi Tg islets showed better integrity and insulin release after in vitro culture. In vivo, b-cell proliferation was detectable in Tg but not wild type pancreata. At age above 12 months, Tg pancreata contained giant islets. Tg mice displayed better glucose tolerance than the controls. Tg islets were more potent in lowering blood glucose when transplanted into syngeneic mice with streptozotocin-induced diabetes, and these transplanted islets also underwent regeneration. Our results indicate that TGFbi is a vital trophic factor promoting islet survival, function and regeneration. At least some of its beneficial effect was mediated by signalling through FAK. **Overall design:** Batch 6: YF050524MOT06, YF050524MOT12, YF050524MOT18

Background corr dist: KL-Divergence = 0.1987, L1-Distance = 0.0462, L2-Distance = 0.0047, Normal std = 0.3324

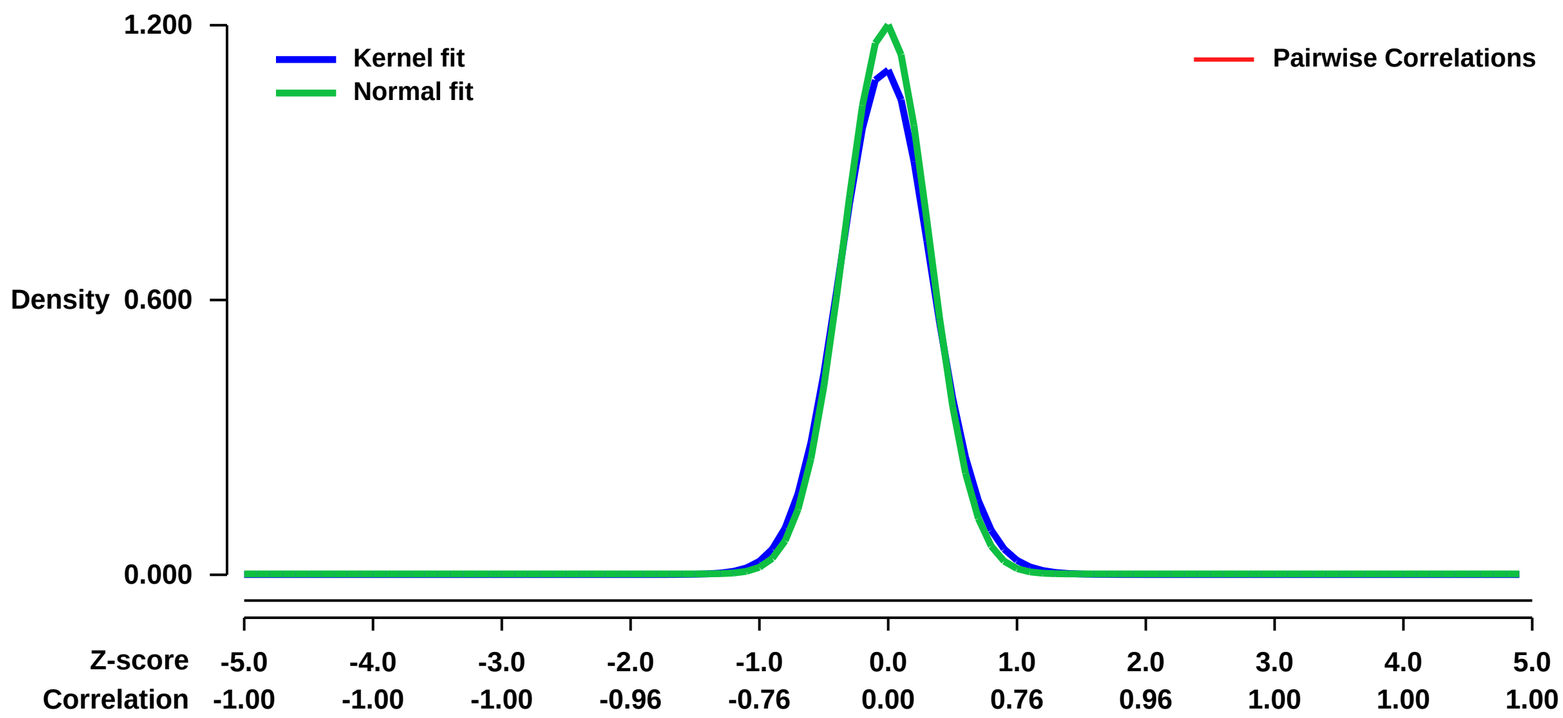

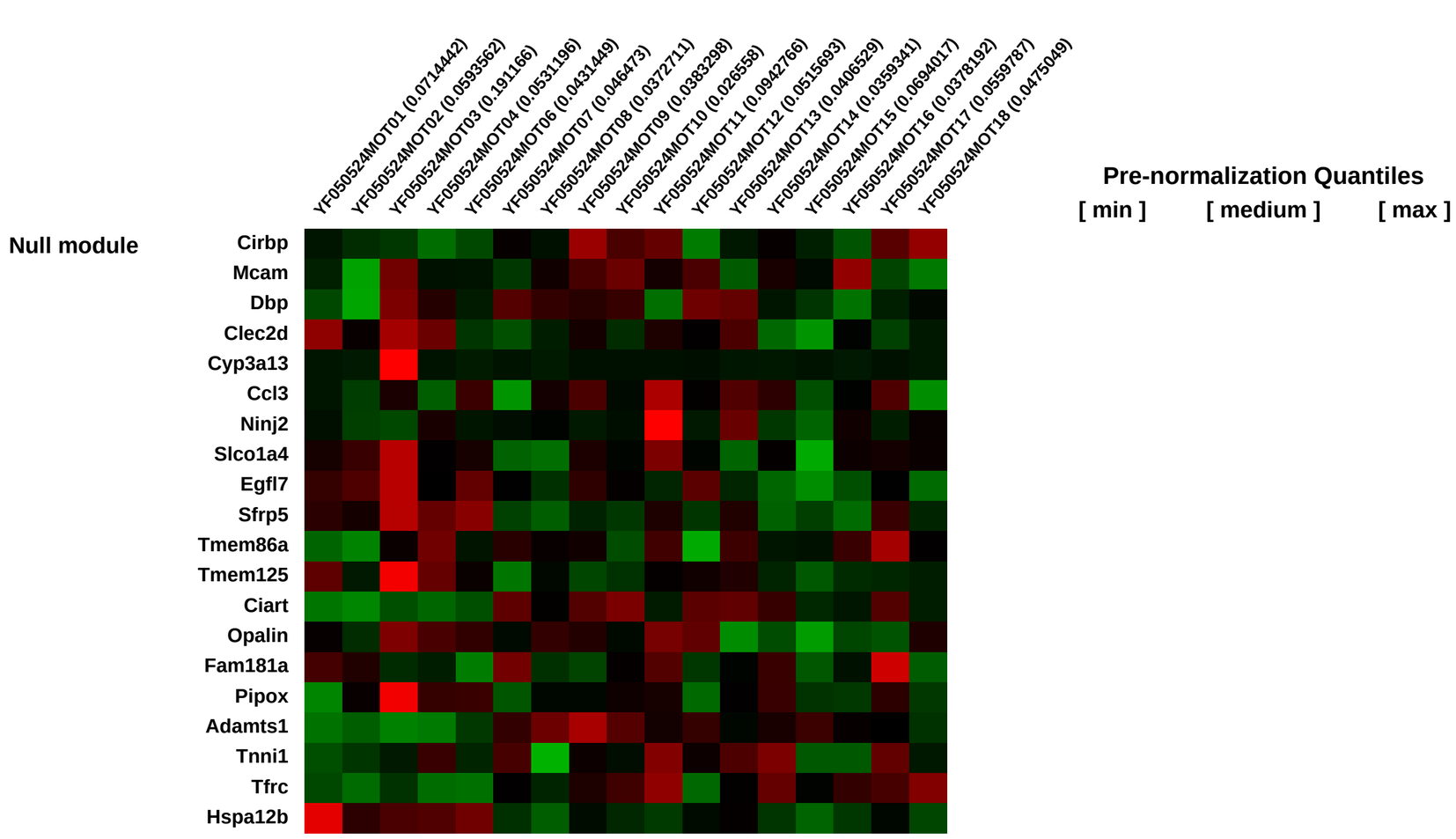

GEO Series "GSE27563" Expression Profiles

Num of samples in this series: 93

Scale of expression profile Z-scores

-3.0 -2.0 -1.0 0.0 1.0 2.0 3.0

GEO Link: http://www.ncbi.nlm.nih.gov/geo/query/acc.cgi?acc=GSE27563
Status: Public on Mar 01 2011
Title: Expression data from murine PBCs from mice with advanced mammary tumors and their tumor-free counterparts.
Organism: Mus musculus
Experiment type: Expression profiling by array
Platform: GPL1261
Pubmed ID: 21781289

Summary & Design:

Summary:
Female MMTV/c-MYC transgenic mice expressed the c-MYC proto-oncogene or a more stable point mutation variant (T58A) of the gene under the control of the hormone-responsive MMTV long terminal repeat (LTR) in an FVB/NJ background (Jackson Laboratories, Bar Harbor, ME). The hormones released during pregnancy and lactation have been shown to enhance expression of the oncogene. Thus, the mice were maintained in a continuous breeding program. Mice were monitored twice weekly for tumor development by palpation and tumors were measured twice weekly. Once the tumors reached 3cm3 the animals were sacrificed and tissue was obtained to confirm the tumors by histological analysis. As a control, female mice of the same age and background strain were maintained in the same facility and under the same breeding conditions as their transgenic counterparts.

Overall design:
Blood (50-250 ¡L, based on weight of the mouse) was collected from MMTV/c-MYC female mice and controls at regular intervals (approximately once per month) and again prior to euthanization (average age 431 days).

Background corr dist: KL-Divergence = 0.2402, L1-Distance = 0.0631, L2-Distance = 0.0109, Normal std = 0.3116

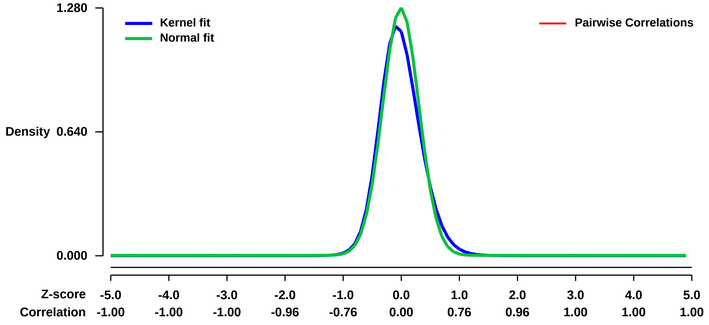

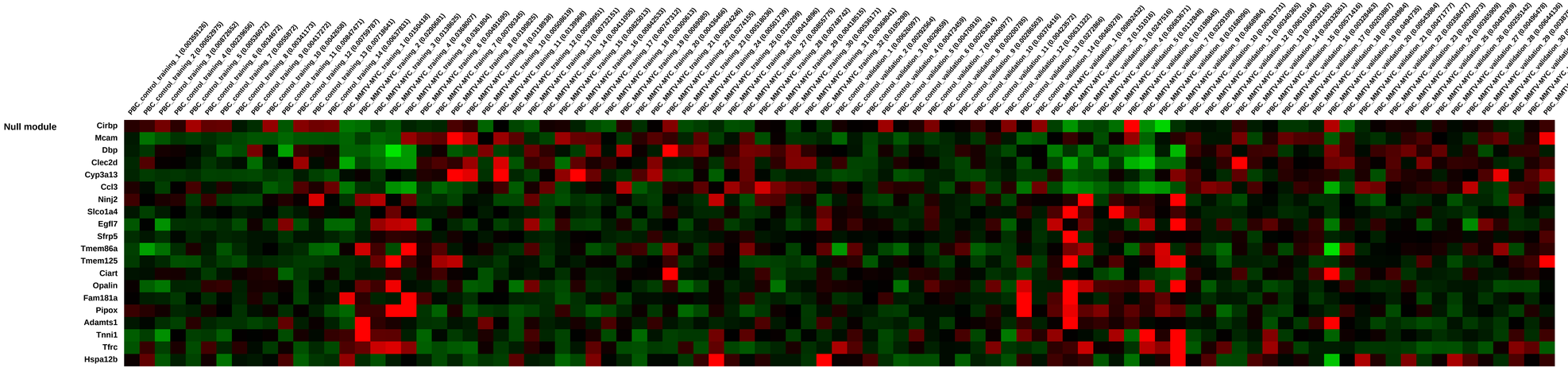

GEO Series "GSE27568" Expression Profiles

Num of samples in this series: 16

Scale of expression profile Z-scores

-3.0 -2.0 -1.0 0.0 1.0 2.0 3.0

GEO Link:	http://www.ncbi.nlm.nih.gov/geo/query/acc.cgi?acc=GSE27568
Status:	Public on Feb 28 2011
Title:	Ubb Knockout Mouse Testis
Organism:	Mus musculus
Experiment type:	Expression profiling by array
Platform:	GPL1261
Pubmed ID:	21542049
Summary & Design:	**Summary:** Analysis of Ubb knockout mouse testes at 7, 4, 21, and 28 dpp. Ubiquitin (Ub) is an essential protein found in all eukaryotic cells and plays important roles in a variety of cellular functions including germ cell development. Targeted disruption of the polyubiquitin gene Ubb results in male and female infertility in mice with germ cells arrested at meiotic prophase I. **Overall design:** Whole testes from wild-type (WT) and Ubbâ /â (KO) mice were harvested at 7, 14, 21, and 28 days postpartum. Total RNA was extracted and hybridized to Affymetrix Mouse Genome 430 2.0 arrays.

Background corr dist: KL-Divergence = 0.0537, L1-Distance = 0.0652, L2-Distance = 0.0066, Normal std = 0.6280

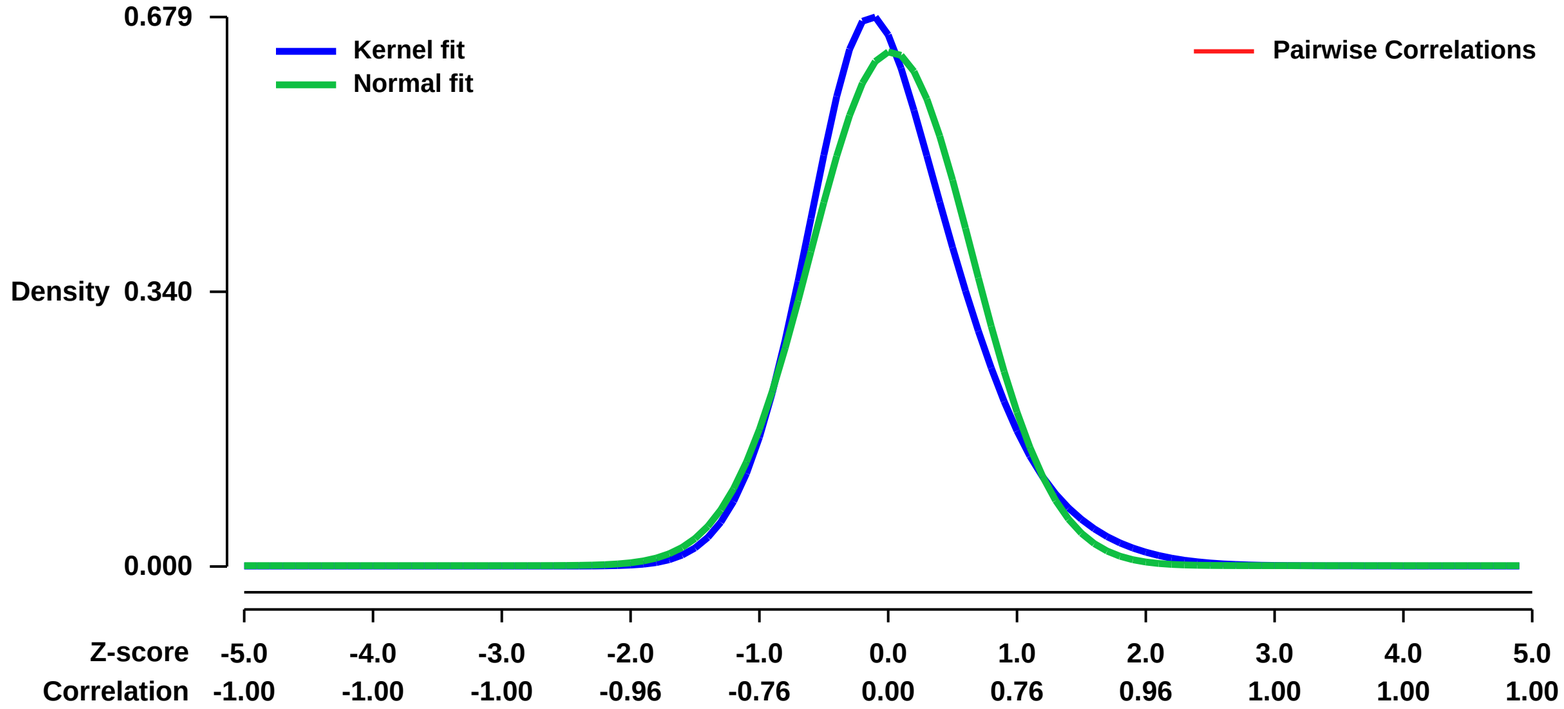

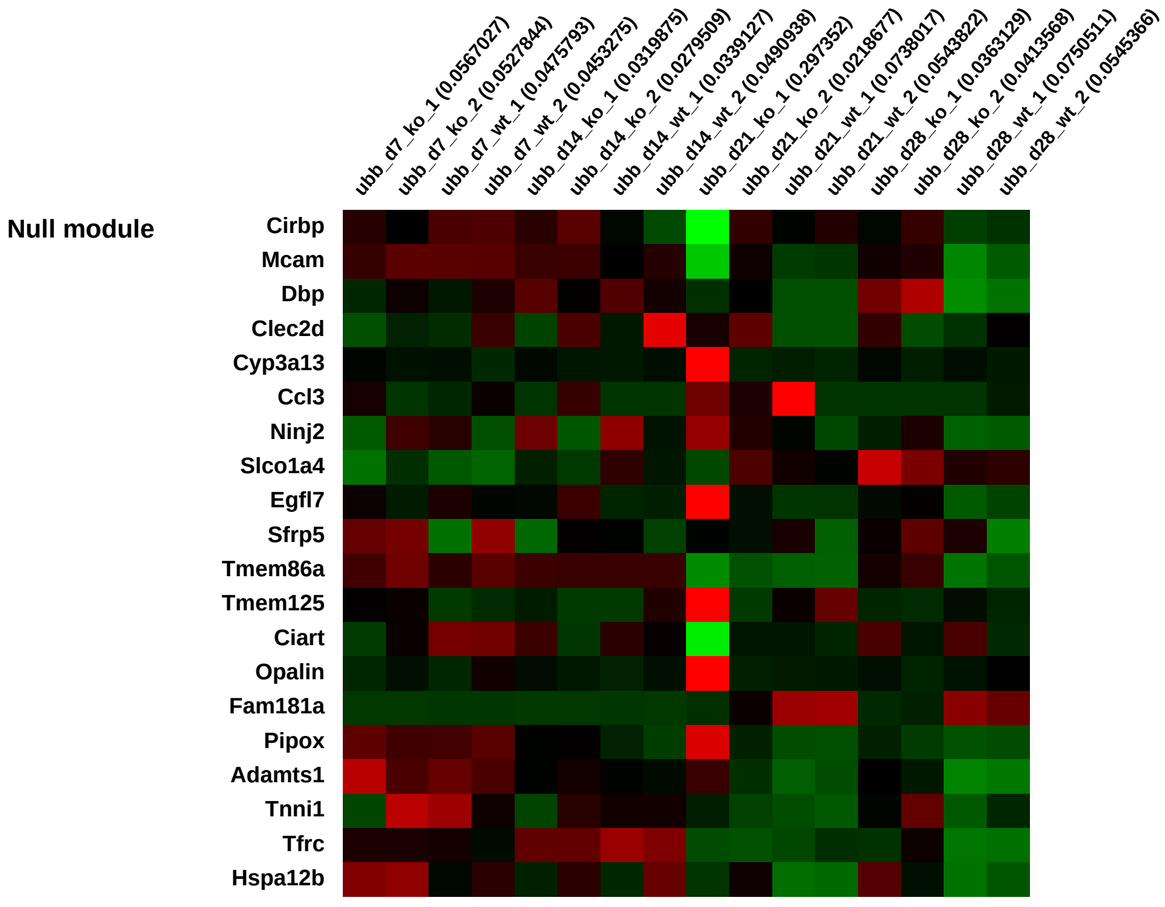

GEO Series "GSE27605" Expression Profiles

Num of samples in this series: 8

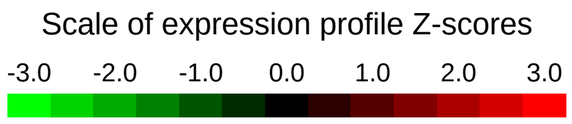

GEO Link:	http://www.ncbi.nlm.nih.gov/geo/query/acc.cgi?acc=GSE27605
Status:	Public on Mar 14 2011
Title:	The intestinal stem cell signature identifies colorectal cancer stem cells and predicts disease relapse
Organism:	Mus musculus
Experiment type:	Expression profiling by array
Platform:	GPL1261
Pubmed ID:	21419747
Summary & Design:	**Summary:** **Using EphB2 or the ISC marker Lgr5, we have FACS-purified and profiled intestinal stem cells (ISCs), crypt proliferative progenitors and late transient amplifying cells to define a gene expression program specific for normal ISCs.** **A frequent complication in colorectal cancer (CRC) is regeneration of the tumor after therapy. The intestinal stem cell signature predicts disease relapse in CRC and identifies a stem cell-like population that displays robust tumor- initiating capacity in immunodeficient mice as well as long-term self-renewal potential.** **Overall design:** **We FACS purified mouse intestinal crypt cells according to their EphB2 or Lgr5 contents. We used Affymetrix chips to hybridize 2 samples from EphB2 high, 2 samples from EphB2 medium and 2 samples from EphB2 low cells (one sample from each group in a first hybridization on February 2009 plus an additional sample from each group on March 2009). Additionally, we hybridized one sample from Lgr5-EGFP high and one sample from Lgr5-EGFP low cells, obtained from Lgr5-EGFP knock-in mice (Barker et al., 2007).**

Background corr dist: KL-Divergence = 0.0298, L1-Distance = 0.0338, L2-Distance = 0.0014, Normal std = 0.6870

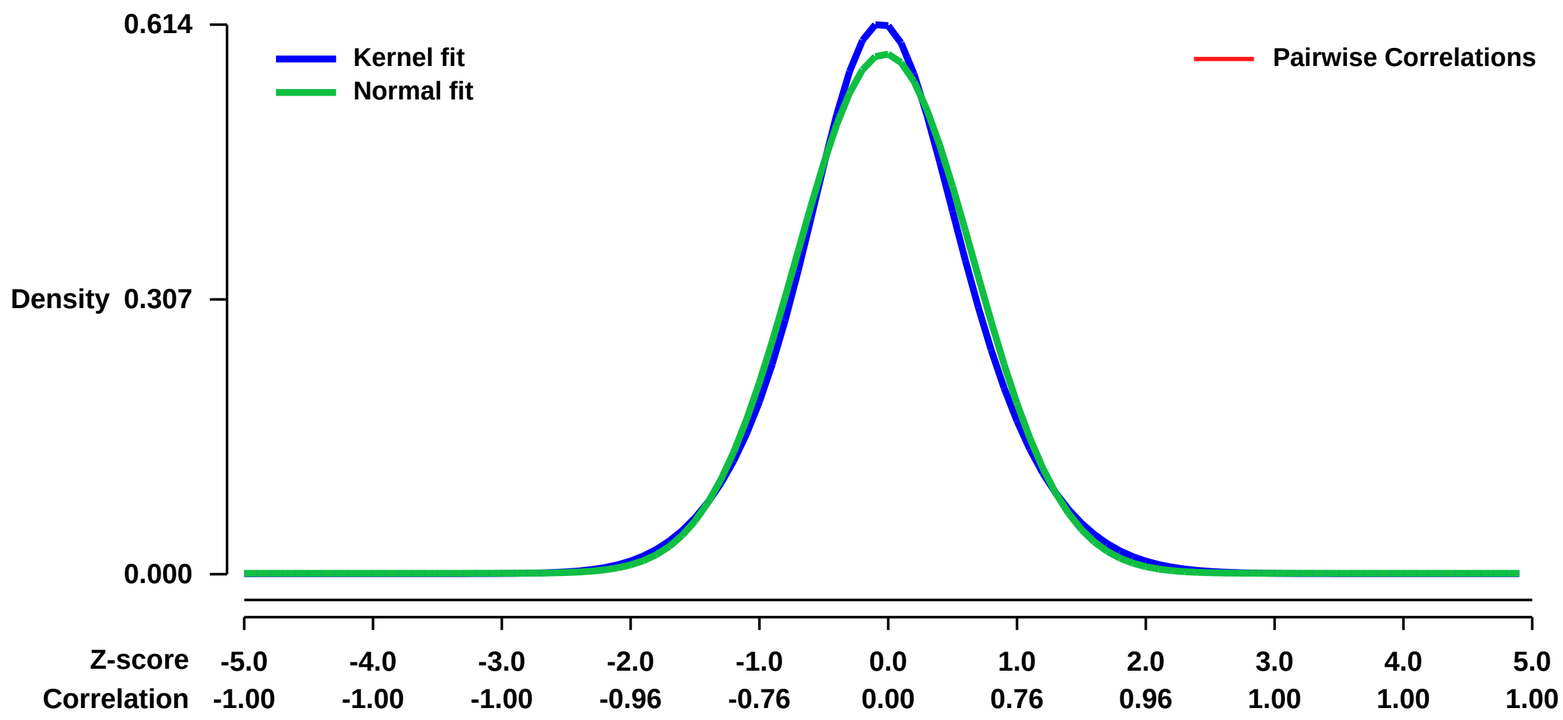

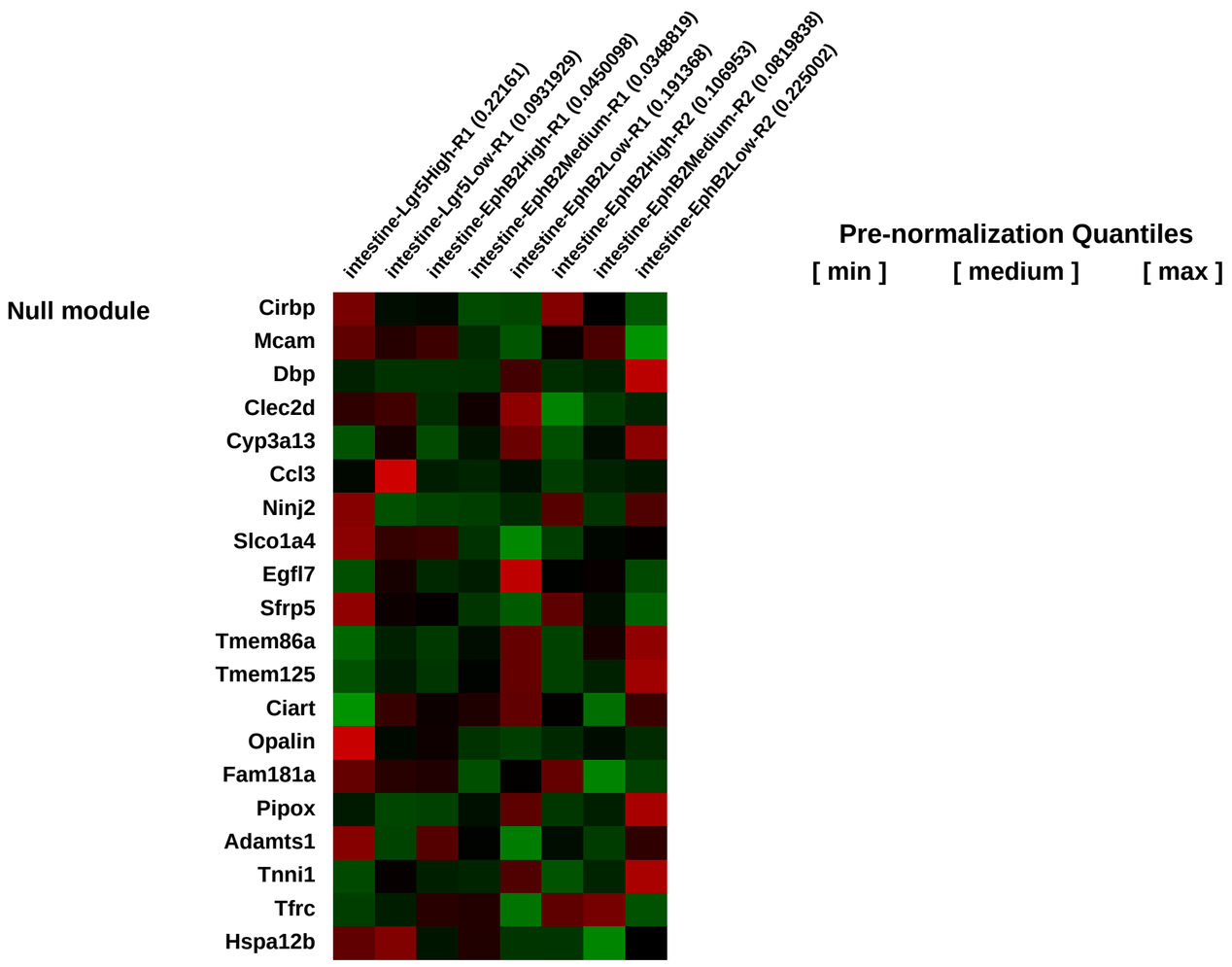

GEO Series "GSE27630" Expression Profiles

Num of samples in this series: 8

Scale of expression profile Z-scores

-3.0 -2.0 -1.0 0.0 1.0 2.0 3.0

GEO Link:	http://www.ncbi.nlm.nih.gov/geo/query/acc.cgi?acc=GSE27630
Status:	Public on Feb 05 2013
Title:	The transcription factor Otx2 regulates choroid plexus development and function
Organism:	Mus musculus
Experiment type:	Expression profiling by array
Platform:	GPL1261
Pubmed ID:	23364326
Summary & Design:	**Summary:** The choroid plexuses (ChPs) are the main regulators of cerebrospinal fluid (CSF) composition and thereby also control the composition of a principal source of signaling molecules that is in direct contact with neural stem cells in the developing brain. The regulators of ChP development mediating the acquisition of a fate that differs from the neighboring neuroepithelial cells are poorly understood. Here, we demonstrate in mice a crucial role for the transcription factor Otx2 in the development and maintenance of ChP cells. Deletion of Otx2 by the Otx2-CreERT2 driver line at E9 resulted in a lack of all ChPs, whereas deletion by the Gdf7-Cre driver line affected predominately the hindbrain ChP, which was reduced in size, primarily owing to an increase in apoptosis upon Otx2 deletion. Strikingly, Otx2 was still required for the maintenance of hindbrain ChP cells at later stages when Otx2 deletion was induced at E15, demonstrating a central role of Otx2 in ChP development and maintenance. Moreover, the predominant defects in the hindbrain ChP mediated by Gdf7-Cre deletion of Otx2 revealed its key role in regulating early CSF composition, which was altered in protein content, including the levels of Wnt4 and the Wnt modulator Tgm2. Accordingly, proliferation and Wnt signaling levels were increased in the distant cerebral cortex, suggesting a role of the hindbrain ChP in regulating CSF composition, including key signaling molecules. Thus, Otx2 acts as a master regulator of ChP development, thereby influencing one of the principal sources of signaling in the developing brain, the CSF. **Overall design:** We performed gene expression microarray analysis of fourth ventricular choroid plexus tissue from Otx2 k.o. mice compared to wildtype mice from the same litters.

Background corr dist: KL-Divergence = 0.0475, L1-Distance = 0.0207, L2-Distance = 0.0005, Normal std = 0.5785

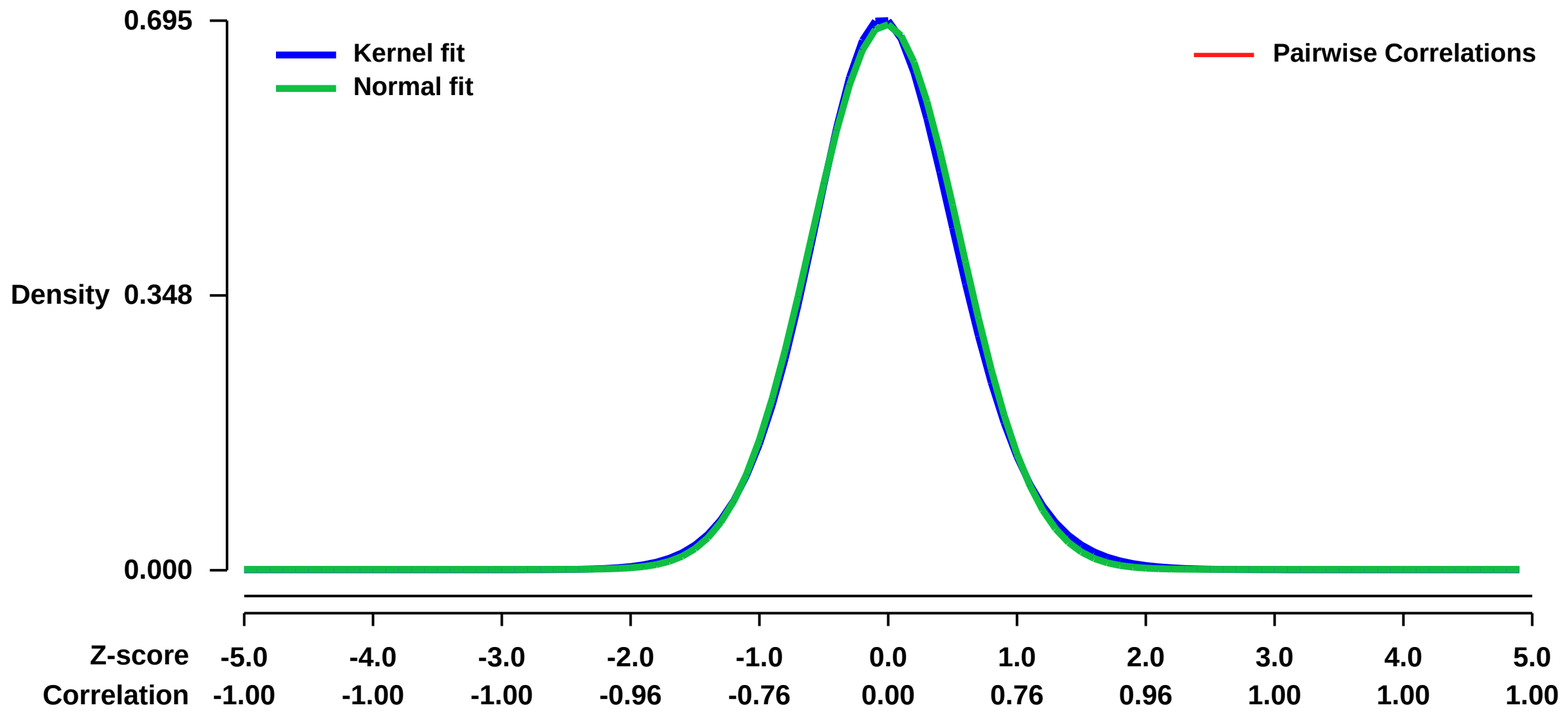

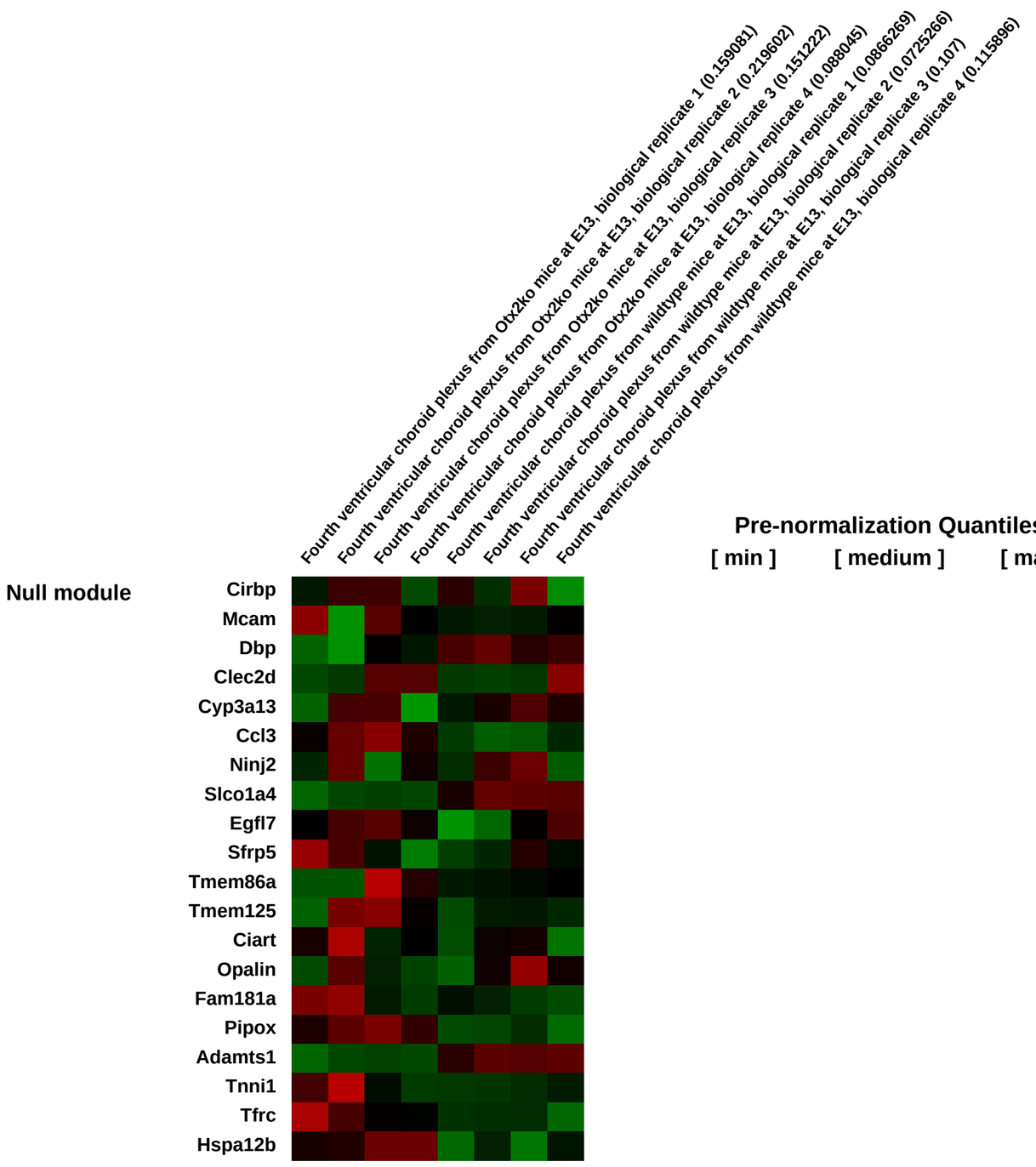

GEO Series "GSE27708" Expression Profiles

Num of samples in this series: 9

Scale of expression profile Z-scores

-3.0 -2.0 -1.0 0.0 1.0 2.0 3.0

GEO Link:	http://www.ncbi.nlm.nih.gov/geo/query/acc.cgi?acc=GSE27708
Status:	Public on Aug 01 2011
Title:	esBAF facilitates pluripotency by conditioning the genome for LIF/STAT3 signaling and by regulating Polycomb function
Organism:	Mus musculus
Experiment type:	Expression profiling by array
Platform:	GPL1261
Pubmed ID:	21785422
Summary & Design:	**Summary:** Signaling by the cytokine LIF and its downstream transcription factor, STAT3, prevents differentiation of pluripotent embryonic stem cells (ESCs) by opposing MAP kinase signaling. This contrasts with most cell types where STAT3 signaling induces differentiation. We find that STAT3 binding across the pluripotent genome is dependent upon Brg, the ATPase subunit of a specialized chromatin remodeling complex (esBAF) found in ESCs. Brg is required to establish chromatin accessibility at STAT3 binding targets, in essence preparing these sites to respond to LIF signaling. Moreover, Brg deletion leads to rapid Polycomb (PcG) binding and H3K27me3-mediated silencing of many Brg-activated targets genome-wide, including the target genes of the LIF signaling pathway. Hence, one crucial role of Brg in ESCs involves its ability to potentiate LIF signaling by opposing PcG. Contrary to expectations, Brg also facilitates PcG function at classical PcG target including all four Hox loci, reinforcing their repression in ESCs. These findings reveal that esBAF does not simply antagonize PcG, but rather, the two chromatin regulators act both antagonistically and synergistically with the common goal of supporting pluripotency. **Overall design:** ChIP-Seq was used to detect and measure STAT3 occupancy and levels of H3K27me3 in the genome before and after the removal of the SWI/SNF ATPase Brg in mouse ESCs. Total of 4 samples (WT and KO STAT3; WT and KO H3K27me3). Input DNA was sequenced as control.

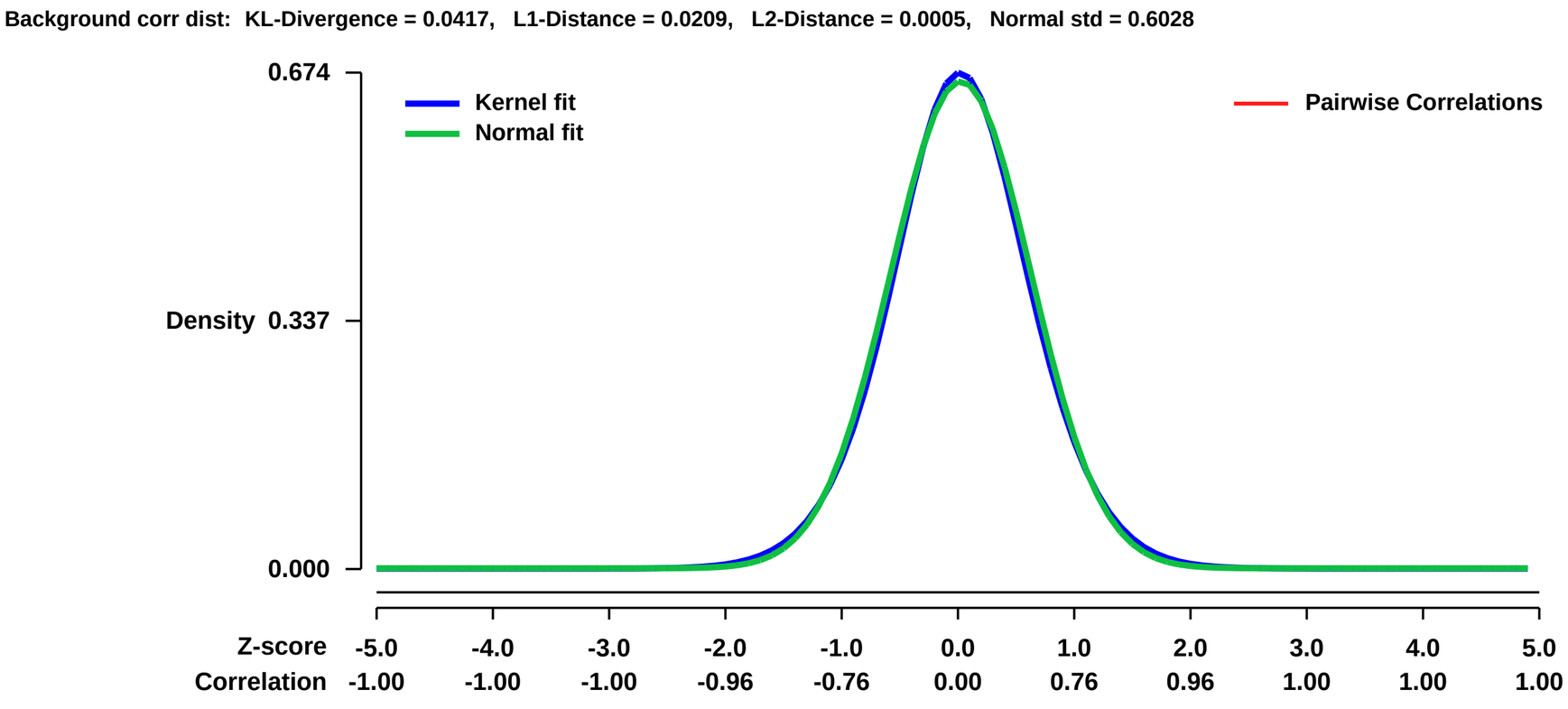

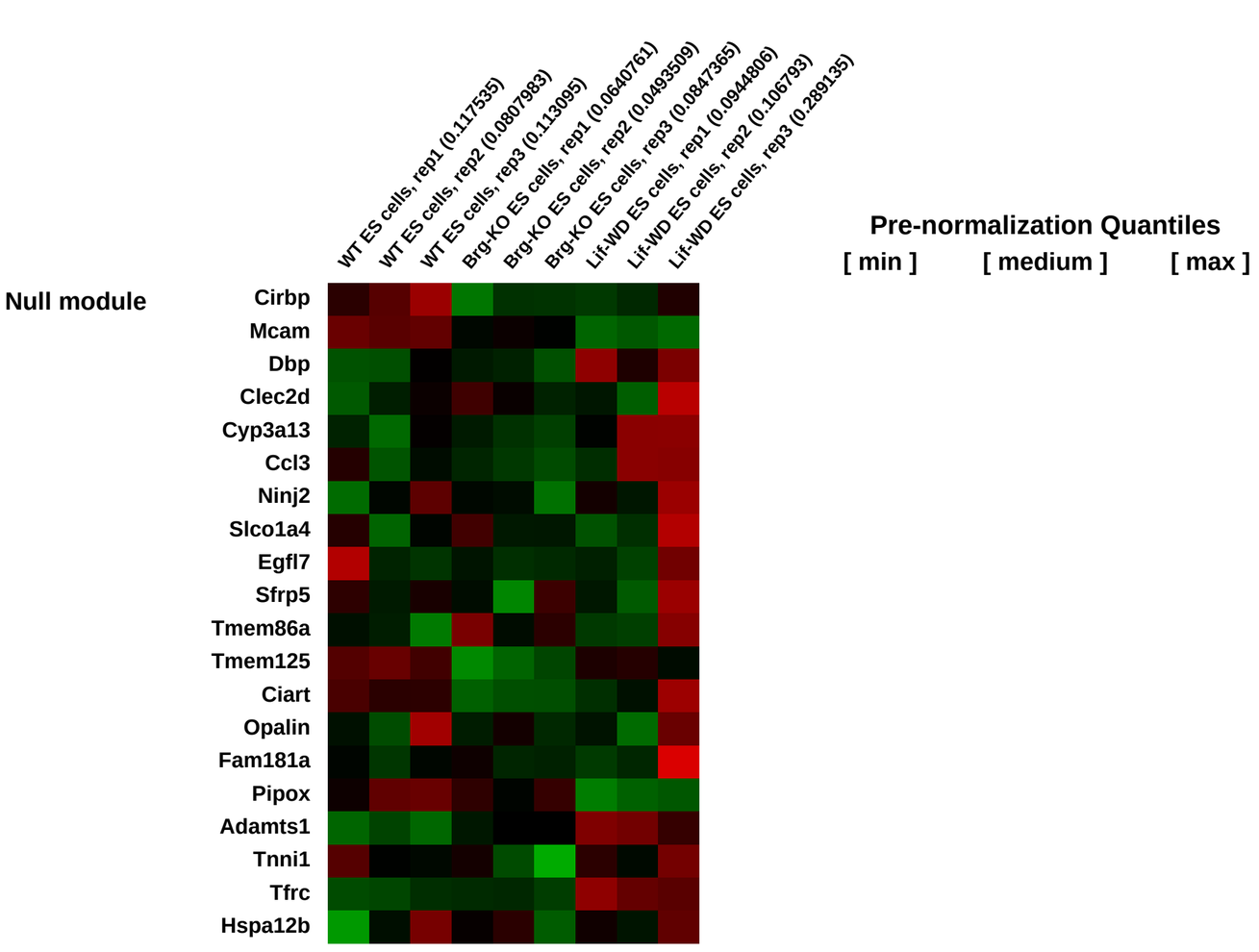

GEO Series "GSE27713" Expression Profiles

Num of samples in this series: 7

Scale of expression profile Z-scores

-3.0 -2.0 -1.0 0.0 1.0 2.0 3.0

GEO Link:	http://www.ncbi.nlm.nih.gov/geo/query/acc.cgi?acc=GSE27713
Status:	Public on Aug 07 2012
Title:	Genome-wide analysis of gene expression patterns in mir-122 knockout mice livers
Organism:	Mus musculus
Experiment type:	Expression profiling by array
Platform:	GPL1261
Pubmed ID:	22820290
Summary & Design:	**Summary:** To invesigate the physiology roles of mir-122 in liver, we performed expression profiling of mir-122 knockout mice and the control B6/129 mice. **Overall design:** Total RNA was extracted from four mir-122 knockout mice and three control mice of 2 months of age. Gene expression was quantified by robust multi-array analysis (RMA) using the Genomic Suite software from Partek.

Background corr dist: KL-Divergence = 0.0468, L1-Distance = 0.0155, L2-Distance = 0.0003, Normal std = 0.5728

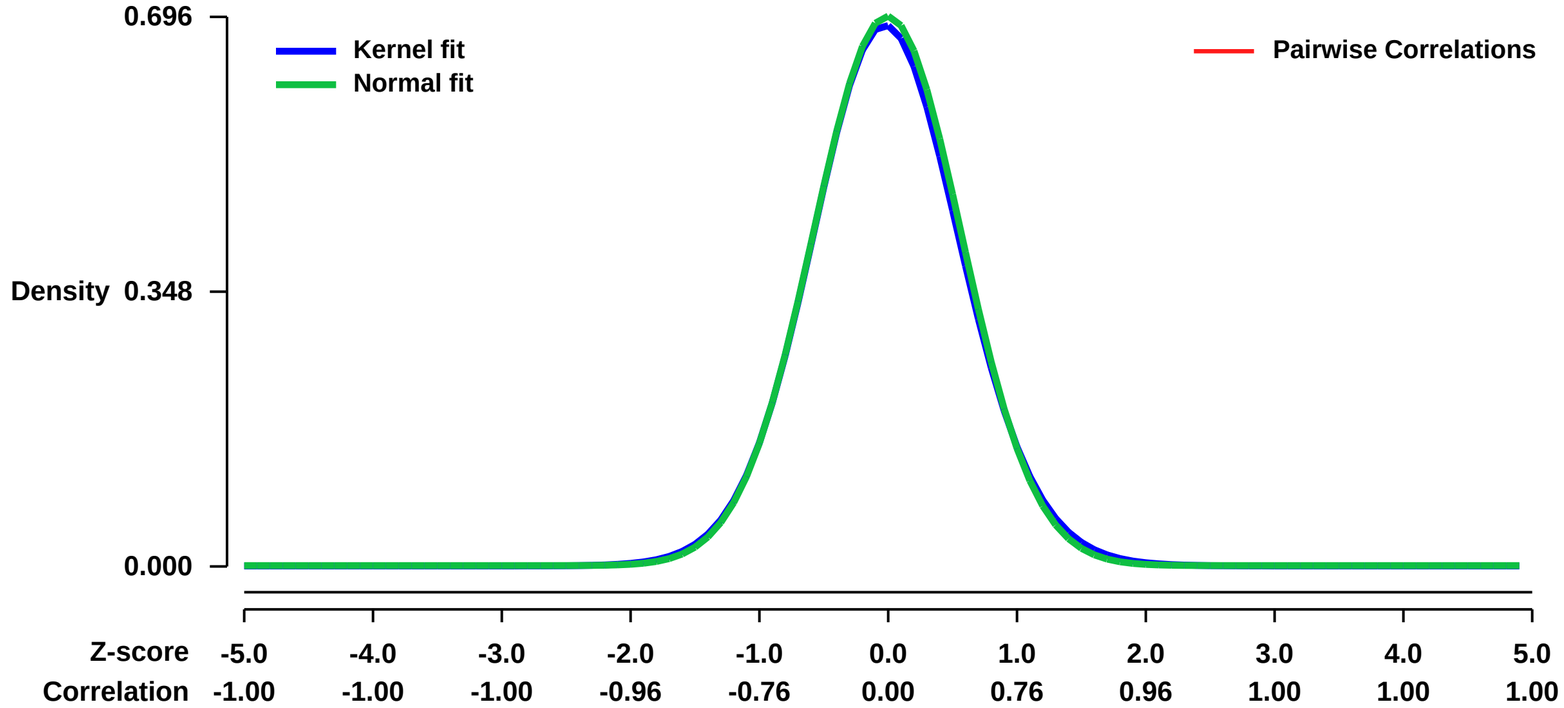

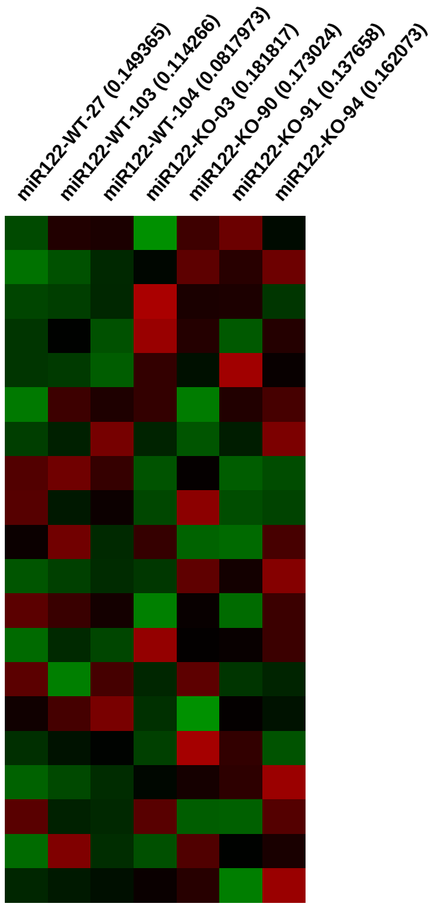

GEO Series "GSE27717" Expression Profiles

Num of samples in this series: 11

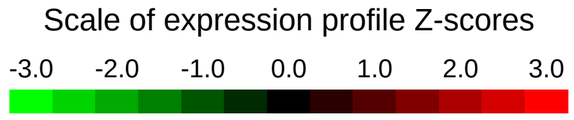

GEO Link:	http://www.ncbi.nlm.nih.gov/geo/query/acc.cgi?acc=GSE27717
Status:	Public on Sep 15 2011
Title:	Expression data from lung tumors of KrasTgfbr2 -/- mouse model
Organism:	Mus musculus
Experiment type:	Expression profiling by array
Platform:	GPL1261
Pubmed ID:	21911454
Summary & Design:	**Summary:** Recent data suggests that repression of the Type II TGF-B Receptor (Tgfr2) repression in human lung adenocarcinoma is important for progression from noninvasive to invasive adenocarcinoma. To test this hypothesis in a animal model of non-invasive lung cancer, we generated an inducible, lung specific Tgfbr2 knockout model in the oncogenic Kras mouse. LSL-KrasG12D positive mice were simultaneously backcrossed to C57/Bl6 mice and to the Tgfbr2 flox/flox mice. To induce tumors, 100 _l of saline containing 3x10e10 particles of an adenovirus containing the Cre recombinase (Ad.Cre) was administered to each LSL-KrasG12D mouse intra-nasally. **Overall design:** Mice were sacrificed at 7 weeks after administration of Adeno-Cre. We used laser capture microdissection to acquire tumor cells from KrasTgfbr2-/- and KrasTgfbr2 wt mouse tumors.

Background corr dist: KL-Divergence = 0.0666, L1-Distance = 0.0266, L2-Distance = 0.0011, Normal std = 0.5027

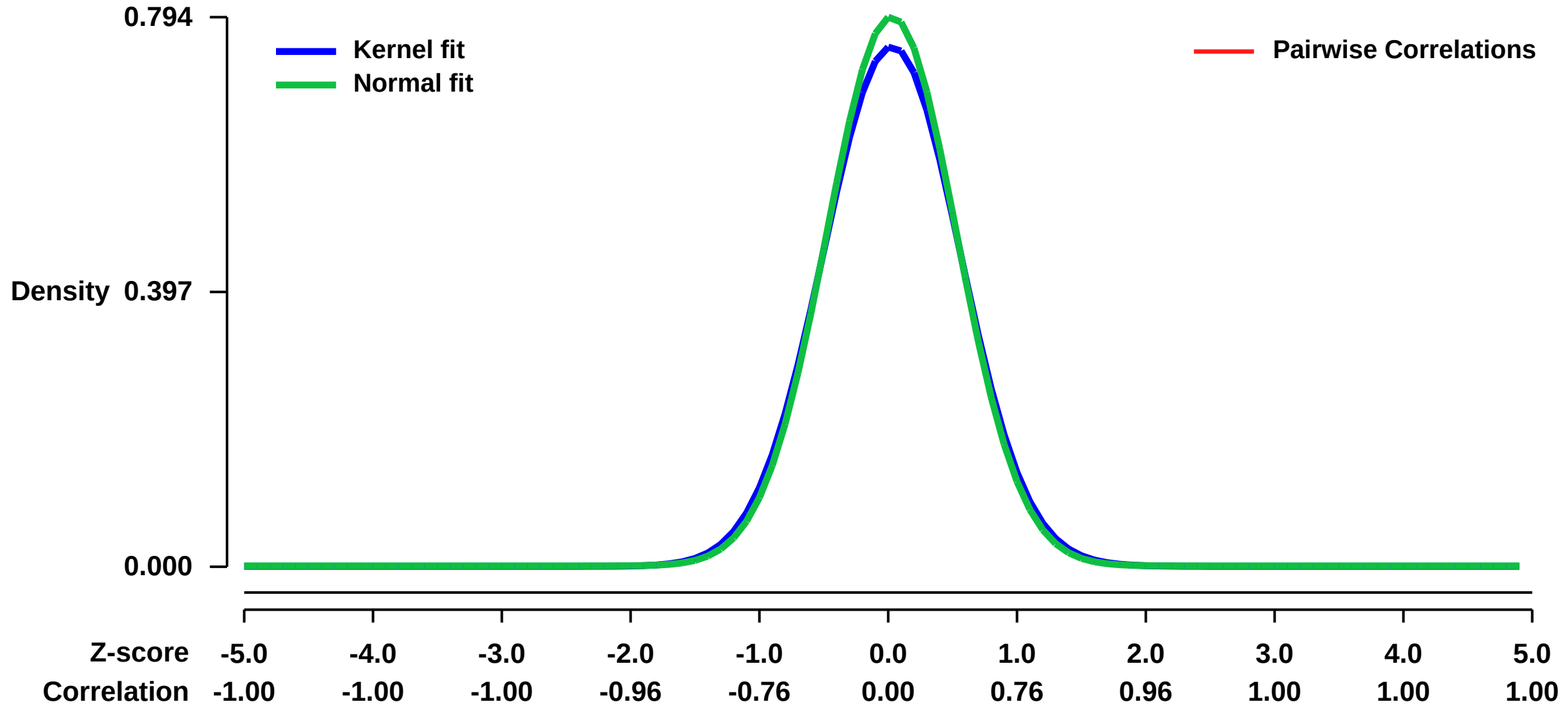

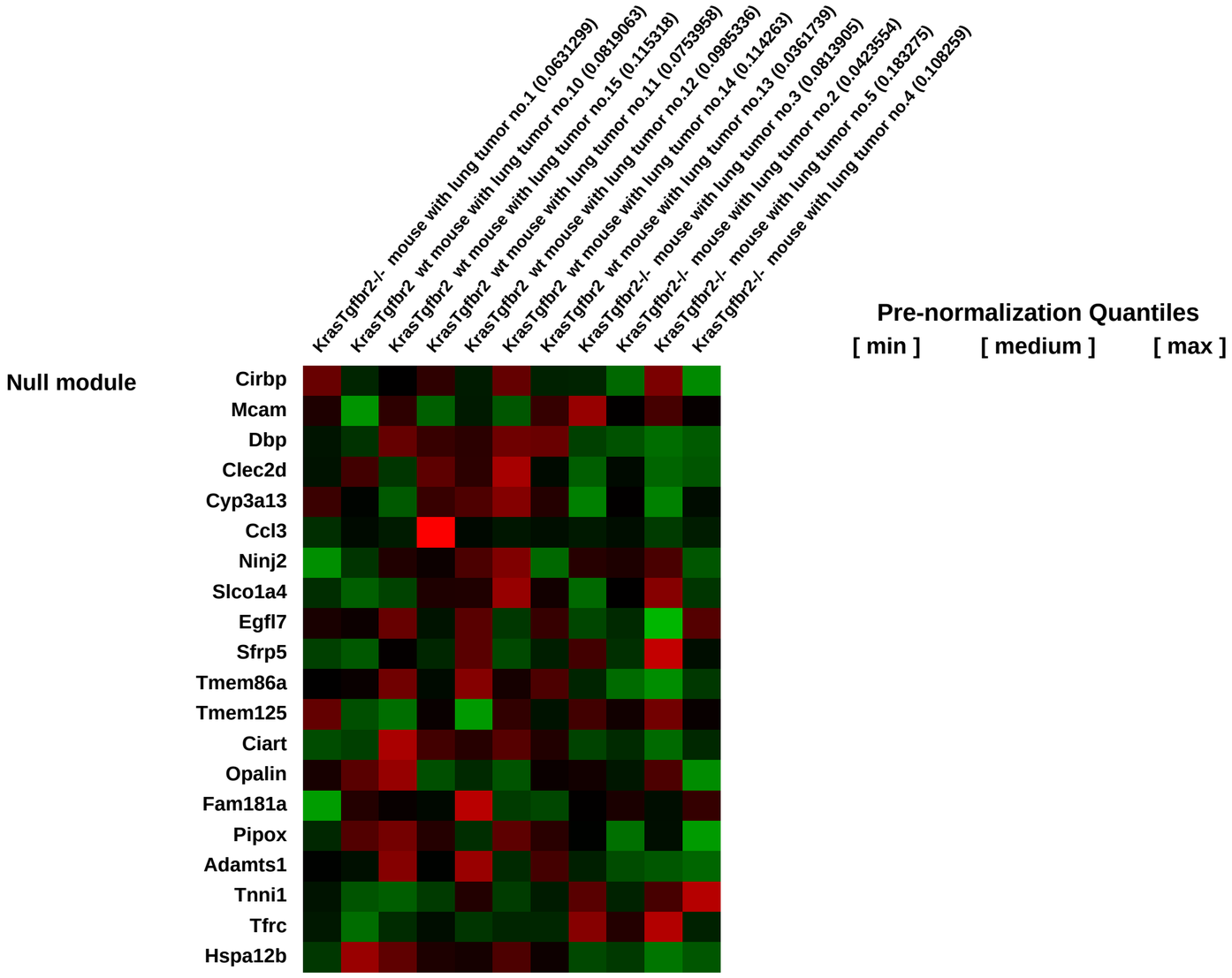

GEO Series "GSE27720" Expression Profiles

Num of samples in this series: 6

Scale of expression profile Z-scores

-3.0 -2.0 -1.0 0.0 1.0 2.0 3.0

GEO Link:	http://www.ncbi.nlm.nih.gov/geo/query/acc.cgi?acc=GSE27720
Status:	Public on Jan 06 2012
Title:	AMPK stimulation and PGC-1 alpha suppression in peroxisome deficient hepatocytes favor catabolic over anabolic carbohydrate metabolism
Organism:	Mus musculus
Experiment type:	Expression profiling by array
Platform:	GPL1261
Pubmed ID:	22002056
Summary & Design:	**Summary:** These arrays contain data from the livers of 10 week old L-Pex5 -/- male mice **Overall design:** 6 arrays, 3 biological replicates

Background corr dist: KL-Divergence = 0.0148, L1-Distance = 0.0326, L2-Distance = 0.0017, Normal std = 0.8076

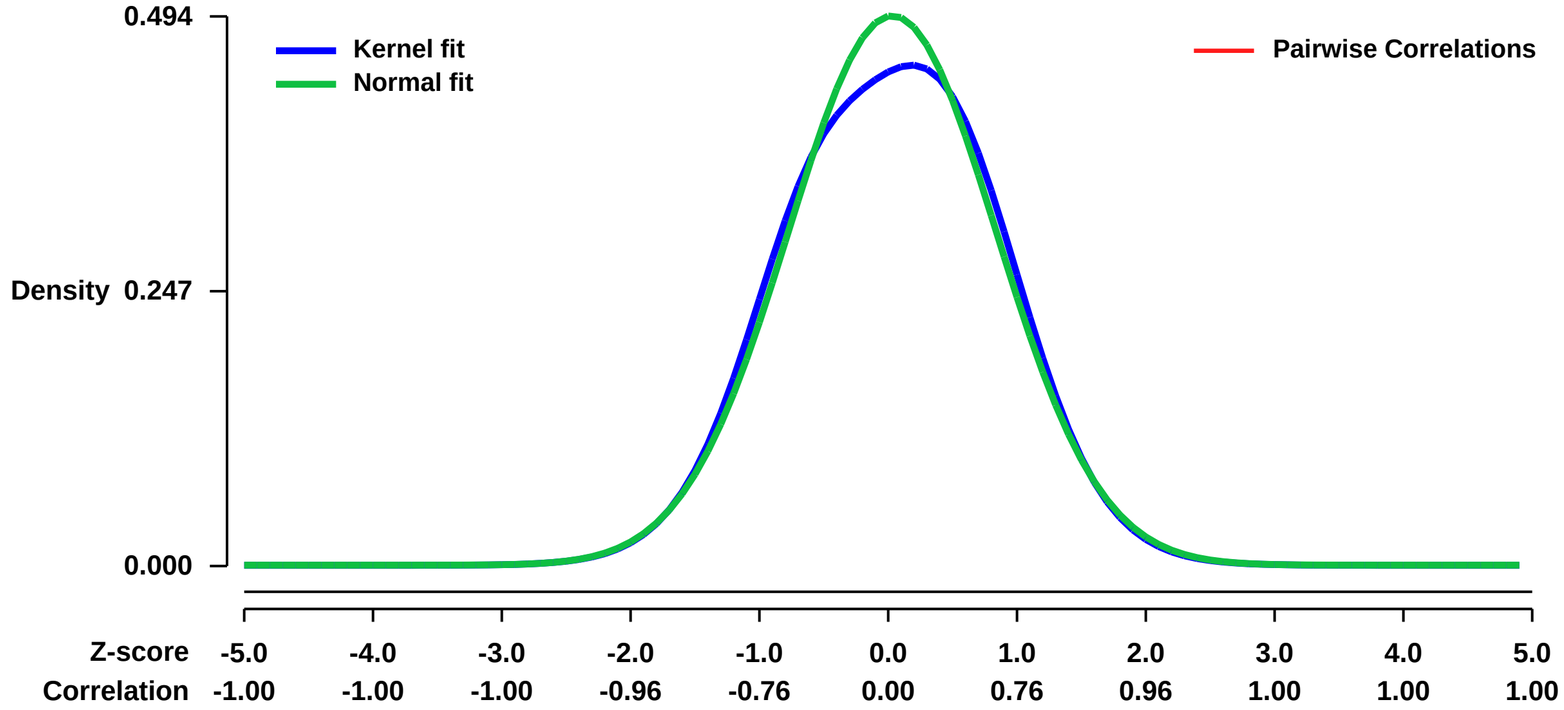

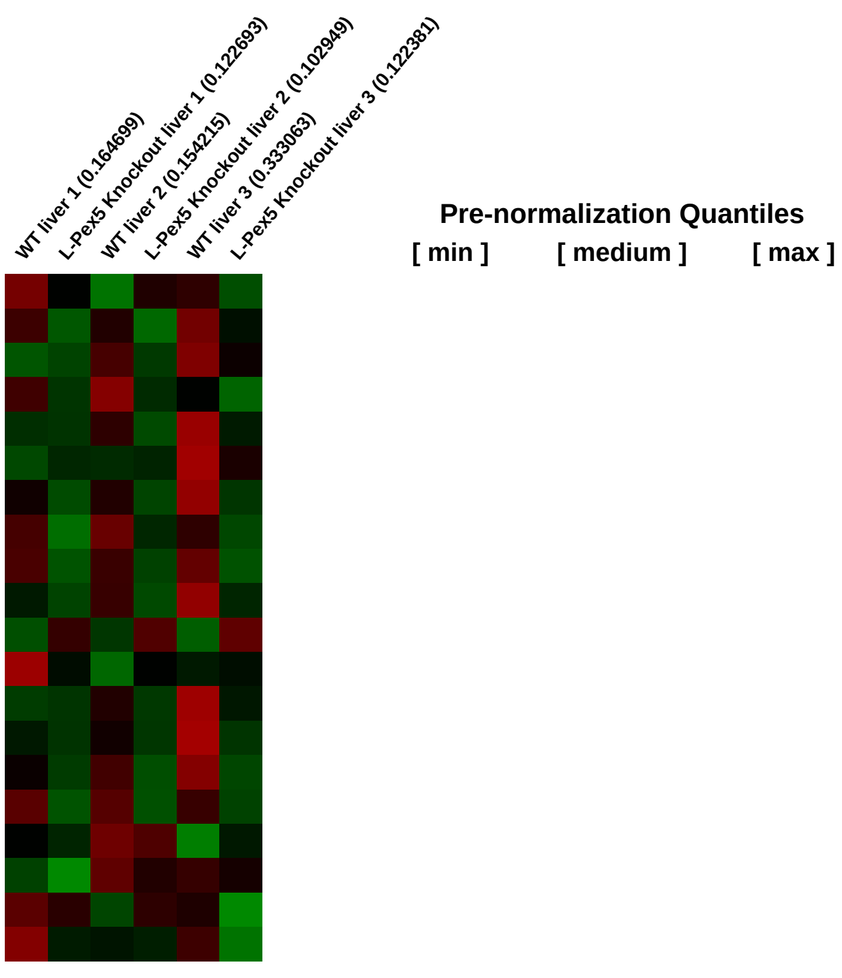

GEO Series "GSE27799" Expression Profiles

Num of samples in this series: 6

Scale of expression profile Z-scores

-3.0 -2.0 -1.0 0.0 1.0 2.0 3.0

GEO Link:	http://www.ncbi.nlm.nih.gov/geo/query/acc.cgi?acc=GSE27799
Status:	Public on May 12 2011
Title:	Expression data from LSK WT and LSK N1-C+
Organism:	Mus musculus
Experiment type:	Expression profiling by array
Platform:	GPL1261
Pubmed ID:	21562564
Summary & Design:	**Summary:** Notch signaling is one of the central regulators of differentiation in a variety of organisms and tissue types. Within the hematopoietic system, Notch is essential for the emergence of definitive HSC during fetal life and controls adult HSC differentiation to the T-cell lineage. Notch activation is controlled by the gamma-secretase complex complex, composed of presenilin, nicastrin (Ncstn), anterior pharynx-1 (Aph1), and presenilin enhancer-2 To determine other role of Notch signaling in HSC we designed a conditional mouse model of Notch activation. WT and N1-IC+ HSC were analysed to determined genes controlled by Notch signaling. **Overall design:** Bone marrow lineage negative, cKit+, Sca1+ cells were sorted from WT and N1-IC+ littermates for RNA extraction and hybridization on Affymetrix microarrays

Background corr dist: KL-Divergence = 0.0326, L1-Distance = 0.0169, L2-Distance = 0.0003, Normal std = 0.6534

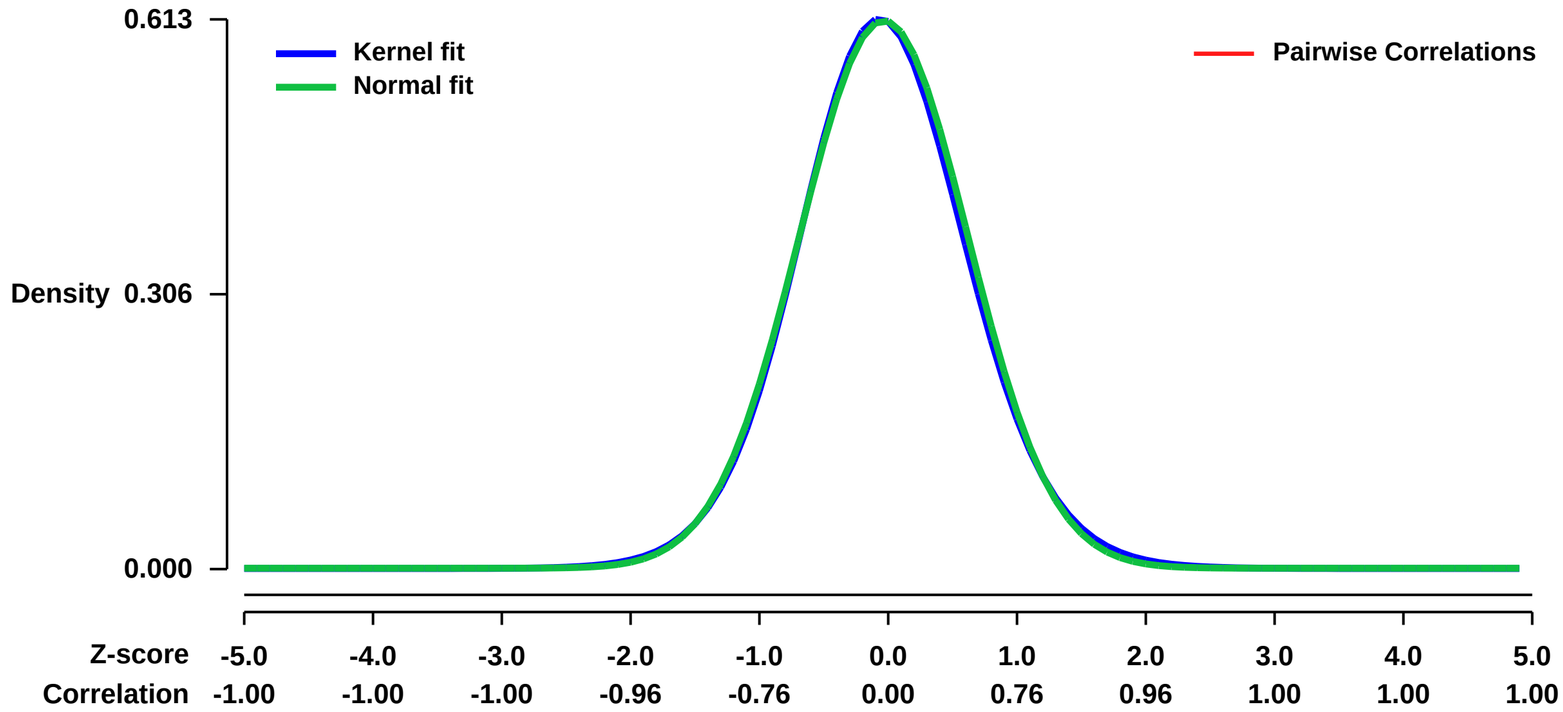

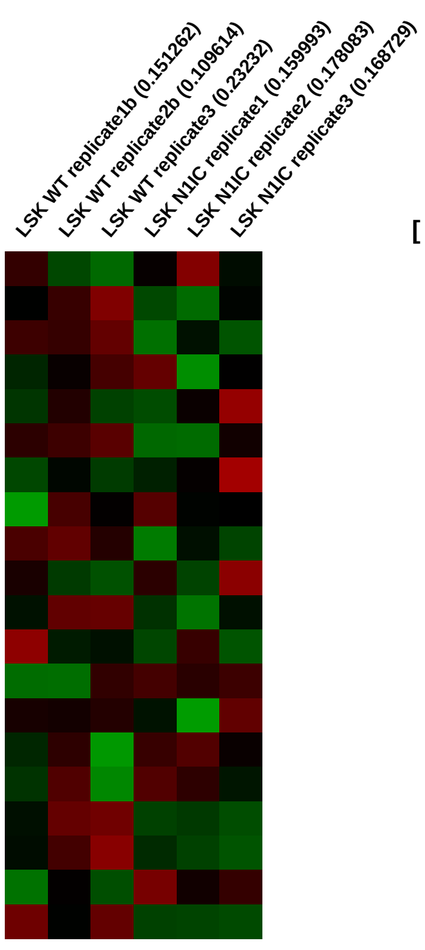

GEO Series "GSE27816" Expression Profiles

Num of samples in this series: 14

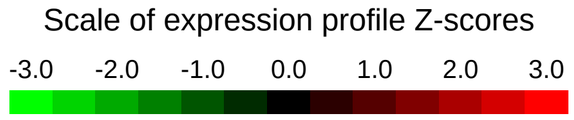

GEO Link:	**http://www.ncbi.nlm.nih.gov/geo/query/acc.cgi?acc=GSE27816**
Status:	**Public on Jul 01 2011**
Title:	**Tet2 loss leads to increased hematopoietic stem cell self-renewal and myeloid transformation**
Organism:	**Mus musculus**
Experiment type:	**Expression profiling by array**
Platform:	**GPL1261**
Pubmed ID:	**21723200**
Summary & Design:	**Summary:** **Recurrent somatic mutations in TET2 and in other genes that regulate the epigenetic state have been identified in patients with myeloid malignancies and in other cancers. However, the in vivo effects of Tet2 loss have not been delineated. We report here that Tet2 loss leads to increased stem-cell self-renewal and to progressive stem cell expansion. Consistent with human mutational data, Tet2 loss leads to myeloproliferation in vivo, notable for splenomegaly and monocytic proliferation. In addition, haploinsufficiency for Tet2 confers increased self-renewal and myeloproliferation, suggesting that the monoallelic TET2 mutations found in most TET2-mutant leukemia patients contribute to myeloid transformation. This work demonstrates that absent or reduced Tet2 function leads to enhanced stem cell function in vivo and to myeloid transformation.** **These studies show that a ubiquitin ligase-substrate pair can orchestrate the molecular program of HSC differentitiation** **Overall design:** **Gene expression profiles from WT and Tet2-/- sorted LSK and myeloid progenitors (CMP and GMP) were compared using genome wide mRNA expression profiling by Affymetrix genechip arrays (Mouse 430 2.0) and key targets were validated by chromatin immunoprecipitation experiments.**

Background corr dist: KL-Divergence = 0.1358, L1-Distance = 0.0335, L2-Distance = 0.0019, Normal std = 0.4092

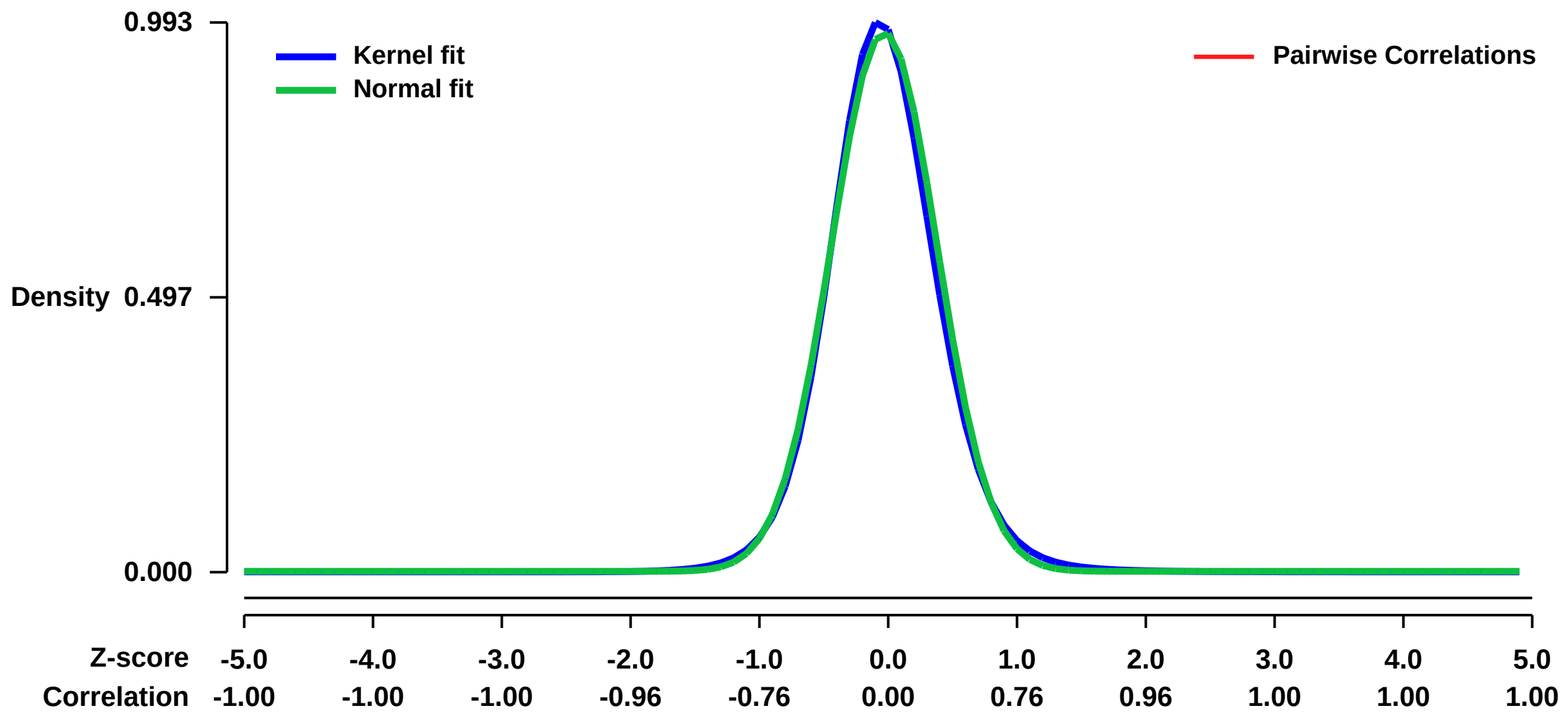

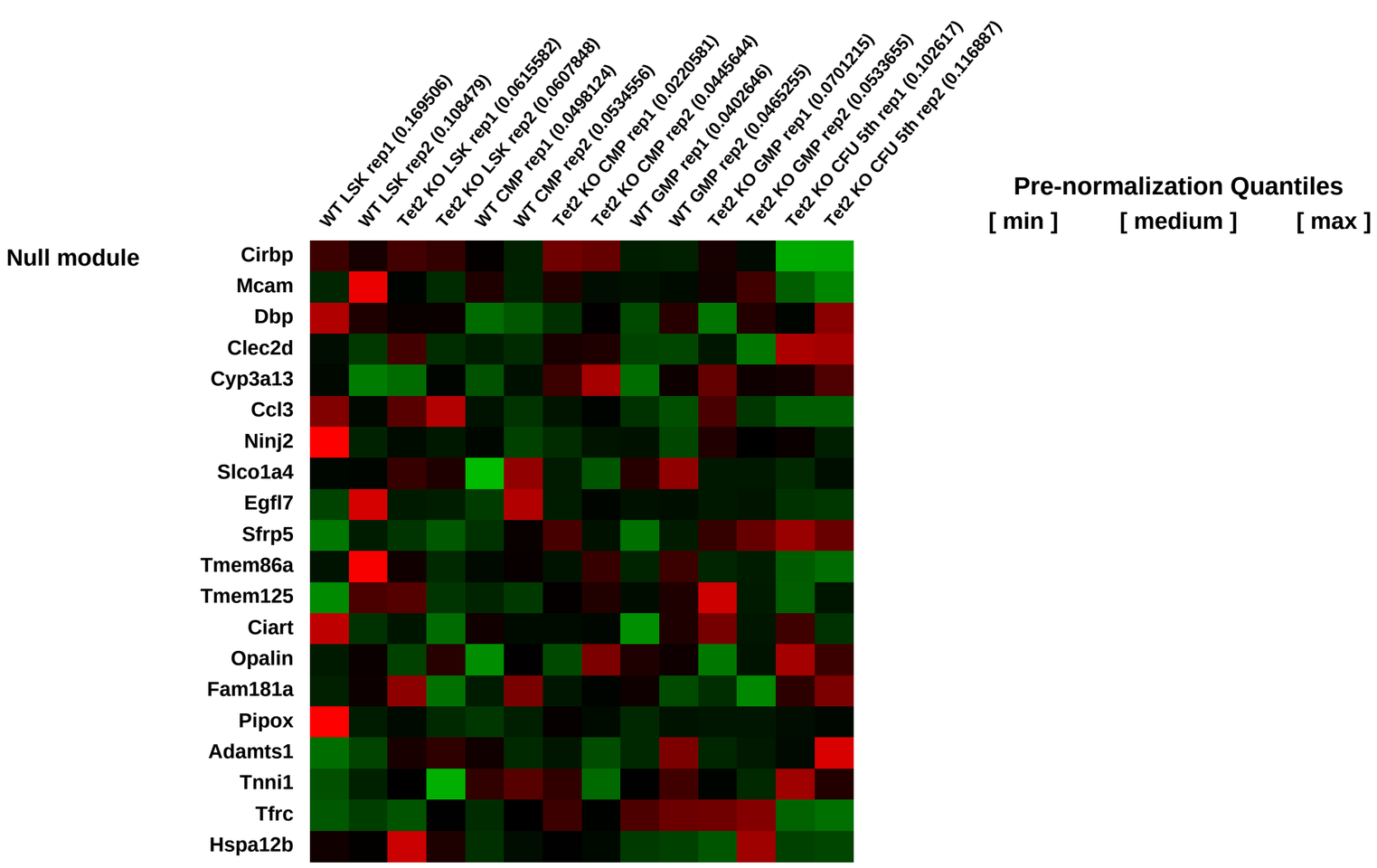

GEO Series "GSE27848" Expression Profiles

Num of samples in this series: 16

Scale of expression profile Z-scores

-3.0 -2.0 -1.0 0.0 1.0 2.0 3.0

GEO Link:	http://www.ncbi.nlm.nih.gov/geo/query/acc.cgi?acc=GSE27848
Status:	Public on Oct 02 2011
Title:	Dietary heme stimulates epithelial cell turnover by downregulating feedback inhibitors of proliferation in murine colon (part 2)
Organism:	Mus musculus
Experiment type:	Expression profiling by array
Platform:	GPL1261
Pubmed ID:	23239972
Summary & Design:	**Summary:** The risk for colon cancer is associated with nutrition, especially high fat and low calcium diets high in red meat. Red meat contains the iron porphyrin pigment heme, which induces cytotoxicity of the colon contents and epithelial hyperproliferation. Using a mouse model, we showed that heme caused damage to the colonic surface epithelium and induced compensatory hyperproliferation. Expression levels of heme- and stress-related genes show that heme affects surface cells and not directly crypt cells. Therefore, injured surface cells should signal to crypt TA cells to induce compensatory hyperproliferation. Surface-specific downregulated inhibitors of proliferation were Wnt inhibitory factor 1, Indian Hedgehog, Bone morphogenic protein 2 and possibly Interleukin-15. Heme also upregulated Amphiregulin, Epiregulin and Cyclooxygenase-2 mRNA in the surface cells, however, their protein/metabolite levels were not increased as heme induced surface-specific translation repression by increasing 4E-BP1. Therefore, we conclude that heme induced colonic hyperproliferation and hyperplasia by repressing feedback inhibition of proliferation. **Overall design:** C57BL/6 mice received a Westernized high fat and low calcium diet with or without heme (the polyporphyrin pigment of red meat). Mice received control or heme diet for 14 days. After 14 days, mice were sacrificed and colons were taken out. RNA was isolated from colon scrapings and subjected to gene expression profiling (n=7 control mice and n=9 heme-fed mice).

Background corr dist: KL-Divergence = 0.1483, L1-Distance = 0.0281, L2-Distance = 0.0012, Normal std = 0.3797

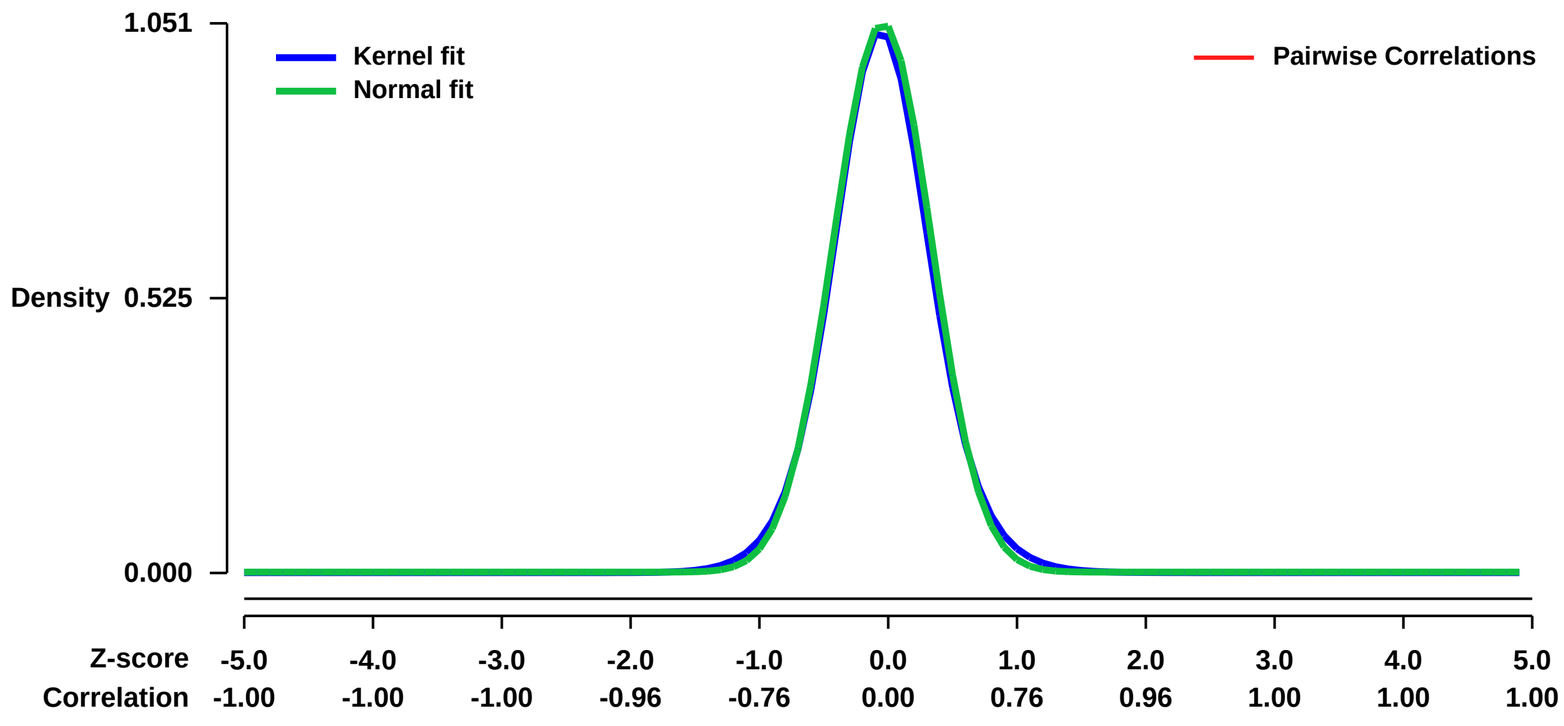

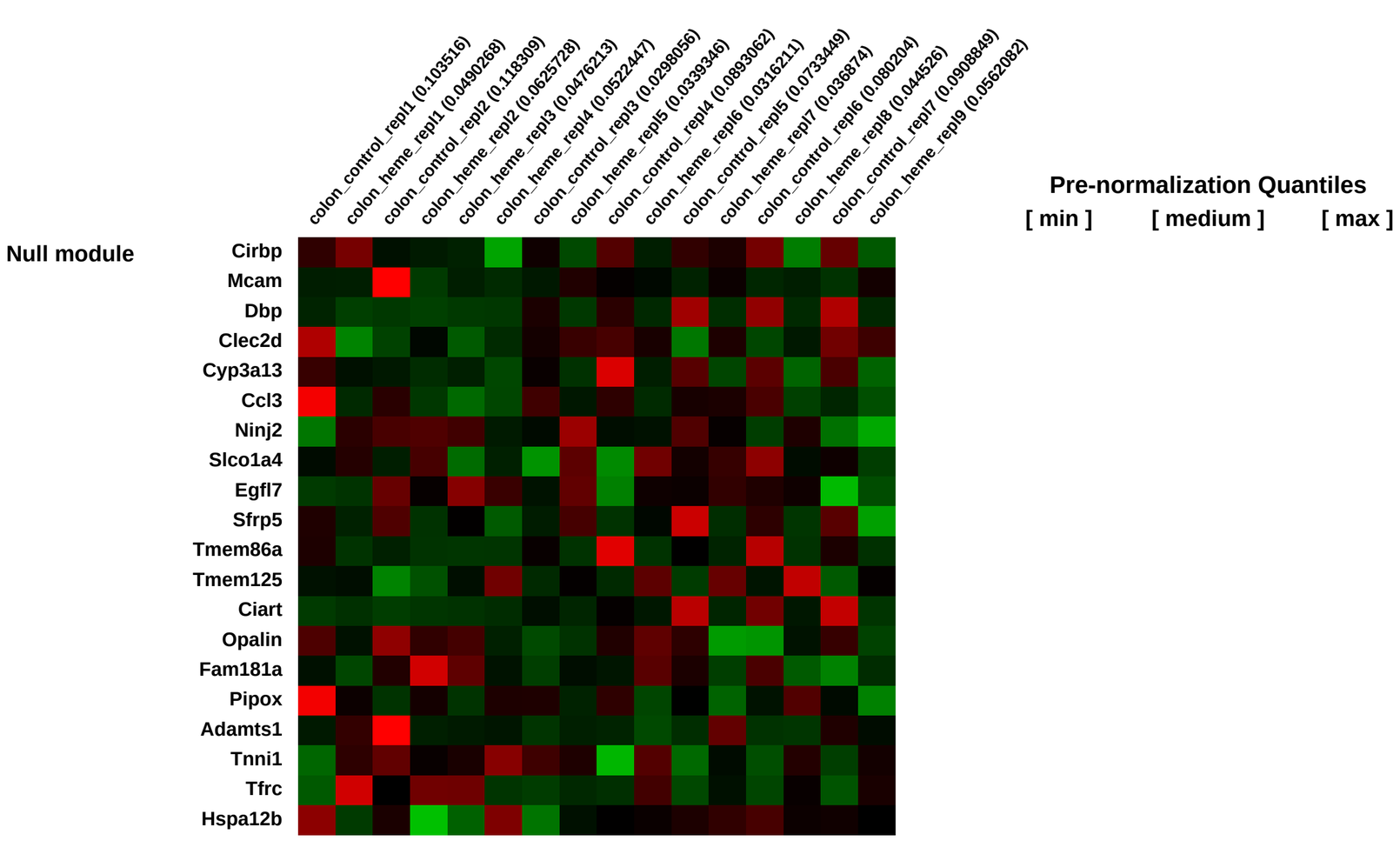

GEO Series "GSE27972" Expression Profiles

Num of samples in this series: 6

Scale of expression profile Z-scores

-3.0 -2.0 -1.0 0.0 1.0 2.0 3.0

GEO Link: http://www.ncbi.nlm.nih.gov/geo/query/acc.cgi?acc=GSE27972
Status: Public on Dec 31 2011
Title: Mouse bone marrow-derived macrophages infected with T. gondii (Type I, RH strain) for 6 hr
Organism: Mus musculus
Experiment type: Expression profiling by array
Platform: GPL1261
Pubmed ID:

Summary & Design:

Summary:
Toxoplasma gondii is a globally distributed parasite pathogen that infects virtually all warm-blooded animals. A hallmark of immunity to acute infection is the production of IFN-¿‡ and IL-12, followed by a protective T cell response that is critical for parasite control. Naˆflve T cell activation requires both TCR stimulation and the engagement of costimulatory receptors. Because of their important function in activating T cells, the expression of co-stimulatory ligands is believed to be under tight control. The molecular mechanisms governing their induction during microbial stimulation, however, are not well understood. We found that all three strains of T. gondii (Types I, II, and III) up-regulated the expression of B7-2, but not B7-1, on the surface of mouse bone marrow-derived macrophages. This induction occurred at the transcriptional level, required active parasite invasion, and was not dependent on MyD88 or TRIF. Genome-wide transcriptional analysis comparing infected and uninfected macrophages revealed the activation of MAPK signaling in infected cells. Using specific inhibitors against MAPKs, we determined that parasite-induced B7-2 is dependent on JNK, but not ERK or p38 signaling. We also observed that T. gondii-induced B7-2 expression on human peripheral blood monocytes is dependent on JNK signaling, indicating that a common mechanism of B7-2 regulation by T. gondii may exist in both humans and mice.

We used microarrays to examine genome-wide changes in host cell gene expression during T. gondii infection at an early time point (6 hpi).

Overall design:
BMdM were mock-treated or infected with T. gondii (Type I, RH strain) at an MOI of 2 and cultured for 6 hours. Biological triplicates were performed. Total RNA was harvested and used for cDNA synthesis, labeling, and hybridization to Affymetrix mouse 430 2.0 expression arrays.

Background corr dist: KL-Divergence = 0.0242, L1-Distance = 0.0274, L2-Distance = 0.0007, Normal std = 0.7449

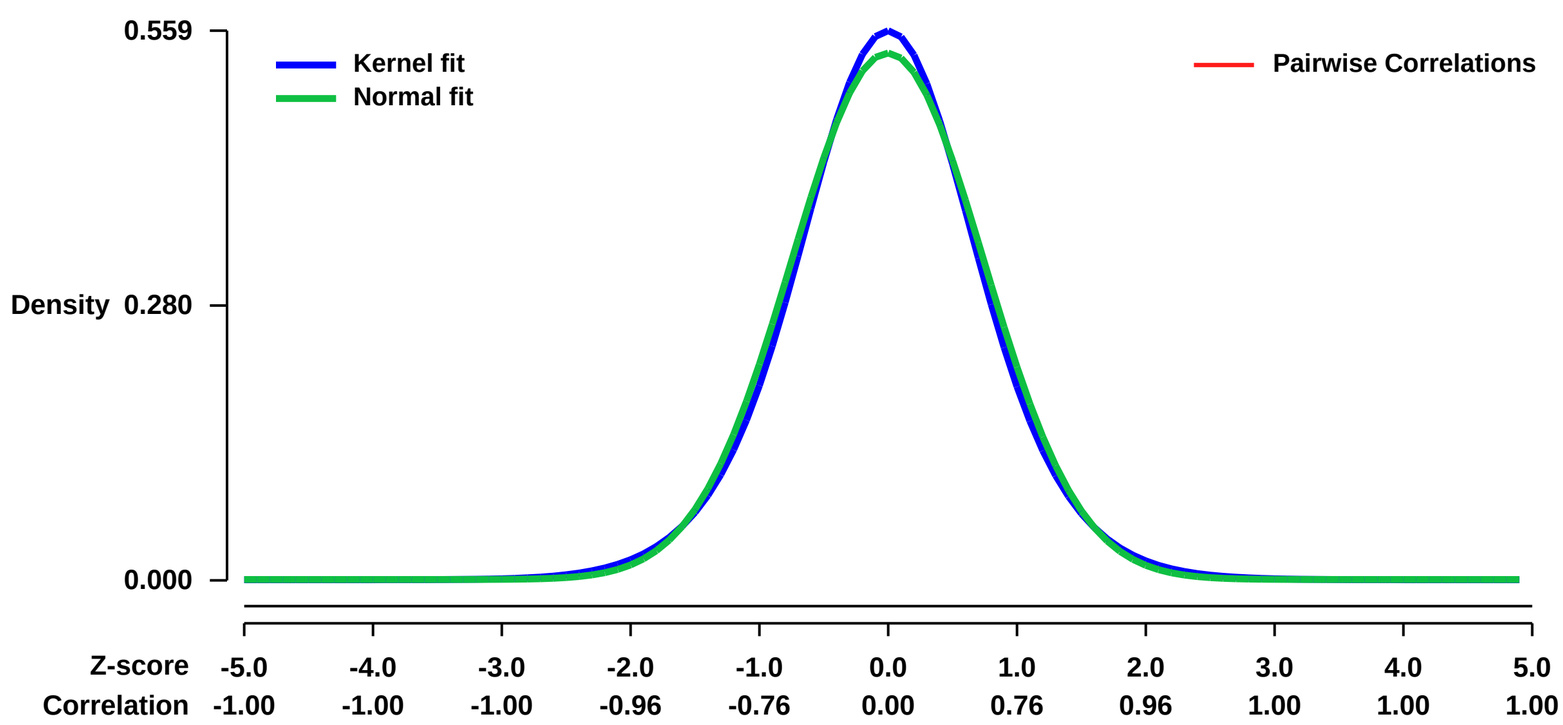

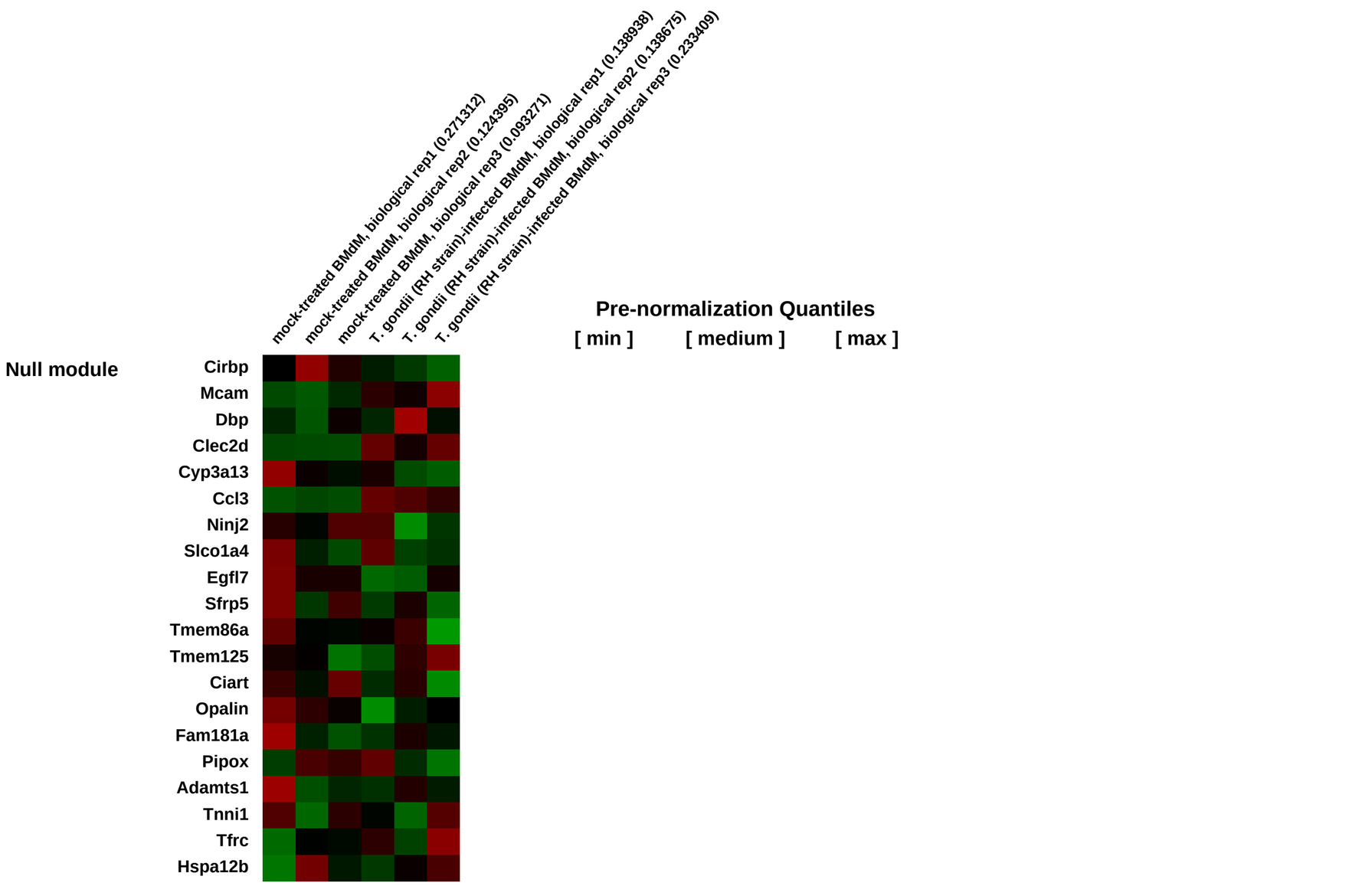

GEO Series "GSE27975" Expression Profiles

Num of samples in this series: 6

Scale of expression profile Z-scores

-3.0 -2.0 -1.0 0.0 1.0 2.0 3.0

GEO Link:	http://www.ncbi.nlm.nih.gov/geo/query/acc.cgi?acc=GSE27975
Status:	Public on Mar 16 2011
Title:	HL-1 cardiomyocyte response to hypoxia
Organism:	Mus musculus
Experiment type:	Expression profiling by array
Platform:	GPL1261
Pubmed ID:	21670500
Summary & Design:	**Summary:** Expression profiling of cultured HL-1 cardiomyocytes subjected to hypoxia for 8 hours. **Overall design:** Three samples from each condition were analyzed

Background corr dist: KL-Divergence = 0.0443, L1-Distance = 0.0247, L2-Distance = 0.0007, Normal std = 0.6032

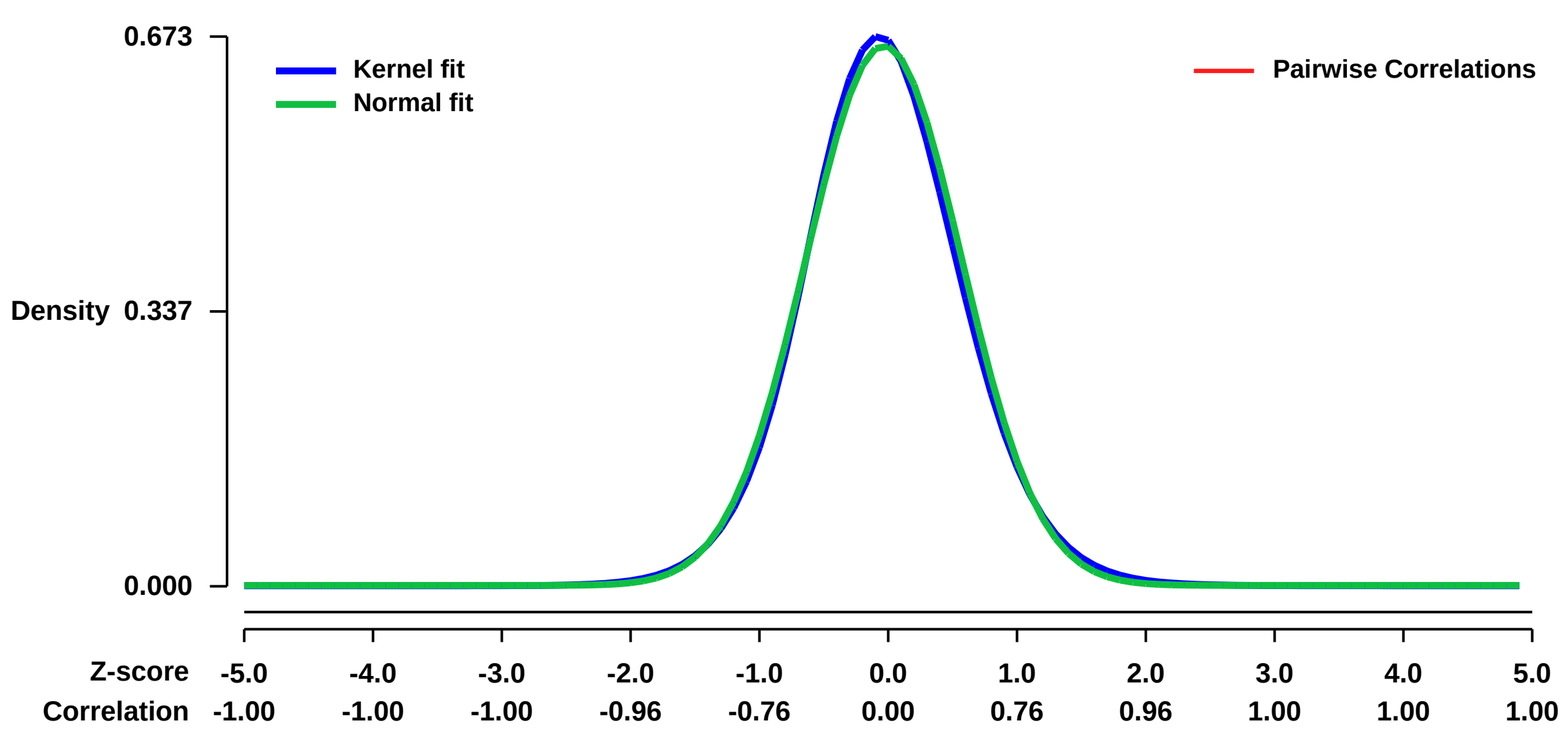

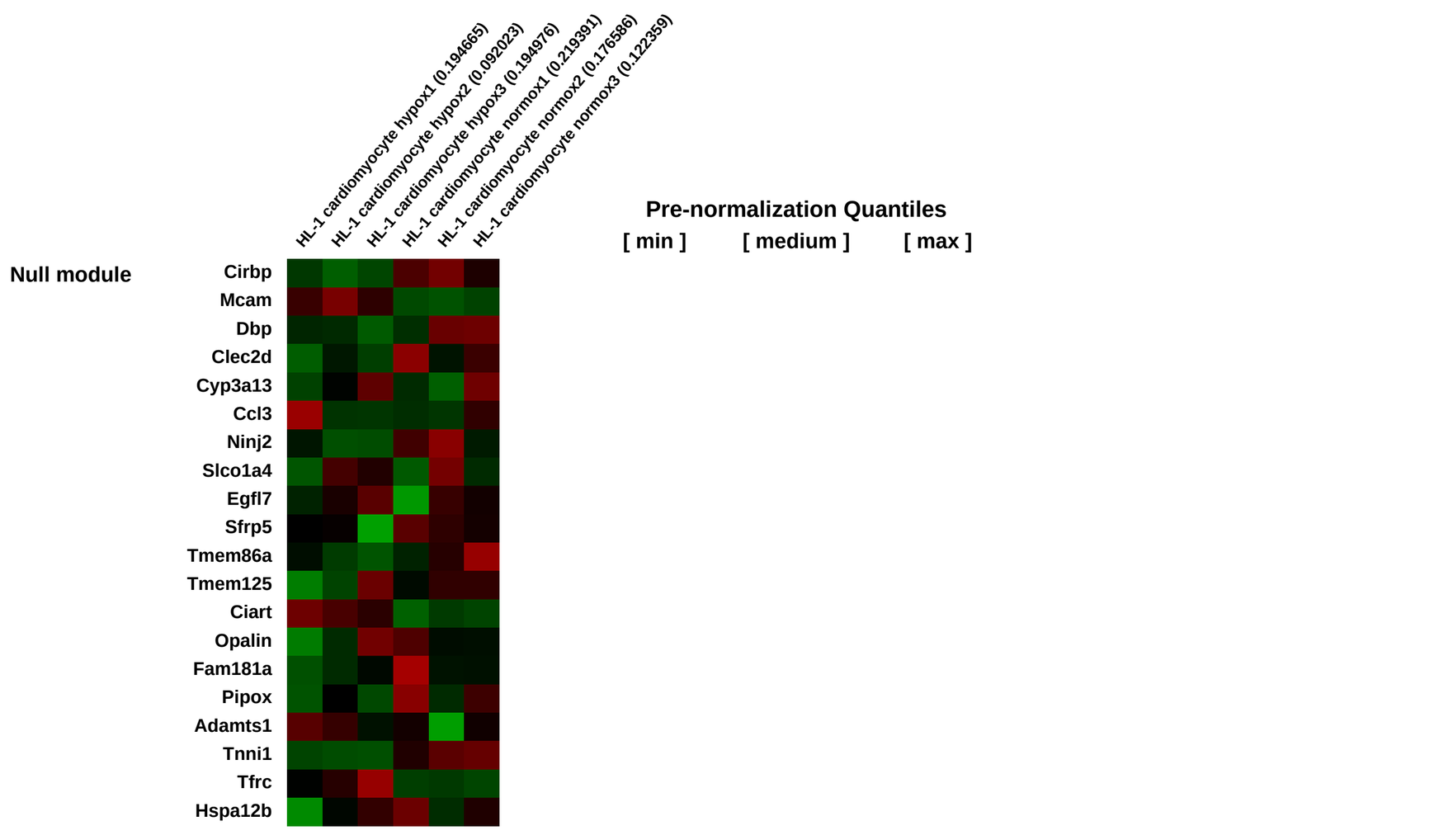

GEO Series "GSE28025" Expression Profiles

Num of samples in this series: 18

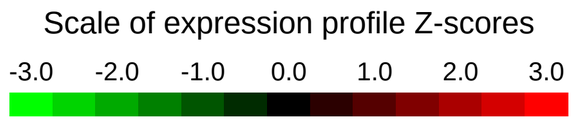

GEO Link:	http://www.ncbi.nlm.nih.gov/geo/query/acc.cgi?acc=GSE28025
Status:	Public on Oct 19 2011
Title:	Comparative gene expression analysis of repro9/repro9 and wild type testes from 14 and 17 day mice
Organism:	Mus musculus
Experiment type:	Expression profiling by array
Platform:	GPL1261
Pubmed ID:	21750041
Summary & Design:	**Summary:** Repro9 in an allele of Mybl1 (A-Myb) transcription factor obtained in ENU screen to identify alleles causing mouse infertility. Repro9/repro9 mutant males are infertile due to meiotic arrest at pachytene stage. Mutants show wide range of abnormalities including inefficient chromosome synapsis, sex body formation and progression through meiotic cycle. Females are unaffected. To determine genes transcriptionally regulated by MYBL1 we analyzed gene expression profiles of wild type and repro9/repro9 mutant testis at 14 and 17 days postpartum. Analysis revealed many misregulated genes, in majority downregulated, at day 14 pp and even more at day 17 pp, probably due to secondary effects of meiotic arrest. Significantly misregulated genes were characterized by Gene Ontology. Comparative gene expression analysis uncovered potential targets of MYBL1 regulation that play roles in regulation of transcription, cell cycle, apoptosis, protein phosphorylation and ubiquitination, chromosome organization and others. **Abstract:**The transcriptional regulation of mammalian meiosis is poorly characterized, due to few genetic and ex vivo models. From a genetic screen, we identify the transcription factor MYBL1 as a male-specific master regulator of several critical meiotic processes. Spermatocytes bearing a novel separation-of-function allele (Mybl1repro9) had subtle defects in autosome synapsis in pachynema, a high incidence of unsynapsed sex chromosomes, incomplete double strand break (DSB) repair on synapsed pachytene chromosomes, and a lack of crossing-over. MYBL1 protein appears in pachynema, and its mutation caused specific alterations in expression of diverse genes, including some translated postmeiotically. These data, coupled with chromatin immunoprecipitation (ChIP-chip) experiments and bioinformatic analysis of promoters, identified direct targets of MYBL1 regulation. Meiosis in mutant females appears unaffected. These results reveal that MYBL1 is a master regulator of meiotic genes that are involved in multiple processes in spermatocytes, including chromosome synapsis, recombination, and cell cycle progression through pachynema. **Overall design:** RNA was extracted from wt and repro9/repro9 mutant testis from 14 and 17 days old mice. This two time points were selected for sample enrichment in early/midpachytene and latepachytene/diplotene spermatocytes, respectively. Total testis RNA from wild-type (â¥3) and mutant (â¥3) mice was reverse-transcribed into double stranded cDNA, and biotin-labeled cRNA (GeneChip IVT labeling kit, Affymetrix, Santa Clara, CA) was hybridized to Affymetrix mouse genome 430 2.0 GeneChips containing. The raw data was processed using Affymetrix GCOS software. Two-way ANOVA analysis resolved differentially expressed (DE) genes either between genotypes and/or days using MeV(version 4.6.1) on log2-transformed expression values. Results were multiple test corrected with the Benjamini-Hochberg method to control the false discovery rate (FDR) in R. ~800 genes significant at FDR<=0.025 were selected as differentially expressed for downstream analysis.

Background corr dist: KL-Divergence = 0.0601, L1-Distance = 0.0440, L2-Distance = 0.0033, Normal std = 0.5461

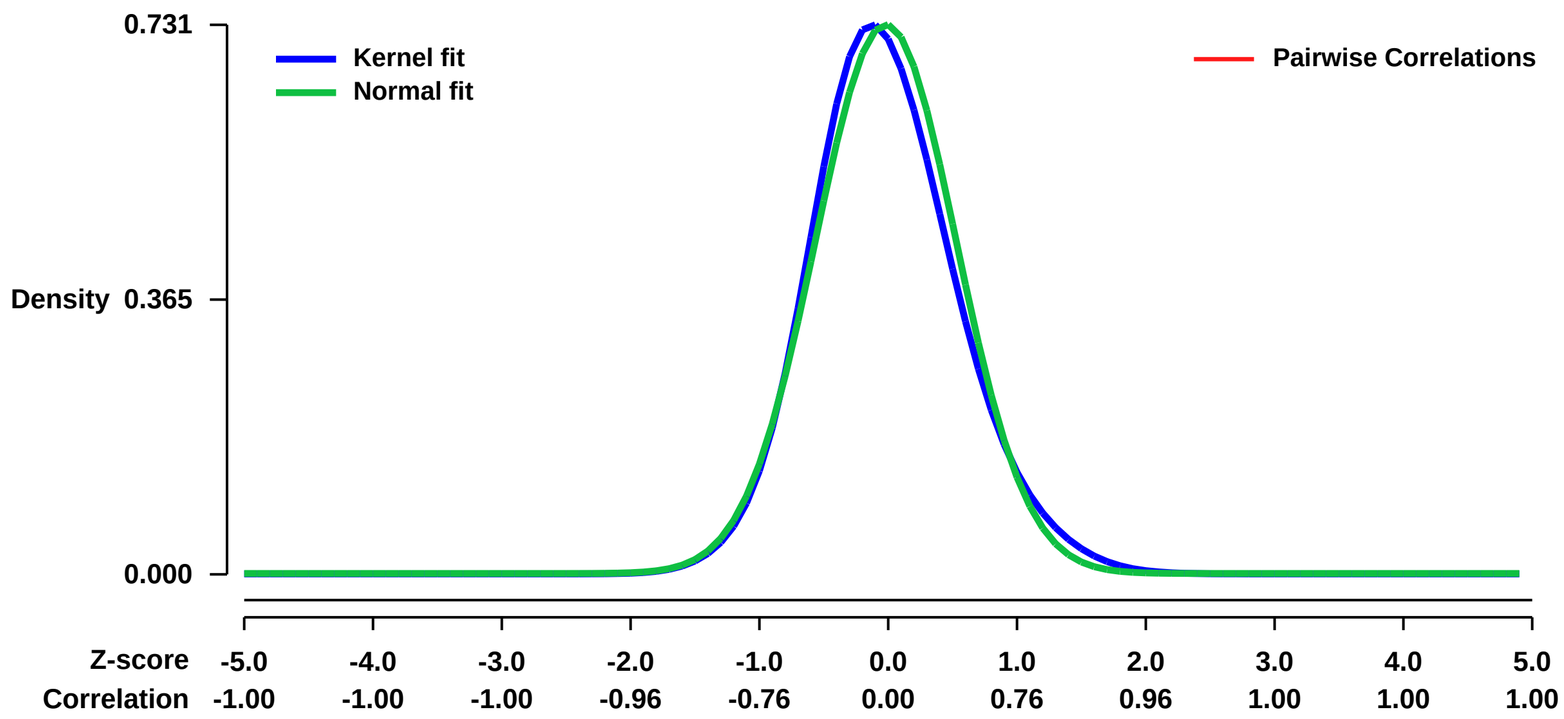

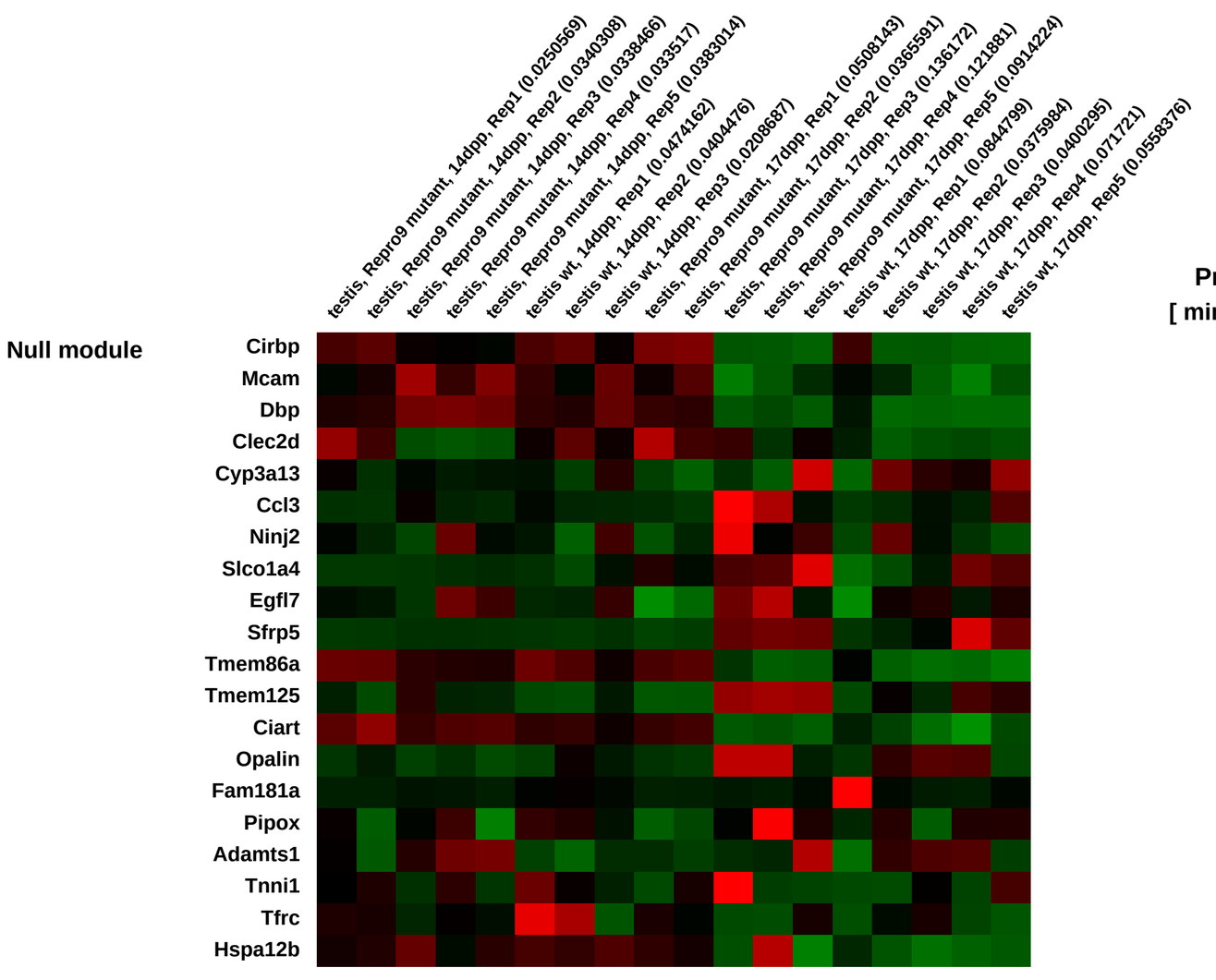

GEO Series "GSE28031" Expression Profiles

Num of samples in this series: 6

Scale of expression profile Z-scores

-3.0 -2.0 -1.0 0.0 1.0 2.0 3.0

GEO Link:	http://www.ncbi.nlm.nih.gov/geo/query/acc.cgi?acc=GSE28031
Status:	Public on Mar 18 2011
Title:	Microarray gene expression profiling of heart failure induced in apolipoprotein E-deficient mice by treatment with rosiglitazone
Organism:	Mus musculus
Experiment type:	Expression profiling by array
Platform:	GPL1261
Pubmed ID:	
Summary & Design:	**Summary:** The anti-diabetic drug and agonist of the peroxisome proliferator-activated receptor gamma (Pparg), rosiglitazone, was recently withdrawn in many countries because the drug use was associated with an increased risk of heart failure. To investigate underlying pathomechanisms, we chose 6-month-old apolipoprotein E (apoE)-deficient mice, which are prone to atherosclerosis and insulin resistance, and thereby mimic the risk profile of patients with cardiovascular disease. After 8 weeks of rosiglitazone treatment (30 mg/kg/day), echocardiography and histology analyses demonstrated that rosiglitazone had induced heart failure with cardiac dilation. Concomitantly, cardiac lipid overload and lipid-induced cardiomyocyte death developed. The microarray gene expression study of heart tissue from rosiglitazone-treated apoE-deficient mice relative to untreated apoE-deficient mice and non-transgenic B6 mice identified cardiac Pparg-dependent lipid metabolism genes in rosiglitazone-treated mice, which seem to trigger a major heart failure promoting pathway. **Overall design:** Microarray gene expression profiling was performed with heart tissue isolated from three study groups: (i) rosiglitazone-treated 8-month-old apolipoprotein (apoE)-deficient mice with symptoms of heart failure, (ii) untreated 8-month-old apoE-deficient mice, and (iii) age-matched, untreated, non-transgenic B6 control mice.

Background corr dist: KL-Divergence = 0.0373, L1-Distance = 0.0241, L2-Distance = 0.0006, Normal std = 0.6413

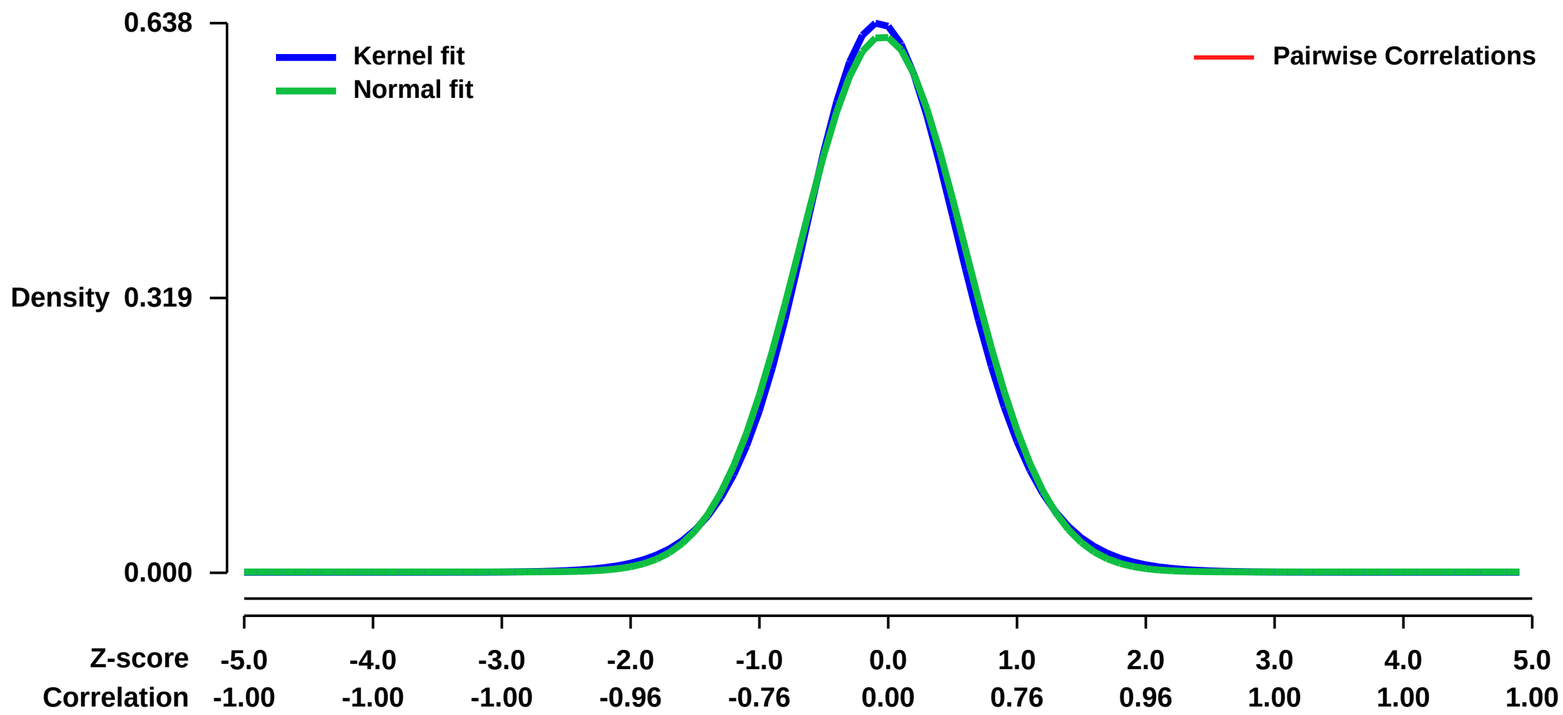

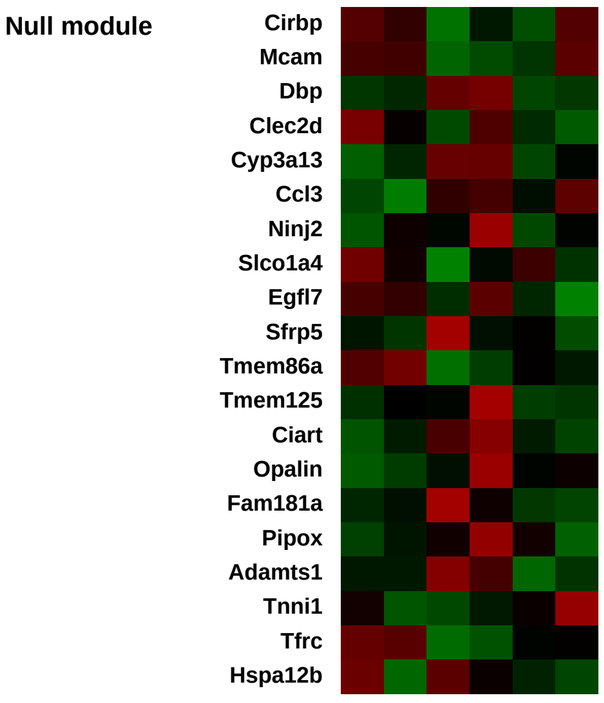

GEO Series "GSE28035" Expression Profiles

Num of samples in this series: 9

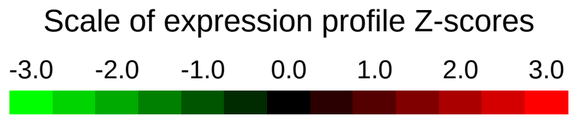

GEO Link:	http://www.ncbi.nlm.nih.gov/geo/query/acc.cgi?acc=GSE28035
Status:	Public on Mar 19 2011
Title:	Expression data from mouse oral keratinocyte
Organism:	Mus musculus
Experiment type:	Expression profiling by array
Platform:	GPL1261
Pubmed ID:	21676921
Summary & Design:	**Summary:** Keratinocytes are the major constituent of epithelial cells at mucosal surfaces and skin, which cover organs, internal cavities and the body. Traditionally, keratinocytes have been considered as an inert component of the multilayered epithelium to protect the subepithelial compartments from the pathogenic microorganisms, toxic stimuli and physical trauma. However, accumulated researches of the airway, gastrointestinal tract and skin have demonstrated that keratinocytes function in the development of the immune system, promotion of pathologic inflammation and even impose diverse decisions on immune cells. We used microarrays to detail the global gene expression of oral keratinocyte during oral adaptive immune response. **Overall design:** Oral keratinocyte were collected at three time points (control, 48h and 96h) in oral adaptive immune response for RNA extraction and hybridization on Affymetrix microarrays

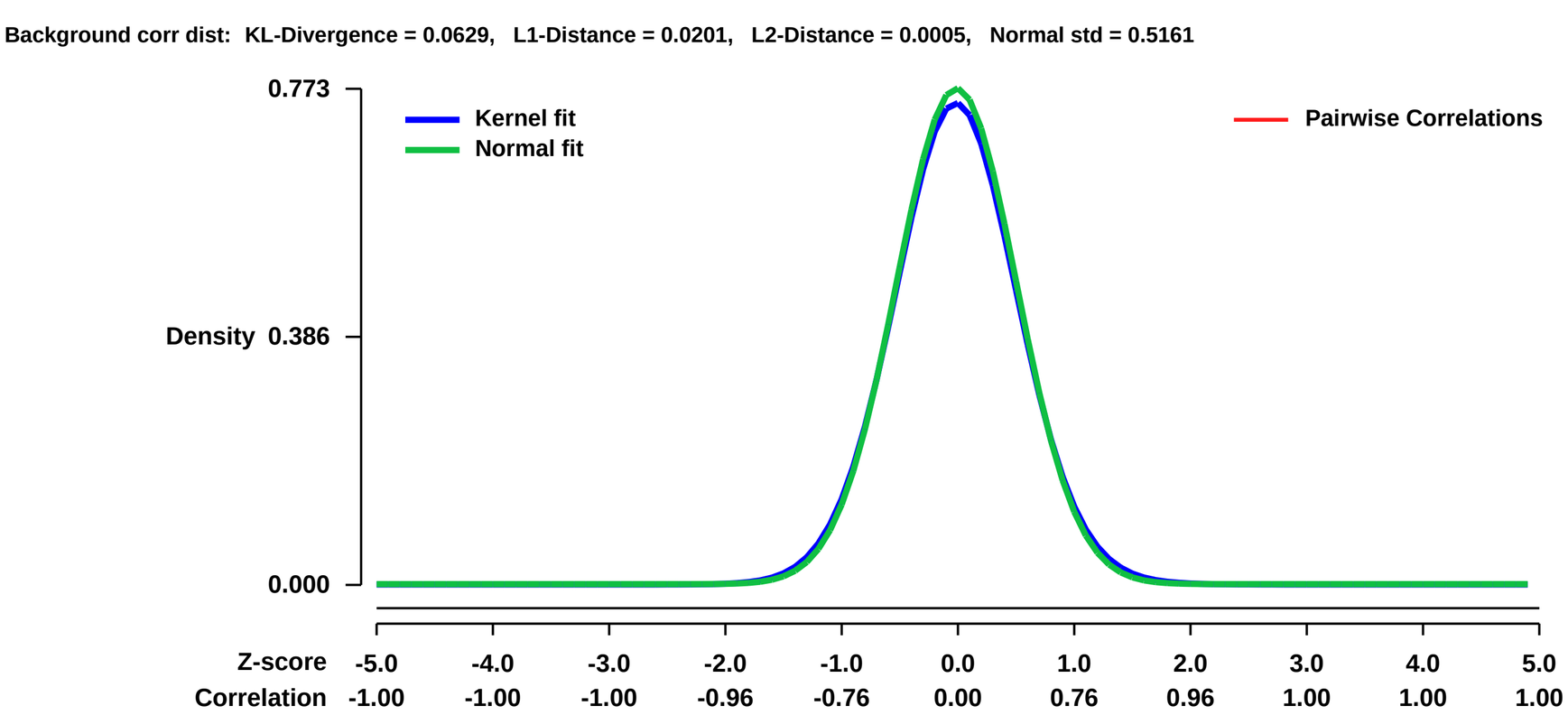

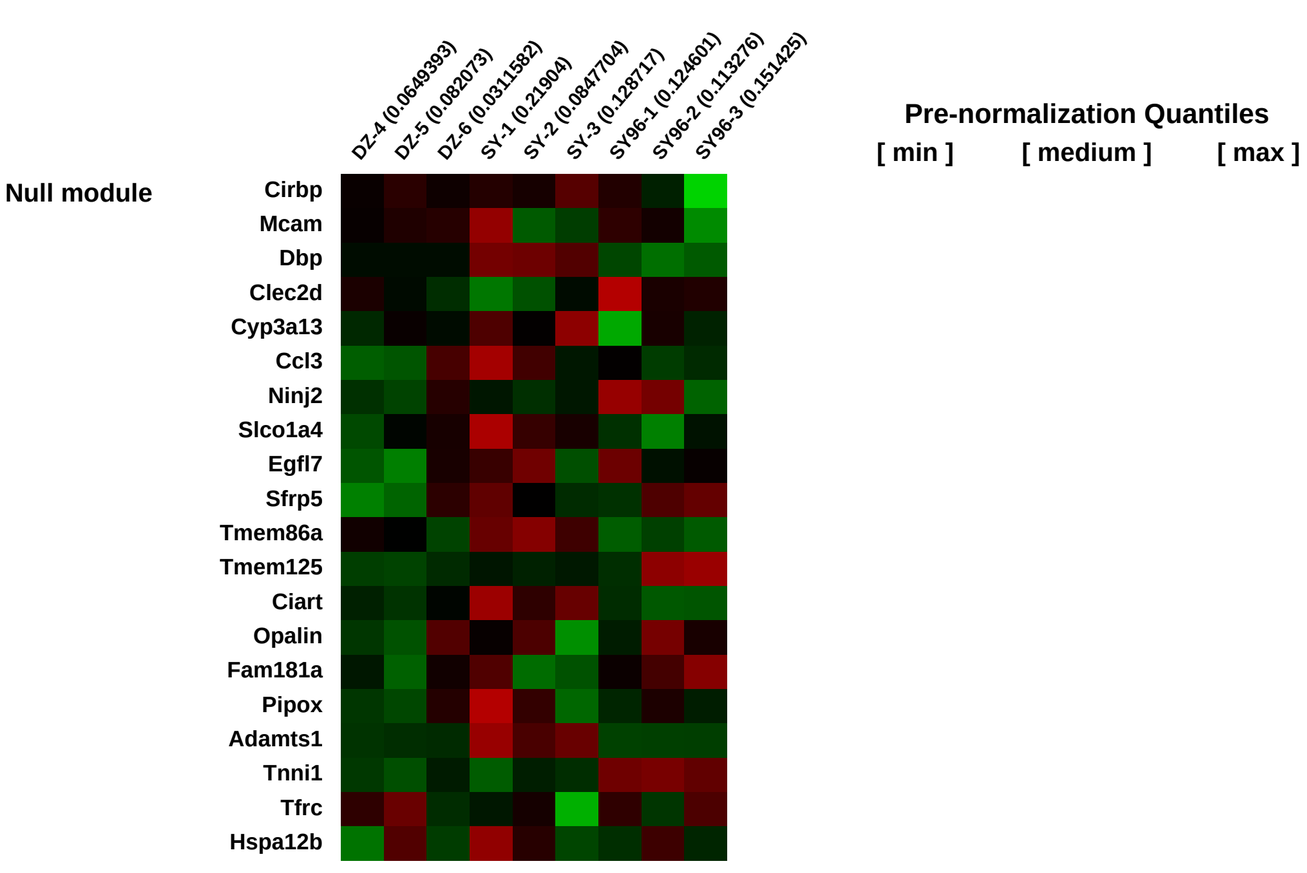

GEO Series "GSE28203" Expression Profiles

Num of samples in this series: 9

Scale of expression profile Z-scores

-3.0 -2.0 -1.0 0.0 1.0 2.0 3.0

GEO Link:	**http://www.ncbi.nlm.nih.gov/geo/query/acc.cgi?acc=GSE28203**
Status:	**Public on Mar 31 2012**
Title:	**Mouse oral tumors induced by activation of Ras and p53 mutations**
Organism:	**Mus musculus**
Experiment type:	**Expression profiling by array**
Platform:	**GPL1261**
Pubmed ID:	
Summary & Design:	**Summary:** **The p53 gain of function p53R172H promotes accelerated tumor growth and progression to carcinoma. To identify gene expression changes associated with the oncogenic function of mutant p53 we compared the expression profiles of oral tumors induced by activation of oncogenic K-ras and p53 gain- or loss-of-function mutations** **Oral tumors were induced by activation of endogenous oncogenic K-rasG12D and p53 loss- or gain-of-function mutations (p53R172H)** **Overall design:** **Oral tumors from mice carrying the p53R172H mutation or deletion of p53 were collected for gene expression analysis**

Background corr dist: **KL-Divergence = 0.0700, L1-Distance = 0.0257, L2-Distance = 0.0011, Normal std = 0.5020**

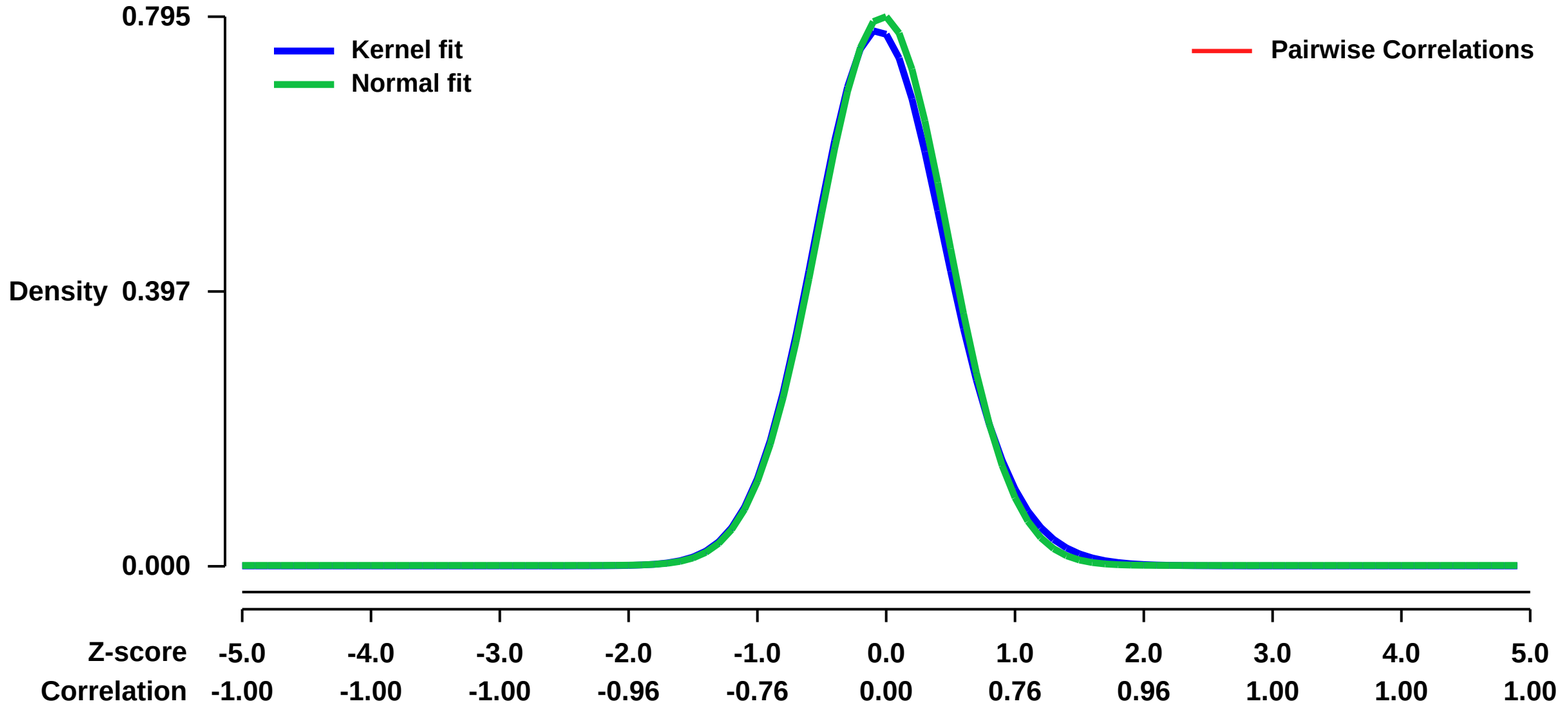

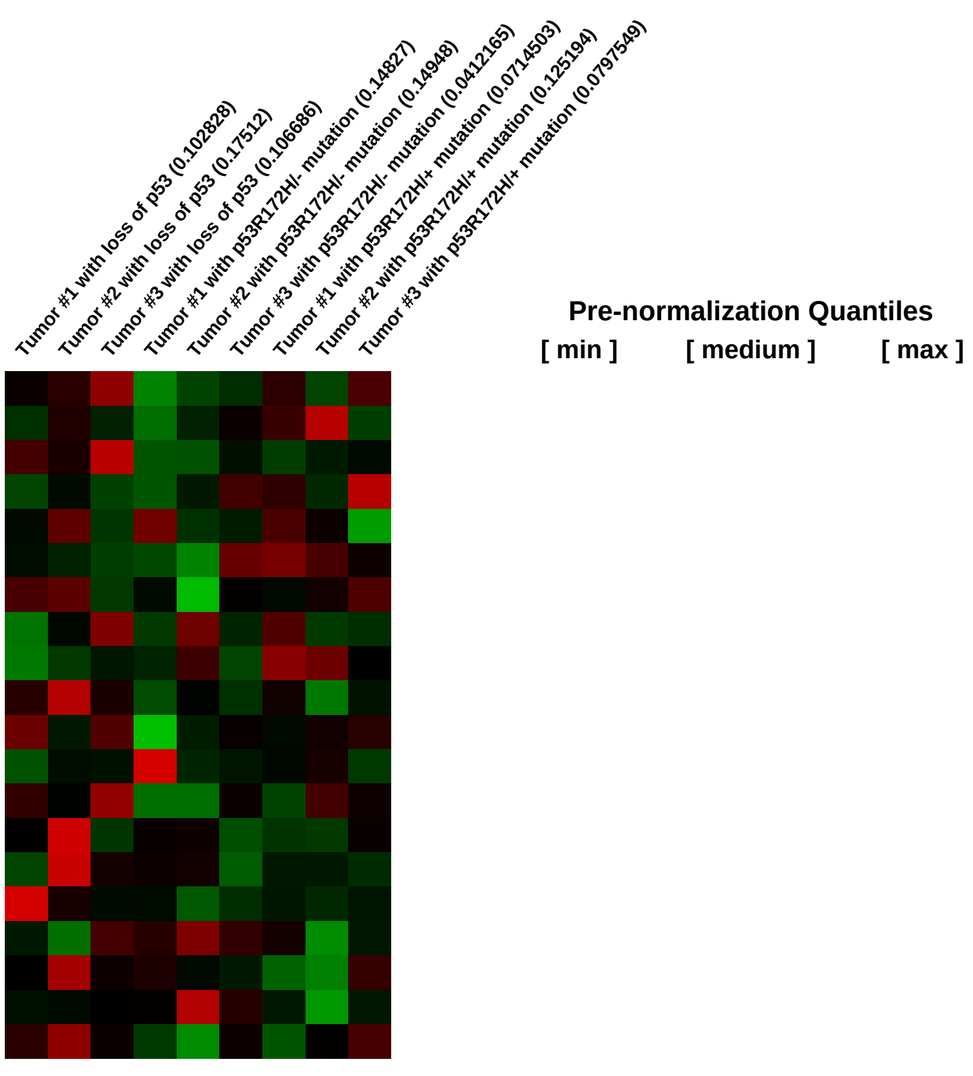

GEO Series "GSE28261" Expression Profiles

Num of samples in this series: 72

Scale of expression profile Z-scores

-3.0 -2.0 -1.0 0.0 1.0 2.0 3.0

GEO Link: http://www.ncbi.nlm.nih.gov/geo/query/acc.cgi?acc=GSE28261
Status: Public on Mar 30 2011
Title: Whole blood gene expression in female Balb/c mice following 2-week Pb exposure and subsequent 2-week recovery period
Organism: Mus musculus
Experiment type: Expression profiling by array
Platform: GPL1261
Pubmed ID:

Summary & Design:

Summary:
Background: Current evidence indicates that even low-level lead (Pb) exposure can have detrimental effects, especially in children. We tested the hypothesis that Pb exposure alters gene expression patterns in peripheral blood cells and that these changes reflect dose-specific alterations in the activity of particular pathways.

Methodology/Principal Finding: Using Affymetrix Mouse Genome 430 2.0 arrays, we examined gene expression changes in the peripheral blood of female Balb/c mice following exposure to per os lead acetate trihydrate or plain drinking water for two weeks and after a two-week recovery period. Data sets were RMA-normalized and dose-specific signatures were generated using established methods of supervised classification and binary regression. Pathway activity was analyzed using the ScoreSignatures module from GenePattern.

Conclusions/Significance: The low-level Pb signature was 93% sensitive and 100% specific in classifying samples a leave-one-out crossvalidation. The high-level Pb signature demonstrated 100% sensitivity and specificity in the leave-one-out crossvalidation. These two signatures exhibited dose-specificity in their ability to predict Pb exposure and had little overlap in terms of constituent genes. The signatures also seemed to reflect current levels of Pb exposure rather than past exposure. Finally, the two doses showed differential activation of cellular pathways. Low-level Pb exposure increased activity of the interferon-gamma pathway, whereas high-level Pb exposure increased activity of the E2F1 pathway.

Overall design:
We isolate total RNA from 72 mouse whole blood samples. These included samples following a 2-week exposure to lead acetate trihydrate (untreated controls = 7; Low Pb 5ug/mL drinking water = 15; High Pb 50ug/mL drinking water = 15) and additional samples following a 2-week recovery period with plain drinking water (untreated controls = 7; Low Pb group = 15; High Pb group = 13).

Background corr dist: KL-Divergence = 0.1437, L1-Distance = 0.0741, L2-Distance = 0.0158, Normal std = 0.3837

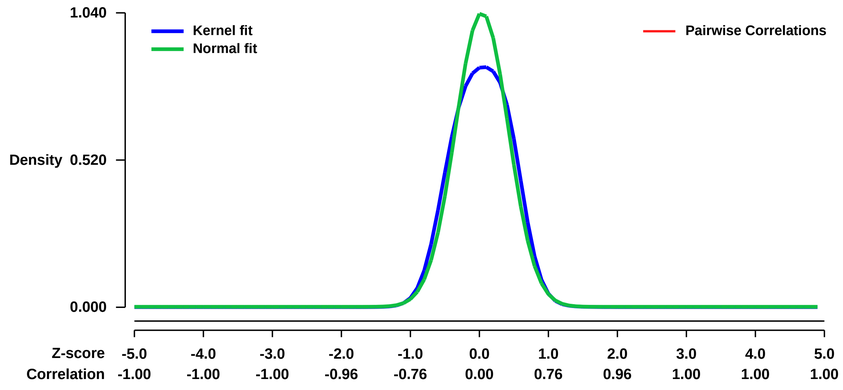

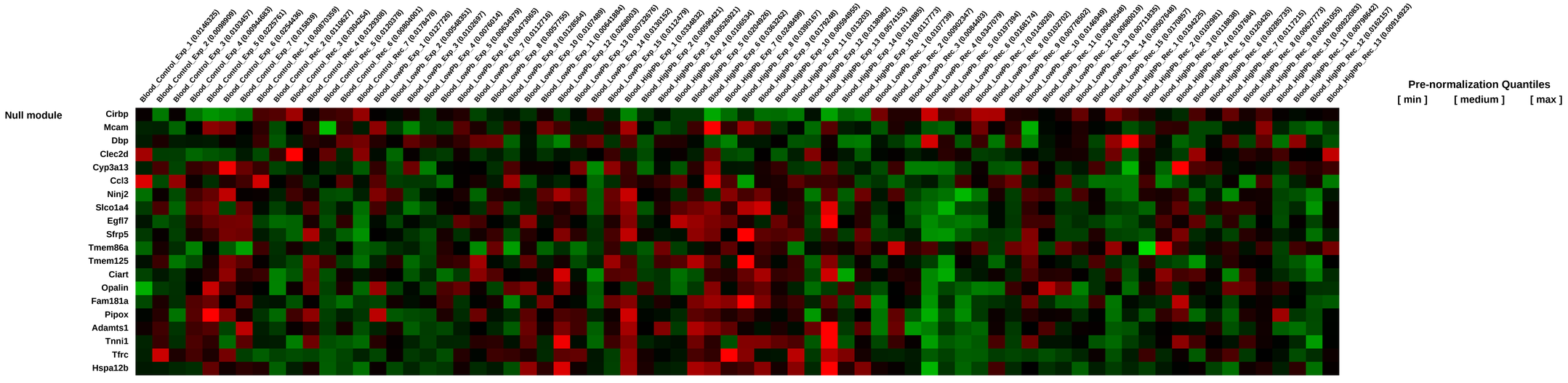

GEO Series "GSE28277" Expression Profiles

Num of samples in this series: 10

Scale of expression profile Z-scores

-3.0 -2.0 -1.0 0.0 1.0 2.0 3.0

GEO Link:	http://www.ncbi.nlm.nih.gov/geo/query/acc.cgi?acc=GSE28277
Status:	Public on Jun 01 2011
Title:	Altered Gene Expression in Placentae from a Mouse Model of Diabetic Pregnancy
Organism:	Mus musculus
Experiment type:	Expression profiling by array
Platform:	GPL1261
Pubmed ID:	21491160
Summary & Design:	**Summary:** **AIMS/HYPOTHESIS: Pregnancies complicated by diabetes have a higher risk of adverse outcomes for mothers and children, including predisposition to disease later in life, such as metabolic syndrome and hypertension. We hypothesized that adverse outcomes from diabetic pregnancies may be linked to compromised placental function. Our goal in this study was to identify cellular and molecular abnormalities in diabetic placenta.** **METHODS: Using a mouse model of diabetic pregnancy, placental gene expression was assayed at midgestation and cellular composition was analyzed at various stages. Genome-wide expression profiling was validated by quantitative PCR, and tissue localization studies were performed to identify cellular correlates of altered gene expression in diabetic placenta.** **RESULTS: We detected significantly altered gene expression in diabetic placenta for genes expressed in the maternal as well as those in the embryonic compartments. We also found altered cellular composition of the decidual compartment. Furthermore, the junctional and labyrinth layers were reduced in diabetic placenta, accompanied by aberrant differentiation of spongiotrophoblast cells.** **CONCLUSIONS/INTERPRETATION: Diabetes during pregnancy alters transcriptional profiles in the murine placenta, affecting cells of both embryonic and maternal origin, and involving several genes not previously implicated in diabetic pregnancies. The molecular changes and abnormal differentiation of multiple cell types precede impaired growth of junctional zone and labyrinth, and placenta overall. Whether these changes represent direct responses to hyperglycaemia or physiological adaptations, they are likely to play a role in pregnancy complications and outcomes, and have implications for developmental origins of adult disease.** **Overall design:** **The STZ diabetic mouse model was used to investigate gene expression changes in diabetic placentae at E10.5. Placentae were dissected from 5 different FVB dams at embryonic day 10.5 under diabetic conditions and from 5 control dams. Gene expression profiles from five individual placentae from independent pregnancies per group were compared.**

Background corr dist: KL-Divergence = 0.0896, L1-Distance = 0.0222, L2-Distance = 0.0008, Normal std = 0.4569

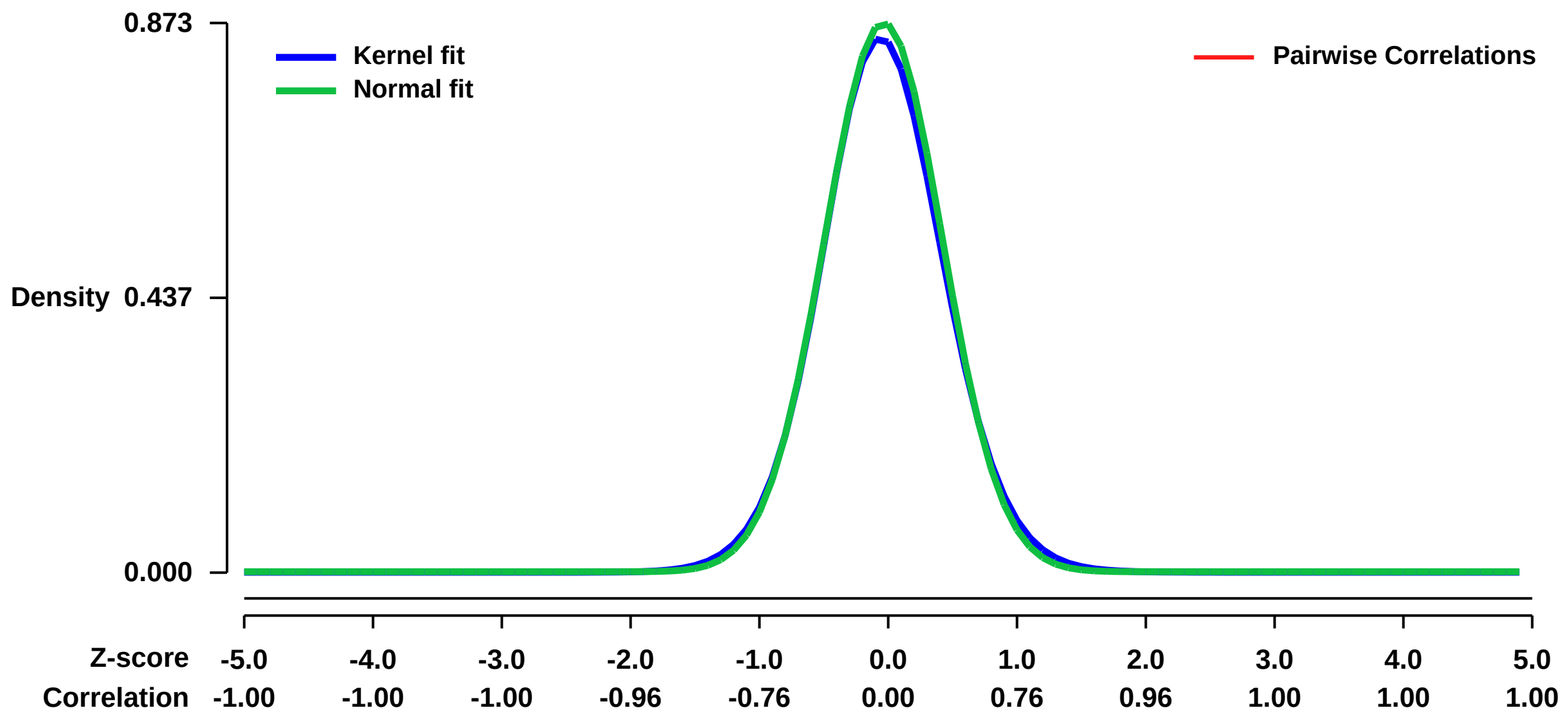

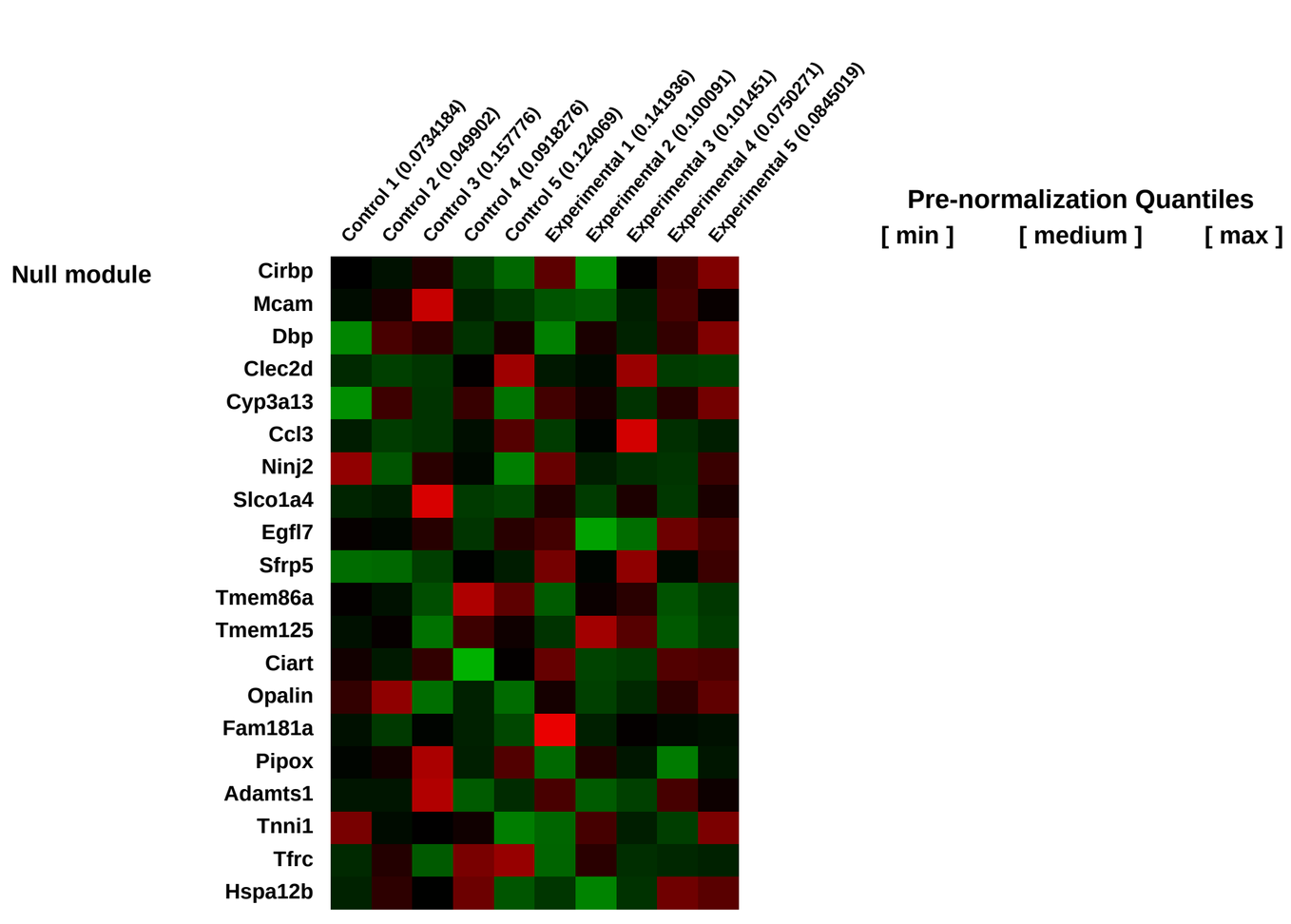

GEO Series "GSE28333" Expression Profiles

Num of samples in this series: 6

Scale of expression profile Z-scores

-3.0 -2.0 -1.0 0.0 1.0 2.0 3.0

GEO Link:	http://www.ncbi.nlm.nih.gov/geo/query/acc.cgi?acc=GSE28333
Status:	Public on Mar 22 2012
Title:	Expression data from BCL11A-null and wild-type bone marrow erythroid pregenitors
Organism:	Mus musculus
Experiment type:	Expression profiling by array
Platform:	GPL1261
Pubmed ID:	21998251
Summary & Design:	**Summary:** BCL11A is a critical mediator of hemoglobin switching and gamma-globin silencing. In this study, we showed the BCL11A is required in vivo for developmental silencing of gamma-globin genes in adult animals. We used microarray to determine the changes in gene expression profile after loss of BCL11A in adult erythroid cells **Overall design:** CD71+Ter119+ erythroid progenitor cells were FACS-sorted from bone marrows of 6-week old control (Bcl11a +/+) and BCL11A knockout (Bcl11a fl/fl EpoR-Cre+) mice.

Background corr dist: KL-Divergence = 0.0415, L1-Distance = 0.0210, L2-Distance = 0.0005, Normal std = 0.6102

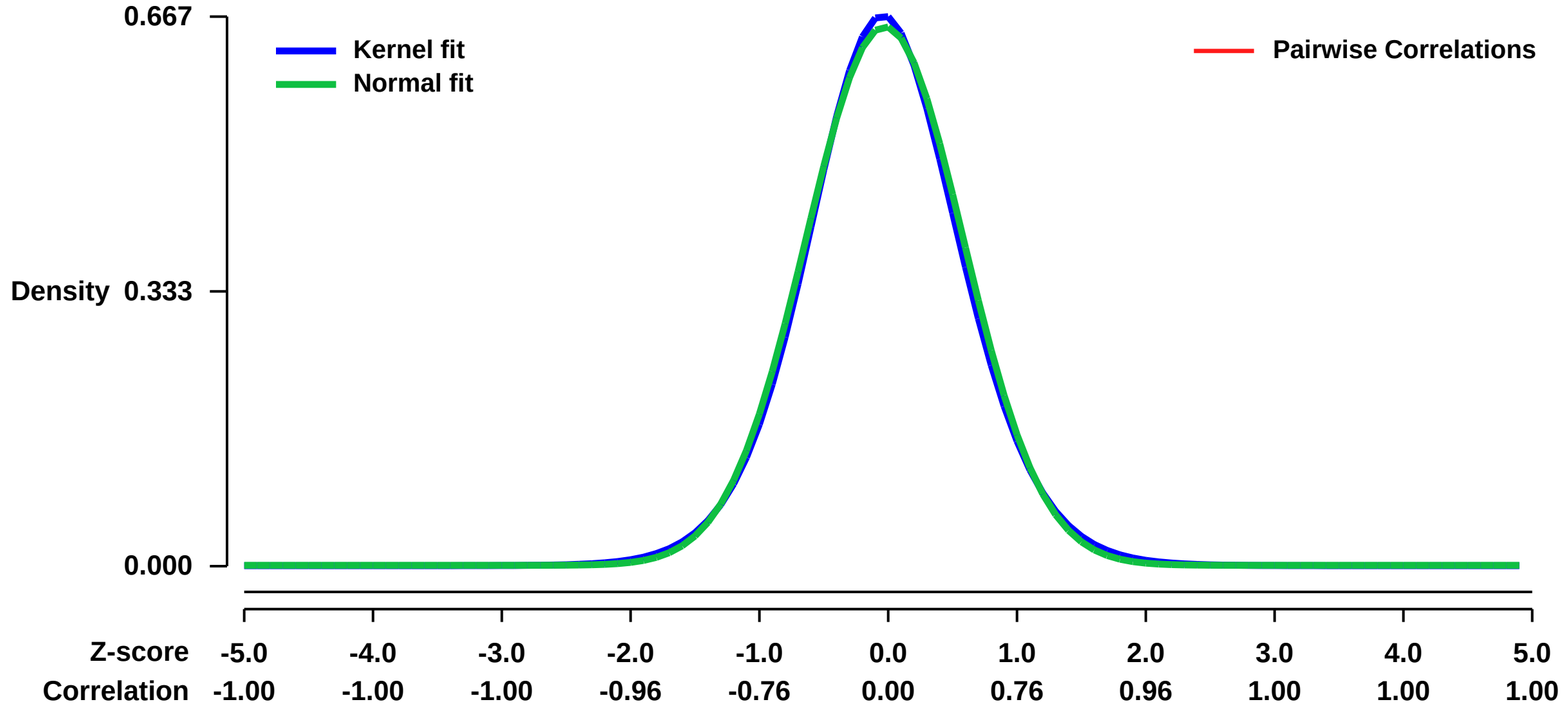

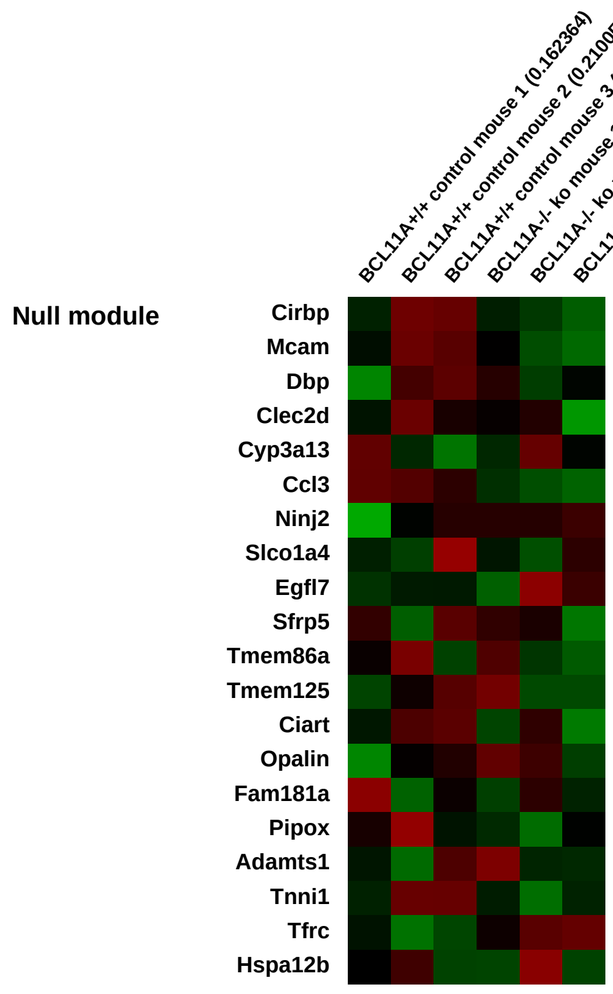

GEO Series "GSE28389" Expression Profiles

Num of samples in this series: 20

Scale of expression profile Z-scores

-3.0 -2.0 -1.0 0.0 1.0 2.0 3.0

GEO Link:	http://www.ncbi.nlm.nih.gov/geo/query/acc.cgi?acc=GSE28389
Status:	Public on Apr 05 2011
Title:	[E-MTAB-368] Transcription profiling by array of mouse embryos at 8 different stages
Organism:	Mus musculus
Experiment type:	Expression profiling by array
Platform:	GPL1261
Pubmed ID:	21427719
Summary & Design:	**Summary:** **Transcription profiling of mouse development** **The experiment were perfomed as a part of our Vertebrate Evo-Devo project. The aim of the project is to compare transcription profiles of normal (unmanipulated, wild-type, whole embryo) vertebrate embryos.** **Overall design:** **Total RNA was collected from wild type C57BL/6 mice, whole embryos at 8 different stages (Stages:E7.5, E8.5, E9.5, E10.5, E12.5, E14.5, E16.5, E18.5), and hybridized to Affymetrix Mouse Genome 430 2.0 Array. All the stages contains data from 2 to 3 biological replications. Each staged-samples consists of pooled total RNA from several whole embryos.**

Background corr dist: **KL-Divergence = 0.0441, L1-Distance = 0.0355, L2-Distance = 0.0018, Normal std = 0.5966**

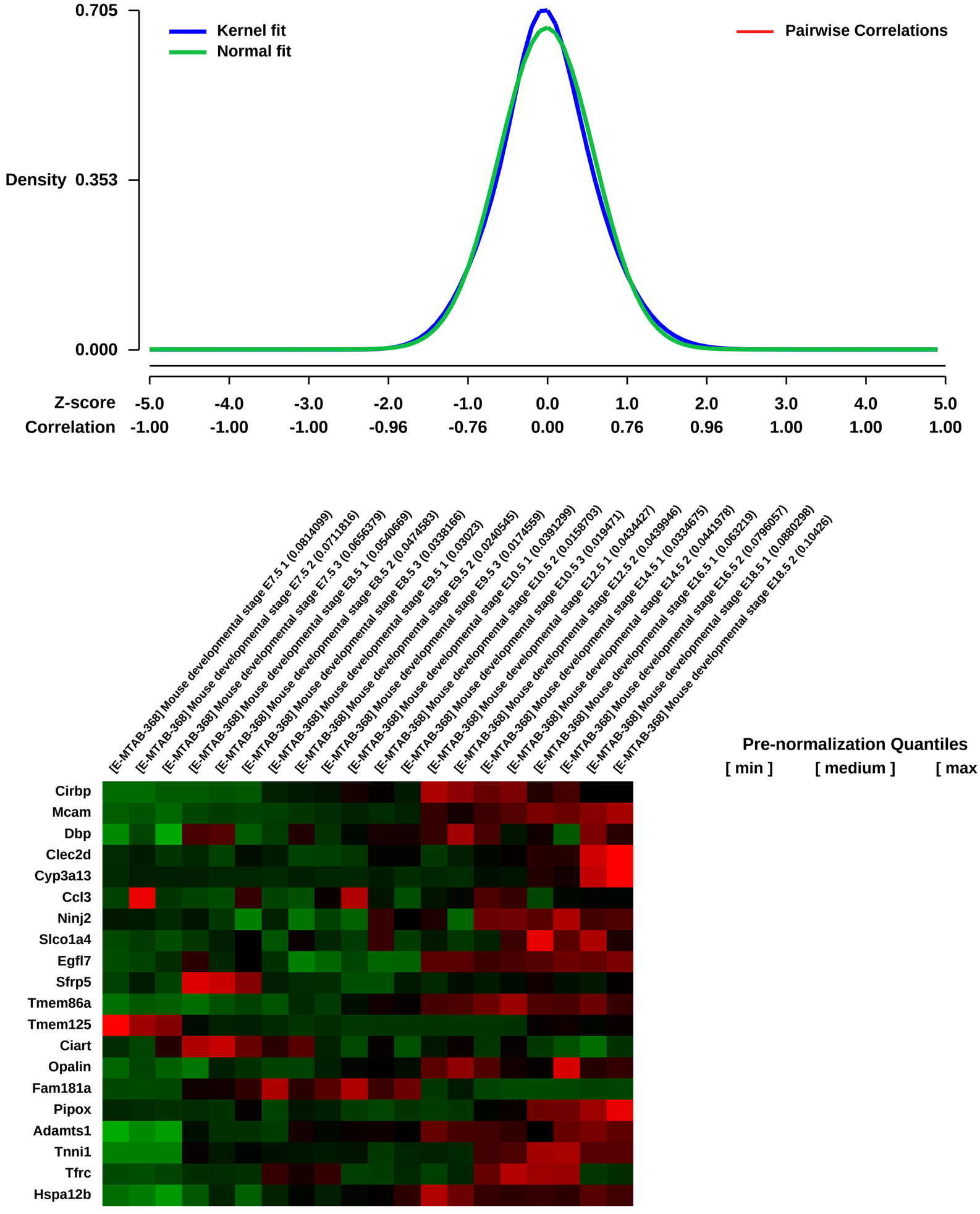

GEO Series "GSE28408" Expression Profiles

Num of samples in this series: 6

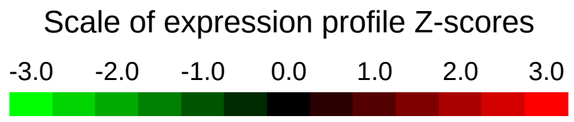

GEO Link:	**http://www.ncbi.nlm.nih.gov/geo/query/acc.cgi?acc=GSE28408**
Status:	**Public on Feb 01 2013**
Title:	**Expression data from Ly6G+ and Ly6G- dendritic cells (DC)**
Organism:	**Mus musculus**
Experiment type:	**Expression profiling by array**
Platform:	**GPL1261**
Pubmed ID:	**23305731**
Summary & Design:	**Summary:** **To investigate the functional properties of Ly6G+ DC, we employed GeneChip analysis to compare the gene expression profiles between Ly6G+ DC and Ly6C- DC.** **Overall design:** **Crude bone marrow (BM) cells prepared from C57BL/6 mice were cultured in the presence of GM-CSF. On day 6, CD11c+/MHC II+/Ly6G+ cells and CD11c+/MHC II+/Ly6G- cells were simultaneously sorted from the same cultures by FACSAria. Total RNA were extracted and hybridized on Affymetrix microarrays.**

Background corr dist: **KL-Divergence = 0.0392, L1-Distance = 0.0299, L2-Distance = 0.0012, Normal std = 0.6277**

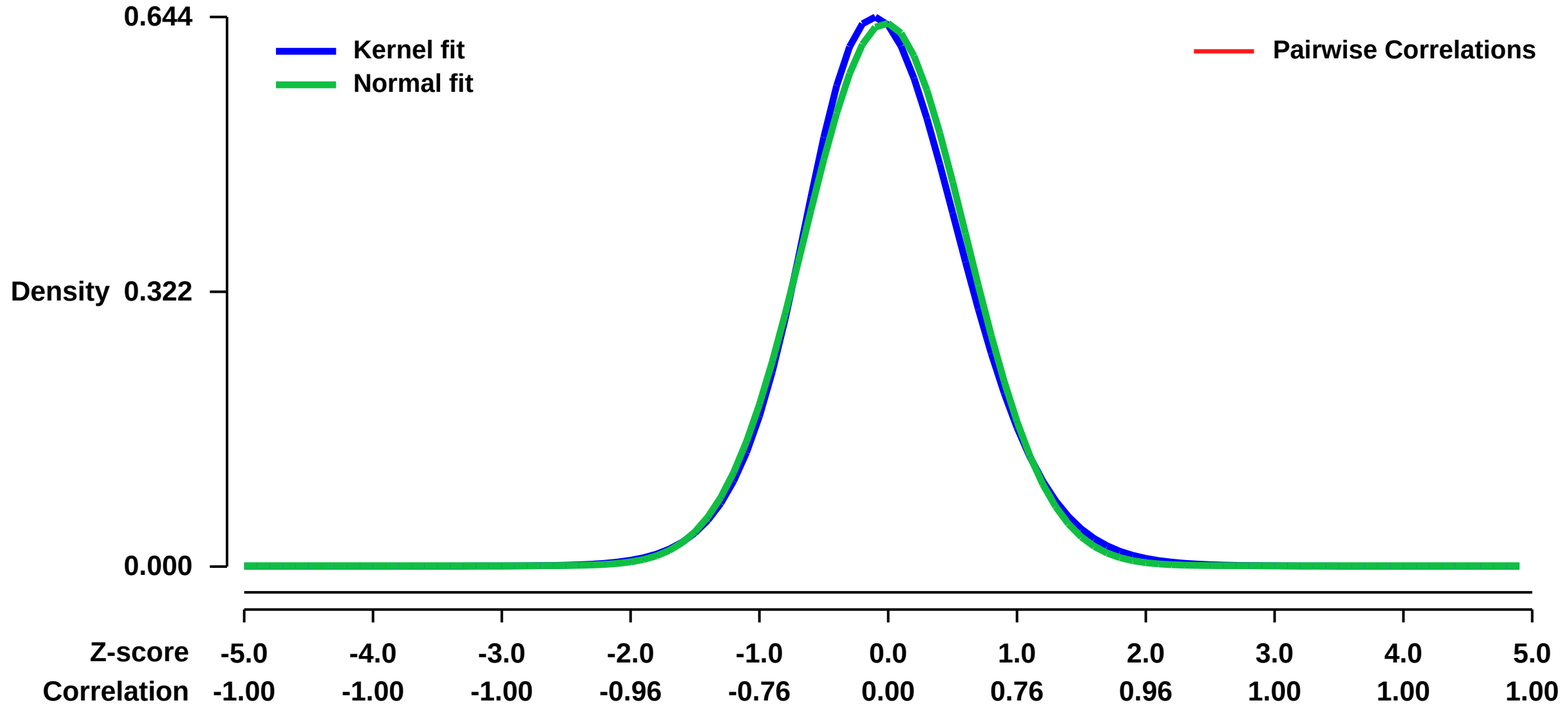

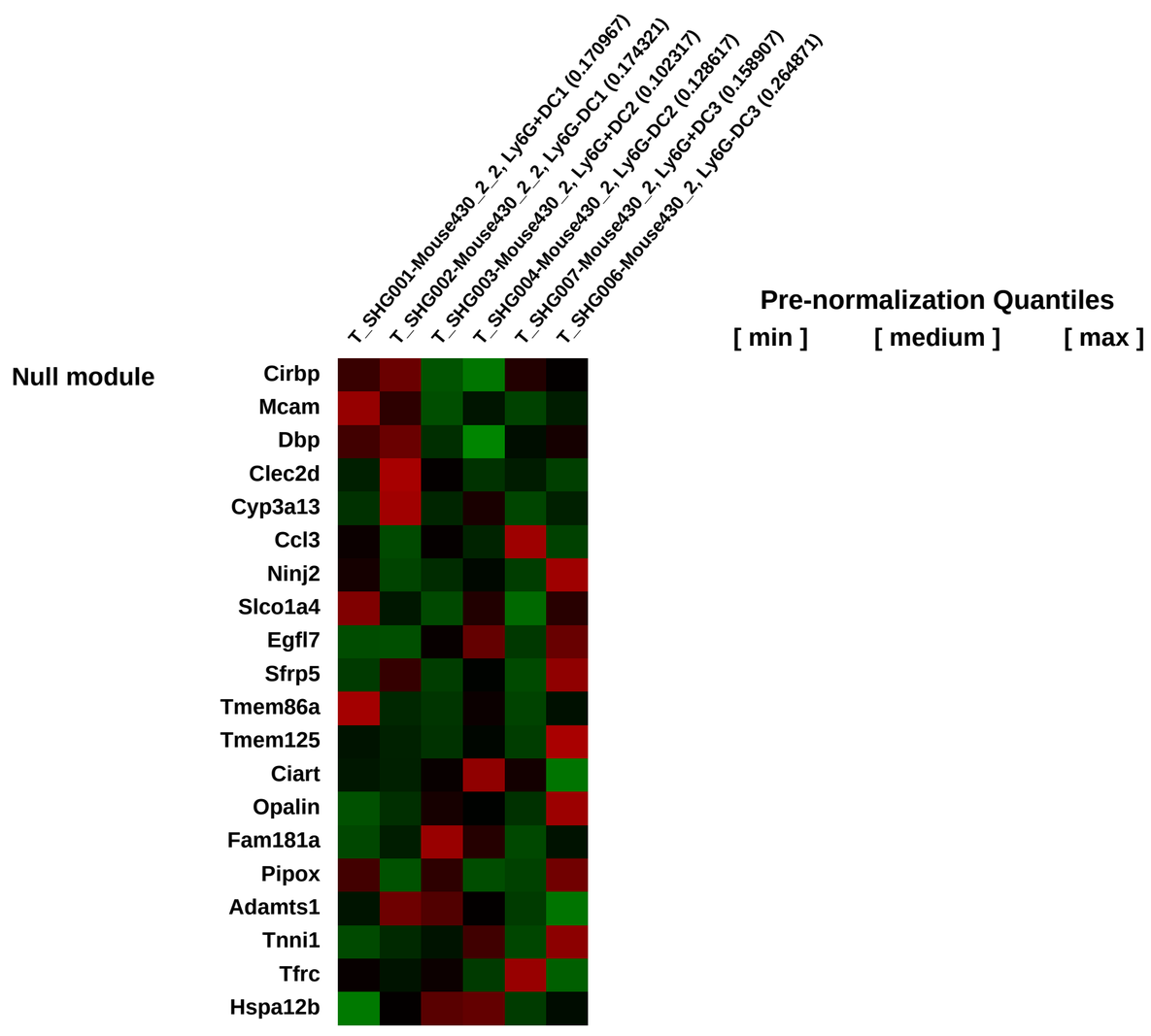

GEO Series "GSE28457" Expression Profiles

Num of samples in this series: 24

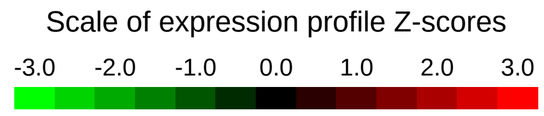

GEO Link:	http://www.ncbi.nlm.nih.gov/geo/query/acc.cgi?acc=GSE28457
Status:	Public on May 31 2012
Title:	Gene expression profile of E1A infected C2C12 myotubes
Organism:	Mus musculus
Experiment type:	Expression profiling by array
Platform:	GPL1261
Pubmed ID:	23027903
Summary & Design:	**Summary:** Proliferating C2C12 myoblasts were induced to differentiate into myotubes and then infected with adenovirus expressing E1A (Ad-E1A), which induces cell cycle re-entry and dedifferentiation. We analyzed the transcriptional profile of E1A infected C2C12-myotubes through the Affymetrix Mouse Genome 430 2.0 Array, searching for genes that were significantly regulated between two independent biological replicates at two different time points (24h and 36h after infection with Ad-E1A). In addition, we took advantage of the E1A mutant known as YH47/dl928 (hereafter referred as YH47), which bears two mutations in the pocket-binding region of E1A (Y48H, C124G) able to disrupt the interaction with Rb and its cognate proteins and to impair cell-cycle re-entry phenotype. YH47 mutant was used to identify the Rb independent transcriptional reprogramming of C2C12. **Overall design:** C2C12 cells were differentiated in vitro to myotubes as previously described. Myotubes were, then, infected with an adenovirus carrying the 12S form of E1A (dl520), with the YH47 E1A mutant (dl928) or with a control adenovirus (CTR) expressing a deletion of essentially the entire E1A gene (dl312). Two different time points after infection were considered (24 hours and 36 hours) to evaluate changes in C2C12 cells expression profile. Technical (A or B) and biological replicates (EXP1 or EXP2) were done for each condition.

Background corr dist: KL-Divergence = 0.1997, L1-Distance = 0.0314, L2-Distance = 0.0016, Normal std = 0.3411

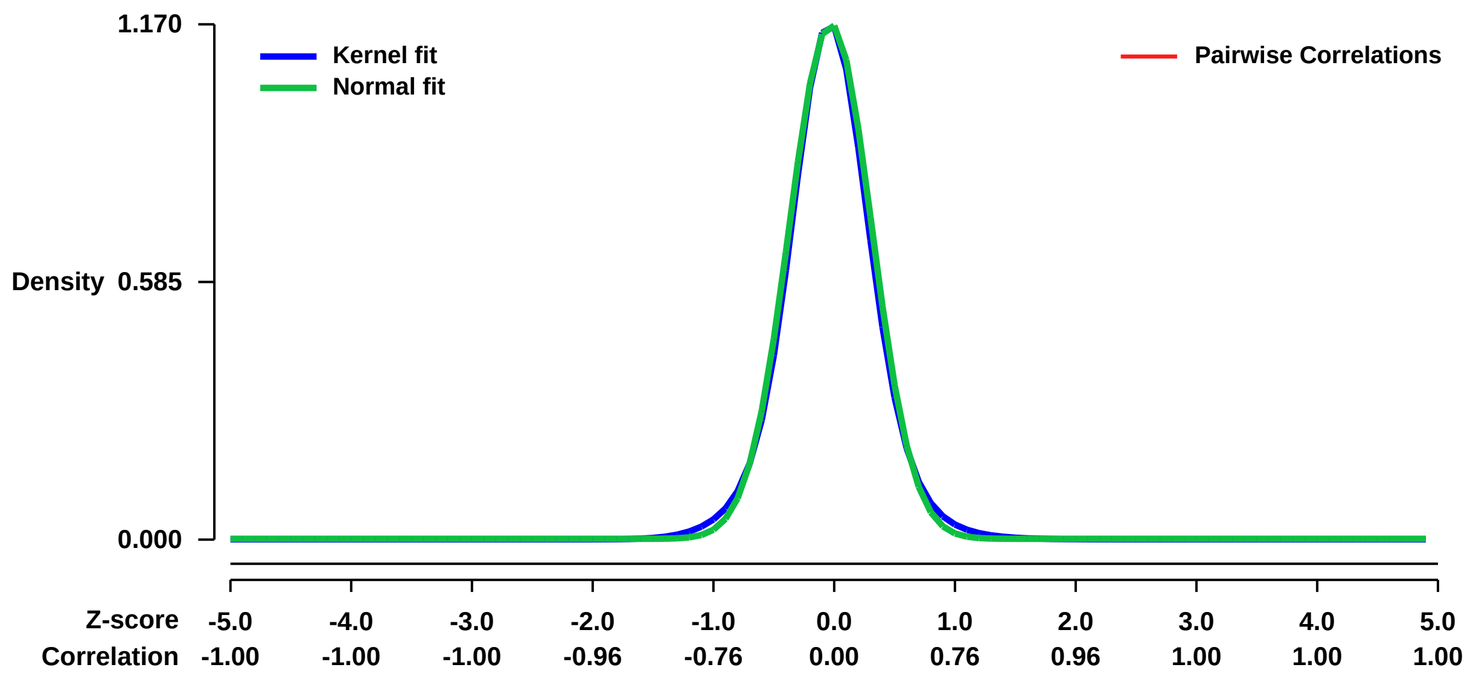

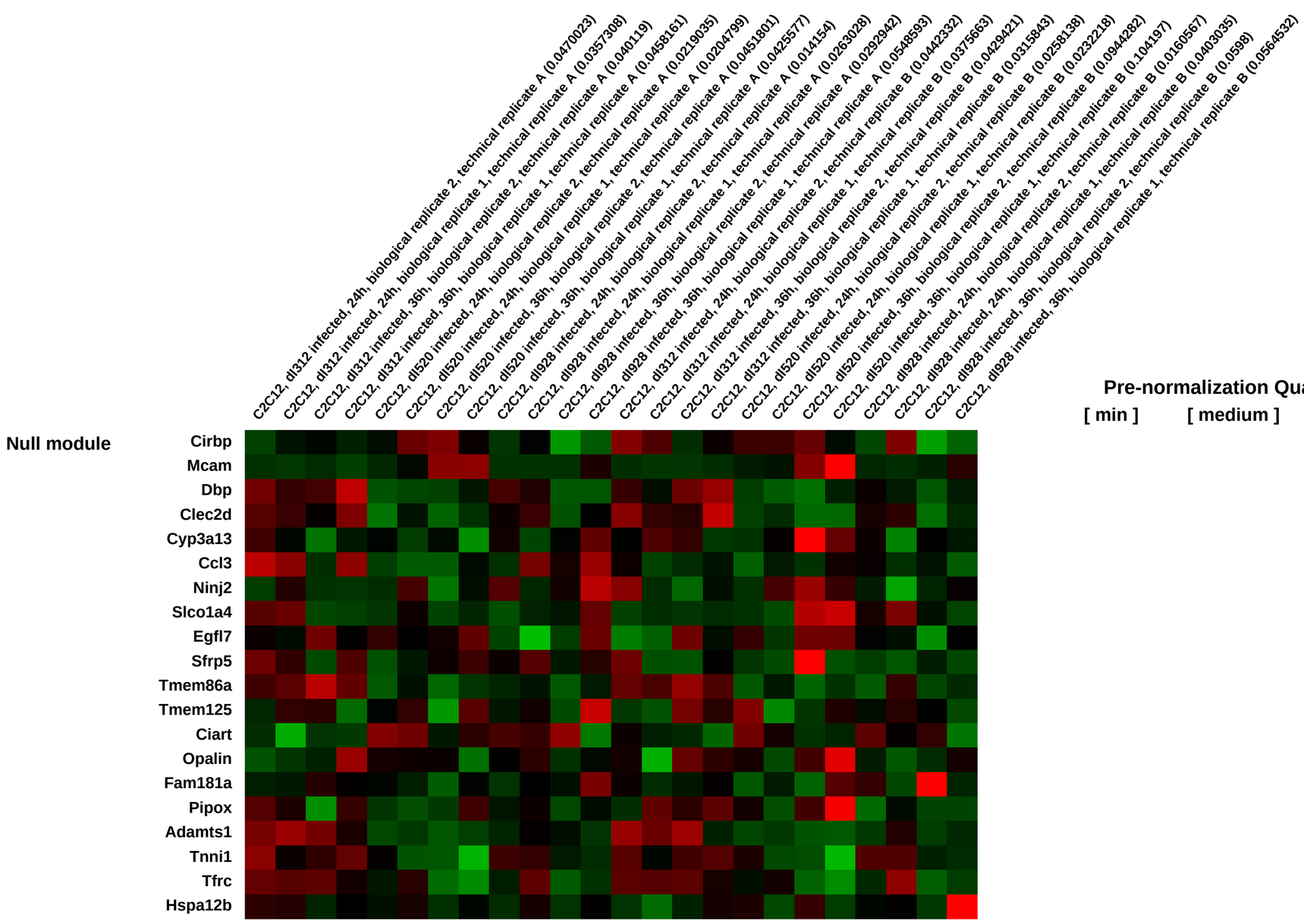

GEO Series "GSE28515" Expression Profiles

Num of samples in this series: 66

Scale of expression profile Z-scores

-3.0 -2.0 -1.0 0.0 1.0 2.0 3.0

GEO Link:	http://www.ncbi.nlm.nih.gov/geo/query/acc.cgi?acc=GSE28515
Status:	Public on Dec 01 2011
Title:	Effect of acute ethanol on medidal prefrontal cortex across BXD genetic mapping panel and progenitors.
Organism:	Mus musculus
Experiment type:	Expression profiling by array
Platform:	GPL1261
Pubmed ID:	22511924
Summary & Design:	**Summary:** In order to elucidate the molecular mechanisms underlying individual variation in sensitivity to ethanol we profiled the prefrontal cortex transcriptomes of two inbred strains that exhibit divergent responses to acute ethanol, the C57BL6/J (B6) and DBA/2J (D2) strains, as well as 27 members of the BXD recombinant inbred panel, which was derived from a B6 x D2 cross. With this dataset we were able to identify several gene co-expression networks that were robustly altered by acute ethanol across the BXD panel. These ethanol-responsive gene-enriched networks were heavily populated by genes regulating synaptic transmission and neuroplasticity, and showed strong genetic linkage to discreet chromosomal loci. Network-based measurements of node importance identified several hub genes as established regulators of ethanol response phenotypes, while other hubs represent novel candidate modulators of ethanol responses. **Overall design:** Animals were injected intraperitoneally (IP) with saline or 1.8 g/kg of ethanol. As part of a parallel study of ethanol induced anxiolysis, all mice underwent behavioral testing that included 15 minutes of restraint in a 50 mL conical tube followed by 10 minutes in a light-dark chamber. Mice were killed by cervical dislocation four hours following IP injection. Immediately thereafter, brains were extracted and chilled for 1 minute in iced phosphate buffer before being microdissected into 8 constituent regions, including the medial prefrontal cortex. Samples were randomly assigned to batch groups prior to total RNA extraction, cRNA synthesis and hybridization. Each microarray represent a pooling of 4-5 animals.

Background corr dist: KL-Divergence = 0.4180, L1-Distance = 0.0881, L2-Distance = 0.0251, Normal std = 0.2427

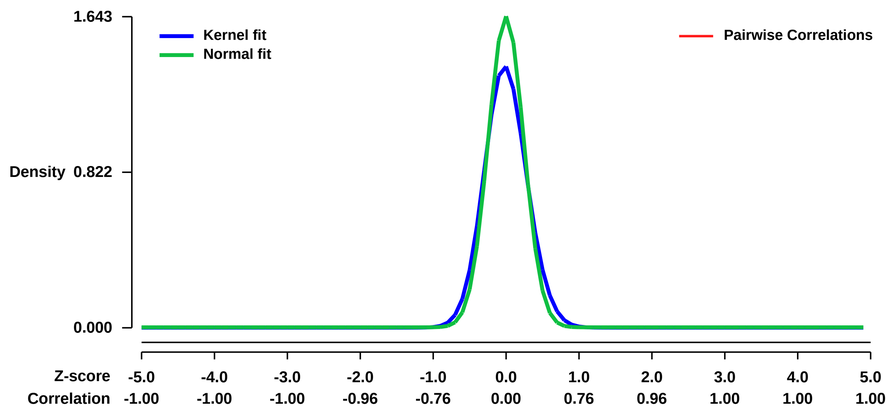

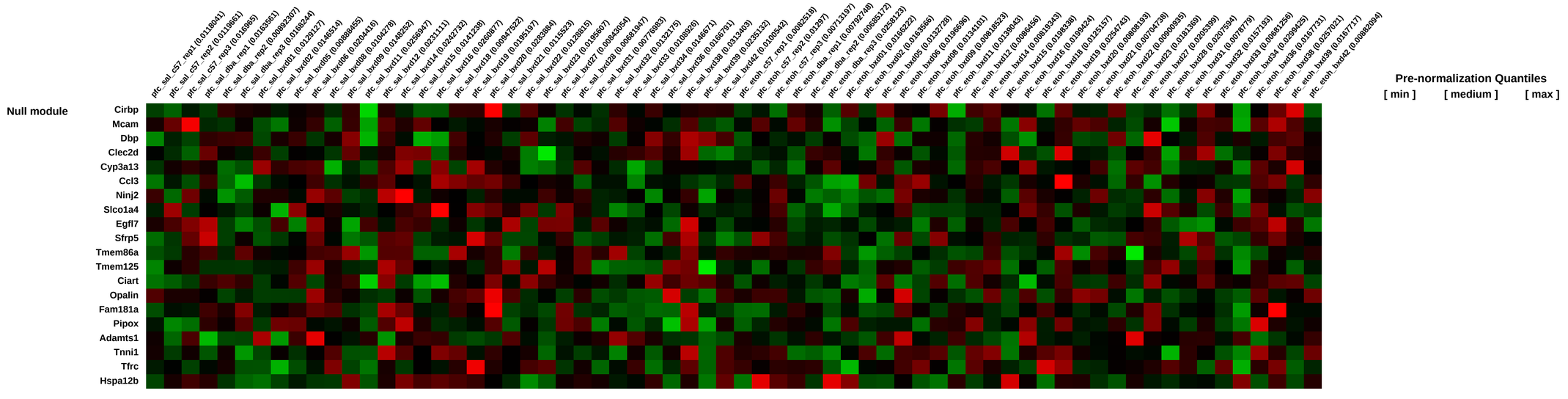

GEO Series "GSE28593" Expression Profiles

Num of samples in this series: 9

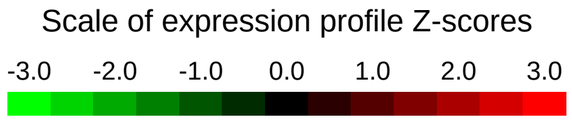

GEO Link:	http://www.ncbi.nlm.nih.gov/geo/query/acc.cgi?acc=GSE28593
Status:	Public on Apr 15 2011
Title:	KMT1E Mediated H3K9 Methylation Is Required for the Maintenance of Embryonic Stem Cells by Repressing Trophectoderm Differentiation
Organism:	Mus musculus
Experiment type:	Expression profiling by array
Platform:	GPL1261
Pubmed ID:	20014010
Summary & Design:	**Summary:** Dynamic regulation of histone methylation by methyltransferases and demethylases plays a central role in regulating the fate of embryonic stem (ES) cells. The histone H3K9 methyltransferase KMT1E, formerly known as ESET or Setdb1, is essential to embryonic development as the ablation of the Setdb1 gene results in peri-implantation lethality and prevents the propagation of ES cells. However, Setdb1- null blastocysts do not display global changes in H3K9 methylation or DNA methylation, arguing against a genome- wide defect. Here we show that conditional deletion of the Setdb1 gene in ES cells results in the upregulation of lineage differentiation markers, especially trophectoderm-specific factors, similar to effects observed upon loss of Oct3/4 expression in ES cells. We demonstrate that KMT1E deficiency in ES cells leads to a decrease in histone H3K9 methylation at and derepression of trophoblast-associated genes such as Cdx2. Furthermore, we find genes that are derepressed upon Setdb1 deletion to overlap with known targets of polycomb mediated repression, suggesting that KMT1E mediated H3K9 methylation acts in concert with polycomb controlled H3K27 methylation. Our studies thus demonstrate an essential role for KMT1E in the control of developmentally regulated gene expression programs in ES cells. **Overall design:** Analysis of KMT1E-deficiency in mouse embryonic stem cells using a Setdb1 conditional allele and tamoxifen-inducible Cre/loxP recombination

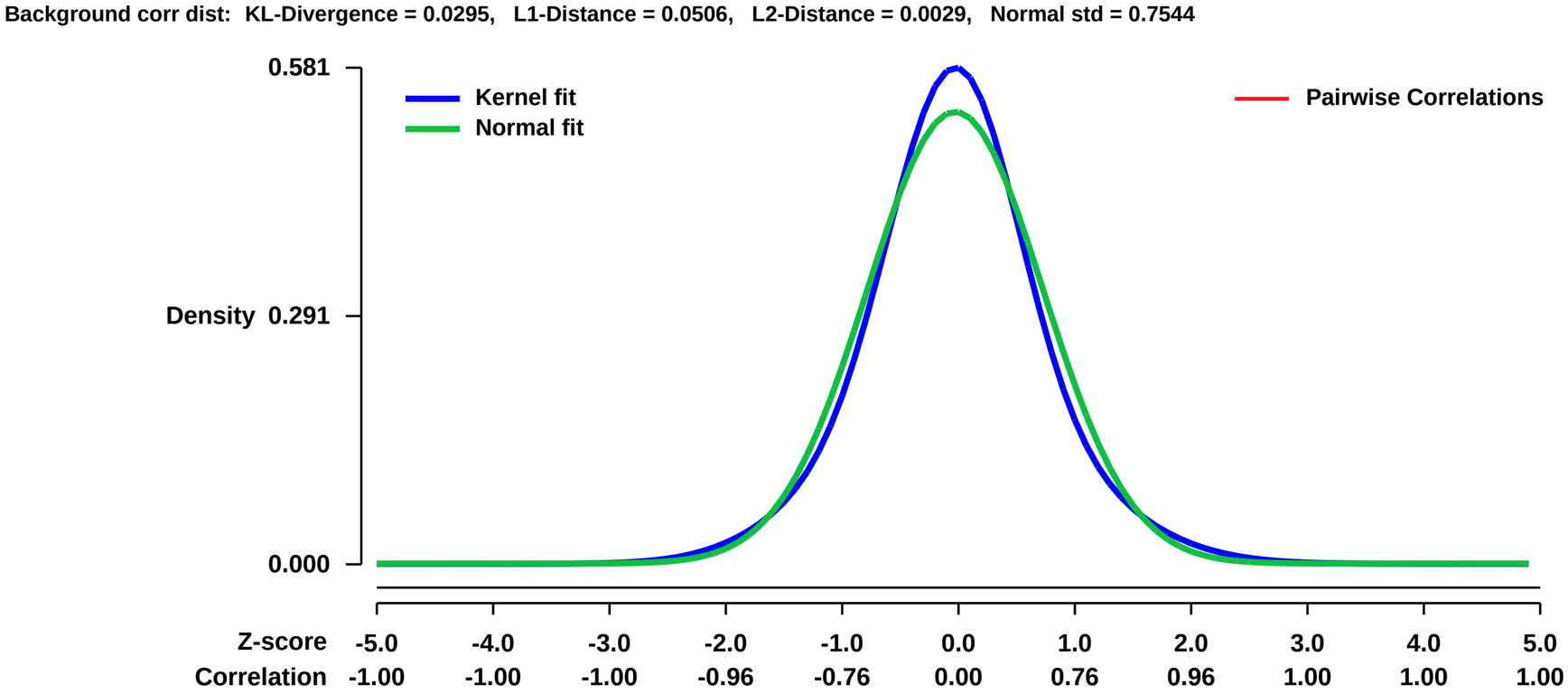

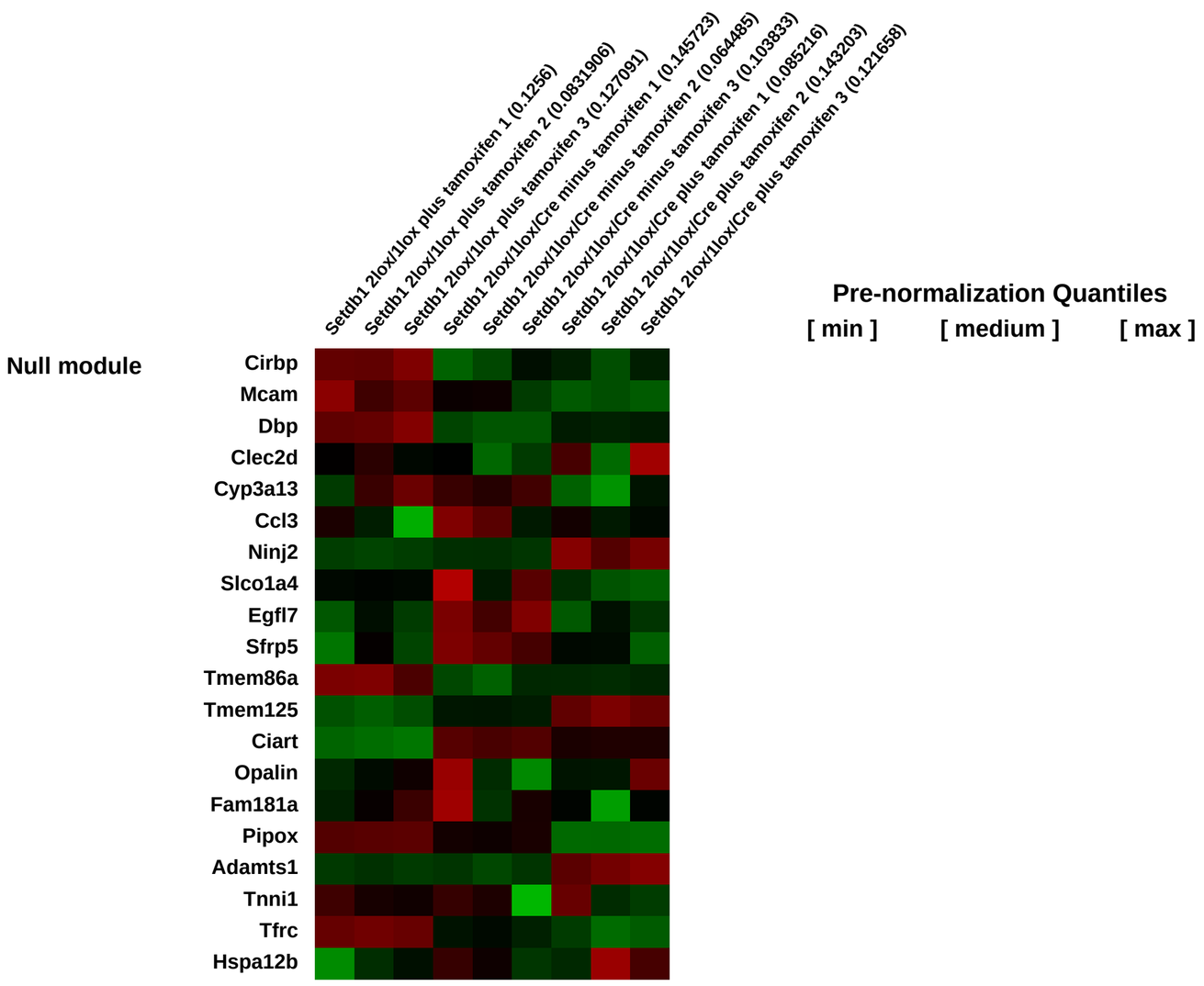

GEO Series "GSE28621" Expression Profiles

Num of samples in this series: 21

Scale of expression profile Z-scores

-3.0 -2.0 -1.0 0.0 1.0 2.0 3.0

GEO Link:	http://www.ncbi.nlm.nih.gov/geo/query/acc.cgi?acc=GSE28621
Status:	Public on May 09 2014
Title:	Transcriptional profiles of macrophages in resolving inflammation
Organism:	Mus musculus
Experiment type:	Expression profiling by array
Platform:	GPL1261
Pubmed ID:	24762537
Summary & Design:	**Summary:** We have performed a comprehensive transcriptional analysis of specific monocyte and macrophage (Mˆ) subsets during an acute self-resolving inflammatory insult. Following initial induction of acute inflammation, tissue resident (Resident) Mˆ are rapidly â clearedâ from the inflammatory foci, only becoming recoverable as inflammation resolves. Monocytes are recruited to the inflammatory lesion where they differentiate into Mˆ. We term these monocyte-derived Mˆ â inflammation-associatedâ to distinguish them from Resident Mˆ which are present throughout the inflammatory response and can renew during the resolution of inflammation by proliferation. Comparative analysis of the Mo and Mˆ populations (both â inflammation-associatedâ and Resident Mˆ) identifies select genes expressed in subsets of â inflammation-associatedâ and Resident Mˆ that play important roles in the resolution of inflammation and/or for immunity, including molecules involved in antigen presentation, cell cycle and others associated with â immaturityâ and Mˆ activation. **Overall design:** We purified monocyte and macrophage populations from the peritoneal cavity of C57BL/6 mice 4, 18, 72 and 168 hours after the induction of inflammation with intraperitoneal administration of zymosan (2x10^7 particles). We also purified tissue resident macrophages and Ly-6B+ bone marrow monocytes from naive mice as reference populations.

Background corr dist: KL-Divergence = 0.1827, L1-Distance = 0.0365, L2-Distance = 0.0024, Normal std = 0.3564

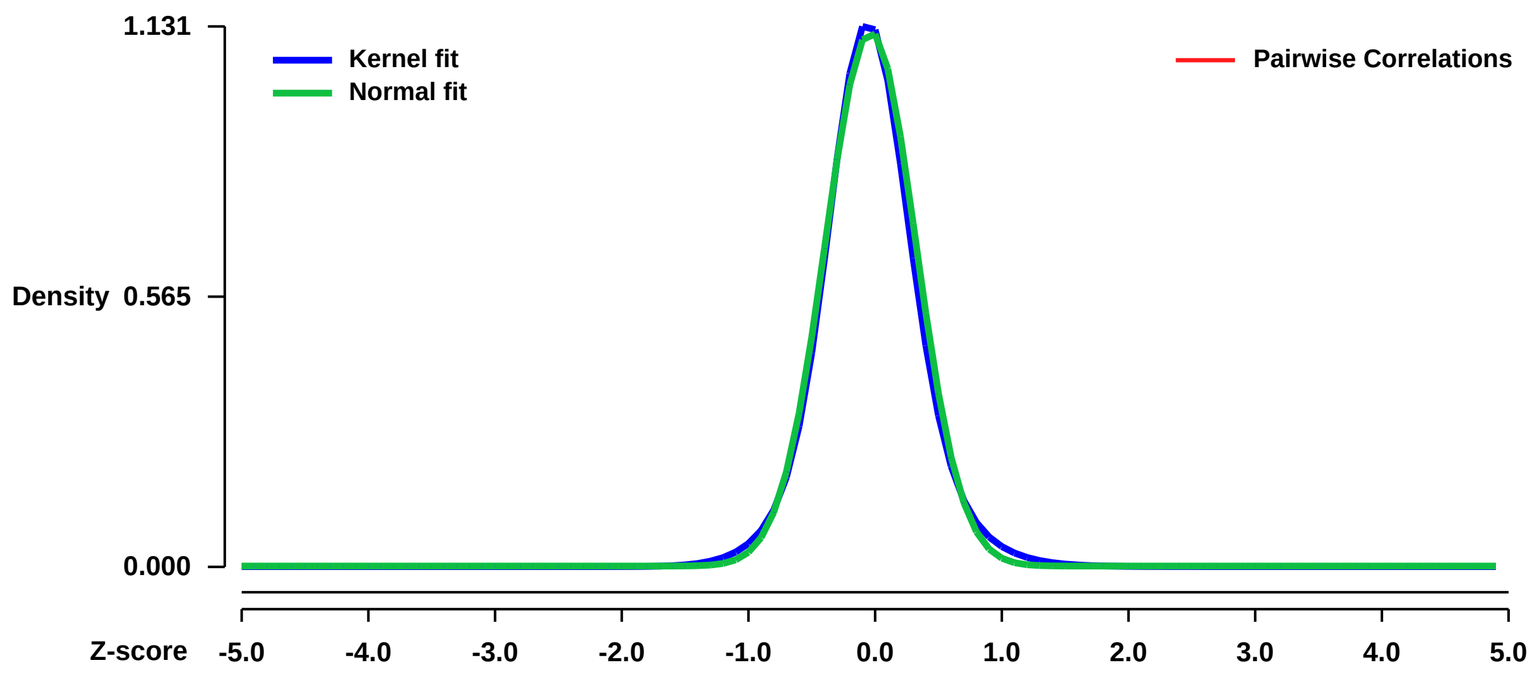

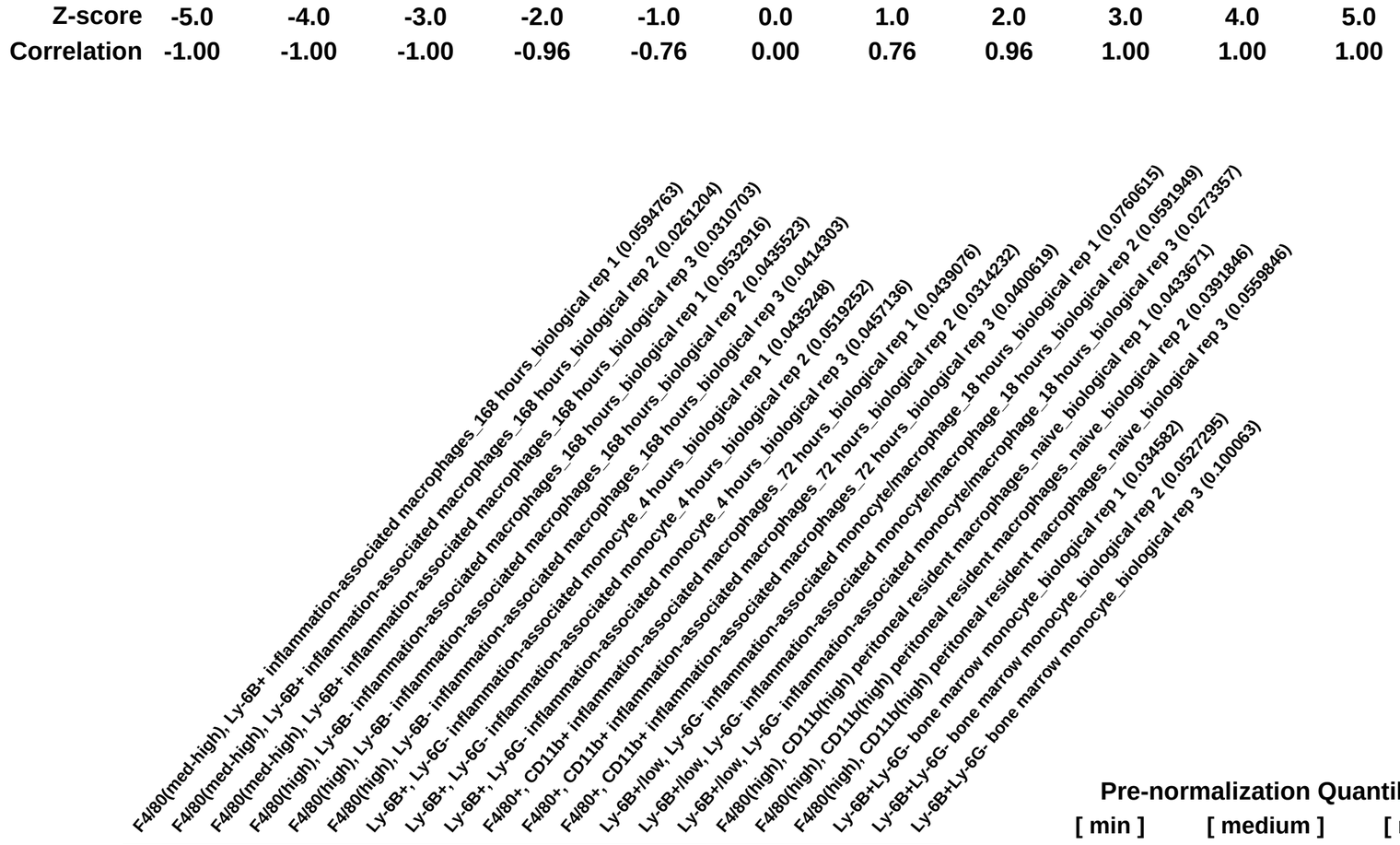

GEO Series "GSE28644" Expression Profiles

Num of samples in this series: 60

Scale of expression profile Z-scores

-3.0 -2.0 -1.0 0.0 1.0 2.0 3.0

GEO Link:	http://www.ncbi.nlm.nih.gov/geo/query/acc.cgi?acc=GSE28644
Status:	Public on Aug 31 2011
Title:	Gene Expression Data Following Chronic Vehicle or Fluoxetine Treatment in Thirty Mouse Inbred Lines
Organism:	Mus musculus
Experiment type:	Expression profiling by array
Platform:	GPL1261
Pubmed ID:	22113448
Summary & Design:	**Summary:** In order to understand how biochemical and genetic differences correlate with treatment response, we measured depressive-like behavior, gene expression and the levels of thirty-six neurobiochemical analytes across a panel of genetically-diverse mouse inbred lines after chronic treatment with vehicle or fluoxetine. Neurobiochemical markers were chosen based on their putative molecular function within pathways proposed to underlie depression, which include neuronal transmission, HPA-axis regulation, and neuroimmune processes. The goal of this study is to establish genetic and biochemical biomarkers that can predict treatment response and to propose a molecular pathway that is critical in mediating anti-depressant response. **Overall design:** Thirty mouse inbred strains (129S1/SvImJ, A/J, AKR/J, BALB/cJ, BTBRT T(+) tf/J, BUB/BnJ, C3H/HeJ, C57BL/6J, C57BLKS/J, C57BR/cdJ, C58/J, CBA/J, CE/J, DBA/2J, FVB/NJ, I/LnJ, LG/J, LP/J, MA/MyJ, MRL/MpJ, NOD/LtJ, NOR/LtJ, NZB/BINJ, NZW/LacJ, P/J, PL/J, RIIIS/J, SJL/J, SM/J, and SWR/J) aged 5-6 weeks old were obtained from The Jackson Laboratory (Bar Harbor, ME). Male mice were kept in polycarbonate cages on a 12-hour light/dark cycle (lights on at 0700h) with access to food and water ad libitum. Following one week of habituation, mice were randomized to either control or treatment group (n=12 male mice per strain per treatment group). Mean water intake for each strain was determined previously by measuring daily water consumption for three weeks (n=12 mice per strain). This information, along with average weight measurements for each strain, was used to determine the amount of fluoxetine required to provide a daily oral dose of 0 or 18 mg/kg per mouse. After chronic administration of 0 or 18 mg/kg of fluoxetine for 21 days, mice aged 9-10 weeks were tested in a tail-suspension and open field apparatus. Upon completion of the study, mice were sacrificed by cervical dislocation and decapitation between 0900h and 1300h. Trunk blood was quickly collected and allowed to clot on ice. Following centrifugation, serum samples were collected and stored at -20C for determination of fluoxetine and norfluoxetine levels using liquid chromatography-mass spectrometry/mass spectrometry (LC-MS/MS). Micro-dissections of individual regions were performed on serial coronal brain sections (approximately 10 ´µm) that were placed on a cold metal block. Cortex was taken from the same section for each animal and immediately snaps frozen on dry ice. Samples were stored at -80C until analysis.

Background corr dist: KL-Divergence = 0.3730, L1-Distance = 0.0800, L2-Distance = 0.0212, Normal std = 0.2917

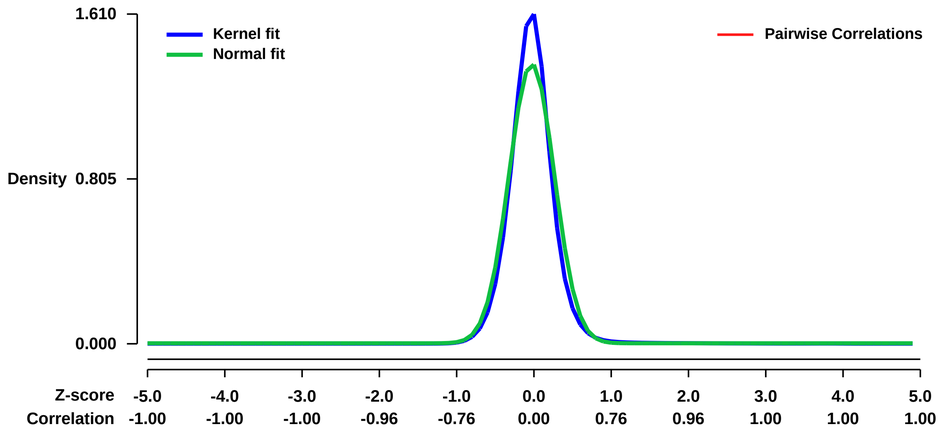

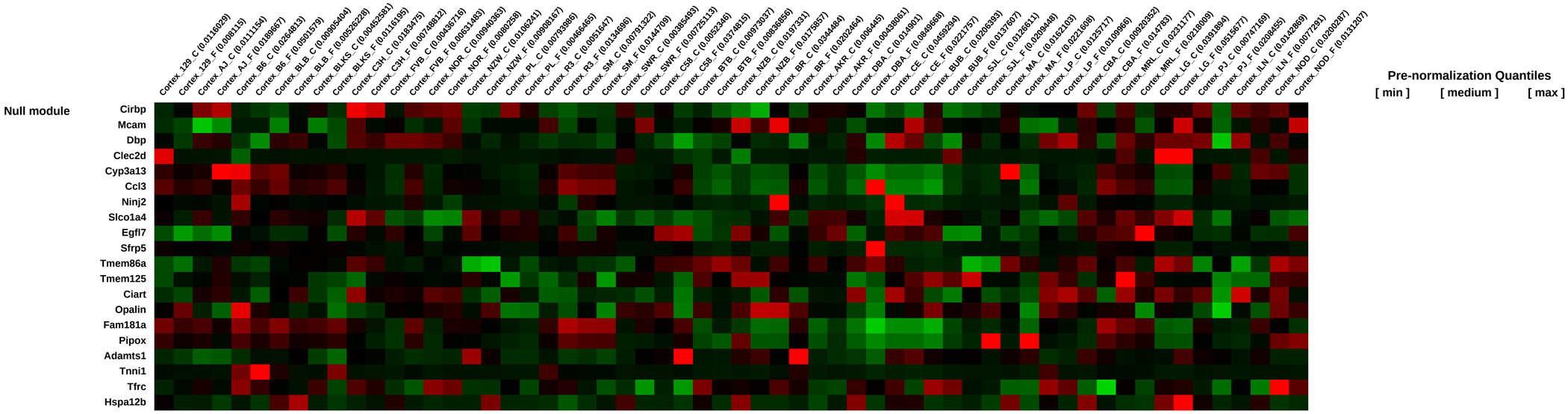

GEO Series "GSE28664" Expression Profiles

Num of samples in this series: 17

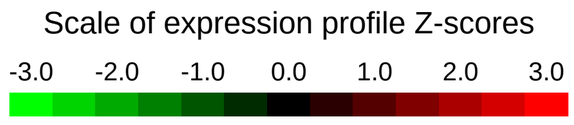

GEO Link:	http://www.ncbi.nlm.nih.gov/geo/query/acc.cgi?acc=GSE28664
Status:	Public on Sep 04 2011
Title:	Akt1 is critical in Maintaining the Blood-Testis Barrier Following Exposure to the Neonatal Goitrogen, 6-N-Propylthiouracil (PTU)
Organism:	Mus musculus
Experiment type:	Expression profiling by array
Platform:	GPL1261
Pubmed ID:	
Summary & Design:	**Summary:** Akt1 plays a protective role in the postnatal C57BL6 mouse testis following lactational exposure to the neonatal goitrogen, propylthiouracil (PTU). To elucidate the transcriptional profile mediating this phenotypic effect, we monitored changes in testicular gene expression at postnatal days (PNDs) 15 and 25 in Akt1+/+, Akt1+/-, and Akt1-/- testes following exposure to 0.01% PTU allowing us to determine changes in gene expression due to 1.) genotype effects; 2.) exposure effects; and 3.) genotype-by-exposure interactions. Early PTU-dependent gene changes included genes involved in lipid metabolism, spermatid differentiation, meiosis and adhesion. Early Akt1-dependent effects were associated with germ cell development, spermatid development and differentiation, and sperm motility. By PND25, the Akt1 gene-environment interaction had pronounced effects on genes associated with Sertoli cell (SC) differentiation and claudin-associated junctional formation suggesting delayed formation of the blood-testis barrier (BTB). To confirm these observations, biotin tracer experiments demonstrated a permeable blood-testis barrier in PTU-exposed PKBalpha/Akt1-/- tubules as late as PND25 compared to PTU-exposed Akt1+/+ seminiferous tubules. Transmission electron microscopy demonstrated altered SC morphology, aberrant SC localization, and disorganized actin bundle formation. Taken together, loss of Akt1 coupled with postnatal exposure to the neonatal goitrogen, PTU, in the testis contributes to a transcriptional profile associated with impaired integrity of the blood-testis barrier. In summary, the Akt1-/- mouse represents a potentially important model to study BTB formation and reassembly in response to male reproductive toxicants and the various signaling networks which mediate these responses. **Overall design:** The microarray analysis employed a balanced factorial design, with one chip created for each of three mice under each experimental condition: mouse genotype (Akt1+/+, Akt1+/-, and Akt1-/-), exposure (PTU and Control), and age (sacrificed at PND15 and 25), with a total of 36 mice and 36 chips. MoGene 1.0 st v1 arrays were used for the samples from PND 15 and Mouse Genome 430 2.0 arrays were used for the samples from PND 25. One chip, PTU-exposed, Akt1-/-, PND25, was determined to not be of high quality and was not included in the analysis or provided here.

Background corr dist: KL-Divergence = 0.0331, L1-Distance = 0.0207, L2-Distance = 0.0005, Normal std = 0.6440

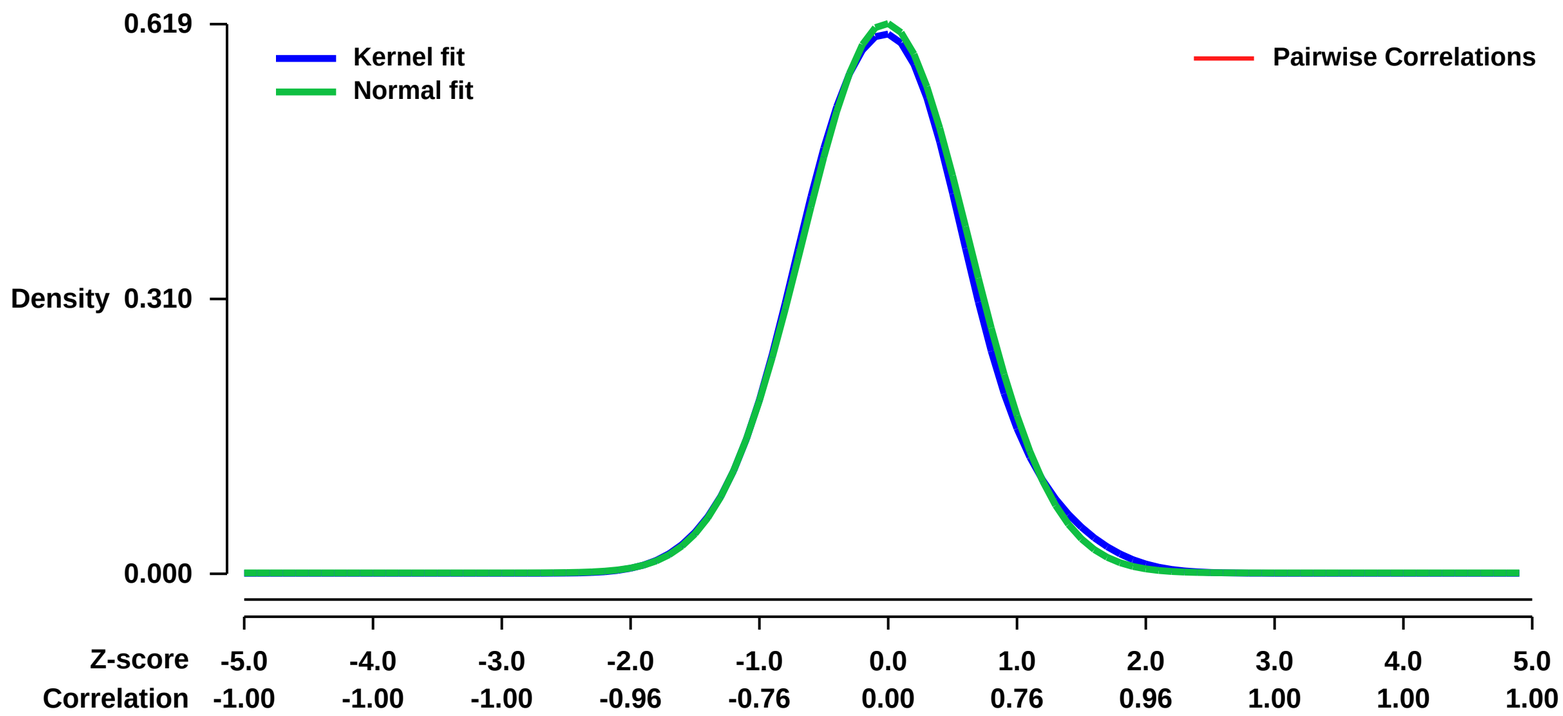

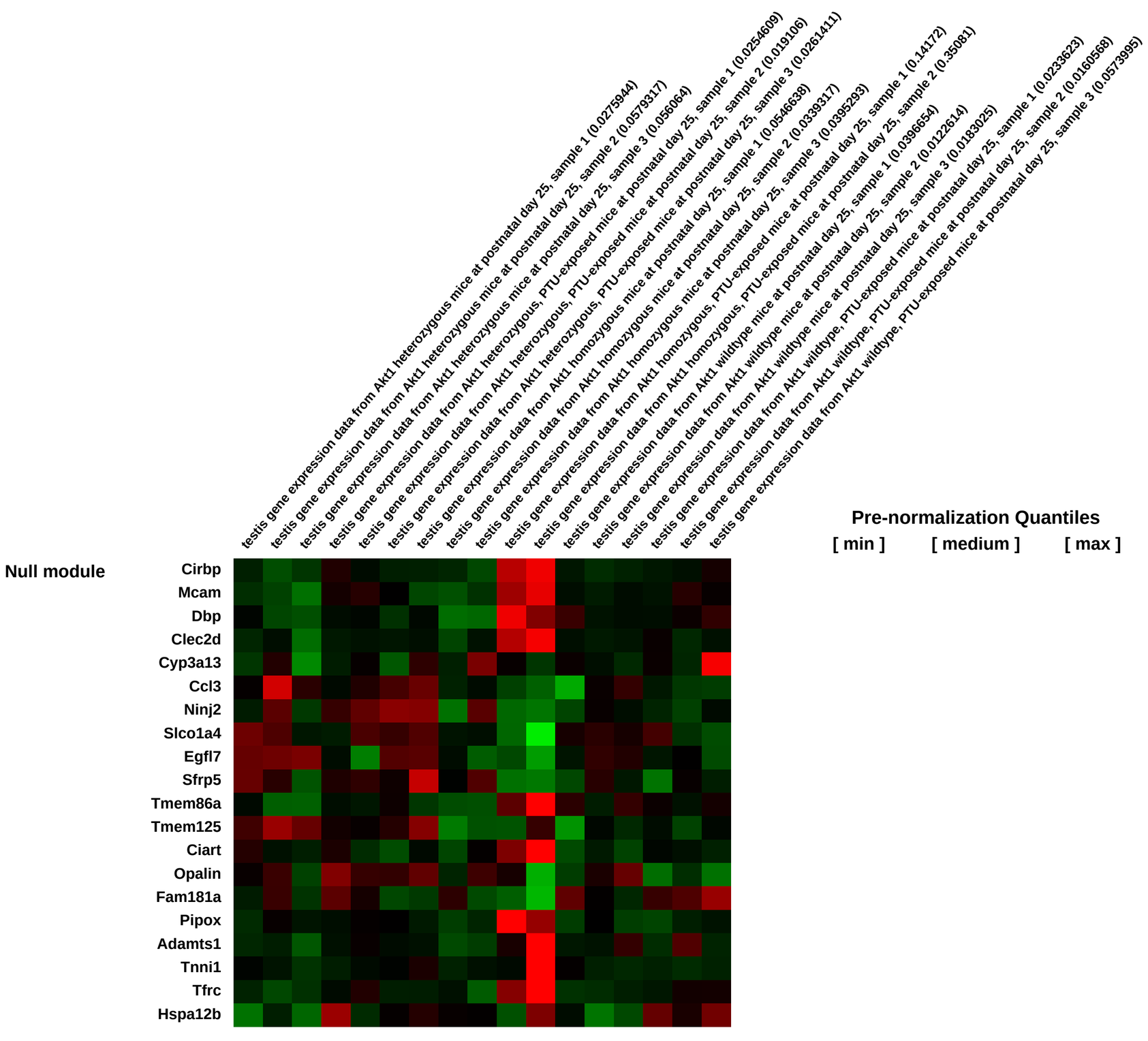

GEO Series "GSE28687" Expression Profiles

Num of samples in this series: 10

Scale of expression profile Z-scores

-3.0 -2.0 -1.0 0.0 1.0 2.0 3.0

GEO Link:	http://www.ncbi.nlm.nih.gov/geo/query/acc.cgi?acc=GSE28687
Status:	Public on Oct 01 2011
Title:	Defective K-Ras Oncoproteins Initiate Cancer In Vivo and Evolve to Overcome Impaired Effector Binding
Organism:	Mus musculus
Experiment type:	Expression profiling by array
Platform:	GPL1261
Pubmed ID:	23637129
Summary & Design:	**Summary:** The oncogenic proteins expressed in human cancer cells are exceedingly difficult targets for drug discovery due to intrinsic properties of the Ras GTPase switch. As a result, recent efforts have largely focused on inhibiting Ras-regulated kinase effector cascades, particularly the Raf/MEK/ERK and PI3 kinase/Akt/mTOR pathways. We constructed murine stem cell leukemia virus (MSCV) vectors encoding oncogenic K-RasD12 with additional â second siteâ amino acid substitutions that that impair PI3 kinase/Akt or Raf/MEK/ERK activation and performed bone marrow transduction/transplantation experiments in mice. In spite of attenuated signaling properties, defective K-Ras oncoproteins induced aggressive clonal T lineage acute lymphoblastic leukemia (T-ALL). These leukemias exhibited a high frequency of somatic Notch1 mutations, which is also true of human T-ALL. Multiple independent T-ALLs restored full oncogenic Ras activity by acquiring â third siteâ mutations within the viral KrasD12 transgenes. Other leukemias with undetectable PTEN and elevated phosphoryated Akt levels showed a similar gene expression profile to human early T progenitor (ETP) T-ALL. Expressing oncoproteins that are defective for specific functions is a general strategy for assessing requirements for tumor maintenance and uncovering potential mechanisms of drug resistance in vivo. In addition, our observation that defective Kras oncogenes regain potent cancer initiating activity strongly supports simultaneously targeting distinct components of Ras signaling networks in the substantial fraction of cancers with RAS mutations. **Overall design:** WT Balb/c mice were lethally irradiated and transplanted with WT Balb/c bone marrow cells transduced with MSCV-IRES-Kras mutant-GFP vectors. Mice developed T-cell lymphoproliferative disease.

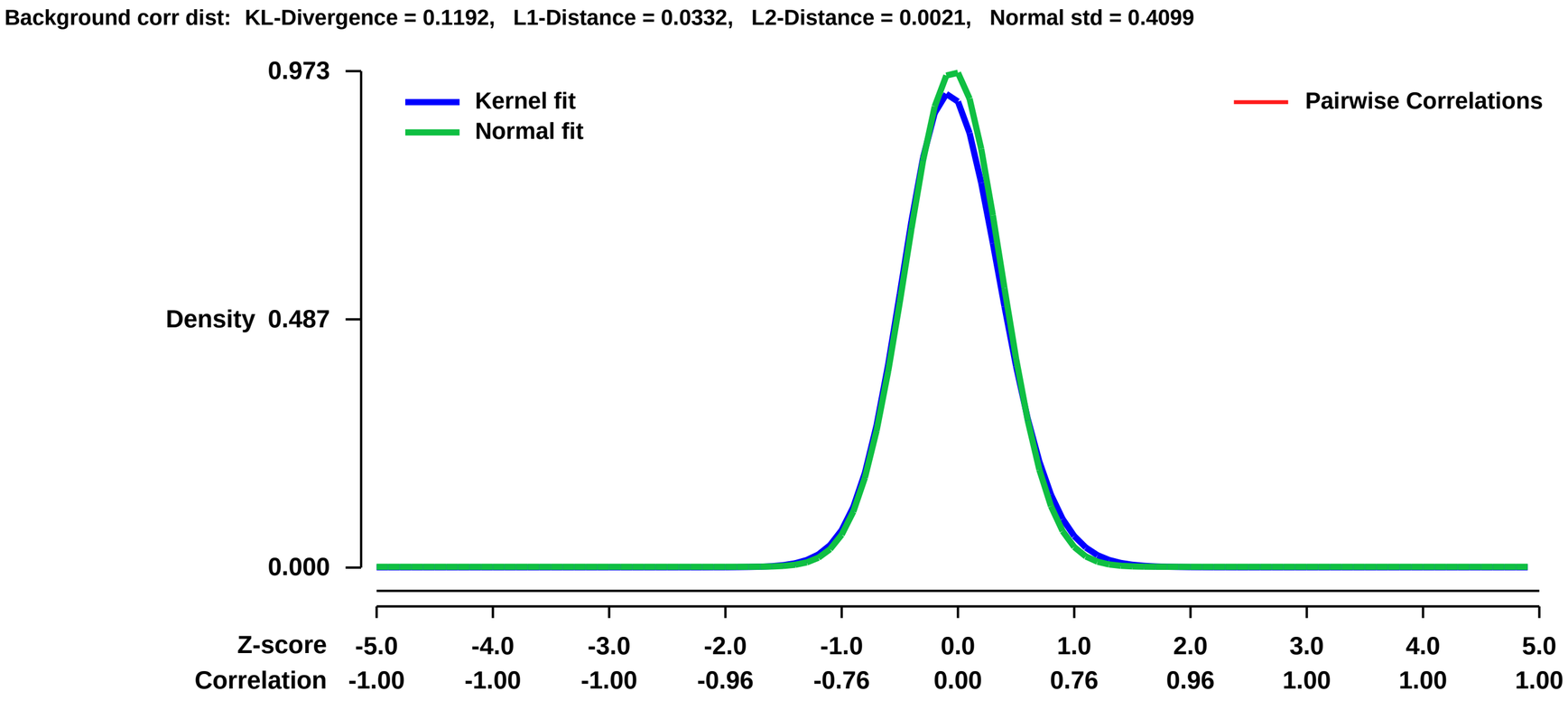

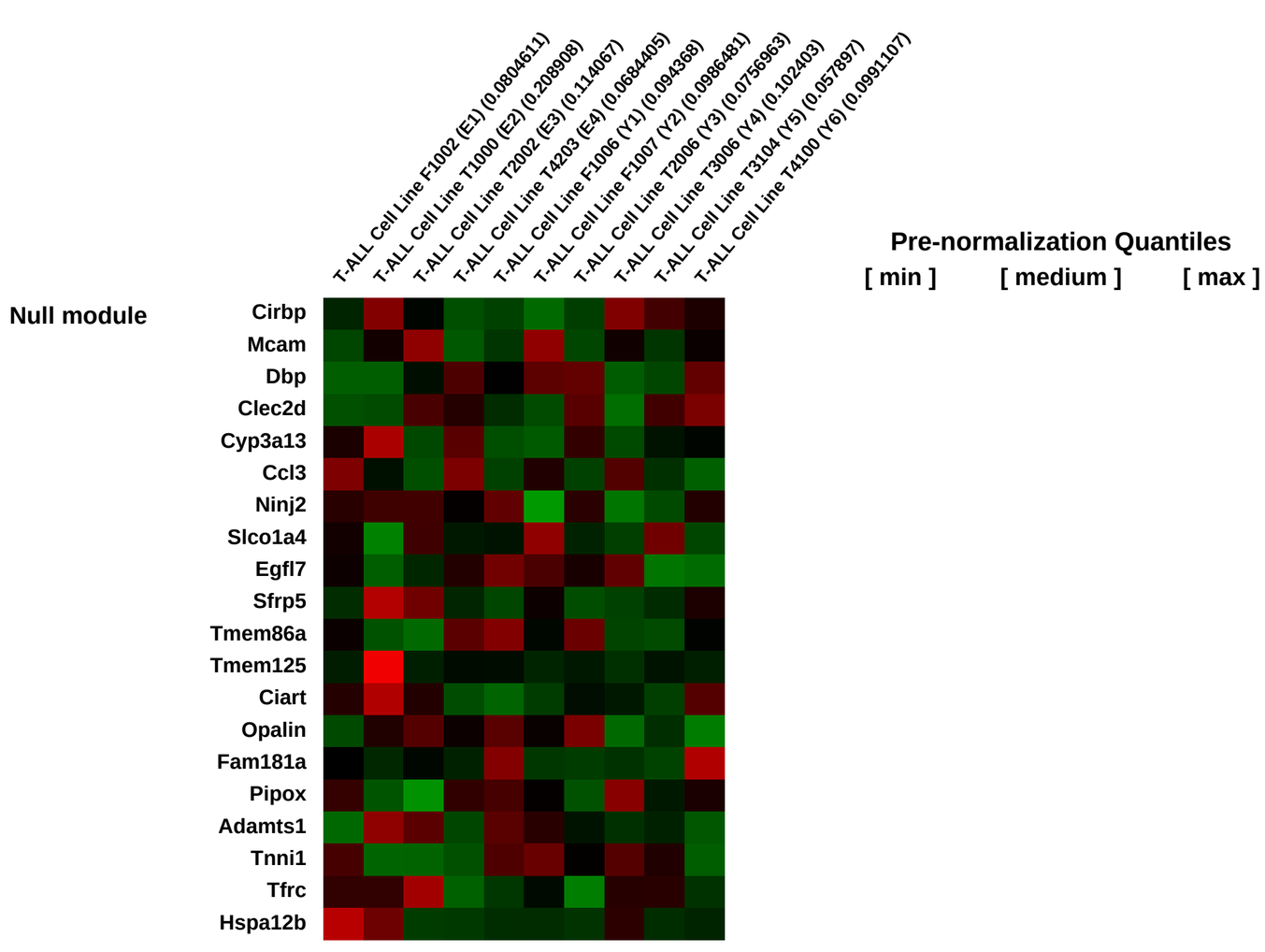

GEO Series "GSE2869" Expression Profiles

Num of samples in this series: 8

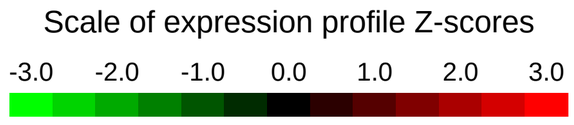

GEO Link:	**http://www.ncbi.nlm.nih.gov/geo/query/acc.cgi?acc=GSE2869**
Status:	**Public on Jul 06 2005**
Title:	**Rosenfeld-5R01NS034934-14**
Organism:	**Mus musculus**
Experiment type:	**Expression profiling by array**
Platform:	**GPL1261**
Pubmed ID:	

Summary & Design:

Summary:
Using targeted gene deletion, we have firmly established that the Class IV POU domain transcription factor Brn-3.2 controls a developmental program regulating axon pathfinding in the mouse visual system. We have isolated and identified downstream gene targets of Brn-3.2, using Representational Difference Analysis (RDA), on cDNA populations derived from wildtype and Brn-3.2-/- retina at the appropriate embryonic stage. One of these candidate genes, the Homeodomain Interacting Protein Kinase 2 (HIPK2), is postulated to be a transcriptional coregulator, based on its in vitro interactions with repressor homeodomain proteins of the NK class, as well as other components of repressor complexes. HIPK2 has also been shown to be involved in post-translational modification of two major transcriptional regulators, p53 and CtBP. Expression of a dominant-negative form of HIPK2 in sensory neurons affects the innervation patterns of their target tissues, suggesting an axon pathfinding defect.

The aim of this project is to identify targets for the Homeodomain Interacting Protein Kinase 2 (HIPK2), that we isolated as a downstream gene target of the class IV POU domain transcription factor Brn-3.2, and to investigate their function in the Brn-3.2 dependent pathway regulating axon pathfinding.

We hypothesize that the genes regulated by HIPK2 will play a critical role in axon pathfinding and that the results of this study will provide novel insights into the molecular mechanisms of axon pathfinding, and possibly neural plasticity and regeneration, and therefore, be of great interest to the field of neurobiology in general.

In order to uncover potential biological role(s) of HIPK2 in neural development, and particularly axon pathfinding, we generated transgenic mouse models for in vivo studies. Our preliminary observations in transgenic mice, indicate that a form of the molecule expected to act as a dominant-negative and designed to be expressed in sensory neurons, affects the innervation patterns of their target tissues, suggesting an axon pathfinding defect. We plan to take advantage of this model to identify genes regulated by HIPK2, and which are likely to be involved in axon pathfinding. To this end, we will compare gene expression profiles in sensory neurons isolated wild-type and transgenic mice. In our experimental paradigm, the trigeminal ganglion represents the ideal sensory structure in which to perform such an analysis: 1) High levels of transgene can be expressed in the trigeminal ganglion, as assessed by the expression of LacZ from the bicistronic construct which contains IRES-LacZ downstream of a dominant negative form of HIPK2. 2) The trigeminal ganglion can be dissected at embryonic day 13.5, when the phenotype is apparent, with ease and free of contamination from surrounding tissues. 3) The amounts of RNA that can be isolated from a single ganglion are in the range of 200-300 ng, which should be sufficient for microarray analysis following linear amplification of RNA. One series will be carried out with transgenic embryos and a control series will be carried out with wildtype littermates. Animals will be prepared and sacrificed by a standard protocol. Tissue will be rapidly dissected from E13.5 trigeminal ganglion, frozen in liquid nitrogen, and stored at -80C until RNA is extracted. RNA will be prepared using RNeasy Micro Kit. We will be providing 4 tissue samples for each of the wildtype and transgenic animals to mitigate any expression differences resulting from mouse to mouse variation.

Keywords: other

Overall design:
as above

Background corr dist: KL-Divergence = 0.0910, L1-Distance = 0.0235, L2-Distance = 0.0008, Normal std = 0.4529

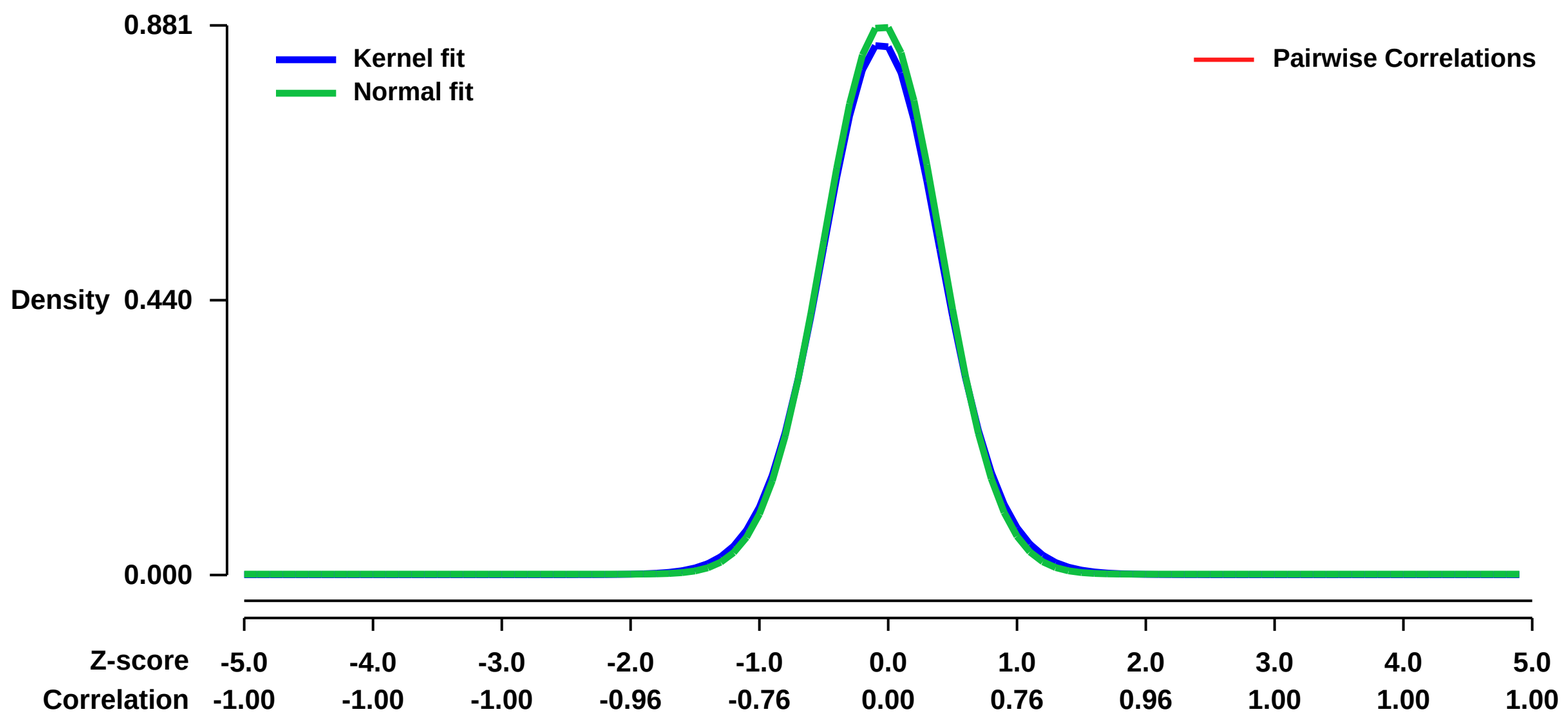

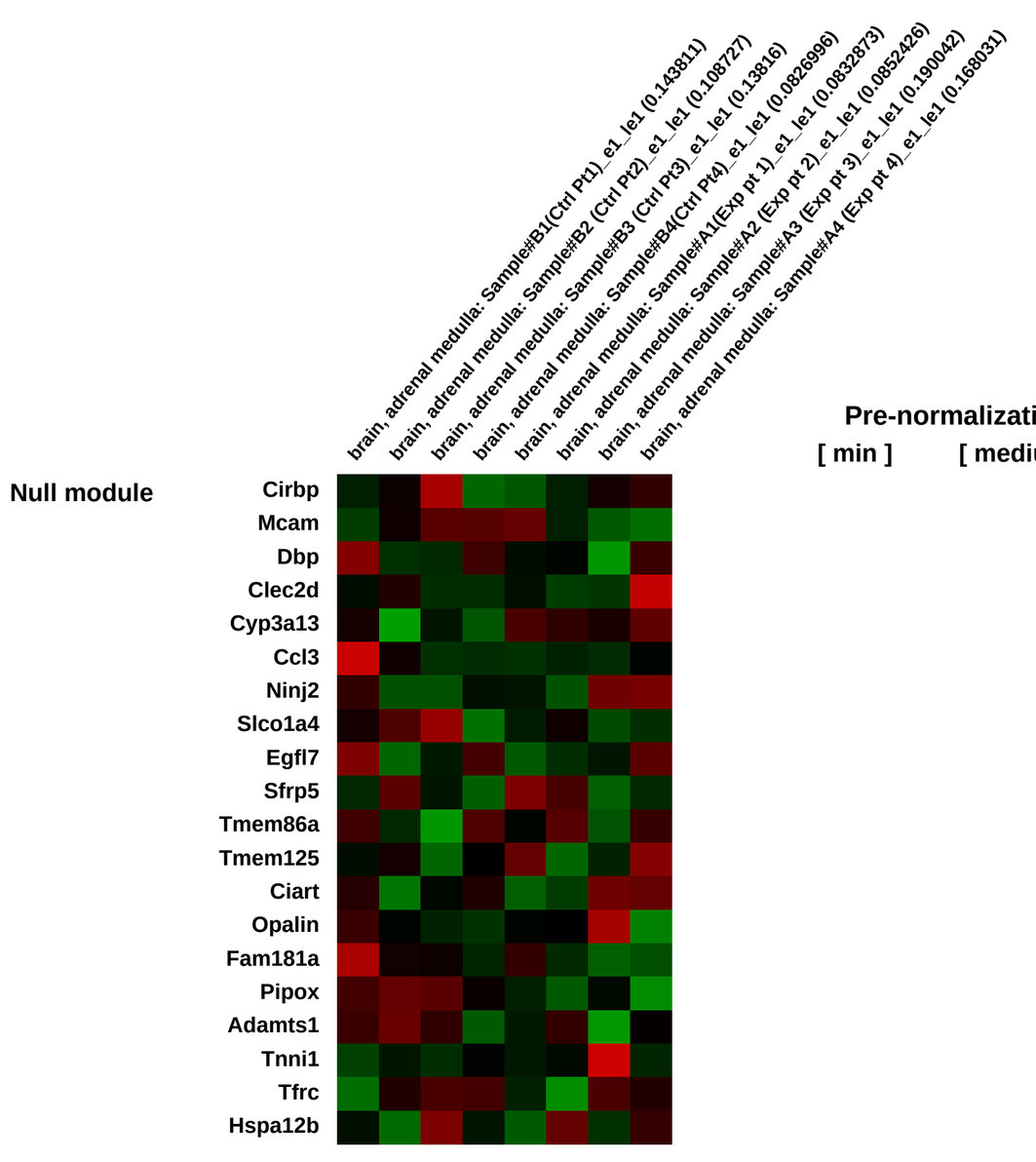

GEO Series "GSE28731" Expression Profiles

Num of samples in this series: 10

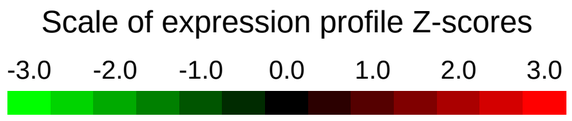

GEO Link:	http://www.ncbi.nlm.nih.gov/geo/query/acc.cgi?acc=GSE28731
Status:	Public on Jan 11 2013
Title:	Effects of Hsp72 on astrocyte activation following stroke in the mouse
Organism:	Mus musculus
Experiment type:	Expression profiling by array
Platform:	GPL1261
Pubmed ID:	22940431
Summary & Design:	**Summary:** **Astrogliosis is a hallmark of the response to brain ischemia, comprised of changes in gene expression and morphology. Hsp72 protects from cerebral ischemia, and although several mechanisms of protection have been investigated, effects on astrocyte activation are unknown. To identify potential mechanisms of protection, gene expression was assessed in mice subjected to middle cerebral artery (MCAO) or sham surgery, of either wildtype (WT) or Hsp72-overexpressing (Hsp72Tg) mice. After stroke, both genotypes exhibited genes related to cell death, stress response, and immune response. Furthermore, genes indicative of astrocyte activation, including cytoskeletal proteins and cytokines, were upregulated. To measure astrocyte activation after stroke, detailed histological and morphological analyses were performed in the cortical penumbra after stroke using unbiased stereology. Consistent with other reports, we observed a marked and persistent increase in glial fibrillary acidic protein (GFAP) as soon as 3 hours after MCAO. In contrast, vimentin immunoreactivity appeared 12-24 hours after stroke, peaked at 72 hours, and returned to baseline after 30 days. Surprisingly, no change in overall astrocyte number was observed based on glutamine synthetase (GS) immunoreactivity. To determine if Hsp72Tg mice exhibited altered astrocyte activation compared to WT controls, morphological evaluation by fractal analysis was used. Overexpression of Hsp72 reduced astrocyte cell area, arbor area, and to a lesser extent fractal dimension, 72 hours following stroke. In conclusion, in vivo overexpression of Hsp72 alters gene expression following stroke, including genes involved in astrocyte activation, and decreases astrocyte activation acutely following MCAO. Thus, modulation of astrogliosis may be a neuroprotective mechanism exerted by Hsp72 after ischemia.** **Overall design:** **A total of 10 samples were analyzed, with 5 of each genotype, wildtype (WT) and Hsp72-overexpressing (Hsp72Tg) mice. Of the 5 in each group, 3 received middle cerebral artery occlusion (MCAO) and 2 received a sham surgery. The sham samples serve as the controls for the MCAO samples in each genotype. All samples were taken from the ischemic or control hemisphere 24 hours after surgery.**

Background corr dist: KL-Divergence = 0.0829, L1-Distance = 0.0224, L2-Distance = 0.0006, Normal std = 0.4685

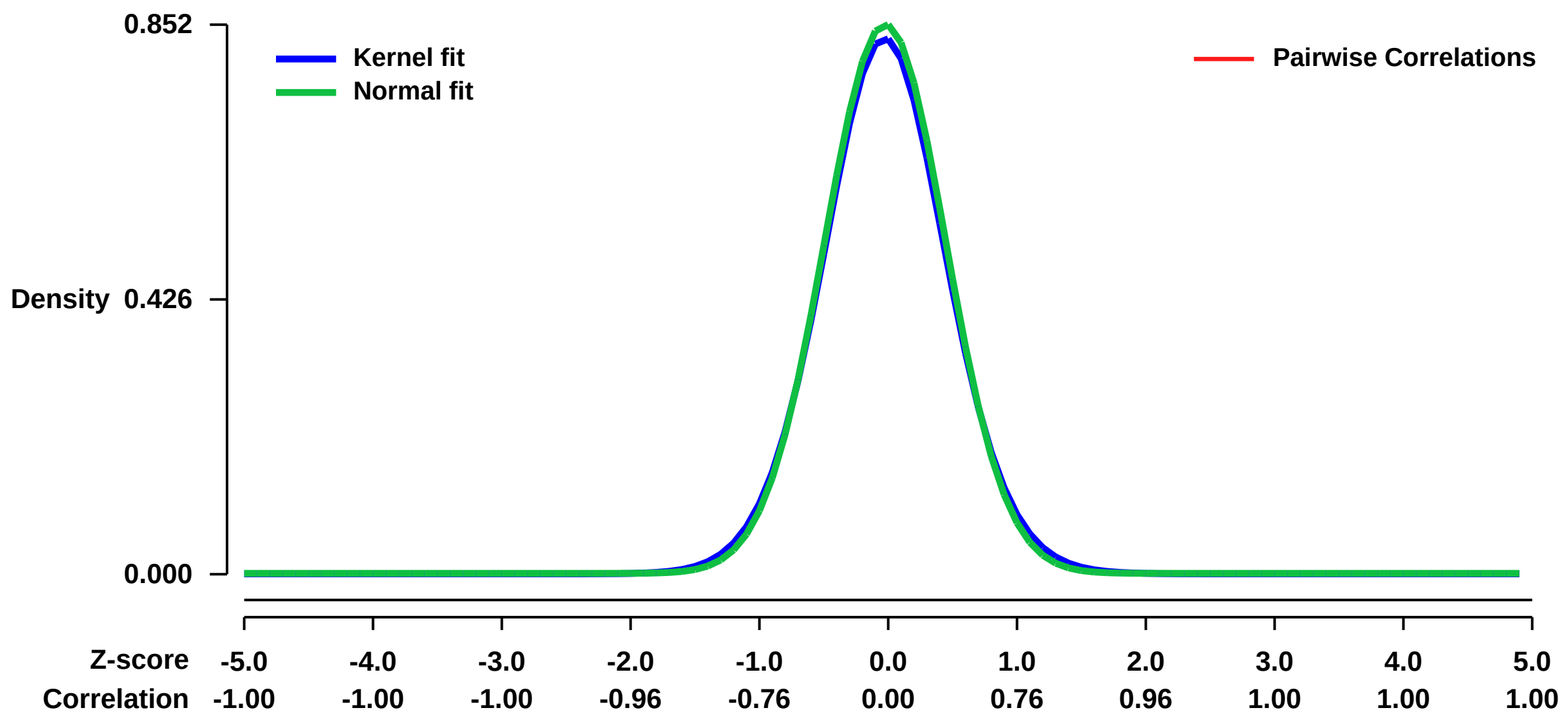

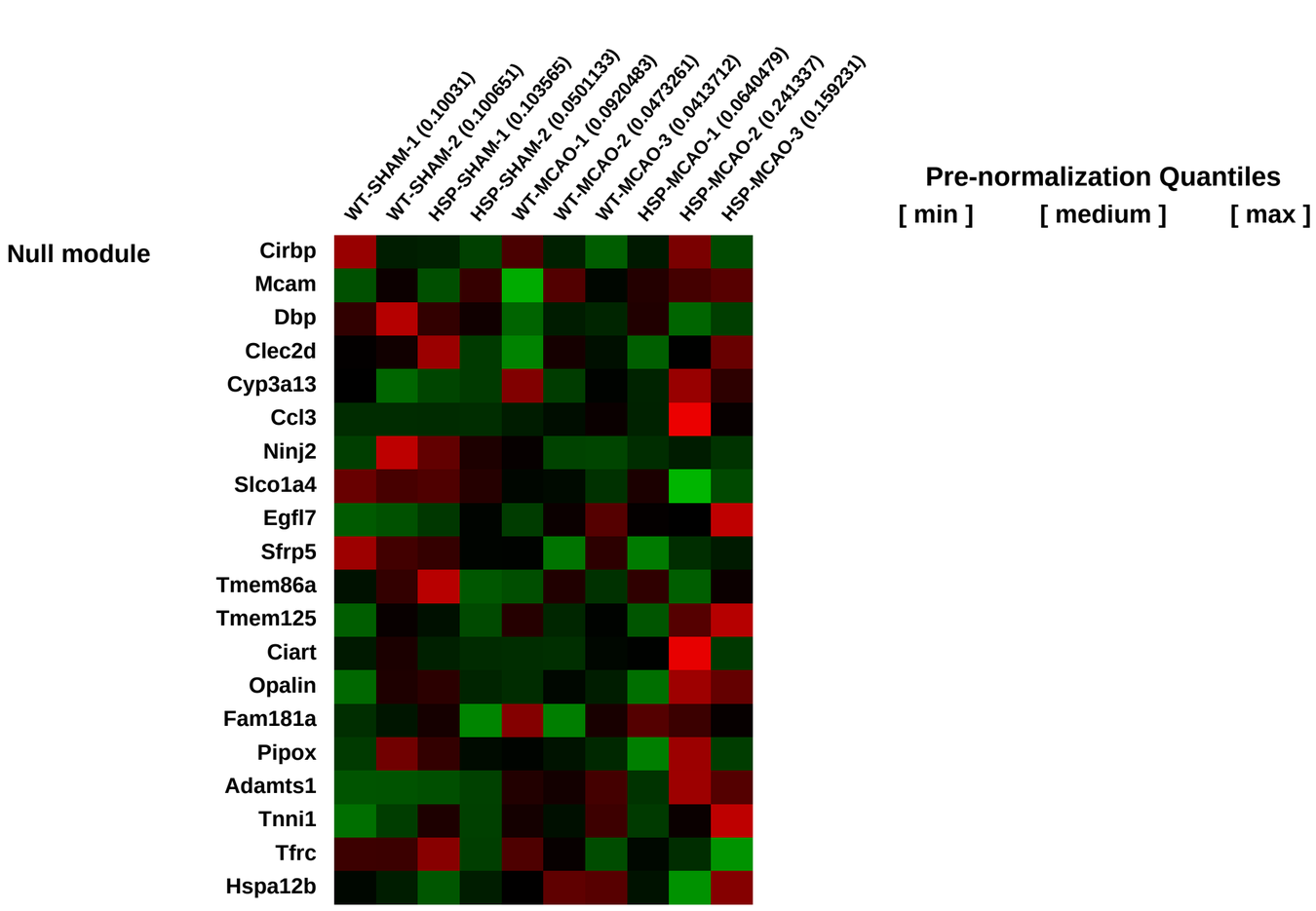

GEO Series "GSE28783" Expression Profiles

Num of samples in this series: 12

Scale of expression profile Z-scores

-3.0 -2.0 -1.0 0.0 1.0 2.0 3.0

GEO Link:	http://www.ncbi.nlm.nih.gov/geo/query/acc.cgi?acc=GSE28783
Status:	Public on May 20 2011
Title:	Effect of anti-miR-33 treatment on gene expression in mouse macrophages from atherosclerotic plaques.
Organism:	Mus musculus
Experiment type:	Expression profiling by array
Platform:	GPL1261
Pubmed ID:	21646721
Summary & Design:	**Summary:** Inhibition of miR-33 results in increased cholesterol efflux and HDL-cholesterol levels in mice. In this study we examined the effect of miR-33 inhibition in a mouse model of atherosclerosis and observed significant reduction in atherosclerotic plaque size. At the end of the study, gene expression in macrophages from the atherosclerotic plaques was assessed. The results demonstrated a reduction in inflammatory gene expression and increased levels of mRNAs containing miR-33 binding sites. **Overall design:** LDLR-/- mice on a Western diet with established atherosclerosis were switched to normal chow and treated with anti-miR-33, control anti-miR, or saline (n=4/group) for 4 weeks. Gene expression profiling was performed on macrophages in aortic plaques isolated at the end of the treatment period by laser capture microdissection.

Background corr dist: KL-Divergence = 0.1533, L1-Distance = 0.0402, L2-Distance = 0.0035, Normal std = 0.3721

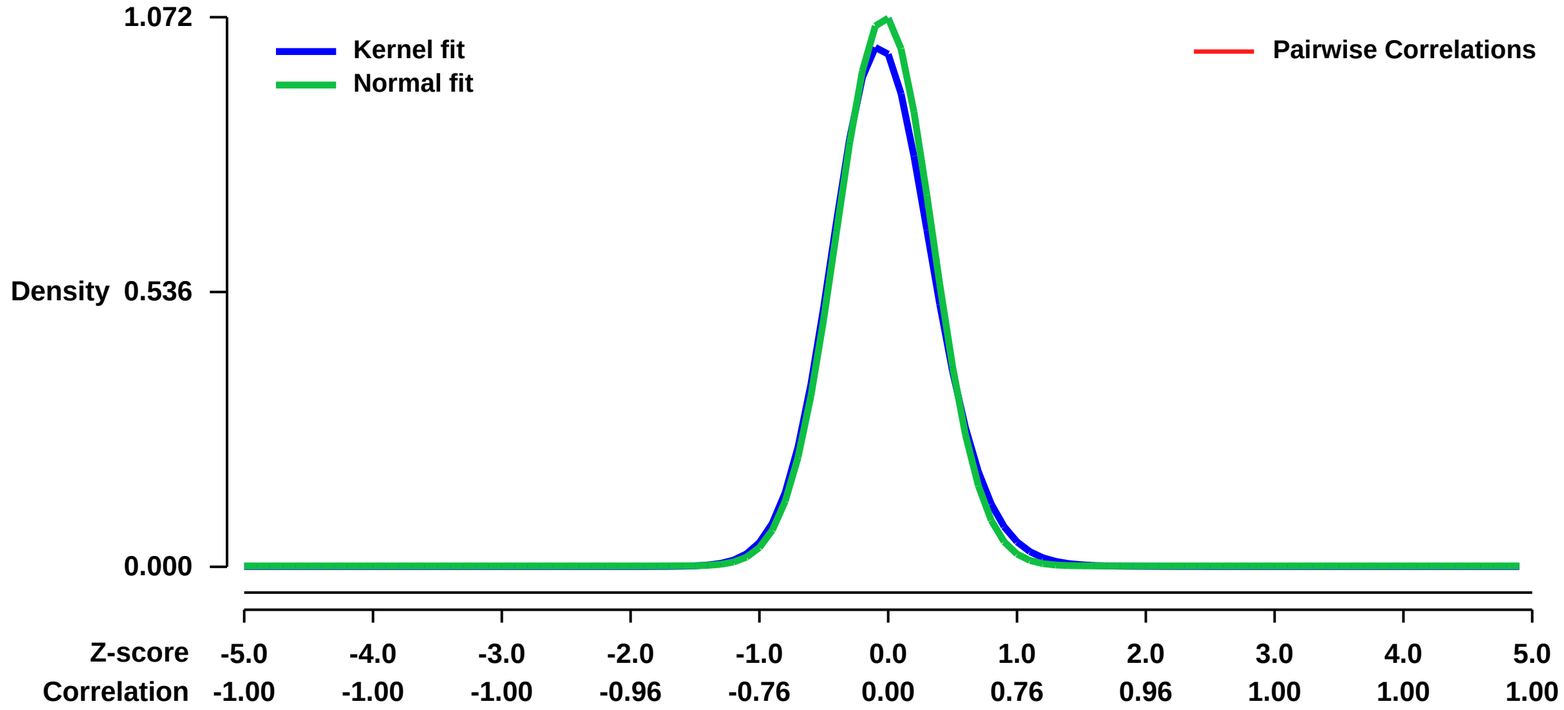

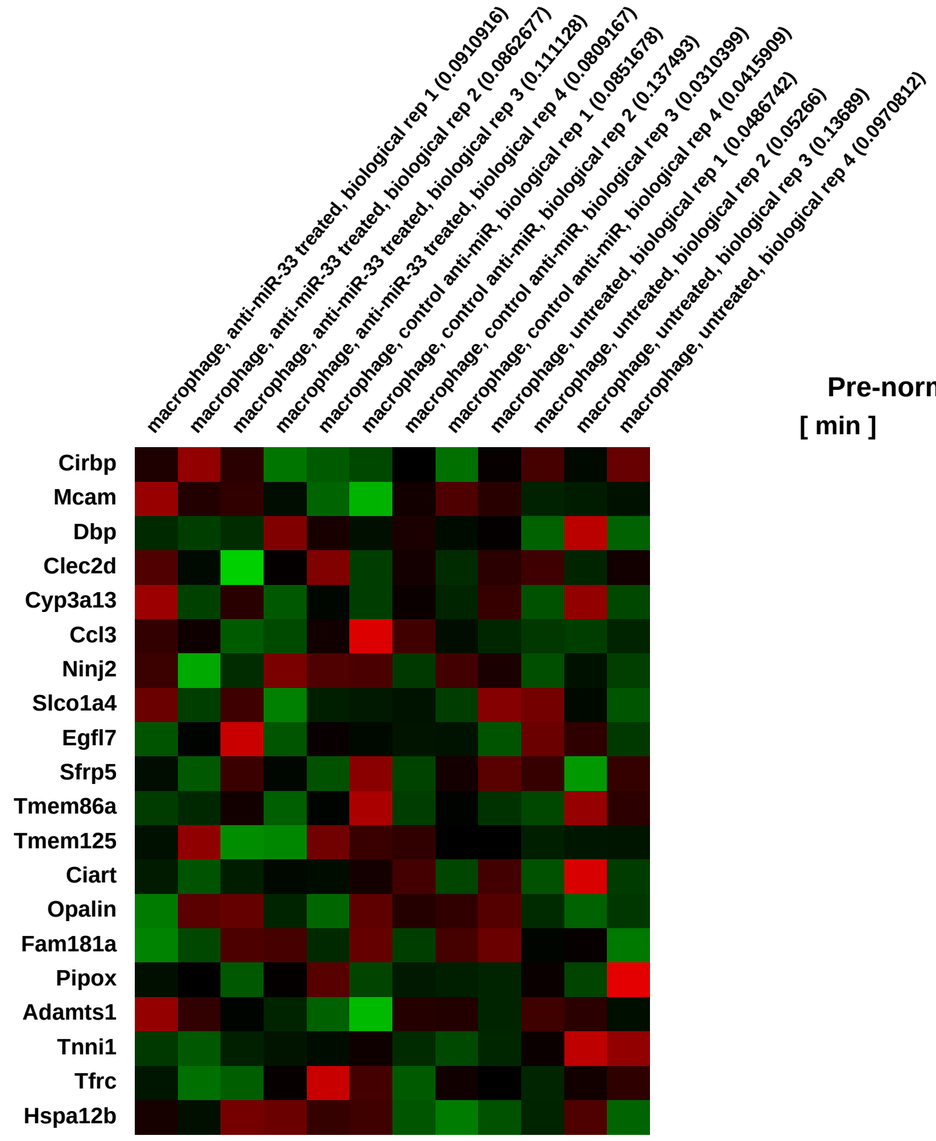

GEO Series "GSE28830" Expression Profiles

Num of samples in this series: 9

Scale of expression profile Z-scores

-3.0 -2.0 -1.0 0.0 1.0 2.0 3.0

GEO Link:	**http://www.ncbi.nlm.nih.gov/geo/query/acc.cgi?acc=GSE28830**
Status:	**Public on Dec 01 2013**
Title:	**Differential gene expression in CD11b+ splenocytes from mice subject to social threat vs. control (II)**
Organism:	**Mus musculus**
Experiment type:	**Expression profiling by array**
Platform:	**GPL1261**
Pubmed ID:	
Summary & Design:	**Summary:** **Gene expression profiling was carried out on splenocyte mRNA samples collected from 6 animals subject to repeated social threat and 6 animals subject to non-threatening control conditions (pooled into 3 groups of 2). The primary research question is whether gene expression differs in CD11b+ splenocytes from animals exposed to social threat vs non-threatening control conditions.** **Keywords: Risk prediction** **Overall design:** **This study provides an additional body of data from the same general protocol used in Series GSE16661, and will support more extensive analyses than the original study.**

Background corr dist: **KL-Divergence = 0.0554, L1-Distance = 0.0377, L2-Distance = 0.0018, Normal std = 0.5796**

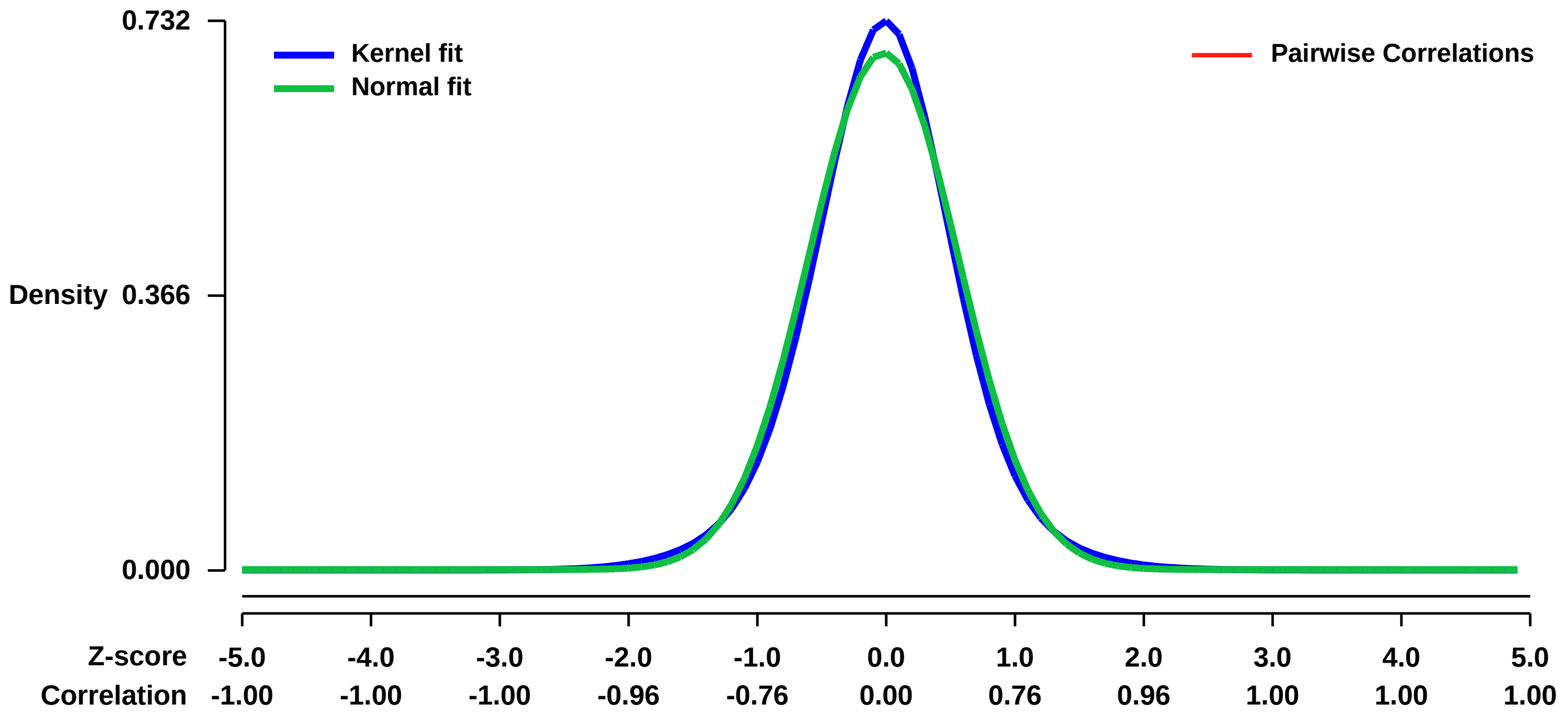

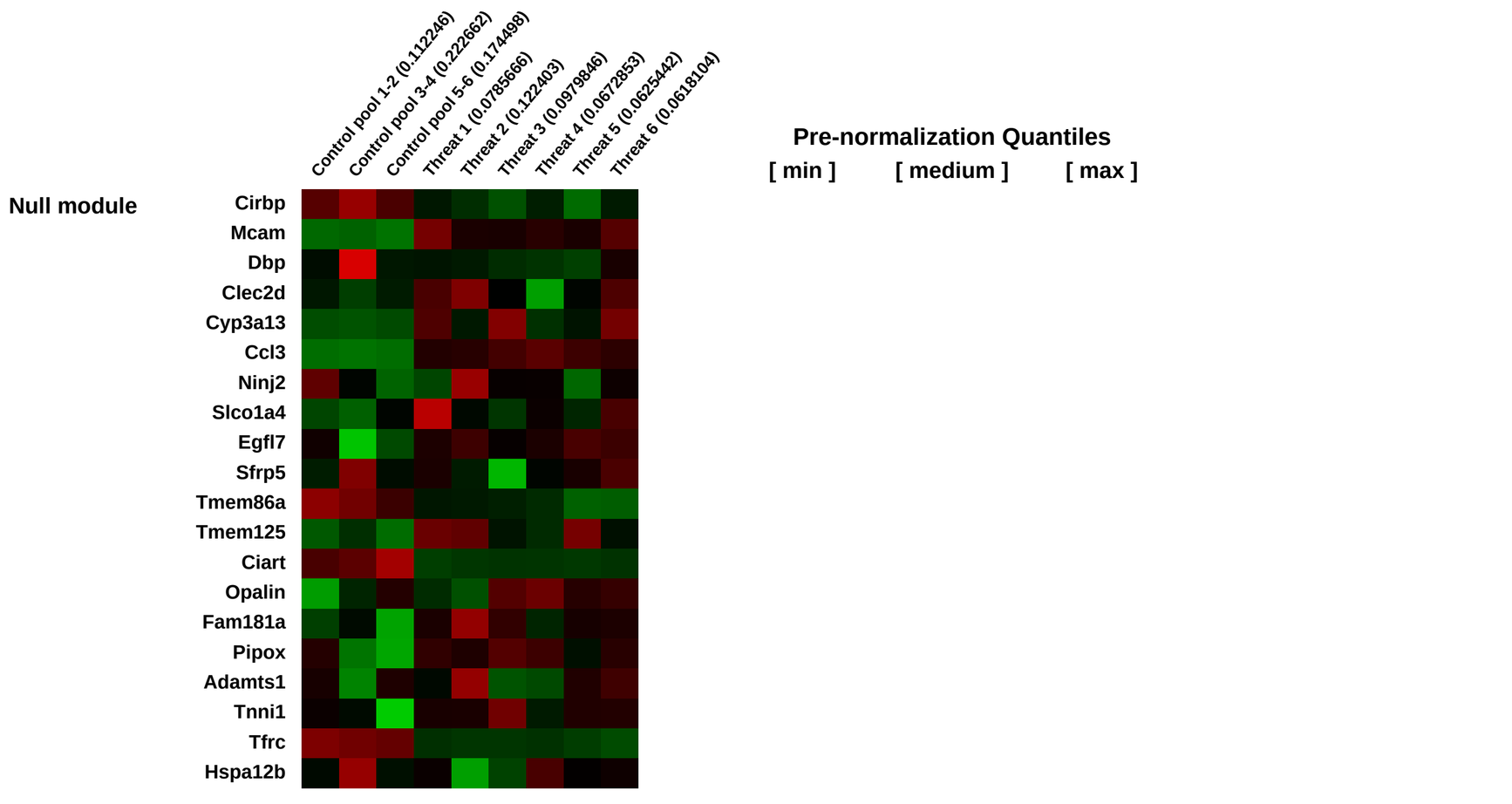

GEO Series "GSE29045" Expression Profiles

Num of samples in this series: 12

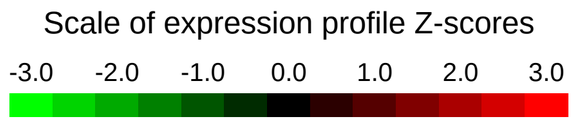

GEO Link: http://www.ncbi.nlm.nih.gov/geo/query/acc.cgi?acc=GSE29045

Status: Public on May 01 2012

Title: Genetic modification of STAT5 levels reveals dose-dependent and isoform-specific requirement for cell lineage progression and differentiation.

Organism: Mus musculus

Experiment type: Expression profiling by array

Platform: GPL1261

Pubmed ID:

Summary & Design:

Summary:
Two highly conserved transcription factors STAT5A and STAT5B play an identical role in the intracellular signaling pathway upon cytokine stimulation, while gene deletion experiments have revealed separable and overlapping functions of STAT5. This questions whether the phenotypic differences in the organ development observed in the individual knockout mice result from isoform-specific functions or quantitative differences in the expression levels of each STAT5 isoform among tissues. To elucidate the redundancy and isoform-specificity of STAT5 for development at molecular levels, mice carrying only a single allele of either Stat5a or Stat5b were generated. Both of these mice overcame the lethal anemia observed in Stat5ab-null mice, indicating that development of erythroid cell lineage was totally dependent on the dosage of STAT5. The blocked progression of B cell lineage at the pre-pro B cell stage in Stat5ab-/- mice was rescued in the presence of a single allele of either Stat5a or Stat5b, while the number of total B220+ cells in bone marrow was smaller in Stat5abnull/Stat5b- mice than Stat5abnull/Stat5a- mice. The paucity of alveolar progenitor cells in the Stat5ab-null mammary epithelium was rescued by a single allele of either Stat5a but not Stat5b, suggesting cell-type dependent isoform-specific function. Genome-wide gene expression analyses revealed that different steps of cell lineage progression require different gene sets which expression requires the different isoform of STAT5 in a dose-dependent manner in the mammary epithelium. Taken together, this study demonstrates that dose-dependent isoform specificity of STAT5A and STAT5B controls progression and differentiation of each cell lineage.

Overall design:
Six days after observation of a plug, mammary tissues from three of each Stat5a-/- mice, Stat5ab+/null mice, Stat5abnull/Stat5b- and Stat5abnull/Stat5a- mice were collected, frozen in liquid nitrogen, and stored at -70 ´C

Background corr dist: KL-Divergence = 0.0195, L1-Distance = 0.0454, L2-Distance = 0.0028, Normal std = 0.7810

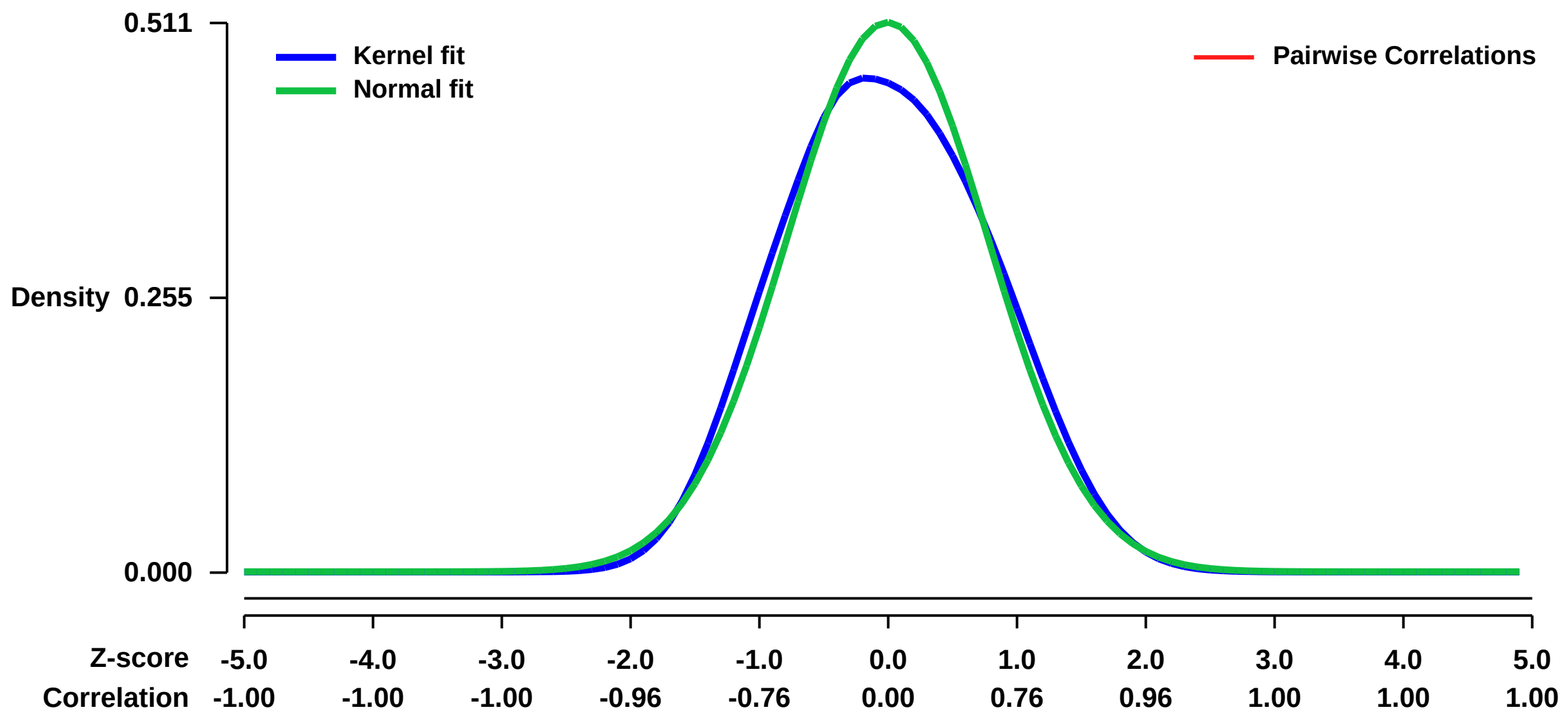

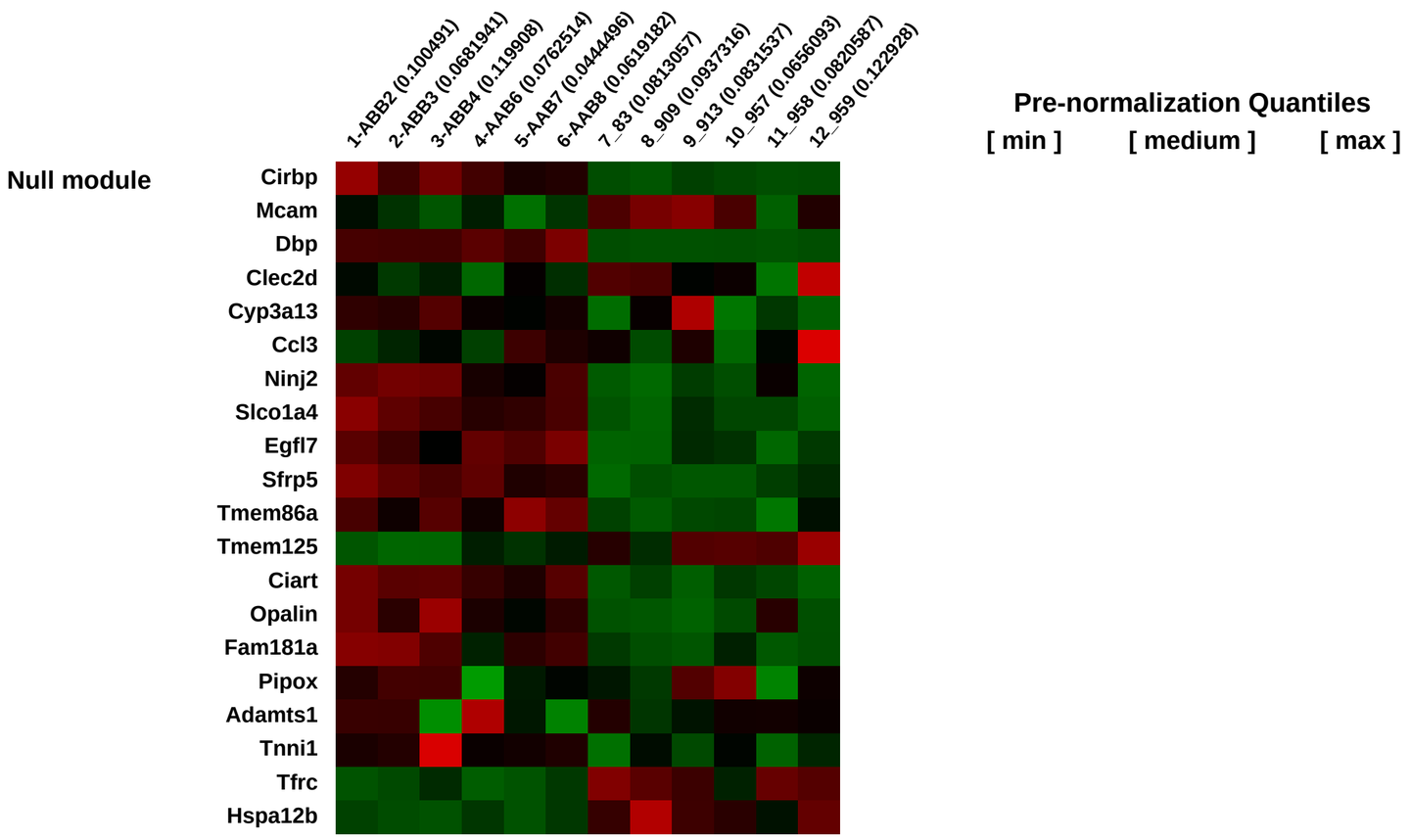

GEO Series "GSE29048" Expression Profiles

Num of samples in this series: 8

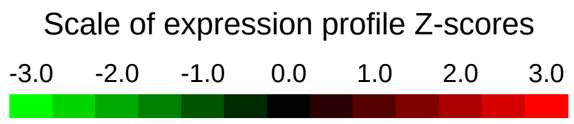

GEO Link:	http://www.ncbi.nlm.nih.gov/geo/query/acc.cgi?acc=GSE29048
Status:	Public on Jan 12 2012
Title:	Expression Profiling Identifies Novel Gene Targets and Functions for Pdx1 in the Duodenum of Mature Mice
Organism:	Mus musculus
Experiment type:	Expression profiling by array
Platform:	GPL1261
Pubmed ID:	22135308
Summary & Design:	**Summary:** Transcription factor pancreatic and duodenal homeobox 1 (Pdx1) plays an essential role in the pancreas to regulate its development and maintain proper islet function. However, less is known about the function of Pdx1 in the small intestine. We aim to investigate the role of Pdx1 in mature proximal small intestine by profiling the expression of genes differentially regulated in response to Pdx1 inactivation restricted to the intestinal epithelium in mice. **Overall design:** Pdx1 was conditionally inactivated in the intestinal epithelium of Pdx1flox/flox;VilCre mice, by crossing mutant mice homozygous for loxP site-flanked Pdx1 alleles with transgenic mice expressing Cre recombinase under the control of the mouse villin 1 gene promoter. Total RNA was isolated from the first five centimeters of the small intestine from adult Pdx1flox/flox;VilCre and littermate control mice. Microarray analysis was performed to investigate genome-wide transcriptional profiles in the proximal small intestine.

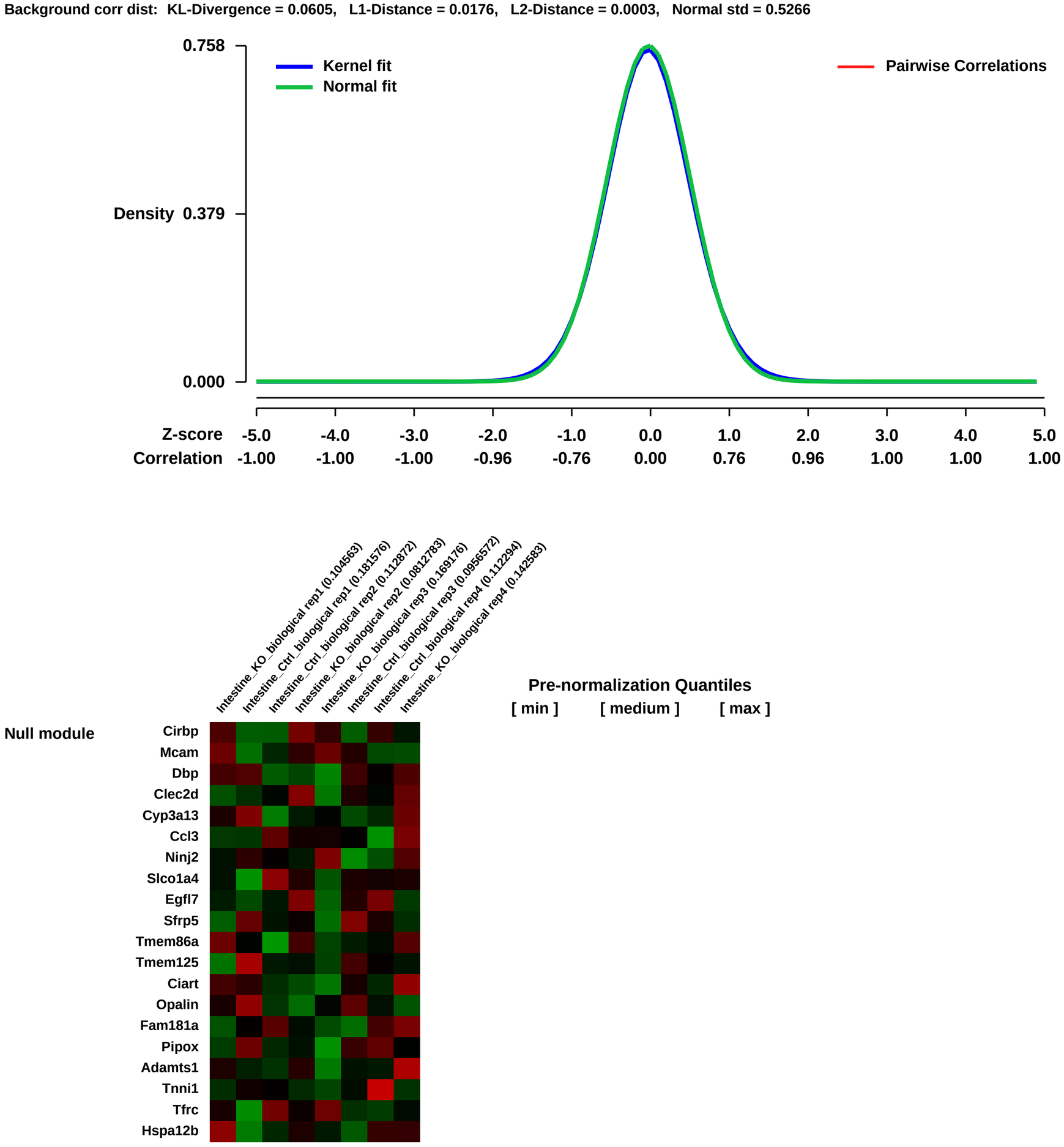

GEO Series "GSE29072" Expression Profiles

Num of samples in this series: 18

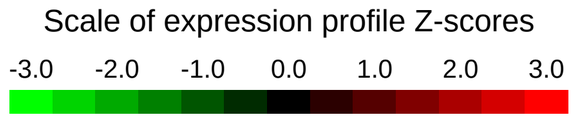

GEO Link:	**http://www.ncbi.nlm.nih.gov/geo/query/acc.cgi?acc=GSE29072**
Status:	**Public on May 05 2011**
Title:	**Zebularine effect on mouse embryonic stem cells manifested as cardiod-myogenic potential: testable hypothesis generation using microarray data**
Organism:	**Mus musculus**
Experiment type:	**Expression profiling by array**
Platform:	**GPL1261**
Pubmed ID:	
Summary & Design:	**Summary:** **Lineage commitment during Embryonic Stem Cells (ESCs) differentiation is controlled not only by a gamut of transcription factors but also by epigenetic events, mainly histone deacetylation and promoter DNA methylation. Moreover, the DNA demethylation agent 5â†-Aza-2â†-deoxycytidine (AzadC) has been widely described in the literature as an effective chemical stimulus used to promote cardiomyogenic differentiation in various stem cell types; however, its toxicity and instability complicate its use. Thus, the purpose of this study was to examine the effects of zebularine, a stable and non-toxic DNA cytosine methylation inhibitor, on ESCs differentiation. Herein are the Affymetrix Expression data obtained from RNA of murine ESCs treated with zebularine.** **Overall design:** **9 control samples (replicates) and 9 zebularine samples (replicates).**

Background corr dist: **KL-Divergence = 0.1776, L1-Distance = 0.0403, L2-Distance = 0.0032, Normal std = 0.3481**

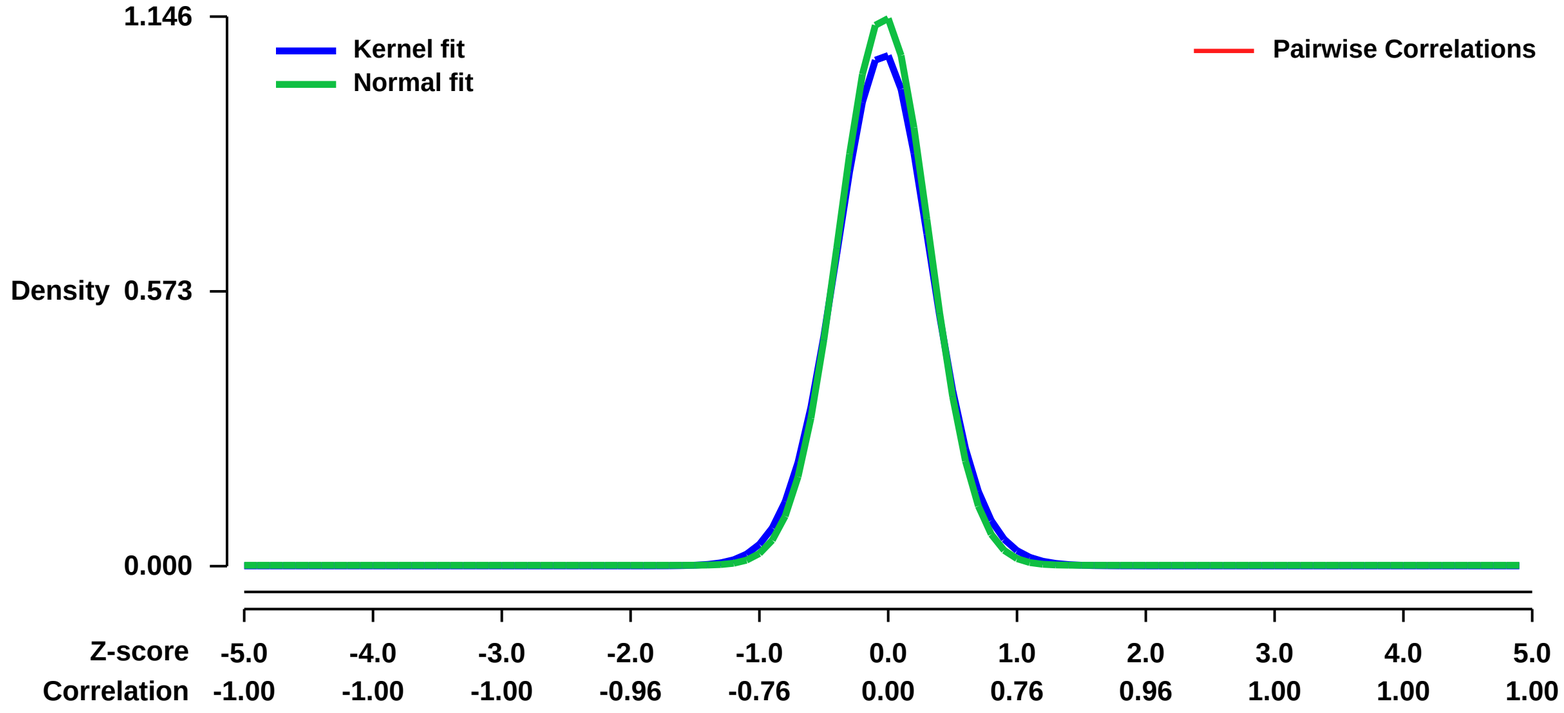

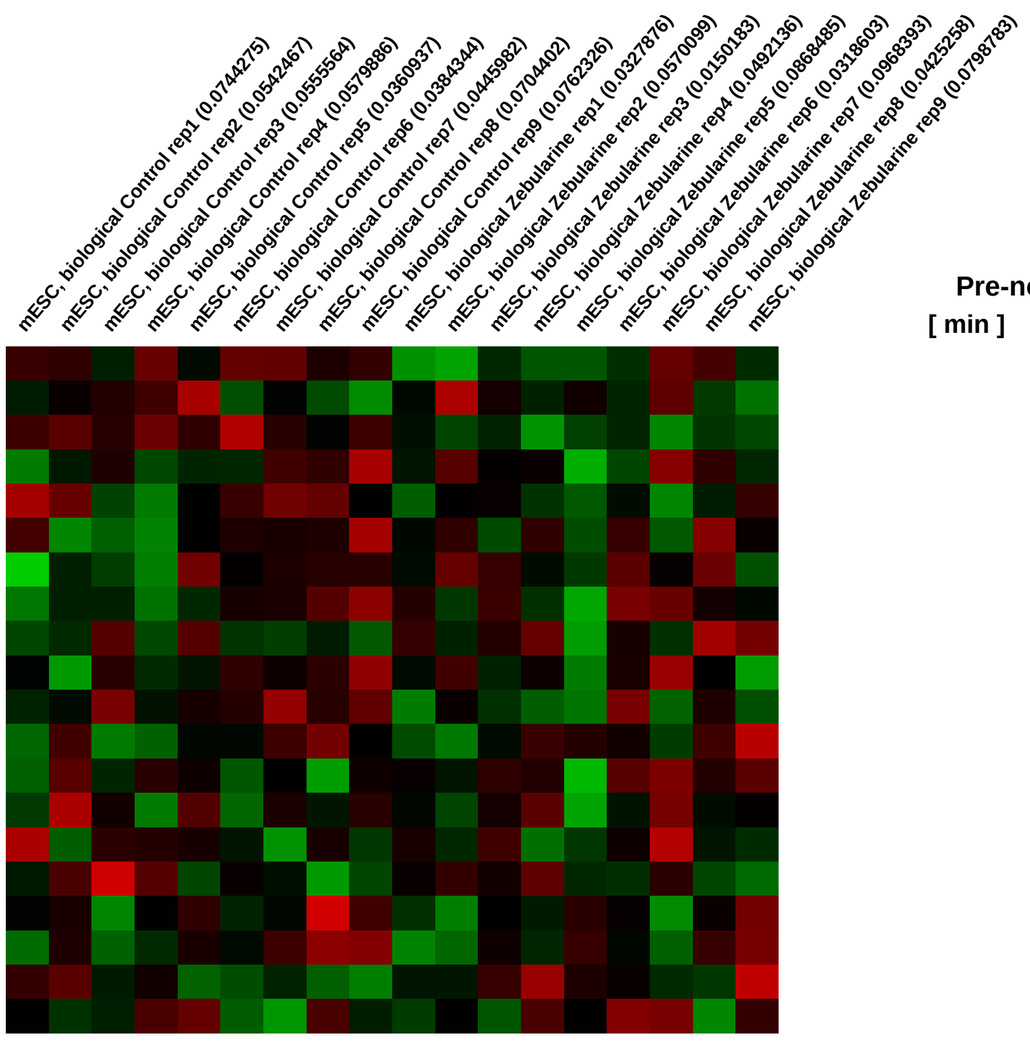

GEO Series "GSE29081" Expression Profiles

Num of samples in this series: 6

Scale of expression profile Z-scores

-3.0 -2.0 -1.0 0.0 1.0 2.0 3.0

GEO Link:	http://www.ncbi.nlm.nih.gov/geo/query/acc.cgi?acc=GSE29081
Status:	Public on Sep 13 2011
Title:	Cerebellar gene expression analysis of Gb5-deficient mice
Organism:	Mus musculus
Experiment type:	Expression profiling by array
Platform:	GPL1261
Pubmed ID:	21883221
Summary & Design:	**Summary:** Gb5 is a divergent, evolutionarily-conserved, member of the heterotrimeric G protein b subunit family that is expressed principally in brain and neuronal tissue. Among Gb isoforms, Gb5 is unique in its ability to heterodimerize with members of the R7 subfamily of the regulator of G protein signaling (RGS) proteins that contain G protein-g like (GGL) domains. Previous studies employing Gb5 knockout mice have shown that Gb5 is an essential stabilizer of GGL domain-containing RGS proteins and regulates the deactivation of retinal phototransduction and the proper functioning of retinal bipolar cells. The purpose of this study is to better understand the functions of Gb5 in the brain outside the visual system by employing molecular biology, immunohistochemistry and confocal imaging technologies. We show here that mice lacking Gb5 have a markedly abnormal neurologic phenotype that includes neurobehavioral developmental delay, wide-based gait, motor learning and coordination deficiencies, and hyperactivity. Using immunohistochemical analysis and a green fluorescent reporter of Purkinje cell maturation we show that the phenotype of Gb5-deficient mice includes, in part, delayed development of the cerebellar cortex, an abnormality that likely contributes to the neurobehavioral phenotype. Multiple neuronally-expressed genes are dysregulated in cerebellum of Gb5 KO mice. **Overall design:** Brain tissues from WT and KO with three biological replications of mice were collected, frozen in liquid nitrogen, and stored at -70 ´℃

Background corr dist: KL-Divergence = 0.0327, L1-Distance = 0.0161, L2-Distance = 0.0003, Normal std = 0.6500

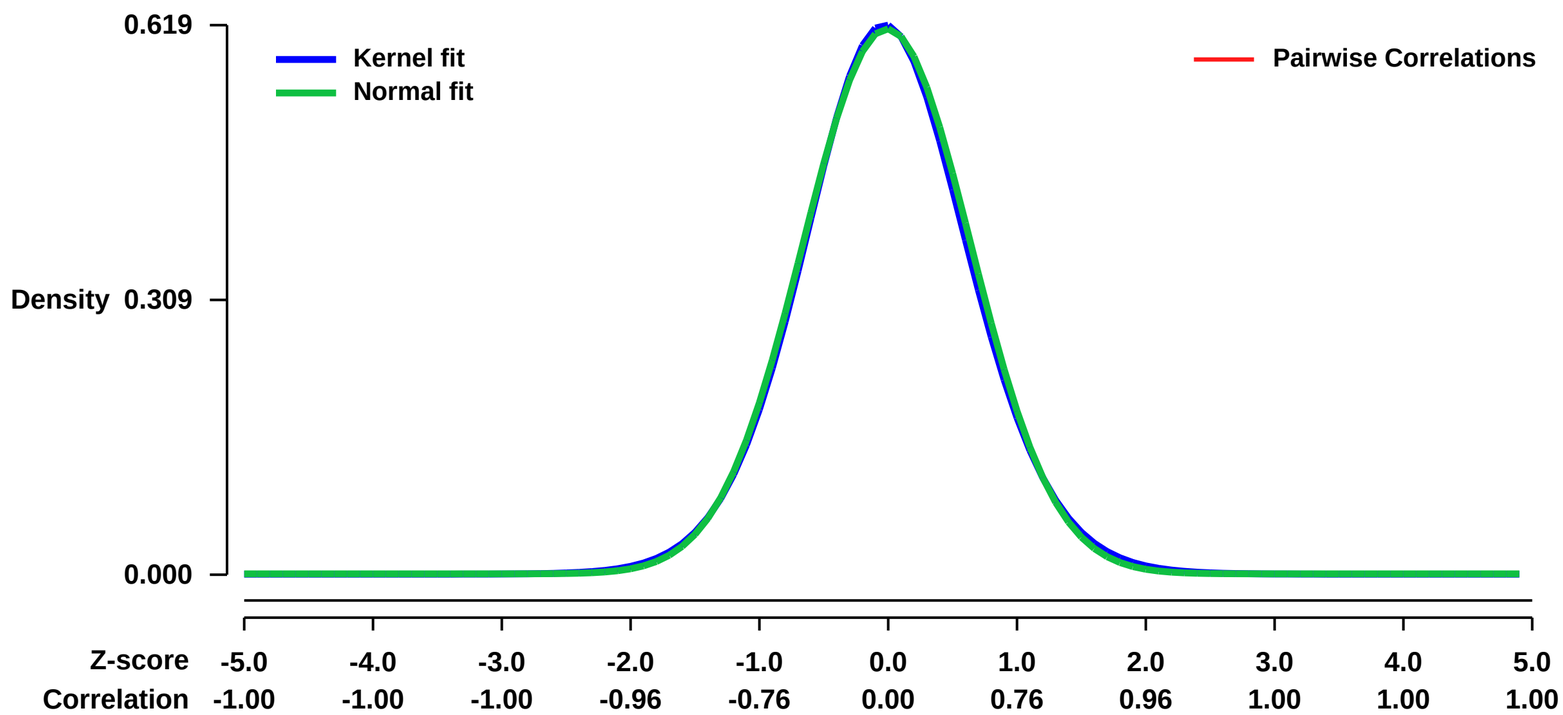

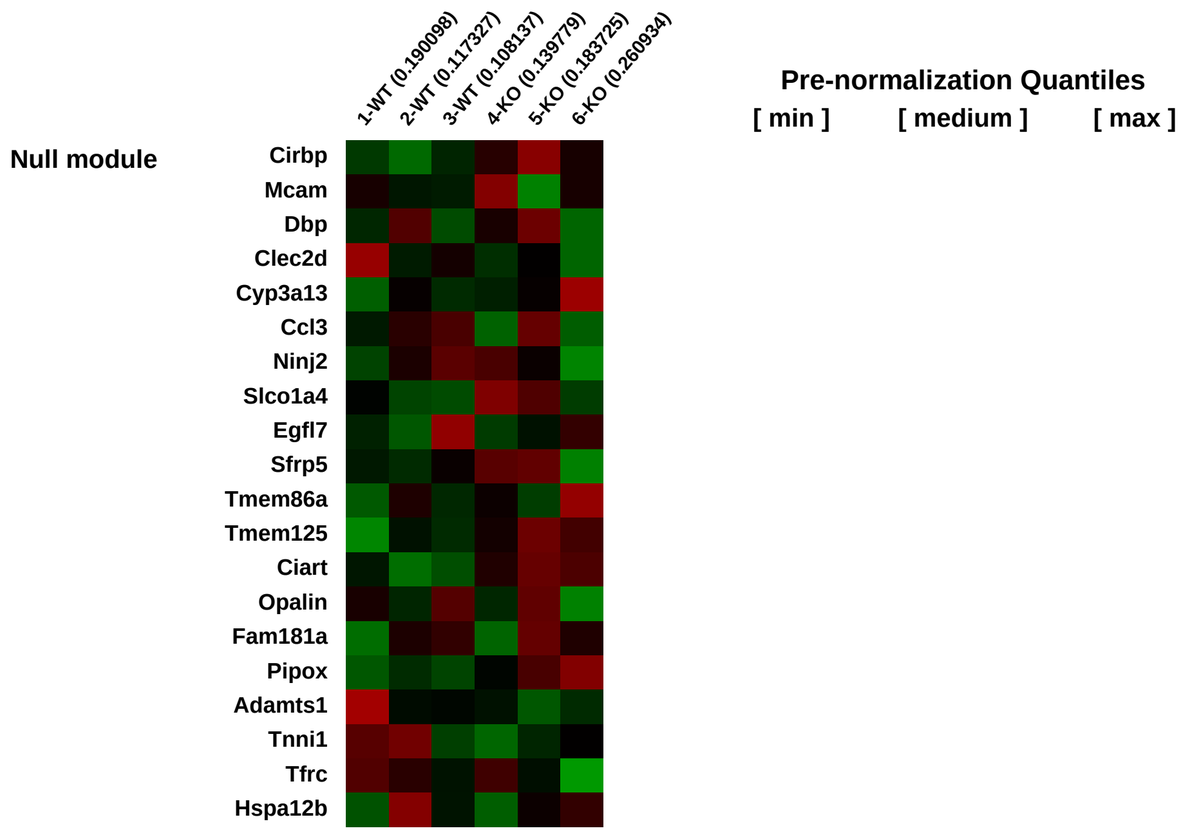

GEO Series "GSE29082" Expression Profiles

Num of samples in this series: 6

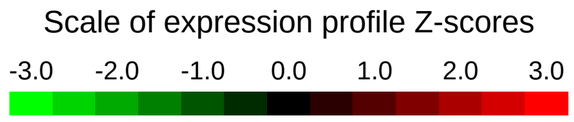

GEO Link:	http://www.ncbi.nlm.nih.gov/geo/query/acc.cgi?acc=GSE29082
Status:	Public on Sep 13 2011
Title:	Gene expression analysis of non-cerebellar portion of Gb5-deficient mice brain
Organism:	Mus musculus
Experiment type:	Expression profiling by array
Platform:	GPL1261
Pubmed ID:	21883221
Summary & Design:	**Summary:** Gb5 is a divergent, evolutionarily-conserved, member of the heterotrimeric G protein b subunit family that is expressed principally in brain and neuronal tissue. Among Gb isoforms, Gb5 is unique in its ability to heterodimerize with members of the R7 subfamily of the regulator of G protein signaling (RGS) proteins that contain G protein-g like (GGL) domains. Previous studies employing Gb5 knockout mice have shown that Gb5 is an essential stabilizer of GGL domain-containing RGS proteins and regulates the deactivation of retinal phototransduction and the proper functioning of retinal bipolar cells. The purpose of this study is to better understand the functions of Gb5 in the brain outside the visual system by employing molecular biology, immunohistochemistry and confocal imaging technologies. We show here that mice lacking Gb5 have a markedly abnormal neurologic phenotype that includes neurobehavioral developmental delay, wide-based gait, motor learning and coordination deficiencies, and hyperactivity. Using immunohistochemical analysis and a green fluorescent reporter of Purkinje cell maturation we show that the phenotype of Gb5-deficient mice includes, in part, delayed development of the cerebellar cortex, an abnormality that likely contributes to the neurobehavioral phenotype. Multiple neuronally-expressed genes are dysregulated in non-cerebellar portion of Gb5 KO mice. **Overall design:** Brain tissues(non-cerebellar portion of brain) from WT and KO with three biological replications of mice were collected, frozen in liquid nitrogen, and stored at -70 ´℃

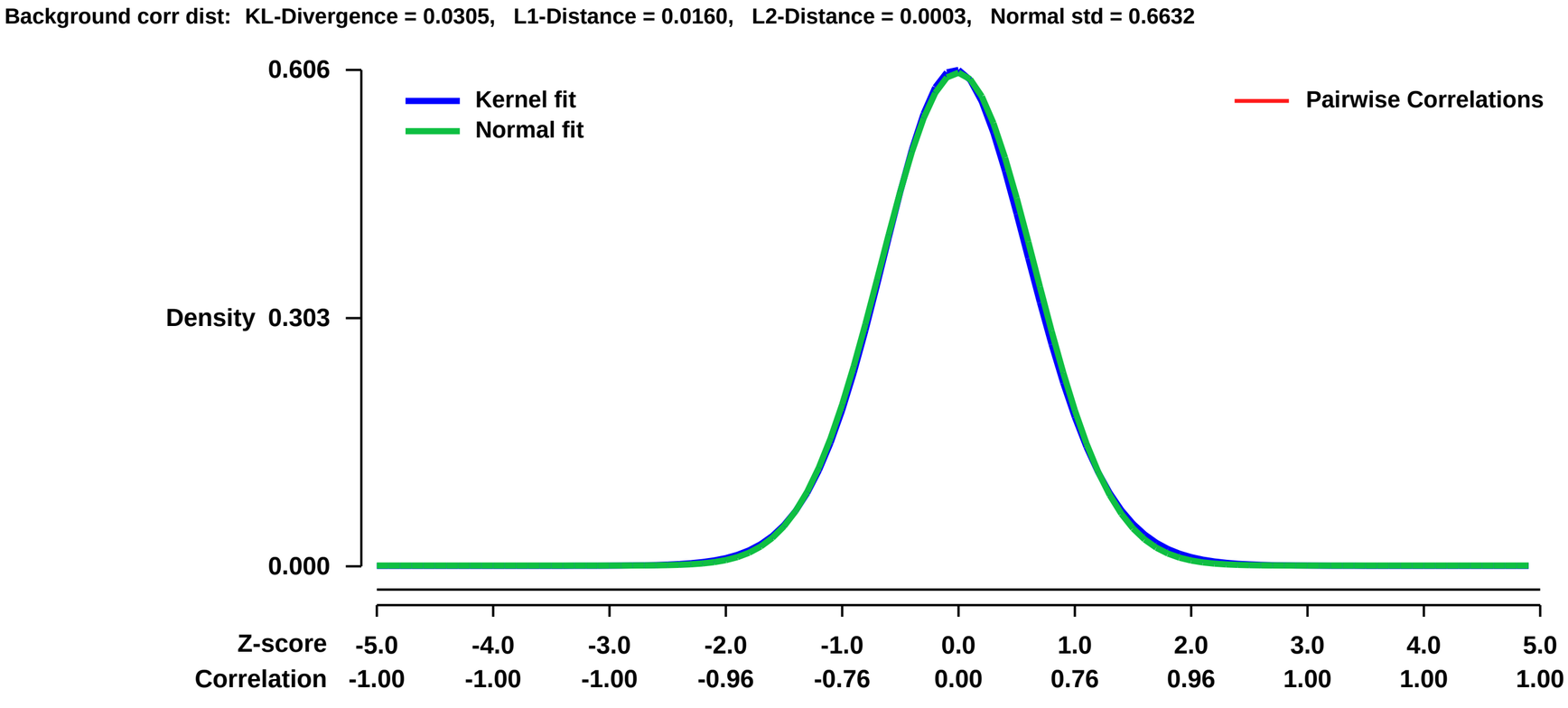

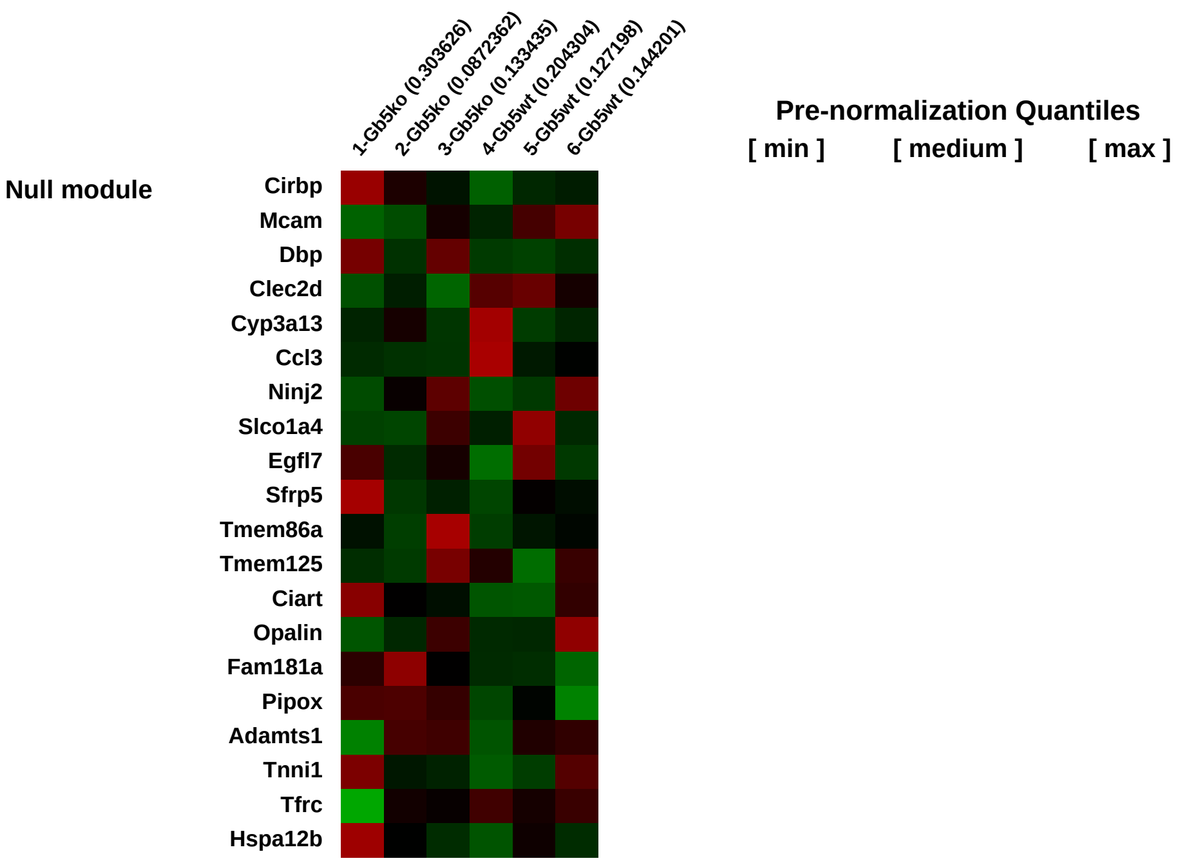

GEO Series "GSE29097" Expression Profiles

Num of samples in this series: 18

Scale of expression profile Z-scores

-3.0 -2.0 -1.0 0.0 1.0 2.0 3.0

GEO Link:	**http://www.ncbi.nlm.nih.gov/geo/query/acc.cgi?acc=GSE29097**
Status:	**Public on May 06 2011**
Title:	**Gene expression between high and low altitude Mus musculus domesticus**
Organism:	**Mus musculus domesticus**
Experiment type:	**Expression profiling by array**
Platform:	**GPL1261**
Pubmed ID:	
Summary & Design:	**Summary:** **Analysis of gene expression profiles is an attractive method for discovering how animals respond to environmental challenges in nature. Compared to low altitudes, high altitudes are characterized by reduced partial pressures of oxygen (hypoxia) and cooler ambient temperatures** **To better understand how mammals cope with high altitudes, we trapped wild house mice (Mus musculus domesticus) from 3 populations in La Paz, Bolivia (3000 - 3600 m) and 3 populations in Lima, Peru (0 â 200 m). Affymetrix GeneChip´fi Mouse Genome 430 2.0 Arrays were use to measure mRNA abundance in the livers of these mice.** **Overall design:** **Eighteen male house mice were trapped from three different locations (3 mice per location)at high alttiude (La Paz, Bolivia, 3600 m) and from three locations at low altiditude (Lima, Peru, 100 m). Total mRNA was extracted from the livers and used for hybridization of Affymetrix GeneChip Mouse expression set 420.**

Background corr dist: **KL-Divergence = 0.1874, L1-Distance = 0.0537, L2-Distance = 0.0069, Normal std = 0.3400**

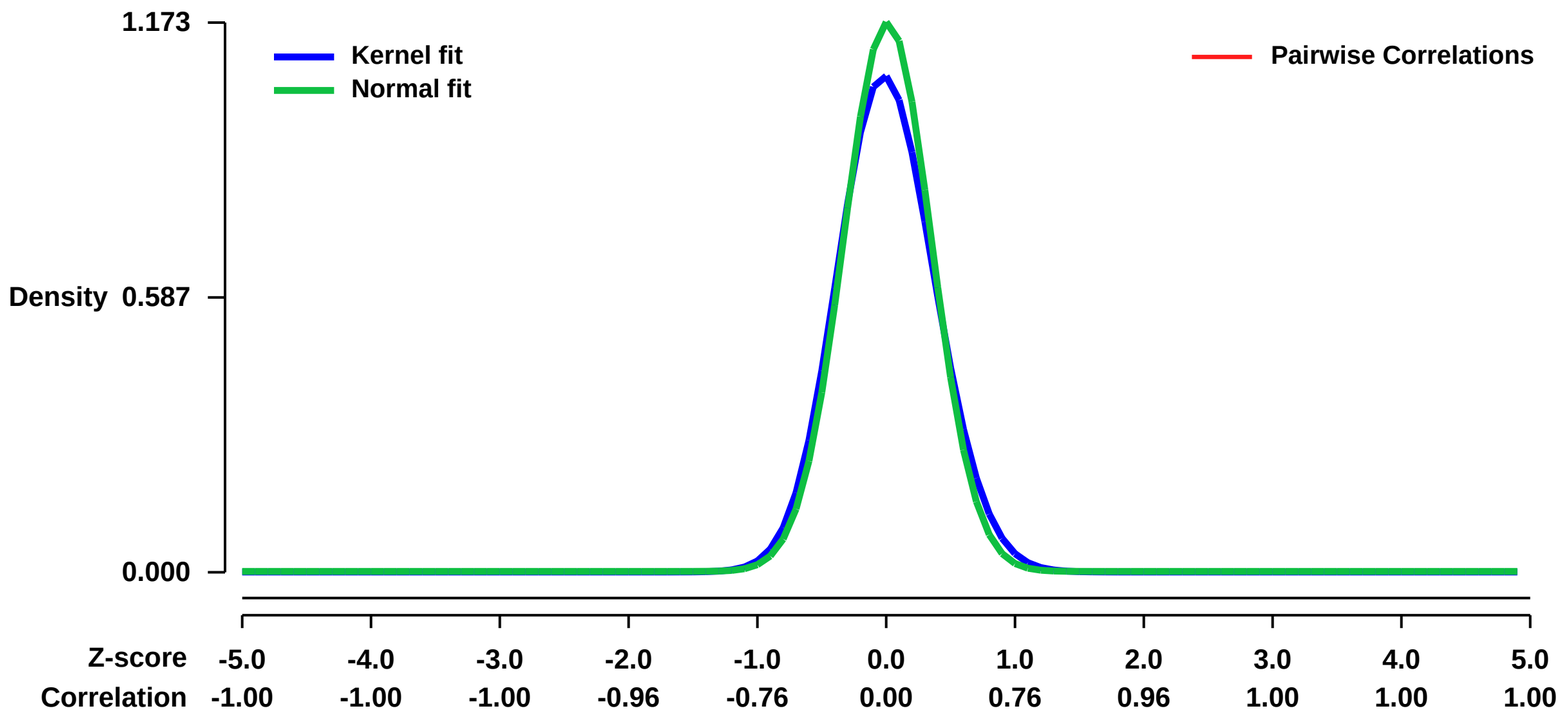

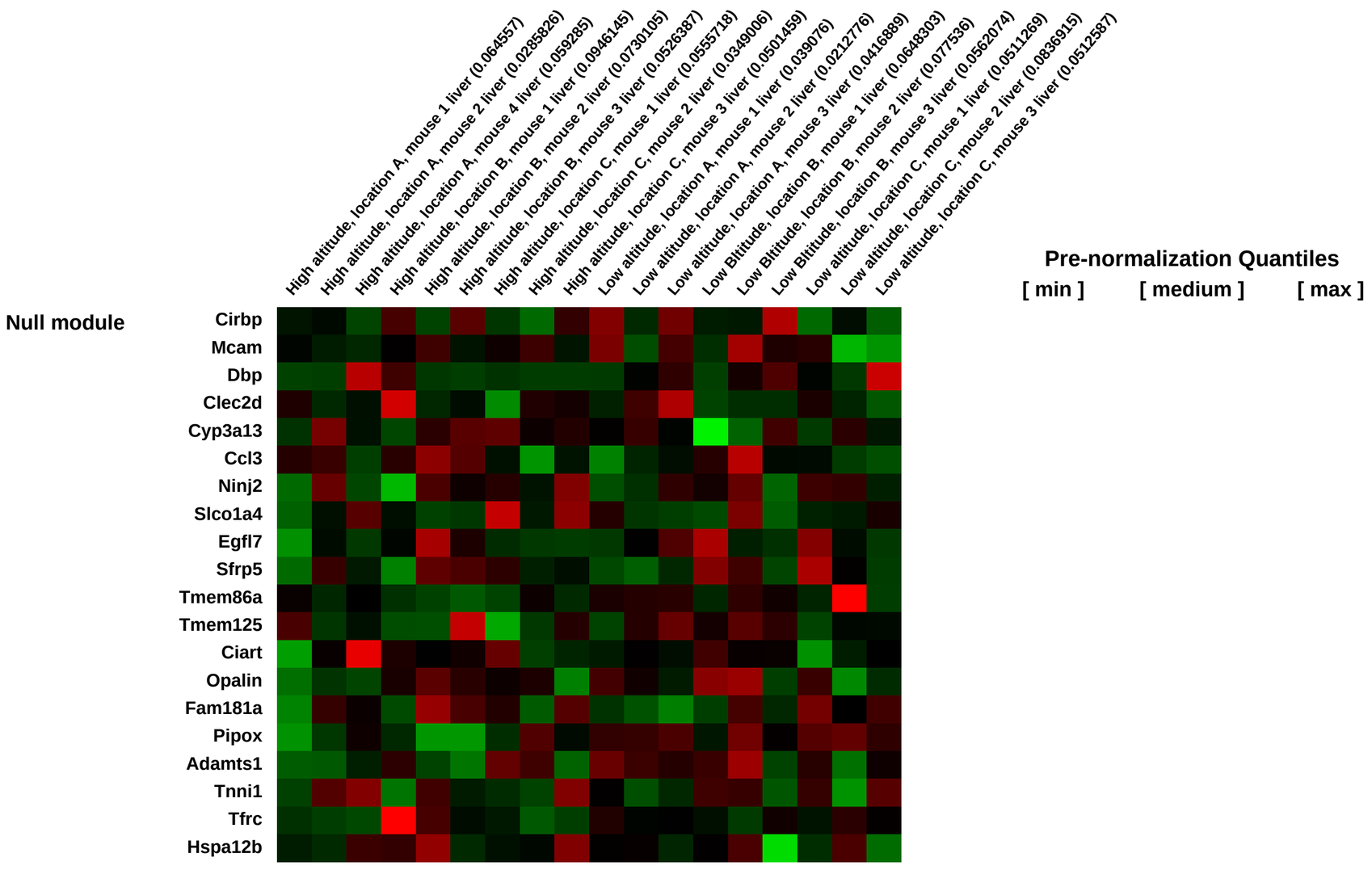

GEO Series "GSE29145" Expression Profiles

Num of samples in this series: 10

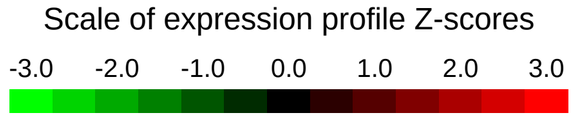

GEO Link:	http://www.ncbi.nlm.nih.gov/geo/query/acc.cgi?acc=GSE29145
Status:	Public on Jan 10 2012
Title:	PKCz-mediated Gaq stimulation of the ERK5 pathway is involved in cardiac hypertrophy
Organism:	Mus musculus
Experiment type:	Expression profiling by array
Platform:	GPL1261
Pubmed ID:	22232556
Summary & Design:	**Summary:** **Background: Gq-coupled G protein-coupled receptors (GPCR) mediate the actions of a variety of messengers that are key regulators of cardiovascular function. Enhanced Gaq-mediated signaling plays an important role in cardiac hypertrophy and in the transition to heart failure. We have recently described that Gaq acts as an adaptor protein that facilitates PKCz-mediated activation of ERK5 in epithelial cells. Since the ERK5 cascade is known to be involved in cardiac hypertrophy, we have investigated the potential relevance of this pathway in Gq-dependent signaling in cardiac cells.** **Methodology/Principal Findings: We have explored the mechanisms involved in Gq-coupled GPCR-mediated stimulation of the ERK5 pathway and its functional consequences in cardiac hypertrophy using both cultured cardiac cells and an animal model of angiotensin-dependent induction of cardiac hypertrophy in wild-type and PKCz knockout mice. We find that PKC¸¶ is required for the activation of the ERK5 pathway by Gq-coupled GPCR in cardiomyocytes and in cardiac fibroblasts. Stimulation of ERK5 by angiotensin II is blocked upon pharmacological inhibition or siRNA-mediated silencing of PKCz in primary cultures of cardiac cells and in cardiomyocytes isolated from PKCz-deficient mice. Moreover, these mice do not develop cardiac hypertrophy upon chronic challenge with angiotensin II, as assessed by morphological, biomarker, electrocardiographic and global gene expression pattern analysis.** **Conclusion/Significance: Our data put forward that PKC¸¶ is essential for Gq- dependent ERK5 activation in cardiac cells and indicate a key cardiac physiological role for this recently described Gaq/PKCz/MEK5 signaling axis.** **Overall design:** **Littermate wild-type and PKCz -/- male mice (32 weeks of age) were subjected to continuous infusion of angiotensin II (or PBS as a control) for 14 days, a well established model for the induction of cardiac hypertrohy**

Background corr dist: KL-Divergence = 0.0510, L1-Distance = 0.0437, L2-Distance = 0.0038, Normal std = 0.5596

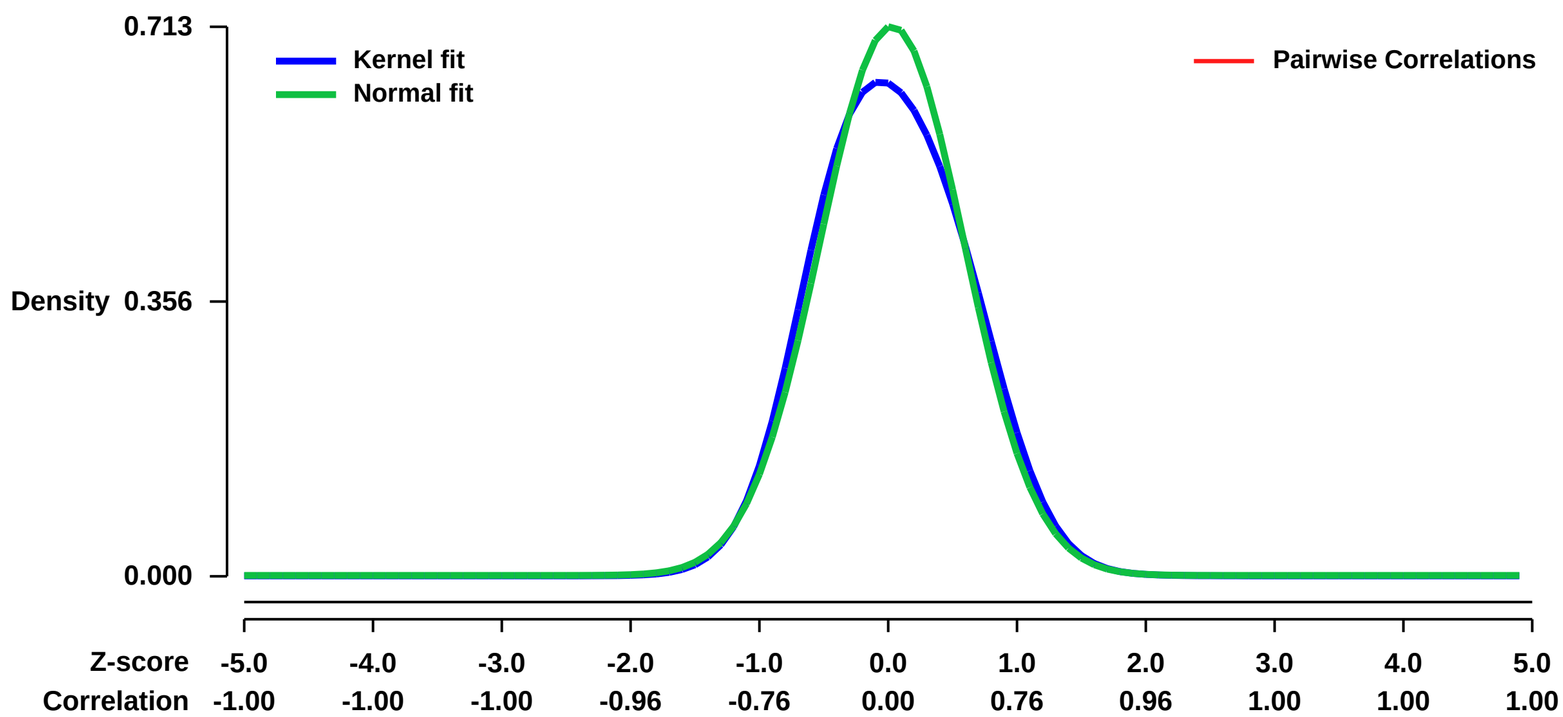

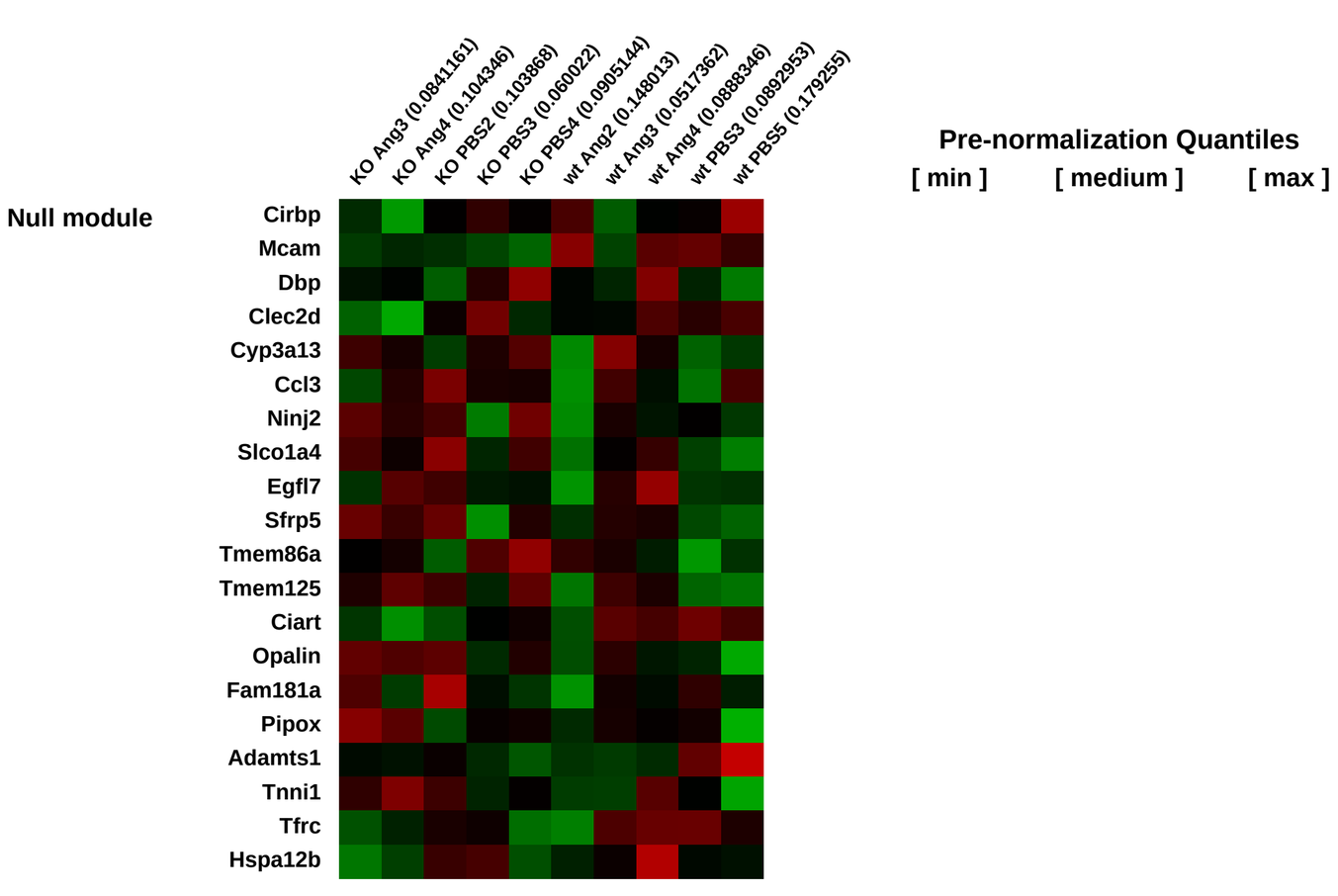

GEO Series "GSE2917" Expression Profiles

Num of samples in this series: 20

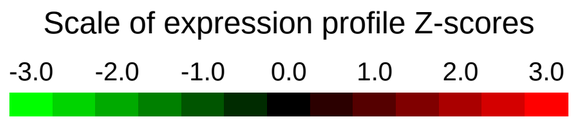

GEO Link:	http://www.ncbi.nlm.nih.gov/geo/query/acc.cgi?acc=GSE2917
Status:	Public on Dec 21 2005
Title:	Profiling of visceral sensory neurons in dorsal root and nodose ganglia in BALB/c mice.
Organism:	Mus musculus
Experiment type:	Expression profiling by array
Platform:	GPL1261
Pubmed ID:	16303873
Summary & Design:	**Summary:** Vagal afferent neurons are thought to convey primarily physiological information, whereas spinal afferents transmit noxious signals from the viscera to the central nervous system. In order to elucidate molecular identities for these different properties, we compared gene expression profiles of neurons located in nodose ganglia (NG) and dorsal root ganglia (DRG) in mice. Intraperitoneal administration of Alexa Fluor-488 conjugated Cholera toxin B allowed identification of neurons projecting to the viscera. Fluorescent neurons in DRG (from T10 to T13) and NG were isolated using laser capture microdissection. Gene expression profiles of visceral afferent neurons, obtained by microarray hybridization, were analysed using multivariate spectral map analysis, SAM algorithm (Significance Analysis of Microarray data) and fold-difference filtering. A total of 1996 genes were found to be differentially expressed in DRG versus NG, including 41 G-protein coupled receptors and 60 ion channels. Expression profiles obtained on laser-captured neurons were contrasted to those obtained on whole ganglia demonstrating striking differences and the need for microdissection when studying visceral sensory neurons because of dilution of the signal by somatic sensory neurons. Furthermore, a detailed catalogue of all adrenergic and cholinergic, GABA, glutamate, serotonin and dopamine receptors, voltage-gated potassium, sodium and calcium channels and transient receptor potential cation channels present in visceral afferents is provided. Our genome-wide expression profiling data provide novel insight into molecular signatures that underlie both functional differences and similarities between NG and DRG visceral sensory neurons. Moreover, these findings will offer novel insight into mode of action of pharmacologic agents modulating visceral sensation. **Keywords:** Cell type comparison **Overall design:** Three separate experiments were performed. First, 5 whole dorsal root ganglia were compared to 7 whole nodose ganglia. Second, Laser captured visceral neurons derived from 5 dorsal root ganglia and 5 nodose ganglia were compared on MG-U74Av2. Third, Laser captured visceral neurons derived from 9 dorsal root ganglia and 11 nodose ganglia were compared on Mouse430_2.

Background corr dist: KL-Divergence = 0.2526, L1-Distance = 0.0551, L2-Distance = 0.0075, Normal std = 0.3012

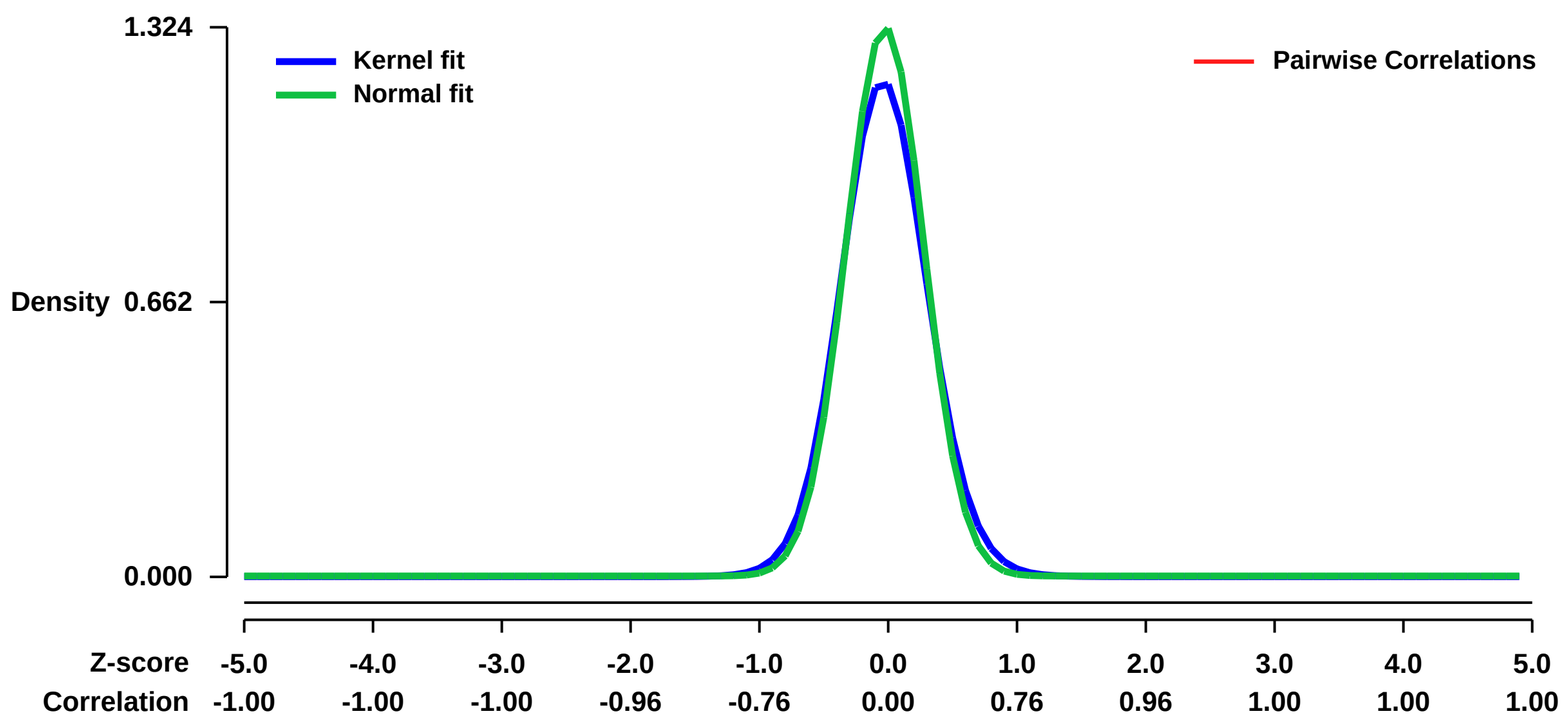

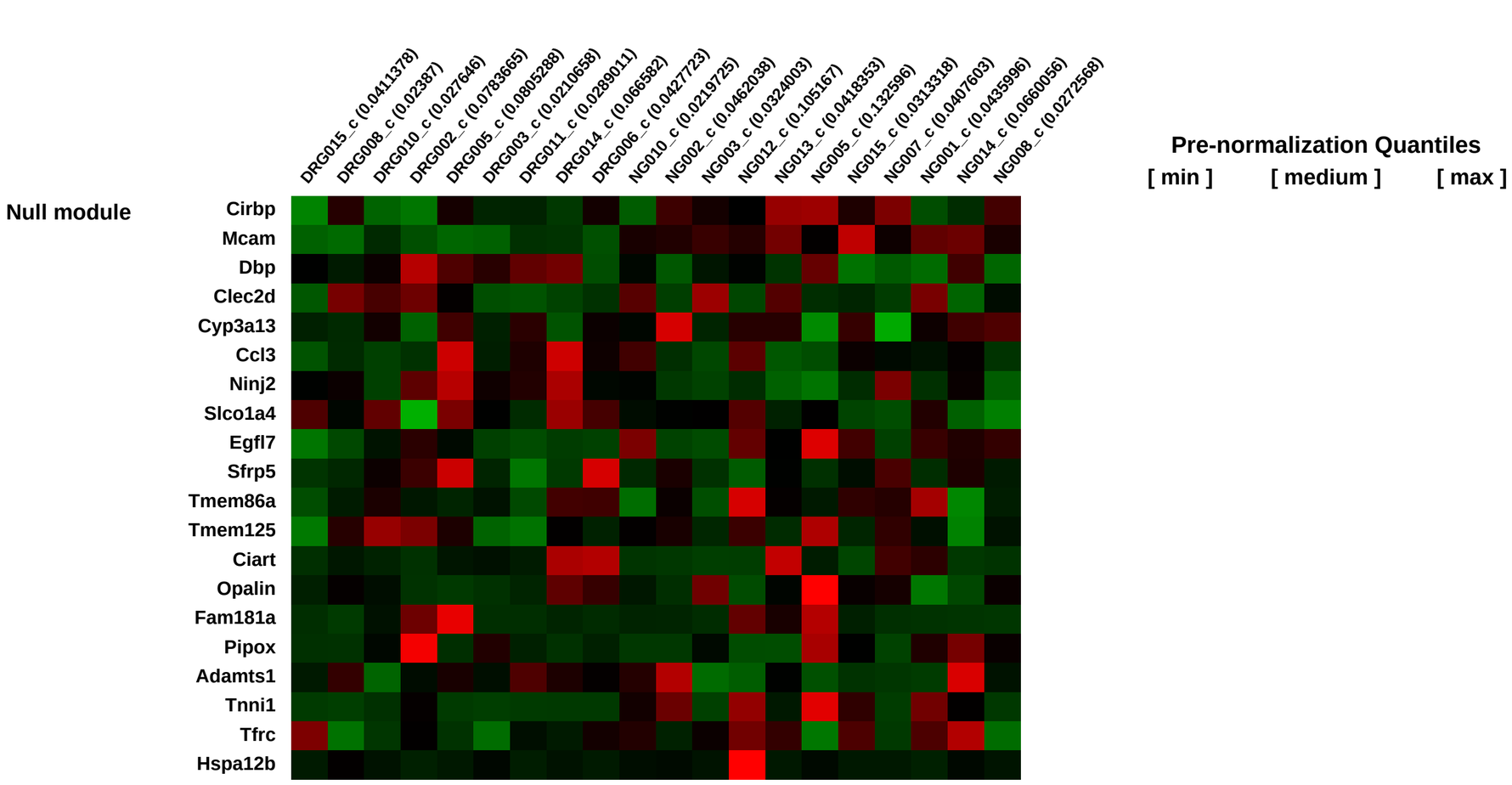

GEO Series "GSE29318" Expression Profiles

Num of samples in this series: 9

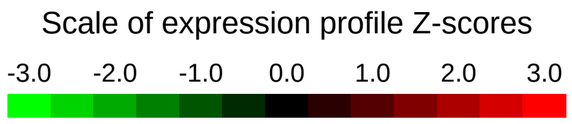

GEO Link:	http://www.ncbi.nlm.nih.gov/geo/query/acc.cgi?acc=GSE29318
Status:	Public on Jul 12 2011
Title:	Expression profile of FAC-sorted murine retinal cells
Organism:	Mus musculus
Experiment type:	Expression profiling by array
Platform:	GPL1261
Pubmed ID:	21743009
Summary & Design:	**Summary:** Microarray experiments were performed using FAC-sorted young photoreceptors to analyze their transcriptome in comparison to remaining retinal cells at same developmental stage and retinal progenitors. **Overall design:** For each replicate, retinae of 6 to 8 postnatal day 0 pNestin-GFP or postnatal day 4 rhoEGFP mice were dissected and FAC-sorted based on GFP expression. RNA of fractions was isolated and subsequently analyzed with microarray experiment.

Background corr dist: KL-Divergence = 0.0360, L1-Distance = 0.0199, L2-Distance = 0.0006, Normal std = 0.6174

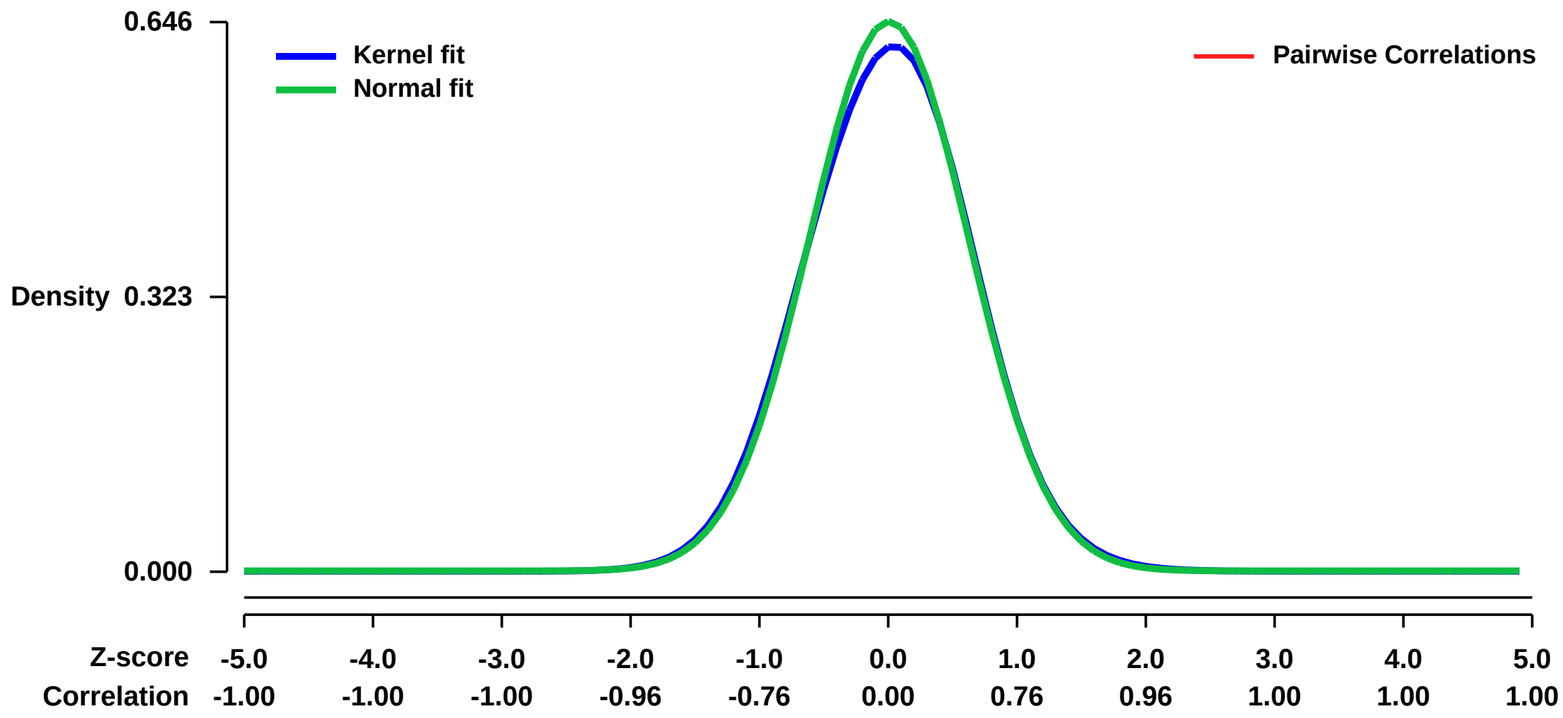

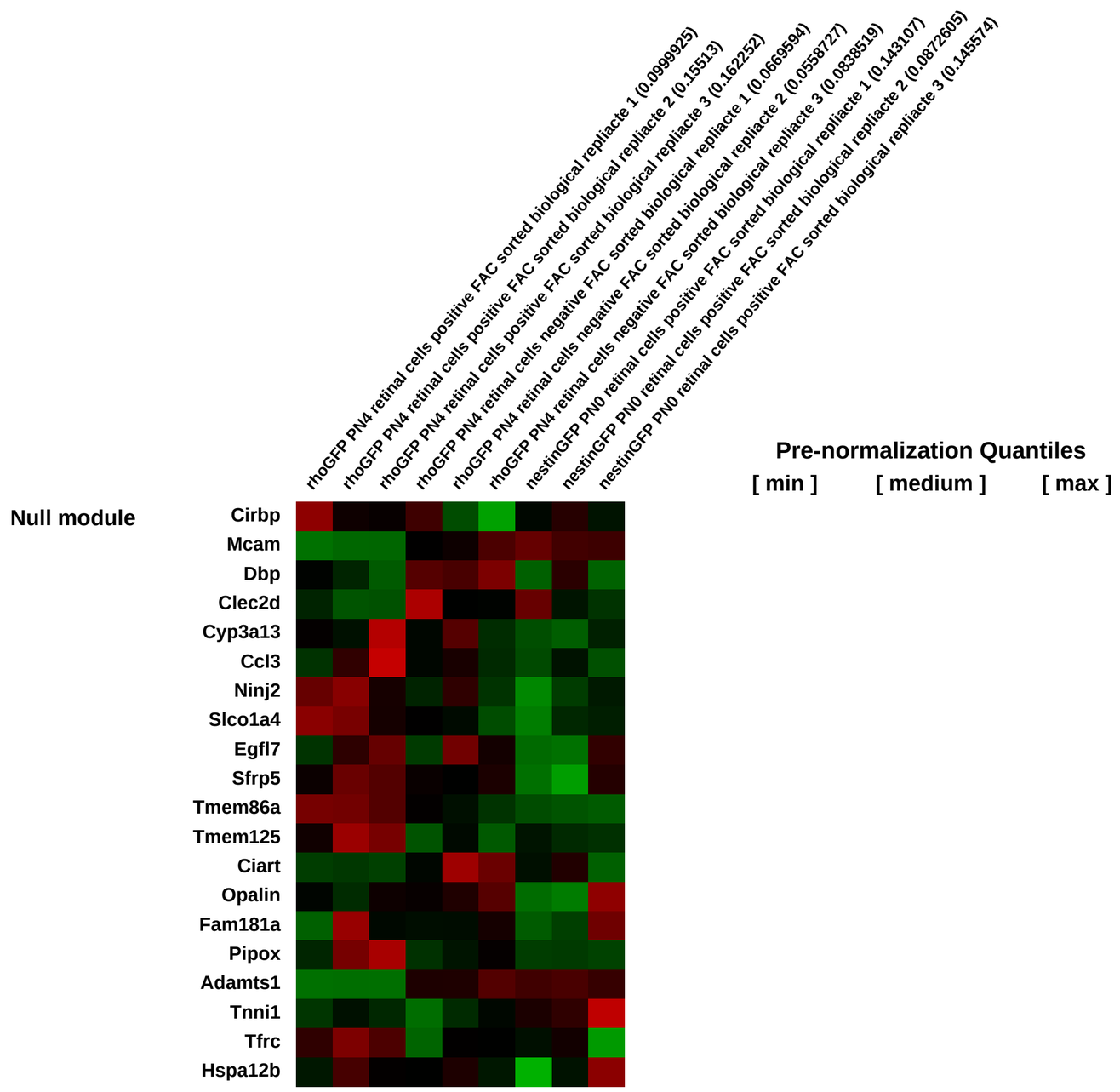

GEO Series "GSE29485" Expression Profiles

Num of samples in this series: 12

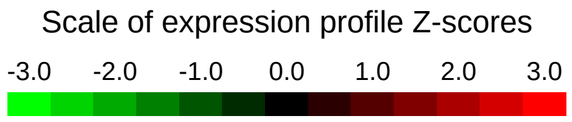

GEO Link:	**http://www.ncbi.nlm.nih.gov/geo/query/acc.cgi?acc=GSE29485**
Status:	**Public on Jul 01 2011**
Title:	**Expression data from Mouse embryo**
Organism:	**Mus musculus**
Experiment type:	**Expression profiling by array**
Platform:	**GPL1261**
Pubmed ID:	**22186409**
Summary & Design:	**Summary:** **Mice lacking the function of the PcG protein CBX2 (also known as M33) show defects in gonadal, adrenal, and splenic development. In particular, XY knockout mice develop ovaries but not testes, and the gonads are hypoplastic in both sexes.** **To clarify the molecular basis of the defects, RNA prepared from both wild type and KO gonads were subjected to microarray analyses.** **Overall design:** **Mouse embryonic gonads of Cbx2 knockout (KO) were sectioned and recovered at E11.5 for RNA extraction and hybridization on Affymetrix microarrays. Four different genotypes of embryos at E11.5 (XY WT, XX WT, XY Cbx2 KO, and XX Cbx2 KO) were frozen in OCT compound without fixation. They were sectioned to 30 ¿…m slices and stained with hematoxylin. The developing gonadal cells localized by GATA4 immunostaining and morphology were prepared using a Laser Microdissection System. The specimens prepared from two or three individuals were combined into one group, and three groups were prepared for each genotype.**

Background corr dist: KL-Divergence = 0.0809, L1-Distance = 0.0245, L2-Distance = 0.0009, Normal std = 0.4711

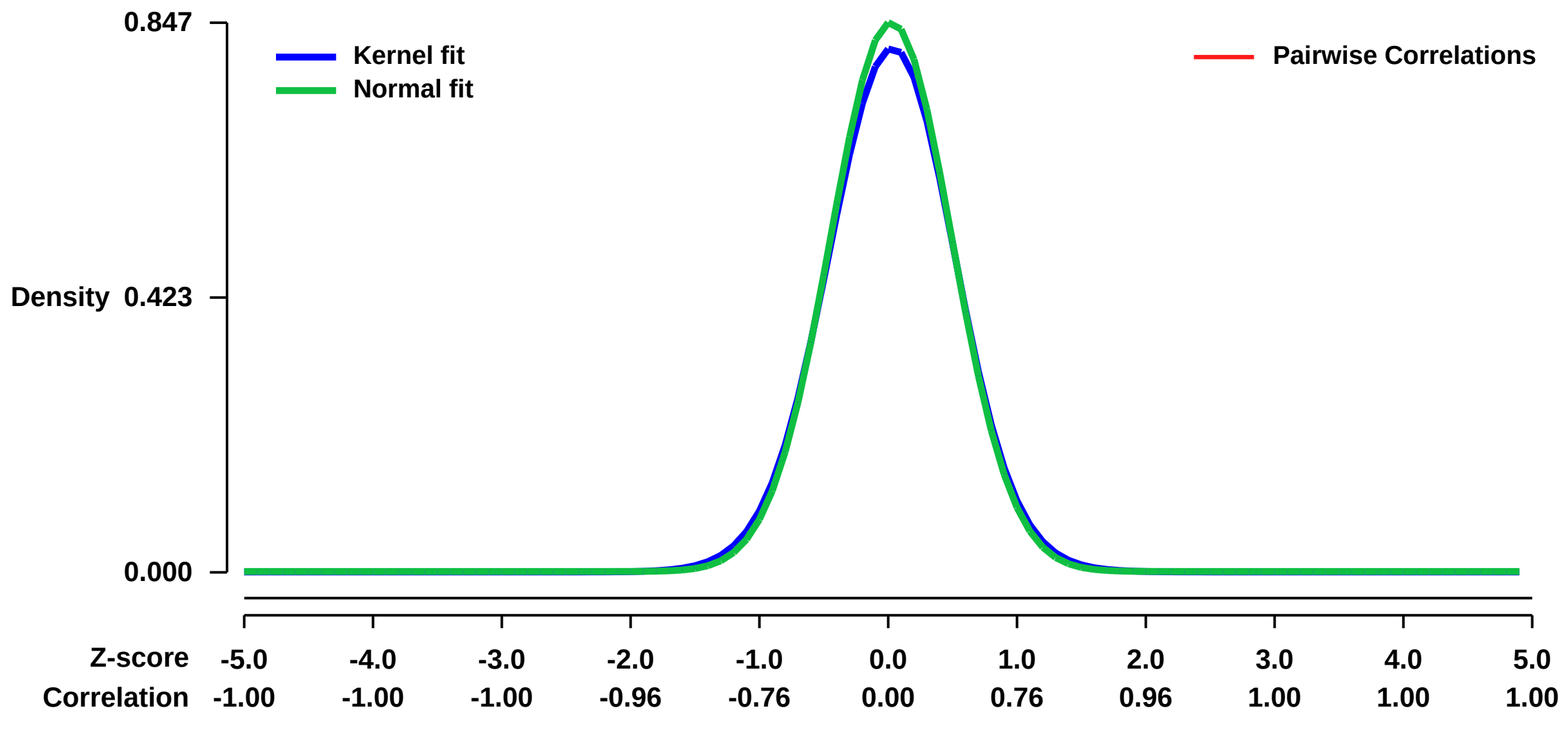

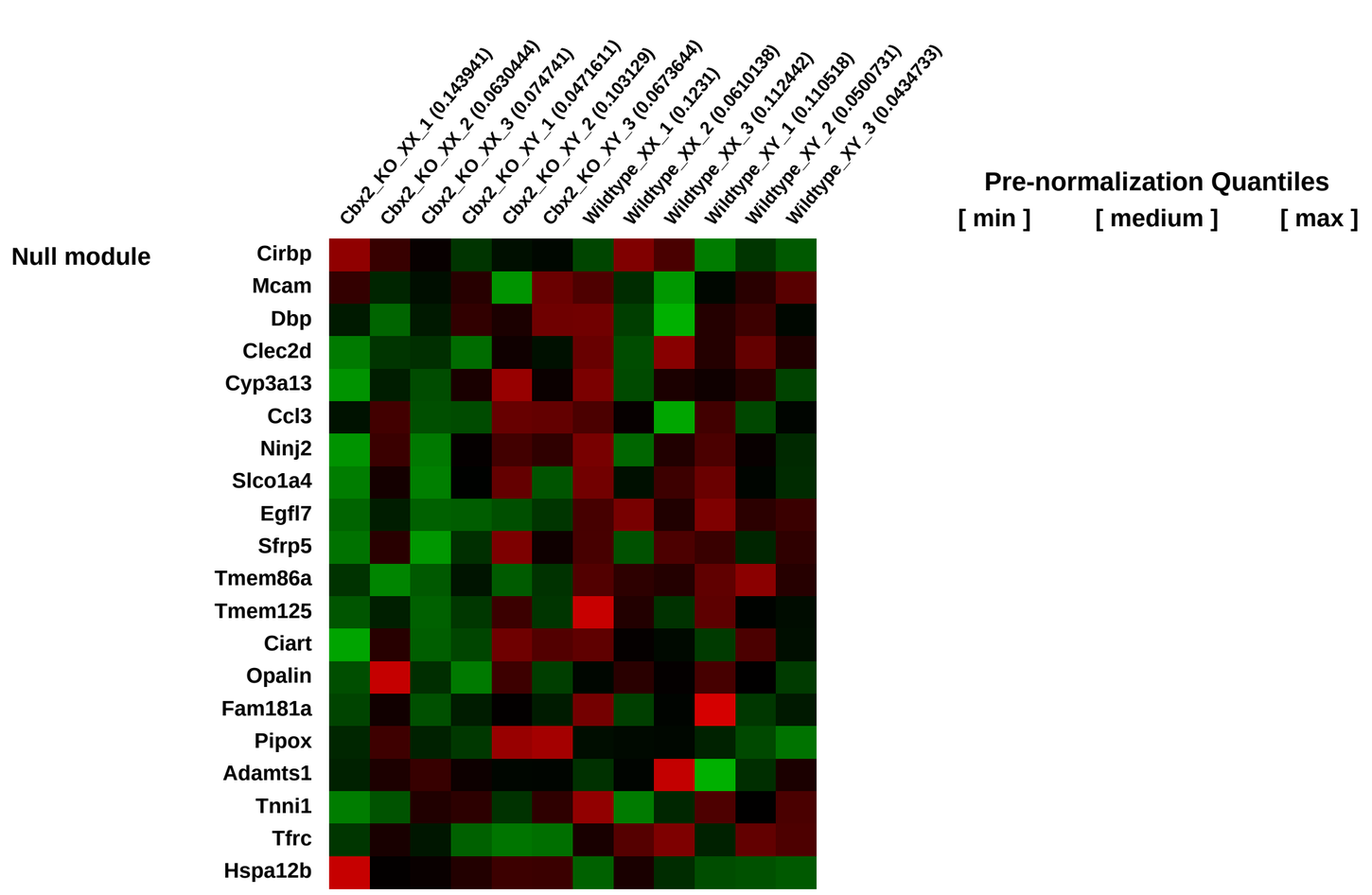

GEO Series "GSE29572" Expression Profiles

Num of samples in this series: 21

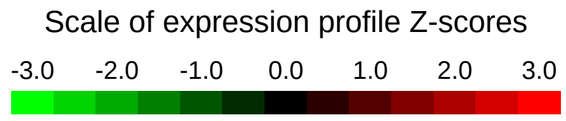

GEO Link:	**http://www.ncbi.nlm.nih.gov/geo/query/acc.cgi?acc=GSE29572**
Status:	**Public on Jul 22 2011**
Title:	**Differential effects of krill oil and fish oil on the hepatic transcriptome in mice**
Organism:	**Mus musculus**
Experiment type:	**Expression profiling by array**
Platform:	**GPL1261**
Pubmed ID:	
Summary & Design:	**Summary:** **Dietary supplementation with ˇ-3 polyunsaturated fatty acids (ˇ-3 PUFAs), specifically the fatty acids docosahexaenoic acid (DHA; 22:6 ˇ-3) and eicosapentaenoic acid (EPA; 20:5 ˇ-3), is known to have beneficial health effects including improvements in glucose and lipid homeostasis and modulation of inflammation. To evaluate the efficacy of two different sources of ˇ-3 PUFAs, we performed gene expression profiling in the liver of mice fed diets supplemented with either fish oil or krill oil. We found that ˇ-3 PUFA supplements derived from a phospholipid krill fraction (krill oil) downregulated the activity of pathways involved in hepatic glucose production as well as lipid and cholesterol synthesis. The data also suggested that krill oil-supplementation increases the activity of the mitochondrial respiratory chain. Surprisingly, an equimolar dose of EPA and DHA derived from fish oil modulated fewer pathways than a krill oil-supplemented diet and did not modulate key metabolic pathways regulated by krill oil, including glucose metabolism, lipid metabolism and the mitochondrial respiratory chain. Moreover, fish oil upregulated the cholesterol synthesis pathway, which was the opposite effect of krill supplementation. Neither diet elicited changes in plasma levels of lipids, glucose or insulin, probably because the mice used in this study were young and were fed a low fat diet. Further studies of krill oil supplementation using animal models of metabolic disorders and/or diets with a higher level of fat may be required to observe these effects.** **Overall design:** **Twenty-one microarrays: three diets (CO, FO, KO) x seven mice per diet x one microarray per mouse**

Background corr dist: KL-Divergence = 0.1248, L1-Distance = 0.0276, L2-Distance = 0.0012, Normal std = 0.4084

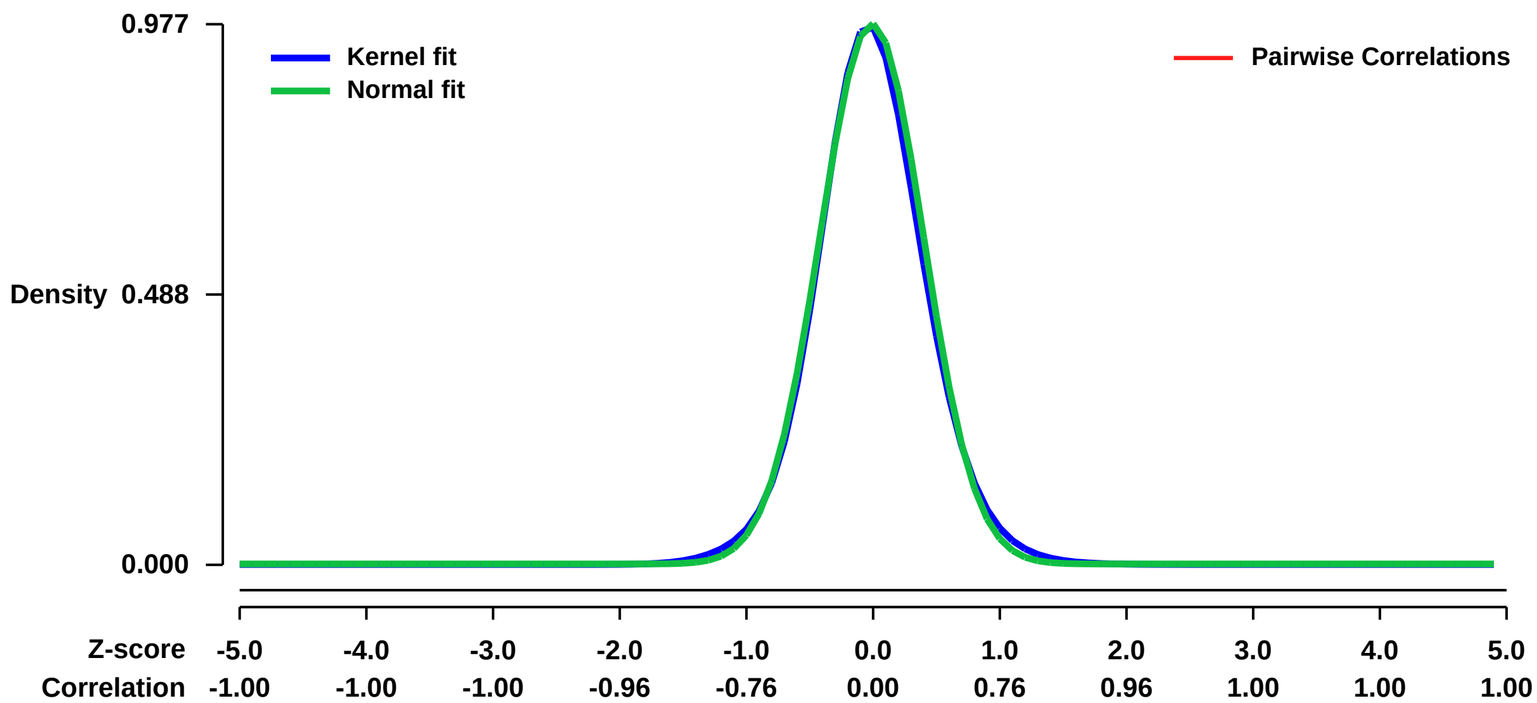

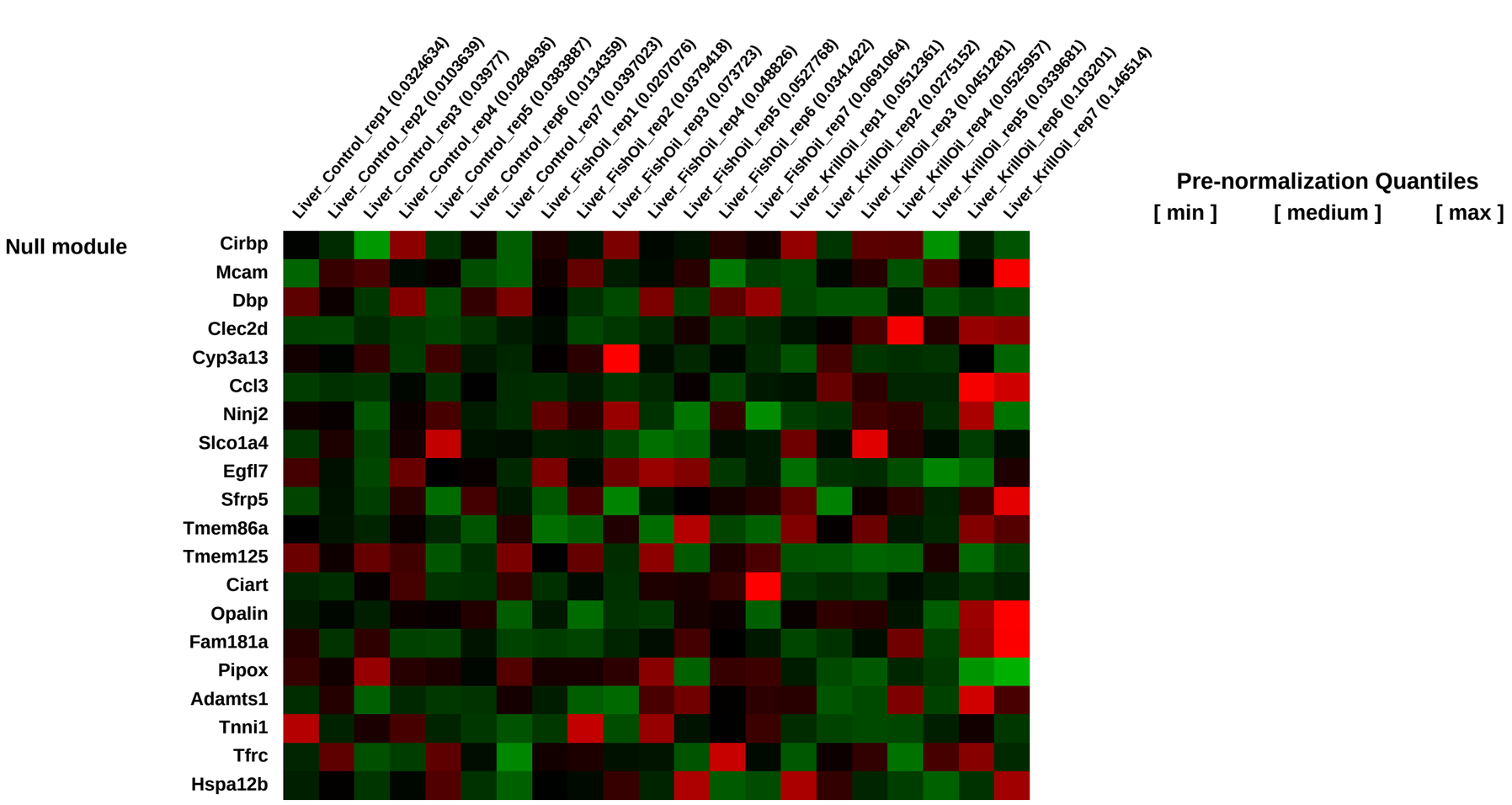

GEO Series "GSE29632" Expression Profiles

Num of samples in this series: 42

Scale of expression profile Z-scores

-3.0 -2.0 -1.0 0.0 1.0 2.0 3.0

GEO Link: http://www.ncbi.nlm.nih.gov/geo/query/acc.cgi?acc=GSE29632
Status: Public on May 25 2012
Title: Effect of Nrf2 deletion in postnatal lung development and BPD phenotype in newborn mice
Organism: Mus musculus
Experiment type: Expression profiling by array
Platform: GPL1261
Pubmed ID:

Summary & Design:

Summary:
Background: Nrf2 is an essential cytoprotective transcription factor. However, association of Nrf2 in organ development and neonatal disease is rarely examined. Hyperoxia exposure to newborn rodents generates pulmonary phenotypes which resemble bronchopulmonary dysplasia (BPD) of prematurity.

Methods: To investigate the role of Nrf2 in lung maturation and BPD pathogenesis, Nrf2-deficient (Nrf2-/-) and wild-type (Nrf2+/+) neonates were exposed to air or hyperoxia (O2). Transcriptome analysis determined Nrf2-directed mechanisms in premature lung. Lung injury was assessed by bronchoalveolar lavage analysis and histopathology.

Results: In Nrf2-/- neonates, basal expression of cell cycle machinery, redox balance, and lipid/carbohydrate metabolism genes were suppressed while immunity genes were overexpressed compared to Nrf2+/+ pups. O2-induced mortality and pulmonary inflammation/injury were significantly higher in Nrf2-/- than in Nrf2+/+. Lung DNA lesion and oxidation were greater in Nrf2-/- than in Nrf2+/+, constitutively and after O2. Nrf2-dependent genes modulated cellular growth/proliferation, defense, immunity, and lipid metabolism against hyperoxia. Bioinformatic elucidation of Nrf2 binding motifs and augmented O2-induced inflammation in genetically deficient neonates validated Gpx2 and Marco as Nrf2 effectors.

Conclusion: Overall, Nrf2 in underdeveloped lungs orchestrated cell cycle, morphogenesis, and immunity as well as cellular defense constitutively and under oxidant stress. Results provide putative molecular mechanisms of Nrf2-directed lung alveolarization and BPD of prematurity.

Overall design:
PARALLEL study design with 42 samples comparing 14 groups of age (P1 to P4 corresponding to day 0 to day 3 animals), gene, and exposure: (4 groups Nrf+/+ wild type P1-P4 air exposure) (4 groups Nrf -/- knockout P1-P4 air exposure), (3 groups Nrf+/+ wild type P2-P4 with 100 percent O2 (hyperoxia exposure) and 3 groupsNrf -/- knockout P2-P4 with 100 percent O2 (hyperoxia exposure)) Biological replicates: 3 per group

Background corr dist: KL-Divergence = 0.2661, L1-Distance = 0.0498, L2-Distance = 0.0062, Normal std = 0.2972

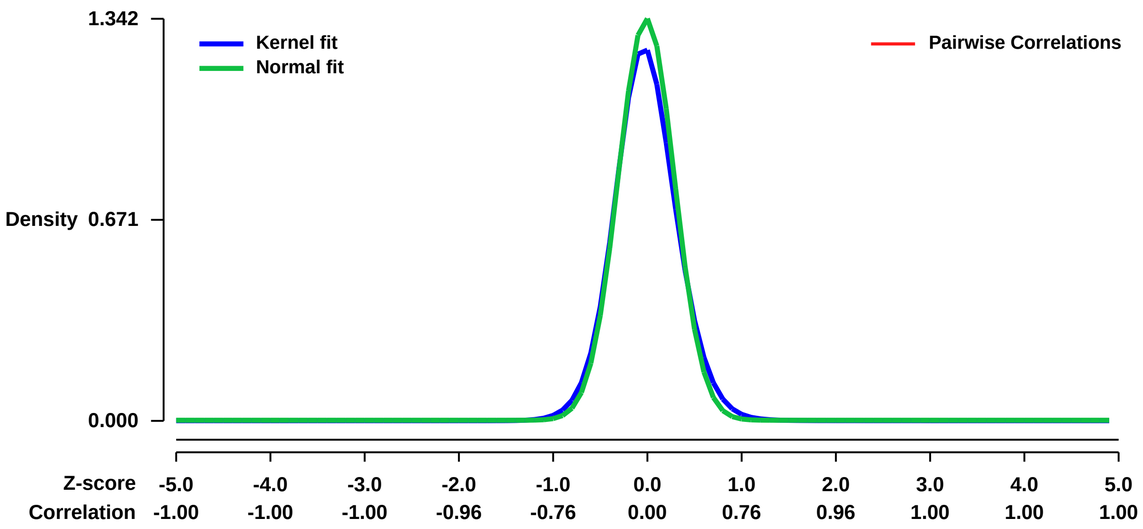

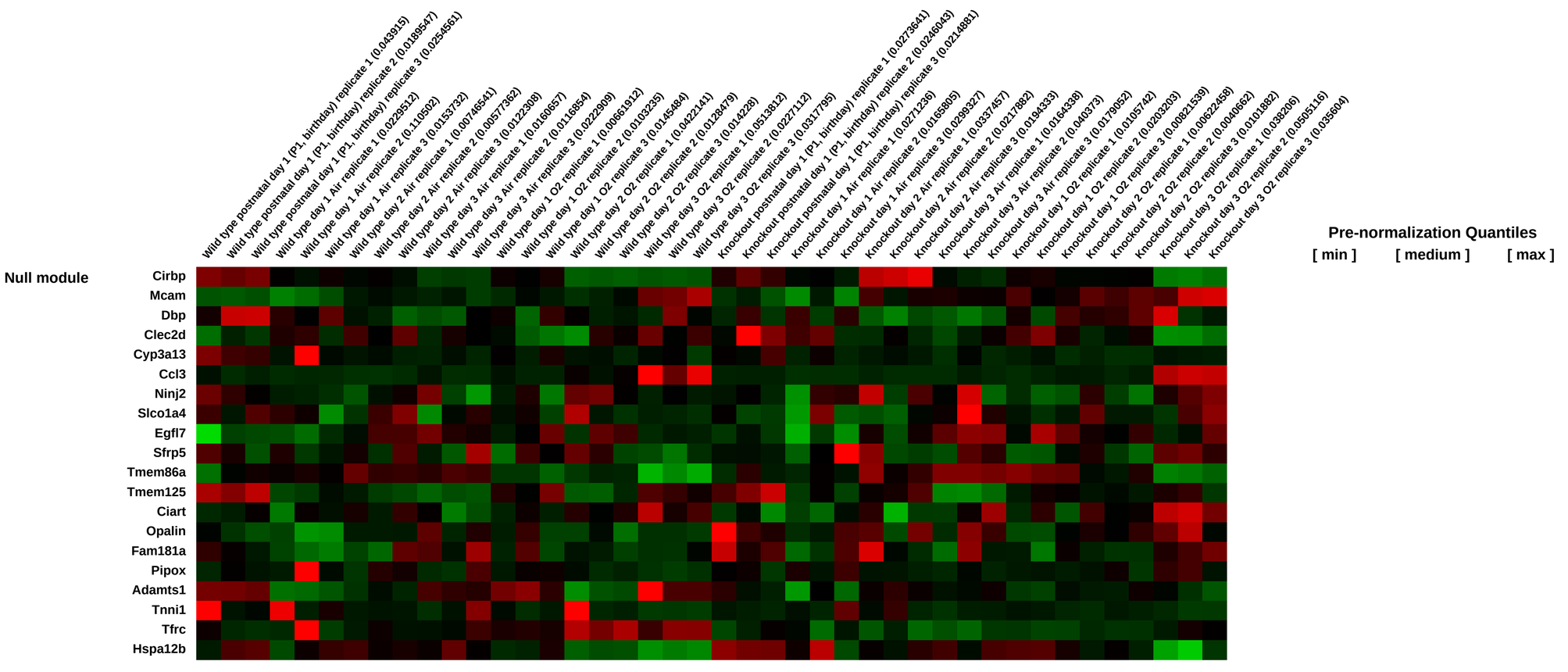

GEO Series "GSE29648" Expression Profiles

Num of samples in this series: 10

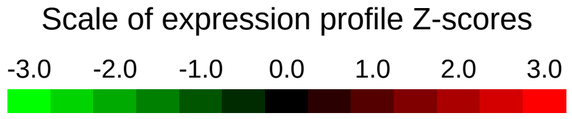

GEO Link:	http://www.ncbi.nlm.nih.gov/geo/query/acc.cgi?acc=GSE29648
Status:	Public on Jun 02 2011
Title:	The impact of a phytoestrogen-rich diet on cardiac gene expression in the context of HCM
Organism:	Mus musculus
Experiment type:	Expression profiling by array
Platform:	GPL1261
Pubmed ID:	22778230
Summary & Design:	**Summary:** A soy diet worsens the progression of an inherited form of hypertrophic cardiomyopathy (HCM) in male mice when compared to casein-fed mice. Females are largely resistant to this diet effect and better preserve cardiac function. We hypothesized that the abundant phytoestrogens found in soy are mainly responsible for this diet-dependent phenotype. Indeed, feeding male mice a phytoestrogen-supplemented casein-based diet can recapitulate the negative outcome seen when male mice are fed a standard soy-based diet. To gain mechanistic insights into disease pathogenesis, we used Affymetrix microarrays to profile gene expression in left ventricular tissue from 2 month old HCM male and female mice as well as wild-type littermate controls. These mice were fed a phytoestrogen (genistein + daidzein)-supplemented casein-based diet. We identified a number of molecular pathways that could explain both the male and female phenotypes. **Overall design:** Hearts from male and female wild-type or HCM C57BL/6 mice fed a phytoestrogen-supplemented (genistein and daidzein mix) casein-based diet were excised at 2 months of age. Total RNA was extracted from left ventricles. Biotin-labeled amplified RNA was hybridized to Affymetrix Mouse Genome 430 2.0 microarrays.

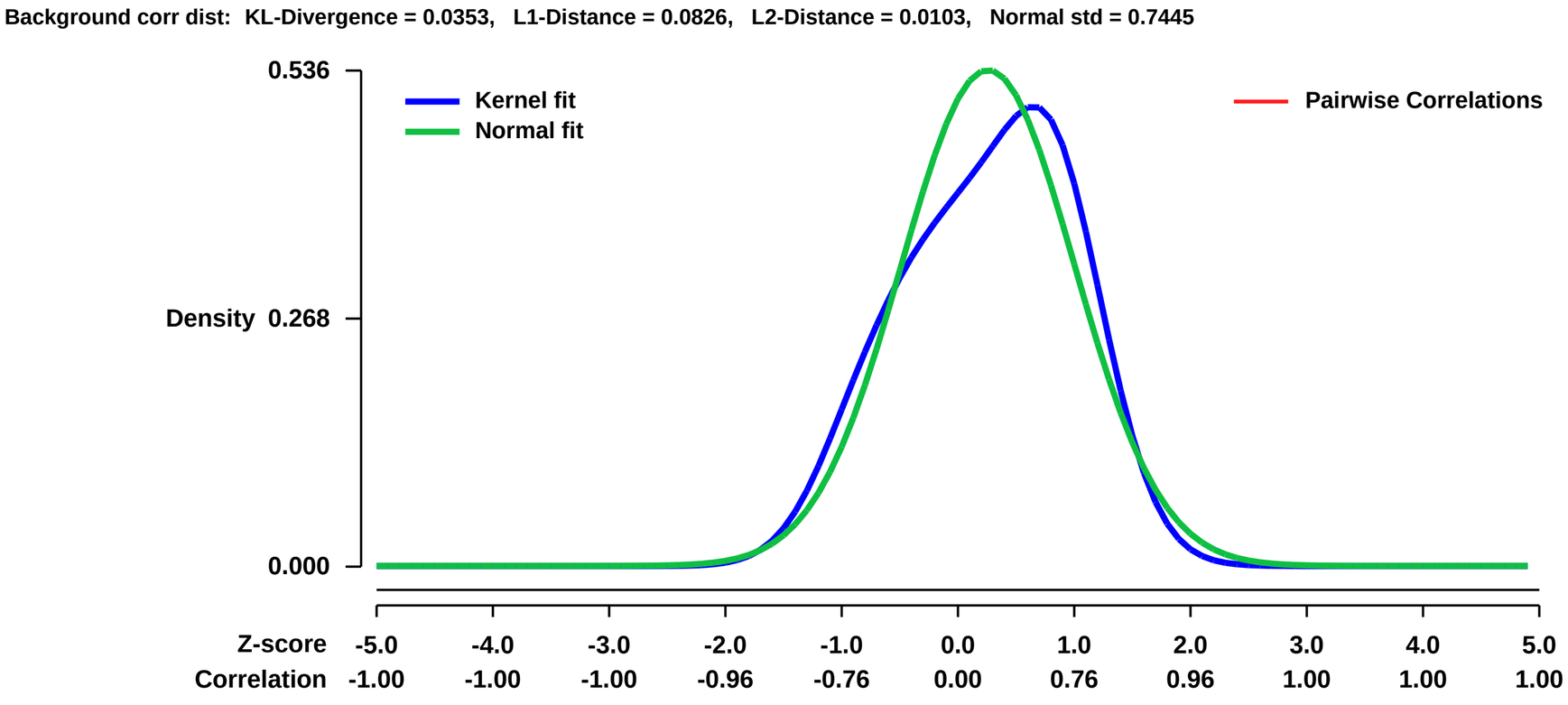

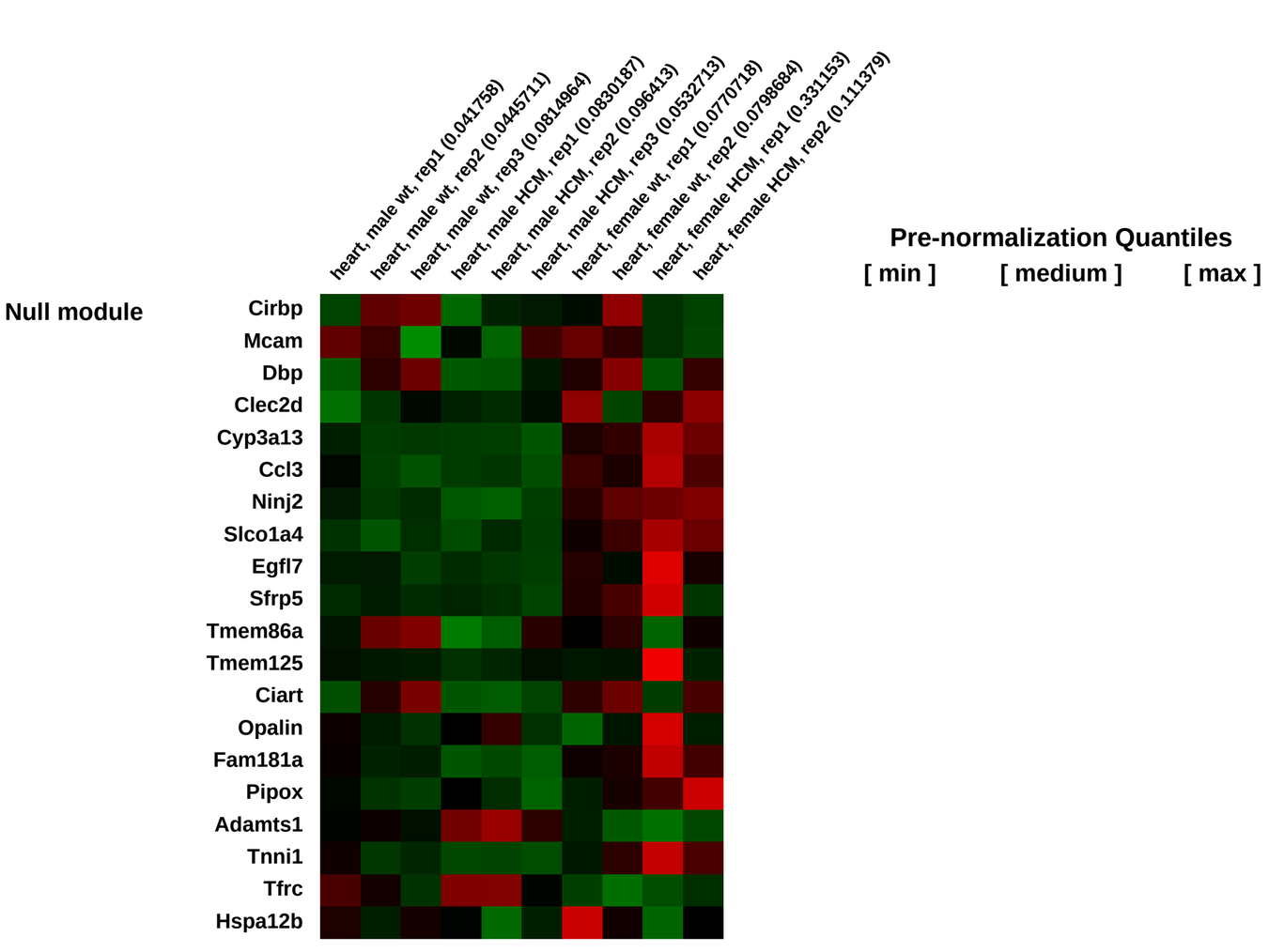

GEO Series "GSE29681" Expression Profiles

Num of samples in this series: 32

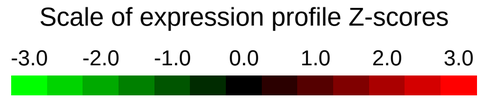

GEO Link:	http://www.ncbi.nlm.nih.gov/geo/query/acc.cgi?acc=GSE29681
Status:	Public on Jun 01 2014
Title:	Expression data from WT and R6/2 mice treated with HSP90 inhibitor NVP-HSP990
Organism:	Mus musculus
Experiment type:	Expression profiling by array
Platform:	GPL1261
Pubmed ID:	
Summary & Design:	**Summary:** Huntingtonâ s disease (HD) is a neurodegenerative disorder that is associated with the deposition of proteinaceous aggregates in the brains of HD patients and mouse models. Previous studies have suggested that wide-scale disruption of protein homeostasis occurs in protein folding diseases. Protein homeostasis can be maintained by activation of the heat shock response (HSR) via the transcription factor heat shock factor 1 (HSF1), the pharmacological activation of which can be achieved by Hsp90 inhibition and has been demonstrated to be beneficial in cell and invertebrate models of HD. Whether the HSR is functional in HD and whether its activation has therapeutic potential in mammalian HD models is currently unknown. To address these issues, we used a novel, brain penetrant Hsp90 inhibitor to activate the HSR in brain after systemic administration. Microarrays, quantitative PCR and western blotting showed that the HSR becomes impaired with disease progression in two mouse models of HD and that this originates at the level of transcription. Huntingtonâ s disease (HD) is a neurodegenerative disorder that is associated with the deposition of proteinaceous aggregates in the brains of HD patients and mouse models. Previous studies have suggested that wide-scale disruption of protein homeostasis occurs in protein folding diseases. Protein homeostasis can be maintained by activation of the heat shock response (HSR) via the transcription factor heat shock factor 1 (HSF1), the pharmacological activation of which can be achieved by Hsp90 inhibition and has been demonstrated to be beneficial in cell and invertebrate models of HD. Whether the HSR is functional in HD and whether its activation has therapeutic potential in mammalian HD models is currently unknown. To address these issues, we used a novel, brain penetrant Hsp90 inhibitor to activate the HSR in brain after systemic administration. Microarrays, quantitative PCR and western blotting showed that the HSR becomes impaired with disease progression in two mouse models of HD and that this originates at the level of transcription. **Overall design:** mRNA expression analysis was performed by microarray in 12 week old R6/2 and WT mice treated with vehicle or HSP990 for 4h (12mg/kg).The following number of replicates was analysed for each genotype: 7 for WT+vehicle, 10 for WT+HSP990, 7 for R6/2+vehicle and 8 for R6/2+HSP990. Microarray quality control was performed using the software package provided on RACE (http://race.unil.ch).

Background corr dist: KL-Divergence = 0.2496, L1-Distance = 0.0430, L2-Distance = 0.0036, Normal std = 0.3048

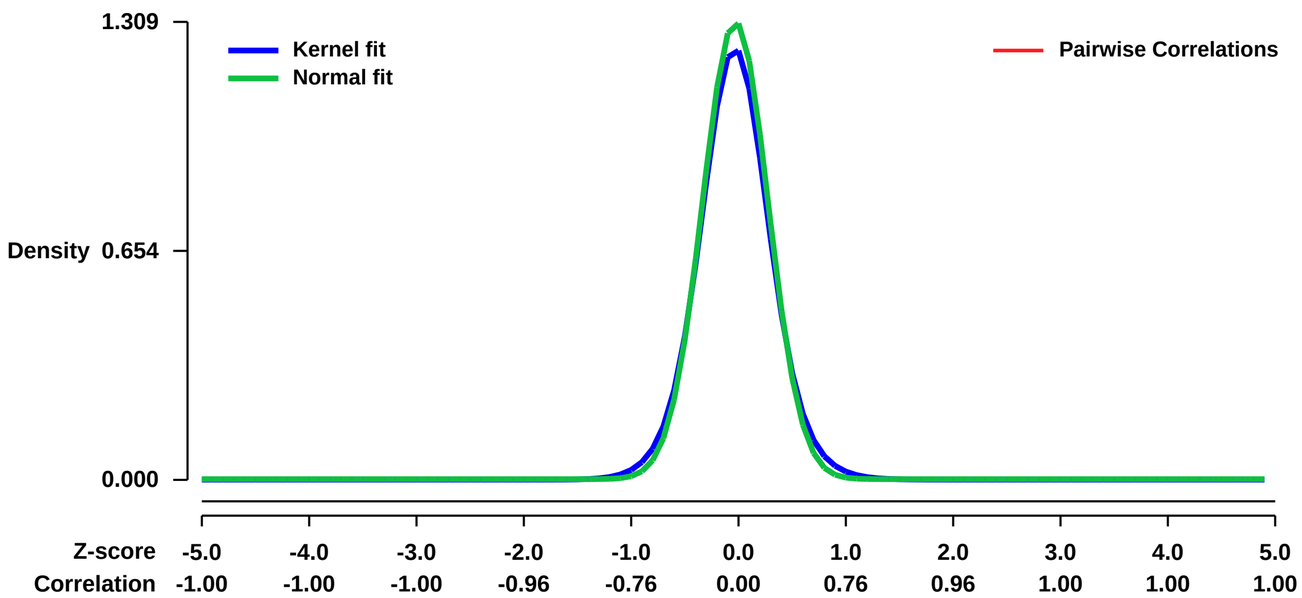

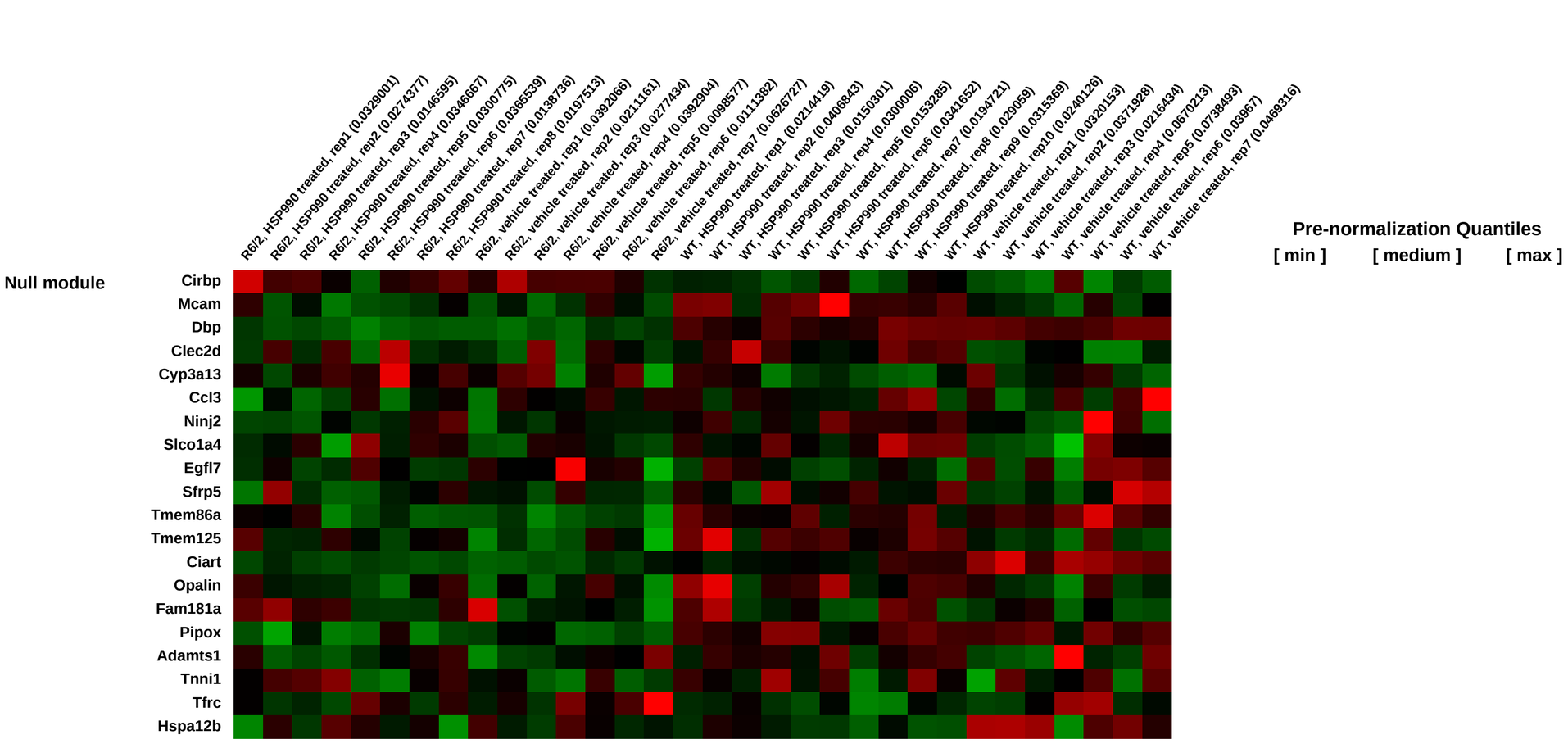

GEO Series "GSE29685" Expression Profiles

Num of samples in this series: 132

Details of this dataset are not shown due to large number of samples and the page size limit.

Find details in http://www.ncbi.nlm.nih.gov/geo/query/acc.cgi?acc=GSE29685

Background corr dist: KL-Divergence = 0.3964, L1-Distance = 0.0812, L2-Distance = 0.0207, Normal std = 0.2500

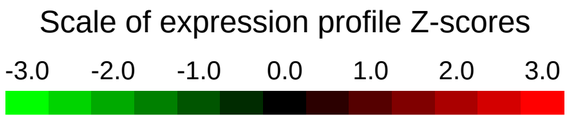

GEO Series "GSE29798" Expression Profiles

Num of samples in this series: 6

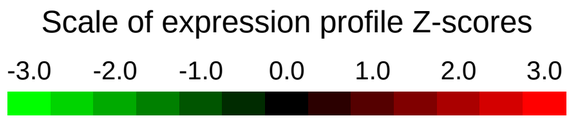

GEO Link:	http://www.ncbi.nlm.nih.gov/geo/query/acc.cgi?acc=GSE29798
Status:	Public on Feb 15 2012
Title:	A combined RNAi and localization approach for dissecting long noncoding RNAs reveals a function of Panct1 in ES cells
Organism:	Mus musculus
Experiment type:	Expression profiling by array
Platform:	GPL1261
Pubmed ID:	22327834
Summary & Design:	**Summary:** Long non-coding RNAs (lncRNAs) regulate diverse biological pathways. Unlike protein coding genes, where methods to comprehensibly study their functional roles in cellular systems are available, techniques to systematically investigate lncRNAs have largely remained unexplored. Here, we report a technology for combined Knockdown and Localization Analysis of Non-coding RNAs (c-KLAN) that merges phenotypic characterization and localization approaches to study lncRNAs. Using a library of endoribonuclease prepared short interfering RNAs (esiRNAs) coupled with a pipeline for synthesizing labeled riboprobes for RNA fluorescence in situ hybridization (FISH), we demonstrate the utility of c-KLAN by identifying a novel transcript Panct1 (Pluripotency associated non-coding transcript 1) that regulates embryonic stem cell identity. We postulate that c-KLAN should be generally useful in the discovery of lncRNAs implicated in various biological processes. **Overall design:** In this experiment, the levels of Panct1(AK156552) have been depleted by RNAi and the expression levels of all genes have been monitored 72 hours post transfection with esiRNAs against Panct1. An esiRNA against non-targeting Luciferase was used as a negative control.

Background corr dist: KL-Divergence = 0.0258, L1-Distance = 0.0248, L2-Distance = 0.0006, Normal std = 0.7131

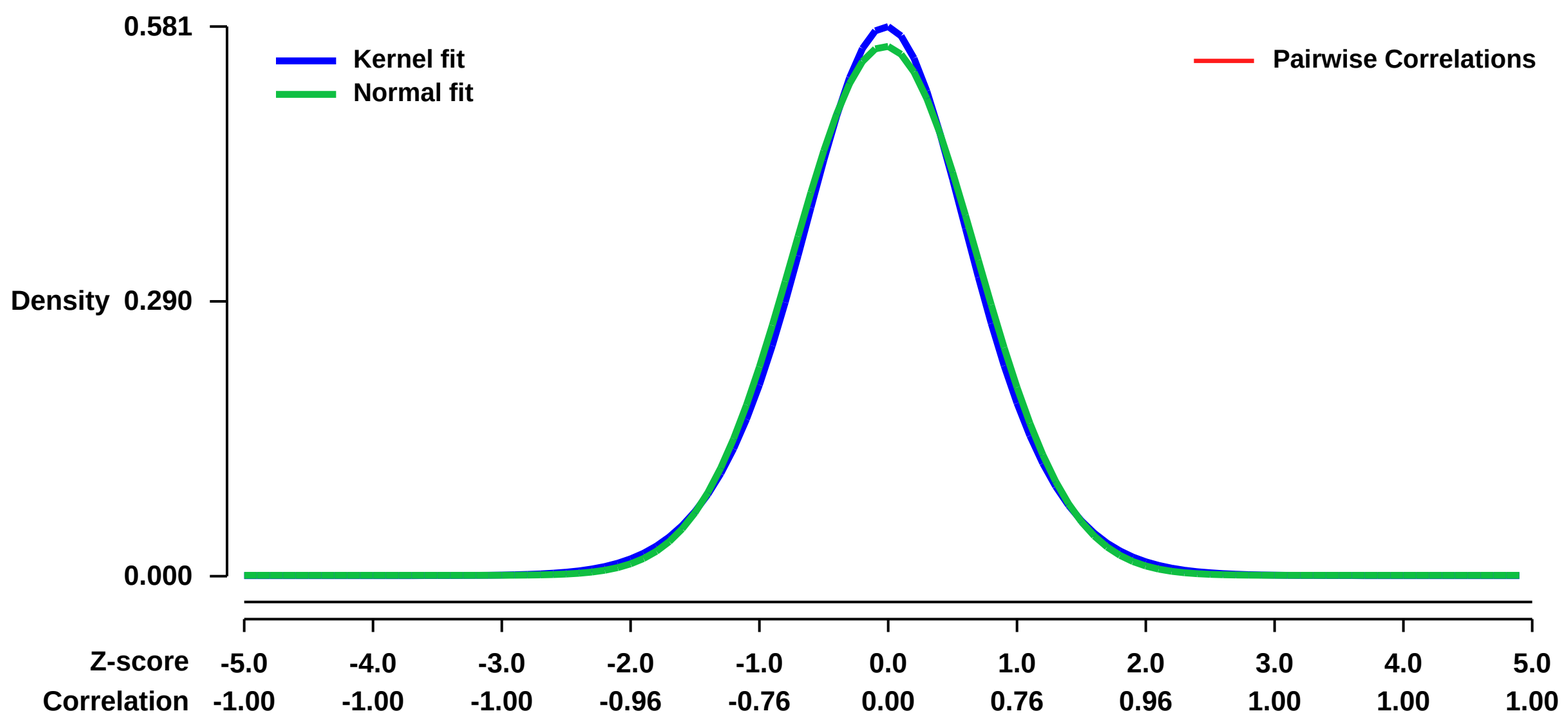

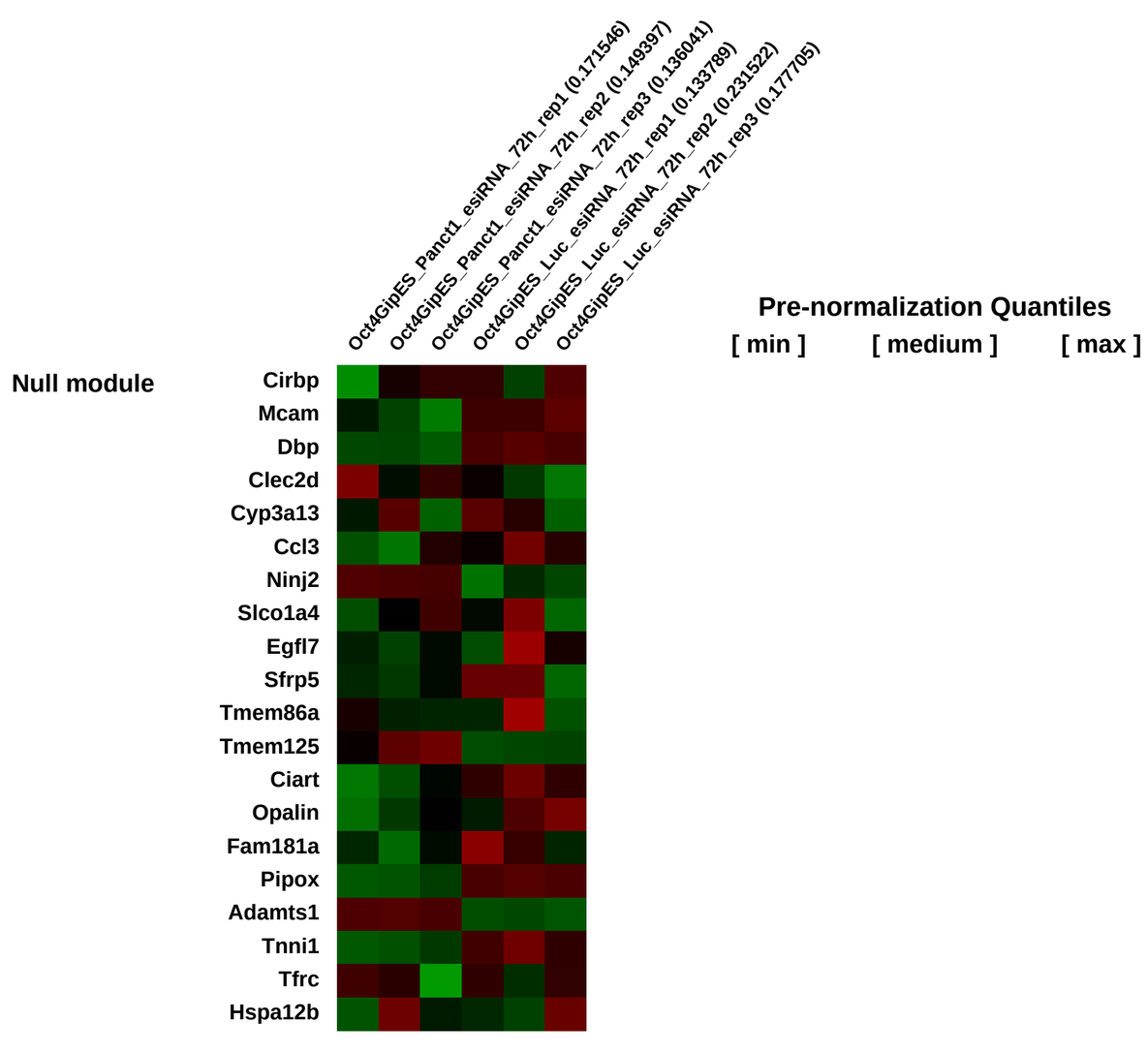

GEO Series "GSE29813" Expression Profiles

Num of samples in this series: 18

Scale of expression profile Z-scores

-3.0 -2.0 -1.0 0.0 1.0 2.0 3.0

GEO Link:	http://www.ncbi.nlm.nih.gov/geo/query/acc.cgi?acc=GSE29813
Status:	Public on Dec 07 2012
Title:	Global gene expression profiling of hepatocellular carcinomas in B6C3F1 mice induced by Ginkgo biloba extract by gavage for two years
Organism:	Mus musculus
Experiment type:	Expression profiling by array
Platform:	GPL1261
Pubmed ID:	23262642
Summary & Design:	**Summary:** Ginkgo biloba leaf extract (GBE) has been used for centuries in traditional Chinese medicine and today is used as an herbal supplement for various indications such as improving neural function, anti-oxidant and anti-cancer effects. As part of the herbal supplement industry, these compounds are largely unregulated, and may be consumed in large concentrations over extended periods of time. This is of particular concern, because the long-term effects in terms of toxicity and carcinogenicity data is lacking for many herbal products, including GBE. The 2-year B6C3F1 mouse carcinogenicity bioassay indicated a marked dose-related increase in hepatocellular carcinoma (HCC) development associated with exposure to GBE. We have shown that the mechanism of this increase in tumorigenesis is related to a marked increase in the incidence of ˛†-catenin mutation, and report a novel mechanism of constitutive ˛†-catenin activation through post-translational modification leading to constitutive Wnt signaling and unregulated growth signaling and oncogenesis. Furthermore, using global gene expression profiling, we show that GBE-induced HCC exhibit overrepresentation of gene categories associated with human cancer and HCC signaling including upregulation of relevant oncogenes and suppression of critical tumor suppressor genes, as well as chronic oxidative stress, a known inducer of calpain-mediated degradation and promoter of hepatocarcinogenesis in humans. These data provide a molecular mechanism to GBE-induced HCC in B6C3F1 mice that is relevant to human cancer, and provides relevant molecular data that will provide the groundwork for further risk assessment of unregulated compounds, including herbal supplements. **Overall design:** Six hepatocellular carcinomas induced by GBE, six spontaneous hepatocellular carcinomas, and six normal liver samples, three technical replicates each.

Background corr dist: KL-Divergence = 0.2189, L1-Distance = 0.0448, L2-Distance = 0.0045, Normal std = 0.3213

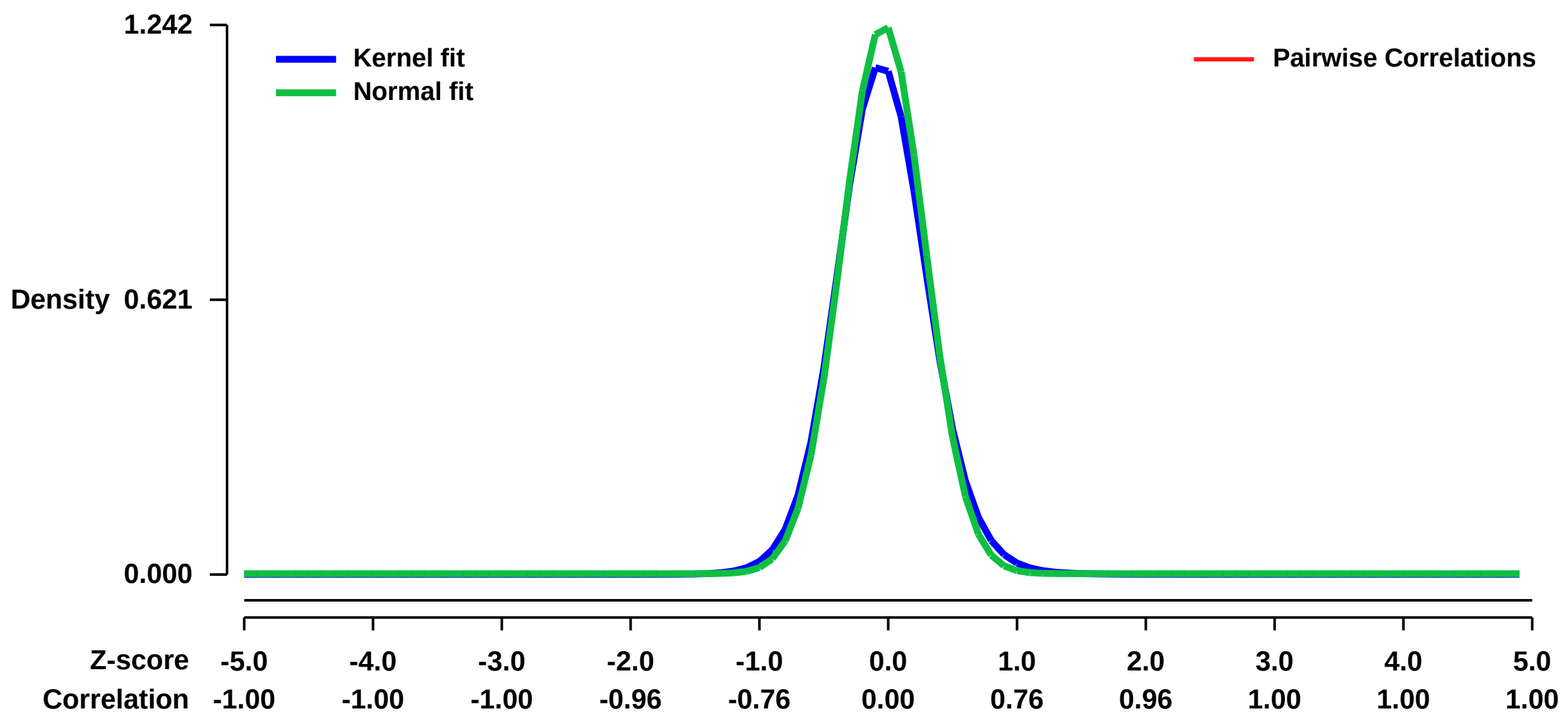

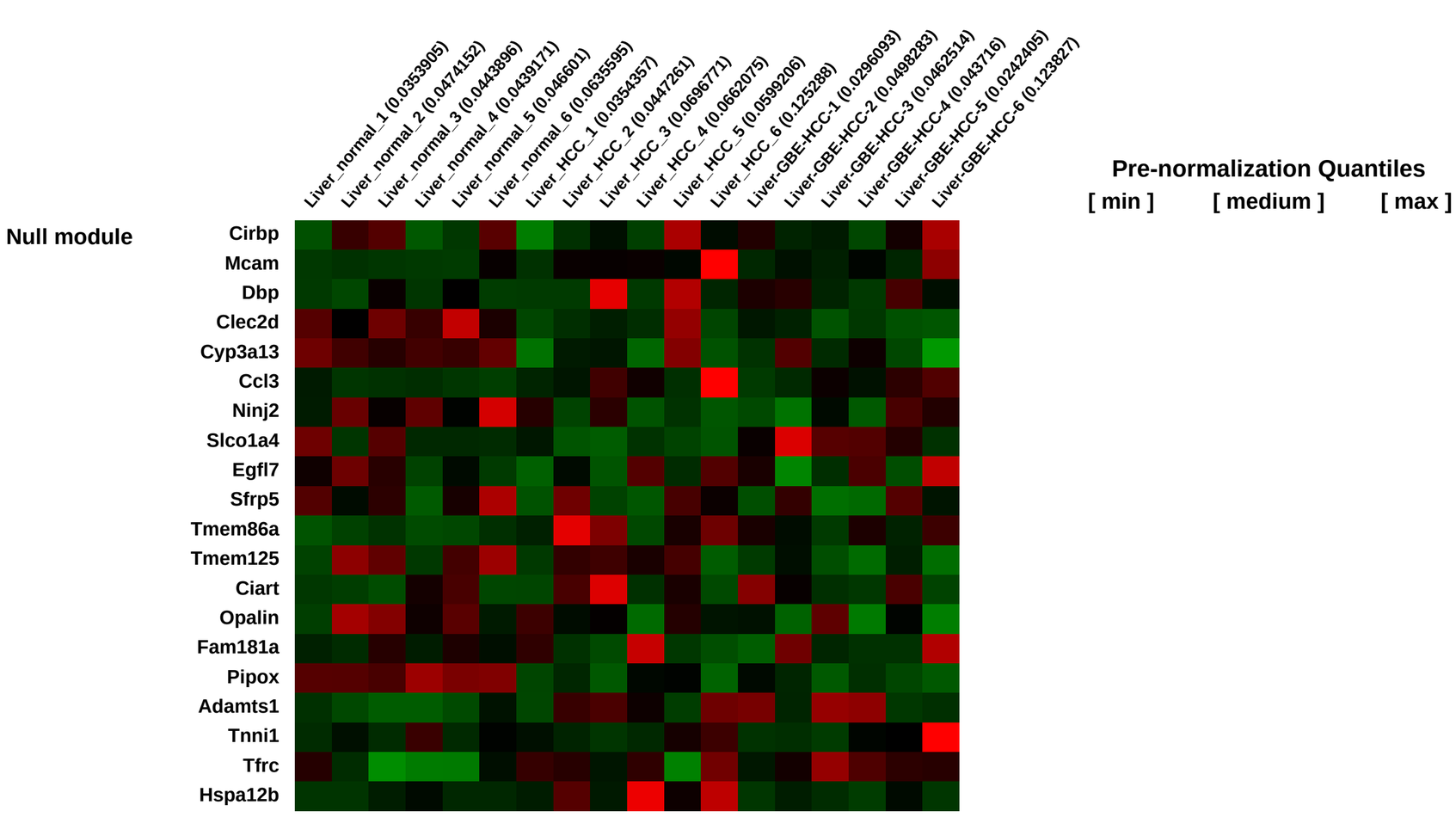

GEO Series "GSE29848" Expression Profiles

Num of samples in this series: 18

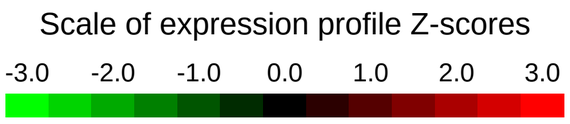

GEO Link:	http://www.ncbi.nlm.nih.gov/geo/query/acc.cgi?acc=GSE29848
Status:	Public on Jul 01 2011
Title:	Microarray data of differentiating embryonic stem cells overexpressing the transcription factor Msgn1
Organism:	Mus musculus
Experiment type:	Expression profiling by array
Platform:	GPL1261
Pubmed ID:	21750544
Summary & Design:	**Summary:** During mammalian gastrulation, pluripotent epiblast stem cells migrate through the primitive streak to form the multipotent progenitors of the mesoderm and endoderm germ layers. Msgn1 is a bHLH transcription factor and is a direct target gene of the Wnt/bcatenin signaling pathway. Msgn1 is expressed in the mesodermal compartment of the primitive streak and is necessary for the proper development of the mesoderm. Msgn1 mutants show defects in somitogenesis leading to a lack of trunk skeletal muscles, vertebra and ribs. To study the molecular and cellular function of Msgn1 in Embryonic Stem Cells (ESC), we have generated doxycycline inducible gain-of-function ESC to overexpress Msgn1 in ESC. In order to identify Msgn1 targets, we performed transcriptional profiling of Msgn1 expressing ES cells and found that upon induction of Msgn1, multiple genes in the Notch pathway were differentially expressed compared to the uninduced cells. Moreover, Whole Mount Insitu Hybridization analysis in Msgn1 null mutants revealed that these Notch pathway genes required Msgn1 for their proper expression in vivo. Our studies demonstrate that Msgn1 is a critical effector of the Wnt pathway during mammalian somitogenesis, mediating crosstalk between the Wnt and Notch pathways. **Overall design:** Inducible A2lox-Flag Msgn1 ES cells were differentiated to form Embryoid bodies (EBs) for 2 days. Flag-Msgn1 was induced on day 2 with doxycycline and samples were collected at three time points, 12h, 24h and 48h after addition of doxycycline. Uninduced cells were used as controls. Experiments were performed in triplicate

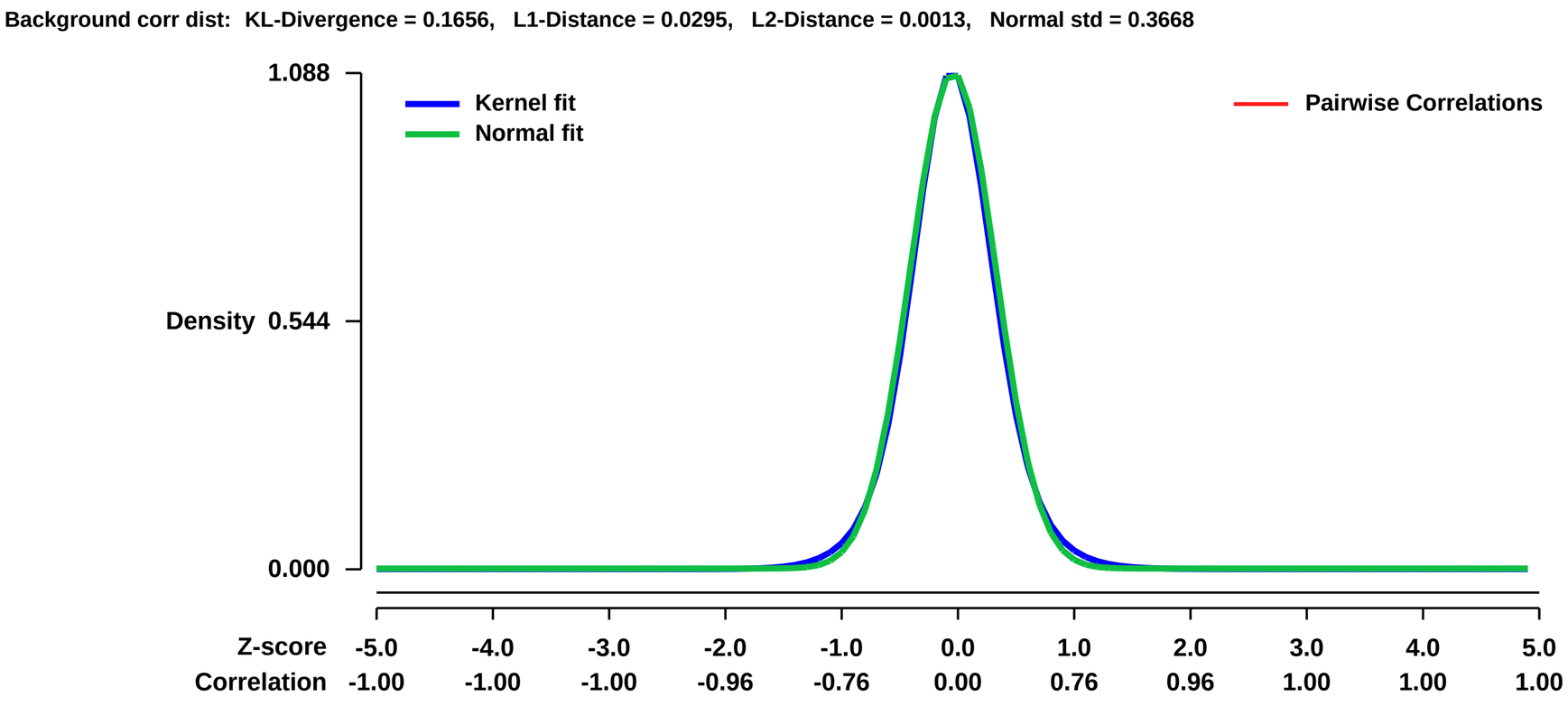

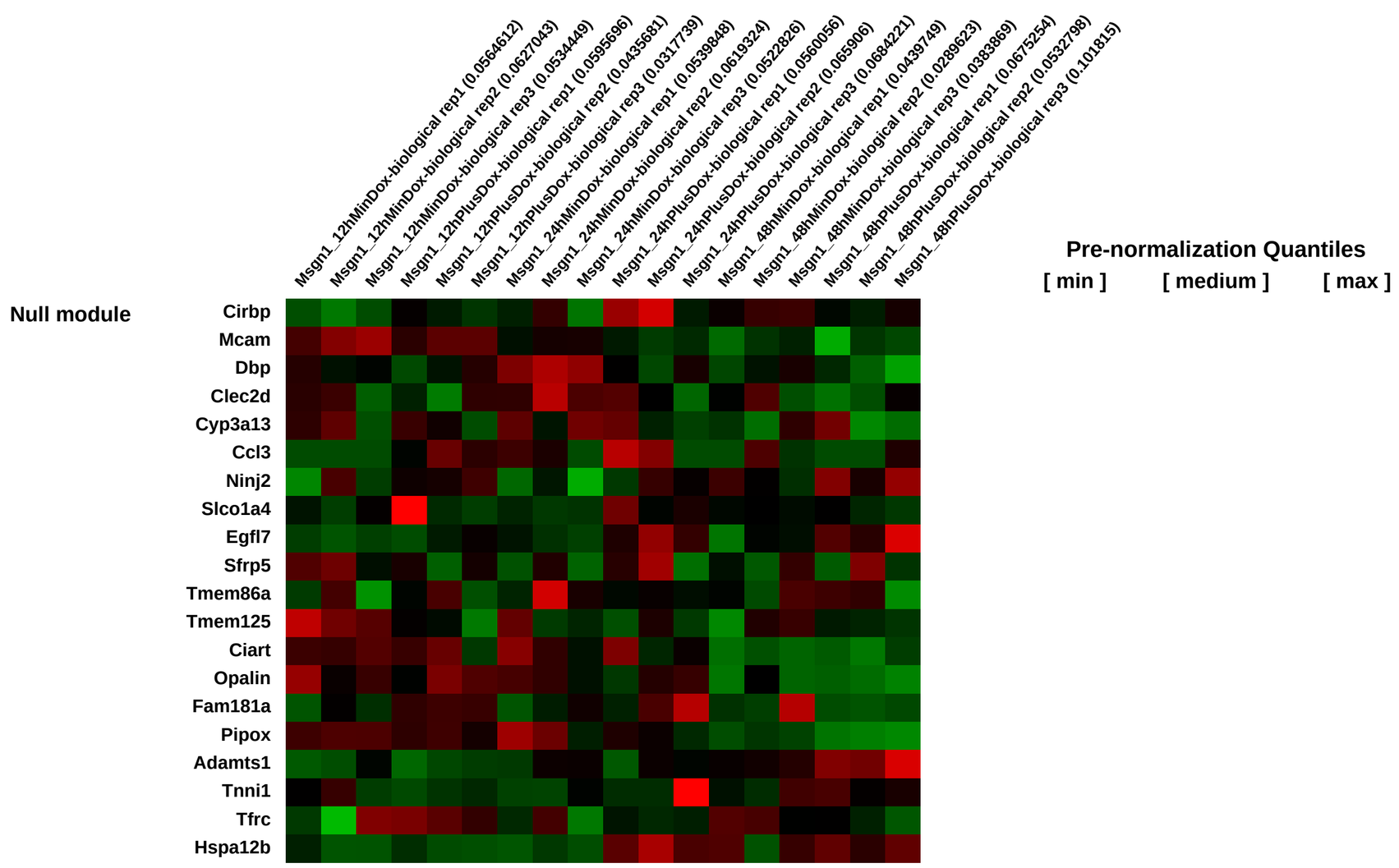

GEO Series "GSE29929" Expression Profiles

Num of samples in this series: 14

Scale of expression profile Z-scores

-3.0 -2.0 -1.0 0.0 1.0 2.0 3.0

GEO Link:	http://www.ncbi.nlm.nih.gov/geo/query/acc.cgi?acc=GSE29929
Status:	Public on Jan 20 2012
Title:	The eIF2 kinase PERK and the integrated stress response facilitate activation of ATF6 during endoplasmic reticulum stress
Organism:	Mus musculus
Experiment type:	Expression profiling by array
Platform:	GPL1261
Pubmed ID:	21917591
Summary & Design:	**Summary:** Disruptions of the endoplasmic reticulum (ER) that perturb protein folding cause ER stress and elicit an unfolded protein response (UPR) that involves translational and transcriptional changes in gene expression aimed at expanding the ER processing capacity and alleviating cellular injury. Three ER stress sensors PERK, ATF6, and IRE1 implement the UPR. PERK phosphorylation of eIF2 during ER stress represses protein synthesis, which prevents further influx of ER client proteins, along with preferential translation of ATF4, a transcription activator of the integrated stress response. In this study we show that the PERK/eIF2¸–~P/ATF4 pathway is required not only for translational control, but also activation of ATF6 and its target genes. The PERK pathway facilitates both the synthesis of ATF6 and trafficking of ATF6 from the ER to the Golgi for intramembrane proteolysis and activation of ATF6. As a consequence, liver-specific depletion of PERK significantly reduces both the translational and transcriptional phases of the UPR, leading to reduced protein chaperone expression, disruptions of lipid metabolism, and enhanced apoptosis. These findings show that the regulatory networks of the UPR are fully integrated, and helps explain the diverse pathologies associated with loss of PERK. **Overall design:** Comparison of gene expression profiles for treated vs control in wildtype and knock-out.

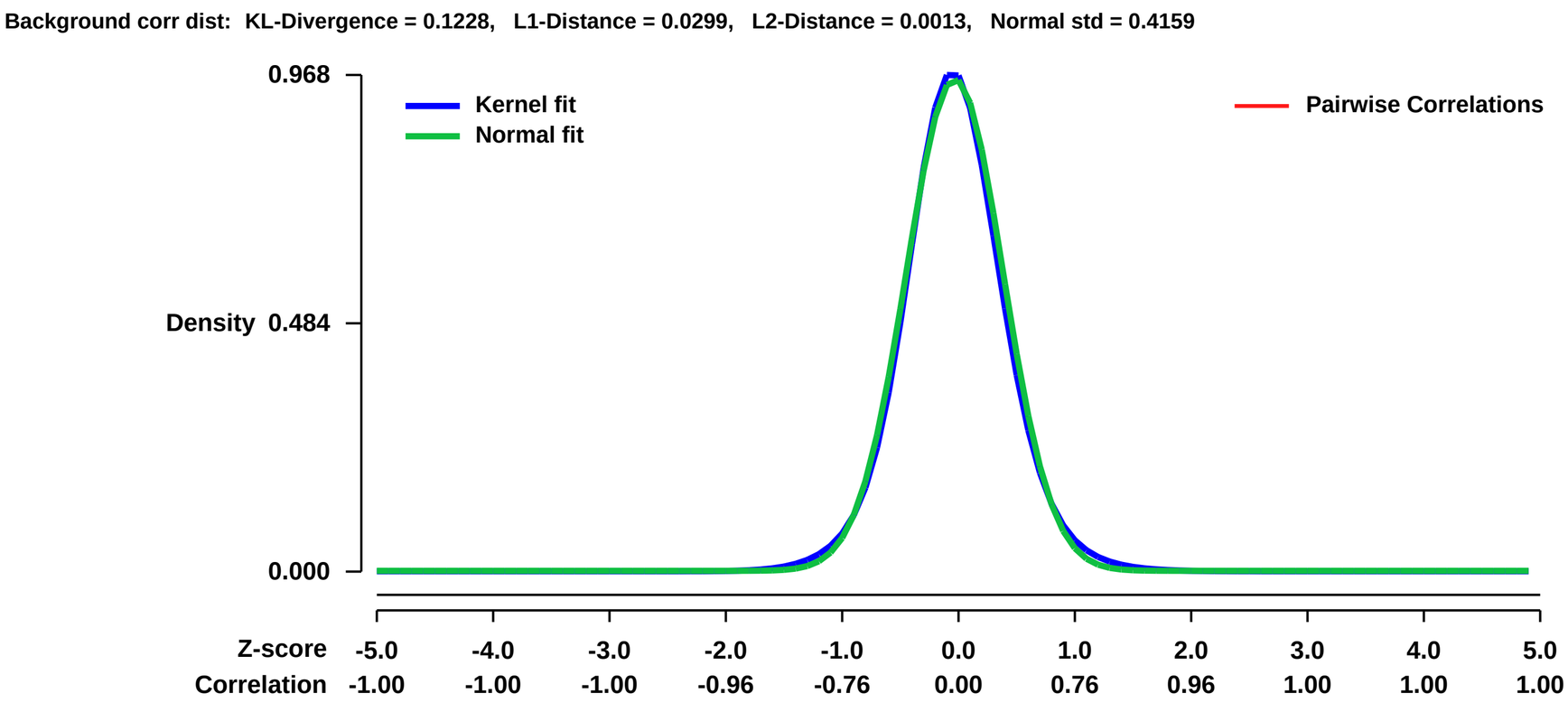

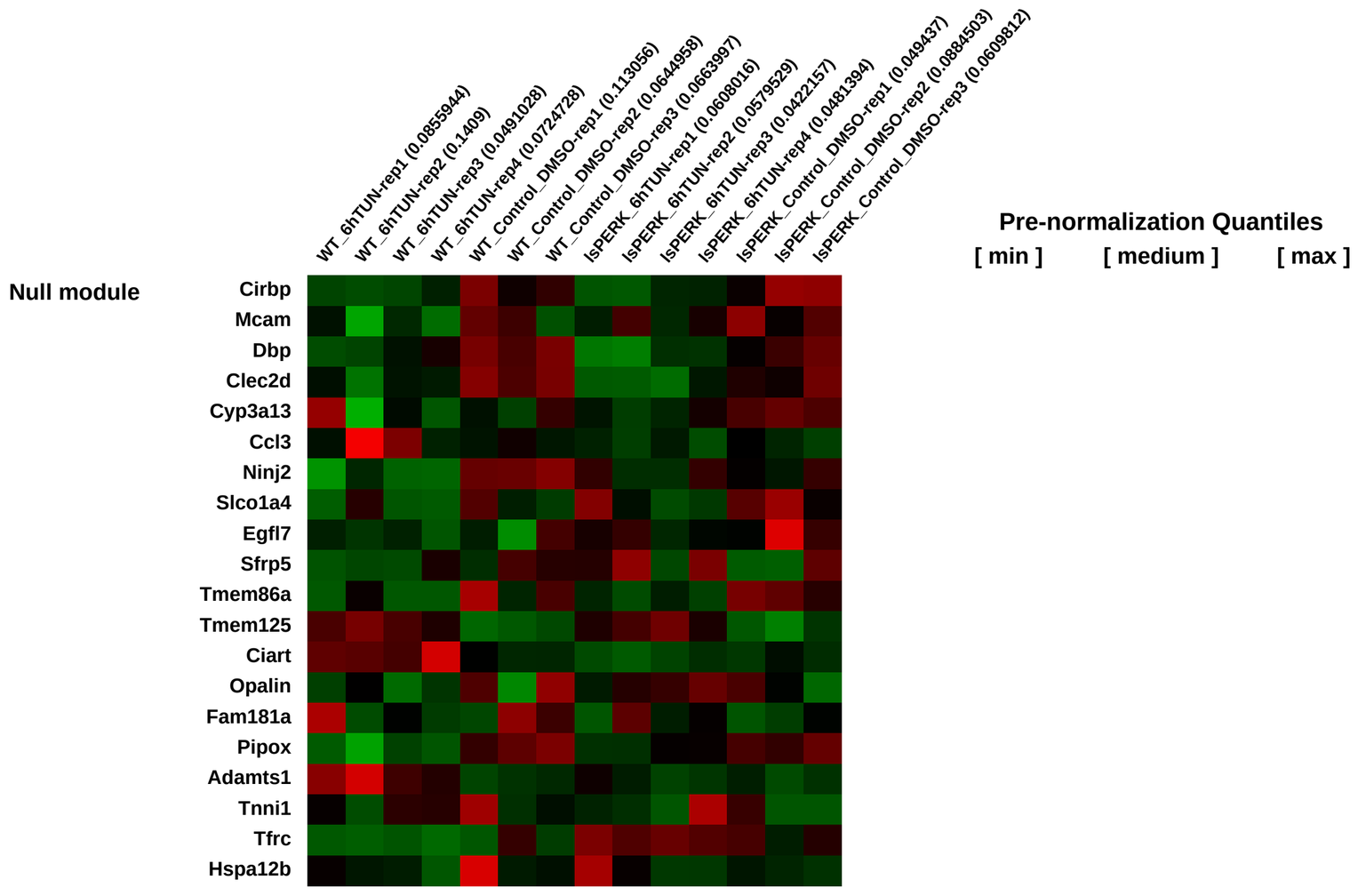

GEO Series "GSE29975" Expression Profiles

Num of samples in this series: 6

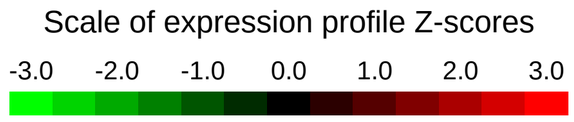

GEO Link:	http://www.ncbi.nlm.nih.gov/geo/query/acc.cgi?acc=GSE29975
Status:	Public on Jun 28 2011
Title:	Expression data from FOG1+/- (or FOG1+/+) and FOG1 ki/ki mouse megakaryocyte (Meg)
Organism:	Mus musculus
Experiment type:	Expression profiling by array
Platform:	GPL1261
Pubmed ID:	21989988
Summary & Design:	**Summary:** The transcription co-factor FOG1 interacts with the chromatin remodeling complex NuRD to mediate gene activation and gene repression during hematopoiesis. We have generated mice with a targeted mutation in the endogenous Fog1 locus that results in an N-ternimal mutation in FOG1 that disrupts the interaction with NuRD. We used gene expression microarrays to explore the global transcriptional programs regulated by FOG1 and NuRD in megakaryocytic cells to aid in understanding its role during hematopoiesis. **Overall design:** Bovine serum albumin (BSA) gradient centrifugation was used to isolate maturated megakaryocutes from mouse

Background corr dist: KL-Divergence = 0.0481, L1-Distance = 0.0629, L2-Distance = 0.0077, Normal std = 0.6379

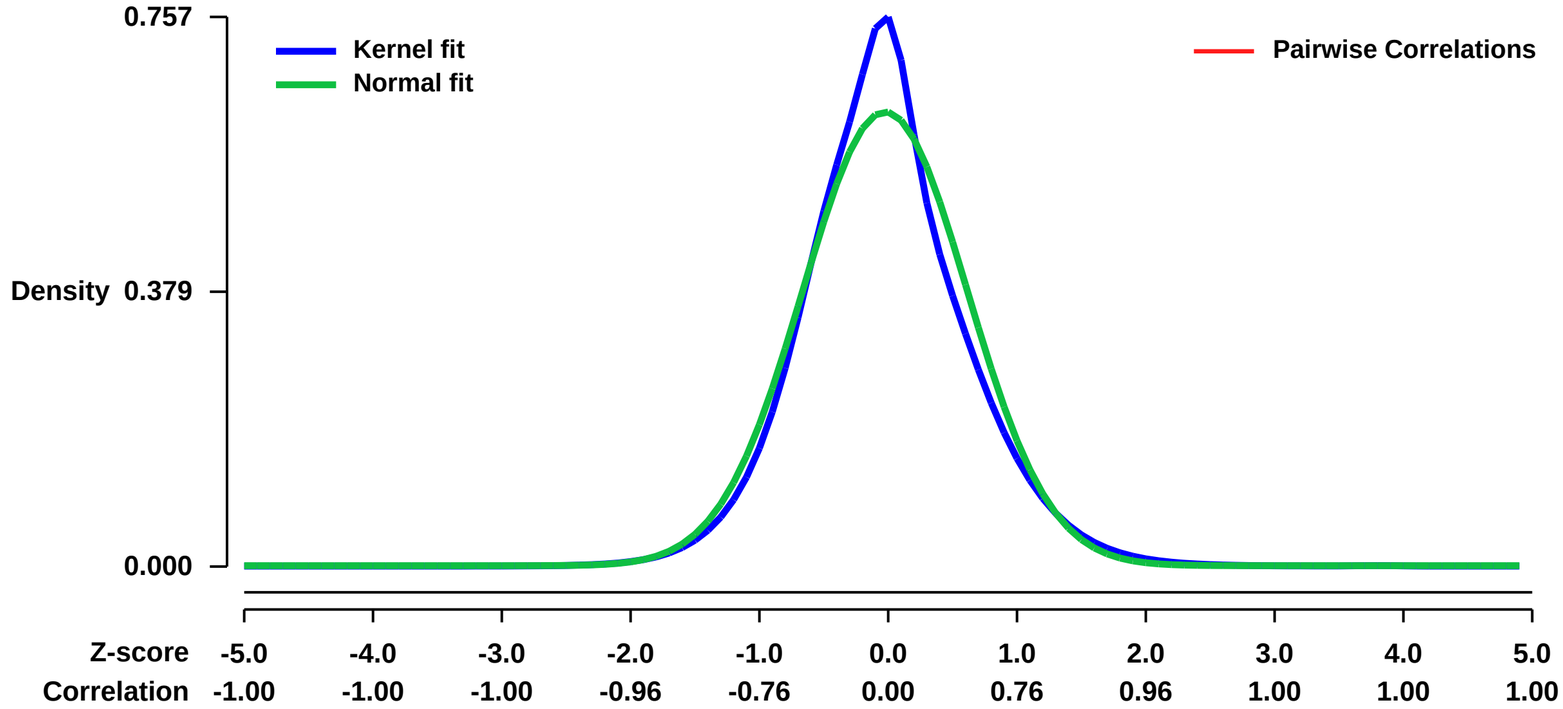

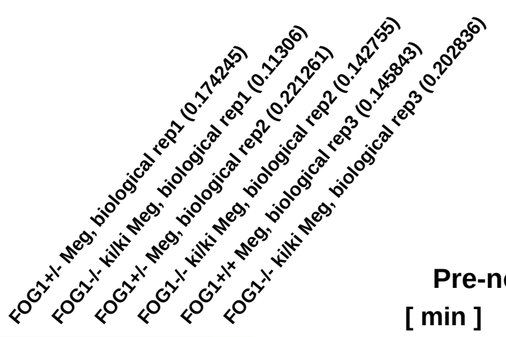

Pre-normalization Quantiles

[min] [medium] [max]

Null module

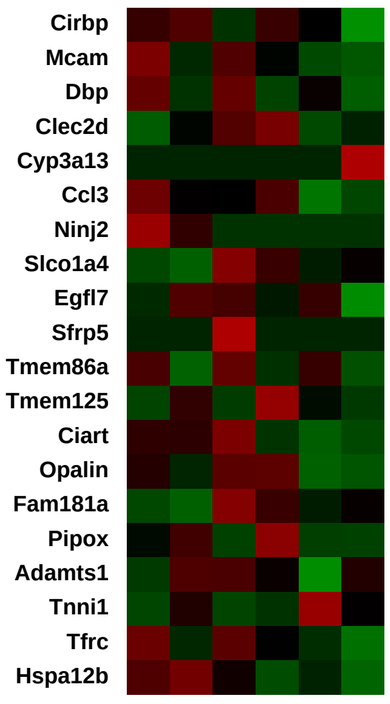

GEO Series "GSE29995" Expression Profiles

Num of samples in this series: 6

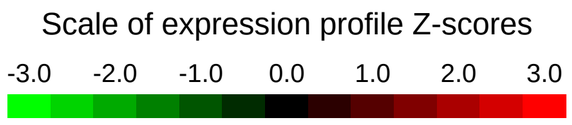

GEO Link:	http://www.ncbi.nlm.nih.gov/geo/query/acc.cgi?acc=GSE29995
Status:	Public on Jun 30 2011
Title:	Expression data from the node and primitive streak (NPS) regions from WT and Wnt3a null embryos
Organism:	Mus musculus
Experiment type:	Expression profiling by array
Platform:	GPL1261
Pubmed ID:	21750544
Summary & Design:	**Summary:** The goal of this project was to elucidate the target genes and transcriptional networks activated by Wnt3a during gastrulation, a complex morphogenetic process in which the embryonic germ layers are formed and the vertebrate body plan is established. **Overall design:** To identify downstream targets of Wnt3a, transcriptional profiling was performed using Affymetrix GeneChips on both wildtype and Wnt3a null embryos at embryonic days (E) 7.75-8. In order to maximize the likelihood of identifying direct target genes of Wnt3a, RNA was isolated from the node and primitive streak (NPS) region, an area where Wnt3a is highly expressed and at a time 12-18 hours before the morpholical phenotype of Wnt3a mutants becomes apparent.

Background corr dist: KL-Divergence = 0.0464, L1-Distance = 0.0222, L2-Distance = 0.0006, Normal std = 0.5907

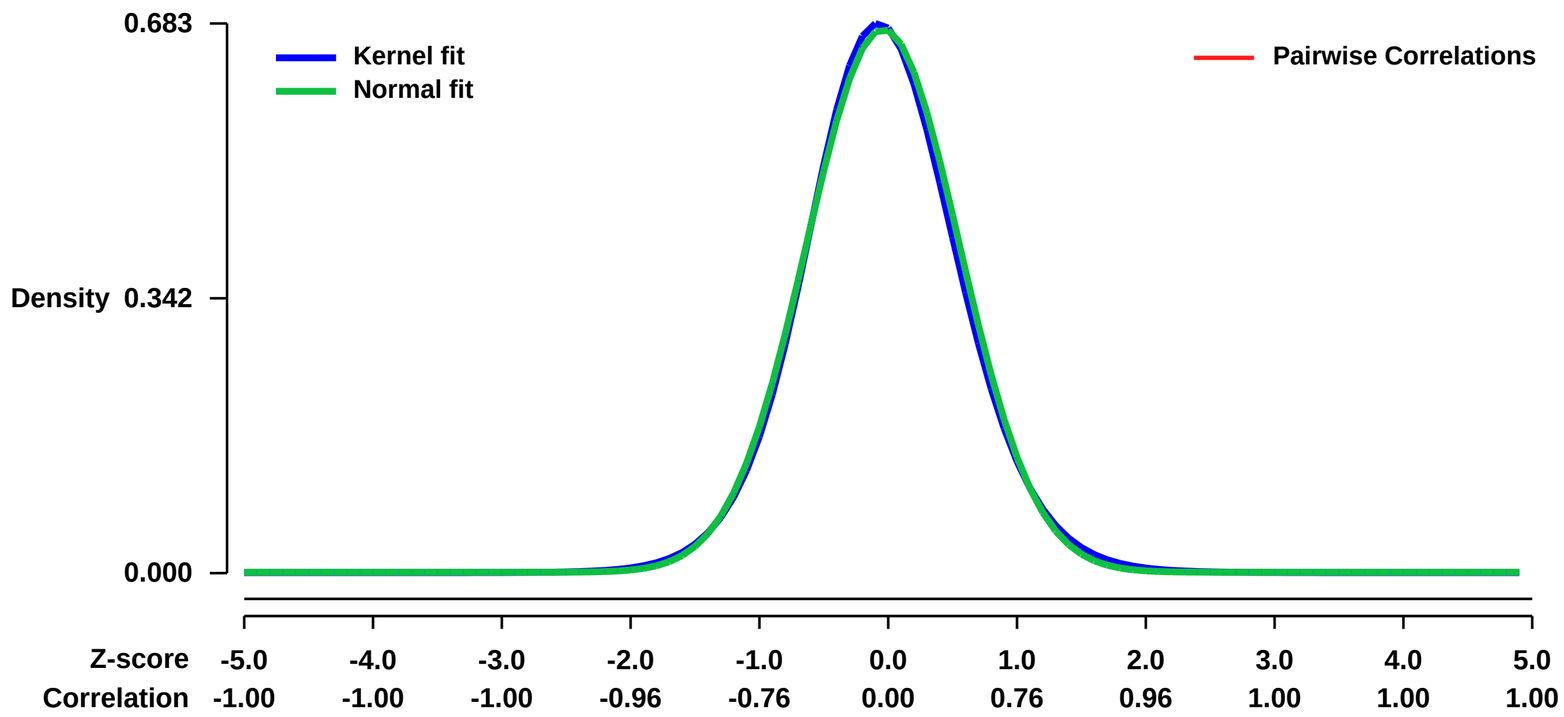

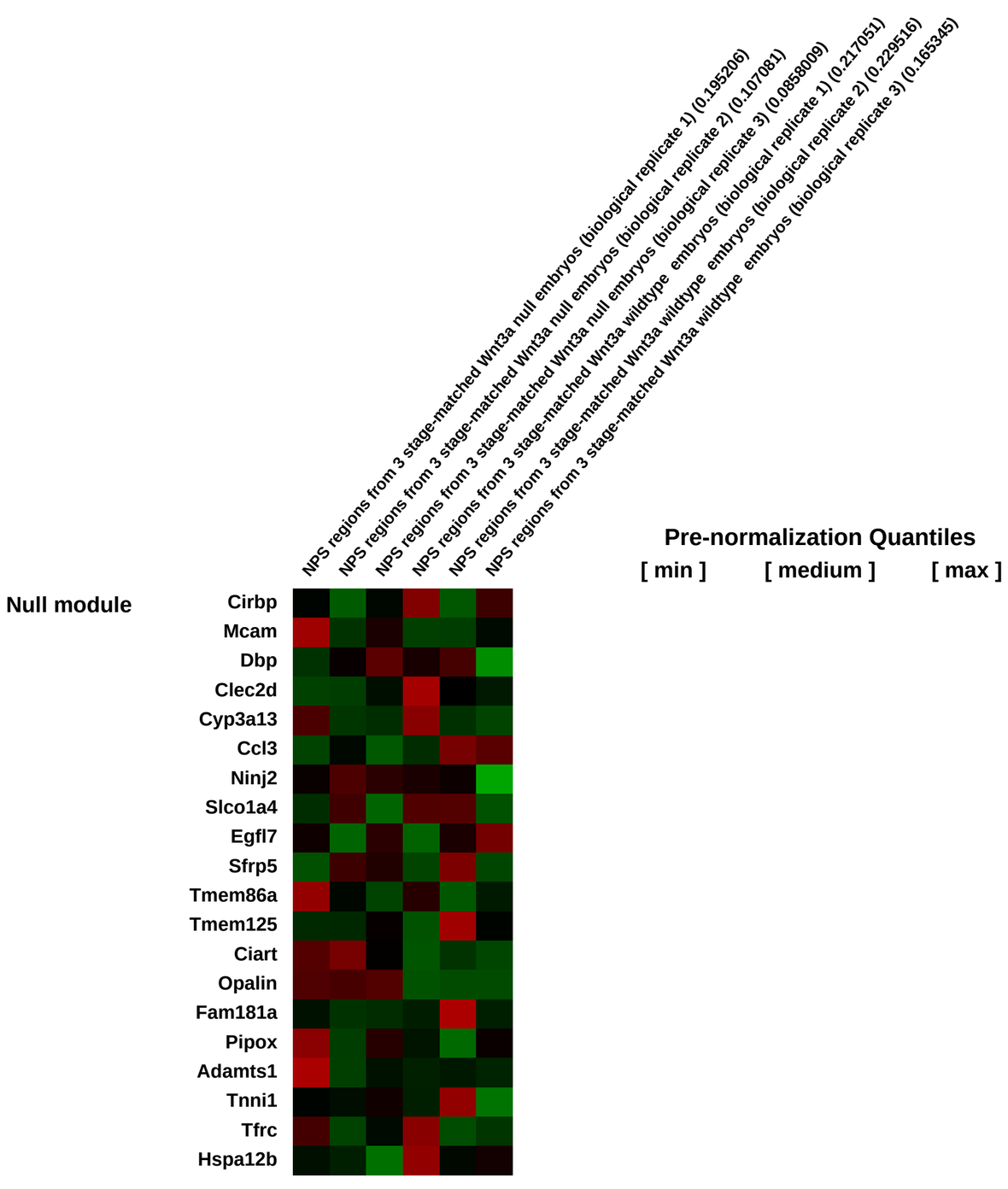

GEO Series "GSE30012" Expression Profiles

Num of samples in this series: 6

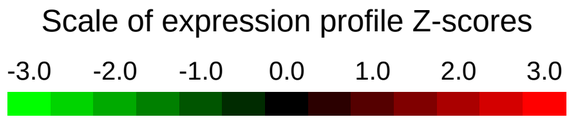

GEO Link:	**http://www.ncbi.nlm.nih.gov/geo/query/acc.cgi?acc=GSE30012**
Status:	**Public on Jun 18 2011**
Title:	**A latent pro-survival function for the mir-290-295 cluster in mouse embryonic stem cells.**
Organism:	**Mus musculus**
Experiment type:	**Expression profiling by array**
Platform:	**GPL1261**
Pubmed ID:	
Summary & Design:	**Summary:** **MicroRNAs (miRNAs) post-transcriptionally regulate the expression of thousands of distinct mRNAs. While some regulatory interactions help to maintain basal cellular functions, others are likely relevant in more specific settings, such as response to stress. Here we describe such a role for the mir-290-295 cluster, the dominant miRNA cluster in mouse embryonic stem cells (mESCs). Examination of a target list generated from bioinformatic prediction, as well as expression data following miRNA loss, revealed strong enrichment for apoptotic regulators, two of which we validated directly: Caspase 2, the most highly conserved mammalian caspase, and Ei24, a p53 transcriptional target. Consistent with these predictions, mESCs lacking miRNAs were more likely to initiate apoptosis following genotoxic exposure to gamma irradiation or doxorubicin. Knockdown of either candidate partially rescued this pro-apoptotic phenotype, as did transfection of members of the mir-290-295 cluster. These findings were recapitulated in a specific mir-290-295 deletion line, confirming that they reflect miRNA functions at physiological levels. In contrast to the basal regulatory roles previously identified, the pro-survival phenotype shown here may be most relevant to stressful gestations, where pro-oxidant metabolic states induce DNA damage. Similarly, this cluster may mediate chemotherapeutic resistance in a neoplastic context, making it a useful clinical target.** **Overall design:** **Three replicates of mouse embryonic stem cells with Dicer (CTRL) compared to three replicates of mouse embryonic stem cells lacking Dicer (CRE)**

Background corr dist: KL-Divergence = 0.0342, L1-Distance = 0.0179, L2-Distance = 0.0003, Normal std = 0.6434

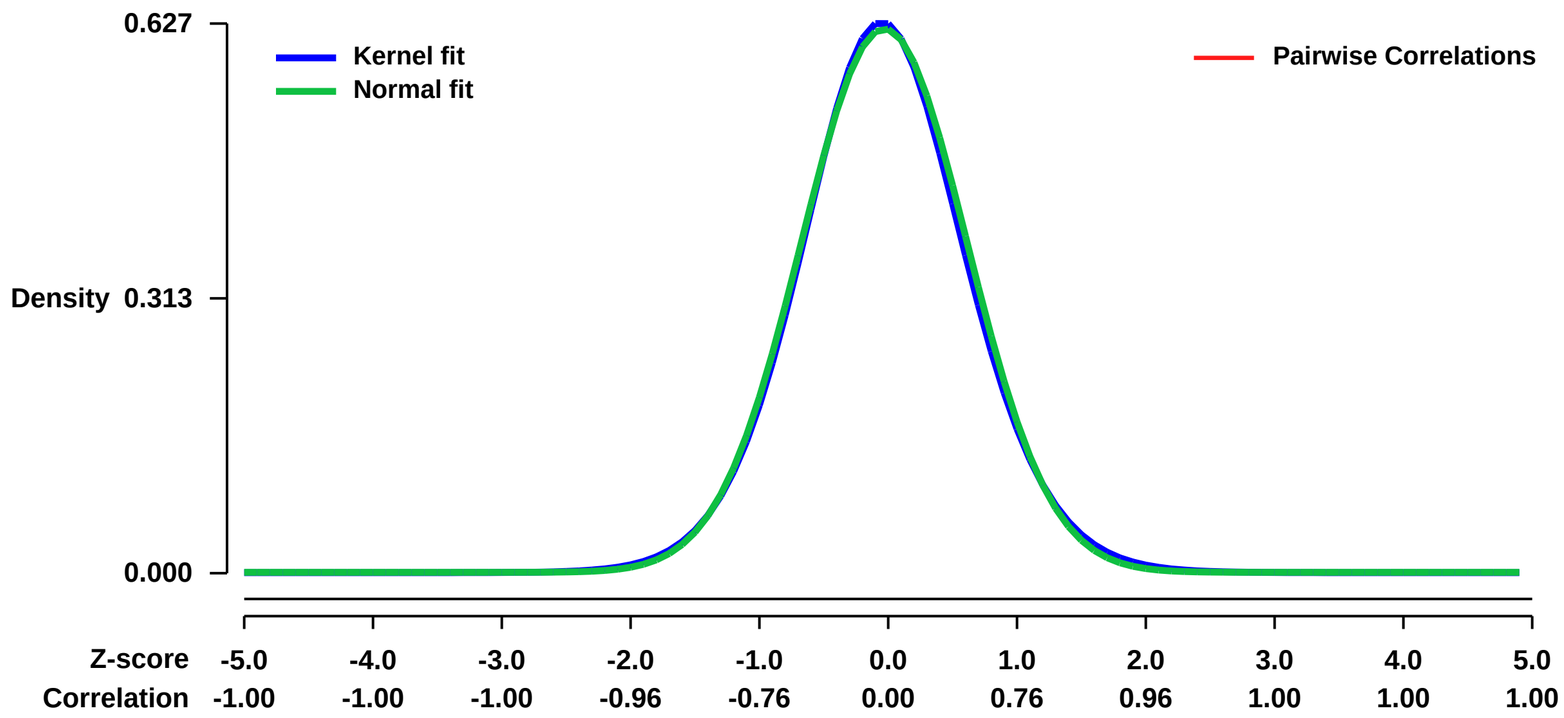

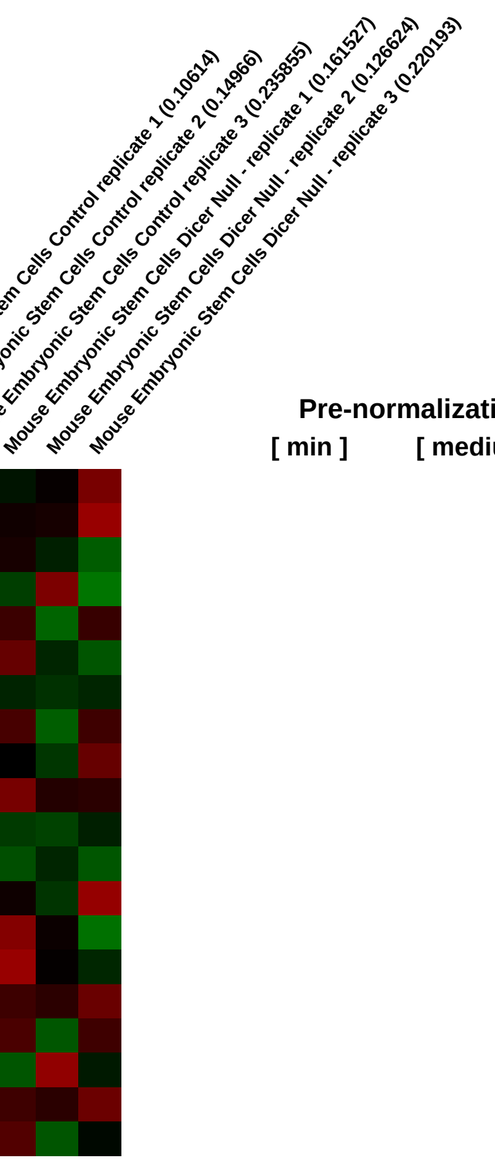

GEO Series "GSE30083" Expression Profiles

Num of samples in this series: 12

Scale of expression profile Z-scores

-3.0 -2.0 -1.0 0.0 1.0 2.0 3.0

GEO Link:	http://www.ncbi.nlm.nih.gov/geo/query/acc.cgi?acc=GSE30083
Status:	Public on Feb 13 2012
Title:	Expression data from CD4 single positive thymocyte subsets from C57BL/6 mice of 6-8 wks of age
Organism:	Mus musculus
Experiment type:	Expression profiling by array
Platform:	GPL1261
Pubmed ID:	22022412
Summary & Design:	**Summary:** After positive selection in the thymus, the newly generated single positive (SP) thymocytes are phenotypically and functionally immature and undergo apoptosis upon antigen stimulation. In the thymic medullary microenvironment, SP cells progressively acquire immunocompetence. Negative selection to remove autoreactive T cells also occur at this stage. We have defined four subsets of CD4 SP, namely, SP1, SP2, SP3, and SP4 that follow a functional maturation program and a sequential emergence during mouse ontogeny. We used microarray to detail the global programm of gene expression during the maturation of murine CD4 single positive thymocytes **Overall design:** Four subsets of CD4+CD8-CD25-NK1.1- thymocytes from C57BL/6 mice of 6-8 wks of age were purified for RNA extraction and hybridization on Affymetrix microarrays, namely, SP1 (Qa-2-6C10+CD69+), SP2 (Qa-2-6C10-CD69+), SP3 (Qa-2-6C10-CD69-), SP4 (Qa-2+6C10-CD69-).

Background corr dist: KL-Divergence = 0.0812, L1-Distance = 0.0208, L2-Distance = 0.0005, Normal std = 0.4748

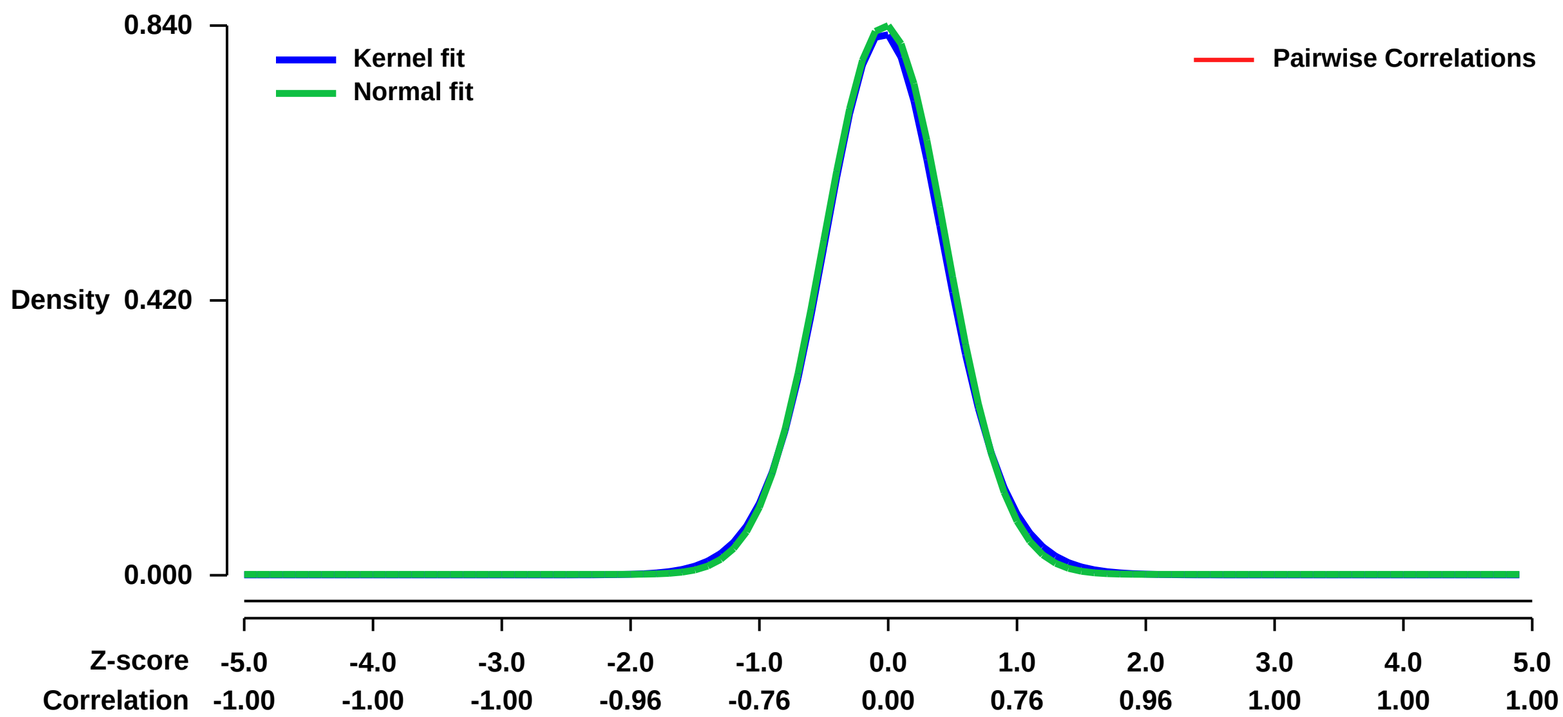

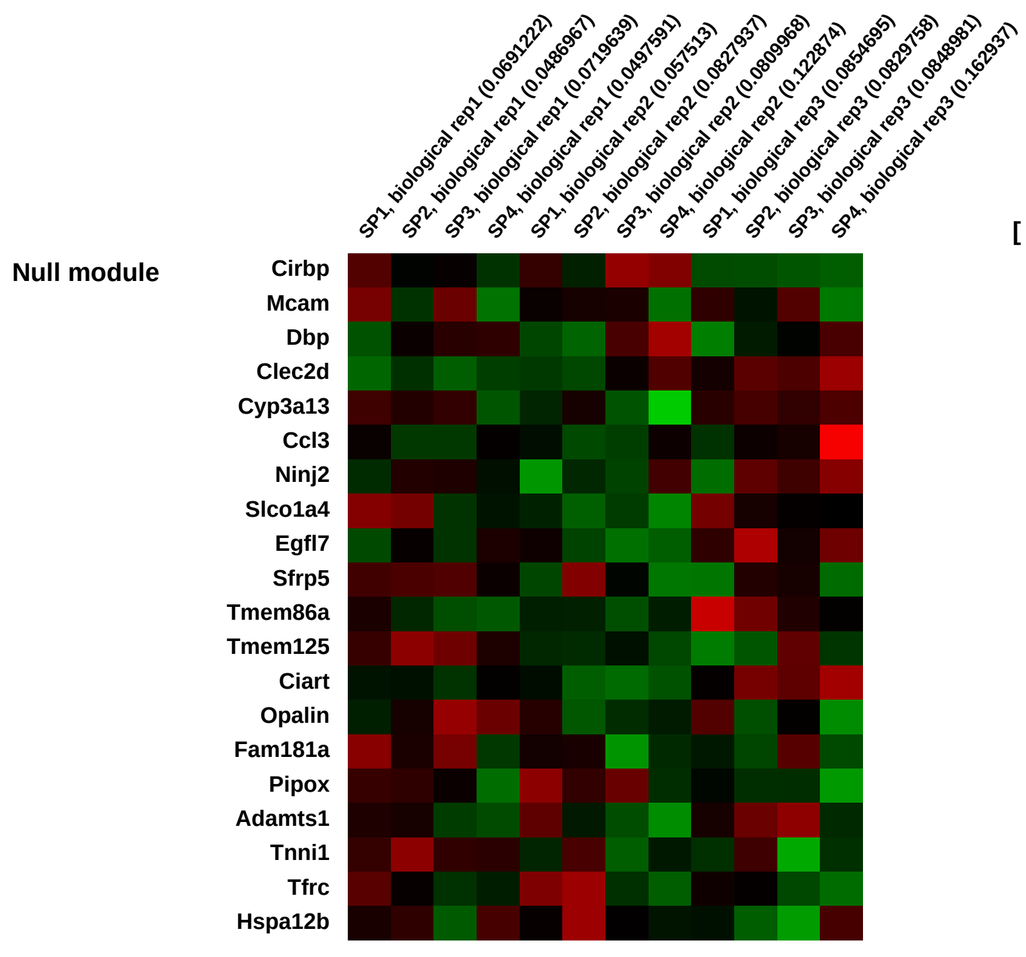

GEO Series "GSE30160" Expression Profiles

Num of samples in this series: 6

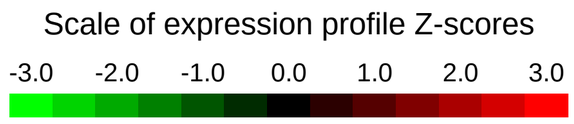

GEO Link:	**http://www.ncbi.nlm.nih.gov/geo/query/acc.cgi?acc=GSE30160**
Status:	**Public on Jul 05 2011**
Title:	**The RANK IVVY Motif-regulated Genes in Osteoclastogenesis**
Organism:	**Mus musculus**
Experiment type:	**Expression profiling by array**
Platform:	**GPL1261**
Pubmed ID:	
Summary & Design:	**Summary:** **By carrying out a systematic structure/function study of the RANK cytoplasmic domain, we previously identified a specific 4-a.a. RANK motif (IVVY535-538) which plays a critical role in osteoclastogenesis by mediating commitment of macrophages to the osteoclast lineage. We have recently validated the role of this IVVY motif in osteoclastogenesis in vivo by generating knockin (KI) mice bearing inactivating mutations in the RANK IVVY motif. This microarray experiment was performed to determine whether the IVVY motif is involved in regulating gene expression in osteoclastogenesis.** **We used microarrays to detail the global programme of gene expression underlying cellularisation and identified distinct classes of up-regulated genes during this process.** **Overall design:** **Bone marrow macrophages isolated from wild-type (WT) or knockin (KI) mice were plated in 60-mm tissue culture dishes and treated with M-CSF (44ng/ml) and RANKL (100ng/ml) for 24 hours. Each genotype has three triplicates. Total RNA was isolated for microarray analysis using mouse chips (type 430.2.0) at the Microarray Shared Facility at the University of Alabama at Birmingham.**

Background corr dist: KL-Divergence = 0.0193, L1-Distance = 0.0421, L2-Distance = 0.0019, Normal std = 0.8277

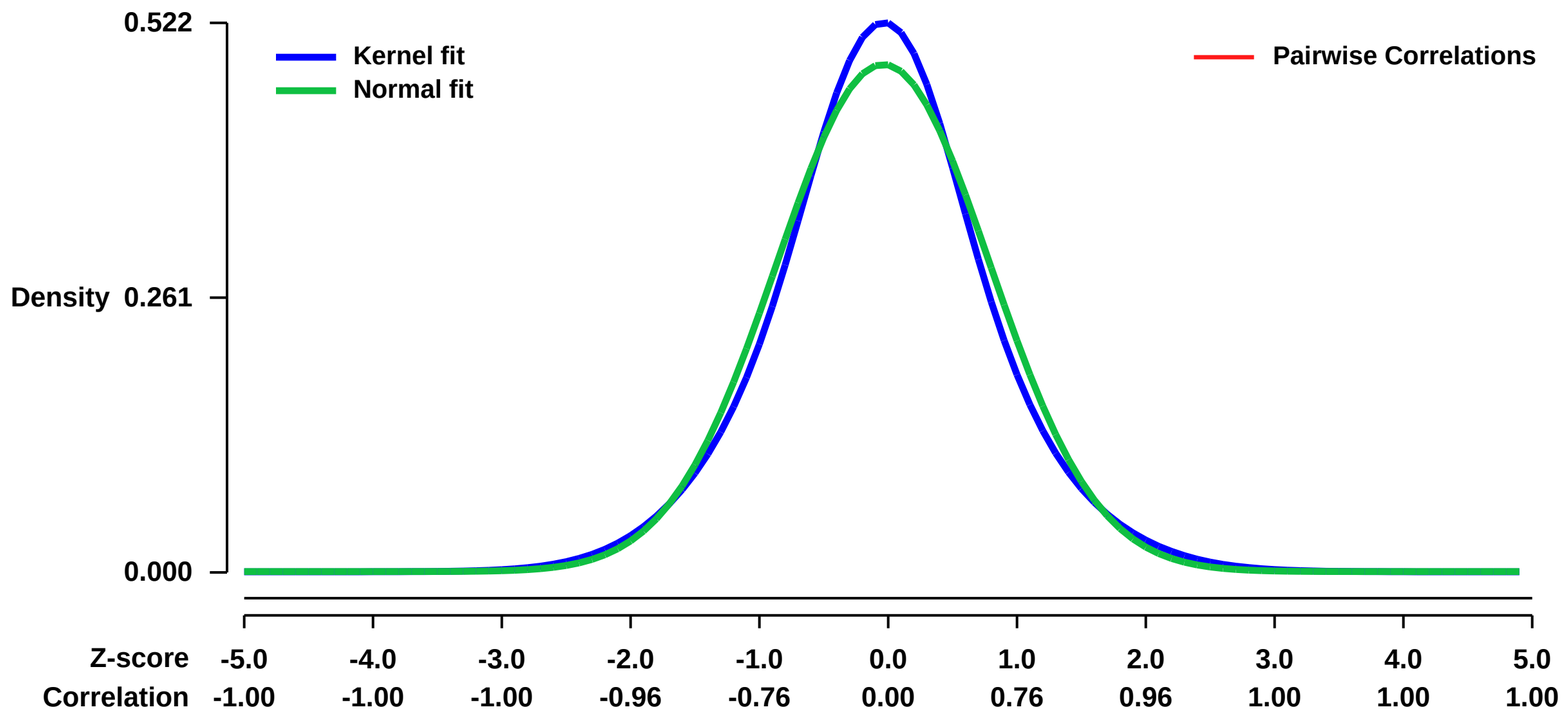

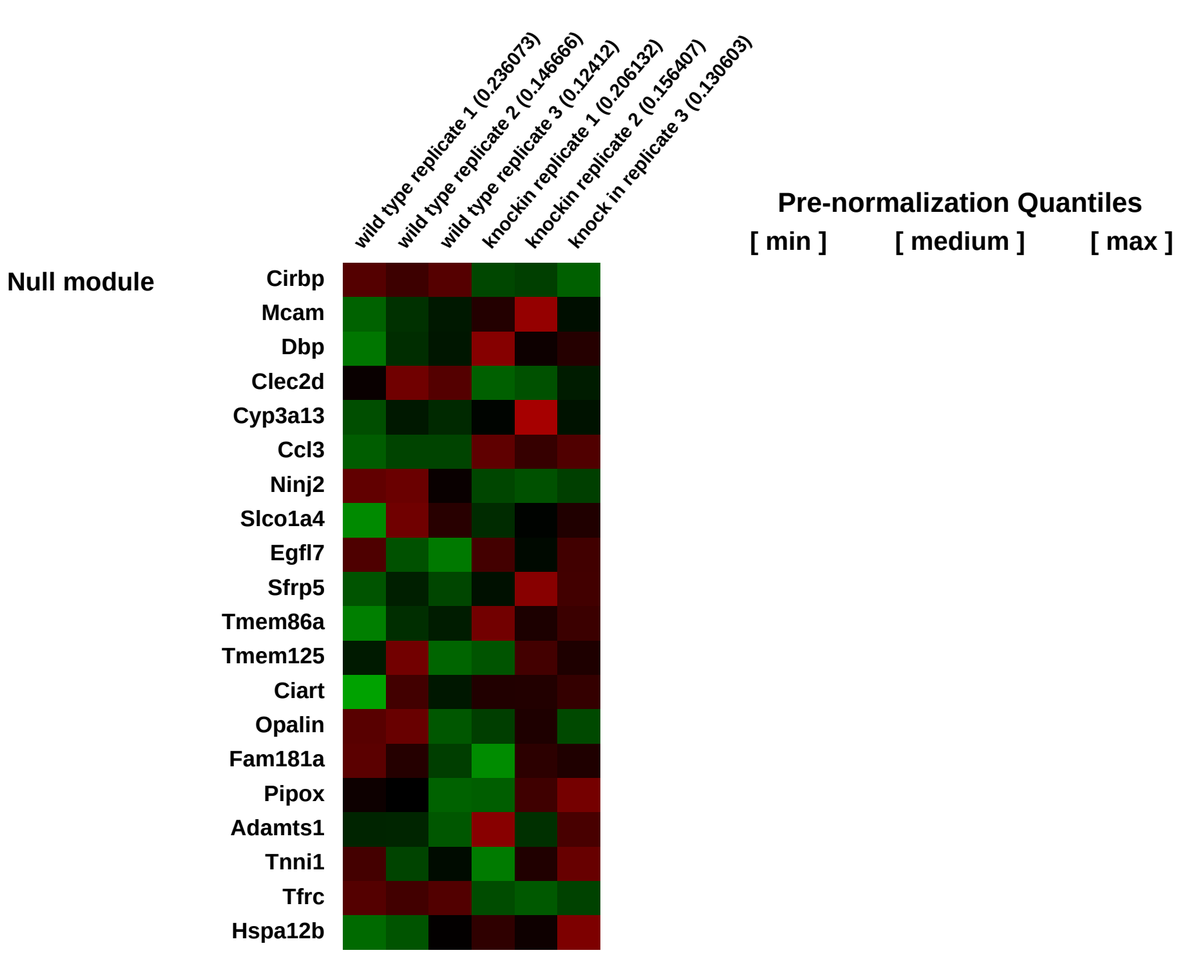

GEO Series "GSE30164" Expression Profiles

Num of samples in this series: 23

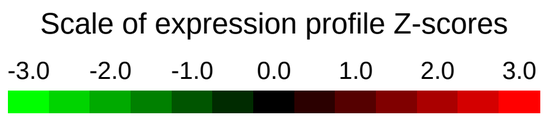

GEO Link:	http://www.ncbi.nlm.nih.gov/geo/query/acc.cgi?acc=GSE30164
Status:	Public on Jun 23 2011
Title:	Transcriptome transfer provides a model for understanding the phenotype of cardiomyocytes
Organism:	Mus musculus
Experiment type:	Expression profiling by array
Platform:	GPL1261
Pubmed ID:	21730152
Summary & Design:	**Summary:** We show that the transfer of the adult ventricular myocyte (AVM) transcriptome into either a fibroblast or an astrocyte converts the host cell into a cardiomyocyte. Transcriptome-effected cardiomyocytes (tCardiomyocytes) display morphologies, immunocytochemical properties, and expression profiles of postnatal cardiomyocytes. Cell morphology analysis shows that tCardiomyoctes are elongated and have a similar length-to-width ratio as AVMs. These global phenotypic changes occur in a time-dependent manner and confer electroexcitability to the tCardiomyocytes. tCardiomyocyte generation does not require continuous overexpression of specific transcription factors; for example, the expression level of transcription factor Mef2c is higher in tCardiomyocytes than in fibroblasts, but similar in tCardiomyocytes and AVMs. These data highlight the dominant role of the gene expression profile in developing and maintaining cellular phenotype. The transcriptomeinduced phenotype remodelingâ generated tCardiomyocyte has significant implications for understanding and modulating cardiac disease development. **Overall design:** Transcriptome transfer can change one cell type to another cell type. We transfect cardiomyocyte transciptome into fibroblast and astrocyte. Transcriptomes from single cells are isolated and amplified and then hybridize on Affymetrix array.

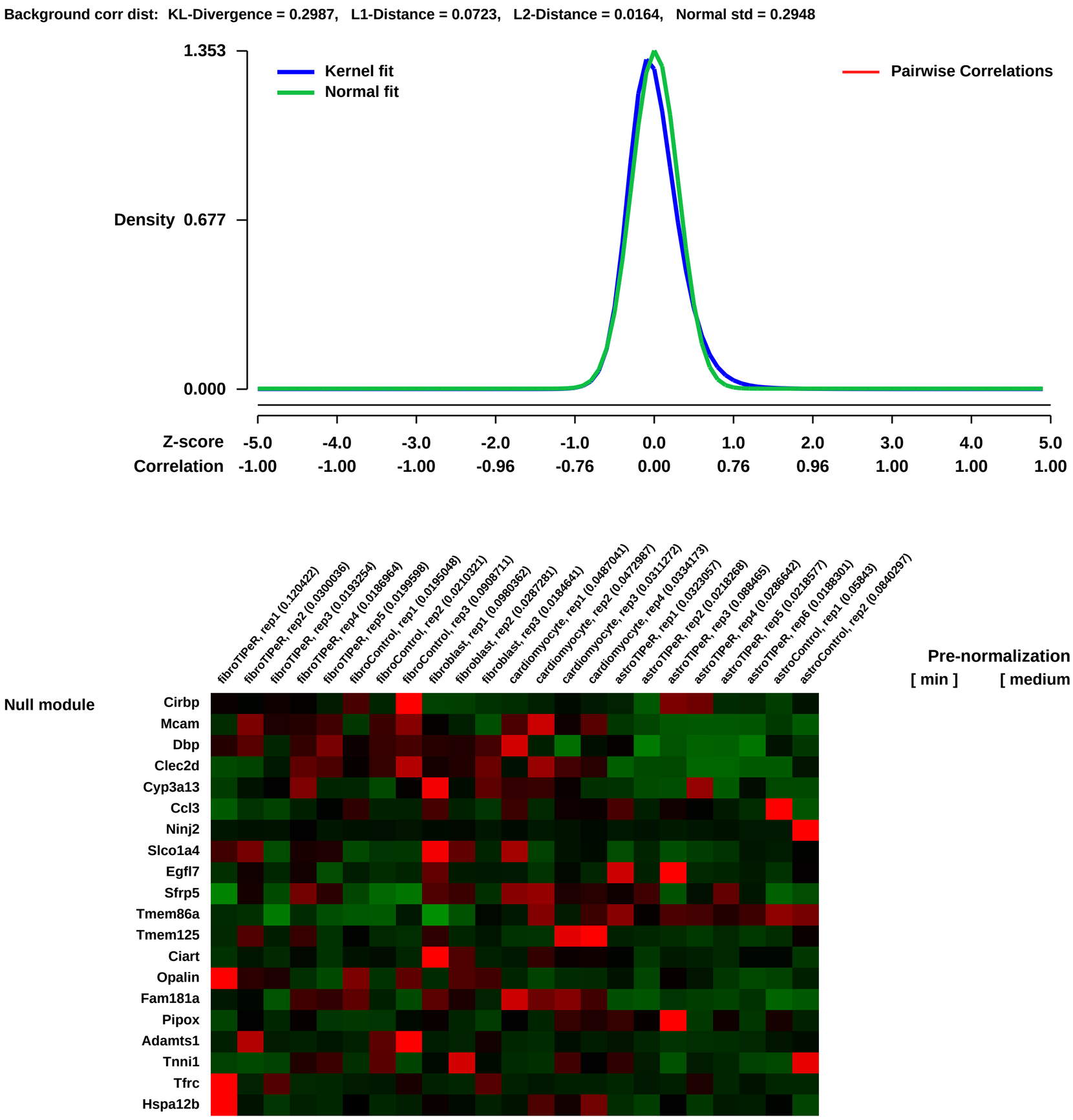

GEO Series "GSE30176" Expression Profiles

Num of samples in this series: 12

Scale of expression profile Z-scores

-3.0 -2.0 -1.0 0.0 1.0 2.0 3.0

GEO Link:	**http://www.ncbi.nlm.nih.gov/geo/query/acc.cgi?acc=GSE30176**
Status:	**Public on Jul 19 2011**
Title:	**Retinoic acid (RA) induction time-course to profile gene expression during mES cell differentiation.**
Organism:	**Mus musculus**
Experiment type:	**Expression profiling by array**
Platform:	**GPL1261**
Pubmed ID:	**21764852**
Summary & Design:	**Summary:** **Murine ES cell gene expression before RA induction are used to compare gene expression for time-points of 2, 4, 6hrs post-induction.** **Overall design:** **KH2 ES Cell RA Differentiation Time-course**

Background corr dist: **KL-Divergence = 0.0719, L1-Distance = 0.0287, L2-Distance = 0.0010, Normal std = 0.5040**

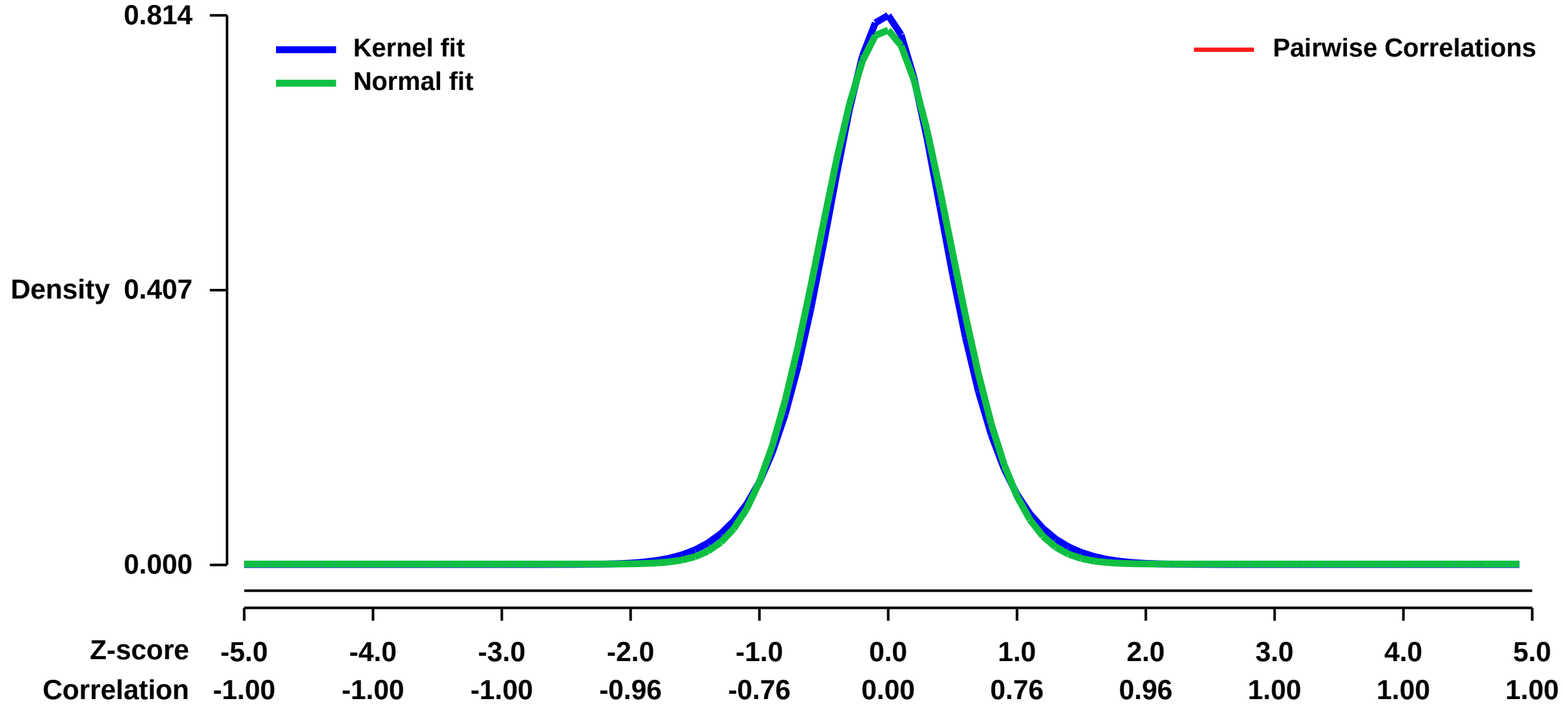

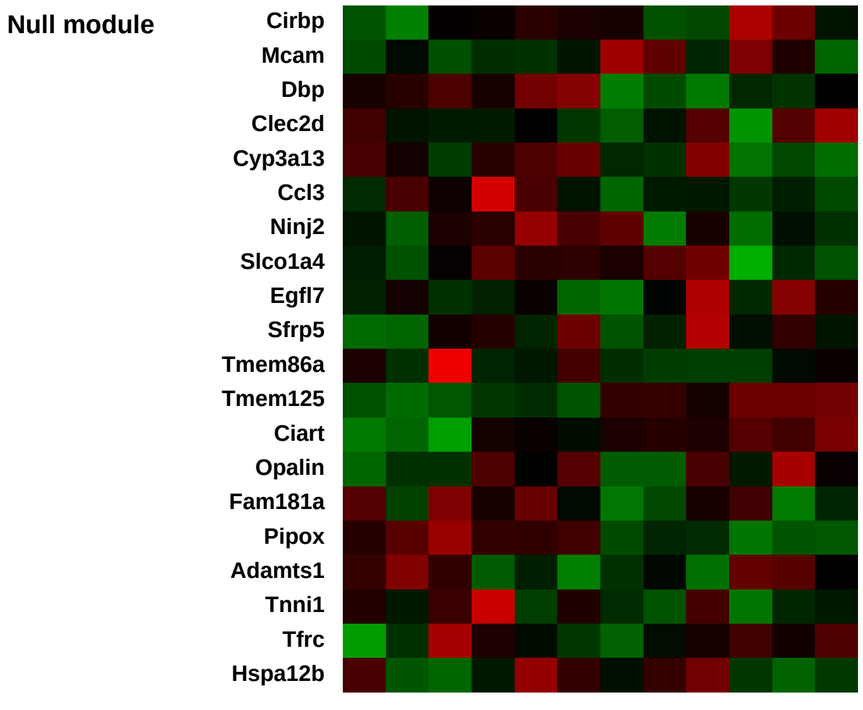

GEO Series "GSE30192" Expression Profiles

Num of samples in this series: 6

Scale of expression profile Z-scores

-3.0 -2.0 -1.0 0.0 1.0 2.0 3.0

GEO Link:	http://www.ncbi.nlm.nih.gov/geo/query/acc.cgi?acc=GSE30192
Status:	Public on Jan 01 2012
Title:	Effect of 5-azacytidine on gene expression in C2C12 myoblasts
Organism:	Mus musculus
Experiment type:	Expression profiling by array
Platform:	GPL1261
Pubmed ID:	21795504
Summary & Design:	**Summary:** Mesenchymal progenitor cells can be differentiated in vitro into myotubes that exhibit many characteristic features of primary mammalian skeletal muscle fibers. However, in general, they do not show the functional excitation-contraction coupling or the striated sarcomere arrangement typical of mature myofibers. Epigenetic modifications have been shown to play a key role in regulating the progressional changes in transcription necessary for muscle differentiation. In this study, we demonstrate that treatment of murine C2C12 mesenchymal progenitor cells with 10 ´µM of the DNA methylation inhibitor 5-azacytidine (5AC) promotes myogenesis, resulting in myotubes with enhanced maturity as compared to untreated myotubes. Specifically, 5AC treatment resulted in the upregulation of muscle genes at the myoblast stage while at later stages nearly 50 % of the 5AC-treated myotubes displayed a mature, well-defined sarcomere organization as well as spontaneous contractions that coincided with action potentials and intracellular calcium transients. Both the percentage of striated myotubes and their contractile activity could be inhibited by 20 nM TTX, 10 ´µM ryanodine and 100 ´µM nifedipine, suggesting that action potential-induced calcium transients are responsible for these characteristics. Our data suggest that genomic demethylation induced by 5AC overcomes an epigenetic barrier that prevents untreated C2C12 myotubes from reaching full maturity. **Overall design:** C2C12 cells were plated at 1500 cells/cm2 (day -1), cultured for 1 day in DMEM 10%NCS, then treated (d0) with or without 10uM 5-azacytidine (5AC) for an additional 3 days. RNA was extracted on day 3 and hybridized to GeneChip Mouse Genome 430 2.0 array (Affymetrix).

Background corr dist: KL-Divergence = 0.0286, L1-Distance = 0.0590, L2-Distance = 0.0044, Normal std = 0.7900

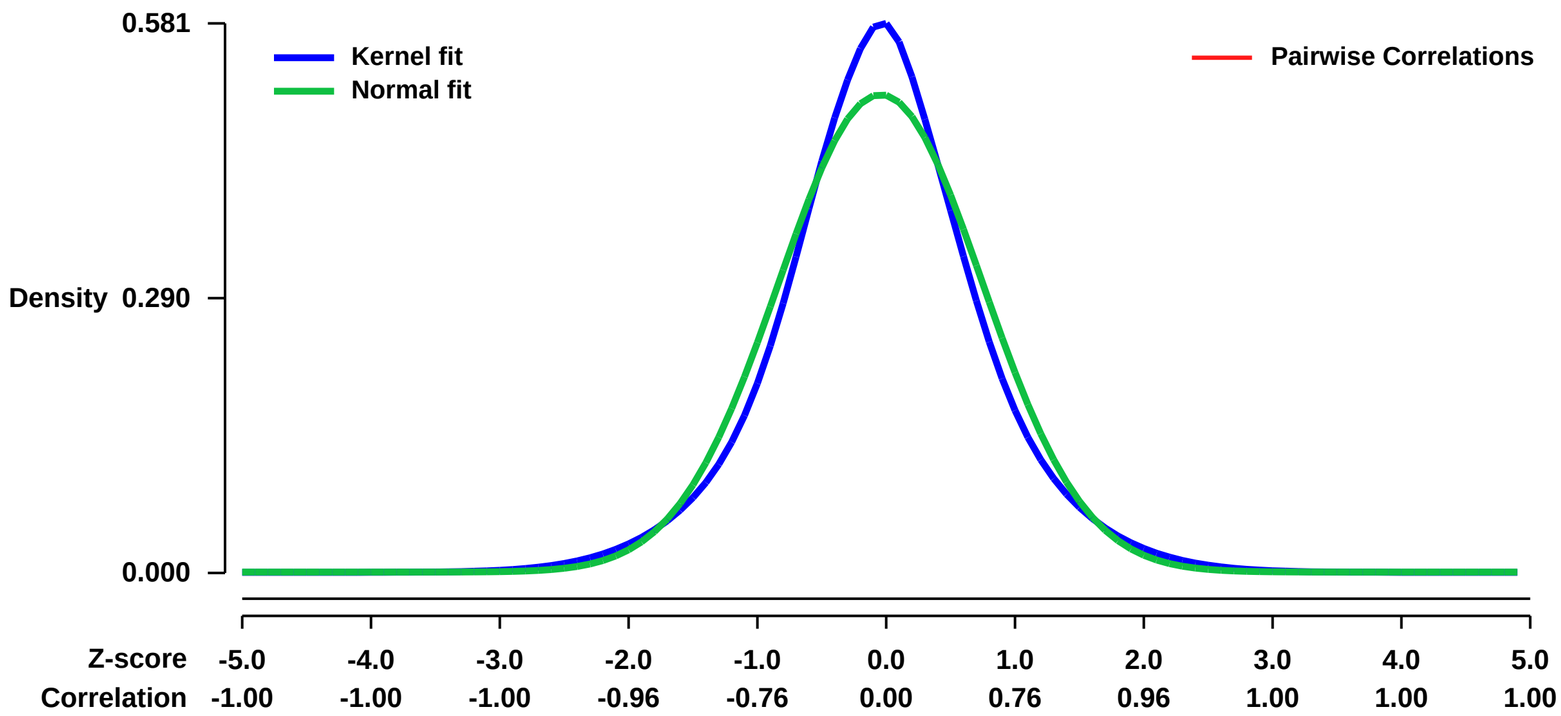

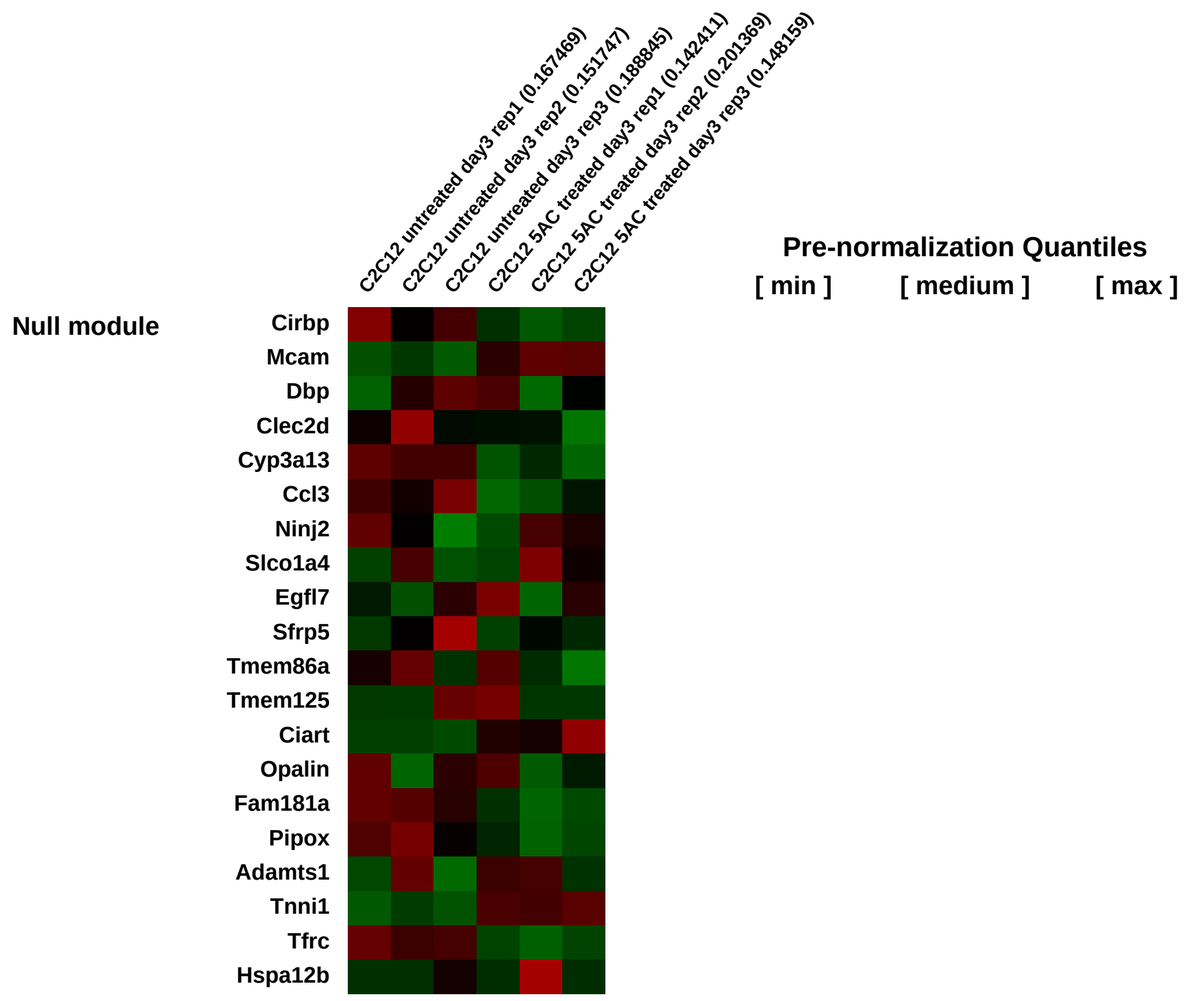

GEO Series "GSE30247" Expression Profiles

Num of samples in this series: 16

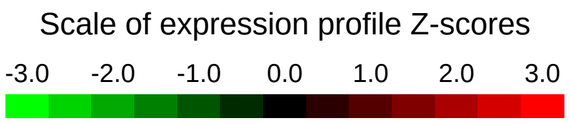

GEO Link:	http://www.ncbi.nlm.nih.gov/geo/query/acc.cgi?acc=GSE30247
Status:	Public on Dec 21 2012
Title:	High Fat Diet Triggers SIRT1 Cleavage in Adipose Tissue Providing a Link between Dietary Stress and Metabolic Dysfunction.
Organism:	Mus musculus
Experiment type:	Expression profiling by array
Platform:	GPL1261
Pubmed ID:	22883230
Summary & Design:	**Summary:** Adipose tissue plays an important role in storing excess nutrients and preventing ectopic lipid accumulation in other organs. Obesity leads to excess lipid storage in adipocytes, resulting in the generation of stress signals and the derangement of metabolic functions. SIRT1 is an important regulatory sensor of nutrient availability in many metabolic tissues. Here we report that SIRT1 functions in adipose tissue to protect from the development of inflammation and obesity under normal feeding conditions, and the progression to metabolic dysfunction under dietary stress. Genetic ablation of SIRT1 from adipose tissue leads to gene expression changes that highly overlap with changes induced by high fat diet in wild type mice, suggesting that dietary stress signals inhibit the activity of SIRT1. Indeed, we show that high fat diet induces the cleavage of SIRT1 in adipose tissue by the inflammation-activated caspase-1, providing a link between dietary stress and predisposition to metabolic dysfunction. **Overall design:** Four replicates from four different biological conditions: 1) SIRT1 wild-type fed low fat diet, 2) SIRT1 wild-type fed high fat diet, 3) SIRT1 knock-out fed low fat diet, 4) SIRT1 knock-out fed high fat diet

Background corr dist: KL-Divergence = 0.1238, L1-Distance = 0.0283, L2-Distance = 0.0017, Normal std = 0.4093

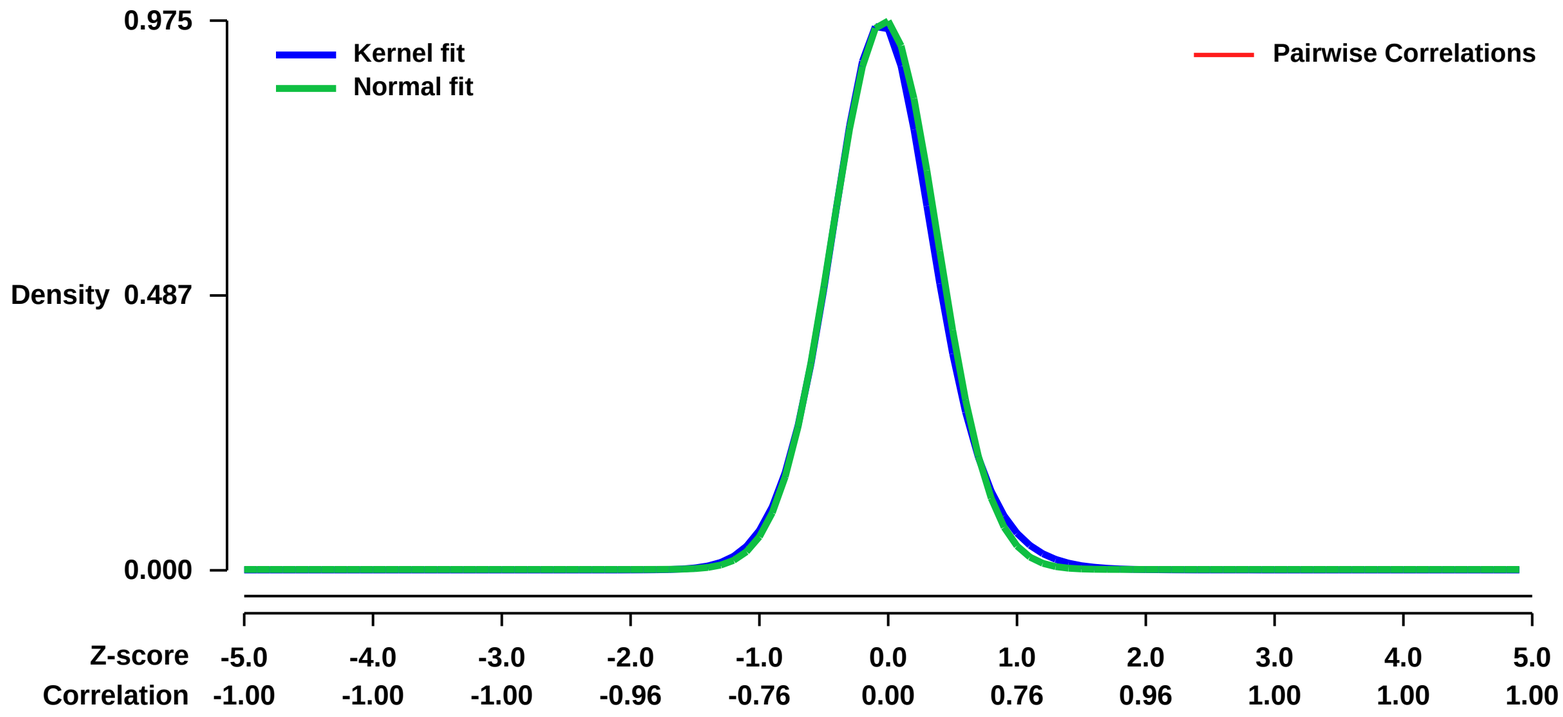

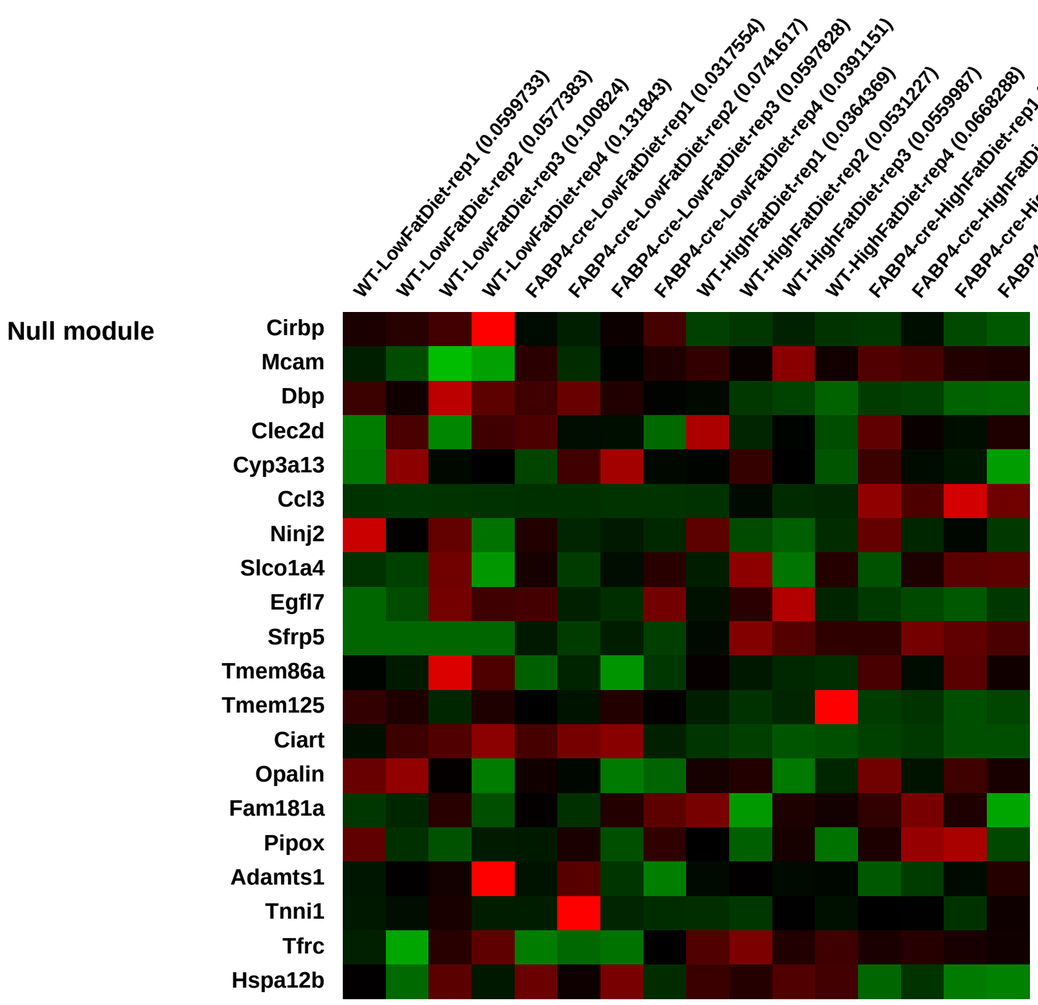

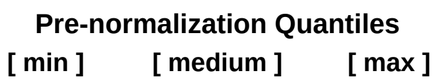

GEO Series "GSE30293" Expression Profiles

Num of samples in this series: 8

Scale of expression profile Z-scores

-3.0 -2.0 -1.0 0.0 1.0 2.0 3.0

GEO Link:	**http://www.ncbi.nlm.nih.gov/geo/query/acc.cgi?acc=GSE30293**
Status:	**Public on Dec 01 2011**
Title:	**Zfp281 Functions as a Transcriptional Repressor for Pluripotency of Mouse Embryonic Stem Cells**
Organism:	**Mus musculus**
Experiment type:	**Expression profiling by array**
Platform:	**GPL1261**
Pubmed ID:	
Summary & Design:	**Summary:** **Zfp281 is a partner protein of Nanog. To identify potential target genes of Zfp281, we generated Zfp281 null ESCs using gene targeting, and compared transcriptomic changes between multiple lines of wildtype, heterozygous and null ESCs.** **Overall design:** **Total 8 ESC lines: 3 wildtype lines, 2 heterozygous lines, and 3 null lines.**

Background corr dist: **KL-Divergence = 0.0694, L1-Distance = 0.0217, L2-Distance = 0.0007, Normal std = 0.5013**

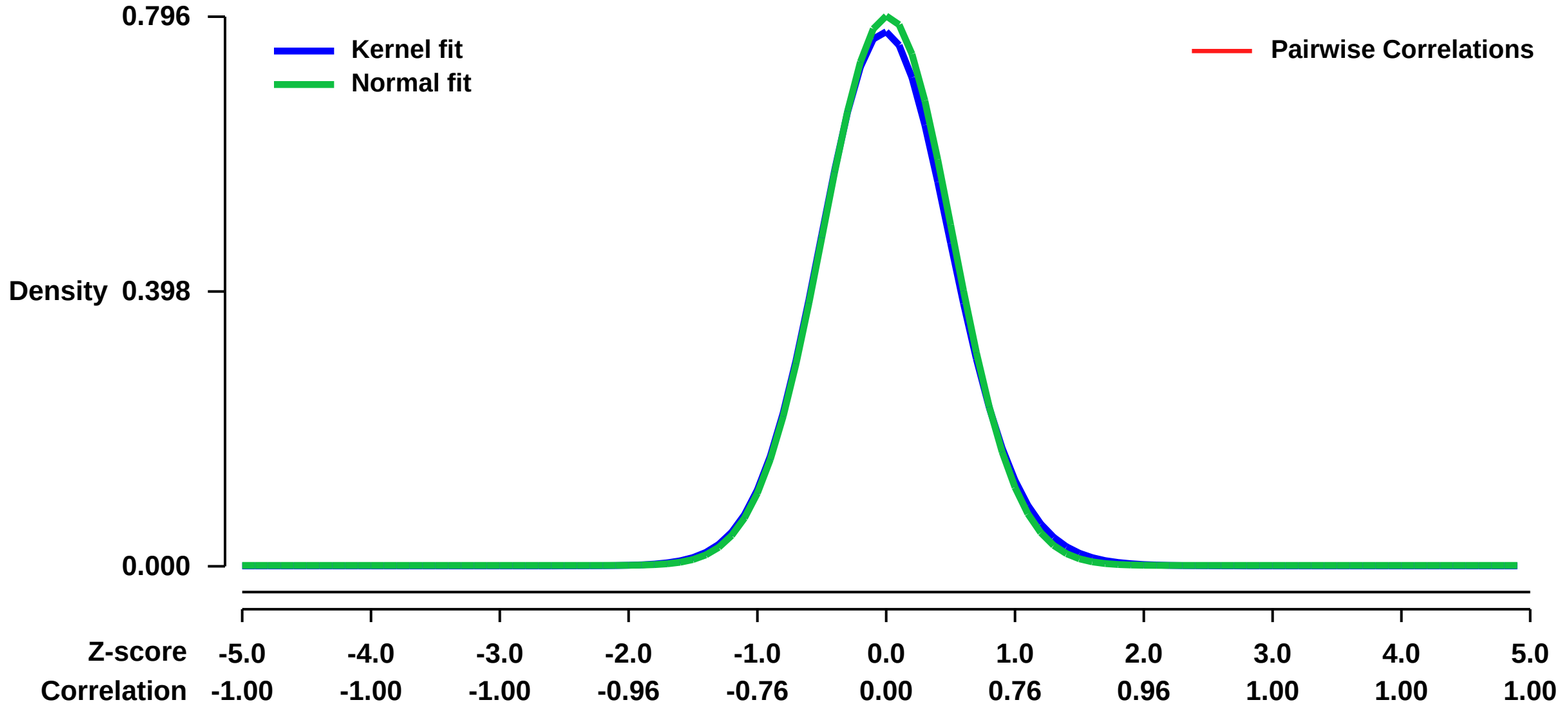

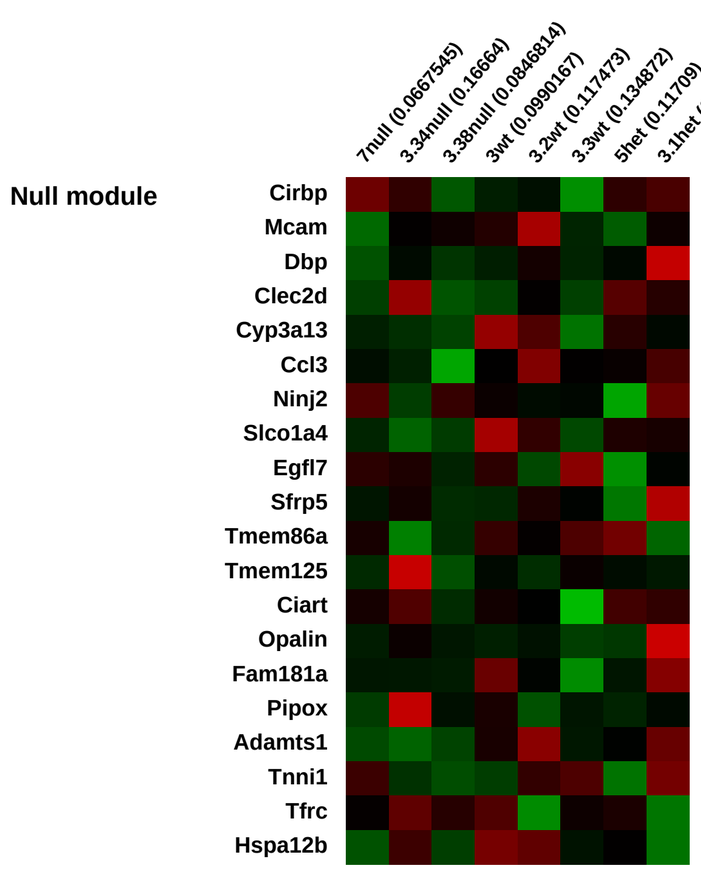

GEO Series "GSE30318" Expression Profiles

Num of samples in this series: 12

Scale of expression profile Z-scores

-3.0 -2.0 -1.0 0.0 1.0 2.0 3.0

GEO Link:	http://www.ncbi.nlm.nih.gov/geo/query/acc.cgi?acc=GSE30318
Status:	Public on May 23 2012
Title:	Expression data from murine Fancc-deficient hematopoietic stem and progenitor cells
Organism:	Mus musculus
Experiment type:	Expression profiling by array
Platform:	GPL1261
Pubmed ID:	22653977
Summary & Design:	**Summary:** We used gene expression microarrays to identify genes whose expression was influenced differently by TNFa in Fancc-deficient mice compared to wild type (WT) mice. To identify genes whose expression was directly or indirectly influenced by Fancc, we looked in particular for genes either suppressed or induced by TNF in WT cells that were not affected by TNF in Fancc-deficient cells. **Overall design:** Enriched populations of KSL cells (marrow mononuclear cells sorted for the c-Kit+/Sca-1+/Lineage (Lin)- fraction from WT and Fancc-deficient mice were exposed for 24 hours in vitro to either hematopoietic growth factors alone (IL-6, IL-11, Flt3L, and SCF) or to those factors plus TNFa (10 ng/ml) after which RNA was prepared and hybridized to Affymetrix microarrays (MOE430 2.0).

Background corr dist: KL-Divergence = 0.1174, L1-Distance = 0.0288, L2-Distance = 0.0013, Normal std = 0.4109

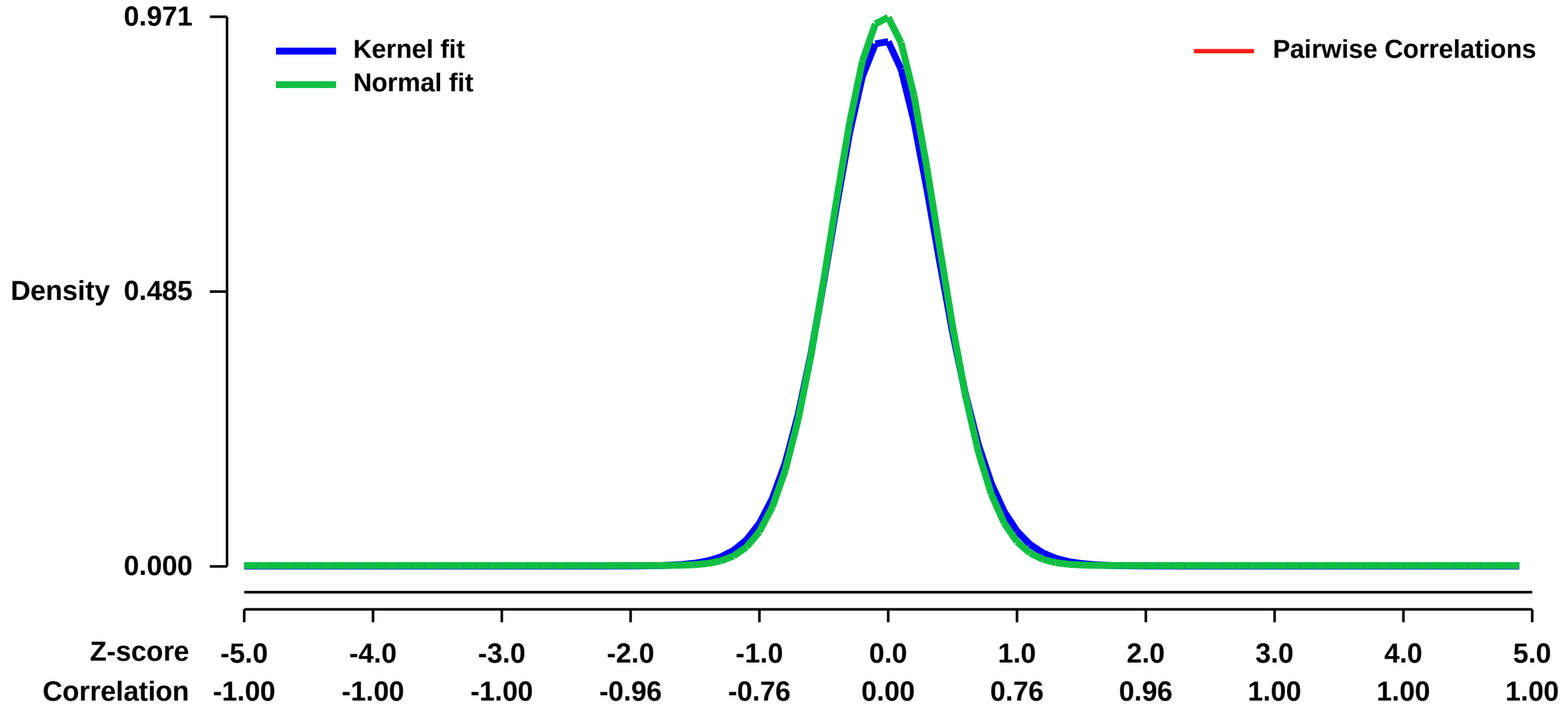

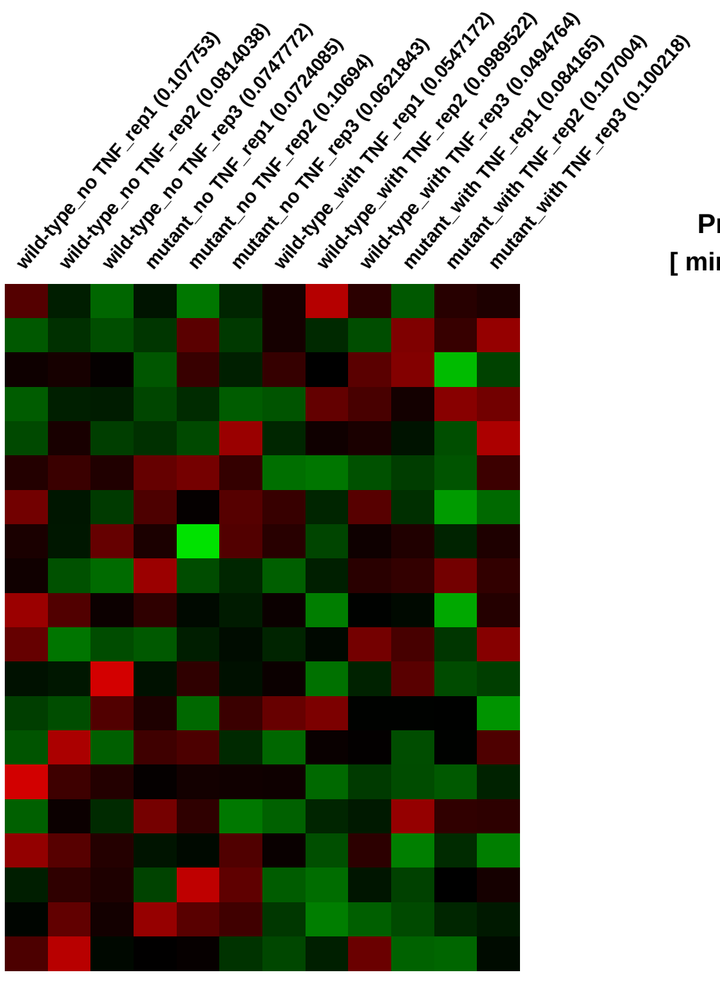

GEO Series "GSE30485" Expression Profiles

Num of samples in this series: 15

Scale of expression profile Z-scores

-3.0 -2.0 -1.0 0.0 1.0 2.0 3.0

GEO Link:	http://www.ncbi.nlm.nih.gov/geo/query/acc.cgi?acc=GSE30485
Status:	Public on Jul 04 2014
Title:	Gene expression accompanying the promotion of hepatocellular carcinoma by intestinal microbiota and Tlr4 in mice.
Organism:	Mus musculus
Experiment type:	Expression profiling by array
Platform:	GPL1261
Pubmed ID:	
Summary & Design:	**Summary:** The effect of Tlr4P712H mutation (rendering TLR4 non-functional), or gut-sterilization by antibiotics, on the induction of tumorgenesis by CCl4 and diethylnitrosamine (DEN) was characterized. Affymetrix Mouse 430 2.0 gene expression measurements were used to characterize the transcriptomic basis of the effects of the above treatments and genotypes on tumorgenesis. **Overall design:** Gene expression of mouse livers of A. WT C3H/HeOuJ mice, B. WT C3H/HeOuJ mice treated with CCl4 and DEN, C. TLR4-mutant C3H/HeJ mice (Tlr4P712H) treated with CCl4 and DEN and D. WT C3H/HeOuJ mice treated with antibiotics (a combination of ampicillin (1 g/l), neomycin [1 g/l], metronidazole[1 g/l] and vancomycin [500 mg/l] in drinking water) and CCl4 and DEN were characterized.

Background corr dist: KL-Divergence = 0.1032, L1-Distance = 0.0263, L2-Distance = 0.0011, Normal std = 0.4349

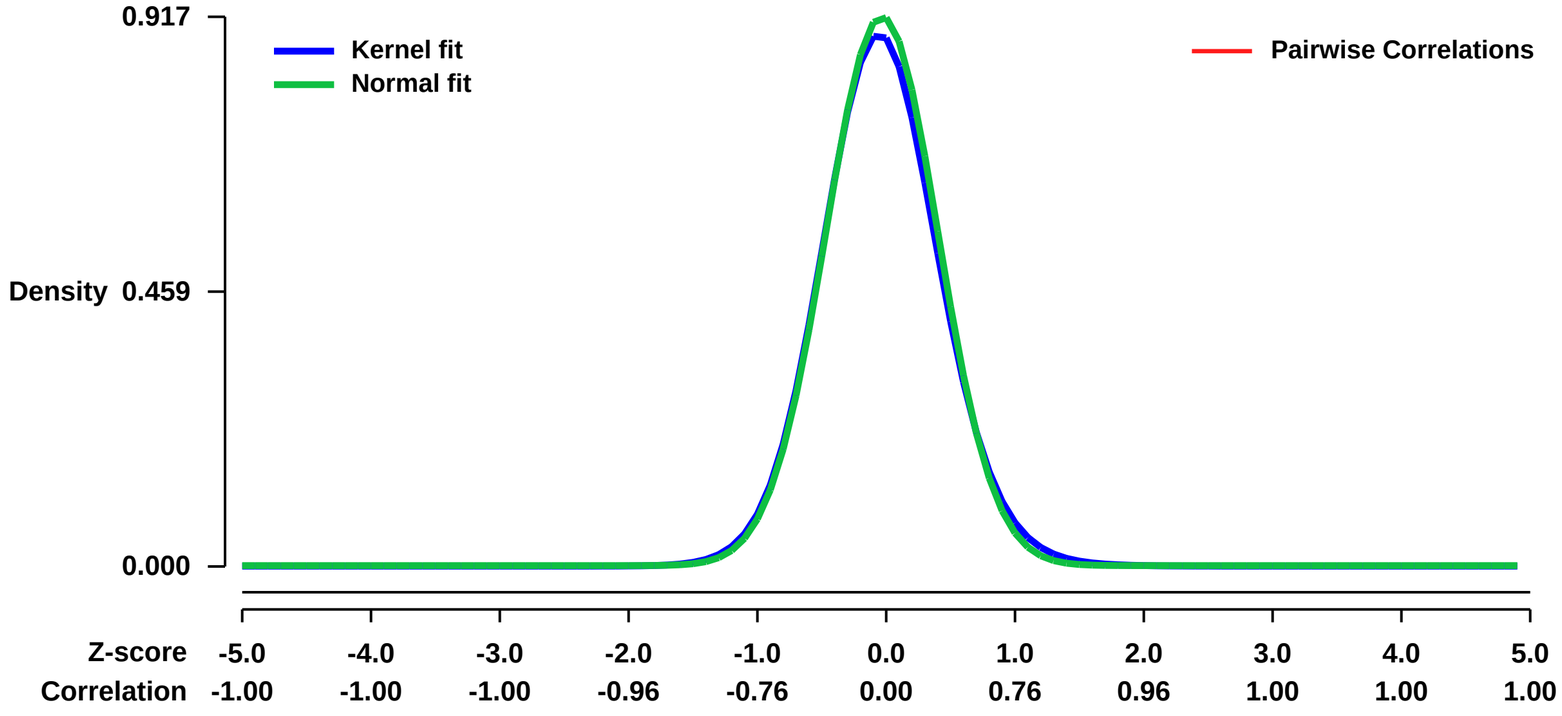

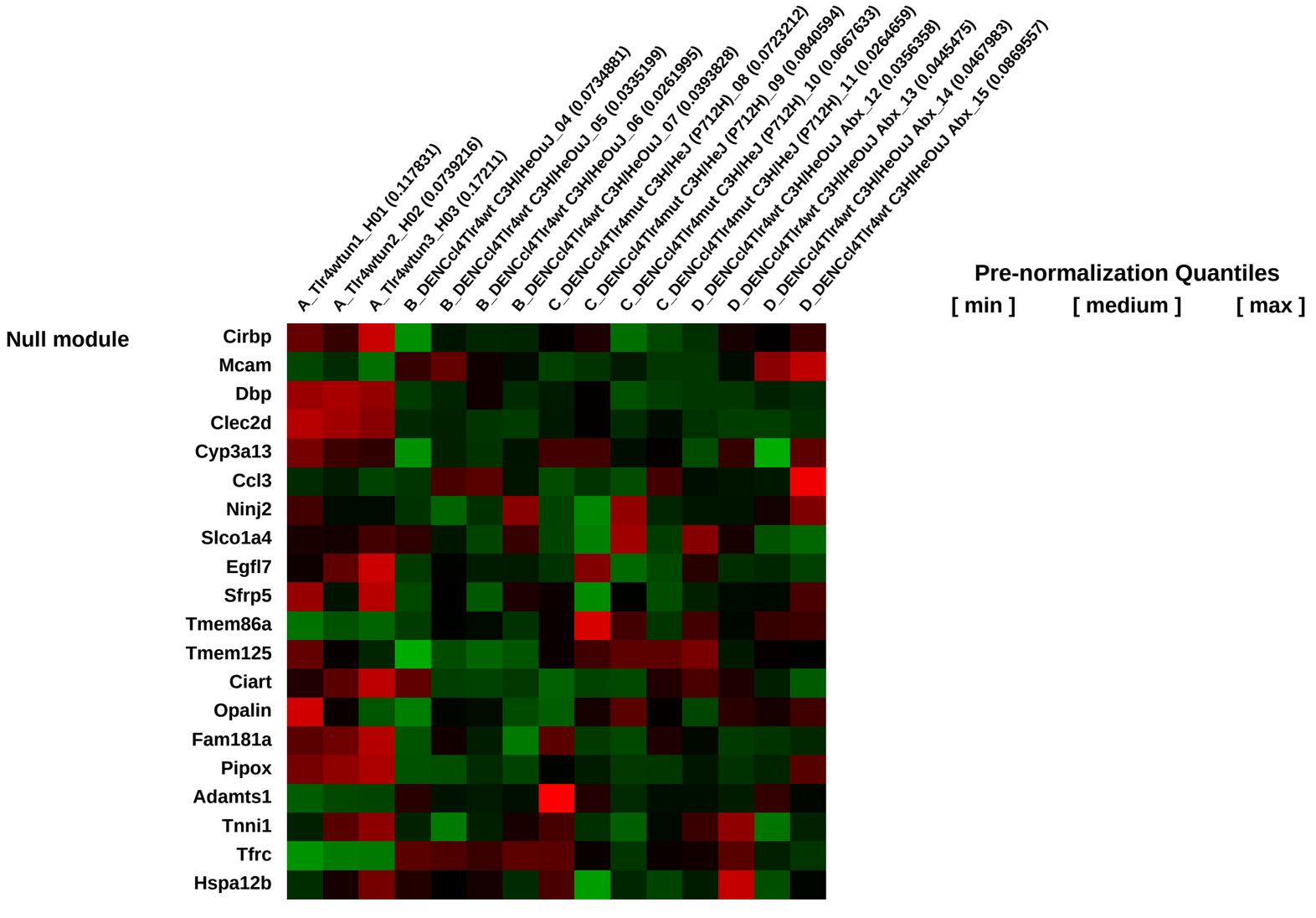

GEO Series "GSE30498" Expression Profiles

Num of samples in this series: 12

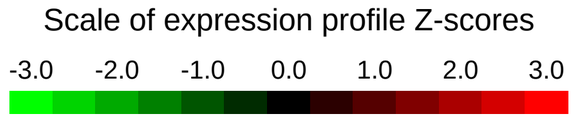

GEO Link:	**http://www.ncbi.nlm.nih.gov/geo/query/acc.cgi?acc=GSE30498**
Status:	**Public on Jul 07 2012**
Title:	**Expression data from superior cervical ganglion cultured cells and whole tissue**
Organism:	**Mus musculus**
Experiment type:	**Expression profiling by array**
Platform:	**GPL1261**
Pubmed ID:	
Summary & Design:	**Summary:** **A transcriptomic expression comparison was done among superior cervical ganglion (SCG) cells cultured on 2D substrates, 3D porous polystyrene scaffolds, and in freshly dissected tissue (in vivo surrogate), with the goal of assessing the feasibility of establishing the meaning of 3D and associated physiological relevance at the molecular level** **Overall design:** **SCG cells were cultured on 2D surfaces and in 3D scaffolds. Chemical cues are controlled by coating. Only spacial properties of the culture systems were compared. Cells from freshly dissected tissue were used as in vivo surrogates for positive control of 3D cells.**

Background corr dist: **KL-Divergence = 0.0255, L1-Distance = 0.0692, L2-Distance = 0.0061, Normal std = 0.8184**

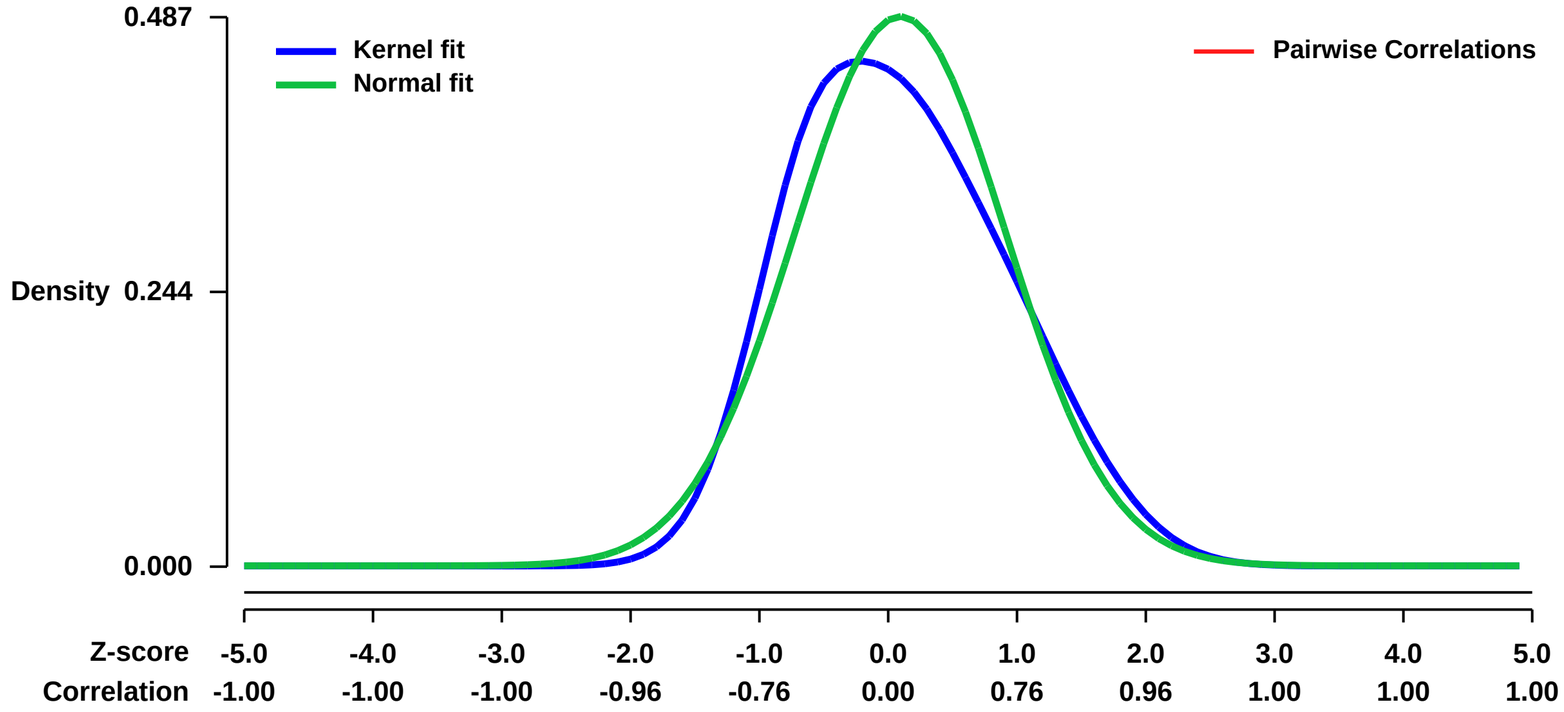

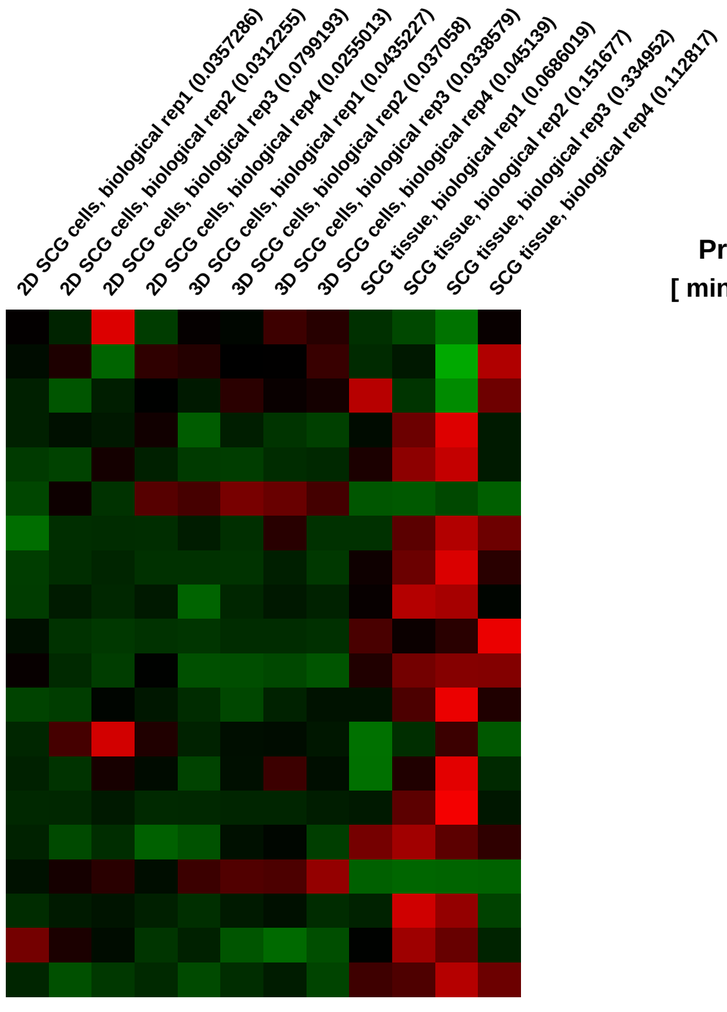

GEO Series "GSE30503" Expression Profiles

Num of samples in this series: 23

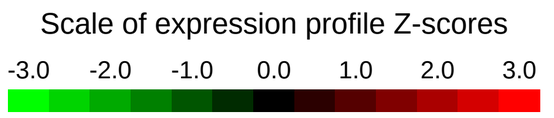

GEO Link:	http://www.ncbi.nlm.nih.gov/geo/query/acc.cgi?acc=GSE30503
Status:	Public on May 10 2012
Title:	Integrin alpha-6 (CD49f) defines a novel and distinct subset of CD4+ regulatory T cells with potent suppression activity.
Organism:	Mus musculus
Experiment type:	Expression profiling by array
Platform:	GPL1261
Pubmed ID:	
Summary & Design:	**Summary:** A common method used both in vitro and in vivo, to identify Tregs in CD4+ T cells is through the characterization of surface marker CD25. Although CD25 expression is well correlated with regulatory activity in vitro, CD4+CD25+ T cells are not the only regulatory CD4+ T cells in vivo. Studies suggest that in many situations, CD4+CD25â T cells are as effective as CD4+CD25+ T cells in controlling T cell mediated disease. Therefore, CD25 is not a uniquely specific cell surface marker for the identification of Tregs. CD49f is an ¸–6-integrin subunit which dimerizes with either the ¸†1 or ¸†4 subunit to form receptors for various laminin isoforms. We found that CD4+ T cells from NOD mice express CD49f, and old non-diabetic NOD mice had an increase of CD4+CD49f+ T cells in the spleen and peripheral lymph node when compared to both young and diabetic mice. This study was conducted to further characterize CD4+CD49f+ Treg cell subpopulation in NOD mice. It was found that CD4+CD49f+T cells possess suppressive ability and only one third of CD4+CD49f+ T cells expressing CD25. Based on the expression of CD49f and CD25, CD4+ T cells was divided into four populations , CD25+CD49f+ ,CD25+CD49f- ,CD25-CD49f+ but CD25-CD49f- are of suppressive ability, and we further found that Foxp3 expression was highly correlated with the suppressive ability of these three Treg populations. In conclusion our data indicate that CD49f marks a CD4+ CD25+ Treg subset with more potent suppression activity and identifies a CD25-CD4+ T cell population with suppression function in a Foxp3+ expression dependent manner. **Overall design:** We divided CD4+ T cells into four populations: CD25+CD49f+, CD25+CD49f-, CD25-CD49f+, CD25-CD49f-; Microarray technology was used to determine gene expression differences among these four groups.

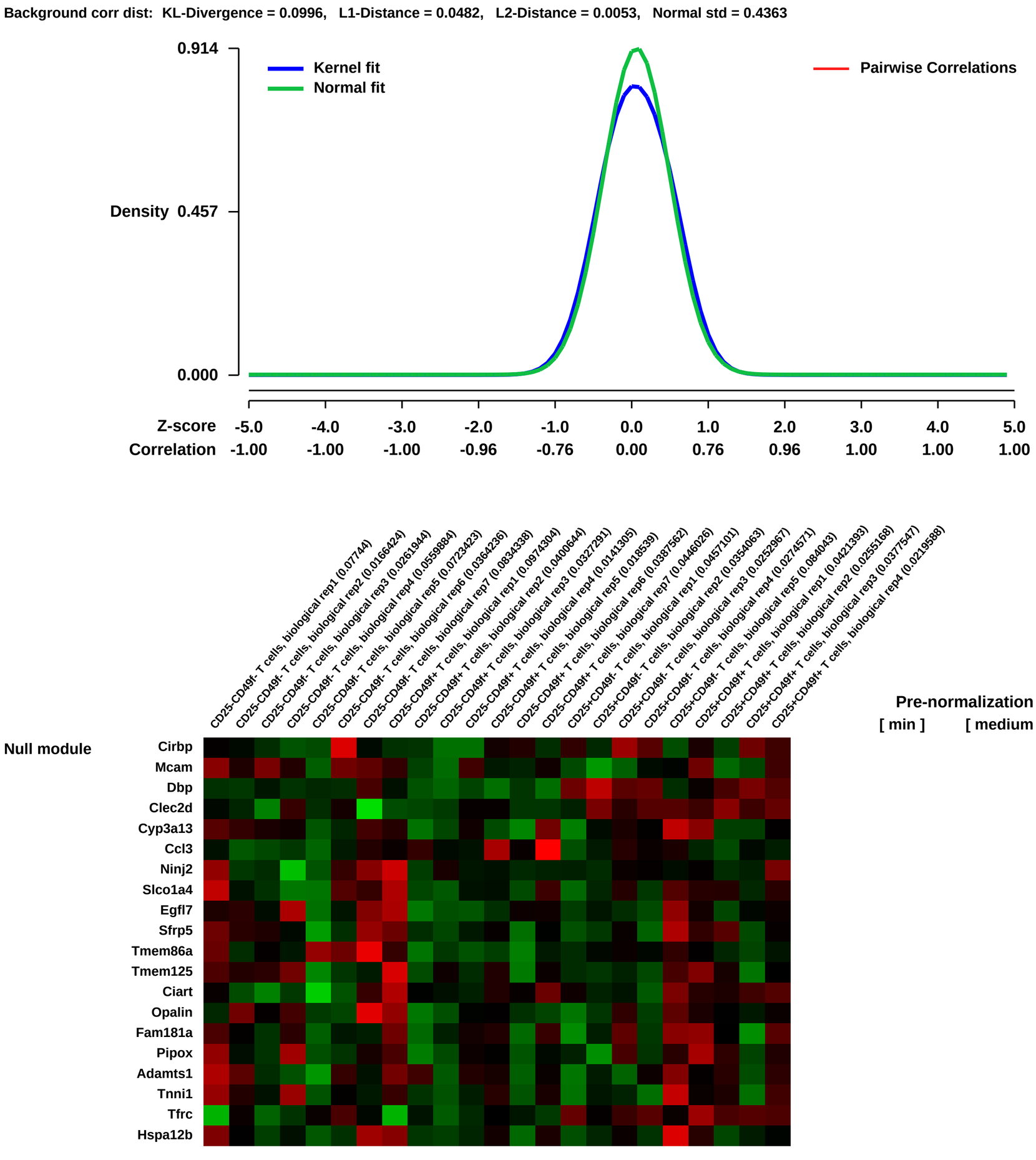

GEO Series "GSE30561" Expression Profiles

Num of samples in this series: 6

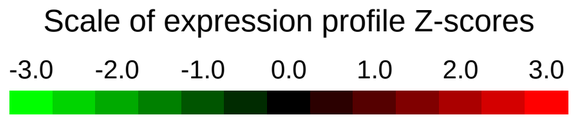

GEO Link:	**http://www.ncbi.nlm.nih.gov/geo/query/acc.cgi?acc=GSE30561**
Status:	**Public on Nov 01 2011**
Title:	**Expression data from mouse embryonic stem cells lacking the Alkbh1 gene**
Organism:	**Mus musculus**
Experiment type:	**Expression profiling by array**
Platform:	**GPL1261**
Pubmed ID:	
Summary & Design:	**Summary:** **AlkB homolog 1 (ALKBH1) is one of nine members of the AlkB homologs in mammals. Most Alkbh1-deficient mice die during embryonic development, and survivors have severe defects in tissues originating from the ectodermal lineage. We hypothesized the phenotype to rely upon aberrant epigenetic regulation and provided evidence for ALKBH1 to be a histone H2A demethylase. We used a whole genome expression microarray to detail differentially expressed genes in embryonic stem cells lacking the Alkbh1 gene and identified distinct classes of up- and down-regulated genes during this process.** **Overall design:** **Wild type and Alkbh-/- embryonic stem cells were established to identify differentially expressed genes at day 0, undifferentiated cells. We sought to obtain a subset of genes possibly explaining the observed phenotype. Total RNA was extracted and hybridized on Affymetrix GeneChips. 3 parallels were analyzed from each of the two genotypes.**

Background corr dist: **KL-Divergence = 0.0310, L1-Distance = 0.0211, L2-Distance = 0.0004, Normal std = 0.6731**

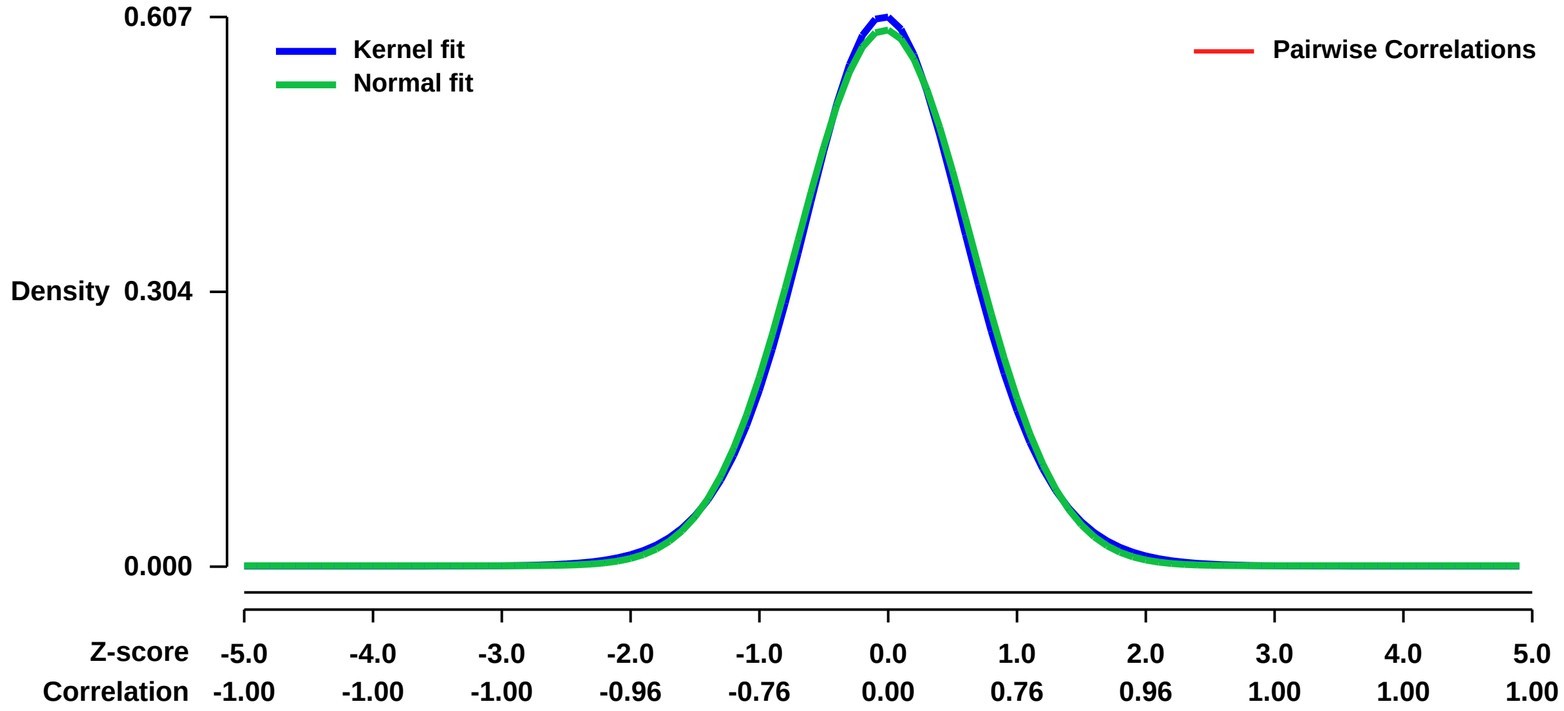

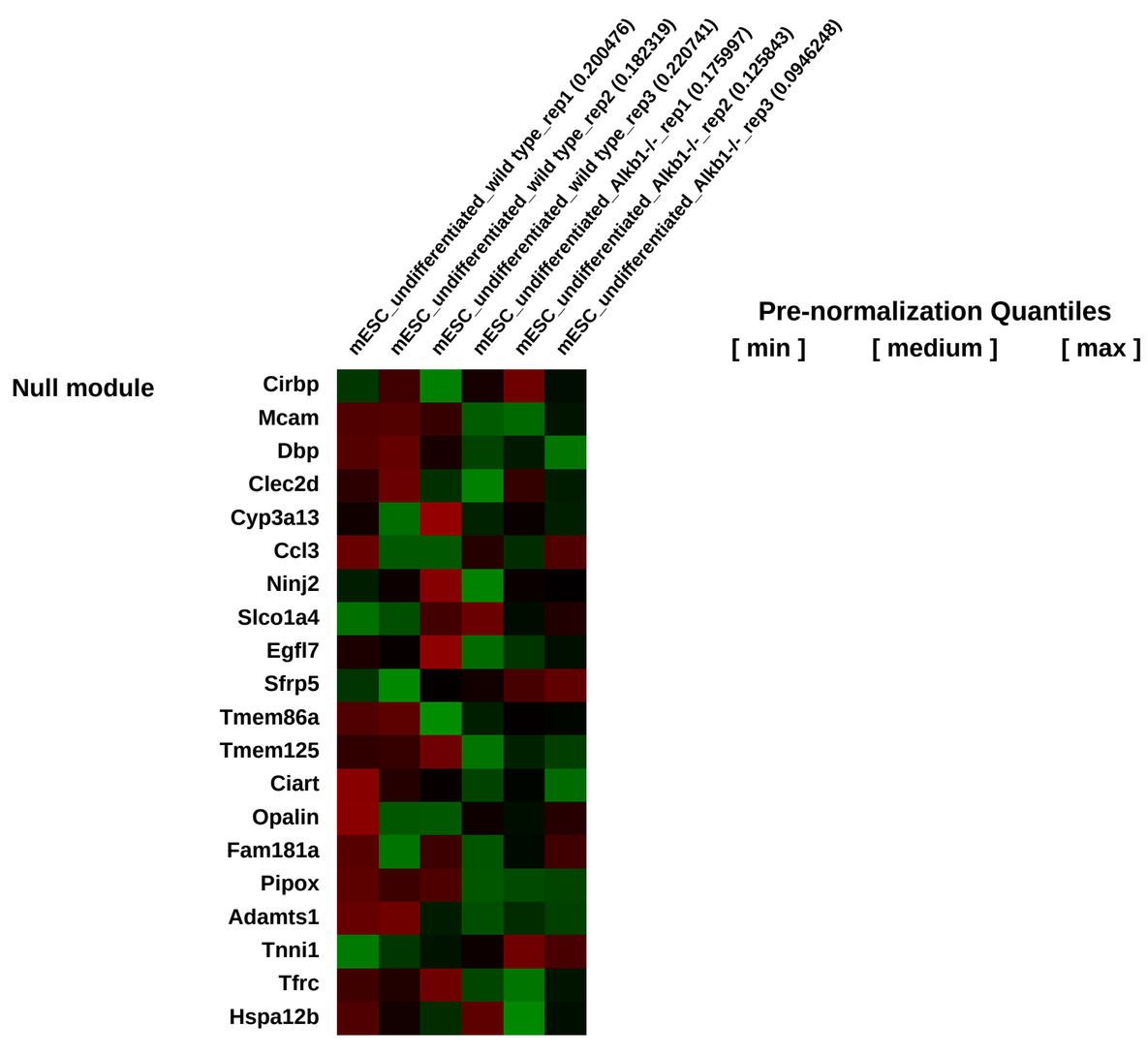

GEO Series "GSE30655" Expression Profiles

Num of samples in this series: 35

Scale of expression profile Z-scores

-3.0 -2.0 -1.0 0.0 1.0 2.0 3.0

GEO Link:	http://www.ncbi.nlm.nih.gov/geo/query/acc.cgi?acc=GSE30655
Status:	Public on Jul 14 2014
Title:	Mice Lacking the ¸†2 Adrenergic Receptor Have a Unique Genetic Profile Before and After Focal Brain Ischemia
Organism:	Mus musculus
Experiment type:	Expression profiling by array
Platform:	GPL1261
Pubmed ID:	
Summary & Design:	**Summary:** The role of the beta2 adrenergic receptor (¸†2AR) after stroke is unclear as pharmacological manipulations of the ¸†2AR have produced contradictory results. We previously showed that mice deficient in the ¸†2AR (¸†2KO) had smaller infarcts compared to wild-type mice (FVB) after middle cerebral artery occlusion (MCAO), a model of stroke. To elucidate mechanisms of this neuroprotection, we evaluated changes in gene expression using microarrays comparing differences before and after MCAO, and differences between genotypes. Genes associated with inflammation and cell death were enriched after MCAO in both genotypes, and we identified several genes not previously shown to increase following ischemia (Ccl9, Gem, and Prg4). In addition to networks that were similar between genotypes, one network with a central node of G protein-coupled receptor and including biological functions carbohydrate metabolism, small molecule biochemistry and inflammation was identified in FVB mice but not in ¸†2KO mice. Analysis of differences between genotypes revealed 11 genes differentially expressed by genotype in all conditions. We demonstrate greater Glo1 protein levels and lower Pmaip/Noxa mRNA levels in ¸†2KO mice. As both genes are implicated in NF¸"B signaling, we measured p65 activity and tumor necrosis factor alpha (TNF¸–) levels 24h after MCAO. MCAO-induced p65 activation and post-ischemic TNF¸– production were both greater in FVB compared to ¸†2KO mice. These results suggest that loss of ¸†2AR signaling results in a neuroprotective phenotype in part due to decreased NF¸"B signaling, decreased inflammation, and decreased apoptotic signaling in the brain. **Overall design:** A total of 15 naˆflve samples were analyzed, with 7-8 of each genotype, wild-type (FVB) and beta2 adrenergic receptor deficient (B2) mice. The naive samples were normalized independently of the MCAO and sham surgery samples.

Background corr dist: KL-Divergence = 0.0829, L1-Distance = 0.0426, L2-Distance = 0.0038, Normal std = 0.4716

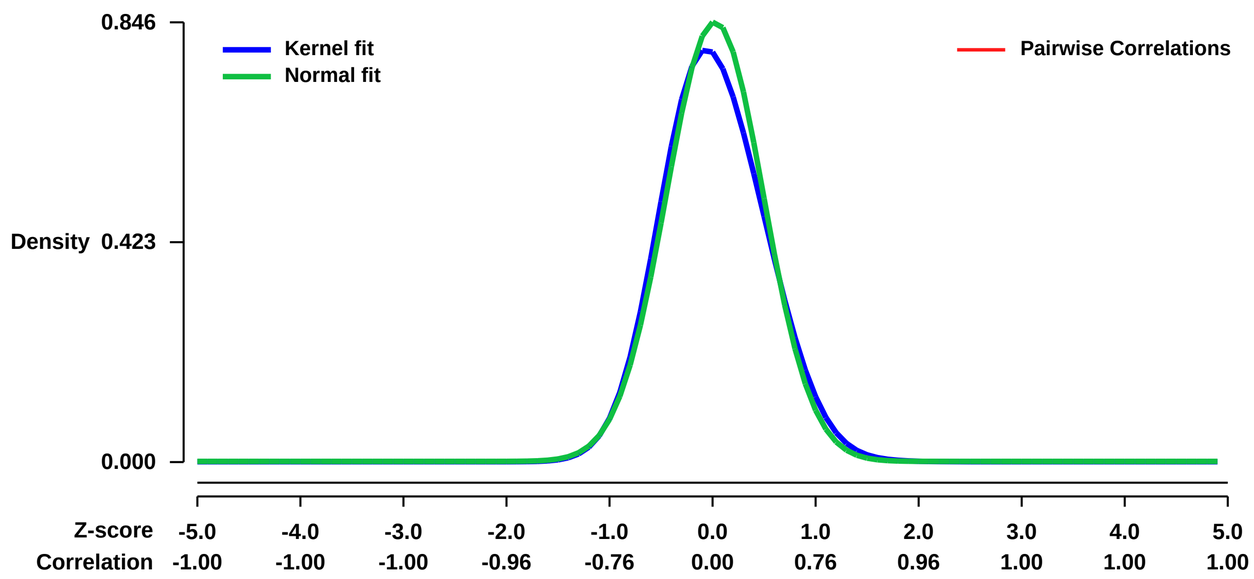

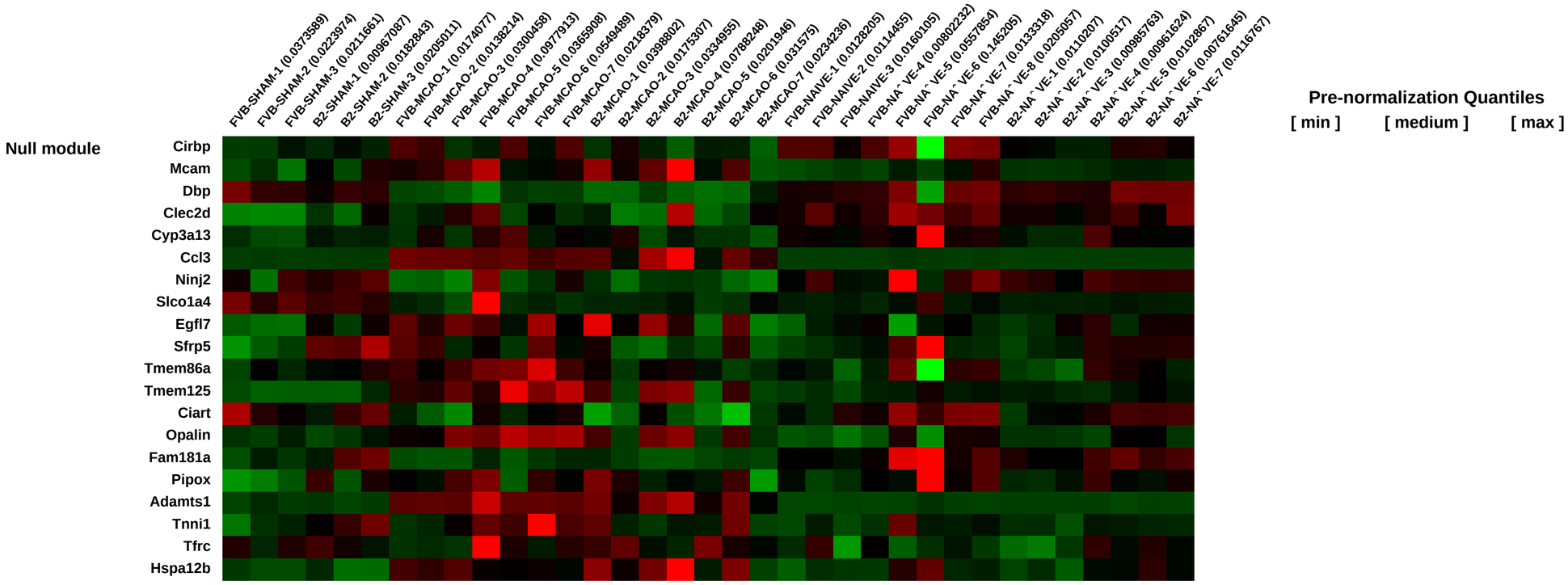

GEO Series "GSE3067" Expression Profiles

Num of samples in this series: 28

Scale of expression profile Z-scores

-3.0 -2.0 -1.0 0.0 1.0 2.0 3.0

GEO Link:	http://www.ncbi.nlm.nih.gov/geo/query/acc.cgi?acc=GSE3067
Status:	Public on Sep 26 2005
Title:	Resistance to thyroid hormone (RTH) and PPARa activation
Organism:	Mus musculus
Experiment type:	Expression profiling by array
Platform:	GPL1261
Pubmed ID:	16985257
Summary & Design:	**Summary:** In this study we used the d337T TRb transgenic mouse that has been created to reproduce the human genetic disease known as resistance to thyroid hormone (RTH) as a model to determine if the d337T TRb mutation would have an effect on PPARa activation. A single amino acid deletion (d337T) abrogates thyroid hormone (T3) binding and transforms the thyroid hormone receptor (TRb) into a constitutive repressor. The principle goal was to determine if T3 regulates myocardial energy metabolism through its nuclear receptors. We introduced a known PPARa activator (WY14, 643) into control and d337T TRb transgenic mice then examined cardiac gene expression using Affymetrix 430_2 expression arrays and RT-PCR. We compared the gene expression of PPARa, RXRb and TRa,b and three PPARa target genes among four studies groups [control, control with WY14, 643, d337T TRb, and d337T TRb with WY14, 643] consisting of seven mice per group. Microarray analysis revealed that these genes responded to the WY14, 643 treatments of control and d337T TRb mice. Analysis of the array and RT-PCR data indicates that mRNA expression levels of PPARa and mRXRb decrease after a six hour drug treatment in both control and d337T TRb mice (P<0.01) as did the array mRNA expression levels for TRa & b (P<0.025). Three target genes (AMPD3, PDK4 and UCP3) of PPARa were up regulated in control and down regulated in the d337T TRb transgenic mouse, indicating a direct action on these metabolic genes when the TRb becomes a repressor. In conclusion, PPARa activation by WY14, 643 has a positive effect on control mice and a negative effect on the TRb transgenic mice which supports our hypothesis that T3 regulates myocardial energy metabolism through its nuclear receptors. **Keywords:** treatment and deletion effects **Overall design:** 7 control, 7 deletion strain individuals, 7 controls with a PPARalpha activator, 7 deletion strain individuals with a PPARalpha activator

Background corr dist: KL-Divergence = 0.4896, L1-Distance = 0.0956, L2-Distance = 0.0315, Normal std = 0.2267

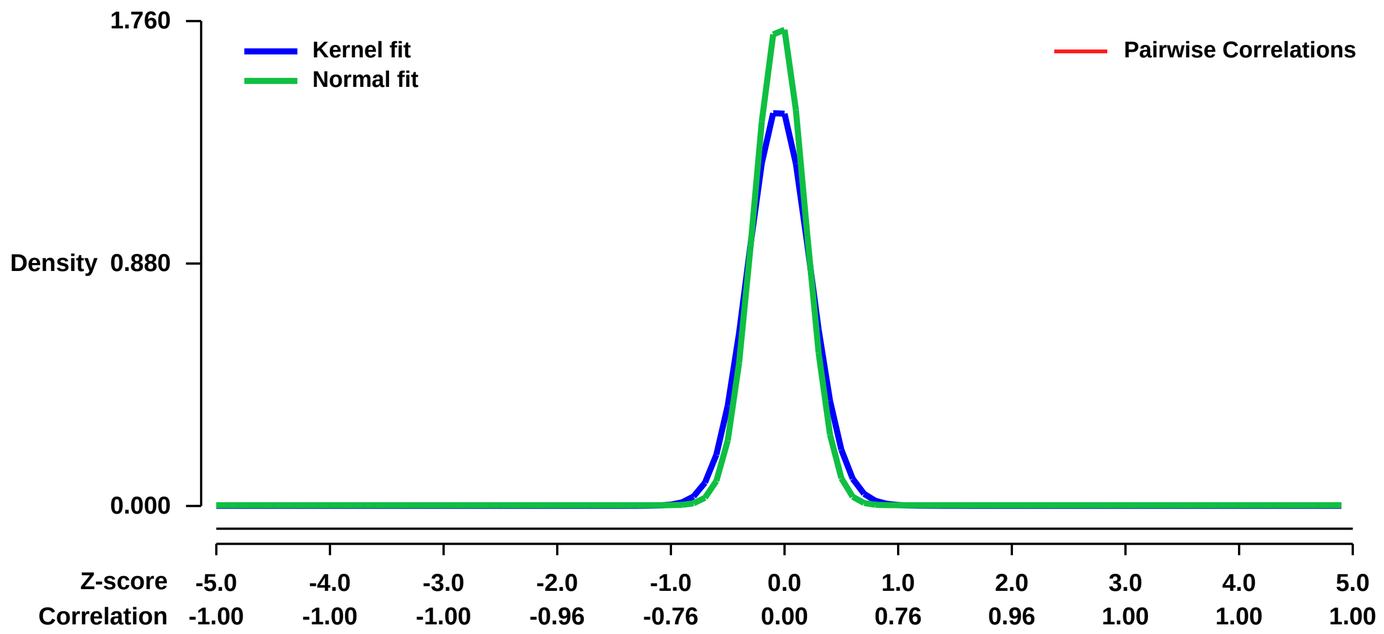

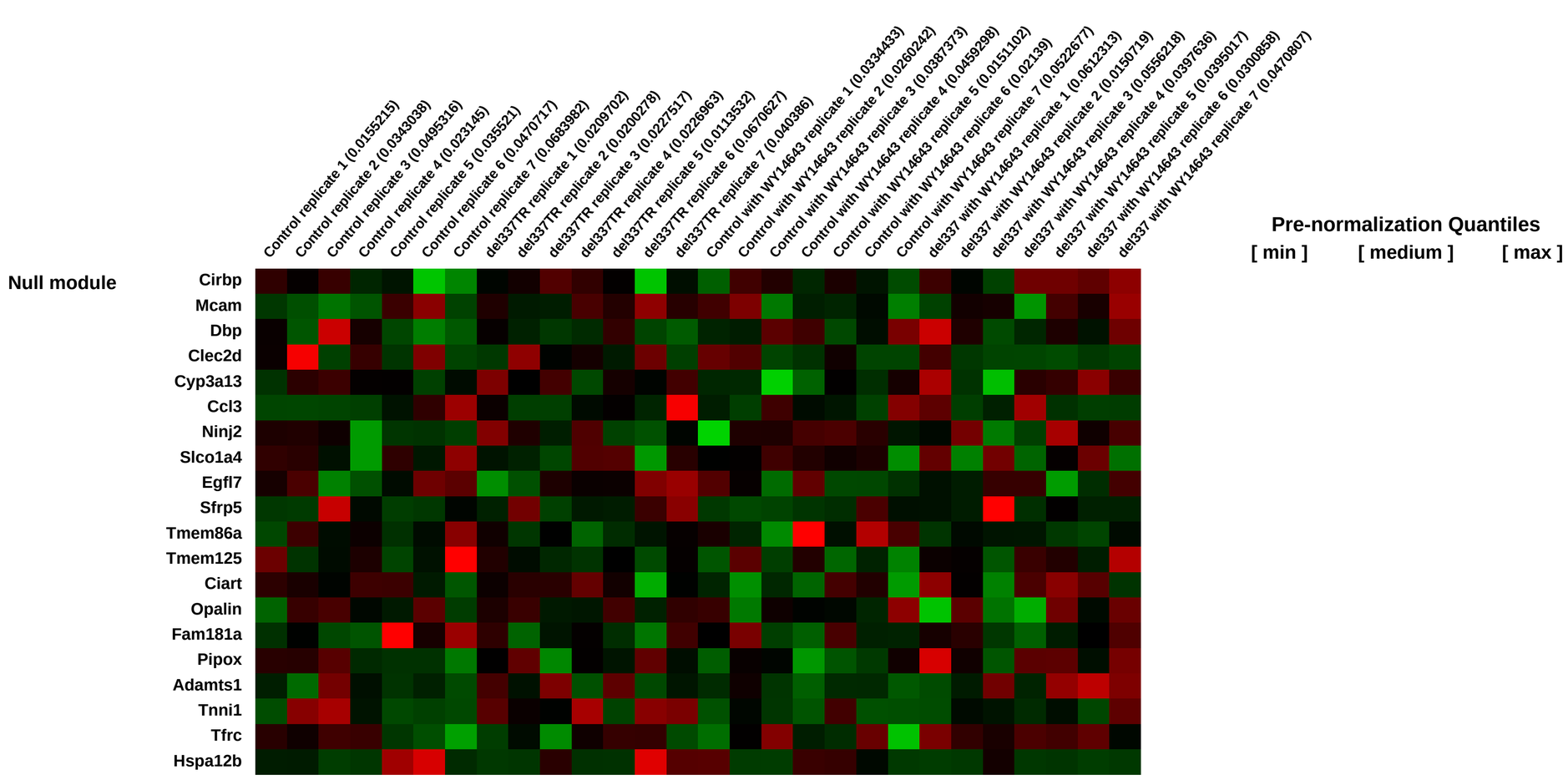

GEO Series "GSE30684" Expression Profiles

Num of samples in this series: 6

Scale of expression profile Z-scores

-3.0 -2.0 -1.0 0.0 1.0 2.0 3.0

GEO Link:	http://www.ncbi.nlm.nih.gov/geo/query/acc.cgi?acc=GSE30684
Status:	Public on Feb 16 2012
Title:	Stem Cell Antigen-1 (Sca-1) Regulates Mammary Tumor Development and Cell Migration
Organism:	Mus musculus
Experiment type:	Expression profiling by array
Platform:	GPL1261
Pubmed ID:	22140470
Summary & Design:	**Summary:** Stem cell antigen-1 (Sca-1 or Ly6A) is a member of the Ly6 family of glycosyl phostidylinositol (GPI)-anchored cell surface proteins. To determine the potential mechanisms by which Sca-1 regulates cell migration, adhesion, and tumor development; we performed an Affymetrix mouse genome 430A 2.0 array on cDNA comparing shLuc and shSca-1 from cells grown in vitro. **Overall design:** We performed an Affymetrix mouse genome 430A 2.0 array on cDNA comparing shLuc and shSca-1 from cells grown in vitro. Experimental groups were profiled in biological triplicate.

Background corr dist: KL-Divergence = 0.0380, L1-Distance = 0.0371, L2-Distance = 0.0017, Normal std = 0.6765

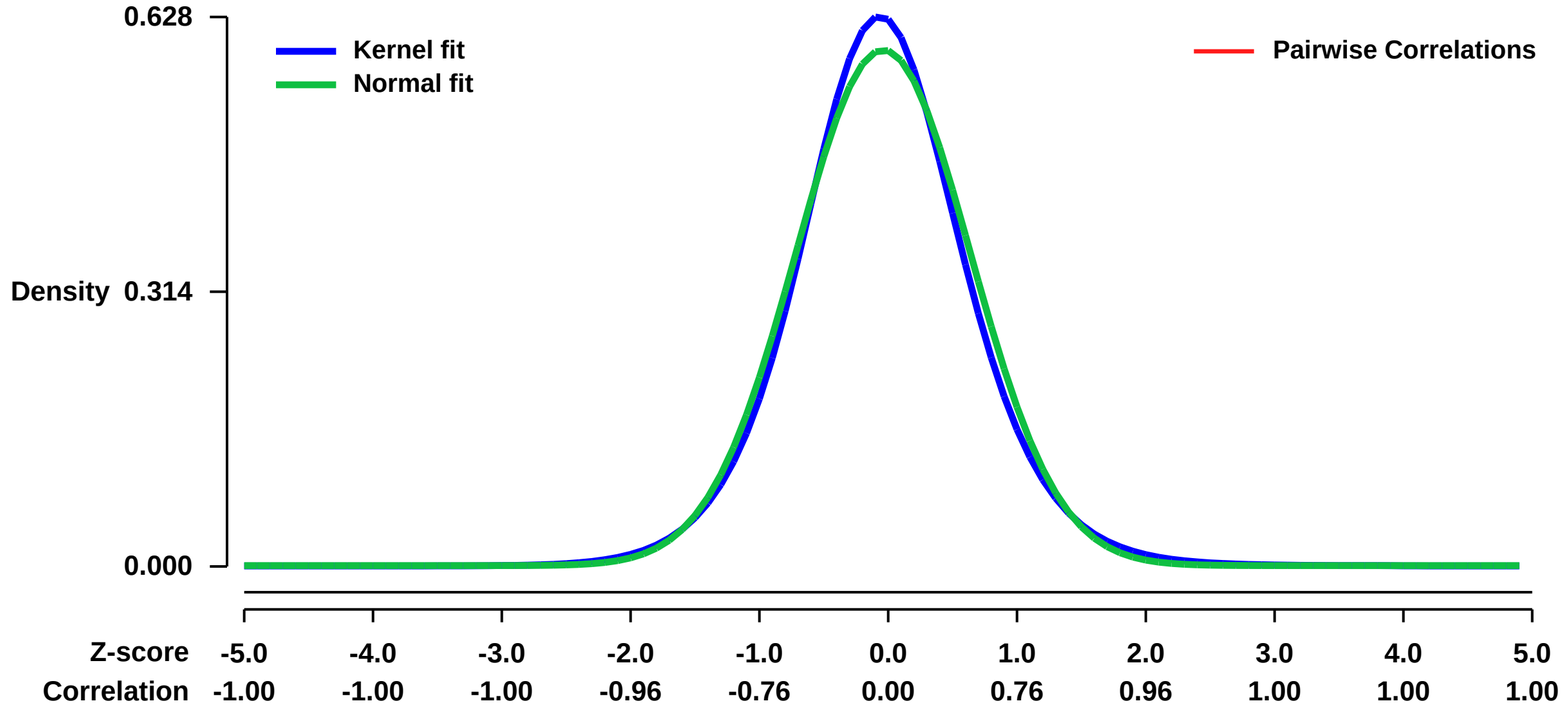

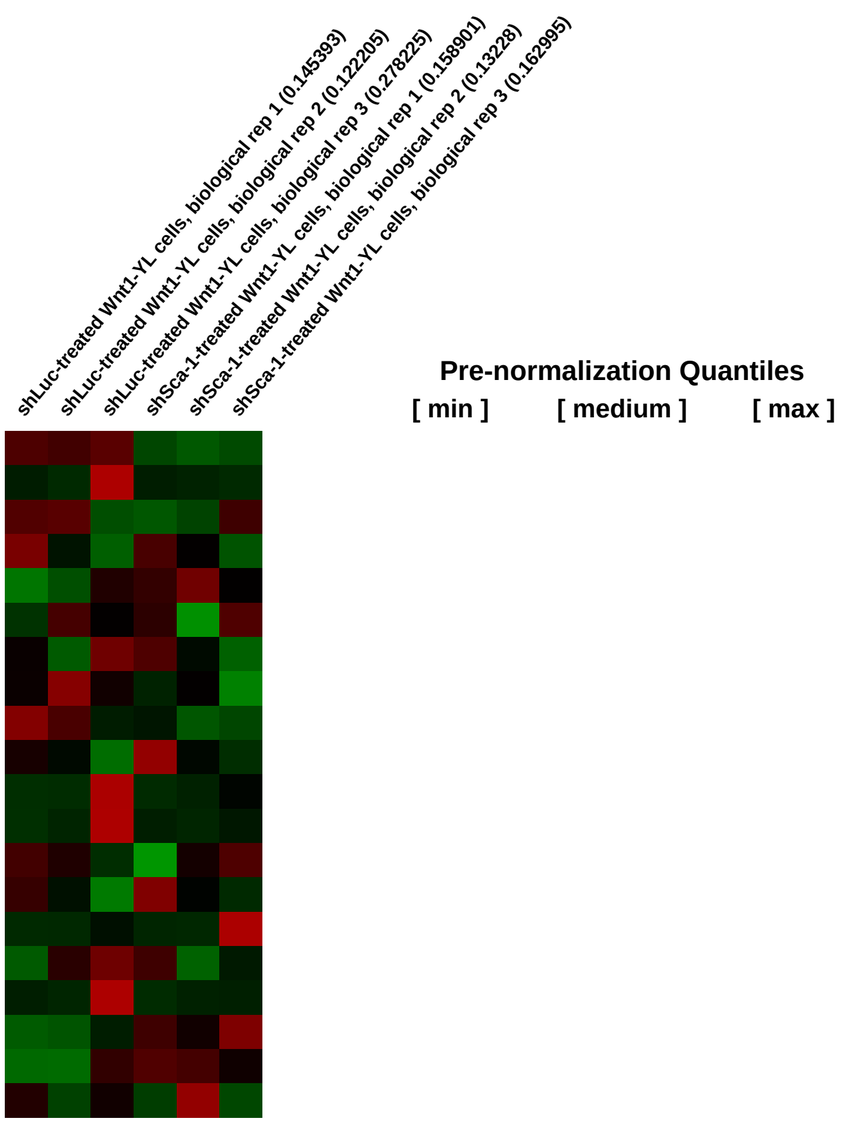

GEO Series "GSE30688" Expression Profiles

Num of samples in this series: 9

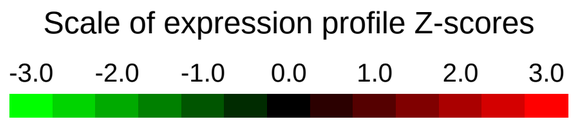

GEO Link:	**http://www.ncbi.nlm.nih.gov/geo/query/acc.cgi?acc=GSE30688**
Status:	**Public on Jul 15 2011**
Title:	**Gene expression profiles of mouse sentinel lymph nodes (SLNs) in xenotransplanted and non tumor bearing CB17 SCID.**
Organism:	**Mus musculus**
Experiment type:	**Expression profiling by array**
Platform:	**GPL1261**
Pubmed ID:	
Summary & Design:	**Summary:** **Cutaneous melanoma first metastasizes into sentinel lymph nodes that control the lymphatic drain from the area of the primary tumor. This observation is used clinically for melanoma patients with primary melanomas thicker than 1mm (tumor stage â¥T2a), for these patients sentinel lymph node biopsy has become an important and routinely performed diagnostic procedure. The importance of sentinel node analysis is reflected by a significant better prognosis of melanoma patients with tumor free sentinel nodes compared to patients with metastatic sentinel nodes. Although intensively studied, not much is known about mechanisms responsible for the development of melanoma metastasis.To analyze gene expression in mouse SLNs of M24met tumor bearing animals as compared to tumor free control animals, SLNs were taken at different time points and analyzed for the presence of human M24met to classify SLNs into control, negative, macro metastatic SLN. After categorized SLNs were subjected to microarray analysis.** **Overall design:** **To analyze gene expression in mouse SLNs of human M24met tumor bearing animals as compared to tumor free control animals, SLNs were taken at different time points and analyzed for the presence of human M24met to classify SLNs into control, negative, macro metastatic SLN. Briefly, explanted SLNs were stored in RNA later (Ambion, Austin, TX) and DNA as well as RNA was extracted using AllPrep DNA/RNA Mini Kit and RNeasy Micro Kit (Qiagen, Valencia, CA) according to manufacturerâ s instructions. To detect human cells in mouse SLNs we used a polymerase chain reaction method for the detection of a human-specific 850-bp fragment of the alpha-satellite DNA on human chromosome 17. For analysis of gene expression RNA from control SLN from tumor free animals (control), RNA from tumor negative SLN (negative), and RNA from macro metastatic SLN (positive) from tumor bearing animals was used to analyze gene expression on Mouse Genome 430A 2.0 Arrays (Affymetrix, Santa Clara, CA)**

Background corr dist: KL-Divergence = 0.0518, L1-Distance = 0.0285, L2-Distance = 0.0014, Normal std = 0.5507

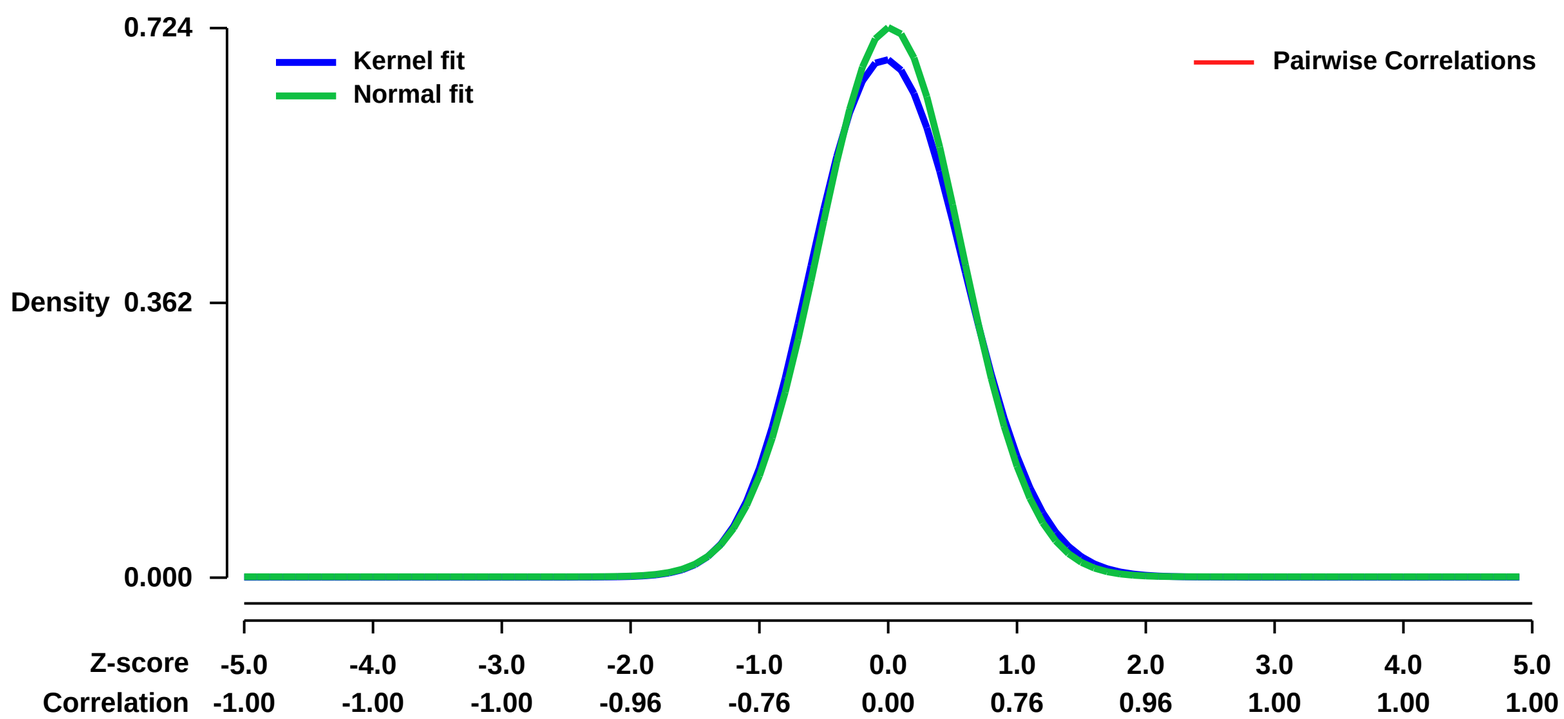

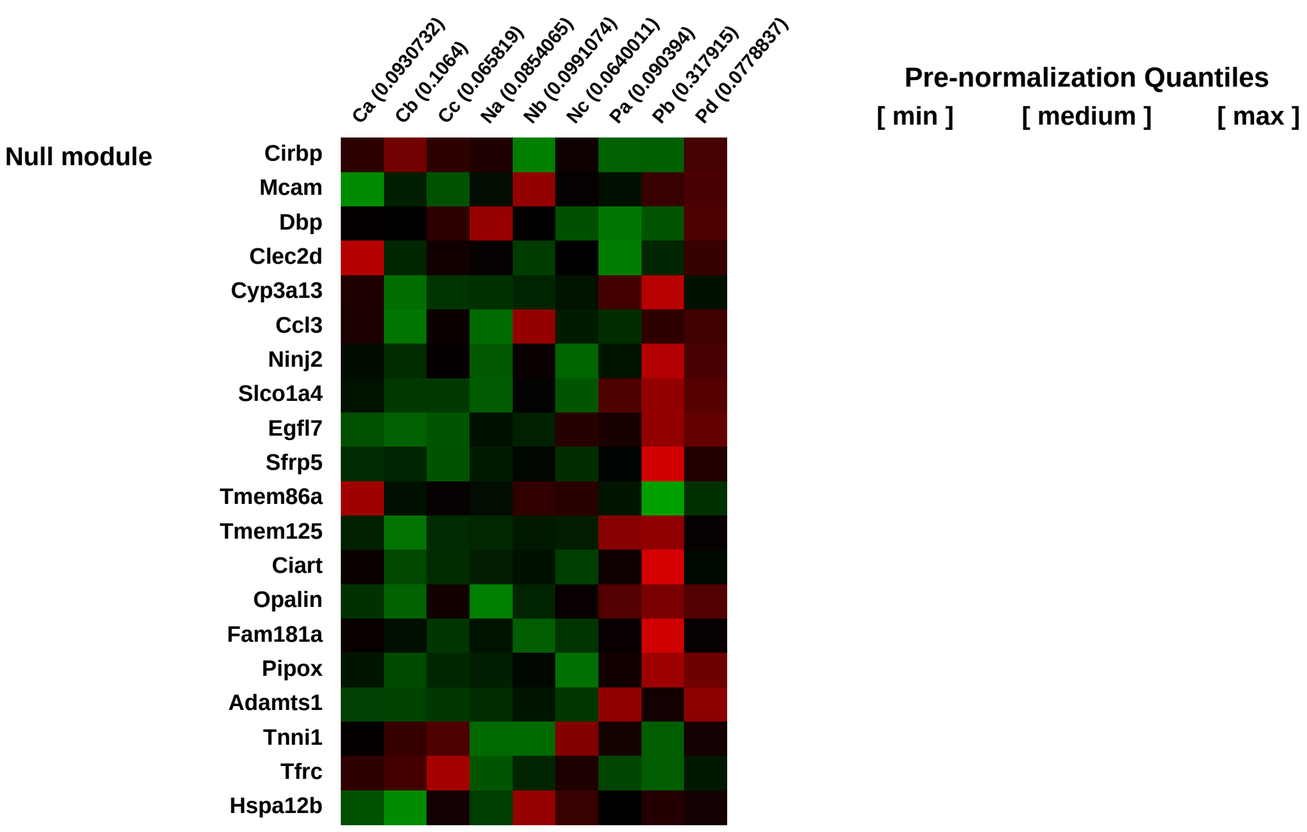

GEO Series "GSE30744" Expression Profiles

Num of samples in this series: 6

Scale of expression profile Z-scores

-3.0 -2.0 -1.0 0.0 1.0 2.0 3.0

GEO Link:	http://www.ncbi.nlm.nih.gov/geo/query/acc.cgi?acc=GSE30744
Status:	Public on Jul 23 2011
Title:	Expression analysis of haploid and diploid ES cells in 2i medium
Organism:	Mus musculus
Experiment type:	Expression profiling by array
Platform:	GPL1261
Pubmed ID:	21900896
Summary & Design:	**Summary:** gene expression differences were analysed between haploid and diploid ES cells **Overall design:** biological triplicates of haploid and diploid ES cell lines were analysed on an Affymetrix GeneChip 430 array

Background corr dist: KL-Divergence = 0.0237, L1-Distance = 0.0121, L2-Distance = 0.0002, Normal std = 0.7036

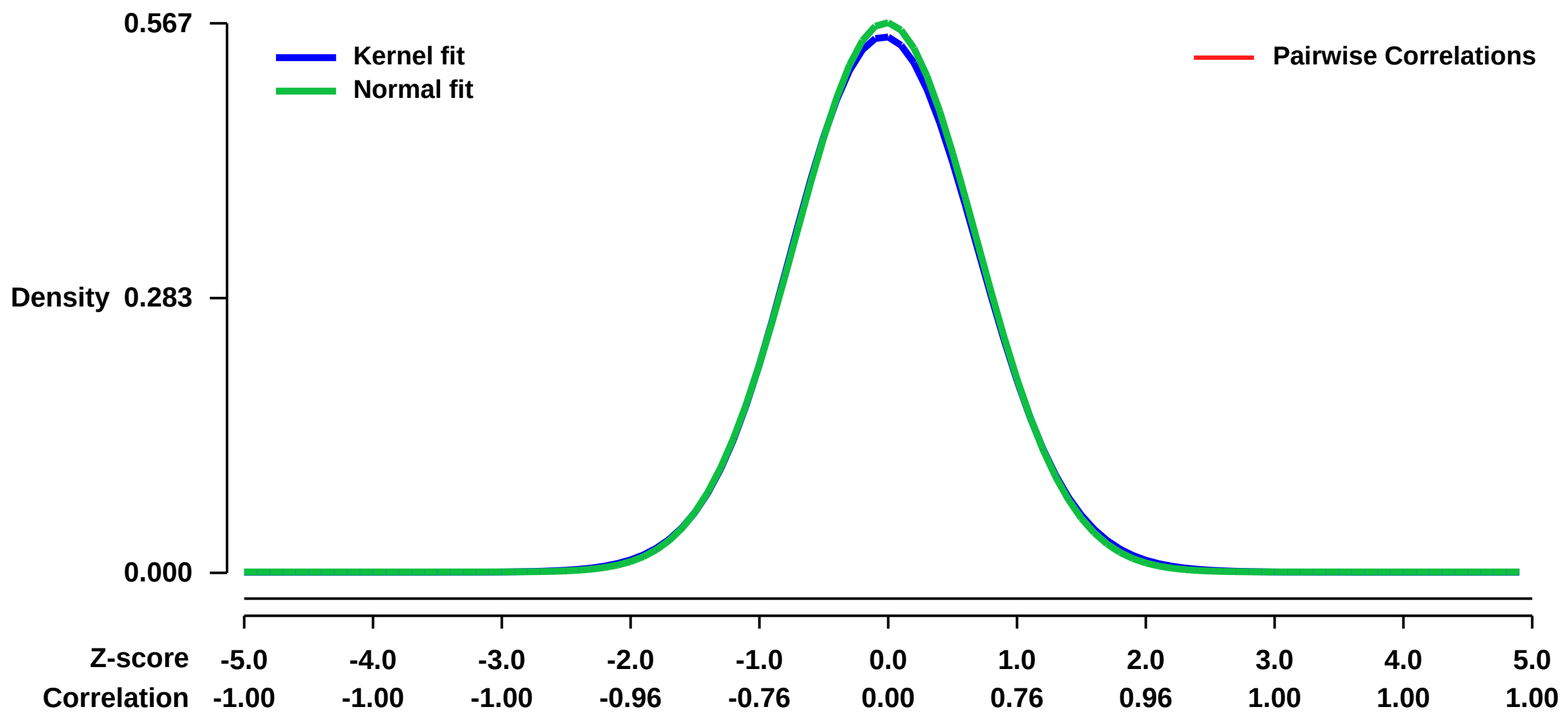

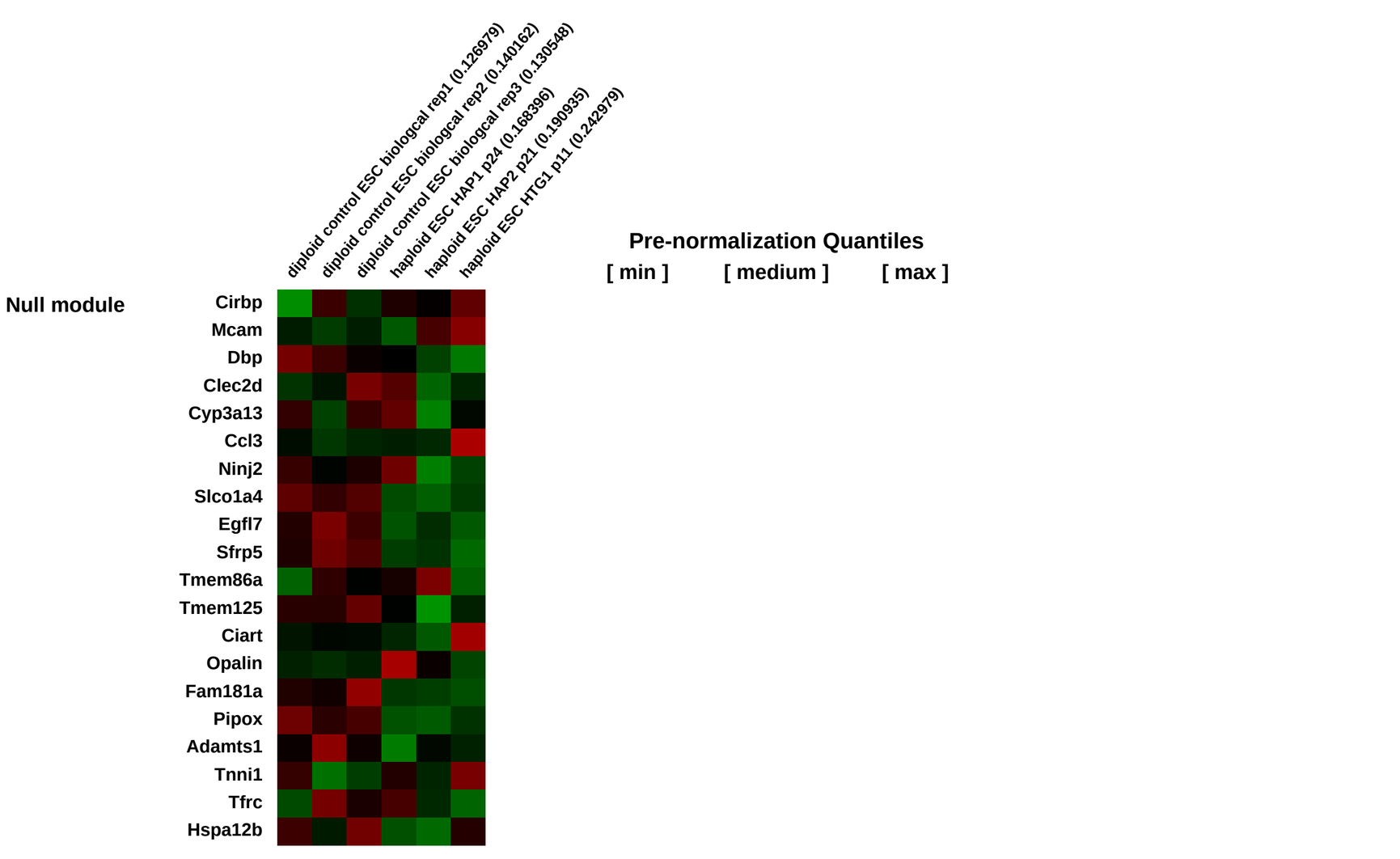

GEO Series "GSE30746" Expression Profiles

Num of samples in this series: 16

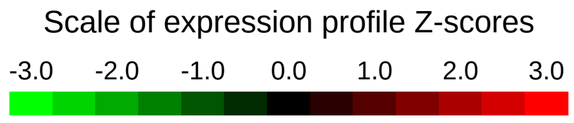

GEO Link:	http://www.ncbi.nlm.nih.gov/geo/query/acc.cgi?acc=GSE30746
Status:	Public on Aug 05 2011
Title:	Expression data from murine Tet-off MLL-AF9/Ras acute myeloid leukemia cell lines following withdrawal of MLL-AF9
Organism:	Mus musculus
Experiment type:	Expression profiling by array
Platform:	GPL1261
Pubmed ID:	21828272
Summary & Design:	**Summary:** To explore oncogene addiction programs in a genetically defined leukemia context we developed an AML mouse model driven by a conditional MLL-AF9 allele together with oncogenic Ras, which enabled us to examine the consequences of MLL-AF9 inhibition in established disease. In order to produce a tightly regulated system that was easy to monitor, we constructed two retroviral vectors containing dsRed-linked MLL-AF9 under control of a tetracycline response element promoter, and KrasG12D or NrasG12D linked to the â Tet-offâ tet-transactivator, which activates TRE expression in a doxycycline repressible manner. Leukemias were generated by retroviral cotransduction of both vectors into hematopoietic stem and progenitor cells, which were transplanted into syngeneic mice. Cells harboring both constructs induced aggressive myelomonocytic leukemia. Five independent primary leukemia cell lines were established from bone marrow of terminal mice. Treatment of these lines with doxycycline rapidly turned off MLL-AF9 expression, and induced terminal myeloid differentiation and complete disease remission in vivo. To identify molecular mechanisms underlying addiction to MLL-AF9, we analyzed global gene expression changes following doxycycline-induced suppression of MLL-AF9. **Overall design:** Independent primary acute myeloid leukemia lines induced by cotransduction of Tet-off MLL-AF9 together with either KrasG12D or NrasG12D were grown in culture and treated with doxycycline for 6 days to inactivate MLL-AF9 expression. In addition, primary acute myeloid leukemia lines with constitutive MLL-AF9 and KrasG12D were included to control for the effects of doxycycline. Untreated and treated cells were harvested for RNA extraction and hybridization to Affymetrix arrays.

Background corr dist: KL-Divergence = 0.0602, L1-Distance = 0.0548, L2-Distance = 0.0054, Normal std = 0.5458

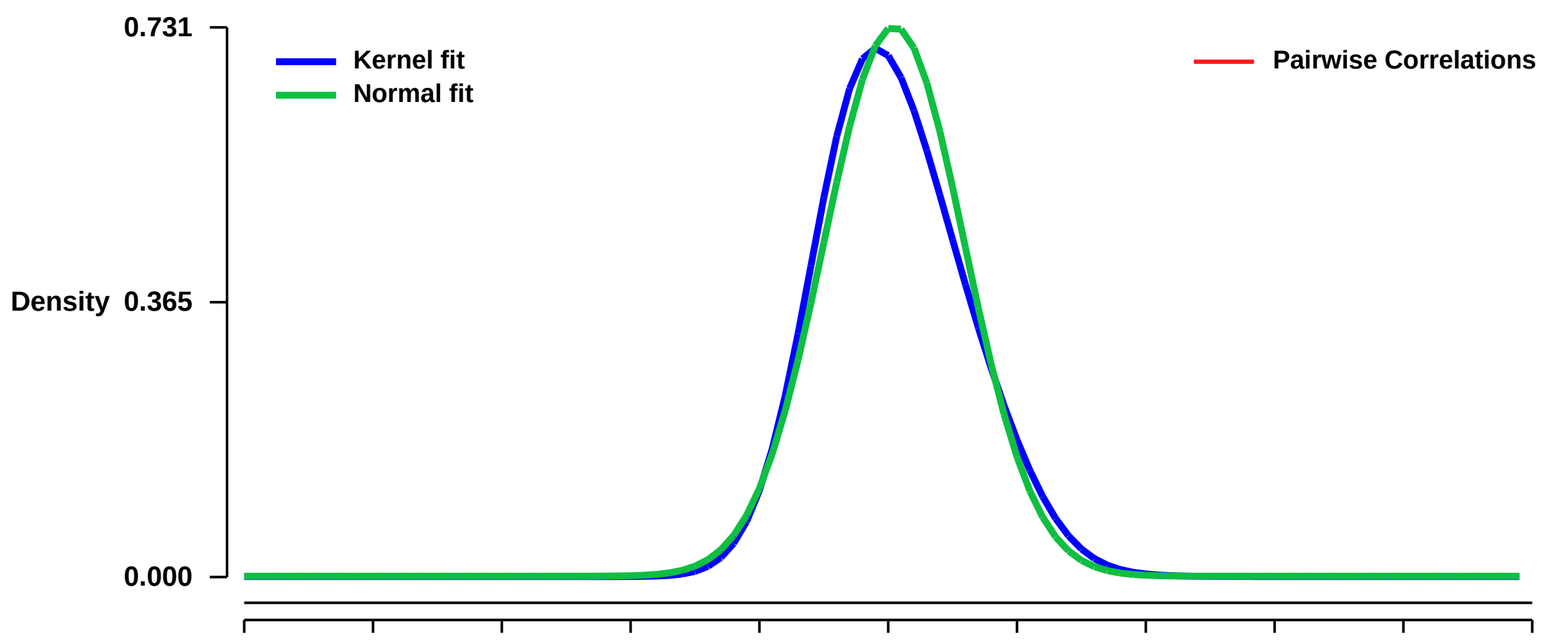

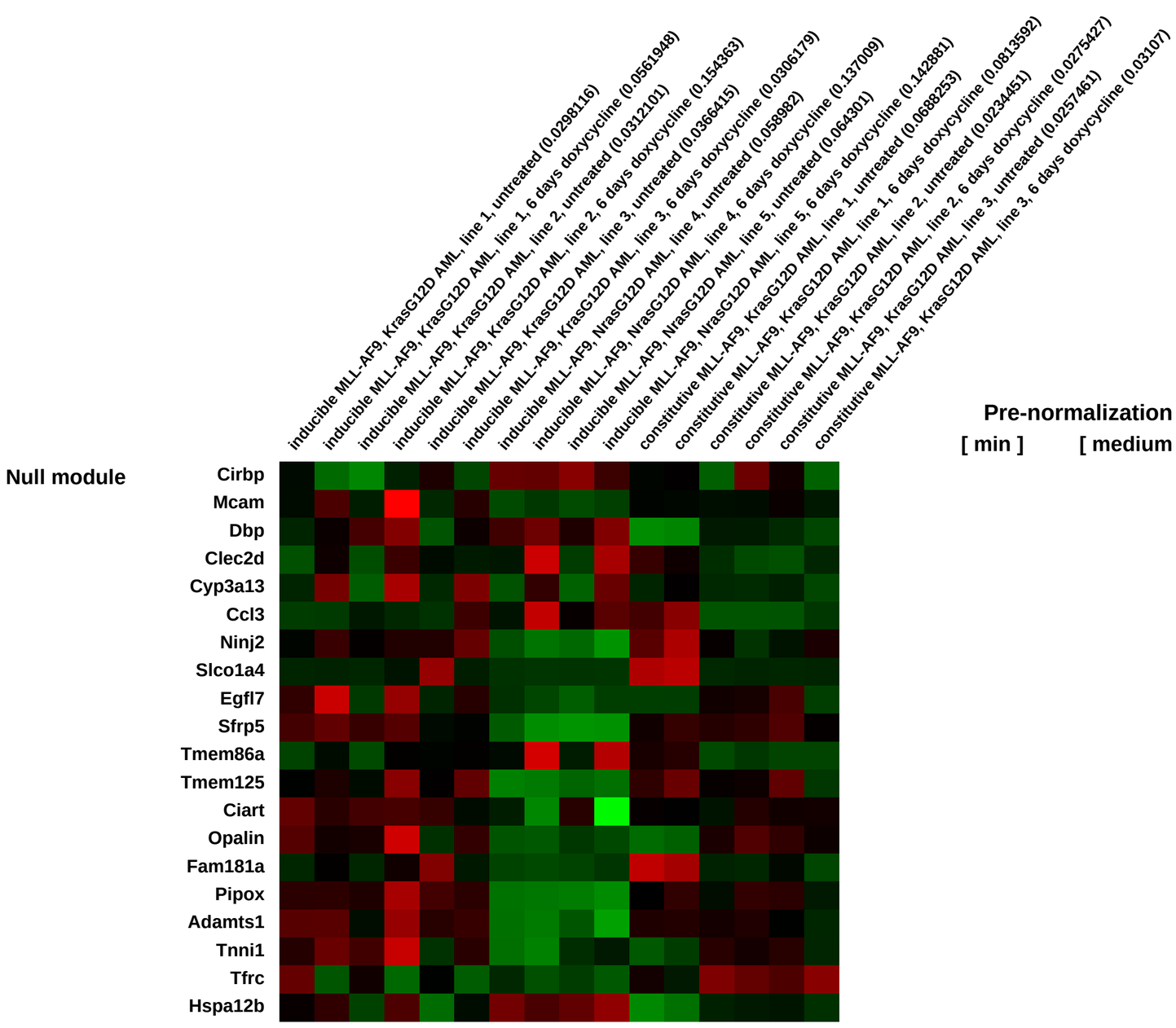

GEO Series "GSE30767" Expression Profiles

Num of samples in this series: 8

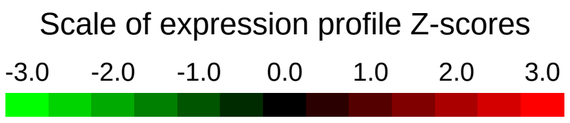

GEO Link:	http://www.ncbi.nlm.nih.gov/geo/query/acc.cgi?acc=GSE30767
Status:	Public on Dec 01 2011
Title:	Vascular endothelial growth factor (VEGF) isoform regulation of early forebrain development
Organism:	Mus musculus
Experiment type:	Expression profiling by array
Platform:	GPL1261
Pubmed ID:	21803034
Summary & Design:	**Summary:** This work was designed to determine the role of the vascular endothelial growth factor A (VEGF) isoforms during early neuroepithelial development in the mammalian central nervous system (CNS), specifically in the forebrain. An emerging model of interdependence between neural and vascular systems includes VEGF, with its dual roles as a potent angiogenesis factor and neural regulator. Although a number of studies have implicated VEGF in CNS development, little is known about the role that the different VEGF isoforms play in early neurogenesis. We used a mouse model of disrupted VEGF isoform expression that eliminates the predominant brain isoform, VEGF164, and expresses only the diffusible form, VEGF120. We tested the hypothesis that VEGF164 plays a key role in controlling neural precursor populations in developing cortex. We used microarray analysis to compare gene expression differences between wild type and VEGF120 mice at E9.5, the primitive stem cell stage of the neuroepithelium. We quantified changes in PHH3-positive nuclei, neural stem cell markers (Pax6 and nestin) and the Tbr2-positive intermediate progenitors at E11.5 when the neural precursor population is expanding rapidly. Absence of VEGF164 (and VEGF188) leads to reduced proliferation without an apparent effect on the number of Tbr2-positive cells. There is a corresponding reduction in the number of mitotic spindles that are oriented parallel to the ventricular surface relative to those with a vertical or oblique angle. These results support a role for the VEGF isoforms in supporting the neural precursor population of the early neuroepithelium. **Overall design:** Four samples each of E9.5 wildtype or VEGF120 mouse forebrain were analyzed with the Mouse 430 2.0 Affymetrix GeneChip

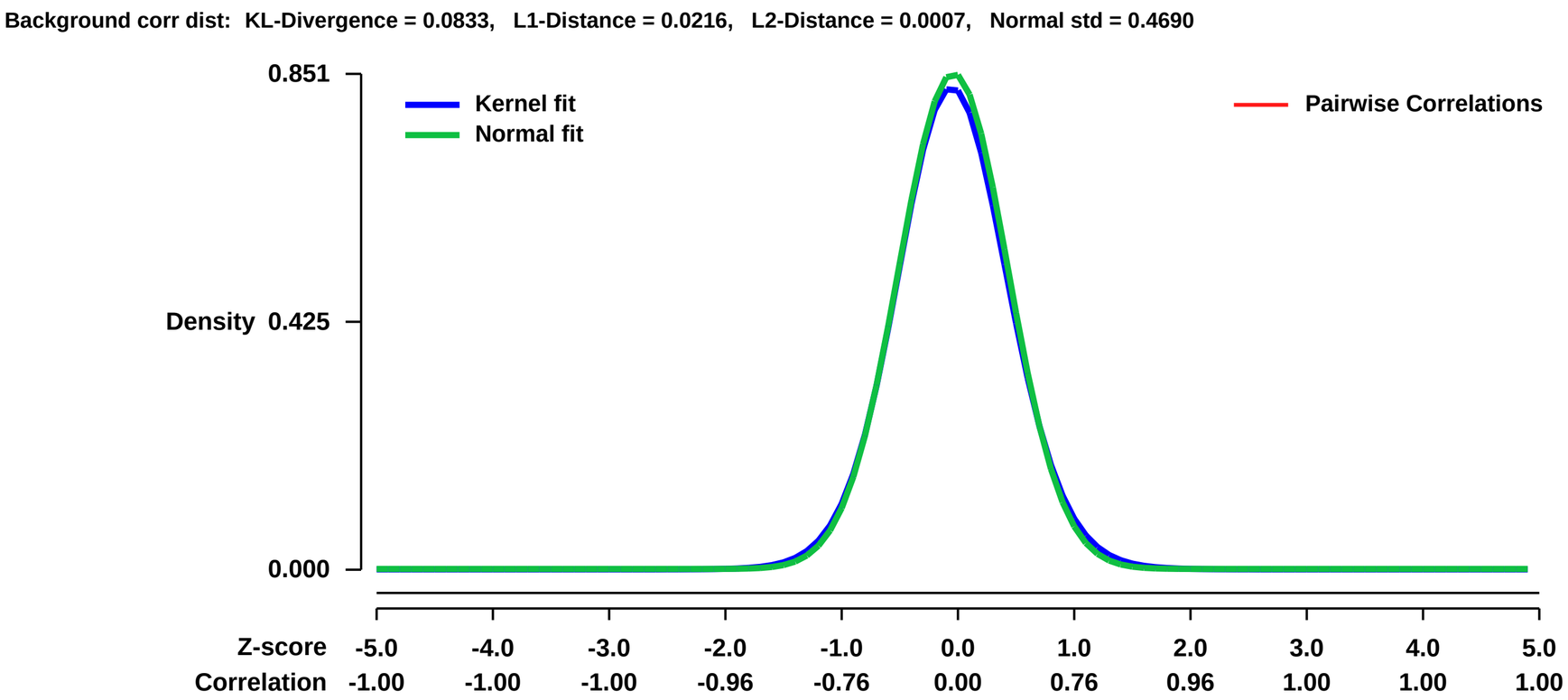

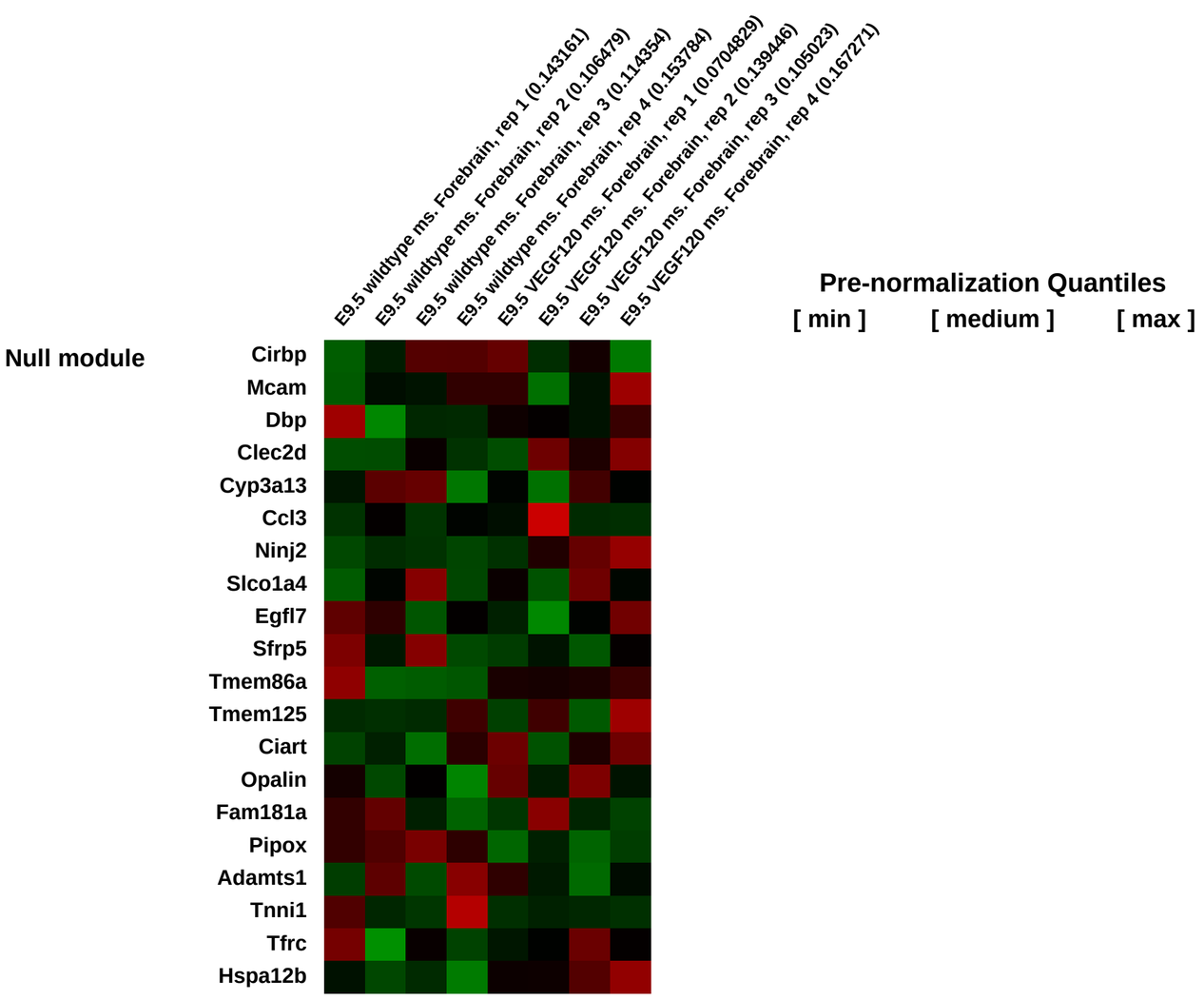

GEO Series "GSE30852" Expression Profiles

Num of samples in this series: 6

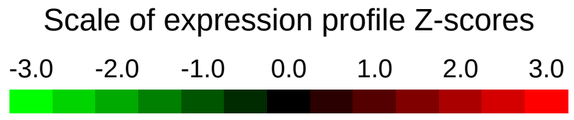

GEO Link:	http://www.ncbi.nlm.nih.gov/geo/query/acc.cgi?acc=GSE30852
Status:	Public on Sep 02 2011
Title:	Expression data from Bmi1 mutant versus wild-type lung cells
Organism:	Mus musculus
Experiment type:	Expression profiling by array
Platform:	GPL1261
Pubmed ID:	21885022
Summary & Design:	**Summary:** **Bmi1 is an important stem cell regulator in multiple tissues, including the lung.** **We used microarrays to analyze the dysregulation of gene expression in the absence of Bmi1 in the lung, to identify pathways important in Bmi1-dependent lung stem cell regulation** **Overall design:** **Primary lung cells (CD31-negative, CD45-negative) were FACS-isolated from Bmi1 wild-type or mutant mice; RNA was then extracted, amplified, and analyzed using Affymetrix Mouse Genome 430 2.0 Arrays.**

Background corr dist: **KL-Divergence = 0.0439, L1-Distance = 0.0208, L2-Distance = 0.0005, Normal std = 0.5988**

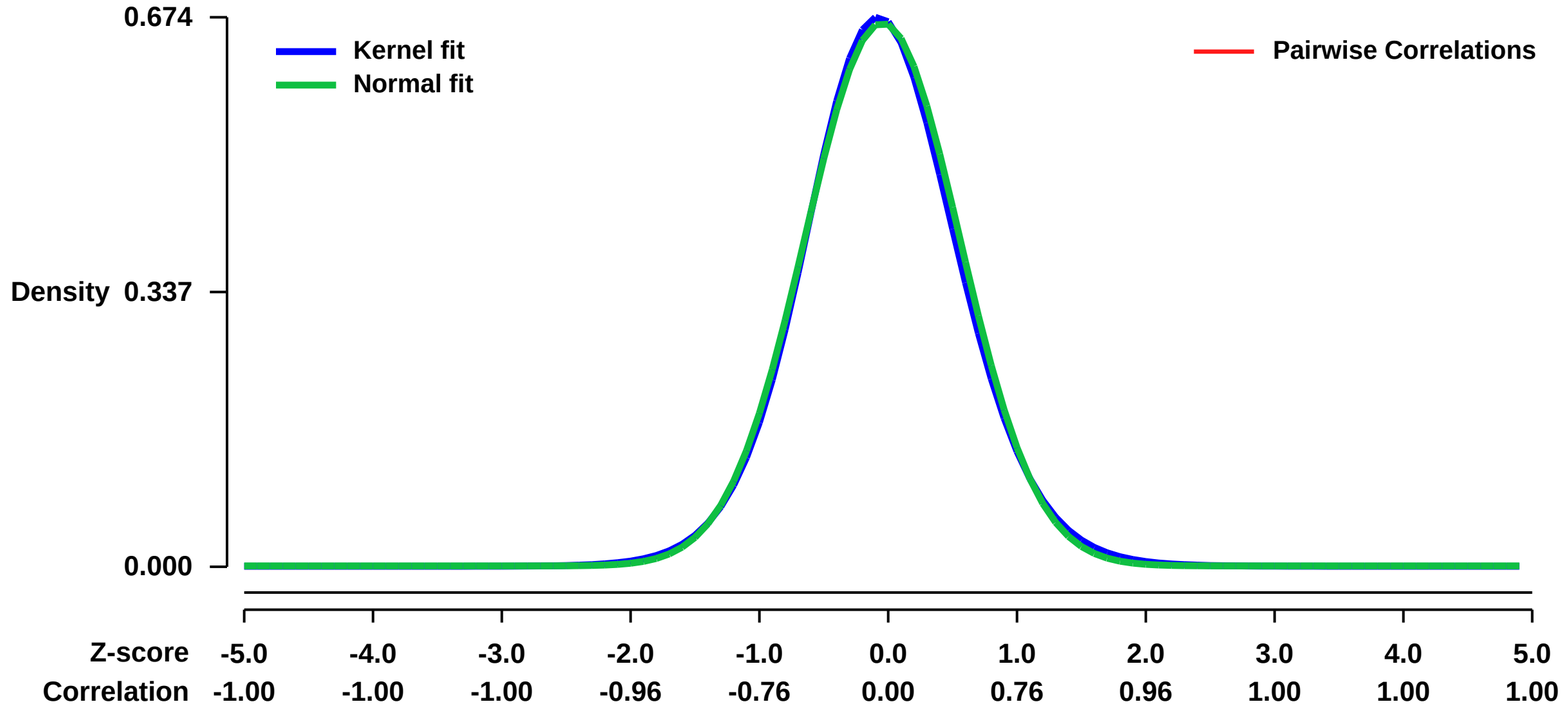

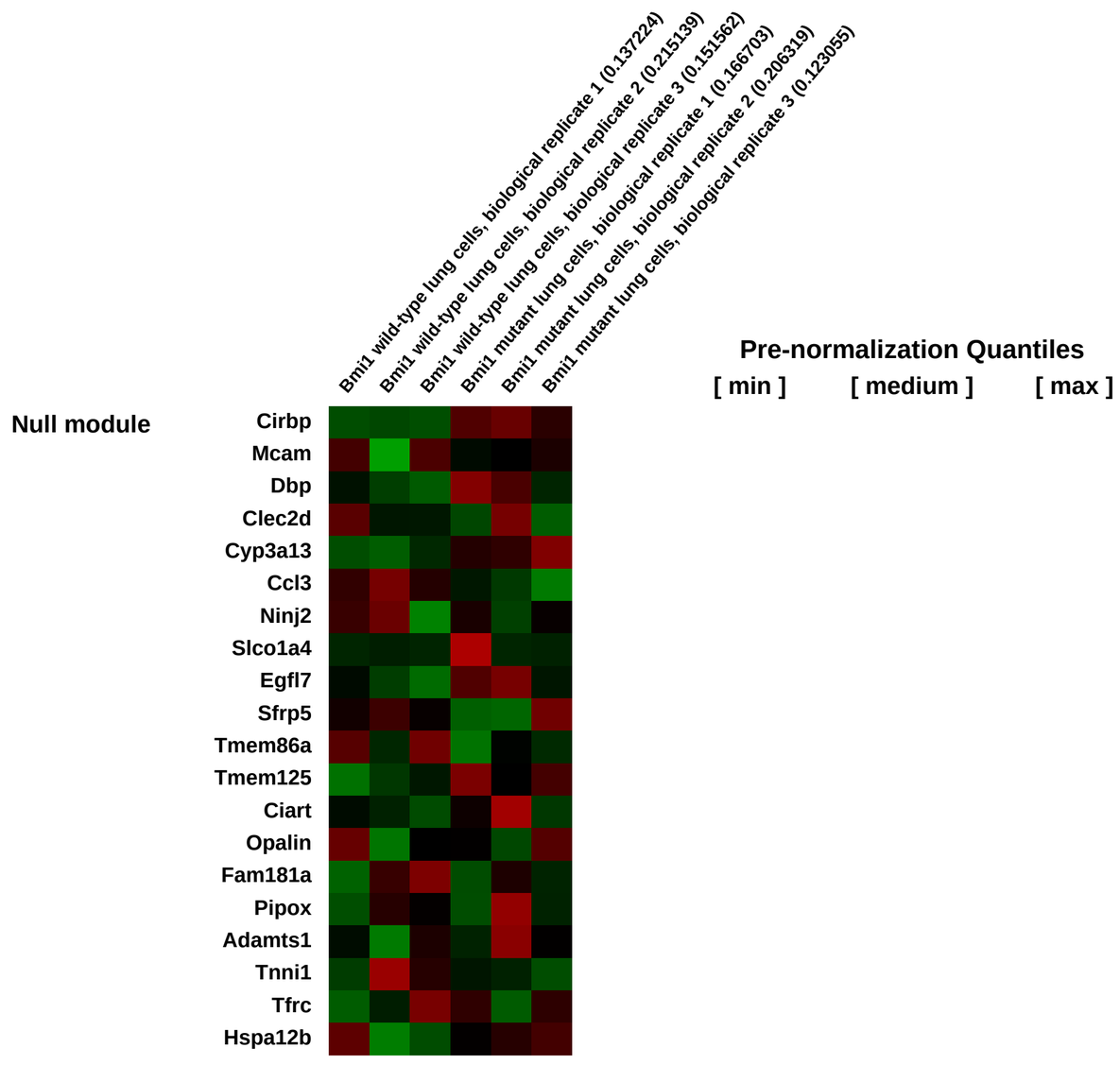

GEO Series "GSE30855" Expression Profiles

Num of samples in this series: 6

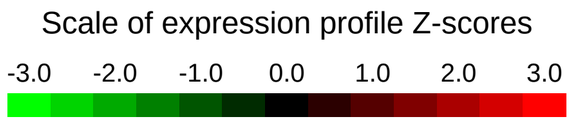

GEO Link:	http://www.ncbi.nlm.nih.gov/geo/query/acc.cgi?acc=GSE30855
Status:	Public on Sep 01 2011
Title:	Establishment of Enhancer Repertoires that Orchestrate the Myeloid and Lymphoid Cell Fates (gene expression dataset 1)
Organism:	Mus musculus
Experiment type:	Expression profiling by array
Platform:	GPL1261
Pubmed ID:	21903424
Summary & Design:	**Summary:** Recent studies have documented genome-wide binding patterns of transcriptional regulators and their associated epigenetic marks in hematopoietic cell lineages. In order to determine how epigenetic marks are established and maintained during developmental progression, we have generated long-term cultures of hematopoietic progenitors by enforcing the expression of the E-protein antagonist Id2. Hematopoietic progenitors that express Id2 are multipotent and readily differentiate upon withdrawal of Id2 expression into committed B lineage cells, thus indicating a causative role for E2A in promoting the B cell fate. Genome-wide analyses revealed that a substantial fraction of lymphoid and myeloid enhancers are pre-marked by H3K4me1 in multipotent progenitors. However, H3K4me1 levels at a subset of enhancers are elevated during developmental progression, resulting in evolving enhancer repertoires that we propose orchestrate the myeloid and B cell fates. **Overall design:** To characterize Id2-HPCs, we performed microarray analysis using RNA derived from cultured E2A-deficient cells, EBF-deficient cells and Id2-HPCs. Id2-HPC cells were cultured in IMDM medium supplemented with 10% FCS/2% PSG/¸†-me and IL7, Flt3-ligand, and SCF cytokines on S17 feeder cells in a humidified incubator at 37 degrees C with 5% CO2. Id2-HPC expanded cells were depleted of small (<1-5%) numbers of CD19-, CD25- and CD11b-positive cells by auto-MACS. E2A -/- and EBF -/- cells were cultured in IMDM supplemented with 10% FCS/2% PSG/¸†-me on S17 feeder cells in the presence of IL-7, Flt3-ligand, and SCF cytokines in a humidified incubator at 37 degree C with 5% CO2.

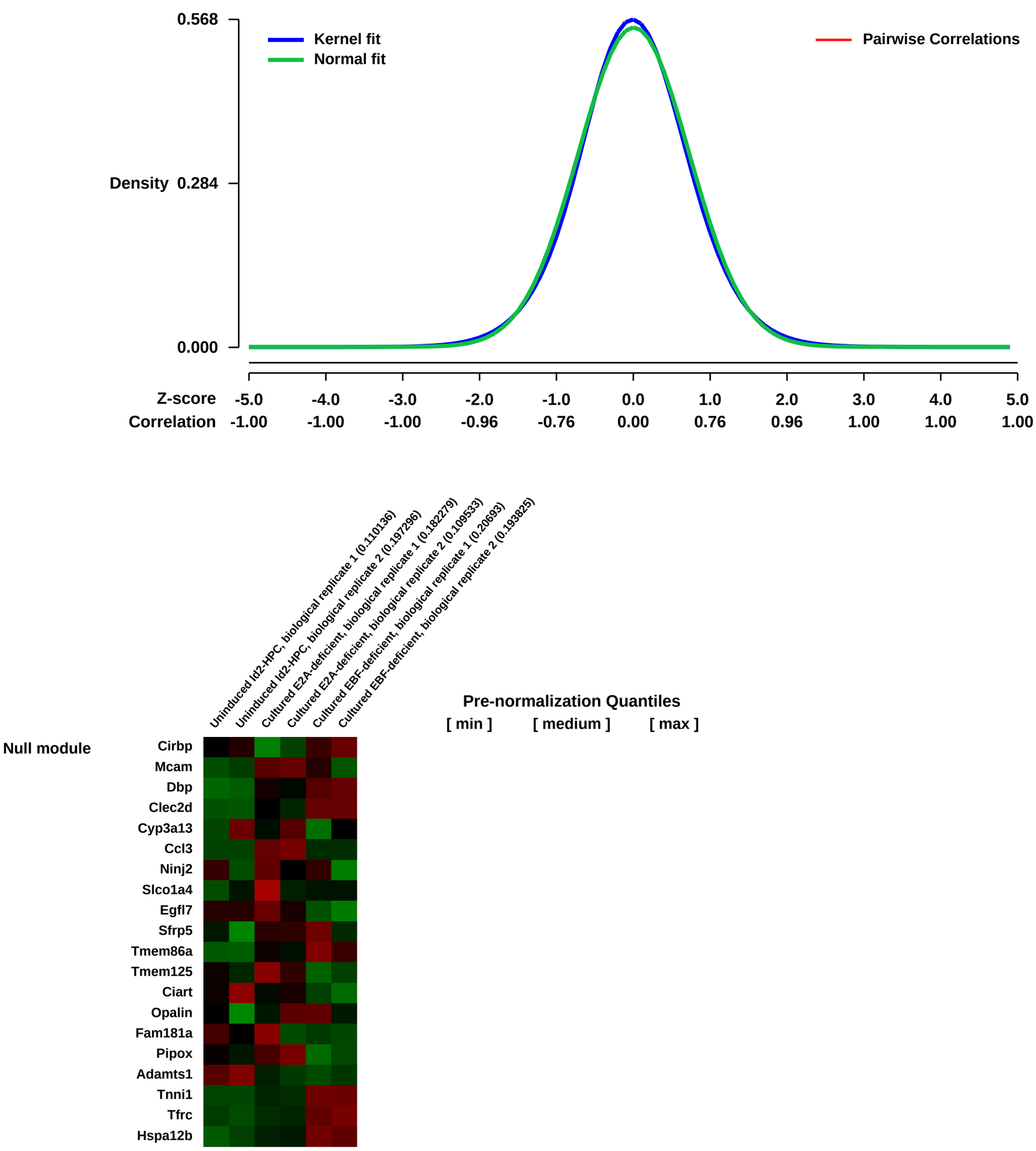

GEO Series "GSE30861" Expression Profiles

Num of samples in this series: 35

Scale of expression profile Z-scores

-3.0 -2.0 -1.0 0.0 1.0 2.0 3.0

GEO Link:	http://www.ncbi.nlm.nih.gov/geo/query/acc.cgi?acc=GSE30861
Status:	Public on Aug 01 2011
Title:	Pathways identified by toxicogenomics analysis reveal the size and dose independency of silica particles-induced toxicity in mice.
Organism:	Mus musculus
Experiment type:	Expression profiling by array
Platform:	GPL1261
Pubmed ID:	
Summary & Design:	**Summary:** Understanding the interactions of nanostructures with biological systems is essential to nanotoxicological research. Using a microarray-based toxicogenomics approach at early stage, this study investigated the relationship between particle size and toxicity of silica particles (SP) with diameters of 30, 70, and 300 nm (SP30, SP70, and SP300) as well as the mechanism of injury in mice. **Overall design:** Two experiments with SiO2 particles of different sizes were considered in mice. One was aimed to investigate the dose-response relationship of SP70 toxicity at a dose of 10, 20, or 40 mg/kg (experiment 1), and the other set to study the size-response relationship of SP-induced toxicity using SP30, SP70, or SP300 (experiment 2). In experiment 2, two dosages each of SP30, SP70, and SP300 were performed. One was 10 mg/kg at three particle sizes, and the other was toxic doses of the three particle sizes, i.e., 10 mg/kg for SP30, 40 mg/kg for SP70, and 200 mg/kg for SP300. The toxic doses of the three particle sizes of SP were decided on the basis of the results of histopathological examinations and serum biochemical analysis in our previous study.n = 5

Background corr dist: KL-Divergence = 0.3288, L1-Distance = 0.0438, L2-Distance = 0.0037, Normal std = 0.2739

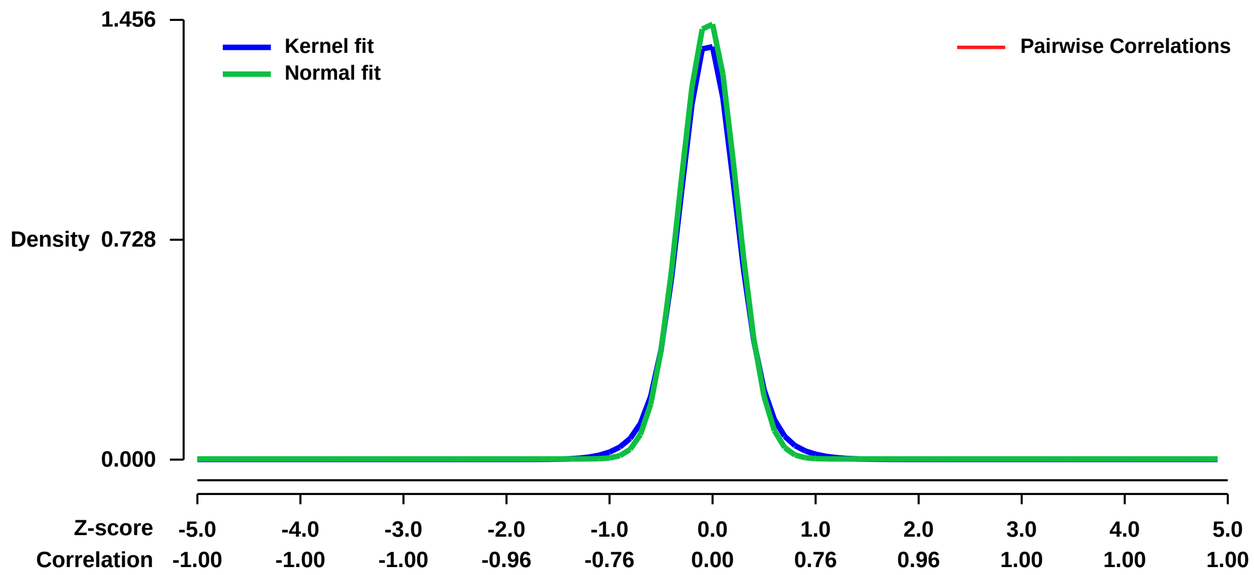

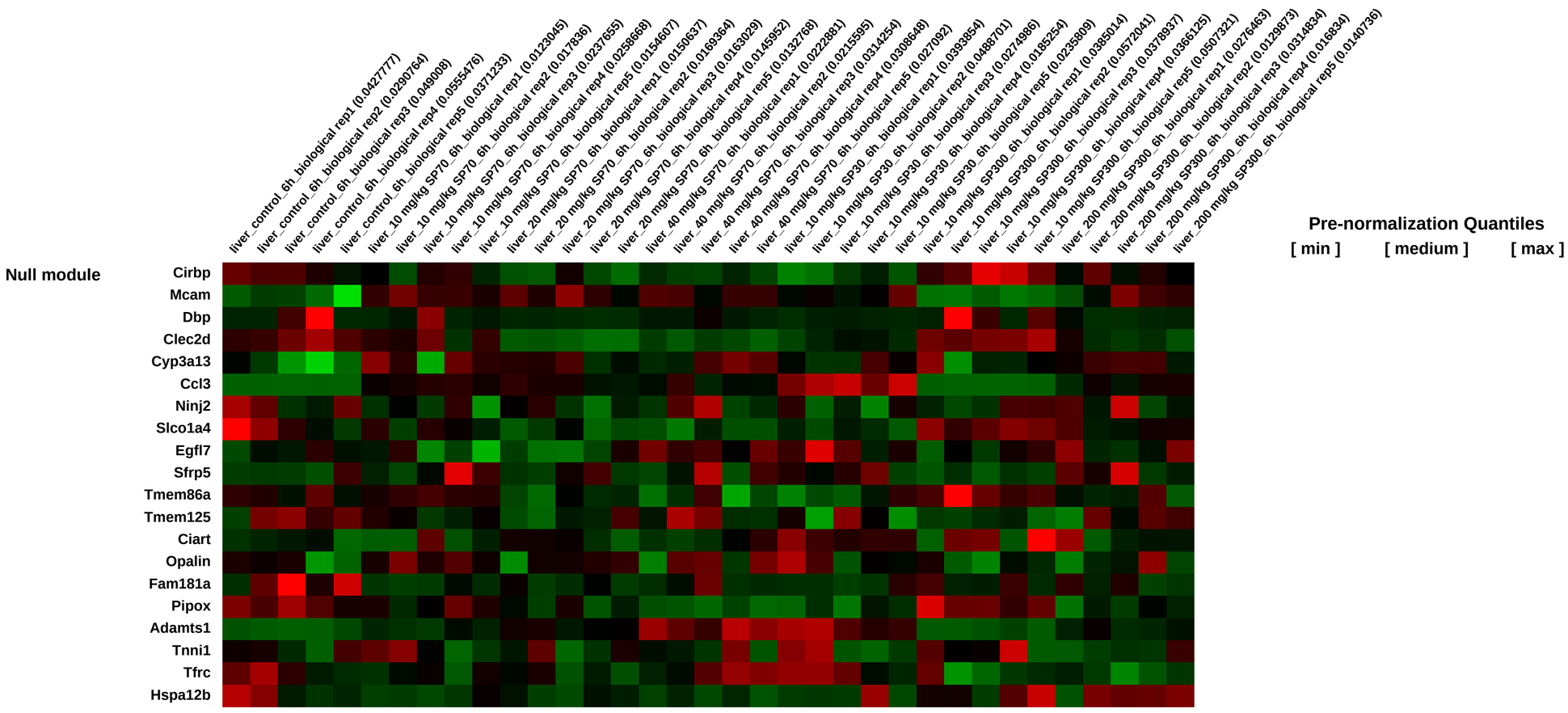

GEO Series "GSE30863" Expression Profiles

Num of samples in this series: 20

Scale of expression profile Z-scores

-3.0 -2.0 -1.0 0.0 1.0 2.0 3.0

GEO Link:	**http://www.ncbi.nlm.nih.gov/geo/query/acc.cgi?acc=GSE30863**
Status:	**Public on Dec 14 2011**
Title:	**Candidate Genes for Panhypopituitarism identified by gene expression profile**
Organism:	**Mus musculus**
Experiment type:	**Expression profiling by array**
Platform:	**GPL1261**
Pubmed ID:	
Summary & Design:	**Summary:** **Prop1 controls the expression of genes besides Pit1 that are important for cell mgration, survival and differentiation in the mouse and human pituitary gland.** **Microarray analysis was used to compare pituitary RNA from newborn Prop1 and Pit1 mutants and their wild type littermates.** **Overall design:** **Total RNA was collected and pooled from Prop1df/df, Porp1+/+, Pit1dw/dw, and Pit+/+ at the age of P1. 5 pools per genotype were hybridized to the Affymetrix Mouse Genome 430 2.0 array.**

Background corr dist: **KL-Divergence = 0.1694, L1-Distance = 0.0448, L2-Distance = 0.0044, Normal std = 0.3551**

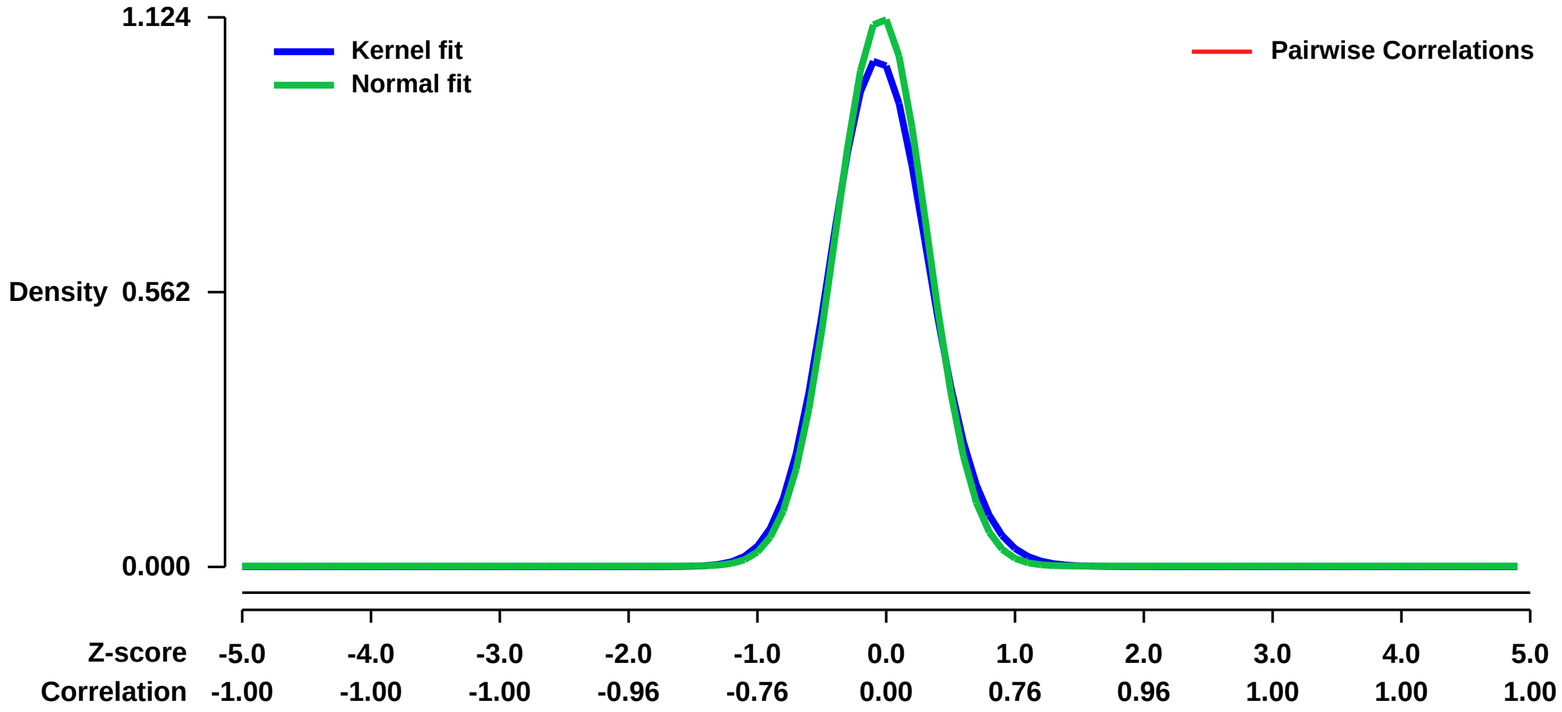

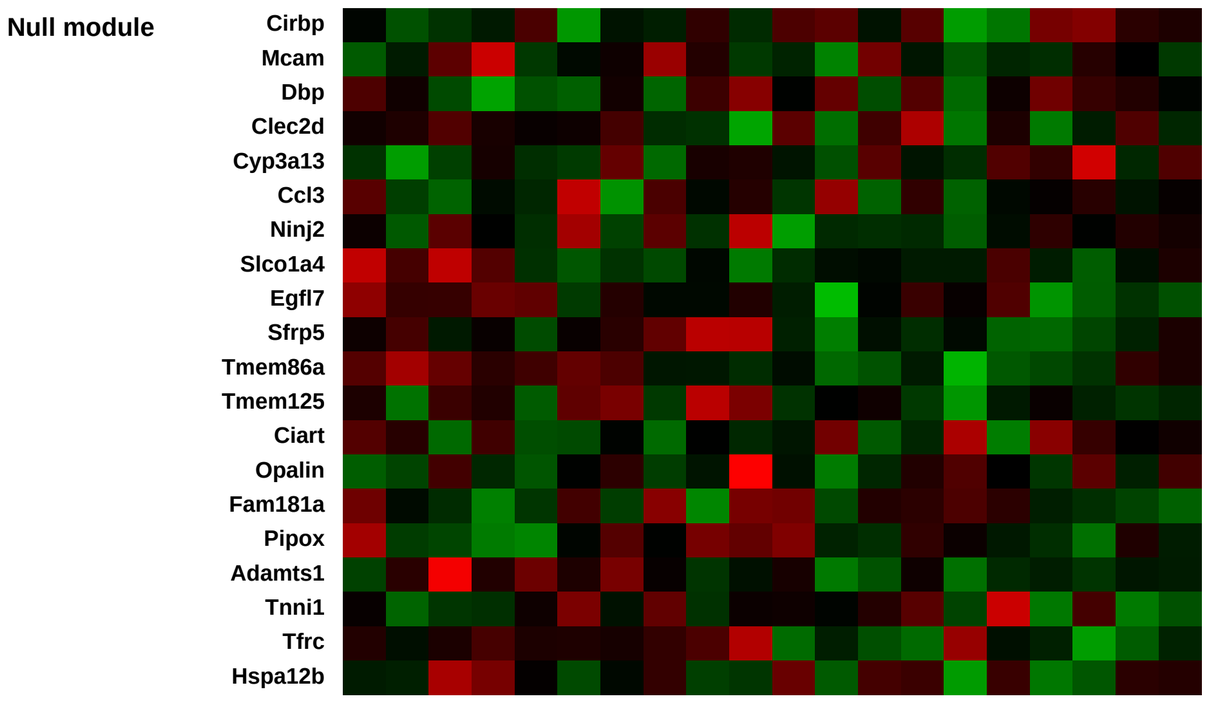

GEO Series "GSE30865" Expression Profiles

Num of samples in this series: 68

Scale of expression profile Z-scores

-3.0 -2.0 -1.0 0.0 1.0 2.0 3.0

GEO Link:	http://www.ncbi.nlm.nih.gov/geo/query/acc.cgi?acc=GSE30865
Status:	Public on Jul 22 2011
Title:	Gene expression of polyoma middle T antigen induced mammary tumors [NZB x PyMT]
Organism:	Mus musculus
Experiment type:	Expression profiling by array
Platform:	GPL1261
Pubmed ID:	22308418
Summary & Design:	**Summary:** Mouse genetic crosses were established between the PyMT model of metastatic breast cancer and NZB strain. Tumors were harvested from the animals for gene expression analysis to identify genes and network modules associated with progression to distant metastatic disease. **Overall design:** Gene expression of 68 samples from the NZB crosses were assayed on Affymetrix chips

Background corr dist: KL-Divergence = 0.0881, L1-Distance = 0.0712, L2-Distance = 0.0127, Normal std = 0.4866

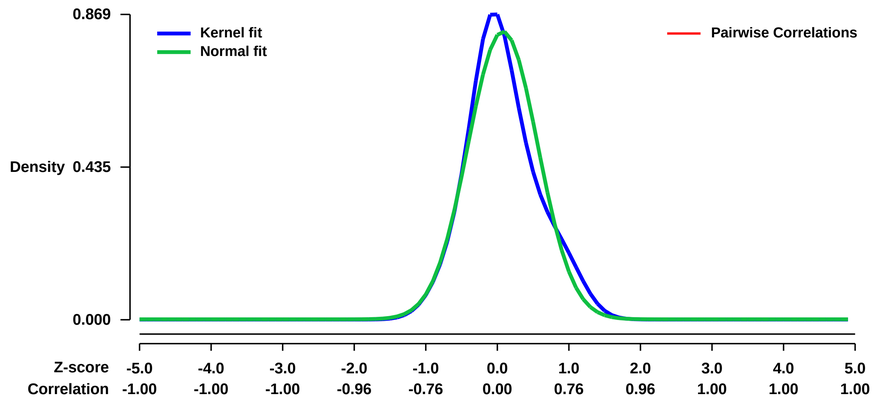

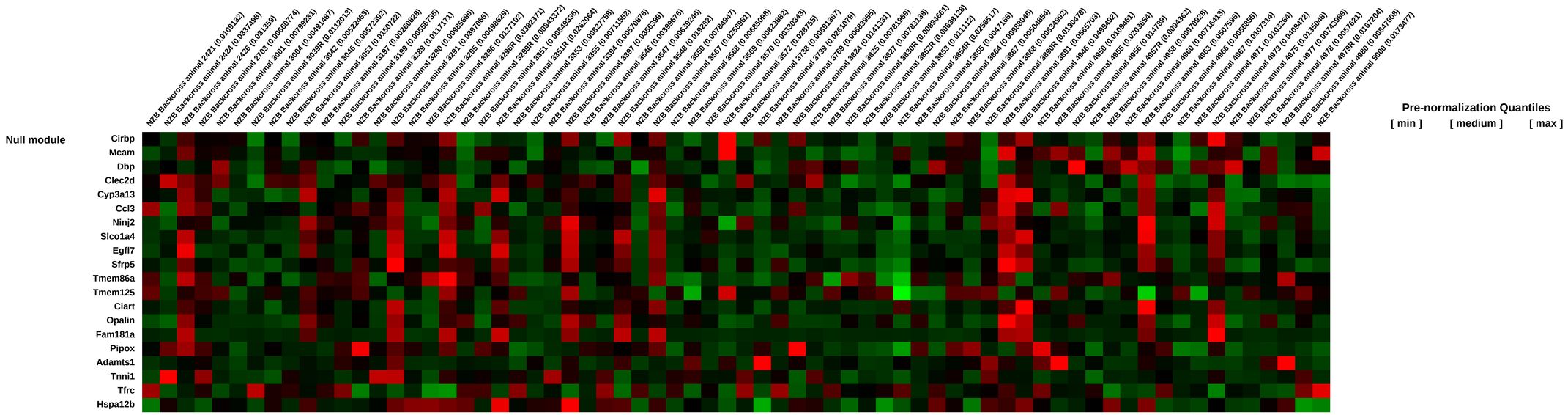

GEO Series "GSE30873" Expression Profiles

Num of samples in this series: 6

Scale of expression profile Z-scores

-3.0 -2.0 -1.0 0.0 1.0 2.0 3.0

GEO Link:	http://www.ncbi.nlm.nih.gov/geo/query/acc.cgi?acc=GSE30873
Status:	Public on Jul 23 2011
Title:	Effects of caspase-8 deletion in the intestinal epithelium
Organism:	Mus musculus
Experiment type:	Expression profiling by array
Platform:	GPL1261
Pubmed ID:	21921917
Summary & Design:	**Summary:** Caspase-8 is a cystein protease involved in regulating apoptosis. The function of caspase-8 was studied in the intestinal epithelium, using mice with an intestinal epithelial cell specific deletion of caspase-8. We used microarrays to investigate the difference of the global programme of gene expression in intestinal epithelial cells of control and caspase-8 deficient mice. **Overall design:** Intestinal epithelial cells were isolated from 3 control mice and 3 mice with a conditional deletion of caspase-8 in the intestinal epithelium. RNA was isolated and subjected to Affymetrix gene chip analysis.

Background corr dist: KL-Divergence = 0.0388, L1-Distance = 0.0228, L2-Distance = 0.0006, Normal std = 0.6268

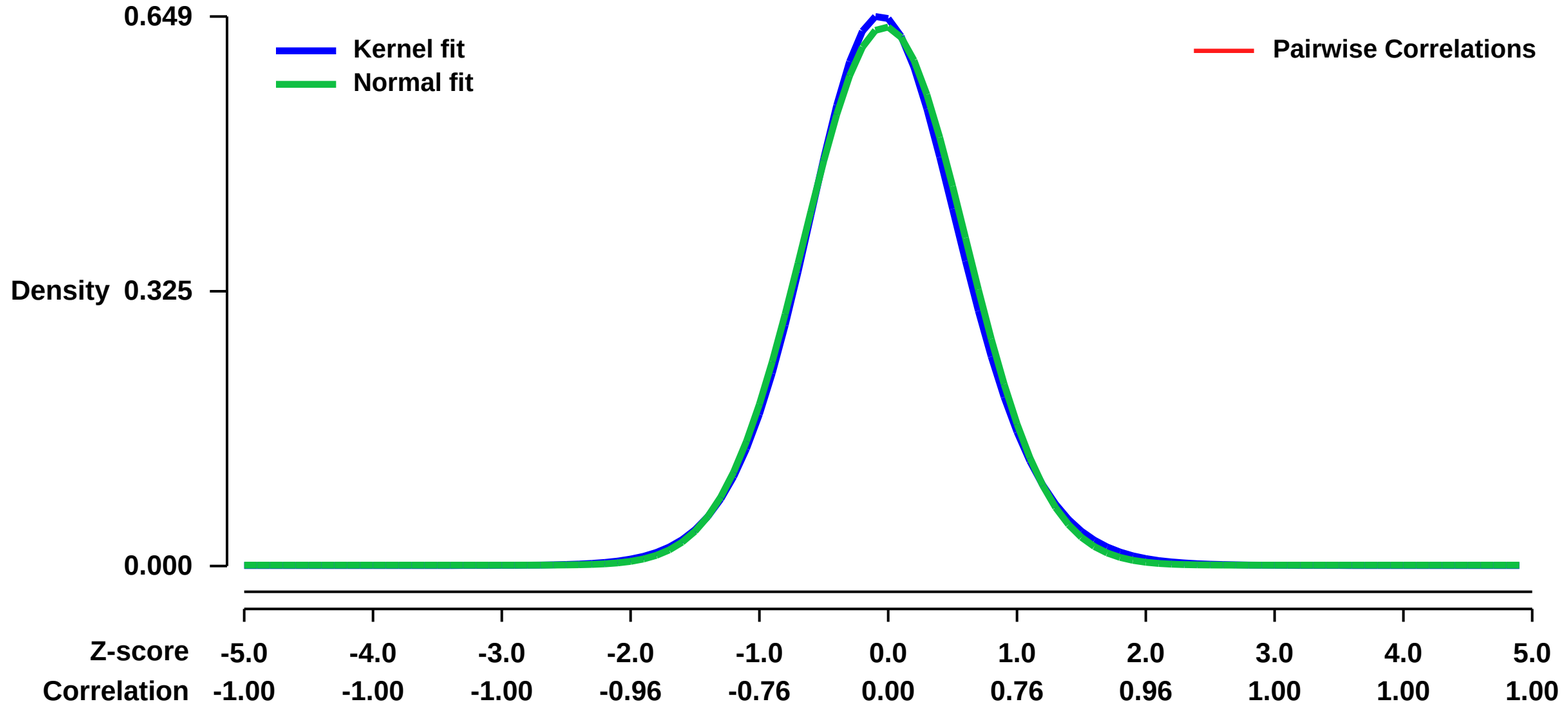

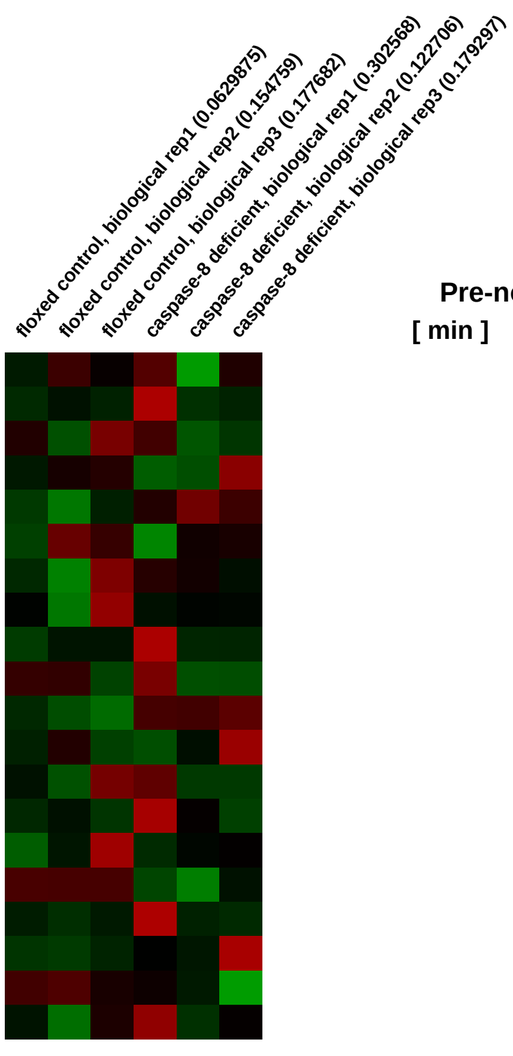

GEO Series "GSE30962" Expression Profiles

Num of samples in this series: 16

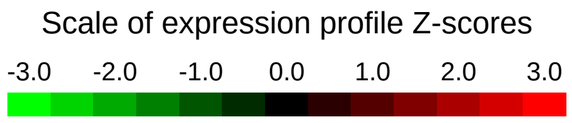

GEO Link:	**http://www.ncbi.nlm.nih.gov/geo/query/acc.cgi?acc=GSE30962**
Status:	**Public on Aug 23 2011**
Title:	**Primary and secondary CD8 T cells during acute and chronic LCMV infection**
Organism:	**Mus musculus**
Experiment type:	**Expression profiling by array**
Platform:	**GPL1261**
Pubmed ID:	**21856186**
Summary & Design:	**Summary:** **Understanding the response of memory CD8 T cells to persistent antigen re-stimulation and the role of CD4 T cell help is critical to the design of successful vaccines for chronic diseases. However, studies comparing the protective abilities and qualities of memory and naˆflve cells have been mostly performed in acute infections, and little is known about their roles during chronic infections. Herein, we show that memory cells dominate over naˆflve cells and are protective when present in large enough numbers to quickly reduce infection. In contrast, when infection is not rapidly reduced, memory cells are quickly lost, unlike naˆflve cells. This loss of memory cells is due to (i) an early block in cell proliferation, (ii) selective regulation by the inhibitory receptor 2B4, and (iii) increased reliance on CD4 T cell help. These findings have important implications towards the design of T cell vaccines against chronic infections and tumors.** **Overall design:** **16 samples are analyzed: 3 replicates of secondary effector CD8 P14 T cells at day 8 post-acute lymphocytic choriomeningitis virus (LCMV) infection; 4 replicates of secondary effector CD8 P14 T cells at day 8 post-chronic LCMV infection; 4 replicates of primary effector CD8 P14 T cells at day 8 post-acute LCMV infection; and 5 replicates of primary effector CD8 P14 T cells at day 8 post-chronic LCMV infection.**

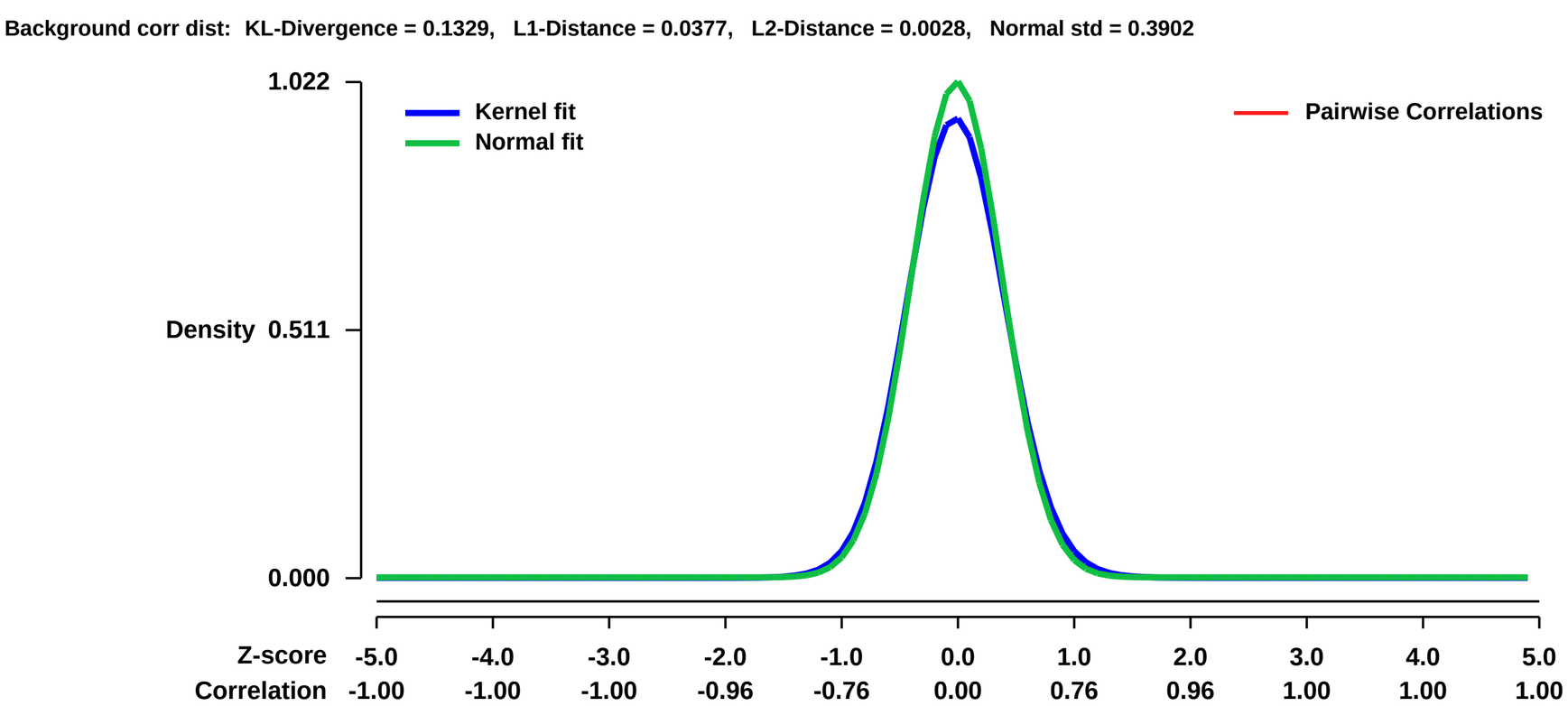

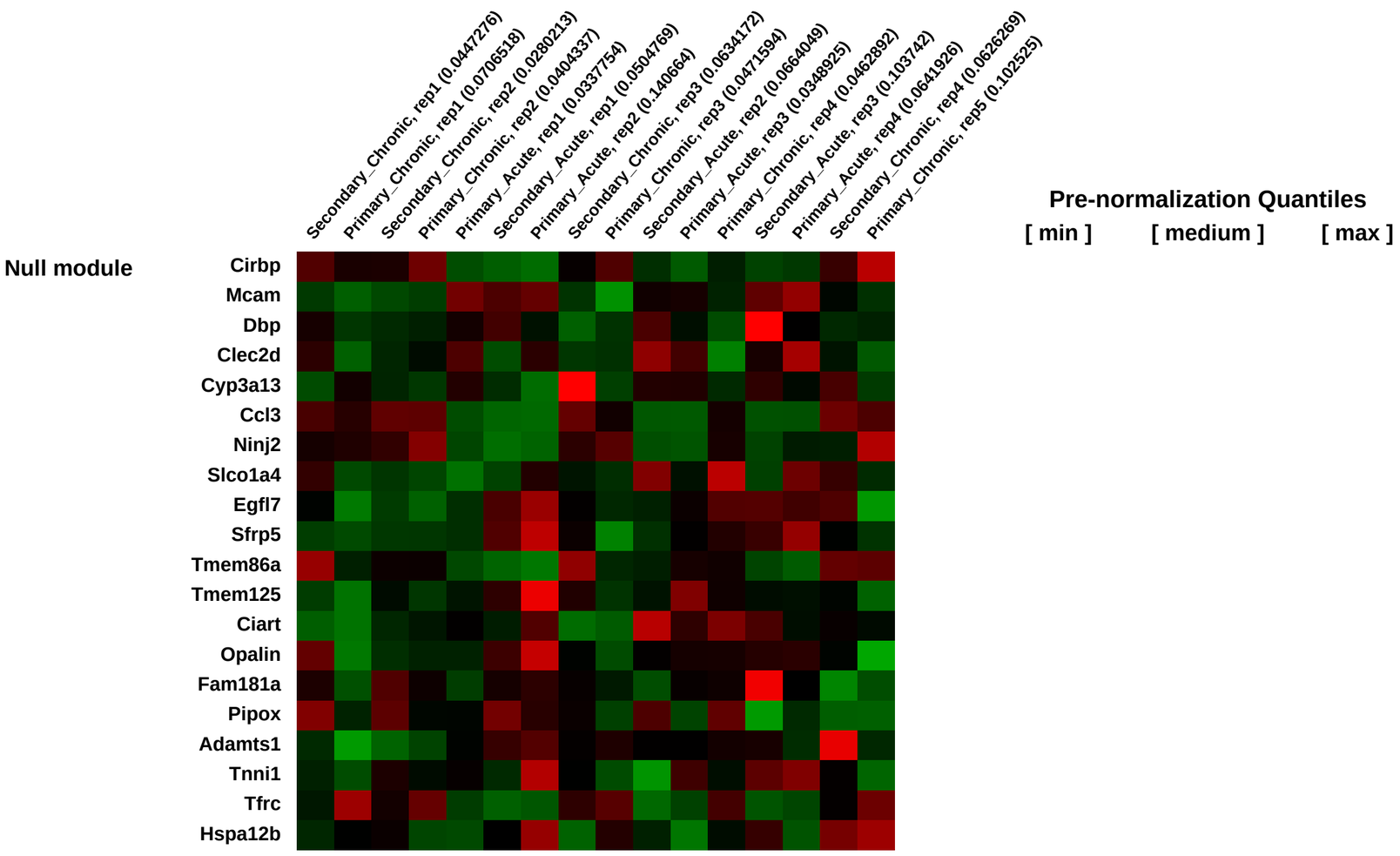

GEO Series "GSE30980" Expression Profiles

Num of samples in this series: 6

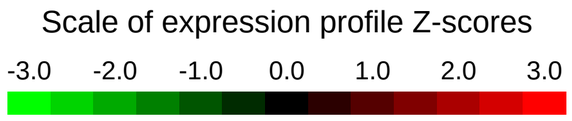

GEO Link:	http://www.ncbi.nlm.nih.gov/geo/query/acc.cgi?acc=GSE30980
Status:	Public on May 21 2014
Title:	Gene profiling on mandibular arches (MdPA1) from Tbx1+/+ and Tbx1-/- mouse embryos
Organism:	Mus musculus
Experiment type:	Expression profiling by array
Platform:	GPL1261
Pubmed ID:	24705356
Summary & Design:	**Summary:** Velo-cardio-facial syndrome/DiGeorge syndrome/22q11.2 deletion syndrome (22q11DS) patients have a submucous cleft palate, velo-pharyngeal insufficiency associated with hypernasal speech, facial muscle hypotonia and feeding difficulties. Inactivation of both alleles of mouse Tbx1, encoding a T-box transcription factor, deleted on 22q11.2, results in a cleft palate and a reduction or loss of branchiomeric muscles. To identify genes downstream of Tbx1 for myogenesis, gene profiling was performed on mandibular arches (MdPA1) from Tbx1+/+ and Tbx1-/- mouse embryos. **Overall design:** To obtain enough RNA for microarray hybridization experiments, dissected mandibular arches from three Tbx1+/+ and three Tbx1-/- E10.5 embryos were pooled according to genotype, with three microarrays performed in total per genotype. The tissue was homogenized in Buffer RLT (QIAGEN). Total RNA was isolated with the RNeasy Micro Kit according to the manufacturerâ s protocol. Quality and quantity of total RNA was determined using an Agilent 2100 Bioanalyzer (Agilent) and an ND-1000 Spectrophotometer (NanoDrop), respectively. Biotinylated single-stranded cDNA targets were amplified from 100 nanograms (ng) starting total RNA using the Ovation RNA Amplification System V2 and FL- Ovation cDNA Biotin Module V2 (NuGEN). A total of 3.75 ¸…g of cDNA from the last step was hybridized to the GeneChip Test3 array (Affymetrix) to test the quality of the labeled target. Nucleic acid samples that passed quality control were then hybridized to the GeneChip Mouse Genome 430 2.0 Arrays (Affymetrix). Hybridization, washing, staining and scanning were performed in the Genomics Core at Einstein (http://www.einstein.yu.edu/genetics/CoreFacilities.aspx?id=23934) according to the Affymetrix manual.

Background corr dist: KL-Divergence = 0.0413, L1-Distance = 0.0184, L2-Distance = 0.0004, Normal std = 0.6119

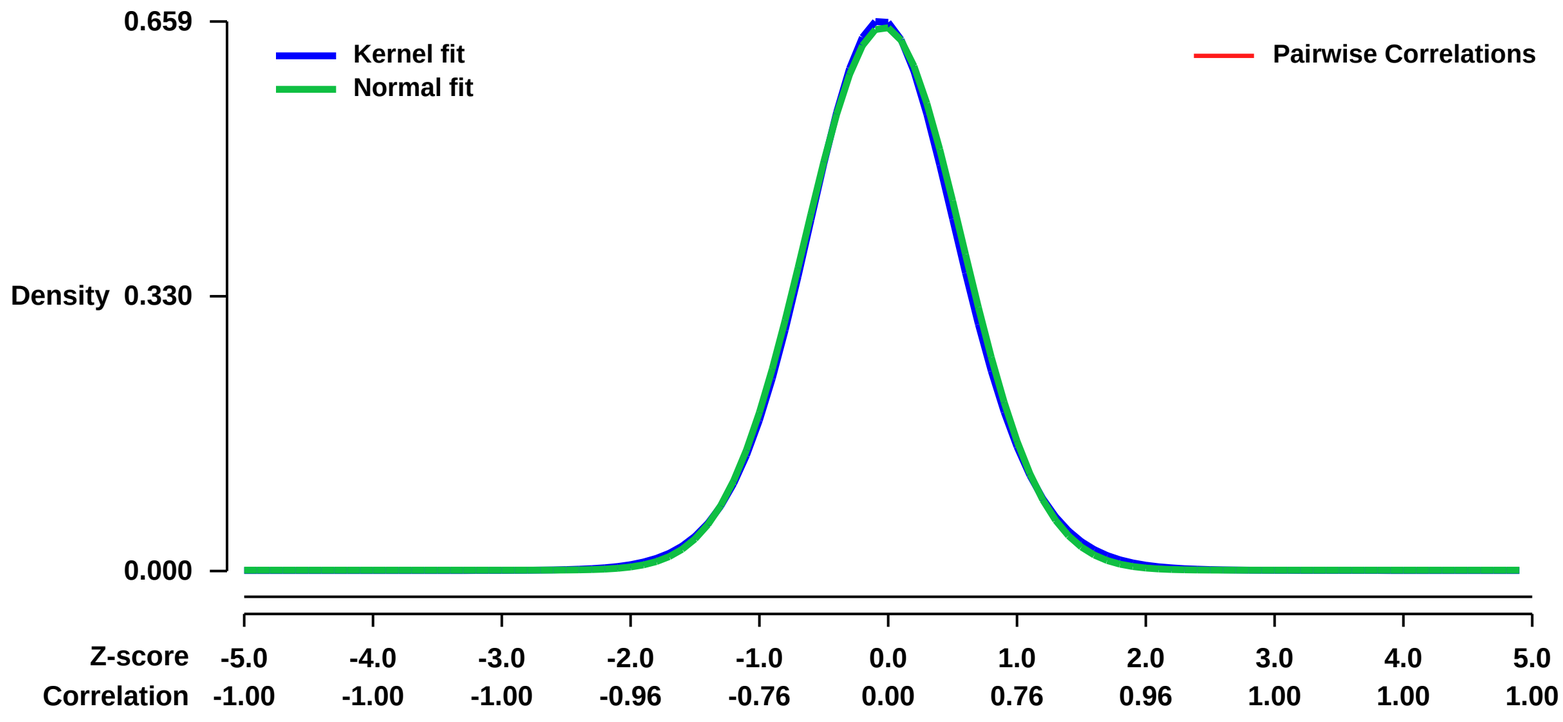

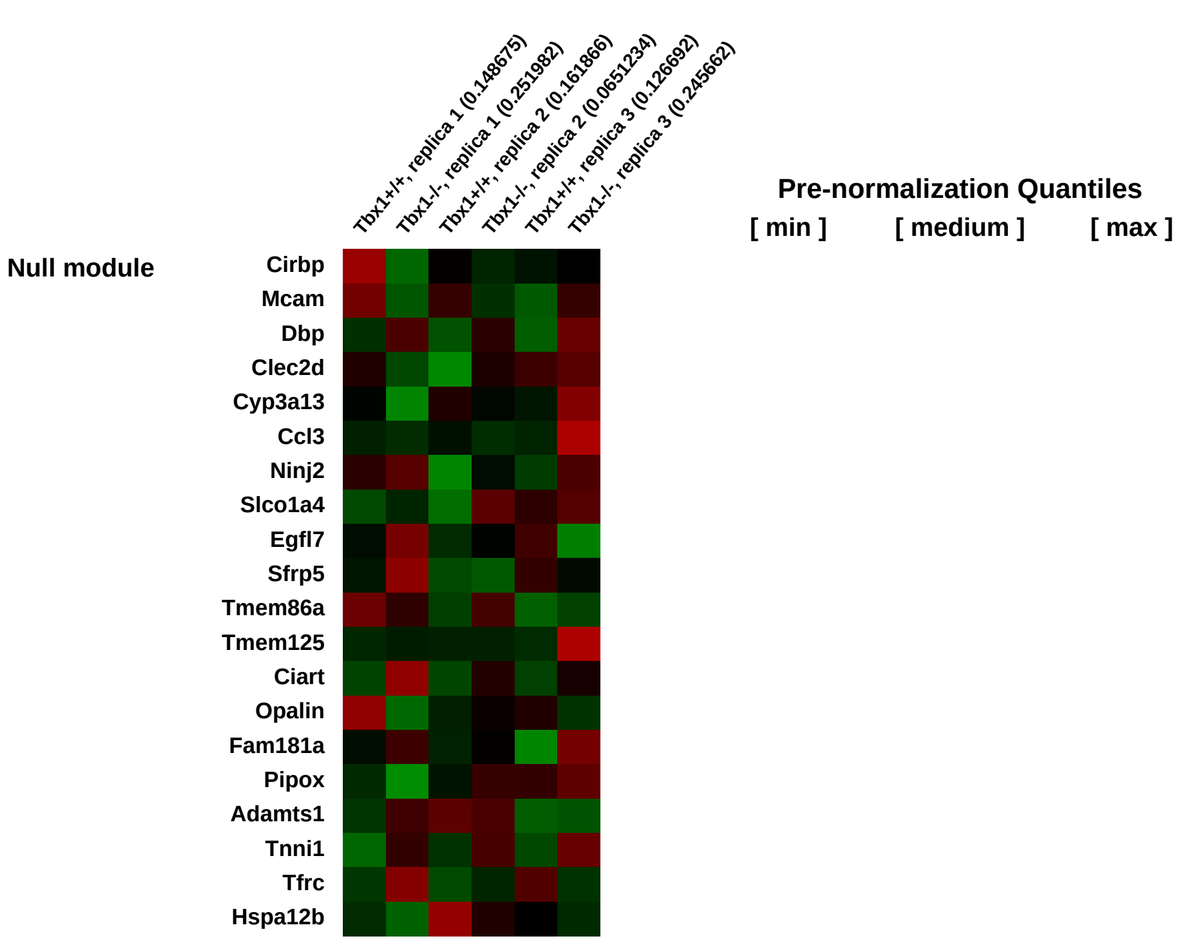

GEO Series "GSE31004" Expression Profiles

Num of samples in this series: 8

Scale of expression profile Z-scores

-3.0 -2.0 -1.0 0.0 1.0 2.0 3.0

GEO Link:	**http://www.ncbi.nlm.nih.gov/geo/query/acc.cgi?acc=GSE31004**
Status:	**Public on Dec 15 2011**
Title:	**Effects of Nicotine on the Fetal Mouse Palate Development and Transcriptome**
Organism:	**Mus musculus**
Experiment type:	**Expression profiling by array**
Platform:	**GPL1261**
Pubmed ID:	
Summary & Design:	**Summary:** **Nonsyndromic cleft palate is a common birth defect (1:700) with a complex etiology involving both genetic and environmental risk factors. Nicotine, a major teratogen present in tobacco products, was shown to cause alterations and delays in the developing fetus. To demonstrate the effect of nicotine on craniofacial development, particularly palatogenesis, we delivered three different doses of nicotine (1.5, 3.0 and 4.5 mg/kg/day) into pregnant BALB/c mice throughout their entire pregnancy using subcutaneous osmotic mini-pump. We assessed the pups for morphological anomalies, as well as genome-wide mRNA (transcriptome) microarray analysis. Consistent administration of nicotine caused developmental retardation, still birth, low birth weight, and significant palatal size and shape abnormality in the pups. However, it did not cause obvious cleft palate. The microarray data analysis using IPA identified differential expression of genes involved in various biological pathways, particularly cancer, genetic diseases, and tissue development in response to consistent nicotine exposure. 6232 up-regulated and 6310 down-regulated genes were detected in nicotine-treated groups compared to the control. Moreover, 45% of the genes associated with cleft palate were found to be affected by nicotine. Alterations of a subset of differentially expressed genes were illustrated with hierarchal clustering and RT-PCR. We concluded that consistent nicotine exposure during pregnancy interferes with normal growth and development of the fetus including palatogenesis; however, this interference does not result in cleft palate, rather smaller palate size with persistent MES. To our knowledge, this is the first experiment revealing the impact of nicotine on the fetal palate transcriptome in mice.** **Overall design:** **Total 8 samples were analyzed. Using an osmotic minipump, duplicate samples from palates of either sterile physiological saline or nicotine (1.5 mg/kg/day, 3.0 mg/kg/day, or 4.5 mg/kg/day)-treated newborn pups.**

Background corr dist: KL-Divergence = 0.0673, L1-Distance = 0.0308, L2-Distance = 0.0016, Normal std = 0.5256

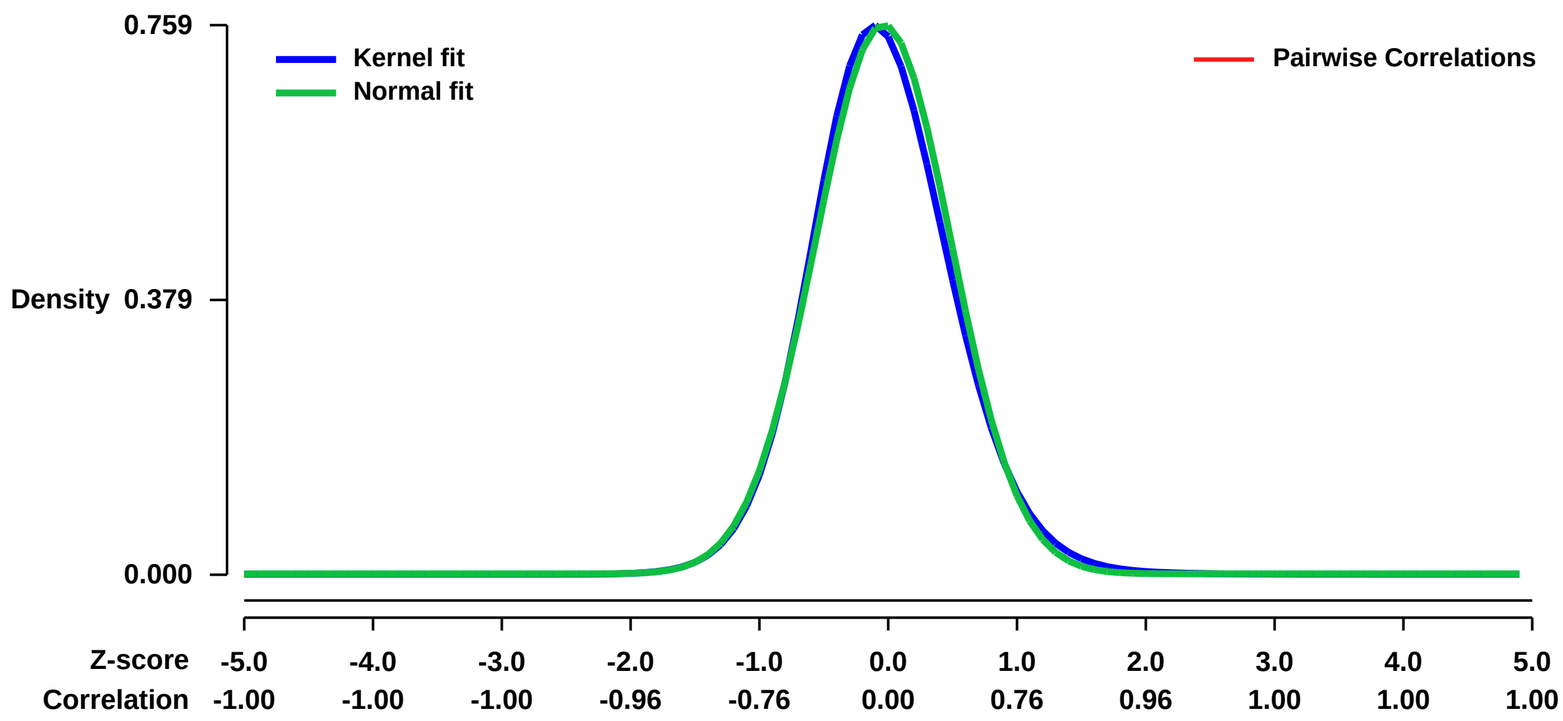

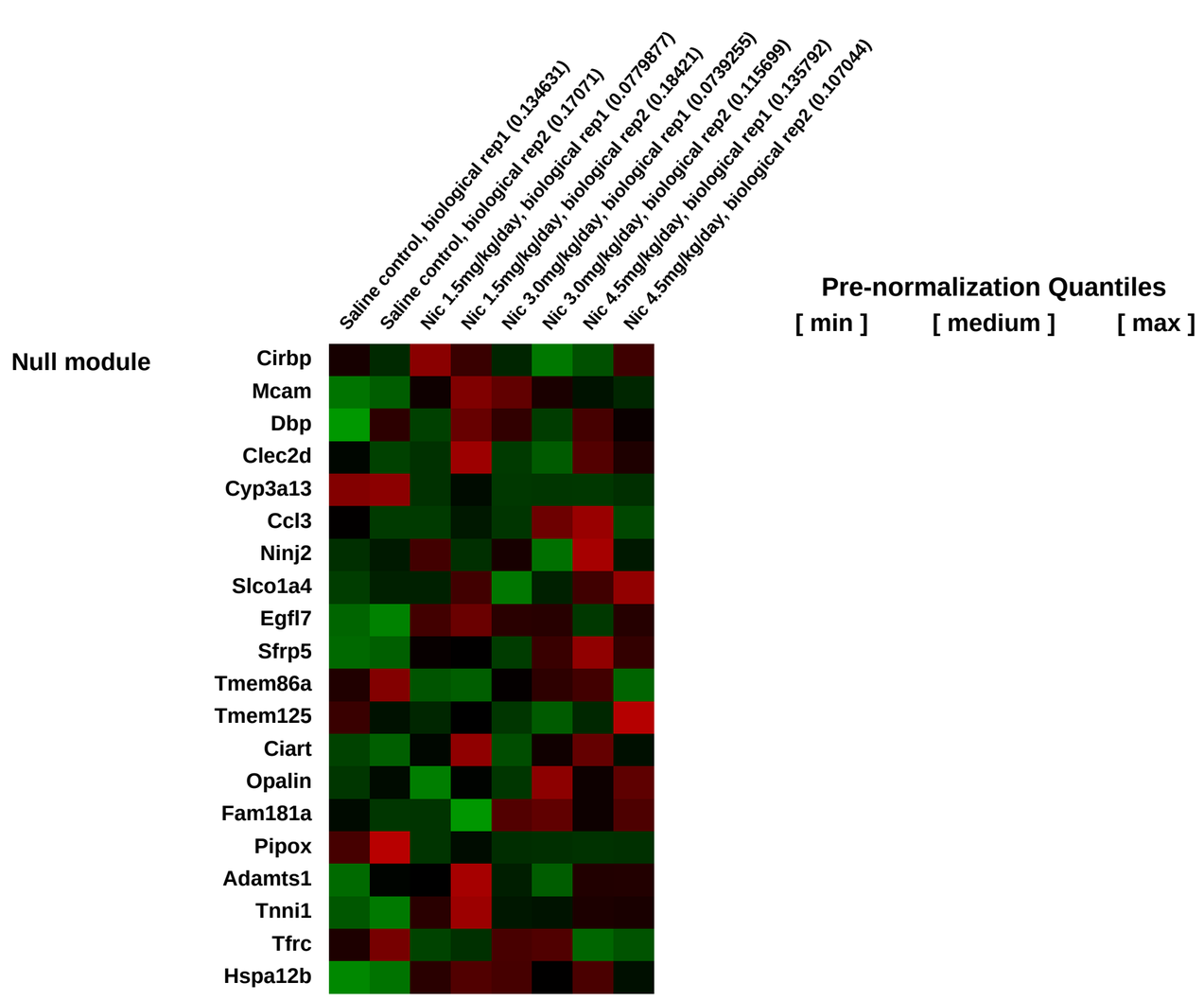

GEO Series "GSE31013" Expression Profiles

Num of samples in this series: 12

Scale of expression profile Z-scores

-3.0 -2.0 -1.0 0.0 1.0 2.0 3.0

GEO Link:	http://www.ncbi.nlm.nih.gov/geo/query/acc.cgi?acc=GSE31013
Status:	Public on Jun 22 2012
Title:	Global Differential Gene Expression Analysis of Spontaneous Lung Tumors in B6C3F1 Mice: Comparison to Human Non-Small Cell Lung Cancer
Organism:	Mus musculus
Experiment type:	Expression profiling by array
Platform:	GPL1261
Pubmed ID:	22688403
Summary & Design:	**Summary:** Introduction: Lung cancer is the leading cause of cancer-related death in people. There are several chemically induced and genetically modified mouse models used to study lung cancer. We hypothesized that spontaneous murine (B6C3F1) lung tumors can serve as a model to study human non-small cell lung cancer (NSCLC). Methods: RNA was extracted from untreated 2-year-old B6C3F1 mouse spontaneous lung (SL) tumors and age-matched normal lung tissue from a chronic inhalation NTP study. Global gene expression analysis was performed using Affymetrix Mouse Genome 430 2.0 GeneChip´fi arrays. After data normalization, for each probe set, pairwise comparisons between groups were made using a bootstrap t-test while controlling the mixed directional false discovery rate (mdFDR) to generate a differential gene expression list. IPA, KEGG, and EASE software tools were used to evaluate the overrepresented cancer genes and pathways. Results: MAPK and TGF-beta pathways were overrepresented within the dataset. Almost all of the validated genes by quantitative real time RT-PCR had comparable directional fold changes with the microarray data. The candidate oncogenes included Kras, Braf, Raf1, Id2, Hmga1, Cks1b, and Foxf1. The candidate tumor suppressor genes included Rb1, Cdkn2a, Hnf4a, Tcf21, Ptprd, Hpgd, Hopx, Ogn, Id4, Hoxa5, Smad6, Smad7, Zbtb16, Cyr61, Dusp4, and Ifi16. In addition, several genes important in lung development were also differentially expressed, such as Smad6, Hopx, Sox4, Sox9 and Mycn. Conclusion: In this study, we have demonstrated that several cancer genes and signaling pathways relevant for human NSCLC were similarly altered in spontaneous murine lung tumors. **Overall design:** Six spontaneous lung tumors and six normal lungs (as controls) from 2-year-old B6C3F1 mice.

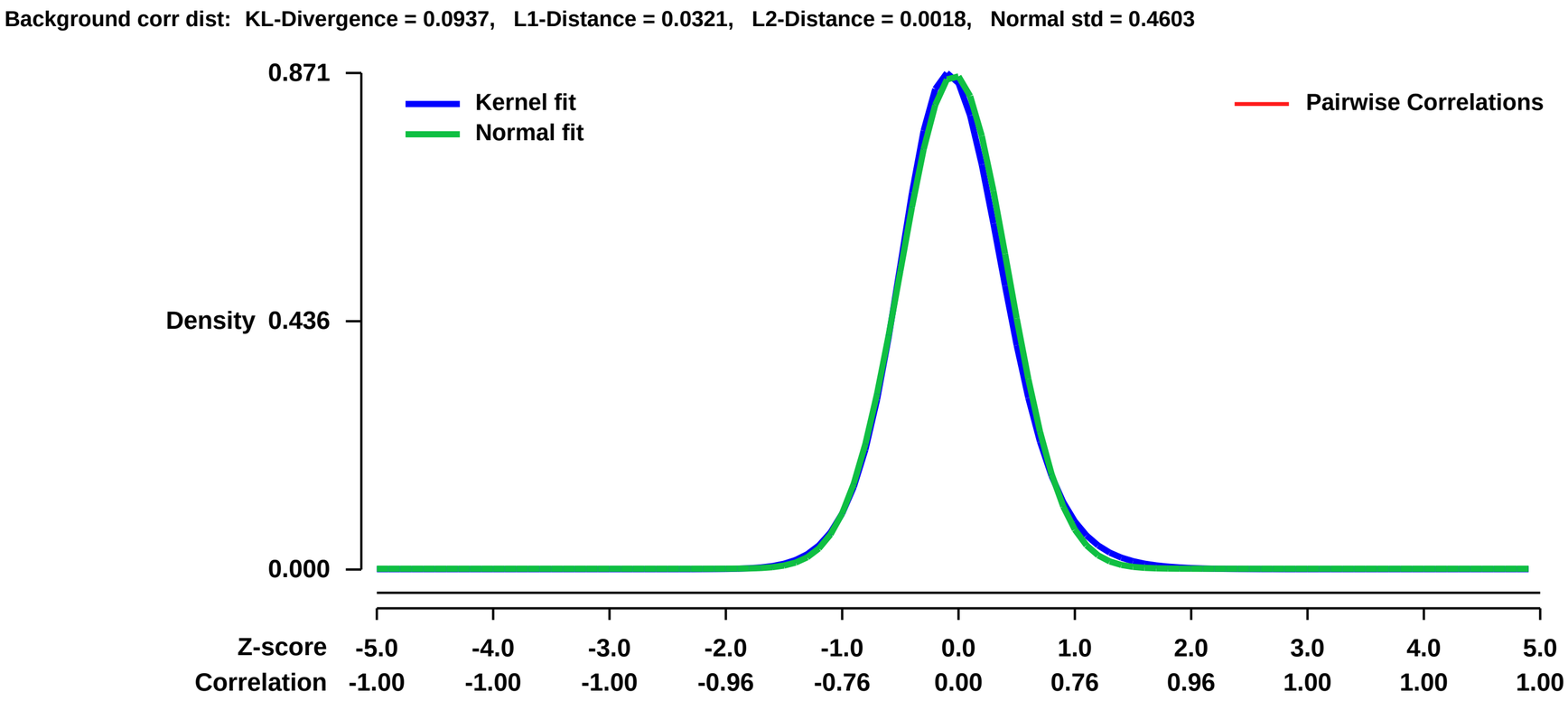

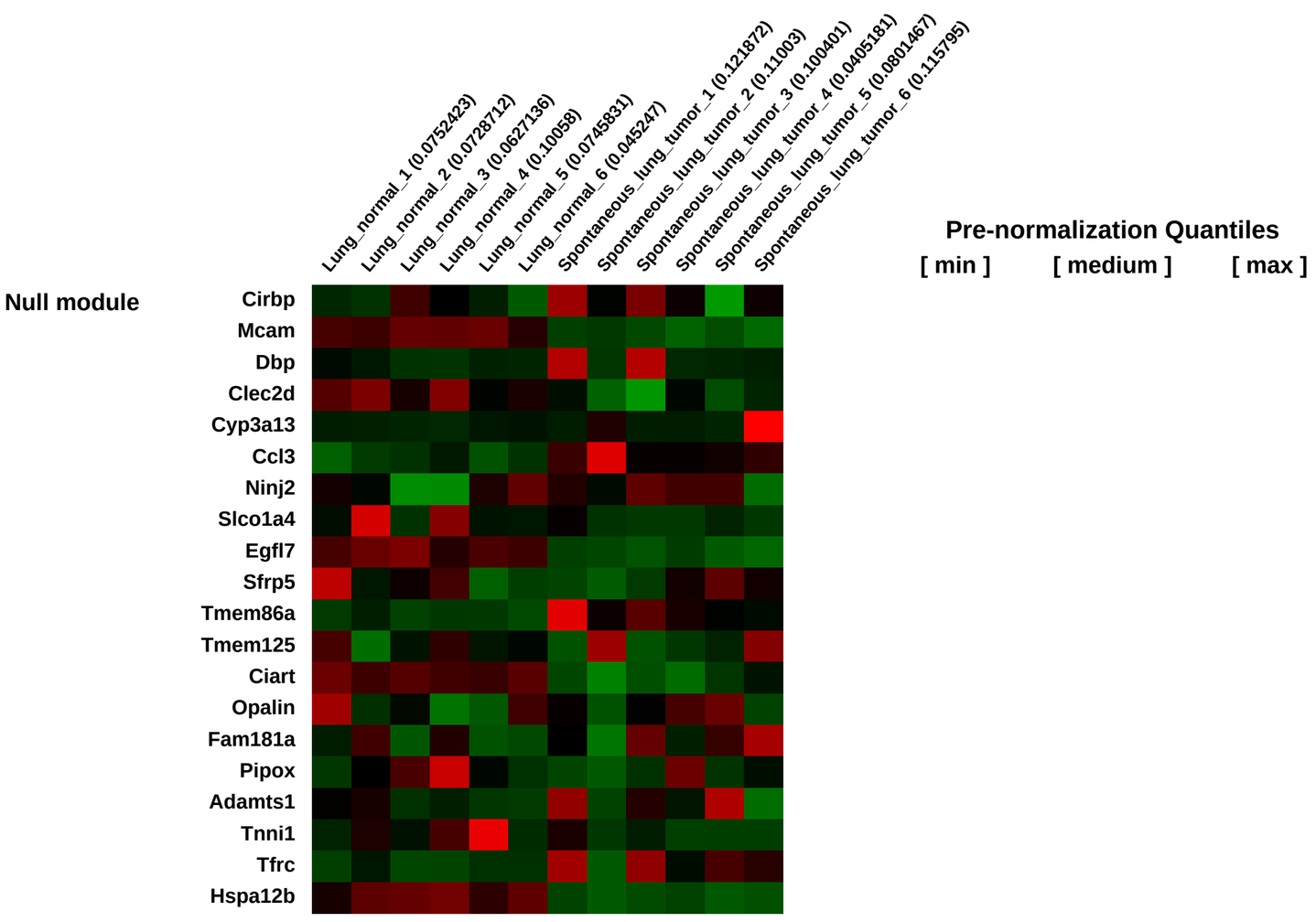

GEO Series "GSE31042" Expression Profiles

Num of samples in this series: 6

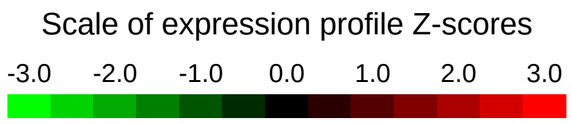

GEO Link:	**http://www.ncbi.nlm.nih.gov/geo/query/acc.cgi?acc=GSE31042**
Status:	**Public on Dec 30 2013**
Title:	**Expression data of mouse hematopoietic cells, Nr4a1/3 wild type and double mutant**
Organism:	**Mus musculus**
Experiment type:	**Expression profiling by array**
Platform:	**GPL1261**
Pubmed ID:	
Summary & Design:	**Summary:** **We investigate the cellular and molecular mechanisms of tumor suppression by NR4A1 and NR4A3, and show a cell intrinsic essential function in maintenance of hematopoietic stem cell (HSC) homeostasis. In the absence of Nr4a1/3, HSC lost quiescence, became highly proliferative leukemia-stem cell (LSC) that transplanted AML to recipient mice.´ We further revealed that loss of NR4A1/3 leads to deregulated expression of the key cell cycle regulator Cdkn1c (P57), c-Myc oncogene, and glucose metabolic genes leading to enhanced aerobic glycolysis or â Warburg effectâ in LSCs.´ Reintroduction of Nr4a1 in LSCs restored HSC quiescence, and reversed Nr4a1/3 deficiency induced P57 suppression and c-Myc overexpression. Collectively, we identify an essential role of Nr4a1/3 in coordinately regulating cell cycle entry and glucose metabolism to prevent uncontrolled stem cell proliferation and AML transformation. These results have major implications for designing therapeutic strategies in AML.** **Overall design:** **To identify NR4A-dependent molecular signaling pathways that may control HSC homeostasis, we performed genome-wide transcript profiling of Lin-Sca1+ (LS) cells from WT and DKO mice. For Affymetrix analysis, we generated three independent pools of RNA from sorted LS cells from 10-20 WT or DKO (2- to 3-week-old) mice per sample.**

Background corr dist: KL-Divergence = 0.0491, L1-Distance = 0.0294, L2-Distance = 0.0012, Normal std = 0.5845

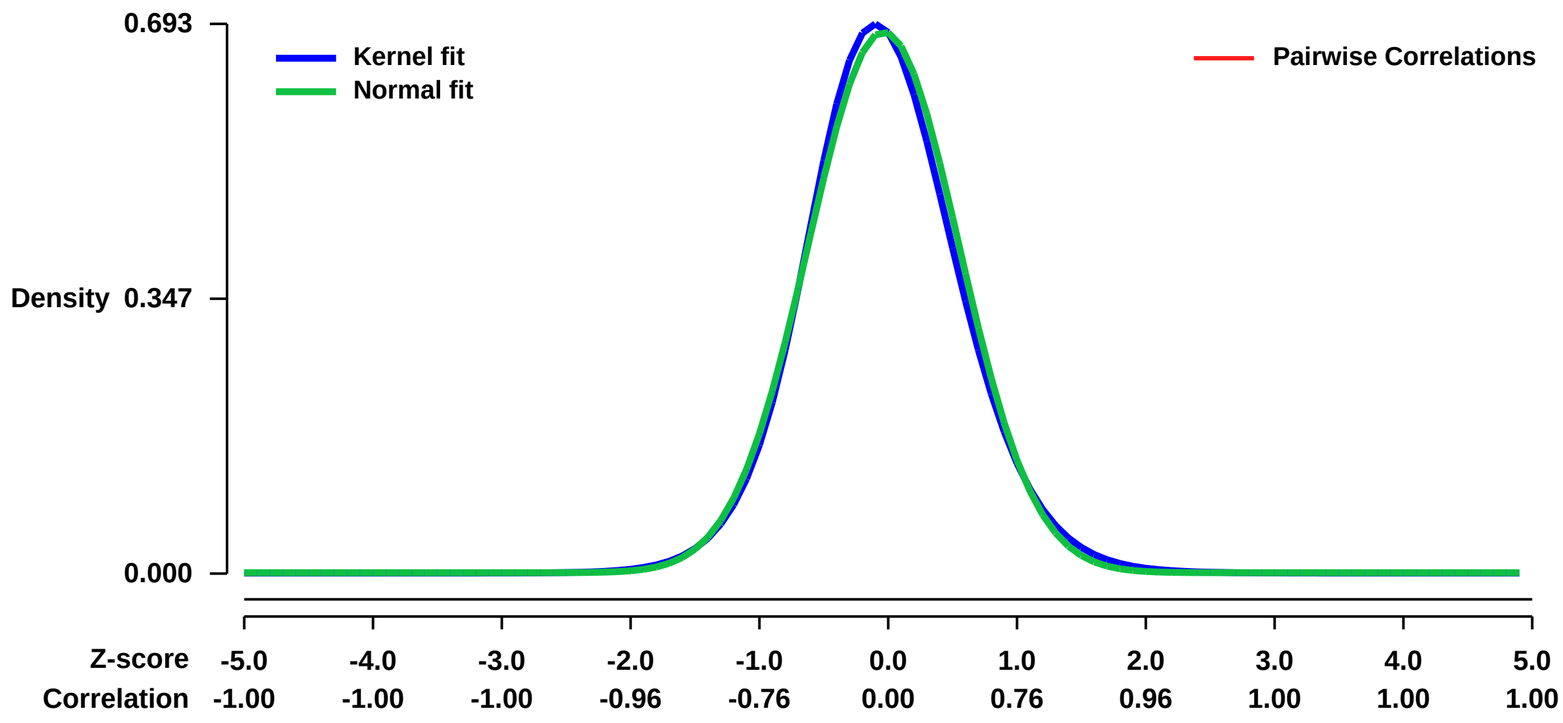

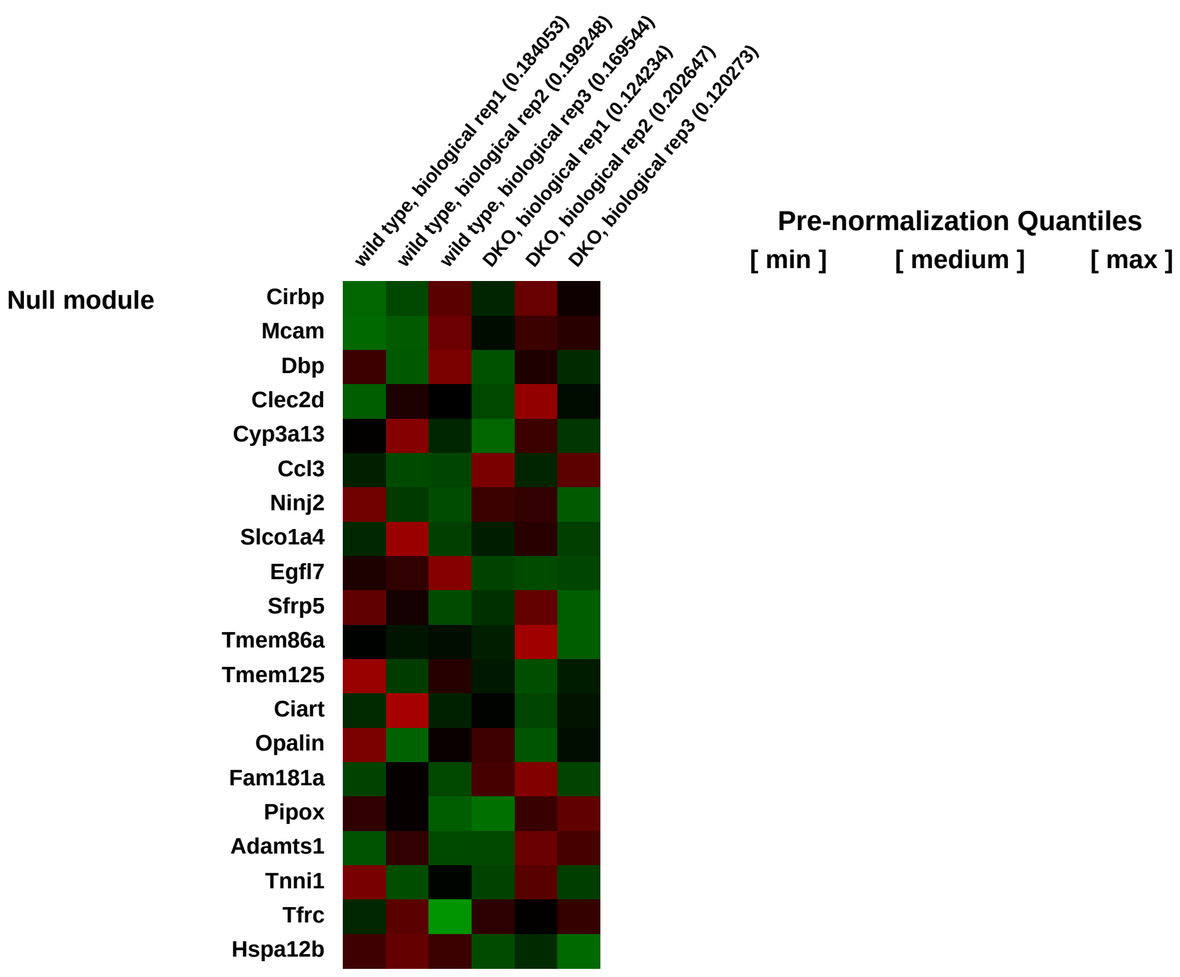

GEO Series "GSE31086" Expression Profiles

Num of samples in this series: 6

Scale of expression profile Z-scores

-3.0 -2.0 -1.0 0.0 1.0 2.0 3.0

GEO Link:	**http://www.ncbi.nlm.nih.gov/geo/query/acc.cgi?acc=GSE31086**
Status:	**Public on Feb 08 2012**
Title:	**Expression data from Bmi1-null common myeloid progenitor (CMP)**
Organism:	**Mus musculus**
Experiment type:	**Expression profiling by array**
Platform:	**GPL1261**
Pubmed ID:	**22351929**
Summary & Design:	**Summary:** **Bmi1 is a component of polycomb repressive complex 1 and its role in the inheritance of the stemness of adult somatic stem cells has been well characterized. Bmi1 maintains the self-renewal capacity of adult stem cells, at least partially, by repressing the Ink4a/Arf locus that encodes a cyclin-dependent kinase inhibitor, p16Ink4a, and a tumor suppressor, p19Arf 14. Deletion of both Ink4a and Arf in Bmi1-deficient mice substantially restored the defective self-renewal capacity of HSCs and neural stem cells.** **Overall design:** **Purified CMP from BM of recipient mice repopulated with wild-type, Ink4a-/-Arf-/-, and Bmi1-/- Ink4a-/-Arf-/- BM cells were subjected to RNA extraction and hybridization on Affymetrix microarrays.**

Background corr dist: **KL-Divergence = 0.0491, L1-Distance = 0.0270, L2-Distance = 0.0010, Normal std = 0.5869**

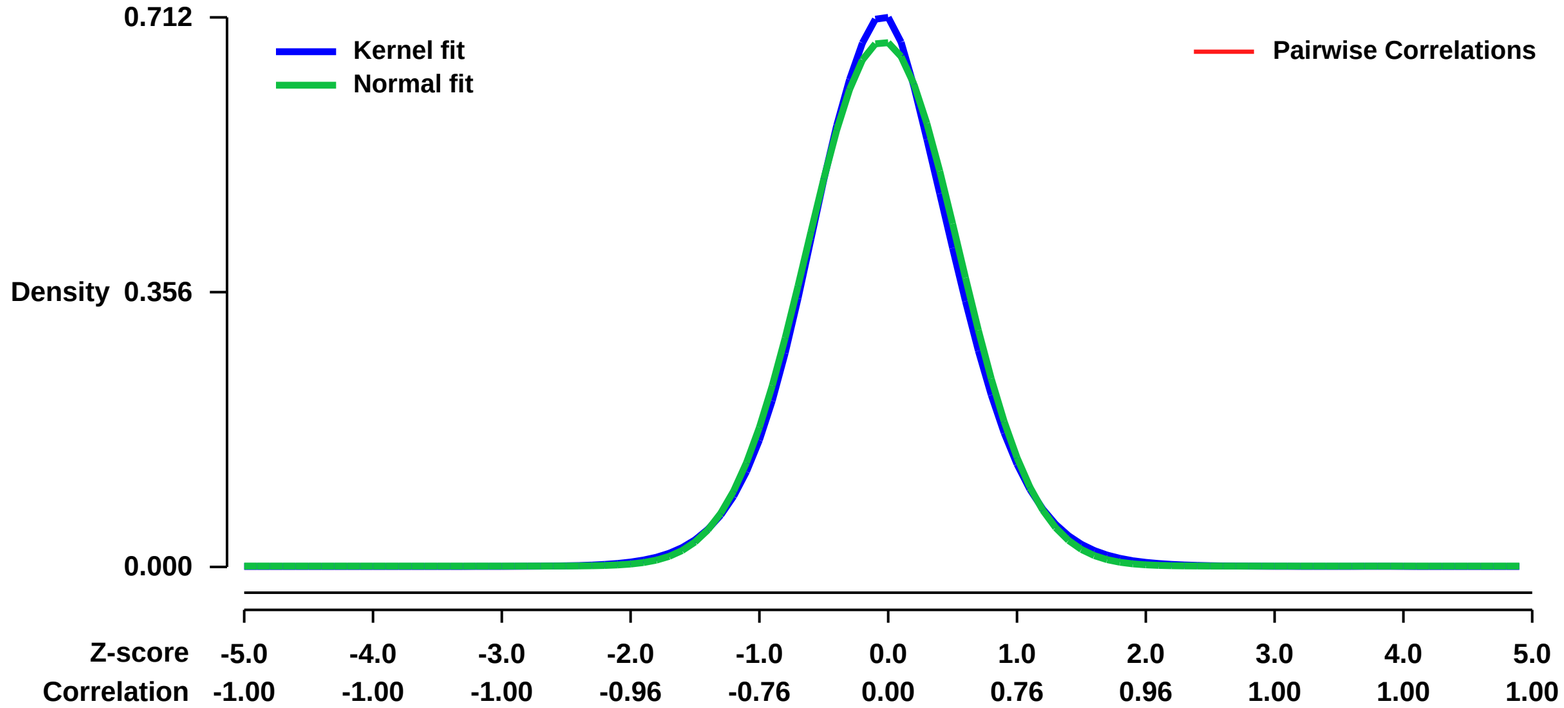

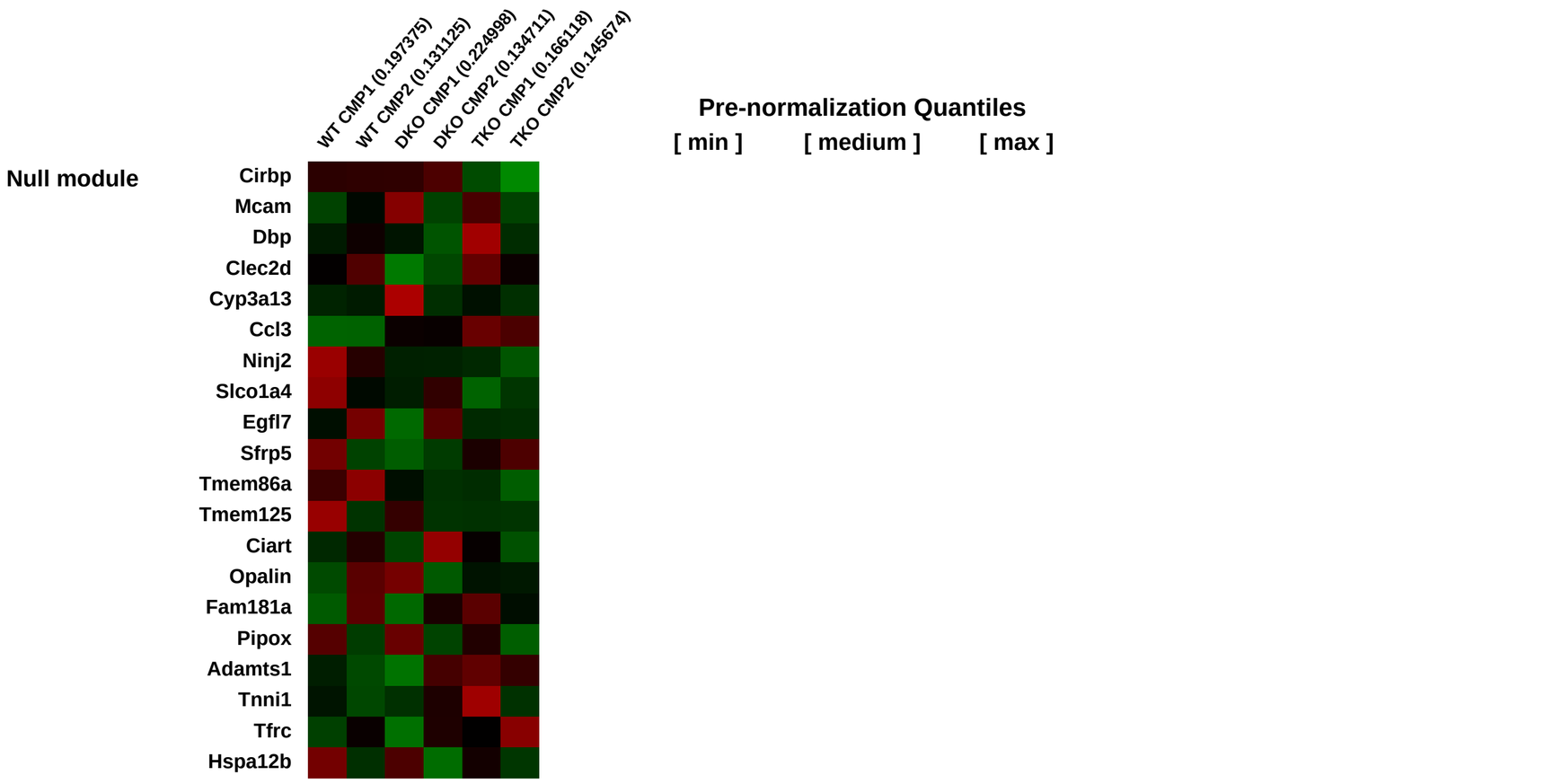

GEO Series "GSE31099" Expression Profiles

Num of samples in this series: 24

Scale of expression profile Z-scores

-3.0 -2.0 -1.0 0.0 1.0 2.0 3.0

GEO Link:	http://www.ncbi.nlm.nih.gov/geo/query/acc.cgi?acc=GSE31099
Status:	Public on Nov 21 2011
Title:	Expression data from treatment-induced senescence in mouse Emu-myc B-cell lymphoma model
Organism:	Mus musculus
Experiment type:	Expression profiling by array
Platform:	GPL1261
Pubmed ID:	23945590
Summary & Design:	**Summary:** Treatment induced senescence (TIS) is a terminal cell cycle arrest program, increasingly recognized as a tumor suppressor mechanism complementing apoptosis in response to standard chemotherapy regimens. In particular cells with blocked apoptotic pathways rely on senescence as the only remaining failsafe mechanism to keep the neoplastic growth in check. However, little is known about biological properties, long-term fate of senescent tumor cells and their impact on the microenvironment. We used global gene expression profiling by microarrays to gain insight in the molecular programme underlying the treatment-induced senescence in Emu-myc transgenic B-cell lymphomas (apoptosis protected by Bcl2 overexpression), which robustly enter senescence in response to DNA-damaging anticancer agents such as Adriamycin (ADR). **Overall design:** Primary lymphoma cells isolated from lymph nodes of Emu-Myc transgenic mice were used. In this model the the c-Myc oncogene is constitutively expressed in the cells of B-cell lineage, leading to spontaneous development of aggressive B-cell lymphomas, resembling Burkitt lymphoma in humans. In order to bring up the senescence as the main failsafe mechanism, primary lymphoma cells are protected from apoptosis by retroviral over-expression of a strong antiapoptotic protein Bcl2. These cells (Myc;Bcl2) massively undergo senescence upon DNA-damaging treatment. Adriamycin (ADR) is a cytostatic drug, used as a standard part of several lymphoma treatment regimens. In this study, transcriptional profiles of matched pairs of untreated vs. 5 days ADR treated Myc;Bcl2 lymphomas were analysed.

Background corr dist: KL-Divergence = 0.2224, L1-Distance = 0.0463, L2-Distance = 0.0050, Normal std = 0.3219

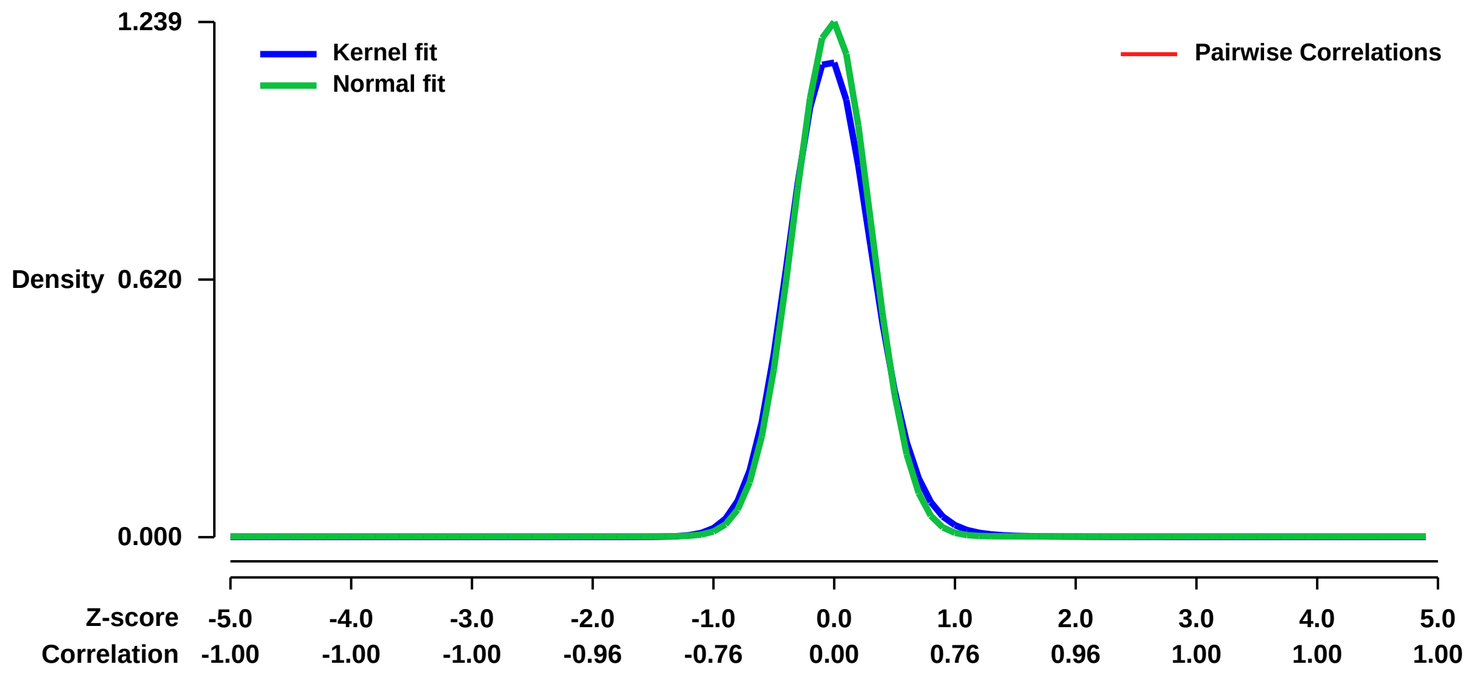

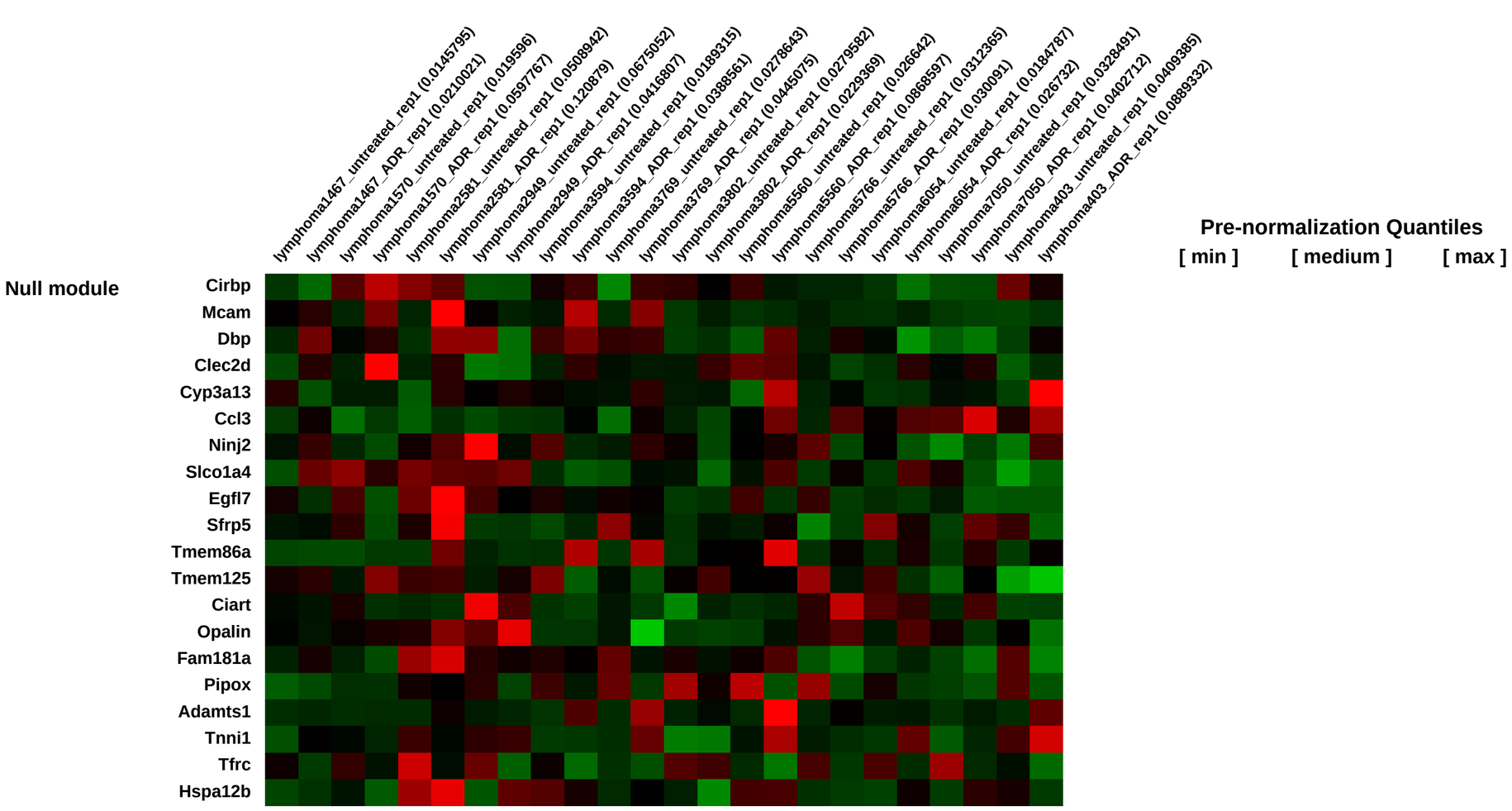

GEO Series "GSE31150" Expression Profiles

Num of samples in this series: 6

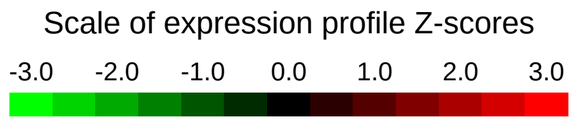

GEO Link:	http://www.ncbi.nlm.nih.gov/geo/query/acc.cgi?acc=GSE31150
Status:	Public on Nov 19 2012
Title:	The role of Raf-1 kinase inhibitor protein in the regulation of pancreatic beta cell proliferation in mice
Organism:	Mus musculus
Experiment type:	Expression profiling by array
Platform:	GPL1261
Pubmed ID:	22926403
Summary & Design:	**Summary:** **AIMS/HYPOTHESIS: Manoeuvres aimed at increasing beta cell mass have been proposed as regenerative medicine strategies for diabetes treatment. Raf-1 kinase inhibitor protein 1 (RKIP1) is a common regulatory node of the mitogen-activated protein kinase (MAPK) and nuclear factor ¸”B (NF-¸”B) pathways and therefore may be involved in regulation of beta cell homeostasis. The aim of this study was to investigate the involvement of RKIP1 in the control of beta cell mass and function.** **METHODS: Rkip1 (also known as Pebp1) knockout (Rkip1 (-/-)) mice were characterised in terms of pancreatic and glucose homeostasis, including morphological and functional analysis. Glucose tolerance and insulin sensitivity were examined, followed by assessment of glucose-induced insulin secretion in isolated islets and beta cell mass quantification through morphometry. Further characterisation included determination of endocrine and exocrine proliferation, apoptosis, MAPK activation and whole genome gene expression assays. Capacity to reverse a diabetic phenotype was assessed in adult Rkip1 (-/-) mice after streptozotocin treatment.** **RESULTS: Rkip1 (-/-) mice exhibit a moderately larger pancreas and increased beta cell mass and pancreatic insulin content, which correlate with an overall improvement in whole body glucose tolerance. This phenotype is established in young postnatal stages and involves enhanced cellular proliferation without significant alterations in cell death. Importantly, adult Rkip1 (-/-) mice exhibit rapid reversal of streptozotocin-induced diabetes compared with control mice.** **CONCLUSIONS/INTERPRETATION: These data implicate RKIP1 in the regulation of pancreatic growth and beta cell expansion, thus revealing RKIP1 as a potential pharmacological target to promote beta cell regeneration.** **Overall design:** **Pancreatic gene expression of Rkip-1 (Raf kinase inhibitor 1) knockout (KO) and wild type (WT) mice, including three biological replicates in each group.**

Background corr dist: KL-Divergence = 0.0457, L1-Distance = 0.0163, L2-Distance = 0.0003, Normal std = 0.5868

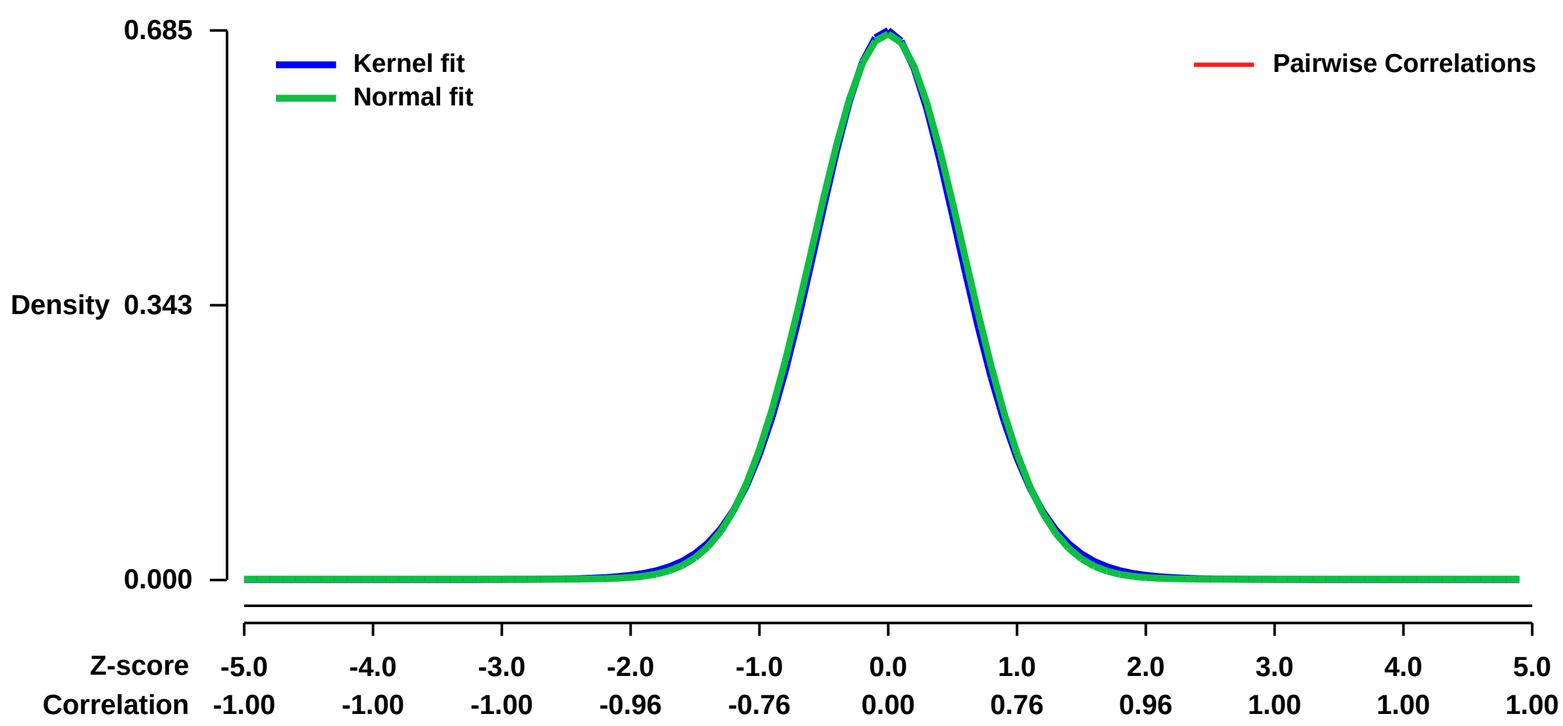

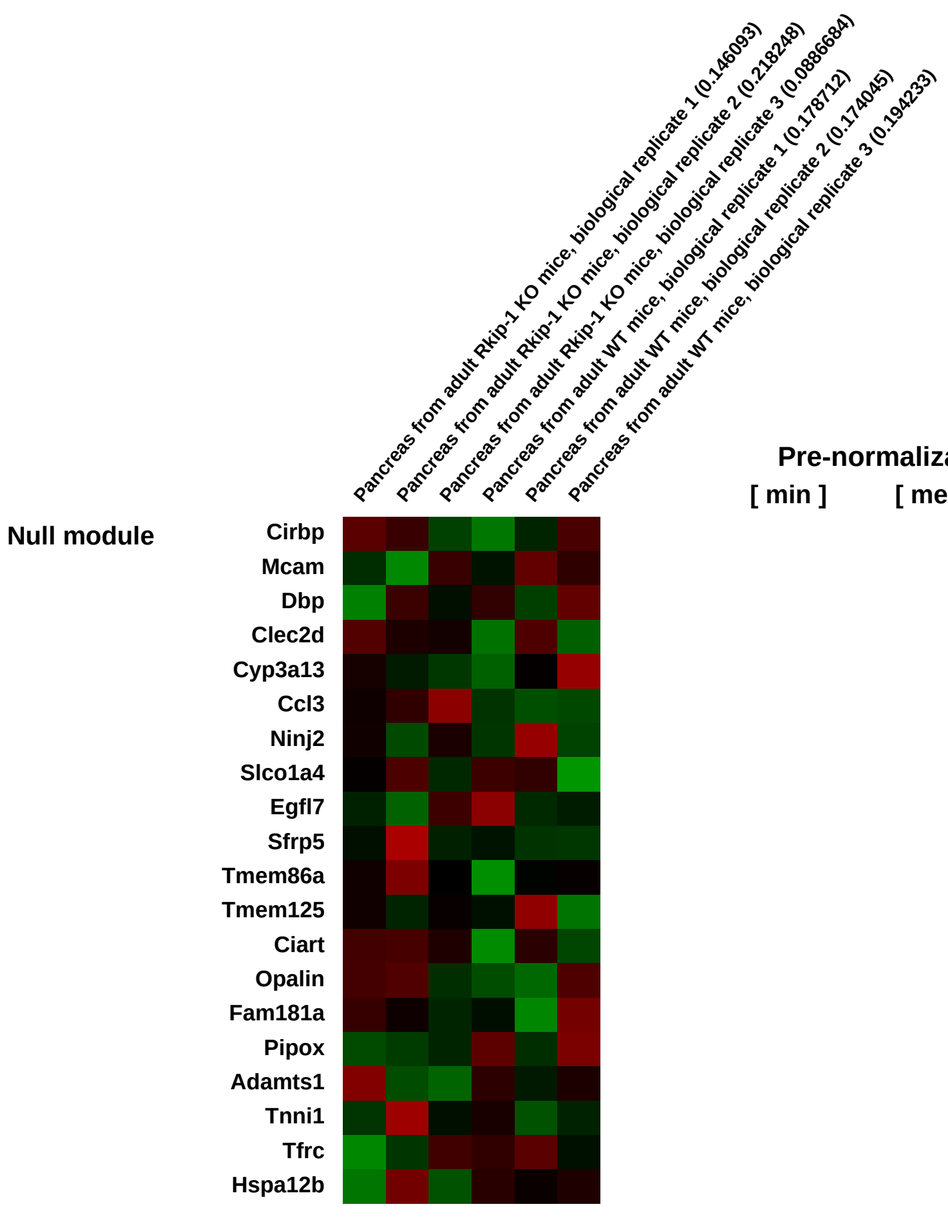

GEO Series "GSE31166" Expression Profiles

Num of samples in this series: 6

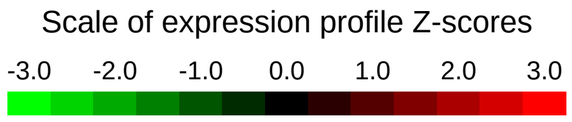

GEO Link:	http://www.ncbi.nlm.nih.gov/geo/query/acc.cgi?acc=GSE31166
Status:	Public on Dec 13 2012
Title:	Expression data from inducible ES stable cell line
Organism:	Mus musculus
Experiment type:	Expression profiling by array
Platform:	GPL1261
Pubmed ID:	23180766
Summary & Design:	**Summary:** **In order to identify the effects of the induction of the gene of interest on the mouse ES transcriptome, we performed Affymetrix Gene-Chip hybridization experiments for the inducible not-tagged cell line.** **Transcriptome analysis of the inducible transgenic mouse ES cell line.** **The E13 inducible cell lines derived from parental EB3 cell line. The cell line EB3 was obtained from the laboratory of Dr Hitoshi Niwa as previously described in (Masui S et al., 2005).** **Tthe specific mouse gene is E130012A19Rik.** **Overall design:** **For the analysis on the inducible not-tagged cell line, total RNA was extracted from three biological replicates grown in medium deprived of Tetracycline for 48 hours; RNA extracted from un-induced clones was used as control.**

Background corr dist: KL-Divergence = 0.0196, L1-Distance = 0.0228, L2-Distance = 0.0005, Normal std = 0.7644

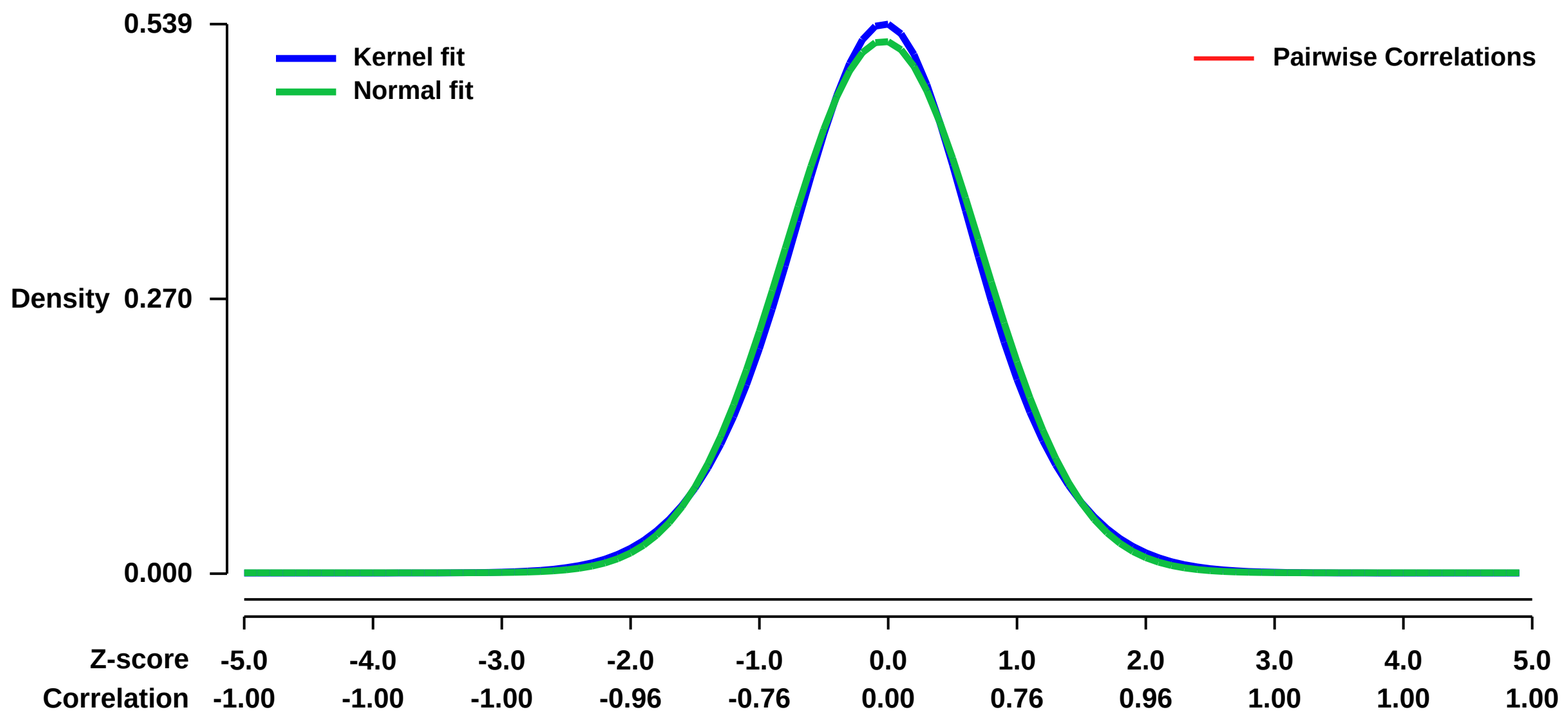

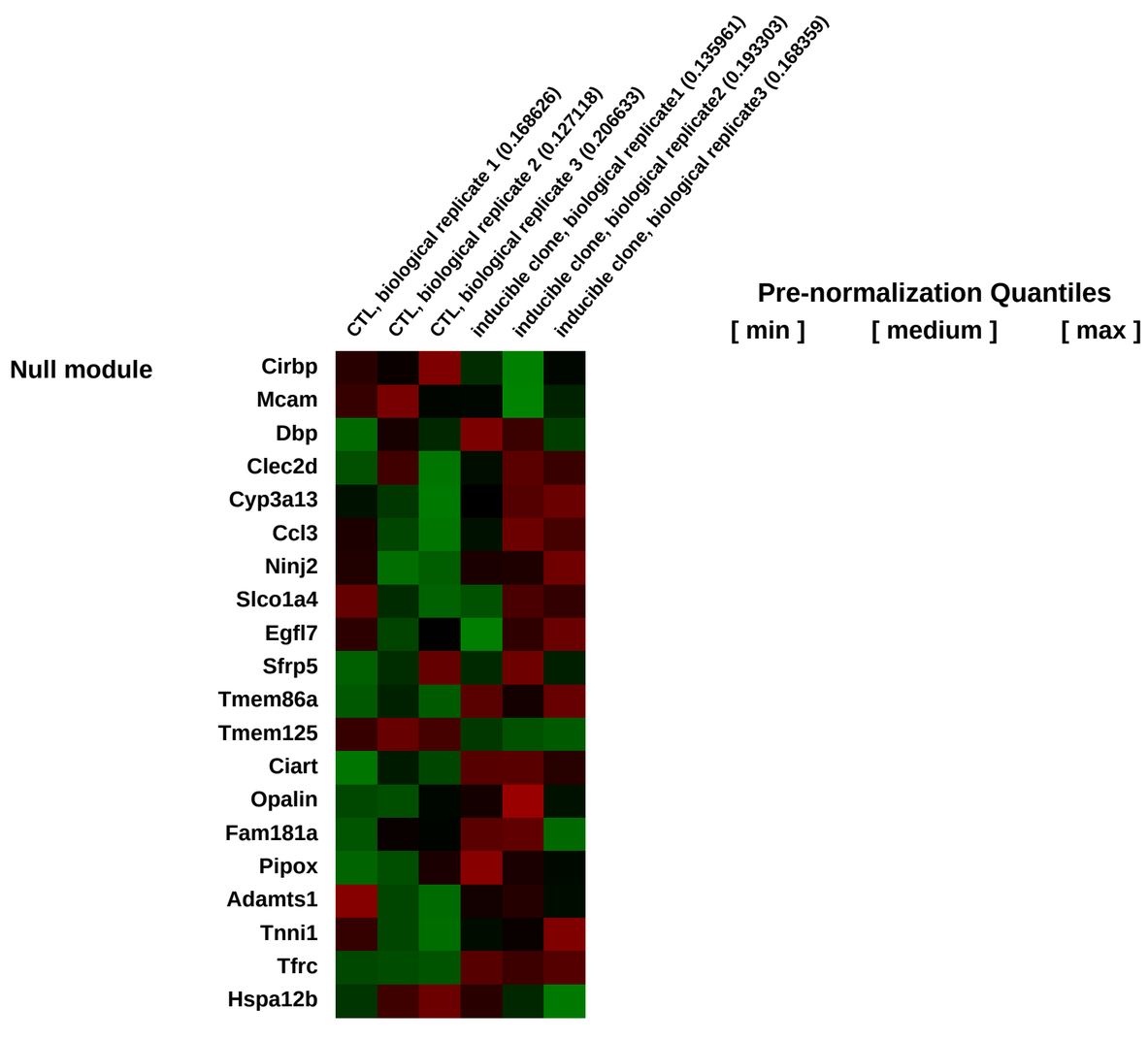

GEO Series "GSE31208" Expression Profiles

Num of samples in this series: 8

Scale of expression profile Z-scores

-3.0 -2.0 -1.0 0.0 1.0 2.0 3.0

GEO Link:	**http://www.ncbi.nlm.nih.gov/geo/query/acc.cgi?acc=GSE31208**
Status:	**Public on Dec 31 2011**
Title:	**Expression data of MCK conditional frataxin knock-out mice**
Organism:	**Mus musculus**
Experiment type:	**Expression profiling by array**
Platform:	**GPL1261**
Pubmed ID:	
Summary & Design:	**Summary:** **Frataxin deficiency in human is the cause of Friedreich's ataxia (FA), a lethal neuro- and cardio-degenerative disease. Knock-out (KO) mice of this mouse model of FA exhibit classical cardiomyopathy of the patients. The onset of FA phenotypes in the KO mice is approximately 6-7 weeks of age. This genearray analysis was conducted to examine the changes in gene expression in the heart of KO mice relative to their wild-type (WT) littermates at 4- and 10-weeks of age. At 10-weeks of age, the KO mice begin to die from severe cardiomyopathy.** **Overall design:** **RNA from the heart of four female 4-week-old MCK littermates (two WT and two KO) and four female 10-week-old MCK littermates (two WT and two KO) was extracted and hybridised to Affymetrix Mouse Genome 430 2.0 Array.**

Background corr dist: KL-Divergence = 0.0279, L1-Distance = 0.0409, L2-Distance = 0.0027, Normal std = 0.6823

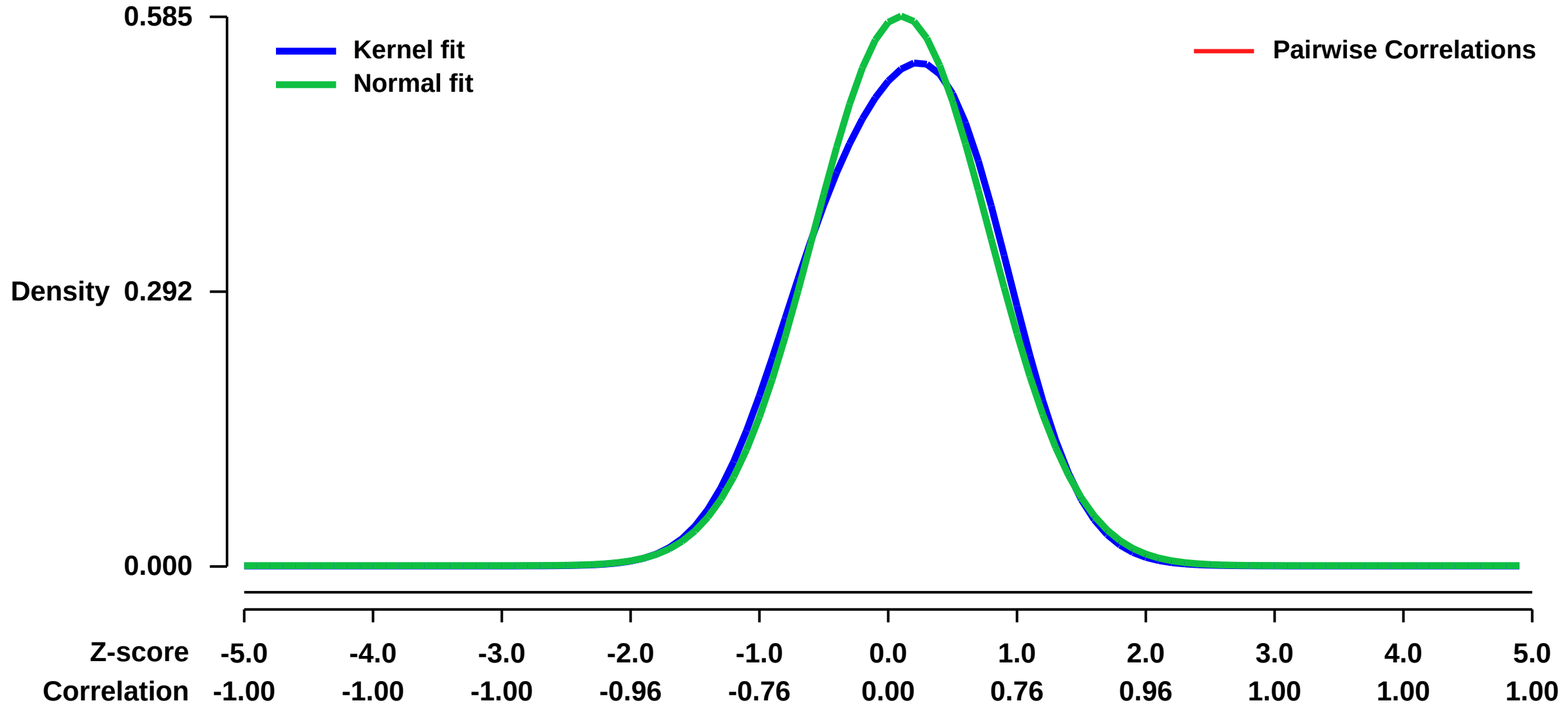

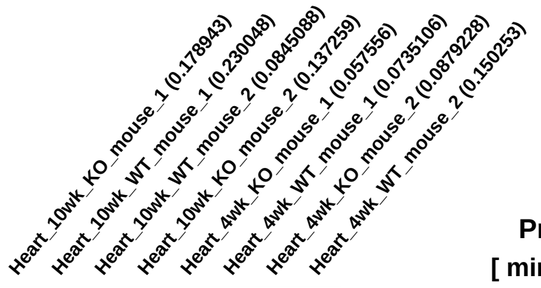

Pre-normalization Quantiles

[min] [medium] [max]

Null module

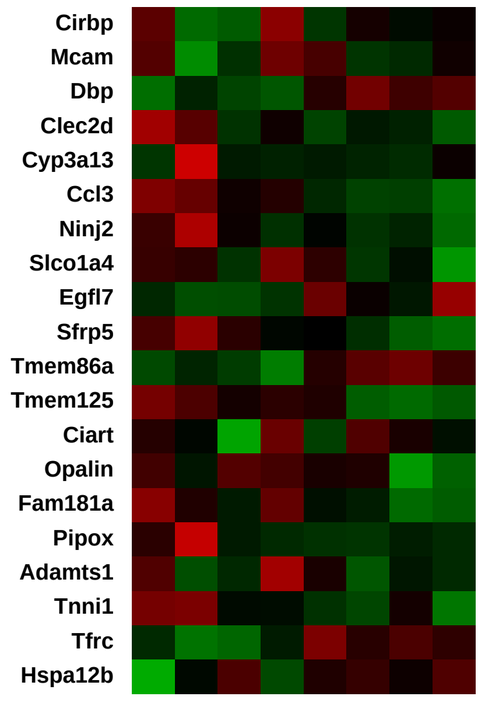

GEO Series "GSE31244" Expression Profiles

Num of samples in this series: 6

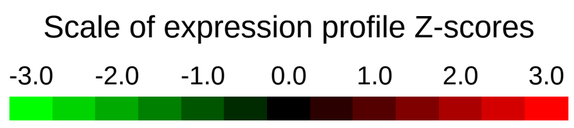

GEO Link:	http://www.ncbi.nlm.nih.gov/geo/query/acc.cgi?acc=GSE31244
Status:	Public on Aug 09 2011
Title:	Notch1 mediates cell fate decisions in the mouse uterus and is critical for complete decidualization
Organism:	Mus musculus
Experiment type:	Expression profiling by array
Platform:	GPL1261
Pubmed ID:	21990372
Summary & Design:	**Summary:** Uterine receptivity implies a dialogue between the hormonally primed maternal endometrium and the free-floating blastocyst. Endometrial stromal cells proliferate, avert apoptosis, and undergo decidualization in preparation for implantation; however, the molecular mechanisms that underlie differentiation into the decidual phenotype remain largely undefined. The Notch family of transmembrane receptors transduce extracellular signals responsible for cell survival, cell-to-cell communication, and trans-differentiation, all fundamental processes for decidualization and pregnancy. Using a murine artificial decidualization model, pharmacological inhibition of Notch signaling by gamma-secretase inhibition resulted in significantly decreased deciduoma. Furthermore, a progesterone receptor (PR)-Cre Notch1 bigenic (Notch1d/d) confirmed a Notch1-dependant hypomorphic decidual phenotype. Microarray and pathway analysis, following Notch1 ablation, demonstrated significantly altered signaling repertoire. Concomitantly, hierarchical clustering demonstrated Notch1-dependent differences in gene expression. Uteri deprived of Notch1 signaling demonstrated decreased cellular proliferation; namely, reduced proliferation-specific antigen, Ki67, altered p21, cdk6, and cyclinD activity, and increased apoptotic-profile, augmented cleaved caspase-3, Bad, and attenuated Bcl2. Demonstrated here, the pre-implantation uterus relies on Notch signaling to inhibit apoptosis of stromal fibroblasts and regulate cell cycle progression, which together promotes successful decidualization. In summary, Notch1 signaling modulates multiple signaling mechanisms crucial for decidualization and we provide greater perspective to the coordination of multiple signaling modalities required during decidualization **Overall design:** RNA samples from 3-5 separate mice were extracted. All mRNA quantities were normalized against 18S gene expression. Gene expression levels were measured by real-time RT-PCR SYBR Green analysis using the ABI Prism 7700 Sequence Detector System according to manufacturerâ s instructions (Applied Biosystems).

Background corr dist: KL-Divergence = 0.0271, L1-Distance = 0.0121, L2-Distance = 0.0002, Normal std = 0.6810

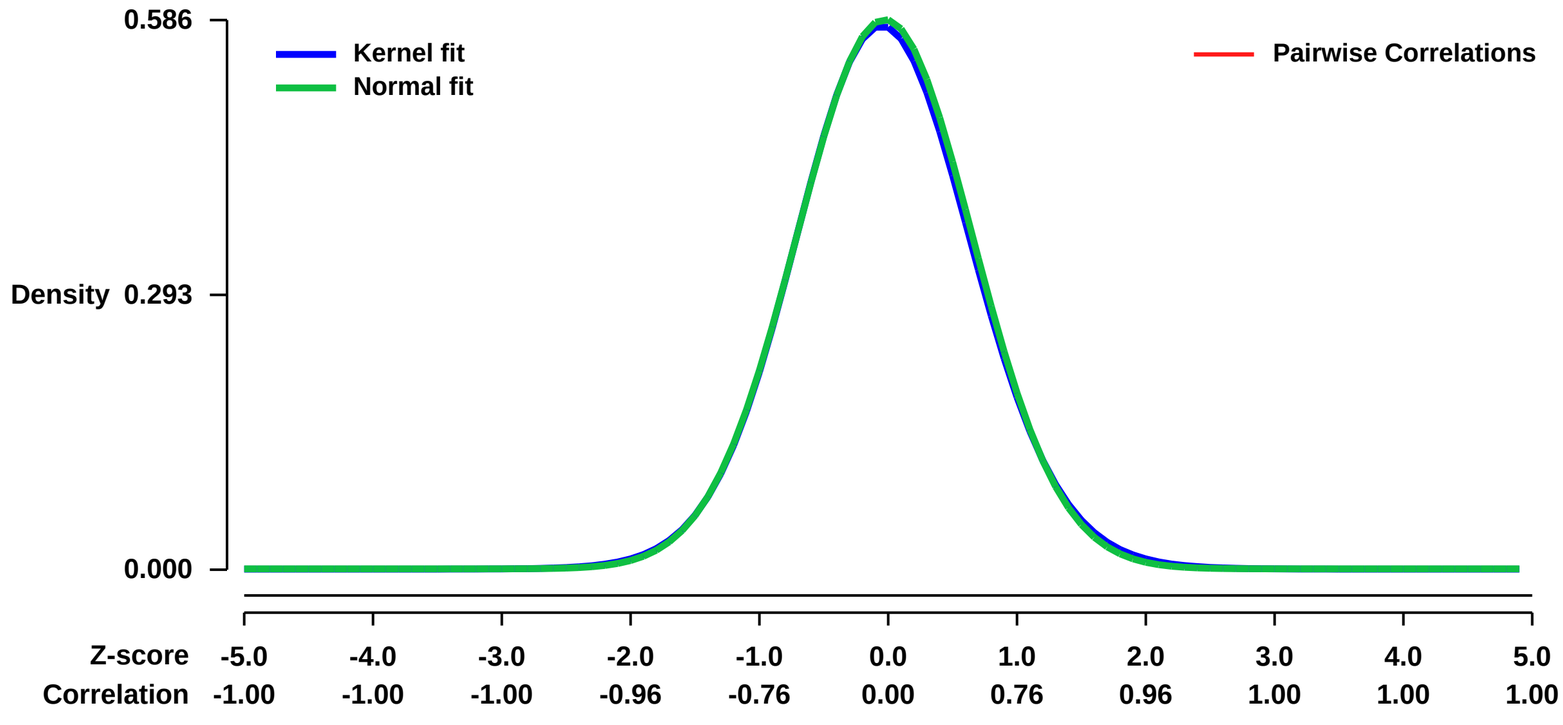

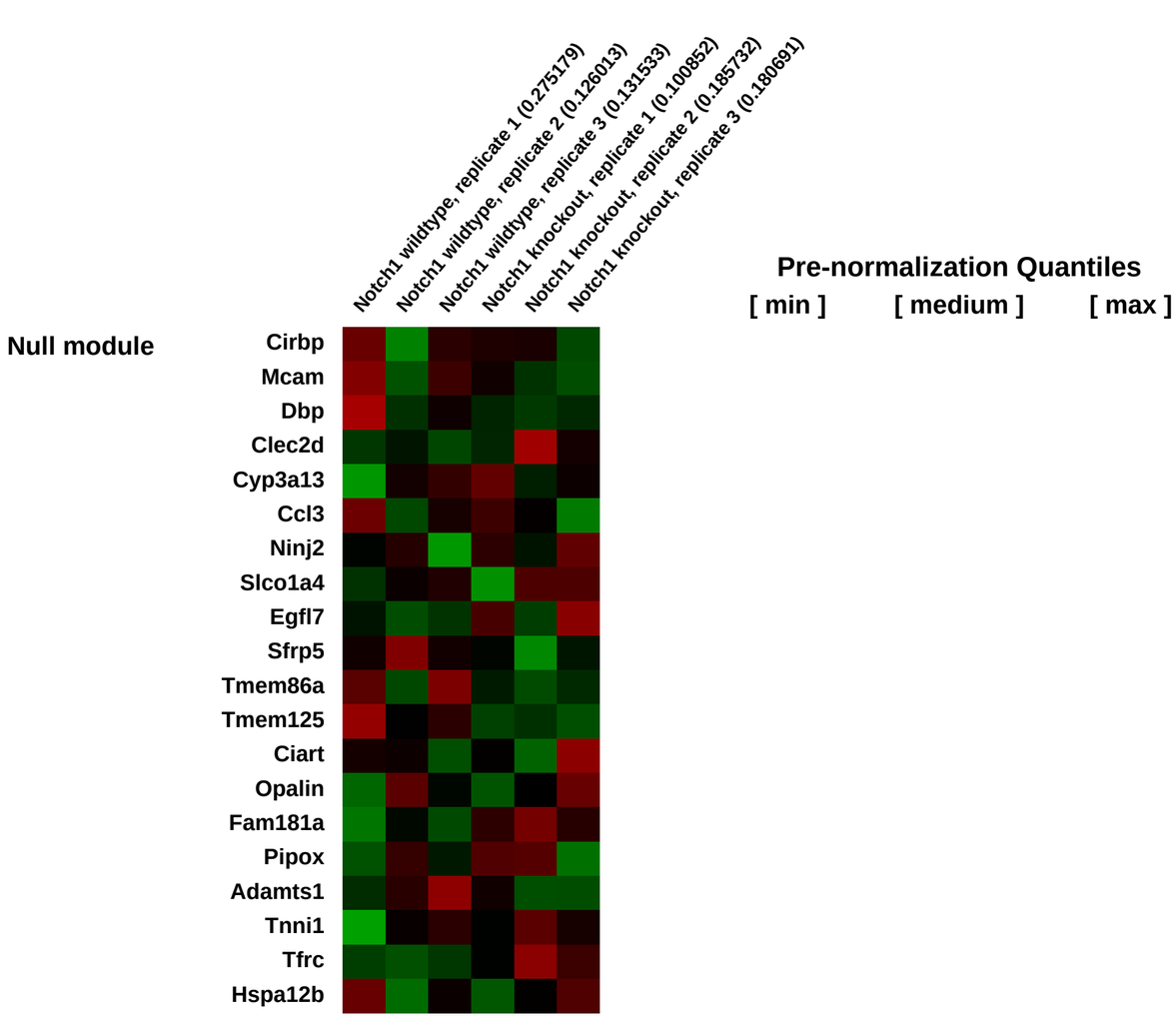

GEO Series "GSE31246" Expression Profiles

Num of samples in this series: 12

Scale of expression profile Z-scores

-3.0 -2.0 -1.0 0.0 1.0 2.0 3.0

GEO Link:	http://www.ncbi.nlm.nih.gov/geo/query/acc.cgi?acc=GSE31246
Status:	Public on Aug 08 2012
Title:	Expression data from SP and non-SP sorted anti-EpCAM treated A2C12 cells
Organism:	Mus musculus
Experiment type:	Expression profiling by array
Platform:	GPL1261
Pubmed ID:	
Summary & Design:	**Summary:** Targeted therapies against cancer stem cells which are enriched in side populations (SP) involves interruption of Wnt-signalling. Furthermore, EpCAM is a SP marker and modulator of Wnt-signalling. Therefore, the effects of an anti-EpCAM treatment on SP-cells and WNT/¸†-catenin signalling was studied. SP of the murine lung adenocarcinoma cell line A2C12 was obtained by fluorescence activated cell sorting and whole genome scans helped to define their molecular phenotype after anti-EpCAM antibody treatment. **Overall design:** Anti-EpCAM treated and untreated A2C12 cells were subjected to Hoechst 33342 dye exclusion assay and sorted to SP and non-SP fractions by FACS. Three biological replicates.

Background corr dist: KL-Divergence = 0.0751, L1-Distance = 0.0299, L2-Distance = 0.0015, Normal std = 0.4823

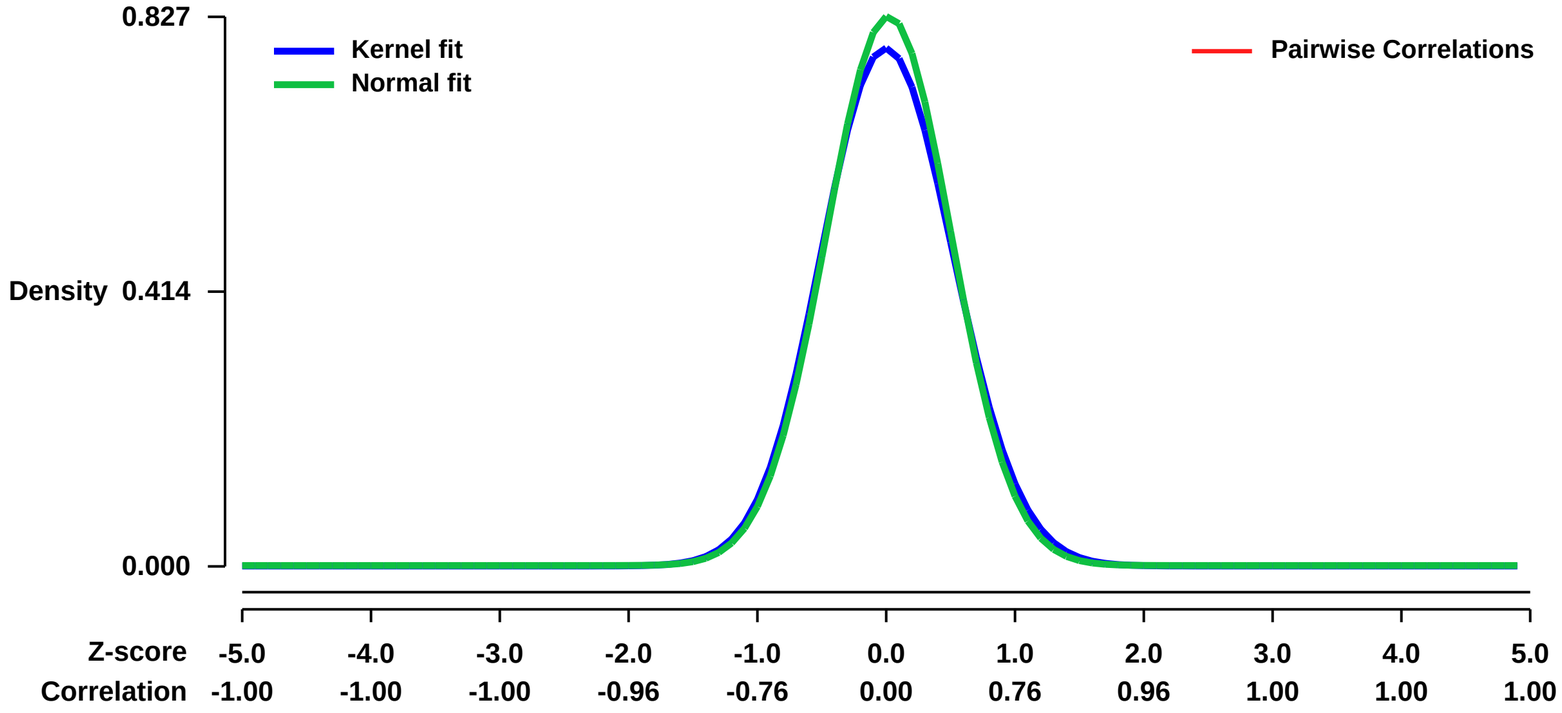

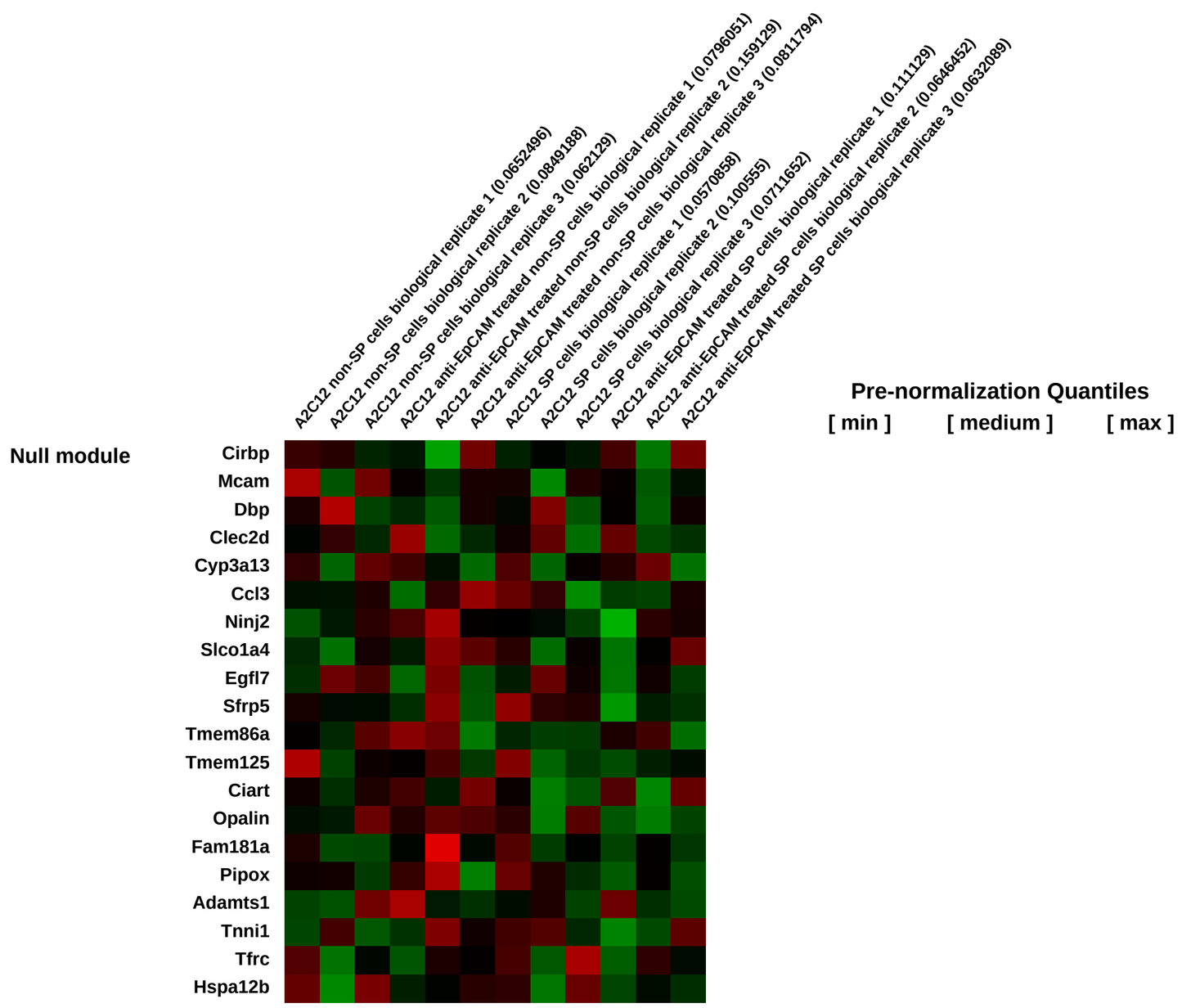

GEO Series "GSE3126" Expression Profiles

Num of samples in this series: 6

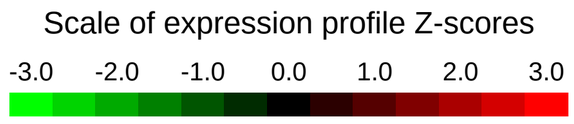

GEO Link:	**http://www.ncbi.nlm.nih.gov/geo/query/acc.cgi?acc=GSE3126**
Status:	**Public on Dec 31 2005**
Title:	**Comparison of HNF4 null mouse embryonic livers with control mouse embryonic livers**
Organism:	**Mus musculus**
Experiment type:	**Expression profiling by array**
Platform:	**GPL1261**
Pubmed ID:	**16714383**
Summary & Design:	**Summary:** **To study the role of hepatic nuclear factor alpha (HNF4a in hepatogenesis, we used loxP-Cre technology to eliminate it from developing mouse livers.** **A comparison of control and experimental livers revealed that hepatocytes lacking HNF4a_failed to fully differentiate. Specifically, HNF4a null liver cells failed to express genes that are markers of mature hepatocytes including Gys2, Pck1, and G6pc. These cells also failed to form normal cellular junctions, which are critical for establishment of the hepatic epithelium [Parviz et al. (2003) Nat.Genet. 34, 292-96]. Because HNF4a functions as a transcription factor, we hypothesized that it regulates liver development by controlling the expression of genes whose products are essential in executing cellular differentiation and morphogenesis. To identify these genes, we compared expression profiles between HNF4a null and wild type E18.5 fetal livers using Affymetrix gene arrays. We identified 564 genes whose expression was decreased by at least 2.5-fold and 34 genes whose expression was increased by at least 2.5-fold when HNF4a was eliminated from hepatocytes. These represent genes involved in diverse molecular pathways, reflecting the pleiotropic phenotype of HNF4a null livers. Our goal was to use the information from the gene arrays to define the mechanisms through which HNF4a controls the generation of the hepatic epithelium. We identified 27 genes from our list of downregulated genes with either defined or predicted roles in cellular junctions and/or adhesion. Most striking was that loss of HNF4a altered the expression of genes encoding proteins involved in virtually all types of cellular junctions including tight junctions (Cldn1, Cldn-2, Cldn-12, Ocln, F11r/Jam1, Cxadr, Crb3), adherens junctions (Cdh1), desmosomes (Dsc2, Pkp2, Krt2-8), and gap junctions (Gjb1, Gjb2). Using immunoblotting and immunohistochemistry, we found that the expression of proteins representing each of these junction types was reduced or absent. Analysis of these genes for the presence of putative HNF4a binding sites revealed that 25 of 27 contain such sites. We have used chromatin immunoprecipitation to confirm that HNF4a occupies several of these sites in vivo, including Cdh1, Cldn1, and F11r/Jam1. From these data, we conclude that HNF4a is a central mediator of the fully differentiated hepatocyte gene expression program and that it orchestrates the expression of cell junction and adhesion proteins required for establishing the hepatic epithelium.** **Keywords: E18.5 fetal hnf4 null and control mouse livers** **Overall design:** **comparison of three hnf4 null livers to three control**

Background corr dist: KL-Divergence = 0.0251, L1-Distance = 0.0111, L2-Distance = 0.0001, Normal std = 0.6969

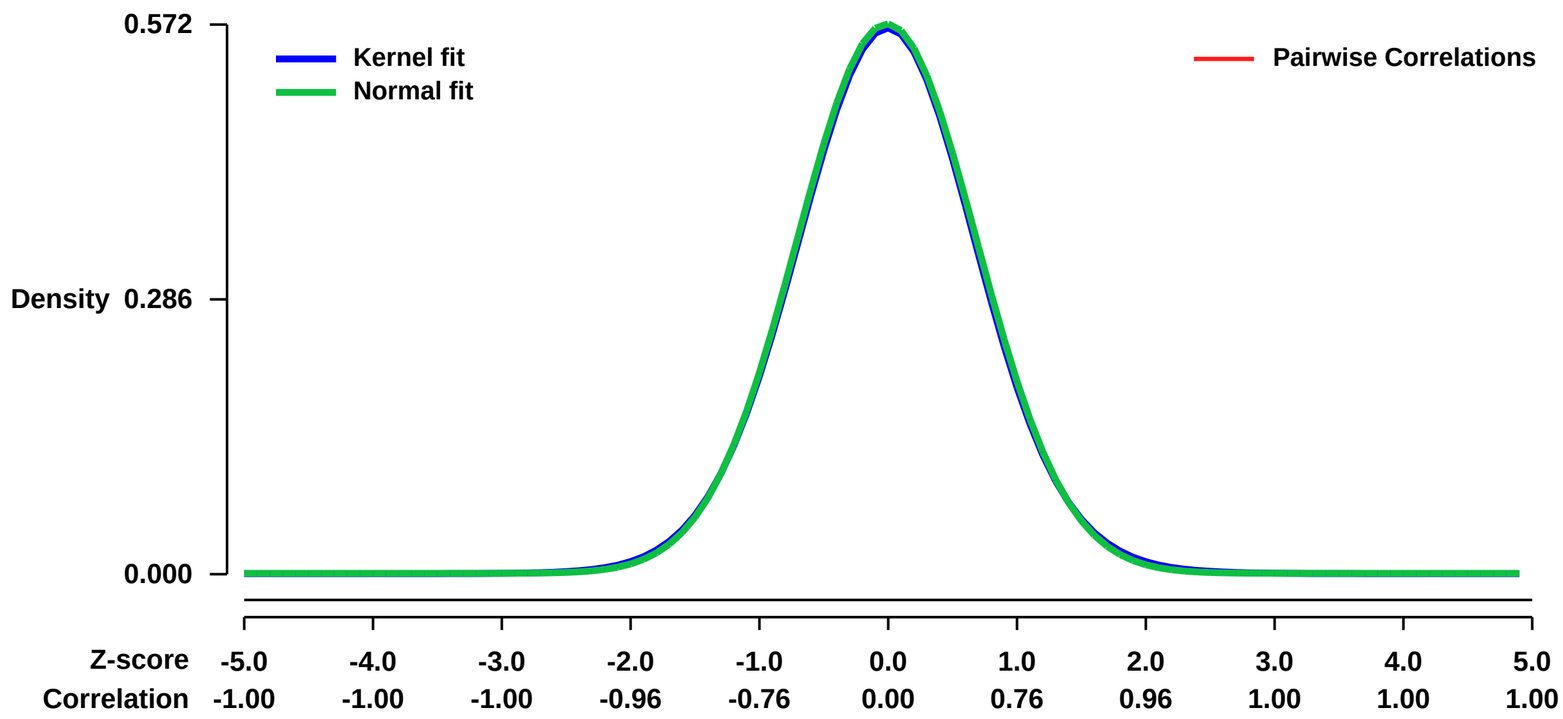

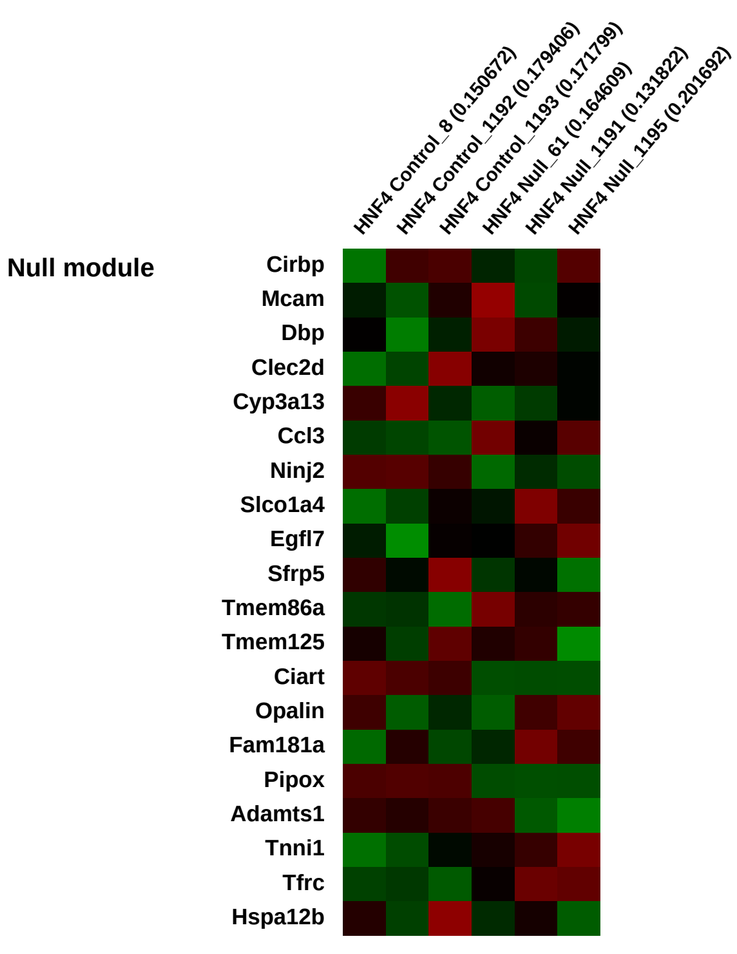

GEO Series "GSE31359" Expression Profiles

Num of samples in this series: 8

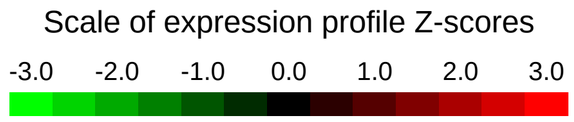

GEO Link:	**http://www.ncbi.nlm.nih.gov/geo/query/acc.cgi?acc=GSE31359**
Status:	**Public on Aug 13 2011**
Title:	**Expression data from mouse EMT-induced and non-induced cells**
Organism:	**Mus musculus**
Experiment type:	**Expression profiling by array**
Platform:	**GPL1261**
Pubmed ID:	
Summary & Design:	**Summary:** **The conversion of an epithelial cell to a mesenchymal cell is critical to vertebrate embryogenesis and a defining structural feature of organ development, such as forming fibroblasts in injured tissues, or in initiating metastases in epithelial cancer. From a general perspective, EMT is about disaggregating epithelial units and reshaping epithelia for movement. This phenotypic conversion requires the molecular reprogramming of epithelia with new biochemical instructions. It is known that commonly used molecular markers for EMT include increased expression of N-cadherin and vimentin, nuclear localization of beta-catenin, and increased production of the transcription factors such as Snail, Twist, and SIP1/ZEB2. Much of this conversion, however, has been studied during experiments that expose new transduction and signaling pathways in epithelia, and more recently in fibrogenic tissues. It is not yet clear whether the fibroblast transition of EMT is an expected middle phase of transdifferentiating epithelia, or whether EMT producing fibroblasts is an arrested form of transdifferentiation. EMT is easily engaged by a combination of cytokines associated with proteolytic digestion of basement membranes upon which epithelia reside. We analyzed PCA and hierarchical clustering method of the gene expression pattern of the renal tubular cells and mammary gland cells. We then identified the genes which discriminate between the renal tubular and the mammary gland epithelial cells (PC1), or EMT-induced and non-induced cells (PC3). Undergoing EMT identifies the genes that discriminate between the renal tubular and the mammary gland epithelial cells(PC1), or EMT-induced and non-induced cells (PC3).** **Overall design:** **Affymetrix GeneChip Mouse Genome 430 2.0 Array was used to transcriptionally profile to compare mouse EMT-induced cells and non-induced cells.**

Background corr dist: KL-Divergence = 0.0562, L1-Distance = 0.0330, L2-Distance = 0.0017, Normal std = 0.5554

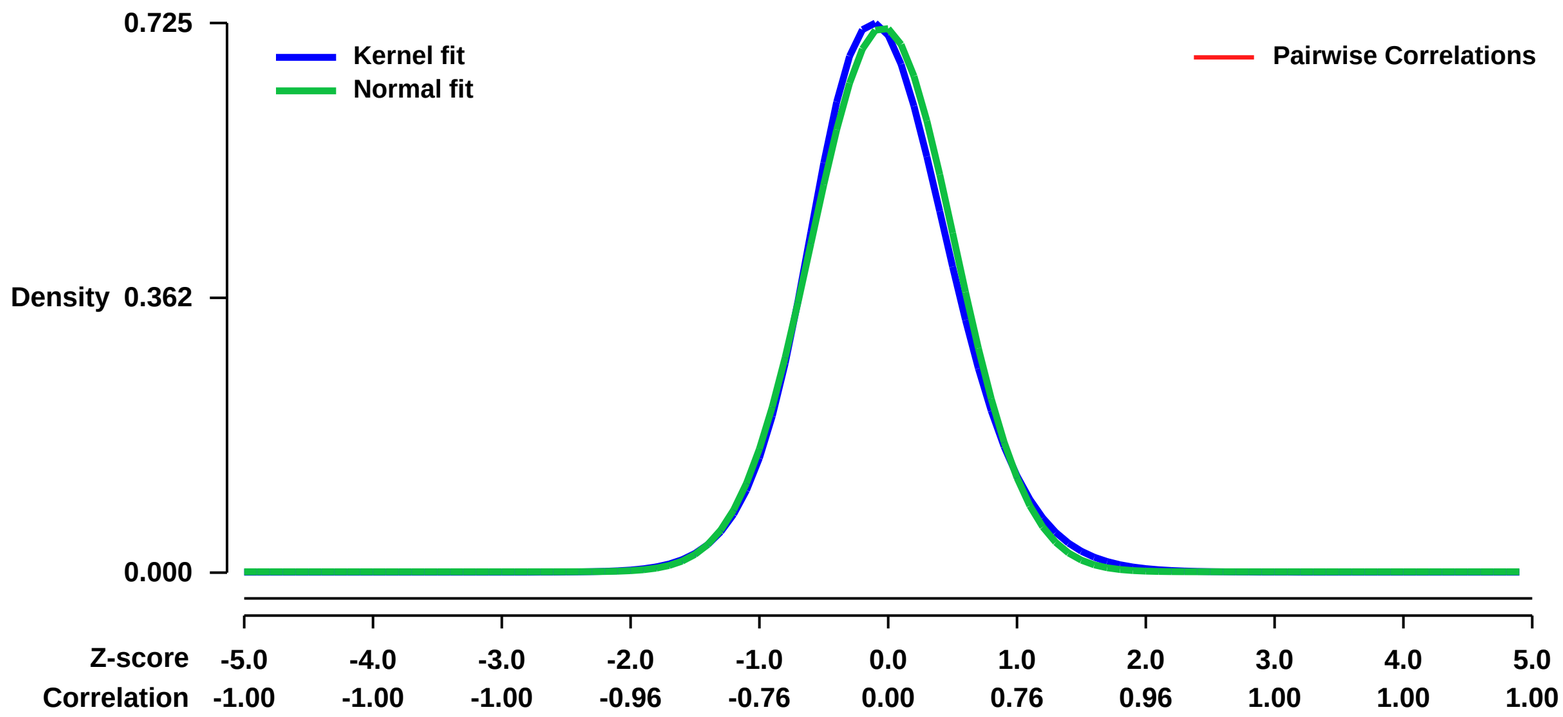

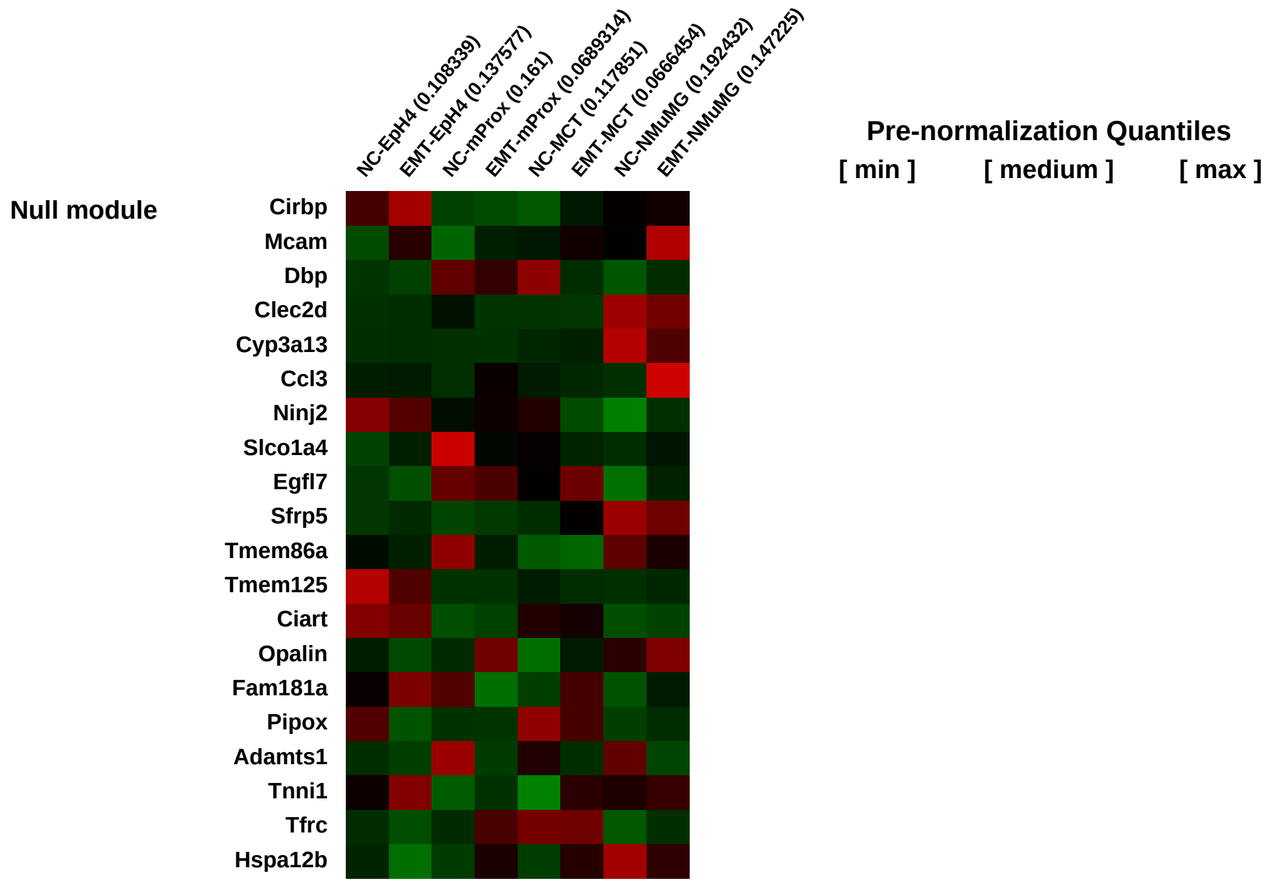

GEO Series "GSE31378" Expression Profiles

Num of samples in this series: 9

Scale of expression profile Z-scores

-3.0 -2.0 -1.0 0.0 1.0 2.0 3.0

GEO Link:	http://www.ncbi.nlm.nih.gov/geo/query/acc.cgi?acc=GSE31378
Status:	Public on Aug 16 2013
Title:	Host cell gene expression in Human respiratory syncytial virus (HRSV) infected mouse macrophage cells at 4, 24 hours post infection
Organism:	Mus musculus
Experiment type:	Expression profiling by array
Platform:	GPL1261
Pubmed ID:	23506210
Summary & Design:	**Summary:** We used the microarray data to analyze host cells response on mouse macrophage cells infected with HRSV **Overall design:** The HRSV infected mouse macrophage cells were harvested at 4 and 24 hpi and RNA extraction was performed using standard protocol as described by Affymetrix. The aim of this experiment is to analyze host cell response to HRSV infection.

Background corr dist: KL-Divergence = 0.0597, L1-Distance = 0.0481, L2-Distance = 0.0032, Normal std = 0.5745

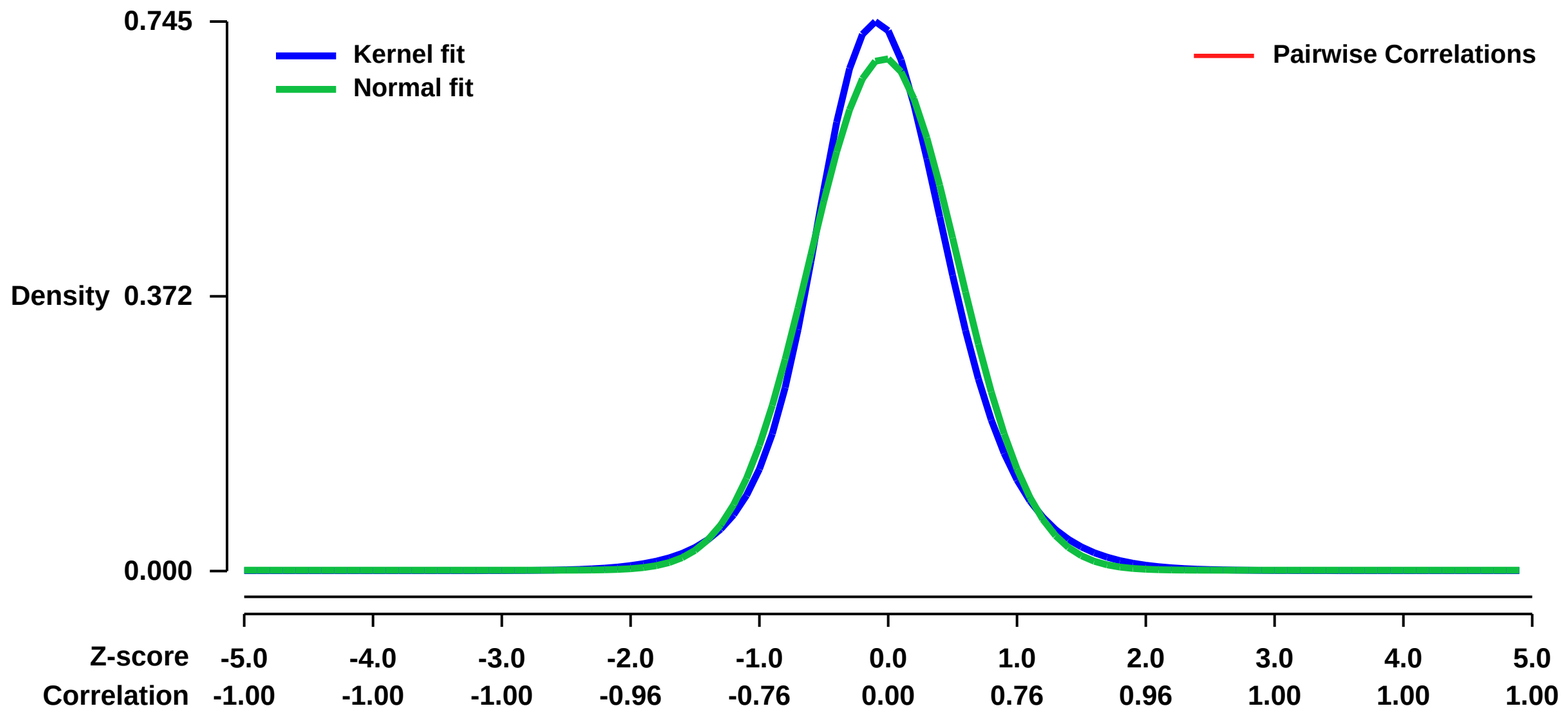

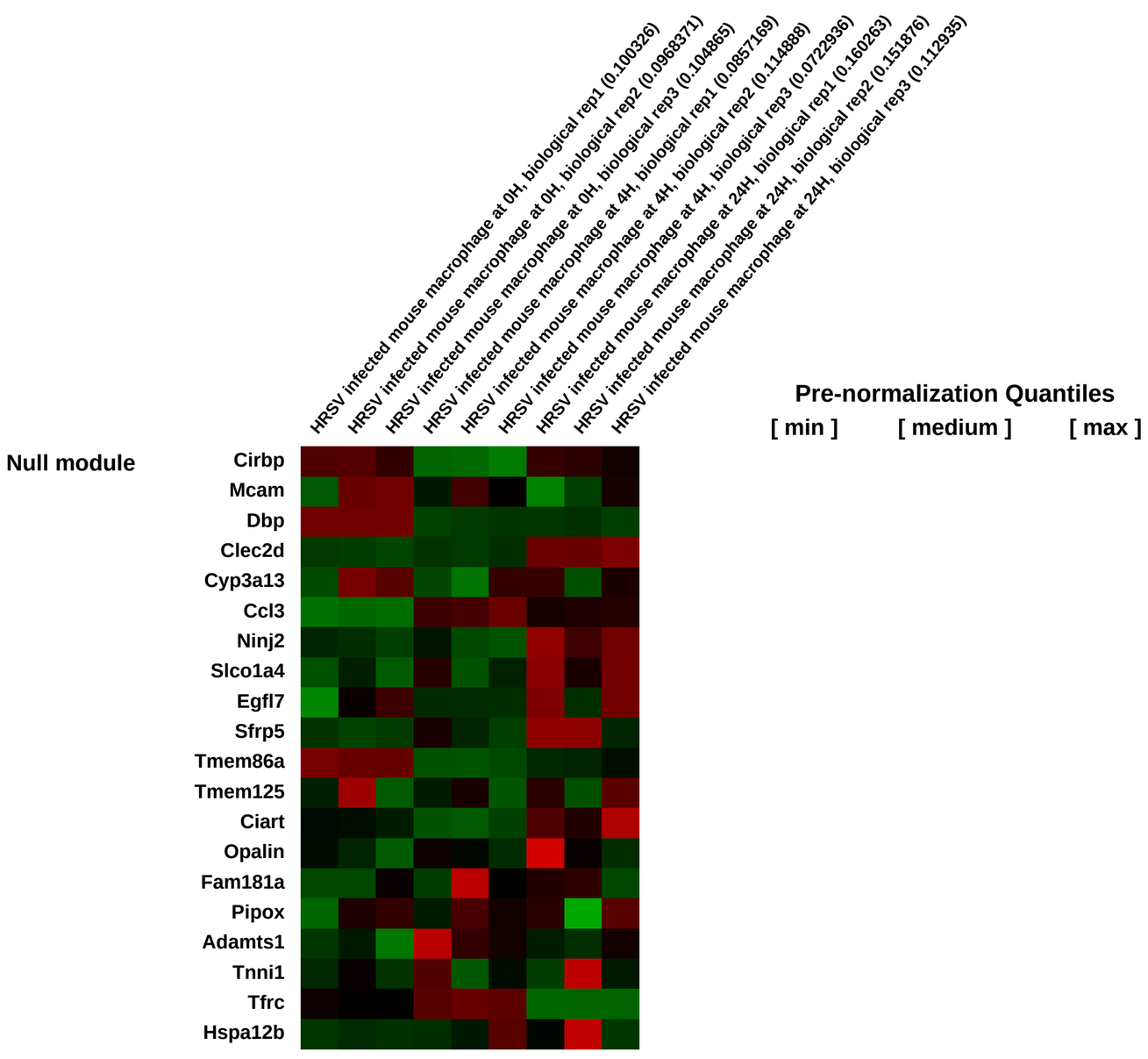

GEO Series "GSE31406" Expression Profiles

Num of samples in this series: 12

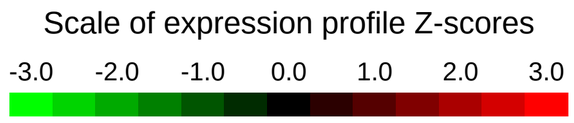

GEO Link:	http://www.ncbi.nlm.nih.gov/geo/query/acc.cgi?acc=GSE31406
Status:	Public on Apr 01 2014
Title:	Gene expression analyses of PR action in the uteri of SRC-2 mutant mice
Organism:	Mus musculus
Experiment type:	Expression profiling by array
Platform:	GPL1261
Pubmed ID:	24571987
Summary & Design:	**Summary:** Ovarian estrogen (E2) and progesterone (P4) are indispensable for embryo-implantation and endometrial stromal decidualization; however, the molecular mechanisms that underpin these reproductive processes are unclear. Steroid receptor coregulator-2 (SRC-2) belongs to the multifunctional SRC/p160 family which also includes SRC-1 and SRC-3. Sharing strong sequence homology, all three SRCs exert diverse regulatory effects by modulating the transcriptional potency of nuclear receptor family members, including the estrogen and progesterone receptor (ER and PR respectively). Importantly, absence of SRC-2 in PR positive cells in the epithelial, stromal, and myometrial compartments of the murine uterus results in a striking infertility defect. This reproductive phenotype highlights a key role for SRC-2 in uterine function which is not shared with other coregulators. Intriguingly, abrogation of uterine SRC-2 does not block embryo apposition or attachment to the apical surface of luminal epithelial cells of the endometrium but rather prevents P4-dependent local decidualization of the sub-epithelial stroma. Remarkably, epithelial-specific ablation of SRC-2 in the murine uterus does not compromise endometrial functionality, again underscoring the unique importance of stromal derived SRC-2 in uterine function. The stromal decidualization defect resulting from SRC-2 ablation is reflected at the molecular level by a marked attenuation in P4 responsive target genes known to be critical for P4 dependent decidualization (i.e. ERBB receptor feedback inhibitor 1, Follistatin and Fkbp5). Conversely, the induction of E2 or P4 target genes involved in embryo implantation (i.e. leukemia inhibitory factor (LIF) and Indian hedgehog (Ihh) respectively) is not affected by SRC-2â s absence. As with mouse studies, decidualization of primary human stromal cells (HESCs) in culture is blocked by SRC-2 knockdown; however, HESC decidualization is unaffected by knockdown of SRC-1 or SRC-3. As a consequence of SRC-2 knockdown, molecular studies disclose a striking decrease in the induction of a subset of P4 target genes (i.e. WNT4 and FKBP5) which are essential for the stromal-epithelioid transformation step, the cellular hallmark of endometrial decidualization. Collectively, these studies not only showcase the evolutionary importance of SRC-2 in endometrial biology but also suggest that deregulation of this coregulator may underpin a spectrum of hormone-dependent uterine pathologies such as endometriosis and endometrial cancer. **Overall design:** multiple group comparison

Background corr dist: KL-Divergence = 0.0933, L1-Distance = 0.0314, L2-Distance = 0.0013, Normal std = 0.4618

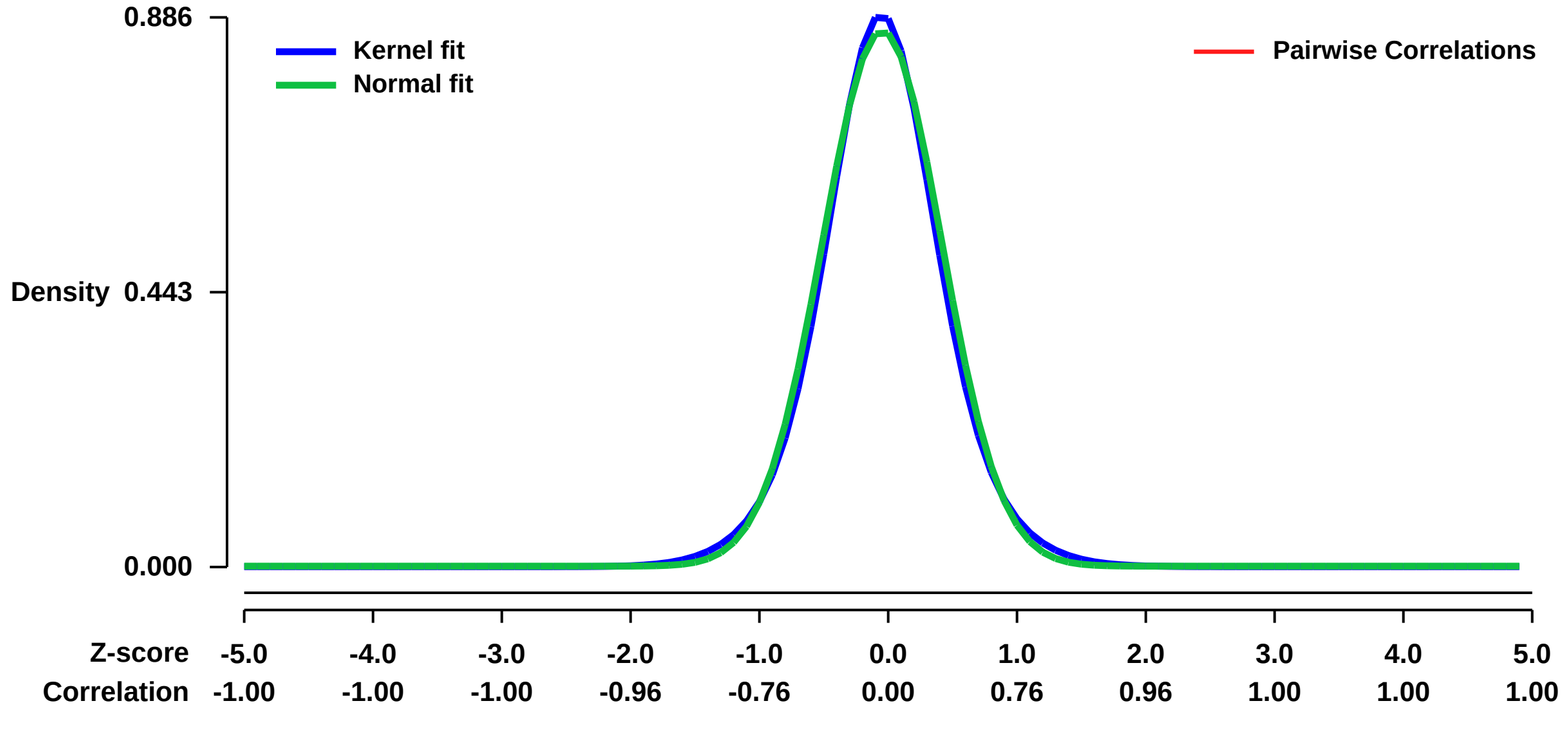

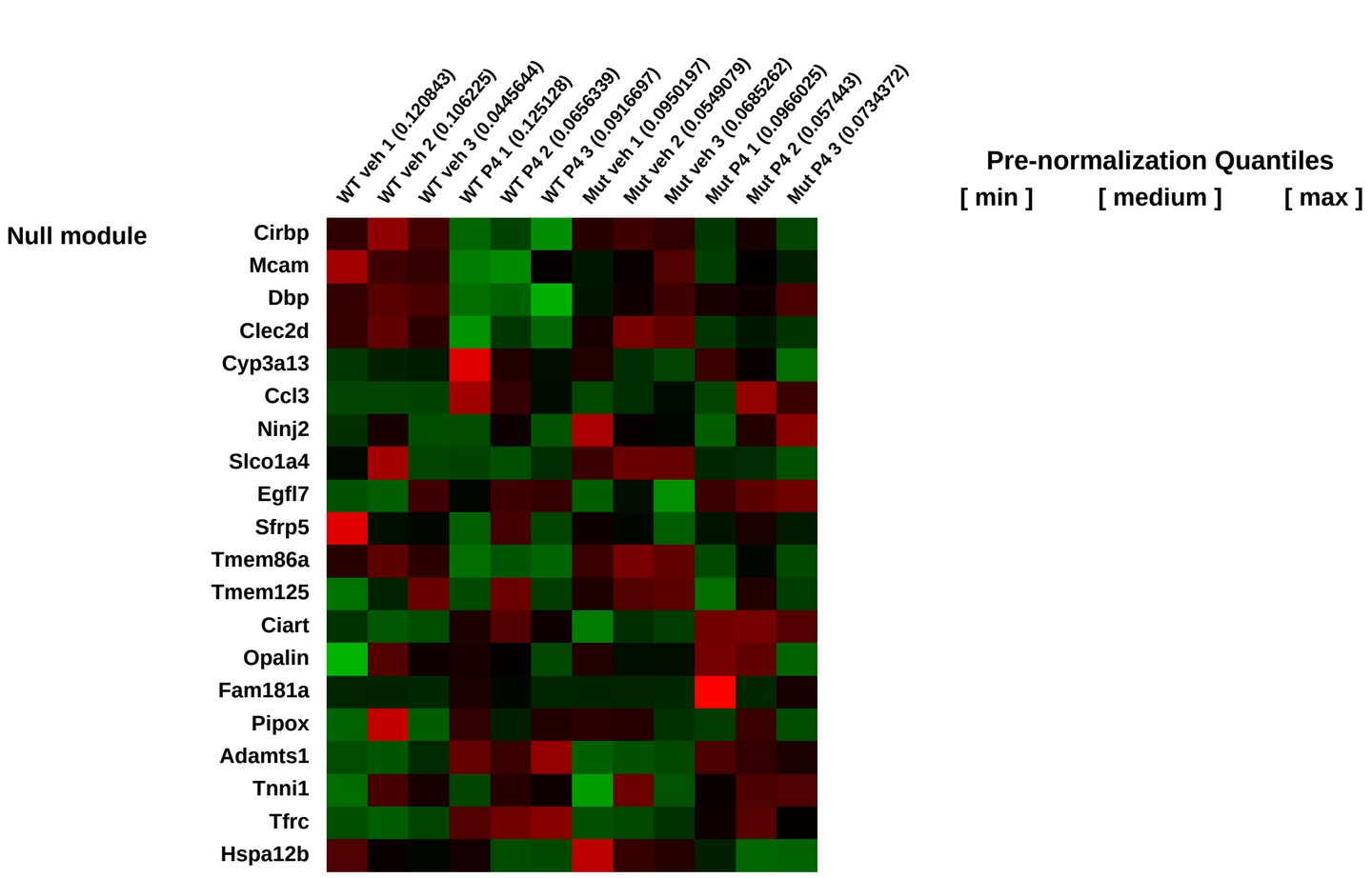

GEO Series "GSE31453" Expression Profiles

Num of samples in this series: 13

Scale of expression profile Z-scores

-3.0 -2.0 -1.0 0.0 1.0 2.0 3.0

GEO Link:	http://www.ncbi.nlm.nih.gov/geo/query/acc.cgi?acc=GSE31453
Status:	Public on Aug 07 2012
Title:	Genome-wide analysis of gene expression patterns in the liver tumors of mir-122 knockout mice
Organism:	Mus musculus
Experiment type:	Expression profiling by array
Platform:	GPL1261
Pubmed ID:	22820290
Summary & Design:	**Summary:** To invesigate the physiological roles of mir-122 in hepatocarcinogenesis, we performed expression profiling of the liver tumors of mir-122 knockout mice and the liver tissues of the control B6/129 mice. **Overall design:** Total RNA was extracted from three tumors of mir-122 knockout mice and liver tissues of two control mice of 11 months of age; five tumors of mir-122 knockout mice and the liver tissues of three control mice of 14 months of age. Gene expression was quantified by robust multi-array analysis (RMA) using the Genomic Suite software from Partek.

Background corr dist: KL-Divergence = 0.0913, L1-Distance = 0.0362, L2-Distance = 0.0026, Normal std = 0.4497

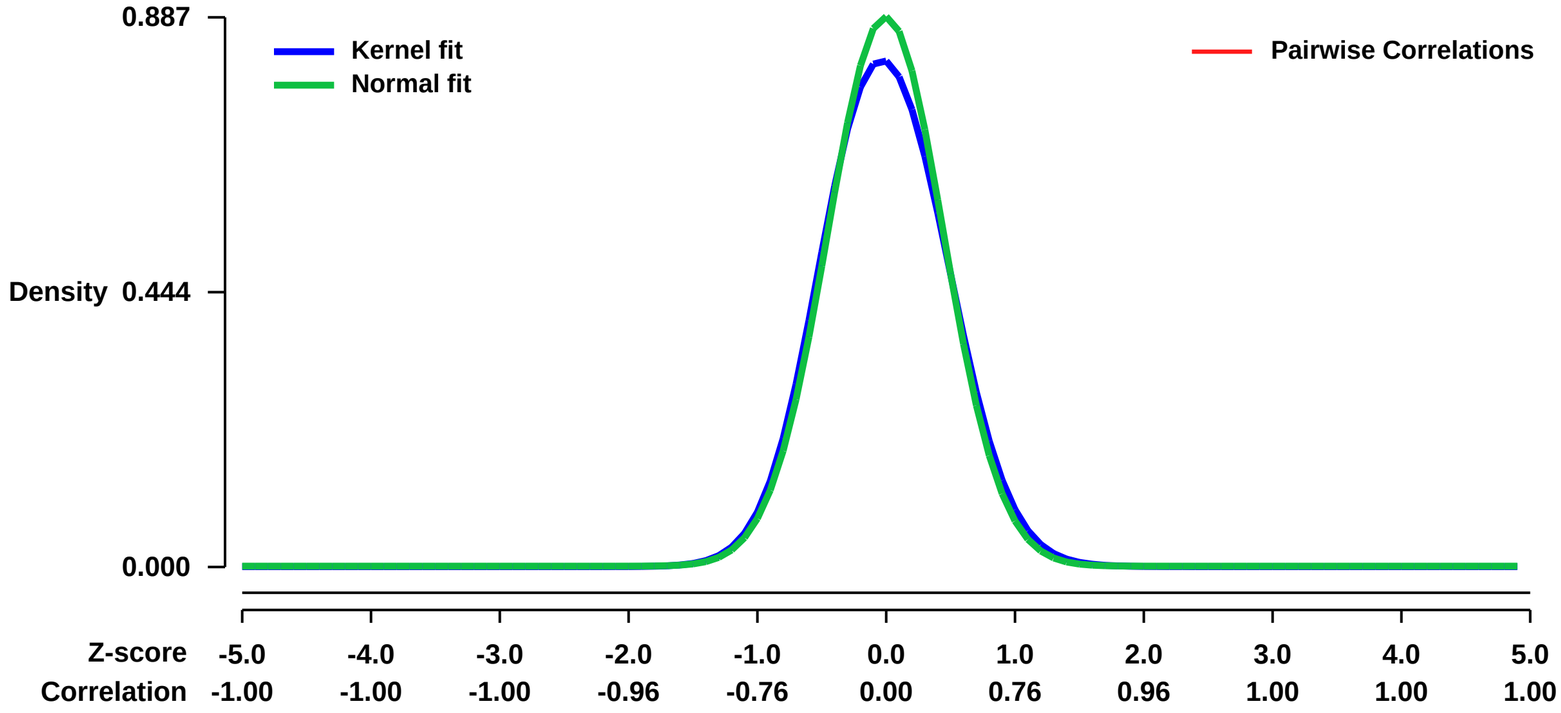

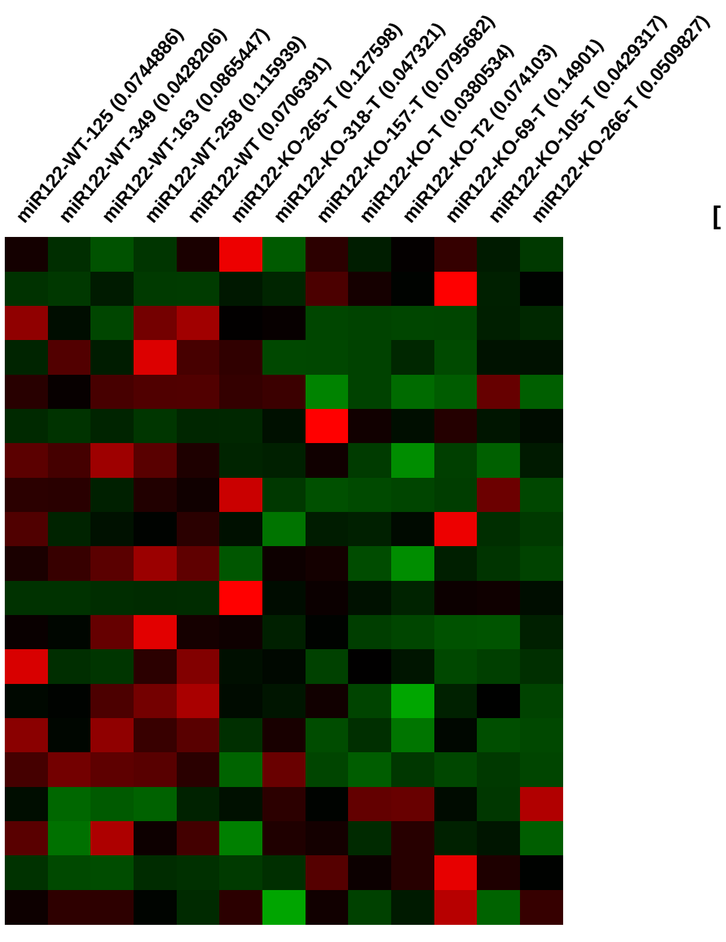

GEO Series "GSE31638" Expression Profiles

Num of samples in this series: 15

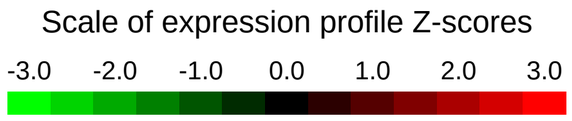

GEO Link:	http://www.ncbi.nlm.nih.gov/geo/query/acc.cgi?acc=GSE31638
Status:	Public on Aug 31 2011
Title:	Expression data from primary hepatocytes knocking down or overexpressing IRE1a
Organism:	Mus musculus
Experiment type:	Expression profiling by array
Platform:	GPL1261
Pubmed ID:	21911379
Summary & Design:	**Summary:** The ER-resident protein kinase/endoribonuclease IRE1 is activated through trans-autophosphorylation in response to protein folding overload in the ER lumen and maintains ER homeostasis by triggering a key branch of the unfolded protein response. Here we show that mammalian IRE1a in liver cells is also phosphorylated by a kinase other than itself in response to metabolic stimuli. Glucagon stimulated protein kinase PKA, which in turn phosphorylated IRE1a at Ser724, a highly conserved site within the kinase activation domain. Blocking Ser724 phosphorylation impaired the ability of IRE1a to augment the upregulation by glucagon signaling of the expression of gluconeogenic genes. Moreover, hepatic IRE1a was highly phosphorylated at Ser724 by PKA in mice with obesity, and silencing hepatic IRE1a markedly reduced hyperglycemia and glucose intolerance. Hence, these results suggest that IRE1a integrates signals from both the ER lumen and the cytoplasm in the liver and is coupled to the glucagon signaling in the regulation of glucose metabolism. We used DNA microarray to analyze the transcriptomic change upon IRE1a overexpression or IRE1a depletion in primary hepatocytes, to study the changes related to IRE1a **Overall design:** Primary hepatocytes were infected with the desired adenoviruses (Ad-EGFP, Ad-WT, Ad-S724A, Ad-shCON, Ad-shIRE1a#2) or treated with glucagon. Total cellular RNA was isolated with TRIzol (Invitrogen) and subjected to analysis by Affymetrix Mouse Genome 430 2.0 Arrays. Three experiments were independently conducted.

Background corr dist: KL-Divergence = 0.1161, L1-Distance = 0.0361, L2-Distance = 0.0027, Normal std = 0.4128

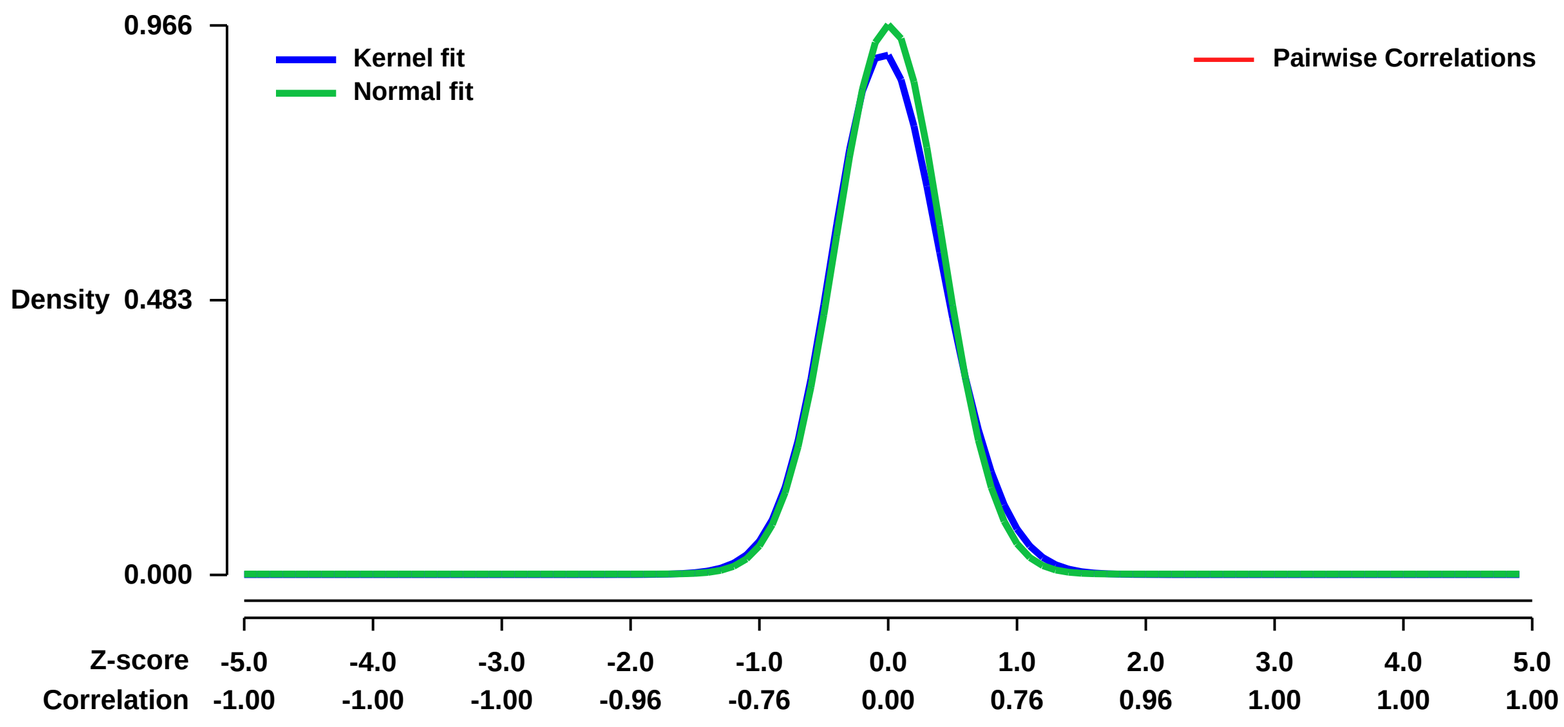

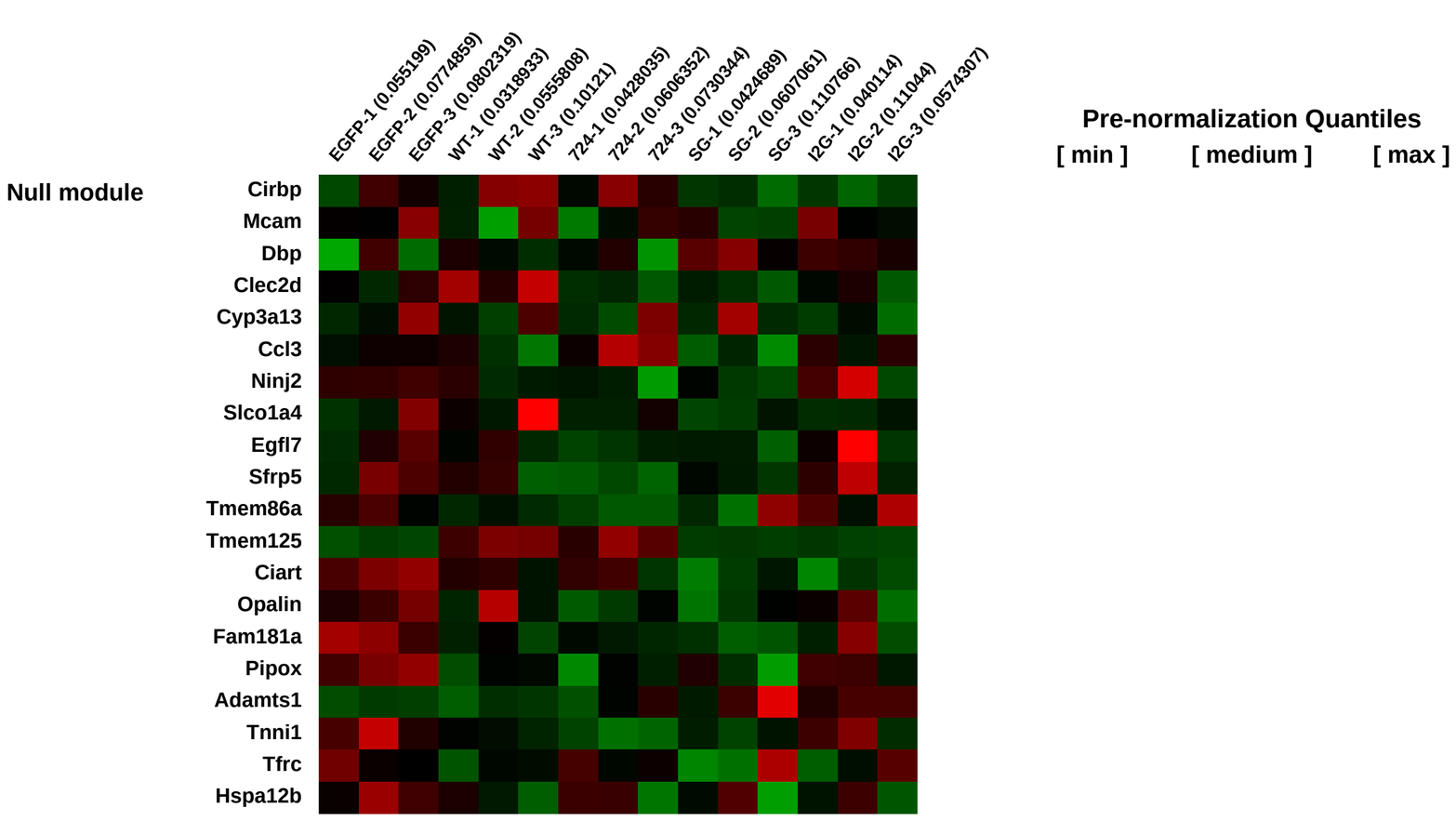

GEO Series "GSE31646" Expression Profiles

Num of samples in this series: 11

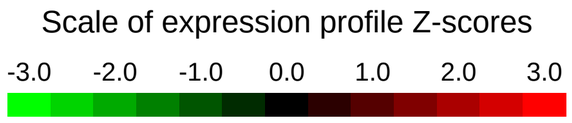

GEO Link:	http://www.ncbi.nlm.nih.gov/geo/query/acc.cgi?acc=GSE31646
Status:	Public on Mar 31 2012
Title:	Adipose tissue in the presence or absence of kinin B1 receptors
Organism:	Mus musculus
Experiment type:	Expression profiling by array
Platform:	GPL1261
Pubmed ID:	
Summary & Design:	**Summary:** We studied adipose tissue from wild type mice, kinin B1 receptor knockout mice (B1KO), and B1KO mice with rescued expression of kinin B1 receptor selectively in fat. We used microarrays to detail the gene expression profile of the epididymal fat of these mice. **Overall design:** Three-month-old mice were killed and tissue was collected for RNA processing and microarray analysis.

Background corr dist: KL-Divergence = 0.1556, L1-Distance = 0.0390, L2-Distance = 0.0031, Normal std = 0.3671

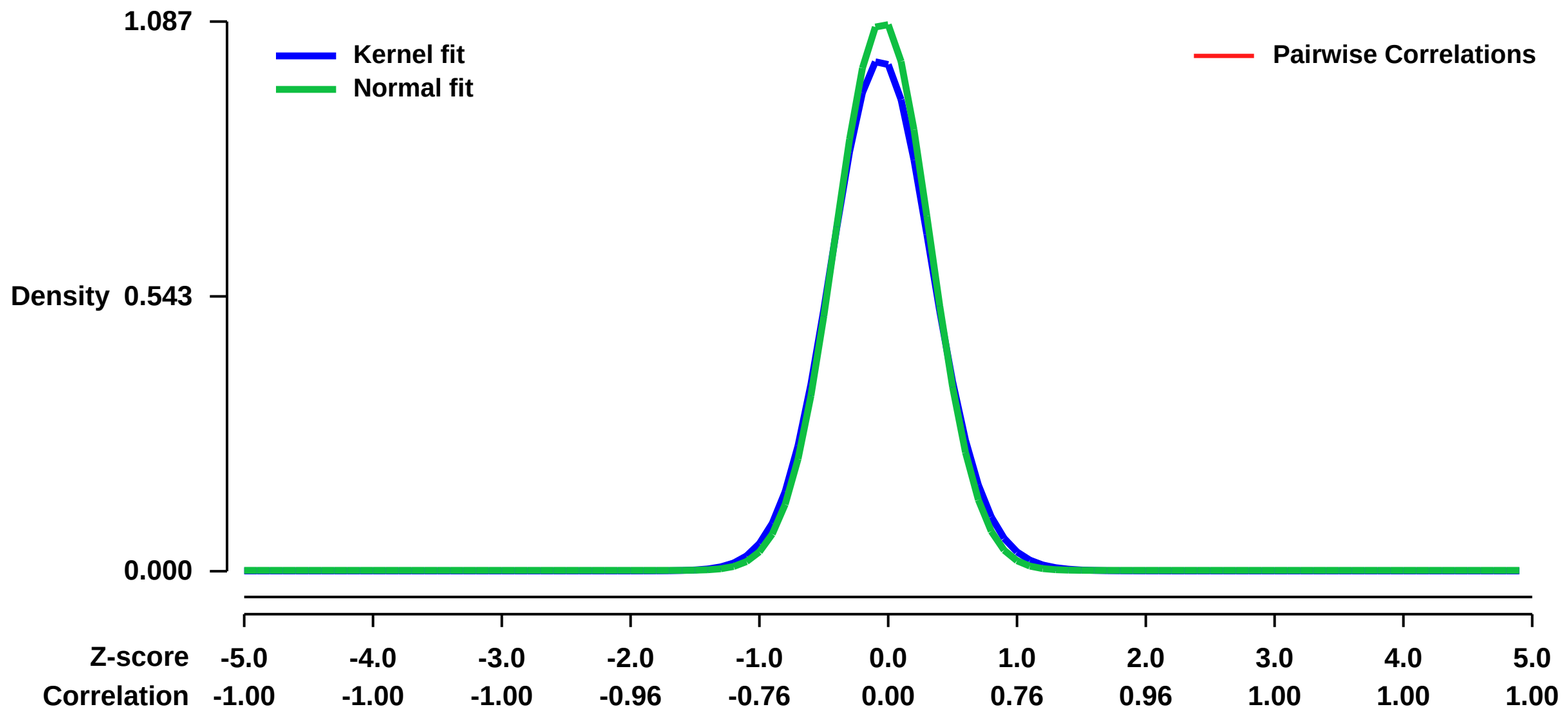

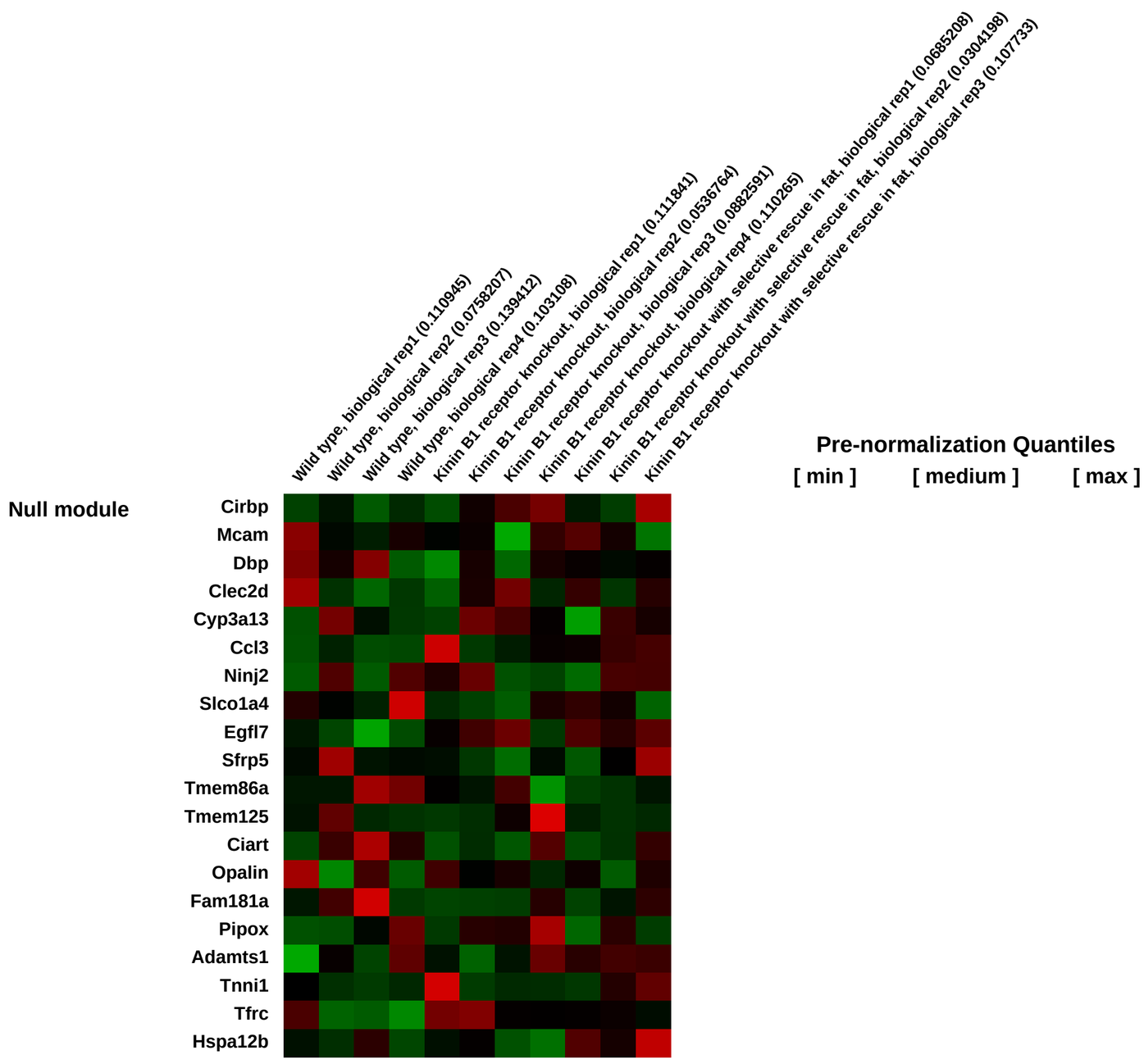

GEO Series "GSE31702" Expression Profiles

Num of samples in this series: 10

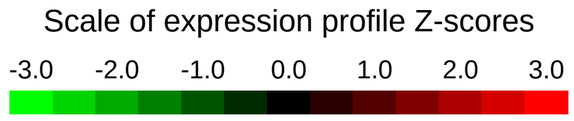

GEO Link:	http://www.ncbi.nlm.nih.gov/geo/query/acc.cgi?acc=GSE31702
Status:	Public on Aug 30 2011
Title:	CD4+ T cell gene expression in B6 vs B6.Sle1c2 mice
Organism:	Mus musculus
Experiment type:	Expression profiling by array
Platform:	GPL1261
Pubmed ID:	22711888
Summary & Design:	**Summary:** **Sle1c is a sublocus of the NZM2410-derived Sle1 major susceptibility locus. We have previously shown that Sle1c contributes to lupus pathogenesis by conferring CD4+ T cell-intrinsic hyperactivation and increased susceptibility to chronic graft-versus-host disease (cGVHD) that mapped to the centromeric portion of the locus. In this study, we have refined the centromeric sublocus to a 675Kb interval, termed Sle1c2. Recombinant congenic strains expressing Sle1c2 exhibited a T cell-intrinsic CD4+ T cell hyperactivation and cGVHD susceptibility, similar to mice with the parental Sle1c.** **We performed a microarray analysis on CD4+ T cells to gain insights into the transcriptional programs that regulate the hyperactivation conferred by Sle1c2.** **Overall design:** **CD4+ T cell cDNA was prepared from spenocytes from 5 mice from each strain and B6.Sle1c2 gene expression was compared to B6 gene expresion.**

Background corr dist: KL-Divergence = 0.0810, L1-Distance = 0.0213, L2-Distance = 0.0006, Normal std = 0.4784

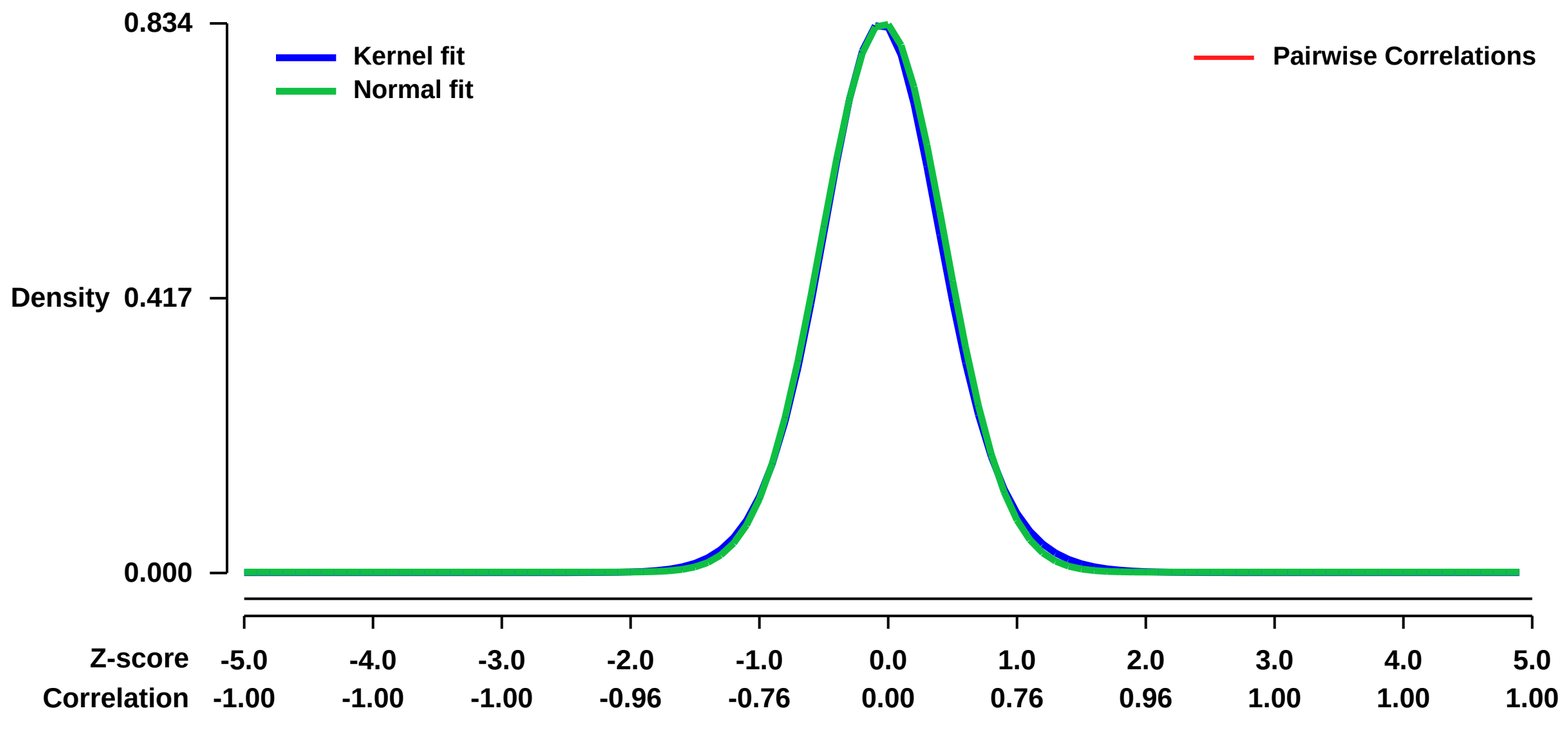

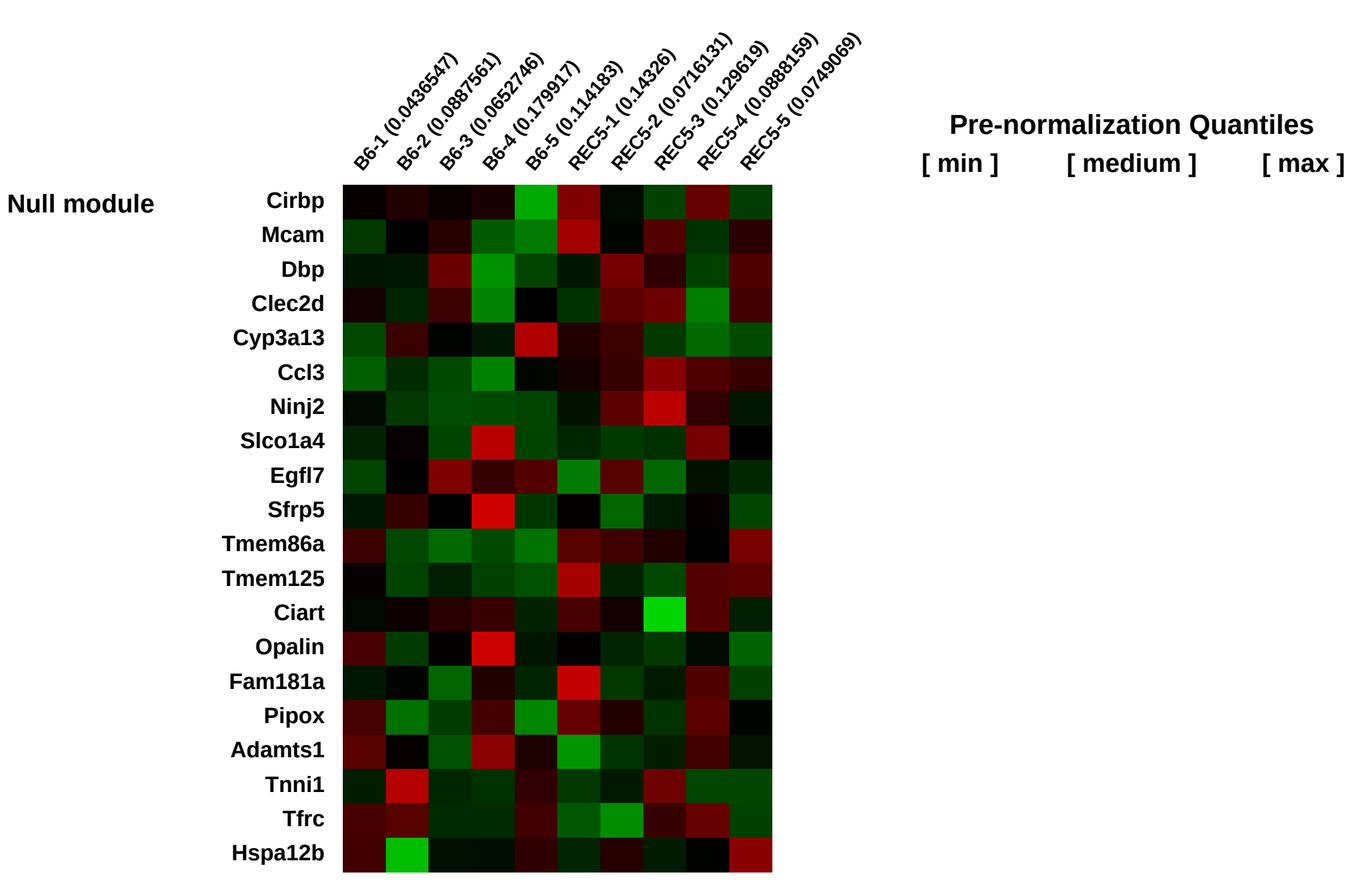

GEO Series "GSE31752" Expression Profiles

Num of samples in this series: 6

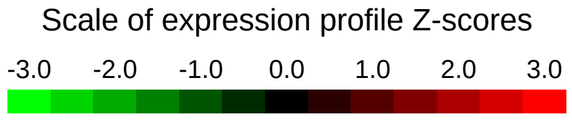

GEO Link:	**http://www.ncbi.nlm.nih.gov/geo/query/acc.cgi?acc=GSE31752**
Status:	**Public on Aug 31 2011**
Title:	**Mig-6 plays a critical role in the regulation of cholesterol homeostasis and bile acid synthesis.**
Organism:	**Mus musculus**
Experiment type:	**Expression profiling by array**
Platform:	**GPL1261**
Pubmed ID:	
Summary & Design:	**Summary:** **The disruption of cholesterol homeostasis leads to an increase in cholesterol levels which results in the development of cardiovascular disease. Mitogen Inducible Gene 6 (Mig-6) is an immediate early response gene that can be induced by various mitogens, stresses, and hormones. To identify the metabolic role of Mig-6 in the liver, we conditionally ablated Mig-6 in the liver using the Albumin-Cre mouse model (Albcre/+Mig-6f/f; Mig-6d/d). Mig-6d/d mice exhibit hepatomegaly and fatty liver. Serum levels of total, LDL, and HDL cholesterol and hepatic lipid were significantly increased in the Mig-6d/d mice. The daily excretion of fecal bile acids was significantly decreased in the Mig-6d/d mice. DNA microarray analysis of mRNA isolated from the livers of these mice showed alterations in genes that regulate lipid metabolism, bile acid, and cholesterol synthesis, while the expression of genes that regulate biliary excretion of bile acid and triglyceride synthesis showed no difference in the Mig-6d/d mice compared to Mig-6f/f controls. These results indicate that Mig-6 plays an important role in cholesterol homeostasis and bile acid synthesis. Mice with liver specific conditional ablation of Mig-6 develop hepatomegaly and increased intrahepatic lipid and provide a novel model system to investigate the genetic and molecular events involved in the regulation of cholesterol homeostasis and bile acid synthesis. Defining the molecular mechanisms by which Mig-6 regulates cholesterol homeostasis will provide new insights into the development of more effective ways for the treatment and prevention of cardiovascular disease.** **Overall design:** **Eight week old Mig-6f/f vs Mig-6d/d male mice after undergoing a 24 hour fast**

Background corr dist: KL-Divergence = 0.0256, L1-Distance = 0.0139, L2-Distance = 0.0002, Normal std = 0.6931

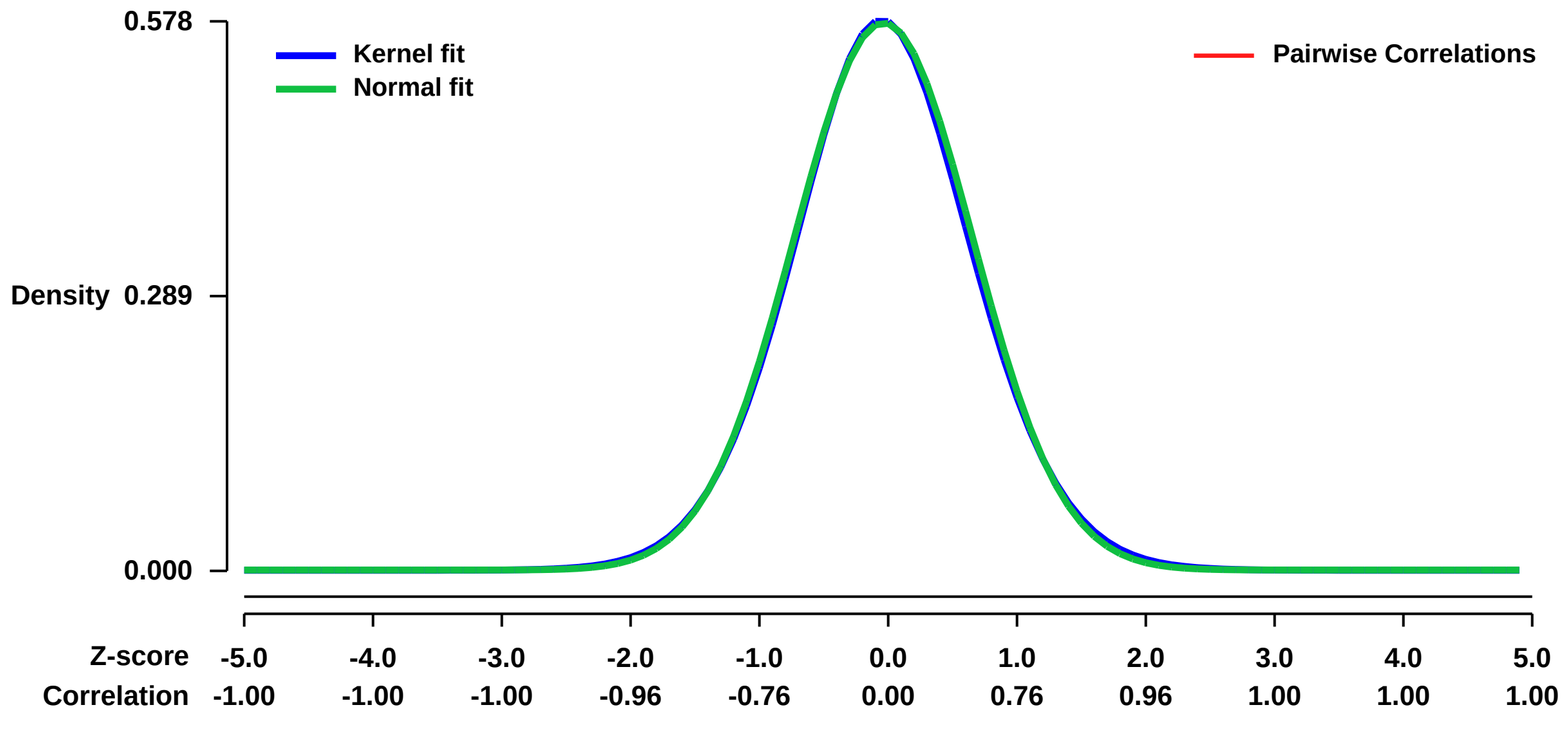

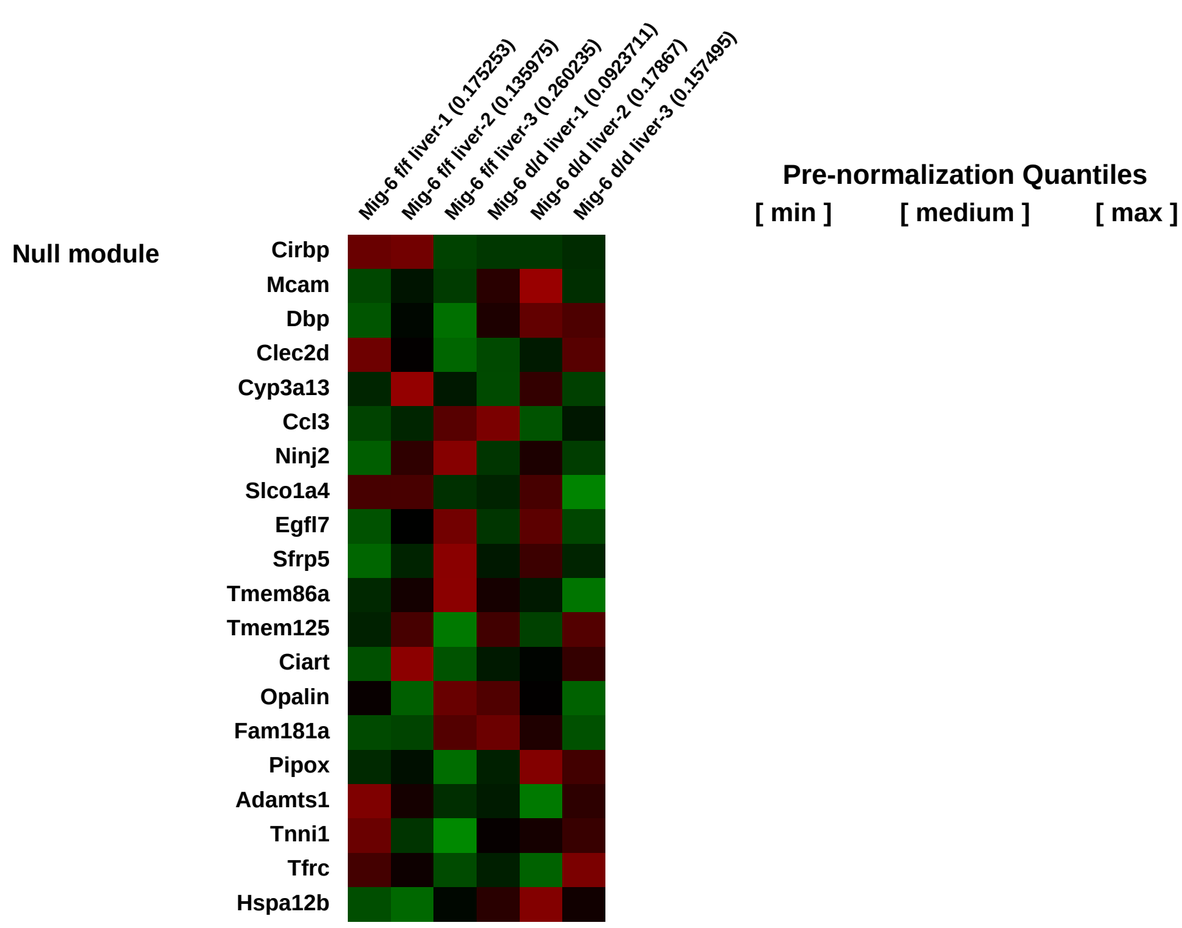

GEO Series "GSE31792" Expression Profiles

Num of samples in this series: 18

Scale of expression profile Z-scores

-3.0 -2.0 -1.0 0.0 1.0 2.0 3.0

GEO Link:	http://www.ncbi.nlm.nih.gov/geo/query/acc.cgi?acc=GSE31792
Status:	Public on Jul 01 2012
Title:	Distinct and Overlapping Gene Regulatory Networks in BMP- and HDAC-Controlled Cell Fate Determination in the Embryonic Forebrain
Organism:	Mus musculus
Experiment type:	Expression profiling by array
Platform:	GPL1261
Pubmed ID:	22748179
Summary & Design:	**Summary:** Both bone morphogenetic proteins (BMPs) and histone deacetylases (HDACs) have previously been established to play a role in the development of the three major cell types of the central nervous system: neurons, astrocytes, and oligodendrocytes. We have previously established a connection between these two protein families, showing that HDACs suppress BMP-promoted astrogliogenesis in the embryonic striatum. Since HDACs act in the nucleus to effect changes in transcription, an unbiased analysis of their transcriptional targets could shed light on their downstream effects on BMP-signaling. Using neurospheres from the embryonic striatum as an in vitro system to analyze this phenomenon, we have performed microarray expression profiling on BMP2- and trichostatin A (TSA)-treated cultures, followed by validation of the findings with quantitative RT-PCR and protein analysis. **Overall design:** Neurospheres from the embryonic striatum were used to analyze cellular differentiation into neurons and astrocytes in vitro. To analyze the role of BMP2 and the HDAC-inhibitor TSA in this system, neurospheres were treated with TSA or BMP2 for 24 h, and mRNA was extracted after 6 and 24 h of the respective treatment.

Background corr dist: KL-Divergence = 0.1556, L1-Distance = 0.0355, L2-Distance = 0.0026, Normal std = 0.3698

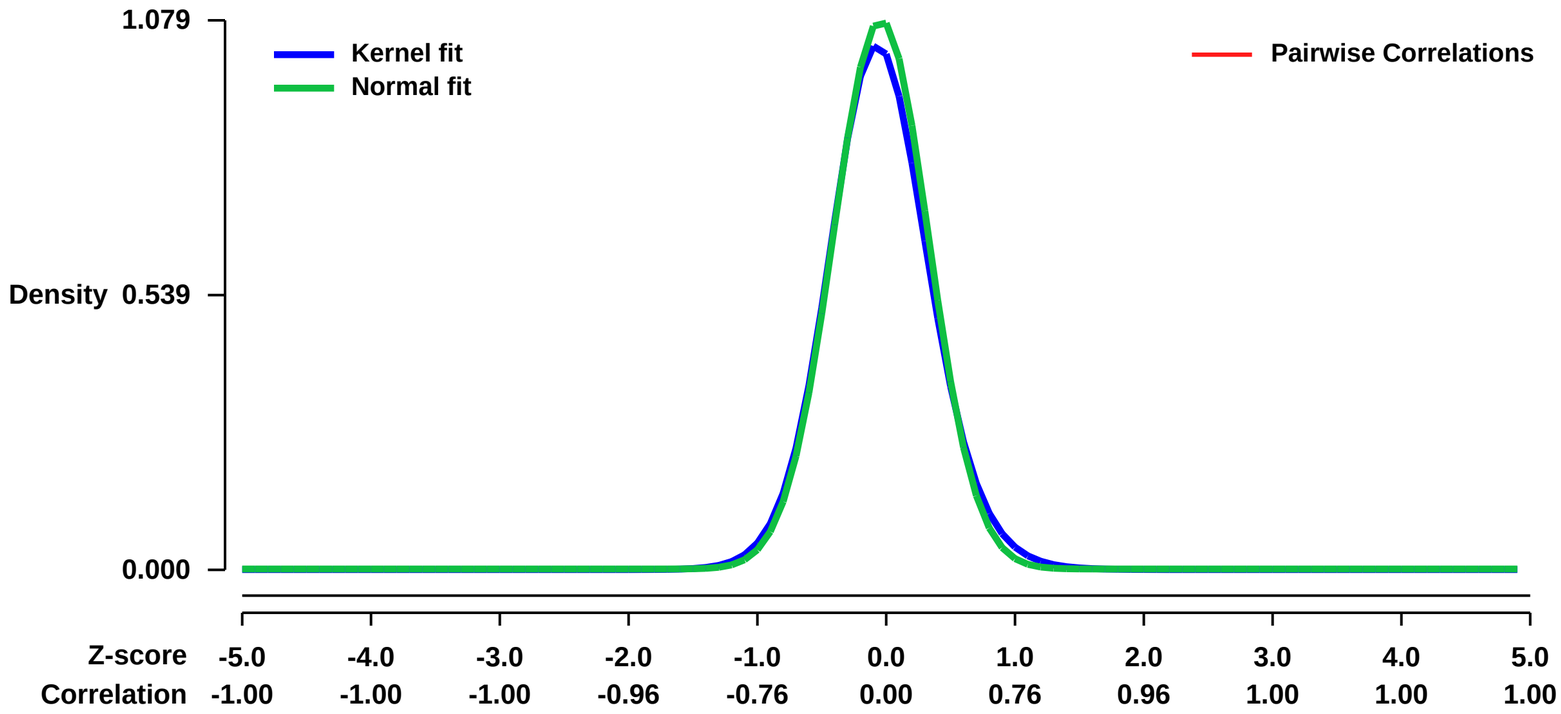

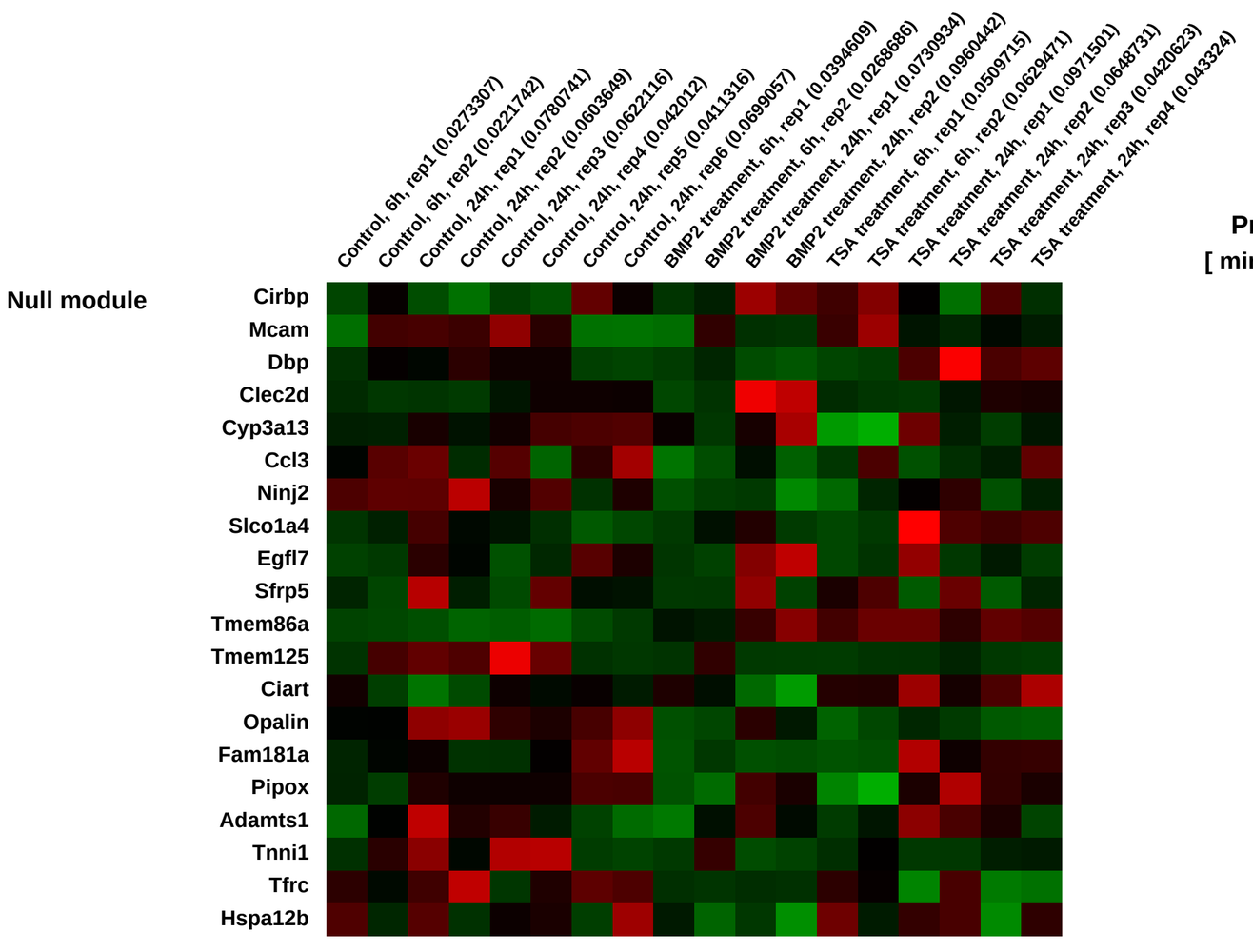

GEO Series "GSE31797" Expression Profiles

Num of samples in this series: 6

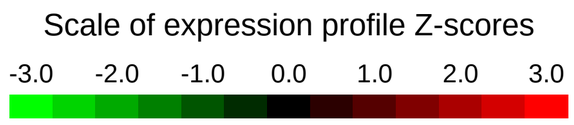

GEO Link:	http://www.ncbi.nlm.nih.gov/geo/query/acc.cgi?acc=GSE31797
Status:	Public on Mar 01 2012
Title:	Activation of SREBP in Alveolar Type II Cells Enhances Lipogenesis Causing Pulmonary Lipotoxicity
Organism:	Mus musculus
Experiment type:	Expression profiling by array
Platform:	GPL1261
Pubmed ID:	22267724
Summary & Design:	**Summary:** **Background: Lung function is dependent upon the precise regulation of the synthesis, storage, and catabolism of tissue and alveolar lipids.** **Results: Activation of SREBP (Sterol Response Element Binding Protein) induced lipogenesis in alveolar epithelial cells, causing neutral lipid accumulation, lung inflammation, and tissue remodeling.** **Conclusions: The accumulation of neutral lipids in type II epithelial cells and alveolar macrophages caused lung inflammation, consistent with findings in lipid storage disorders.** **Significance: Pulmonary lipotoxicity may contribute to the pathogenesis of lung dysfunction associated with diabetes, obesity, and other metabolic disorders.** **Overall design:** **Genome-wide transcription profiling comparison between doxycycline-exposed SFTPC-rtTAWT/Tg/(tetO)7CMV-CreWT/Tg/Insig1flox/flox/Insig2-/- mice (i.e., Insig1/2â /â) and Insig1flox/flox/Insig2-/- . Three independent pooled RNA from isolated lung type 2 cells of each genotype were used.**

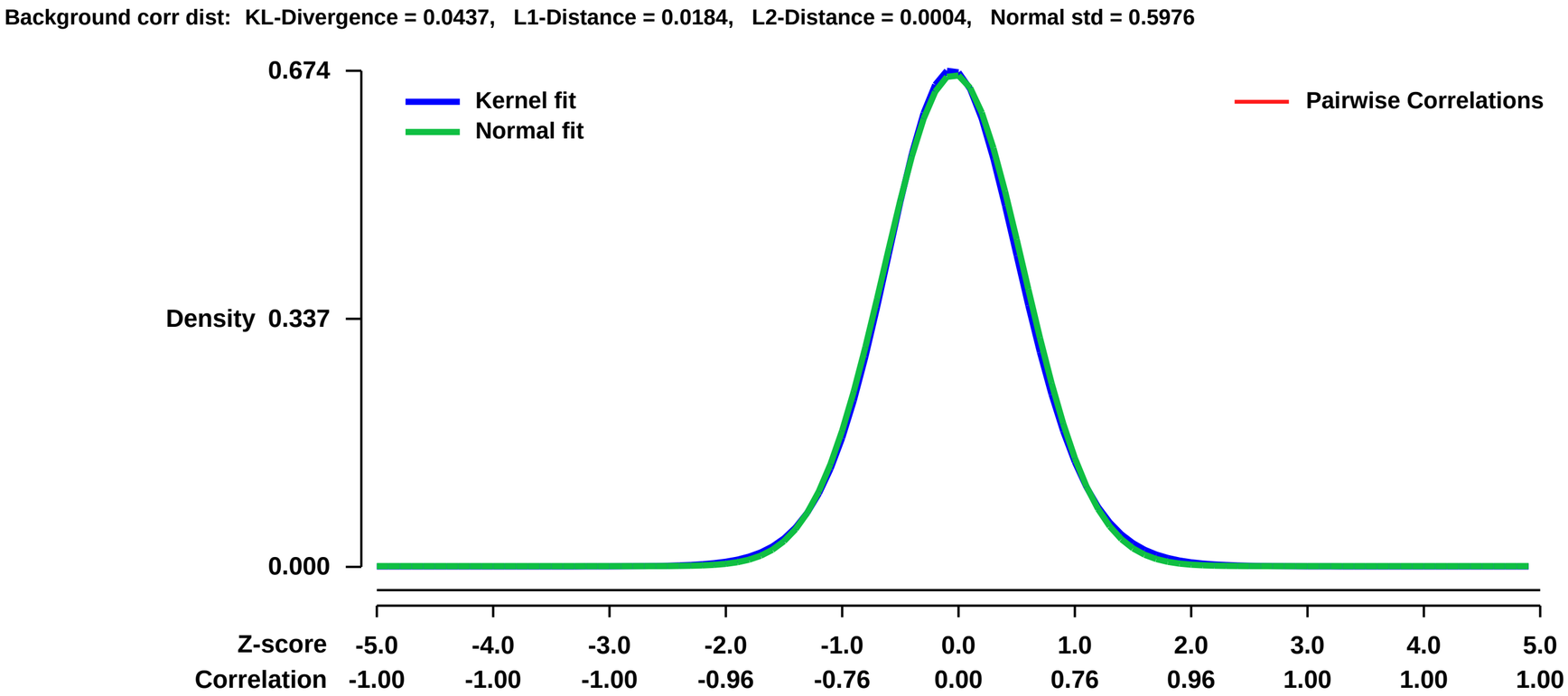

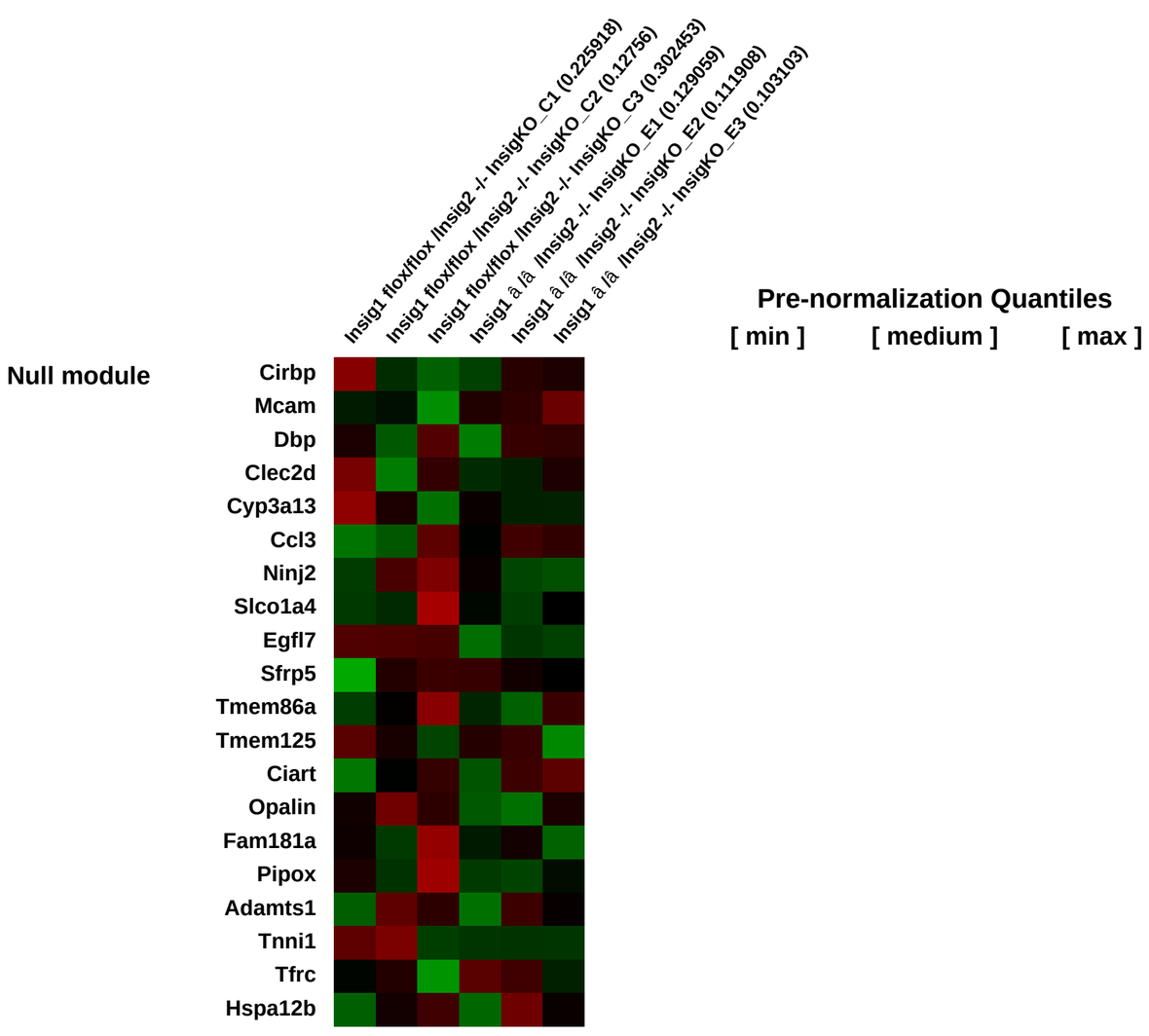

GEO Series "GSE3181" Expression Profiles

Num of samples in this series: 6

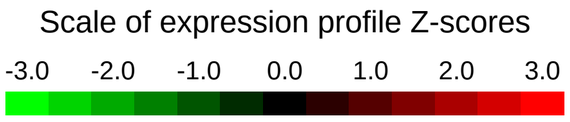

GEO Link:	**http://www.ncbi.nlm.nih.gov/geo/query/acc.cgi?acc=GSE3181**
Status:	**Public on Dec 21 2005**
Title:	**SRF-null neonatal cardiomyocytes**
Organism:	**Mus musculus**
Experiment type:	**Expression profiling by array**
Platform:	**GPL1261**
Pubmed ID:	**16368687**
Summary & Design:	**Summary:** **Serum Response Factor (SRF) is a transcriptional regulator required for mesodermal development. Numerous studies have implicated SRF as a central regulator of muscle gene expression and myogenesis. In this present study we used a loss of function approach to delineate the role of SRF in cardiac myocyte gene expression and function. In SRF null neonatal cardiomyocytes, we observe severe defects in the contractile apparatus, including Z-disc and stress fiber formation, as well as mislocalization and/or attenuation of sarcomeric proteins. Consistent with this, gene array and RT-PCR analyses show downregulation of genes encoding key cardiac transcriptional regulatory factors and proteins required for the maintenance of sarcomeric structure, function, and regulation. Chromatin IP analysis reveals that at least a subset of these proteins are likely regulated directly by SRF. Together the results presented here reveal new cellular and genetic mechanisms through which SRF exacts control over the contractile apparatus in cardiac myocytes.** **Keywords: genetic modification** **Overall design:** **There are three control replicates (cardiomyocytes transduced with Adeno-GFP virus) and three experimental replicates (cardiomyocytes transduced with Adeno-CRE to excise SRF).**

Background corr dist: KL-Divergence = 0.0178, L1-Distance = 0.0149, L2-Distance = 0.0003, Normal std = 0.7593

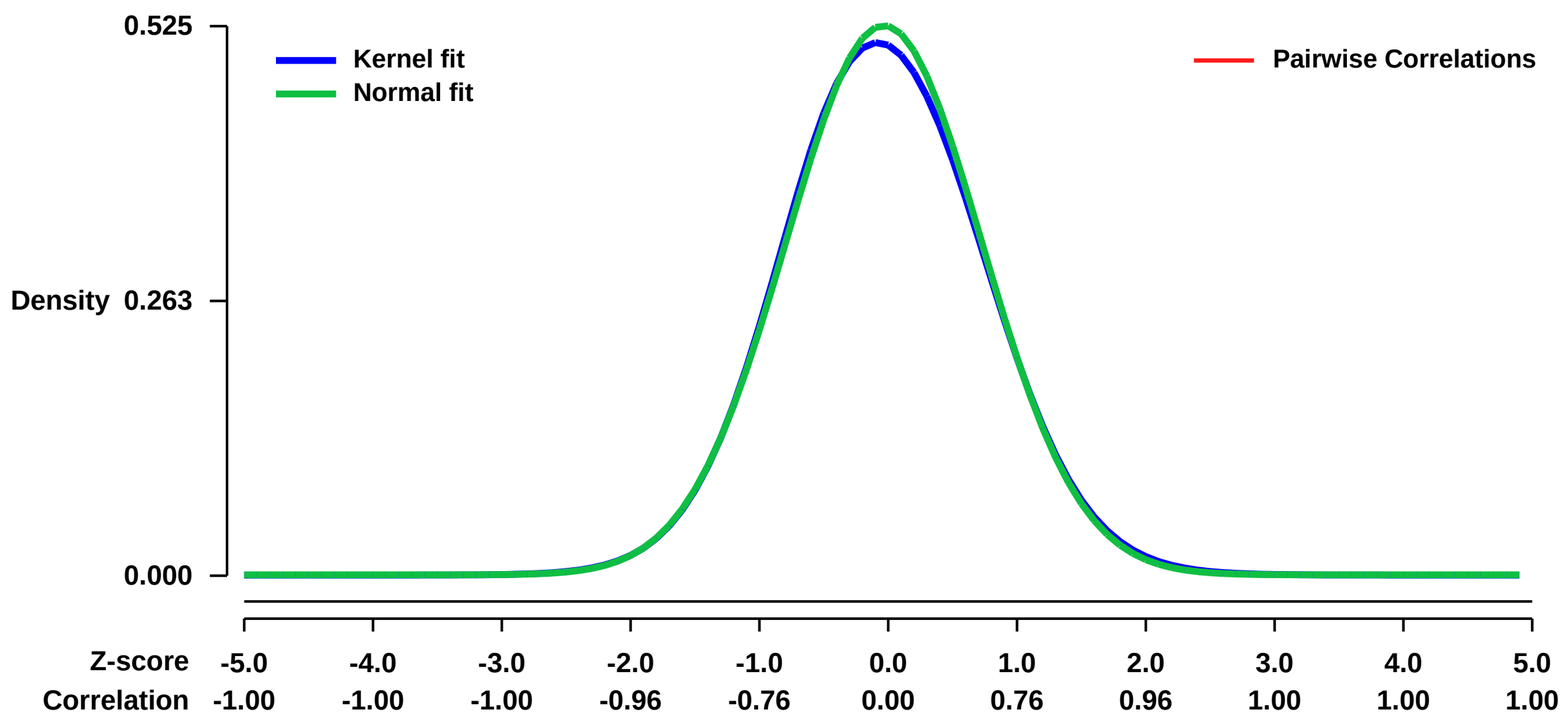

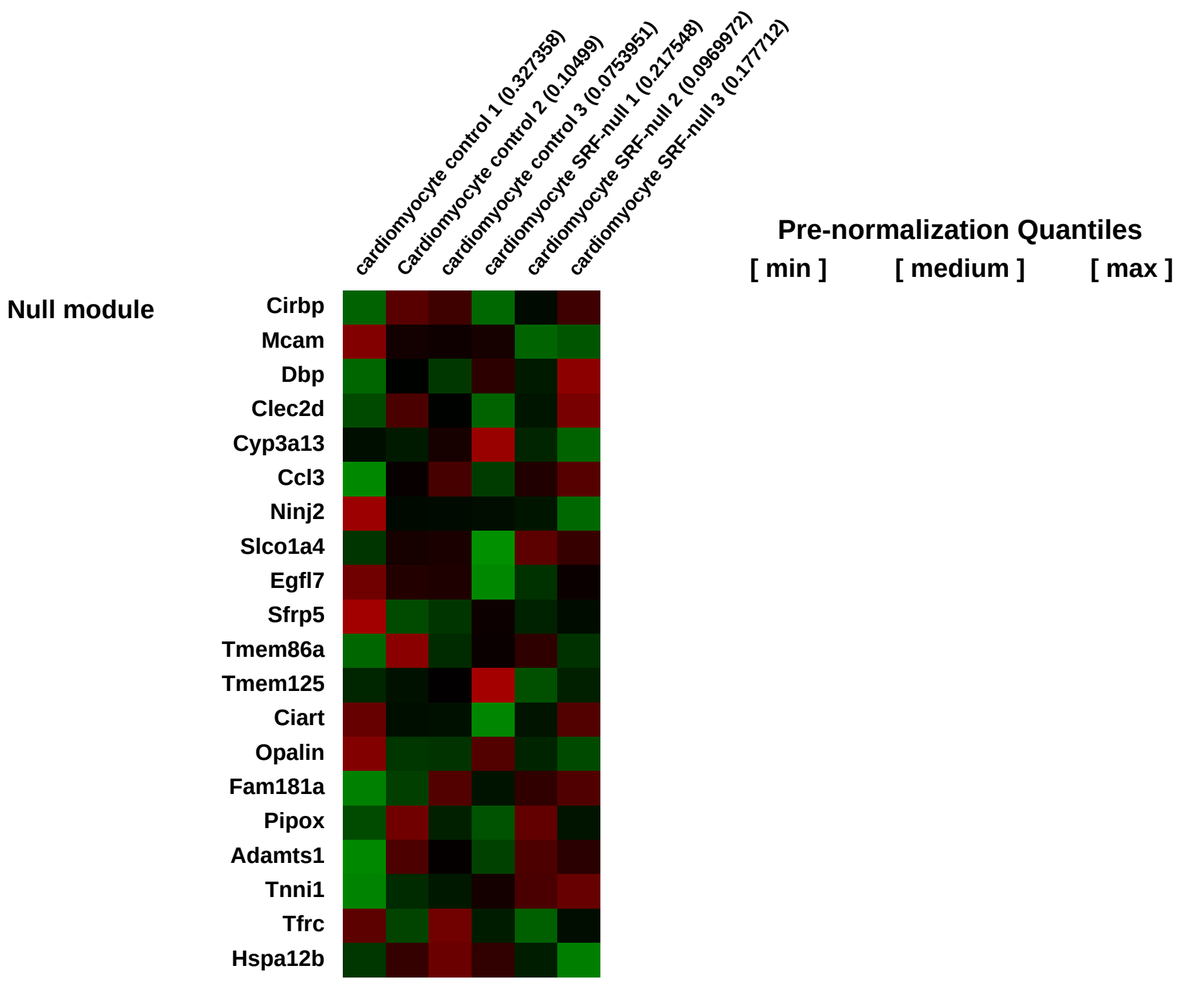

GEO Series "GSE31938" Expression Profiles

Num of samples in this series: 8

Scale of expression profile Z-scores

-3.0 -2.0 -1.0 0.0 1.0 2.0 3.0

GEO Link:	**http://www.ncbi.nlm.nih.gov/geo/query/acc.cgi?acc=GSE31938**
Status:	**Public on Mar 01 2012**
Title:	**Hypothalamus**
Organism:	**Mus musculus**
Experiment type:	**Expression profiling by array**
Platform:	**GPL1261**
Pubmed ID:	
Summary & Design:	**Summary:** **These arrays contain data from hypthalamus tissue of nestin-Pex5 -/- male mice** **Overall design:** **Gene expression in biological replicates from hypothalamus of 4 wild type mice was compared with 4 NestinPex5-/- mice. In the latter, functional peroxisomes were deleted from all neural cells.**

Background corr dist: **KL-Divergence = 0.0553, L1-Distance = 0.0186, L2-Distance = 0.0004, Normal std = 0.5391**

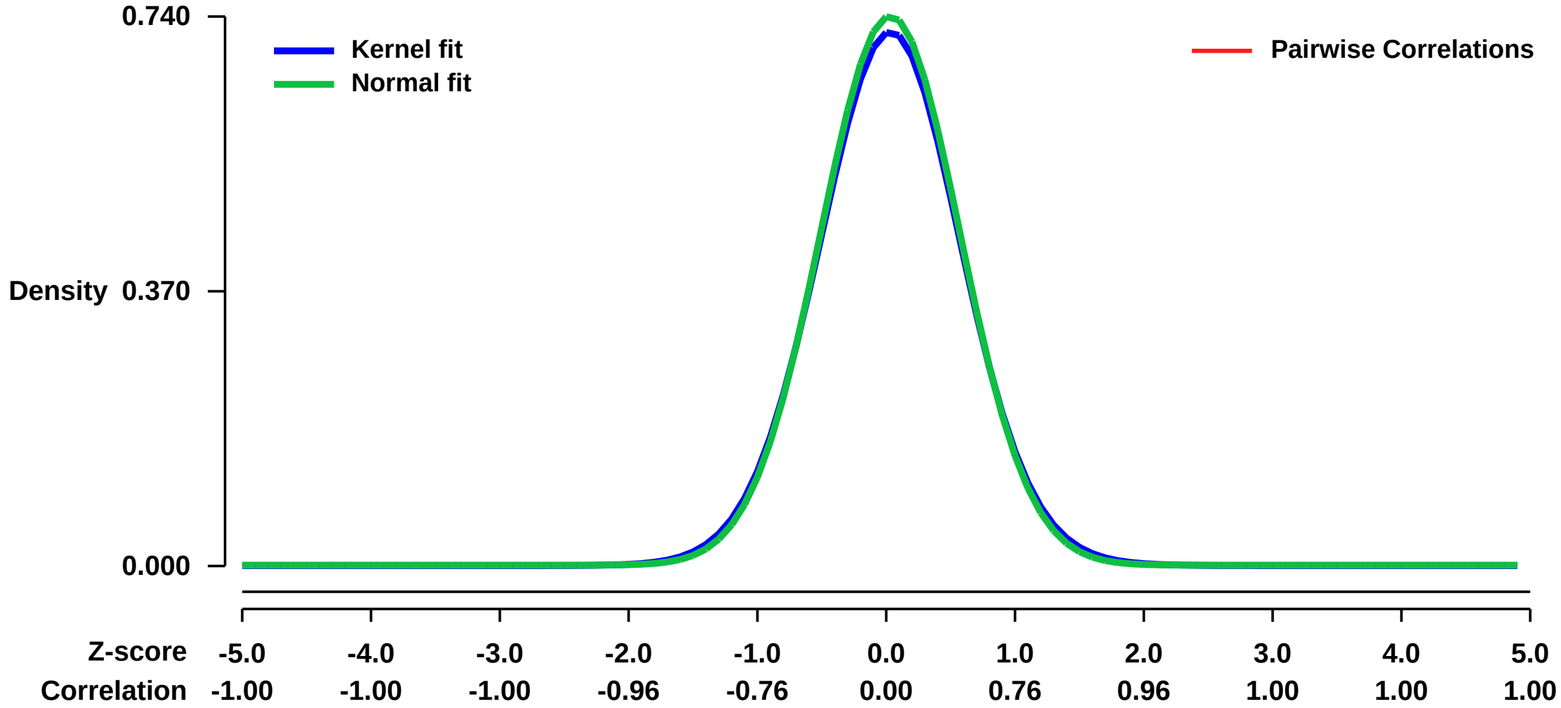

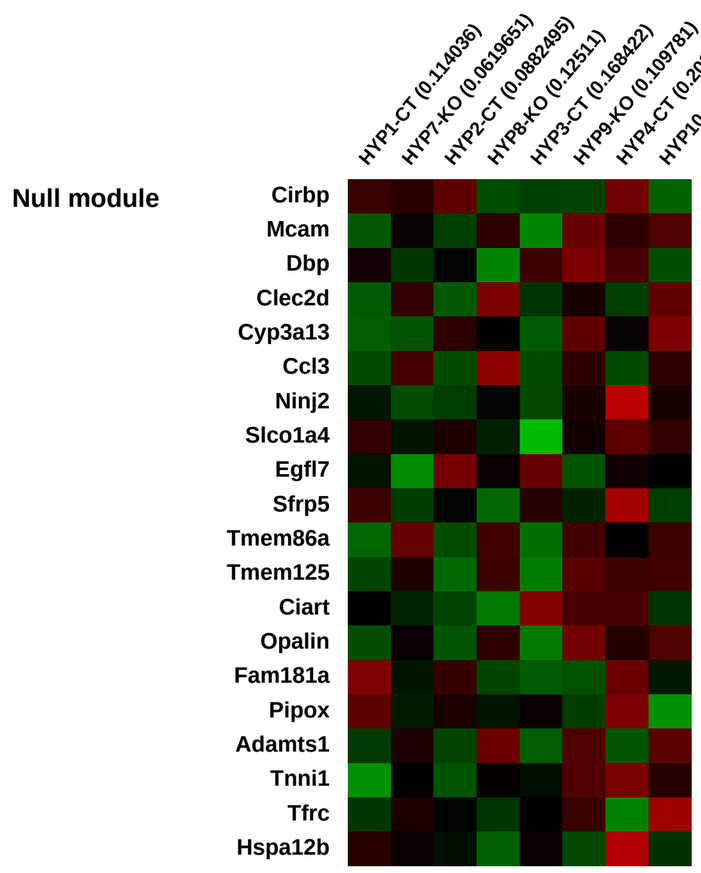

GEO Series "GSE31940" Expression Profiles

Num of samples in this series: 8

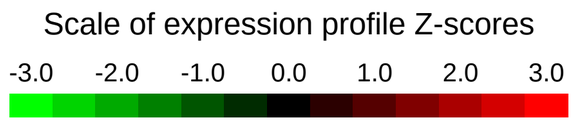

GEO Link:	**http://www.ncbi.nlm.nih.gov/geo/query/acc.cgi?acc=GSE31940**
Status:	**Public on Mar 01 2012**
Title:	**White adipose tissue from aP2-Pex5 knockout and control mice**
Organism:	**Mus musculus**
Experiment type:	**Expression profiling by array**
Platform:	**GPL1261**
Pubmed ID:	
Summary & Design:	**Summary:** **These arrays contain data from gonodal adipose tissue of aP2-Pex5 -/- male mice** **Overall design:** **4 arrays from gonadal adipose tissue from control mice (Swiss background) are compared with 4 arrays from gonadal adipose tissue of aP2-Pex5 knockout mice. The latter lack functional peroxisomes in adipose tissue.**

Background corr dist: **KL-Divergence = 0.0585, L1-Distance = 0.0201, L2-Distance = 0.0006, Normal std = 0.5314**

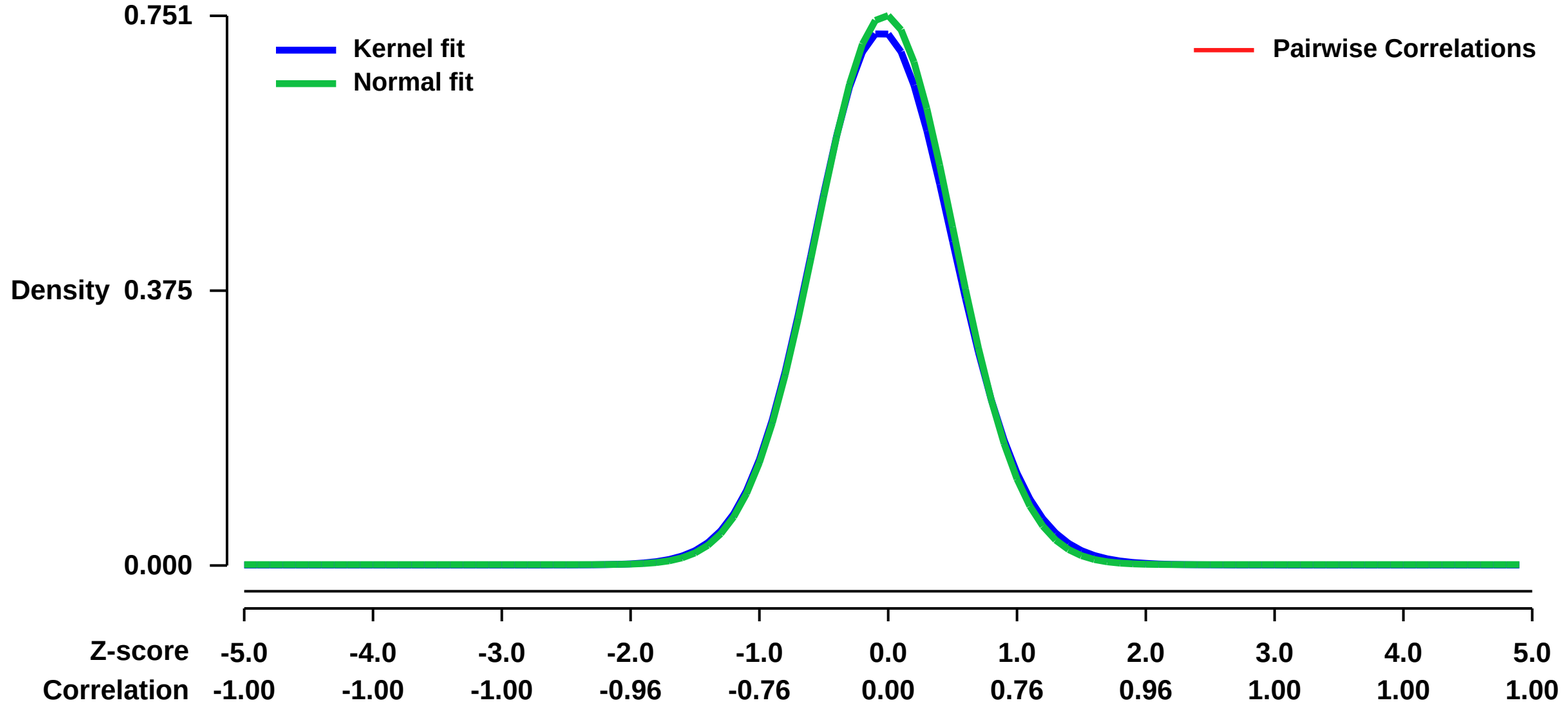

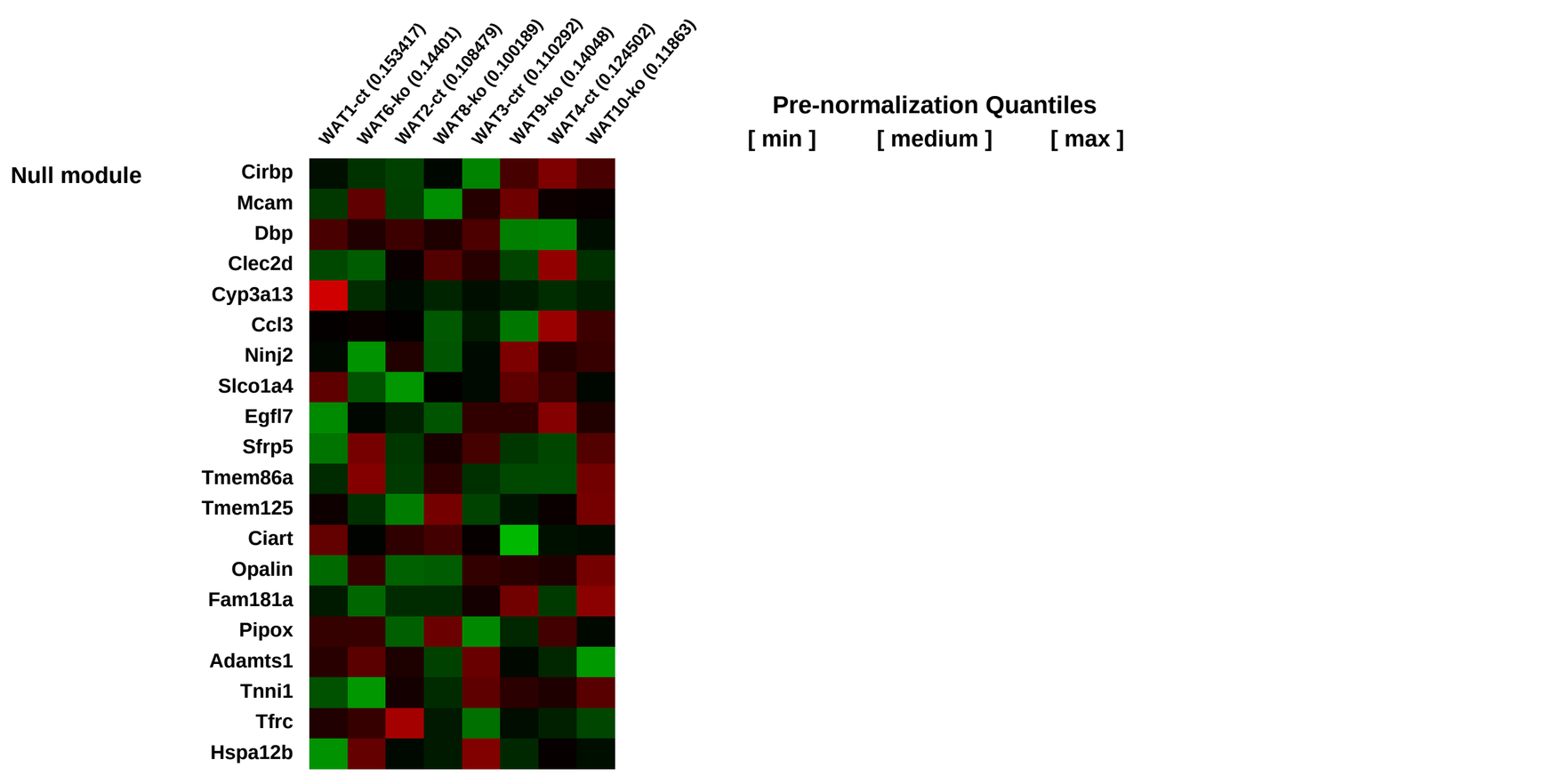

GEO Series "GSE3196" Expression Profiles

Num of samples in this series: 12

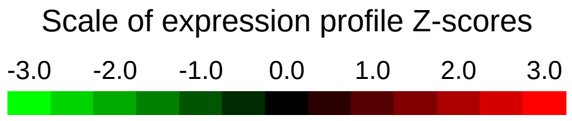

GEO Link:	**http://www.ncbi.nlm.nih.gov/geo/query/acc.cgi?acc=GSE3196**
Status:	**Public on Oct 24 2005**
Title:	**Gene expression in hypoxic MEFs having only p300 and CBP with deleted CH1 domains**
Organism:	**Mus musculus**
Experiment type:	**Expression profiling by array**
Platform:	**GPL1261**
Pubmed ID:	**16237459**
Summary & Design:	**Summary:** **The CH1 protein interaction domain of the transcriptional coactivators p300 and CBP is thought to interact with HIF-1alpha and this interaction is thought to be critical to the expression of HIF-1alpha target genes in response to hypoxia. To test the requirement of the CH1 domain for gene expression in response to hypoxia, rimary mouse embryonic fibroblasts (MEFs) were generated from C57Bl/6x129/Sv F2 e14.5 embryos that contain a deletion in the CH1 domain of three of four alleles of CBP and p300. The remaining allele of p300 or CBP was a conditional knock out allele. Control MEFs with only a single conditional knockout allele of p300 or CBP were also generated. At passage 3 MEFs were infected with Cre Adenovirus and grown until they had expanded at least 100 fold. Subconfluent MEFs were treated with 21% oxygen (normoxia) or 0.1% oxygen (hypoxia) with 5% carbon dioxide at 37 C in a humid chamber for 6hrs. At the start of treatment, medium was removed and replaced with medium (DMEM+10% FBS+pen-strep+ l-glu) that had been preequilibrated overnight in normoxia or hypoxia as appropriate. Immediately after treatment, cells were lysed in Trizol for RNA extraction.** **Keywords: genetic modification, dose response** **Overall design:** **12 samples; 4 genotypes [CBP+/flox (flox1), p300 +/flox (flox2), CBP CH1/flox;p300 CH1/CH1 (triCH1flox1),CBP CH1/CH1;p300 CH1/flox (triCH1flox2)] , 2 treatments (normoxia and hypoxia).**

Background corr dist: KL-Divergence = 0.1522, L1-Distance = 0.0360, L2-Distance = 0.0026, Normal std = 0.3713

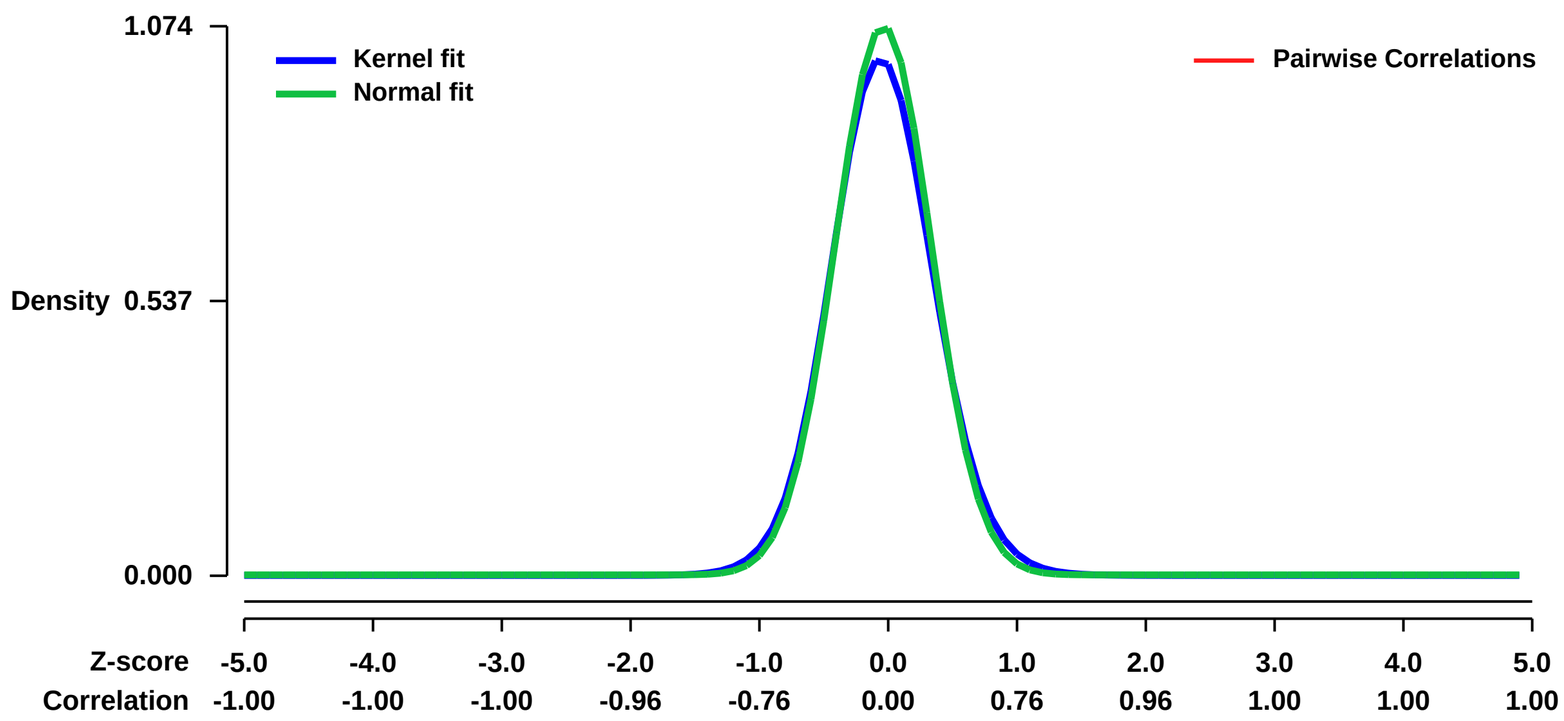

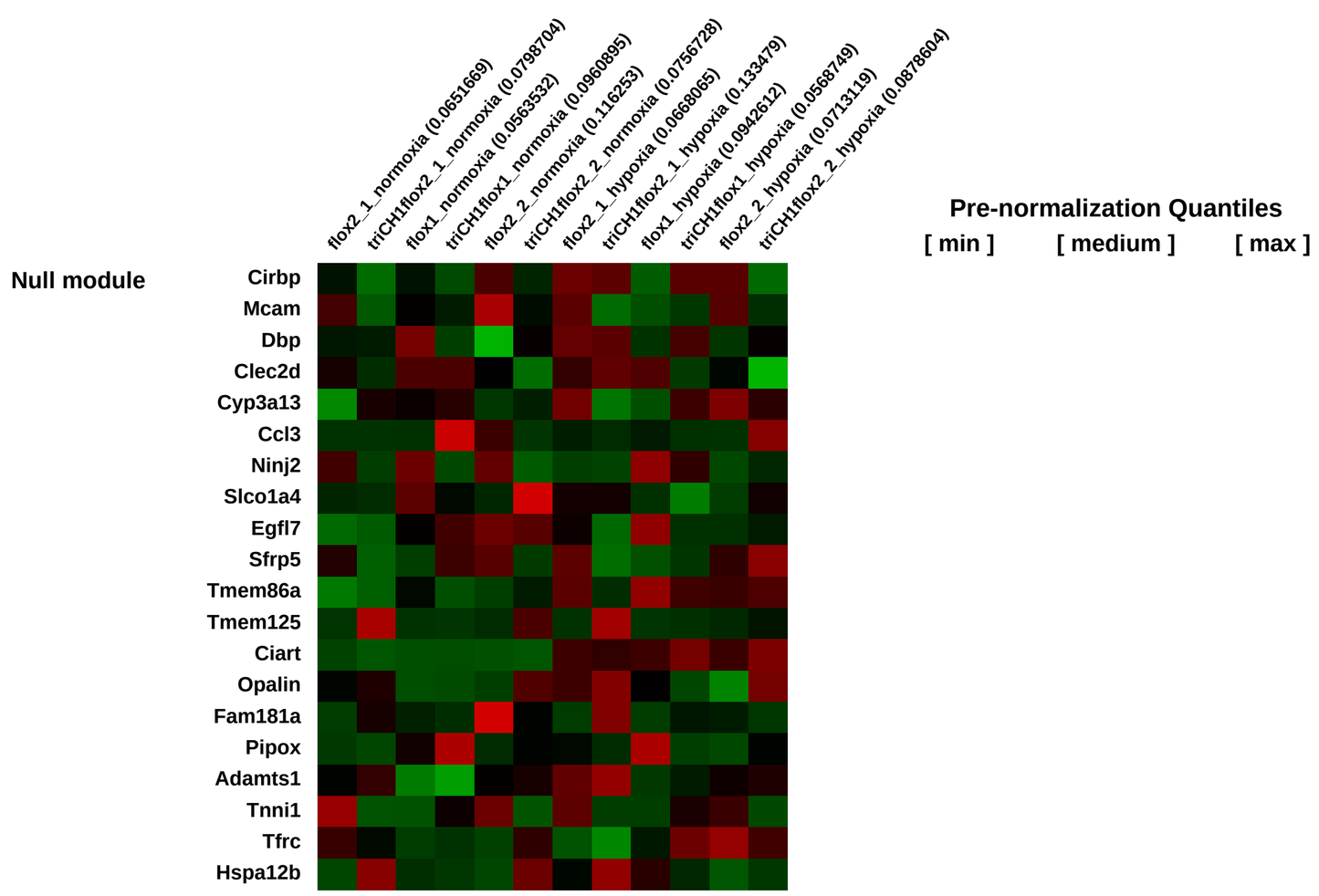

GEO Series "GSE31972" Expression Profiles

Num of samples in this series: 6

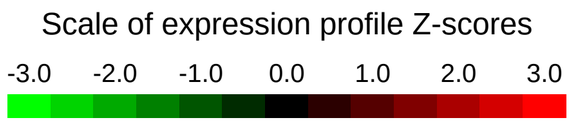

GEO Link:	**http://www.ncbi.nlm.nih.gov/geo/query/acc.cgi?acc=GSE31972**
Status:	**Public on Dec 07 2011**
Title:	**Transcriptional profiling of ICAM-positive and -negative cells from the mouse olfactory epithelium**
Organism:	**Mus musculus**
Experiment type:	**Expression profiling by array**
Platform:	**GPL1261**
Pubmed ID:	
Summary & Design:	**Summary:** **We used trasncriptional profiling of fluorescent activated cell sorting (FACS) purified ICAM1-positive and negative cells from the olfactory epithelium (OE) of three-week old mice to identify genes enriched in the horizontal basal cells.** **Overall design:** **The olfactory epithelia from P21-P25 CD1 mice (Charles River Laboratories, Wilmington, MA), were isolated, dissociated, and then purified by FACS using a FITC-conjugated antibody for ICAM1 (CD54). ICAM1-positive and negative cell populations were collected and compared. RNA was purified with TRIzol reagent (Invitrogen, Carlsbad, CA), subjected to two rounds of amplification, labeled, and hybridized to Affymetrix Mouse Genome 430.2 GeneChip microarrays (Affymetrix Inc., Santa Clara, CA, USA) using Affymetrix reagents and protocols (http://www.affymetrix.com). There were three experimental replicates, each consisting of the ICAM1 (+) and ICAM1 (-) FACS purified cell populations from individual litters of mice that were dissected/dissociated/FACS-purified using an ICAM1-FITC conjugated antibody; one microarray was used for each ICAM1 (+) and ICAM1 (-) sample for a total of six microarrays. Microarray data were normalized using GCRMA.**

Background corr dist: **KL-Divergence = 0.0145, L1-Distance = 0.0398, L2-Distance = 0.0017, Normal std = 0.8821**

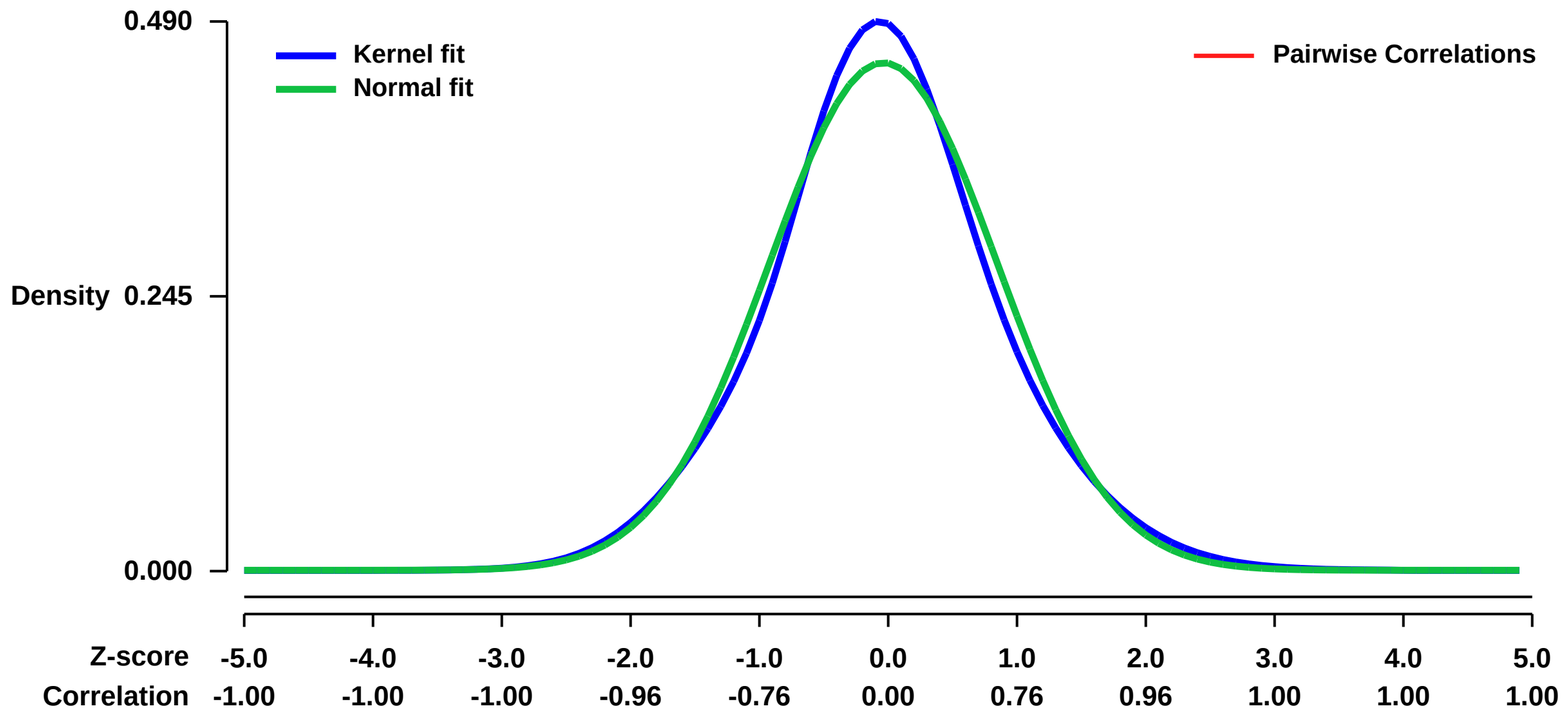

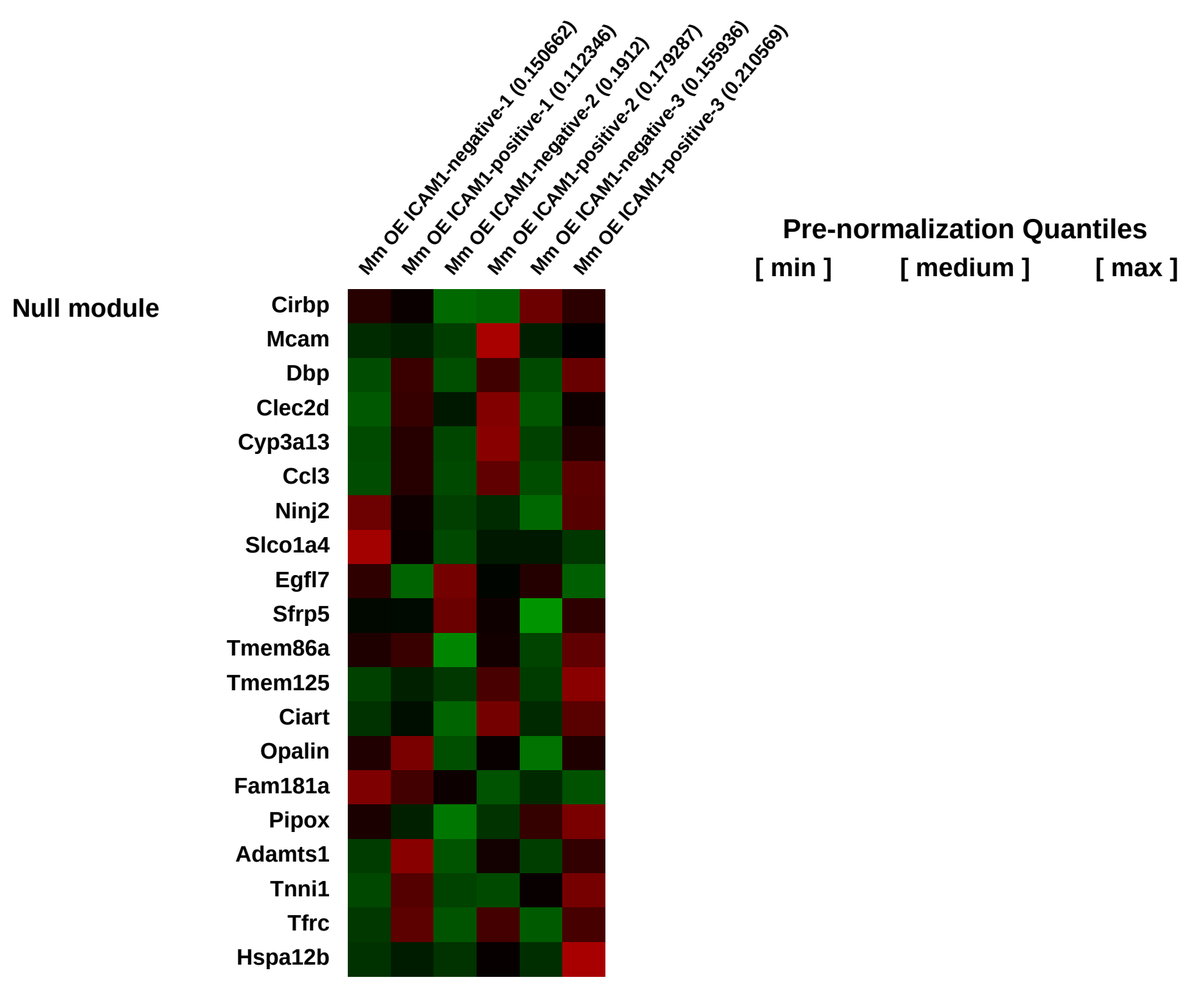

GEO Series "GSE32015" Expression Profiles

Num of samples in this series: 51

Scale of expression profile Z-scores

-3.0 -2.0 -1.0 0.0 1.0 2.0 3.0

GEO Link:	http://www.ncbi.nlm.nih.gov/geo/query/acc.cgi?acc=GSE32015
Status:	Public on Dec 03 2012
Title:	Expression data from inducible ES stable cell lines
Organism:	Mus musculus
Experiment type:	Expression profiling by array
Platform:	GPL1261
Pubmed ID:	23180766
Summary & Design:	**Summary:** In order to identify the effects of the induction of the gene of interest on the mouse ES transcriptome, we performed Affymetrix Gene-Chip hybridization experiments for the different inducible cell lines Transcriptome analysis of the inducible transgenic mouse ES cell lines **Overall design:** For the analysis on the different inducible cell lines, total RNA was extracted from three biological replicates grown in medium deprived of Tetracycline for 17 and 24 hours; RNA extracted from un-induced clones was used as control. Total RNA extracted from parental cell line EBRTcH3 (EB3) was used as additional control.

Background corr dist: KL-Divergence = 0.3818, L1-Distance = 0.0747, L2-Distance = 0.0167, Normal std = 0.2525

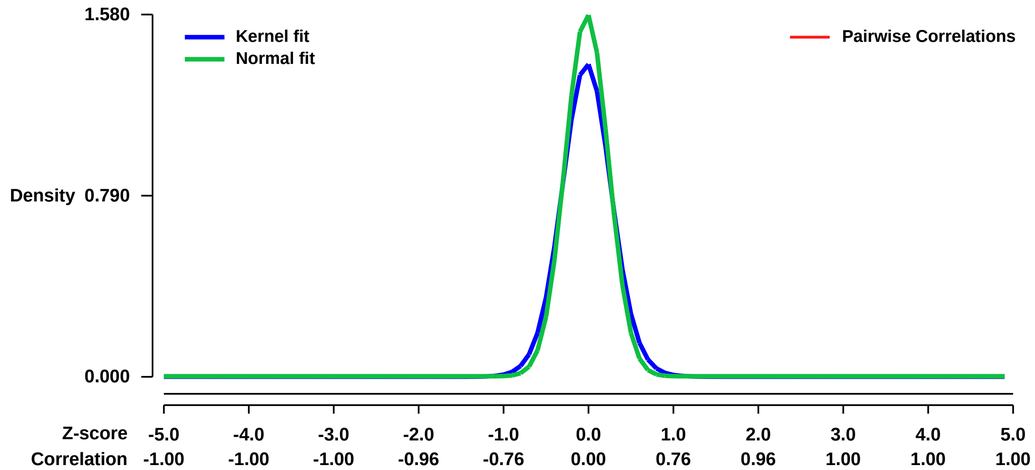

Z-score	-5.0	-4.0	-3.0	-2.0	-1.0	0.0	1.0	2.0	3.0	4.0	5.0
Correlation	-1.00	-1.00	-1.00	-0.96	-0.76	0.00	0.76	0.96	1.00	1.00	1.00

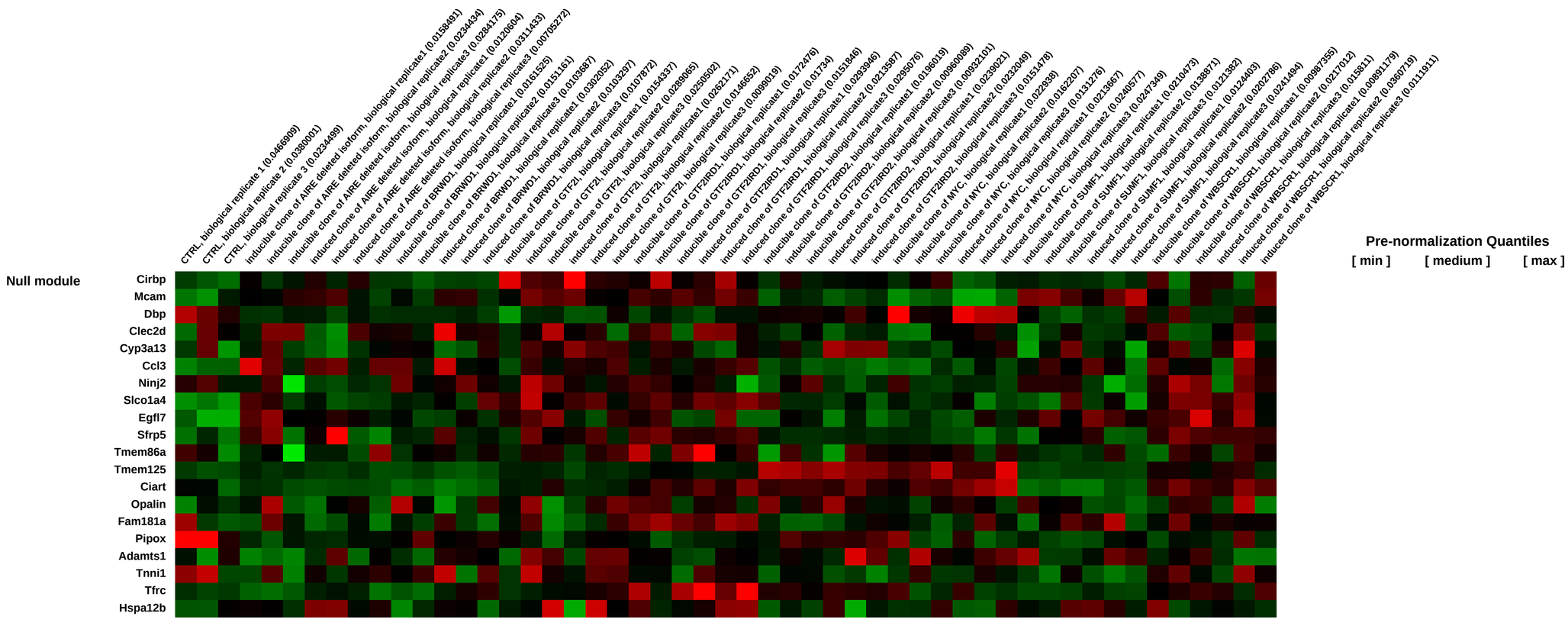

GEO Series "GSE3203" Expression Profiles

Num of samples in this series: 16

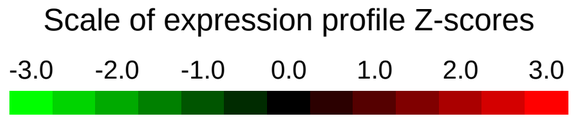

GEO Link:	http://www.ncbi.nlm.nih.gov/geo/query/acc.cgi?acc=GSE3203
Status:	Public on Aug 26 2006
Title:	Influenza virus infection-induced gene expression changes of regional B cells are mediated in part through type I IFN
Organism:	Mus musculus
Experiment type:	Expression profiling by array
Platform:	GPL1261
Pubmed ID:	17237394
Summary & Design:	**Summary:** **Influenza virus infection-induced gene expression changes of regional B cells are mediated at least in part through type I Interferon:** **Our objective is to determine whether the influenza virus-infection induced gene expression changes in regional lymph node B cells are facilitated at least in part through type I interferon. Our specific aim is to compare the gene expression profile of highly FACS-purified B cells in the regional lymph nodes of wildtype and IFNR-/- mice prior to and 48h following infection with influenza virus infection and to contrast this expression profile with that of FACS-purified wildtype B cells activated in vitro with IFN-beta +/- anti-CD86 for 12h.** **Keywords: Infection-induced responses** **Overall design:** **We analyzed gene expression from mouse lymph node B cells purified by flow cytometric sorting using single channel oligonucleotide microarrays. There were 4 groups: 1) wild type uninfected mice (control group), 2) wild type mice infected with influenza (flu) for 2 days, 3) IFNR-/- mice infected with flu for 2 days, 4) cells stimulated with IFN-b in vitro for 17 h. Each group contained 4 biological replicates obtained from independent experiments. There were 16 total samples and each was measured on a separate array.**

Background corr dist: KL-Divergence = 0.0926, L1-Distance = 0.0269, L2-Distance = 0.0011, Normal std = 0.4486

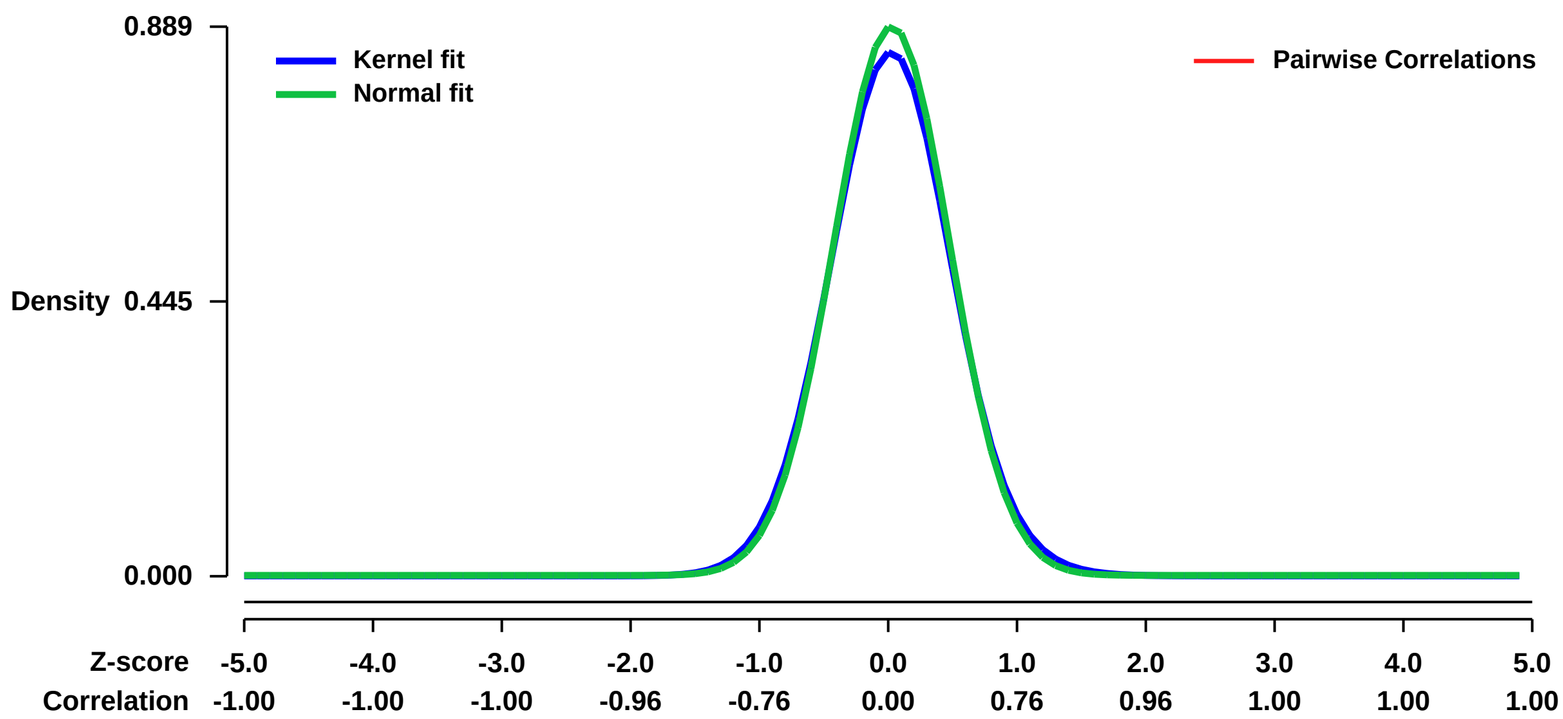

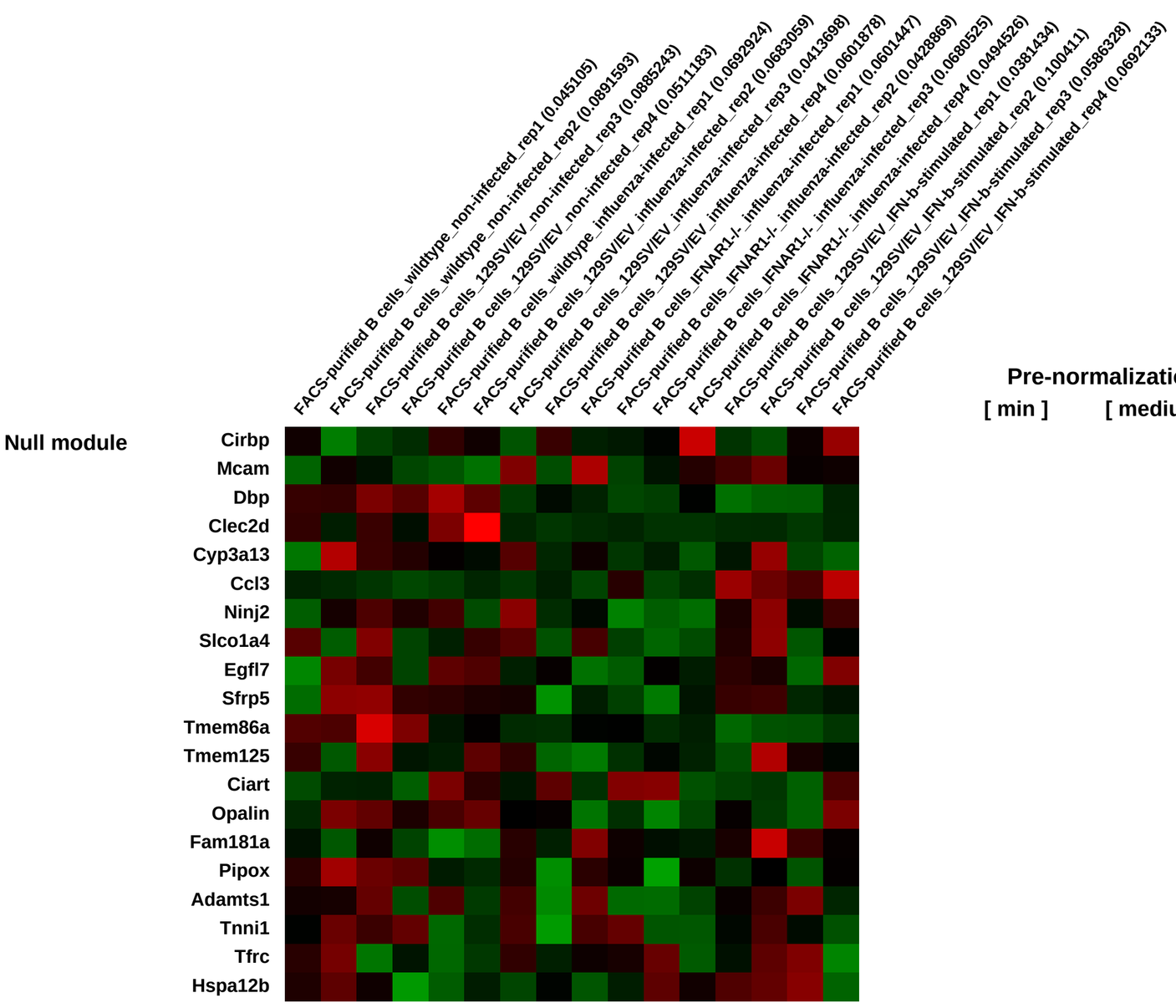

GEO Series "GSE32034" Expression Profiles

Num of samples in this series: 14

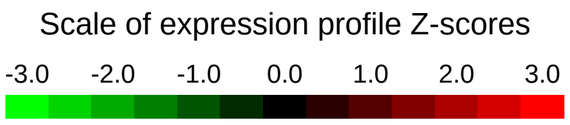

GEO Link:	http://www.ncbi.nlm.nih.gov/geo/query/acc.cgi?acc=GSE32034
Status:	Public on Oct 03 2012
Title:	Tissue-specific differences in PPAR‹‡ control of macrophage function.
Organism:	Mus musculus
Experiment type:	Expression profiling by array
Platform:	GPL1261
Pubmed ID:	22855714
Summary & Design:	**Summary:** PPAR‹‡ is known for its anti-inflammatory actions in macrophages. However, which macrophage populations express PPAR‹‡ in vivo and how it regulates tissue homeostasis in the steady state and during inflammation is not completely understood. We show that lung and spleen macrophages constitutively expressed PPAR‹‡, while other macrophage populations did not. Recruitment of monocytes to sites of inflammation was associated with induction of PPAR‹‡ as they differentiated to macrophages. Its absence in these macrophages led to failed resolution of inflammation, characterized by persistent, low-level recruitment of leukocytes. Conversely, PPAR‹‡ agonists supported an earlier cessation in leukocyte recruitment during resolution of acute inflammation and likewise suppressed monocyte recruitment to chronically inflamed atherosclerotic vessels. In the steady state, PPAR‹‡ deficiency in macrophages had no obvious impact in the spleen but profoundly altered cellular lipid homeostasis in lung macrophages. Reminiscent of pulmonary alveolar proteinosis, LysM-Cre x PPAR‹‡flox/flox mice displayed mild leukocytic inflammation in the steady-state lung and succumbed faster to mortality upon infection with S. pneumoniae. Surprisingly, this mortality was not due to overly exuberant inflammation, but instead to impaired bacterial clearance. Thus, in addition to its anti-inflammatory role in promoting resolution of inflammation, PPAR‹‡ sustains functionality in lung macrophages and thereby has a pivotal role in supporting pulmonary host defense. **Overall design:** The two major subsets of monocytes (Ly-6C+ and Ly-6Clo) from 12-week old C57Bl/6 mice were sorted and the RNA extracted and hybridized to Affymetrix GeneChip´fi 430 2.0 arrays. We pooled leukocytes from 5 mice for each sort and sorted 3 to 4 separate times for 3 to 4 biological replicates.

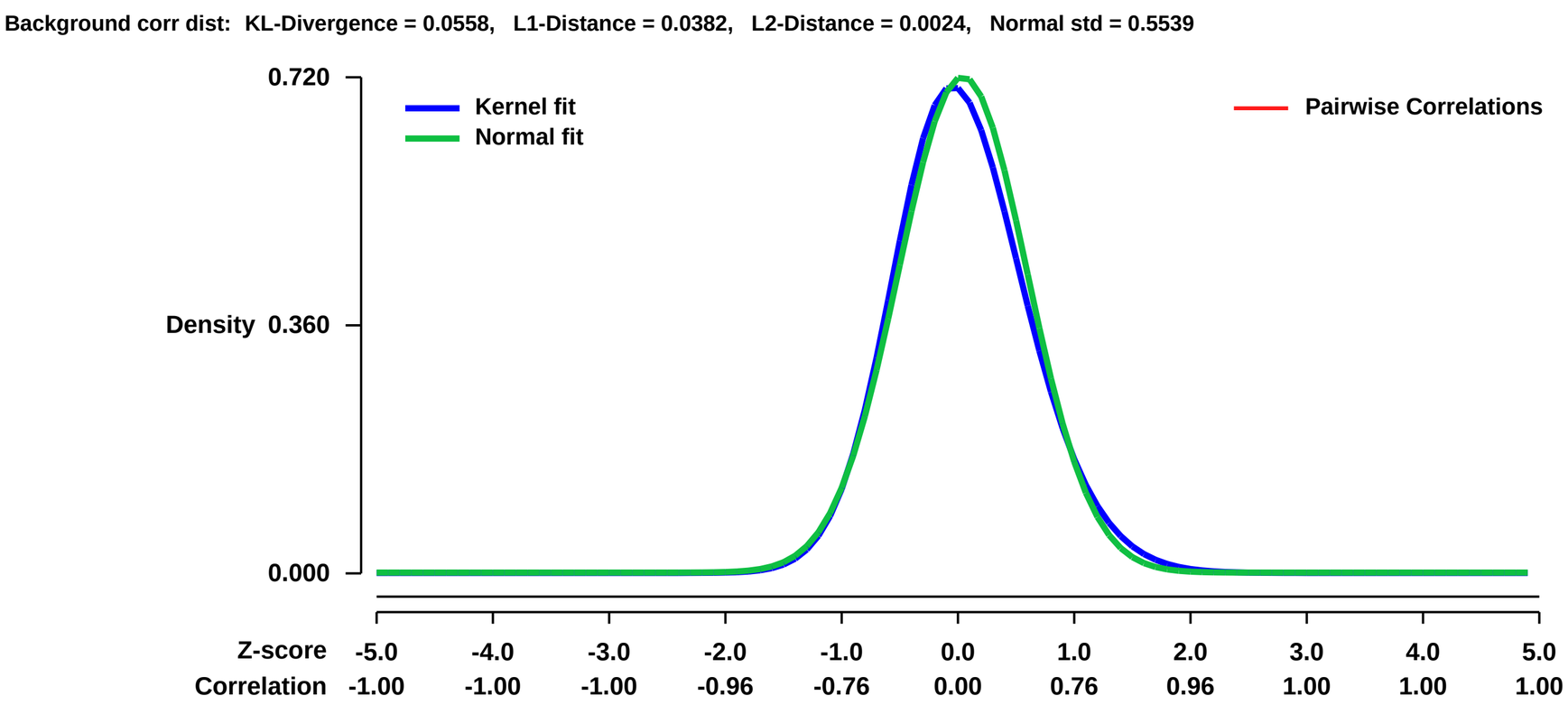

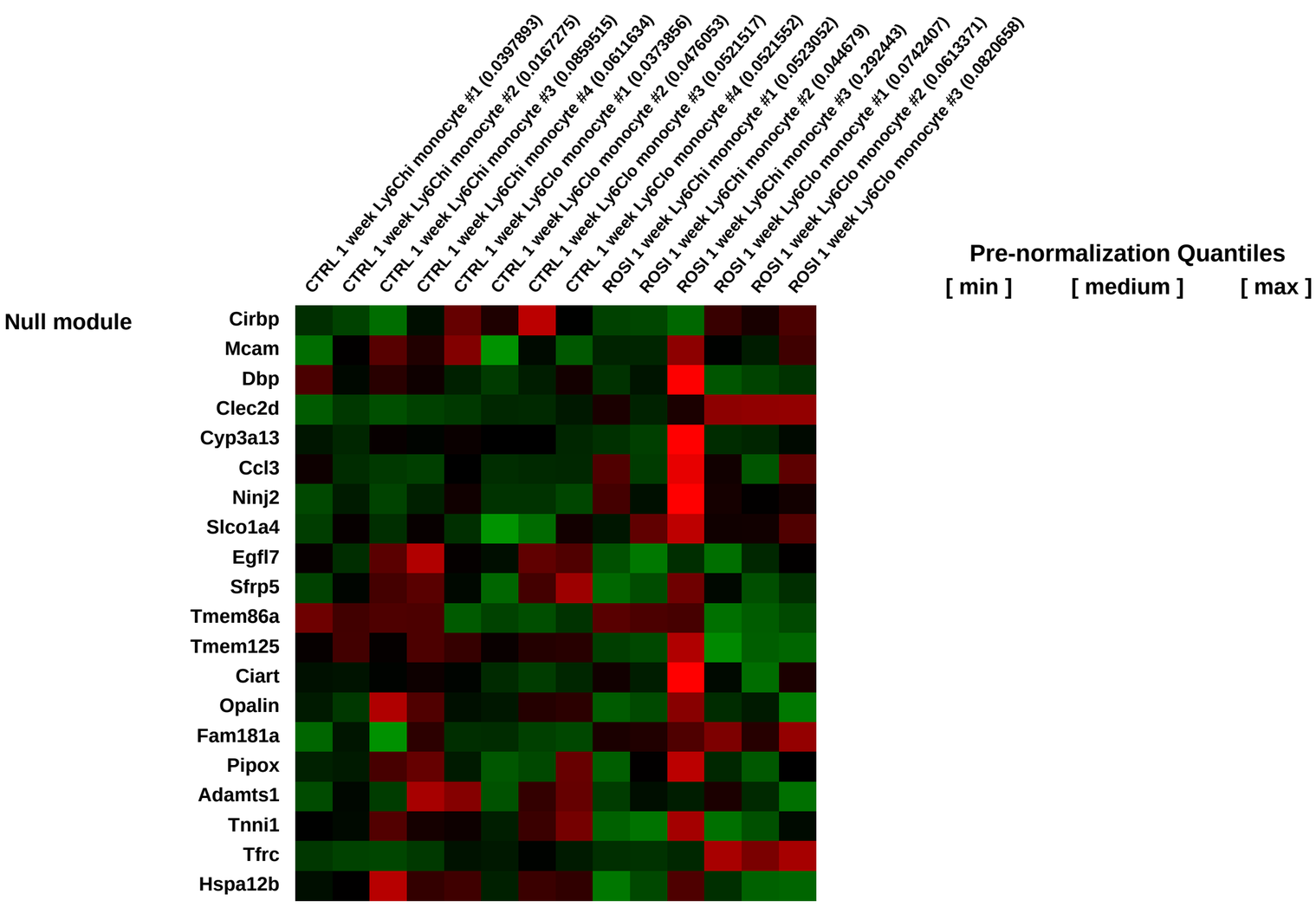

GEO Series "GSE32078" Expression Profiles

Num of samples in this series: 12

Scale of expression profile Z-scores

-3.0 -2.0 -1.0 0.0 1.0 2.0 3.0

GEO Link:	http://www.ncbi.nlm.nih.gov/geo/query/acc.cgi?acc=GSE32078
Status:	Public on Sep 14 2011
Title:	Differential gene expression profiles during embryonic heart development in diabetic mice pregnancy
Organism:	Mus musculus
Experiment type:	Expression profiling by array
Platform:	GPL1261
Pubmed ID:	23287646
Summary & Design:	**Summary:** Congenital heart defects (CHD) are one of the most common defects in offspring of diabetic mothers. There is a clear association between maternal diabetes and CHD; however the underlying molecular mechanism remains unknown. We hypothesized that maternal diabetes affects with the expression of early developmental genes that regulate the essential developmental processes of the heart, thereby resulting in the pathogenesis of CHD. We analyzed genome-wide expression profiling in the developing heart of embryos from diabetic and control mice by using the oligonucleotide microarray. Microarray analysis revealed that a total of 878 genes exhibited more than 1.5 fold changes in expression level in the hearts of experimental embryos in either E13.5 or E15.5 compared with their respective controls. Expression pattern of genes that is differentially expressed in the developing heart was further examined by the real-time reverse transcriptase-polymerase chain reaction. Several genes involved in a number of molecular signaling pathways such as apoptosis, proliferation, migration and differentiation in the developing heart were differentially expressed in embryos of diabetic pregnancy. It is concluded that altered expression of several genes involved in heart development may contribute to CHD in offspring of diabetic mothers. **Overall design:** Embryos with heart malformations from diabetic mice were used as the experimental samples. At least three or four embryos each from three or four different litters of diabetic or control groups were used for each microarray experiment (n = 3). Total RNA was extracted from the pooled embryonic heart tissues at E13.5 and E15.5 of diabetic and control groups using RNeasy micro kit (Qiagen, CA, USA). RNA was quantified by Nanodrop 1000 (Thermo Scientific, MA, USA) and its quality was determined using a Bioanalyzer (Agilent, CA, USA). For each sample, 100 ng of total RNA was used for the 3â IVT Express assay according to Origen Labs SOP (Origen Labs, Singapore). The extracted total RNA was transcribed into cDNA, which was then used as a template to synthesize biotin-labeled aRNA (amplified RNA). The aRNA was then fragmented and hybridized to Affymetrix Mouse Genome 430 2.0 array(Affymetrix, CA, USA) for 16 hours at 45´”C with rotation at 60 rpm. Arrays were then washed and stained using the FS450_0004 fluidics protocol on 3 fluidics stations and scanned using an Affymetrix 3000 7G scanner (Affymetrix, CA, USA). The scanned images were inspected for hybridization efficiency. The raw data (CEL) files generated from GCOS (GeneChip Operating Software, Affymetrix, CA, USA) were imported into Expression Console (EC) 1.1 (Affymetrix, CA, USA) to perform the Mas5 normalization and generate the quality control (QC) metrics.

Background corr dist: KL-Divergence = 0.1298, L1-Distance = 0.0323, L2-Distance = 0.0018, Normal std = 0.3944

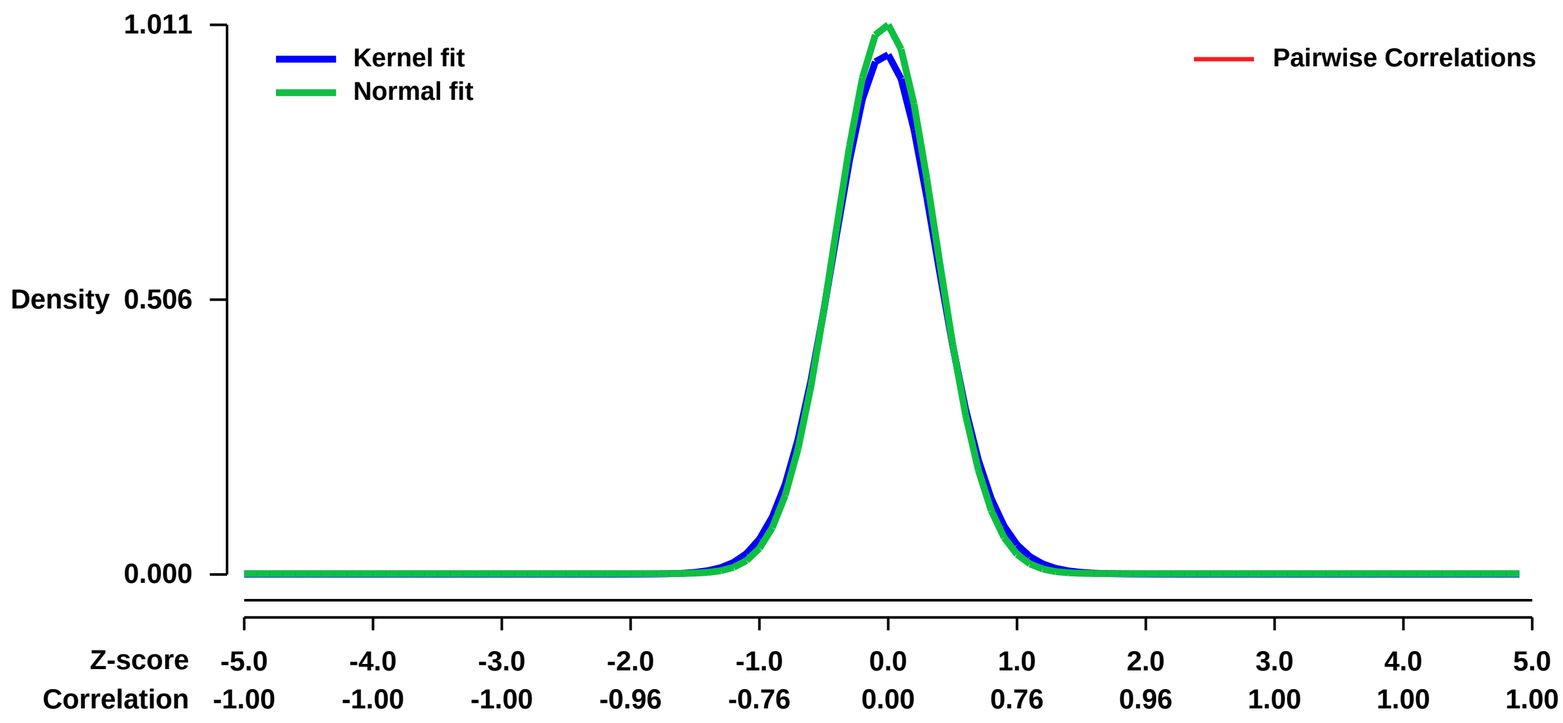

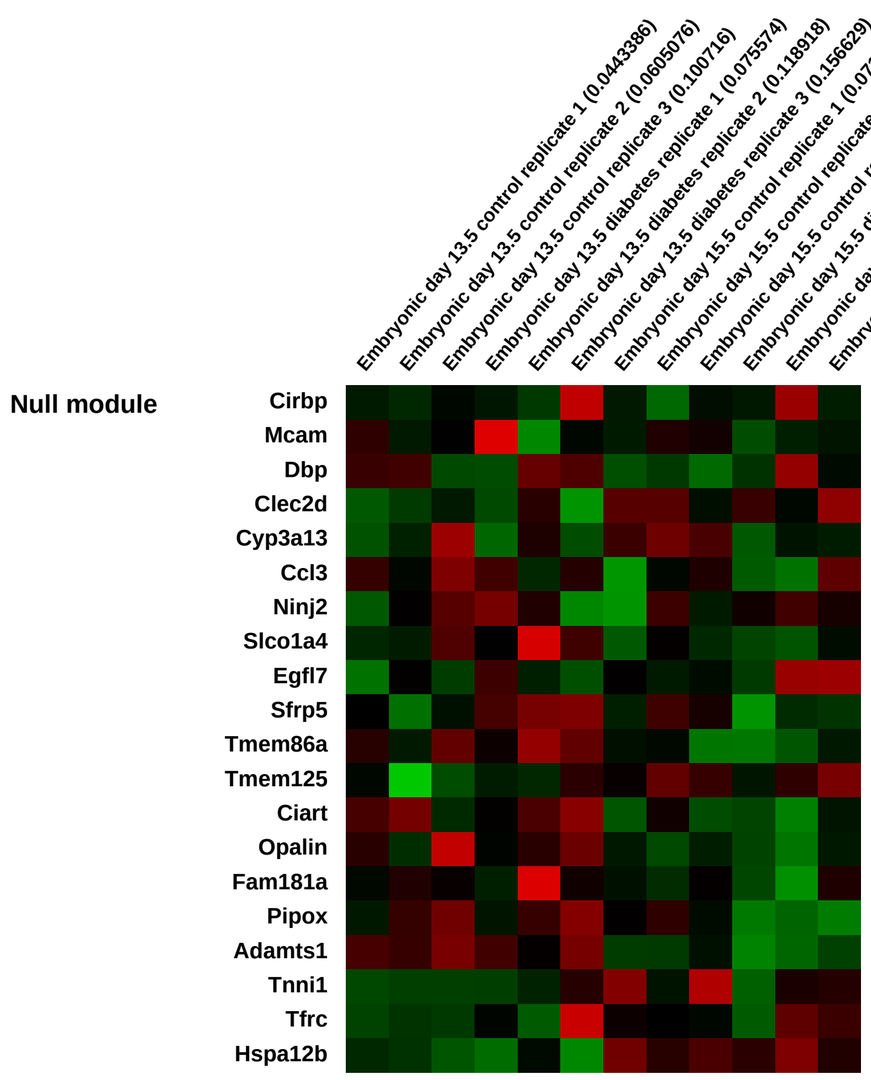

GEO Series "GSE32093" Expression Profiles

Num of samples in this series: 6

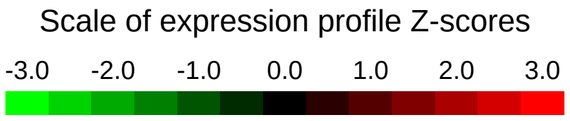

GEO Link:	**http://www.ncbi.nlm.nih.gov/geo/query/acc.cgi?acc=GSE32093**
Status:	**Public on Apr 01 2012**
Title:	**Expression data from E12.5 embryonic kidneys isolated from wild-type and Ret-deficient mice**
Organism:	**Mus musculus**
Experiment type:	**Expression profiling by array**
Platform:	**GPL1261**
Pubmed ID:	
Summary & Design:	**Summary:** **To better understand the signaling and transcriptional events involved in the GDNF-independent emergence of the ureteric bud from the Wolffian duct, microarray expression analysis was performed on embryonic kidneys from wild-type and Ret-deficient mice. Microarray data was used to identify genes and gene networks involved in the GDNF-independent outgrowth of the ureteric bud.** **Overall design:** **Whole embryonic kidneys from E12.5 Ret mutant and wild-type mice were isolated. Isolated kidneys were lysed and RNA was extracted with the Qiagen RNEasy Micro kit. The RNA was amplified using the NuGEn Ovation kit and hybridized to the Affymetrix GeneChip Mouse Whole Genome 430 2.0 microarray. Three biological replicates for Ret-knockout and wild-type kidneys were performed.**

Background corr dist: **KL-Divergence = 0.0400, L1-Distance = 0.0258, L2-Distance = 0.0008, Normal std = 0.6234**

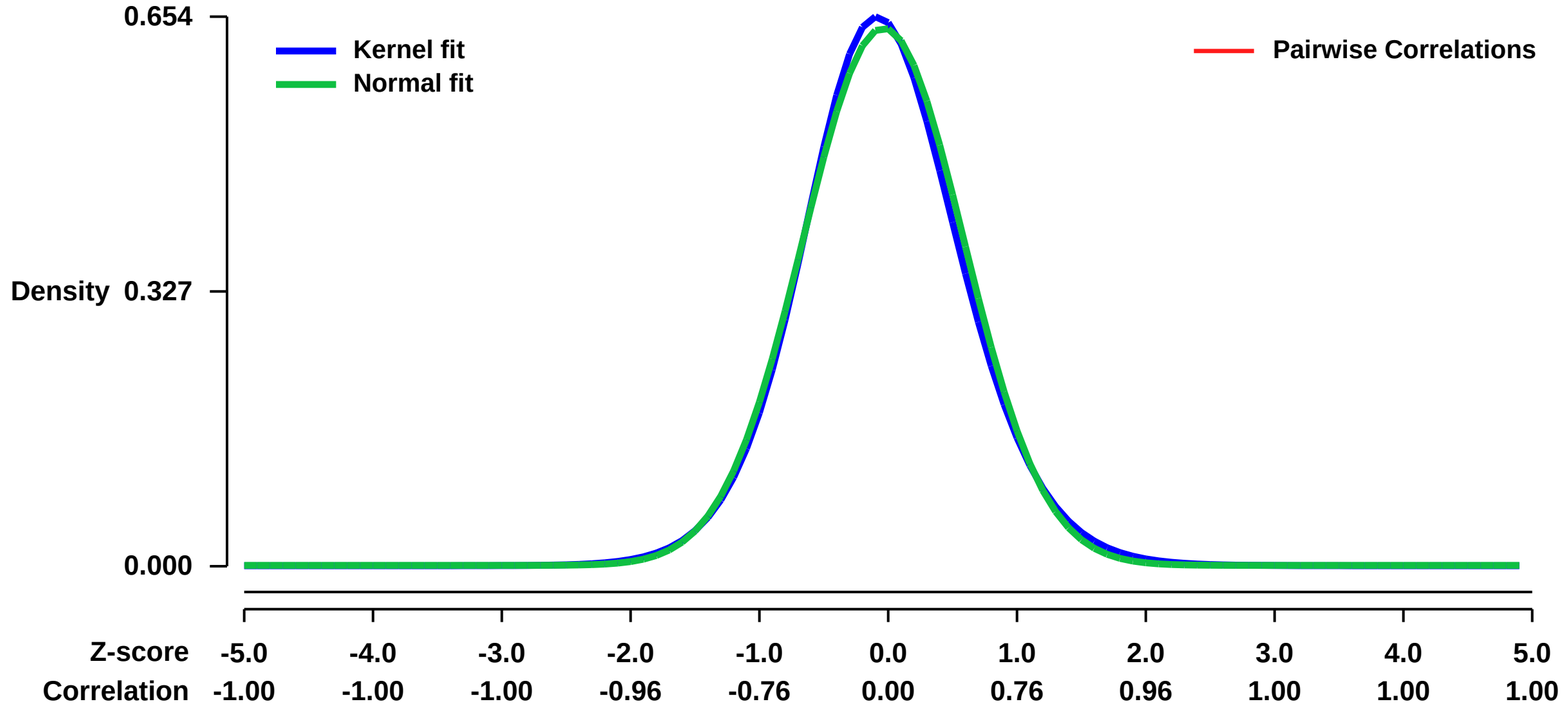

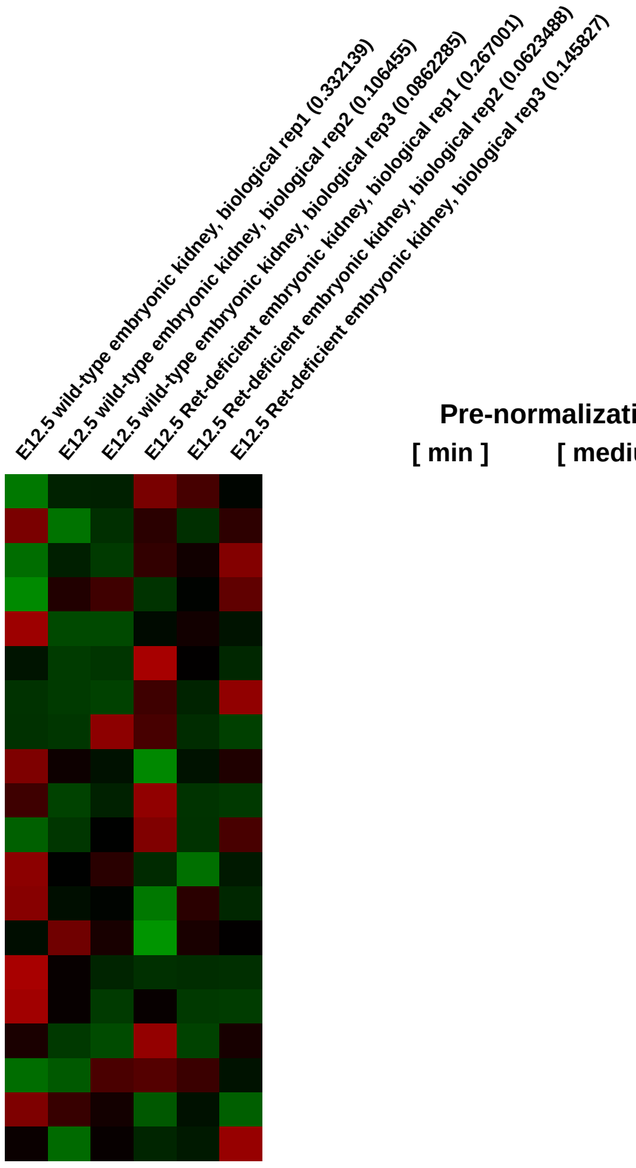

GEO Series "GSE32102" Expression Profiles

Num of samples in this series: 49

Scale of expression profile Z-scores

-3.0 -2.0 -1.0 0.0 1.0 2.0 3.0

GEO Link:	http://www.ncbi.nlm.nih.gov/geo/query/acc.cgi?acc=GSE32102
Status:	Public on Sep 15 2011
Title:	Arsenate Sub-chronic Drinking Water Study
Organism:	Mus musculus
Experiment type:	Expression profiling by array
Platform:	GPL1261
Pubmed ID:	21795629
Summary & Design:	**Summary:** **Concentration- and time-dependent genomic changes in the mouse urinary bladder following exposure to arsenate in drinking water for up to twelve weeks.** **Inorganic arsenic (Asi) is a known human bladder carcinogen. The objective of this study was to examine the concentration dependence of the genomic response to Asi in the urinary bladders of mice. C57BL/6J mice were exposed for 1 or 12 weeks to arsenate in drinking water at concentrations of 0.5, 2, 10, and 50 mg As/L. Urinary bladders were analyzed using gene expression microarrays. A consistent reversal was observed in the direction of gene expression change: from predominantly decreased expression at 1 week to predominantly increased expression at 12 weeks. These results are consistent with evidence from in vitro studies of an acute adaptive response that is suppressed on longer exposure due to down-regulation of Fos. Pathways with the highest enrichment in gene expression changes were associated with epithelial-to-mesenchymal transition, inflammation, and proliferation. Benchmark dose (BMD) analysis determined that the lowest median BMD values for pathways were above 5 mg As/L, despite the fact that pathway enrichment was observed at the 0.5 mg As/L exposure concentration. This disparity may result from the non-monotonic nature of the concentration-responses for the expression changes of a number of genes, as evidenced by the much fewer gene expression changes at 2 mg As/L compared to lower or higher concentrations. Pathway categories with concentration-related gene expression changes included cellular morphogenesis, inflammation, apoptosis/survival, cell cycle control, and DNA damage response. The results of this study provide evidence of a concentration-dependent transition in the mode of action for the subchronic effects of Asi in mouse bladder cells in the vicinity of 2 mg Asi/L.** **Overall design:** **Female C57Bl/J mice will be exposed to COLD Arsenate in drinking water. One week interium sac on 7/18/06. 100 samples including liver, lung, kidney and bladder. Bladder will be analyzed with microarrays, 24 samples. Twelve week terminal sac on 10/05/06. 75 total samples including lung, kidney, and bladder. Bladdler will be analyzed by microarray, 25 samples. Drinking water containing As will be prepared weekly with monitoring to determine amount used by mice. Following tissues will be available for genomic study: Bladder, liver, lung, and kidney.**

Background corr dist: KL-Divergence = 0.4036, L1-Distance = 0.0614, L2-Distance = 0.0095, Normal std = 0.2485

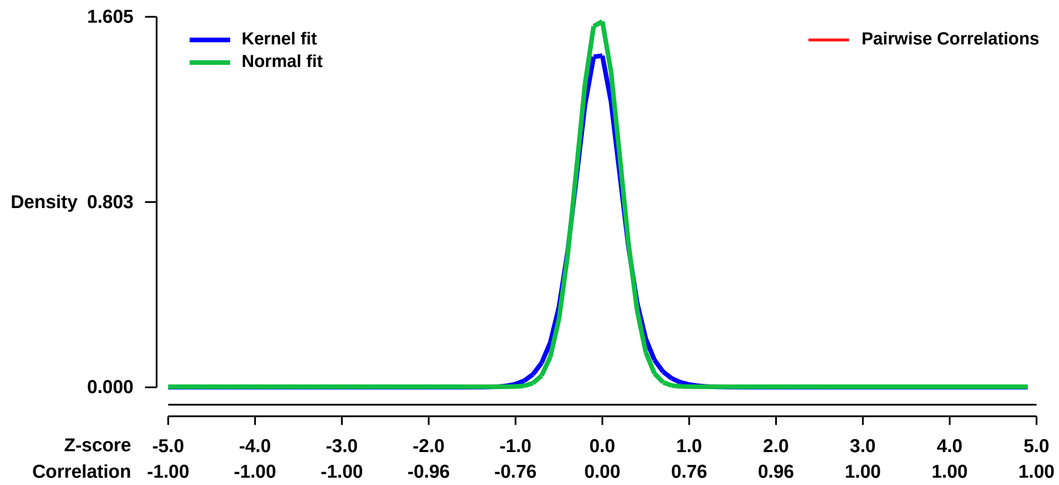

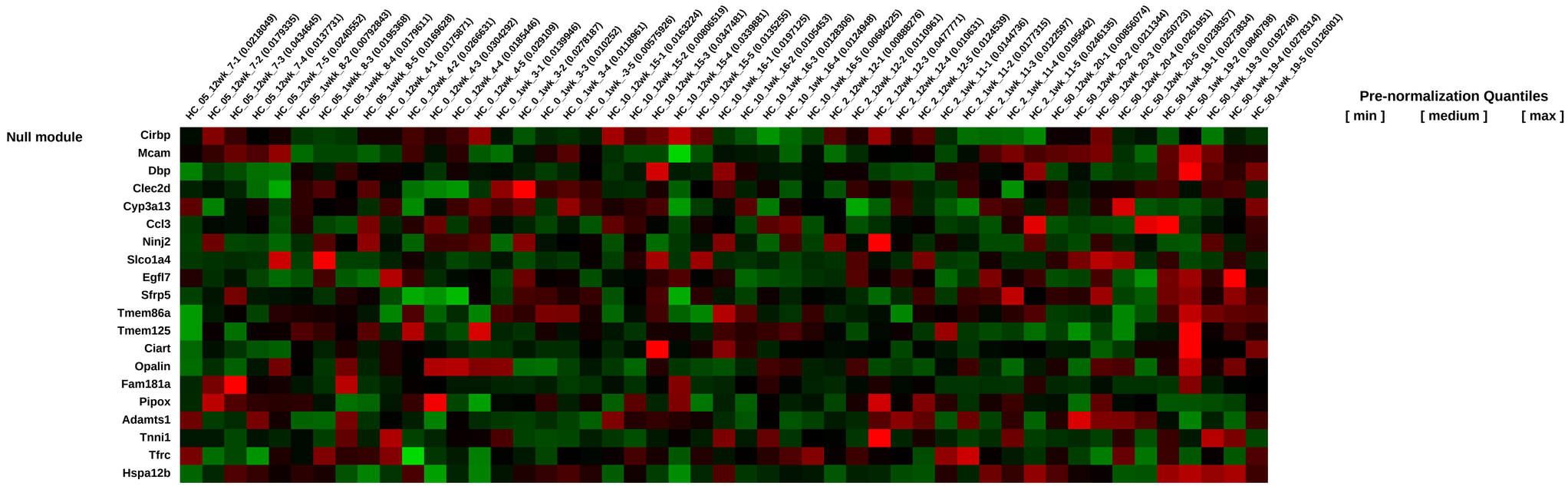

GEO Series "GSE32103" Expression Profiles

Num of samples in this series: 6

Scale of expression profile Z-scores

-3.0 -2.0 -1.0 0.0 1.0 2.0 3.0

GEO Link:	http://www.ncbi.nlm.nih.gov/geo/query/acc.cgi?acc=GSE32103
Status:	Public on Sep 01 2012
Title:	Expression data from mice mammary glands from Elf5 knockout (KO) and wildtype controls
Organism:	Mus musculus
Experiment type:	Expression profiling by array
Platform:	GPL1261
Pubmed ID:	23086238
Summary & Design:	**Summary:** We developed conditional knockout mice where the transcription factor Elf5 (also called ESE-2) is deleted in the mammary glands. Loss of Elf5 results in block in alveologenesis and epithelial differentiation defects. Mammary gland samples from Elf5 knockout and wild type animals were analyzed for global transcriptome changes. **Overall design:** We used microarrays to performing transcriptional profiling of Elf5KO and control mammary glands at Lac1 (Lactation day 1)

Background corr dist: KL-Divergence = 0.0299, L1-Distance = 0.0253, L2-Distance = 0.0009, Normal std = 0.6722

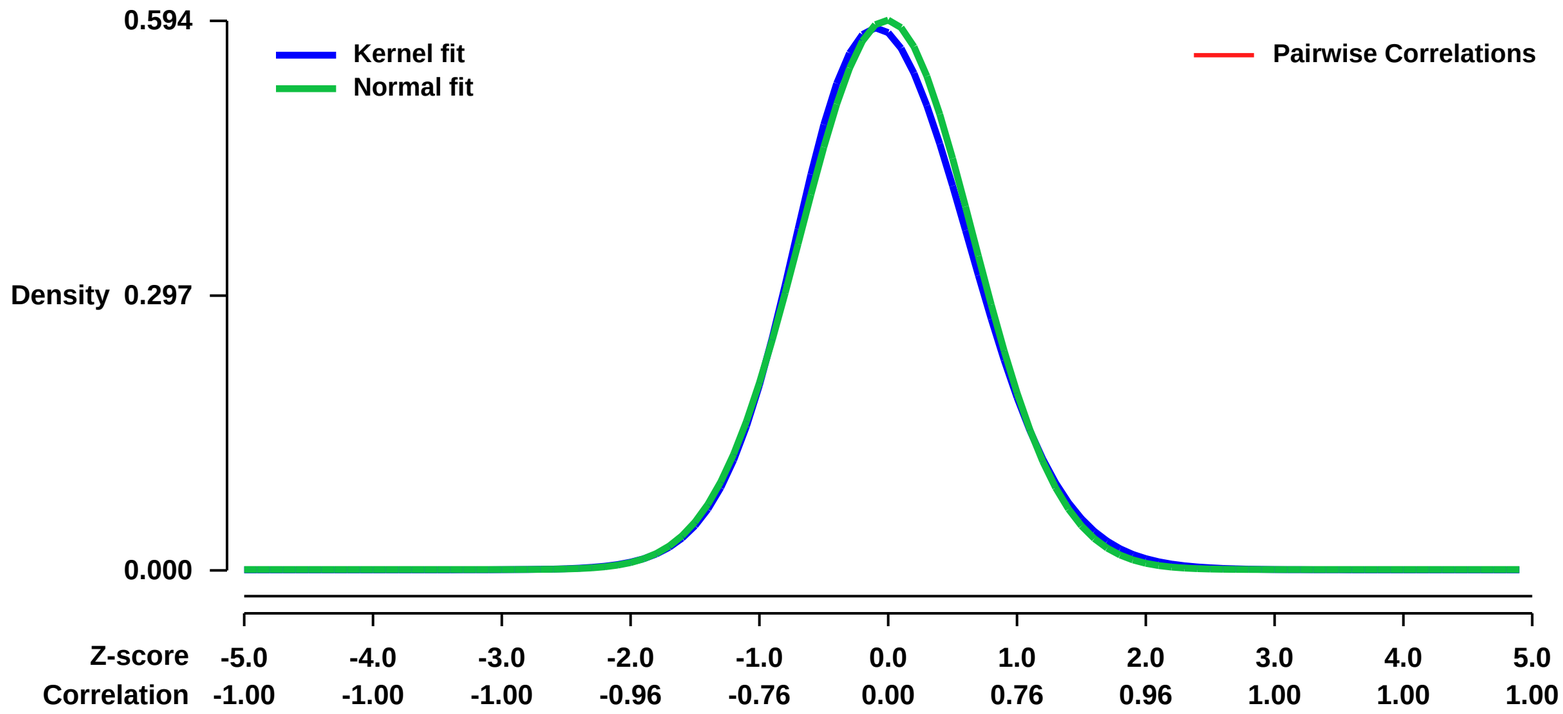

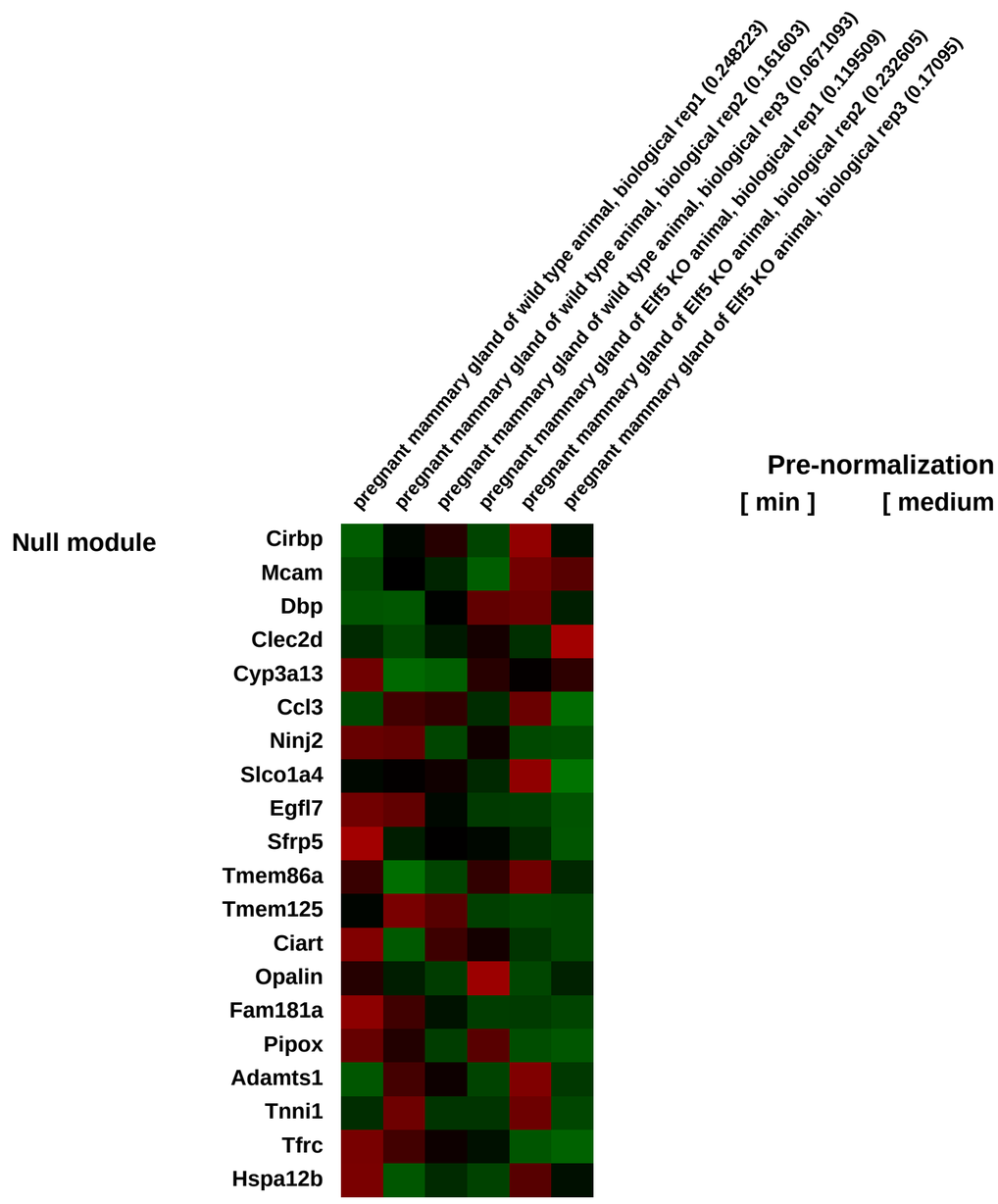

GEO Series "GSE32214" Expression Profiles

Num of samples in this series: 6

Scale of expression profile Z-scores

-3.0 -2.0 -1.0 0.0 1.0 2.0 3.0

GEO Link:	http://www.ncbi.nlm.nih.gov/geo/query/acc.cgi?acc=GSE32214
Status:	Public on Oct 31 2011
Title:	Expression profiling of erythroid developmental subsets isolated from mouse fetal liver.
Organism:	Mus musculus
Experiment type:	Expression profiling by array
Platform:	GPL1261
Pubmed ID:	22076376
Summary & Design:	**Summary:** The S1 and S3 erythroid developmental subsets were isolated using flow cytometry and the cell surface markers CD71 and Ter119 as described by Pop et. al. 2010 (PMID: 20877475) Expression profiles for S1 and S3 subsets were generated using Affymetrix GeneChips. Results were used to identify genes that are differentially expressed during erythropoiesis. **Overall design:** Single cell suspensions were prepared by mechanically dissociating whole fetal livers obtained from E12.5 to E13.5 Balb/C mouse embryos. Cells were stained for CD71, Ter119, and a cocktail containing lineage-specific antibodies. S1 and S3 erythroid developmental subsets were identified and isolated using flow cytometric sorting as described by Pop et. al. 2010 (PMID: 20877475). S1 and S3 subsets were isolated on 3 seperate days to generate total RNA (biological replicates). 20 ng of total RNA from each biological replicate was converted to cDNA, linearly amplified and biotinylated using Ovation reagents (Nugen, San Carlos, CA). Samples were hybridized to Mouse Genome 430 2.0 Arrays (Affymetrix, Santa Clara, CA). Microarray suite 5 (MAS5) processed sample data were normalized to the average of 18SRNA (AFFX-18SRNAMur/X00686_M_at), GAPDH (AFFX-GapdhMur/M32599_3_at) and ¸†-actin (1419734_at) expression values. These gene expression profiles were performed as part of the manuscript by Shearstone et. al. Global DNA Demethylation During Erythropoiesis In Vivo

Background corr dist: KL-Divergence = 0.0491, L1-Distance = 0.0863, L2-Distance = 0.0176, Normal std = 0.6771

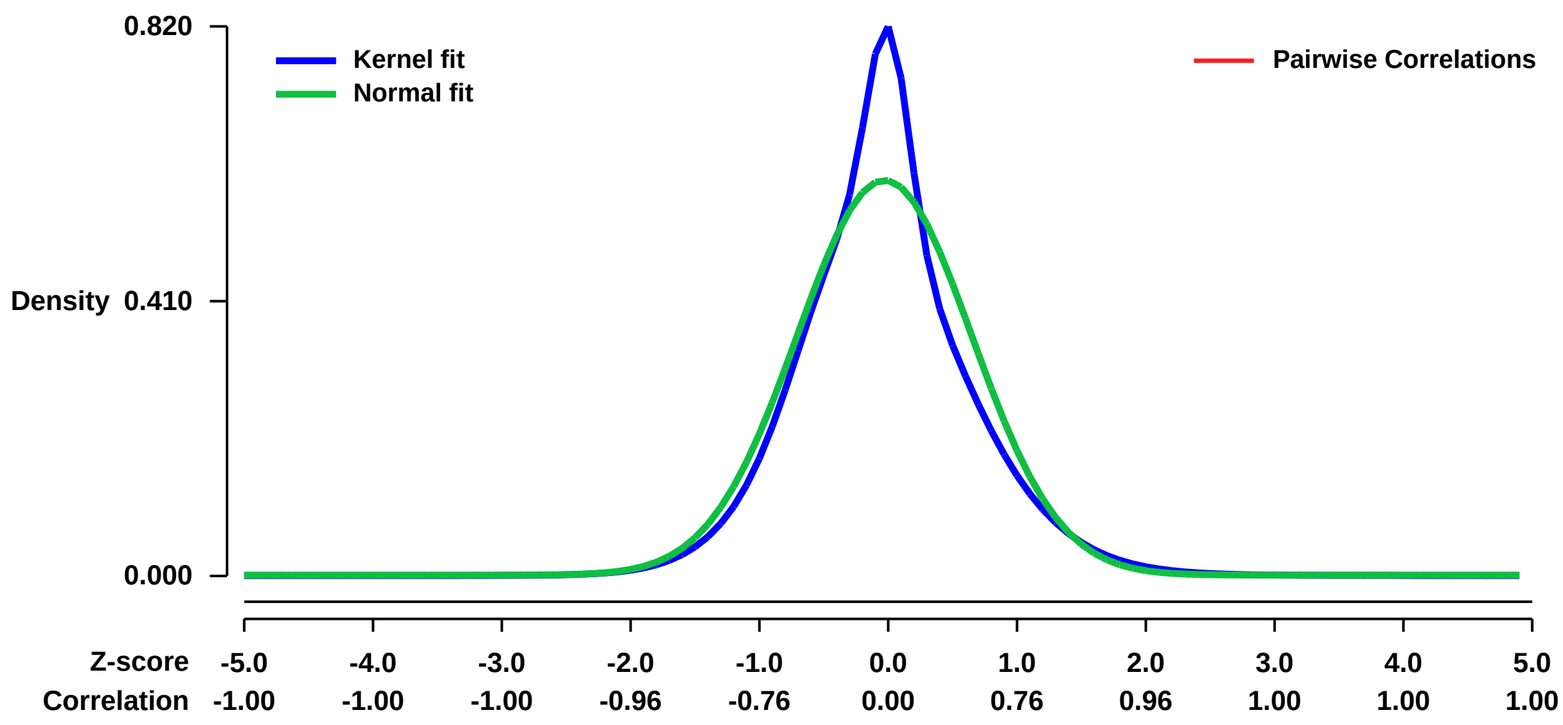

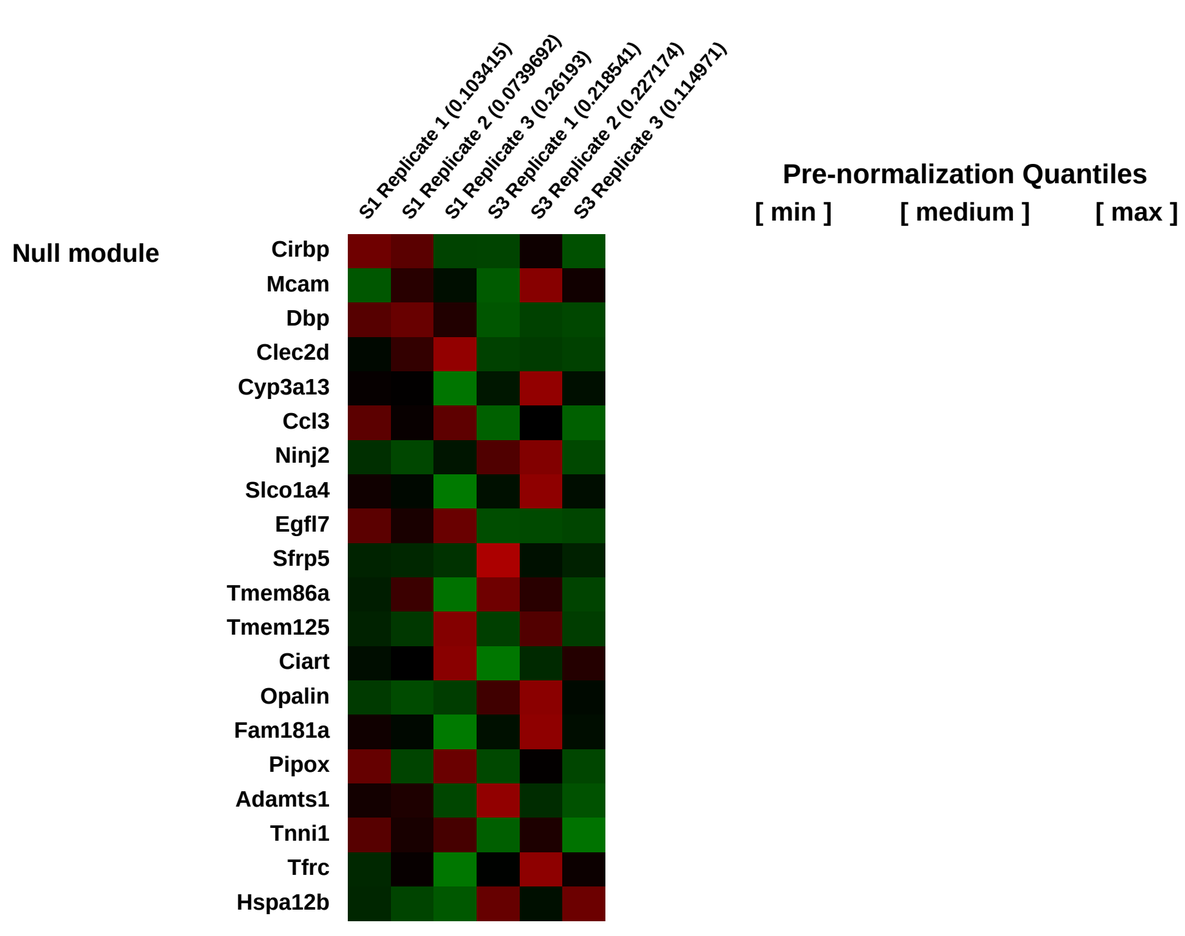

GEO Series "GSE32223" Expression Profiles

Num of samples in this series: 12

Scale of expression profile Z-scores

-3.0 -2.0 -1.0 0.0 1.0 2.0 3.0

GEO Link:	http://www.ncbi.nlm.nih.gov/geo/query/acc.cgi?acc=GSE32223
Status:	Public on Nov 02 2011
Title:	Transcriptional profile of ER71 EYFP positive/negative cells in ER71 WT and MT embryos
Organism:	Mus musculus
Experiment type:	Expression profiling by array
Platform:	GPL1261
Pubmed ID:	21989919
Summary & Design:	**Summary:** ER71 mutant embryos are nonviable and lack hematopoietic and endothelial lineages. To further define the functional role for ER71 in cell lineage decisions, we generated genetically modified mouse models. We engineered an ER71-EYFP transgenic mouse model by fusing the 3.9 kb ER71 promoter to the EYFP reporter gene. Using FACS and transcriptional profiling, we examined the EYFP+ populations of cells in ER71 mutant and wildtype littermates. In the absence of ER71, we observed an increase in the number of EYFP expressing cells, increased expression of the cardiac molecular program and decreased expression of the hemato-endothelial program compared to the wildtype littermate controls. We have also generated a novel ER71-Cre transgenic mouse model using the same 3.9 kb ER71 promoter. Genetic fate mapping studies revealed that the ER71 expressing cells daughter hematopoietic and endothelial lineages in the wildtype background. In the absence of ER71, these cell populations contributed to alternative mesodermal lineages including the cardiac lineage. To extend these analyses, we used an inducible ES/EB system and observed that ER71 overexpression repressed cardiogenesis. Together, these studies identify ER71 as a critical regulator of mesodermal fate decisions, acting to specify the hematopoietic and endothelial lineages at the expense of cardiac lineages. This enhances our understanding of the mechanisms that govern mesodermal fate decisions early during embryogenesis. **Overall design:** 12samples were analyzed, including triplicates of WT; EYFP positive, WT EYFP negative, ER71 MT; EYFP positive and ER71 MT; EYFP negative cells

Background corr dist: KL-Divergence = 0.1330, L1-Distance = 0.0360, L2-Distance = 0.0025, Normal std = 0.3907

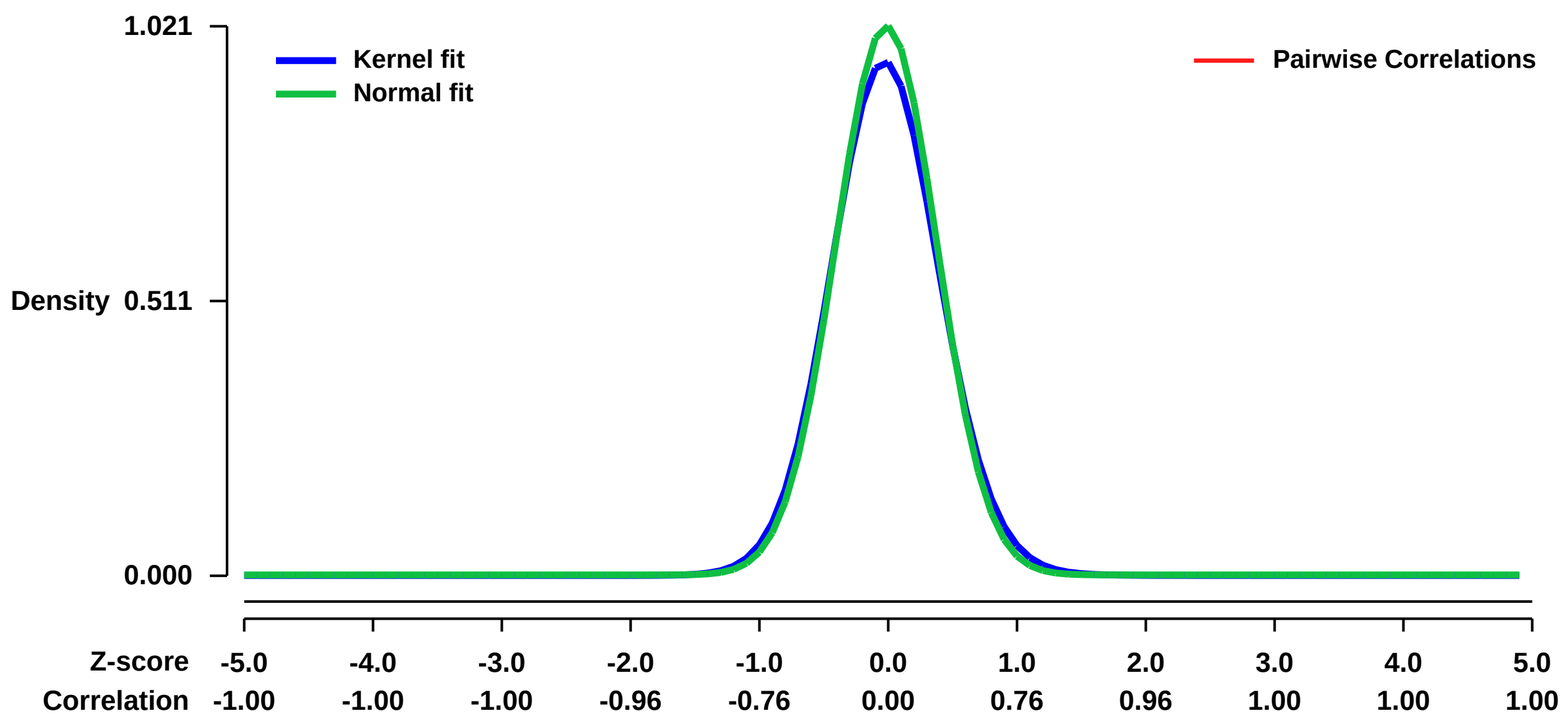

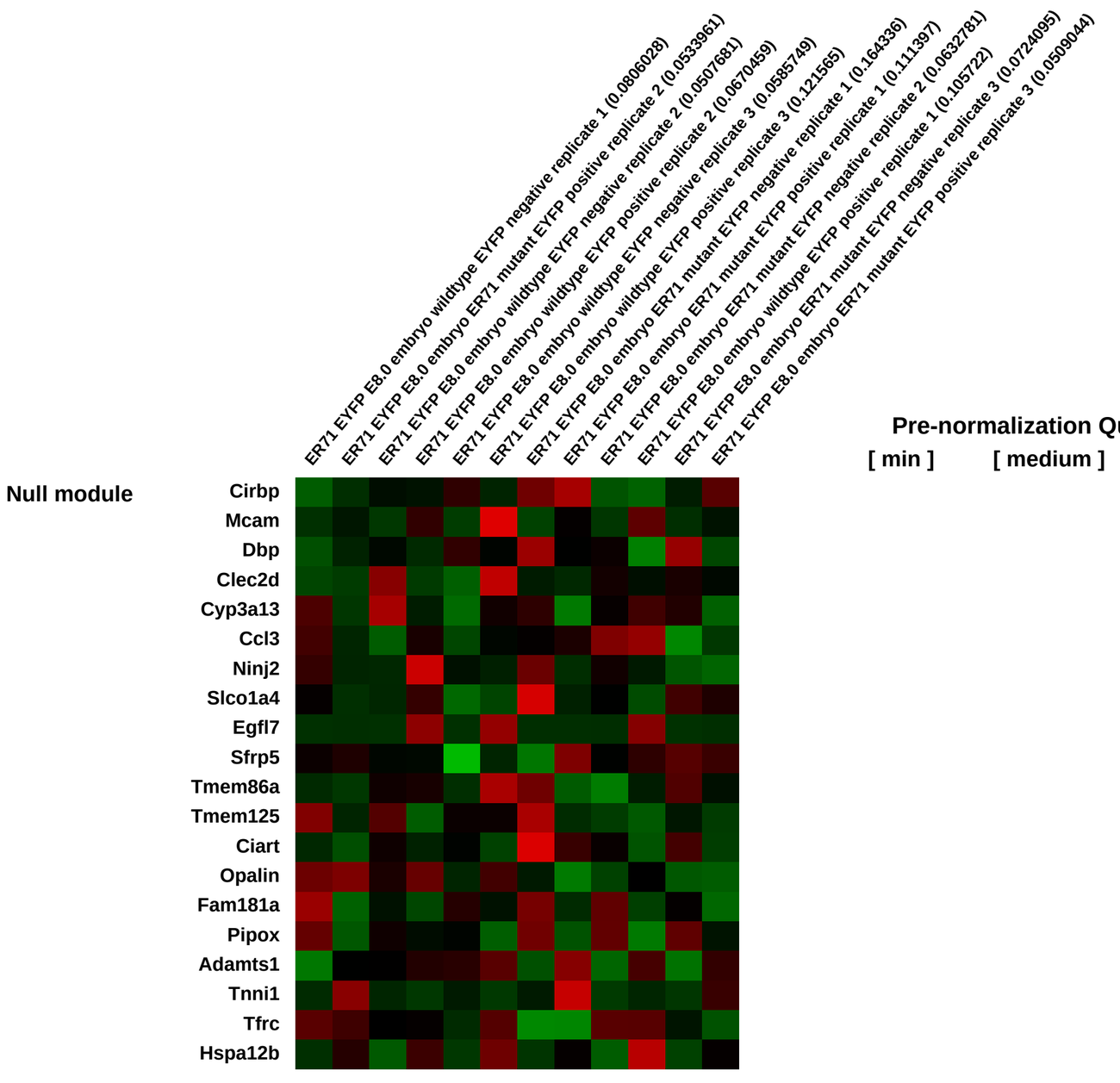

GEO Series "GSE32265" Expression Profiles

Num of samples in this series: 6

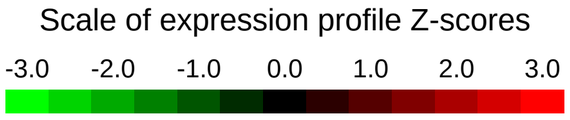

GEO Link:	http://www.ncbi.nlm.nih.gov/geo/query/acc.cgi?acc=GSE32265
Status:	Public on Sep 19 2012
Title:	Gene-expression changes resulting from loss of the mTORC1 component Raptor in murine hematopoietic stem and progenitor cell-enriched populations (HSPC)
Organism:	Mus musculus
Experiment type:	Expression profiling by array
Platform:	GPL1261
Pubmed ID:	22958934
Summary & Design:	**Summary:** We investigated the role of mTORC1 in murine hematopoiesis by conditionally deleting the Raptor gene in murine hematopoietic stem cells. We observed mutliple alterations evoked by Raptor loss in hematopoiesis and profiled gene-expression alterations induced by raptor loss in Flt3-Lin-Sca1+cKit+ hematopoietic stem and progenitor enriched cell populations, 5 weeks post Raptor deletion. **Overall design:** Flt3-Lin-Sca1+cKit+ cells were flow sorted from mice containing homozygous floxed alleles for exon 6 of the Raptor gene in the presence (MT group) or absence (WT group) of the MxCre transgene, which was induced with injections of mice with pIpC 5 weeks before cell isolation.

Background corr dist: KL-Divergence = 0.0270, L1-Distance = 0.0296, L2-Distance = 0.0012, Normal std = 0.6994

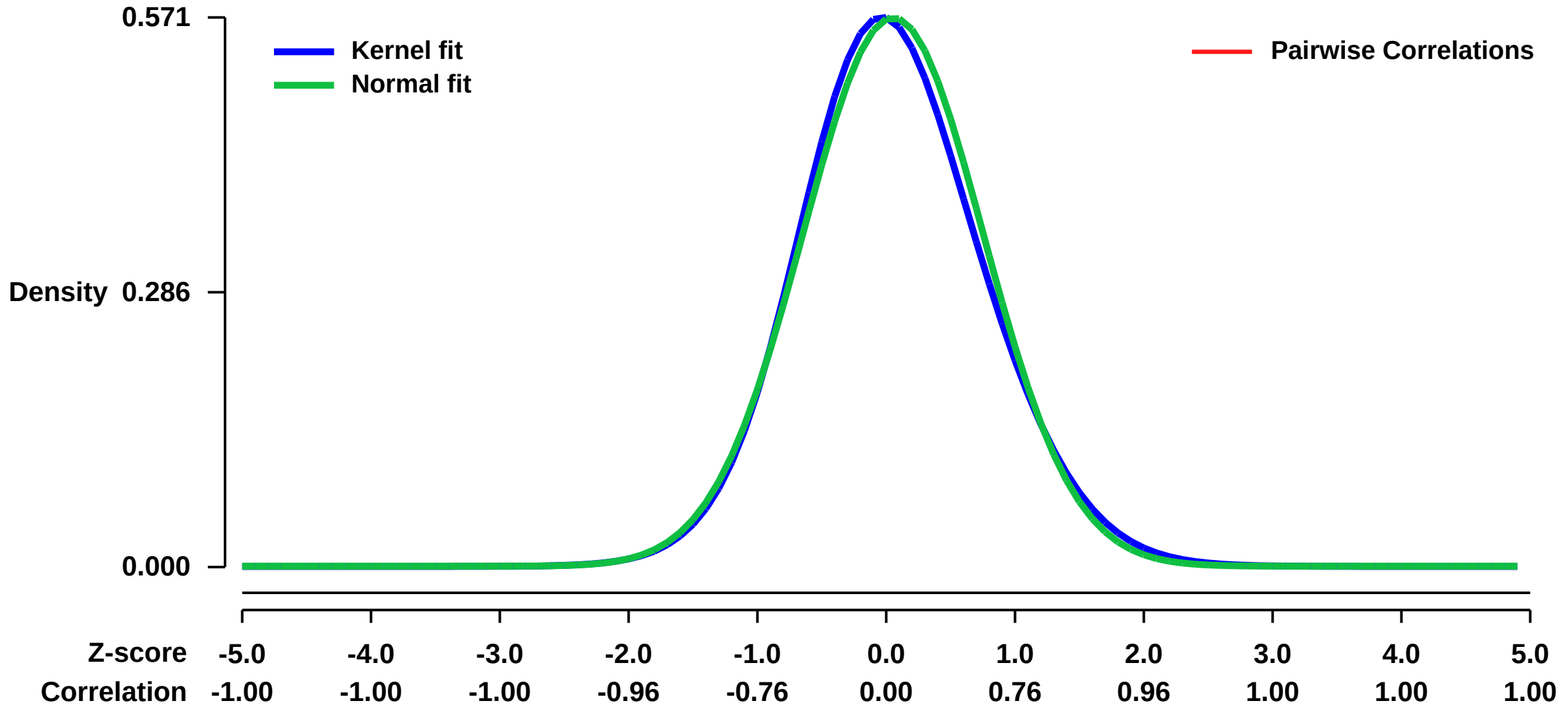

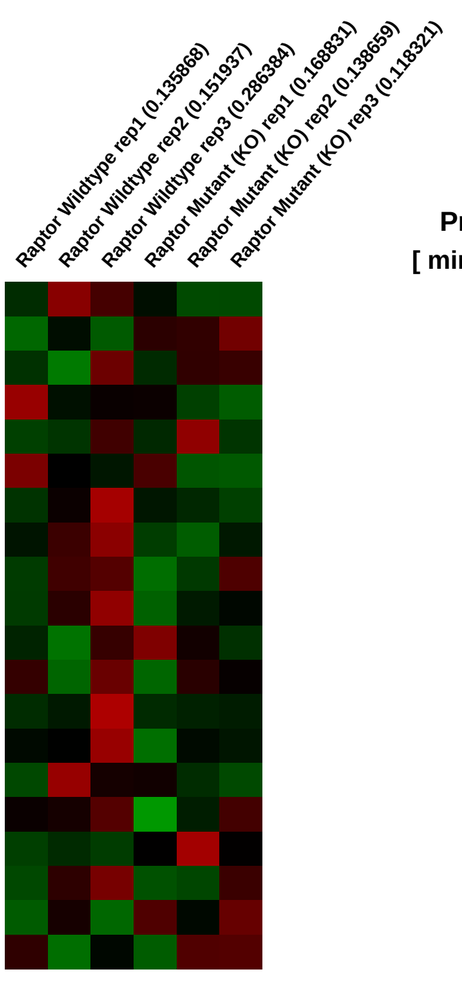

GEO Series "GSE32287" Expression Profiles

Num of samples in this series: 16

Scale of expression profile Z-scores

-3.0 -2.0 -1.0 0.0 1.0 2.0 3.0

GEO Link:	http://www.ncbi.nlm.nih.gov/geo/query/acc.cgi?acc=GSE32287
Status:	Public on Apr 04 2012
Title:	Expression data from wild-type and Rybp-deficient ES cells
Organism:	Mus musculus
Experiment type:	Expression profiling by array
Platform:	GPL1261
Pubmed ID:	22269950
Summary & Design:	**Summary:** We used microarrays to investigate a global change in gene expression by conditional depletion of Rybp in mouse ES cells. **Overall design:** Total RNAs were extracted from wild-type and Rybp-deficient ES cells, and were subjected to microarray analysis using Affymetrix GeneChip Mouse Genome 430A 2.0 arrays

Background corr dist: KL-Divergence = 0.1704, L1-Distance = 0.0323, L2-Distance = 0.0018, Normal std = 0.3569

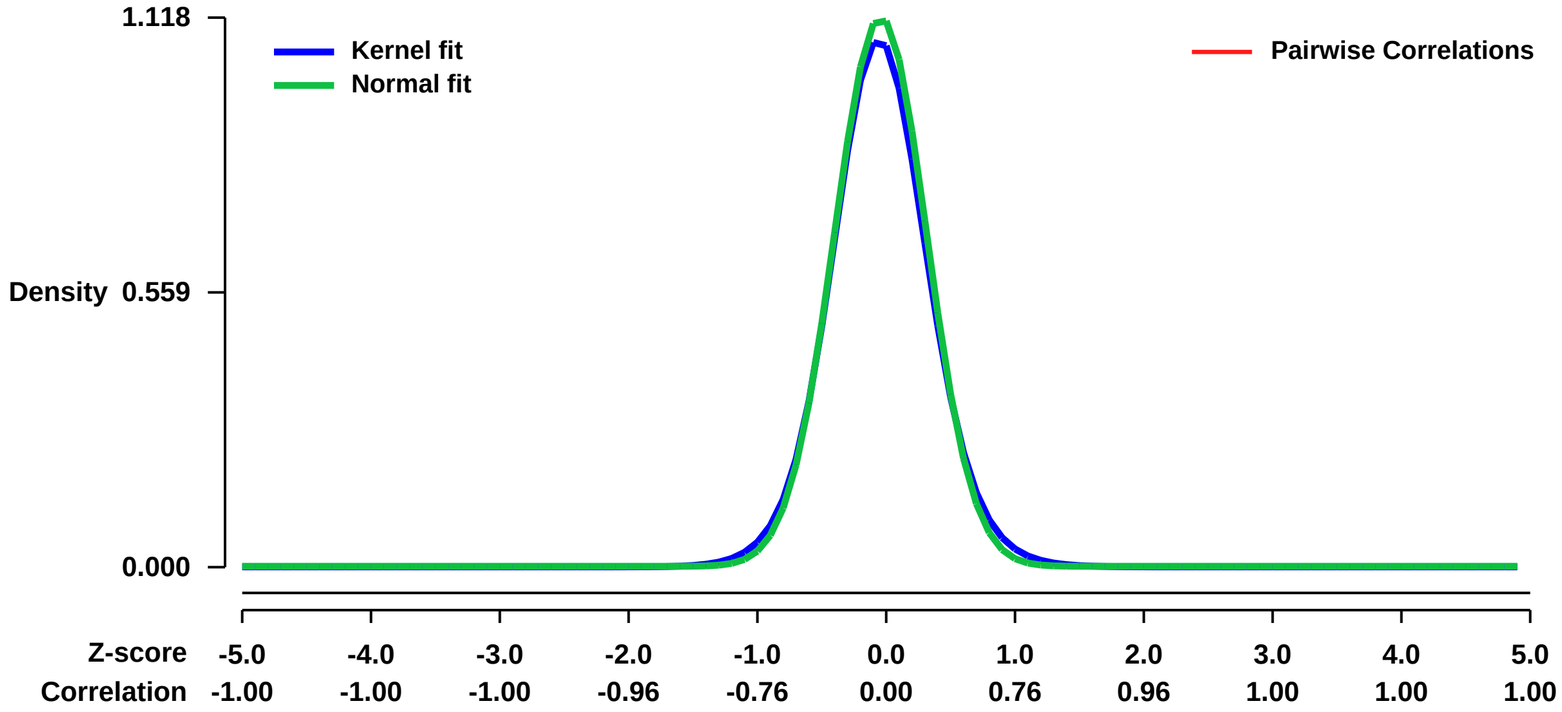

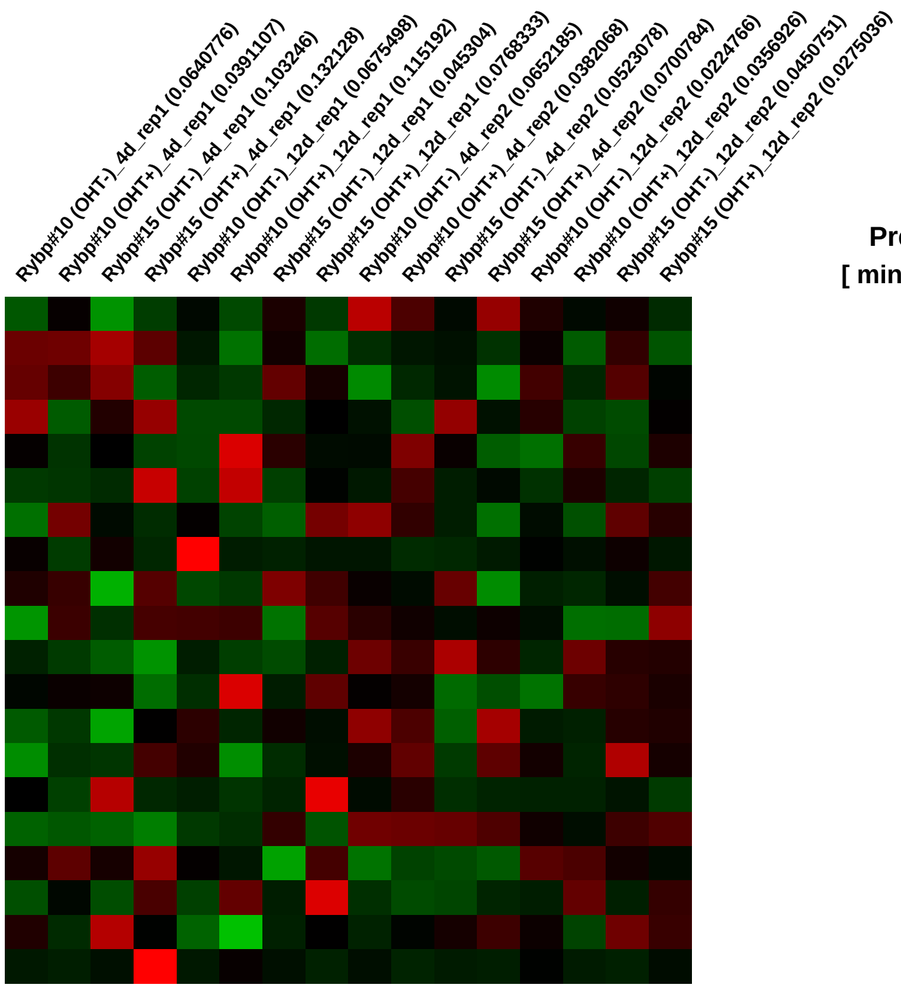

GEO Series "GSE32288" Expression Profiles

Num of samples in this series: 6

Scale of expression profile Z-scores

-3.0 -2.0 -1.0 0.0 1.0 2.0 3.0

GEO Link:	**http://www.ncbi.nlm.nih.gov/geo/query/acc.cgi?acc=GSE32288**
Status:	**Public on Apr 04 2012**
Title:	**Gene expression profile in Yaf2 KD and/or RYBP KO ES cells.**
Organism:	**Mus musculus**
Experiment type:	**Expression profiling by array**
Platform:	**GPL1261**
Pubmed ID:	**22269950**
Summary & Design:	**Summary:** **Gene expression change by Yaf2 KD in wild type or RYBP KO ES cells.** **Overall design:** **Total RNAs were extracted from the respective ES cells, and were subjected to microarray analysis using Affymetrix GeneChip Mouse Genome 430A 2.0 arrays**
Background corr dist:	**KL-Divergence = 0.0452, L1-Distance = 0.0174, L2-Distance = 0.0003, Normal std = 0.5903**

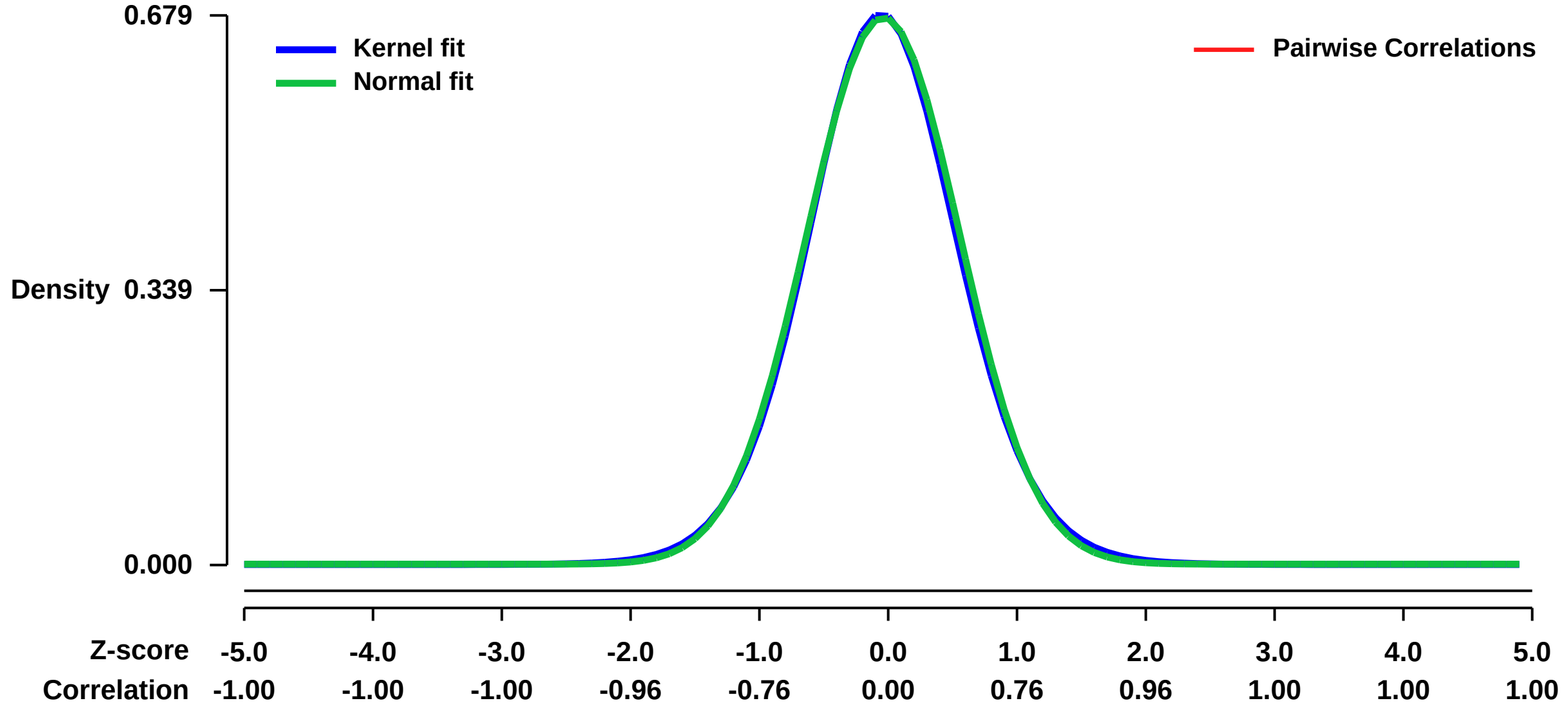

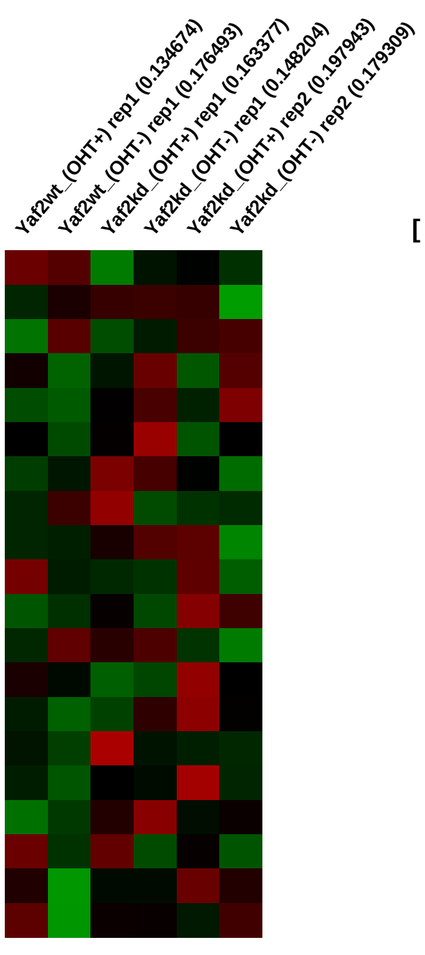

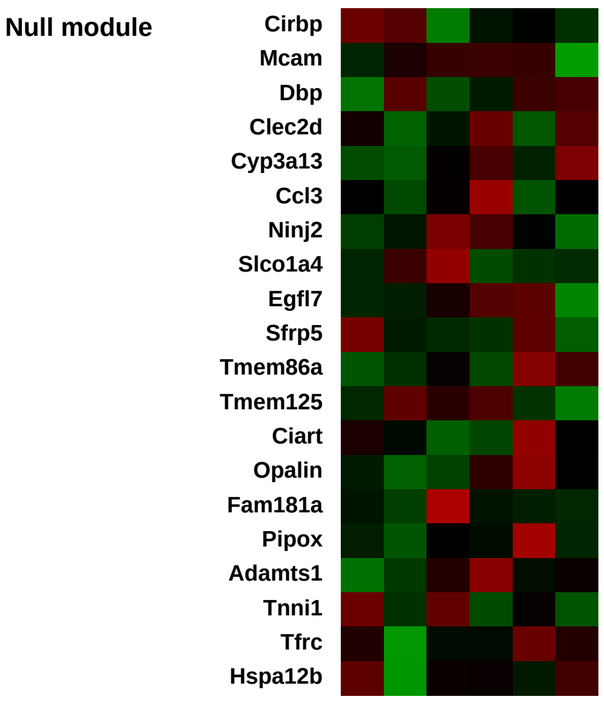

GEO Series "GSE32316" Expression Profiles

Num of samples in this series: 12

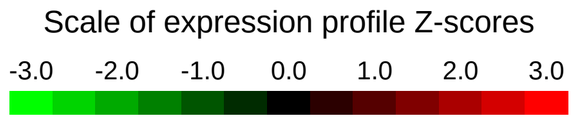

GEO Link:	**http://www.ncbi.nlm.nih.gov/geo/query/acc.cgi?acc=GSE32316**
Status:	**Public on Jan 06 2012**
Title:	**FGFR1 target genes in brown adipose tissues**
Organism:	**Mus musculus**
Experiment type:	**Expression profiling by array**
Platform:	**GPL1261**
Pubmed ID:	**22174314**
Summary & Design:	**Summary:** **We aimed to identify genes that are regulated by FGFR1 in brown adipose tissues of adult male ob/ob mice by injecting 1 mg/kg anti-FGFR1 agonistic antibody.** **Overall design:** **Brown adipose tissues were isolated from adult male ob/ob mice at day 4 after a single intraperitoneal injection of 1 mg/kg anti-FGFR1 agonistic antibody or pair-fed mice injected with control IgG. N=6 mice per each group.**

Background corr dist: **KL-Divergence = 0.1245, L1-Distance = 0.0368, L2-Distance = 0.0026, Normal std = 0.3996**

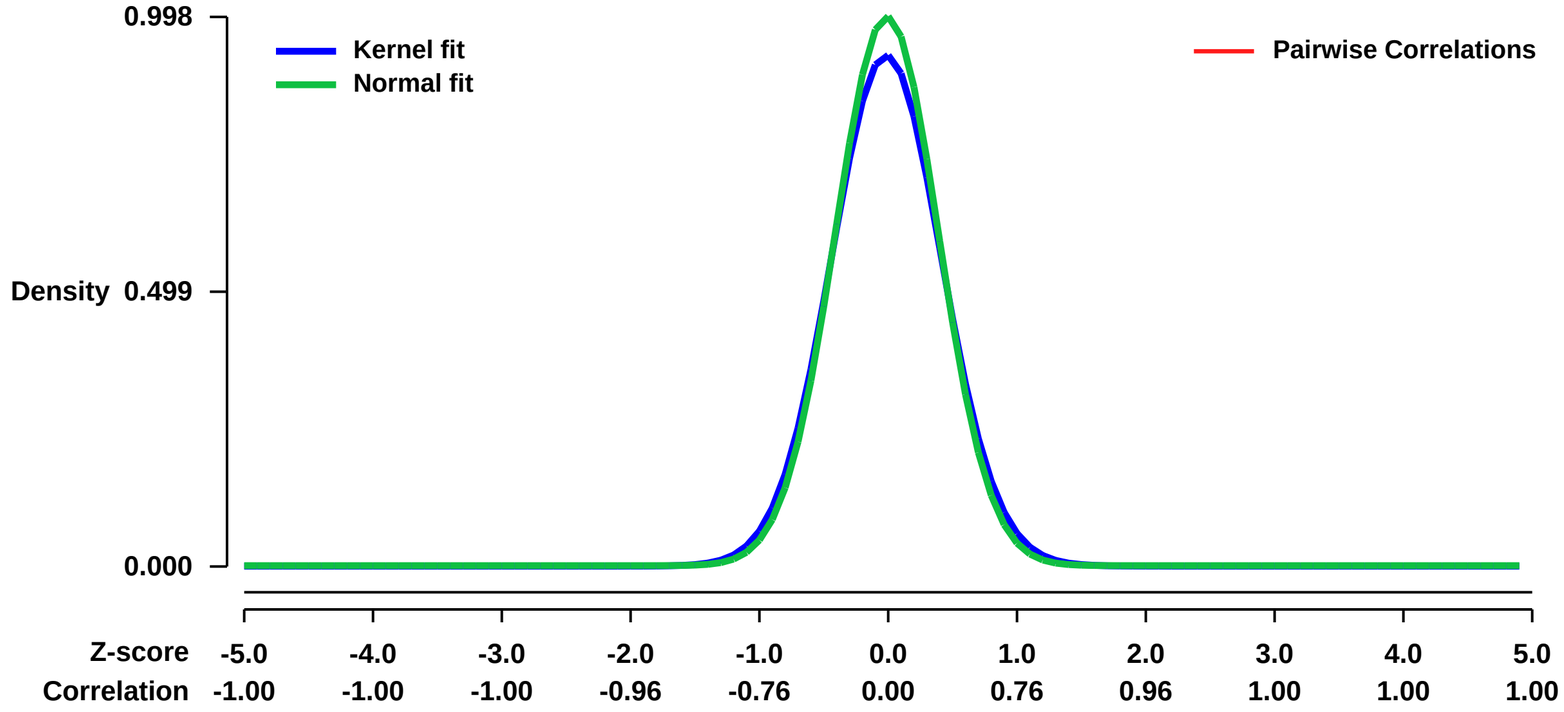

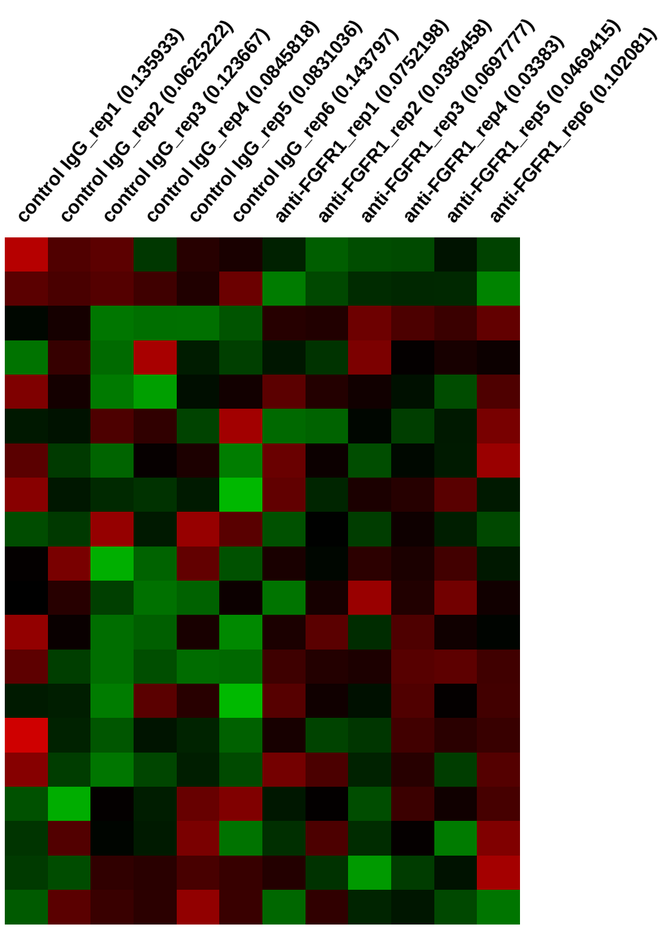

GEO Series "GSE32386" Expression Profiles

Num of samples in this series: 13

Scale of expression profile Z-scores

-3.0 -2.0 -1.0 0.0 1.0 2.0 3.0

GEO Link:	http://www.ncbi.nlm.nih.gov/geo/query/acc.cgi?acc=GSE32386
Status:	Public on Apr 01 2012
Title:	Expression profiling of murine neuroblastoma in transgenic mice
Organism:	Mus musculus
Experiment type:	Expression profiling by array
Platform:	GPL1261
Pubmed ID:	22764207
Summary & Design:	**Summary:** Neuroblastoma is an embryonal tumor arising from the neural crest. It can be mimicked in mice by neural crest-specific overepxression of oncogenes such as MYCN or mutated ALK. **Overall design:** Expression profiling of murine neuroblastoma driven by MYCN were compared to those driven by mutated ALK or both oncogenes. Mouse normal adrenal tissue served as a control.

Background corr dist: KL-Divergence = 0.0643, L1-Distance = 0.0382, L2-Distance = 0.0025, Normal std = 0.5410

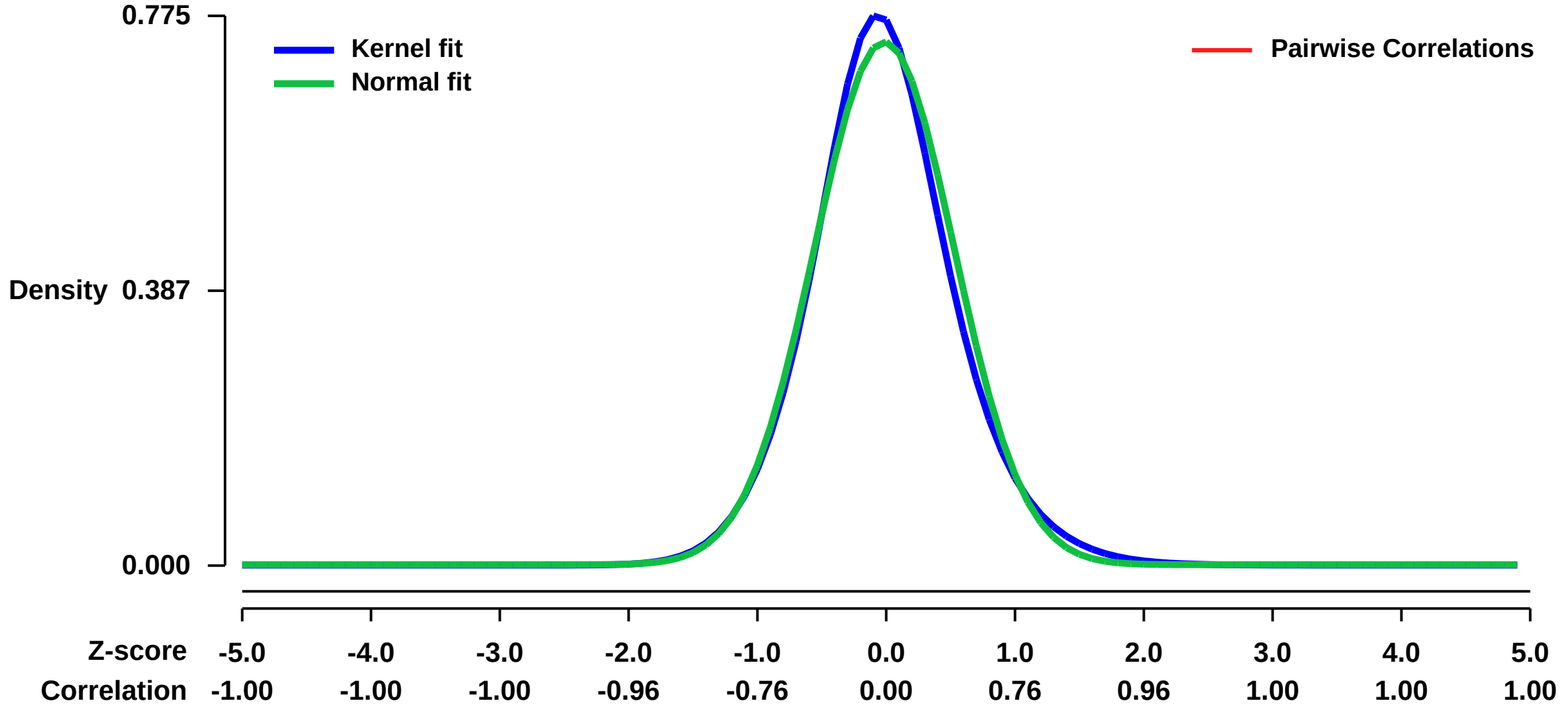

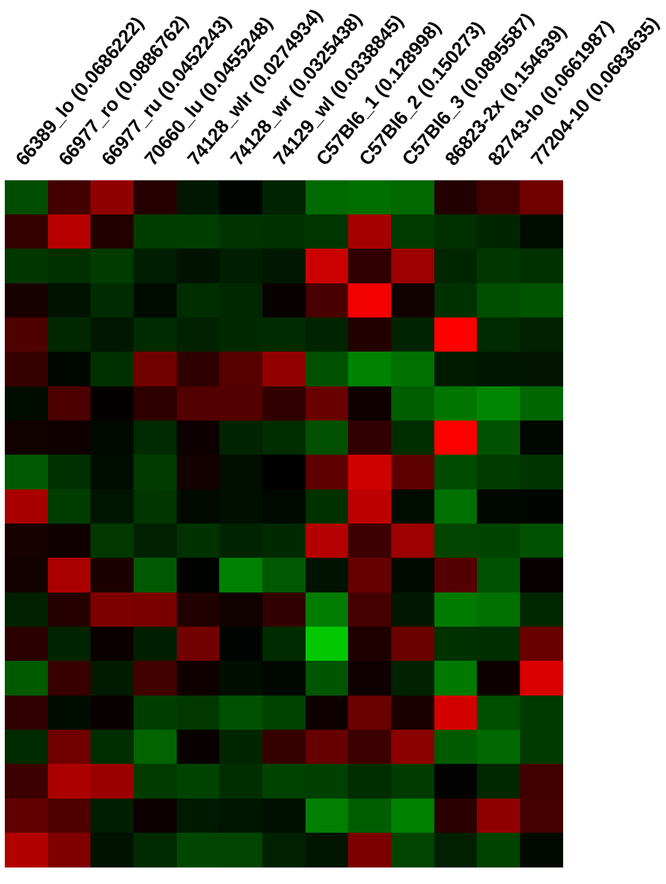

GEO Series "GSE32422" Expression Profiles

Num of samples in this series: 6

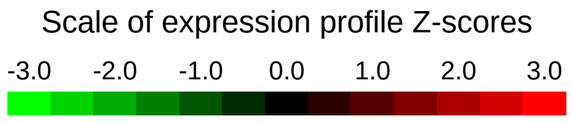

GEO Link:	http://www.ncbi.nlm.nih.gov/geo/query/acc.cgi?acc=GSE32422
Status:	Public on Jan 06 2013
Title:	Expression data from the dorsal and lateral lobes of the prostates of TRAMP mice treated with OSU-CG5
Organism:	Mus musculus
Experiment type:	Expression profiling by array
Platform:	GPL1261
Pubmed ID:	23275006
Summary & Design:	**Summary:** Cells undergoing malignant transformation often shift their cellular metabolism from primarily oxidative phosphorylation to aerobic glycolysis (the Warburg effect). Energy restriction-mimetic agents (ERMAs), such as 2-deoxyglucose and resveratrol, that target this shift in cellular metabolism have been effective in inhibiting cancer cell growth in vitro, and xenograft tumor growth in vivo. We recently developed a novel ERMA, OSU-CG5, that exhibits higher in vivo activity than previously described ERMAs. In this study, we investigated the effect of OSU-CG5 on global gene expression in the dorsal and lateral lobes of the prostate of transgenic adenocarcinoma of the mouse prostate (TRAMP) mice, and on its ability to suppress lesion progression in these mice. **Overall design:** Intact male TRAMP mice were randomized into 2 groups and treated for 4-weeks (from age 6 to 10 weeks) with a vehicle or 100 mg/kg/day OSU-CG5 via oral gavage. At the end of the study, the urogenital tracts were collected and prostates microdissected. RNA was extracted from the dorsal and lateral lobes of the prostates from 3 mice per group, and Affymetrix microarrays were performed.

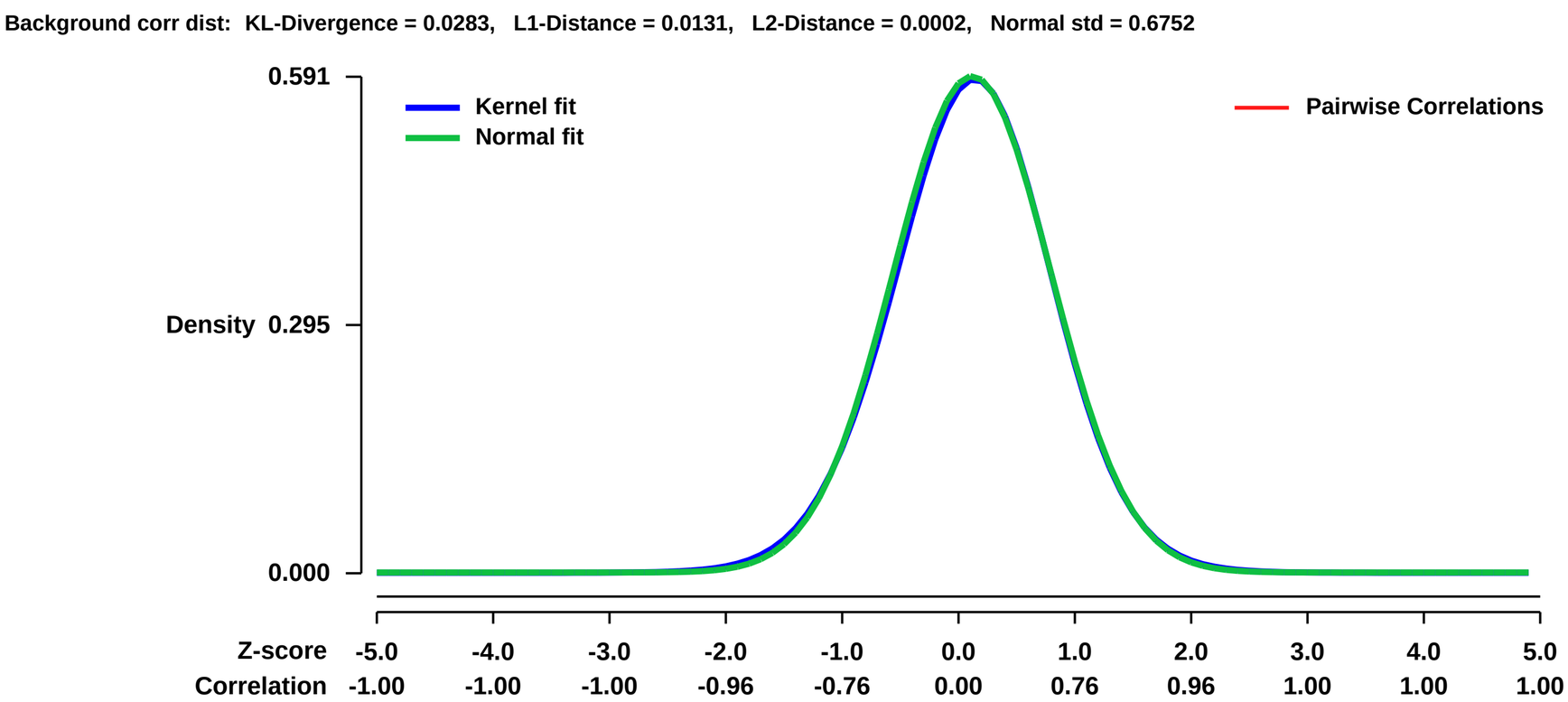

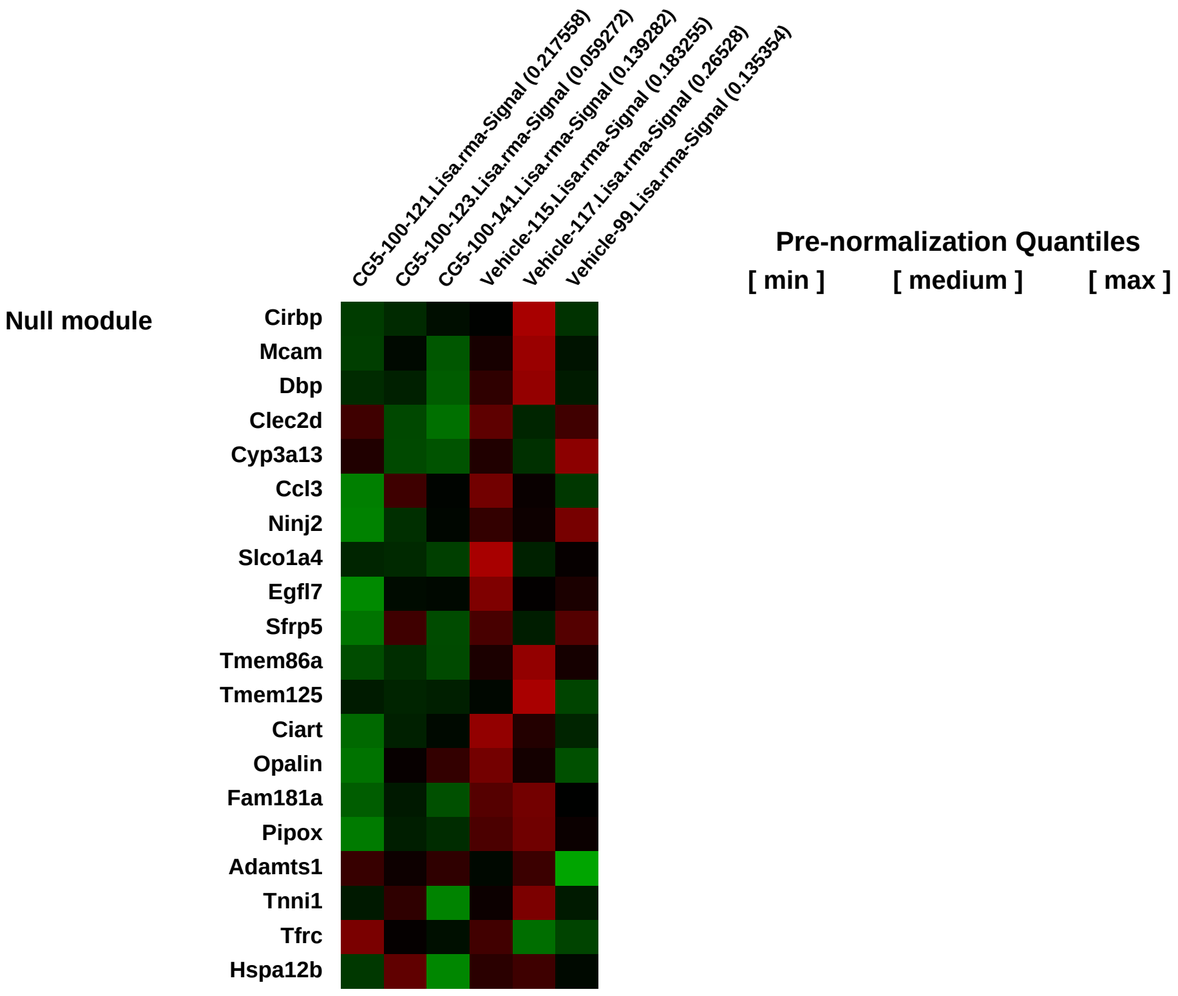

GEO Series "GSE3253" Expression Profiles

Num of samples in this series: 12

Scale of expression profile Z-scores

-3.0 -2.0 -1.0 0.0 1.0 2.0 3.0

GEO Link:	http://www.ncbi.nlm.nih.gov/geo/query/acc.cgi?acc=GSE3253
Status:	Public on Sep 12 2005
Title:	Exaggerated neuroinflammation and sickness behavior in aged mice after activation of the peripheral innate immune system
Organism:	Mus musculus
Experiment type:	Expression profiling by array
Platform:	GPL1261
Pubmed ID:	15919760
Summary & Design:	**Summary:** **Acute cognitive impairment (i.e., delirium) is common in elderly emergency department patients and frequently results from infections that are unrelated to the central nervous system. Since** **activation of the peripheral innate immune system induces brain microglia to produce inflammatory cytokines that are responsible for behavioral deficits, we investigated if aging exacerbated neuroinflammation and sickness behavior after peripheral injection of** **lipopolysaccharide (LPS). Microarray analysis revealed a transcriptional profile indicating the presence of primed or activated microglia and increased inflammation in the aged brain.** **Furthermore, aged mice had a unique gene expression profile in the brain after an intraperitoneal injection of LPS, and the LPS-induced elevation in the brain inflammatory cytokines and oxidative stress was both exaggerated and prolonged compared with adults. Aged mice were anorectic longer and lost more weight than adults after peripheral LPS administration. Moreover, reductions in both locomotor and social behavior remained 24 h later in aged mice, when adults had fully recovered, and the exaggerated neuroinflammatory response in aged mice was not reliably paralleled by increased circulating cytokines in the periphery. Taken together, these data** **establish that activation of the peripheral innate immune system leads to exacerbated neuroinflammation in the aged as compared with adult mice. This dysregulated link between the** **peripheral and central innate immune system is likely to be involved in the severe behavioral deficits that frequently occur in older adults with systemic infections.** **Keywords: Aging, cytokines, brain, inflammation, behavior** **Overall design:** **In this study, adult and aged mice were injected intraperitoneal with sterile saline or Escherichia coli LPS (0.33 mg/kg, ~10 ´¦g/mouse; serotype 0127:B8, Sigma). This dosage of LPS was used because it induces a mild transient sickness behavior in young adults. Mice were killed 4 h after saline or LPS injection by CO2 asphyxiation. Blood samples were collected and brains were removed, separated in half at the longitudinal fissure, frozen in liquid nitrogen, and stored (-80´℃) until assaying. Total RNA was later isolated from some brain samples for microarray analysis (n=3).**

Background corr dist: KL-Divergence = 0.1805, L1-Distance = 0.0447, L2-Distance = 0.0044, Normal std = 0.3453

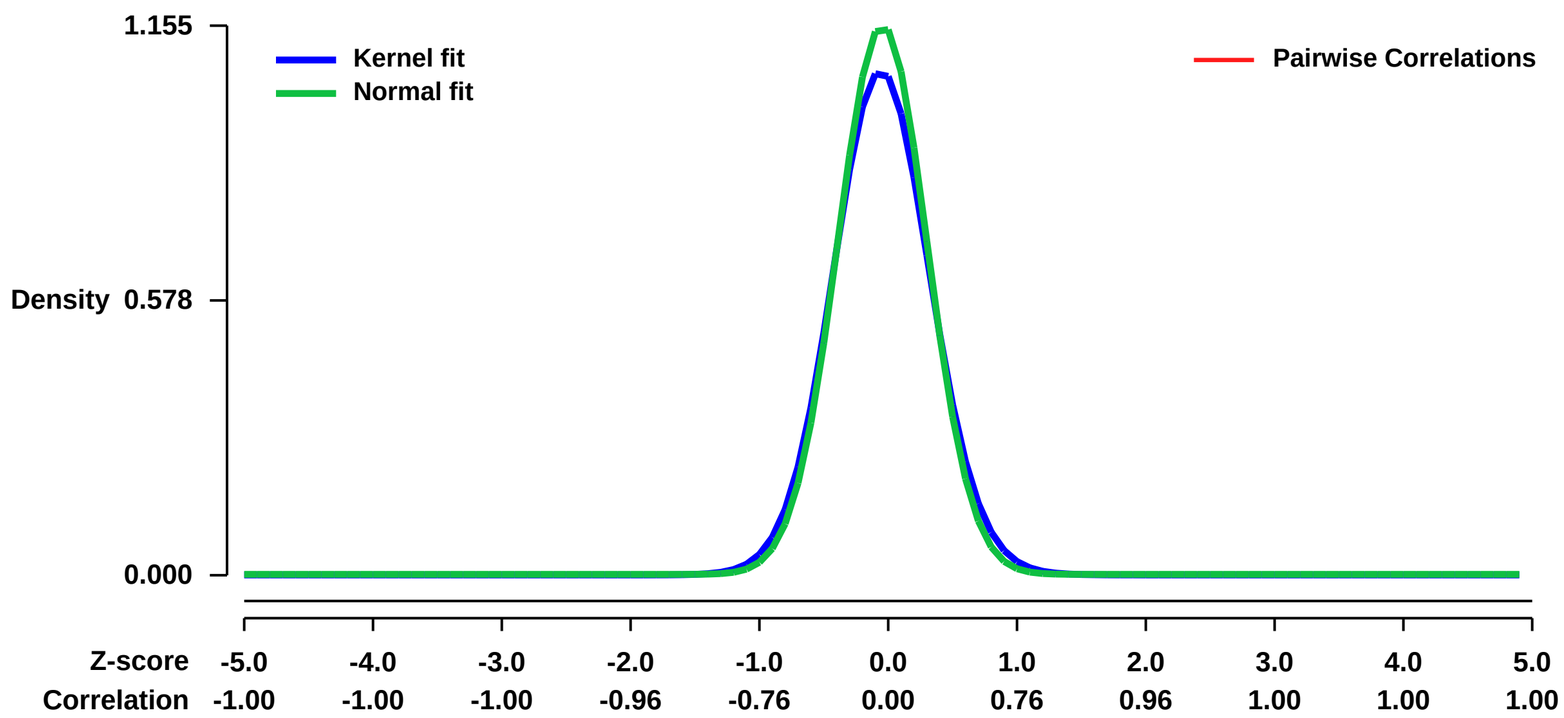

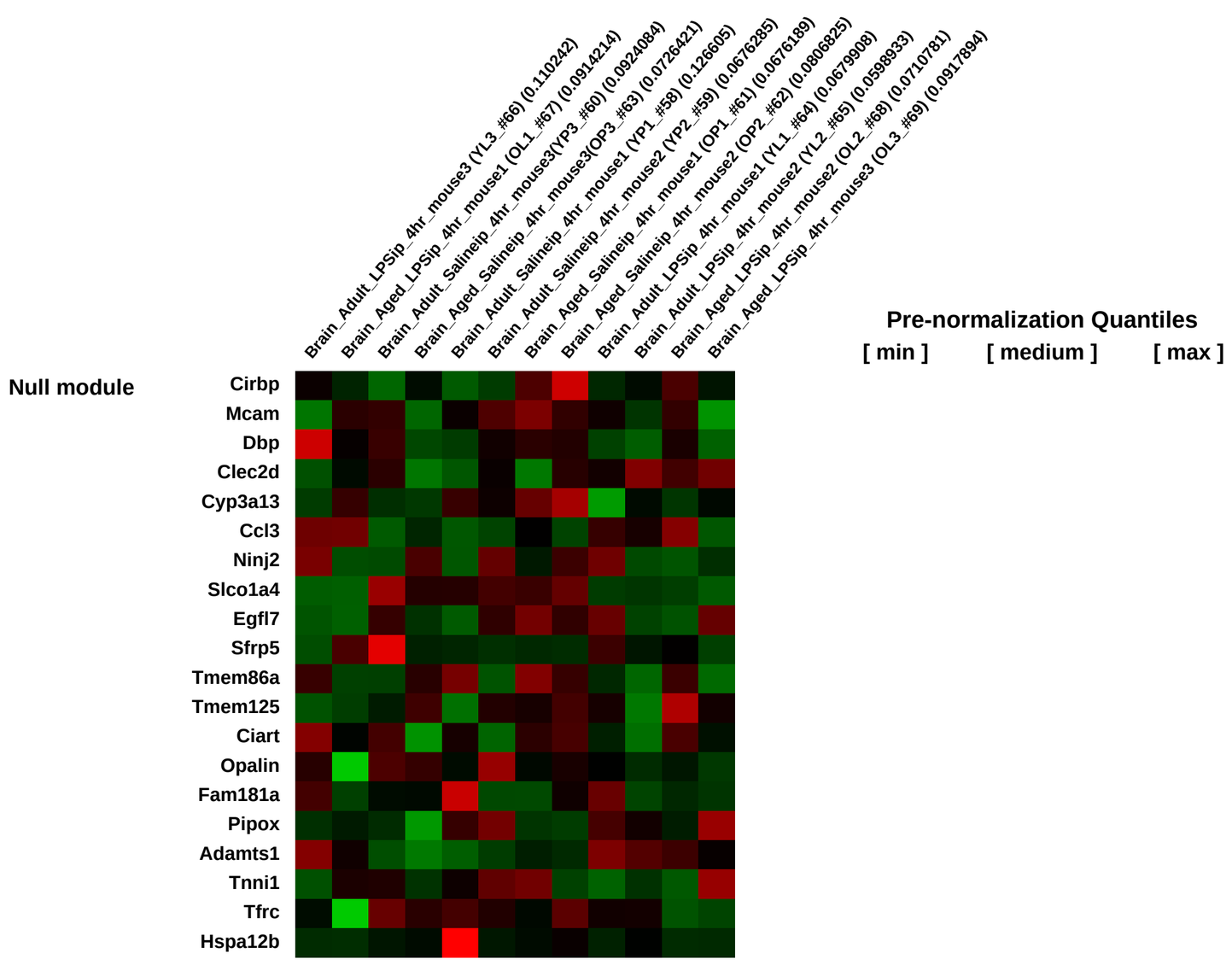

GEO Series "GSE32615" Expression Profiles

Num of samples in this series: 10

Scale of expression profile Z-scores

-3.0 -2.0 -1.0 0.0 1.0 2.0 3.0

GEO Link:	**http://www.ncbi.nlm.nih.gov/geo/query/acc.cgi?acc=GSE32615**
Status:	**Public on Jun 30 2014**
Title:	**Expression data of mouse Ewing’s sarcoma**
Organism:	**Mus musculus**
Experiment type:	**Expression profiling by array**
Platform:	**GPL1261**
Pubmed ID:	
Summary & Design:	**Summary:** **Ewingâ s sarcoma is highly malignant bone tumor that involves childhood and adolescent, and its nature has not been well understood. To clarify its cellular origin and the mechanisms of tumorigenesis, we used ex vivo approach to create a murine model for Ewingâ s sarcoma. The osteochondrogenic progenitors derived from the facial zone (FZ) of murine long bones at late gestation were purified by microdissection, introduced with EWS-FLI1 or EWS-ERG retroviruses and transplanted into nude mice. Ewingâ s sarcoma-like small round cell sarcoma developed at 100% penetrance, whereas tumor induction was less effective when growth place (GP)-derived cells were used. The different response of gene expression to EWS-FLI1 between FZ and GP cells suggests importance of the specific cellular context for EWS-FLI1 to induce Ewingâ s sarcoma. The Wnt/˛†-catenin pathway was involved in close relationship to the cellular context, with Dkk2 and Wipf1 as important downstream modulators. Furthermore, gene expression profiling revealed similarity between our models and human Ewingâ s sarcoma. These results indicate that Ewingâ s sarcoma originates from the embryonic osteochondrogenic progenitor.** **Overall design:** **For comparing with human Ewing’s sarcoma, we used expression databases E-MEXP-533 (Henderson SR et al, Genome Biol 6:R76, 2005) and E-MEXP-1142 (Schaefer KL et al, Eur J Cancer 44:699, 2008). In addition, the data sets for other sarcomas that include GSE6481 (Nakayama R et al, Mod Pathol 20:749, 2007), GSE7529 (Albino D et al, Cancer 113:1412, 2008) and GSE21122 (Barretina J et al, Nat Genet 42:715, 2010) were used for clustering analysis.**

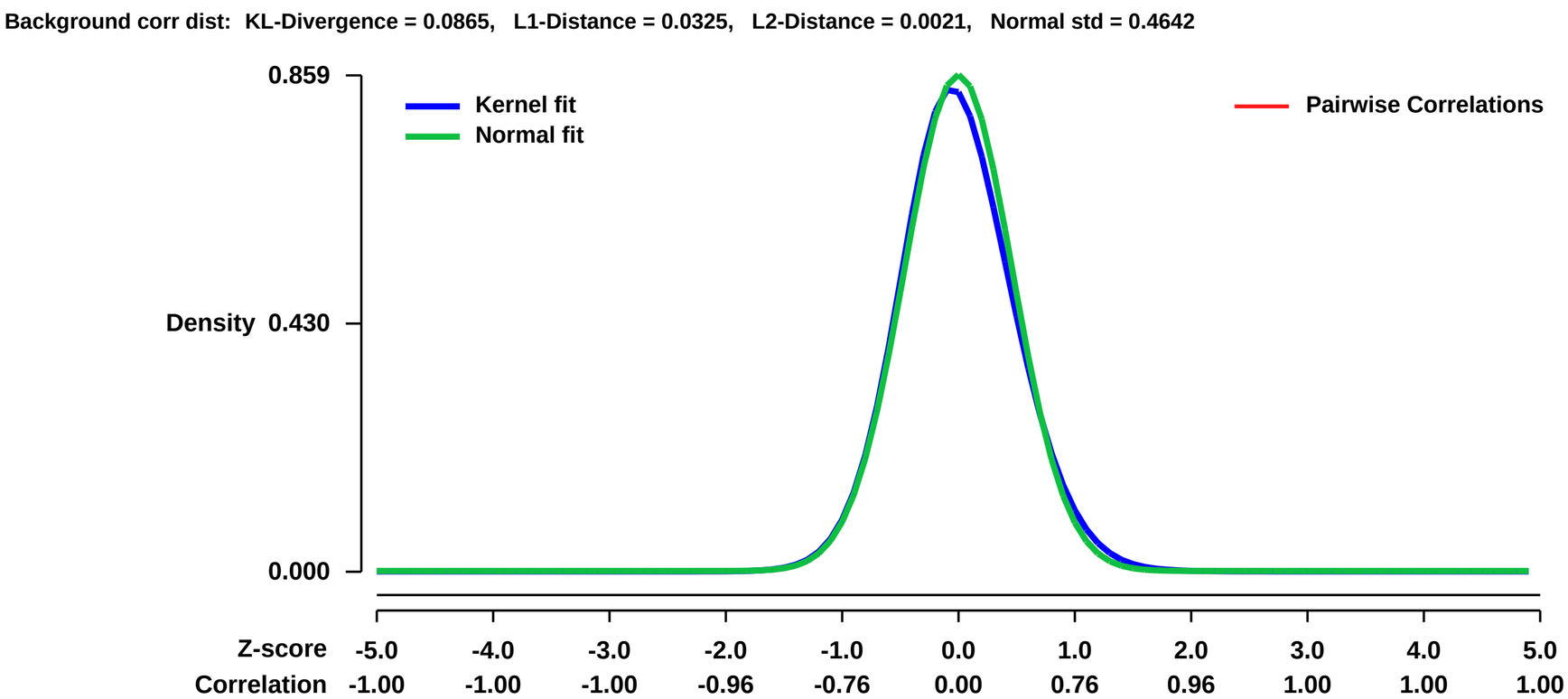

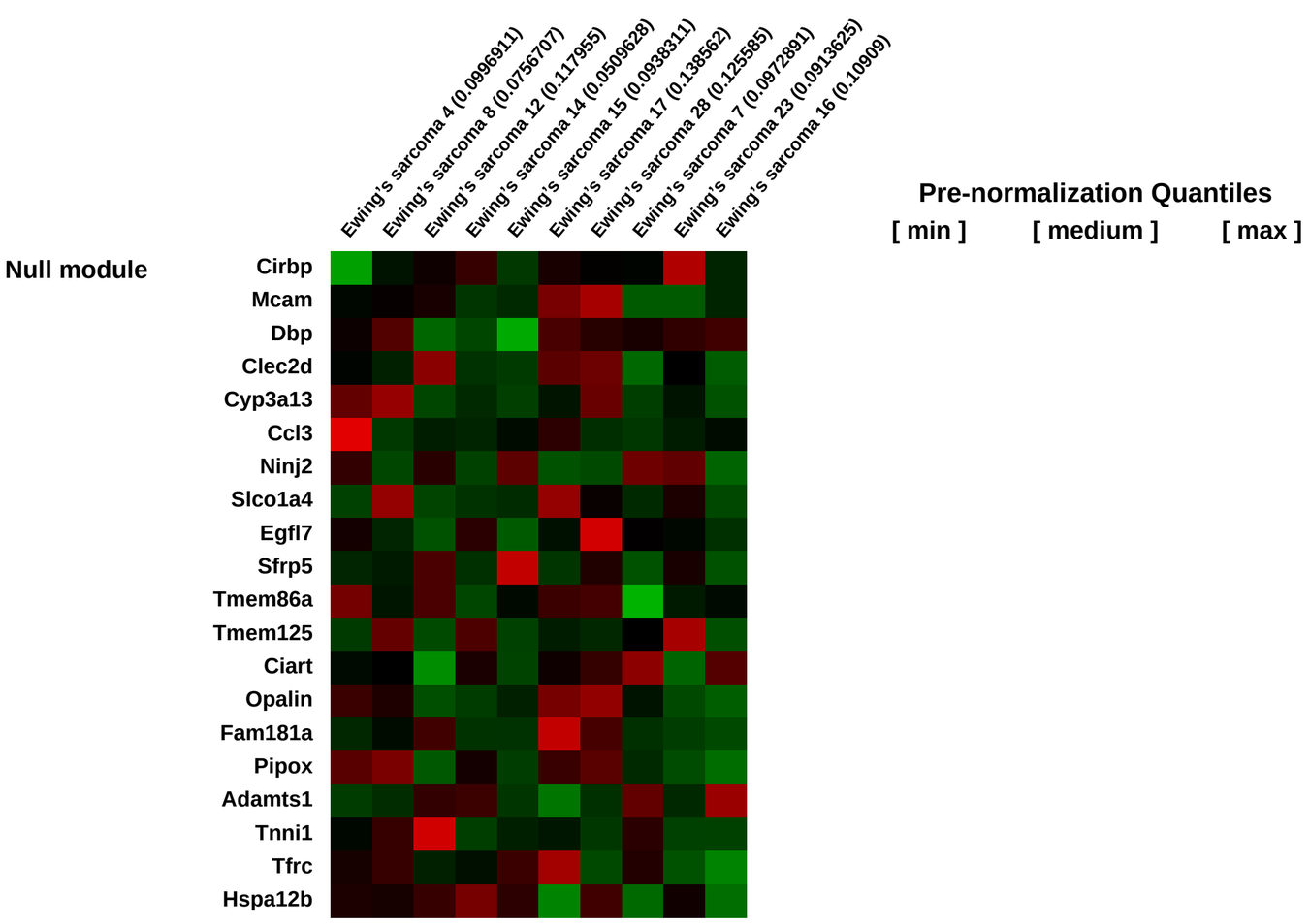

GEO Series "GSE32624" Expression Profiles

Num of samples in this series: 6

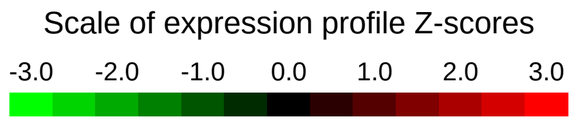

GEO Link:	http://www.ncbi.nlm.nih.gov/geo/query/acc.cgi?acc=GSE32624
Status:	Public on Dec 06 2011
Title:	Functional and epigenetic studies reveal multistep differentiation and plasticity of in vitro and in vivo follicular T helper cells.
Organism:	Mus musculus
Experiment type:	Expression profiling by array
Platform:	GPL1261
Pubmed ID:	22018472
Summary & Design:	**Summary:** Follicular T helper cells (Tfh) are critical for providing help to B cells for germinal center (GC) formation. Mutations affecting SAP prevent GC formation due to defective T:B cell interactions, yet effects on Tfh cell differentiation remain unclear. We describe the in vitro differentiation of functionally competent â Tfh-likeâ cells that expressed IL-21, Tfh markers, and Bcl6, and rescued GC formation in SAP-deficient hosts substantially better than other T helper (Th) cells. SAP-deficient Tfh-like cells appeared virtually indistinguishable from wildtype, yet failed to support GCs in vivo. Interestingly, both Tfh-like and in vivo-derived Tfh cells could produce effector cytokines in response to polarizing conditions. Moreover, other Th cell populations could be reprogrammed to obtain Tfh characteristics. ChIP-Seq analyses revealed positive epigenetic markings on Tbx21, Gata3 and Rorc in Tfh-like and ex vivo Tfh cells, and Bcl6 in other Th cells, supporting the concept of plasticity between Tfh and other Th populations. We describe the in vitro differentiation of functionally competent IL-21-producing cells with Tfh-like properties. Importantly, transfer of low numbers of these cells induced GC formation in SAP-deficient hosts more effectively than other in vitro differentiated Th cells, suggesting they represent bona fide Tfh cell precursors. We have chosen the name â Tfh-likeâ cells for these in vitro differentiated IL-21 producing cells as they exhibit Tfh characteristics, but do not reside within B cell follicles. SAP-deficient Tfh-like cells were virtually indistinguishable from WT, yet nonetheless, failed to effectively contribute to Tfh cells and rescue GC formation in vivo. Evaluation of cytokine production as well as epigenetic chromatin modifications of genes encoding Th cell-specific transcription factors from either in vitro-generated Tfh-like cells or Tfh cells isolated directly ex vivo provided evidence for plasticity between Tfh-like and other Th cell populations. Our results provide insight into the requirements for differentiation and plasticity of Tfh cells, which are critical for the generation of effective long-term humoral immunity. **Overall design:** RNA was prepared from subconfluent asynchronously proliferating cells using TRIZOL and purified by RNeasy MinElute Cleanup kit (Qiagen). Hybridization to Affymetrix GeneChip Mouse Genome 430 2.0 arrays was used to generate gene expression profiles of WT Tfh-like and SAP-deficient Tfh-like cells.

Background corr dist: KL-Divergence = 0.0264, L1-Distance = 0.0124, L2-Distance = 0.0001, Normal std = 0.6898

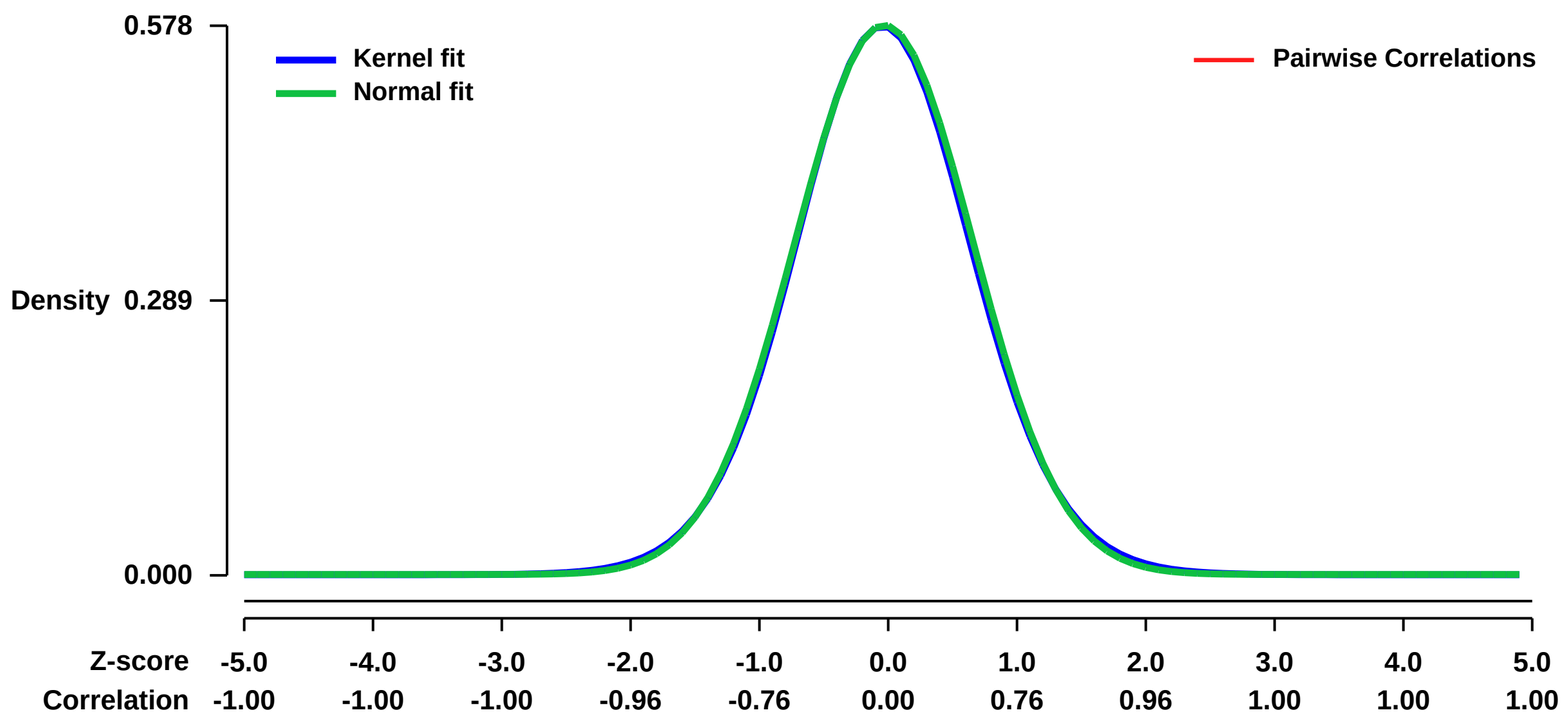

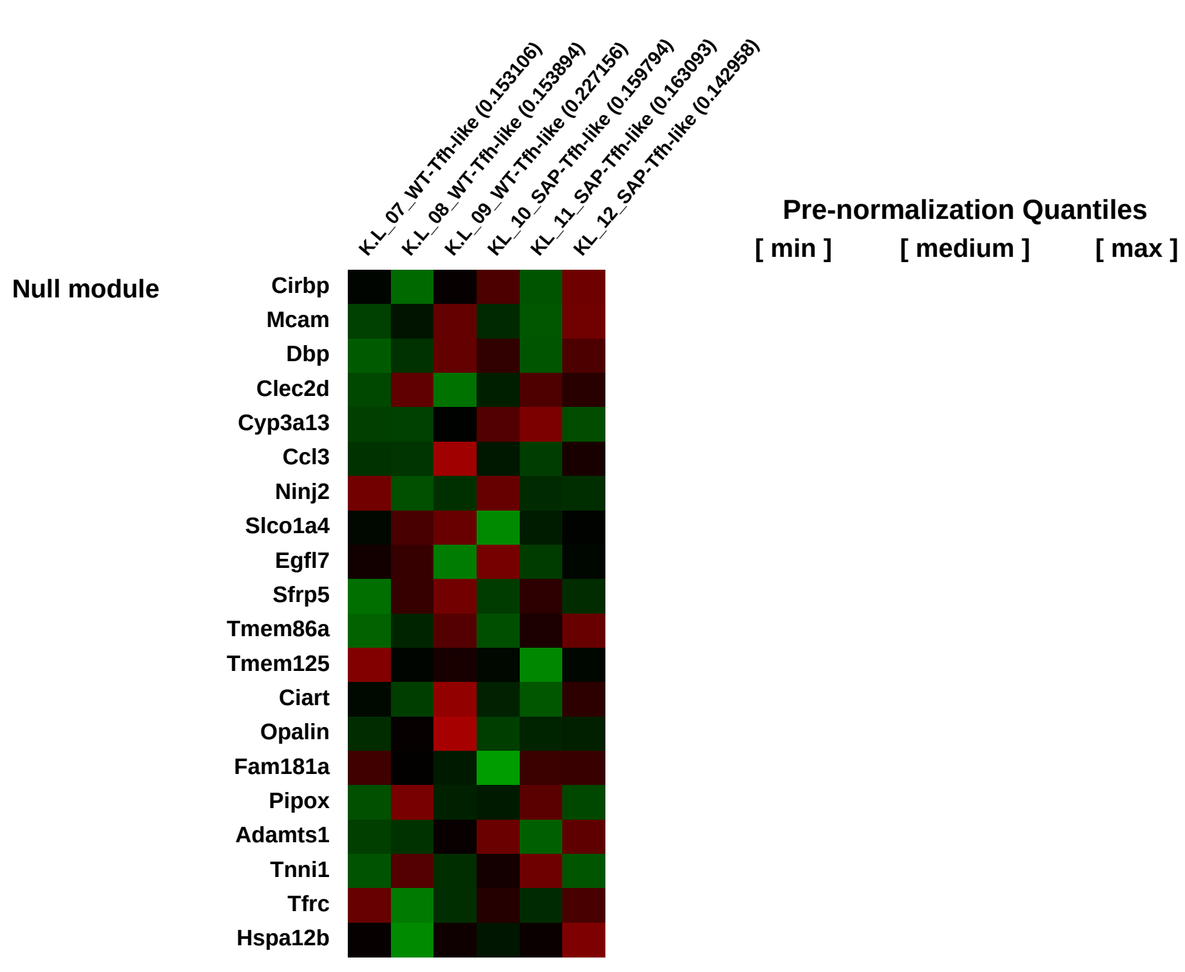

GEO Series "GSE32653" Expression Profiles

Num of samples in this series: 6

Scale of expression profile Z-scores

-3.0 -2.0 -1.0 0.0 1.0 2.0 3.0

GEO Link:	http://www.ncbi.nlm.nih.gov/geo/query/acc.cgi?acc=GSE32653
Status:	Public on Mar 07 2013
Title:	Hlxb9 regulated genes in pancreatic beta cells
Organism:	Mus musculus
Experiment type:	Expression profiling by array
Platform:	GPL1261
Pubmed ID:	23419452
Summary & Design:	**Summary:** Hlxb9 is a differentiation factor important for neuronal, and pancreatic beta cell differentiation. It is a transcription factor that represses transcription. It's target genes are unknown. The mouse pancreatic beta cell line MIN6 was used to assess the expression of genes de-repressed upon Hlxb9 knockdown. **Overall design:** Several independent transfections of MIN6 cells were performed with scrambled negative control siRNA (Qiagen) or with mouse Hlxb9 siRNA (Dharmacon). The cells were processed for RNA isolation and whole cell protein extracts, 72 hours post-transfection. The level of Hlxb9 knockdown was assessed by western blot analysis. RNA preps from those samples that showed more than 75% knockdown were used for microarray analysis.

Background corr dist: KL-Divergence = 0.0259, L1-Distance = 0.0136, L2-Distance = 0.0002, Normal std = 0.6933

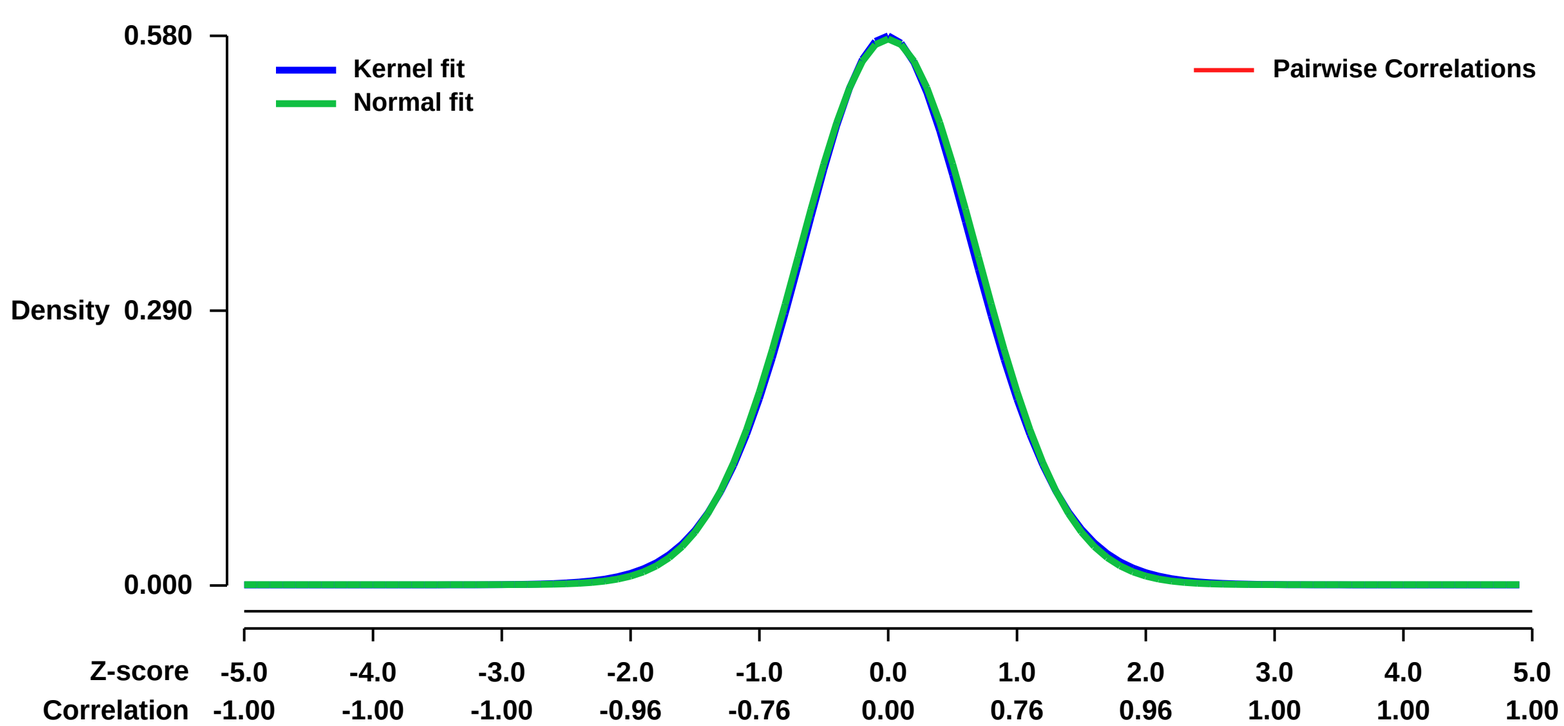

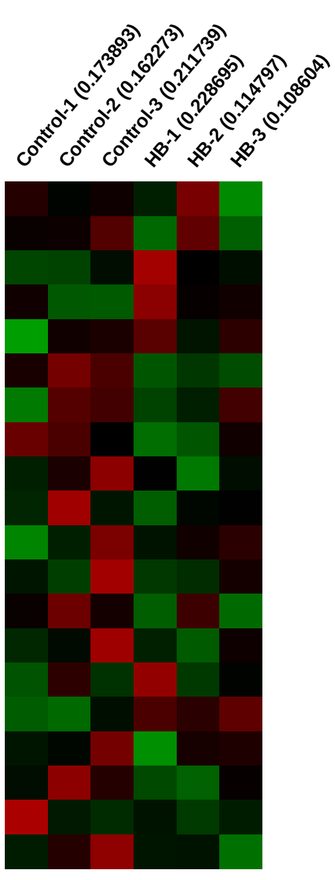

GEO Series "GSE32706" Expression Profiles

Num of samples in this series: 33

Scale of expression profile Z-scores

-3.0 -2.0 -1.0 0.0 1.0 2.0 3.0

GEO Link:	http://www.ncbi.nlm.nih.gov/geo/query/acc.cgi?acc=GSE32706
Status:	Public on Oct 08 2011
Title:	Comparative transcriptomics and metabolomic analysis of fenofibrate and fish oil treatments in mice
Organism:	Mus musculus
Experiment type:	Expression profiling by array
Platform:	GPL1261
Pubmed ID:	21954454
Summary & Design:	**Summary:** Elevated circulating triglycerides, which are considered a risk factor for cardiovascular disease, can be targeted by treatment with fenofibrate or fish oil. To gain insight into underlying mechanisms, we carried out a comparative transcriptomics and metabolomics analysis of the effect of 2 week treatment withfenofibrate and fish oil in mice. Plasma triglycerides were significantly decreased byfenofibrate (-49.1%) and fish oil (-21.8%), whereas plasma cholesterol was increased by fenofibrate (+29.9%) and decreased by fish oil (-32.8%). Levels of various phospholipid species were specifically decreased by fish oil, while levels of Krebs cycle intermediates were increased specifically by fenofibrate. Plasma levels of many amino acids were altered by fenofibrate and to a lesser extent by fish oil. Both fenofibrate and fish oil upregulated genes involved in fatty acid metabolism, and downregulated genes involved in blood coagulation and fibrinolysis. Significant overlap in gene regulation by fenofibrate and fish oil was observed, reflecting their property as high or low affinity agonist for PPAR$_{\alpha}$–, respectively. Fenofibrate specifically downregulated genes involved in complement cascade and inflammatory response. Fish oil specifically downregulated genes involved in cholesterol and fatty acid biosynthesis, and upregulated genes involved in amino acid and arachidonic acid metabolism. Taken together, the data indicate that despite being similarly potent towards modulating plasma free fatty acids, cholesterol and triglyceride levels, fish oil causes modest changes in gene expression likely via activation of multiple mechanistic pathways, whereas fenofibrate causes pronounced gene expression changes via a single pathway, reflecting the key difference between nutritional and pharmacological intervention. **Overall design:** Expression profiling of liver from mice fed control diet, fish oil or fenofibrate for 2 weeks.

Background corr dist: KL-Divergence = 0.4473, L1-Distance = 0.0814, L2-Distance = 0.0210, Normal std = 0.2363

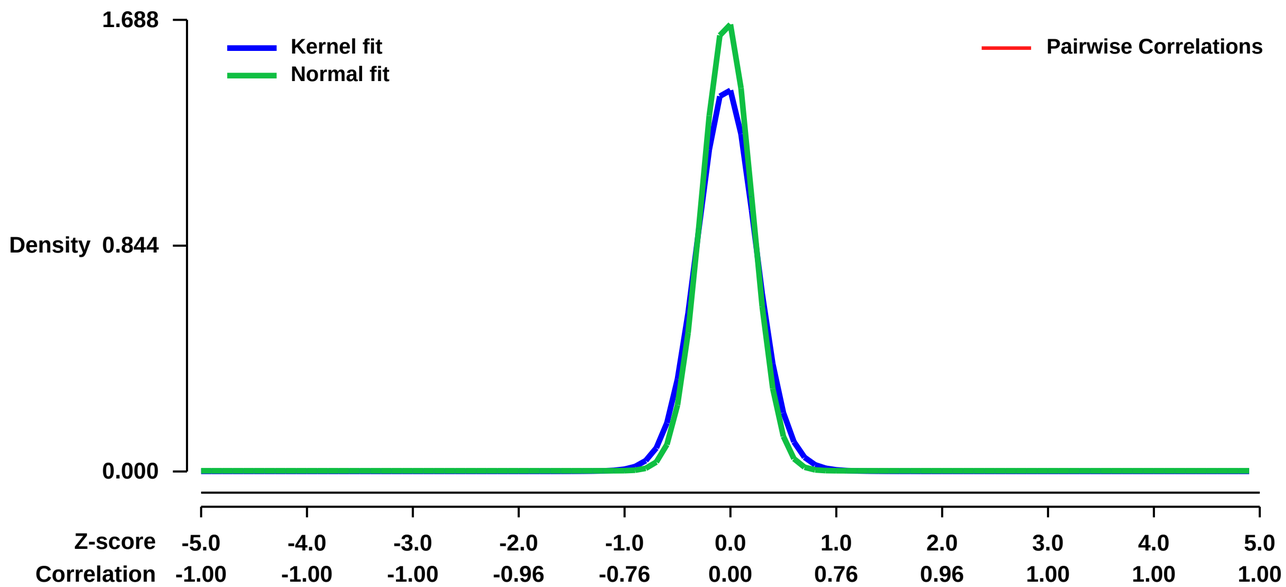

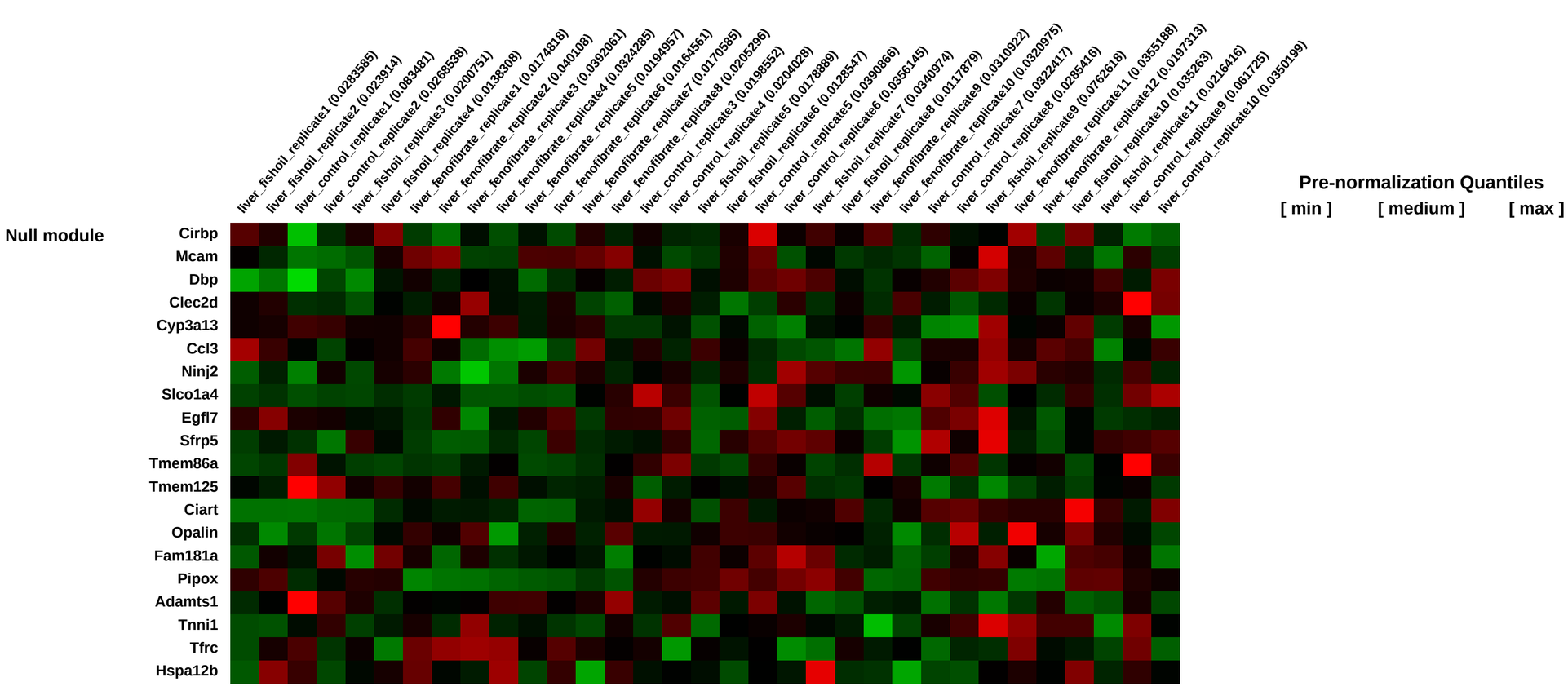

GEO Series "GSE3293" Expression Profiles

Num of samples in this series: 8

Scale of expression profile Z-scores

-3.0 -2.0 -1.0 0.0 1.0 2.0 3.0

GEO Link:	http://www.ncbi.nlm.nih.gov/geo/query/acc.cgi?acc=GSE3293
Status:	Public on Dec 31 2005
Title:	Leptin Regulated Mouse Gallbladder Genes
Organism:	Mus musculus
Experiment type:	Expression profiling by array
Platform:	GPL1261
Pubmed ID:	17463181
Summary & Design:	**Summary:** Gallstone disease is a major contributor to health care costs in the United States. Approximately 12 % of the U.S. population has gallstones. As a result, more than 700,000 cholecystectomies are performed in this country each year. Many of these patients are obese and have a positive family history; but surprisingly, little is known about the link between obesity, genetics and gallstone formation. Obese individuals have been shown to have supersaturated bile, larger gallbladder fasting volumes and impaired gallbladder emptying. We have recently demonstrated that leptin plays a role in gallbladder motility. In an effort to understand the genetic basis for these observations, we tested the hypothesis that leptin would alter gallbladder gene expression. Methods: Affymetrix oligonucleotide microarrays 430 2.0 were used to compare gallbladder gene expression profiles from 12 week old control saline-treated leptin-deficient (Lep ob) and from leptin-treated Lep ob female mice. Analyses were performed on pooled RNA (n=4) from the gallbladders of 12 saline-treated Lep ob mice and from 12 Lep ob mice which were administered daily IP 5 ug/g of recombinant murine leptin for 4 weeks. Resulting data were analyzed utilizing Gene Chip Operating Software or MAS 5.0. Results: Of the genes analyzed 314 were upregulated and 108 were downregulated by leptin administration. Numerous genes related to gallstone pathogenesis, gallbladder absorption/secretion, inflammatory cytokines, and insulin resistance were altered by leptin. **Keywords: comparitive response to leptin** **Overall design:** Female B6.V-lepob obese mice (n=24) aged 7 weeks were obtained from The Jackson Laboratory (Bar Harbor, ME). Upon arrival, mice were placed on a standard chow diet and were allowed to acclimate for 1 week before starting the experiment. For leptin treatments, mice received daily intraperitoneal injections of either recombinant mouse leptin (R&D Systems, Minneapolis, MN) (n=12) at a dose of 5 ´¡g/g body weight or with saline as a control (n=12) for 4 weeks. At 12 weeks of age, mice were fasted overnight with free access to water. The following morning the mice underwent cholecystectomy. Three gallbladders were pooled to create 4 pools in each treatment and total RNA was isolated. Affymetrix murine 430 2.0 arrays were utilized to examine altered gallbladder gene expression as a result of leptin administration. The resulting data was analyzed utlizing Gene Chip Operating Software or MAS 5.0.

Background corr dist: KL-Divergence = 0.0763, L1-Distance = 0.0225, L2-Distance = 0.0008, Normal std = 0.4847

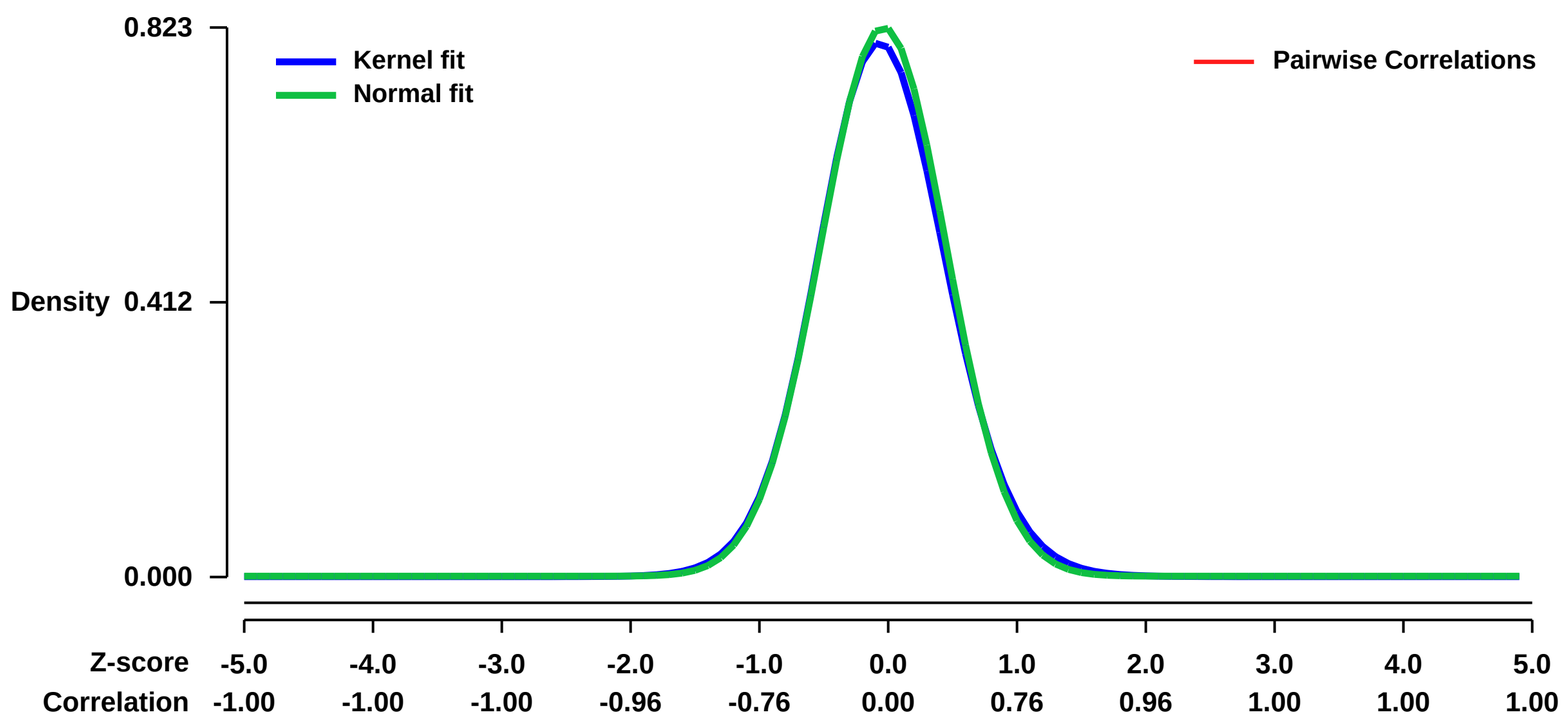

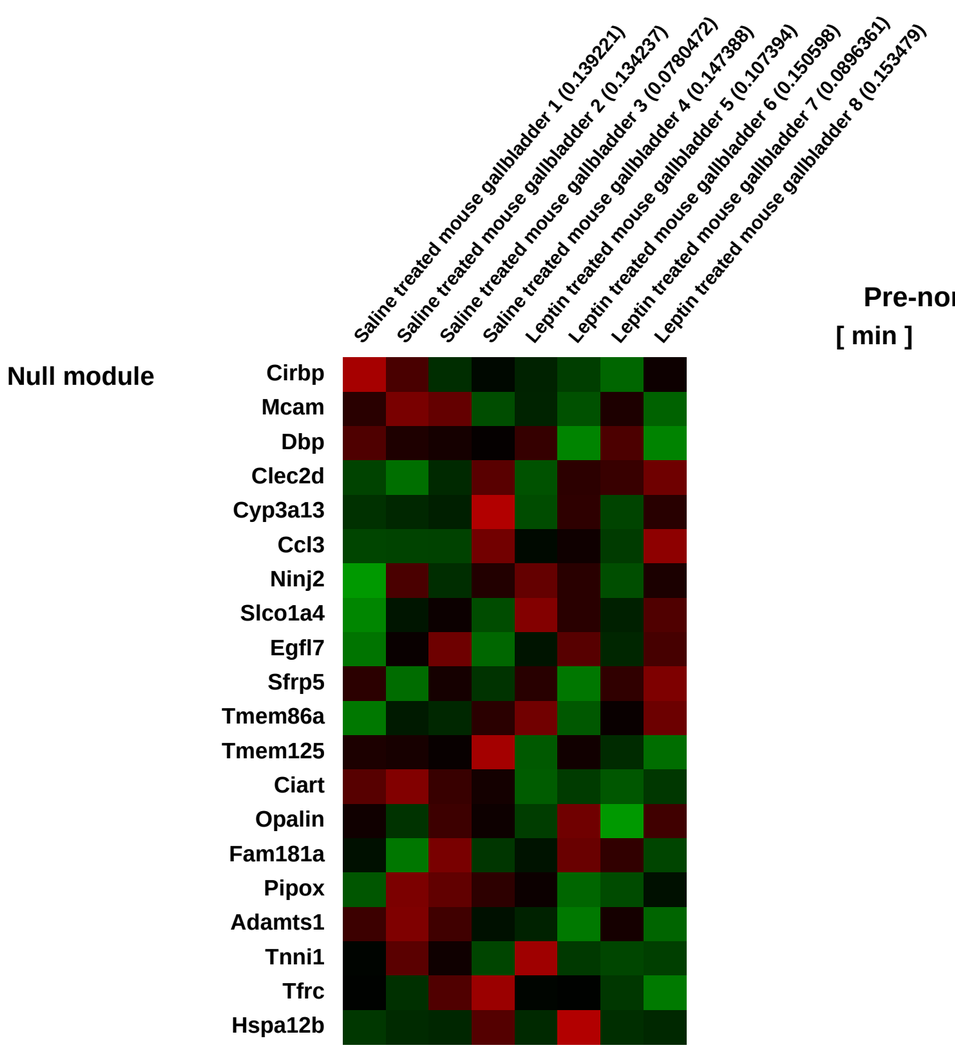

GEO Series "GSE32937" Expression Profiles

Num of samples in this series: 8

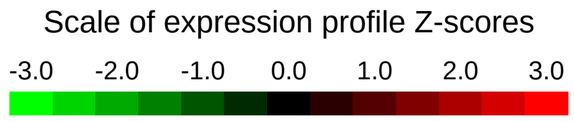

GEO Link:	**http://www.ncbi.nlm.nih.gov/geo/query/acc.cgi?acc=GSE32937**
Status:	**Public on Oct 13 2011**
Title:	**MicroRNA-29 in Aortic Dilation: Implications for Aneurysm Formation**
Organism:	**Mus musculus**
Experiment type:	**Non-coding RNA profiling by array**
Platform:	**GPL1261**
Pubmed ID:	**21903938**
Summary & Design:	**Summary:** **We compared the aorta of 6-weeks-old mice (young) with 18-months-old mice (old). Using the publicly available tools Sylamer and DIANA-mirExTra, we identified an enrichment for miR-29 binding sites in the 3'UTR of genes downregulated in the aged aortas. We subsequently showed that inhibition of miR-29 in aged mice prevented dilation of the aorta.** **Overall design:** **aortas of 6 week old and 18 month old mice**

Background corr dist: **KL-Divergence = 0.0766, L1-Distance = 0.0196, L2-Distance = 0.0005, Normal std = 0.4847**

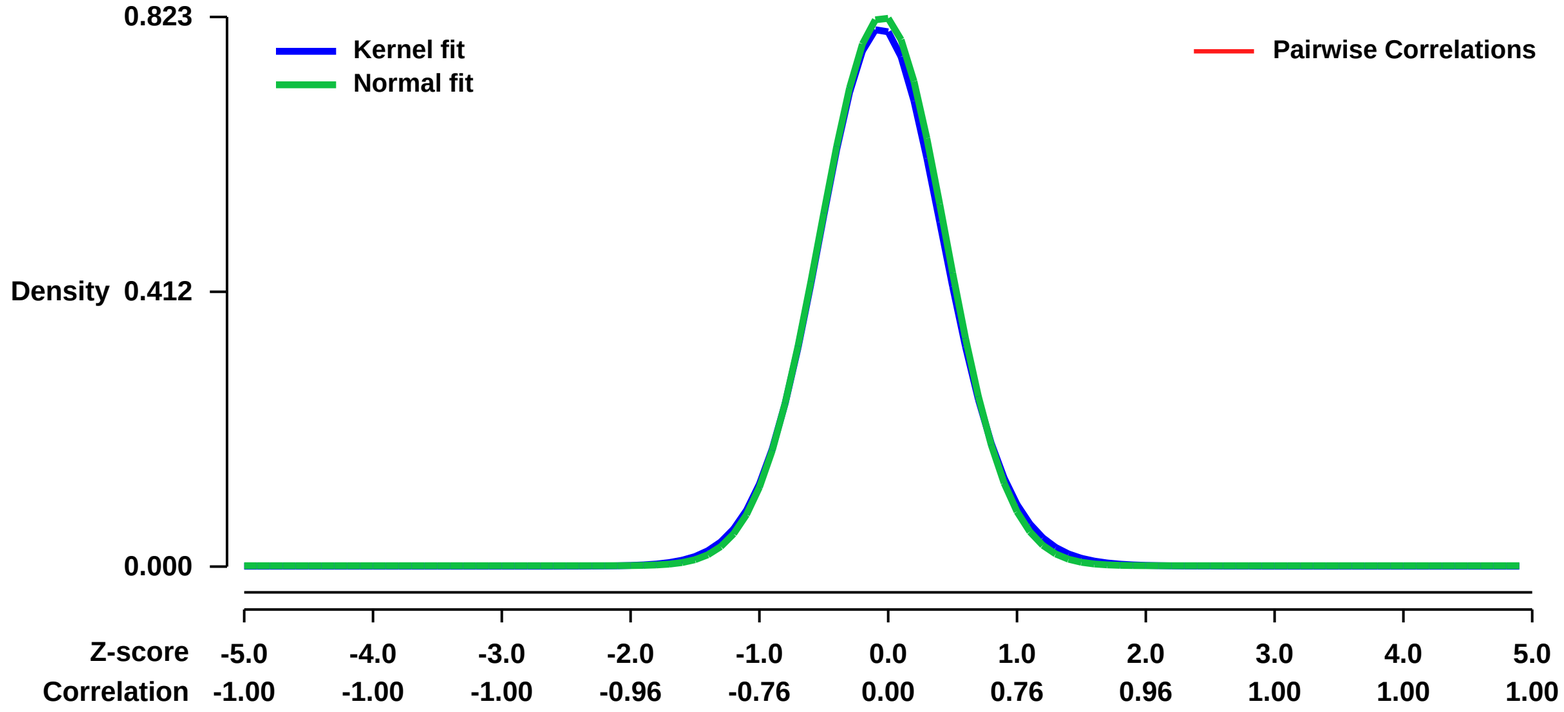

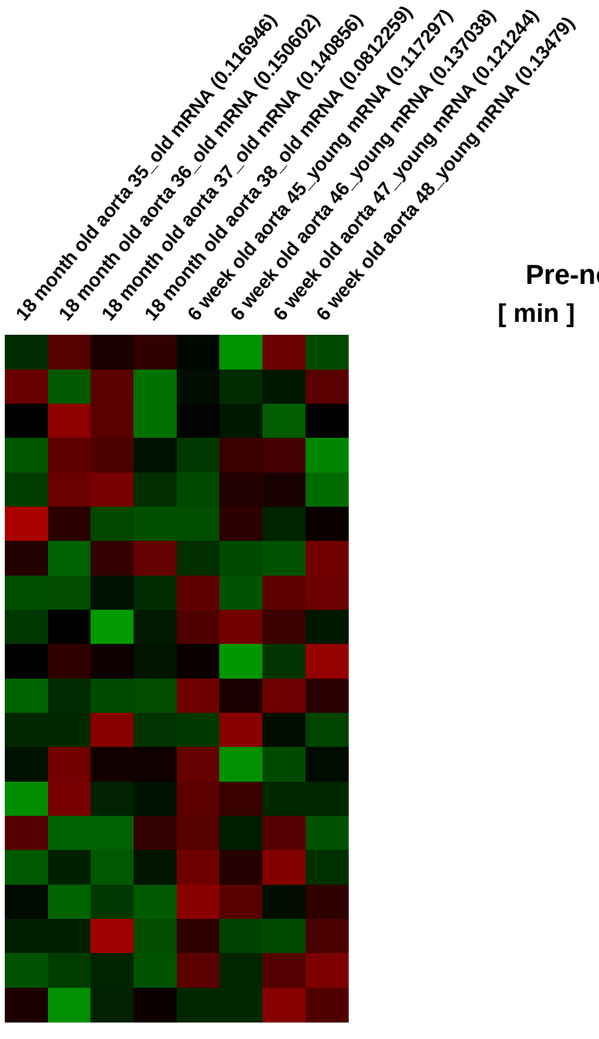

GEO Series "GSE32963" Expression Profiles

Num of samples in this series: 6

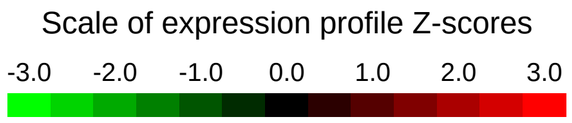

GEO Link:	http://www.ncbi.nlm.nih.gov/geo/query/acc.cgi?acc=GSE32963
Status:	Public on Jan 01 2012
Title:	Gene expression profile in the developing and adult mouse cochlear sensory epithelia
Organism:	Mus musculus
Experiment type:	Expression profiling by array
Platform:	GPL1261
Pubmed ID:	22900075
Summary & Design:	**Summary:** To understand the molecular control of development and regeneration in the mammalian cochlear sensory epithelia, we performed a comparative study of gene expression patterns between postnatal day-3 (P3) and adult stages using a microarrays approach. **Overall design:** Two inner ear development stages were used in this study, Post-natal day three and eight-week-old adult. A total number of sixty Swiss mice were exploited for each stage. The cochlear sensory epithelia (CSE) were collected from the inner ears and immediately placed in RNA later solution. A total of six independent dissection experiments were carried out separately in order to obtain three biological replicates for each stage. In each experiment, the CSE from 20 mice were pooled. Total RNA was purified from each biological sample separately using RNAeasy Mini Kit and the RNA integrity was assessed by the Nanodrop 2000

Background corr dist: KL-Divergence = 0.0318, L1-Distance = 0.0515, L2-Distance = 0.0038, Normal std = 0.7289

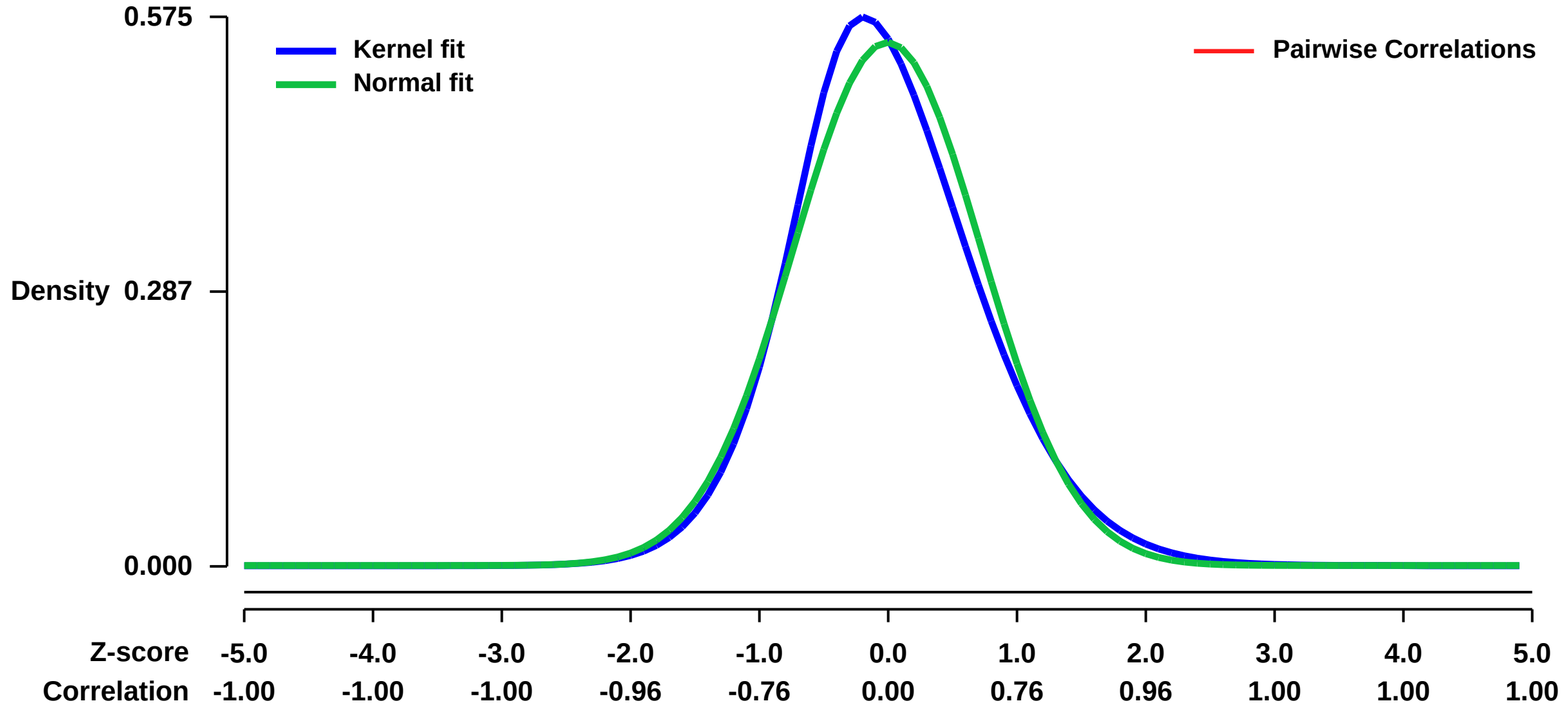

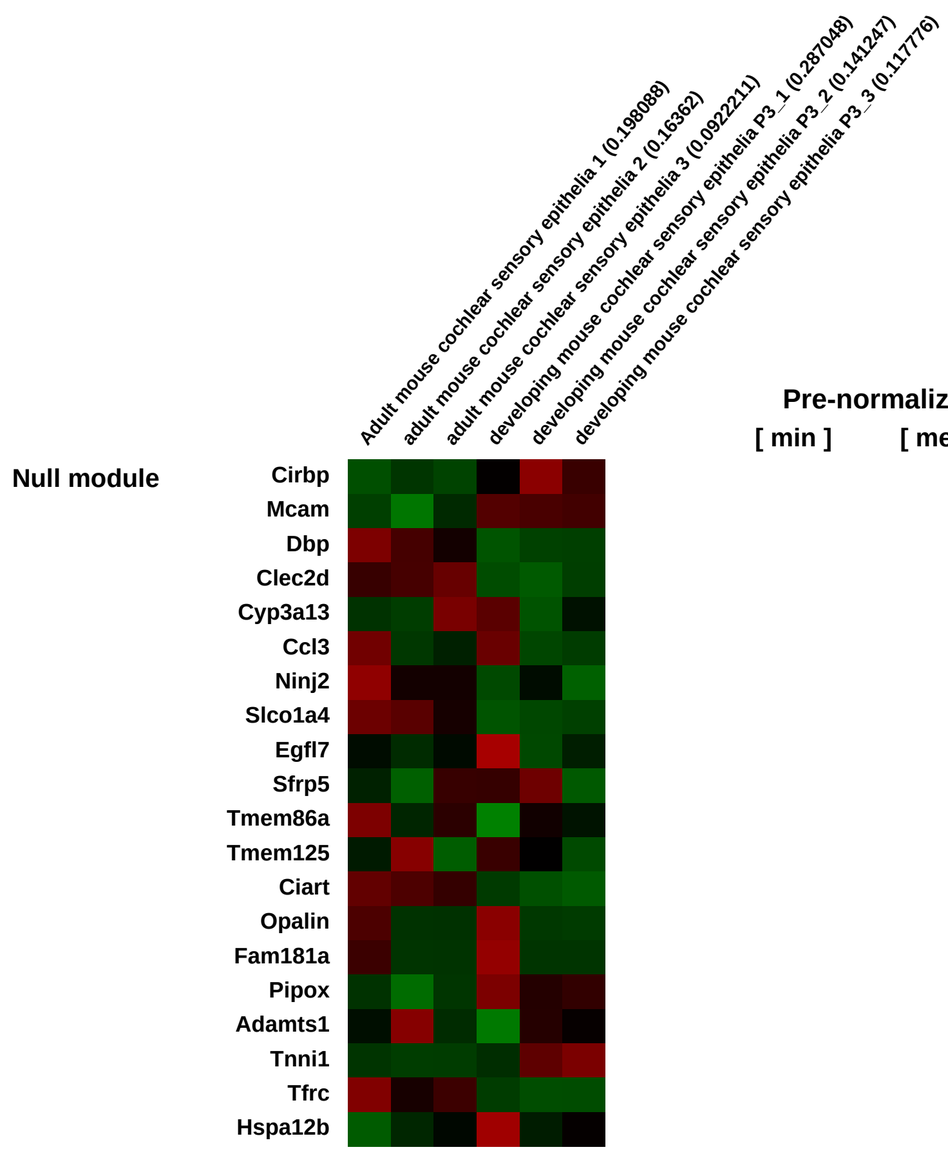

GEO Series "GSE32986" Expression Profiles

Num of samples in this series: 18

Scale of expression profile Z-scores

-3.0 -2.0 -1.0 0.0 1.0 2.0 3.0

GEO Link:	http://www.ncbi.nlm.nih.gov/geo/query/acc.cgi?acc=GSE32986
Status:	Public on Oct 15 2011
Title:	Synergism between curdlan and GM-CSF in mouse dendritic cells
Organism:	Mus musculus
Experiment type:	Expression profiling by array
Platform:	GPL1261
Pubmed ID:	22250091
Summary & Design:	**Summary:** A simultaneous engagement of different pathogen recognition receptors provides a tailor made adaptive immunity for an efficient defence against distinct pathogens. For example, cross talk of TLR and c-type lectin signalling effectively shapes distinct gene expression patterns by integrating the signals at the level of NF-¸”B. Here, we extend this principle to a strong synergism between the Dectin-1 agonist, curdlan, and an inflammatory growth factor, GM-CSF. Both together act in synergy in inducing a strong inflammatory signature which converts immature DCs to potent effector DCs. A variety of cytokines (IL-1¸†, IL-6, TNF-¸–, IL-2 and IL-12p70), costimulatory molecules (CD80, CD86, CD40 and CD70), chemokines (CxCl1, CxCl2, CxCl3, CCl12, CCl17) as well as receptors and molecules involved in fugal recognition and immunity such as Mincle, Dectin-1, Dectin-2 and Pentraxin 3 are strongly up-regulated in DC treated simultaneously with curdlan and GM-CSF. The synergistic effect of both stimuli resulted in strong IKB¸– phosphorylation, in its rapid degradation and in enhanced nuclear translocation of all NF-¸”B subunits. We further identified MAPK ERK, as one possible integration site of both signals, since its phosphorylation was clearly augmented when curdlan was co-applied with GM-CSF. Our data demonstrate that the immunomodulatory activity of curdlan requires an additional signal provided by GM-CSF to successfully initiate a robust ¸†-glucan specific cytokine and chemokine response. The integration of both signals clearly prime and tailor a more effective innate and adaptive response against invading microbes and fungi. **Overall design:** CD11b+ fraction of FLT3L generated BM DCs (3-4 x106) were stimulated for 4 hours with 100 or 1 ¸…g/ml curdlan in presence or absence of 5 ng/ml GM-CSF in triplicates.

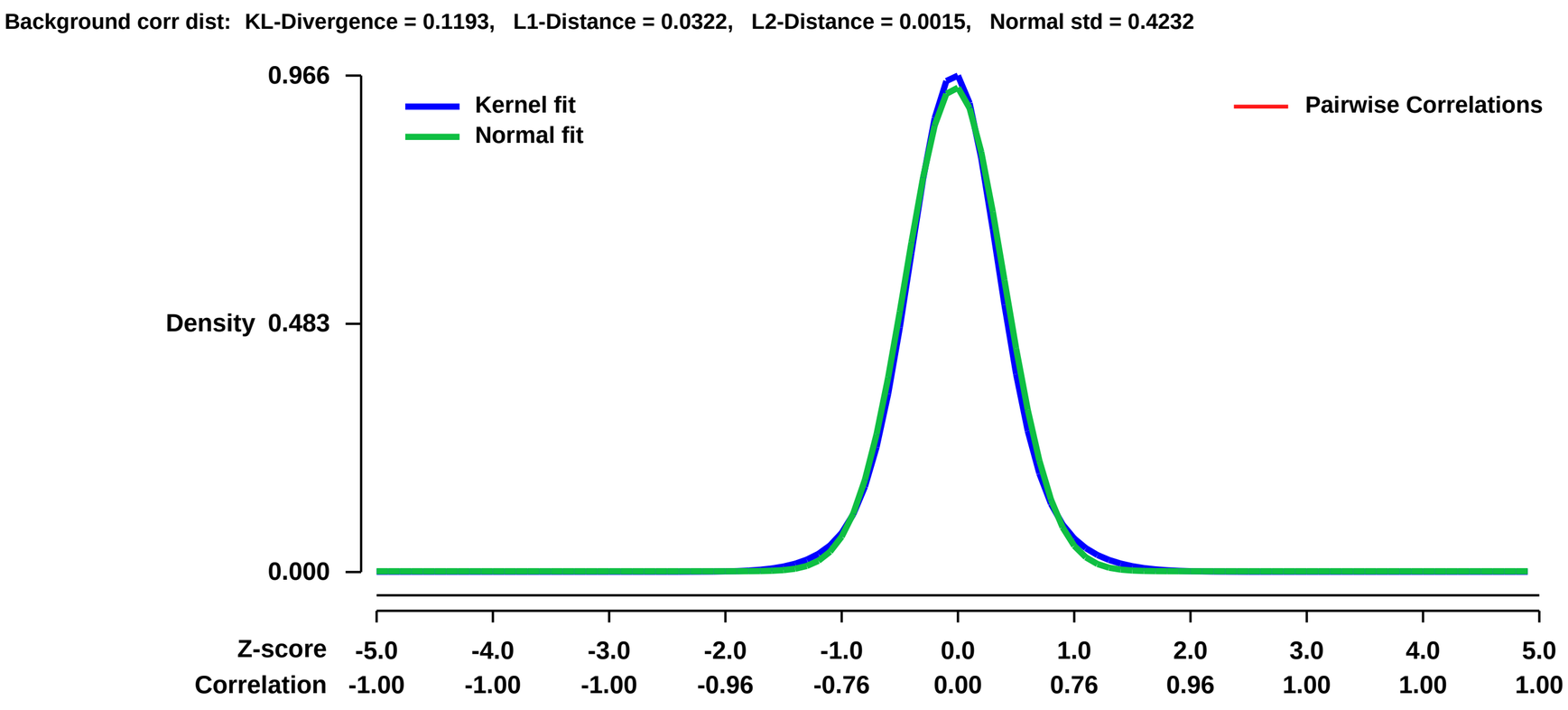

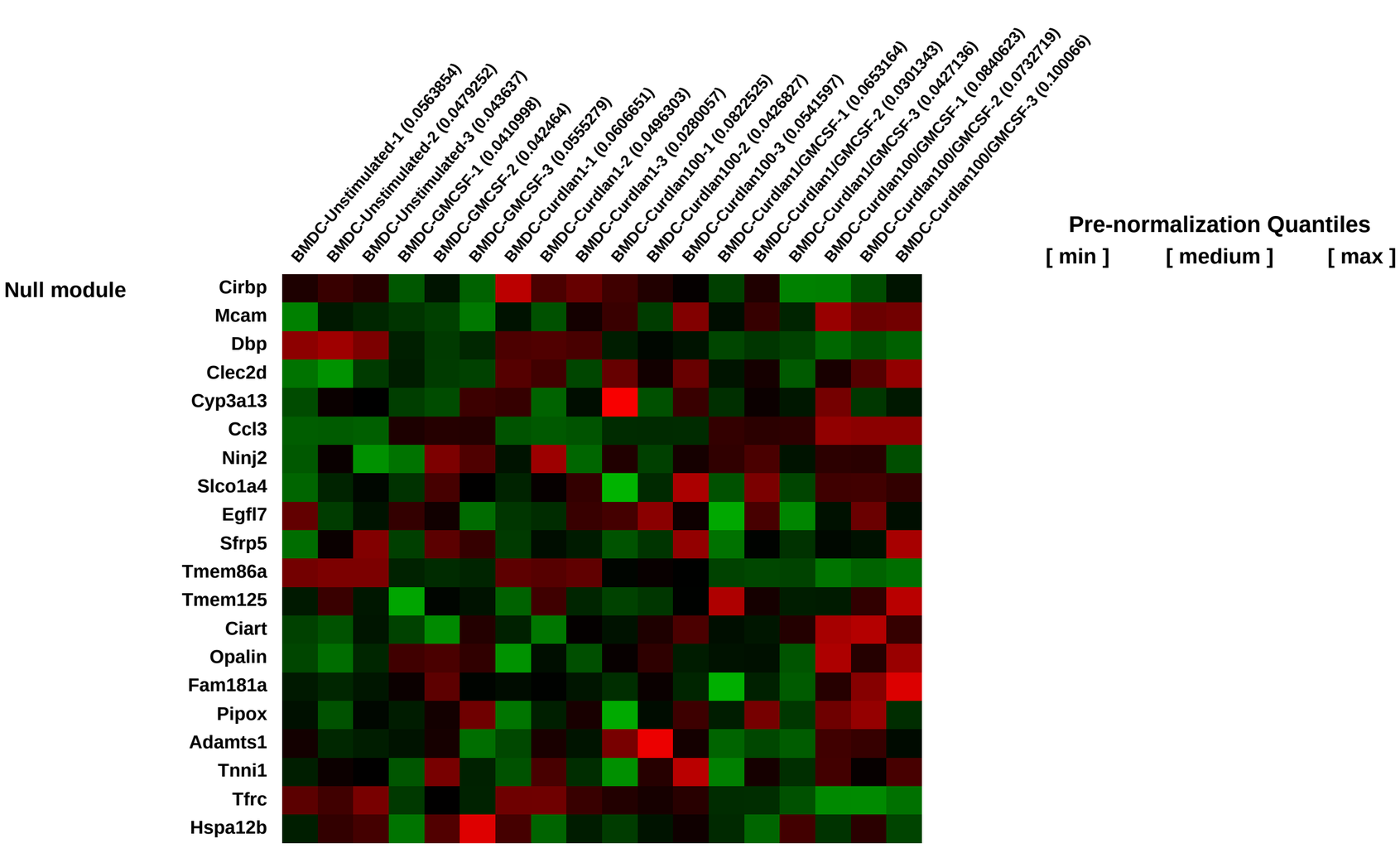

GEO Series "GSE33031" Expression Profiles

Num of samples in this series: 6

Scale of expression profile Z-scores

-3.0 -2.0 -1.0 0.0 1.0 2.0 3.0

GEO Link:	http://www.ncbi.nlm.nih.gov/geo/query/acc.cgi?acc=GSE33031
Status:	Public on Dec 01 2011
Title:	PU.1 restricts adult hematopoietic stem cell proliferation via cell specific autoregulation
Organism:	Mus musculus
Experiment type:	Expression profiling by array
Platform:	GPL1261
Pubmed ID:	23395001
Summary & Design:	**Summary:** To guarantee blood supply throughout adult life hematopoietic stem cells (HSCs) need to carefully balance between self-renewing cell divisions and quiescence. Identification of genes controlling HSC self-renewal is of utmost importance given that HSCs are the only stem cells with broad clinical applications. Transcription factor PU.1 is one of the major regulators of myeloid and lymphoid development. Recent reports suggest that PU.1 mediates its functions via gradual expression level changes rather than binary on/off states. So far, this has not been considered in any study of HSCs and thus, PU.1â s role in HSC function has remained largely unclear. Here we demonstrate using hypomorphic mice with an engineered disruption of an autoregulatory feedback loop that decreased PU.1 levels resulted in loss of key HSC functions, all of which could be fully rescued by restoration of proper PU.1 levels via a human PU.1 transgene. Mechanistically, we found excessive HSC cell divisions and altered expression of cell cycle regulators whose promoter regions were bound by PU.1 in normal HSCs. Adequate PU.1 levels were maintained by a mechanism of direct autoregulation restricted to HSCs through a physical interaction of a -14kb enhancer with the proximal promoter. Our findings identify PU.1 as novel regulator controling the switch between cell division and quiescence in order to prevent exhaustion of HSCs. Given that even moderate level changes greatly impact stem cell function, our data suggest important therapeutic implications for leukemic patients with reduced PU.1 levels. Moreover, we provide first proof, that autoregulation of a transcription factor, PU.1, has a crucial function in vivo. We anticipate that our concept of how autoregulation forms an active chromosomal conformation will impact future research on transcription factor networks regulating stem cell fate. **Overall design:** HSCs of Pu.1 knock-in (PU.1ki/ki) mice were used for RNA extraction and hybridization on Affymetrix microarrays. We compared these microarray samples with the corresponding wild type.

Background corr dist: KL-Divergence = 0.0424, L1-Distance = 0.0588, L2-Distance = 0.0056, Normal std = 0.6556

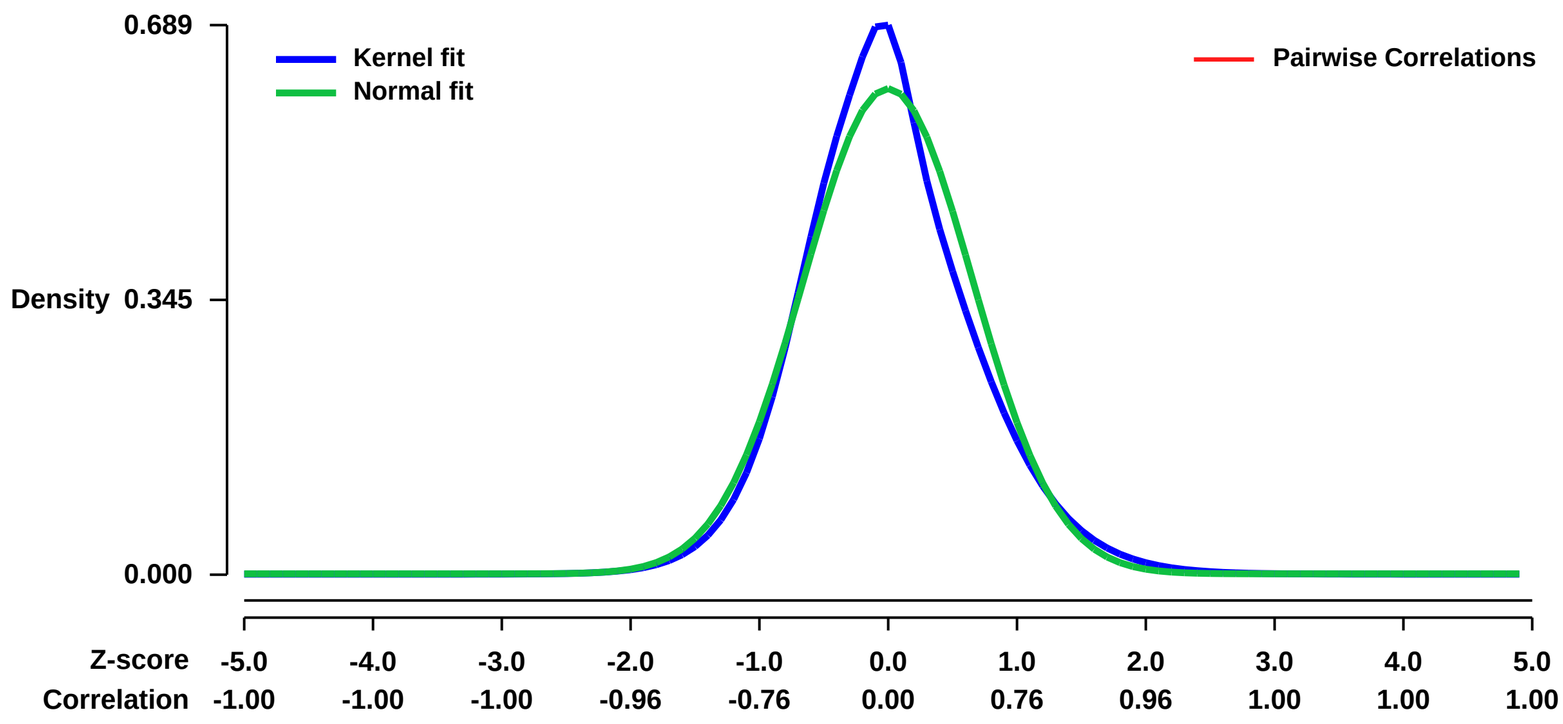

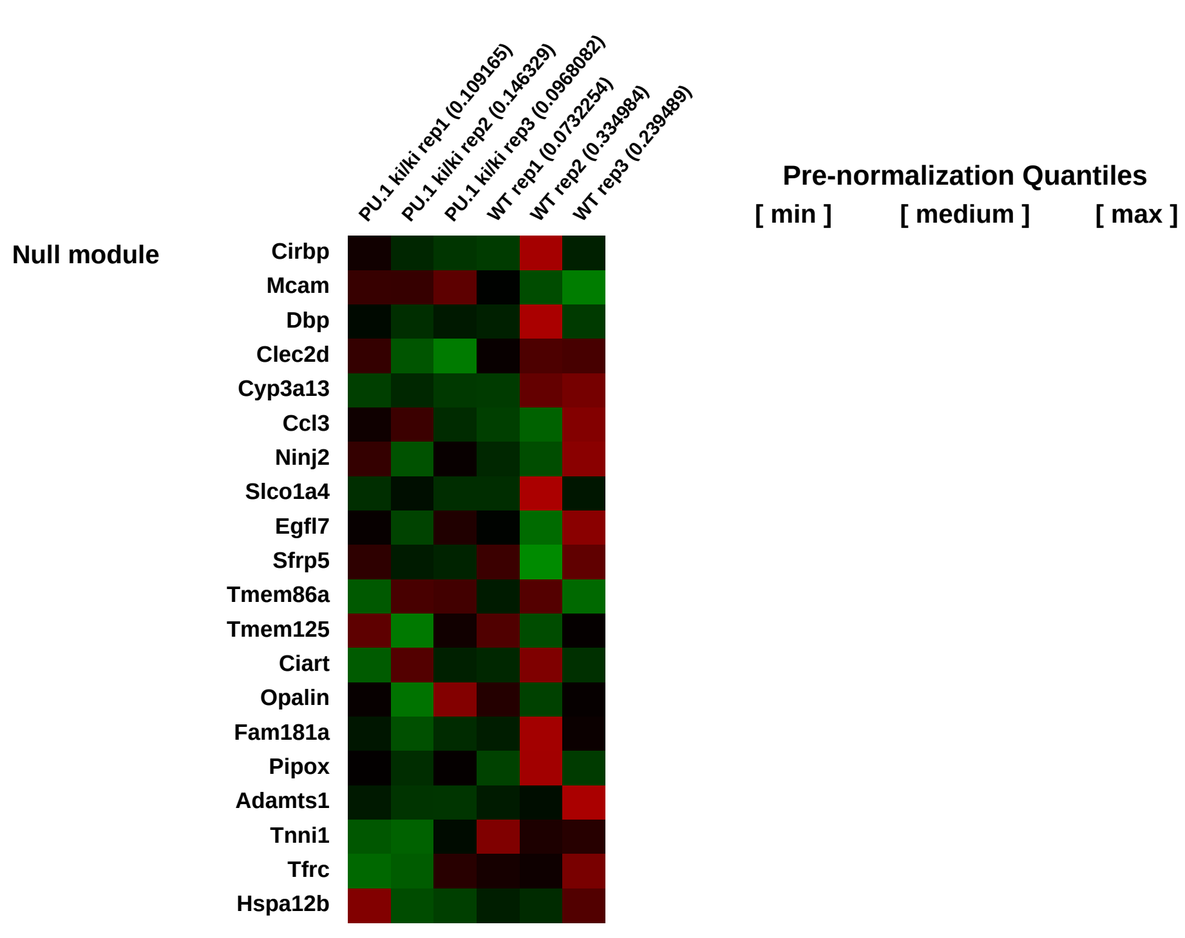

GEO Series "GSE33064" Expression Profiles

Num of samples in this series: 18

Scale of expression profile Z-scores

-3.0 -2.0 -1.0 0.0 1.0 2.0 3.0

GEO Link:	http://www.ncbi.nlm.nih.gov/geo/query/acc.cgi?acc=GSE33064
Status:	Public on Apr 04 2012
Title:	Expression data from a Tbx1 gene allelic series
Organism:	Mus musculus
Experiment type:	Expression profiling by array
Platform:	GPL1261
Pubmed ID:	22367967
Summary & Design:	**Summary:** This study was aimed at identifying Tbx1 dosage-dependent genes in vivo, so we performed a transcriptome analysis of Tbx1 mutants with nine different genotypes corresponding to different Tbx1 mRNA dosages. **Overall design:** Tbx1 gene dosage

Background corr dist: KL-Divergence = 0.1151, L1-Distance = 0.0368, L2-Distance = 0.0028, Normal std = 0.4198

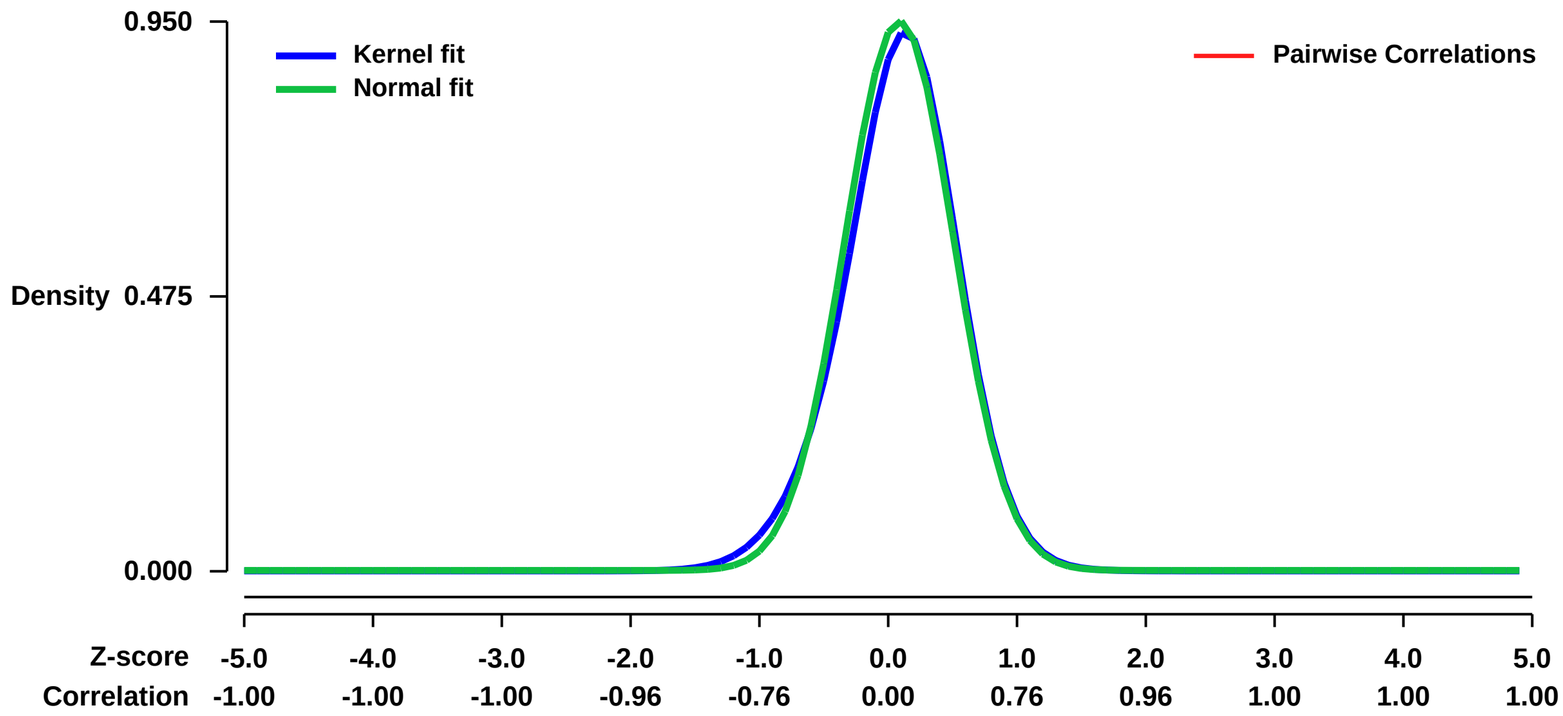

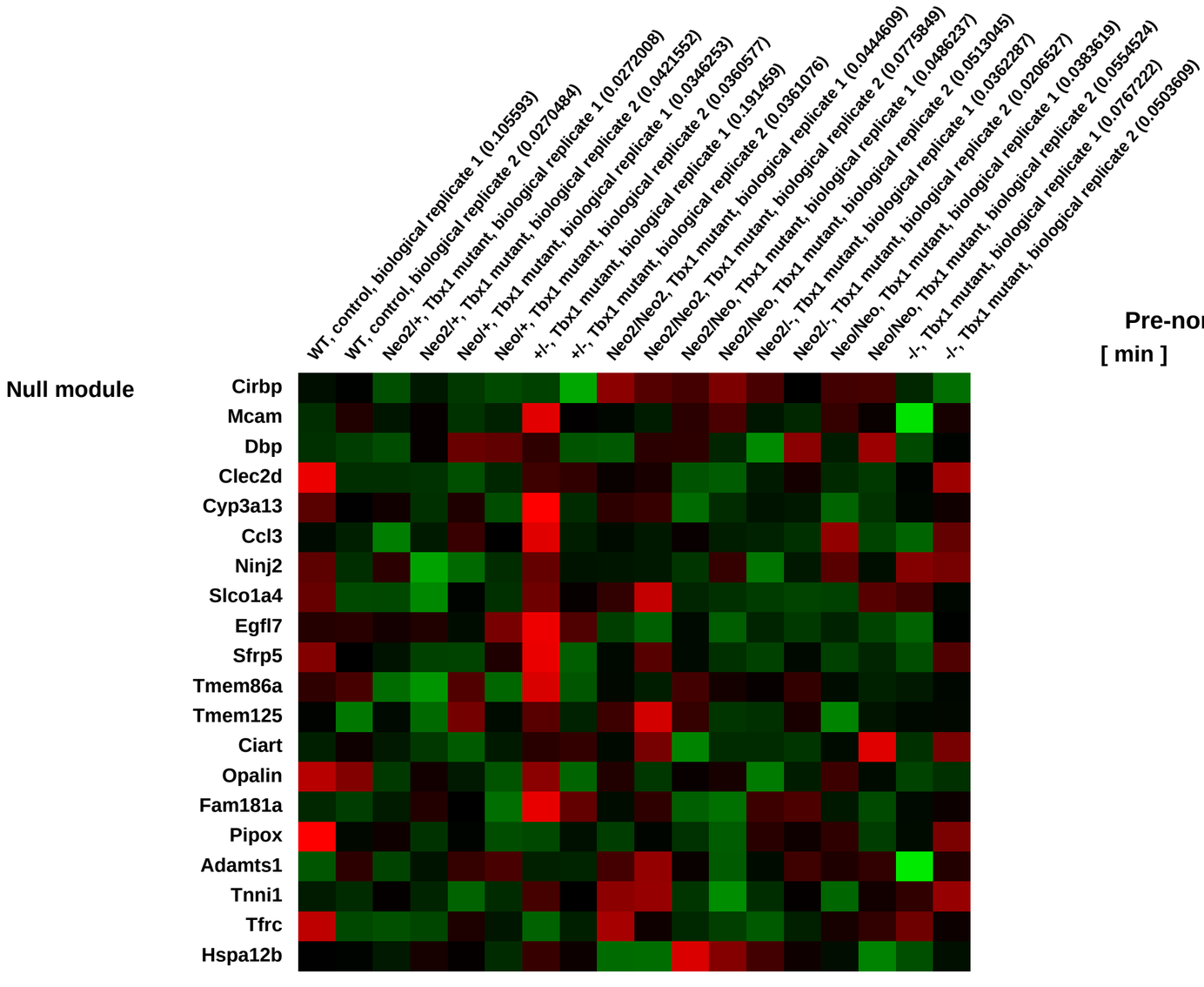

GEO Series "GSE33101" Expression Profiles

Num of samples in this series: 8

Scale of expression profile Z-scores

-3.0 -2.0 -1.0 0.0 1.0 2.0 3.0

GEO Link:	http://www.ncbi.nlm.nih.gov/geo/query/acc.cgi?acc=GSE33101
Status:	Public on Dec 01 2011
Title:	Gene expression profiles in Sirt1/PPARalpha bigenic mice
Organism:	Mus musculus
Experiment type:	Expression profiling by array
Platform:	GPL1261
Pubmed ID:	22055503
Summary & Design:	**Summary:** Cardiac-specific PPARalpha transgenic (Tg-PPARalpha) mice show mild cardiac hypertrophy and systolic dysfunction. The failing heart phenotypes observed in Tg-PPARalpha are exacerbated by crossing with cardiac-specific Sirt1 transgenic (Tg-Sirt1) mice, whereas Tg-Sirt1 mice themselves do not show any cardiac hypertrophy or systolic dysfunction. To investigate the mechanism leading to the failing heart phenotypes in TgPPARalpha/Tg-Sirt1 bigenic mice, microarray analyses were performed. The microarray analyses revealed that many ERR target genes were downregulated in Tg-PPARalpha and in Tg-Sirt1, and they were further downregulated in the Tg-PPARalpha/Tg-Sirt1 bigenic mice. **Overall design:** Four groups of cardiac-specific transgenic mice were used for the study, i.e., control, PPARalpha, Sirt1 and PPARalpha/Sirt1. Hearts were dissected after 10-11 weeks of male FVB background transgenic mice. Total RNA was prepared from the hearts to conduct the microarray analyses.

Background corr dist: KL-Divergence = 0.0486, L1-Distance = 0.0164, L2-Distance = 0.0003, Normal std = 0.5638

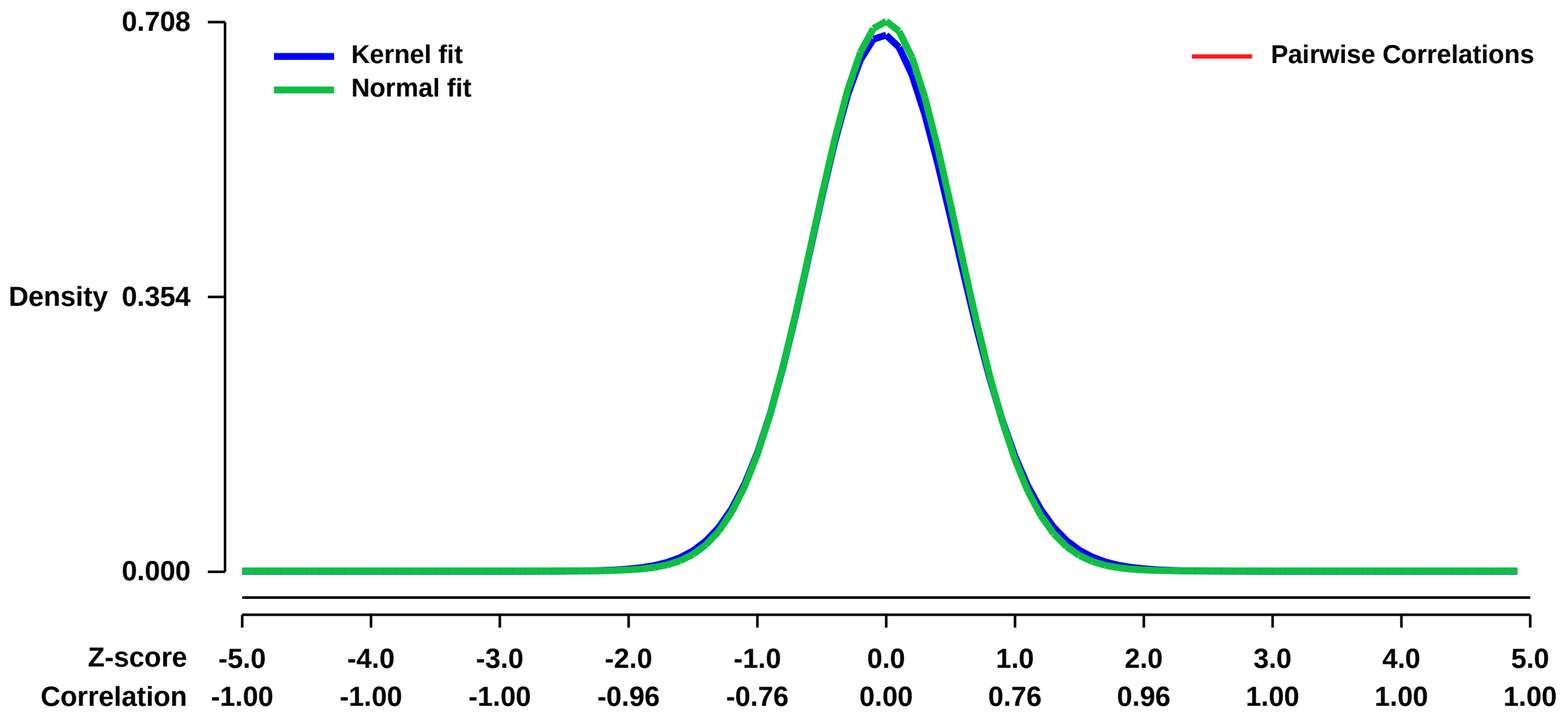

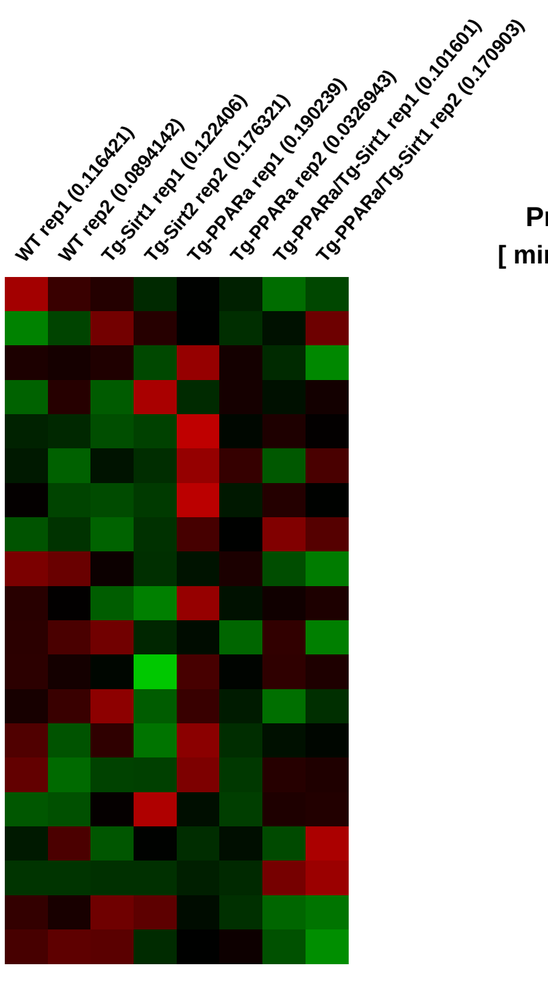

GEO Series "GSE3313" Expression Profiles

Num of samples in this series: 24

Scale of expression profile Z-scores

-3.0 -2.0 -1.0 0.0 1.0 2.0 3.0

GEO Link:	http://www.ncbi.nlm.nih.gov/geo/query/acc.cgi?acc=GSE3313
Status:	Public on Jun 30 2014
Title:	Impaired revascularization in a mouse model of diabetes associated with dysregulation of angiogenic-regulatory network.
Organism:	Mus musculus
Experiment type:	Expression profiling by array
Platform:	GPL1261
Pubmed ID:	15920034
Summary & Design:	**Summary:** Diabetes is a risk factor for the development of cardiovascular diseases that are associated with impaired angiogenesis or increased endothelial cell apoptosis. Here is it shown that angiogenic repair of ischemic hind limbs was impaired in Lepr db/db mice, a leptin receptor deficient model of diabetes, compared to wild-type C57BL/6 (WT) mice as evaluated by laser Doppler flow and capillary density analyses. To identify molecular targets associated with this disease process, hind limb cDNA expression profiles were created from adductor muscle of Lepr db/db and WT mice before and after hind limb ischemia using Affymetrix GeneChip´fi Mouse Expression Set microarrays. The expression patterns of numerous angiogenesis related proteins were altered in Lepr db/db versus WT mice following ischemic injury. These transcripts included neuropilin-1, VEGF-A, placental growth factor, elastin and matrix metalloproteinases that are implicated in blood vessel growth and maintenance of vessel wall integrity. These data illustrate that impaired ischemia-induced neovascularization in type 2 diabetes is associated with the dysregulation of a complex angiogenesis-regulatory network. **Keywords:** Diabetes, ischemia, angiogenesis, microarrays **Overall design:** Gene expression data for adductor muscle in the ischemic limb from wild type mice and Lepr db/db mice of 4 time points (before hind limb ischemia, 1 day, 7 days and 14 days after hind limb ischemia surgery). Three independent experimental replicates of each condition for each time point.

Background corr dist: KL-Divergence = 0.1724, L1-Distance = 0.0358, L2-Distance = 0.0026, Normal std = 0.3616

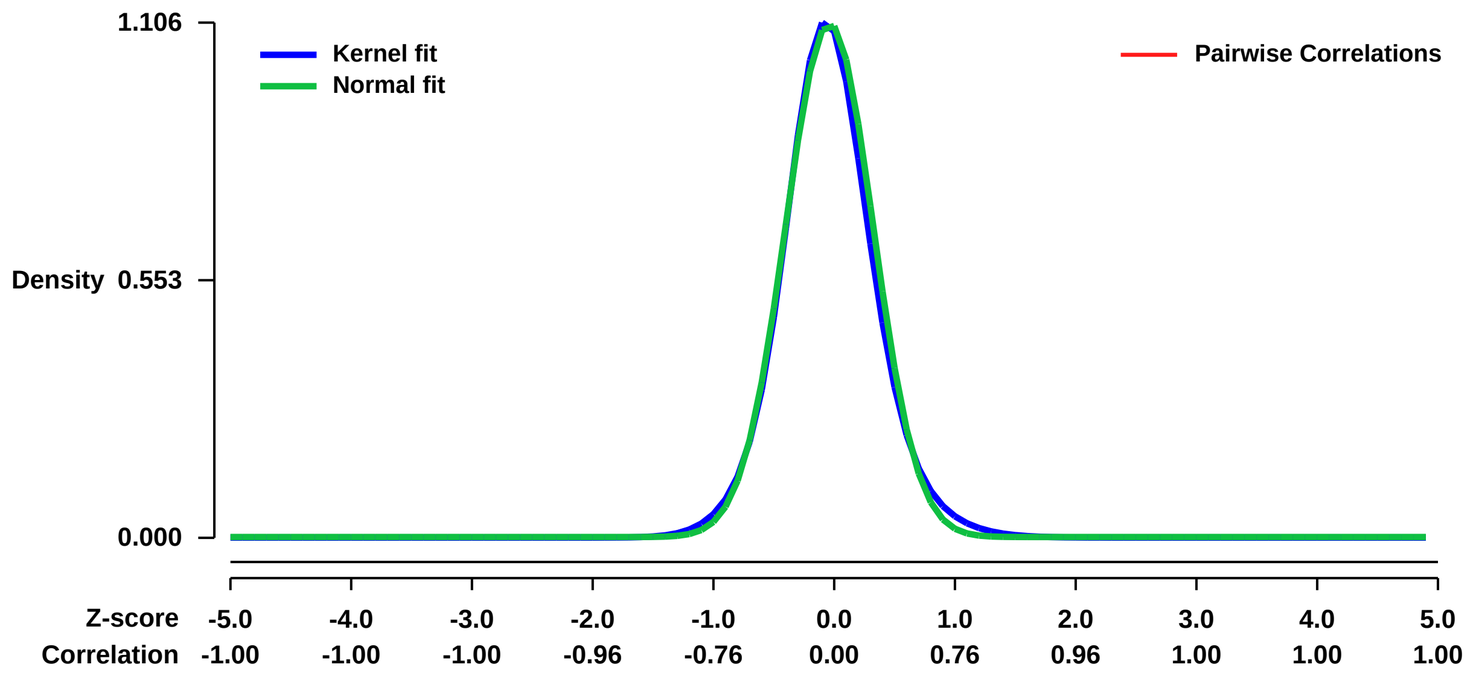

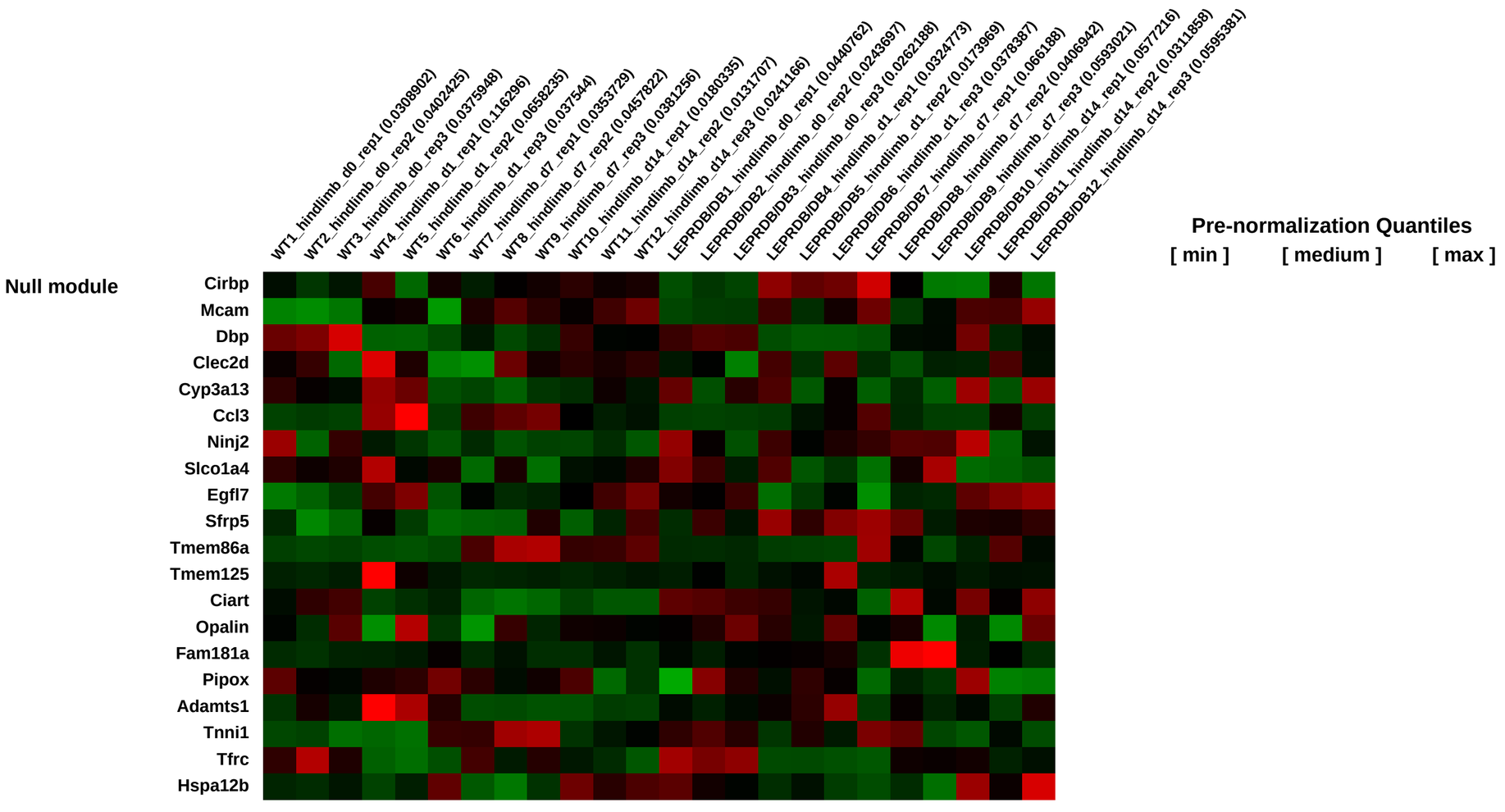

GEO Series "GSE33132" Expression Profiles

Num of samples in this series: 8

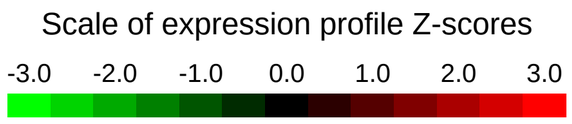

GEO Link:	http://www.ncbi.nlm.nih.gov/geo/query/acc.cgi?acc=GSE33132
Status:	Public on Oct 21 2011
Title:	Expression data from purified control and Brdt˛ BD1 round spermatids.
Organism:	Mus musculus
Experiment type:	Expression profiling by array
Platform:	GPL1261
Pubmed ID:	22570411
Summary & Design:	**Summary:** Brdt is a testis specific member of a family of chromatin interacting proteins. All of the family members have been shown to regulate transcription. Brdt is highly expressed in round spermatids, and may play a role in transcriptional regulation in these cells. We investigated transcriptional changes in mutant round spermatids that were homozygous for a mutation in which the first bromodomain of Brdt was removed. **Overall design:** Round spermatids were purified from seven adult animals of each genotype for each Affymetrix microarray. Purity of round spermatids was assessed by propidium iodide staining.

Background corr dist: KL-Divergence = 0.0577, L1-Distance = 0.0221, L2-Distance = 0.0007, Normal std = 0.5318

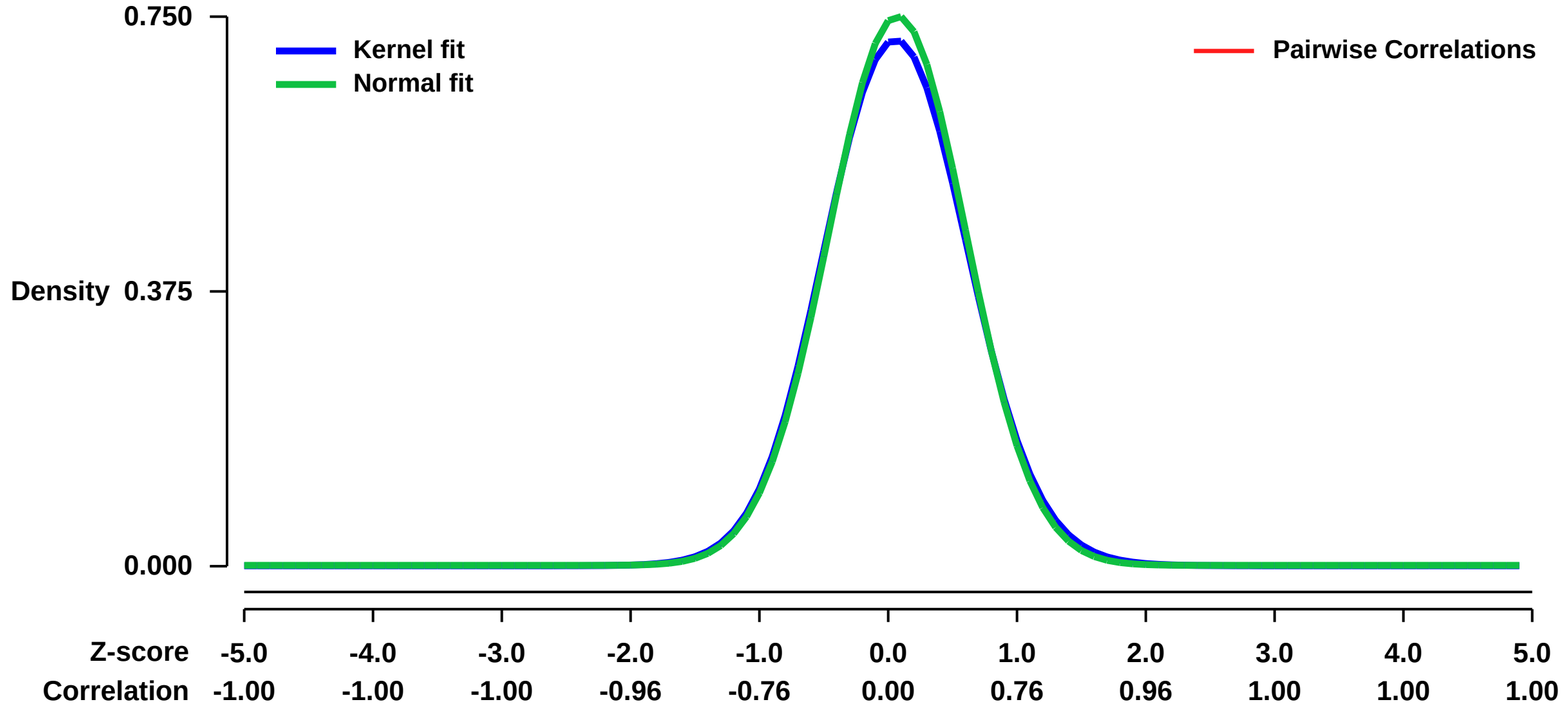

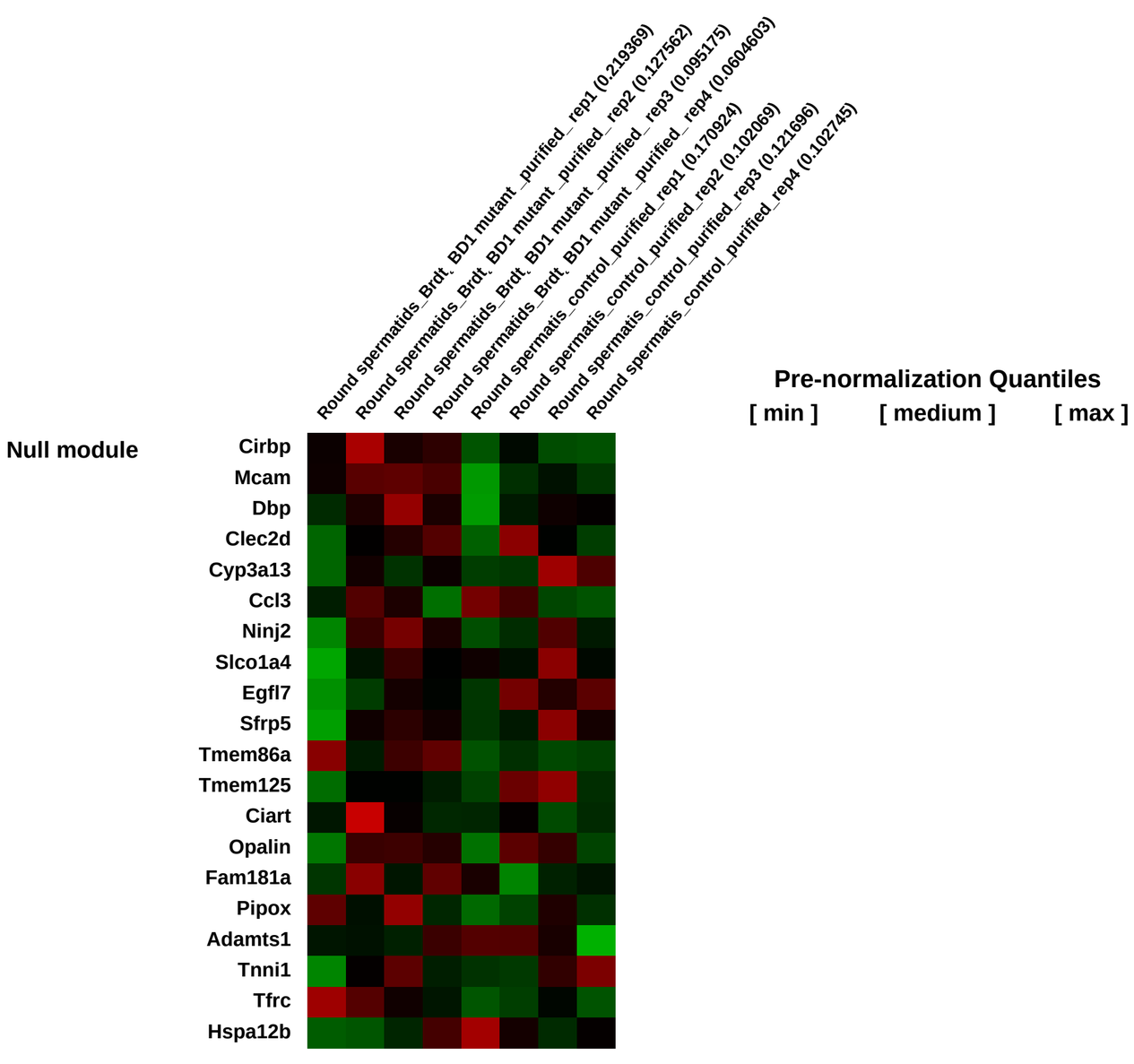

GEO Series "GSE33134" Expression Profiles

Num of samples in this series: 31

Scale of expression profile Z-scores

-3.0 -2.0 -1.0 0.0 1.0 2.0 3.0

GEO Link:	http://www.ncbi.nlm.nih.gov/geo/query/acc.cgi?acc=GSE33134
Status:	Public on Dec 31 2011
Title:	Protective gene expression changes elicited by an inherited defect in photoreceptor structure.
Organism:	Mus musculus
Experiment type:	Expression profiling by array
Platform:	GPL1261
Pubmed ID:	
Summary & Design:	**Summary:** To investigate pathogenic mechanisms in such instances, we have characterized rod photoreceptor and retinal gene expression changes in response to a defined insult to photoreceptor structure, using the retinal degeneration slow (rds) mouse model. Global gene expression profiling was performed on flow-sorted rds and wild-type rod photoreceptors immediately prior and subsequent to times at which OSs are normally elaborated. Dysregulated genes were identified via microarray hybridization, and selected candidates were validated using quantitative PCR analyses. We identified a single key gene, Egr1, that was dysregulated in a sustained fashion in rds rod photoreceptors and in the retina. Egr1 upregulation was associated with microglial activation and migration, into the outer retina at times subsequent to the major peak of photoreceptor cell death. Interestingly, this response was accompanied by neurotrophic factor upregulation. We hypothesize that activation of Egr1 and neurotrophic factors represents a protective immune mechanism, contributing to the characteristically slow retinal degeneration of the rds mouse model. **Overall design:** We had two conditions WT and Rds-KO at 4 different time points: postnatal (P) 6, P9, P14 and P21.

Background corr dist: KL-Divergence = 0.0735, L1-Distance = 0.0832, L2-Distance = 0.0128, Normal std = 0.6445

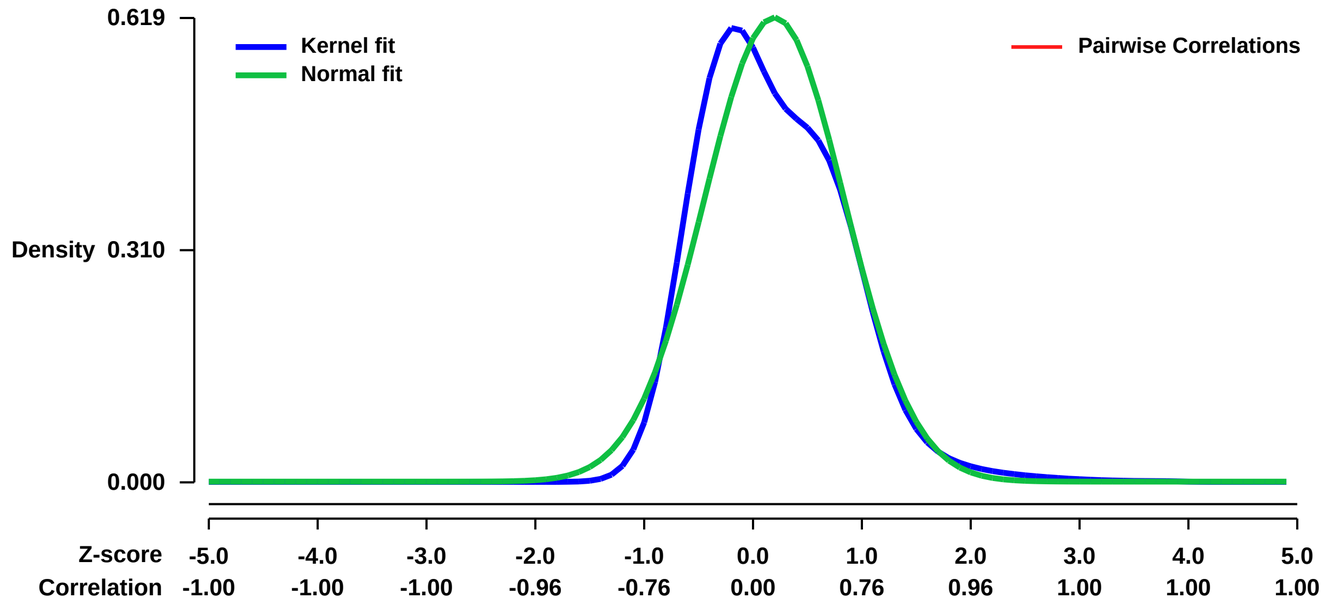

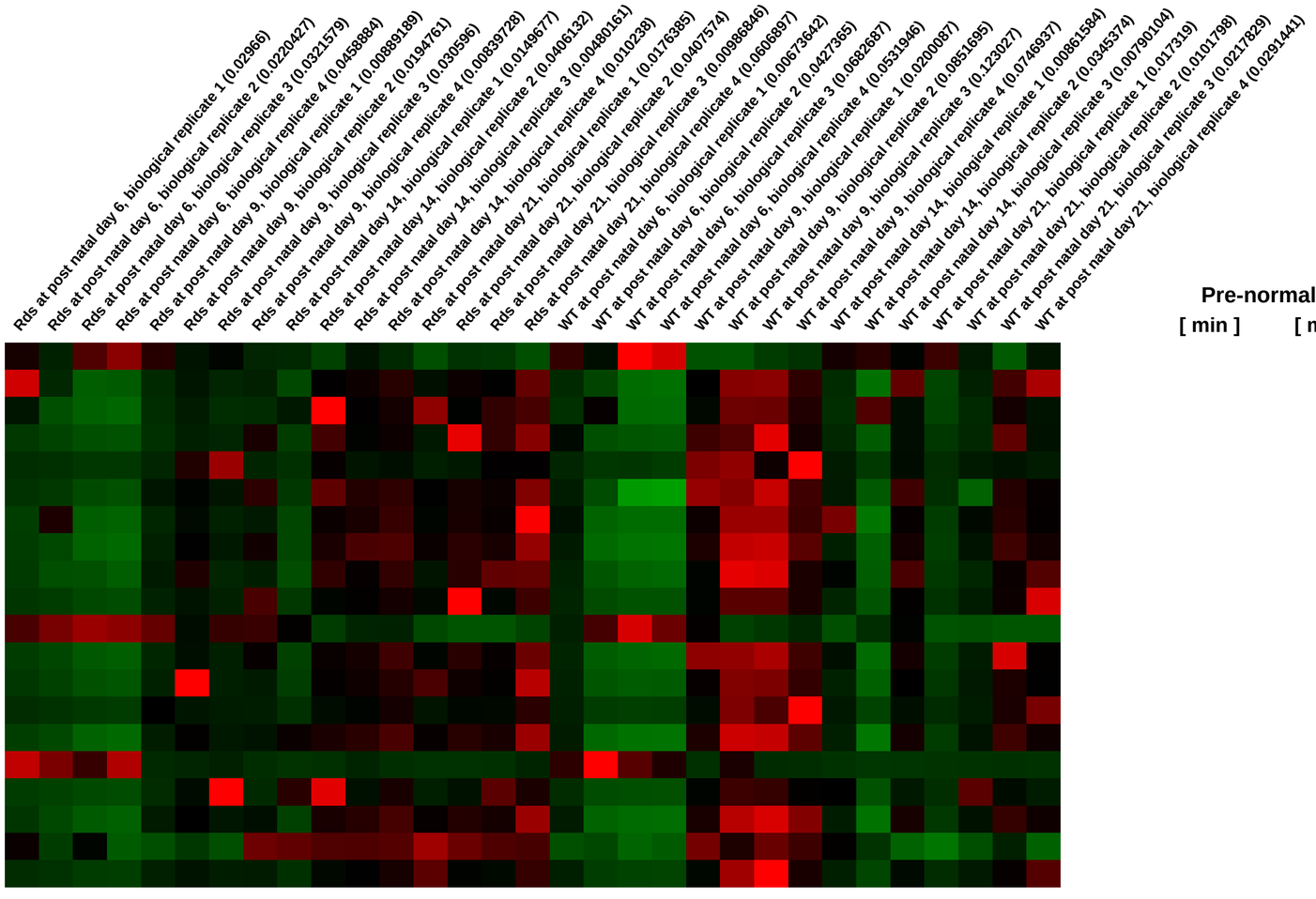

GEO Series "GSE33156" Expression Profiles

Num of samples in this series: 18

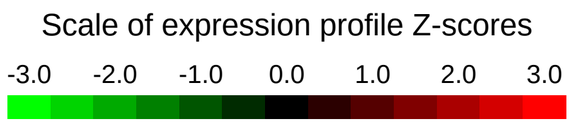

GEO Link:	http://www.ncbi.nlm.nih.gov/geo/query/acc.cgi?acc=GSE33156
Status:	Public on Jan 01 2013
Title:	Hedgehog signaling in T cell differentiation
Organism:	Mus musculus
Experiment type:	Expression profiling by array
Platform:	GPL1261
Pubmed ID:	23408837
Summary & Design:	**Summary:** **Despite Hedgehogâ s influence on T-cell activation and proliferation, the transcriptional targets of Gli2 in lymphocytes are not known. We therefore examined the Hedgehog-dependent transcriptional response of resting and early-stage activated T-cells in order to define their transcriptional response to Hedgehog pathway activation.** **We have established transgenic models where transcription of target genes by Gli2 is either constitutively activated or repressed in cells of the T-lineage. Gli2 has an N-terminal repressor domain and a C-terminal activator domain. Lck-Gli2¸ N2 (Gli2A) mice carry a transgene encoding a truncated form of Gli2 that acts as a permanent transcriptional activator of Hh target genes. Conversely, Lck-Gli2¸ C2 (Gli2R) mice express a repressor of Gli2-dependent transcription, which by binding to Gli binding sites inhibits physiological Hh-dependent transcription, and hence Hh signal transduction, in the cell. These transgenes are driven by the Lck promoter and are only expressed in T-lineage cells** **Overall design:** **Purified fresh, resting CD4 cells (unstimulated) and from CD4 cells stimulated with anti-CD3/CD28 for 6h (stimulated) were analysed in order to obtain transcriptional profiles before and during the early stages of T-cell activation.**

Background corr dist: KL-Divergence = 0.0709, L1-Distance = 0.0778, L2-Distance = 0.0097, Normal std = 0.5606

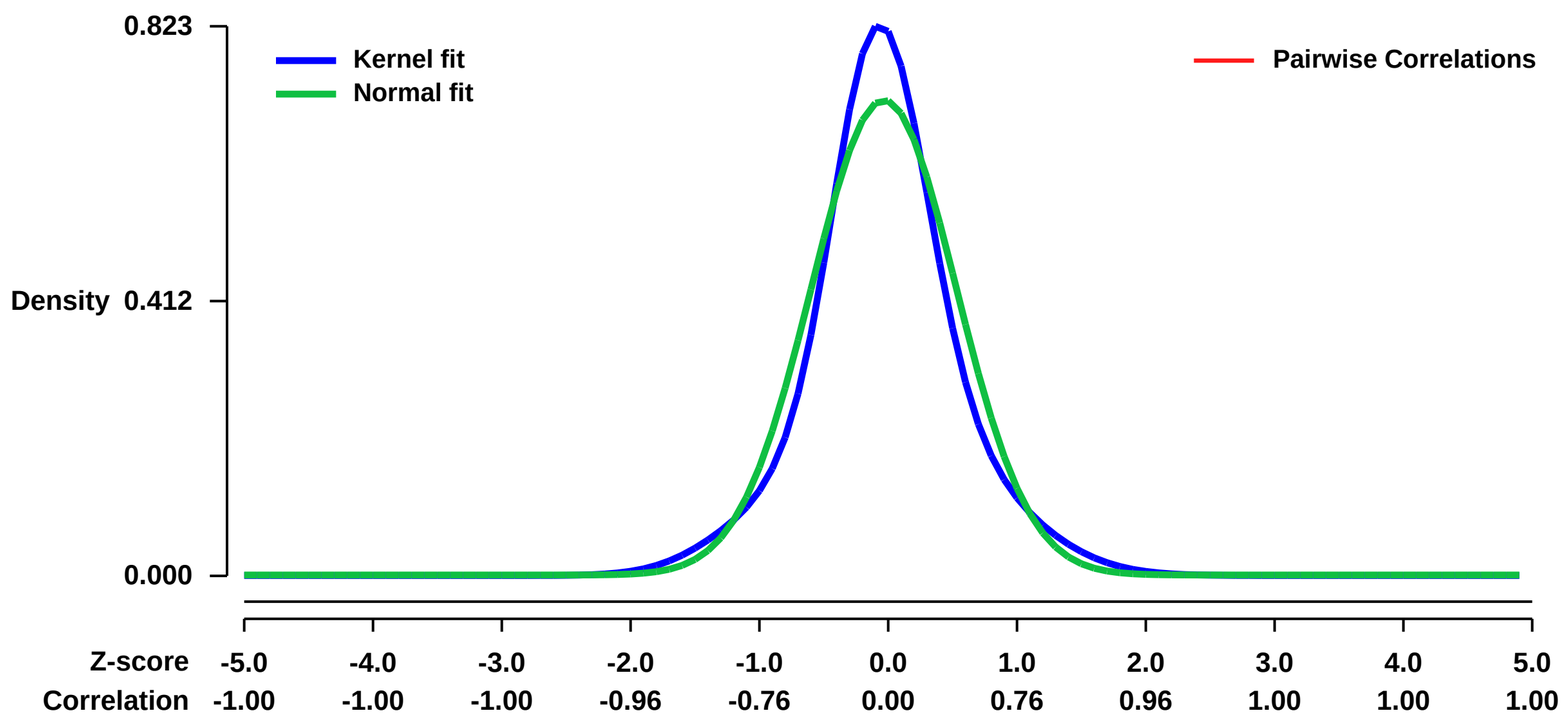

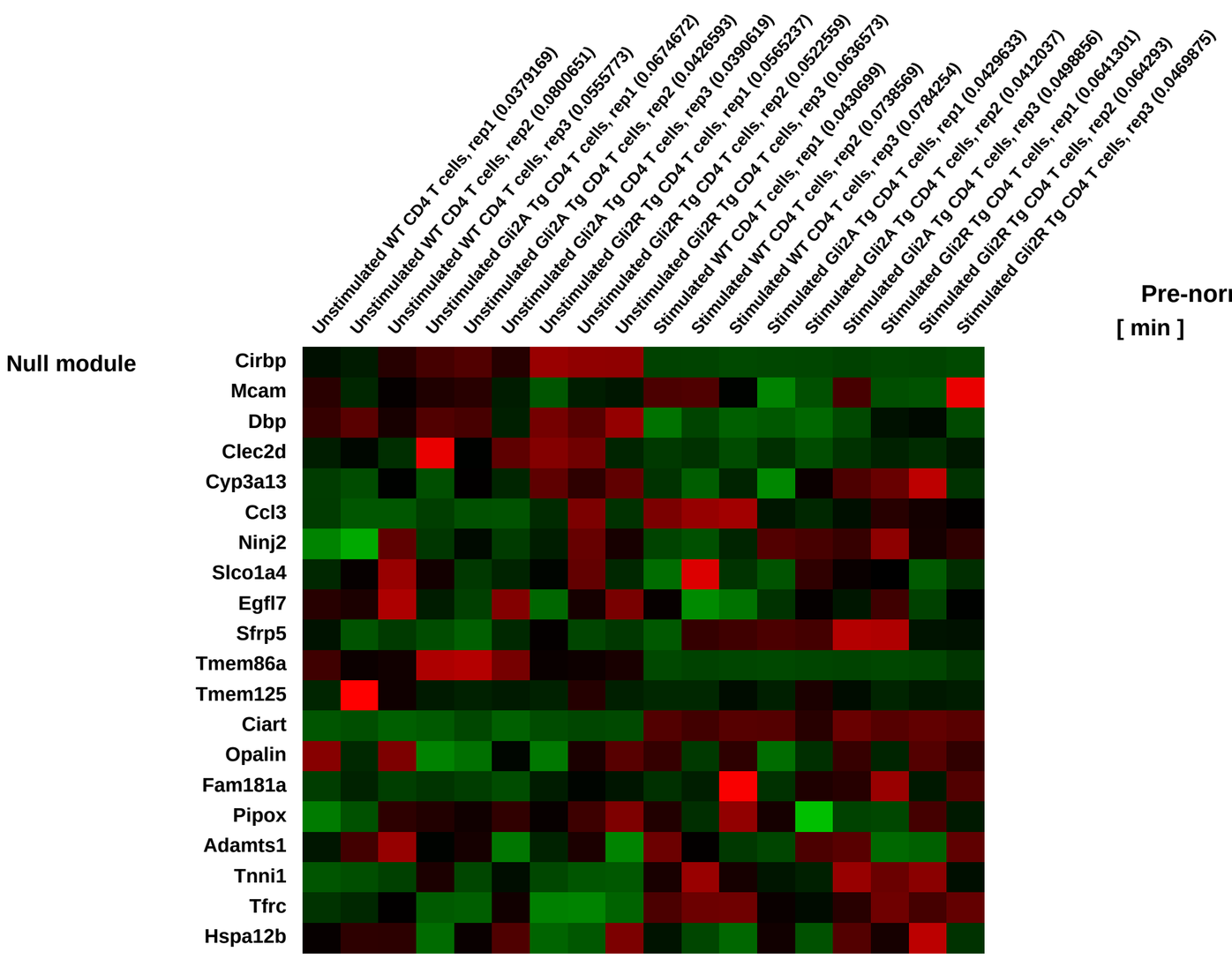

GEO Series "GSE33199" Expression Profiles

Num of samples in this series: 64

Scale of expression profile Z-scores

-3.0 -2.0 -1.0 0.0 1.0 2.0 3.0

GEO Link:	http://www.ncbi.nlm.nih.gov/geo/query/acc.cgi?acc=GSE33199
Status:	Public on Feb 29 2012
Title:	A mouse model of the most aggressive subgroup of human medulloblastoma [Mouse430_2]
Organism:	Mus musculus
Experiment type:	Expression profiling by array
Platform:	GPL1261
Pubmed ID:	22340591
Summary & Design:	**Summary:** Mouse models of medulloblastoma are compared to human subgroups through microarray expression and other measures **Overall design:** This study contrasts mouse medullablastomas from a range of mouse genetic models. For Shh-type medulloblastoma [dka001-005, 009, 033 and 034] and [dka050-057], spontaneous medulloblastomas from [Cdkn2c-/-; Trp53FlFl; Nestin-Cre] and [Cdkn2c-/-; Ptch1+/-] (Uziel et al.,2005 Genes Dev) were used, respectively. For Myc [dka010-022, 037, 046, 049 and 058-71] and Mycn [dka023-032, 036 and 047] were generated by orthotopic injection of either Myc or Mycn overexpression in Cdkn2c-/-, Trp53-/- cerebellar cells into immunocompromised nude mice. For Wnt-type medulloblastomas [pgr003, 016 and 066], spontaneously developed tumors from CTNNB1+/lox (ex3); BLBP-Cre; Trp53FlFl (Gibson et al., Nature, 2010) were removed for RNA extraction.

Background corr dist: KL-Divergence = 0.3359, L1-Distance = 0.0564, L2-Distance = 0.0083, Normal std = 0.2699

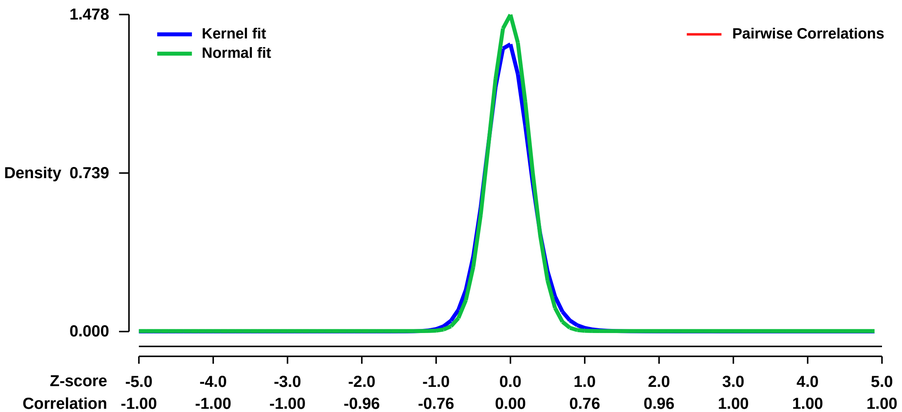

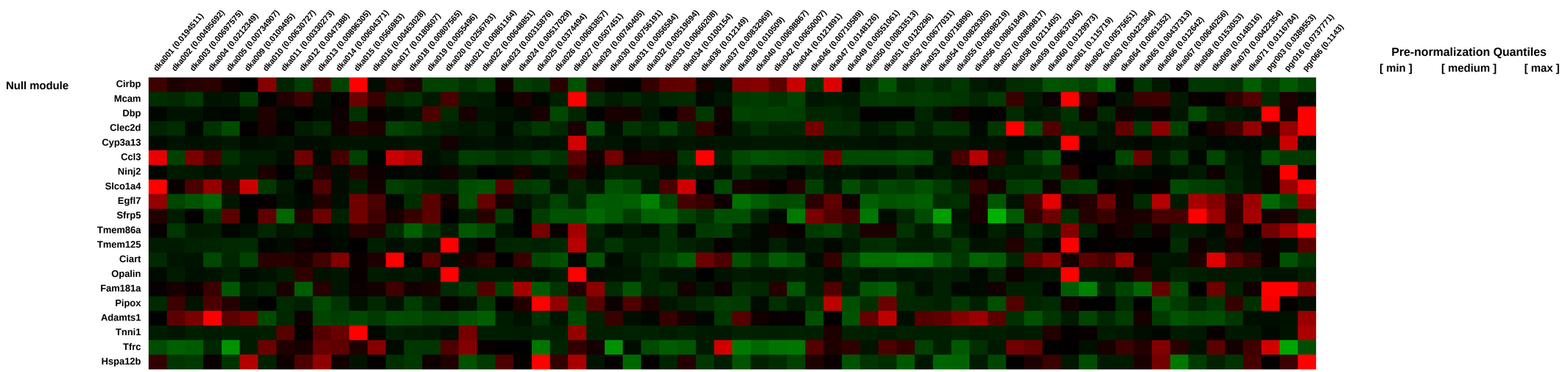

GEO Series "GSE33302" Expression Profiles

Num of samples in this series: 17

Scale of expression profile Z-scores

-3.0 -2.0 -1.0 0.0 1.0 2.0 3.0

GEO Link:	http://www.ncbi.nlm.nih.gov/geo/query/acc.cgi?acc=GSE33302
Status:	Public on Sep 06 2012
Title:	Expression data from sleep deprivation experiment in mouse hippocampus
Organism:	Mus musculus
Experiment type:	Expression profiling by array
Platform:	GPL1261
Pubmed ID:	22930738
Summary & Design:	**Summary:** We used microarrays to detail the global programme of gene expression underlying the effect of sleep deprivation in the mouse hippocampus and identified distinct classes of regulated genes during this process. **Overall design:** Hippocampal tissue was taken from sleep deprived mice and time-matched non-sleep-deprived control animals that were left undisturbed in their home cages during the sleep deprivation period for a total of 8 and 9 replicates per group. RNA was isolated and cDNA was synthesized from hippocampal tissue, and the sample from each animal was hybridized to a separate Affymetrix Mouse 430_2 microarray

Background corr dist: KL-Divergence = 0.1760, L1-Distance = 0.0517, L2-Distance = 0.0063, Normal std = 0.3479

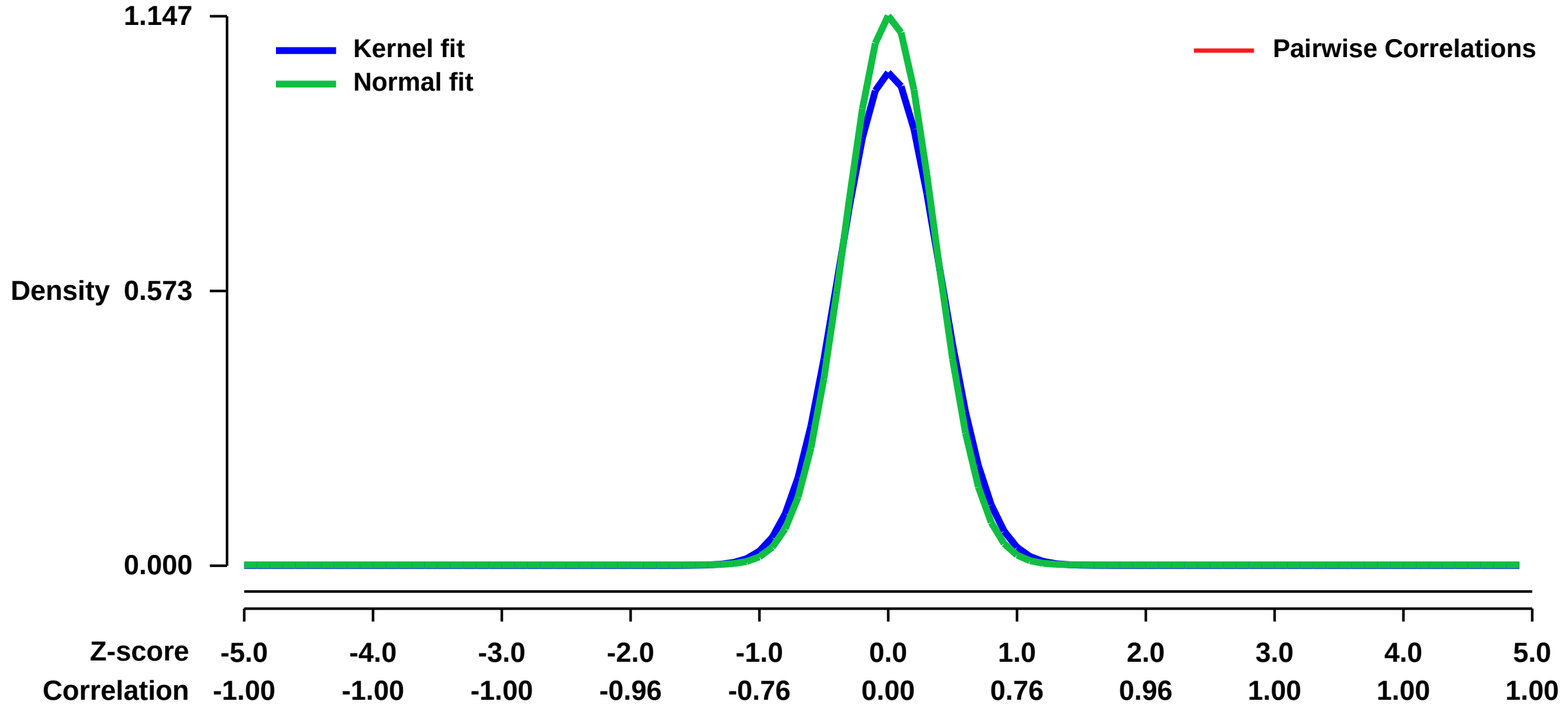

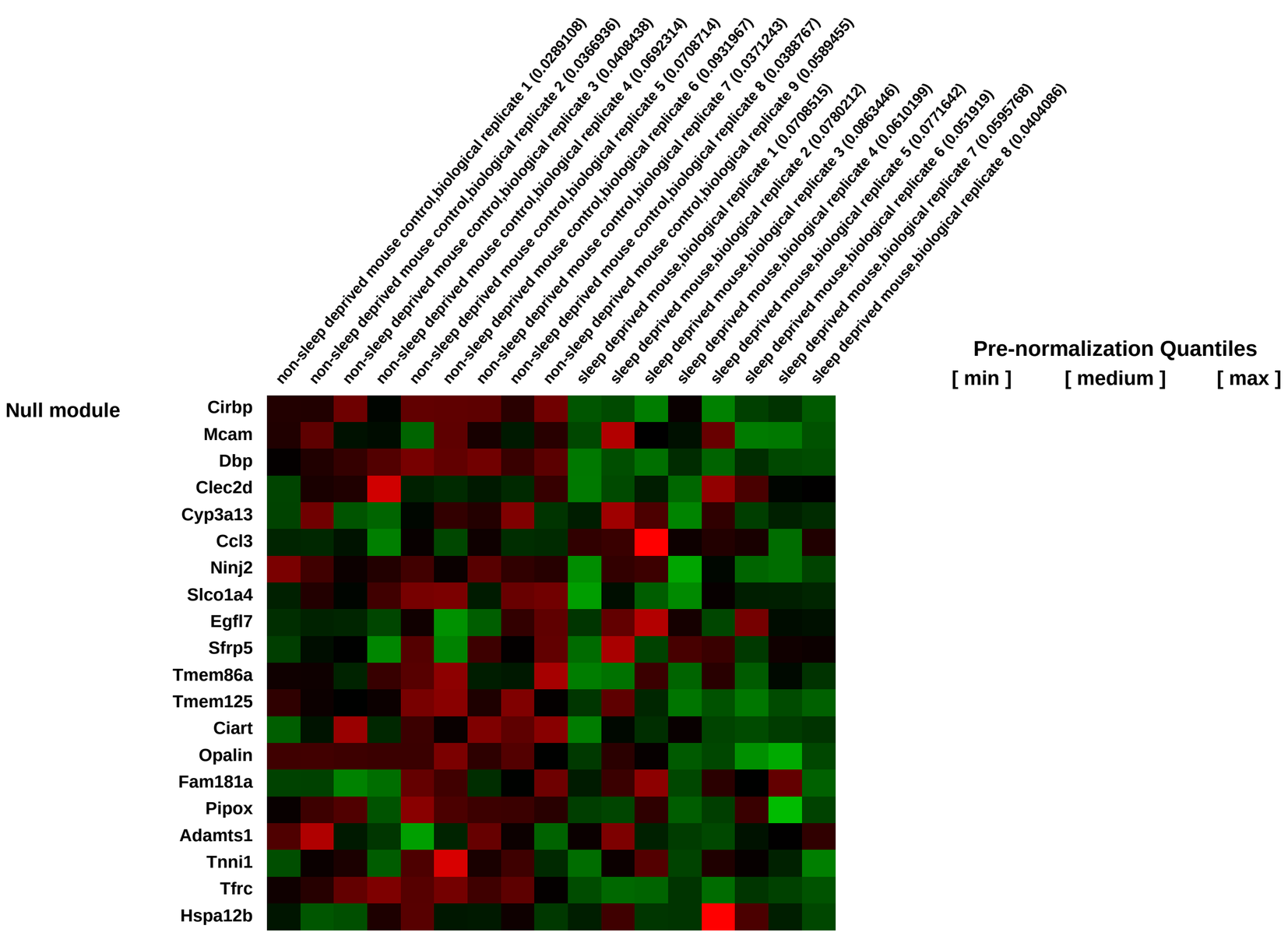

GEO Series "GSE33308" Expression Profiles

Num of samples in this series: 10

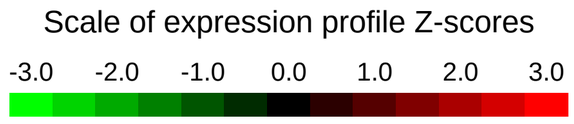

GEO Link:	http://www.ncbi.nlm.nih.gov/geo/query/acc.cgi?acc=GSE33308
Status:	Public on Jan 01 2013
Title:	Keratinocyte Growth Factor and Dexamethasone Plus Elevated cAMP Levels Synergistically Support Pluripotent Stem Cell Differentiation into Alveolar Epithelial Type II Ce
Organism:	Mus musculus
Experiment type:	Expression profiling by array
Platform:	GPL1261
Pubmed ID:	23176317
Summary & Design:	**Summary:** Alveolar epithelial type II (ATII)-like cells can be generated from murine embryonic stem cells (ESCs), although to date, no robust protocols applying specific differentiation factors are established. We hypothesized that the keratinocyte growth factor (KGF), an important mediator of lung organogenesis and primary ATII cell maturation and proliferation, together with dexamethasone, 8-bromoadenosine-cAMP, and isobutylmethylxanthine (DCI), which induce maturation of primary fetal ATII cells, also support the alveolar differentiation of murine ESCs. Here we demonstrate that the above stimuli synergistically potentiate the alveolar differentiation of ESCs as indicated by increased expression of the surfactant proteins (SP-) C and SP-B. This effect is most profound if KGF is supplied not only in the late stage, but at least also during the intermediate stage of differentiation. Our results indicate that KGF most likely does not enhance the generation of (mes)endodermal or NK2 homeobox 1 (Nkx2.1) expressing progenitor cells but rather, supported by DCI, accelerates further differentiation/maturation of respiratory progeny in the intermediate phase and maturation/proliferation of emerging ATII cells in the late stage of differentiation. Ultrastructural analyses confirmed the presence of ATII-like cells with intracellular composite and lamellar bodies. Finally, induced pluripotent stem cells (iPSCs) were generated from transgenic mice with ATII cell-specific lacZ reporter expression. Again, KGF and DCI synergistically increased SP-C and SP-B expression in iPSC cultures, and lacZ expressing ATII-like cells developed. In conclusion, ATII cell-specific reporter expression enabled the first reliable proof for the generation of murine iPSC-derived ATII cells. In addition, we have shown KGF and DCI to synergistically support the generation of ATII-like cells from ESCs and iPSCs. Combined application of these factors will facilitate more efficient generation of stem cell-derived ATII cells for future basic research and potential therapeutic application. **Overall design:** mESCs at d24 of differentiation with KGF and DCI treatment

Background corr dist: KL-Divergence = 0.0344, L1-Distance = 0.0193, L2-Distance = 0.0005, Normal std = 0.6401

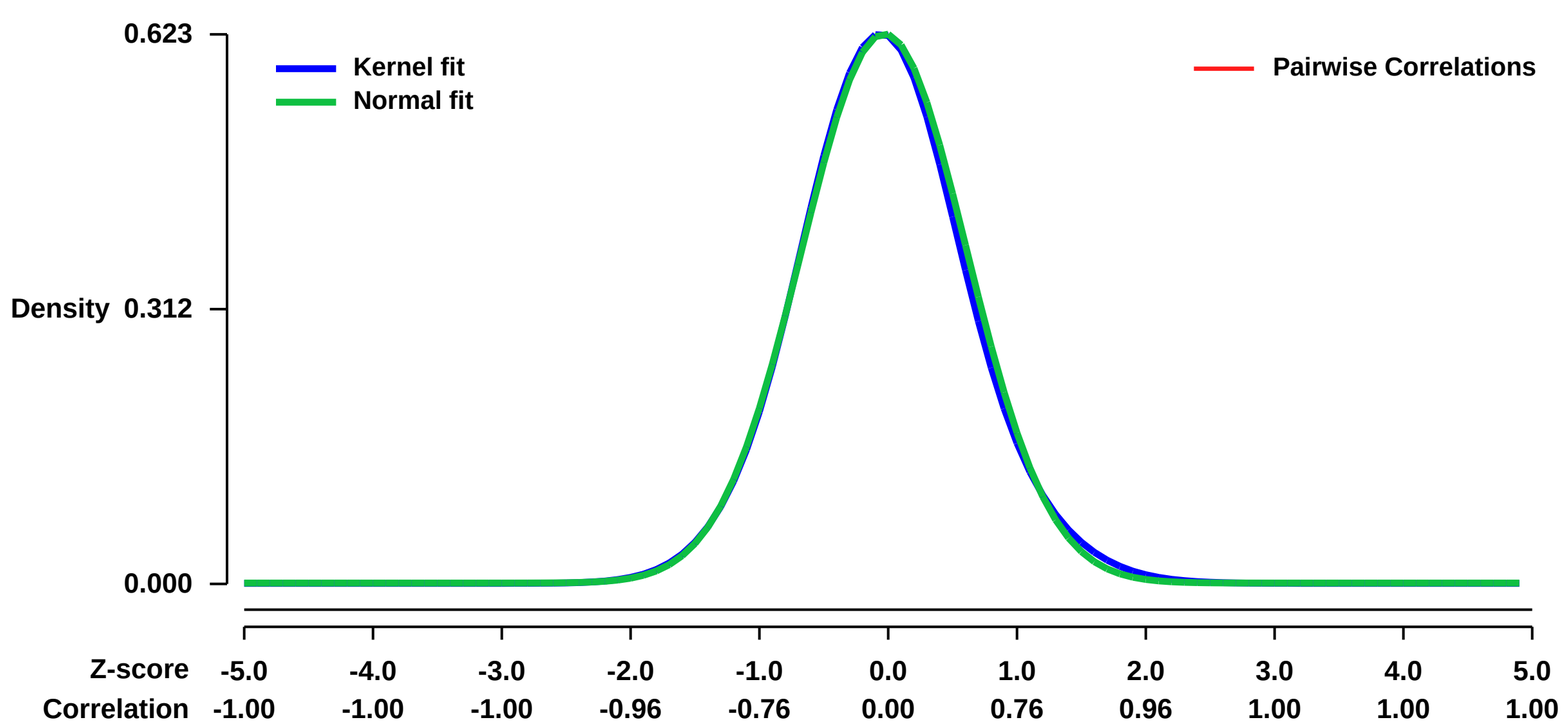

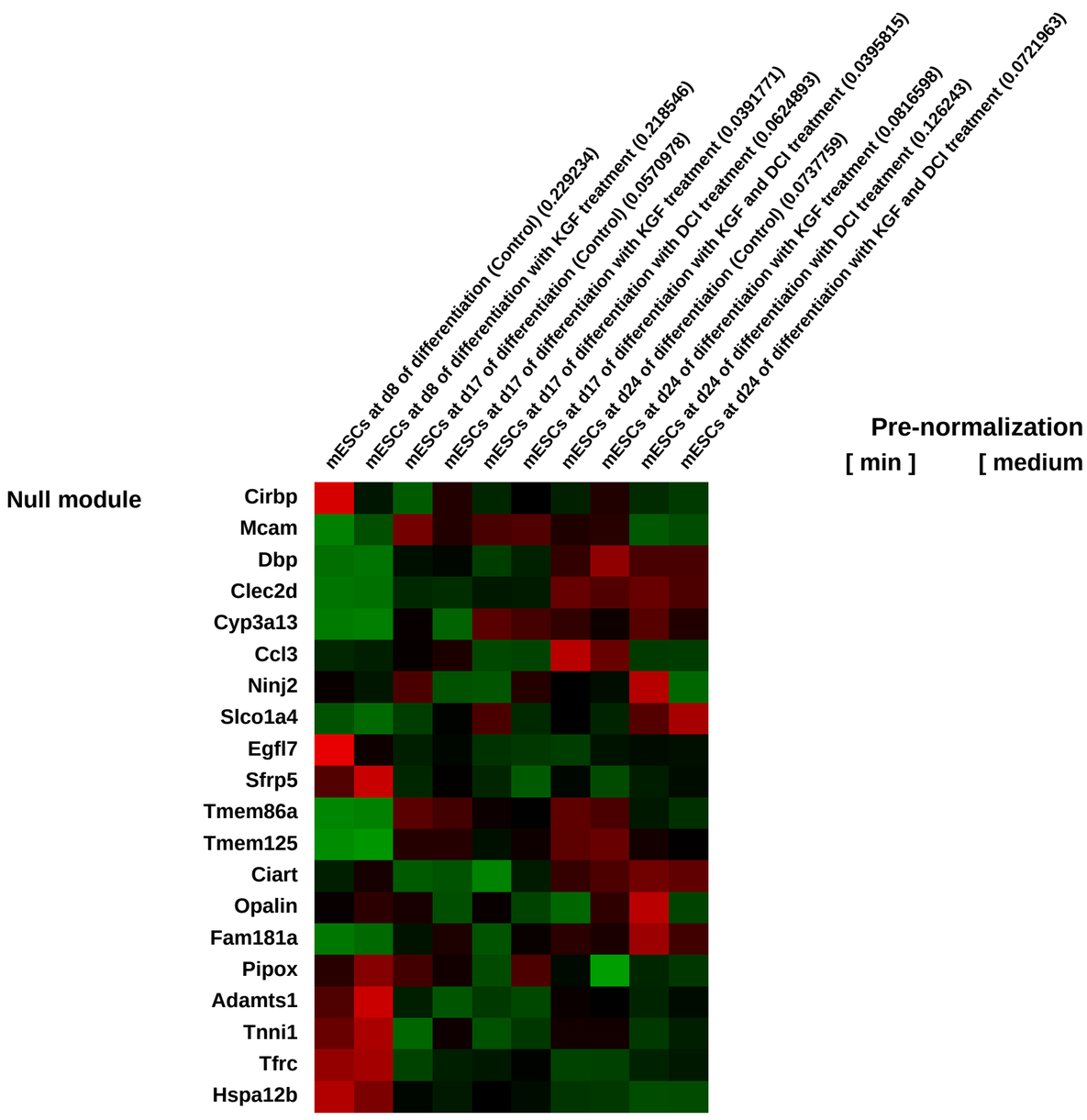

GEO Series "GSE33341" Expression Profiles

Num of samples in this series: 227

Details of this dataset are not shown due to large number of samples and the page size limit.

Find details in http://www.ncbi.nlm.nih.gov/geo/query/acc.cgi?acc=GSE33341

Background corr dist: KL-Divergence = 0.2132, L1-Distance = 0.0887, L2-Distance = 0.0240, Normal std = 0.3326

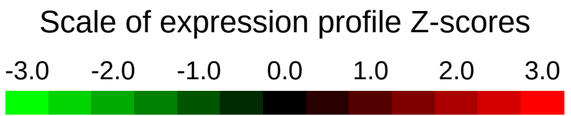

GEO Series "GSE33446" Expression Profiles

Num of samples in this series: 18

Scale of expression profile Z-scores

-3.0 -2.0 -1.0 0.0 1.0 2.0 3.0

GEO Link:	http://www.ncbi.nlm.nih.gov/geo/query/acc.cgi?acc=GSE33446
Status:	Public on Jan 03 2013
Title:	Gene expression accompanying the promotion of hepatocellular carcinoma by intestinal microbiota and Tlr4 in mice.
Organism:	Mus musculus
Experiment type:	Expression profiling by array
Platform:	GPL1261
Pubmed ID:	22516259
Summary & Design:	**Summary:** The effect of Tlr4P712H mutation (rendering TLR4 non-functional), or gut-sterilization by antbiotics, on the induction of tumorgenesis by CCl4 and diethylnitrosamine (DEN) was characterized. Affymetrix Mouse 430 2.0 gene expression measurements were used to characterize the transcriptomic basis of the effects of the above treatments and genotypes on tumorgenesis. **Overall design:** Gene expression of mouse livers of A. Normal liver from WT C3H/HeOuJ mice, B. HCC from WT C3H/HeOuJ mice treated with CCl4 and DEN, C.HCC from TLR4-mutant C3H/HeJ mice (Tlr4P712H) treated with CCl4 and DEN and D.HCC from WT C3H/HeOuJ mice treated with antibiotics (a combination of ampicillin (1 g/l), neomycin [1 g/l], metronidazole[1 g/l] and vancomycin [500 mg/l] in drinking water) and CCl4 and DEN were characterized.

Background corr dist: KL-Divergence = 0.2105, L1-Distance = 0.0448, L2-Distance = 0.0045, Normal std = 0.3261

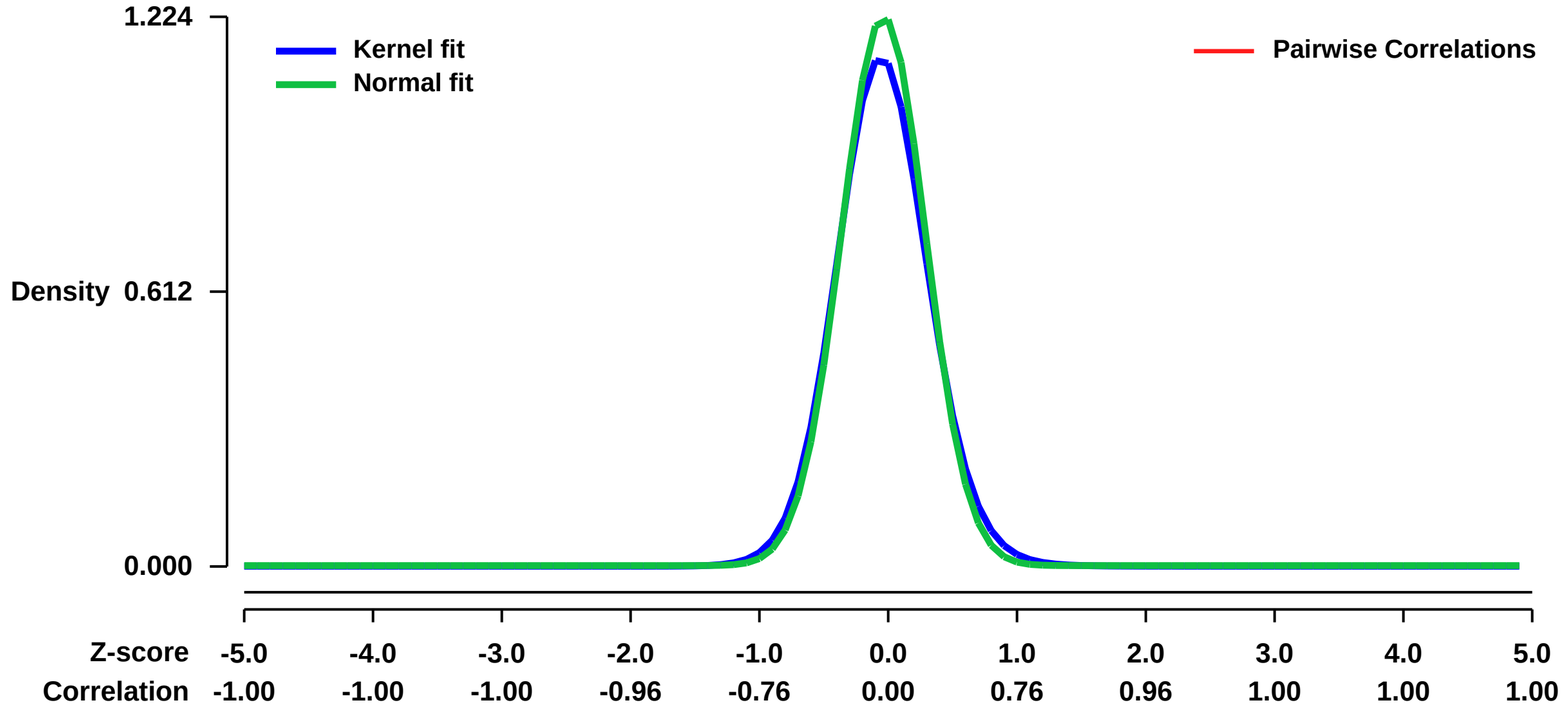

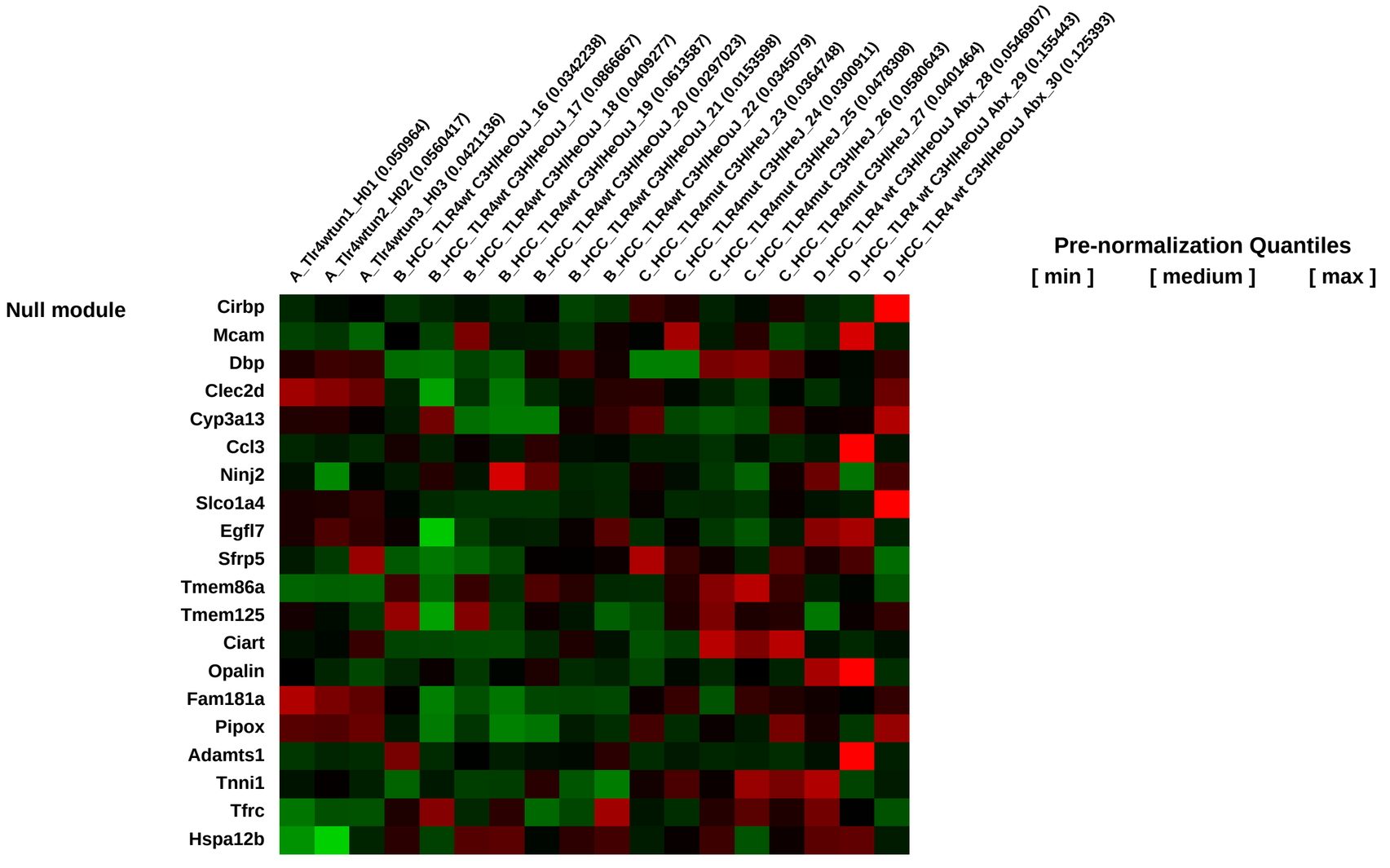

GEO Series "GSE33513" Expression Profiles

Num of samples in this series: 6

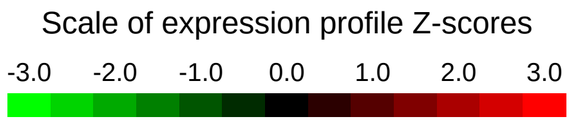

GEO Link:	http://www.ncbi.nlm.nih.gov/geo/query/acc.cgi?acc=GSE33513
Status:	Public on Dec 06 2011
Title:	T cell factor 1 is a gatekeeper for T-cell specification in response to Notch signaling
Organism:	Mus musculus
Experiment type:	Expression profiling by array
Platform:	GPL1261
Pubmed ID:	22109558
Summary & Design:	**Summary:** Although transcriptional programs associated with T-cell specification and commitment have been described, the functional hierarchy and the roles of key regulators in structuring/ orchestrating these programs remain unclear. Activation of Notch signaling in uncommitted precursors by the thymic stroma initiates the T-cell differentiation program. One regulator first induced in these precursors is the DNA binding protein Tcf-1, a T-cell specific mediator of Wnt signaling. Yet the specific contribution of Tcf-1 to early T-cell development and the signals inducing it in these cells remain unclear. Here we assign functional significance to Tcf-1 as a gatekeeper of T-cell fate. We show that Tcf-1 is directly activated by Notch signals. Tcf-1 is required at the earliest phase of Tcell determination for progression beyond the early thymic progenitor (ETP) stage. The global expression profile of Tcf-1 deficient progenitors indicates that basic processes of DNA metabolism are downregulated in its absence and the blocked T-cell progenitors become abortive and die by apoptosis. Our data thus add an important functional relationship to the roadmap of T-cell development. We used microarrays to detail the global programme of gene expression of mouse ETP thymocyte after Ikaros inactivation with dominant negative of Ik at different stage. **Overall design:** 6 samples (mouse ETP thymocytes from wt, and Tcf1 inactivation) are analyzed Mouse Microarray Expression platforms, Affymetrix Mouse 430 2.0,

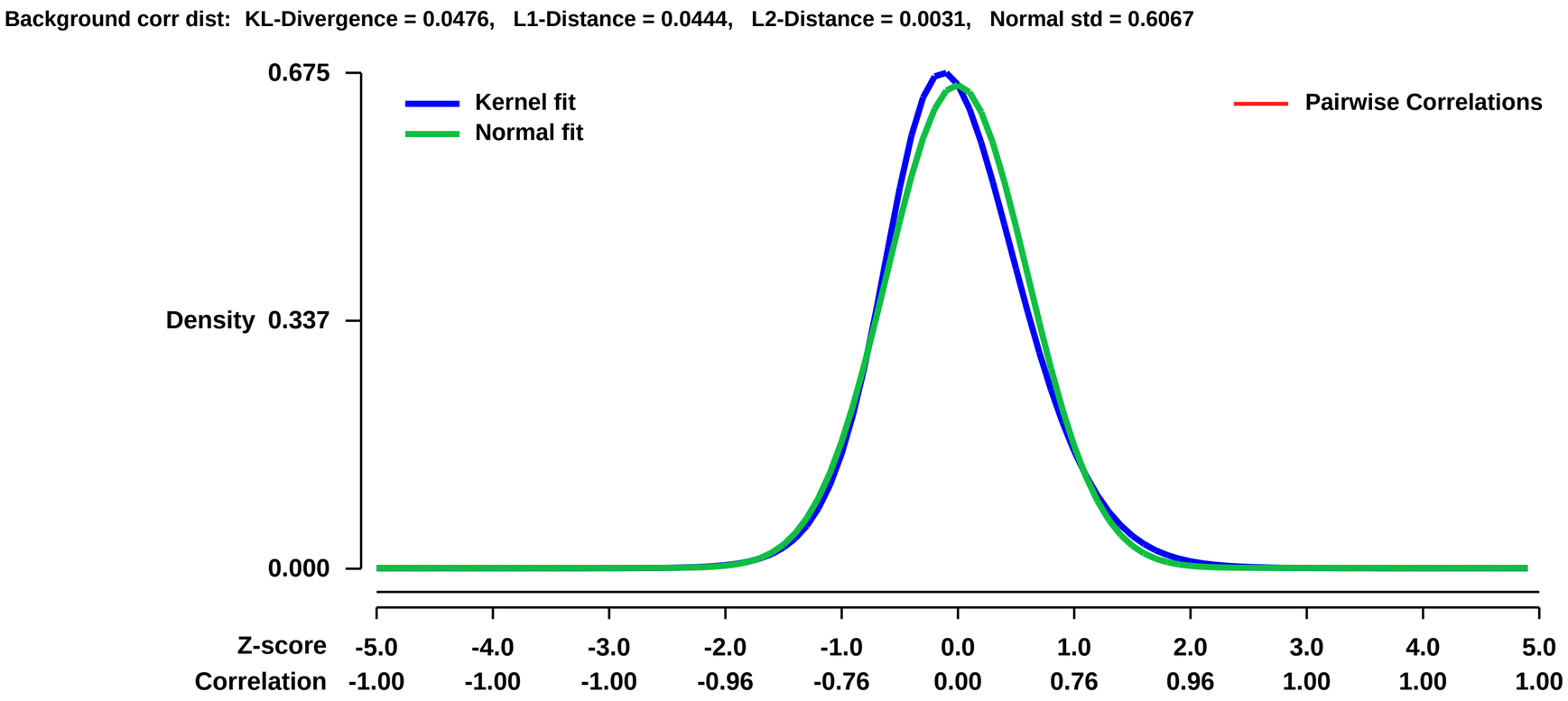

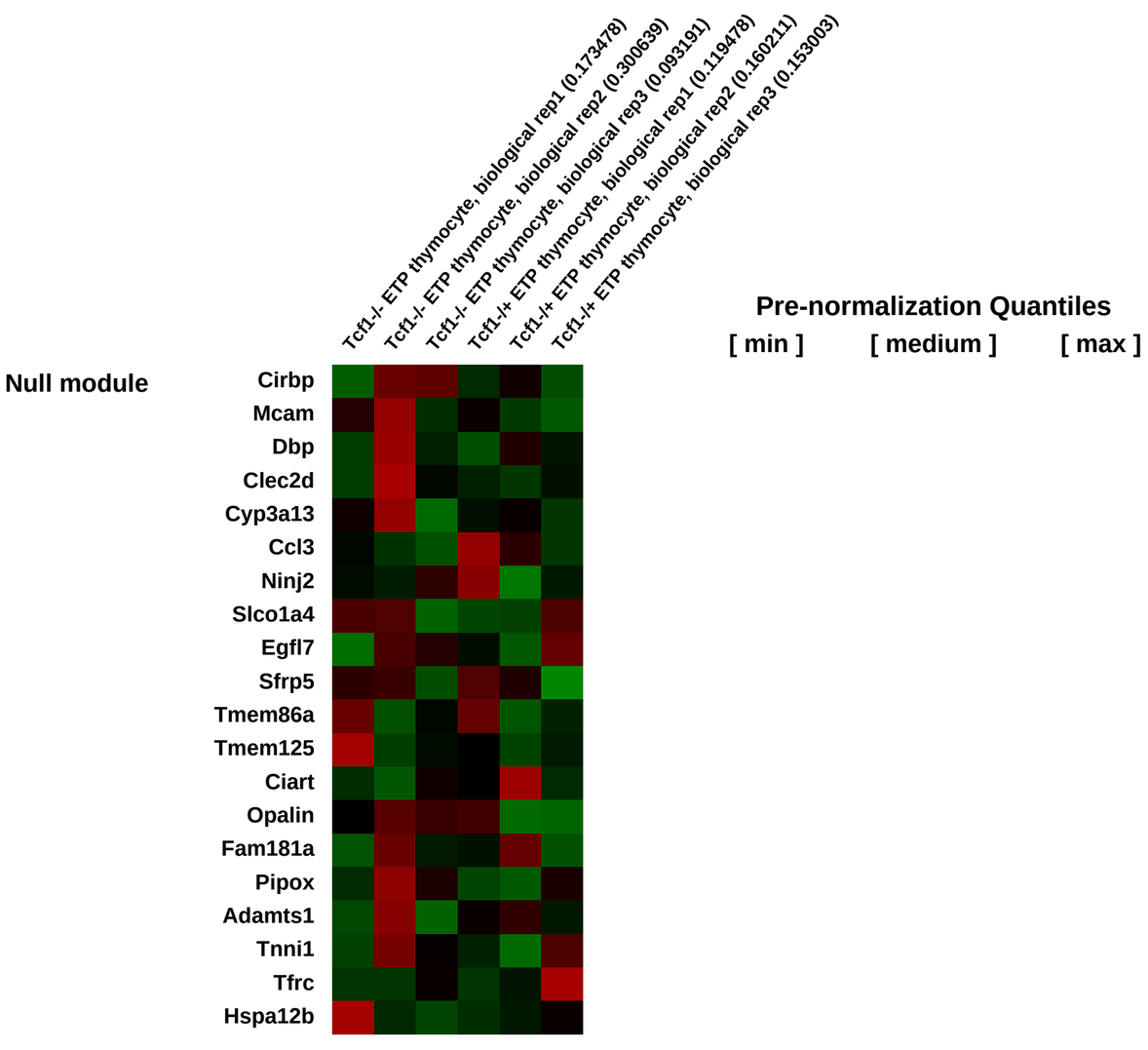

GEO Series "GSE33659" Expression Profiles

Num of samples in this series: 9

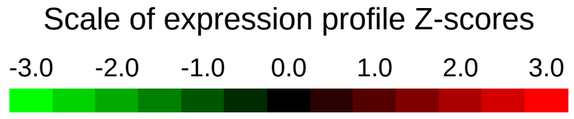

GEO Link:	http://www.ncbi.nlm.nih.gov/geo/query/acc.cgi?acc=GSE33659
Status:	Public on Feb 10 2012
Title:	Direct Recruitment of Polycomb Repressive Complex 1 (PRC1) to Chromatin by Core Binding Transcription Factors (microarray)
Organism:	Mus musculus
Experiment type:	Expression profiling by array
Platform:	GPL1261
Pubmed ID:	22325351
Summary & Design:	**Summary:** Polycomb repressive complexes (PRCs) play key roles in developmental epigenetic regulation. Yet the mechanisms that target PRCs to specific loci in mammalian cells remain incompletely understood. In this study, we show that Bmi1, a core component of Polycomb Repressive Complex 1 (PRC1), binds directly to the Runx1/CBFbeta transcription factor complex. Genome-wide studies in megakaryocytic cells demonstrate considerable chromatin occupancy overlap between the PRC1 core component Ring1b and Runx1/CBFbeta and functional regulation of a significant fraction of commonly bound genes. Bmi1/Ring1b and Runx1/CBFbeta deficiency generate partial phenocopies of one another in vivo. We also show that Ring1b occupies key Runx1 binding sites in primary murine thymocytes and that this occurs via Polycomb Repressive Complex 2 (PRC2) independent mechanisms. Genetic depletion of Runx1 results in reduced Ring1b binding at these sites in vivo. These findings provide evidence for site-specific PRC1 chromatin recruitment by core binding transcription factors in mammalian cells. **Overall design:** shRNA mediated knockdown of CBFb, Ring1b and control in biological triplicate

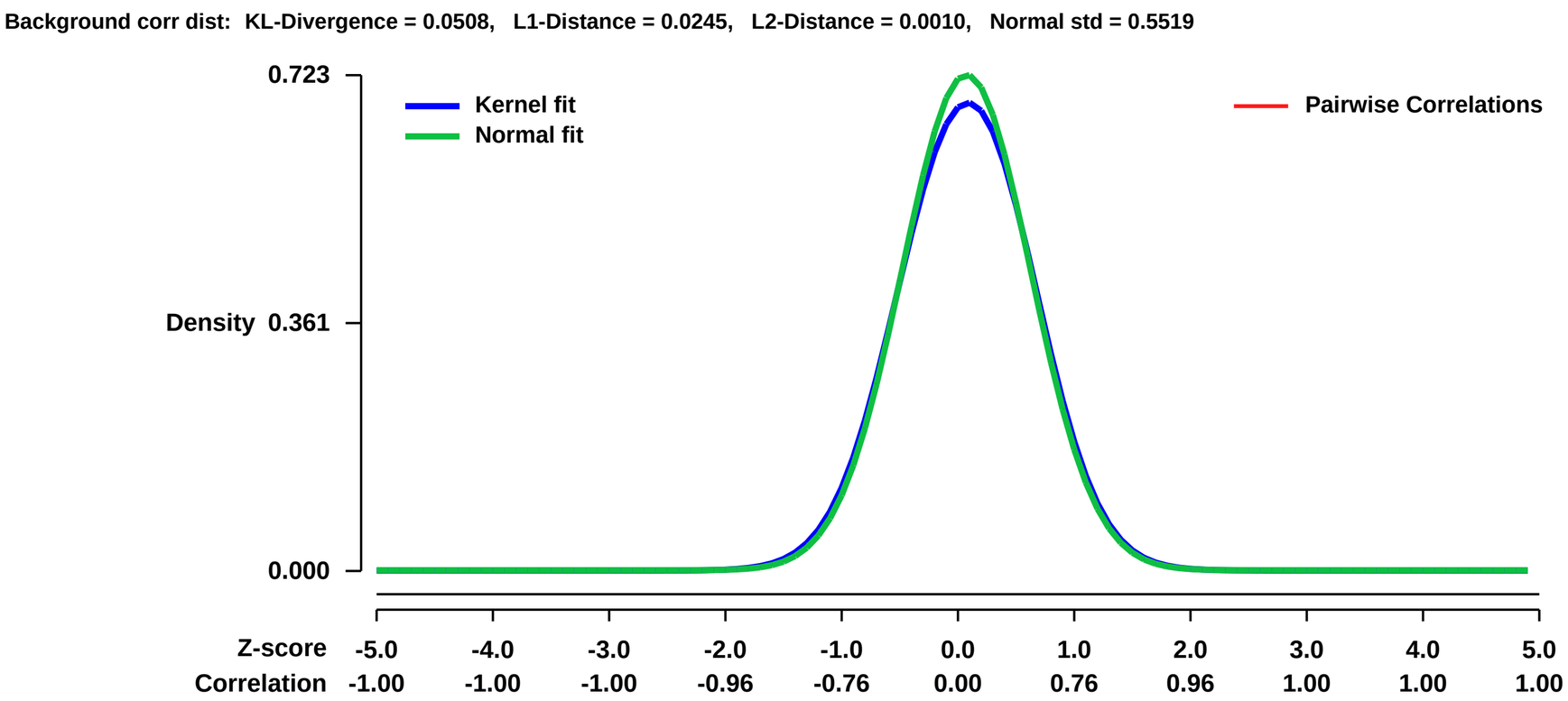

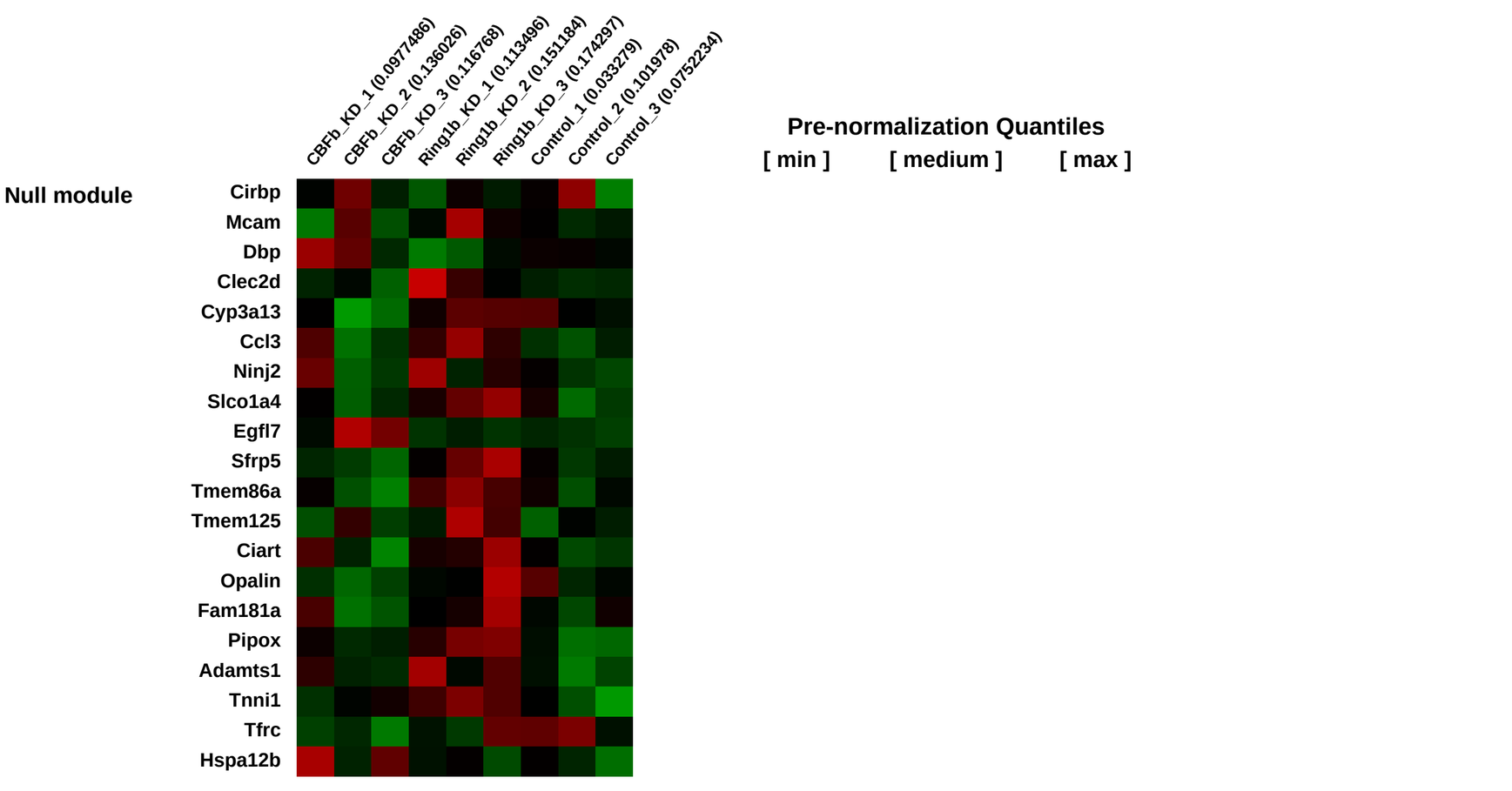

GEO Series "GSE33770" Expression Profiles

Num of samples in this series: 8

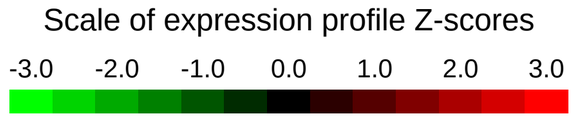

GEO Link:	**http://www.ncbi.nlm.nih.gov/geo/query/acc.cgi?acc=GSE33770**
Status:	**Public on Nov 12 2013**
Title:	**Microarray Studies on the STAT5A MUTANT.**
Organism:	**Mus musculus**
Experiment type:	**Expression profiling by array**
Platform:	**GPL1261**
Pubmed ID:	
Summary & Design:	**Summary:** **Stat5+/- mice were bred into the C57BL/6 background. Stat5+/- mice were intercrossed and mouse embryonic fibroblasts (MEFs) were isolated from 12.5-13.5-day WT or Stat5-/- fetuses. The retroviral-expression vector carrying a DNA binding domain mutant Stat5A (E437/E438?AA) or tyrosine-phosphorylated Stat5A Y694F mutation based on an MSCV-IRES-GFP backbone (gift from Richard Moriggl, Ludwig-Boltzmann Institute, Vienna, Austria) was infected into Stat5-/- MEFs. FACS was used to select GFP+ cells. After 5 hours starvation in serum free medium with 0.1% of BSA, MEFs were treated with growth hormone for 2 hours. Total cellular RNA from each group of the MEFs was extracted with TRIzol reagent (Invitrogen) according to the manufacturer's instructions. Microarray analyses were performed using Affymetrix Mouse Genome 430 2.0 GeneChips (Affymetrix, Santa Clara, CA) (four groups, biological replicates for each group). Expression values were determined with GeneChip Operating Software (GCOS) v1.1.1 software. RMA signals were summarized using GeneSpring GX 10.0.1 (Agilent) and normalized by quantile normalization. All data analysis was performed with GeneSpring software GX 10.01.** **Overall design:** **Total 4 groups (EA, EA_GH, YF, YF_GH), biological duplicate replication for each group**

Background corr dist: KL-Divergence = 0.0380, L1-Distance = 0.0916, L2-Distance = 0.0110, Normal std = 0.7913

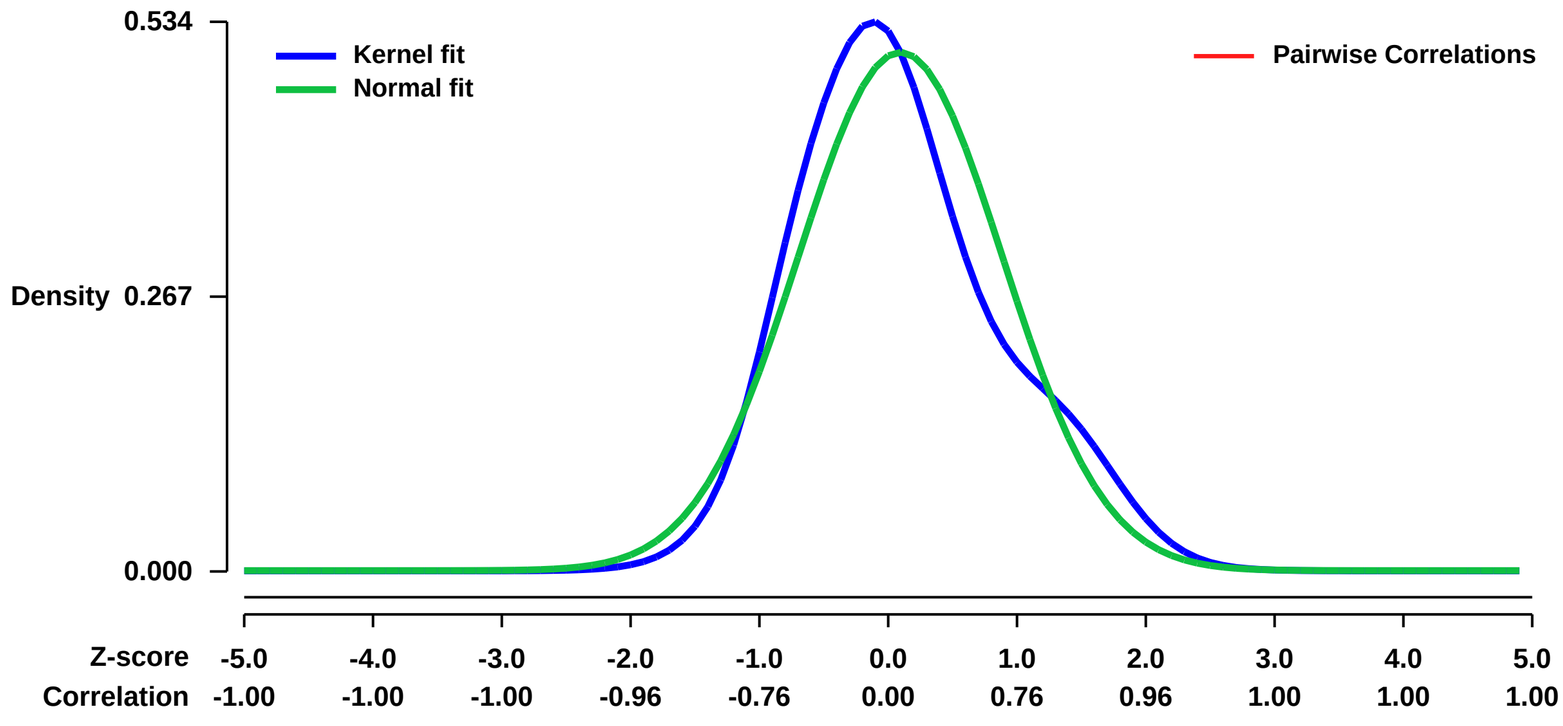

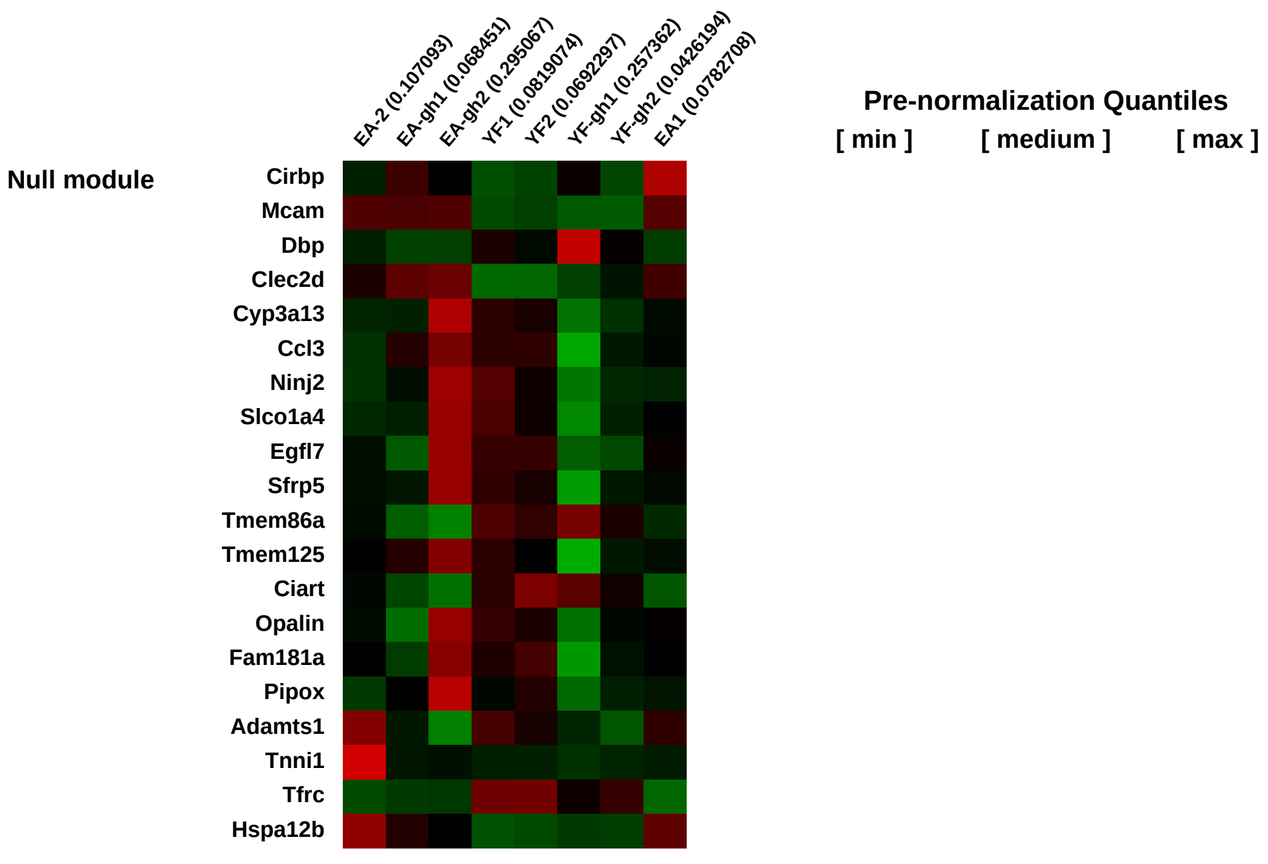

GEO Series "GSE33942" Expression Profiles

Num of samples in this series: 12

Scale of expression profile Z-scores

-3.0 -2.0 -1.0 0.0 1.0 2.0 3.0

GEO Link:	**http://www.ncbi.nlm.nih.gov/geo/query/acc.cgi?acc=GSE33942**
Status:	**Public on Feb 29 2012**
Title:	**Role of PKD2 in TCR-induced transcriptional reprogramming of naˆflve T cells**
Organism:	**Mus musculus**
Experiment type:	**Expression profiling by array**
Platform:	**GPL1261**
Pubmed ID:	**23525088**
Summary & Design:	**Summary:** **Comparison of transcriptional profile of TCR stimulated P14-TCR wild-type and P14-PKD2 null murine lymph node cells** **Overall design:** **Lymph node cells from 3 biological replicates (3 wild-type and 3 PKD2 null mice) were isolated and left unstimulated or stimulated for 4 hours with antigenic peptide (gp33-41) prior to RNA extraction and hybridization to Affymetrix microarray.**

Background corr dist: **KL-Divergence = 0.0765, L1-Distance = 0.0838, L2-Distance = 0.0107, Normal std = 0.5803**

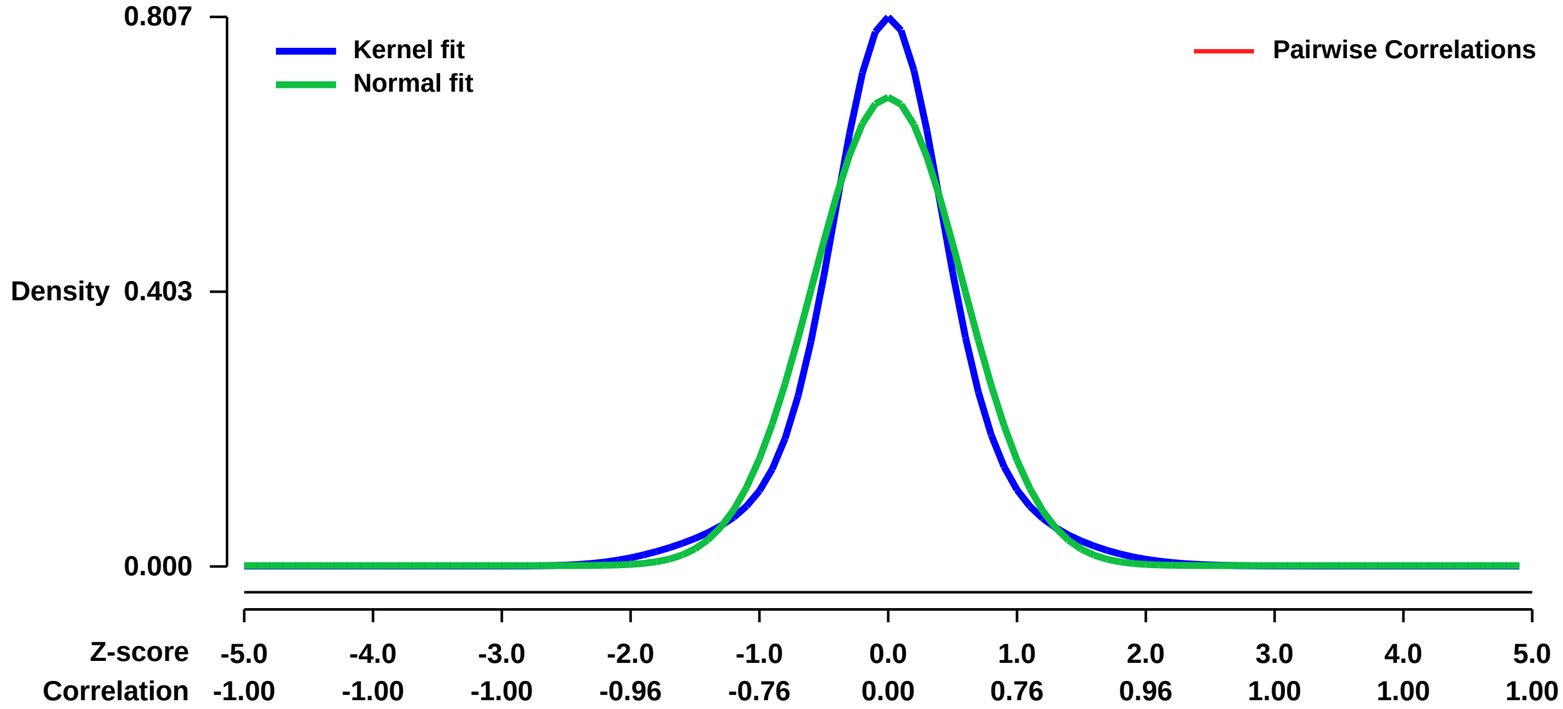

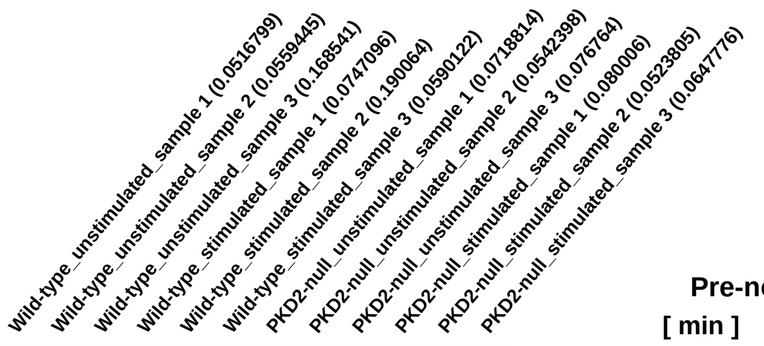

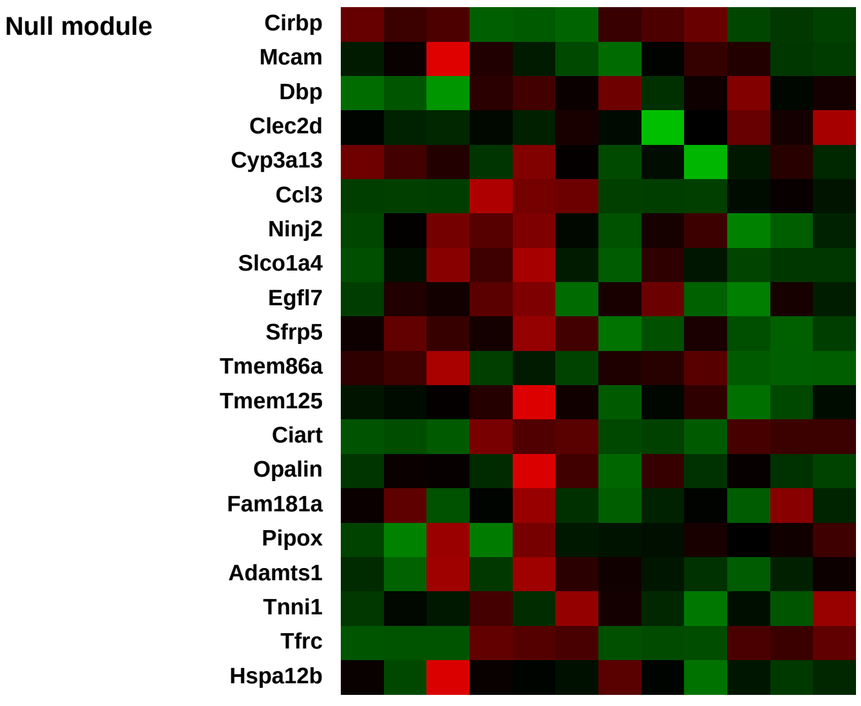

GEO Series "GSE34064" Expression Profiles

Num of samples in this series: 6

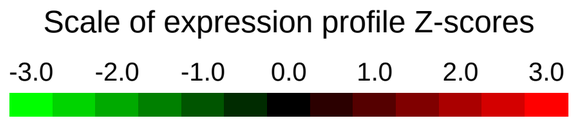

GEO Link:	**http://www.ncbi.nlm.nih.gov/geo/query/acc.cgi?acc=GSE34064**
Status:	**Public on Jan 01 2013**
Title:	**Expression data from mesodermal Tbx1-knockout otic vesicles at E11.5**
Organism:	**Mus musculus**
Experiment type:	**Expression profiling by array**
Platform:	**GPL1261**
Pubmed ID:	
Summary & Design:	**Summary:** **The T-box transcription factor Tbx1 is expressed in the otic vesicle and surrounding periotic mesenchyme during inner ear development. Mesenchymal Tbx1 is essential for inner ear development, with conditional mutants displaying defects in both auditory and vestibular systems. We have previously identified reduced expression of retinoic acid metabolic genes in the periotic mesenchyme of mesoderm conditional Tbx1 mutants, using the T-Cre mouse line, implicating retinoic acid in mesenchymal-epithelial signaling downstream of Tbx1 in the periotic mesenchyme.** **In order to identify downstream effectors of mesenchymal-epithelial signaling downstream of mesenchymal Tbx1, we have utilized a gene profiling approach comparing embryonic day 11.5 otic vesicle tissue from T-Cre-mediated conditional Tbx1 mutants (Mest-KO) and conditional heterozygous control litter mates (control).** **Overall design:** **E11.5 T-Cre-mediated conditional Tbx1 mutants (Mest-KO) and control (T-Cre conditional Tbx1 heterozygotes) embryos were microdissected to isolate the otic vesicle. Left and right ears from 3 embryos of the same genotype were pooled for each chip.**

Background corr dist: KL-Divergence = 0.0459, L1-Distance = 0.0284, L2-Distance = 0.0011, Normal std = 0.5991

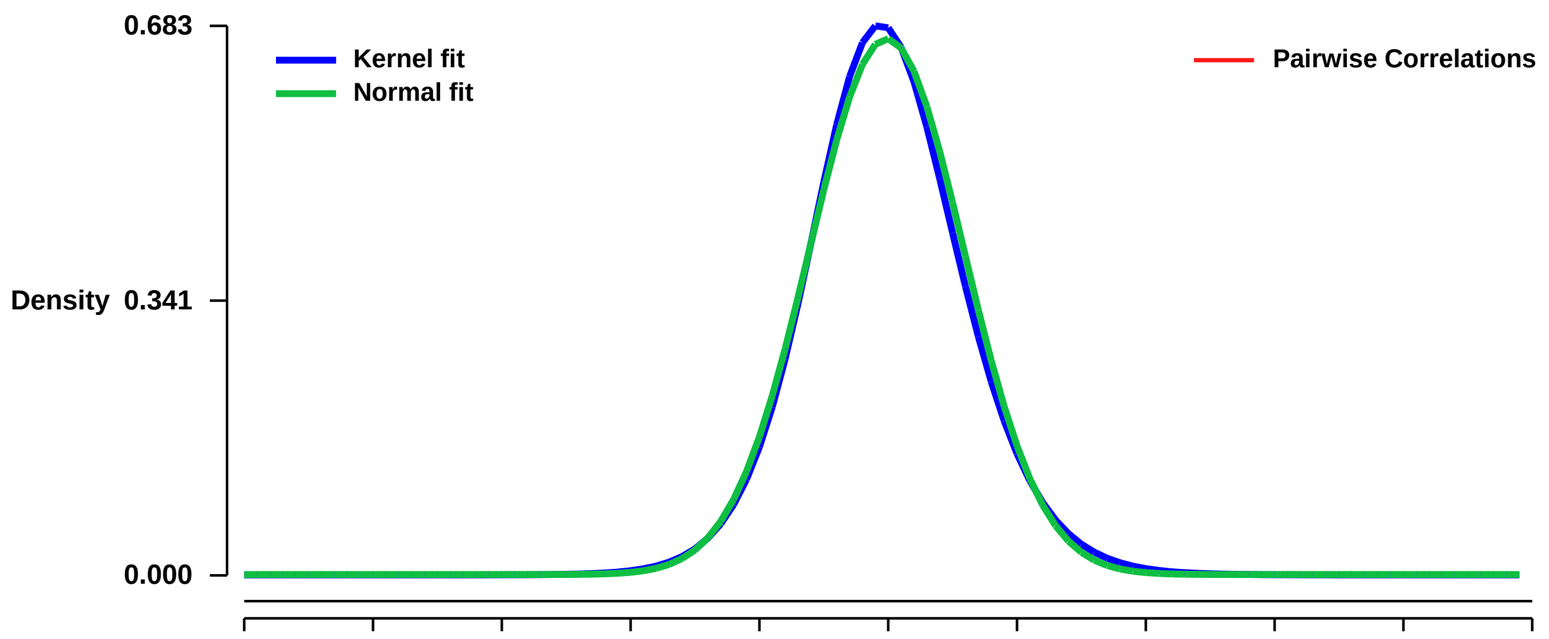

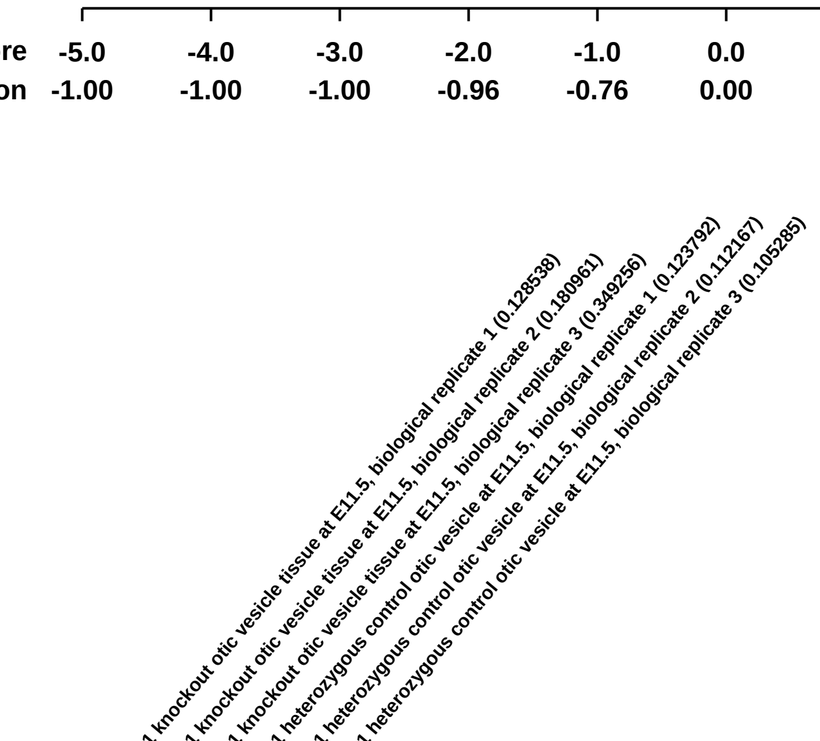

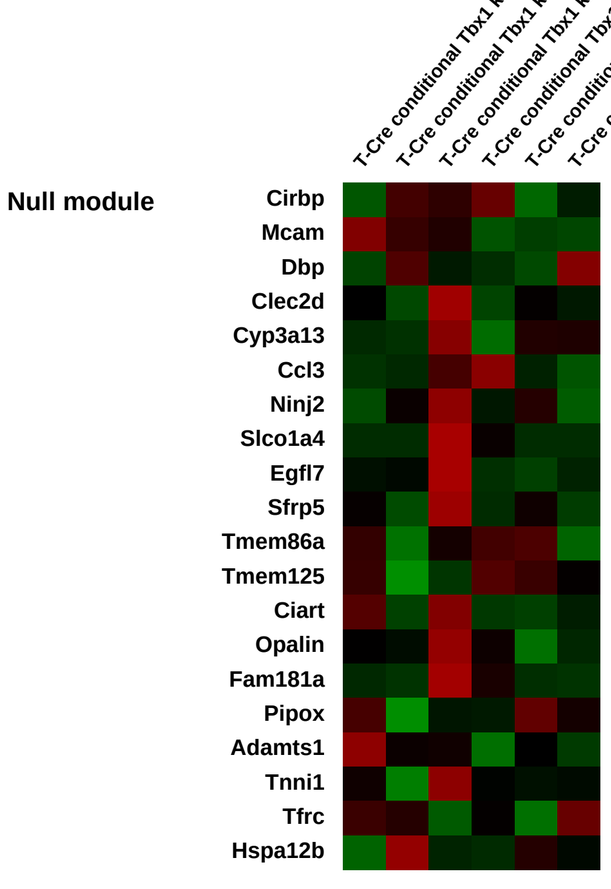

GEO Series "GSE34065" Expression Profiles

Num of samples in this series: 6

Scale of expression profile Z-scores

-3.0 -2.0 -1.0 0.0 1.0 2.0 3.0

GEO Link:	http://www.ncbi.nlm.nih.gov/geo/query/acc.cgi?acc=GSE34065
Status:	Public on Jan 01 2013
Title:	Expression data from mesodermal Tbx1-knockout otic vesicles and periotic mesenchyme at E11.5
Organism:	Mus musculus
Experiment type:	Expression profiling by array
Platform:	GPL1261
Pubmed ID:	
Summary & Design:	**Summary:** **The T-box transcription factor Tbx1 is expressed in the otic vesicle and surrounding periotic mesenchyme during inner ear development. Mesenchymal Tbx1 is essential for inner ear development, with conditional mutants displaying defects in both auditory and vestibular systems. We have previously identified reduced expression of retinoic acid metabolic genes in the periotic mesenchyme of mesoderm conditional Tbx1 mutants, using the T-Cre mouse line, implicating retinoic acid in mesenchymal-epithelial signaling downstream of Tbx1 in the periotic mesenchyme.** **In order to identify downstream effectors of mesenchymal-epithelial signaling downstream of mesenchymal Tbx1, we have utilized a gene profiling approach comparing embryonic day 11.5 otic vesicle and surrounding periotic mesenchyme from T-Cre-mediated conditional Tbx1 mutants (Mest-KO) and conditional heterozygous control litter mates (control). This data was used in conjunction with OV-only data (GSE34064) to identify expression changes within the periotic mesenchyme.** **Overall design:** **E11.5 T-Cre-mediated conditional Tbx1 mutants (Mest-KO) and control (T-Cre conditional Tbx1 heterozygotes) embryos were microdissected to isolate the otic vesicle and surrounding periotic mesenchyme. Left and right ears from 3 embryos of the same genotype were pooled for each chip, and 3 biological replicates of each chip were performed.**

Background corr dist: KL-Divergence = 0.0473, L1-Distance = 0.0220, L2-Distance = 0.0006, Normal std = 0.5858

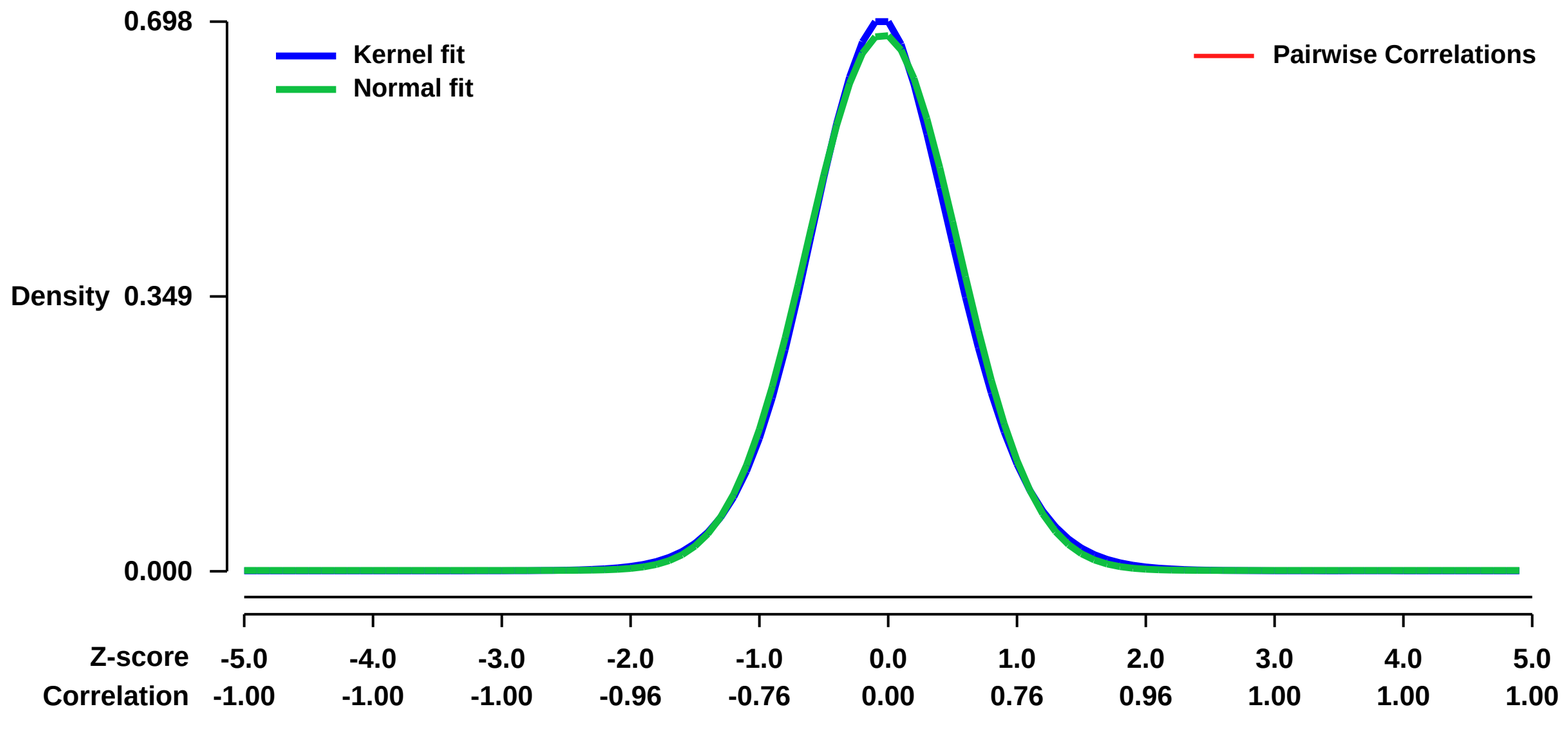

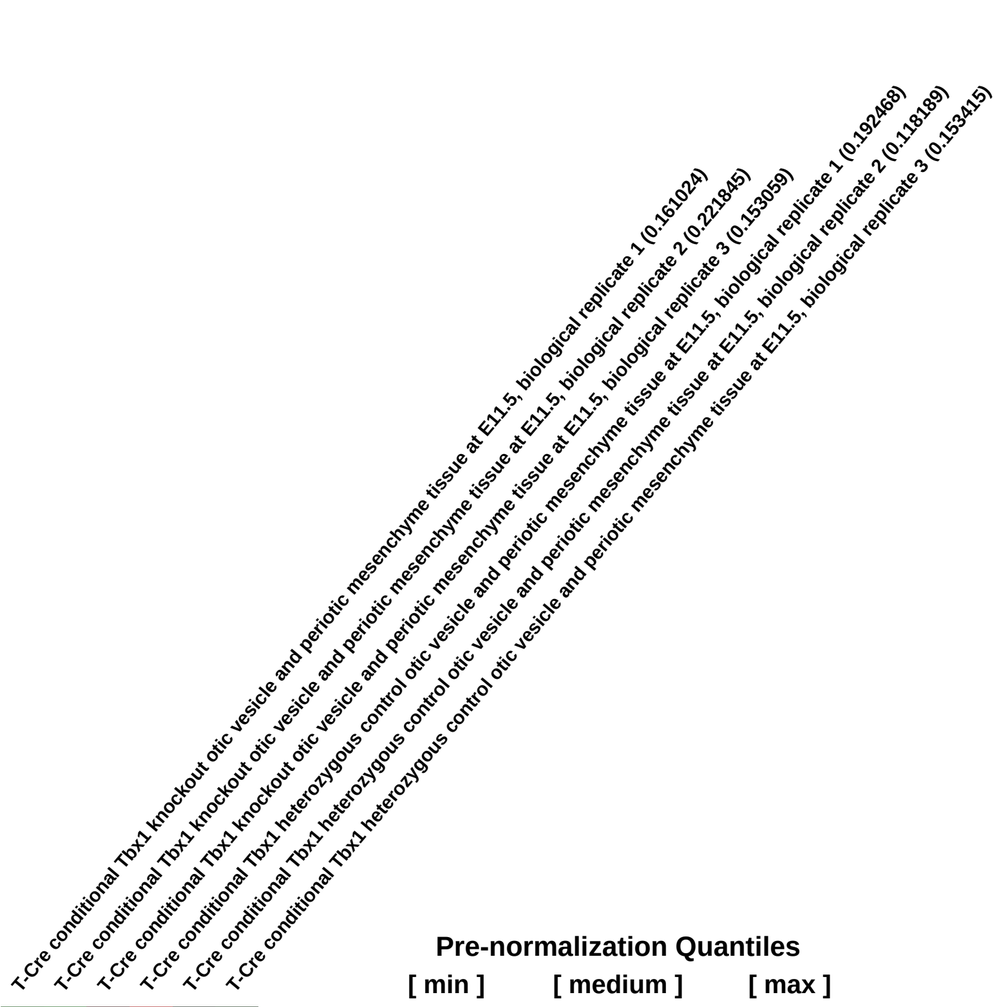

Pre-normalization Quantiles

[min] [medium] [max]

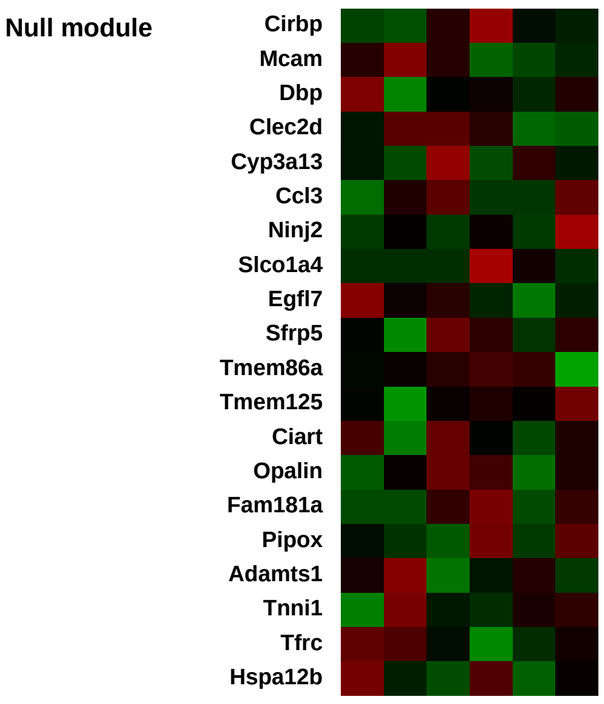

GEO Series "GSE34091" Expression Profiles

Num of samples in this series: 8

Scale of expression profile Z-scores

-3.0 -2.0 -1.0 0.0 1.0 2.0 3.0

GEO Link:	**http://www.ncbi.nlm.nih.gov/geo/query/acc.cgi?acc=GSE34091**
Status:	**Public on Jul 25 2012**
Title:	**Nucleosome dynamics specifies genome-wide binding of the male germ cell gene regulator CTCFL and of CTCF [Mouse430_2 Expression]**
Organism:	**Mus musculus**
Experiment type:	**Expression profiling by array**
Platform:	**GPL1261**
Pubmed ID:	**22709888**
Summary & Design:	**Summary:** **The effect of CTCFL mutation on the transcriptional program in testes** **Overall design:** **Testis RNA extracted from CTCFL wildtype and mutant mice was hybridized on Affymetrix Mouse430_2 arrays**

Background corr dist: **KL-Divergence = 0.0649, L1-Distance = 0.0180, L2-Distance = 0.0003, Normal std = 0.5147**

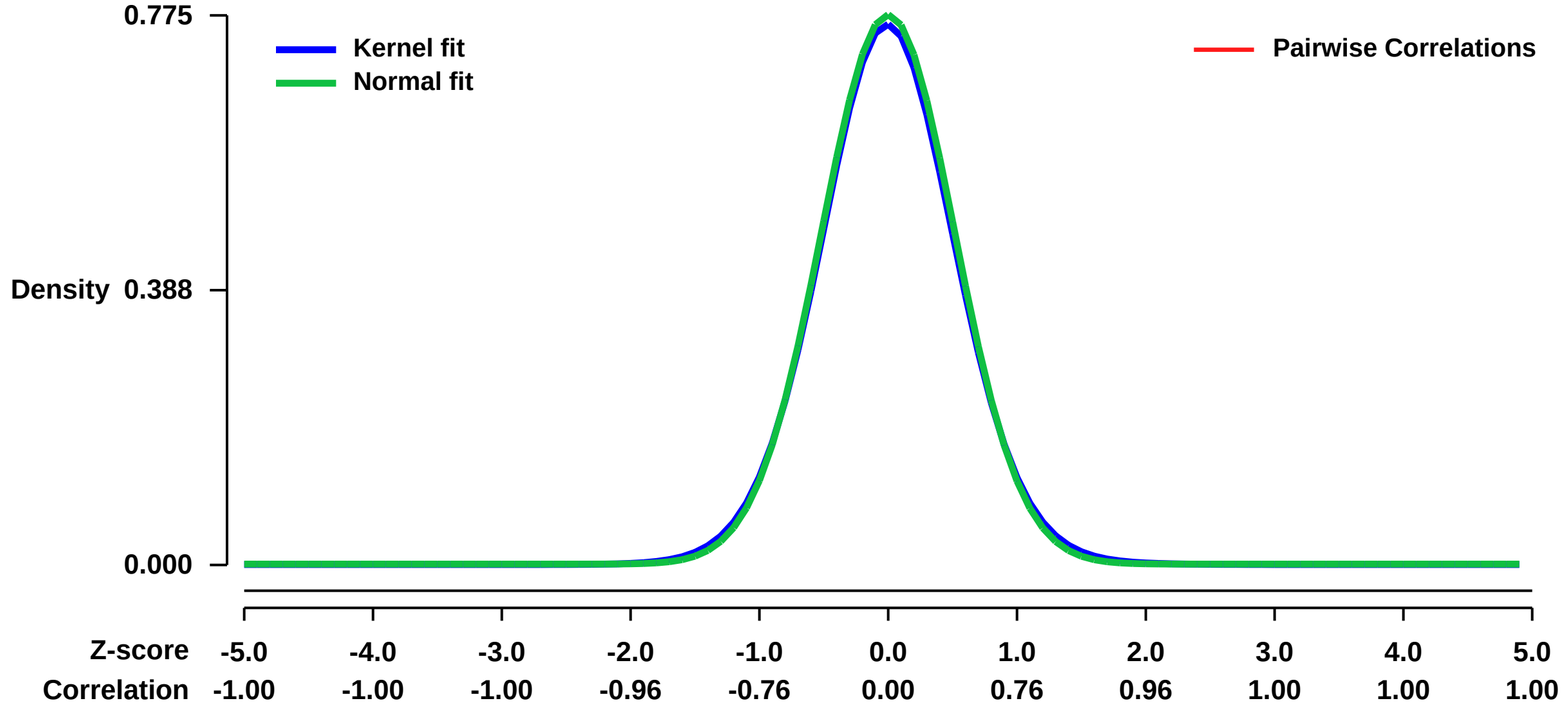

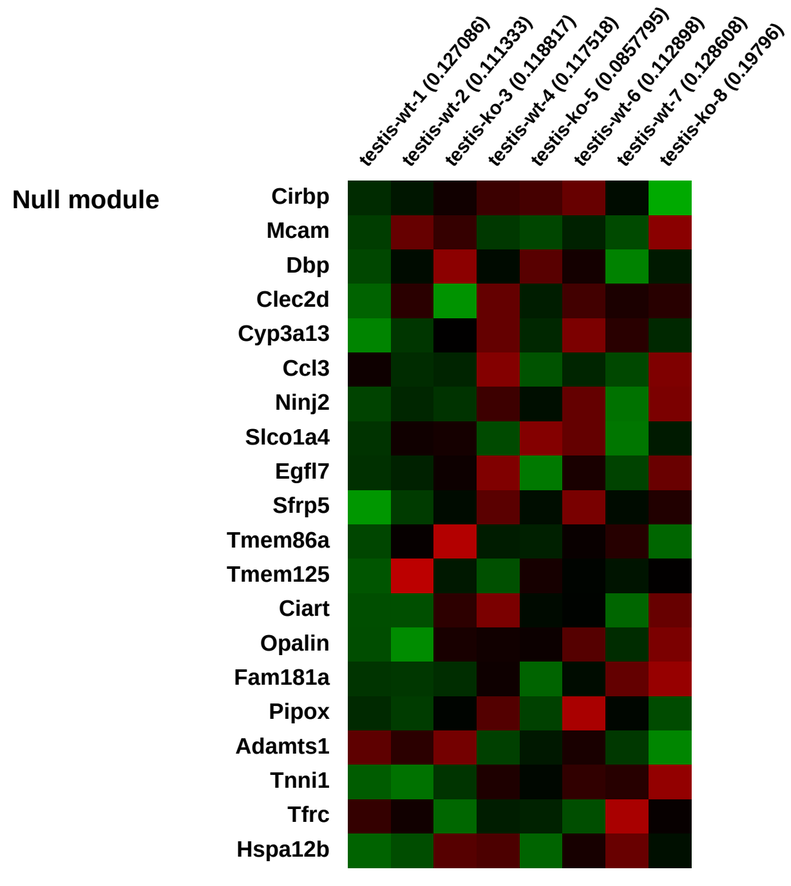

GEO Series "GSE34114" Expression Profiles

Num of samples in this series: 12

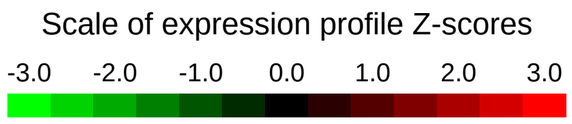

GEO Link:	**http://www.ncbi.nlm.nih.gov/geo/query/acc.cgi?acc=GSE34114**
Status:	**Public on Dec 30 2012**
Title:	**Temporal response of mouse peritoneal cells to a non-pathogenic E. coli infection**
Organism:	**Mus musculus**
Experiment type:	**Expression profiling by array**
Platform:	**GPL1261**
Pubmed ID:	
Summary & Design:	**Summary:** **Analysis of early and late changes in the mouse peritoneal cells in response to E. coli induced sepis. Result provide an insight into the molecular function and pathways expressed at these different time points.** **Overall design:** **The mice were divided in two groups; the first group of mice were not treated with E. coli and was referred to as the naive group. Each mouse of the second group was injected with 2 X108 cells of a non- pathogenic isolate of E. coli suspended in a phosphate buffered saline (PBS) solution. After 1h, 2h and 18h of E. coli administration, peritoneal lavage fluid was obtained from two mice each for E. coli treated group at 1 and 2h and three mice of both groups (control and E. coli treated) at 18h. A common naive group of 2 mice harvested at 2h served as a control for both 1h and 2h.**

Background corr dist: **KL-Divergence = 0.0819, L1-Distance = 0.0275, L2-Distance = 0.0011, Normal std = 0.4862**

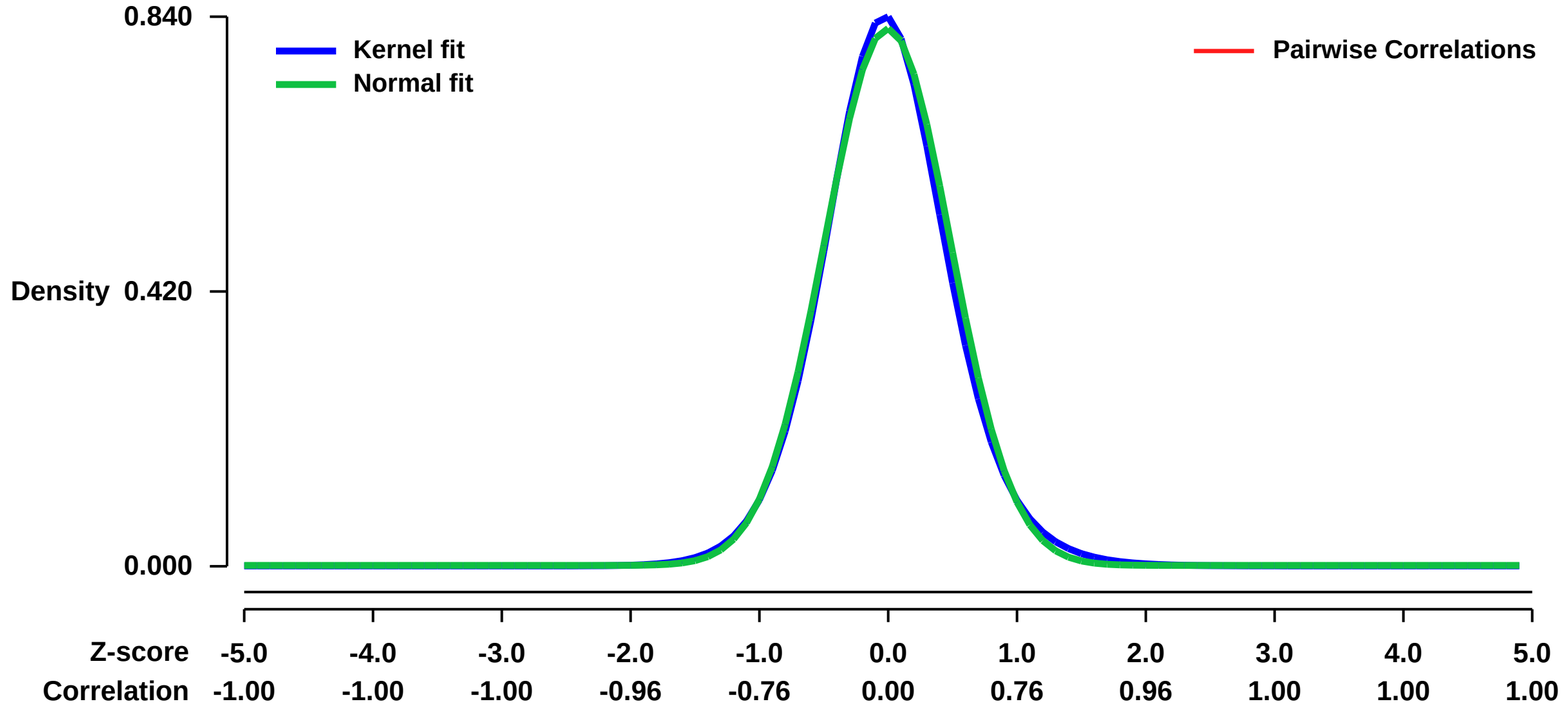

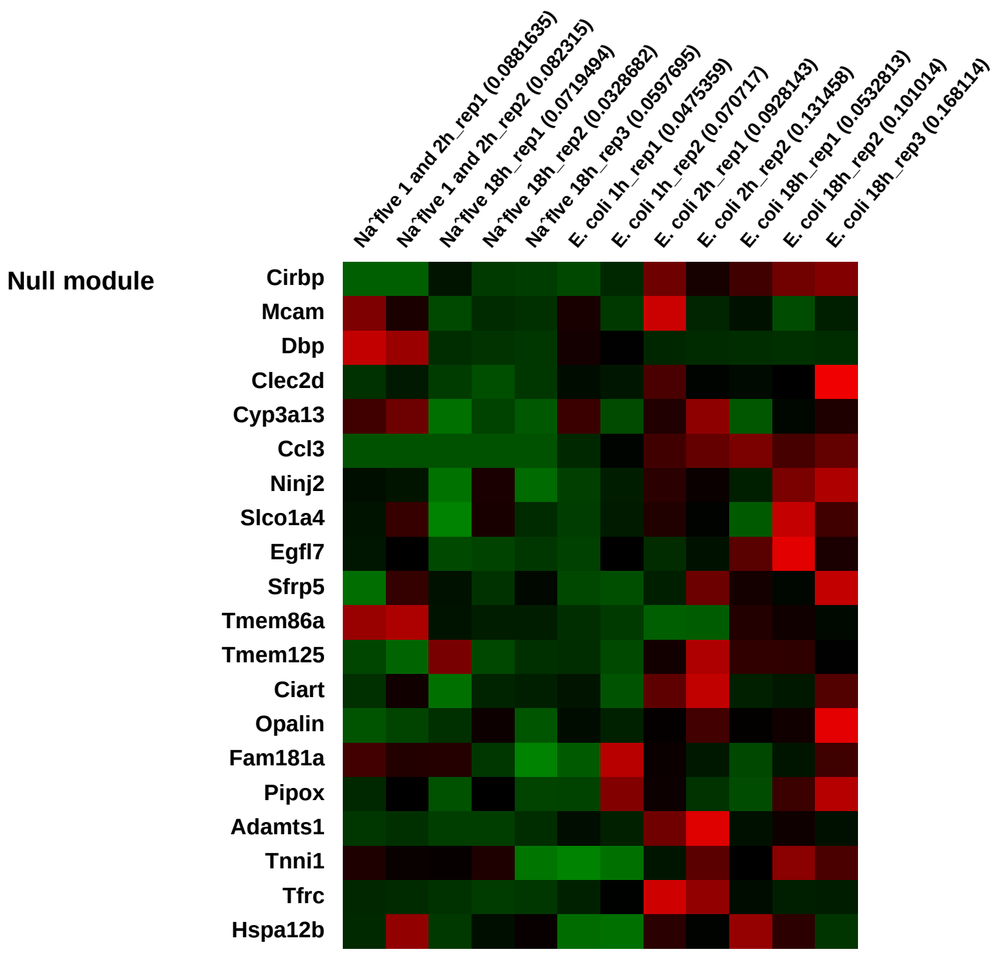

GEO Series "GSE34189" Expression Profiles

Num of samples in this series: 6

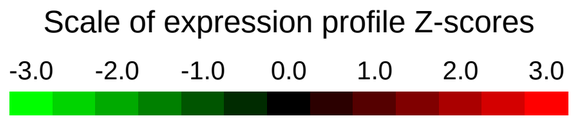

GEO Link:	**http://www.ncbi.nlm.nih.gov/geo/query/acc.cgi?acc=GSE34189**
Status:	**Public on Dec 07 2011**
Title:	**Neural invasion induces cachexia via astrocytic activation of neural route in pancreatic cancer**
Organism:	**Mus musculus**
Experiment type:	**Expression profiling by array**
Platform:	**GPL1261**
Pubmed ID:	
Summary & Design:	**Summary:** **Pancreatic cancer is characterized by a high frequency of cachexia, pain and neural invasion (N-inv). Neural damage is occurred by N-inv and modulates pain and muscle atrophy via the activation of astrocyte in the connected spine. The activated astrocyte by N-inv, thus, may affect cachexia in pancreatic cancer. Clinical studies in patients and autopsy cases with pancreatic cancer have revealed that N-inv is related to cachexia and astrocytic activation. We established a novel murine model of cancer cachexia using N-inv of human pancreatic cancer cells. Mice with N-inv showed a loss of body weight, skeletal muscle, and fat mass without appetite loss, which are compatible with an animal model of cancer cachexia. Activation of astrocytes in the spinal cord connected with N-inv was observed in our model. Experimental cachexia was suppressed by disrupting neural routes or inhibiting the activation of astrocytes. These data provide the first evidence that N-inv induces cachexia via astrocytic activation of neural route in pancreatic cancer.** **Overall design:** **We produced neural invasion (N-inv) model using intraneural injection of Capan-1 cells to left sciatic nerve of male SCID mouse. For controls, subcutaneous model (SC) and PBS model were produced. Microarray analysis was performed using the first lumbar cord (L1) from PBS, SC, and N-inv mice at 6 w (n = 2 each).**

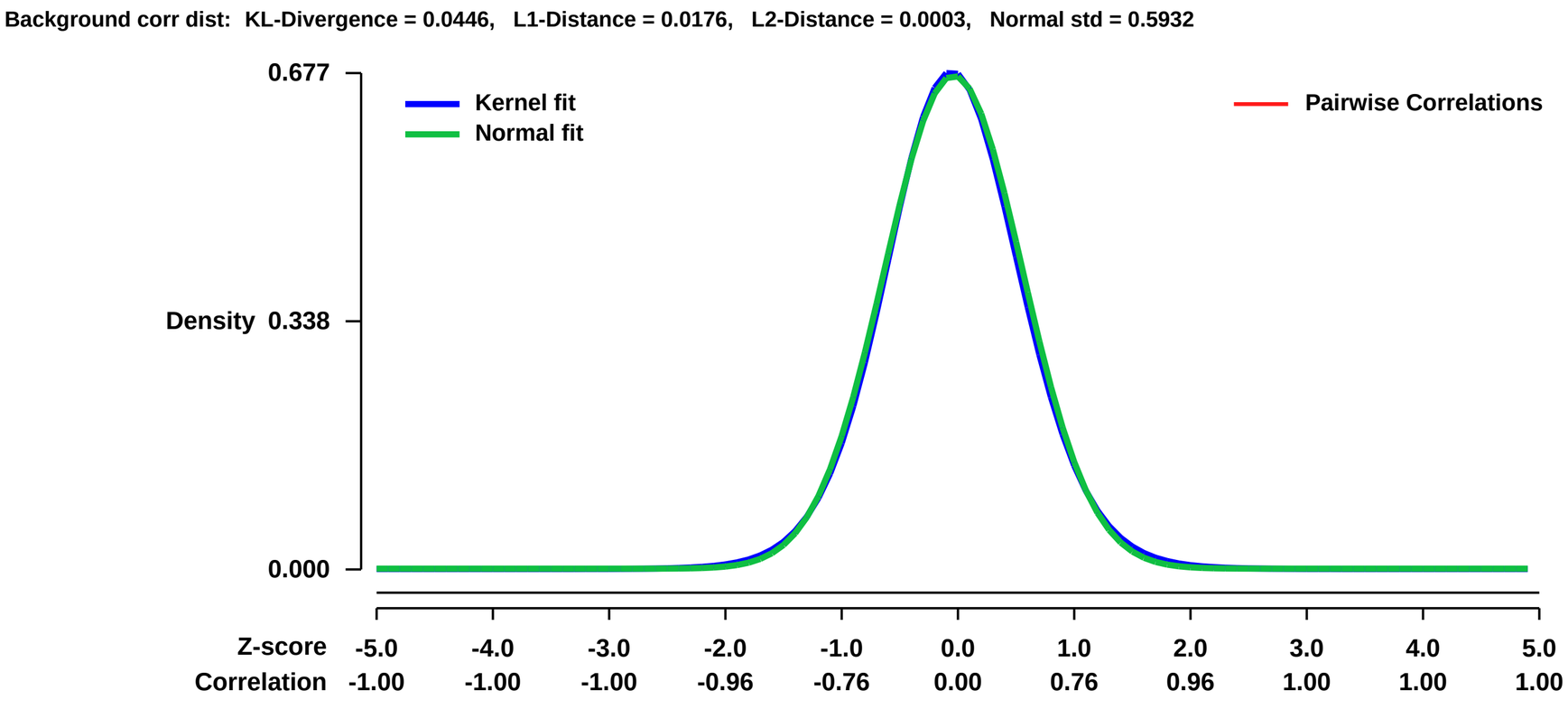

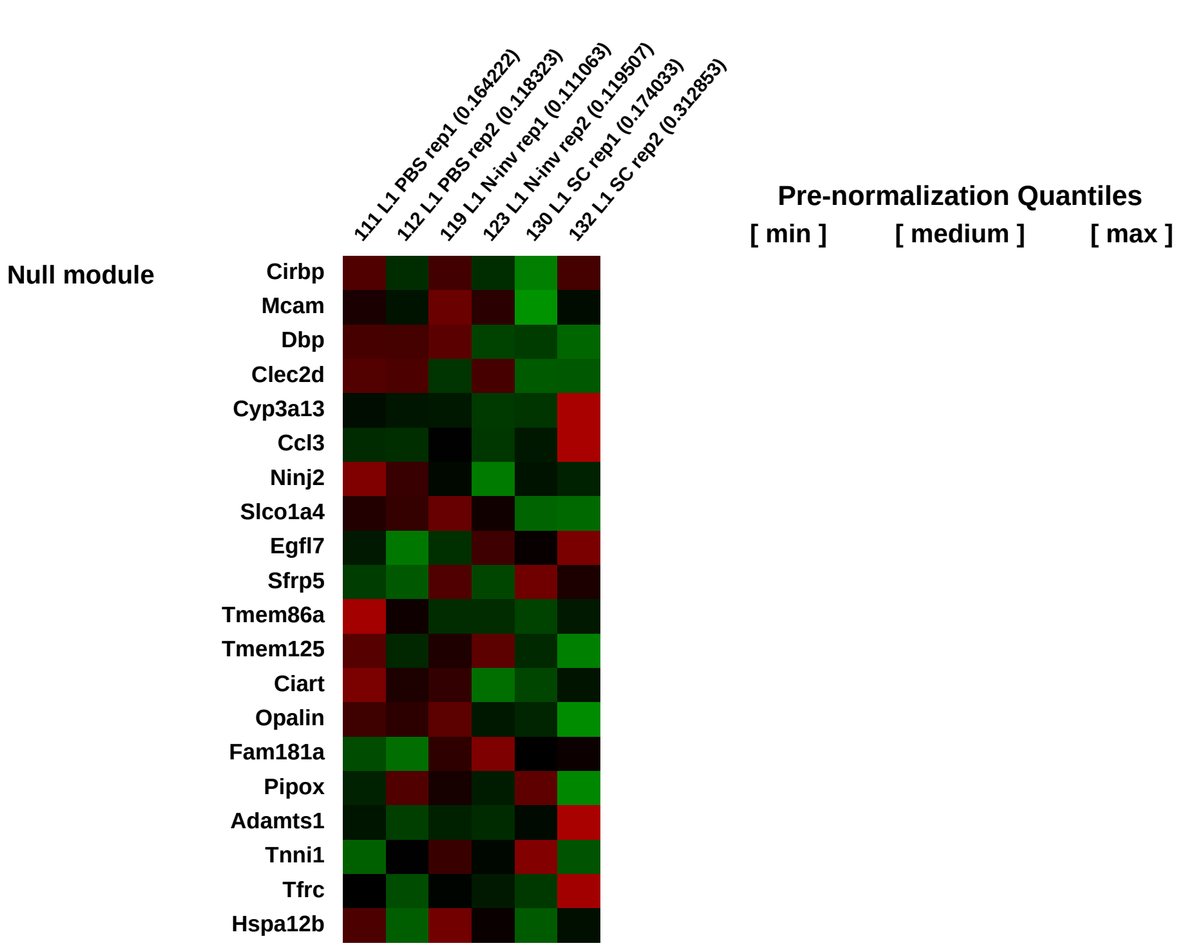

GEO Series "GSE34206" Expression Profiles

Num of samples in this series: 8

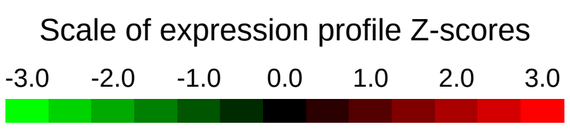

GEO Link:	http://www.ncbi.nlm.nih.gov/geo/query/acc.cgi?acc=GSE34206
Status:	Public on Dec 07 2011
Title:	Gene regulation in macrophages from irradiated tumors
Organism:	Mus musculus
Experiment type:	Expression profiling by array
Platform:	GPL1261
Pubmed ID:	22761754
Summary & Design:	**Summary:** Tumors engender an environment dominated by M2 differentiated tumor macrophages that support tumor invasion, metastases and escape from immune control. In this study, we demonstrate that following radiation therapy of tumors in mice there is an influx of tumor macrophages that polarize towards wound repair and immune suppression. To investigate changes in the phenotype of tumor macrophages following radiation therapy, we FACS sorted tumor macrophages from Panc02 tumors. We have previously shown that we can distinguish mature tumor macrophages from immature myeloid and MDSC populations by expression of Gr1 and IA (MHC class II). To isolate these sub-populations, we first gated CD11b+ cells in the untreated or irradiated tumors, then sorted the CD11b+IA+ macrophage population and the CD11b+Gr1hi MDSC population. Cytospins of the sorted populations demonstrates that the CD11b+Gr1hi MDSC predominantly have a granulocyte morphology and the CD11b+IA+ cells have a macrophage morphology in both the untreated and irradiated tumors. RNA was purified from CD11b+IA+ macrophages from untreated or irradiated tumors 1 day or 7 days following radiation therapy and Gene Expression Microarray analysis was performed. **Overall design:** There are untreated and irradiated samples at time points 1 day and 7 days following radiation therapy. The experiment was repeated in entirety, generating a second gene array sample for each. For analysis, the untreated samples of 1 day and 7 days were grouped together.

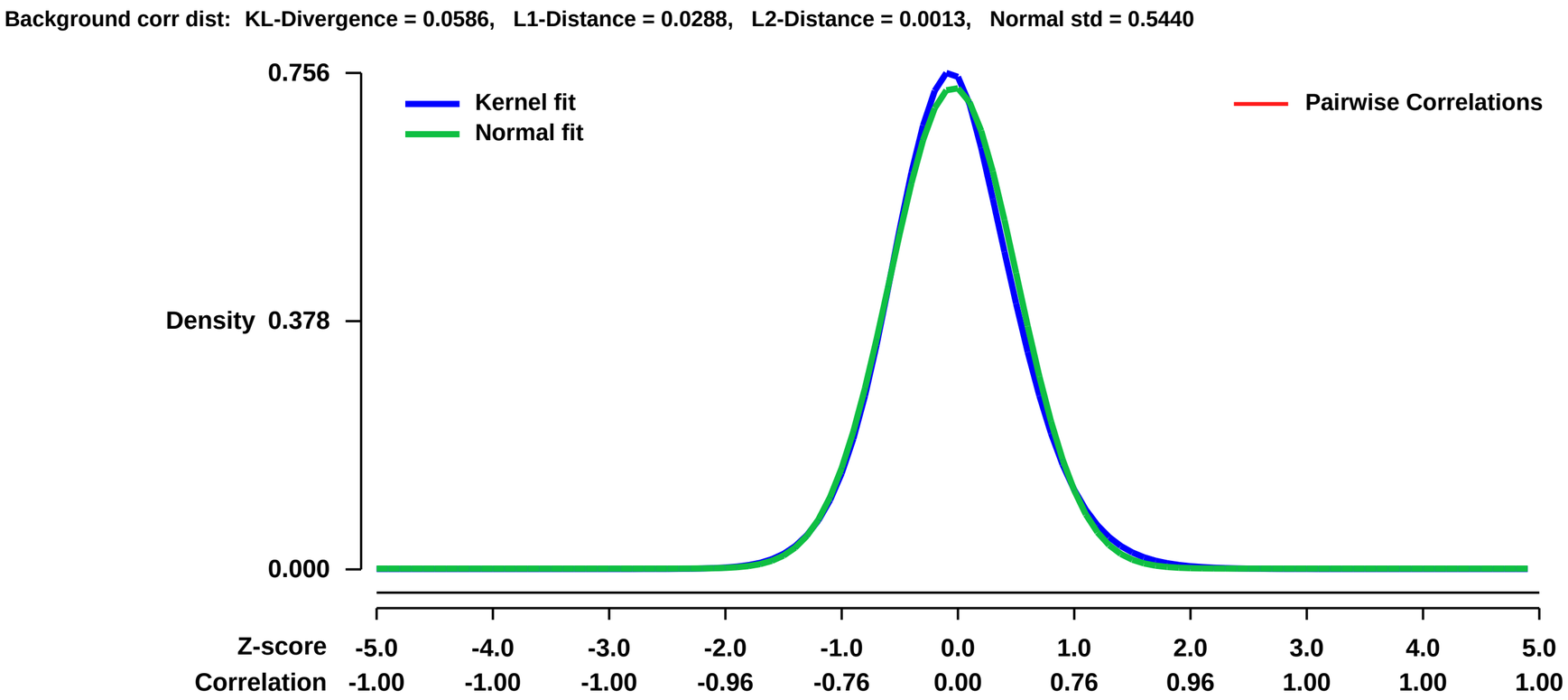

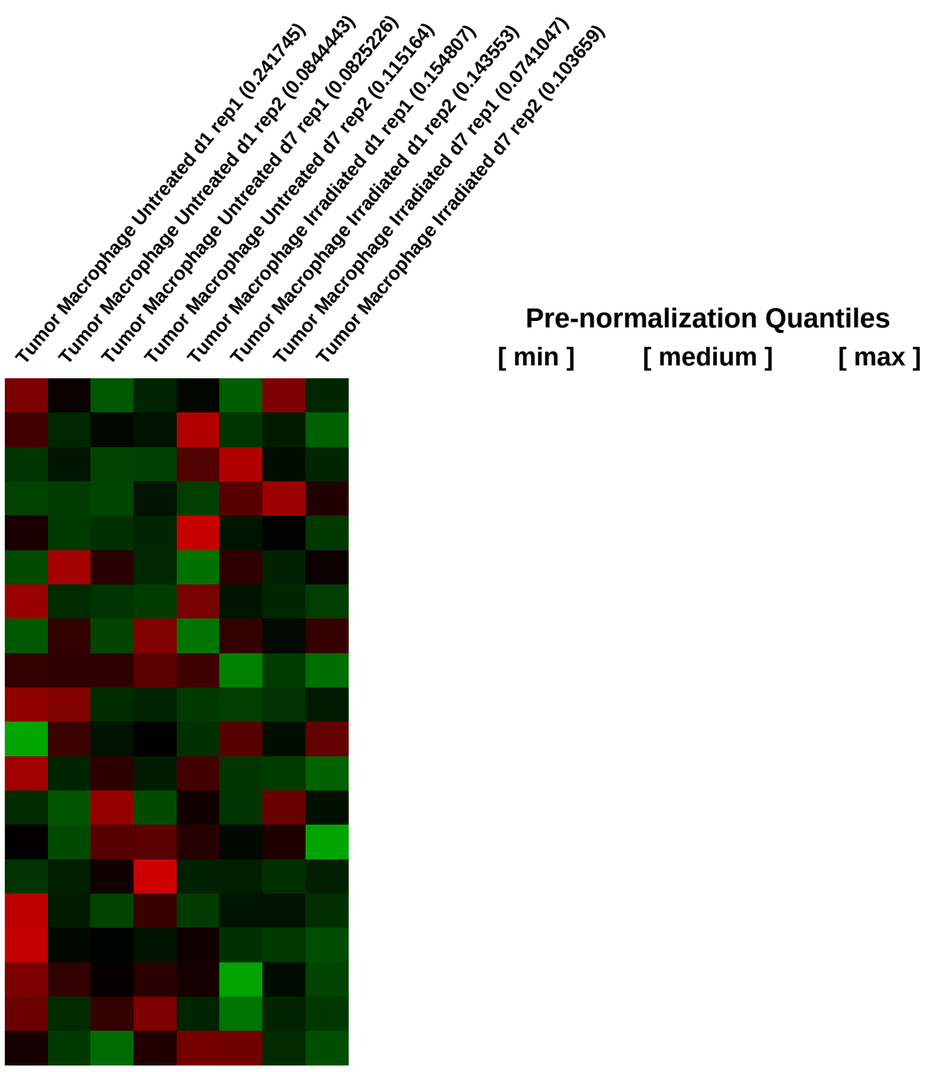

GEO Series "GSE34215" Expression Profiles

Num of samples in this series: 6

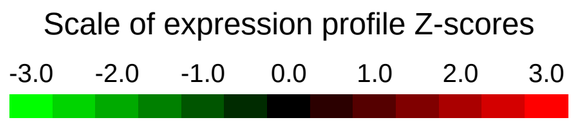

GEO Link:	http://www.ncbi.nlm.nih.gov/geo/query/acc.cgi?acc=GSE34215
Status:	Public on Dec 06 2012
Title:	Knockout of GPx4 gene in mouse keratinocyte
Organism:	Mus musculus
Experiment type:	Expression profiling by array
Platform:	GPL1261
Pubmed ID:	23364477
Summary & Design:	**Summary:** Comparative analysis of gene expression in cultured primary keratinocytes isolated from newborn control (K14-cre; GPx4fl/+) and knockout (K14-cre; GPx4fl/fl) mice. Selenoproteins are essential for skin function, as targeted abolition of selenoproteins in epidermal tissue results in newborn mice manifesting gross abnormalities of skin and hair, accompanied by retarded growth and premature death. To investigate whether lack of a single selenoprotein could induce similar phenotypic effect in mice, we generated keratinocyte-specific knockout mice lacking glutathione peroxidase 4 (GPx4), an essential selenoprotein in skin, to examine phenotypic changes resulting from the lack of GPx4 in skin. Ablation of GPx4 results in focal alopecia and disturbed hair follicle morphogenesis, with GPx4 being essential during early stages of hair follicle morphogenesis as well as for keratinocyte adhesion and proliferation in culture. **Overall design:** We have generated mice with selective removal of the GPx4 gene in keratinocytes under the control of Keratin-14-cre (K14-cre) promoter. Comparative microarray analysis was performed on RNA samples taken from pooled primary keratinocytes from knockout and control mice from the same litter. Array replicates were performed using RNA samples from three different litters.

Background corr dist: KL-Divergence = 0.0401, L1-Distance = 0.0263, L2-Distance = 0.0009, Normal std = 0.6210

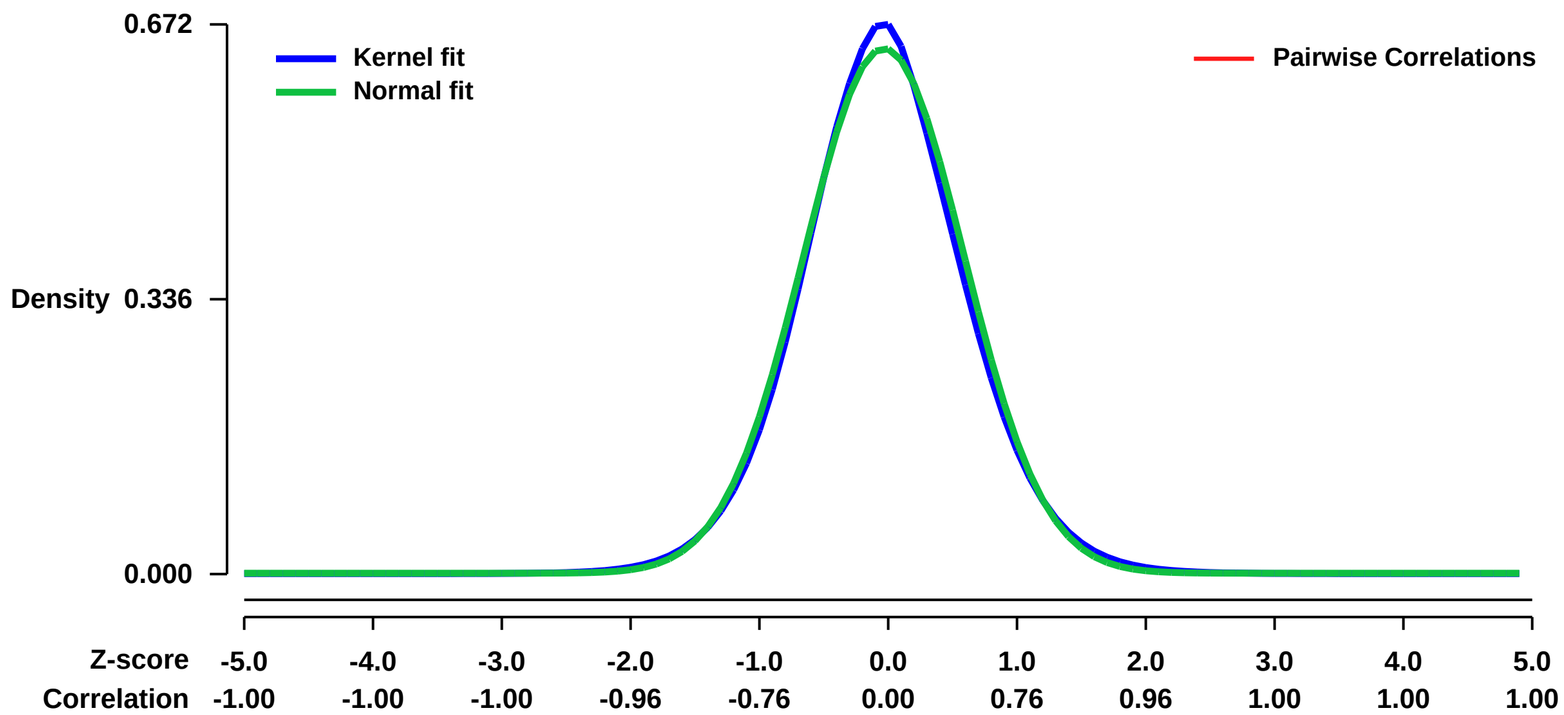

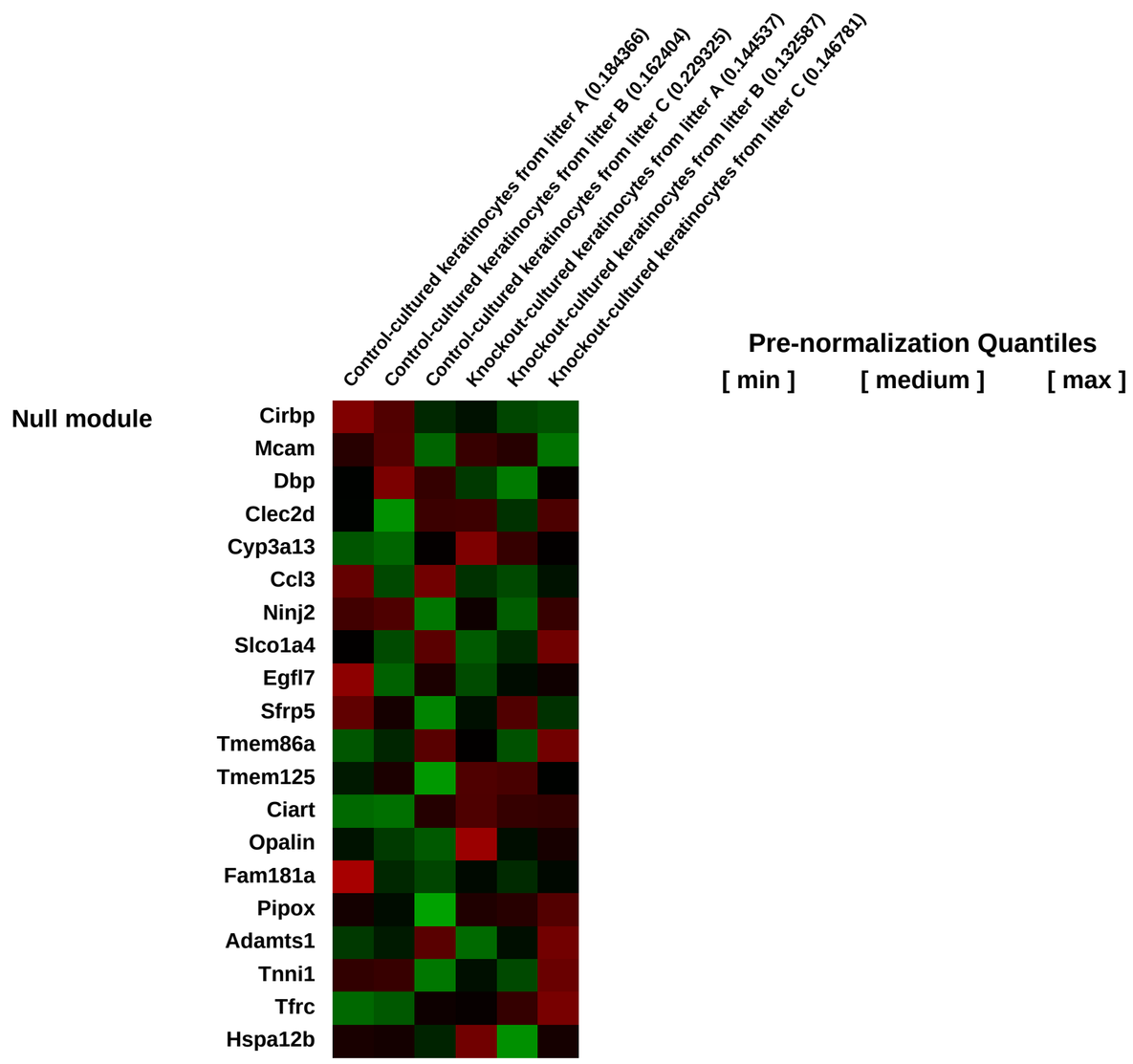

GEO Series "GSE34217" Expression Profiles

Num of samples in this series: 7

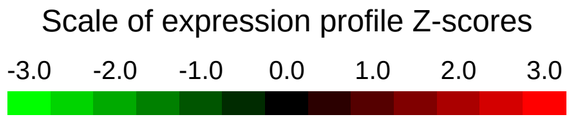

GEO Link:	http://www.ncbi.nlm.nih.gov/geo/query/acc.cgi?acc=GSE34217
Status:	Public on Jun 05 2012
Title:	Expression profile of miR-17-92a-MSCV-IRES-Thy1.1 transduced P14 CD8+ T cells
Organism:	Mus musculus
Experiment type:	Expression profiling by array
Platform:	GPL1261
Pubmed ID:	22665768
Summary & Design:	**Summary:** During acute viral infections, effector CD8+ T cells differentiate into memory precursors or short-lived terminal effectors. miR-17-92a over-expression skews CD8+ effector cells to the terminal differentiation. We used microarray to identify the genes that are differentially expressed caused by miR-17-92a over-expression. **Overall design:** CD8+ T cells from P14 TCR transgenic mice were infected with miR-17-92a-MSCV-IRES-Thy1.1 vector and transfer to C57BL6 recipients. Chimeras were infected with LCMV Armstrong. Thy1.1+ miR-17-92a-MSCV-IRES-Thy1.1 transduced P14 cells and Thy1.1- non-transduced P14 cells were sorted by FACS. RNA was extracted from samples, labeled, and hybridized to Affymetrix microarrays.

Background corr dist: KL-Divergence = 0.0441, L1-Distance = 0.0242, L2-Distance = 0.0007, Normal std = 0.5956

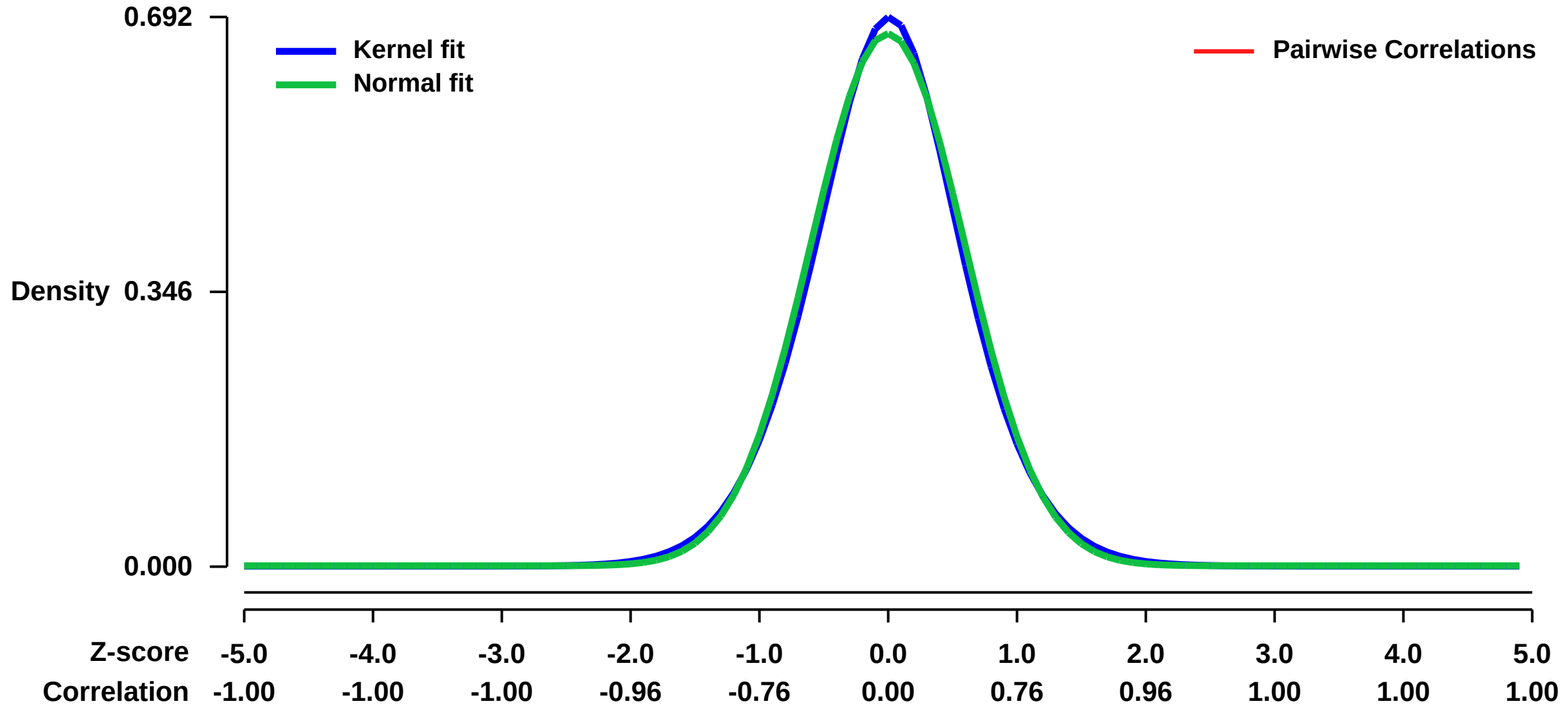

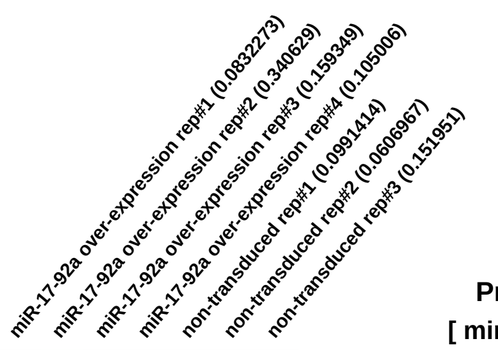

Pre-normalization Quantiles

[min] [medium] [max]

Null module

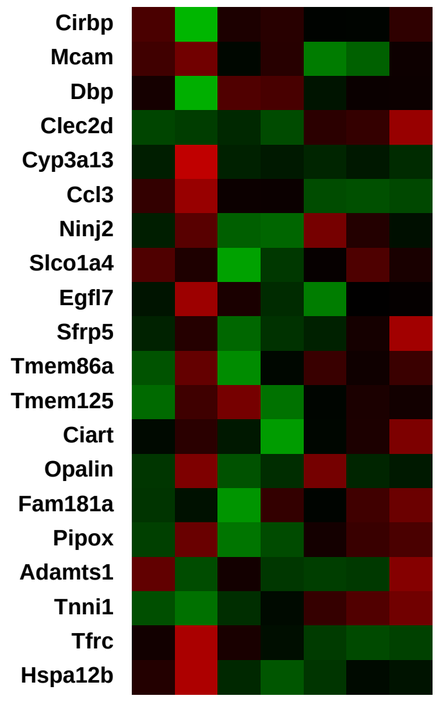

GEO Series "GSE34279" Expression Profiles

Num of samples in this series: 30

Scale of expression profile Z-scores

-3.0 -2.0 -1.0 0.0 1.0 2.0 3.0

GEO Link:	http://www.ncbi.nlm.nih.gov/geo/query/acc.cgi?acc=GSE34279
Status:	Public on Dec 20 2012
Title:	Retinoic acid (RA) induction time-course to profile gene expression during mES cell differentiation
Organism:	Mus musculus
Experiment type:	Expression profiling by array
Platform:	GPL1261
Pubmed ID:	23260668
Summary & Design:	**Summary:** Murine ES cell gene expression before RA induction are used to compare gene expression for time-points of 8, 12, 16, 24, 36, 48, 60 and 72 hours post-induction. **Overall design:** KH2 ES Cell RA Differentiation Time-course

Background corr dist: KL-Divergence = 0.0761, L1-Distance = 0.0220, L2-Distance = 0.0006, Normal std = 0.4833

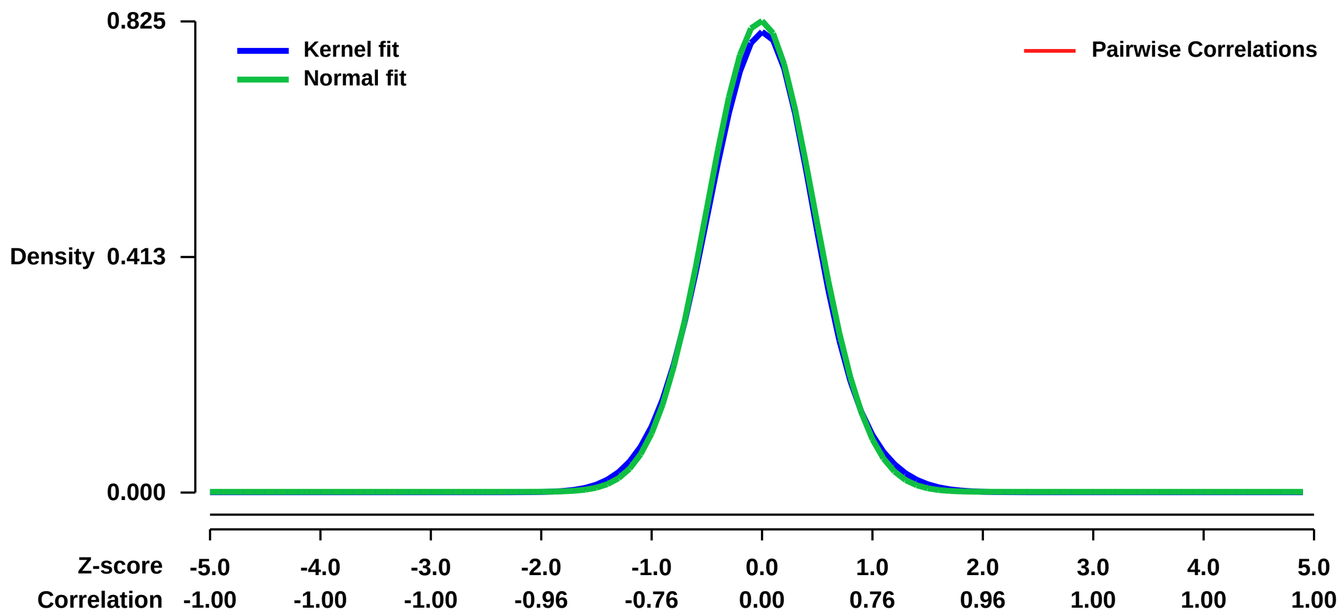

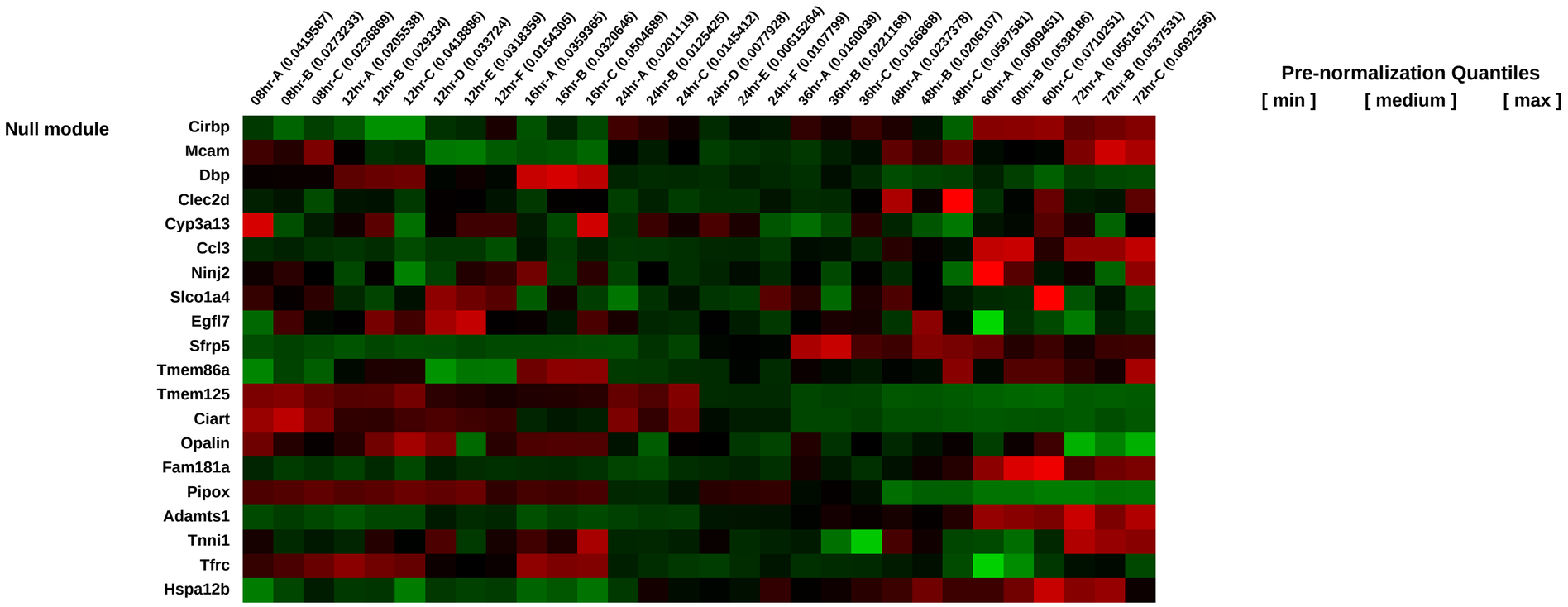

GEO Series "GSE34324" Expression Profiles

Num of samples in this series: 12

Scale of expression profile Z-scores

-3.0 -2.0 -1.0 0.0 1.0 2.0 3.0

GEO Link:	**http://www.ncbi.nlm.nih.gov/geo/query/acc.cgi?acc=GSE34324**
Status:	**Public on Feb 26 2013**
Title:	**Gene expression by Retinoic Acid in mouse Dendritic Cells**
Organism:	**Mus musculus**
Experiment type:	**Expression profiling by array**
Platform:	**GPL1261**
Pubmed ID:	**23322377**
Summary & Design:	**Summary:** **The purpose of this study was to determine and clarify the retinoic effect on the gene expression profile for mouse dendritic cells.** **Overall design:**

Background corr dist: **KL-Divergence = 0.0982, L1-Distance = 0.0355, L2-Distance = 0.0026, Normal std = 0.4484**

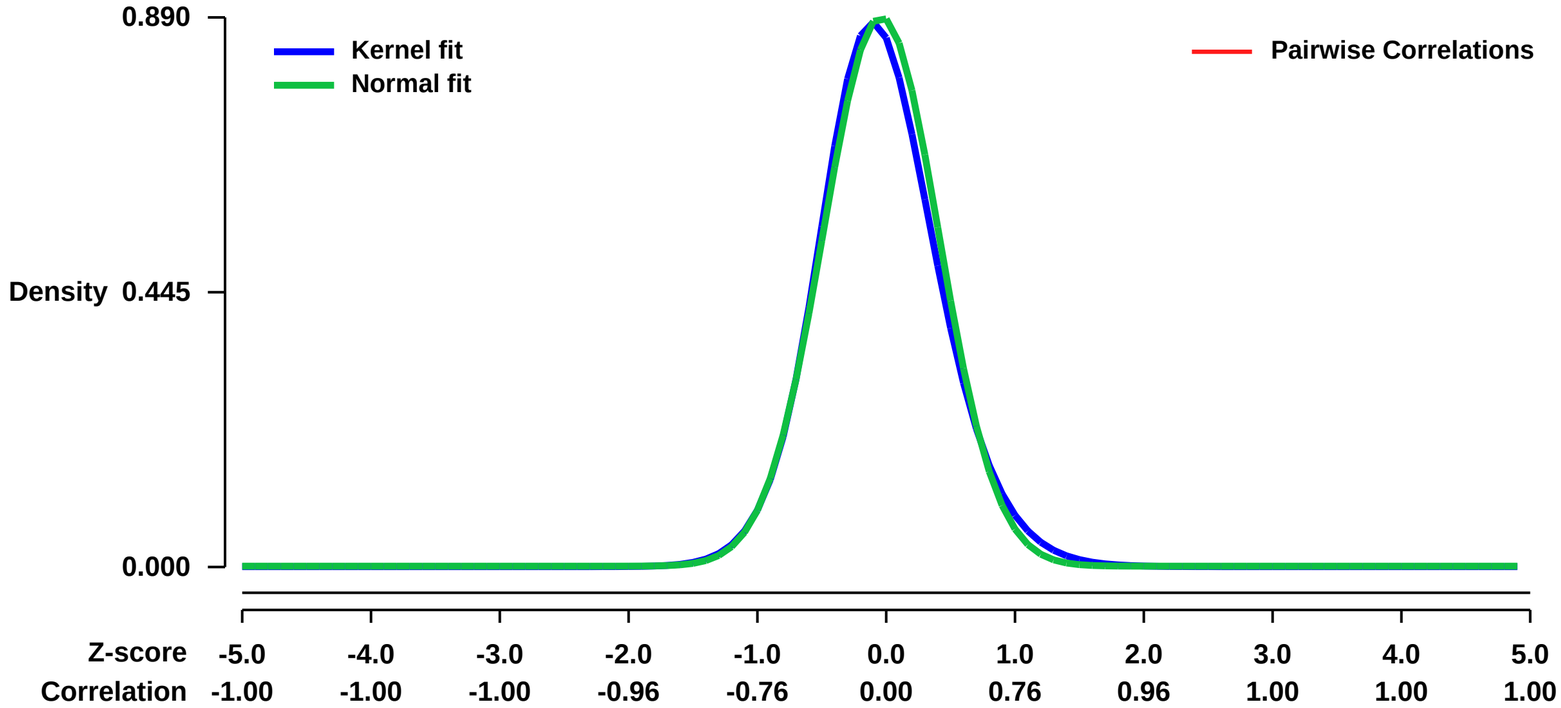

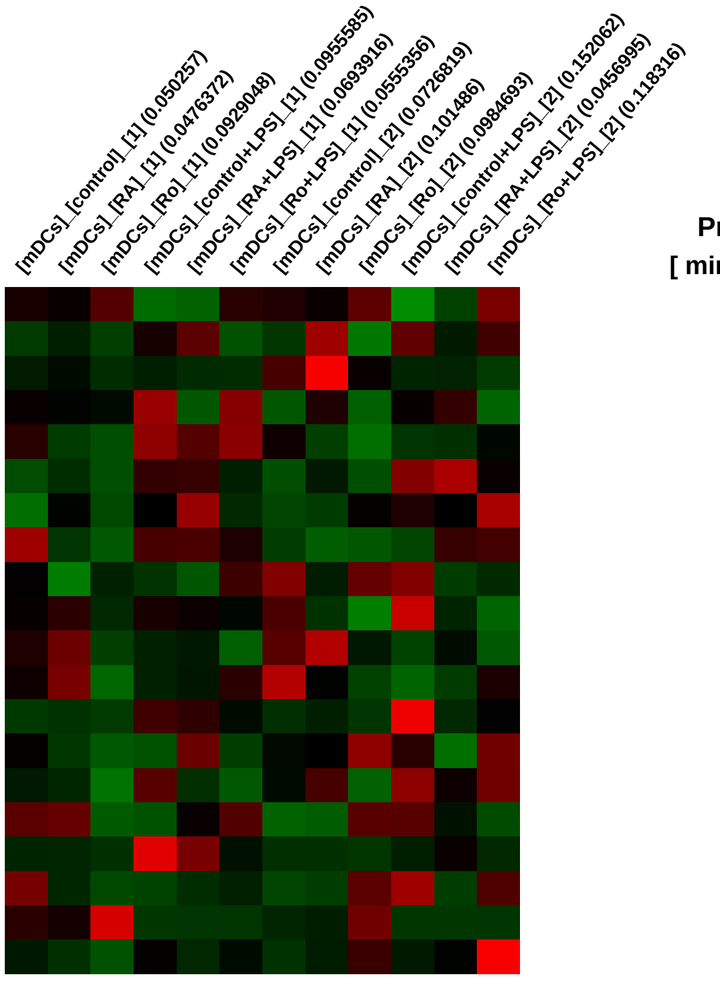

GEO Series "GSE34351" Expression Profiles

Num of samples in this series: 12

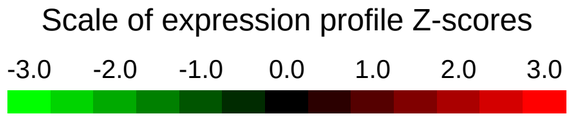

GEO Link:	http://www.ncbi.nlm.nih.gov/geo/query/acc.cgi?acc=GSE34351
Status:	Public on Aug 15 2012
Title:	Gene expression profile on ischemic kidneys from wildtype C57BL/10 and TLR4 null C57BL/10ScNJ mice
Organism:	Mus musculus
Experiment type:	Expression profiling by array
Platform:	GPL1261
Pubmed ID:	22895517
Summary & Design:	**Summary:** TLR4 deficiency attenuates kidney injury after ischemic reperfusion as measured by both renal function and morphology. To better understand the role of TLR4 during the acute kidney injury, we used DNA microarray to identify genes that were differentially expressed on kidneys in wildtype B10 mice and TLR4 null mice during the early stage of injury. **Overall design:** A murine ischemic reperfusion injury model was established. After right nephrectomy, the left pedicle was clamped for 23min followed by 4hr reperfusion. Sham mice were used as controls. 6 WT males and 6 TLR4 null males were included with 3 ischemic and 3 shams in each group.

Background corr dist: KL-Divergence = 0.1223, L1-Distance = 0.0249, L2-Distance = 0.0008, Normal std = 0.4083

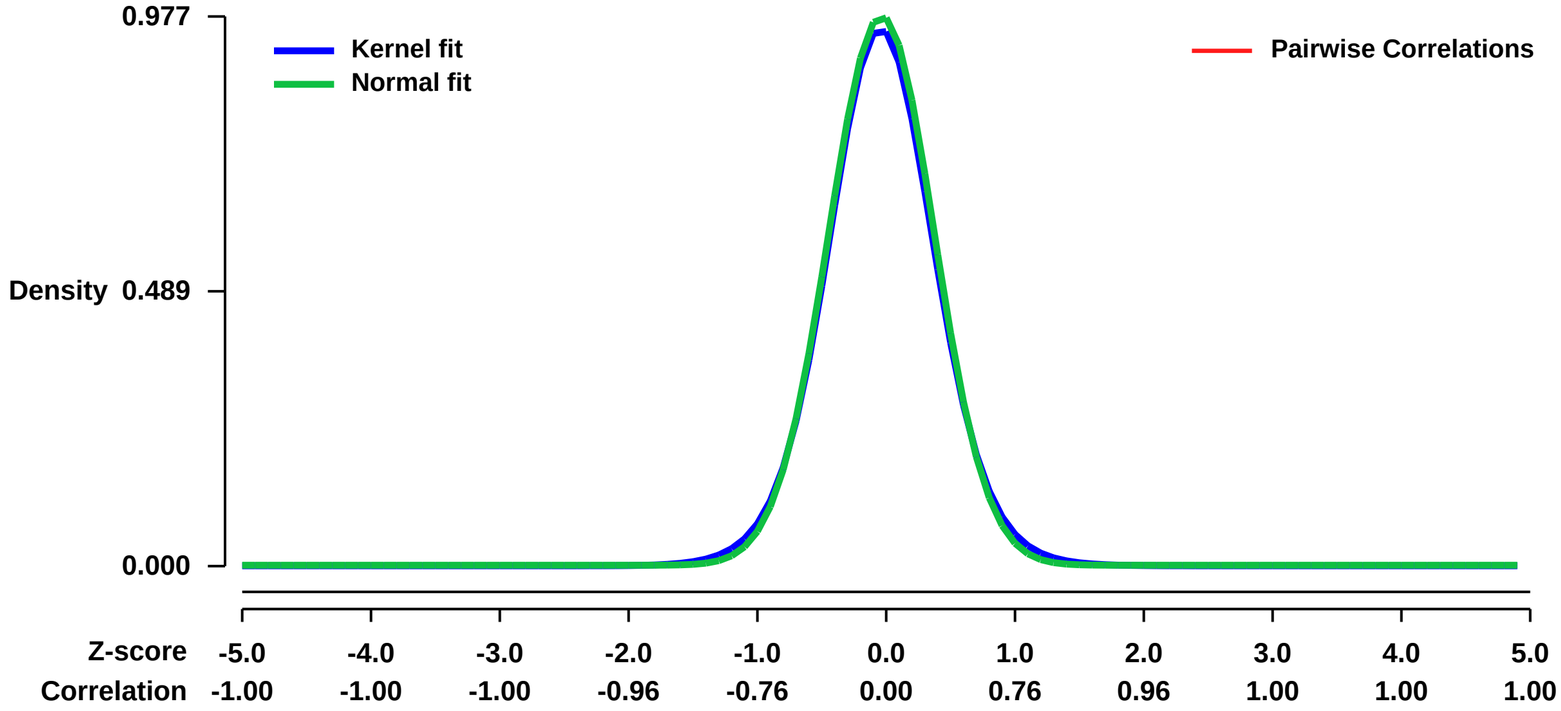

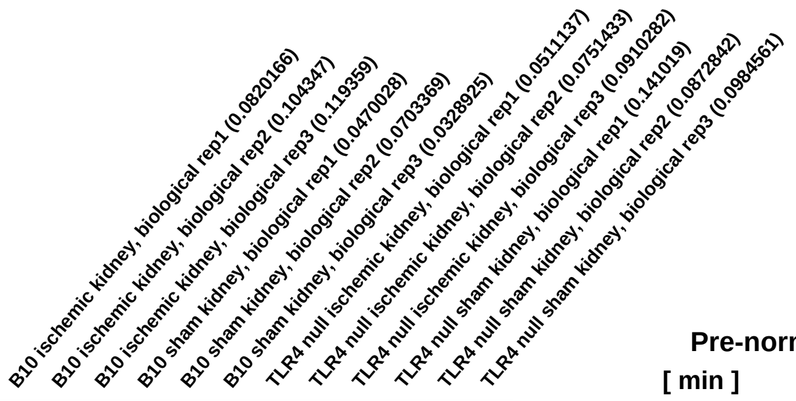

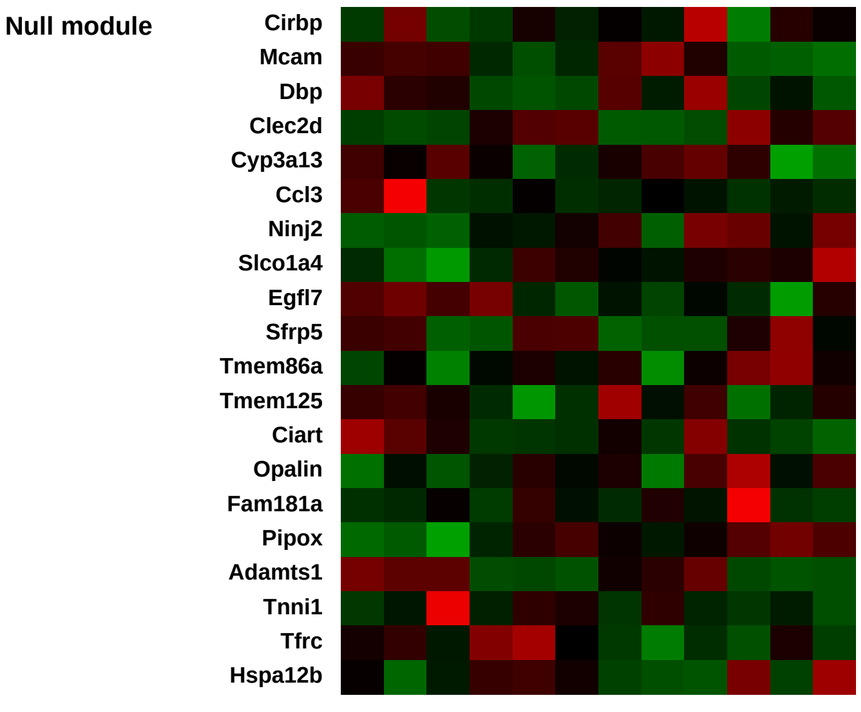

GEO Series "GSE3440" Expression Profiles

Num of samples in this series: 15

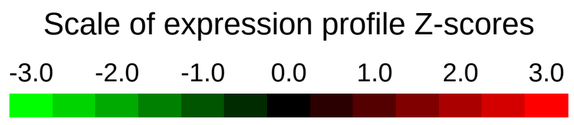

GEO Link:	http://www.ncbi.nlm.nih.gov/geo/query/acc.cgi?acc=GSE3440
Status:	Public on Nov 01 2005
Title:	Effect of aldosterone on gene expression in the heart
Organism:	Mus musculus
Experiment type:	Expression profiling by array
Platform:	GPL1261
Pubmed ID:	16601137

Summary & Design:

Summary:
Aldosterone is known to have a number of direct adverse effects on the heart, including fibrosis and myocardial inflammation. However, genetic mechanisms of aldosterone action on the heart remain unclear.

This experiment investigated of temporal changes in gene expression profile of the whole heart induced by acute administration of a physiologic dose of aldosterone in the mouse. mRNA levels of 34,000 known mouse genes were measured at eight time points after aldosterone administration using oligonucleotide microarrays and compared to those of the control animals who underwent a sham injection. A novel software tool (CAGED) designed for analysis of temporal microarray experiments using a Bayesian approach was used to identify genes differentially expressed between the aldosterone-injected and control group.

CAGED analysis identified twelve genes as having significant differences in their temporal profiles between aldosterone-injected and control groups. All of these genes exhibited a decrease in expression level 1-3 hours after aldosterone injection followed by a brief rebound and a return to baseline. These findings were validated by quantitative RT-PCR. The differentially expressed genes included phosphatases, regulators of steroid biosynthesis, inactivators of reactive oxygen species, and structural proteins. Several of these genes are known to functionally mediate biochemical phenomena previously observed to be triggered by aldosterone administration, such as phosphorylation of ERK1/2. These results provide the first description of cardiac genetic response to aldosterone and identify several potential mediators of known biochemical sequelae of aldosterone administration in the heart.

Methods:

Male C57BL6 mice were injected with aldosterone 10 mcg/kg (experimental group) or vehicle (control group) at time 0. Five animals were sacrificed at each of the following time points in each group: 0, 0.5, 1, 2, 3, 4, 5, and 12 hours from injection. Hearts were removed and total RNA extracted from the hearts of all five animals at each time point / experimental condition was pooled for gene expression analysis.

Keywords: time series

Overall design:
Time series of effect of aldosterone on gene expression in the mouse heart

Background corr dist: **KL-Divergence = 0.1782, L1-Distance = 0.0443, L2-Distance = 0.0043, Normal std = 0.3474**

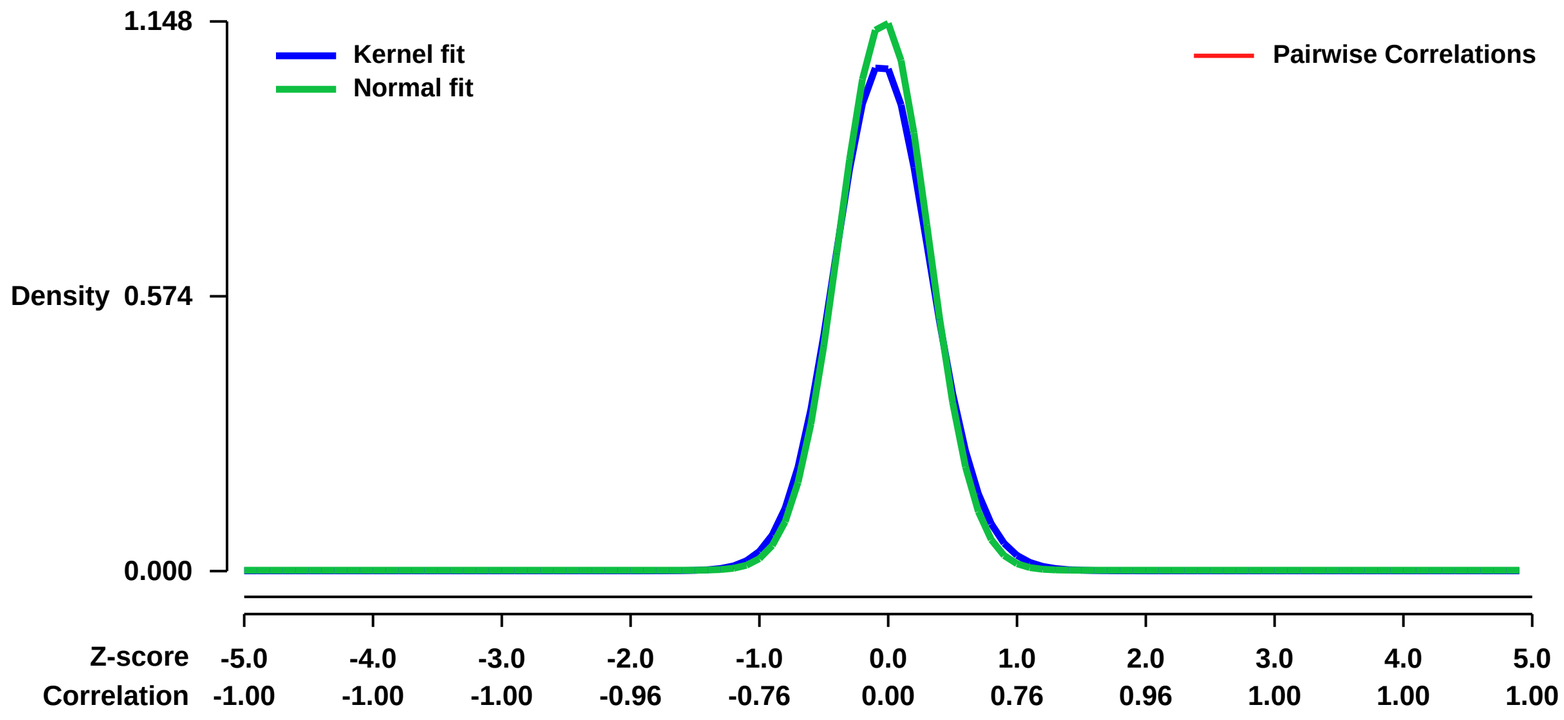

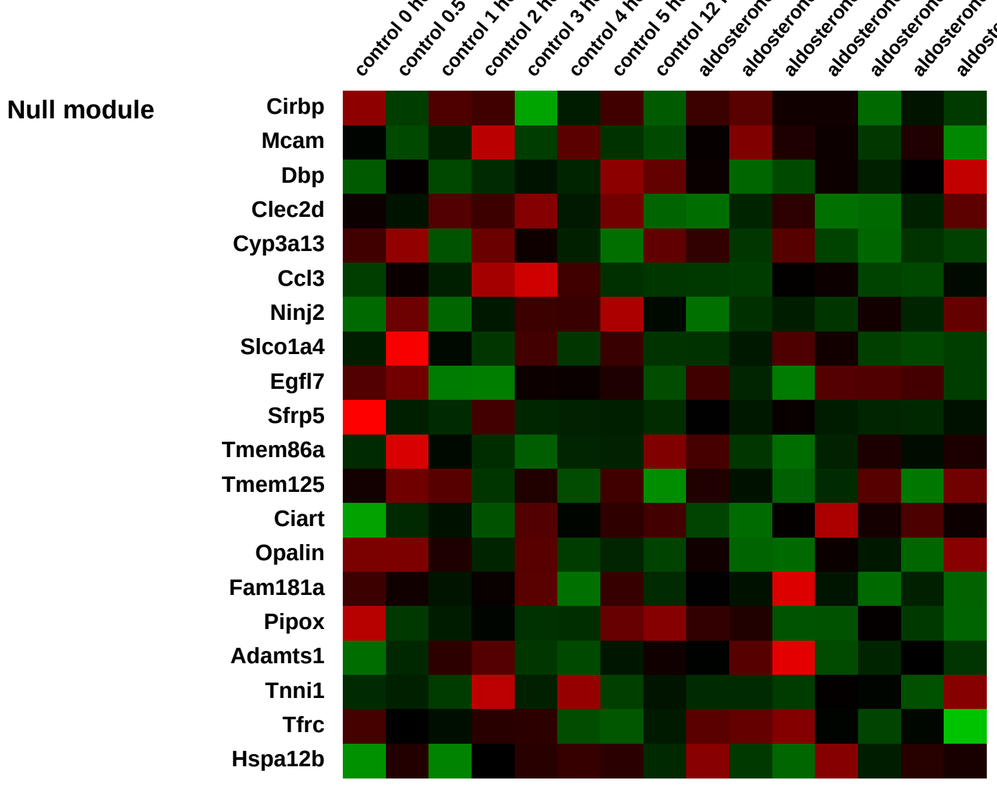

GEO Series "GSE34552" Expression Profiles

Num of samples in this series: 10

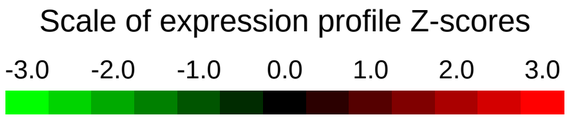

GEO Link:	http://www.ncbi.nlm.nih.gov/geo/query/acc.cgi?acc=GSE34552
Status:	Public on Nov 05 2012
Title:	Expression data from mouse kidney tissue
Organism:	Mus musculus
Experiment type:	Expression profiling by array
Platform:	GPL1261
Pubmed ID:	22791343
Summary & Design:	**Summary:** **The role of the renin-angiotensin system in chronic kidney disease involves multiple peptides and receptors. Exerting antipodal pathophysiological mechanisms, renin inhibition and AT1 antagonism ameliorate renal damage.** **This is a comparison between the renin inhibitor aliskiren with the At1 antagonist losartan in mice with chronic kidney disease due to renal ablation.** **Overall design:** **Renal tissue from ablated mice was used after 6-week treatment with either 500 mg/l losartan or 50 mg/kg aliskiren per day (n = 5)**

Background corr dist: **KL-Divergence = 0.0759, L1-Distance = 0.0208, L2-Distance = 0.0006, Normal std = 0.4855**

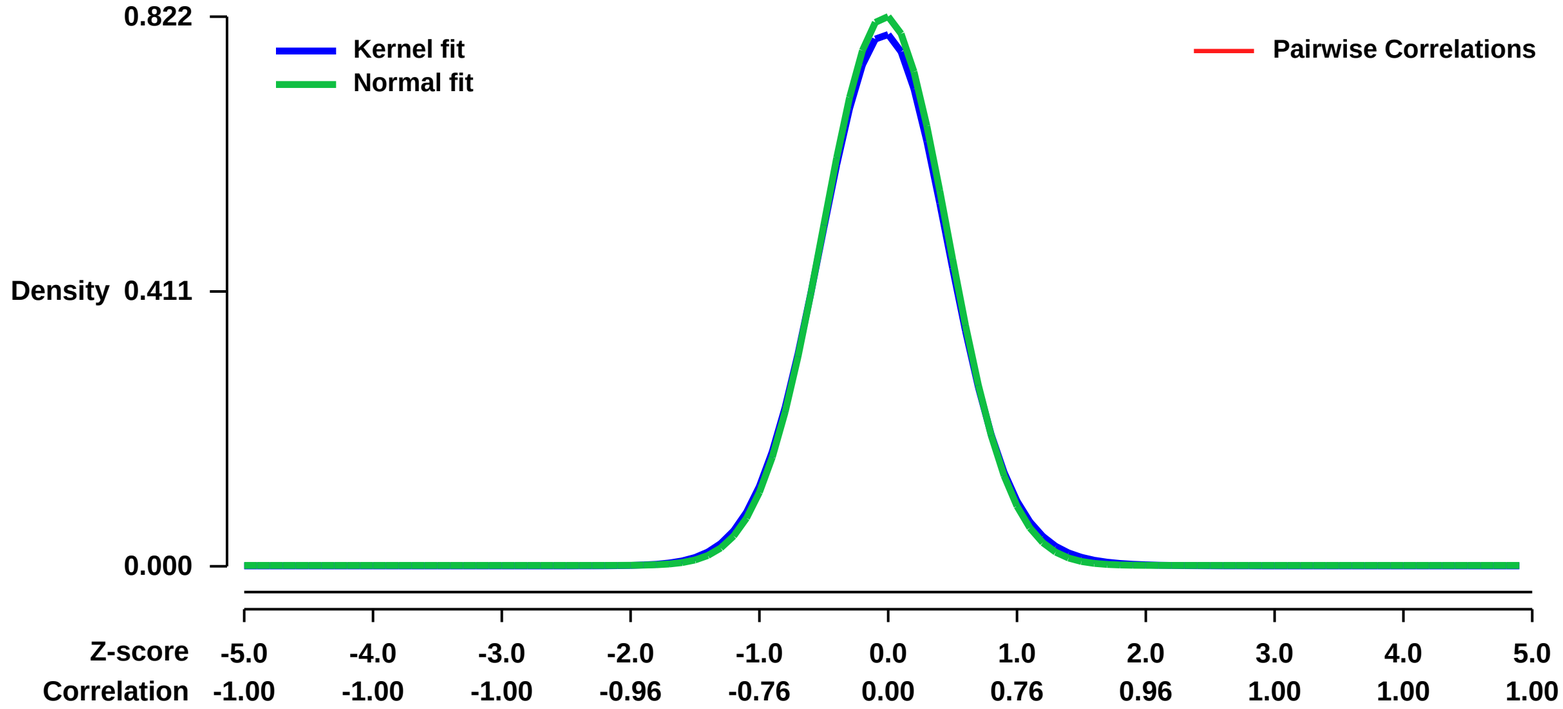

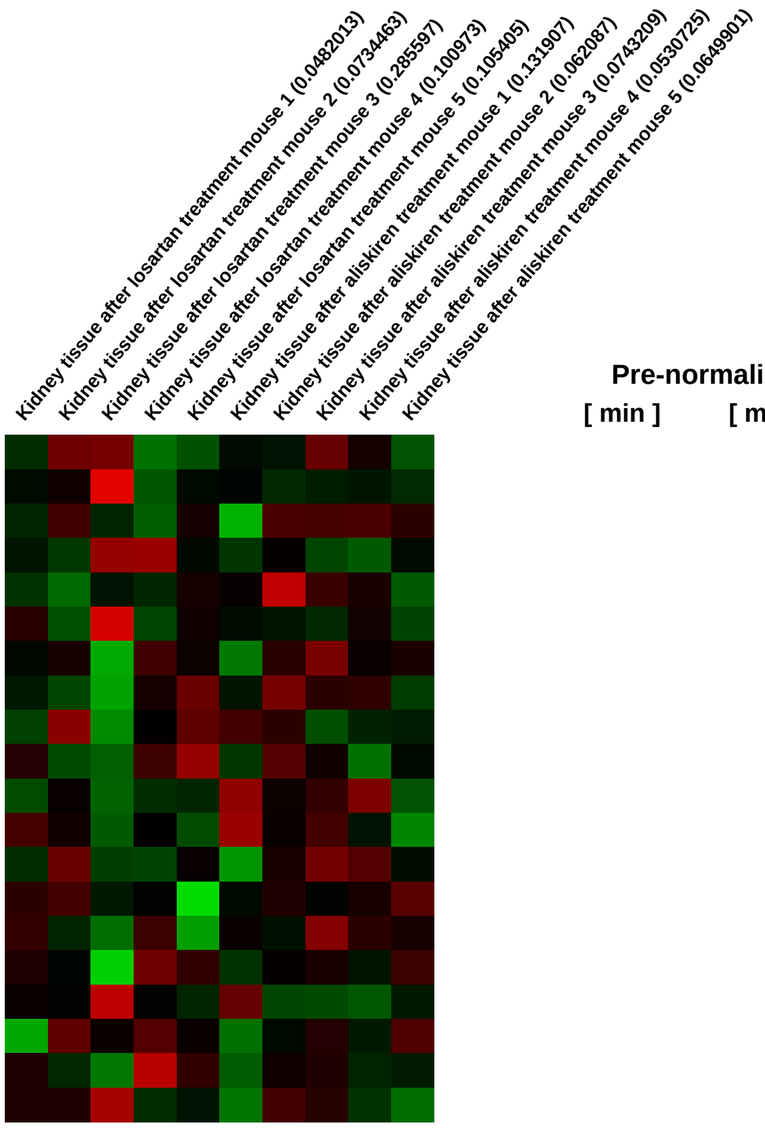

GEO Series "GSE34618" Expression Profiles

Num of samples in this series: 7

Scale of expression profile Z-scores

-3.0 -2.0 -1.0 0.0 1.0 2.0 3.0

GEO Link:	http://www.ncbi.nlm.nih.gov/geo/query/acc.cgi?acc=GSE34618
Status:	Public on May 02 2012
Title:	Expression data from CD8+ Central memory T cells after different time periods of Concanavalin A in vitro activation.
Organism:	Mus musculus
Experiment type:	Expression profiling by array
Platform:	GPL1261
Pubmed ID:	22567129
Summary & Design:	**Summary:** CD8+ tumor infiltrating T cells (TIL) lack effector-phase functions due to defective proximal TCR-mediated signaling shown to result from inactivation of p56lck kinase. We identify a novel interacting partner for p56lck in nonlytic TIL, Protocadherin-18 (â pcdh18â), and show that pcdh18 is transcribed upon in vitro or in vivo activation of CD8+ central memory T cells (CD44+CD62LhiCD127+) coincident with conversion into effector memory cells (CD44+CD62LloCD127+). Expression of pcdh18 in primary CD8+ effector cells induces the phenotype of nonlytic TIL: defective; proximal TCR signaling, cytokine secretion, and cytolysis; and enhanced AICD. pcdh18 contains a motif (centered at Y505) shared with src kinases (QGQYQP) which is required for the inhibitory phenotype. Thus, pcdh18 is a novel marker of CD8+ effector memory T cells expressed upon cell activation that can function as a negative regulator by restricting the effector phase. We used microarrays to detail the global programme of gene expression underlying CD8+ 'Central memory' T cells activation and identified distinct transcriptional pattern clusters. **Overall design:** Ten spleens were pooled from 62 week old C57BL/6 male mice and enriched for CD8+ T cells by negative selection using a cocktail of biotinylated antibodies to deplete CD4, CD11c, CD11b, MHC-II, B220, and NK cells. Cells were then stained for CD8, CD44, CD62L, and CD127 and sorted (using a iCyt Reflection parallel cell sorter). Cells were collected and cultured (0.5 x106 cells/well) in 10% complete RPMI media supplemented with 0.005 ugr Con A and RNA prepared using TRIZOL and the 'RNeasy clean-up kit' (Invitrogen) after activation for different times. We established single transcriptional profiles for 6 time points after T cell activation (4, 6, 8, 16, 20, 24 h) including a control zero h time point (prior to activation). RNA was isolated by standard procedures and its quality was assessed by the NYU Center for Health Informatics and Bioinformatics. cDNAs were hybridized to GeneSpring arrays using the mouse genome MOE430 2.0 array (Affymetrix) which interrogates ~45,000 transcripts.

Background corr dist: KL-Divergence = 0.0627, L1-Distance = 0.0842, L2-Distance = 0.0115, Normal std = 0.6392

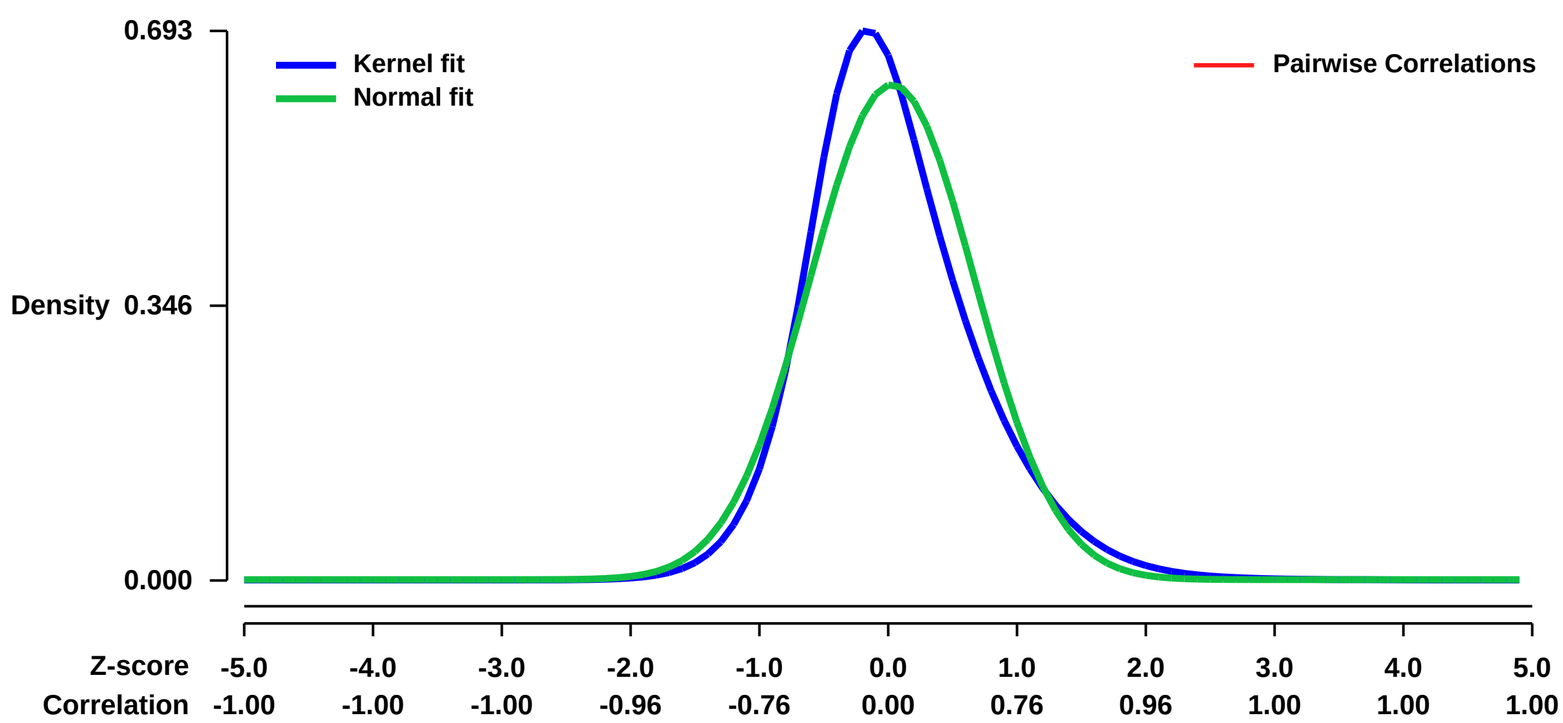

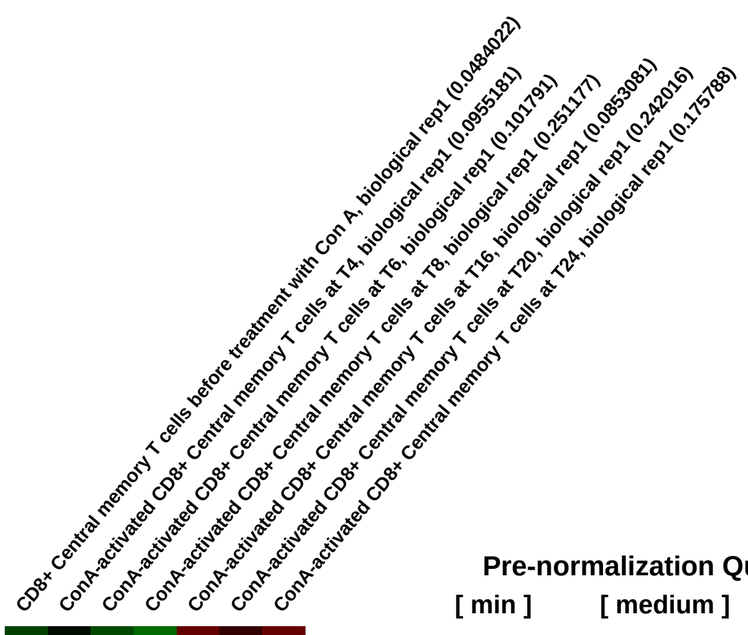

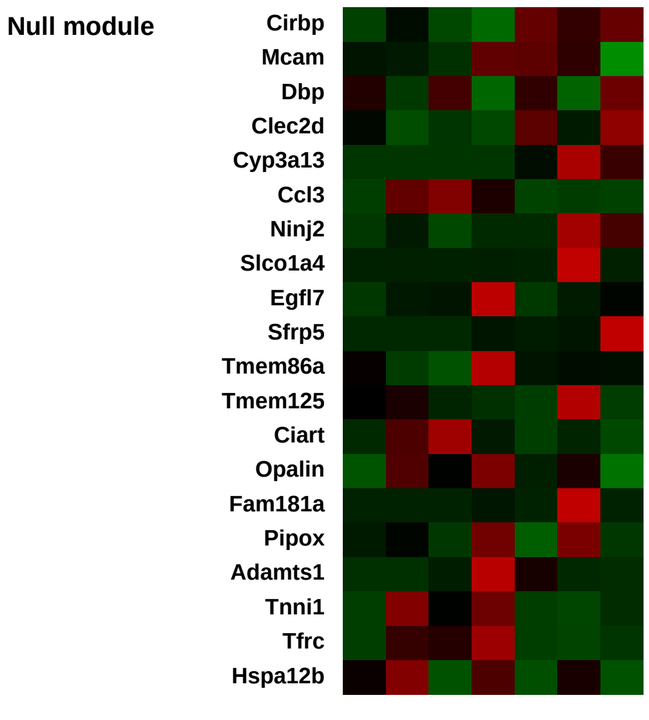

GEO Series "GSE34629" Expression Profiles

Num of samples in this series: 6

Scale of expression profile Z-scores

-3.0 -2.0 -1.0 0.0 1.0 2.0 3.0

GEO Link:	**http://www.ncbi.nlm.nih.gov/geo/query/acc.cgi?acc=GSE34629**
Status:	**Public on Dec 22 2012**
Title:	**Comparing expression profiles of NIH3T3 cells with and without LPAR1 mutation**
Organism:	**Mus musculus**
Experiment type:	**Expression profiling by array**
Platform:	**GPL1261**
Pubmed ID:	
Summary & Design:	**Summary:** **To explore the signaling pathways of mutant LPAR1, we performed gene expression profiling for NIH3T3 cells expressing wild-type and mutant LPAR1 receptors using Affymetrix mouse 430 2.0 arrays** **Overall design:** **6 RNA samples from the same cell line. 3 samples contained LPAR1 mutant and 3 samples were wild-type. Cells were harvested at 0, 60, and 120 minutes.**

Background corr dist: **KL-Divergence = 0.0350, L1-Distance = 0.0225, L2-Distance = 0.0005, Normal std = 0.6473**

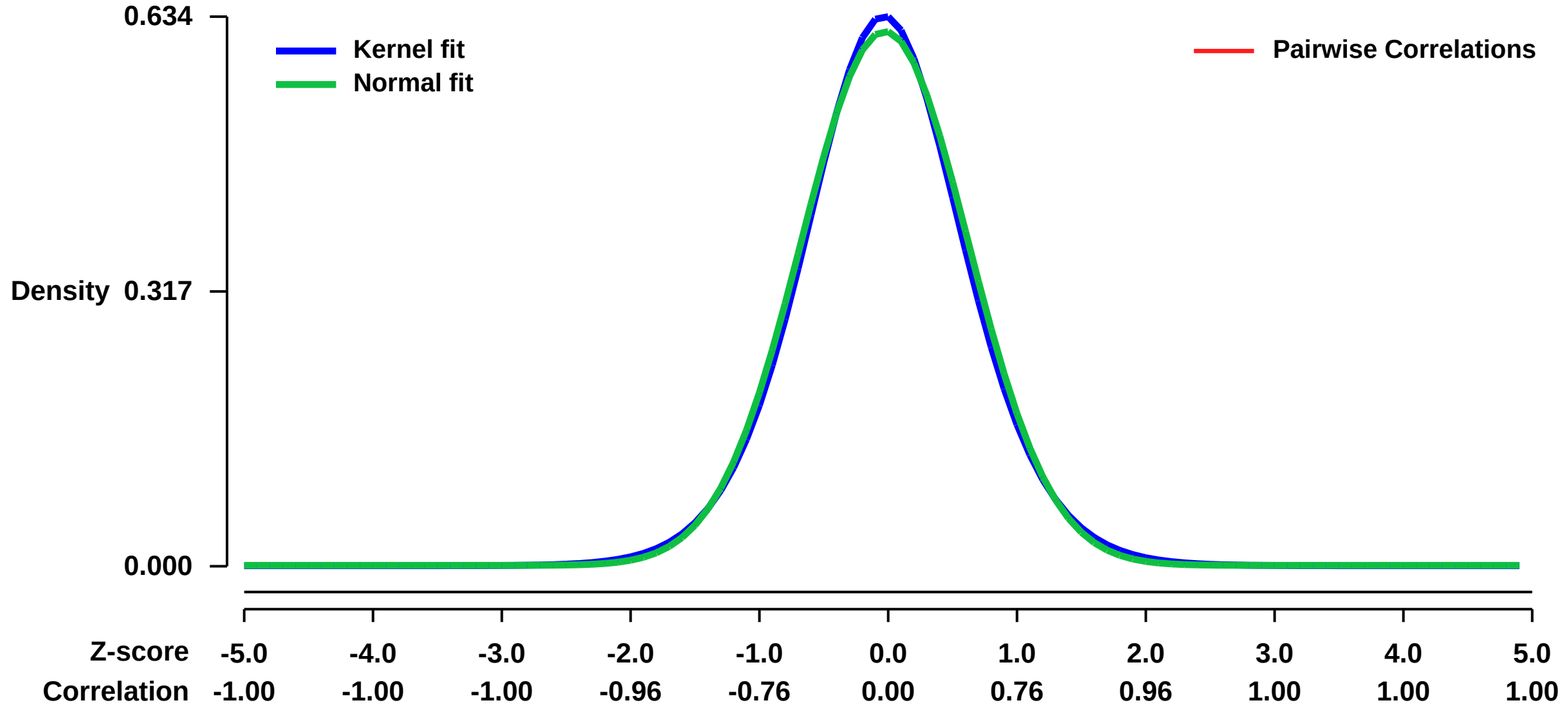

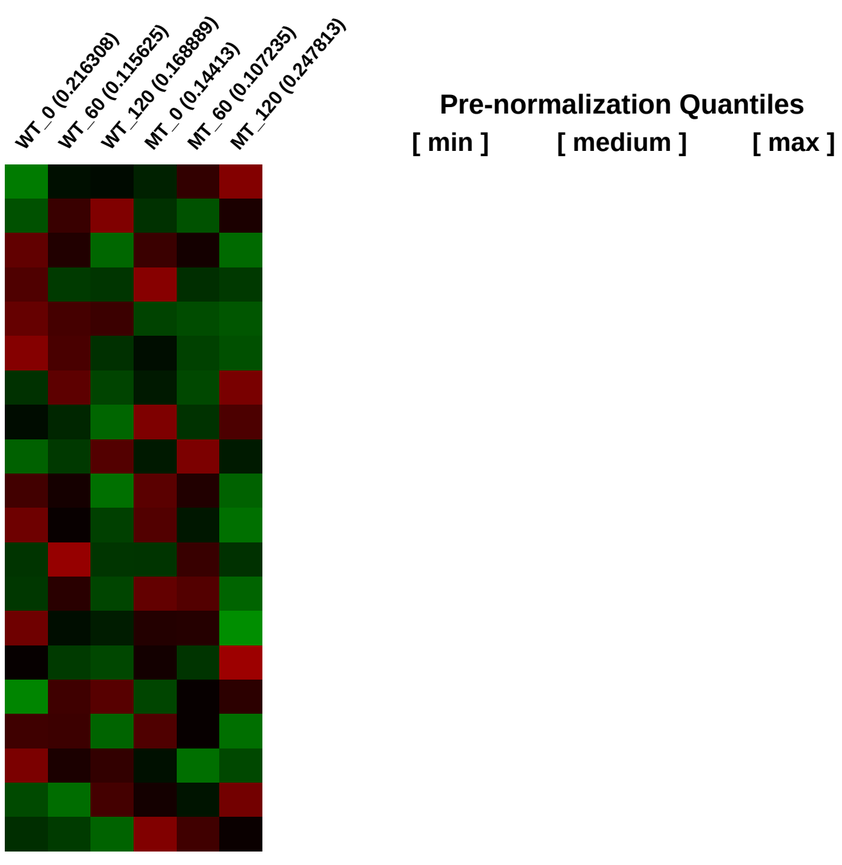

GEO Series "GSE3463" Expression Profiles

Num of samples in this series: 12

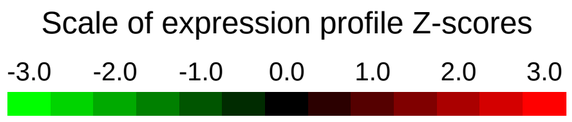

GEO Link:	http://www.ncbi.nlm.nih.gov/geo/query/acc.cgi?acc=GSE3463
Status:	Public on Dec 17 2005
Title:	Expression profiling of mouse gonadal somatic cells
Organism:	Mus musculus
Experiment type:	Expression profiling by array
Platform:	GPL1261
Pubmed ID:	16399799
Summary & Design:	**Summary:** Gene expression profiling of FACS sorted GFP+ve cells from sexed gonads of transgenic pSF1-eGFP mice **Keywords: Time course and comparison of sexes** **Overall design:** Experiment is both a time course and an assesment of sex specific expression in SF1+ve somatic gonadal cells. Each time point and sex has been profiled in triplicate

Background corr dist: KL-Divergence = 0.0488, L1-Distance = 0.0488, L2-Distance = 0.0033, Normal std = 0.6164

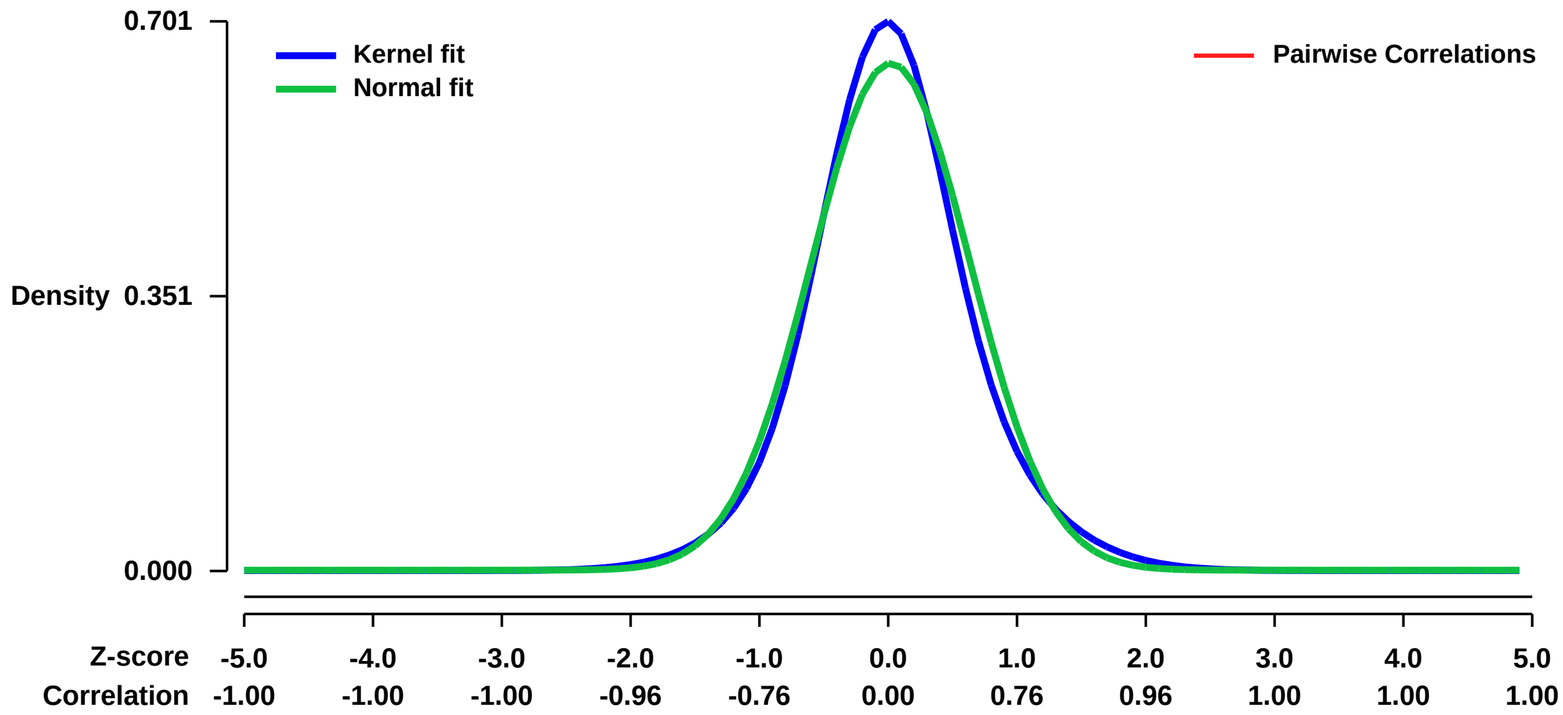

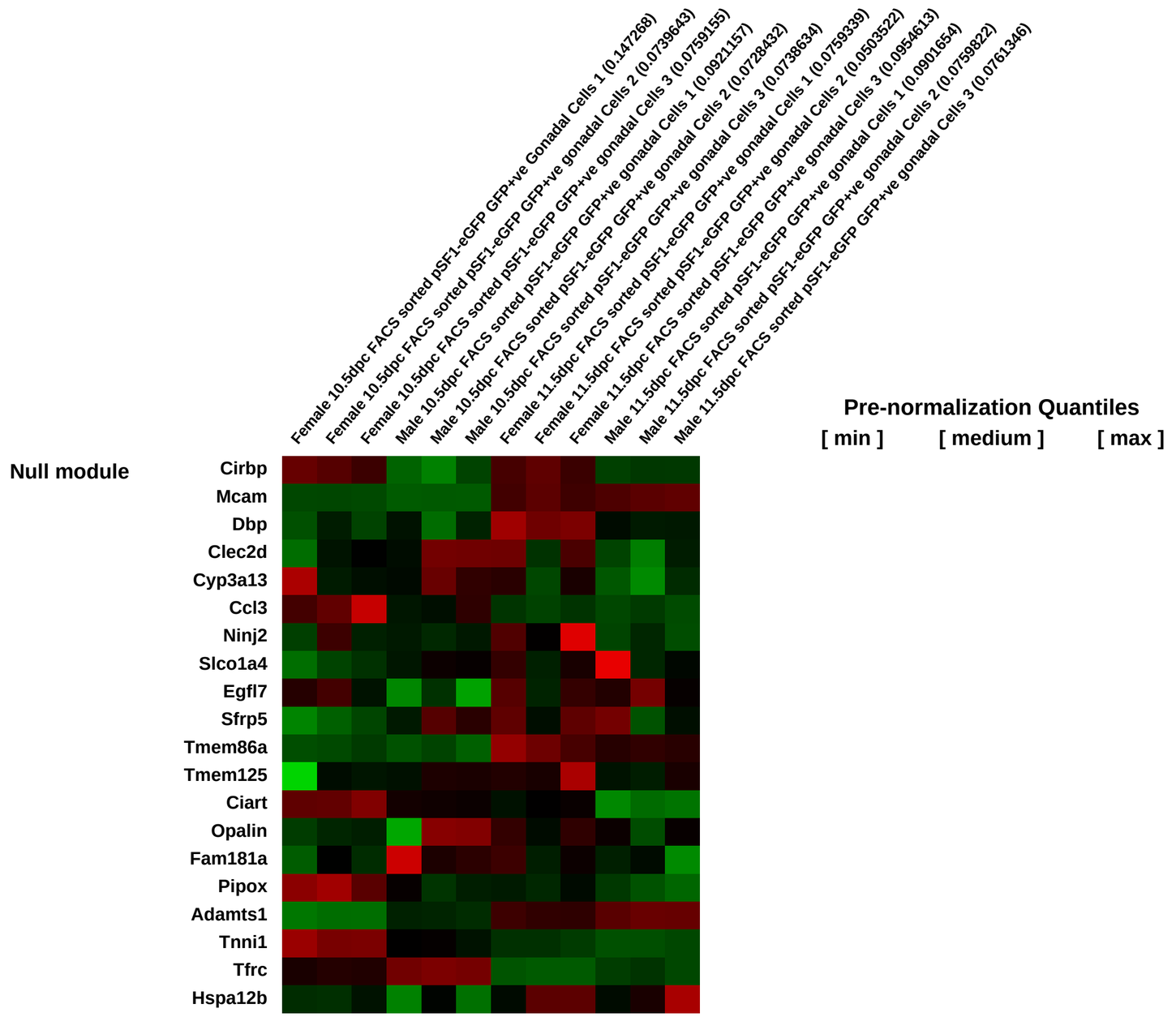

GEO Series "GSE34729" Expression Profiles

Num of samples in this series: 6

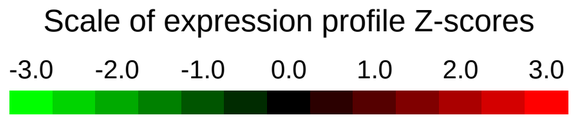

GEO Link:	http://www.ncbi.nlm.nih.gov/geo/query/acc.cgi?acc=GSE34729
Status:	Public on Jan 09 2013
Title:	Gene expression changes induced by overexpression of EVI1 in Lin- hematopoietic cells [Lin]
Organism:	Mus musculus
Experiment type:	Expression profiling by array
Platform:	GPL1261
Pubmed ID:	23212151
Summary & Design:	**Summary:** The transcription factor Evi1 is essential for the formation and maintenance of hematopoietic stem cells, and induces clonal dominance with malignant progression upon constitutive activation by chromosomal rearrangements or transgene integration events. To understand the immediate and adaptive response of primary murine hematopoietic cells to the transcriptional upregulation of Evi1, we developed an inducible lentiviral vector system with a robust expression switch. We found that Evi1 delays differentiation and promotes survival in myeloid culture conditions, orchestrating a battery of genes involved in stemness (Aldh1a1, Ly6a [Sca1], Abca1, Epcam, among others). Importantly, Evi1 suppresses Cyclins and Cyclin-dependent kinases (Cdk), while it upregulates Cdk inhibitors, inducing quiescence in various proliferation-inducing cytokine conditions and operating in a strictly dose-dependent manner. Hematopoietic cells with persisting Evi1-induction tend to adopt a relatively low expression level. We thus classify Evi1 as a dormancy-inducing oncogene, likely requiring epigenetic and genetic compensation for cell expansion and malignant progression. **Overall design:** Lin- Rosa26rtTA cells were isolated, transduced in S3F11 cytokines, induced the next day with DOX [1 ¸…g/ml] and 20 hours later sorted for negative/low or highly EGFP expressing cells, from which total RNA was extraced and subjected to Microarray Analysis

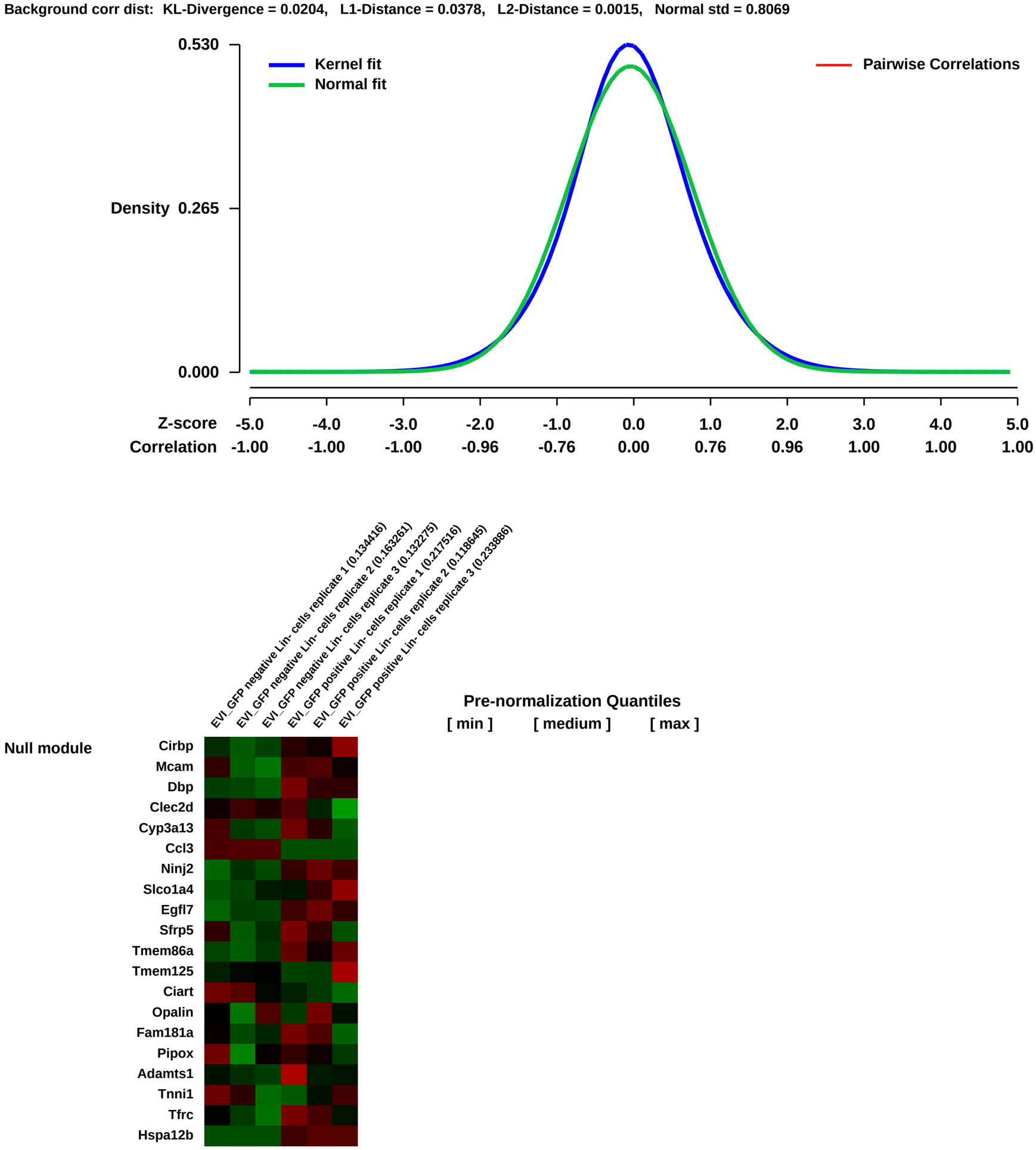

GEO Series "GSE34732" Expression Profiles

Num of samples in this series: 12

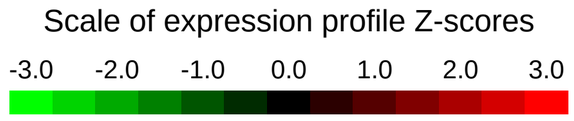

GEO Link:	**http://www.ncbi.nlm.nih.gov/geo/query/acc.cgi?acc=GSE34732**
Status:	**Public on May 22 2012**
Title:	**Differenetial Gene Expression in Limbs of Wild Type and Lmx1b KO mice during limb dorsalization (e11.5, e12.5 & e13.5)**
Organism:	**Mus musculus**
Experiment type:	**Expression profiling by array**
Platform:	**GPL1261**
Pubmed ID:	
Summary & Design:	**Summary:** **Lmx1b regulates dorsalization of limb fates, but the mechanism of this regulation has not been characterized. To identify candidate genes regulated by Lmx1b we compared the limbs from Lmx1b KO mice to wild type mice during limb dorsalization (e11.5-13.5). Differentially expressed genes that we common to all three stages examined were considered to be likely candidates for Lmx1b regulation and further evaluated.** **Overall design:** **At 11.5 and 12.5 dpc, embryos were harvested and the limb buds with the limb girdles were isolated. Embryos at 13.5dpc were also harvested and their distal limb buds (zeugopods and autopods) were isolated. Embryos were genotyped to confirm Lmx1b homozygosity (-/- or +/+). RNA from embryonic forelimbs and hindlimbs of wild type (WT) and Lmx1b KO mice was harvested using the Rneasy Kit (Qiagen). RNA was pooled to decrease genetic variability, i.e., six limbs at 11.5 dpc, three limbs at 12.5 dpc and six limbs at 13.5 dpc. Duplicate samples were generated using different embryos for each stage and then hybridized to the Affymetrix GeneChip´fi Mouse Genome 430 2.0 Array (UCI, Irvine, CA).**

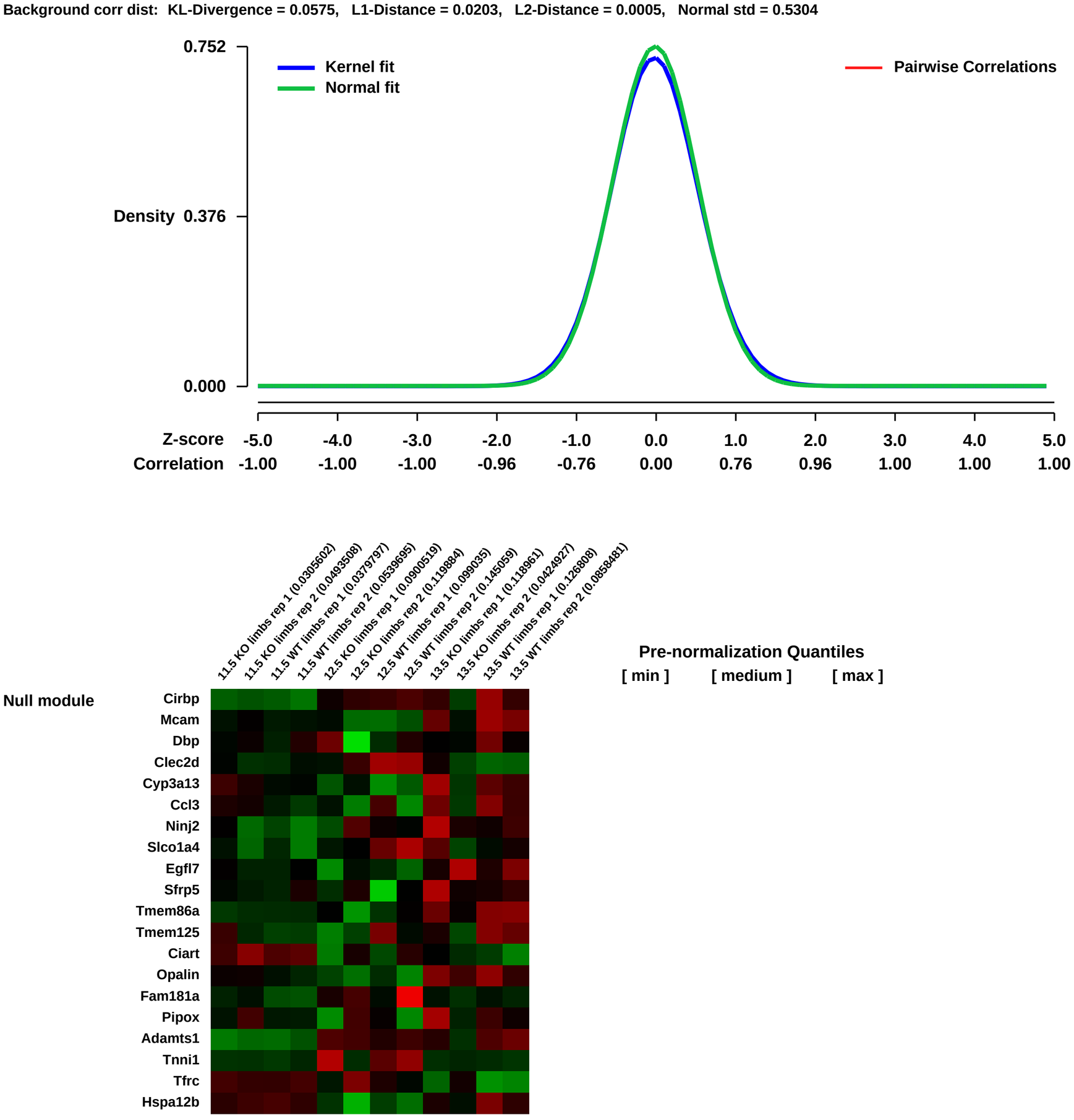

GEO Series "GSE34755" Expression Profiles

Num of samples in this series: 6

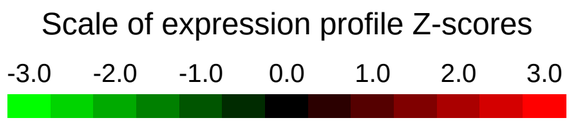

GEO Link:	**http://www.ncbi.nlm.nih.gov/geo/query/acc.cgi?acc=GSE34755**
Status:	**Public on May 01 2014**
Title:	**Gene expression changes induced by Evi1 withdrawal in Evi1 dependent myeloid clone C6**
Organism:	**Mus musculus**
Experiment type:	**Expression profiling by array**
Platform:	**GPL1261**
Pubmed ID:	
Summary & Design:	**Summary:** **The transcription factor Evi1 is essential for the formation and maintenance of hematopoietic stem cells, and induces clonal dominance with malignant progression upon constitutive activation by chromosomal rearrangements or transgene integration events. To understand the immediate and adaptive response of primary murine hematopoietic cells to the transcriptional upregulation of Evi1, we developed an inducible lentiviral vector system with a robust expression switch. We found that Evi1 delays differentiation and promotes survival in myeloid culture conditions, orchestrating a battery of genes involved in stemness (Aldh1a1, Ly6a [Sca1], Abca1, Epcam, among others). Importantly, Evi1 suppresses Cyclins and Cyclin-dependent kinases (Cdk), while it upregulates Cdk inhibitors, inducing quiescence in various proliferation-inducing cytokine conditions and operating in a strictly dose-dependent manner. Hematopoietic cells with persisting Evi1-induction tend to adopt a relatively low expression level. We thus classify Evi1 as a dormancy-inducing oncogene, likely requiring epigenetic and genetic compensation for cell expansion and malignant progression.** **Overall design:** **Evi1 dependent myeloid clone C6 cells expressing a Doxycyclin inducible codon-optimized murine Evi1 were harvested at day 2 after DOX withdrawal and compared to C6 cells under Doxycyclin 1 ug/ml**

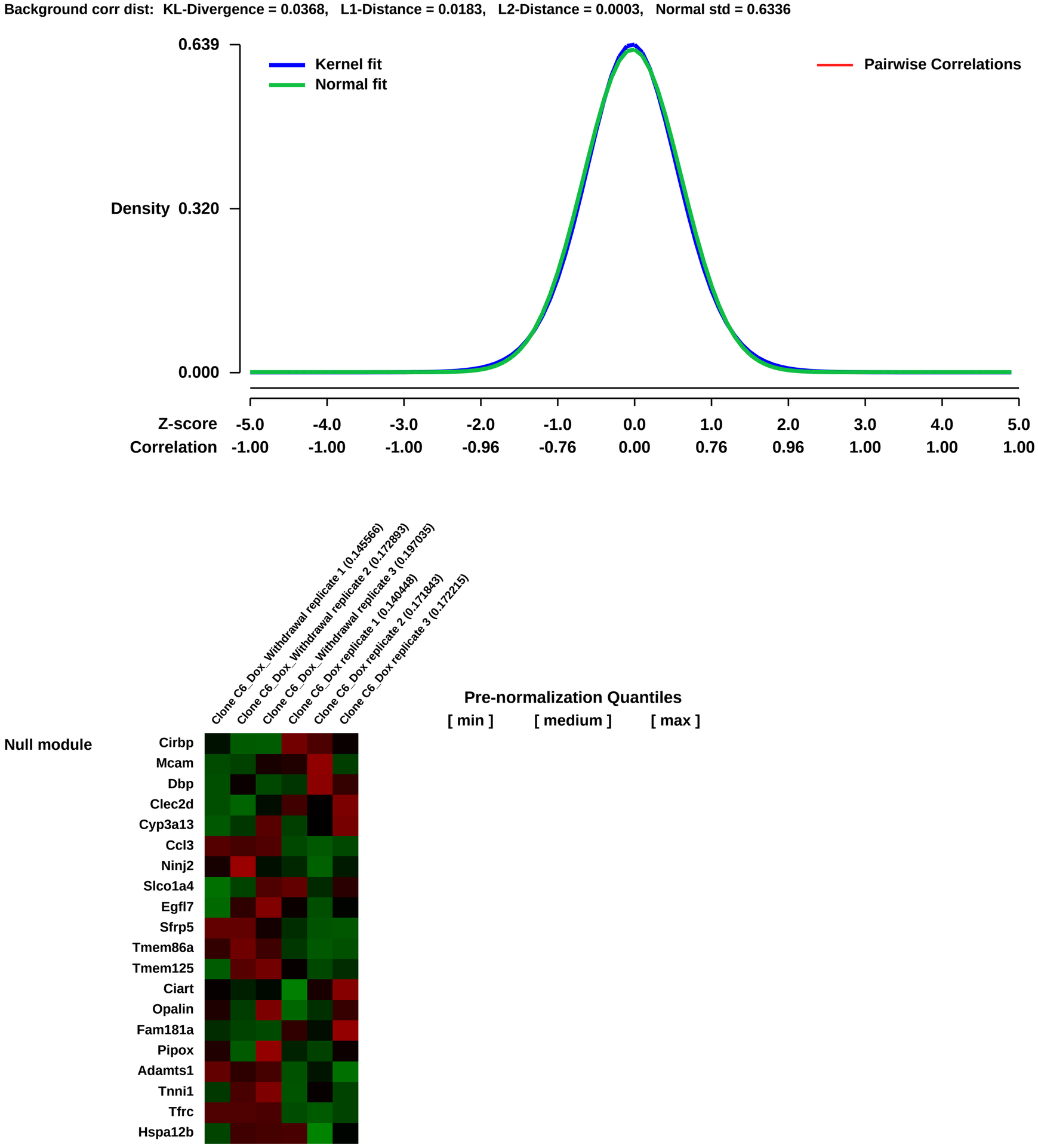

GEO Series "GSE34761" Expression Profiles

Num of samples in this series: 8

Scale of expression profile Z-scores

-3.0 -2.0 -1.0 0.0 1.0 2.0 3.0

GEO Link:	http://www.ncbi.nlm.nih.gov/geo/query/acc.cgi?acc=GSE34761
Status:	Public on Feb 01 2012
Title:	All-iPS cell mice generated from terminally differentiated B cells
Organism:	Mus musculus
Experiment type:	Expression profiling by array
Platform:	GPL1261
Pubmed ID:	22387999
Summary & Design:	**Summary:** The generation of induced pluripotent stem cells (iPSCs) often results in aberrant silencing of the imprinted Dlk1-Dio3 gene cluster, which compromises their ability to generate entirely iPSC-derived mice (â all-iPSC miceâ). Here, we show that reprogramming in the presence of ascorbic acid attenuates hypermethylation of Dlk1-Dio3 by enabling a chromatin configuration at its imprint control region that interferes with abnormal binding of the DNA methyltransferase Dnmt3a. This approach allowed us to generate adult all-iPSC mice from mature B cells, which have thus far failed to support the development of exclusively iPSC-derived postnatal mice. Our data demonstrate that factor-mediated reprogramming can endow a defined, terminally differentiated cell type with a developmental potential equivalent to that of embryonic stem cells. More generally, these findings indicate that the choice of culture conditions used for transcription factor-mediated reprogramming can strongly influence the epigenetic and biological properties of resultant iPSCs. **Overall design:** iPS cells were generated from MEFs of the Col-OKSM reprogrammable mice. In the presence of doxycycline, the reprogramming transcription factors Oct4, Sox2, Klf4, and cMyc were induced in MEFs to derivate iPS cells. Total RNA was isolated from iPS cells derivated in the presence or absence of ascorbic acid in culture medium.

Background corr dist: KL-Divergence = 0.0891, L1-Distance = 0.0231, L2-Distance = 0.0007, Normal std = 0.4564

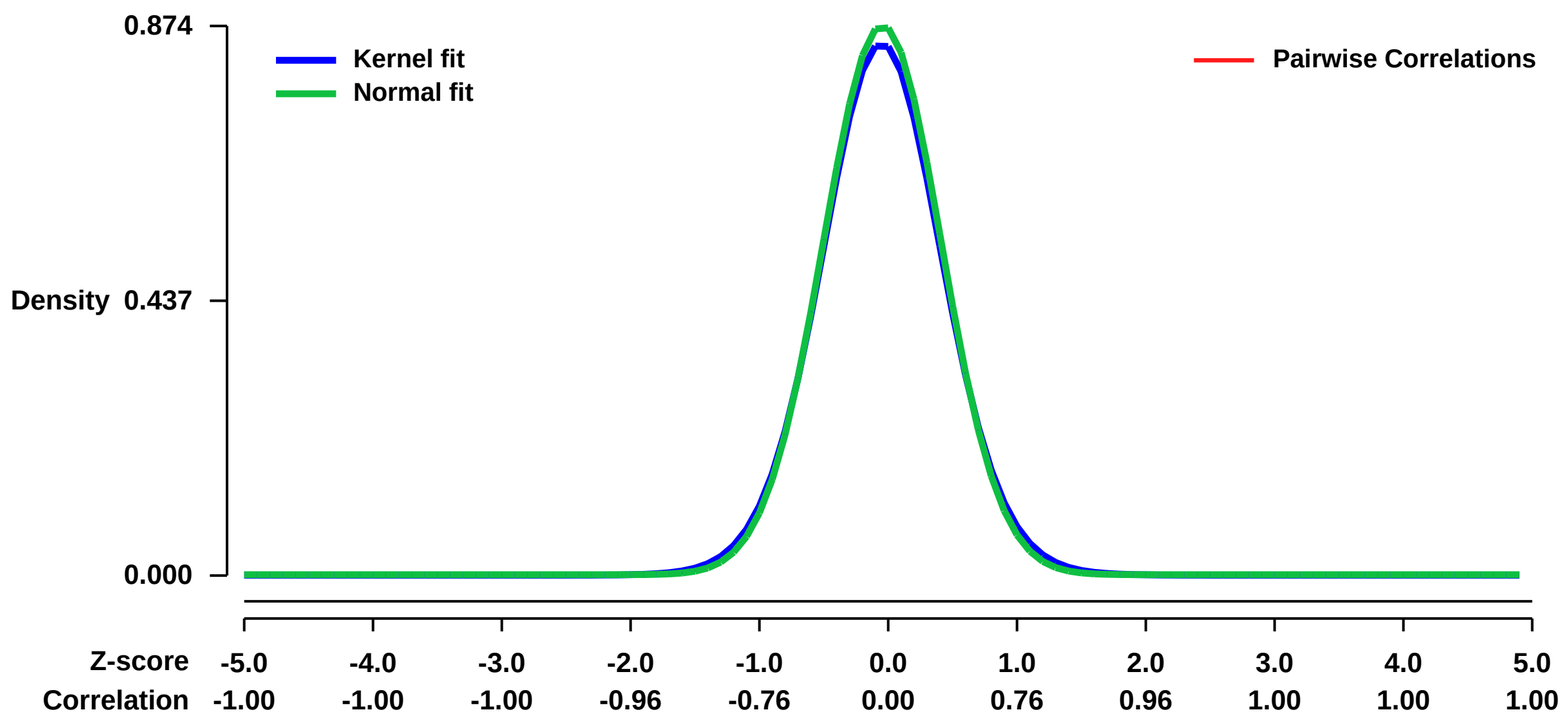

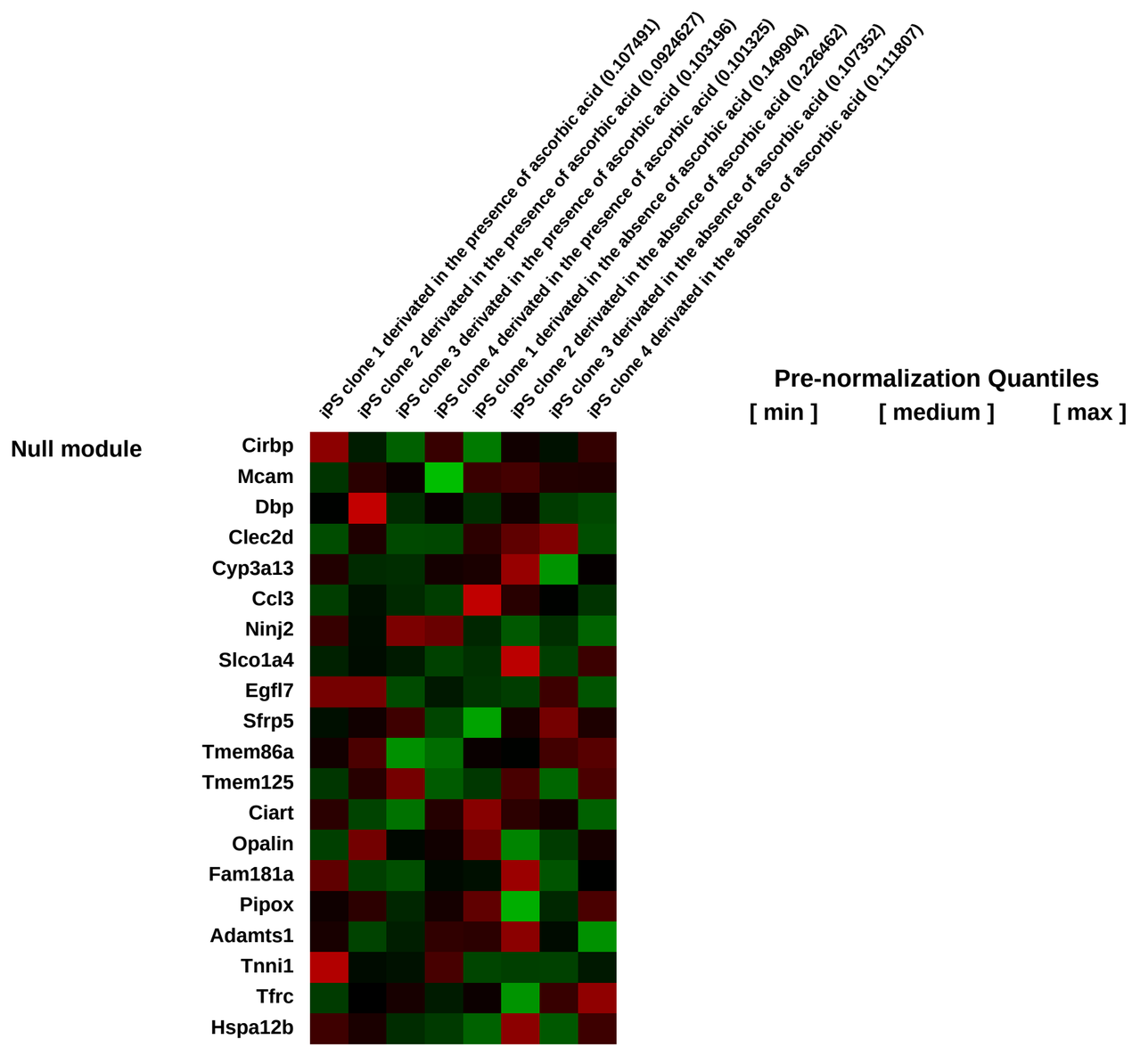

GEO Series "GSE34765" Expression Profiles

Num of samples in this series: 6

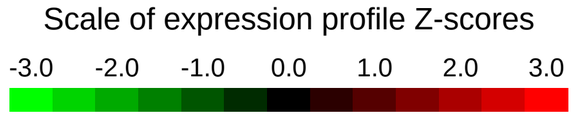

GEO Link:	http://www.ncbi.nlm.nih.gov/geo/query/acc.cgi?acc=GSE34765
Status:	Public on Sep 30 2012
Title:	Transcriptomic analysis of the cerebellum of daDREAM mice
Organism:	Mus musculus
Experiment type:	Expression profiling by array
Platform:	GPL1261
Pubmed ID:	22563308
Summary & Design:	**Summary:** DREAM (downstream regulatory element antagonist modulator) is a Ca2+-binding protein that binds DNA and represses transcription in a Ca2+-dependent manner. Previous studies have shown a role for DREAM in cerebellar function regulating the expression of the sodium/calcium exchanger3 (NCX3) in cerebellar granules to control Ca2+ homeostasis and survival of these neurons. To achieve a more global view of the genes regulated by DREAM in the cerebellum, we performed a genome-wide analysis in transgenic cerebellum expressing a Ca2+-insensitive/CREB-independent dominant active mutant DREAM (daDREAM). Our results indicate that DREAM is a major transcription factor in the cerebellum that regulates genes important for cerebellar development. **Overall design:** We used Affymetrix microarrays (GeneChip Mouse Genome 430 2.0) to compare global gene expression in wild type (WT) versus transgenic cerebellum cells. For ech type of sample three hybridizations were carried-out (independent biological replicates).

Background corr dist: KL-Divergence = 0.0144, L1-Distance = 0.0300, L2-Distance = 0.0013, Normal std = 0.8079

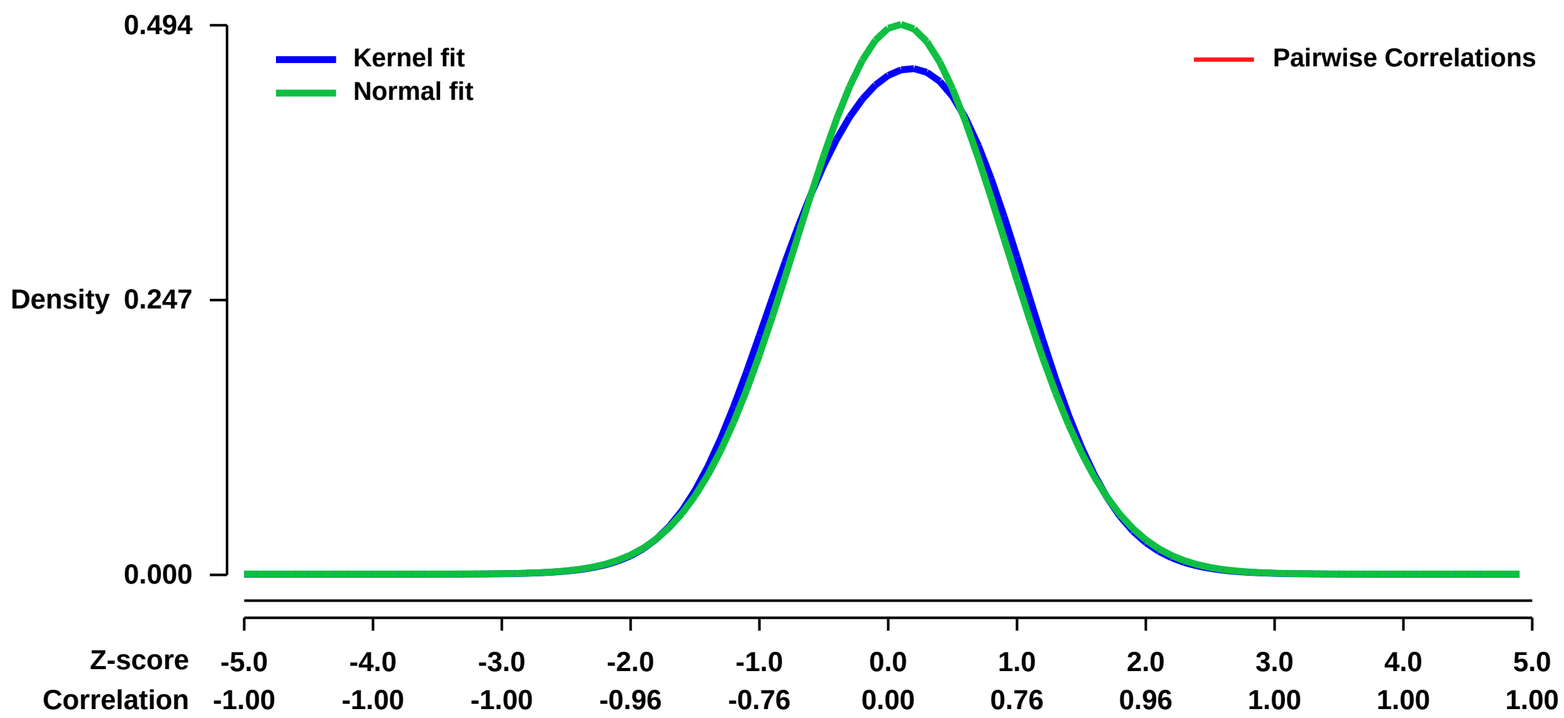

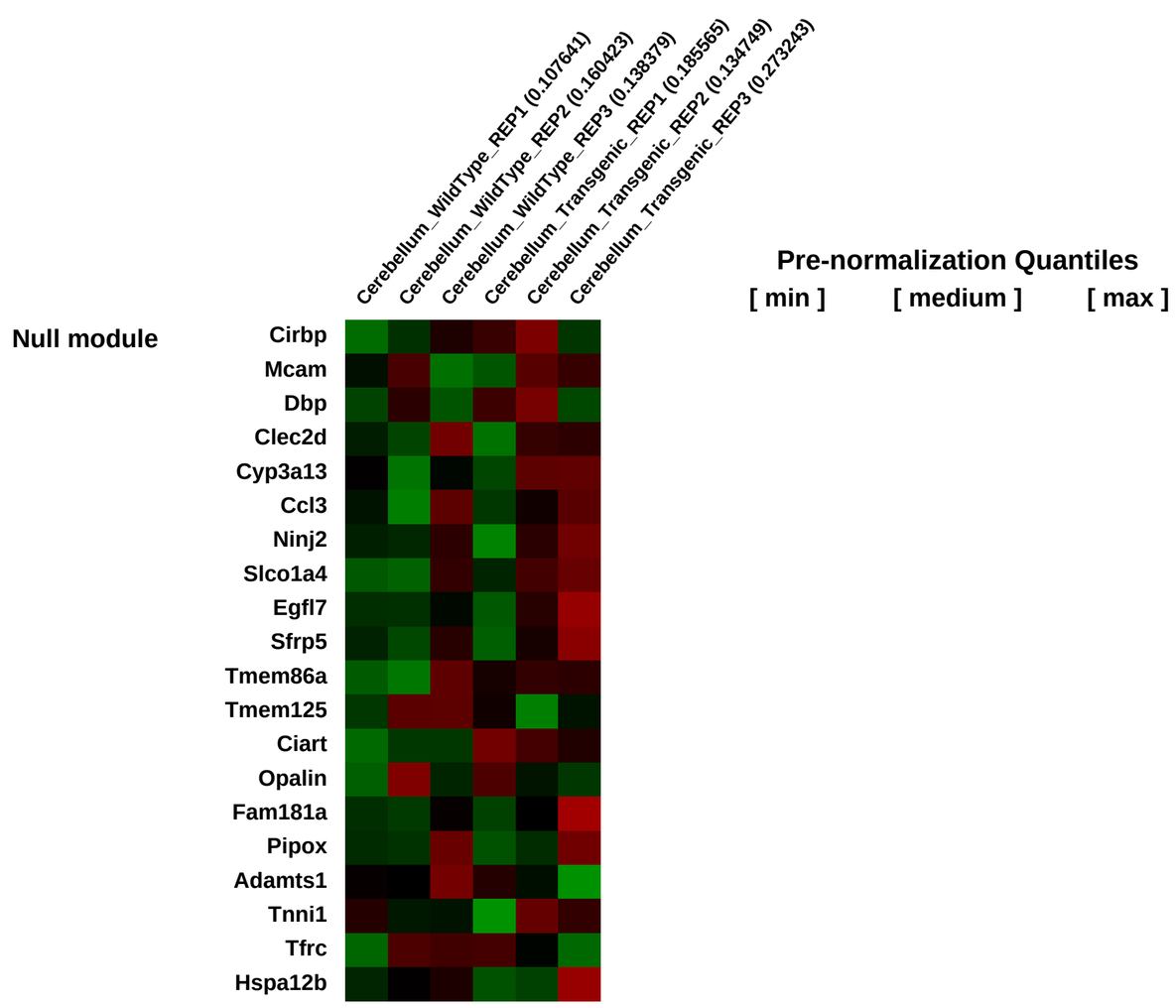

GEO Series "GSE34773" Expression Profiles

Num of samples in this series: 26

Scale of expression profile Z-scores

-3.0 -2.0 -1.0 0.0 1.0 2.0 3.0

GEO Link:	http://www.ncbi.nlm.nih.gov/geo/query/acc.cgi?acc=GSE34773
Status:	Public on Feb 04 2012
Title:	Skeletal muscle PGC-1a mediates mitochondrial, but not metabolic, changes during calorie restriction.
Organism:	Mus musculus
Experiment type:	Expression profiling by array
Platform:	GPL1261
Pubmed ID:	22308395
Summary & Design:	**Summary:** Calorie restriction (CR) is a dietary intervention that extends lifespan and healthspan in a variety of organisms. CR improves mitochondrial energy production, fuel oxidation and reactive oxygen species scavenging in skeletal muscle and other tissues, and these processes are thought to be critical to the benefits of CR. PGC-1a is a transcriptional coactivator that regulates mitochondrial function and is induced by CR. Consequently, many of the mitochondrial and metabolic benefits of CR are attributed to increased PGC-1a activity. To test this model for the first time, we examined the metabolic and mitochondrial response to CR in mice lacking skeletal muscle PGC-1a (MKO). Surprisingly, MKO mice demonstrated a normal improvement in glucose homeostasis in response to CR, indicating that skeletal muscle PGC-1a is dispensable for the whole-body benefits of CR. In contrast, gene expression profiling and electron microscopy demonstrated that PGC-1a is required for the full CR-induced increases in mitochondrial gene expression and mitochondrial density in skeletal muscle. These results demonstrate that PGC-1a is a major regulator of the mitochondrial response to CR in skeletal muscle, but surprisingly show that neither PGC-1a nor mitochondrial biogenesis in skeletal muscle are required for the metabolic benefits of CR. **Overall design:** Control (FLOX) and PGC-1a skeletal muscle specific knock out (MKO) mice were placed on a control diet [C] or a calorie restriction diet [CR] for 12 weeks. RNA was isolated from TA/EDL muscles for microarray analysis. The following numbers of mice were analyzed from each group: C FLOX: n = 6; C MKO: n = 7; CR FLOX: n = 6; CR MKO: n = 7. Mice were mixed C57/BL6 and 129 background.

Background corr dist: KL-Divergence = 0.2204, L1-Distance = 0.0535, L2-Distance = 0.0068, Normal std = 0.3180

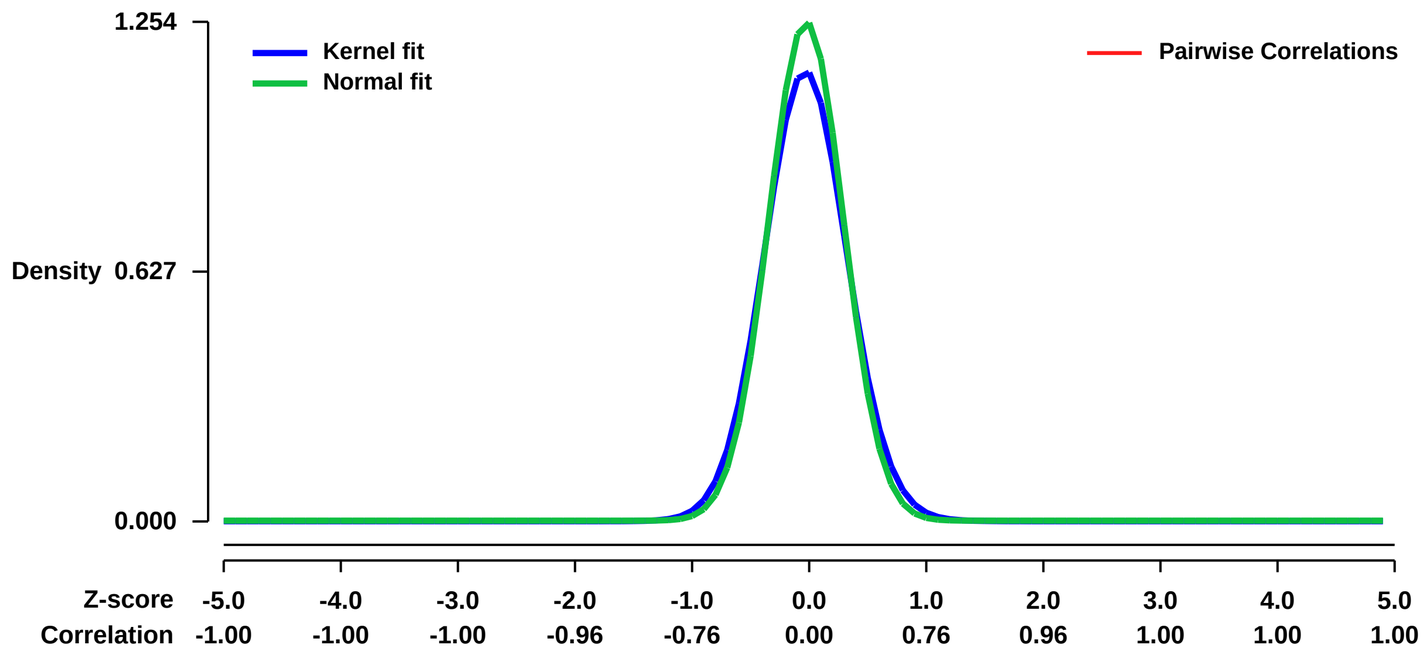

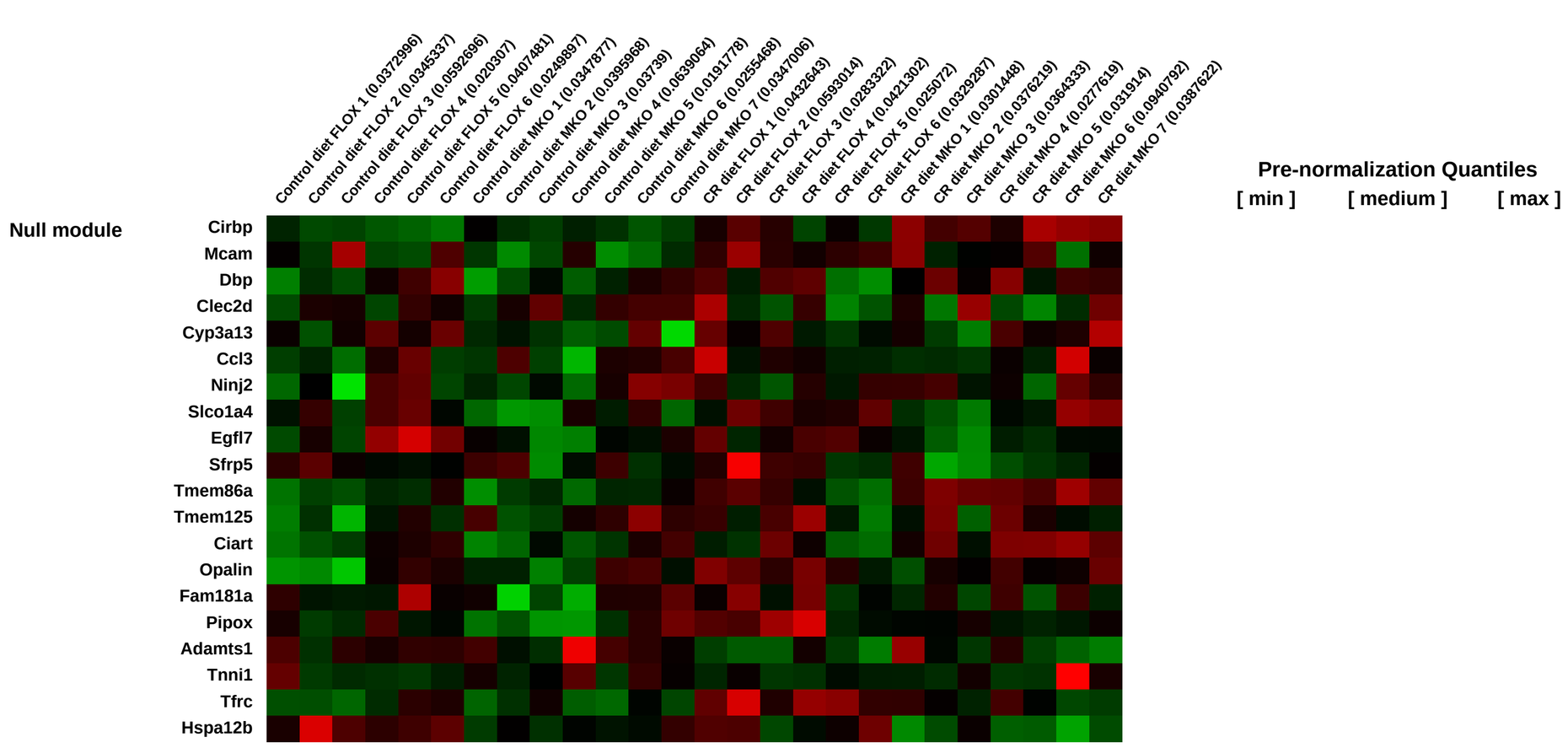

GEO Series "GSE34807" Expression Profiles

Num of samples in this series: 20

Scale of expression profile Z-scores

-3.0 -2.0 -1.0 0.0 1.0 2.0 3.0

GEO Link:	**http://www.ncbi.nlm.nih.gov/geo/query/acc.cgi?acc=GSE34807**
Status:	**Public on Dec 20 2012**
Title:	**The estrogen receptor ¸– is required and sufficient to maintain physiological glucose uptake in the mouse heart**
Organism:	**Mus musculus**
Experiment type:	**Expression profiling by array**
Platform:	**GPL1261**
Pubmed ID:	
Summary & Design:	**Summary:** **Rationale: Estrogens attenuate cardiac hypertrophy and increase cardiac contractility via their cognate receptors ER¸– and ER¸†. Since female sex hormones enhance global glucose utilization and because myocardial function and mass are tightly linked to cardiac glucose metabolism we tested the hypothesis that expression and activation of the estrogen receptor ¸– (ER¸–) might be required and sufficient to maintain physiological cardiac glucose uptake in the murine heart. Methods and Results: Cardiac glucose uptake quantified in vivo by 18F-fluorodeoxyglucose positron emission tomography (FDG-PET) was strongly impaired in ovarectomized compared to gonadal intact female C57BL/6JO mice. The selective ER¸– agonist 16¸–-LE2 and the non-selective ER¸– and ER¸† agonist 17¸†-estradiol completely restored cardiac glucose uptake in ovarectomized mice. Cardiac FDG uptake was strongly decreased in female ER¸– knockout mice (ERKO) compared to wild type littermates. Biochemical assays, affymetrix cDNA array analysis, western blotting and immuno-staining of cardiac glucose transporters revealed a positive correlation of ER¸– dependent cardiac FDG uptake with preserved cardiac glucose transporter-1 expression and micro-vascular localization. Conclusions: Systemic activation of the ER¸– estrogen receptor is sufficient and its expression is required to maintain physiological glucose uptake in the murine heart, which is likely to contribute to known cardio-protective estrogen effects.** **Overall design:** **total samples analysed are 20**

Background corr dist: KL-Divergence = 0.0902, L1-Distance = 0.0670, L2-Distance = 0.0084, Normal std = 0.4873

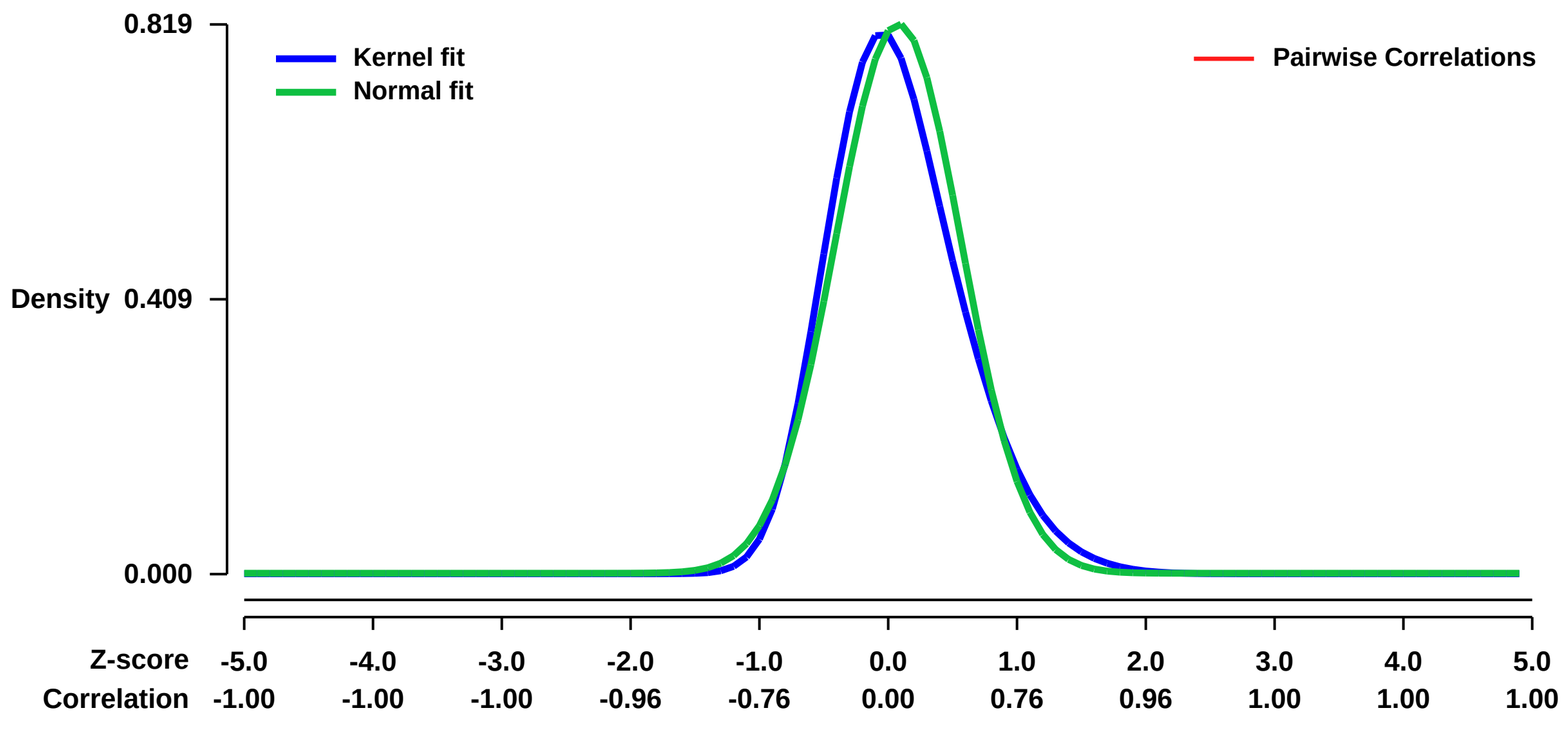

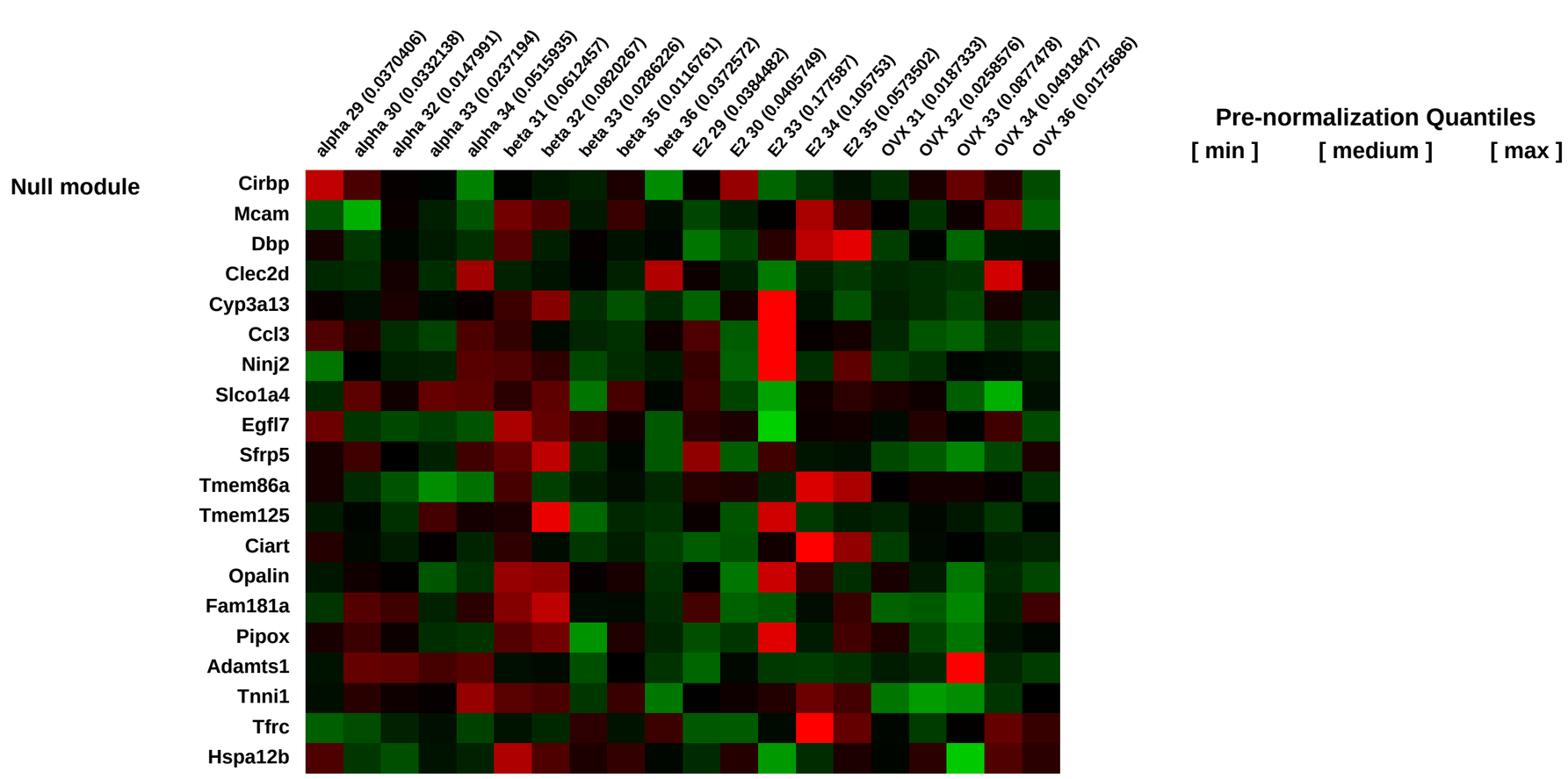

GEO Series "GSE34839" Expression Profiles

Num of samples in this series: 6

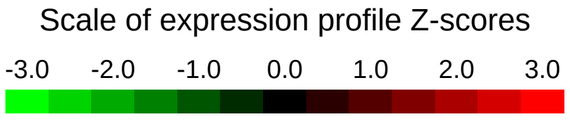

GEO Link:	http://www.ncbi.nlm.nih.gov/geo/query/acc.cgi?acc=GSE34839
Status:	Public on Feb 28 2012
Title:	Pten loss and RAS/MAPK activation cooperate to promote EMT and prostate cancer metastasis initiated from stem/progenitor cells
Organism:	Mus musculus
Experiment type:	Expression profiling by array
Platform:	GPL1261
Pubmed ID:	22350410
Summary & Design:	**Summary:** PTEN loss or PI3K/AKT signaling pathway activation correlates with human prostate cancer progression and metastasis. However, in preclinical murine models, deletion of Pten alone fails to mimic the significant metastatic burden that frequently accompanies the end stage of human disease. To identify additional pathway alterations that cooperate with PTEN loss in prostate cancer progression, we surveyed human prostate cancer tissue microarrays and found that the RAS/MAPK pathway is significantly elevated both in primary and metastatic lesions. In an attempt to model this event, we crossed conditional activatable K-rasG12D/WT mice with the prostate conditional Pten deletion model we previously generated. Although RAS activation alone cannot initiate prostate cancer development, it significantly accelerated progression caused by PTEN loss, accompanied by epithelial-to-mesenchymal transition (EMT) and macrometastasis with 100% penitence. A novel stem/progenitor subpopulation with mesenchymal characteristics was isolated from the compound mutant prostates, which was highly metastatic upon orthotopic transplantation. Importantly, inhibition of RAS/MAPK signaling by PD325901, a MEK inhibitor, significantly reduced the metastatic progression initiated from transplanted stem/progenitor cells. Collectively, these data indicate that activation of RAS/MAPK signaling serves as a potentiating second hit to alteration of the PTEN/PI3K/AKT axis and co-targeting both pathways is highly effective in preventing the development of metastatic prostate cancers. **Overall design:** Murine mutants with prostate specific loss of Pten and K-ras activation (K-rasG12D) under regulation of the probasin promoter developed high grade, invasive prostate cancer. RNA was extracted from dissected prostate lobes from individual mutants with pathology thought to closely mimic human disease. Prostate tissue was subject to RNA extraction and hybridization on Affymetrix cDNA microarrays.

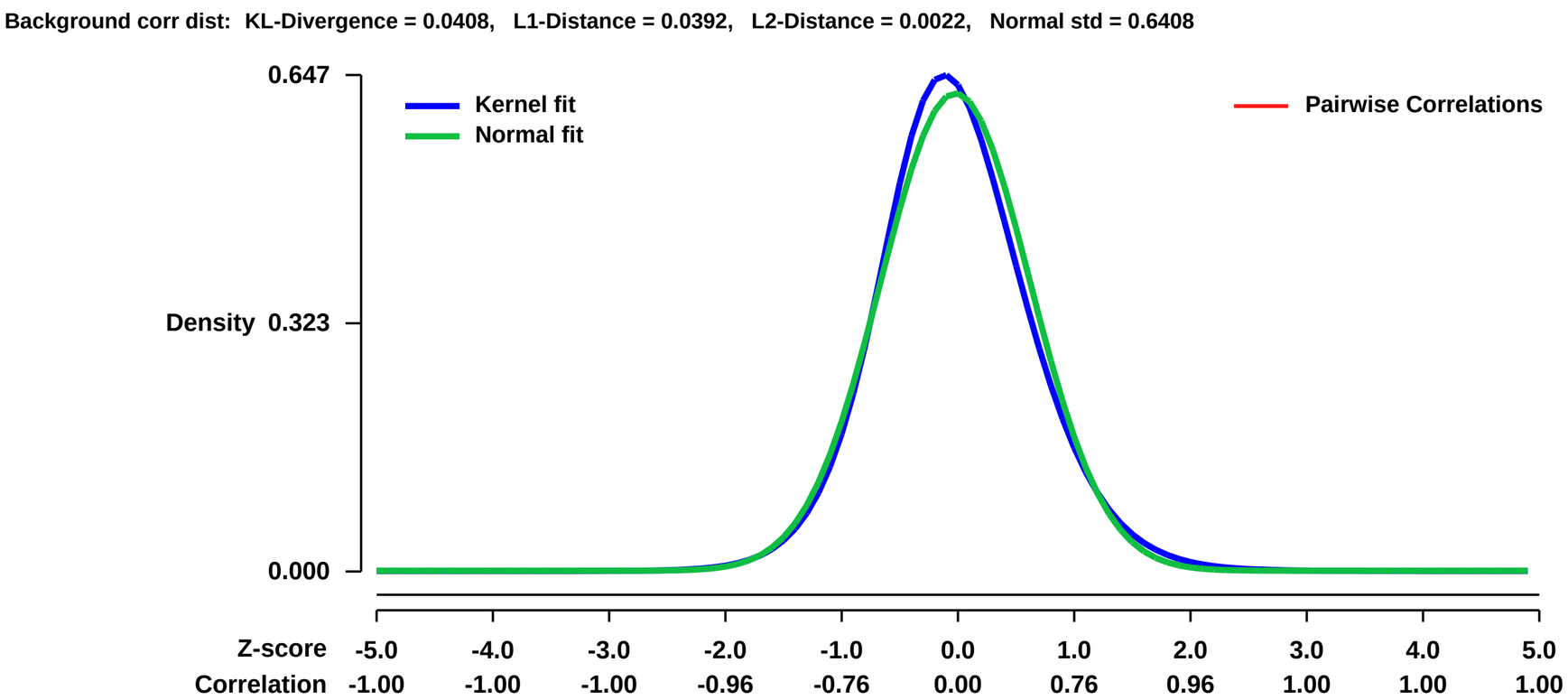

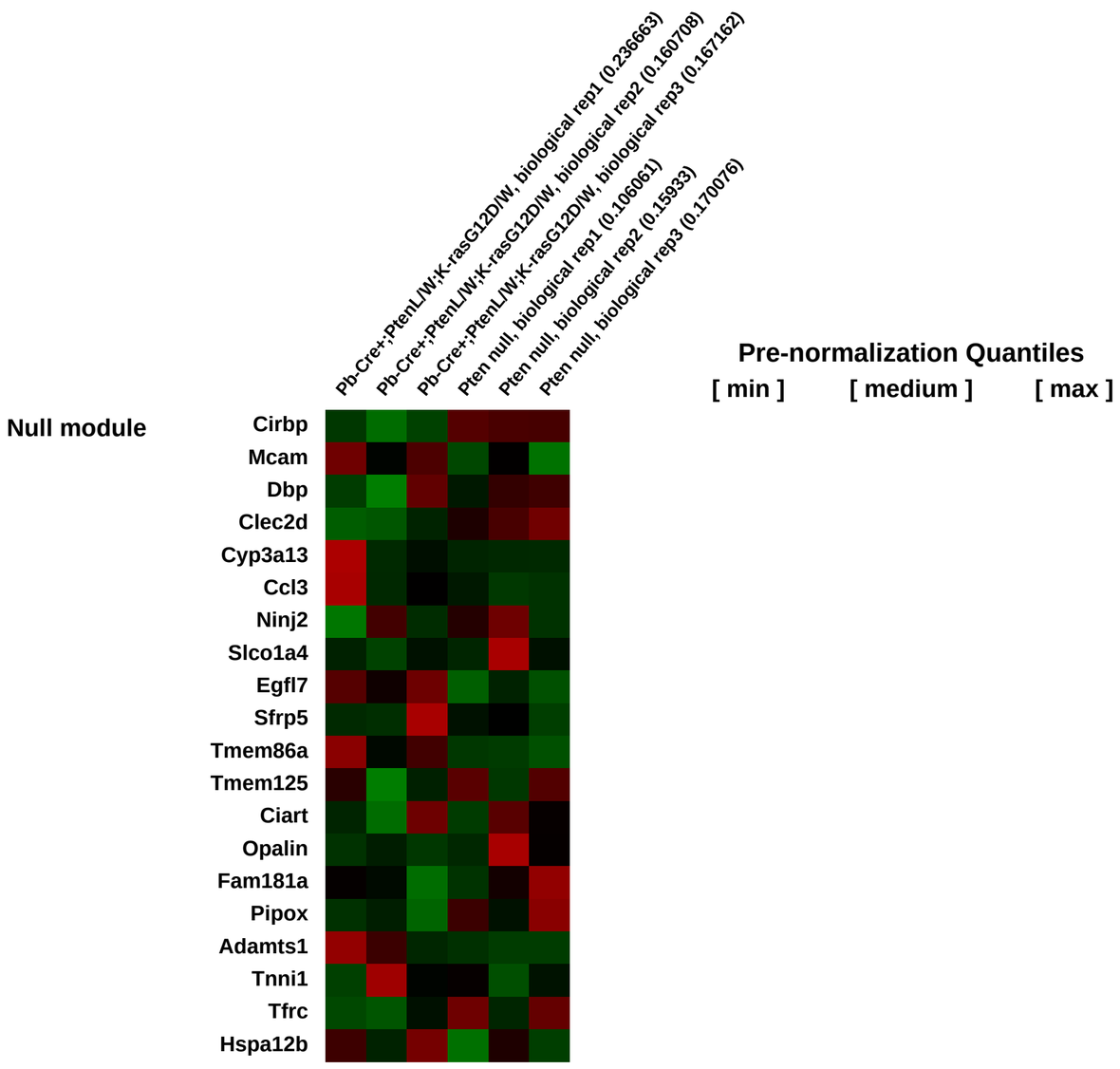

GEO Series "GSE34902" Expression Profiles

Num of samples in this series: 6

Scale of expression profile Z-scores

-3.0 -2.0 -1.0 0.0 1.0 2.0 3.0

GEO Link:	http://www.ncbi.nlm.nih.gov/geo/query/acc.cgi?acc=GSE34902
Status:	Public on Sep 06 2012
Title:	Genome-wide Profiling of Progesterone Receptor and GATA2 Binding in the Mouse Uterus [Affymetrix]
Organism:	Mus musculus
Experiment type:	Expression profiling by array
Platform:	GPL1261
Pubmed ID:	22638070
Summary & Design:	**Summary:** Progesterone (P4) signaling through its nuclear transcription factor, the progesterone receptor (PR), is essential for normal uterine function. Although deregulation of PR mediated signaling is known to underscore uterine dysfunction and a number of endometrial pathologies, the early molecular mechanisms of this deregulation are unclear. To address this issue, we have defined the genome-wide PR and GATA2 cistrome in the murine uterus using chromatin immunoprecipitation followed by massively parallel sequencing (ChIP-seq). In uteri of ovariectomized mice, we identified 6367 PR binding sites in the absence of P4 ligand; however, this number increased at nearly three fold (18,432) following acute P4 exposure. Sequence analysis revealed that approximately 73% of these binding sites contain a progesterone response element (PRE) or a half-site motif recognized by the PR. Many previously identified P4 target genes known to regulate uterine function were found to contain PR binding sites, confirming the validity of our methodology. In addition we identified 46,183 GATA2 binding sites in P4 treatment conditions with 7,954 binding sites overlapping that of the PR. **Overall design:** Gene expression data from ovariectomized Oil and P4 treated Gata2 f/f uterus horn

Background corr dist: KL-Divergence = 0.0332, L1-Distance = 0.0192, L2-Distance = 0.0004, Normal std = 0.6535

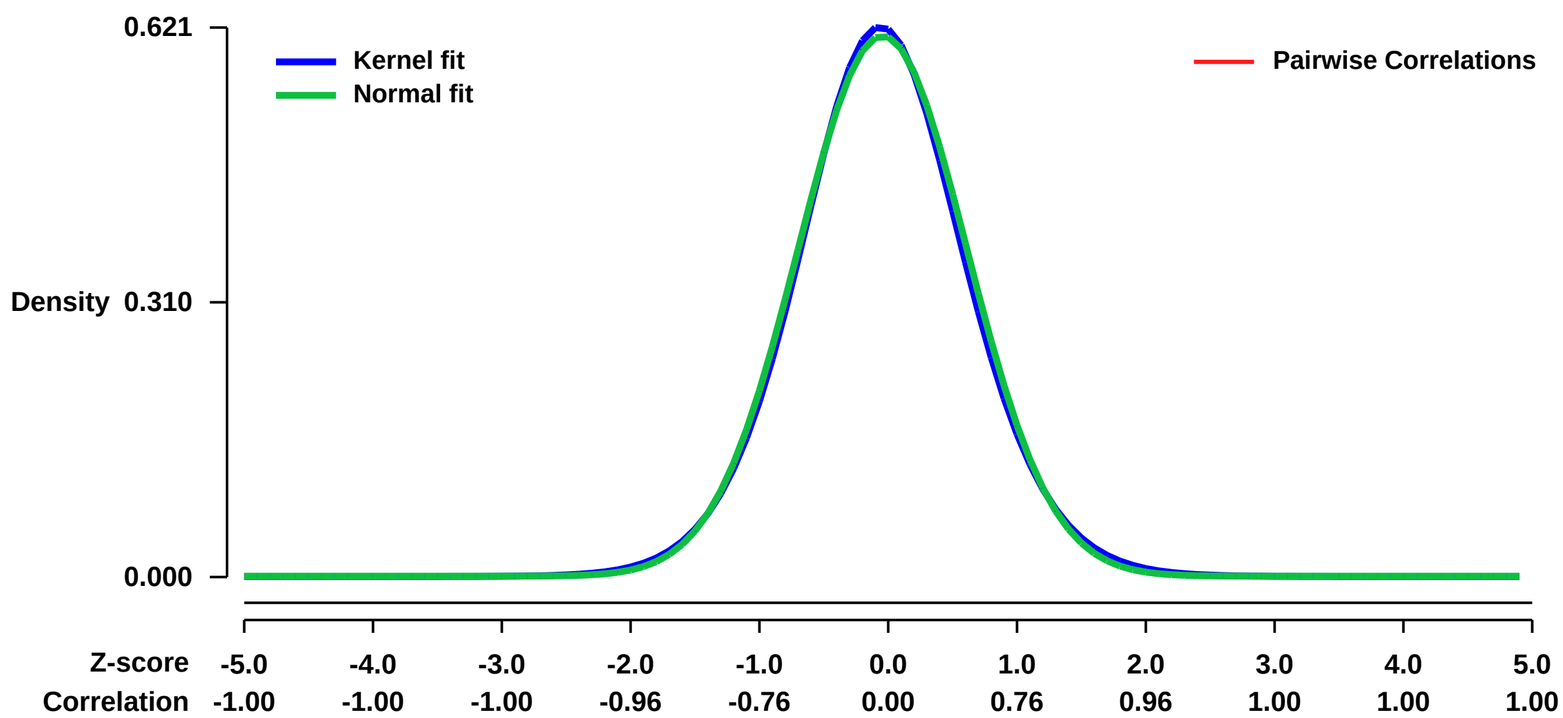

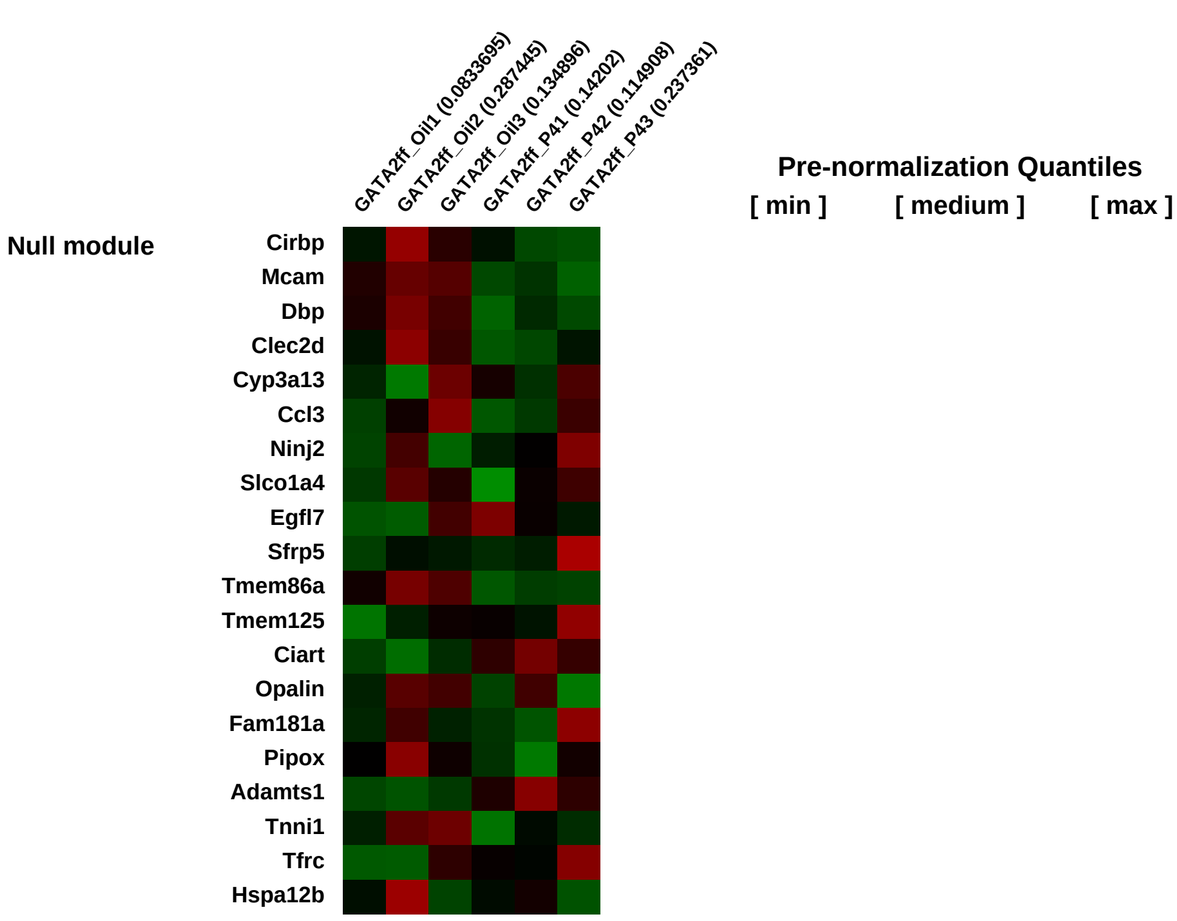

GEO Series "GSE34959" Expression Profiles

Num of samples in this series: 10

Scale of expression profile Z-scores

-3.0 -2.0 -1.0 0.0 1.0 2.0 3.0

GEO Link:	http://www.ncbi.nlm.nih.gov/geo/query/acc.cgi?acc=GSE34959
Status:	Public on Feb 22 2012
Title:	Expression profiling of primary wild type (WT), Ezh2-null and Eed-null murine MLL-AF9 AML
Organism:	Mus musculus
Experiment type:	Expression profiling by array
Platform:	GPL1261
Pubmed ID:	22396593
Summary & Design:	**Summary:** We evaluated gene expression changes in murine leukemia caused by retroviral overexpression of MLL-AF9. We compared wild-type (WT) leukemia cells with mutant leukemia cells after cre-mediated inactivation of homozygous conditional alleles for Ezh2 or Eed, both of which are components of the Polycomb Repressive Complex2. **Overall design:** For WT cells, 3 biological replicates were hybridized. For Ezh2-null cells, 4 biological replicates were hybridized. For Eed-cells, 3 biological replicates were hybridized.

Background corr dist: KL-Divergence = 0.0919, L1-Distance = 0.0330, L2-Distance = 0.0021, Normal std = 0.4512

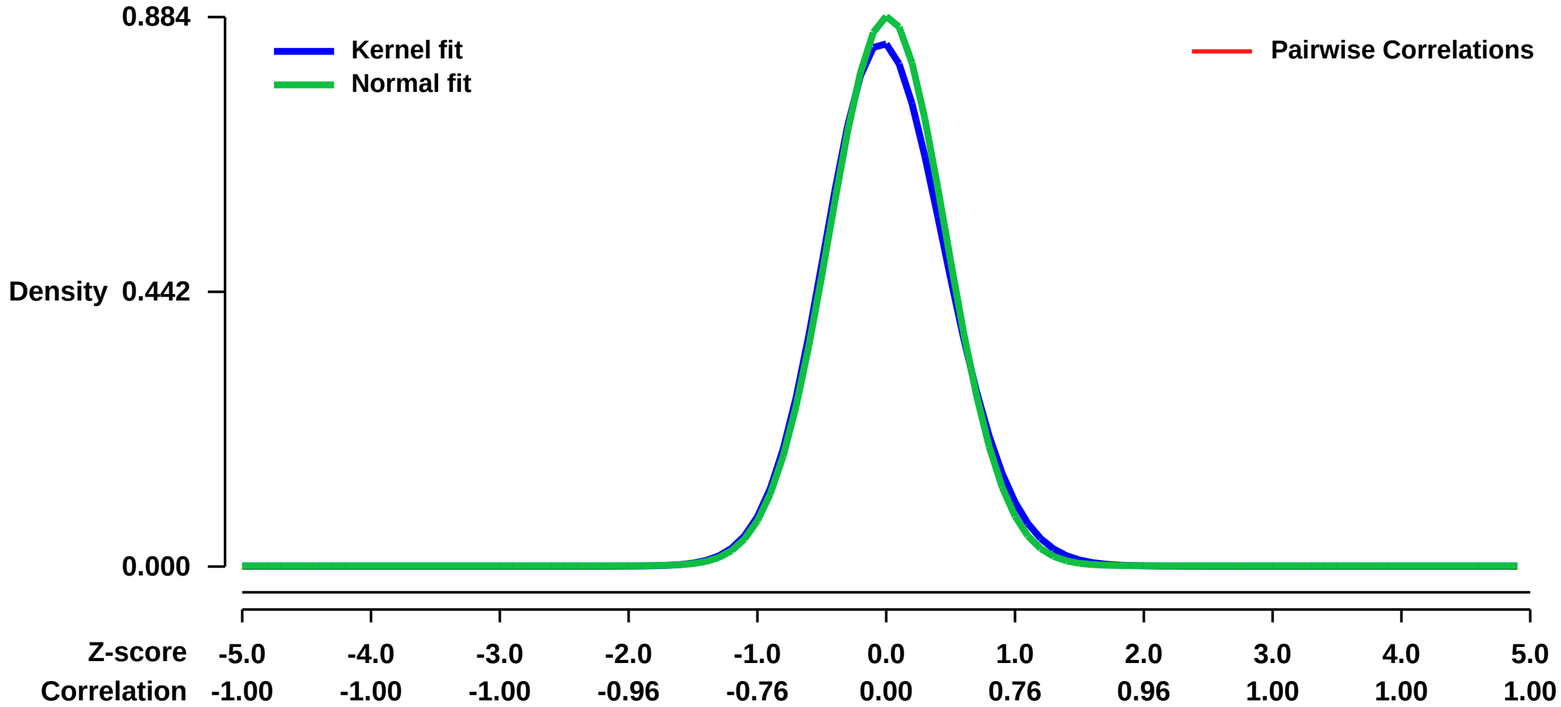

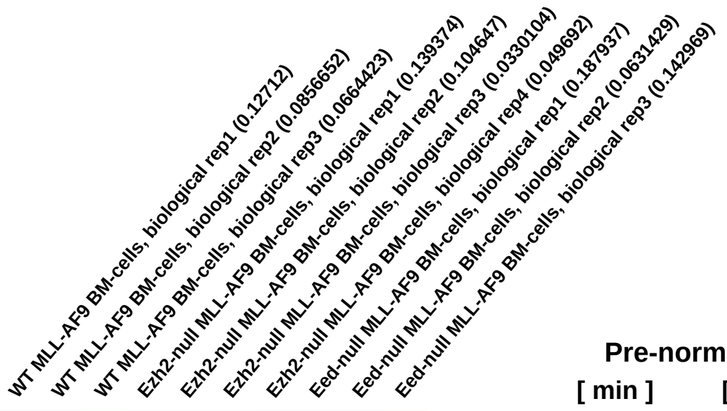

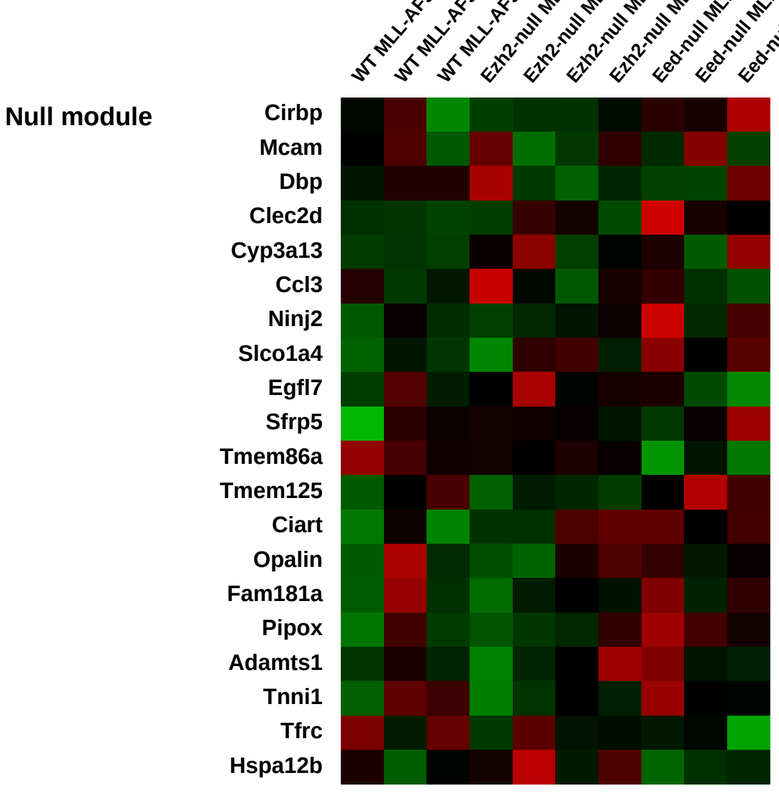

GEO Series "GSE34961" Expression Profiles

Num of samples in this series: 9

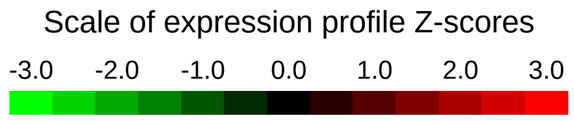

GEO Link:	http://www.ncbi.nlm.nih.gov/geo/query/acc.cgi?acc=GSE34961
Status:	Public on Feb 22 2012
Title:	Expression profiling of secondary wild type (WT) and Ezh2-null murine MLL-AF9 AML
Organism:	Mus musculus
Experiment type:	Expression profiling by array
Platform:	GPL1261
Pubmed ID:	22396593
Summary & Design:	**Summary:** We evaluated gene expression changes in secondary recipient murine leukemia caused by retroviral overexpression of MLL-AF9. We compared wild-type (WT) leukemia cells with mutant leukemia cells after cre-mediated inactivation of a homozygous conditional allele for Ezh2, a component of the Polycomb Repressive Complex2. **Overall design:** For WT cells, 4 biological replicates were hybridized. For Ezh2-null cells, 5 biological replicates were hybridized.

Background corr dist: KL-Divergence = 0.0622, L1-Distance = 0.0284, L2-Distance = 0.0014, Normal std = 0.5159

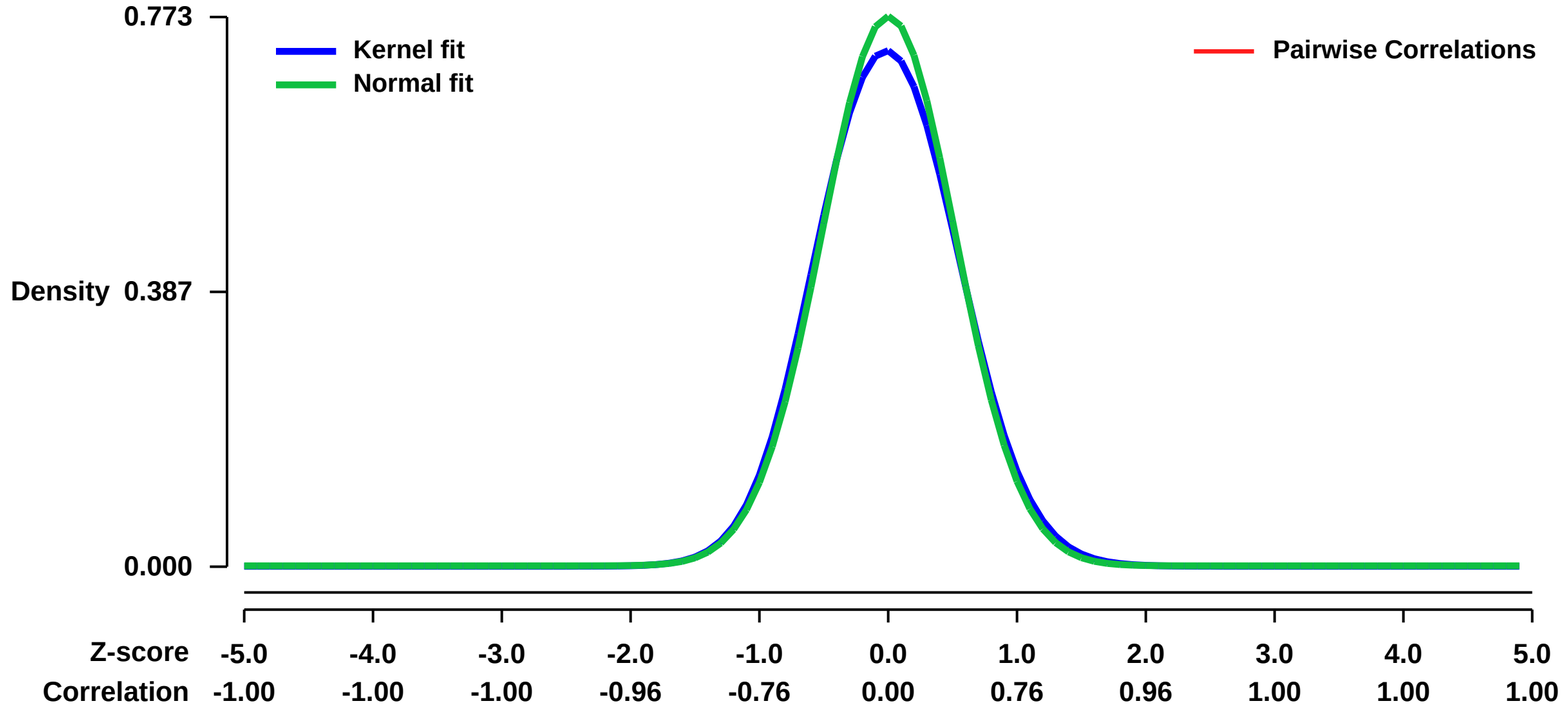

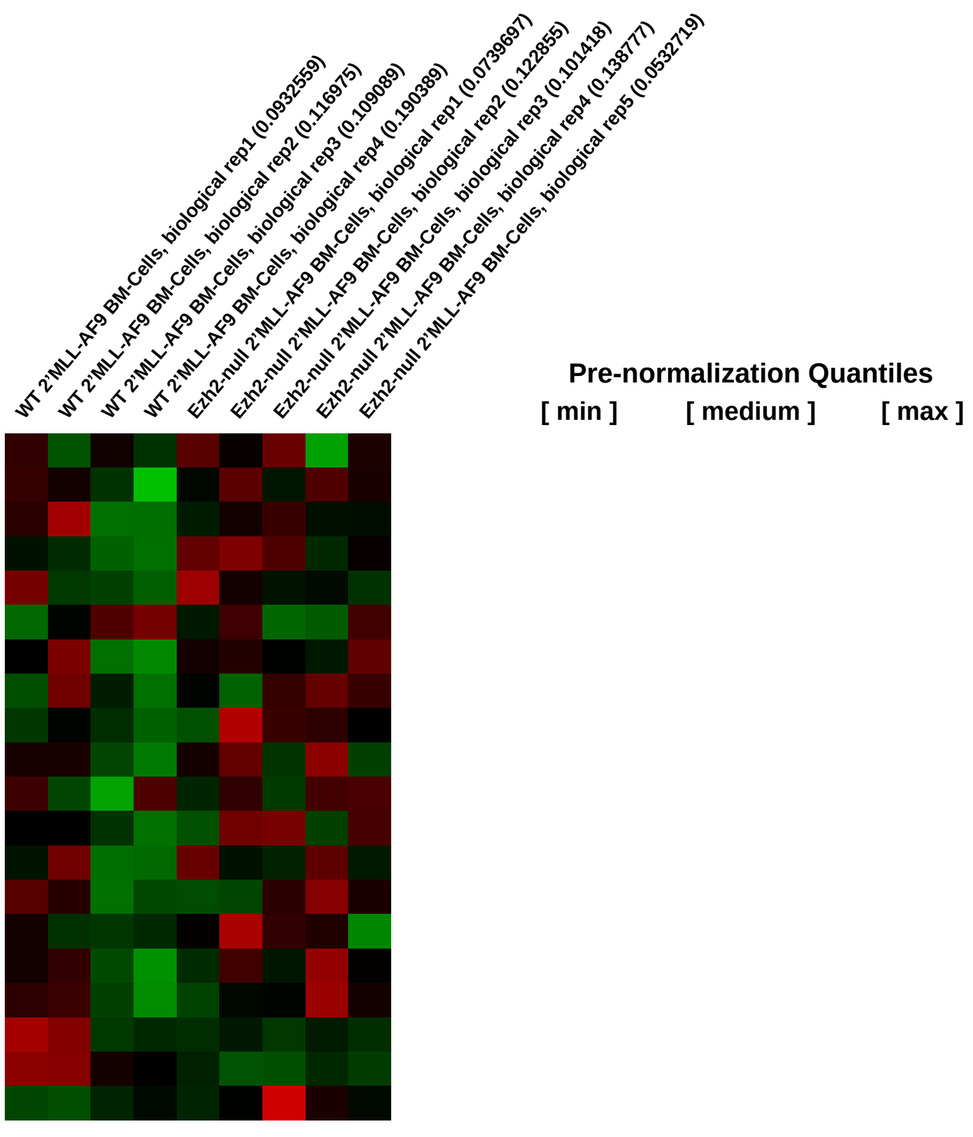

GEO Series "GSE3501" Expression Profiles

Num of samples in this series: 6

Scale of expression profile Z-scores

-3.0 -2.0 -1.0 0.0 1.0 2.0 3.0

GEO Link:	http://www.ncbi.nlm.nih.gov/geo/query/acc.cgi?acc=GSE3501
Status:	Public on Jan 01 2006
Title:	Comparative analysis of 10 week and 5 week Bitransgenic mice (LH mouse crossed with MMTV-neu mouse)
Organism:	Mus musculus
Experiment type:	Expression profiling by array
Platform:	GPL1261
Pubmed ID:	16434967
Summary & Design:	**Summary:** To identify genes that may facilitate early steps of ErbB2/Neu-mediated mammary tumorigenesis, we performed comparative microarray analysis of 5- and 10-week bitransgenic mammary glands (LHxMMTV-neu) in triplicate. **Keywords: transgenic mouse, erbB2, MMTV-neu, HER2, mammary tumor, breast cancer** **Overall design:** We analyzed 3 pooled RNA samples that represented 3 animals for each time point so that a total of 9 bitransgenic mice were analyzed per time point.

Background corr dist: **KL-Divergence = 0.0235, L1-Distance = 0.0195, L2-Distance = 0.0004, Normal std = 0.7222**

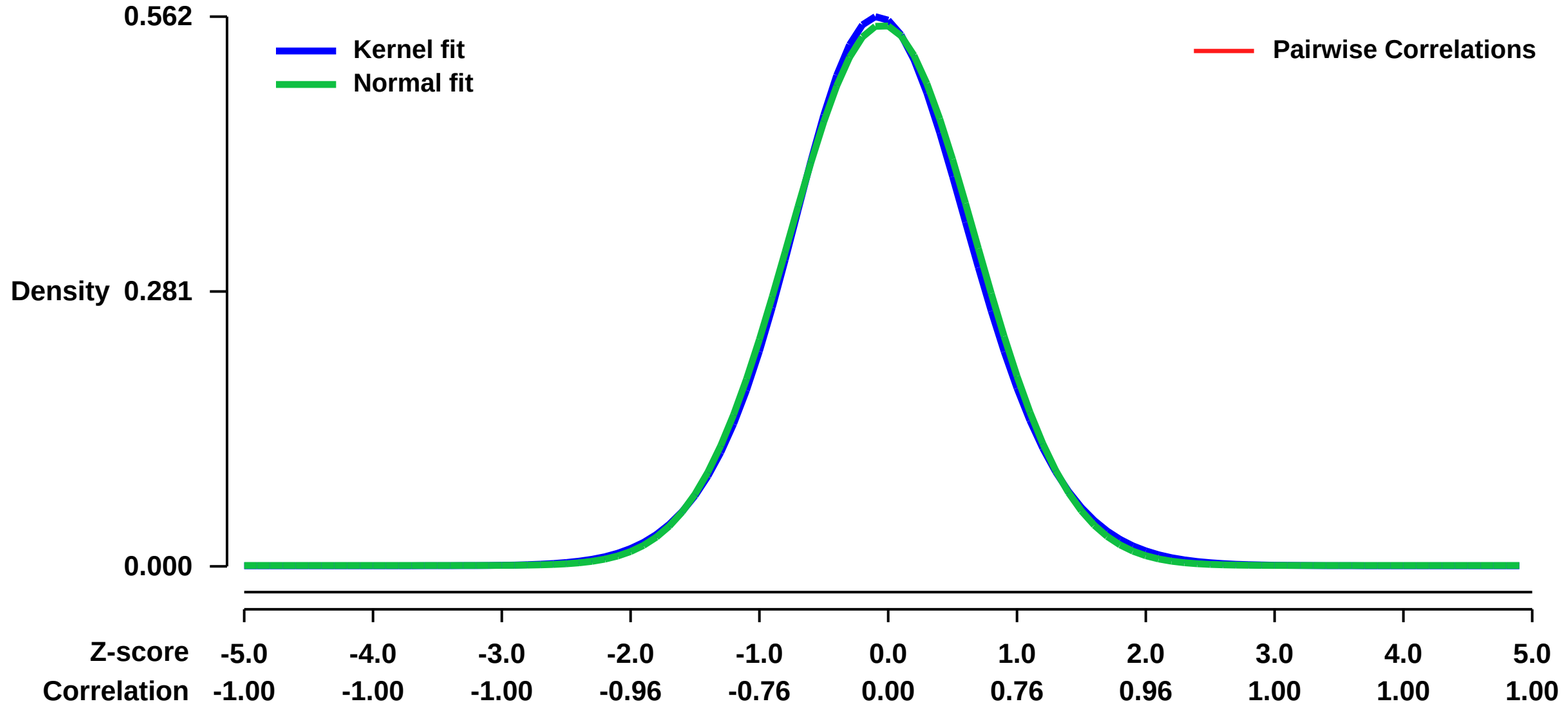

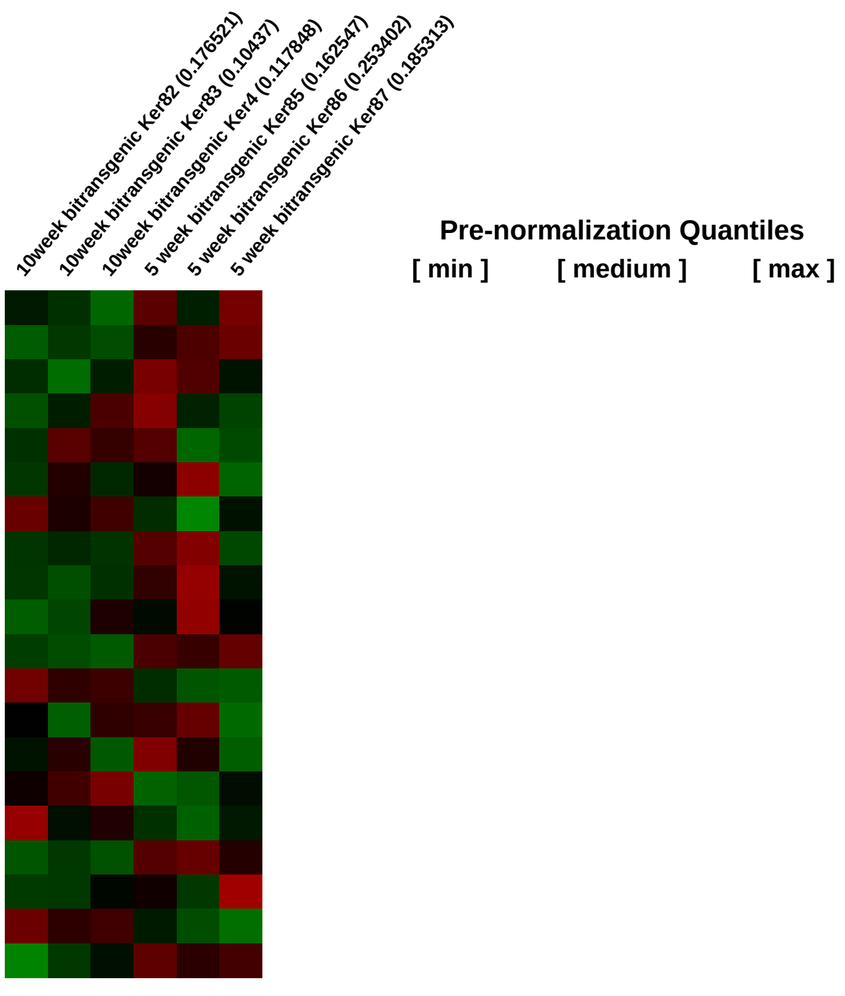

GEO Series "GSE35044" Expression Profiles

Num of samples in this series: 9

Scale of expression profile Z-scores

-3.0 -2.0 -1.0 0.0 1.0 2.0 3.0

GEO Link:	http://www.ncbi.nlm.nih.gov/geo/query/acc.cgi?acc=GSE35044
Status:	Public on Jan 17 2012
Title:	Expression profiles of Telomerase+ vs. ALT+ G3 Atm-/-TERT-ER T-cell lymphomas
Organism:	Mus musculus
Experiment type:	Expression profiling by array
Platform:	GPL1261
Pubmed ID:	22341440
Summary & Design:	**Summary:** We used microarray profiling to document the difference between telomerase+ vs. ALT+ T-cell lymphomas developed on G3 Atm-/-TERT-ER genetic background. **Overall design:** T-cell lymphomas were developed in G3 Atm-/-TERT-ER mice with 4-OHT treatment. These cells were either maintained on SCID mice treated with 4-OHT or vehicle. Cells maintained on vehicle eventually developed ALT-dependent resistance. We used microarray to profile telomerase+ tumors vs. ALT+ tumors from the same parental lines.

Background corr dist: KL-Divergence = 0.0830, L1-Distance = 0.0208, L2-Distance = 0.0006, Normal std = 0.4711

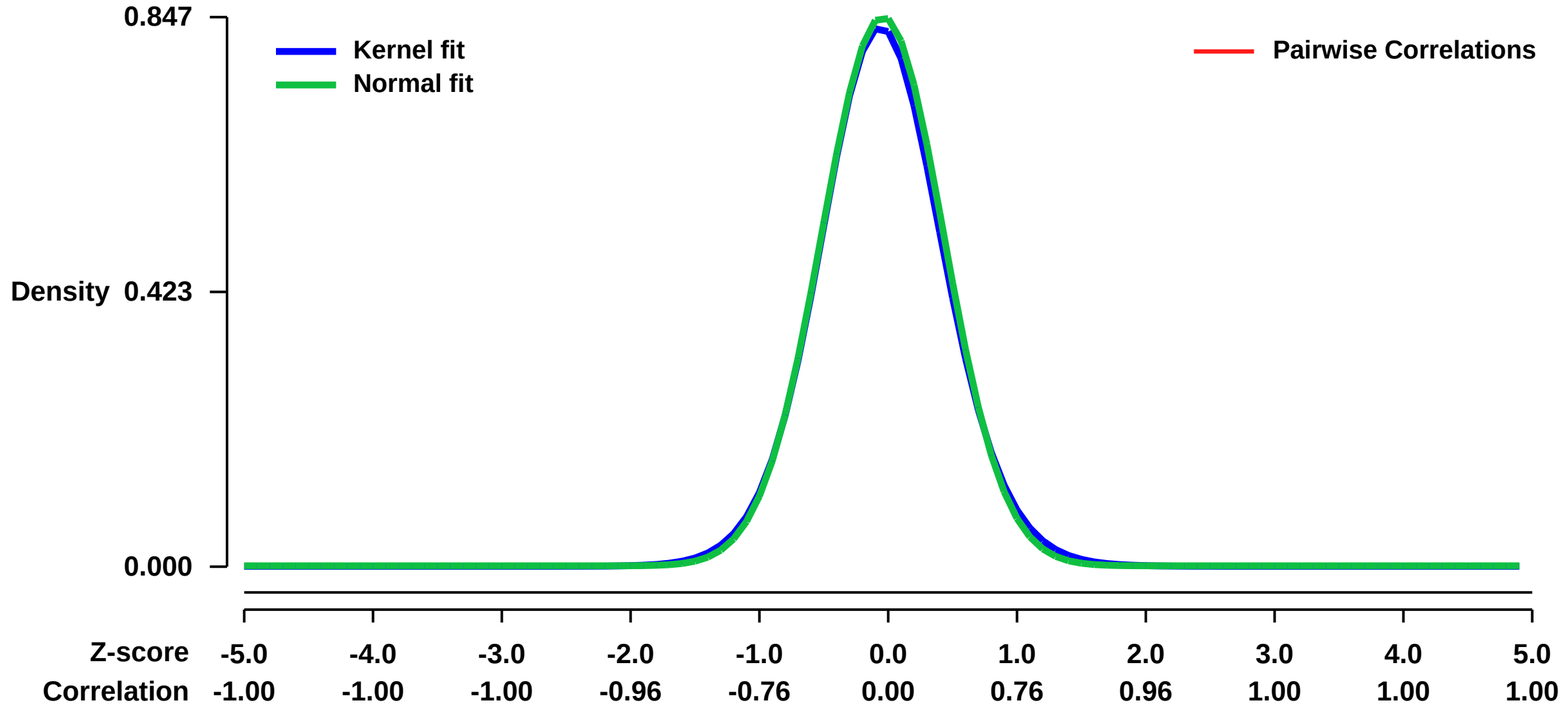

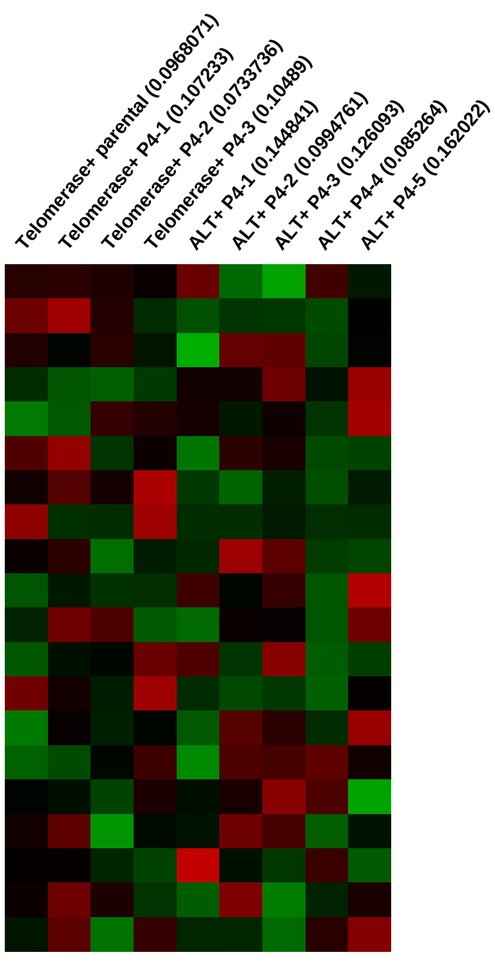

GEO Series "GSE35106" Expression Profiles

Num of samples in this series: 9

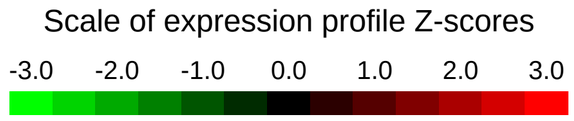

GEO Link:	http://www.ncbi.nlm.nih.gov/geo/query/acc.cgi?acc=GSE35106
Status:	Public on Jan 14 2012
Title:	Polysome-bound mRNA during oocyte maturation
Organism:	Mus musculus
Experiment type:	Expression profiling by array
Platform:	GPL1261
Pubmed ID:	21460039
Summary & Design:	**Summary:** Oocyte maturation, fertilization, and early embryonic development occur in the absence of gene transcription. Therefore, it is critical to understand at a global level the post-transcriptional events that are driving these transitions. Here, we have used a systems approach by combining polysome mRNA profiling and bioinformatics to identify RNA binding motifs in mRNAs that either enter or exit the polysome pool during mouse oocyte maturation. Association of mRNA with the polysomes correlates with active translation. **Overall design:** Forty-eight hours (h) after PMSG injection, mice were stimulated with hCG for 0, 4, or 14 h, and GV-, MI- and MII-stage oocytes were collected. Polysome-bound mRNAs were purified, reverse-transcribed and linearly amplified with the WT-Ovation FFPE RNA Amplification System V2 (NuGEN). 5´µg cDNA were fragmented and hybridized with Affymetrix Mouse Genome 430.2 array chips. Experiments were done using 3 independent sample sets.

Background corr dist: KL-Divergence = 0.1068, L1-Distance = 0.0773, L2-Distance = 0.0124, Normal std = 0.4711

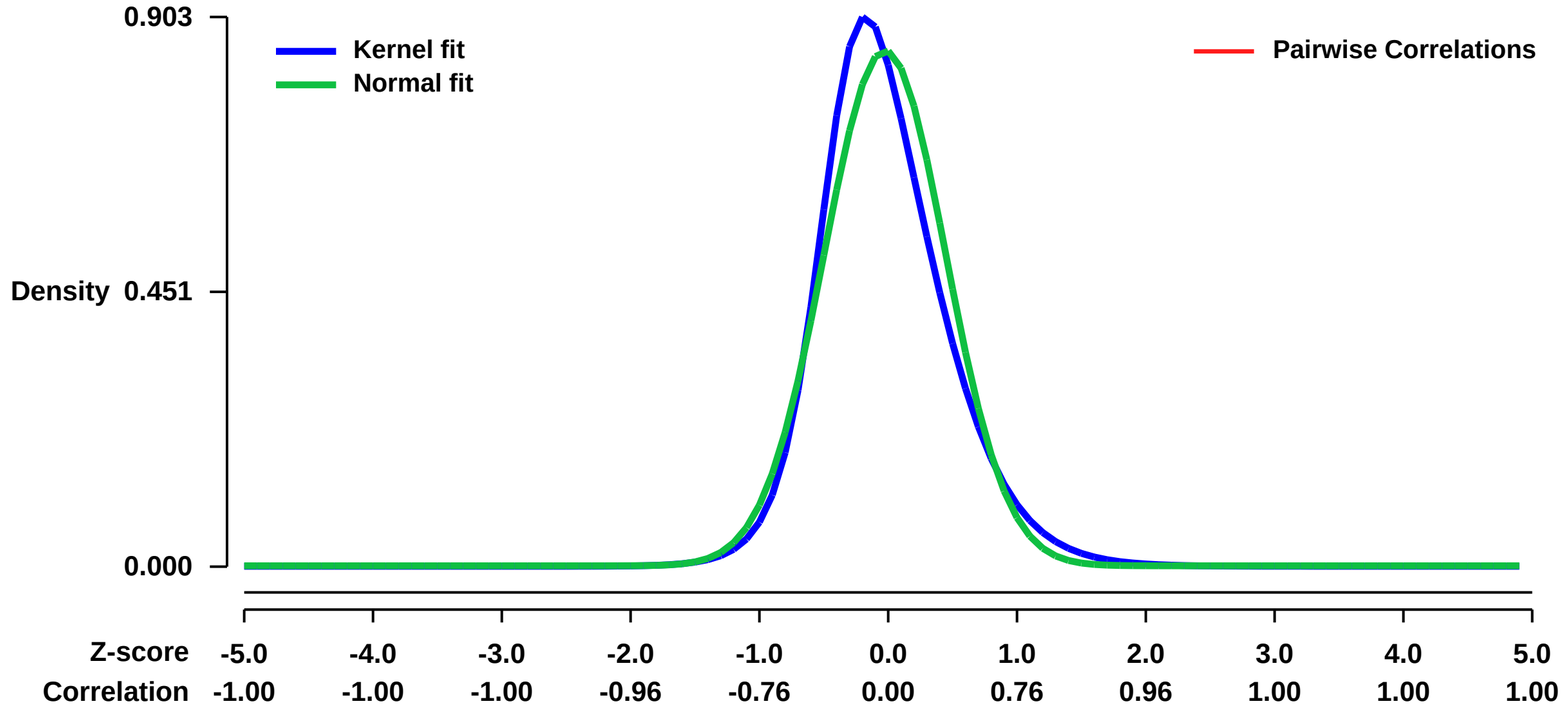

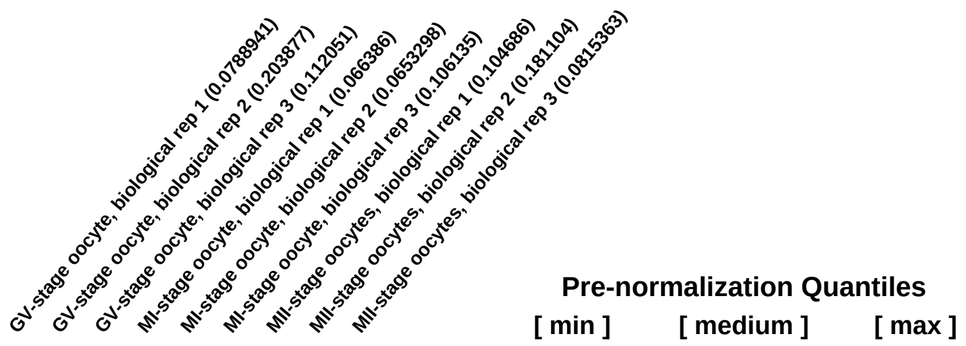

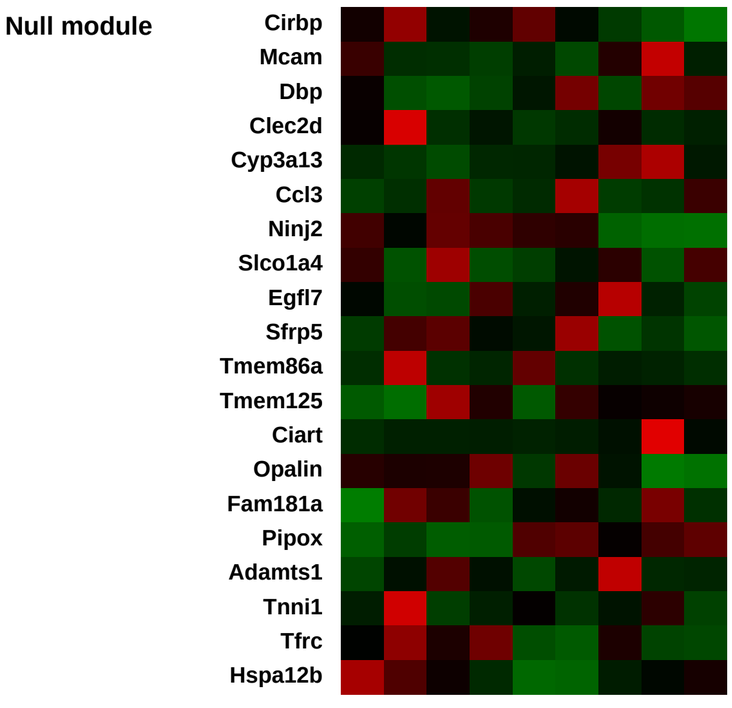

GEO Series "GSE35160" Expression Profiles

Num of samples in this series: 6

Scale of expression profile Z-scores

-3.0 -2.0 -1.0 0.0 1.0 2.0 3.0

GEO Link:	http://www.ncbi.nlm.nih.gov/geo/query/acc.cgi?acc=GSE35160
Status:	Public on Feb 01 2012
Title:	Functional analysis of the cytoprotective transcription factor Nrf2 in skin morphogenesis and disease: Identification of Nrf2 target genes
Organism:	Mus musculus
Experiment type:	Expression profiling by array
Platform:	GPL1261
Pubmed ID:	22383093
Summary & Design:	**Summary:** The Nrf2 transcription factor is a key player in the cellular stress response, which regulates the expression of important antioxidant enzymes and other cytoprotective proteins. We recently generated a novel transgenic mouse model to determine the function of Nrf2 in the skin. These mice revealed interesting phenotypic abnormalities, including hyperkeratosis and acanthosis. To gain insight into the underlying molecular mechanisms, we wanted to identify genes, which are differentially expressed in the skin of wild-type and mutant mice before the onset of phenotypic abnormalities. **Overall design:** RNA from whole skin of 3 single P2.5 K5cre-caNrf2 (tg/tg) and 3 single P2.5 K5cre-wt (tg/wt=control) mice were used

Background corr dist: KL-Divergence = 0.0365, L1-Distance = 0.0130, L2-Distance = 0.0001, Normal std = 0.6269

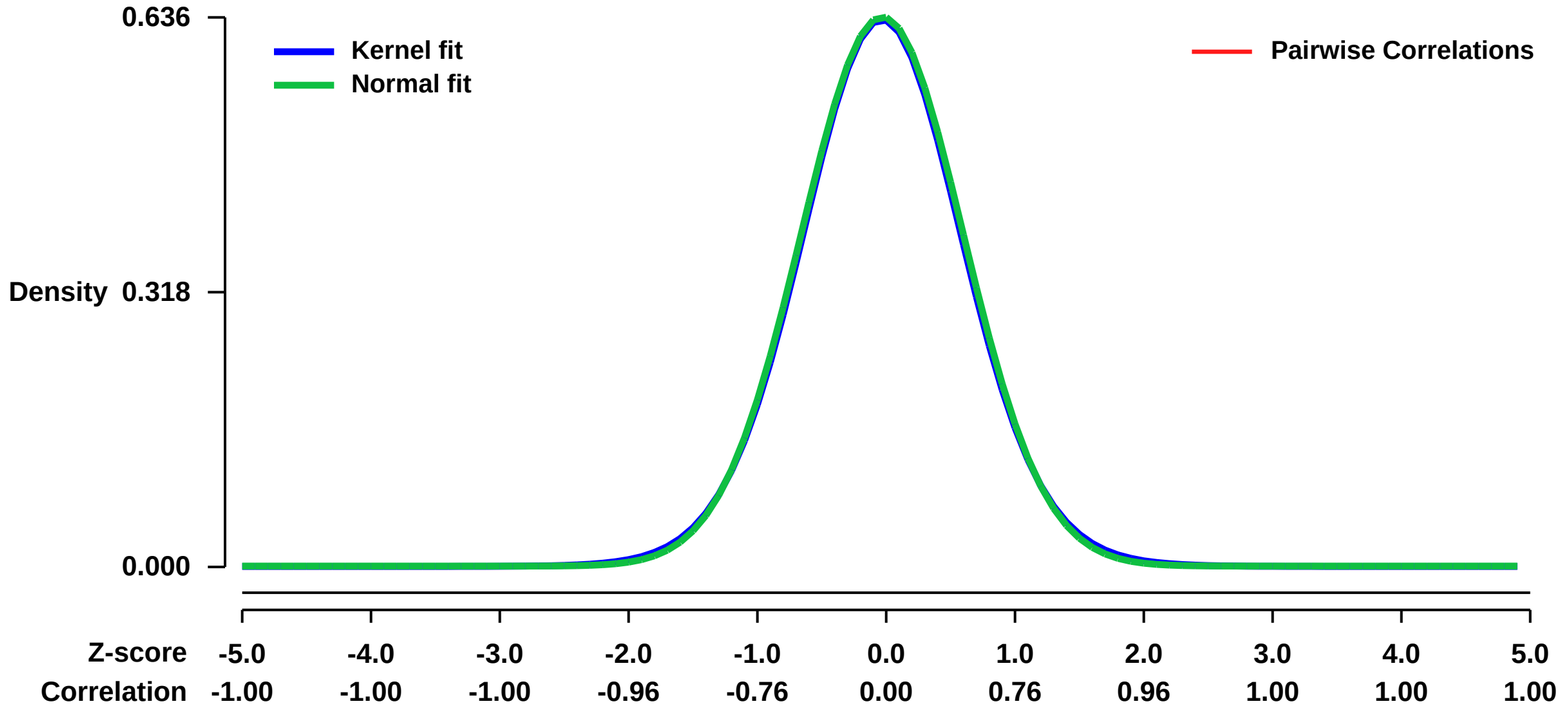

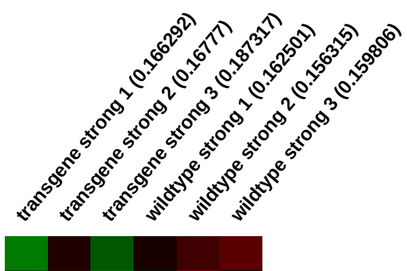

Pre-normalization Quantiles

[min] [medium] [max]

Null module

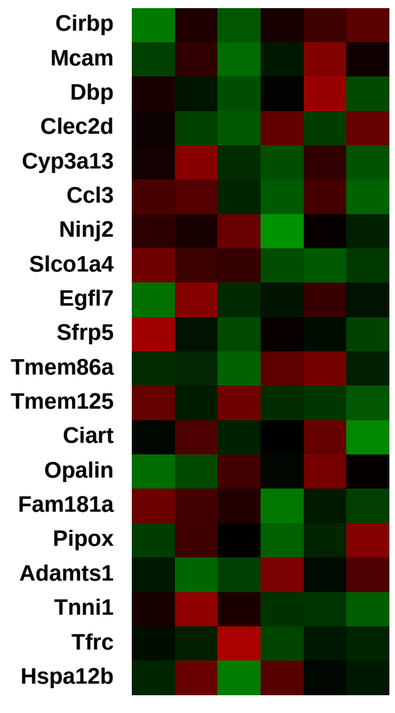

GEO Series "GSE35206" Expression Profiles

Num of samples in this series: 14

Scale of expression profile Z-scores

-3.0 -2.0 -1.0 0.0 1.0 2.0 3.0

GEO Link:	http://www.ncbi.nlm.nih.gov/geo/query/acc.cgi?acc=GSE35206
Status:	Public on Dec 05 2012
Title:	Specific transcriptional response of four blockers of estrogen receptors on estradiol-modulated genes in the mouse mammary gland
Organism:	Mus musculus
Experiment type:	Expression profiling by array
Platform:	GPL1261
Pubmed ID:	22678160
Summary & Design:	**Summary:** The efficacy and exceptionally good tolerance of estrogen blockade in the treatment of breast cancer is well recognized but novel agents are required, especially to take advantage of the multiple consecutive responses obtained in breast cancer progressing following previous hormone therapy, thus delaying the use of cytotoxic chemotherapy with its usually serious side effects. Acolbifene (ACOL) is a novel and unique antiestrogen completely free of estrogen-like activity in both the mammary gland and uterus while preventing bone loss. From the preclinical and clinical data so-far available, this new antiestrogen represents a unique opportunity for a highly potent and specific blockade of estrogen action in the mammary gland and uterus while exerting estrogen-like beneficial effects in other tissues (selective estrogen receptor modulator or SERM activity). In order to better understand the specificity of action of acolbifene, we have used Affymetrix GeneChips containing 45,000 probe sets to analyze 34,000 genes to determine the specificity of this compound compared to the pure antiestrogen fulvestrant, as well as the mixed antagonists/agonists tamoxifen and raloxifene to block the effect of estradiol (E2) and to induce effects of their own on gene expression in the mouse mammary gland. The genes modulated by E2 were those identified in two separate experiments and validated by quantitative real-time PCR (Q_RT-PCR). Three hours after the single subcutaneous injection of E2 (0.05 ug), the simultaneous administration of acolbifene, fulvestrant, tamoxifen and raloxifene blocked by 98%, 62%, 43% and 92% the number of E2-upregulated genes, respectively. On the other hand, 70%, 10%, 25% and 55% of the genes down-regulated by E2 were blocked by the same compounds. Acolbifene was also the compound which, when used alone, modulated the smallest number of genes also influenced by E2, namely 4%, thus possibly explaining the potent tumoricidal action of this compound in human breast cancer xenografts where 61% of tumors disappeared, thus bringing a new paradigm in the hormonal therapy of breast cancer. **Overall design:** Female C57BL6 mice were ovariectomized (OVX). One week after OVX, mice were treated with EM-652.HCl (acolbifene), tamoxifen citrate, raloxifene or ICI 182780 (fulvestrant). Compounds were administered to OVX mice or to OVX mice simultaneously treated with 17b-estradiol (E2). Control groups received an injection of the vehicle alone. All animals were sacrificed after 3h of treatment.Mammary glands from all mice of the same group were collected and pooled. Total mRNA was isolated and converted to biotinylated cRNA.A microarray analysis was performed using Murine U74Av2 Affymetrix microarrays.

Background corr dist: KL-Divergence = 0.1067, L1-Distance = 0.0402, L2-Distance = 0.0033, Normal std = 0.4237

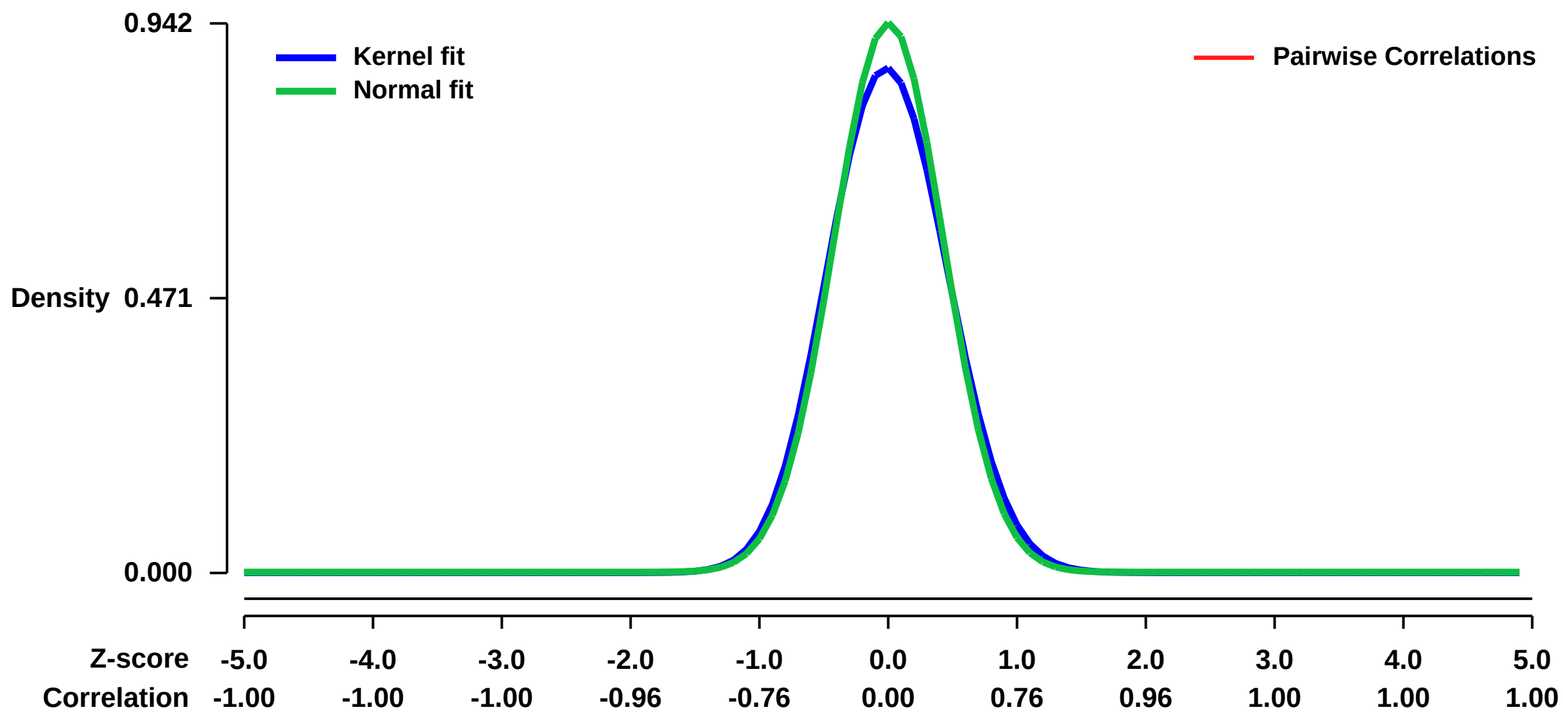

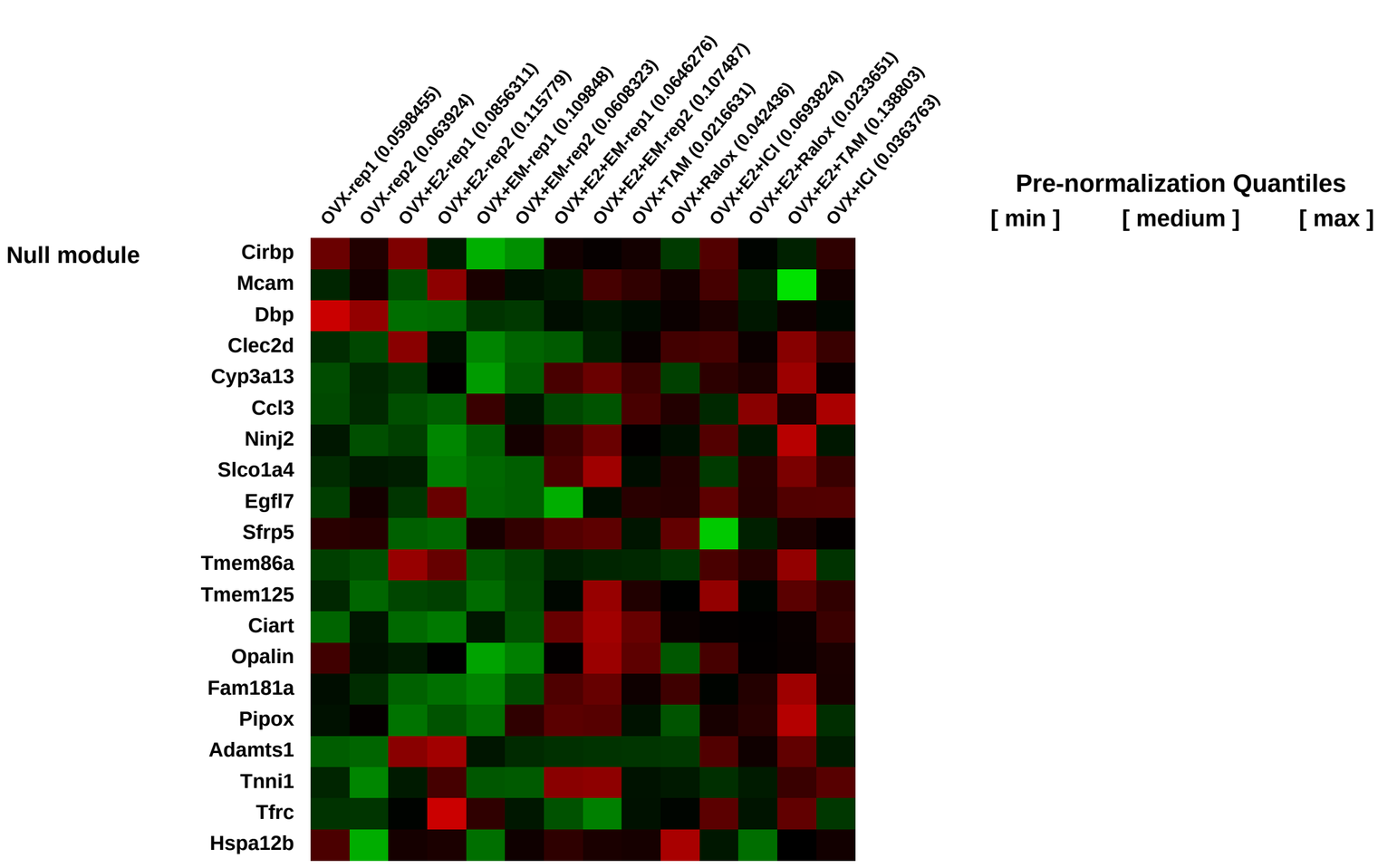

GEO Series "GSE35219" Expression Profiles

Num of samples in this series: 6

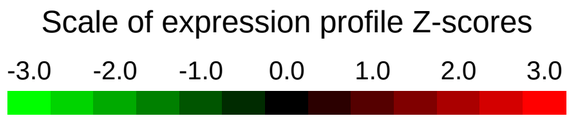

GEO Link:	http://www.ncbi.nlm.nih.gov/geo/query/acc.cgi?acc=GSE35219
Status:	Public on Aug 14 2012
Title:	Synergy between PI3K Signaling and MYC in Burkitt Lymphomagenesis
Organism:	Mus musculus
Experiment type:	Genome variation profiling by SNP array
Platform:	GPL1261
Pubmed ID:	22897848
Summary & Design:	**Summary:** In Burkitt lymphoma (BL), an aggressive germinal-center (GC) derived non-Hodgkin B-cell lymphoma characterized by MYC translocations as early transforming event, the apoptotic properties of MYC must have been overcome by pro-survival signals. Whereas activation of the pro-survival factor NFkappaB is not eminent in BL, PI3K signalling, which mediates B cell receptor associated survival signals in mature B cells, might be the cooperating event. Here we prove this hypothesis by the generation of BL in mice upon concordant expression of MYC and activation of PI3K in GC B cells. Unlike existing murine BL-like models, our tumour model fully phenocopies primary human BL and reflects the complexity of the disease with regard to histological appearance, surface marker expression, and characteristic gene expression profiles. Like in human BL, tumour monoclonality indicated a multistep pathogenesis underlining MYC and PI3K as predisposing events that invariably lead to GC-derived BL formation. In accordance, copy number alteration analysis revealed genomic regions involved in BL pathogenesis. **Overall design:** All samples were obtained from murine lymphomas (Cgamma1-cre; R26StopFLMYC;R26StopFLP110* animals). Cells used for microarray analysis were sorted reporter positive cells. Tumour cells were compared to a matched germline DANN sample to identify acquired aberrations.

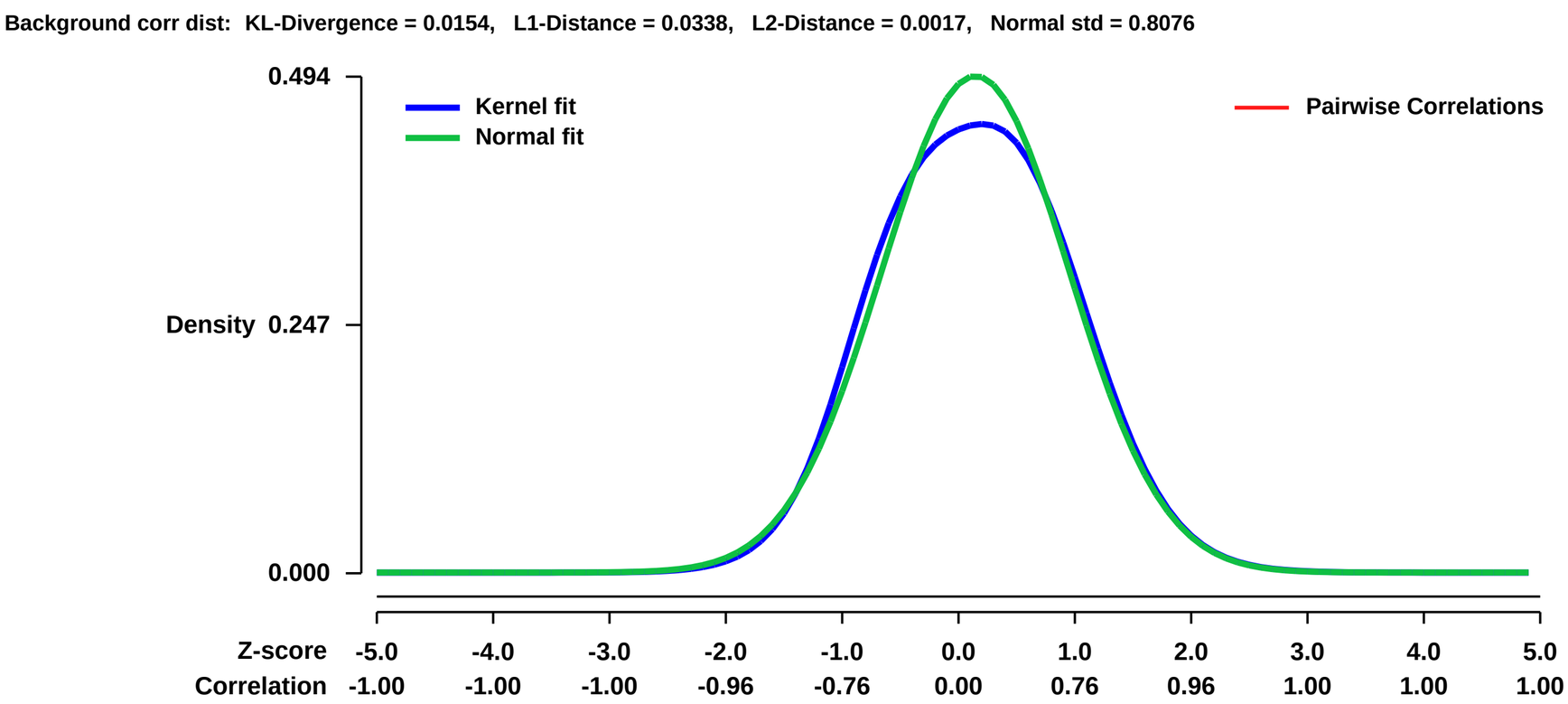

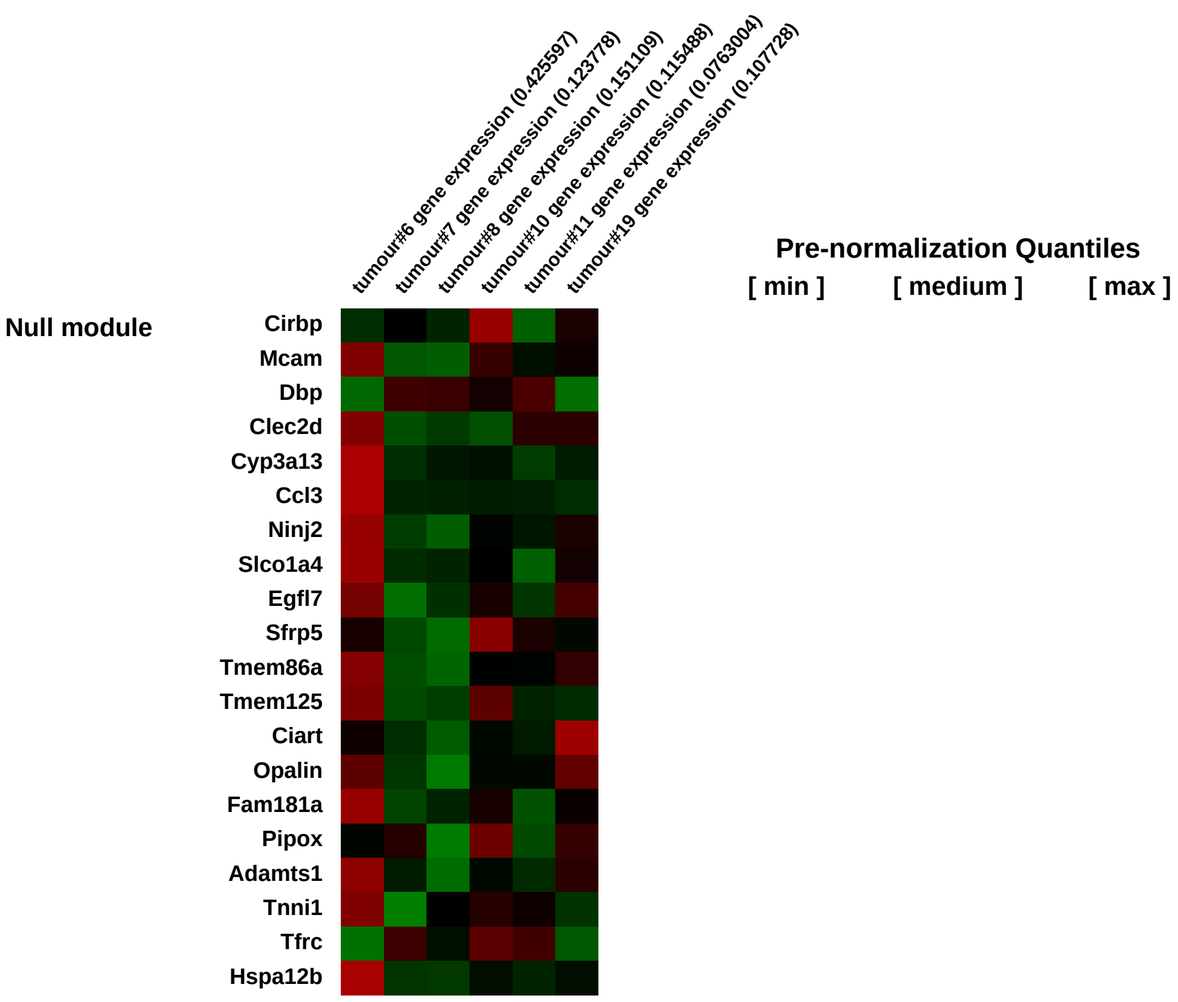

GEO Series "GSE35226" Expression Profiles

Num of samples in this series: 12

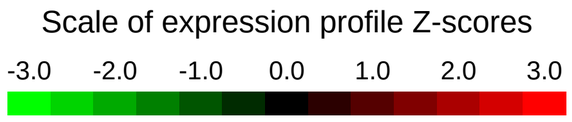

GEO Link:	**http://www.ncbi.nlm.nih.gov/geo/query/acc.cgi?acc=GSE35226**
Status:	**Public on Feb 01 2012**
Title:	**Systems approach identifies HIPK2 as a critical regulator of kidney tubulointerstitial fibrosis**
Organism:	**Mus musculus**
Experiment type:	**Expression profiling by array**
Platform:	**GPL1261**
Pubmed ID:	**22406746**
Summary & Design:	**Summary:** **We used an integrated computational/experimental systems biology approach to identify upstream protein kinases that regulate gene expression changes in kidneys of HIV-1 transgenic mice (Tg26), which have significant tubulo-interstitial fibrosis (TIF) and glomerulosclerosis (GS). We identified the homeo-domain interacting protein kinase 2 (HIPK2) as a key regulator of TIF and GS. HIPK2 was upregulated in kidneys of Tg26 and patients with various kidney diseases. HIV infection increased the protein level of HIPK2 by promoting oxidative stress, which inhibited Siah1-mediated proteasomal degradation of HIPK2.** **The data contain two sets: kidney corticies from WT and Tg26 mice and HEK293 transfected with HIPK2, HIPK2-DN and wild type.** **Overall design:** **Gene expression comparison between kidney cortecies of Tg26 HIV mouse model and wild type. Gene expression comparison between 293 HEK cells with HIPK-DN, HIPK-KO and normal.**

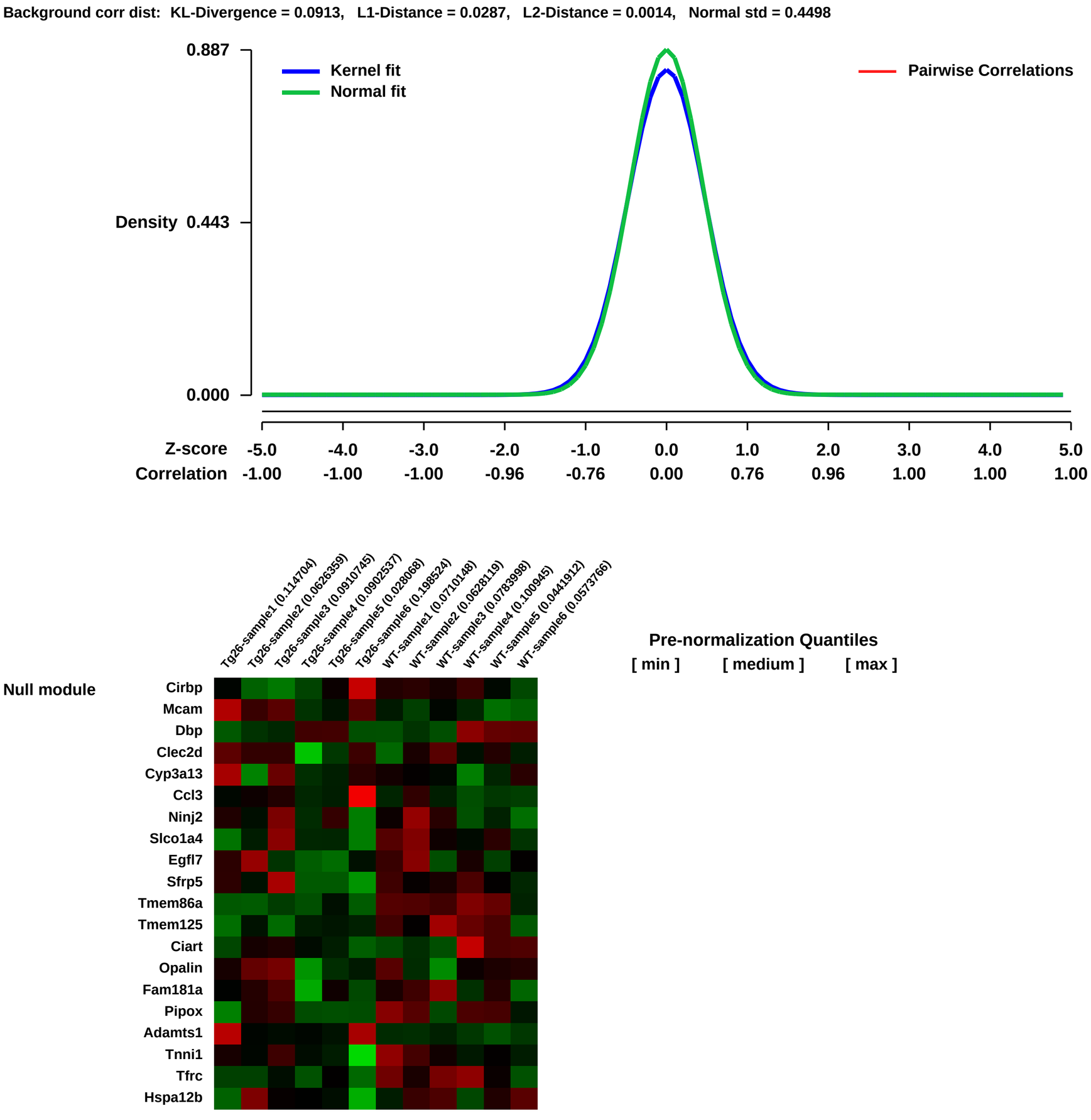

GEO Series "GSE35247" Expression Profiles

Num of samples in this series: 15

Scale of expression profile Z-scores

-3.0 -2.0 -1.0 0.0 1.0 2.0 3.0

GEO Link:	http://www.ncbi.nlm.nih.gov/geo/query/acc.cgi?acc=GSE35247
Status:	Public on Jan 21 2012
Title:	Genome unstable murine prostate cancers acquire genomic aberrations and bone metastatic features of the human disease
Organism:	Mus musculus
Experiment type:	Genome variation profiling by genome tiling array
Platform:	GPL1261
Pubmed ID:	22341455
Summary & Design:	**Summary:** Gene copy numbers of prostate tumors of G3 and G4 generations of LSL-mTert PB-Pten/p53 mouse model **Overall design:** Prostate tumors were developed in G3 and G4 generations of LSL-mTert PB-Pten/p53 mice. These tumors were profiled with affy and aCGH. We used affy gene expression to correlate with the copy number alterations in the mouse prostate tumors.

Background corr dist: KL-Divergence = 0.2052, L1-Distance = 0.0483, L2-Distance = 0.0055, Normal std = 0.3318

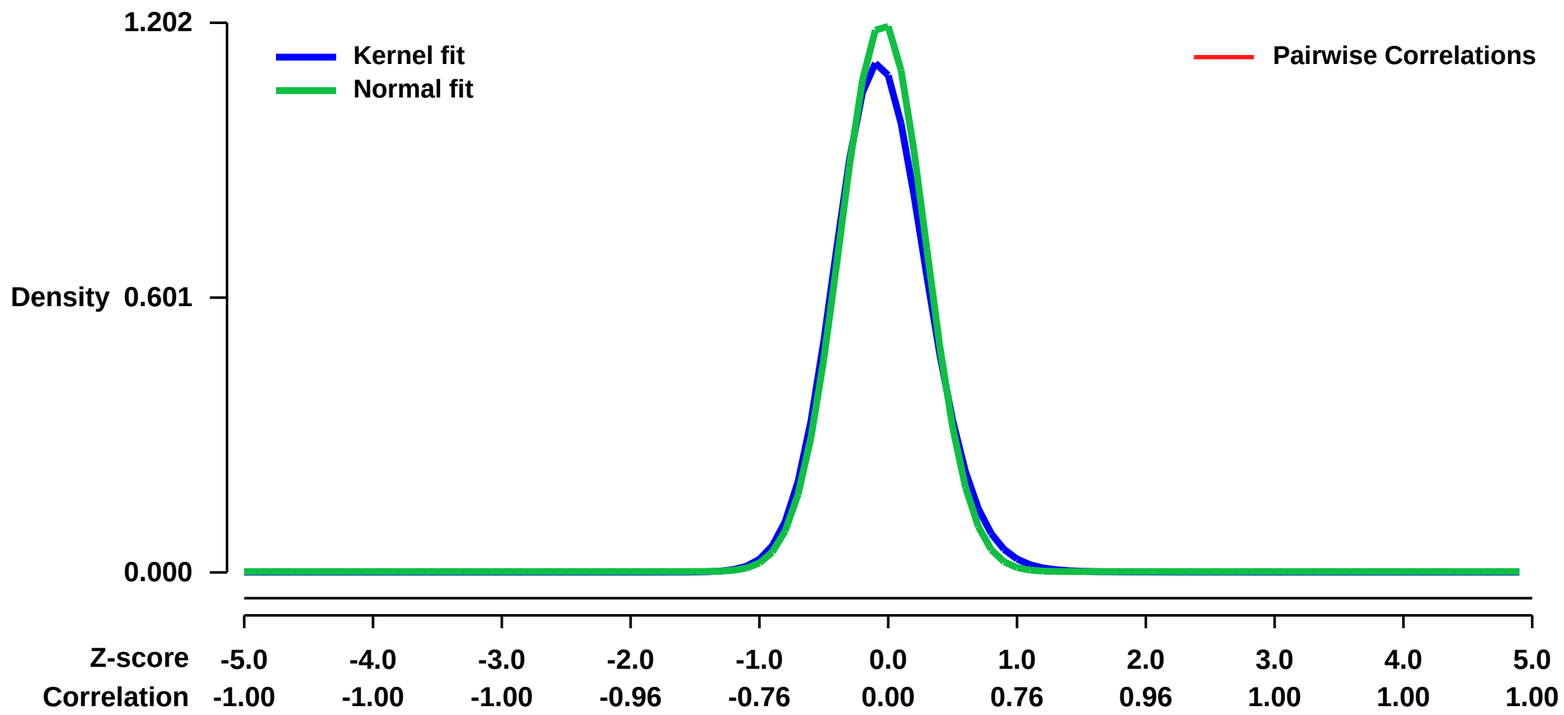

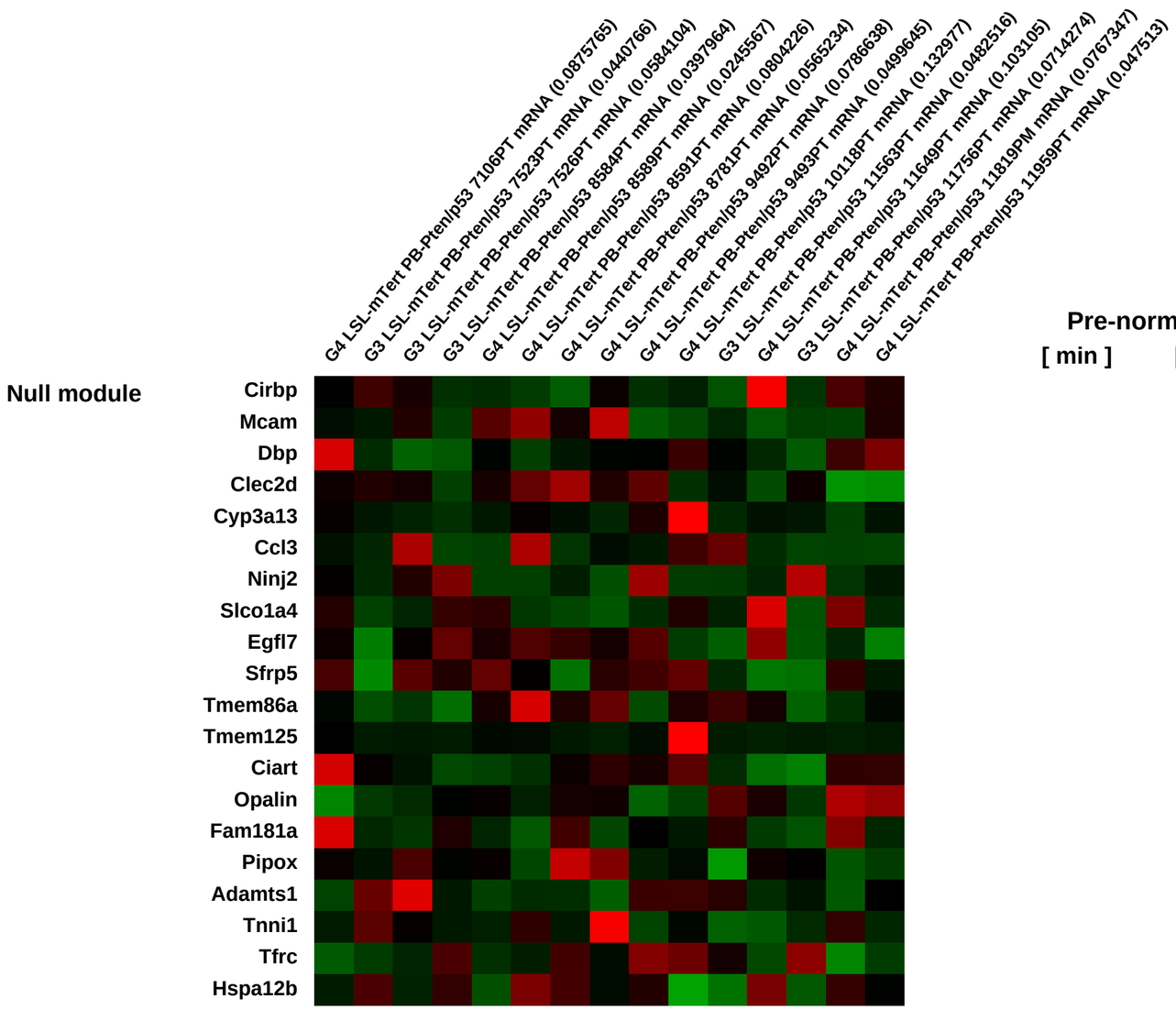

GEO Series "GSE35260" Expression Profiles

Num of samples in this series: 21

Scale of expression profile Z-scores

-3.0 -2.0 -1.0 0.0 1.0 2.0 3.0

GEO Link:	http://www.ncbi.nlm.nih.gov/geo/query/acc.cgi?acc=GSE35260
Status:	Public on Mar 19 2013
Title:	Functional dissection of the Paired domain of Pax6 â distinct roles of subdomains in neurogenesis and proliferation
Organism:	Mus musculus
Experiment type:	Expression profiling by array
Platform:	GPL1261
Pubmed ID:	23404109
Summary & Design:	**Summary:** The transcription factor Pax6 acts as a key developmental regulator in various organs. In the developing brain Pax6 regulates patterning, neurogenesis and proliferation, but how these diverse effects are mediated at the molecular level is not well understood. As Pax6 regulates forebrain development including neurogenesis, proliferation and patterning, almost exclusively by one of its DNA-binding domains, the bipartite paired domain, we examined the role of its respective DNA-binding subdomains (PAI and RED). Using mice with point mutations in the PAI (Pax6Leca4, N50K) and RED (Pax6Leca2, R128C) subdomains we unravelled opposing roles of mutations in these subdomains in regulating genes that control proliferation in the developing cerebral cortex. Mutation of the PAI domain reduced proliferation of both apical and basal progenitors, while the RED domain mutation significantly increased proliferation. Conversely, neurogenesis was affected only by the PAI domain mutation phenocopying the neurogenic defects observed in full Pax6 mutants. Genome-wide expression analysis supported the molecularly distinct signature upon mutation of these subdomains unravelling the key neurogenic signature mediated by the PAI domain. The altered expression of genes identified as direct Pax6 targets by chromatin immunoprecipitation allowed to further identify regulatory elements whose function was impaired by each individual Pax6 mutated protein. Thus, Pax6 achieves its key roles in the developing forebrain by utilizing distinct subdomains to regulate neurogenesis and exert opposing effects on proliferation, while Pax6-target genes involved in patterning tolerate either subdomain mutation. **Overall design:** We performed gene expression microarray analysis of Pax6 mutant mice (Leca2, Leca4, Sey) and control mice

Background corr dist: KL-Divergence = 0.0555, L1-Distance = 0.0286, L2-Distance = 0.0013, Normal std = 0.5344

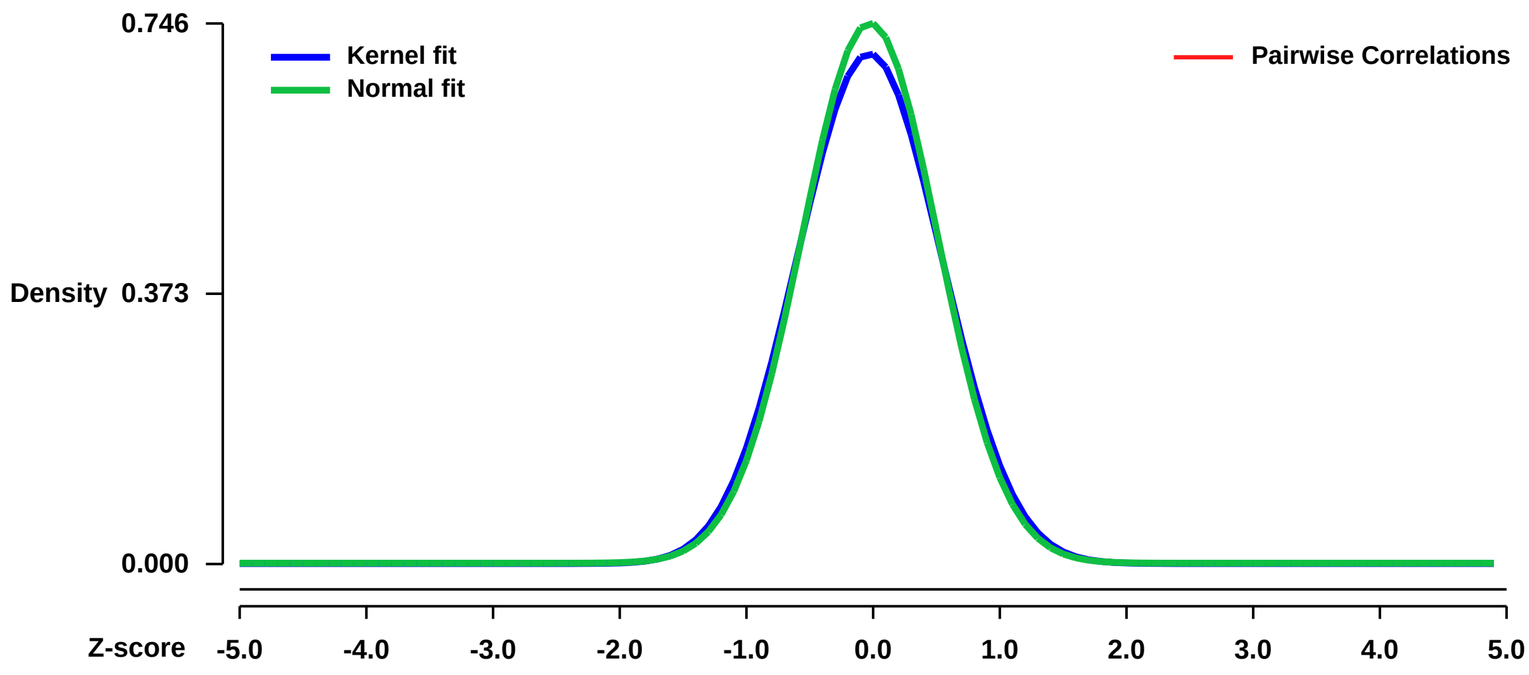

Correlation -1.00 -1.00 -1.00 -0.96 -0.76 0.00 0.76 0.96 1.00 1.00 1.00

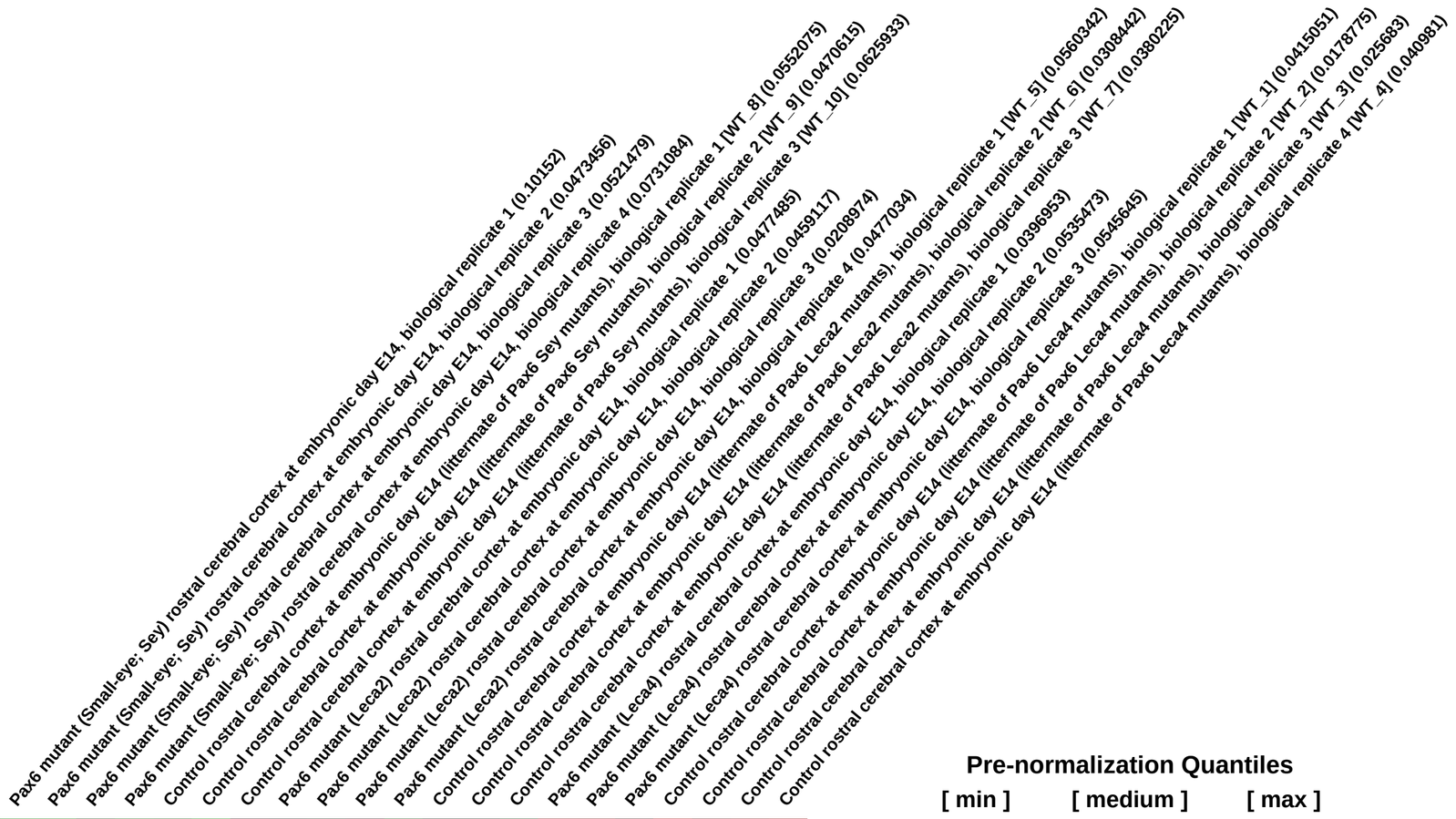

Null module

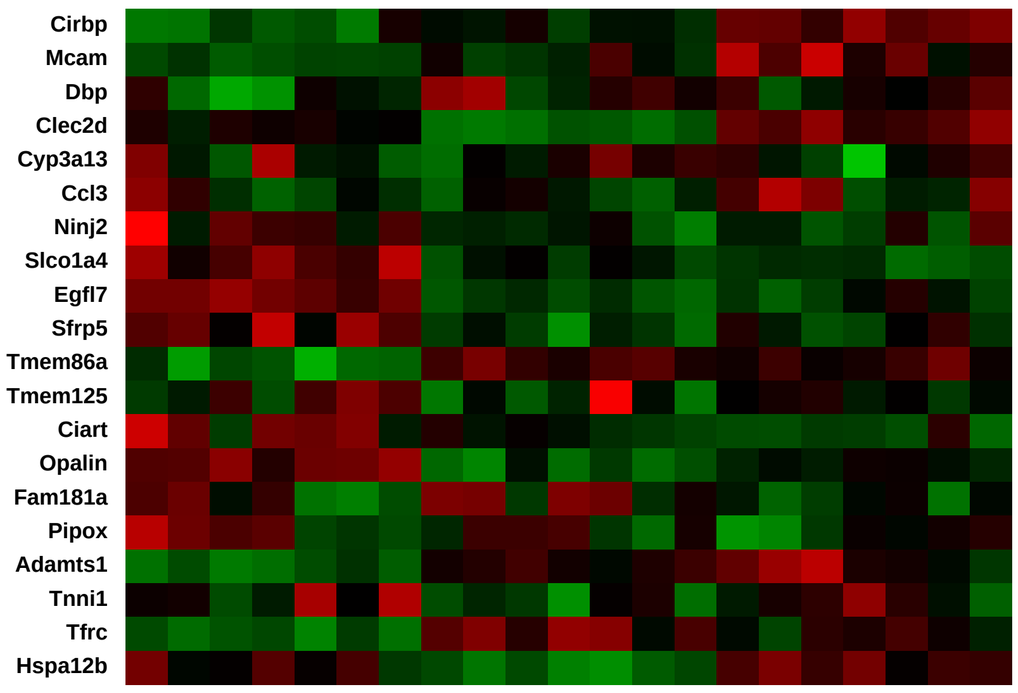

GEO Series "GSE35299" Expression Profiles

Num of samples in this series: 8

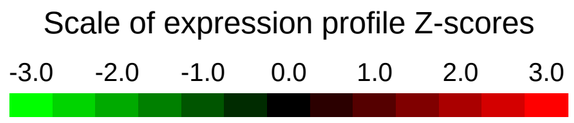

GEO Link:	http://www.ncbi.nlm.nih.gov/geo/query/acc.cgi?acc=GSE35299
Status:	Public on Jan 01 2013
Title:	Implantation Failure of Blastocysts Derived from Oocyte-directed Connexin 43 depleted Mice is Associated with Impaired Ribosomal and Translational Machinery Gene Exp
Organism:	Mus musculus
Experiment type:	Expression profiling by array
Platform:	GPL1261
Pubmed ID:	

Summary & Design:

Summary:
Oocyte quality is a well- established determinant of embryonic fate. However, the molecular participants and biological markers that affect and predict adequate embryonic development are largely elusive. We have previously reported that oocyte- directed Connexin 43 (Cx43) depletion leads to embryo implantation defects, although both the morphology of the oocyte and processes presiding embryo implantation appear to undergo normally. In the context of previous data determining Cx43 indispensability to oocyte and embryonic development, we show here that the timing of Cx43 depletion from the oocyte and the ovarian follicle is crucial in determining the severity of subsequent embryonic defects. Specifically, we show that the implantation defects of blastocysts resulting from oocyte- directed Cx43-depleted follicles (depletion occurs at day 3 postnatal), is not due to maternal luteal insufficiency but rather depends solely on the defective blastocysts. Gene expression microarray analysis revealed global defects in the expression of ribosomal proteins, translation initiation factors and other genes associated with cellular biosynthetic and metabolic processes in these defective oocytes and specifically blastocysts. We therefore propose that timely expression of Cx43 in the oocyte and ovarian follicles is a major determinant of oocyte developmental competence, by determining the ability of the resulting blastocyst to facilitate biomass expansion and undergo adequate embryo implantation

Overall design:
To study the effect of CX43 on the transcriptom of the pre implantation stages, we compared CX43 KO oocytes to the WT oocytes in three different stages of the very early development. First comparison MII oocytes, second comparison blastocysts, third comparison implantation site.

Background corr dist: KL-Divergence = 0.0632, L1-Distance = 0.0559, L2-Distance = 0.0053, Normal std = 0.5652

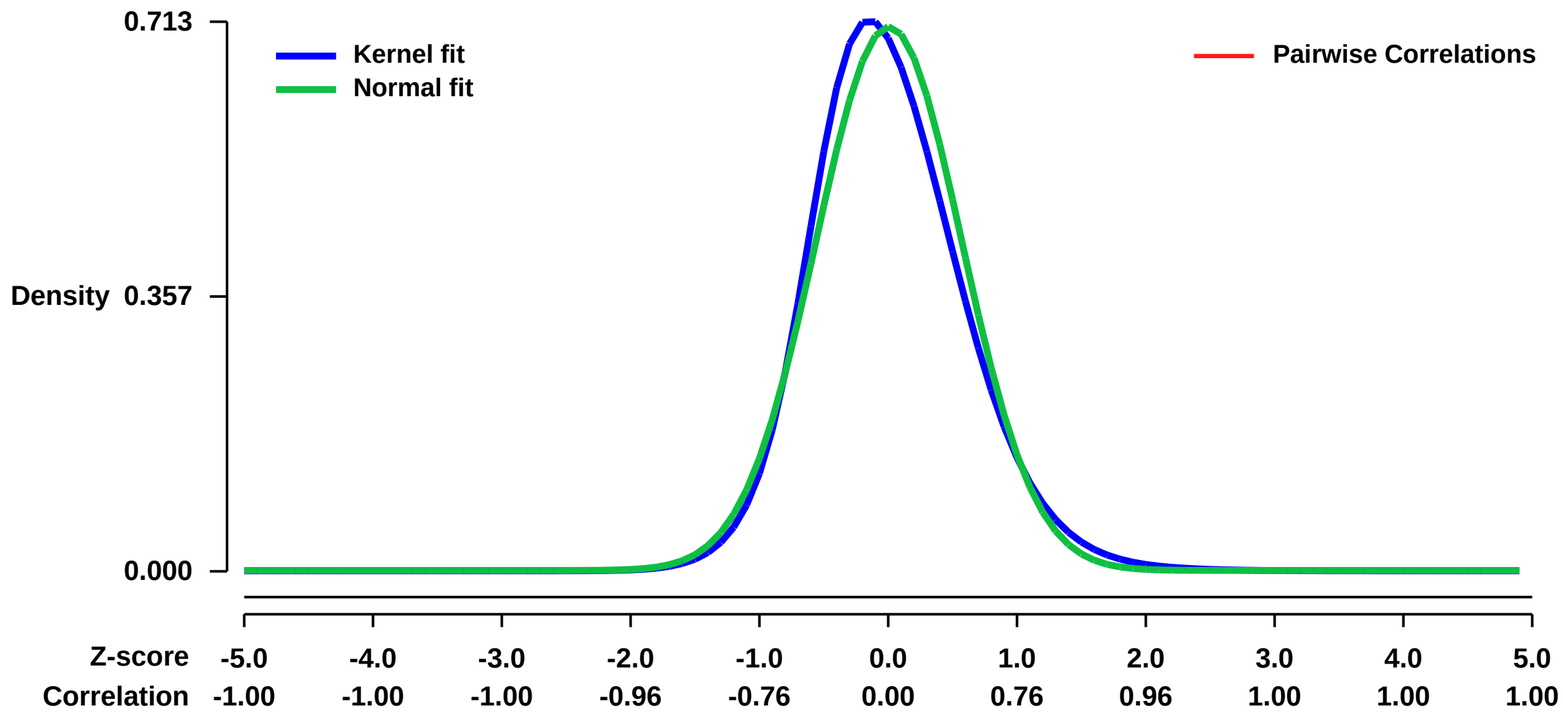

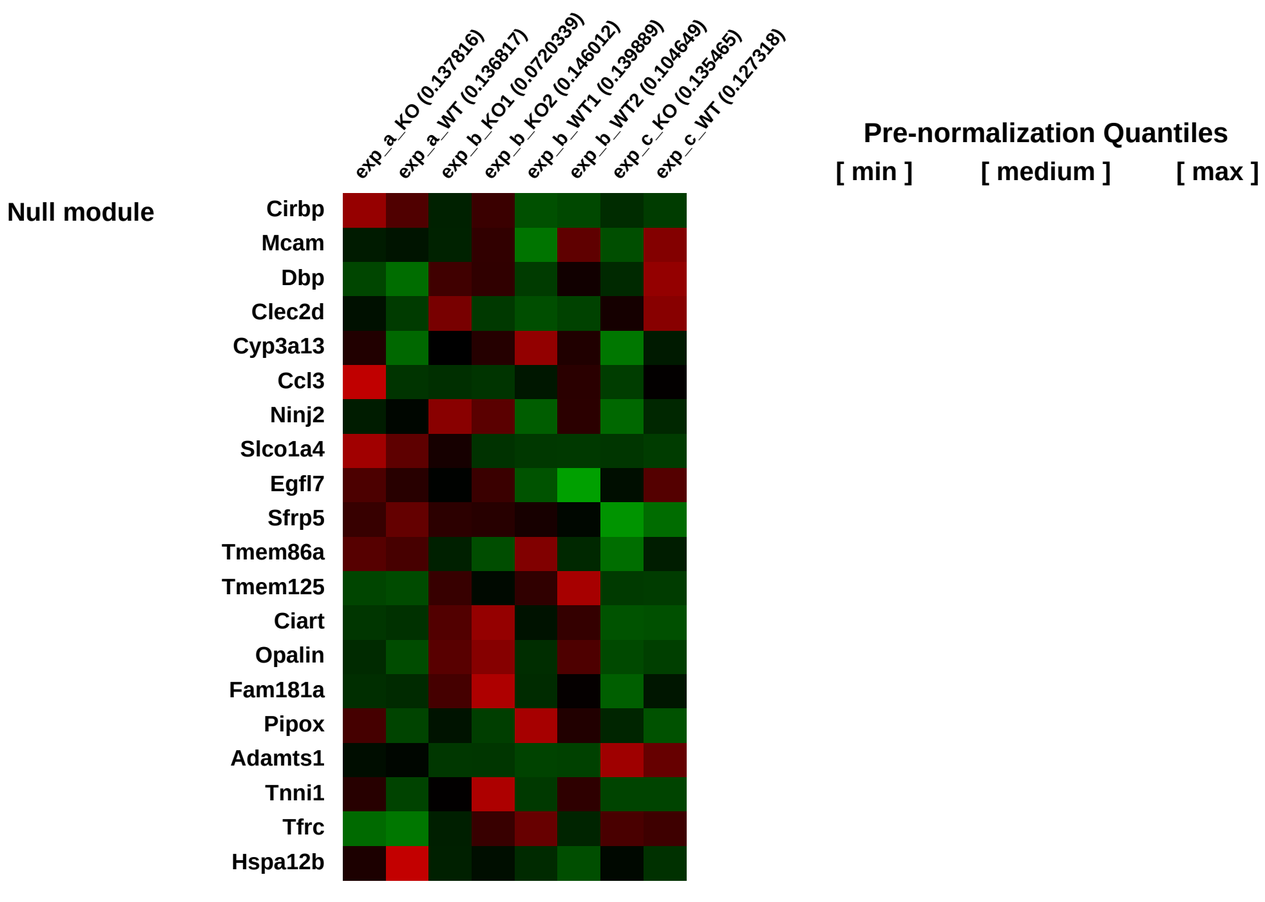

GEO Series "GSE35318" Expression Profiles

Num of samples in this series: 12

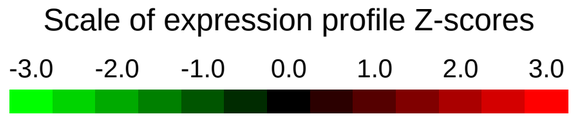

GEO Link:	http://www.ncbi.nlm.nih.gov/geo/query/acc.cgi?acc=GSE35318
Status:	Public on Jul 10 2012
Title:	p38a-dependent gene expression in dendritic cells
Organism:	Mus musculus
Experiment type:	Expression profiling by array
Platform:	GPL1261
Pubmed ID:	22615377
Summary & Design:	**Summary:** Gene expression in wild-type and p38a-knockout dendritic cells (DCs) were compared. Lymph node dendritic cells were isolated from mice, and left unstimulated and stimulated with Pam3CSK4, a toll-like receptor 2 agonist. C57BL/6 wild-type mice, and dendritic cell-specific p38a-knockout mice on a C57BL/6 background were used for isolation of primary DCs. **Overall design:** Gene expression 0, 2, and 4 h after stimulation was analyzed with each time point in duplicate.

Background corr dist: KL-Divergence = 0.1423, L1-Distance = 0.0306, L2-Distance = 0.0017, Normal std = 0.3824

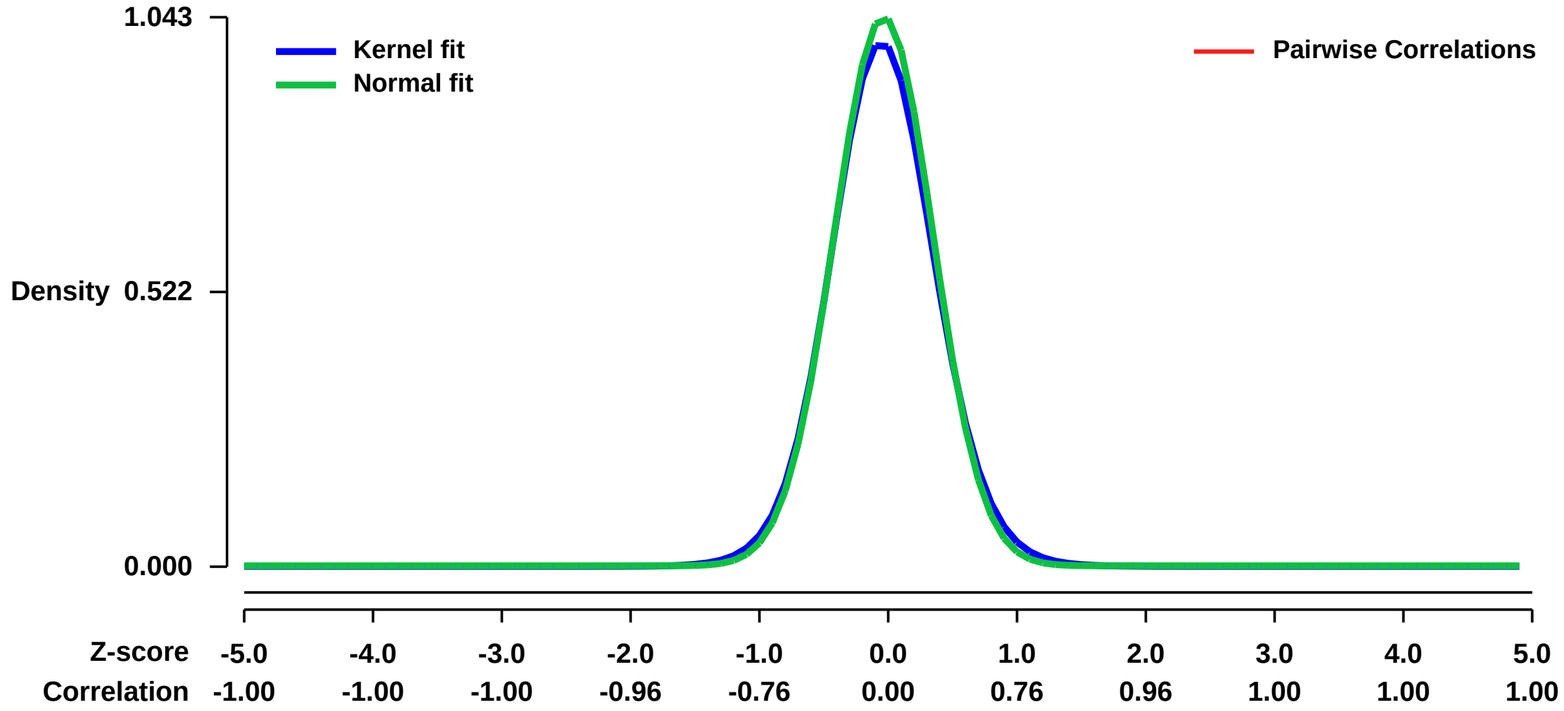

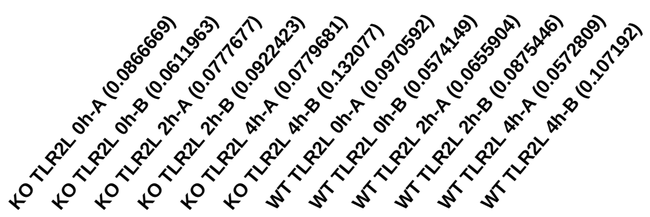

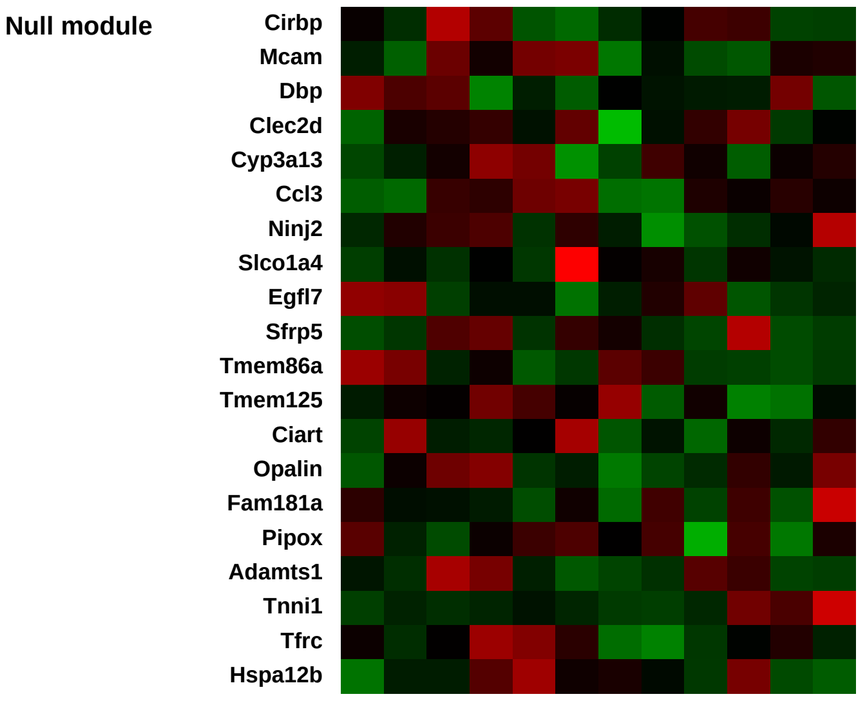

GEO Series "GSE35332" Expression Profiles

Num of samples in this series: 12

Scale of expression profile Z-scores

-3.0 -2.0 -1.0 0.0 1.0 2.0 3.0

GEO Link:	http://www.ncbi.nlm.nih.gov/geo/query/acc.cgi?acc=GSE35332
Status:	Public on May 02 2012
Title:	Stem cell factor programs the mast cell activation phenotype
Organism:	Mus musculus
Experiment type:	Expression profiling by array
Platform:	GPL1261
Pubmed ID:	22529299
Summary & Design:	**Summary:** Mast cells, activated by antigen via the high affinity receptor for IgE (Fc$_\epsilon$RI), release an array of pro-inflammatory mediators that contribute to allergic disorders such as asthma and anaphylaxis. The KIT ligand, stem cell factor (SCF), is critical for mast cell expansion, differentiation and survival, and, under acute conditions, enhances mast cell activation. However, extended SCF exposure in vivo conversely protects against fatal antigen-mediated anaphylaxis. In investigating this dichotomy, we identified a novel mode of regulation of the mast cell activation phenotype through SCF-mediated programming. We found that mouse bone marrow-derived mast cells chronically exposed to SCF displayed a marked attenuation of Fc$_\epsilon$RI-mediated degranulation and cytokine production. The hypo-responsive phenotype was not a consequence of altered signals regulating calcium flux or protein kinase C, but of ineffective cytoskeletal reorganization, with evidence implicating a down-regulation of expression of the Src kinase Hck. Collectively, these findings demonstrate a major role for SCF in the homeostatic control of mast cell activation with potential relevance to mast cell-driven disease and the development of novel approaches for the treatment of allergic disorders. **Overall design:** Mouse bone marrow-derived mast cells were treated with IL3 or IL3+SCF. Six replicates each.

Background corr dist: KL-Divergence = 0.1206, L1-Distance = 0.0248, L2-Distance = 0.0008, Normal std = 0.4115

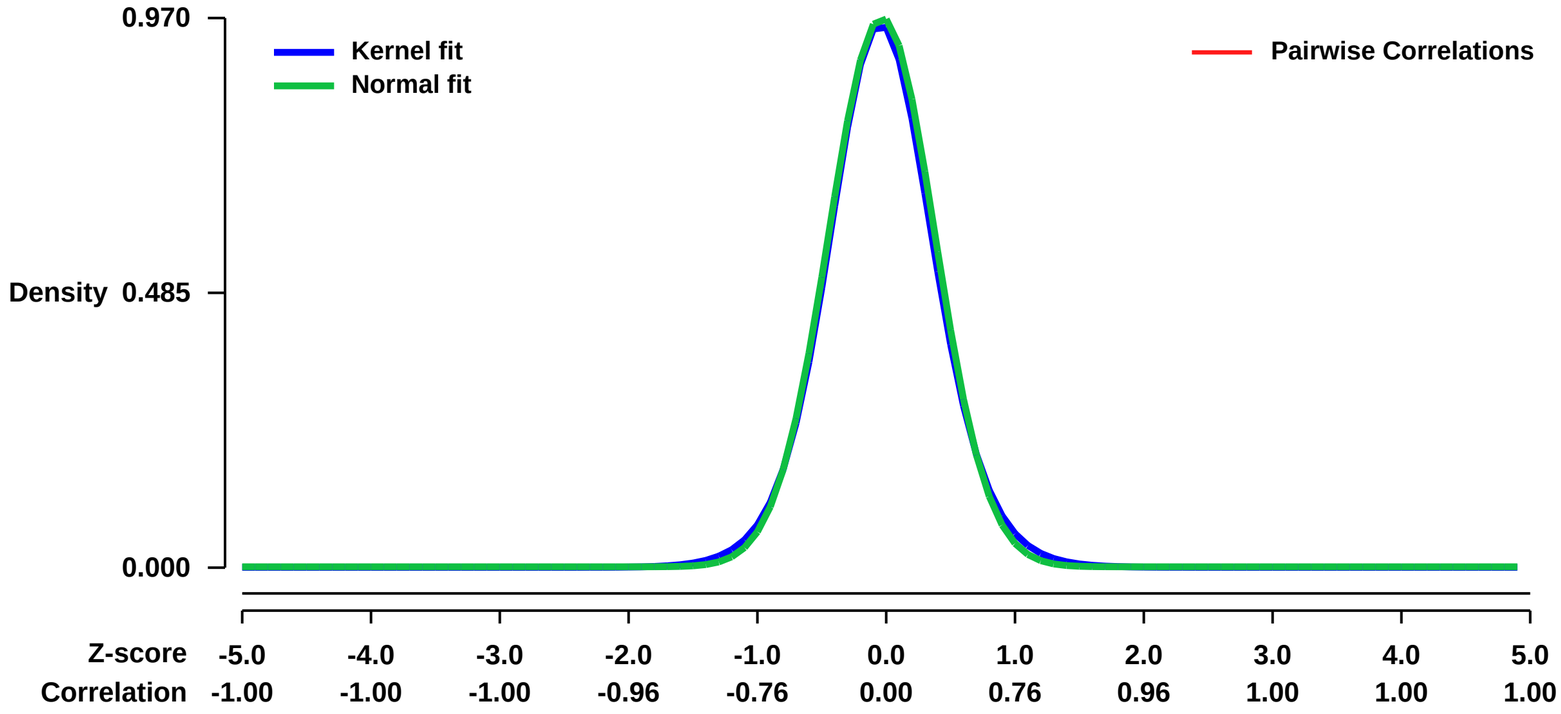

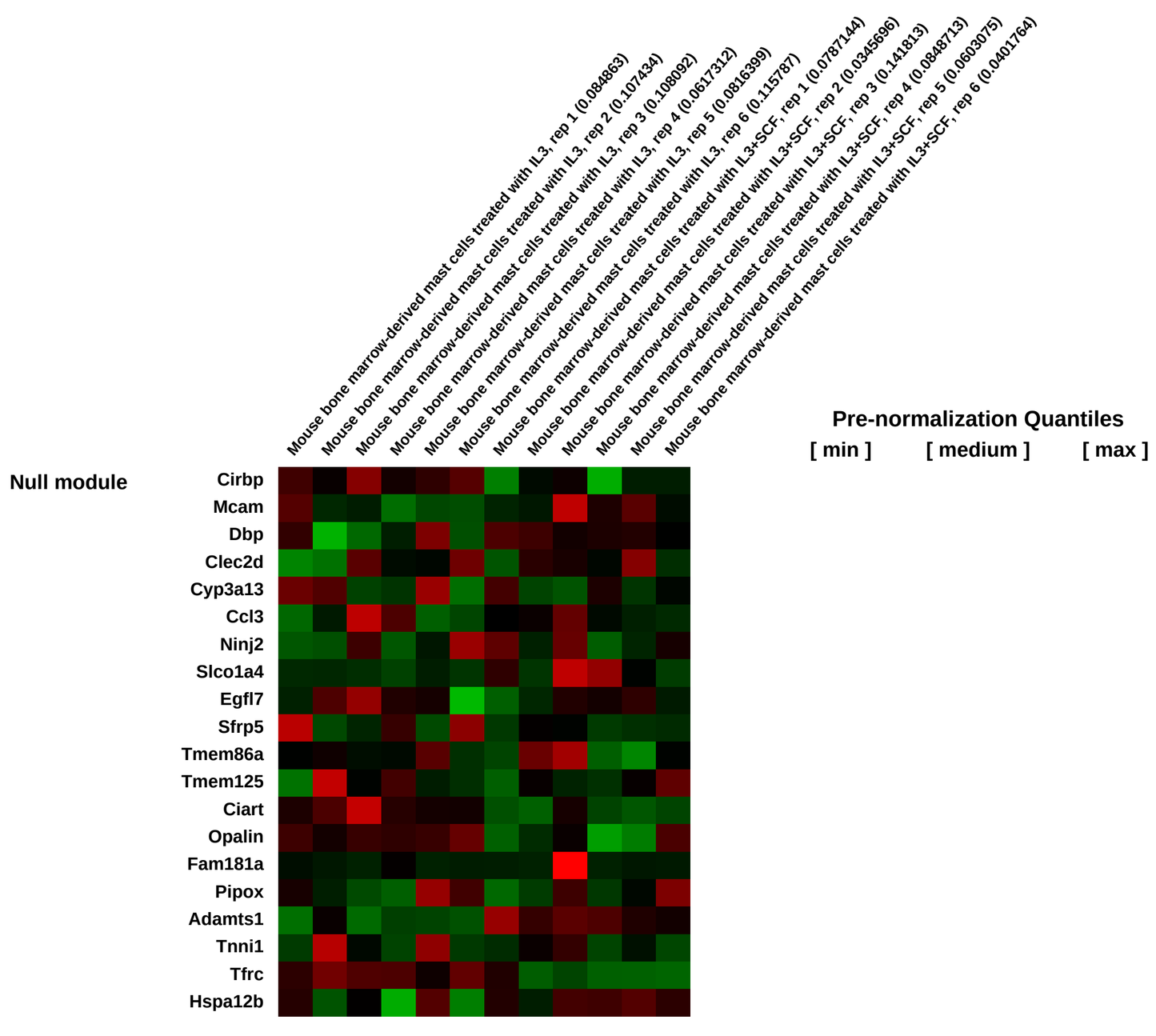

GEO Series "GSE35338" Expression Profiles

Num of samples in this series: 30

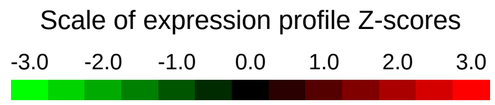

GEO Link:	http://www.ncbi.nlm.nih.gov/geo/query/acc.cgi?acc=GSE35338
Status:	Public on May 02 2012
Title:	Expression data from reactive astrocytes acutely purified from young adult mouse brains
Organism:	Mus musculus
Experiment type:	Expression profiling by array
Platform:	GPL1261
Pubmed ID:	22553043
Summary & Design:	**Summary:** Reactive astrogliosis is characterized by a profound change in astrocyte phenotype in response to all CNS injuries and diseases. To better understand the reactive astrocyte state, we used Affymetrix GeneChip arrays to profile gene expression in populations of reactive astrocytes isolated at various time points after induction using two different mouse injury models, ischemic stroke and neuroinflammation. **Overall design:** Young adult male mice underwent middle cerebral artery occlusion (MCAO) to produce ischemic stroke or control sham surgery. Young adult mice were injected intraperitoneally with 5 mg/kg lipopolysaccharide (LPS) to produce neuroinflammation or saline for control. Astrocytes were acutely purified from control and injured brains at 1 day after injury for LPS/saline injection and 1, 3 days and 7 days after MCAO/sham surgeries.
Background corr dist:	KL-Divergence = 0.1320, L1-Distance = 0.0498, L2-Distance = 0.0057, Normal std = 0.3941

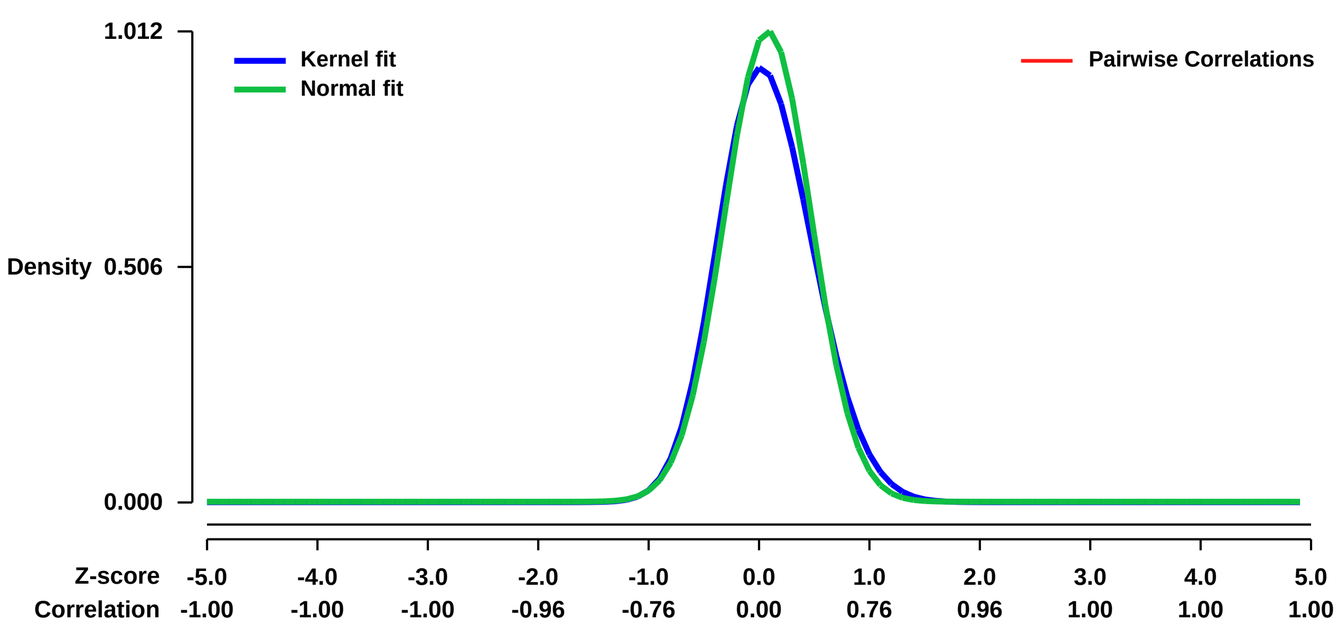

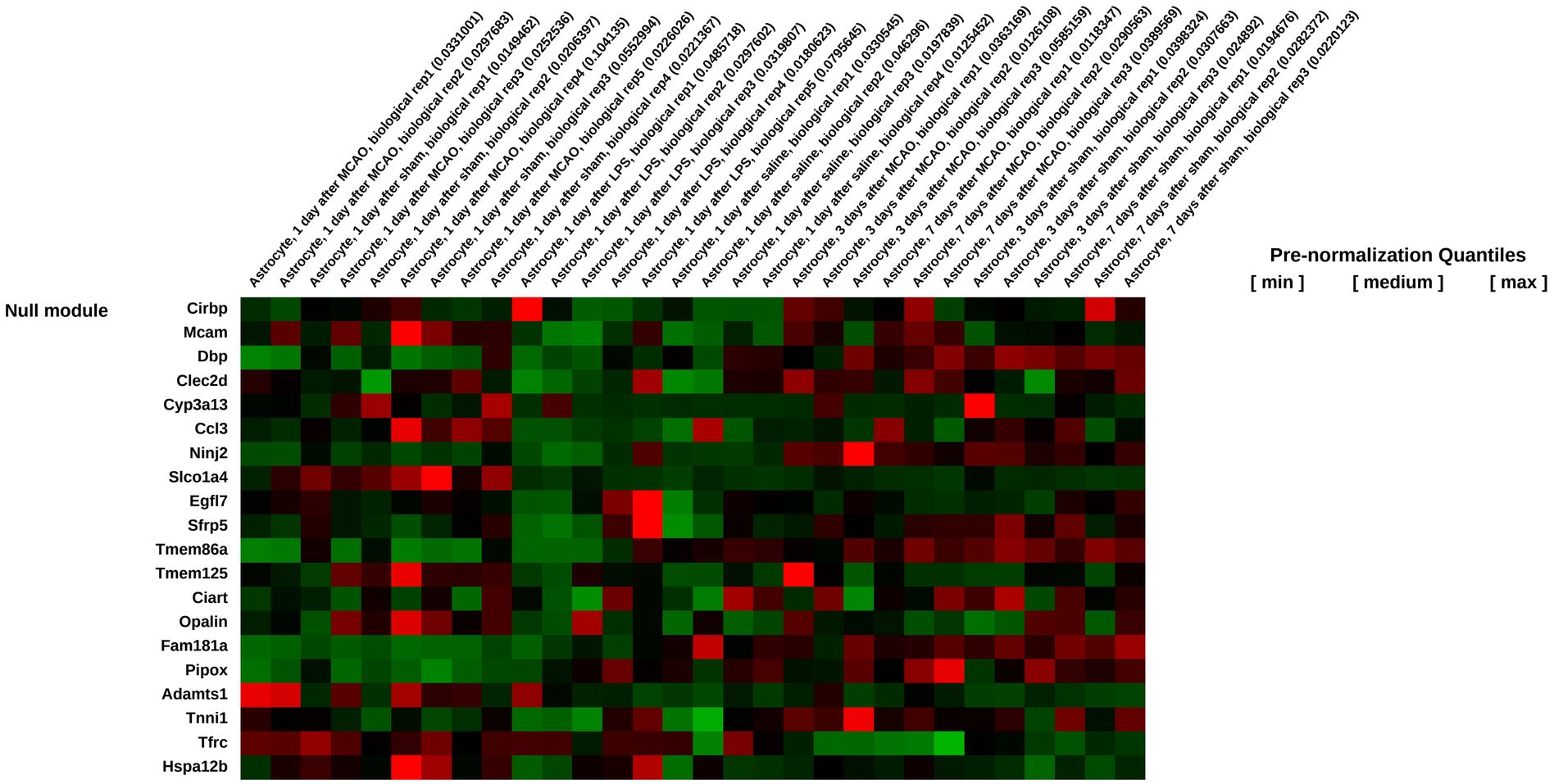

GEO Series "GSE35357" Expression Profiles

Num of samples in this series: 12

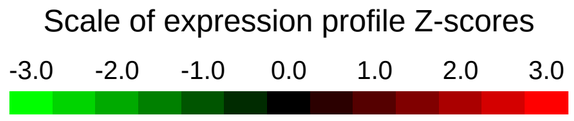

GEO Link:	http://www.ncbi.nlm.nih.gov/geo/query/acc.cgi?acc=GSE35357
Status:	Public on Feb 03 2012
Title:	Gene expression profiling of Myf5-Cre;Smad4flox/flox mouse models of tongue development
Organism:	Mus musculus
Experiment type:	Expression profiling by array
Platform:	GPL1261
Pubmed ID:	22438570
Summary & Design:	**Summary:** We investigated Smad4-mediated TGF-beta signaling in the development of occipital somite-derived myogenic progenitors during tongue morphogenesis by comparing the transcriptomes of tongue derived from Myf5-Cre;Smad4flox/flox mutant and Myf5-Cre;Smad4flox/+ control mice at day E13.5. Based on gene expression profiles and functional studies, we elucidated the influences Smad4 activity and TGF-beta signaling have on the gene expression profiles underlying tongue development. The data are consistent with the hypothesis that TGF-beta-Smad4-FGF6 signaling cascade plays a crucial role in myogenic cell fate determination and lineage progression during tongue myogenesis. **Overall design:** We obtained RNA samples from tongue tissues of mutant and control mouse embryos (C57BL/6J) at day E13.5 RNA and subjected them to analysis on Affymetrix GeneChip Mouse Genome 430 2.0 Arrays.

Background corr dist: KL-Divergence = 0.1151, L1-Distance = 0.0296, L2-Distance = 0.0014, Normal std = 0.4133

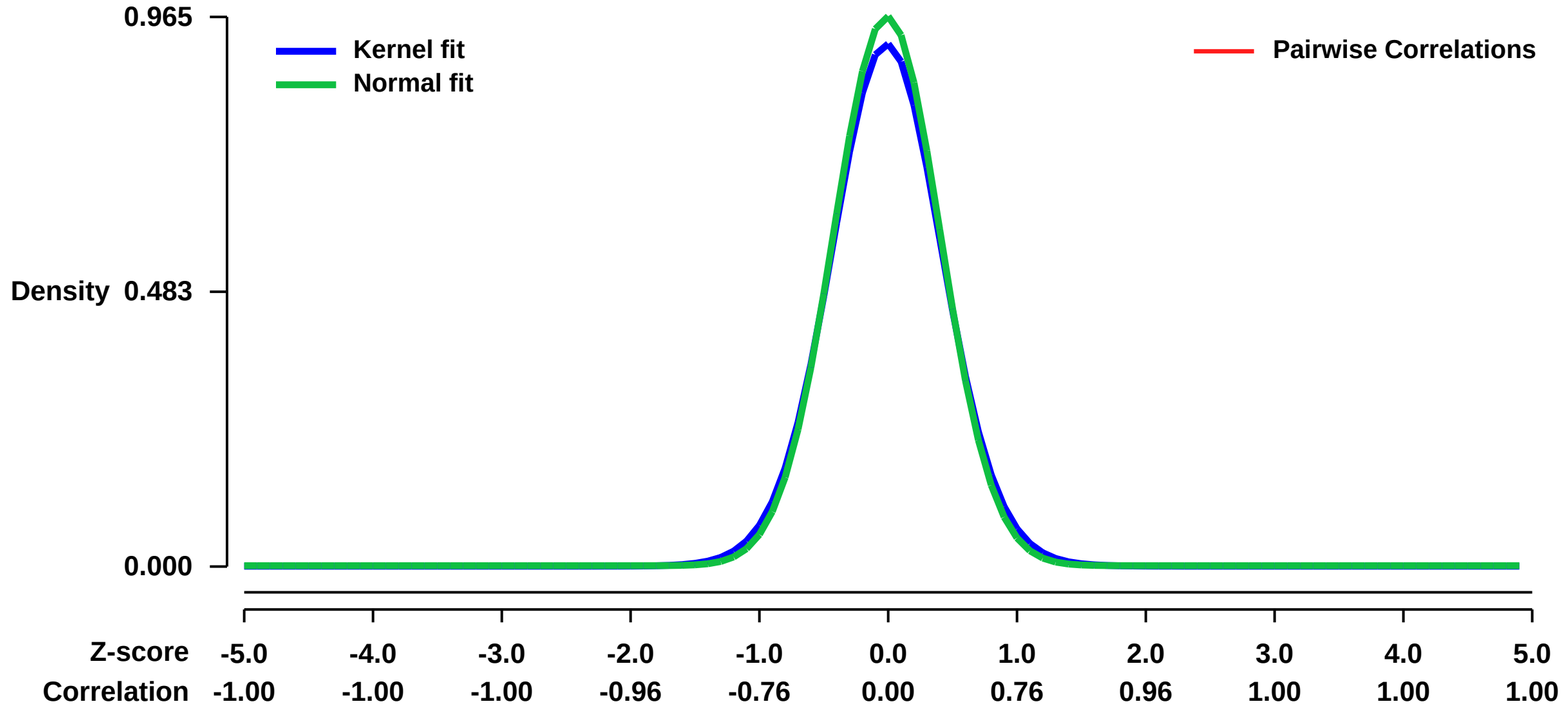

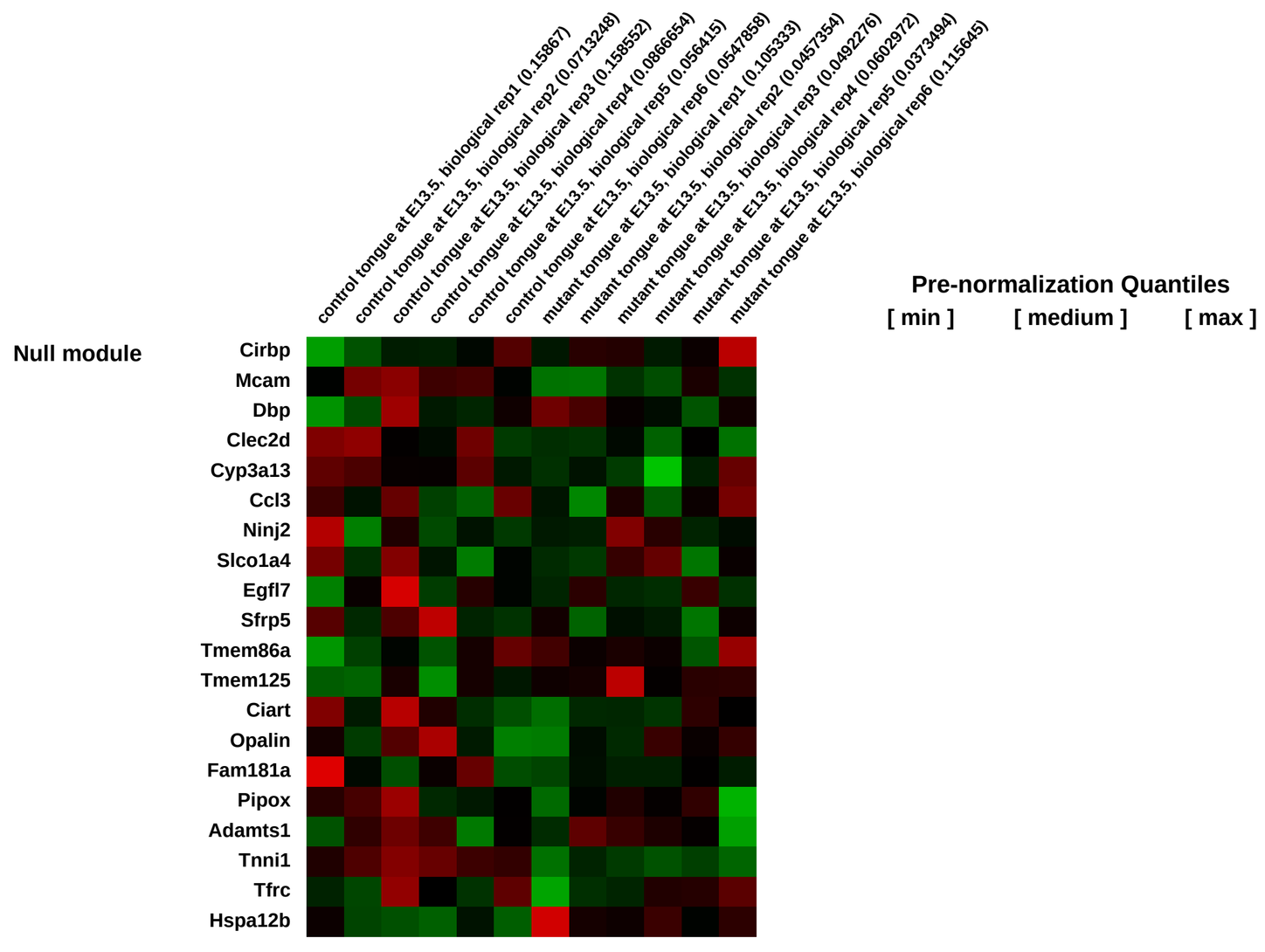

GEO Series "GSE35435" Expression Profiles

Num of samples in this series: 6

Scale of expression profile Z-scores

-3.0 -2.0 -1.0 0.0 1.0 2.0 3.0

GEO Link:	http://www.ncbi.nlm.nih.gov/geo/query/acc.cgi?acc=GSE35435
Status:	Public on Sep 29 2012
Title:	Genome-wide analysis of mouse macrophages stimulated with IL-4 (bone marrow macrophages) (Affymetrix)
Organism:	Mus musculus
Experiment type:	Expression profiling by array
Platform:	GPL1261
Pubmed ID:	23293084
Summary & Design:	**Summary:** Analysis of alternative activation of macrophages at gene expression level. The study forms part of a wider study where we compare the effects of IL-4 in different human and mouse macrophages. Our results support the notion that in vitro culture conditions greatly affect the macrophage response to IL-4. Total RNA obtained from bone marrow derived macrophages upon exposure to 20 ng/ml of IL-4 for 18 hours. **Overall design:** Bone marrow derived macrophages were stimulated with the Th2 cytokine IL-4, for RNA extraction and hybridization on Affymetrix microarrays.

Background corr dist: KL-Divergence = 0.0170, L1-Distance = 0.0428, L2-Distance = 0.0029, Normal std = 0.8007

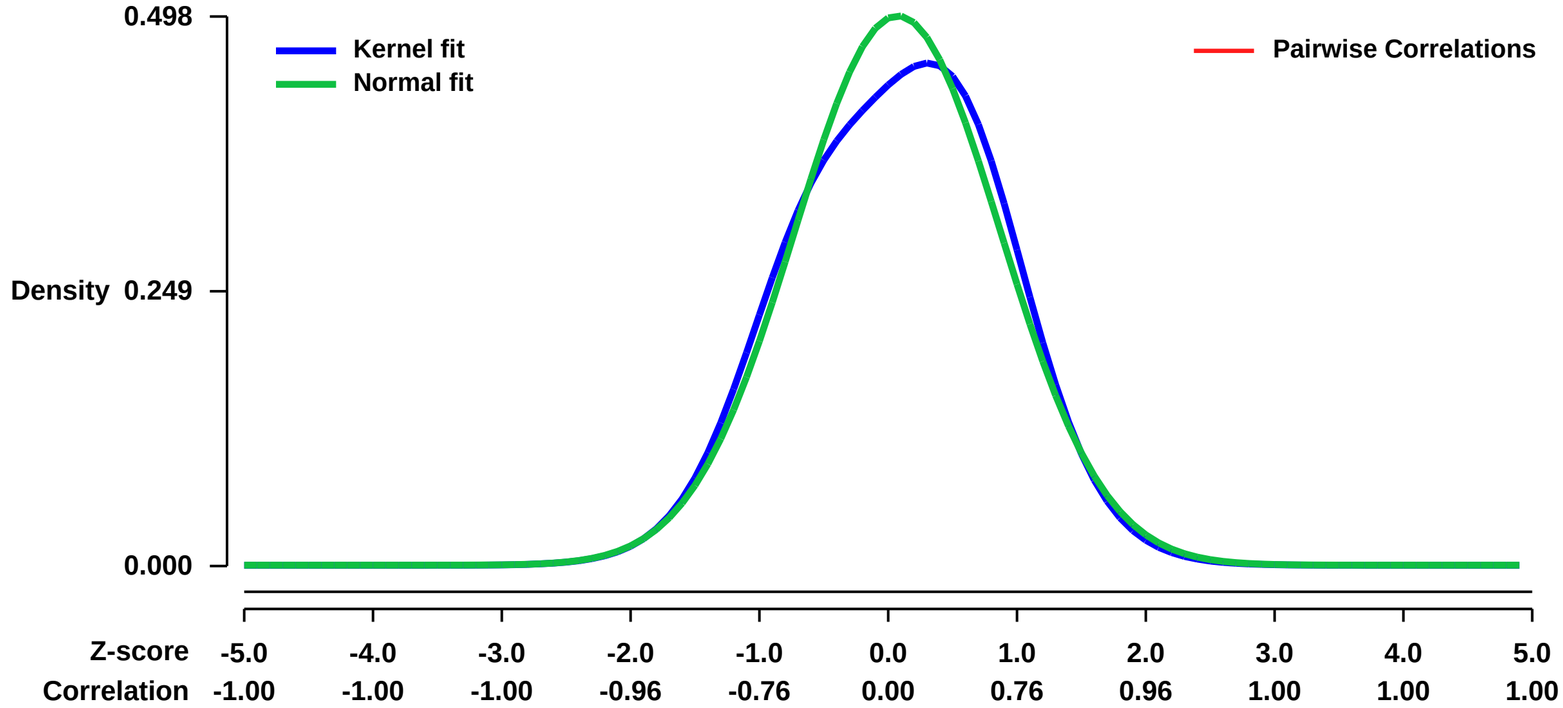

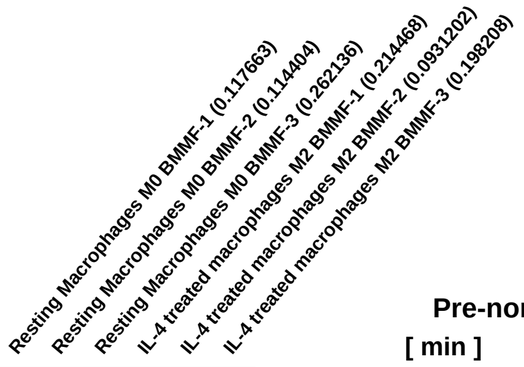

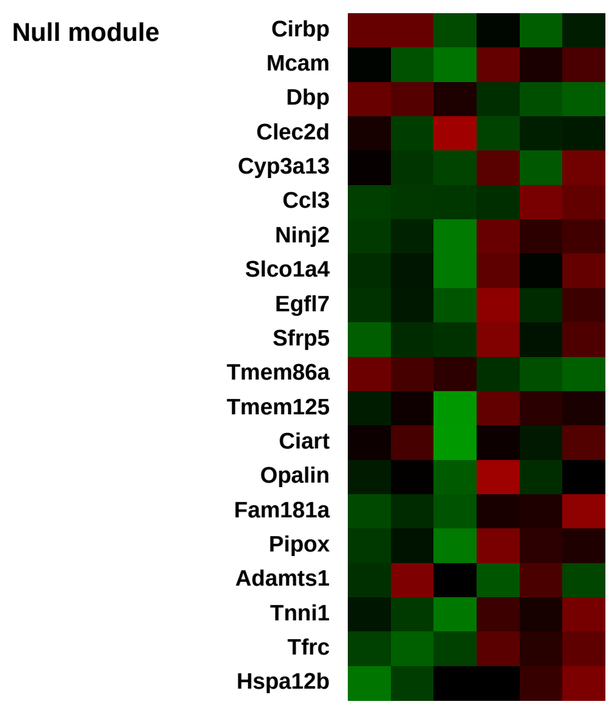

GEO Series "GSE3554" Expression Profiles

Num of samples in this series: 6

Scale of expression profile Z-scores

-3.0 -2.0 -1.0 0.0 1.0 2.0 3.0

GEO Link:	http://www.ncbi.nlm.nih.gov/geo/query/acc.cgi?acc=GSE3554
Status:	Public on Nov 04 2005
Title:	Microarray Analysis of Retinal Gene Expression in the DBA/2J Model of Glaucoma
Organism:	Mus musculus
Experiment type:	Expression profiling by array
Platform:	GPL1261
Pubmed ID:	16505032
Summary & Design:	**Summary:** **Purpose: The DBA/2J mouse is a model for secondary angle-closure glaucoma due to iris atrophy and pigment dispersion, which ultimately leads to increased intraocular pressure (IOP). We sought to correlate changes in retinal gene expression with glaucoma-like pathology by performing microarray analysis of retinal RNA from DBA/2J mice at 3 months before disease onset, and at 8 months, after IOP elevation. Methods: IOP was monitored monthly in DBA/2J animals by Tono-Pen and animals with normal (3 months) or elevated IOP (8 months) were identified. RNA was prepared from 3 individual retinas at each age, and the RNA was amplified and used to generate biotin-labeled probe for high density mouse Affymetrix arrays (U430.2). A subset of genes was selected for confirmation by quantitative RT-PCR using independent retina samples from DBA/2J animals at 3, 5 and 8 months of age, and compared to retinas from C57BL/6J control animals at 3 and 8 months. Results: There were changes in expression of 68 genes, with 32 genes increasing and 36 genes decreasing at 8 months versus 3 months. Upregulated genes were associated with immune response, glial activation, signaling and gene expression, while down-regulated genes included multiple crystallin genes. Significant changes in 9 upregulated genes and 2 downregulated genes were confirmed by quantitative RT-PCR, with some showing changes in expression by 5 months. Conclusions: DBA/2J retina shows evidence for glial activation and an immune-related response following IOP elevation, similar to what has been reported following acute elevation of IOP in other models.** **Keywords: retina, glaucoma, DBA/2J, elevated intraocular pressure** **Overall design:** **IOP was monitored monthly in DBA/2J animals by Tono-Pen and animals with normal (3 months) or elevated IOP (8 months) were identified. RNA was prepared from 3 individual retinas at each age, and the RNA was amplified and used to generate biotin-labeled probe for high density mouse Affymetrix arrays (U430.2). A subset of genes was selected for confirmation by quantitative RT-PCR using independent retina samples from DBA/2J animals at 3, 5 and 8 months of age, and compared to retinas from C57BL/6J control animals at 3 and 8 months.**

Background corr dist: **KL-Divergence = 0.0472, L1-Distance = 0.0372, L2-Distance = 0.0019, Normal std = 0.6520**

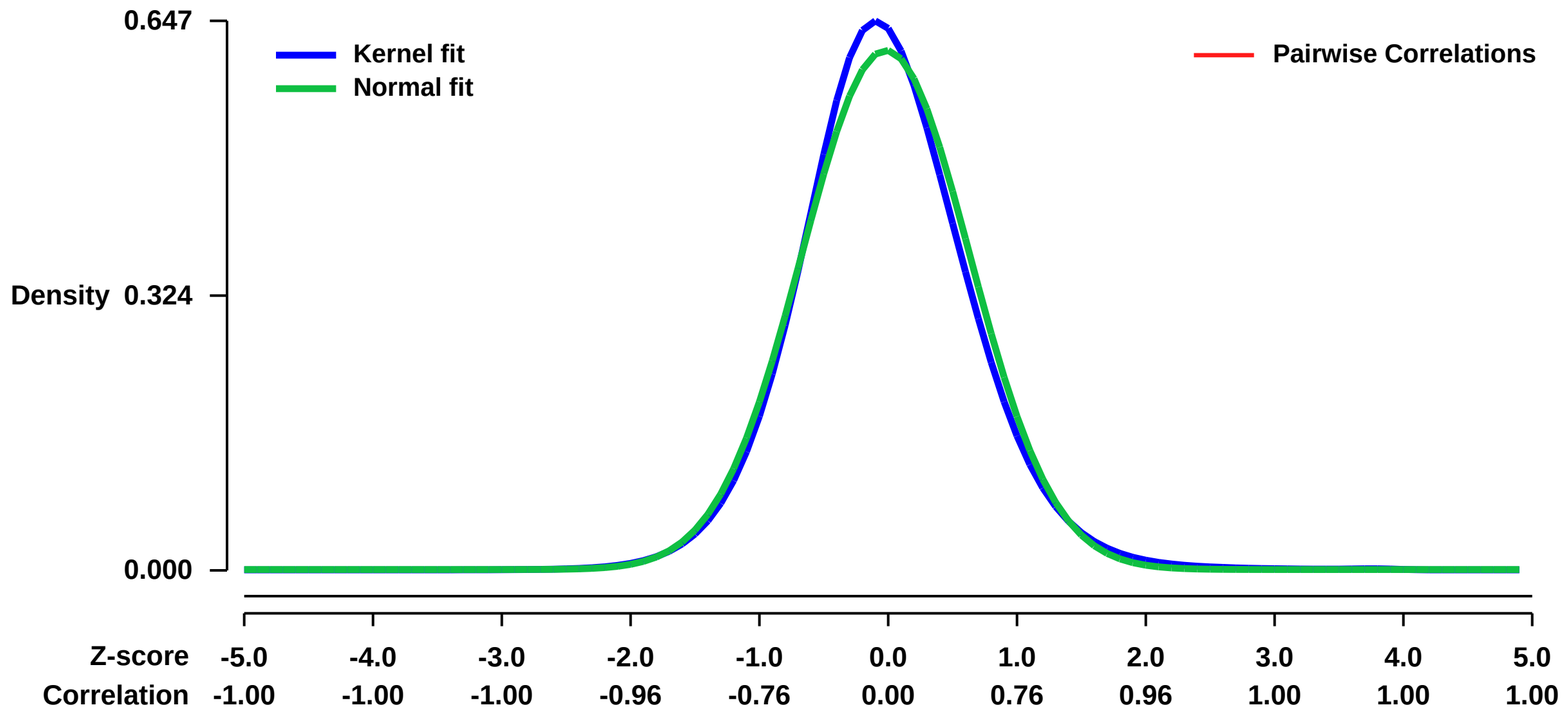

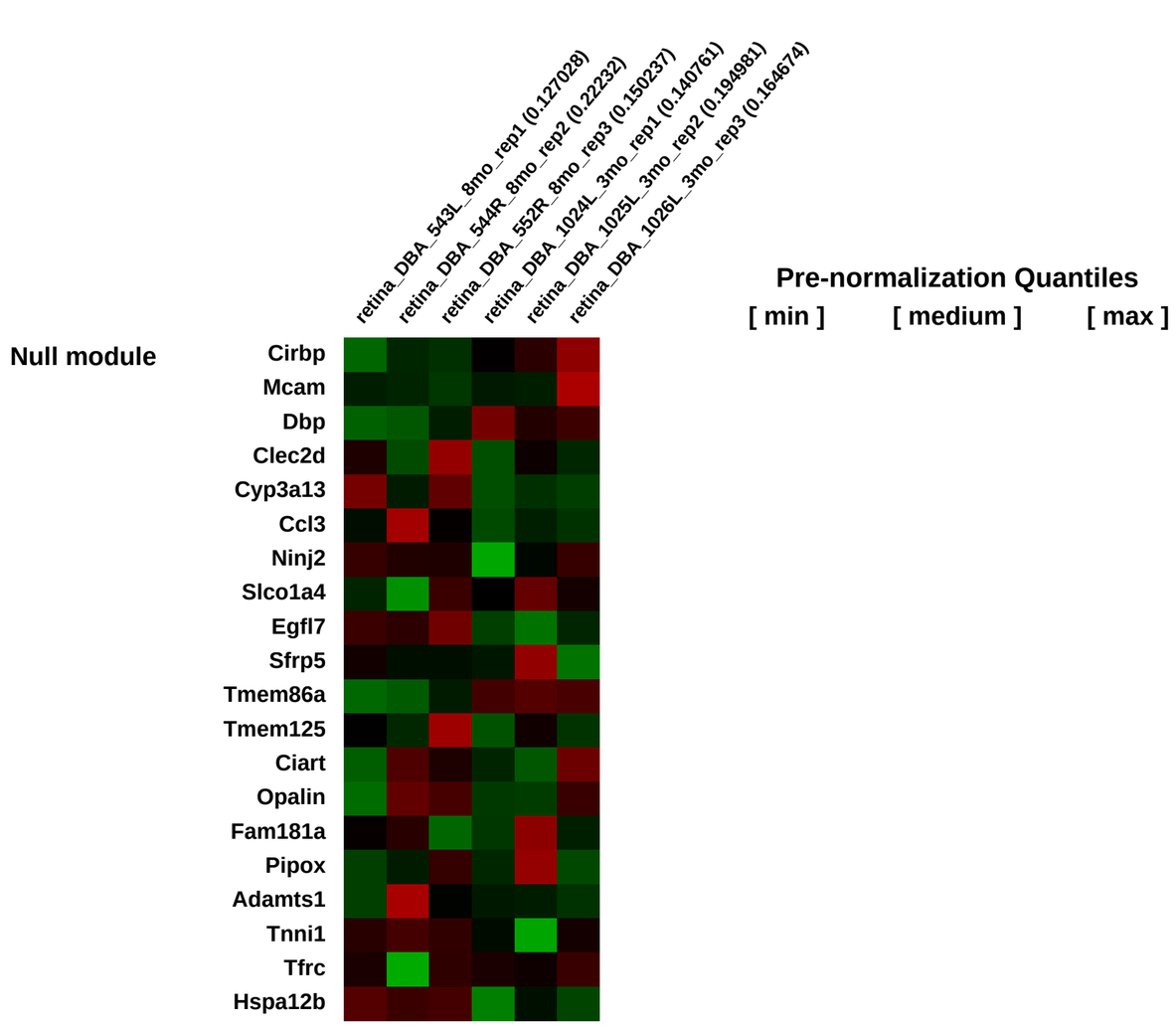

GEO Series "GSE35593" Expression Profiles

Num of samples in this series: 6

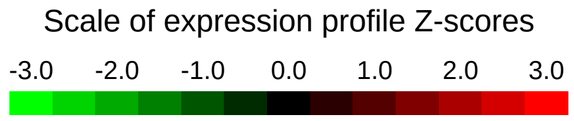

GEO Link:	http://www.ncbi.nlm.nih.gov/geo/query/acc.cgi?acc=GSE35593
Status:	Public on Feb 16 2013
Title:	Foxo1/3 depletion in granulosa cells reveals novel mechanisms controlling follicle growth and death and endocrine regulation of pituitary FSH.
Organism:	Mus musculus
Experiment type:	Expression profiling by array
Platform:	GPL1261
Pubmed ID:	23322722
Summary & Design:	**Summary:** The Foxo transcription factors regulate multiple cellular functions. Foxo1 and Foxo3 are highly expressed in granulosa cells of ovarian follicles. Selective depletion of the Foxo1 and Foxo3 genes in granulosa cells revealed a novel ovarian-pituitary endocrine feedback loop characterized by: 1) undetectable levels of serum FSH but not LH, 2) reduced expression of the pituitary Fshb gene and its transcriptional regulators and 3) ovarian production of a factor(s) that suppresses pituitary cell Fshb. Equally notable and independent of FSH, depletion of Foxo1/3 altered the expression of specific genes associated with follicle growth versus apoptosis by disrupting critical regulatory interactions of Foxo1/3 with the activin and BMP2 pathways, respectively. As a consequence, granulosa cell proliferation and apoptosis were decreased. These data provide the first evidence that Foxo1/3 divergently regulate follicle growth or death by interacting with the activin and BMP pathways in granulosa cells and by modulating pituitary FSH production. **Overall design:** A direct comparison of ovarian granulosa cells from wild type d25, Foxo1/3 dKO d25 and Foxo1/3 dKO 2 month mice.

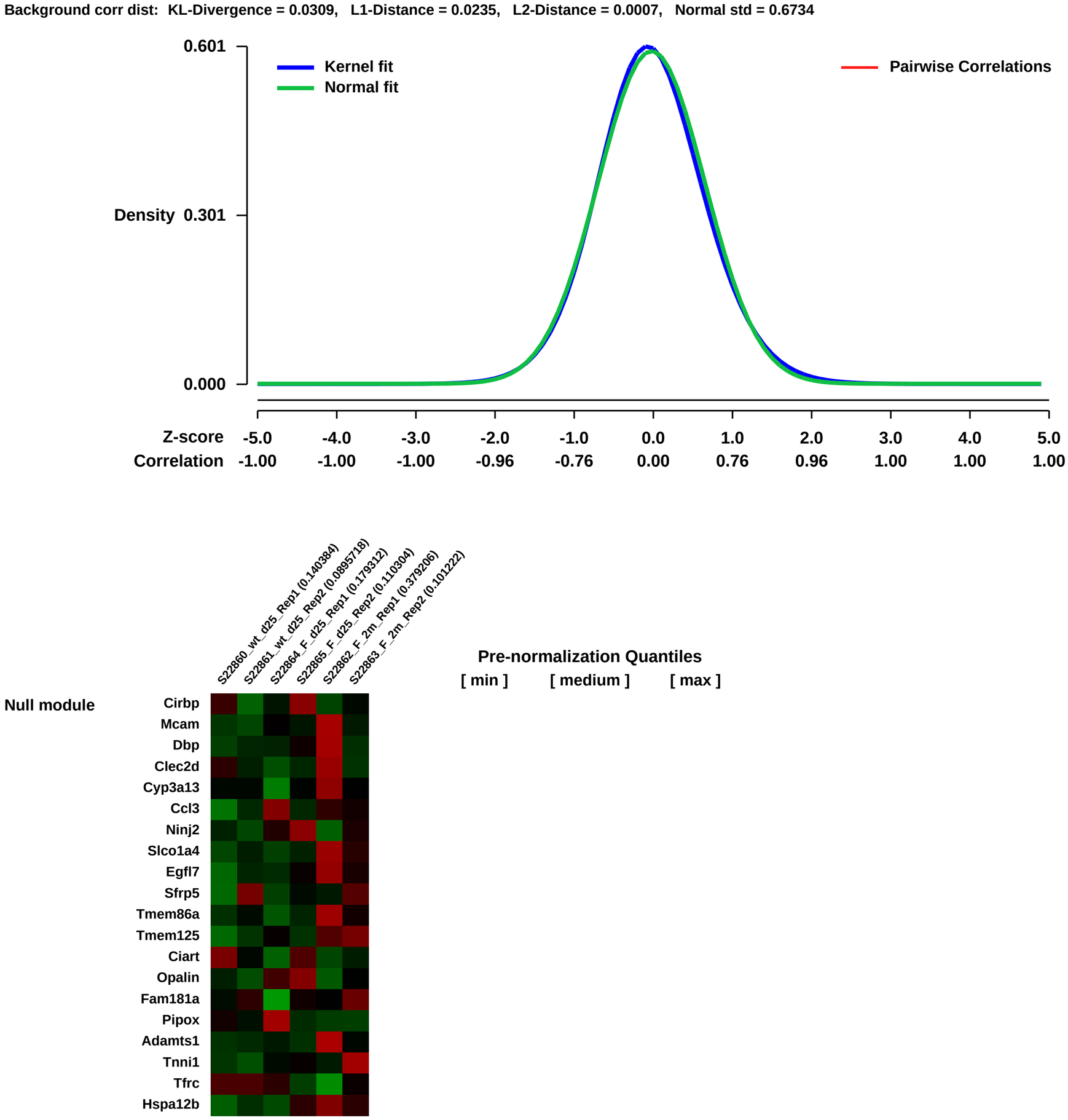

GEO Series "GSE35761" Expression Profiles

Num of samples in this series: 6

Scale of expression profile Z-scores

-3.0 -2.0 -1.0 0.0 1.0 2.0 3.0

GEO Link:	http://www.ncbi.nlm.nih.gov/geo/query/acc.cgi?acc=GSE35761
Status:	Public on Jun 01 2012
Title:	Effect of fluoxetine treatment on translational profiles of S100a10 cortical pyramidal cells
Organism:	Mus musculus
Experiment type:	Expression profiling by array
Platform:	GPL1261
Pubmed ID:	22632977
Summary & Design:	**Summary:** Molecular phenotyping of cell types and neural circuits underlying pathological neuropsychiatric conditions and their responses to therapy provides one avenue for the development of more specific and effective treatments. In this study, we identify a cell population in the cerebral cortex that shows robust and specific molecular adaptations following long-term SSRI treatment. We employed the bacTRAP strategy, which uses BAC transgenic mice expressing EGFP-tagged ribosomal protein L10a in specific cell populations, to affinity purify polysome-bound mRNAs from S100a10-expressing corticostriatal projection neurons. We show that the S100a10 cells are a unique population of cortical cells that are strongly and specifically responsive to chronic SSRI administration and that this response requires p11 (the protein product of S100a10). Our data demonstrate that the beneficial actions of antidepressant therapy can be mediated by a single cell type that is positioned to normalize activity between cortical and subcortical sites, and suggest that development of drugs that specifically target the activity of these cells may result in improved therapies to treat depression. **Overall design:** S100a10 bacTRAP mice were administered either fluoxetine (FLX) or vehicle (VEH) in their drinking water for 15-18 days. Three independent TRAP replicates from the cortex of each group were then collected. Total RNA from the immunoprecipitates was amplified and hybridized. Data were normalized with the GCRMA algorithm and replicates were averaged across conditions. We recommend filtering data to remove probe sets with normalized expression values less than 50 in at least one condition. Because the S100a10 BAC labels some non-neuronal cells, we recommend only probe sets listed in Table S1 of the accompanying paper be included in the analysis.

Background corr dist: KL-Divergence = 0.0516, L1-Distance = 0.0503, L2-Distance = 0.0038, Normal std = 0.6364

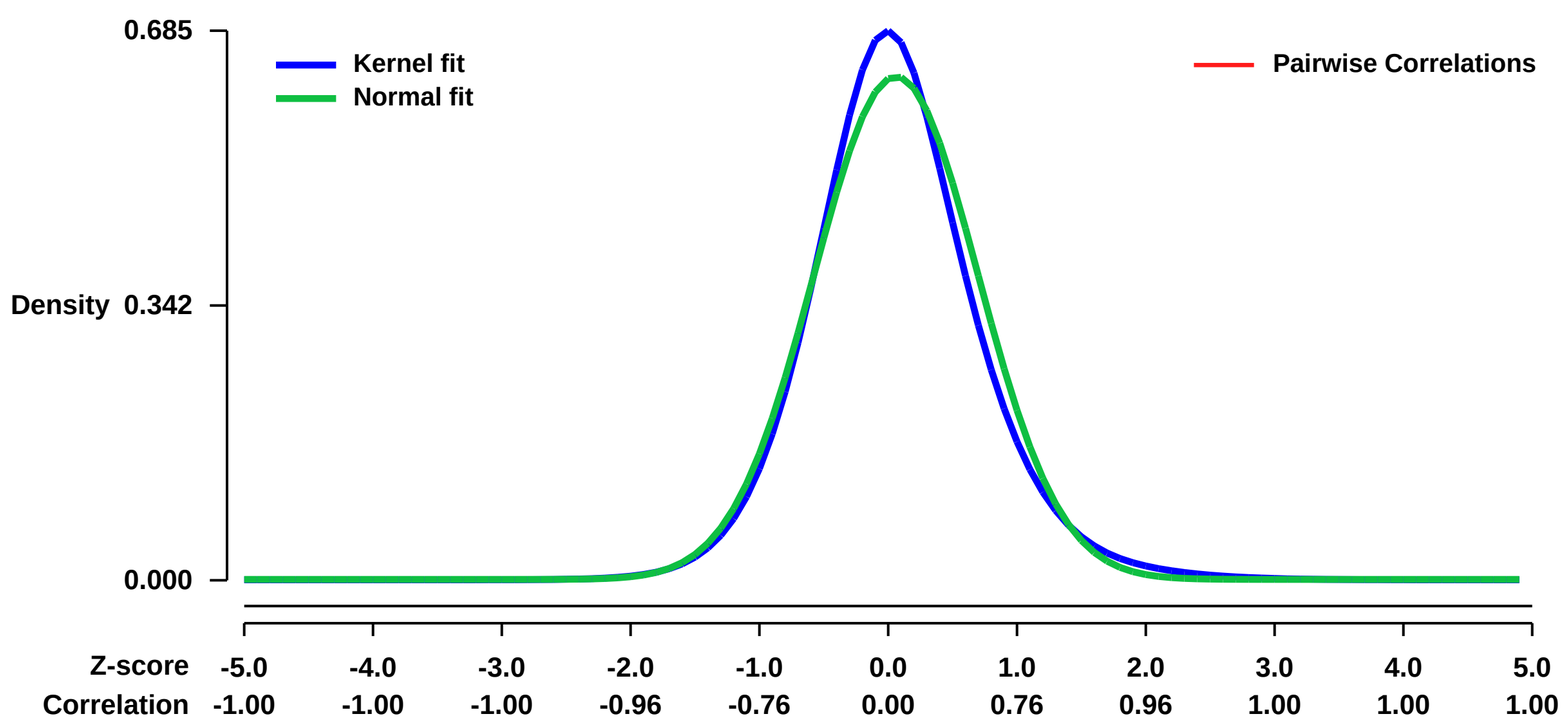

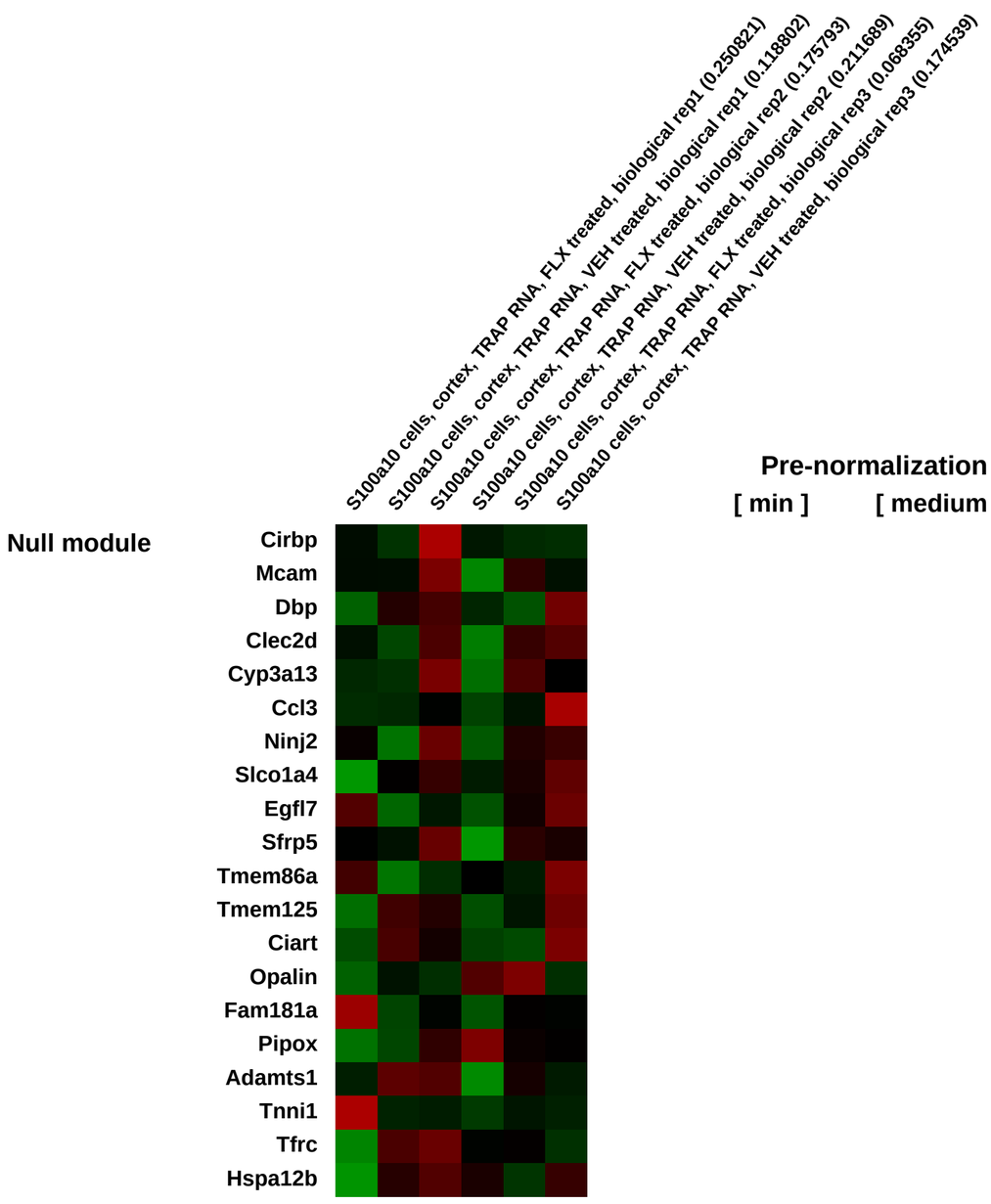

GEO Series "GSE35763" Expression Profiles

Num of samples in this series: 6

Scale of expression profile Z-scores

-3.0 -2.0 -1.0 0.0 1.0 2.0 3.0

GEO Link:	http://www.ncbi.nlm.nih.gov/geo/query/acc.cgi?acc=GSE35763
Status:	Public on Jun 01 2012
Title:	Effect of fluoxetine treatment on translational profiles of Glt25d2 cortical pyramidal cells
Organism:	Mus musculus
Experiment type:	Expression profiling by array
Platform:	GPL1261
Pubmed ID:	22632977
Summary & Design:	**Summary:** Molecular phenotyping of cell types and neural circuits underlying pathological neuropsychiatric conditions and their responses to therapy provides one avenue for the development of more specific and effective treatments. In this study, we identify a cell population in the cerebral cortex that shows robust and specific molecular adaptations following long-term SSRI treatment. We employed the bacTRAP strategy, which uses BAC transgenic mice expressing EGFP-tagged ribosomal protein L10a in specific cell populations, to affinity purify polysome-bound mRNAs from S100a10-expressing corticostriatal projection neurons. We show that the S100a10 cells are a unique population of cortical cells that are strongly and specifically responsive to chronic SSRI administration and that this response requires p11 (the protein product of S100a10). Our data demonstrate that the beneficial actions of antidepressant therapy can be mediated by a single cell type that is positioned to normalize activity between cortical and subcortical sites, and suggest that development of drugs that specifically target the activity of these cells may result in improved therapies to treat depression. **Overall design:** Glt25d2 bacTRAP mice were administered either fluoxetine (FLX) or vehicle (VEH) in their drinking water for 15-18 days. Three independent TRAP replicates from cortex of each group were then collected. Total RNA from the immunoprecipitates was amplified and hybridized. Data were normalized with the GCRMA algorithm and replicates were averaged across conditions. We recommend filtering data to remove probe sets with normalized expression values less than 50 in at least one condition. Because the S100a10 BAC labels some non-neuronal cells, we recommend only probe sets listed in Table S1 of the accompanying paper be included in the analysis.

Background corr dist: KL-Divergence = 0.0307, L1-Distance = 0.0183, L2-Distance = 0.0004, Normal std = 0.6655

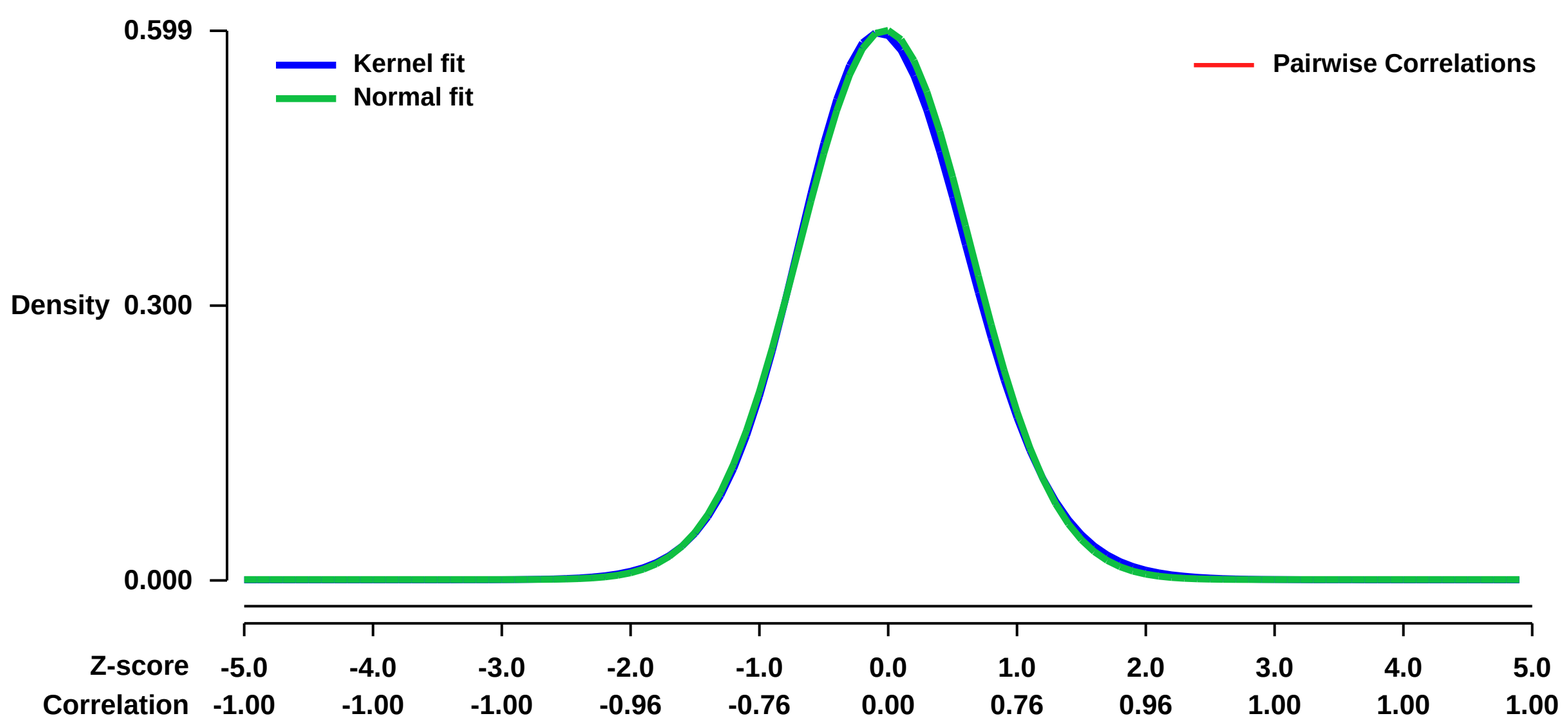

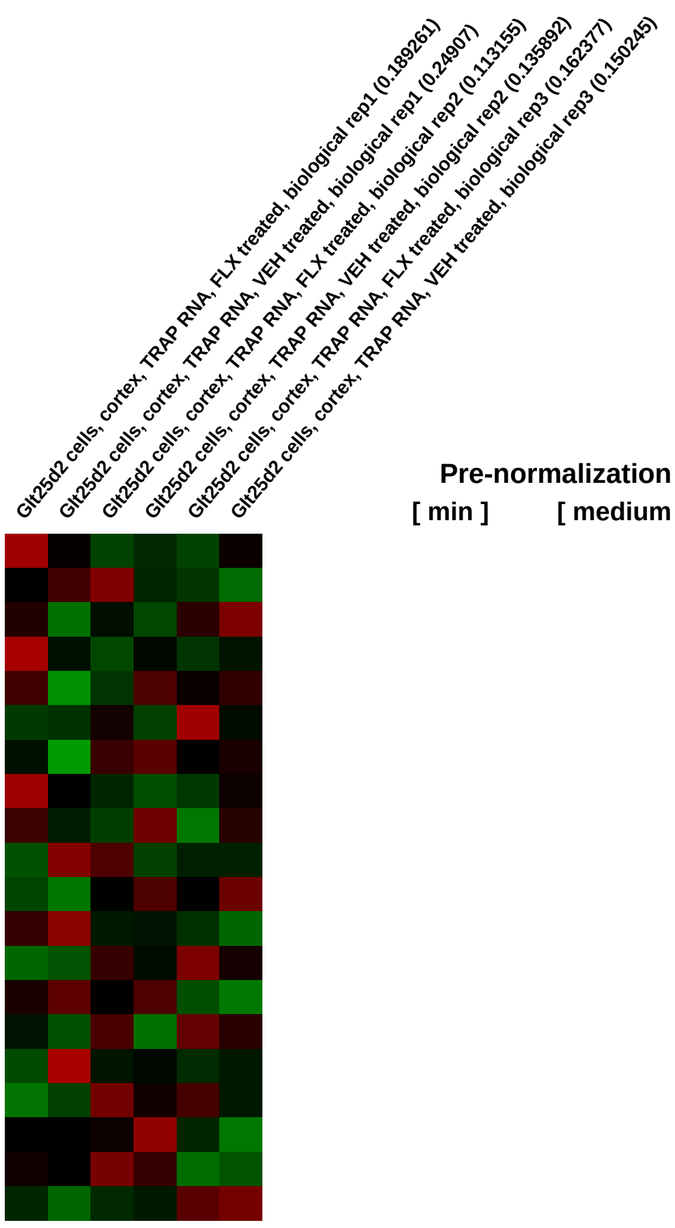

GEO Series "GSE3583" Expression Profiles

Num of samples in this series: 9

Scale of expression profile Z-scores

-3.0 -2.0 -1.0 0.0 1.0 2.0 3.0

GEO Link:	http://www.ncbi.nlm.nih.gov/geo/query/acc.cgi?acc=GSE3583
Status:	Public on Jun 20 2007
Title:	Huntington’s disease: Gene expression changes caused by Hdh CAG mutation or 3-nitropropionic acid in striatal cells
Organism:	Mus musculus
Experiment type:	Expression profiling by array
Platform:	GPL1261
Pubmed ID:	17708681
Summary & Design:	**Summary:** Affymetrix MG430 2.0 expression levels of wild-type (STHdhQ7/Q7), 3NP-treated wild-type (STHdhQ7/Q7+3-NP), and mutant (STHdhQ111/Q111) striatal cells **Keywords: Pharmacological and genetic HD cell culture models** **Overall design:** Investigation of HD disease mechanism by gene expression profiling of two HD model systems

Background corr dist: KL-Divergence = 0.0454, L1-Distance = 0.0173, L2-Distance = 0.0003, Normal std = 0.5904

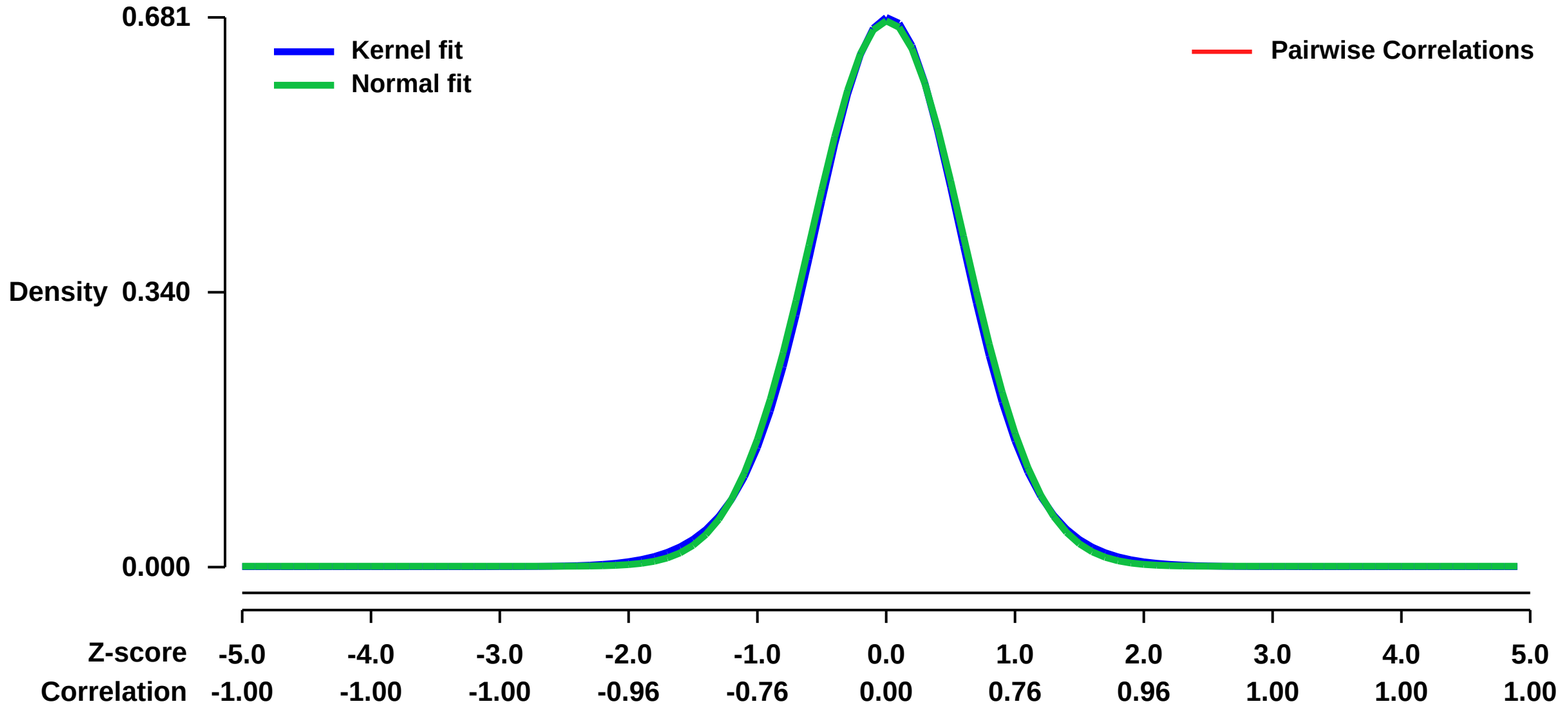

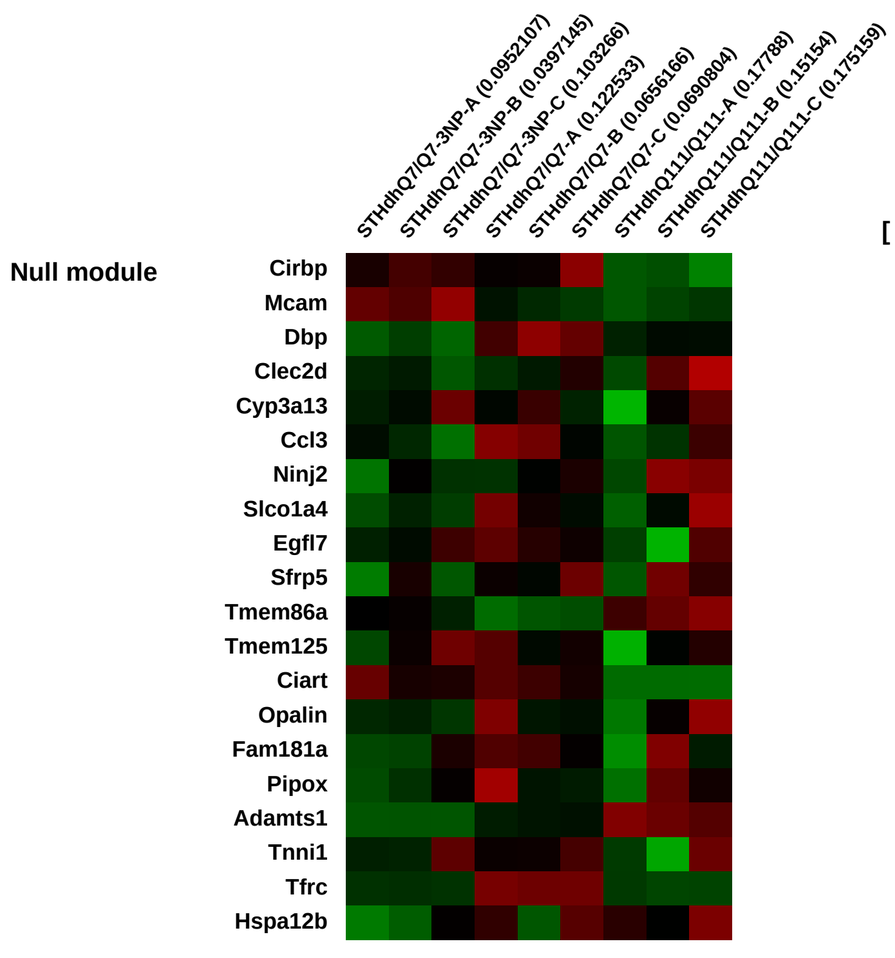

GEO Series "GSE35844" Expression Profiles

Num of samples in this series: 9

Scale of expression profile Z-scores

-3.0 -2.0 -1.0 0.0 1.0 2.0 3.0

GEO Link:	http://www.ncbi.nlm.nih.gov/geo/query/acc.cgi?acc=GSE35844
Status:	Public on Jun 18 2012
Title:	Dicer1 deletion in myeloid-committed progenitors causes neutrophil dysplasia and blocks macrophage/dendritic cell development in mice
Organism:	Mus musculus
Experiment type:	Expression profiling by array
Platform:	GPL1261
Pubmed ID:	22353998
Summary & Design:	**Summary:** MiRNAs have the potential to regulate cellular differentiation programs. However, miRNA-deficiency in primary hematopoietic stem cells (HSCs) results in HSC depletion in mice, leaving the question of whether miRNAs play a role in early-lineage decisions unanswered. To address this issue, we deleted Dicer1, which encodes an essential RNaseIII enzyme for miRNA biogenesis, in murine CCAAT/enhancer-binding protein alpha (C/EBPA)-positive myeloid-committed progenitors in vivo. In contrast to the results in HSCs, we found that miRNA depletion affected neither the number of myeloid progenitors nor the percentage of C/EBPA-positive progenitor cells. Analysis of gene-expression profiles from wild type and Dicer1-deficient granulocyte-macrophage progenitors (GMPs) revealed that 20 miRNA families were active in GMPs. Of the derepressed miRNA targets in Dicer1-null GMPs, 27% are normally exclusively expressed in HSCs or are specific for multi-potent progenitors and erythropoiesis, indicating an altered gene-expression landscape. Dicer1-deficient GMPs were defective in myeloid development in vitro and exhibited an increased replating capacity, indicating a regained self-renewal potential of these cells. In mice, Dicer1 deletion blocked monocytic differentiation, depleted macrophages and caused myeloid dysplasia with morphological features of Pelger-Huˆ«t anomaly. These results provide evidence for a miRNA-controlled switch for a cellular program of self-renewal and expansion towards myeloid differentiation in GMPs. **Overall design:** To generate Cebpa-Cre;R26-LSL-Eyfp;Dicer1wt/fl/Dicer1fl/fl mice, we crossed mice that contain floxed Dicer1 alleles (Dicer1fl) with Cebpa-Cre;R26-LSL-Eyfp reporter mice 2. Fetal livers were obtained on embryonic day (E) 13.5. Routine genotyping of Dicer1; Cebpa-Cre;R26-LSL-Eyfp mice was performed by PCR assays of DNA from tail or toe biopsies. For transplantation, 6 to 8-week-old recipient mice (C57Bl/6, Jackson Laboratories) were irradiated (8.5 Gy) and tail-vein injected with fetal liver single-cell suspensions. Typically, cells from each fetal liver were transplanted into two recipient mice. Hematopoietic tissues were analyzed 6-10 weeks post transplantation. EYFP positive GMPs from the bone marrow of Dicer wt control (n=3), Dicer -/wt (n=3 and Dicer fl/fl (n=3) were sorted and analyzed for gene expression profiles.

Background corr dist: KL-Divergence = 0.1010, L1-Distance = 0.0231, L2-Distance = 0.0009, Normal std = 0.4374

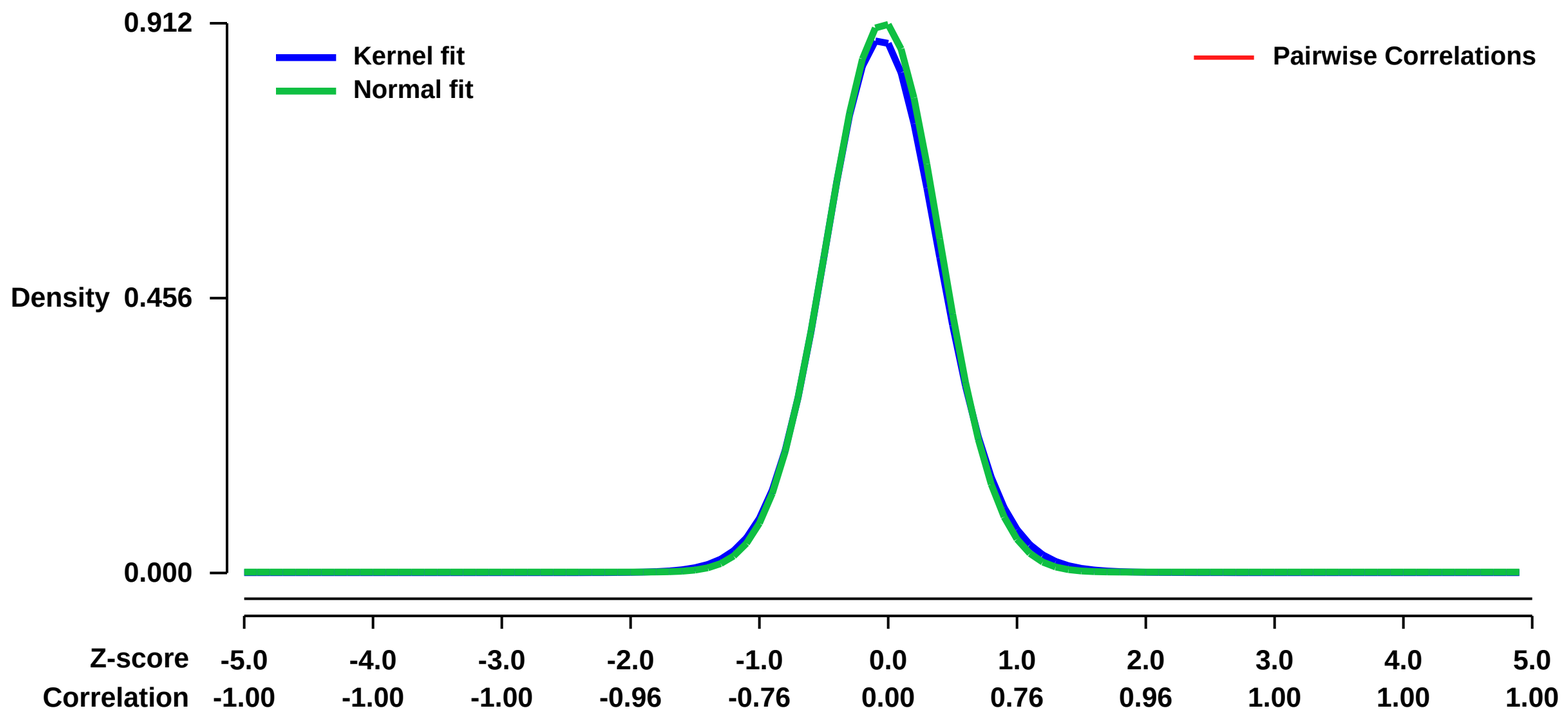

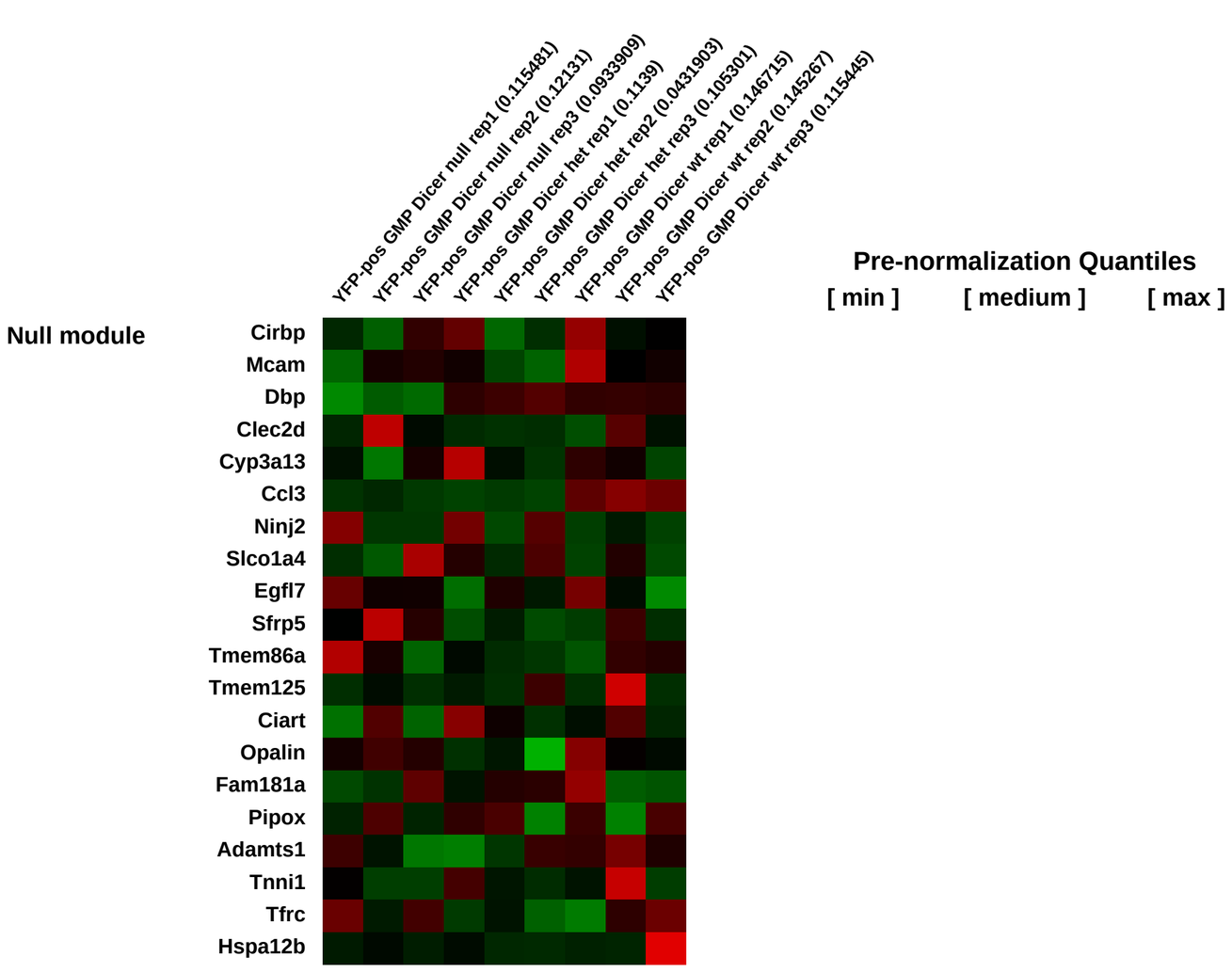

GEO Series "GSE35899" Expression Profiles

Num of samples in this series: 15

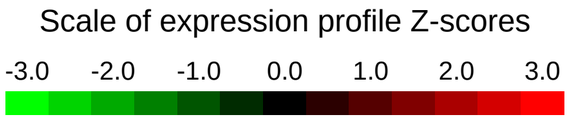

GEO Link:	**http://www.ncbi.nlm.nih.gov/geo/query/acc.cgi?acc=GSE35899**
Status:	**Public on Feb 18 2014**
Title:	**Expression data from Mammospheres**
Organism:	**Mus musculus**
Experiment type:	**Expression profiling by array**
Platform:	**GPL1261**
Pubmed ID:	**24290754**
Summary & Design:	**Summary:** **The combined activation of Wnt/^ -catenin and MET/HGF is required for mammary cancer stem cell (MaCSC) maintenance. We generated mammospheres derived from tumors of mice harboring Wnt/Met signaling mutations on which we performed microarray analysis to evaluate gene expression signatures controlled by Wnt and MET pathways. We used the gene expression profiles to dissect the role and the functions of these pathways in MaCSCs.** **Overall design:** **We treated mammospheres with Wnt and MET pathway inhibitors alone or in combination. Samples treated with DMSO were used as vehicle control.**

Background corr dist: **KL-Divergence = 0.0642, L1-Distance = 0.0265, L2-Distance = 0.0012, Normal std = 0.5104**

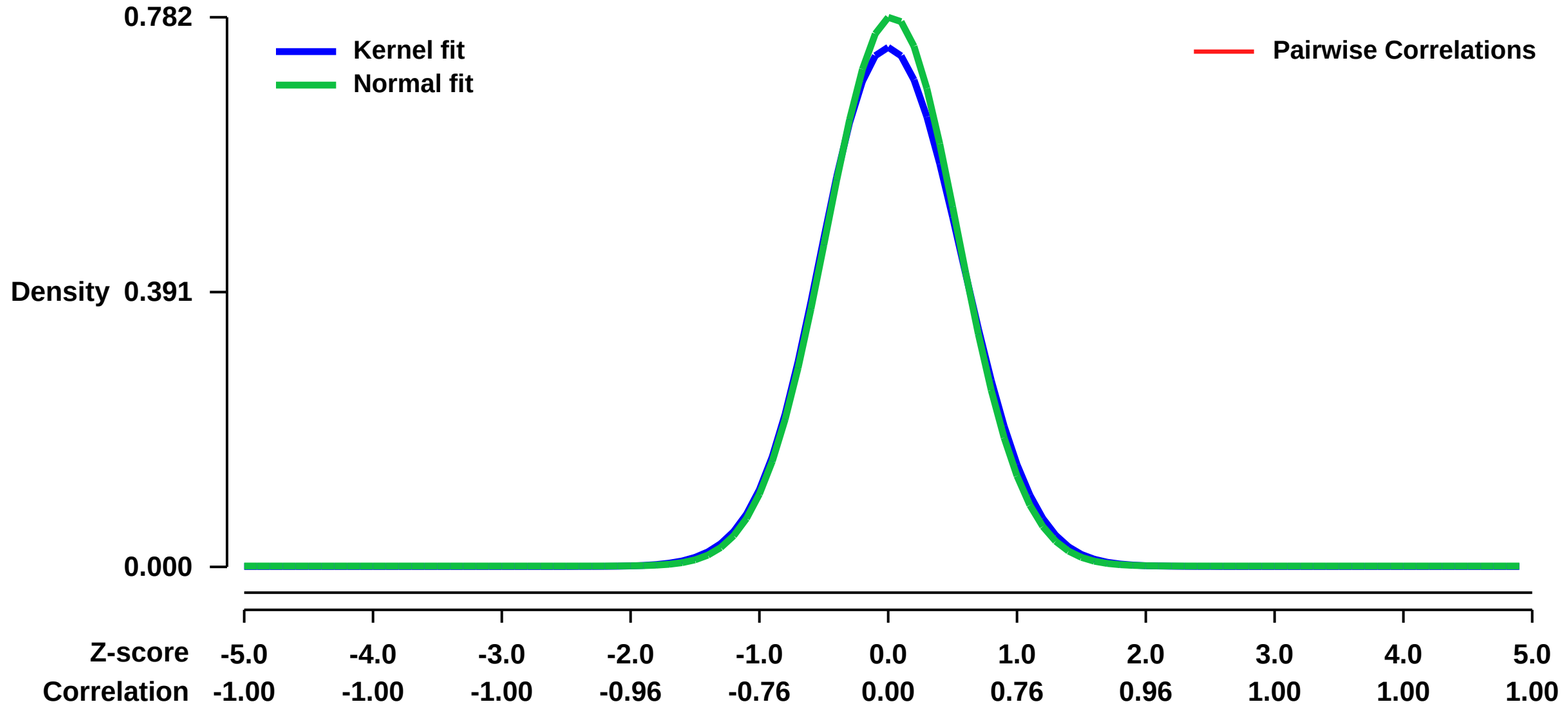

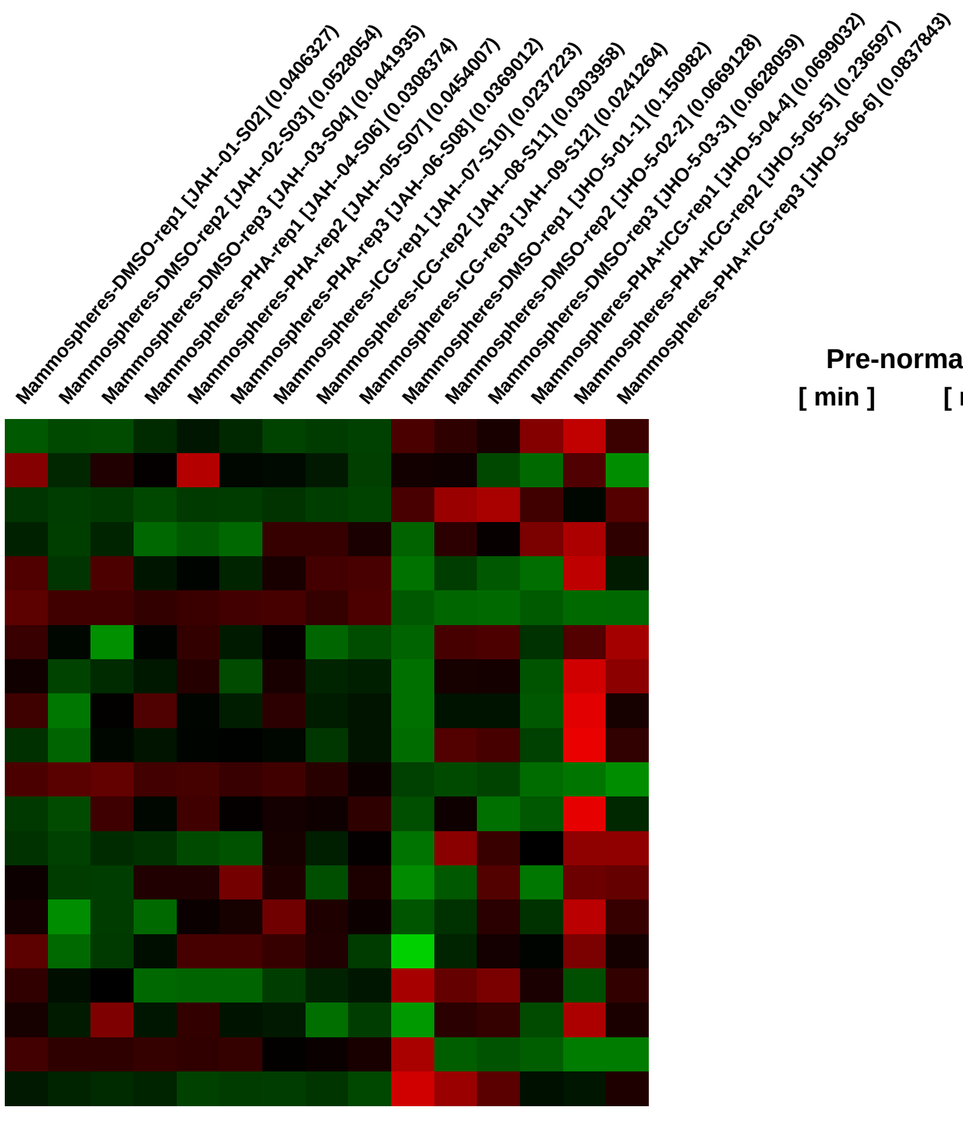

GEO Series "GSE3595" Expression Profiles

Num of samples in this series: 6

Scale of expression profile Z-scores

-3.0 -2.0 -1.0 0.0 1.0 2.0 3.0

GEO Link:	http://www.ncbi.nlm.nih.gov/geo/query/acc.cgi?acc=GSE3595
Status:	Public on Jun 10 2006
Title:	Identification of potential KLF7 target genes in olfactory sensory neurons
Organism:	Mus musculus
Experiment type:	Expression profiling by array
Platform:	GPL1261
Pubmed ID:	17123745
Summary & Design:	**Summary:** KLF7 null mice show profound axonal growth defects in the olfactory epithelium. The goal of this study was the identification of potential KLF7 target genes in olfactory sensory neurons. Keywords: Molecular analysis of knockout mice. **Overall design:** Olfactory epithelia were isolated from 3 wildtype and 3 mutant 1 day old pups and the RNA isolated, labeled and hybridized to one chip each.

Background corr dist: KL-Divergence = 0.0329, L1-Distance = 0.0446, L2-Distance = 0.0027, Normal std = 0.6976

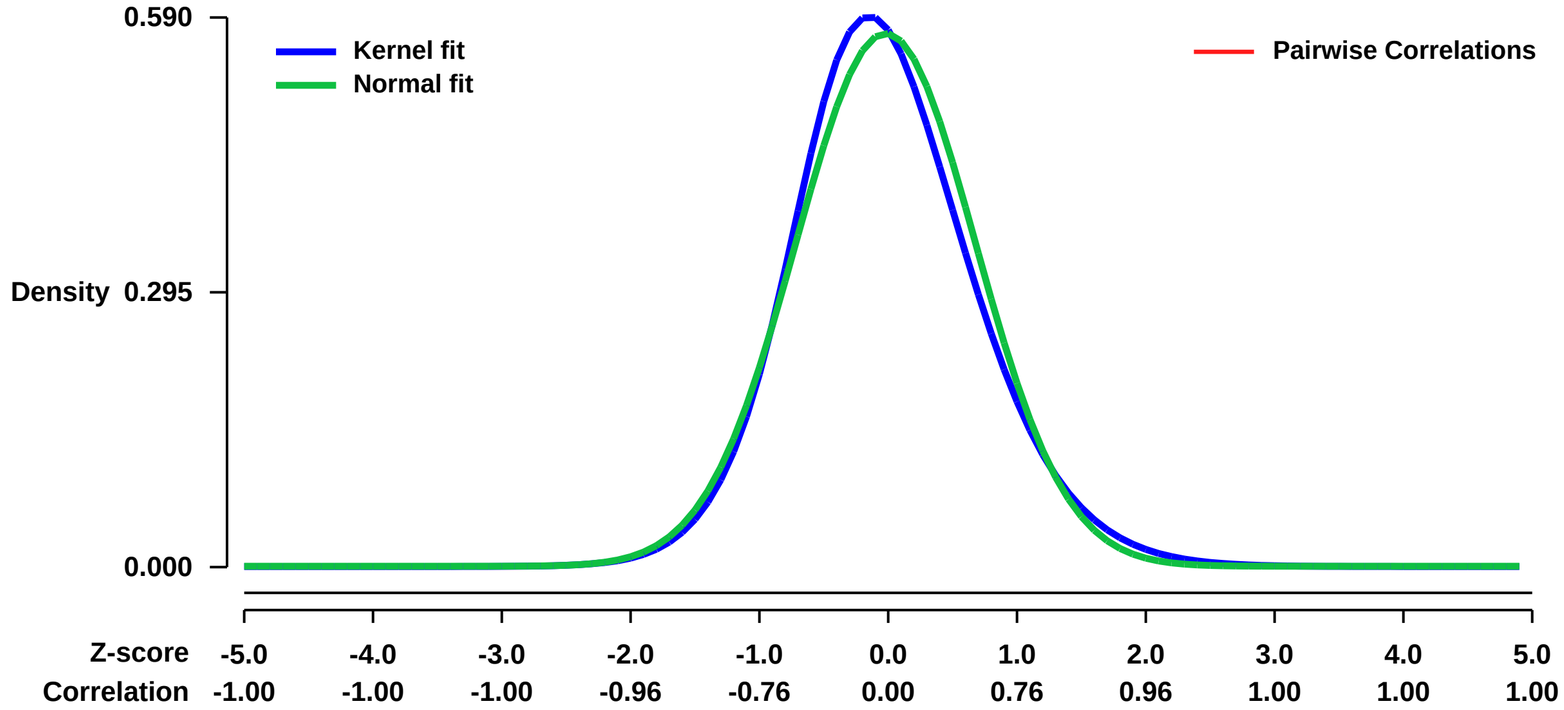

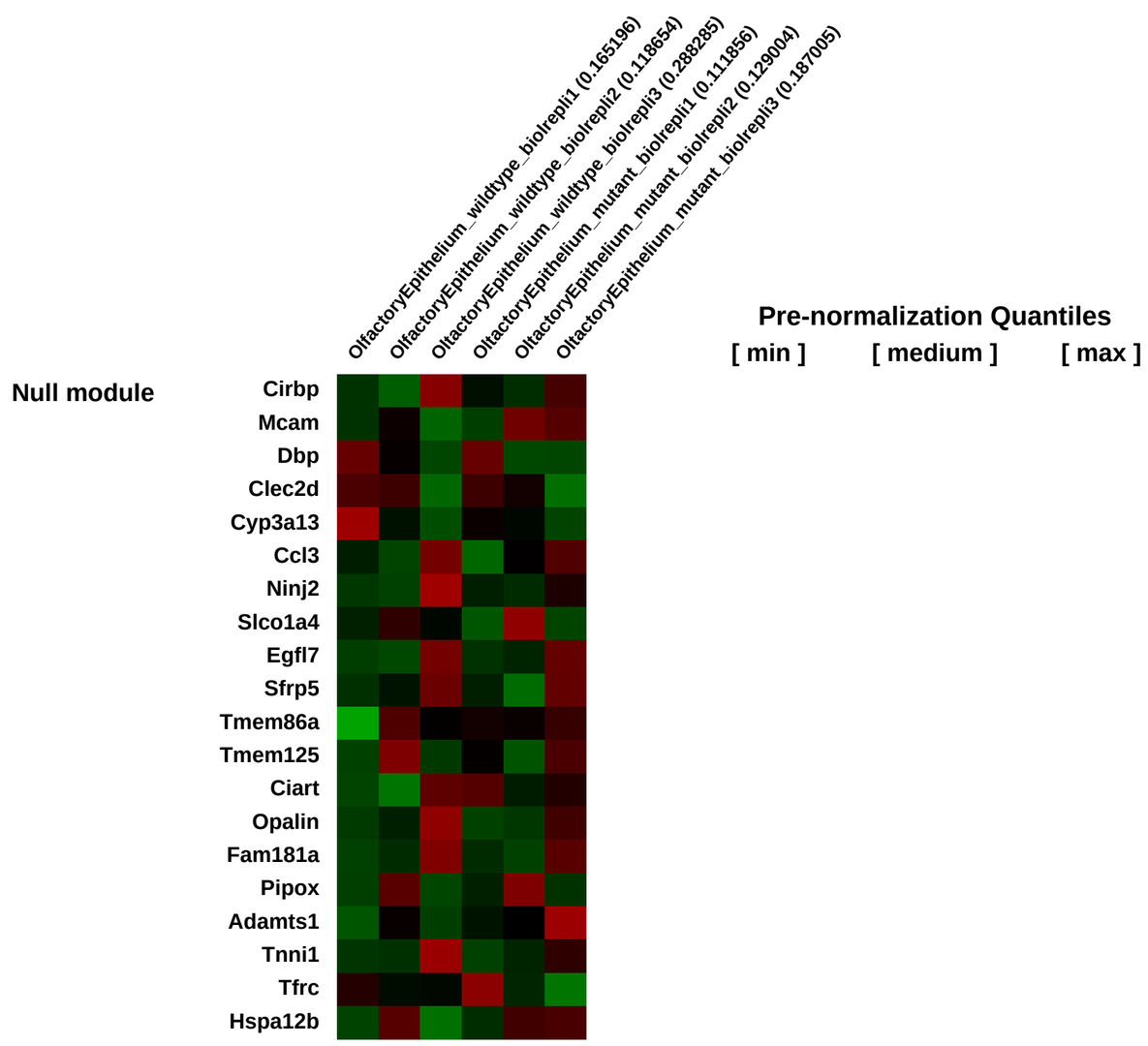

GEO Series "GSE35961" Expression Profiles

Num of samples in this series: 12

Scale of expression profile Z-scores

-3.0 -2.0 -1.0 0.0 1.0 2.0 3.0

GEO Link:	http://www.ncbi.nlm.nih.gov/geo/query/acc.cgi?acc=GSE35961
Status:	Public on Feb 21 2012
Title:	Expression data from mouse liver treated with metformin
Organism:	Mus musculus
Experiment type:	Expression profiling by array
Platform:	GPL1261
Pubmed ID:	23028442
Summary & Design:	**Summary:** **Optimal treatment for nonalcoholic steatohepatitis (NASH) has not yet been established, particularly for individuals without diabetes.** **We examined the effects of metformin, commonly used to treat patients with type 2 diabetes, on liver pathology in a non-diabetic NASH mouse model.** **Overall design:** **Eight-week-old C57BL/6 mice were fed a methionine- and choline-deficient (MCD) + high fat (HF) diet with or without 0.1% metformin for 8 weeks.**

Background corr dist: **KL-Divergence = 0.0889, L1-Distance = 0.0223, L2-Distance = 0.0007, Normal std = 0.4619**

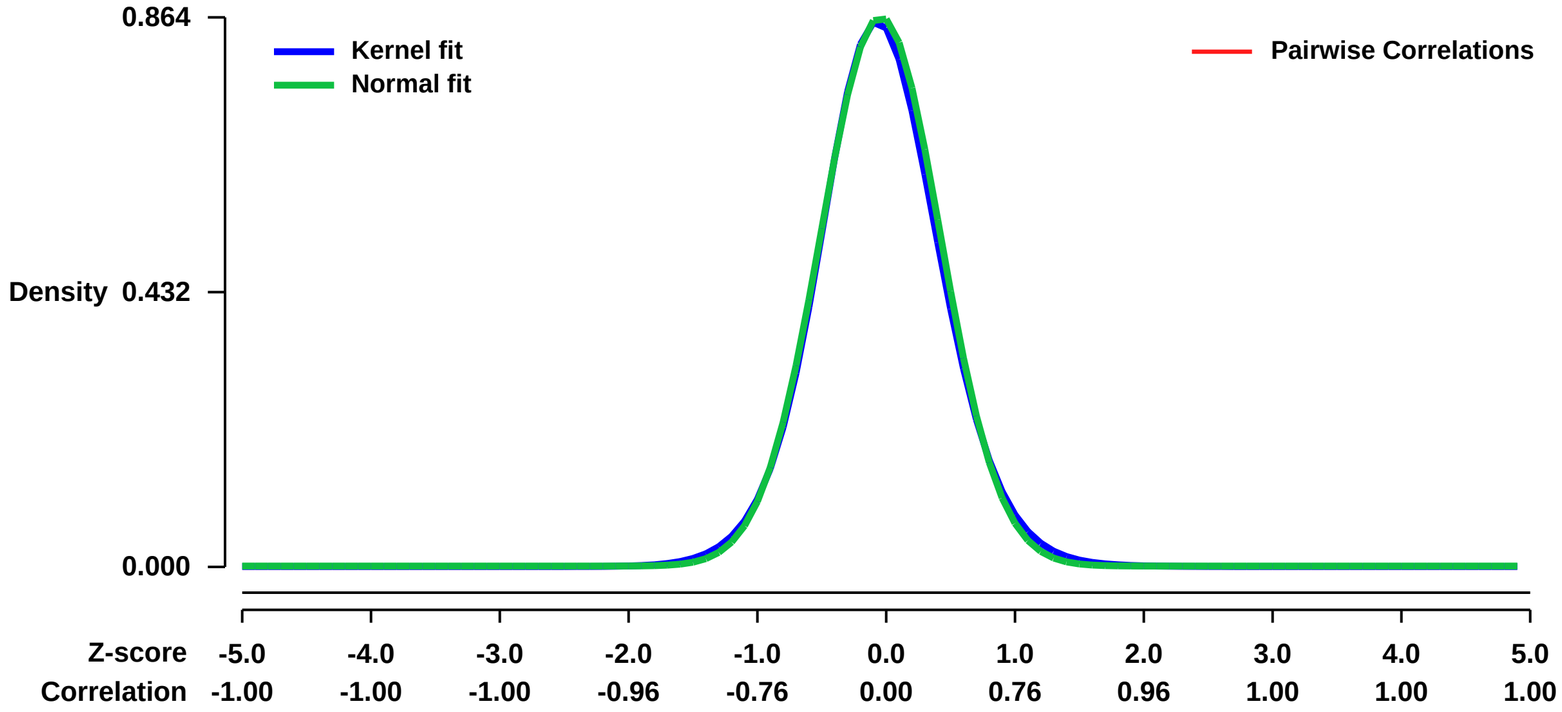

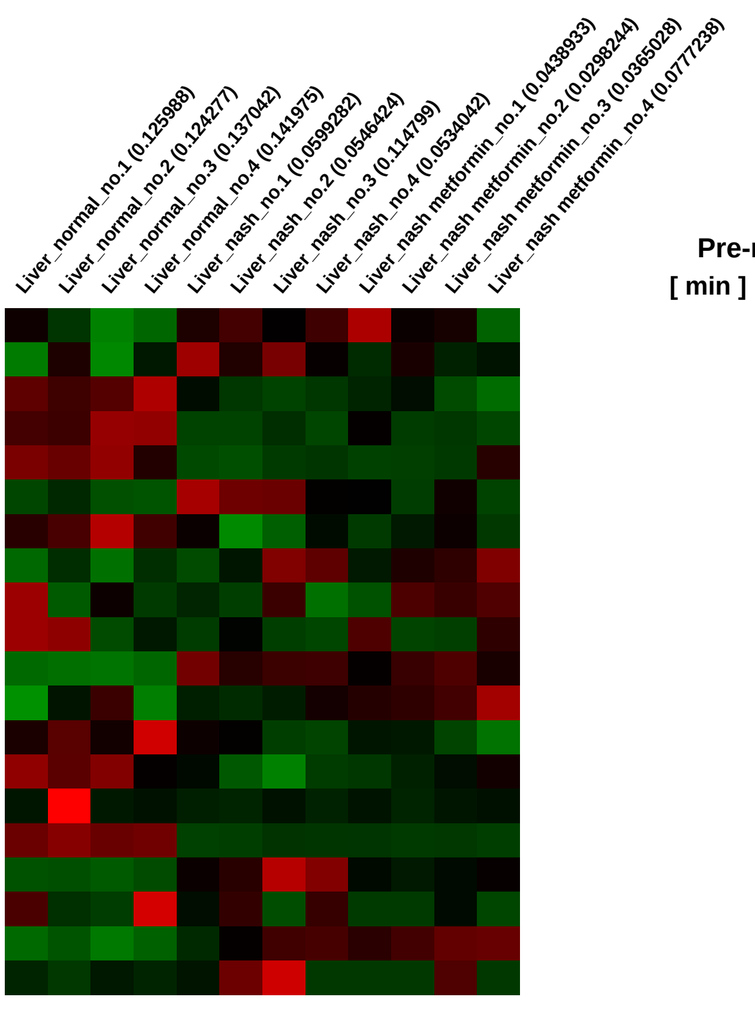

GEO Series "GSE35979" Expression Profiles

Num of samples in this series: 6

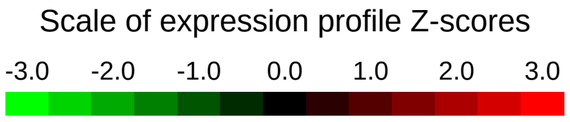

GEO Link:	http://www.ncbi.nlm.nih.gov/geo/query/acc.cgi?acc=GSE35979
Status:	Public on Feb 23 2012
Title:	Gene expression data from IL13-induced allergic airway inflammation of mice lungs
Organism:	Mus musculus
Experiment type:	Expression profiling by array
Platform:	GPL1261
Pubmed ID:	22611474
Summary & Design:	**Summary:** Asthma is a common chronic inflammatory airway condition with a strong genetic and inheritability component, as siblings and first-degree relatives of those with the disease are often affected. For our studies, we used a well-characterized transgenic mouse model of allergic airway inflammation induced by IL13. In this model, IL13 is conditionally overexpressed in the mouse lung when treated with doxycycline. Upon IL13 induction, these mice showed inflammatory cell infiltration, pronounced emphysema, increased pulmonary compliance, lung volume enlargement, mucus metaplasia, and increased expression of matrix metalloproteinases and cathepsins in the lung. We performed gene expression microarray to examine the changes in gene expression during IL13-induced allergic airway inflammation. **Overall design:** The CC10-rtTA-IL13 transgenic (TG) and wildtype (WT) mice were treated with doxycycline for seven days. Mice were euthanized and the left upper lobes from all mice were removed for RNA extraction using the TRIzol method.

Background corr dist: KL-Divergence = 0.0277, L1-Distance = 0.0161, L2-Distance = 0.0003, Normal std = 0.6879

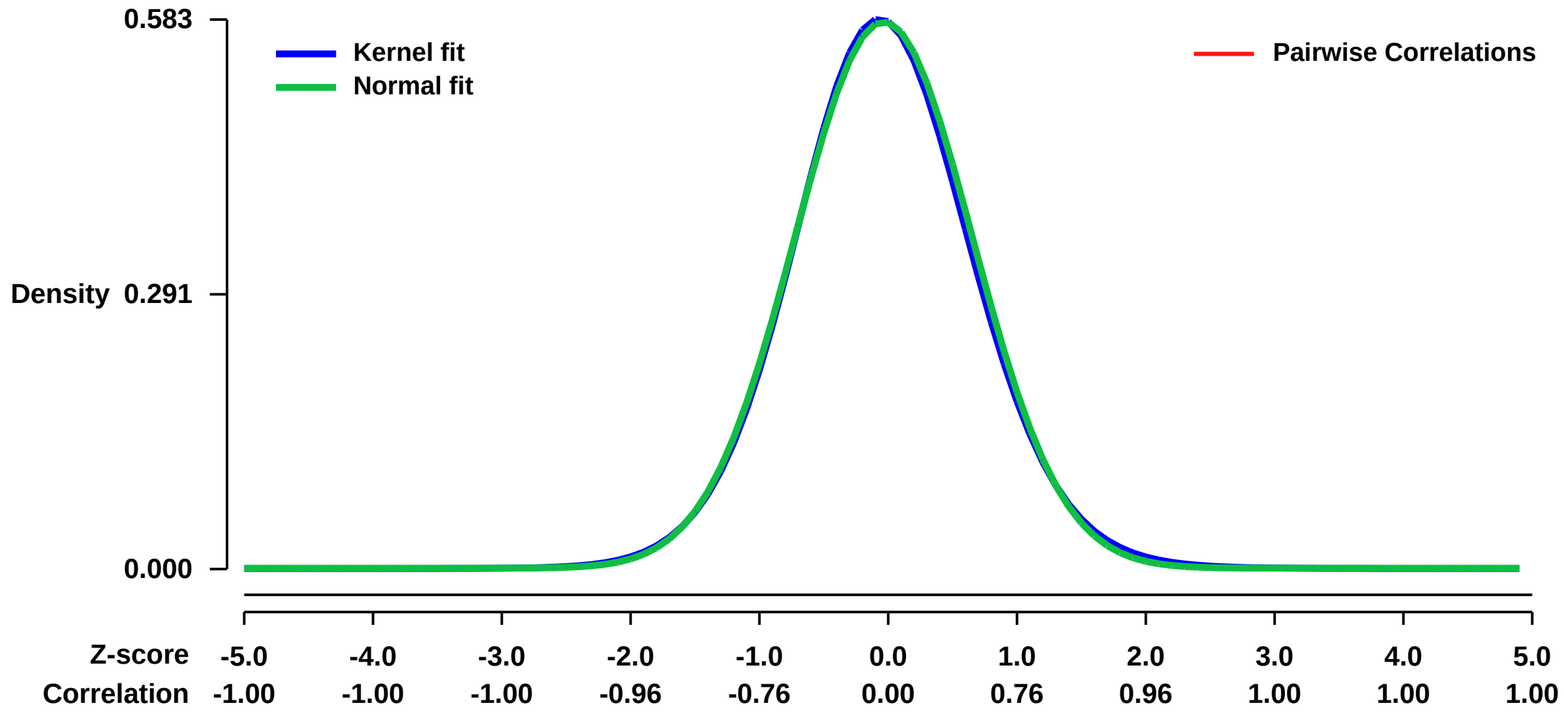

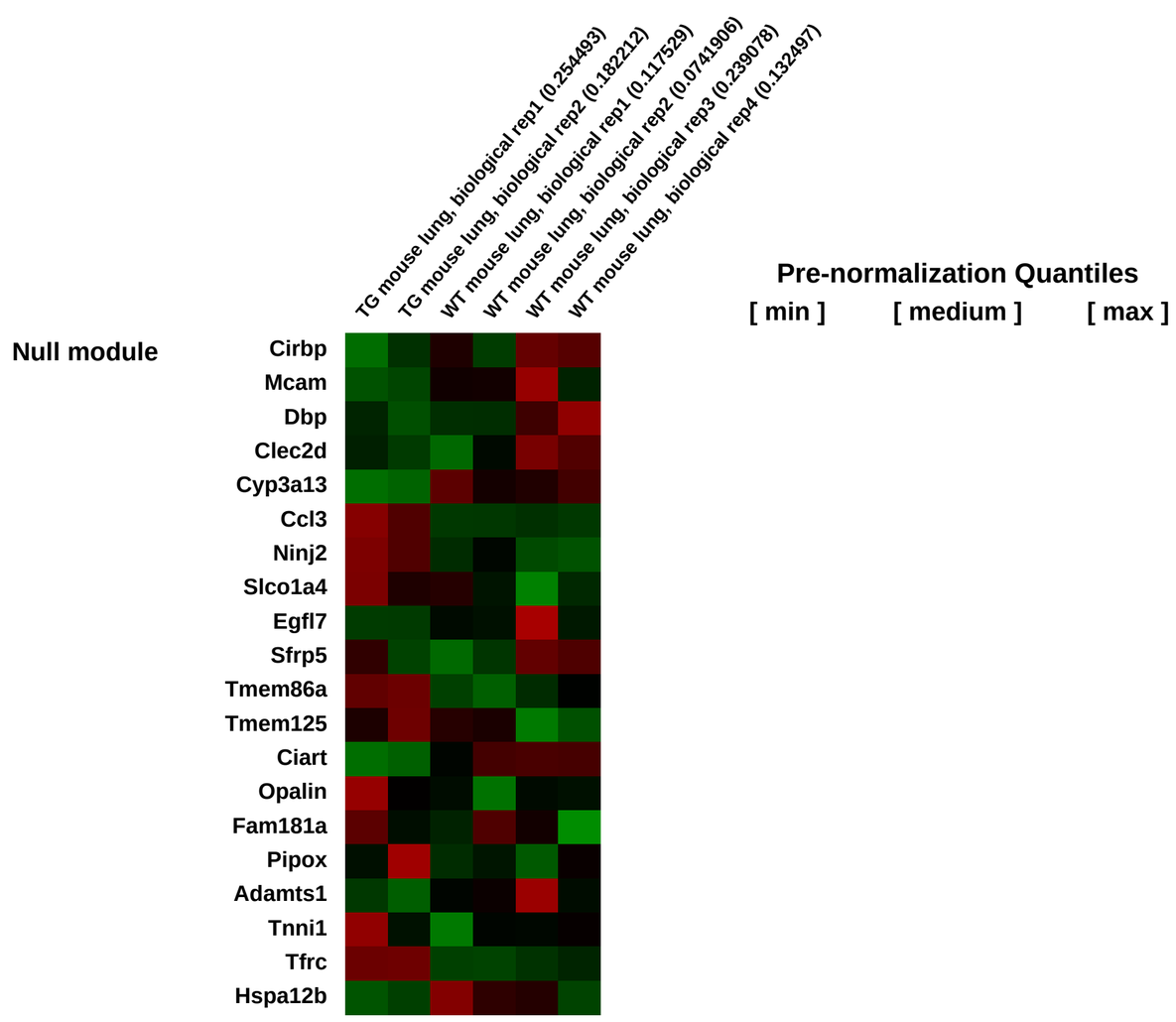

GEO Series "GSE36209" Expression Profiles

Num of samples in this series: 9

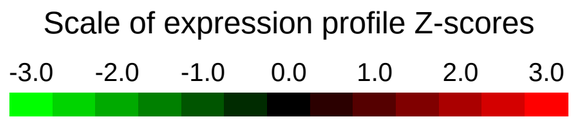

GEO Link:	**http://www.ncbi.nlm.nih.gov/geo/query/acc.cgi?acc=GSE36209**
Status:	**Public on Mar 02 2012**
Title:	**Expression data for OVE26 diabetic mouse podocyte**
Organism:	**Mus musculus**
Experiment type:	**Expression profiling by array**
Platform:	**GPL1261**
Pubmed ID:	
Summary & Design:	**Summary:** **Podocytes form filtration barrier through foot process around glomerualar basement membrane and selectively permit permeability of molecular smaller than albumin. Diabetes can cause podocyte pathological changes leading to high urine albumin level. Diabetic mouse model OVE26 has extremly high urine albumin and previously studies indicated its podocyte damaged.** **Here we try to find the key genes change in OVE26 diabetic mouse model podocyte by microarray assay while normal FVB mouse podocyte set as control.** **Overall design:** **Podocyte eGFP transgenic mice were made on FVB background and crossbred to OVE26 diabetic model. Glomeruli isolated from OVE-GFP mice were digested by trypsin into signal cell. Podocytes with GFP were sorting out by FACS.**

Background corr dist: **KL-Divergence = 0.0948, L1-Distance = 0.0240, L2-Distance = 0.0010, Normal std = 0.4481**

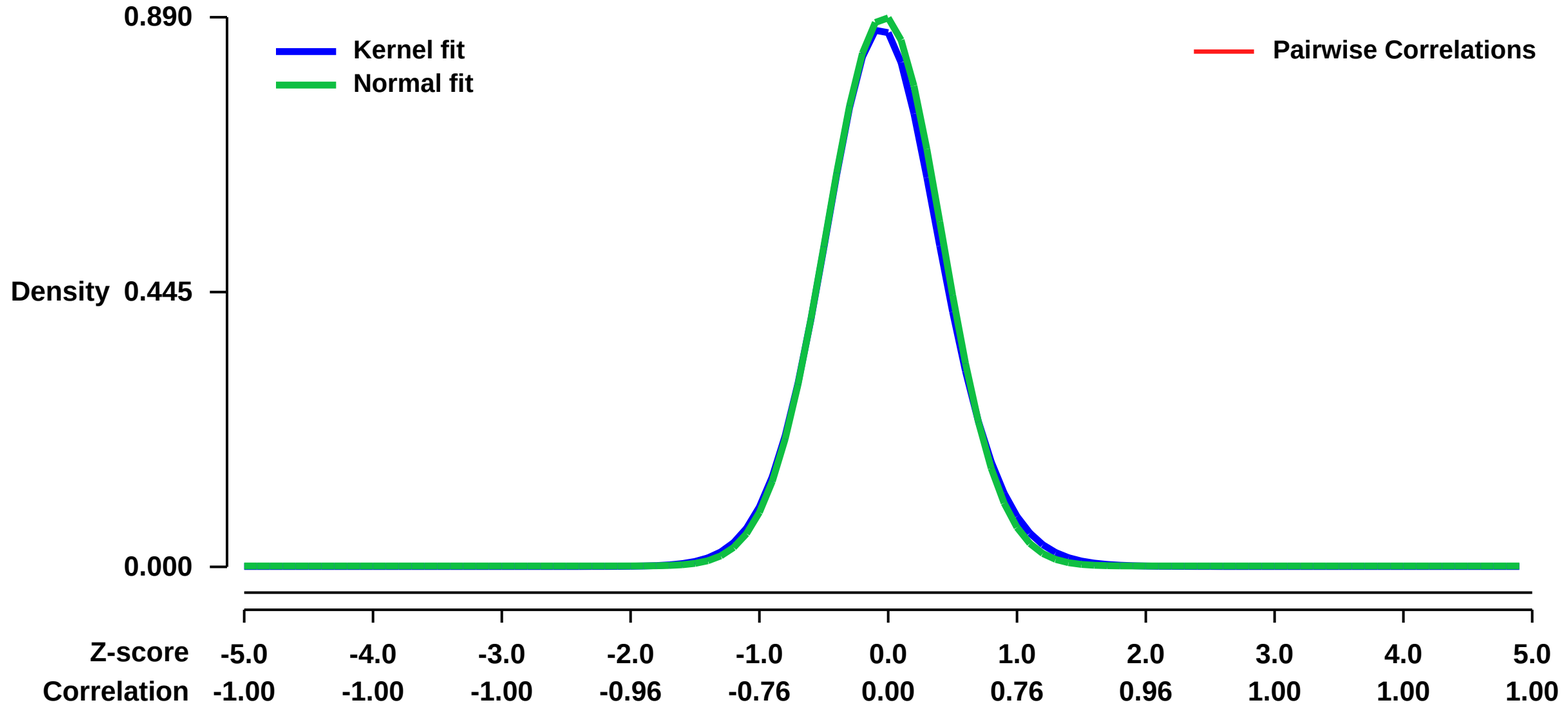

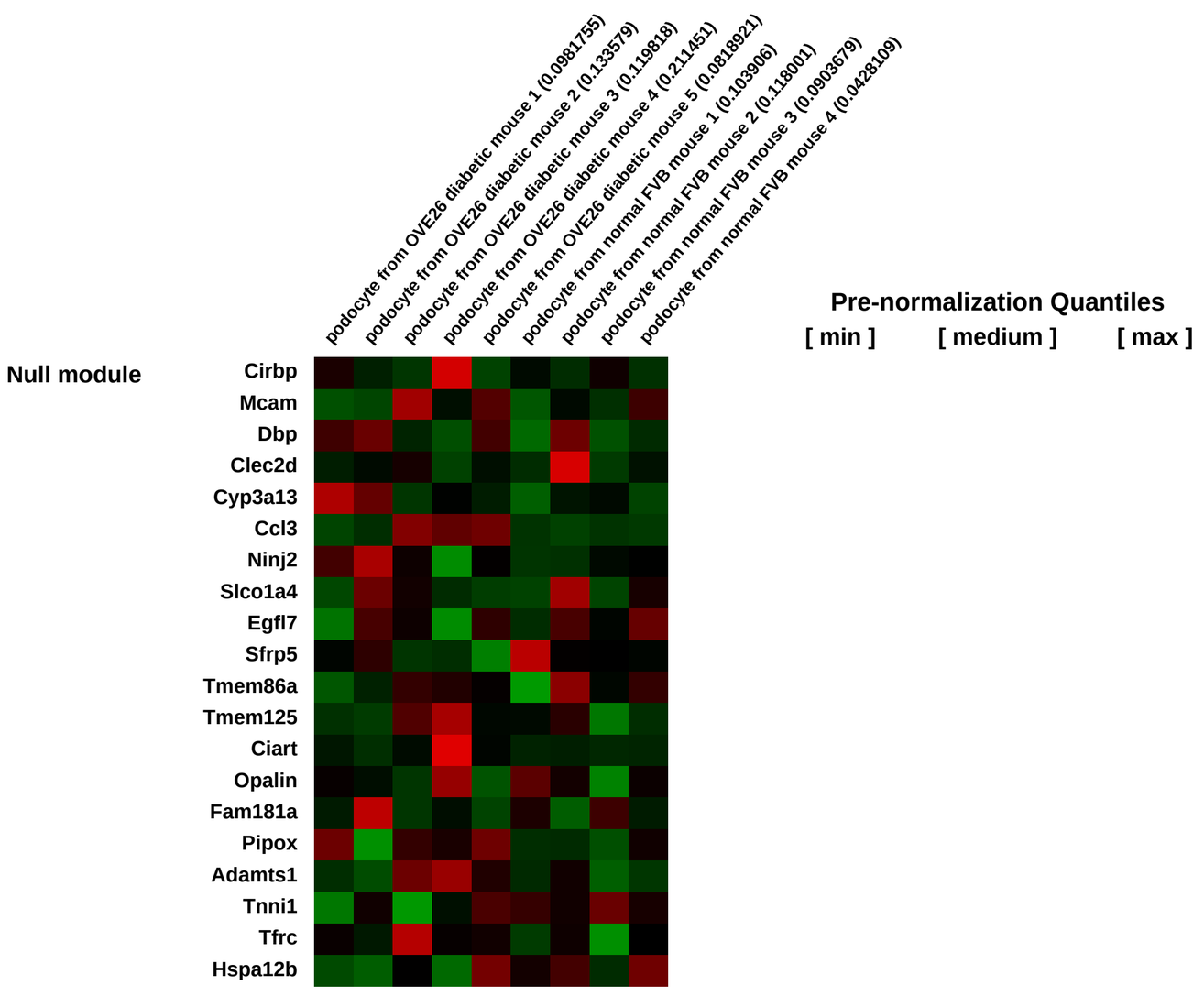

GEO Series "GSE3621" Expression Profiles

Num of samples in this series: 18

Scale of expression profile Z-scores

-3.0 -2.0 -1.0 0.0 1.0 2.0 3.0

GEO Link:	http://www.ncbi.nlm.nih.gov/geo/query/acc.cgi?acc=GSE3621
Status:	Public on Jul 31 2007
Title:	R6/1 brain hemisphere time series gene expression
Organism:	Mus musculus
Experiment type:	Expression profiling by array
Platform:	GPL1261
Pubmed ID:	17696994
Summary & Design:	**Summary:** HD R6/1 transgenic mouse line brain hemispheres dissected. RNA targets were created for transgenics and wildtypes at time points 18, 22 and 27 weeks. Profiles and data analysis performed using the Bioconductor software and linear model contrasts using LIMMA on RMA probeset summarys. **Keywords: timecourse** **Overall design:** 18 samples extracted, 3 transgenic plus 3 littermate controls analysed at each timepoint.

Background corr dist: KL-Divergence = 0.2701, L1-Distance = 0.0575, L2-Distance = 0.0085, Normal std = 0.2927

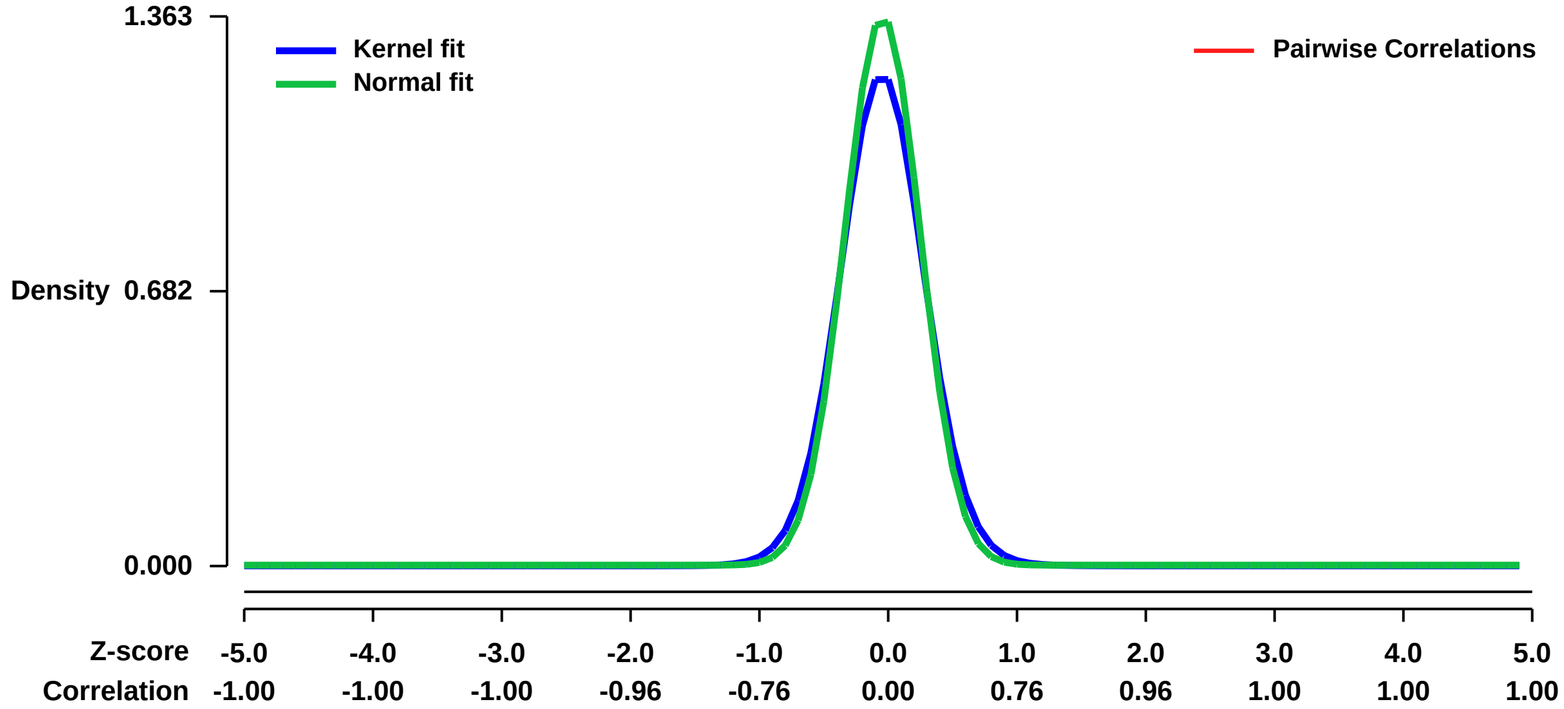

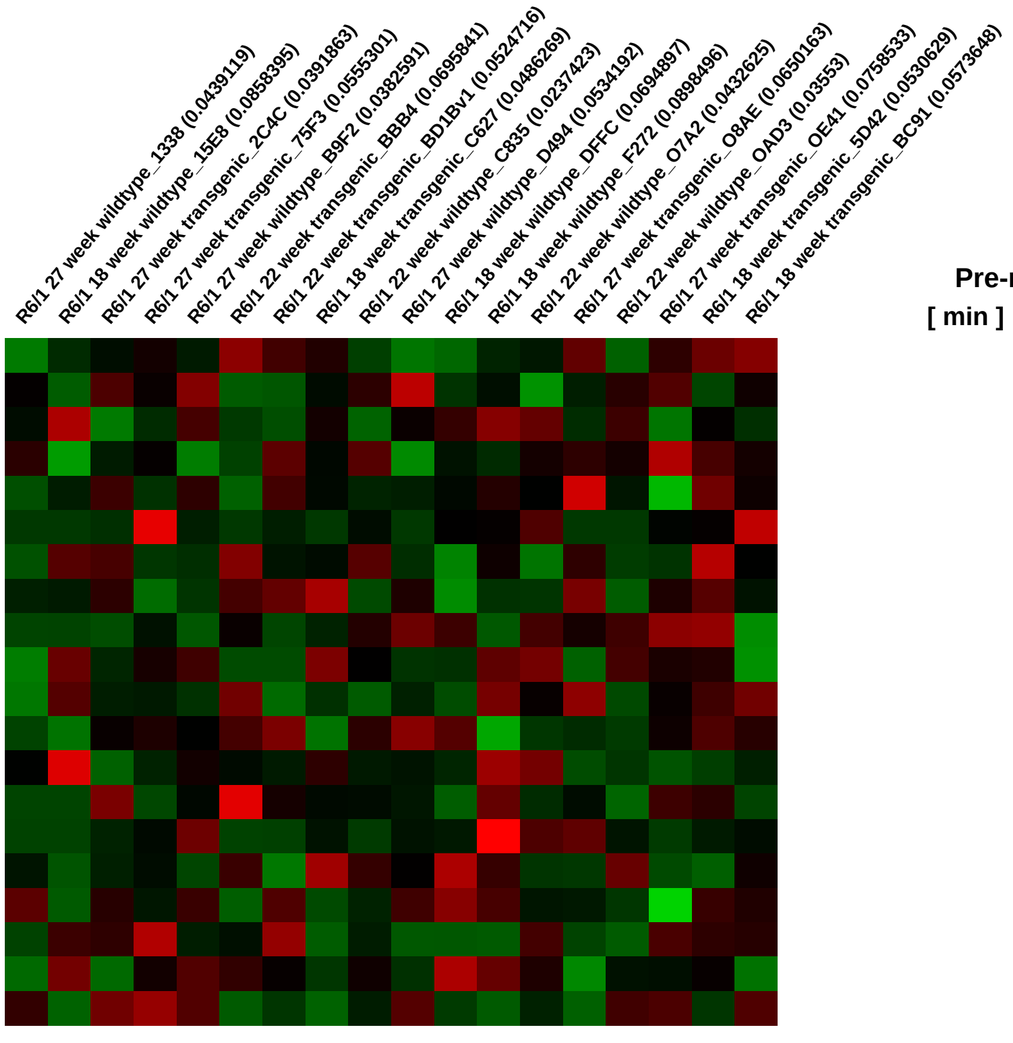

GEO Series "GSE36237" Expression Profiles

Num of samples in this series: 64

Scale of expression profile Z-scores

-3.0 -2.0 -1.0 0.0 1.0 2.0 3.0

GEO Link: http://www.ncbi.nlm.nih.gov/geo/query/acc.cgi?acc=GSE36237
Status: Public on Mar 09 2012
Title: Tg2576 and wild-type mice treated with PDE9A-inhibitor
Organism: Mus musculus
Experiment type: Expression profiling by array
Platform: GPL1261
Pubmed ID:

Summary & Design:

Summary:
Many forms of synaptic plasticity are critically dependent upon production of cGMP to trigger activity-dependent increases in synaptic size and strength. Phosphodiesterase 9A (PDE9A) is a high affinity, cGMP-specific phosphodiesterase with widespread distribution in the central nervous system. Inhibition of PDE9A results in significant accumulation of cGMP in brain tissue and cerebrospinal fluid (CSF) of rodents, and increases CSF cGMP in human volunteers. We hypothesized that chronic exposure to a PDE9A inhibitor, and the associated elevations in brain cGMP could provide a therapeutic benefit to vulnerable synapses chronically exposed to A$_L$† in transgenic mice over-expressing human mutant amyloid precursor protein (Tg2576 mice). A total of N=20 animals per group of 4 month old Tg2576 mice and non-transgenic littermates (WT) were implanted with Alzet osmotic minipumps to deliver vehicle or the PDE9A inhibitor PF-04447943. Neurobehavioral outcomes were measured as conditioned fear response after 28 days of treatment and subsequently brains were harvested for measurement of A$_L$†, gene expression profiling or synaptic density as assessed by Golgi staining of dendrites. Dendritic spine density on apical dendrites of CA1 neurons exhibited a small but significant deficit in the density of dendritic spines in vehicle treated Tg2576 mice as compared to WT mice. This deficit was ameliorated by 30 days of exposure to PF-04447943. No significant drug effect was observed in WT mice. No significant effects of drug treatment were observed on A$_L$† levels in Tg2576 mice. Behavioral analysis of Tg2576 mice showed deficits in fear conditioning as early as 2 months old, and therefore were considered unlikely to be due to the accumulation of oligomeric A$_L$†. These deficits were not affected by drug treatment. Transcriptional profiles of Tg2576 mice treated with drug compared to vehicle showed evidence of regulation of pathways related to synaptic plasticity and remodeling of the dendritic cytoskeleton, consistent with stabilization of vulnerable spine structure. These data supports the hypothesis that PDE9A inhibition can stabilize vulnerable synapses early in the Alzheimerâ s disease process.

Overall design:
4-month old Tg2576 mice and non-transgenic (WT) littermates were implanted with minipumps to deliver vehicle or the PDE9A-inhibitor, PF-04447943, for 28 days. At the end of the study, hippocampus and frontal cortex were dissected from n=8 mice per group, RNA was isolated, and hybridized to Affymetrix 430 2.0 mouse whole genome microarray.

Background corr dist: KL-Divergence = 0.1705, L1-Distance = 0.0379, L2-Distance = 0.0029, Normal std = 0.3549

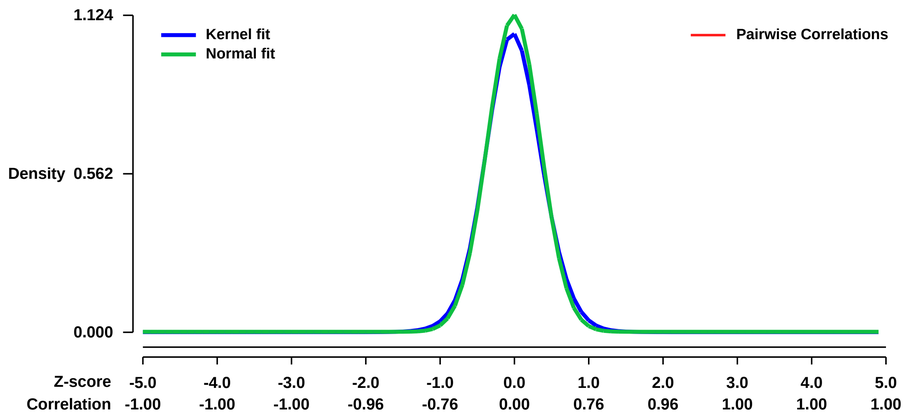

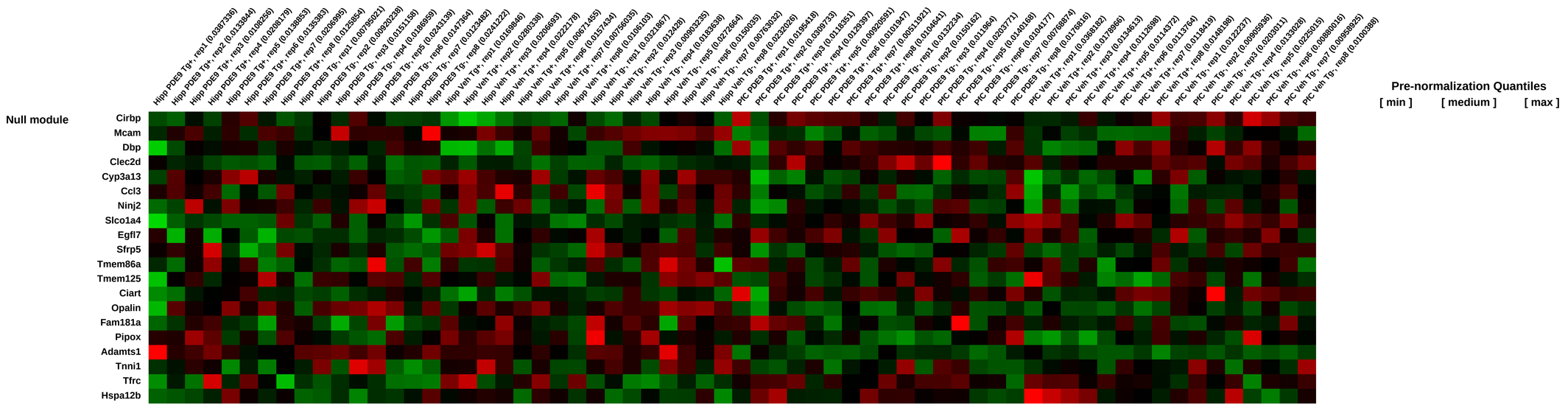

GEO Series "GSE36336" Expression Profiles

Num of samples in this series: 6

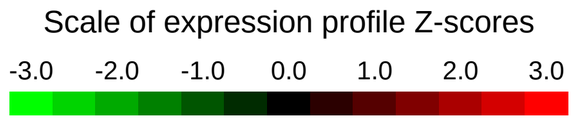

GEO Link:	**http://www.ncbi.nlm.nih.gov/geo/query/acc.cgi?acc=GSE36336**
Status:	**Public on Apr 25 2014**
Title:	**Expression data from kidneys of diabetic WT and T3-/- mice**
Organism:	**Mus musculus**
Experiment type:	**Expression profiling by array**
Platform:	**GPL1261**
Pubmed ID:	
Summary & Design:	**Summary:** **Activation of A Disintegrin and A Metalloprotease Domain17 (ADAM17) is involved in nephropathy, but the role of this metalloprotease and its inhibitor TIMP3 in diabetic kidney disease is unclear. We used microarray profiling to find genes differentially expressed in the 2 genotypes which could explain the more severe diabetic kidney disease features observed in T3-/- mice compared to the WT littermates.** **Overall design:** **Total RNA was extracted from 3 WT and 3 Timp3-/- diabetic kidneys**

Background corr dist: **KL-Divergence = 0.0281, L1-Distance = 0.0112, L2-Distance = 0.0001, Normal std = 0.6704**

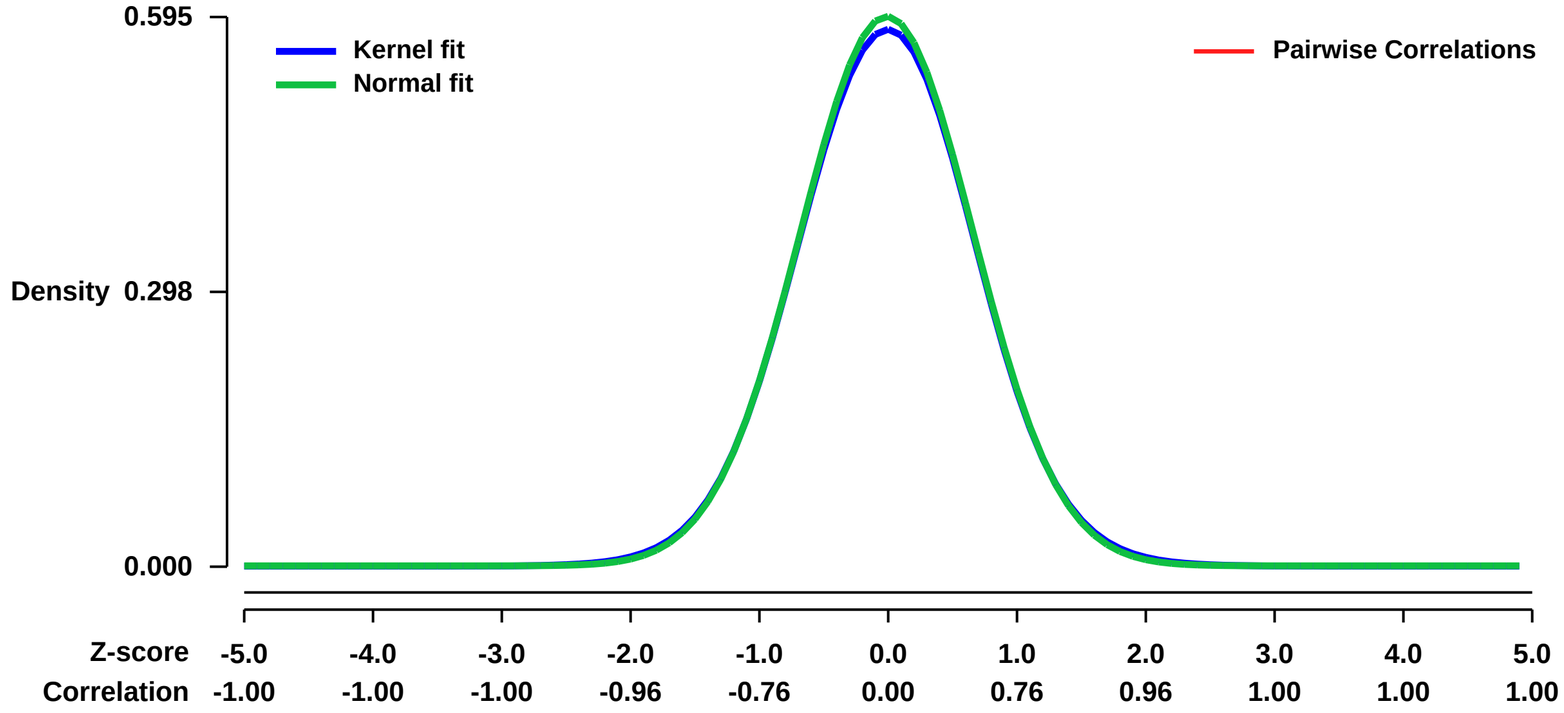

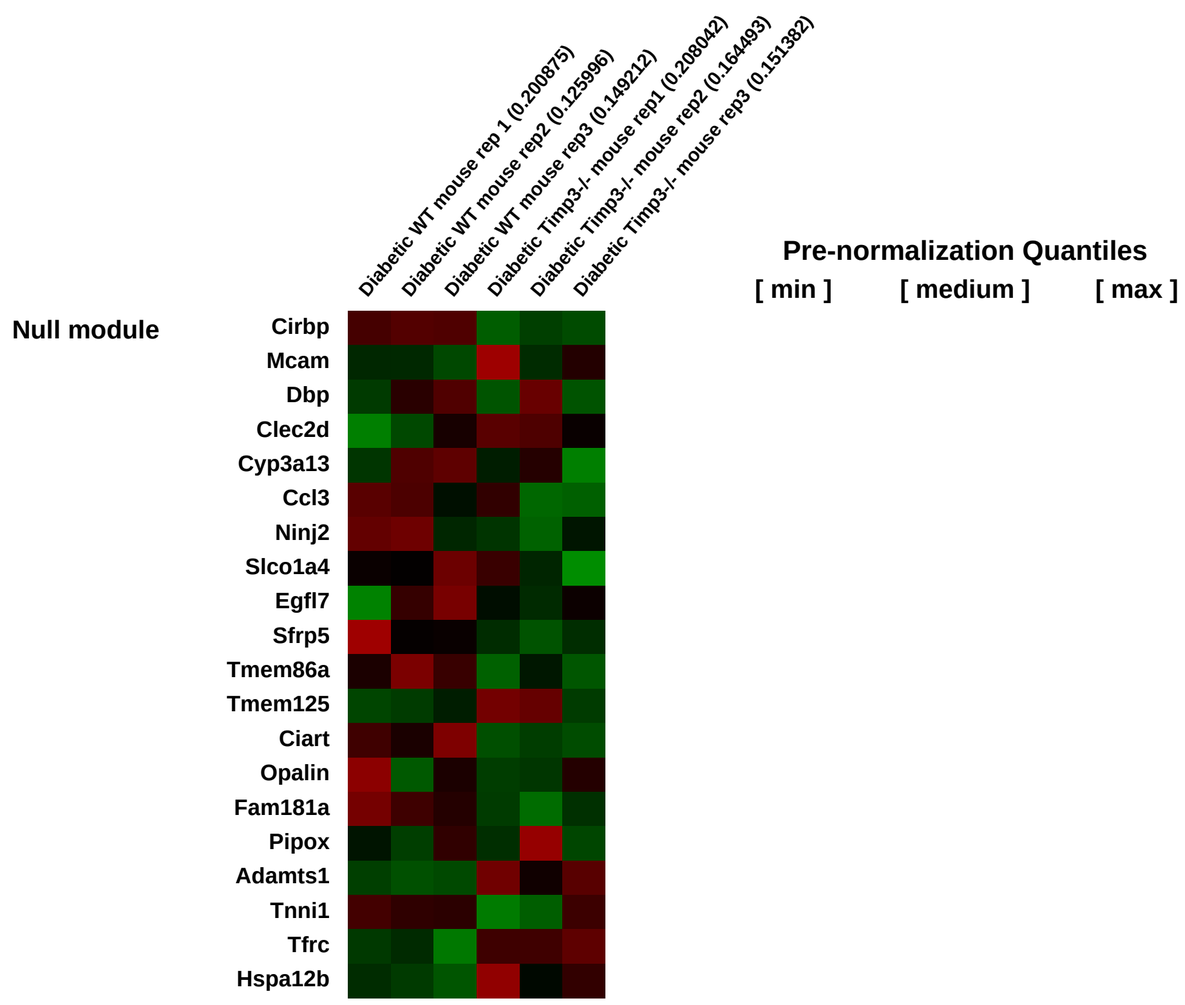

GEO Series "GSE36378" Expression Profiles

Num of samples in this series: 20

Scale of expression profile Z-scores

-3.0 -2.0 -1.0 0.0 1.0 2.0 3.0

GEO Link:	http://www.ncbi.nlm.nih.gov/geo/query/acc.cgi?acc=GSE36378
Status:	Public on Mar 10 2012
Title:	Mapping the Transcriptional Landscape of Autoimmune Targeted Tissues: Transient Alterations in the Extracellular Milieu Precede Innate and Delayed Adaptive Immune Re
Organism:	Mus musculus
Experiment type:	Expression profiling by array
Platform:	GPL1261
Pubmed ID:	
Summary & Design:	**Summary:** **The C57BL/6.NOD-Aec1Aec2 mouse is a model for primary Sjˆ¶grenâ s syndrome and was constructed by introducing two genetic intervals derived from the NOD mouse that confers Sjˆ¶grenâ s syndrome (SjS)-like disease in SjS-non-susceptible C57BL/6 mice.** **To define the chronological interrelationships of biological themes associated with progression from pre- to sub-clinical to overt spontaneous experimental SjS-like disease involving the extracellular milieu (EM) of the salivary glands, we carried out a study utilizing microarray technology in which the parental C57BL/6J mouse was used as the healthy control strain. A bioinformatics-based data analysis methodology designed for comprehensive visualization of global datasets between C57BL/6J and C57BL/6.NOD-Aec1Aec2 mice has permitted a definition of the molecular changes that correlate with onset of stomatitis sicca (xerostomia) in the SjS-susceptible mice. The transcriptome data set of C57BL/6J permitted identification of normal physiological activity.** **Overall design:** **The study was designed to define the changing gene expression profiles within the salivary glands of C57BL/6.NOD-Aec1Aec2 mice at multiple time points representing a pre-disease stage (4 weeks), the early pre-clinical stage (8 weeks), the initial influx of leukocytes into the salivary glands (12 weeks), and the early clinical phase of autoimmunity (16 weeks) to characterize the influence of the extracellular milieu on early development of disease. Because the C57BL/6.NOD-Aec1Aec2 mouse was derived from the C57BL/6J line, C57BL/6J mice were used as the comparative healthy controls. This comparison permitted the identification of disease-associated gene expressions by subtracting out normal physiological processes. This present study represents the C57BL/6J healthy control mice. Series GSE15640 includes the data for the C57BL/6.NOD-Aec1Aec2 mice.**

Background corr dist: KL-Divergence = 0.0794, L1-Distance = 0.0693, L2-Distance = 0.0110, Normal std = 0.4914

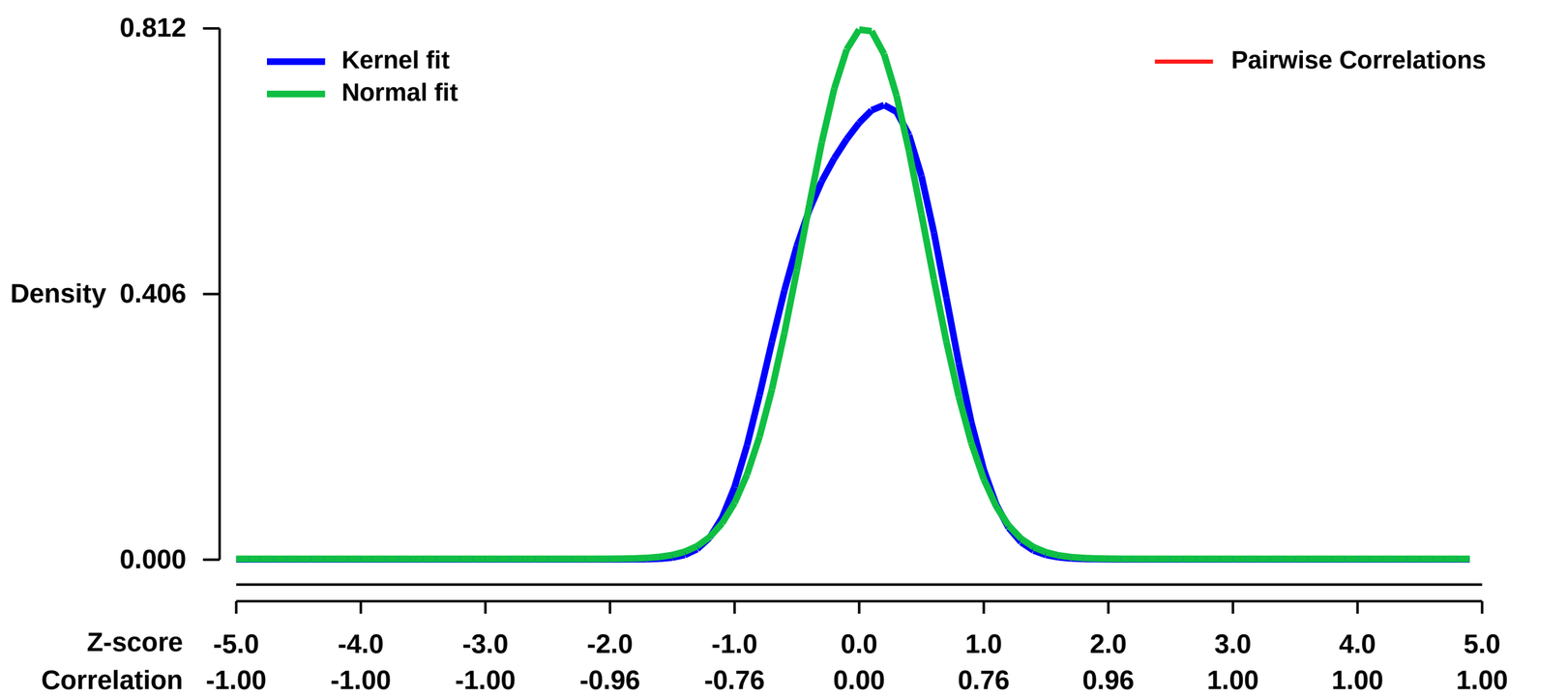

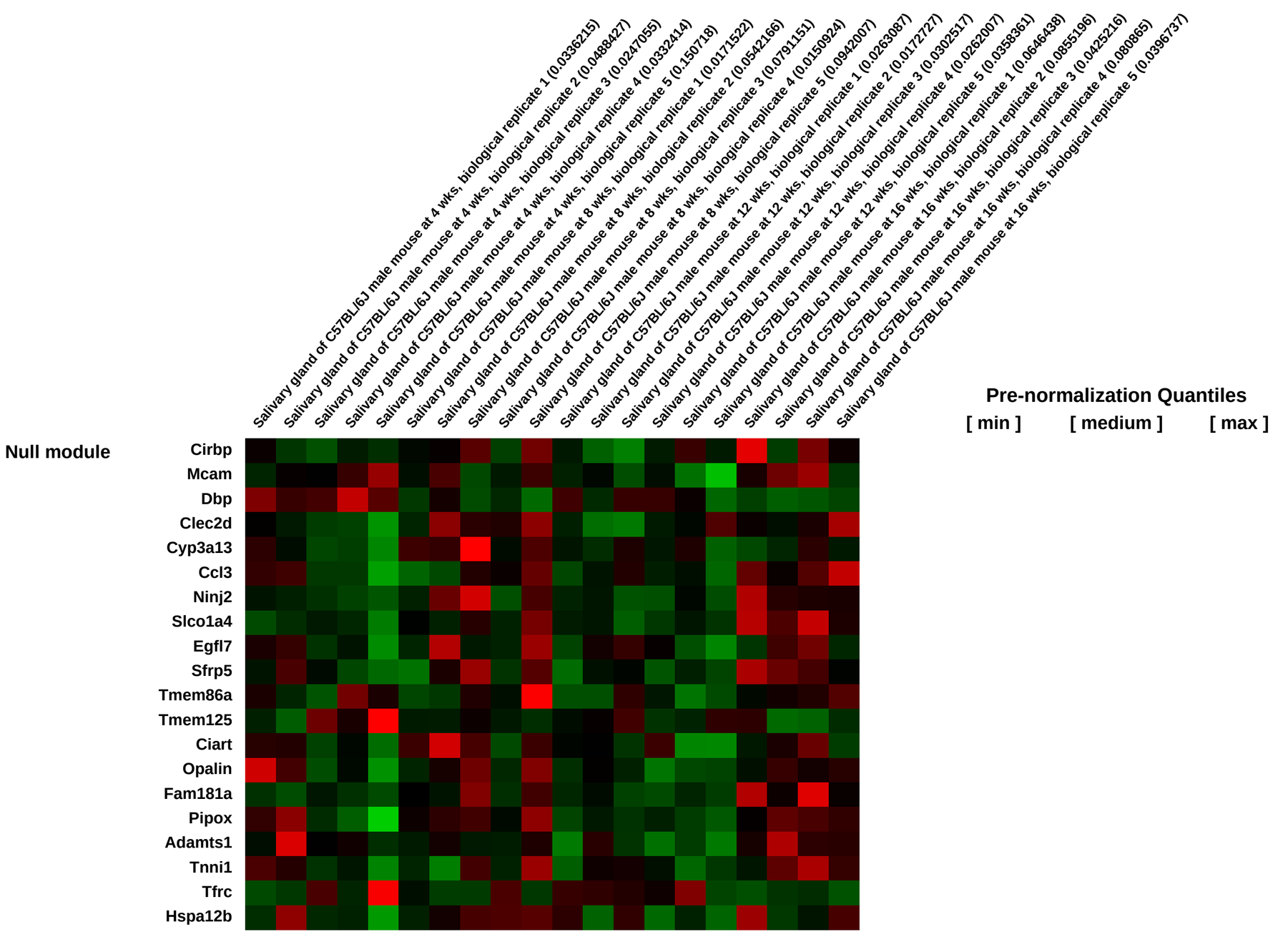

GEO Series "GSE36384" Expression Profiles

Num of samples in this series: 12

Scale of expression profile Z-scores

-3.0 -2.0 -1.0 0.0 1.0 2.0 3.0

GEO Link:	http://www.ncbi.nlm.nih.gov/geo/query/acc.cgi?acc=GSE36384
Status:	Public on Dec 31 2012
Title:	ZNF335 regulates stem cell proliferation and neuronal differentiation via Trithorax complex and REST/NRSF [gene expression]
Organism:	Mus musculus
Experiment type:	Expression profiling by array
Platform:	GPL1261
Pubmed ID:	23178126
Summary & Design:	**Summary:** The progression from stem cell to differentiated neuron is associated with extensive chromatin remodeling that controls gene expression, but the mechanisms that connect chromatin to gene expression are not well defined. Here we show that mutation of ZNF335 causes severe human microcephaly (""small brain""), small somatic size, and neonatal death. Germline Znf335 null mutations are embryonically lethal in mice, whereas RNA-interference studies and postmortem human studies show that Znf335 is essential for neural progenitor self-renewal, neurogenesis, and neuronal differentiation. Znf335 is a component of a vertebrate-specific, trithorax H3K4 methylation complex, while global ChIP-seq and mRNA expression studies show that Znf335 is a previously unsuspected, direct regulator of REST/NRSF, a master regulator of neural gene expression and neural cell fate, as well as other essential neural-specific genes. Our results reveal ZNF335 as an essential link between H3K4 complexes and REST/NRSF, and provide the first direct evidence that this pathway regulates human neurogenesis and neuronal differentiation. **Overall design:** ShRNA knockdown cells were FACS sorted and analyzed for changes in gene expression

Background corr dist: KL-Divergence = 0.0259, L1-Distance = 0.0379, L2-Distance = 0.0021, Normal std = 0.6957

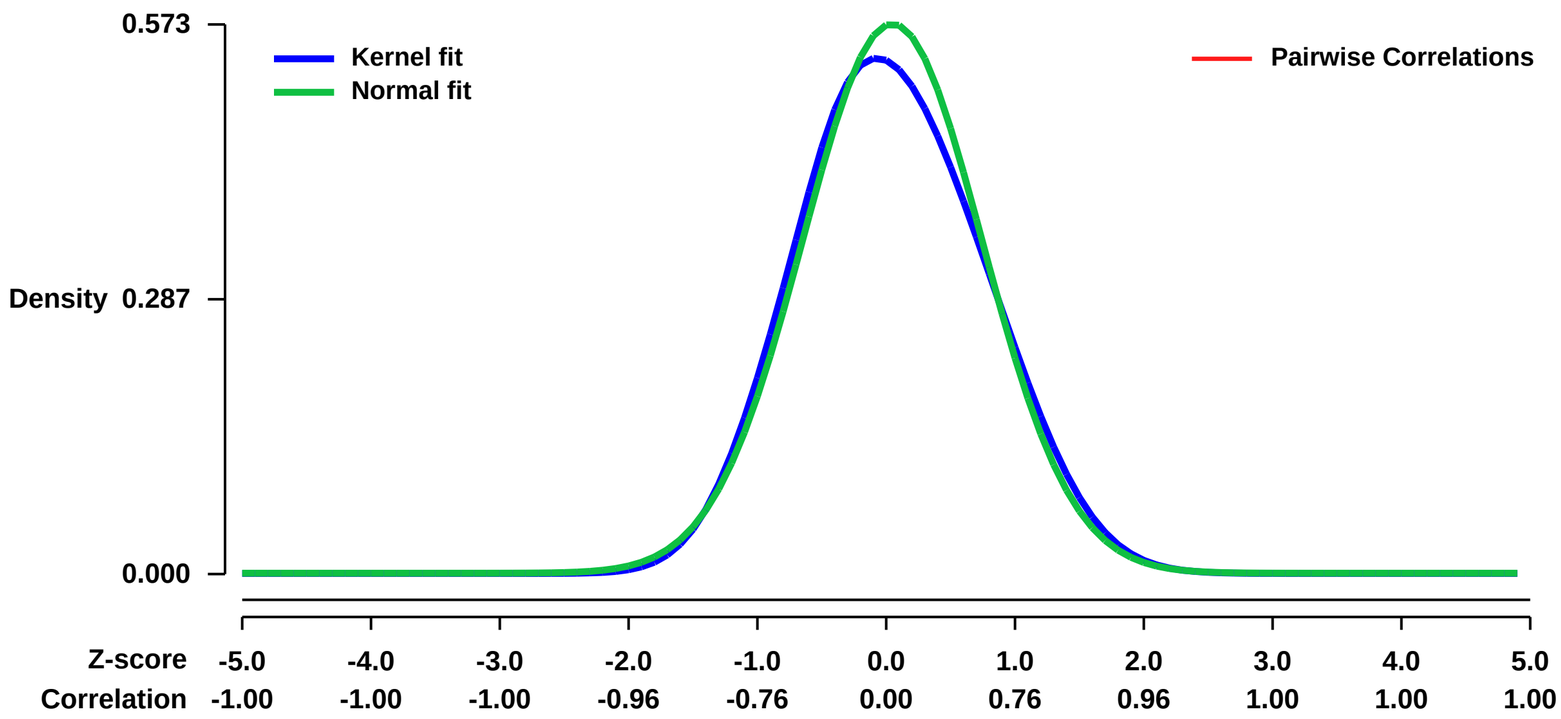

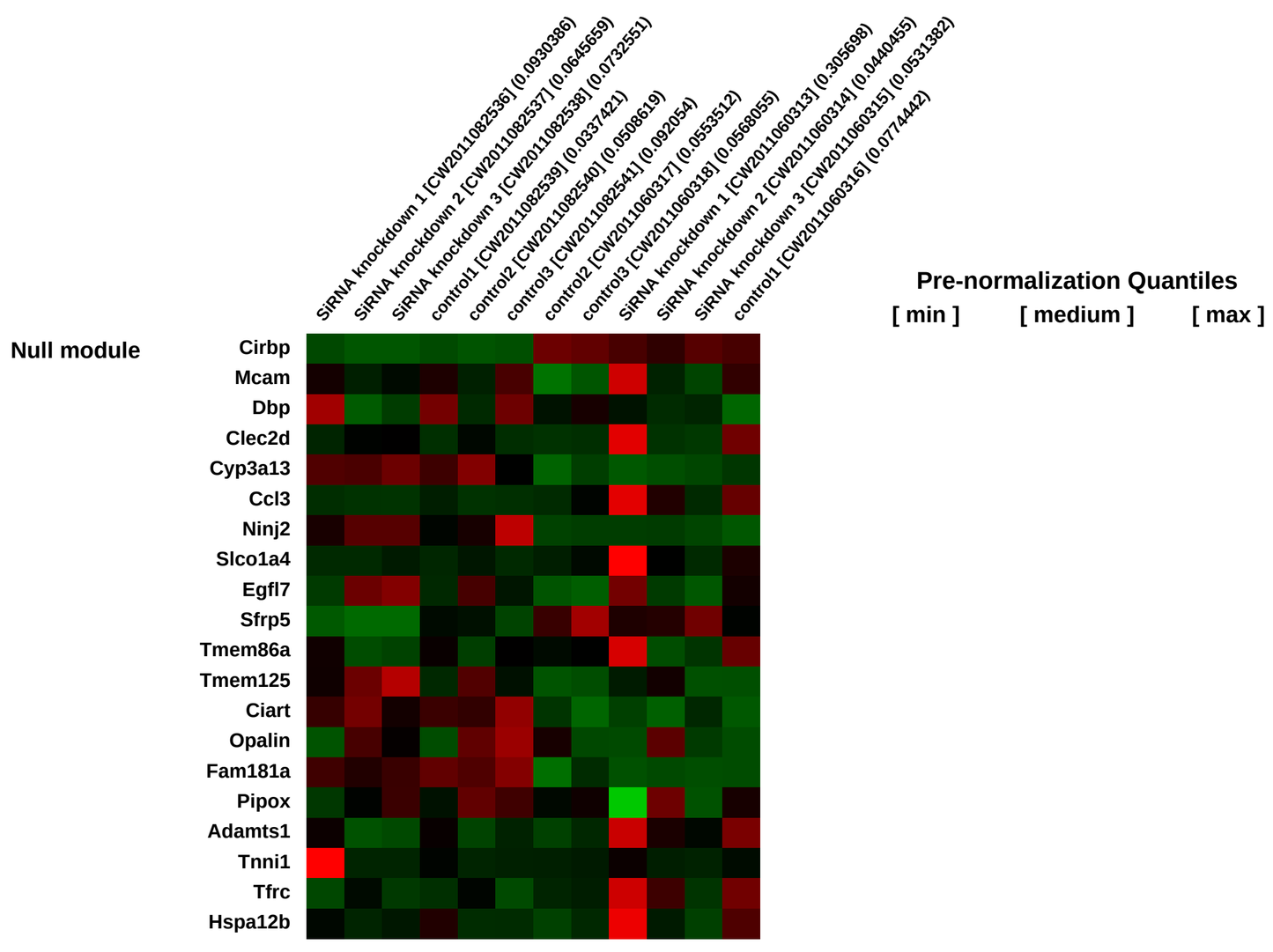

GEO Series "GSE36414" Expression Profiles

Num of samples in this series: 8

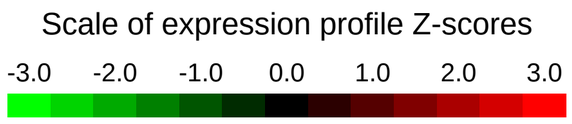

GEO Link:	http://www.ncbi.nlm.nih.gov/geo/query/acc.cgi?acc=GSE36414
Status:	Public on Mar 08 2013
Title:	Gene expression changes induced in the stromal cell line EL08-1D2 by co-culture with leukemic B cells (CLL)
Organism:	Mus musculus
Experiment type:	Expression profiling by array
Platform:	GPL1261
Pubmed ID:	23328482
Summary & Design:	**Summary:** Tumor cell survival critically depends on heterotypic communication with benign cells in the microenvironment. Here we describe a novel survival signaling pathway activated in stromal cells by contact to B-cells from chronic lymphocytic leukemia (CLL) patients. The expression of PKC-¸†II and the subsequent activation of NF-¸”B in bone marrow stromal cells is a prerequisite to support the survival of malignant B-cells. PKC-¸† knockout mice are insusceptible to CLL-transplantations, underscoring the in vivo significance of the PKC-¸†II-NF-¸”B signaling pathway in the tumor microenvironment. Upregulated stromal PKC-¸†II in biopsies from CLL, breast- and pancreatic-cancer patients suggest that this pathway may commonly be activated in a variety of malignancies. We used microarrays to determine gene expression changes induced by co-culturing with leukemic B-cells (CLL) in EL08-1D2 cells. **Overall design:** We compared EL08-1D2 cells co-cultured for 5 days with leukemic B-cells to EL08-1D2 mono-cultured cells by microarray analysis on Affymetrix MG-430_2.0 arrays.

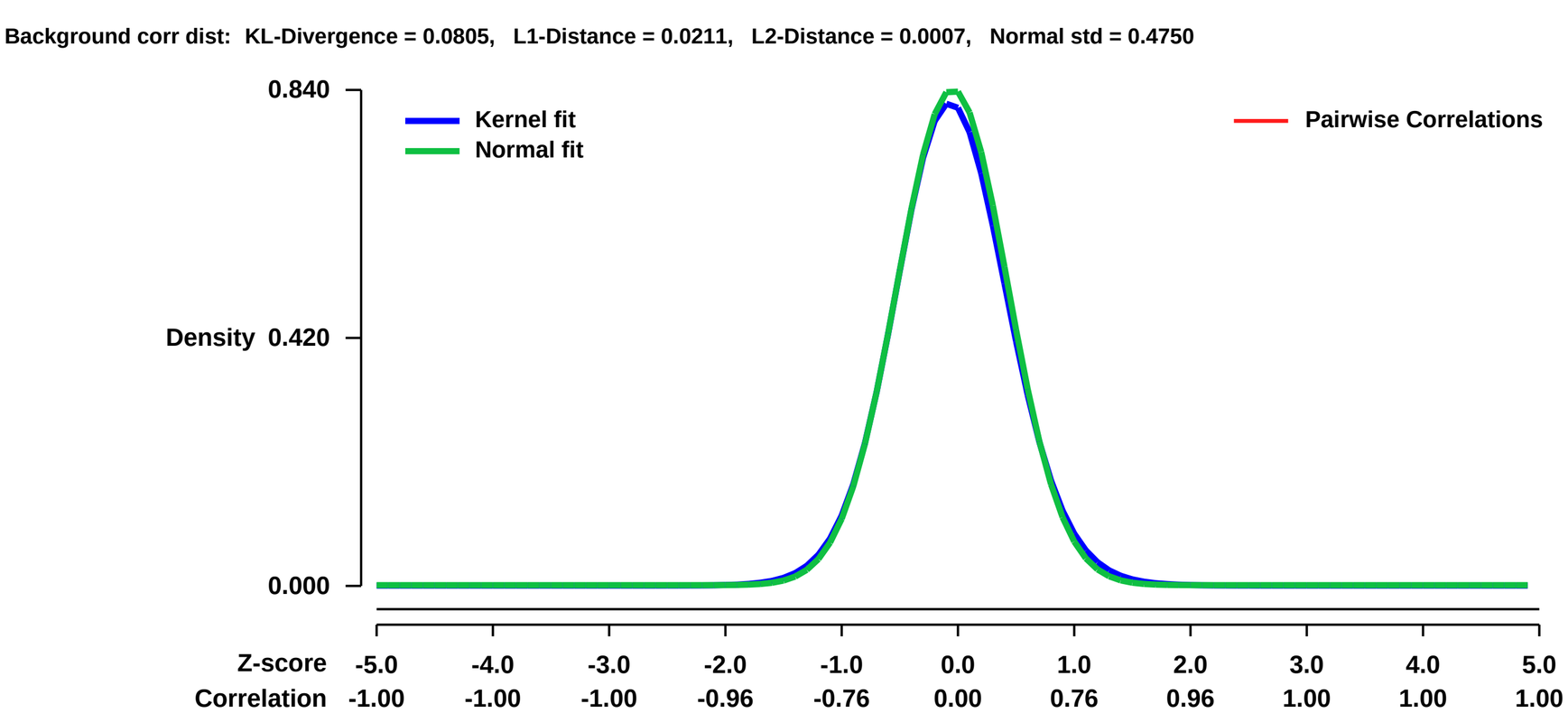

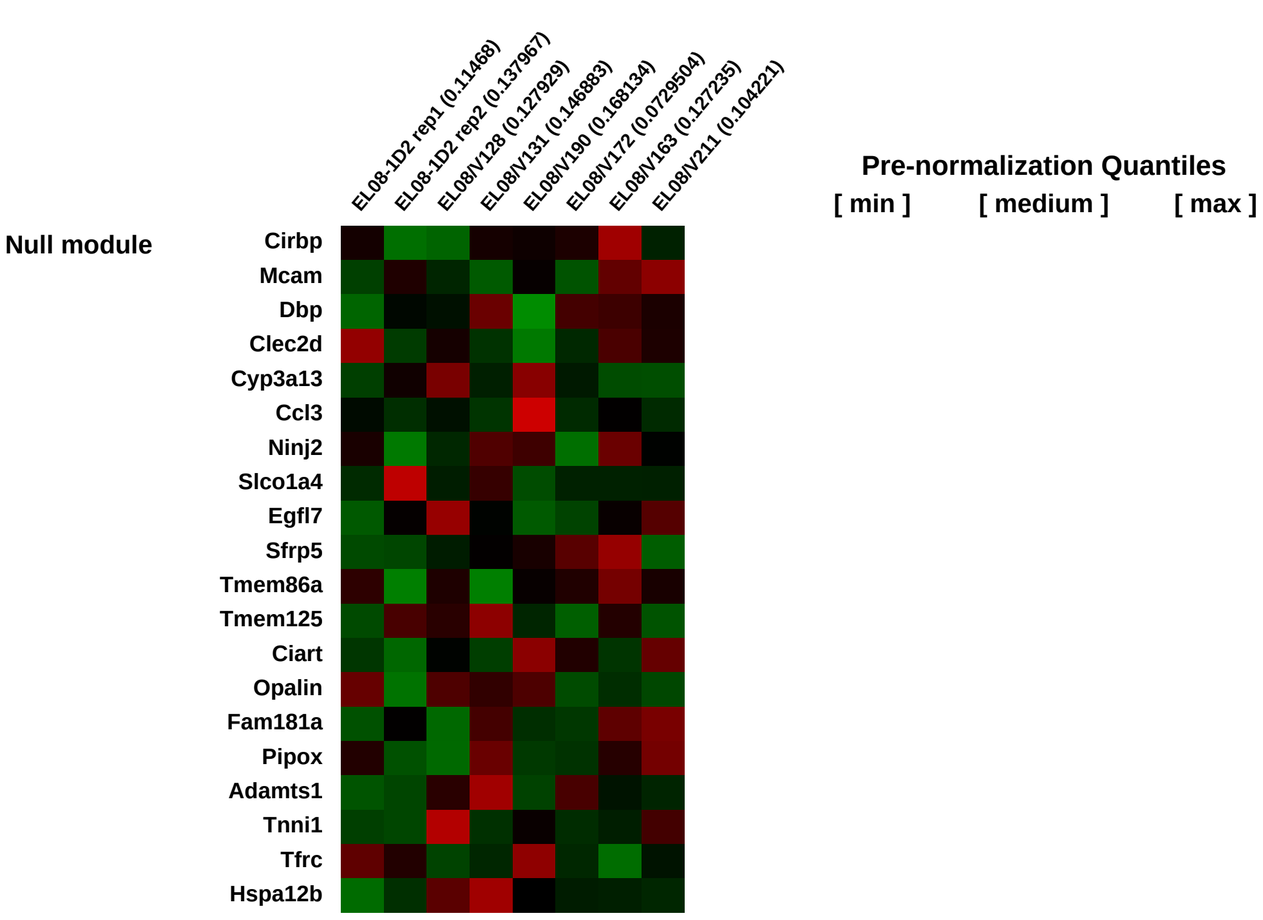

GEO Series "GSE36415" Expression Profiles

Num of samples in this series: 14

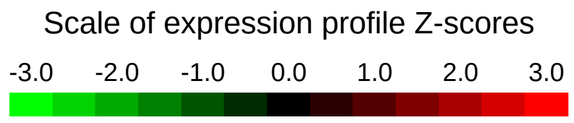

GEO Link:	http://www.ncbi.nlm.nih.gov/geo/query/acc.cgi?acc=GSE36415
Status:	Public on Mar 08 2013
Title:	Effect of NF-kappaB activation in bone marrow stromal cells co-cultured with CLL cells
Organism:	Mus musculus
Experiment type:	Expression profiling by array
Platform:	GPL1261
Pubmed ID:	23328482
Summary & Design:	**Summary:** **Tumor cell survival critically depends on heterotypic communication with benign cells in the microenvironment. Here we describe a novel survival signaling pathway activated in stromal cells by contact to B-cells from chronic lymphocytic leukemia (CLL) patients. The expression of PKC-¸†II and the subsequent activation of NF-¸”B in bone marrow stromal cells is a prerequisite to support the survival of malignant B-cells. PKC-¸† knockout mice are insusceptible to CLL-transplantations, underscoring the in vivo significance of the PKC-¸†II-NF-¸”B signaling pathway in the tumor microenvironment. Upregulated stromal PKC-¸†II in biopsies from CLL, breast- and pancreatic-cancer patients suggest that this pathway may commonly be activated in a variety of malignancies.** **We used microarrays to determine Nemo/ IKK-gamma dependent gene expression changes in bone marrow stromal cells (BMSCs) induced by co-culturing with leukemic B-cells (CLL)** **Overall design:** **We compared mouse BMSC cells from Nemo knockout cells (Nemo+CRE) and Nemo wild type cells (Nemo-CRE) co-cultured for 5 days with leukemic B-cells microarray analysis on Affymetrix MG-430_2.0 arrays..**

Background corr dist: KL-Divergence = 0.0724, L1-Distance = 0.0218, L2-Distance = 0.0007, Normal std = 0.4965

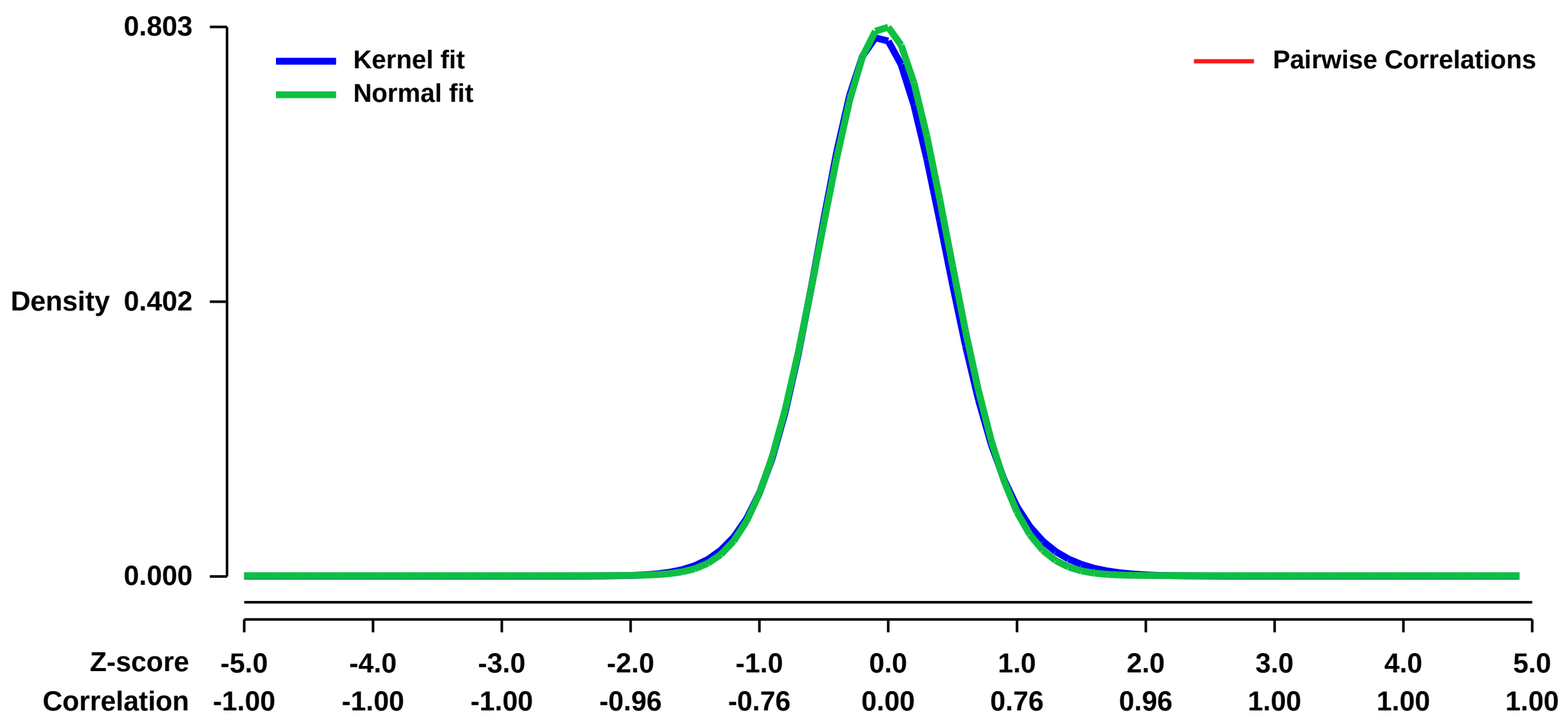

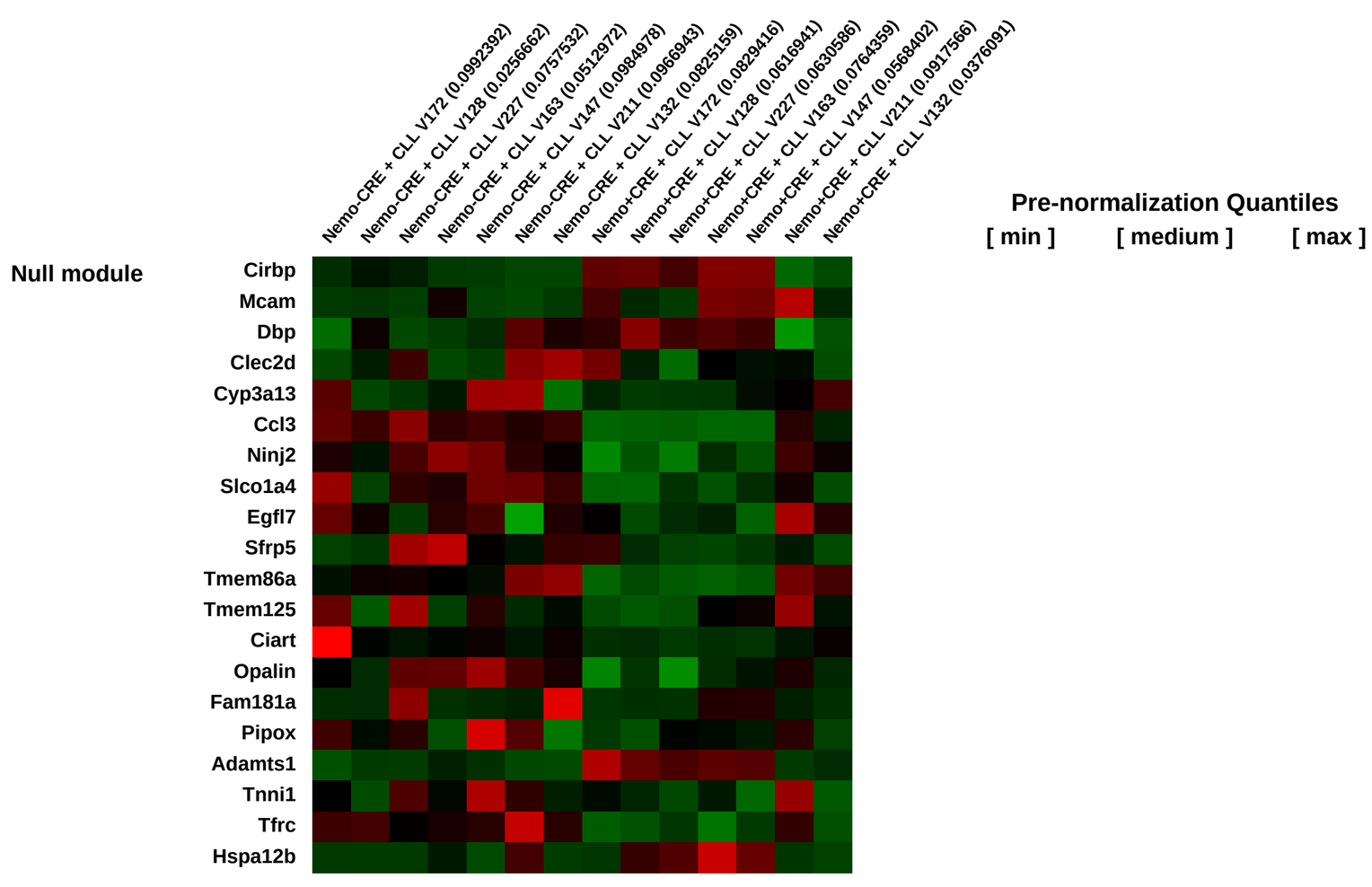

GEO Series "GSE36437" Expression Profiles

Num of samples in this series: 6

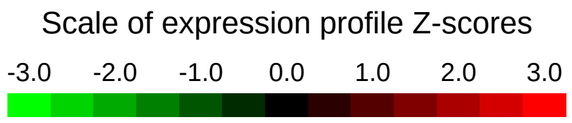

GEO Link:	http://www.ncbi.nlm.nih.gov/geo/query/acc.cgi?acc=GSE36437
Status:	Public on Mar 31 2012
Title:	Expression data from caudal artery of Notch3WT and Notch3KO mice
Organism:	Mus musculus
Experiment type:	Expression profiling by array
Platform:	GPL1261
Pubmed ID:	23117660
Summary & Design:	**Summary:** Notch3 is a transmembrane receptor which is critically important for the structure and myogenic response of distal arteries, particularly cerebral arteries. After activation of the receptor, the intracellular domain translocates in the nucleus to activate target genes transcription. In order to identify Notch3 target genes, we used microarrays to compare gene expression from caudal arteries (Notch3+/+ vs Notch3-/-) and selected down-regulated genes in Notch3-/- arteries. **Overall design:** Caudal arteries were dissected from 1 month old Notch3+/+ and Notch3-/- mice. RNA was prepared with arteries pooled from three (AJ_N3WT_3, AJ_N3WT_4) or four (AJ_N3WT_1, AJ_N3KO_1, AJ_N3KO_2, AJ_N3KO_4) mice and hybridized on Mouse MOE430.2 Affymetrix chips. For each group (Notch3+/+ and Notch3-/-), three biological replicates were performed.

Background corr dist: KL-Divergence = 0.0378, L1-Distance = 0.0194, L2-Distance = 0.0004, Normal std = 0.6262

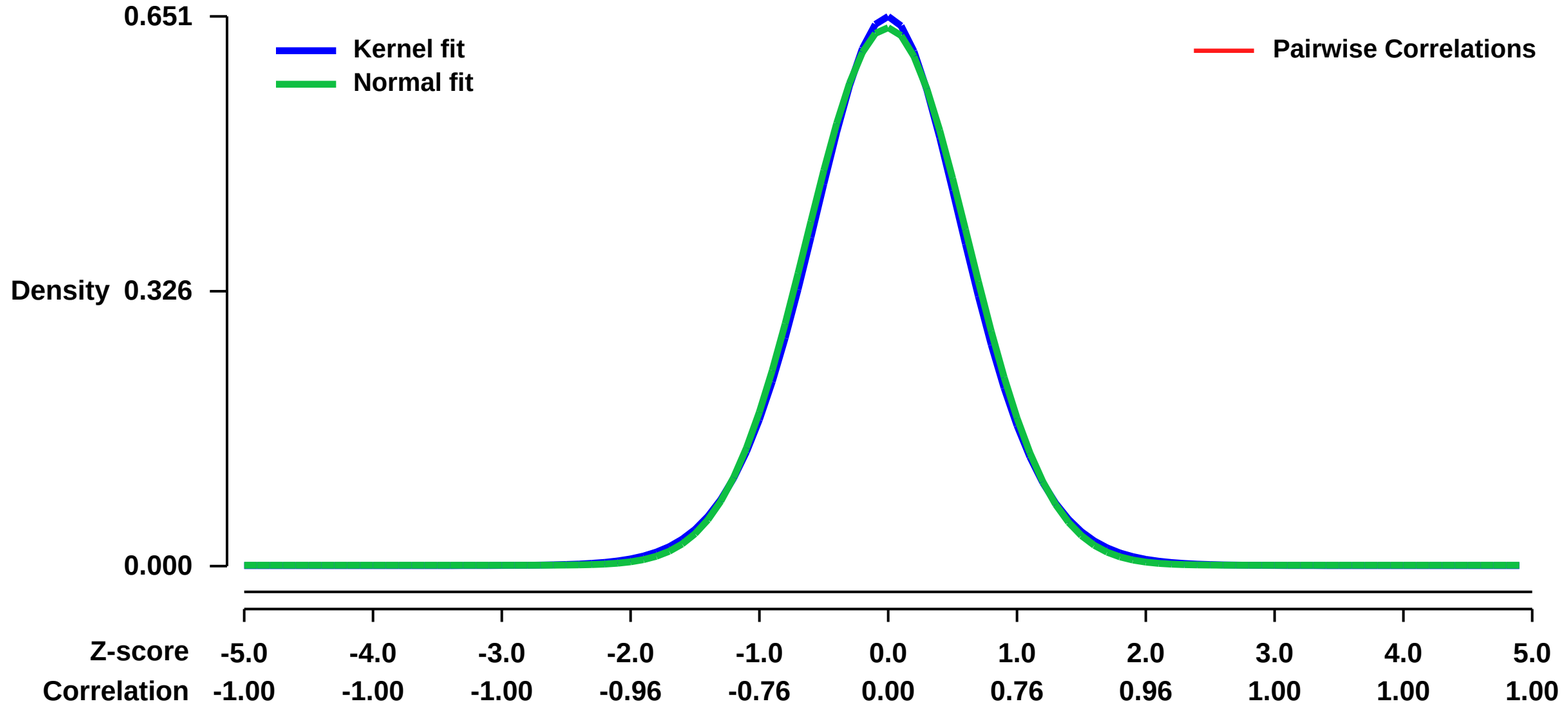

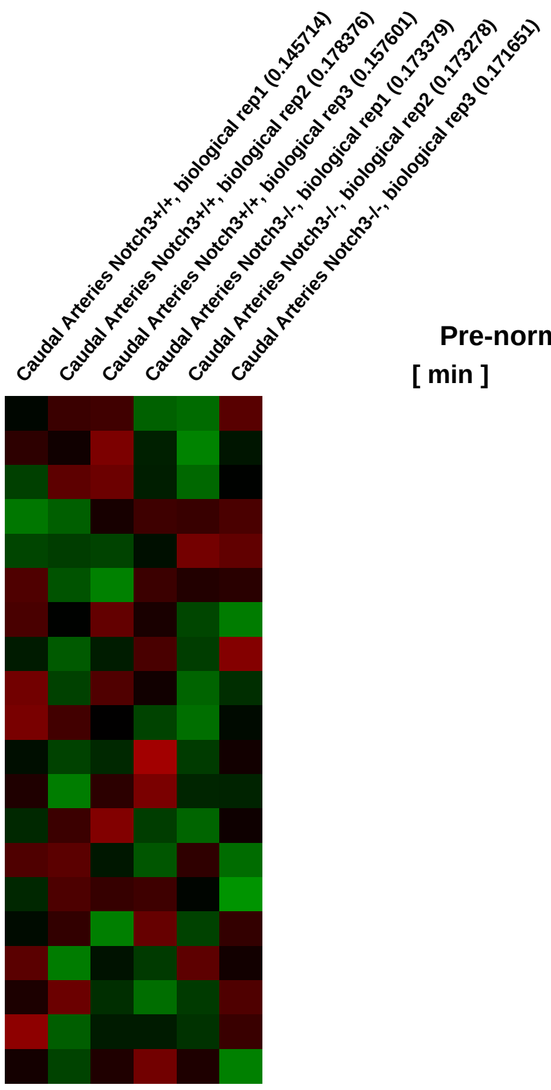

GEO Series "GSE36477" Expression Profiles

Num of samples in this series: 8

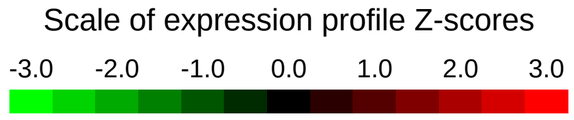

GEO Link:	**http://www.ncbi.nlm.nih.gov/geo/query/acc.cgi?acc=GSE36477**
Status:	**Public on Jun 01 2012**
Title:	**Expression data from mammary macrophages isolated from MMTV-iFGFR1 transgenic mice**
Organism:	**Mus musculus**
Experiment type:	**Expression profiling by array**
Platform:	**GPL1261**
Pubmed ID:	
Summary & Design:	**Summary:** **The goal of this experiment was to profile macrophages from mammary glands isolated from transgenic mice that express inducible FGFR1 in mammary epithelial cells (MMTV-iFGFR1 transgenic mice). The mice were treated with with dimerizer to activates iFGFR1 for 48 hours and 4 weeks to induce mammary hyperplasias. Control mice included non-transgenic littermates treated with dimerizer for the same amount of time.** **Overall design:** **Macrophages were sorted from mammary glands of MMTV-iFGFR1 transgenic mice and non-transgenic mice following dimerizer treatment using Cd11b-PE. Macrophages from 3 mice were pooled for each sample. RNA was extracted and analyzed using the Affymetrix Mouse 2.0 chip.**

Background corr dist: **KL-Divergence = 0.0876, L1-Distance = 0.0270, L2-Distance = 0.0013, Normal std = 0.4631**

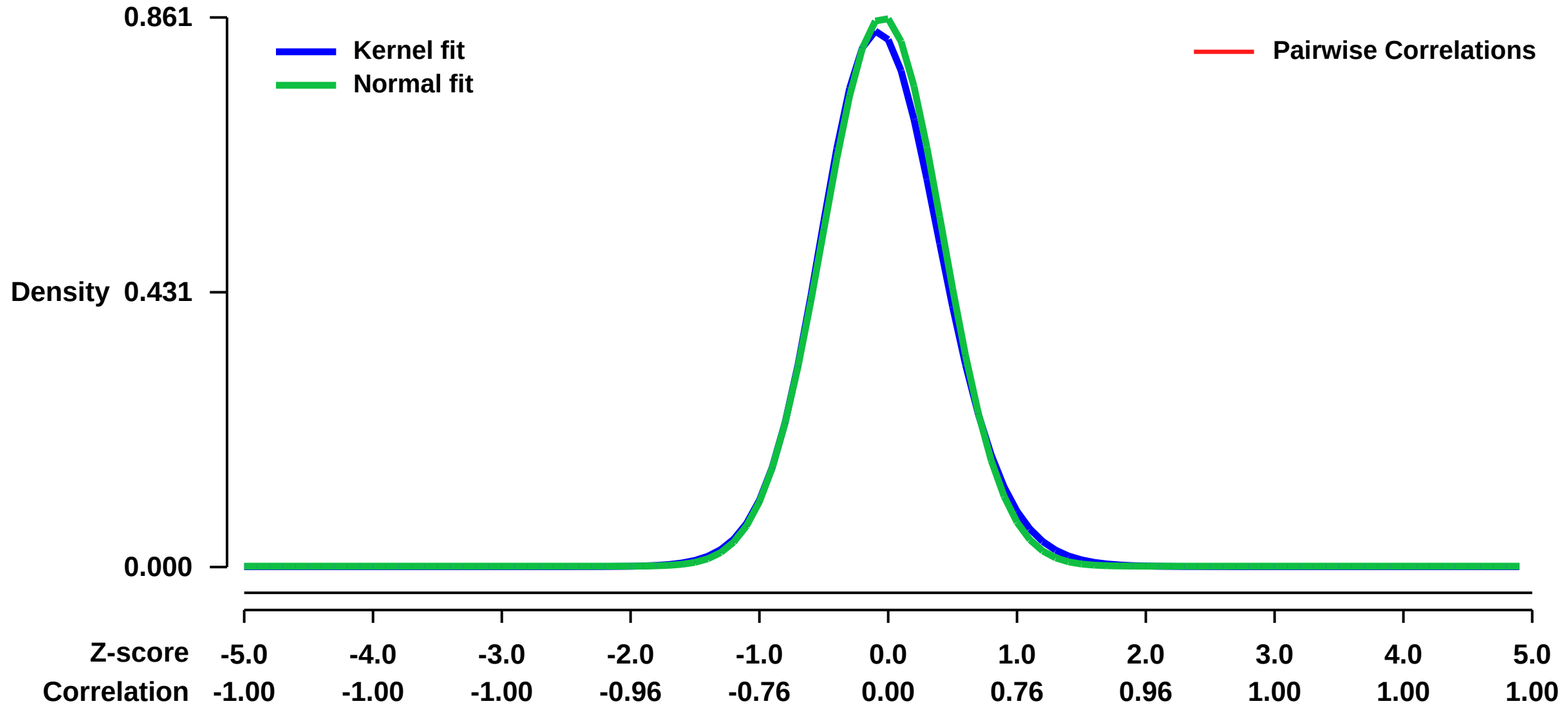

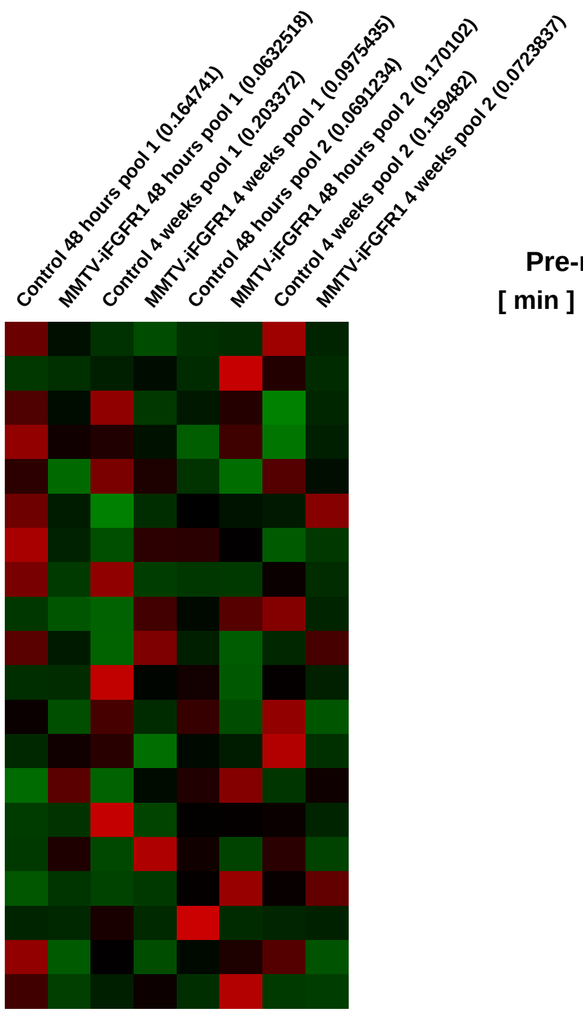

GEO Series "GSE36513" Expression Profiles

Num of samples in this series: 8

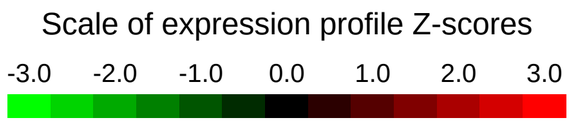

GEO Link:	http://www.ncbi.nlm.nih.gov/geo/query/acc.cgi?acc=GSE36513
Status:	Public on Feb 18 2013
Title:	Long noncoding RNA as regulatory switch of protein turnover
Organism:	Mus musculus
Experiment type:	Expression profiling by array
Platform:	GPL1261
Pubmed ID:	24521543
Summary & Design:	**Summary:** Long intervening noncoding RNAs (lincRNAs) are prevalent genes with poorly understood functions. Here we discover a pathway of lincRNA-regulated proteolysis. The enhancer-like lincRNA HOTTIP extends the half-life of its binding protein WDR5, a subunit of the MLL H3K4 methylase complex, resulting in increased chromatin occupancy and gene activation. LincRNA-mediated stabilization requires direct RNA-protein interaction in a long RNA context, and blocks turnover at a step after target protein poly-ubiquitination. We elucidate the lincRNA binding interface on WDR5. A WDR5 mutant that selectively abrogates lincRNA binding becomes unstable, and is defective in gene activation, maintenance of histone H3 lysine 4 trimethylation, and embryonic stem cell self renewal. The ability to modulate protein turnover may allow lincRNAs to control the lifespan of molecular interactions at chromatin and elsewhere, broadening their scope in epigenetics and cell fate control. **Overall design:** Gene expression analysis: To establish a differentiation signature for mouse V6.5 ES cells infected with anti mouse WDR5 shRNA, rescued with doxycycline inducible WDR5 WT or WDR5 F266A, total RNA was isolated in biologic duplicate from cells in different conditions and hybridized to Affymetrix Mouse 430 2.0 arrays.

Background corr dist: KL-Divergence = 0.0512, L1-Distance = 0.0247, L2-Distance = 0.0007, Normal std = 0.5684

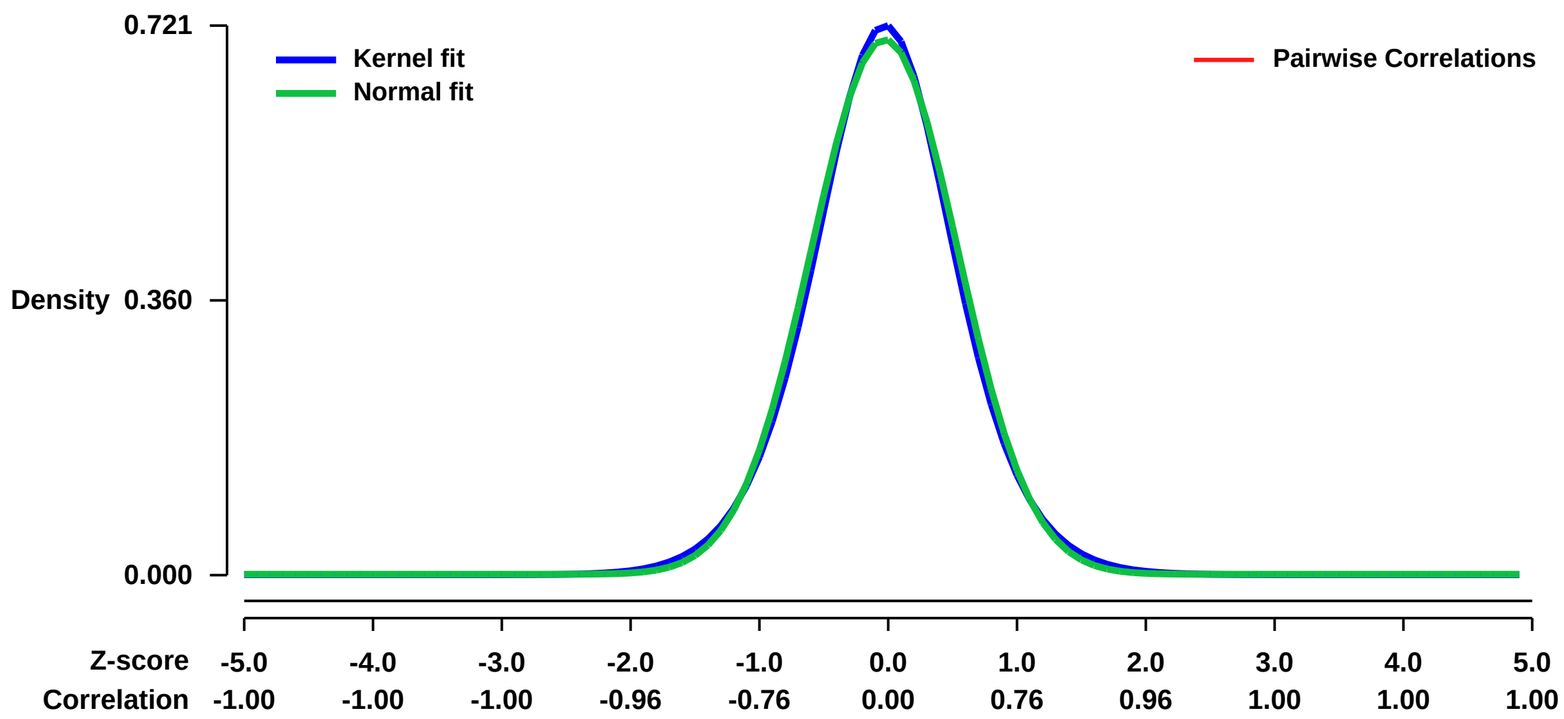

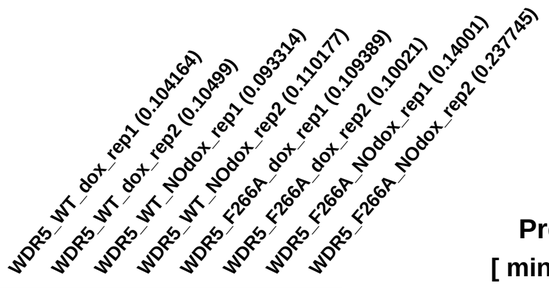

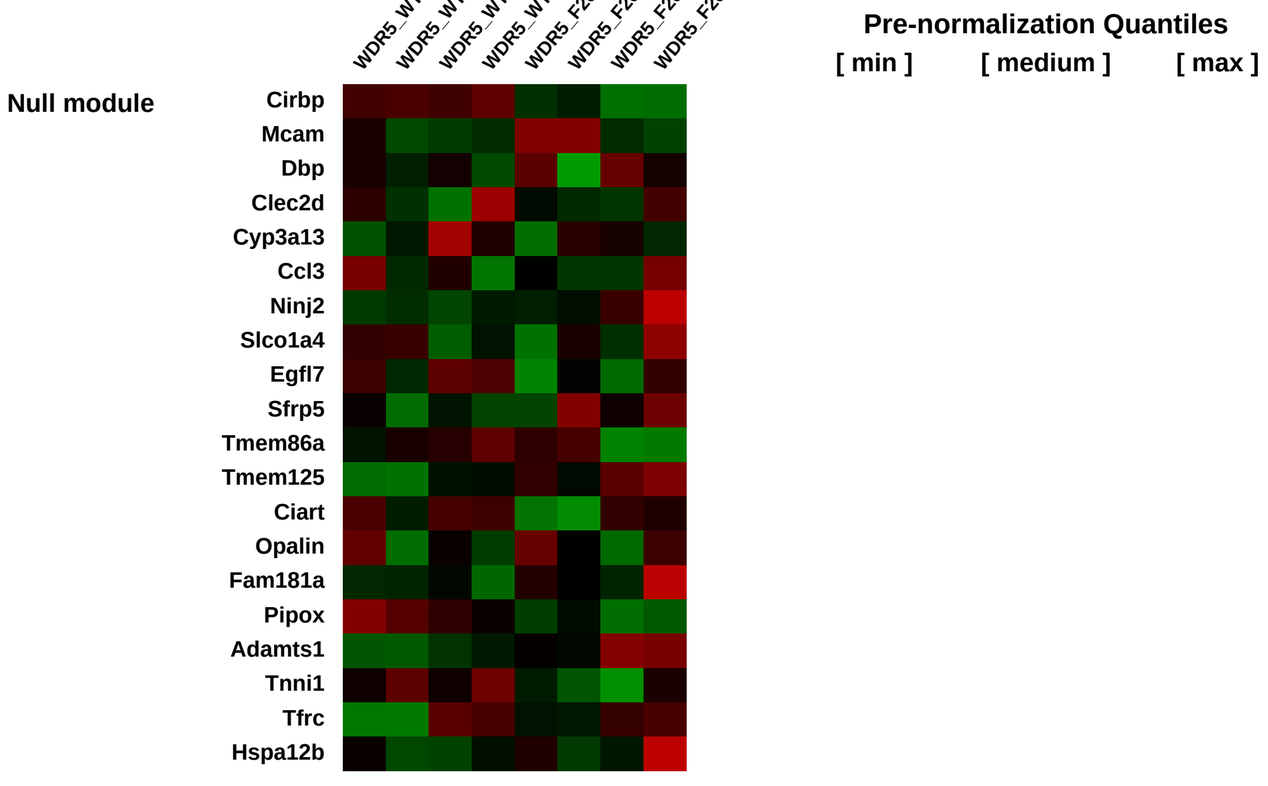

GEO Series "GSE36530" Expression Profiles

Num of samples in this series: 6

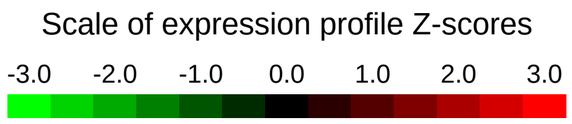

GEO Link:	http://www.ncbi.nlm.nih.gov/geo/query/acc.cgi?acc=GSE36530
Status:	Public on Mar 13 2013
Title:	Expression data for program activation by IR-induced DNA breaks in G1 phase Murine PreB cells
Organism:	Mus musculus
Experiment type:	Expression profiling by array
Platform:	GPL1261
Pubmed ID:	23496831
Summary & Design:	**Summary:** The objective of this set of samples is to identify genes that are differentially expressed following the introduction of DNA double strand breaks (DSBs) by ionizing radiation in wild-type murine pre-B cells. The data generated in this project will be compared to the data generated in GSE9024, in which genes that are differentially expressed following the introduction of DNA double strand breaks (DSBs) by the Rag proteins in murine pre-B cells were examined. In order to understand the differences between the physiologic and genotoxic responses to DSB DNA damage, we need to compare cells that are all in the same compartment of the cell cycle. We are therefore examining the response to IR-induced damage in cells that are arrested in G1, which would correspond to our previous study of G1 arrested cells with Rag-induced breaks. This will illuminate the difference directly, allowing us to better understand the signaling responses to the different types of DNA damage. **Overall design:** Murine v-abl-transformed pre-B cells were treated with 3 uM STI571 for 48 hours. The cell type is Wild type (3 biological replicates). For each wild type cell line, cells were treated with 1 Gy ionizing radiation or no ionizing radiation. Each sample was hybridized once using Affymetrix Mouse Genome 2.0 GeneChip arrays (Mouse 430 v2, Affymetrix, Santa Clara, CA). Data were analyzed using the unirradiated samples as the controls.

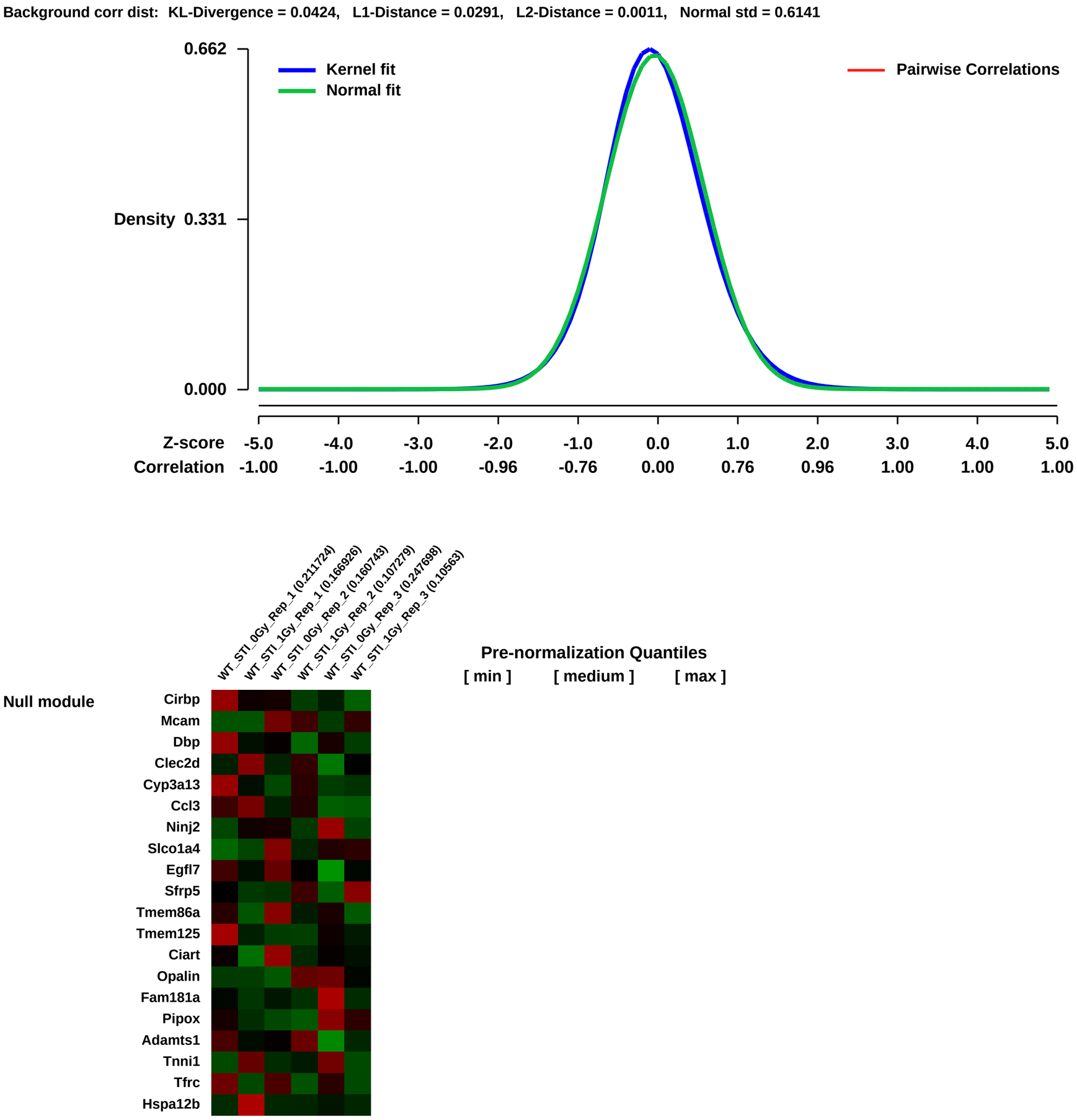

GEO Series "GSE36569" Expression Profiles

Num of samples in this series: 6

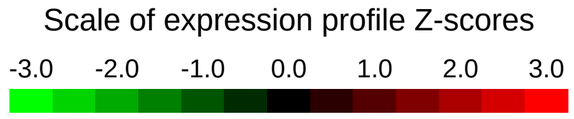

GEO Link:	**http://www.ncbi.nlm.nih.gov/geo/query/acc.cgi?acc=GSE36569**
Status:	**Public on Aug 25 2013**
Title:	**SCFA receptor response**
Organism:	**Mus musculus**
Experiment type:	**Expression profiling by array**
Platform:	**GPL1261**
Pubmed ID:	**23665276**
Summary & Design:	**Summary:** **The purpose of this study was to determine the gene expression patterns of the colon of GPR41 KO and GPR43 KO mice in response to ETOH treatment** **Overall design:** **The mice were treated with rectal injection of ETOH. 24 hours later, the colon tissues were harvested and total RNA was isolated for array experiments.**
Background corr dist:	**KL-Divergence = 0.0439, L1-Distance = 0.0213, L2-Distance = 0.0005, Normal std = 0.6022**

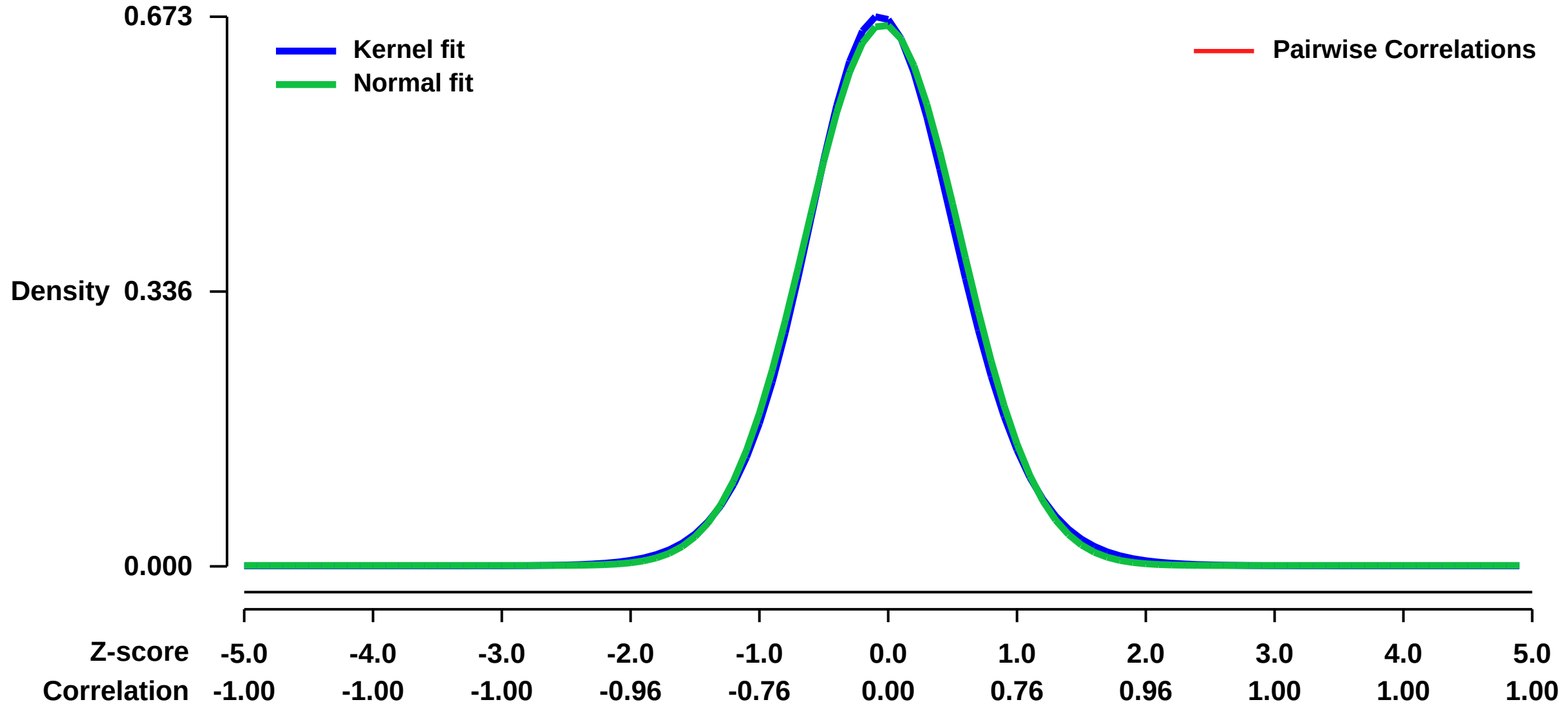

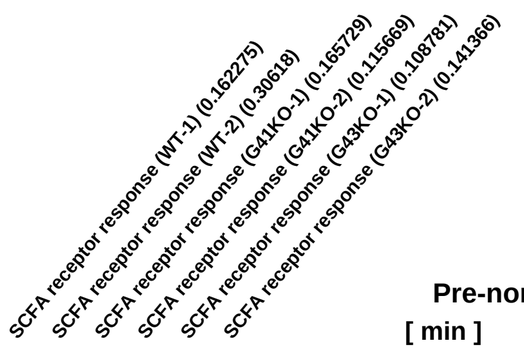

Pre-normalization Quantiles

[min] [medium] [max]

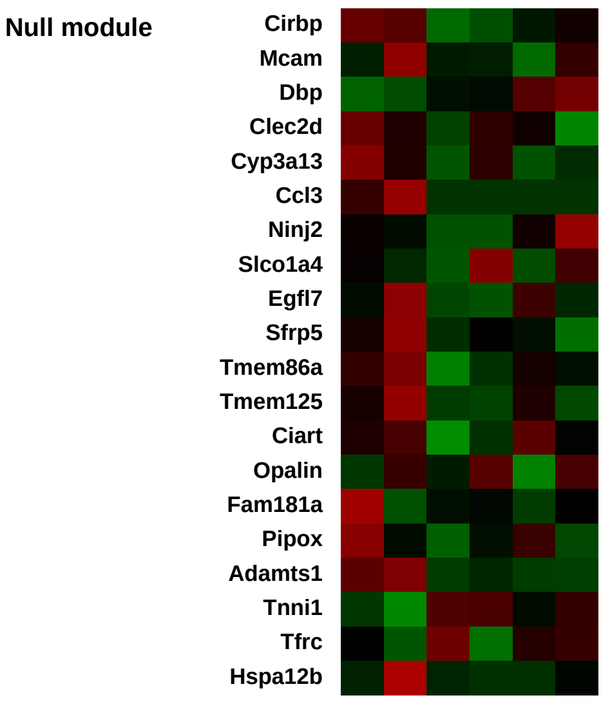

GEO Series "GSE36618" Expression Profiles

Num of samples in this series: 6

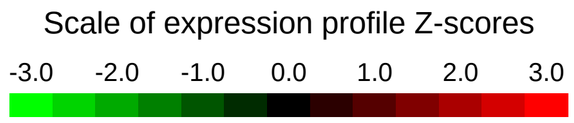

GEO Link:	http://www.ncbi.nlm.nih.gov/geo/query/acc.cgi?acc=GSE36618
Status:	Public on Mar 20 2012
Title:	Mechanisms of terminal erythroid differentiation defect in EKLF-deficient mice
Organism:	Mus musculus
Experiment type:	Expression profiling by array
Platform:	GPL1261
Pubmed ID:	18852285
Summary & Design:	**Summary:** EKLF is a Krˆ…ppel-like transcription factor identified as a transcriptional activator and chromatin modifier in erythroid cells. EKLF-deficient (Eklf -/-) mice die at day 14.5 of gestation from severe anemia. In this study, we demonstrate that early progenitor cells fail to undergo terminal erythroid differention in Eklf -/- embryos. To discover potential EKLF target genes responsible for the failure of erythropoiesis, transcriptional profiling was performed with RNA from wild type and Eklf -/- early erythroid progenitor cells. These analyses identified significant perturbation of a network of genes involved in cell cycle regulation, with the critical regulator of the cell cycle, E2f2, at a hub. E2f2 mRNA and protein levels were markedly decreased in Eklf -/- early erythroid progenitor cells, which showed a delay in the G1-to-S-phase transition. Chromatin immunoprecipitation analysis demonstrated EKLF occupancy at the proximal E2f2 promoter in vivo. Consistent with the role of EKLF as a chromatin modifier, EKLF binding-sites in the E2f2 promoter were located in a region of EKLF-dependent DNase I sensitivity in early erythroid progenitor cells. We propose a model in which EKLF-dependent activation and modification of the E2f2 locus is required for cell cycle progression preceding terminal erythroid differentiation. **Overall design:** RNA was isolated from flow-sorted early erythroid progenitors in 13.5 day old fetal livers from EKLF knock out mice (n=3 fetal livers) and wild-type control mice (n=3 fetal livers) for gene expression analysis

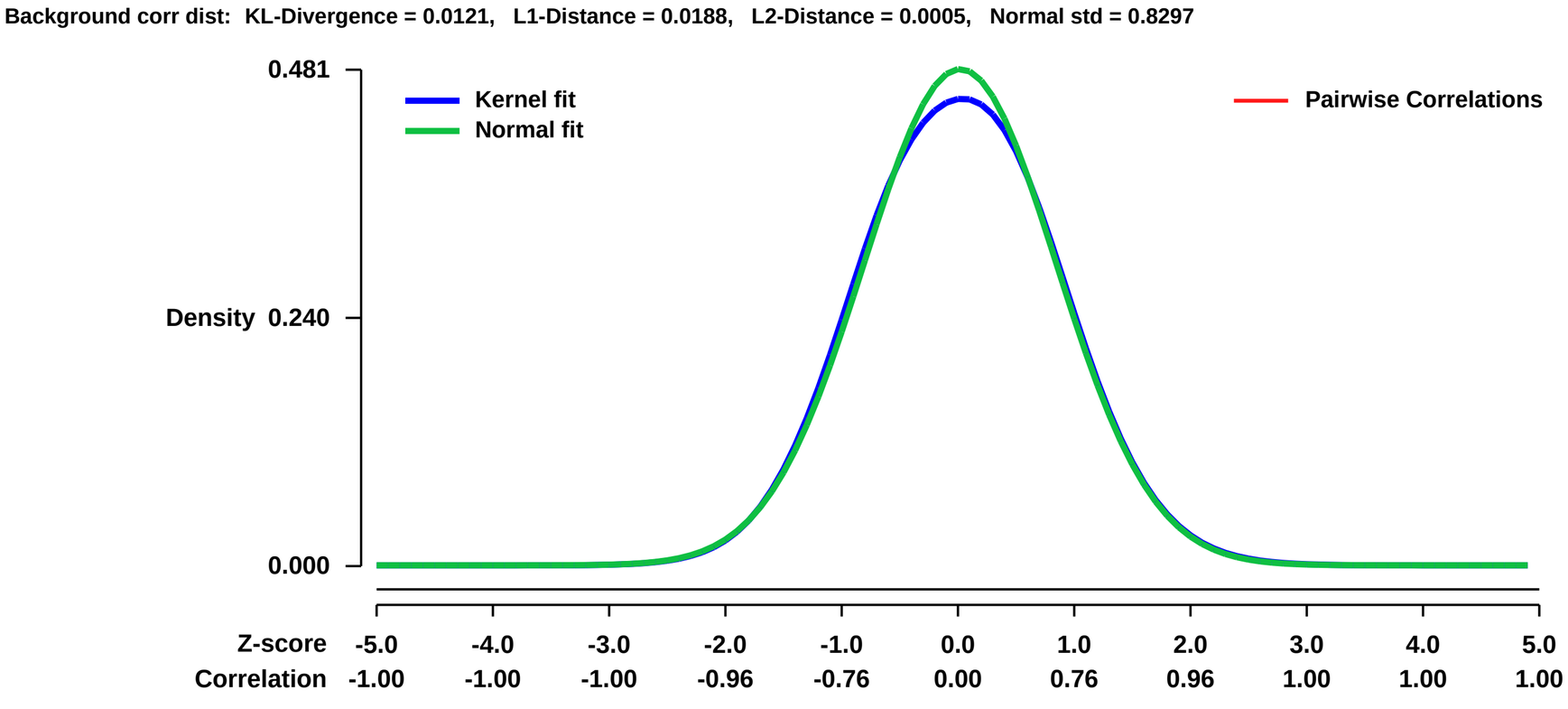

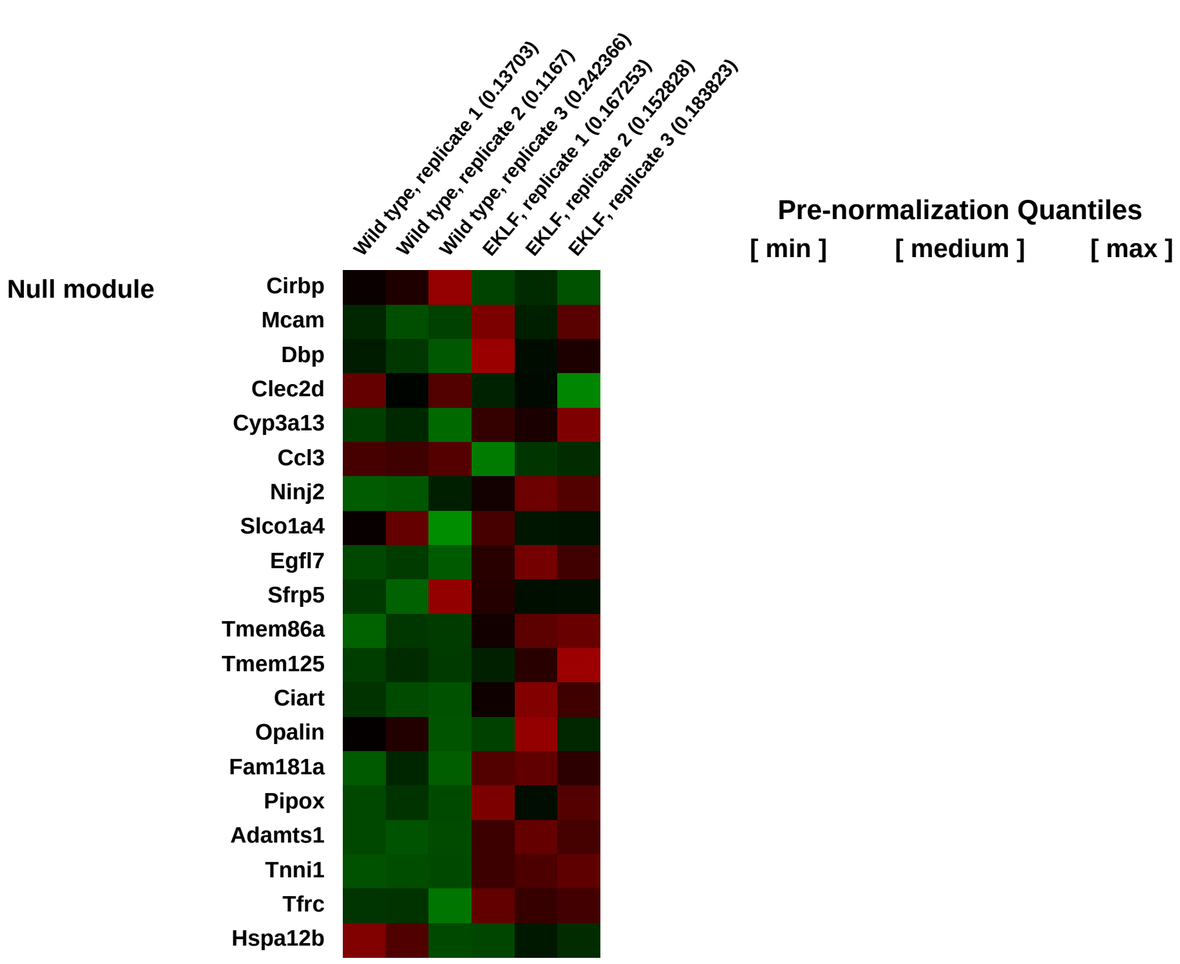

GEO Series "GSE36665" Expression Profiles

Num of samples in this series: 6

Scale of expression profile Z-scores

-3.0 -2.0 -1.0 0.0 1.0 2.0 3.0

GEO Link:	http://www.ncbi.nlm.nih.gov/geo/query/acc.cgi?acc=GSE36665
Status:	Public on Apr 15 2012
Title:	Gene expression profiling of Wwox targeted ablation in mouse mammary epithelial cells
Organism:	Mus musculus
Experiment type:	Expression profiling by array
Platform:	GPL1261
Pubmed ID:	22574198
Summary & Design:	**Summary:** The WWOX gene has been implicated in human cancers, including breast cancer.The development and tumorigenesis between human and mouse mammary glands (MGs) share similar molecular details and signal transduction pathways. We established mouse line that specifically knockout the expression of WWOX gene in the MG epithelial cells (MECs) by crossing BK5-cre mice with our WWOX flox stain. In order to study the gene expression profile in the subpopulation MECs, we isolated the organoids from the 4th MGs of both BK5-cre +; WWOX flox/flox (KO) mice and their WT counterparts (BK5-cre -; WWOX flox/flox), 3 mice each genotype. The total RNA from the mouse MG organoids was extracted and purified by TRIzol/RNeasy Kit and their integrity was checked on Agilent RNA 6000 Nanochip. The goal is to identify the significant perturbation in tumorigenic pathways in these cells induced by WWOX ablation. **Overall design:** Mammary gland epithelial organoids samples and gene expression profiles were deribed from three WWOX-KO mice (BK5-cre +; WWOX flox/flox) and from three WWOX-WT mice (BK5-cre -; WWOX flox/flox)

Background corr dist: KL-Divergence = 0.0345, L1-Distance = 0.0188, L2-Distance = 0.0004, Normal std = 0.6428

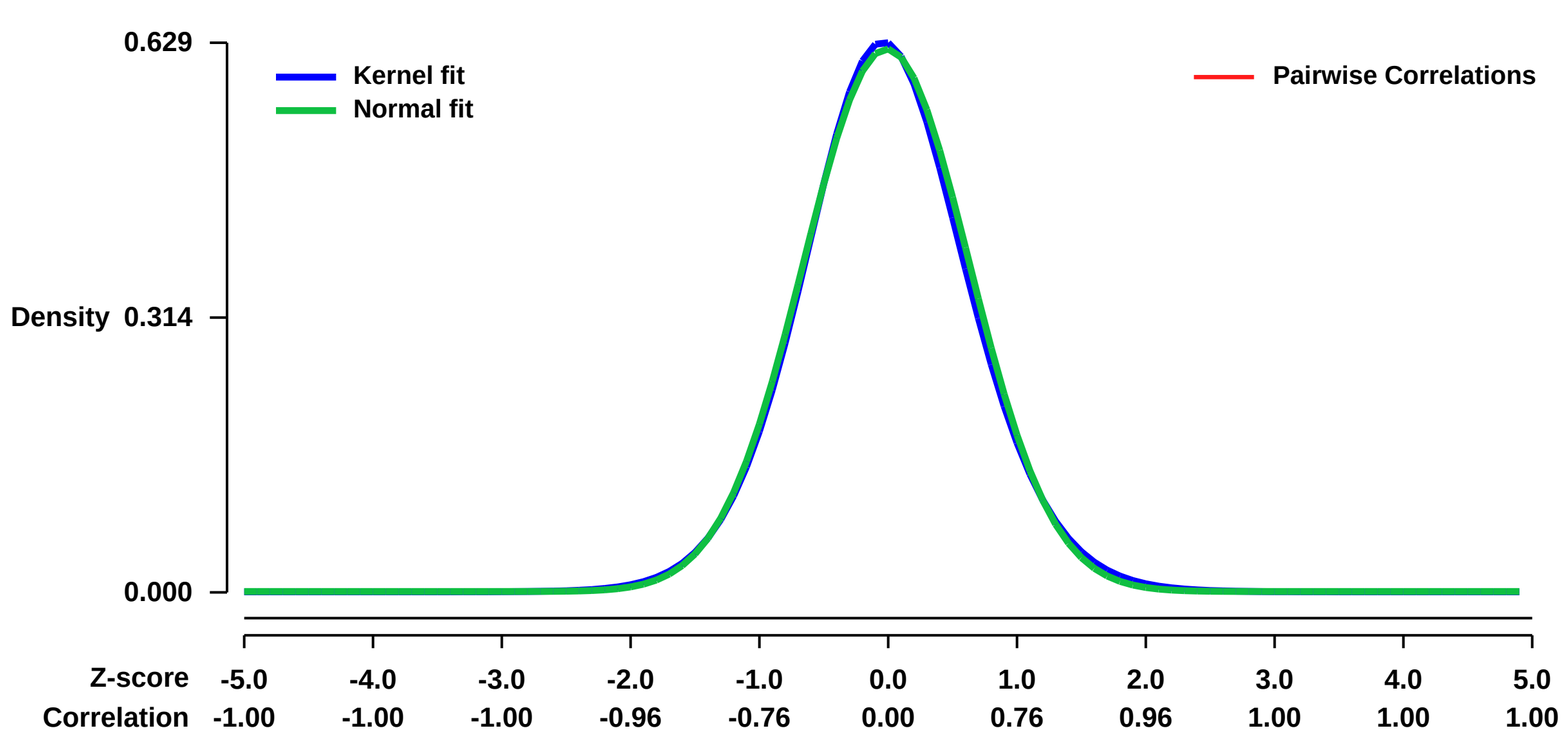

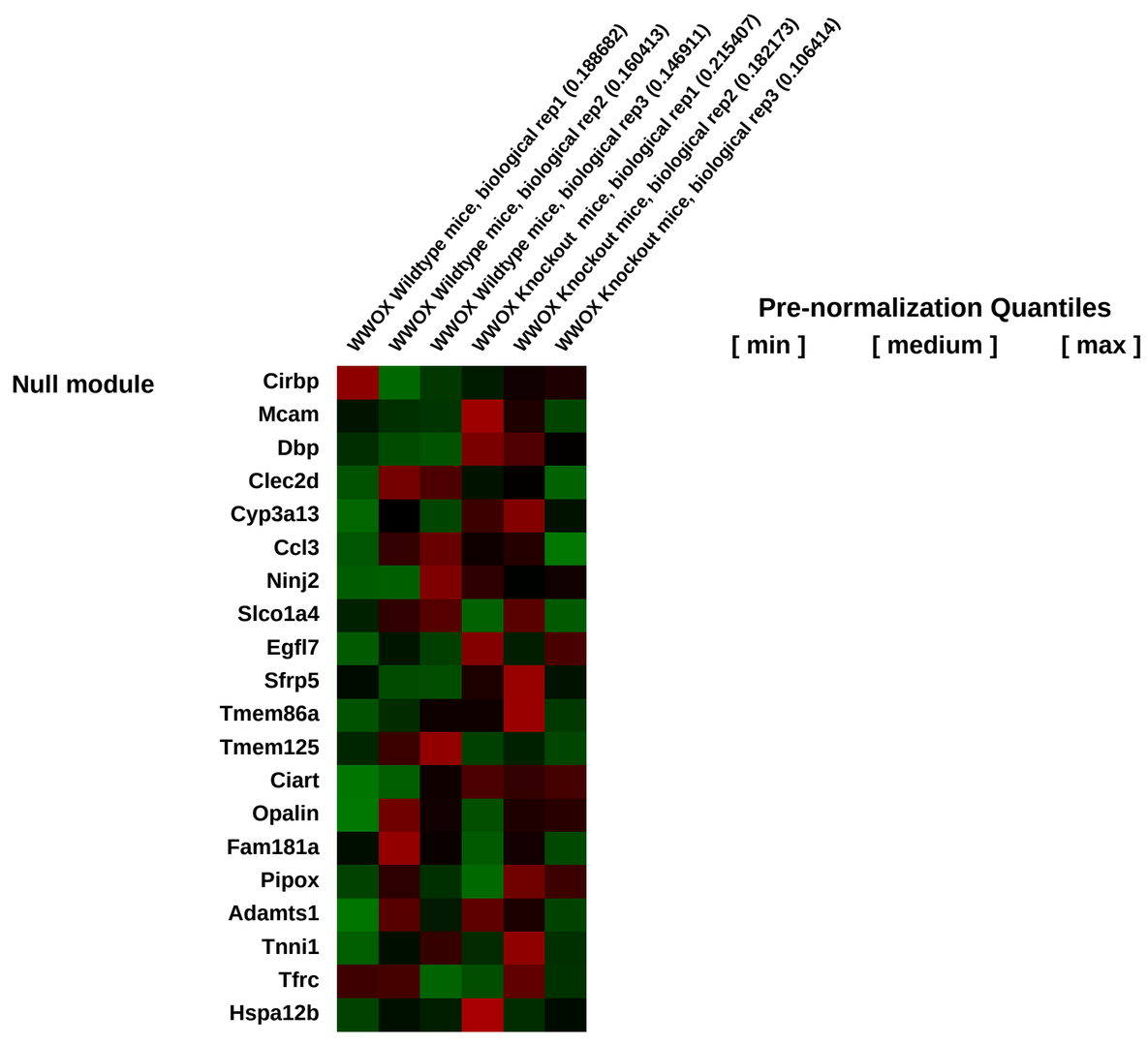

GEO Series "GSE36810" Expression Profiles

Num of samples in this series: 16

Scale of expression profile Z-scores

-3.0 -2.0 -1.0 0.0 1.0 2.0 3.0

GEO Link:	http://www.ncbi.nlm.nih.gov/geo/query/acc.cgi?acc=GSE36810
Status:	Public on Mar 27 2012
Title:	Expression data from mouse lungs exposed in-utero and/or as an adult to second-hand smoke (SHS)
Organism:	Mus musculus
Experiment type:	Expression profiling by array
Platform:	GPL1261
Pubmed ID:	22962063
Summary & Design:	**Summary:** Second-hand smoke (SHS) exposure during pregnancy has adverse effects on offspring. We used microarrays to characterize the gene expression changes caused by in-utero exposure and adult exposure to SHS in adult mouse lungs. **Overall design:** Left lungs from Balb/c male mice were collected at 15 weeks of age for RNA extraction and hybridization on Affymetrix mouse 430 2.0 microarrays. Based on their smoke exposure status, there are 4 groups of mice, each exposed in-utero to filtered-air or SHS and as an adult to filtered-air or SHS. We extracted RNA from 4 animals from each group for microarray analysis (N = 16 samples).

Background corr dist: KL-Divergence = 0.0998, L1-Distance = 0.0238, L2-Distance = 0.0008, Normal std = 0.4416

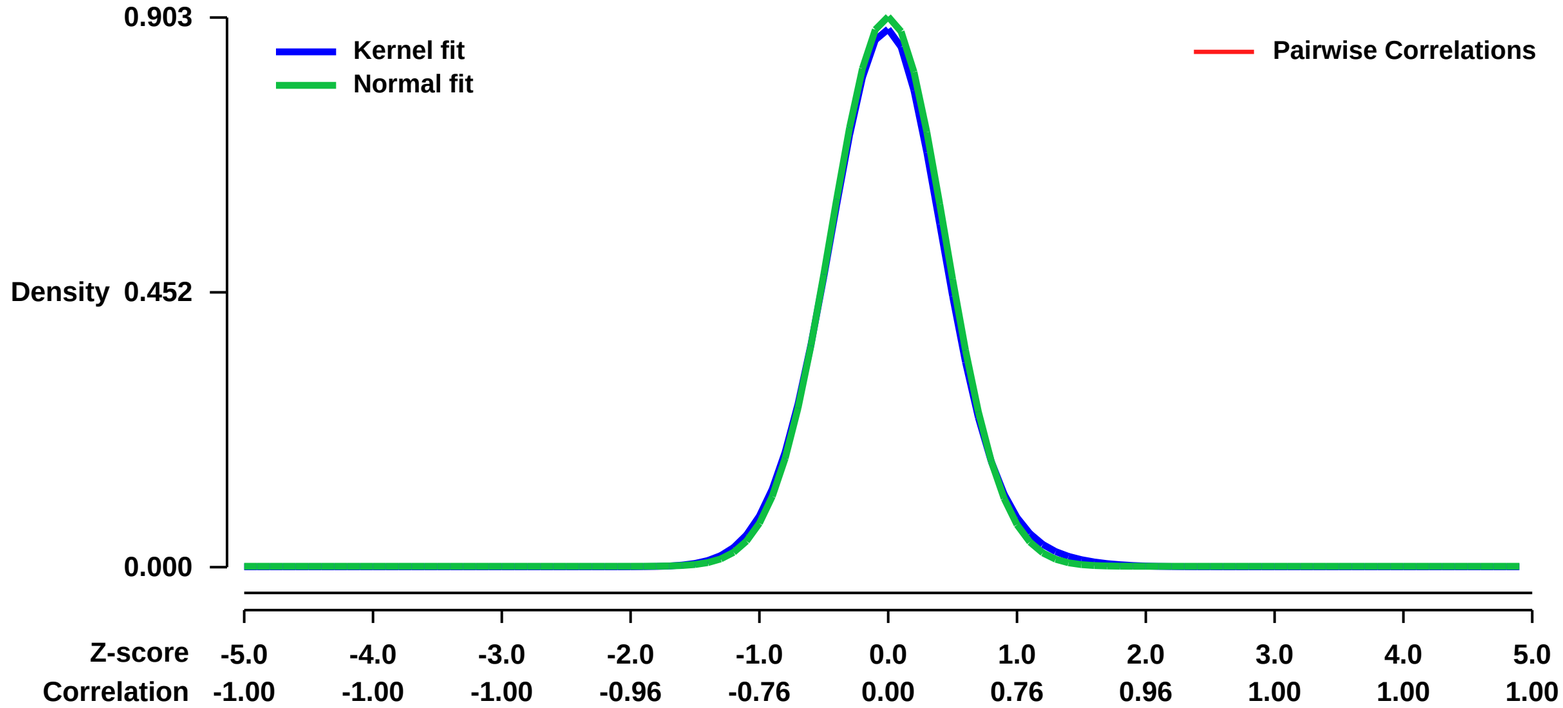

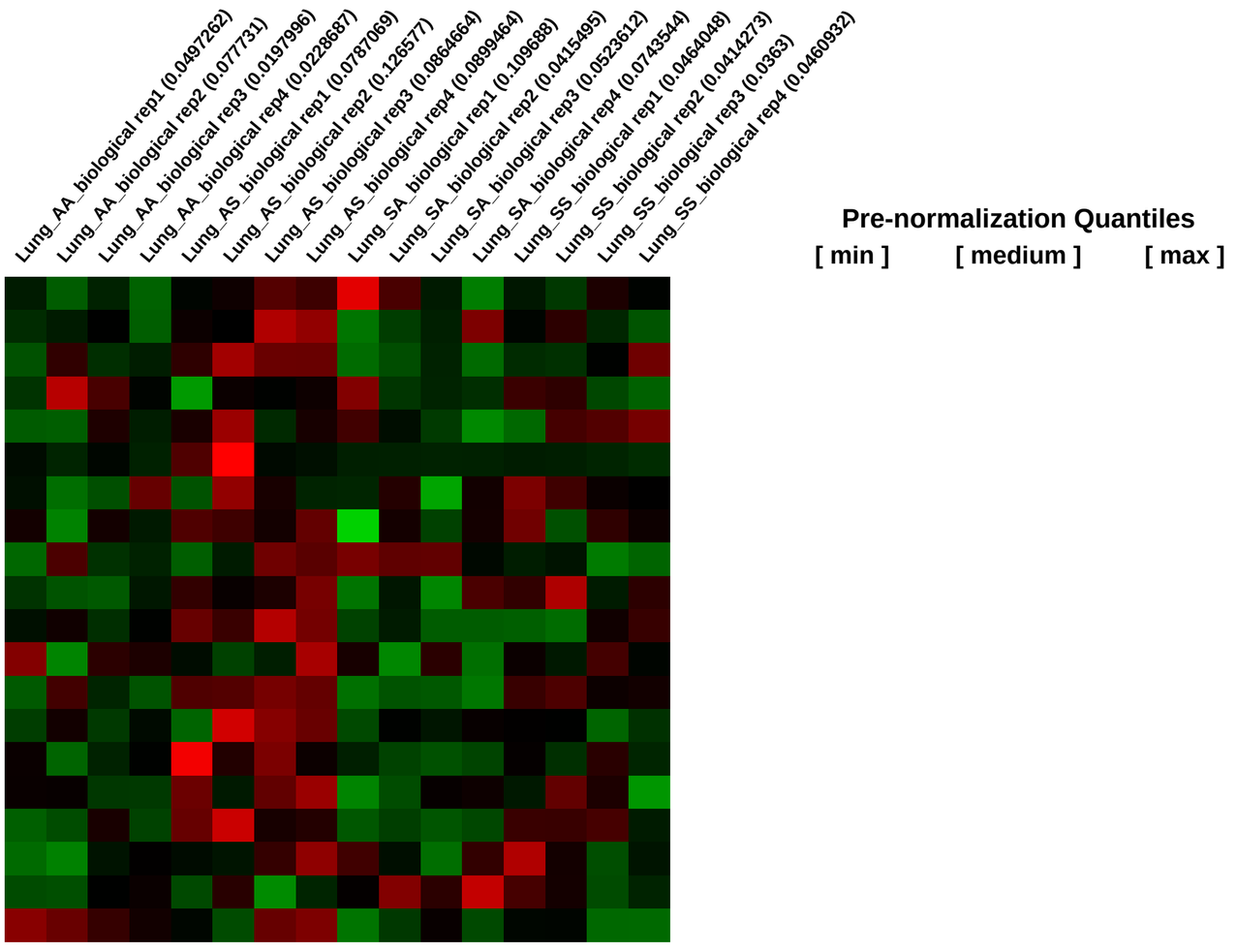

GEO Series "GSE36826" Expression Profiles

Num of samples in this series: 12

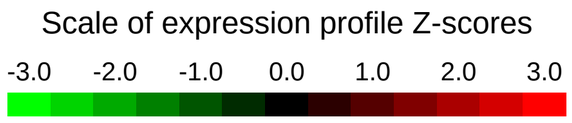

GEO Link:	http://www.ncbi.nlm.nih.gov/geo/query/acc.cgi?acc=GSE36826
Status:	Public on Dec 05 2012
Title:	Neutrophil-derived IL-1¸† is sufficient for abscess formation in immunity against Staphylococcus aureus in mice
Organism:	Mus musculus
Experiment type:	Expression profiling by array
Platform:	GPL1261
Pubmed ID:	23209417
Summary & Design:	**Summary:** Neutrophil abscess formation is critical in innate immunity against many pathogens. Here, the mechanism of neutrophil abscess formation was investigated using a mouse model of Staphylococcus aureus cutaneous infection. Gene expression analysis of S. aureus-infected skin revealed that induction of neutrophil recruitment genes was largely dependent upon IL-1beta/IL-1R activation. Unexpectedly, using IL 1beta reporter mice, neutrophils were identified as the primary source of IL-1beta at the site of infection. Furthermore, IL-1beta-producing neutrophils were necessary and sufficient for abscess formation and bacterial clearance. S. aureus-induced IL 1beta production by neutrophils required TLR2, NOD2, FPRs and the ASC/NLRP3 inflammasome. Taken together, IL-1beta and neutrophil abscess formation during an infection are functionally, spatially and temporally linked as a consequence of direct IL-1beta production by neutrophils. **Overall design:** Lesional skin biopsies obtained from C57BL/6J WT mice or IL-1R-deficient mice at 4 hours post-infection with Staphylococcus aureus. Uninfected skin biopsies were also collected from WT and IL-1R-deficient mice.

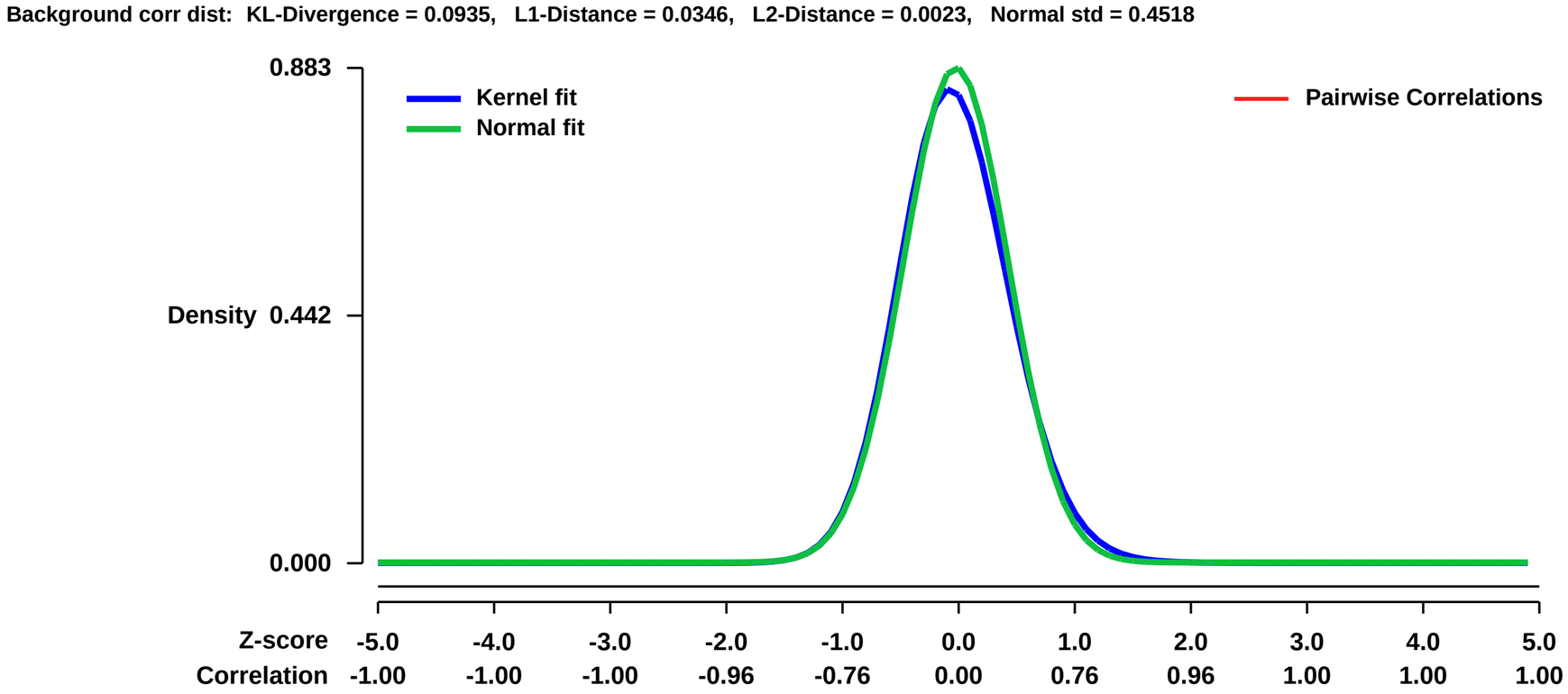

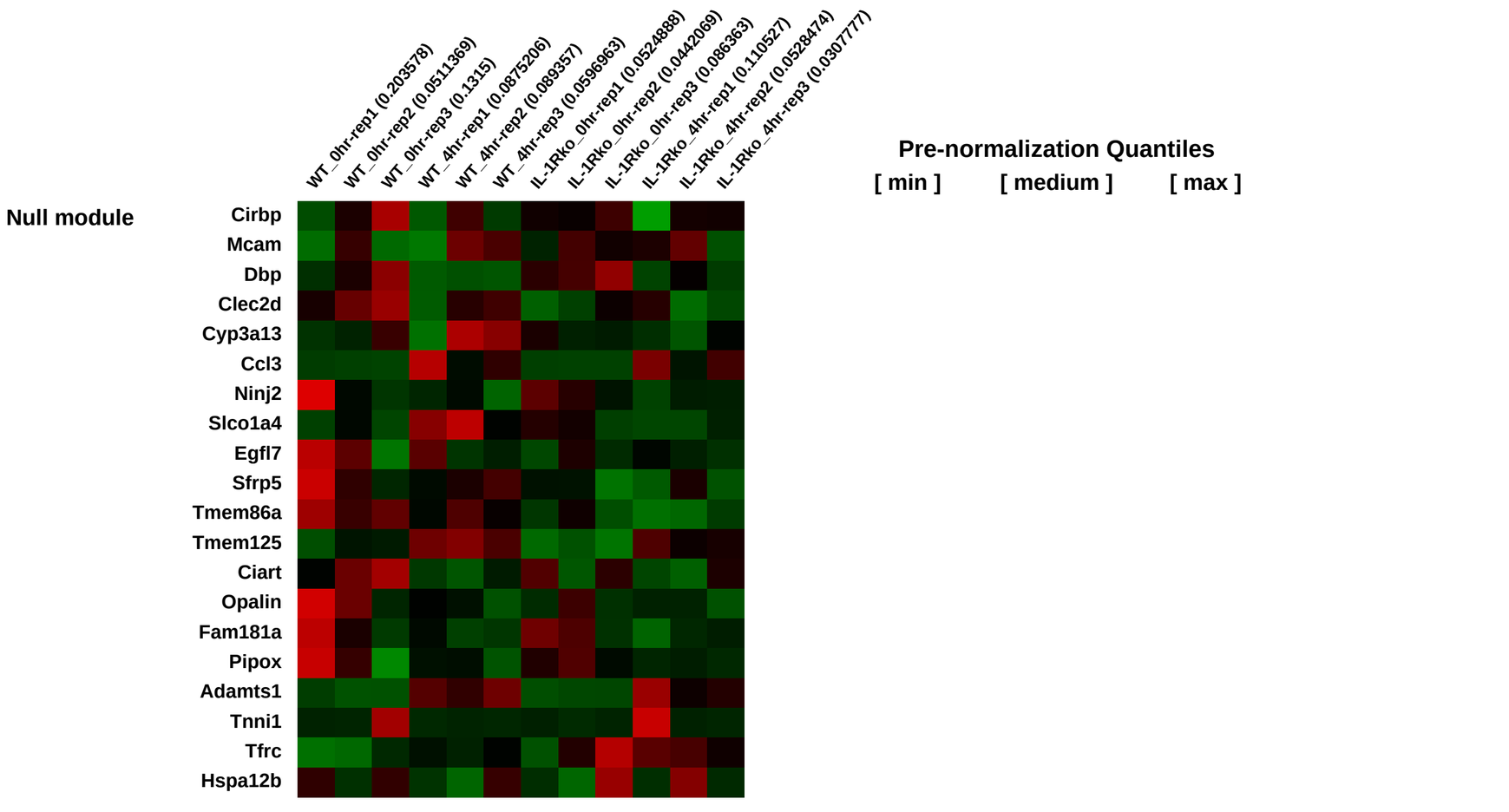

GEO Series "GSE36838" Expression Profiles

Num of samples in this series: 18

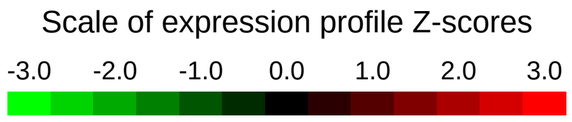

GEO Link:	http://www.ncbi.nlm.nih.gov/geo/query/acc.cgi?acc=GSE36838
Status:	Public on Mar 28 2012
Title:	Expression profiling of the effect of high-fat diet, low-fat diet, CR and exercise on mice liver
Organism:	Mus musculus
Experiment type:	Expression profiling by array
Platform:	GPL1261
Pubmed ID:	22509016
Summary & Design:	**Summary:** Dietary interventions are effective ways to extend or shorten lifespan. By examining midlife hepatic gene expressions in mice under different dietary conditions, which resulted in different lifespans and aging-related phenotypes, we were able to identify genes and pathways that modulate the aging process. We found that pathways transcriptionally correlated with diet-modulated lifespan and physiological changes were enriched for lifespan-modifying genes. **Overall design:** At the age of 5 weeks, animals were randomly assigned to one of the 6 intervention groups (n = 30 for each group): feeding of a low-fat diet (10% fat, D12450B, Research Diets) ad libitum (LF) or with 30% calorie restriction (LF+CR) or with voluntary running exercise (LF+Ex), feeding of a high-fat diet (60% fat, D12492, Research Diets) ad libitum (HF) or with 30% calorie restriction (HF+CR) or with voluntary running exercise (HF+Ex). All mice were housed individually during the study. The daily consumption of food in LF and HF groups was recorded over a week and averaged to determine the amount of food for the following week for the LF+CR and HF+CR groups, respectively. After 1 week acclimation in cage with the locked running wheels, mice in the LF+Ex and HF+Ex groups were allowed free access to a running wheel, and the running distance and time were recorded automatically by the equipment. The hepatic transcriptional level for 3 mice from each intervention group at 62 weeks of age was analyzed using Affymetrix Mouse Genome 430 2.0 Arrays.

Background corr dist: KL-Divergence = 0.1729, L1-Distance = 0.0467, L2-Distance = 0.0048, Normal std = 0.3511

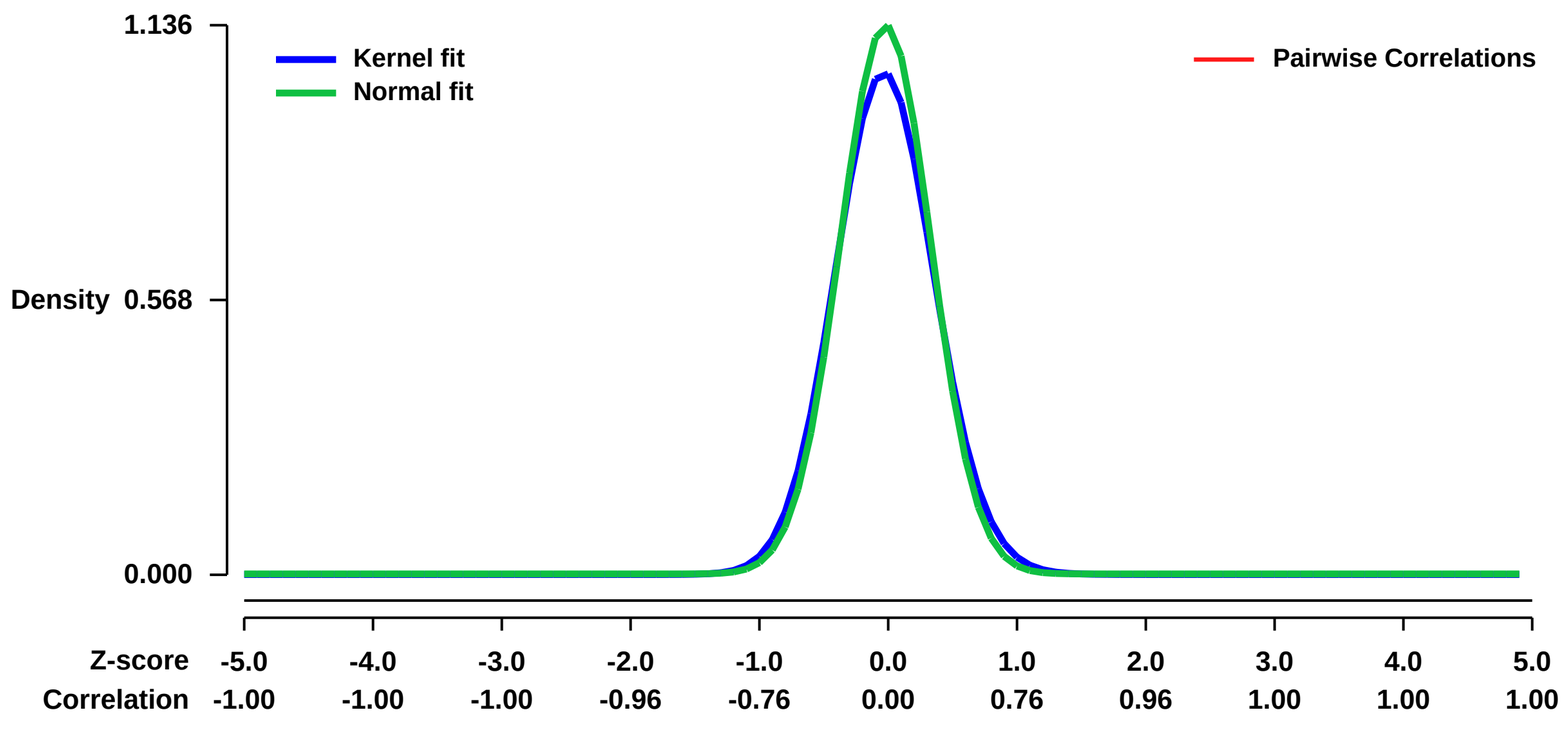

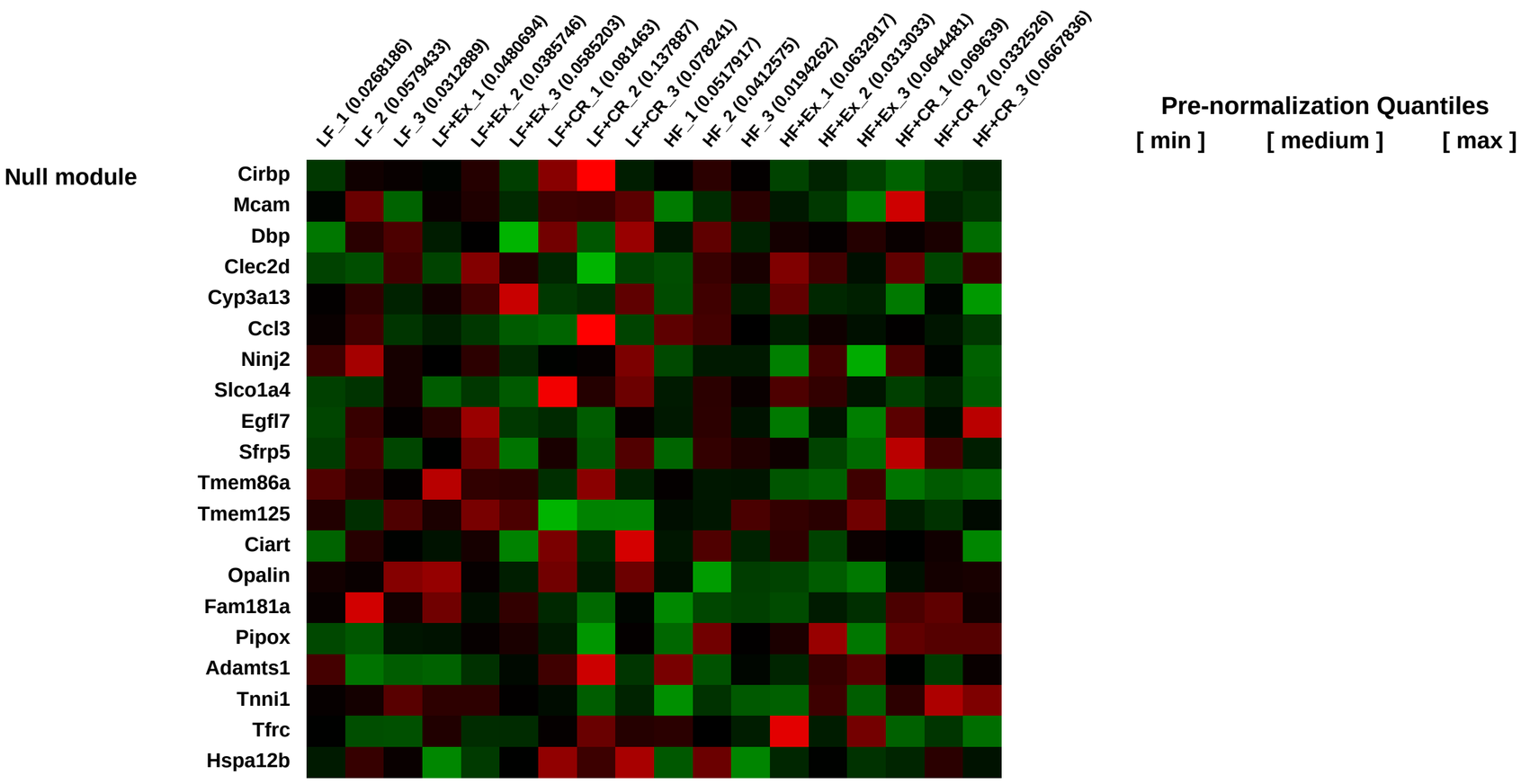

GEO Series "GSE36974" Expression Profiles

Num of samples in this series: 14

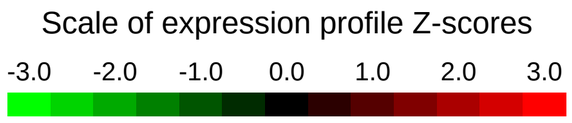

GEO Link:	**http://www.ncbi.nlm.nih.gov/geo/query/acc.cgi?acc=GSE36974**
Status:	**Public on Mar 31 2013**
Title:	**Genotype modulates gene expression profiles in the uterus in response to preconceptual folate supplementation.**
Organism:	**Mus musculus**
Experiment type:	**Expression profiling by array**
Platform:	**GPL1261**
Pubmed ID:	
Summary & Design:	**Summary:** **Periconceptual supplementation of women with folate is considered a great success for public health. Higher folate status, either by supplementation, or via the mandatory fortification of grain products in the United States, has lead to significant reduction in the incidence of neural tube defects. Besides birth defects, folate deficiency has been linked to a variety of morbidities, most notably to increased risk for cancer. However, recent evidence suggests that excess folate may be detrimental - for birth defect incidence or in the progression of cancer. How folate mediates beneficial or detrimental effects is not well understood. It is also unknown what molecular responses are elicited in women taking folate supplements, and thus experience a bolus of folate on top of the status achieved by fortification. To characterize this response, we performed gene expression profiling experiments on uterus tissue of pregnant mice after a preconceptional regimen of supplementation with folinic acid. We suggest that folinic acid supplementation affects expression of genes that contribute to protein synthesis and localization, genes that play a role for mitochondrial biology and oxidative phosphorylation, and genes encoding nucleotide-binding proteins, including protein kinases and GTP-binding intracellular signaling factors. The extent of such a response is strongly modulated by the genetic background. Finally, we suggest that folinic acid supplementation in this paradigm may affect histone methylation status, a potential avenue to mechanisms of gene regulation.** **Overall design:** **Gene expression profiles were generated from uterus tissue. Female mice were either C57BL/6 wildtype, or homozygous for a Folr4 mutation, and received injections of either saline of folininc acid, respectively.**

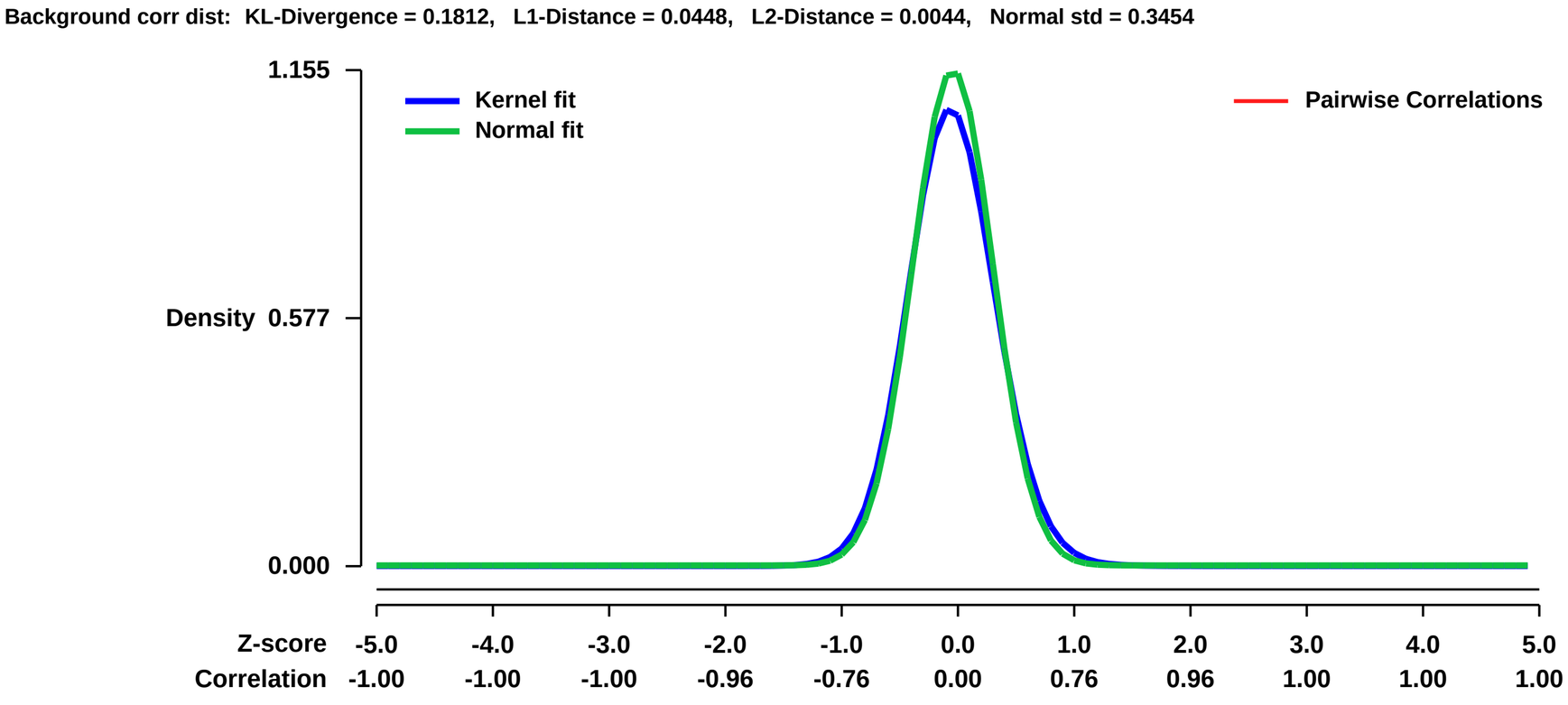

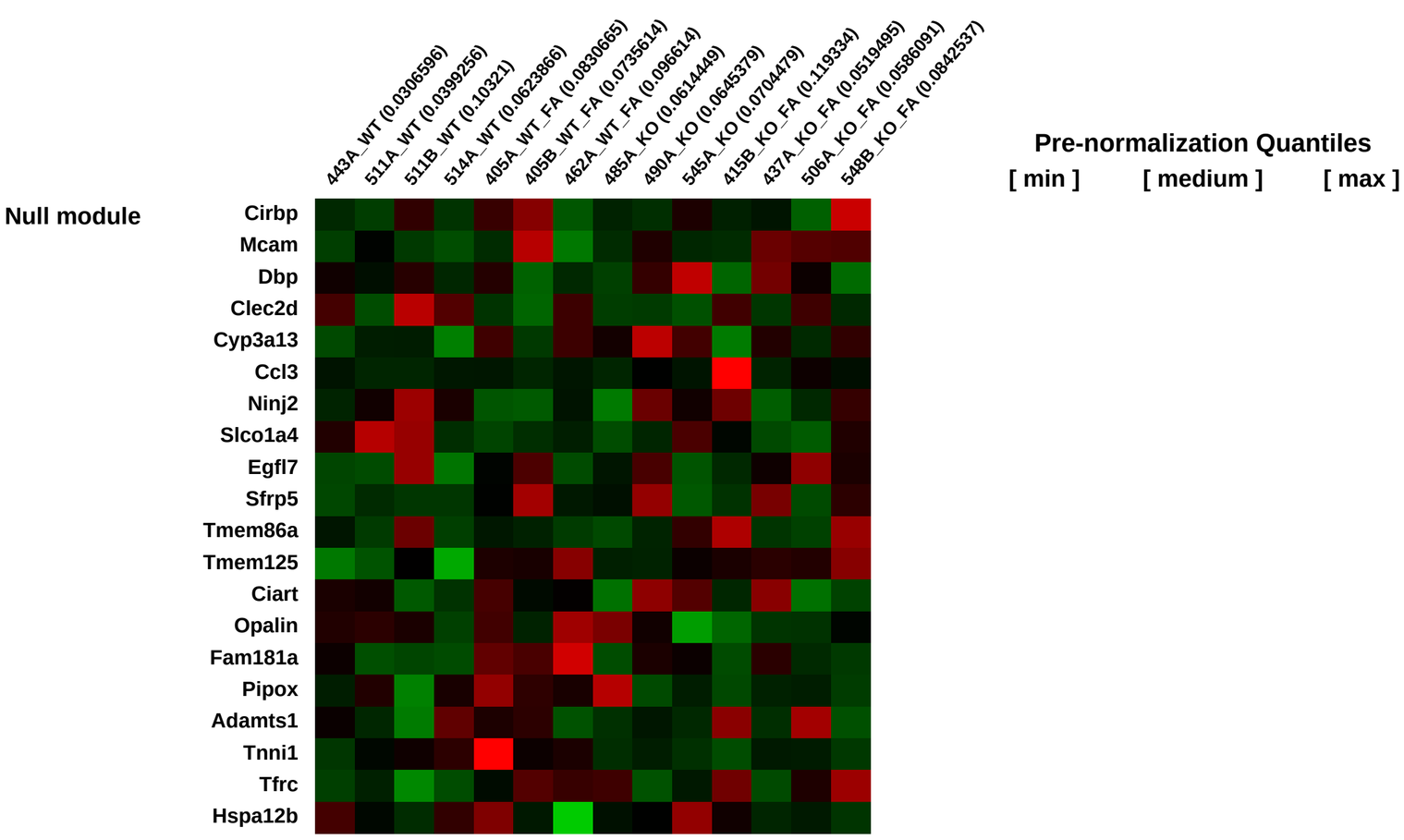

GEO Series "GSE37055" Expression Profiles

Num of samples in this series: 42

Scale of expression profile Z-scores

-3.0 -2.0 -1.0 0.0 1.0 2.0 3.0

GEO Link: http://www.ncbi.nlm.nih.gov/geo/query/acc.cgi?acc=GSE37055
Status: Public on Jul 20 2012
Title: Cell-type specific postnatal developmental expression data from mouse cerebellar Purkinje and Stellate/Basket cells
Organism: Mus musculus
Experiment type: Expression profiling by array
Platform: GPL1261
Pubmed ID: 22754500

Summary & Design:

Summary:
The assembly of neural circuits involves multiple sequential steps such as the specification of cell types, their migration to proper brain locations, morphological and physiological differentiation, and the formation and maturation of synaptic connections. This intricate and often prolonged process is guided by elaborate genetic mechanisms that regulate each developmental event. Evidence from numerous systems suggests that each cell type, once specified, is endowed with a genetic program that directs its subsequent development. This cell intrinsic program unfolds in respond to, and is regulated by, extrinsic signals, including cell-cell and synaptic interactions. To a large extent, the execution of this genetic program is achieved by the expression of specific sets of genes that support distinct developmental processes. Therefore, a comprehensive analysis of the developmental progression of gene expression in synaptic partners of neurons may provide a basis for exploring the genetic mechanisms regulating circuit assembly.

Here we examined the developmental gene expression profiles in well defined cell types in a stereotyped microcircuit of the cerebellar cortex.

Overall design:
Manually sorted pure populations of Purkinje cells and Stellate/Basket cells, 3 biological replicates, from Gad67-GFP bac-transgenic (G42) mice were profiled during postnatal developmental stages P3, P7, P14, P21, P28, P35 and P56 using Affymetrix MOE430.2 expression array

Background corr dist: KL-Divergence = 0.1175, L1-Distance = 0.0758, L2-Distance = 0.0135, Normal std = 0.4253

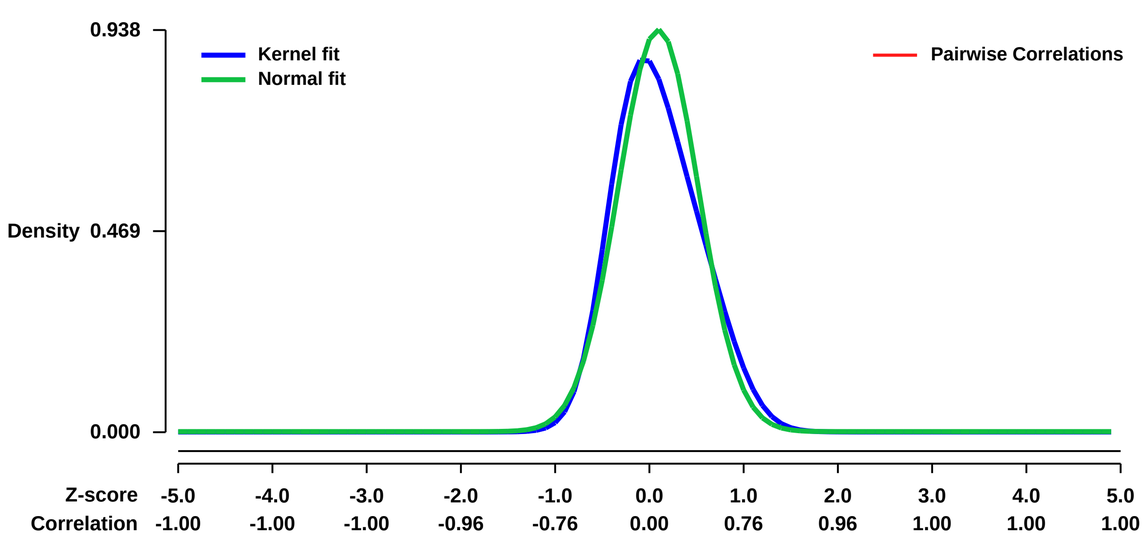

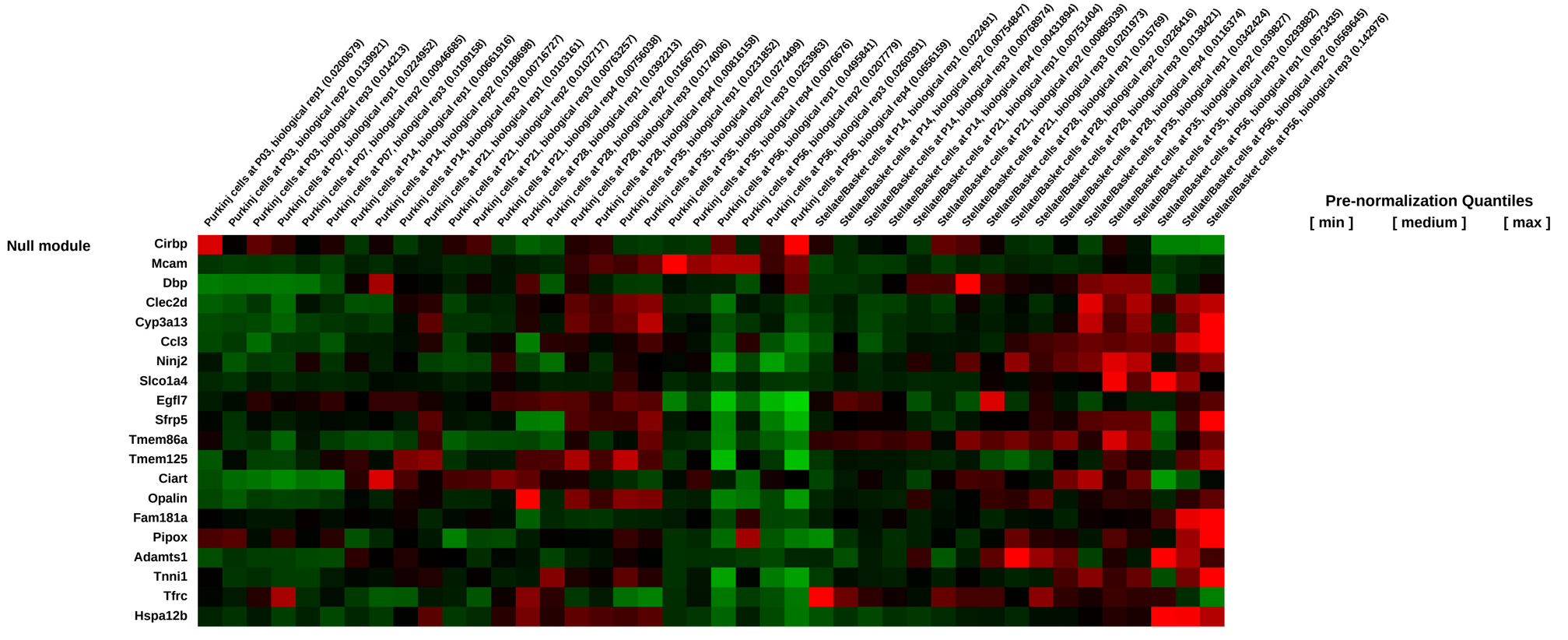

GEO Series "GSE37191" Expression Profiles

Num of samples in this series: 12

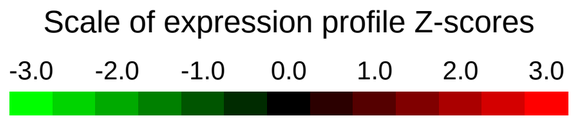

GEO Link:	http://www.ncbi.nlm.nih.gov/geo/query/acc.cgi?acc=GSE37191
Status:	Public on Jan 01 2013
Title:	Gene expression profiling reveals mast cell-dependent inflammation in the meninges in early EAE.
Organism:	Mus musculus
Experiment type:	Expression profiling by array
Platform:	GPL1261
Pubmed ID:	23267561

Summary & Design:

Summary:
The meninges are generally considered relatively inert tissues that house the CSF and provide protection for the brain and spinal cord. However, our previous studies using Kit mutant (Kit W/Wv) mast cell-deficient mice demonstrated that mast cells residing in the dura mater and pia mater exacerbate the severity of experimental autoimmune encephalomyelitis (EAE), the rodent model of the CNS demyelinating disease, multiple sclerosis. These data suggest that the meninges are sites of active immune responses in disease. Gene expression profiles of meningeal tissue from wild type and mast cell deficient mice prior to and at day 6 post-EAE induction were found highly distinct. Increases in both mast cell- and neutrophil-associated transcripts were among the notable disease-related changes observed in wild type mice. Kinetic analyses show that meningeal mast cells are activated within 24 hours of disease induction to express multiple mediators including IL-1b and TNF as well as the neutrophil chemoattractant, CXCL2, an observation corresponding with an influx of neutrophils to the meninges. Neutrophil recruitment as well as the disease-related loss of BBB integrity is dependent on mast cell-derived TNF. These data provide unequivocal evidence that the meninges are sites of early inflammatory events in EAE. Mast cells residing within these tissues promote disease by orchestrating an early and efficient immune cell co-localization resulting in a robust local inflammatory response and a breach of the proximal BBB. We hypothesize that these events reflect an aberrant manifestation of the normal immune surveillance role of the meninges in infection settings.

Overall design:
Immunized WT and Kit W/Wv mice were sacrificed on Day 6 post-immunization and perfused with PBS as were naˆflve littermate control mice. The dura mater was immediately removed from the calvarium of the skull and pooled (10 mice/group, 4 groups). RNA was isolated using SV Total RNA Isolation System (Promega). Each pool was analyzed in technical triplicates. Briefly, cRNA was synthesized and amplified/labeled using the Affymetrix Express Kit, then fragmented and hybridized to the The GeneChip´fi Mouse Genome 430 2.0 Array in accordance to the Affymetrix GeneChip expression analysis technical manual (Affymetrix, Santa Clara, CA). After hybridization, arrays were washed and stained with Affymetrix fluidics protocol FS450_0001 and scanned with a 7G Affymetrix GeneChip Scanner. Image data were analyzed with Affymetrix Expression Consoleâ¢ software and normalized with Robust Multichip Analysis (RMA; www.bioconductor.org/) to determine signal log ratios (CITE: Gentleman, R.C., Carey, V.J., Bates, D.M., Bolstad, B., Dettling, M., Dudoit, S., Ellis, B., Gautier, L., Ge, Y., Gentry, J., et al. (2004). Bioconductor: open software development for computational biology and bioinformatics. Genome Biol 5, R80.). The mean fold change was calculated from 3 independent technical replicates for each of the four experimental conditions and assessed by a non-parametric rank product test (CITE: Hong, F., Breitling, R., McEntee, C.W., Wittner, B.S., Nemhauser, J.L., and Chory, J. (2006). RankProd: a bioconductor package for detecting differentially expressed genes in meta-analysis. Bioinformatics 22, 2825-2827). Heat maps were generated with Genesis (Cite: Sturn, A., Quackenbush, J. and Trajanoski, Z. (2002) Genesis: cluster analysis of microarray data. Bioinformatics, 18, 207-208).

Background corr dist: KL-Divergence = 0.1081, L1-Distance = 0.0249, L2-Distance = 0.0009, Normal std = 0.4256

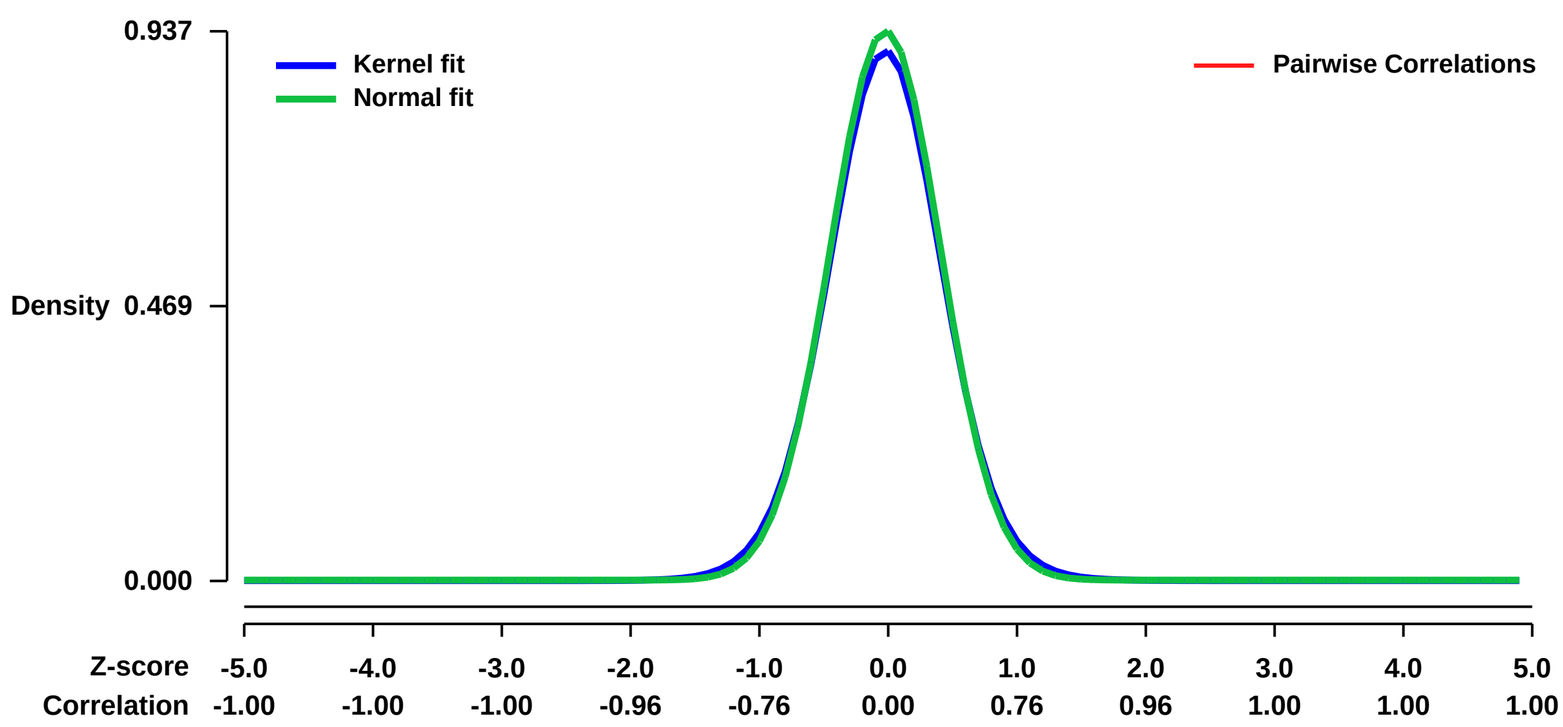

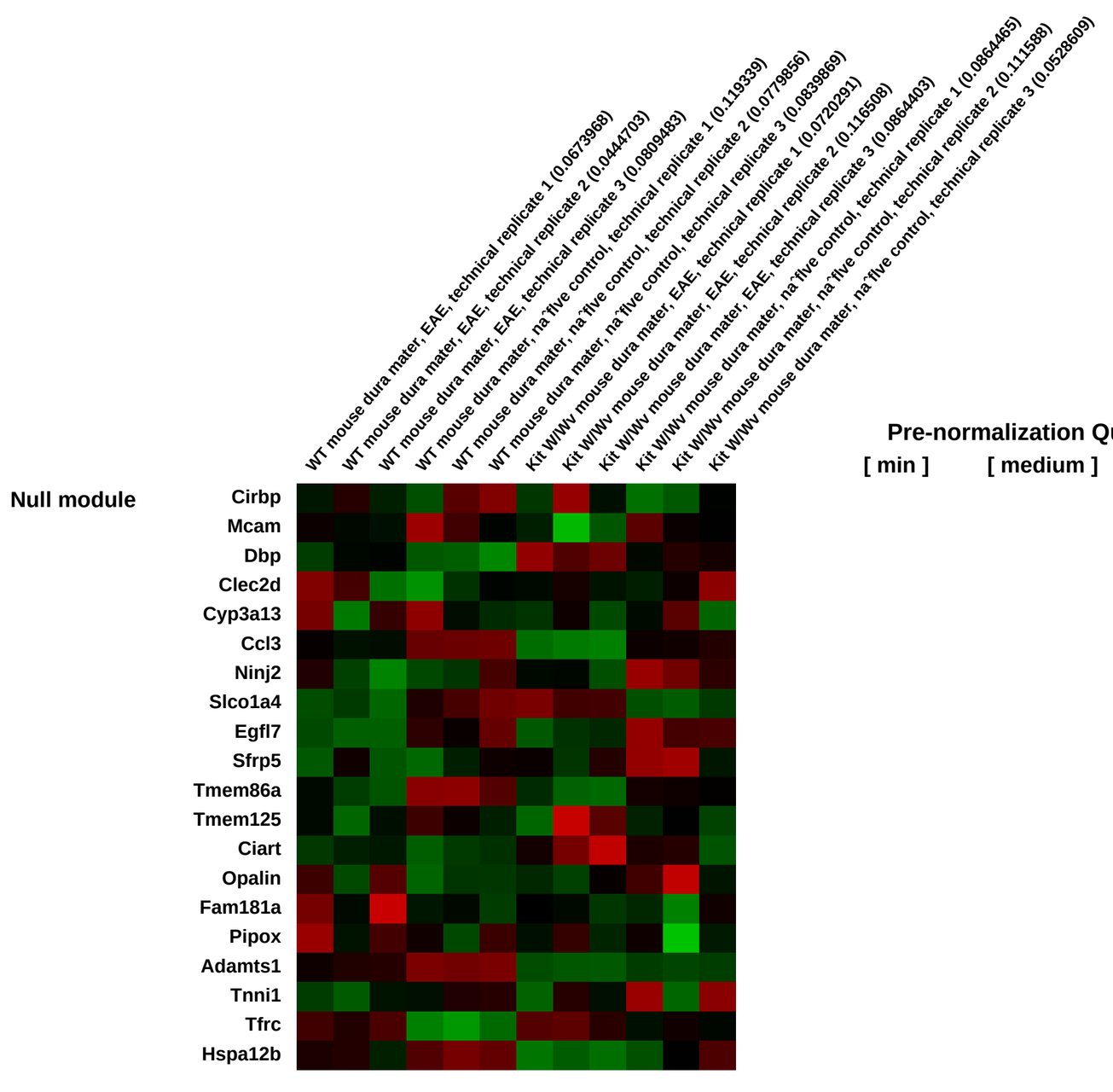

GEO Series "GSE37221" Expression Profiles

Num of samples in this series: 6

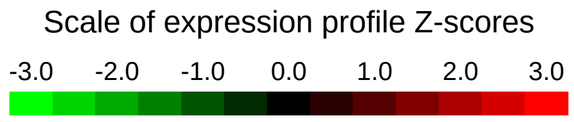

GEO Link:	http://www.ncbi.nlm.nih.gov/geo/query/acc.cgi?acc=GSE37221
Status:	Public on Apr 13 2012
Title:	Fz2-Fz7 double knock-out E8.5 mouse
Organism:	Mus musculus
Experiment type:	Expression profiling by array
Platform:	GPL1261
Pubmed ID:	23095888
Summary & Design:	**Summary:** Fz2Fz7 double knock out mouse microarray (E8.5) **Overall design:** Fz2-Fz7 double KO vs. Fz7 KO

Background corr dist: KL-Divergence = 0.0369, L1-Distance = 0.0220, L2-Distance = 0.0005, Normal std = 0.6370

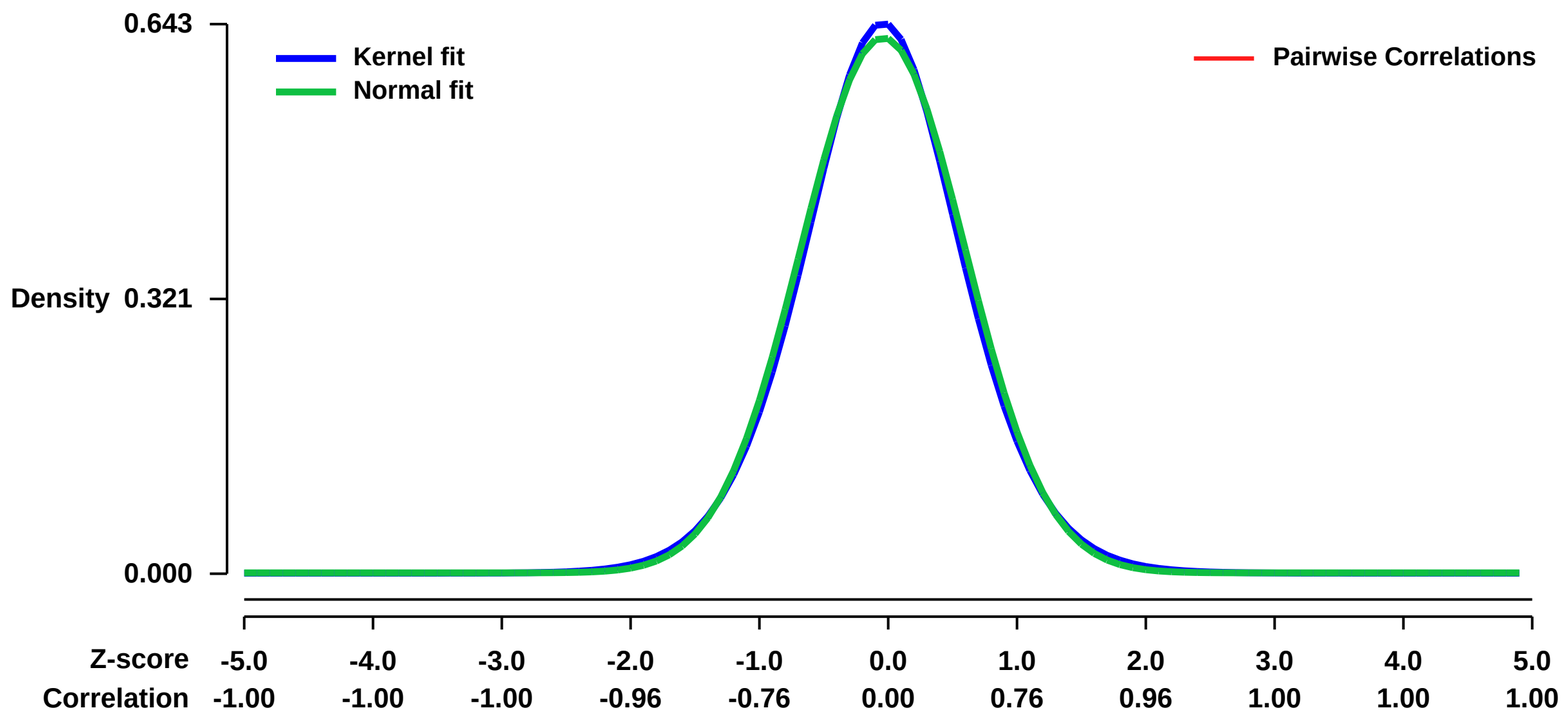

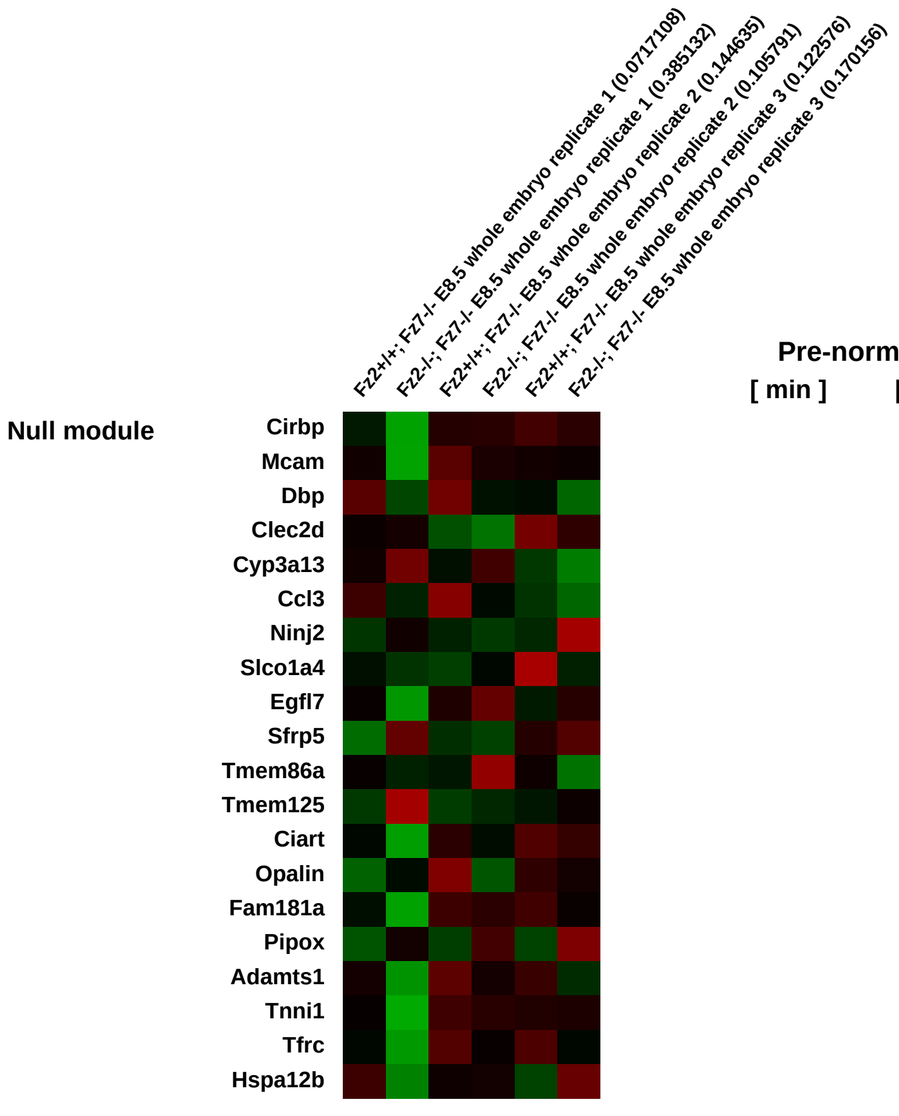

GEO Series "GSE37415" Expression Profiles

Num of samples in this series: 24

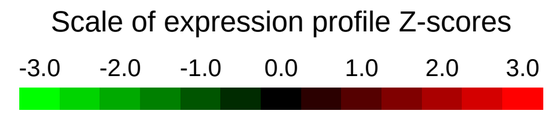

GEO Link:	http://www.ncbi.nlm.nih.gov/geo/query/acc.cgi?acc=GSE37415
Status:	Public on May 18 2012
Title:	Phloridzin reduces blood glucose levels and alters hepatic gene expression in normal BALB/c mice
Organism:	Mus musculus
Experiment type:	Expression profiling by array
Platform:	GPL1261
Pubmed ID:	22538082
Summary & Design:	**Summary:** We previously showed that a diet containing phloridzin suppressed the blood glucose levels in streptozotocin-induced diabetic mice most likely by inhibiting glucose absorption from the small intestine. In this study, we showed that 0.5% and 1% phloridzin diets significantly reduce the blood glucose levels in healthy normal BALB/c mice after 7 days of feeding. To understand the effect of the high continuing intake of dietary phloridzin on normal mouse livers, we analyzed the hepatic gene expressions in mice fed diets containing 0%, 0.1%, 0.5%, or 1% phloridzin for 14 days using DNA microarrays. **Overall design:** Six-week-old male mice were divided into 4 groups of 6 mice each, housed in groups of 3 per cage, and fed a standard purified AIN-93G diet containing 0% (Con), 0.1% (Phlorizin0.1), 0.5% (Phlorizin0.5), or 1% phloridzin (purity > 97%) (Phlorizin1.0) for 2 weeks.

Background corr dist: KL-Divergence = 0.2189, L1-Distance = 0.0354, L2-Distance = 0.0021, Normal std = 0.3236

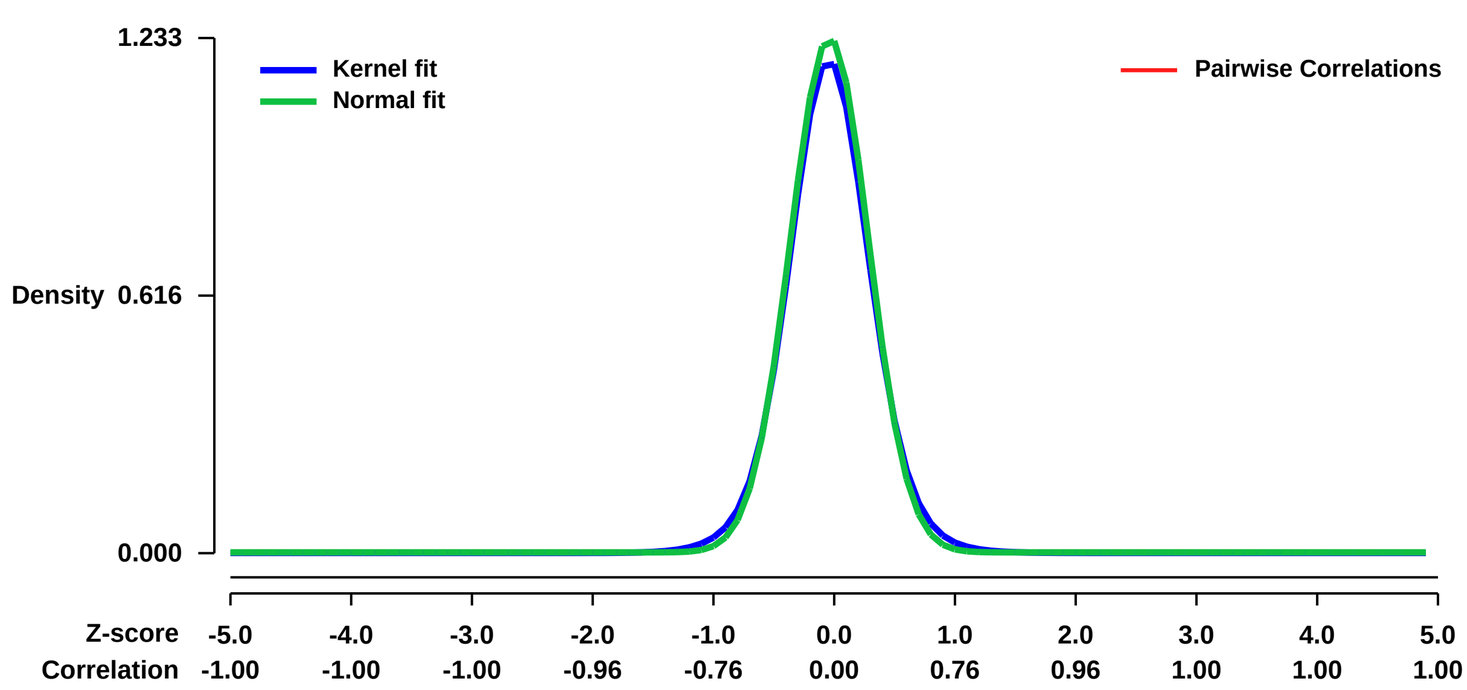

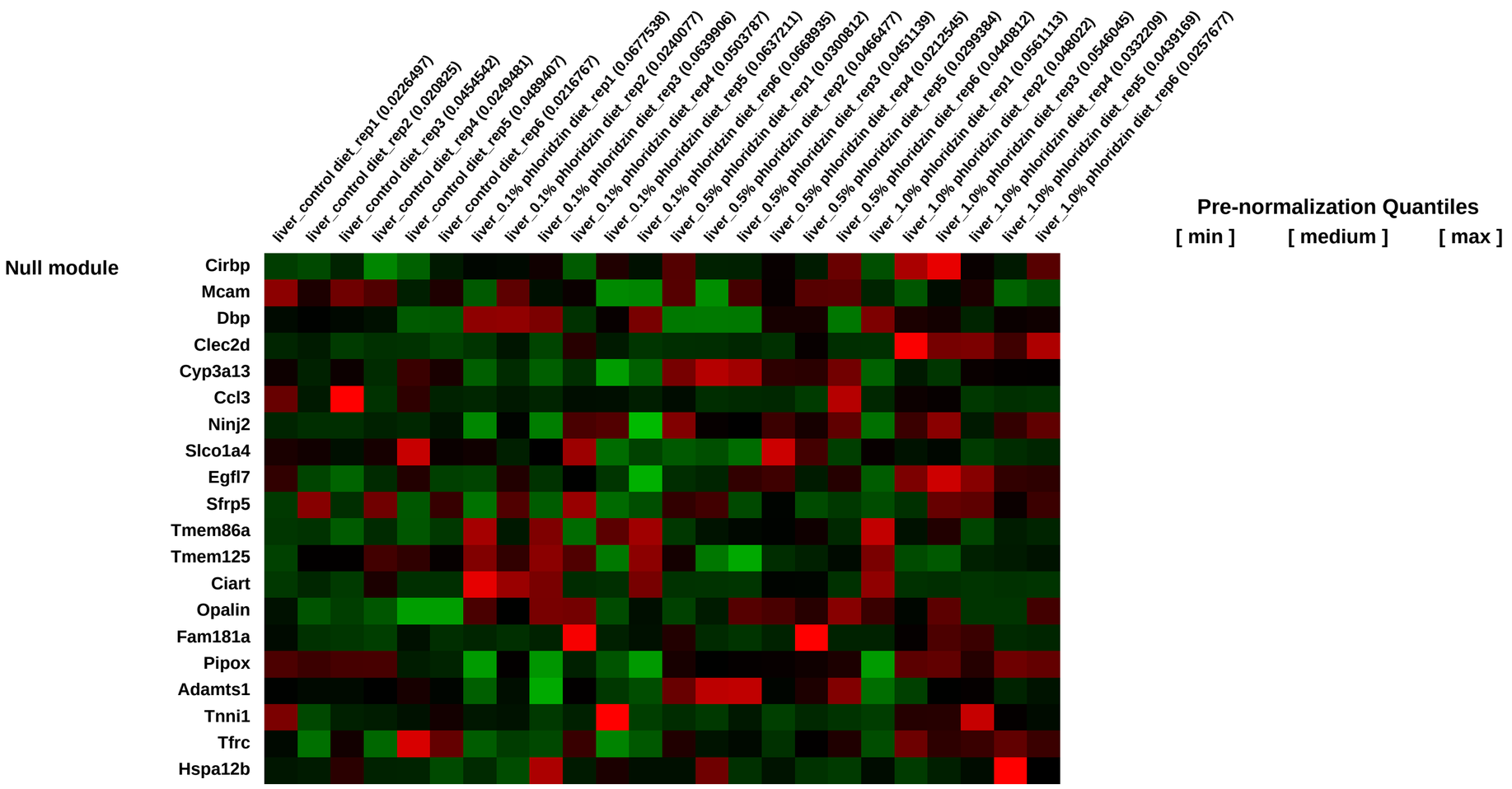

GEO Series "GSE37431" Expression Profiles

Num of samples in this series: 6

Scale of expression profile Z-scores

-3.0 -2.0 -1.0 0.0 1.0 2.0 3.0

GEO Link:	http://www.ncbi.nlm.nih.gov/geo/query/acc.cgi?acc=GSE37431
Status:	Public on Apr 23 2012
Title:	Endothelial cell-enriched genes expression in mouse embryo
Organism:	Mus musculus
Experiment type:	Expression profiling by array
Platform:	GPL1261
Pubmed ID:	22535667
Summary & Design:	**Summary:** The early blood vessels of the embryo and yolk sac in mammals develop by aggregation of de novo forming angioblasts into a primitive vascular plexus, which then undergoes a complex remodeling process. Angiogenesis is also important for disease progression in the adult. However, the precise molecular mechanism of vascular development remains unclear. It is therefore of great interest to determine which genes are specifically expressed in developing endothelial cells.Here, we utilized Flk1-deficient mouse embryos, which lack endothelial cells, to perform a genome-wide survey for genes related to vascular development. **Overall design:** Wild type (WT), Flk1+/GFP and Flk1 KO embryos proper (fetuses) were dissected out at 8.5 dpc. Total RNAs from these embryos were prepared using RNeasy kit. Gene expression analysis was performed by GeneSpring software.

Background corr dist: KL-Divergence = 0.0198, L1-Distance = 0.0371, L2-Distance = 0.0015, Normal std = 0.8138

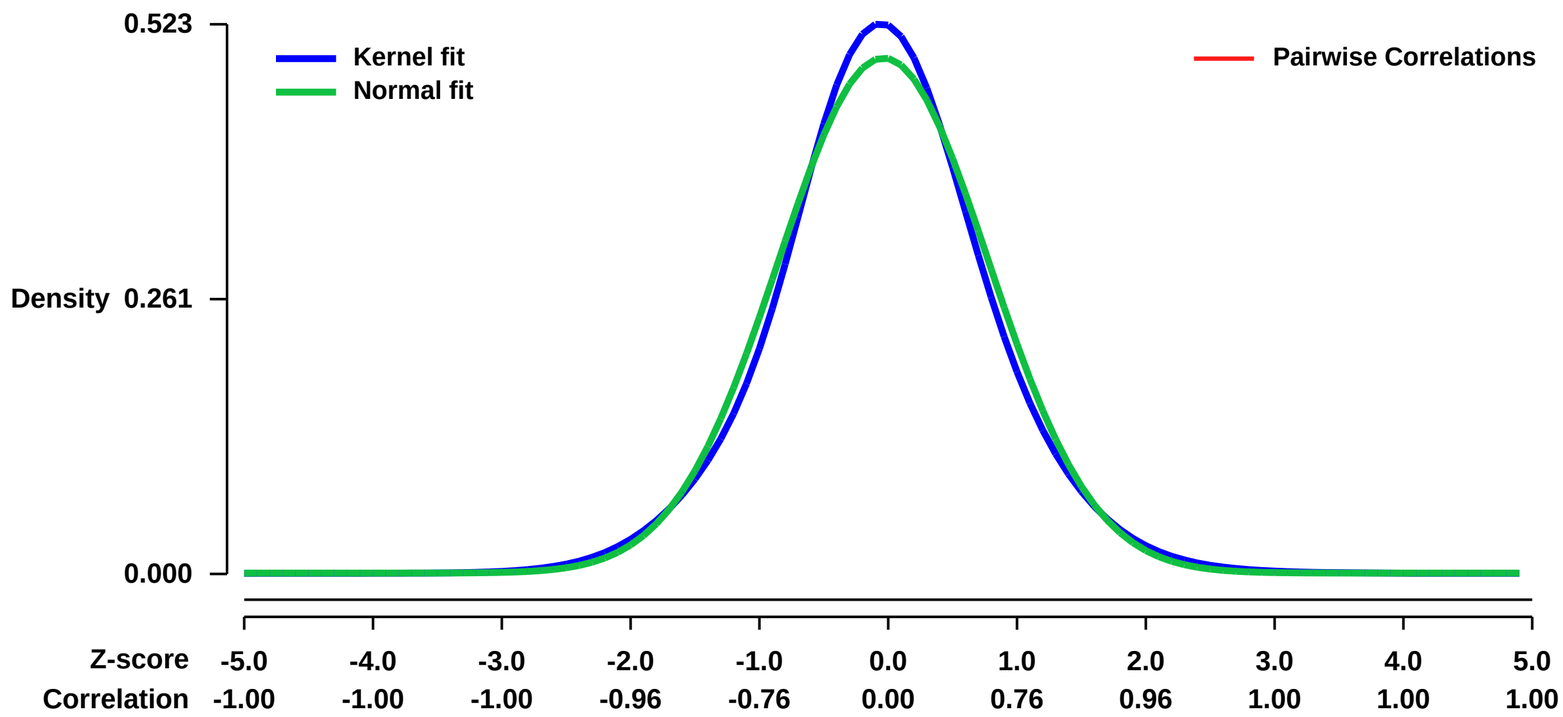

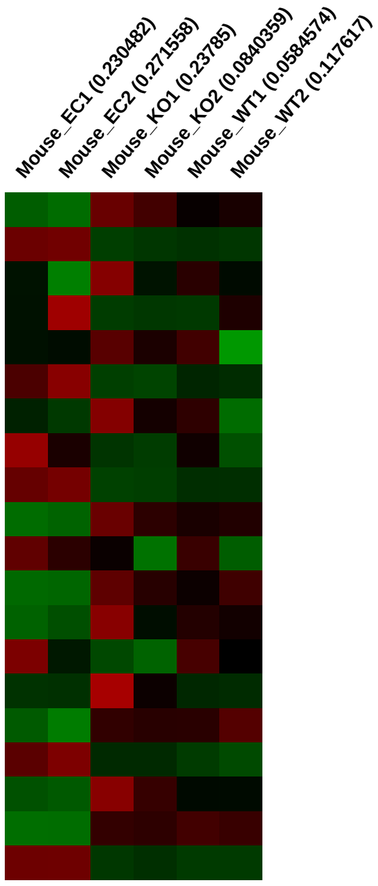

GEO Series "GSE37546" Expression Profiles

Num of samples in this series: 20

Scale of expression profile Z-scores

-3.0 -2.0 -1.0 0.0 1.0 2.0 3.0

GEO Link:	http://www.ncbi.nlm.nih.gov/geo/query/acc.cgi?acc=GSE37546
Status:	Public on Apr 26 2012
Title:	Disturbed Hepatic Carbohydrate Management During High Metabolic Demand in Medium-Chain Acyl-CoA Dehydrogenase (MCAD)-deficient Mice
Organism:	Mus musculus
Experiment type:	Expression profiling by array
Platform:	GPL1261
Pubmed ID:	18459129
Summary & Design:	**Summary:** Medium-chain acyl-coenzyme A (CoA) dehydrogenase (MCAD) catalyzes crucial steps in mitochondrial fatty acid oxidation, a process that is of key relevance for maintenance of energy homeostasis, especially during high metabolic demand. To gain insight into the metabolic consequences of MCAD deficiency under these conditions, we compared hepatic carbohydrate metabolism in vivo in wild-type and MCAD-/- mice during fasting and during a lipopolysaccharide (LPS)-induced acute phase response (APR). MCAD-/- mice did not become more hypoglycemic on fasting or during the APR than wild-type mice did. Nevertheless, microarray analyses revealed increased hepatic peroxisome proliferator-activated receptor gamma coactivator-1a (Pgc-1a) and decreased peroxisome proliferator-activated receptor alpha (Ppar a) and pyruvate dehydrogenase kinase 4 (Pdk4) expression in MCAD-/- mice in both conditions,suggesting altered control of hepatic glucose metabolism. Quantitative flux measurements revealed that the de novo synthesis of glucose-6-phosphate (G6P) was not affected on fasting in MCAD-/- mice. During the APR, however, this flux was significantly decreased (-20%) in MCAD-/- mice compared with wild-type mice. Remarkably, newly formed G6P was preferentially directed toward glycogen in MCAD-/- mice under both conditions. Together with diminished de novo synthesis of G6P, this led to a decreased hepatic glucose output during the APR in MCAD-/- mice; de novo synthesis of G6P and hepatic glucose output were maintained in wild-type mice under both conditions. APR-associated hypoglycemia, which was observed in wild-type mice as well as MCAD-/- mice, was mainly due to enhanced peripheral glucose uptake. Conclusion: Our data demonstrate that MCAD deficiency in mice leads to specific changes in hepatic carbohydrate management on exposure to metabolic stress. This deficiency, however, does not lead to reduced de novo synthesis of G6P during fasting alone, which may be due to the existence of compensatory mechanisms or limited rate control of MCAD in murine mitochondrial fatty acid oxidation. **Overall design:** Total RNA obtained from Liver (20 samples) , where comparing 4 groups, consisting out of 5 biological replicates, all groups where fasted for 12 hrs, and half of them where injected with LPS (100ug/20gr BW) or vehicle

Background corr dist: KL-Divergence = 0.1254, L1-Distance = 0.0278, L2-Distance = 0.0011, Normal std = 0.4081

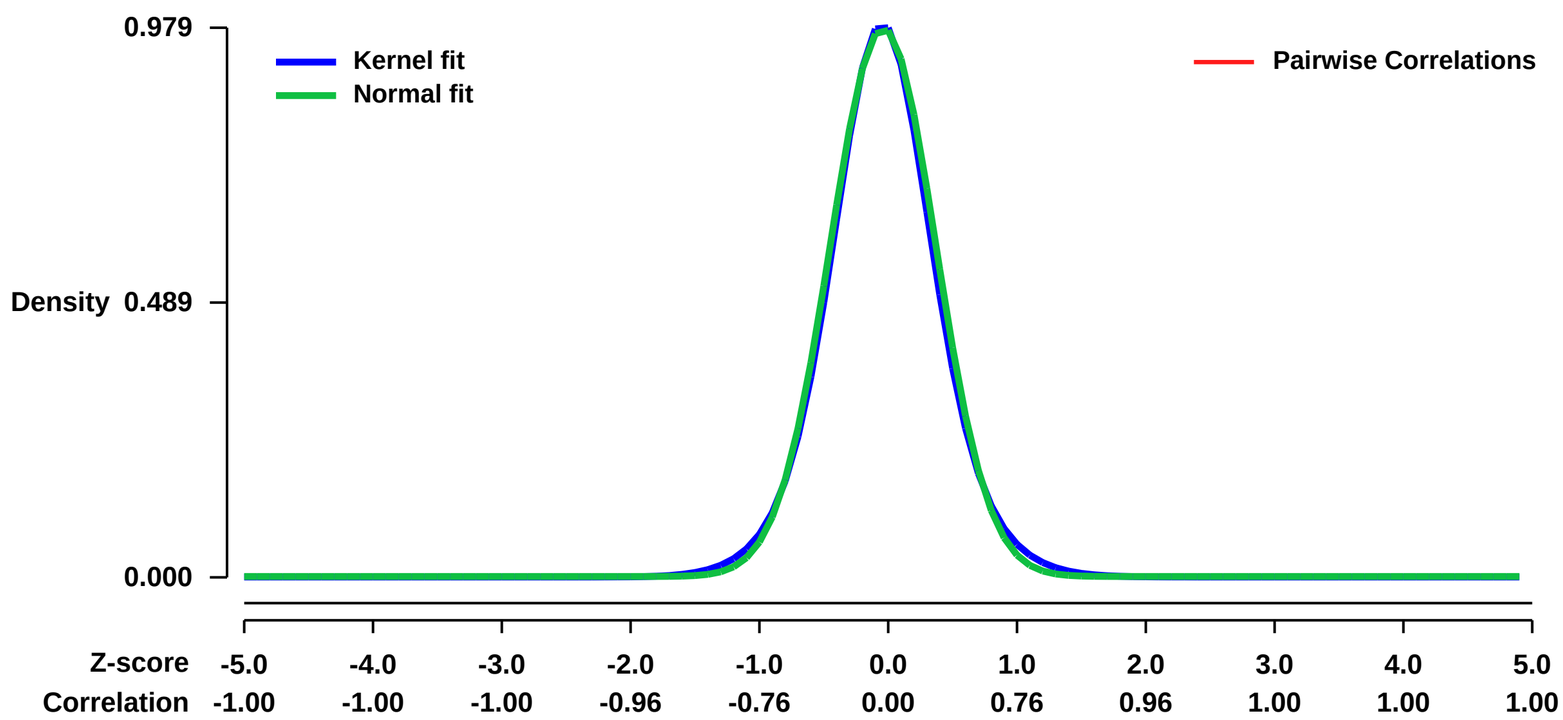

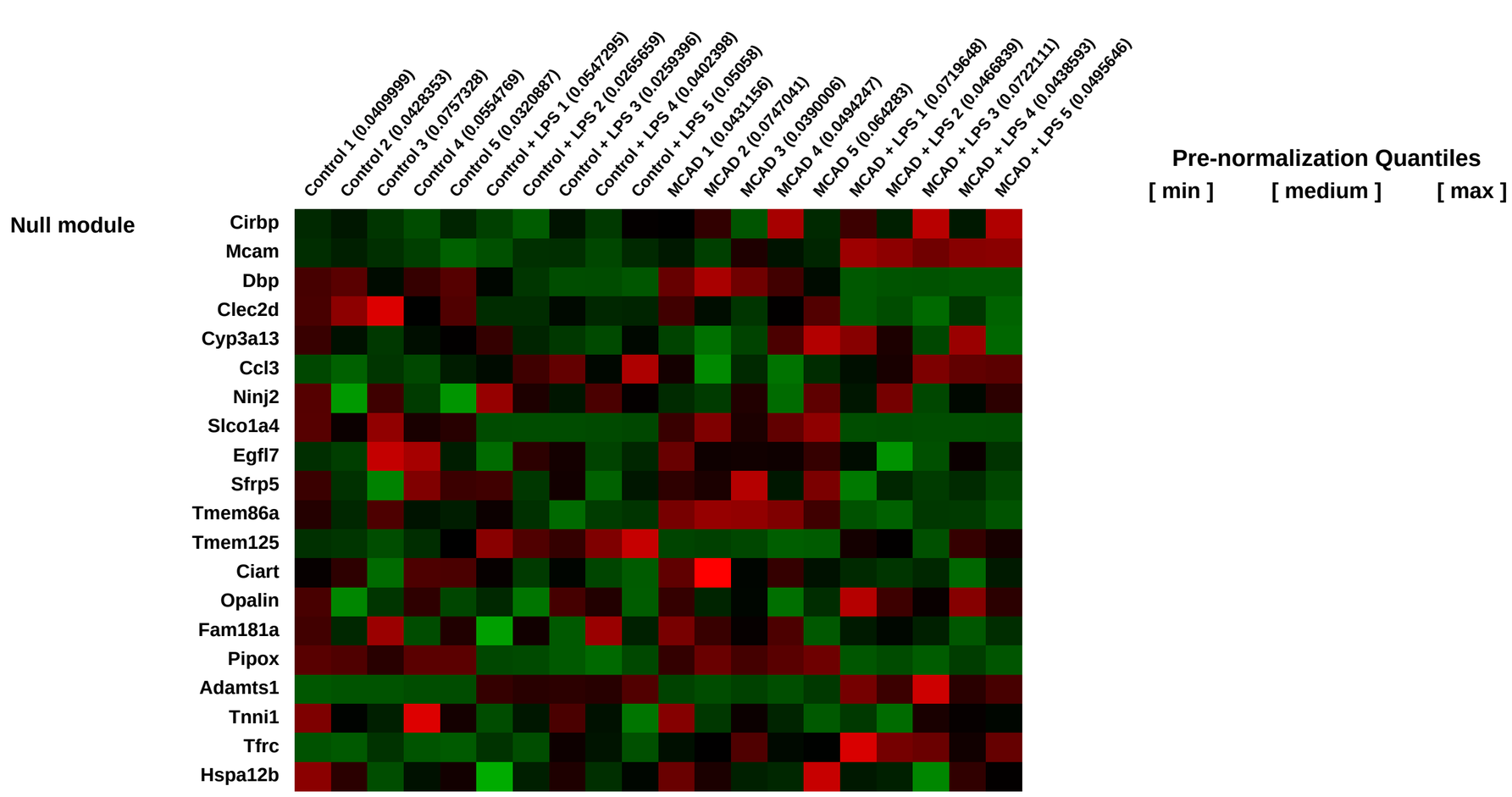

GEO Series "GSE37563" Expression Profiles

Num of samples in this series: 6

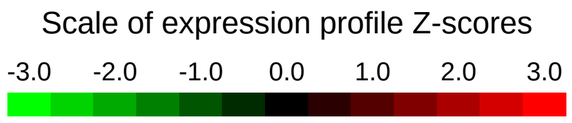

GEO Link:	http://www.ncbi.nlm.nih.gov/geo/query/acc.cgi?acc=GSE37563
Status:	Public on Sep 05 2012
Title:	In vivo gene expression data from wild type and CTLA-4 KO 5C.C7 T cells
Organism:	Mus musculus
Experiment type:	Expression profiling by array
Platform:	GPL1261
Pubmed ID:	22753941
Summary & Design:	**Summary:** CTLA-4 is thought to inhibit effector T cells both intrinsically, by competing with CD28 for B7 ligands, and extrinsically, through the action of regulatory T cells. We studied in vivo responses of normal and CTLA-4-deficient antigen-specific murine effector CD4+ T cells. In order to do these studies in a physiological model of immunity to foreign antigen, we transferred small numbers of congenically marked RAG2-deficient 5C.C7 T cells with either a normal or knockout allele of CTLA-4 into normal syngeneic B10.A recipient mice. The T cells were then activated by immunization with MCC peptide and LPS. To look for transcriptional signatures of negative regulation of T cell responses by CTLA-4, we used microarray analysis to compare transcripts in wild type and CTLA-4 KO 5C.C7 T cells four days after immunization. This is the first instance in which differences are observed in extent of accumulation of wild type and CTLA-4 KO 5C.C7 T cells. #!# **Overall design:** To compare the gene expression profile between wild type and CTLA-4 KO adoptively transferred T cells 4 days after immunization.

Background corr dist: KL-Divergence = 0.0451, L1-Distance = 0.0197, L2-Distance = 0.0004, Normal std = 0.5927

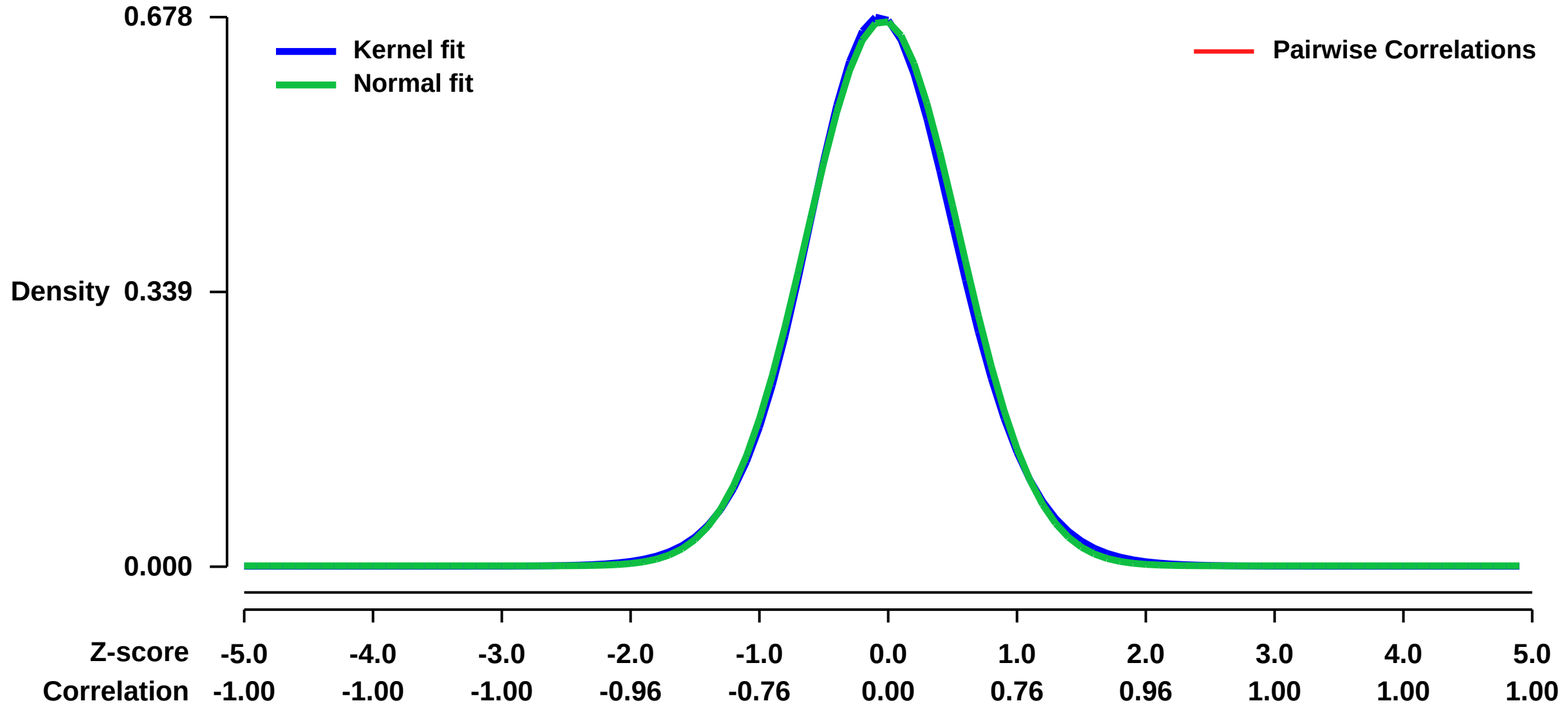

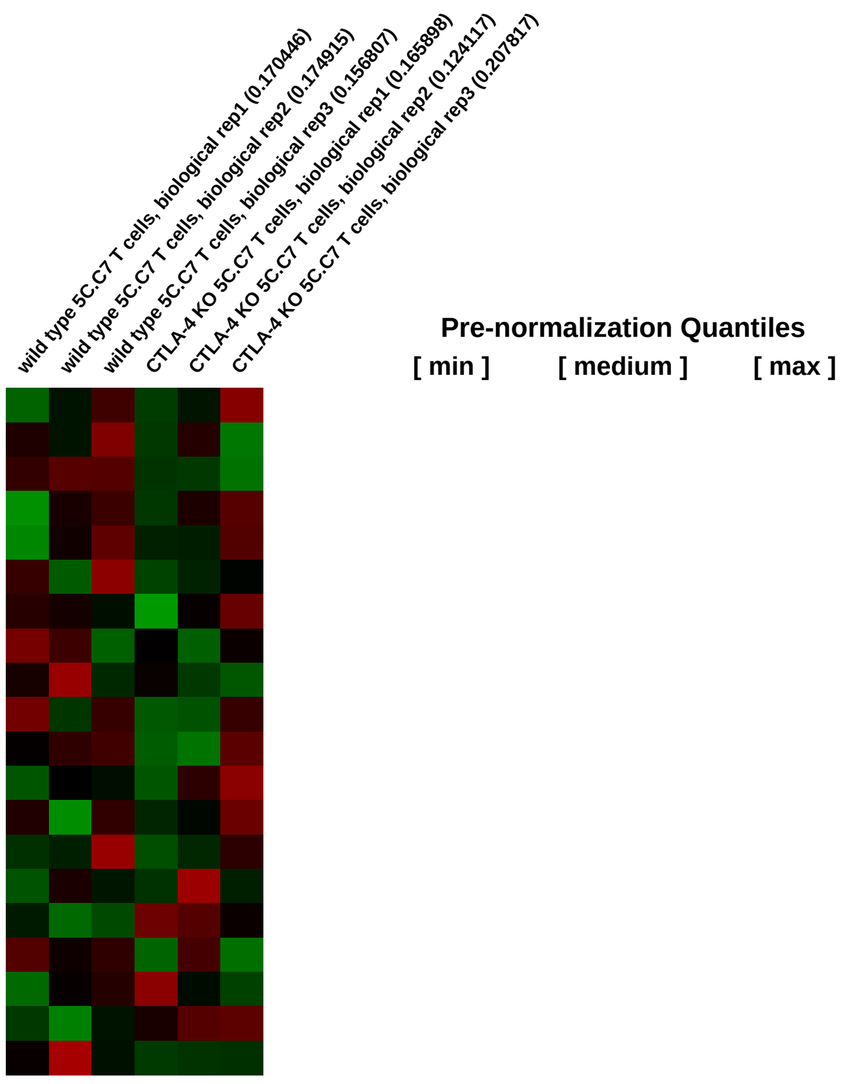

GEO Series "GSE37658" Expression Profiles

Num of samples in this series: 6

Scale of expression profile Z-scores

-3.0 -2.0 -1.0 0.0 1.0 2.0 3.0

GEO Link:	http://www.ncbi.nlm.nih.gov/geo/query/acc.cgi?acc=GSE37658
Status:	Public on Jul 04 2012
Title:	Gene expression analysis of inducible ES cells overexpressing Etv2 (induced for 12 hours at day 3 of differentiation)
Organism:	Mus musculus
Experiment type:	Expression profiling by array
Platform:	GPL1261
Pubmed ID:	22628281
Summary & Design:	**Summary:** During embryogenesis, the endothelial and the hematopoietic lineages first appear during gastrulation in the blood island of the yolk sac. We have previously reported that an Ets variant gene 2 (Etv2/ER71) mutant embryo lacks hematopoietic and endothelial lineages, however, the precise roles of Etv2 in yolk sac development remains unclear. We carried out a transcriptome analysis using an ES cell line that can inducibly express Etv2. Cells were induced for 12 hours at day 3 of differentiation. **Overall design:** An ES cell line (dervied from mouse of background strain 129P2/Ola) with a doxycycline inducible expression casette of Etv2 (ER71 A2Lox.cre) was differentiated in hanging drops. At 3 days of differentiation, cells were treated with doxycycline for 12 hours, and subsequently Flk1(+) cells were sorted. Experiment was done in triplicate and untreated cells were used for control.

Background corr dist: KL-Divergence = 0.0250, L1-Distance = 0.0262, L2-Distance = 0.0010, Normal std = 0.7073

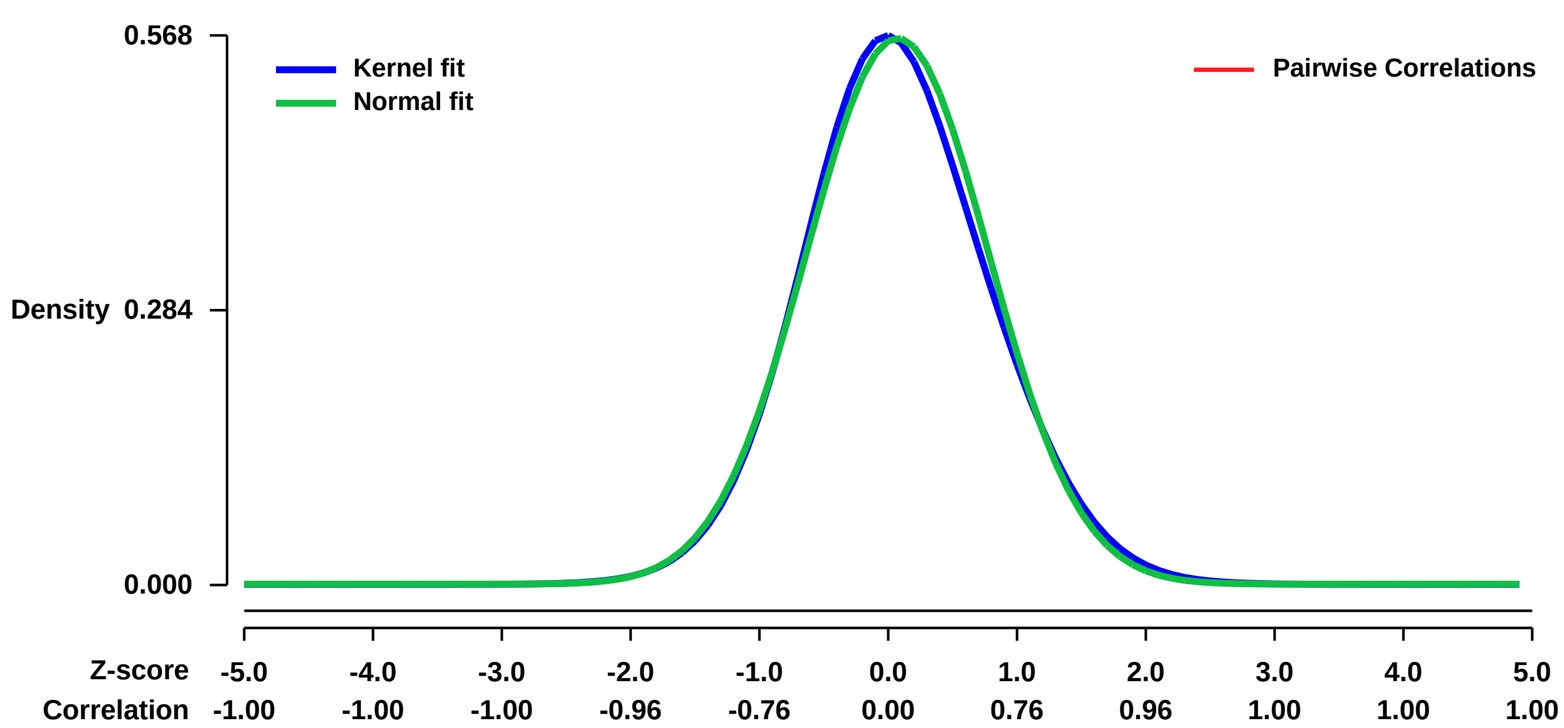

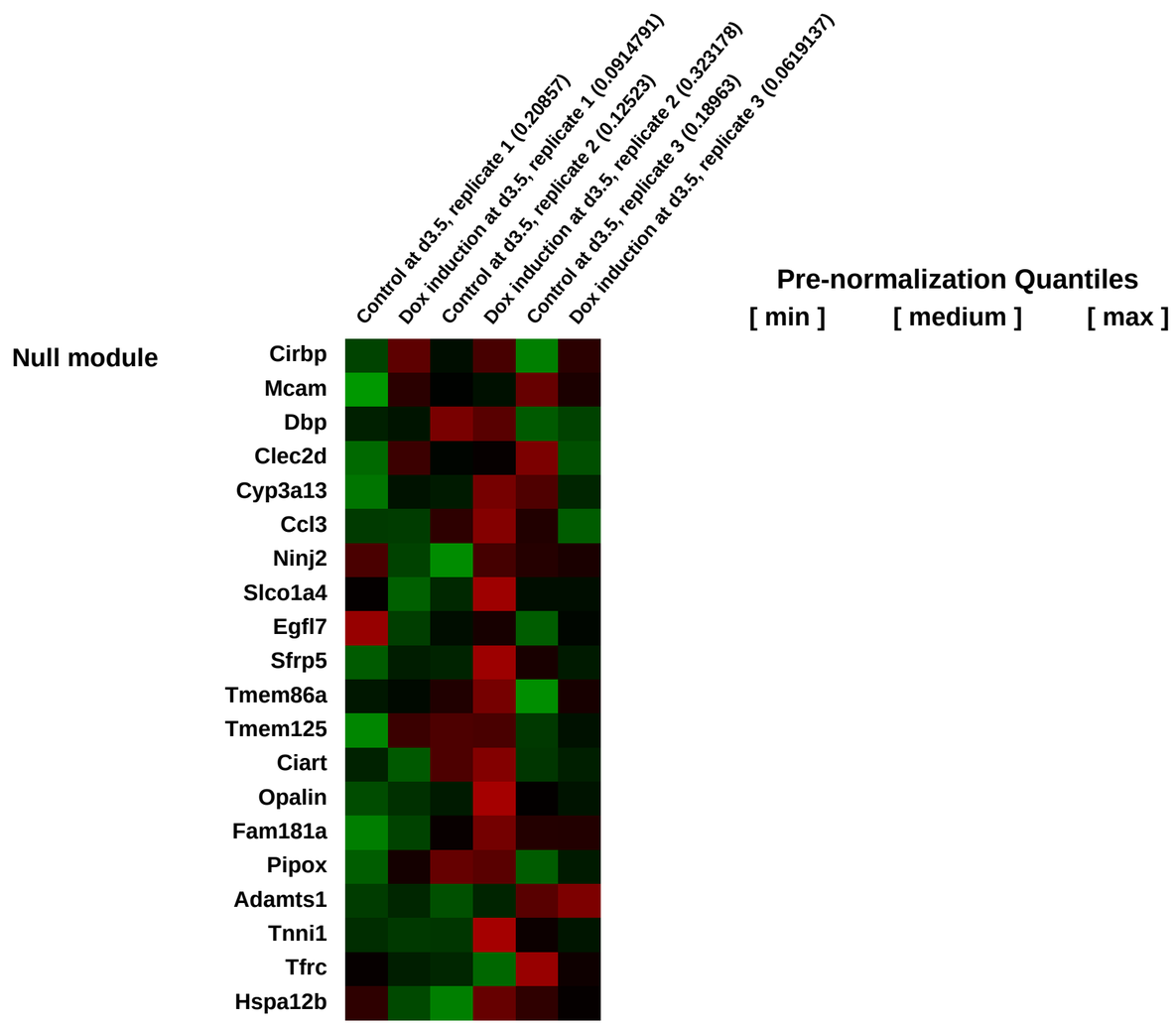

GEO Series "GSE37676" Expression Profiles

Num of samples in this series: 6

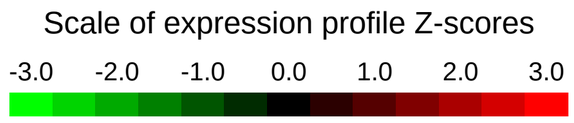

GEO Link:	http://www.ncbi.nlm.nih.gov/geo/query/acc.cgi?acc=GSE37676
Status:	Public on May 02 2012
Title:	Expression data from control and Ascorbic Acid (AA) stimulated Mc-3T3-E1 osteoblasts
Organism:	Mus musculus
Experiment type:	Expression profiling by array
Platform:	GPL1261
Pubmed ID:	23740245
Summary & Design:	**Summary:** Despite advances in investigating functional aspects of osteoblast (OB) differentiation, especially studies on how bone proteins are deposited and mineralized, there has been little research on the intracellular trafficking of bone proteins during OB differentiation. Collagen synthesis and secretion is markedly upregulated upon Ascorbic Acid (AA) stimulation. Understanding the mechanism by which collagen is mobilized in specialized OB cells is important for both basic cell biology and diseases involving defects in bone secretion and deposition. RabGTPases are major regulators on protein trafficking throughout the cell. In this study, we identified the Rab GTPases that are upregulated during 5-day AA differentiation of OBs using microarray analysis, namely Rab1, Rab3d and Rab27b. We used microarrays to detail the global programme of gene expression underlying procollagen production and trafficking and identified up-regulated genes during this process. **Overall design:** Control Mc3T3-E1 cells and 5 day Ascorbic Acid stimulated cells were processed for RNA extraction and hybridization on Affymetrix microarrays.

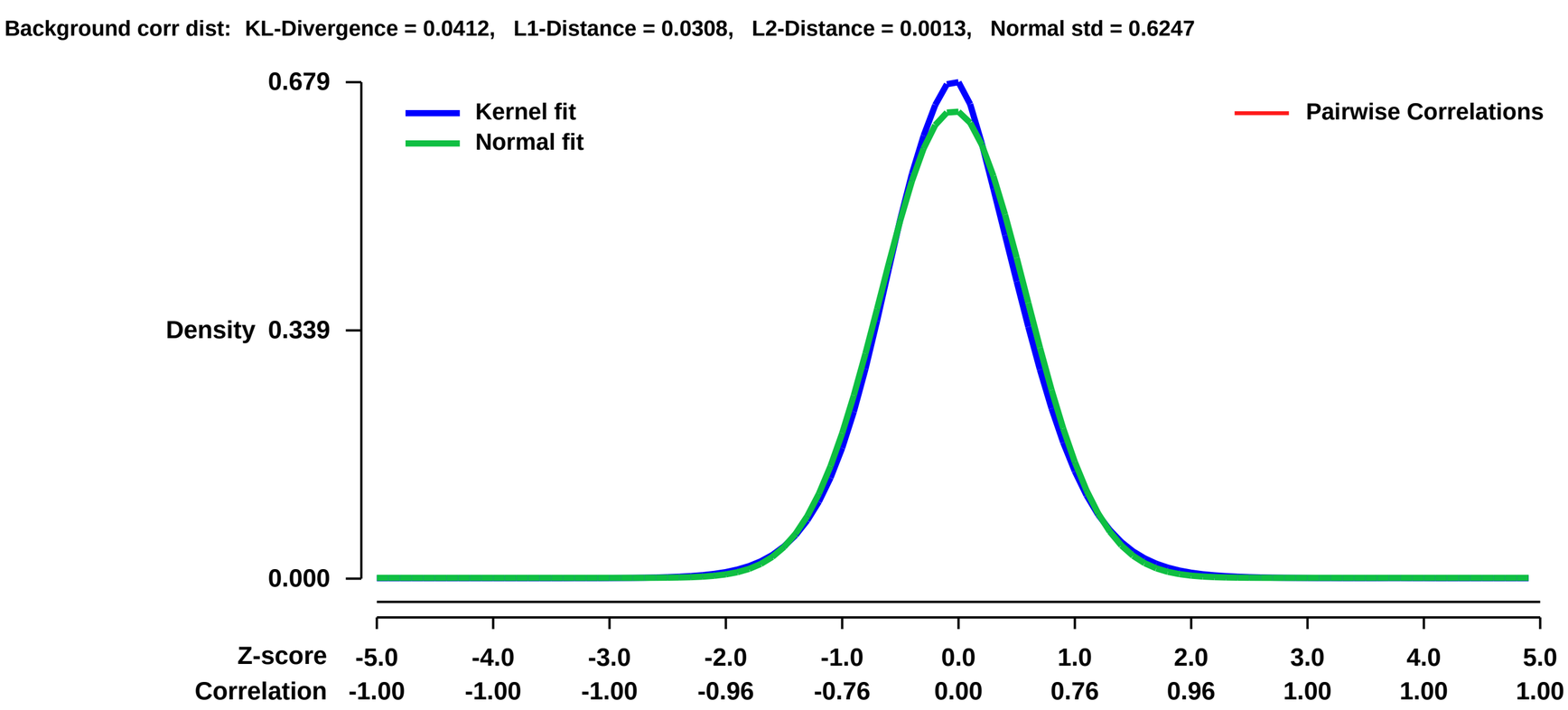

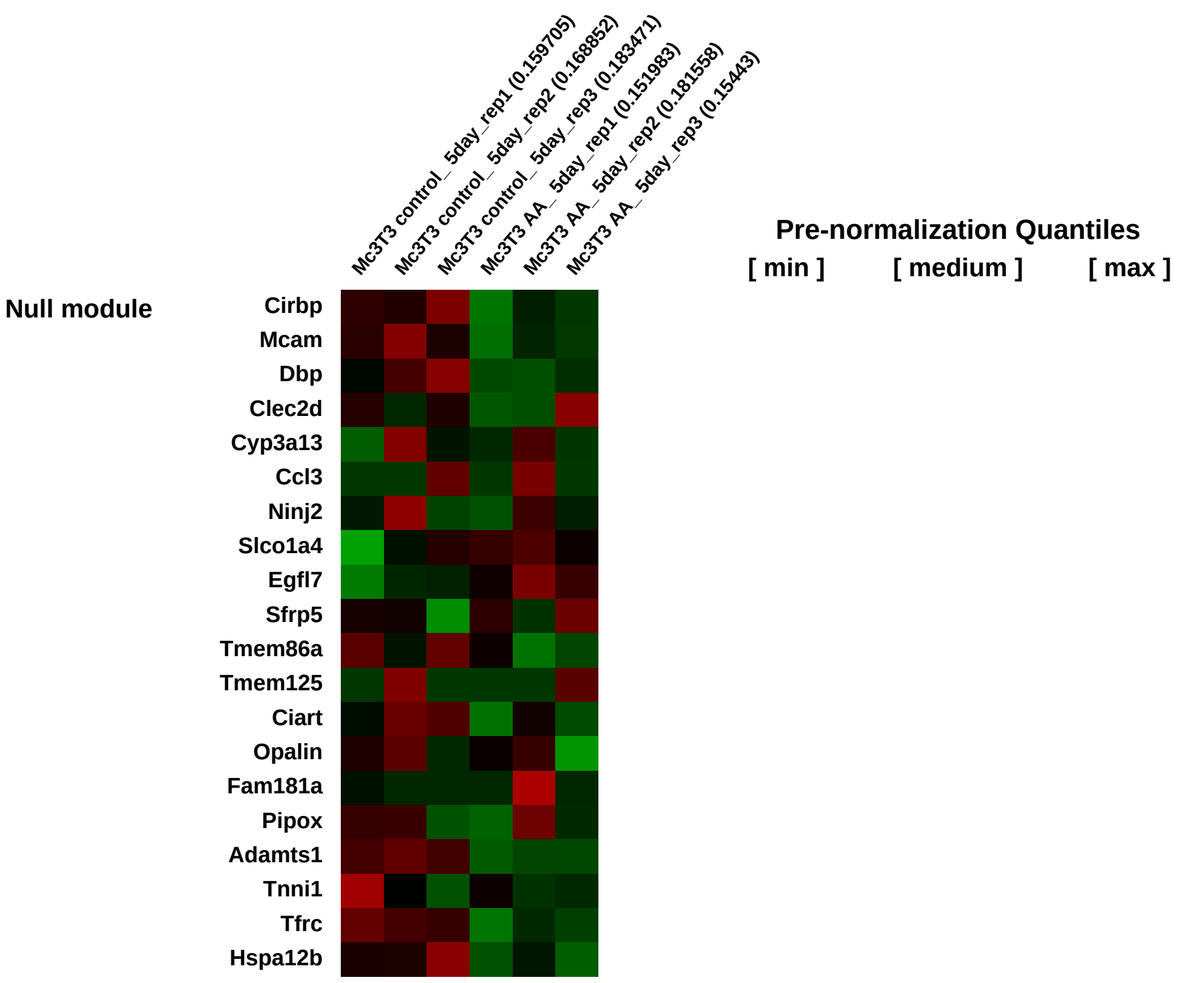

GEO Series "GSE37975" Expression Profiles

Num of samples in this series: 8

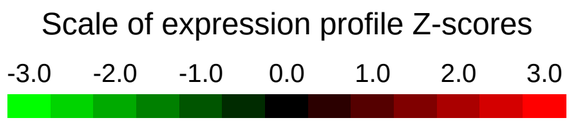

GEO Link:	http://www.ncbi.nlm.nih.gov/geo/query/acc.cgi?acc=GSE37975
Status:	Public on Jul 18 2012
Title:	Comparison of matched primary and metastasis 4T1.2 syngeneic mammary tumor model of spontaneous bone metastasis
Organism:	Mus musculus
Experiment type:	Expression profiling by array
Platform:	GPL1261
Pubmed ID:	22820642
Summary & Design:	**Summary:** Breast cancer metastasis to bone is a critical determinant of long-term survival after treatment of primary tumors. We used a mouse model of spontaneous bone metastasis to determine new molecular mechanisms. Differential transcriptome comparisons of primary and metastatic tumor cells revealed that a substantial set of genes suppressed in bone metastases were highly enriched for promoter elements for the type I interferon (IFN) regulatory factor, Irf7, itself suppressed in mouse and human metastases. The critical function of the Irf7 pathway was demonstrated by restoration of exogenous Irf7 or systemic interferon administration, which significantly reduced bone metastases and prolonged metastasis-free survival. Using mice deficient in the type I receptor (Ifnar1-/-) or mature B, T and NK cell responses (NOD Scid IL-2r‚‡-/- mice), we demonstrated that Irf7-driven suppression of metastasis was reliant on IFN signaling to host immune cells. Metastasis suppression correlated with decreased accumulation of myeloid-derived suppressor cells and increased CD4++, CD8 T cells and NK cells in the peripheral blood and was reversed by depletion of CD8+ cells and NK cells. Clinical importance of our findings was demonstrated as increased primary tumor Irf7 expression predicted prolonged bone and lung metastasis-free survival. Thus we report for the first time, a novel innate immune pathway, intrinsic to breast cancer cells, whose suppression in turn restricts systemic immunosurveillance to enable metastasis. This pathway may constitute a novel therapeutic target for restricting breast cancer metastases. **Overall design:** Microarrays were used to profile transcriptional alterations inherent in tumor cells growing in bone when compared to matched primary tumor cells in the 4T1.2 murine mammary tumor model. Primary and metastasized tumor were isolated from the same mouse with 4 independent biological replicates.

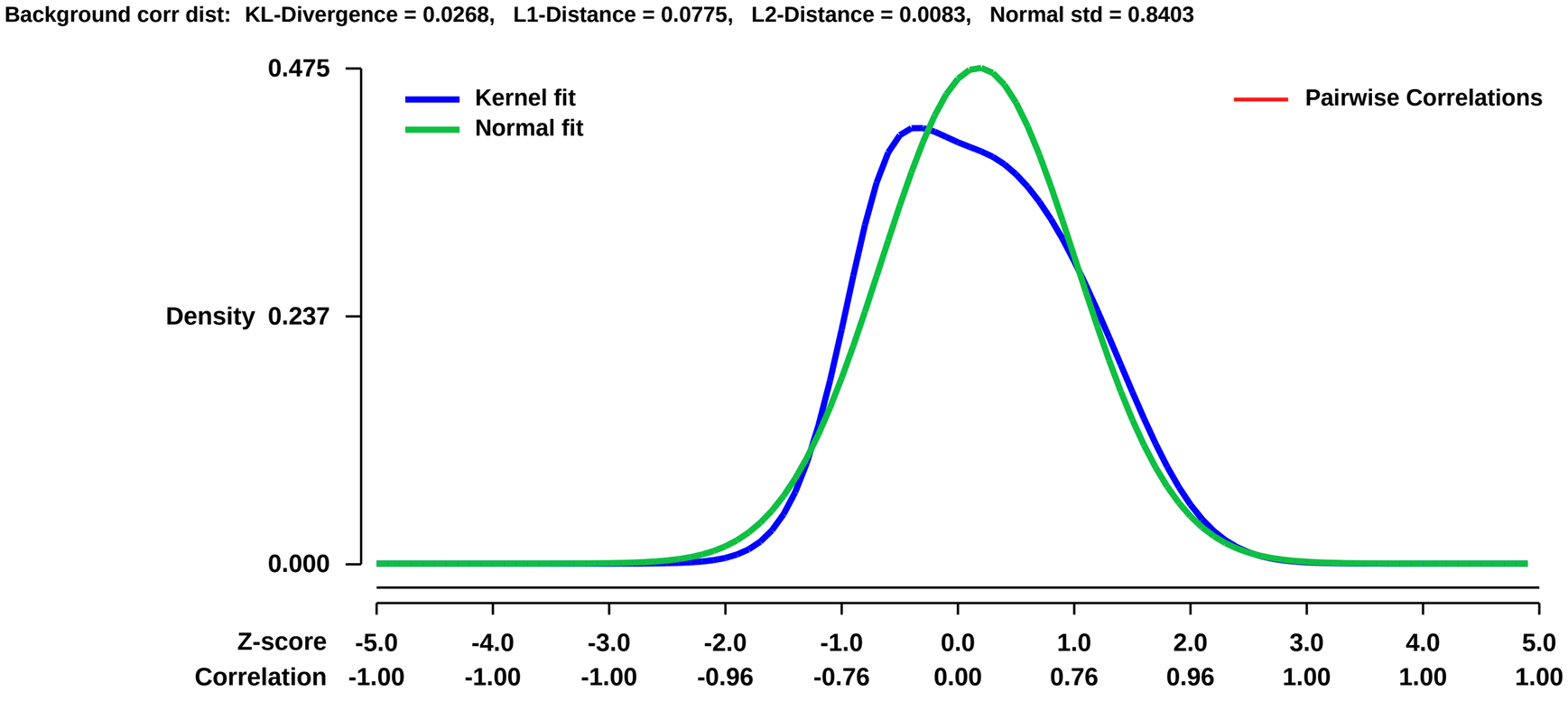

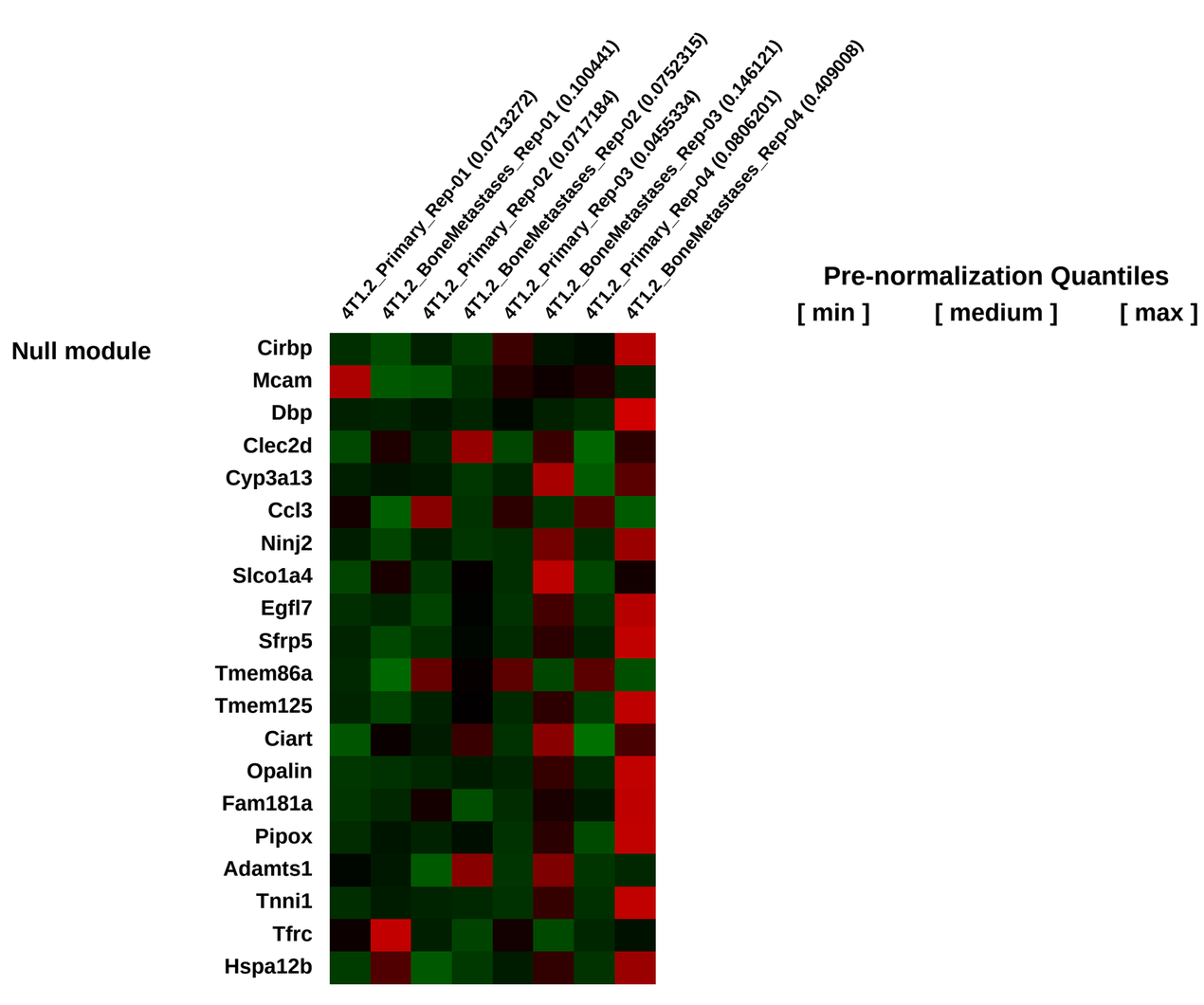

GEO Series "GSE38001" Expression Profiles

Num of samples in this series: 12

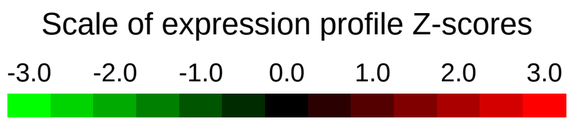

GEO Link:	**http://www.ncbi.nlm.nih.gov/geo/query/acc.cgi?acc=GSE38001**
Status:	**Public on Jun 19 2012**
Title:	**Polyglutamine expanded huntingtin dramatically alters the genome-wide binding of HSF1 (mRNA)**
Organism:	**Mus musculus**
Experiment type:	**Expression profiling by array**
Platform:	**GPL1261**
Pubmed ID:	
Summary & Design:	**Summary:** **In Huntingtonâ s disease (HD), polyglutamine expansions in the huntingtin (Htt) protein cause subtle changes in cellular functions that, over-time, lead to neurodegeneration and death. Studies have indicated that activation of the heat shock response can reduce many of the effects of mutant Htt in disease models, suggesting that the heat shock response is impaired in the disease. To understand the basis for this impairment, we have used genome-wide chromatin immunoprecipitation followed by massively parallel sequencing (ChIP-Seq) to examine the effects of mutant Htt on the master regulator of the heat shock response, HSF1. We find that, under normal conditions, HSF1 function is highly similar in cells carrying either wild-type or mutant Htt. However, polyQ-expanded Htt severely blunts the HSF1-mediated stress response. Surprisingly, we find that the HSF1 targets most affected upon stress are not directly associated with proteostasis, but with cytoskeletal binding, focal adhesion and GTPase activity. Our data raise the intriguing hypothesis that the accumulated damage from life-long impairment in these stress responses may contribute significantly to the etiology of Huntington's disease.** **Overall design:** **Affymetrix MG430 2.0 expression levels of wild-type (STHdhQ7/Q7) and mutant (STHdhQ111/Q111) striatal cells under growth condition (33˚C) and upon heat shock (42˚C for six hours)**

Background corr dist: KL-Divergence = 0.0496, L1-Distance = 0.0405, L2-Distance = 0.0027, Normal std = 0.5782

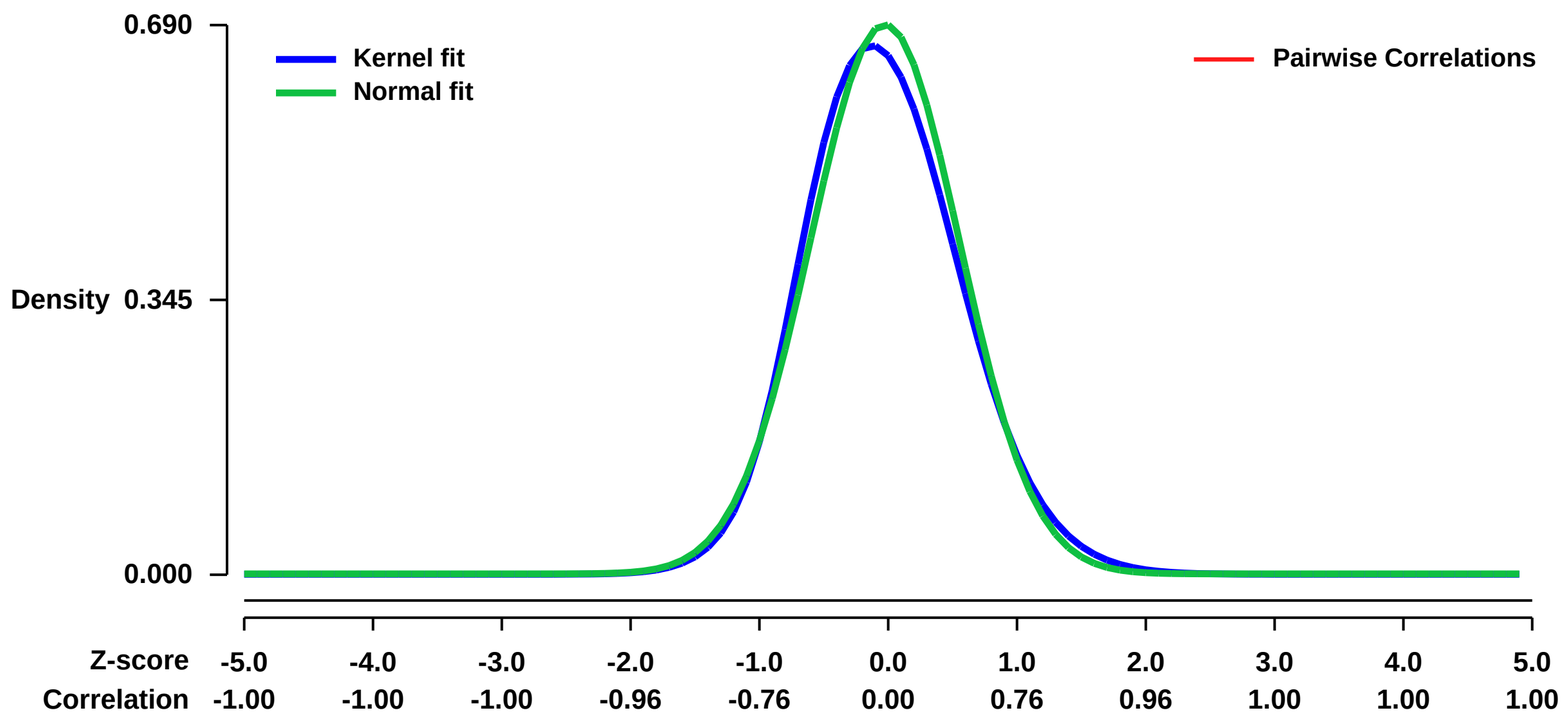

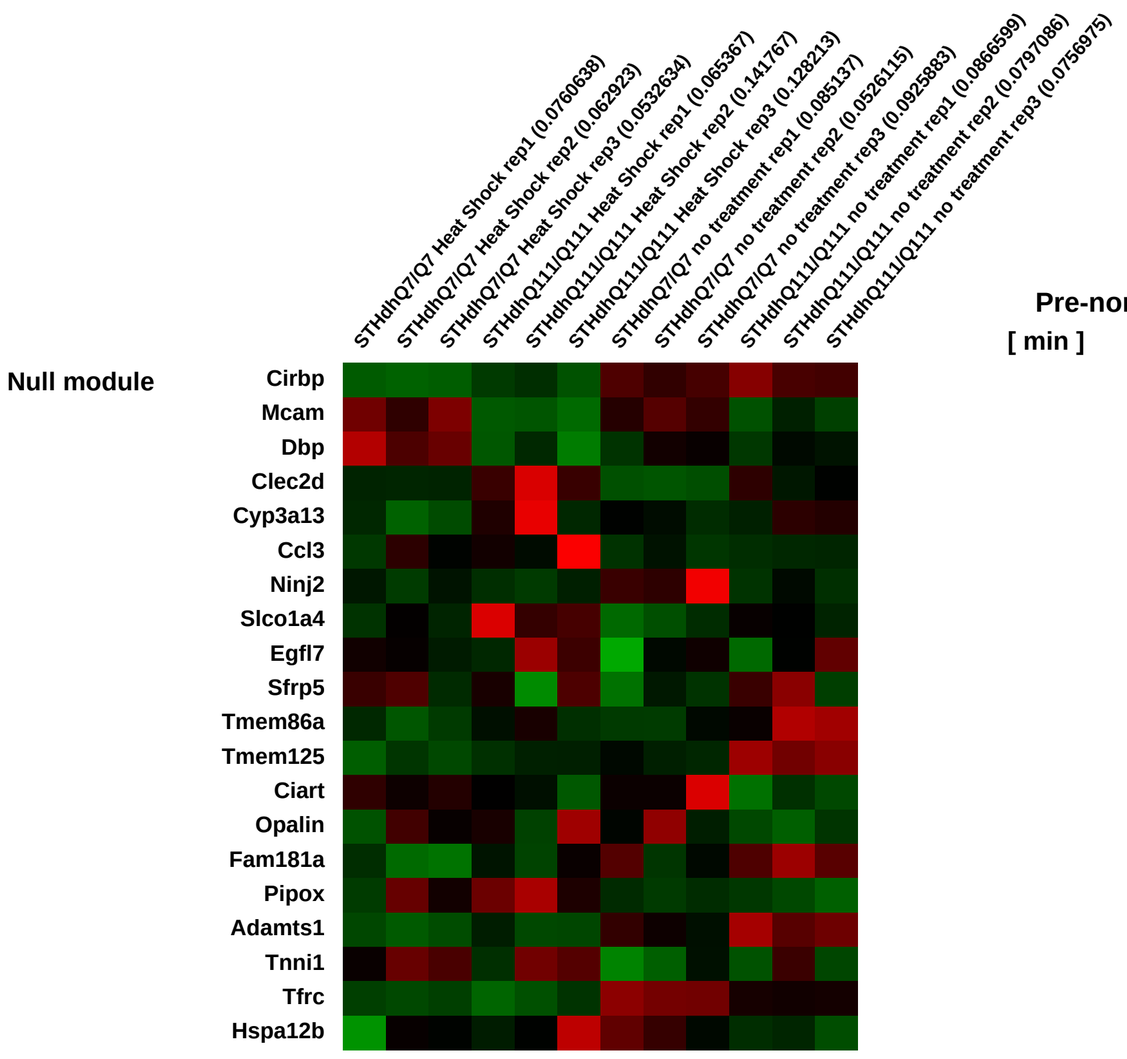

GEO Series "GSE38031" Expression Profiles

Num of samples in this series: 8

Scale of expression profile Z-scores

-3.0 -2.0 -1.0 0.0 1.0 2.0 3.0

GEO Link:	http://www.ncbi.nlm.nih.gov/geo/query/acc.cgi?acc=GSE38031
Status:	Public on Jul 25 2013
Title:	DNA damage-induced differentiation of NSC
Organism:	Mus musculus
Experiment type:	Expression profiling by array
Platform:	GPL1261
Pubmed ID:	24052948
Summary & Design:	**Summary:** Murine ES-derived neural stem cells (NSC) were not irradiated (ctrl) or irradiated with 10Gy and cultured for 7 days (irr). The goal was to study the gene expression changes in NSC at d7 after irradiation. **Overall design:** Total RNA was extracted from 4 ctrl and 4 irr samples (biological quadruplicates).

Background corr dist: KL-Divergence = 0.0114, L1-Distance = 0.0339, L2-Distance = 0.0011, Normal std = 0.9128

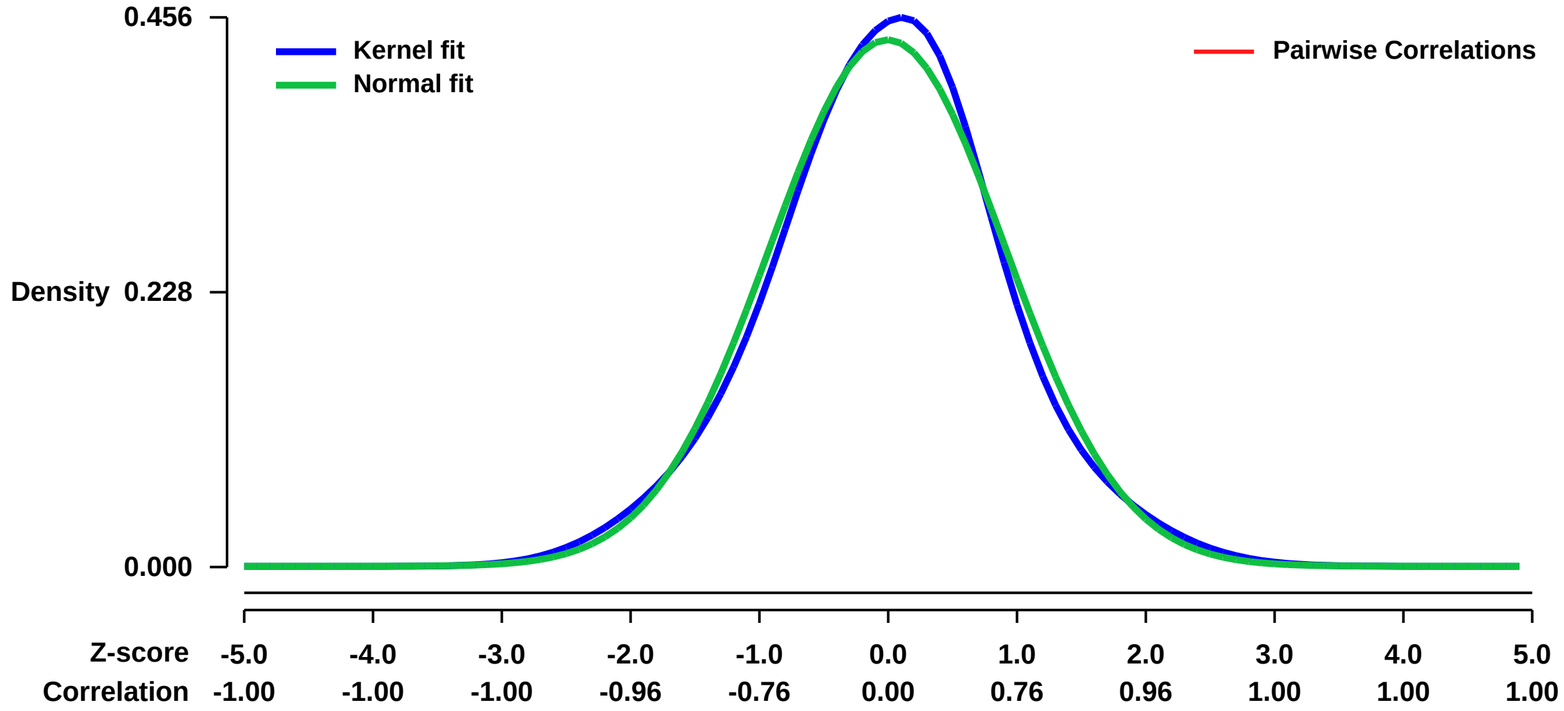

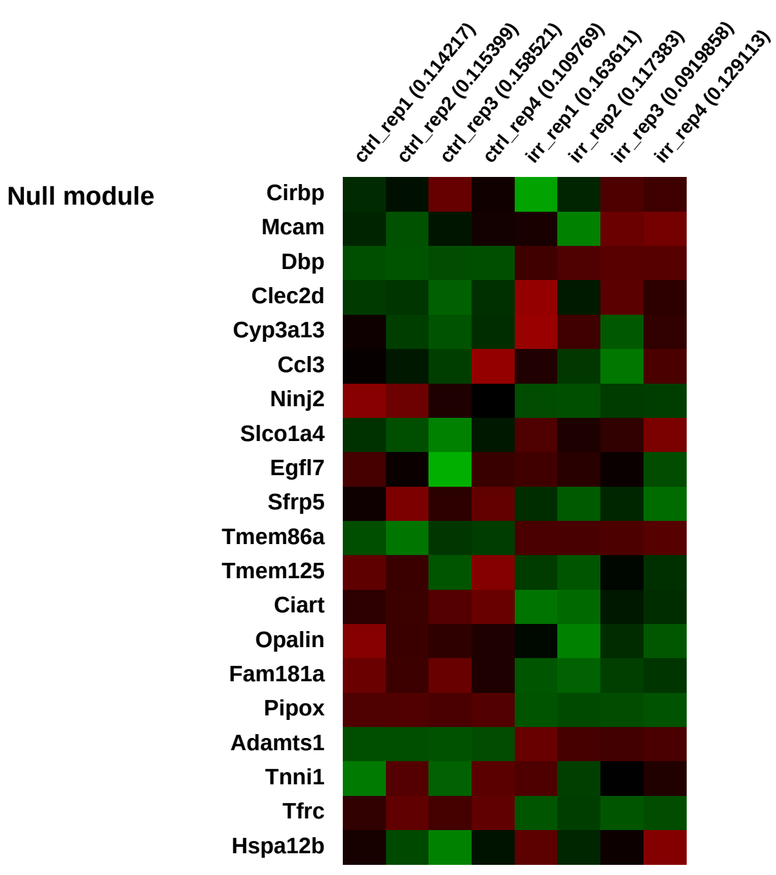

GEO Series "GSE38044" Expression Profiles

Num of samples in this series: 6

Scale of expression profile Z-scores

-3.0 -2.0 -1.0 0.0 1.0 2.0 3.0

GEO Link:	http://www.ncbi.nlm.nih.gov/geo/query/acc.cgi?acc=GSE38044
Status:	Public on Mar 13 2013
Title:	Gene activation by Rag-mediated DNA double-strand breaks in G1-phase murine pre-B cells
Organism:	Mus musculus
Experiment type:	Expression profiling by array
Platform:	GPL1261
Pubmed ID:	23496831
Summary & Design:	**Summary:** The objective is to identify genes that are differentially expressed following the introduction of DNA double-strand breaks (DSBs) by the Rag proteins in murine pre-B cells. Cells lacking Artemis are used since the Rag-induced DSBs will not be repaired, and thus, will provide a continuous stimulus to the cell. **Overall design:** Murine v-abl-transformed pre-B cells were treated with 3 uM STI571 for 48 hours. Cell types included RAG-2-deficient (3 biological replicates) and Artemis-deficient (3 biological replicates) G1-phase pre-B cells. Each sample was hybridized once using Affymetrix Mouse Genome 2.0 GeneChip arrays (Mouse 430 v2, Affymetrix, Santa Clara, CA). Data were analyzed using the RAG-2-deficient samples as the controls.

Background corr dist: KL-Divergence = 0.0469, L1-Distance = 0.0246, L2-Distance = 0.0007, Normal std = 0.5897

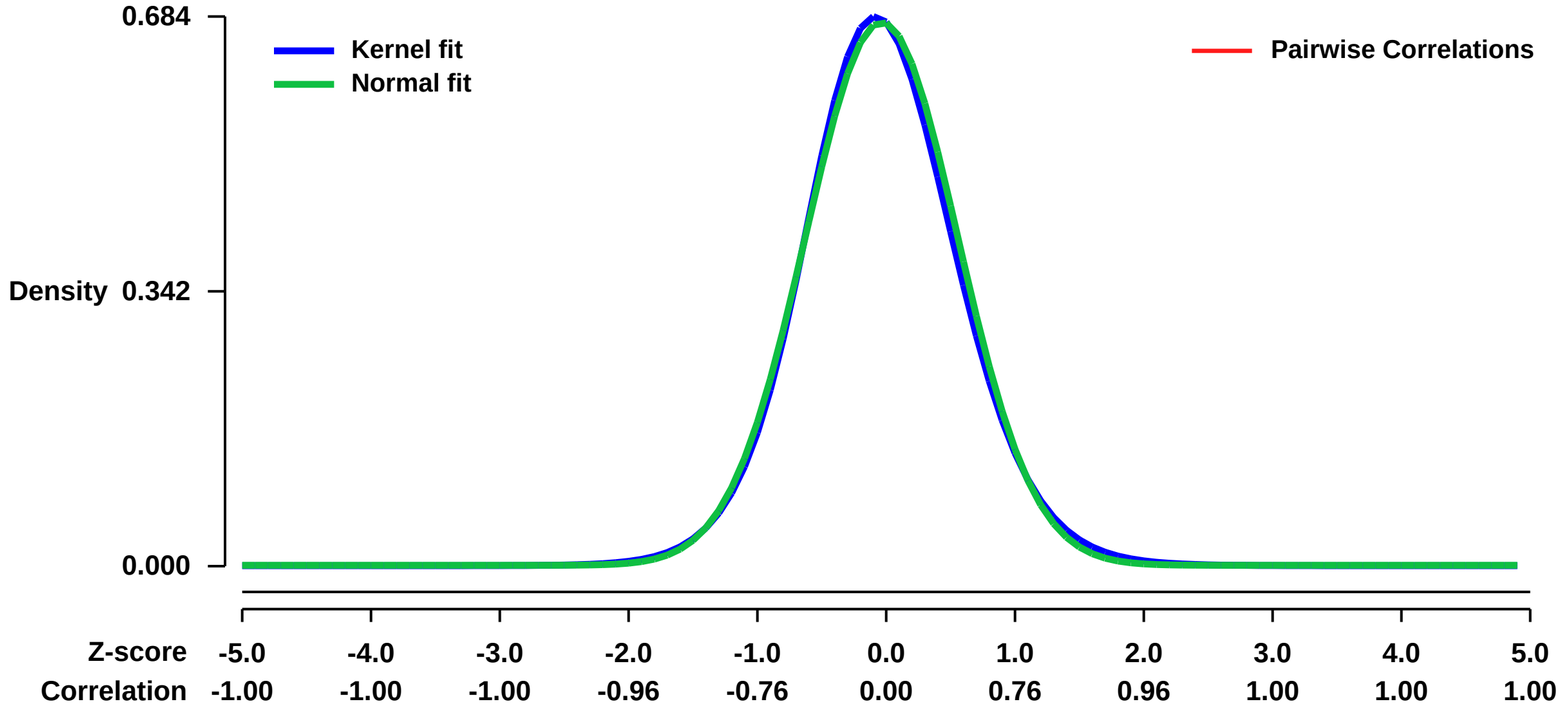

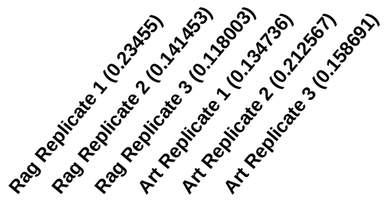

Pre-normalization Quantiles

[min] [medium] [max]

Null module

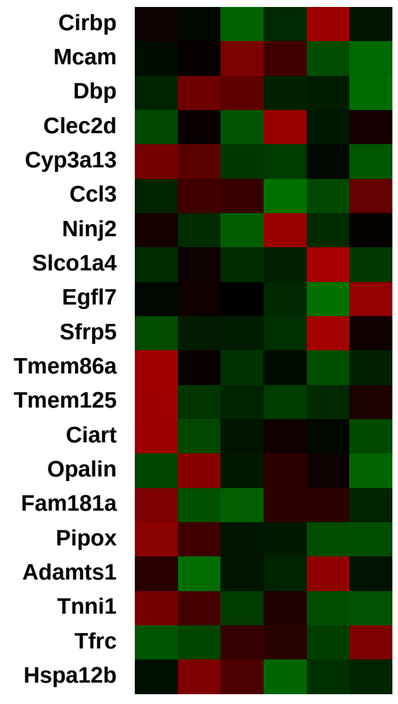

GEO Series "GSE38067" Expression Profiles

Num of samples in this series: 24

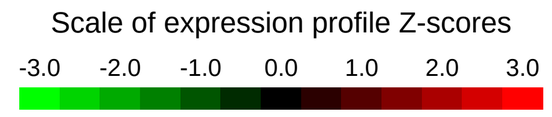

GEO Link:	http://www.ncbi.nlm.nih.gov/geo/query/acc.cgi?acc=GSE38067
Status:	Public on May 23 2012
Title:	Hepatic gene expression in streptozotocin-induced diabetic mice fed a quercetin diet
Organism:	Mus musculus
Experiment type:	Expression profiling by array
Platform:	GPL1261
Pubmed ID:	19496084
Summary & Design:	**Summary:** Quercetin is a food component that may ameliorate the diabetic symptoms. We examined hepatic gene expression of BALB/c mice with streptozotocin (STZ)-induced diabetes to elucidate the mechanism of the protective effect of dietary quercetin on diabetes-associated liver injury. We fed STZ-induced diabetic mice with diets containing 0.1% or 0.5% quercetin for 2 weeks and compared the patterns of hepatic gene expression in these groups of mice using a DNA microarray. Diets containing 0.1% or 0.5% quercetin lowered the STZ-induced increase in blood glucose levels and improved plasma insulin levels. A cluster analysis of the hepatic gene expressions showed that 0.5% quercetin diet suppressed STZ-induced alteration of gene expression. Gene set enrichment analysis (GSEA) and quantitative RT-PCR analysis showed that the quercetin diets had their greatest suppressive effect on the STZ-induced elevation of expression of cyclin dependent kinase inhibitor p21(WAF1/Cip1) (Cdkn1a). **Overall design:** Six-week-old male mice were divided into 4 groups of 6 mice each, housed in groups of 3 per cage. After 1 week mice were intraperitoneally injected with STZ. Mice (n=6) in the untreated control group did not receive any treatment. After 1 week, 18 mice showing non-fasting blood glucose levels of 230-400 mg/dL were divided into 3 groups: one group was fed with AIN93G only (control group), the others with an AIN93G diet containing 0.1% or 0.5% quercetin (Funakoshi, Tokyo, Japan) for 2 weeks.

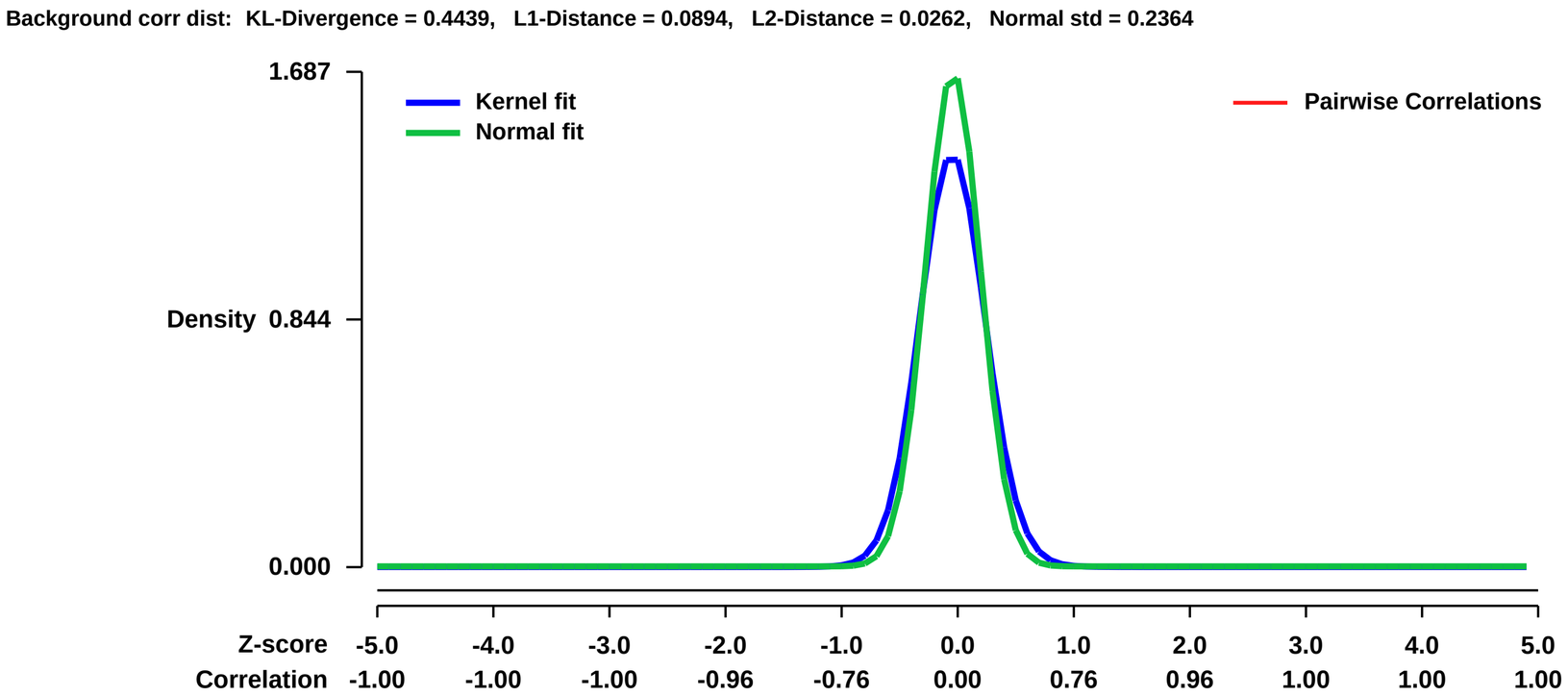

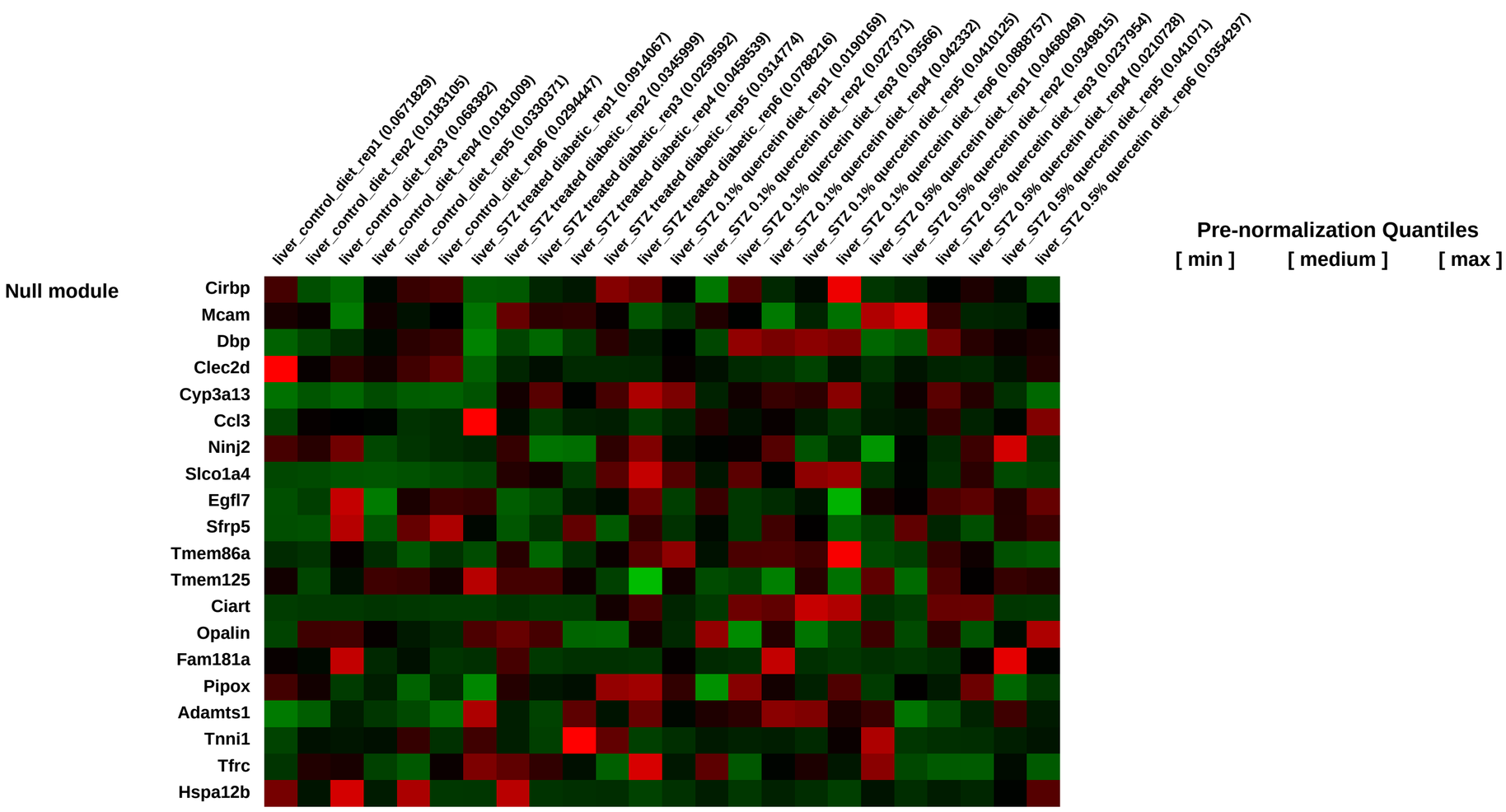

GEO Series "GSE38136" Expression Profiles

Num of samples in this series: 24

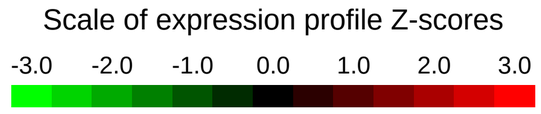

GEO Link:	http://www.ncbi.nlm.nih.gov/geo/query/acc.cgi?acc=GSE38136
Status:	Public on May 30 2012
Title:	Hepatic gene expression in BALB/c mice fed a quercetin diet
Organism:	Mus musculus
Experiment type:	Expression profiling by array
Platform:	GPL1261
Pubmed ID:	19496084
Summary & Design:	**Summary:** We showed that diets containing 0.1% or 0.5% quercetin lowered the STZ-induced increase in blood glucose levels and improved plasma insulin levels. A cluster analysis of the hepatic gene expressions showed that 0.5% quercetin diet suppressed STZ-induced alteration of gene expression. Gene set enrichment analysis (GSEA) and quantitative RT-PCR analysis showed that the quercetin diets had their greatest suppressive effect on the STZ-induced elevation of expression of cyclin dependent kinase inhibitor p21(WAF1/Cip1) (Cdkn1a). In this experiment, we determined the effect of quercetin on healthy control BALB/c mice that were fed the AIN93G diet containing 0, 0.1, 0.5 or 1% quercetin for 2 weeks. GSEA and one-way ANOVA did not detect any significant changes in hepatic gene expression in normal mice as a result of a quercetin diet. Using a linear modeling approach and the empirical Bayes statistics, we found that Ubc were significantly reduced by both the 0.5% and 1% quercetin. **Overall design:** Six-week-old male mice were divided into 4 groups of 6 mice each, housed in groups of 3 per cage, and fed a standard purified AIN-93G diet containing 0% (Control), 0.1% (0.1), 0.5% (0.5), or 1% quercertin (1.0) for 2 weeks.

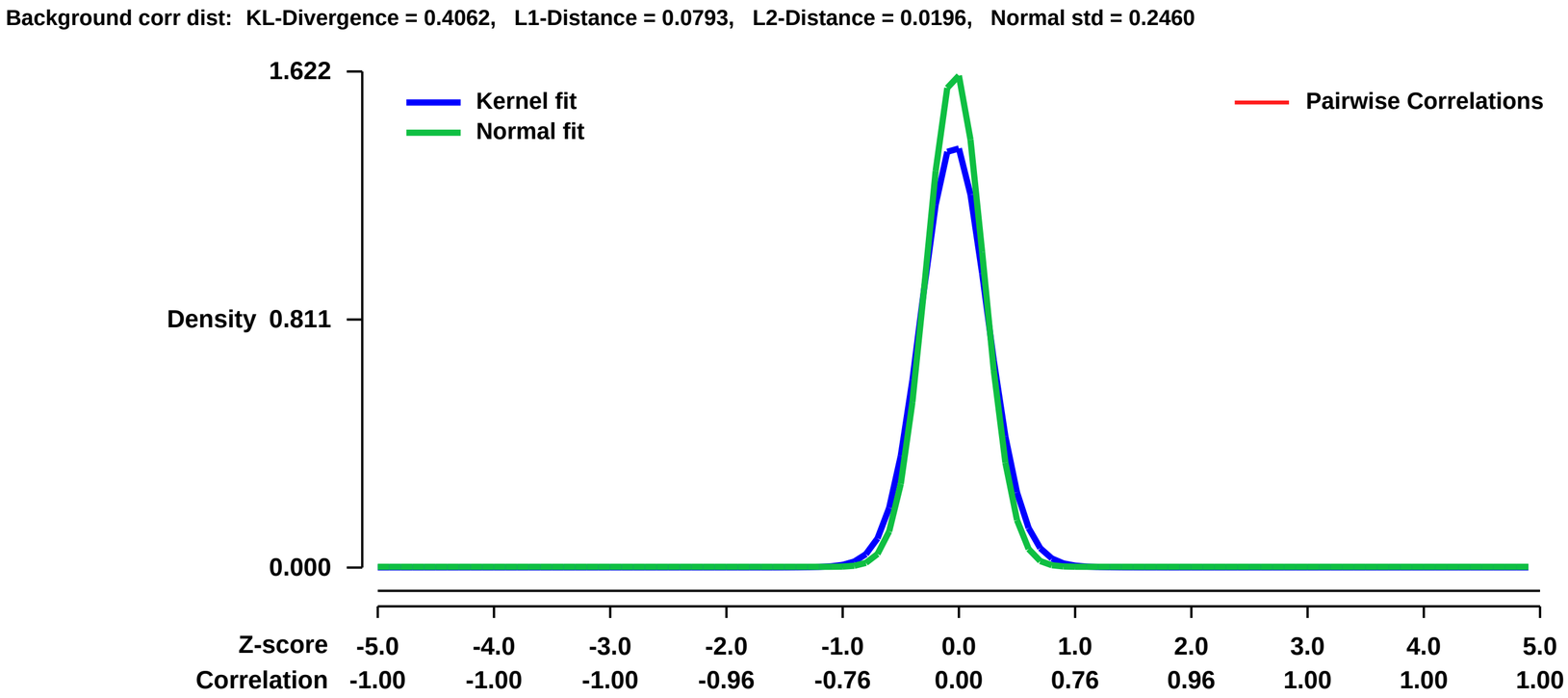

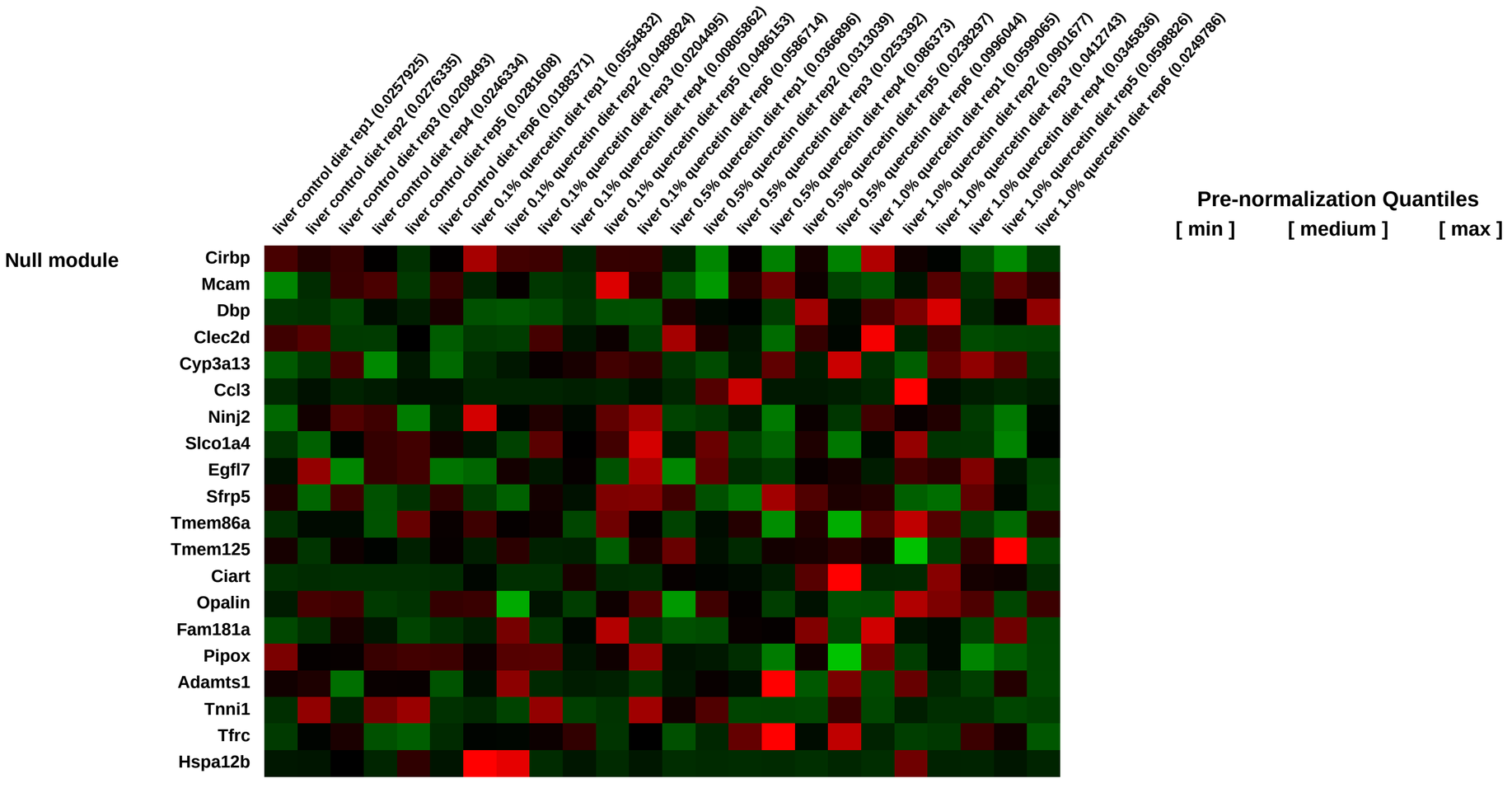

GEO Series "GSE38138" Expression Profiles

Num of samples in this series: 20

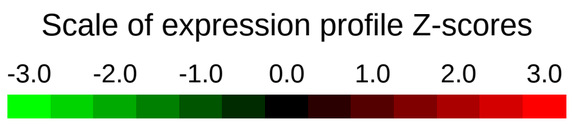

GEO Link:	http://www.ncbi.nlm.nih.gov/geo/query/acc.cgi?acc=GSE38138
Status:	Public on May 30 2012
Title:	Hepatic gene expression in streptozotocin-induced diabetic mice fed a phloridzin diet
Organism:	Mus musculus
Experiment type:	Expression profiling by array
Platform:	GPL1261
Pubmed ID:	19413312
Summary & Design:	**Summary:** Phloridzin is a dihydrochalcone typically contained in apples. A diet containing 0.5 % phloridzin significantly improves hyperglycemia but not hypoinsulinemia and tissue lipid peroxidation in streptozotocin (STZ)-induced diabetic mice after 14 days. The phloridzin diet has no effect on the alteration of hepatic gene expression in STZ-induced diabetic mice. A quantitative RT-PCR analysis showed a reversal of the STZ induction of the sodium/glucose cotransporter gene Sglt1 and the drug-metabolizing enzyme genes Cyp2b10 and Ephx1 in the small intestine of mice fed a 0.5% phloridzin diet. These mice also showed a reversal of the STZ-mediated renal induction of the glucose-regulated facilitated glucose transporter gene Glut2. Dietary phloridzin improved the abnormal elevations in blood glucose level and the overexpression of Sglt1, Cyp2b10 and Ephx1 in the small intestine of STZ-induced diabetic mice. **Overall design:** Six-week-old male mice were divided into 4 groups of 6 mice each, housed in groups of 3 per cage. After 1 week mice were intraperitoneally injected with STZ. Mice (n=6) in the untreated control group did not receive any treatment. After 1 week, 18 mice showing non-fasting blood glucose levels of 330-590 mg/dL were divided into 3 groups: one group was fed with AIN93G only (control group), the others with an AIN93G diet containing 0.1% or 0.5% phloridzin (Funakoshi, Tokyo, Japan) for 2 weeks.

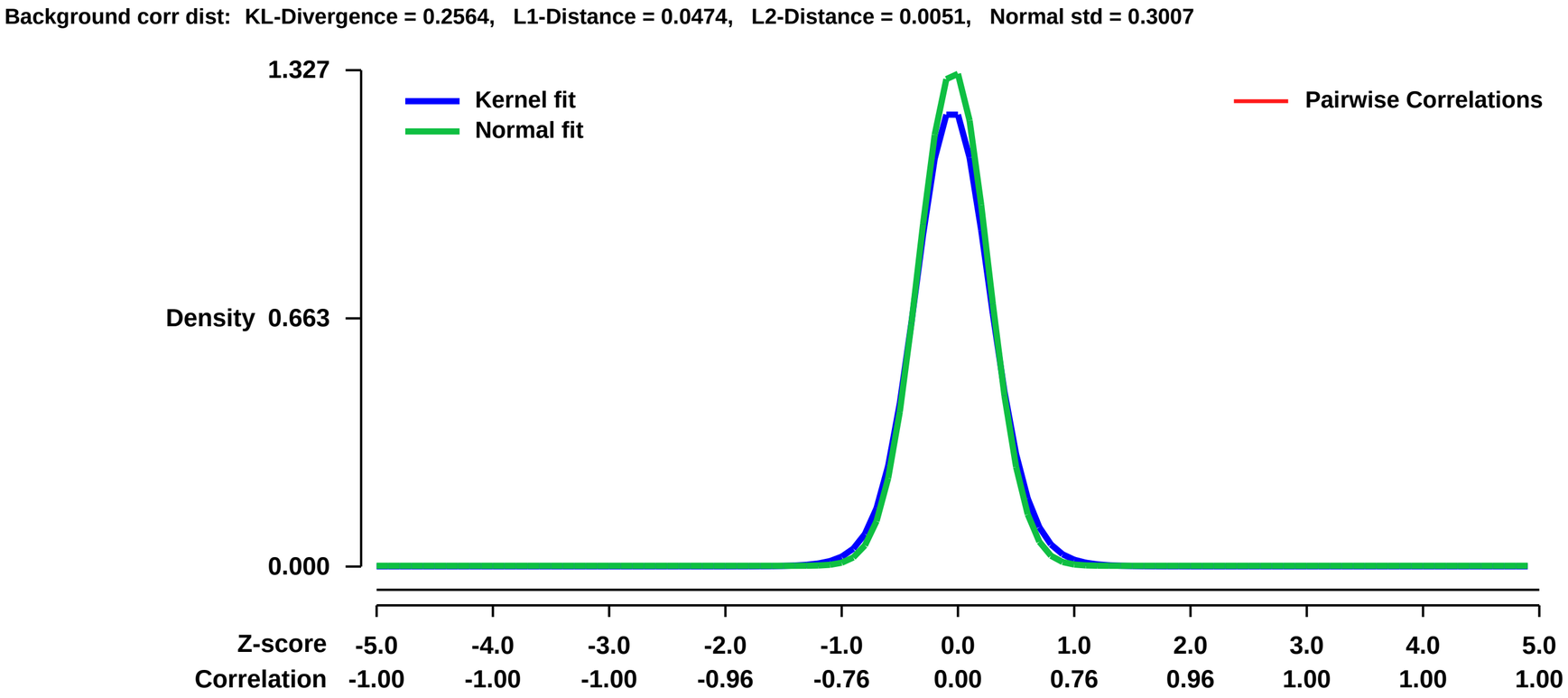

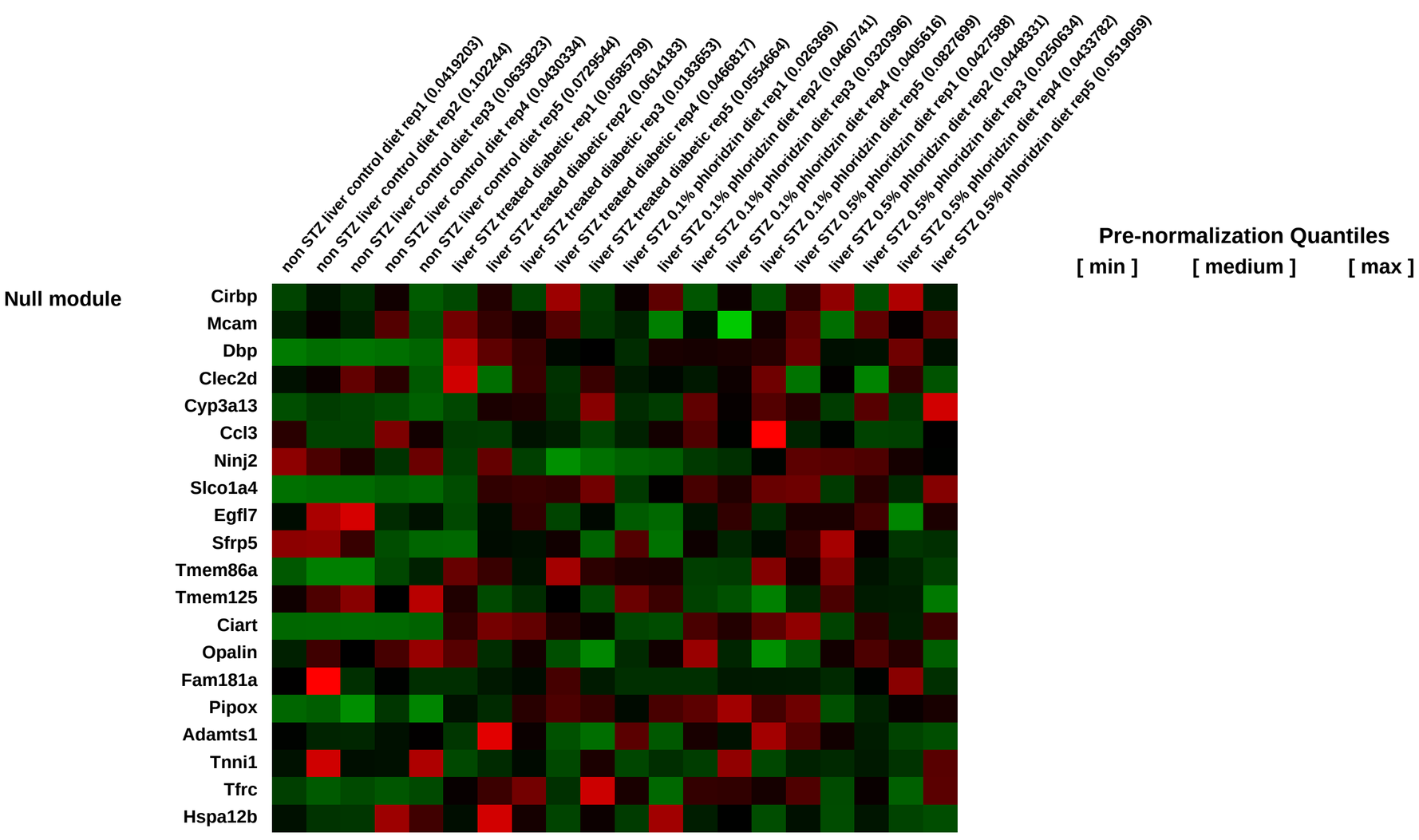

GEO Series "GSE38141" Expression Profiles

Num of samples in this series: 18

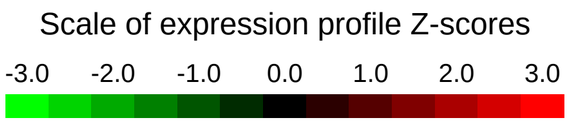

GEO Link:	http://www.ncbi.nlm.nih.gov/geo/query/acc.cgi?acc=GSE38141
Status:	Public on May 30 2012
Title:	Chronic dietary intake of quercetin alleviates hepatic fat accumulation associated with consumption of a Western-style diet in C57/BL6J mice
Organism:	Mus musculus
Experiment type:	Expression profiling by array
Platform:	GPL1261
Pubmed ID:	21462320
Summary & Design:	**Summary:** To determine the effect of consumption of a quercetin-rich diet on obesity and dysregulated hepatic gene expression, C56BL/6J mice were fed for 20 weeks on control or a Western diet high in fat, cholesterol and sucrose, both with or without 0.05% quercetin. Chronic dietary intake of quercetin reduced body weight gain and visceral and liver fat accumulation, and improved hyperglyceamia, hyperinsulinaemia, dyslipidaemia in mice fed a Western-style diet. Feeding a Western-style diet altered expression of genes related to inflammatory responses, lipid metabolism and oxidative phosphorylation in C57BL/6J mice after 20 weeks. The results from exhaustive gene expression analysis showed that quercetin minimally influenced hepatic gene expression in mice fed the Western diet. The gene screening results (GSEA) were consistent with the notion that it did improve mitochondrial function to some extent. Quantitative RT-PCR analysis indicated that quercetin did influence important regulators of fat accumulation and metabolic disorders. Our results suggest that quercetin reduces fat accumulation presumably through decreasing oxidative stress and increasing PPAR¸– expression, and the following improvement of gene expression related to steatosis in the liver. **Overall design:** C56BL/6J mice were fed for 20 weeks on AIN93G (con) or a Western diet high in fat, cholesterol and sucrose, both with or without 0.05% quercetin for 20 weeks.

Background corr dist: KL-Divergence = 0.2400, L1-Distance = 0.0510, L2-Distance = 0.0061, Normal std = 0.3079

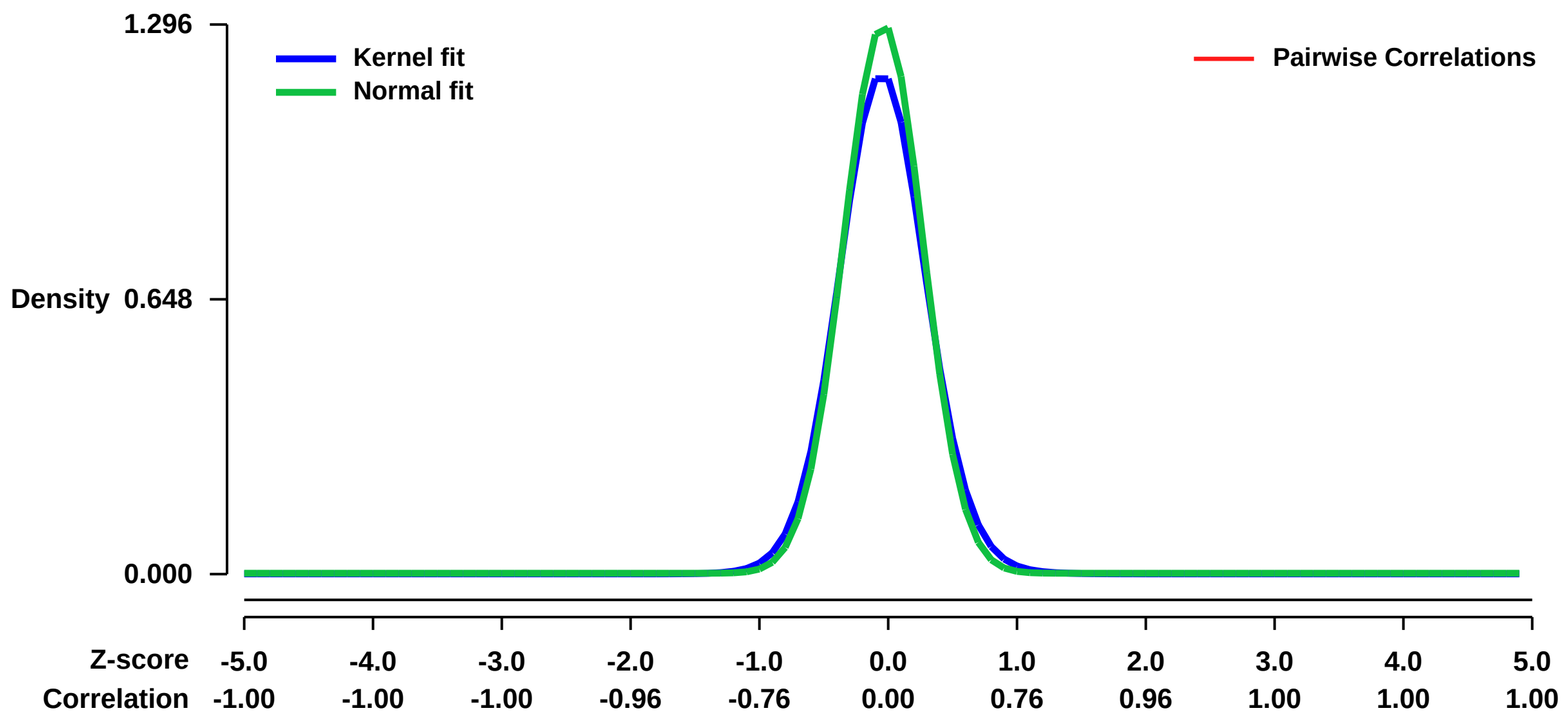

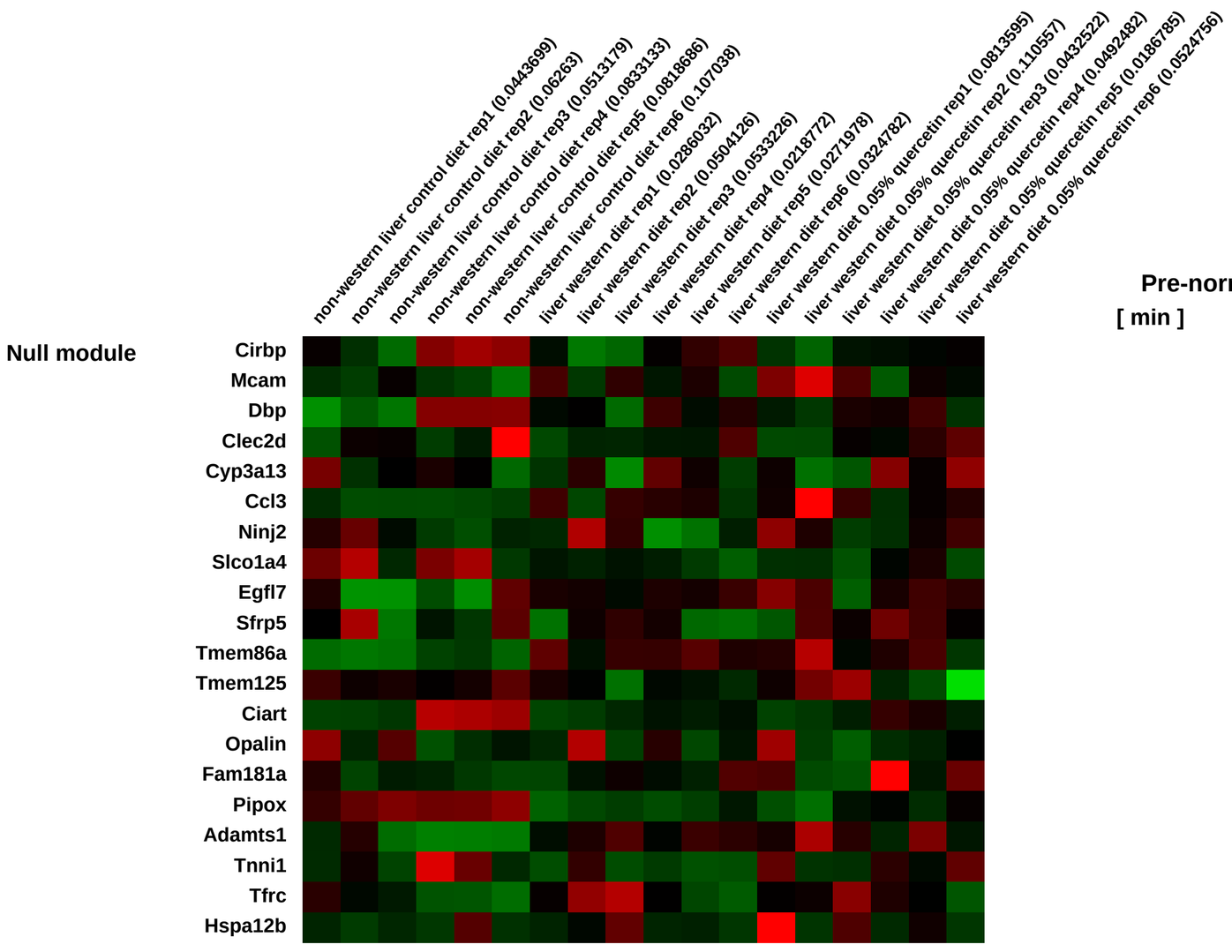

GEO Series "GSE38215" Expression Profiles

Num of samples in this series: 11

Scale of expression profile Z-scores

-3.0 -2.0 -1.0 0.0 1.0 2.0 3.0

GEO Link:	http://www.ncbi.nlm.nih.gov/geo/query/acc.cgi?acc=GSE38215
Status:	Public on Jun 01 2013
Title:	Expression analysis of control and low protein fed mouse offspring subsequently treated with multiple low doses of STZ
Organism:	Mus musculus
Experiment type:	Expression profiling by array
Platform:	GPL1261
Pubmed ID:	23986224
Summary & Design:	**Summary:** Low protein (LP) during gestation leads to low birth weight and poor fetal growth, with altered islet development and glucose intolerance in adulthood. Additionally, LP offspring fail to regenerate their ¸†-cells following depletion with streptozotocin (STZ), in contrast to control-fed offspring that are capable of ¸†-cell regeneration. Our objective was to identify genes and signalling pathways that may be critically altered in LP offspring rendering them susceptible to develop long term glucose intolerance and decreased ¸†-cell plasticity. **Overall design:** Pregnant Balb/C mice were place on a control (20% protein) or isocaloric low protein (8%) diet for the period of gestation, and then all dams were switch to the control diet at birth. Female offspring were injected with streptozotocin (35 mg/kg body weight; sodium citrate buffer 0.1 mol/L, pH 4.5) or vehicle (sham). Total RNA was extracted from pancreas of 30 day old female offspring (n=3) and hybridized to Affymetrix GeneChips.

Background corr dist: KL-Divergence = 0.0800, L1-Distance = 0.0381, L2-Distance = 0.0029, Normal std = 0.4716

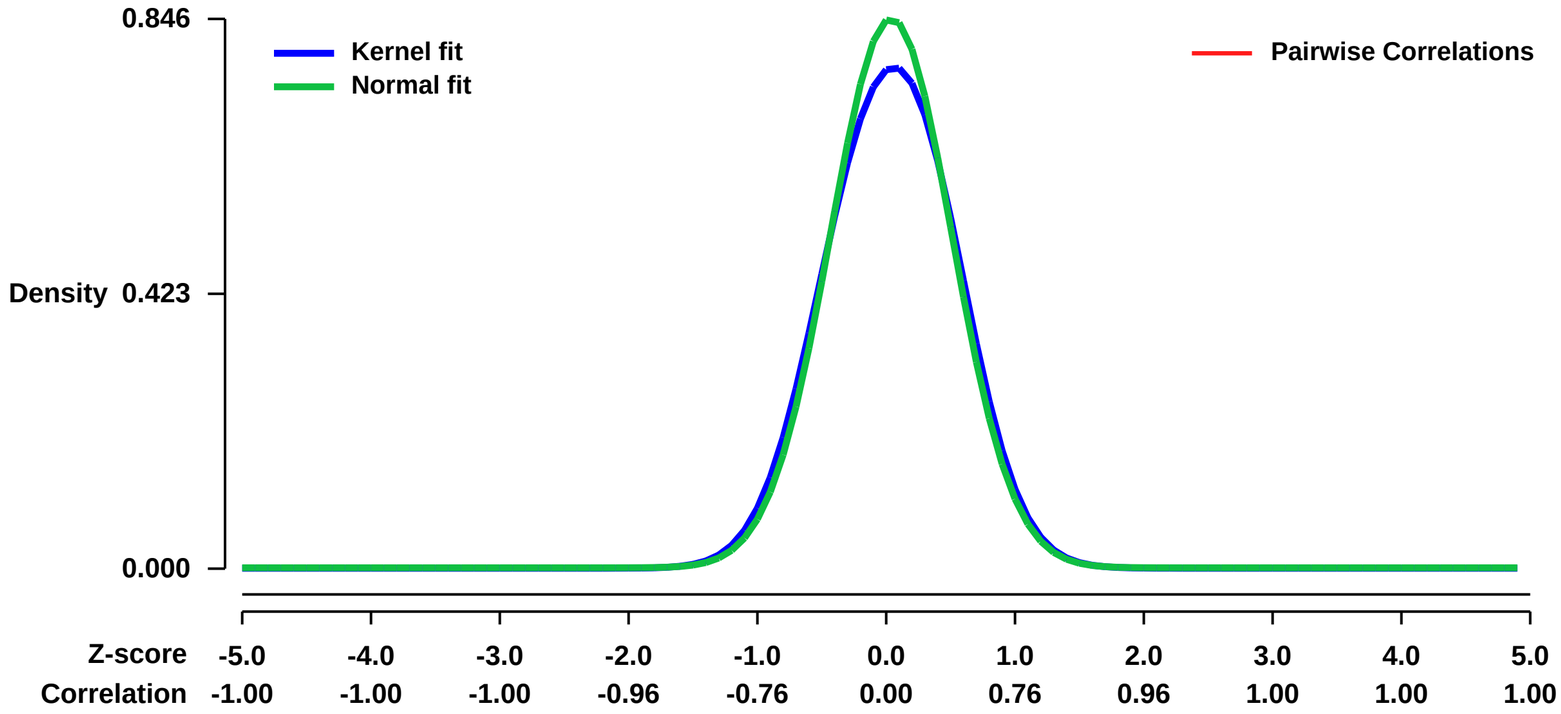

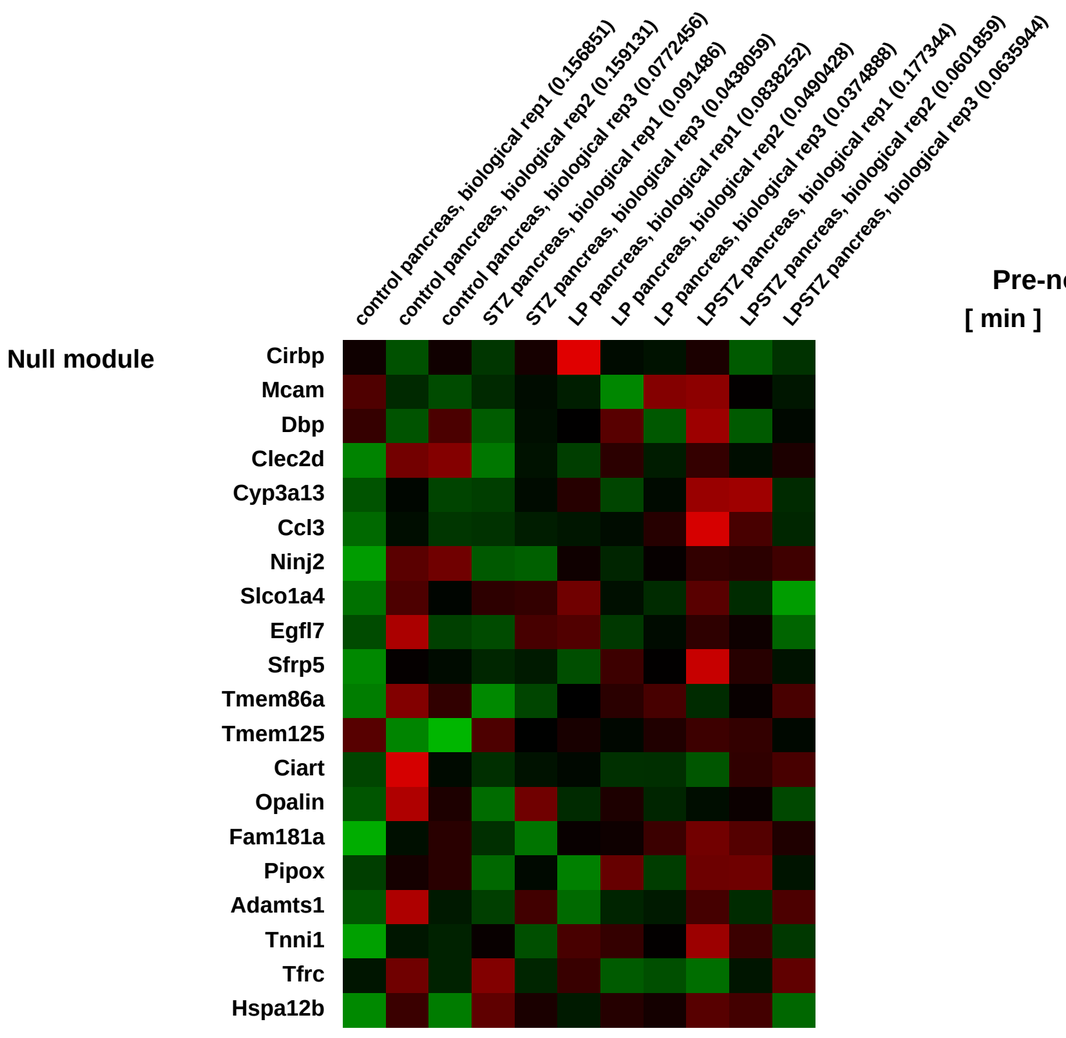

GEO Series "GSE38224" Expression Profiles

Num of samples in this series: 12

Scale of expression profile Z-scores

-3.0 -2.0 -1.0 0.0 1.0 2.0 3.0

GEO Link:	http://www.ncbi.nlm.nih.gov/geo/query/acc.cgi?acc=GSE38224
Status:	Public on Jun 11 2012
Title:	Expression data from Ring1A(-/-);Ring1B(fl/fl);R26::CreERT2 ES cells expressing either of mock, WT or mutant Ring1B construct before or after OHT treatment
Organism:	Mus musculus
Experiment type:	Expression profiling by array
Platform:	GPL1261
Pubmed ID:	22844243
Summary & Design:	**Summary:** We used microarrays to investigate the restoration of repression of PRC1 target gene expression in Ring1A/B-dKO ES cells stably expressing either of mock, WT or mutant Ring1B construct. **Overall design:** Total RNAs were extracted from the respective ES cells, and were subjected to microarray analysis using Affymetrix GeneChip Mouse Genome 430A 2.0 arrays

Background corr dist: KL-Divergence = 0.1261, L1-Distance = 0.0314, L2-Distance = 0.0017, Normal std = 0.3993

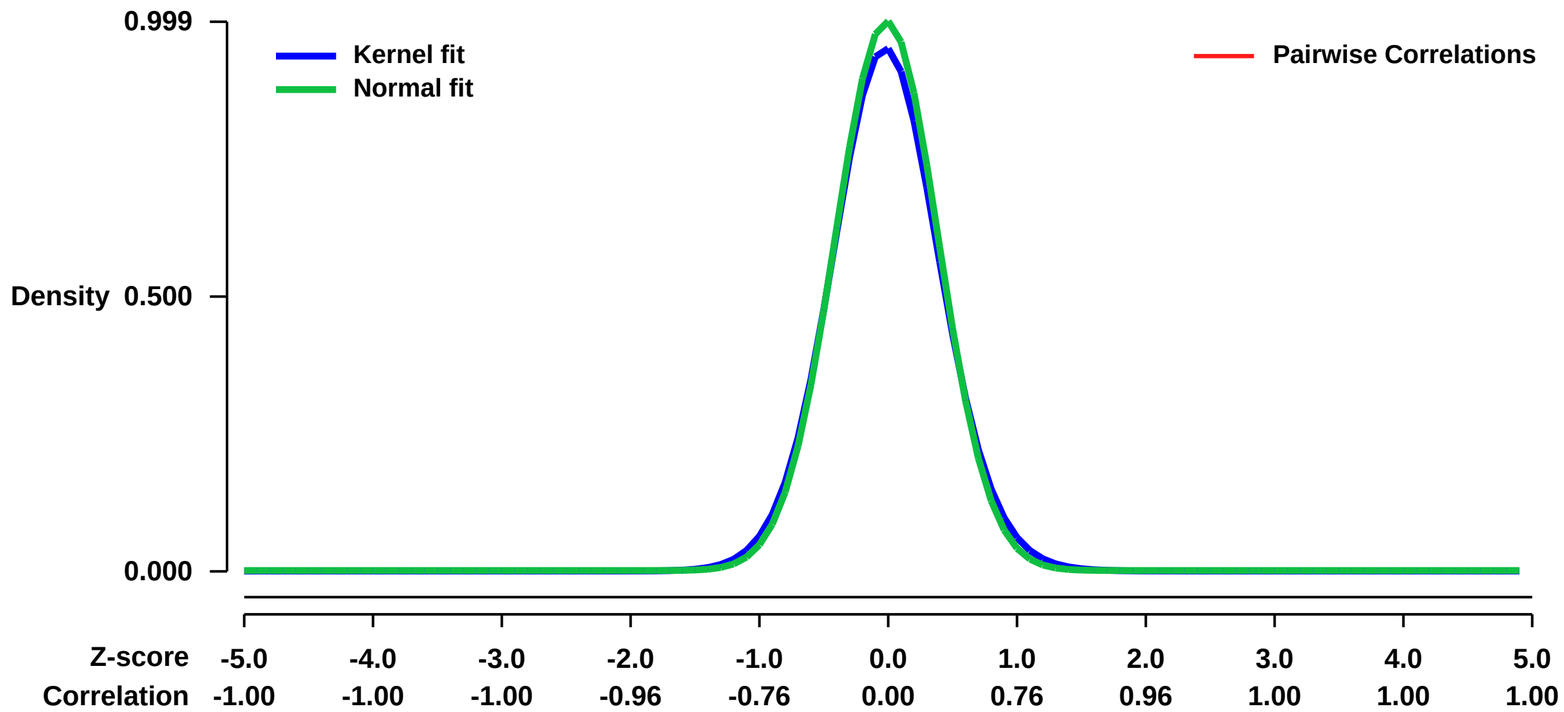

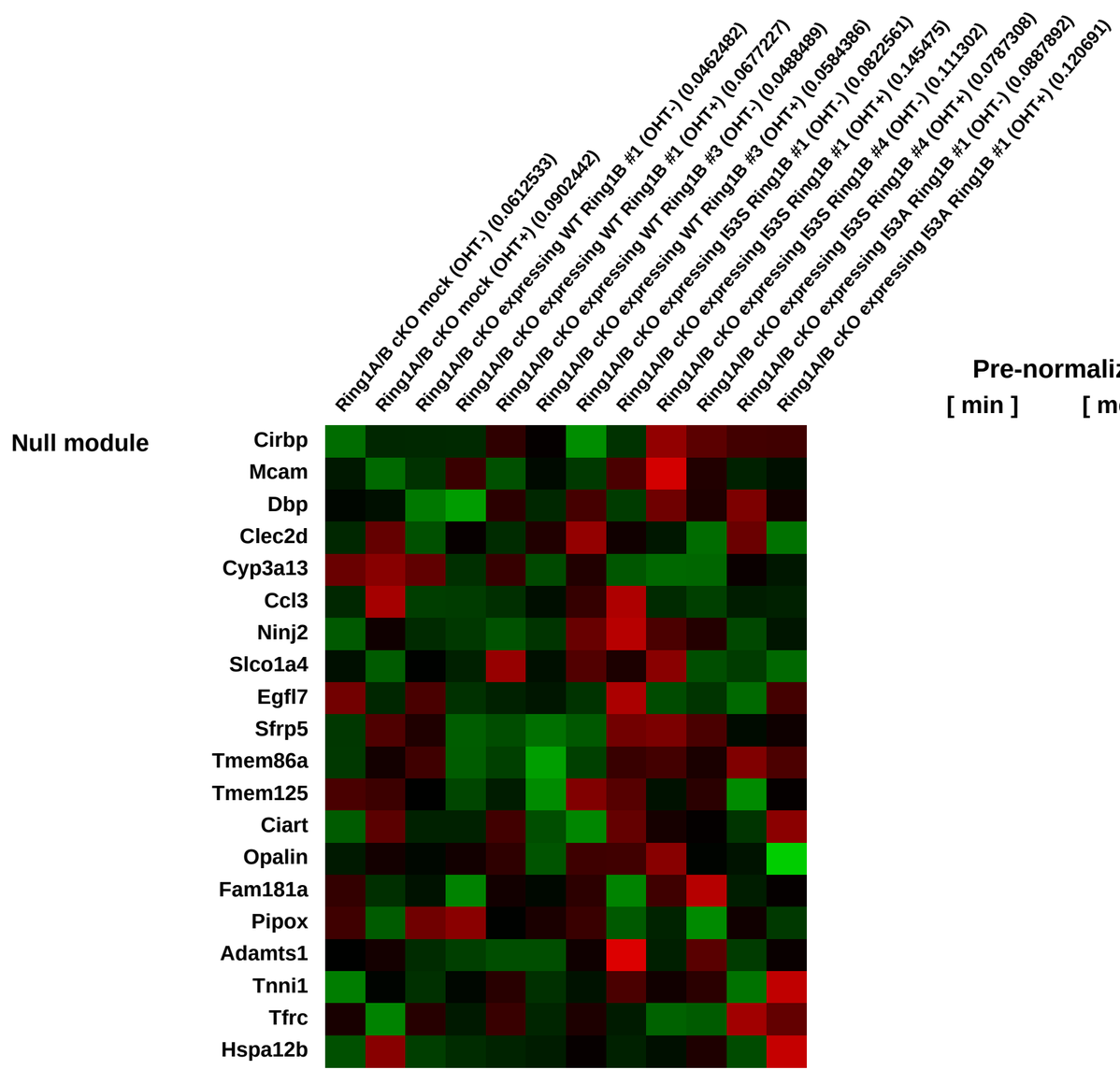

GEO Series "GSE38257" Expression Profiles

Num of samples in this series: 14

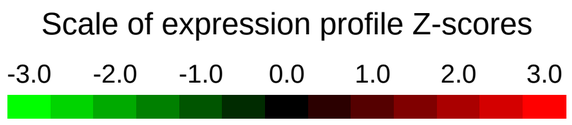

GEO Link:	http://www.ncbi.nlm.nih.gov/geo/query/acc.cgi?acc=GSE38257
Status:	Public on Dec 21 2012
Title:	A Novel Tumor suppressor network in squamous malignancies
Organism:	Mus musculus
Experiment type:	Expression profiling by array
Platform:	GPL1261
Pubmed ID:	23145321
Summary & Design:	**Summary:** The specific ablation of Rb1 gene in stratified epithelia (RbF/F;K14cre) promotes proliferation and altered differentiation but is insufficient to produce spontaneous tumors. The pRb relative, p107, compensates some of the functions of pRb in these tissues, however RbF/F;K14cre;p107-/- mice die postnatally. Acute pRb loss in stratified epithelia, using an inducible mouse model (RbF/F;K14creERTM), shows that p107 exerts specific tumor suppressor functions in its absence. After simultaneous absence of pRb and p107, p53 transcriptional function is impaired and Pten expression is reduced. All mutant mice develop spontaneous squamous tumors carcinomas rapidly. Gene expression analysis of mouse tumors, besides supporting the impaired p53 function and the susceptibility to Akt/mTOR inhibitors, also revealed significant overlap with human squamous carcinomas. Thus, RbF/F;K14creERTM;p107-/- may constitute a new mouse model for these malignancies. Collectively, these data demonstrate the existence of a previously unreported functional connection between pRb, Pten and p53 tumor suppressors, through p107, of a particular relevance in squamous tumor development. **Overall design:** Gene expression was compared between normal mouse skin and carcinomas arising in the skin of RbF/F;K14creERTM;p107-/- mouse. All mice were treated with tamoxifen.

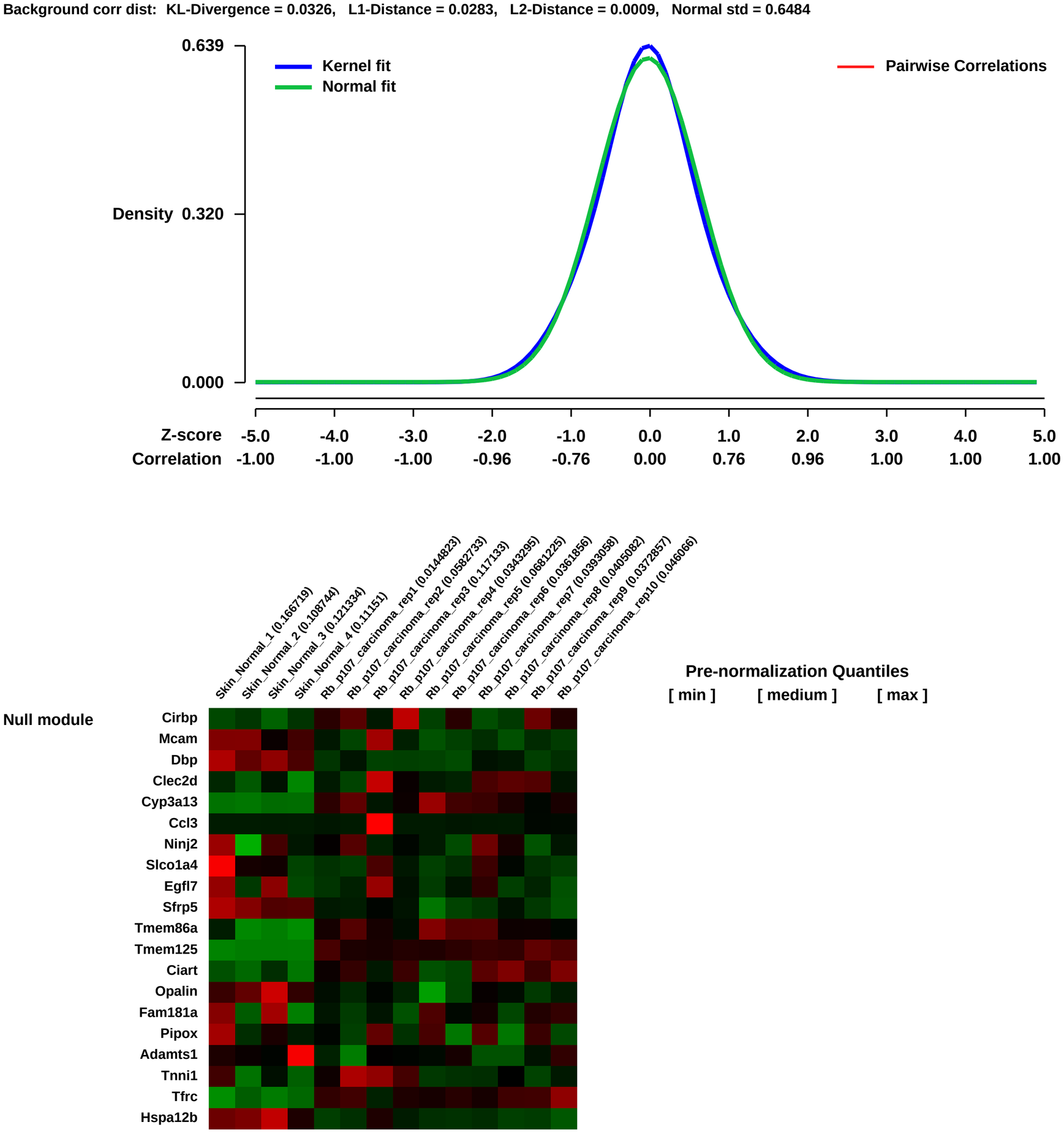

GEO Series "GSE38277" Expression Profiles

Num of samples in this series: 18

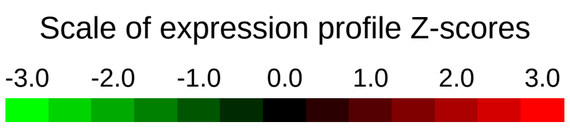

GEO Link:	http://www.ncbi.nlm.nih.gov/geo/query/acc.cgi?acc=GSE38277
Status:	Public on Jan 17 2014
Title:	Lsd1 coordinates trophoblast development by retaining stem cells in their niche and directing cell fate
Organism:	Mus musculus
Experiment type:	Expression profiling by array
Platform:	GPL1261
Pubmed ID:	24448552
Summary & Design:	**Summary:** Stem cells reside in specific niches providing stemness-maintaining environments. Thus, the regulated migration from these niches is associated with differentiation onset. However, mechanisms retaining stem cells in their niche remain poorly understood. Here, we show that the epigenetic regulator lysine-specific demethylase 1 (Lsd1) organises the trophoblast niche of the early mouse embryo by coordinating migration and invasion of trophoblast stem cells (TSCs). Lsd1 deficiency leads to the depletion of the stem cell pool resulting from precocious migration of TSCs. Migration is induced by premature expression of the transcription factor Ovol2 that is repressed by Lsd1 in undifferentiated wild-type TSCs. Increasing Ovol2 levels suffices to recapitulate the migration phenotype. Furthermore, Lsd1-deficient TSCs exhibit a developmental bias towards cells of the syncytiotrophoblast and impaired spongiotrophoblast and trophoblast giant cell differentiation. In summary, we describe that the epigenetic modifier Lsd1 coordinates placental development by retaining TSCs in their niche and directing trophoblast differentiation. **Overall design:** Mouse trophoblast stem cells (TSCs) were isoloated from a single conditional Lsd1-deficient mouse (Lsd1tm1Schˆ…le). Deletion of Lsd1 was induced eight days before the collection of RNA by addition of 0.2 ´¡M 4OH-tamoxife. Cells were isolated at successive stages of differentiation for total RNA extraction and hybridization on Affymetrix microarrays. To that end, we harvested cells at three time-points: before induction of differentiation (d0), two days after induction of differentiation (d2), and four days after induction of differentiation (d4). Three replicates (1, 2, 3) for control (-) and Lsd1-deficeint (+) cells were included for each differentiation stage.

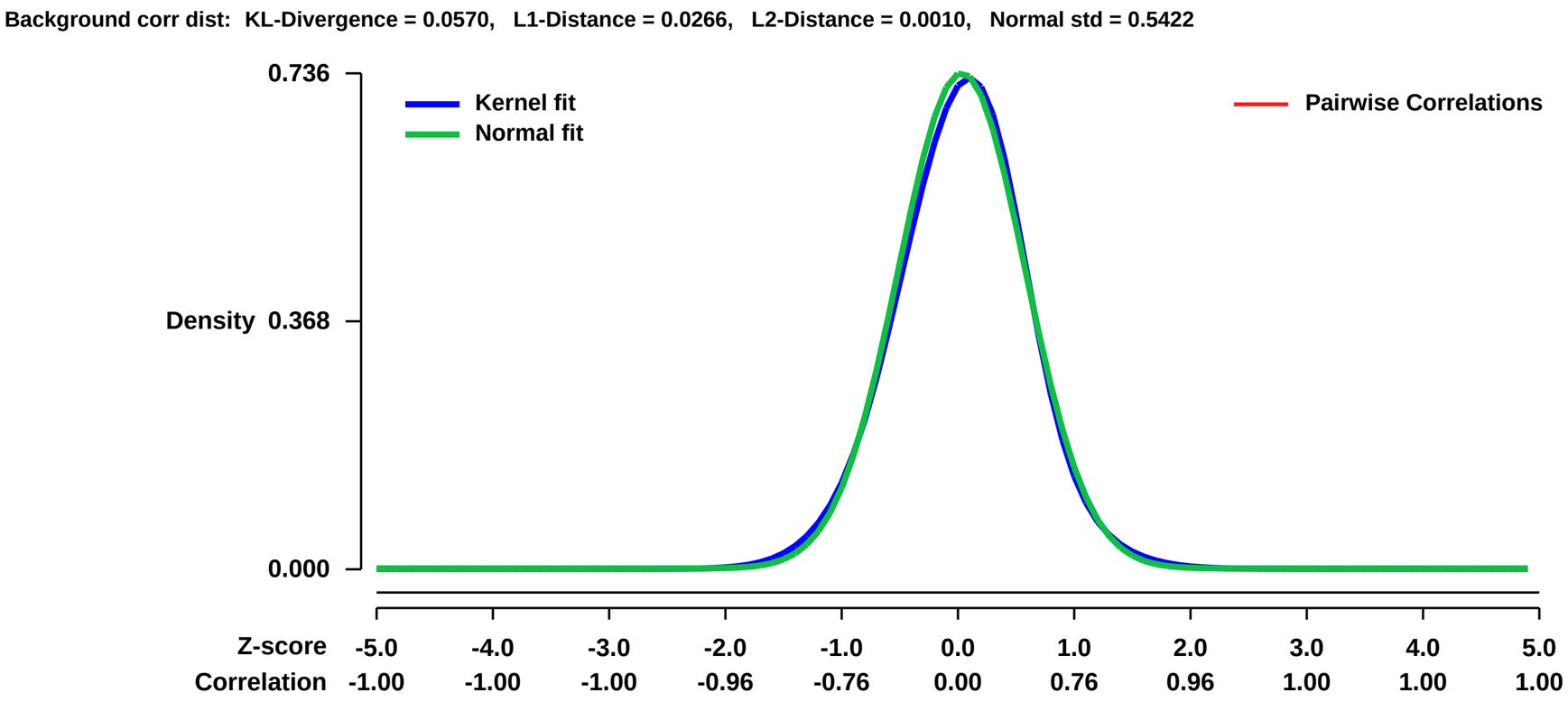

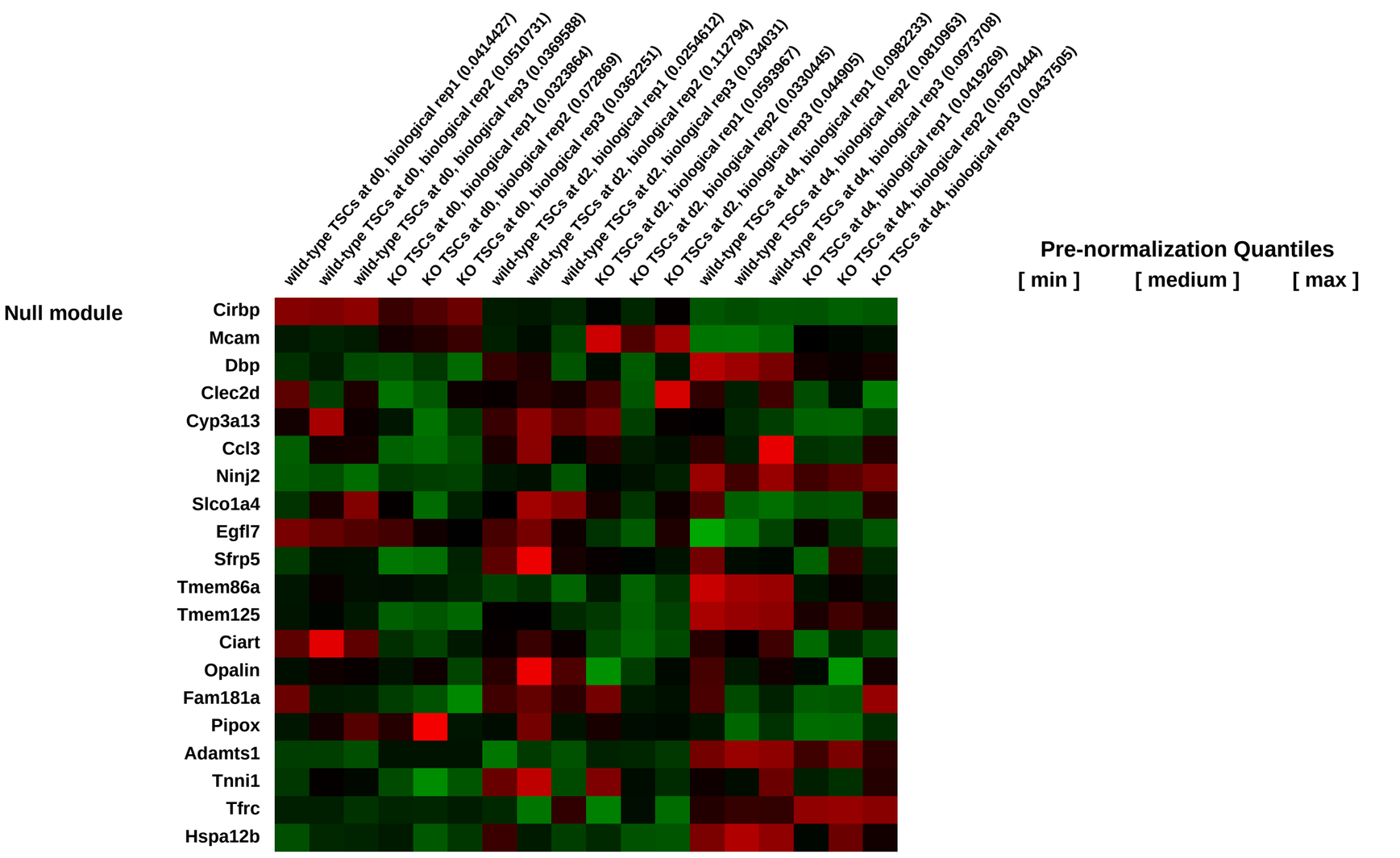

GEO Series "GSE38283" Expression Profiles

Num of samples in this series: 7

Scale of expression profile Z-scores

-3.0 -2.0 -1.0 0.0 1.0 2.0 3.0

GEO Link:	http://www.ncbi.nlm.nih.gov/geo/query/acc.cgi?acc=GSE38283
Status:	Public on May 28 2012
Title:	Expression data from normal brain/glioma associated macrophages
Organism:	Mus musculus
Experiment type:	Expression profiling by array
Platform:	GPL1261
Pubmed ID:	24371228
Summary & Design:	**Summary:** Tumor associated macrophages are contributing to local invasion, angiogensis, and metastasis during the progression of many kinds of tumor including glioma We used microrray to study the difference of expression of glioma associated macrophages and normal brain tissue associated macrophages **Overall design:** The macrophgages were isolated based on the markers of GFP and F4/80+ from Gl261 glioma and normal brain, RNA were extracted for microarray analysis

Background corr dist: KL-Divergence = 0.0613, L1-Distance = 0.0320, L2-Distance = 0.0017, Normal std = 0.5371

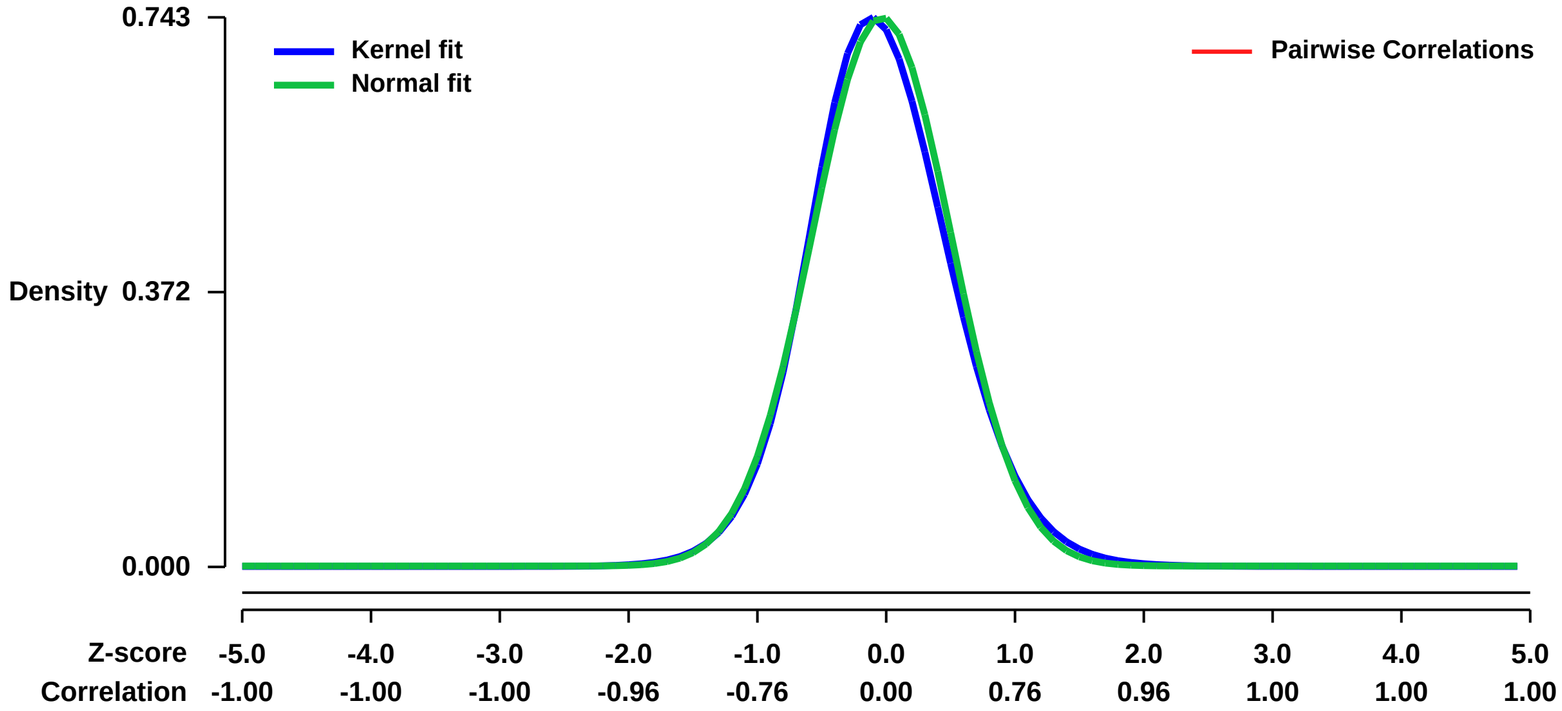

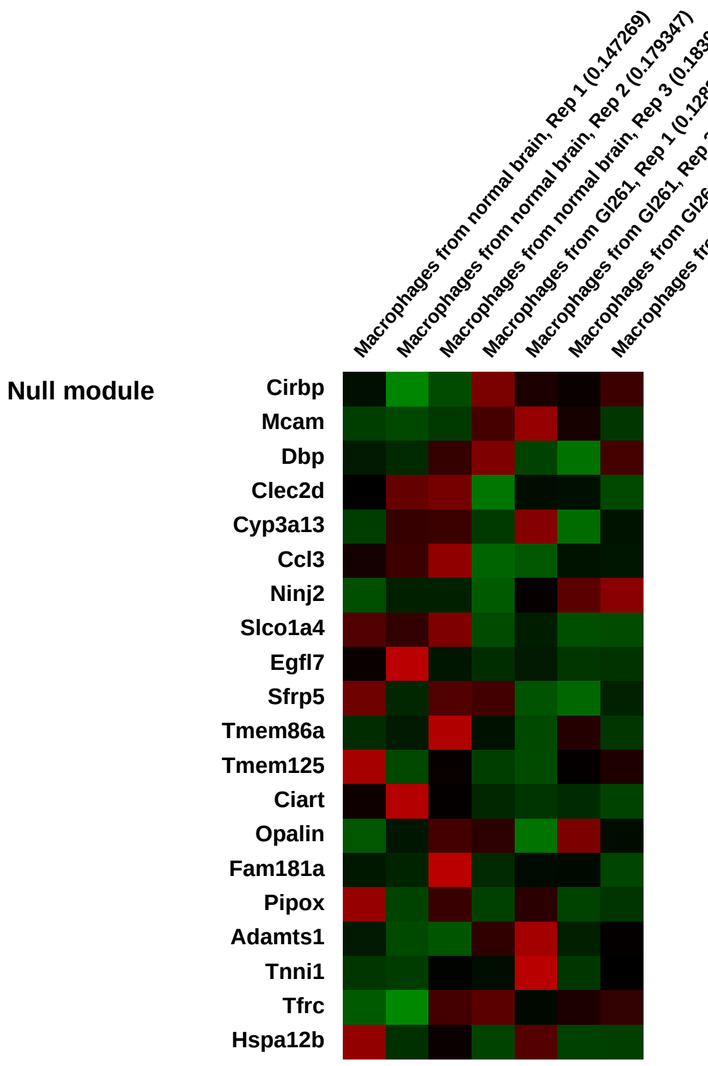

GEO Series "GSE38304" Expression Profiles

Num of samples in this series: 8

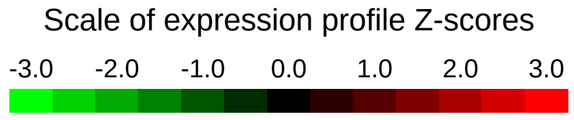

GEO Link:	http://www.ncbi.nlm.nih.gov/geo/query/acc.cgi?acc=GSE38304
Status:	Public on Sep 24 2012
Title:	Gene Expression Profiles of MYC+ and MYC- mouse Germinal Center B cells
Organism:	Mus musculus
Experiment type:	Expression profiling by array
Platform:	GPL1261
Pubmed ID:	23001145
Summary & Design:	**Summary:** Germinal centers (GC) arise within B cell follicles upon antigenic challenge. In the dark zones (DZ) of GCs, B cells proliferate and hypermutate their immunoglobulin genes, and mutants with increased affinity are positively selected in the light zone (LZ) to either differentiate into plasma and memory cells, or re-enter the DZ for further refinement. However, the molecular circuits governing GC positive selection are not known. Here, we show that the GC reaction requires the biphasic regulation of c-MYC expression, involving its transient induction during early GC commitment, its repression by BCL6 in DZ B cells, and its re-induction in a subpopulation of positively selected LZ B cells destined to DZ re-entry. Accordingly, acute disruption of MYC function in vivo leads to GC collapse, indicating an essential role in GC physiology. These results have implications for our understanding of GC selection and the role of MYC deregulation in B cell lymphomas. We used microarrays to determine the global gene expression programs that distinguish MYC+ GC B cells from their MYC- negative counterparts. **Overall design:** GFPMYC+ and GFPMYC- GC B cell subpopulations were collected by Fluorescence Activated Cell Sorting (FACS) from B cell enriched fractions of splenic mononuclear cell pools of GFPMYC knock-in mice (12 days after SRBC immunization). 5-20ng of total RNA (RIN>9) for each sample was used as a template for linear cDNA amplification (Ovation RNA amplification Kit, NuGen). cDNA was labeled using the Encore Biotin Labeling Kit (NuGen) and hybridized to Affymetrix Mouse 430.2 gene expression arrays.

Background corr dist: KL-Divergence = 0.0656, L1-Distance = 0.0311, L2-Distance = 0.0016, Normal std = 0.5216

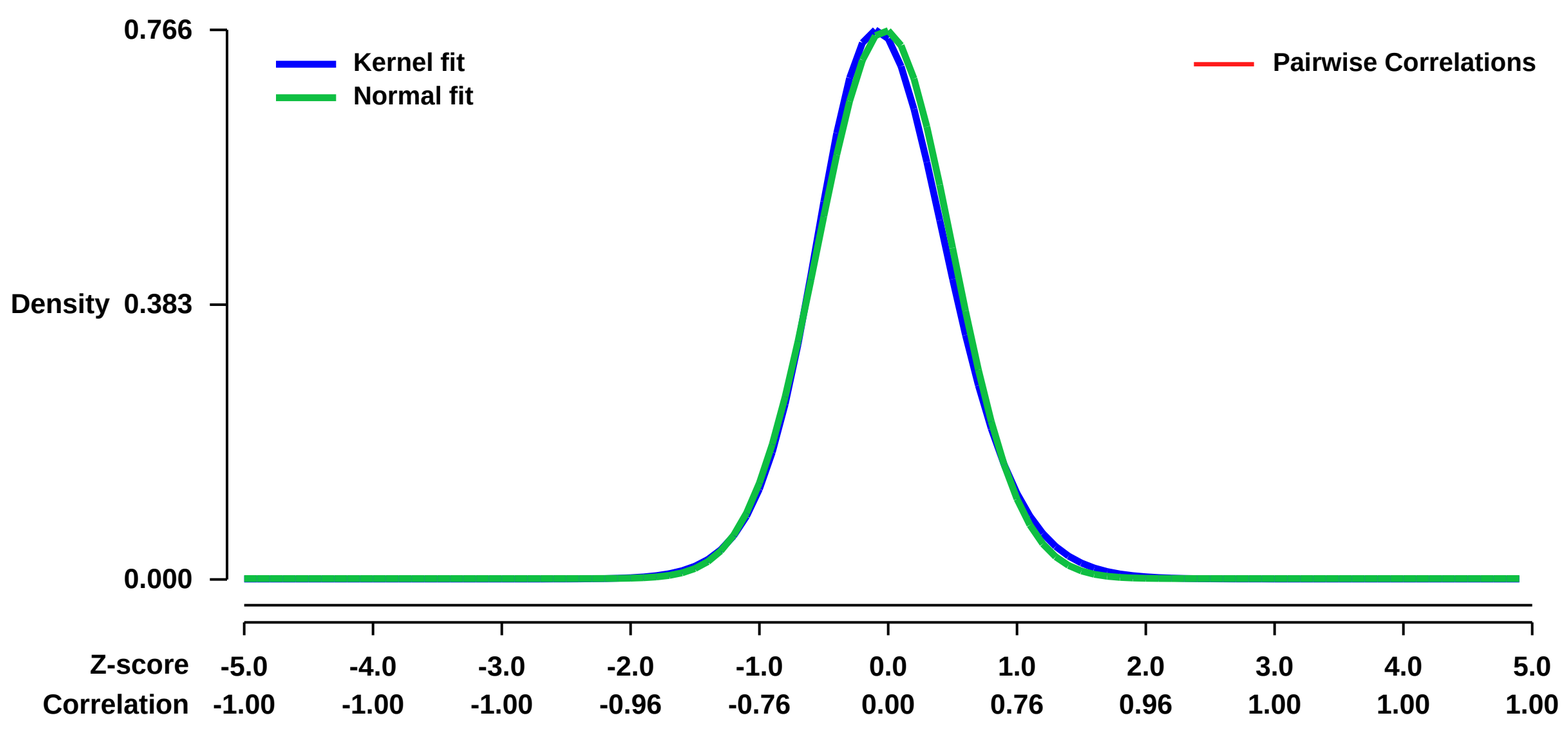

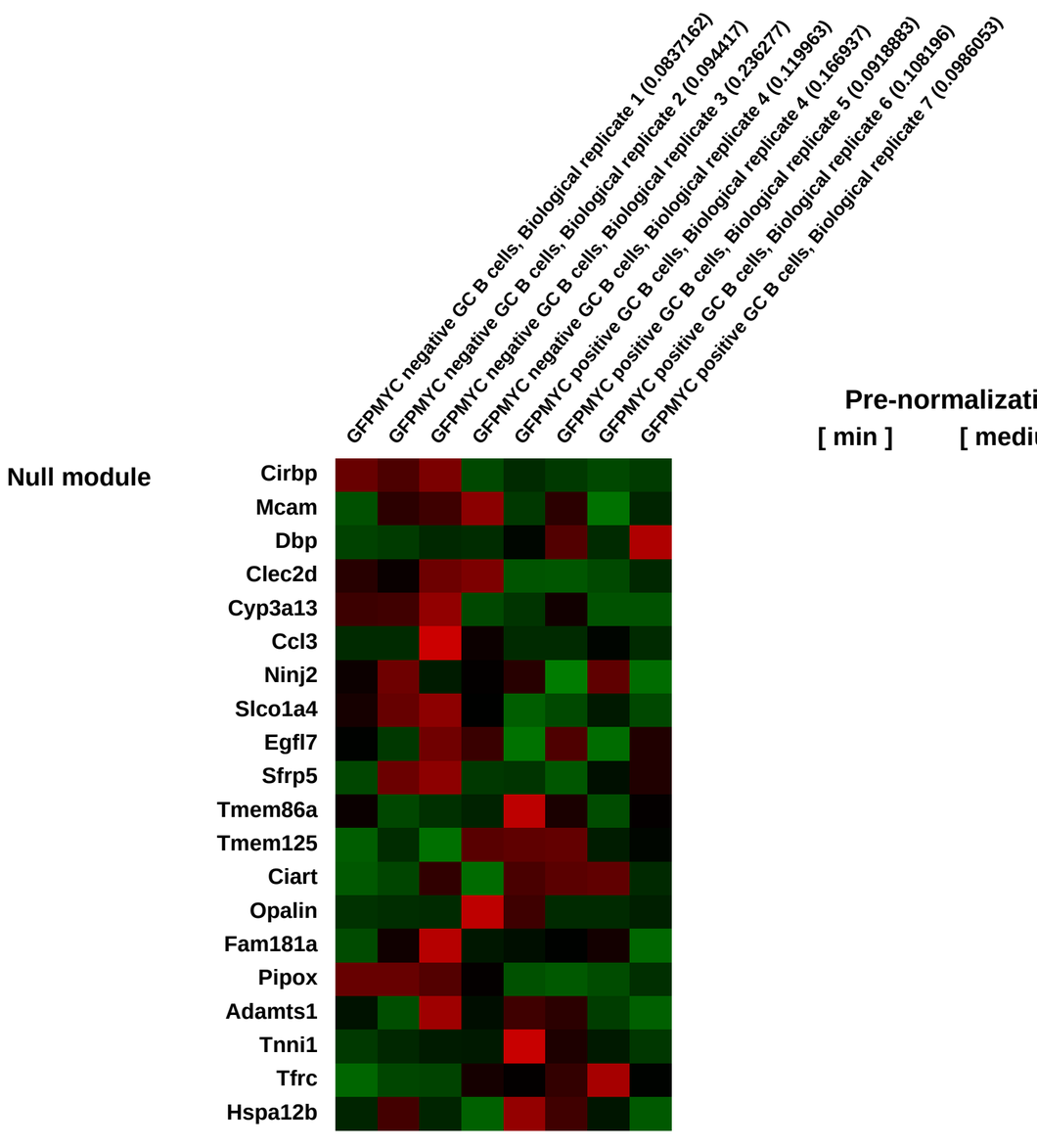

GEO Series "GSE3837" Expression Profiles

Num of samples in this series: 12

Scale of expression profile Z-scores

-3.0 -2.0 -1.0 0.0 1.0 2.0 3.0

GEO Link:	http://www.ncbi.nlm.nih.gov/geo/query/acc.cgi?acc=GSE3837
Status:	Public on Oct 31 2006
Title:	Methylglyoxal treatment of MH-S cell line induces apoptosis and immune response
Organism:	Mus musculus
Experiment type:	Expression profiling by array
Platform:	GPL1261
Pubmed ID:	17183656
Summary & Design:	**Summary:** Mycobacteria-induced apoptosis of macrophages plays an important role in modulation of the host immune response involving TNF-alpha as major cytokine. The underlying mechanisms are still ill-defined. Here, we show for the first time that methylglyoxal (MG) and AGEs levels were elevated during mycobacterial infection of macrophages and that their increased levels mediated mycobacteria-induced apoptotic and immune response of macrophages. Moreover, we show that high levels of AGEs were formed at the sites of pulmonary tuberculosis. This observation represents the first evidence of the potential involvement of AGEs in tuberculosis and in infectious diseases in general. Global gene expression profiling of MG-treated macrophages reveals diversified potential roles of MG in cellular processes, including apoptosis, immune response, and growth regulation. The results of this study provide new insights into intervention strategies to develop therapeutic tools against infectious diseases in which MG and AGE production plays critical roles. **Keywords:** time course, replicates, immune response, apoptosis **Overall design:** MH-S cells (ATCC Number: CRL-2019), an alveolar macrophage cell line, was treated with 0.8 mM MG. At different time points after treatment (30 min, 4 h, and 8 h) the cells were harvested for total RNA preparation. As negative control the cells without treatment were included. RNA preparation was performed using Trizol method. Totally three independent experiments were performed, so that each time point consists of biological triplicates.

Background corr dist: KL-Divergence = 0.1074, L1-Distance = 0.0377, L2-Distance = 0.0029, Normal std = 0.4288

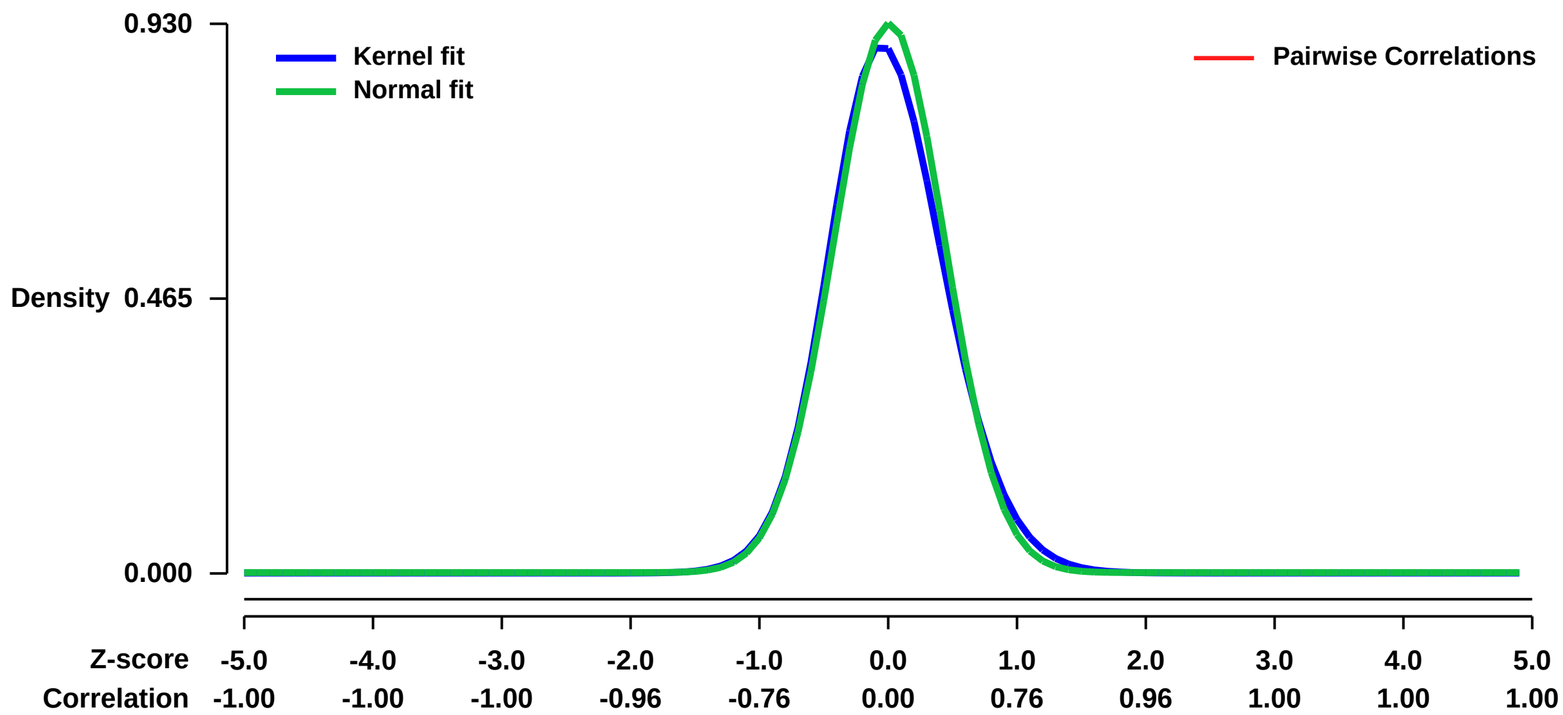

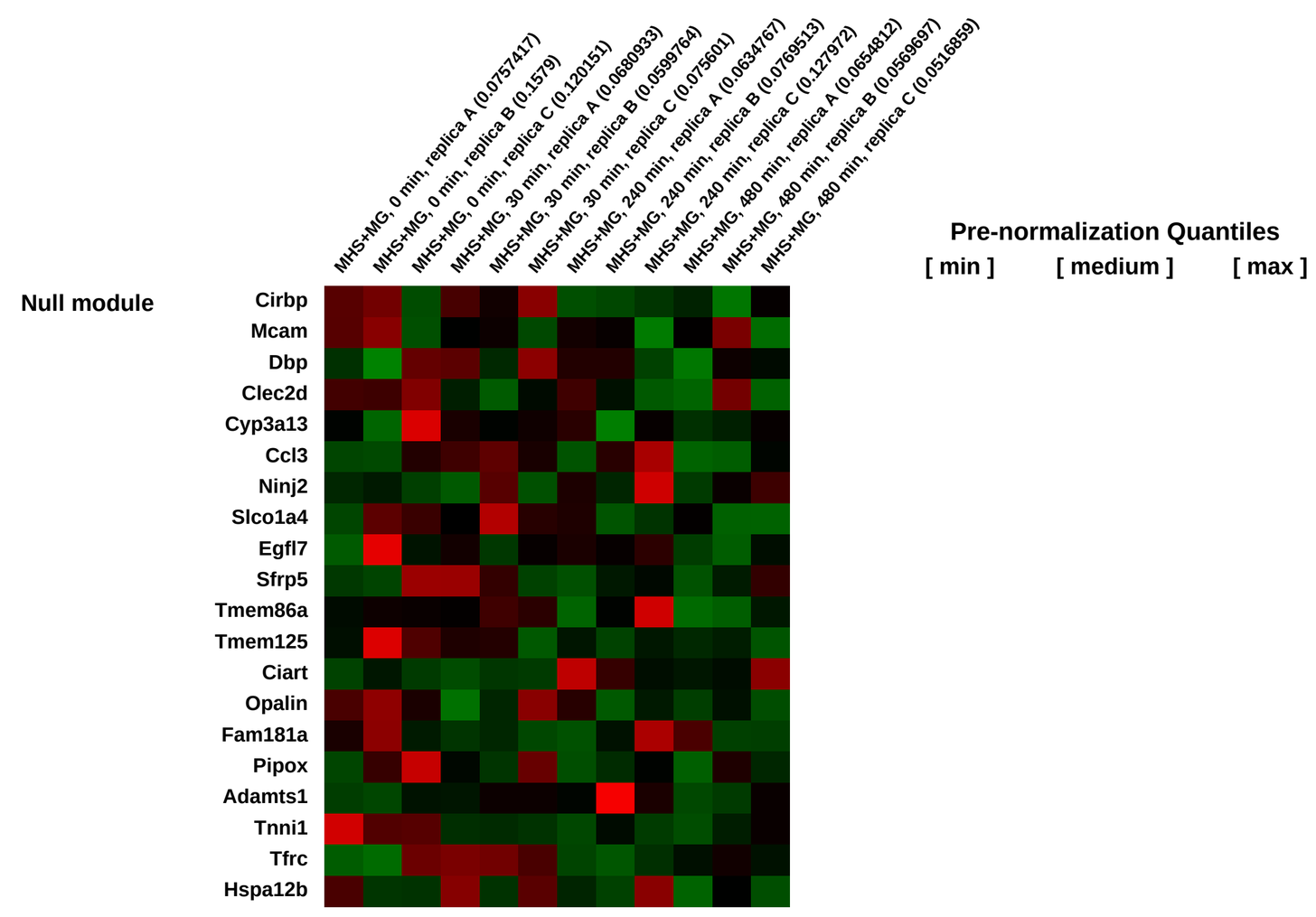

GEO Series "GSE38375" Expression Profiles

Num of samples in this series: 27

Scale of expression profile Z-scores

-3.0 -2.0 -1.0 0.0 1.0 2.0 3.0

GEO Link:	http://www.ncbi.nlm.nih.gov/geo/query/acc.cgi?acc=GSE38375
Status:	Public on Jul 01 2012
Title:	Interleukin-27 priming of T cells controls Interleukin-17-production in trans via induction of Programmed cell death ligand 1
Organism:	Mus musculus
Experiment type:	Expression profiling by array
Platform:	GPL1261
Pubmed ID:	
Summary & Design:	**Summary:** Interleukin (IL)-27 is a key immunosuppressive cytokine that counters T helper 17 (Th17) cell-mediated pathology. To identify mechanisms by which IL-27 might exert its immunosuppressive effect, we analyzed genes in T cells rapidly induced by IL-27. We found that IL-27 priming of naˆflve T cells upregulated expression of programmed death ligand 1 (PD-L1) in a signal transducer and activator of transcription (STAT)1-dependent manner. When co-cultured with naˆflve CD4+ T cells, IL-27-primed T cells inhibited the differentiation of Th17 cells in trans through a PD-1-PD-L1 interaction. In vivo, co-administration of naˆflve TCR transgenic T cells (2D2 T cells) with IL-27-primed T cells expressing PD-L1 inhibited the development of Th17 cells and protected from severe autoimmune encephalomyelitis. Thus, these data identify a suppressive activity of IL-27, by which CD4+ T cells can restrict differentiation of Th17 cells in trans. **Overall design:** The roles of IL-6 and IL-27 in naˆflve CD4+ T cells was investigated by comparing global gene expression by Affymetrix Mouse Genome 430 2.0 Arrays. The functional outcome of STAT proteins was further evaluated by profiling gene expression changes between WT and STAT-deficient T cells in naˆflve CD4+ T cells with specific stimulation. All condition were done in biological triplicate.

Background corr dist: KL-Divergence = 0.2235, L1-Distance = 0.0477, L2-Distance = 0.0049, Normal std = 0.3169

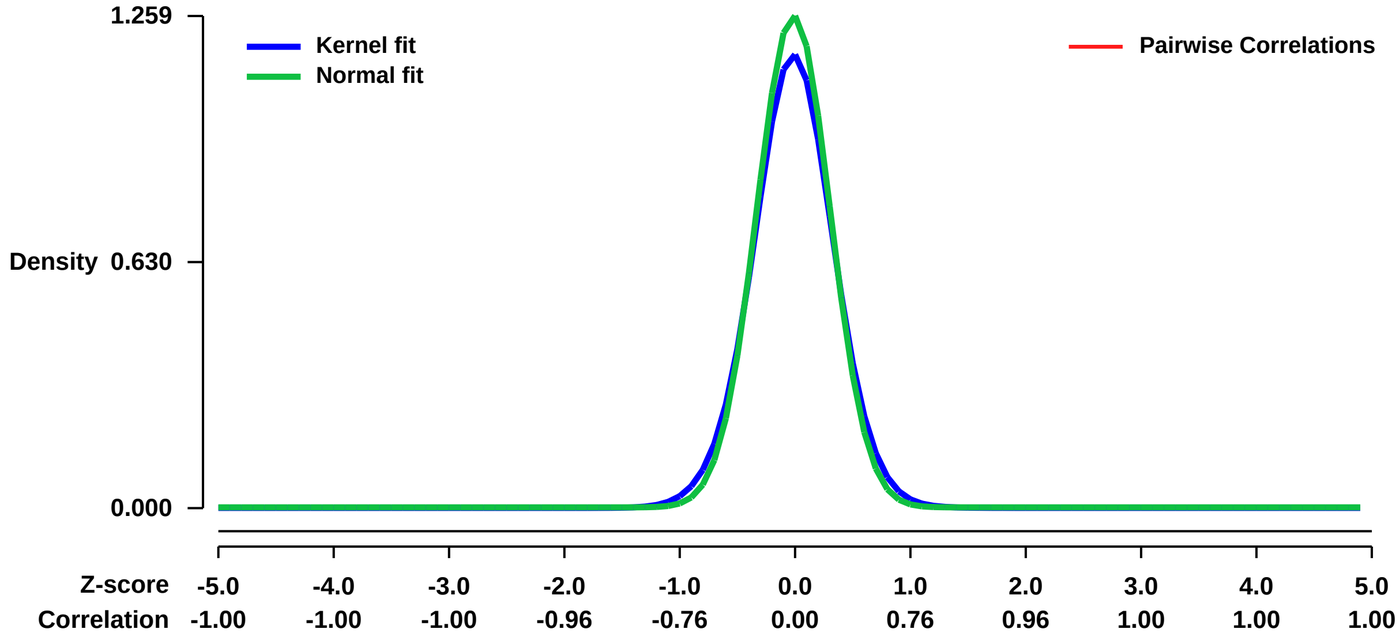

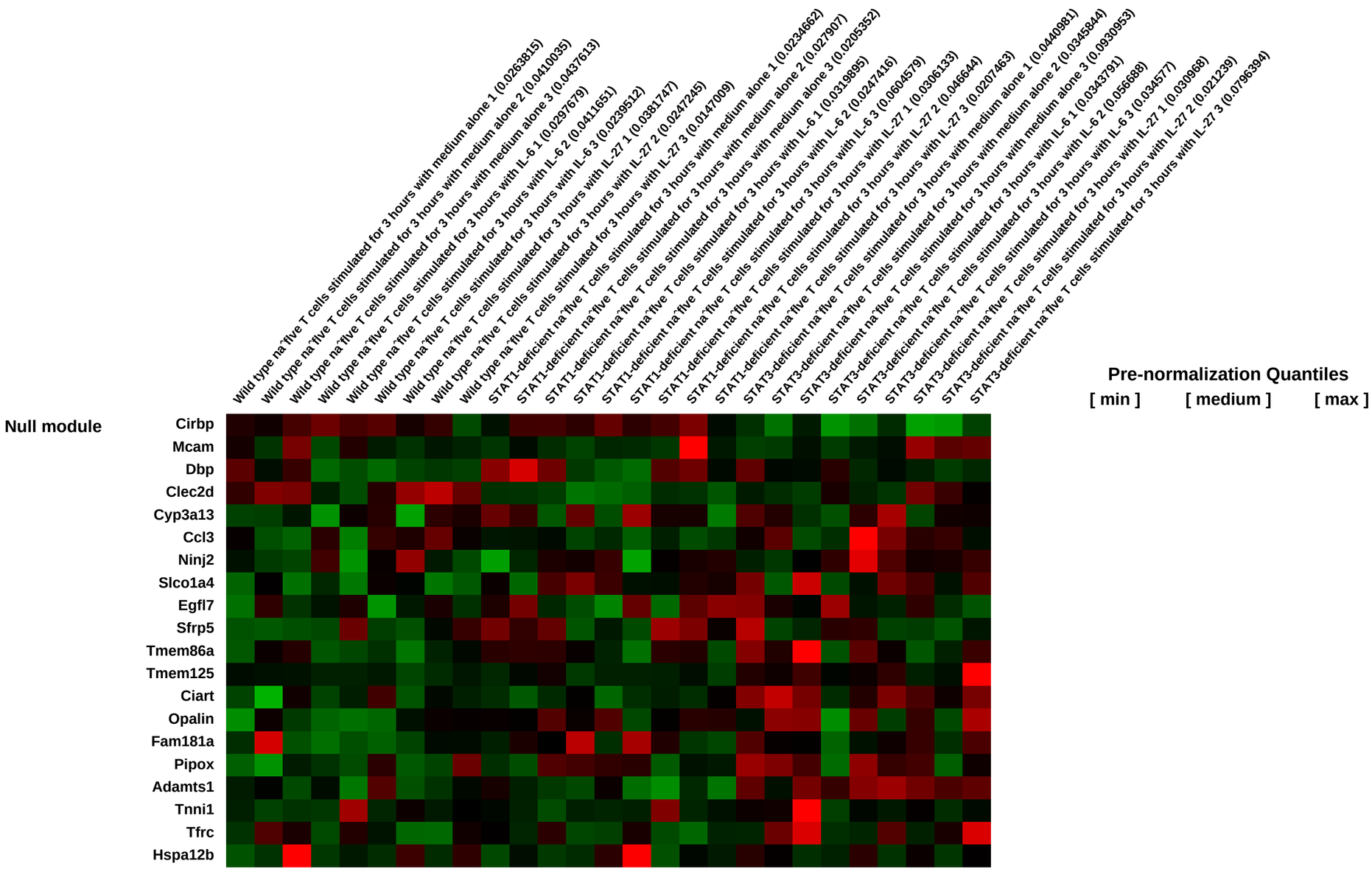

GEO Series "GSE38409" Expression Profiles

Num of samples in this series: 16

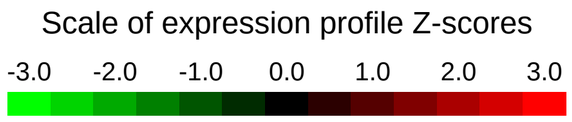

GEO Link:	http://www.ncbi.nlm.nih.gov/geo/query/acc.cgi?acc=GSE38409
Status:	Public on Jun 02 2012
Title:	Expression data from mouse lungs, exposed in-utero to second-hand smoke (SHS) and challenged with ovalbumin (OVA) as adults.
Organism:	Mus musculus
Experiment type:	Expression profiling by array
Platform:	GPL1261
Pubmed ID:	23898987
Summary & Design:	**Summary:** SHS exposure during pregnancy has adverse effects on offspring. We used microarrays to characterize the gene expression changes caused by in-utero SHS exposure and adult (19-23 weeks) OVA challenge in 23-week mouse lungs. **Overall design:** Left lungs from Balb/c male and female mice were collected at 23 weeks of age for RNA extraction and hybridization on Affymetrix mouse 430 2.0 microarrays. Based on the gender differences and in-utero exposure status, there are 4 groups of mice, females and males, exposed in-utero to filtered-air or SHS. All were exposure to OVA (19-23 weeks). We extracted RNA from 4 animals from each group for microarray analysis (total N = 16 samples).

Background corr dist: KL-Divergence = 0.0488, L1-Distance = 0.0396, L2-Distance = 0.0021, Normal std = 0.5850

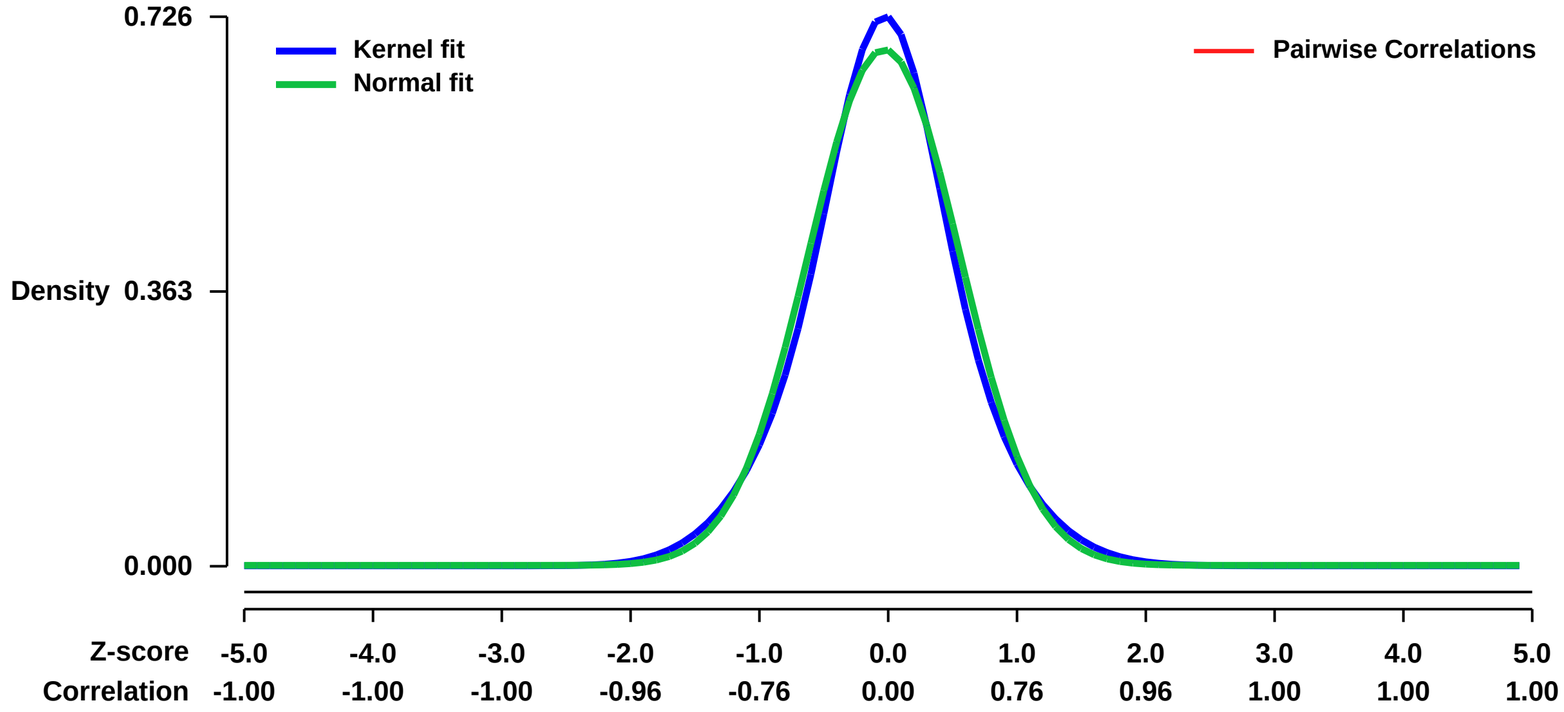

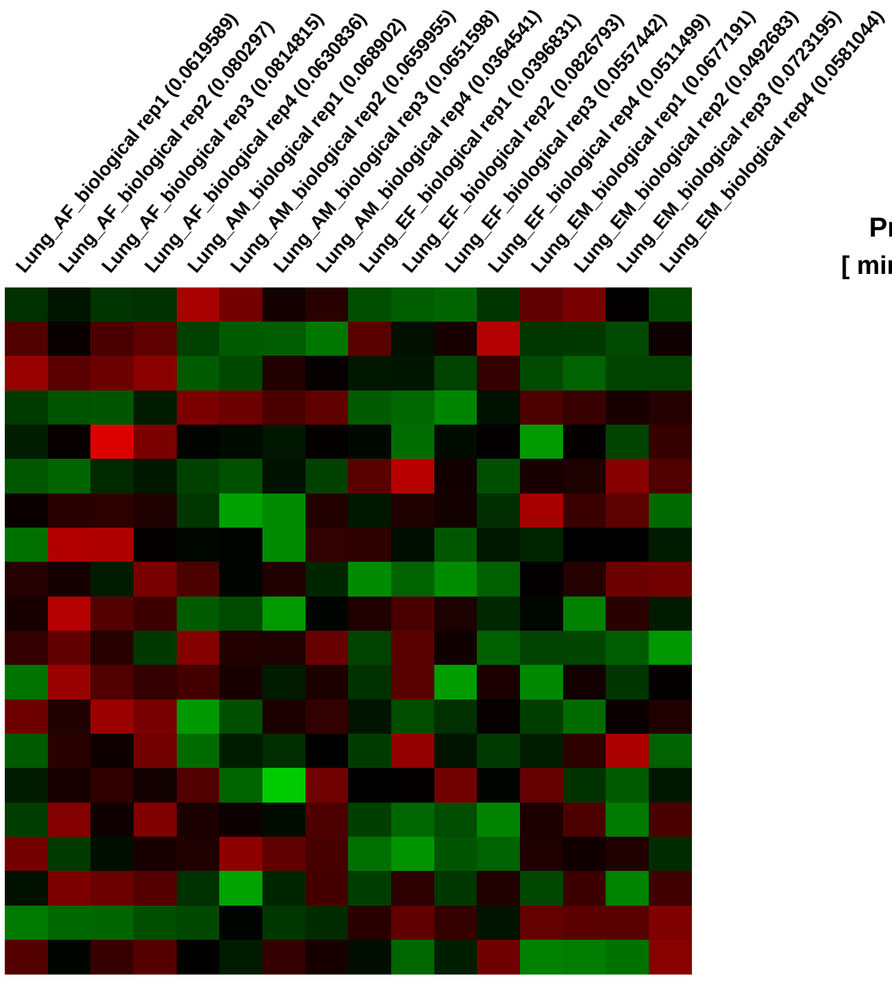

GEO Series "GSE3843" Expression Profiles

Num of samples in this series: 8

Scale of expression profile Z-scores

-3.0 -2.0 -1.0 0.0 1.0 2.0 3.0

GEO Link:	http://www.ncbi.nlm.nih.gov/geo/query/acc.cgi?acc=GSE3843
Status:	Public on Dec 22 2005
Title:	Targeted disruption of glycerol kinase gene in mice: expression analysis in liver
Organism:	Mus musculus
Experiment type:	Expression profiling by array
Platform:	GPL1261
Pubmed ID:	16368706
Summary & Design:	**Summary:** Glycerol kinase deficiency (GKD) is an X-linked inborn error of metabolism with metabolic and neurologic crises. Liver shows the highest level of glycerol kinase (GK) activity in humans and mice. Absence of genotype-phenotype correlations in patients with GKD indicate the involvement of modifier genes, including other network partners. To understand the molecular pathogenesis of GKD, we performed microarray analysis on liver mRNA from neonatal glycerol kinase (Gyk) knockout (KO) and wild type (WT) mice. Unsupervised learning revealed the overall gene expression profile of the KO mice was different from that of WT. Real time PCR confirmed differences for selected genes. Functional gene enrichment analysis was used to find 56 increased and 37 decreased gene functional categories. Pathway Assist analysis identified changes in gene expression levels of genes involved in organic acid metabolism indicating that GK was part of the same metabolic network which correlates well with the patients with GKD having metabolic acidemia during their episodic crises. Network component analysis (NCA) showed that transcription factors SREBP-1c, ChREBP, HNF-4alpha, and PPAR-alpha, had increased activity in the Gyk KO mice compared with WT mice; while SREBP-2 was less active in the Gyk KO mice. These studies show that Gyk deletion causes alterations in gene expression of genes in several regulatory networks and is the first time NCA has been used to expand on microarray data from a mouse knockout model of a human disease. **Keywords:** Glycerol kinase (Gyk) knockout mouse; mouse model of human Glycerol Kinase Deficiency; Gyk KO versus WT liver expression analysis; Affymetrix mus 430 2.0 GeneChip **Overall design:** Male WT and KO mouse pups were sacrificed on day of life (dol) 3 and each liver was harvested. Total RNA from 4 KO and 4 WT livers was isolated individually. cDNA was synthesized from the poly(A)+ mRNA in the total RNA, Biotin-tagged and fragmented to an average strand length of 100 bases (range 35-200 bases). Ten ´µg of each cRNA was hybridized onto an Affymetrix mus 430 2.0 GeneChip to analyze differences in liver gene expression between KO and WT mice. Day of life three was chosen because the mice are phenotypically symptomatic with statistically different parameters for hypoglycemia, acidosis; low bicarbonate and decreased base excess. On day of life 2 they are not significantly different from wild type in all of these important clinical phenotypes.

Background corr dist: KL-Divergence = 0.0646, L1-Distance = 0.0186, L2-Distance = 0.0005, Normal std = 0.5135

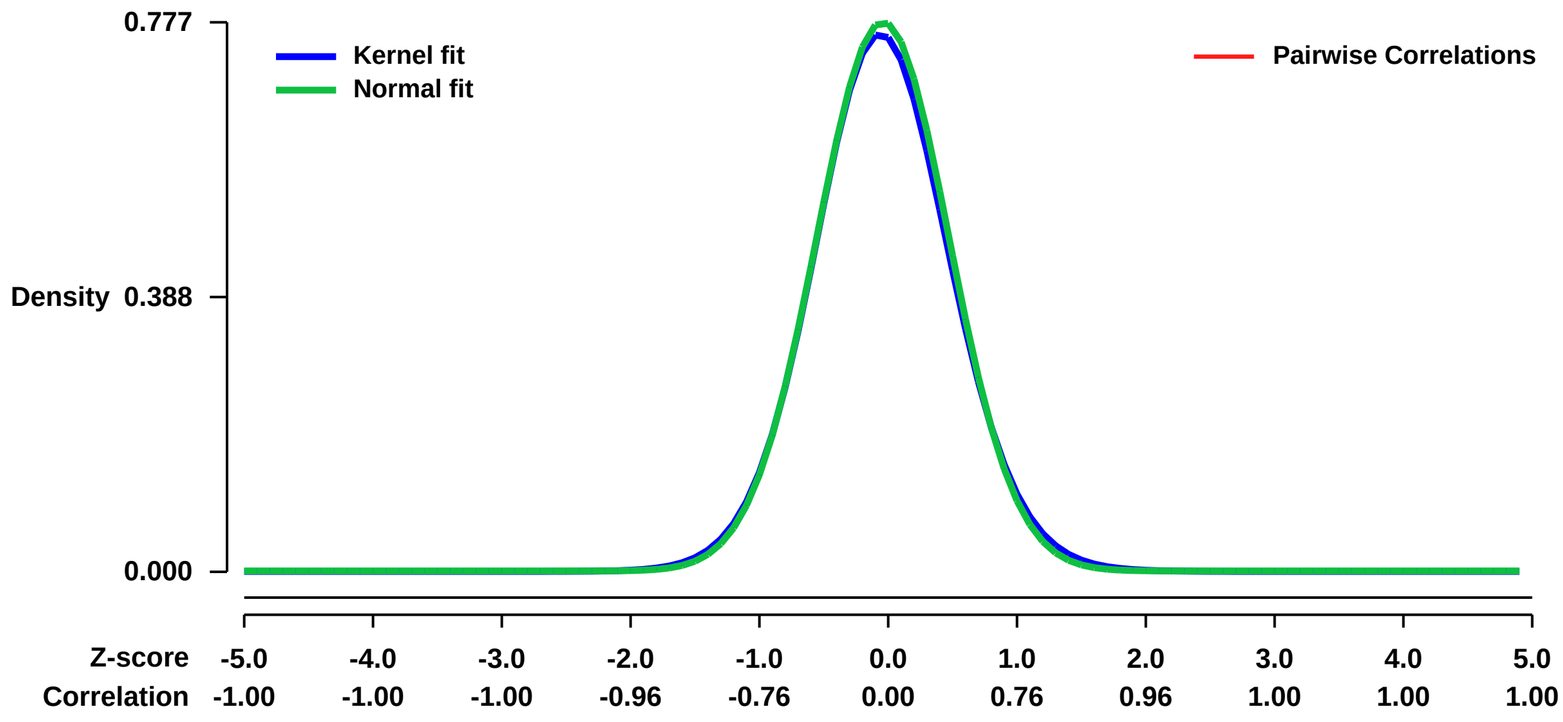

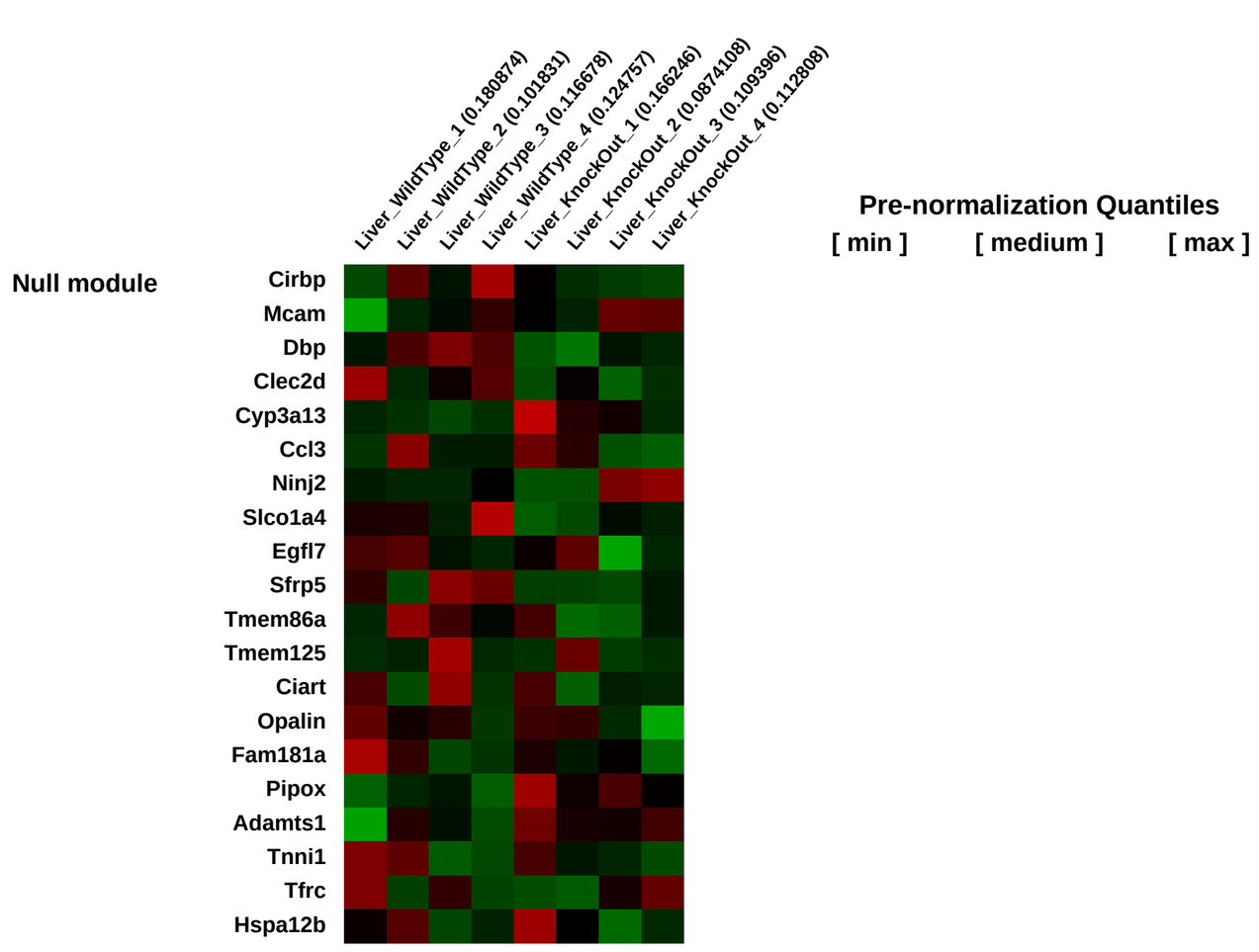

GEO Series "GSE38463" Expression Profiles

Num of samples in this series: 41

Scale of expression profile Z-scores

-3.0 -2.0 -1.0 0.0 1.0 2.0 3.0

GEO Link:	http://www.ncbi.nlm.nih.gov/geo/query/acc.cgi?acc=GSE38463
Status:	Public on Jan 14 2013
Title:	Gene expression profiling of mouse B cell progenitors
Organism:	Mus musculus
Experiment type:	Expression profiling by array
Platform:	GPL1261
Pubmed ID:	23334668
Summary & Design:	**Summary:** Gene expression profiling was performed of Pax5 wild type bone marrow subsets from common lymphoid progenitors through to Hardy stage F cells. These cells were obtained by flow sorting of bone marrow. **Overall design:** SNP & Sequencing data: dbGaP phs000341.v1.p1

Background corr dist: KL-Divergence = 0.2990, L1-Distance = 0.0620, L2-Distance = 0.0107, Normal std = 0.2837

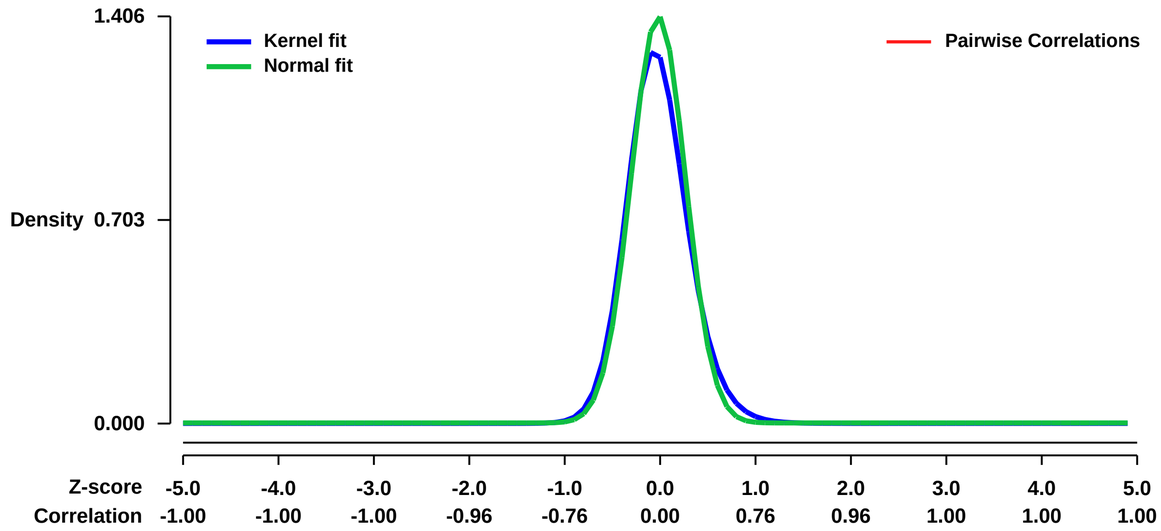

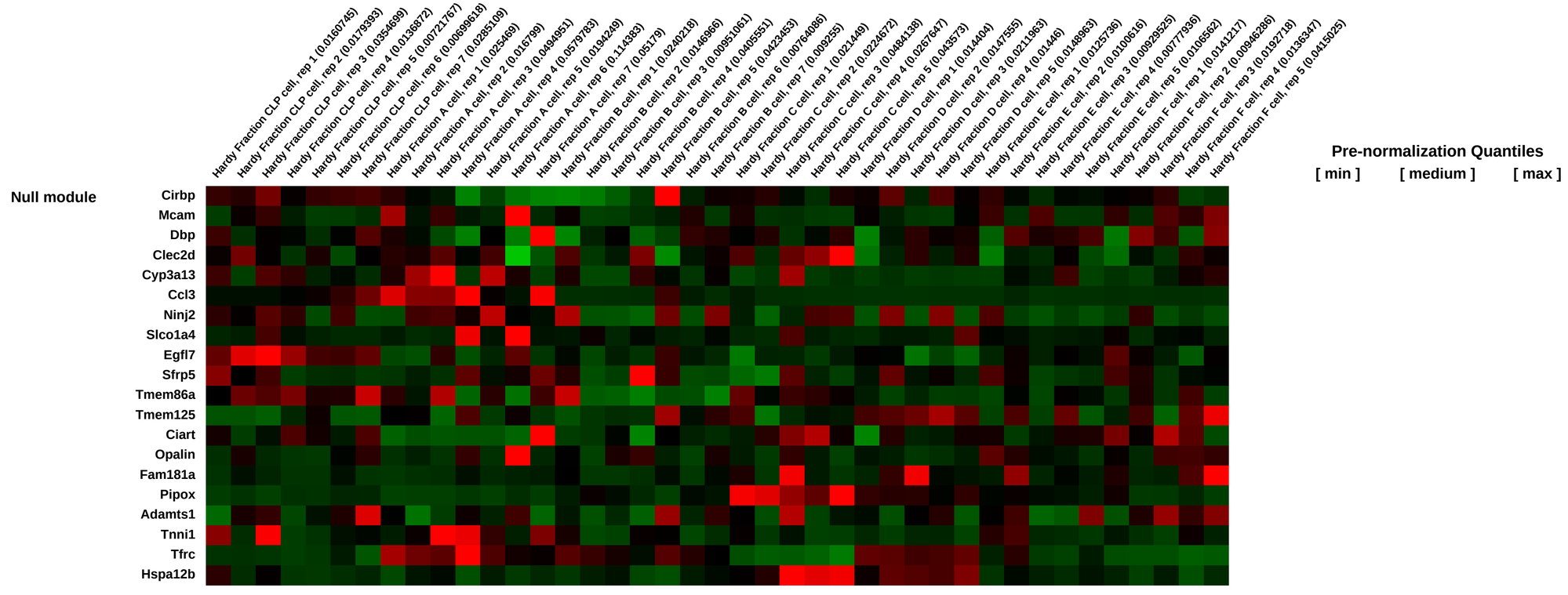

GEO Series "GSE38538" Expression Profiles

Num of samples in this series: 6

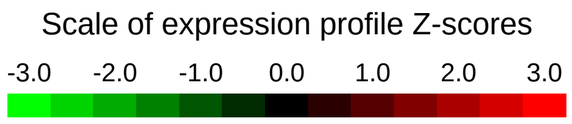

GEO Link:	http://www.ncbi.nlm.nih.gov/geo/query/acc.cgi?acc=GSE38538
Status:	Public on Jun 07 2012
Title:	Expression data from E12.5 NSP cells, CTL v REST shRNA
Organism:	Mus musculus
Experiment type:	Expression profiling by array
Platform:	GPL1261
Pubmed ID:	22791895
Summary & Design:	**Summary:** REST is a master regulator of genes that are involved in the acqusition of neuronal fate. The role of REST is not well understood so we attempted to investigate the role of REST in the development of neural cells by analysing the genes that are upregulated when REST is knocked down via shRNA We used microarrays to assess the genes which were up and down regulated after REST is knocked down **Overall design:** E12.5 NSP cells were infected with either control or REST shRNA expressing lentiviruses and collected after 6 days for RNA extraction

Background corr dist: KL-Divergence = 0.0362, L1-Distance = 0.0235, L2-Distance = 0.0007, Normal std = 0.6399

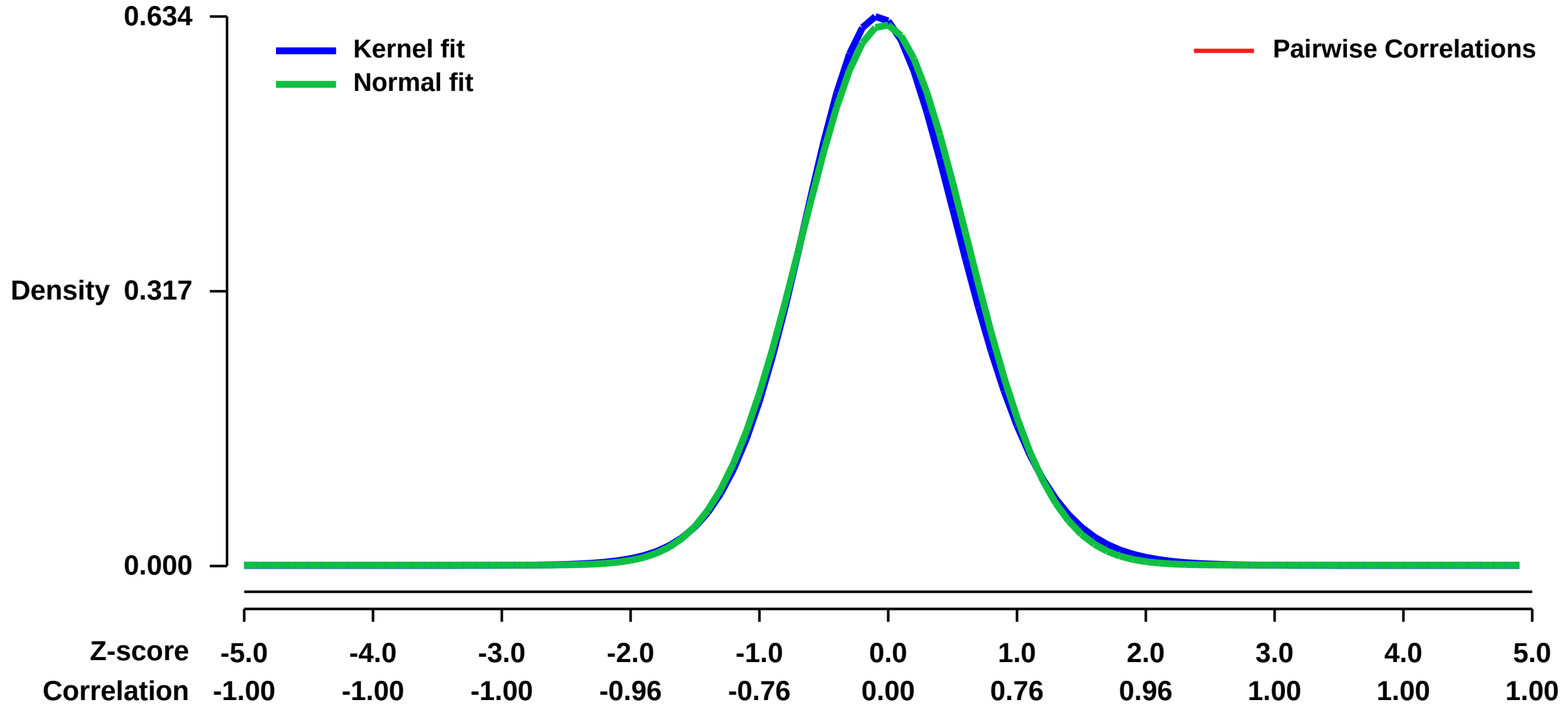

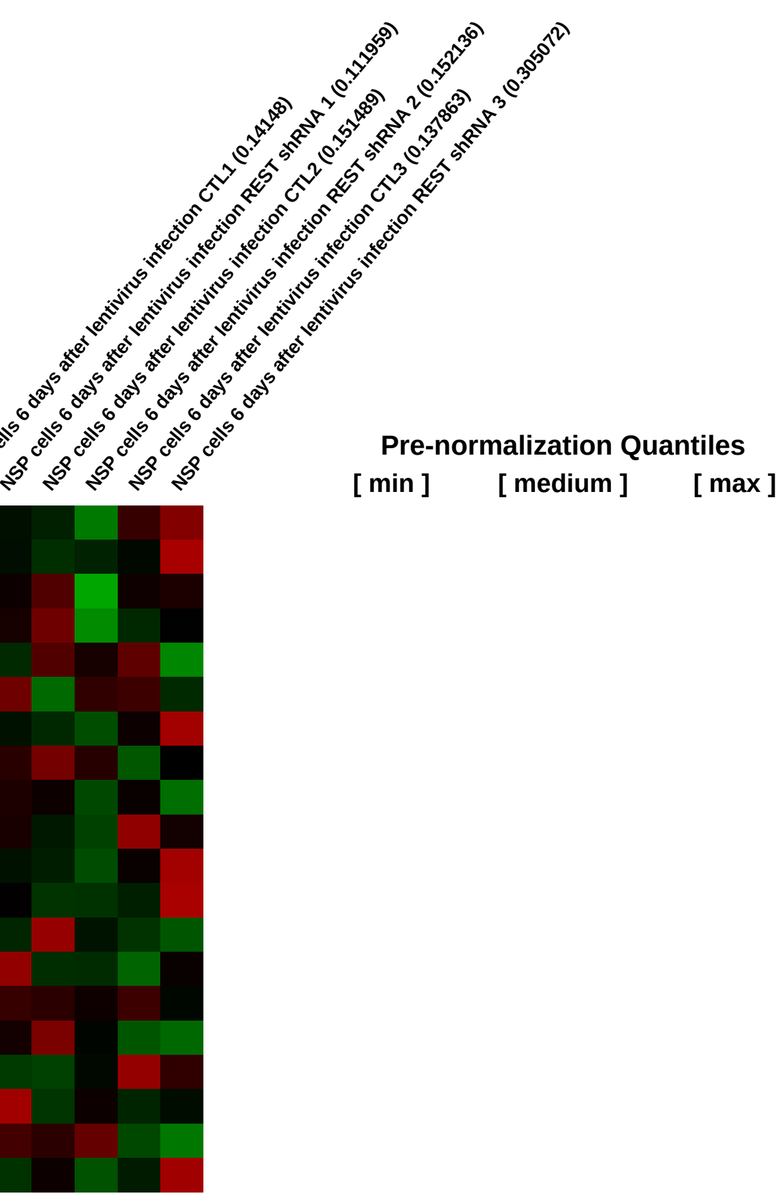

GEO Series "GSE38574" Expression Profiles

Num of samples in this series: 32

Scale of expression profile Z-scores

-3.0 -2.0 -1.0 0.0 1.0 2.0 3.0

GEO Link:	http://www.ncbi.nlm.nih.gov/geo/query/acc.cgi?acc=GSE38574
Status:	Public on Jun 08 2012
Title:	Gene expression data from Ldlr-/-, Apob100/100, Mttp flox/flox Mx1-Cre mice at different stages of atherosclerosis development
Organism:	Mus musculus
Experiment type:	Expression profiling by array
Platform:	GPL1261
Pubmed ID:	18369455
Summary & Design:	**Summary:** Gene expression profiles from the aortic arch of Ldlr-/-Apob100/100 Mttpflox/flox Mx1-Cre mice at different stages of atherosclerosis development **Overall design:** Total RNAs from the aortic arch were collected at different time points during atherosclerosis development (10, 20, 30, 40, 50, and 60 weeks of age), 4-7 mice per time point.

Background corr dist: KL-Divergence = 0.3656, L1-Distance = 0.0660, L2-Distance = 0.0123, Normal std = 0.2582

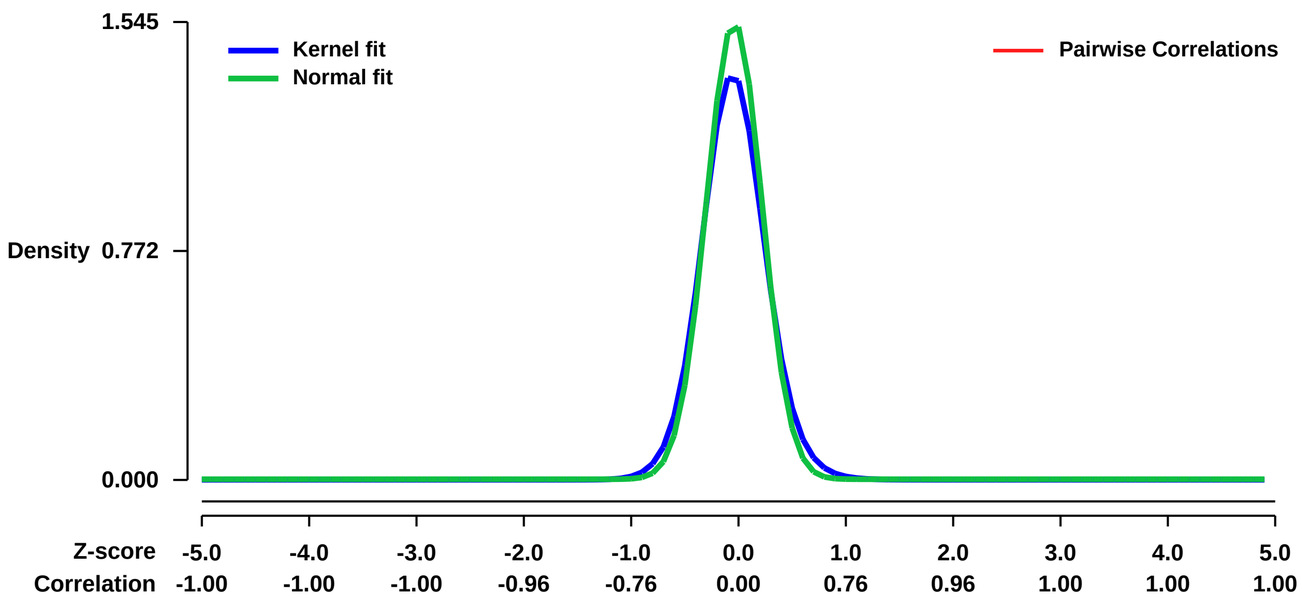

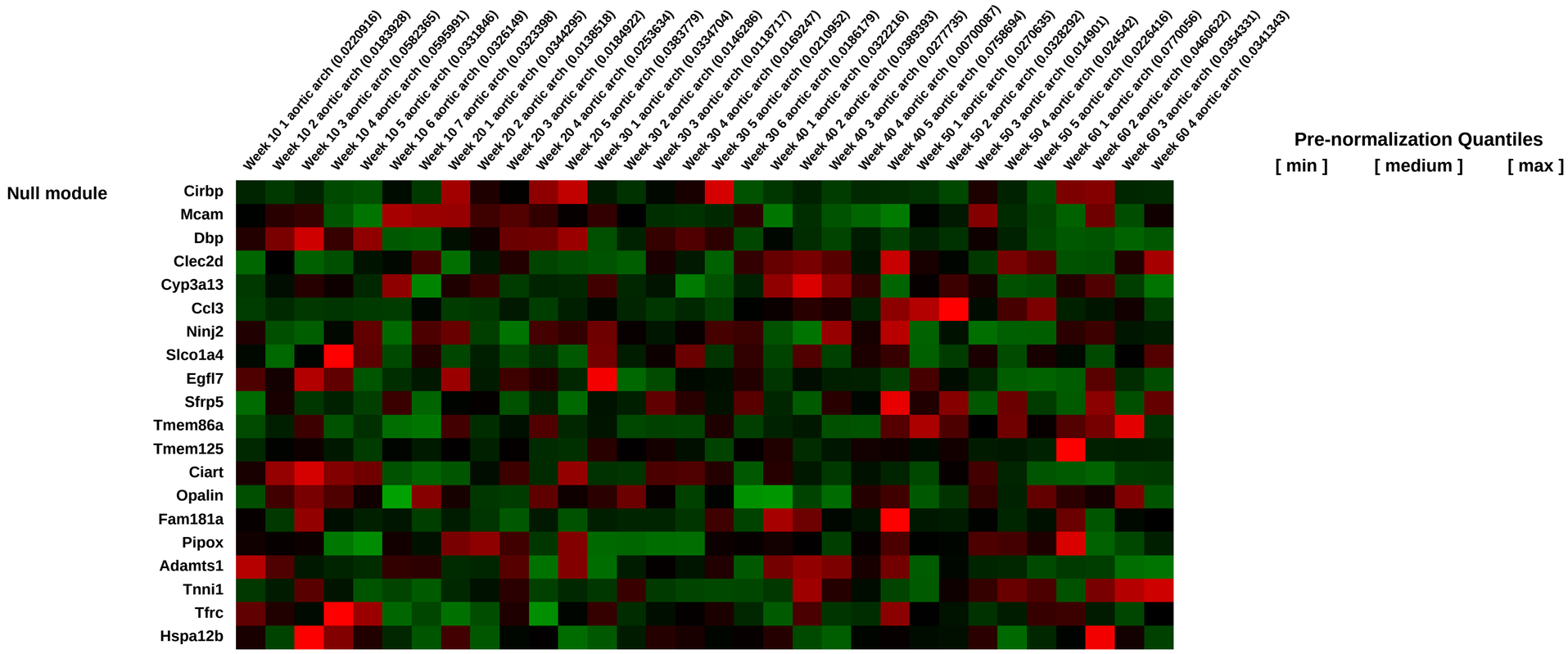

GEO Series "GSE3861" Expression Profiles

Num of samples in this series: 6

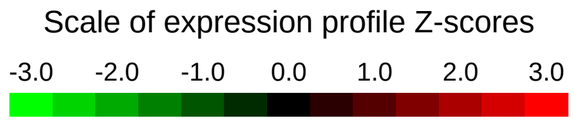

GEO Link:	http://www.ncbi.nlm.nih.gov/geo/query/acc.cgi?acc=GSE3861
Status:	Public on Mar 20 2006
Title:	Distinct hematopoietic cell fates regulated by graded expression of HOXA10
Organism:	Mus musculus
Experiment type:	Expression profiling by array
Platform:	GPL1261
Pubmed ID:	

Summary & Design:

Summary:
The homeobox (Hox) transcription factor HOXA10 has been implicated in regulation of hematopoietic cell fate. Here, using a transgenic mouse model where expression of HOXA10 is tightly regulated in a graded, doxycyclin-dependent manner we demonstrate that several key commitment steps in hematopoietic differentiation have distinctly different outcomes depending on the expression level of HOXA10. Similarly, HOXA10 regulates hematopoietic stem cell (HSC) proliferation in a dose dependent manner, since intermediate levels of HOXA10 generated a 4.5-fold increase in long-term repopulating capacity after 13 days of liquid culture, whereas high levels reduced proliferation of HSCs. Interestingly, the effects on HSC proliferation were associated with altered expression of several known regulators of stem cell self-renewal. Taken together, our findings reveal entirely novel functional and molecular aspects of HOXA10 in regulation of hematopoiesis and emphasize the need for tightly regulated production of HOX proteins in possible future applications of stem cell expansion.

Keywords: Affymetrix

Overall design:
LSK cells were sorted from rtTA-HA10 and cultured for 72 hours in complete serum free medium in three different concentrations of doxycycline (0, 0.1 and 0.5 ´¡g/ml doxycycline). RNA was extracted using RNeasy Mini kit, Qiagen, labeled and amplified according to AffymetrixTM Two Cycle Target Labeling Protocol. Hybridization and washing was performed according to AffymetrixTM GeneChip Expression protocol. Chips were scanned using an AffymetrixTM GeneChip Scanner 3000. The Affymetrix software GCOS was used to generate cell intensity data files (CEL) from two independent experiments. The CEL file data was then imported into the GeneSpring´fi software version 7.2 (Silicon Genetics, Redwood City, CA). The GC-RMA method was used for normalization and data was processed as follows: values below 0.01 were set to 0.01. All of the genes in each sample were divided by the median of the specified list of 100 positive control genes present on the MOE430 v2 chip. All samples were then normalized against the median of the untreated control samples. Each measurement for each gene in the treated samples was divided by the median of that gene's measurements in the corresponding control samples. We judged genes to be differentially expressed when the difference in expression between two conditions was at least 2-fold.

Background corr dist: KL-Divergence = 0.0353, L1-Distance = 0.0186, L2-Distance = 0.0004, Normal std = 0.6391

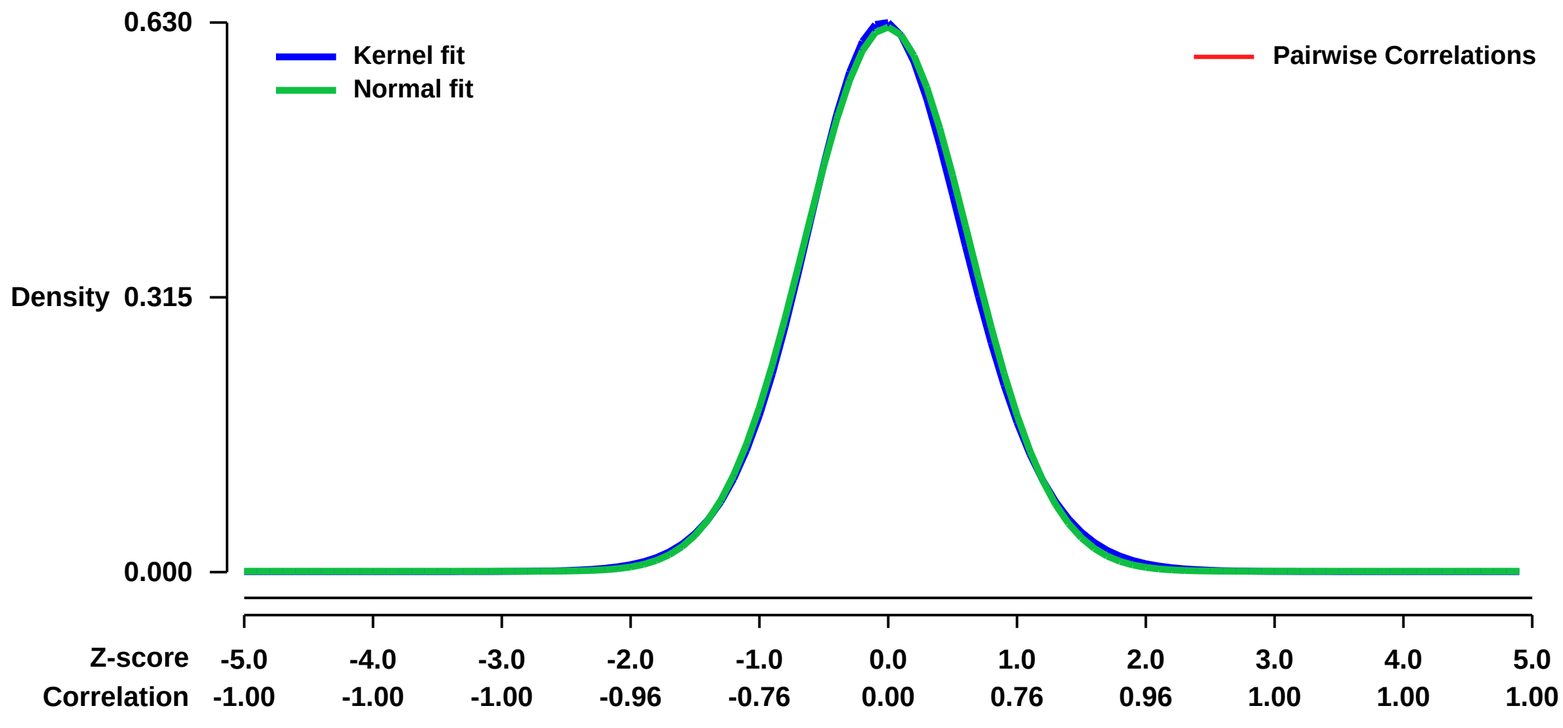

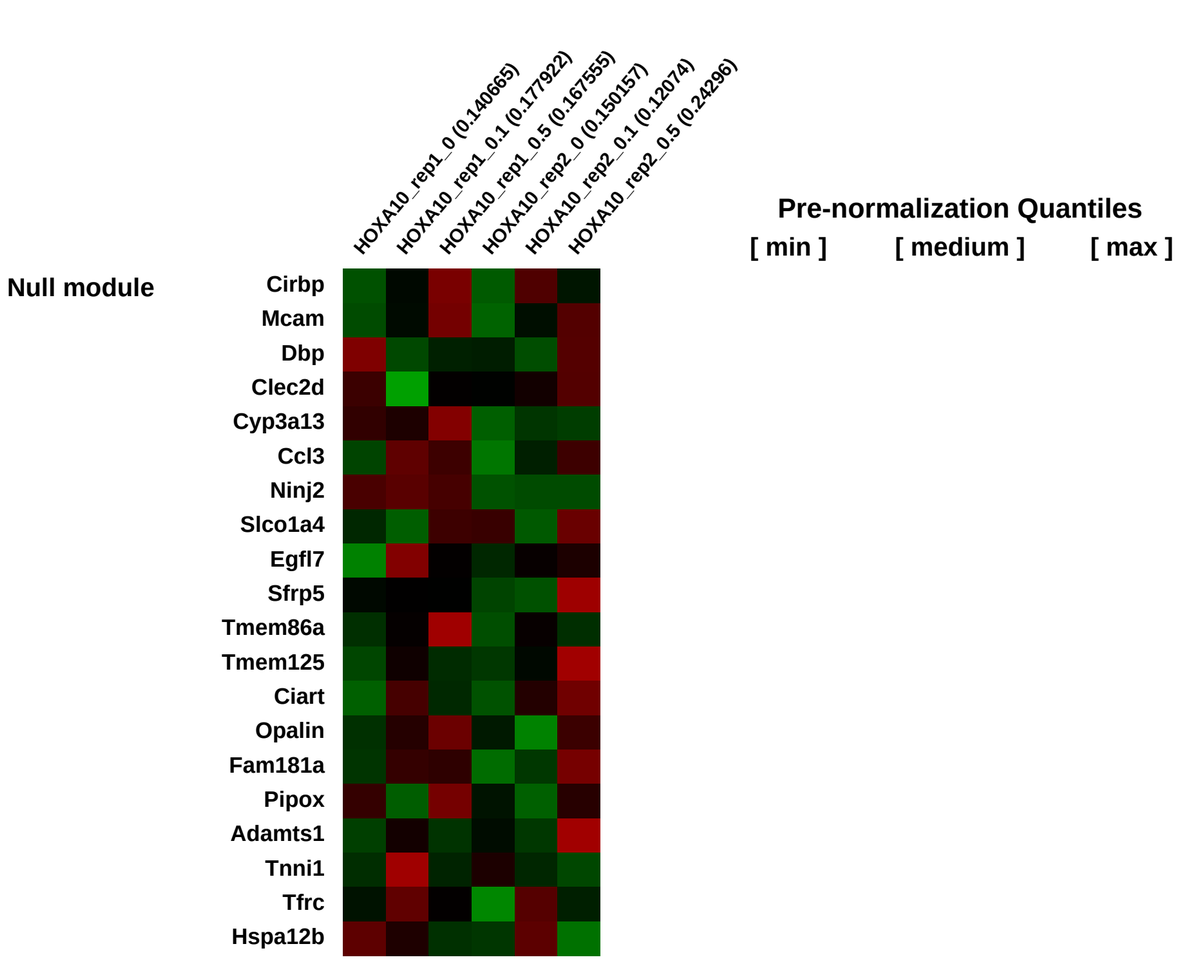

GEO Series "GSE38672" Expression Profiles

Num of samples in this series: 6

Scale of expression profile Z-scores

-3.0 -2.0 -1.0 0.0 1.0 2.0 3.0

GEO Link:	http://www.ncbi.nlm.nih.gov/geo/query/acc.cgi?acc=GSE38672
Status:	Public on Nov 16 2012
Title:	Deletion of miRNA processing enzyme Dicer in POMC-expressing cells leads to neurodegeneration and development of obesity
Organism:	Mus musculus
Experiment type:	Expression profiling by array
Platform:	GPL1261
Pubmed ID:	
Summary & Design:	**Summary:** The activity of the endoribonuclease Dicer is crucial to produce the mature form of most microRNAs (miRNAs). Recent studies indicate that lack of miRNAs in different neuronal types results in a range of anatomical and behavioural phenotypes. In the present study we aimed to investigate the developmental and metabolic consequences of miRNA ablation in hypothalamic POMC neurons studying mice with a conditional deletion of Dicer in this population of neurons (POMCDicerKO). These mice exhibited a progressive obese phenotype characterized by hyperphagia, increased adiposity, hyperleptinemia, defective glucose metabolism and alterations in the pituitary-adrenal axis. The development of the obese phenotype was paralleled by a POMC neuron degenerative process that was complete by 6 weeks of age. Furthermore, immunohistochemistry and gene expression studies in control C57Bl/6 adult mice showed that Dicer was expressed in relevant hypothalamic areas and neurons implicated in energy balance, and that its expression was regulated by nutrient availability. Collectively, our results highlight a crucial role for miRNAs in POMC neuron survival and the consequent development of neurodegenerative obesity. **Overall design:** Total RNA was extracted from hypothalamic microdissections of 2-week old control and POMCDicerKO mice using the RNeasy micro spin columns (Qiagen, Venlo, The Netherlands). Ten micrograms of total RNA were converted into cRNA, biotinylated, fragmented, and hybridized to GeneChip Mouse Genome 430 2.0 (Affymetrix, Santa Clara, CA). Six microarrays were hybridized with three independent samples from control and POMCDicerKO mice.

Background corr dist: KL-Divergence = 0.0435, L1-Distance = 0.0161, L2-Distance = 0.0002, Normal std = 0.5962

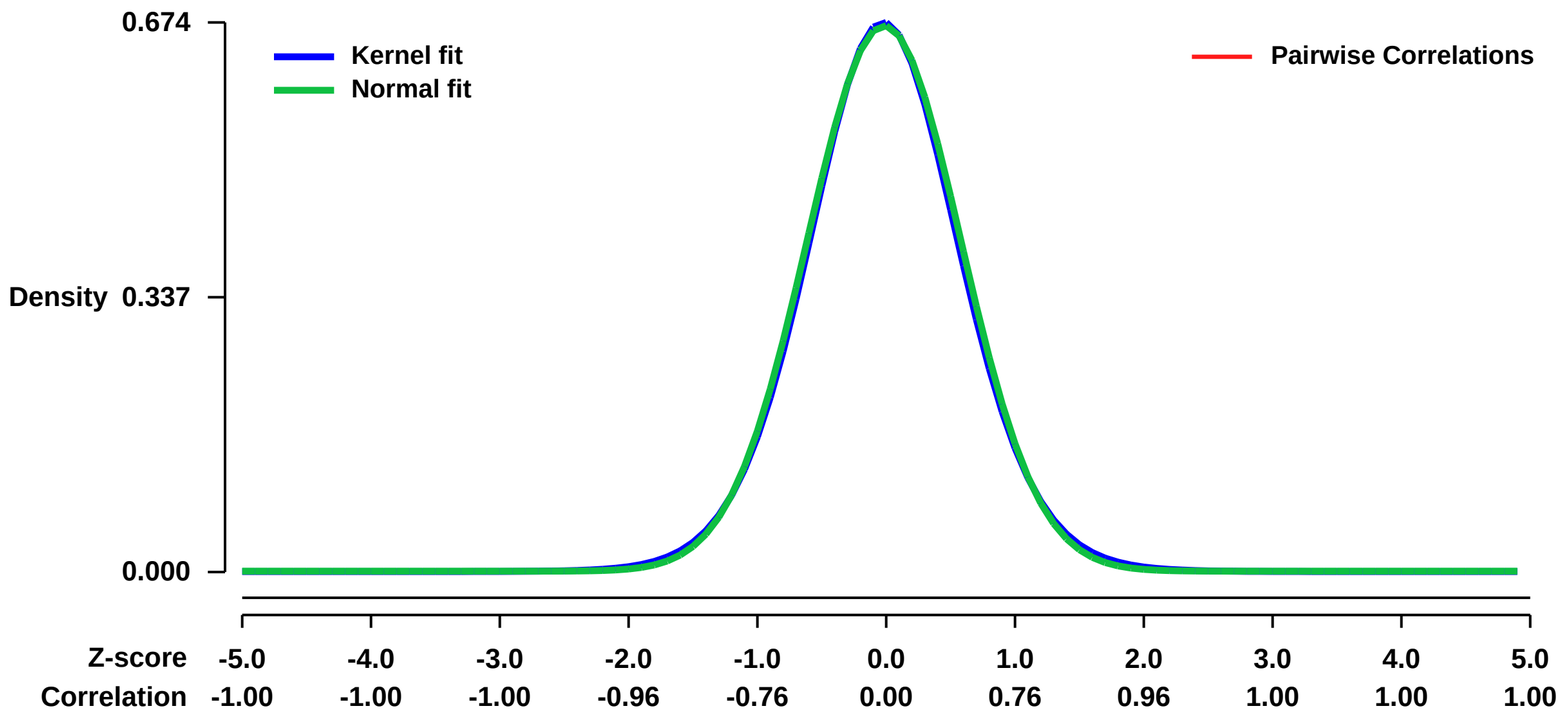

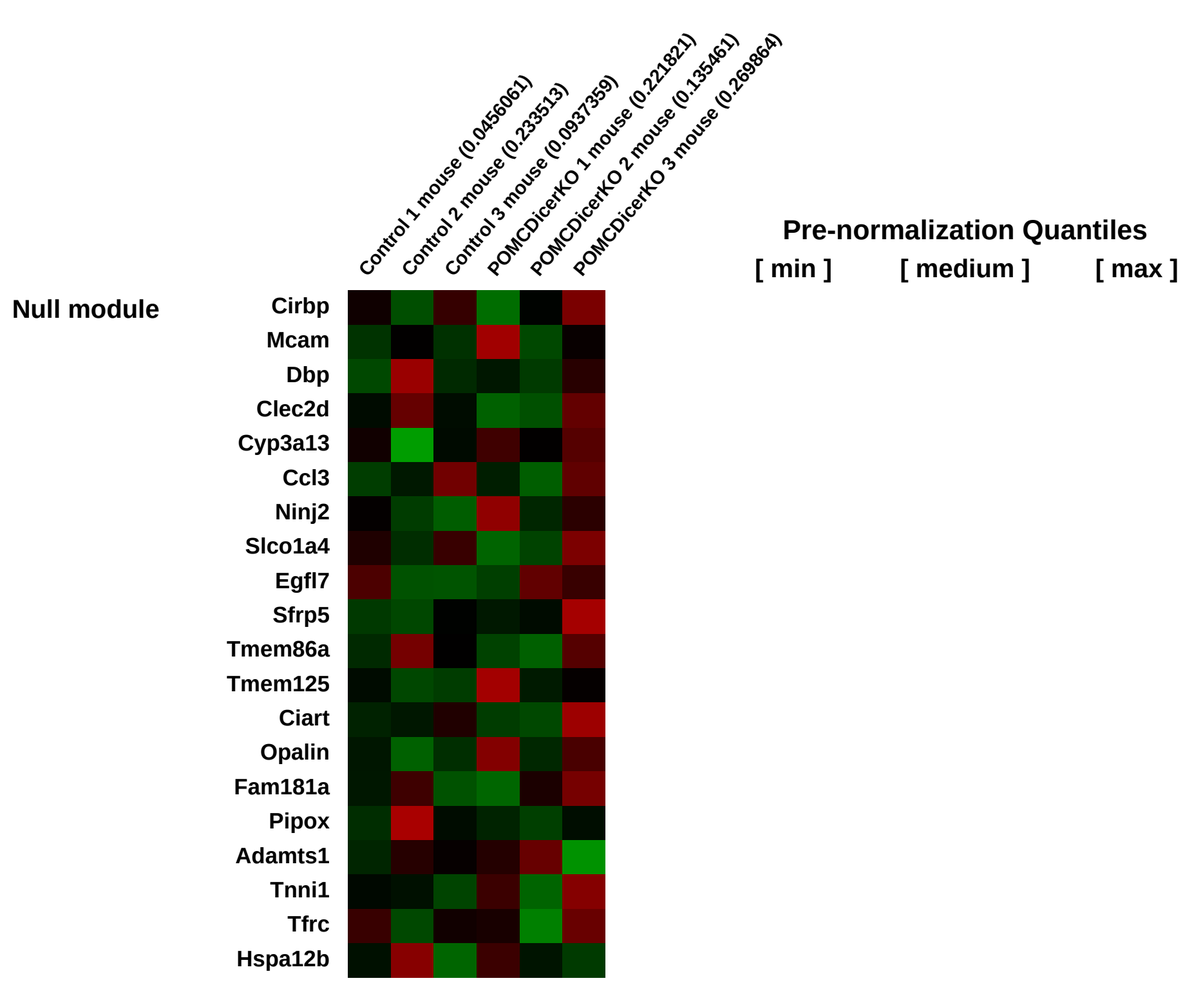

GEO Series "GSE38693" Expression Profiles

Num of samples in this series: 8

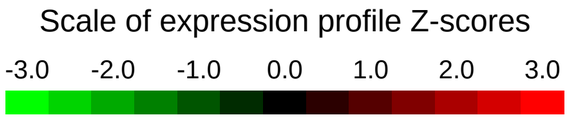

GEO Link:	**http://www.ncbi.nlm.nih.gov/geo/query/acc.cgi?acc=GSE38693**
Status:	**Public on Jun 14 2012**
Title:	**c-JUN REPROGRAMS SCHWANN CELLS OF INJURED NERVES TO GENERATE A REPAIR CELL ESSENTIAL FOR REGENERATION**
Organism:	**Mus musculus**
Experiment type:	**Expression profiling by array**
Platform:	**GPL1261**
Pubmed ID:	
Summary & Design:	**Summary:** **The striking PNS regenerative response to injury rests on the plasticity of adult Schwann cells and their ability to transit between differentiation states, a highly unusual feature in mammals. Using mice with inactivation of Schwann cell c-Jun, we show that the injury response involves c-Jun dependent natural reprograming of differentiated cells to generate a distinct Schwann cell state specialized to promote regeneration. Transected distal stumps of c-Jun mutants show 172 disregulated genes, resulting in abnormal expression of growth factors, adhesion molecules and cytoskeletal changes that lead to neuronal death, inhibition of axon growth and striking failures of functional repair after injury. These observations provide a molecular basis for understanding Schwann cell plasticity and nerve regeneration. They offer conclusive support for the notion that Schwann cells control repair in the PNS, using dedicated transcriptional controls to generate a distinct repair cell, a transition that shows similarities to transdifferentiation seen in other systems.** **Overall design:** **Total RNA was purified from a 10mm segment of the distal stump and uninjured contralateral nerve from c-Jun mutants and control mice 7 days after nerve cut. For each condition (injured/uninjured) and genotype (control/ knock-out) 2 independent samples (replicates) were generated from pooled nerves of 4/6 mice resulting in a total of 8 samples: CTRL.cut.R1, CTRL.cut.R2, CTRL.uncut.R1, CTRL.uncut.R2, KO.cut.R1, KO.cut.R2, KO.uncut.R1,KO.uncut.R2.**

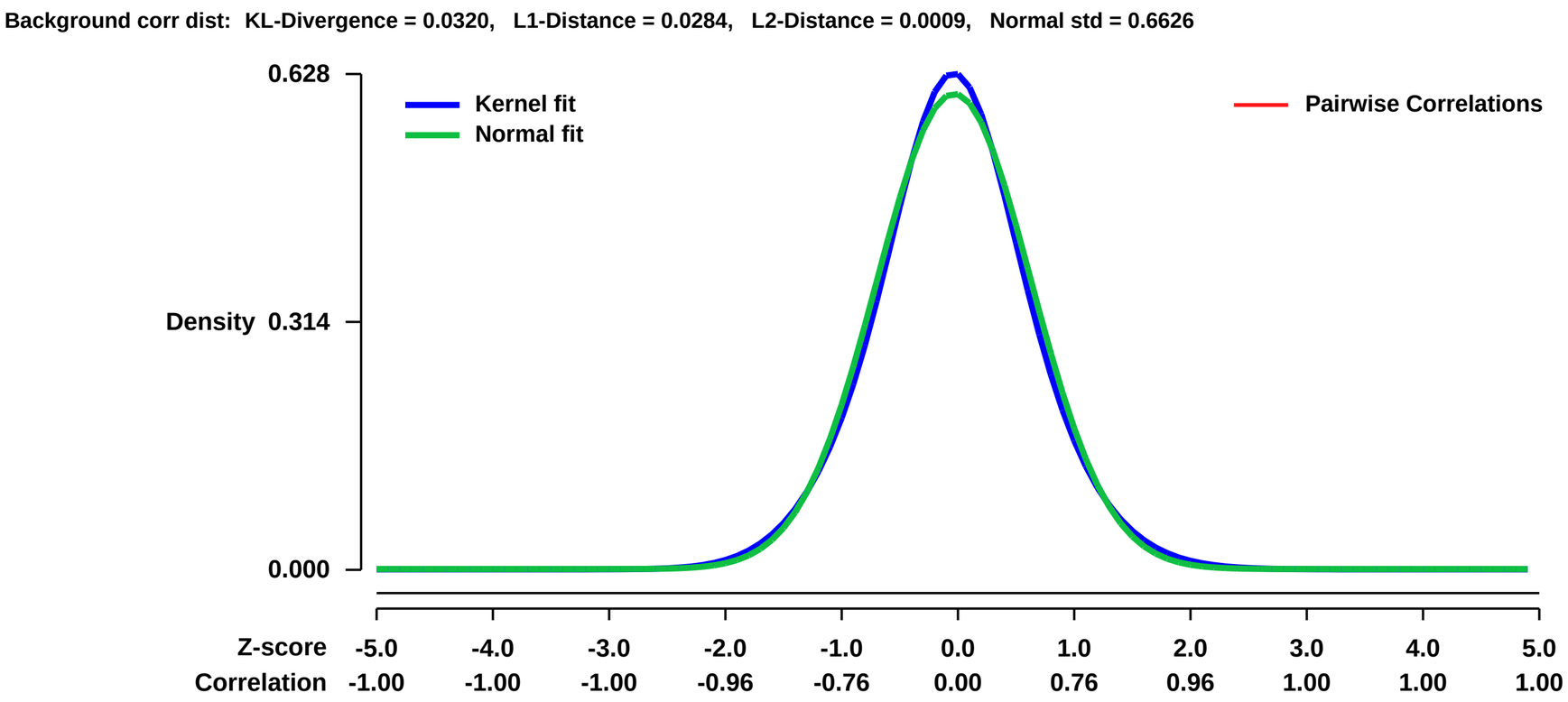

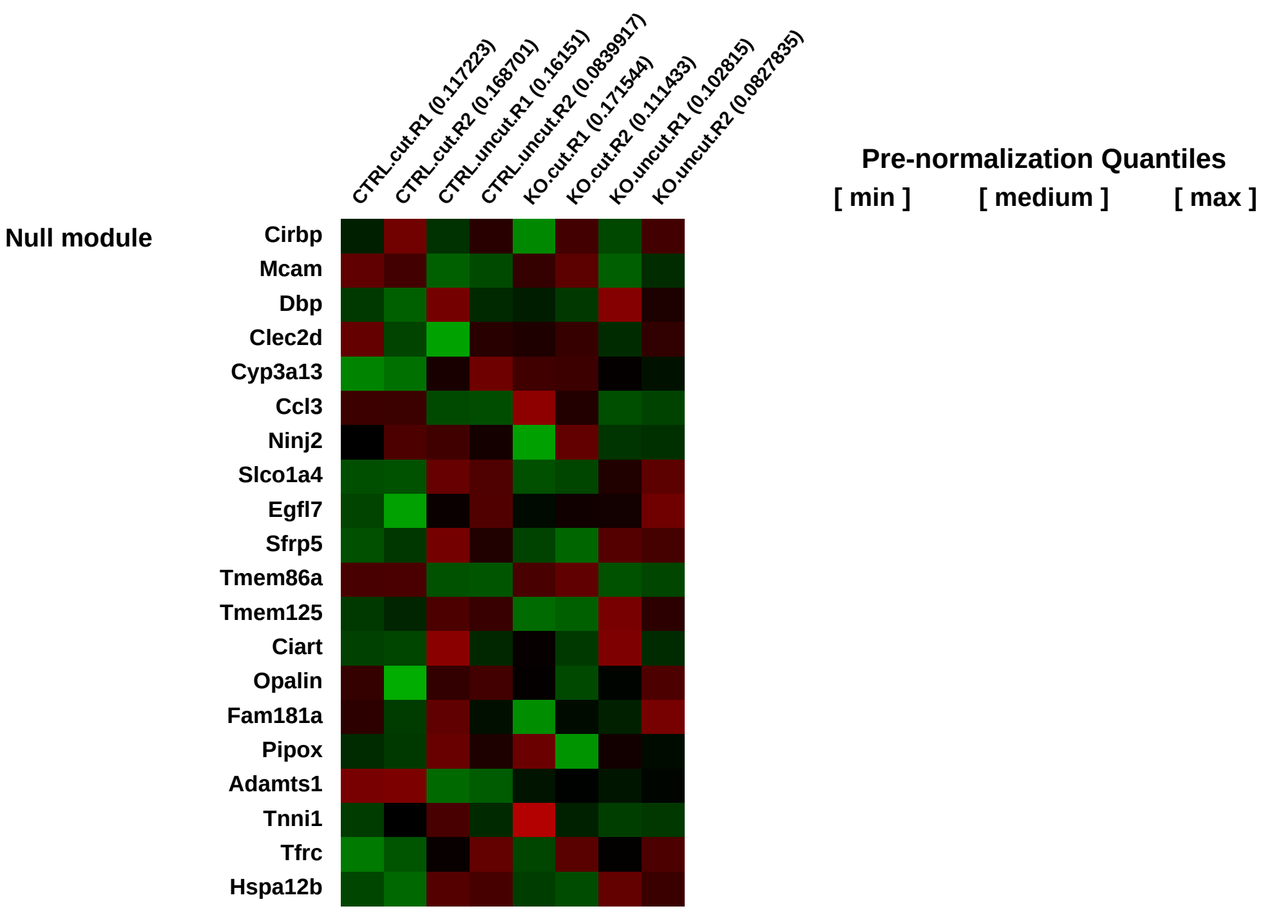

GEO Series "GSE38696" Expression Profiles

Num of samples in this series: 8

Scale of expression profile Z-scores

-3.0 -2.0 -1.0 0.0 1.0 2.0 3.0

GEO Link:	http://www.ncbi.nlm.nih.gov/geo/query/acc.cgi?acc=GSE38696
Status:	Public on Jun 14 2012
Title:	Gene expression in mouse germinal center light zone and dark zone B cells
Organism:	Mus musculus
Experiment type:	Expression profiling by array
Platform:	GPL1261
Pubmed ID:	22740445
Summary & Design:	**Summary:** Microarrays of gene expression in mouse germinal center light zone and dark zone B cells sorted according to the expression of cell surface molecules CD83 and CXCR4 We used microarray data to identify genes differentially expressed by B cells in the light and dark zones of germinal centers from mouse skin-draining lymph nodes 12 days after subcutaneous immunization with NP-OVA in alum. **Overall design:** Germinal center B cells (B220+CD38-CD95+) were sorted from immunized mouse lymph nodes into light zone (CXCR4hi/CD83lo) and dark zone (CXCR4lo/CD83hi) populations, from which RNA was extracted

Background corr dist: KL-Divergence = 0.0538, L1-Distance = 0.0239, L2-Distance = 0.0006, Normal std = 0.5628

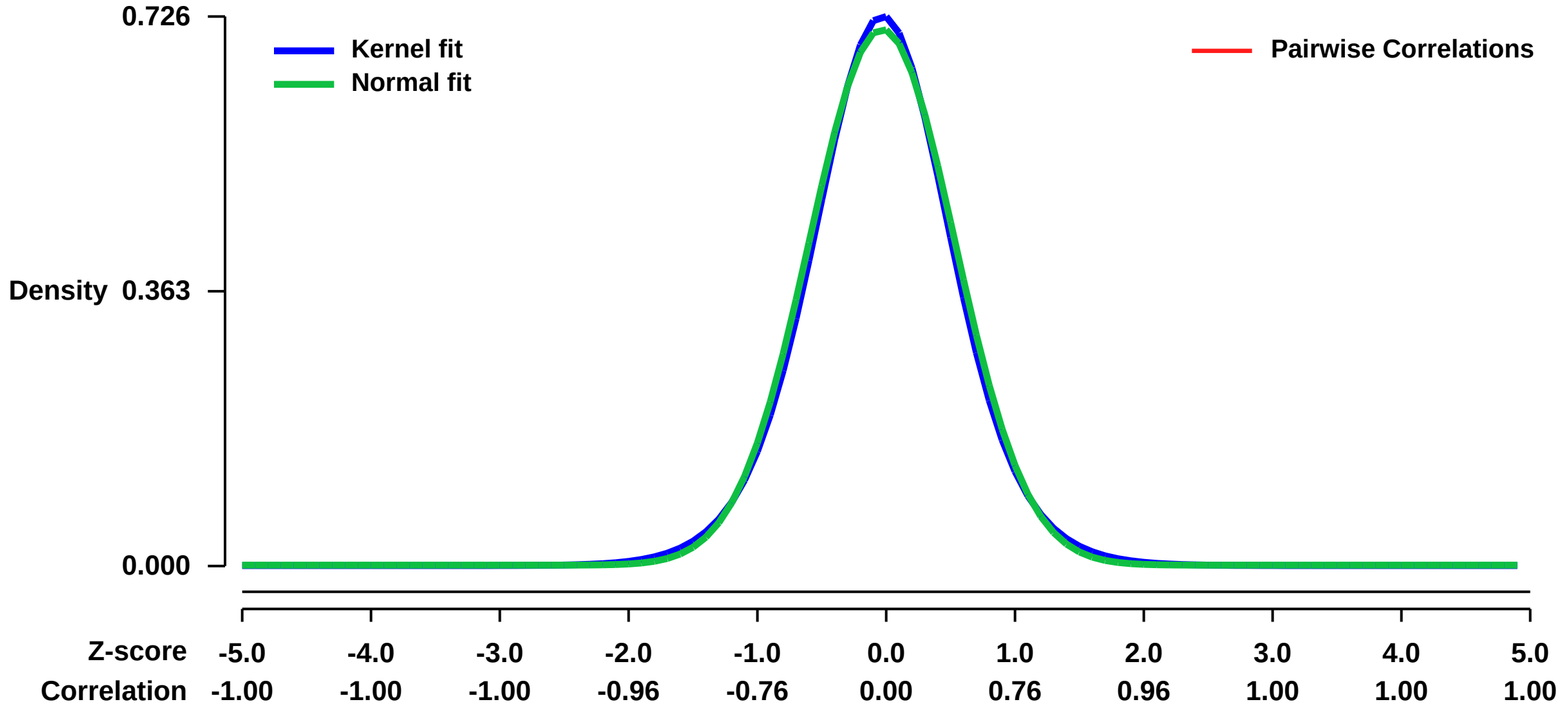

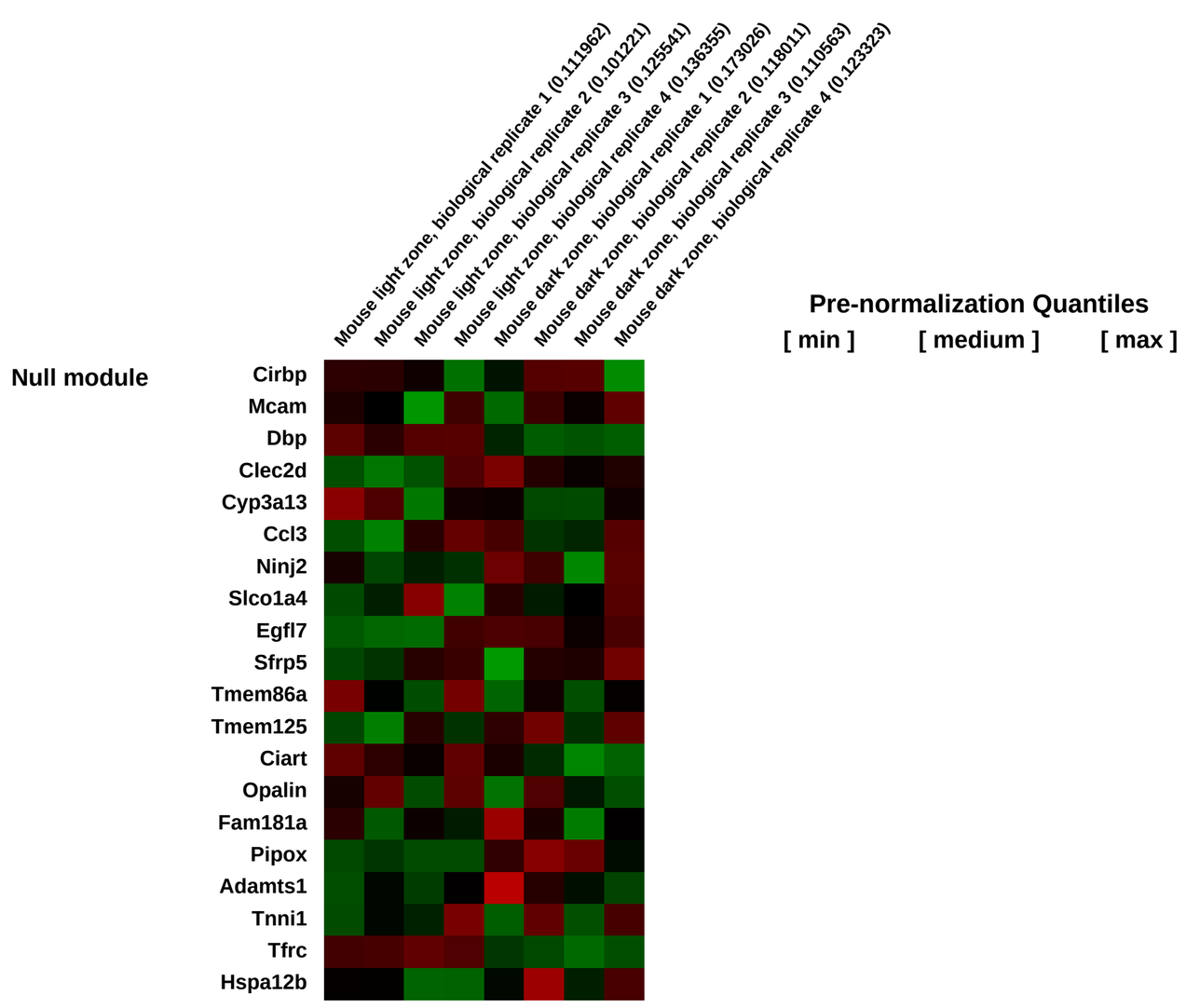

GEO Series "GSE38797" Expression Profiles

Num of samples in this series: 16

Scale of expression profile Z-scores

-3.0 -2.0 -1.0 0.0 1.0 2.0 3.0

GEO Link:	http://www.ncbi.nlm.nih.gov/geo/query/acc.cgi?acc=GSE38797
Status:	Public on Jul 16 2012
Title:	Expression values from wild-type retinas and retinas with a mutant Rhodopsin transgene (Tg(RHO P347S)) with and without Endothelin-2 (EDN2)
Organism:	Mus musculus
Experiment type:	Expression profiling by array
Platform:	GPL1261
Pubmed ID:	
Summary & Design:	**Summary:** Expression of the Endothelin-2 (Edn2) mRNA is greatly increased in the photoreceptors (PRs) of mouse models of inherited PR degeneration. To identify retinasl gene whose expression is directly or indirectly regulated by EDN2 in the presence of the Tg(RHO P347S) mutant allele, we defined mRNAs that were differentially expressed in Edn2+/+, Edn2-/-, Tg(RHO P347S) Edn2+/+, and Tg(RHO P347S) Edn2-/- retinas. **Overall design:** RNA was extracted from Edn2+/+, Edn2-/-, Tg(RHO P347S) Edn2+/+, and Tg(RHO P347S) Edn2-/- retinas at postnatal day 21 (PN21) and hybridized to Affymetrix arrays

Background corr dist: KL-Divergence = 0.1800, L1-Distance = 0.0456, L2-Distance = 0.0046, Normal std = 0.3454

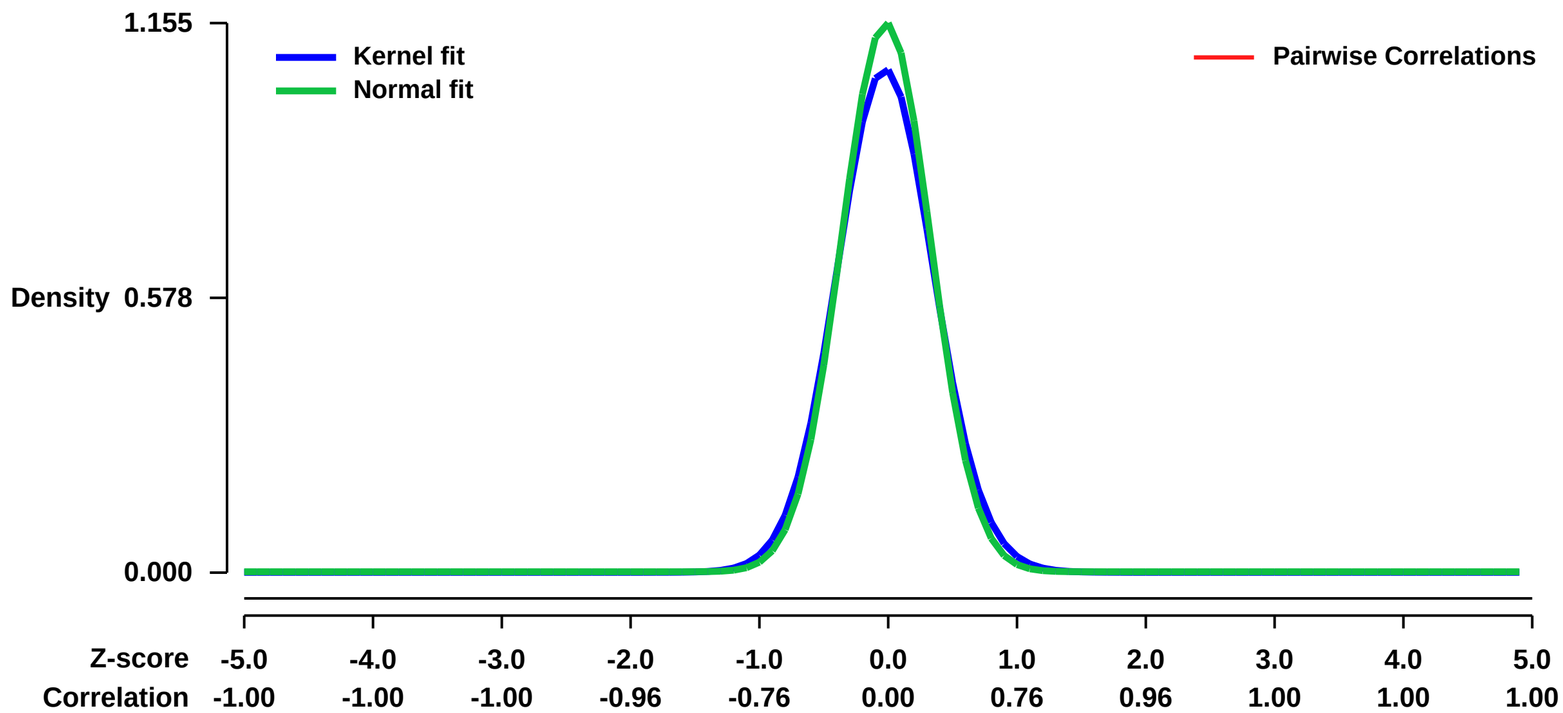

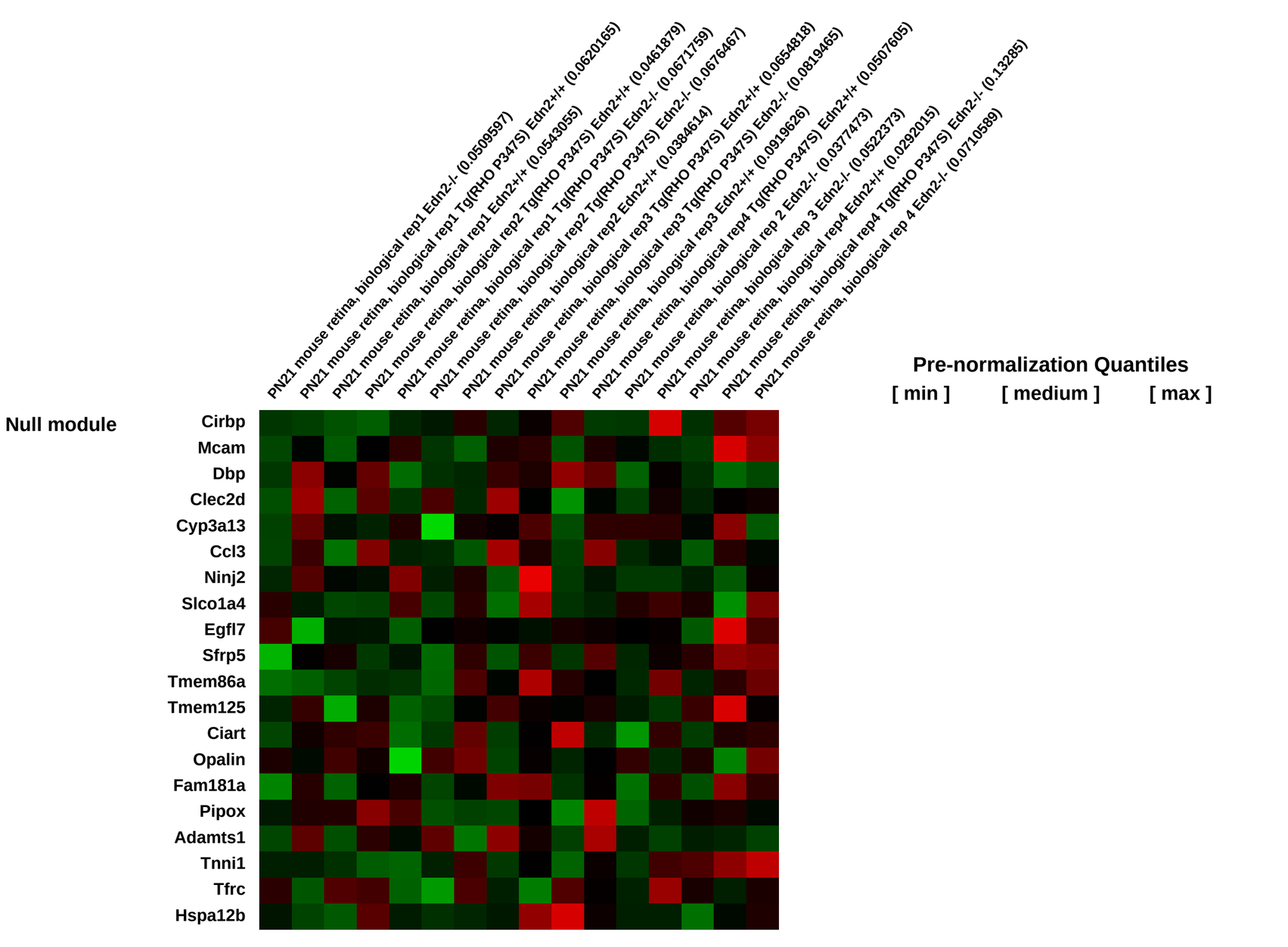

GEO Series "GSE38822" Expression Profiles

Num of samples in this series: 22

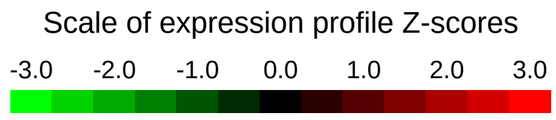

GEO Link:	http://www.ncbi.nlm.nih.gov/geo/query/acc.cgi?acc=GSE38822
Status:	Public on Aug 08 2012
Title:	Gene expression profiling of experimental granulation tissue in Mmp13-/- mice compared to wild type mice
Organism:	Mus musculus
Experiment type:	Expression profiling by array
Platform:	GPL1261
Pubmed ID:	22880047
Summary & Design:	**Summary:** Proteinases play a pivotal role in wound healing by degrading molecular barriers, regulating cell-matrix interactions and availability of bioactive molecules. Matrix metalloproteinase-13 (MMP-13, collagenase-3) is a wide spectrum proteinase. Its expression and function is linked to the growth and invasion of many epithelial cancers such as squamous cell carcinoma. Moreover, the physiologic expression of MMP-13 is associated e.g. to scarless healing of human fetal skin and adult gingival wounds. While MMP-13 is not found in the normally healing skin wounds in human adults, it is expressed in mouse skin during wound healing. Thus, mouse wound healing models can be utilized for studying the role of MMP-13 in the events of wound healing. As the processes such as the migration and proliferation of keratinocytes, angiogenesis, inflammation and activation of fibroblasts are components of wound repair as well as of cancer, many results received from wound healing studies are also adaptable to cancer research. Classically, the process of wound healing can be devided into three phases which are histologically and functionally separate but temporally overlapping: 1) hemostasis and inflammation, 2) re-epithelialization and granulation tissue formation, and 3) matrix remodeling. Granulation tissue is formed into the wound via fibroplasia, angiogenesis and extracellular matrix (ECM) deposition by fibroblasts. Granulation tissue is rich in inflammatory cells, fibroblasts, myofibroblasts and blood vessels. After epidermal recovery, the granulation tissue is resolved via matrix remodeling and cell apoptosis. A sterile viscose cellulose sponge (VCS) characterized by defined size and structure can be used to experimentally induce formation of subcutaneous granulation tissue. Compared to normal granulation tissue, this model allows easy examination of the granulation tissue in its entirety but leaving out epidermal keratinocytes in the sample preparation. In this study, we studied the role of MMP-13 in the formation of mouse VCS-induced granulation tissue. We performed gene expression profiling of the granulation tissue samples of Mmp13-/- (KO) and wild type (WT) mice harvested at day 7, day 14 and day 21 after VCS implantation. **Overall design:** Mmp13-/- (KO) mice were generated as described (Inada et al. 2004, PNAS, 101: 17192-17197) and used in these experiments after backcrossing at least seven generations into C57BL6 mice. The WT mice were generated from the backcrossed heterozygote Mmp13-/- (KO) mice. Granulation tissues were harvested at three time points (7d, 14d, 21d) from Mmp13-/- (KO) and WT mice. One sample of each mouse was analyzed (n=3, 7d; n=4, 14d; n=4, 21d; for each genotype). The samples were processed for RNA extraction and Affymetrix 3'IVT DNA microarray gene expression analysis.

Background corr dist: KL-Divergence = 0.1290, L1-Distance = 0.0326, L2-Distance = 0.0019, Normal std = 0.3952

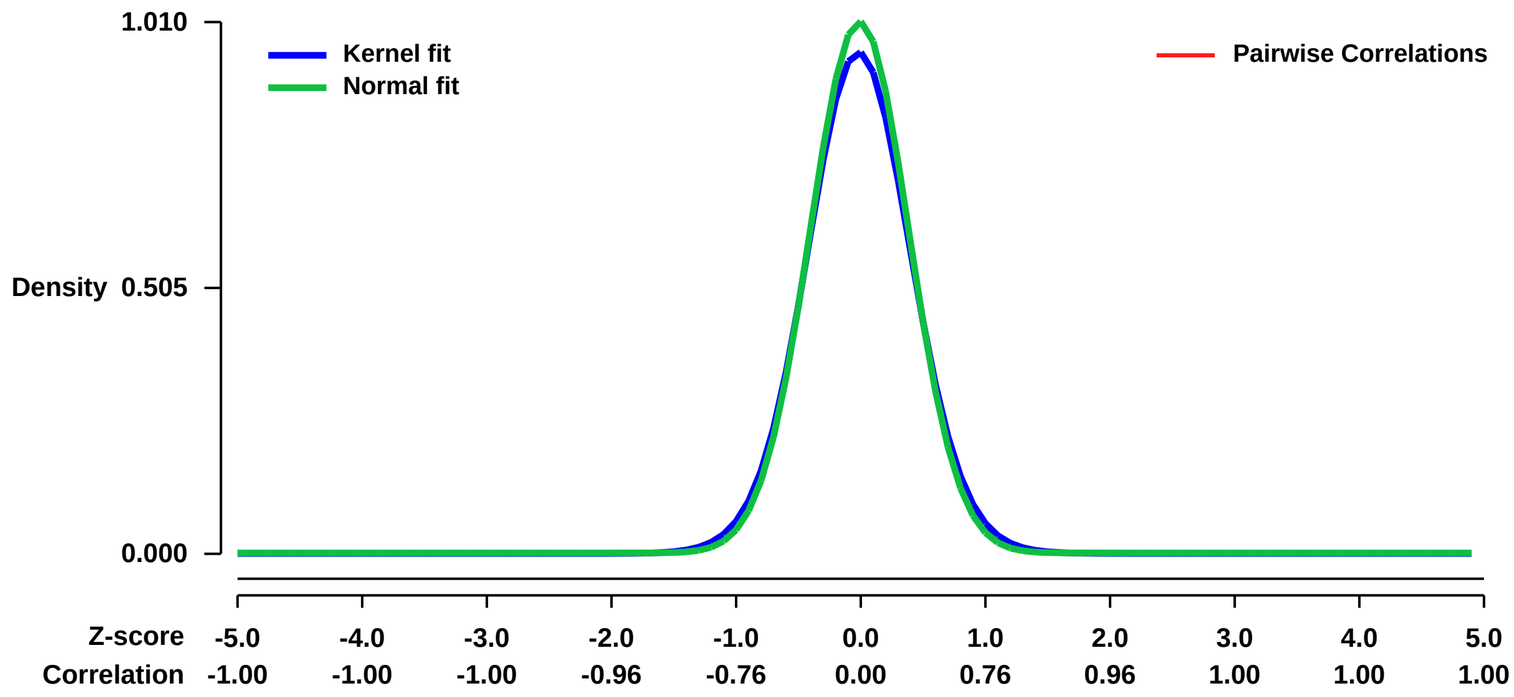

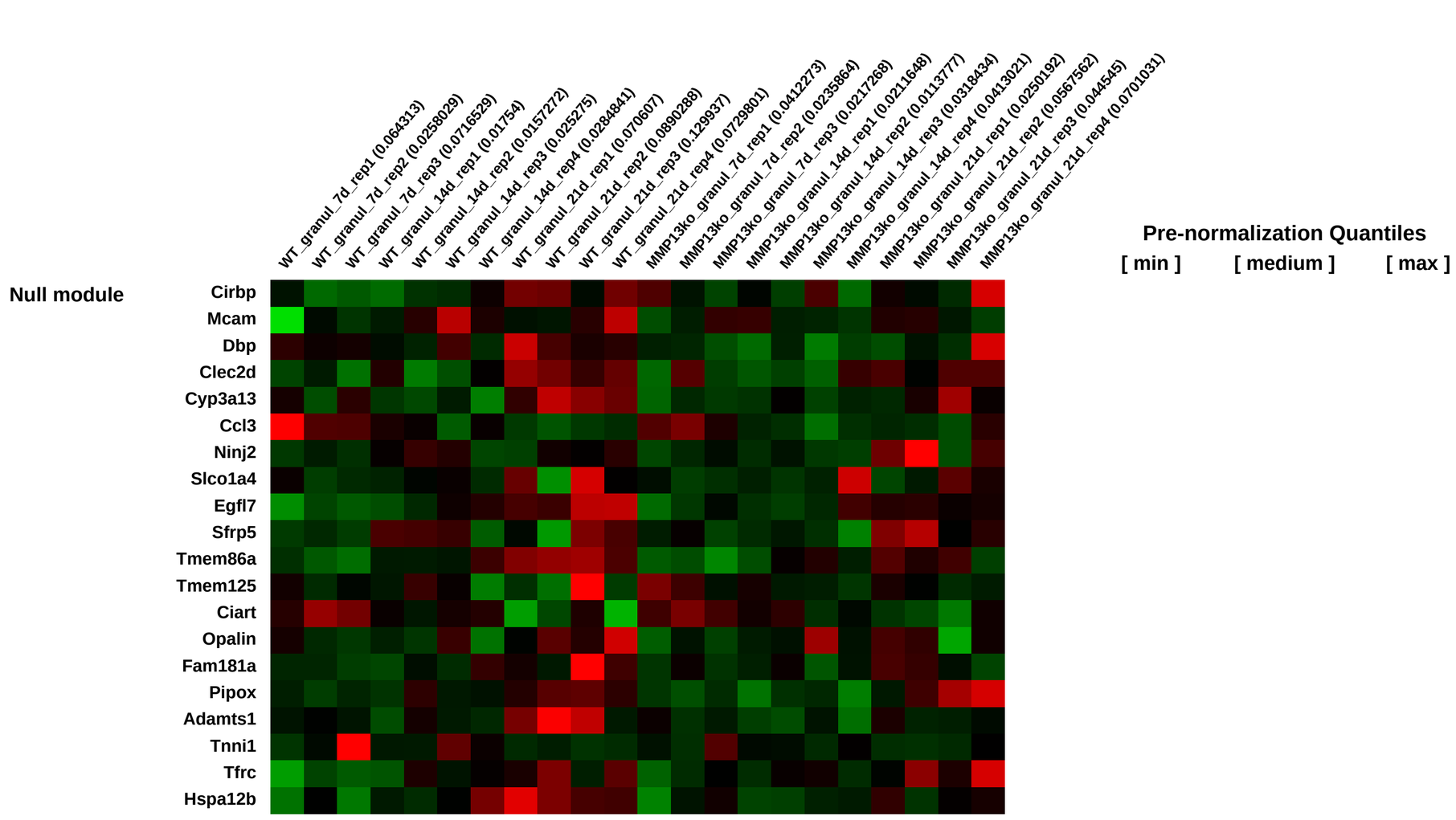

GEO Series "GSE38831" Expression Profiles

Num of samples in this series: 7

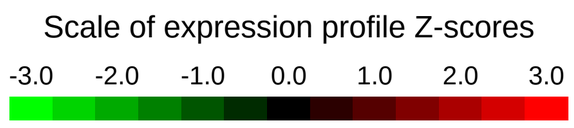

GEO Link:	http://www.ncbi.nlm.nih.gov/geo/query/acc.cgi?acc=GSE38831
Status:	Public on Dec 22 2013
Title:	Deciphering genomic alterations in colorectal cancer through transcriptional subtype-based network analysis
Organism:	Mus musculus
Experiment type:	Expression profiling by array
Platform:	GPL1261
Pubmed ID:	24260186
Summary & Design:	**Summary:** High-throughput genomic studies have identified thousands of genetic alterations in colorectal cancer (CRC). Distinguishing driver from passenger mutations is critical for developing rational therapeutic strategies. Because only a few transcriptional subtypes exist in previously studied tumor types, we hypothesize that highly heterogeneous genomic alterations may converge to a limited number of distinct mechanisms that drive unique gene expression patterns in different transcriptional subtypes. In this study, we defined transcriptional subtypes for CRC and identified driver networks/pathways for each subtype, respectively. Applying consensus clustering to a patient cohort with 1173 samples identified three transcriptional subtypes, which were validated in an independent cohort with 485 samples. The three subtypes were characterized by different transcriptional programs related to normal adult colon, early colon embryonic development, and epithelial mesenchymal transition, respectively. They also showed statistically different clinical outcomes. For each subtype, we mapped somatic mutation and copy number variation data onto an integrated signaling network and identified subtype-specific driver networks using a random walk-based strategy. We found that genomic alterations in the Wnt signaling pathway were common among all three subtypes; however, unique combinations of pathway alterations including Wnt, VEGF, Notch and TGF-beta drove distinct molecular and clinical phenotypes in different CRC subtypes. Our results provide a coherent and integrated picture of human CRC that links genomic alterations to molecular and clinical consequences, and which provides insights for the development of personalized therapeutic strategies for different CRC subtypes. **Overall design:** To characterize the embryonic development of colon, we conducted a time course microarray study using the inbred C57BL/6 (Jackson Laboratories, Bar Harbor, ME) mice. Seven samples corresponding to the mouse colonic development from E13.5 to E18.5 and adult (eight week post-natal) were collected. RNA samples were submitted to the Vanderbilt Functional Genomics Shared Resource (FSGR, http://array.mc.vanderbilt.edu), where RNA was hybridized to the Affymetrix Mouse Genome 430 2.0 GeneChip Expression Arrays (Santa Clara, CA) according to manufacturerâ s instructions. The RMA algorithm was used for data normalization. Mouse gene symbols were mapped to human gene symbols by the Human and Mouse Orthology list available from the Mouse Genome Informatics (http://www.informatics.jax.org/).

Background corr dist: KL-Divergence = 0.0290, L1-Distance = 0.0333, L2-Distance = 0.0015, Normal std = 0.7069

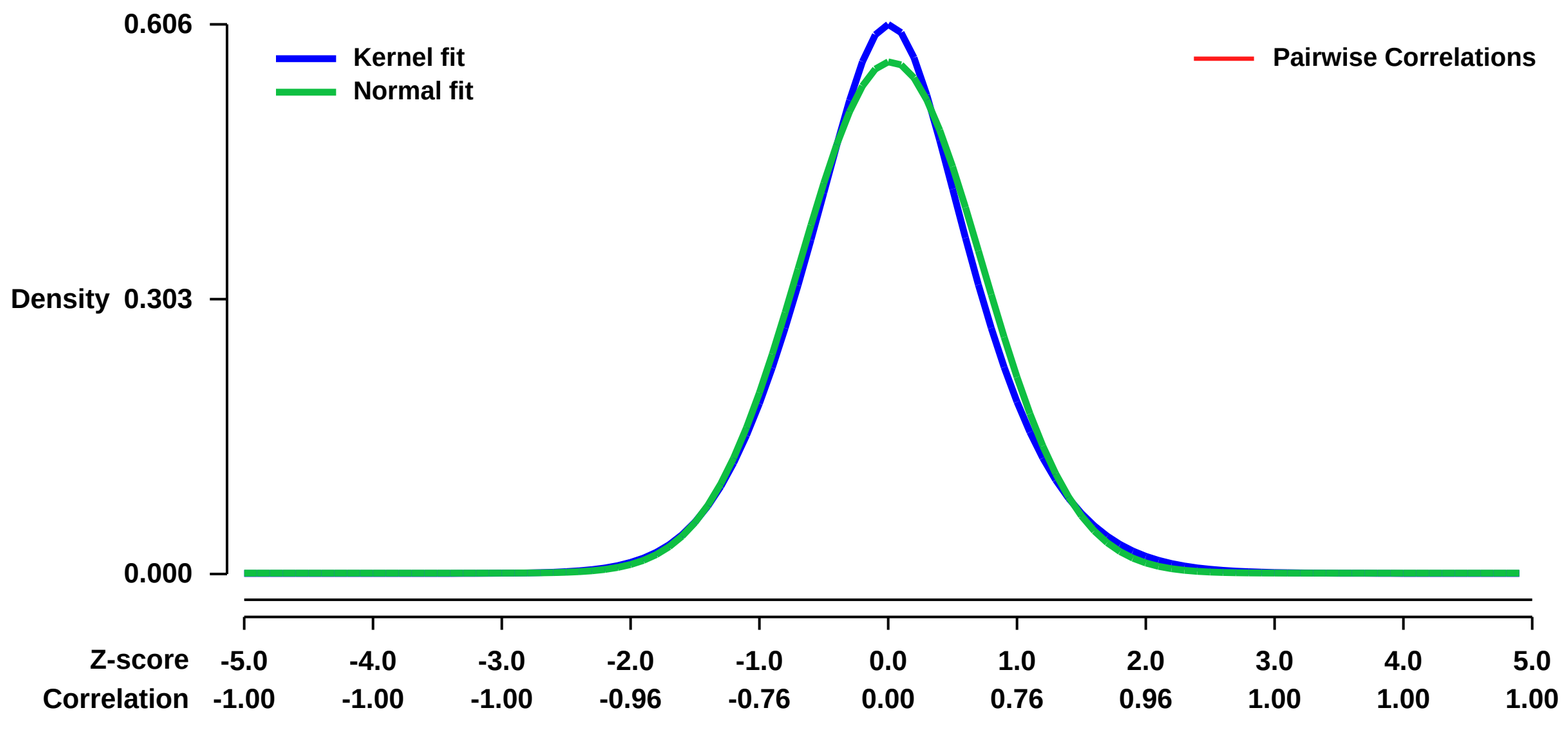

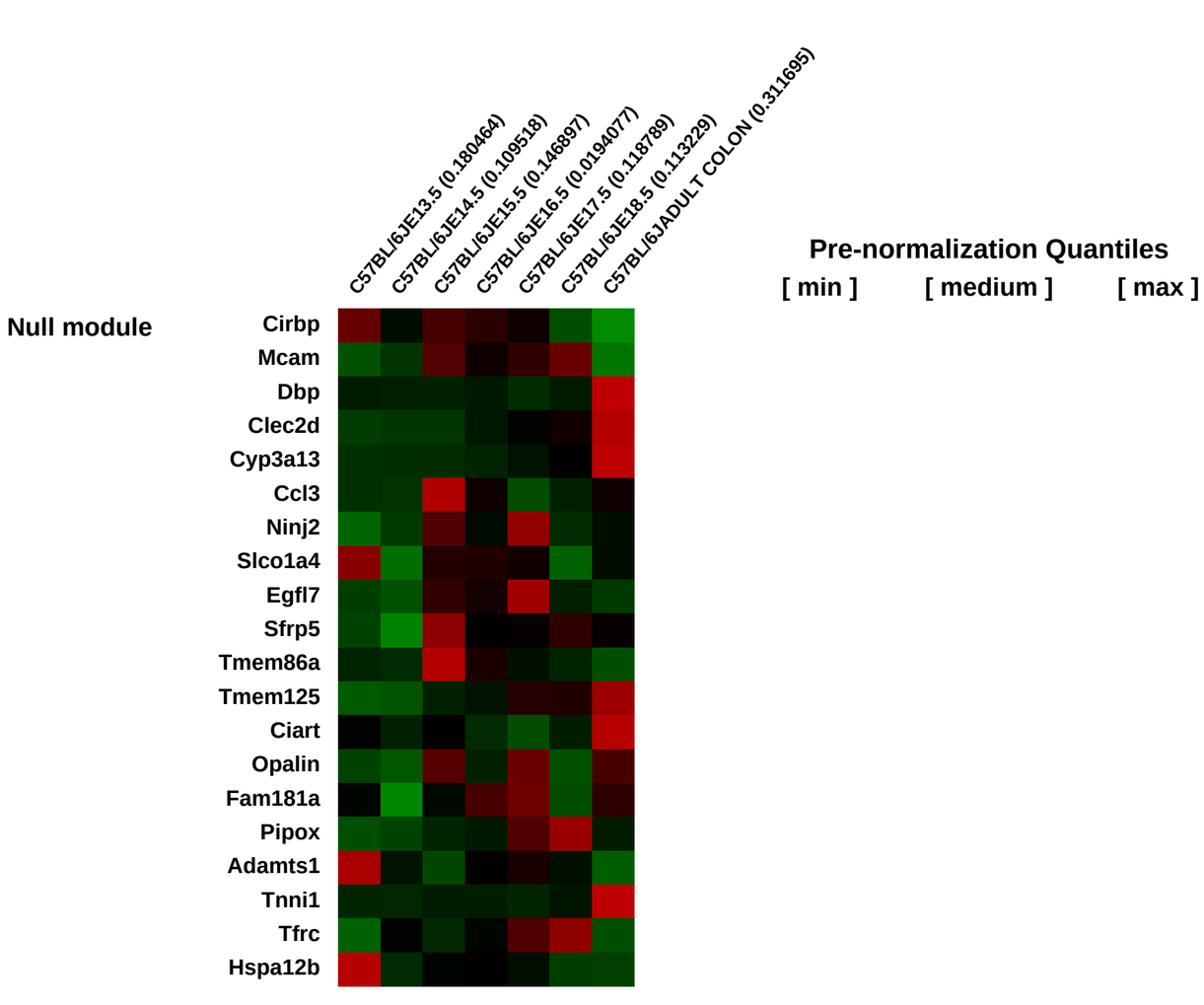

GEO Series "GSE38837" Expression Profiles

Num of samples in this series: 6

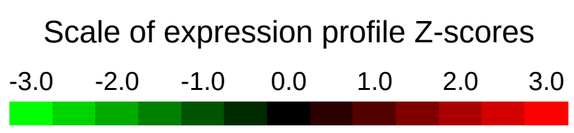

GEO Link:	http://www.ncbi.nlm.nih.gov/geo/query/acc.cgi?acc=GSE38837
Status:	Public on Apr 11 2014
Title:	Zbtb20-mediated repression of genes in developing CA1 pyramidal neurons
Organism:	Mus musculus
Experiment type:	Expression profiling by array
Platform:	GPL1261
Pubmed ID:	23283686
Summary & Design:	**Summary:** The transcriptional repressor Zbtb20 is essential for specification of hippocampal CA1 pyramidal neurons. Moreover, ectopic expression of Zbtb20 is sufficient to transform subicular and retrosplenial areas of D6/Zbtb20S mice to CA1. We used microarrays to identify genes that are repressed by Zbtb20 in developing CA1 pyramidal neurons in the CA1-transformed cortex of D6/Zbtb20S mice. **Overall design:** For RNA extraction and hybridization on Affymetrix microarrays, we isolated the CA1-transformed subiculum and retrosplenial cortex from postnatal day 1 D6/Zbtb20S mice, as well as corresponding areas from their wildtype littermates. Total RNA was extracted using the RNeasy Lipid Tissue Mini Kit (Qiagen). Each RNA sample represents a pool of RNA obtained from dissected tissues of seven animals.

Background corr dist: KL-Divergence = 0.0353, L1-Distance = 0.0136, L2-Distance = 0.0002, Normal std = 0.6349

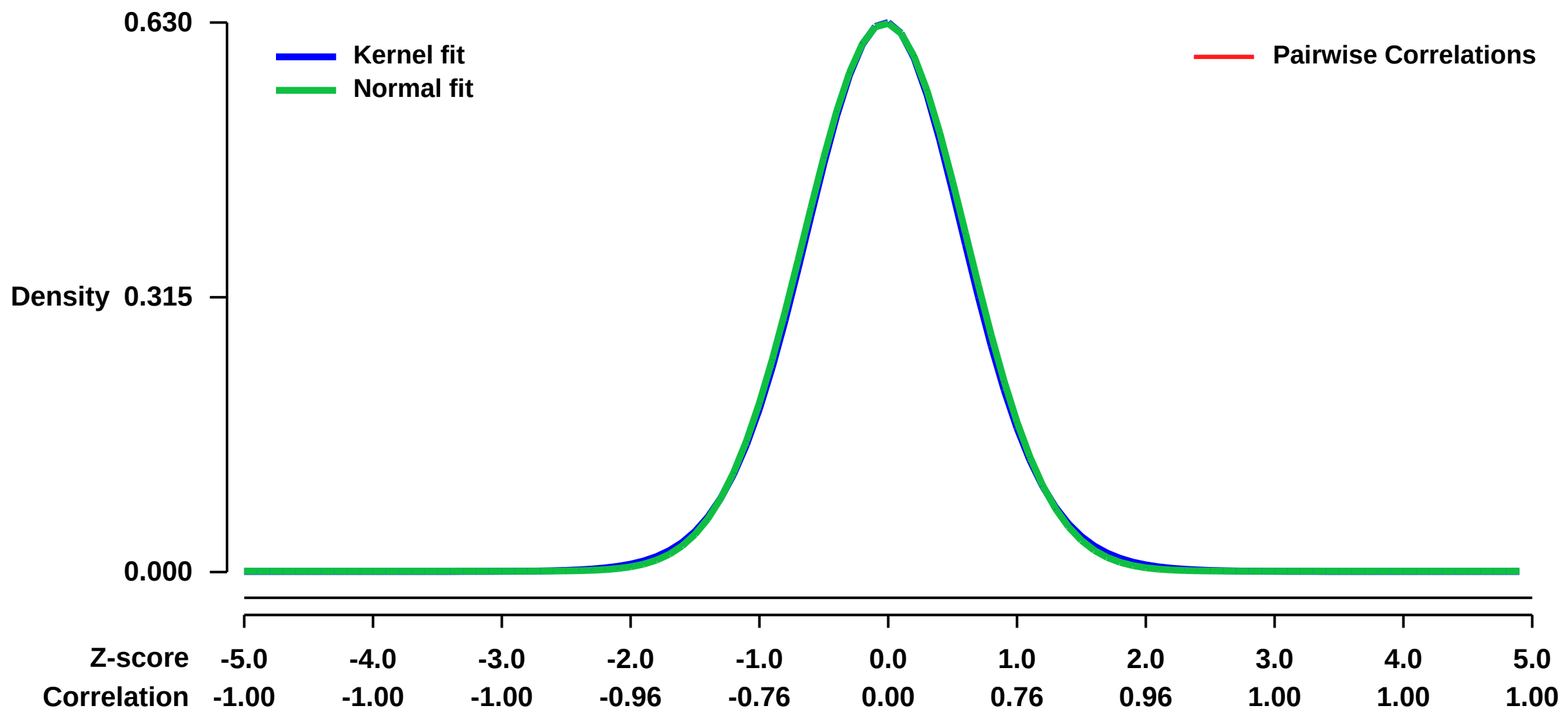

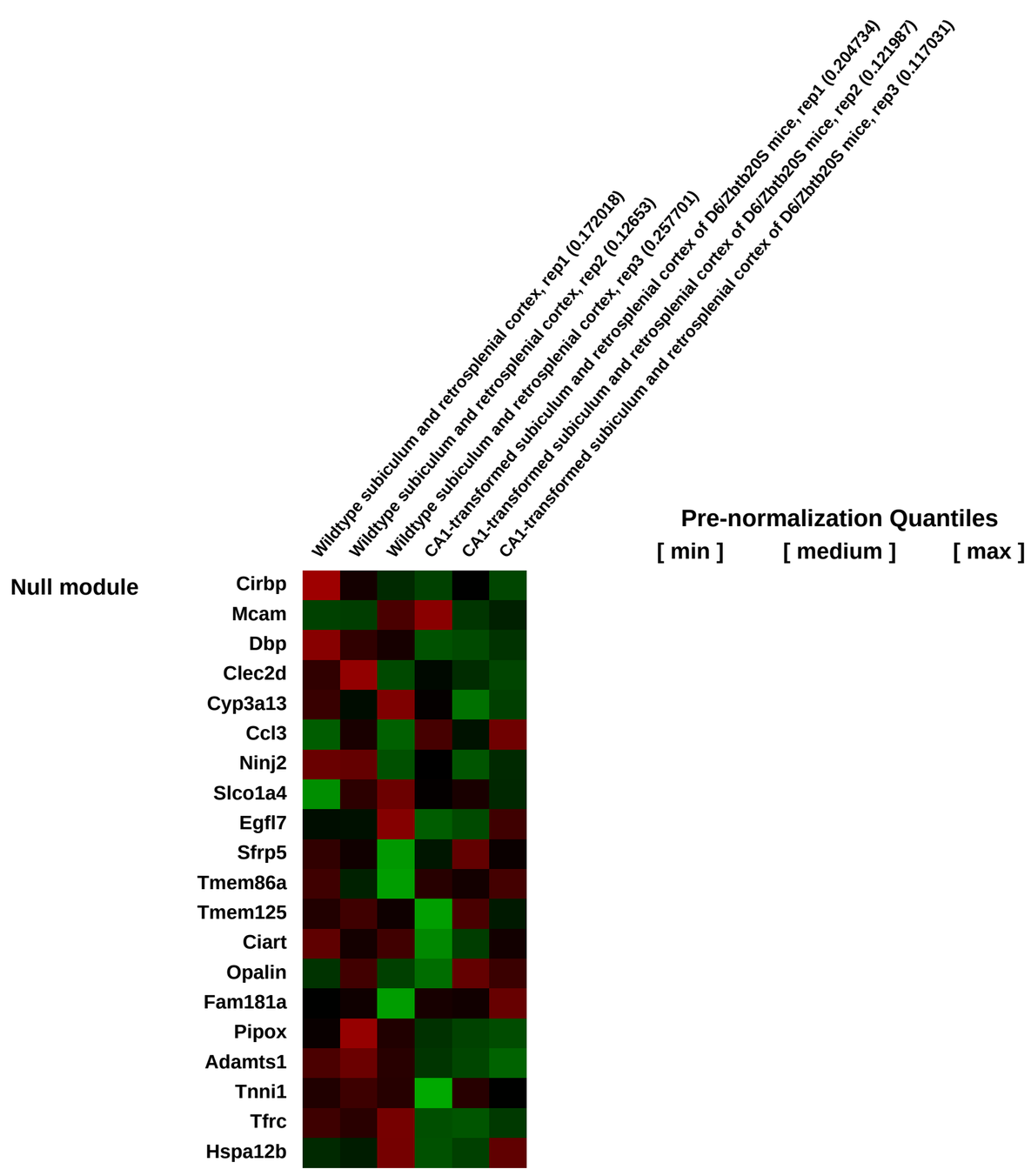

GEO Series "GSE38880" Expression Profiles

Num of samples in this series: 12

Scale of expression profile Z-scores

-3.0 -2.0 -1.0 0.0 1.0 2.0 3.0

GEO Link:	**http://www.ncbi.nlm.nih.gov/geo/query/acc.cgi?acc=GSE38880**
Status:	**Public on Jul 01 2012**
Title:	**Subtherapeutic antibiotics alter the murine colonic microbiome and early life adiposity**
Organism:	**Mus musculus**
Experiment type:	**Expression profiling by array**
Platform:	**GPL1261**
Pubmed ID:	
Summary & Design:	**Summary:** **Early life exposure to antibiotics alters the gut microbiome. These alterations lead to changes in metabolic homeostasis and an increase in host adiposity. We used microarrays to identify metabolic genes that may be up- or down-regulated secondary to antibiotic exposure.** **Low dose antibiotics have been widely used as growth promoters in the agricultural industry since the 1950â s, yet the mechanisms for this effect are unclear. Because antimicrobial agents of different classes and varying activity are effective across several vertebrate species, we hypothesized that such subtherapeutic administration alters the population structure of the gut microbiome as well as its metabolic capabilities. We generated a model of adiposity by giving subtherapeutic antibiotic therapy (STAT) to young mice and evaluated changes in the composition and capabilities of the gut microbiome. STAT administration increased adiposity in young mice and altered hormones related to metabolism. We observed substantial taxonomic changes in the microbiome, changes in copies of key genes involved in the metabolism of carbohydrates to short-chain fatty acids (SCFA), increases in colonic SCFA levels, and alterations in the regulation of hepatic metabolism of lipids and cholesterol. In this model, we demonstrate the alteration of early life murine metabolic homeostasis through antibiotic manipulation.** **Overall design:** **C57BL6 mice were divided into low-dose penicillin or control groups. Given antibiotics via drinking water after weaning. Sacrificed and liver sections collected for RNA extraction.**

Background corr dist: KL-Divergence = 0.1531, L1-Distance = 0.0396, L2-Distance = 0.0031, Normal std = 0.3687

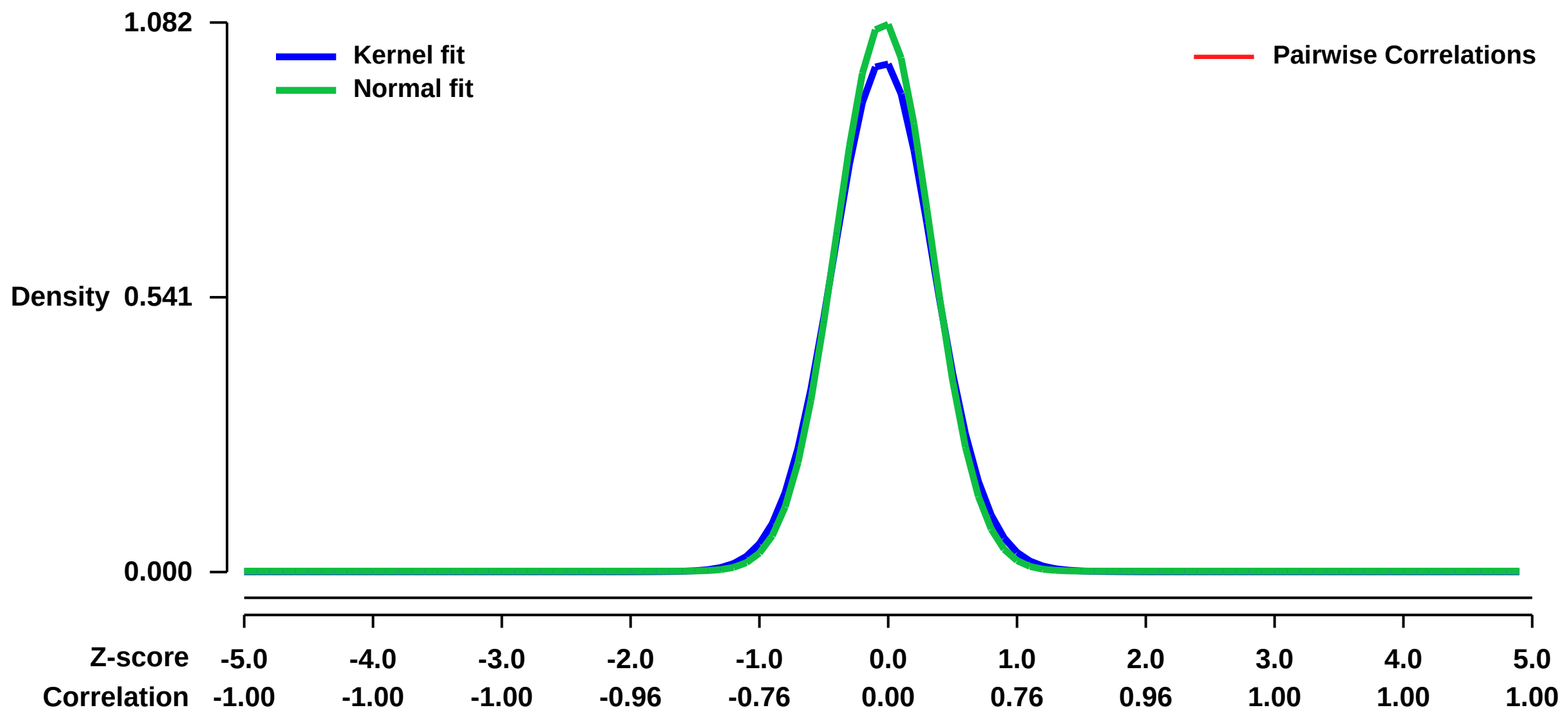

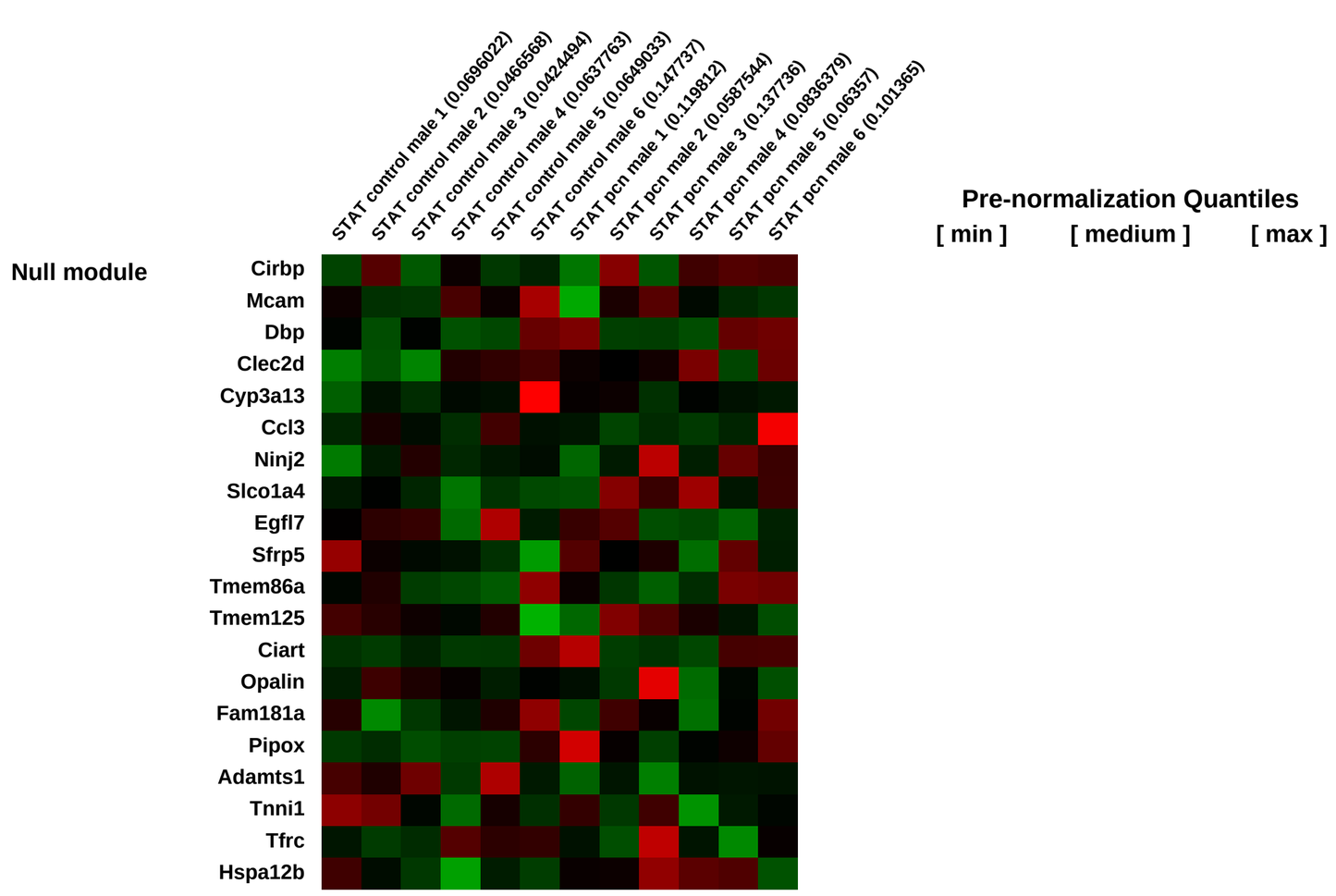

GEO Series "GSE3889" Expression Profiles

Num of samples in this series: 20

Scale of expression profile Z-scores

-3.0 -2.0 -1.0 0.0 1.0 2.0 3.0

GEO Link:	http://www.ncbi.nlm.nih.gov/geo/query/acc.cgi?acc=GSE3889
Status:	Public on Dec 23 2005
Title:	Scd1 Knockout Mice on very low fat diet
Organism:	Mus musculus
Experiment type:	Expression profiling by array
Platform:	GPL1261
Pubmed ID:	17005996
Summary & Design:	**Summary:** Stearoyl-CoA desaturase 1-deficient (SCD1-/-) mice have impaired monounsaturated fatty acid (MUFA) synthesis. When maintained on a very low-fat, high-carbohydrate (VLF-HC) diet, SCD1-/- mice develop severe hypercholesterolemia characterized by an increase in apolipoprotein B-containing lipoproteins and the appearance of lipoprotein-X. Additionally, high-density lipoprotein cholesterol is dramatically reduced in VLF-HC SCD1-/- mice. The concomitant presence of elevated plasma bile acids, bilirubin and aminotransferases in the VLF-HC SCD1-/- mouse are indicative of hepatic dysfunction. Supplementation of the VLF-HC diet with unsaturated fat (canola oil), but not saturated fat (coconut oil), prevents these plasma phenotypes. However, dietary oleate was not as effective as canola oil in reducing low-density lipoprotein cholesterol, signifying an additional role for dietary polyunsaturated fatty acid deficiency in the development of this phenotype. These results indicate that lack of SCD1 results in an increased requirement for dietary unsaturated fat to compensate for impaired MUFA synthesis and to prevent hypercholesterolemia and hepatic dysfunction. **Keywords: repeat (genotype and diet)** **Overall design:** We used Affymetrix Mouse430v2.0 microarray chips to search for gene expression changes unique to the VLF-HC SCD1-/- group. These chips contain 45,101 probe sets representing over 39,000 transcripts and variants from over 34,000 mouse genes. We studied SCD1+/+ and SCD1-/- mice on chow or the VLF-HC diet, analyzing five individual livers from each subgroup for a total of twenty microarrays.

Background corr dist: KL-Divergence = 0.0559, L1-Distance = 0.0742, L2-Distance = 0.0112, Normal std = 0.5746

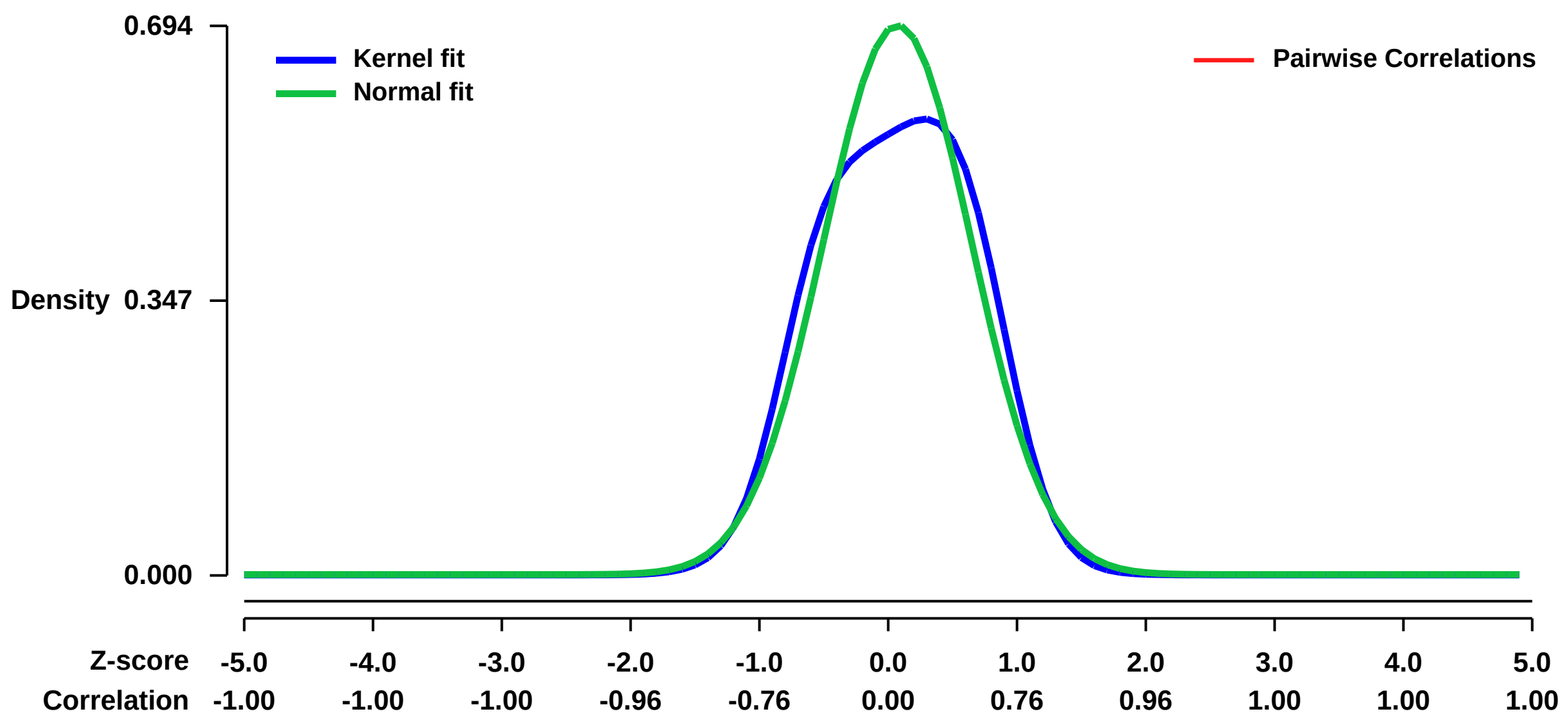

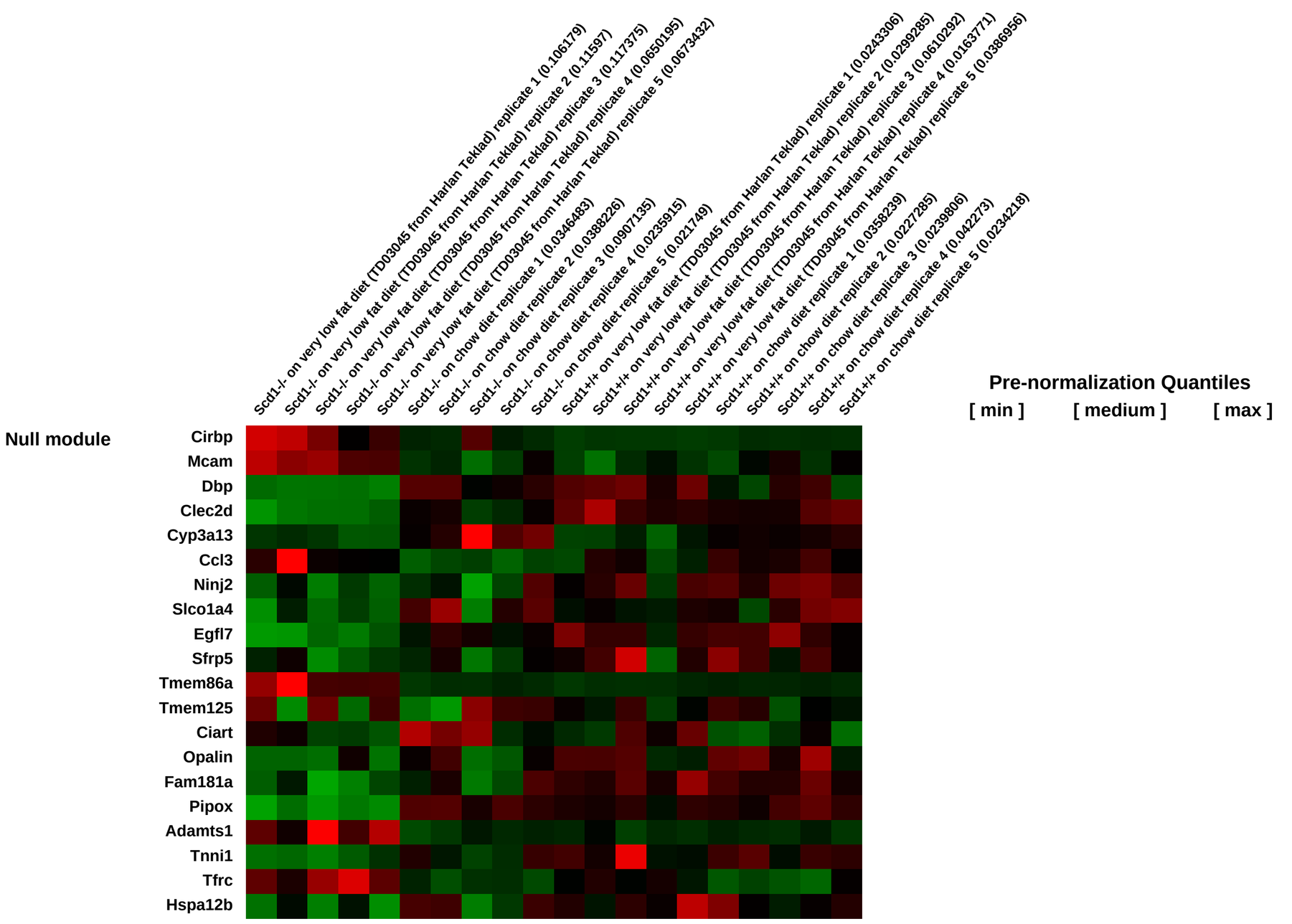

GEO Series "GSE39030" Expression Profiles

Num of samples in this series: 6

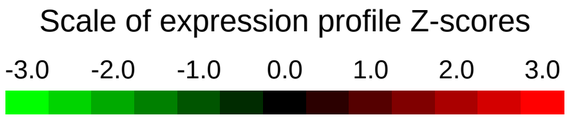

GEO Link:	http://www.ncbi.nlm.nih.gov/geo/query/acc.cgi?acc=GSE39030
Status:	Public on Oct 29 2013
Title:	Impact of ectopic expression of SNAIL2, ZEB2, ZEB1 or TWIST1 on BRAF-target genes in the murine melanocytic melan-a cell line
Organism:	Mus musculus
Experiment type:	Expression profiling by array
Platform:	GPL1261
Pubmed ID:	24075834
Summary & Design:	**Summary:** We have demonstrated that the oncogenic activation of B-RAF (using a truncated delta-BRAF-ER version inducible with tamoxifen) in the melan-a melanocyte cell line triggers the activation of Zeb1 and Twist1 at the expanse of Zeb2 and Snail2. Enforced maintenance of Zeb2 or Snail2 expression reduces the B-RAF oncogenic potential while ectopic expression of Zeb1 or Twist1 cooperates with B-RAF in melan-a cell transformation. To get an insight into the properties of these embryonic transcription factors, gene expression profiles of melan-a-derived cell lines either expressing a non-activated B-RAF (- tamoxifen) or an activated BRAF (+ tamoxifen) alone or in combination with Snail2, Zeb2, Twist1 or Zeb1 have been established. **Overall design:** Ectopic expression of SNAIL2, ZEB2, ZEB1 or TWIST1 on BRAF-target genes in the murine melanocytic melan-a cell line.

Background corr dist: KL-Divergence = 0.0343, L1-Distance = 0.0304, L2-Distance = 0.0011, Normal std = 0.6606

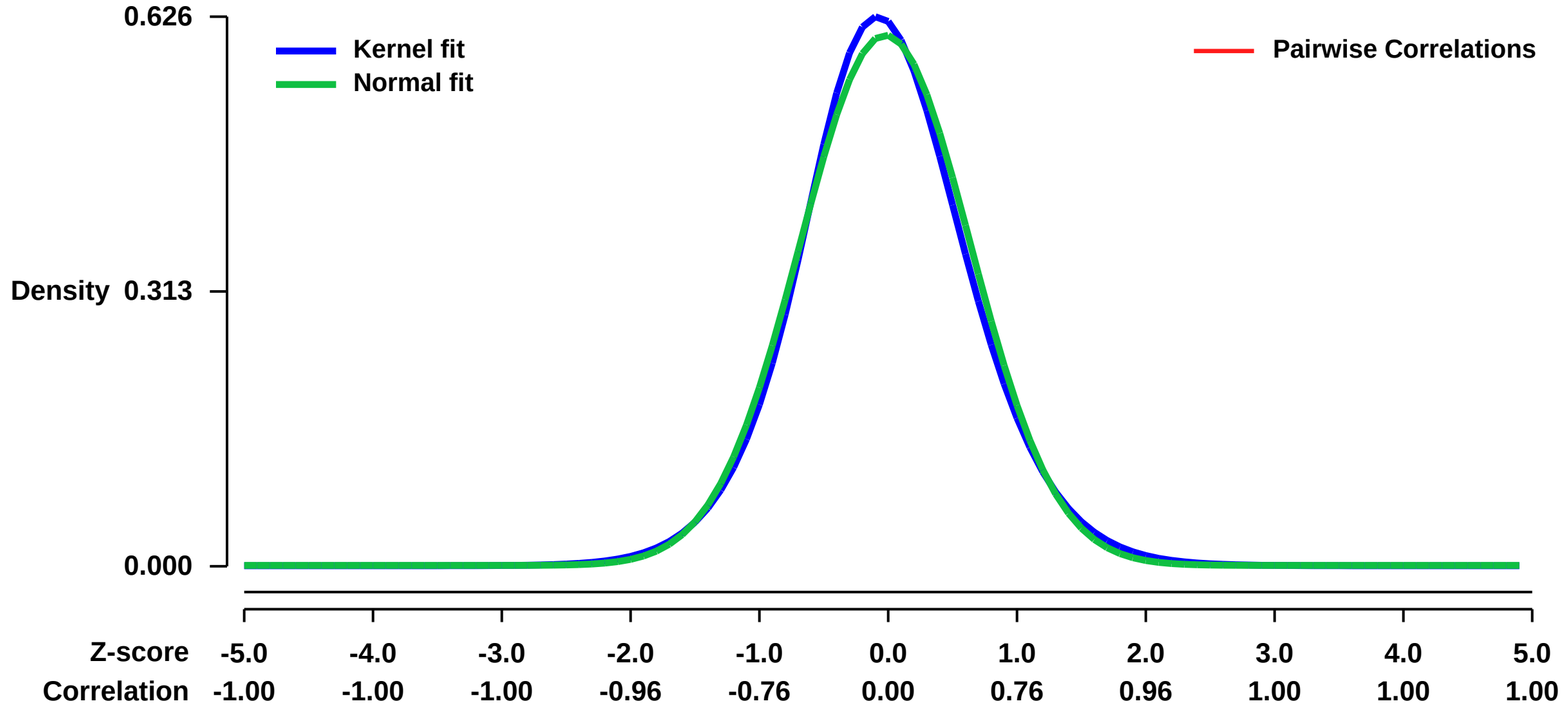

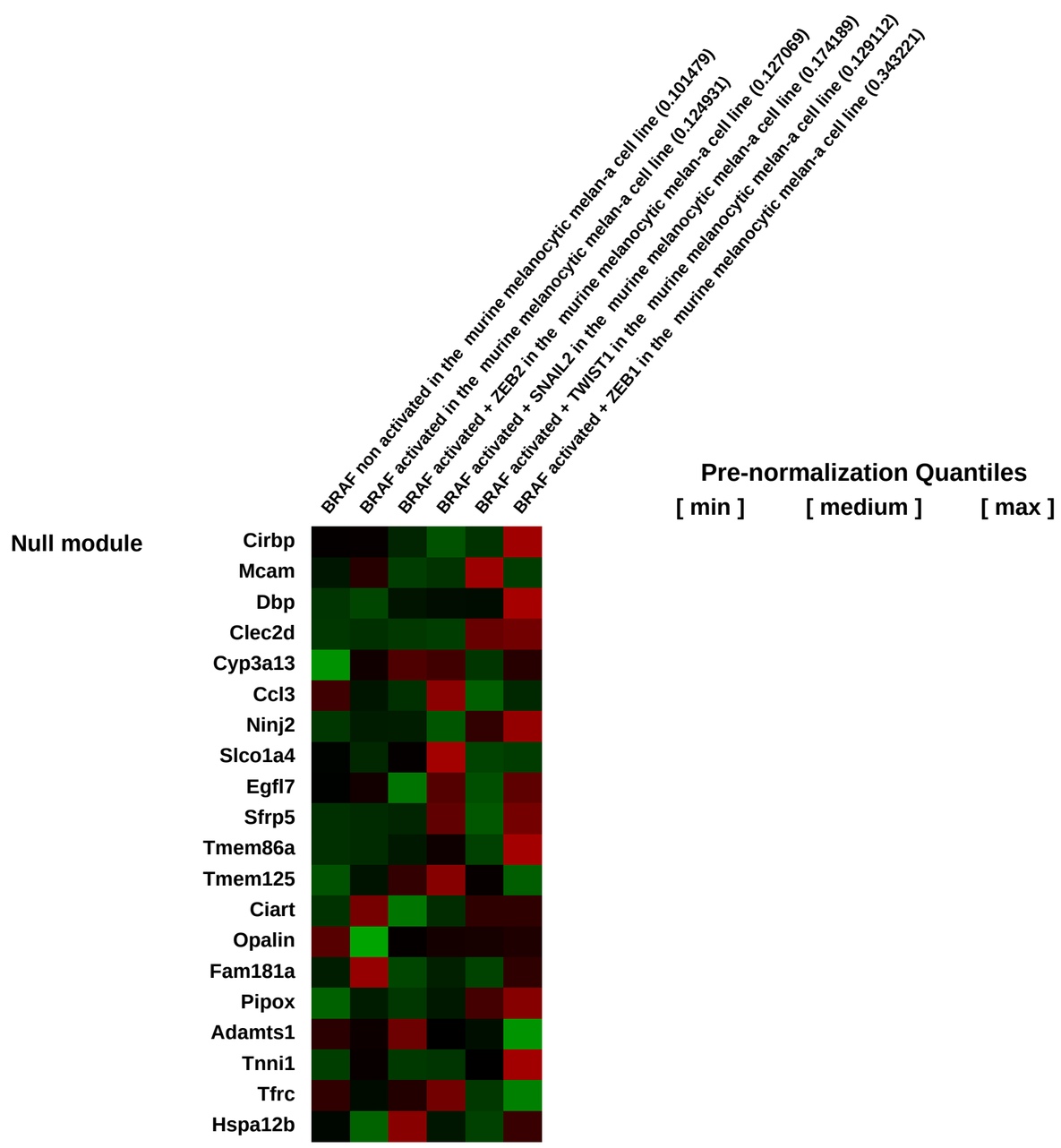

GEO Series "GSE39034" Expression Profiles

Num of samples in this series: 9

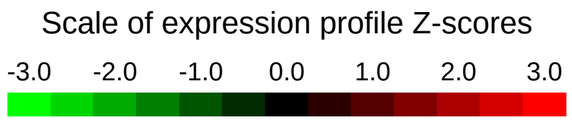

GEO Link:	http://www.ncbi.nlm.nih.gov/geo/query/acc.cgi?acc=GSE39034
Status:	Public on Nov 29 2012
Title:	Mammalian cells acquire epigenetic hallmarks of human cancer during immortalization
Organism:	Mus musculus
Experiment type:	Expression profiling by array
Platform:	GPL1261
Pubmed ID:	23143272
Summary & Design:	**Summary:** Progression to malignancy requires cells to overcome senescence and switch to an immortal phenotype. Thus, exploring the genetic and epigenetic changes that occur during senescence/immortalization may help elucidate crucial events that lead to cell transformation. In the present study, we have globally profiled DNA methylation in relation to gene expression in primary, senescent and immortalized mouse embryonic fibroblasts. **Overall design:** Primary, senescent and immortalized mouse fibroblasts obtained from three independent embryos. Compare immortalized versus primary and senescent versus primary cells.

Background corr dist: KL-Divergence = 0.0790, L1-Distance = 0.0213, L2-Distance = 0.0007, Normal std = 0.4801

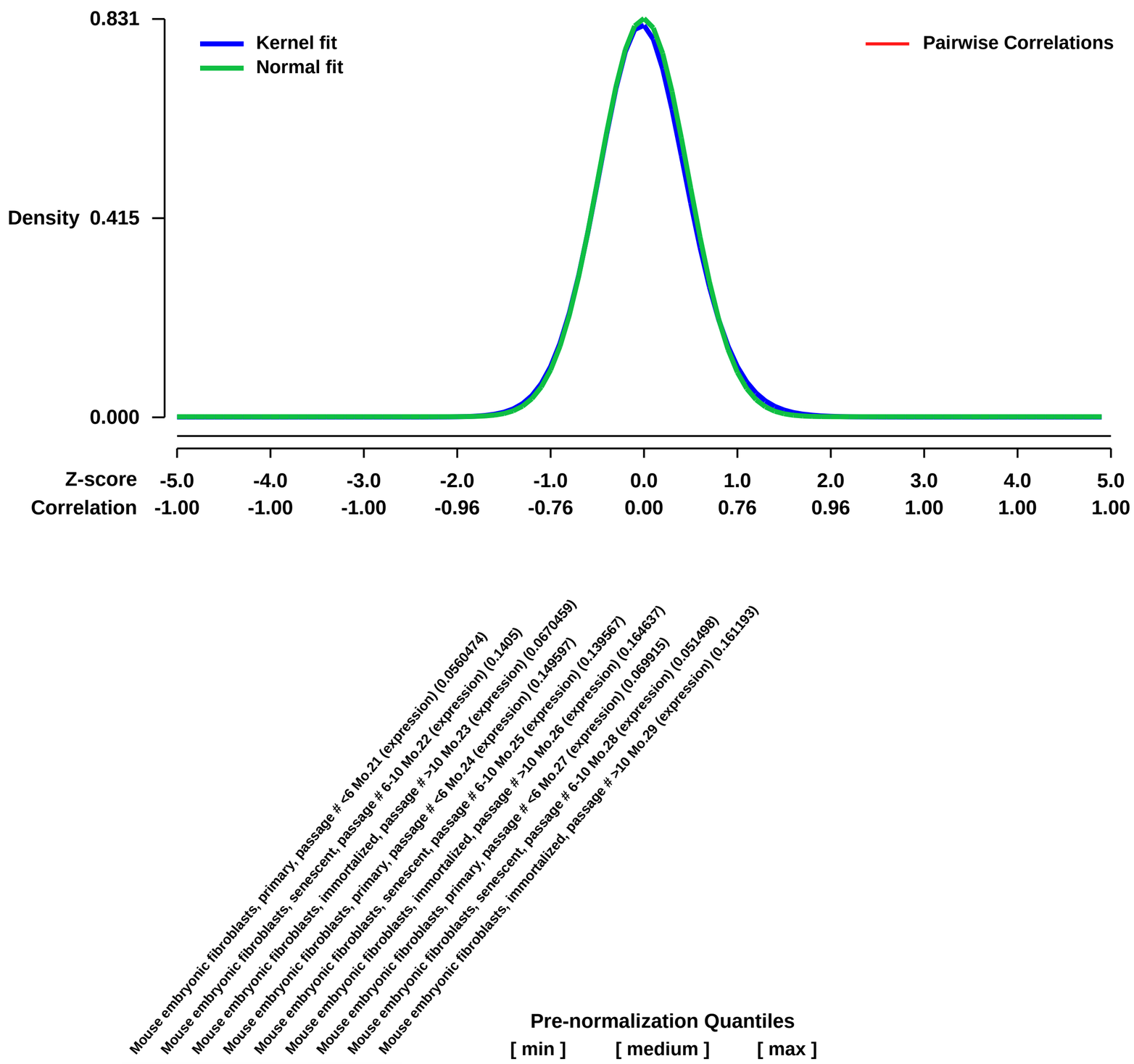

GEO Series "GSE39082" Expression Profiles

Num of samples in this series: 6

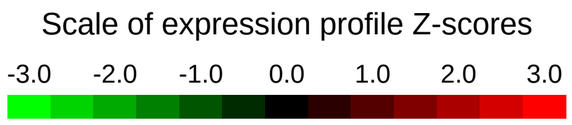

GEO Link:	**http://www.ncbi.nlm.nih.gov/geo/query/acc.cgi?acc=GSE39082**
Status:	**Public on Jul 04 2012**
Title:	**Expression data from cultured c-Kit+Sca-1+Lin- (KSL)cells**
Organism:	**Mus musculus**
Experiment type:	**Expression profiling by array**
Platform:	**GPL1261**
Pubmed ID:	
Summary & Design:	**Summary:** **The Notch signaling pathway plays a critical role in regulating the proliferation and differentiation of stem and progenitor cells including hematopoietic stem and progenitor cells (HSPCs). Notch receptors and ligands are expressed in BM stromal and hematopoietic cells. A large body of evidence has demonstrated that activating Notch signaling enhances HSCs self-renewal and facilitates its expansion ex vivo. We report that an endothelium-targeted soluble Notch ligand, the DSL domain of mouse Delta-like 1 fused with a RGD motif (mD1R), efficiently promotes the expansion ex vivo of mouse bone marrow HSPCs in a Notch signaling and endocytosis dependent manner. HSPCs expanded in the presence of mD1R kept long-term HSPC repopulation capacity.** **We used microarrays to compare the gene expression profiles of HSPCs expanded in the presence of PBS and mD1R.** **Overall design:** **KSL cells were plated on Human umbilical vein endothelial cells (HUVECs) and cultured in a serum-free medium supplemented with a cocktail containing 5 types of mouse cytokines (m5GF) in the presence of PBS or mD1R for 7 days. Then KSL cells were sorted from these cultured hematopoietic cells for RNA extraction and hybridization on Affymetrix microarrays. The experiments were repeated 3 times.**

Background corr dist: KL-Divergence = 0.0342, L1-Distance = 0.0284, L2-Distance = 0.0010, Normal std = 0.6605

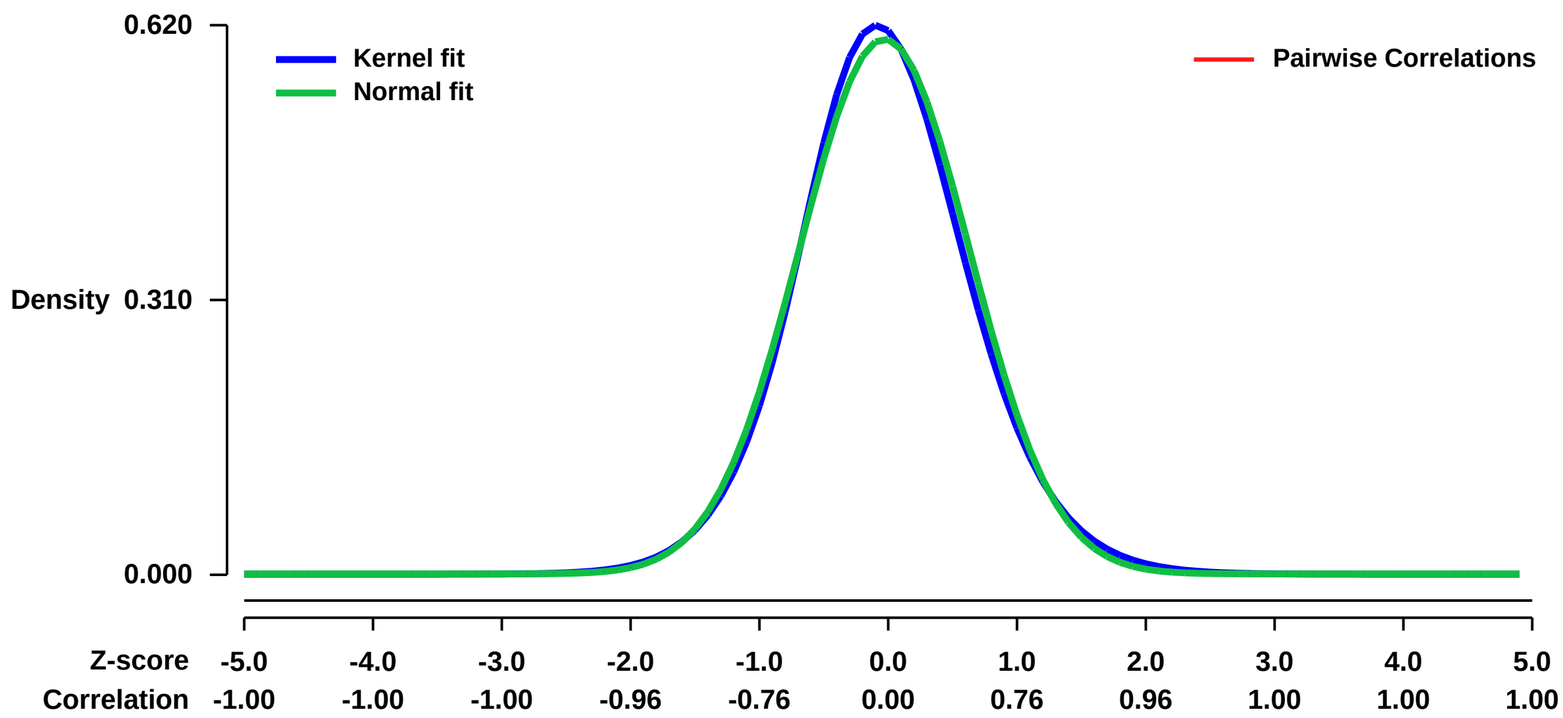

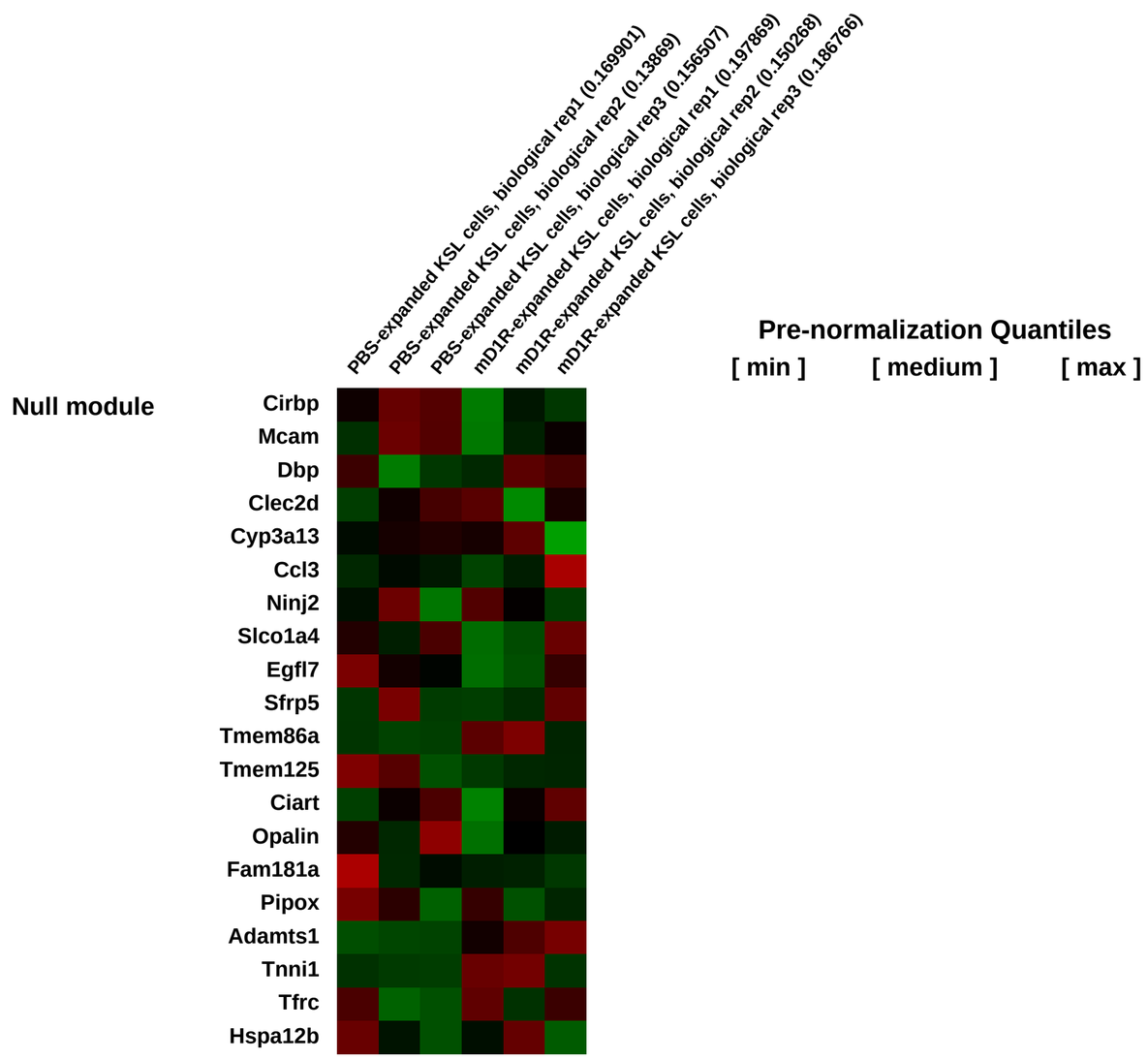

GEO Series "GSE39273" Expression Profiles

Num of samples in this series: 6

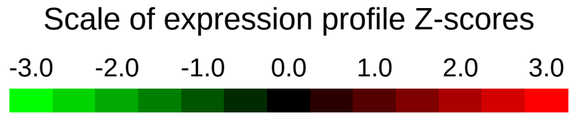

GEO Link:	**http://www.ncbi.nlm.nih.gov/geo/query/acc.cgi?acc=GSE39273**
Status:	**Public on Jan 11 2013**
Title:	**Effect of transgenic human IL8 on gene expression in mouse colon cancer tumors**
Organism:	**Mus musculus**
Experiment type:	**Expression profiling by array**
Platform:	**GPL1261**
Pubmed ID:	**23041326**
Summary & Design:	**Summary:** **mRNA expression in colon cancer tumores** **of CBA/C57BL/6 transgenic mice** **bearing a BAC which contains the human IL8 gene and promoter** **was compared to that of CBA/C57BL/6 controls.** **Overall design:** **B. human IL8 transgenic CBA/C57BL/6 mice (n=3).**

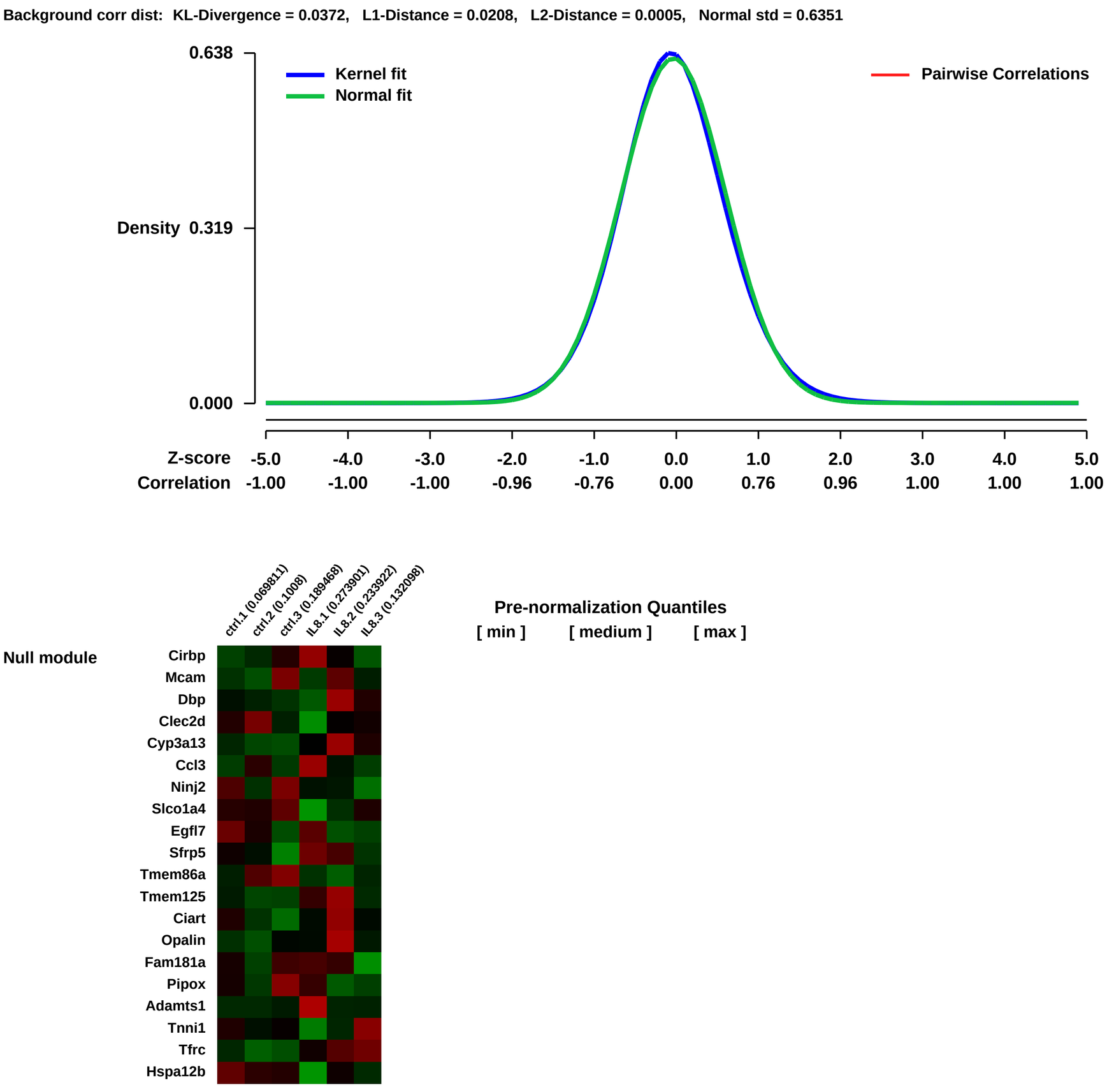

GEO Series "GSE39355" Expression Profiles

Num of samples in this series: 7

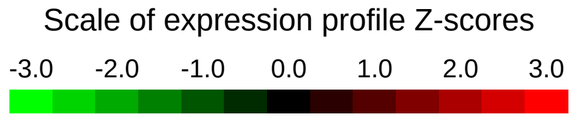

GEO Link:	**http://www.ncbi.nlm.nih.gov/geo/query/acc.cgi?acc=GSE39355**
Status:	**Public on Mar 01 2013**
Title:	**Expression profiling of mouse primary prostate luminal cells from WT and T-ETV1 mice, which contains human ETV1 cDNA under the endogenous Tmprss2 promoter.**
Organism:	**Mus musculus**
Experiment type:	**Expression profiling by array**
Platform:	**GPL1261**
Pubmed ID:	**23512661**
Summary & Design:	**Summary:** **Chromosomal rearrangements involving ETS factors, ERG and ETV1, occur frequently in prostate cancer. We here examine mouse prostate cells from WT mice with s with T-ETV1 mice, which contains express the truncated human ETV1 under the endogenous Tmprss2 promoter. ETV1 expression can be tracked by GFP expression.** **Overall design:** **Primary prostate cells were isolated and luminal prostate cells were FACS-sorted by CD49F+ Sca1- from the lineage (CD31, CD45, Ter119) negative fraction. Total RNA was extracted from three biological replicates, and amplified using NuGEN V2cDNA amplification kit. This was used to hybridize to Affymetrix expression arrays using the Mouse Genome 430 2.0 platform.**

Background corr dist: **KL-Divergence = 0.0642, L1-Distance = 0.0279, L2-Distance = 0.0012, Normal std = 0.5311**

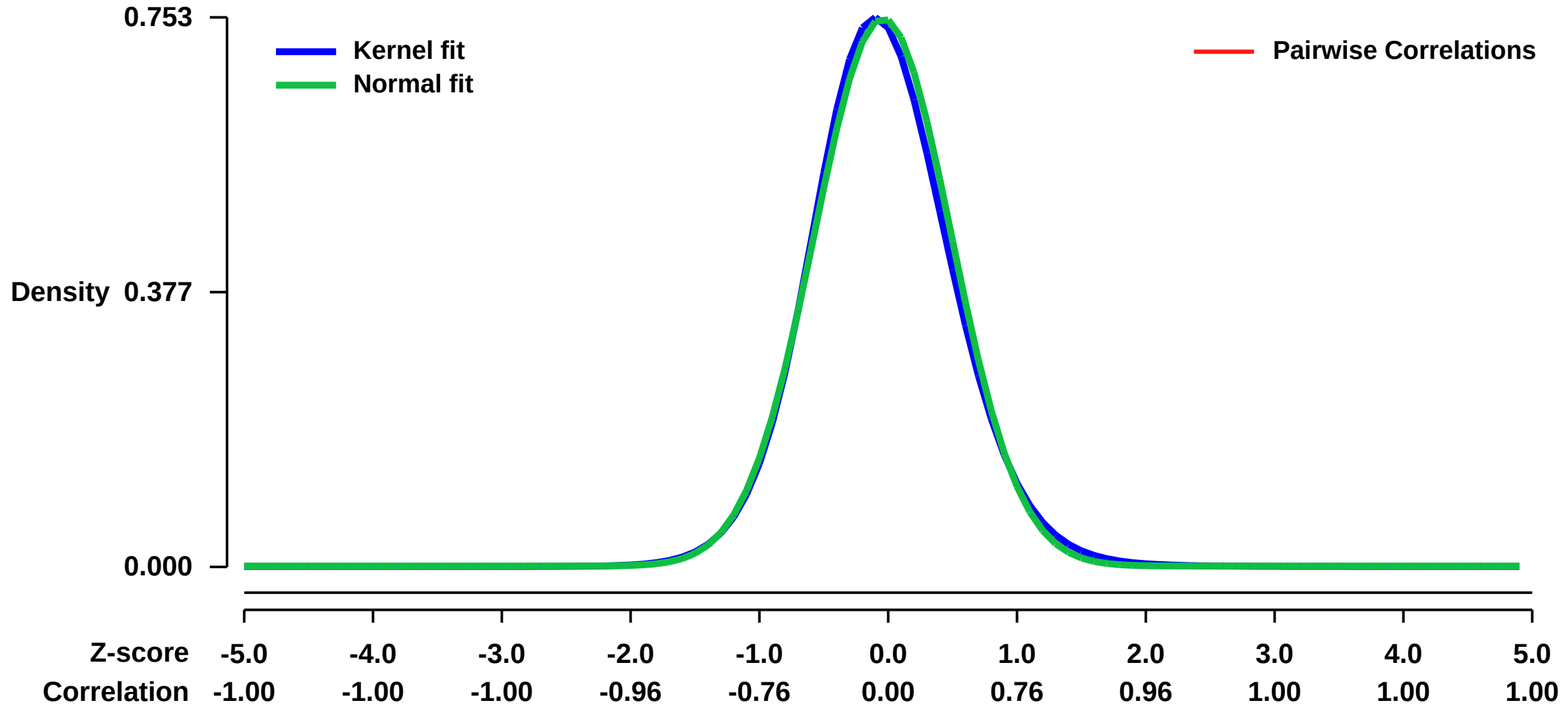

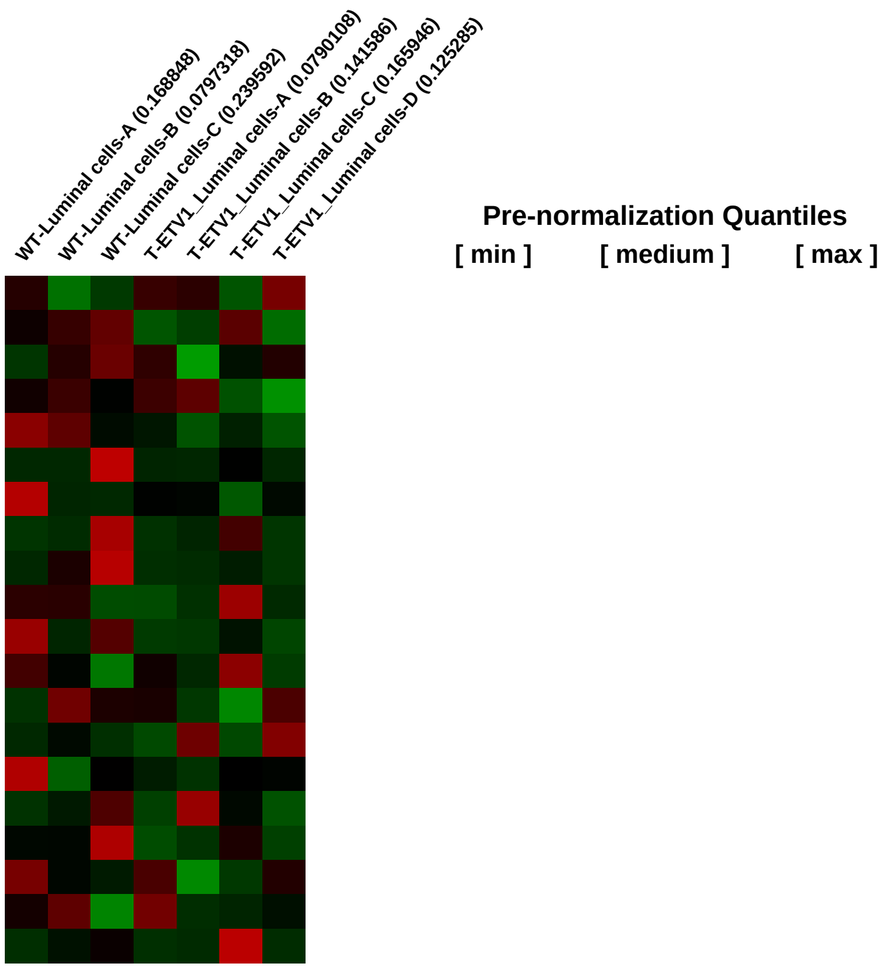

GEO Series "GSE39375" Expression Profiles

Num of samples in this series: 10

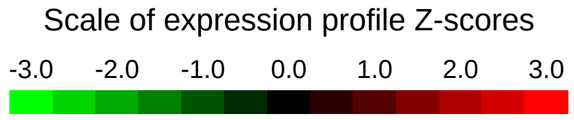

GEO Link:	**http://www.ncbi.nlm.nih.gov/geo/query/acc.cgi?acc=GSE39375**
Status:	**Public on Sep 01 2012**
Title:	**Polysome profiling in liver identifies dynamic regulation of endoplasmic reticulum translatome by obesity and fasting**
Organism:	**Mus musculus**
Experiment type:	**Other**
Platform:	**GPL1261**
Pubmed ID:	**22927828**
Summary & Design:	**Summary:** **Obesity-associated metabolic complications are generally considered to emerge from abnormalities in carbohydrate and lipid metabolism, whereas the status of protein metabolism is not well studied. Here, we performed comparative polysome and associated transcriptional profiling analyses to study the dynamics and functional implications of endoplasmic reticulum (ER)-associated protein synthesis in the mouse liver under conditions of obesity and nutrient deprivation.** **Overall design:** **lean wild type and genetically obese (ob/ob) mice with or without overnight fasting were sacrificed with their liver tissues removed. ER-associated polysomes were purified and analyzed by microarray.**

Background corr dist: **KL-Divergence = 0.1087, L1-Distance = 0.0301, L2-Distance = 0.0017, Normal std = 0.4250**

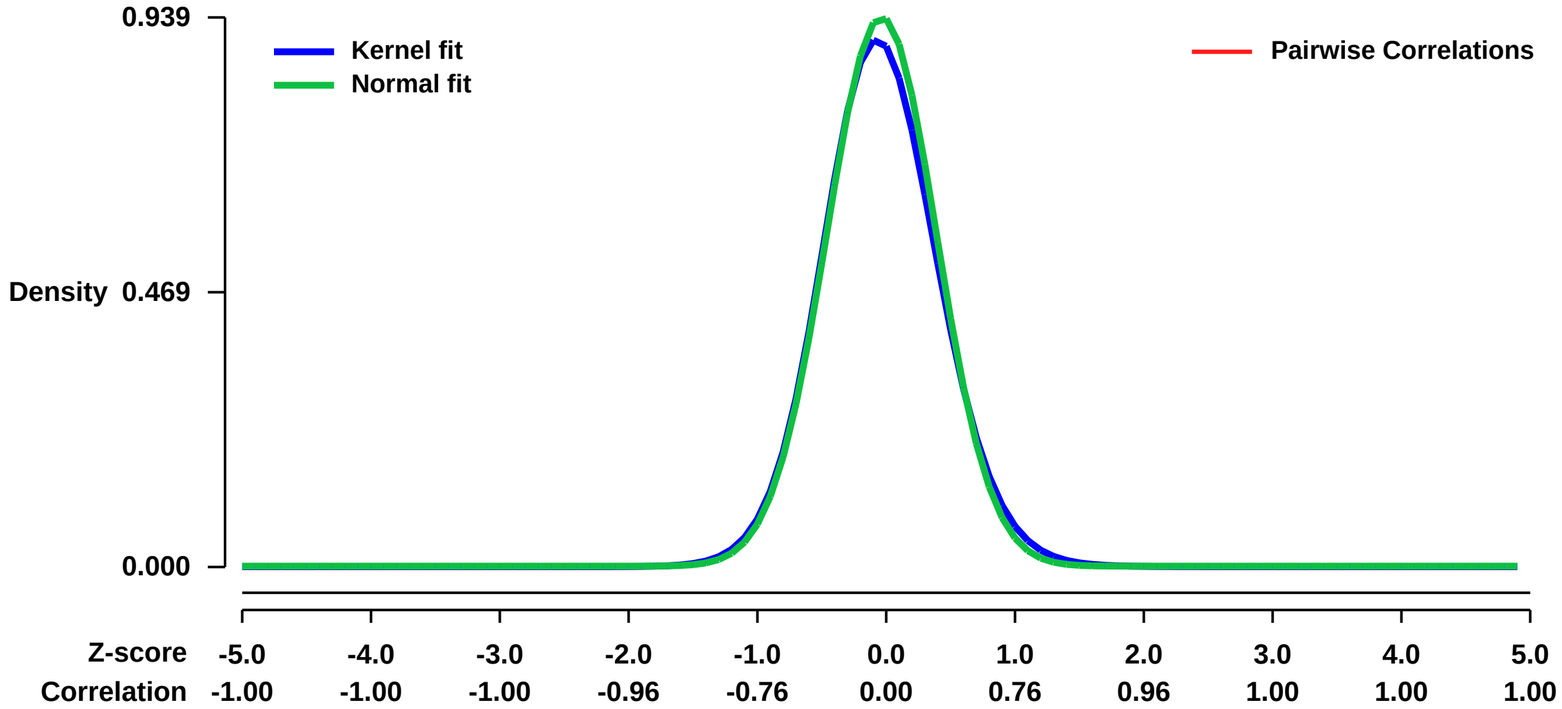

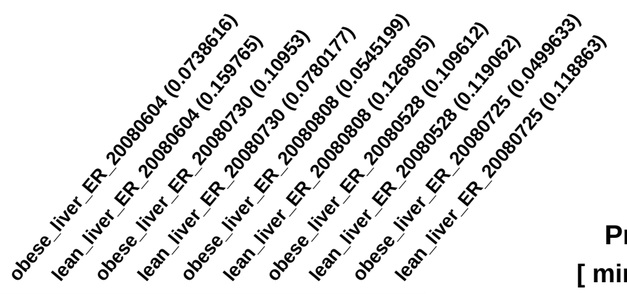

Pre-normalization Quantiles

[min] [medium] [max]

Null module

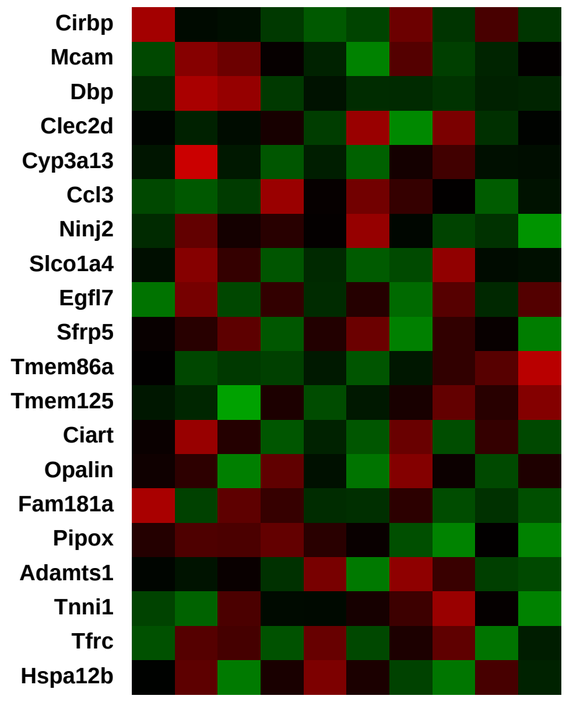

GEO Series "GSE39391" Expression Profiles

Num of samples in this series: 21

Scale of expression profile Z-scores

-3.0 -2.0 -1.0 0.0 1.0 2.0 3.0

GEO Link:	http://www.ncbi.nlm.nih.gov/geo/query/acc.cgi?acc=GSE39391
Status:	Public on Aug 30 2012
Title:	Gene expression data from ahES cells, ES cells, MEF cells and round sperm
Organism:	Mus musculus
Experiment type:	Expression profiling by array
Platform:	GPL1261
Pubmed ID:	23023130
Summary & Design:	**Summary:** Haploid stem cells offer an easy-to-manipulate genetic system and therefore have great values for studies of recessive phenotypes. Here, we show that mouse androgenetic haploid ES (ahES) cell lines can be established by transferring sperm into enucleated oocyte. The ahES cells maintain haploidy and stable growth over 30 passages, express pluripotent markers, possess the ability to differentiate into all three germ-layers in vitro and in vivo, and contribute to germline of chimeras when injected into blastocysts. Although epigenetically distinct from sperm cells, the ahES cells can produce viable and fertile progenies after intracytoplasmic injection into mature oocytes. The oocyte injection procedure can also produce viable transgenic mice from genetically engineered ahES cells. We used microarrays to compare the global programme of gene expression among ahES cells, normal diploid ES cells, MEF cells and round sperm cells and found that gene expression pattern of ahES cells was highly similar with ES cells but was distinct from MEF cells and round sperms. **Overall design:** Androgenetic haploid ES cells were FACS sorted to harvest the G0/G1 phase haploid cells. Total RNA were extracted from three ahES cell lines (AH129-5, AH129-N1, AH129-NC1, all 129Sv genetic background), two ES cell lines (CS1-1, R1, 129Sv background), MEF cells and round sperm and hybridized with Affymetrix GeneChip 430 2.0 array. Data were collected and analyzed to compare their gene expression pattern.

Background corr dist: KL-Divergence = 0.0710, L1-Distance = 0.0949, L2-Distance = 0.0148, Normal std = 0.6873

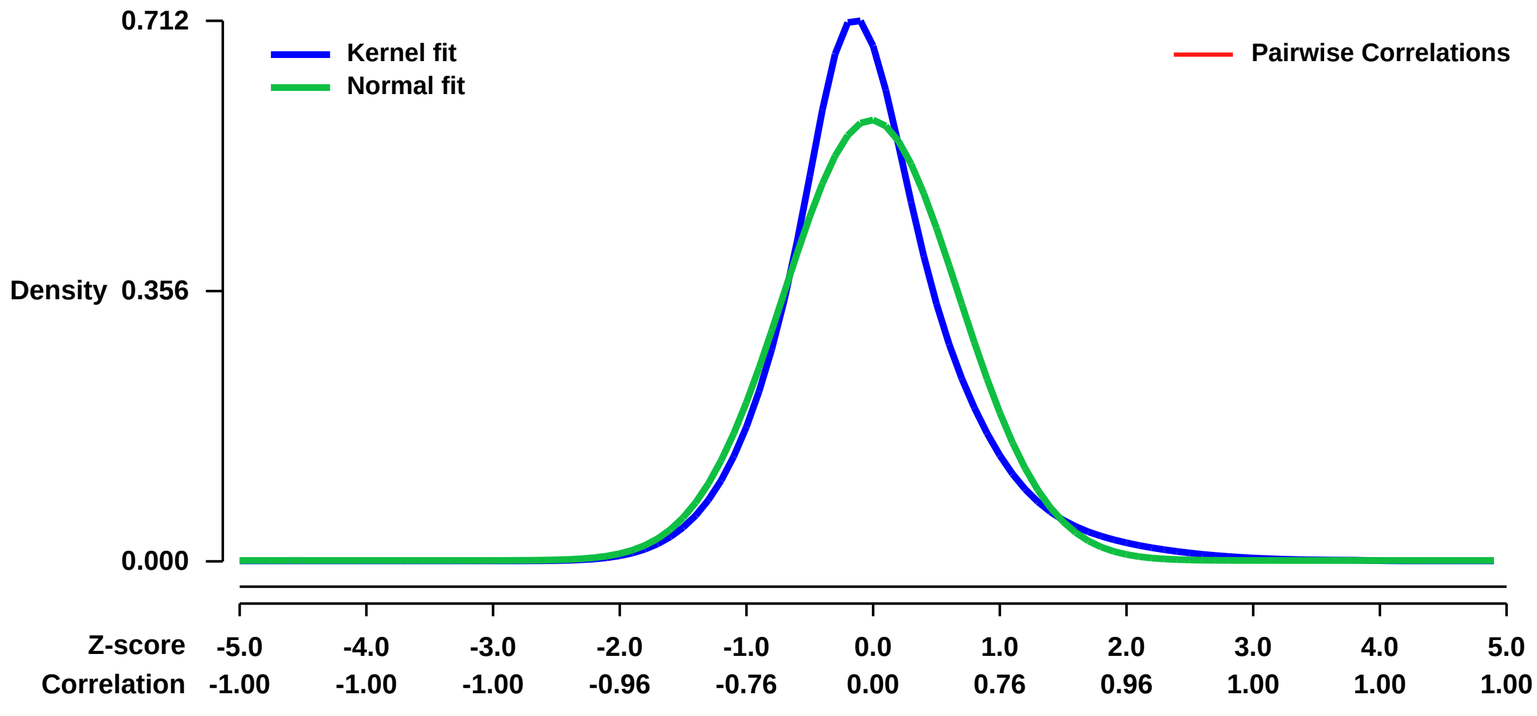

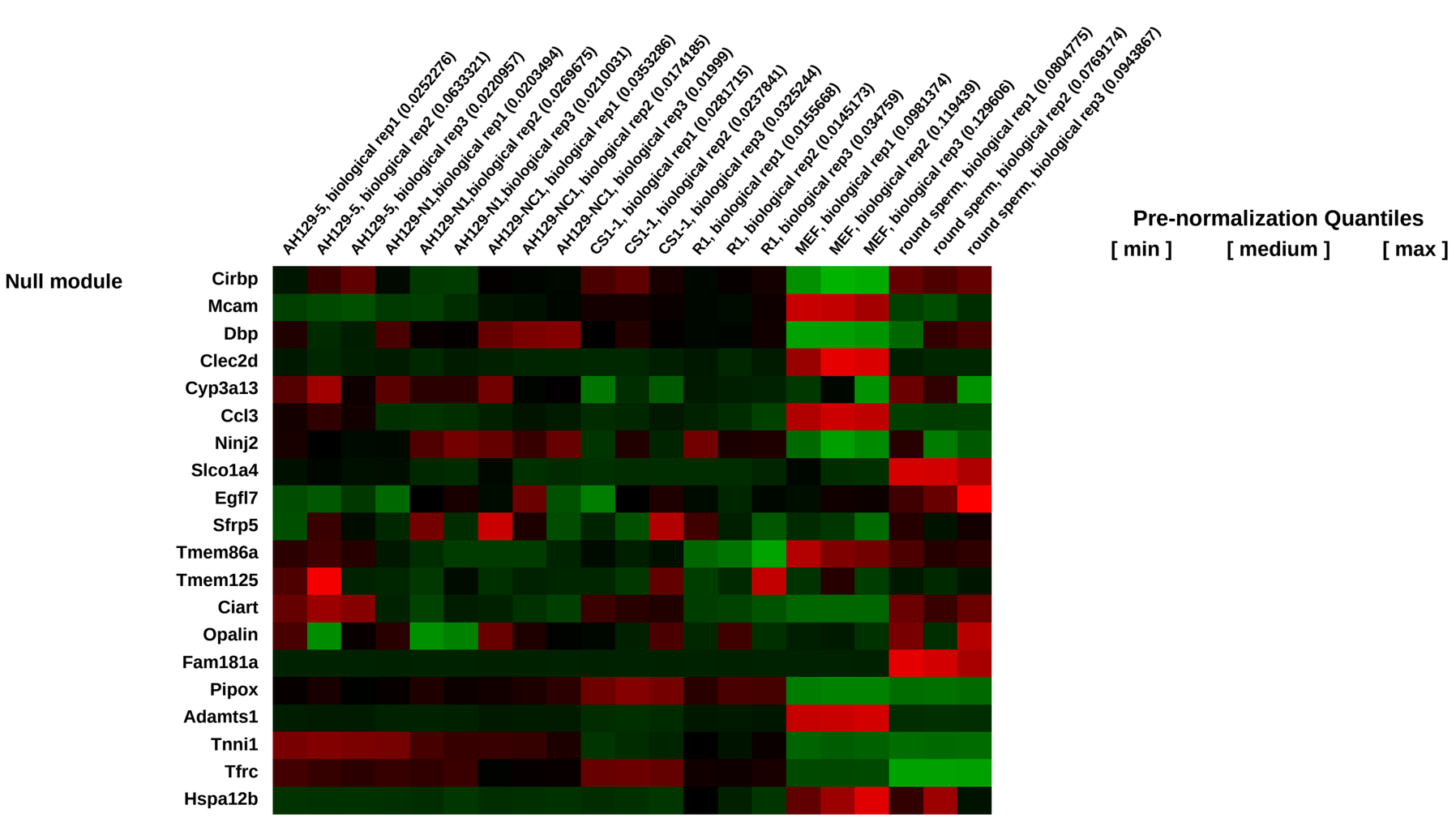

GEO Series "GSE39449" Expression Profiles

Num of samples in this series: 6

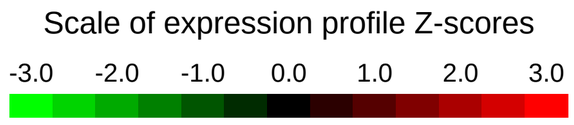

GEO Link:	http://www.ncbi.nlm.nih.gov/geo/query/acc.cgi?acc=GSE39449
Status:	Public on Feb 25 2014
Title:	Differentially activated CD8 T cells in liver and gut
Organism:	Mus musculus
Experiment type:	Expression profiling by array
Platform:	GPL1261
Pubmed ID:	19265543
Summary & Design:	**Summary:** **Naˆflve, liver- and gut-activated CD8 OT-I T cells show differential migration behaviour. To analyze which genes could be responsible for different migration patterns, naˆflve, liver-activated and gut-activated CD8 T cells were isolated and compared for their gene expression profile.** **Overall design:** **After total RNA extraction, reverse transcription, cDNA extraction, the biotinylated cRNA was transcribed, fragmented, and 15 ´µg cRNA hybridized in duplicates for each of the three groups to the GeneChip arrays. Group1: naˆflve, Group2: liver-activated Group3: gut-activated. Lists of differentially regulated genes were created using High Performance Chip Data Analysis (HPCDA) with Bioretis database (http://www.bioretis-analysis.de). Worldwide data sharing is possible via Bioretis, please ask the authors.**

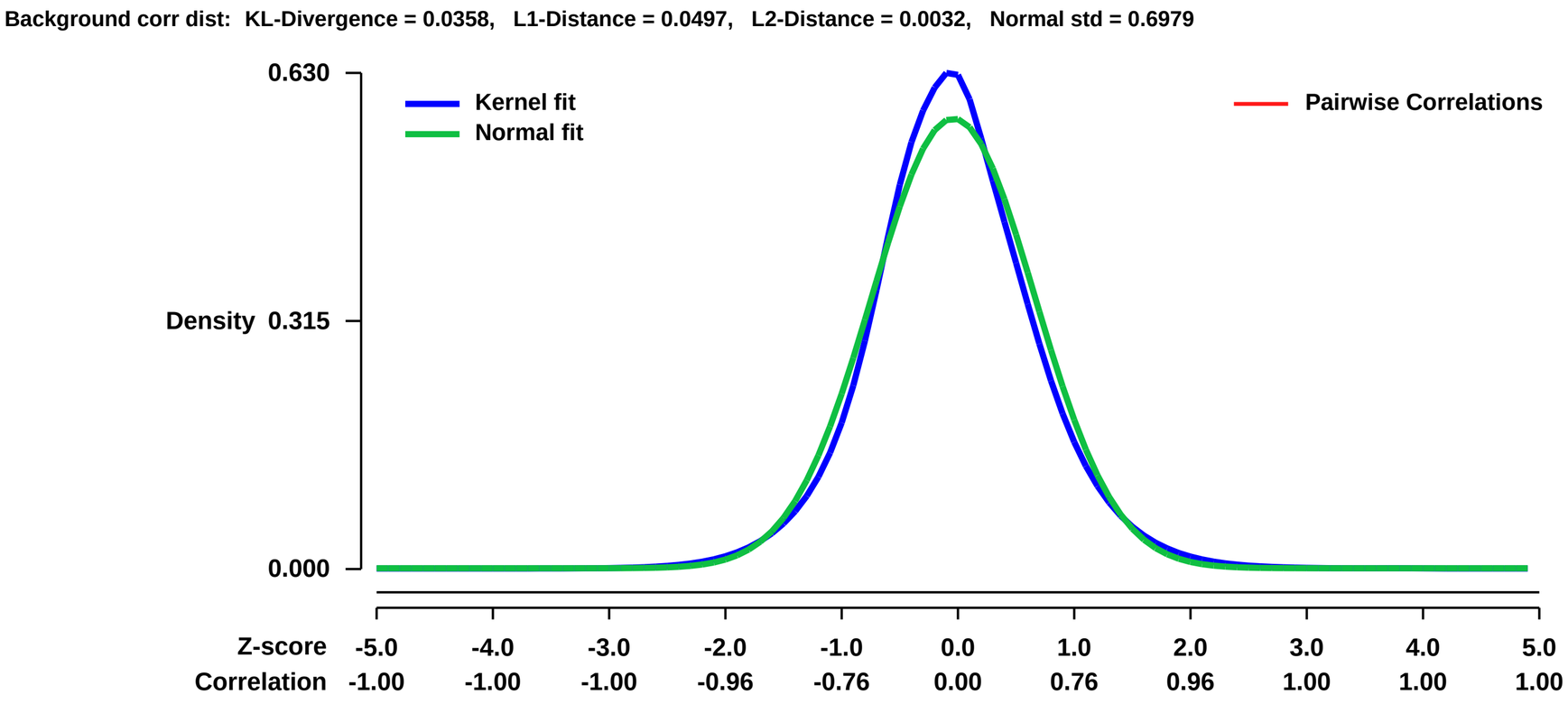

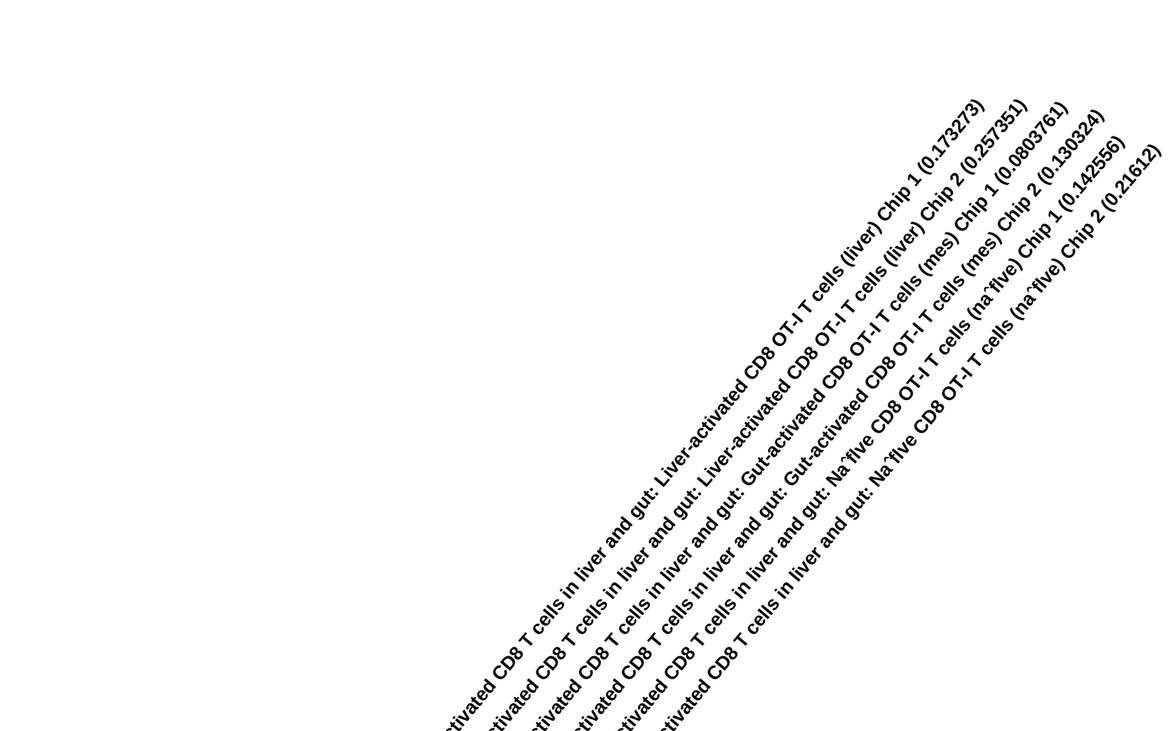

GEO Series "GSE39557" Expression Profiles

Num of samples in this series: 15

Scale of expression profile Z-scores

-3.0 -2.0 -1.0 0.0 1.0 2.0 3.0

GEO Link:	**http://www.ncbi.nlm.nih.gov/geo/query/acc.cgi?acc=GSE39557**
Status:	**Public on Jul 02 2013**
Title:	**Expression data from genetically engineered mouse models (GEMMs)**
Organism:	**Mus musculus**
Experiment type:	**Expression profiling by array**
Platform:	**GPL1261**
Pubmed ID:	**23403635**
Summary & Design:	**Summary:** **3 Cell lines from Apc, p53 (AP) GEMMs were compared to 12 cell lines from Apc, Kras, p53 (AKP) GEMMs.** **Mouse 430 2.0 arrays were used to determine genomic expression differences between the two genotypes (AP and AKP).** **Overall design:** **RNA was extracted from 3 AP and 10 AKP cell lines using the Qiagen RNEasy kit, and hybridized to individual Affymetrix mouse 430 2.0 chips as per manufacturer's instructions**

Background corr dist: **KL-Divergence = 0.1709, L1-Distance = 0.0613, L2-Distance = 0.0093, Normal std = 0.3784**

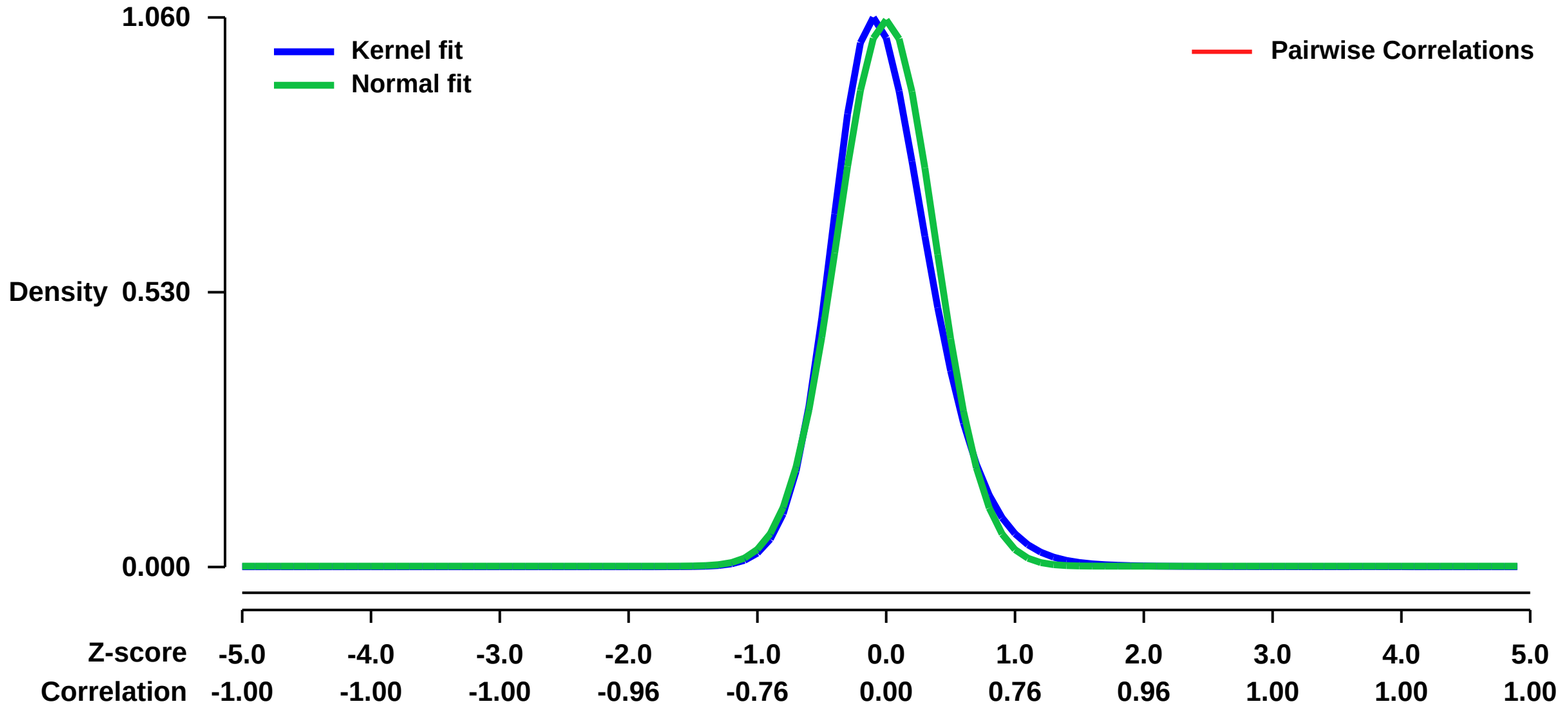

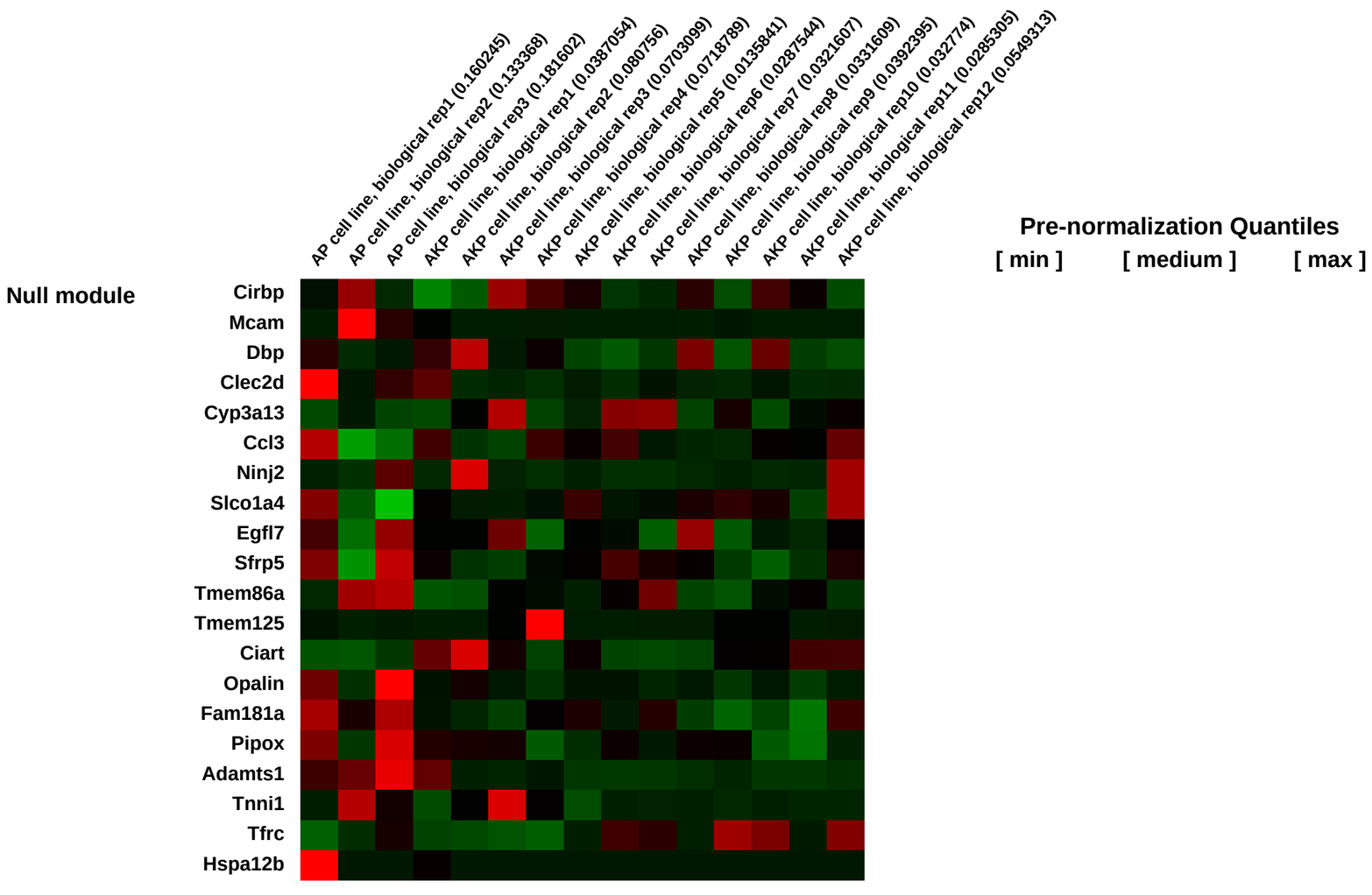

GEO Series "GSE39562" Expression Profiles

Num of samples in this series: 26

Scale of expression profile Z-scores

-3.0 -2.0 -1.0 0.0 1.0 2.0 3.0

GEO Link:	http://www.ncbi.nlm.nih.gov/geo/query/acc.cgi?acc=GSE39562
Status:	Public on Jul 24 2012
Title:	Immortalized clonal brown, beige and white adipose cell lines
Organism:	Mus musculus
Experiment type:	Expression profiling by array
Platform:	GPL1261
Pubmed ID:	22796012
Summary & Design:	**Summary:** Brown fat generates heat via the mitochondrial uncoupling protein UCP1, defending against hypothermia and obesity. Recent data suggest that there are two distinct types of brown fat: classical brown fat derived from a myf-5 cellular lineage and UCP1-positive cells that emerge in white fat from a non-myf-5 lineage. Here, we report the isolation of â beigeâ cells from murine white fat depots. **Overall design:** Microarray analysis of the differentiated clonal inguinal and interscapular adipocytes in the presence of forskolin (10microM). These samples were profiled using Affymetrix mouse 430 2.0 arrays, 26 samples in total.

Background corr dist: KL-Divergence = 0.3735, L1-Distance = 0.0779, L2-Distance = 0.0186, Normal std = 0.2548

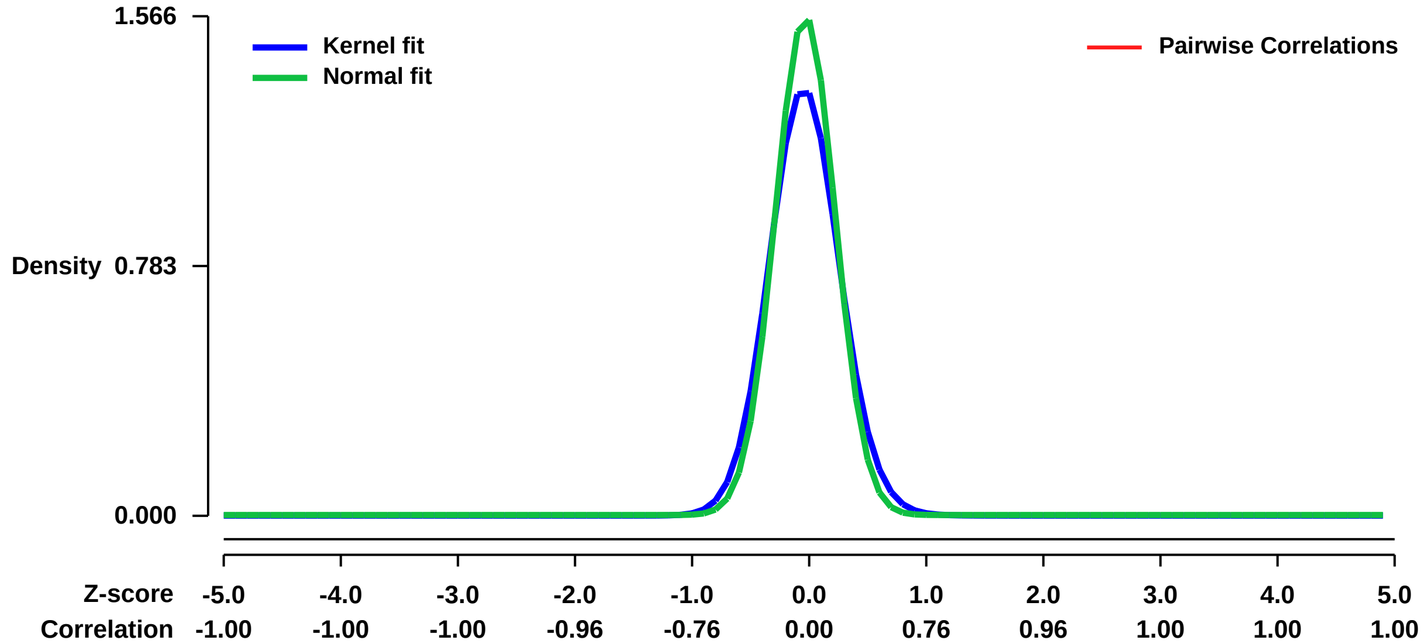

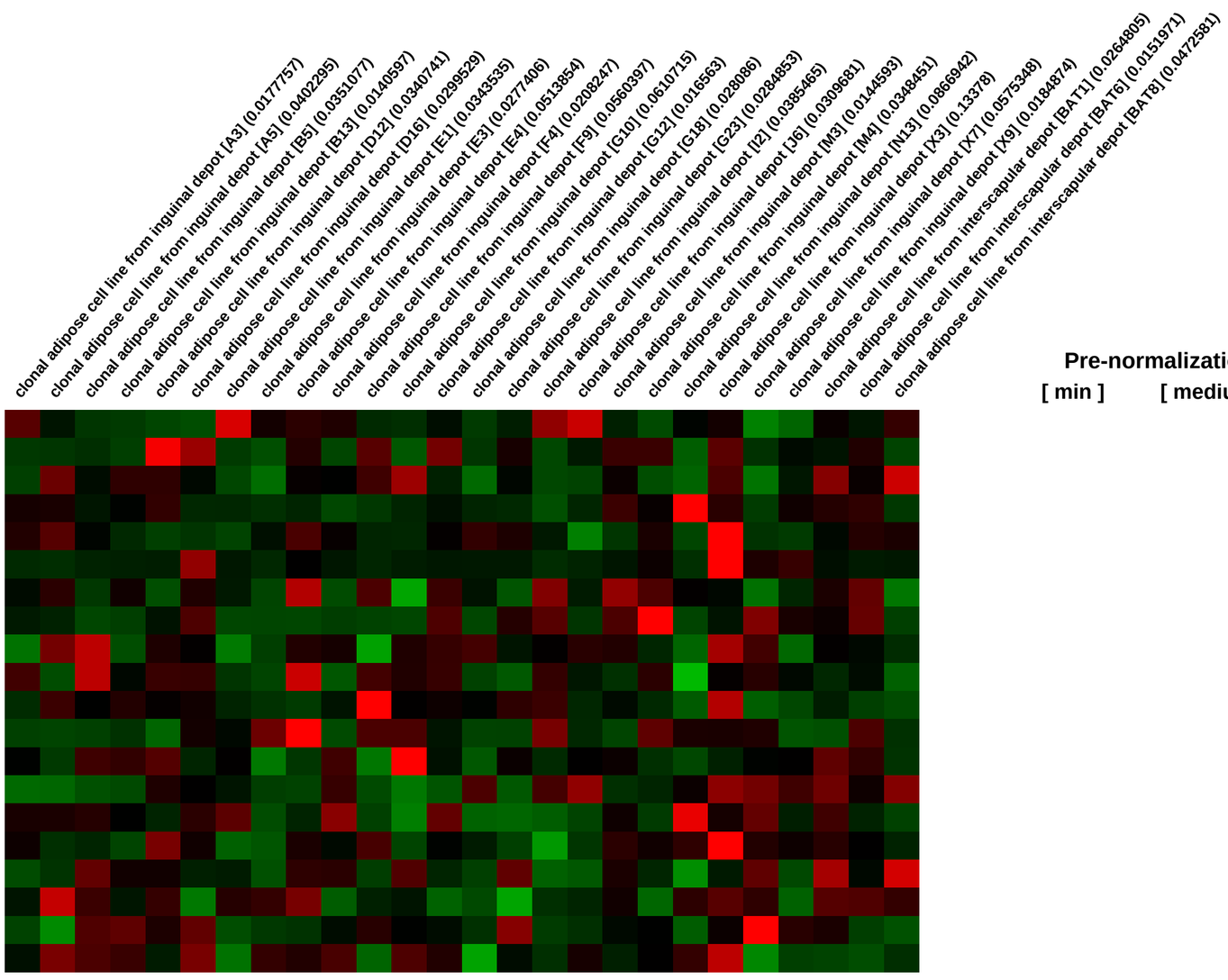

GEO Series "GSE39592" Expression Profiles

Num of samples in this series: 8

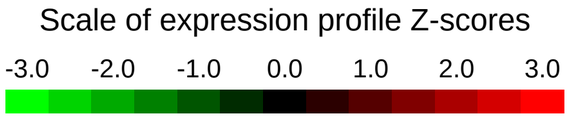

GEO Link:	**http://www.ncbi.nlm.nih.gov/geo/query/acc.cgi?acc=GSE39592**
Status:	**Public on Jul 24 2012**
Title:	**Expression data from cAMP-treated WT or IFN-gR1-deficient T cells**
Organism:	**Mus musculus**
Experiment type:	**Expression profiling by array**
Platform:	**GPL1261**
Pubmed ID:	
Summary & Design:	**Summary:** **cAMP inhibits TCR signaling, T cell proliferation, cytokine production and T cell function.** **We used microarrays to detail the global programme of gene expression in TCR-activated WT or IFN-gR1-deficient CD4+ T cells by db-cAMP.** **Overall design:** **CD4+ T cells were purified from spleens of WT or IFN-gR1-deficient mice by autoMACS, and activated with anti-CD3 plus anti-CD28 for 15 h. db-cAMP or vehicle control (med) was added into cultures for the last 3 h.**

Background corr dist: **KL-Divergence = 0.0621, L1-Distance = 0.0240, L2-Distance = 0.0007, Normal std = 0.5343**

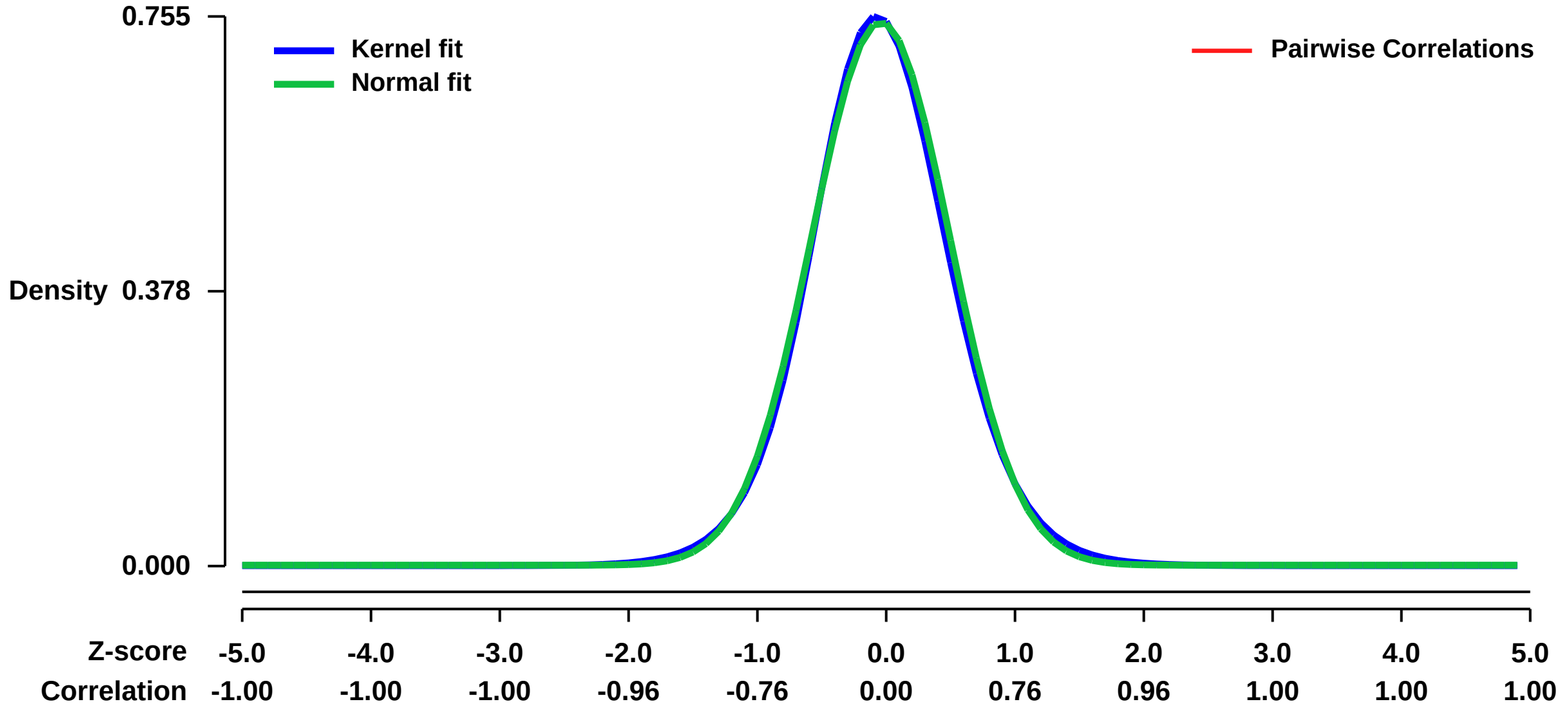

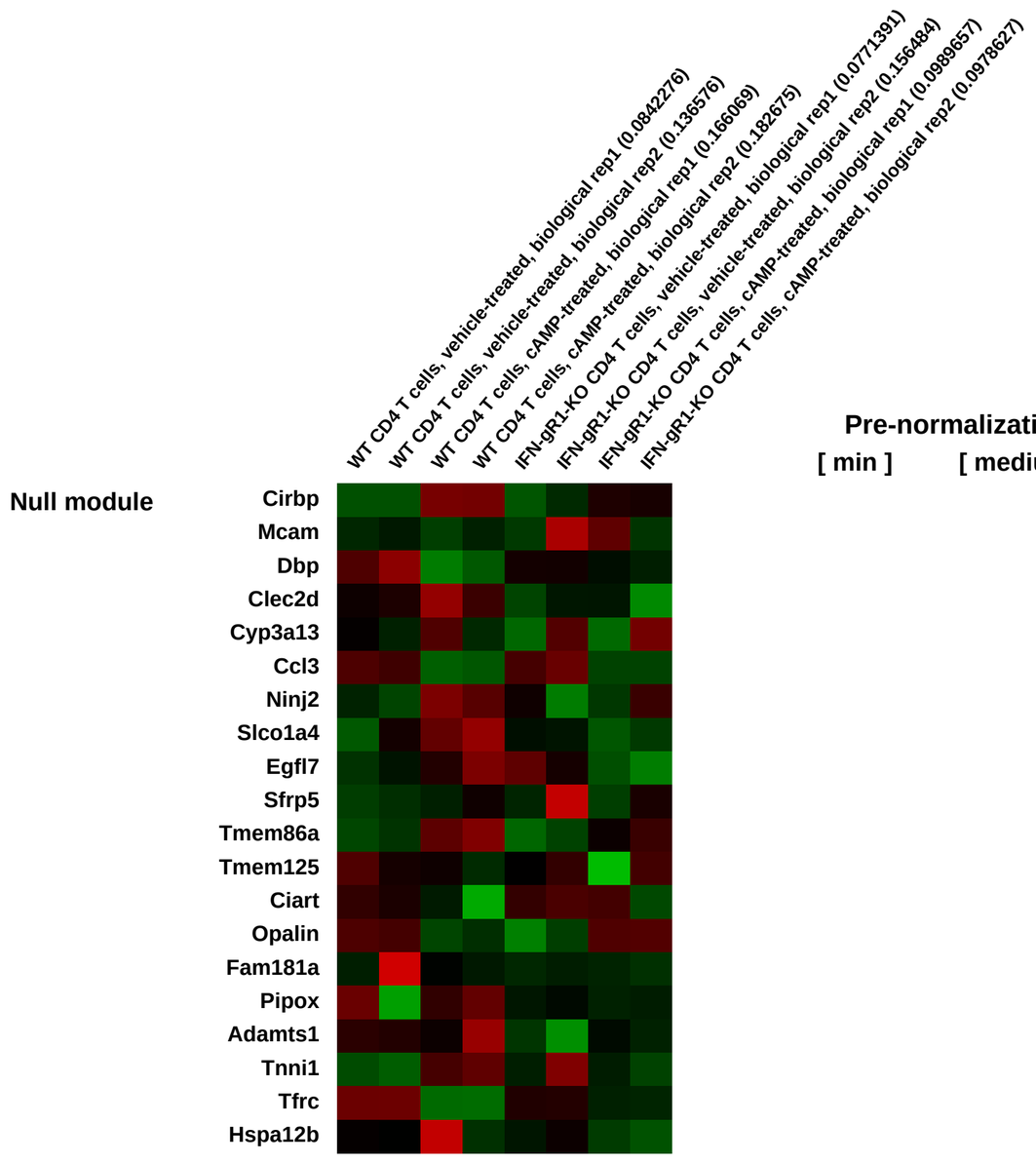

GEO Series "GSE39766" Expression Profiles

Num of samples in this series: 6

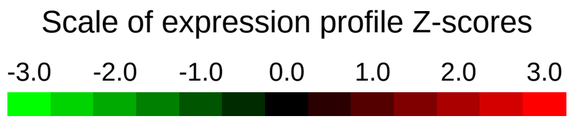

GEO Link:	**http://www.ncbi.nlm.nih.gov/geo/query/acc.cgi?acc=GSE39766**
Status:	**Public on Aug 10 2012**
Title:	**Blockade of TNF‹– after ischemia reperfusion injury ameliorates renal prognosis**
Organism:	**Mus musculus**
Experiment type:	**Expression profiling by array**
Platform:	**GPL1261**
Pubmed ID:	
Summary & Design:	**Summary:** **Recently, acute kidney injury (AKI) is thought to develop a predisposition toward chronic kidney disease. But the detailed mechanism of the disease progression after AKI is unknown. We made two ischemia-reperfusion injury (IRI) mice models, repaired kidney model and atrophic kidney model, and studied the mechanism that kidney after IRI became atrophy. We found that the atrophy kidney model had two peaks of apoptosis 3 and 14 days after IRI, whereas the repaired kidney model had only one apoptosis peak 3 days after IRI. We showed that the second apoptosis is responsible for the kidney atrophy. Moreover, apoptotic ligands, TNF‹– and FasL were upregulated at the same time of two apoptosis peaks on the atrophic kidney, and blockade of them before IRI prevented kidney from falling into atrophy. Surprisingly, inhibition of the second apoptosis by anti-TNF‹– antibody protected from renal atrophy. We propose that apoptosis might play a major role in AKI progression and blockade of TNF‹– after IRI will be a new therapeutic approach for AKI.** **Overall design:** **Mice were subjected for 0, 45, and 60 min of unilateral IRI. Mice kidneys were collected at day 1 and 3 after IRI for RNA extraction and hybridization on Affymetrix microarrays. There are 6 samples, 1day IRI45(1), 1day IRI60(2), 1day IRI0(3), 3day IRI45(4), 3day IRI60(5), 3day IRI0(6).**

Background corr dist: KL-Divergence = 0.0415, L1-Distance = 0.0215, L2-Distance = 0.0005, Normal std = 0.6111

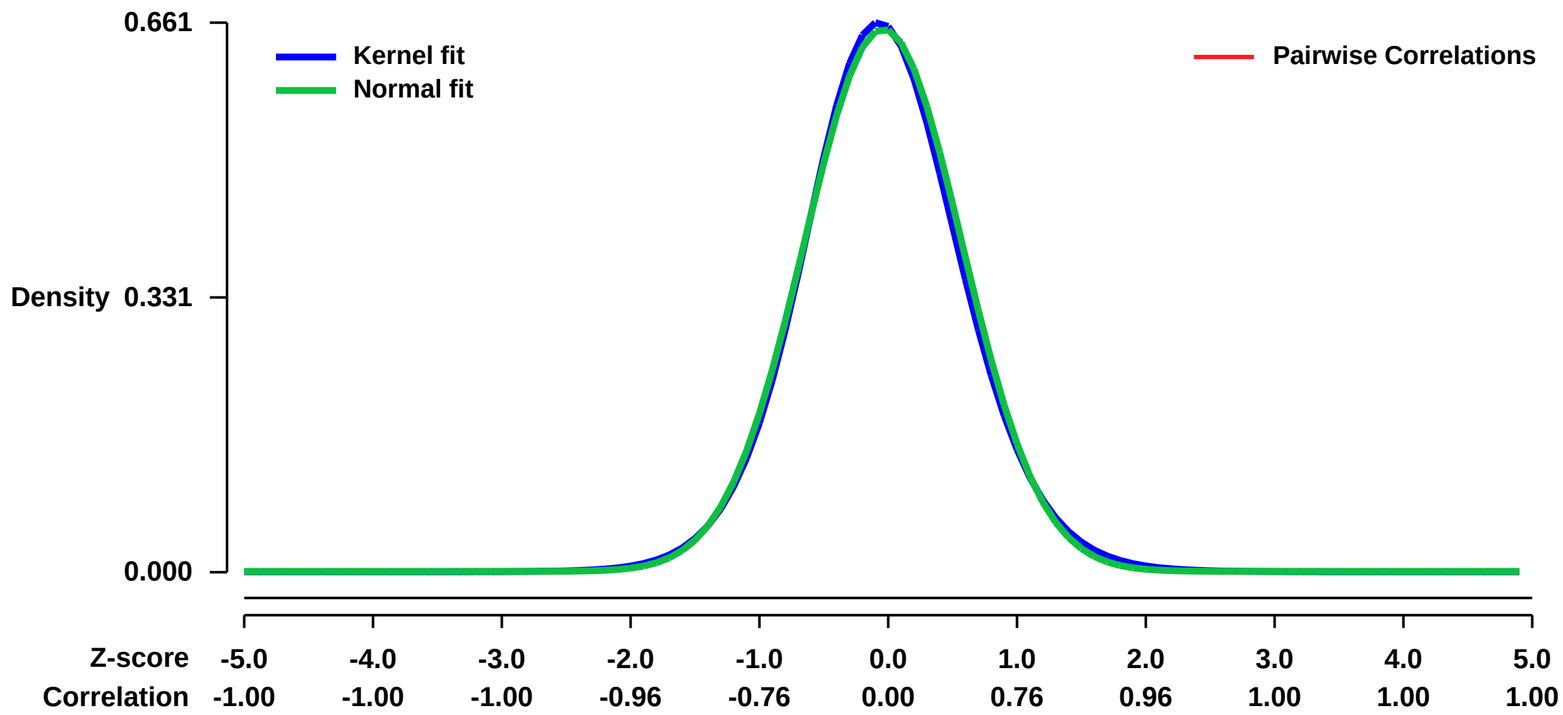

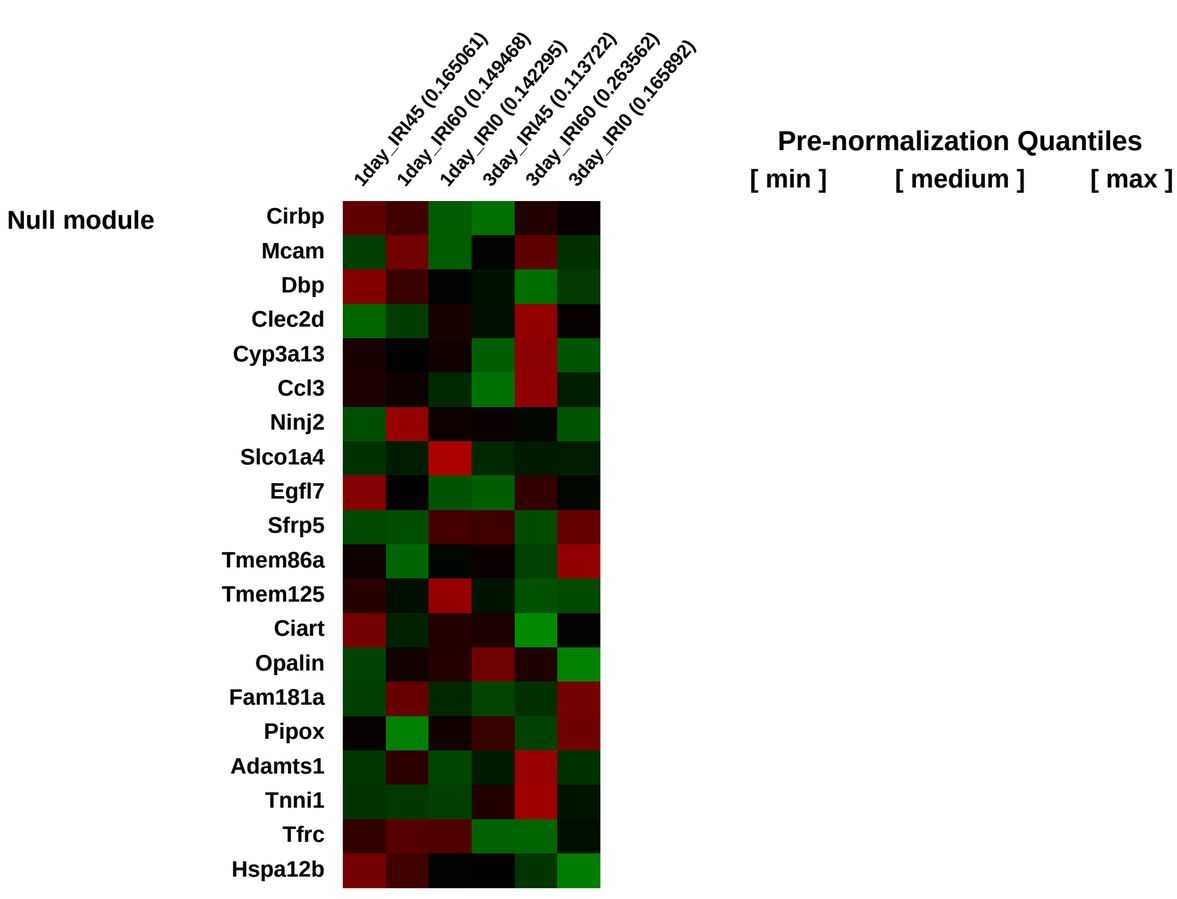

GEO Series "GSE39770" Expression Profiles

Num of samples in this series: 10

Scale of expression profile Z-scores

-3.0 -2.0 -1.0 0.0 1.0 2.0 3.0

GEO Link:	http://www.ncbi.nlm.nih.gov/geo/query/acc.cgi?acc=GSE39770
Status:	Public on Aug 01 2012
Title:	Expression data from embryonic stem cells following siRNA transfection of UPS members [Differentiation_ES]
Organism:	Mus musculus
Experiment type:	Expression profiling by array
Platform:	GPL1261
Pubmed ID:	23103054
Summary & Design:	**Summary:** While transcriptional regulation of stem cell self-renewal and differentiation has been extensively studied, only a small number of studies have addressed the roles for post-translational modifications in these processes. A key mechanism of post-translational modification is ubiquitination by the ubiquitin-proteasome system (UPS). Using UPS-targeted RNAi screens, we identify novel regulators of pluripotency and differentiation. We focus on two of these proteins, the deubiquitinating enzyme, Psmd14, and the E3 ligase, Fbxw7, and characterize their importance in ES cell pluripotency and cellular reprogramming. **Overall design:** Embryonic stem cells were reverse transfected with siRNA, and differentiated for 48hrs in conditions with retinoic acid, 48 hrs post transfection cells were isloated for RNA extraction and hybridization on Affymetrix microarrays

Background corr dist: KL-Divergence = 0.0856, L1-Distance = 0.0226, L2-Distance = 0.0006, Normal std = 0.4634

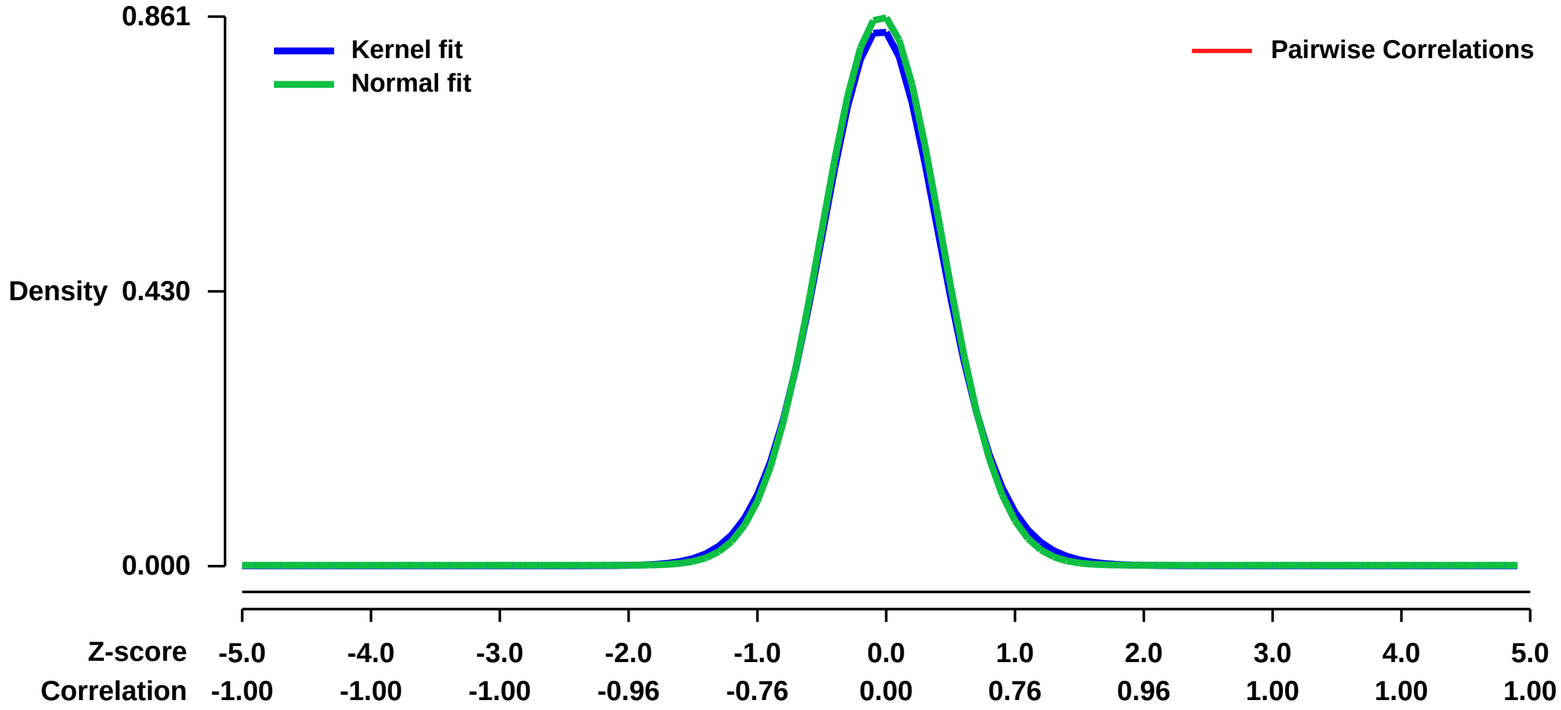

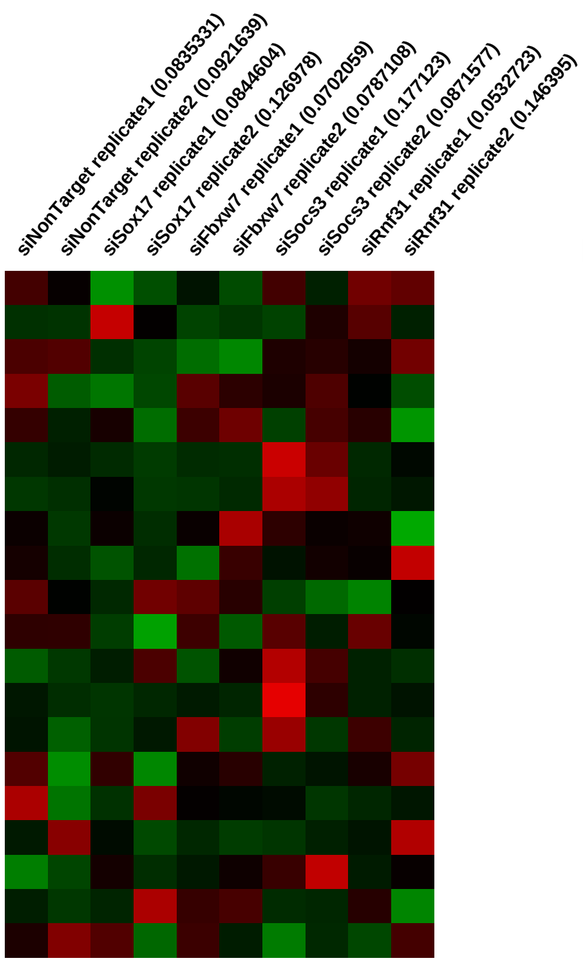

GEO Series "GSE39771" Expression Profiles

Num of samples in this series: 10

Scale of expression profile Z-scores

-3.0 -2.0 -1.0 0.0 1.0 2.0 3.0

GEO Link:	http://www.ncbi.nlm.nih.gov/geo/query/acc.cgi?acc=GSE39771
Status:	Public on Aug 01 2012
Title:	Expression data from embryonic stem cells following siRNA transfection of UPS members [self_renewal]
Organism:	Mus musculus
Experiment type:	Expression profiling by array
Platform:	GPL1261
Pubmed ID:	23103054
Summary & Design:	**Summary:** While transcriptional regulation of stem cell self-renewal and differentiation has been extensively studied, only a small number of studies have addressed the roles for post-translational modifications in these processes. A key mechanism of post-translational modification is ubiquitination by the ubiquitin-proteasome system (UPS). Using UPS-targeted RNAi screens, we identify novel regulators of pluripotency and differentiation. We focus on two of these proteins, the deubiquitinating enzyme, Psmd14, and the E3 ligase, Fbxw7, and characterize their importance in ES cell pluripotency and cellular reprogramming. **Overall design:** Embryonic stem cells were reverse transfected with siRNA, 48 hrs post transfection cells were isloated for RNA extraction and hybridization on Affymetrix microarrays

Background corr dist: KL-Divergence = 0.0991, L1-Distance = 0.0239, L2-Distance = 0.0008, Normal std = 0.4406

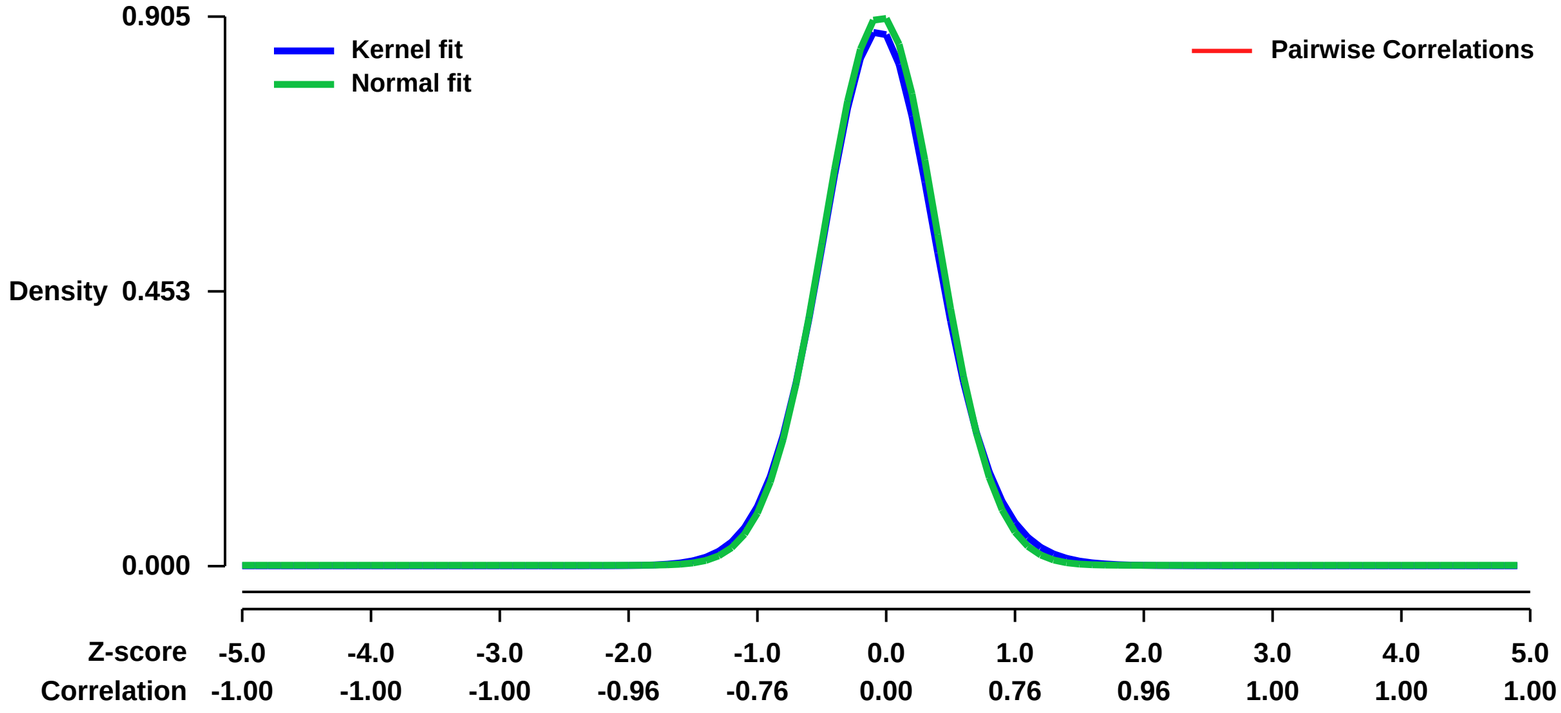

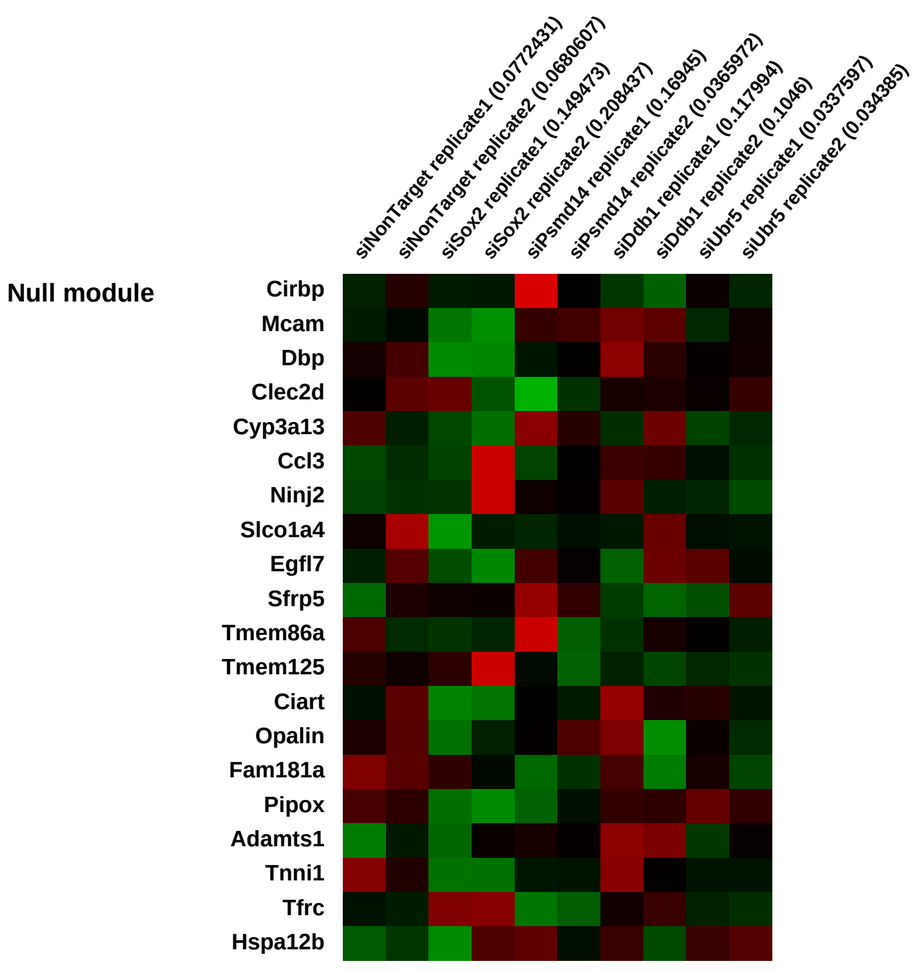

GEO Series "GSE39820" Expression Profiles

Num of samples in this series: 22

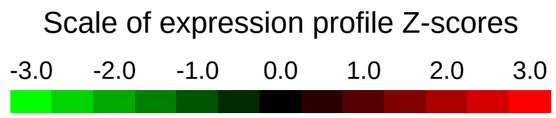

GEO Link:	**http://www.ncbi.nlm.nih.gov/geo/query/acc.cgi?acc=GSE39820**
Status:	**Public on Sep 01 2012**
Title:	**Induction and molecular signature of pathogenic Th17 cells**
Organism:	**Mus musculus**
Experiment type:	**Expression profiling by array**
Platform:	**GPL1261**
Pubmed ID:	**22961052**
Summary & Design:	**Summary:** **TGF-beta3 produced by developing Th17 cells induces highly pathogenic T cells that are functionally and molecularly distinct from TGF-beta1-induced Th17 cells. The microarray data represent a distinct molecular signature for pathogenic versus non-pathogenic Th17 cells.** **Overall design:** **NOCYTO: no cytokines**

Background corr dist: **KL-Divergence = 0.0991, L1-Distance = 0.0309, L2-Distance = 0.0017, Normal std = 0.4374**

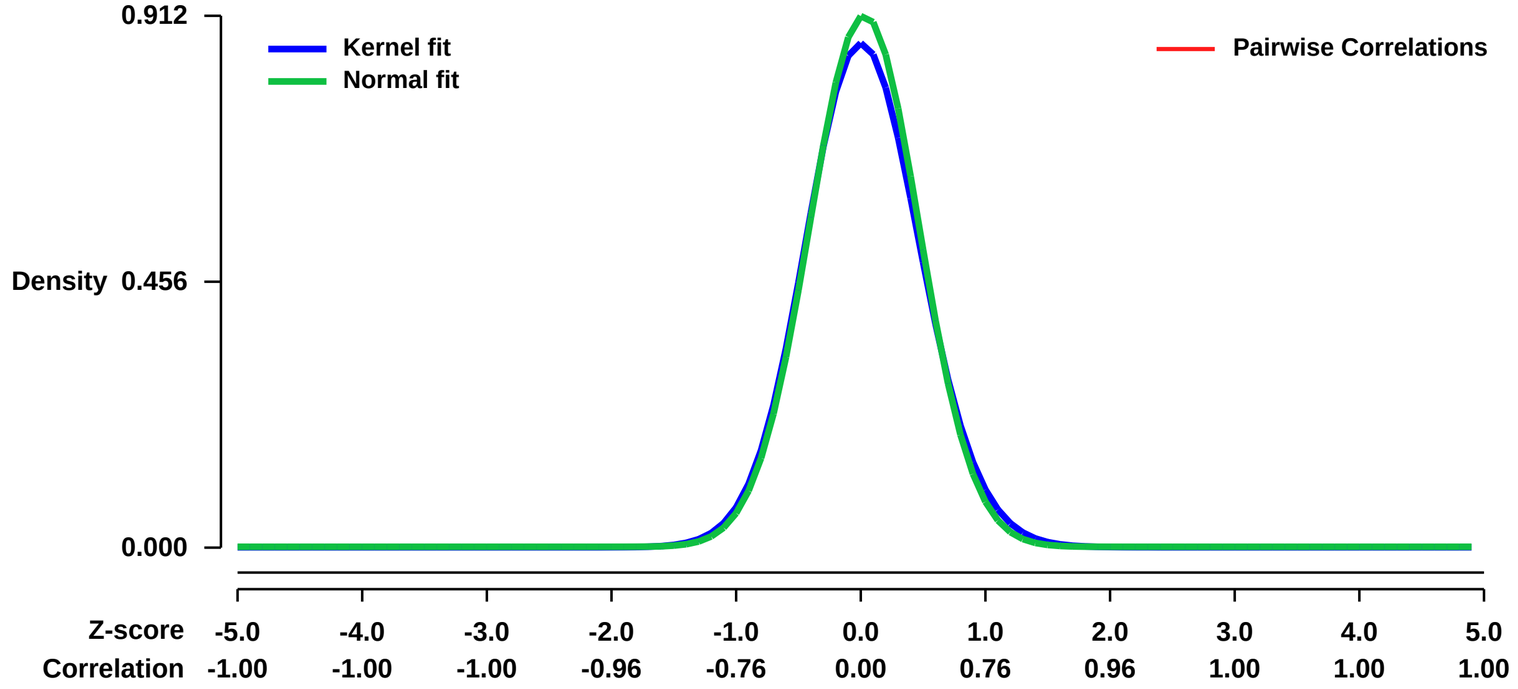

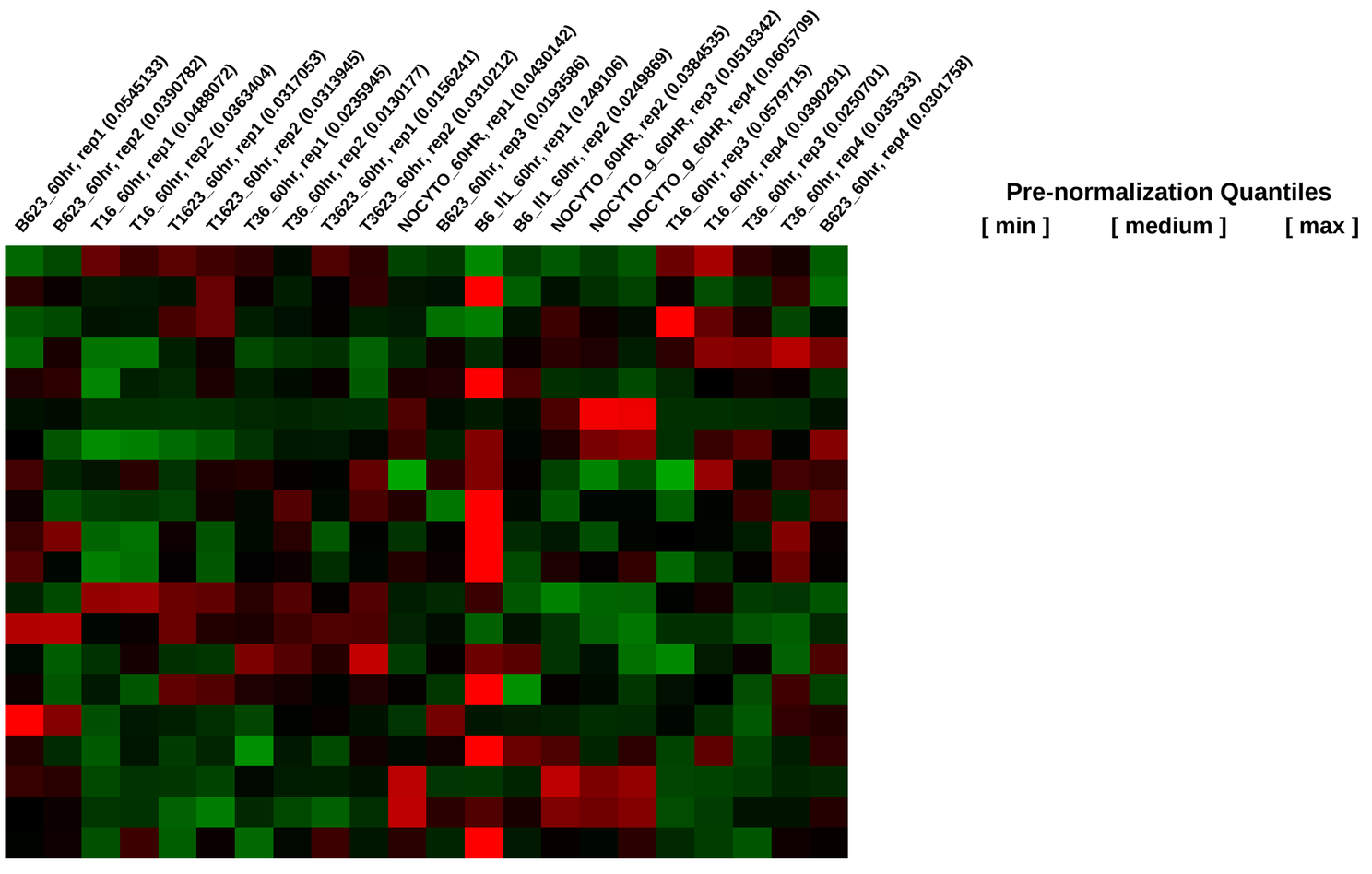

GEO Series "GSE39865" Expression Profiles

Num of samples in this series: 21

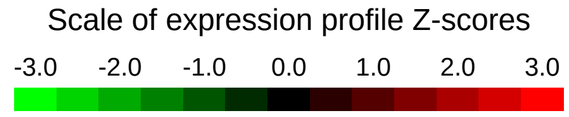

GEO Link:	http://www.ncbi.nlm.nih.gov/geo/query/acc.cgi?acc=GSE39865
Status:	Public on Aug 04 2012
Title:	The gene expression analysis of the spinal cord of SBMA (Spinal Bulbar Muscular Atrophy) model mice
Organism:	Mus musculus
Experiment type:	Expression profiling by array
Platform:	GPL1261
Pubmed ID:	23023499
Summary & Design:	**Summary:** To identify the gene expression changes that are specific to SBMA, we prepared total mRNA samples from the spinal cords of transgenic mice carrying a full-length human AR with 97 CAGs (AR-97Q), transgenic mice bearing a wild-type allele of AR with 24 CAGs (AR-24Q), and the wild-type littermates of the AR-97Q mice (C57BL/6). We used AR-97Q (Line #7-8) male mice because they show progressive muscular atrophy and weakness as well as SBMA-like pathology such as the accumulation of the pathogenic androgen receptor in the nucleus of motor neurons. Using microarray analysis, we identified the genes with significantly altered expression among the three types of mice. **Overall design:** For each group, we examined the male mice at 7-9, 10-12, and 13-15 weeks of age. These stages were chosen because the AR-97Q mice are generally asymptomatic at 7-9 weeks of age (before-onset stage), present with mild motor impairment at 10-12 weeks (early stage), and are severely weakened with profound muscle atrophy at 13-15 weeks (advanced stage). RNA from the total spinal cord, excluding the dorsal root ganglia, was isolated from three mice of each genotype at each stage. For wild-type, pooled sample for three mice were used in each stage.

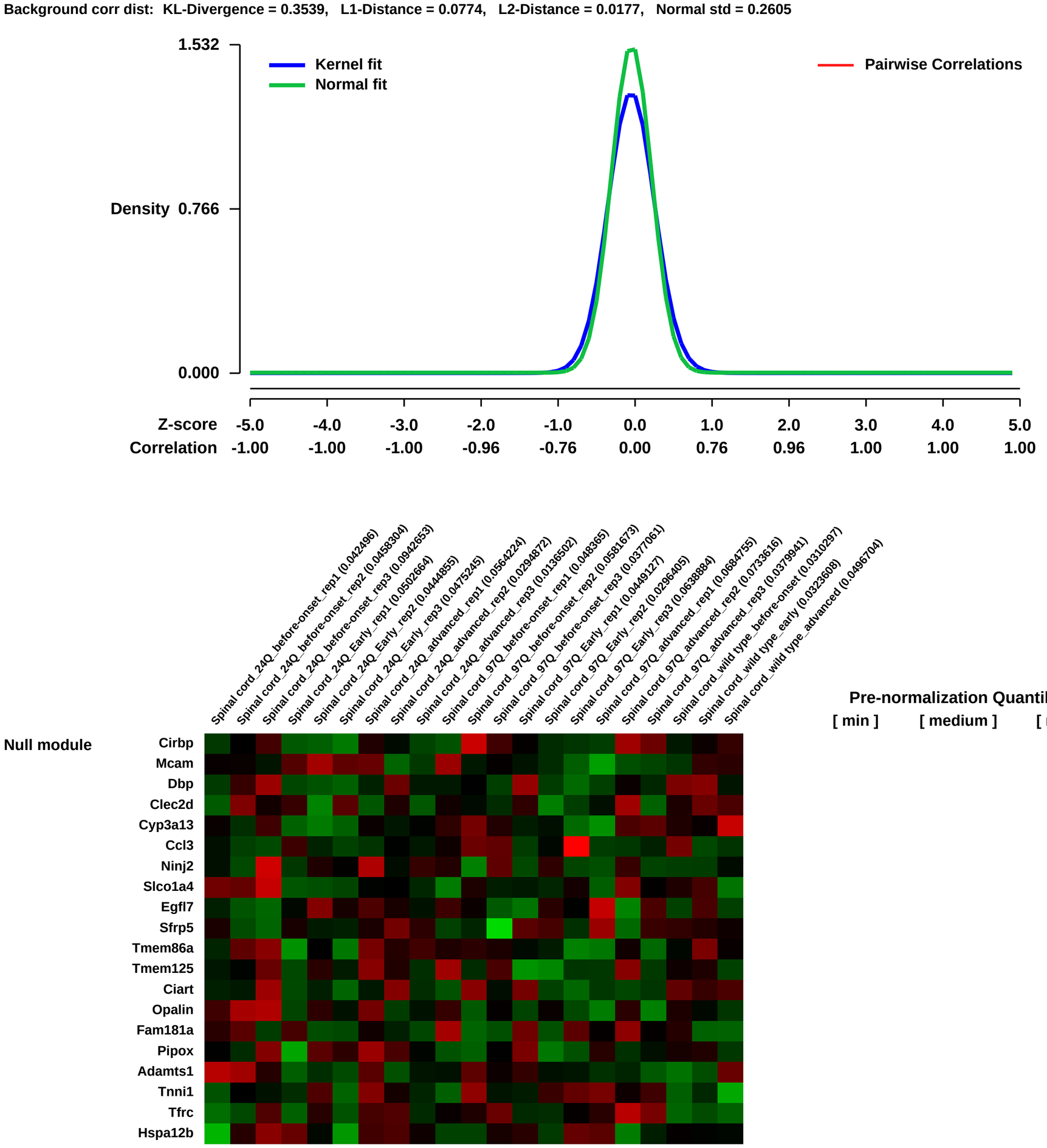

GEO Series "GSE39886" Expression Profiles

Num of samples in this series: 24

Scale of expression profile Z-scores

-3.0 -2.0 -1.0 0.0 1.0 2.0 3.0

GEO Link:	http://www.ncbi.nlm.nih.gov/geo/query/acc.cgi?acc=GSE39886
Status:	Public on Aug 04 2012
Title:	Selective inhibition of CD4+ T-cell cytokine production and autoimmunity by BET protein and c-Myc inhibitors
Organism:	Mus musculus
Experiment type:	Expression profiling by array
Platform:	GPL1261
Pubmed ID:	22912406
Summary & Design:	**Summary:** Bromodomain-containing proteins bind acetylated lysine residues on histone tails and are involved in the recruitment of additional factors that mediate histone modifications and enable transcription. A compound, I-BET-762, that inhibits binding of an acetylated histone peptide to BRD4 and other proteins of the BET (bromodomain and extra-terminal domain) family, was previously shown to suppress the production of pro-inflammatory proteins by macrophages and block acute inflammation in mice. Here we investigate the effect of I-BET-762 on T cell function. We show that treatment of naˆflve CD4+ T cells with I-BET-762 during early differentiation modulates subsequent cytokine production, and inhibits the ability of Th1-skewed cells to induce autoimmune pathogenesis in a model of experimental autoimmune encephalomyelitis (EAE) in vivo. The suppressive effects of I-BET-762 on T-cell mediated inflammation were not due to inhibition of expression of the pro-inflammatory cytokines, IFN-. or IL-17, but correlated with the ability to suppress GM-CSF production from CNS-infiltrating T cells, resulting in decreased recruitment of macrophages and granulocytes. The effects of I-BET-762 were distinct from those of the fumarate ester, dimethyl fumarate (DMF), a candidate drug for treatment of multiple sclerosis (MS). Our data suggest that I-BET and DMF could have complementary roles in the treatment of MS, and provide a strong rationale for inhibitors of BET-family proteins in the treatment of autoimmune diseases, based on their dual ability to suppress granulocyte and macrophage recruitment by T cells as well as production of pro-inflammatory proteins by macrophages. **Overall design:** RNA from resting or activated CD4+ T cells grown in the presence of a control substance (DMSO or Control-768) or two different concentrations of I-BET-762, was hybridized to the chip. There are 3 biological replicates for a total of 2 (cell states) x 4 (conditions) x 3 (replicates) = 24 samples.

Background corr dist: KL-Divergence = 0.1425, L1-Distance = 0.0653, L2-Distance = 0.0080, Normal std = 0.4122

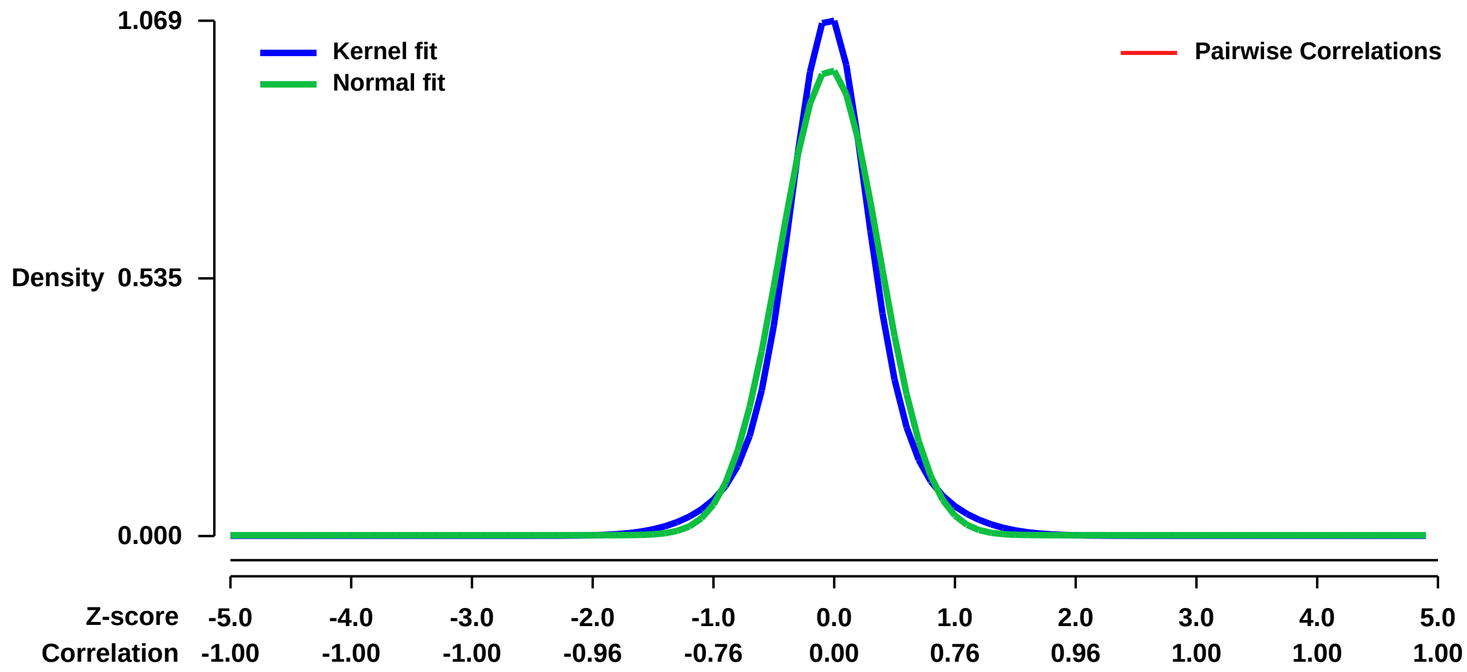

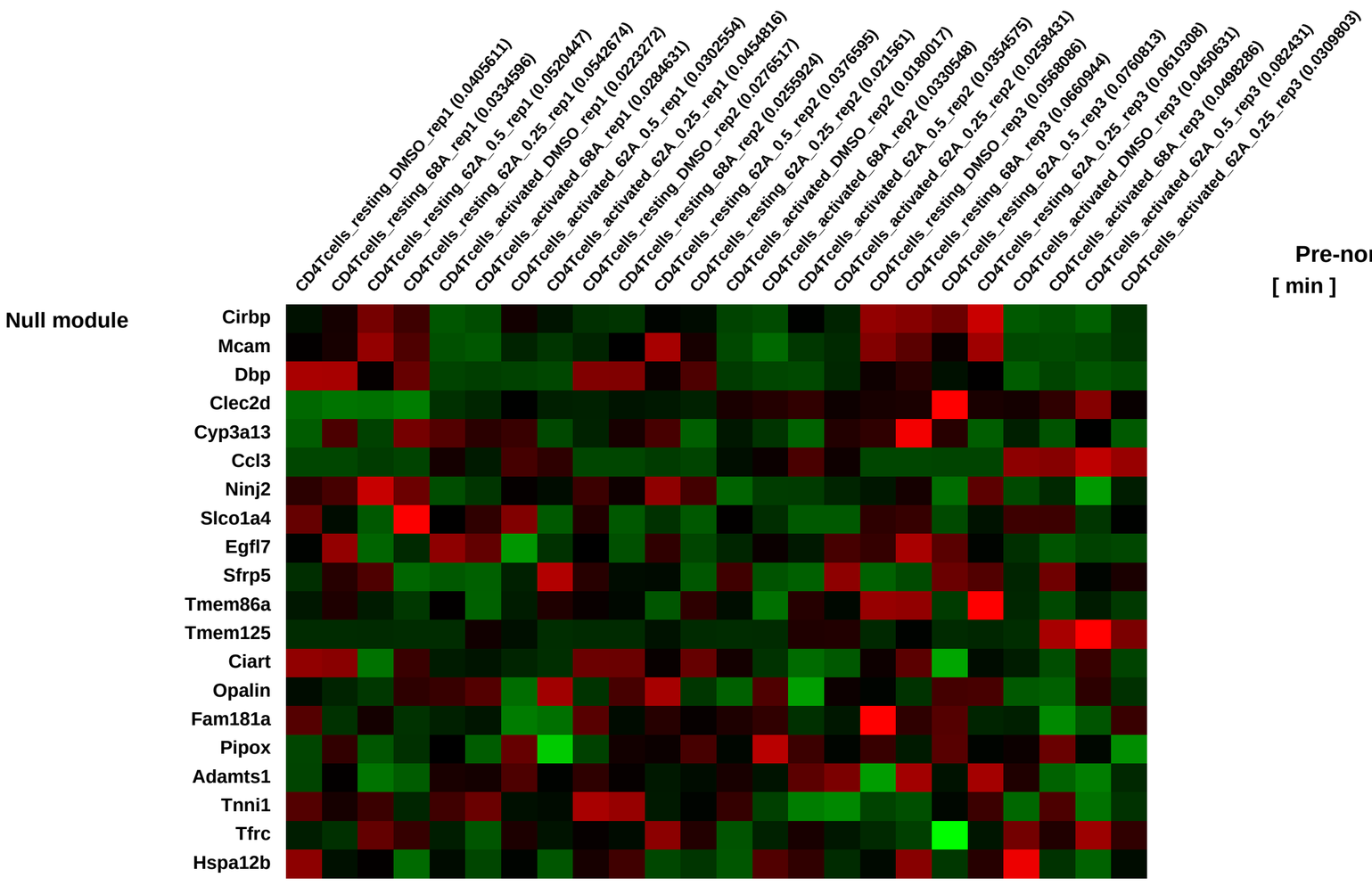

GEO Series "GSE39897" Expression Profiles

Num of samples in this series: 36

Scale of expression profile Z-scores

-3.0 -2.0 -1.0 0.0 1.0 2.0 3.0

GEO Link:	http://www.ncbi.nlm.nih.gov/geo/query/acc.cgi?acc=GSE39897
Status:	Public on Sep 11 2013
Title:	Expression data for mouse embryogenesis from oocyte to newborn
Organism:	Mus musculus
Experiment type:	Expression profiling by array
Platform:	GPL1261
Pubmed ID:	23961710
Summary & Design:	**Summary:** Studies in mouse have led to enormous progress in our understanding of early human development. The identification of genes and the signaling pathways involved in mouse embryogenesis have helped us to better understand fertilization, morulation, gastrulation, organogenesis and embryonic development in mammals. We report a detailed analysis of the global gene expression profiles from oocyte to the end of organogenesis in mouse. Our studies revealed distinct temporal regulation patterns for genes belonging to different functional categories, supporting their roles during organogenesis. **Overall design:** Mouse embryos were selected at successive stage for for RNA extraction and hybridization on Affymetrix microarrays. We sought to obtain homogeneous populations of embryos at each developmental stage in order to increase the temporal resolution of expression profiles. To that end, we hand-selected embryos according to morphological criteria at 12 time-points from embryos to newborn

Background corr dist: KL-Divergence = 0.0939, L1-Distance = 0.0418, L2-Distance = 0.0040, Normal std = 0.4636

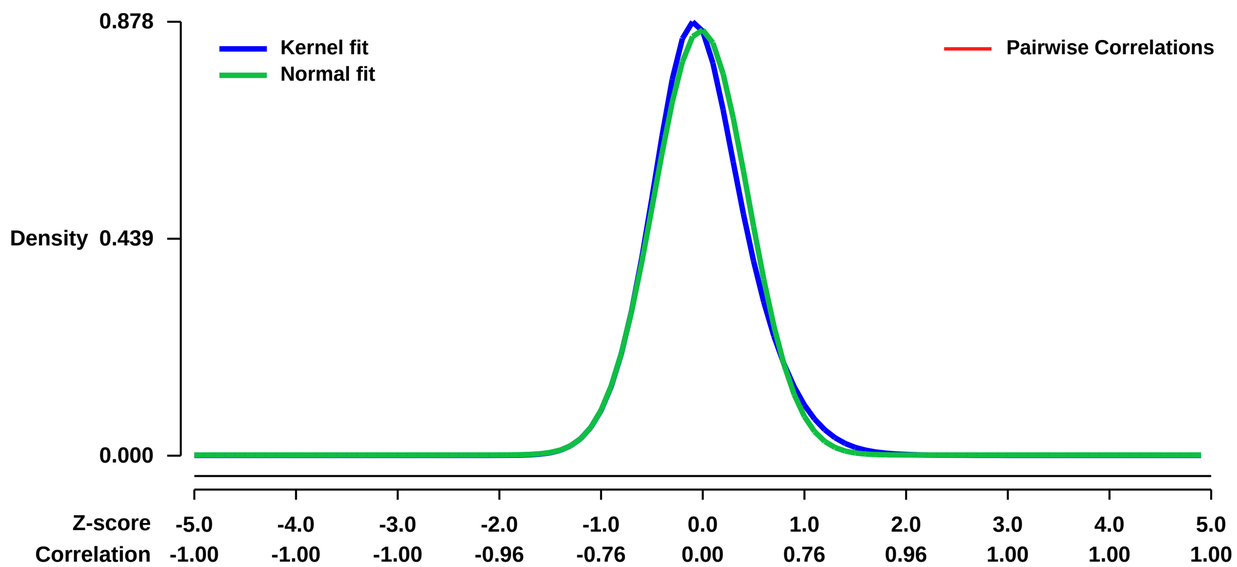

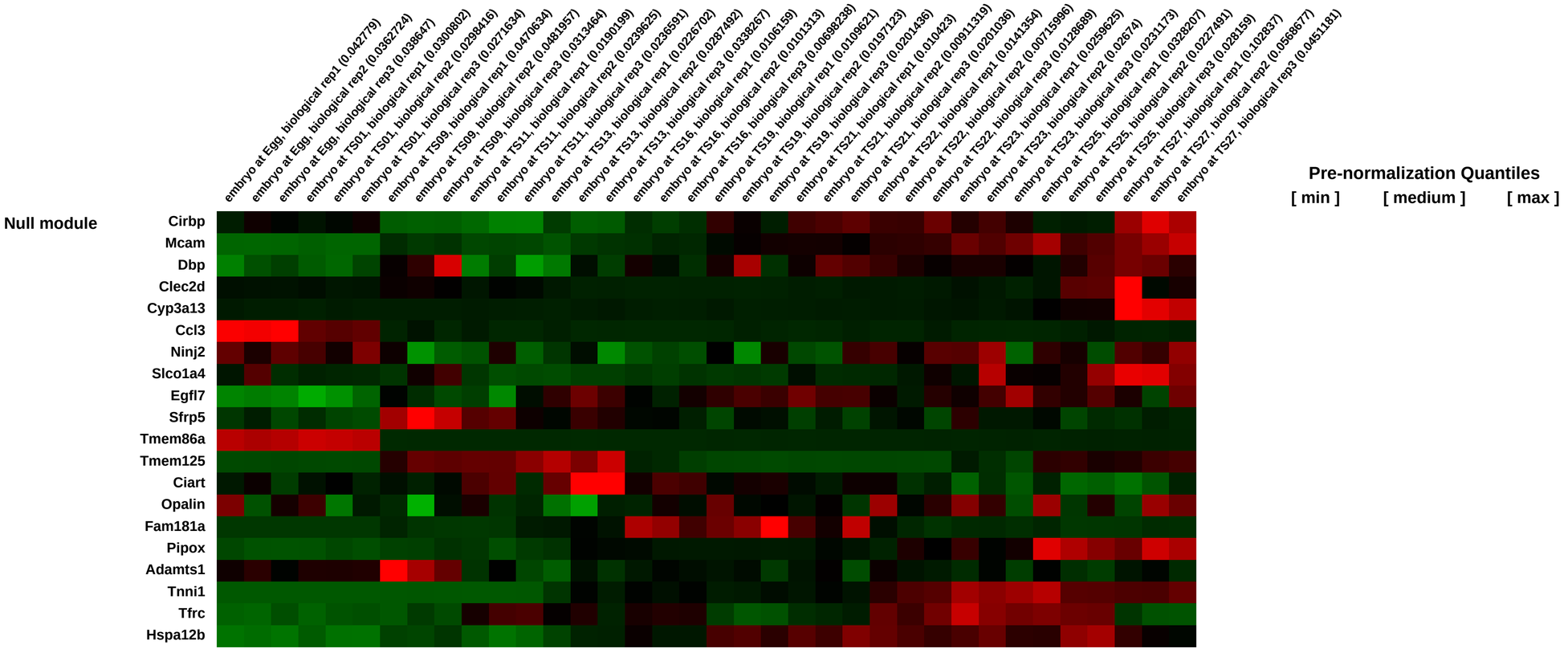

GEO Series "GSE39984" Expression Profiles

Num of samples in this series: 18

Scale of expression profile Z-scores

-3.0 -2.0 -1.0 0.0 1.0 2.0 3.0

GEO Link:	http://www.ncbi.nlm.nih.gov/geo/query/acc.cgi?acc=GSE39984
Status:	Public on Aug 09 2012
Title:	Comparison of the genetic extinction of NRAS to pharmacological MEK inhibition in an inducible mouse model of melanoma
Organism:	Mus musculus
Experiment type:	Expression profiling by array
Platform:	GPL1261
Pubmed ID:	22983396
Summary & Design:	**Summary:** Since direct pharmacological inhibition of RAS has thus far been unsuccessful, we explored system biology approaches to identify synergistic drug combination(s) that can mimic direct RAS inhibition. Leveraging an inducible mouse model of NRAS-mutant melanoma, we compare pharmacological MEK inhibition to complete NRAS-Q61K extinction in vivo. NRAS-Q61K extinction leads to a complete and durable tumor regression by enhancing both apoptosis and cell cycle arrest. By contrast, MEK inhibition only produces tumor stasis at best and we find that it robustly activates apoptosis but does not significantly impede proliferation. We used microarrays to determine which transcripts were affected by NRAS-Q61K extinction but insufficiently by MEK inhibition. We selected a single comparative timepoint, 4 days post-treatment. Downstream analyses included GSEA and TRAP algorithms, leading to the identification of a differentially affected CDK4-driven proliferation network. Immune genes were also identified as significant, but control experiments determined these to be largely the off-target effects of doxycycline and not of NRAS-Q61K extinction. **Overall design:** The iNRAS-475 mouse melanoma cell line was injected intradermally into nude mice which were fed 2mg/ml doxycycline water. Tumors were allowed to reach 200-500mm3 after 6 weeks. Mice were then treated with vehicle or 100mg/kg of the AZD6244 MEK inhibitor, or doxycyline was withdrawn from the diet. Each sample represents a distinct tumor and thus provide six biological, not technical replicates per cohort.

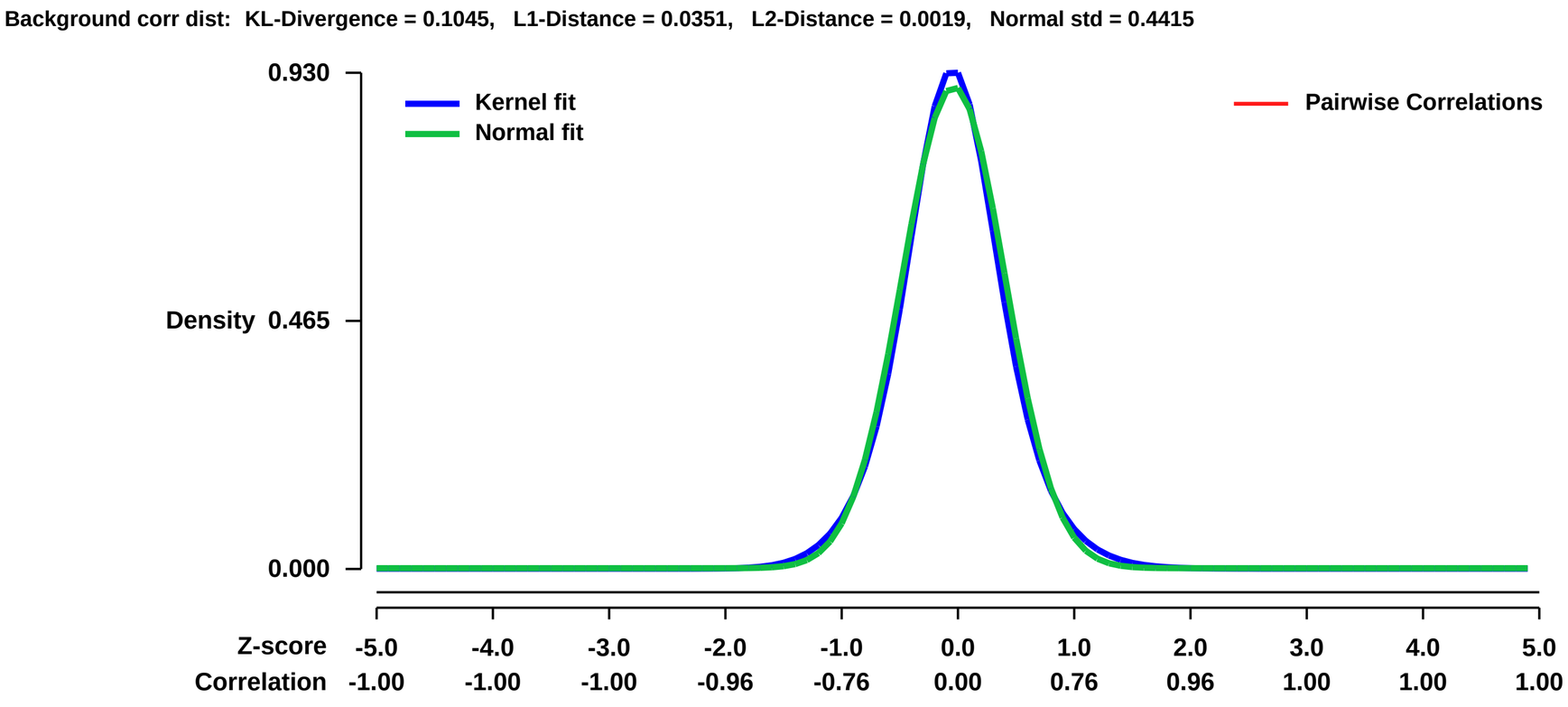

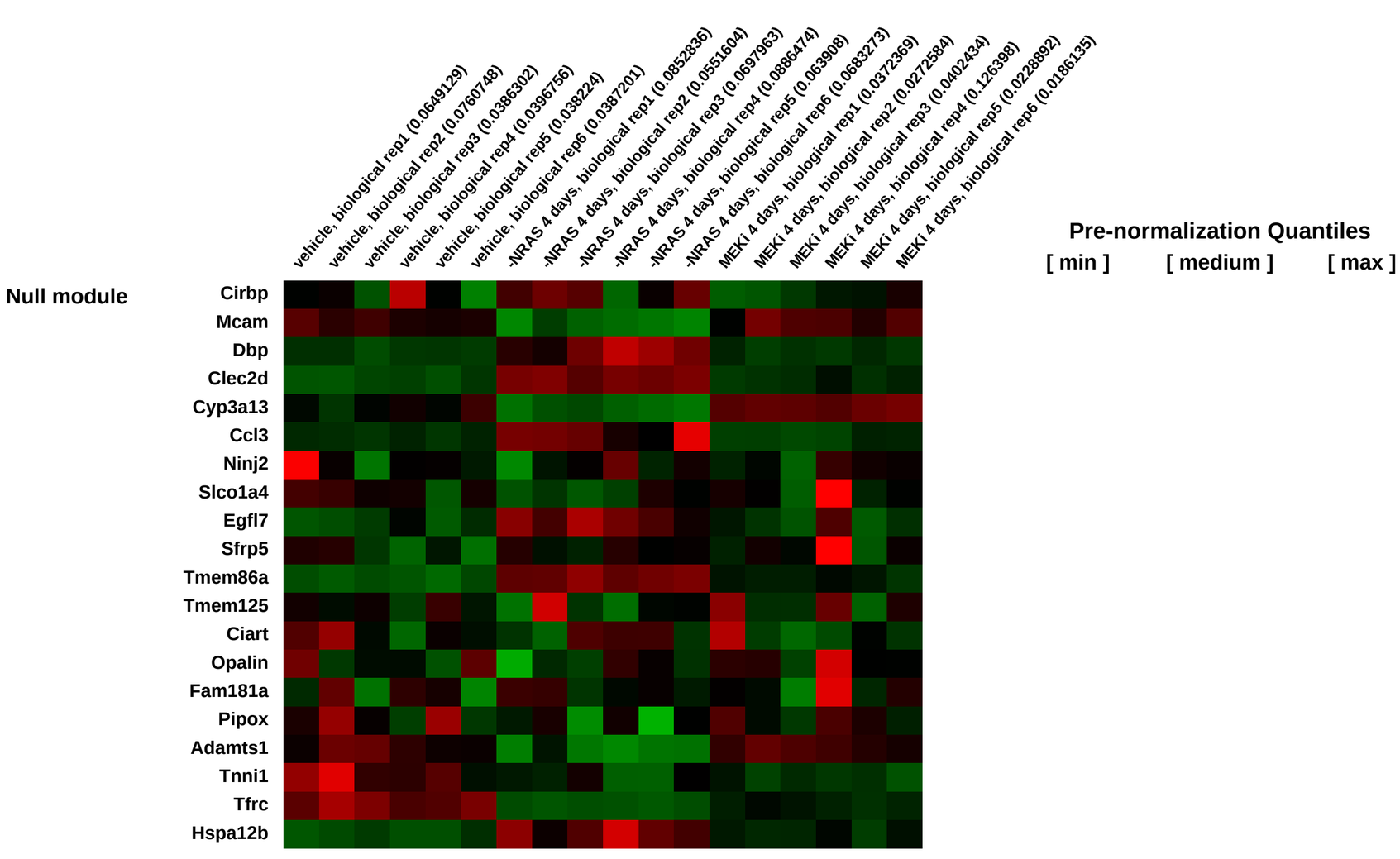

GEO Series "GSE40087" Expression Profiles

Num of samples in this series: 15

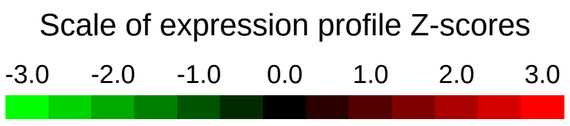

GEO Link:	**http://www.ncbi.nlm.nih.gov/geo/query/acc.cgi?acc=GSE40087**
Status:	**Public on Nov 13 2012**
Title:	**Expression data from Middle Ear Mucosal Metaplasia in Mice**
Organism:	**Mus musculus**
Experiment type:	**Expression profiling by array**
Platform:	**GPL1261**
Pubmed ID:	
Summary & Design:	**Summary:** **Chronic Otitis Media (OM) develops after sustained inflammation and is characterized by secretory middle ear epithelial metaplasia and effusion, most frequently mucoid. Non-typeable Haemophilus influenzae (NTHi), the most common acute OM pathogen, is known to activate inflammation and mucin expression in vitro and in animal models of OM. The goals of this study were to: examine expression profiling epithelial effects of NTHi challenge in murine middle ears.** **We used microarrays to detail examine the global programme of gene expression underlying epithelial effects of NTHi challenge in murine middle ears during this study.** **Overall design:** **Weekly transtympanic inoculation of Balb/c mice with 300 ´µg/ml of NTHi lysates vs saline was performed. Bacteria were grown on chocolate agar at 37´”C in 5% CO2 overnight and inoculated in brain heart infusion (BHI) broth supplemented with 3.5 mg of nicotinamide adenine dinucleotide per ml. After overnight incubation, bacteria were subcultured into 5 ml of fresh brain heart infusion (BHI) and upon reaching log phase growth, NTHi were washed and suspended in phosphate-buffered saline (PBS) followed by sonication for lysis. Three transtympanic inoculation of 6 Balb/c mice middle ears (3 animals, 6 ears) with 50 uL of 300 ug/ml of NTHi bacterial lysate and 6 Balb/c mice middle ears (3 animals, 6 ears) with 50 uL of 1X phosphate buffered saline (PBS) were carried out weekly over 4 weeks (injection on days 7, 14, and 21). On day 28, the mice were euthanized and their bullae harvested. Expression microarray analysis was performed at 1 and 7 days. Microarray findings were validated in independent animal samples and in a cultured murine middle ear epithelial cell (mMEEC) line.**

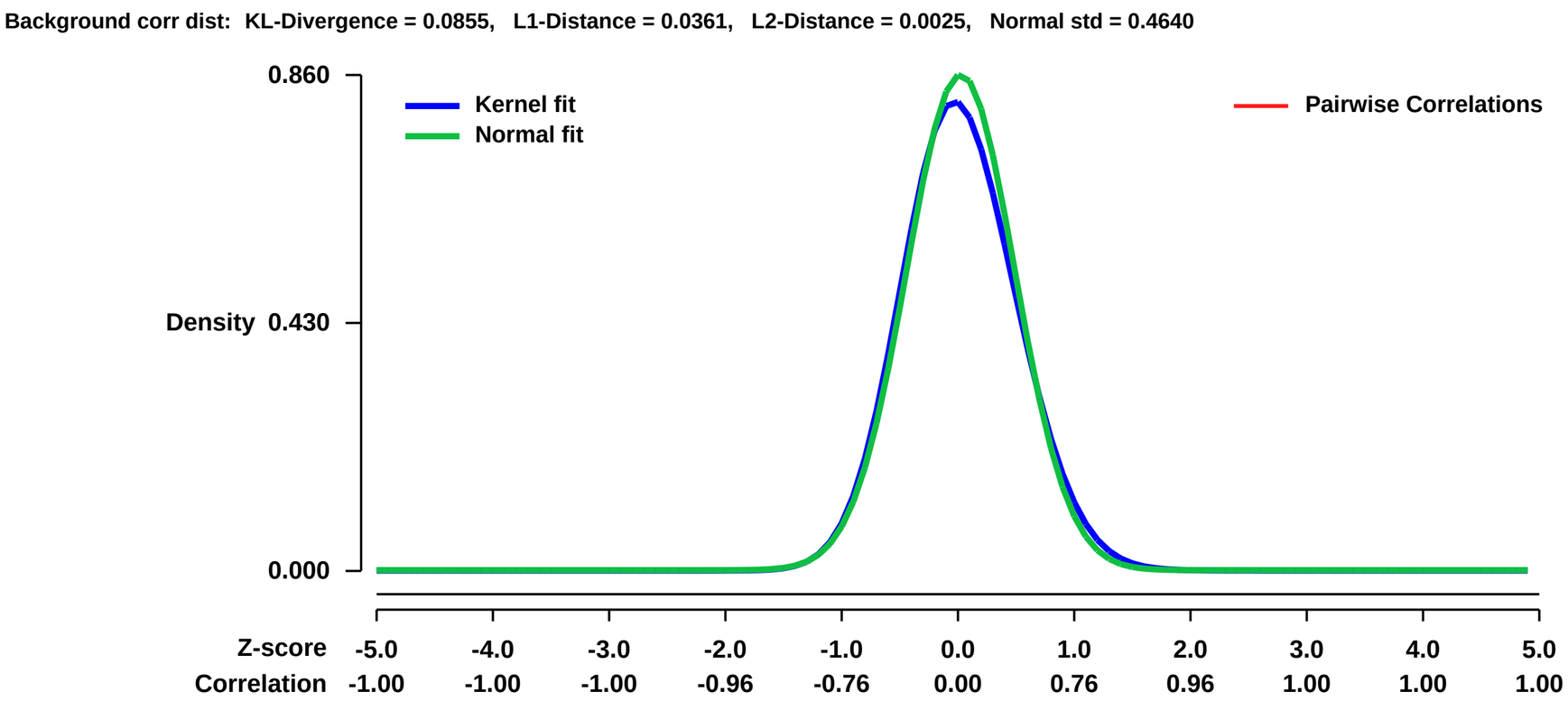

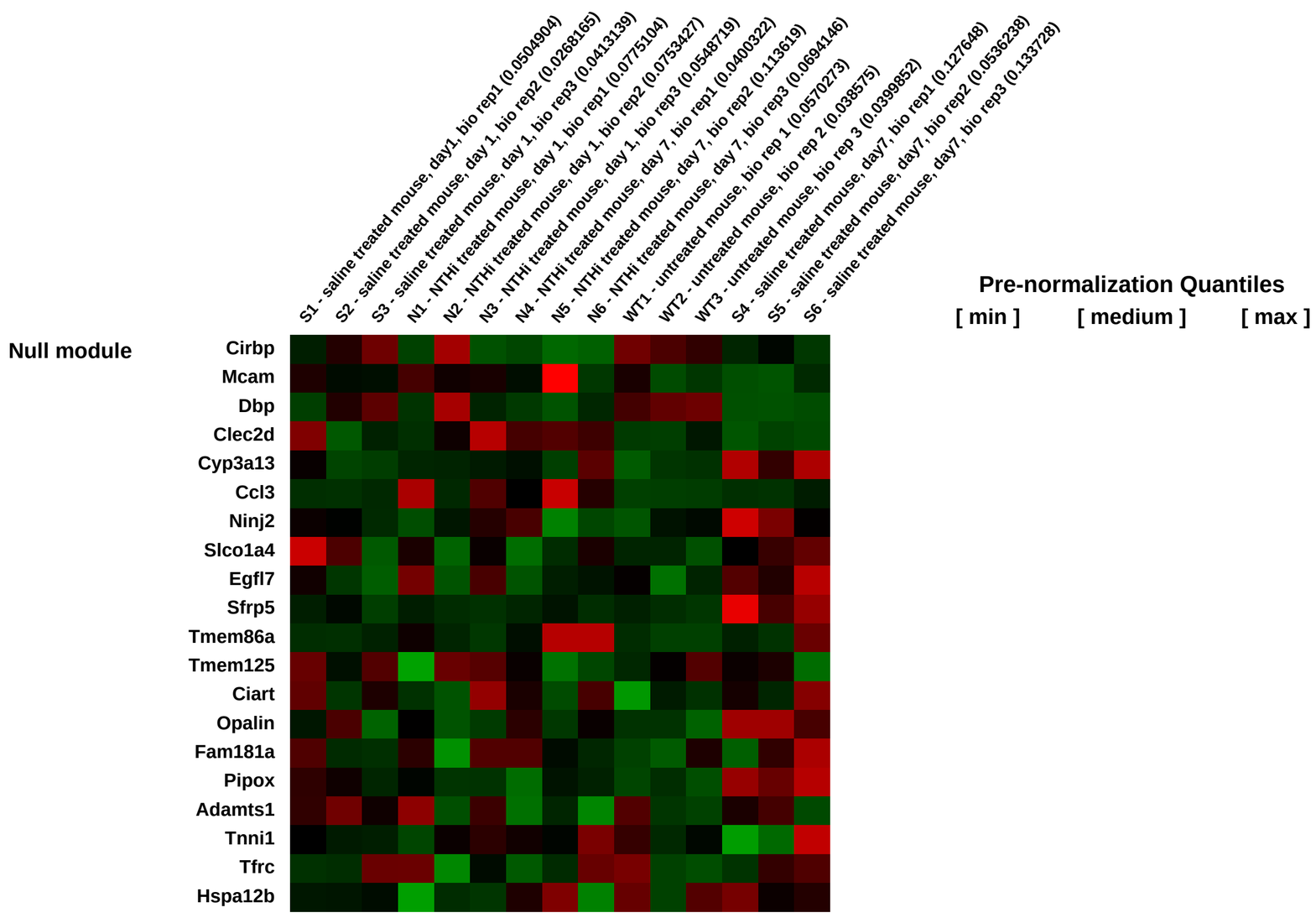

GEO Series "GSE40284" Expression Profiles

Num of samples in this series: 6

Scale of expression profile Z-scores

-3.0 -2.0 -1.0 0.0 1.0 2.0 3.0

GEO Link:	http://www.ncbi.nlm.nih.gov/geo/query/acc.cgi?acc=GSE40284
Status:	Public on Jun 25 2013
Title:	Gene expression data of Lsd1fl/fl and Lsd1fl/fl Mx1Cre CD150+ CD48- lin- c-Kit+ Sca-1+ LT-HSCs
Organism:	Mus musculus
Experiment type:	Expression profiling by array
Platform:	GPL1261
Pubmed ID:	23795291
Summary & Design:	**Summary:** We discovered that mice that lack Lsd1 in hematopoietic cells were exhibited increased frequencies of CD150+ CD48- lin- c-Kit+ Sca-1+ LT-HSCs, but completely lacked the lin- c-Kit+ Sca-1- myeloid progenitor compartment. To determine the genes altered by Lsd1-loss, CD150+ CD48- lin- c-Kit+ Sca-1+ LT-HSCs from Lsd1fl/fl and Lsd1fl/fl Mx1Cre mice were FACS-purified to be analyzed by gene expression profiling. **Overall design:** Primary CD150+ CD48- lin- c-Kit+ Sca-1+ LT-HSCs were isolated by FACS-sorting, from the bone marrow of Lsd1fl/fl and Lsd1fl/fl Mx1Cre animals, one week after the final p(I:C) dose. Total RNA from three biological replicates per genotype was extracted with the RNeasy Micro Kit (QIAGEN), treated with DNaseI, reverse transcribed. RNA extracted from CD150+ CD48- lin- c-Kit+ Sca-1+ cells was amplified with the Ovation Pico WTA RNA Amplification System 2 (NuGEN Technologies). Single-stranded cDNA amplification products were purified using QIAquick PCR Purification Kit (QIAGEN) and labeled with the FL-Ovation cDNA Biotin Module V2 (NuGEN). The Biotin-labeled cDNA was used to hybridize to Affymetrix expression arrays using the Mouse Genome 430 2.0 array platform. Primary CD150+ CD48- lin- c-Kit+ Sca-1+ LT-HSCs were isolated by FACS-sorting, from the bone marrow of Lsd1fl/fl and Lsd1fl/fl Mx1Cre animals, one week after the final p(I:C) dose. Total RNA from three biological replicates per genotype was extracted with the RNeasy Micro Kit (QIAGEN), treated with DNaseI, reverse transcribed. RNA extracted from CD150+ CD48- lin- c-Kit+ Sca-1+ cells was amplified with the Ovation Pico WTA RNA Amplification System 2 (NuGEN Technologies). Single-stranded cDNA amplification products were purified using QIAquick PCR Purification Kit (QIAGEN) and labeled with the FL-Ovation cDNA Biotin Module V2 (NuGEN). The Biotin-labeled cDNA was used to hybridize to Affymetrix expression arrays using the Mouse Genome 430 2.0 array platform.

Background corr dist: KL-Divergence = 0.0508, L1-Distance = 0.0643, L2-Distance = 0.0068, Normal std = 0.6243

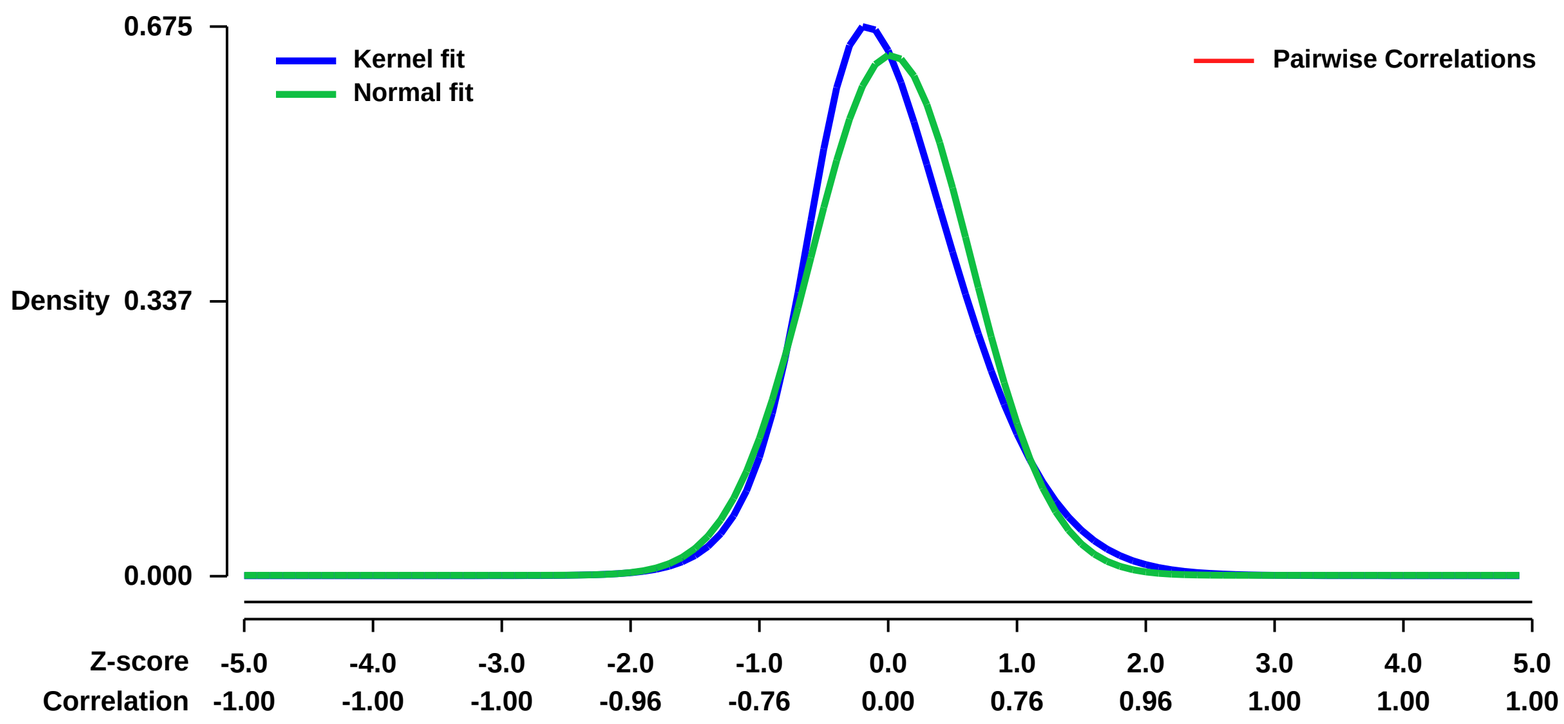

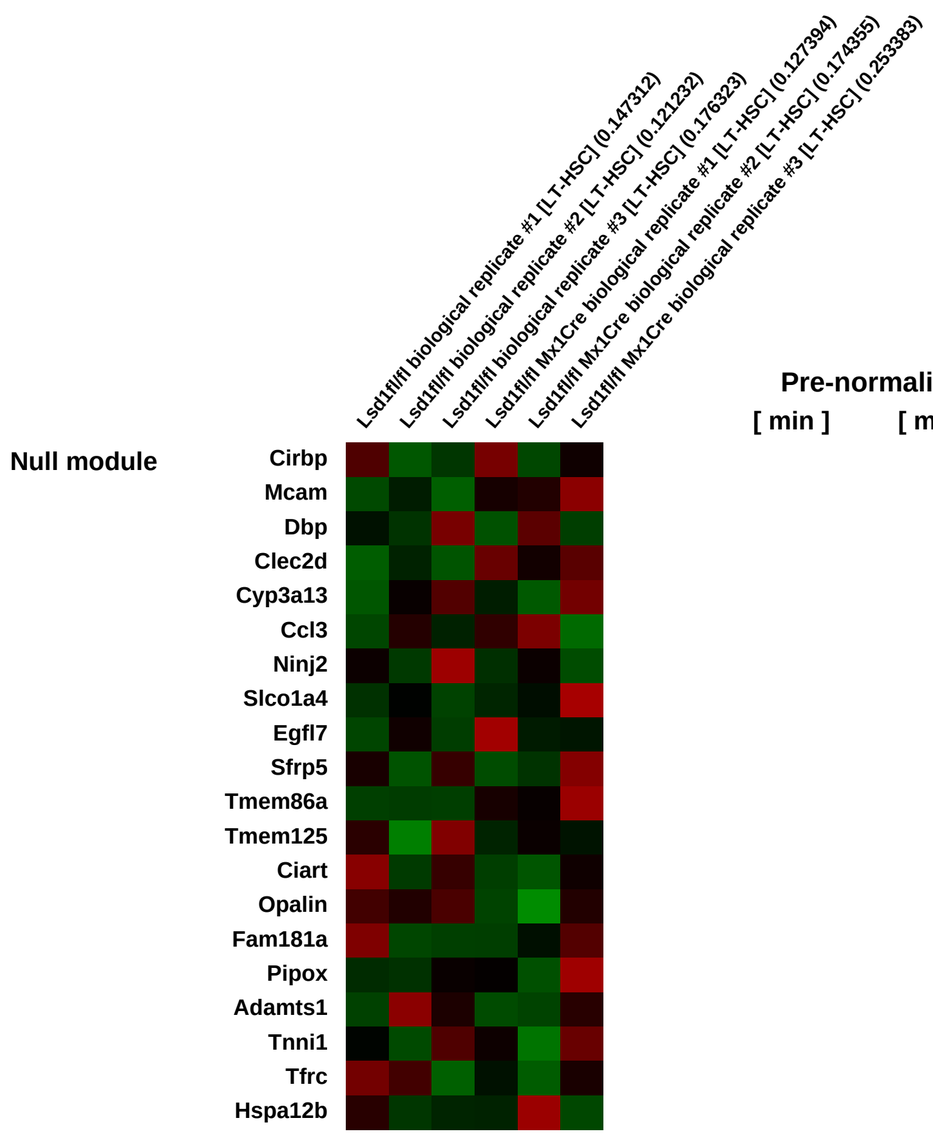

GEO Series "GSE4029" Expression Profiles

Num of samples in this series: 10

Scale of expression profile Z-scores

-3.0 -2.0 -1.0 0.0 1.0 2.0 3.0

GEO Link:	**http://www.ncbi.nlm.nih.gov/geo/query/acc.cgi?acc=GSE4029**
Status:	**Public on May 01 2006**
Title:	**Basonuclin: A novel mammalian maternal effect gene**
Organism:	**Mus musculus**
Experiment type:	**Expression profiling by array**
Platform:	**GPL1261**
Pubmed ID:	**16624857**
Summary & Design:	**Summary:** **Keywords: RNAi knockdown** **Overall design:** **Basonuclin-deficient oocytes were created by a mouse transgenic RNAi approach, which knocks down basonuclin mRNA level specifically in oocytes. Microarray analysis was performed on total RNA from four non-transgenic (control) and six transgenic (basonuclin-deficient) oocyte samples (approximately 50 oocytes per sample).**

Background corr dist: **KL-Divergence = 0.0734, L1-Distance = 0.0871, L2-Distance = 0.0111, Normal std = 0.6253**

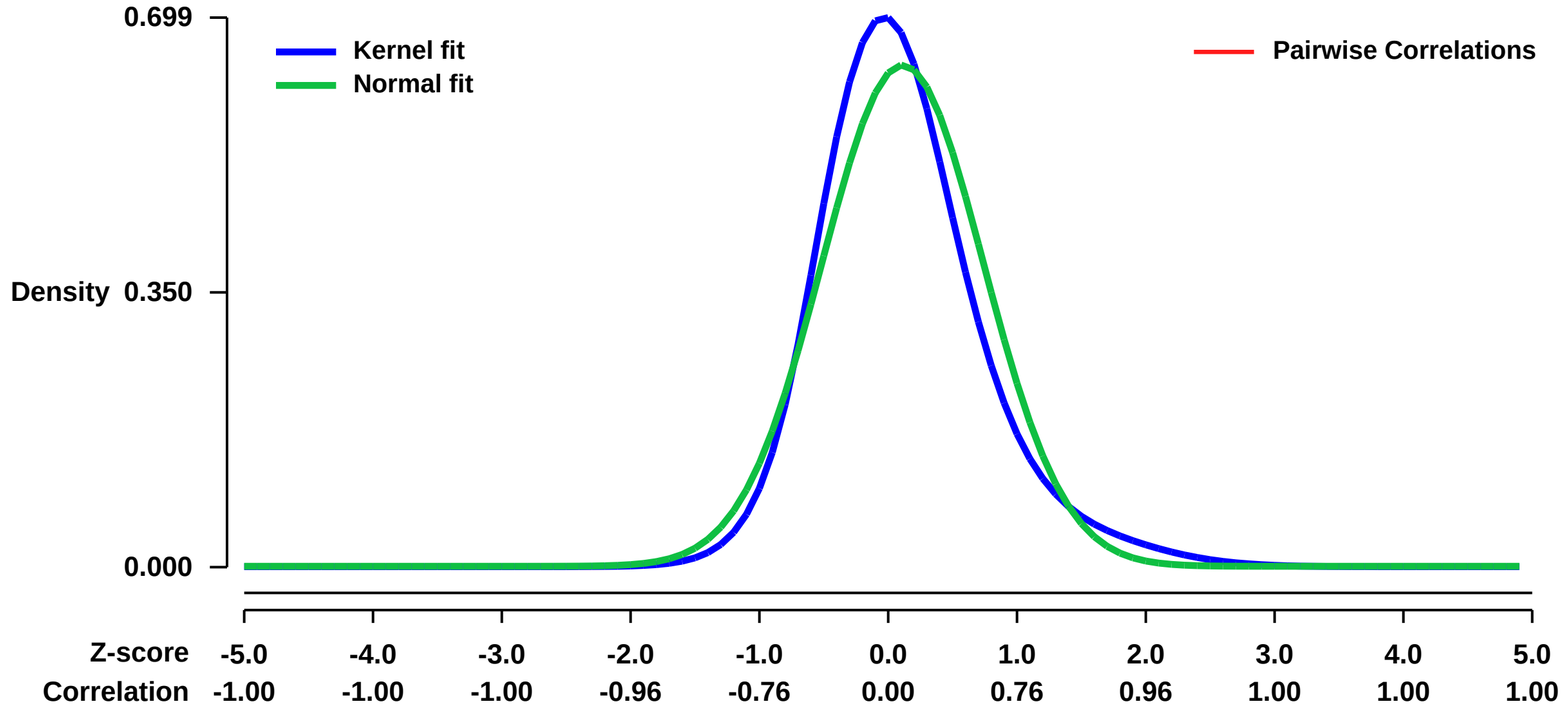

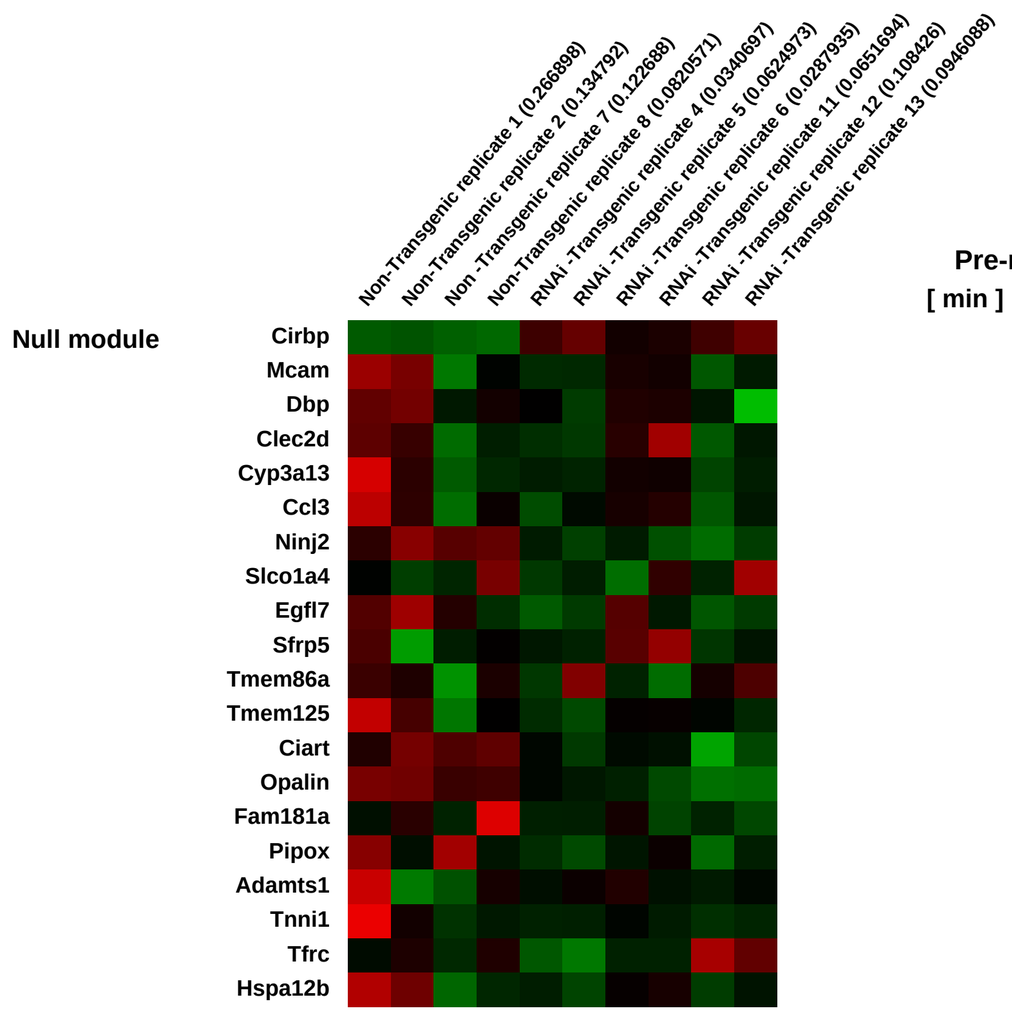

GEO Series "GSE40296" Expression Profiles

Num of samples in this series: 6

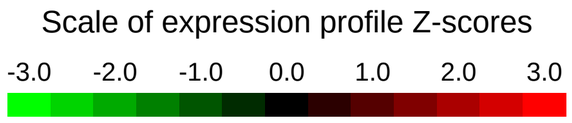

GEO Link:	**http://www.ncbi.nlm.nih.gov/geo/query/acc.cgi?acc=GSE40296**
Status:	**Public on Aug 23 2012**
Title:	**Essential roles of the histone methyltransferase ESET in the epigenetic control of neural progenitor cells during development**
Organism:	**Mus musculus**
Experiment type:	**Expression profiling by array**
Platform:	**GPL1261**
Pubmed ID:	**22991445**
Summary & Design:	**Summary:** **In the developing brain, neural progenitor cells (NPCs) switch the differentiation competency via changing gene expression profiles that are governed partly by epigenetic control such as histone modification, although the precise mechanism is unknown. Here we found that ESET/Setdb1/KMT1E, a histone H3 Lys-9 (H3K9) methyltransferase, was highly expressed at early stages of brain development but down-regulated over time, and that ablation of ESET led to decreased H3K9 trimethylation and misregulation of genes, resulting in severe brain defects and early lethality. In the mutant brain, endogenous retrotransposons were derepressed, and non-neural gene expression was activated. Furthermore, early neurogenesis was most severely impaired, while astrocyte formation was enhanced. We conclude that there is an epigenetic role of ESET in temporal and tissue-specific gene regulation in the developing brain.** **We used microarrays to identify genes up- or down- regulated when ESET is ablated in the dorsal telencephalon.** **Overall design:** **We used 3 WT and 3 cKO male E14.5 embryo for each analysis**

Background corr dist: KL-Divergence = 0.0404, L1-Distance = 0.0189, L2-Distance = 0.0004, Normal std = 0.6141

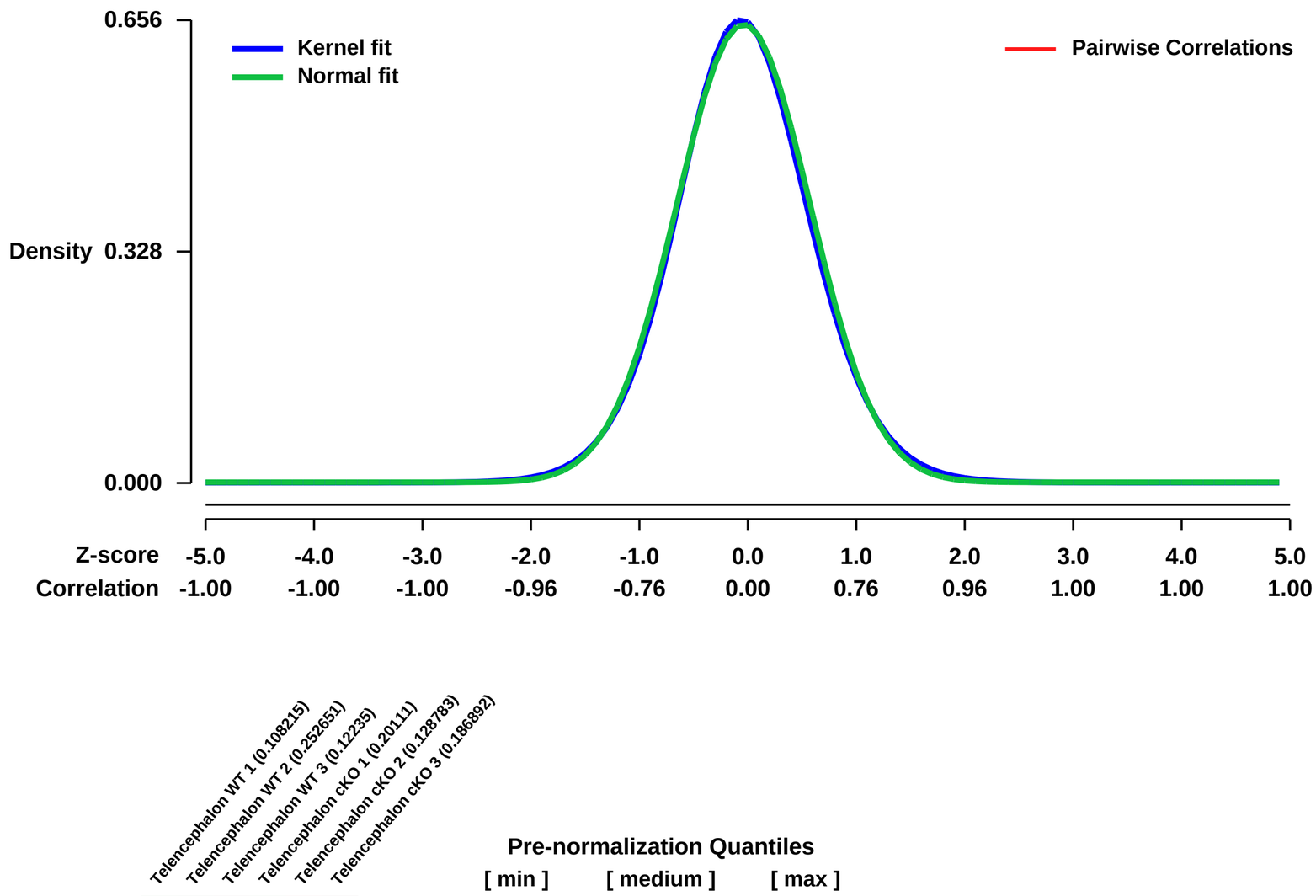

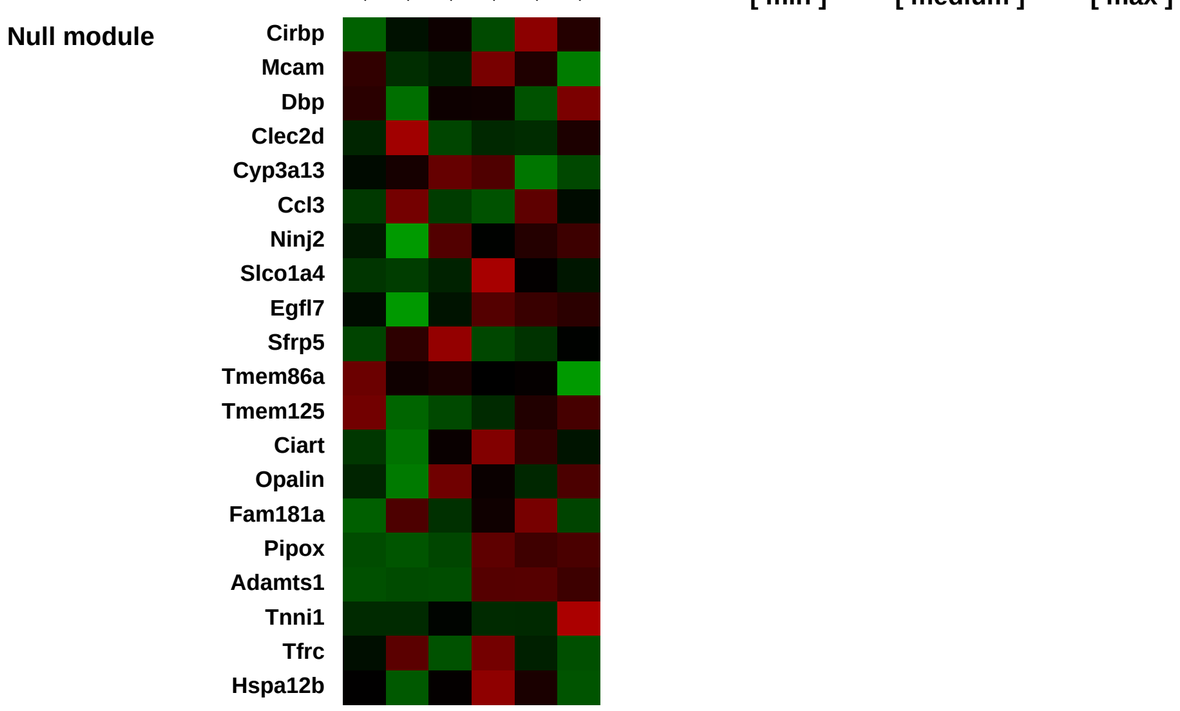

GEO Series "GSE40368" Expression Profiles

Num of samples in this series: 10

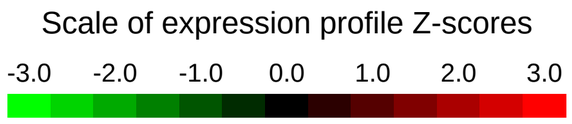

GEO Link:	http://www.ncbi.nlm.nih.gov/geo/query/acc.cgi?acc=GSE40368
Status:	Public on Aug 09 2013
Title:	Sphingosine-1-phosphate phosphatase 1 regulates keratinocyte differentiation and epidermal homeostasis
Organism:	Mus musculus
Experiment type:	Expression profiling by array
Platform:	GPL1261
Pubmed ID:	23637227
Summary & Design:	**Summary:** Sphingosine 1-phosphate (S1P) is a bioactive lipid whose levels are tightly regulated by its synthesis and degradation. Intracellularly, S1P is dephosphoryled by the actions of two S1P-specific phosphatases, sphingosine 1-phosphate phosphatase 1 and 2. To identify the physiologic functions of S1P phosphatase 1, we have studied mice with its gene, Sgpp1, deleted. Sgpp1-/- mice appeared normal at birth but during the first week of life, they exhibited stunted growth, suffered desquamation, and most died before weaning. Interestingly, the epidermal permeability barrier developed normally during embryogenesis. Sgpp1 -/- pups and surviving adults exhibited epidermal hyperplasia and abnormal expression of keratinocyte differentiation markers. Keratinocytes isolated from Sgpp1 -/- skin had increased intracellular S1P levels, and expressed a gene expression profile that indicated enhanced differentiation. The results reveal S1P metabolism as a regulator of keratinocyte differentiation and epidermal homeostasis. **Overall design:** Comparison of KO vs. WT with five replications per treatment sample

Background corr dist: KL-Divergence = 0.0632, L1-Distance = 0.0318, L2-Distance = 0.0018, Normal std = 0.5180

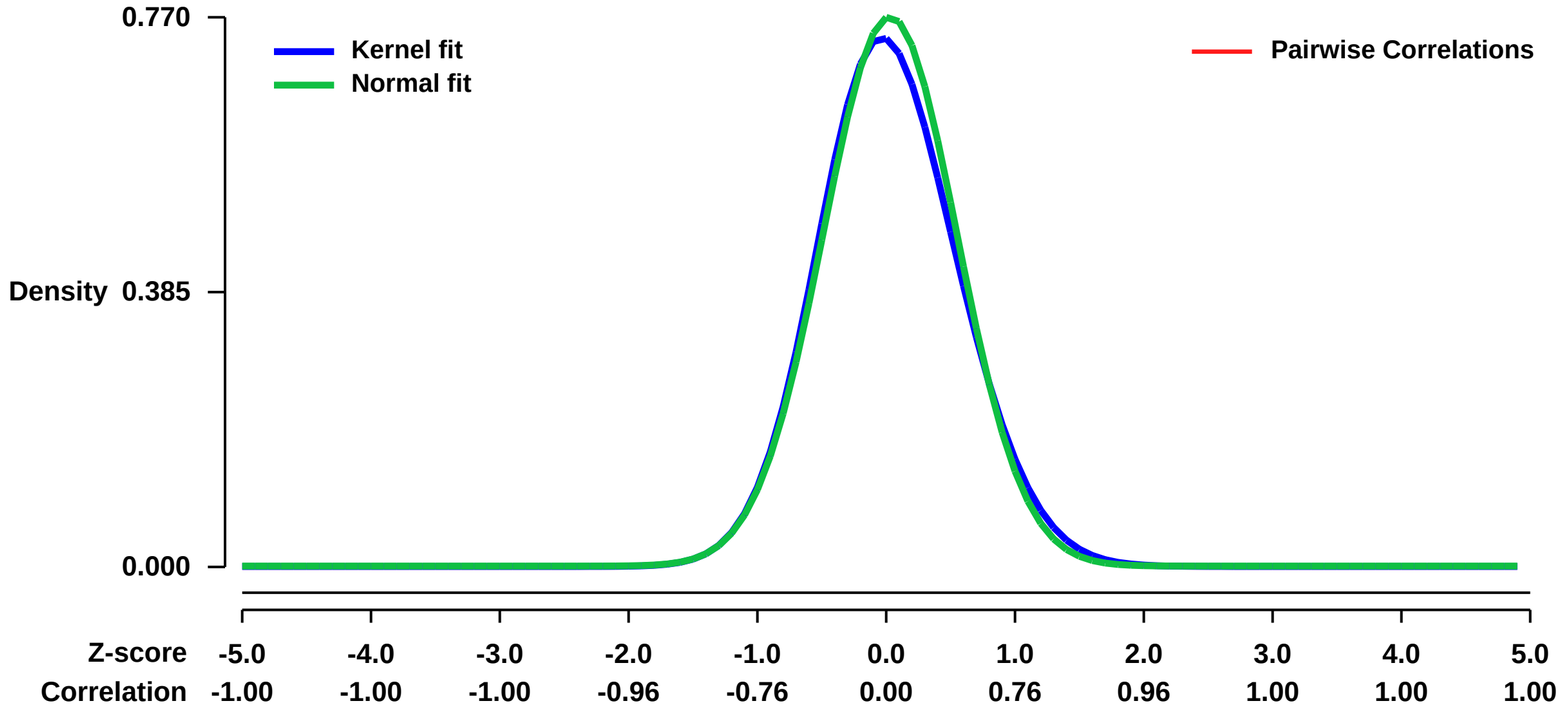

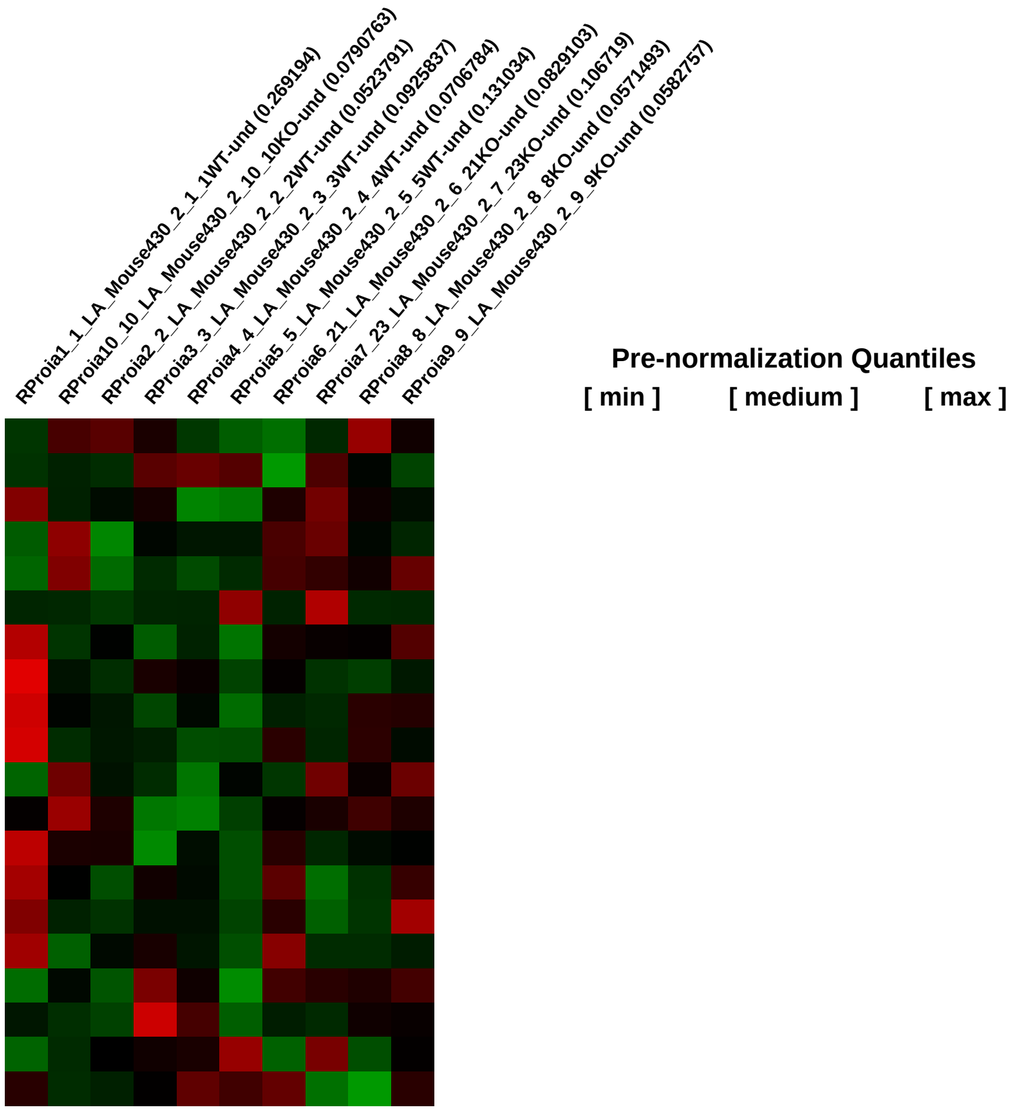

GEO Series "GSE4040" Expression Profiles

Num of samples in this series: 6

Scale of expression profile Z-scores

-3.0 -2.0 -1.0 0.0 1.0 2.0 3.0

GEO Link:	**http://www.ncbi.nlm.nih.gov/geo/query/acc.cgi?acc=GSE4040**
Status:	**Public on Jan 13 2006**
Title:	**sikes-affy-mouse-84486**
Organism:	**Mus musculus**
Experiment type:	**Expression profiling by array**
Platform:	**GPL1261**
Pubmed ID:	
Summary & Design:	**Summary:** **Reversible phosphorylation is a critical step in the control of cellular signaling events. The protein phosphatase 1 (PP1) regulates neuronal proteins by mediating their de-phosphorylation. PP1 selectivity and subcellular localization is conferred via association with a panel of interacting proteins. We have extensively characterized the association of PP1 with inhibitor-1, an interacting protein widely expressed in brain and heart. Inhibitor-1 deletion results in a persistently active PP1 phosphatase in vitro. Inhibitor-1 overexpression results in increased transformation of cultured cells and enhances the rate of learning and memory in mouse models through largely unknown mechanisms. Significantly, inhibitor-1 activation is cAMP-sensitive. The genes regulated by inhibitor-1/PP1 signals have not been characterized. Identification of these genes is expected to provide key insights into the role of inhibitor-1/PP1 escape from cellular homeostasis and regulation of neuronal learning and memory.** **We will determine gene expression patterns in hippocampus of wild-type and inhibitor-1 knock-out mice. The results of these studies of constitutive expression will be used as a baseline for future studies aimed to determine the role cAMP-mediated gene expression in I-1 knock-out mice.** **We hypothesize that the genes regulated by the inhibitor-1/PP1 holoenzyme are critical to cellular growth commitment including resistance to growth arrest and neuronal learning and memory** **We will examine the role of inhibitor-1 in regulating hippocampal gene expression using total RNA isolated from whole hippocampi of inhibitor-1 knockout (I-1-/-) animals and parental C57Bl6 controls under non-stimulated conditions. Animals will be sacrificed by a standard protocol. Hippocampal tissue will be rapidly dissected from several animals, flash frozen within 1 minute of extraction, pooled, and total RNA will be processed immediately using TriZol.** **Keywords: dose response** **Overall design:**

Background corr dist: **KL-Divergence = 0.0489, L1-Distance = 0.0183, L2-Distance = 0.0003, Normal std = 0.5764**

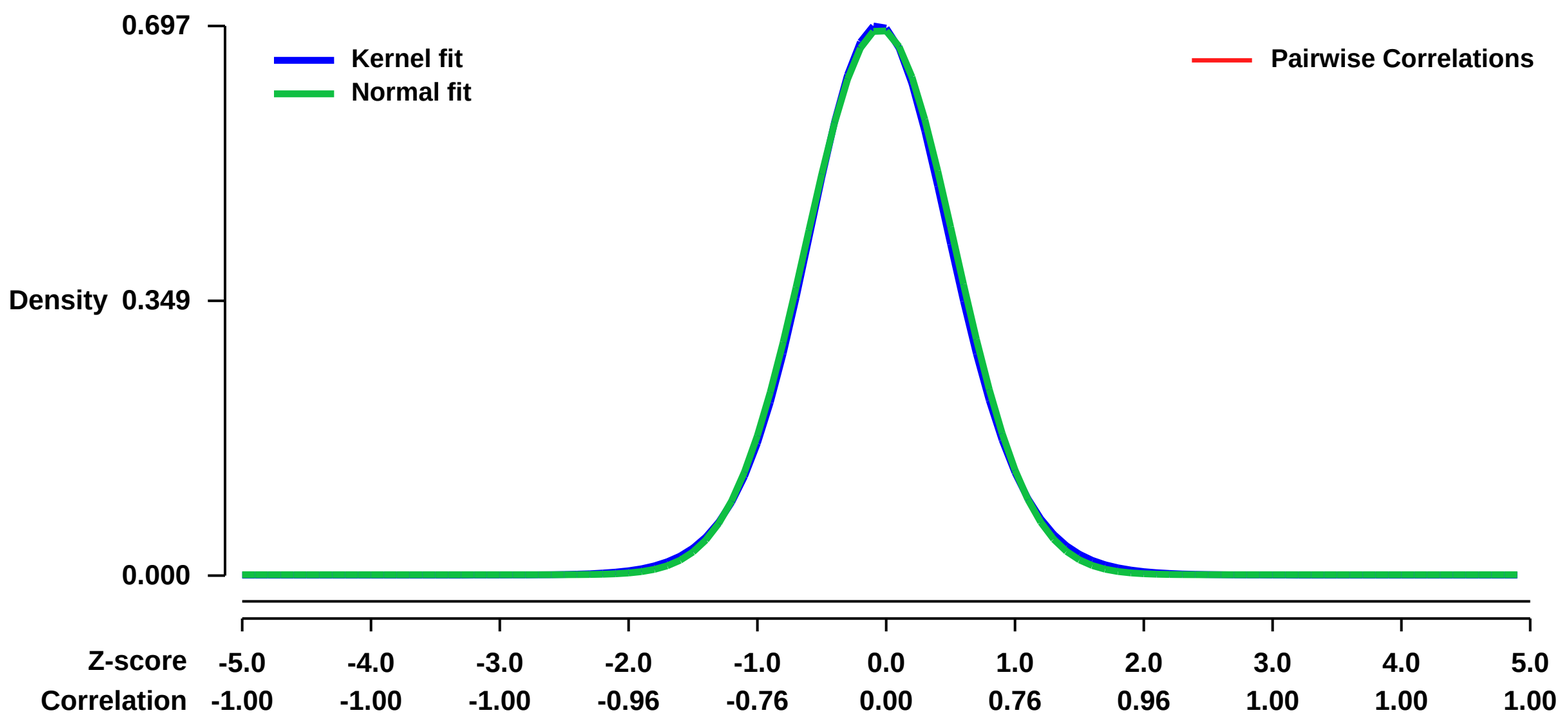

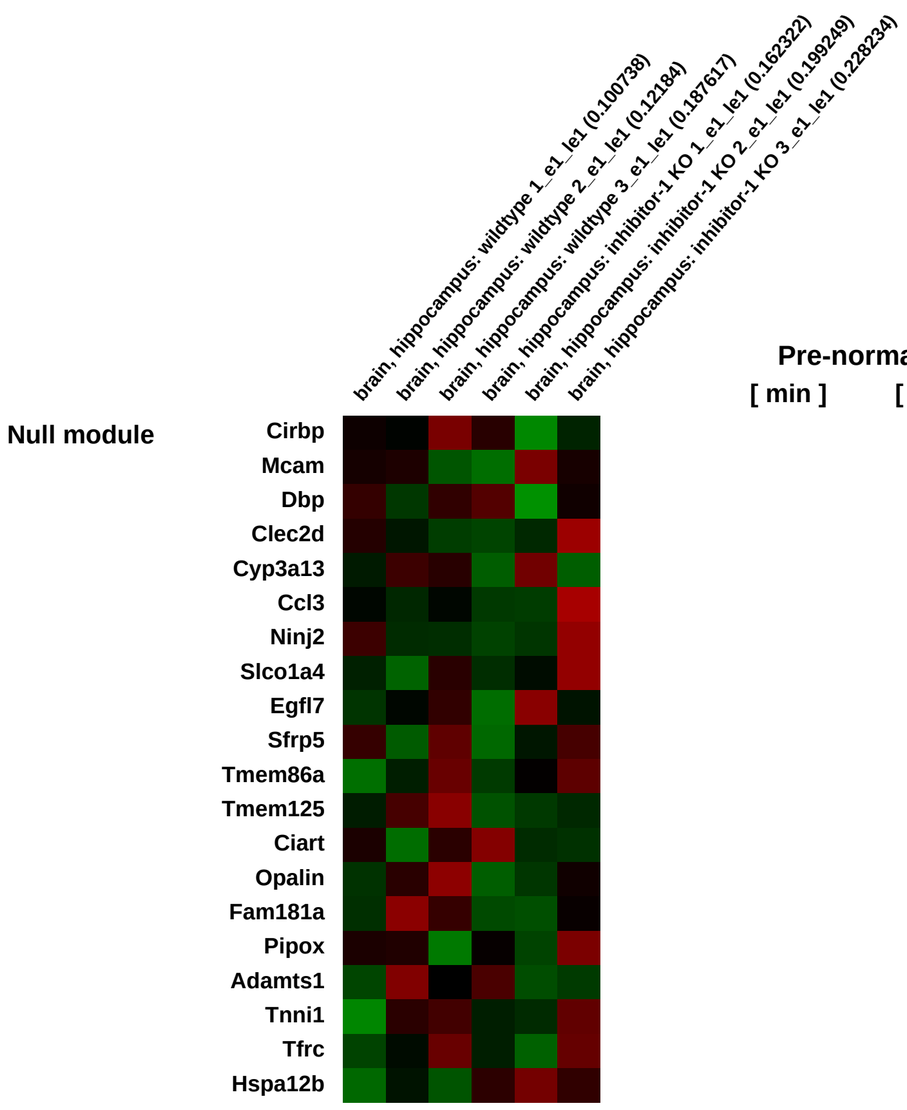

GEO Series "GSE4041" Expression Profiles

Num of samples in this series: 6

Scale of expression profile Z-scores

-3.0 -2.0 -1.0 0.0 1.0 2.0 3.0

GEO Link:	**http://www.ncbi.nlm.nih.gov/geo/query/acc.cgi?acc=GSE4041**
Status:	**Public on Jan 13 2006**
Title:	**zhang-affy-mouse-200705**
Organism:	**Mus musculus**
Experiment type:	**Expression profiling by array**
Platform:	**GPL1261**
Pubmed ID:	
Summary & Design:	**Summary:** **In our original grant we proposed to use the NR3B-null mouse model to study the role of NR3B subunit in motor neuron function. We have now successfully generated NR3B null mice. Interestingly, NR3B-null mice invariably die at age P4-P8. Our preliminary examination indicates that the motor strength of these mice is severely impaired prior to death. As we continue to explore the cause of death in NR3B null mice, we propose to conduct gene profiling experiments to search for transcription changes in the brain related to ablation of the NR3B gene. We have used the facility provided by the NINDS/NIMH Microarray Consortium to identify genes that show abnormal expression patterns in these mice. We would like to compare these changes with that opccured in SOD1 mice, a mouse model of motor neuron diseases. Analysis of these genes will help to identify changes in networks and pathways that may cause the death of NR3B-null mice. These studies will further help to elucidate the functional role of NR3B in motor neurons.** **We will compare samples from motor neurons of wild type and SOD1 mice to identify genes that show abnormal expression patterns, which may be implicated in the death of SOD1 mice and shared with the same changes in NR3B-null mice.** **We hypothesize that genes with their transcription level changing significantly by ablation of NR3B will be associated with the molecular mechanism underlying the death of motor neurons in NR3B null mice.** **As NR3B is expressed primarily in the motor neurons of hindbrain and spinal cord, we have first collected and analyzed the spinal cord samples from NR3B null mice and wild-type controls in P4, an age of disease onset. We like to compare motor neuron smaples from SOD1 mice at the age around the disease onset. Total RNA from total 6 samples will be purified from ~200 motor neurons obtained by Laser Capture Microdissection. Extracted RNAs will be subjected to two rounds of amplification and the obtained cRNA will be biotinylated. The purified cRNA will be sent to the NINDS/NIMH Microarray Consortium be used to hybridize the GeneChip Mouse Genome 430 2.0 Array. The hybridization, scanning, and initial data analysis of these GeneChips will be conducted by the Consortium staff. We will analyze the collected data further after data collection. We will first identify genes that show significant changes between wild-type and SOD1 mice and then compare that with the result from NR3B null mice.** **Keywords: other** **Overall design:**

Background corr dist: **KL-Divergence = 0.0458, L1-Distance = 0.0243, L2-Distance = 0.0007, Normal std = 0.5932**

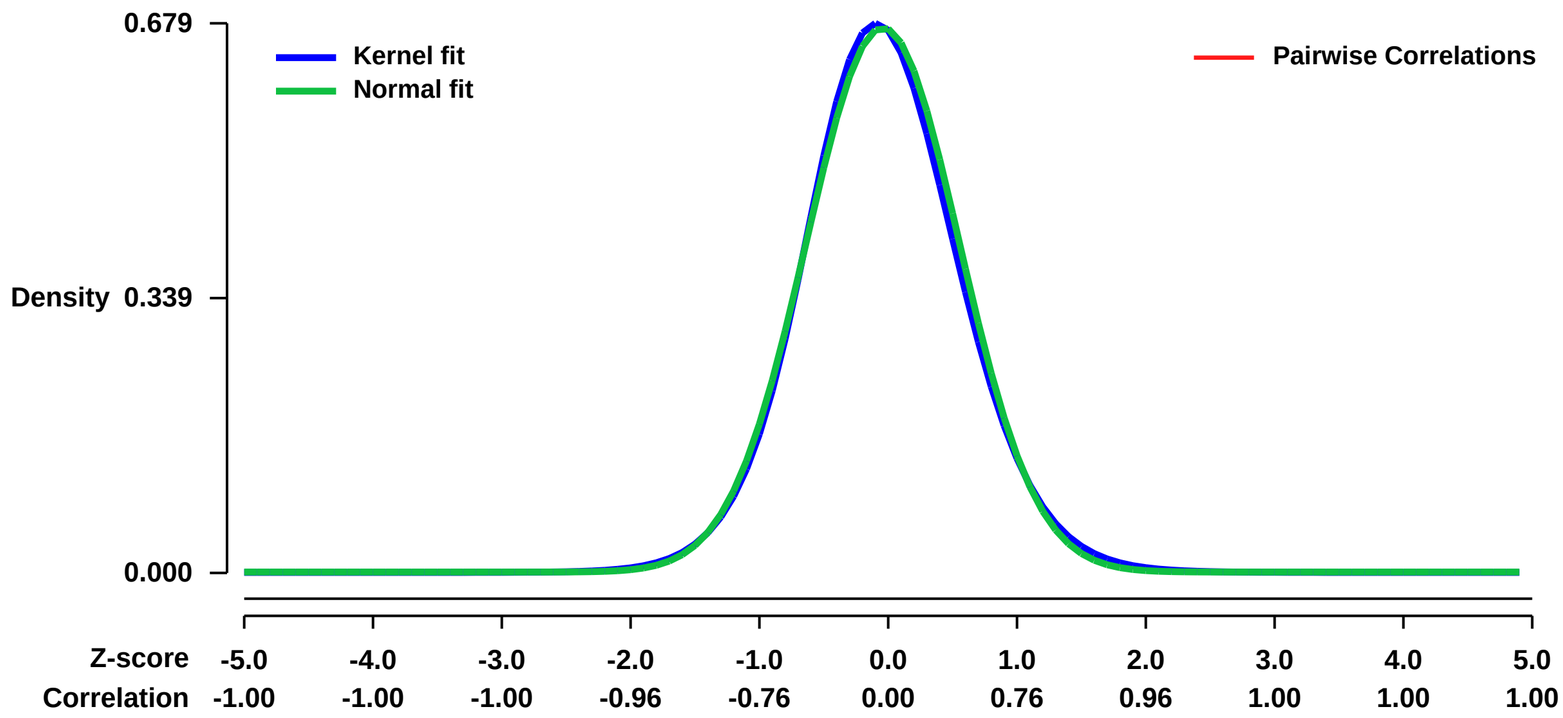

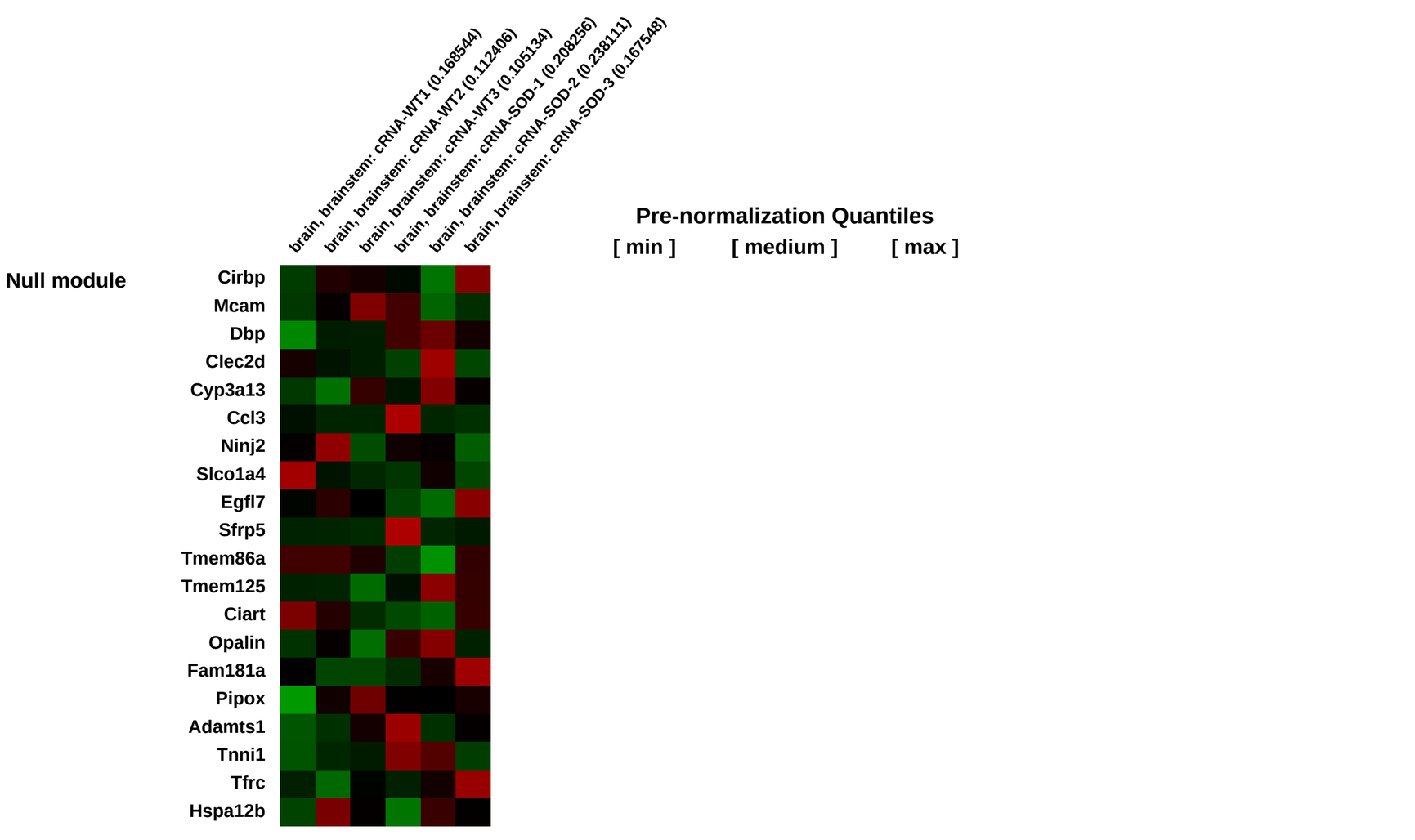

GEO Series "GSE40412" Expression Profiles

Num of samples in this series: 14

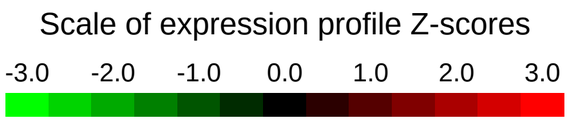

GEO Link:	http://www.ncbi.nlm.nih.gov/geo/query/acc.cgi?acc=GSE40412
Status:	Public on Mar 04 2013
Title:	Replication-coupled passive DNA demethylation for the erasure of genome imprints in mice
Organism:	Mus musculus
Experiment type:	Expression profiling by array
Platform:	GPL1261
Pubmed ID:	23241950
Summary & Design:	**Summary:** Genome-wide DNA demethylation, including the erasure of genome imprints, in primordial germ cells (PGCs), is critical as a first step for creating the totipotent epigenome in the germ line. Here, we provide evidence that contrary to the prevailing model involving active DNA demethylation, imprint erasure in mouse PGCs occurs in a manner consistent with replication-coupled passive DNA demethylation: PGCs erase imprints during their rapid proliferation with little de novo as well as maintenance DNA methylation potential and no major chromatin alterations. Our findings necessitate the re-evaluation of and provide novel insights into the mechanism of genome-wide DNA demethylation in PGCs. **Overall design:** We performed expression analysis of primordial germ cells (PGCs) at embryonic days 10.5-13.5. Because the number of PGCs available at these stages were low, cDNAs were amplified by the method that we previously published (Kurimoto et al. 2006, NAR 34: e42 (PMID 16547197)). To include analysis of PGC gene expression at E9.5, we re-normalized the data from our E9.5 PGC samples (GSM744103, GSM744104) from our previous publication (Hayashi et al., 2011, Cell 146: 519-32 (PMD 21820164)) together with the data from this submission.

Background corr dist: KL-Divergence = 0.1317, L1-Distance = 0.0284, L2-Distance = 0.0016, Normal std = 0.3977

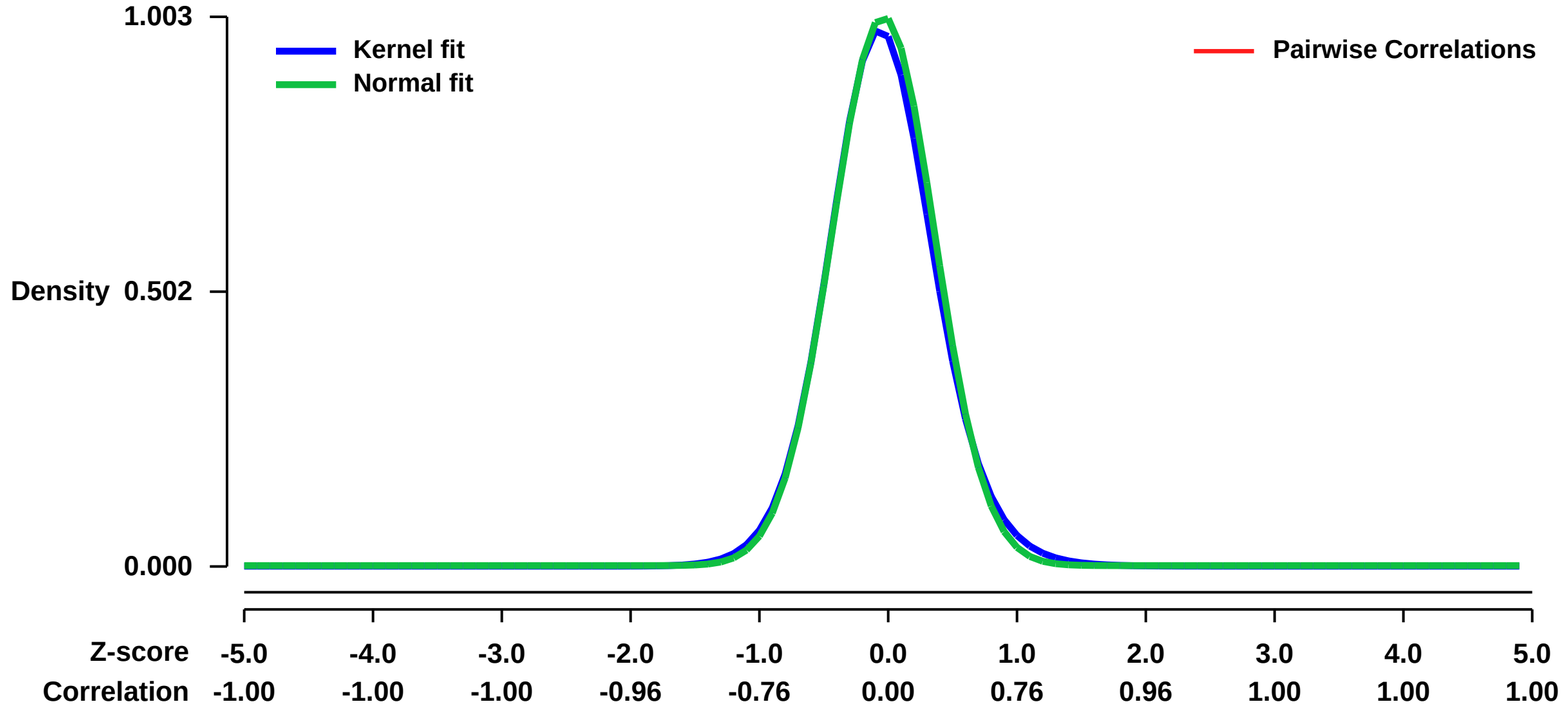

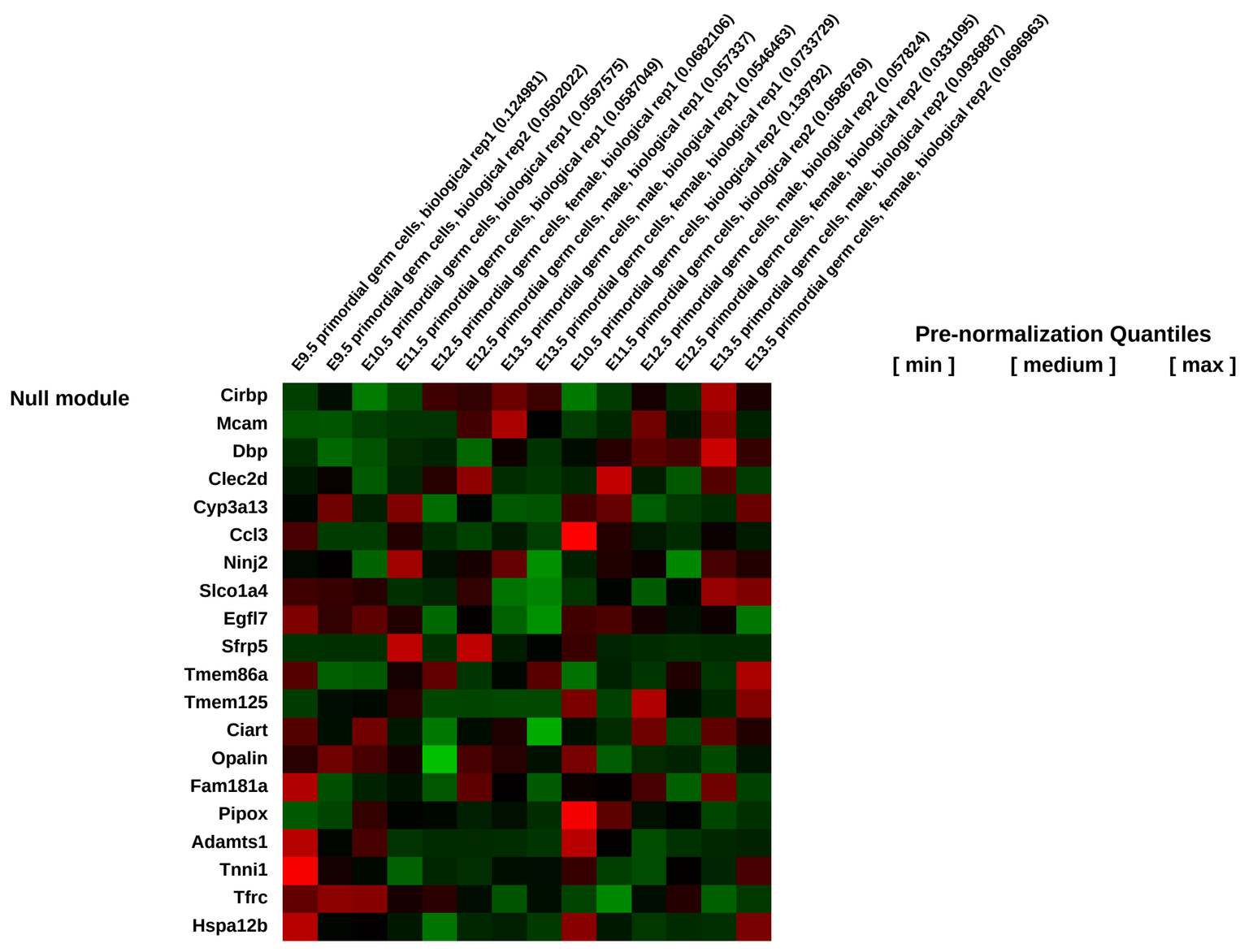

GEO Series "GSE4043" Expression Profiles

Num of samples in this series: 6

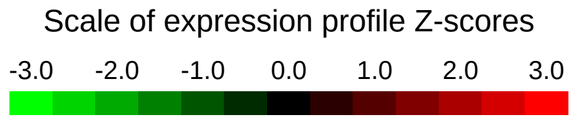

GEO Link:	http://www.ncbi.nlm.nih.gov/geo/query/acc.cgi?acc=GSE4043
Status:	Public on Mar 07 2006
Title:	Gene profiling analysis of Src chemical rescue
Organism:	Mus musculus
Experiment type:	Expression profiling by array
Platform:	GPL1261
Pubmed ID:	16513984
Summary & Design:	**Summary:** **The restoration of catalytic activity to mutant enzymes by small molecules is well-established for in vitro systems. Here we show that the protein tyrosine kinase Src R388A mutant can be rescued in live cells using the small molecule imidazole. Cellular rescue of a v-Src homolog was rapid and reversible and conferred predicted oncogenic properties. Using chemical rescue in combination with mass spectrometry, six known Src kinase substrates were confirmed, and several new protein targets identified. Chemical rescue data suggests that c-Src is active under basal conditions. Rescue of R388A c-Src also allowed contributions of Src to the MAP kinase pathway to be clarified. This chemical rescue approach is likely to be of broad utility in cell signaling.** **We were also interested in examining the impact of Src rescue on the kinetics of gene expression. Chronic gene expression changes in v-Src transformed colon cancer and NIH3T3 cells have been reported, but the chemical rescue method permits insights into rapid kinetic changes. We used gene microarray analysis of imidazole activated Src, 1 h after imidazole treatment of 8A7F cells as well as 6N7F control cells, a set of several genes show increases (>1.7-fold) at 1 h in the 8A7F cells and another set show decreases (>1.7-fold) at 1 h with minimal changes in 6N7F control cells. Thirteen of these genes were further analyzed using real-time RT-PCR and most of the genes tested showed similar changes using both techniques. These gene changes were not reported in cells chronically transformed with v-Src or rapidly stimulated with growth factors suggesting that rapid initiation of Src-mediated tyrosine phosphorylation may induce a specialized pattern of gene expression changes. However, these earlier experiments were done under different conditions which may also contribute to gene effects.** **Keywords: time course, cell type comparison** **Overall design:** **using Murine Genome MOE430 2.0 GeneChips as described in the Affymetrix website.**

Background corr dist: KL-Divergence = 0.0386, L1-Distance = 0.0241, L2-Distance = 0.0006, Normal std = 0.6315

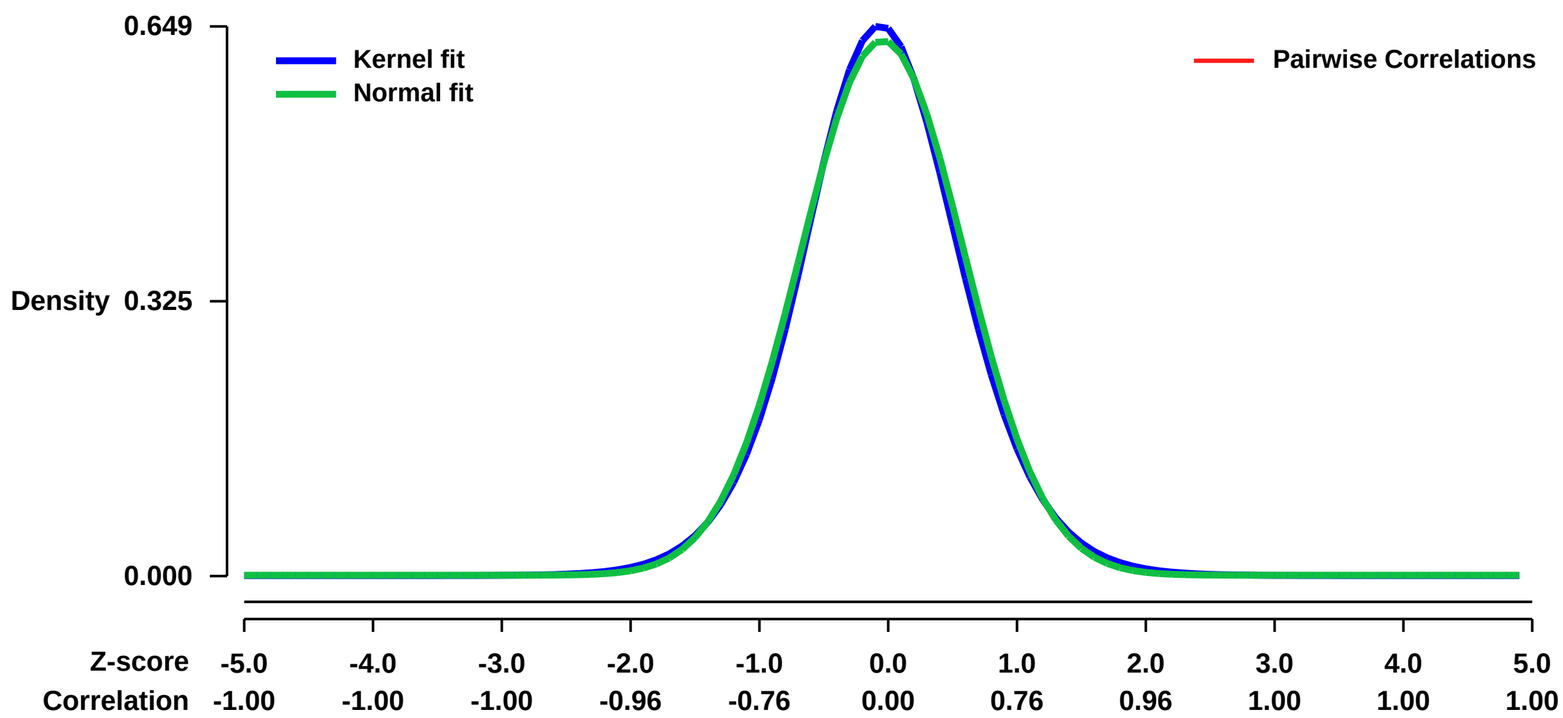

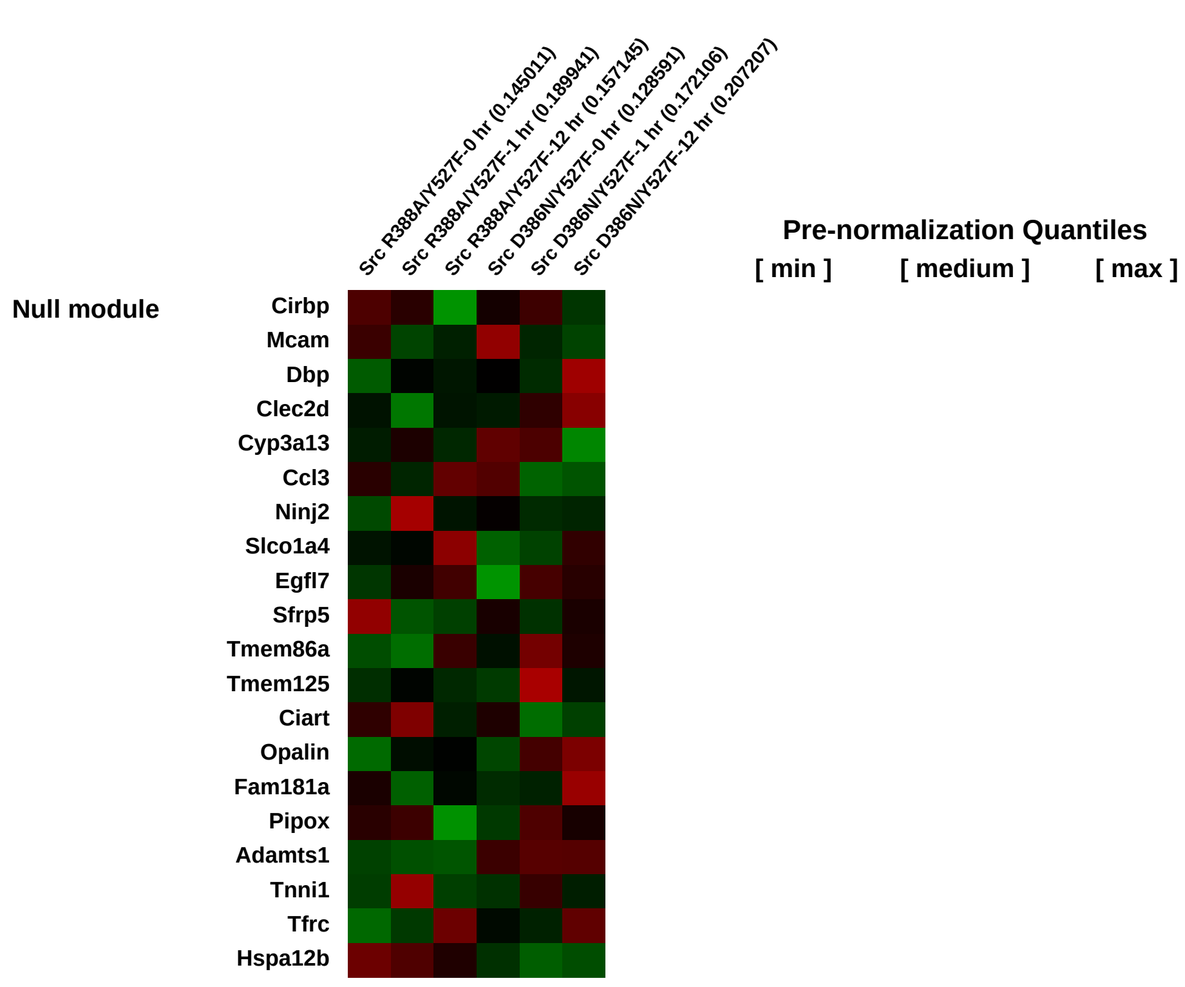

GEO Series "GSE40443" Expression Profiles

Num of samples in this series: 6

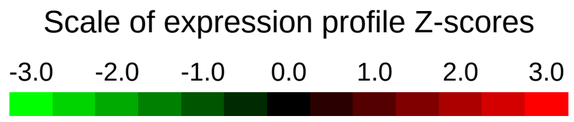

GEO Link:	**http://www.ncbi.nlm.nih.gov/geo/query/acc.cgi?acc=GSE40443**
Status:	**Public on Aug 30 2012**
Title:	**iTreg cells compared to WT Total Treg**
Organism:	**Mus musculus**
Experiment type:	**Expression profiling by array**
Platform:	**GPL1261**
Pubmed ID:	**22966001**
Summary & Design:	**Summary:** **iTreg cells from Tbmc mLN mice treated with one week of 1% Oral Ova were compared to Total Treg from WT mice.** **Overall design:** **CD4+ Foxp3+ cells were also sorted from WT Foxp3 GFP Balb/c mice.**

Background corr dist: **KL-Divergence = 0.0492, L1-Distance = 0.0369, L2-Distance = 0.0020, Normal std = 0.5956**

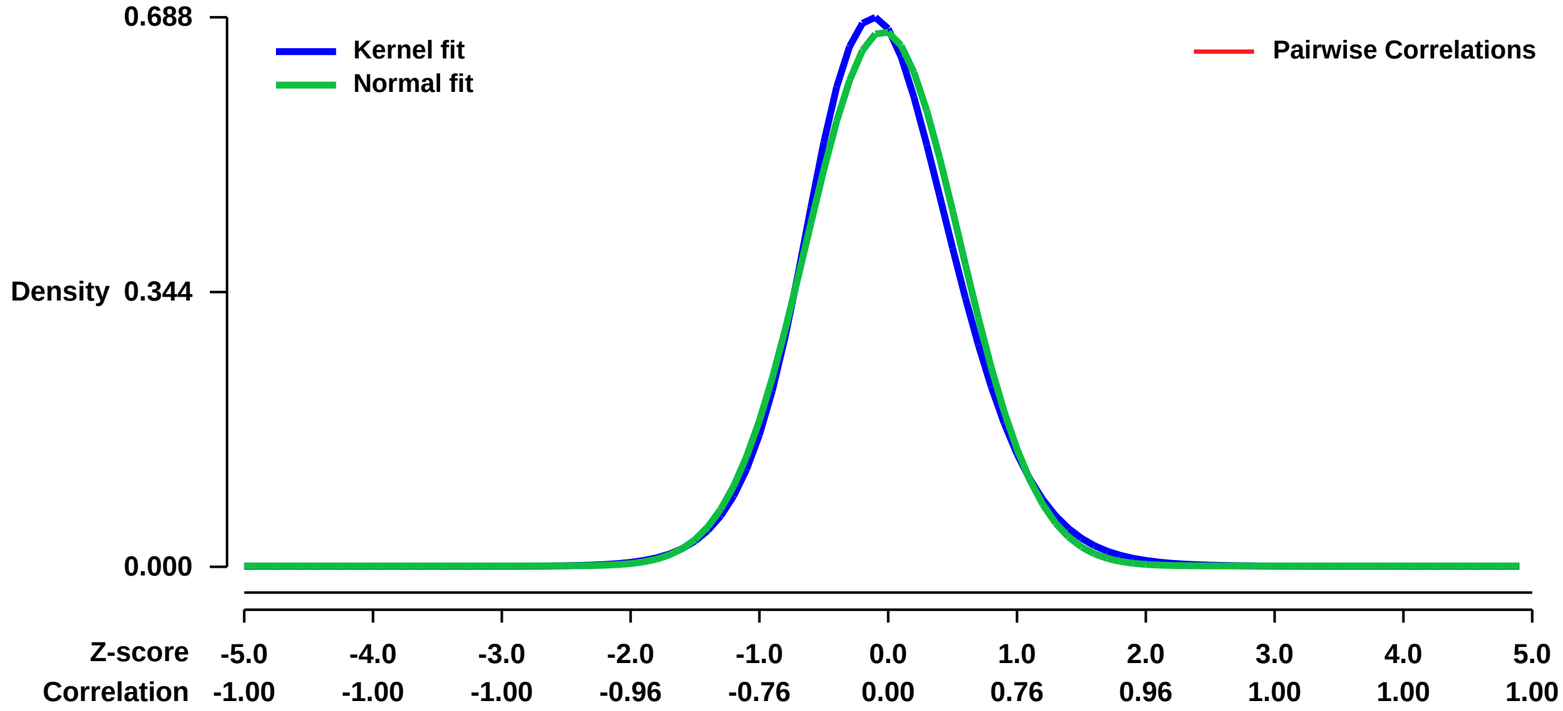

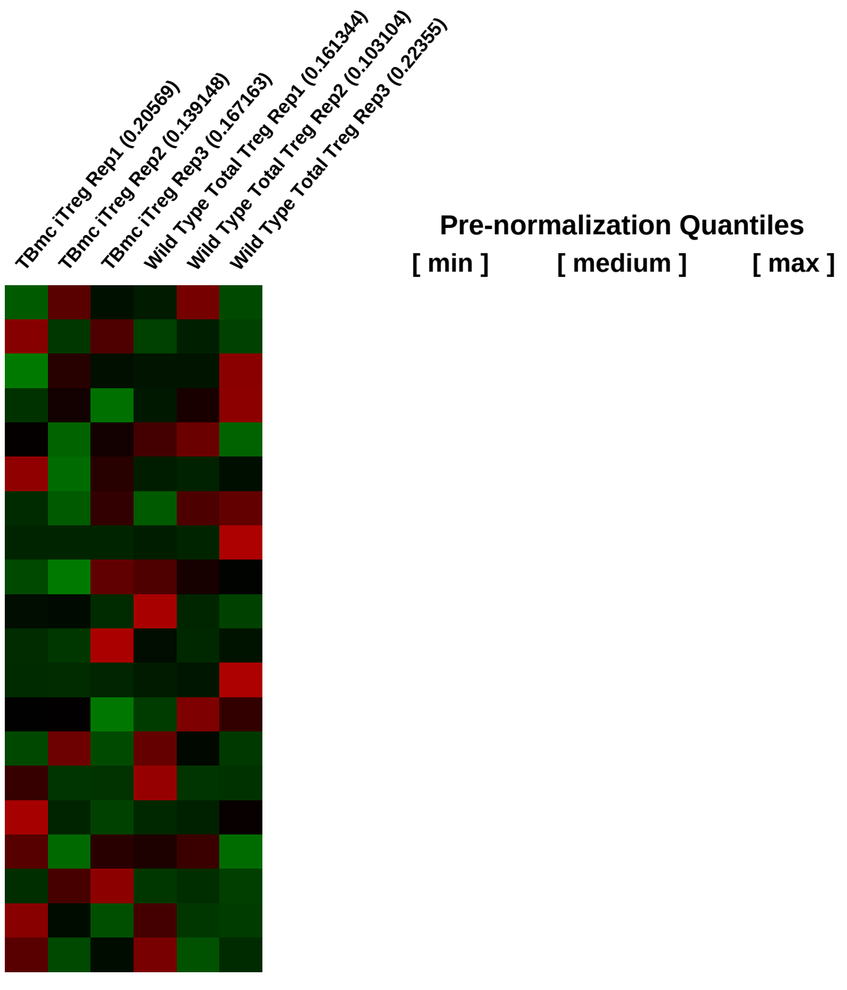

GEO Series "GSE40513" Expression Profiles

Num of samples in this series: 6

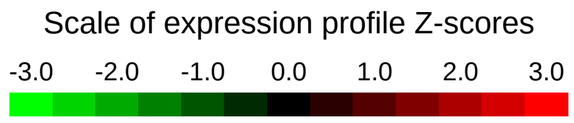

GEO Link:	http://www.ncbi.nlm.nih.gov/geo/query/acc.cgi?acc=GSE40513
Status:	Public on Oct 16 2012
Title:	Gene expression profile of mouse breast cancer V720 cells treated with vehicle or PD 0332991
Organism:	Mus musculus
Experiment type:	Expression profiling by array
Platform:	GPL1261
Pubmed ID:	23079655
Summary & Design:	**Summary:** D-cyclins represent components of cell cycle machinery. To test the efficacy of targeting D-cyclins in cancer treatment, we engineered mouse strains which allow acute and global ablation of individual D-cyclins in a living animal. Ubiquitous shutdown of cyclin D1 or inhibition of cyclin D associated kinase activity in mice bearing ErbB2-driven mammary carcinomas halted cancer progression and triggered tumor-specific senescence, without compromising the animals' health. Ablation of cyclin D3 in mice bearing T-cell acute lymphoblastic leukemias (T-ALL) triggered tumorspecific apoptosis. Such selective killing of leukemic cells can be also achieved by inhibiting cyclin D associated kinase activity in mouse and human T-ALL models. Hence, contrary to what one might expect from ablation of a cell cycle protein, acute shutdown of a D-cyclin leads not only to cell cycle arrest, but it also triggers tumor cell senescence or apoptosis, and it affects different tumor types through distinct cellular mechanisms. Inhibiting cyclin D-activity represents a highly-selective anticancer strategy which specifically targets cancer cells without significantly affecting normal tissues. **Overall design:** Mouse breast cancer V720 cells were cultured in the presence of the CDK4/6 inhibitor PD 0332991 (PD; 1 microM) or vehicle (VO) for 24 hrs. Experiment was done in biological triplicate. A total of 6 RNA samples (3 vehicle treated and 3 PD 0332991 treated samples) were used for microarray expression analysis.

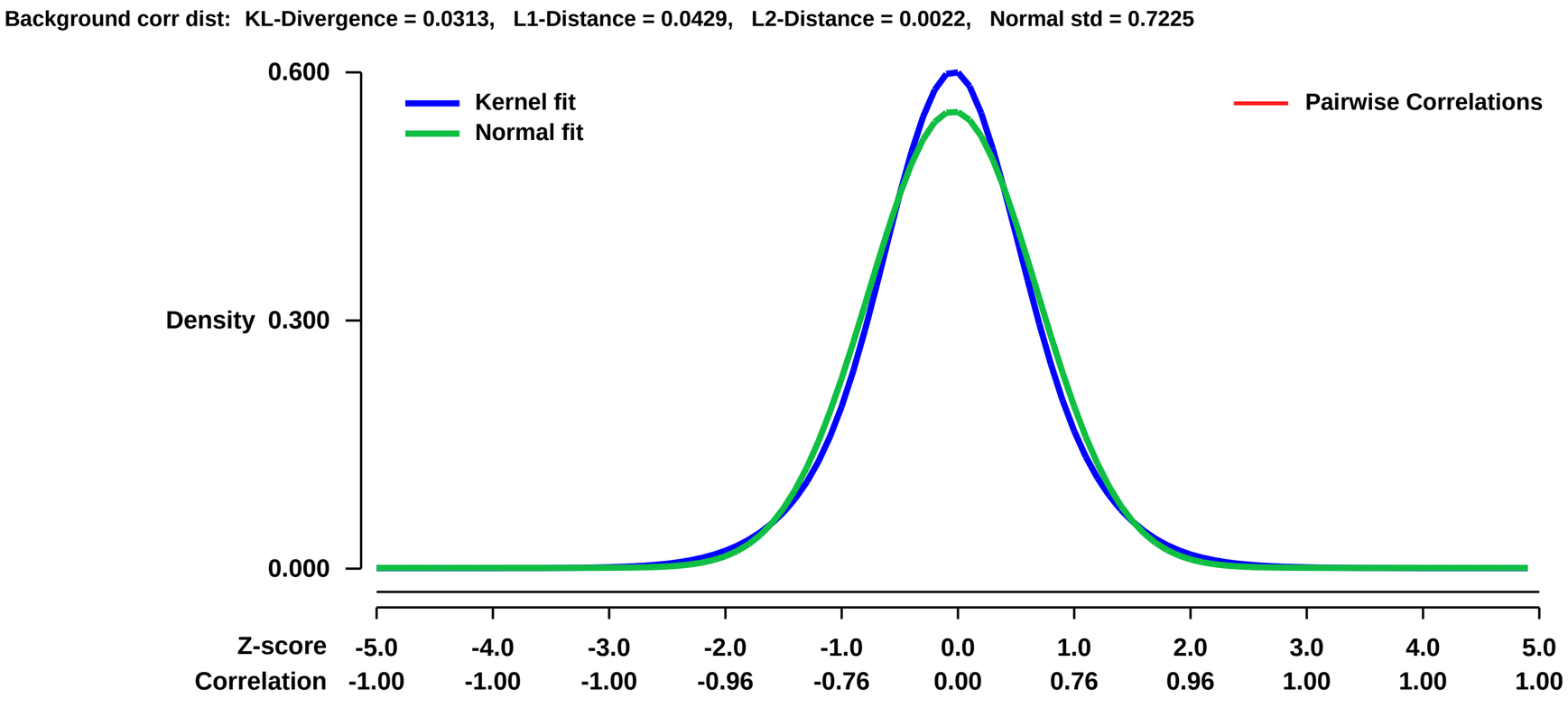

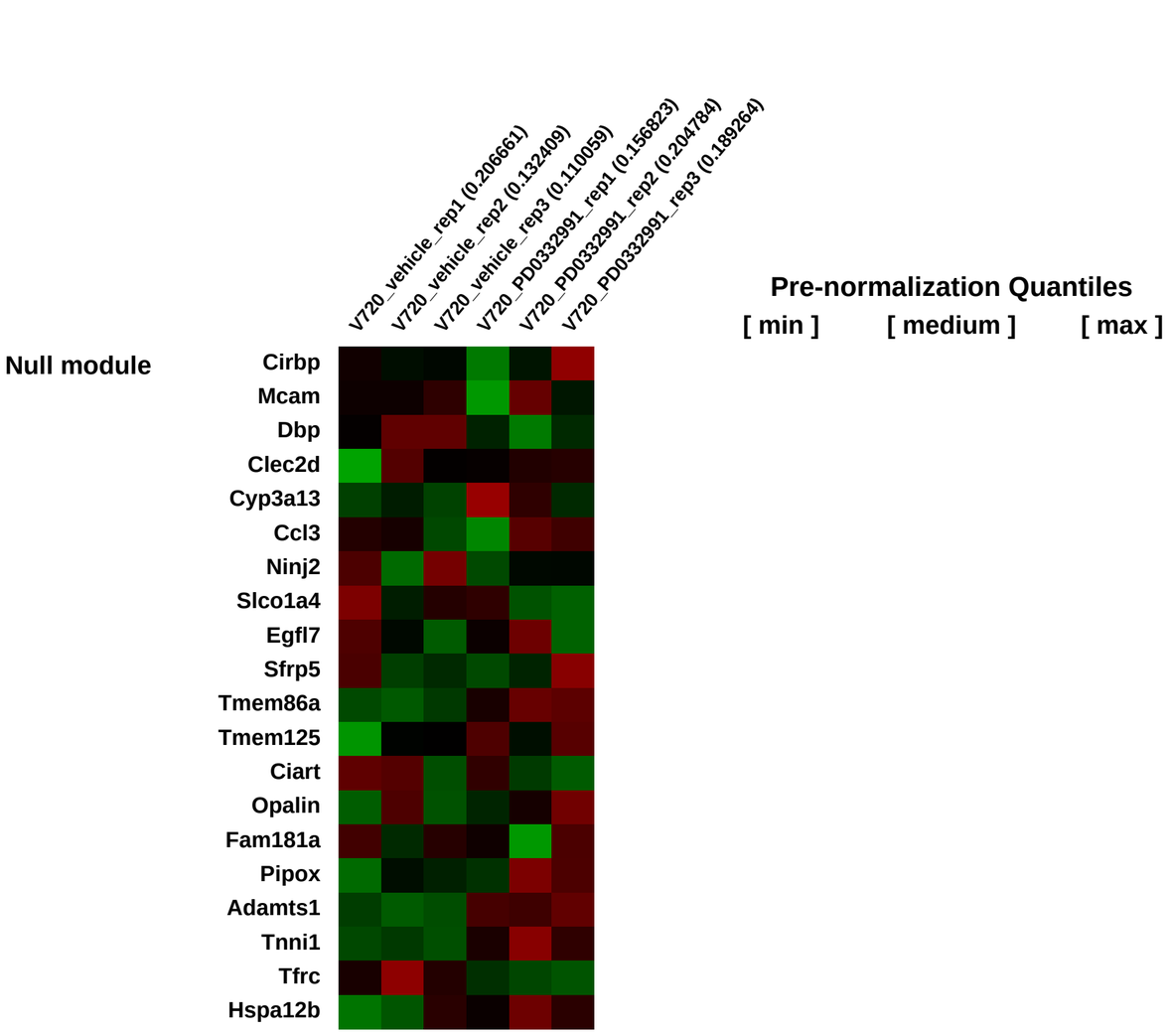

GEO Series "GSE40609" Expression Profiles

Num of samples in this series: 28

Scale of expression profile Z-scores

-3.0 -2.0 -1.0 0.0 1.0 2.0 3.0

GEO Link:	http://www.ncbi.nlm.nih.gov/geo/query/acc.cgi?acc=GSE40609
Status:	Public on Sep 06 2012
Title:	Murine PDAC cell lines
Organism:	Mus musculus
Experiment type:	Expression profiling by array
Platform:	GPL1261
Pubmed ID:	
Summary & Design:	**Summary:** Expression profiles of 28 murine pancreatic cancer cell lines isolated from a KrasG12D-based mouse model of pancreatic cancer **Overall design:** mRNA of 28 low passaged murine pancreatic cancer cell lines was extracted and hybridized to Affymetrix microarrays

Background corr dist: KL-Divergence = 0.2861, L1-Distance = 0.0675, L2-Distance = 0.0126, Normal std = 0.2853

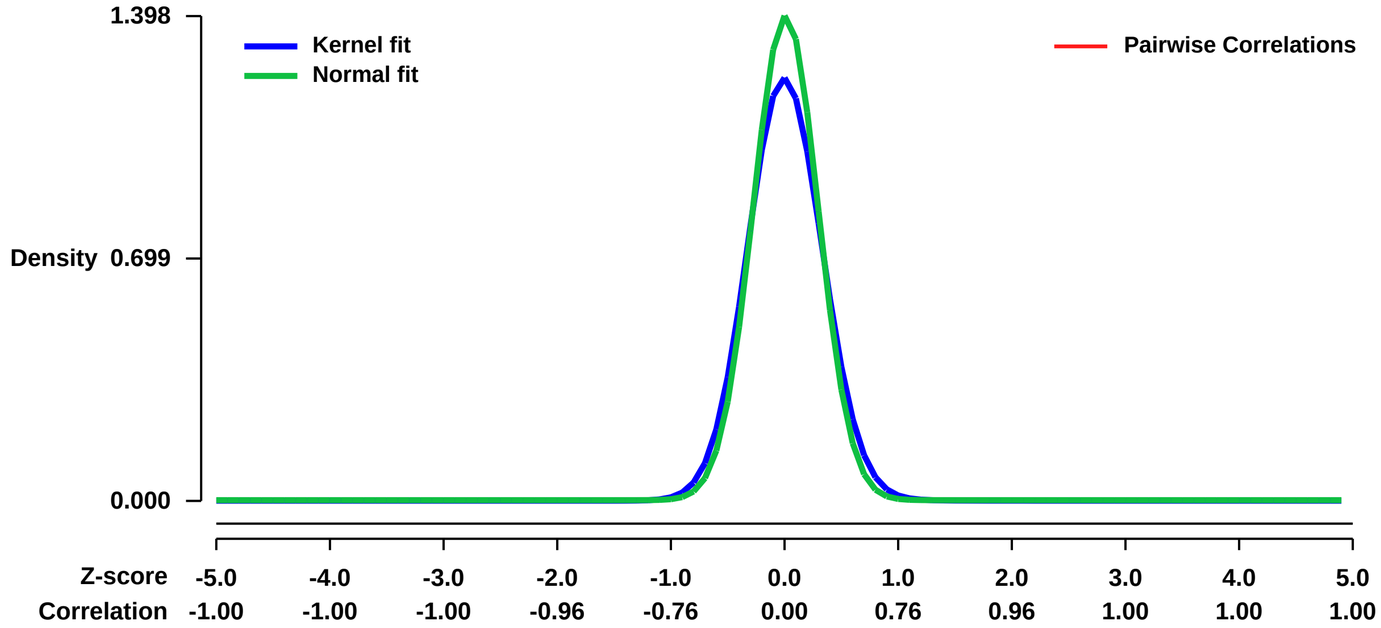

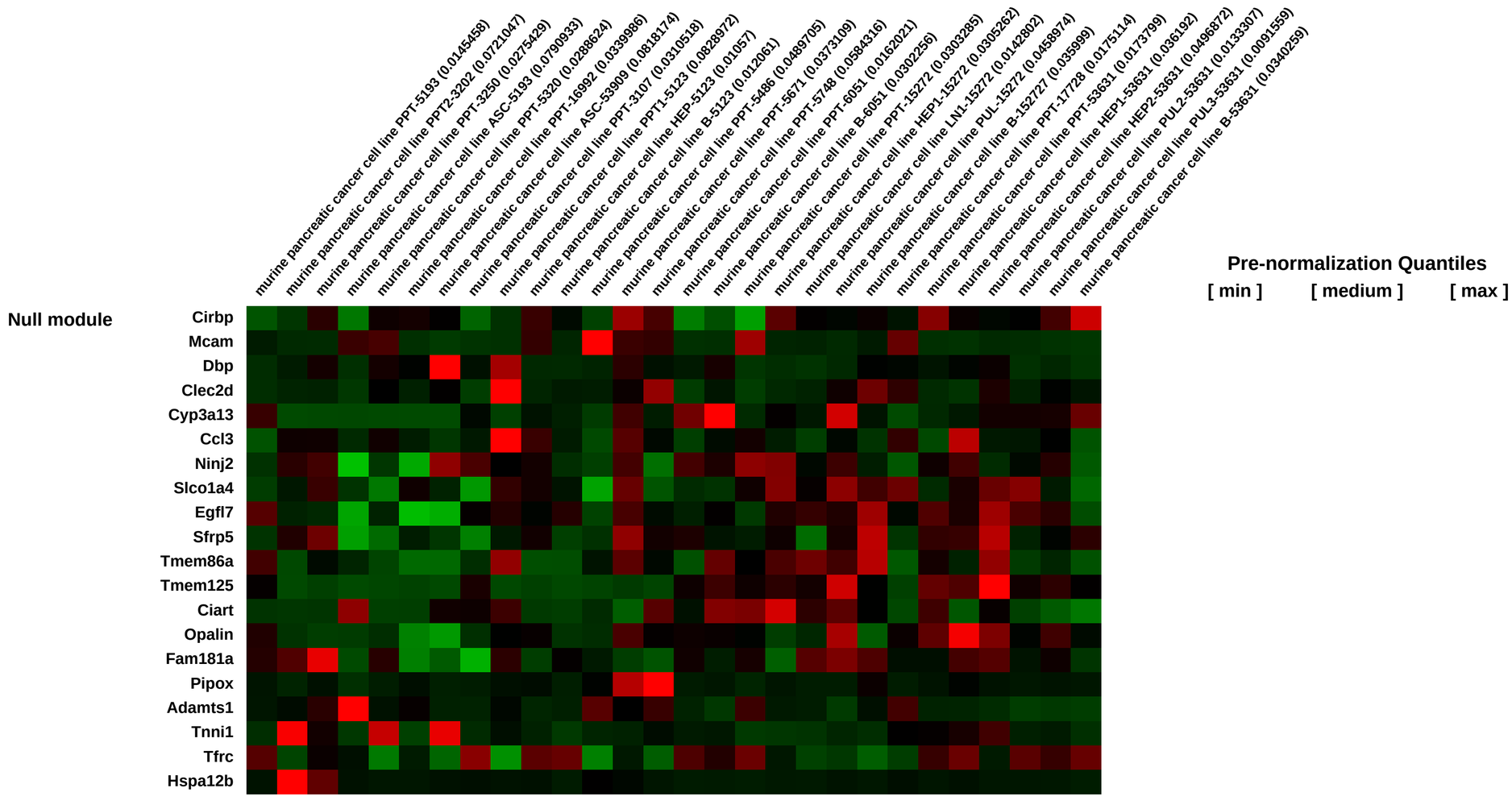

GEO Series "GSE40660" Expression Profiles

Num of samples in this series: 6

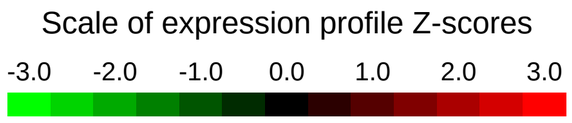

GEO Link:	**http://www.ncbi.nlm.nih.gov/geo/query/acc.cgi?acc=GSE40660**
Status:	**Public on Jan 01 2014**
Title:	**Gata2 is a master regulator of endometrial function and progesterone signaling [Affymetrix]**
Organism:	**Mus musculus**
Experiment type:	**Expression profiling by array**
Platform:	**GPL1261**
Pubmed ID:	
Summary & Design:	**Summary:** **The role of Gata2 in regulating uterine function including fertility, implantation, decidualization and P4 signaling in the mouse was investigated by the conditional ablation of Gata2 in the uterus using the (PR-cre) mouse and ChIP-seq for in vivo GATA2 binding sites in the murine uterus upon acute P4 administration.** **Overall design:** **Gata2 gene ablation was confirmed by real-time PCR analysis in the PR-cre; Gata2fl/fl (termed Gata2d/d) uterus. While littermate controls are fertile, Gata2d/d females are completely infertile. Analysis of the infertility indicates that implantation does not occur, and the uterine stroma is incapable of undergoing the decidual reaction to support further embryonic development. Measure of P4 target genes including PR itself indicate a block in P4 target gene induction and that Gata2 regulates PR expression directly. Microarray analysis demonstrates that ablation of Gata2 leads to specific gene changes, including disruption of the Wnt signaling pathway, Progesterone receptor (PR) signaling, and Ihh signaling pathway. In addition we identified 46,183 GATA2 binding sites in P4 treatment conditions with 7,954 binding sites overlapping that of the PR.Taken together, these data demonstrate that Gata2 is a critical regulator of gene expression and function in the murine uterus.**

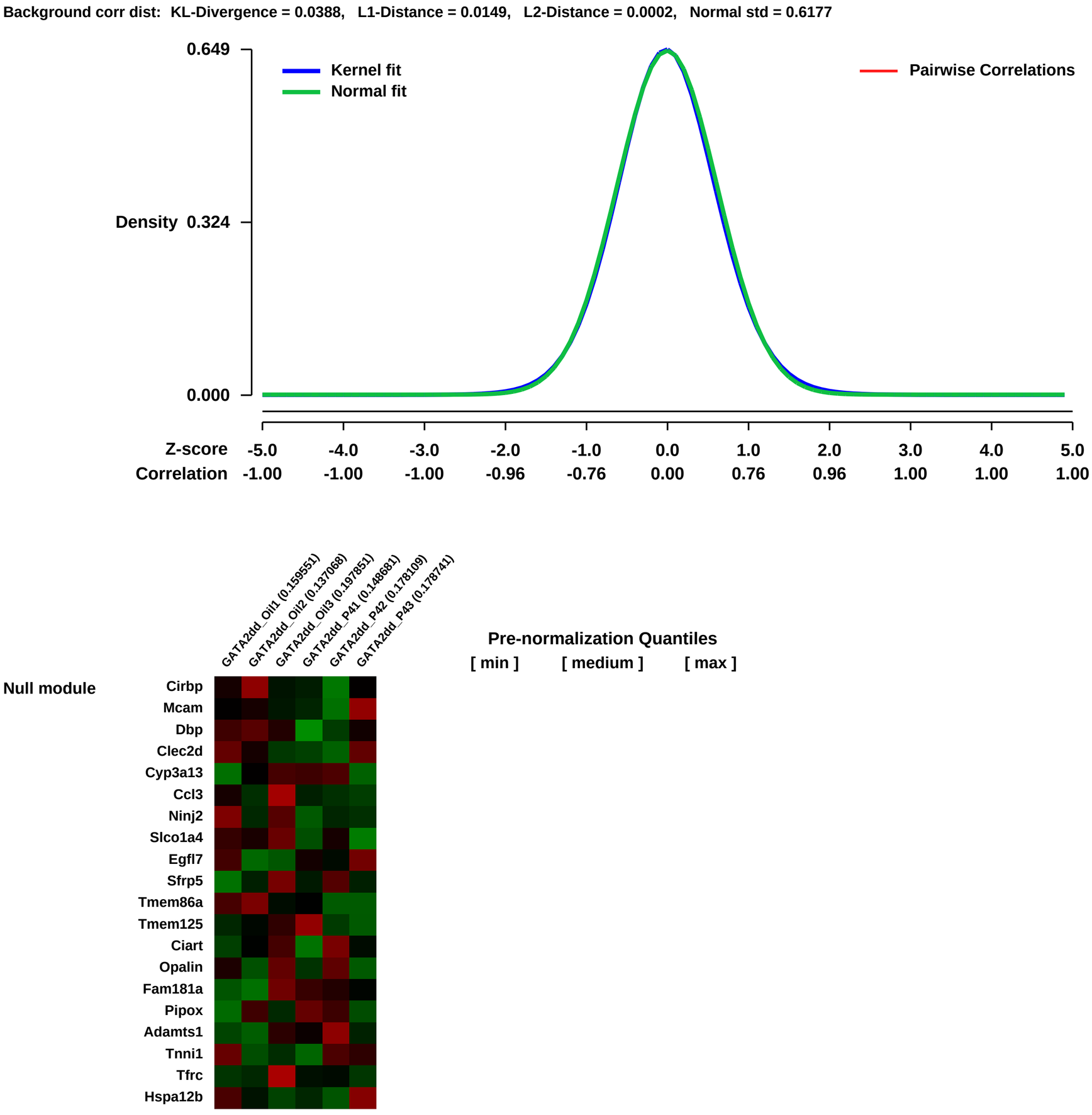

GEO Series "GSE40685" Expression Profiles

Num of samples in this series: 11

Scale of expression profile Z-scores

-3.0 -2.0 -1.0 0.0 1.0 2.0 3.0

GEO Link:	**http://www.ncbi.nlm.nih.gov/geo/query/acc.cgi?acc=GSE40685**
Status:	**Public on Sep 28 2012**
Title:	**Foxp3 exploits a preexistent enhancer landscape for regulatory T cell lineage specification [Expression]**
Organism:	**Mus musculus**
Experiment type:	**Expression profiling by array**
Platform:	**GPL1261**
Pubmed ID:	**23021222**
Summary & Design:	**Summary:** **Regulatory T (Treg) cells, whose identity and function are defined by the transcription factor Foxp3, are indispensable for immune homeostasis. It is unclear whether Foxp3 exerts its Treg lineage specification function through active modification of the chromatin landscape and establishment of new enhancers or by exploiting a pre-existing enhancer landscape. Analysis of the chromatin accessibility of Foxp3-bound enhancers in Treg and Foxp3-negative T cells showed that Foxp3 was bound overwhelmingly to pre-accessible enhancers occupied by its cofactors in precursor cells or a structurally related predecessor. Furthermore, the bulk of Foxp3-bound Treg cell enhancers inaccessible in Foxp3- CD4+ cells became accessible upon T cell receptor activation prior to Foxp3 expression with only a small subset associated with several functionally important genes being exclusively Treg cell-specific. Thus, in a late cellular differentiation process Foxp3 defines Treg cell functionality in an â opportunisticâ manner by largely exploiting the preformed enhancer network instead of establishing a new enhancer landscape.** **Overall design:** **Array expression. Three cell types with 3-5 replicates each.**

Background corr dist: KL-Divergence = 0.0865, L1-Distance = 0.0219, L2-Distance = 0.0007, Normal std = 0.4629

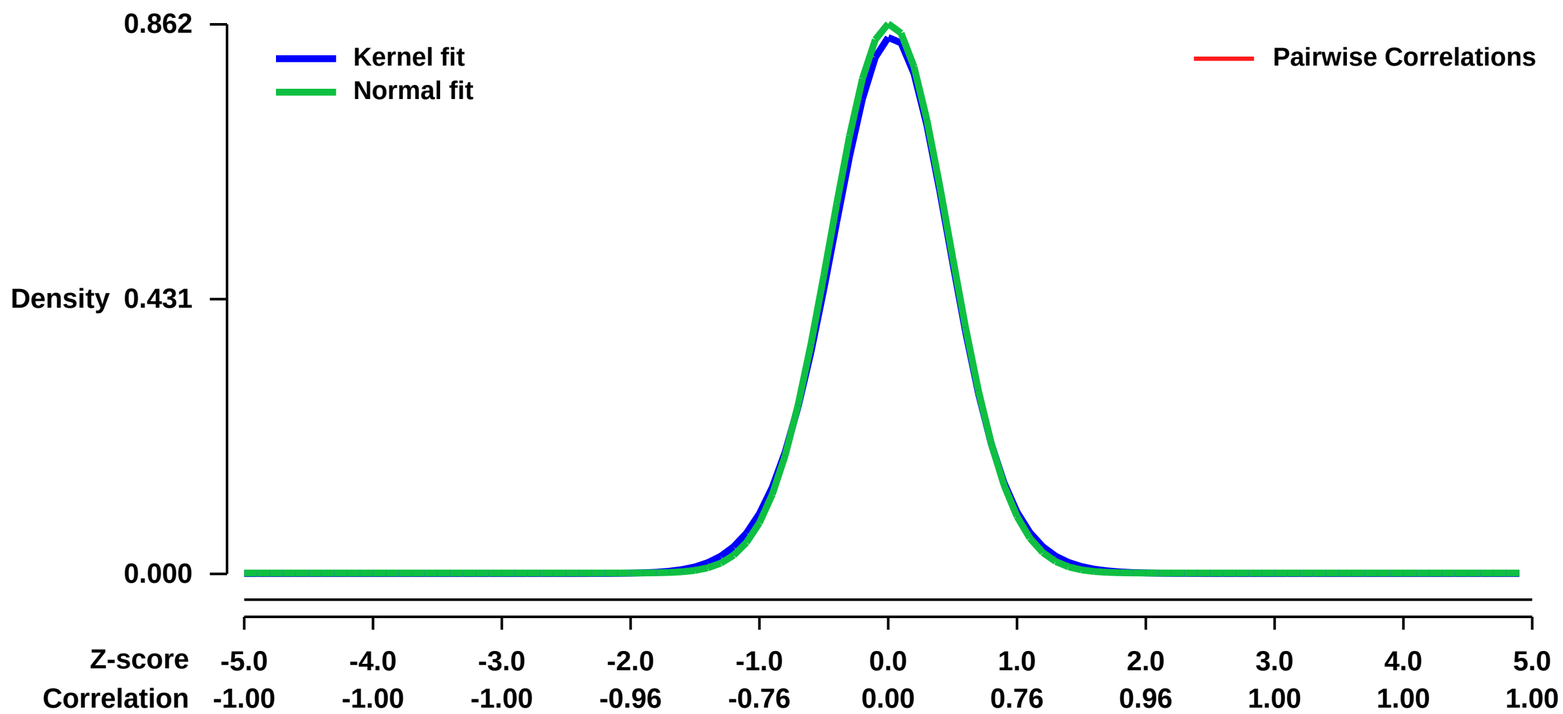

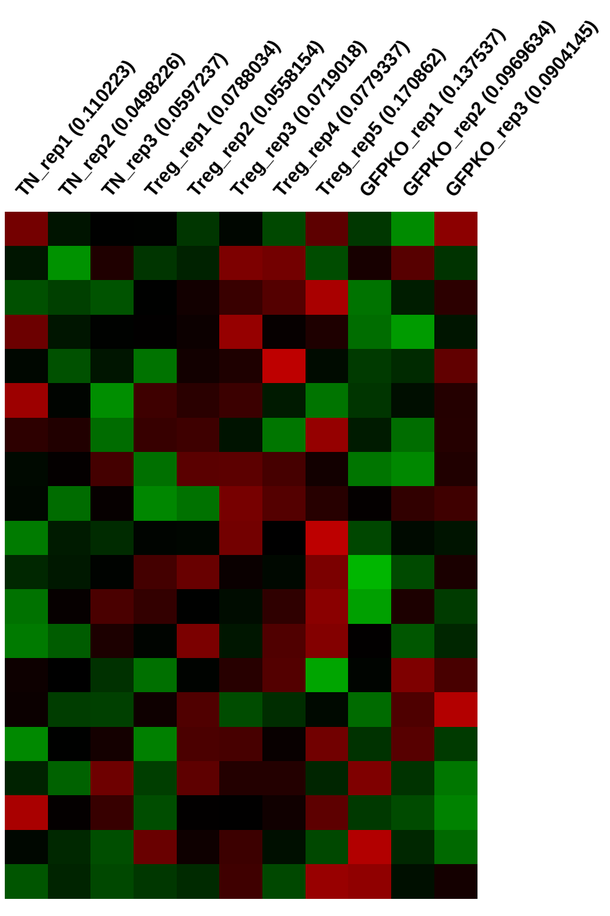

GEO Series "GSE40773" Expression Profiles

Num of samples in this series: 10

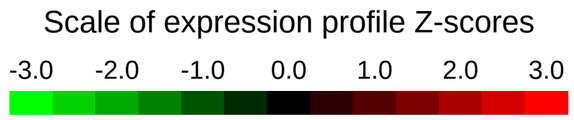

GEO Link:	**http://www.ncbi.nlm.nih.gov/geo/query/acc.cgi?acc=GSE40773**
Status:	**Public on Sep 12 2012**
Title:	**Dynamic changes in liver 5-hydroxymethylcytosine profiles upon non-genotoxic carcinogen exposure**
Organism:	**Mus musculus**
Experiment type:	**Expression profiling by array**
Platform:	**GPL1261**
Pubmed ID:	**23598998**
Summary & Design:	**Summary:** **29-32 days old male mice where either treated with Phenobarbital or untreated** **Overall design:** **Replicated control vs. pb treated study**

Background corr dist: **KL-Divergence = 0.0669, L1-Distance = 0.0246, L2-Distance = 0.0009, Normal std = 0.5027**

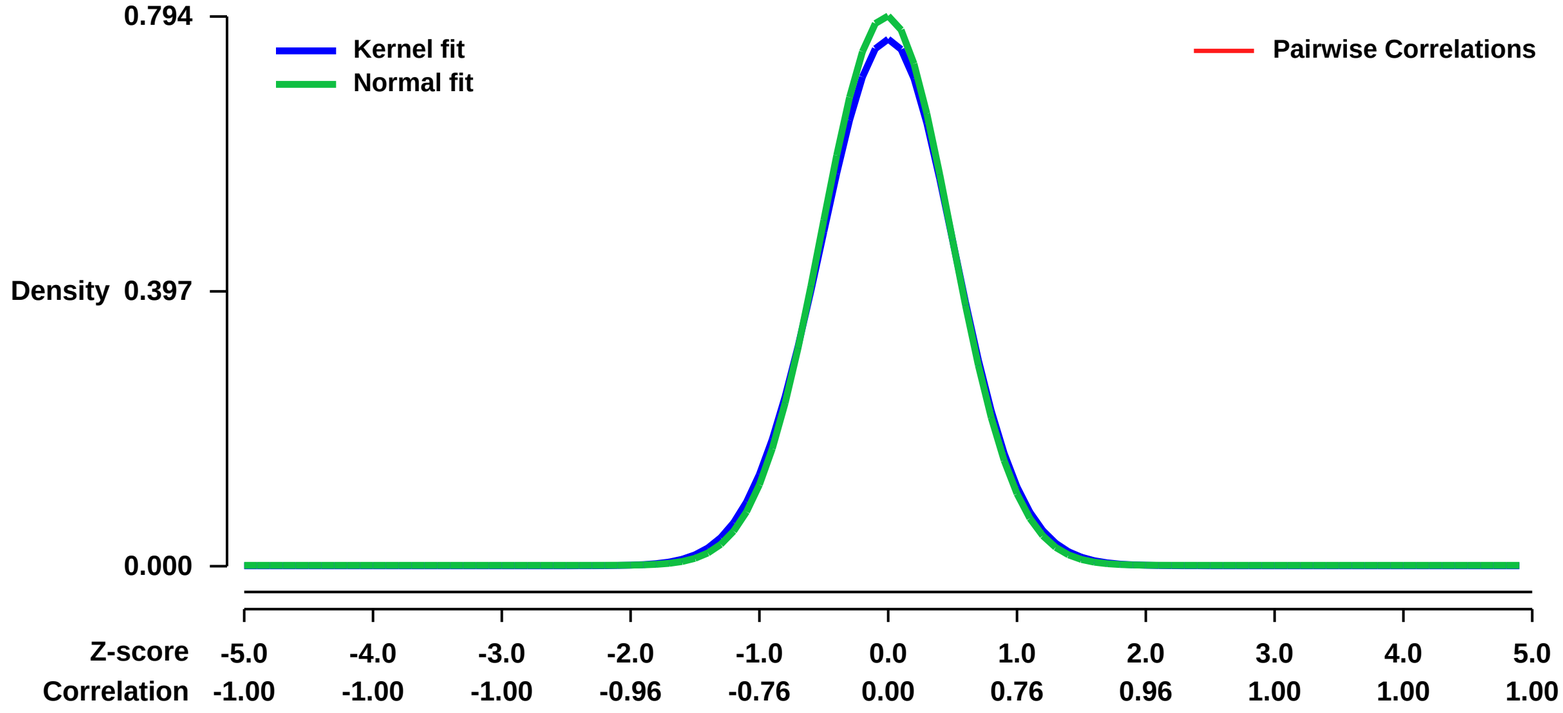

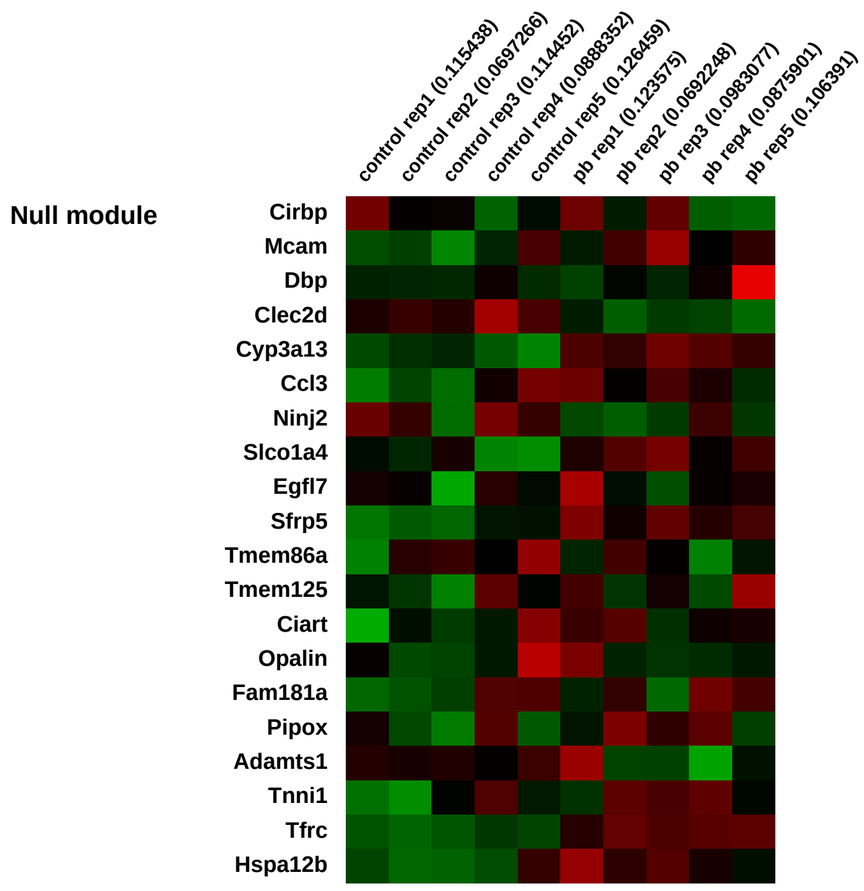

GEO Series "GSE40795" Expression Profiles

Num of samples in this series: 50

Scale of expression profile Z-scores

-3.0 -2.0 -1.0 0.0 1.0 2.0 3.0

GEO Link:	http://www.ncbi.nlm.nih.gov/geo/query/acc.cgi?acc=GSE40795
Status:	Public on Oct 12 2012
Title:	Transcriptomic Dose Response Changes in Female Mouse and Rat Lungs following Chloroprene Exposure
Organism:	Mus musculus
Experiment type:	Expression profiling by array
Platform:	GPL1261
Pubmed ID:	23125180
Summary & Design:	**Summary:** ˆ-chloroprene (2-chloro-1,3-butadiene), a monomer used in the production of neoprene elastomers, is of regulatory interest due to the production of multi-organ tumors in mouse and rat cancer bioassays. A significant increase in female mouse lung tumors was observed at the lowest exposure concentration of 12.8 ppm while a small, but not statistically significant, increase was observed in female rats only at the highest exposure concentration of 80 ppm. The metabolism of chloroprene results in the generation of reactive epoxides and the rate of overall chloroprene metabolism is highly species dependent. To identify potential key events in the mode-of-action of chloroprene lung tumorigenesis, dose response and time course gene expression microarray measurements were made in the lungs of female mice and female rats. The gene expression changes were analyzed using both a traditional analysis of variance approach followed by pathway enrichment analysis and a pathway-based benchmark dose (BMD) analysis approach. Pathways related to glutathione biosynthesis and metabolism were the primary pathways consistent with cross-species differences in tumor incidence and transcriptional BMD values for the pathway were more similar to differences in tumor response than were estimated target tissue dose surrogates based on the total amount of chloroprene metabolized per unit mass of lung tissue per day. The closer correspondence of the transcriptional changes with the tumor response are likely due to their reflection of the overall balance between metabolic activation and detoxication reactions whereas the current tissue dose surrogate reflects only oxidative metabolism. **Overall design:** Female mice (B6C3F1/Crl) were exposed to chloroprene (CAS 126-99-8) by whole-body inhalation exposure at 0, 0.3, 2, 13, or 90 ppm. Exposures were performed for 6 hr/day, 5 days per week. The animals were sacrified at 5 days or 19 days (15 exposure days) post initiation of exposure. The right lung was excised and gene expression microarray analysis was performed using Affymetrix Mouse 430_2 arrays. Female rats (F344/NCrl) were exposed to chloroprene (CAS 126-99-8) by whole-body inhalation exposure at 0, 5, 30, 90, or 200 ppm. Exposures were performed for 6 hr/day, 5 days per week. The animals were sacrified at 5 days or 19 days (15 exposure days) post initiation of exposure. The right lung was excised and gene expression microarray analysis was performed using Affymetrix Rat 230_2 arrays.

Background corr dist: KL-Divergence = 0.1693, L1-Distance = 0.0369, L2-Distance = 0.0026, Normal std = 0.3558

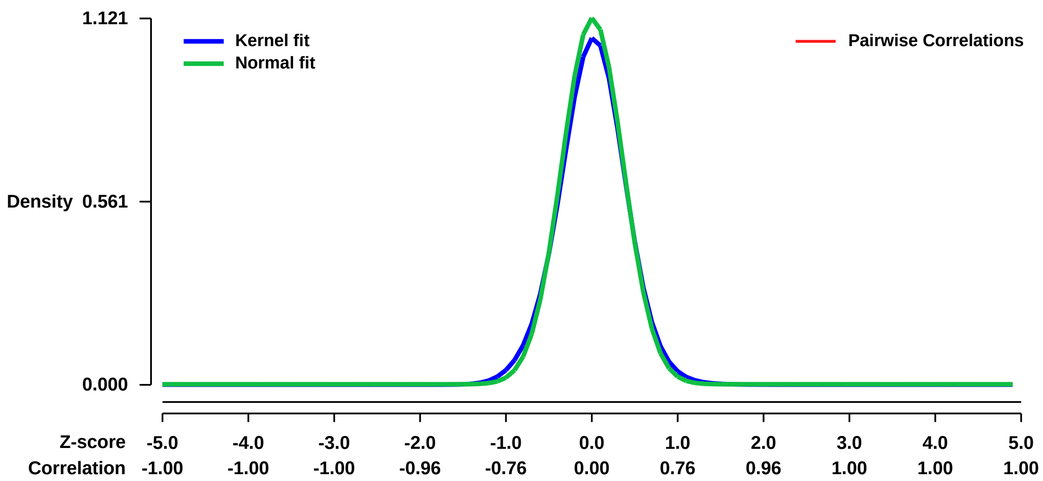

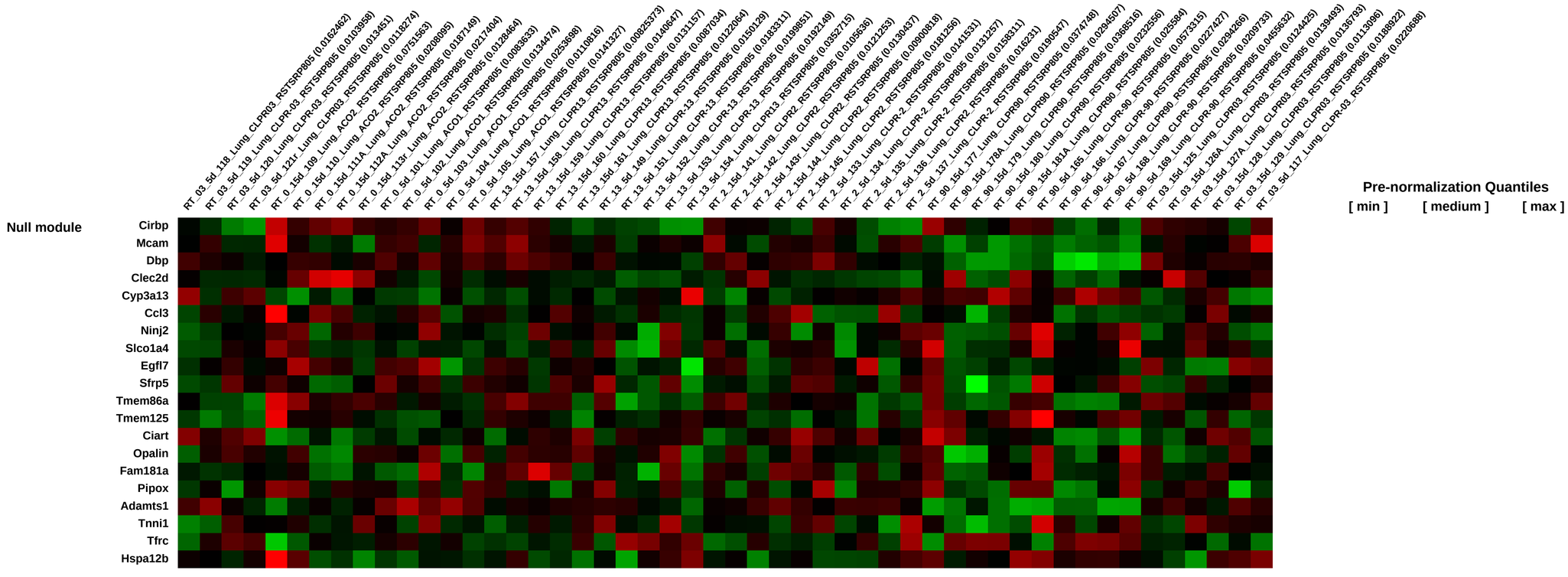

GEO Series "GSE40856" Expression Profiles

Num of samples in this series: 8

Scale of expression profile Z-scores

-3.0 -2.0 -1.0 0.0 1.0 2.0 3.0

GEO Link:	http://www.ncbi.nlm.nih.gov/geo/query/acc.cgi?acc=GSE40856
Status:	Public on Apr 01 2013
Title:	Non-tumor/tumor intestinal tissue of control or intestine-specific HAI-1 deficient Apc(Min/+) mice
Organism:	Mus musculus
Experiment type:	Expression profiling by array
Platform:	GPL1261
Pubmed ID:	23447577
Summary & Design:	**Summary:** To analyse roles of HAI-1/Spint1 in intestinal tumorigenesis, we examined the effect of intestine-specific deletion of Spint1 gene on Apc(Min/+) mice. The loss of Hai-1/Spint1 significantly accelerated tumor formation in ApcMin/+ mice and shortened their survival periods. Mouse small intestine tumor tissue or background mucosa lacking macroscopically visible tumors were proceeded to RNA extraction and hybridization on microarrays (Affymetrix Mouse Genome 430 2.0 Array). **Overall design:** Non-tumor or tumor intestinal mucosa tissues of Apc (Min/+)/Spint1 (flox/flox) mice and non-tumor or tumor intestinal mucosa tissues of Apc (Min/+)/Spint1 (flox/flox)/Vil-Cre mice were analysed. The experiment was repeated respectively.

Background corr dist: KL-Divergence = 0.0508, L1-Distance = 0.0245, L2-Distance = 0.0009, Normal std = 0.5637

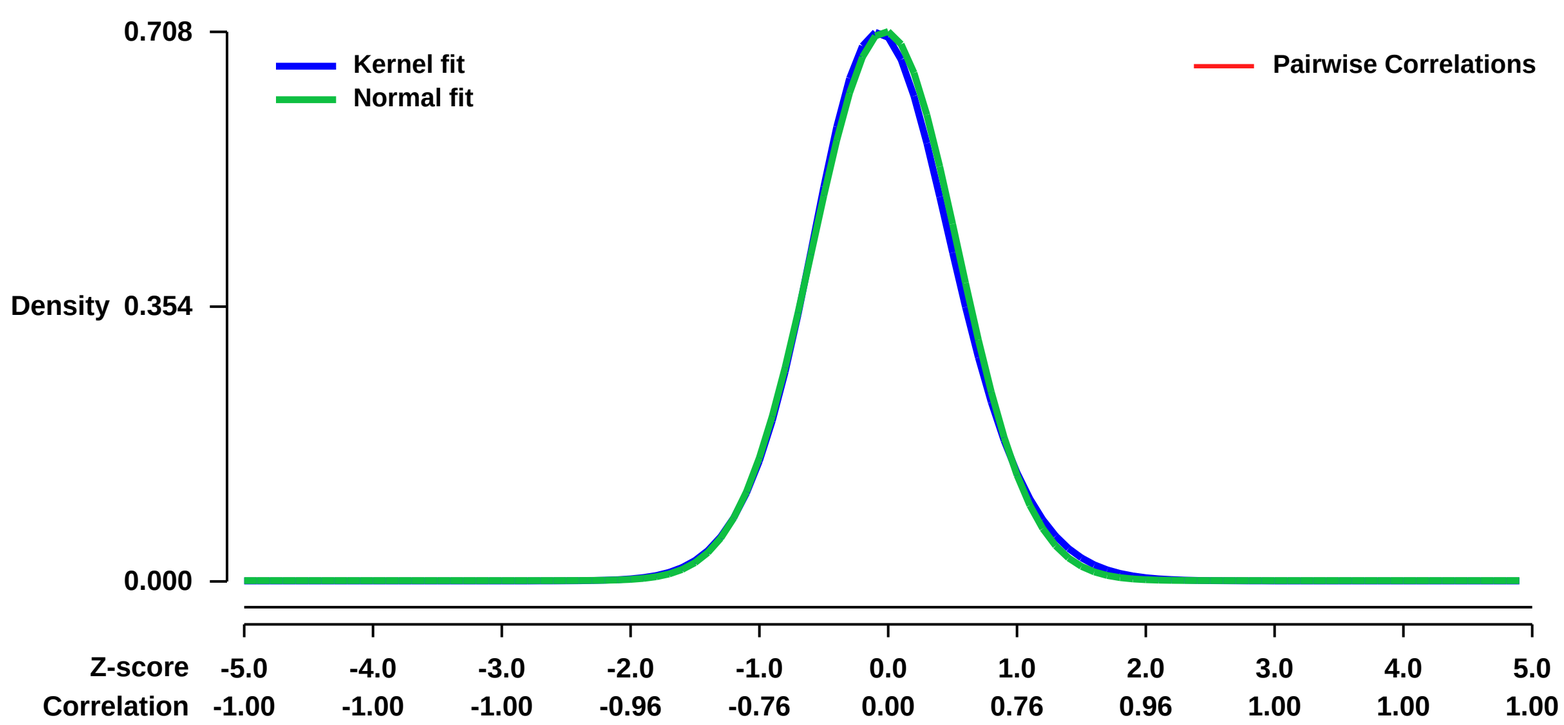

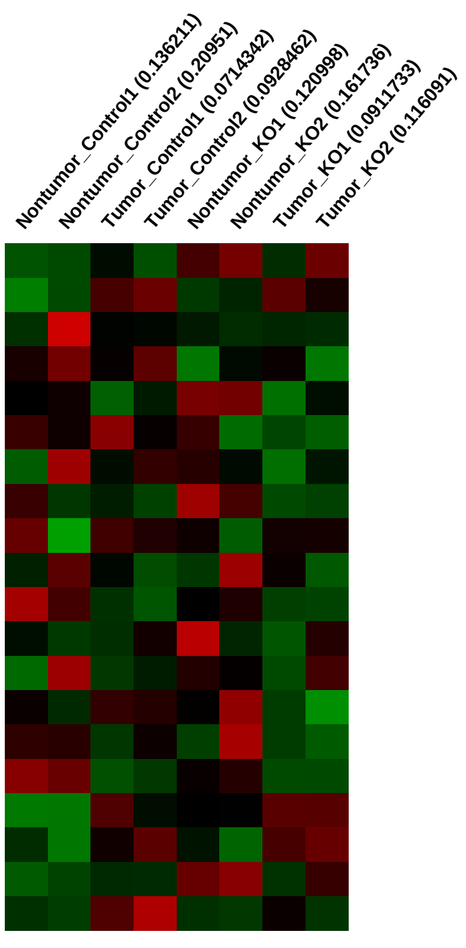

GEO Series "GSE4098" Expression Profiles

Num of samples in this series: 16

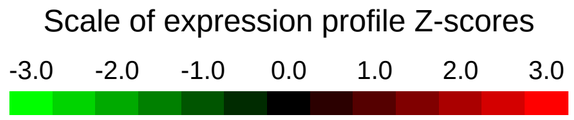

GEO Link:	**http://www.ncbi.nlm.nih.gov/geo/query/acc.cgi?acc=GSE4098**
Status:	**Public on Jan 27 2006**
Title:	**Mouse limbal epithelial basal cells vs. corneal epithelial basal cell gene expression profile**
Organism:	**Mus musculus**
Experiment type:	**Expression profiling by array**
Platform:	**GPL1261**
Pubmed ID:	**16675456**
Summary & Design:	**Summary:** **Limbal vs. corneal epithelial basal cell gene expression patterns were identified and compared** **Keywords: repeat** **Overall design:** **8 limbal and 8 corneal epithelial basal cells samples from 8 mice were dissected and mRNAs were isolated and amplified for microarray analysis**

Background corr dist: **KL-Divergence = 0.1724, L1-Distance = 0.0608, L2-Distance = 0.0095, Normal std = 0.3604**

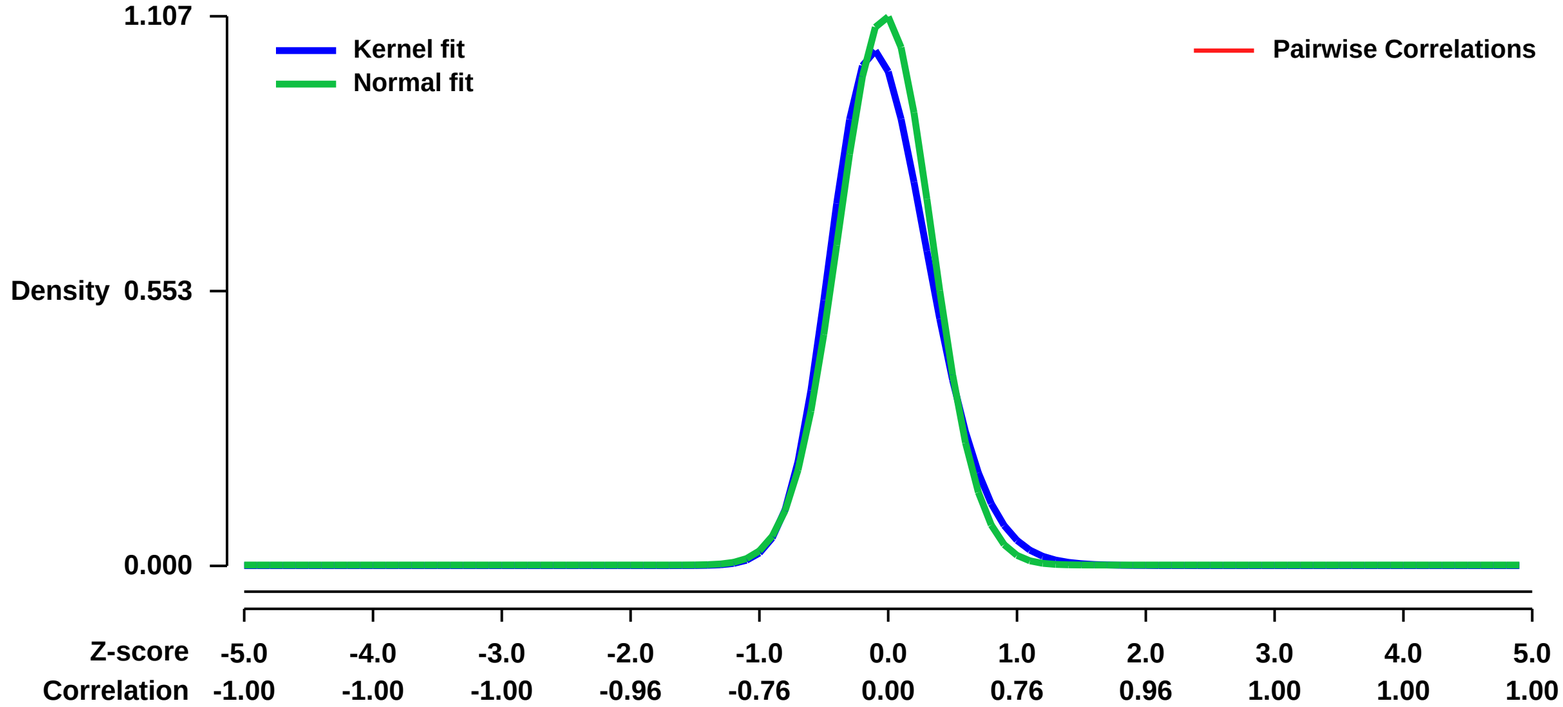

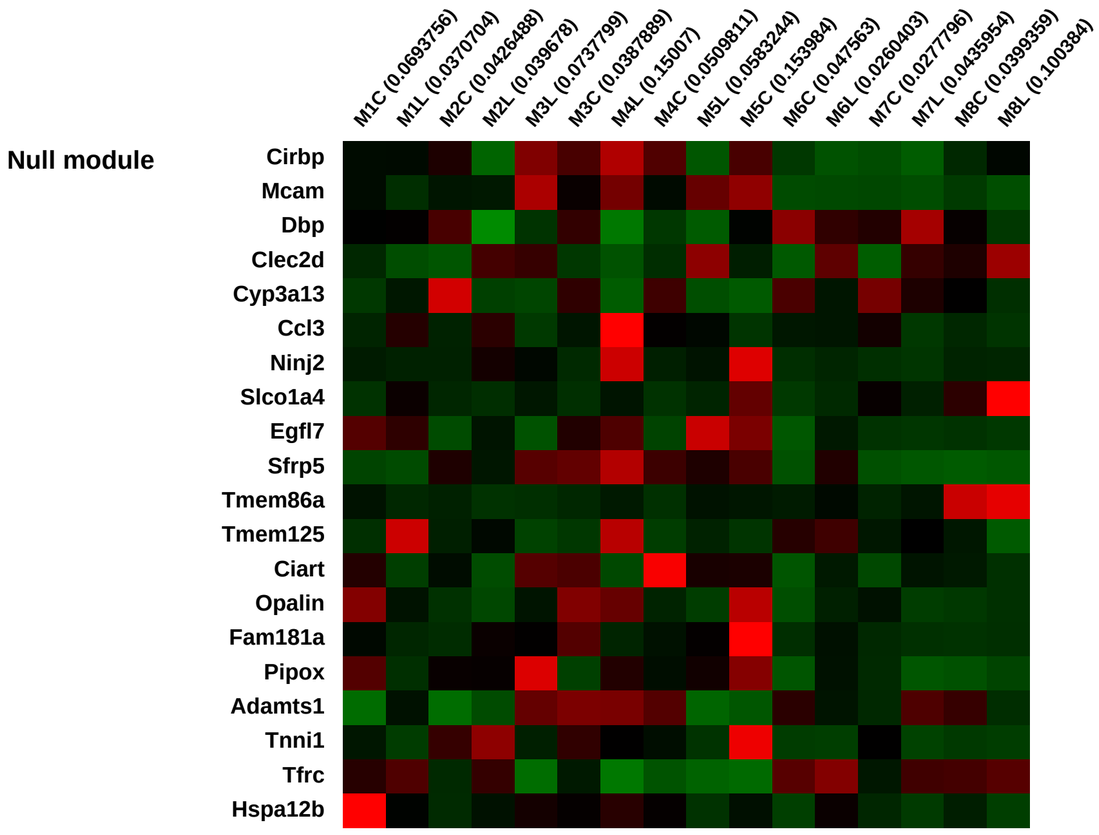

GEO Series "GSE41005" Expression Profiles

Num of samples in this series: 8

Scale of expression profile Z-scores

-3.0 -2.0 -1.0 0.0 1.0 2.0 3.0

GEO Link:	http://www.ncbi.nlm.nih.gov/geo/query/acc.cgi?acc=GSE41005
Status:	Public on Sep 20 2012
Title:	HSF1 mediated Gene regulation in T cells at normal (37C) and febrile (40C) temperatures
Organism:	Mus musculus
Experiment type:	Expression profiling by array
Platform:	GPL1261
Pubmed ID:	24043900
Summary & Design:	**Summary:** HSF1 is a major transcriptional regulator of heat shock responses. Many cells activate HSF1 in response to heat shock temperatures (>42oC) and other cellular stress causing agents. Unlike other cell types, T cells activate HSF1 in response to T cell activation or when exposed to febrile (40oC) temperatures, suggesting a role for HSF1 beyond the heat-shock response. We used microarray analysis and HSF1 knock-out mice to study the HSF1 mediated gene regulation in activated T cells under normal and fever temperatures. **Overall design:** T cells were purifed from spleen and lymphnodes using miltenyi anti-CD3 magnetic beads and were activated for 5 hr with plate bound anti-CD3 at normal (37oC) and febrile(40oC) temperatures in triplicate cultures. Total RNA from triplicate cultures were extracted, pooled and processed for hybridization on to whole mouse genome 430 2.0 affymetrix microarray chips.

Background corr dist: KL-Divergence = 0.0781, L1-Distance = 0.0198, L2-Distance = 0.0005, Normal std = 0.4824

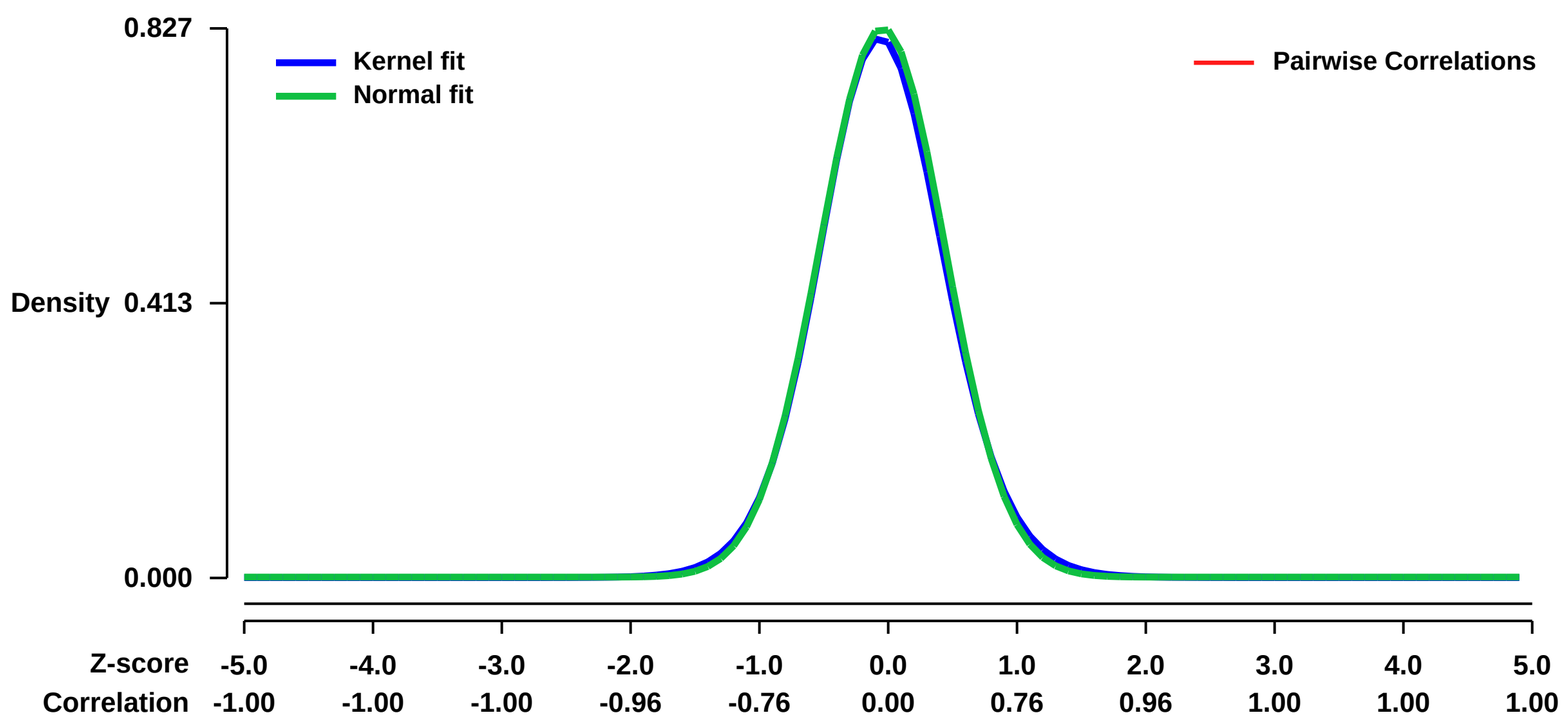

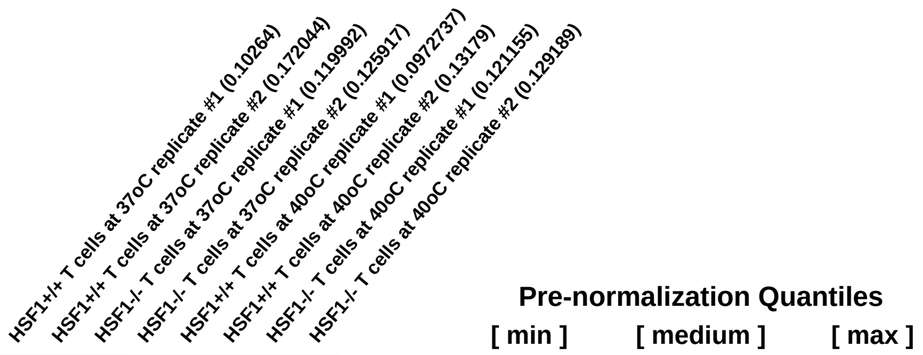

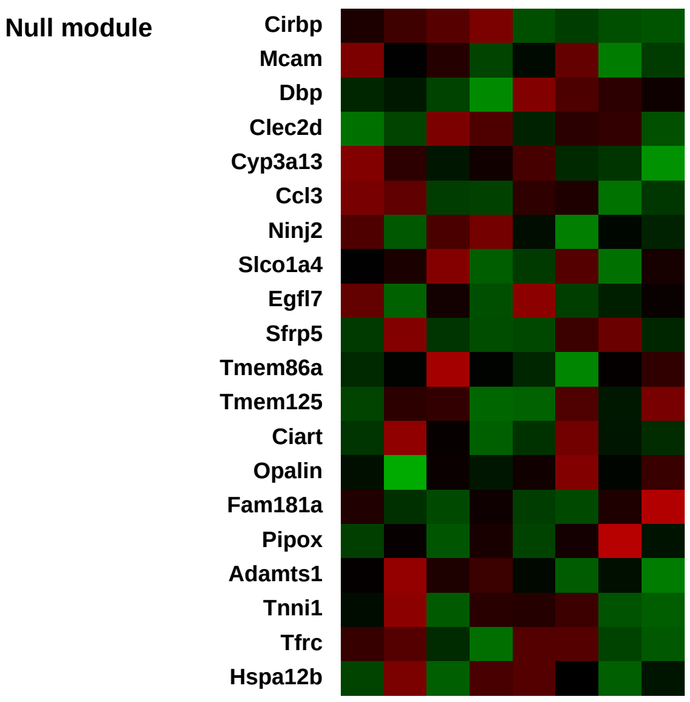

GEO Series "GSE41084" Expression Profiles

Num of samples in this series: 6

Scale of expression profile Z-scores

-3.0 -2.0 -1.0 0.0 1.0 2.0 3.0

GEO Link:	http://www.ncbi.nlm.nih.gov/geo/query/acc.cgi?acc=GSE41084
Status:	Public on Jul 01 2013
Title:	Expression data after irradiating mMSCs for 12 hours with broadband terahertz source
Organism:	Mus musculus
Experiment type:	Expression profiling by array
Platform:	GPL1261
Pubmed ID:	23378916
Summary & Design:	**Summary:** We report that terahertz (THz) irradiation of mouse mesenchymal stem cells with a pulsed broadband (centered at 10 THz) source, or a single-frequency, 2.52 THz, (SF) laser source, both with weak average power (<1mW/cm2), results in specific heterogenic changes in gene expression. The insignificant differential expression of heat shock and stress related genes as well as our temperature measurements imply a non-thermal response. The microarray survey and RT-PCR experiments demonstrate that at different irradiation conditions distinct groups of genes are activated. Stem cells irradiated for 12 hours with the broadband THz source exhibit an accelerated differentiation toward adipose phenotype, while the 2-hour (broadband or SF) irradiation affects genes transcriptionally active in pluripotent stem cells. Phenotypic and gene expression differences suggest that the THz effect depends on irradiation parameters such as duration and type of THz source, and on the level of stem cell differentiation. Computer simulations of the core promoters of two pluripotency markers reveal association between gene upregulation and propensity for DNA breathing. We propose that THz radiation has potential for non-contact control of cellular gene expression. **Overall design:** Growing in petri dish mouse mesenchymal stem cell cultures are irradiated for 12 hours with pulsed ultrafast (35 fs) broadband (centered at ~10 THz) source. Three independent biological experiments were conducted. In each experiment, a control mMSC culture was placed adjacent to the irradiated sample, and the temperature was kept at 26-27´”C for both the control and the irradiated sample. Immediately after completing the irradiation, total RNA was extracted from the irradiated sample and the control, and microarrays were used to identify differential changes in gene expression between the irradiated sample and its respective control. In each experiment, the mMSC cultures were synchronized to be at the same differentiation time point immediately before the irradiation.

Background corr dist: KL-Divergence = 0.0339, L1-Distance = 0.0126, L2-Distance = 0.0001, Normal std = 0.6395

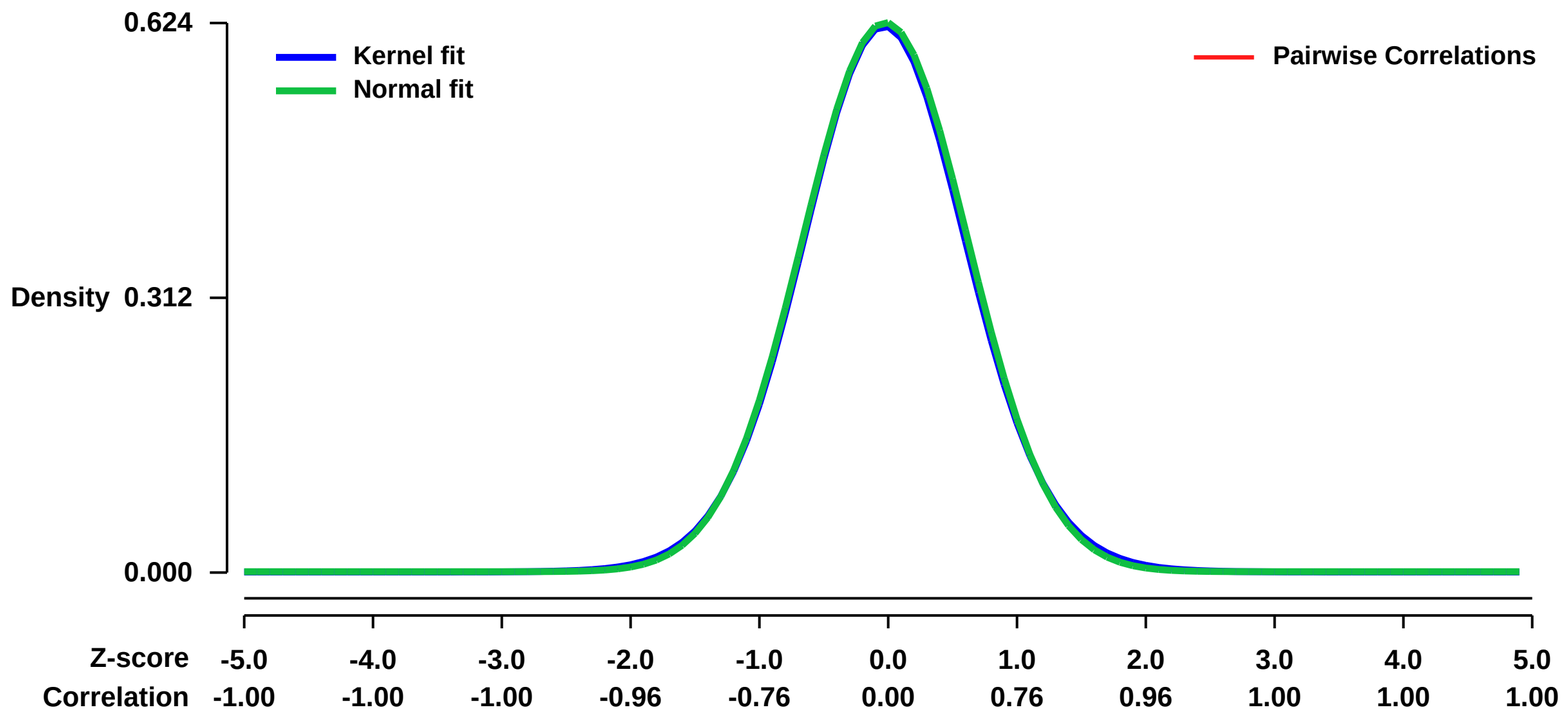

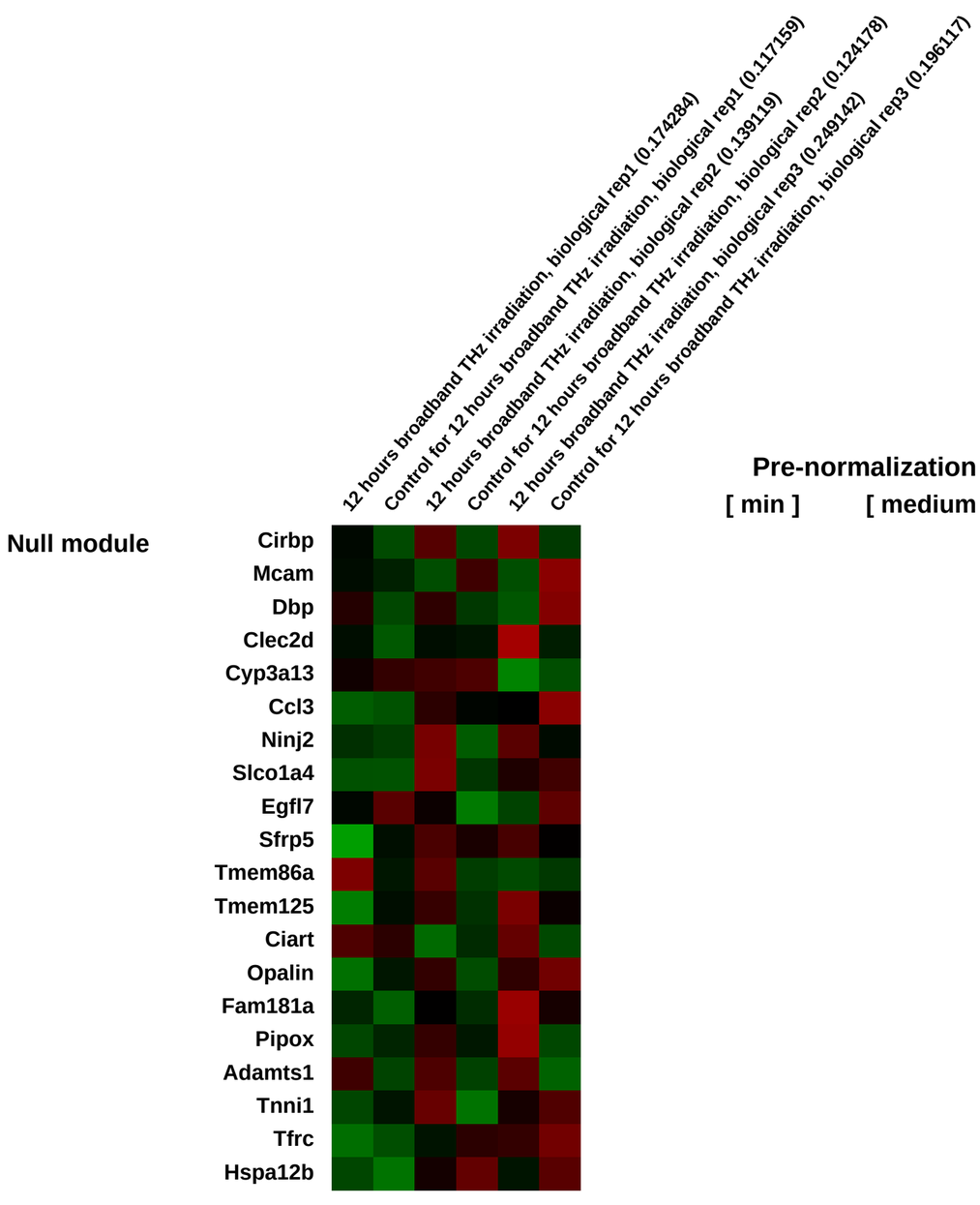

GEO Series "GSE41085" Expression Profiles

Num of samples in this series: 6

Scale of expression profile Z-scores

-3.0 -2.0 -1.0 0.0 1.0 2.0 3.0

GEO Link:	http://www.ncbi.nlm.nih.gov/geo/query/acc.cgi?acc=GSE41085
Status:	Public on Jul 01 2013
Title:	Expression data after irradiating mMSCs for 2 hours with single frequency terahertz laser source
Organism:	Mus musculus
Experiment type:	Expression profiling by array
Platform:	GPL1261
Pubmed ID:	23378916
Summary & Design:	**Summary:** We report that terahertz (THz) irradiation of mouse mesenchymal stem cells with a pulsed broadband (centered at 10 THz) source, or a single-frequency, 2.52 THz, (SF) laser source, both with weak average power (<1mW/cm2), results in specific heterogenic changes in gene expression. The insignificant differential expression of heat shock and stress related genes as well as our temperature measurements imply a non-thermal response. The microarray survey and RT-PCR experiments demonstrate that at different irradiation conditions distinct groups of genes are activated. Stem cells irradiated for 12 hours with the broadband THz source exhibit an accelerated differentiation toward adipose phenotype, while the 2-hour (broadband or SF) irradiation affects genes transcriptionally active in pluripotent stem cells. Phenotypic and gene expression differences suggest that the THz effect depends on irradiation parameters such as duration and type of THz source, and on the level of stem cell differentiation. Computer simulations of the core promoters of two pluripotency markers reveal association between gene upregulation and propensity for DNA breathing. We propose that THz radiation has potential for non-contact control of cellular gene expression. **Overall design:** Growing in petri dish mouse mesenchymal stem cell cultures are irradiated for 2 hours with a single-frequency (2.52 THz) CW laser source. Three independent biological experiments were conducted. In each experiment, a control mMSC culture was placed adjacent to the irradiated sample, and the temperature was kept at 26-27´"C for both the control and the irradiated sample. Immediately after completing the irradiation, total RNA was extracted from the irradiated sample and the control, and microarrays were used to identify differential changes in gene expression between the irradiated sample and its respective control. In each experiment, the mMSC cultures were synchronized to be at the same differentiation time point immediately before the irradiation.

Background corr dist: KL-Divergence = 0.0484, L1-Distance = 0.0181, L2-Distance = 0.0003, Normal std = 0.5774

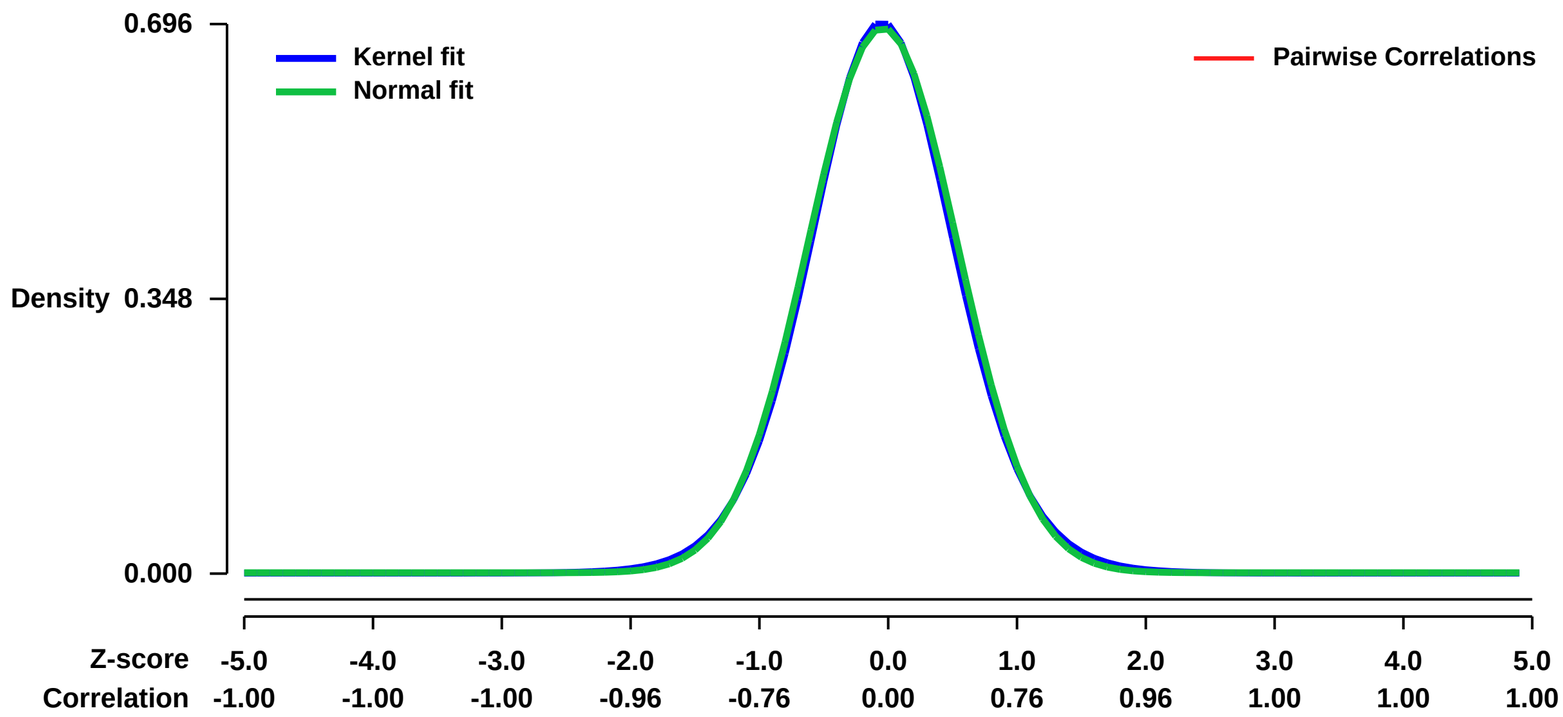

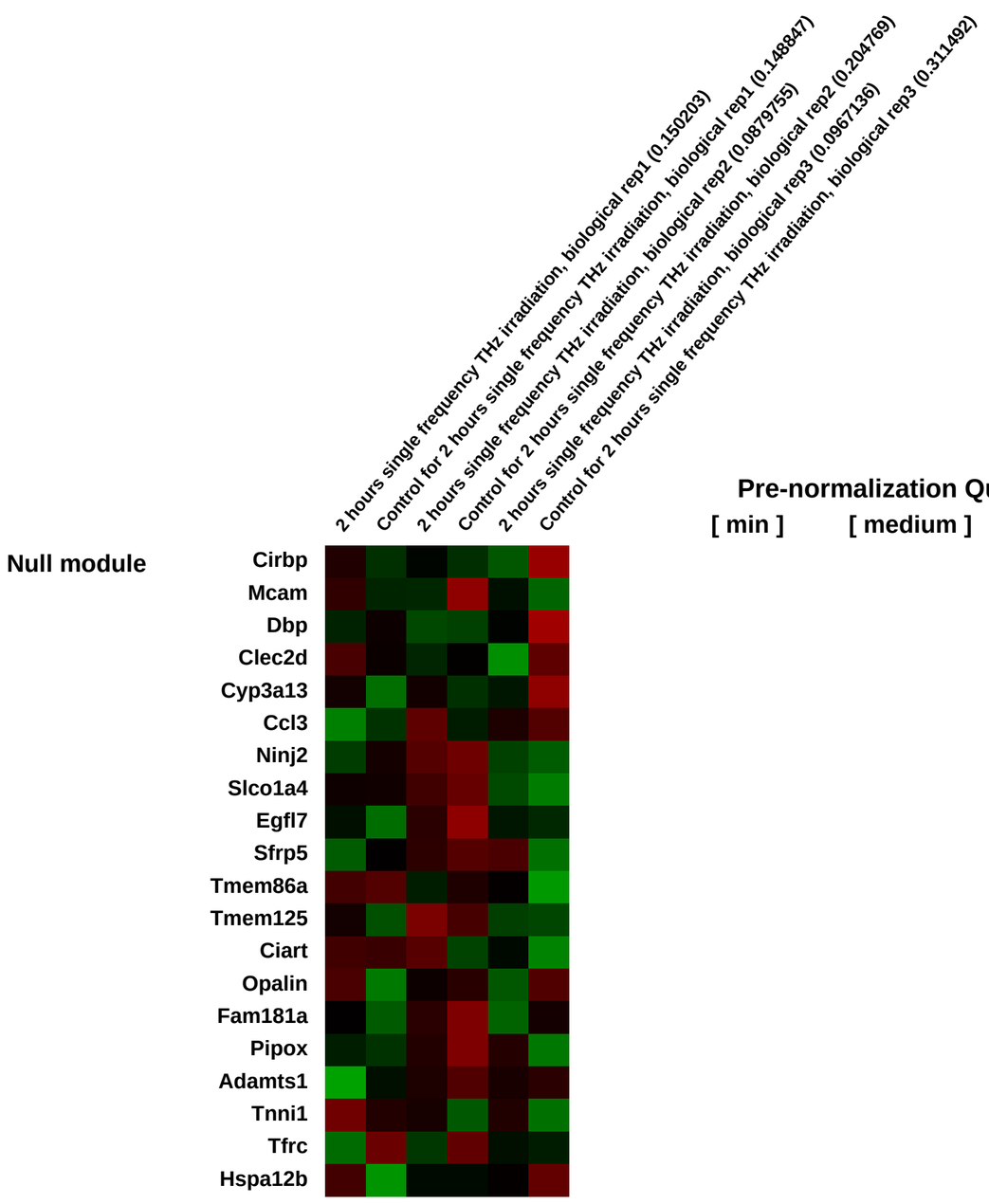

GEO Series "GSE41095" Expression Profiles

Num of samples in this series: 6

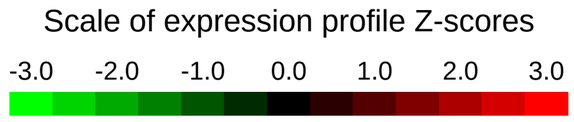

GEO Link:	**http://www.ncbi.nlm.nih.gov/geo/query/acc.cgi?acc=GSE41095**
Status:	**Public on Sep 25 2012**
Title:	**Maternal diabetes alters transcriptional programs in the developing embryo.**
Organism:	**Mus musculus**
Experiment type:	**Expression profiling by array**
Platform:	**GPL1261**
Pubmed ID:	**19538749**
Summary & Design:	**Summary:** **Exposure to maternal diabetes during pregnancy alters transcriptional profiles in the developing embryo. The enrichment, within the set of de-regulated genes, of those encoding transcriptional regulatory molecules provides support for the hypothesis that maternal diabetes affects specific developmental programs.** **We compared E10.5 cntrol embryos to E10.5 embryos from diabetic pregnancies in the FVB mouse strain.** **Overall design:** **Diabetes was induced in 7-9 week old female FVB mice by streptozotocin. Dams whose blood glucose levels exceeded 250 mg/dl were set up for mating. Embryos were dissected at E10.5 and total RNA was isolated. Equal amounts of RNA prepared from 3 individual embryos were pooled into one sample; each embryo was from a different pregnancy. Three pools were constructed for a total of nine embryos from diabetic pregnancies, and independently three pools for control embryos.**

Background corr dist: **KL-Divergence = 0.0201, L1-Distance = 0.0326, L2-Distance = 0.0011, Normal std = 0.7805**

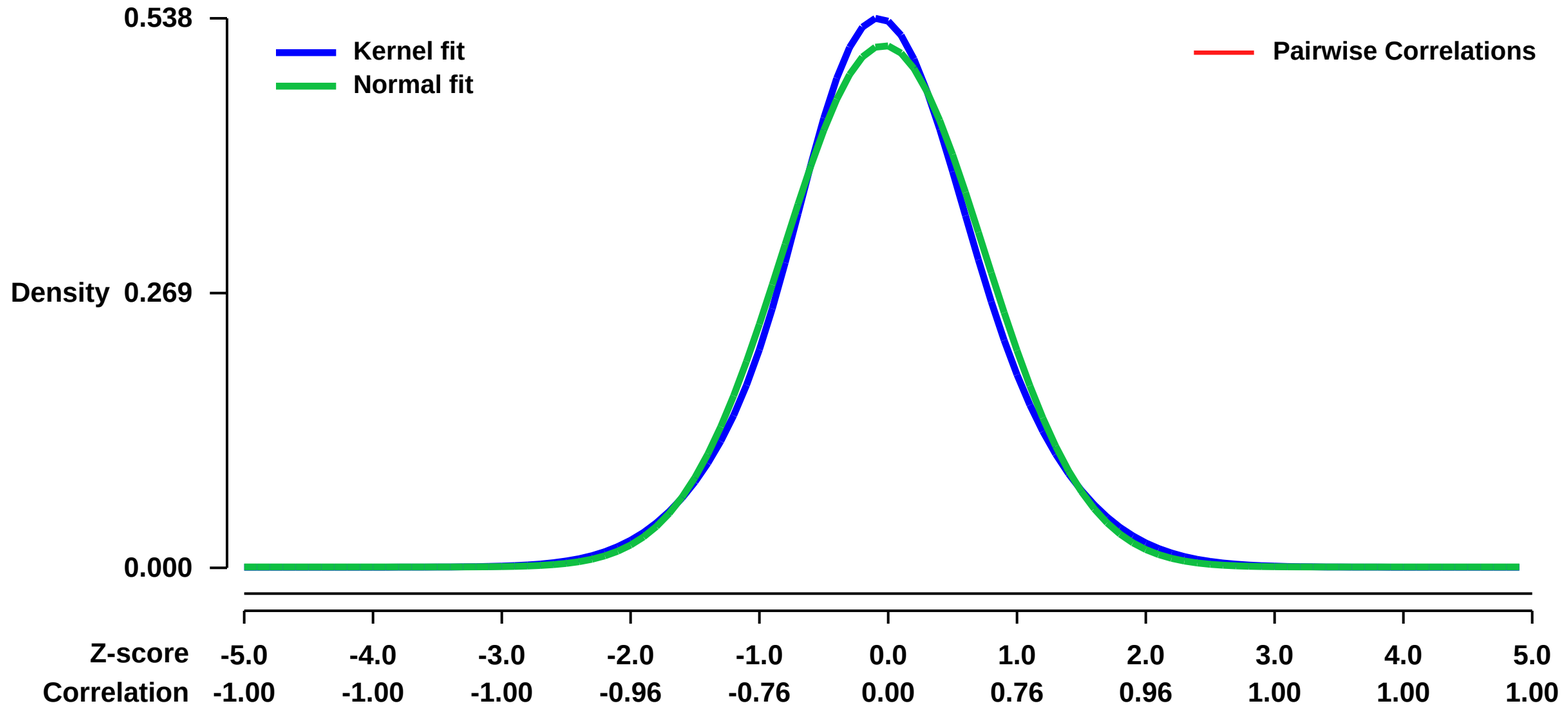

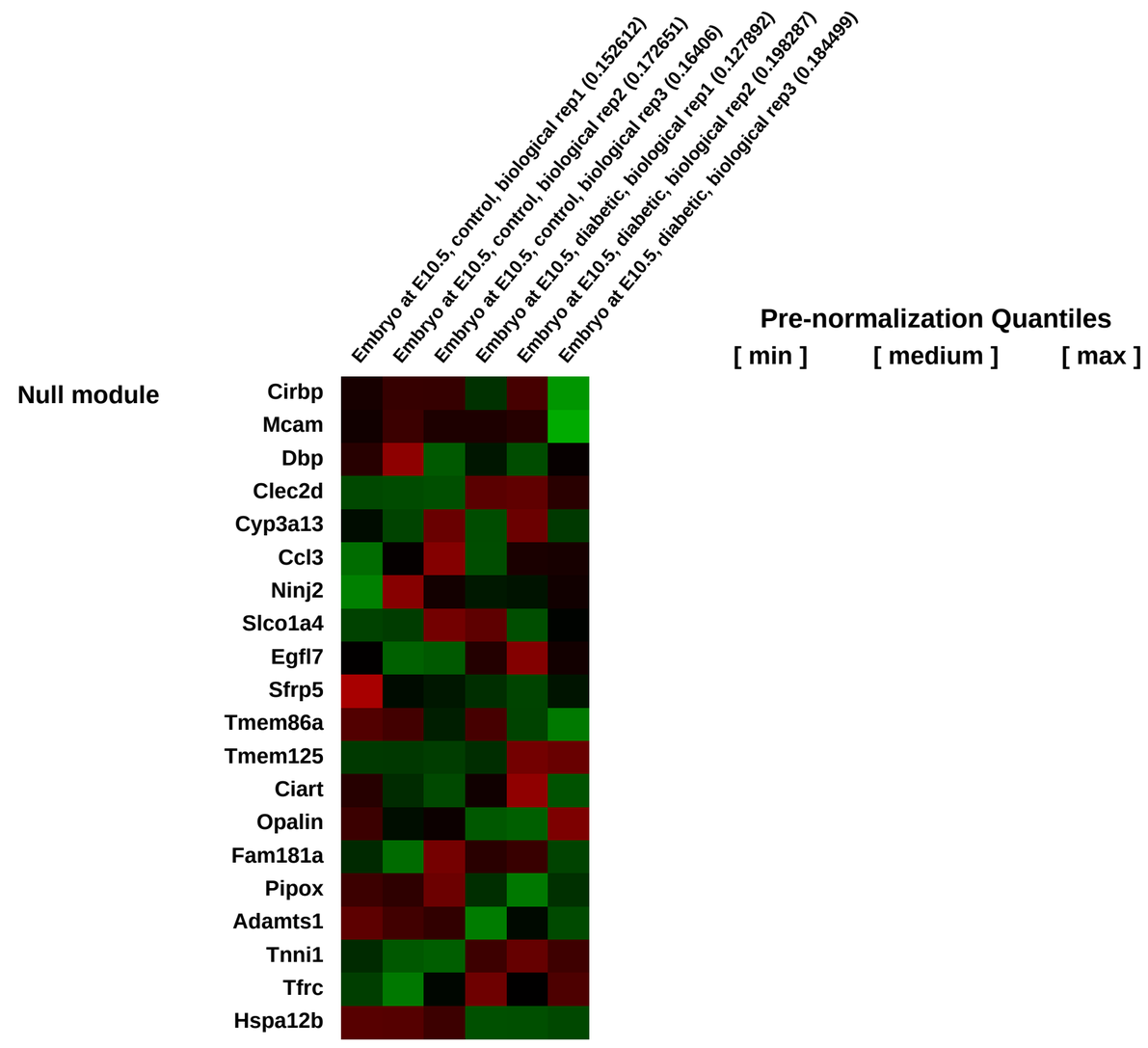

GEO Series "GSE41185" Expression Profiles

Num of samples in this series: 8

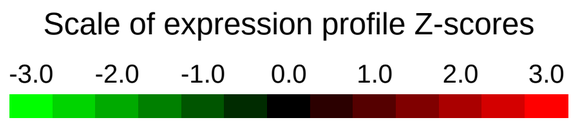

GEO Link:	**http://www.ncbi.nlm.nih.gov/geo/query/acc.cgi?acc=GSE41185**
Status:	**Public on Sep 06 2013**
Title:	**Potentiation of regulatory T cell stability and function via a neuropilin-1:semaphorin-4a axis**
Organism:	**Mus musculus**
Experiment type:	**Expression profiling by array**
Platform:	**GPL1261**
Pubmed ID:	**23913274**
Summary & Design:	**Summary:** **Regulatory T cells (Treg) represent a critical immunoregulatory component of the immune system. The signals that maintain Treg stability and potentiate their function remain obscure. Here we show that the immune cell surface ligand semaphorin-4a (Sema4a)** **Overall design:** **Sema treated and NRP1 knock outs were compared to untreated wild type T cell controls**

Background corr dist: **KL-Divergence = 0.0434, L1-Distance = 0.0294, L2-Distance = 0.0015, Normal std = 0.5876**

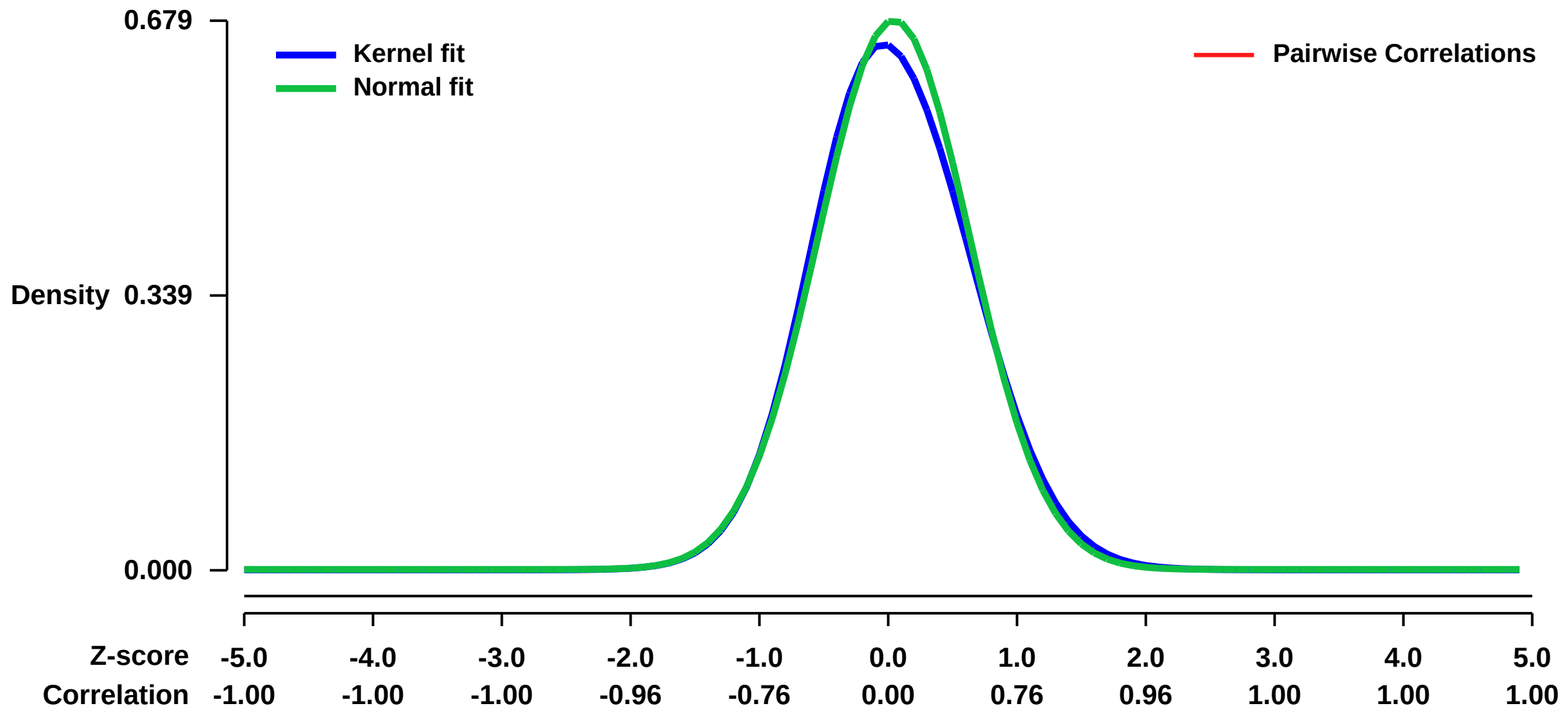

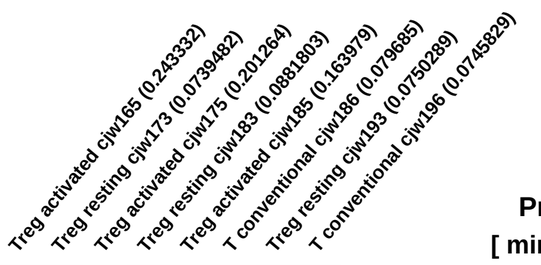

Pre-normalization Quantiles

[min] [medium] [max]

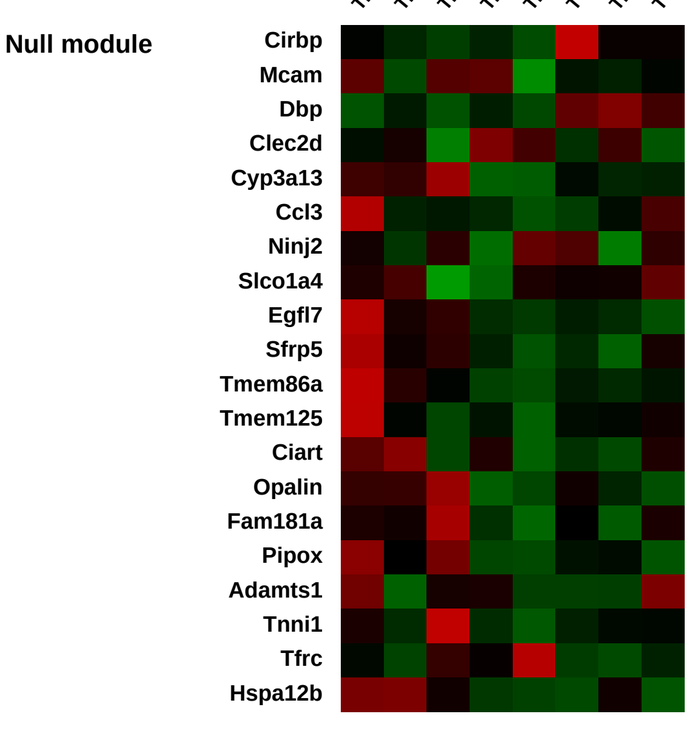

GEO Series "GSE41260" Expression Profiles

Num of samples in this series: 6

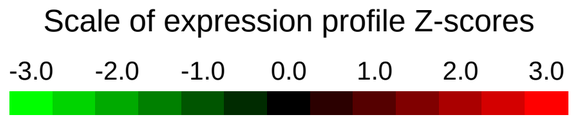

GEO Link:	http://www.ncbi.nlm.nih.gov/geo/query/acc.cgi?acc=GSE41260
Status:	Public on Oct 02 2012
Title:	Expression Profiles of E11.5 Mouse Optic Fissure
Organism:	Mus musculus
Experiment type:	Expression profiling by array
Platform:	GPL1261
Pubmed ID:	23147794
Summary & Design:	**Summary:** Mice that are mutant for both Fgfr1 and Fgfr2 specifically in the developing retina develop coloboma. To analyze the transcripts that are affected by defective FGF signaling, we micro-dissected the optic fissure region from the control and FGFR condtional mutant mice and did microarray analysis. **Overall design:** E11.5 control and Six3Cre+; Fgfr1fx/fx;Fgfr2 fx/fx optic fissures are dissected using laser-assisted micro-dissection microscope, RNAs are extracted and labelled and hybridyzed to chips

Background corr dist: KL-Divergence = 0.0386, L1-Distance = 0.0255, L2-Distance = 0.0007, Normal std = 0.6295

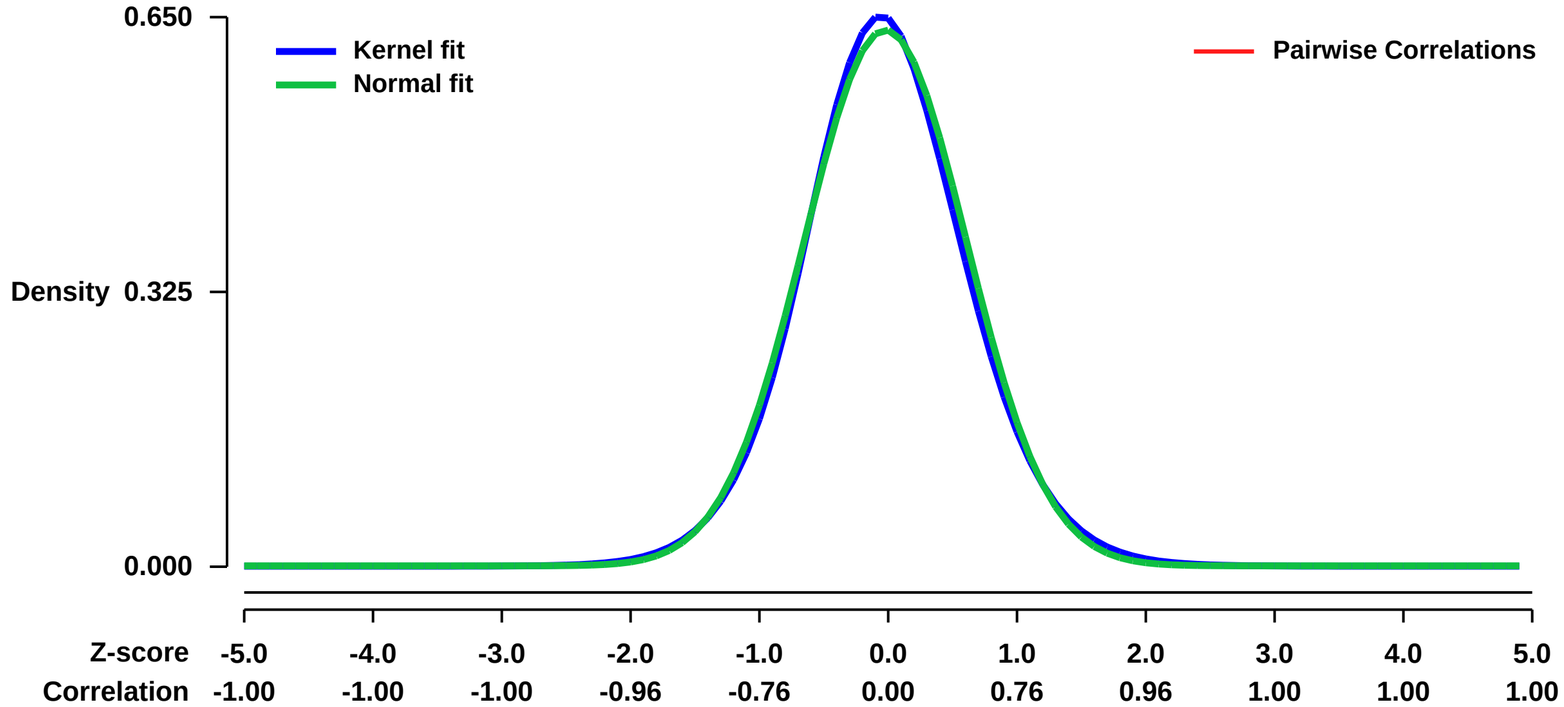

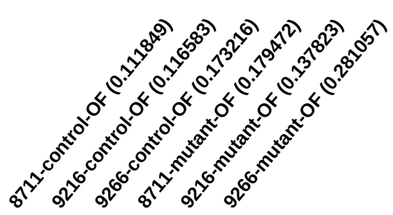

Pre-normalization Quantiles

[min] [medium] [max]

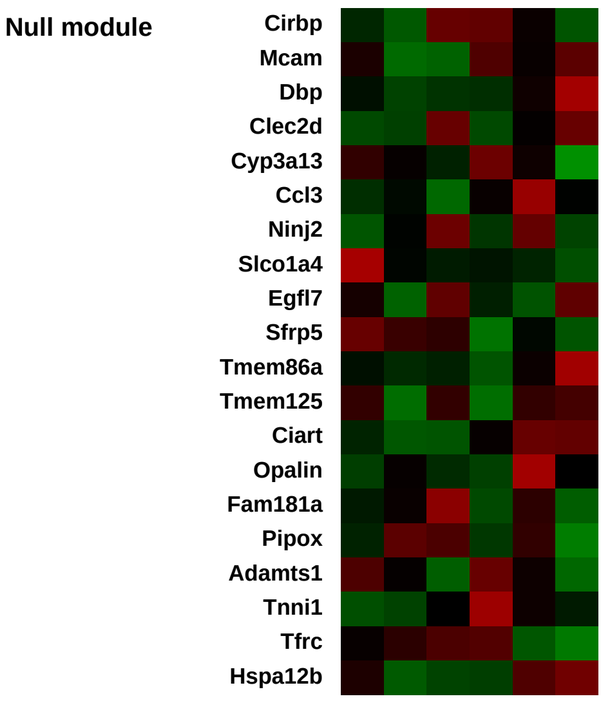

GEO Series "GSE41307" Expression Profiles

Num of samples in this series: 8

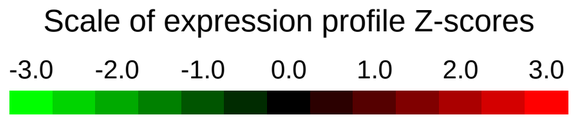

GEO Link:	**http://www.ncbi.nlm.nih.gov/geo/query/acc.cgi?acc=GSE41307**
Status:	**Public on Aug 13 2013**
Title:	**Gene expression microarray analysis on hippocampus of Schnurri-2 knockout and wild-type control mice**
Organism:	**Mus musculus**
Experiment type:	**Expression profiling by array**
Platform:	**GPL1261**
Pubmed ID:	**23389689**
Summary & Design:	**Summary:** **Schnurri-2 (Shn-2), an NF-kappa B site-binding protein, tightly binds to the enhancers of major histocompatibility complex (MHC) class I genes and inflammatory cytokines, which have been shown to harbor common variant single nucleotide polymorphisms associated with schizophrenia. Shn-2 knockout mice show behavioral abnormalities that strongly resemble those of schizophrenics. We performed gene expression microarray analysis of hippocampi from Shn-2 knockout and wild-type control mice.** **Overall design:** **Hippocampal RNA isolated from four Shn-2 knockout and four control wild-type mice were compared.**

Background corr dist: **KL-Divergence = 0.0637, L1-Distance = 0.0203, L2-Distance = 0.0005, Normal std = 0.5131**

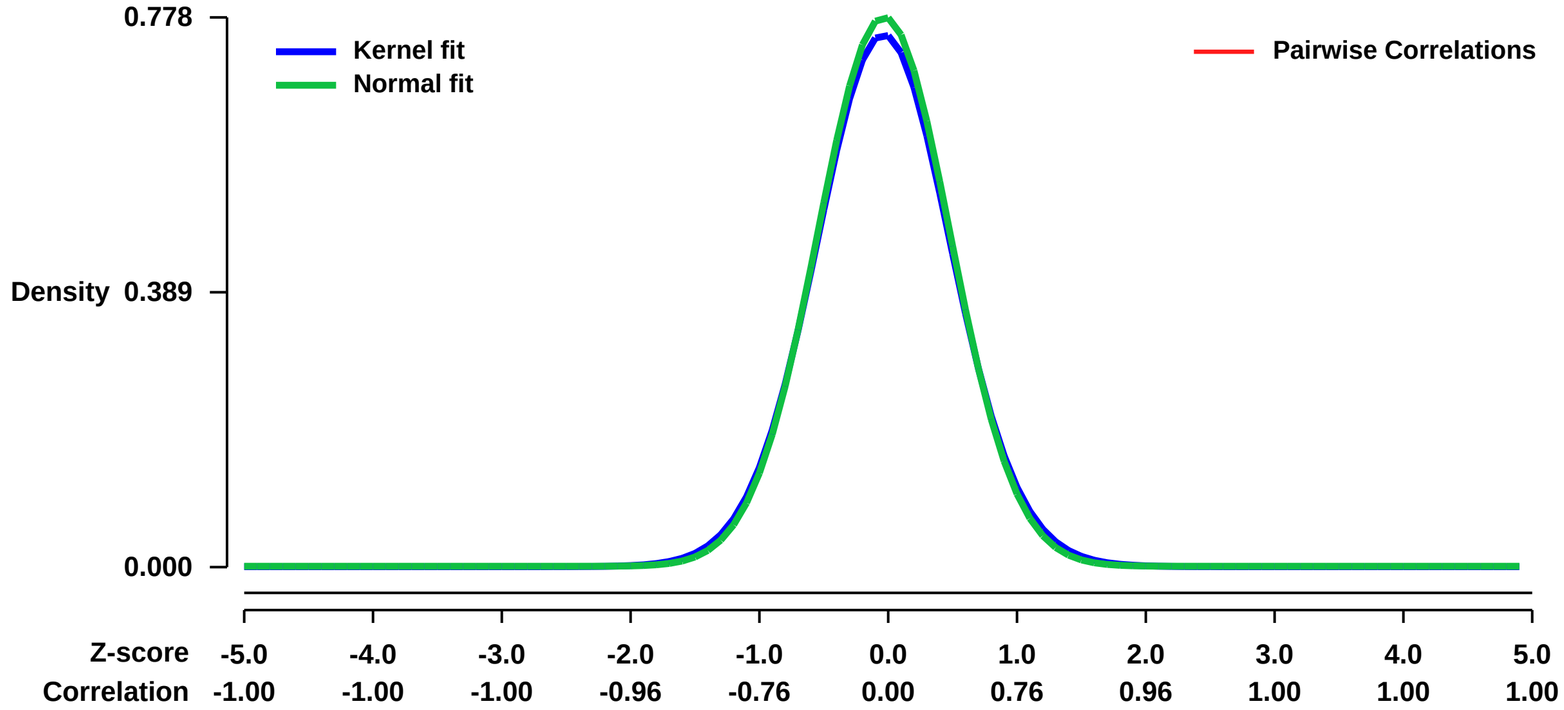

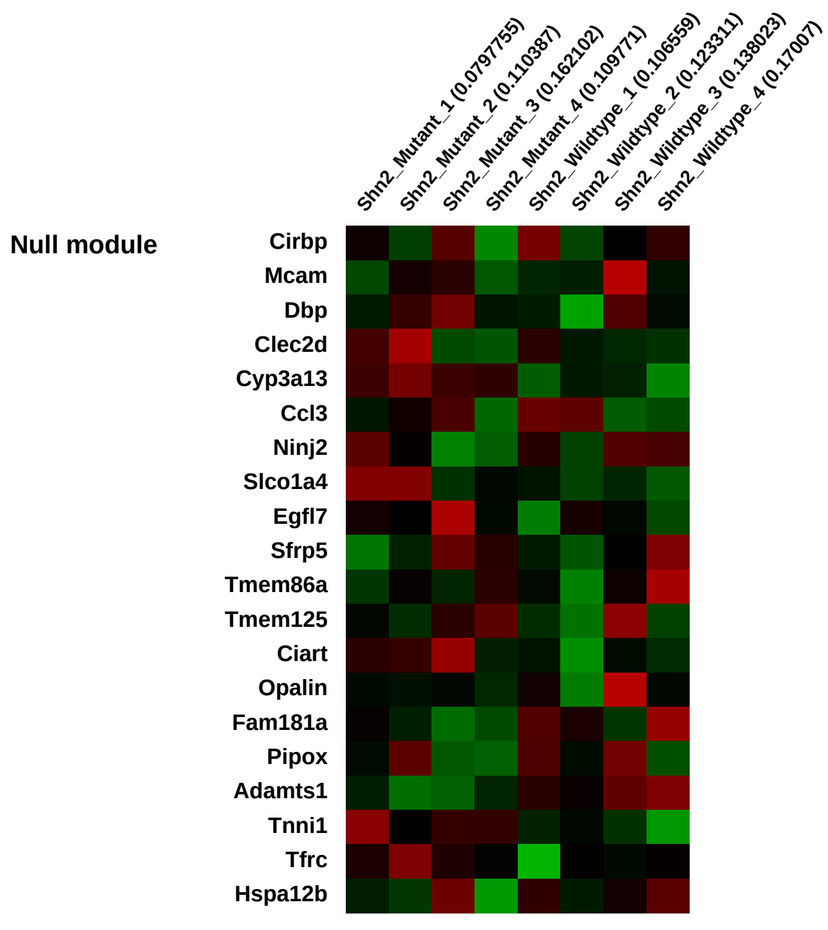

GEO Series "GSE41342" Expression Profiles

Num of samples in this series: 26

Scale of expression profile Z-scores

-3.0 -2.0 -1.0 0.0 1.0 2.0 3.0

GEO Link:	http://www.ncbi.nlm.nih.gov/geo/query/acc.cgi?acc=GSE41342
Status:	Public on Nov 01 2012
Title:	Data from a time course study of gene expression in a mouse model of osteoarthritis
Organism:	Mus musculus
Experiment type:	Expression profiling by array
Platform:	GPL1261
Pubmed ID:	23382930
Summary & Design:	**Summary:** The purpose of this study was to characterize the histologic development of OA in a mouse model where OA is induced by destabilization of the medial meniscus (DMM model) and to identify genes regulated during different stages of the disease, using RNA isolated from the joint â organâ and analyzed using microarrays.427 genes from the microarrays passed consistency and significance filters. There was an initial up-regulation at 2 and 4 weeks of genes involved in morphogenesis, differentiation, and development, including growth factor and matrix genes, as well as transcription factors including Atf2, Creb3l1, and Erg. Most genes were off or down-regulated at 8 weeks with the most highly down-regulated genes involved in cell division and the cytoskeleton. Gene expression increased at 16 weeks, in particular extracellular matrix genes including Prelp, Col3a1 and fibromodulin.The results support a phasic development of OA with early matrix remodelling and transcriptional activity followed by a more quiescent period that is not maintained. **Overall design:** RNA was pooled prior to microarray analysis such that 3 randomly selected samples from each surgical group and time point were pooled to create each biological replicate. Because 9 mice were used for each experimental group, a total of three biological replicates per group were analyzed using the Affymetrix Mouse Genome 430 2.0 oligonucleotide arrays as described. One replicate pool, which was from week two DMM mice, did not meet the RNA integrity level needed for microarray analysis; thus, this pool was not analyzed further, leaving two pools for the week two DMM mice.

Background corr dist: KL-Divergence = 0.1052, L1-Distance = 0.0242, L2-Distance = 0.0007, Normal std = 0.4325

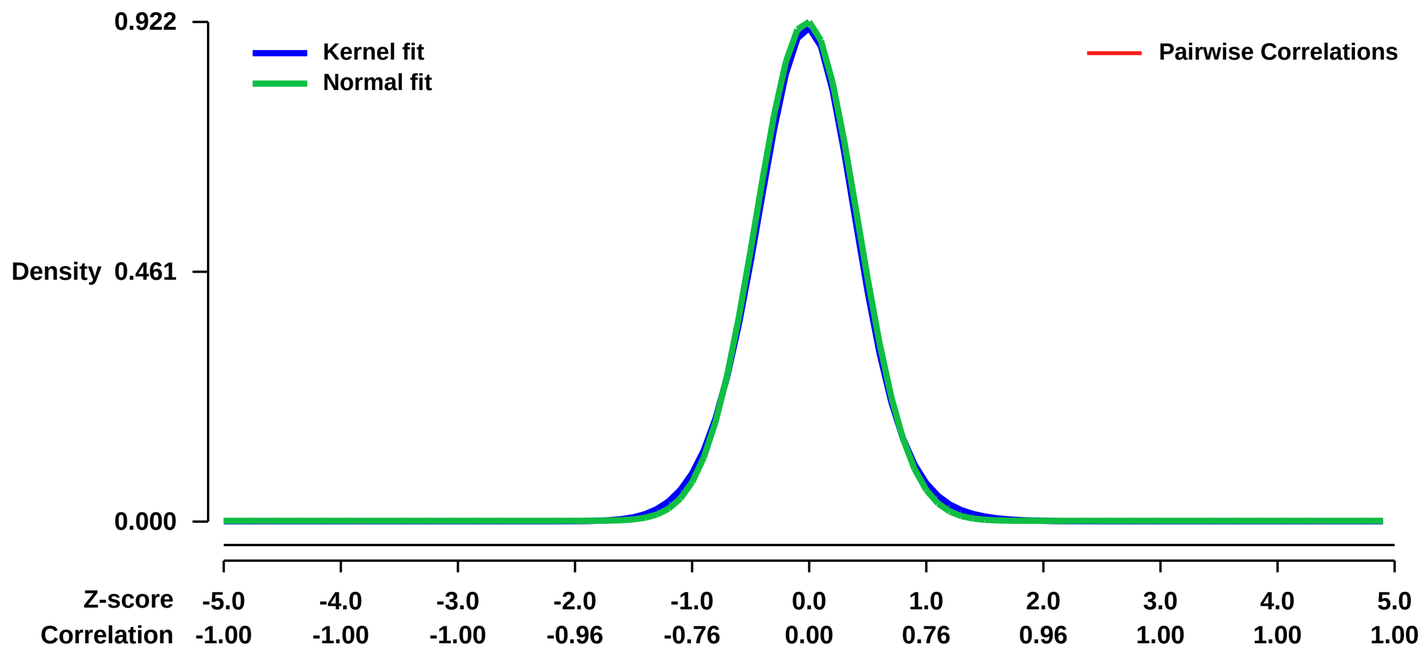

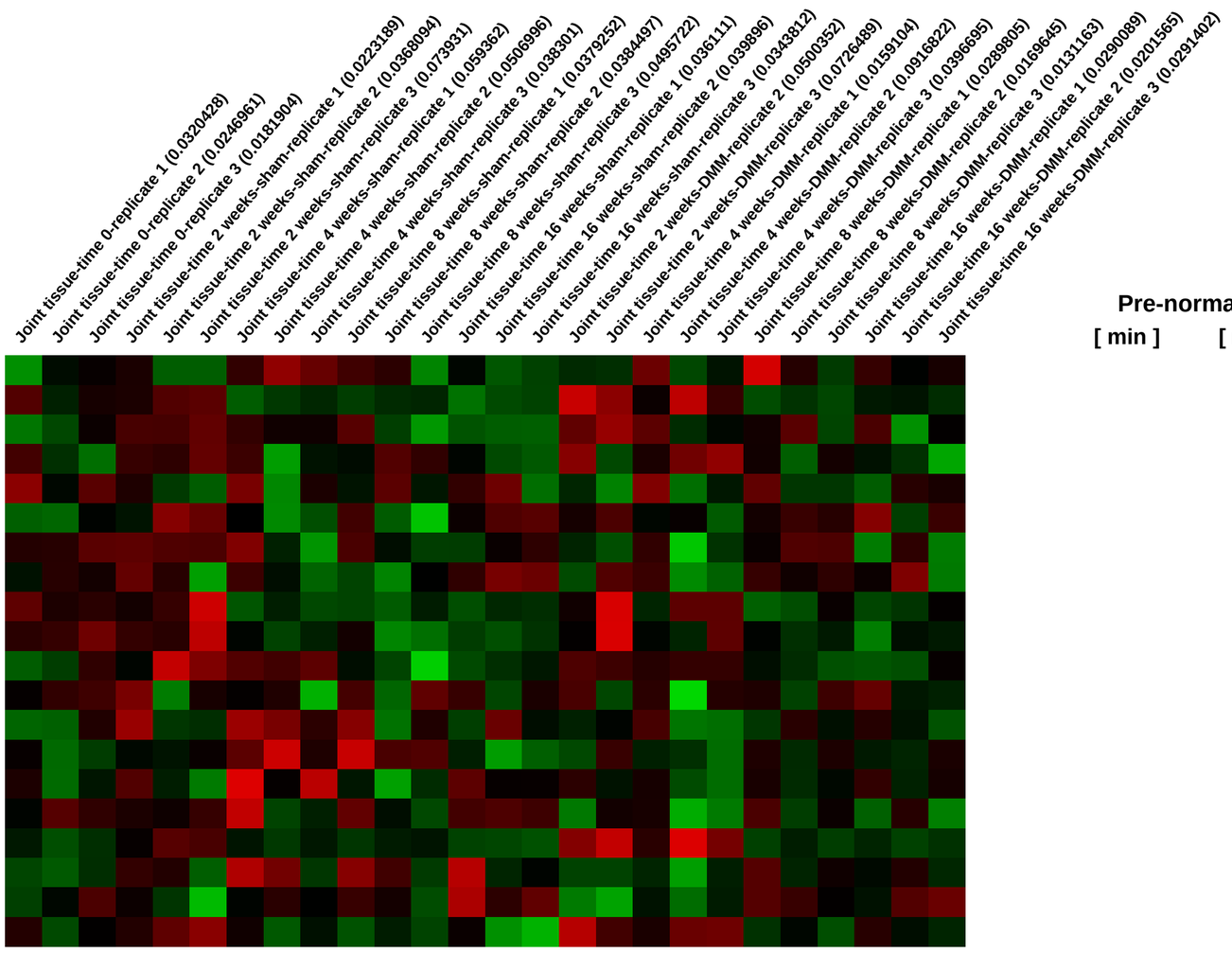

GEO Series "GSE41558" Expression Profiles

Num of samples in this series: 8

Scale of expression profile Z-scores

-3.0 -2.0 -1.0 0.0 1.0 2.0 3.0

GEO Link:	http://www.ncbi.nlm.nih.gov/geo/query/acc.cgi?acc=GSE41558
Status:	Public on Oct 13 2012
Title:	SRC-2 Coactivator Deficiency Decreases Functional Reserve in Response to Pressure Overload of Mouse Heart
Organism:	Mus musculus
Experiment type:	Expression profiling by array
Platform:	GPL1261
Pubmed ID:	23300926
Summary & Design:	**Summary:** A major component of the cardiac stress response is the simultaneous activation of several gene regulatory networks. Interestingly, the transcriptional regulator steroid receptor coactivator-2, SRC-2 is often decreased during cardiac failure in humans. We postulated that SRC-2 suppression plays a mechanistic role in the stress response and that SRC-2 activity is an important regulator of the adult heart gene expression profile. Genome-wide microarray analysis, confirmed with targeted gene expression analyses revealed that genetic ablation of SRC-2 activates the â fetal gene programâ in adult mice as manifested by shifts in expression of a) metabolic and b) sarcomeric genes, as well as associated modulating transcription factors. While these gene expression changes were not accompanied by changes in left ventricular weight or cardiac function, imposition of transverse aortic constriction (TAC) predisposed SRC-2 knockout (KO) mice to stress-induced cardiac dysfunction. In addition, SRC-2 KO mice lacked the normal ventricular hypertrophic response as indicated through heart weight, left ventricular wall thickness, and blunted molecular signaling known to activate hypertrophy. Our results indicate that SRC-2 is involved in maintenance of the steady-state adult heart transcriptional profile, with its ablation inducing transcriptional changes that mimic a stressed heart. These results further suggest that SRC-2 deletion interferes with the timing and integration needed to respond efficiently to stress through disruption of metabolic and sarcomeric gene expression and hypertrophic signaling, the three key stress responsive pathways. **Overall design:** For microarray analysis, 250ng of RNA isolated from total heart (RNeasy kit, Qiagen) for each sample was labeled using the new standard Affymetrix linear amplification protocol using the 3' IVT Express Kit. This was reverse-transcribed and cRNA was produced and biotinylated via in vitro transcription. A hybridization cocktail containing Affymetrix spike-in controls and 15 ¸…g fragmented, labeled cRNA was loaded onto a GeneChip´fi Mouse 430 2.0 array. The array was hybridized for 16 hours at 45´ºC with rotation at 60 rpm then washed and stained with a strepavidin, R-phycoerythrin conjugate stain using the FS 450_0001 Fluidics protocol setting. Signal amplification was done using biotinylated antistreptavidin. The stained array was scanned on the Affymetrix GeneChip´fi Scanner 3000. The images were analyzed and quality control metrics recorded using Affymetrix Command Console v3. Experiments were run using Affymetrix MG 430 2.0 chip with 45,101 probesets representing 20,757 unique genes. There were 8 experiments in 2 groups: WT-unstressed â 4 experiments, and KO-unstressed â 4 experiments. QC parameters for all experiments were within the acceptable limits. We used the following software packages for data QC, statistical analysis and presentation of the results: Affymetrix Expression Console (www.affymetrix.com), Partek (www.partek.com), BRB Array Tools (linus.nci.nih.gov/BRB-ArrayTools.html), and dChip (biosun1.harvard.edu/complab/dchip). Expressions were estimated using the RMA (Multi-Array Analysis) method [38] with Partek software. Differentially expressed genes were found using the RVM (Random Variance Model) t-test, which is designed for small sample size experiments [39]. We used BRB Array Tools software, developed by Dr. Richard Simon and the BRB-ArrayTools Development Team. All genes were included in the comparison. For the genes represented by more than one probeset, we used the most highly expressed probeset. The cutoffs for differentially expressed genes were False Discovery Rate (FDR) = 0.05 [40].

Background corr dist: KL-Divergence = 0.0856, L1-Distance = 0.0220, L2-Distance = 0.0008, Normal std = 0.4644

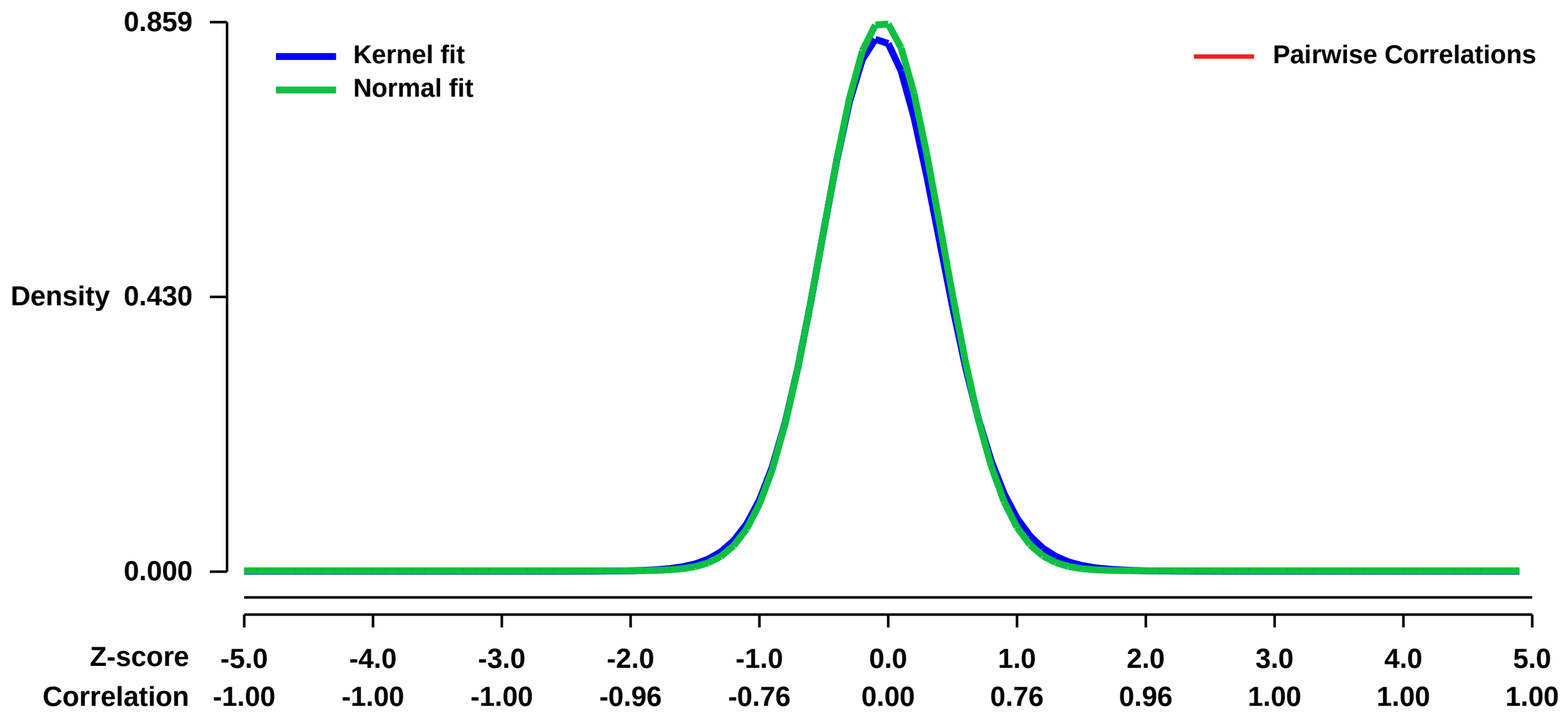

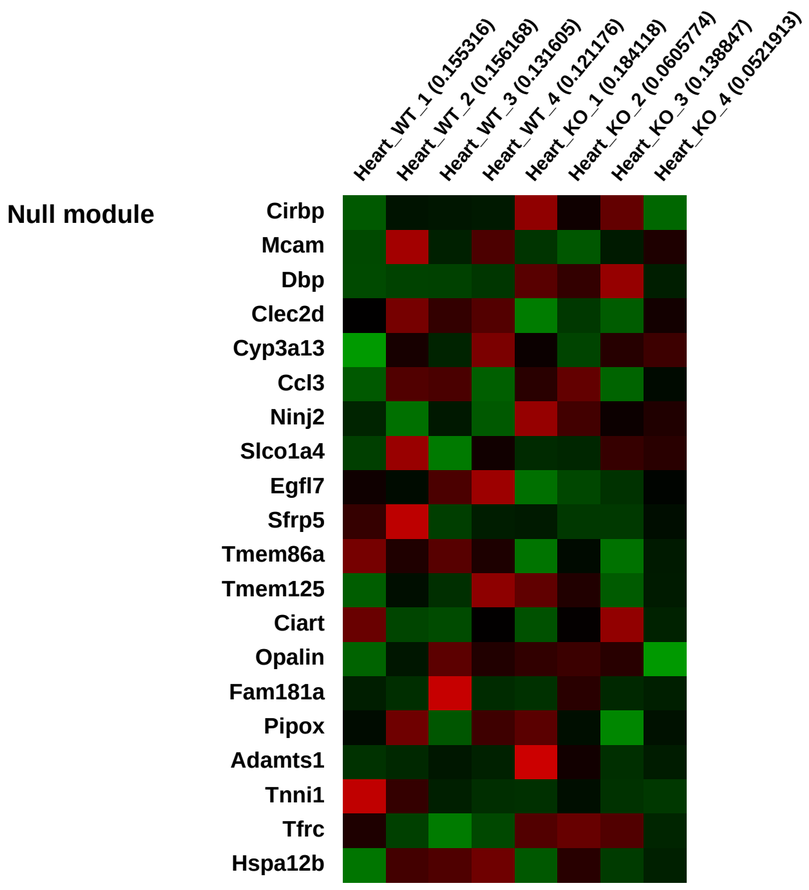

GEO Series "GSE41706" Expression Profiles

Num of samples in this series: 6

Scale of expression profile Z-scores

-3.0 -2.0 -1.0 0.0 1.0 2.0 3.0

GEO Link:	http://www.ncbi.nlm.nih.gov/geo/query/acc.cgi?acc=GSE41706
Status:	Public on Oct 20 2012
Title:	Expression data from adult (9 month-old) hearts from GRK2 heterozygous C57BL/6J mice and its wild type littermates
Organism:	Mus musculus
Experiment type:	Expression profiling by array
Platform:	GPL1261
Pubmed ID:	
Summary & Design:	**Summary:** G protein-coupled receptor kinase 2 (GRK2) has emerged as a key regulator of cardiac function and myocardial structure. Cardiac GRK2 is increased in heart failure and ischemia in humans, whereas genetic inhibition of GRK2 is cardioprotective in animal models of these pathologies. However, the mechanistic basis underlying these effects are not fully understood. We have used adult GRK2 hemizygous mice (GRK2+/-) as a model to assess the effects of a sustained systemic inhibition of GRK2 in heart tissue with age. We used microarrays to determine the global programme of gene expression underlying cardioprotection in GRK2 hemizygous mice. **Overall design:** 9 month-old mice hearts were collected for RNA extraction and hybridization on Affymetrix microarrays.

Background corr dist: KL-Divergence = 0.0396, L1-Distance = 0.0137, L2-Distance = 0.0002, Normal std = 0.6109

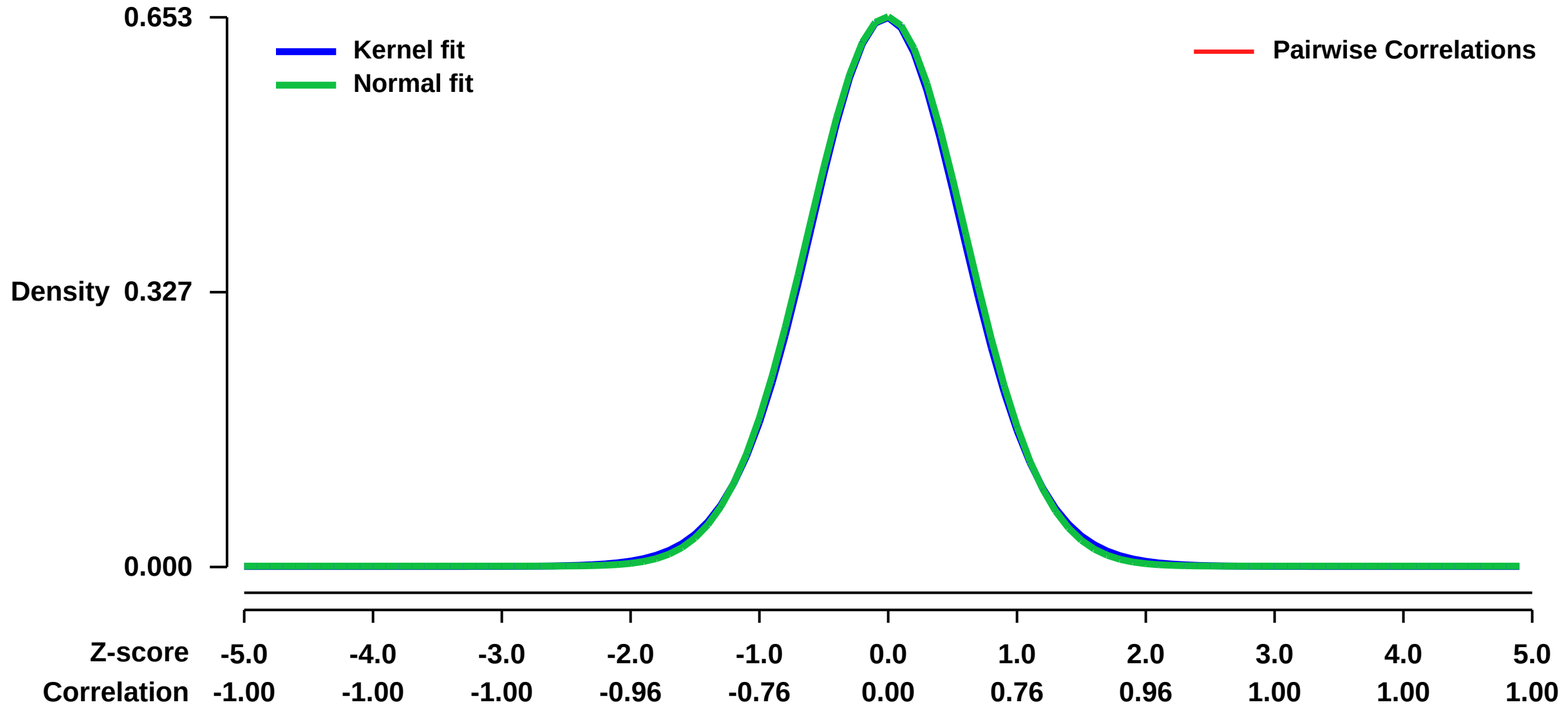

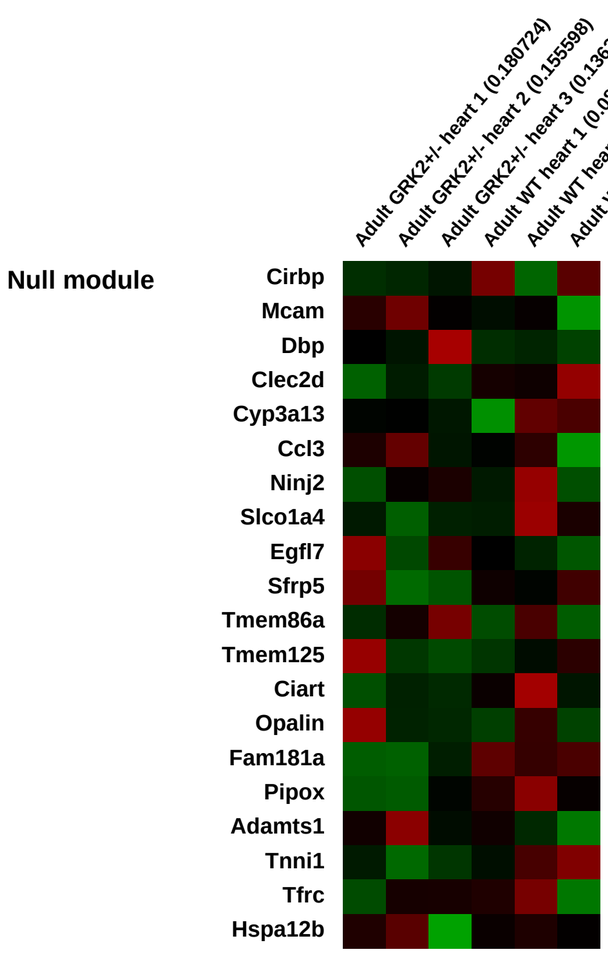

GEO Series "GSE41746" Expression Profiles

Num of samples in this series: 18

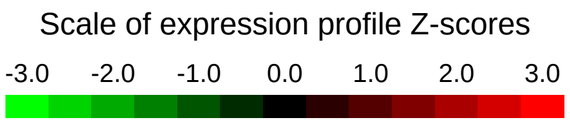

GEO Link:	**http://www.ncbi.nlm.nih.gov/geo/query/acc.cgi?acc=GSE41746**
Status:	**Public on Oct 23 2012**
Title:	**Comparative expression data of PD21 Pik3cd+/- and Pik3cd-/- female mice ovaries responsed to exogenous gonadotropins.**
Organism:	**Mus musculus**
Experiment type:	**Expression profiling by array**
Platform:	**GPL1261**
Pubmed ID:	
Summary & Design:	**Summary:** **The Pik3cd null females are subfertile and have less growing follicles than their heterozygous littermates in the ovary. These mice poorly respond to the exogenous gonadotropins and ovulate much less oocytes than controls. In addition, the estrodial stimulated GC proliferation in preantral follicles is also impaired in Pik3cd null ovaries. FSH and E2 dramatically activates PI3K/AKT pathway in GCs of wild type mice, but not in the Pik3cd null mice.** **we used microarray to identify those genes regulated by Pik3cd in response to PMSG (Pregnant Mare Serum Gonadotropin) and E2 treatment in ovary.** **Overall design:** **We set 3 treatment groups of both Pik3cd+/- and Pik3cd-/- female mice, including PD21 untreatment, PD21 after PMSG administration for 44 hours, PD21 after E2 administration for 72 hours, each group contained three biological repeats. The genes up/down-regulated significantly (not less than 2 fold change) in Pik3cd+/- mice after PMSG and E2 treatment were listed out as PMSG or E2 target genes, in which, those had not the same change trends in Pik3cd-/- were considered as Pik3cd-dependent genes.**

Background corr dist: **KL-Divergence = 0.1591, L1-Distance = 0.0396, L2-Distance = 0.0032, Normal std = 0.3654**

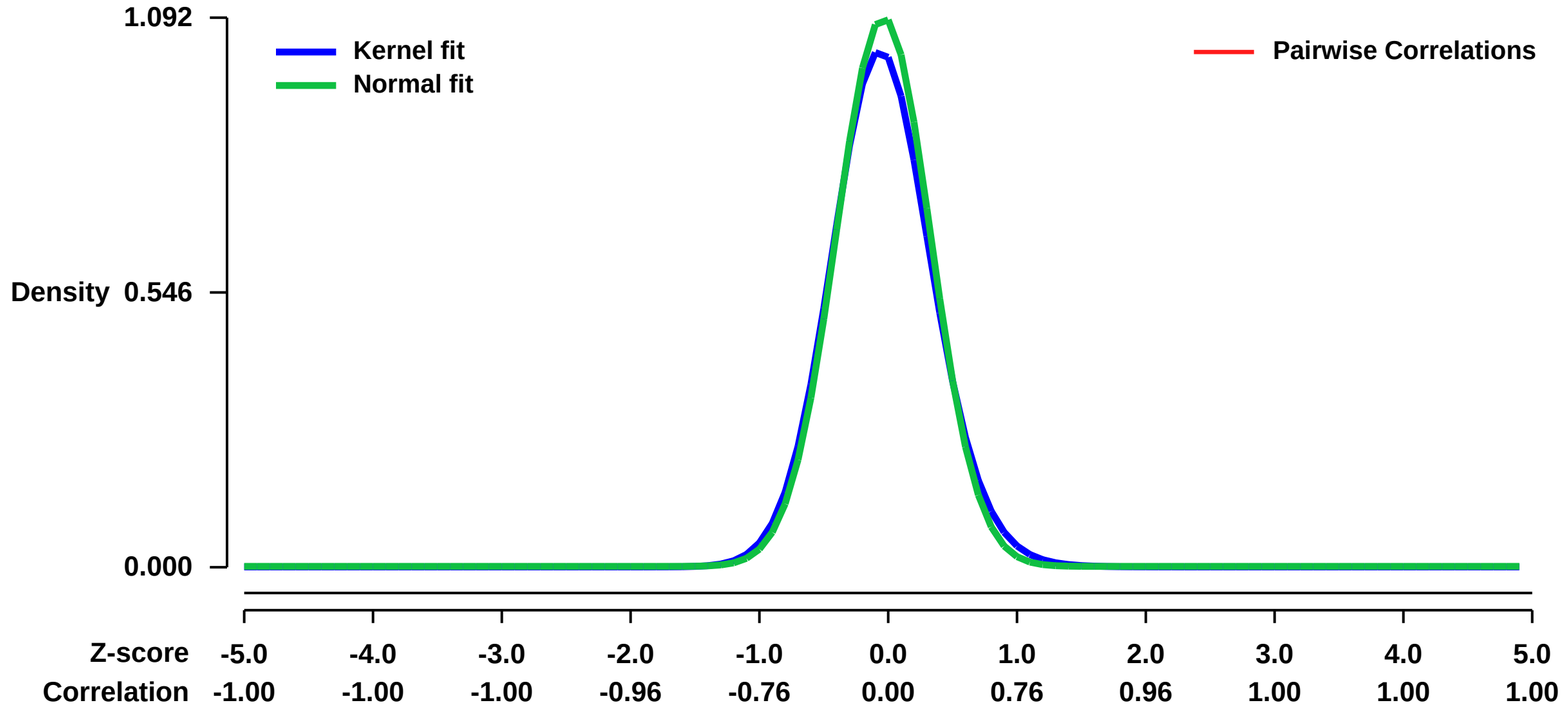

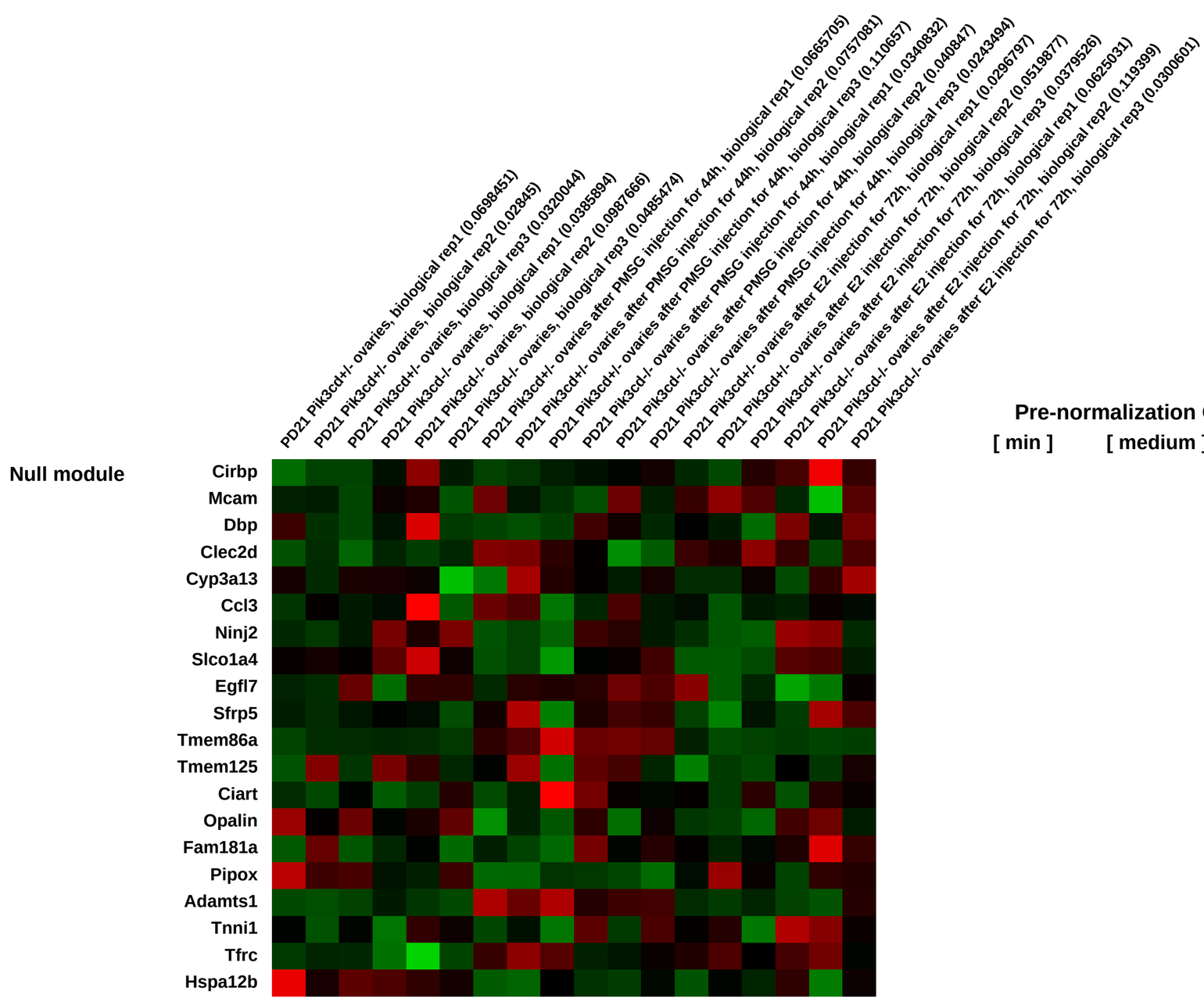

GEO Series "GSE41789" Expression Profiles

Num of samples in this series: 45

Scale of expression profile Z-scores

-3.0 -2.0 -1.0 0.0 1.0 2.0 3.0

GEO Link:	http://www.ncbi.nlm.nih.gov/geo/query/acc.cgi?acc=GSE41789
Status:	Public on Nov 01 2013
Title:	Senescence gene signature of radiation fibrosis
Organism:	Mus musculus
Experiment type:	Expression profiling by array
Platform:	GPL1261
Pubmed ID:	24052614
Summary & Design:	**Summary:** Radiation lung injury is characterized by early inflammation and late fibrosis. The causes underlying the chronic, progressive nature of radiation injury are poorly understood. Here, we report that the gene expression of irradiated lung tissue correlates with that observed in the lungs in aged animals. We demonstrate that NOX4 expression and superoxide elaboration is increased in irradiated lungs and pneumocytes in a dose dependent fashion. We used microarrays to detail the global programme of gene expression and report that irradiated lung tissue correlates with that observed in the lungs in aged animals. **Overall design:** Female C57Bl/Ncr mice, aged 10 weeks were treated with/ without radiation to the thorax with a X-RAD 320 x-ray irradiator at a dose rate of 2.61 Gy/minute. An age-matched cohort of mice received no IR while additional cohorts received 5 Gy in a single dose, 17.5 Gy in a single dose. RNA was extracted and hybridization done on Affymetrix Mouse430_2 microarrays.

Background corr dist: KL-Divergence = 0.2852, L1-Distance = 0.0589, L2-Distance = 0.0090, Normal std = 0.2862

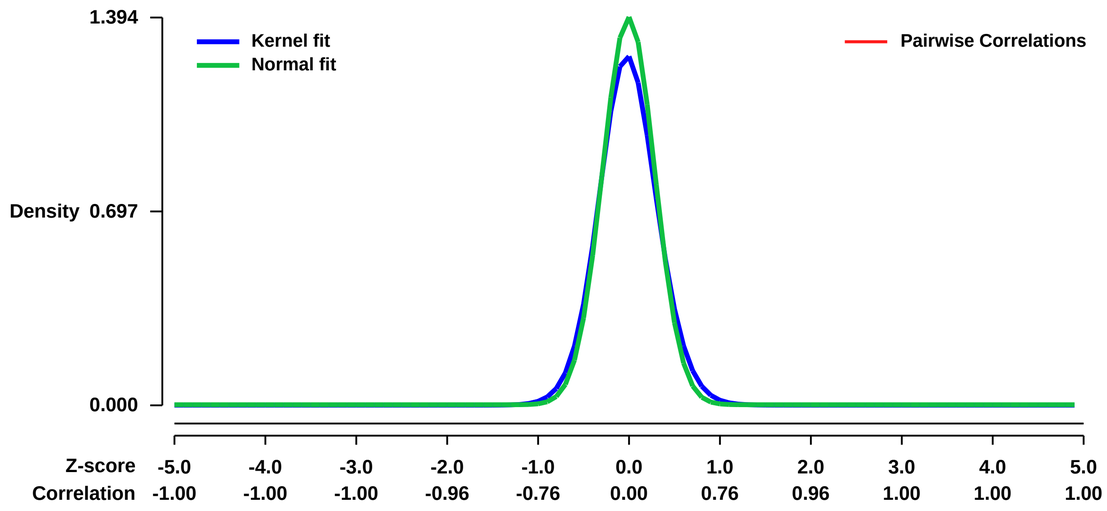

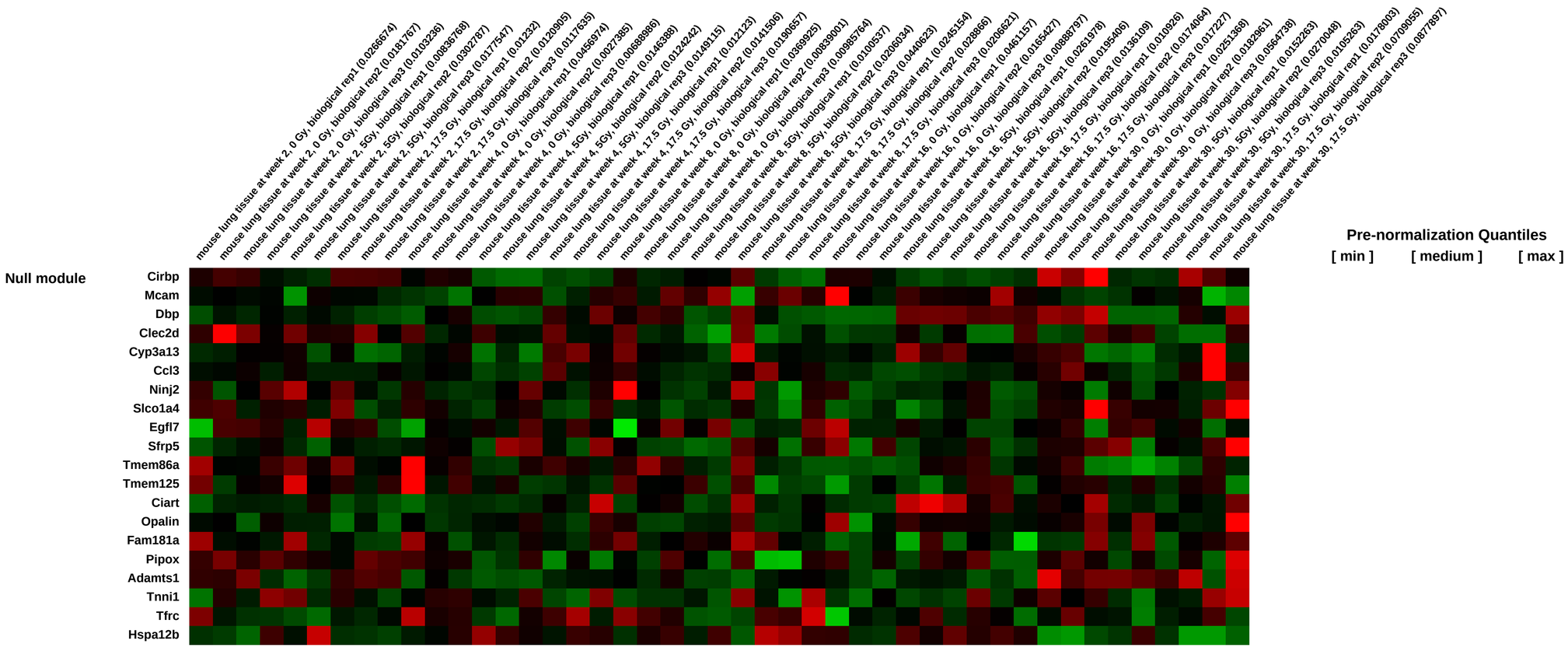

GEO Series "GSE41807" Expression Profiles

Num of samples in this series: 6

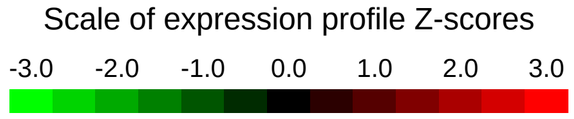

GEO Link:	**http://www.ncbi.nlm.nih.gov/geo/query/acc.cgi?acc=GSE41807**
Status:	**Public on Oct 25 2012**
Title:	**Expression data from adult (9 month-old) and young (4 month-old) hearts from C57BL/6J mice**
Organism:	**Mus musculus**
Experiment type:	**Expression profiling by array**
Platform:	**GPL1261**
Pubmed ID:	
Summary & Design:	**Summary:** **G protein-coupled receptor kinase 2 (GRK2) has emerged as a key regulator of cardiac function and myocardial structure. Cardiac GRK2 is increased in heart failure and ischemia in humans, whereas genetic inhibition of GRK2 is cardioprotective in animal models of these pathologies. However, the mechanistic basis underlying these effects are not fully understood. We have used adult GRK2 hemizygous mice (GRK2+/-) as a model to assess the effects of a sustained systemic inhibition of GRK2 in heart tissue with age.** **We used microarrays to determine the global programme of gene expression underlying cardioprotection with age in GRK2 hemizygous mice in comparation with their wild-type littermates.** **Overall design:** **9 month-old and 4 month-old mice hearts were collected for RNA extraction and hybridization on Affymetrix microarrays.**

Background corr dist: **KL-Divergence = 0.0358, L1-Distance = 0.0129, L2-Distance = 0.0001, Normal std = 0.6285**

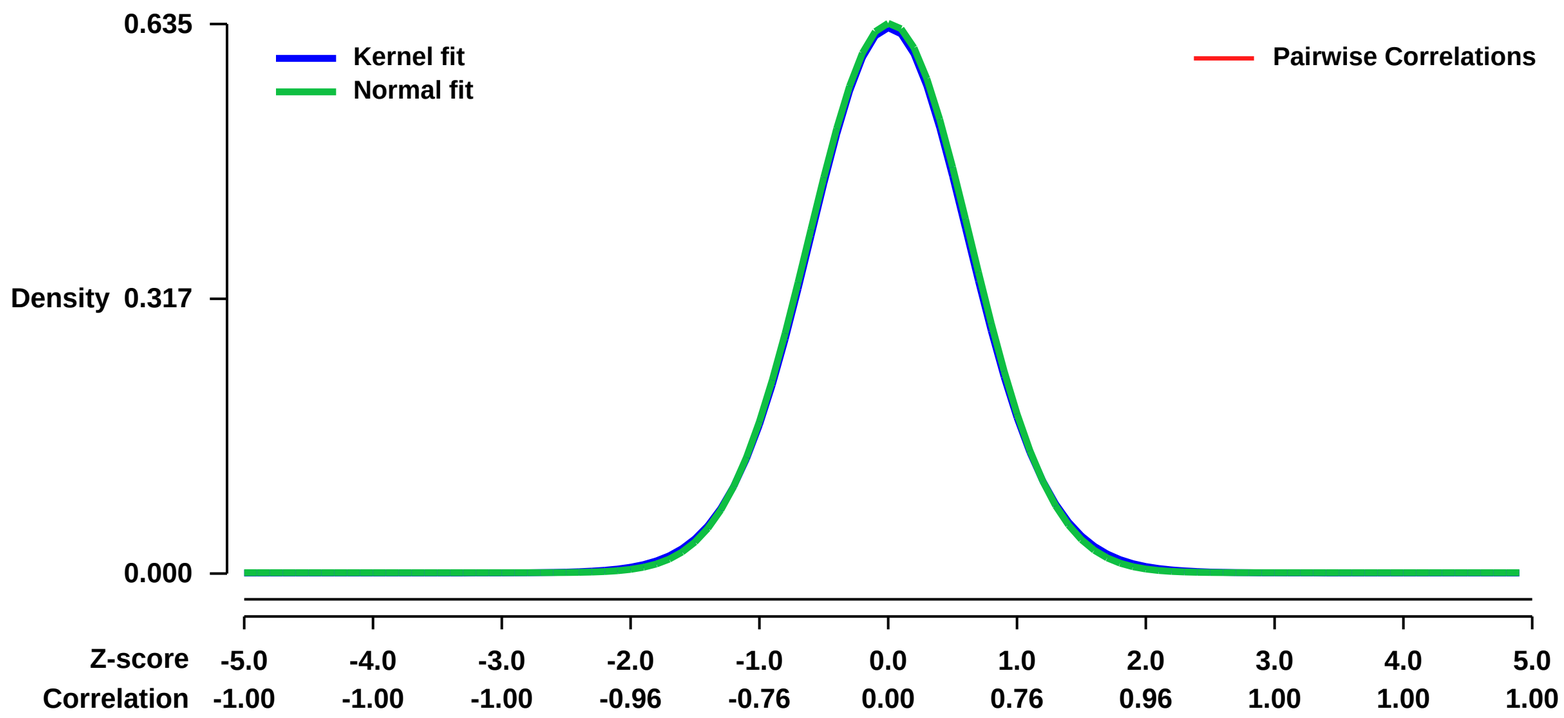

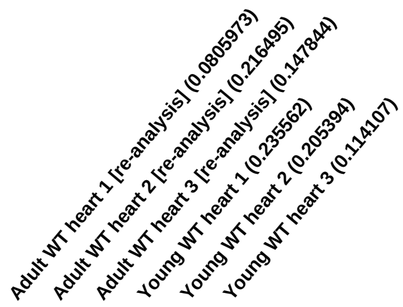

Pre-normalization Quantiles

[min] [medium] [max]

Null module

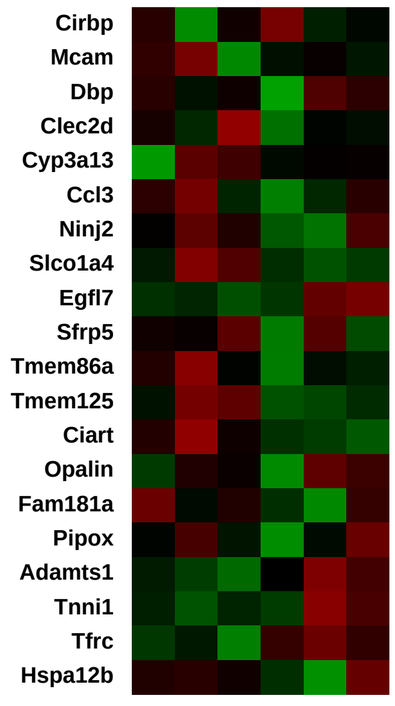

GEO Series "GSE41808" Expression Profiles

Num of samples in this series: 6

Scale of expression profile Z-scores

-3.0 -2.0 -1.0 0.0 1.0 2.0 3.0

GEO Link:	http://www.ncbi.nlm.nih.gov/geo/query/acc.cgi?acc=GSE41808
Status:	Public on Oct 25 2012
Title:	Expression data from adult (9 month-old) and young (4 month-old) hearts from GRK2 heterozygous C57BL/6J mice.
Organism:	Mus musculus
Experiment type:	Expression profiling by array
Platform:	GPL1261
Pubmed ID:	
Summary & Design:	**Summary:** G protein-coupled receptor kinase 2 (GRK2) has emerged as a key regulator of cardiac function and myocardial structure. Cardiac GRK2 is increased in heart failure and ischemia in humans, whereas genetic inhibition of GRK2 is cardioprotective in animal models of these pathologies. However, the mechanistic basis underlying these effects are not fully understood. We have used adult GRK2 hemizygous mice (GRK2+/-) as a model to assess the effects of a sustained systemic inhibition of GRK2 in heart tissue with age. We used microarrays to determine the global programme of gene expression underlying cardioprotection in GRK2 hemizygous mice with age. **Overall design:** 9 month-old and 4 month-old mice hearts were collected for RNA extraction and hybridization on Affymetrix microarrays.

Background corr dist: KL-Divergence = 0.0467, L1-Distance = 0.0166, L2-Distance = 0.0003, Normal std = 0.5832

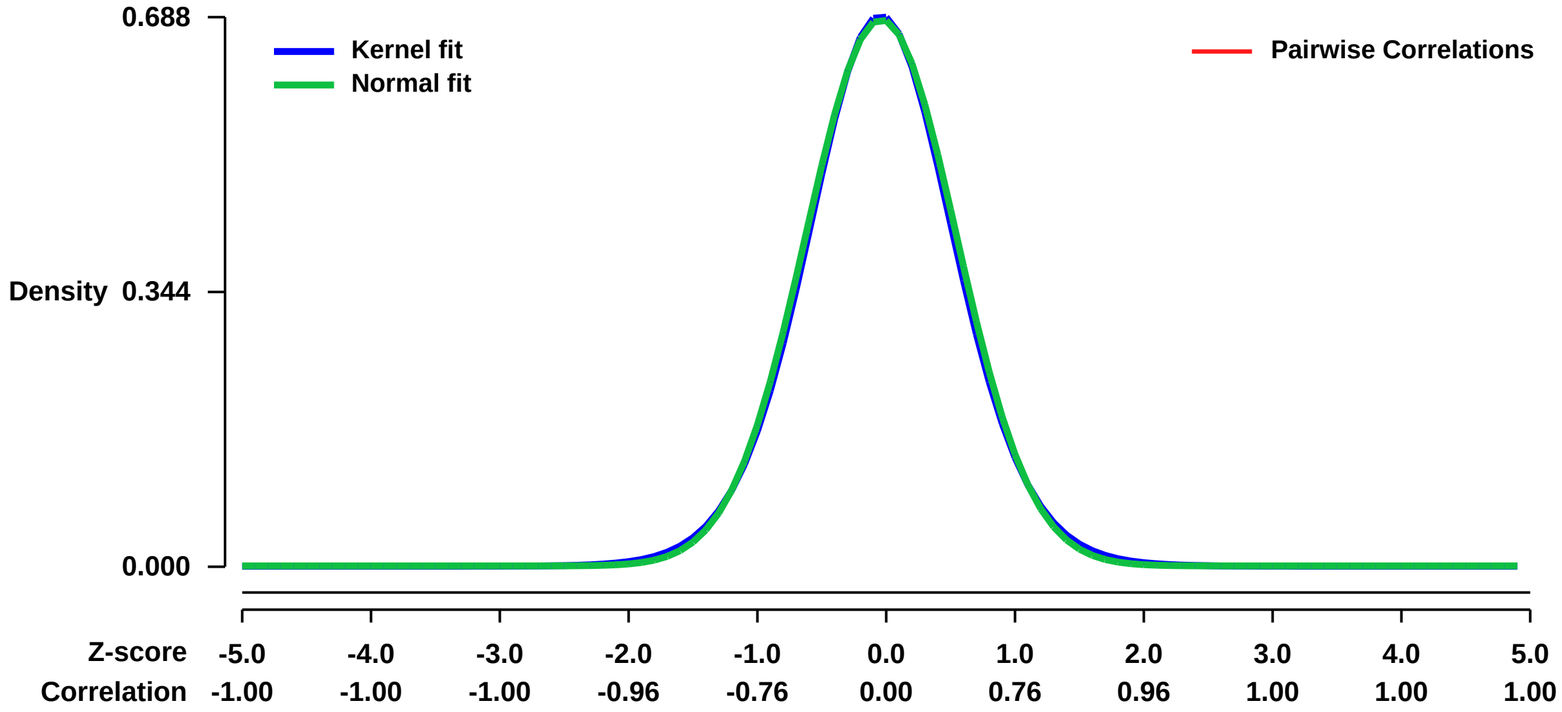

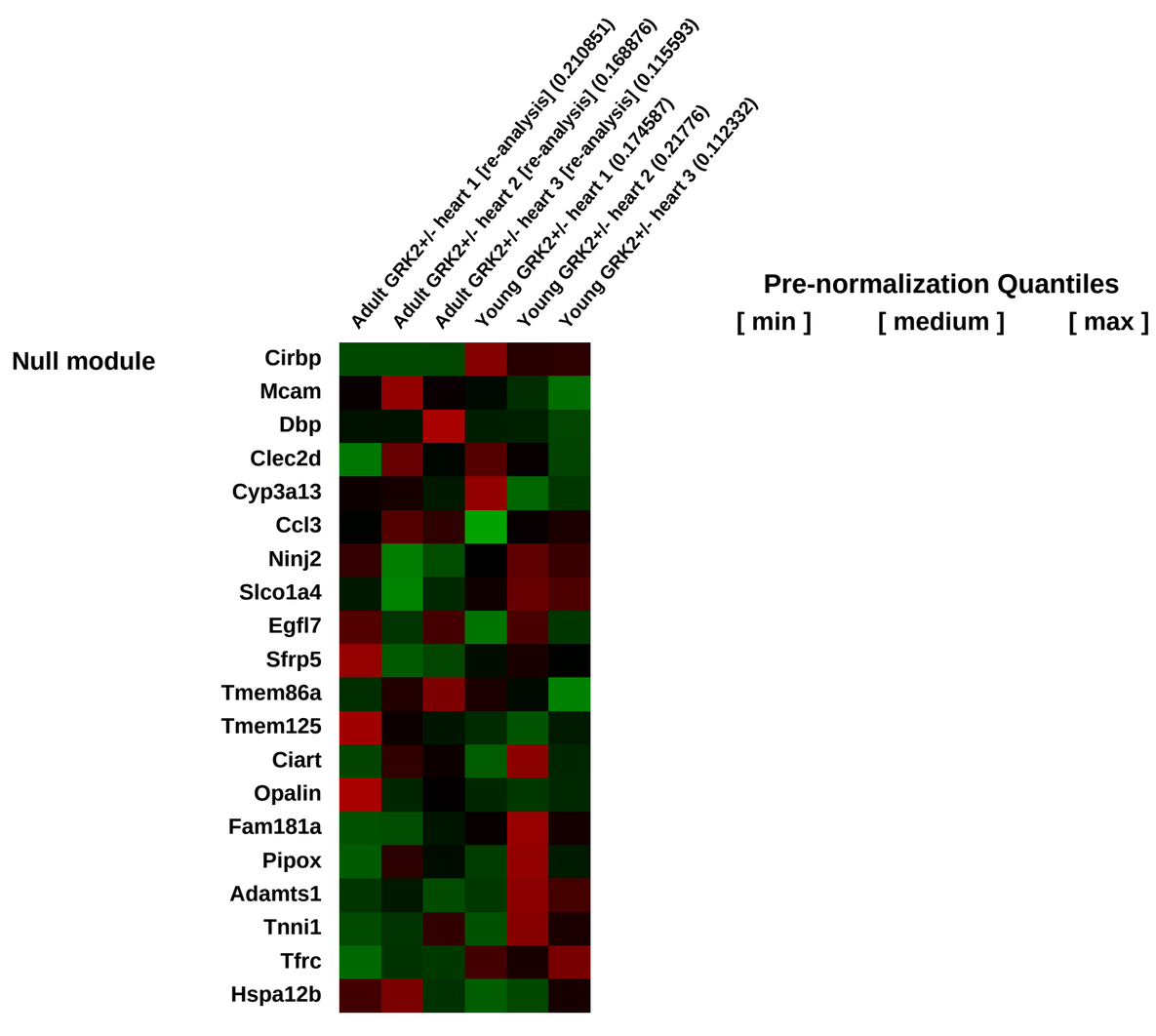

GEO Series "GSE41895" Expression Profiles

Num of samples in this series: 12

Scale of expression profile Z-scores

-3.0 -2.0 -1.0 0.0 1.0 2.0 3.0

GEO Link:	http://www.ncbi.nlm.nih.gov/geo/query/acc.cgi?acc=GSE41895
Status:	Public on Jan 01 2014
Title:	Dmrt1 (doublesex and mab-3 related transcription factor 1) conditional knockout expression analysis of E15.5 testes.
Organism:	Mus musculus
Experiment type:	Expression profiling by array
Platform:	GPL1261
Pubmed ID:	
Summary & Design:	**Summary:** Dmrt1 (doublesex and mab-3 related transcription factor 1) is a conserved transcriptional regulator of male differentiation required for testicular development in vertebrates. This study examines the result of conditional removal of Dmrt1 in E15.5 testes tissue in B6 and 129Sv strains. **Overall design:** This study examines the result of conditional removal of Dmrt1 in E15.5 testes tissue in B6 and 129Sv strains.

Background corr dist: KL-Divergence = 0.0803, L1-Distance = 0.0298, L2-Distance = 0.0015, Normal std = 0.4748

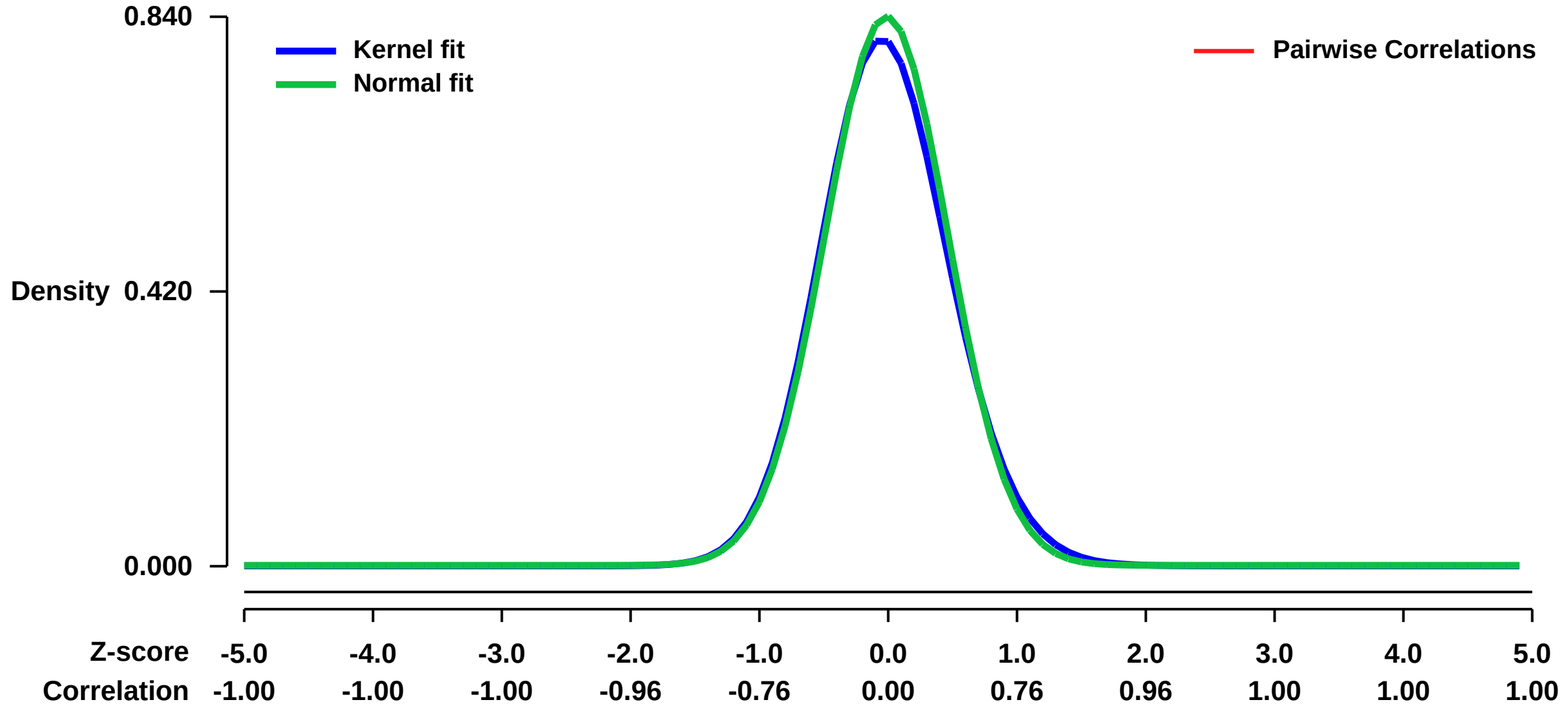

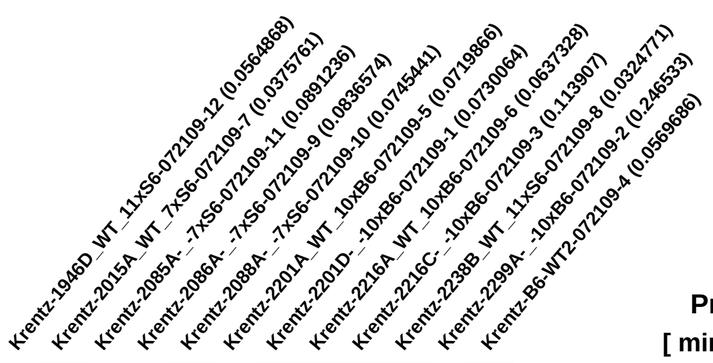

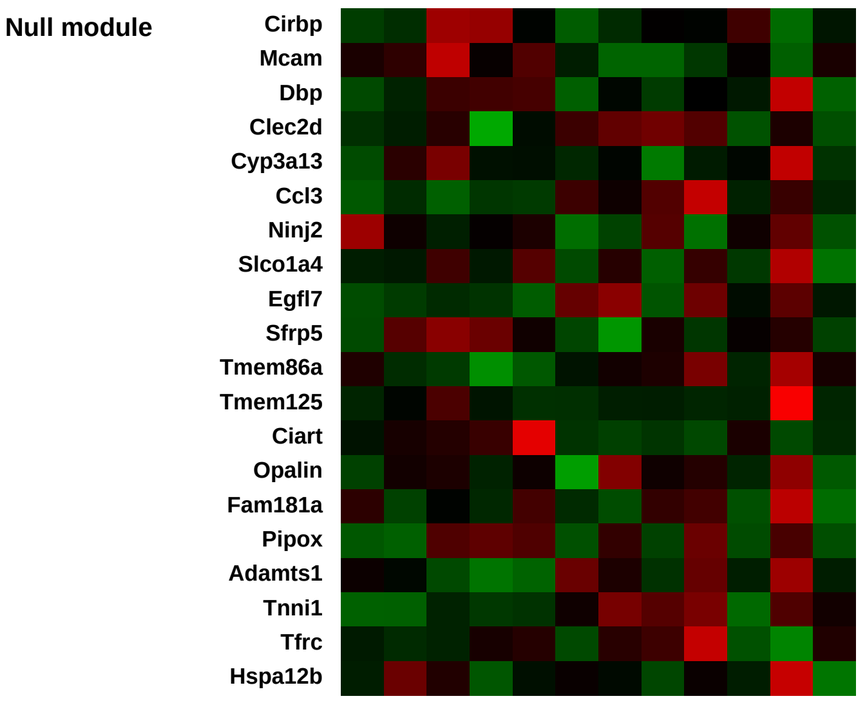

GEO Series "GSE41896" Expression Profiles

Num of samples in this series: 6

Scale of expression profile Z-scores

-3.0 -2.0 -1.0 0.0 1.0 2.0 3.0

GEO Link:	http://www.ncbi.nlm.nih.gov/geo/query/acc.cgi?acc=GSE41896
Status:	Public on Jan 01 2014
Title:	Dmrt1 (doublesex and mab-3 related transcription factor 1) conditional knockout expression analysis of E15.5 ovaries.
Organism:	Mus musculus
Experiment type:	Expression profiling by array
Platform:	GPL1261
Pubmed ID:	
Summary & Design:	**Summary:** Dmrt1 (doublesex and mab-3 related transcription factor 1) is a conserved transcriptional regulator of male differentiation required for testicular development in vertebrates. This study examines the result of conditional removal of Dmrt1 in E15.5 ovaries. **Overall design:** This study examines the result of conditional removal of Dmrt1 in E15.5 ovaries.

Background corr dist: KL-Divergence = 0.0396, L1-Distance = 0.0172, L2-Distance = 0.0003, Normal std = 0.6145

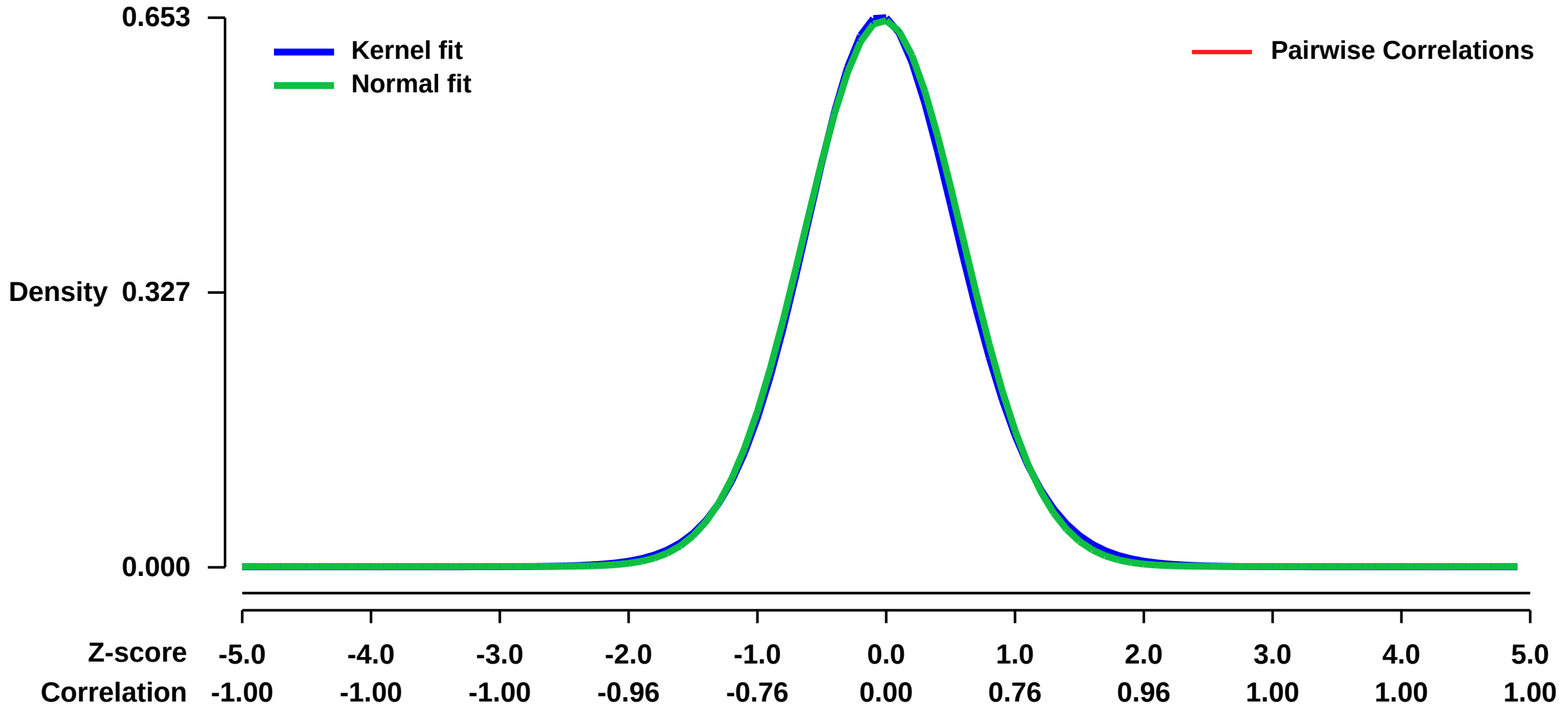

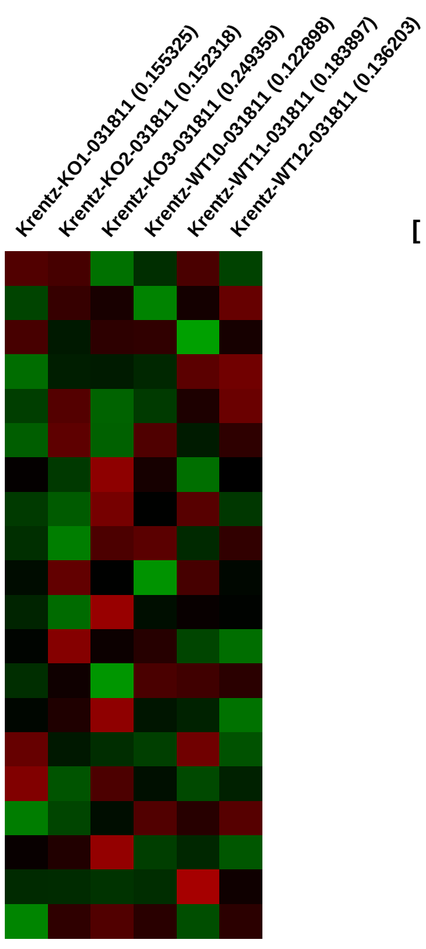

GEO Series "GSE41907" Expression Profiles

Num of samples in this series: 7

Scale of expression profile Z-scores

-3.0 -2.0 -1.0 0.0 1.0 2.0 3.0

GEO Link:	http://www.ncbi.nlm.nih.gov/geo/query/acc.cgi?acc=GSE41907
Status:	Public on Dec 01 2012
Title:	Transcriptional regulation of myoblasts in HMGA2 KO mice
Organism:	Mus musculus
Experiment type:	Expression profiling by array
Platform:	GPL1261
Pubmed ID:	23177649
Summary & Design:	**Summary:** We sought to identify critical factors regulating muscle stem cell activation and commitment, and determined through loss-of-function analyses that HMGA2 (high mobility group AT-hook 2) is a key regulator of myogenesis both in vitro and in vivo. **Overall design:** mRNAs were isolated from Hmga2 -/- and Hmga2 +/+ mice myoblasts, and a microarray experiment was performed.

Background corr dist: KL-Divergence = 0.0533, L1-Distance = 0.0165, L2-Distance = 0.0003, Normal std = 0.5505

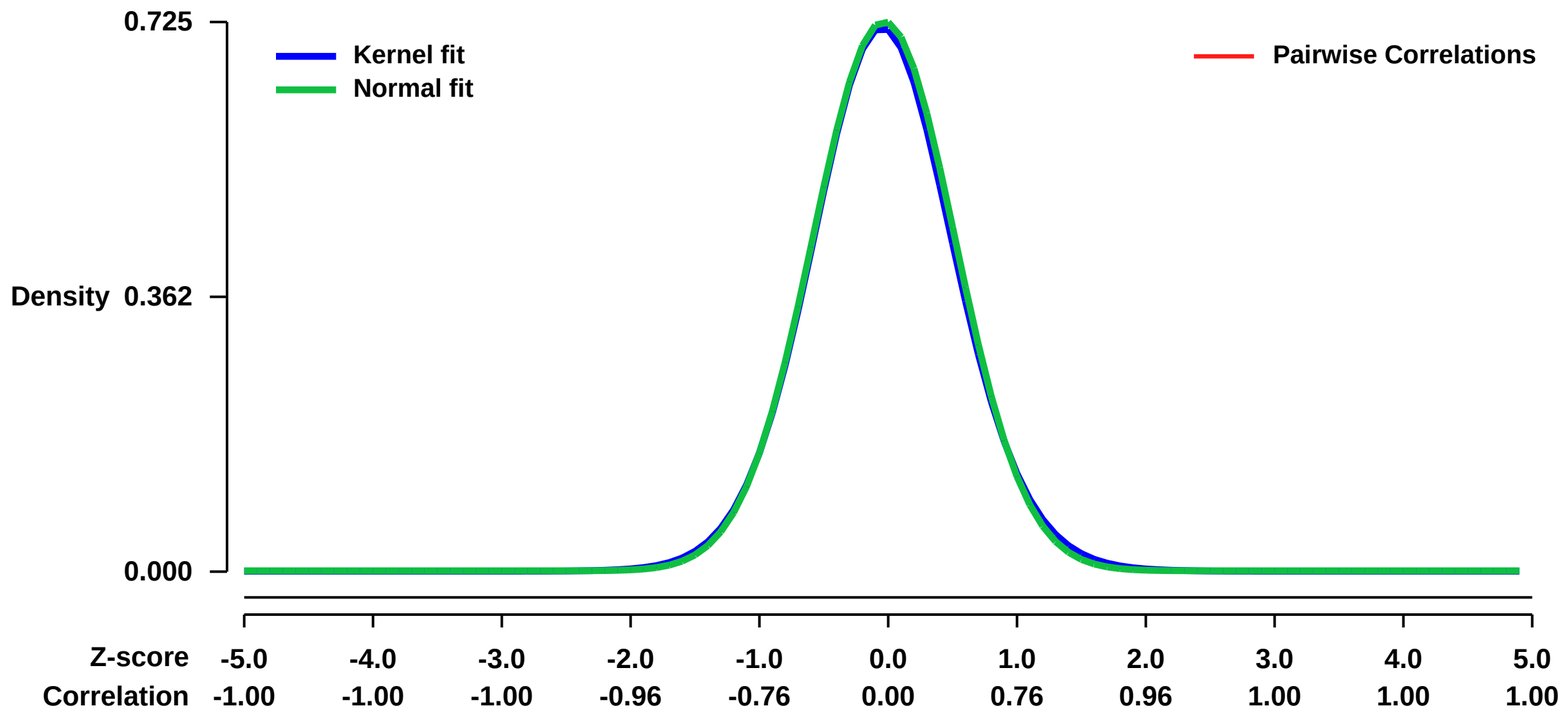

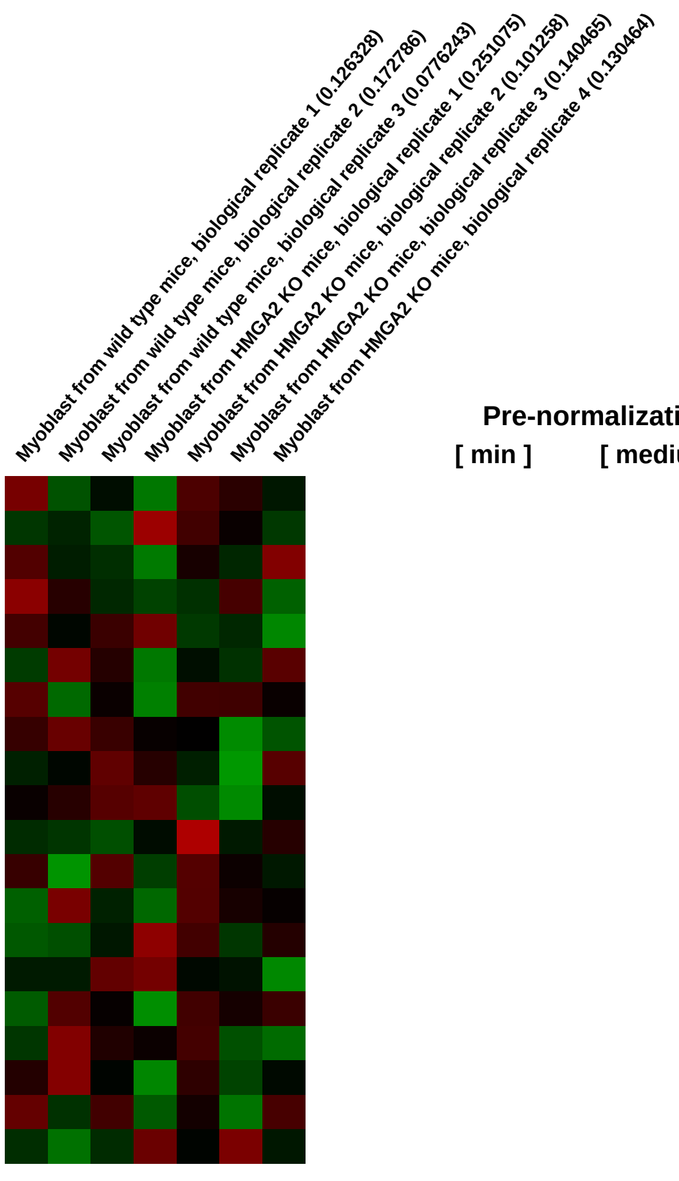

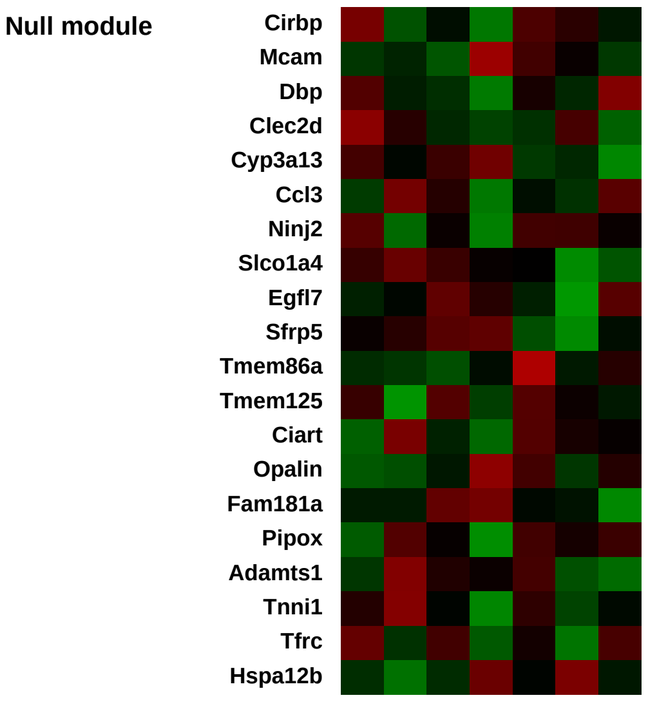

GEO Series "GSE41910" Expression Profiles

Num of samples in this series: 12

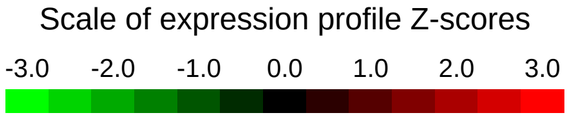

GEO Link:	http://www.ncbi.nlm.nih.gov/geo/query/acc.cgi?acc=GSE41910
Status:	Public on Feb 19 2013
Title:	Gene expression profiling of gastrocnemius of mini muscle mice
Organism:	Mus musculus
Experiment type:	Expression profiling by array
Platform:	GPL1261
Pubmed ID:	23362141
Summary & Design:	**Summary:** Few studies have investigated heterogeneity of selection response in replicate lines subjected to equivalent selection. We developed 4 replicate lines of mice based on high levels of voluntary wheel running (high runner or HR lines) while also maintaining 4 non-selected control lines. This led to the unexpected discovery of the HR mini-muscle (HRmini) phenotype, recognized by a 50% reduction in hindlimb muscle mass, which became fixed in 1 of the 4 HR selected lines. Here, we report genome-wide expression profiling describing transcriptome differences between HRnormal and HRmini medial gastrocnemius. This work provides a resource for understanding differences in muscle phenotypes in populations exhibiting high running capacity. **Overall design:** Male mice were used from an animal model of 4 closed lines selectively bred for high voluntary wheel-running behaviour (HR) and 4 control lines bred without intentional selection, described in Swallow et al. Animals used in the current work were sampled from generation 37 at a mean age of 84 days (range = 79-86). For microarray analysis, we used gastrocnemius muscles (including both lateral and medial portions) from HRmini line #3 and HRnormal line #8 (n = 6, in each group). To obtain sufficient RNA, gastrocnemius samples of HRmini were pooled from left and right limbs from each animal, whereas HRnormal gastrocnemius was sampled from either left or right limb only.

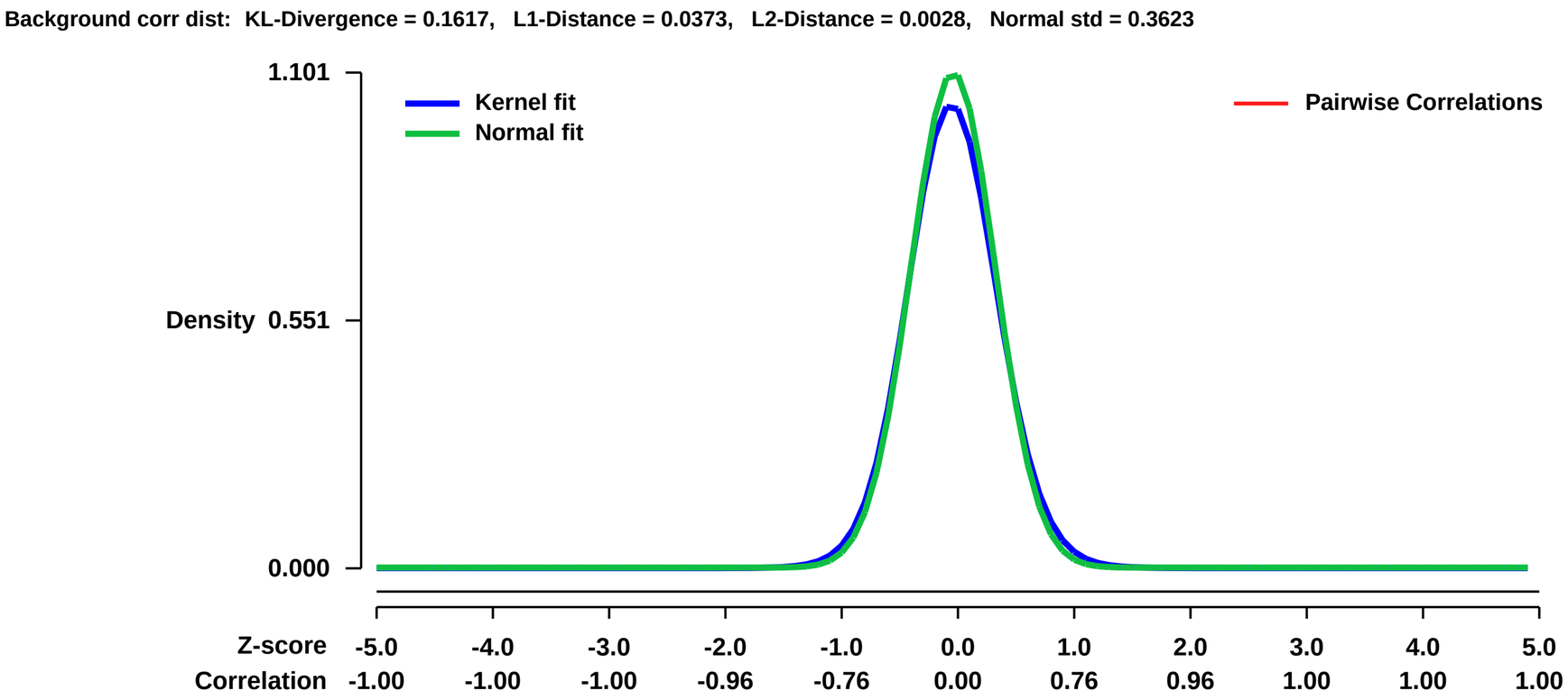

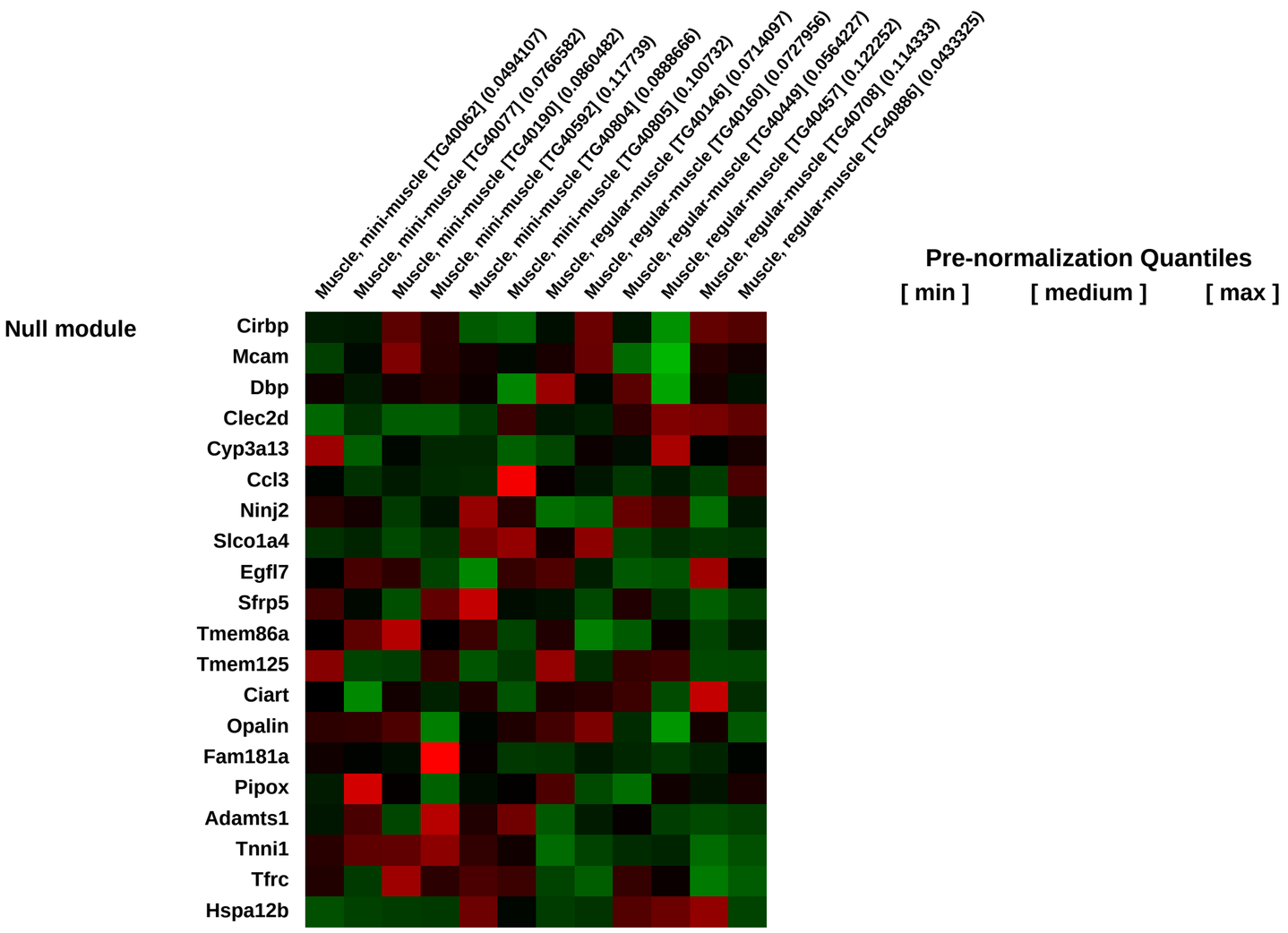

GEO Series "GSE41942" Expression Profiles

Num of samples in this series: 6

Scale of expression profile Z-scores

-3.0 -2.0 -1.0 0.0 1.0 2.0 3.0

GEO Link:	**http://www.ncbi.nlm.nih.gov/geo/query/acc.cgi?acc=GSE41942**
Status:	**Public on Nov 01 2012**
Title:	**Overexpression of miR-9 and miR-9* in 32D cells**
Organism:	**Mus musculus**
Experiment type:	**Expression profiling by array**
Platform:	**GPL1261**
Pubmed ID:	
Summary & Design:	**Summary:** **Overexpression of miR-9 and miR-9* in 32D cells, cells grown under IL-3 conditions and miR-9 and miR-9* were introduced with retroviral vectors containing about ~150 bp up and downstream of mmu-mir-9-2.** **Expression was determined to find out the effect of miR-9/9*overexpression on the transcriptome level compared to introduction of empty vector control.** **Overall design:** **Transcriptome levels were determined for 32D cells expressing miR-9 and miR-9* and empty vector control. Experiment performed in three independent replicates.**

Background corr dist: **KL-Divergence = 0.0444, L1-Distance = 0.0310, L2-Distance = 0.0014, Normal std = 0.6092**

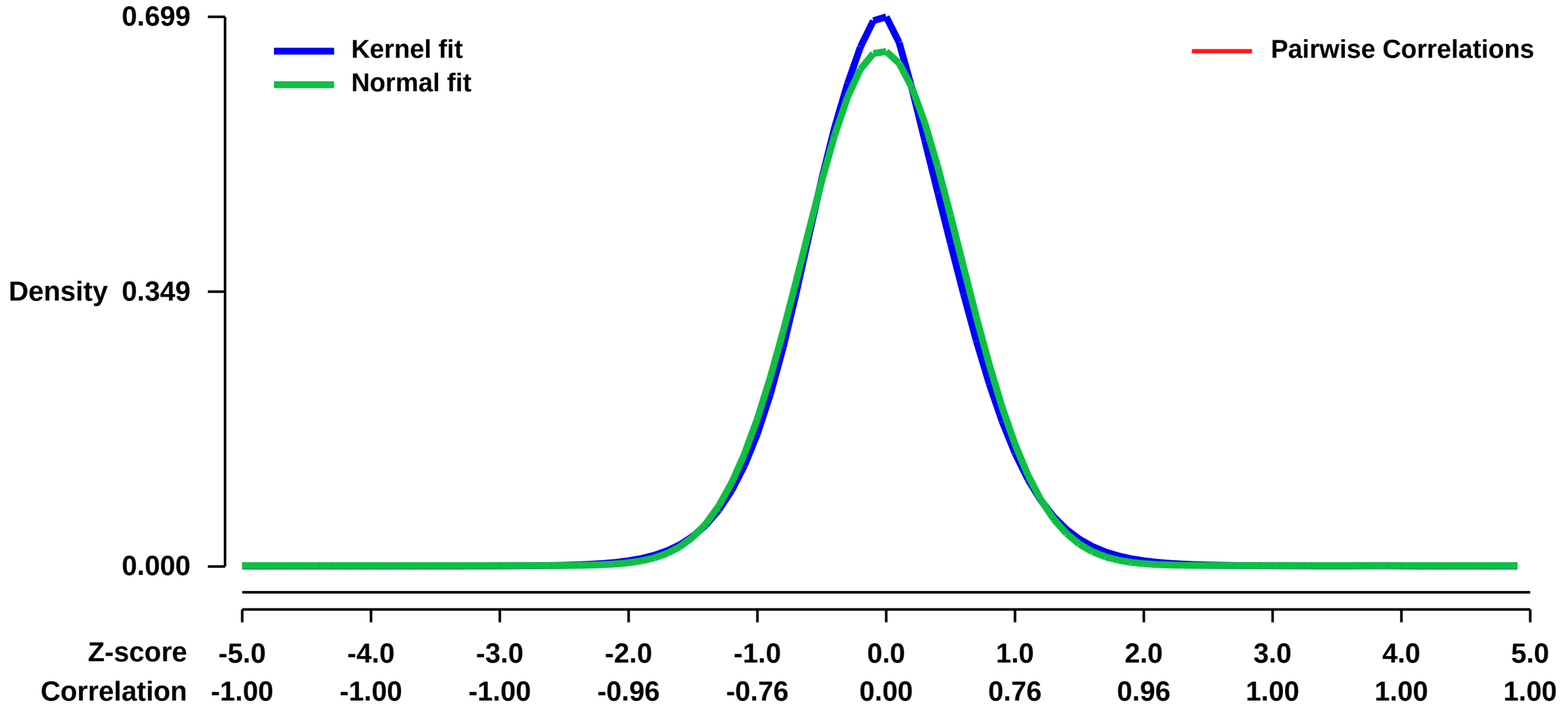

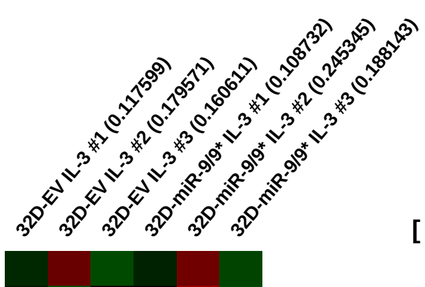

Pre-normalization Quantiles

[min] [medium] [max]

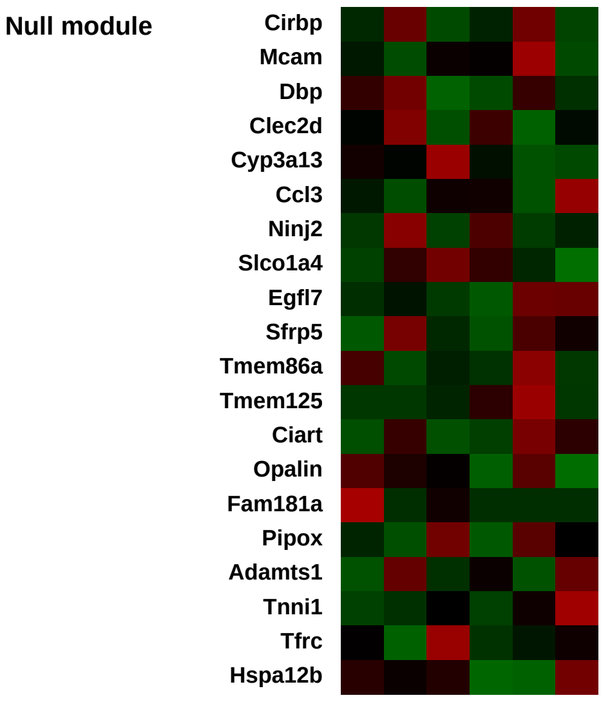

GEO Series "GSE41997" Expression Profiles

Num of samples in this series: 6

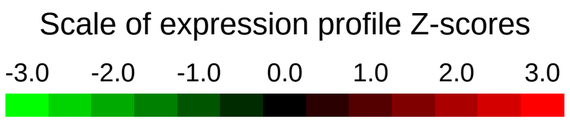

GEO Link:	http://www.ncbi.nlm.nih.gov/geo/query/acc.cgi?acc=GSE41997
Status:	Public on Dec 12 2013
Title:	Expression data from Dmp1-GFP sorted osteocytes
Organism:	Mus musculus
Experiment type:	Expression profiling by array
Platform:	GPL1261
Pubmed ID:	24333171
Summary & Design:	**Summary:** Estrogens are well known steroid hormones necessary to maintain bone health. In addition, mechanical loading, which estrogen signaling may intersect with the Wnt/¸†-catenin pathway, is also essential for bone health. As osteocytes are known as the major mechanosensory cells embedded in mineralized bone matrix, osteocyte ER¸– deletion mice (ER¸–¸ Ocy/¸ Ocy) were generated by mating ER¸– floxed mice with Dmp1-Cre mice to determine functions of ER¸– in osteocytes. Trabecular bone mineral density of female, but not male ER¸–¸ Ocy/¸ Ocy mice was significantly decreased. Bone formation parameters in ER¸–¸ Ocy/¸ Ocy were significantly decreased while osteoclast parameters were unchanged. This suggests that ER¸– in osteocytes exerts osteoprotective function by positively controlling bone formation. To identify potential targets of ER¸–, gene array analysis of Dmp1-GFP osteocytes FACS sorted from ER¸–¸ Ocy/¸ Ocy and control mice was performed. Expression of Mdk and Sostdc1, both known inhibitors of Wnt, were significantly increased without alteration of the mature osteocyte marker Sost or ¸†-catenin. Hindlimb unloading exacerbated the trabecular bone loss, but surprisingly cortical bone was resistant. These studies show that ER¸– in osteocytes has osteoprotective effects in trabecular bone through regulating expression of Wnt antagonists, but conversely plays a negative role in cortical bone loss due to unloading. **Overall design:** Wild type and osteocyte-specific Estrogen Receptor alpha knock-out mice were generated. The number of both genotypes of mice was three. Calvarial osteocytes of both genotypes harboring Dmp1-GFP were extracted by sequential enzymatic digestion, followed by FACS Aria sorting and total RNAs were purified for Affymetix GeneChip microarray analysis without pooling.

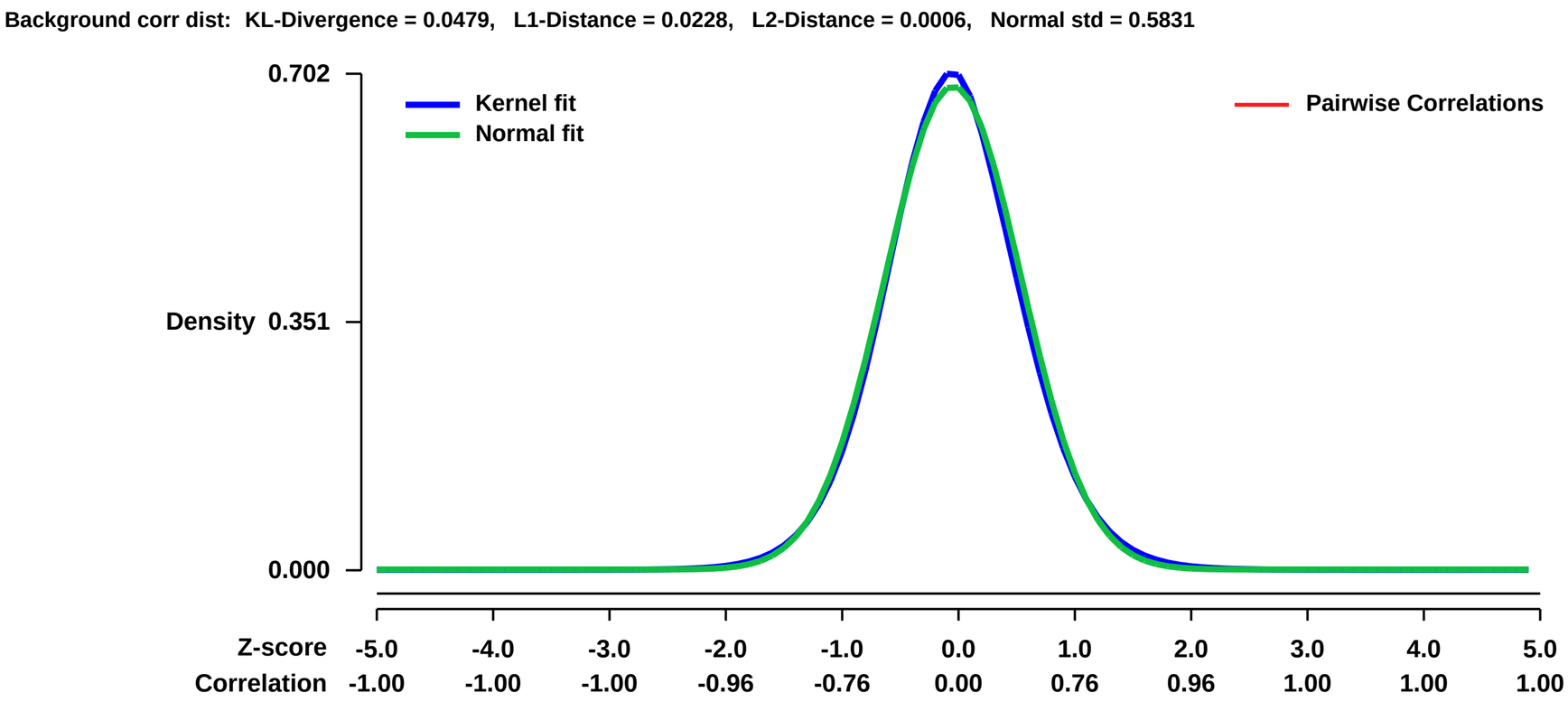

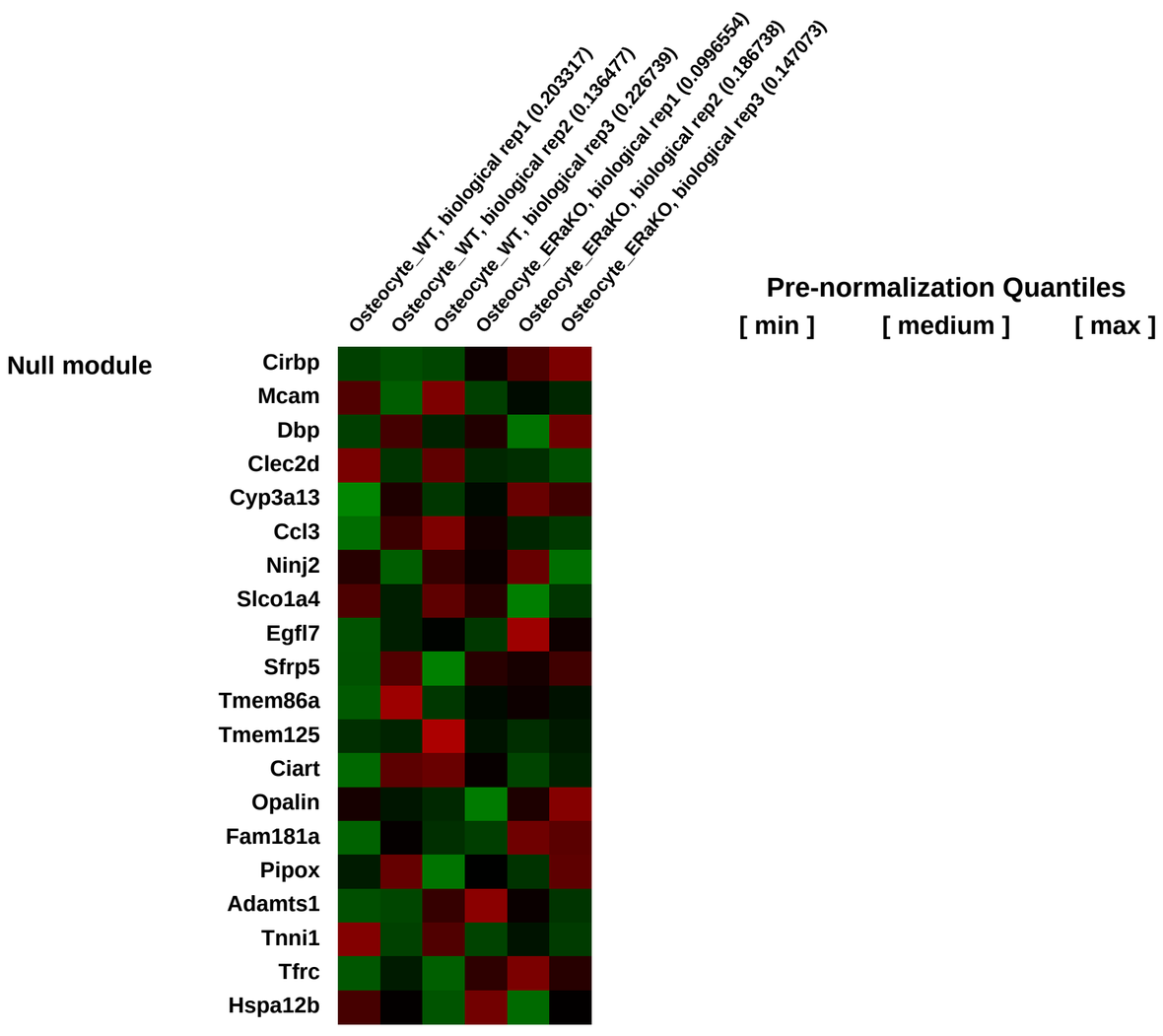

GEO Series "GSE42008" Expression Profiles

Num of samples in this series: 6

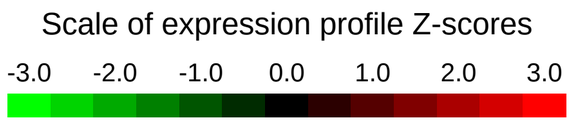

GEO Link:	http://www.ncbi.nlm.nih.gov/geo/query/acc.cgi?acc=GSE42008
Status:	Public on Jul 01 2013
Title:	Expression data from NcGFP ki/+, NcGFP ki/ki and wt (W4) ES cells
Organism:	Mus musculus
Experiment type:	Expression profiling by array
Platform:	GPL1261
Pubmed ID:	24036274
Summary & Design:	**Summary:** We generated a gene replacement allele of the E-cadherin locus that express an N-cadherin-GFP fusion in ES cells. Expression profiles of homozygous and heterozygous knock-in ES cells were analyzed in comparison to wt ES cells. The GEO Samples were compared to published data of E-cadherin knock-out ES cells (ArrayExpress, accession number E-MEXP-2836). The comparison data are linked below. **Overall design:** RNA was extracted from two independent experiments per genotype, data analysis was performed using the R/Bioconductor Limma software. Quality of the data set was controlled by the simpleaffy package and normalized by quantile normalization with the GCRMA alogrithm.

Background corr dist: KL-Divergence = 0.0266, L1-Distance = 0.0110, L2-Distance = 0.0001, Normal std = 0.6873

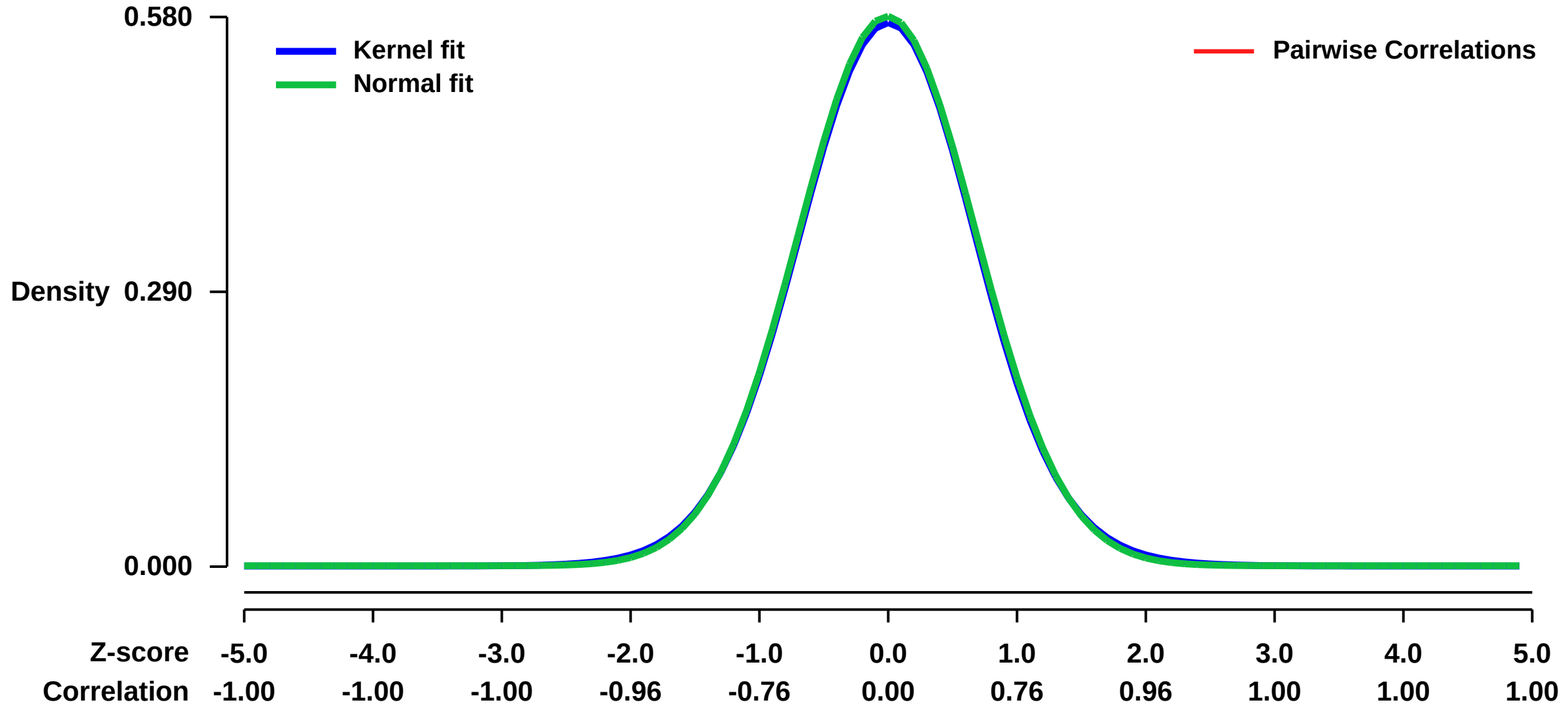

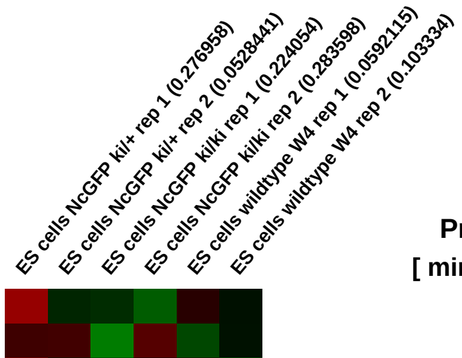

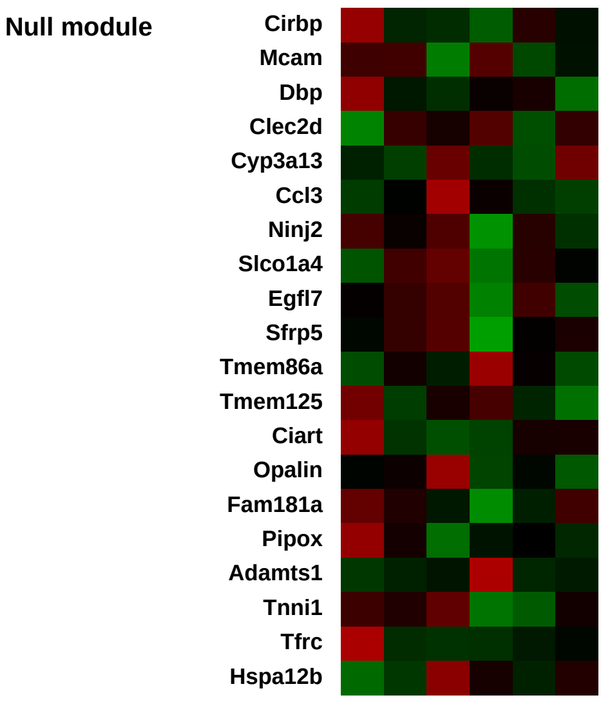

GEO Series "GSE42018" Expression Profiles

Num of samples in this series: 8

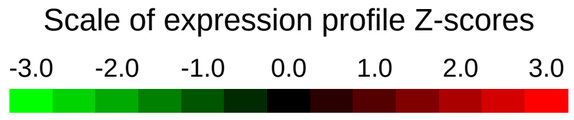

GEO Link:	**http://www.ncbi.nlm.nih.gov/geo/query/acc.cgi?acc=GSE42018**
Status:	**Public on Nov 07 2012**
Title:	**Cerebellar Granule Neuron Temporal-NFI Microarray Data**
Organism:	**Mus musculus**
Experiment type:	**Expression profiling by array**
Platform:	**GPL1261**
Pubmed ID:	**23407945**
Summary & Design:	**Summary:** **Dendrite and synapse development are critical for establishing appropriate neuronal circuits, and disrupted timing of these events can alter connectivity leading to disordered neural function.** **In early postnatal development of cerebellar granule neurons (CGNs), the expression of many genes is temporally regulated. Further, NFI (Nuclear Factor I) proteins have been shown to play important roles in the regulation of gene expression in developing CGNs.** **To identify NFI-regulated genome-wide targets involved in late maturation of mouse CGNs, we performed two groups of microarray expression analysis: (1) temporal expression arrays using 1.5 and 6 day cultures of mouse CGNs representing immature and more mature CGNs, respectively, which identified 844 Temporal-Up or Down genes; and (2) NFI-regulated genes in 6 day CGN cultures that were infected at the time of plating with lentiviral vectors expressing either NFI dominant repressor (NFI-EnR) or EnR control protein. This identified 686 NFI-Up (NFI-EnR down-regulated) or NFI-Down (NFI-EnR up-regulated) genes.** **Overlap analysis identified 212 temporal genes that were regulated by NFI. These results indicated that NFI plays a pivotal role in the regulation of late CGN maturation.** **Overall design:** **For temporal arrays, mouse CGN progenitors were purified from P6 mouse cerebellum and cultured for either 1.5 or 6 days. Three biological replicates were analyzed for each time point. For NFI arrays, CGN progenitors from P6 mice were transduced upon plating with either NFI-EnR or EnR control lentivirus and cultured 6 days. Four pairs of biological replicates were performed.**

Background corr dist: **KL-Divergence = 0.0420, L1-Distance = 0.0198, L2-Distance = 0.0006, Normal std = 0.5872**

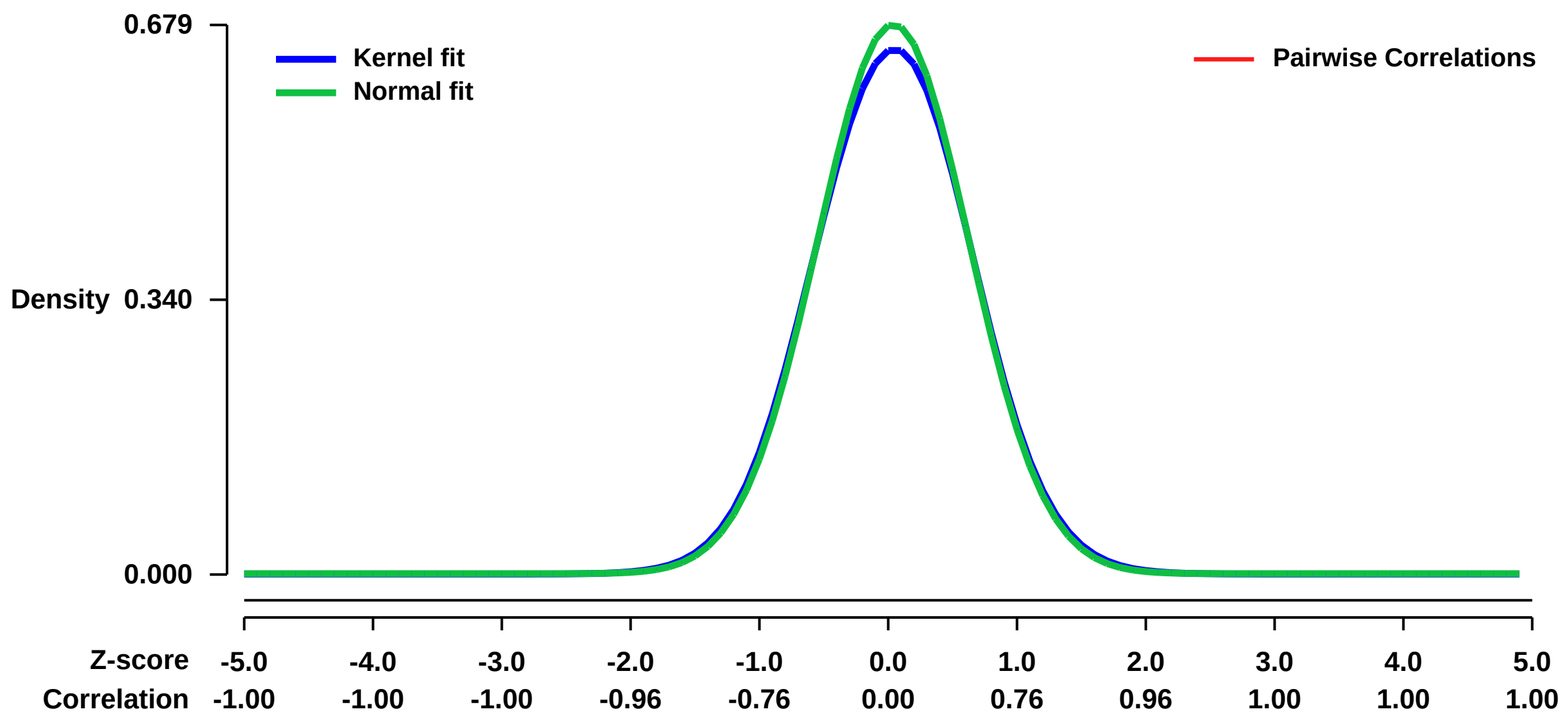

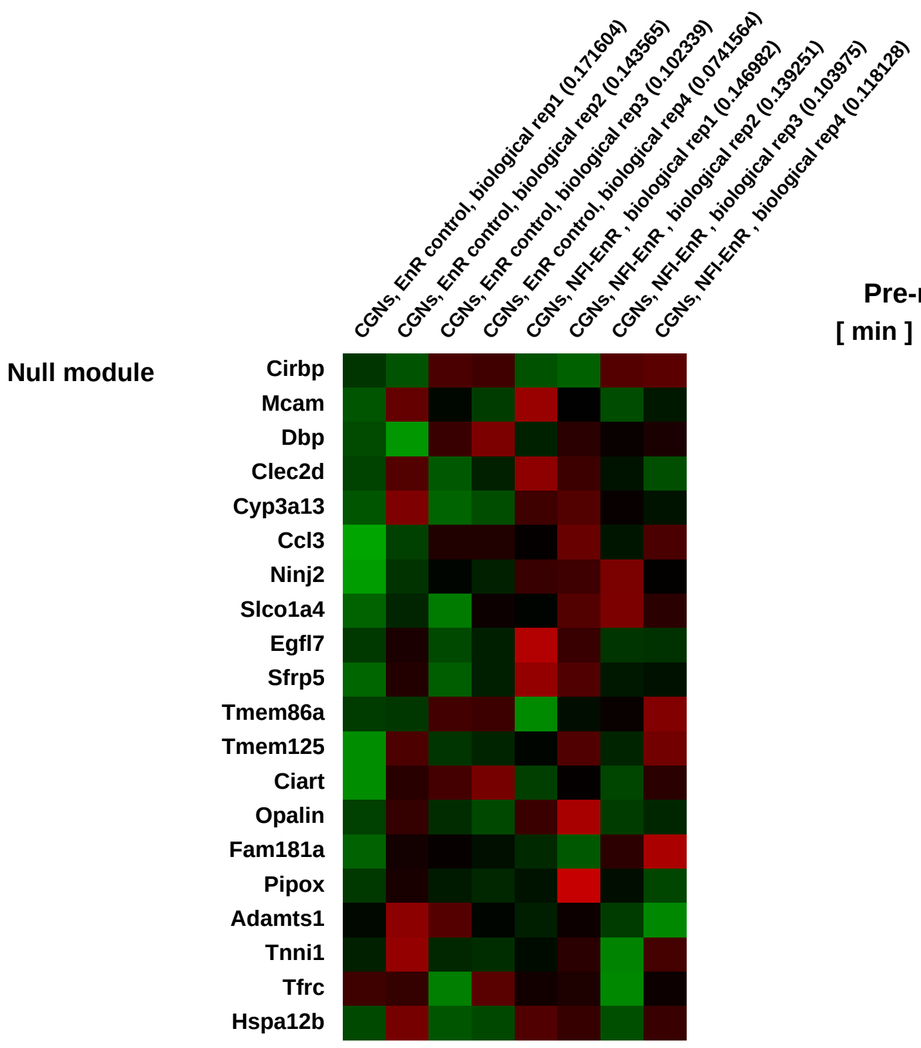

GEO Series "GSE42021" Expression Profiles

Num of samples in this series: 27

Scale of expression profile Z-scores

-3.0 -2.0 -1.0 0.0 1.0 2.0 3.0

GEO Link:	http://www.ncbi.nlm.nih.gov/geo/query/acc.cgi?acc=GSE42021
Status:	Public on Mar 07 2013
Title:	Gene expression profiles of CD4SP Foxp3GFP-CD25+ Treg precursors and Foxp3GFP-CD25- thymocytes
Organism:	Mus musculus
Experiment type:	Expression profiling by array
Platform:	GPL1261
Pubmed ID:	23420886
Summary & Design:	**Summary:** We investigated at which stage of maturation commitment to a stable Foxp3-expressing phenotype takes place. We assessed stability of Foxp3 expression in thymic Foxp3+ Treg subsets of different maturity, defined by CD24 expression. Next we compared gene expression profiles of Foxp3+ Treg subsets (+) of different maturity (24lo, 24int, 24hi) and could identify a set of genes that were specifically up or downregulated in Foxp3+ Tregs, but not in Foxp3- conventional T cells, in a maturation-dependent manner. **Overall design:** Gene expression of Foxp3+ Treg subsets (+) of different maturity (24lo, 24int, 24hi) compared to their Foxp3- conventional Tcell subsets (-) counterpart.

Background corr dist: KL-Divergence = 0.2463, L1-Distance = 0.0487, L2-Distance = 0.0055, Normal std = 0.3050

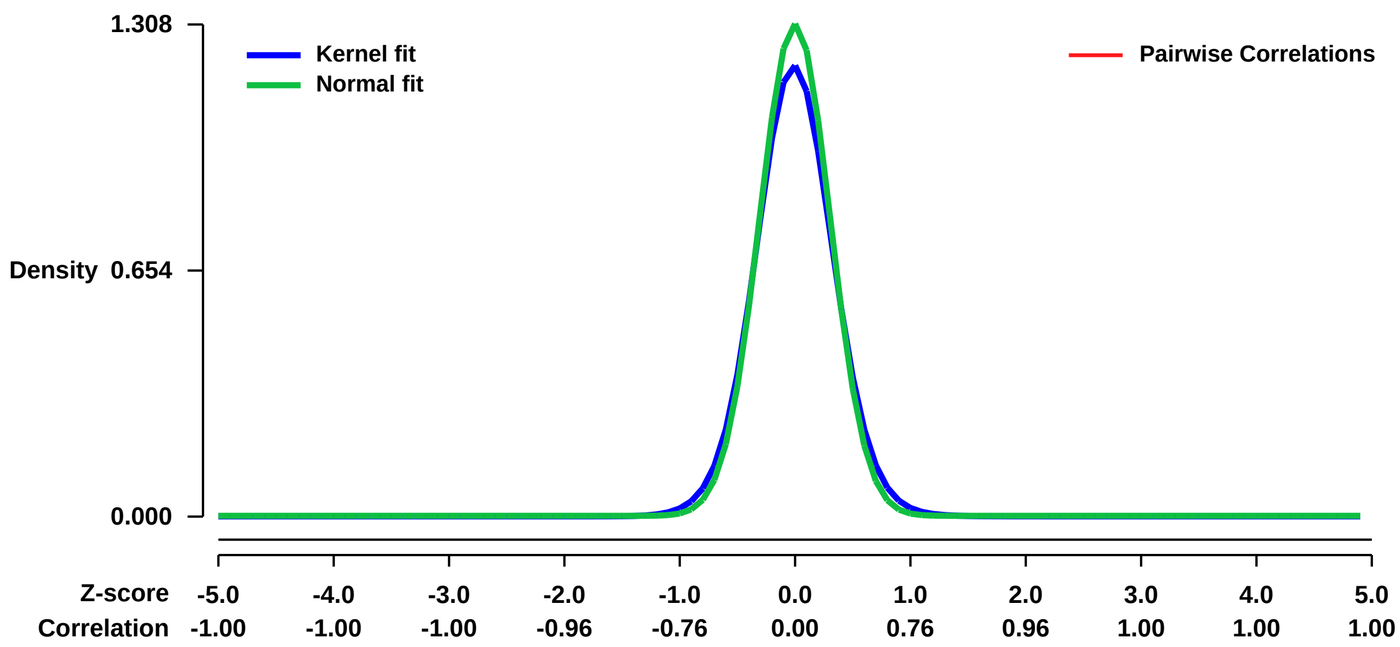

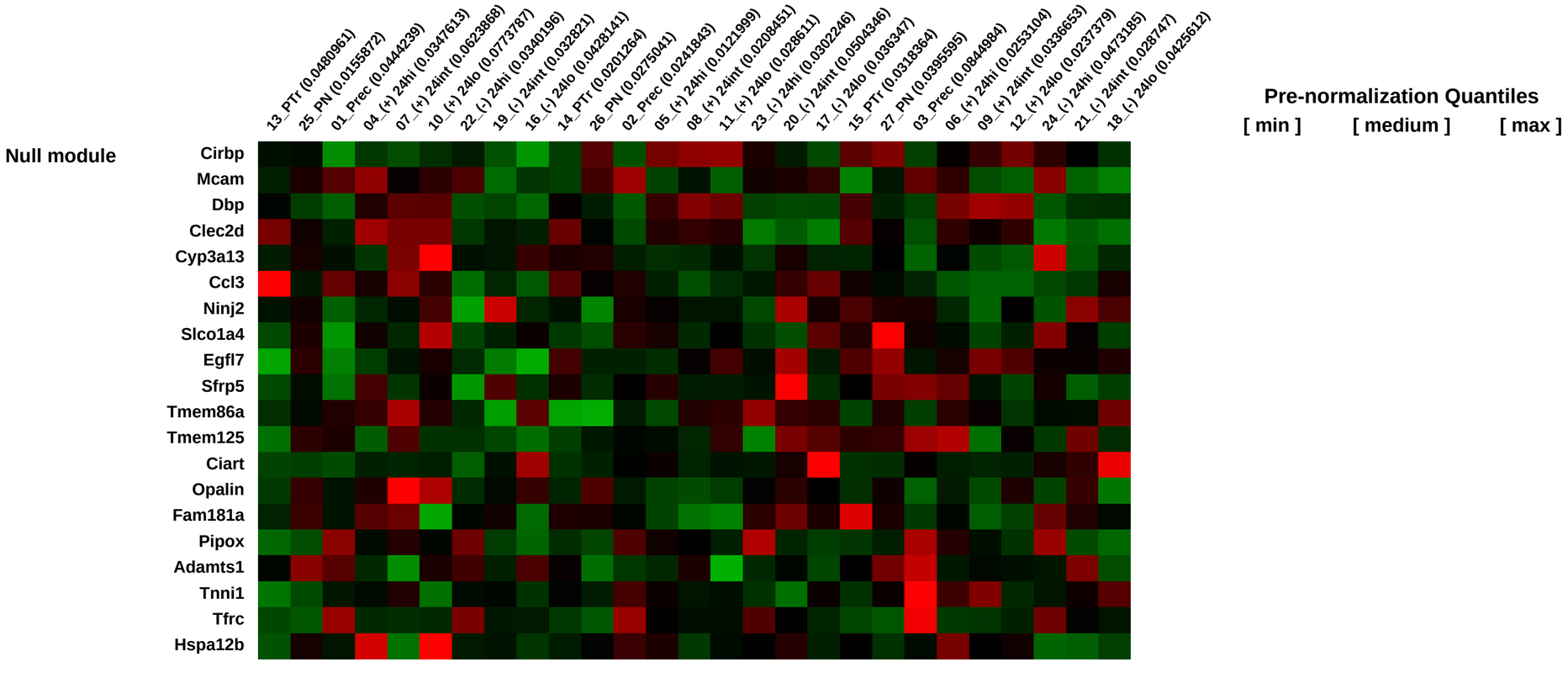

GEO Series "GSE42047" Expression Profiles

Num of samples in this series: 24

Scale of expression profile Z-scores

-3.0 -2.0 -1.0 0.0 1.0 2.0 3.0

GEO Link:	http://www.ncbi.nlm.nih.gov/geo/query/acc.cgi?acc=GSE42047
Status:	Public on Oct 04 2013
Title:	TWEAK-treated time course in Pan02 cells
Organism:	Mus musculus
Experiment type:	Expression profiling by array
Platform:	GPL1261
Pubmed ID:	23974006
Summary & Design:	**Summary:** Tumor necrosis factor-related weak inducer of apoptosis, TWEAK, is a TNF superfamily member that mediates signaling through its receptor fibroblast growth factor inducible-14, Fn14. In tumor cell lines, TWEAK induces proliferation, survival and NF-kappaB signaling and gene expression that promote tumor growth and suppress antitumor immune responses. Anti-TWEAK antibody, RG7212, inhibits tumor growth in vivo with decreases in pathway activation markers and modulation of tumor, blood and spleen immune cell composition. Candidate response prediction markers, including Fn14, have been identified in mouse models. Phase I pharmacodynamic data from patients are consistent with preclinical results. TWEAK:Fn14 signaling is upregulated in human cancer and pathway activation induces tumor proliferation and survival signaling. Blockade with anti-TWEAK mAb, RG7212, inhibits tumor growth in multiple models in mice. TWEAK induces changes that suppress anti-tumor immune responses and RG7212 blocks these effects resulting in changes in tumor immune cell composition and decreases in cytokines that promote immunosuppression. Antitumor efficacy in mice was observed in a range of Fn14 expressing models with pathway activation and expressing either wild-type or mutant p53, BRAF or KRAS suggesting both a patient selection strategy and potential broad clinical applicability. Preclinical mechanism of action hypotheses are supported by Phase I clinical data, with decreases in proliferation markers and increased tumor T cell infiltration. **Overall design:** Pan02 cells untreated or treated with 1090-TW (TWEAK) for 4 hours, 8 hours, or 24 hours. Four replicates for each condition were performed.

Background corr dist: KL-Divergence = 0.2309, L1-Distance = 0.0329, L2-Distance = 0.0016, Normal std = 0.3208

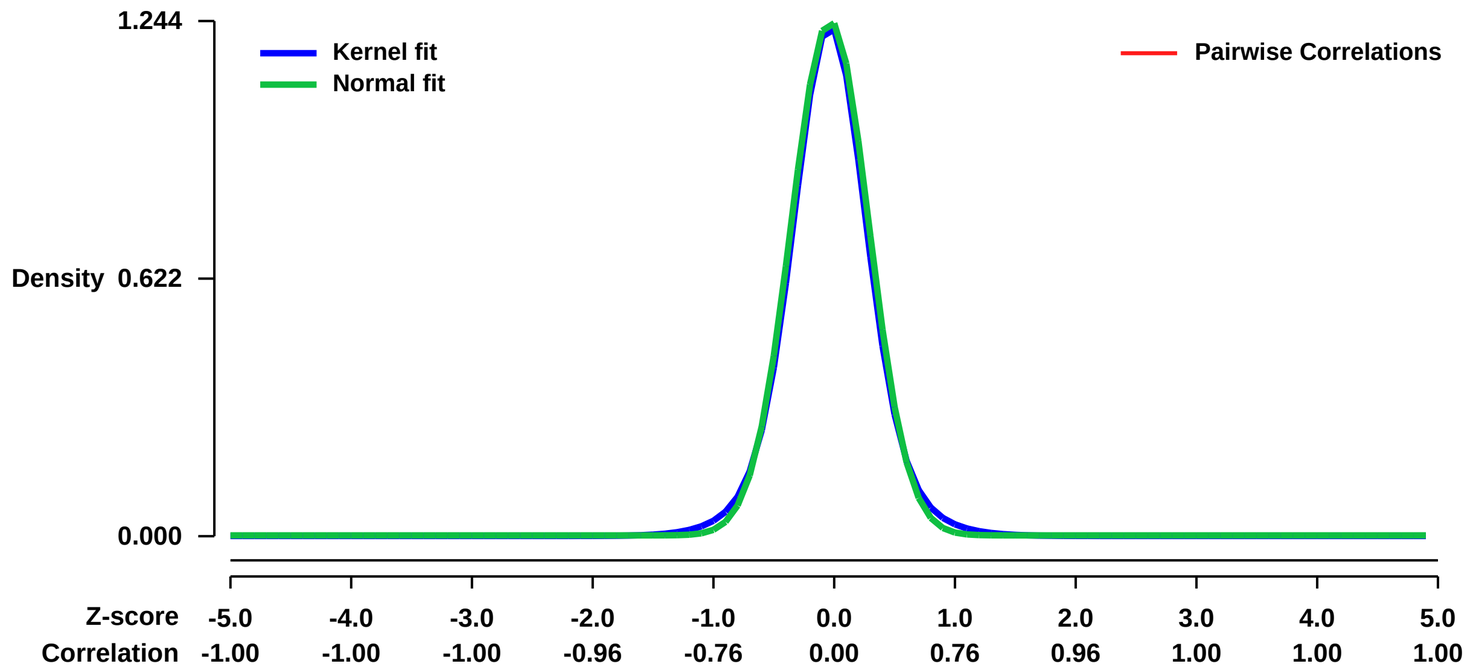

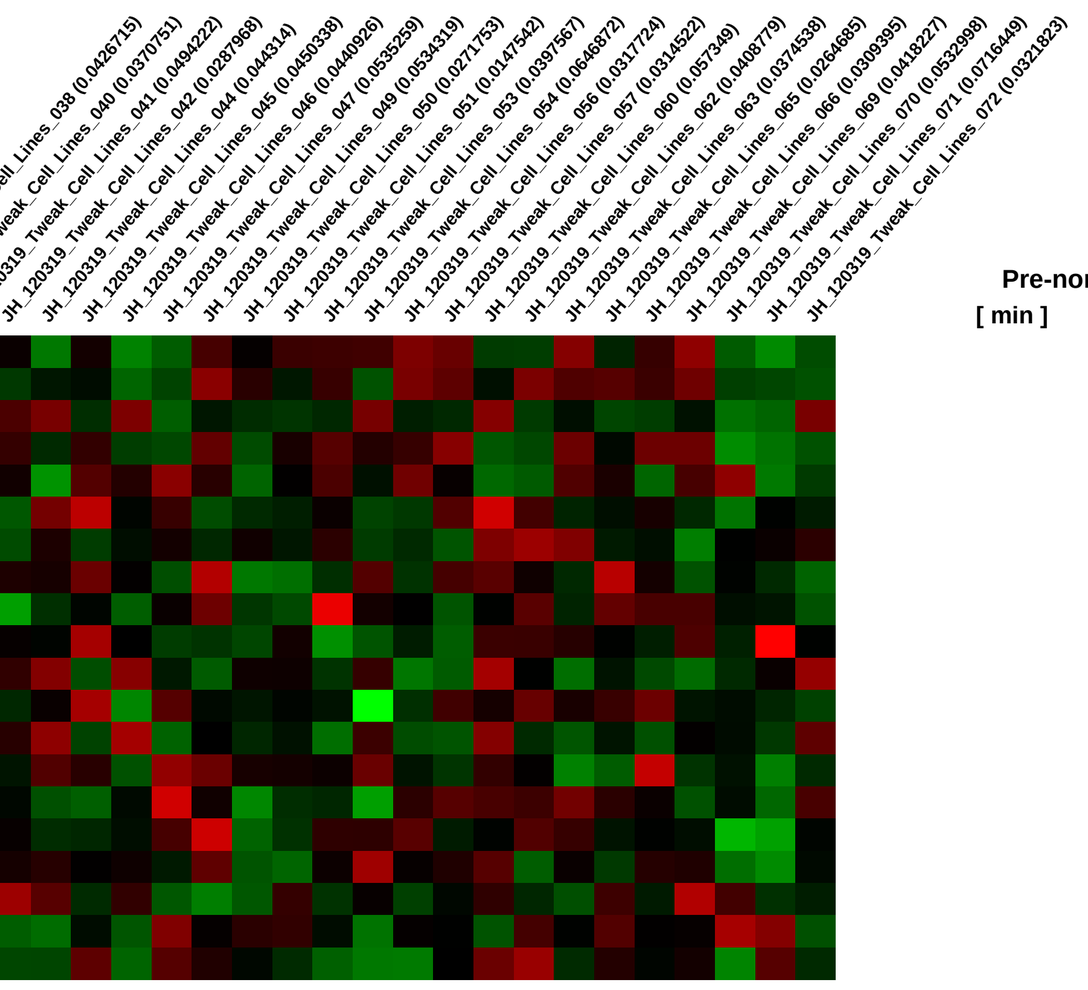

GEO Series "GSE42049" Expression Profiles

Num of samples in this series: 8

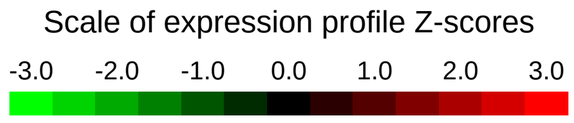

GEO Link:	http://www.ncbi.nlm.nih.gov/geo/query/acc.cgi?acc=GSE42049
Status:	Public on Oct 04 2013
Title:	TWEAK-treated time course in CAKI cells grown as xenografts
Organism:	Homo sapiens
Experiment type:	Expression profiling by array
Platform:	GPL1261
Pubmed ID:	23974006
Summary & Design:	**Summary:** Tumor necrosis factor-related weak inducer of apoptosis, TWEAK, is a TNF superfamily member that mediates signaling through its receptor fibroblast growth factor inducible-14, Fn14. In tumor cell lines, TWEAK induces proliferation, survival and NF-kappaB signaling and gene expression that promote tumor growth and suppress antitumor immune responses. Anti-TWEAK antibody, RG7212, inhibits tumor growth in vivo with decreases in pathway activation markers and modulation of tumor, blood and spleen immune cell composition. Candidate response prediction markers, including Fn14, have been identified in mouse models. Phase I pharmacodynamic data from patients are consistent with preclinical results. TWEAK:Fn14 signaling is upregulated in human cancer and pathway activation induces tumor proliferation and survival signaling. Blockade with anti-TWEAK mAb, RG7212, inhibits tumor growth in multiple models in mice. TWEAK induces changes that suppress anti-tumor immune responses and RG7212 blocks these effects resulting in changes in tumor immune cell composition and decreases in cytokines that promote immunosuppression. Antitumor efficacy in mice was observed in a range of Fn14 expressing models with pathway activation and expressing either wild-type or mutant p53, BRAF or KRAS suggesting both a patient selection strategy and potential broad clinical applicability. Preclinical mechanism of action hypotheses are supported by Phase I clinical data, with decreases in proliferation markers and increased tumor T cell infiltration. **Overall design:** CAKI cells impanted as xenografts in Athymic, Nu/Nu nude mice, treated with anti-TWEAK antibody (TW212) or Vehicle for 24 hours. Four replicates for each condition were performed. RNA was extracted from xenografts, processed and hybridized to human and mouse chips.

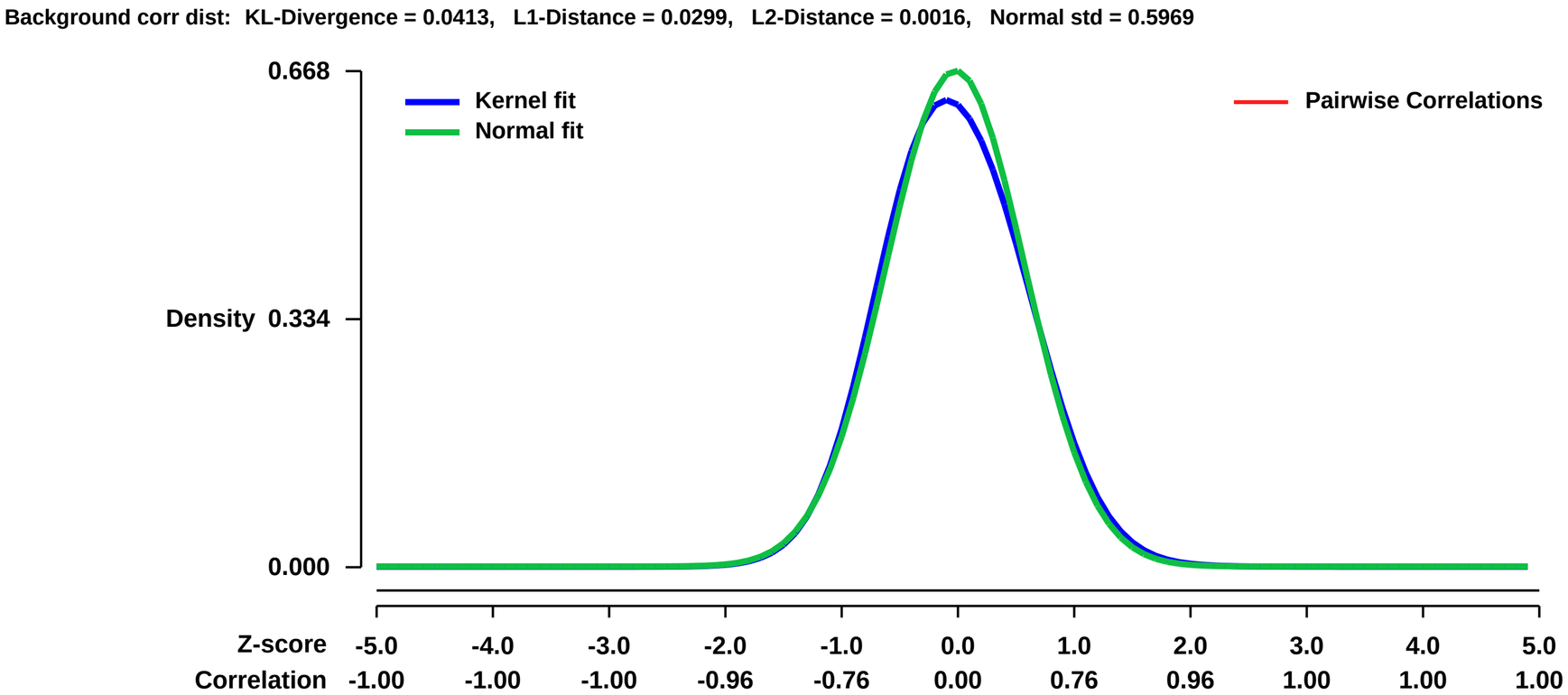

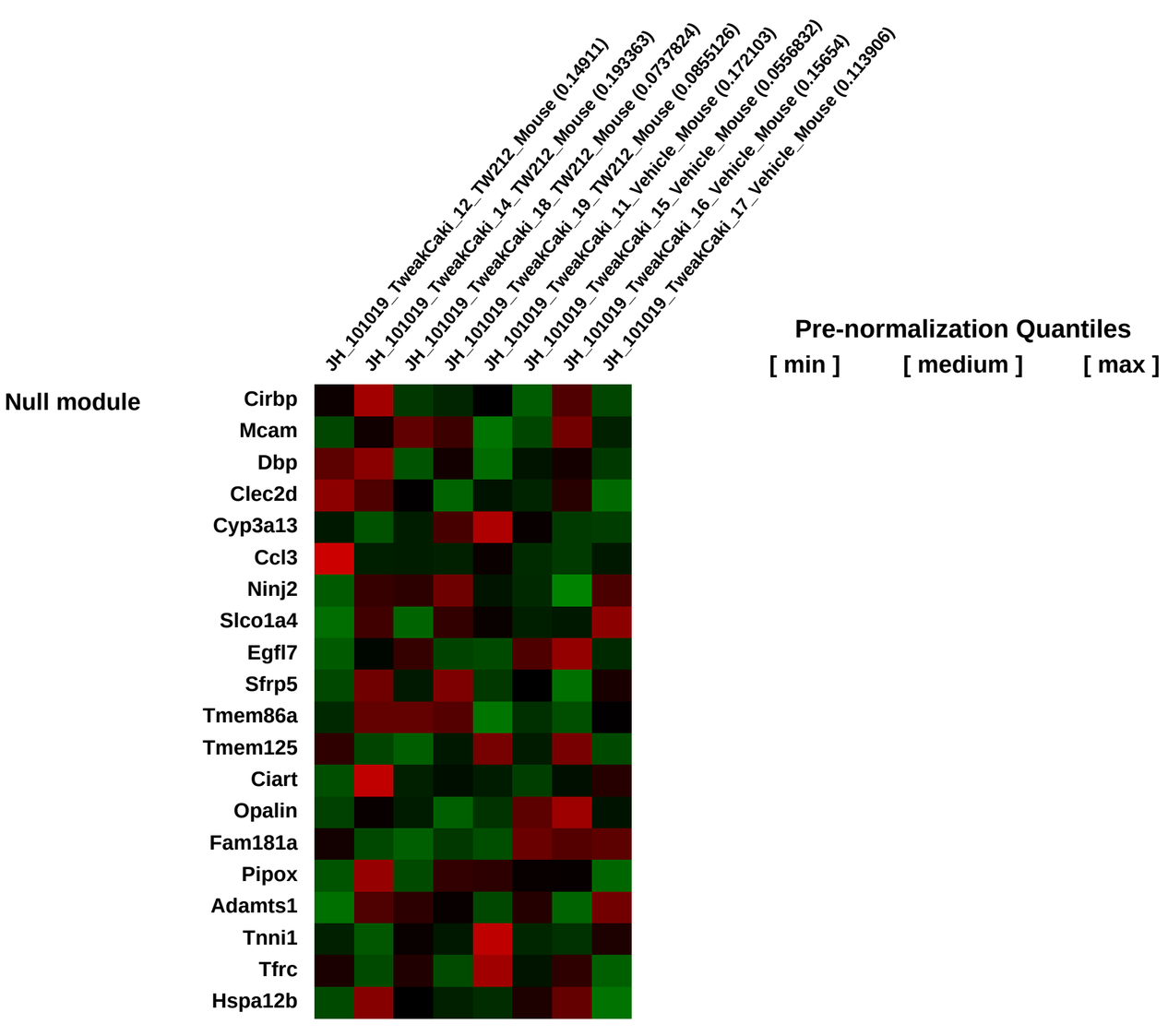

GEO Series "GSE42061" Expression Profiles

Num of samples in this series: 12

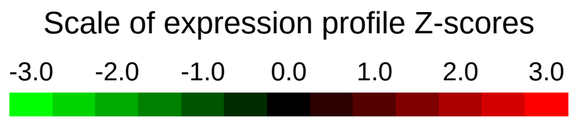

GEO Link:	**http://www.ncbi.nlm.nih.gov/geo/query/acc.cgi?acc=GSE42061**
Status:	**Public on Nov 07 2012**
Title:	**hyperlipidemia impaired innate response**
Organism:	**Mus musculus**
Experiment type:	**Expression profiling by array**
Platform:	**GPL1261**
Pubmed ID:	
Summary & Design:	**Summary:** **To explore the effect of hyperlipidemia on macrophages' innate immune response to Porphyromonas gingivalis invasion** **Overall design:** **12 samples, 3 replicates in 4 groups, with cells from hyperlipidemic ApoE deficient mice and nonhyperlipidemic C57BL/6 mice stimulate with or without P.gingivalis(Pg)**

Background corr dist: **KL-Divergence = 0.0969, L1-Distance = 0.0429, L2-Distance = 0.0028, Normal std = 0.4676**

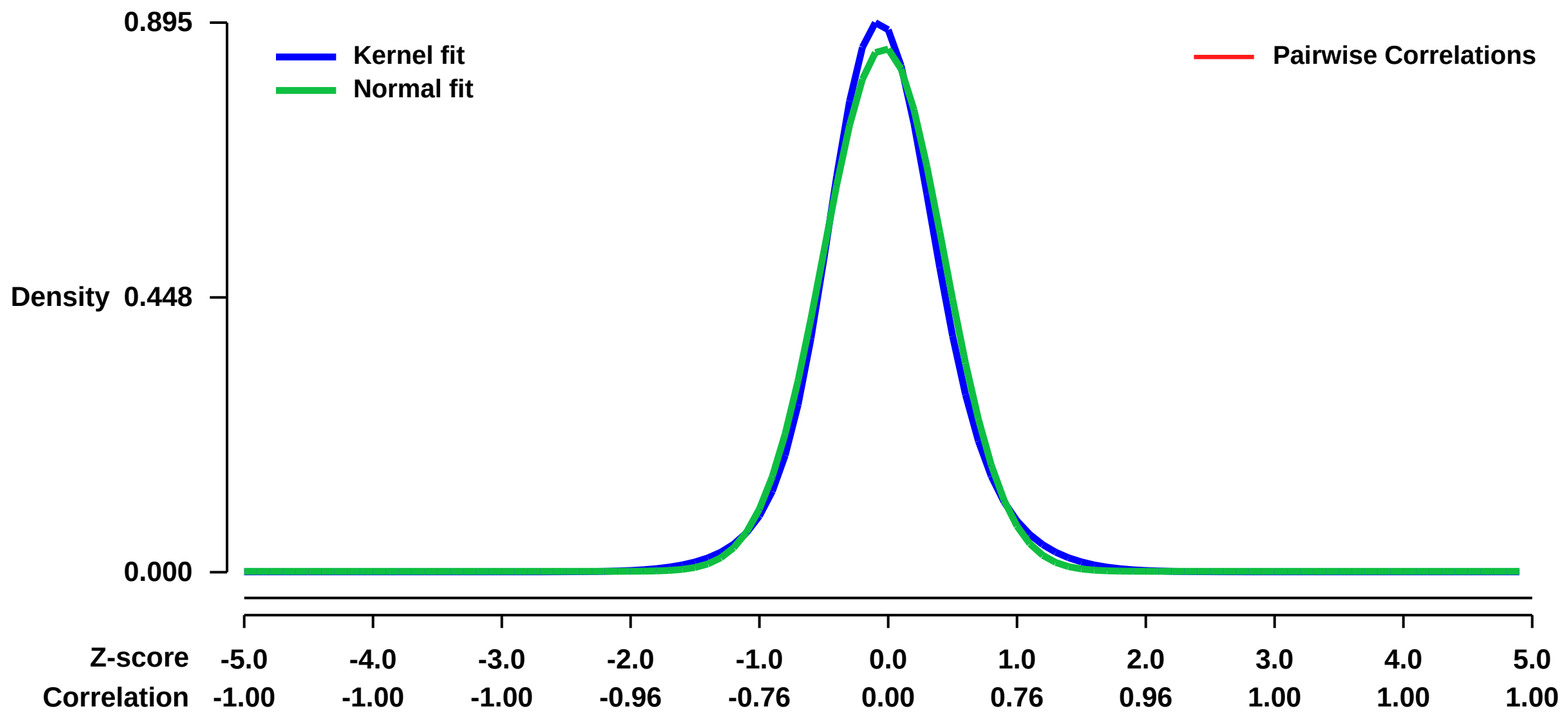

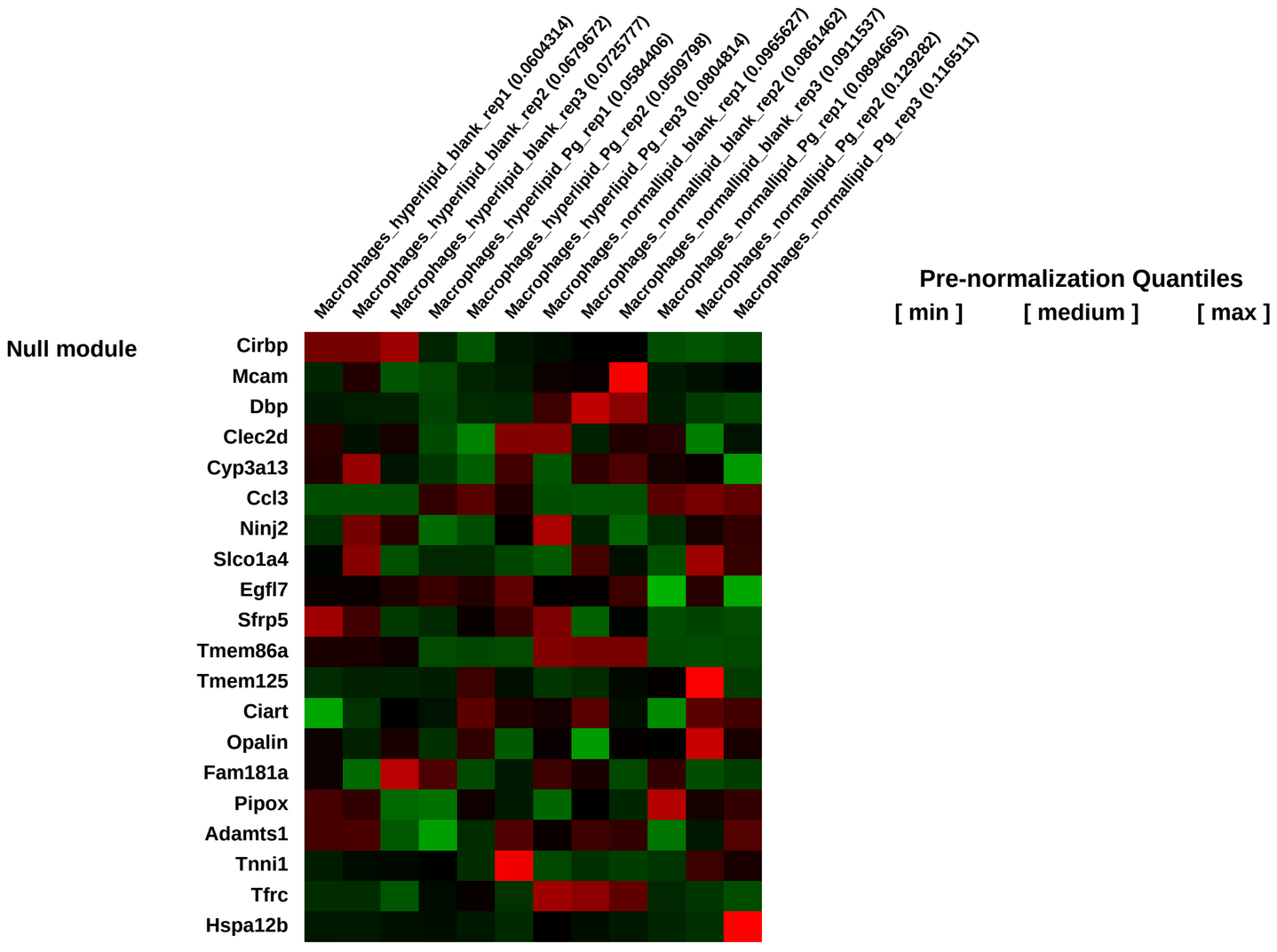

GEO Series "GSE42103" Expression Profiles

Num of samples in this series: 9

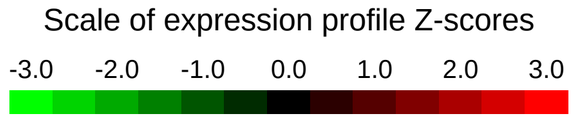

GEO Link:	**http://www.ncbi.nlm.nih.gov/geo/query/acc.cgi?acc=GSE42103**
Status:	**Public on Jan 01 2013**
Title:	**Dual Pten/p53 suppression enhances Notch signaling and sarcoma progression**
Organism:	**Mus musculus**
Experiment type:	**Expression profiling by array**
Platform:	**GPL1261**
Pubmed ID:	
Summary & Design:	**Summary:** **Soft tissue sarcomas (STS) are a heterogeneous group of tumors associated with poor clinical outcome. While a subset of STS are characterized by simple karyotypes and recurrent chromosomal translocations, the mechanisms driving cytogenetically complex sarcomas are largely unknown. Clinical evidence led us to partially inactivate Pten and p53 in the smooth muscle lineage of mice, which developed high-grade undifferentiated pleomorphic sarcomas (HGUPS), leiomyosarcomas (LMS) and carcinosarcomas (CS) that widely recapitulate the human disease, including the aberrant karyotype and metastatic behavior. Pten was found haploinsufficient whereas the wild-type allele of p53 invariably gained point mutations. Gene expression profile showed upregulated Notch signaling in Ptenâ /+p53â /+ tumors compared to Pten+/+p53â /+. Consistently, Pten silencing exacerbated the clonogenic and invasive potential of p53-deficient bone marrow-derived mouse mesenchymal stem cells and tumor cells, while activating the Notch pathway. Moreover, the increased oncogenic behavior of Ptenâ /+p53â /+ and shPten-transduced Pten+/+p53â /+ tumor cells was counteracted by treatment with a gamma secretase inhibitor (GSI), suggesting that the aggressiveness of those tumors can be attributed, at least in part, to enhanced Notch signaling. This study demonstrates a cooperative role for Pten and p53 suppression in complex karyotype sarcomas while establishing Notch as an important functional player in the crosstalk of these pathways during tumor progression. Our results highlight the importance of molecularly subclassifying high-grade sarcoma patients for targeted treatments.** **Compare Ptenâ /+p53â /+ to Pten+/+p53â /+ high-grade undifferentiated pleomorphic sarcomas (HGUPS)** **Overall design:** **Keywords: Differential gene expression.**

Background corr dist: KL-Divergence = 0.0618, L1-Distance = 0.0709, L2-Distance = 0.0081, Normal std = 0.5992

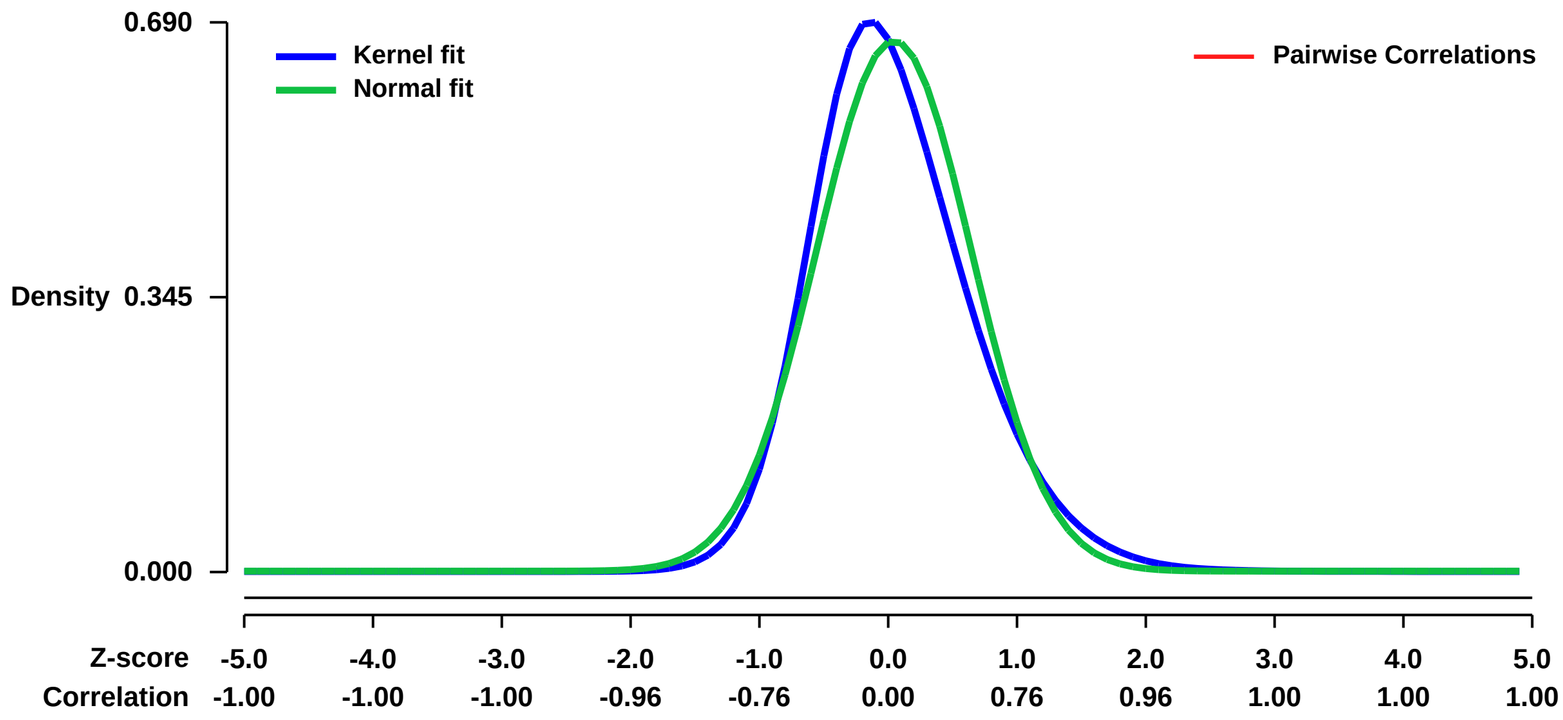

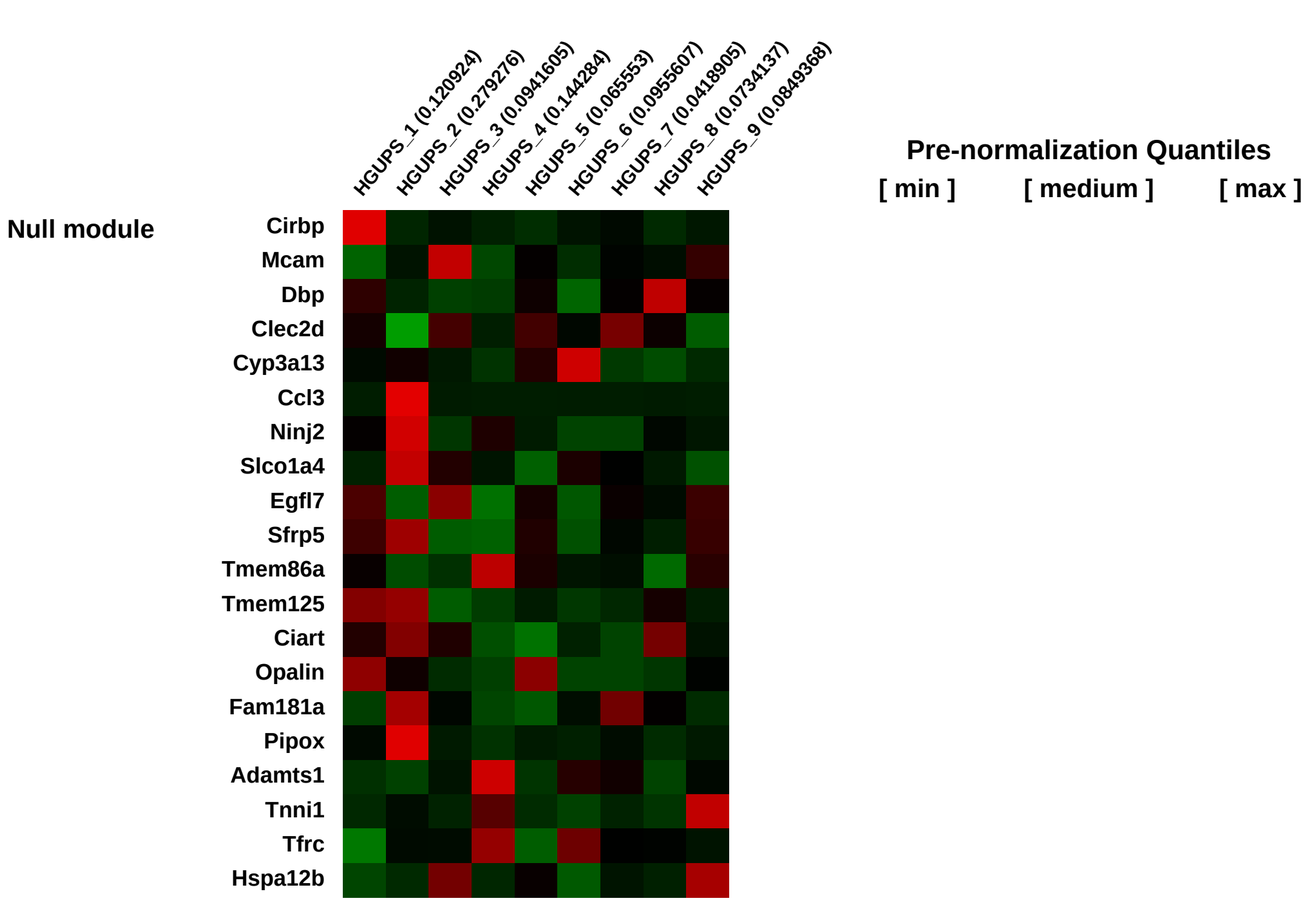

GEO Series "GSE42238" Expression Profiles

Num of samples in this series: 9

Scale of expression profile Z-scores

-3.0 -2.0 -1.0 0.0 1.0 2.0 3.0

GEO Link:	http://www.ncbi.nlm.nih.gov/geo/query/acc.cgi?acc=GSE42238
Status:	Public on Feb 19 2013
Title:	The C-terminus of CBFˆ -SMMHC is required to induce embryonic hematopoietic defects and leukemogenesis.
Organism:	Mus musculus
Experiment type:	Expression profiling by array
Platform:	GPL1261
Pubmed ID:	23152542
Summary & Design:	**Summary:** The C-terminus of CBFˆ -SMMHC, the fusion protein produced by a chromosome 16 inversion in acute myeloid leukemia subtype M4Eo, contains domains for self-mulimerization and transcriptional repression, both of which have been proposed to be important for leukemogenesis by CBFˆ -SMMHC. To test the role of the fusion protein's C-terminus in vivo, we generated knock-in mice expressing a C-terminally truncated CBFˆ -SMMHC (CBFˆ -SMMHC¸ C95). Embryos with a single copy of CBFˆ -SMMHCDC95 were viable and showed no defects in hematopoiesis, while embryos homozygous for the CBFˆ -SMMHC¸ C95 allele had hematopoietic defects and died in mid-gestation, similar to embryos with a single-copy of the full-length CBFˆ -SMMHC¸ C95. To identify gene expression changes induced by CBFˆ -SMMHCDC95, we compared the gene expression profile in the blood cells of Cbfb+/+, Cbfb+/¸ C95, and Cbfb¸ C95/¸ C95 embryonic day 12.5 (E12.5) mice. **Overall design:** Cbfb+/¸ C95 were mated together to generate Cbfb+/+, Cbfb+/¸ C95, and Cbfb¸ C95/¸ C95 embryos. Blood from 8-10 E12.5 embryos of the same genotype was pooled, and RNA was isolated, labeled, and hybridized to Affymetrix Genechip mouse microarray (430 2.0) chips. 3 chips were used for each genotype.

Background corr dist: KL-Divergence = 0.0484, L1-Distance = 0.0351, L2-Distance = 0.0021, Normal std = 0.5825

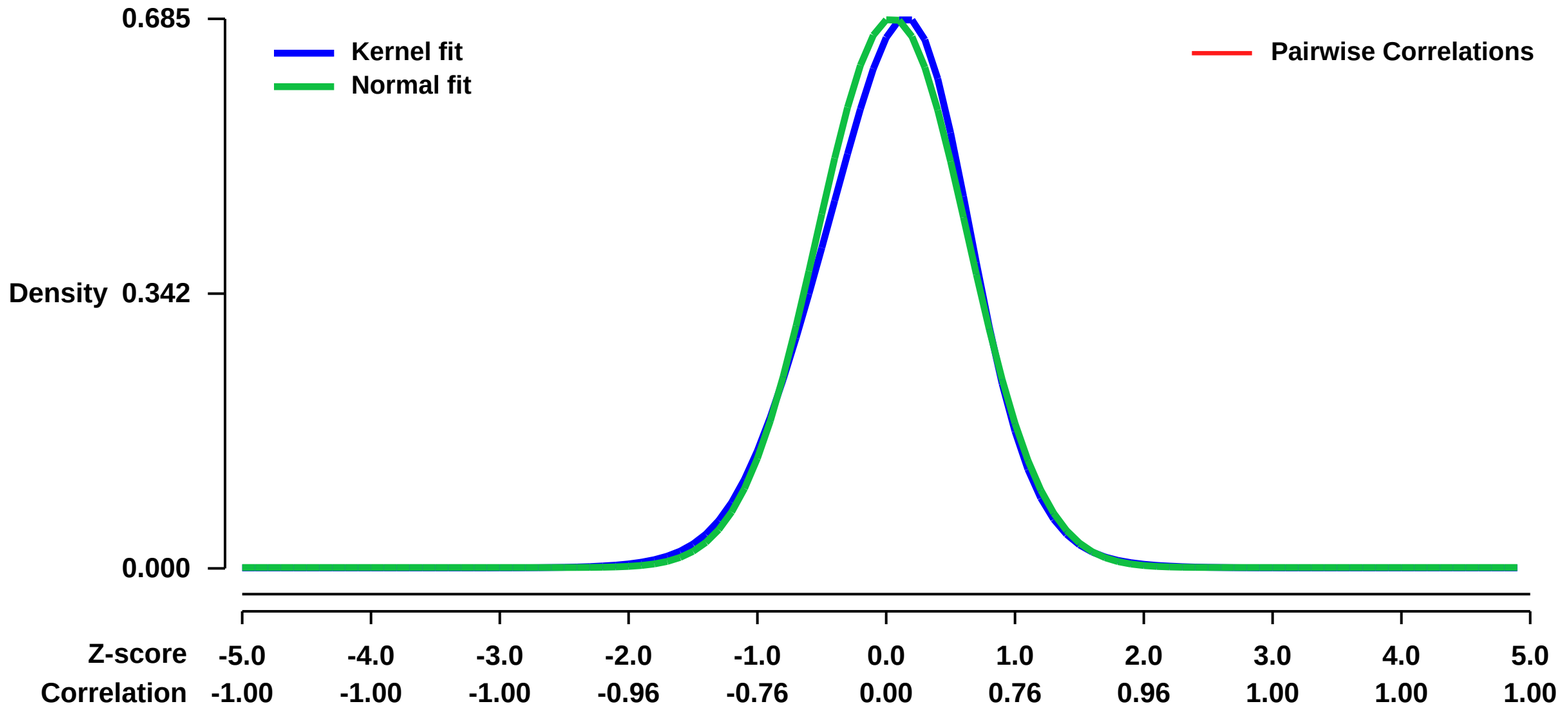

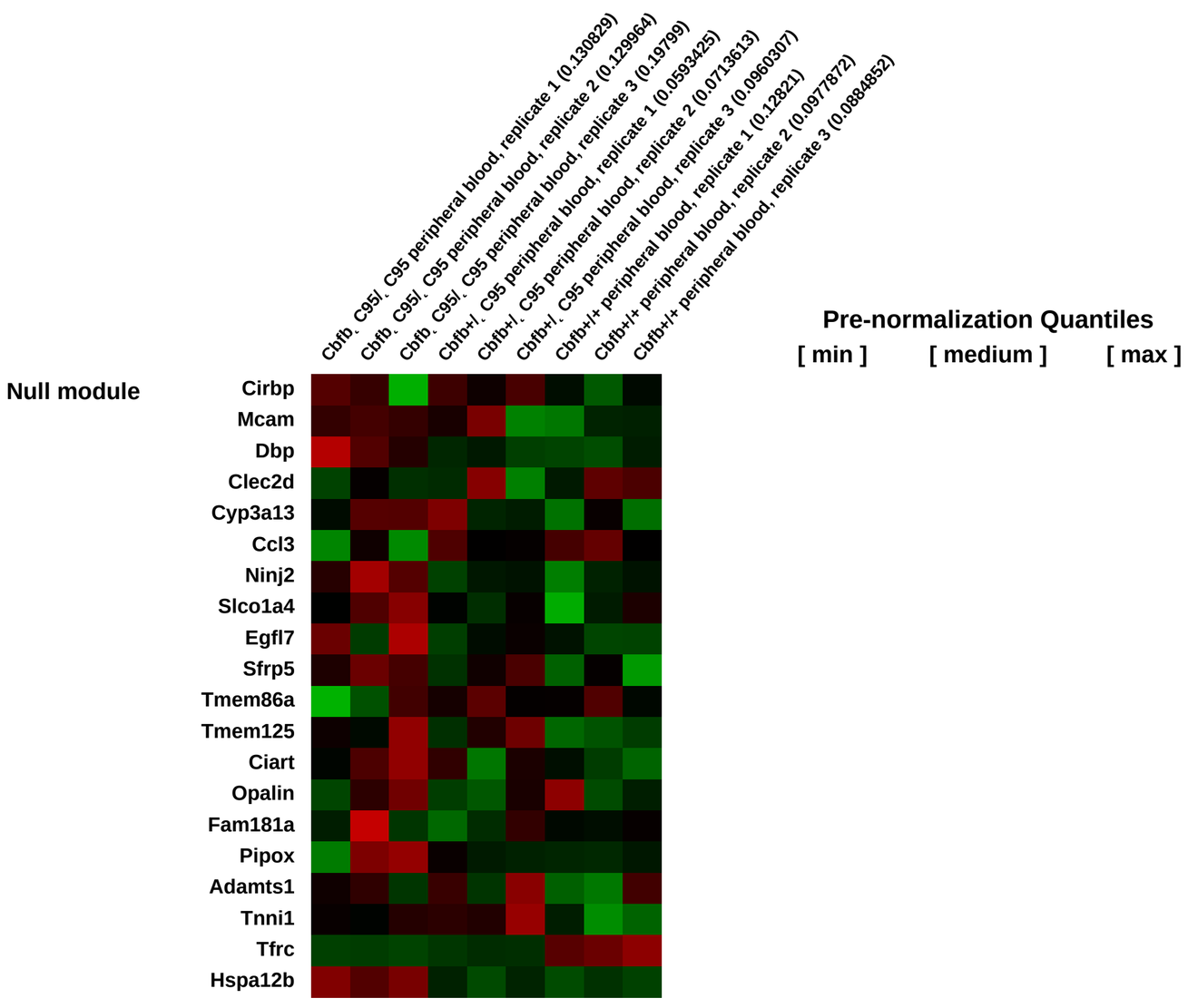

GEO Series "GSE42260" Expression Profiles

Num of samples in this series: 6

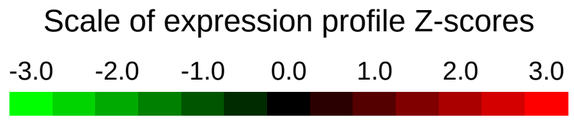

GEO Link:	http://www.ncbi.nlm.nih.gov/geo/query/acc.cgi?acc=GSE42260
Status:	Public on Jan 18 2013
Title:	Notch Pathway Activation Targets AML Cell Homeostasis and Differentiation: MLL-AF9 transformed LGMP
Organism:	Mus musculus
Experiment type:	Expression profiling by array
Platform:	GPL1261
Pubmed ID:	23359070
Summary & Design:	**Summary:** To determine role of Notch signaling in AML leukemia initiating cells we used a conditional mouse knock-in model of Notch1-IC to induce Notch1-IC expression in MLL-AF9 transformed LGMP. WT and Notch1-IC+ LGMP were analyzed to determined genes controlled by Notch signaling. **Overall design:** 12 weeks old wt lethaly irradiated mice were transplanted with 50000 cKit+ MLL-AF9-IRES-YFP infected cells from MLL-AF9 EF1 wt/wt ROSAwt/CreERT2 or MLL-AF9 EF1 wt/lsl-N1-IC ROSAwt/CreERT2 mice + 250000 support wt total bone marrow cells. 4 weeks after transplant mice were injected 2 times with tamoxifen (0.2mg/g body weight) every other day. Mice were sacrificed and analyzed 6 days after last injection. LGMP were flow purified for RNA extraction and hybridization on Affymetrix microarrays.

Background corr dist: KL-Divergence = 0.0405, L1-Distance = 0.0182, L2-Distance = 0.0004, Normal std = 0.6118

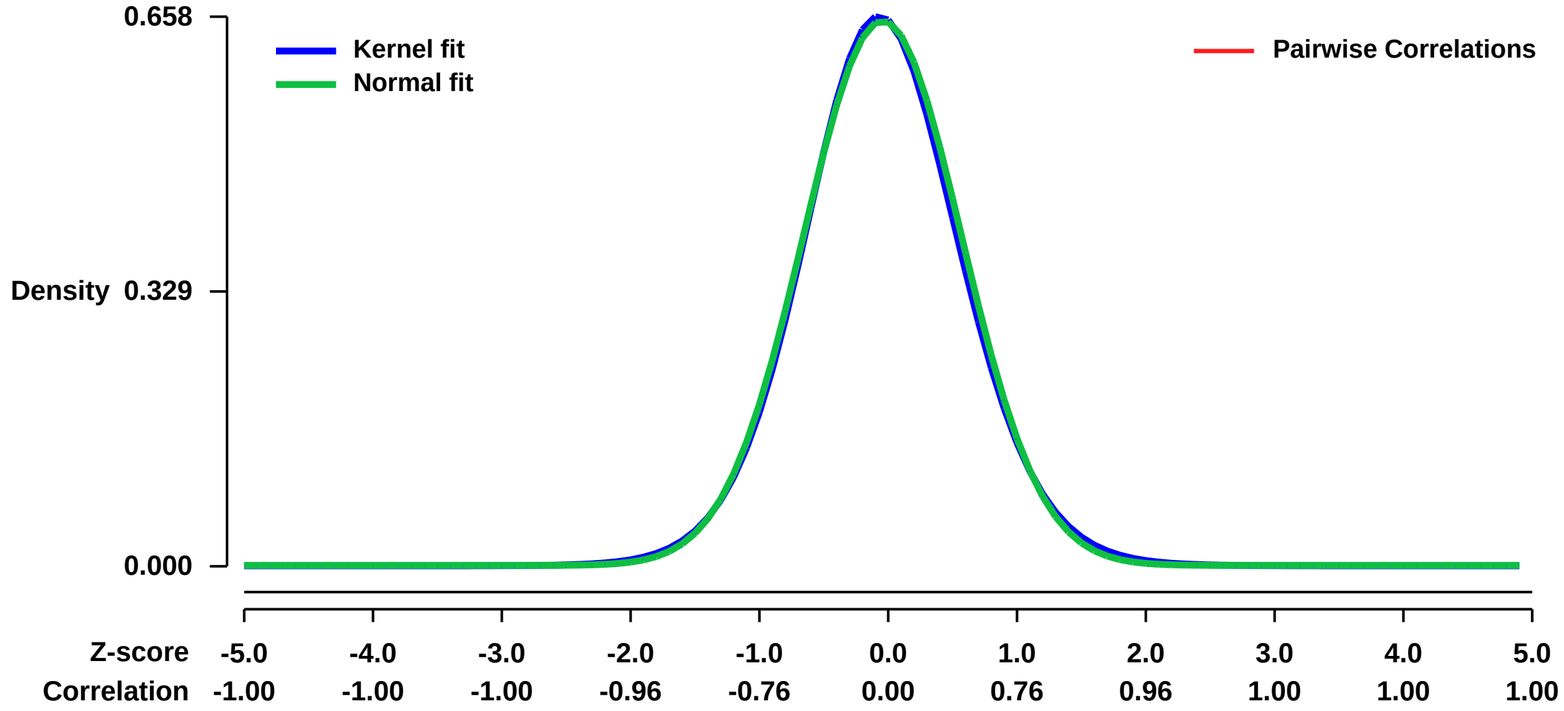

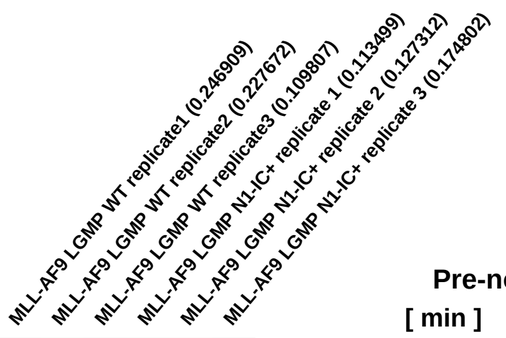

Pre-normalization Quantiles

[min] [medium] [max]

Null module

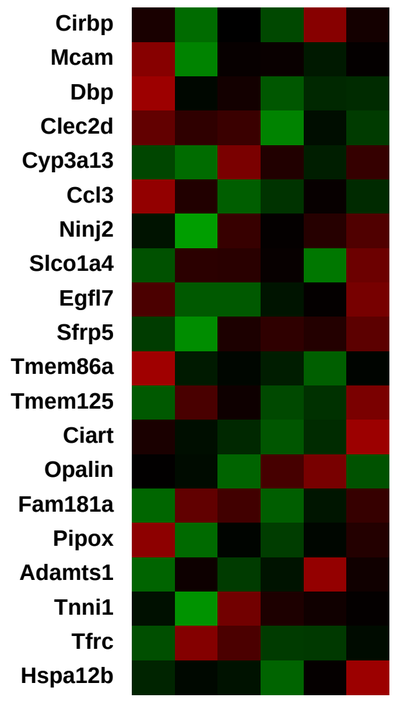

GEO Series "GSE42264" Expression Profiles

Num of samples in this series: 26

Scale of expression profile Z-scores

-3.0 -2.0 -1.0 0.0 1.0 2.0 3.0

GEO Link:	http://www.ncbi.nlm.nih.gov/geo/query/acc.cgi?acc=GSE42264
Status:	Public on Nov 14 2012
Title:	Hsp70 and a Novel Axis of Type 1 Interferon-Dependent Antiviral Immunity in the Measles Virus-Infected Brain
Organism:	Mus musculus
Experiment type:	Expression profiling by array
Platform:	GPL1261
Pubmed ID:	23135720
Summary & Design:	**Summary:** The major inducible 70 kDa heat shock protein (hsp70) is host protective in a mouse model of measles virus (MeV) brain infection. Transgenic constitutive expression of hsp70 in neurons, the primary target of MeV infection, abrogates neurovirulence in neonatal H-2d congenic C57BL/6 mice. A significant level of protection is retained after depletion of T lymphocytes, implicating innate immune mechanisms. Focus of the present work was to elucidate the basis for hsp70-dependent innate immunity using this model. Transcriptome analysis of brains from transgenic (TG) and non-transgenic (NT) mice 5 days after infection identified type 1 interferon (IFN) signaling and macrophage activation/antigen presentation as the main differences linked to survival. The pivotal role for type 1 IFN in hsp70-mediated protection was demonstrated in mice with a genetically disrupted type 1 IFN receptor (IFNAR-/-), where IFNAR-/- eliminated the difference in survival between TG and NT mice. Brain macrophages, not neurons, are the predominant source of type 1 IFN in the virus-infected brain, and in vitro studies provided a mechanistic basis by which MeV-infected neurons can induce IFN-¿† in uninfected microglia in an hsp70-dependent manner. MeV infection induced extracellular release of hsp70 from mouse neuronal cells that constitutively express hsp70, and extracellular hsp70 induced IFN-¿† transcription in mouse microglial cells through Toll-like receptors 2 and 4. Collectively, results support a novel axis of type 1 IFN-dependent antiviral immunity in the virus-infected brain that is driven by hsp70. **Overall design:** Hsp70-overexpressing transgenic (TG) and non-transgenic (NT) mice were infected with MeV intracranially, and total brain mRNA harvested at 5 and 10 days post infection (d.p.i.) was analyzed, sampling the hemisphere opposite the side of viral inoculation. Analysis includes 6 groups: infected TG at 5 d.p.i. (n=4), infected TG at 10 d.p.i. (n=5), infected NT at 5 d.p.i. (n=4), infected NT at 10 d.p.i. (n=5), uninfected TG at 5 d.p.i. (n=4), and uninfected NT at 5 d.p.i. (n=4).

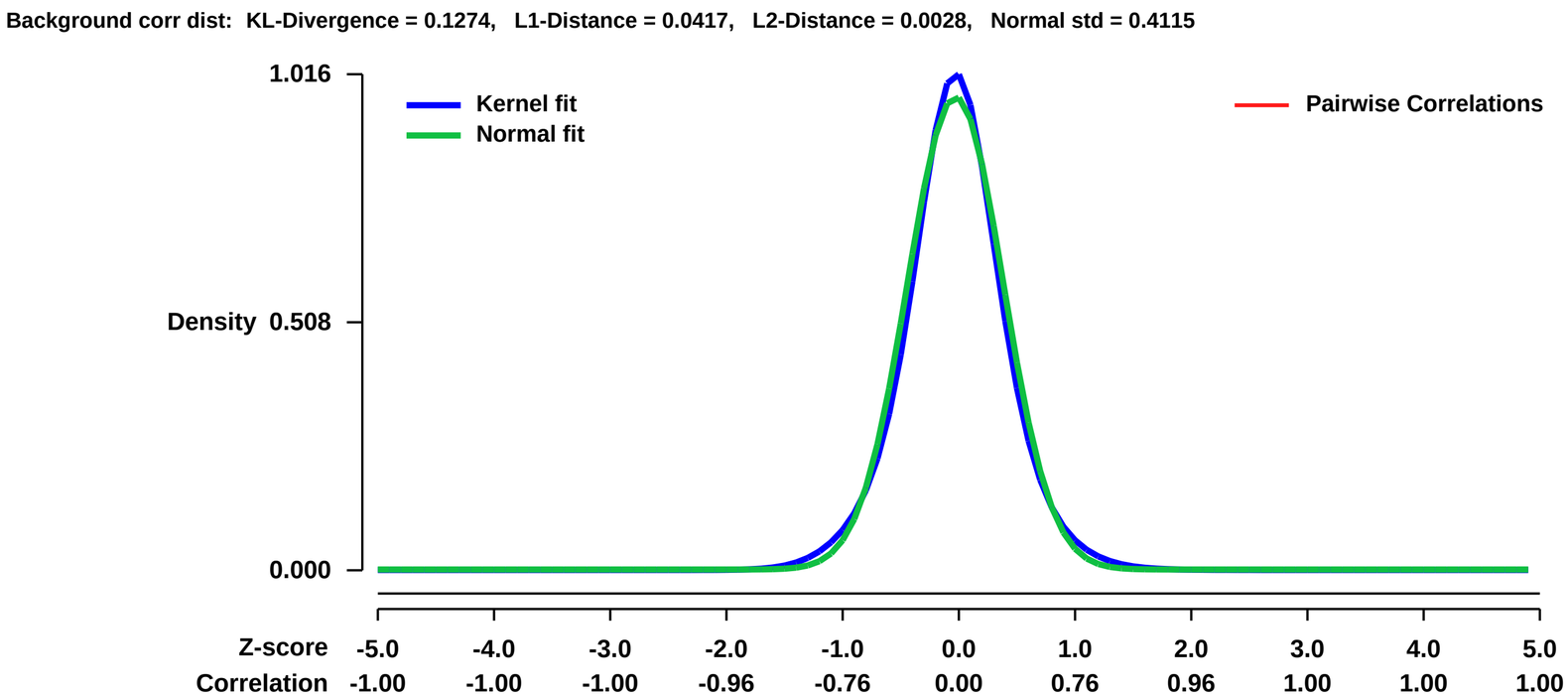

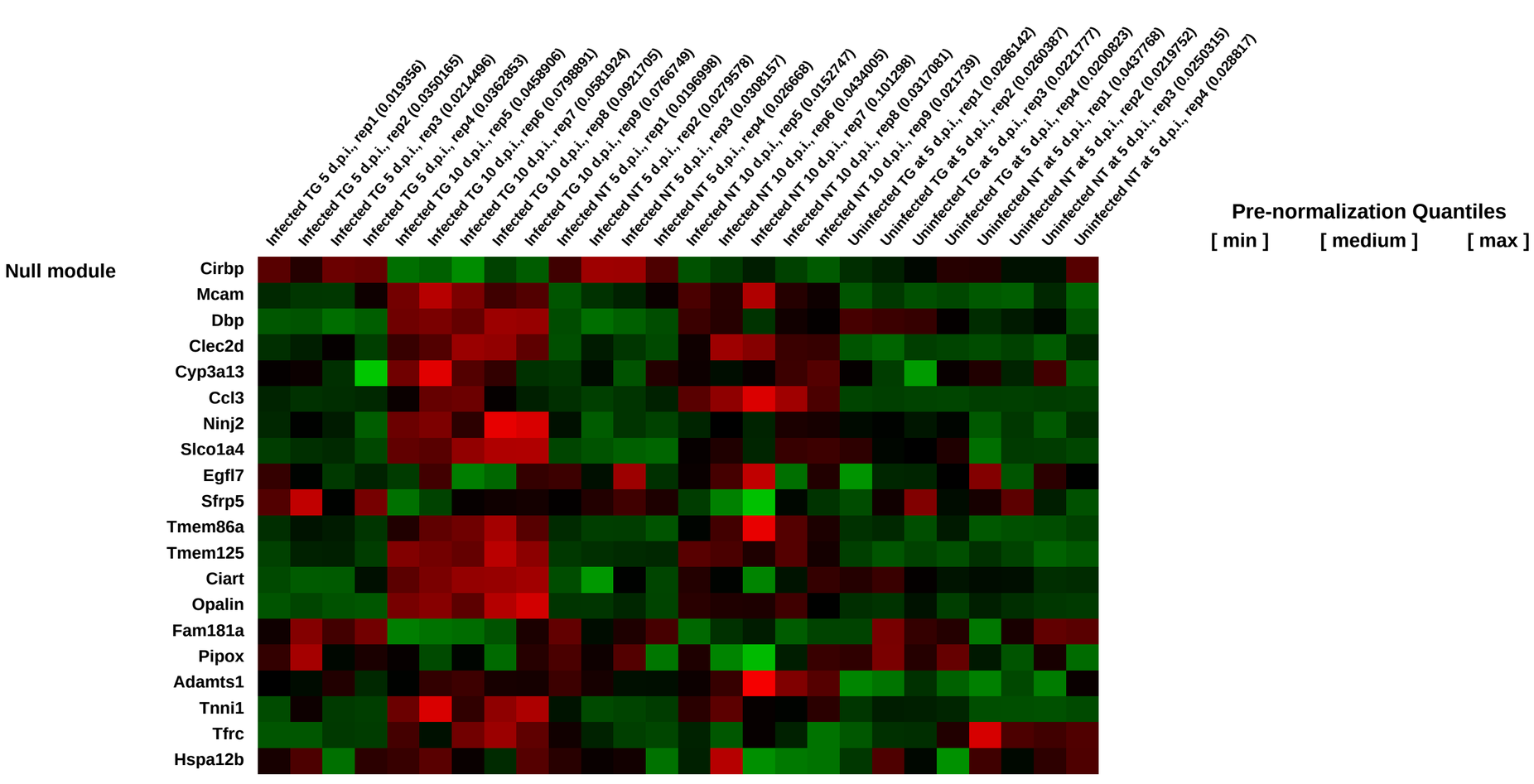

GEO Series "GSE42299" Expression Profiles

Num of samples in this series: 8

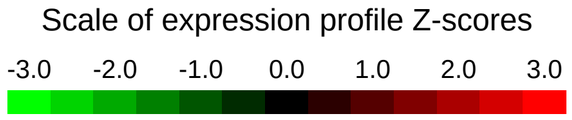

GEO Link:	http://www.ncbi.nlm.nih.gov/geo/query/acc.cgi?acc=GSE42299
Status:	Public on Dec 10 2012
Title:	Expression profiles of C2C12 myotubes in response to PGC-1¸– (peroxisome proliferator-activated receptor gamma, coactivator 1 alpha) overexpression and/or iron chelati
Organism:	Mus musculus
Experiment type:	Expression profiling by array
Platform:	GPL1261
Pubmed ID:	23318259
Summary & Design:	**Summary:** Mitochondria are centers of metabolism and signaling whose content and function must adapt to changing cellular environments. The biological signals that initiate mitochondrial restructuring and the cellular processes that drive this adaptive response are largely obscure. To better define these systems, we performed matched quantitative genomic and proteomic analyses of mouse muscle cells as they performed mitochondrial biogenesis. We find that proteins involved in cellular iron homeostasis are highly coordinated with this process, and that depletion of cellular iron results in a rapid, dose-dependent decrease of select mitochondrial protein levels and oxidative capacity. We further show that this process is universal across a broad range of cell types and fully reversed when iron is reintroduced. Collectively, our work reveals that cellular iron is a key regulator of mitochondrial biogenesis, and provides quantitative datasets that can be leveraged to explore post-transcriptional and post-translational processes that are essential for mitochondrial adaptation. **Overall design:** C2C12 mouse myoblasts were differentiated into myotubes for 3 days, at which point they were infected with adenovirus expressing either green fluorescent protein (GFP) or GFP-tagged PGC-1¸– (GFP-PGC-1¸–) ´– treatment with the iron chelator deferoxamine (DFO) (for 4 treatments total). The cells were grown for three more days, then RNA was extracted and applied to Affymetrix Mouse 430 2.0 arrays. Gene expression was measured in biological duplicate (4 treatments ^ 2 replicates = 8 arrays).

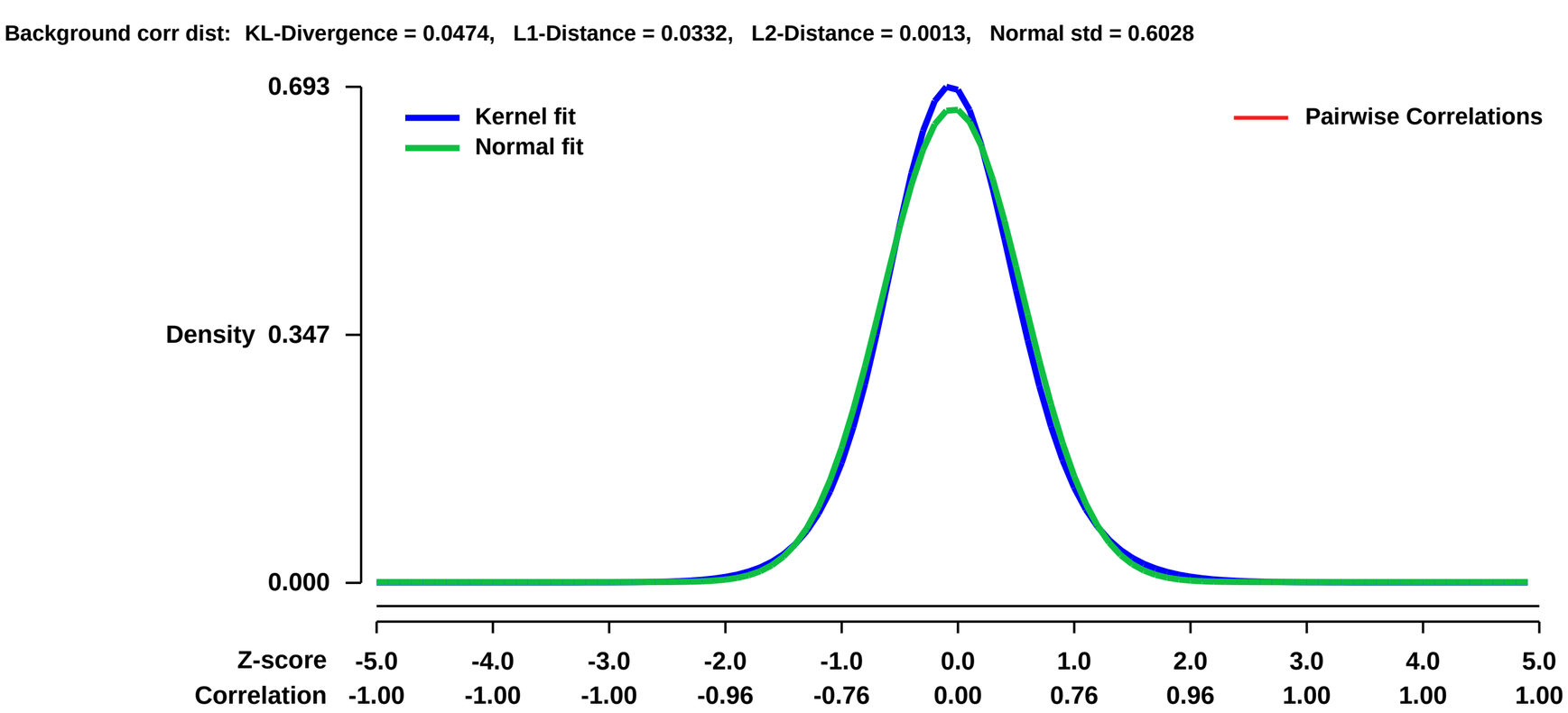

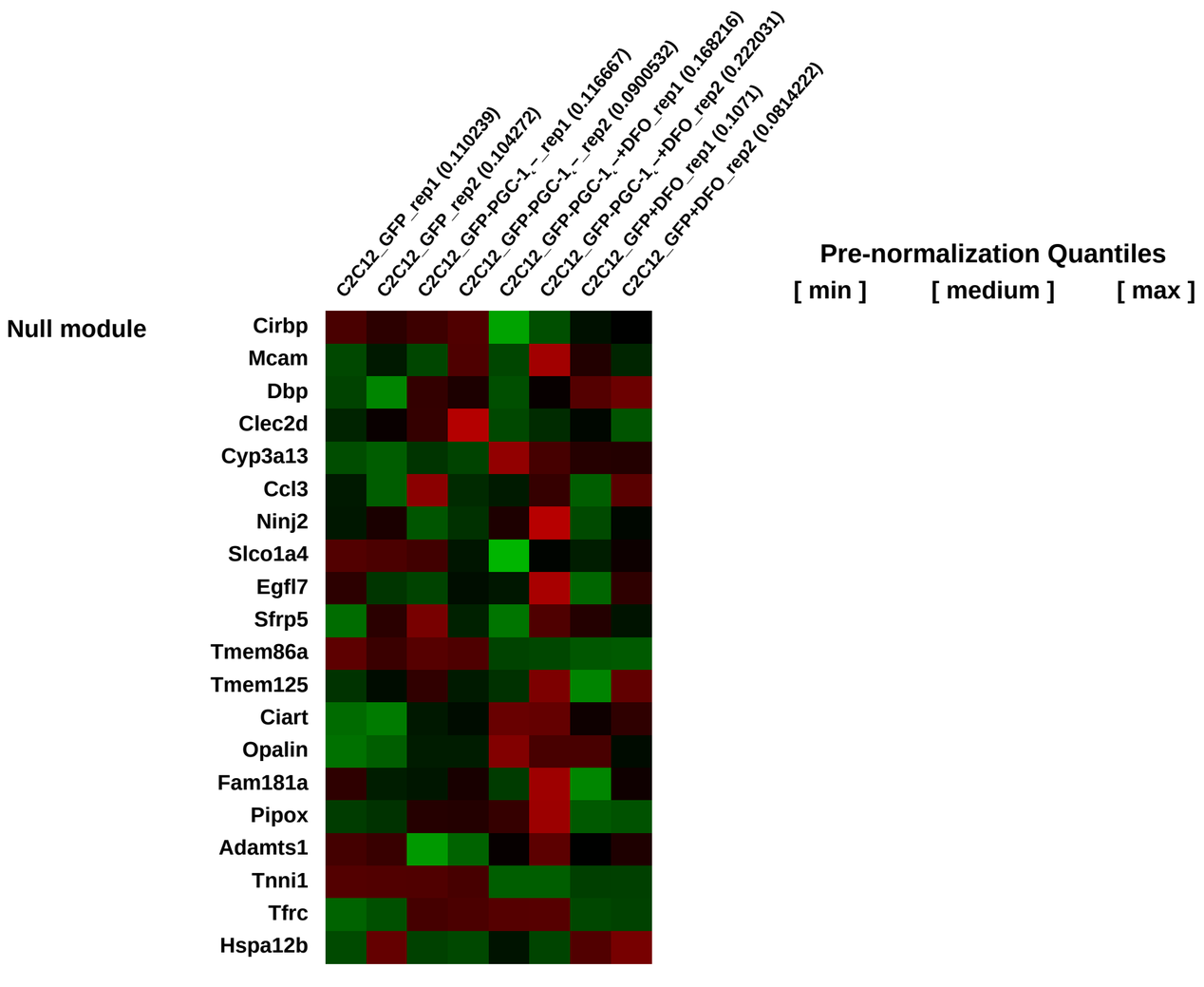

GEO Series "GSE4230" Expression Profiles

Num of samples in this series: 8

Scale of expression profile Z-scores

-3.0 -2.0 -1.0 0.0 1.0 2.0 3.0

GEO Link:	http://www.ncbi.nlm.nih.gov/geo/query/acc.cgi?acc=GSE4230
Status:	Public on Feb 13 2006
Title:	Gene expression profiles in developing nephrons using Lim1 metanephric mesenchyme-specific conditional mutant mice
Organism:	Mus musculus
Experiment type:	Expression profiling by array
Platform:	GPL1261
Pubmed ID:	16464245
Summary & Design:	**Summary:** **BACKGROUND: Lim1 is a homeobox gene that is essential for nephrogenesis. During metanephric kidney development, Lim1 is expressed in the nephric duct, ureteric buds, and the induced metanephric mesenchyme. Conditional ablation of Lim1 in the metanephric mesenchyme blocks the formation of nephrons at the nephric vesicle stage, leading to the production of small, non-functional kidneys that lack nephrons.** **METHODS: In the present study, we used Affymetrix probe arrays to screen for nephron-specific genes by comparing the expression profiles of control and Lim1 conditional mutant kidneys. Kidneys from two developmental stages, embryonic day 14.5 (E14.5) and 18.5 (E18.5), were examined.** **RESULTS: Comparison of E18.5 kidney expression profiles generated a list of 465 nephron-specific gene candidates that showed a more than 2-fold increase in their expression level in control kidney versus the Lim1 conditional mutant kidney. Computational analysis confirmed that this screen enriched for kidney-specific genes. Furthermore, at least twenty-eight of the top fifty (56%) candidates (or their vertebrate orthologs) were previously reported to have a nephron-specific expression pattern. Our analysis of E14.5 expression data yielded 41 candidate genes that are up-regulated in the control kidneys compared to the conditional mutants. Three of them are related to the Notch signaling pathway that is known to be important in cell fate determination and nephron patterning.** **CONCLUSIONS: Therefore, we demonstrate that Lim1 conditional mutant kidneys serve as a novel tissue source for comprehensive expression studies and provide a means to identify nephron-specific genes.** **Keywords: tissue specificity, time course, development, kidney, metanephric mesenchyme, nephron, Lim1, knockout mice, conditional knockout** **Overall design:** **Normalized data were exported in a tab delimited text format. Fold changes of each transcript from different samples were calculated and sorted using Microsoft Excel 5.0 software. Signal obtained from control kidney samples were used as an experiment to compare to the signal obtained from Lim1 conditional mutant kidneys that was designated as a baseline. A 2-fold change in the means of signal obtained from experimental duplicates and those from baseline duplicates was used as the criterion to identify differentially expressed transcripts. To ensure the quality of the data, probe sets that showed a fold change between duplicates greater than between the experimental mean and baseline mean were removed. To study only genes that showed consistent expression on experimental chips, probe sets that did not show consistent present calls in the experimental duplicates were removed. To focus on genes with a significant fold change between the experiment and the baseline, only probe sets that the product of their experimental mean and fold change were more than 100 were retained. To produce a compact differentially expressed gene list, the probe set list was sorted within Microsoft Excel based on Locus Link number and redundant entries were removed. Our experimental design description and the data format provided in the Additional files fulfill the MIAME (minimum information about a microarray experiment) standards.**

Background corr dist: **KL-Divergence = 0.0369, L1-Distance = 0.0151, L2-Distance = 0.0003, Normal std = 0.6203**

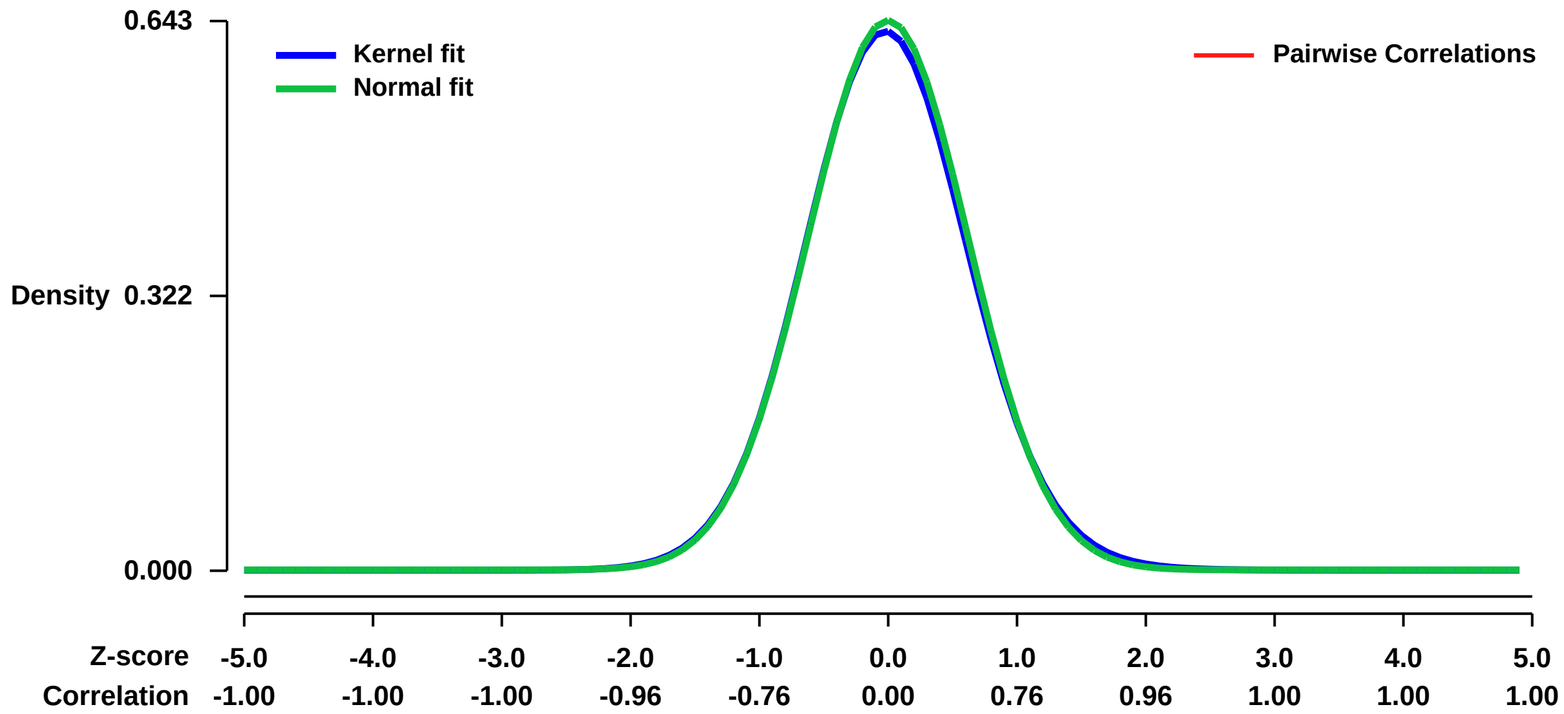

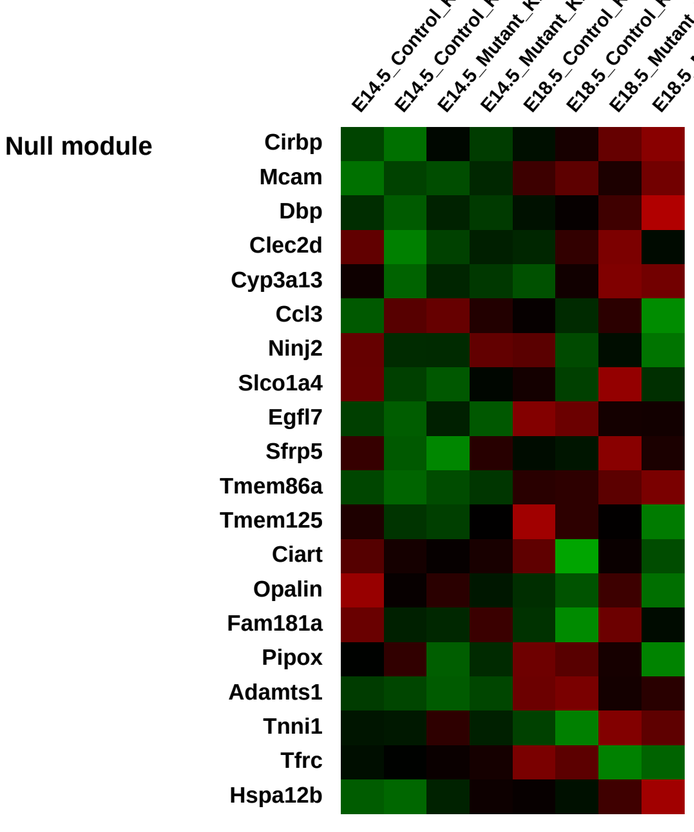

GEO Series "GSE4238" Expression Profiles

Num of samples in this series: 24

Scale of expression profile Z-scores

-3.0 -2.0 -1.0 0.0 1.0 2.0 3.0

GEO Link:	http://www.ncbi.nlm.nih.gov/geo/query/acc.cgi?acc=GSE4238
Status:	Public on Aug 08 2006
Title:	rhythmic transcriptome in the murine wt adrenal
Organism:	Mus musculus
Experiment type:	Expression profiling by array
Platform:	GPL1261
Pubmed ID:	16998155
Summary & Design:	**Summary:** This study was performed to characterize the rhythmic transcirptome of the murine adrenal gland with a focus on the corticosterone synthesis pathway. **Keywords: time course** **Overall design:** LD entrained male animals were released into DD and from the second day on whole adrenals were prepared from 12 time points at 4 hrs intervals.

Background corr dist: KL-Divergence = 0.1034, L1-Distance = 0.0281, L2-Distance = 0.0012, Normal std = 0.4307

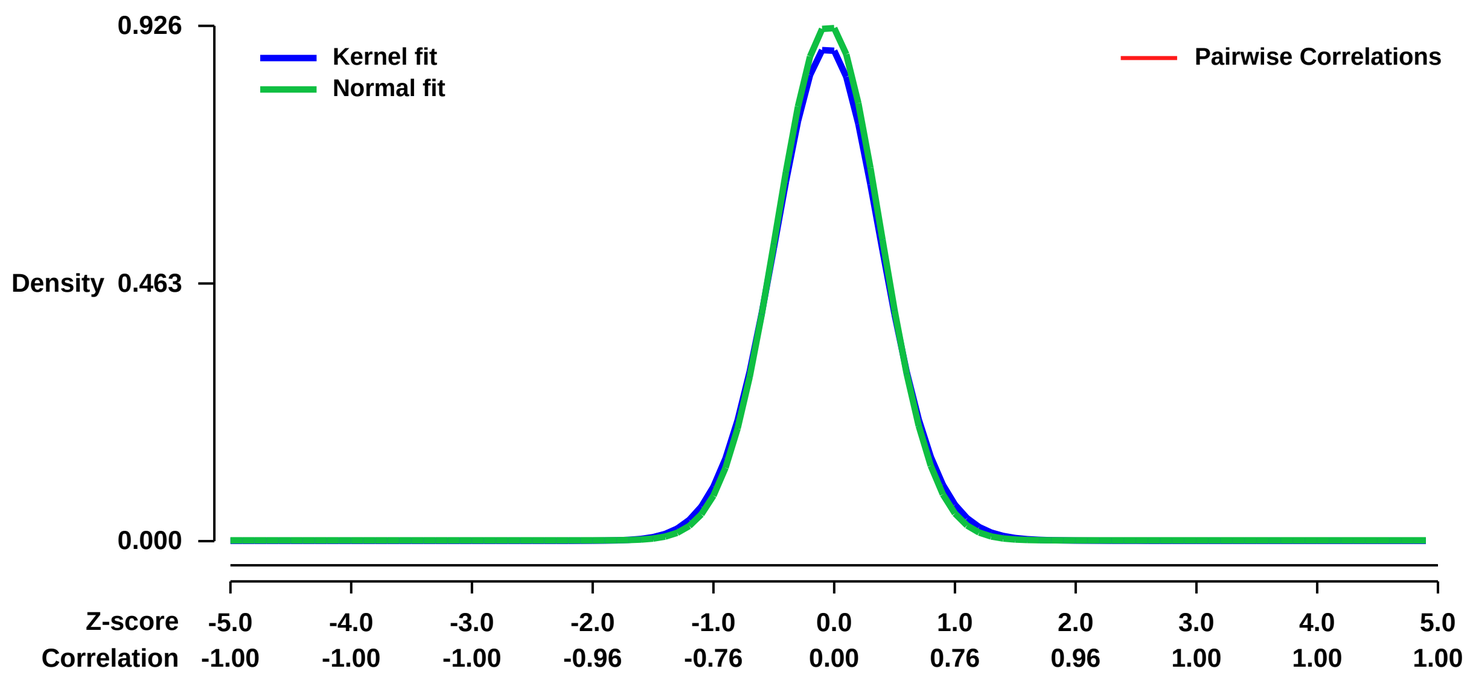

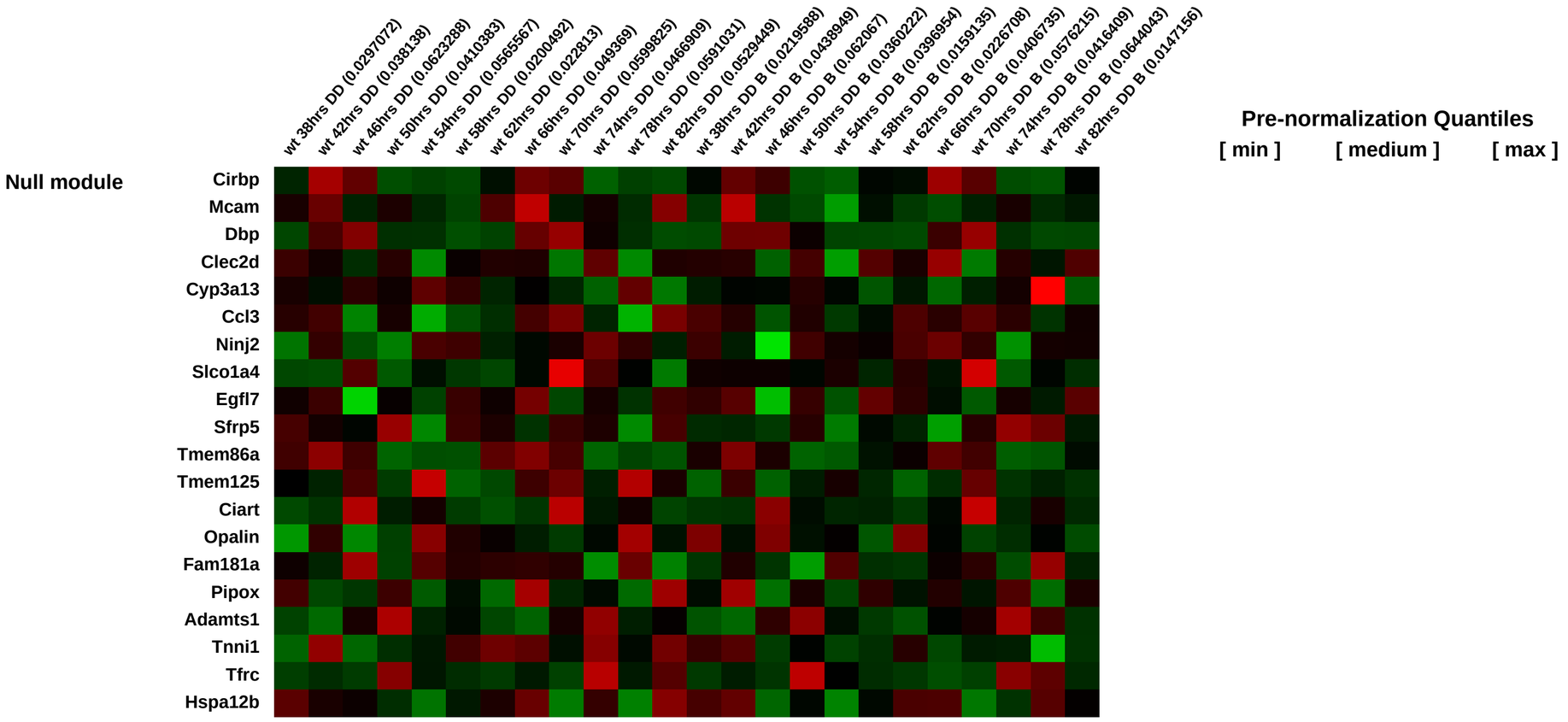

GEO Series "GSE42473" Expression Profiles

Num of samples in this series: 15

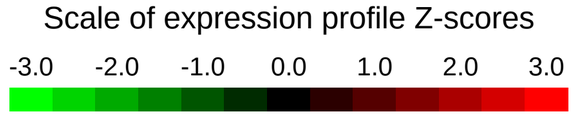

GEO Link:	http://www.ncbi.nlm.nih.gov/geo/query/acc.cgi?acc=GSE42473
Status:	Public on Dec 04 2012
Title:	PGC-1 alpha isoforms and muscle hypertrophy
Organism:	Mus musculus
Experiment type:	Expression profiling by array
Platform:	GPL1261
Pubmed ID:	23217713
Summary & Design:	**Summary:** An alternative promoter of the PGC-1alpha gene gives rise to three new PGC-1alpha isoforms refered to as PGC-1a2 (A2), PGC-1a3 (A3) and PGC-1a4 (A4). The proximal PGC-1 alpha promotor transcribes the canonical PGC-1 alpha which is refered to as PGC-1a1 (A1).G1/G2/G3 samples refer to the Green fluorescent protein (GFP) control samples used in this experiment. Forced expression of the PGC-1a4 isoform results in muslce hypertrophy associated with increased IGF-1 signaling and repression of myostatin signaling. **Overall design:** Mouse primary myoblasts isolated from C57BL/6 mice were differentiated in vitro. Fully differentiated myotubes were transduced with adenoviral vectors expressing GFP (as control) or each of the PGC-1alpha isoforms originating from the proximal or alternative promotor.

Background corr dist: KL-Divergence = 0.1210, L1-Distance = 0.0285, L2-Distance = 0.0011, Normal std = 0.4209

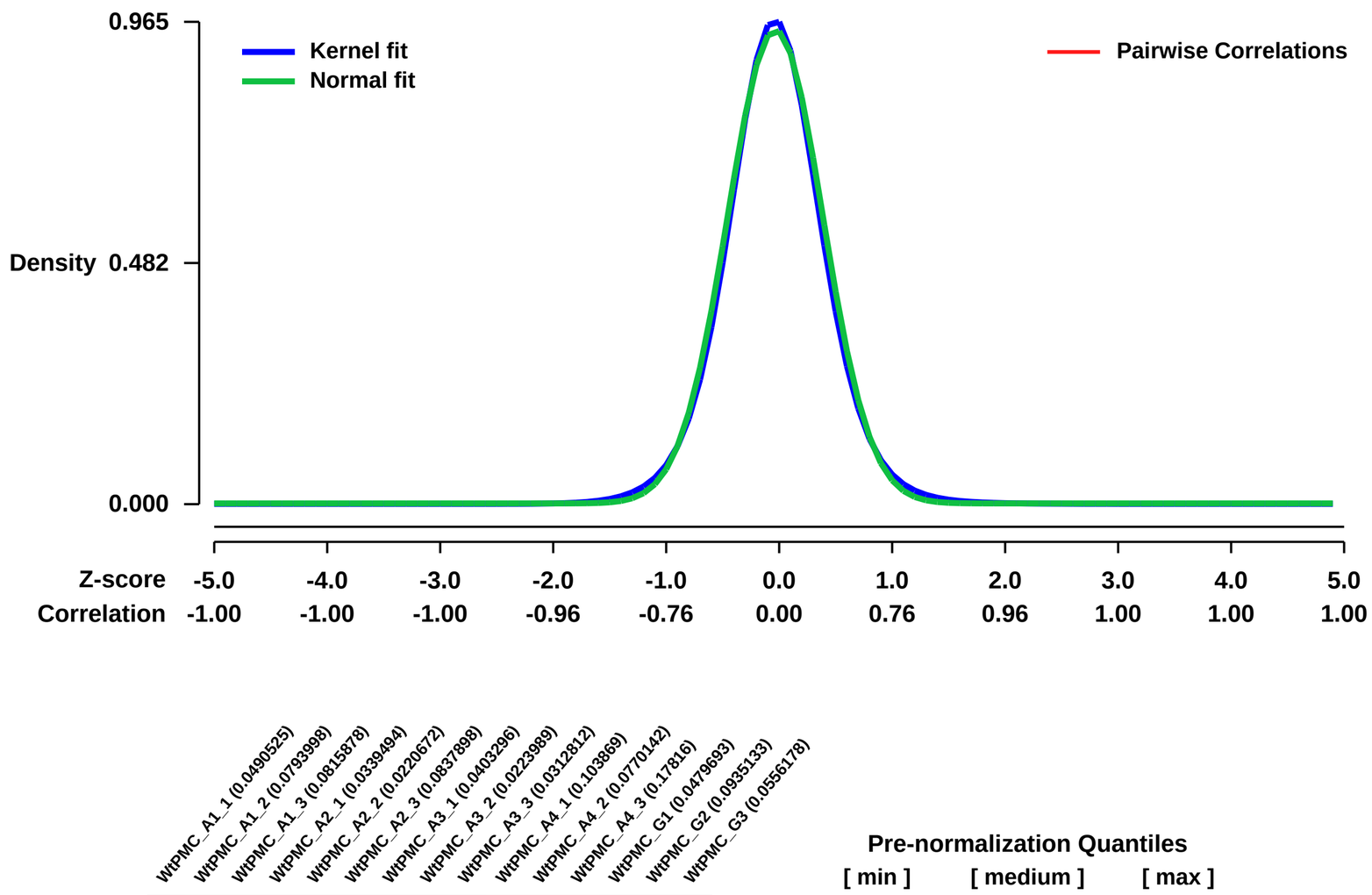

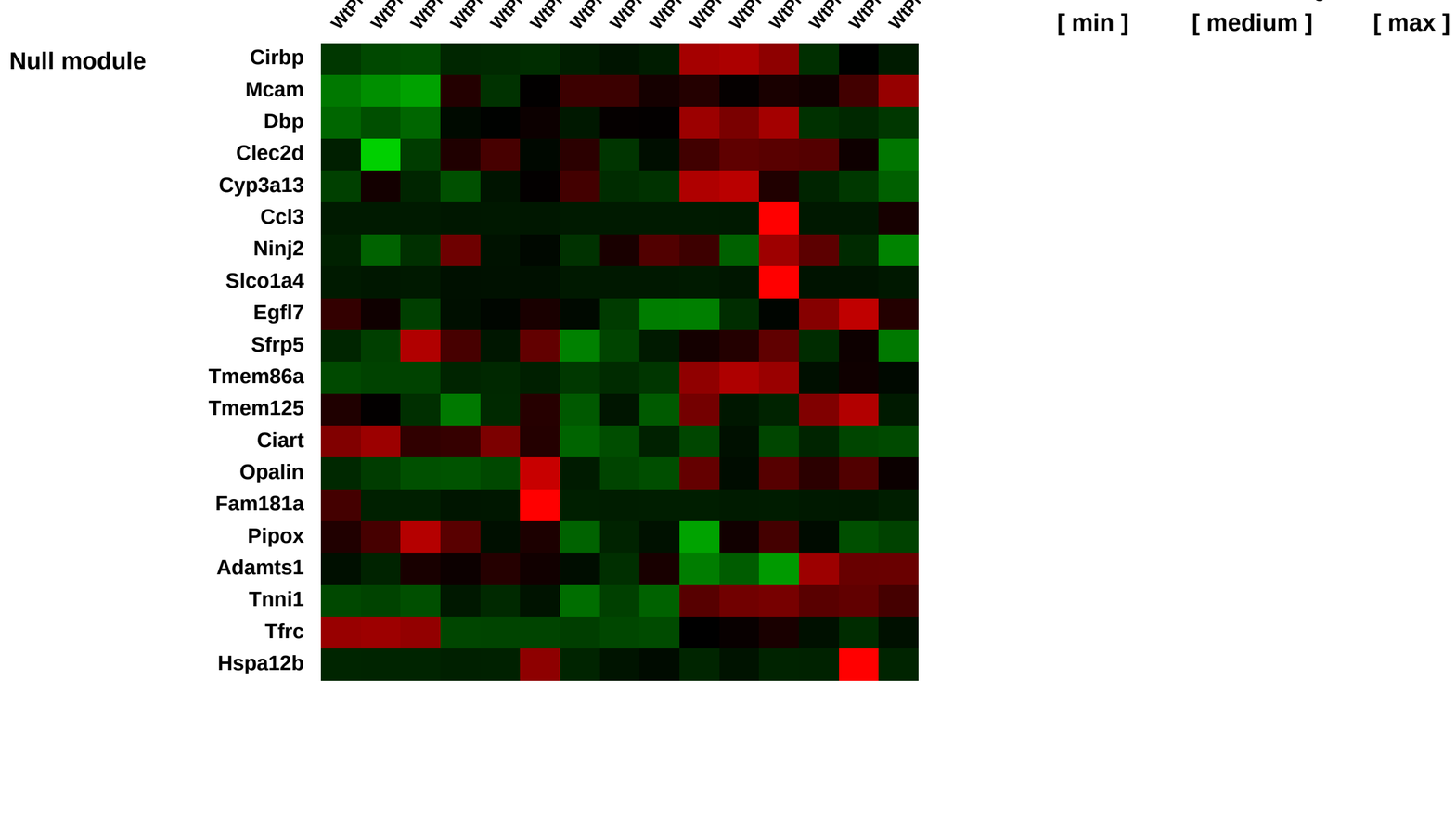

GEO Series "GSE42565" Expression Profiles

Num of samples in this series: 6

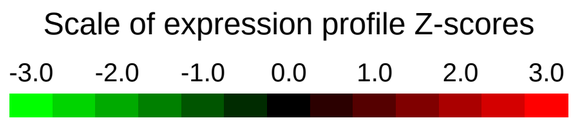

GEO Link:	**http://www.ncbi.nlm.nih.gov/geo/query/acc.cgi?acc=GSE42565**
Status:	**Public on Dec 15 2012**
Title:	**Transcriptional responses to Sonic Hedgehog pathway stimulation in in vitro derived neural progenitors**
Organism:	**Mus musculus**
Experiment type:	**Expression profiling by array**
Platform:	**GPL1261**
Pubmed ID:	**23249739**
Summary & Design:	**Summary:** **The objective of this study was to identify genes regulated by Sonic Hedgehog pathway stimulation in neural progenitors.** **Overall design:** **Paired (parallel culture) triplicates of neuralized embryoid body cultures with and without Shh pathway stimulation (Ag1.3-treatment)**

Background corr dist: **KL-Divergence = 0.0382, L1-Distance = 0.0221, L2-Distance = 0.0005, Normal std = 0.6291**

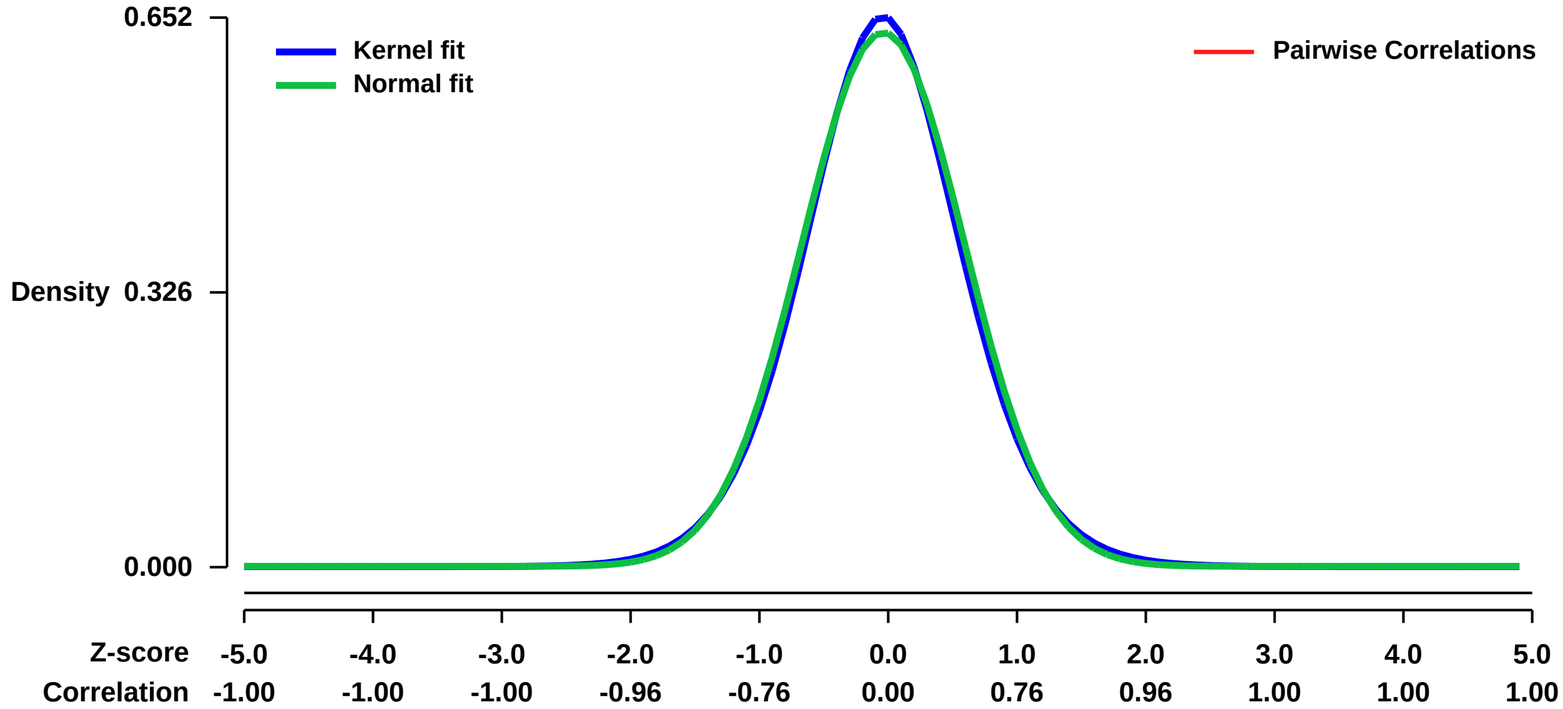

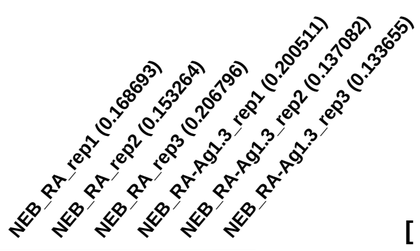

Pre-normalization Quantiles

[min] [medium] [max]

Null module

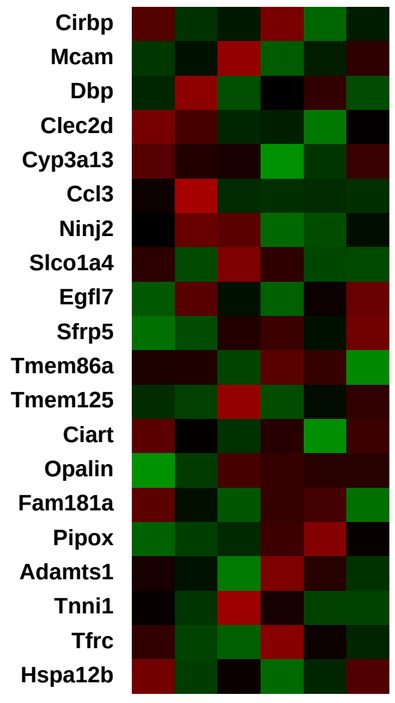

GEO Series "GSE4260" Expression Profiles

Num of samples in this series: 6

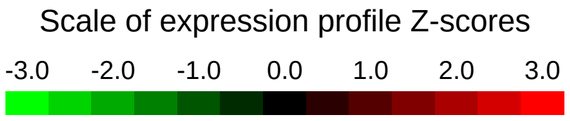

GEO Link:	http://www.ncbi.nlm.nih.gov/geo/query/acc.cgi?acc=GSE4260
Status:	Public on Feb 17 2006
Title:	Cumulus-oocyte complex temporal expression
Organism:	Mus musculus
Experiment type:	Expression profiling by array
Platform:	GPL1261
Pubmed ID:	16455817
Summary & Design:	**Summary:** Cumulus-oocyte complexes were isolated a seperate time-points to generate temporal complexes. Targets from two biological replicates at each time point (0h, 8h, 16h post-hCG treatment) were generated and the expression profiles were determined using Affymetrix GeneChip Mouse Genome 430 2.0 Arrays. Comparisons between the sample groups allow the identification of genes with temporal expression patterns. **Keywords: time course** **Overall design:** 2 eCG-primed (48h) pooled cumulus-oocyte complexes, 2 eCG-primed (48h) hCG-treated (8h) pooled cumulus-oocyte complexes, and 2 eCG-primed (48h) hCG-treated (16h) pooled cumulus-oocyte complexes replicates were analyzed

Background corr dist: KL-Divergence = 0.0244, L1-Distance = 0.0244, L2-Distance = 0.0006, Normal std = 0.7316

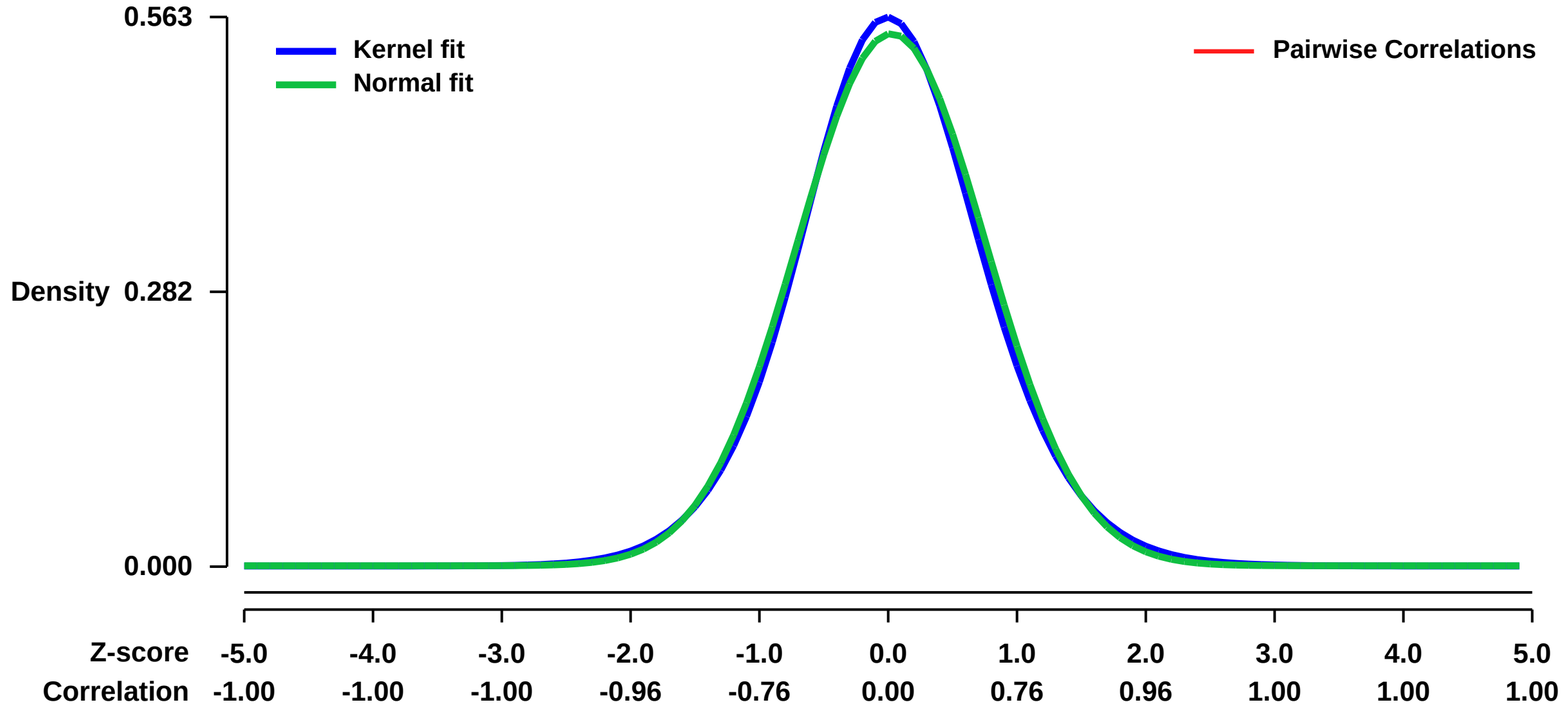

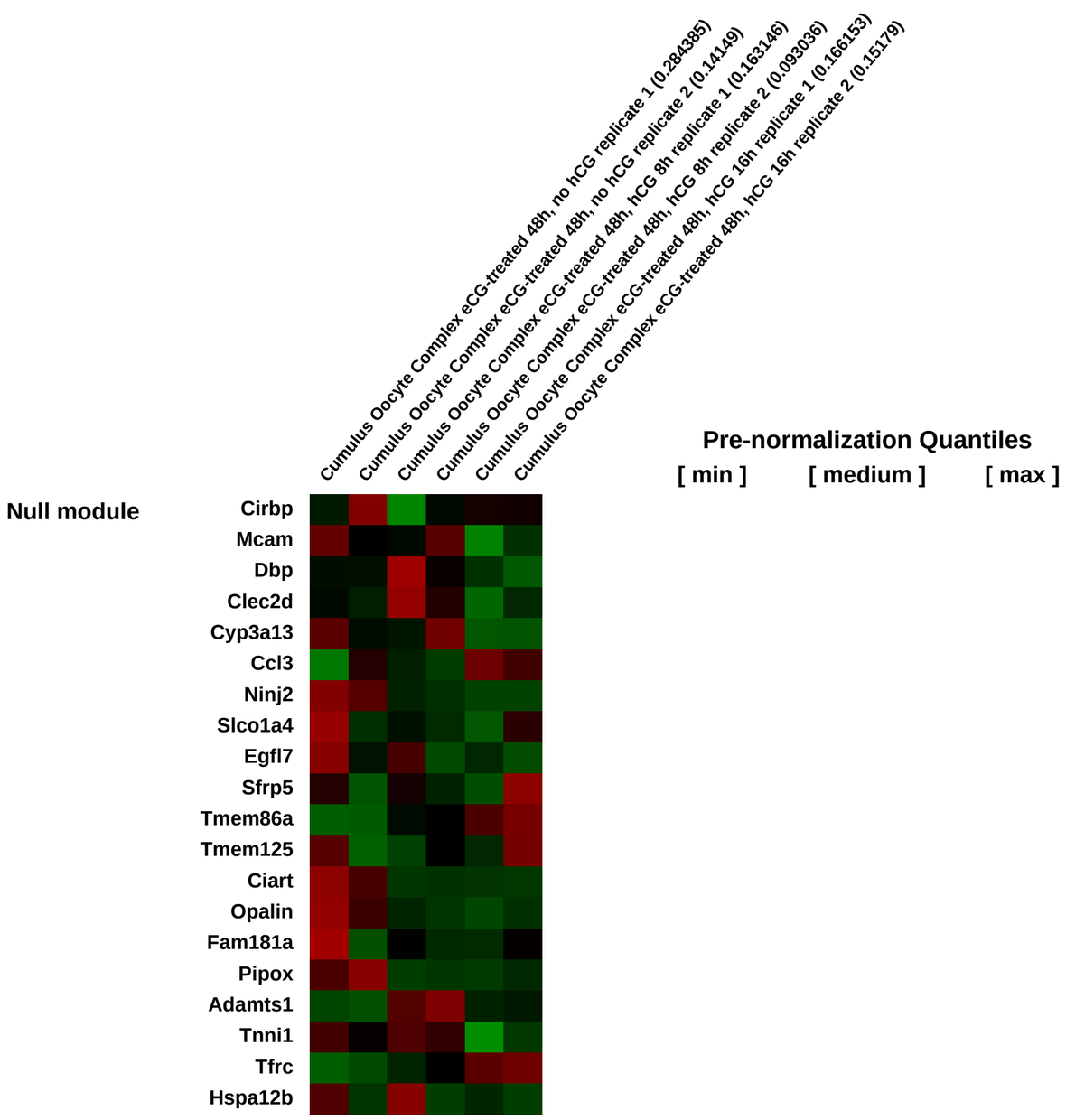

GEO Series "GSE42601" Expression Profiles

Num of samples in this series: 6

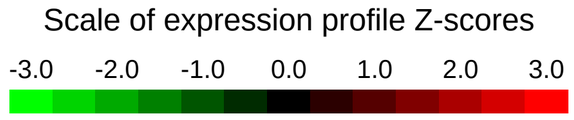

GEO Link:	**http://www.ncbi.nlm.nih.gov/geo/query/acc.cgi?acc=GSE42601**
Status:	**Public on Jun 01 2013**
Title:	**Expression data from wild-type and Dazap1 mutant mouse testes**
Organism:	**Mus musculus**
Experiment type:	**Expression profiling by array**
Platform:	**GPL1261**
Pubmed ID:	**23965306**
Summary & Design:	**Summary:** **Deleted in Azoospermia Associated Protein 1 (DAZAP1) is a ubiquitous RNA-binding protein that is highly expressed in the testis. It is a component of the hnRNP particles and shuttles between the nucleus and the cytoplasm. Mice expressing the DAZAP1-Fn mutant protein manifest both growth retardation and spermatogenic arrest before meiosis I. To elucidate the biological function(s) of DAZAP1 and to search for its natural RNA substrates, we compared the expression profiles of wild-type and Dazap1 mutant testes by cDNA microarrays.** **Overall design:** **We used wild-type and Dazap1 mutant mouse testes. Each genotype has three replicates. 6 total samples were analyzed.**

Background corr dist: **KL-Divergence = 0.0070, L1-Distance = 0.0271, L2-Distance = 0.0008, Normal std = 0.9770**

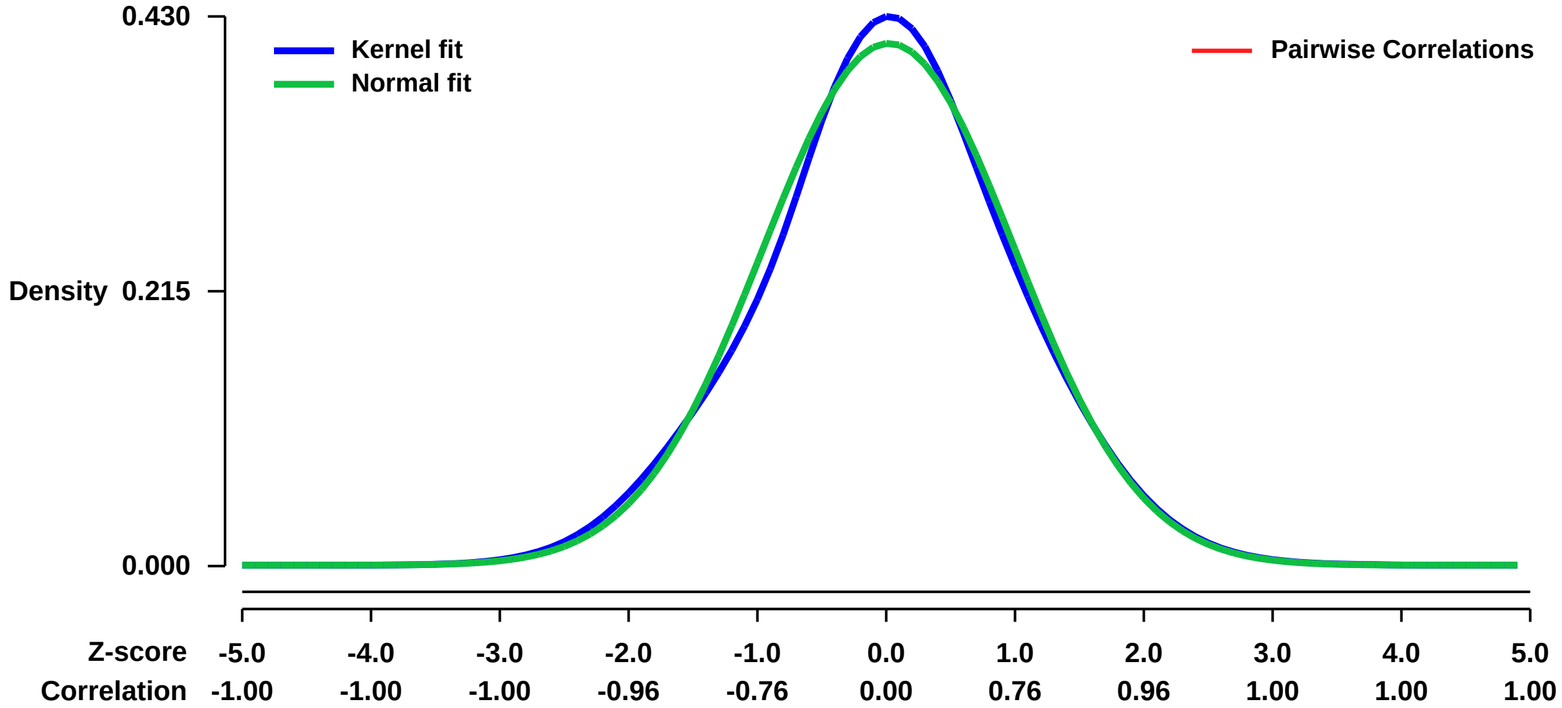

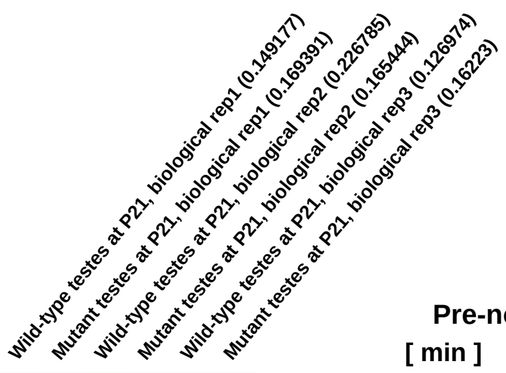

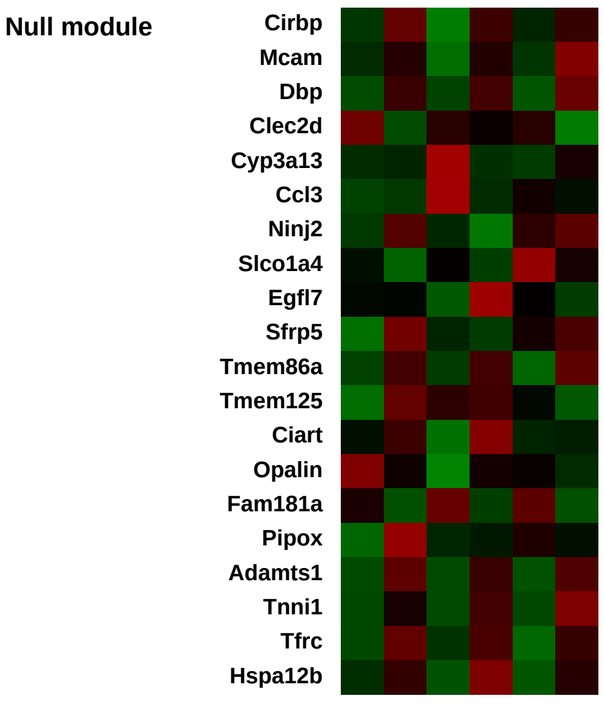

GEO Series "GSE42688" Expression Profiles

Num of samples in this series: 8

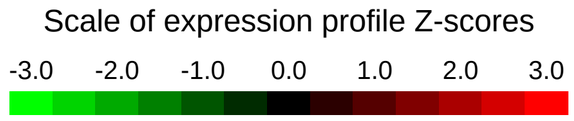

GEO Link:	**http://www.ncbi.nlm.nih.gov/geo/query/acc.cgi?acc=GSE42688**
Status:	**Public on Dec 04 2012**
Title:	**Gene expression analysis of male and female embryonic day 14 genital tubercle (GUDMAP Series ID: 45).**
Organism:	**Mus musculus**
Experiment type:	**Expression profiling by array**
Platform:	**GPL1261**
Pubmed ID:	
Summary & Design:	**Summary:** **The long term objective is to create an encyclopedia of the expression levels of all genes in multiple components of the developing urogenital system. The central thesis is straightforward. The combination of microdissected and laser capture microdissection (LCM) plus Microarray analysis offers a powerful, efficient and effective method for the creation of a global gene expression atlas of the developing urogenital system. Microarrays with essentially complete genome coverage can be used to quantitate expression levels of every gene. The ensuing rapid read-out provides an expression atlas that is more sensitive, more economical and more complete than would be possible by in situ hybridizations alone. The data submitted here represents the gene expression profiles of the embryonic day 14 genital tubercle of the male and the female.** **Overall design:** **The genital tubercle region from E14 (TS22) FVB/N males and females were microdissected and total RNA isolated for gene expression analysis using the Affymetrix MOE430 microarray chip.**

Background corr dist: KL-Divergence = 0.0489, L1-Distance = 0.0248, L2-Distance = 0.0008, Normal std = 0.5759

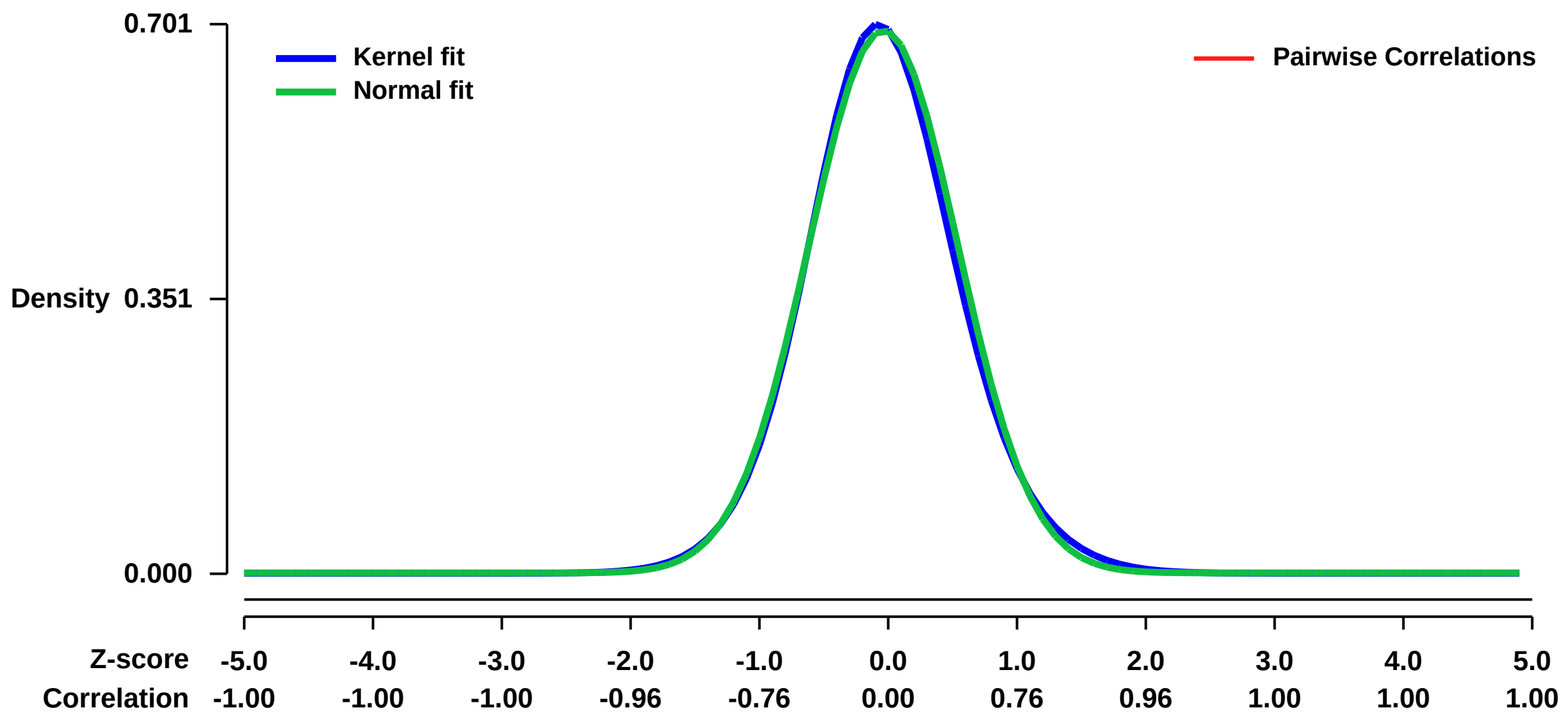

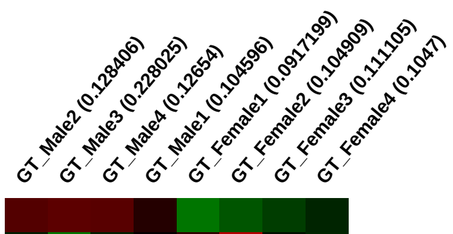

Pre-normalization Quantiles

[min] [medium] [max]

Null module

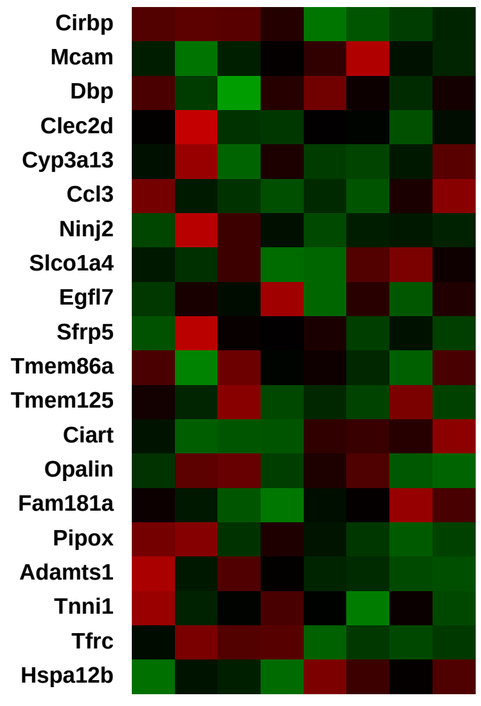

GEO Series "GSE42753" Expression Profiles

Num of samples in this series: 6

Scale of expression profile Z-scores

-3.0 -2.0 -1.0 0.0 1.0 2.0 3.0

GEO Link:	http://www.ncbi.nlm.nih.gov/geo/query/acc.cgi?acc=GSE42753
Status:	Public on Dec 06 2012
Title:	Microarray gene expression profiling of transgenic mice with myocardium-specific expression of RKIP or a GRK-specific peptide inhibitor
Organism:	Mus musculus
Experiment type:	Expression profiling by array
Platform:	GPL1261
Pubmed ID:	23362259
Summary & Design:	**Summary:** The Raf kinase inhibitor protein (RKIP) is a dual inhibitor of the Raf kinase and the G-protein-coupled receptor kinase 2 (GRK2). GRK2 is an indispensable kinase, which exerts a major role in the pathogenesis of heart failure, and inhibition of GRK2 is cardioprotective in experimental models of heart failure. To investigate the cardiac function of RKIP as GRK2 inhibitor, we generated transgenic mice with myocardium-specific expression of RKIP under control of the alpha-MHC promoter. For comparison, mice with myocardium-specific expression of a GRK-specific peptide inhibitor (GRK-Inh) were also generated. Two different transgenic mouse models were established. Transgenic RKIP mice and transgenic GRK-Inh mice were born at Mendelian frequencey and grew to adulthood normally. **Overall design:** Microarray gene expression profiling was performed with heart tissue isolated from three study groups: (i) RKIP-transgenic mice, (ii) GRK-Inh-transgenic mice, and (iii) B6 control mice.

Background corr dist: KL-Divergence = 0.0459, L1-Distance = 0.0191, L2-Distance = 0.0004, Normal std = 0.5905

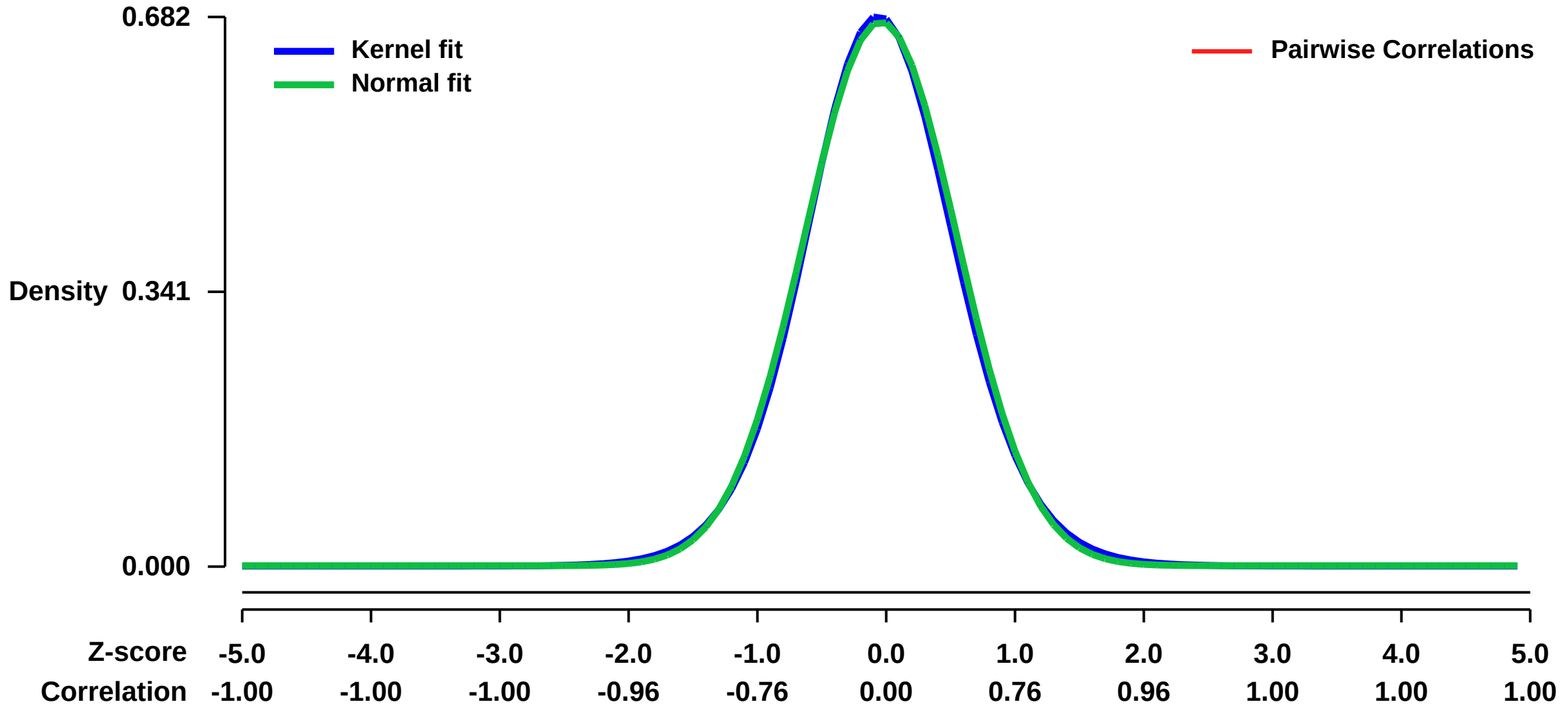

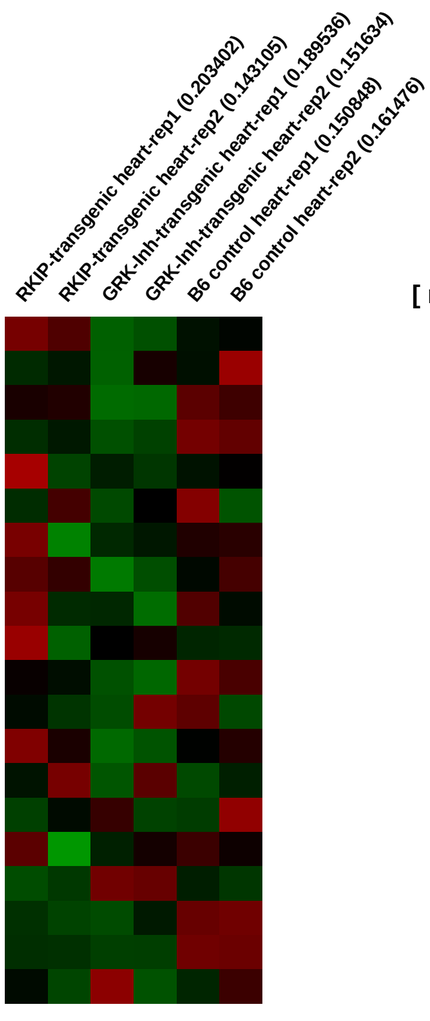

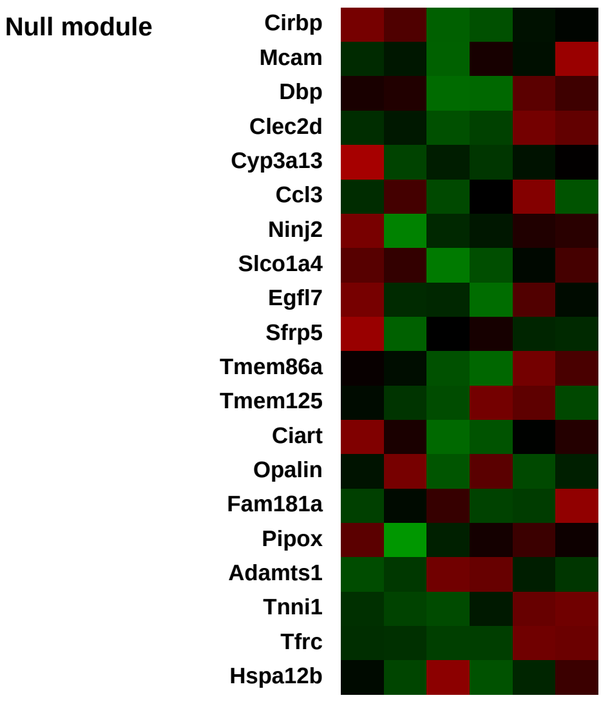

GEO Series "GSE42775" Expression Profiles

Num of samples in this series: 12

Scale of expression profile Z-scores

-3.0 -2.0 -1.0 0.0 1.0 2.0 3.0

GEO Link:	http://www.ncbi.nlm.nih.gov/geo/query/acc.cgi?acc=GSE42775
Status:	Public on Aug 13 2013
Title:	Gene expression microarray analysis on the medial prefrontal cortex of Schnurri-2 knockout and wild-type control mice
Organism:	Mus musculus
Experiment type:	Expression profiling by array
Platform:	GPL1261
Pubmed ID:	23389689
Summary & Design:	**Summary:** Schnurri-2 (Shn-2), an NF-kappa B site-binding protein, tightly binds to the enhancers of major histocompatibility complex (MHC) class I genes and inflammatory cytokines, which have been shown to harbor common variant single nucleotide polymorphisms associated with schizophrenia. Shn-2 knockout mice show behavioral abnormalities that strongly resemble those of schizophrenics. We performed gene expression microarray analysis of prefrontal cortices from Shn-2 knockout and wild-type control mice. **Overall design:** Prefrontal cortex RNA isolated from six Shn-2 knockout and six control wild-type mice were compared.

Background corr dist: KL-Divergence = 0.1296, L1-Distance = 0.0369, L2-Distance = 0.0026, Normal std = 0.3934

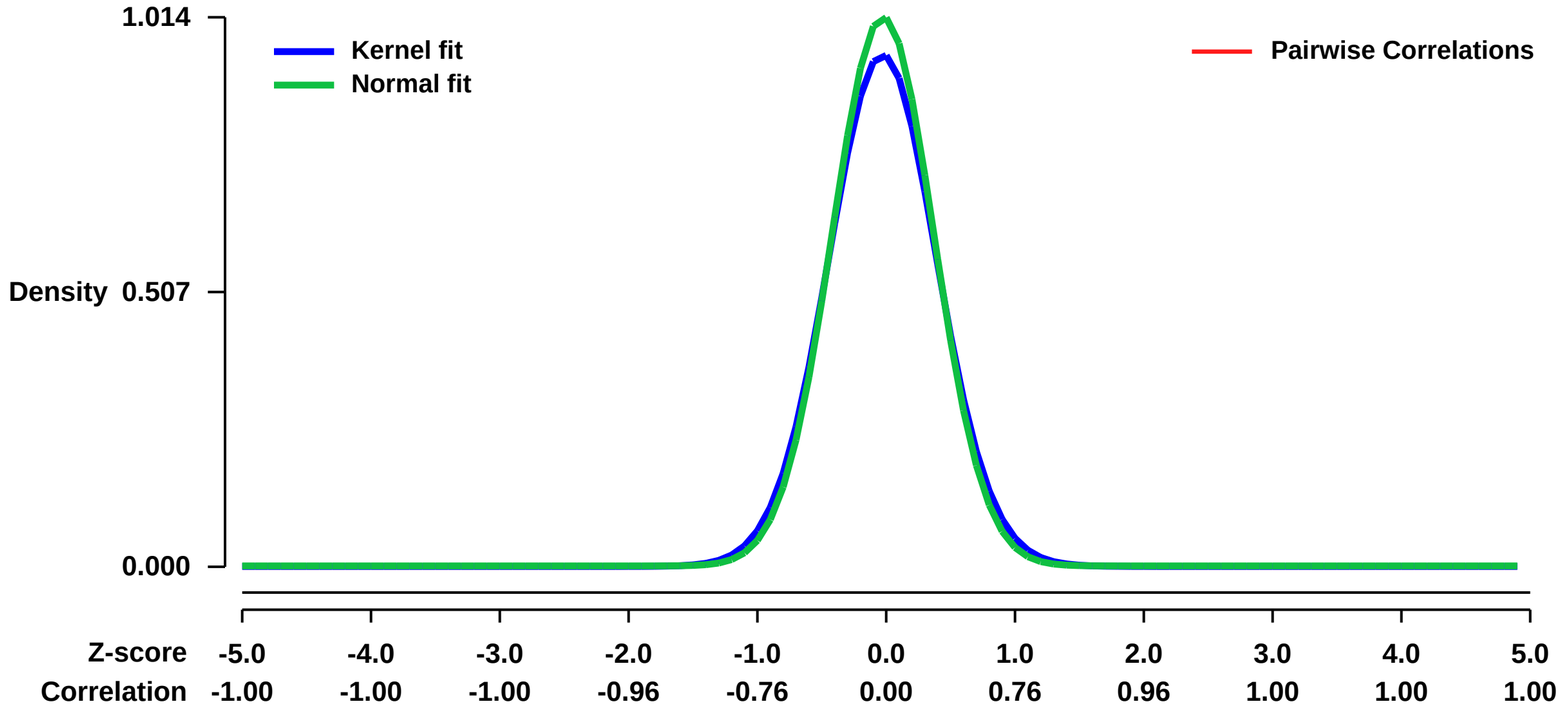

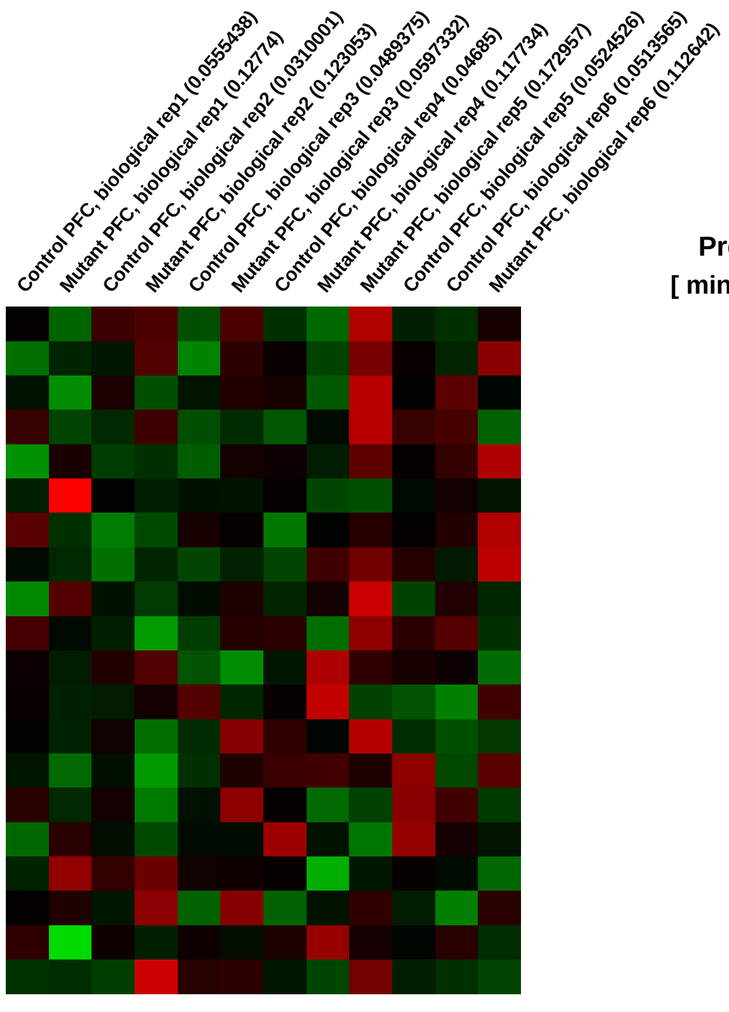

GEO Series "GSE42777" Expression Profiles

Num of samples in this series: 12

Scale of expression profile Z-scores

-3.0 -2.0 -1.0 0.0 1.0 2.0 3.0

GEO Link:	http://www.ncbi.nlm.nih.gov/geo/query/acc.cgi?acc=GSE42777
Status:	Public on Aug 13 2013
Title:	Gene expression microarray analysis on the dentate gyrus of Schnurri-2 knockout and wild-type control mice
Organism:	Mus musculus
Experiment type:	Expression profiling by array
Platform:	GPL1261
Pubmed ID:	23389689
Summary & Design:	**Summary:** Schnurri-2 (Shn-2), an NF-kappa B site-binding protein, tightly binds to the enhancers of major histocompatibility complex (MHC) class I genes and inflammatory cytokines, which have been shown to harbor common variant single nucleotide polymorphisms associated with schizophrenia. Shn-2 knockout mice show behavioral abnormalities that strongly resemble those of schizophrenics. We performed gene expression microarray analysis of dentate gyri from Shn-2 knockout and wild-type control mice. **Overall design:** Dentate gyrus RNA isolated from six Shn-2 knockout and six control wild-type mice were compared.

Background corr dist: KL-Divergence = 0.1212, L1-Distance = 0.0259, L2-Distance = 0.0009, Normal std = 0.4091

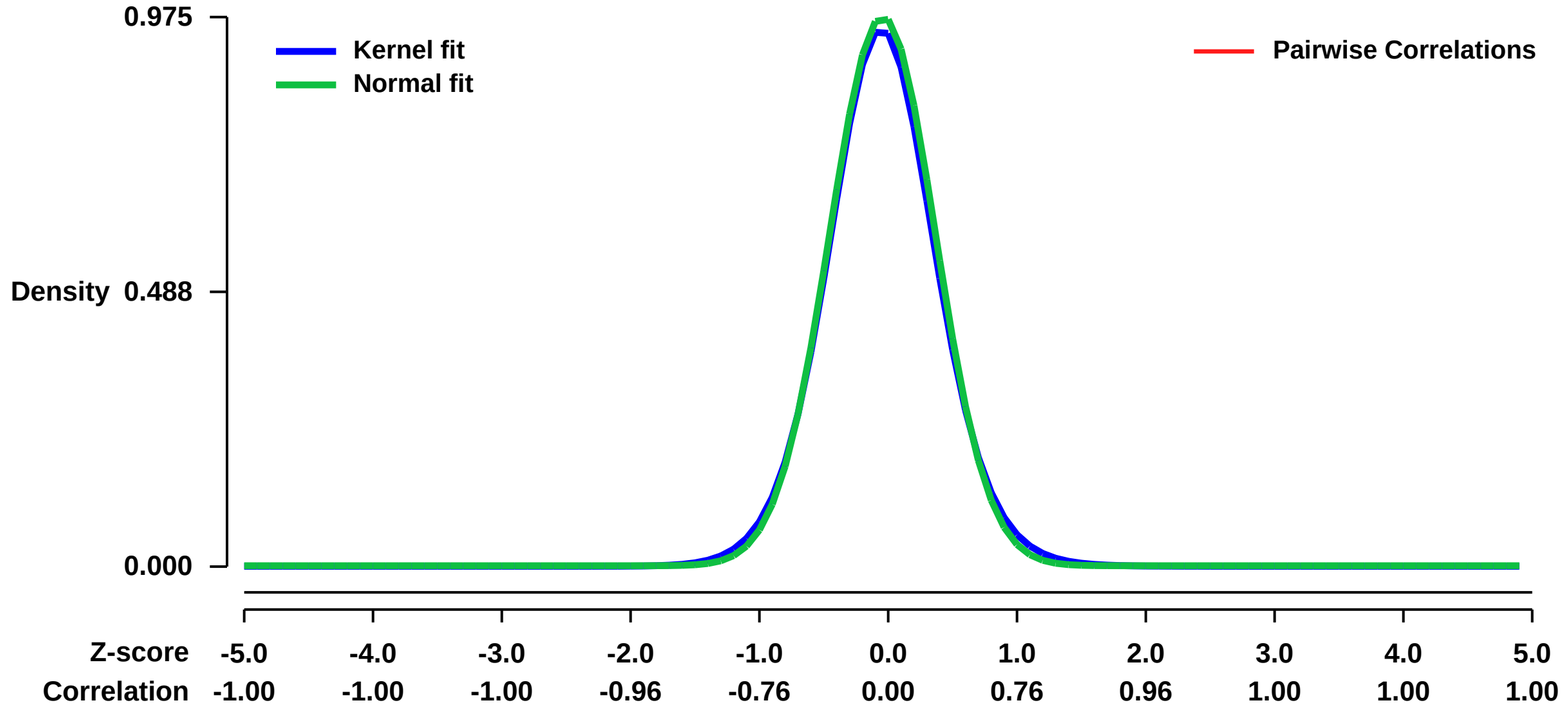

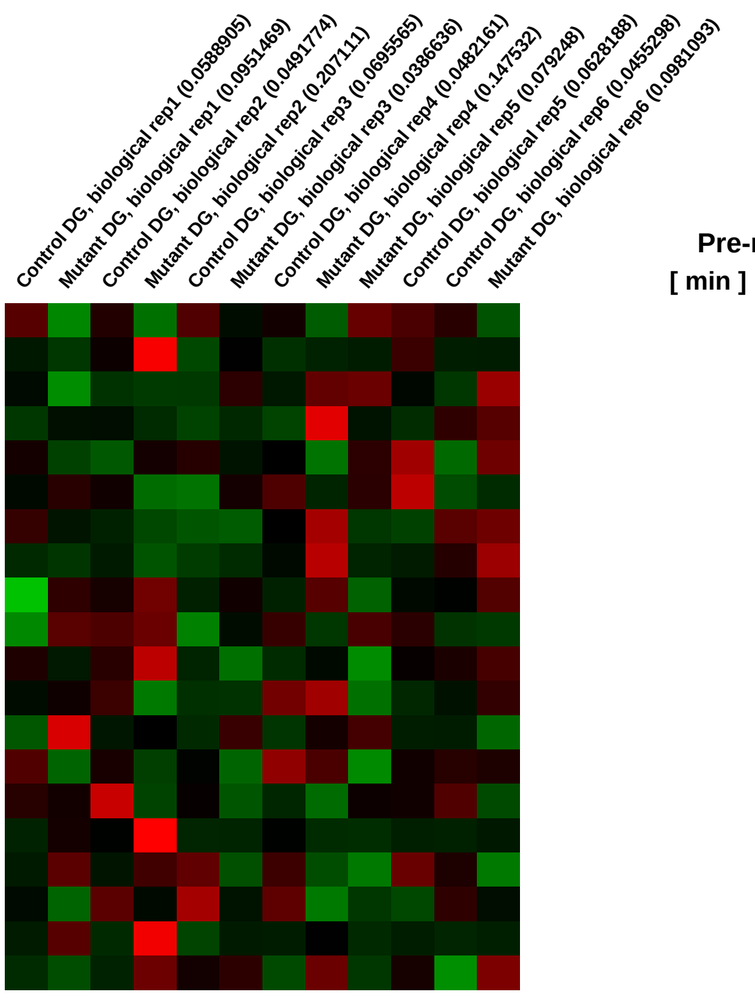

GEO Series "GSE42858" Expression Profiles

Num of samples in this series: 12

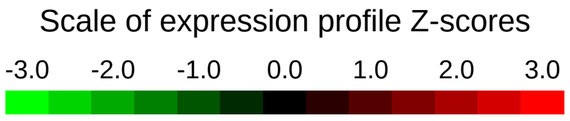

GEO Link:	http://www.ncbi.nlm.nih.gov/geo/query/acc.cgi?acc=GSE42858
Status:	Public on Aug 27 2013
Title:	Progesterone receptor-dependent gene signatures in the mouse mammary gland after acute progesterone treatment
Organism:	Mus musculus
Experiment type:	Expression profiling by array
Platform:	GPL1261
Pubmed ID:	23979845
Summary & Design:	**Summary:** Progesterone (P) acting through its cognate nuclear receptors (PRs) plays an essential role in driving pregnancy-associated branching morphogenesis of the mammary gland. However, the fundamental mechanisms, including global cistromic and acute genomic transcriptional responses that are required to elicit active branching morphogenesis in response to P, have not been elucidated. We used microarray analysis to identify global gene expression signatures that are acutely regulated by PRs in the mouse mammary gland after acute P treatment. **Overall design:** Mammary gland gene expression data from 10-week-old ovariectomized wildtype and progesterone receptor null mice treated subcutaneously with 17¸†-Estradiol for 24 hours and then 17¸†-Estradiol plus Progesterone for 8 or 24 hours. Three replicate pools were tested with three mice per pool.

Background corr dist: KL-Divergence = 0.1073, L1-Distance = 0.0330, L2-Distance = 0.0020, Normal std = 0.4239

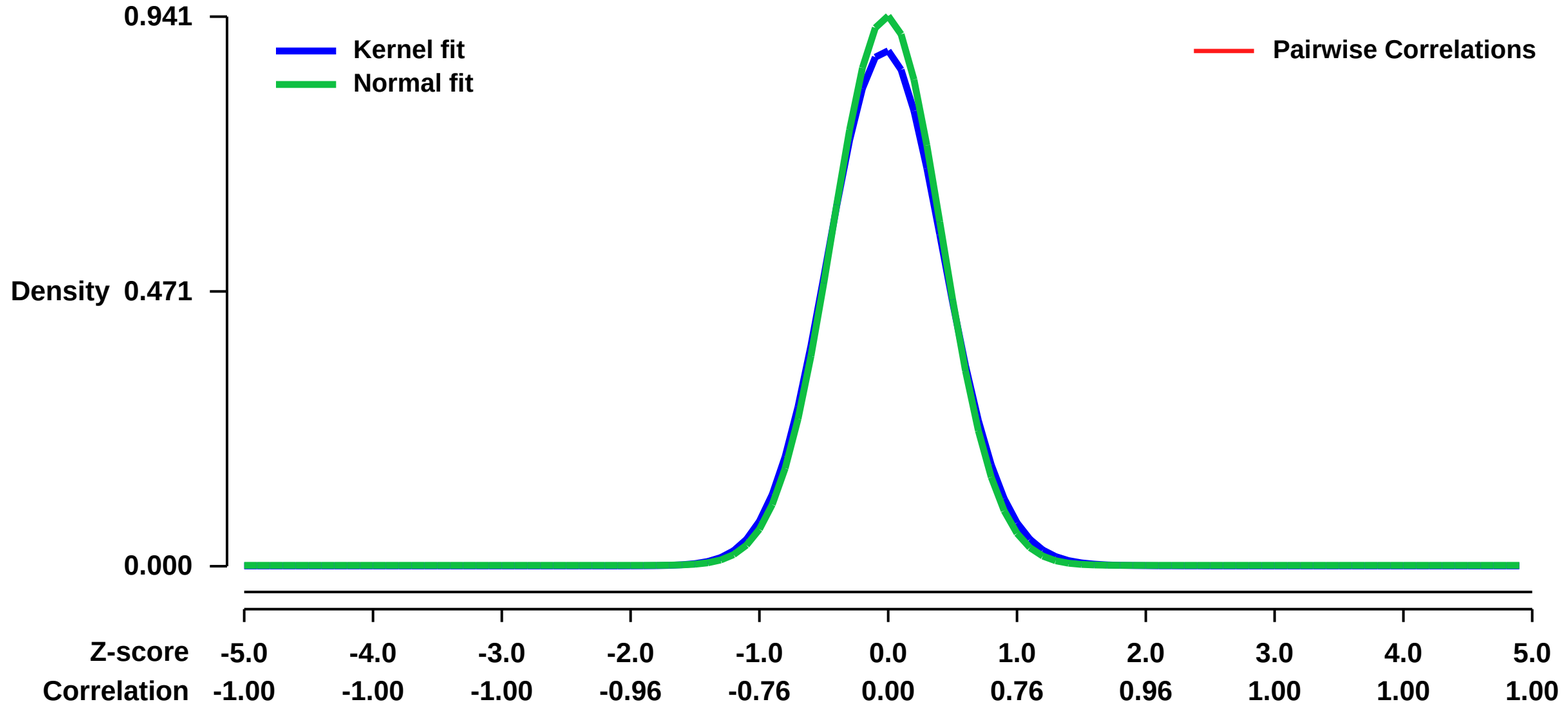

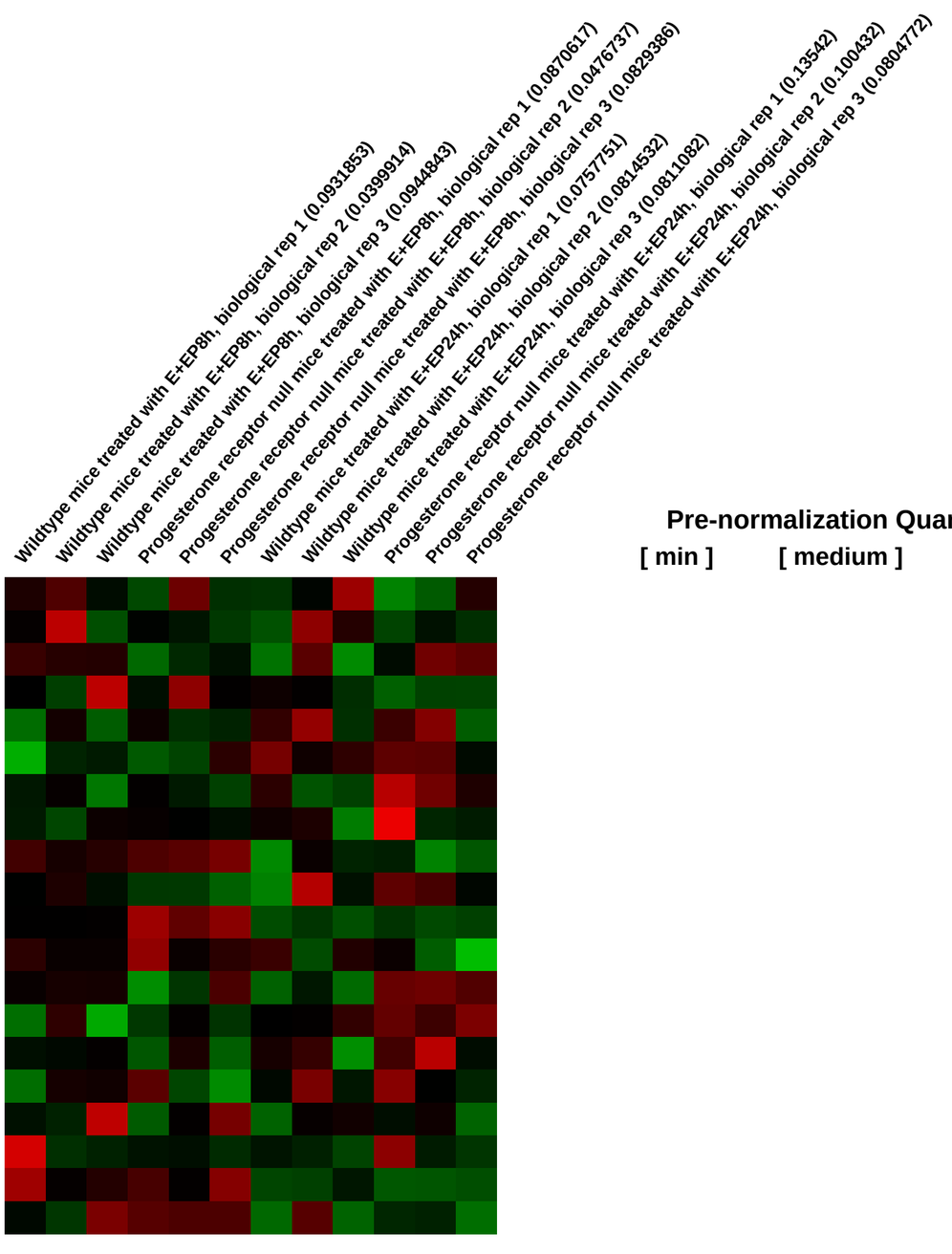

GEO Series "GSE42930" Expression Profiles

Num of samples in this series: 10

Scale of expression profile Z-scores

-3.0 -2.0 -1.0 0.0 1.0 2.0 3.0

GEO Link: http://www.ncbi.nlm.nih.gov/geo/query/acc.cgi?acc=GSE42930
Status: Public on Dec 15 2012
Title: Differential gene expression in APOE3 and APOE4 gene targeted replacement mice
Organism: Mus musculus
Experiment type: Expression profiling by array
Platform: GPL1261
Pubmed ID:

Summary & Design:

Summary:
The aim of the study was to investigate hepatic gene expression profiles differentially regulated by the APOE genotype in gene targeted replacement mice. The APOE4 genotype is associated with increased mortality in the elderly and is an independent risk factor for age-dependent chronic diseases. However, little is known about the underlying mechanisms and molecular targets involved in the APOE4-risk association. As APOE is centrally involved in lipid and cholesterol metabolism and in large part is produced in the liver, we analyzed hepatic RNA profiles of APOE4- and APOE3-expressing mice.

Overall design:
2 groups of 5 animals with 1 liver extract per animal. Mice were homozygous for a human APOE3 or APOE4 gene targeted replacement of the endogenous mouse Apoe gene (B6.129P2-Apoetm2(APOE*3)Mae N8 or B6.129P2-Apoetm3(APOE*4)Mae N8, Taconic Transgenic Modelsâ¢, http://www.taconic.com/wmspage.cfm?parm1=2542), purchased at the age of 6-8 weeks, strain C57BL/6, 3 months old at the performance of the microarray, 6 weeks on a high-fat diet containing 41% energy from milk fat and 2 g/kg cholesterol.

Background corr dist: KL-Divergence = 0.1274, L1-Distance = 0.0331, L2-Distance = 0.0020, Normal std = 0.3974

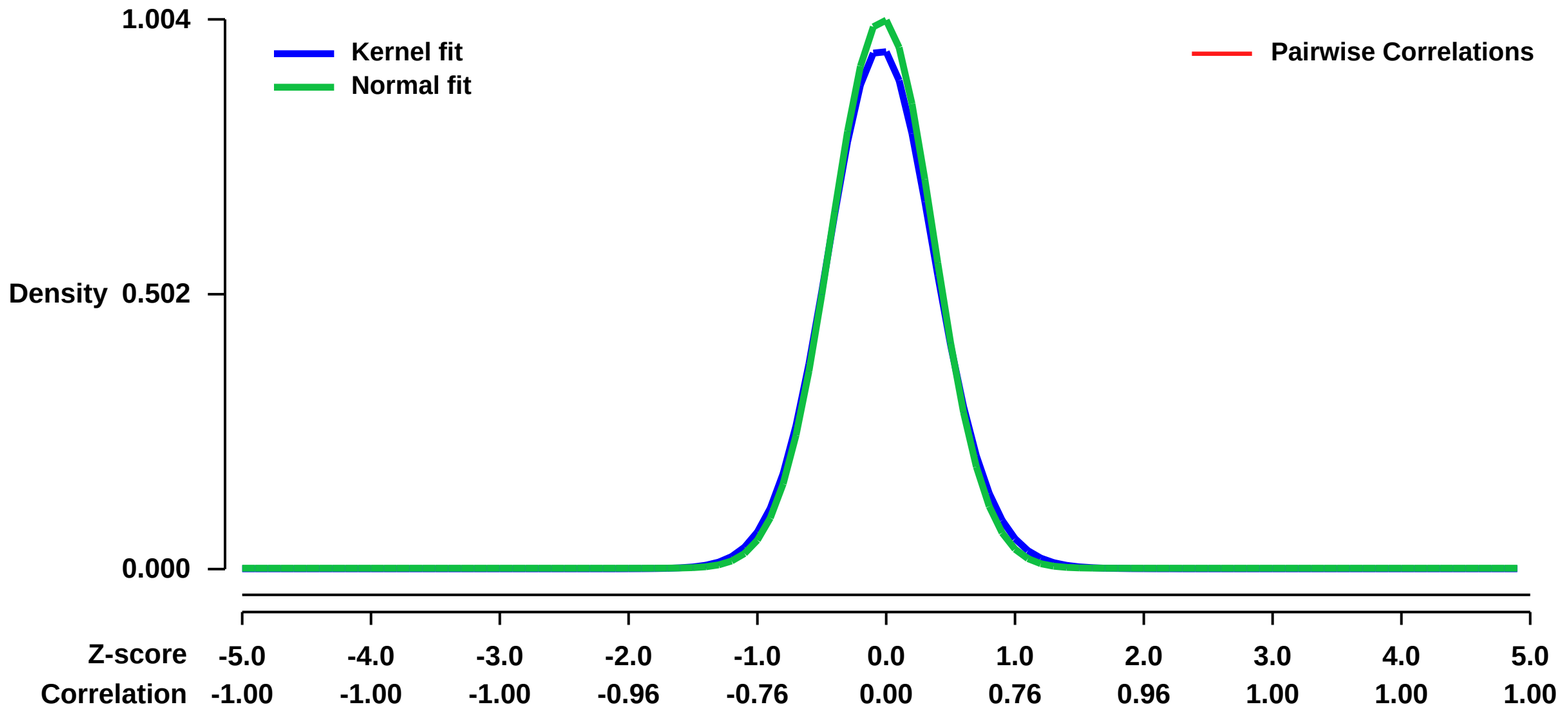

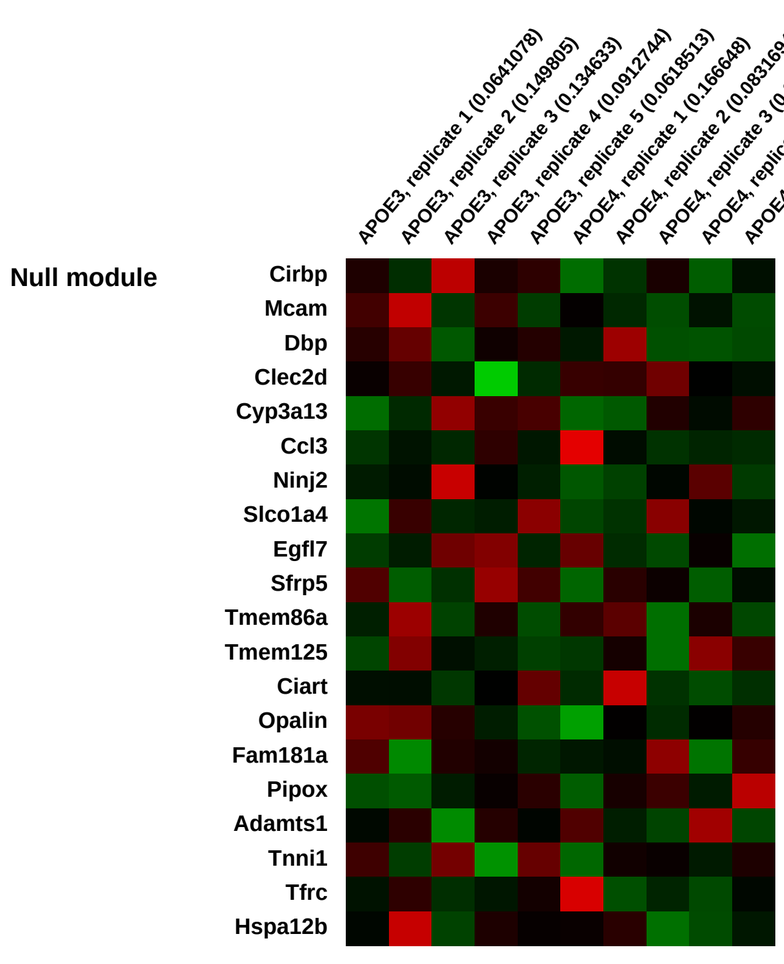

GEO Series "GSE43042" Expression Profiles

Num of samples in this series: 6

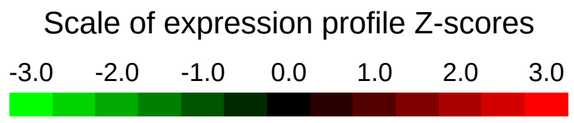

GEO Link:	http://www.ncbi.nlm.nih.gov/geo/query/acc.cgi?acc=GSE43042
Status:	Public on Feb 09 2013
Title:	The role of Ldb1 in hemangioblast development: genome-wide analysis shows that Ldb1 controls essential hematopoietic genes/pathways in mouse early development and
Organism:	Mus musculus
Experiment type:	Expression profiling by array
Platform:	GPL1261
Pubmed ID:	23390196
Summary & Design:	**Summary:** The first site exhibiting hematopoietic activity in mammalian development is the yolk sac blood island, which originates from the hemangioblast. Here we performed differentiation assays, as well as genome-wide molecular and functional studies in BL-CFCs to gain insight into the function of the essential Ldb1 factor in early primitive hematopoietic development. We show that the previously reported lack of yolk sac hematopoiesis and vascular development in Ldb1-/- mouse result from a decreased number of hemangioblasts and a block in their ability to differentiate into erythroid and endothelial progenitor cells. Transcriptome analysis and correlation with the genome wide binding pattern of Ldb1 in hemangioblasts revealed a number of direct target genes and pathways misregulated in the absence of Ldb1. The regulation of essential developmental factors by Ldb1 defines it as an upstream transcriptional regulator of hematopoietic/endothelial development. We show the complex interplay that exists between transcription factors and signaling pathways during the very early stages of hematopoietic/endothelial development and the specific signalling occurring in hemangioblasts in contrast to more advanced hematopoietic developmental stages. Finally, by revealing novel genes and pathways, not previously associated with early development, our study provides novel candidate targets to manipulate the differentiation of hematopoietic and/or endothelial cells. We used microarrays to detail the global programme of gene expression underlying the Ldb1+/+ and Ldb1-/- in Flk1+ cells. **Overall design:** RNA was isolated from Ldb1+/+ and Ldb1-/- Flk1+ cells with the QIAGEN RNeasy Mini Kit and integrity was checked on the Agilent 2100 Bioanalyzer. RNA was converted to biotin-labelled cRNA, hybridised on the Mouse Genome 430 2.0 Array and analyzed with the Affymetrix GeneChip´fi Scanner 3000 according to the manufacturer protocol.

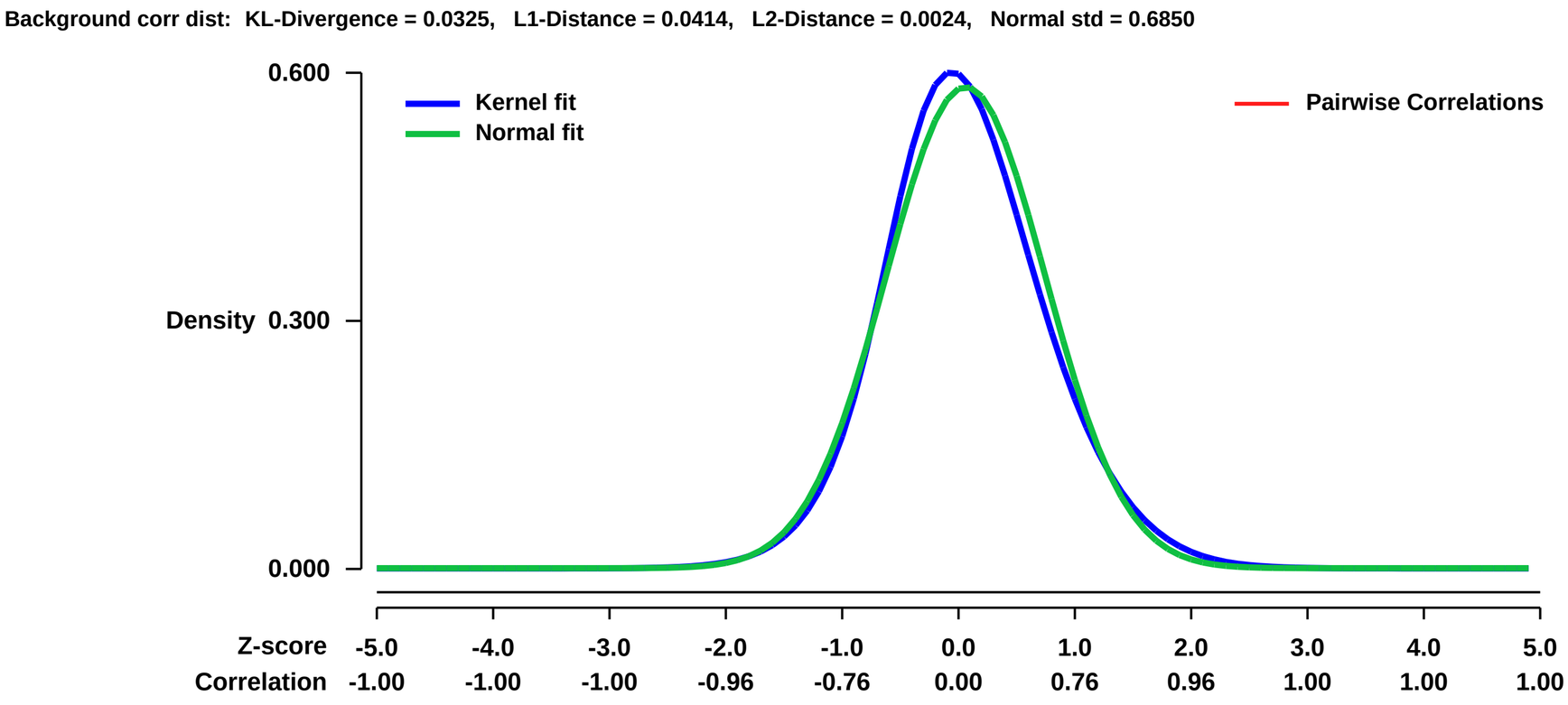

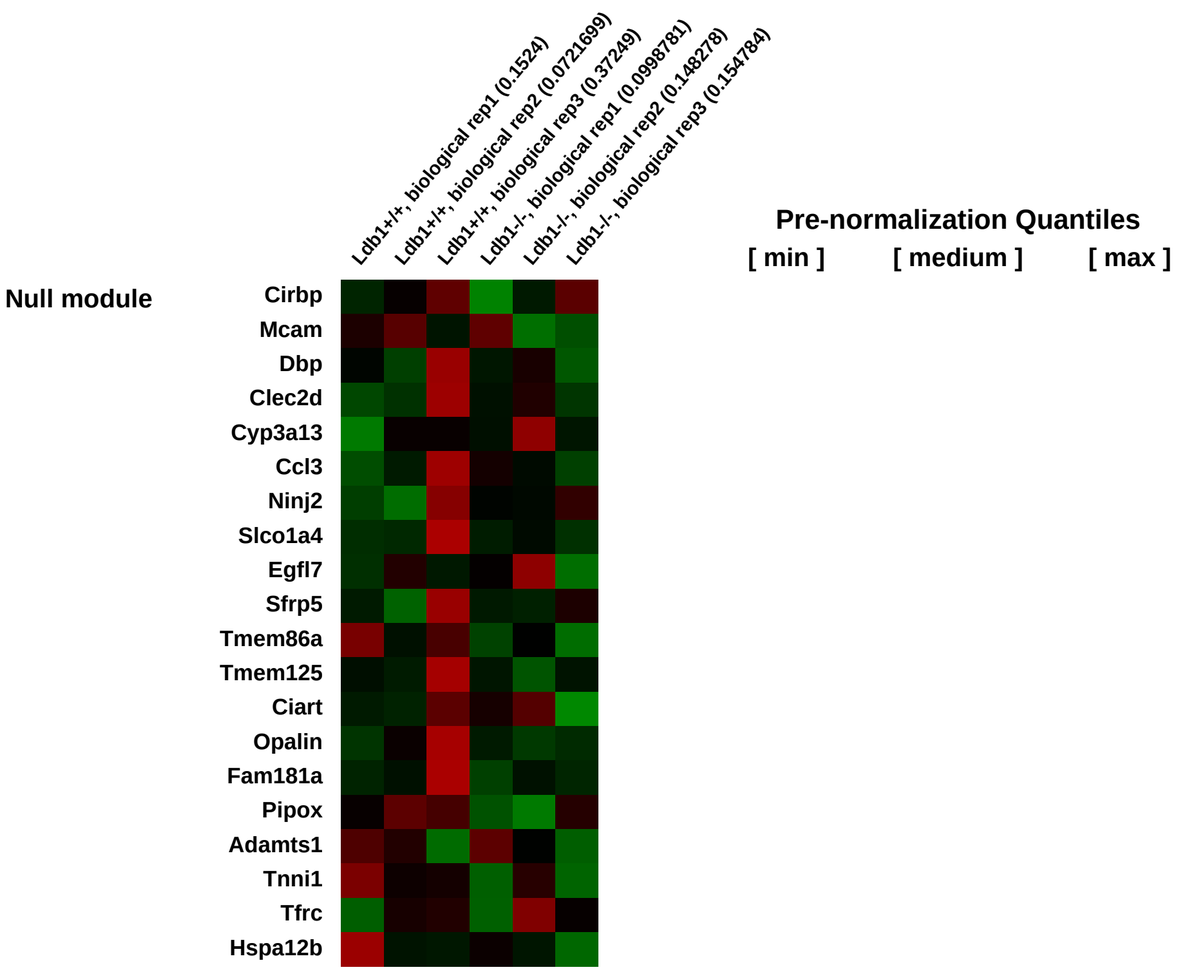

GEO Series "GSE43059" Expression Profiles

Num of samples in this series: 8

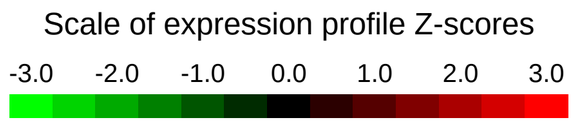

GEO Link:	**http://www.ncbi.nlm.nih.gov/geo/query/acc.cgi?acc=GSE43059**
Status:	**Public on Dec 01 2013**
Title:	**Role of Jmjd2b and Jmjd2c in mESCs identity**
Organism:	**Mus musculus**
Experiment type:	**Expression profiling by array**
Platform:	**GPL1261**
Pubmed ID:	**24361252**
Summary & Design:	**Summary:** **We used microarray to determine the changes in gene expression profile after KD of Jmjd2b and Jmjd2c compared to Anti-GFP KD from mES cells** **Overall design:** **Mouse ES cells were infected with AntiGFP, Jmjd2b and Jmjd2c shRNAs lentivirus, puromycin selected, passage them 2-3 times, collected for RNA isolation and gene expression**

Background corr dist: **KL-Divergence = 0.0472, L1-Distance = 0.0195, L2-Distance = 0.0004, Normal std = 0.5768**

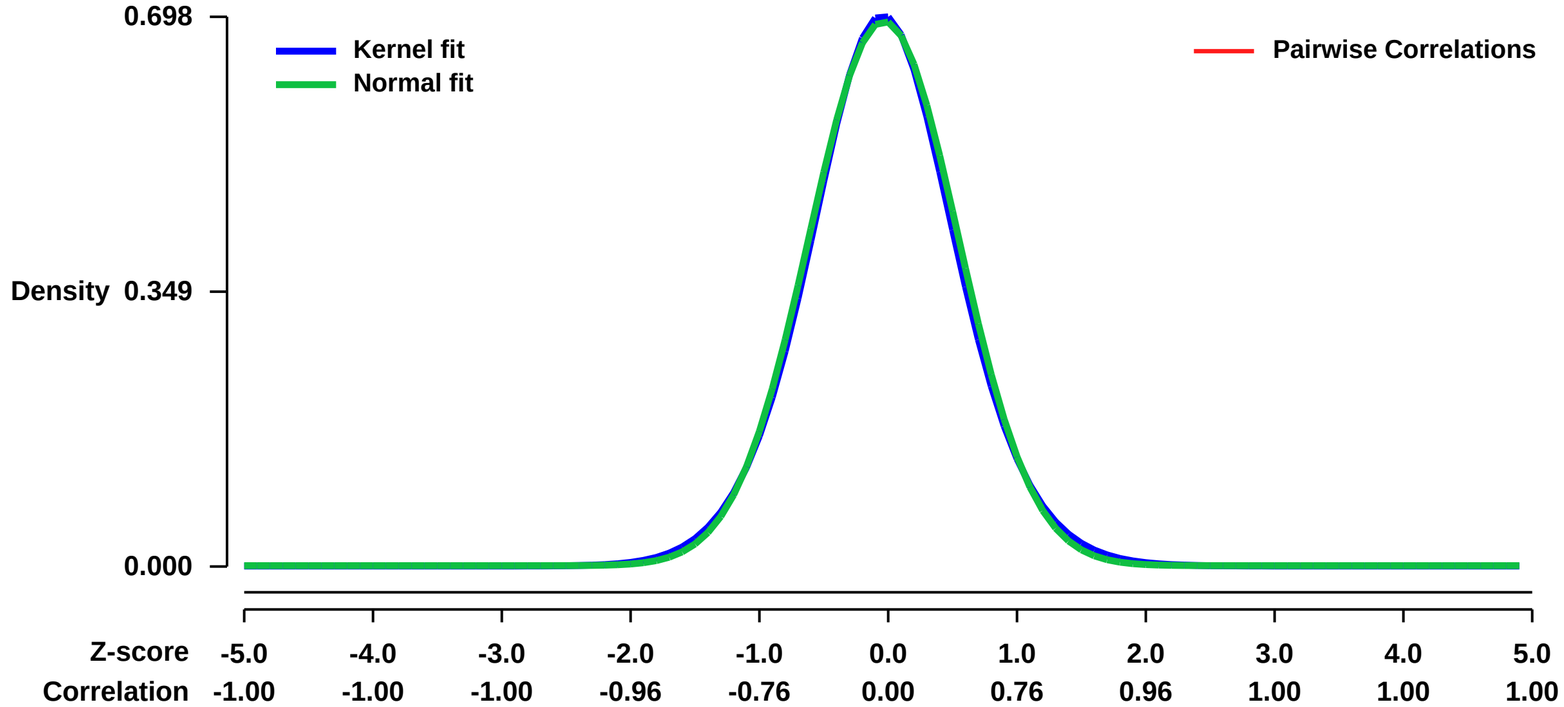

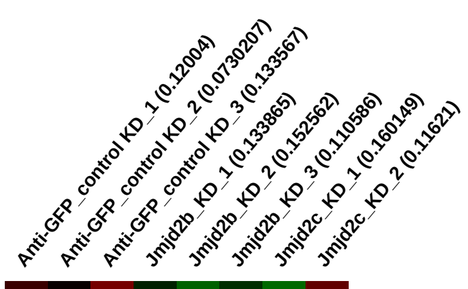

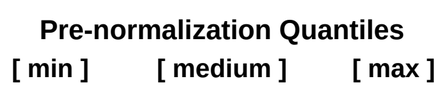

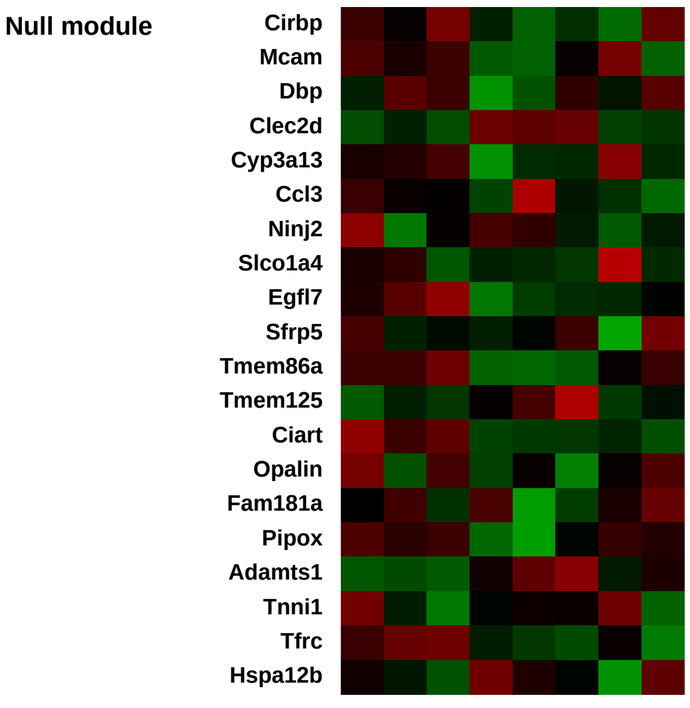

GEO Series "GSE4307" Expression Profiles

Num of samples in this series: 20

Scale of expression profile Z-scores

-3.0 -2.0 -1.0 0.0 1.0 2.0 3.0

GEO Link:	http://www.ncbi.nlm.nih.gov/geo/query/acc.cgi?acc=GSE4307
Status:	Public on Apr 26 2006
Title:	Expression data from single cells from ICMs of mouse blastocysts at E3.5
Organism:	Mus musculus
Experiment type:	Expression profiling by array
Platform:	GPL1261
Pubmed ID:	16547197
Summary & Design:	**Summary:** The inner cell mass (ICM) of the early blastocyst at E3.5, a source of ES cell derivation, is a morphologically homogeneous population of undifferentiated pluripotent cells that give rise to all embryonic lineages. The immediate application of the newly developed V1V3 method to single cells in this stage of mouse embryos revealed the presence of two populations of cells, one with primitive endoderm expression and the other with pluripotent epiblast-like gene expression. The genes expressed differentially between these two populations were well preserved in morphologically differentiated primitive endoderm and epiblast in the embryos one day later (E4.5), demonstrating that the method successfully detects subtle but essential differences in gene expression at the single-cell level among seemingly homogeneous cell populations. This study provides a strategy to analyze biophysical events in medicine as well as in neural, stem cell, and developmental biology, where small numbers of distinctive or diseased cells play critical roles. **Keywords:** Single cell analysis **Overall design:** We isolated blastocysts at E3.5 and dissociated the ICM into single cells by trypsin-EDTA treatment. To prepare cDNA samples, we then randomly picked a total of 55 single cells. cDNAs were synthesized and amplified by the V1V3 method, and screened by gene-specific PCR using Oct4 and Cdx2 to remove trophectoderm cells, and 50 cells were identified as Oct4-positive and Cdx2-negative, ICM cells.

Background corr dist: KL-Divergence = 0.3839, L1-Distance = 0.0784, L2-Distance = 0.0191, Normal std = 0.2531

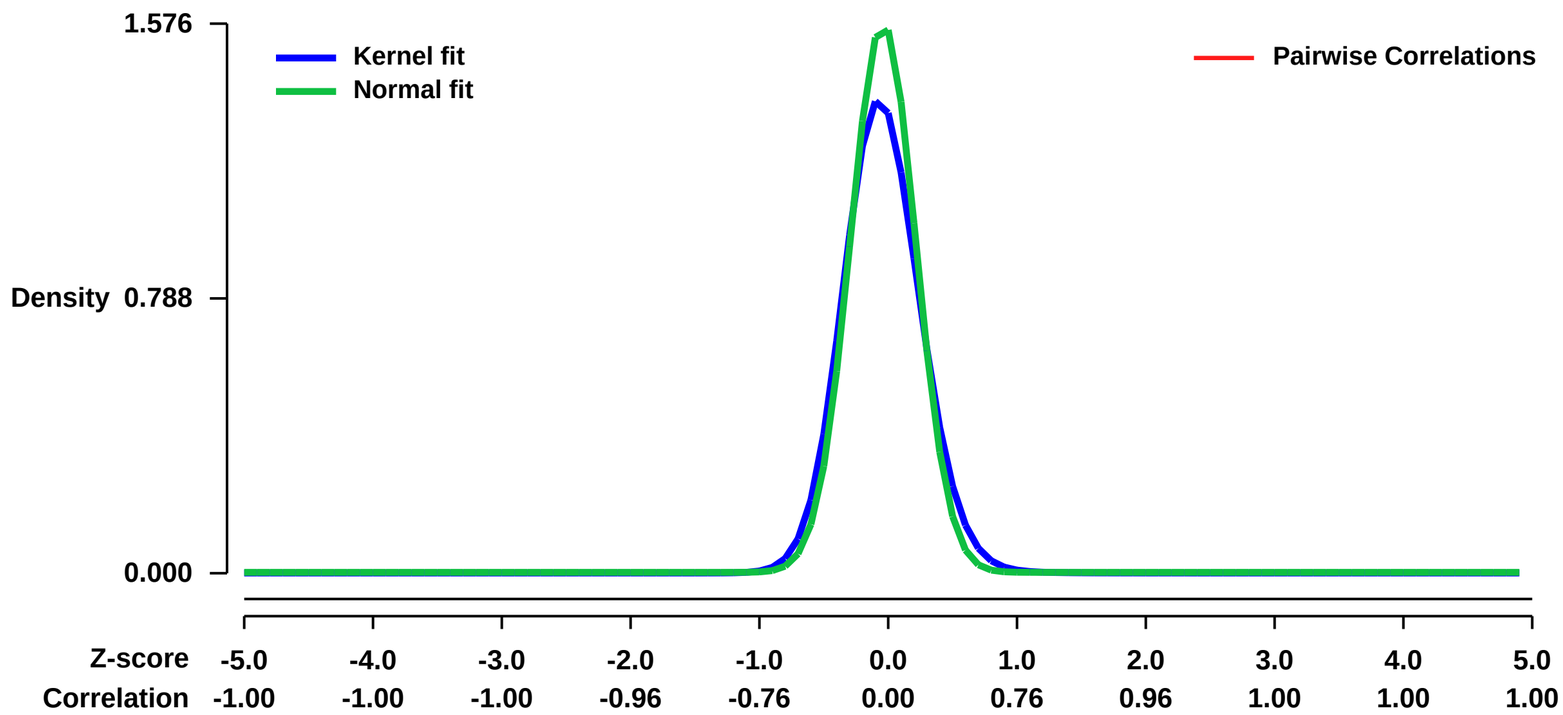

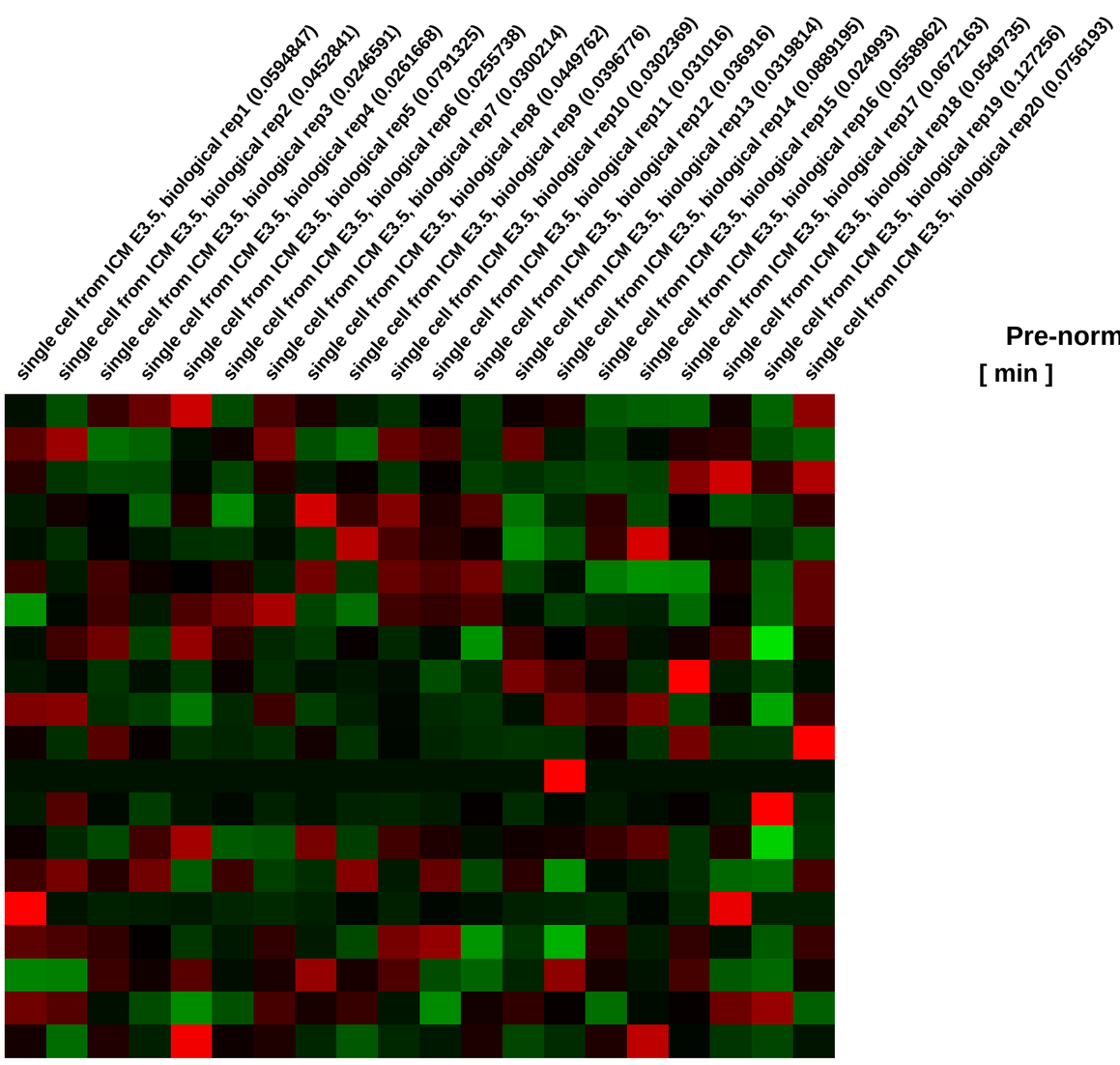

GEO Series "GSE4308" Expression Profiles

Num of samples in this series: 16

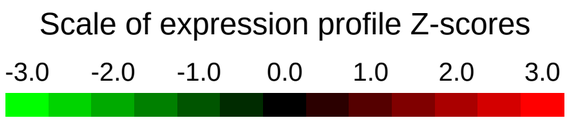

GEO Link:	http://www.ncbi.nlm.nih.gov/geo/query/acc.cgi?acc=GSE4308
Status:	Public on Apr 26 2006
Title:	Expression data for validation of single cell cDNA amplification method (V1V3 method)
Organism:	Mus musculus
Experiment type:	Expression profiling by array
Platform:	GPL1261
Pubmed ID:	16547197
Summary & Design:	**Summary:** A systems-level understanding of a small but essential population of cells in development or adulthood (e.g., somatic stem cells) requires accurate quantitative monitoring of genome-wide gene expression, ideally from single cells. We report here a strategy to globally amplify mRNAs from single cells for highly quantitative high-density oligonucleotide microarray analysis that combines a small number of directional PCR cycles with subsequent linear amplification. Using this strategy, both the representation of gene expression profiles and reproducibility between individual experiments are unambiguously improved from the original method, along with high coverage and accuracy. **Keywords: Method validation** **Overall design:** To verify the ability of the developed method, we prepared total RNA from ES cells and diluted it to the single-cell level (10 pg). Eight array data from the cDNA samples amplified independently from the 10 pg RNA (amplified samples) were compared to each other, and to eight array data from the undiluted 5 ug RNA (nonamplified controls). Since all the materials were the same, all of the observed variations were attributable to the methodogoly.

Background corr dist: KL-Divergence = 0.0712, L1-Distance = 0.0754, L2-Distance = 0.0095, Normal std = 0.5719

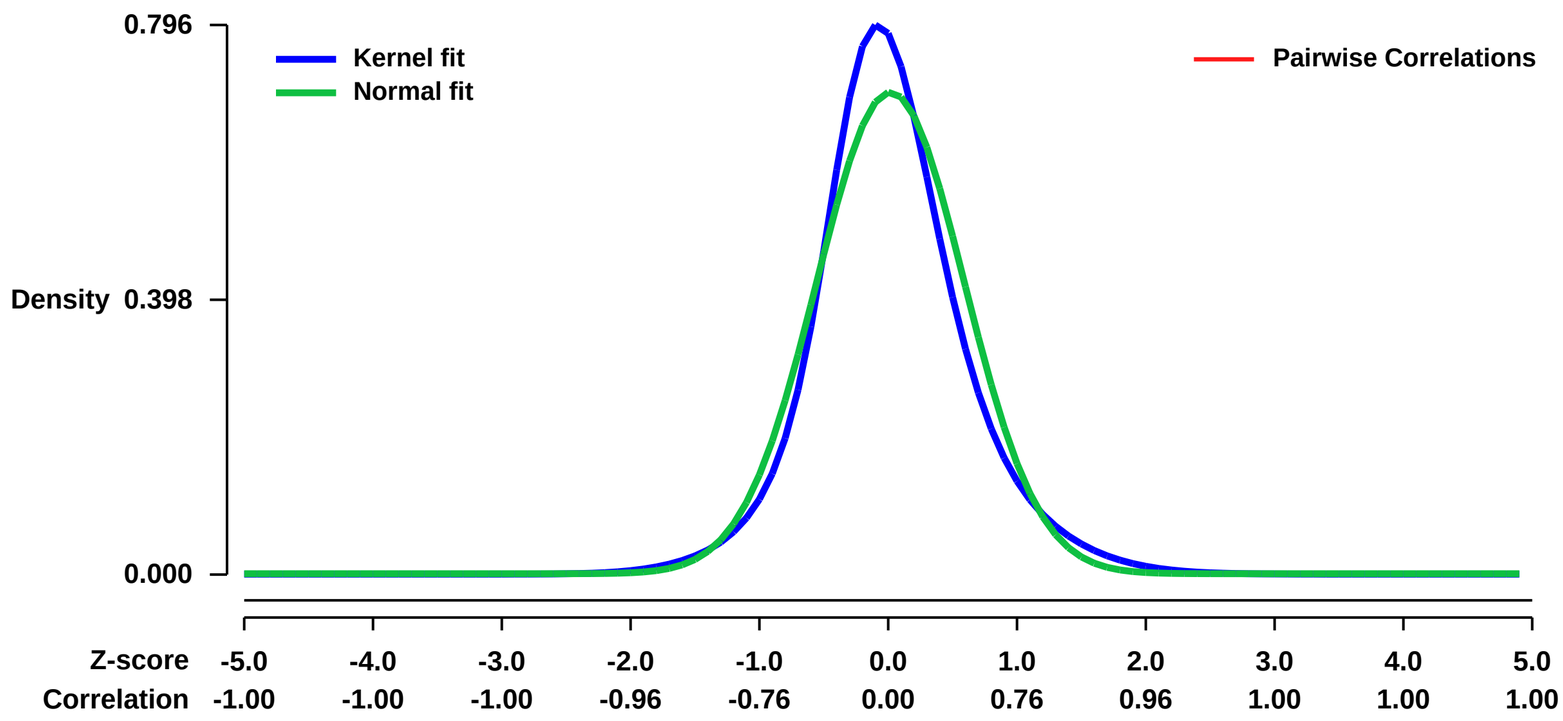

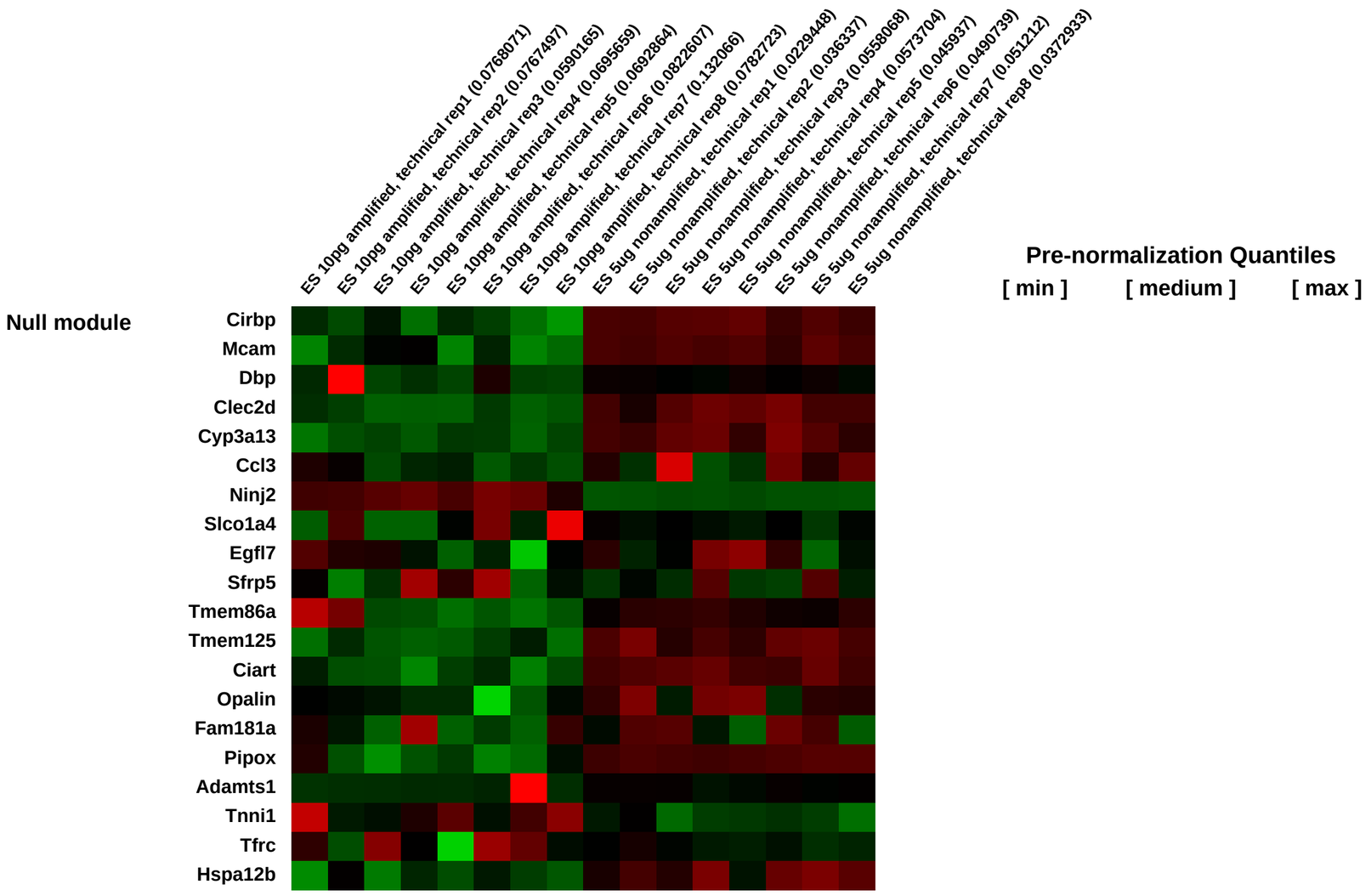

GEO Series "GSE43181" Expression Profiles

Num of samples in this series: 10

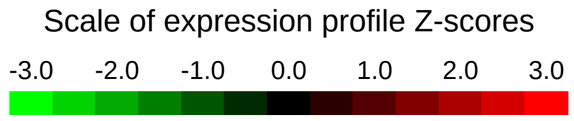

GEO Link:	**http://www.ncbi.nlm.nih.gov/geo/query/acc.cgi?acc=GSE43181**
Status:	**Public on Jan 31 2013**
Title:	**Expression data of mouse preoptic region 5 h after LPS-administration comparing wt and mPGES-1 KO mice.**
Organism:	**Mus musculus**
Experiment type:	**Expression profiling by array**
Platform:	**GPL1261**
Pubmed ID:	
Summary & Design:	**Summary:** **WT mice and mPGES-1 KO mice were treated with 120 mikrogram/kg LPS and sacrificed 5 h later.** **The preoptic region was dissected by LCM and analyzed using GeneChip Mouse Genome 430 2.0 arrays (Affymetrix).** **Overall design:** **Groups: WT LPS-treated versus mPGES-1 KO LPS-treated mice.**

Background corr dist: **KL-Divergence = 0.1163, L1-Distance = 0.0361, L2-Distance = 0.0027, Normal std = 0.4143**

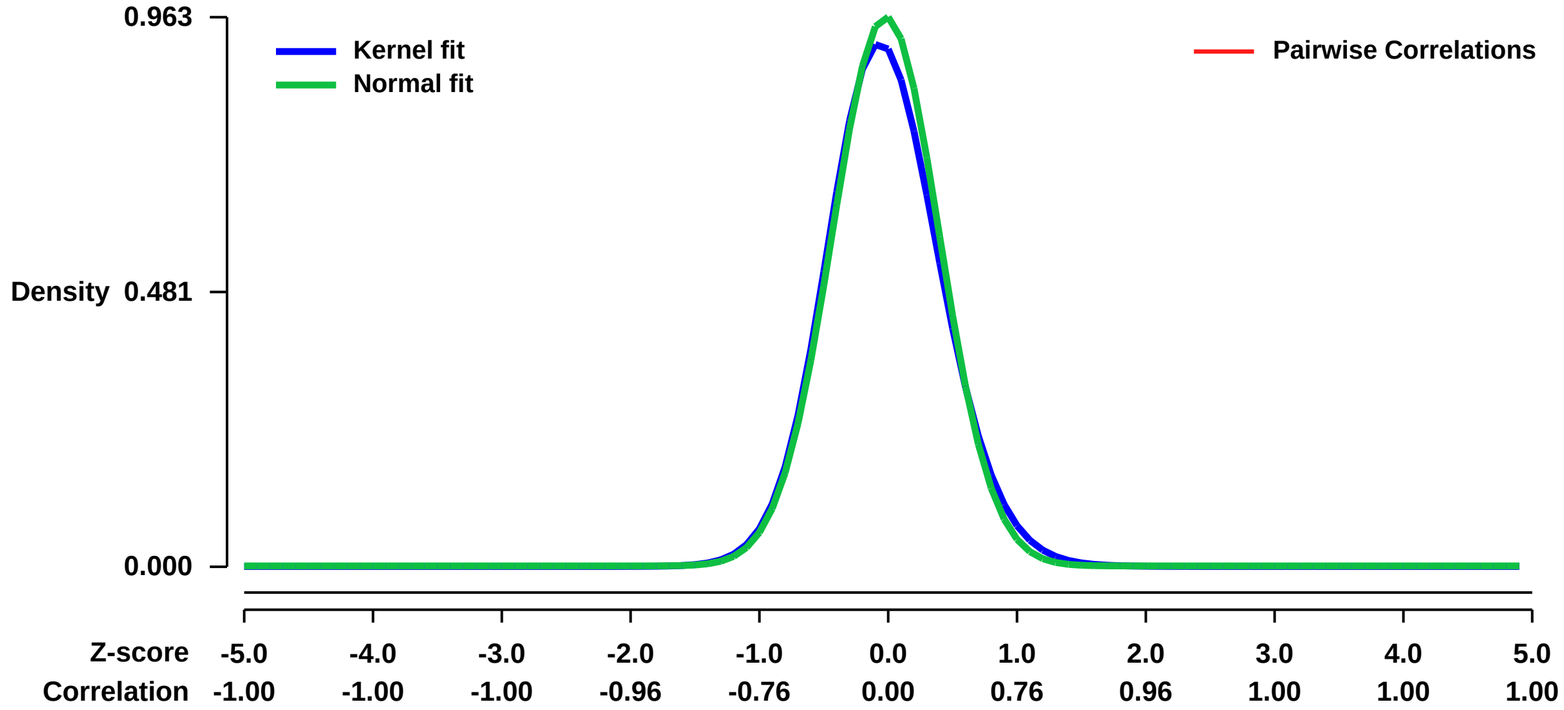

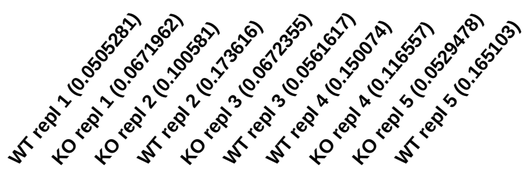

Pre-normalization Quantiles

[min] [medium] [max]

Null module

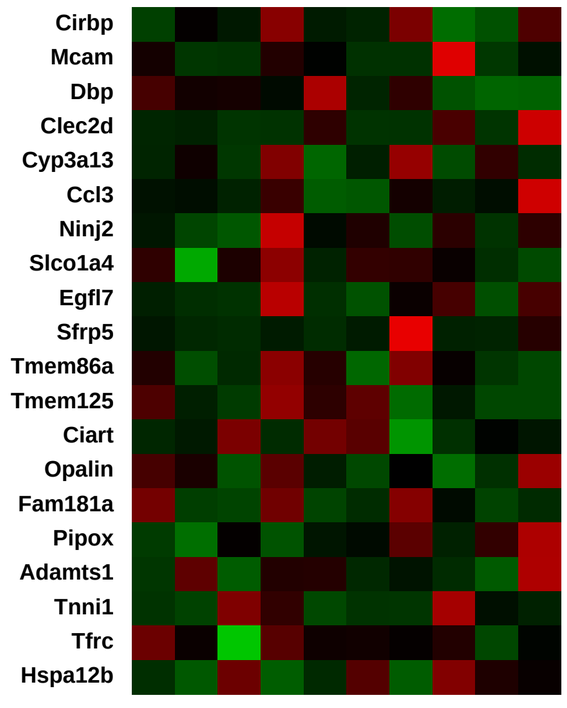

GEO Series "GSE43224" Expression Profiles

Num of samples in this series: 6

Scale of expression profile Z-scores

-3.0 -2.0 -1.0 0.0 1.0 2.0 3.0

GEO Link:	http://www.ncbi.nlm.nih.gov/geo/query/acc.cgi?acc=GSE43224
Status:	Public on Feb 01 2013
Title:	Expression data from WT and E2A-deficient murine DN2 cells
Organism:	Mus musculus
Experiment type:	Expression profiling by array
Platform:	GPL1261
Pubmed ID:	23297135
Summary & Design:	**Summary:** The E2A transcription factors promote the development of thymus-seeding cells but it remains unknown whether these proteins play a role in T lymphocyte lineage specification or commitment. By examining E2A-dependent genes in developing T cells, we will address whether these proteins are involved in these processes. **Overall design:** DN2 cells from WT and E2A-deficient murine fetal thymi were FACS sorted. Subsequently RNA was extracted, labelled and hybridized to Affymetrix microarrays. The goal of this study is to investigate E2A-dependent genes in developing T cells

Background corr dist: KL-Divergence = 0.0381, L1-Distance = 0.0132, L2-Distance = 0.0001, Normal std = 0.6183

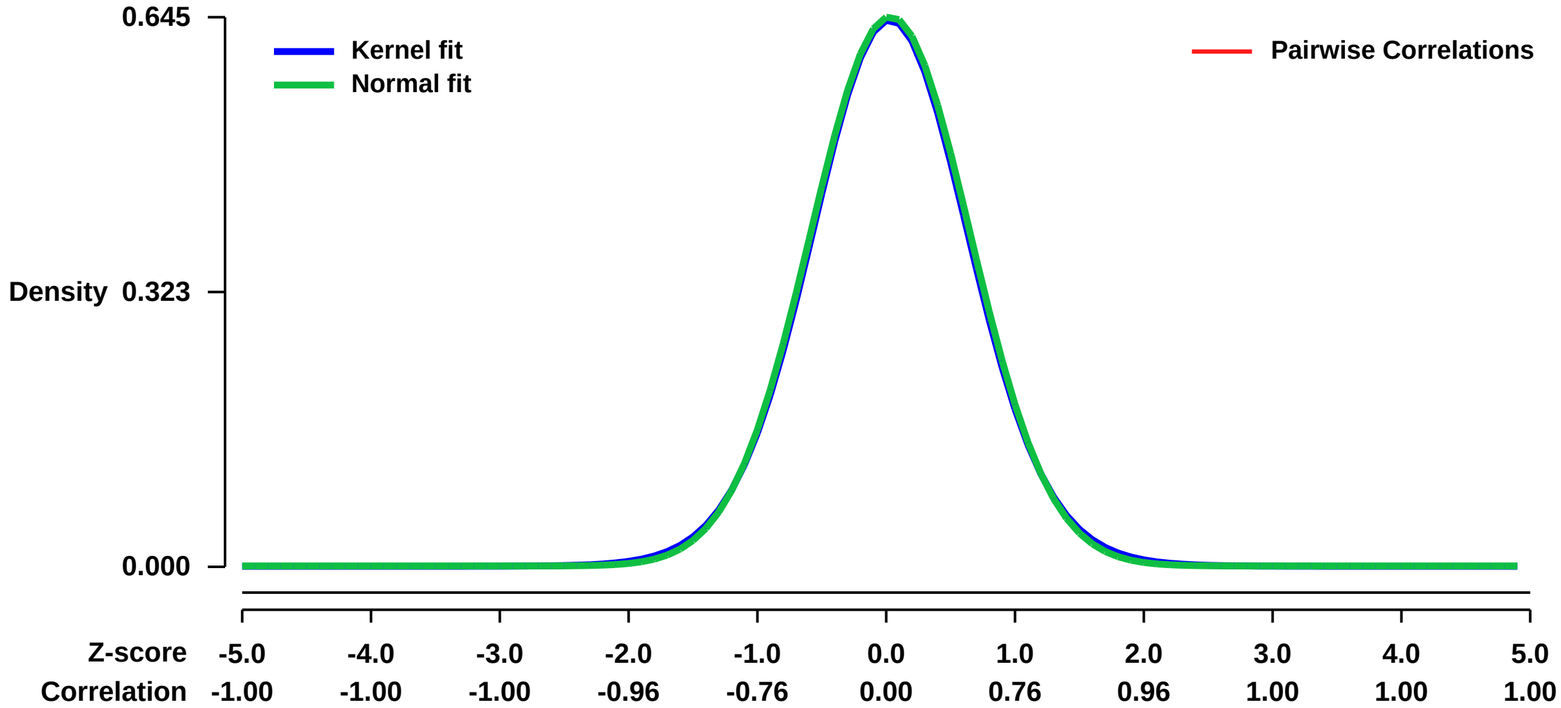

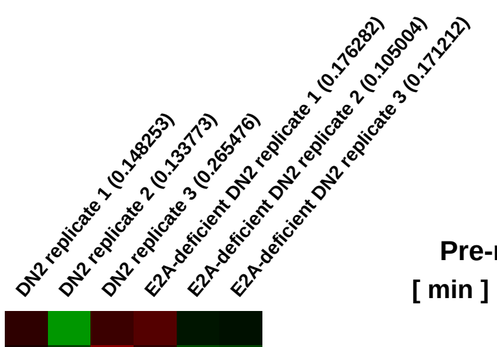

Pre-normalization Quantiles

[min] [medium] [max]

Null module

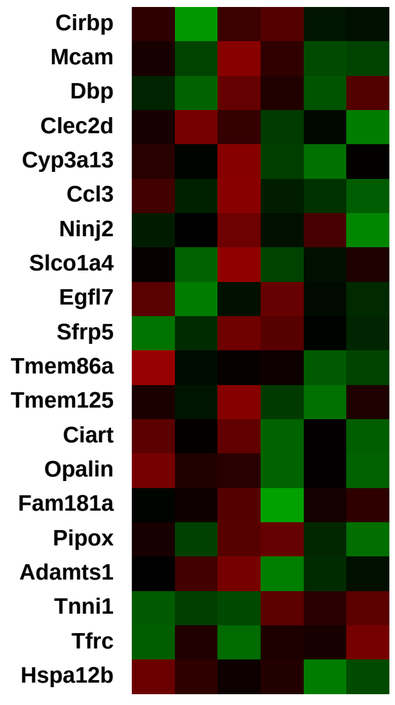

GEO Series "GSE4323" Expression Profiles

Num of samples in this series: 6

Scale of expression profile Z-scores

-3.0 -2.0 -1.0 0.0 1.0 2.0 3.0

GEO Link:	http://www.ncbi.nlm.nih.gov/geo/query/acc.cgi?acc=GSE4323
Status:	Public on Feb 04 2008
Title:	Gene expression changes in FORKO mice
Organism:	Mus musculus
Experiment type:	Expression profiling by array
Platform:	GPL1261
Pubmed ID:	17217615
Summary & Design:	**Summary:** To understand consequences of loss of FSH receptor, we used genetically altered mouse mutants with deletion of this receptor. Follitropin Receptor Knockout (FORKO) mice present various developmental and age-dependent abnormalities such as infertility, senescence and increased tumor incidences in addition to other phenotypes. To explore why the atrophic ovaries of FORKO mice develop ovarian anomalies later in life, we used expression profiling studies to gain a more comprehensive view of genes that are misregulated. Keywords: Comparison of Wildtype and FSH-Receptor Knock out Ovaries at 8 months of age. **Overall design:** Affymetrix 39 K GeneChip´fi Mouse Genome 430 2.0 Array has over 45000 probe sets which analyses 39000+ transcripts and variants from over 34000 well characterized mouse genes. A total of 1 ´µg of double-stranded cDNA was transcribed in vitro using the Bioarray High-Yield RNA Transcript Labeling Kit (Enzo, Farmingdale, NY) according to the manufacturer's instructions using biotinylated CTP and UTP (Enzo, Farmingdale, NY). Following 5-hr incubation at 37´°C, the resultant biotin-labeled cRNA was purified with RNAeasy columns (Qiagen) and eluted in 40 ´µl of RNAse-free water. The concentration of biotin-labeled cRNA was determined by RNA bio-analyzer. Target cRNAs corresponding to either wild type ovary or FORKO ovarian tissue were hybridized to an individual GeneChip from an identical lot of Affymetrix 39 K GeneChip´fi Mouse Genome 430 2.0 array for 16 hr. GeneChip arrays were washed and stained using antibody-mediated signal amplification and the Affymetrix Fluidics Station's standard Eukaryotic GE Wash 2 protocol, using Affymetrix equipment and protocols (Affymetrix, Santa Clara, CA).

Background corr dist: KL-Divergence = 0.0459, L1-Distance = 0.0259, L2-Distance = 0.0008, Normal std = 0.5964

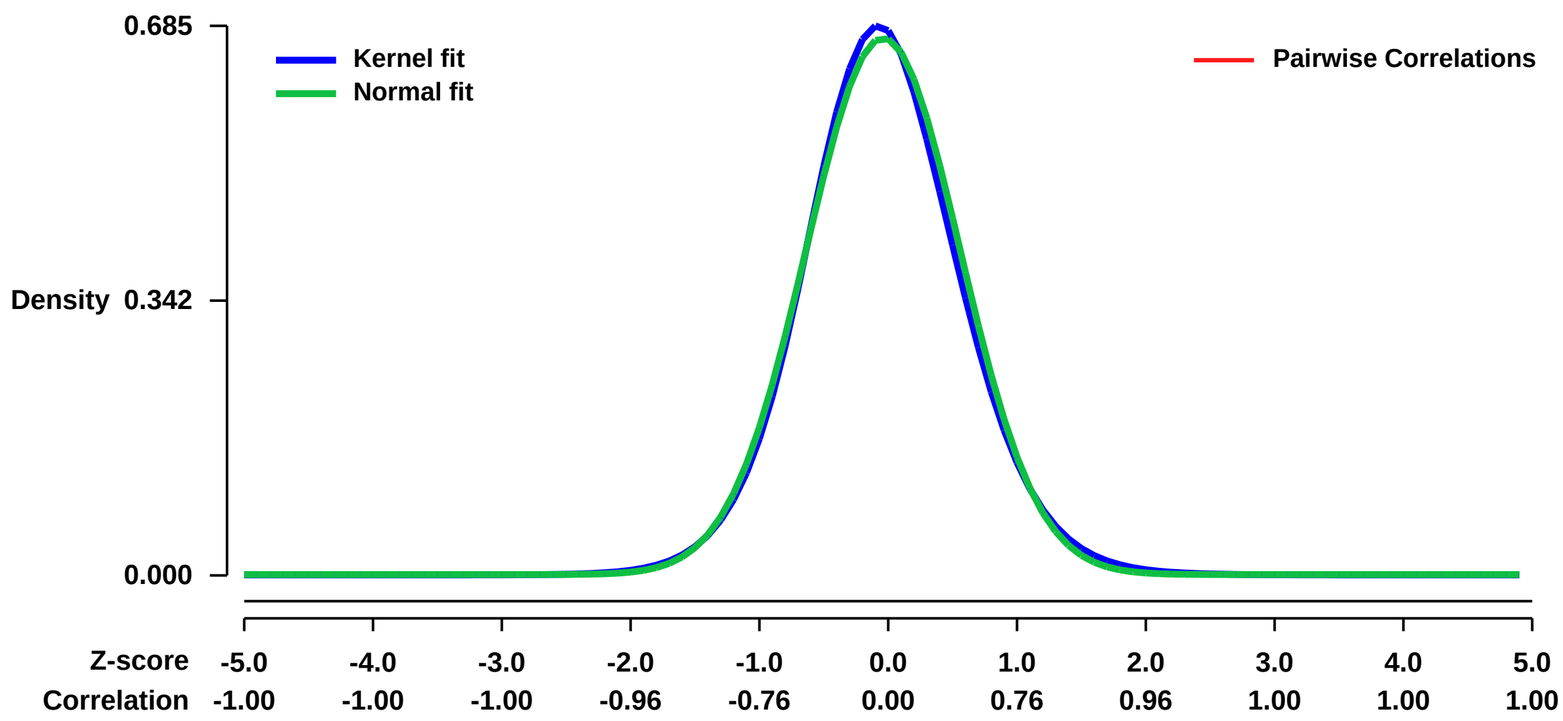

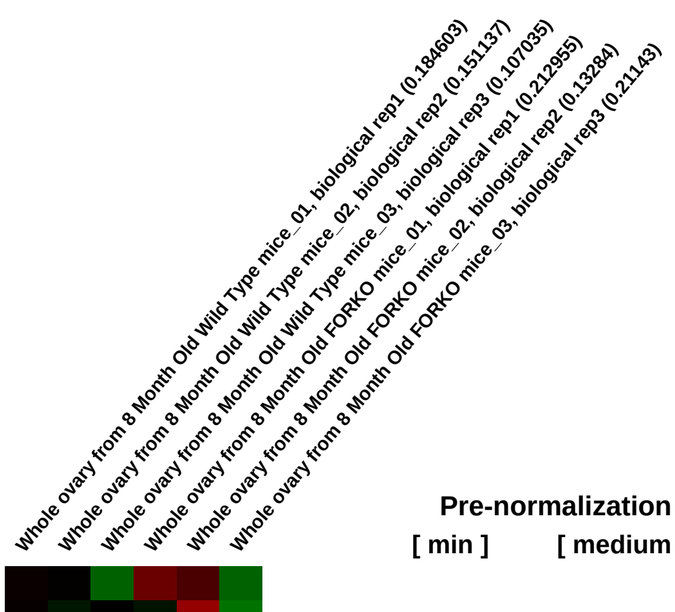

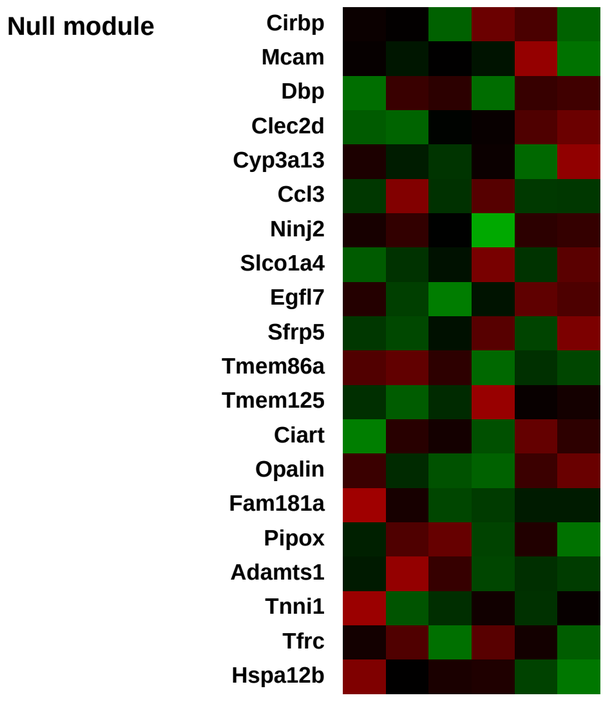

GEO Series "GSE43242" Expression Profiles

Num of samples in this series: 10

Scale of expression profile Z-scores

-3.0 -2.0 -1.0 0.0 1.0 2.0 3.0

GEO Link:	**http://www.ncbi.nlm.nih.gov/geo/query/acc.cgi?acc=GSE43242**
Status:	**Public on Jan 21 2014**
Title:	**Effect of osteoblast-specific constitutive activation of beta-catenin or deletion of FoxO1 on gene expression in mice**
Organism:	**Mus musculus**
Experiment type:	**Expression profiling by array**
Platform:	**GPL1261**
Pubmed ID:	**24429522**
Summary & Design:	**Summary:** **The gene expression of mice with osteoblast-specific beta-catenin activation or FoxO1 deactivation are each compared to that of Wt.** **Overall design:** **C. Osteoblast specific FoxO1 deleted mice (n=3)**

Background corr dist: **KL-Divergence = 0.1216, L1-Distance = 0.0309, L2-Distance = 0.0017, Normal std = 0.4052**

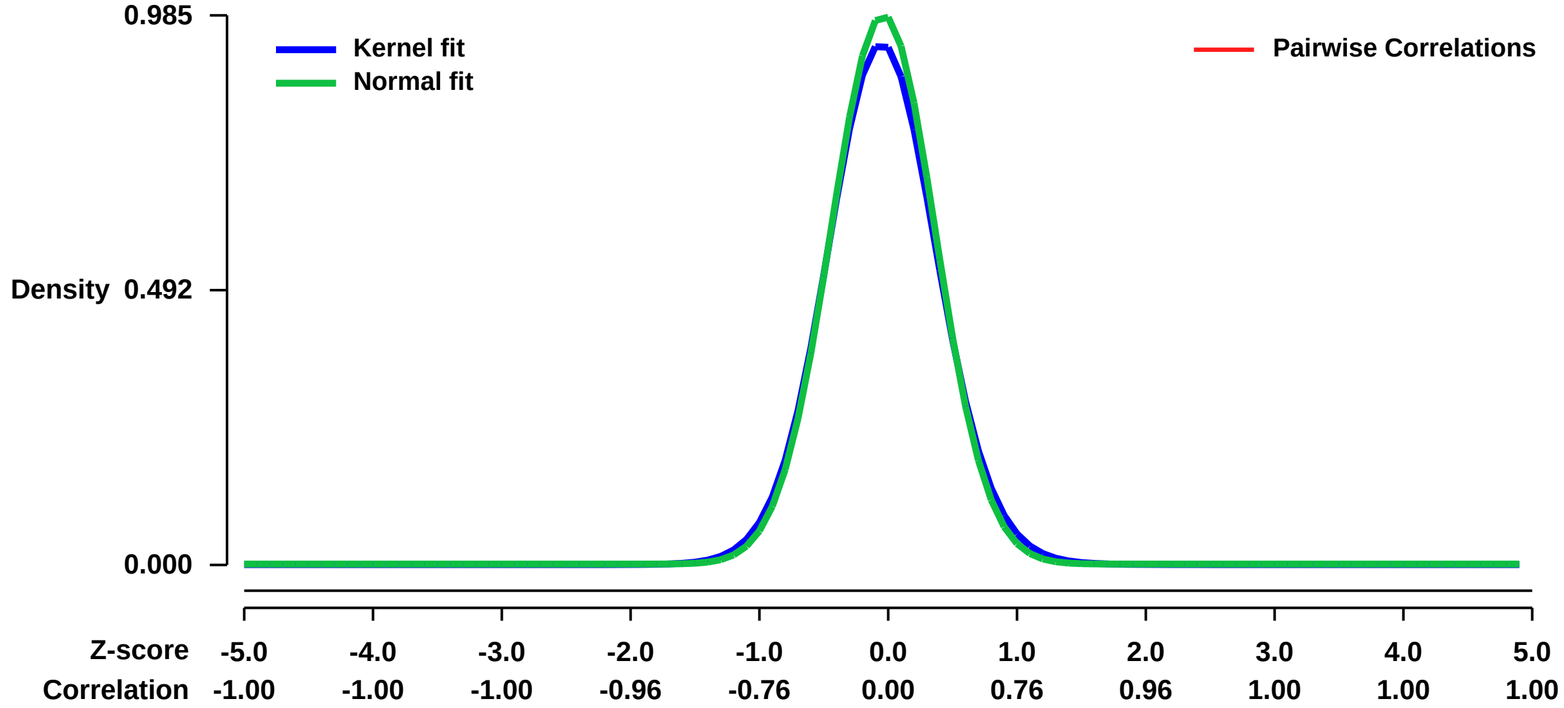

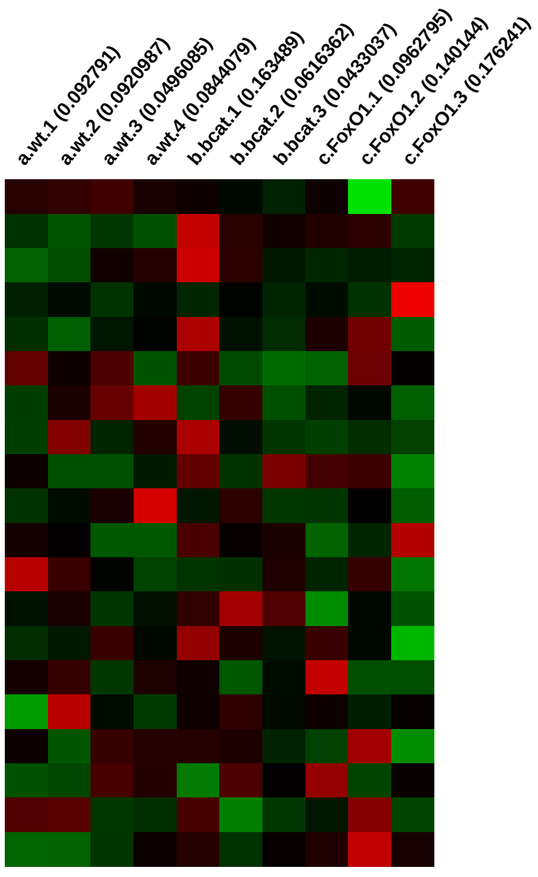

GEO Series "GSE4332" Expression Profiles

Num of samples in this series: 8

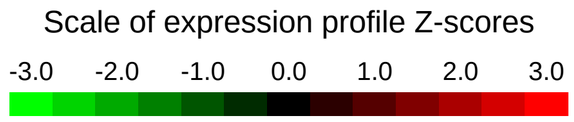

GEO Link:	http://www.ncbi.nlm.nih.gov/geo/query/acc.cgi?acc=GSE4332
Status:	Public on Mar 15 2006
Title:	Cell intrinsic alterations underlie hematopoietic stem cell aging
Organism:	Mus musculus
Experiment type:	Expression profiling by array
Platform:	GPL1261
Pubmed ID:	15967997
Summary & Design:	**Summary:** **Loss of immune function and an increased incidence of myeloid leukemia are two of the most clinically significant consequences of aging of the hematopoietic system. To better understand the mechanisms underlying hematopoietic aging, we evaluated the cell intrinsic functional and molecular properties of highly purified long-term hematopoietic stem cells (LT-HSCs) from young and old mice. We found that LT-HSC aging was accompanied by cell autonomous changes, including increased stem cell self-renewal, differential capacity to generate committed myeloid and lymphoid progenitors, and diminished lymphoid potential. Expression profiling revealed that LT-HSC aging was accompanied by the systemic down-regulation of genes mediating lymphoid specification and function and up-regulation of genes involved in specifying myeloid fate and function. Moreover, LT-HSCs from old mice expressed elevated levels of many genes involved in leukemic transformation. These data support a model in which age-dependent alterations in gene expression at the stem cell level presage downstream developmental potential and thereby contribute to age-dependent immune decline, and perhaps also to the increased incidence of leukemia in the elderly.** **Groups of assays that are related as part of a time series.** **Keywords: time_series_design** **Overall design:** **5 old mice and 3 young mice**

Background corr dist: KL-Divergence = 0.0603, L1-Distance = 0.0196, L2-Distance = 0.0006, Normal std = 0.5299

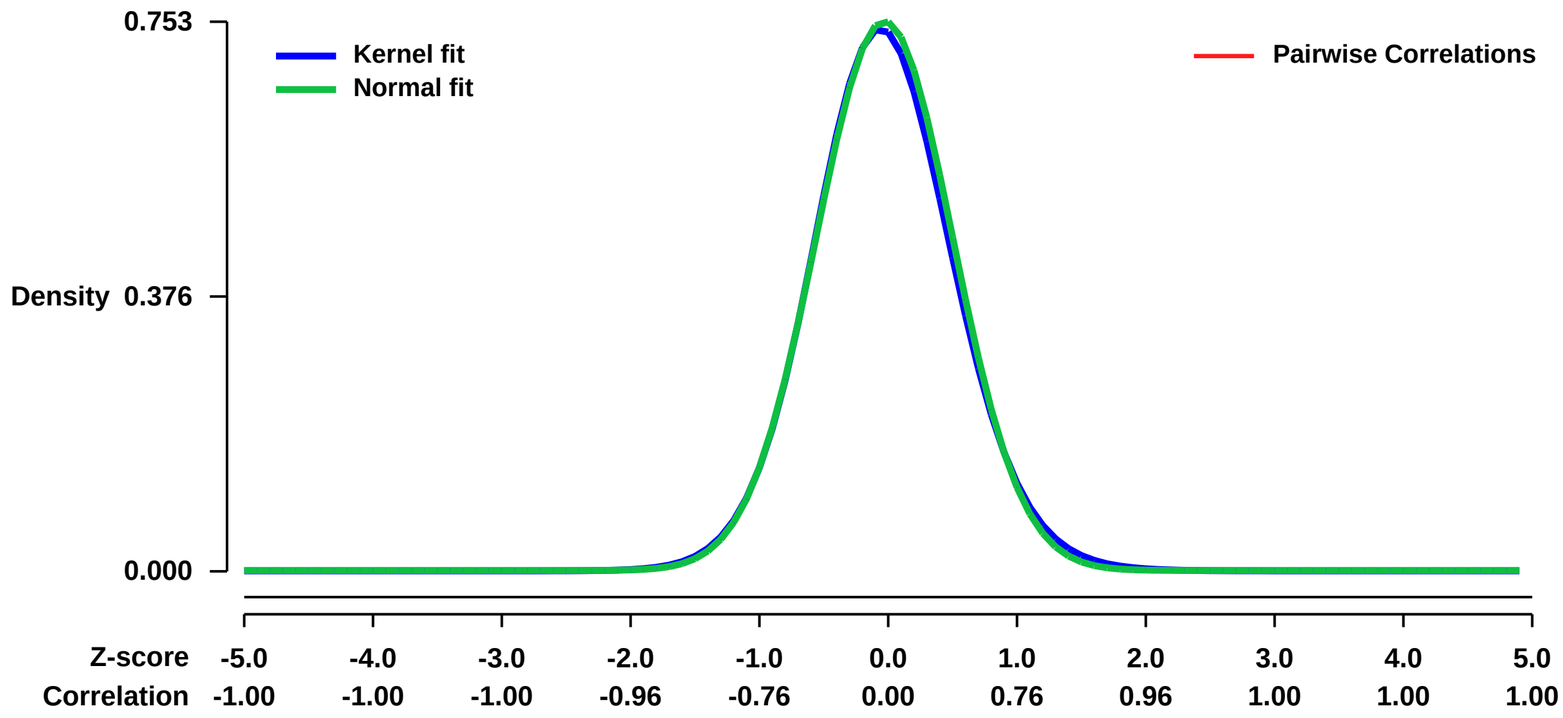

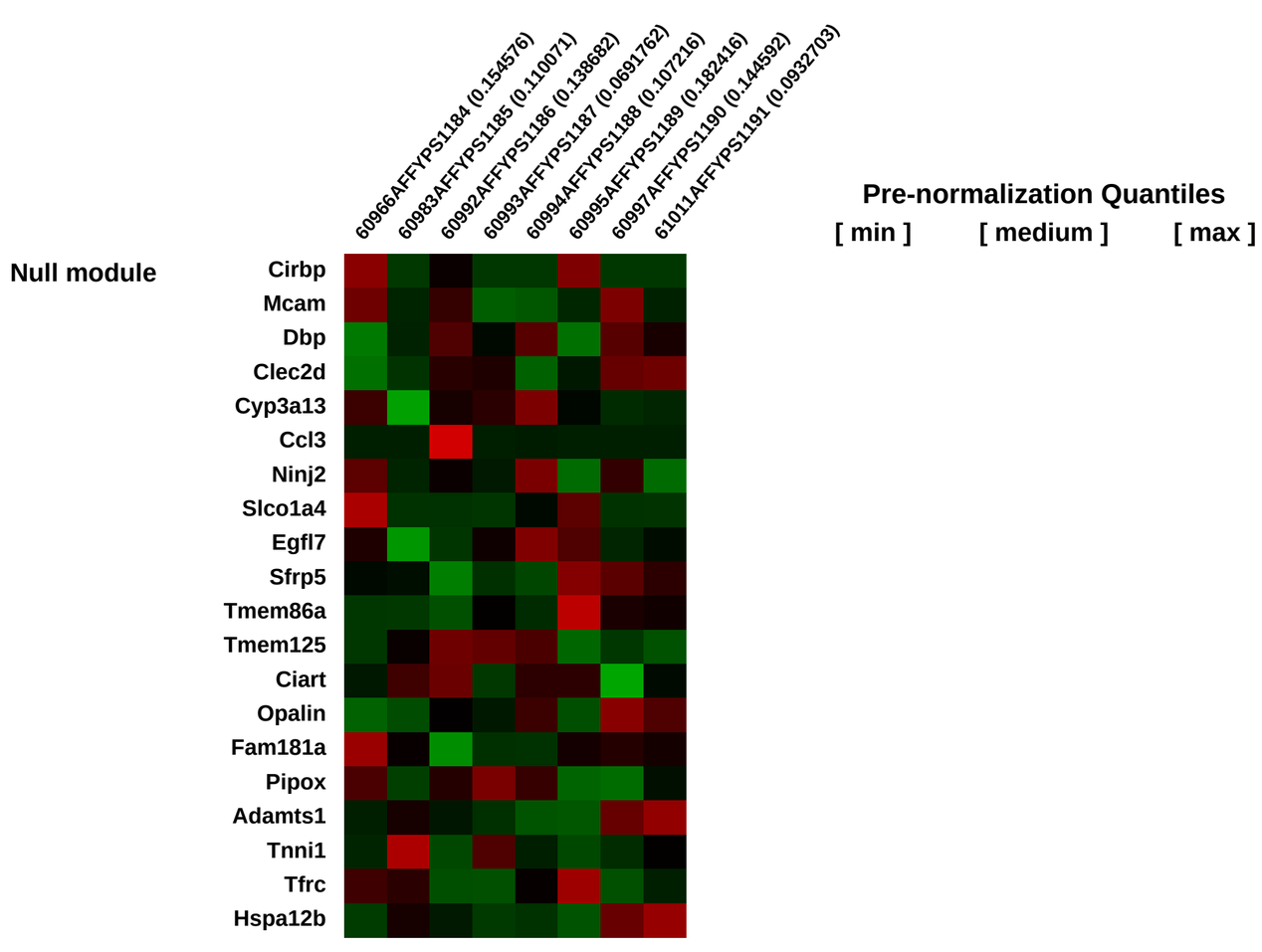

GEO Series "GSE43373" Expression Profiles

Num of samples in this series: 130

Details of this dataset are not shown due to large number of samples and the page size limit.

Find details in http://www.ncbi.nlm.nih.gov/geo/query/acc.cgi?acc=GSE43373

Background corr dist: KL-Divergence = 0.1128, L1-Distance = 0.0557, L2-Distance = 0.0090, Normal std = 0.4228

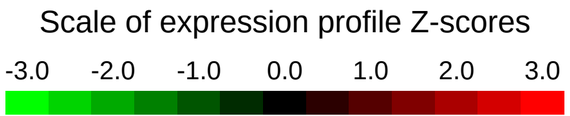

GEO Series "GSE43381" Expression Profiles

Num of samples in this series: 26

Scale of expression profile Z-scores

-3.0 -2.0 -1.0 0.0 1.0 2.0 3.0

GEO Link:	http://www.ncbi.nlm.nih.gov/geo/query/acc.cgi?acc=GSE43381
Status:	Public on Jan 15 2013
Title:	Expression profiling across mouse epithelial tissues
Organism:	Mus musculus
Experiment type:	Expression profiling by array
Platform:	GPL1261
Pubmed ID:	24142692
Summary & Design:	**Summary:** To characterize genes, pathways, and transcriptional regulators enriched in the mouse cornea, we compared the expression profiles of whole mouse cornea, bladder, esophagus, lung, proximal small intestine, skin, stomach, and trachea. **Overall design:** Total RNA was purified from esophagus, lung, proximal small intestine, skin, stomach, and trachea. Data from previous studies in the lab (cornea, GSE43155; bladder, GSE15770; and E18.5 skin, GSE15772) were utilized in the comparison.

Background corr dist: KL-Divergence = 0.0408, L1-Distance = 0.0400, L2-Distance = 0.0029, Normal std = 0.6123

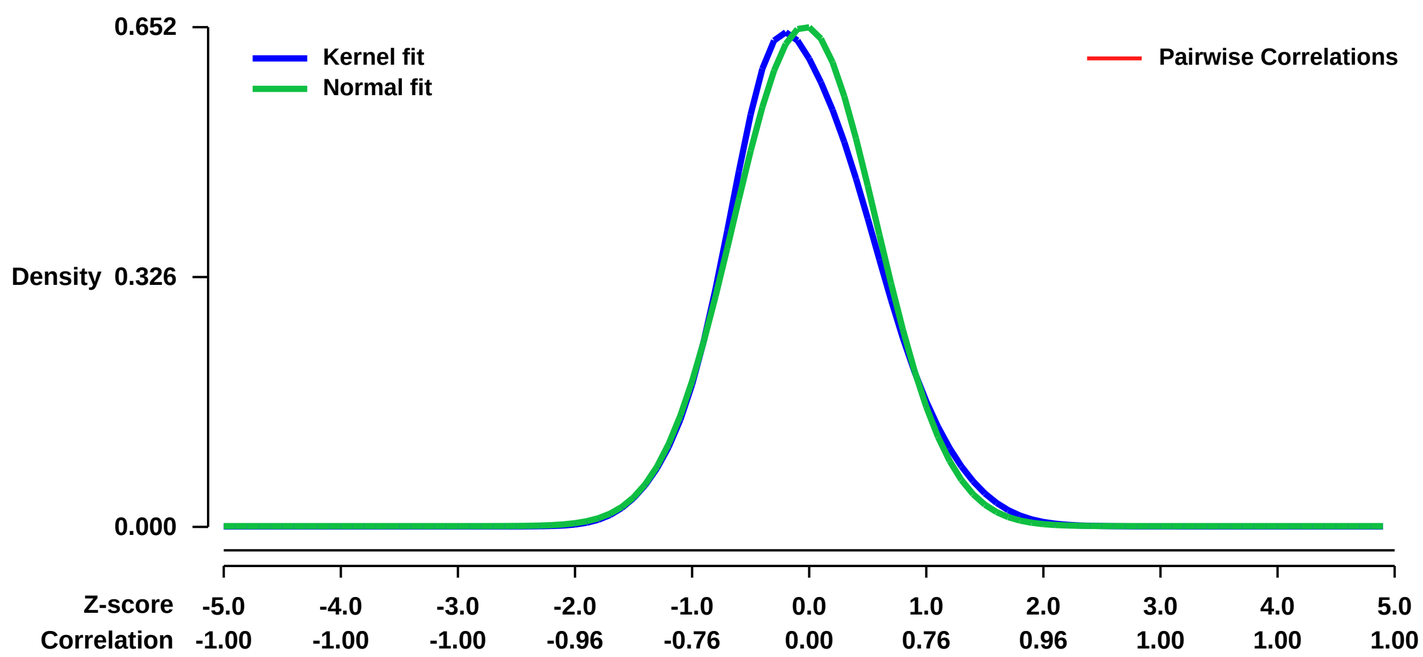

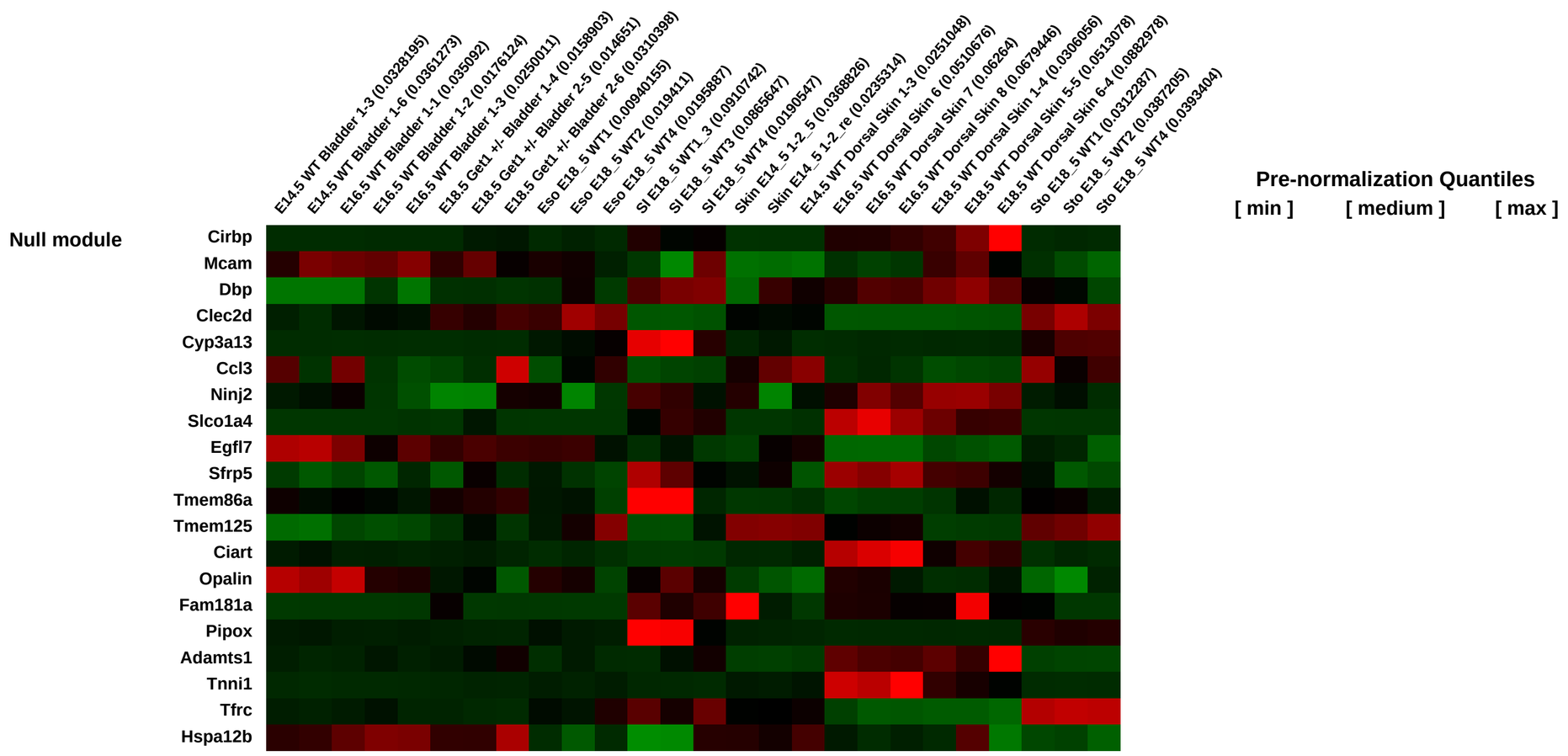

GEO Series "GSE43556" Expression Profiles

Num of samples in this series: 8

Scale of expression profile Z-scores

-3.0 -2.0 -1.0 0.0 1.0 2.0 3.0

GEO Link:	http://www.ncbi.nlm.nih.gov/geo/query/acc.cgi?acc=GSE43556
Status:	Public on Feb 20 2013
Title:	MicroRNA-34a regulates cardiac ageing and function
Organism:	Mus musculus
Experiment type:	Non-coding RNA profiling by array
Platform:	GPL1261
Pubmed ID:	23426265
Summary & Design:	**Summary:** We compared the heart of 6-weeks-old mice (young) with 18-months-old mice (old) **Overall design:** hearts of 6 week old and 18 month old mice

Background corr dist: KL-Divergence = 0.0832, L1-Distance = 0.0207, L2-Distance = 0.0006, Normal std = 0.4697

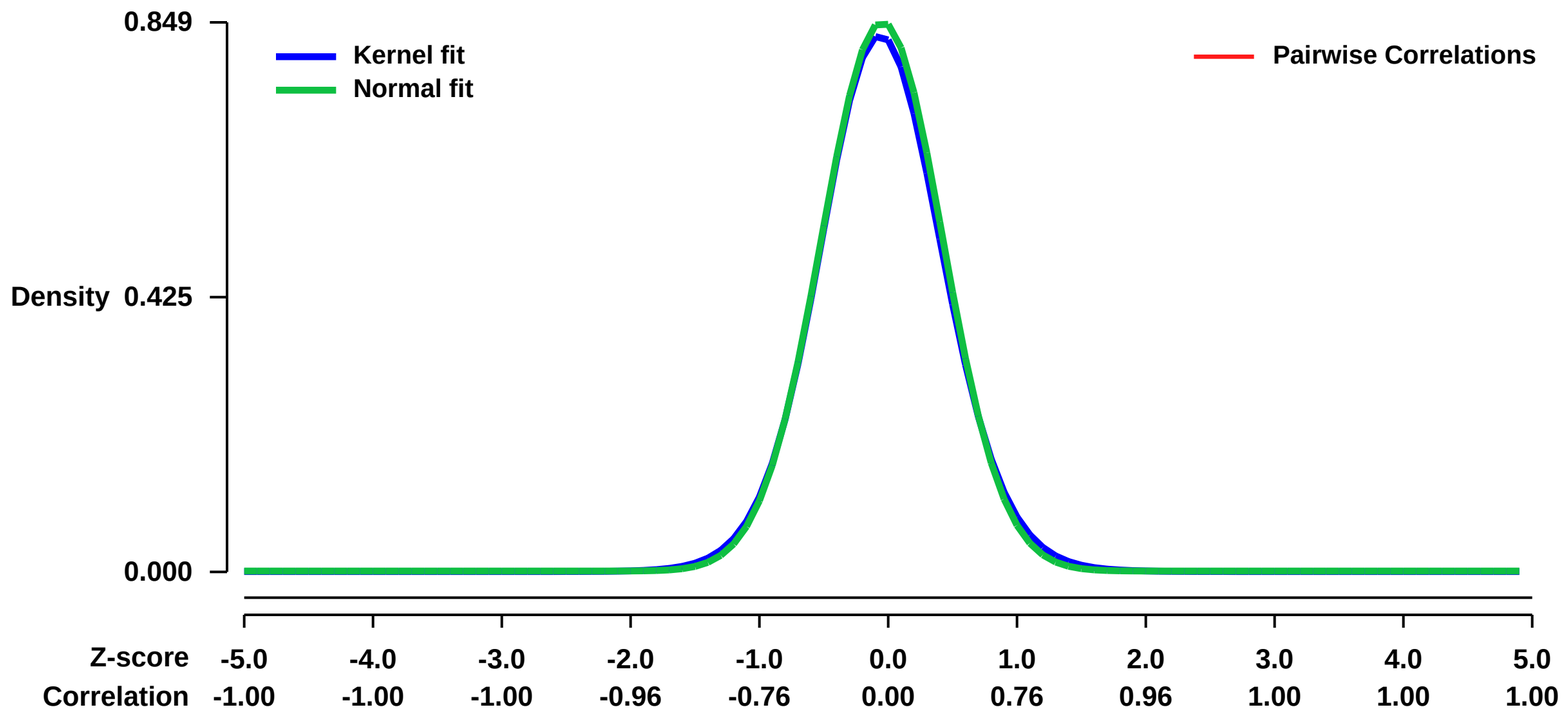

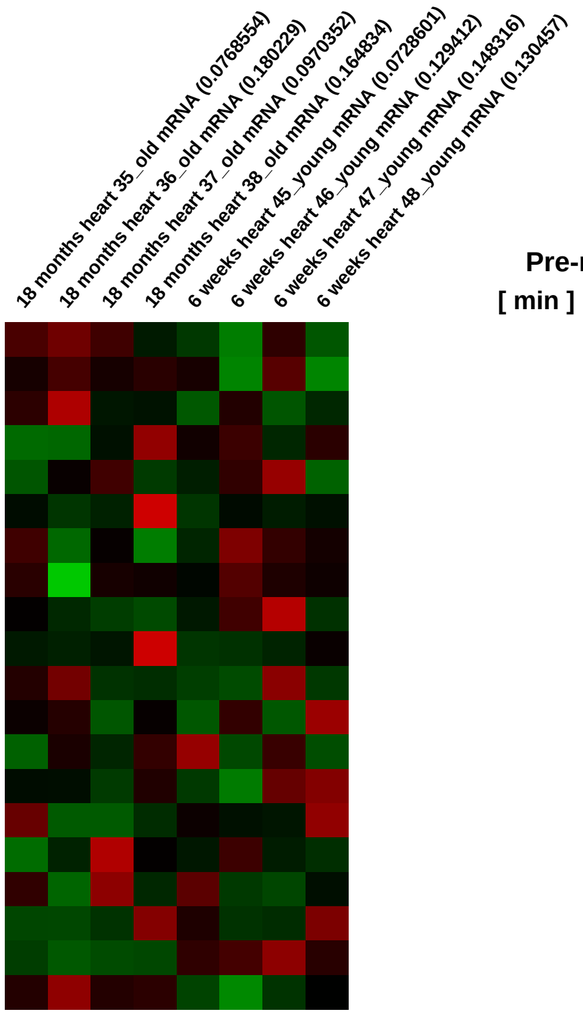

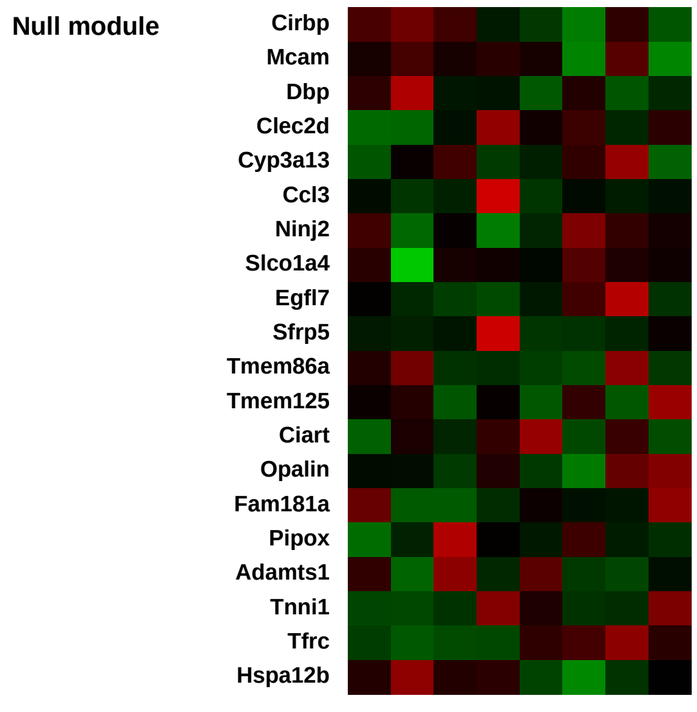

GEO Series "GSE43581" Expression Profiles

Num of samples in this series: 12

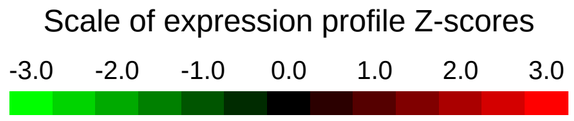

GEO Link:	http://www.ncbi.nlm.nih.gov/geo/query/acc.cgi?acc=GSE43581
Status:	Public on Jan 18 2013
Title:	Hepatic glucose sensing is required to preserve beta-cell glucose competence
Organism:	Mus musculus
Experiment type:	Expression profiling by array
Platform:	GPL1261
Pubmed ID:	23549084
Summary & Design:	**Summary:** We assessed the impact of glucose transporter Glut2 gene inactivation in adult mouse liver (LG2KO mice). This suppressed hepatic glucose uptake but not glucose output. In the fasted state, expression of carbohydrate responsive element-binding protein (ChREBP) and its glycolytic and lipogenic target genes was abnormally elevated. Feeding, energy expenditure, and insulin sensitivity were identical in LG2KO and control mice. Glucose tolerance was normal early after Glut2 inactivation but intolerance developed at later time. This was caused by progressive impairment of glucose-stimulated insulin secretion even though beta-cell mass and insulin content remained normal. Liver transcript profiling revealed a coordinate down-regulation of cholesterol biosynthesis genes in LG2KO mice. This was associated with reduced hepatic cholesterol in fasted mice and a 30 percent reduction in bile acid production. We showed that chronic bile acids or FXR agonist treatment of primary islets increases glucose-stimulated insulin secretion, an effect not seen in islets from fxr-/- mice. Collectively, our data show that glucose sensing by the liver controls beta-cell glucose competence, through a mechanism that likely depends on bile acid production and action on beta-cells. **Overall design:** three replicates each of ps_ctrl_refed, ps_tamox_refed, ps_ctrl_fasted, ps_tamox_fasted

Background corr dist: KL-Divergence = 0.0709, L1-Distance = 0.0372, L2-Distance = 0.0028, Normal std = 0.4933

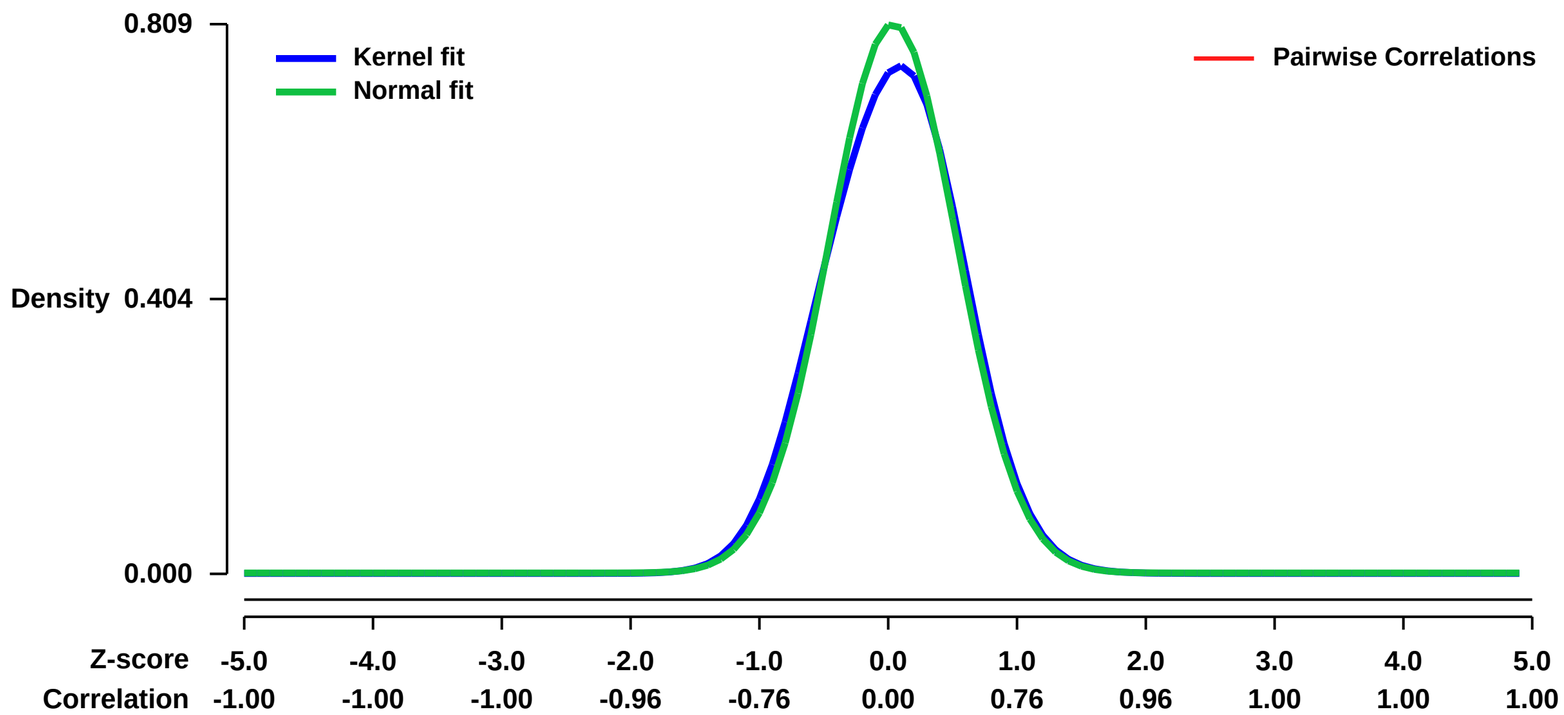

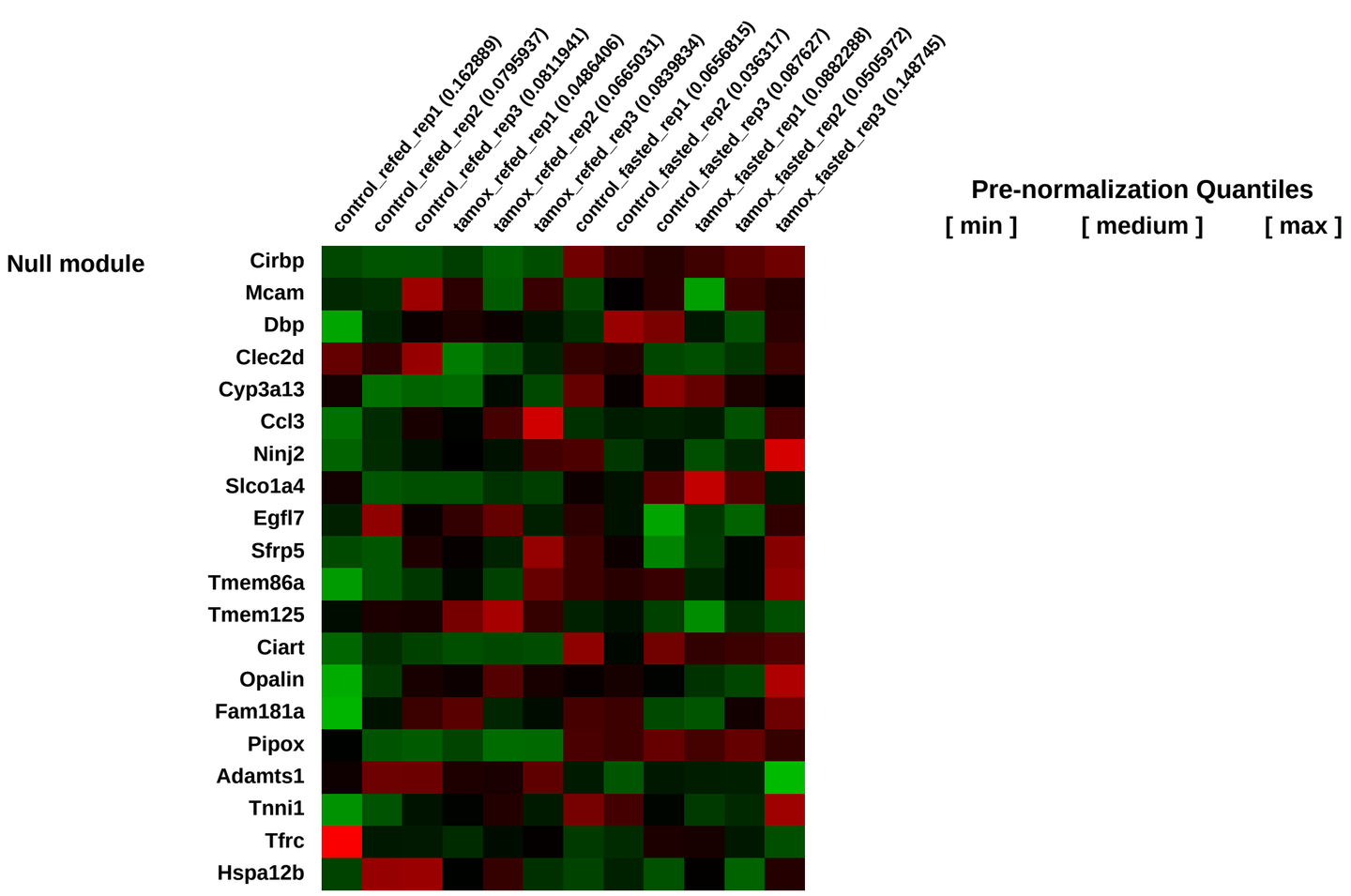

GEO Series "GSE43620" Expression Profiles

Num of samples in this series: 8

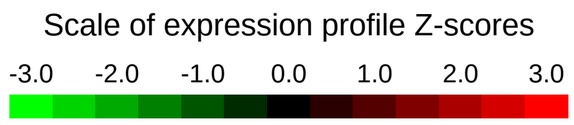

GEO Link:	http://www.ncbi.nlm.nih.gov/geo/query/acc.cgi?acc=GSE43620
Status:	Public on Jan 19 2014
Title:	Effects of sodium tungstate administration in Irs2 -/- mice
Organism:	Mus musculus
Experiment type:	Expression profiling by array
Platform:	GPL1261
Pubmed ID:	24253047
Summary & Design:	**Summary:** **Relative beta cell deficit and increased beta cell apoptosis are hallmarks of type 2 diabetes (T2D). The Insulin/Insulin Growth Factor (Igf) signaling pathway is an established regulator of beta cell survival and is found downregulated in human T2D islets. The Insulin Receptor Substrate 2 (Irs2) plays a central role in the coordination of this pathway in beta cells. Thus, Irs2 knockout mice (Irs2 -/-) exhibit increased beta cell apoptosis that leads to a progressive decline of beta cell mass and hyperglycaemia. In this study, we sought to determine whether the anti-diabetic compound sodium tungstate could prevent the onset of diabetes in Irs2 -/- mice. Oral administration of tungstate resulted in an overall improvement in whole-body glucose tolerance in Irs2 -/- mice which correlated with increased beta cell mass. Enhanced beta cell mass was due to a dramatic reduction of beta cell apoptosis without changes in proliferation. Whole genome gene profiling analysis of islets isolated from treated Irs2 -/- mice confirmed a broad impact of tungstate on cell death pathways. Mechanistically, tungstate induced Erk1/2 phosphorylation in islets in vitro and, in agreement, treated Irs2 -/- islets exhibited increased basal Erk1/2 phosphorylation. Tungstate also downregulated expression of apoptosis-related genes in Irs2-/- islets in vitro, uncovering a direct effect of this compound in islets. All together, our data demonstrate that tungstate can restore beta cell mass and glucose homeostasis in a context of deficient Insulin/Igf signaling. This study underscores the importance of developing strategies specifically designed to arrest beta cell apoptosis as a means to prevent progressive beta cell failure in diabetes.** **Overall design:** **10-week old WT and Irs2 -/- mice were randomly divided into two treatment group, in a total of 4 experimental groups. For 21 days one group received distilled water as drinking water (untreated group) whilst the other received ad libitum a solution of 2mg/ml of sodium tungstate in distilled water (treated group). For each experimental group 2 independent samples were analysed, in a total of 8 samples.**

Background corr dist: KL-Divergence = 0.0481, L1-Distance = 0.0167, L2-Distance = 0.0003, Normal std = 0.5662

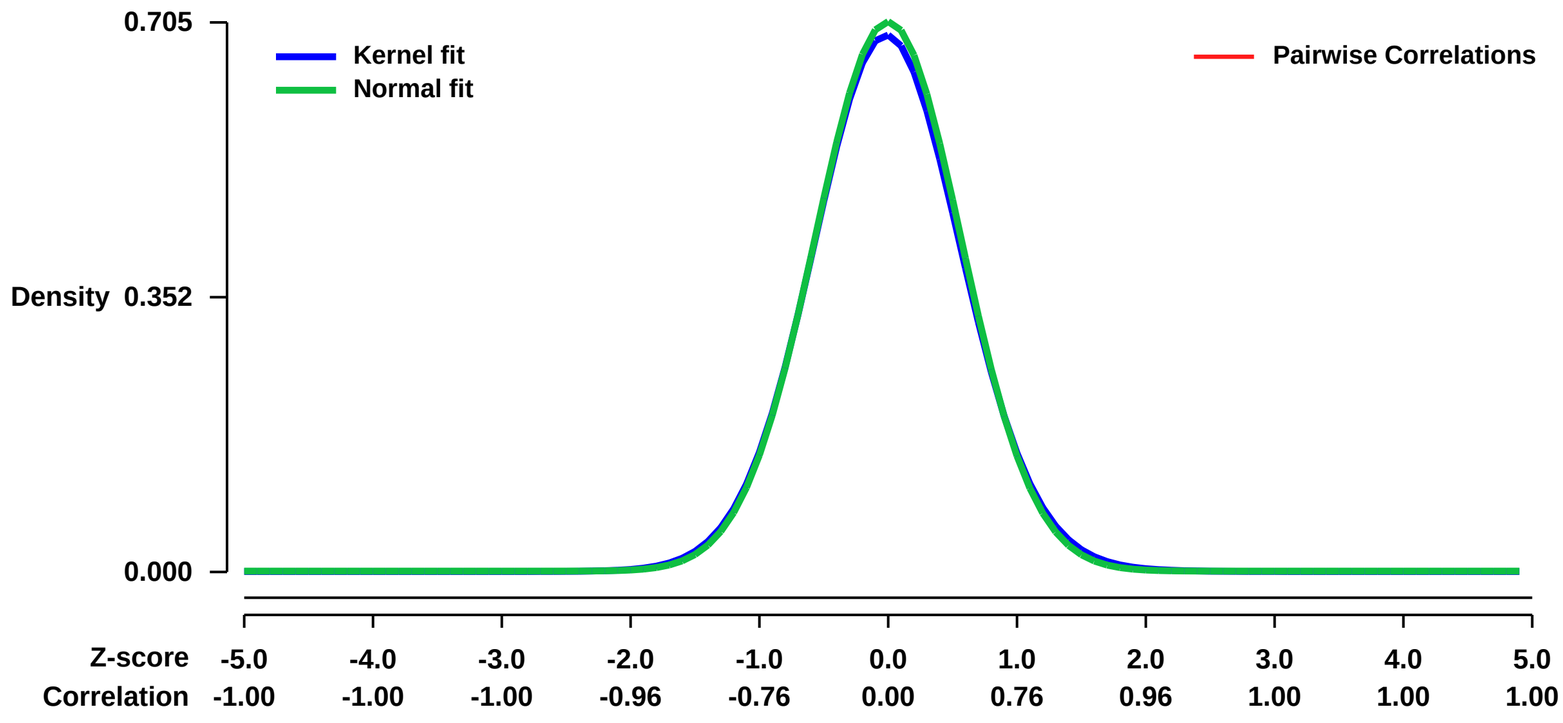

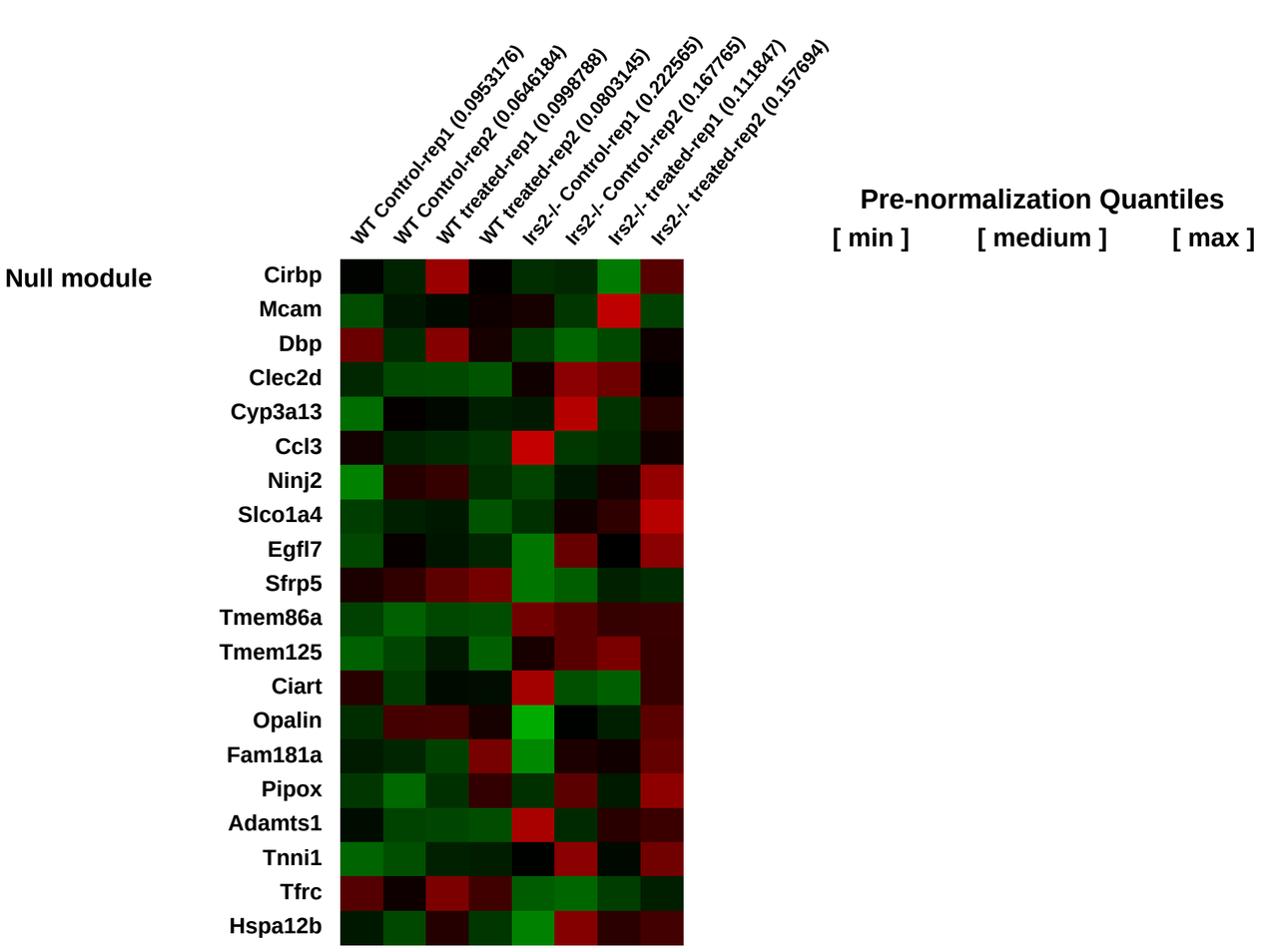

GEO Series "GSE43635" Expression Profiles

Num of samples in this series: 9

Scale of expression profile Z-scores

-3.0 -2.0 -1.0 0.0 1.0 2.0 3.0

GEO Link:	**http://www.ncbi.nlm.nih.gov/geo/query/acc.cgi?acc=GSE43635**
Status:	**Public on Jan 19 2013**
Title:	**Expression data from mouse T cells after CLIP (Crosslinking immunoprecipitation) procedures (mRNA)**
Organism:	**Mus musculus**
Experiment type:	**Expression profiling by array**
Platform:	**GPL1261**
Pubmed ID:	
Summary & Design:	**Summary:** **Molecular networks based on genome-wide mRNA and miRNA expression in activated T cells are interated by co-regulation with miRNA and protein-coding genes during immune responses, however, accurate prediction of miRs and their targets remains a challenge. Furthermore, the specific changes in the expression of miRNAs and/or mRNAs in allogeneic activated T cells during HCT would be distinct from those responding to non-specific stimulation.** **Recently, Ago-CLIP has been demonstrated to provide a robust platform for identification of precise miRNA-mRNA interactions by definitively distinguishing direct from indirect miRNA-target interactions. We utilized CLIP procedure followed by screening with standard microarray platforms for miRNA and mRNA transcripts to demonstrate the miR-mRNA landscape and identify novel molecular targets for modulating T cell responses.** **Overall design:** **Mixed cell culture was performed with T cells in the presence of syngeneic 57BL/6, or allogeneic BALB/c dendritic cells or cultivated with anti-CD3e and anti-CD28 mAB9 for 24 h. Purified T cells were processde for CLIP procedures and followed by RNA isolation (TRIzol LS and miReasy Kit) and hybridization on Affymetrix microarrays and Exiqon 6th generation miRCURY LNA microRNA Arrays . We sought to obtain that the specific changes in the expression of miRNAs and/or mRNAs in allogeneic activated T cells during hematopoietic cells transplantation and that would be distinct from those responding to non-specific stimulation.**

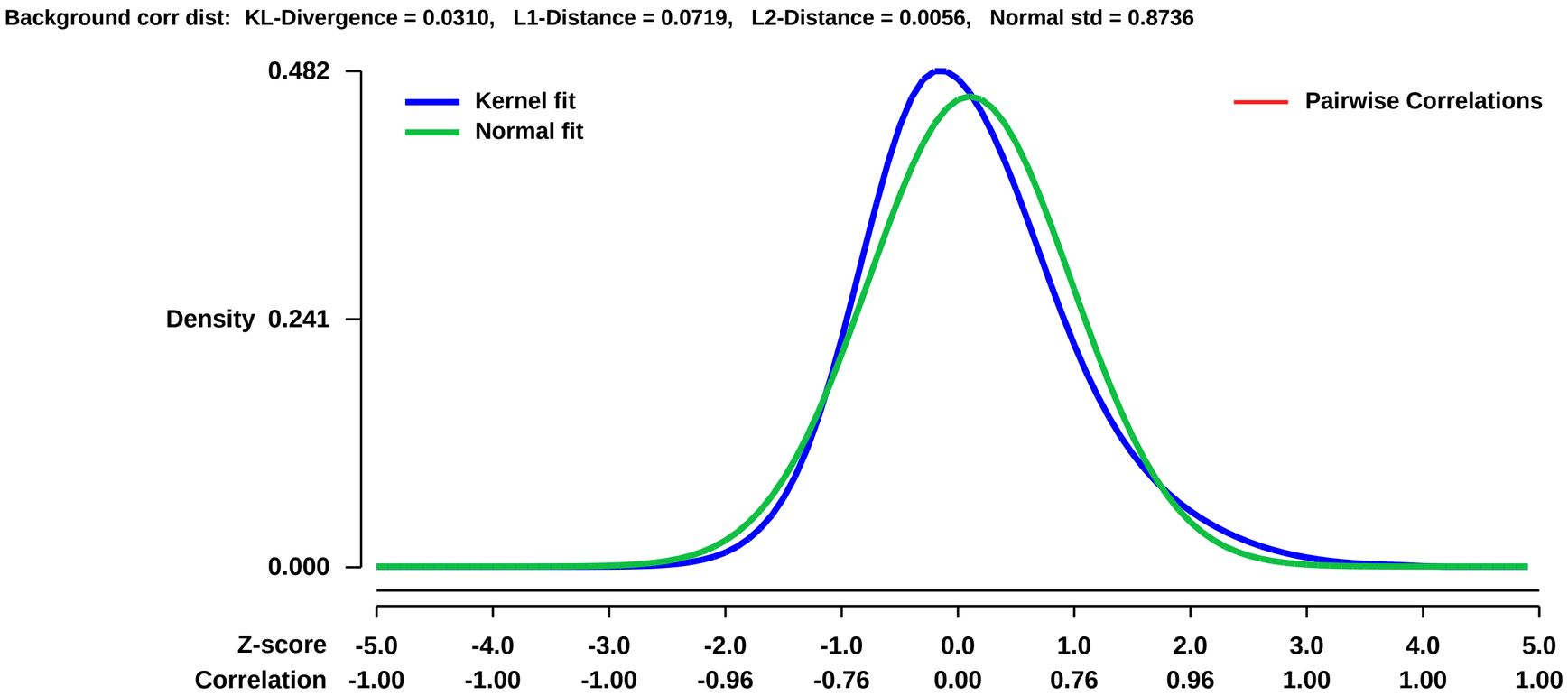

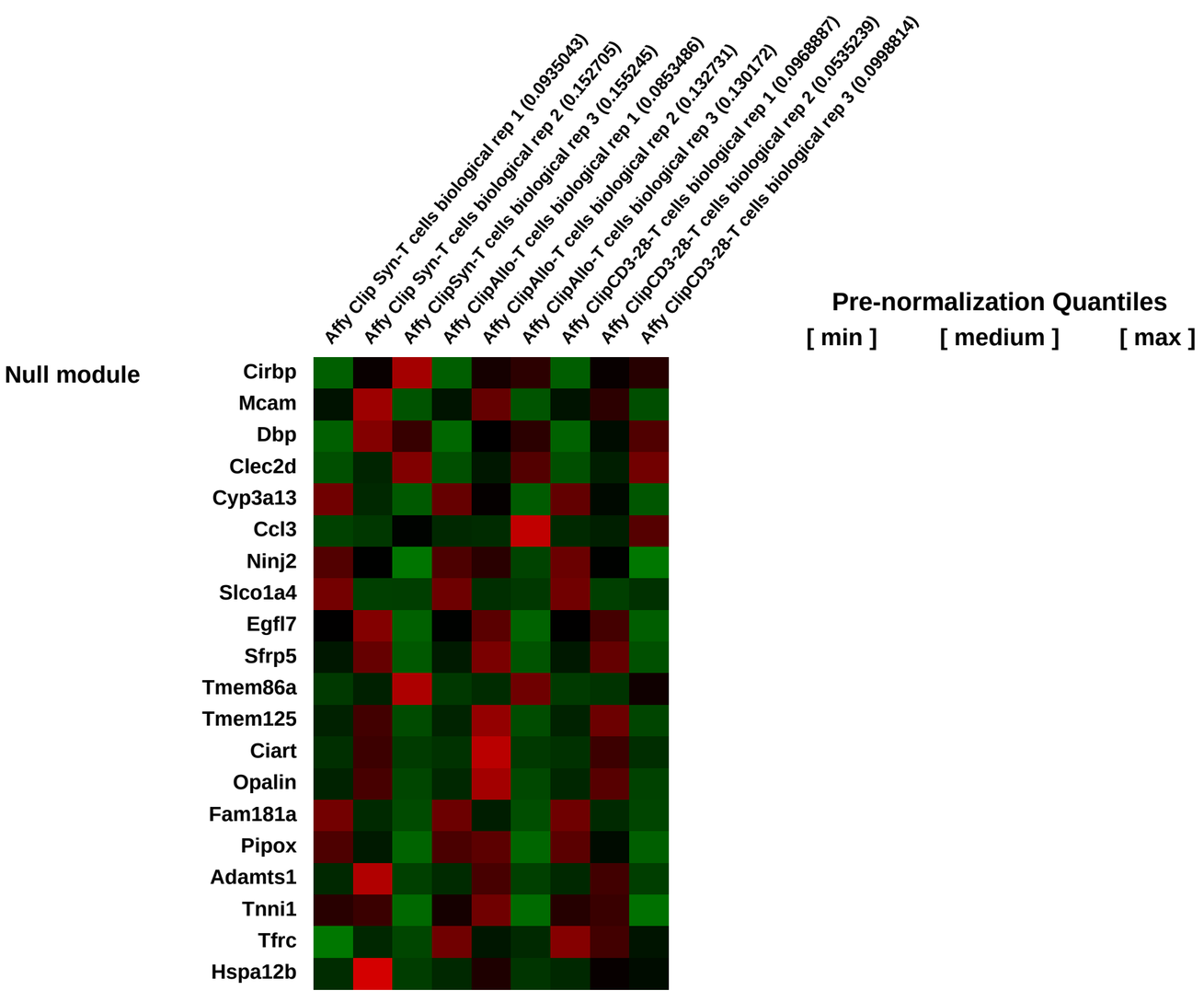

GEO Series "GSE43713" Expression Profiles

Num of samples in this series: 16

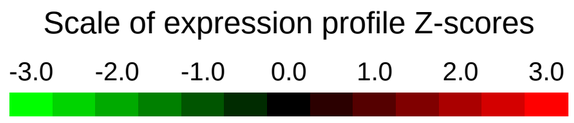

GEO Link:	http://www.ncbi.nlm.nih.gov/geo/query/acc.cgi?acc=GSE43713
Status:	Public on Sep 05 2013
Title:	Microarray to find CHOP dependent genes in response to proteasome inhibition
Organism:	Mus musculus
Experiment type:	Expression profiling by array
Platform:	GPL1261
Pubmed ID:	23761072
Summary & Design:	**Summary:** Environmental stresses that disrupt protein homeostasis induce phosphorylation of eIF2, triggering repression of global protein synthesis coincident with preferential translation of ATF4, a transcriptional activator of the Integrated stress response (ISR). Depending on the extent of protein disruption, ATF4 may not be able to restore proteostatic control and instead switch to a terminal outcome that features elevated expression of the transcription factor CHOP (GADD153/DDIT3). The focus of this study was to define the mechanisms by which CHOP directs gene regulatory networks that determine cell fate. We find that in response to proteasome inhibition, CHOP induces the expression of a collection of genes encoding transcription regulators, including ATF5, which is preferentially translated during eIF2 phosphorylation. Transcriptional expression of ATF5 is directly activated by both CHOP and ATF4. Knock-down of ATF5 increased cell survival in response to proteasome inhibition, supporting the idea that both ATF5 and CHOP have pro-apoptotic functions. Transcriptome analyses of ATF5-dependent genes revealed targets involved in apoptosis, including, NOXA, which is important for inducing cell death during proteasome inhibition. This study suggests that the ISR features a feed-forward loop of stress induced transcriptional regulators, each subject to transcriptional and translational control that can switch cell fate towards apoptosis. **Overall design:** 8 plates (10cm) of WT and and 8 plates (10cm) of CHOP-/- MEF cells were subject to no stress (4 each for a total of 8) or treated for 8 hours with 1uM MG132 (4 each for a total of 8). Unstressed cells were harvested at the same time as the stressed cells

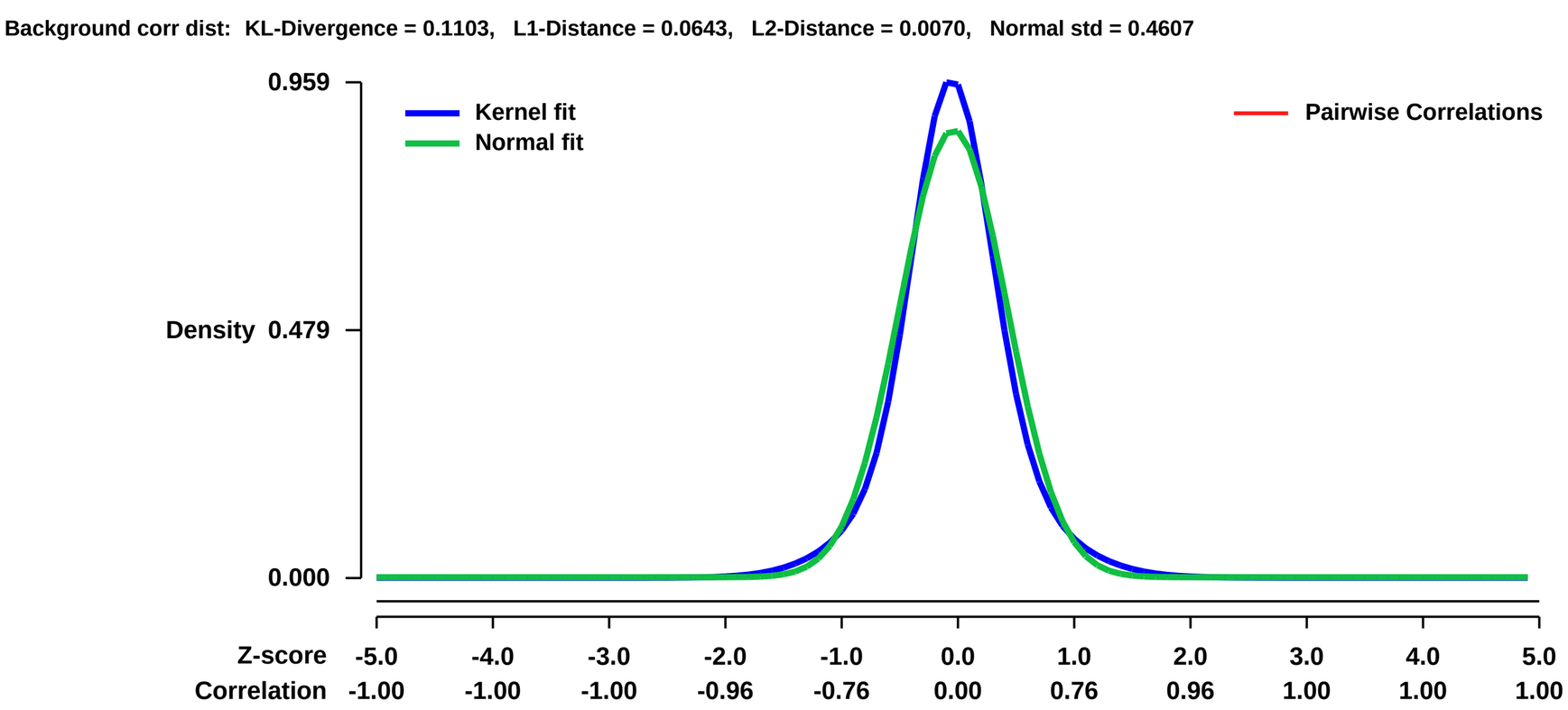

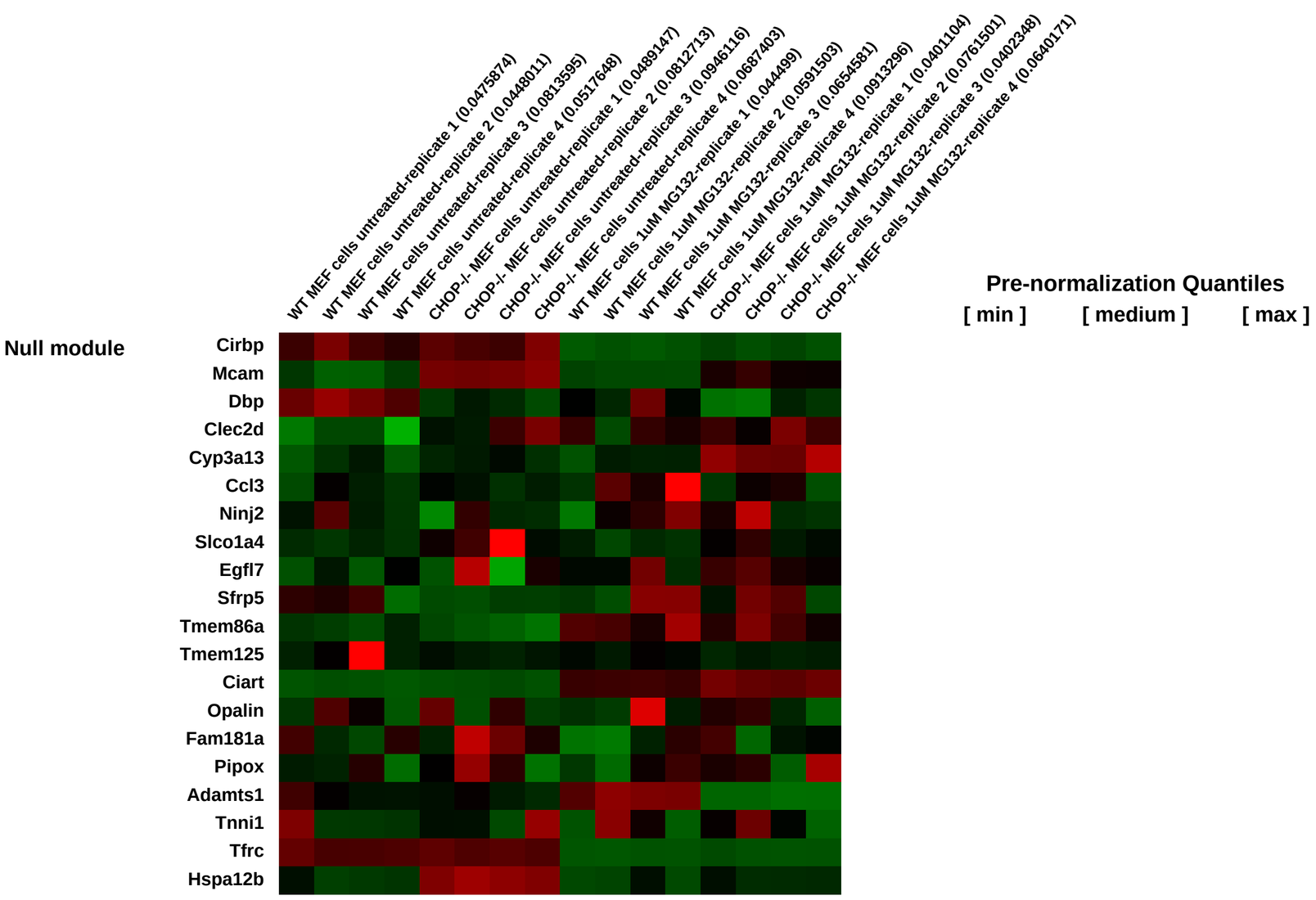

GEO Series "GSE43779" Expression Profiles

Num of samples in this series: 6

Scale of expression profile Z-scores

-3.0 -2.0 -1.0 0.0 1.0 2.0 3.0

GEO Link:	http://www.ncbi.nlm.nih.gov/geo/query/acc.cgi?acc=GSE43779
Status:	Public on Jan 28 2013
Title:	Expression data from 2-amino acetophenone (2-AA) treated mouse Skeletal muscle
Organism:	Mus musculus
Experiment type:	Expression profiling by array
Platform:	GPL1261
Pubmed ID:	
Summary & Design:	**Summary:** Metabolic responses begin promptly upon the initiation of infection, and progress as a series of coordinated events. Mitochondria may play a key role in the development of insulin resistance. Reduced energy production and mitochondrial dysfunctional may further favor infection, and be an important step in the establishment of chronic and persistent infections. We have used mouse skeletal muscle transcriptome data which have led to the hypothesis that 2-AA causes harm to the host by triggering mitochondrial dysfunction in skeletal muscle. **Overall design:** The gastrocnemius muscles were isolated from control and 4days 2-AA treated mouse for RNA extraction and hybridization on Affymetrix microarrays.

Background corr dist: KL-Divergence = 0.0223, L1-Distance = 0.0276, L2-Distance = 0.0011, Normal std = 0.7411

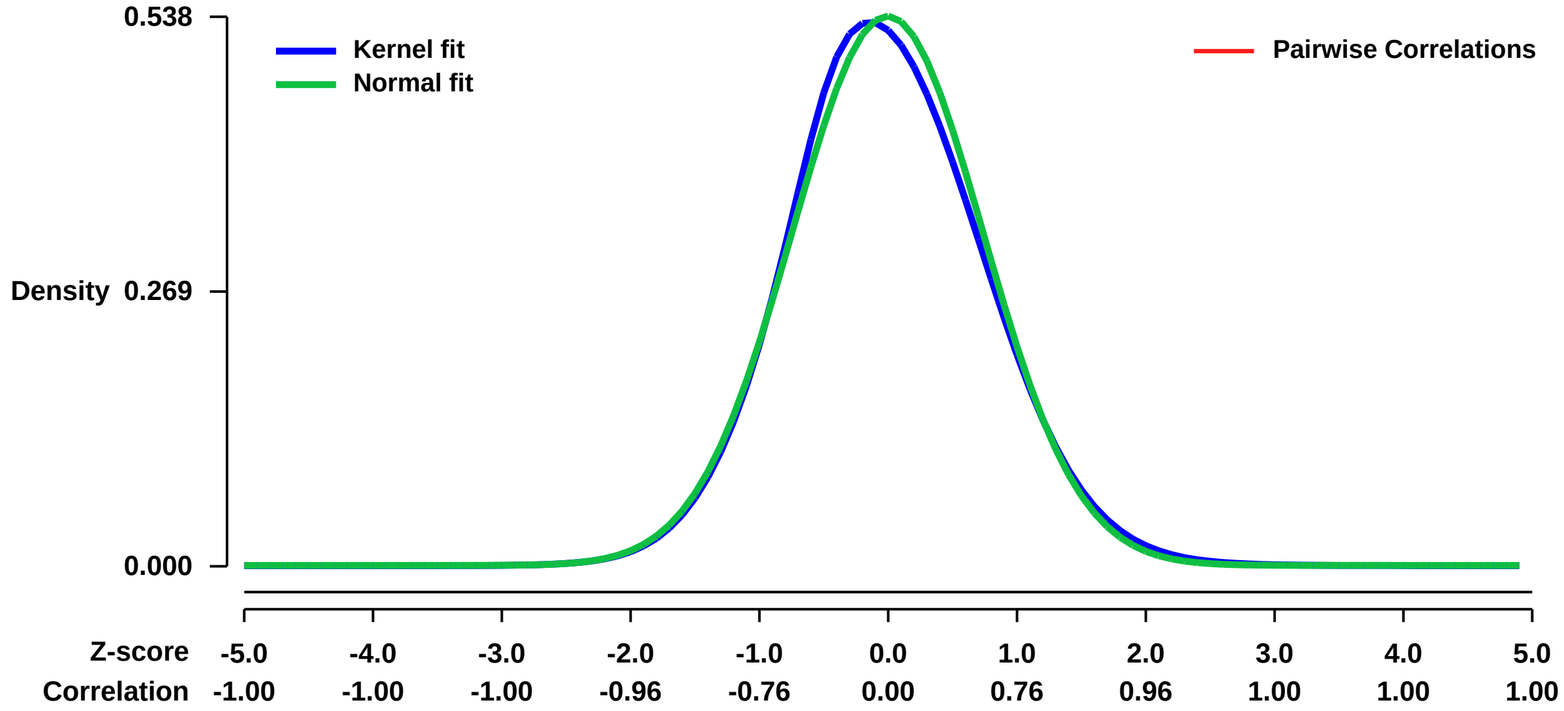

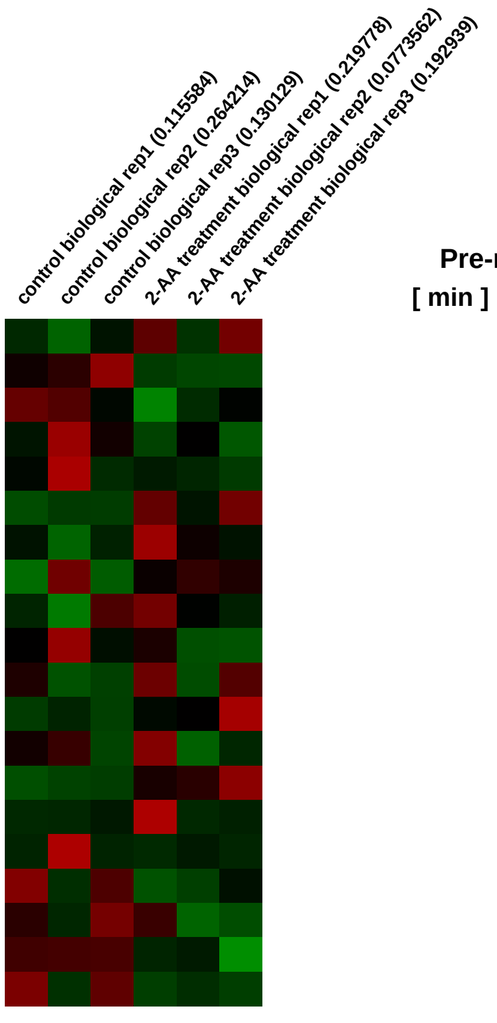

GEO Series "GSE43899" Expression Profiles

Num of samples in this series: 12

Scale of expression profile Z-scores

-3.0 -2.0 -1.0 0.0 1.0 2.0 3.0

GEO Link:	http://www.ncbi.nlm.nih.gov/geo/query/acc.cgi?acc=GSE43899
Status:	Public on Aug 30 2013
Title:	Co-ordinate inhibiton of autism candidate genes by topoisomerase inhibitors [array]
Organism:	Mus musculus
Experiment type:	Expression profiling by array
Platform:	GPL1261
Pubmed ID:	23995680
Summary & Design:	**Summary:** Topoisomerases are necessary for the expression of neurodevelopmental genes, and are mutated in some patients with autism spectrum disorder (ASD). We have studied the effects of inhibitors of Topoisomerase 1 (Top1) and Topoisomerase 2 (Top2) enzymes on mouse cortical neurons. We find that topoisomerases selectively inhibit long genes (>100kb), with little effect on all other gene expression. Using ChIPseq against RNA Polymerase II (Pol2) we show that the Top1 inhibitor topotecan blocks transcriptional elongation of long genes specifically. Many of the genes inhibited by topotecan are candidate ASD genes, leading us to propose that topoisomerase inhibition might contribute to ASD pathology. **Overall design:** 9) cultured mouse cortical neurons treated with topotecan with or without subsequent drug washout, vs vehicle-treated controls.

Background corr dist: KL-Divergence = 0.0306, L1-Distance = 0.0234, L2-Distance = 0.0007, Normal std = 0.6443

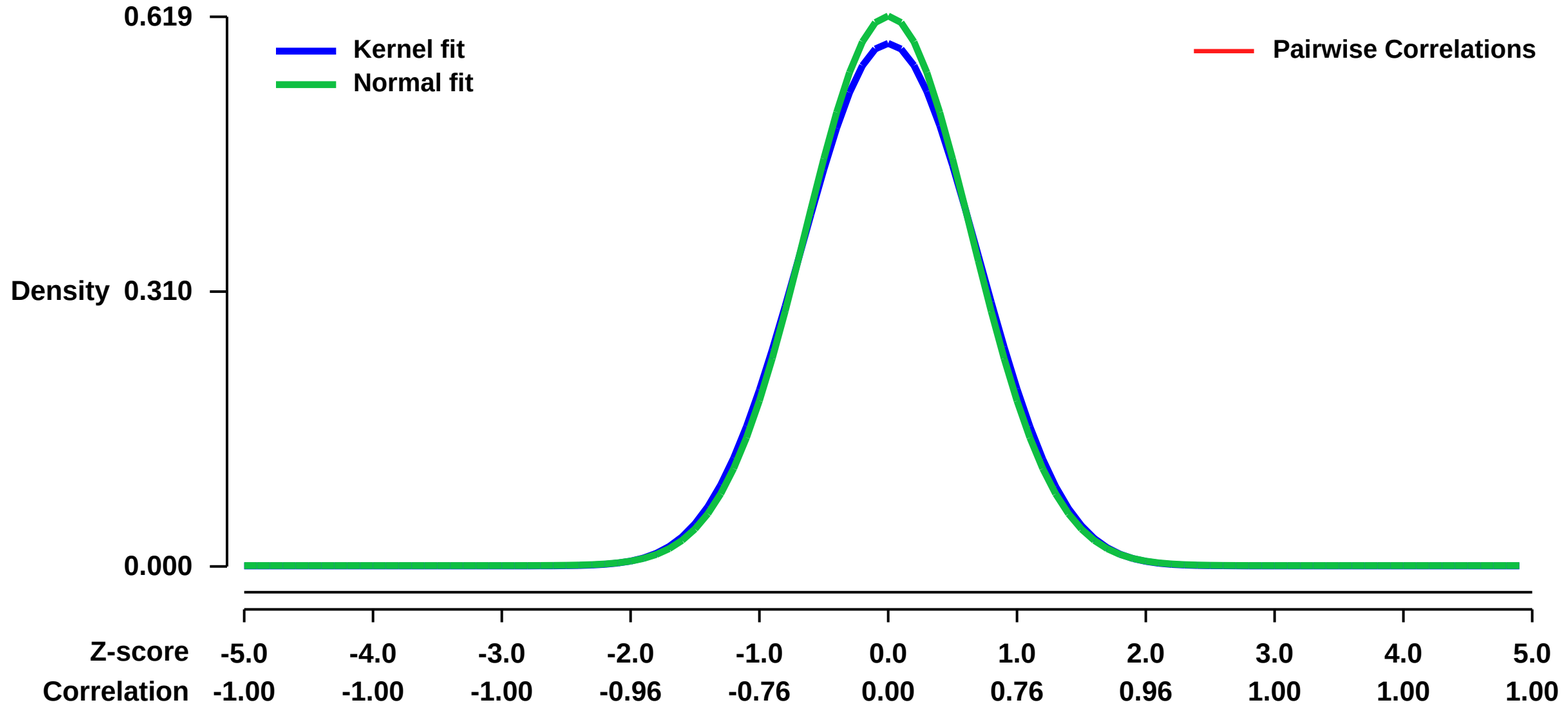

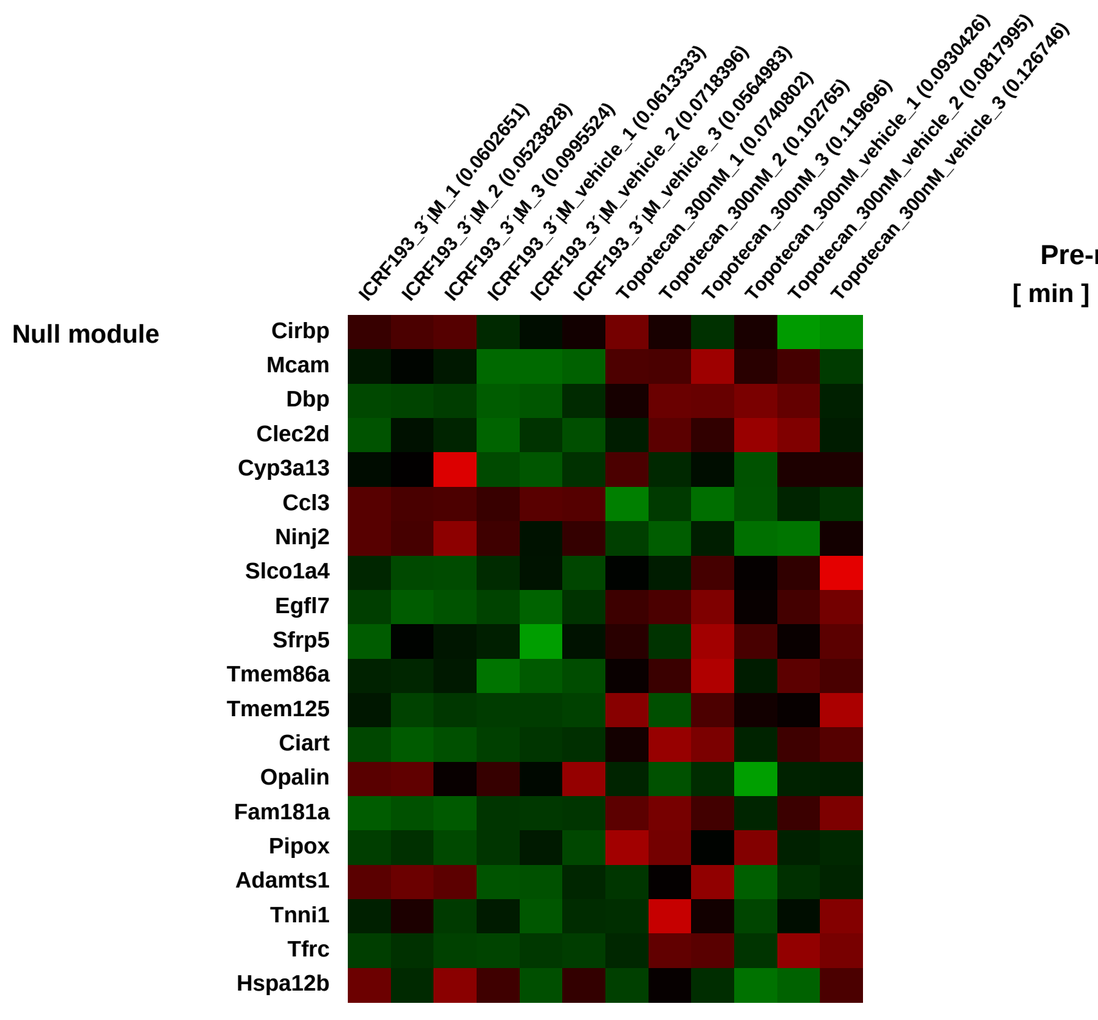

GEO Series "GSE43927" Expression Profiles

Num of samples in this series: 19

Scale of expression profile Z-scores

-3.0 -2.0 -1.0 0.0 1.0 2.0 3.0

GEO Link:	http://www.ncbi.nlm.nih.gov/geo/query/acc.cgi?acc=GSE43927
Status:	Public on Feb 04 2014
Title:	Exposure to Propylthiouracil in Pregnant Mice Potentiates the Transcriptional Response to Thyroid Hormone in the Fetal Cerebral Cortex
Organism:	Mus musculus
Experiment type:	Expression profiling by array
Platform:	GPL1261
Pubmed ID:	24436321
Summary & Design:	**Summary:** **Although the effects of thyroid hormones (TH) on the brain development have been extensively studied perinatally, effects of TH of maternal origin on the fetal brain development have been largely unexplored. We applied a high throughput study on the mouse models with aberrant TH levels on gestation day (GD) 16, before the onset of fetal thyroid function. Although 3 day treatment with methimazole (MMI) and perchlorate significantly decreased TH levels in fetal cerebral cortex, few changes in the abundance of mRNA were revealed by the microarray analysis. Injection TH to dams 12 hours before sacrifice on GD 16 induced 161 genes significantly changed in fetal cortex. Nine out of 10 selected genes were confirmed with RT-PCR, including known TH responsive gene Klf9 and other novel TH responsive genes such as Appbp2, Ppap2b and Fgfr1op2. TH regulation of the expression of these genes was also confirmed with cultured N2a˛† cells. Thyroid responsive elements (TREs) in the promoters of these genes were identified using electrophoresis mobility shift assay. TH effect on microRNA (miRNA) expression in developing cortex on GD 16 and postnatal day (PND) 15 was investigated with microarray and RT-PCR. Some of miRNAs and precursors decreased in fetal cortex from the dams injected with TH on GD 16, including miR-16 and miR-106. Using 3â untranslate region reporter vector, we identified Klf9 is one of the target genes of miR-106, while Ppap2b is the target of miR-16. These results indicated that TH regulation on gene expression could through TR-TRE interaction and through regulating target miRNA expression. This study is the first report to identify TH responsive genes and miRNAs genome wide in the early fetal brain; it provides evidence to further understand the mechanism of TH effect on brain development.** **Overall design:** **1 of 20 samples removed due to poor quality.**

Background corr dist: KL-Divergence = 0.2258, L1-Distance = 0.0571, L2-Distance = 0.0081, Normal std = 0.3144

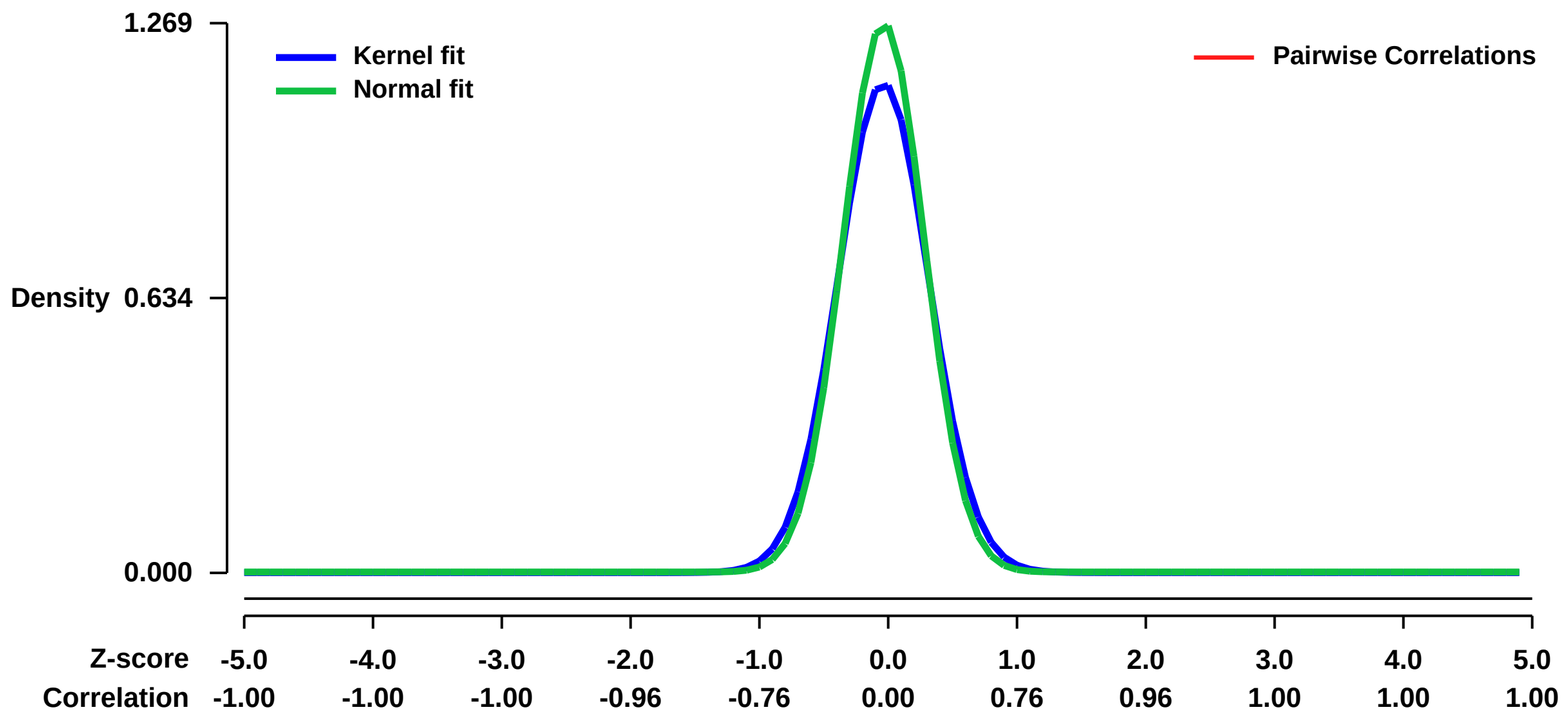

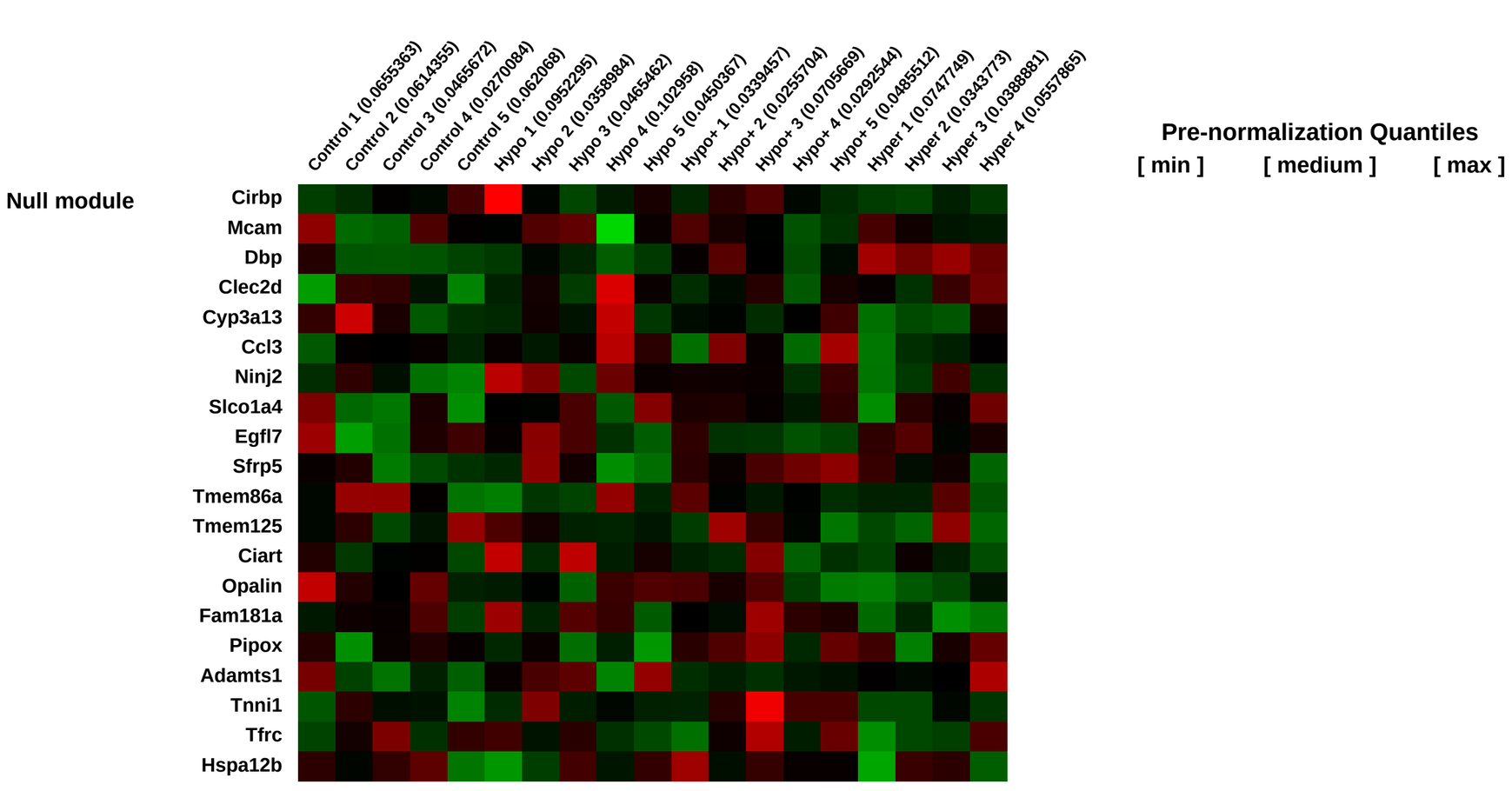

GEO Series "GSE44025" Expression Profiles

Num of samples in this series: 6

Scale of expression profile Z-scores

-3.0 -2.0 -1.0 0.0 1.0 2.0 3.0

GEO Link:	http://www.ncbi.nlm.nih.gov/geo/query/acc.cgi?acc=GSE44025
Status:	Public on Nov 06 2013
Title:	Expression data from Sh2b3 Knock-out NOTCH1-induced leukemias
Organism:	Mus musculus
Experiment type:	Expression profiling by array
Platform:	GPL1261
Pubmed ID:	23908464
Summary & Design:	**Summary:** **To formally address the tumor suppressor activity of Sh2b3 in vivo, we tested the interaction between oncogenic NOTCH1 and Sh2b3 loss in a retroviral- transduction bone marrow transplantation model of NOTCH-induced T-ALL** **Forced expression of activated NOTCH1 in this model typically results in full leukemia transformation 5-10 weeks later.** **Overall design:** **We performed microarray gene expression analysis of Sh2b3 wild type and Sh2b3â /â NOTCH1 induced leukemias**

Background corr dist: **KL-Divergence = 0.0428, L1-Distance = 0.0195, L2-Distance = 0.0004, Normal std = 0.6009**

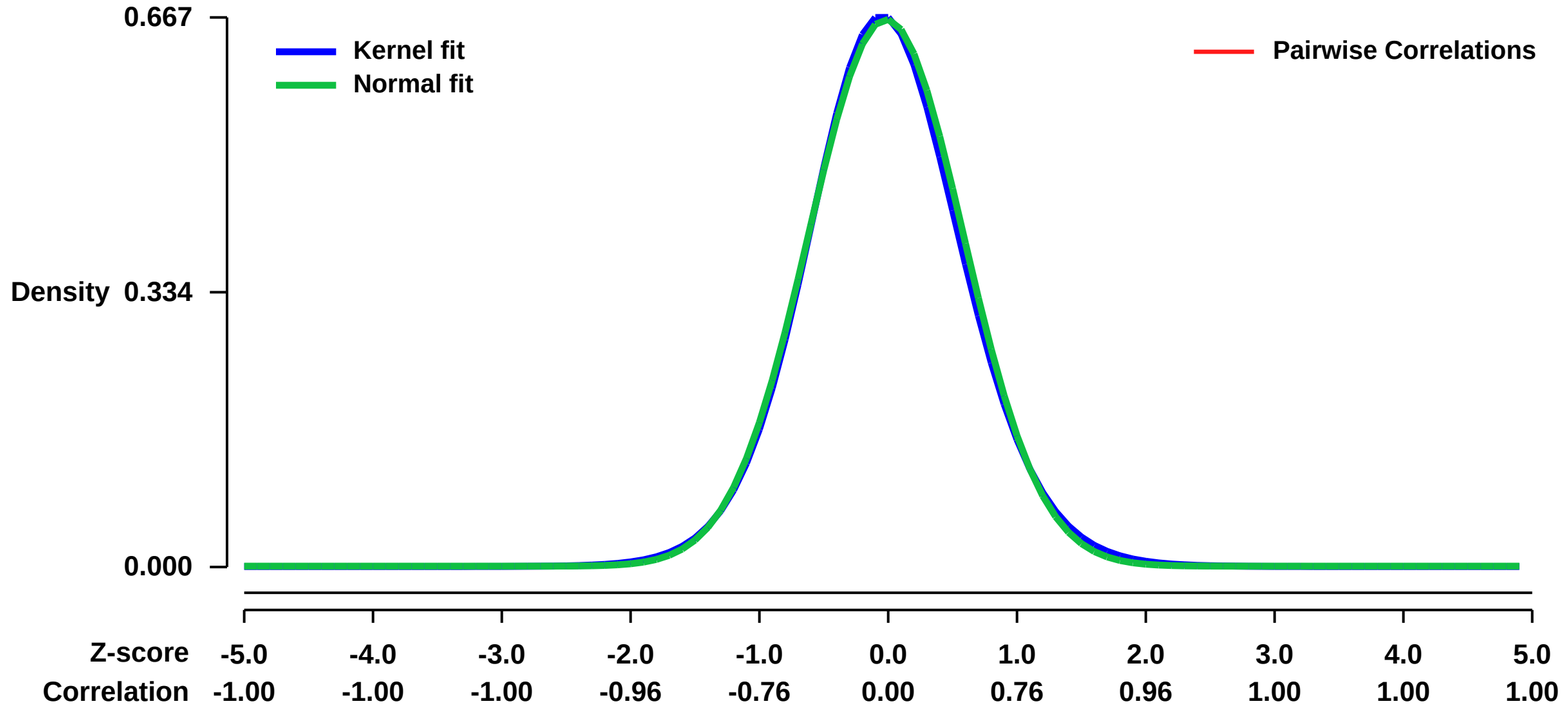

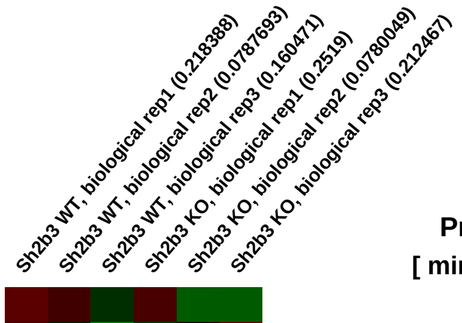

Pre-normalization Quantiles

[min] [medium] [max]

Null module

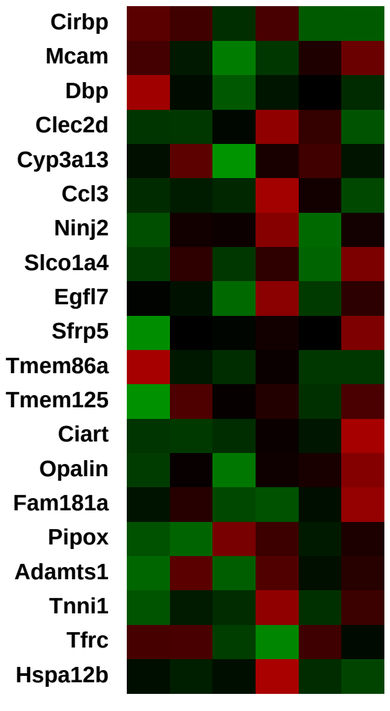

GEO Series "GSE44084" Expression Profiles

Num of samples in this series: 8

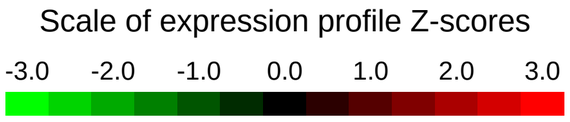

GEO Link:	http://www.ncbi.nlm.nih.gov/geo/query/acc.cgi?acc=GSE44084
Status:	Public on Jun 05 2013
Title:	Expression data from pre-iPSCs with a control, histone methyltransferase or Cbx3 (HP1g) knockdown
Organism:	Mus musculus
Experiment type:	Expression profiling by array
Platform:	GPL1261
Pubmed ID:	23748610
Summary & Design:	**Summary:** Transition from a partially reprogrammed pre-iPSC state to iPSC state can be achieved by modulating levels of histone modifying enzymes or proteins that can bind to histone modifications We used microarrays to determine the gene expression profile of pre-iPSCs depleted for either 3 histone methyltransferases together or the HP1gamma protein **Overall design:** pre-iPSCs were subjected to simultaneous siRNA mediated knockdown of Ehmt1, Ehmt2 and Setdb1- which is the 3XHMT sample that mediate H3k9me2/me3 or Cbx3(HP1gamma) or control siRNA to luciferase

Background corr dist: KL-Divergence = 0.0611, L1-Distance = 0.0178, L2-Distance = 0.0003, Normal std = 0.5259

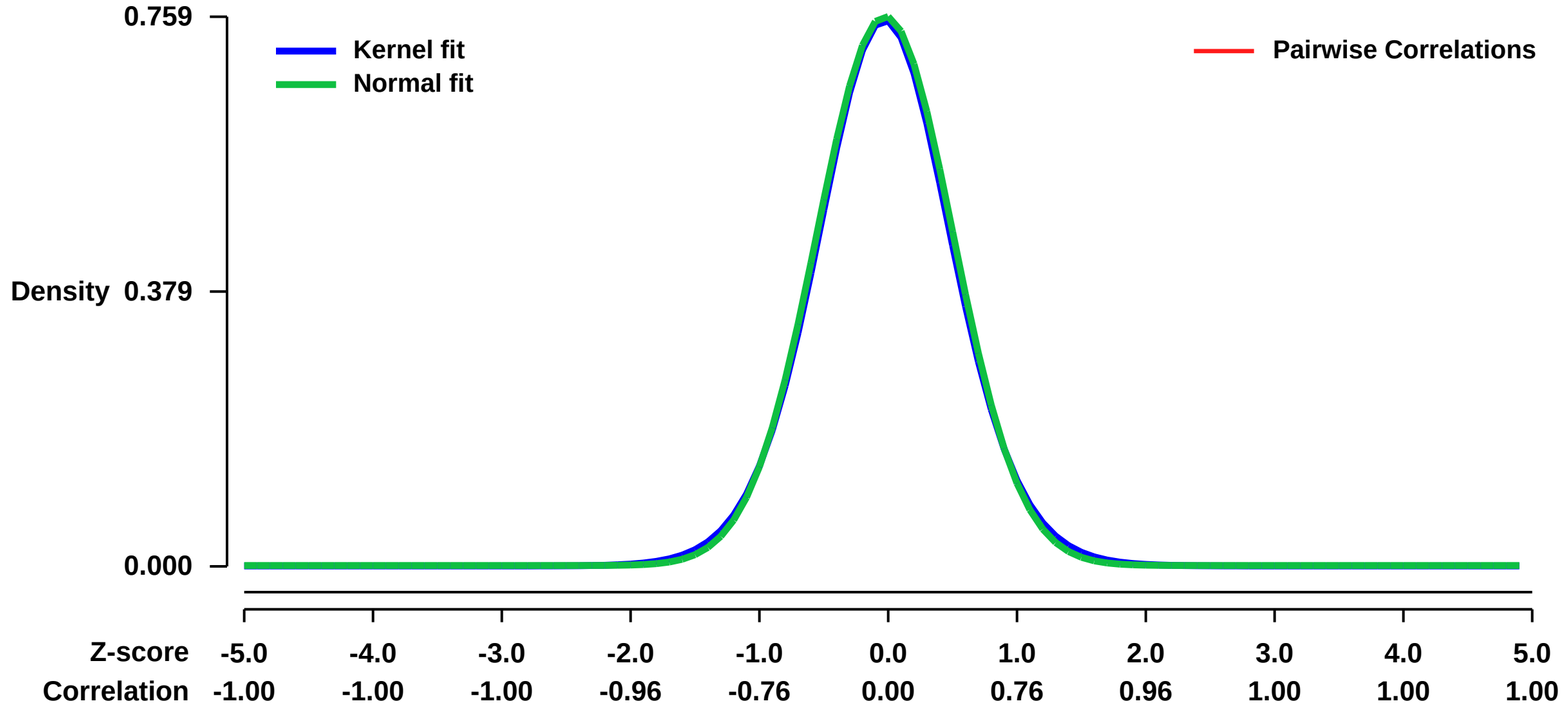

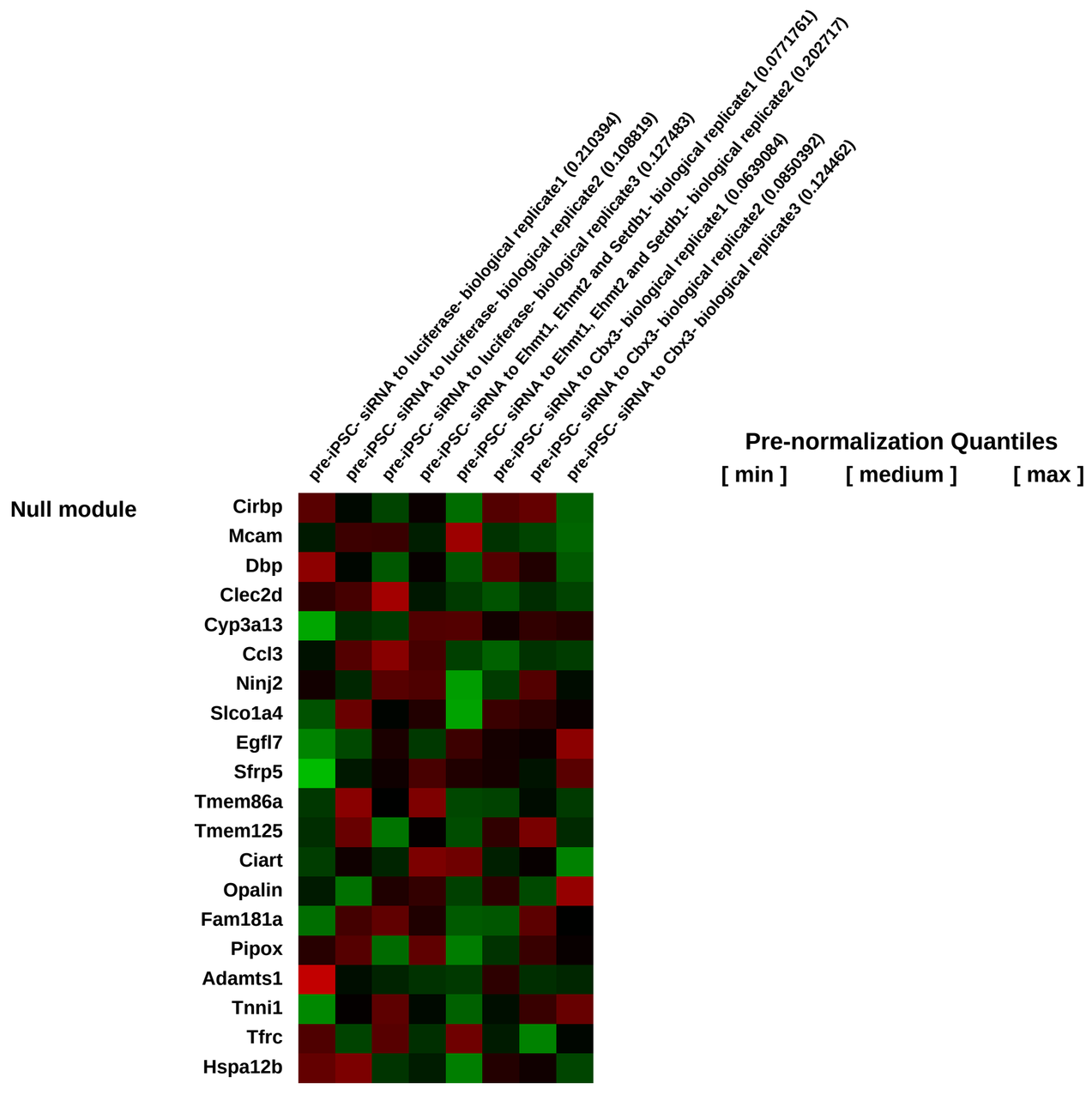

GEO Series "GSE44091" Expression Profiles

Num of samples in this series: 32

Scale of expression profile Z-scores

-3.0 -2.0 -1.0 0.0 1.0 2.0 3.0

GEO Link:	http://www.ncbi.nlm.nih.gov/geo/query/acc.cgi?acc=GSE44091
Status:	Public on Jul 30 2013
Title:	Genome-wide expression of the epithelial layer cells of mice injected with Clostridium difficile Toxin A and B
Organism:	Mus musculus
Experiment type:	Expression profiling by array
Platform:	GPL1261
Pubmed ID:	23897615
Summary & Design:	**Summary:** Toxin A (TcdA) and Toxin B (TcdB), of the pathogen Clostridium difficile, are virulence factors that cause gross pathologic changes (e.g. inflammation, secretion, and diarrhea) in the infected host, yet the molecular and cellular pathways leading to observed host responses are poorly understood. To address this gap, TcdA and/or TcdB were injected into the ceca of mice and the genome-wide transcriptional response of epithelial layer cells was examined. Bioinformatic analysis of gene expression identified sets of cooperatively expressed genes. Further analysis of inflammation associated genes revealed dynamic chemokine responses. **Overall design:** In total, 32 samples were analyzed (one microarray per mouse). The sample groups are separated by two factors: Toxin (TcdA, TcdB, TcdA+TcdB, or Sham injection) and endpoint (2, 6, or 16h). TcdA+B at 16h was not included, leaving 11 sample groups. Each sample group included biological triplicates, except TcdA+TcdB at 6h (one array) and Sham injection at 16h (four arrays).

Background corr dist: KL-Divergence = 0.2592, L1-Distance = 0.0407, L2-Distance = 0.0031, Normal std = 0.3015

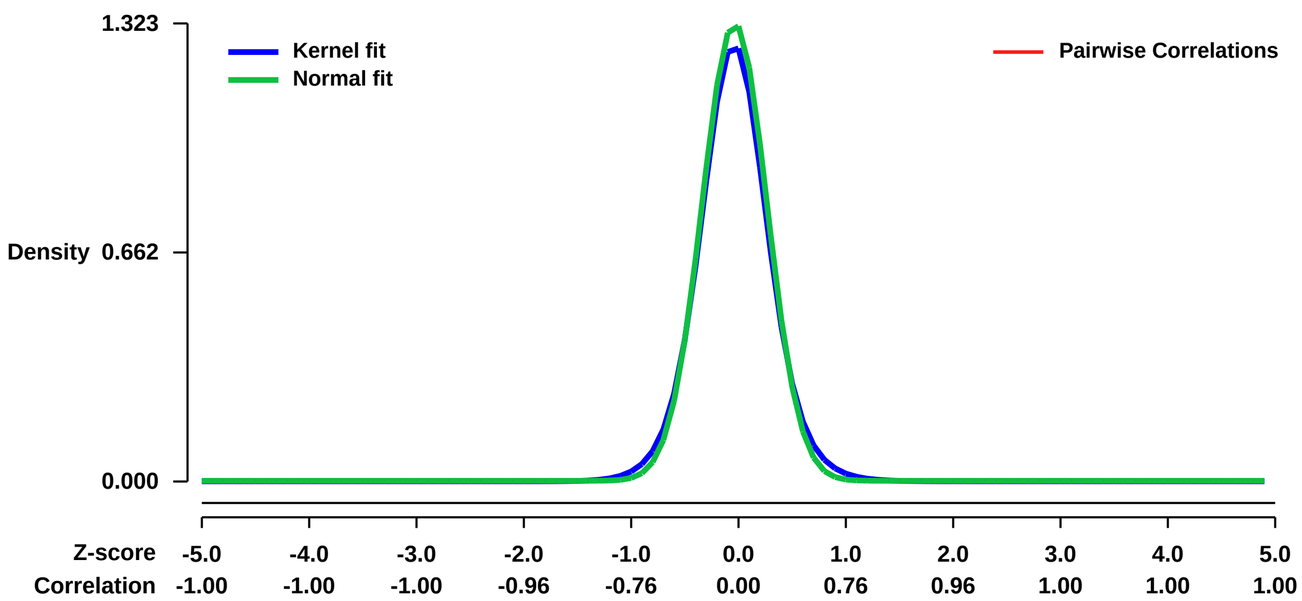

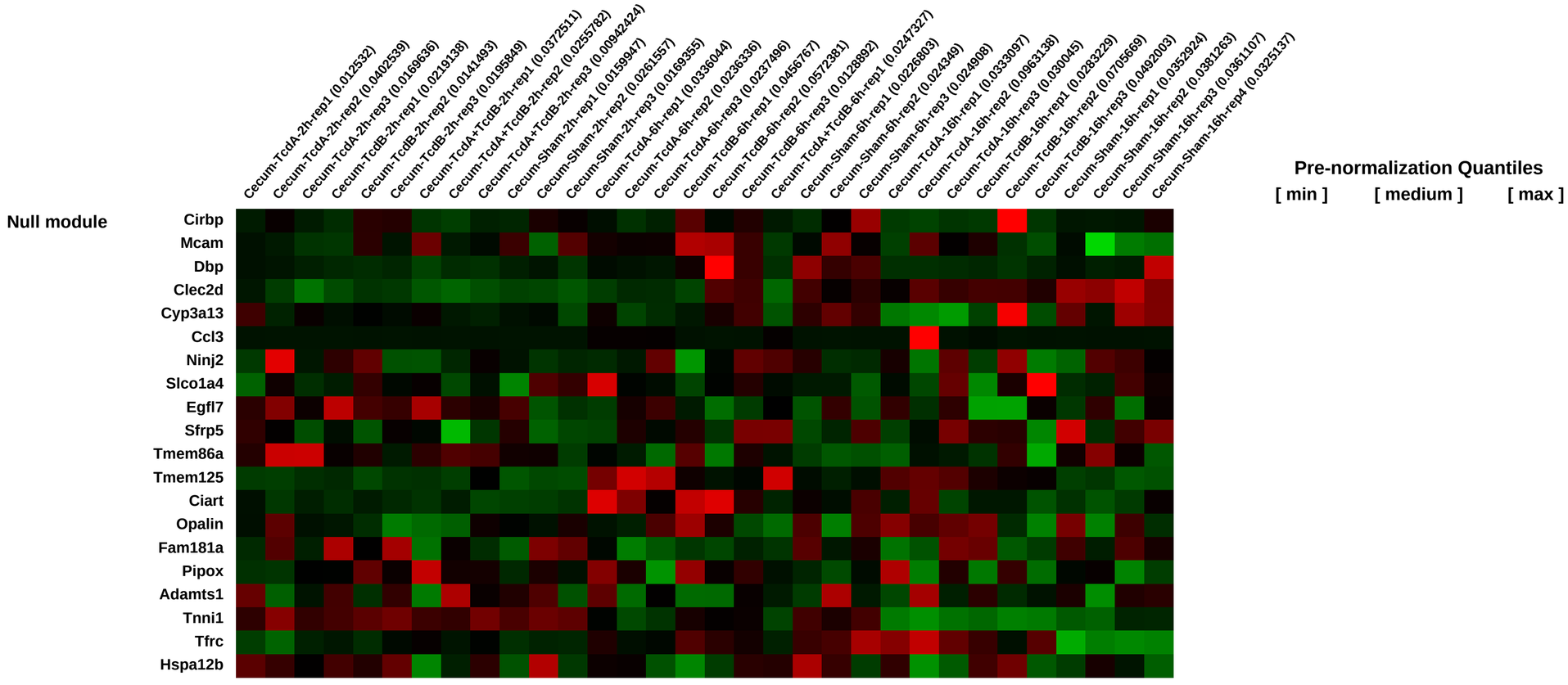

GEO Series "GSE44101" Expression Profiles

Num of samples in this series: 6

Scale of expression profile Z-scores

-3.0 -2.0 -1.0 0.0 1.0 2.0 3.0

GEO Link:	http://www.ncbi.nlm.nih.gov/geo/query/acc.cgi?acc=GSE44101
Status:	Public on Feb 08 2013
Title:	Expression data from Spdef +/+ and Spdef -/- mice
Organism:	Mus musculus
Experiment type:	Expression profiling by array
Platform:	GPL1261
Pubmed ID:	
Summary & Design:	**Summary:** Goblet cell numbers decrease within the conjunctival epithelium in drying and cicatrizing ocular surface diseases. Factors regulating goblet cell differentiation in conjunctival epithelium are unknown. Recent data indicate that the transcription factor SAM-pointed domain epithelial-specific transcription factor (Spdef) is essential for goblet cell differentiation in tracheobronchial and gastrointestinal epithelium of mice. Using Spdef -/- mice, we determined that Spdef is required for conjunctival goblet cell differentiation and that Spdef -/- mice, which lack conjunctival goblet cells, have significantly increased corneal surface fluorescein staining and tear volume, a phenotype consistent with dry eye. Microarray analysis of conjunctival epithelium in Spdef -/- mice identified 43 signficantly upregulated genes and 110 signficantly downregulated genes in the conjunctival epithelium of Spdef -/- mice compared to that of Spdef +/+ control mice (3 fold change, p<0.01). Downregulated genes of particular interested included goblet cell-specific genes (Muc5ac, Tff1, Gcnt3). Upregulated genes included epithelial cell differentiation/keratinization genes (Sprr2h, Tgm1) and pro-inflammatory genes (Il1-¸–, Il-1¸†, Tnf-¸–), all of which are upregulated in dry eye. Interestingly, four Wnt pathway genes were downregulated. **Overall design:** Conjunctival epithelium of Spdef +/+ and Spdef -/- mice was collected by laser capture microdissection for RNA extraction and hybridization on Affymetrix microarrays to determine if gene expression patterns in the conjunctival epithelium of Spdef -/- mice is altered compared to that of Spdef +/+ mice.

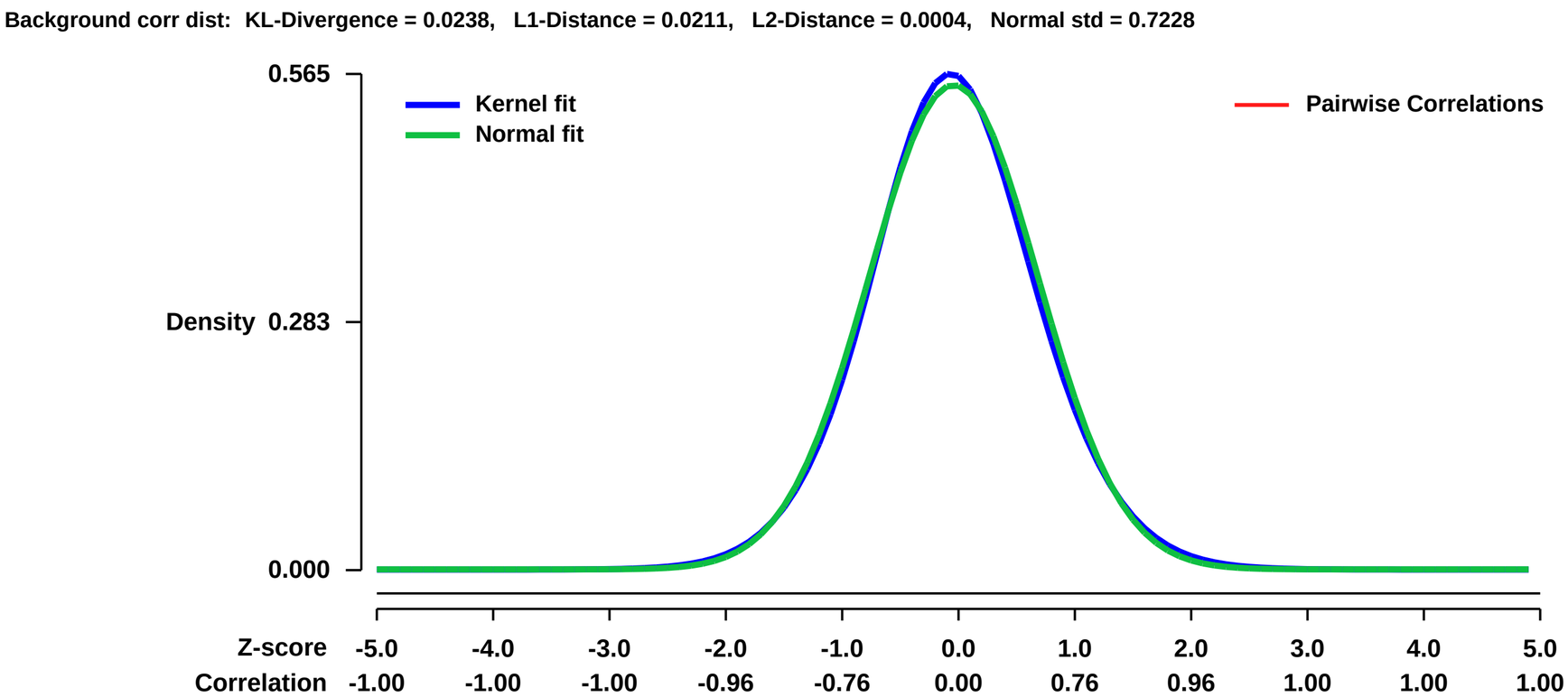

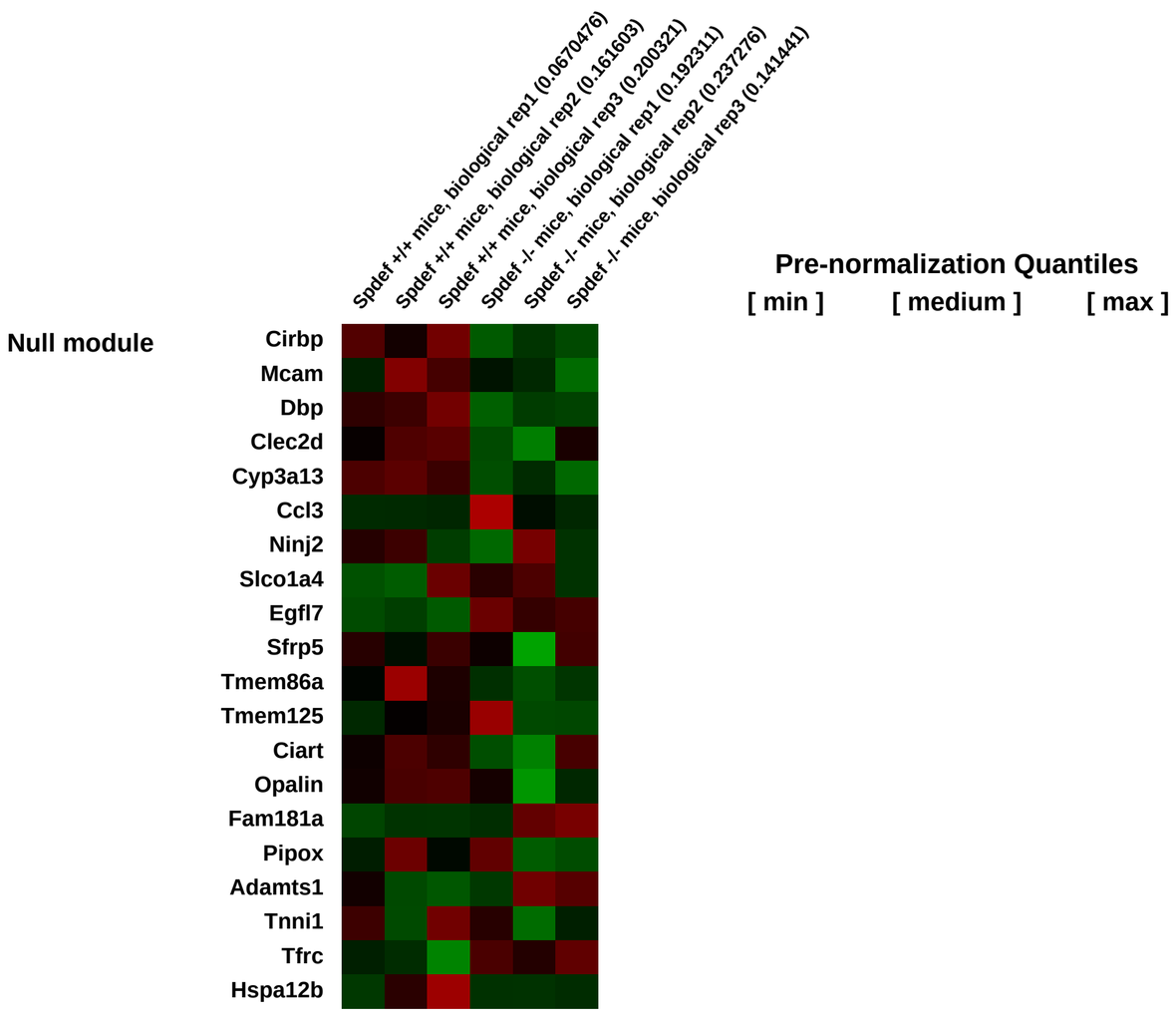

GEO Series "GSE4411" Expression Profiles

Num of samples in this series: 11

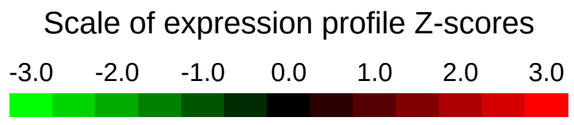

GEO Link:	http://www.ncbi.nlm.nih.gov/geo/query/acc.cgi?acc=GSE4411
Status:	Public on Mar 08 2006
Title:	burde-affy-arabi-64764
Organism:	Mus musculus
Experiment type:	Expression profiling by array
Platform:	GPL1261
Pubmed ID:	16024660
Summary & Design:	**Summary:** In skeletal muscle, the pattern of electrical activity regulates the expression of proteins involved in synaptic transmission, contraction and metabolism. Disruptions in electrical activity, resulting from prolonged bed-rest, cast-immobilization or trauma, inevitably lead to muscle atrophy. The mechanisms that regulate muscle atrophy are poorly understood, but it seems likely that changes in gene expression play a key role in initiating and maintaining a muscle atrophy program. Previously, we found that Runx1, a transcription factor previously termed AML1, was substantially induced in muscle following denervation. More recently, we sought to determine whether this increase in Runx1 expression may be causally related to the morphological changes in skeletal muscle that accompany muscle disuse, notably muscle atrophy. We found that Runx1 is indeed required to sustain muscle and to minimize atrophy following denervation. Experiments described here are designed to identify the genes that are regulated by Runx1 in skeletal muscle with the particular goal of identifying genes that regulate muscle atrophy. We propose to use microarray analysis to identify genes, expressed in skeletal muscle, that are mis-regulated in mice lacking Runx1. We inactivated runx1 selectively in skeletal muscle and found that denervated myofibers in mutant mice atrophy far more (90% atrophy) than in wild-type mice (30% atrophy). We therefore reason that Runx1 activates and/or represses genes that are required to sustain muscle and to minimize atrophy. We generated MCK::cre; runx1f/- and runx1f/- control mice. In normal mice, an increase in runx1 expression is detected by two days after denervation and is maximal by five days after denervation. Muscle atrophy is first evident between one and two weeks after denervation. As we wish to avoid detecting global changes in gene expression that are associated with late stages of muscle atrophy, we plan to denervate muscle for three or five days and to compare gene expression in dissected innervated and denervated muscles from mutant and control mice. We will generate thirty samples for comparison-5 replicates per condition: Samples 1-3 from runx1f/- control mice. (1) innervated tibialis anterior muscles (TA); (2) 3-day-denervated TA; (3) 5-day-denervated TA. Samples 4-6 from MCK::cre; runx1f/- mice. (4) innervated TA; (5) 3-day-denervated TA; (6) 5-day-denervated TA. We obtain sufficient total RNA (10 micrograms) from each dissected muscle to avoid pooling samples. We will analyze adult mice of the same age (~six weeks after birth; most will be littermates) and sex-male. It is difficult to anticipate how many genes will be identified in this screen, as few target genes for Runx1 have been identified in any cell type and none in skeletal muscle. Moreover, although we would prefer to focus our attention on genes that are strongly dependent upon Runx1 expression (e.g. more than 5-fold difference in expression in wild-type and mutant mice), we do not know the extent to which target gene expression will depend upon Runx1. For these reasons, in these experiments, we will analyze expression from five â identicalâ samples, so that we can be confident that even small (e.g. three-fold) differences in expression can be reliably determined. Importantly, in order to confirm results obtained from the microarray data, we will use other assays (RNase protection) to measure RNA expression of candidate genes in innervated and denervated muscles of wild-type and mutant mice. **Keywords:** other **Overall design:**

Background corr dist: KL-Divergence = 0.0801, L1-Distance = 0.0262, L2-Distance = 0.0008, Normal std = 0.4874

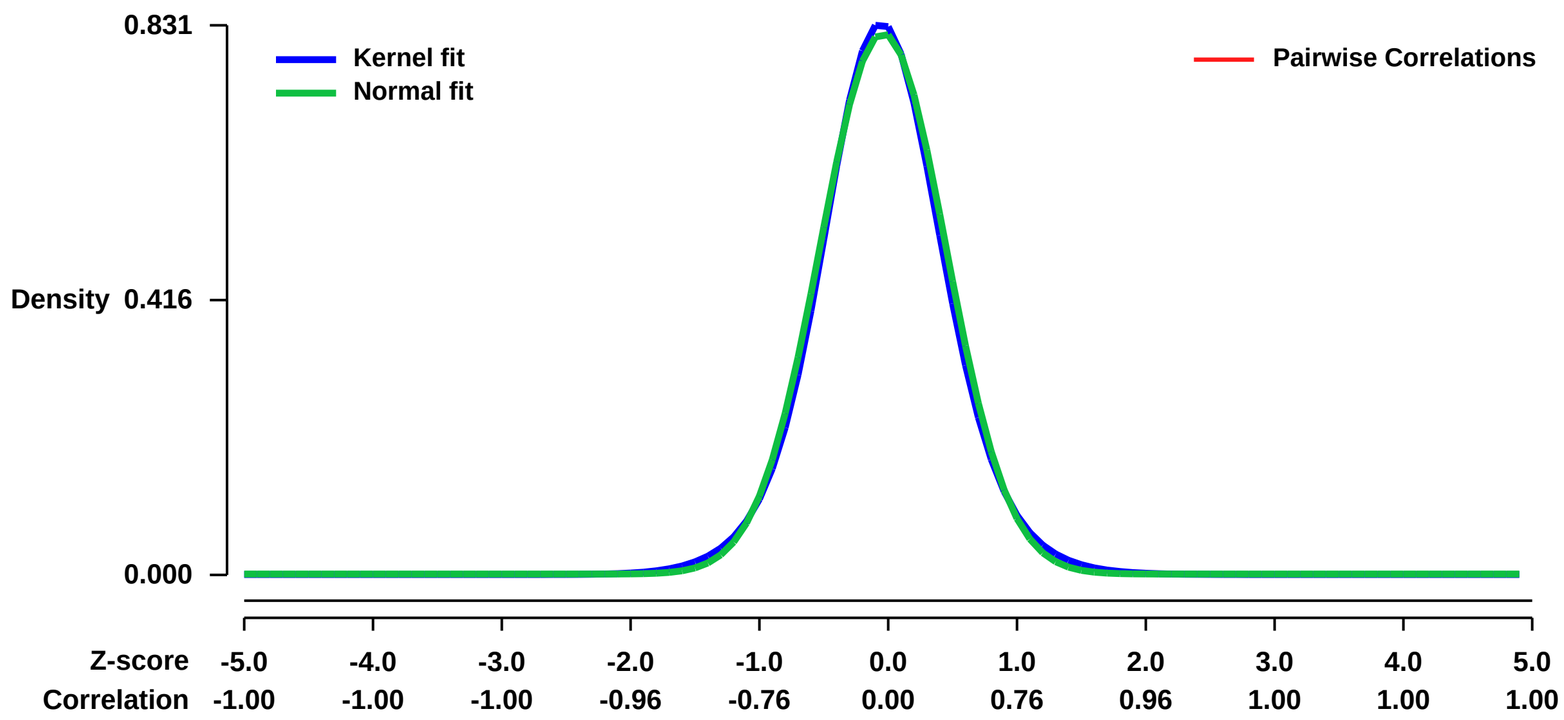

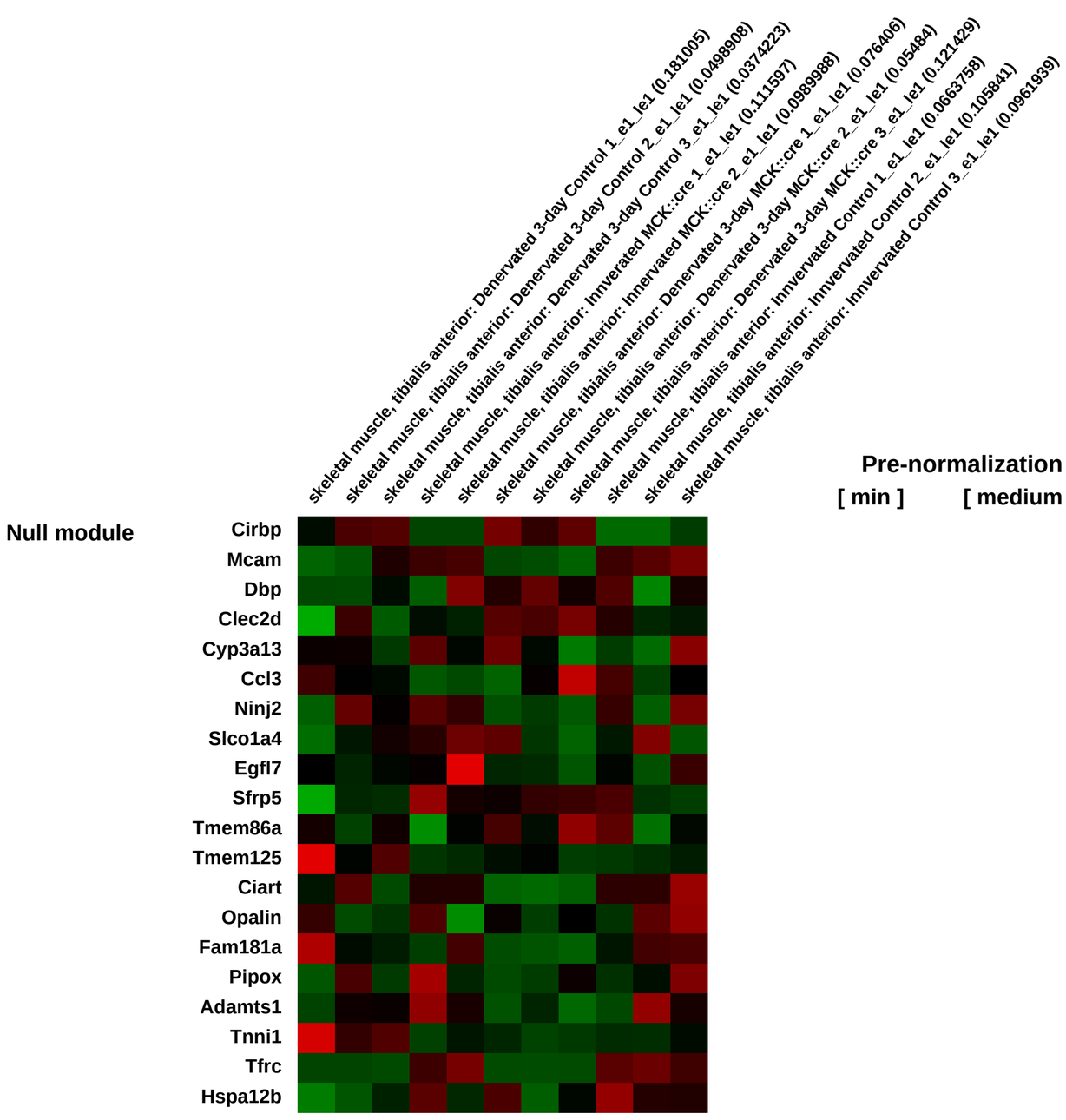

GEO Series "GSE44118" Expression Profiles

Num of samples in this series: 6

Scale of expression profile Z-scores

-3.0 -2.0 -1.0 0.0 1.0 2.0 3.0

GEO Link:	http://www.ncbi.nlm.nih.gov/geo/query/acc.cgi?acc=GSE44118
Status:	Public on Dec 01 2013
Title:	Expression Data from Endothelial Cells as a Consequence of Ets2 Signaling in PyMT Tumor Associated Fibroblasts
Organism:	Mus musculus
Experiment type:	Expression profiling by array
Platform:	GPL1261
Pubmed ID:	23977064
Summary & Design:	**Summary:** Tumor associated fibroblasts are known to play an important role in angiogenesis, however the specific signaling pathways playing an important role in this cross talk remain ill defined. Here, we studied how Ets2 transcrpiton factor signaling in tumor associated fibroblasts effected gene expression in surrounding endothelial cells in the MMTV-PyMT mammary tumor model. Inactivation of Ets2 specifically in fibroblasts using Fsp-cre significantly reduced tumor associated angiogenesis, and was indicated to effect ECM remodeling, cell adhesion and cell chemotaxis processes in neighboring endothelial cells. We have identified Ets2 in fibroblasts as a key signaling molecule to induce tumor associated angiogenesis. Additionally, this function does not rely on the presence of tumor cells, indicating a memory in fibroblasts to induce angiogenesis. **Overall design:** Primary mammary endothelial cells were isolated from mice with or without fibroblast Ets2 in the presence of the PyMT oncogene through sorting with a CD31 antibody. RNA was extracted and samples were submitted for Affymetrix gene expression arrays

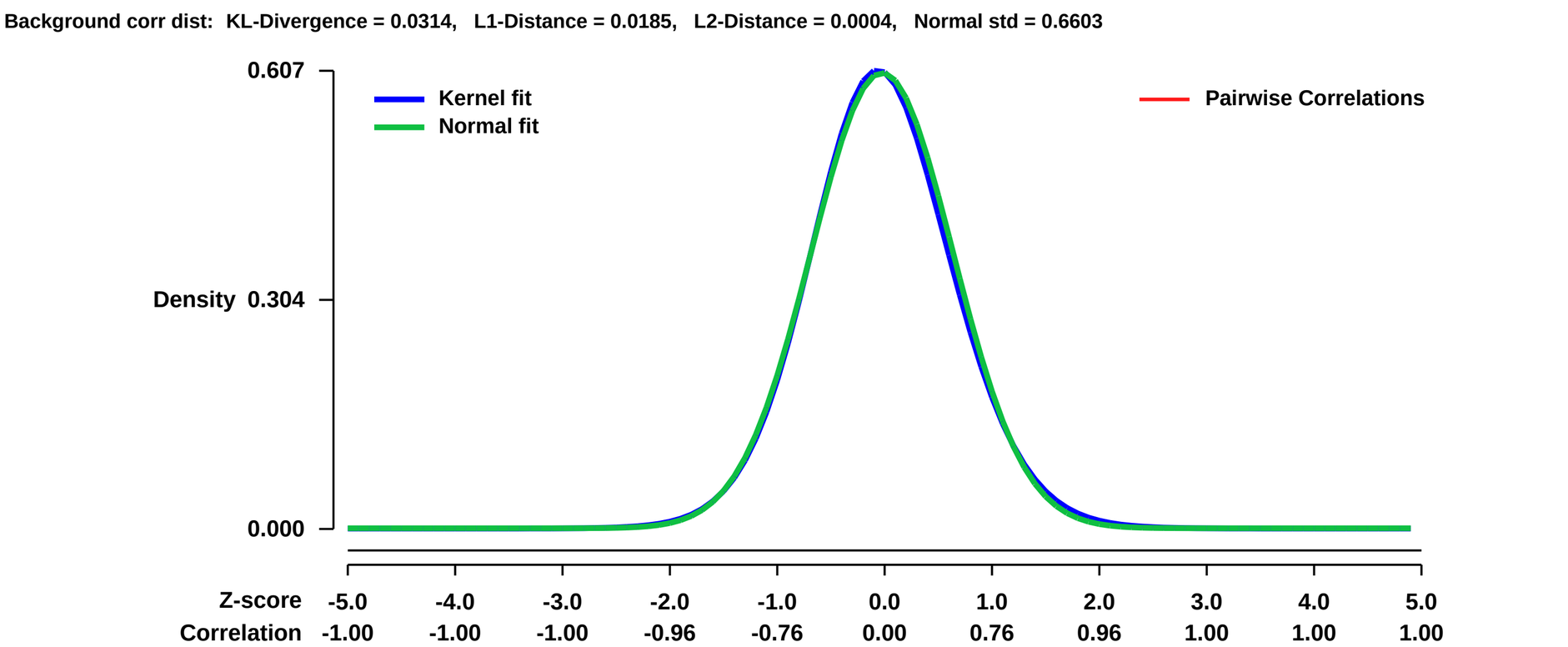

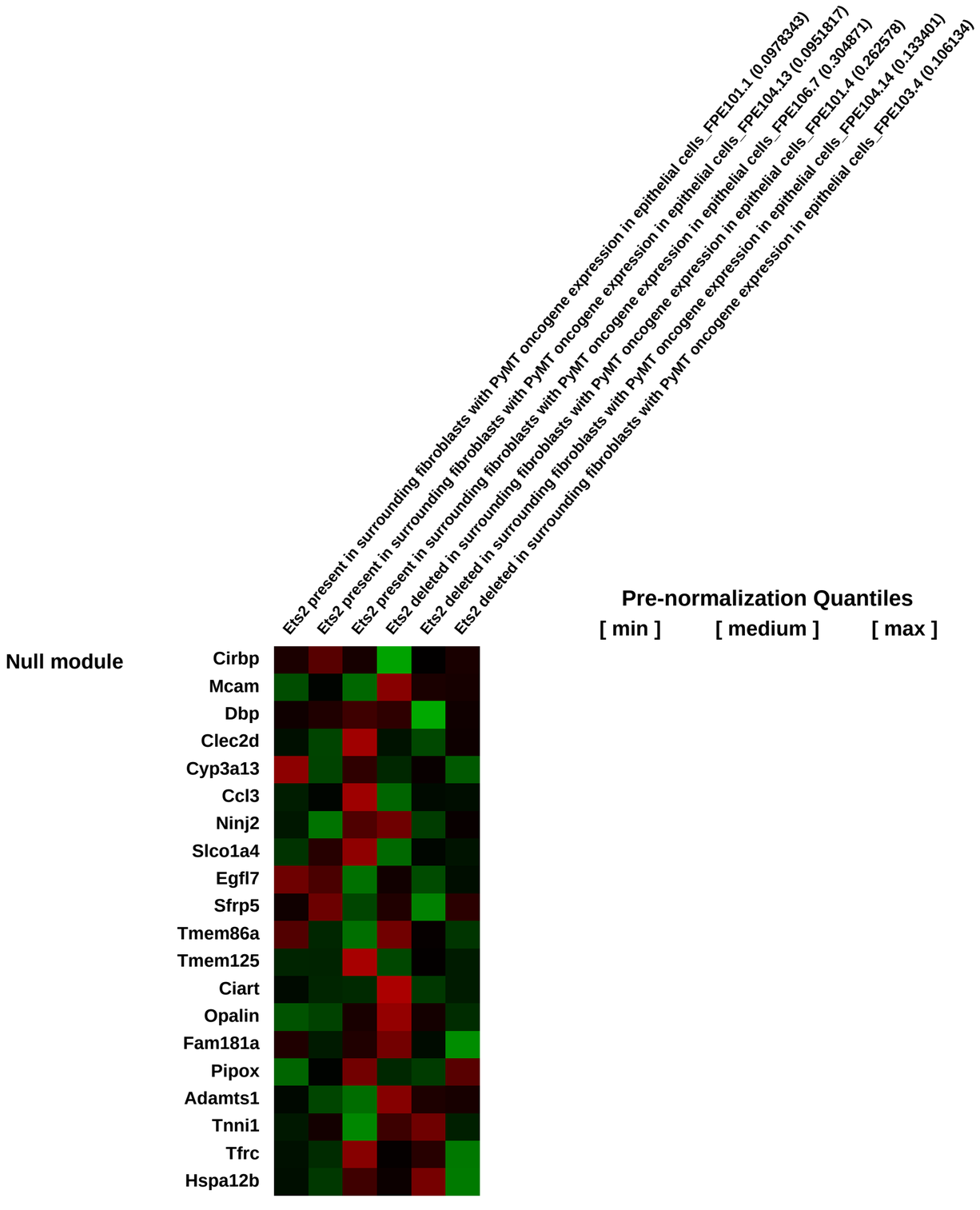

GEO Series "GSE44162" Expression Profiles

Num of samples in this series: 6

Scale of expression profile Z-scores

-3.0 -2.0 -1.0 0.0 1.0 2.0 3.0

GEO Link:	http://www.ncbi.nlm.nih.gov/geo/query/acc.cgi?acc=GSE44162
Status:	Public on Apr 10 2013
Title:	Let-7 represses Nr6a1 and a mid-gestation developmental program in adult fibroblasts [3p arrays]
Organism:	Mus musculus
Experiment type:	Expression profiling by array
Platform:	GPL1261
Pubmed ID:	23630078
Summary & Design:	**Summary:** MicroRNAs (miRNAs) are critical to proliferation, differentiation, and development. Here, we characterize gene expression in murine Dicer-null adult mesenchymal stem cell lines, a fibroblast cell type. Loss of Dicer leads to de-repression of let-7 targets at levels that exceed 10-100 fold with increases in transcription. Direct and indirect targets of this miRNA belong to a mid-gestation embryonic program that encompasses known oncofetal genes as well as oncogenes not previously associated with an embryonic state. Surprisingly, this mid-gestation program represents a distinct period that occurs between the pluripotent state of the inner cell mass at embryonic day 3.5 and the induction of let-7, upon differentiation, at embryonic day 10.5. Within this mid-gestation program, we characterize the let-7 target Nr6a1, an embryonic transcriptional repressor that regulates gene expression in adult fibroblasts following miRNA loss. In total, let-7 is required for the continual suppression of embryonic gene expression in adult cells, a mechanism that may underlie its tumor suppressive function. **Overall design:** Three dicer heterozygotes and 3 dicer null sarcoma cell lines.

Background corr dist: KL-Divergence = 0.0360, L1-Distance = 0.0203, L2-Distance = 0.0005, Normal std = 0.6381

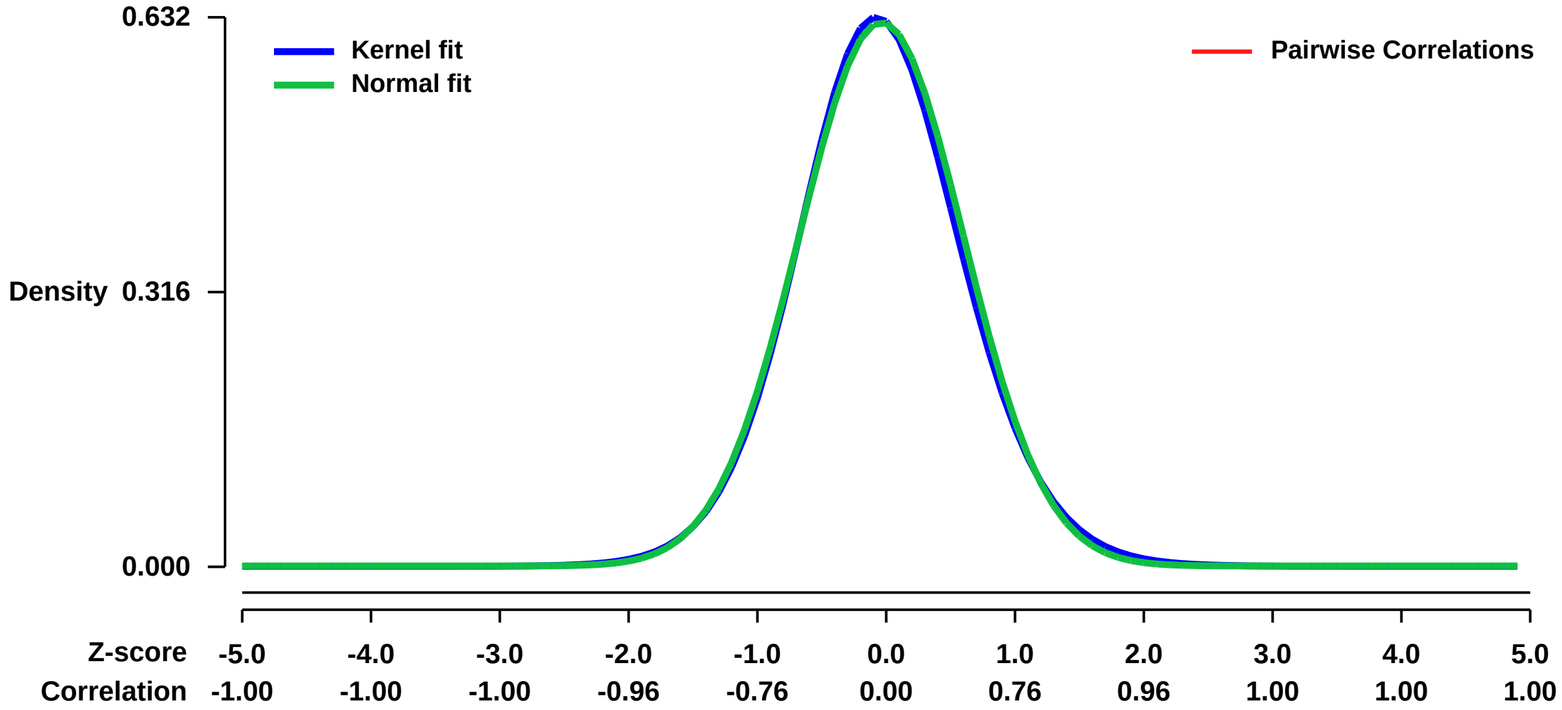

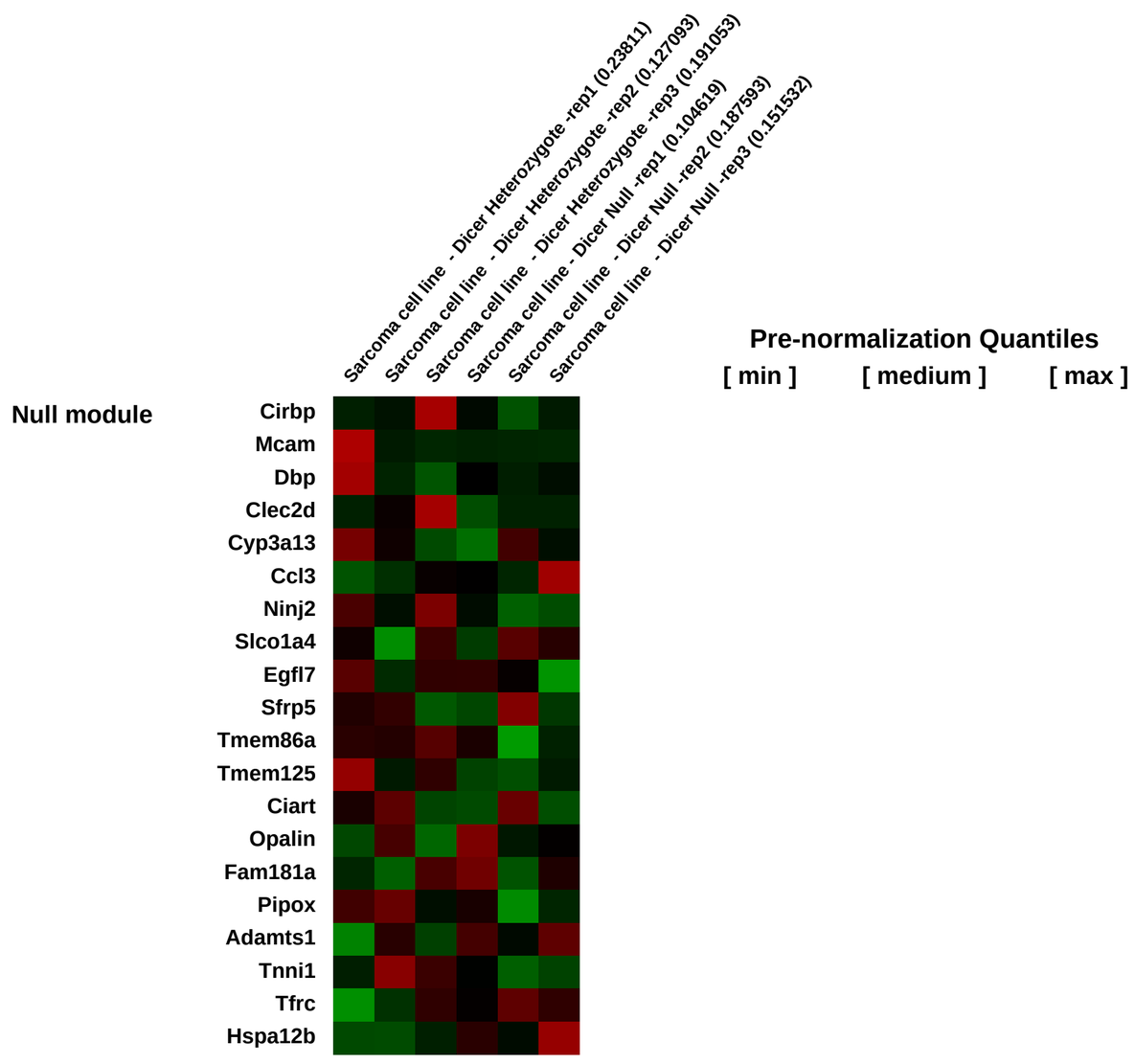

GEO Series "GSE4420" Expression Profiles

Num of samples in this series: 8

Scale of expression profile Z-scores

-3.0 -2.0 -1.0 0.0 1.0 2.0 3.0

GEO Link:	http://www.ncbi.nlm.nih.gov/geo/query/acc.cgi?acc=GSE4420
Status:	Public on Mar 05 2007
Title:	Diabetic mice fat- niacin bound chromium
Organism:	Mus musculus
Experiment type:	Expression profiling by array
Platform:	GPL1261
Pubmed ID:	16940432
Summary & Design:	**Summary:** To study effect of niacin bound chromium in changing genetic profile of subcutaneous fat from diabetic mice **Keywords: nutritional supplemetation, obesity** **Overall design:** Two groups (n=4 each group) of mice were supplemented (oral gavage) with: i) niacin bound chromium (10 mg/kg body wt) in water for 10 wks (5d/wk) or ii) matching volume of water. After 10 wks of supplementation the subcutaneous fat was harvested and gene expression profile was studied using Affymetrix mouse genome 430 v 2.0 chips.

Background corr dist: KL-Divergence = 0.0863, L1-Distance = 0.0220, L2-Distance = 0.0007, Normal std = 0.4630

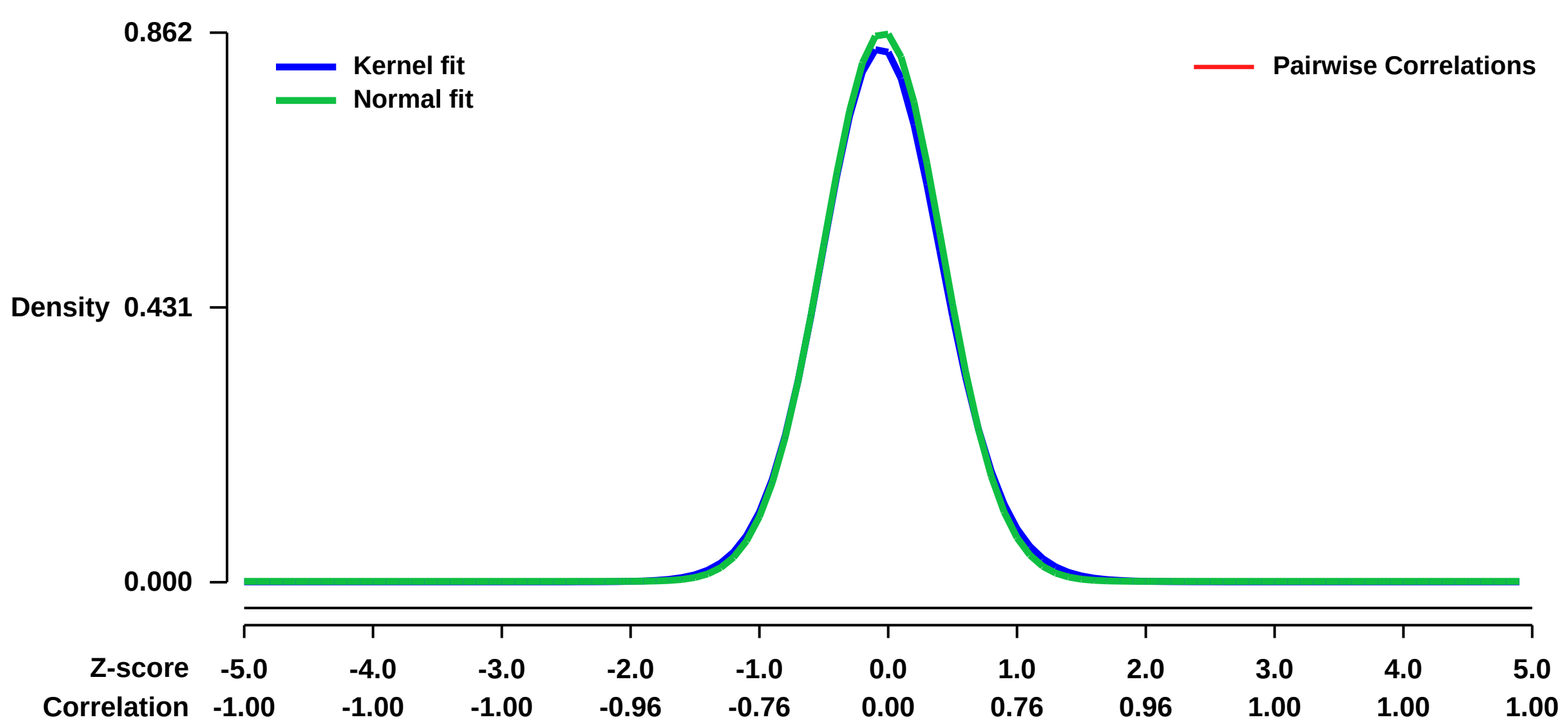

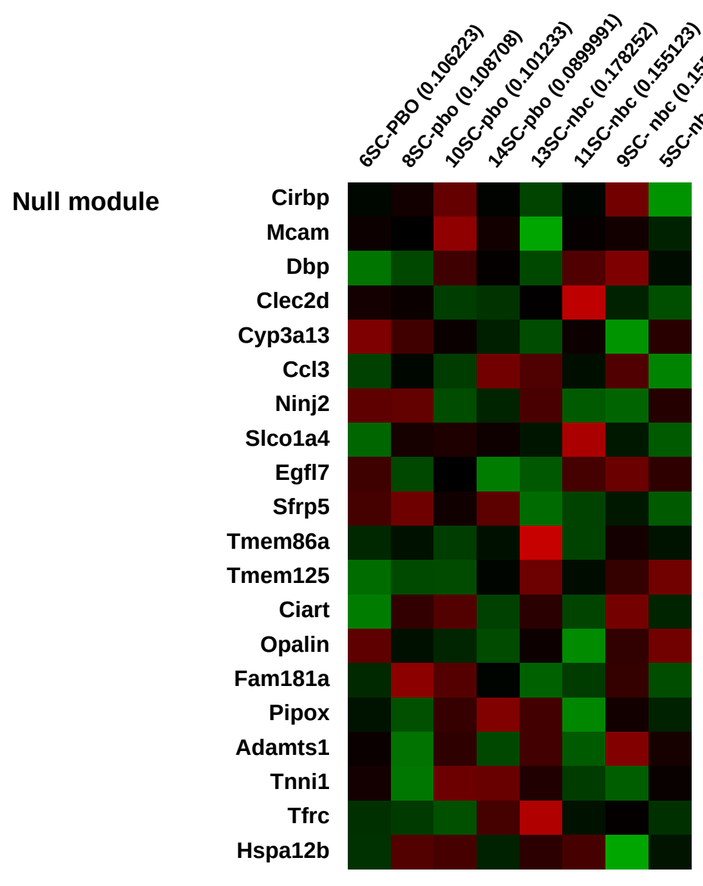

GEO Series "GSE44261" Expression Profiles

Num of samples in this series: 12

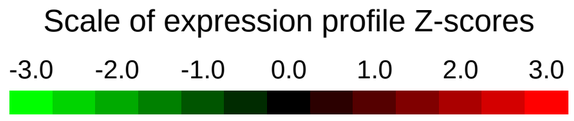

GEO Link:	**http://www.ncbi.nlm.nih.gov/geo/query/acc.cgi?acc=GSE44261**
Status:	**Public on Feb 13 2013**
Title:	**Gene expression data from mouse CD8 T cells**
Organism:	**Mus musculus**
Experiment type:	**Expression profiling by array**
Platform:	**GPL1261**
Pubmed ID:	**23563690**
Summary & Design:	**Summary:** **Determing the influence of lipid metabolism on murine T cell blastogenesis. Gene expression studies from purified spleen and lymph node T cells with conditional deletion of the SREBP Cleavage Activating Protein (SCAP) ex vivo or activated with plate-bound anti-CD3 and CD28 antibodies for 6 h.** **Overall design:** **CD8 T cells were purified from T cell specific Scap deficient mouse spleens (KO, n=3) and control littermate (WT, n=3). The cells from each mouse were used for RNA extraction at either quiescent (T0) or 6 h activation (T6).**

Background corr dist: **KL-Divergence = 0.1140, L1-Distance = 0.0274, L2-Distance = 0.0011, Normal std = 0.4275**

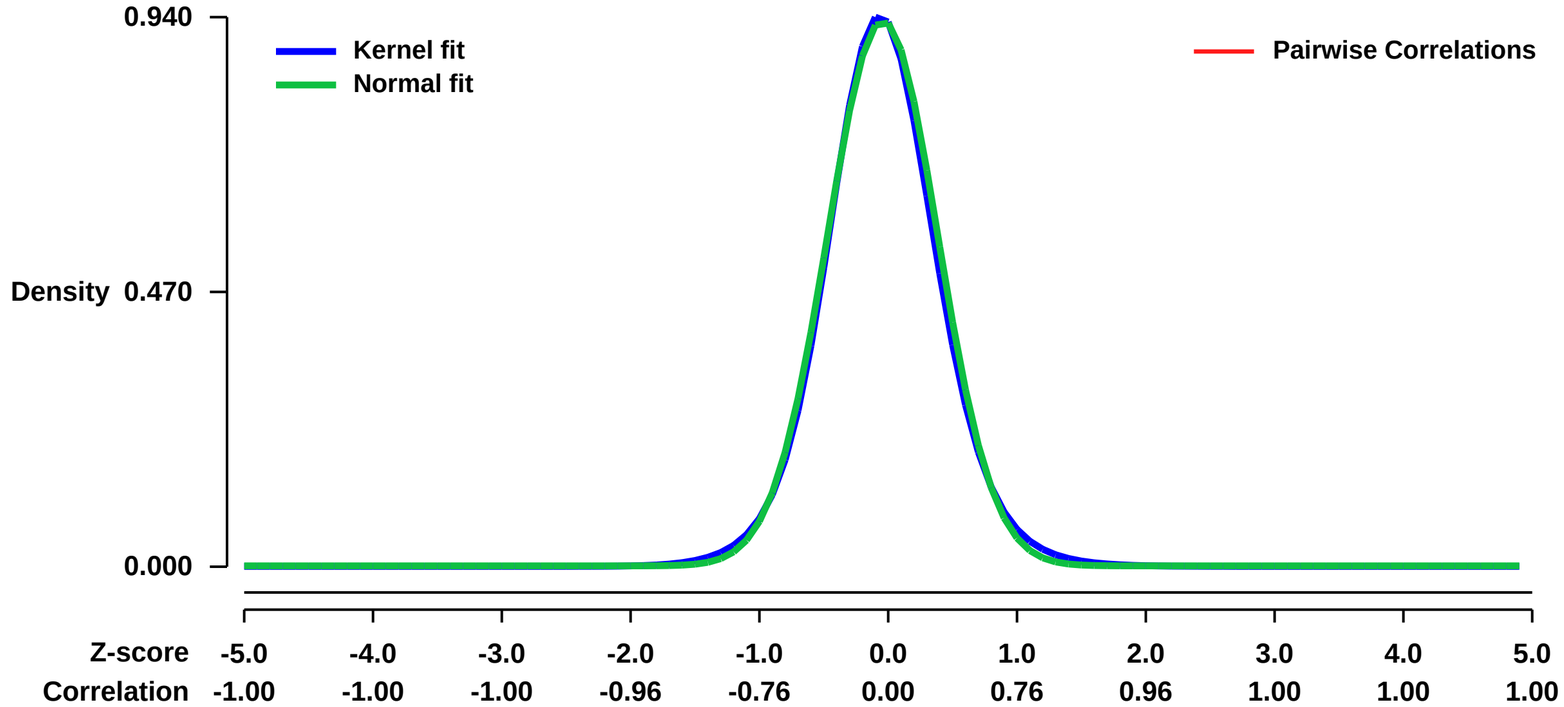

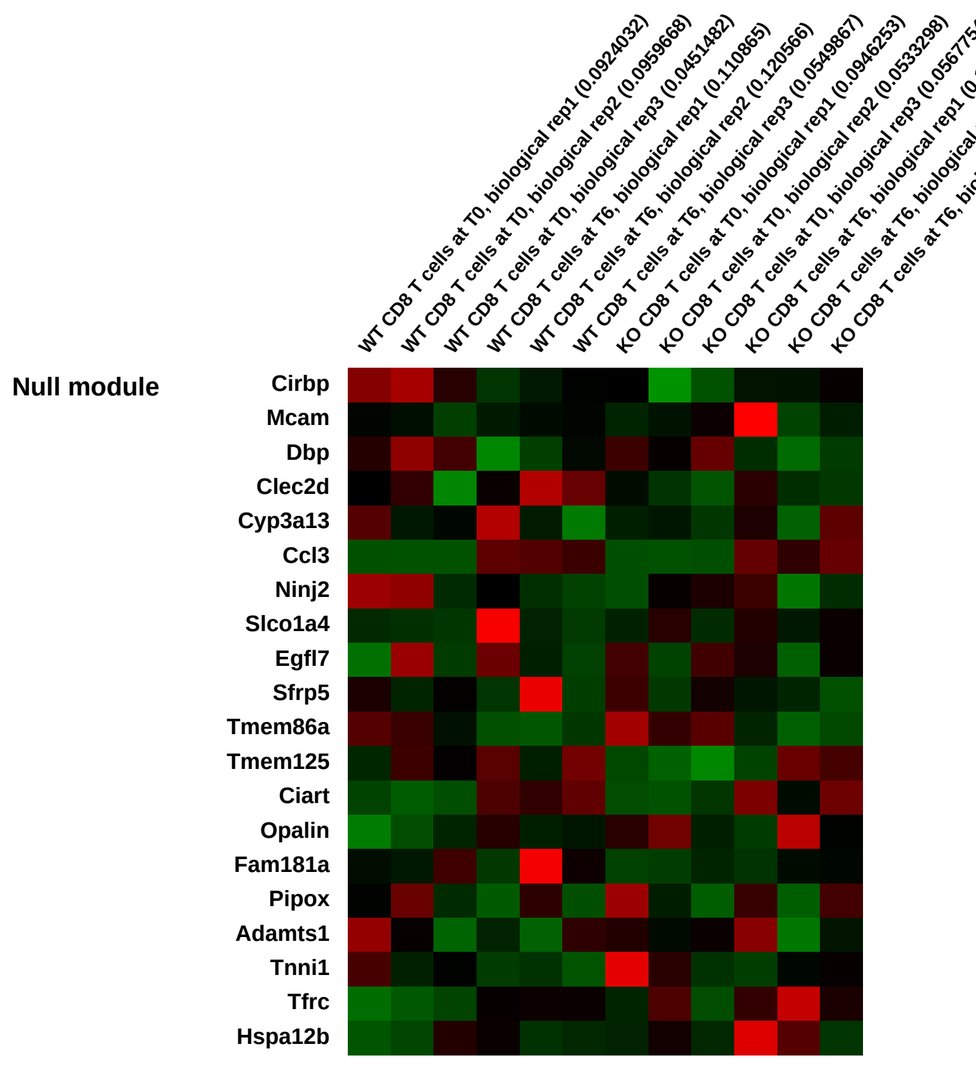

GEO Series "GSE44331" Expression Profiles

Num of samples in this series: 12

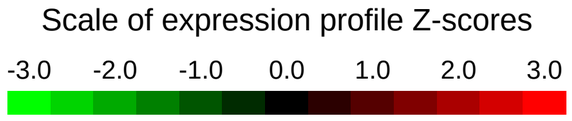

GEO Link:	http://www.ncbi.nlm.nih.gov/geo/query/acc.cgi?acc=GSE44331
Status:	Public on Apr 04 2013
Title:	Expression data from C57BL/6J and C57BL6/J Sarm-deficient mice uninfected or infected with vesicular stomatitis virus (VSV)
Organism:	Mus musculus
Experiment type:	Expression profiling by array
Platform:	GPL1261
Pubmed ID:	23749635
Summary & Design:	**Summary:** Sarm-deficient mice are protected from VSV encephalitis and death. Microarray was done to examine genes contributing to this phenotype **Overall design:** WT and KO mice were infected with VSV and brains were harvested at day 5 post-infection for RNA extraction

Background corr dist: KL-Divergence = 0.1726, L1-Distance = 0.0431, L2-Distance = 0.0039, Normal std = 0.3515

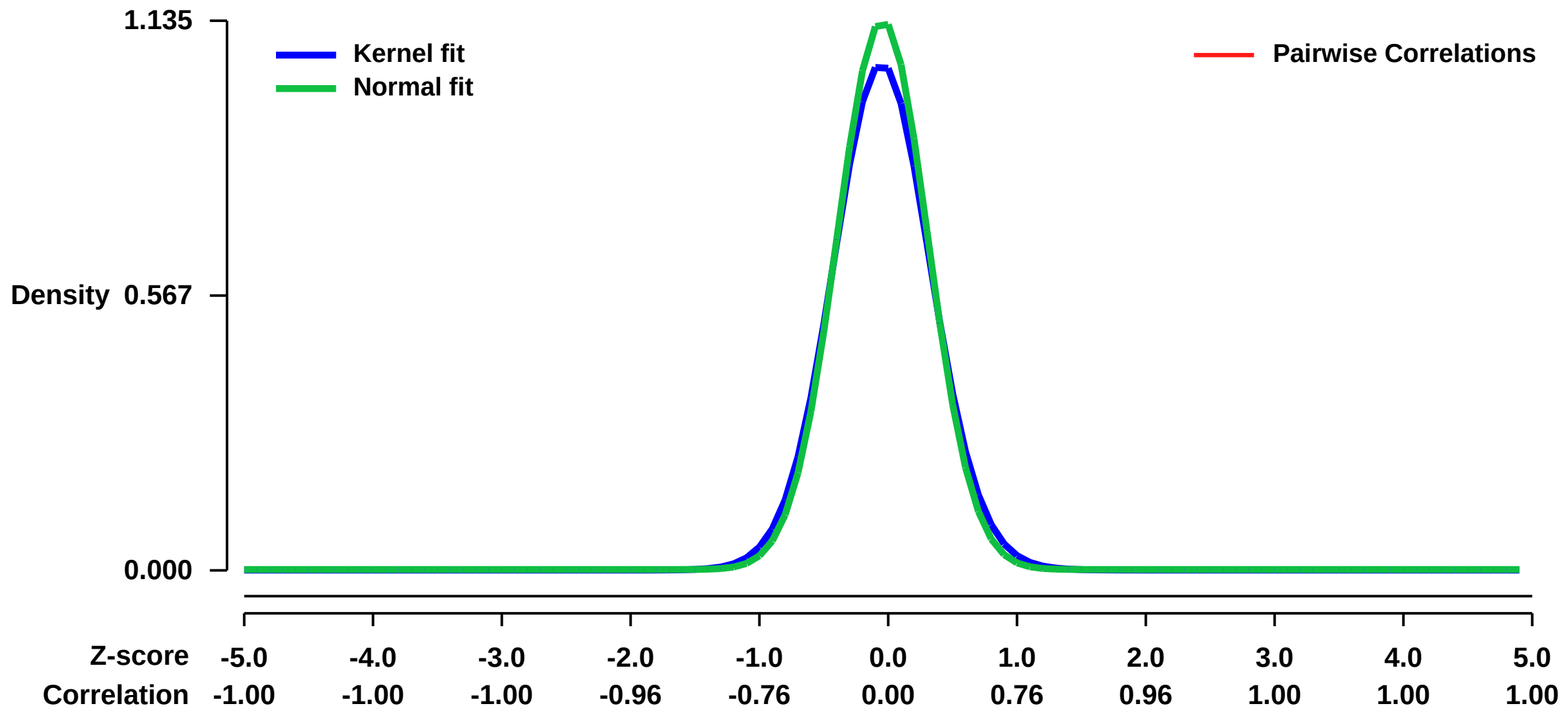

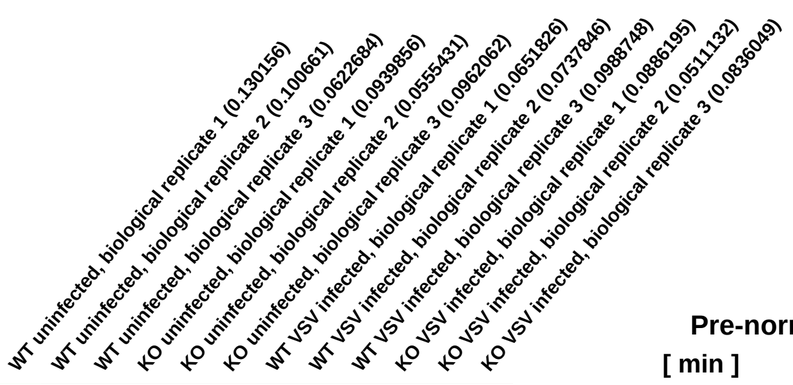

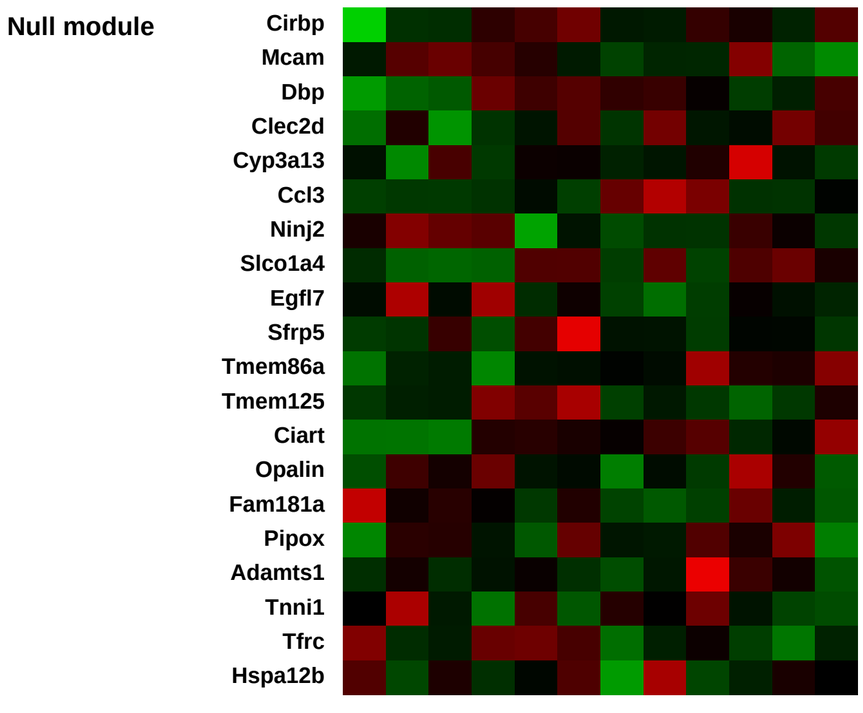

GEO Series "GSE44355" Expression Profiles

Num of samples in this series: 10

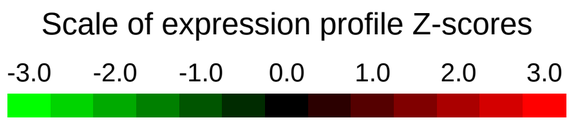

GEO Link:	http://www.ncbi.nlm.nih.gov/geo/query/acc.cgi?acc=GSE44355
Status:	Public on Jul 04 2013
Title:	Expression data from Adriamycin-treated Emu-myc; Suv39h1-/- B-cell lymphoma
Organism:	Mus musculus
Experiment type:	Expression profiling by array
Platform:	GPL1261
Pubmed ID:	23945590
Summary & Design:	**Summary:** Oncogene-induced senescence (OIS), a terminal cell cycle block countering (pre)neoplastic lesions, is characterised on the molecular level by trimethylated histone H3 lysine 9 (h3K9me3), a transcriptionally repressive chromatin mark linked to silencing of S-phase-promoting genes. Whether H3K9-governed chromatin remodelling influences anticancer treatment-induced senescence (TIS) and whether functional control of this mark impacts on treatment outcome is not known. We used global gene expression profiling by microarrays to gain insight into the molecular responses of Emu-myc; Suv39h1-/- B-cell lymphoma cells to senescence-inducing anticancer agent Adriamycin (ADR). **Overall design:** Primary lymphoma cells isolated from lymph nodes of Emu-Myc; Suv39h1-/- mice were used. In this model, the c-Myc oncogene is constitutively expressed in the cells of the B-cell lineage, leading to spontaneous development of aggressive B-cell lymphomas. Adriamycin (ADR), a cytostatic drug used as a standard part of several lymphoma treatment regimens, is known to massively induce TIS in Suv39h1-proficient lymphomas, protected from apoptosis by Bcl-2 over expression (Myc;Bcl2). In order to discern the impact of Suv39h1 to TIS induction under these conditions, we analysed here transcriptional profiles of matched pairs of Emu-myc;Suv39h1-/-;Bcl2 lymphomas, untreated or treated for 5 days with ADR.

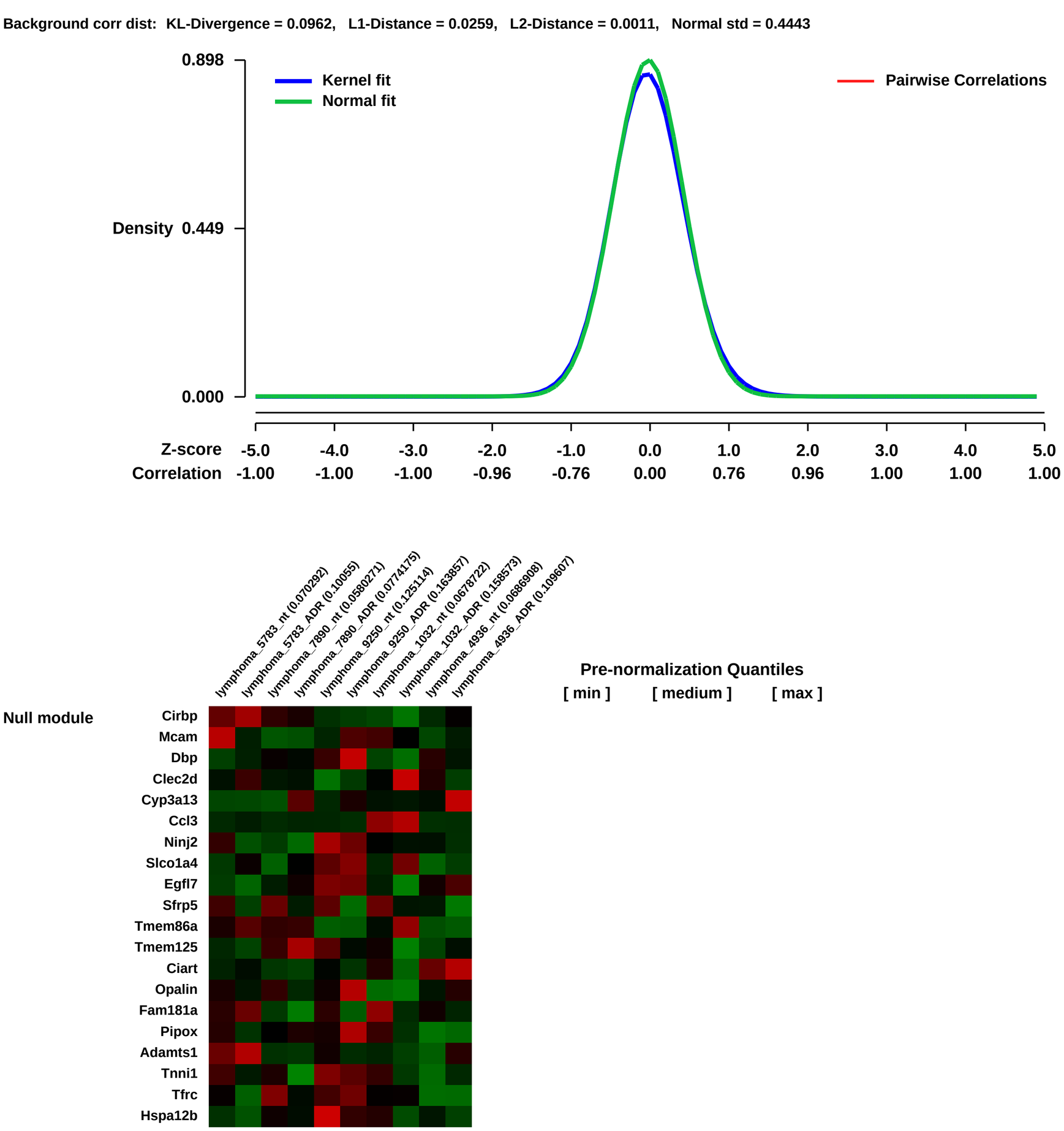

GEO Series "GSE44356" Expression Profiles

Num of samples in this series: 18

Scale of expression profile Z-scores

-3.0 -2.0 -1.0 0.0 1.0 2.0 3.0

GEO Link:	http://www.ncbi.nlm.nih.gov/geo/query/acc.cgi?acc=GSE44356
Status:	Public on Aug 24 2013
Title:	Expression data from wild-type and HMGN1 knockout mice injected with N-nitrosodiethylamine
Organism:	Mus musculus
Experiment type:	Expression profiling by array
Platform:	GPL1261
Pubmed ID:	24296759
Summary & Design:	**Summary:** HMGN1 contributes to the shortened latency of liver tumorigenesis by changing a chromatin structure and expression of relevant genes To assess the molecular mechanisms underlying accelerated tumor development in Hmgn1-/- mice, we performed the gene expression profiling of liver cells at early stages **Overall design:** Expression profiles has been compared between Hmgn1+/+ and Hmgn1-/- mice livers at 4 weeks after birth and at 12 weeks after DEN or saline (control) injection at 4 weeks

Background corr dist: KL-Divergence = 0.2569, L1-Distance = 0.0562, L2-Distance = 0.0079, Normal std = 0.2990

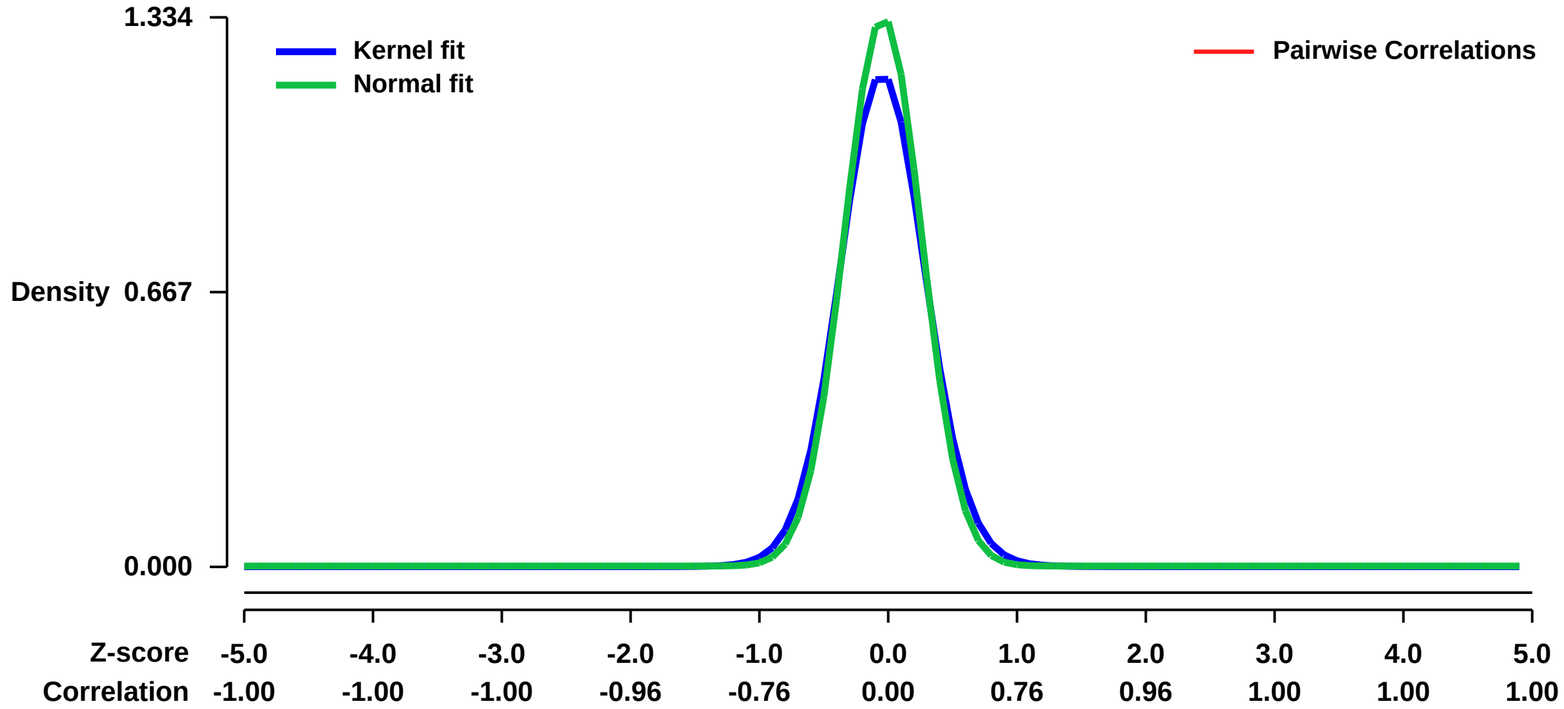

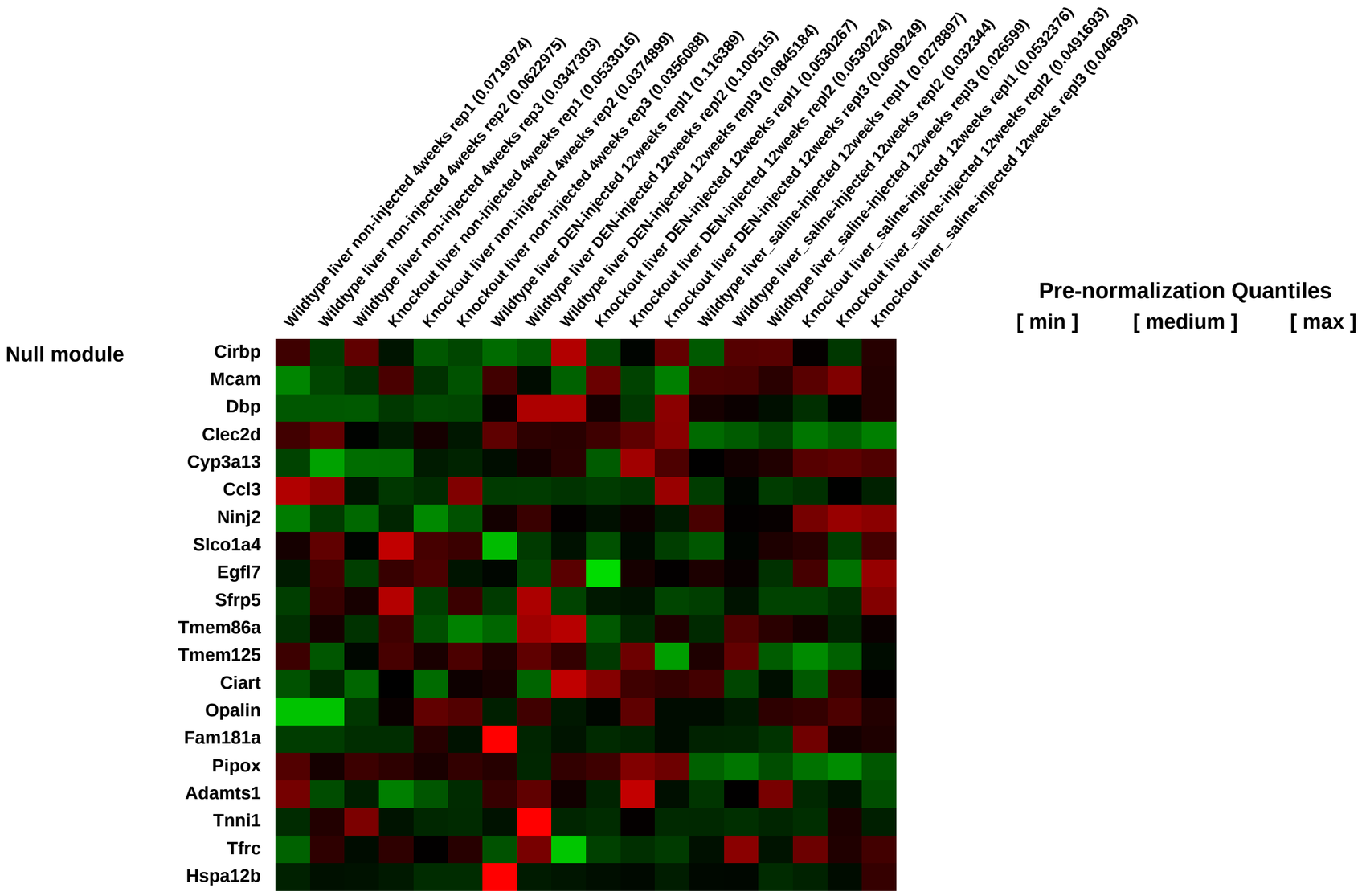

GEO Series "GSE44363" Expression Profiles

Num of samples in this series: 16

Scale of expression profile Z-scores

-3.0 -2.0 -1.0 0.0 1.0 2.0 3.0

GEO Link:	**http://www.ncbi.nlm.nih.gov/geo/query/acc.cgi?acc=GSE44363**
Status:	**Public on May 01 2013**
Title:	**Transcriptomic modulation by adenosine 2A receptors in normal and endotoxemic myocardium**
Organism:	**Mus musculus**
Experiment type:	**Expression profiling by array**
Platform:	**GPL1261**
Pubmed ID:	
Summary & Design:	**Summary:** **Analysis of venticular myocardium from adenosine 2A receptors (A2AR) knockouts following LPS stimulation. Results provide insight into the molecular components of A2AR mediated protection, but also reveal pathogenetic components of endotoxemic myocarditis as a result of LPS exposure. These findings demonstrate that intrinsic A2AR activity exerts limited transcriptional effects in unstressed heart, modifying G-coupled cAMP/PKA signal paths. LPS-dependent injury and dysfunction is associated with profound up-regulation of inflammatory/immune processes, fibrotic and cell death paths, and NF-kB, Erk/MAPK and JAK/Stat signaling, with shifts in multiple determinants of cardiac contraction and survival. Intrinsic A2AR activity modulates key aspects of these inflammatory responses, involving MAPK, JAK/Stat and NF-kB signaling** **Overall design:** **Total RNA obtained from adenosine 2A receptor knockout or wild-type murine ventricular myocardium that were treated for 24 hours with either saline or lipopolysaccharide (n=4/group).**

Background corr dist: **KL-Divergence = 0.1147, L1-Distance = 0.0360, L2-Distance = 0.0019, Normal std = 0.4273**

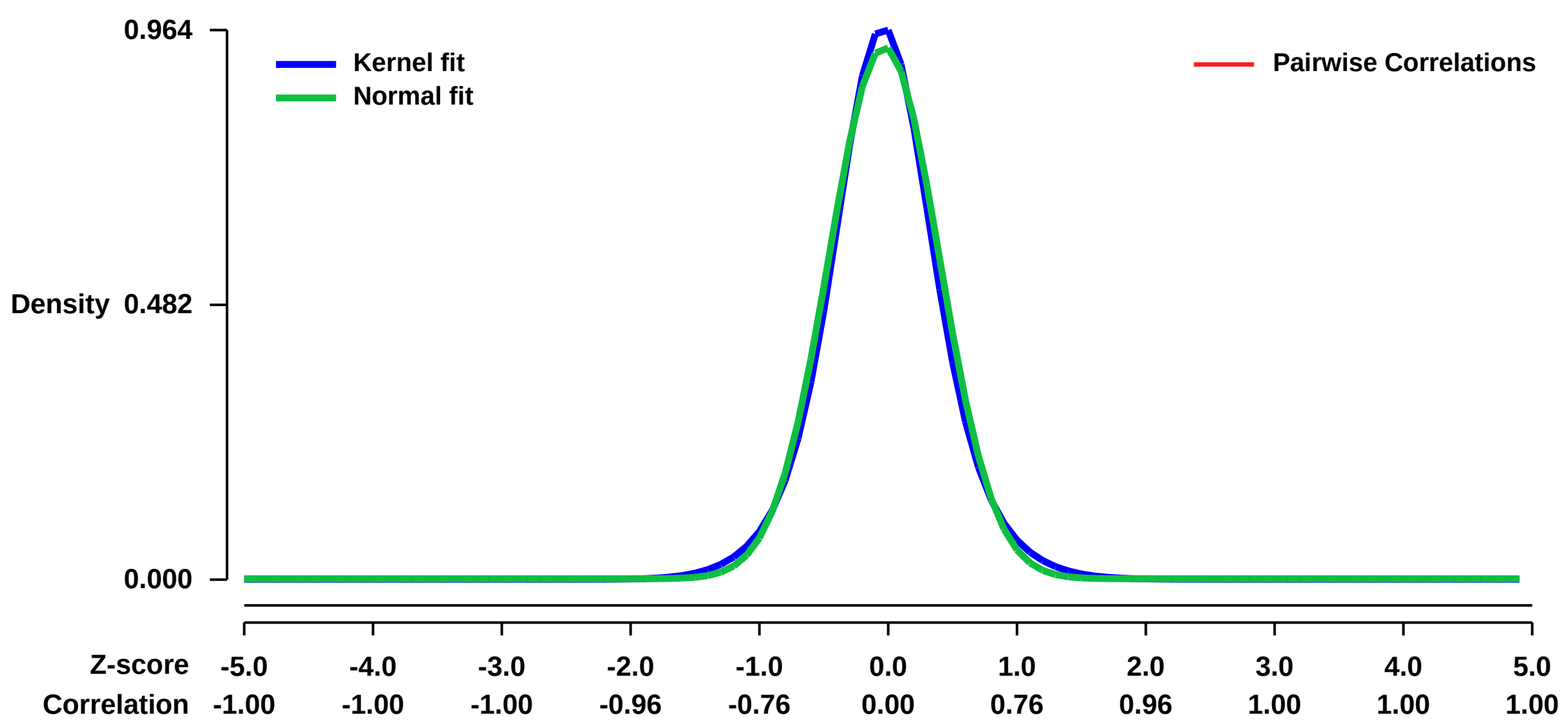

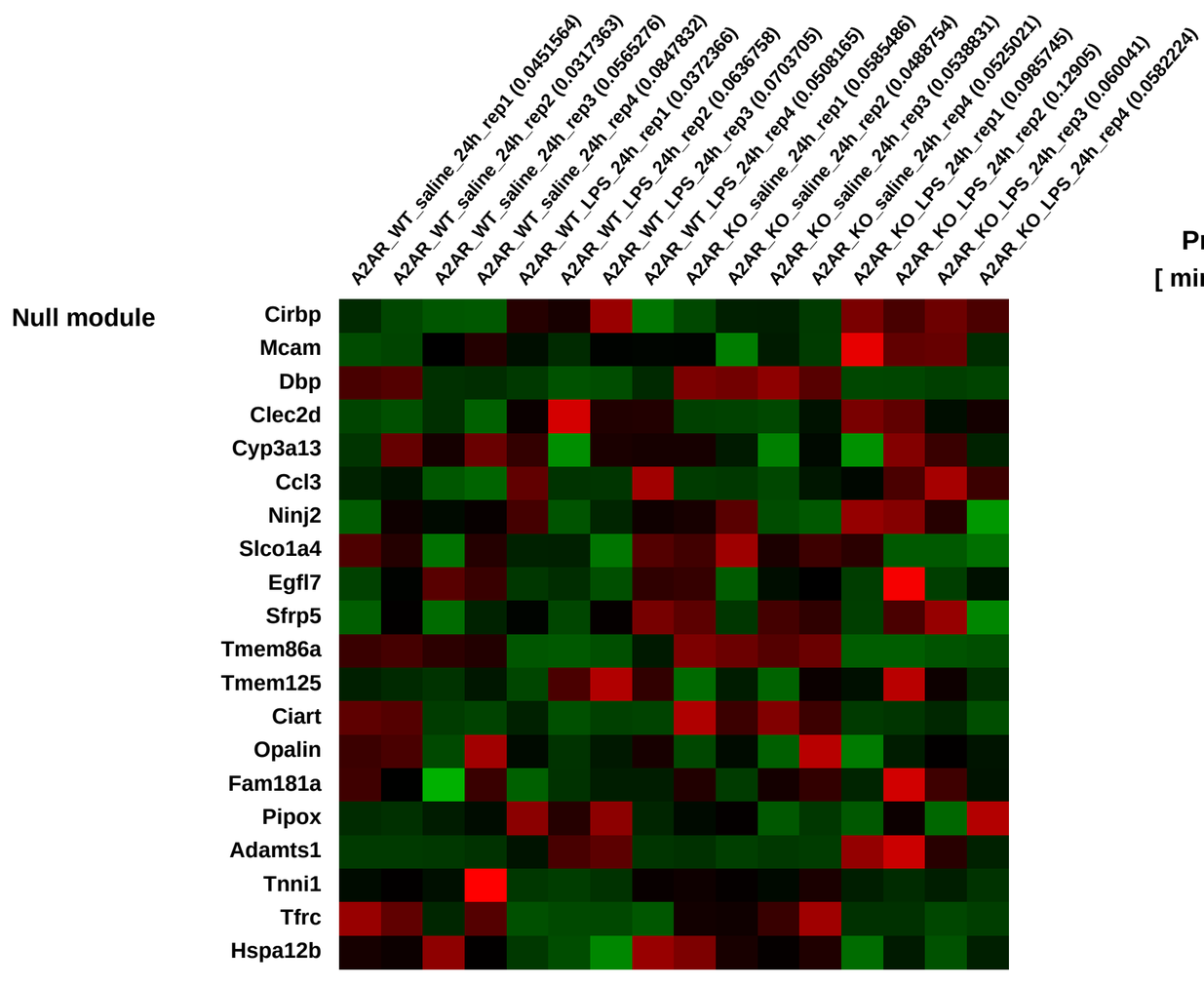

GEO Series "GSE44563" Expression Profiles

Num of samples in this series: 6

Scale of expression profile Z-scores

-3.0 -2.0 -1.0 0.0 1.0 2.0 3.0

GEO Link:	http://www.ncbi.nlm.nih.gov/geo/query/acc.cgi?acc=GSE44563
Status:	Public on Dec 22 2013
Title:	Expression data from C2C12 myotubes infected with RML prions
Organism:	Mus musculus
Experiment type:	Expression profiling by array
Platform:	GPL1261
Pubmed ID:	24244171
Summary & Design:	**Summary:** Prion infection in animals results in neurodegeneration and eventually death. To examine the cellular impact of Prion disease, we profiled non-proliferative fully differentiated C2C12 cells, which can replicate prions to high levels. Results suggest that accumulation of high levels of PrPSc in C2C12 myotubes does not cause any overt cellular dysfunction or molecular pathology. **Overall design:** C2C12 cells were differentiated into confluent myotubes. Cells were infected or not with 100ul of 10% brain homogenate obtained from a C57BL/6 mouse clinically affected with RML prions. 16 days after infection, cells were collected by scraping and RML was purified.

Background corr dist: KL-Divergence = 0.0415, L1-Distance = 0.0144, L2-Distance = 0.0002, Normal std = 0.6034

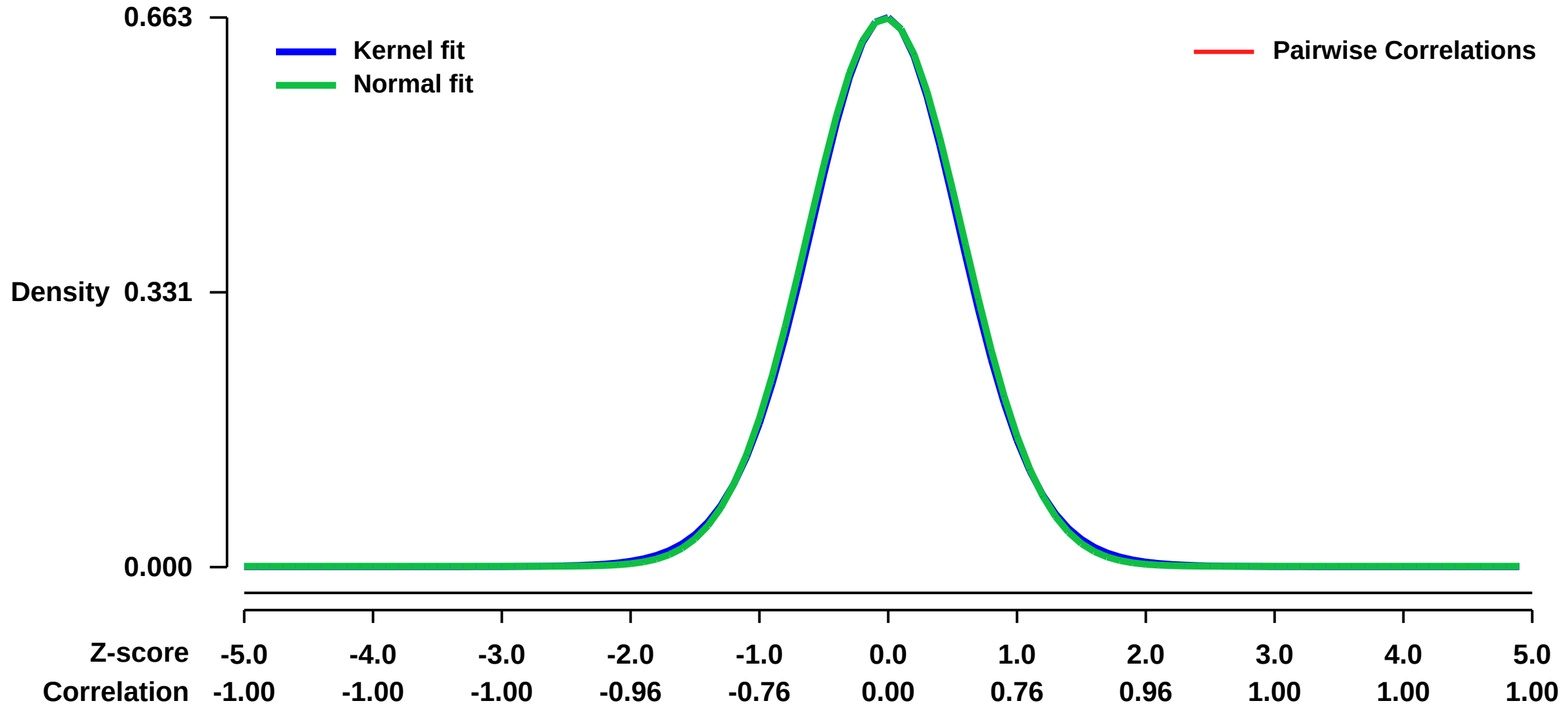

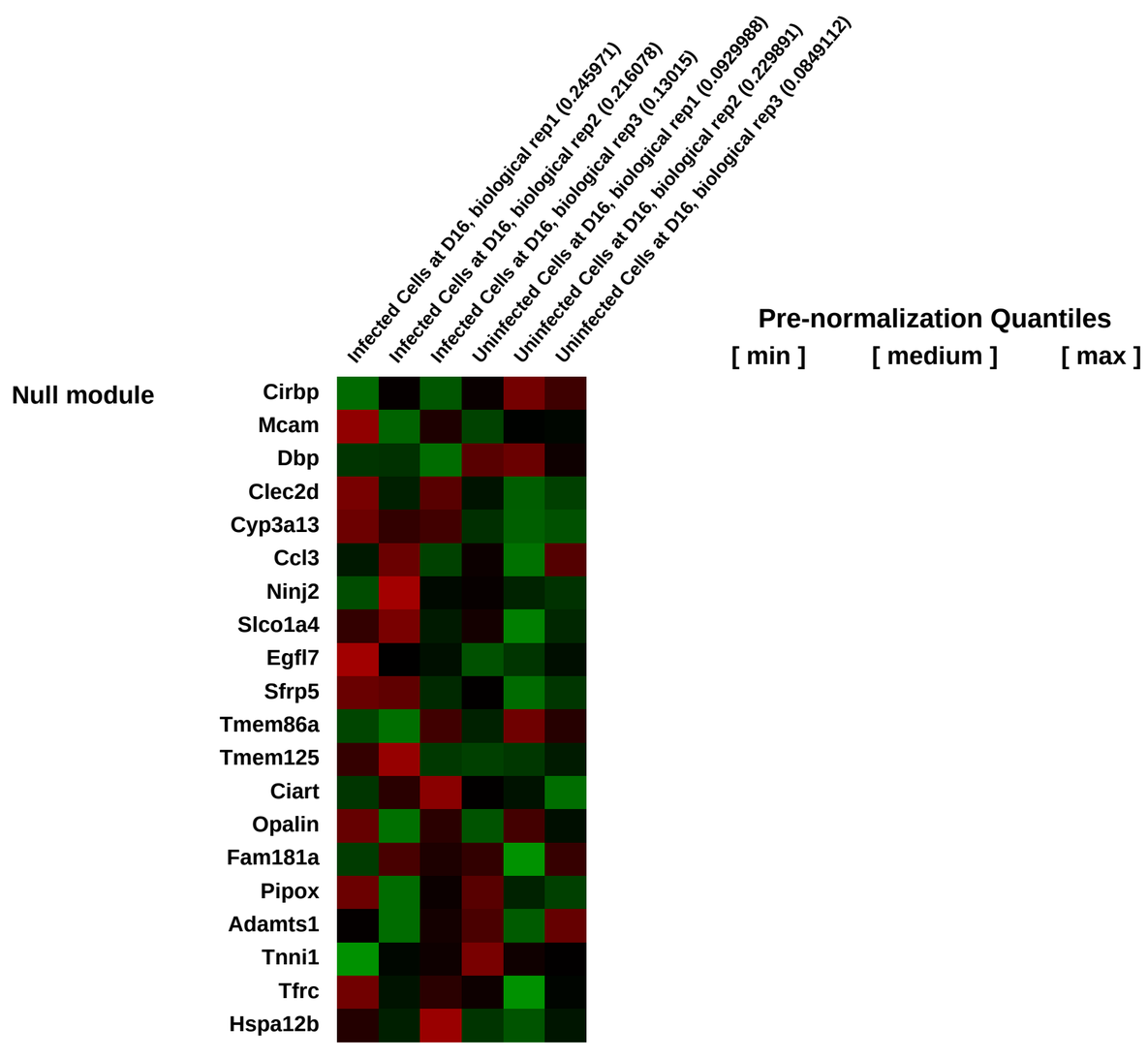

GEO Series "GSE44599" Expression Profiles

Num of samples in this series: 18

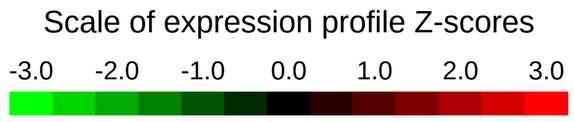

GEO Link:	**http://www.ncbi.nlm.nih.gov/geo/query/acc.cgi?acc=GSE44599**
Status:	**Public on Aug 01 2013**
Title:	**ZNF365 promotes stability of fragile sites and telomeres**
Organism:	**Mus musculus**
Experiment type:	**Expression profiling by array**
Platform:	**GPL1261**
Pubmed ID:	**23776040**
Summary & Design:	**Summary:** **Critically short telomeres activate cellular senescence or apoptosis, as mediated by the tumor suppressor p53, but in the absence of this checkpoint response, telomere dysfunction engenders chromosomal aberrations and cancer. Here, analysis of p53-regulated genes activated in the setting of telomere dysfunction identified Zfp365 (ZNF365 in humans) as a direct p53 target that promotes genome stability. Germline polymorphisms in the ZNF365 locus are associated with increased cancer risk, including those associated with telomere dysfunction. On the mechanistic level, ZNF365 suppresses expression of a subset of common fragile sites (CFS) including telomeres. In the absence of ZNF365, defective telomeres engage in aberrant recombination of telomere ends, leading to increased telomere sister chromatid exchange (T-SCE) and formation of anaphase DNA bridges, including ultra-fine DNA bridges (UFB), and ultimately increased cytokinesis failure and aneuploidy. Thus, the p53-ZNF365 axis contributes to genomic stability in the setting of telomere dysfunction.** **Overall design:** **We expressed an inducible p53 allele encoding a p53-estrogen receptor fusion protein (p53ER) that becomes functional upon addition of 4-hydroxytamoxifen (4-OHT) in TKO cells. We chose a time point of 4 hours post-4-OHT induction to catalog potential direct targets.**

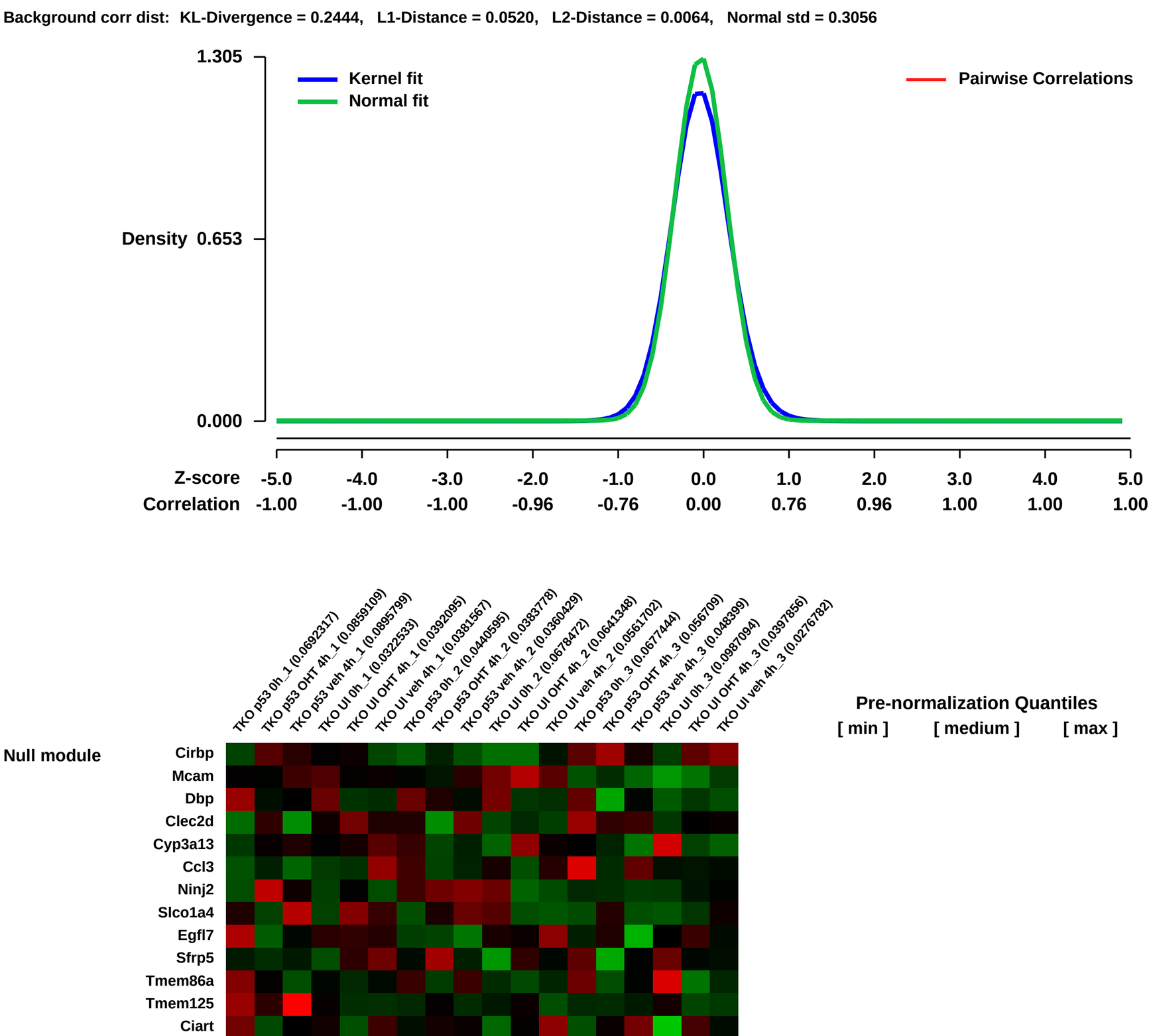

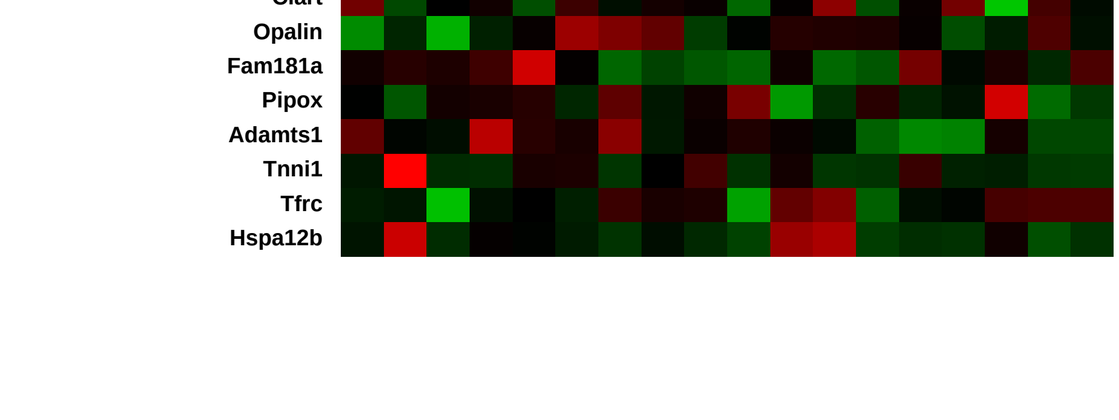

GEO Series "GSE44651" Expression Profiles

Num of samples in this series: 12

Scale of expression profile Z-scores

-3.0 -2.0 -1.0 0.0 1.0 2.0 3.0

GEO Link:	http://www.ncbi.nlm.nih.gov/geo/query/acc.cgi?acc=GSE44651
Status:	Public on Jul 03 2013
Title:	Laser Capture Microdissection isolation of preovulatory granulosa cells from WT and bERKO ovaries
Organism:	Mus musculus
Experiment type:	Expression profiling by array
Platform:	GPL1261
Pubmed ID:	23580569
Summary & Design:	**Summary:** Determining the spatial and temporal expression of genes involved in the ovulatory pathway is critical for the understanding of the role of each estrogen receptor in the modulation of folliculogenesis and ovulation. Estrogen receptor (ER) ¸† is highly expressed in ovarian granulosa cells and mice lacking ER¸† (¸†ERKO) are subfertile due to inefficient ovulation. Previous work has focused on isolated granulosa cells or cultured follicles and while informative, provides confounding results due to the heterogeneous cell types present including granulosa, theca and oocytes and exposure to in vitro conditions. Herein, we isolated preovulatory granulosa cells from WT and ER¸†-null mice using laser capture microdissection to examine the genomic transcriptional response downstream of PMSG (mimicking FSH) and PMSG/hCG (mimicking LH) stimulation. This allows for a direct comparison of in vivo granulosa cells at the same stage of development from both WT and ER¸†-null ovaries. ER¸†-null granulosa cells showed altered expression of genes known to be regulated by FSH (Akap12 and Runx2) as well as not previously reported (Arnt2 and Pou5f1) in WT granulosa cells. Our analysis also identified 304 genes not previously associated with ER¸† in granulosa cells. LH responsive genes including Abcb1b and Fam110c show reduced expression in ER¸†-null granulosa cells; however novel genes including Rassf2 and Megf10 were also identified as being downstream of LH signaling in granulosa cells. Collectively, our data suggests that granulosa cells from ER¸†-null ovaries may not be appropriately differentiated and are unable to respond properly to gonadotropin stimulation We used microarray to compare the gene expression profiles of wiltype (WT) and Erb-null (bERKO) preovulatory granulosa cells as they respond to either PMSG or PMSG+hCG treatments. **Overall design:** Laser microdissection was used to collect a purified population of granulosa cells only from preovulatory follicles. We chose to compre the response to PMSG or PMSG+hCG of granulosa cells collected from either WT and bERKO preovulatory follicles. We chose to collect cells 48h after mice were treated with PMSG to compare the gene expression profile ot preovulatory granulosa cells. We also studied the response of these cells to LH (or hCG) as we collected cells 4h after mice were treated with hCG (peak of transcriptional response to hCG).

Background corr dist: KL-Divergence = 0.1242, L1-Distance = 0.0379, L2-Distance = 0.0031, Normal std = 0.4079

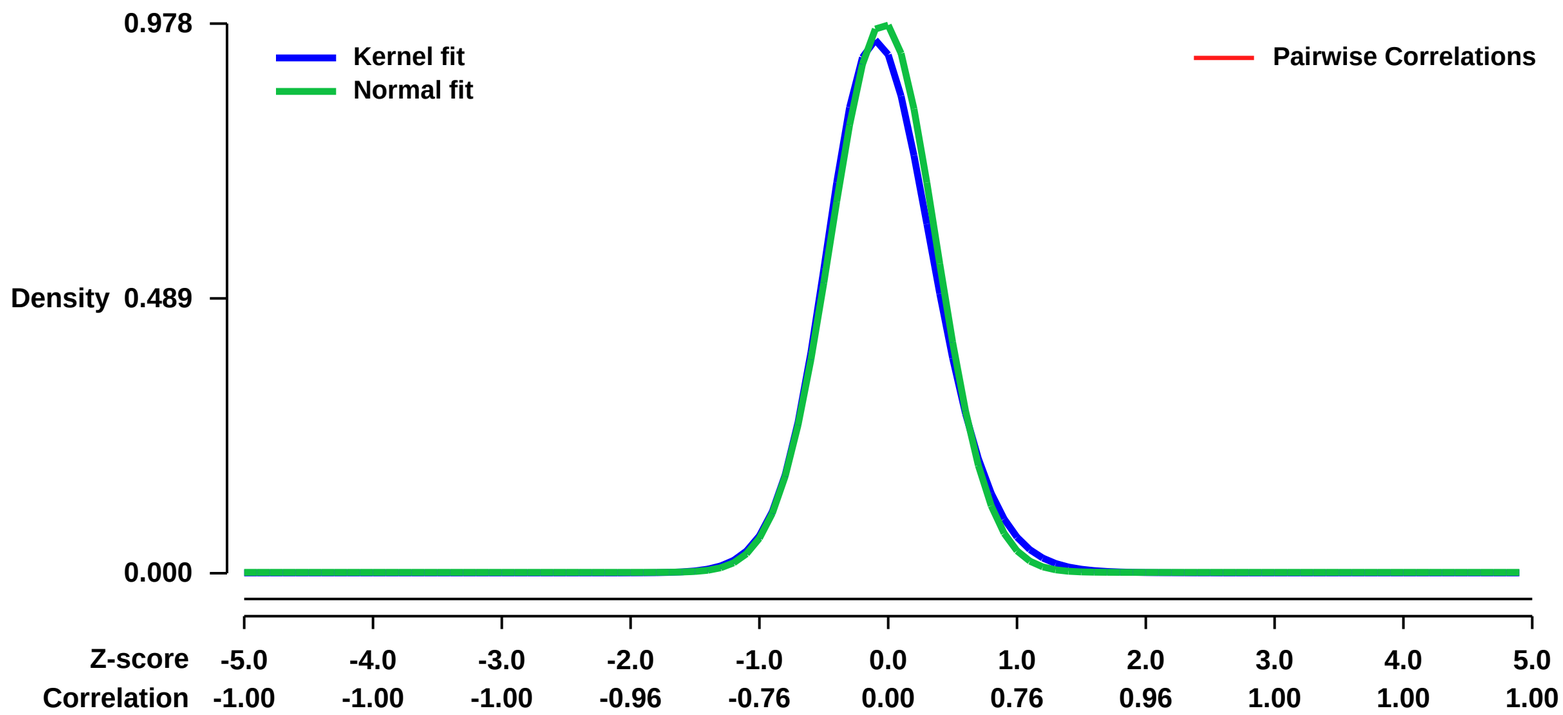

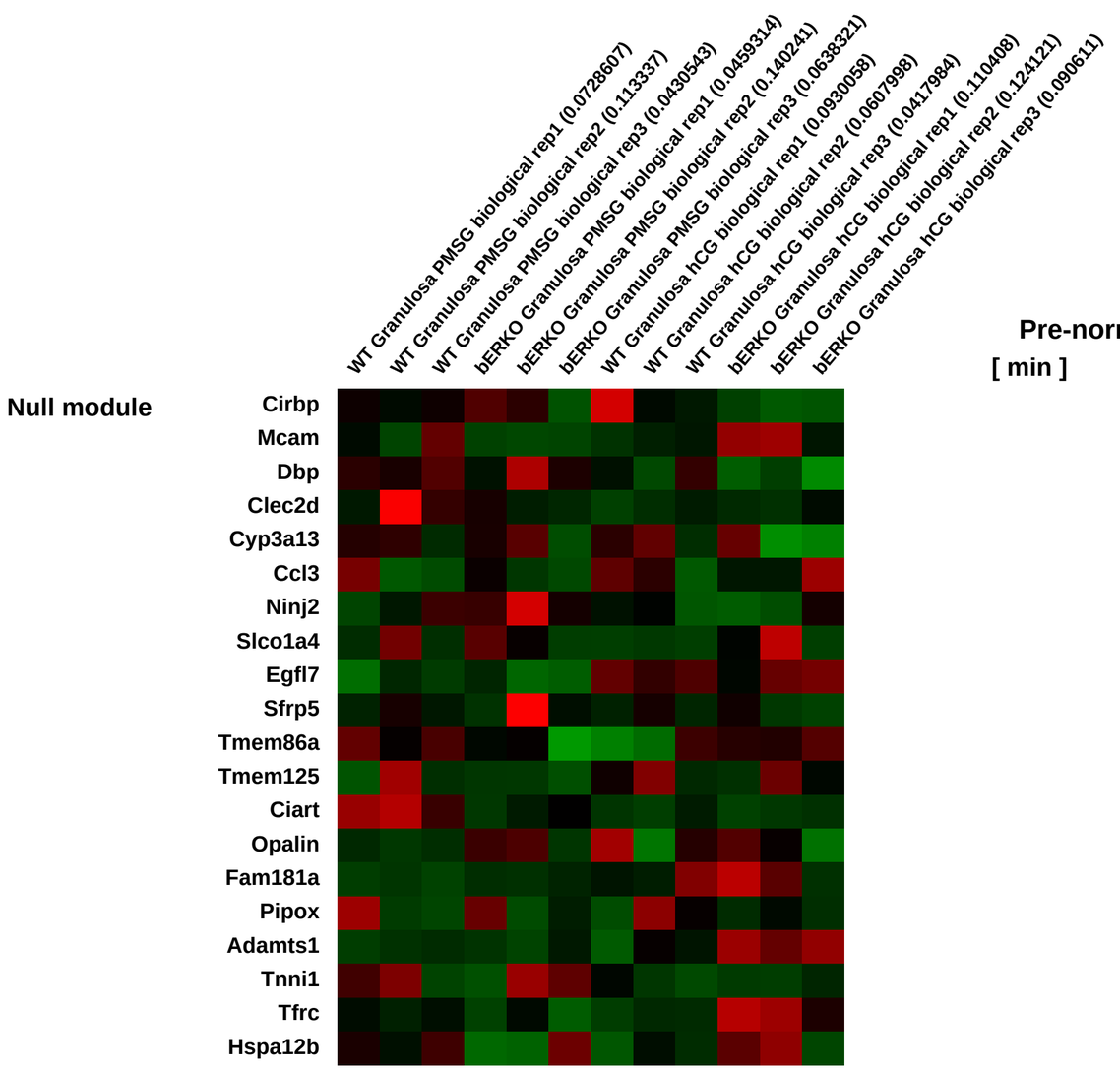

GEO Series "GSE44663" Expression Profiles

Num of samples in this series: 6

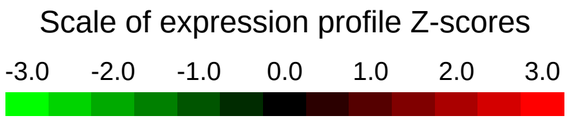

GEO Link:	**http://www.ncbi.nlm.nih.gov/geo/query/acc.cgi?acc=GSE44663**
Status:	**Public on Feb 26 2013**
Title:	**Expression data from adult mouse mesenteric arteries**
Organism:	**Mus musculus**
Experiment type:	**Expression profiling by array**
Platform:	**GPL1261**
Pubmed ID:	
Summary & Design:	**Summary:** **Vascular smooth muscle cells require beta1 integrin for survival. Following the induced deletion of smooth muscle beta1 integrin, smooth muscle cells undergo apoptosis and arteries become fibrotic. This microarray study on mesenteric arteries 2 weeks after the initiation of beta1 integrin deletion specifically in smooth muscle cells of the adult mouse aimed to examine early changes in expression following deletion.** **Overall design:** **Mesenteric arteries from three wild type mixed background and three beta1 integrin smooth muscle knockout mixed background mice are examined.**

Background corr dist: **KL-Divergence = 0.0392, L1-Distance = 0.0238, L2-Distance = 0.0007, Normal std = 0.6246**

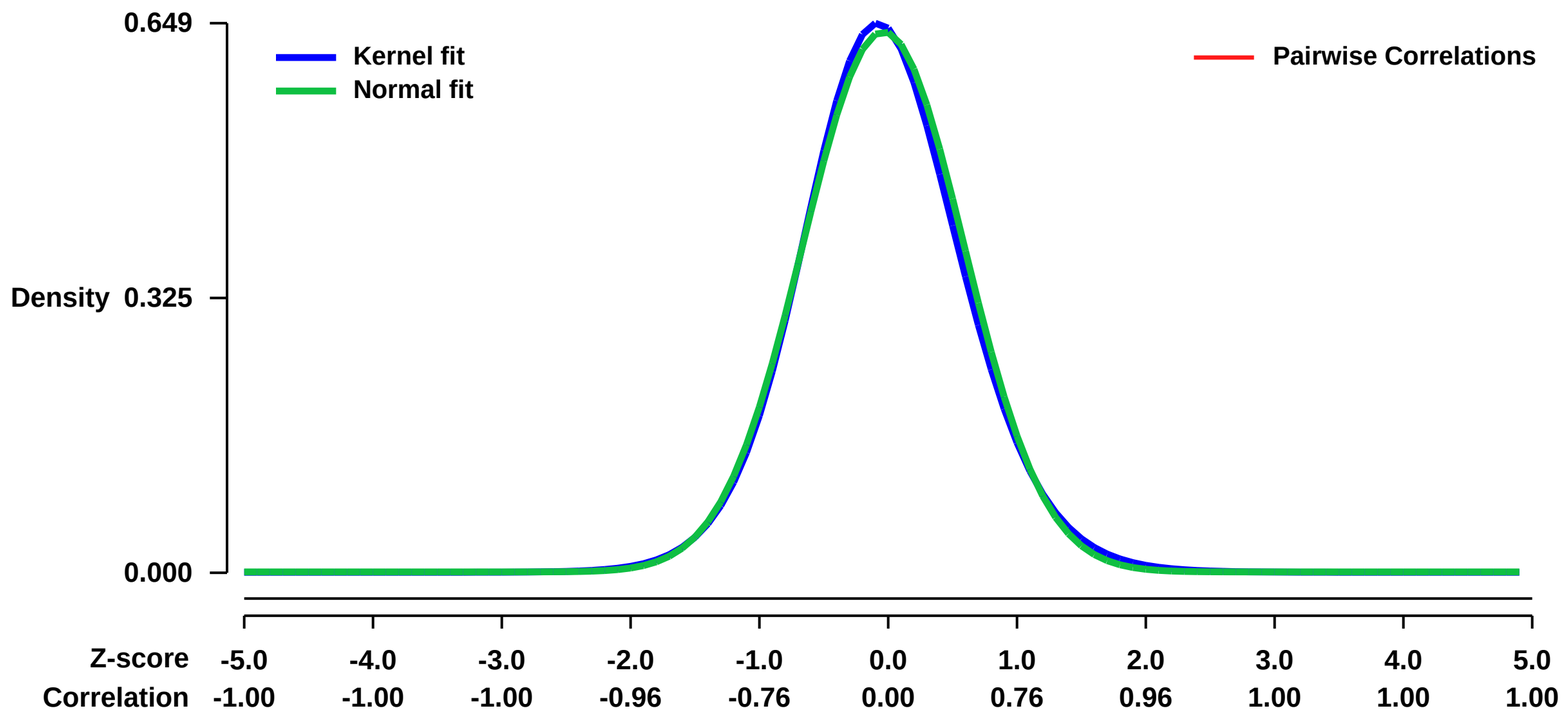

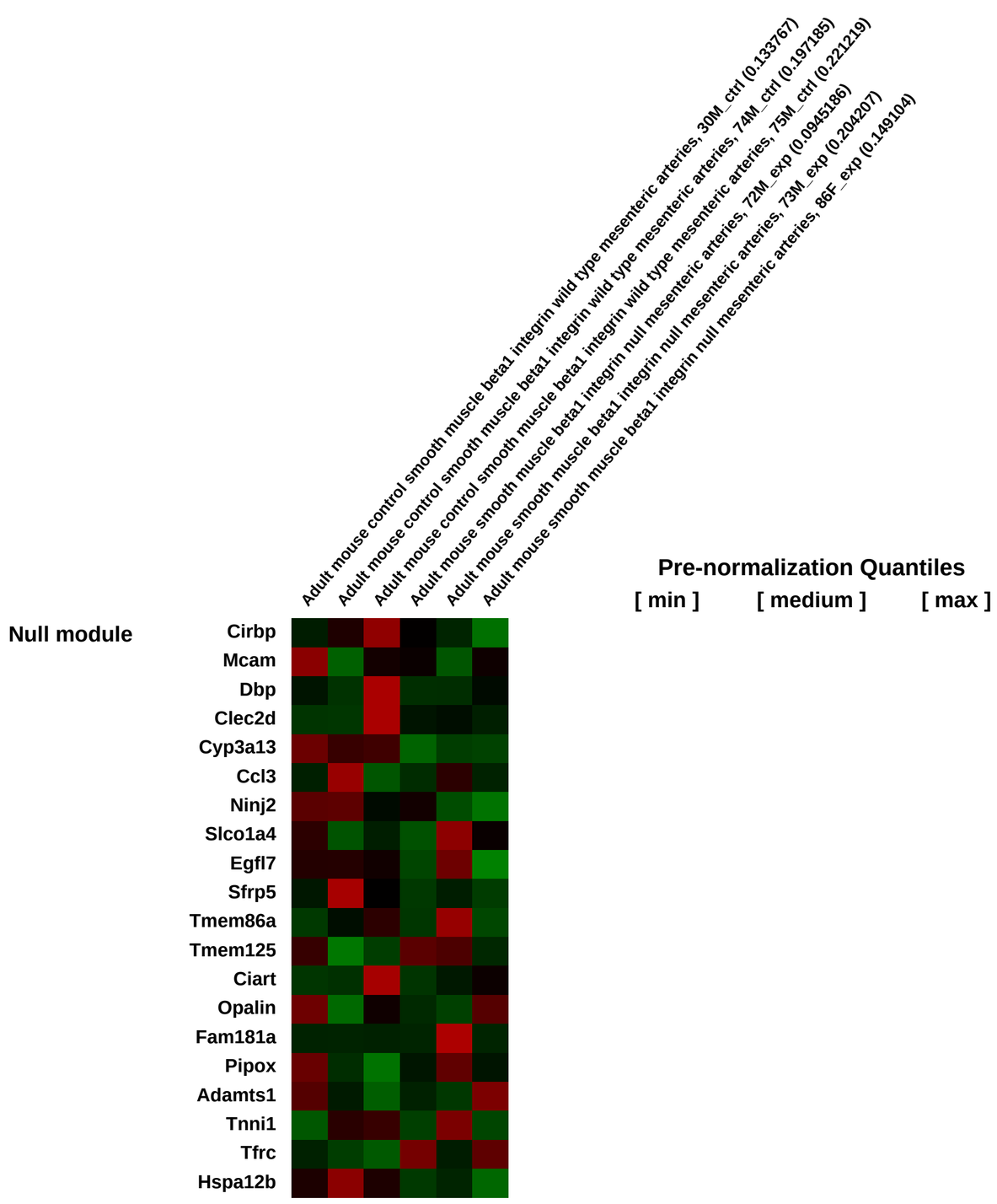

GEO Series "GSE4479" Expression Profiles

Num of samples in this series: 10

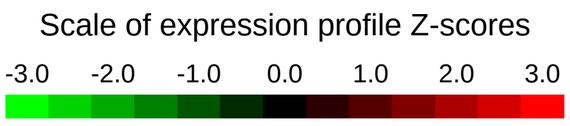

GEO Link:	http://www.ncbi.nlm.nih.gov/geo/query/acc.cgi?acc=GSE4479
Status:	Public on Jun 01 2006
Title:	Expression data from CD4+ splenocytes 6h post-sepsis
Organism:	Mus musculus
Experiment type:	Expression profiling by array
Platform:	GPL1261
Pubmed ID:	16931309
Summary & Design:	**Summary:** Lymphocytes are adversely affected during sepsis. Some CD4+ splenocytes undergo apoptosis while others become Th2 polarized. The molecular determinants of these phenotypic changes are not known. Here we compare the transcriptional response of septic CD4 splenocytes to CD4 splenocytes from sham-manipulated animals 6h after sepsis and identify an early transcriptional component to the septic CD4+ splenocyte phenotype. We used microarrays to detail the global program of gene expression underlying the sepsis-induced changes in CD4+ splenocyte phenotype. Keywords: disease state analysis **Overall design:** CD4+ splenocytes were isolated 6h after the surgical induction of sepsis for RNA extraction and hybridization on Affymetrix microarrays. We sought to obtain a homogeneous cell population in order to reduce any effects of cellular heterogeneity on expression profiles. To that end, immunomagnetic negative selection was used to enrich CD4+ splenocyte populations to ~91%. (n=5 biological replicates each CLP and sham)

Background corr dist: KL-Divergence = 0.0880, L1-Distance = 0.0271, L2-Distance = 0.0012, Normal std = 0.4568

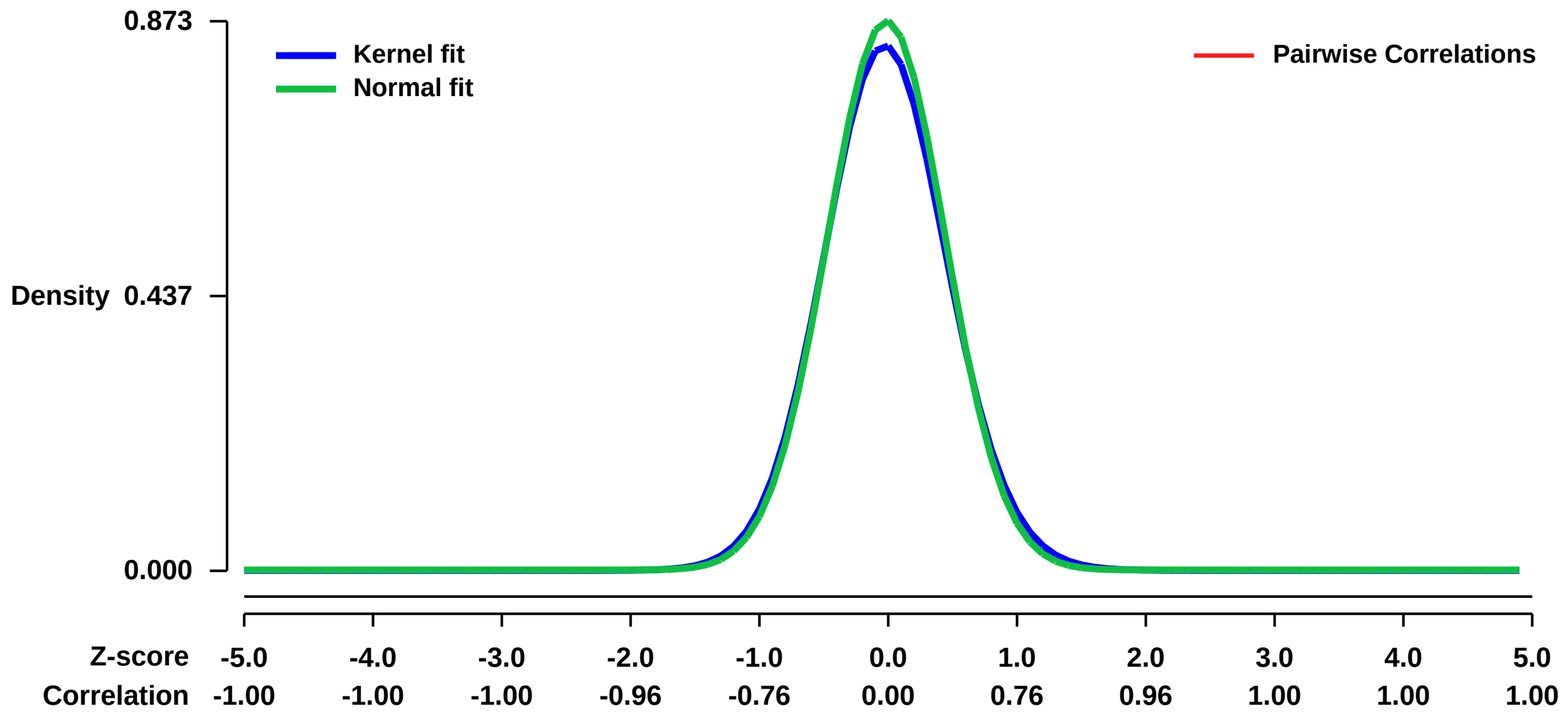

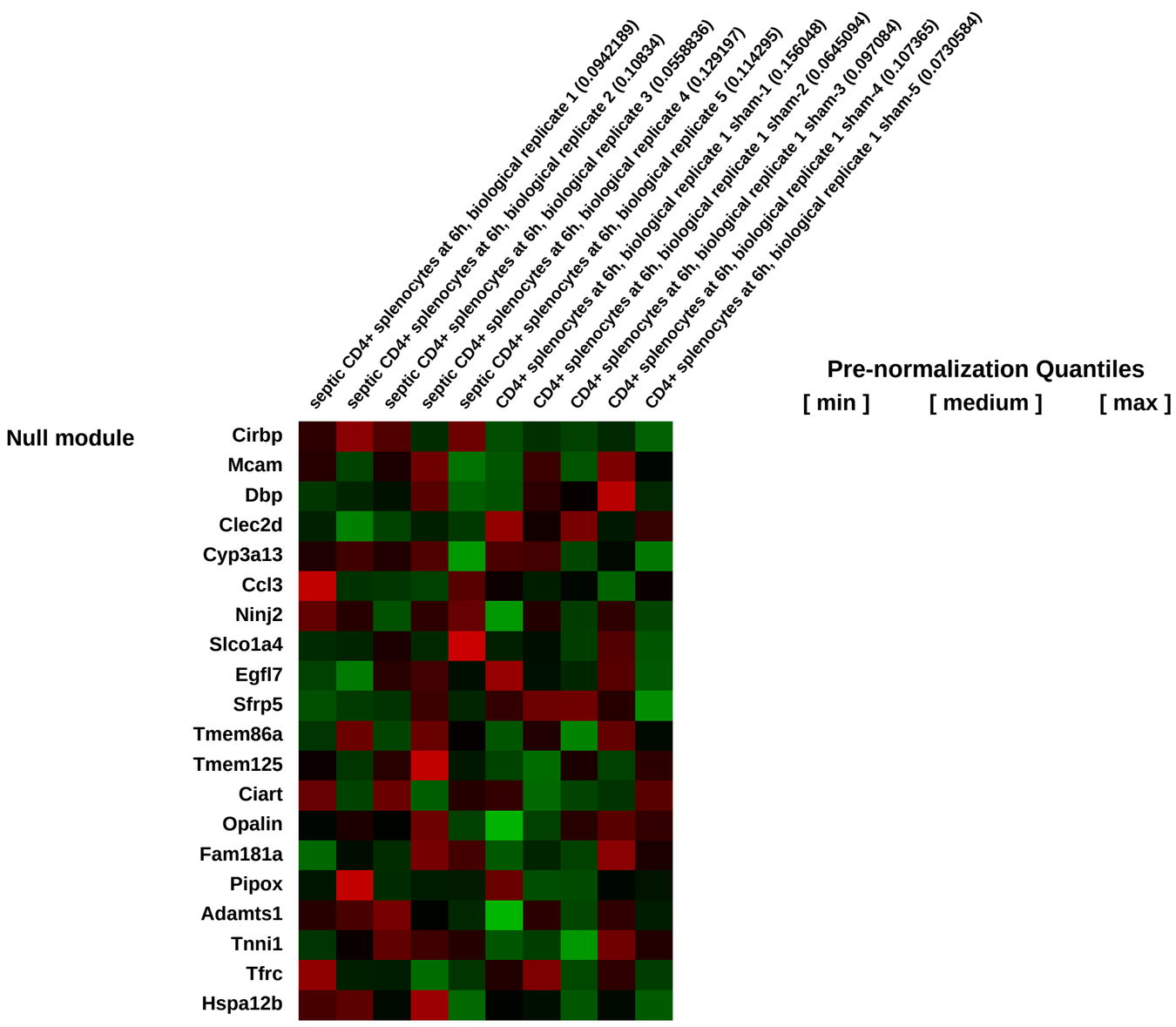

GEO Series "GSE4481" Expression Profiles

Num of samples in this series: 18

Scale of expression profile Z-scores

-3.0 -2.0 -1.0 0.0 1.0 2.0 3.0

GEO Link:	**http://www.ncbi.nlm.nih.gov/geo/query/acc.cgi?acc=GSE4481**
Status:	**Public on Dec 15 2006**
Title:	**C-type natriuretic peptide regulates endochondral ossification through p38 MAP kinase-dependent pathways_2**
Organism:	**Mus musculus**
Experiment type:	**Expression profiling by array**
Platform:	**GPL1261**
Pubmed ID:	
Summary & Design:	**Summary:** **C-type natriuretic peptide (CNP) has been recently identified as an important anabolic regulator of endochondral bone growth, but the molecular mechanism mediating these effects are not completely understood. Here we demonstrate that CNP activates the p38 MAP kinase pathway in chondrocytes and that pharmacological inhibition of p38 blocks the anabolic effects of CNP in a tibia organ culture system. We further show that CNP stimulates endochondral bone growth largely through expansion of the hypertrophic zone of the growth plate, while delaying mineralization. Both effects are reversed by p38 inhibition. We performed Affymetrix microarray analyses to identify CNP target genes in the organ culture system. These studies confirmed that hypertrophic chondrocytes are the main targets of CNP signaling in the growth plate, potentially because cGMP-dependent kinases I and II, important transducers of CNP signaling and are expressed at much higher levels in these cells than in other areas of the tibia. One of the genes most strongly induced by CNP was the Ptgs2 gene, encoding Cox2. Real-time PCR confirmed that Cox2 expression was induced by CNP in hypertrophic chondrocytes, but surprisingly in a p38-independent manner. Moreover, Cox2 inhibition â in contrast to p38 inhibition - did not block the anabolic effects of CNP. In summary, our data identify novel target genes of CNP and demonstrate that the p38 pathway is a novel, essential mediator of CNP effects on endochondral ossification, with potential implications for numerous skeletal diseases.** **Keywords: Growth plate zone comparison and treatment response analysis** **Overall design:** **Tibiae from E15.5 day old embryonic mice were isolated and cultured in minimal media in the presence of vehicle, BSA/HCl (1mM), or C-type natriuretic peptide, CNP (10-6M). On the sixth day of treatment cultured tibias were micro-dissected into the resting/proliferating, hypertrophic, and mineralized areas. Distinct zones from approximately 24 bones were pooled together, from which RNA was isolated using the Qiagen RNeasy Lipid Extraction Kit. Once the quality of total RNA from three independent trials was determined using the Agilent 2100 bioanalyzer, microarray analyses were performed at the London Regional Genomics Centre using MOE430_2.0 Affymetrix arrays. Results were analyzed using GeneSpring 7.2 software.**

Background corr dist: KL-Divergence = 0.1409, L1-Distance = 0.0266, L2-Distance = 0.0011, Normal std = 0.3892

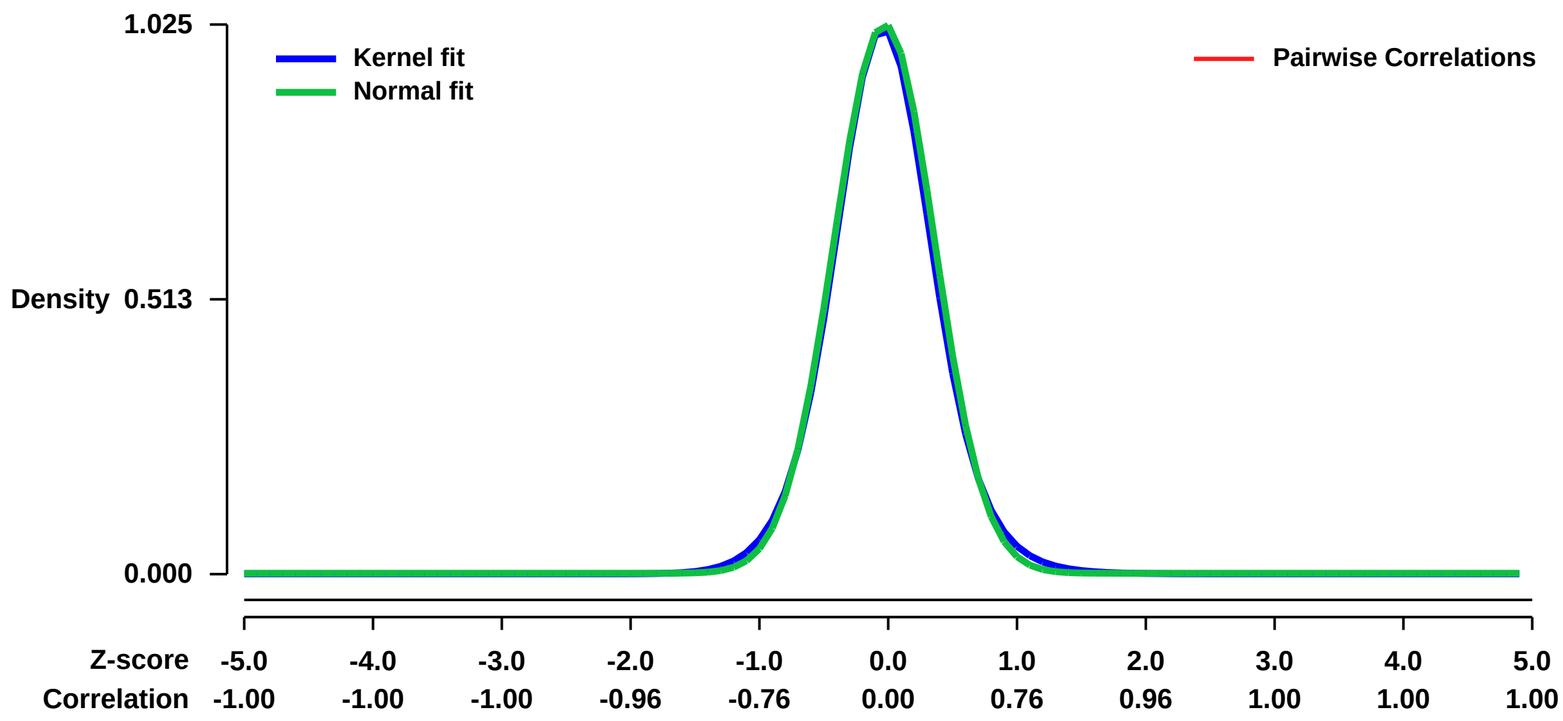

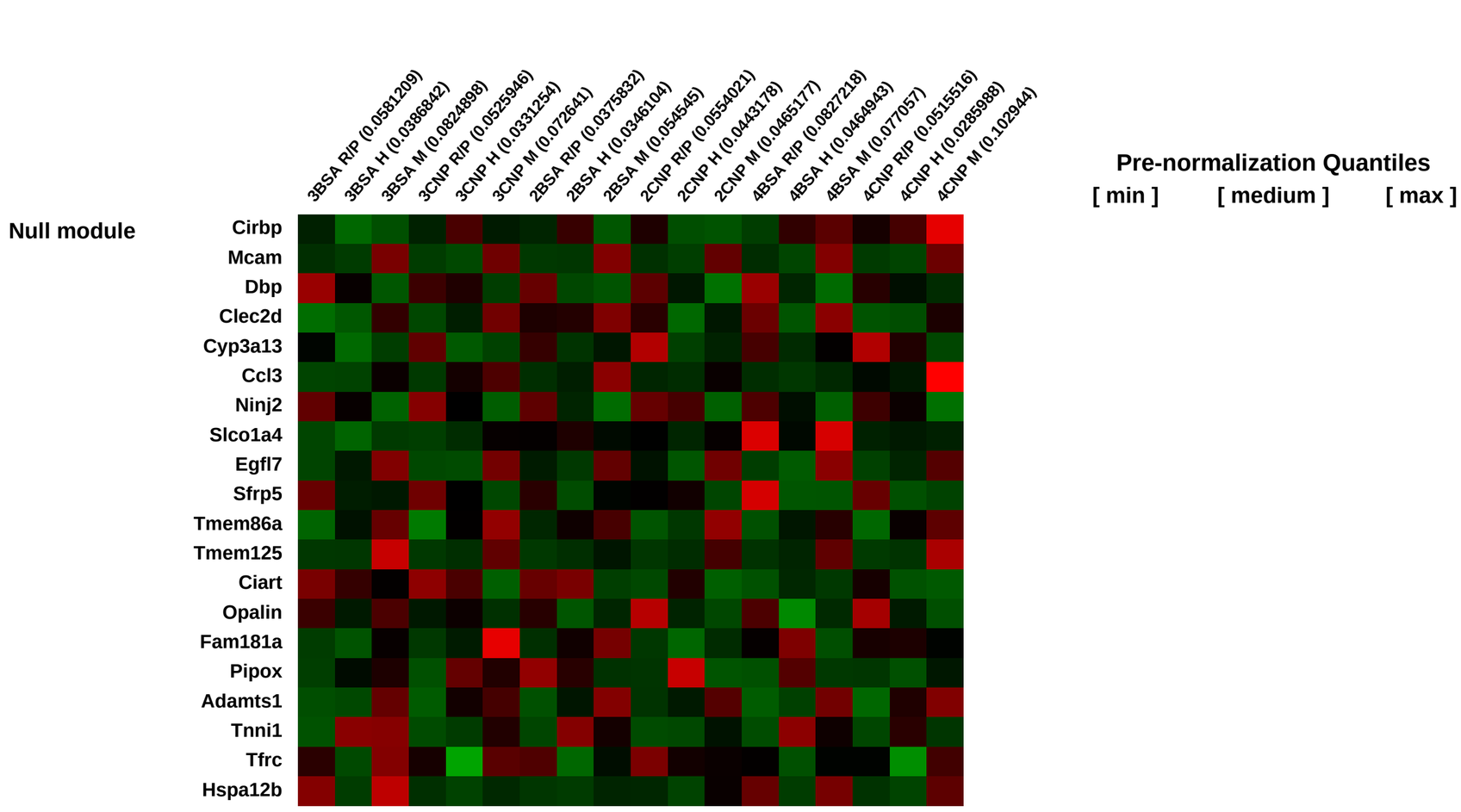

GEO Series "GSE45005" Expression Profiles

Num of samples in this series: 12

Scale of expression profile Z-scores

-3.0 -2.0 -1.0 0.0 1.0 2.0 3.0

GEO Link:	http://www.ncbi.nlm.nih.gov/geo/query/acc.cgi?acc=GSE45005
Status:	Public on Jul 31 2013
Title:	Expression data from renal cortex of ICR-derived Glomerulonephritis (ICGN) mice and ICR mice
Organism:	Mus musculus
Experiment type:	Expression profiling by array
Platform:	GPL1261
Pubmed ID:	23989031
Summary & Design:	**Summary:** ICR-derived glomerulonephritis (ICGN) mice is a novel inbred strain of mice with a hereditary nephrotic syndrome. Deletion mutation of tensin 2 (Tns2), a focal adhesion molecule, has been suggested to be responsible for nephrotic syndrome in ICGN mice, however, existence of other associative factors has been suggested. To identify additional associative factors and to better understand onset mechanism of nephrotic syndrome in ICGN mice, comprehensive gene expression analysis using DNA microarray was conducted. Immune-related pathways were markedly altered in ICGN mice kidney as compared with ICR mice. Furthermore, gene expression level of complement component 1, s subcomponent (C1s), whose human homologue has been reported to associate with lupus nephritis, was markedly low in ICGN mice kidney. **Overall design:** RNA from renal cortex of 4- and 8-week-old ICGN and ICR mice was extracted and processed for hybridization on Affymetrix microarrays (N=3).

Background corr dist: KL-Divergence = 0.1065, L1-Distance = 0.0253, L2-Distance = 0.0010, Normal std = 0.4277

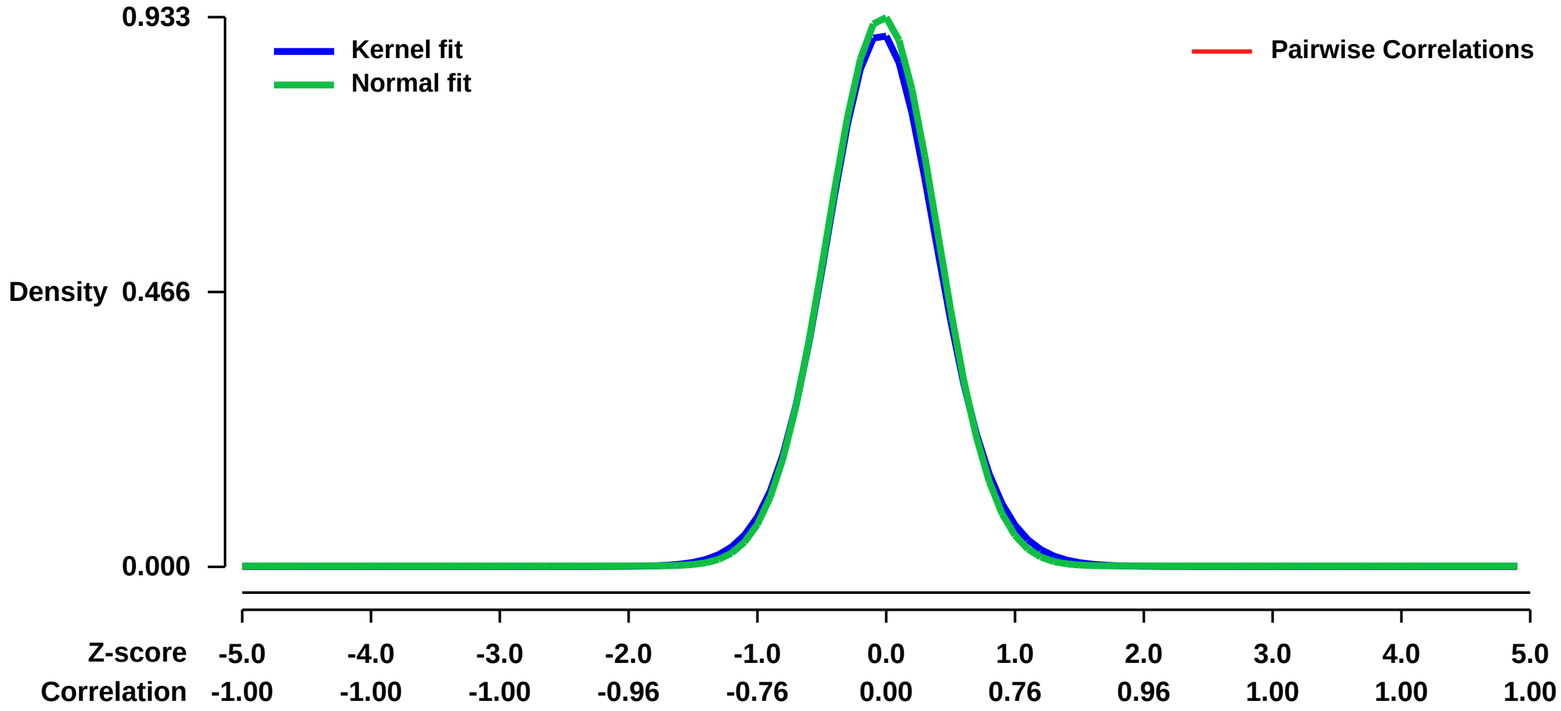

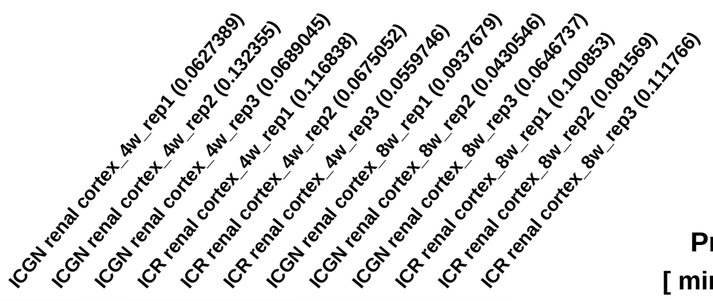

Pre-normalization Quantiles

[min] [medium] [max]

Null module

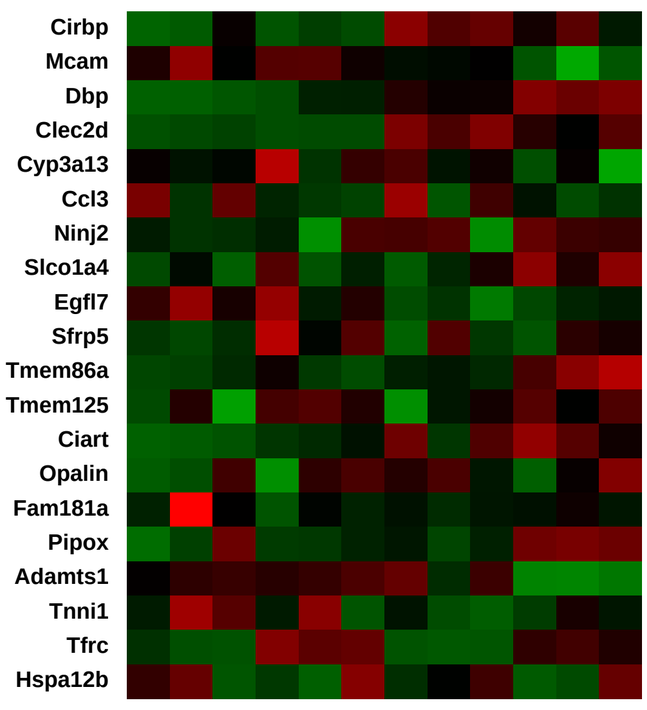

GEO Series "GSE45028" Expression Profiles

Num of samples in this series: 22

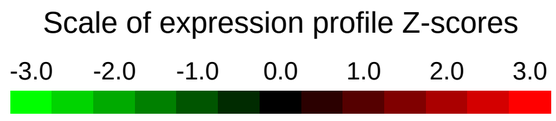

GEO Link:	**http://www.ncbi.nlm.nih.gov/geo/query/acc.cgi?acc=GSE45028**
Status:	**Public on Jul 01 2014**
Title:	**Expression data from NOD and C57BL/6 mouse pancreas CD8ˌ–- Dendritic Cells (DCs) under steady-state and after in-vitro LPS stimulation**
Organism:	**Mus musculus**
Experiment type:	**Expression profiling by array**
Platform:	**GPL1261**
Pubmed ID:	
Summary & Design:	**Summary:** **Abstract Two major dendritic cell (DC) subsets have been described in the islets of mice: The immunogenic CD8ˌ–-CD11b+ DCs and the tolerogenic CD8ˌ–+CD103+ DCs. We have recently reported on reduced numbers of the minor population of tolerogenic CD8ˌ–+CD103+ DCs in the pancreas of 5 week old pre-diabetic non-obese diabetic (NOD) mice. Aim: To analyze also the larger subset of CD11c+CD8ˌ–- DCs isolated from the pancreas of pre-diabetic NOD mice 1) for maturation and tolerance inducing molecules found abnormally expressed on CD8ˌ–+CD103+ DCs, and 2) for genome-wide gene expression to further elucidate abnormalities in underlying gene expression networks. Methods: CD11c+CD8ˌ–- DCs were isolated from 5 week old C57BL/6 and NOD pancreas. Expression of cell surface markers including CD86, CCR5, CD11b, CD103, Clec9a, CD24 and CD200R3 were measured by FACS. Genome-wide gene expression by microarray was assessed during the steady state and after in vitro LPS stimulation. Results: The steady state pancreatic CD11c+ CD8ˌ–- DCs during the pre-diabetic stage showed: 1) A reduced expression of several gene networks important for the prime functions of the cell, such as for cell renewal, immune stimulation and immune tolerance induction, for migration and for the provision of growth factors for beta cell regeneration. This general deficiency state was corroborated by a reduced in vivo proliferation (BrdU incorporation) of the cells and the reduced expression in FACS analysis of CD86, CCR5, CD103, Clec9a, CD24 and CD200R3 on the cells. 2) A hyper reactivity of these cells to LPS correlated with an enhanced pro-inflammatory state characterized by altered expression of a number of classical pro-inflammatory factors and cytokines. Conclusion: The NOD CD11c+CD8ˌ–- DCs seem to be Janus-faced depending on the conditions: Deficient in steady state with reduced immune stimulation capabilities also for tolerance induction; over-inflammatory with a molecular profile suggesting a preferential stimulatory capacity for Th1 cells when encountering a Pathogen-Associated Molecular Pattern (PAMP) in the form of LPS.** **We used microarray gene expression analysis to explain the abnormal expression of several cell surface markers involved in tolerace, migration and maturation in the steady-state and to measure the effect of a PAMP such as LPS** **Overall design:** **We isolated RNA from FACS sorted CD11c+CD8ˌ–- DCs in 10 pooled pancreases from pre-diabetic NOD and non-diabetic C57BL/6 mice at 5 weeks. In addition, we treated in another experiment the isolated pancreas DCs with LPS (and PBS), incubated for 18h and measured gene expression. We compared gene expression between strains NOD vs C57BL/6 under steady-state and after in-vitro LPS/PBS stimulation.**

Background corr dist: KL-Divergence = 0.0365, L1-Distance = 0.0850, L2-Distance = 0.0118, Normal std = 0.7351

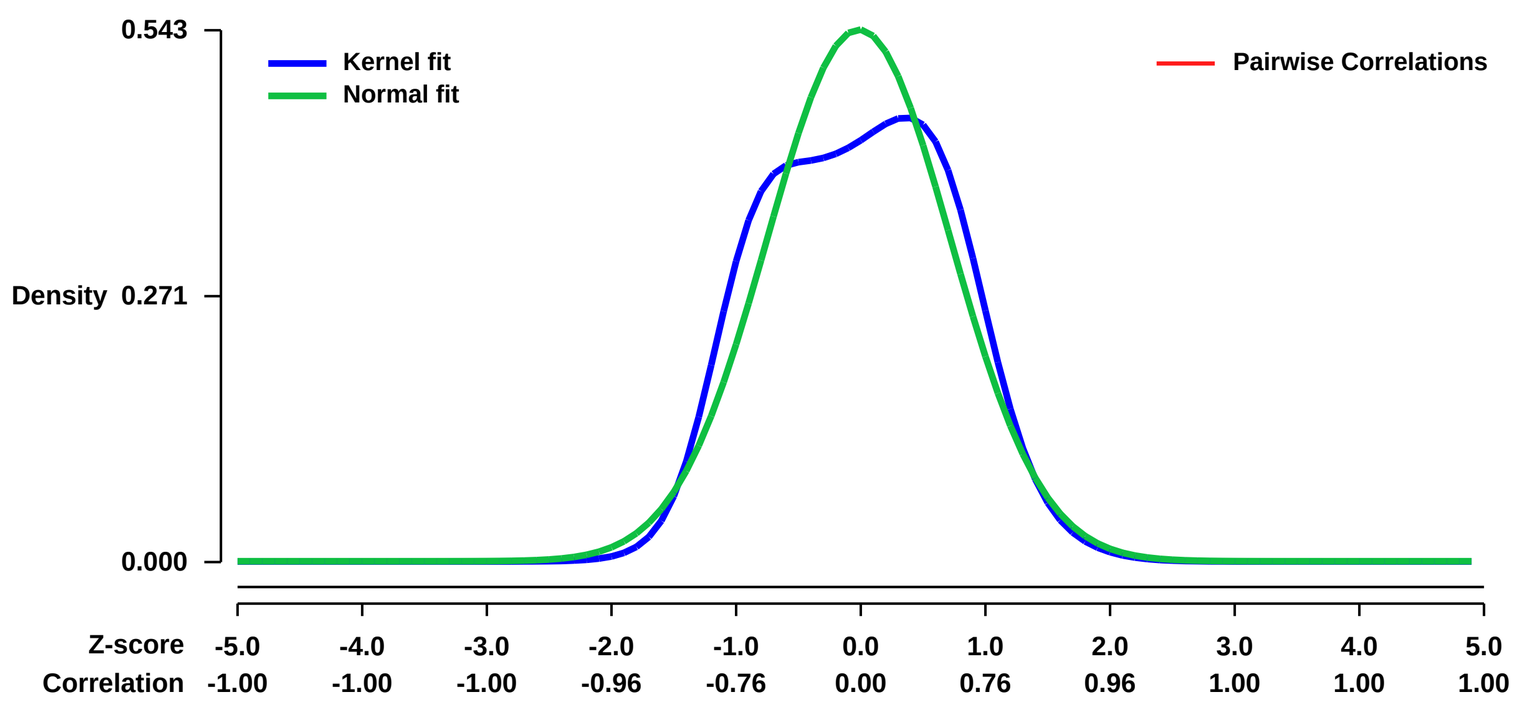

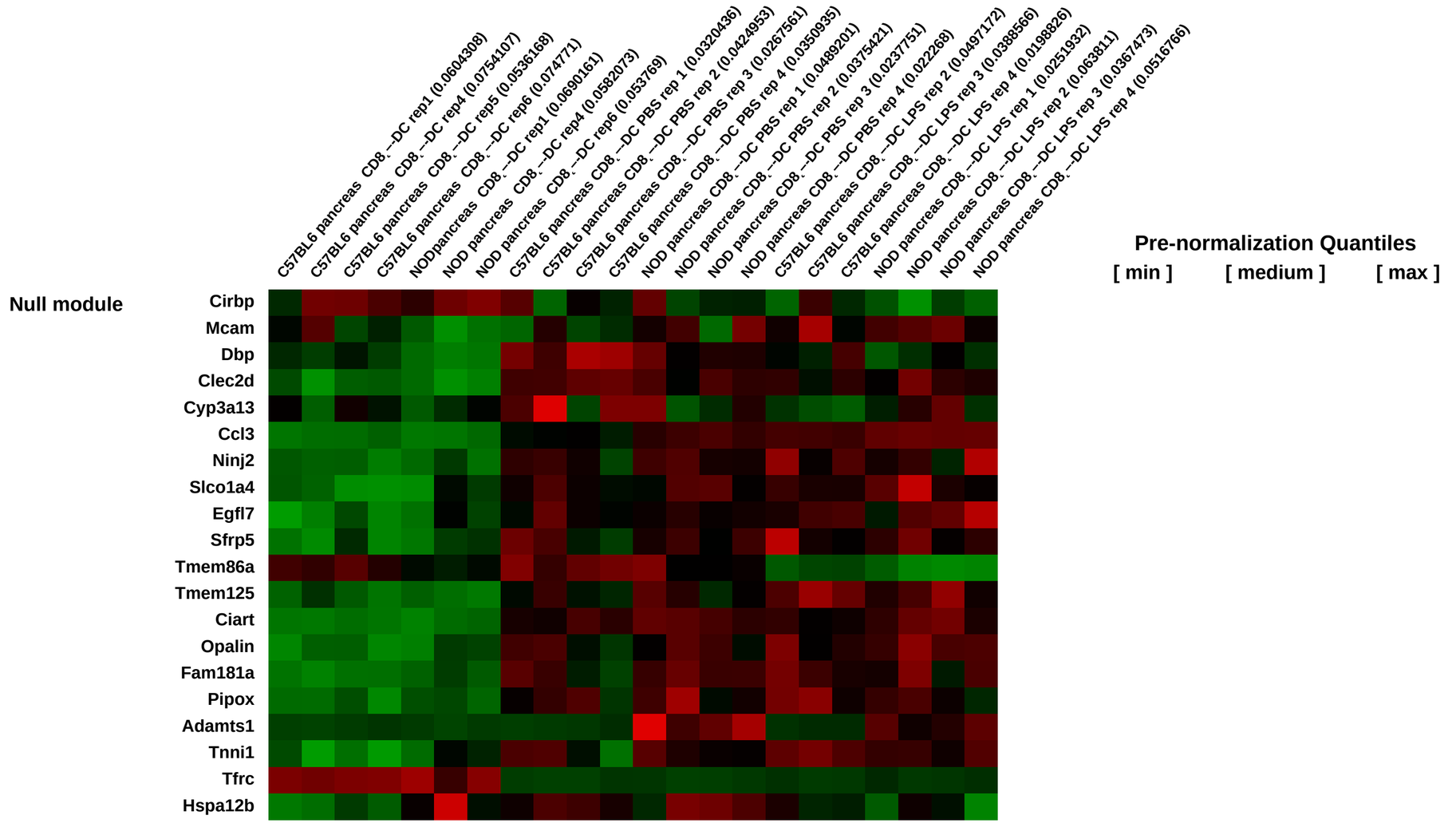

GEO Series "GSE45043" Expression Profiles

Num of samples in this series: 12

Scale of expression profile Z-scores

-3.0 -2.0 -1.0 0.0 1.0 2.0 3.0

GEO Link:	http://www.ncbi.nlm.nih.gov/geo/query/acc.cgi?acc=GSE45043
Status:	Public on May 29 2013
Title:	Age-mediated transcriptomic changes in adult mouse substantia nigra
Organism:	Mus musculus
Experiment type:	Expression profiling by array
Platform:	GPL1261
Pubmed ID:	23638090
Summary & Design:	**Summary:** Substantia nigra pars compacta (SNpc) is highly sensitive to normal aging and selectively degenerates in Parkinson's disease. Until now, molecular mechanisms behind SNpc aging have not been fully investigated using high throughput techniques. Here, aging-associated early changes in transcriptome of SNpc were investigated comparing late middle-aged (18 months old) to young (2 months old) mice. **Overall design:** Three age groups of C57 wild type mice were used in microarray analysis: young (2 months old), middle aged (10 months old), and late-middle aged (18 months old) mice. Four replicates were included in each age group and each replicate was pooled from 4 mice (4 mice/replicate x 4 replicates x 3 age groups). Total RNA was isolated from SNpc for hybridization on Affymetrix microarrays.

Background corr dist: KL-Divergence = 0.0738, L1-Distance = 0.0392, L2-Distance = 0.0021, Normal std = 0.5110

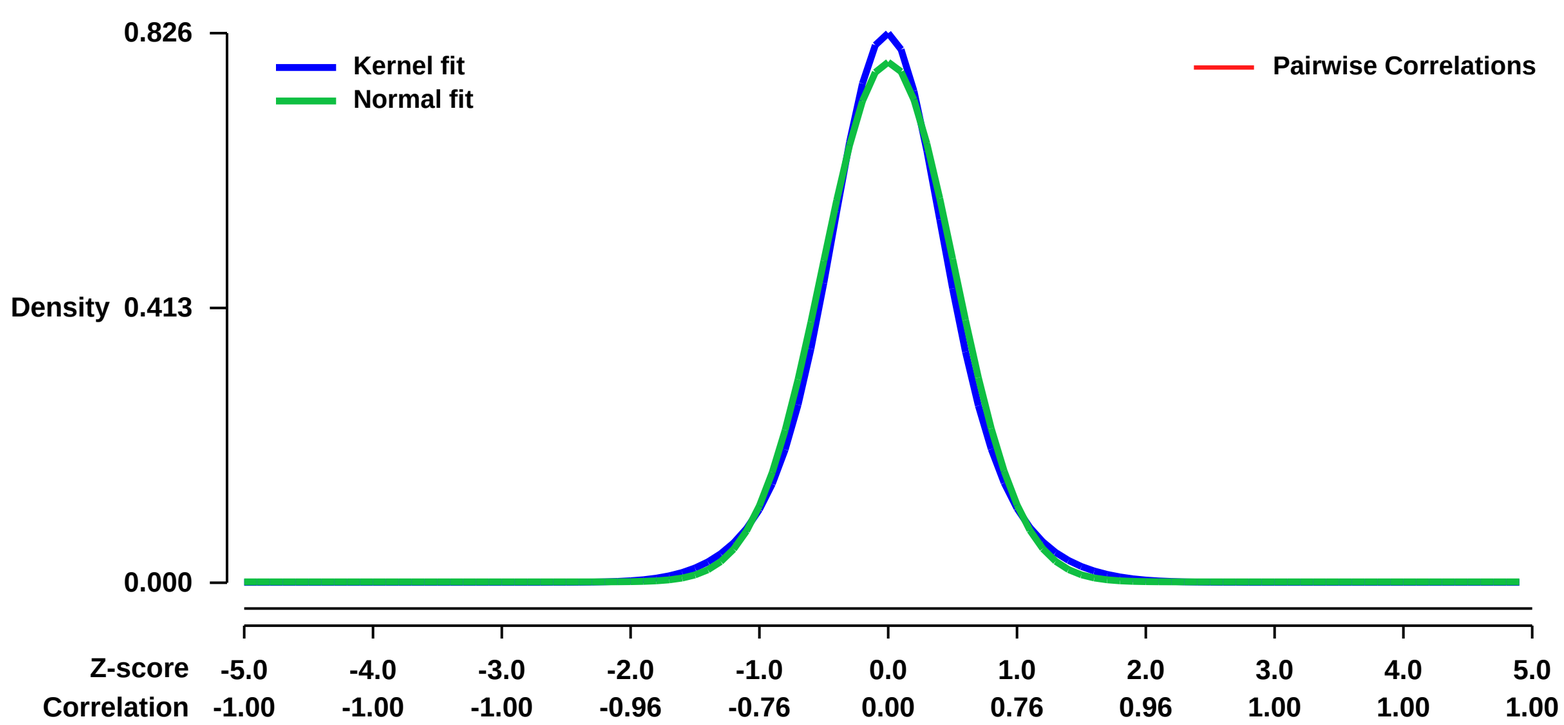

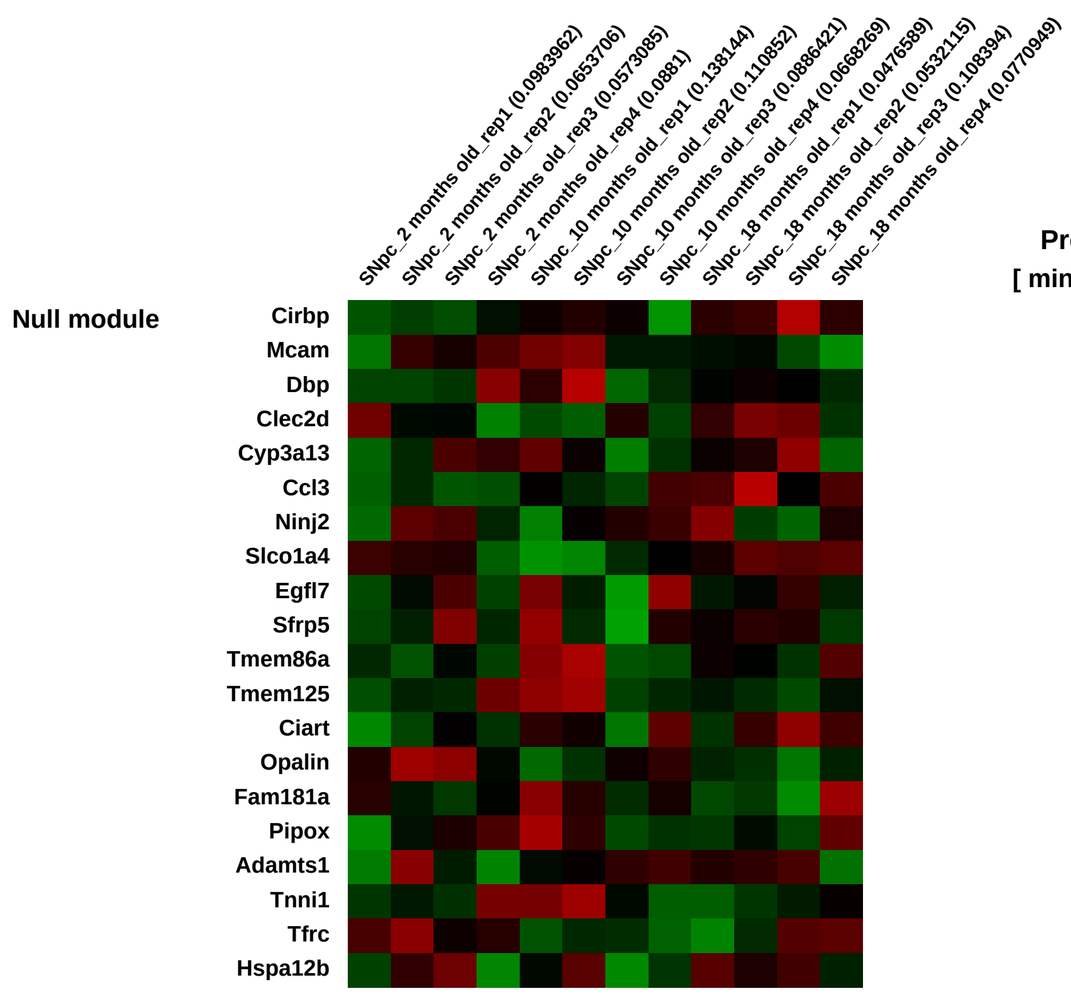

GEO Series "GSE45044" Expression Profiles

Num of samples in this series: 12

Scale of expression profile Z-scores

-3.0 -2.0 -1.0 0.0 1.0 2.0 3.0

GEO Link:	http://www.ncbi.nlm.nih.gov/geo/query/acc.cgi?acc=GSE45044
Status:	Public on May 29 2013
Title:	Age-mediated transcriptomic changes in adult mouse brain ventral tegmental area
Organism:	Mus musculus
Experiment type:	Expression profiling by array
Platform:	GPL1261
Pubmed ID:	23638090
Summary & Design:	**Summary:** Substantia nigra pars compacta (SNpc) is highly sensitive to normal aging and selectively degenerates in Parkinson's disease. However, ventral tegmental area (VTA), a region adjacent to SNpc, is less affected in PD. Until now, molecular mechanisms behind VTA aging have not been fully investigated using high throughput techniques. Here, aging-associated early changes in transcriptome of VTA were investigated comparing late middle-aged (18 months old) to young (2 months old) mice. **Overall design:** Three age groups of C57 wild type mice were used in microarray analysis: young (2 months old), middle aged (10 months old), and late-middle aged (18 months old) mice. Four replicates were included in each age group and each replicate was pooled from 5 mice (5 mice/replicate x 4 replicates x 3 age groups). Total RNA was isolated from VTA for hybridization on Affymetrix microarrays.

Background corr dist: KL-Divergence = 0.0452, L1-Distance = 0.0543, L2-Distance = 0.0056, Normal std = 0.5948

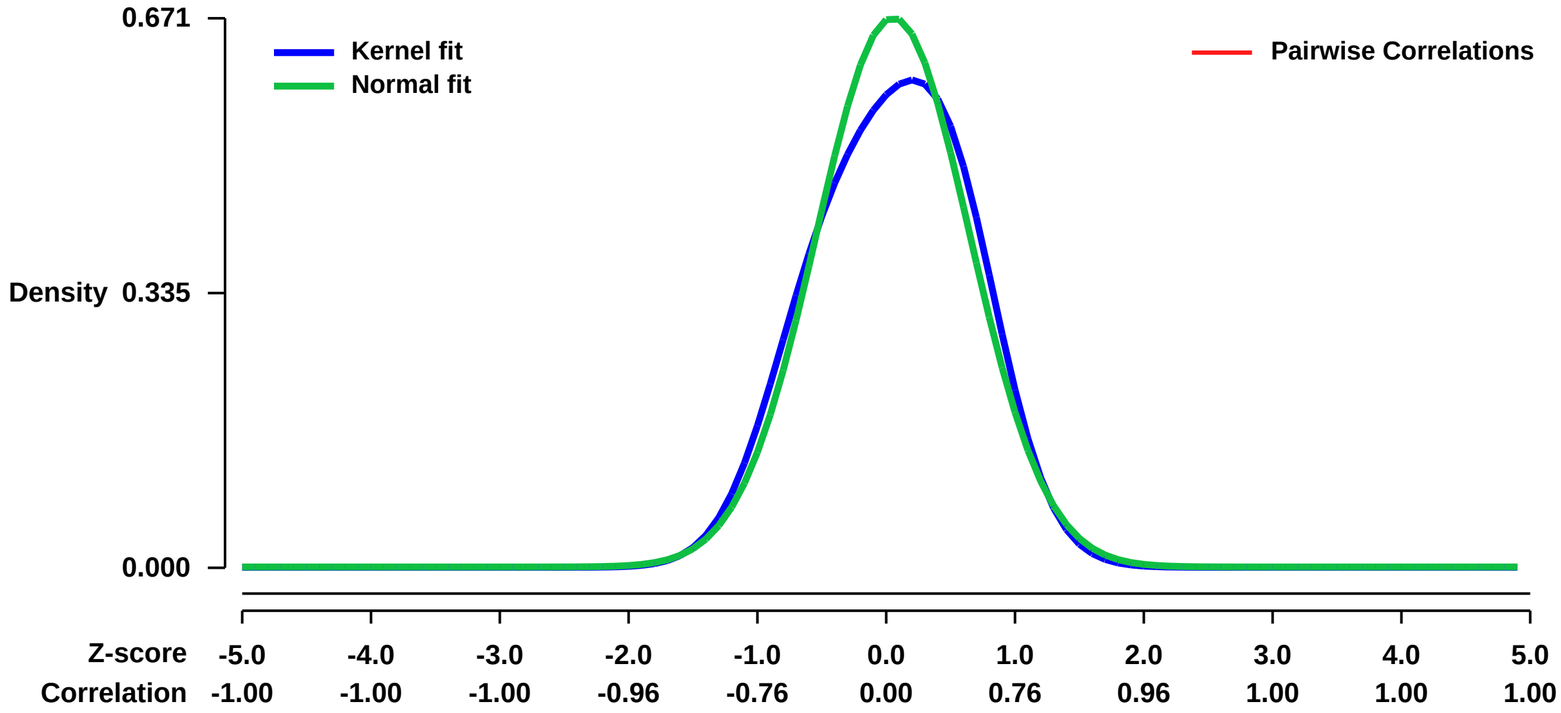

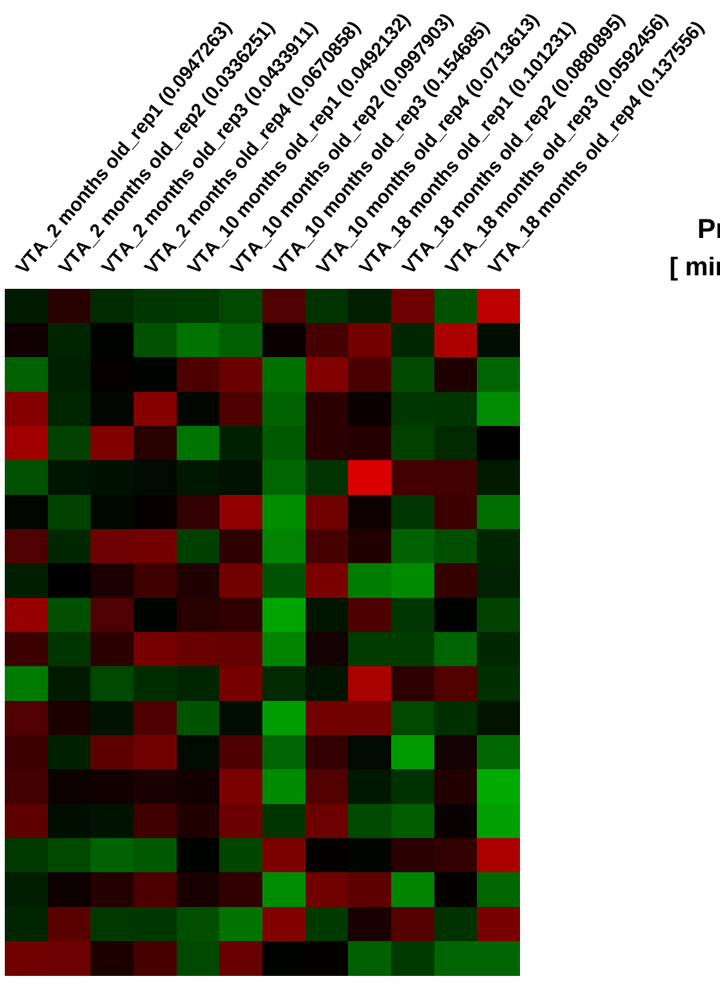

GEO Series "GSE45051" Expression Profiles

Num of samples in this series: 18

Scale of expression profile Z-scores

-3.0 -2.0 -1.0 0.0 1.0 2.0 3.0

GEO Link:	**http://www.ncbi.nlm.nih.gov/geo/query/acc.cgi?acc=GSE45051**
Status:	**Public on Jun 01 2013**
Title:	**Gene expression profile of liver from adult and neonatal Balb/c mice after listeriosis**
Organism:	**Mus musculus**
Experiment type:	**Expression profiling by array**
Platform:	**GPL1261**
Pubmed ID:	
Summary & Design:	**Summary:** **Expression profiling by microarray was used with a murine listeriosis model to better understand increased susceptibility of preterm neonates to infection.** **We used DNA microarray to identify genes that were differentially expressed in liver of adult and neonatal Balb/c mice after listeriosis infection.** **Overall design:** **A murine listeriosis model was established. The methods for culturing and counting the Listeria monocytogenes (strain CNL 85/163) had been described in previous publications. The Listeria was injected intraperitoneally using a 1-mL U-100 insulin syringe with a 30 gauge needle. Doses of Listeria monocytogenes used were based on work by our laboratory showing that similar bacterial colony counts were obtained with 4.2 x 10^5 total Listeria per adult mouse and 150 Listeria per gram for 3 to 5 day old neonatal mice. In neonatal mice, great care was taken to void deep intraperitoneal injection towards the viscera, or across the central abdominal vessels. At specified time points, liver was removed upon animal sacrifice and immediately flash frozen in liquid nitrogen and stored at -80 degrees Centigrade. Three adult mice and three neonatal mice were used at each time point.**

Background corr dist: KL-Divergence = 0.1508, L1-Distance = 0.0278, L2-Distance = 0.0014, Normal std = 0.3783

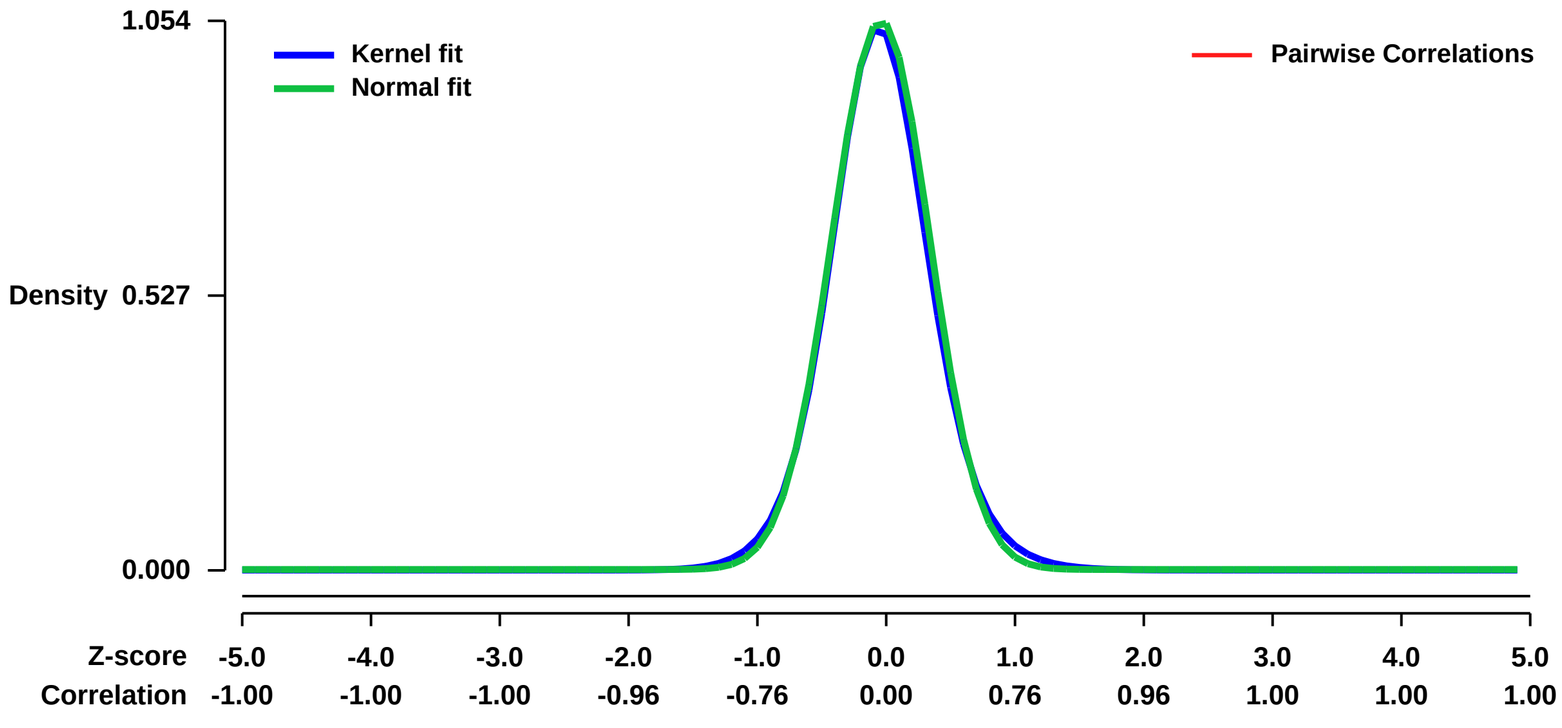

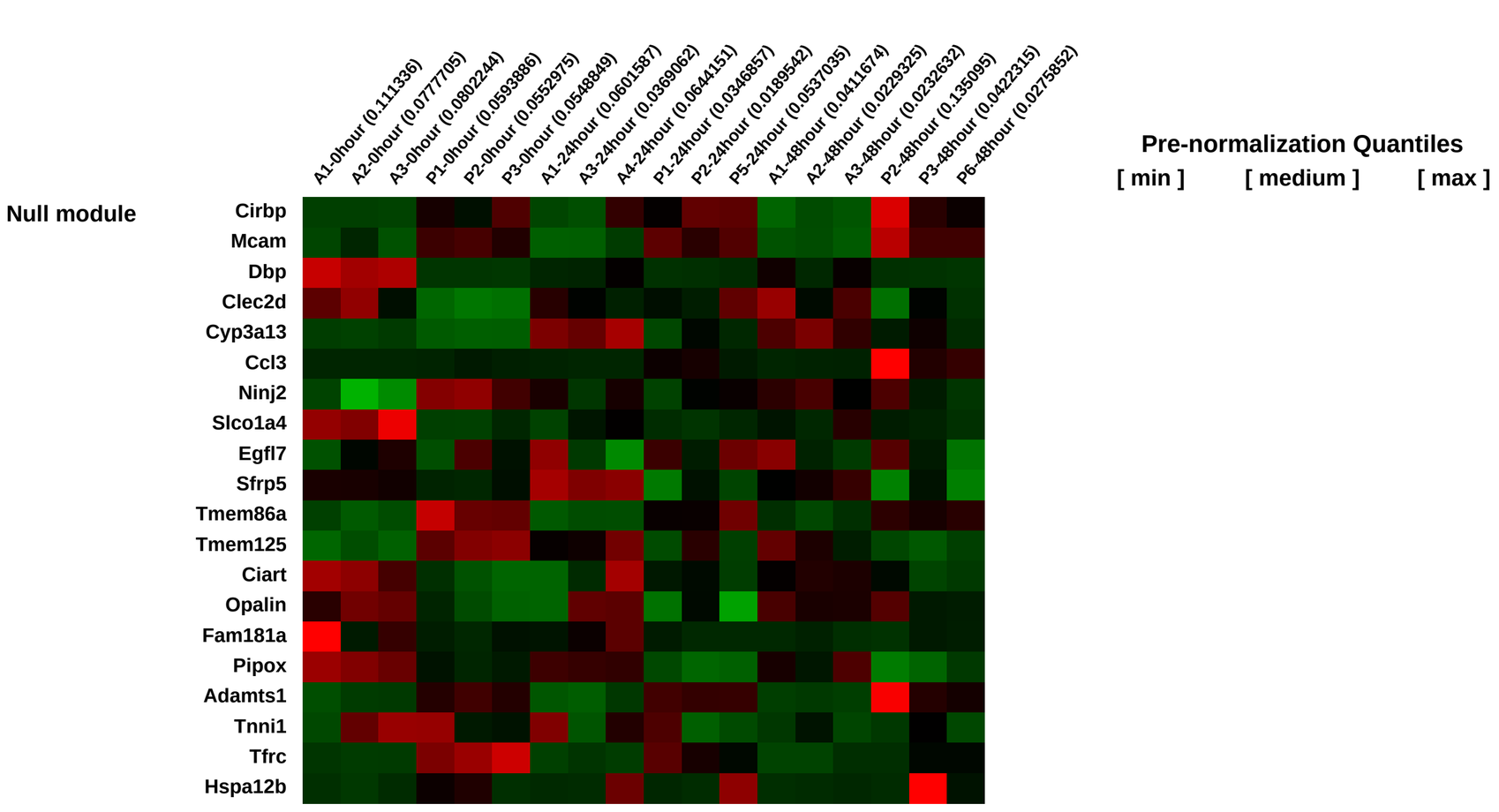

GEO Series "GSE45143" Expression Profiles

Num of samples in this series: 6

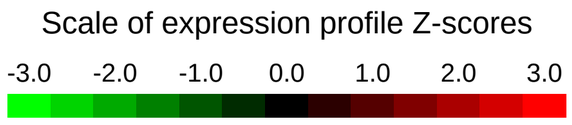

GEO Link:	http://www.ncbi.nlm.nih.gov/geo/query/acc.cgi?acc=GSE45143
Status:	Public on Aug 01 2013
Title:	Pax6 is required for normal cell cycle exit and the differentiation kinetics of retinal progenitor cells.
Organism:	Mus musculus
Experiment type:	Expression profiling by array
Platform:	GPL1261
Pubmed ID:	24073291
Summary & Design:	**Summary:** The coupling between cell-cycle exit and onset of differentiation is a common feature throughout the developing nervous system, but the mechanisms that link these processes are mostly unknown. Although the transcription factor Pax6 was implicated in both proliferation and differentiation of multiple regions within the CNS, its contribution to the transition between these successive states remains elusive. To gain insight into the role of Pax6 during the transition from proliferating progenitors to differentiating precursors, we investigated cell-cycle and transcriptomic changes occurring in Pax6- retinal progenitor cells (RPCs). Our analyses revealed a unique cell-cycle phenotype of the Pax6-deficient RPCs, which included a reduced number of cells in the S phase, an increased number of cells exiting the cell cycle, and delayed differentiation kinetics of Pax6- precursors. These alterations were accompanied by co-expression of factors that promote (Ccnd1, Ccnd2, Ccnd3) and inhibit (P27kip1 and P27kip2) the cell cycle. Further characterization of the changes in transcription profile of the Pax6-deficient RPCs revealed abrogated expression of multiple factors which are known to be involved in regulating proliferation of RPCs, including the transcription factors Vsx2, Nr2e1, Plagl1 and Hedgehog signaling. These findings provide novel insight into the molecular mechanism mediating the pleiotropic activity of Pax6 in RPCs. The results further suggest that rather than conveying a linear effect on RPCs, such as promoting their proliferation and inhibiting their differentiation, Pax6 regulates multiple transcriptional networks which function simultaneously, thereby conferring the capacity to proliferate, assume multiple cell fates and execute the differentiation program into retinal lineages. **Overall design:** The data contains 3 control and 3 Pax6 negative samples representing biological repeats. Each sample was prepared from ~1.8 million cells taken from the distal retina of either E12 alpha-Cre or Pax6 floxed alpha-Cre animals. Distally located retinal progenitors expressing Cre and eGFP were separated using FACS.

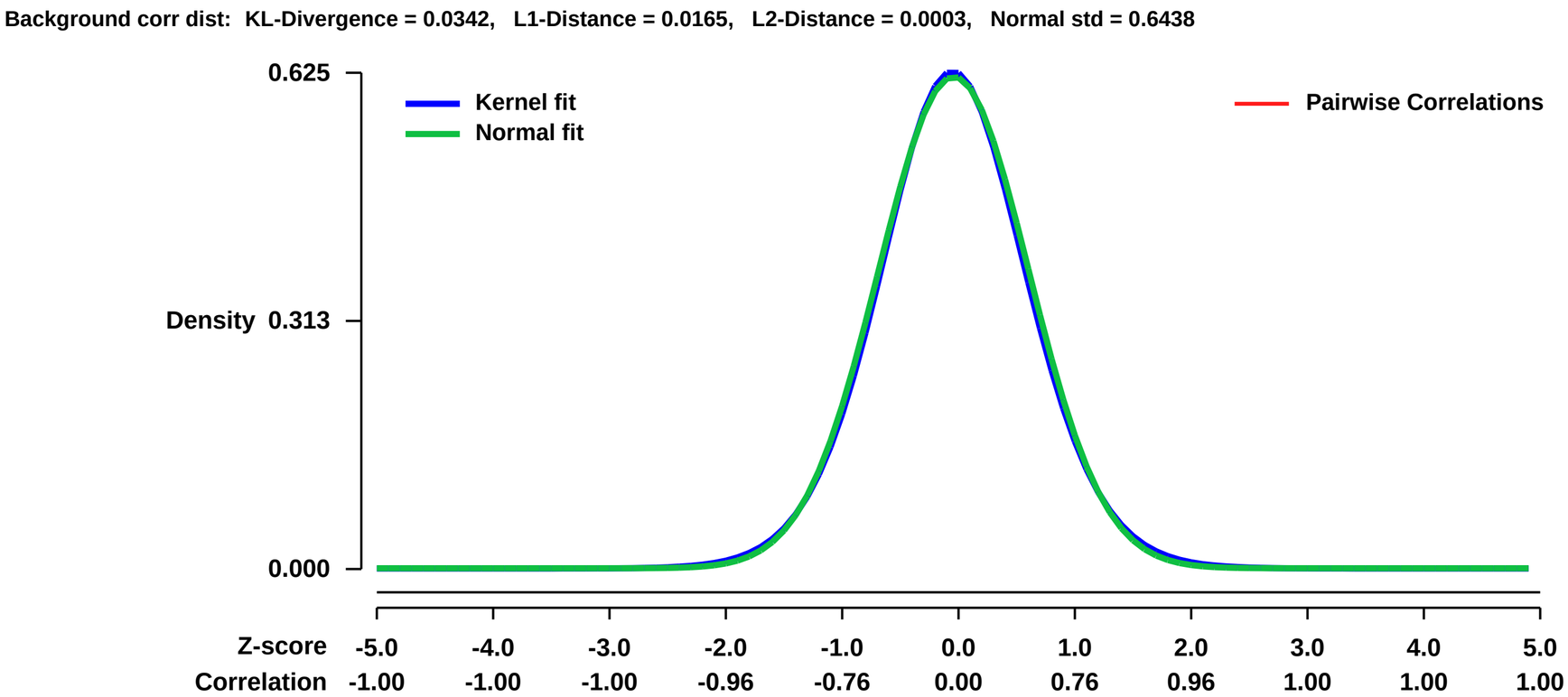

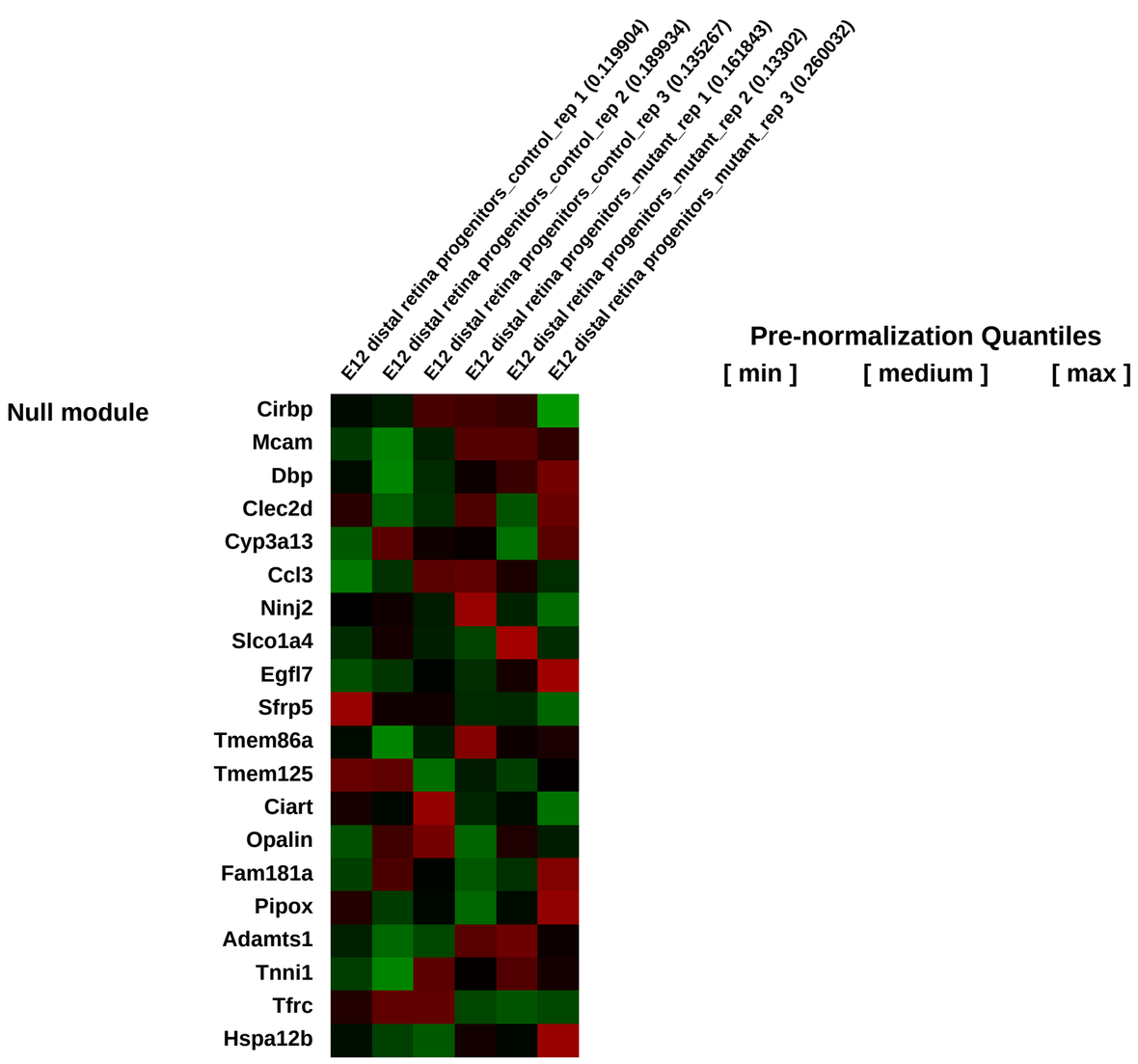

GEO Series "GSE4518" Expression Profiles

Num of samples in this series: 12

Scale of expression profile Z-scores

-3.0 -2.0 -1.0 0.0 1.0 2.0 3.0

GEO Link:	http://www.ncbi.nlm.nih.gov/geo/query/acc.cgi?acc=GSE4518
Status:	Public on Mar 21 2007
Title:	Divergent and Convergent Effects on Gene Expression and Function in Acute versus Chronic Endothelial Activation
Organism:	Mus musculus
Experiment type:	Expression profiling by array
Platform:	GPL1261
Pubmed ID:	17566077
Summary & Design:	**Summary:** Activation of the vascular endothelium with cytokines such as TNF is widely used to study the role of the vasculature in proinflammatory disease. To gain insight into mechanisms of prolonged vascular endothelial activation we compared changes in gene expression induced by continuous activation in stable tmTNFalpha expressing cells with changes due to acute TNFalpha challenge in vitro. Affymetrix Genechip´fi analysis was performed on RNA from control, acute and continuous TNFalpha-activated endothelial cells. Only 36% of the significant changes in gene expression were convergent between the acute and continuously activated endothelial cells in comparison to the control. From the divergently regulated genes, for example the cytokine ENA-78 was specifically induced in chronically activated cells, while E-Selectin, a cell adhesion molecule, was upregulated only in acutely activated endothelial cells. Antioxidant SOD gene induction was noted in acute activation while NADPH oxidase was selectively upregulated in continuous activated endothelium in accordance with significant ROS induction occurred only in these cells. In addition, the anti-angiogenic genes PAI-1 and thrombospondin were upregulated only in acutely activated endothelium, consistent with reduced angiogenic activity observed in acute versus chronically activated endothelial cells in vitro. These data suggest that continuous activation of endothelial cells leads to specific expression and functional changes, consistent with alterations observed in dysfunctional endothelium exposed to or involved in chronic inflammation. **Keywords: Expression profiling** **Overall design:** This experiment compares the response of endothelial cells from newborn mice that were either stably transfected with a non-cleavable transmembrane mutant form of murine TNFalpha, or treated with soluble TNFalpha (20ng/ml) for 4 hours. Each treatment was compared to mock-transfected control cells. Four replicates for each condition were used. Five micrograms of total RNA was assayed per Genechip using standard Affymetrix protocols.

Background corr dist: KL-Divergence = 0.1479, L1-Distance = 0.0409, L2-Distance = 0.0037, Normal std = 0.3783

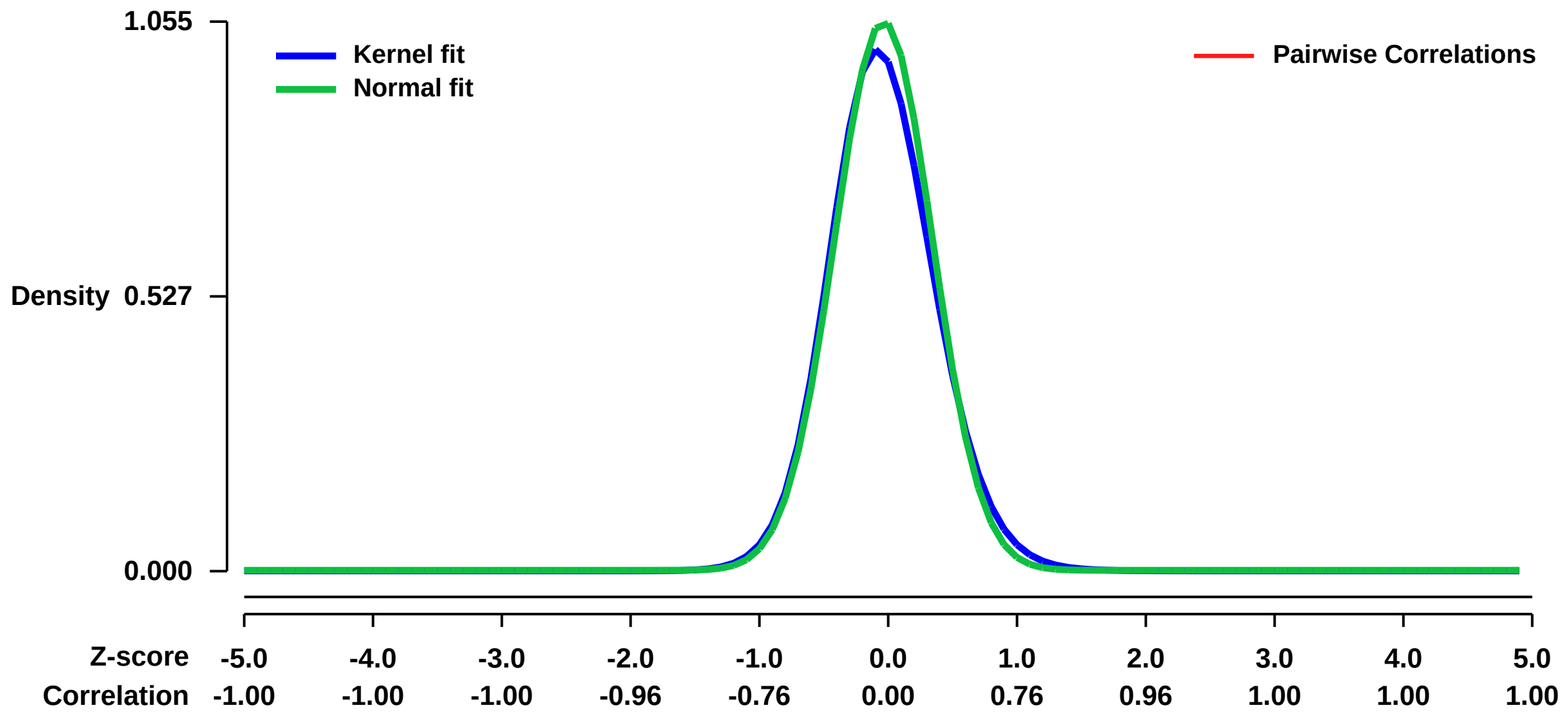

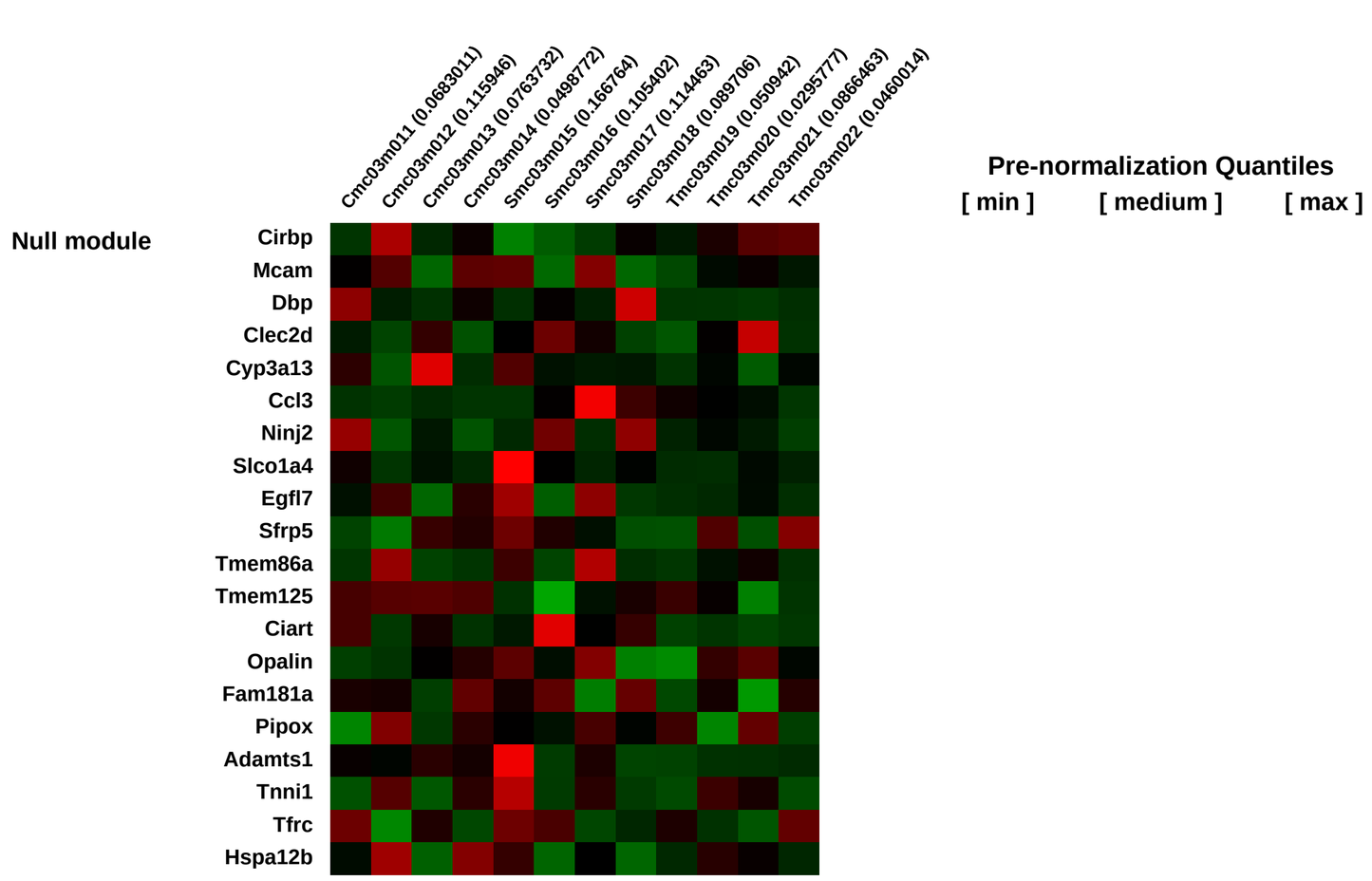

GEO Series "GSE45194" Expression Profiles

Num of samples in this series: 12

Scale of expression profile Z-scores

-3.0 -2.0 -1.0 0.0 1.0 2.0 3.0

GEO Link:	http://www.ncbi.nlm.nih.gov/geo/query/acc.cgi?acc=GSE45194
Status:	Public on Mar 14 2014
Title:	Oncogenic Nras has a bimodal effect on hematopoietic stem cells promoting proliferation and self-renewal
Organism:	Mus musculus
Experiment type:	Expression profiling by array
Platform:	GPL1261
Pubmed ID:	24284627
Summary & Design:	**Summary:** Pre-leukemic mutations are thought to promote clonal expansion of hematopoietic stem cells (HSCs) by increasing self-renewal and competitiveness. However, mutations that increase HSC proliferation tend to reduce competitiveness and self-renewal potential, raising the question of how a mutant HSC can sustainably outcompete wild-type HSCs. Activating mutations in NRAS are prevalent in human myeloproliferative disease and leukemia. Here we show that a single allele of oncogenic NrasG12D increases HSC proliferation but also increases reconstituting and self-renewal potential upon serial transplantation in irradiated mice, all without immortalizing HSCs or causing leukemia in our experiments. NrasG12D also confers long-term self-renewal potential upon multipotent progenitors. To explore the mechanism by which NrasG12D promotes HSC proliferation and self-renewal we assessed HSC cell cycle kinetics using H2B-GFP label retention. We found that NrasG12D had a bimodal effect on HSCs, increasing the proliferation of some HSCs while increasing the quiescence and competitiveness of other HSCs. One signal can therefore increase HSC proliferation, competitiveness, and self-renewal through a bimodal effect that promotes proliferation in some HSCs and quiescence in others. **Overall design:** 12 RNA samples from mouse bone marrows were analyzed. There are three biological replicates for each subtype.

Background corr dist: KL-Divergence = 0.1688, L1-Distance = 0.0830, L2-Distance = 0.0164, Normal std = 0.4092

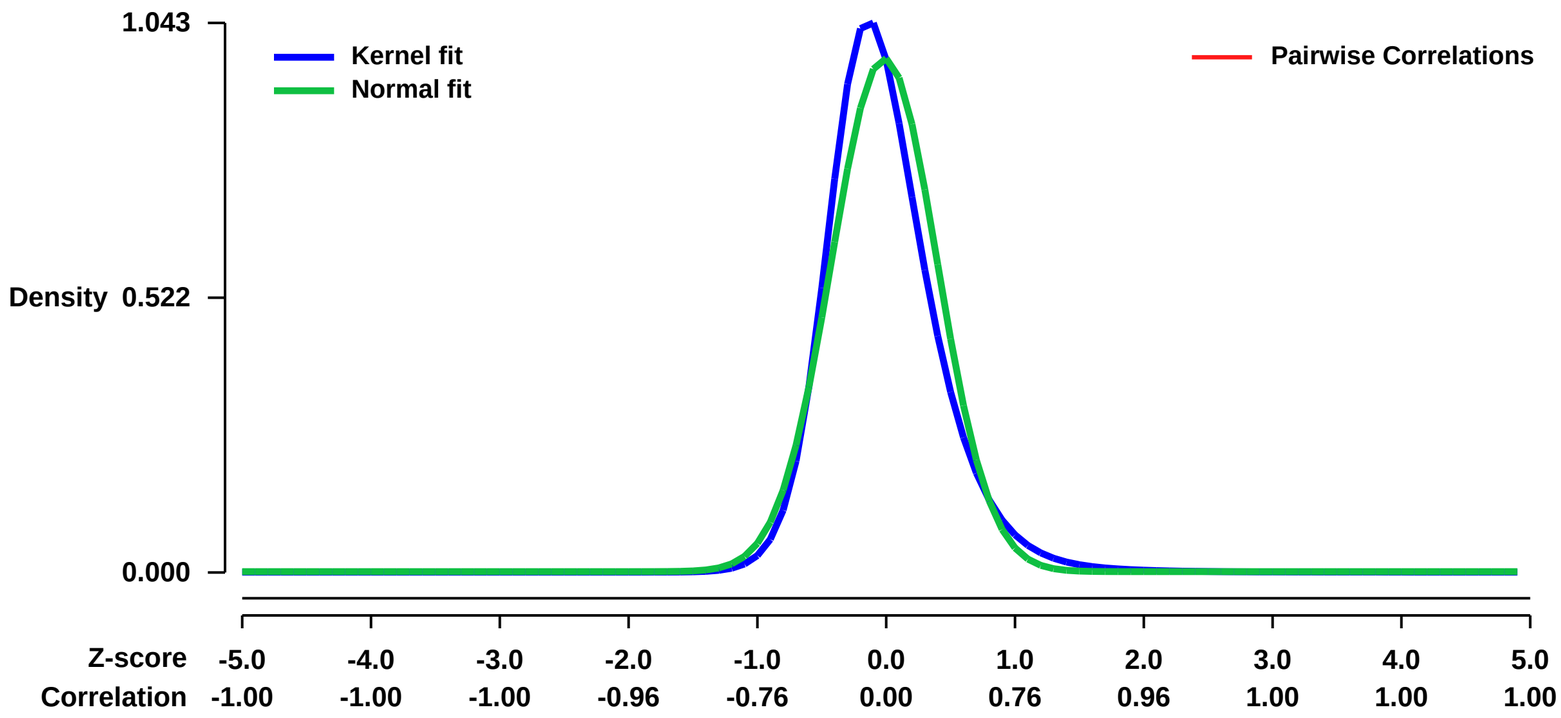

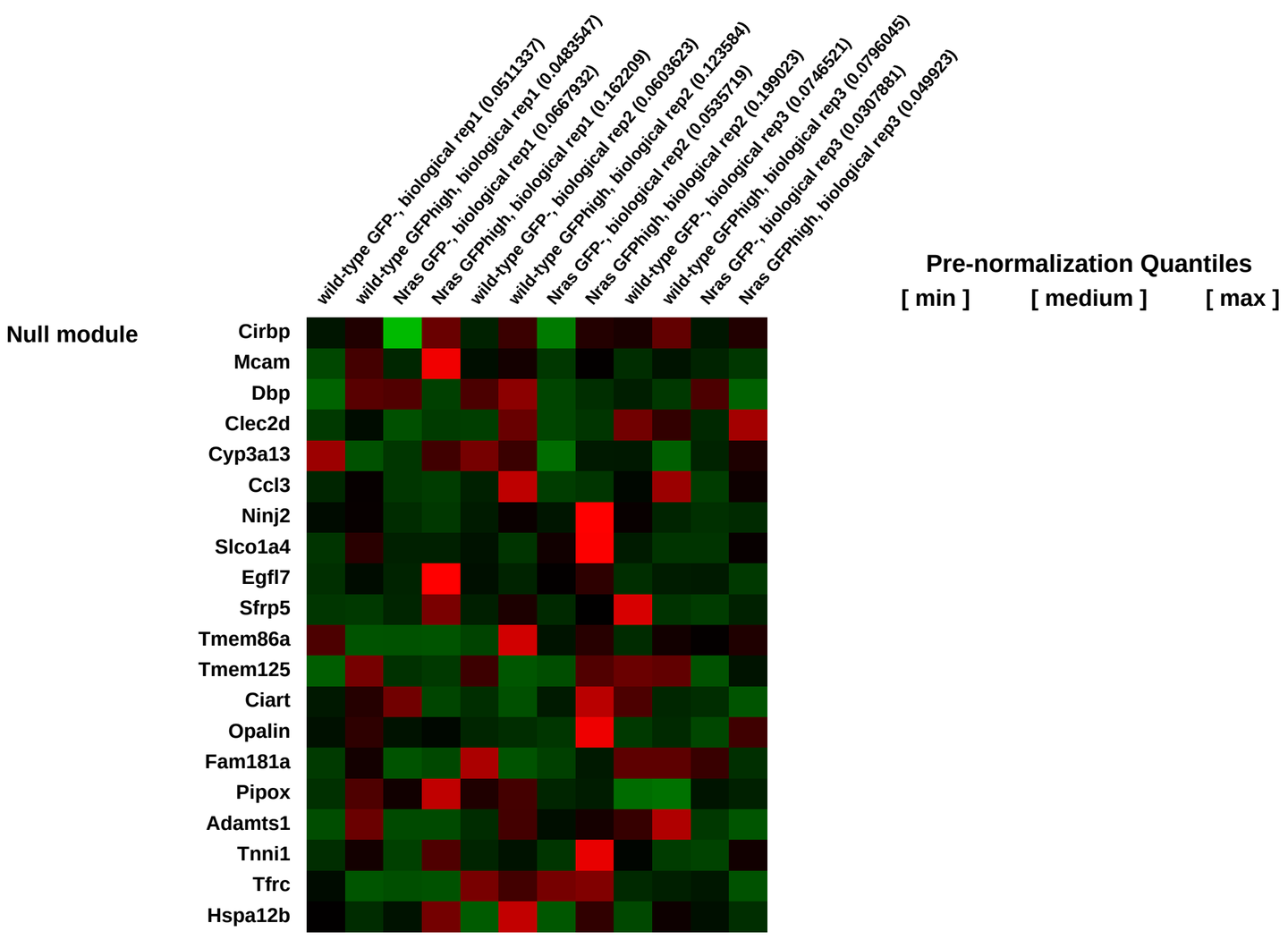

GEO Series "GSE45229" Expression Profiles

Num of samples in this series: 20

Scale of expression profile Z-scores

-3.0 -2.0 -1.0 0.0 1.0 2.0 3.0

GEO Link:	http://www.ncbi.nlm.nih.gov/geo/query/acc.cgi?acc=GSE45229
Status:	Public on Apr 16 2013
Title:	Unique pharmacological actions of atypical neuroleptic quetiapine: possible role in cell cycle/fate control
Organism:	Mus musculus
Experiment type:	Expression profiling by array
Platform:	GPL1261
Pubmed ID:	23549417
Summary & Design:	**Summary:** Quetiapine is an atypical neuroleptic with a pharmacological profile distinct from classic neuroleptics. It is currently approved for treating patients with schizophrenia, major depression and bipolar I disorder. However, its cellular effects remain elusive. We used microarrays to characterize RNA transcript levels in the brains of mice chronically treated with quetiapine, the neuroleptic haloperidol, or vehicle. We further characterized particular RNA transcripts in cortical cell cultures. **Overall design:** Mice were given one of 5 treatments (vehicle, 1 mg/kg haloperidol, 0.3 mg/kg haloperidol, 100 mg/kg quetiapine, 10 mg/kg quetiapine). Pooled tissue samples were used for microarray analysis of gene expression in the frontal cortex (FC) and striatum (STR). Frontal cortex gene targets were subsequently verified with quantitative real-time PCR (qRT-PCR) from the same cohort of mice and an independent cohort.

Background corr dist: KL-Divergence = 0.1111, L1-Distance = 0.0722, L2-Distance = 0.0098, Normal std = 0.4609

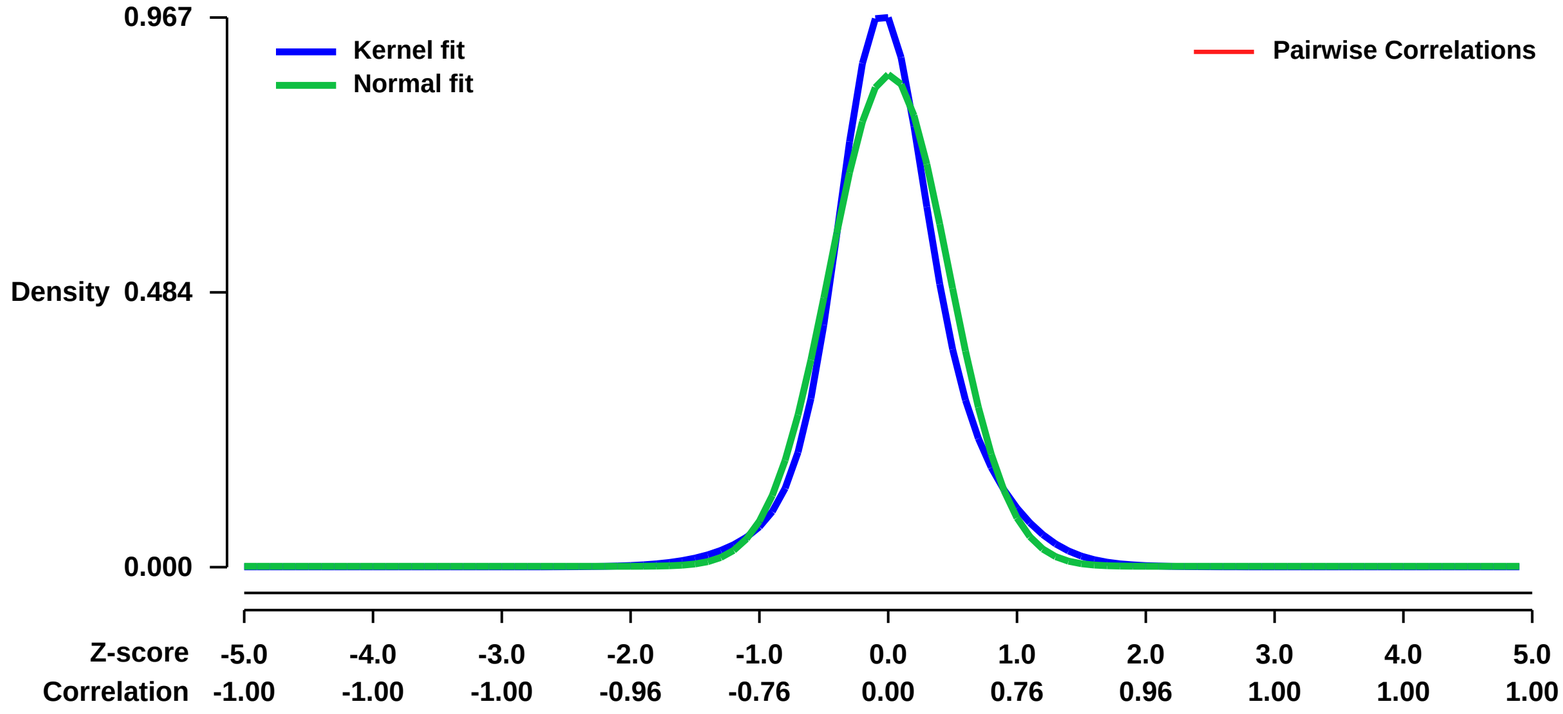

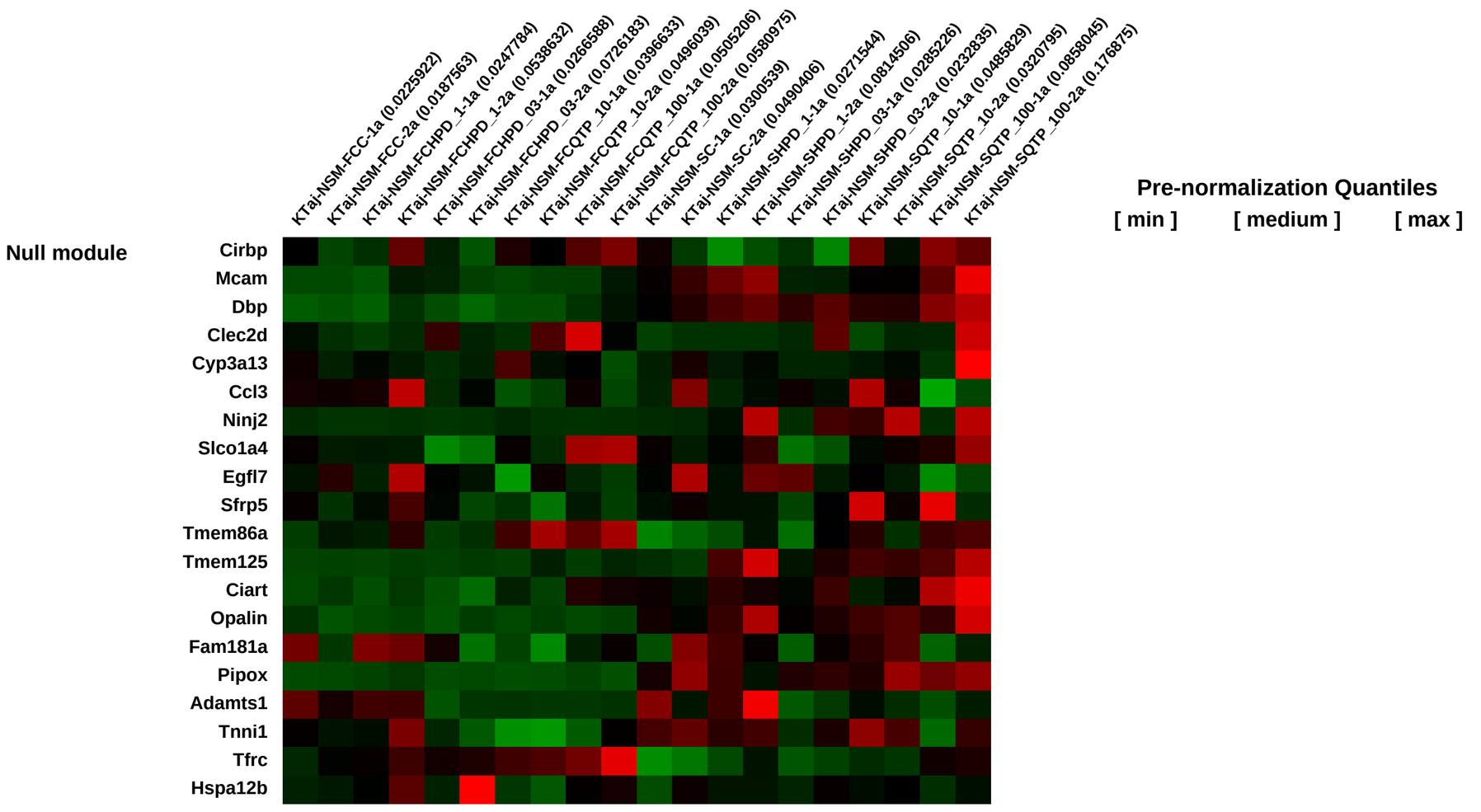

GEO Series "GSE4523" Expression Profiles

Num of samples in this series: 6

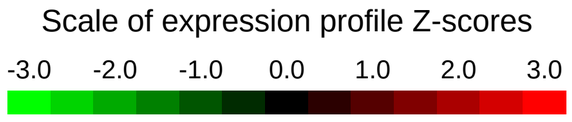

GEO Link:	http://www.ncbi.nlm.nih.gov/geo/query/acc.cgi?acc=GSE4523
Status:	Public on Mar 29 2006
Title:	Expression Studies of Melanotransferrin in Mouse Brain
Organism:	Mus musculus
Experiment type:	Expression profiling by array
Platform:	GPL1261
Pubmed ID:	17449903
Summary & Design:	**Summary:** Melanotransferrin (MTf) or melanoma tumor antigen p97 is an iron (Fe)-binding transferrin homolog expressed highly on melanomas and at lower levels on normal tissues. It has been suggested that MTf is involved in a variety of processes such as Fe metabolism and cellular differentiation. Considering the crucial role of Fe in many metabolic pathways e.g., DNA synthesis, it is important to understand the function of MTf. To define the roles of MTf, a MTf knockout (MTf -/-) mouse model was developed. Examination of the MTf -/- mice demonstrated no phenotypic differences compared to wild-type littermates. However, microarray analysis showed differential expression of molecules involved in proliferation such as Mef2a, Tcf4, Gls and Apod in MTf -/- mice compared to MTf +/+ littermates, suggesting a role for MTf in proliferation and tumorigenesis. **Keywords:** Melanotransferrin, knockout mouse, comparative genomic hybridization **Overall design:** Six 17.5 week old female mice comprising four MTf -/- and two MTf +/+ from the same litter were used. Total RNA was isolated from brain tissue and processed as per standard Affymetrix protocol to obtain final cRNA products that were hybridized to the mouse GeneChip´fi 430 2.0. The mouse GeneChip´fi 430 2.0 consists of greater than 39,000 transcripts and variants from over 34,000 well characterized mouse genes. On completion of hybridization and washing, microarray chips were scanned with the Affymetrix GeneChip´fi Scanner 3000 (Millenium Sciences).

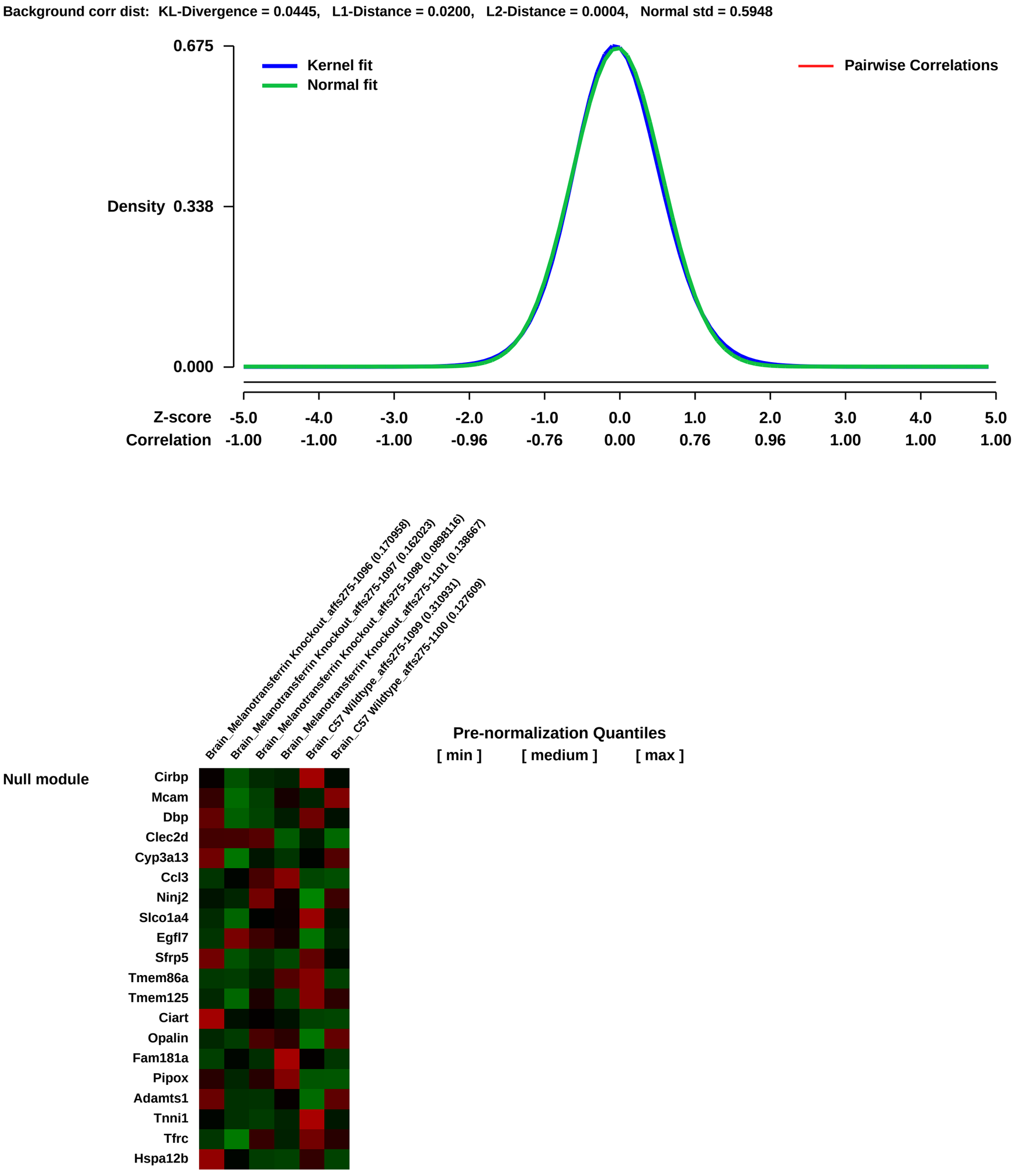

GEO Series "GSE45369" Expression Profiles

Num of samples in this series: 14

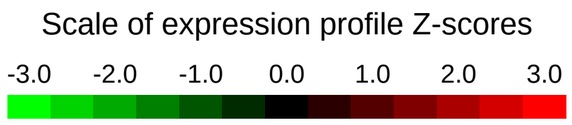

GEO Link: http://www.ncbi.nlm.nih.gov/geo/query/acc.cgi?acc=GSE45369

Status: Public on Mar 22 2013

Title: Mouse lung transcriptional response to flagellin stimulation

Organism: Mus musculus

Experiment type: Expression profiling by array

Platform: GPL1261

Pubmed ID:

Summary & Design:

Summary:
Vaccine adjuvants enhance adaptive immunity to co-administered antigens. Whereas the modes of action are multiple, the activation of antigen-presenting cells (APC) like dendritic cells by adjuvants is a prerequisite. Detection of microbial signals by innate sensors like Toll-like receptors (TLR) is a major mechanism of APC activation. Most candidate or licensed vaccines assume that adjuvant activity of TLR agonists depends on direct effect on APCs. This study addressed whether TLR stimulation of non-hematopoietic cells could contribute to the adjuvant effect. Nasal administration of flagellin enhanced T´ cell- and antibody-mediated immunity to co-administered antigens in a TLR5-dependent but inflammasome-independent manner. We found that lung radioresistant cells were sufficient to promote immunity, thereby suggesting that direct TLR5-mediated APC stimulation is dispensable to adjuvant activity. Consistent with this, radioresistant compartment is essential to stimulate the swift TLR5-dependent transcription. The transcriptional response was restricted to the epithelial compartment and was associated to the production of a narrow set of mediators including the chemokine CCL20, known to promote APC recruitment in mucosal tissues. Besides, flagellin was rapidly degraded in lower airways and was not transported into lung parenchyma or peripheral tissues. This study therefore suggests an unexpected mechanism for how TLR agonists act as adjuvant and how epithelium is instrumental to sense and integrate microbial signals to promote adaptive immunity. In conclusion, the immune-enhancing effect of adjuvants on epithelial cells can be harnessed for improving vaccines.

Overall design:
1 ´µg of flagellin was instillated intranasally to LPS-unresponsive C3H/HeJ mice. Total lung RNA was extracted 1h later and prepare for hybridization on Affymetrix microarrays.

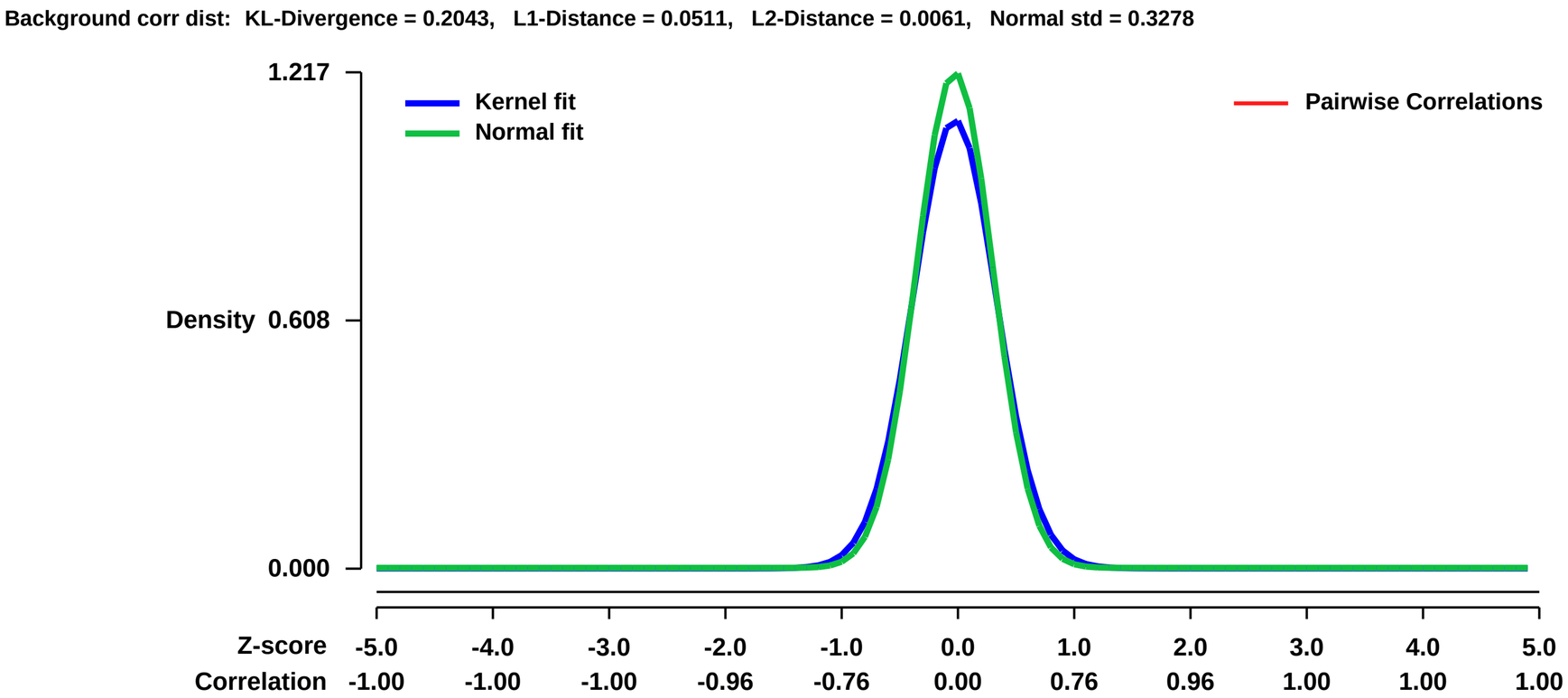

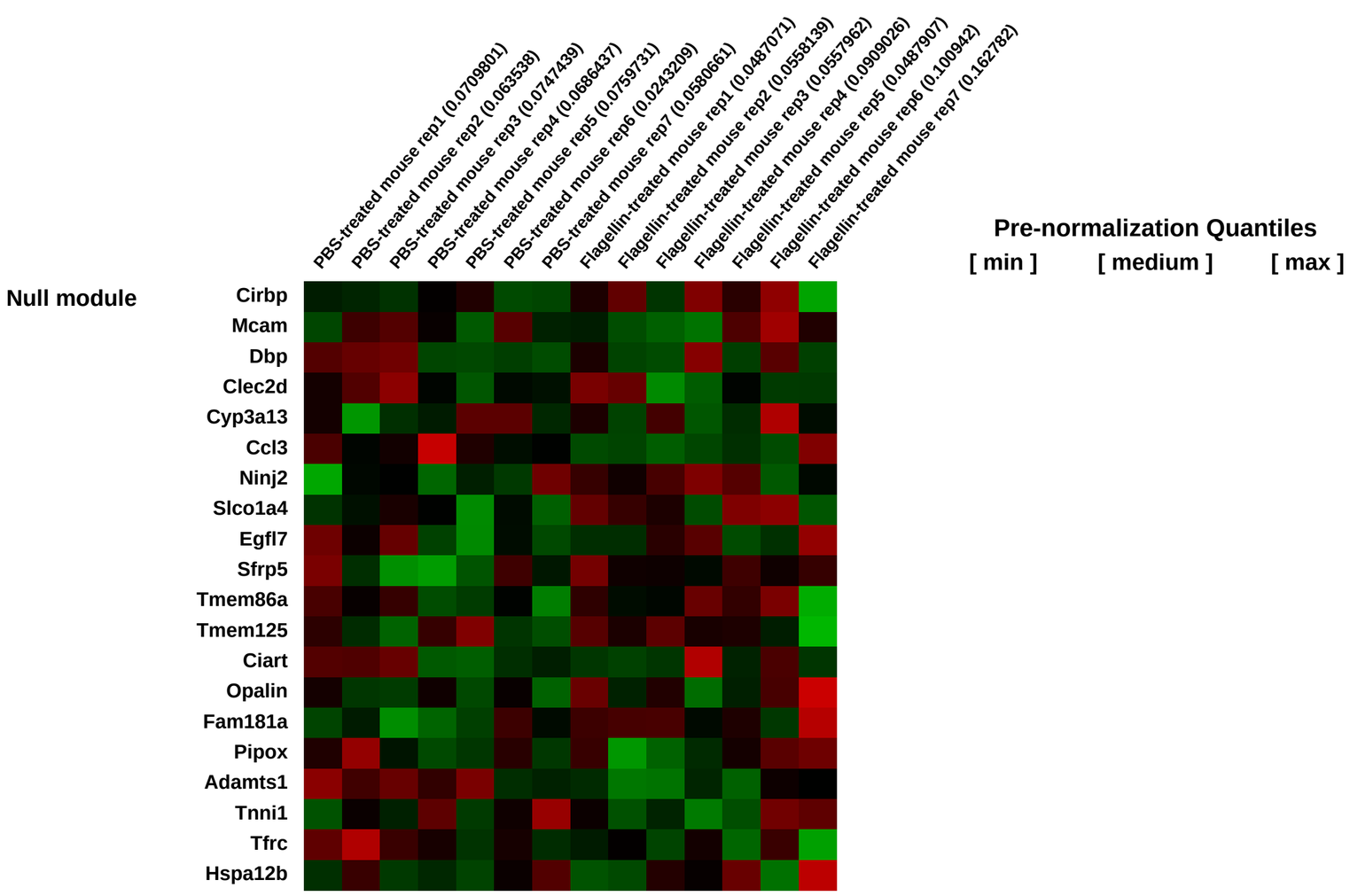

GEO Series "GSE45430" Expression Profiles

Num of samples in this series: 9

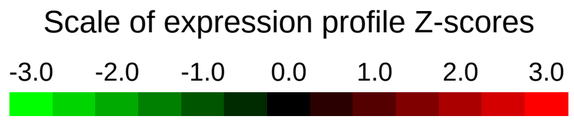

GEO Link:	http://www.ncbi.nlm.nih.gov/geo/query/acc.cgi?acc=GSE45430
Status:	Public on Mar 23 2013
Title:	Sox4 is a key oncogenic target in C/EBP‚Äì mutant Acute Myeloid Leukemia
Organism:	Mus musculus
Experiment type:	Expression profiling by array
Platform:	GPL1261
Pubmed ID:	24183681
Summary & Design:	**Summary:** Mutation or epigenetic silencing of the transcription factor C/EBP‚Äì is observed in ~10% of patients with acute myeloid leukemia (AML). In both cases, a common global gene expression profile is observed, but down-stream targets relevant for leukemogenesis are not known. Here we identify Sox4 as a direct target of C/EBP‚Äì whereby its expression is inversely correlated with C/EBP‚Äì activity. Downregulation of Sox4 abrogated increased self-renewal of leukemic cells and restored their differentiation. Gene expression profiles of leukemia initiating cells (LICs) from both Sox4 overexpression and murine mutant C/EBP‚Äì AML models clustered together, but differed from other types of AML. Our data demonstrate that Sox4 overexpression resulting from C/EBP‚Äì inactivation contributes to the development of leukemias with a distinct LIC phenotype. **Overall design:** K/L (bi-allelic Cebpa mutations) leukemic mice and Sox4 overexprssing leukemic mice were used for RNA extraction and hybridization on Affymetrix microarrays. We compared these microarray samples with the C57/BL6 wild type mice.

Background corr dist: KL-Divergence = 0.0498, L1-Distance = 0.0448, L2-Distance = 0.0033, Normal std = 0.5848

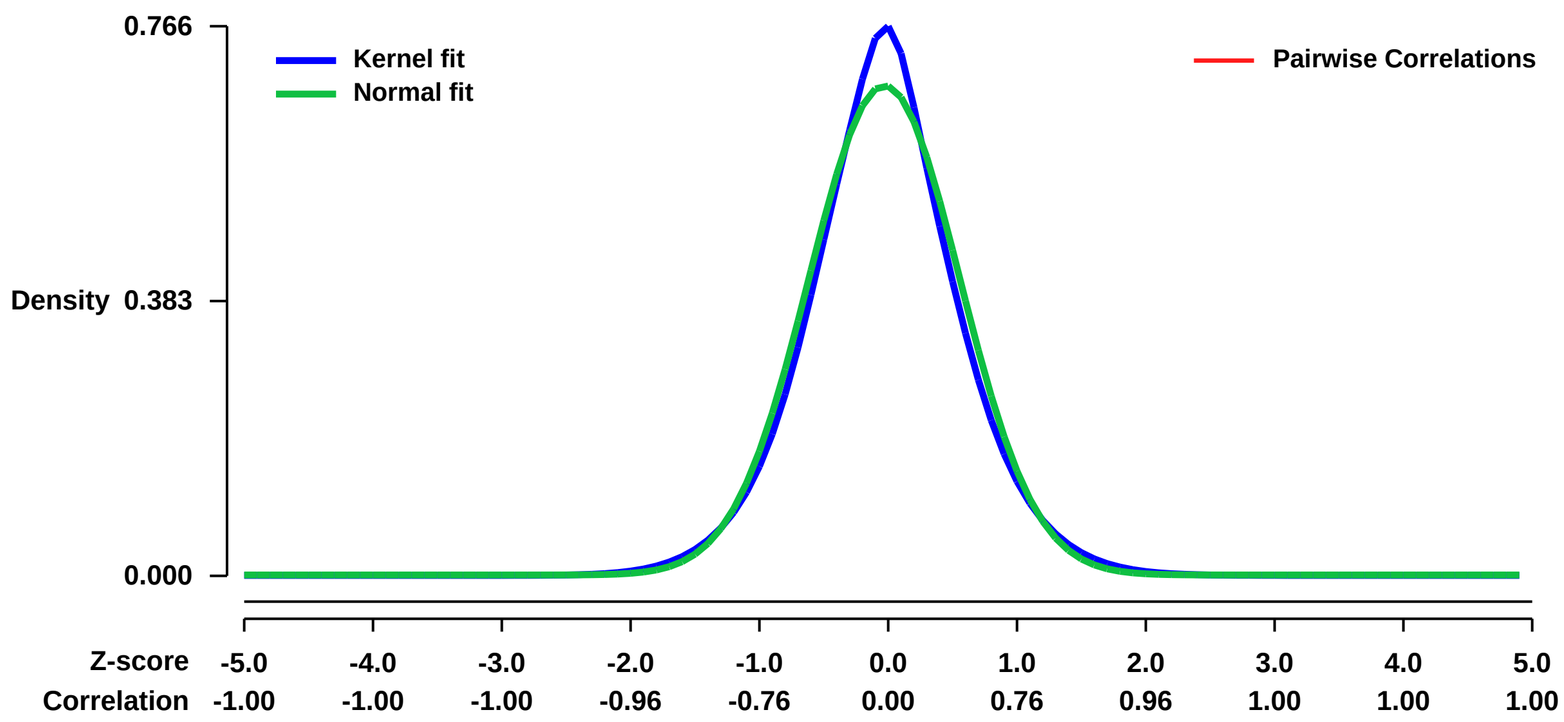

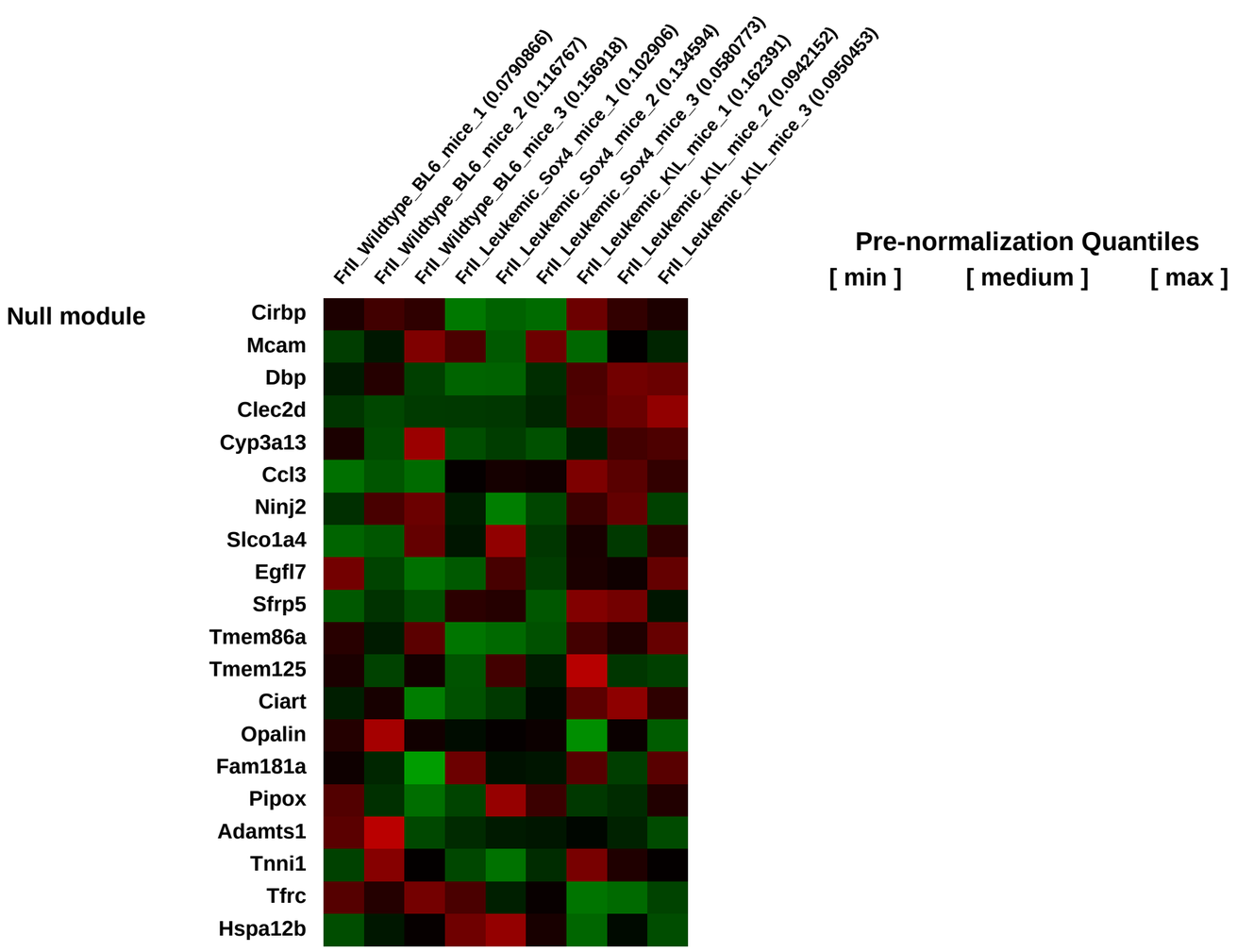

GEO Series "GSE45465" Expression Profiles

Num of samples in this series: 39

Scale of expression profile Z-scores

-3.0 -2.0 -1.0 0.0 1.0 2.0 3.0

GEO Link:	http://www.ncbi.nlm.nih.gov/geo/query/acc.cgi?acc=GSE45465
Status:	Public on Mar 25 2013
Title:	Dynamic changes in liver 5-hydroxymethylcytosine profiles upon non-genotoxic carcinogen exposure [Replicated control vs. pb treated study]
Organism:	Mus musculus
Experiment type:	Expression profiling by array
Platform:	GPL1261
Pubmed ID:	23598998
Summary & Design:	**Summary:** Dynamic changes in the mouse liver DNA methylome associated with short (1 day) and prolonged (7, 28 and 91 days) exposure to the rodent liver non-genotoxic carcinogen (NGC), phenobarbital (PB). **Overall design:** Replicated control vs. pb treated study

Background corr dist: KL-Divergence = 0.2219, L1-Distance = 0.0499, L2-Distance = 0.0058, Normal std = 0.3176

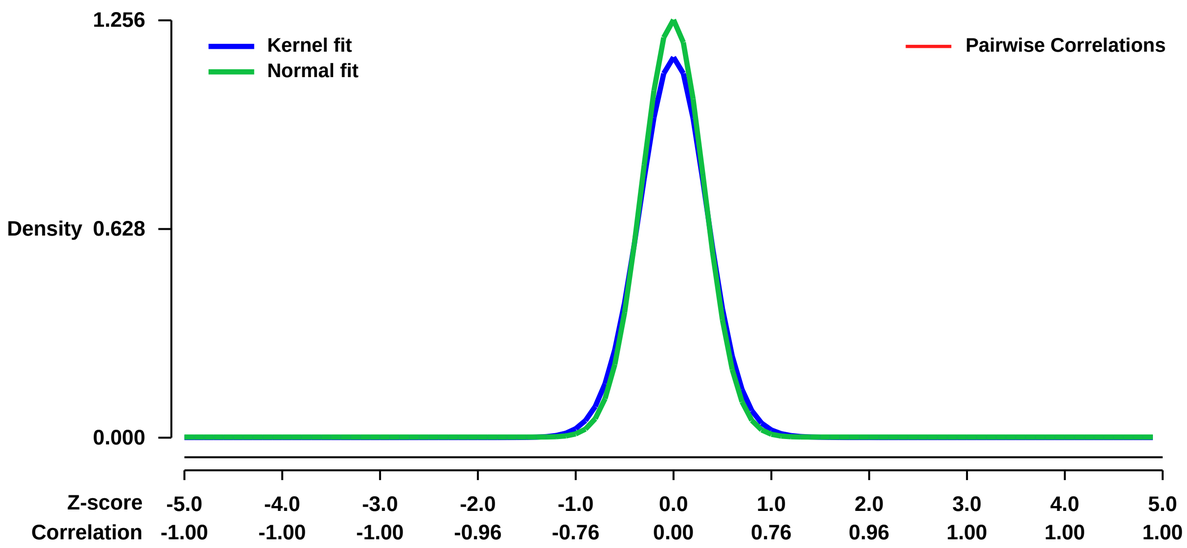

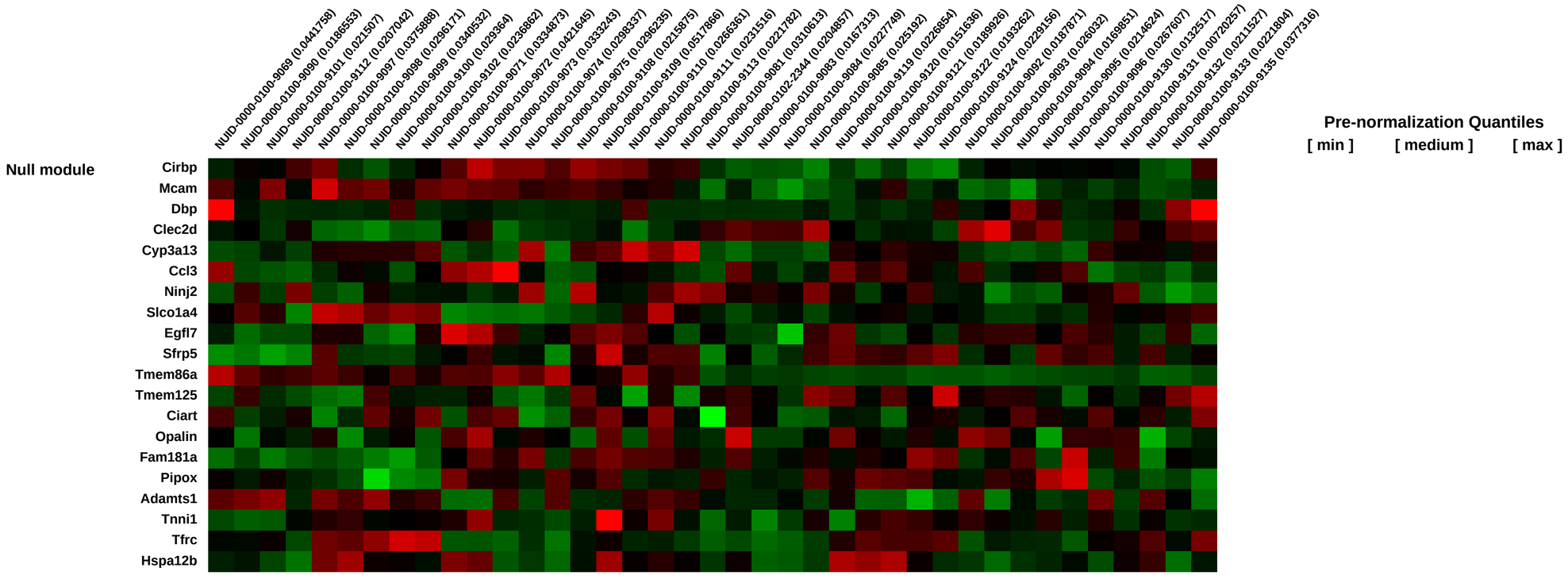

GEO Series "GSE45487" Expression Profiles

Num of samples in this series: 9

Scale of expression profile Z-scores

-3.0 -2.0 -1.0 0.0 1.0 2.0 3.0

GEO Link:	http://www.ncbi.nlm.nih.gov/geo/query/acc.cgi?acc=GSE45487
Status:	Public on Mar 26 2013
Title:	Identification of genes responsive to low-intensity pulsed ultrasound (LIPUS) in MC3T3-E1 preosteoblast cells
Organism:	Mus musculus
Experiment type:	Expression profiling by array
Platform:	GPL1261
Pubmed ID:	24252911
Summary & Design:	**Summary:** Although LIPUS has been shown to enhance fracture healing, the underlying mechanism of LIPUS remains to be fully elucidated. Here, to understand the molecular mechanism underlying cellular responses to LIPUS, we investigated gene expression profiles in mouse MC3T3-E1 preosteoblast cells using a GeneChip´fi system. **Overall design:** The mouse preosteoblast MC3T3-E1cells were treated with LIPUS (30 mW/cm2) for 20 min followed by culturing for 6 and 24 h at 37C. Mock-treated cells were served as control. Total RNA samples were prepared from the cells, and quality of the RNA was analyzed using a Bioanalyzer 2100. Gene expression was monitored by an Affymetrix GeneChip system with a Mouse Genome 430 2.0 array. Sample preparation for array hybridization was carried out as described in the manufacturer's instructions.

Background corr dist: KL-Divergence = 0.0154, L1-Distance = 0.0176, L2-Distance = 0.0004, Normal std = 0.7802

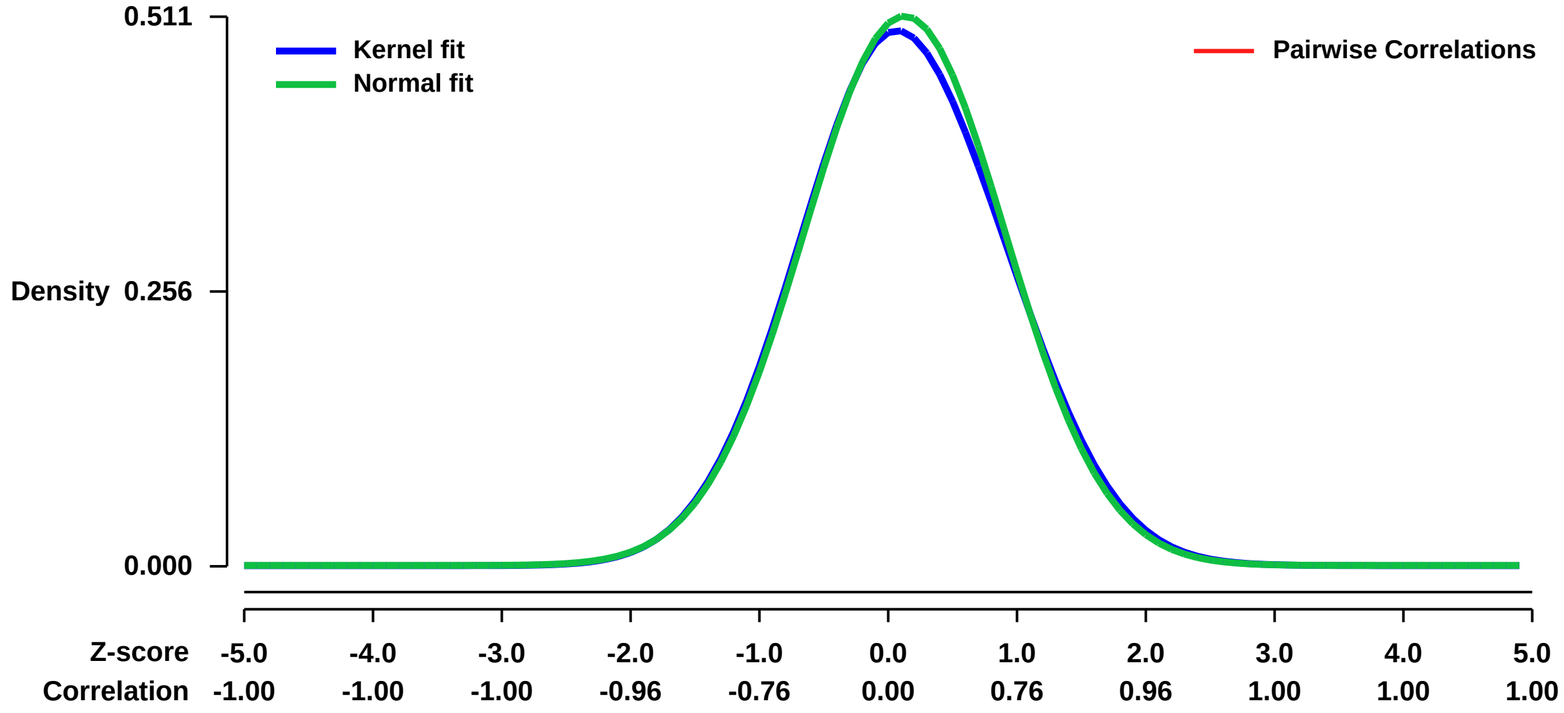

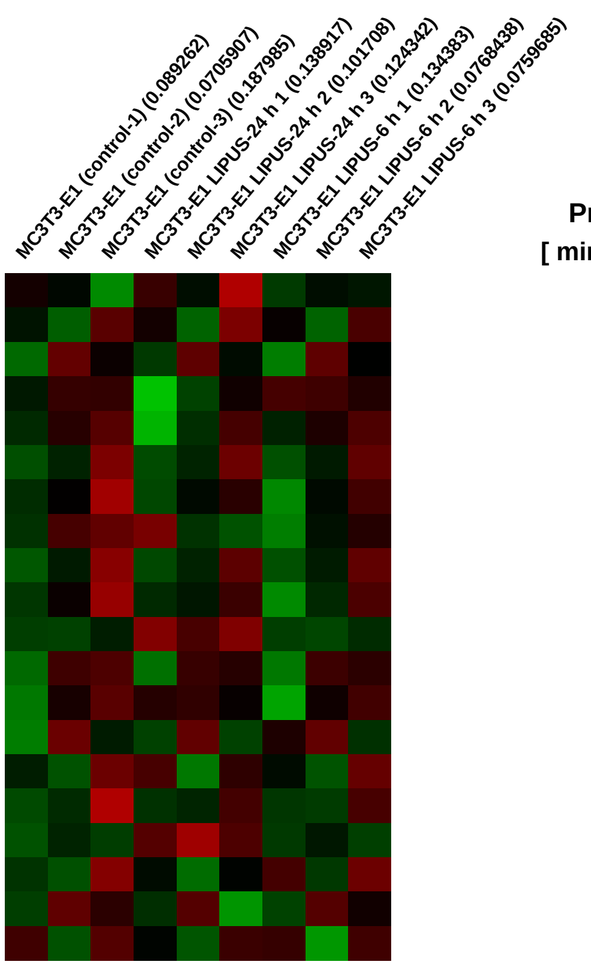

GEO Series "GSE45583" Expression Profiles

Num of samples in this series: 8

Scale of expression profile Z-scores

-3.0 -2.0 -1.0 0.0 1.0 2.0 3.0

GEO Link:	**http://www.ncbi.nlm.nih.gov/geo/query/acc.cgi?acc=GSE45583**
Status:	**Public on Mar 29 2013**
Title:	**A hypomorphic Lsd1 allele results in heart development defects in mice.**
Organism:	**Mus musculus**
Experiment type:	**Expression profiling by array**
Platform:	**GPL1261**
Pubmed ID:	
Summary & Design:	**Summary:** **Microarray characterization of Lsd1 knock-outs compared to littermate controls** **Microarrays were employed to identify transcripts that were differentially modulated in the hearts of wild-type and Lsd1-hypomorphic late-stage embryos.** **Overall design:** **Late-stage embryonic hearts were isolated from wild-type and Lsd1-hypomorphic hearts, in order to isolate RNA for hybridization on Affymetrix microarrays. We sought to identify gene products that are differentially regulated between the two genotypes, in order to explain the observed ventricular septal defects in the hypomorphic animals.**

Background corr dist: **KL-Divergence = 0.0787, L1-Distance = 0.0212, L2-Distance = 0.0005, Normal std = 0.4781**

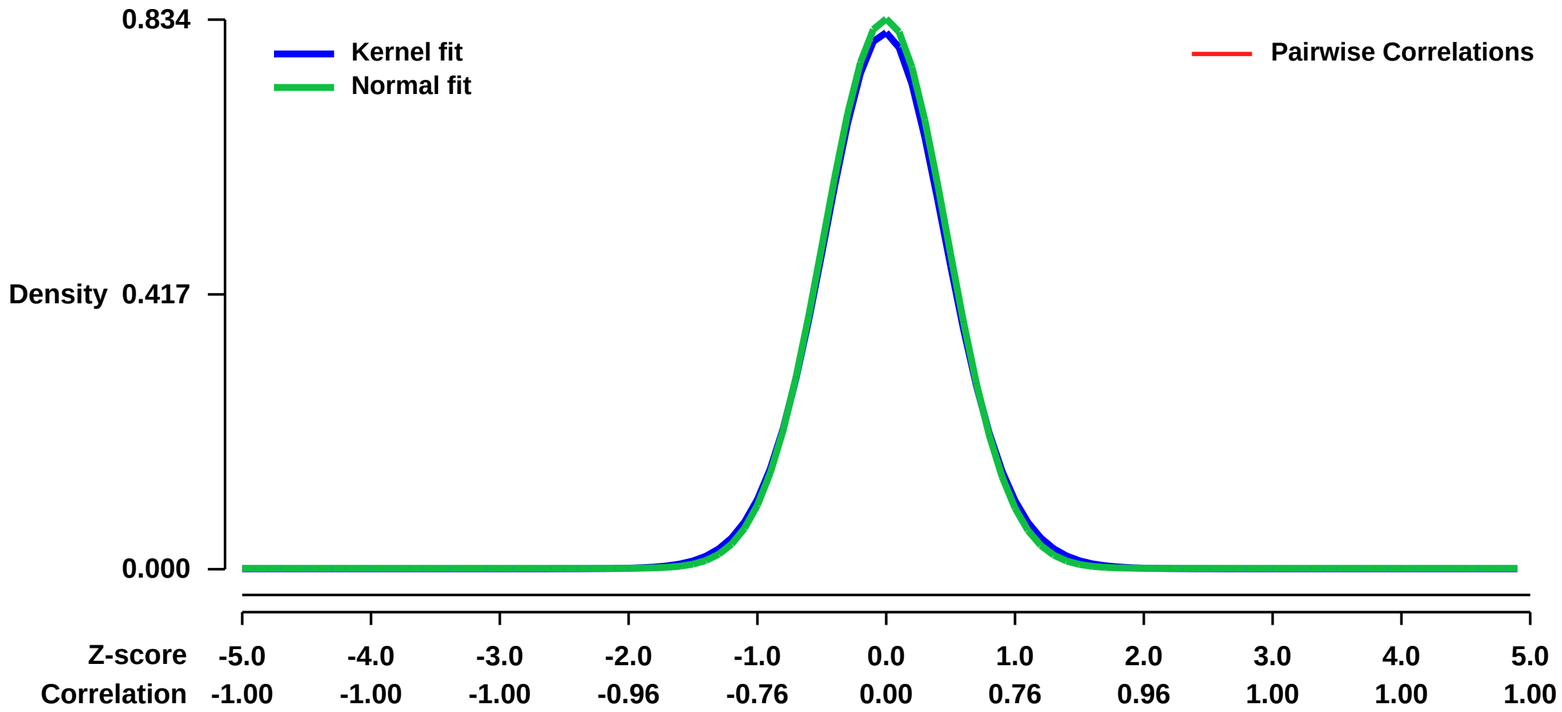

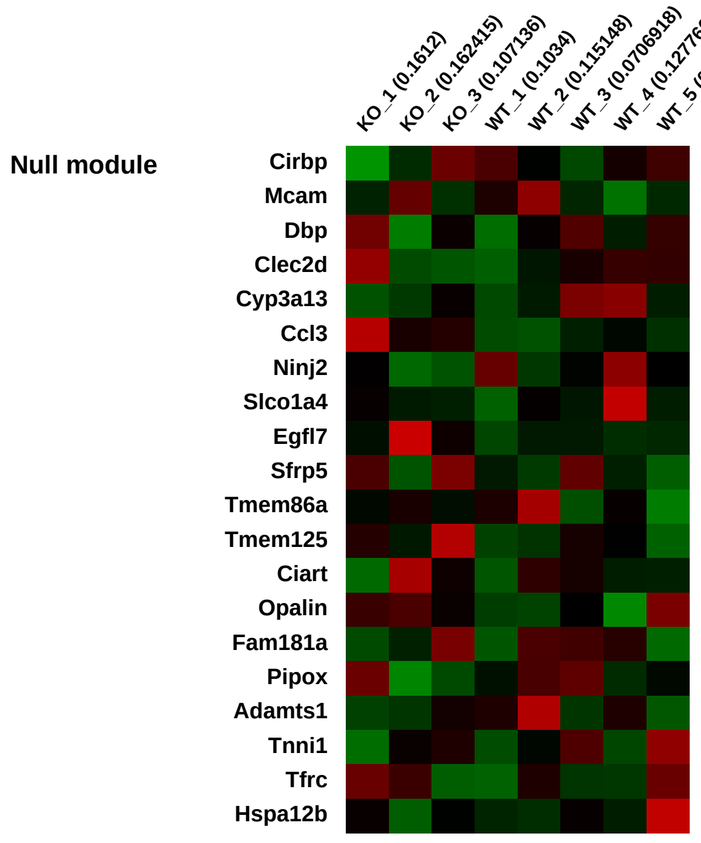

GEO Series "GSE45592" Expression Profiles

Num of samples in this series: 16

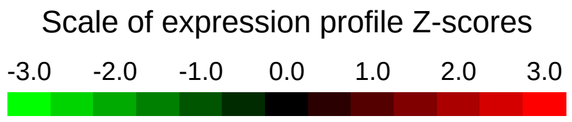

GEO Link:	http://www.ncbi.nlm.nih.gov/geo/query/acc.cgi?acc=GSE45592
Status:	Public on May 01 2013
Title:	Dicer deficiency reveals microRNAs predicted to control gene expression in developing adrenal cortex [array]
Organism:	Mus musculus
Experiment type:	Expression profiling by array
Platform:	GPL1261
Pubmed ID:	23518926
Summary & Design:	**Summary:** MicroRNAs (miRNAs) are small, endogenous, non-protein coding RNAs that are an important means of post-transcriptional gene regulation. Deletion of Dicer, a key miRNA processing enzyme, is embryonic lethal in mice, and tissue-specific Dicer deletion results in developmental defects. Using a conditional knockout model, we generated mice lacking Dicer in the adrenal cortex. These Dicer knockout (KO) mice exhibited perinatal mortality and failure of the adrenal cortex during late gestation between embryonic day 16.5 (E16.5) and E18.5. Further study of Dicer KO adrenals demonstrated a significant loss of Sf1 expressing cortical cells that was histologically evident as early as E16.5 coincident with an increase in p21 and cleaved-caspase 3 staining in the cortex. However, peripheral cortical proliferation persisted in KO adrenals as assessed by anti-PCNA staining. To further characterize the embryonic adrenals from Dicer KO mice, we performed microarray analyses for both gene expression and miRNA on purified RNA isolated from control and KO adrenals of E15.5 and E16.5 embryos. Consistent with the absence of Dicer and the associated loss of miRNA-mediated mRNA degradation, we observed an up-regulation of a small subset of adrenal transcripts in Dicer KO mice, most notably the transcripts coded by the genes Nr6a1 and Acvr1c. Indeed, several miRNAs, including let-7, miR-34c, and miR-21 that are predicted to target these genes for degradation, were also markedly down-regulated in Dicer KO adrenals. Together these data suggest a role for miRNA mediated regulation of a subset of genes that are essential for normal adrenal growth and homeostasis. **Overall design:** Adrenals from control and Dicer KO litter mates were pooled separately from 4 individual litters, resulting in a total of 4 control (cre-) and 4 Dicer KO biological replicates at both E15.5 and E16.5.

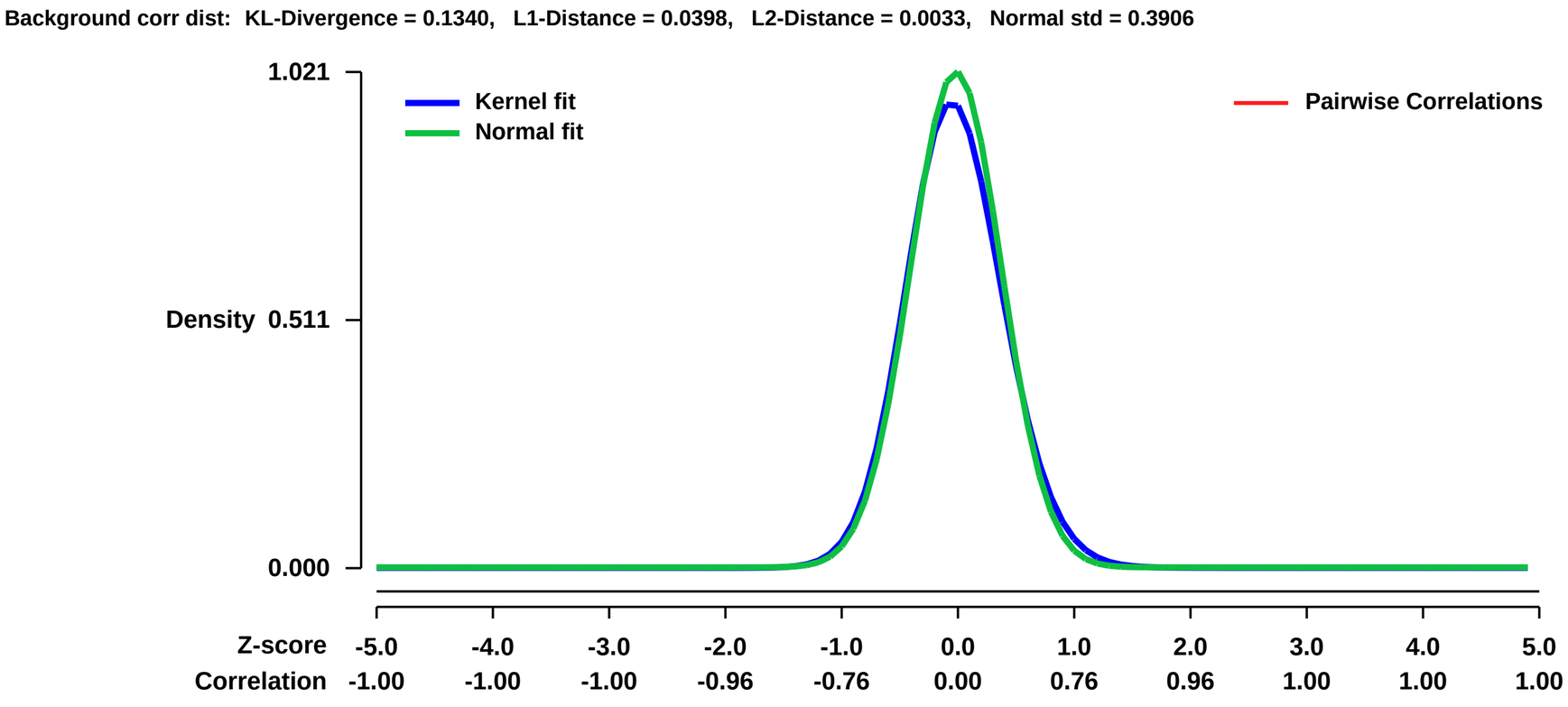

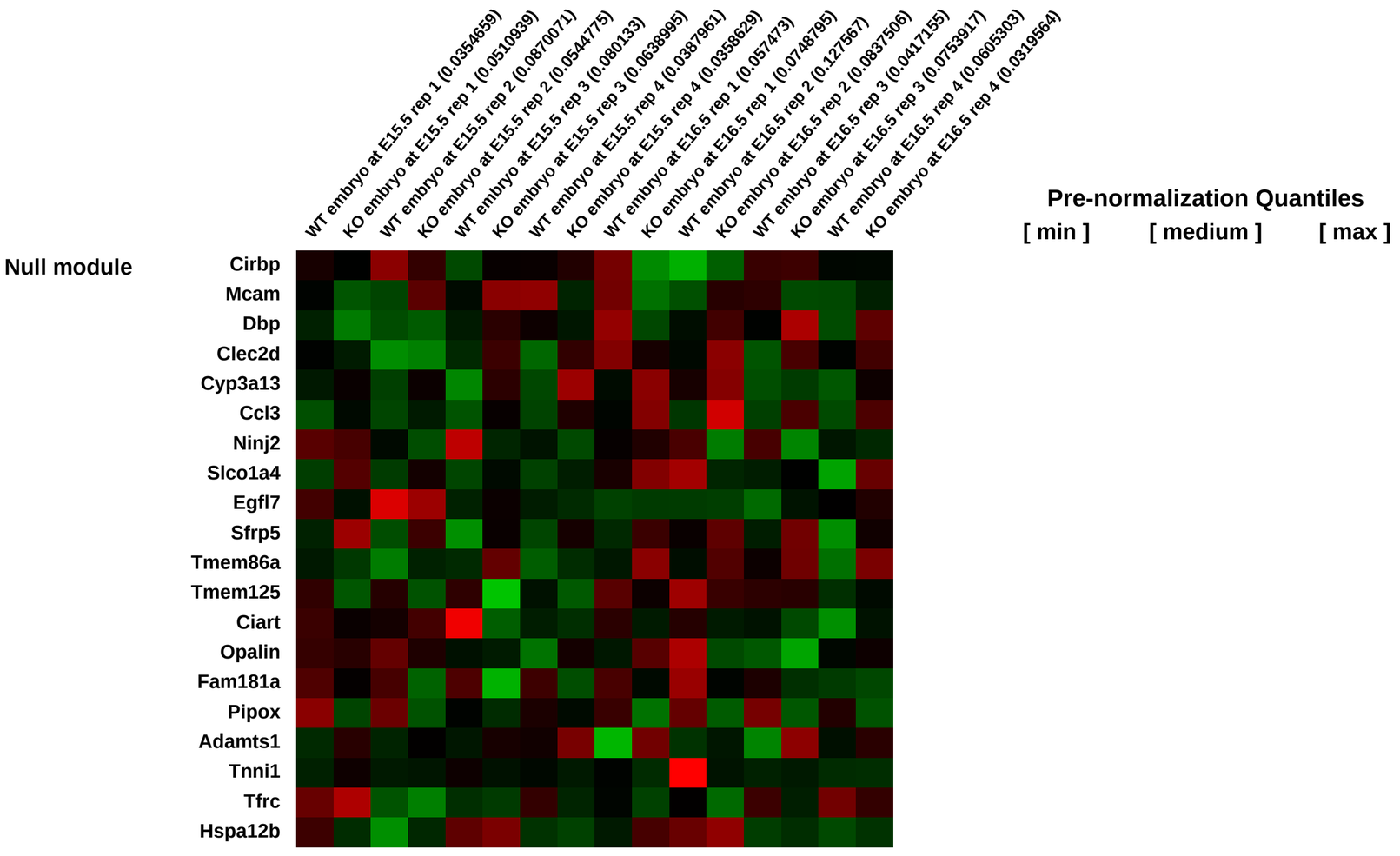

GEO Series "GSE45618" Expression Profiles

Num of samples in this series: 6

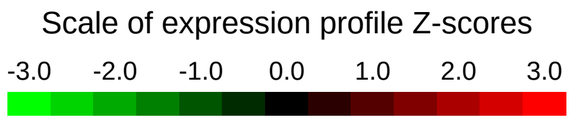

GEO Link:	**http://www.ncbi.nlm.nih.gov/geo/query/acc.cgi?acc=GSE45618**
Status:	**Public on Mar 29 2013**
Title:	**Expression analysis of BL6 murine megakaryocyte progenitors from bone marrow and fetal Liver**
Organism:	**Mus musculus**
Experiment type:	**Expression profiling by array**
Platform:	**GPL1261**
Pubmed ID:	
Summary & Design:	**Summary:** **About 10% of Down syndrome (DS) infants are born with a myeloproliferative disorder (DS-TMD) that spontaneously resolves within the first few months of life. About 20-30% of these infants subsequently develop acute megakaryoblastic leukemia (DS-AMKL). In order to understand differences that may exist between fetal and bone marrow megakaryocyte progenitor cell populations we flow sorted megakaryocyte progenitor cells and performed microarray expression analysis.** **kewywords: Mouse megakaryocyte progenitors** **Overall design:** **Expression data of flow cytometrically isolated murine megakaryocyte progenitor cells (lin-, Sca-1-, c-kit+, CD150+, CD41+) from C57/BL6 murine fetal liver and bone marrow**

Background corr dist: **KL-Divergence = 0.0460, L1-Distance = 0.0371, L2-Distance = 0.0020, Normal std = 0.6078**

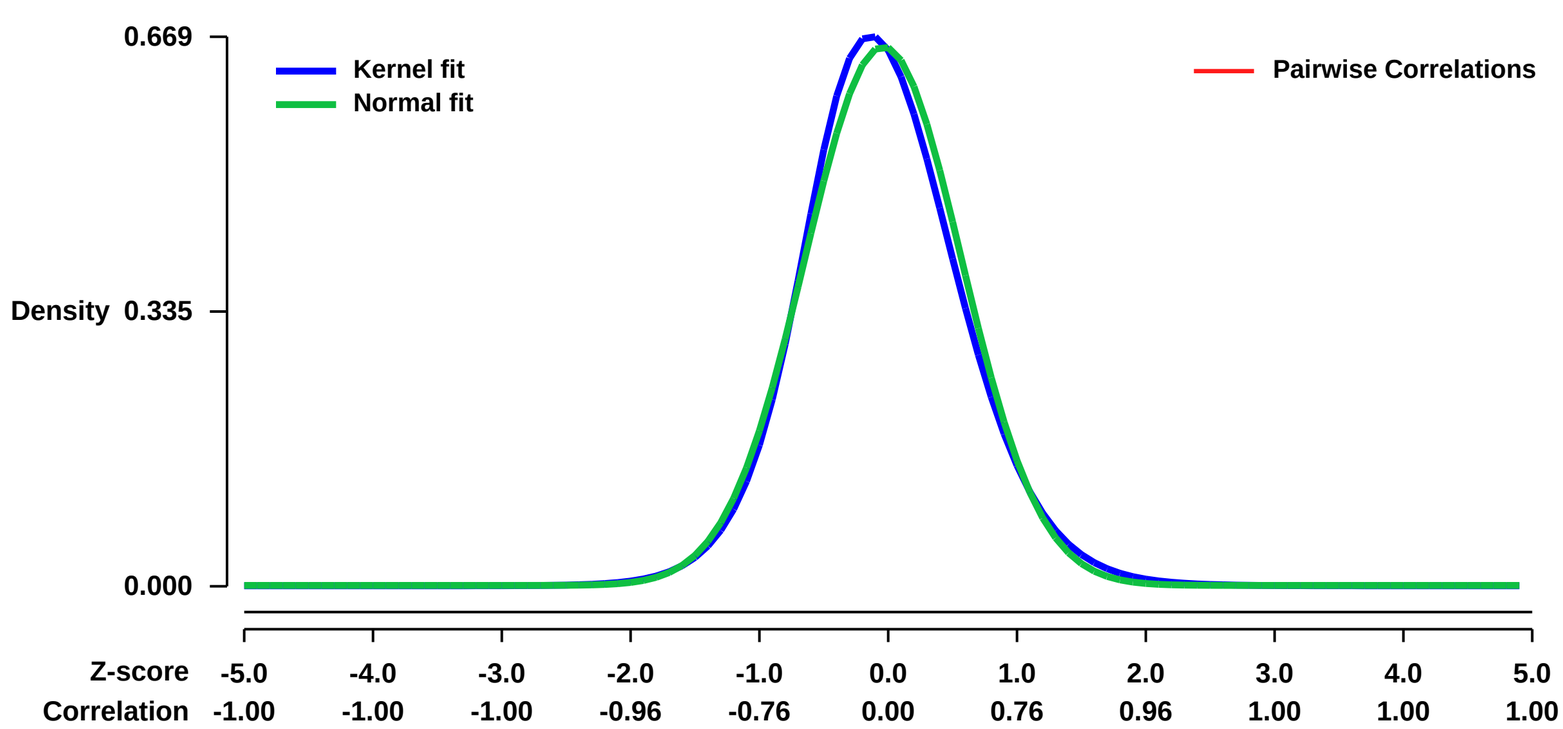

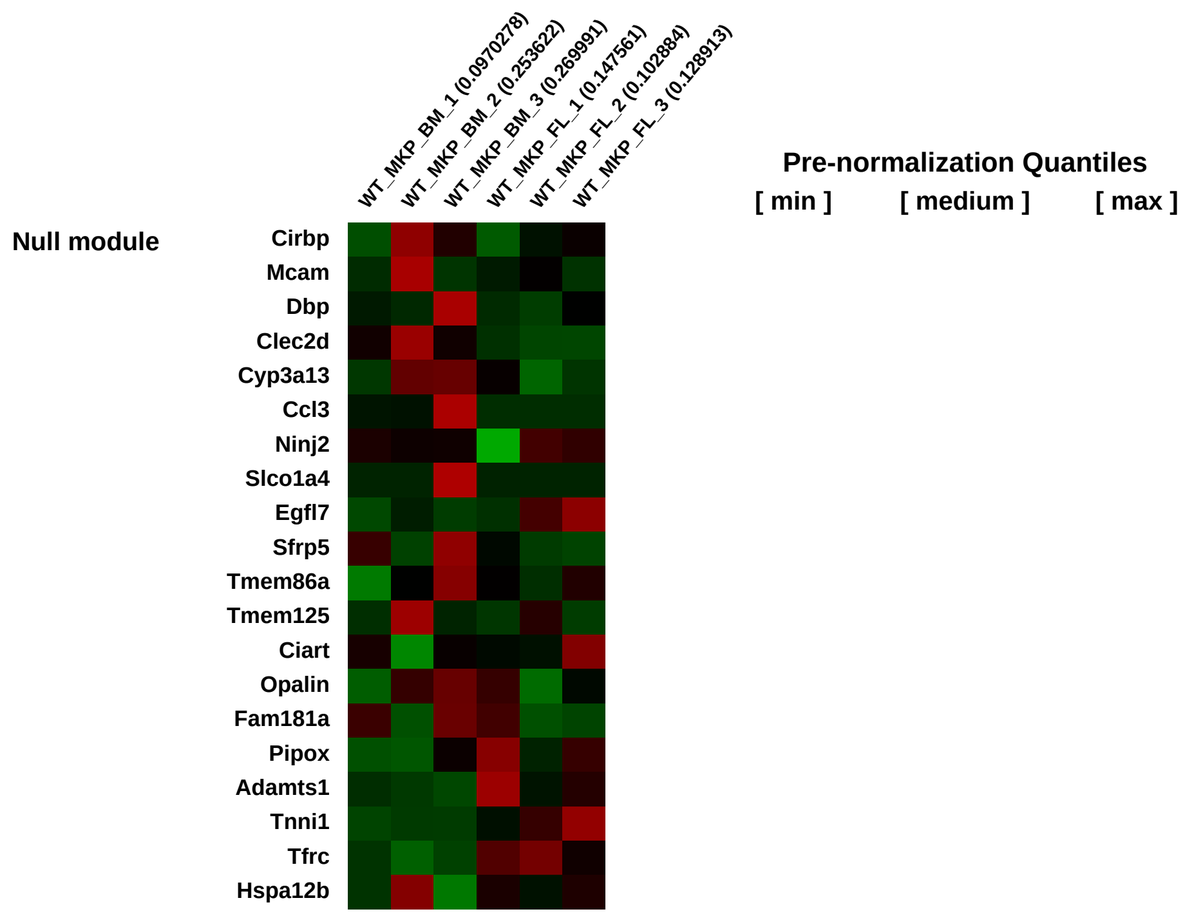

GEO Series "GSE45619" Expression Profiles

Num of samples in this series: 6

Scale of expression profile Z-scores

-3.0 -2.0 -1.0 0.0 1.0 2.0 3.0

GEO Link:	**http://www.ncbi.nlm.nih.gov/geo/query/acc.cgi?acc=GSE45619**
Status:	**Public on Mar 29 2013**
Title:	**Expression analysis of GATA1s murine megakaryocyte progenitors from bone marrow and fetal Liver**
Organism:	**Mus musculus**
Experiment type:	**Expression profiling by array**
Platform:	**GPL1261**
Pubmed ID:	
Summary & Design:	**Summary:** **About 10% of Down syndrome (DS) infants are born with a myeloproliferative disorder (DS-TMD) that spontaneously resolves within the first few months of life. About 20-30% of these infants subsequently develop acute megakaryoblastic leukemia (DS-AMKL). In order to understand differences that may exist between fetal and bone marrow megakaryocyte progenitor cell populations we flow sorted megakaryocyte progenitor cells and performed microarray expression analysis.** **kewywords: Mouse megakaryocyte progenitors** **Overall design:** **Expression data of flow cytometrically isolated murine megakaryocyte progenitor cells (lin-, Sca-1-, c-kit+, CD150+, CD41+) from GATA1s fetal liver and bone marrow**

Background corr dist: **KL-Divergence = 0.0282, L1-Distance = 0.0322, L2-Distance = 0.0012, Normal std = 0.7067**

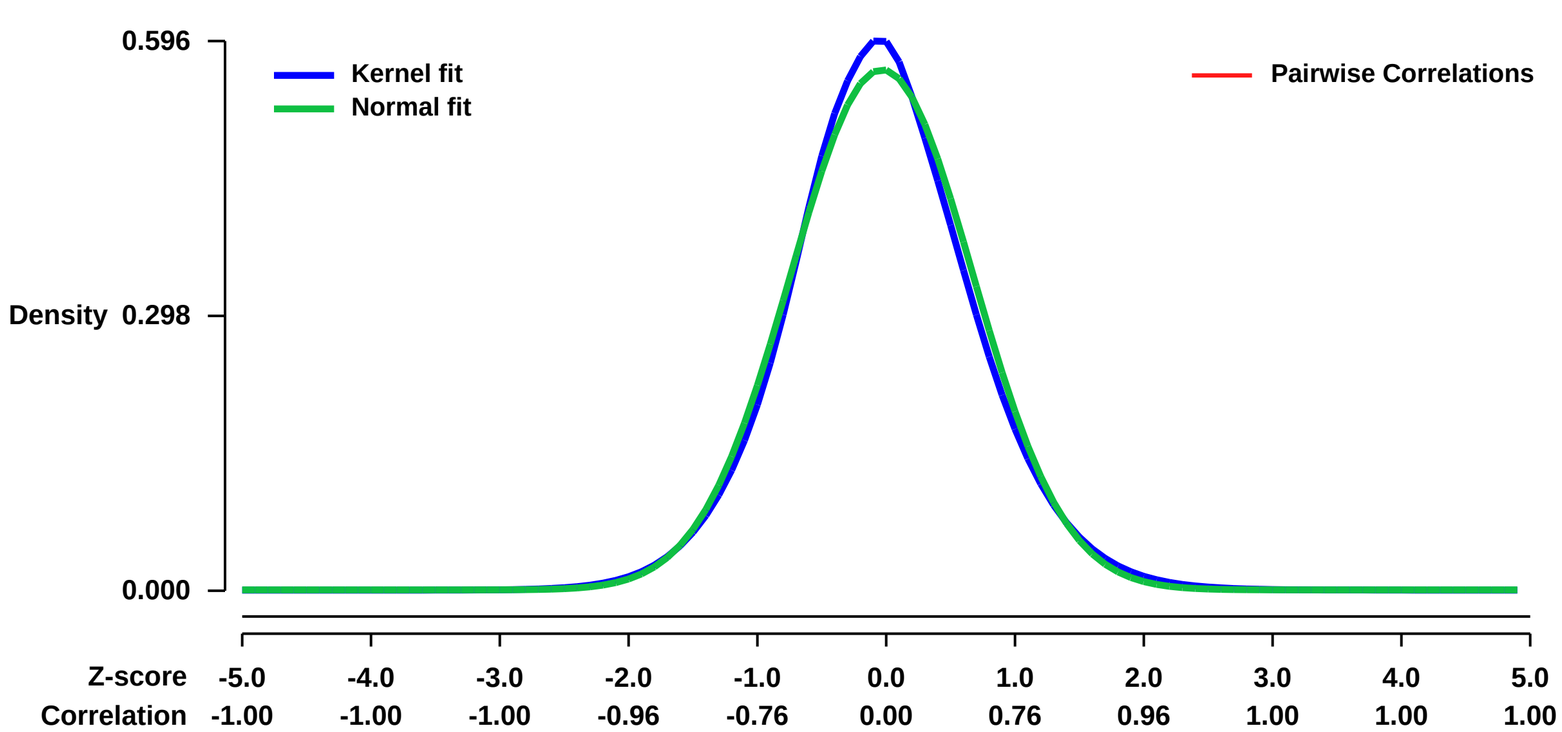

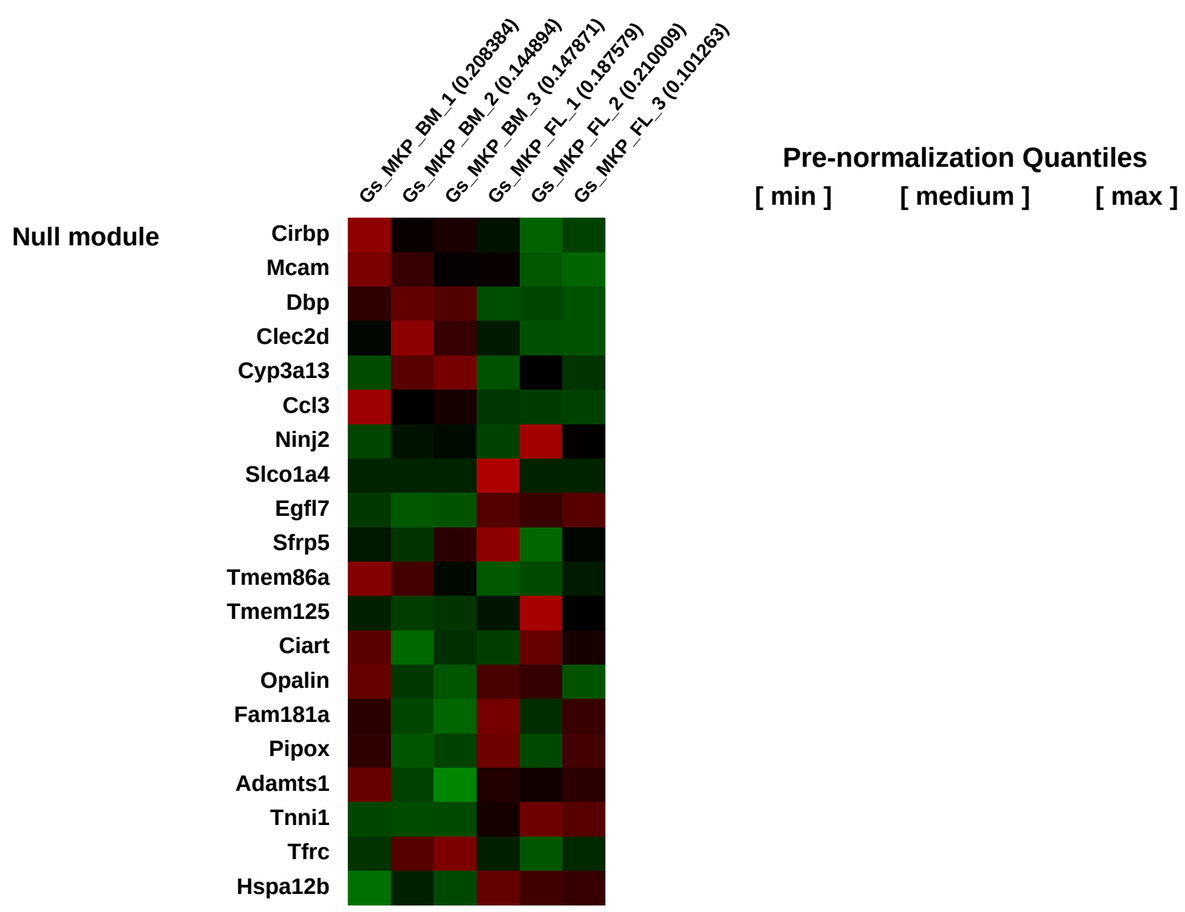

GEO Series "GSE45668" Expression Profiles

Num of samples in this series: 6

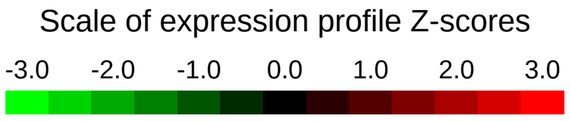

GEO Link: http://www.ncbi.nlm.nih.gov/geo/query/acc.cgi?acc=GSE45668

Status: Public on Apr 02 2013

Title: The presence of the Y-chromosome, not the absence of the second X-chromosome, alters the mRNA levels stored in the fully grown XY mouse oocyte

Organism: Mus musculus

Experiment type: Expression profiling by array

Platform: GPL1261

Pubmed ID:

Summary & Design:

Summary:
The oocytes of B6.Y(TIR) sex-reversed female mouse mature in culture but fail to develop after fertilization because of their cytoplasmic defects. To identify the defective components, we compared the gene expression profiles between the fully-grown oocytes of B6.Y(TIR) (XY) females and those of their XX littermates by cDNA microarray. 173 genes were found to be higher and 485 genes were lower in XY oocytes than in XX oocytes by at least 2-fold. We compared the transcript levels of selected genes by RT-PCR in XY and XX oocytes, as well as in XO oocytes missing paternal X-chromosomes. All genes tested showed comparable transcript levels between XX and XO oocytes, indicating that mRNA accumulation is well adjusted in XO oocytes. By contrast, in addition to Y-encoded genes, many genes showed significantly different transcript levels in XY oocytes. We speculate that the presence of the Y-chromosome, rather than the absence of the second X-chromosome, caused dramatic changes in the gene expression profile in the XY fully-grown oocyte.

Overall design:
Mouse GV oocytes of B6.Y(TIR) were collected for RNA extraction and hybridization to Affymetrix microarray. We sought to extract the differentially expressed genes in the XY oocytes.

Background corr dist: KL-Divergence = 0.0297, L1-Distance = 0.0151, L2-Distance = 0.0002, Normal std = 0.6671

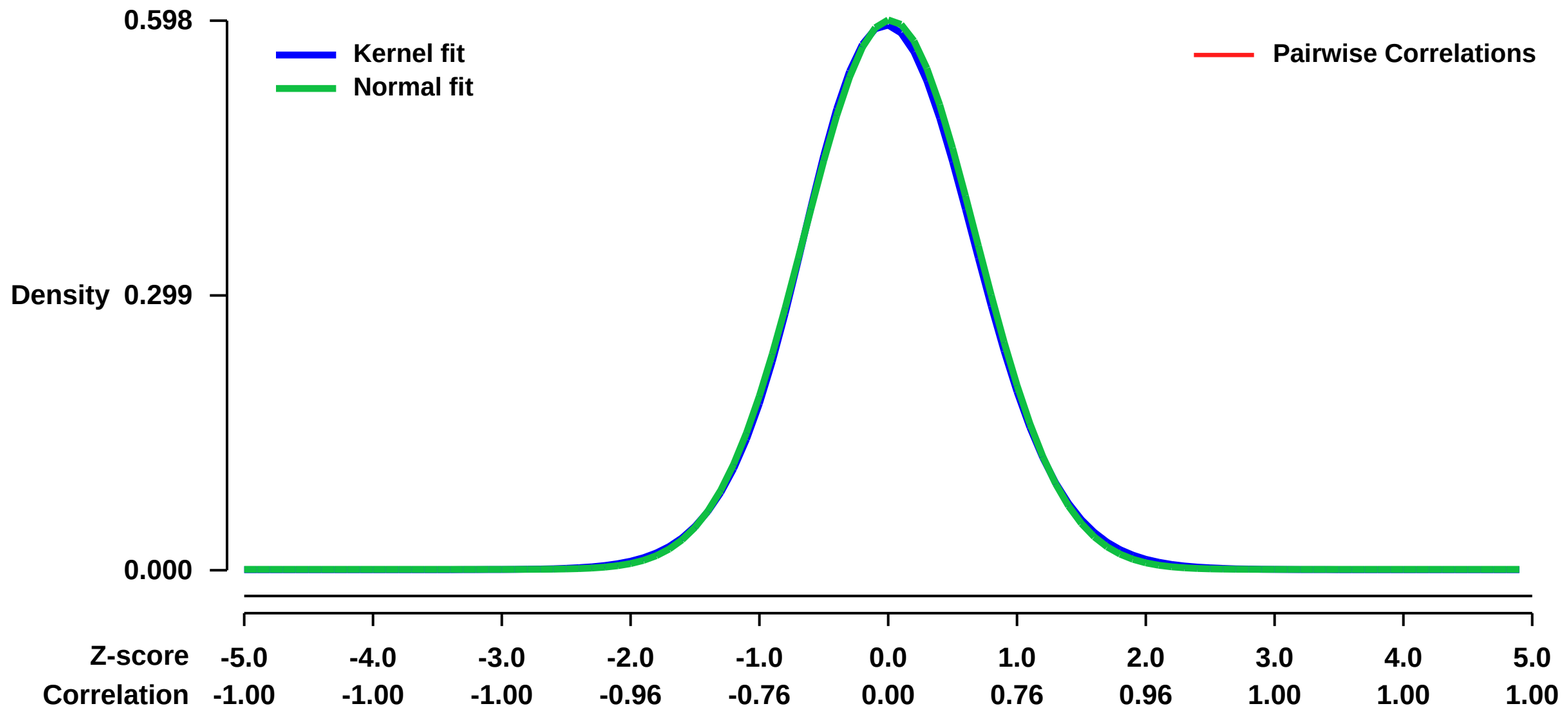

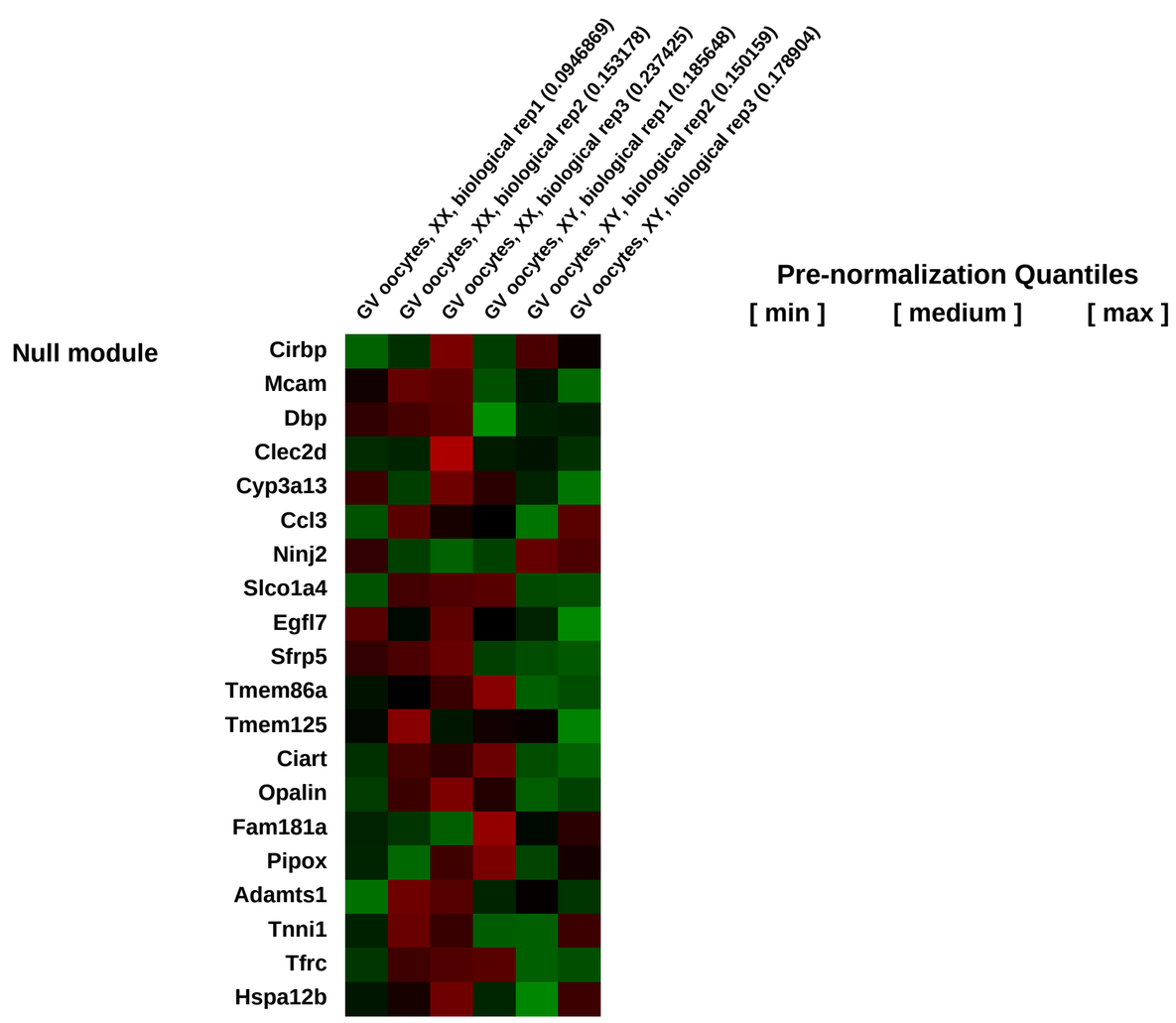

GEO Series "GSE45854" Expression Profiles

Num of samples in this series: 8

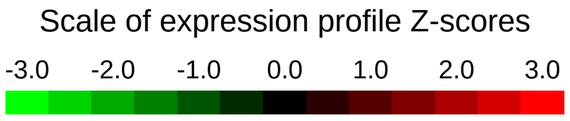

GEO Link:	http://www.ncbi.nlm.nih.gov/geo/query/acc.cgi?acc=GSE45854
Status:	Public on Apr 08 2013
Title:	Expression profiling data of RD and C2C12 cells ectopically expressing DUX4
Organism:	Mus musculus
Experiment type:	Expression profiling by array
Platform:	GPL1261
Pubmed ID:	23717650
Summary & Design:	**Summary:** Transcriptomic changes induced by DUX4 expression were compared between human and mouse cell lines of muscle lineage. We used microarrays to compare transcripts induced in human rhabdmyosarcoma and mouse C2C12 cells ectopically expressing DUX4. **Overall design:** Human rhabdomyosarcoma and mouse C2C12 cells were transfected with DUX4 expression vectors (n=4). Cells transfected with insertless vectors were used as controls. Samples were processed for RNA extraction 16 hours following transfection.

Background corr dist: KL-Divergence = 0.0776, L1-Distance = 0.0214, L2-Distance = 0.0007, Normal std = 0.4846

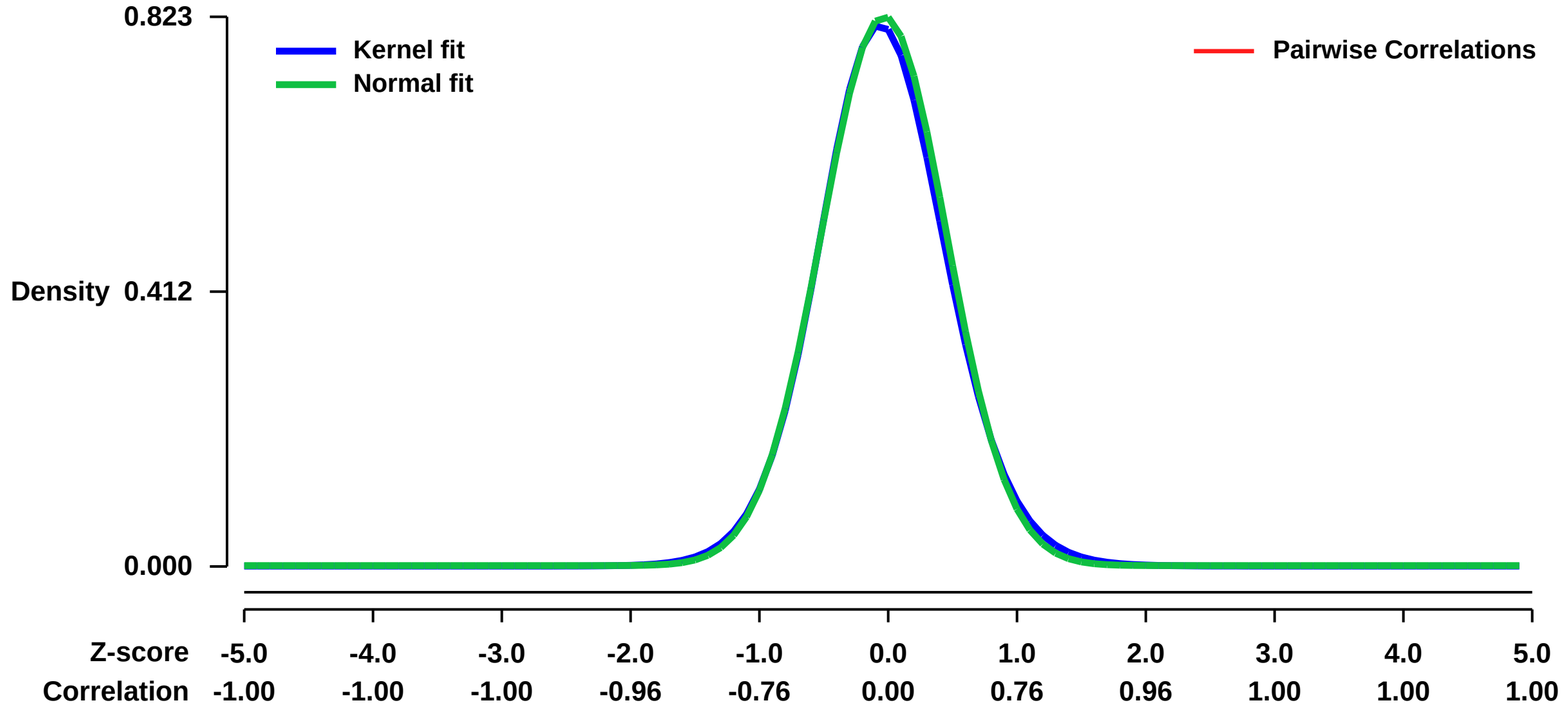

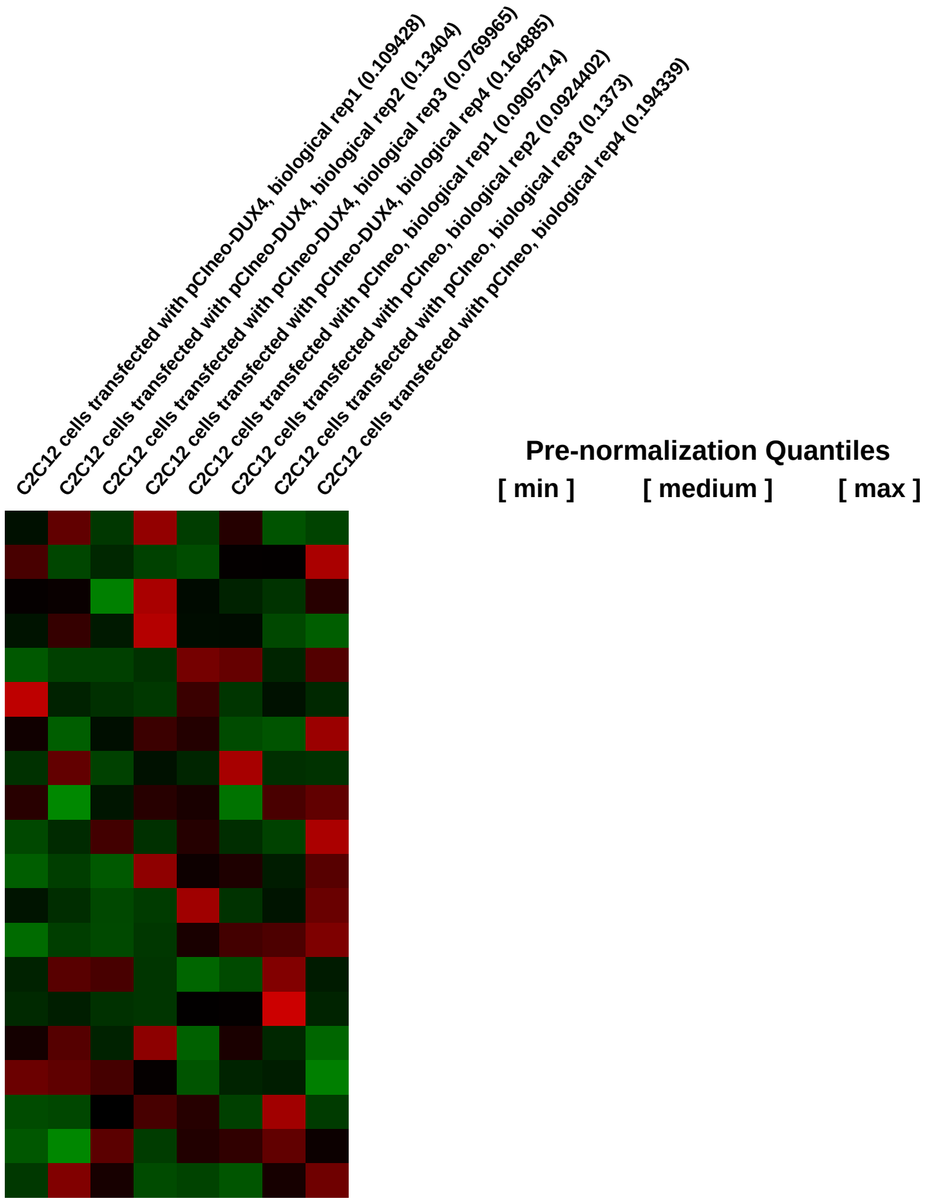

GEO Series "GSE45895" Expression Profiles

Num of samples in this series: 27

Scale of expression profile Z-scores

-3.0 -2.0 -1.0 0.0 1.0 2.0 3.0

GEO Link:	http://www.ncbi.nlm.nih.gov/geo/query/acc.cgi?acc=GSE45895
Status:	Public on Apr 10 2013
Title:	EphrinB2 Regulation by PTH and PTHrP Revealed by Molecular Profiling in Differentiating Osteoblasts
Organism:	Mus musculus
Experiment type:	Expression profiling by array
Platform:	GPL1261
Pubmed ID:	18627264
Summary & Design:	**Summary:** With the aim of identifying new pathways and genes regulated by PTH(1-34) and PTH-related protein 1-141 [PTHrP(1-141)] in osteoblasts, this study was carried out using a mouse marrow stromal cell line, Kusa 4b10, that acquires features of the osteoblastic phenotype in long-term culture conditions. After the appearance of functional PTH receptor 1 (PTHR1) in Kusa 4b10 cells, they were treated with either PTH(1-34) or PTHrP(1-141), and RNA was subjected to Affymetrix whole mouse genome array. **Overall design:** NOTE: This work has been published in 2008 (PMID 18627264); Since the original normalised data for this project is unavailable, the data has been re-normalised using a standard method for GEO submission in 2013. Therefore, the re-normalized data represented in this records may differ slightly from the original normalized data in the publication.

Background corr dist: KL-Divergence = 0.1060, L1-Distance = 0.0288, L2-Distance = 0.0017, Normal std = 0.4275

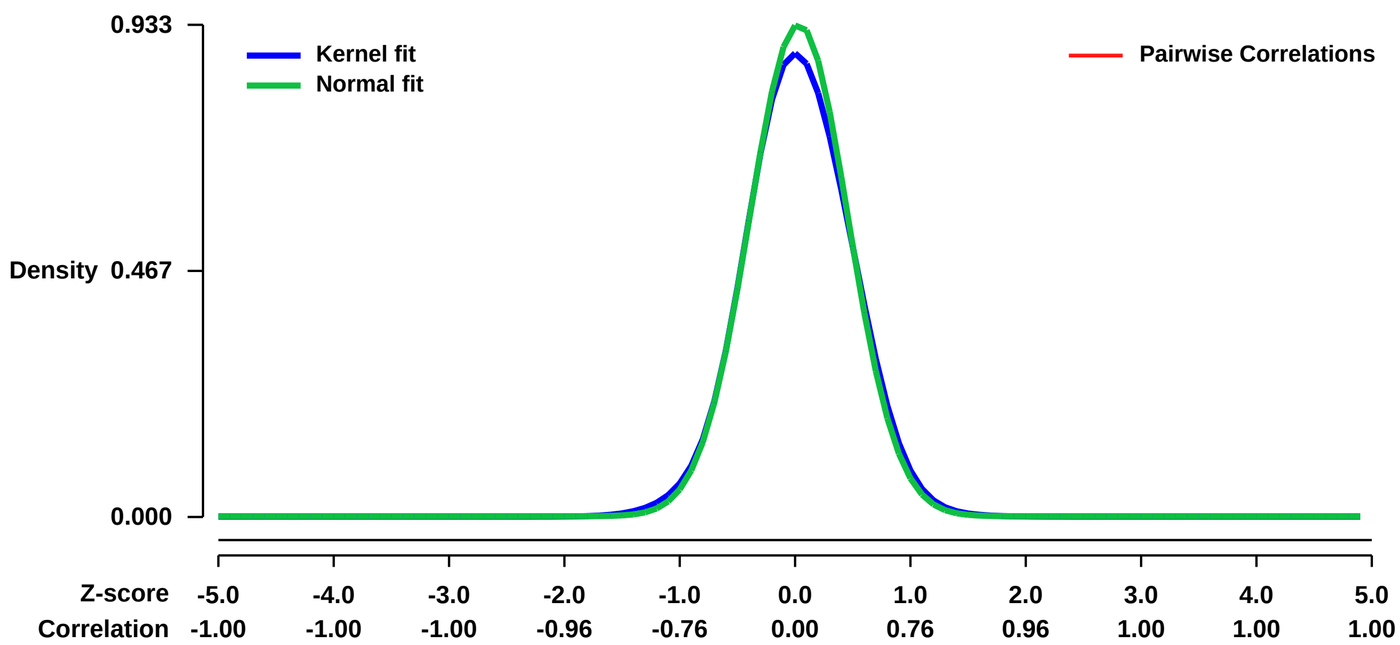

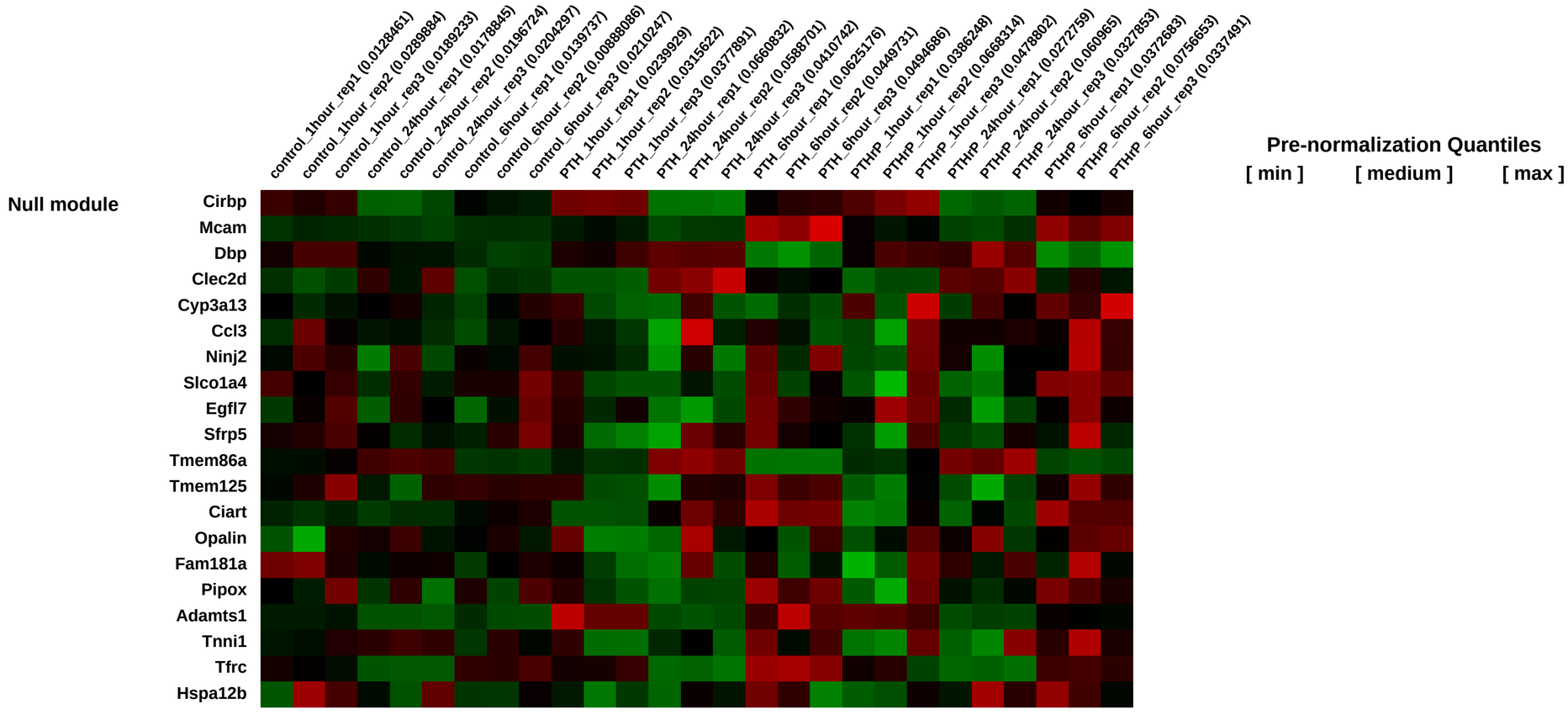

GEO Series "GSE45941" Expression Profiles

Num of samples in this series: 8

Scale of expression profile Z-scores

-3.0 -2.0 -1.0 0.0 1.0 2.0 3.0

GEO Link:	http://www.ncbi.nlm.nih.gov/geo/query/acc.cgi?acc=GSE45941
Status:	Public on Jan 30 2014
Title:	Transcription factor TFAP2C regulates major programs required for murine fetal germ cell maintenance and haploinsufficiency predisposes to teratomas in male mice
Organism:	Mus musculus
Experiment type:	Expression profiling by array
Platform:	GPL1261
Pubmed ID:	23967156
Summary & Design:	**Summary:** Maintenance and maturation of primordial germ cells is controlled by complex genetic and epigenetic cascades, and disturbances in this network lead to either infertility or malignant aberration. Transcription factor Tcfap2c / TFAP2C has been described to be essential for primordial germ cell maintenance and to be upregulated in several human germ cell cancers. Using global gene expression profiling, we identified genes deregulated upon loss of Tcfap2c in primordial germ cell-like cells. We show that loss of Tcfap2c affects many aspects of the genetic network regulating germ cell biology, such as downregulation maturation markers and induction of markers indicative of somatic differentiation, cell cycle, epigenetic remodeling, and pluripotency associated genes. Chromatin-immunoprecipitation analyses demonstrated binding of Tcfap2c to regulatory regions of deregulated genes (Sfrp1, Dmrt1, Nanos3, c-Kit, Cdk6, Cdkn1a, Fgf4, Klf4, Dnmt3b and Dnmt3l) suggesting that these genes are direct transcriptional targets of Tcfap2c in primordial germ cells. Since Tcfap2c deficient primordial germ cell like cells display cancer related deregulations in epigenetic remodeling, cell cycle and pluripotency control, the Tcfap2c-knockout allele was bred onto 129S2/Sv genetic background. There, mice heterozygous for Tcfap2c develop germ cell cancer with high incidence. Precursor lesions can be observed as early as E16.5 in developing testes displaying persisting expression of pluripotency markers. We further demonstrate, that mice with a heterozygous deletion of the Tcfap2c target gene Nanos3 are also prone to develop teratoma. These data highlight Tcfap2c as a critical and dose-sensitive regulator of germ cell fate. **Overall design:** **KO PGC:** Tcfap2c knock-out mouse primordial germ cells (PGCs), 2 biological rep

Background corr dist: KL-Divergence = 0.0560, L1-Distance = 0.0176, L2-Distance = 0.0004, Normal std = 0.5390

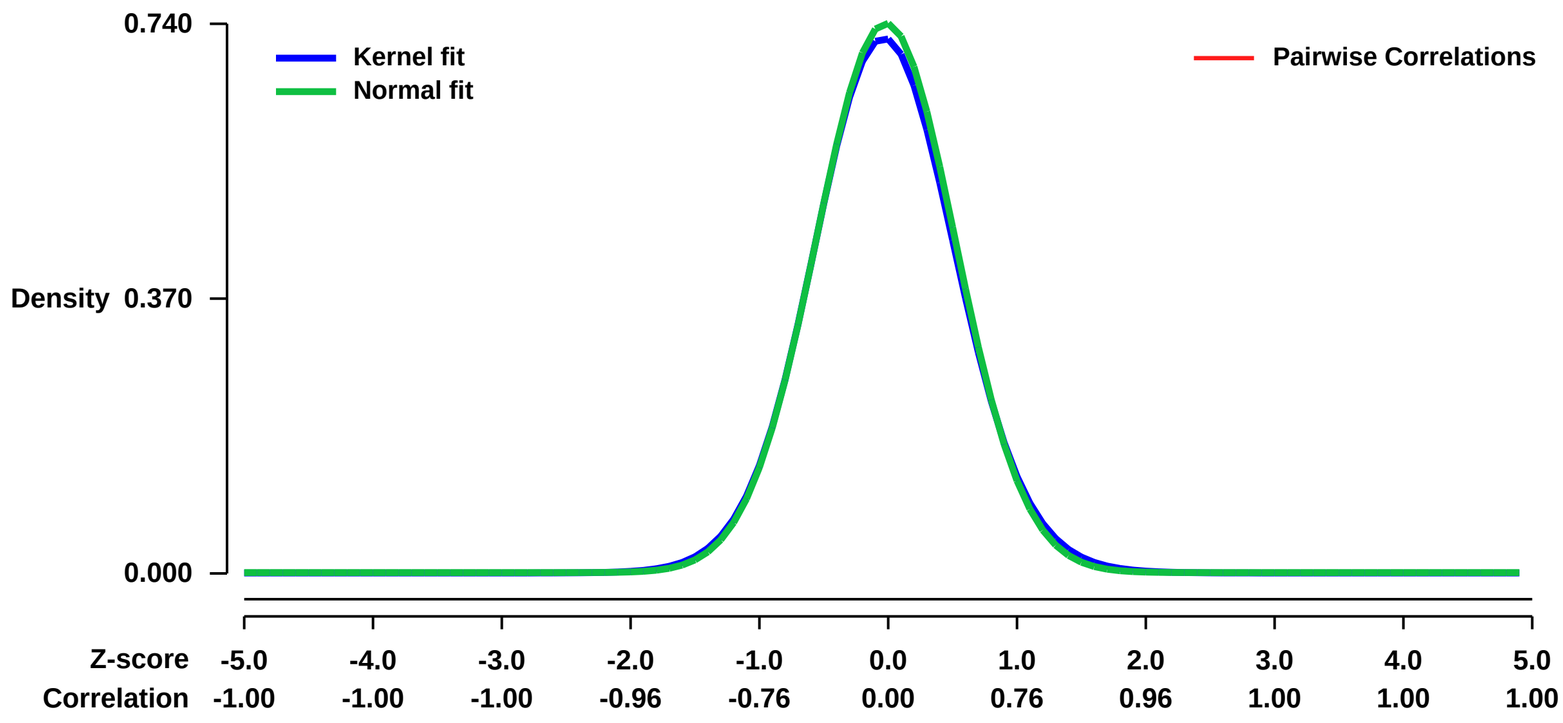

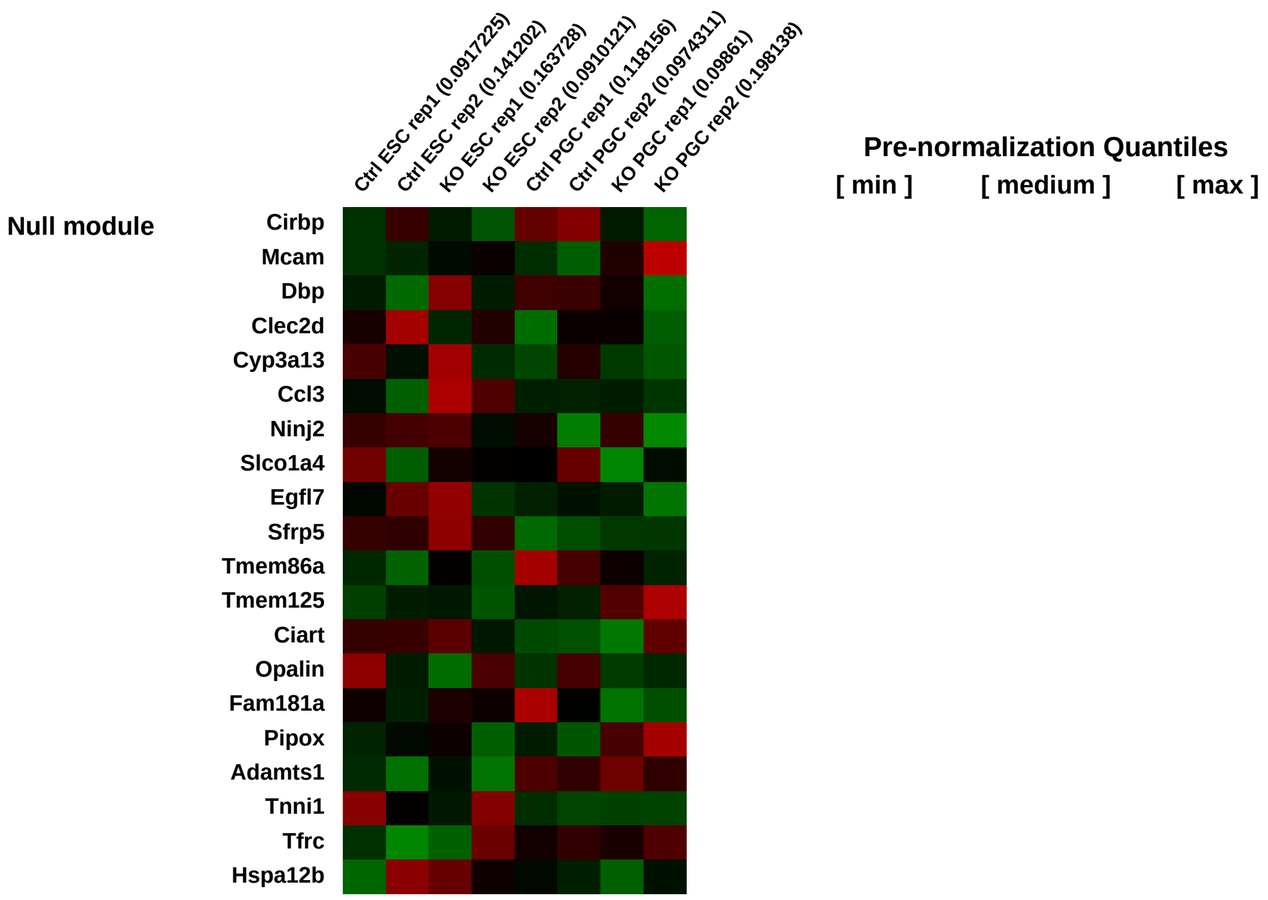

GEO Series "GSE45968" Expression Profiles

Num of samples in this series: 6

Scale of expression profile Z-scores

-3.0 -2.0 -1.0 0.0 1.0 2.0 3.0

GEO Link:	http://www.ncbi.nlm.nih.gov/geo/query/acc.cgi?acc=GSE45968
Status:	Public on Apr 11 2013
Title:	Gene expression profiling of the tongue in Tgfbr2 mutant mouse models
Organism:	Mus musculus
Experiment type:	Expression profiling by array
Platform:	GPL1261
Pubmed ID:	23950180
Summary & Design:	**Summary:** The overall goal of this project is to investigate the role of TGF-beta signaling in tongue development in order to study the contribution of cranial neural crest (CNC) cells towards the patterning of cranial mesoderm for proper tongue formation. Here, we conducted gene expression profiling of embryonic tongue tissue from wild type mice as well as those with a neural crest specific conditional inactivation of the Tgfbr2 gene. The latter mice provide a model of microglossia, a common congenital birth defect which is frequently observed with several syndromic conditions. **Overall design:** To investigate the mechanism of microglossia resulting from dysfunctional TGF-Beta signaling during muscle development, we analyzed neural crest specific conditional inactivation of Tgfbr2 in mice (Tgfbr2fl/fl;Wnt1-Cre). We performed microarray analyses of tongue tissue of Tgfbr2fl/fl;Wnt1-Cre mutant mice and Tgfbr2fl/fl control mice at embryonic day E14.5 (n=3 per genotype) to examine the genes regulated by Tgf-beta during tongue muscle development.

Background corr dist: KL-Divergence = 0.0267, L1-Distance = 0.0183, L2-Distance = 0.0003, Normal std = 0.6951

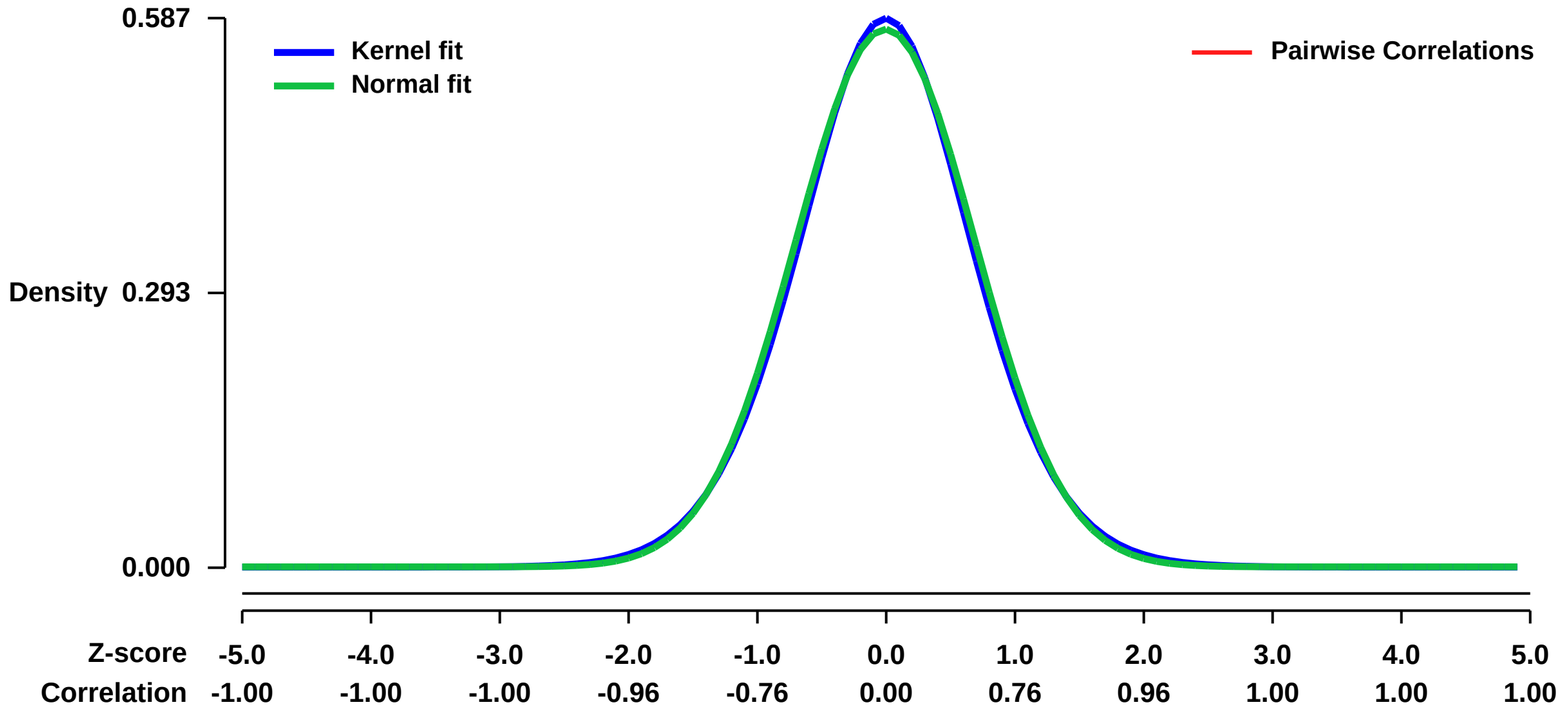

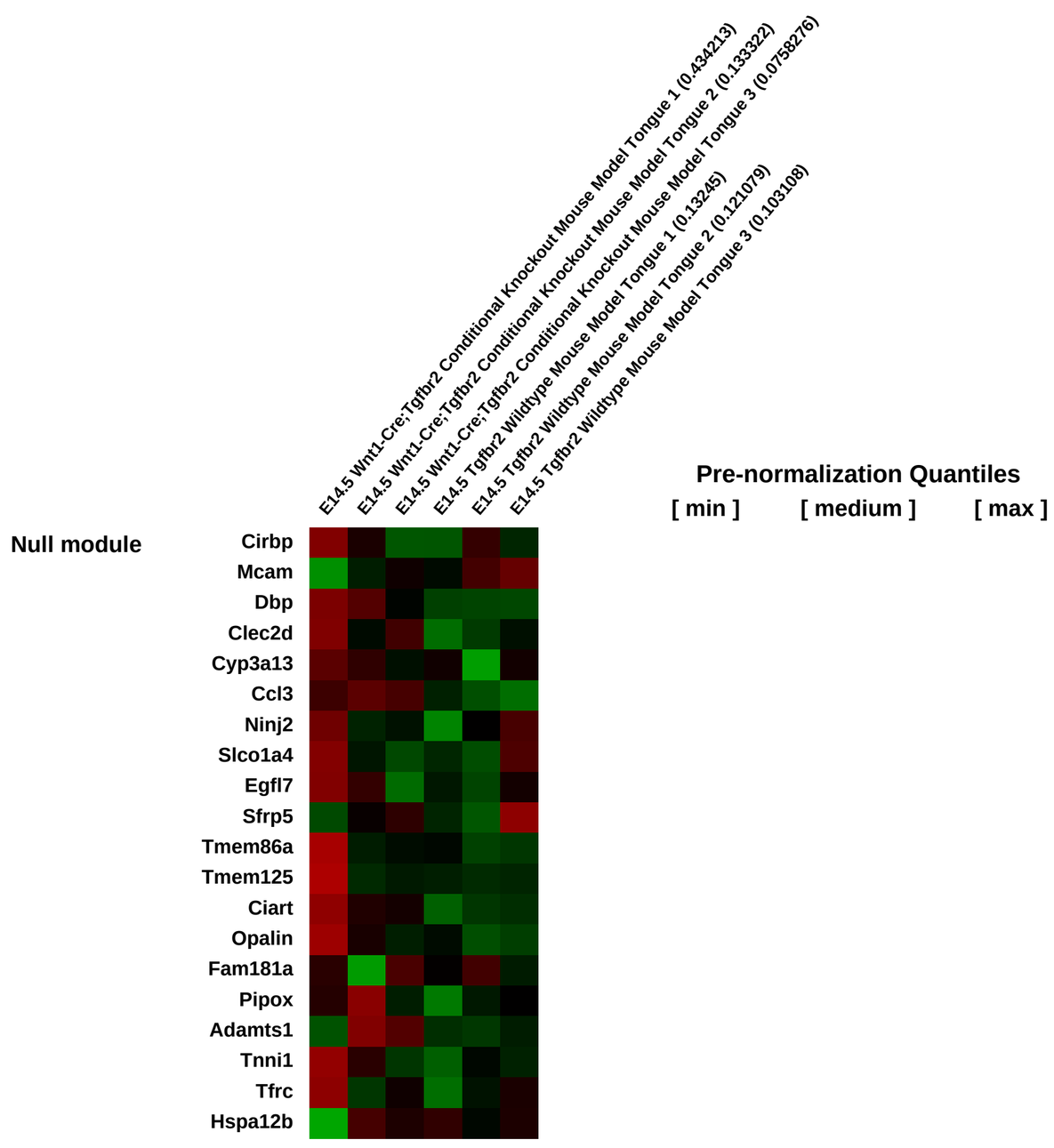

GEO Series "GSE46088" Expression Profiles

Num of samples in this series: 8

Scale of expression profile Z-scores

-3.0 -2.0 -1.0 0.0 1.0 2.0 3.0

GEO Link:	http://www.ncbi.nlm.nih.gov/geo/query/acc.cgi?acc=GSE46088
Status:	Public on Apr 17 2013
Title:	Ikaros responsive genes in the T29 cell line
Organism:	Mus musculus
Experiment type:	Expression profiling by array
Platform:	GPL1261
Pubmed ID:	24643801
Summary & Design:	**Summary:** The mouse Ikaros-deficient thymic lymphoma cell line T29 was transduced with an empty retrovirus (MigR1) or a retrovirus expressing an fusion proein between Ikaros1 and the ligand binding domain of the estrogen receptor. Cells trreated with ethanol or 4-hydroxy-tamoxyfen (4OHT) for 24h were profiled. **Overall design:** We used expression of an inducible ersion of the Ikaros protein in an Ikaros-deficient cell line to identify Ikaros-regulated genes

Background corr dist: KL-Divergence = 0.0639, L1-Distance = 0.0176, L2-Distance = 0.0003, Normal std = 0.5178

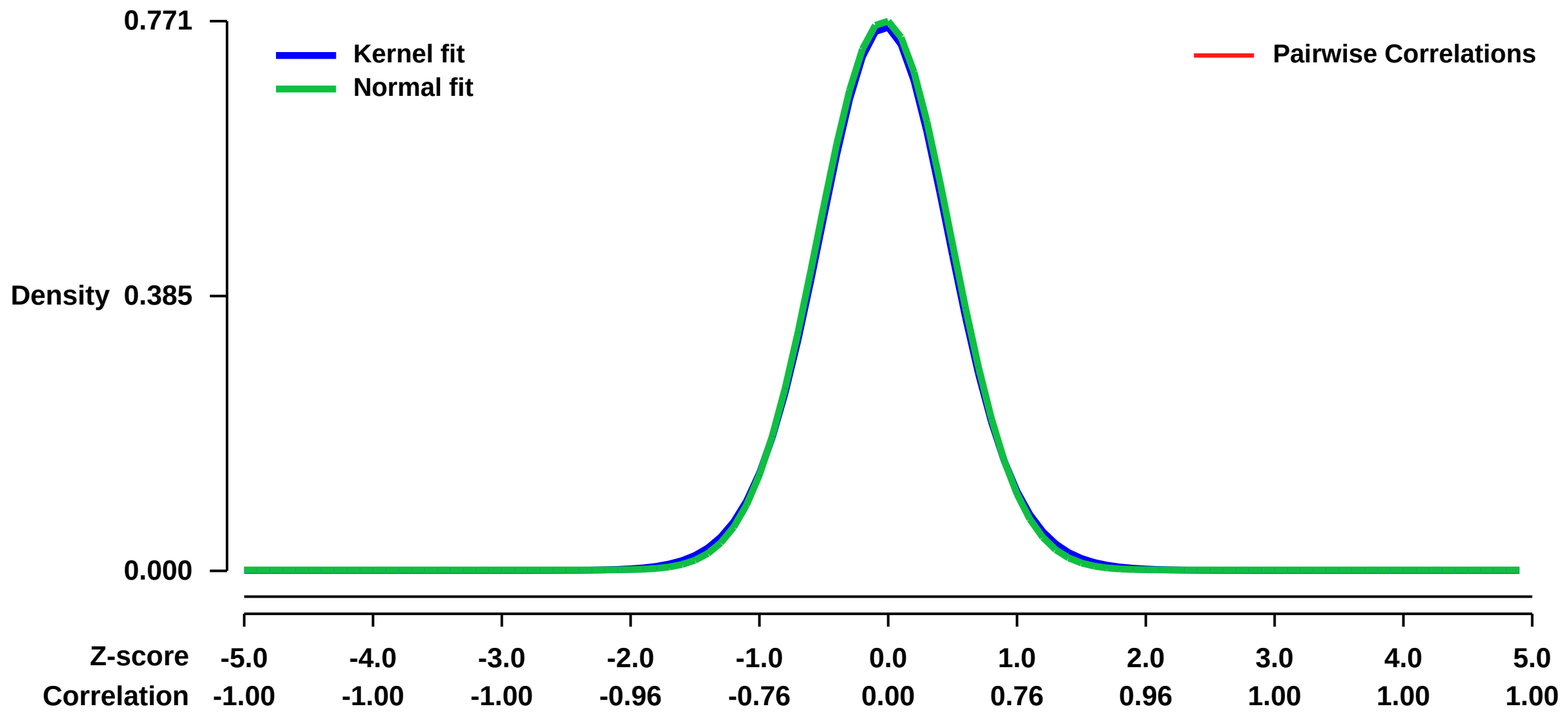

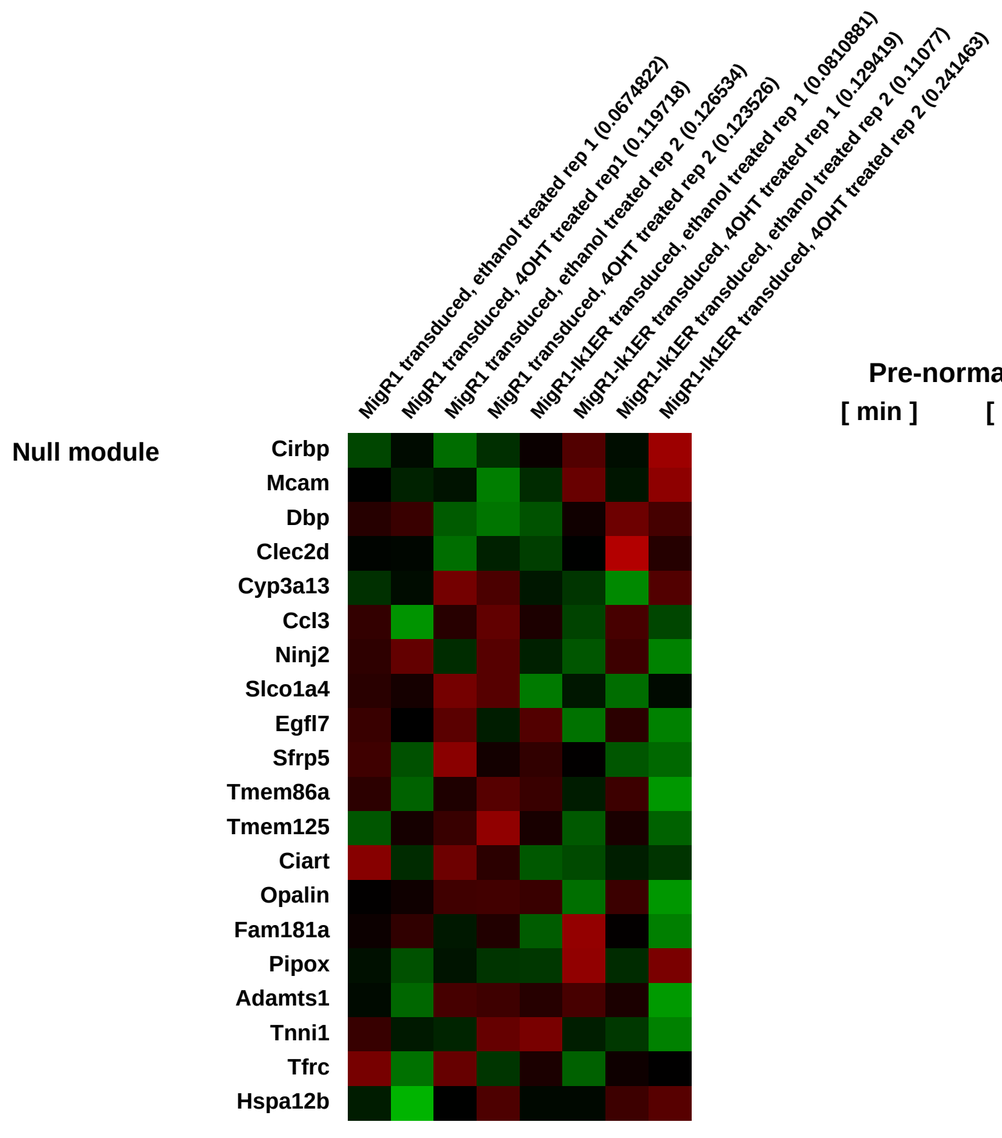

GEO Series "GSE46091" Expression Profiles

Num of samples in this series: 8

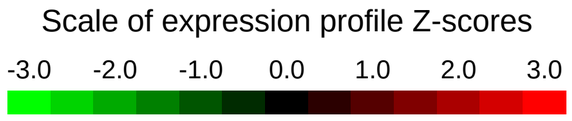

GEO Link:	http://www.ncbi.nlm.nih.gov/geo/query/acc.cgi?acc=GSE46091
Status:	Public on Apr 17 2013
Title:	Genes regulated by the gamma secretase inhibitor in WT and Ikaros deficient DN3 cells
Organism:	Mus musculus
Experiment type:	Expression profiling by array
Platform:	GPL1261
Pubmed ID:	24643801
Summary & Design:	**Summary:** Lineage-negative thymocytes were cultured on OP9-DL1 stromal cells for 16h in the presence of DMSO or the gamma secretase inhibitor MRK-003. DN3 cells cells were then sorted and their transcriptome analyzed. **Overall design:** 8 samples

Background corr dist: KL-Divergence = 0.0511, L1-Distance = 0.0209, L2-Distance = 0.0005, Normal std = 0.5665

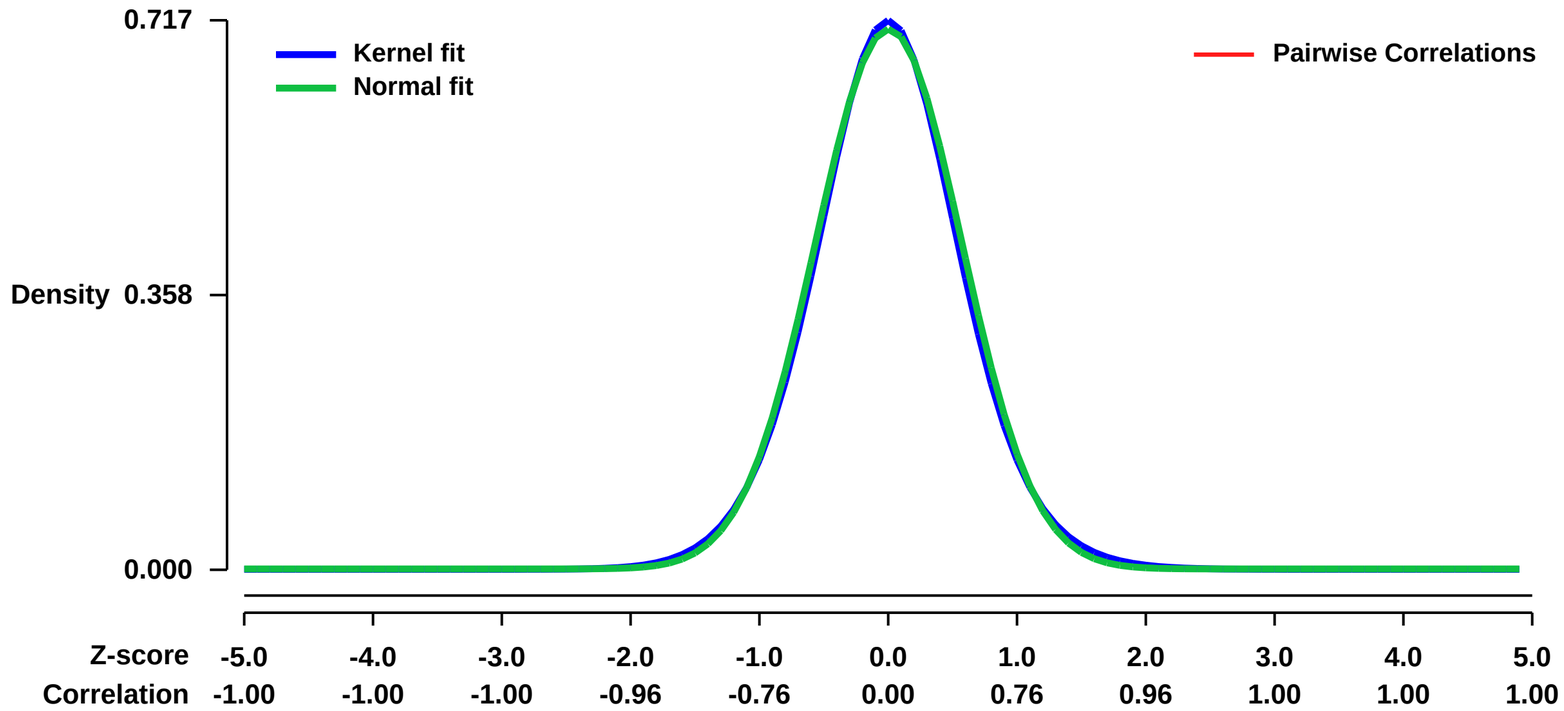

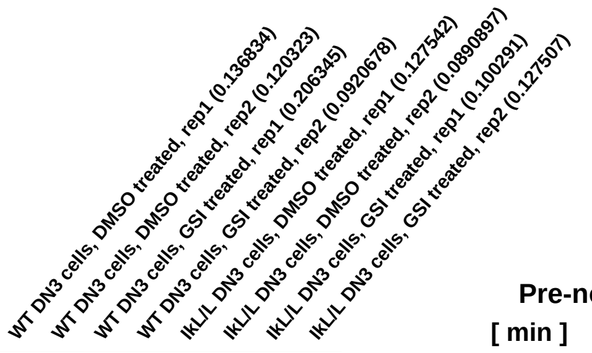

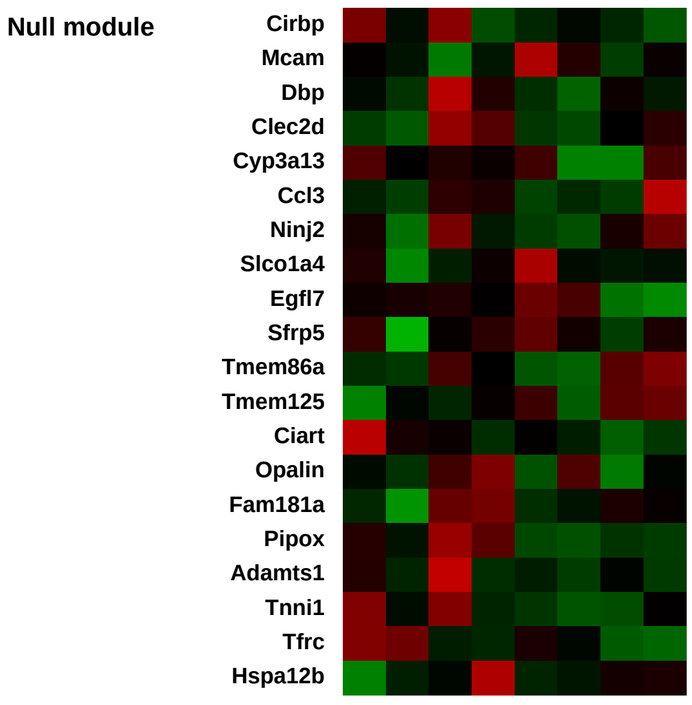

GEO Series "GSE46094" Expression Profiles

Num of samples in this series: 10

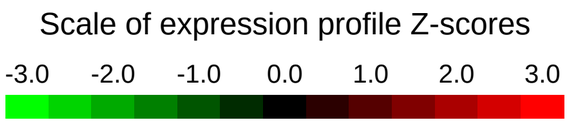

GEO Link:	**http://www.ncbi.nlm.nih.gov/geo/query/acc.cgi?acc=GSE46094**
Status:	**Public on May 01 2014**
Title:	**Expression data from PML-RAR¸– transgenic mouse APL(acute promyelocyte leukemia) cells**
Organism:	**Mus musculus**
Experiment type:	**Expression profiling by array**
Platform:	**GPL1261**
Pubmed ID:	
Summary & Design:	**Summary:** **The differentiation of leukemia stem cells (LSCs) is generally regarded as a one-way alterative process to self-renewal. However, how differentiation impacts LSC stemness has largely been unexplored. Here we show that before reaching terminal differentiation (TD), apical LSCs of mouse acute promyelocytic leukemia passed through a partial differentiation (PD) stage, wherein the leukemia cells re-initiated leukemia via de-differentiation albeit at a reduced rate. Notably, while retinoic acid (RA) preferentially drove the transition of LSC to PD, monocytic Irf8 skewed PD cells to terminal maturation over de-differentiation and/or expansion. Remarkably, the combined use of RA and Irf8 induction depleted the total leukemogenic potential, which indicates that discrete stage- or lineage-specific mechanisms elaborate a step-wise LSC differentiation.** **We used microarrays to detail the global programme of gene expression indicating the molecular mechanisms unerlying the the process of LSC step-wise differentiation.** **Overall design:** **Retroviral GFP-labled mouse APL cells (bone marrow sample) were repopulated in vivo through transplantation into syngenic recipients. At the proper time points, the GFP positive APL bone marrow cells were collected and sorted for UNSC, UNPD and UNTD samples through FACS. RA-PD and RA-TD cells were sorted from bone marrow tissue treated with ATRA (all trans retinoic acid) for 5 days. The freshly isolated samples were then lysed for RNA extration. Each sample had two biological replicates.**

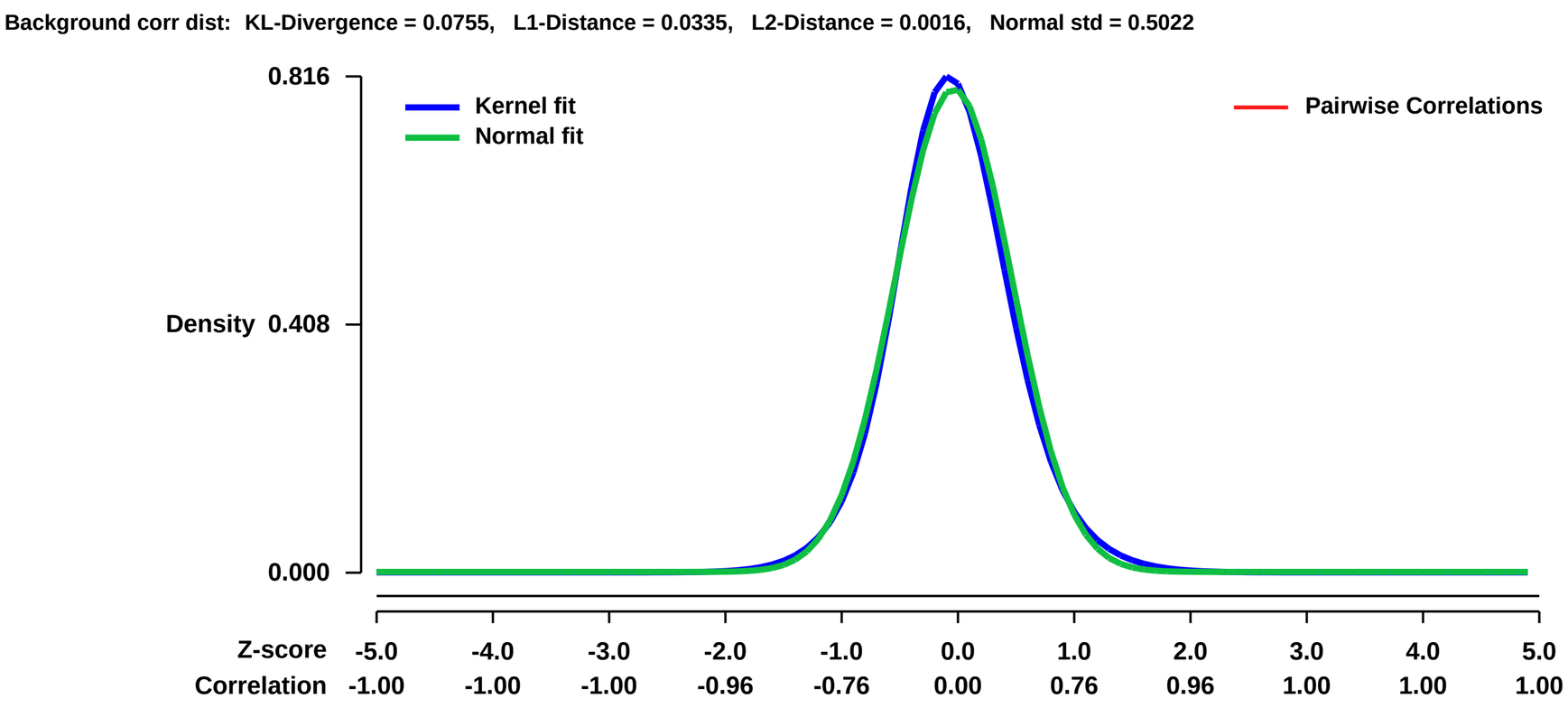

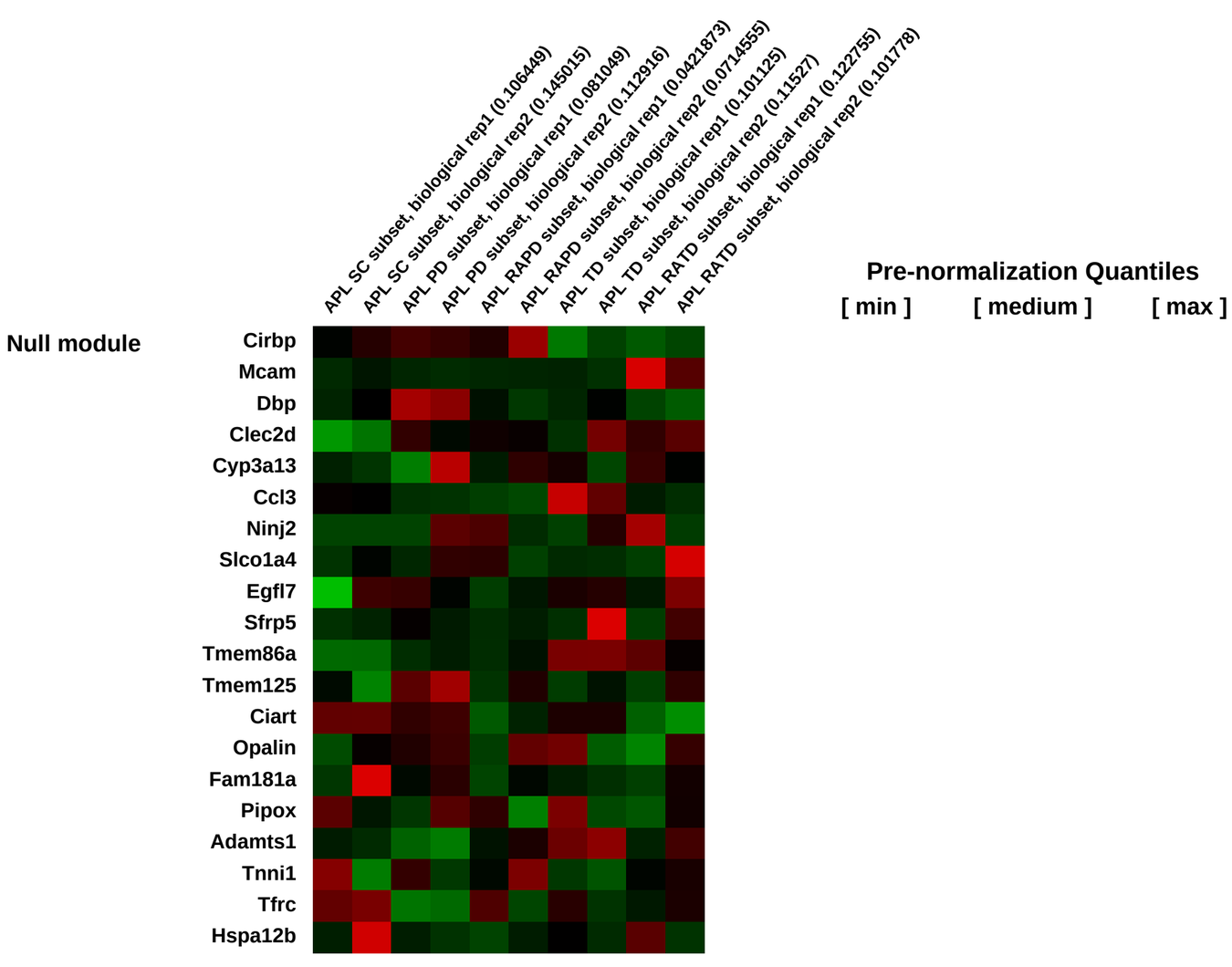

GEO Series "GSE46116" Expression Profiles

Num of samples in this series: 8

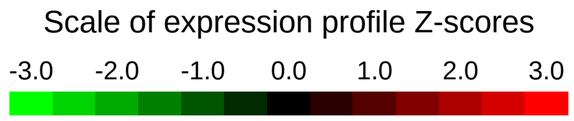

GEO Link:	**http://www.ncbi.nlm.nih.gov/geo/query/acc.cgi?acc=GSE46116**
Status:	**Public on Jul 01 2013**
Title:	**Changes in gene expression upon co-treatment of cells with Dex and E2**
Organism:	**Mus musculus**
Experiment type:	**Expression profiling by array**
Platform:	**GPL1261**
Pubmed ID:	**23803465**
Summary & Design:	**Summary:** **We report changes in gene expression upon co-treatment with Dex and E2 when compared to Dex or E2 treatments alone.** **Overall design:** **We examine expression under four different treatments (unt, Dex, E2, and Dex + E2).**

Background corr dist: **KL-Divergence = 0.0581, L1-Distance = 0.0199, L2-Distance = 0.0005, Normal std = 0.5293**

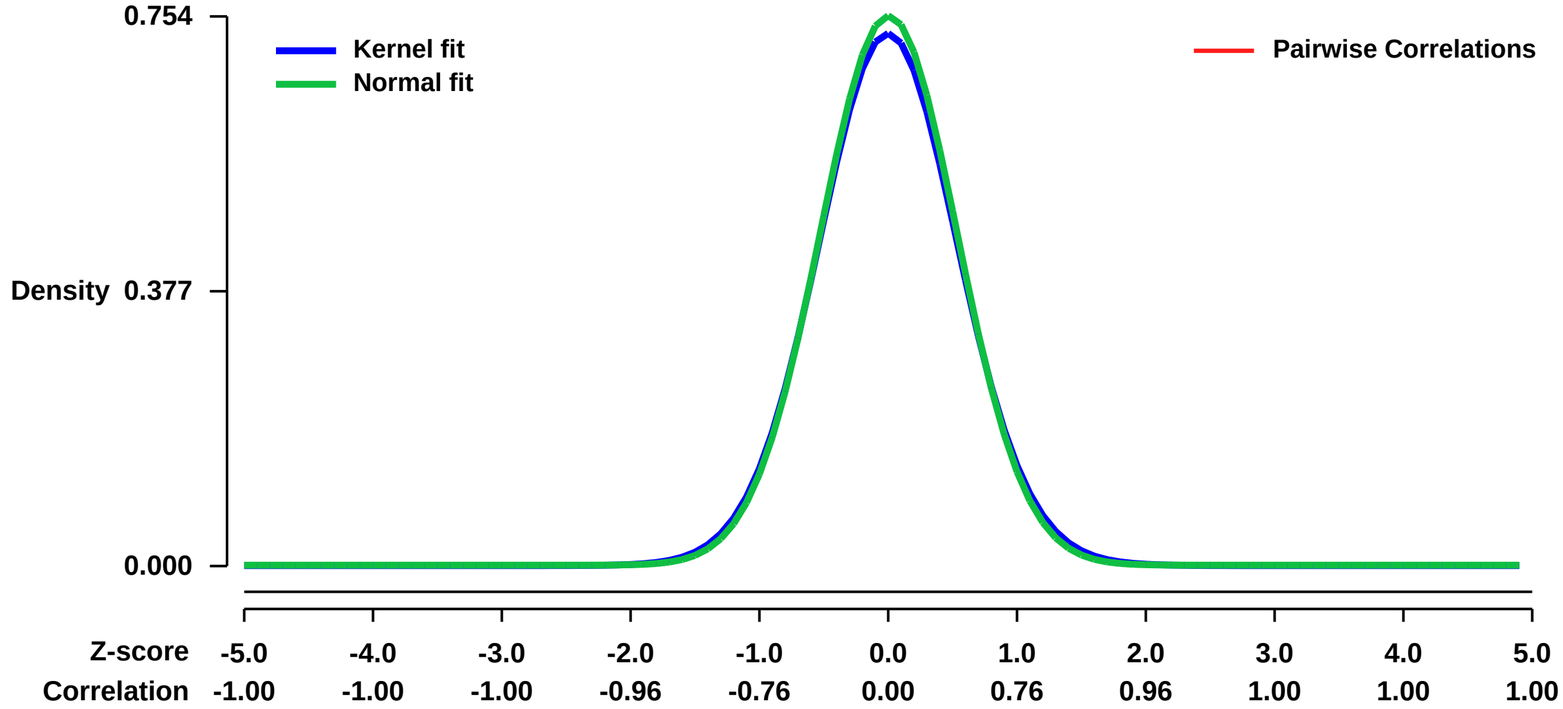

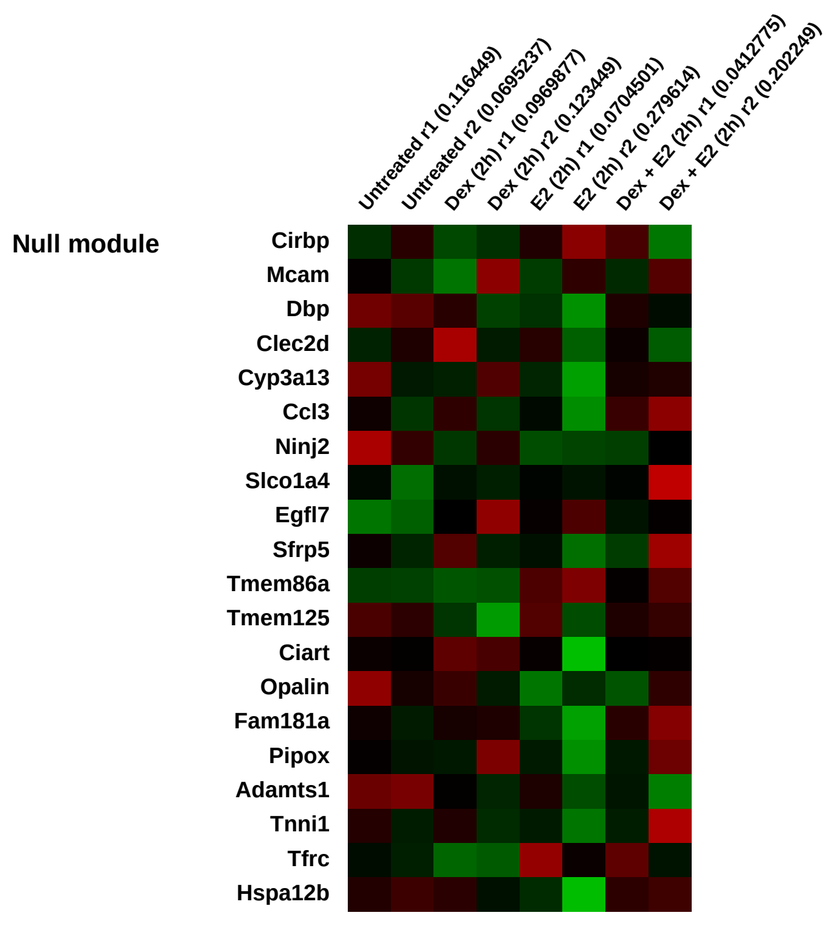

GEO Series "GSE46150" Expression Profiles

Num of samples in this series: 8

Scale of expression profile Z-scores

-3.0 -2.0 -1.0 0.0 1.0 2.0 3.0

GEO Link:	http://www.ncbi.nlm.nih.gov/geo/query/acc.cgi?acc=GSE46150
Status:	Public on Oct 01 2013
Title:	Gene expression profiling of primary mouse embryonic palatal mesenchymal cells in Tgfbr2 mutant mouse models
Organism:	Mus musculus
Experiment type:	Expression profiling by array
Platform:	GPL1261
Pubmed ID:	23975680
Summary & Design:	**Summary:** The overall goal of this project is to investigate the role of TGF-beta signaling in regulating the cellular metabolism of cranial neural crest (CNC) cells during palate development. Here, we conducted gene expression profiling of primary mouse embryonic palatal mesenchymal (MEPM) cells from wild type mice as well as those with a neural crest specific conditional inactivation of the Tgfbr2 gene. The latter mice provide a model of cleft palate, which is among the most common congenital birth defects and observed in many syndromic conditions. **Overall design:** To investigate the adverse effects of dysfunctional TGF-Beta signaling on the cellular metabolism of palatal mesenchyme during palatogenesis, we analyzed mice with a neural crest cell-specific conditional inactivation of Tgfbr2 (Tgfbr2fl/fl;Wnt1-Cre). We performed microarray analyses of primary mouse embryonic palatal mesenchymal cells of Tgfbr2fl/fl;Wnt1-Cre mutant mice and Tgfbr2fl/fl control mice, collected at embryonic day 13.5 (n=4 per genotype) and cultured with standard media (DMEM with supplements). Cells were collected after 2 passages.

Background corr dist: KL-Divergence = 0.0453, L1-Distance = 0.0160, L2-Distance = 0.0003, Normal std = 0.5769

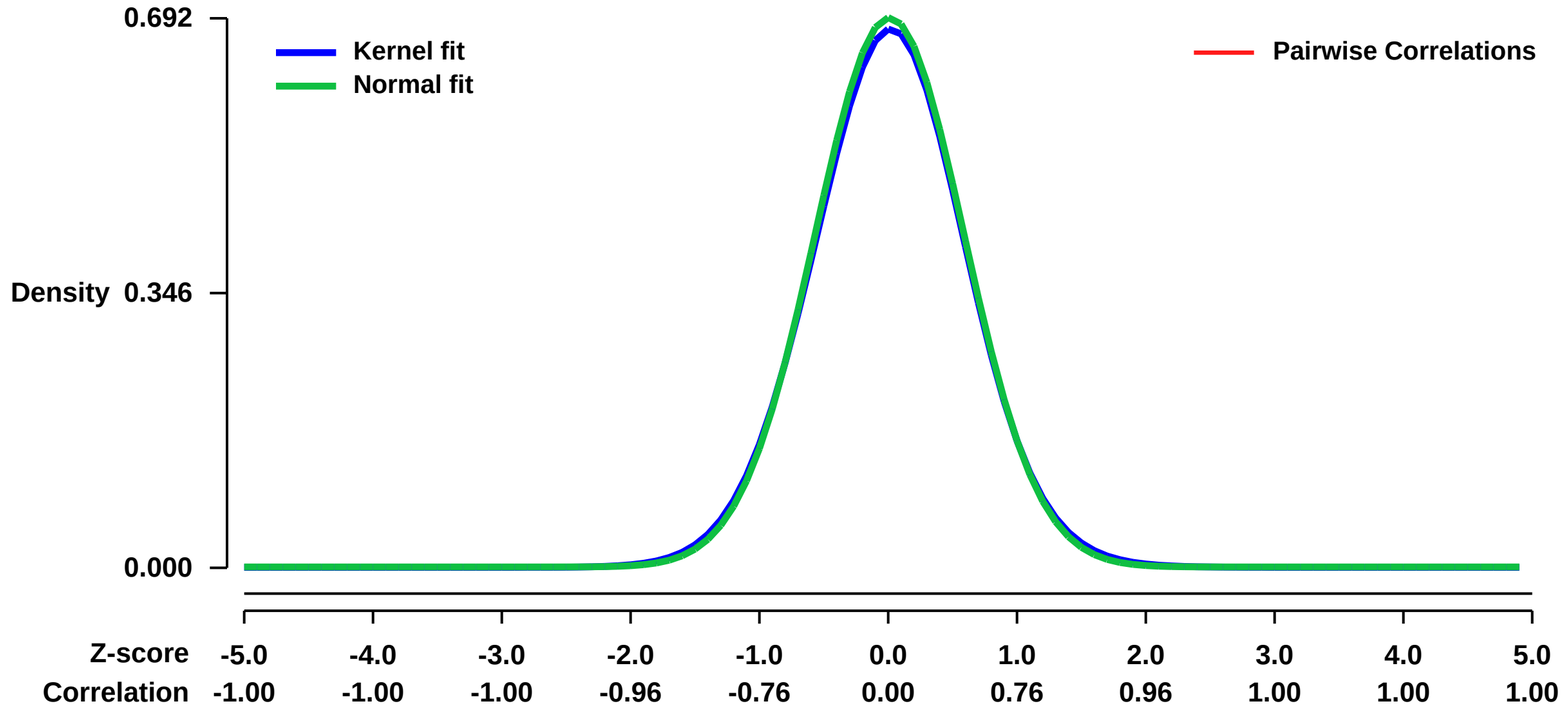

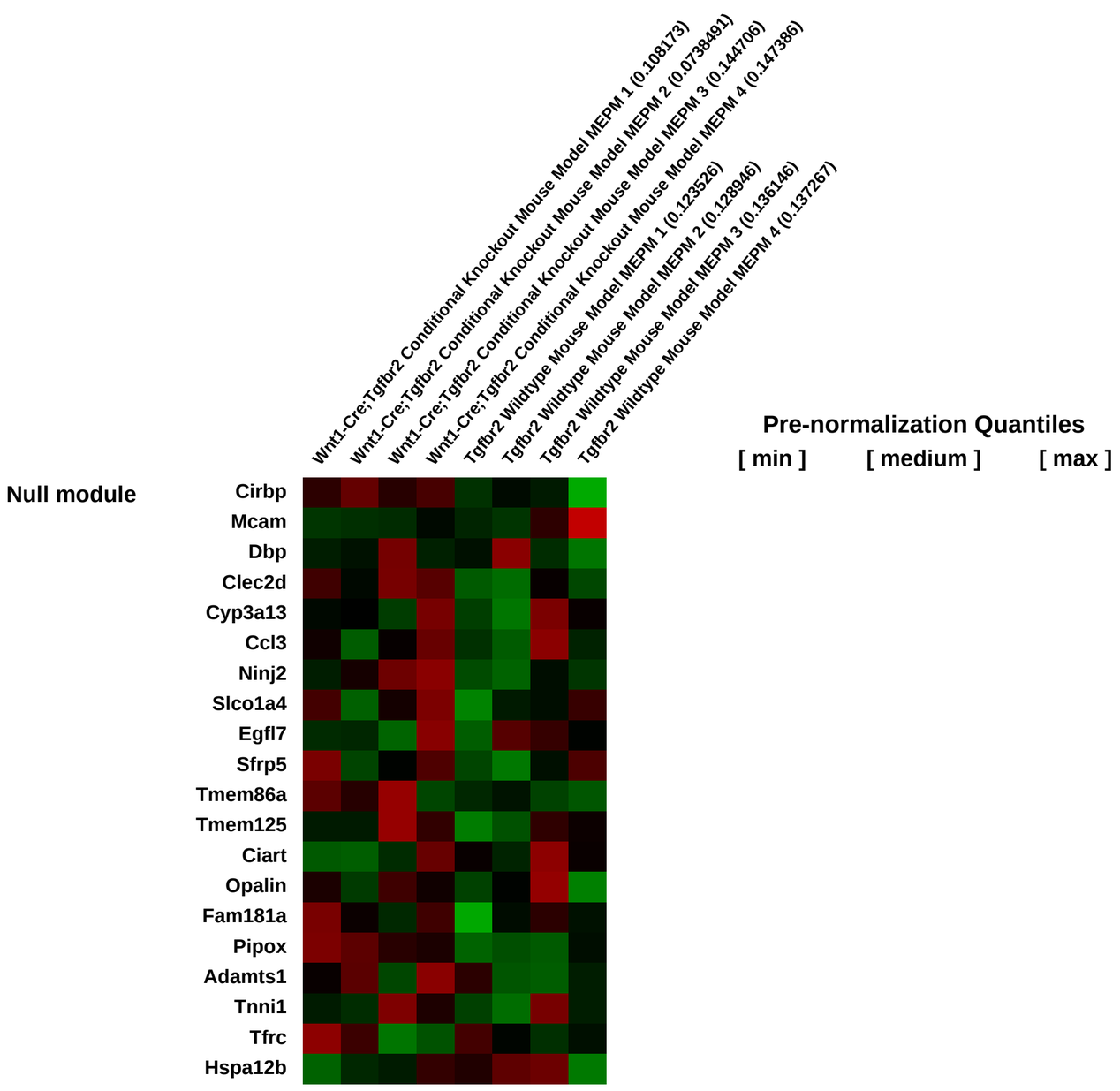

GEO Series "GSE46185" Expression Profiles

Num of samples in this series: 6

Scale of expression profile Z-scores

-3.0 -2.0 -1.0 0.0 1.0 2.0 3.0

GEO Link:	http://www.ncbi.nlm.nih.gov/geo/query/acc.cgi?acc=GSE46185
Status:	Public on Apr 19 2013
Title:	Genome-wide gene expression profiling revealed a critical role for GATA3 in the maintenance of the Th2 cell identity
Organism:	Mus musculus
Experiment type:	Expression profiling by array
Platform:	GPL1261
Pubmed ID:	23824597
Summary & Design:	**Summary:** Functionally polarized CD4+ T helper (Th) cells such as Th1, Th2 and Th17 cells are central to the regulation of acquired immunity. However, the molecular mechanisms governing the maintenance of the polarized functions of Th cells remain unclear. GATA3, a master regulator of Th2 cell differentiation, initiates the expressions of Th2 cytokine genes and other Th2-specific genes. GATA3 also plays important roles in maintaining Th2 cell function and in continuous chromatin remodeling of Th2 cytokine gene loci. However, it is unclear whether continuous expression of GATA3 is required to maintain the expression of various other Th2-specific genes. In this report, genome-wide DNA gene expression profiling revealed that GATA3 expression is critical for the expression of a certain set of Th2-specific genes. We demonstrated that GATA3 dependency is reduced for some Th2-specific genes in fully developed Th2 cells compared to that observed in effector Th2 cells, whereas it is unchanged for other genes. Moreover, effects of a loss of GATA3 expression in Th2 cells on the expression of cytokine and cytokine receptor genes were examined in detail. A critical role of GATA3 in the regulation of Th2-specific gene expression is confirmed in in vivo generated antigen-specific memory Th2 cells. Therefore, GATA3 is required for the continuous expression of the majority of Th2-specific genes involved in maintaining the Th2 cell identity. **Overall design:** Mock-transfected and GATA3 siRNA-transfected Th2 and Th2-4th cells are profiled for mRNA expression

Background corr dist: KL-Divergence = 0.0332, L1-Distance = 0.0373, L2-Distance = 0.0018, Normal std = 0.6839

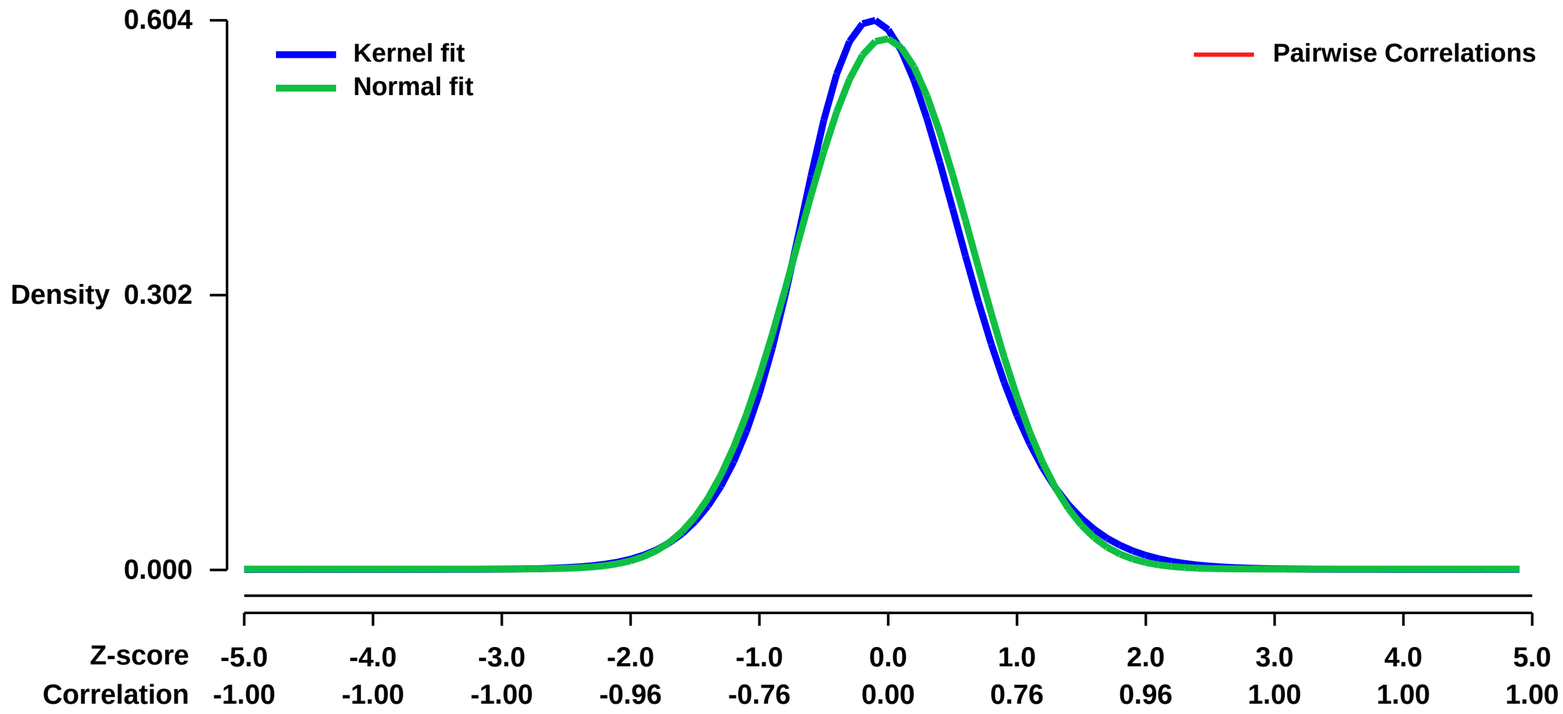

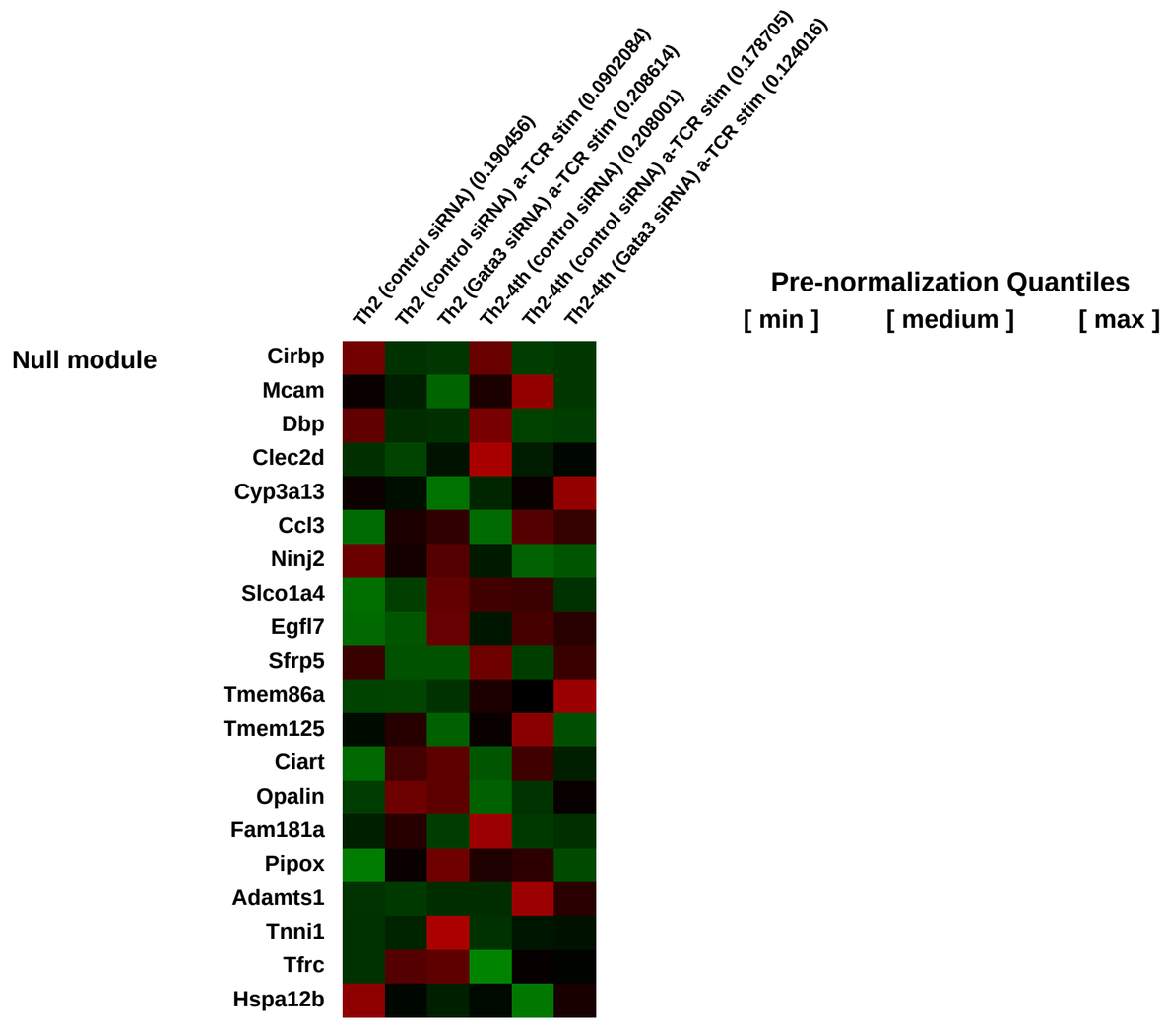

GEO Series "GSE46211" Expression Profiles

Num of samples in this series: 18

Scale of expression profile Z-scores

-3.0 -2.0 -1.0 0.0 1.0 2.0 3.0

GEO Link:	http://www.ncbi.nlm.nih.gov/geo/query/acc.cgi?acc=GSE46211
Status:	Public on Oct 01 2013
Title:	Gene expression profiling of anterior and posterior palatal tissue from Tgfbr2 mutant mouse models
Organism:	Mus musculus
Experiment type:	Expression profiling by array
Platform:	GPL1261
Pubmed ID:	24496627
Summary & Design:	**Summary:** The overall goal of this project is to investigate the role of TGF-beta signaling in epithelial cells as it pertains to the orientation of muscle fibers in the soft palate during embryogenesis. Here, we first conducted gene expression profiling of the anterior and posterior portions of the palate from wild-type mice. In addition, we also conducted gene expression profiling of the posterior palate in mutant mice with an epithelium-specific conditional inactivation of the Tgfbr2 gene. The latter mice provide a model of submucosal cleft palate, which is a congenital birth defect commonly observed in many syndromic conditions. **Overall design:** To investigate the adverse effects of dysfunctional TGF-Beta signaling on tissue-tissue interaction between the palatal epithelium and myofibers during palatogenesis, we analyzed mice with an epithelial cell-specific conditional inactivation of Tgfbr2 (Tgfbr2fl/fl;K14-Cre). We performed microarray analyses of anterior palatal tissue and posterior palatal tissue of E15.5 Tgfbr2fl/fl control mice (n=5, each region), and posterior palatal tissue of Tgfbr2fl/fl;K14-Cre mutant mice, collected at embryonic day 15.5 (n=5). Control samples and mutant samples are from separate litters.

Background corr dist: KL-Divergence = 0.1225, L1-Distance = 0.0338, L2-Distance = 0.0021, Normal std = 0.4035

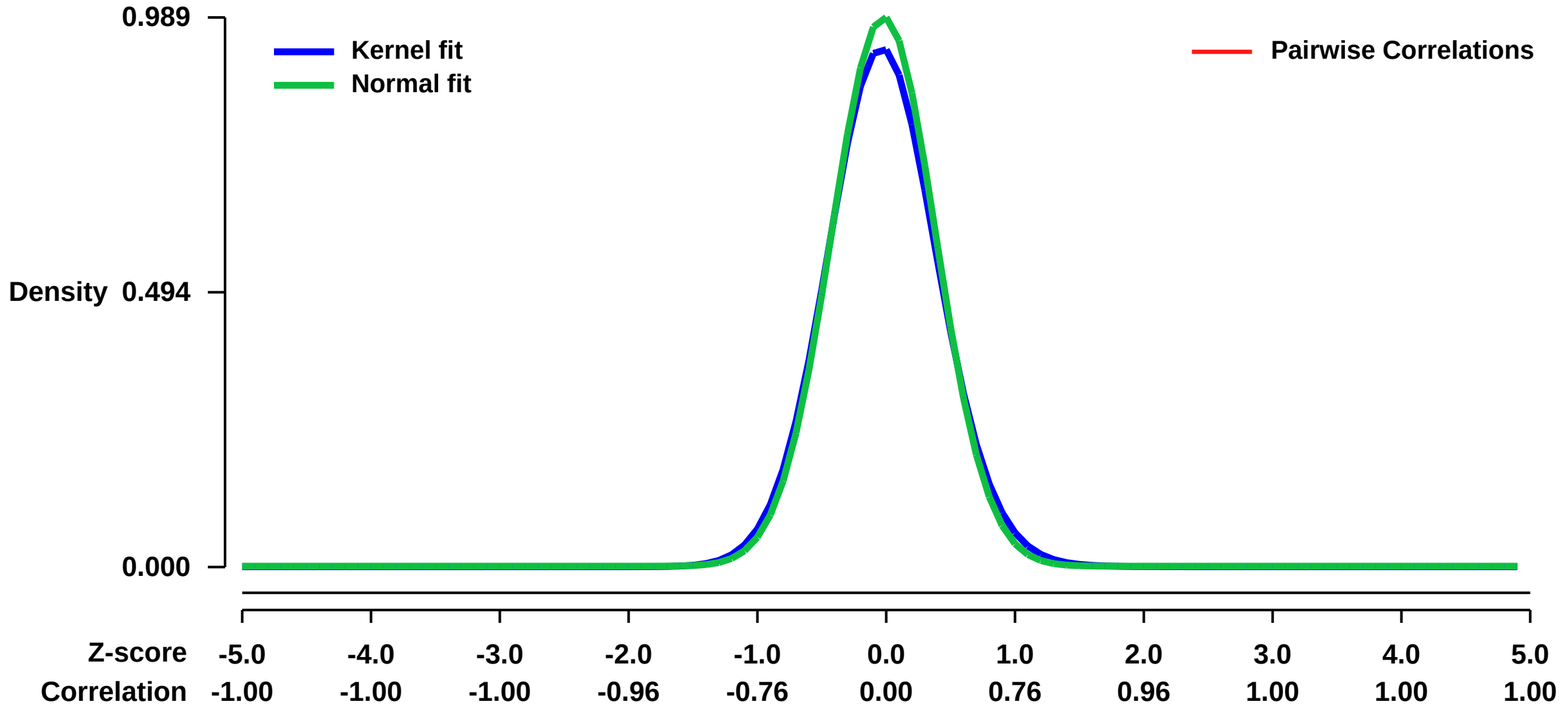

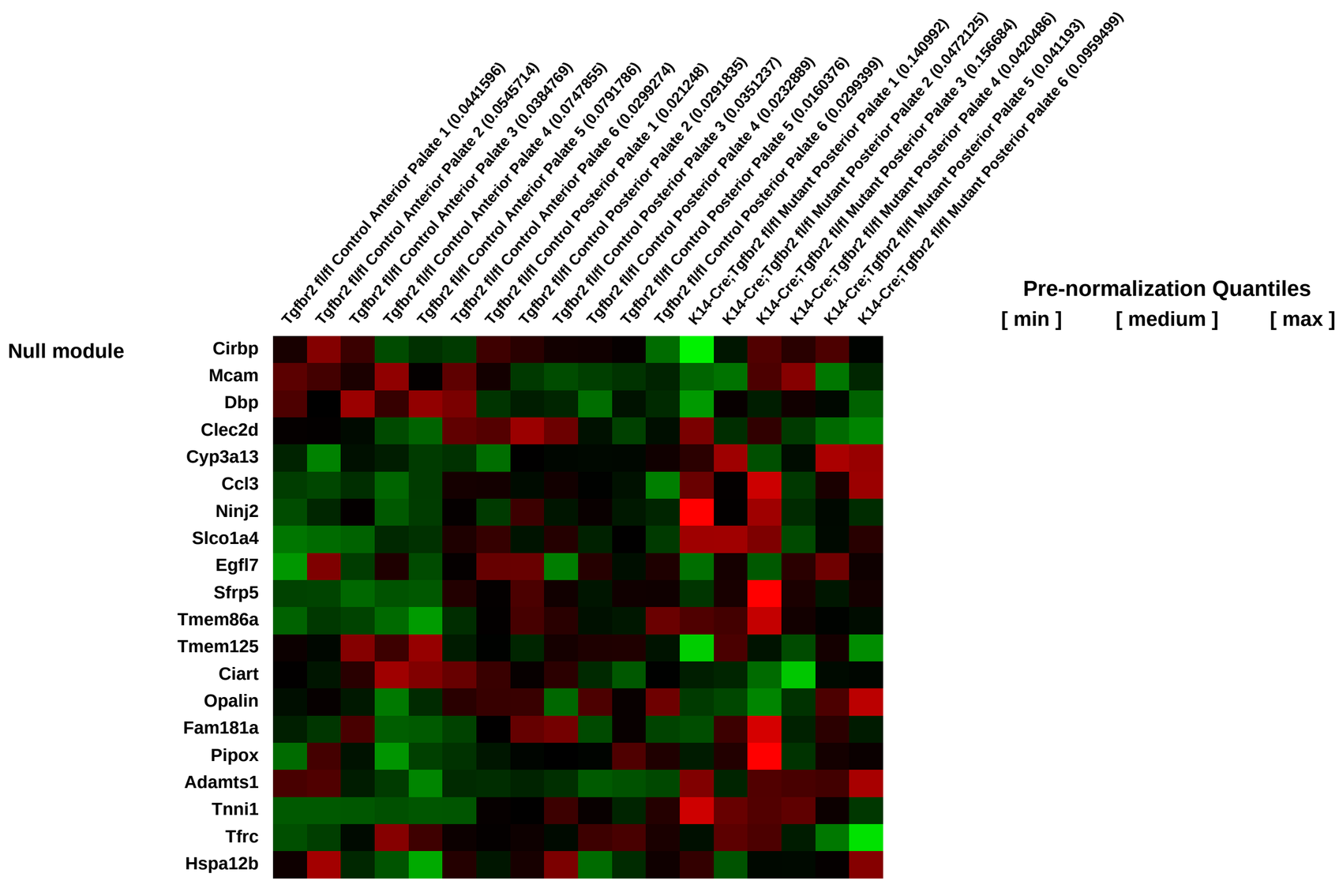

GEO Series "GSE46242" Expression Profiles

Num of samples in this series: 12

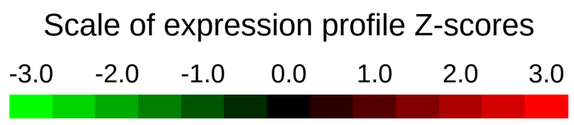

GEO Link:	http://www.ncbi.nlm.nih.gov/geo/query/acc.cgi?acc=GSE46242
Status:	Public on Apr 21 2013
Title:	Egr2-dependent expression in T cell anergy
Organism:	Mus musculus
Experiment type:	Expression profiling by array
Platform:	GPL1261
Pubmed ID:	23548837
Summary & Design:	**Summary:** T cell anergy is one of the mechanisms contributing to peripheral tolerance, particularly in the context of progressively growing tumors and in tolerogenic treatments promoting allograft acceptance. We recently reported that early growth response gene 2 (Egr2) is a critical transcription factor for the induction of anergy in vitro and in vivo, which was identified based on its ability to regulate the expression of inhibitory signaling molecules diacylglycerol kinase (DGK)-a and -z. We reasoned that other transcriptional targets of Egr2 might encode additional factors important for T cell anergy and immune regulation. Thus, we conducted two sets of genome-wide screens: gene expression profiling of wild type versus Egr2-deleted T cells treated under anergizing conditions, and a ChIP-Seq analysis to identify genes that bind Egr2 in anergic cells. Merging of these data sets revealed 49 targets that are directly regulated by Egr2. Among these are inhibitory signaling molecules previously reported to contribute to T cell anergy, but unexpectedly, also cell surface molecules and secreted factors, including lymphocyte-activation gene 3 (Lag3), Class-I-MHC-restricted T cell associated molecule (Crtam), Semaphorin 7A (Sema7A), and chemokine CCL1. These observations suggest that anergic T cells might not simply be functionally inert, and may have additional functional properties oriented towards other cellular components of the immune system. **Overall design:** T cell-specific Egr2 deletion was mediated by use of a Cre-expressing adenovirus and a CAR Tg x Egr2flox/flox mouse in which CAR is expressed exclusively in the T cell compartment from a Lck promoter/CD2 enhancer cassette. OVA-specific Th1 cell clones were generated from CAR Tg x Egr2flox/flox mice. CAR Tg x Egr2flox/flox Th1 T cells were infected with an empty (EV) or a Cre-expressing adenovirus. Upon confirmation of Egr2 deletion by immunoblot, the T cells were left untreated (Control) or anergized (Anergic) by immobilized anti-CD3 for 16 hours, and microarray was conducted after 1 day of rest in culture medium. The microarray analysis was performed three times using three sets of independently manipulated samples

Background corr dist: KL-Divergence = 0.0916, L1-Distance = 0.0260, L2-Distance = 0.0009, Normal std = 0.4594

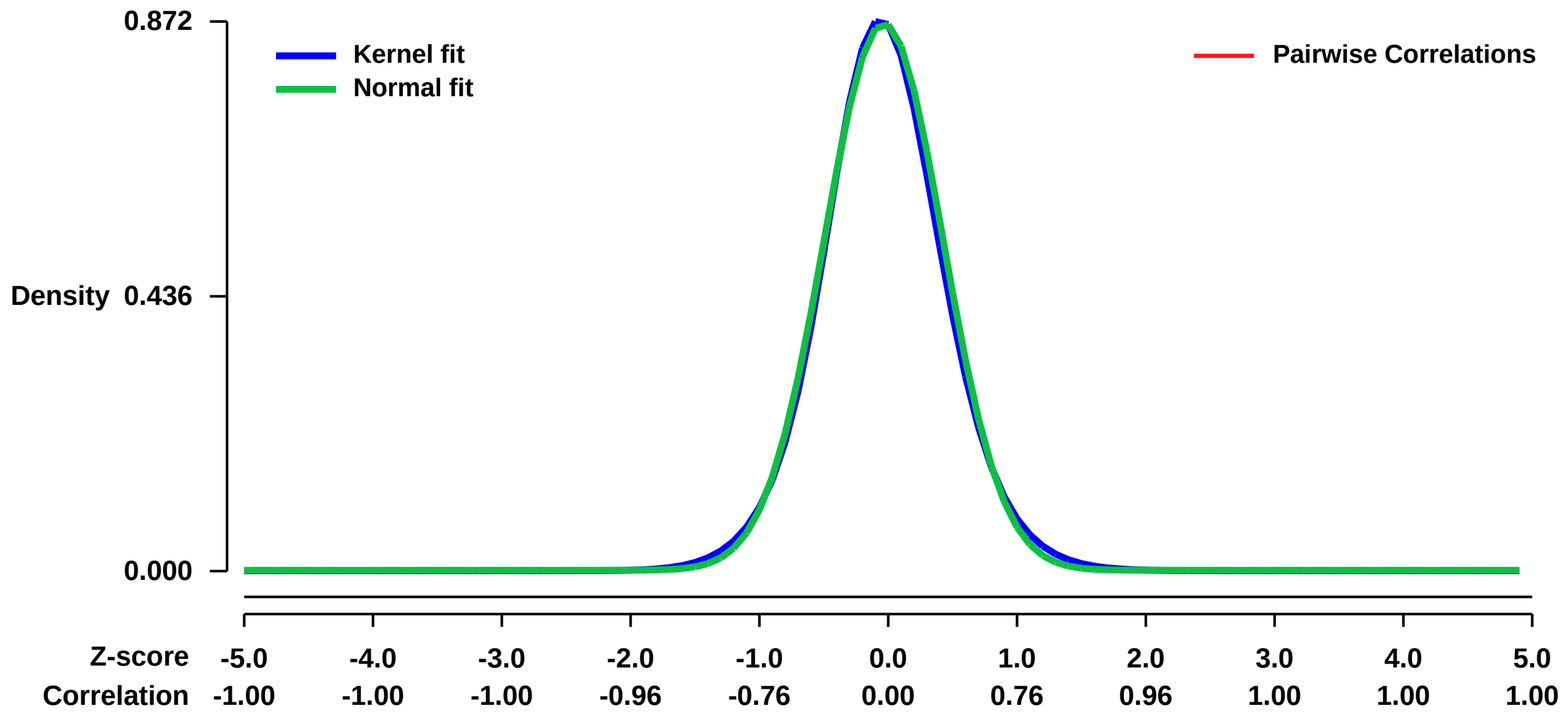

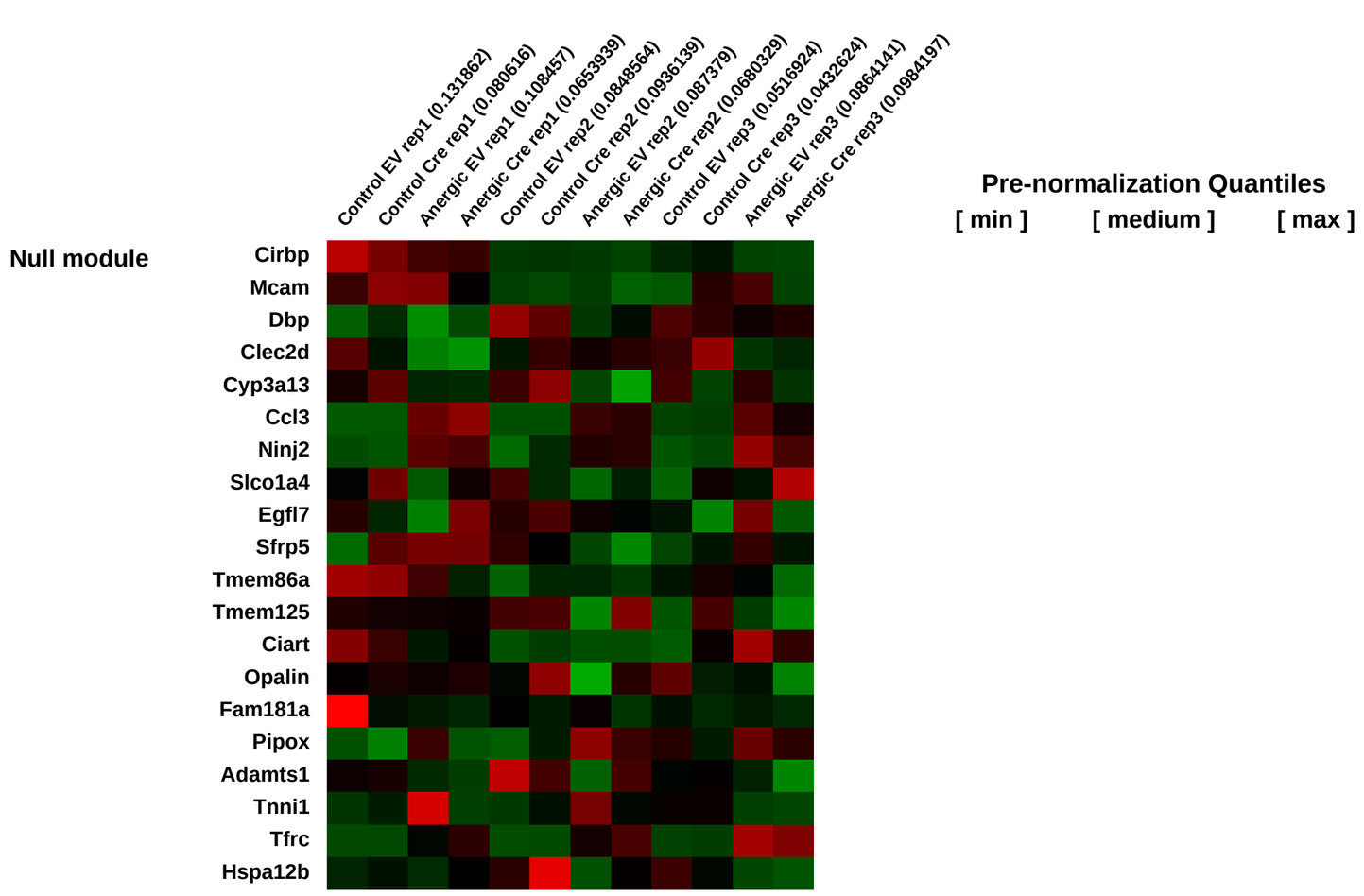

GEO Series "GSE4627" Expression Profiles

Num of samples in this series: 6

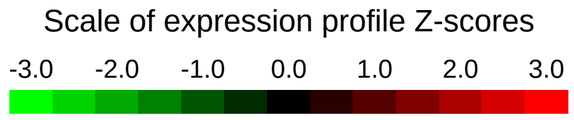

GEO Link:	**http://www.ncbi.nlm.nih.gov/geo/query/acc.cgi?acc=GSE4627**
Status:	**Public on Jul 01 2006**
Title:	**Telomere dysfunction**
Organism:	**Mus musculus**
Experiment type:	**Expression profiling by array**
Platform:	**GPL1261**
Pubmed ID:	
Summary & Design:	**Summary:** **We used microarrays to analyze the prevalence of signalling induced by acute telomere dysfunction (as induced by TRF2DBDM expression = Dataset 1) and in TERC- compared to TERC+ HCC (Dataset 2).** **Keywords: acute telomere dysfunction, hepatocellular cancer** **Overall design:** **Differentially expressed gene clusters were identified using Array Assist 4.0 (Stratagene).**

Background corr dist: **KL-Divergence = 0.0506, L1-Distance = 0.0389, L2-Distance = 0.0023, Normal std = 0.5890**

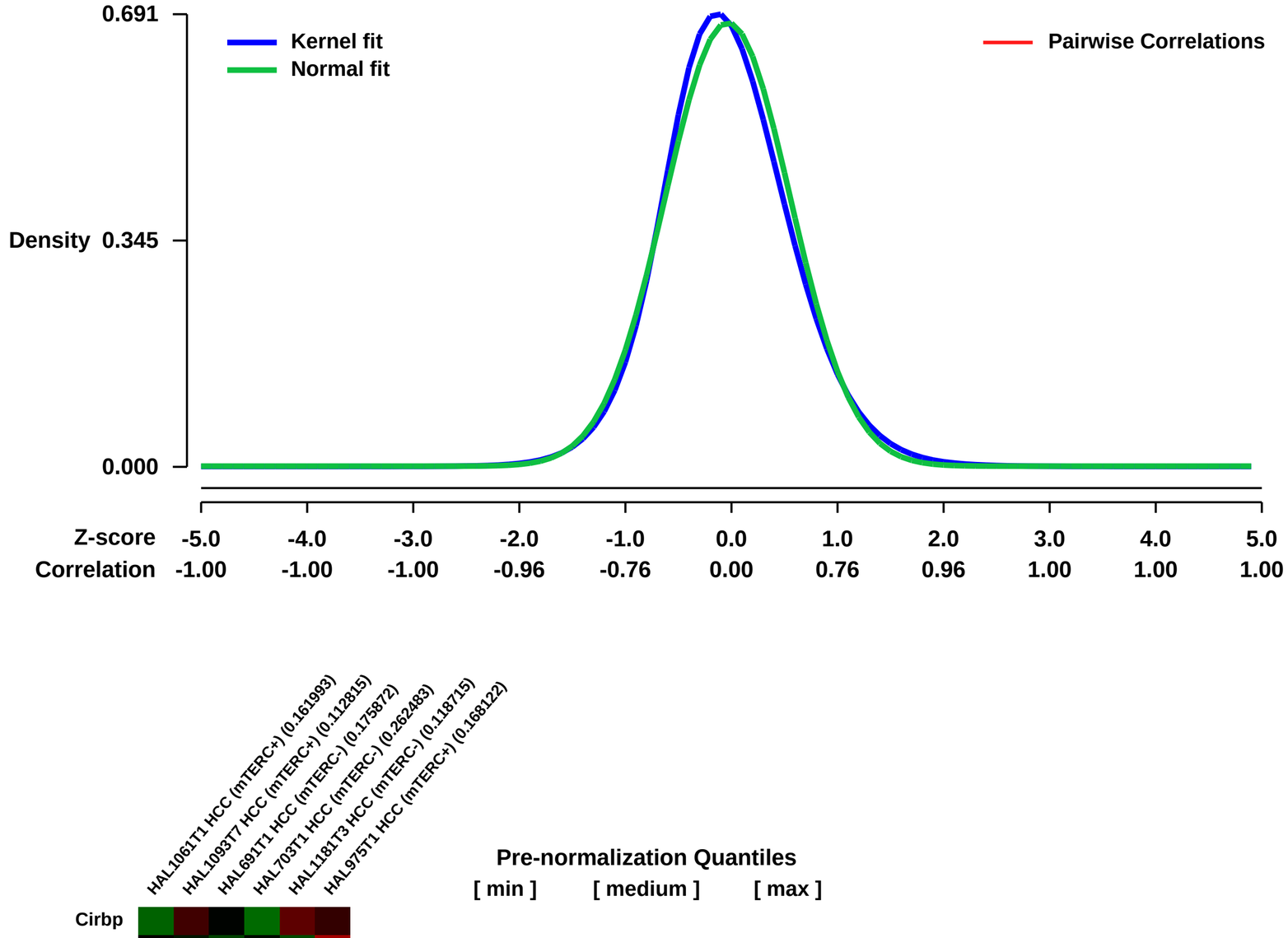

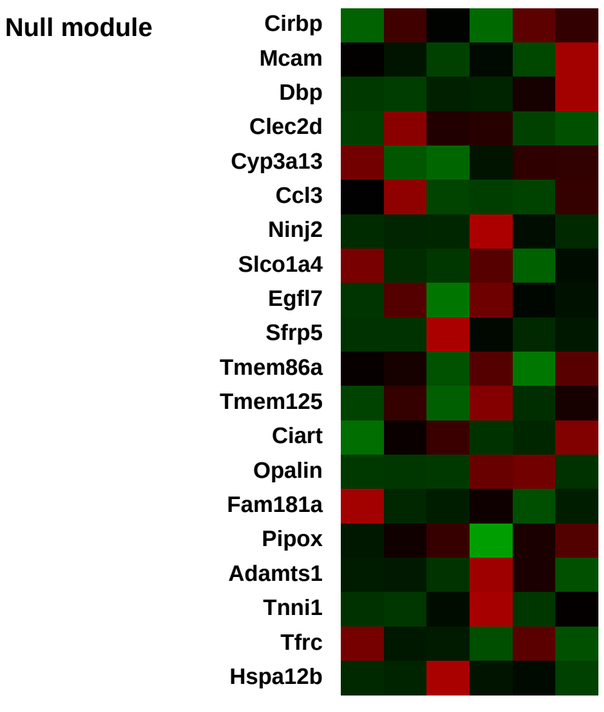

GEO Series "GSE46298" Expression Profiles

Num of samples in this series: 64

Scale of expression profile Z-scores

-3.0 -2.0 -1.0 0.0 1.0 2.0 3.0

GEO Link:	http://www.ncbi.nlm.nih.gov/geo/query/acc.cgi?acc=GSE46298
Status:	Public on Oct 01 2013
Title:	Whole genome transcriptome analysis identifies indices of fast and slow disease progression in two ALS mouse models
Organism:	Mus musculus
Experiment type:	Expression profiling by array
Platform:	GPL1261
Pubmed ID:	24065725
Summary & Design:	**Summary:** Microarray analysis has been applied to the study of ALS in order to investigate gene expression in whole spinal cord homogenates of SOD1 G93A mice and human ALS cases, although the massive presence of glial cells and inflammatory factors has made it difficult to define which gene expression changes were motor neuron specific. Recently, laser capture microdissection (LCM), combined with microarray analysis, has allowed the identification of motor neuron specific changes in gene expression in mouse and human ALS cases. The aim of the present study is to combine LCM and microarray analysis to compare the gene expression profiles of motor neurons from two SOD1G93A mouse strains (129Sv and C57) with different progression of the disease in order to discover the molecular mechanisms that may contribute to the distinct phenotypes and to uncover factors underlying fast and slow disease progression **Overall design:** Motor neurons have been isolated from the spinal cord of 129SvG93A mice, C57G93A mice and non transgenic littermates at different time points and the transcription expression profile of the isolated motor neurons has been analysed

Background corr dist: KL-Divergence = 0.2248, L1-Distance = 0.0369, L2-Distance = 0.0027, Normal std = 0.3165

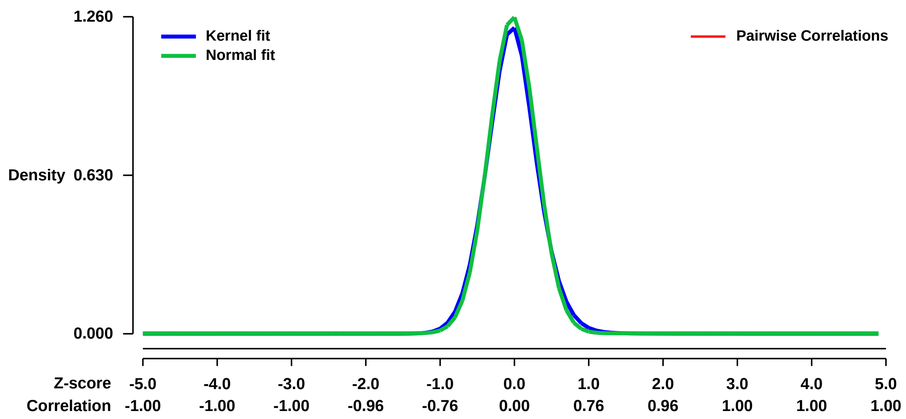

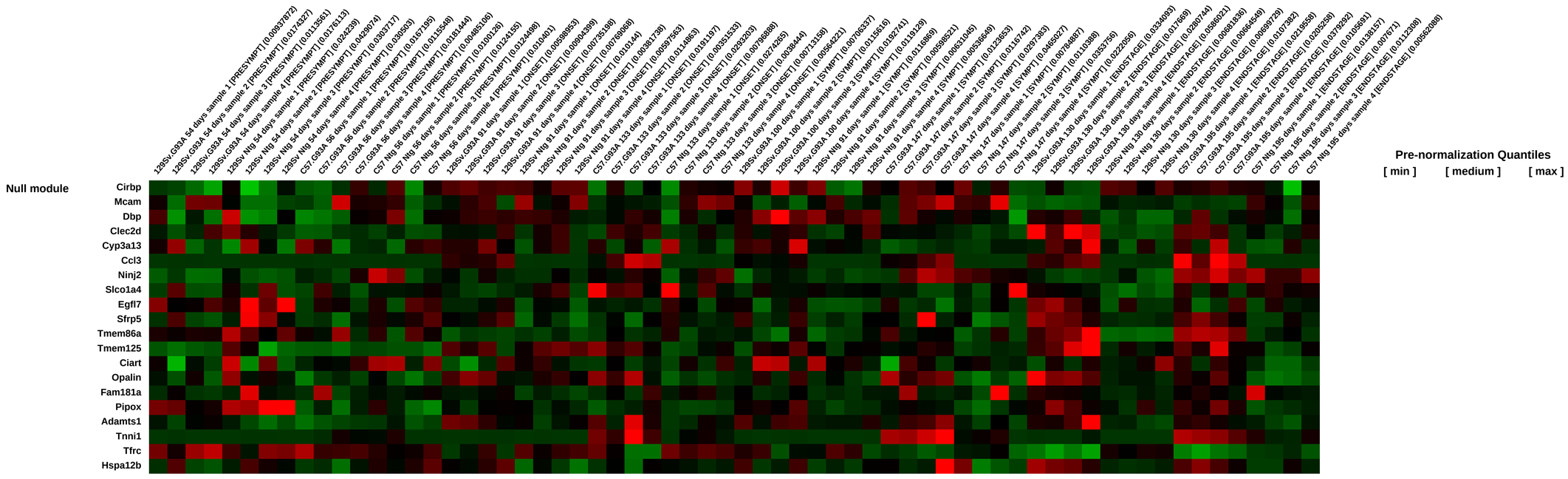

GEO Series "GSE46443" Expression Profiles

Num of samples in this series: 12

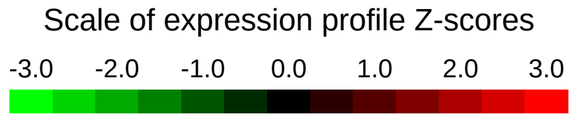

GEO Link:	**http://www.ncbi.nlm.nih.gov/geo/query/acc.cgi?acc=GSE46443**
Status:	**Public on Oct 21 2013**
Title:	**Expression data from mouse cerebral cortex**
Organism:	**Mus musculus**
Experiment type:	**Expression profiling by array**
Platform:	**GPL1261**
Pubmed ID:	**23800850**
Summary & Design:	**Summary:** **Differential gene expression of cerebral cortex might be responsible for distinct neurovascular developments between different mouse strains** **We used Affymetrix microarray to explore the global gene expression patterns of mouse cerebral cortex of different mouse strains at two developmental stages** **Overall design:** **Cerebral cortex from two mouse strains [C57BL/6J(B6) and C3H/J (C3H)] at post-natal day 1 (p1) and post-natal 11 weeks (11 wk) were harvested for microarray experiments**

Background corr dist: **KL-Divergence = 0.0145, L1-Distance = 0.0214, L2-Distance = 0.0004, Normal std = 0.8048**

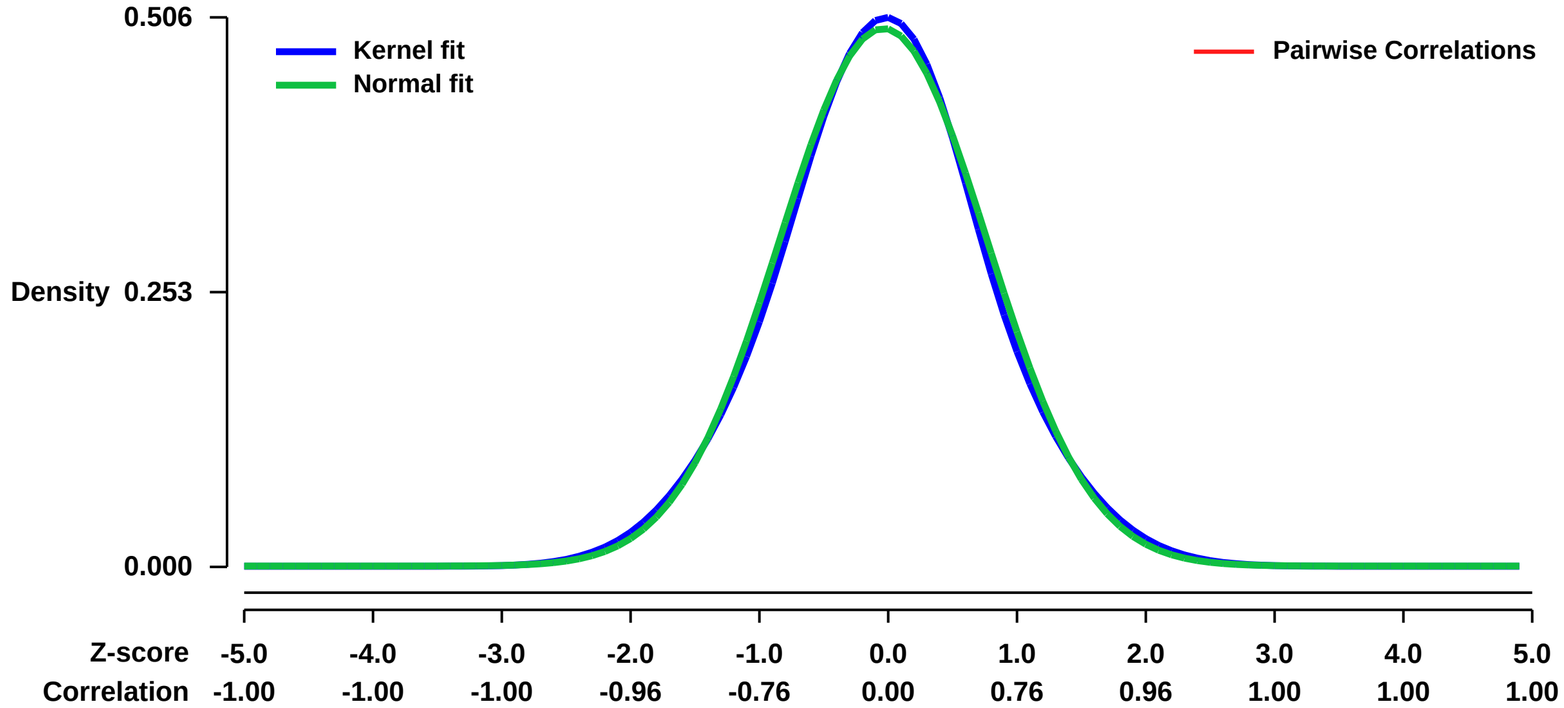

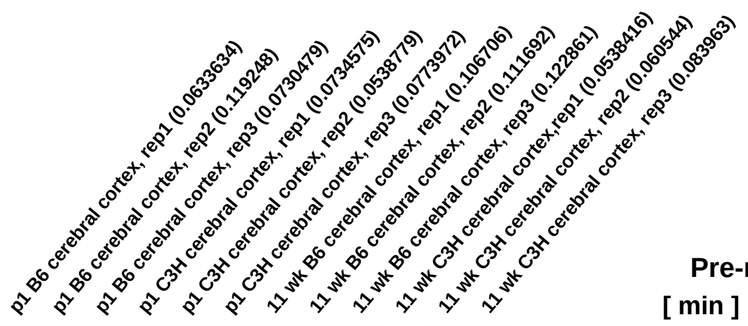

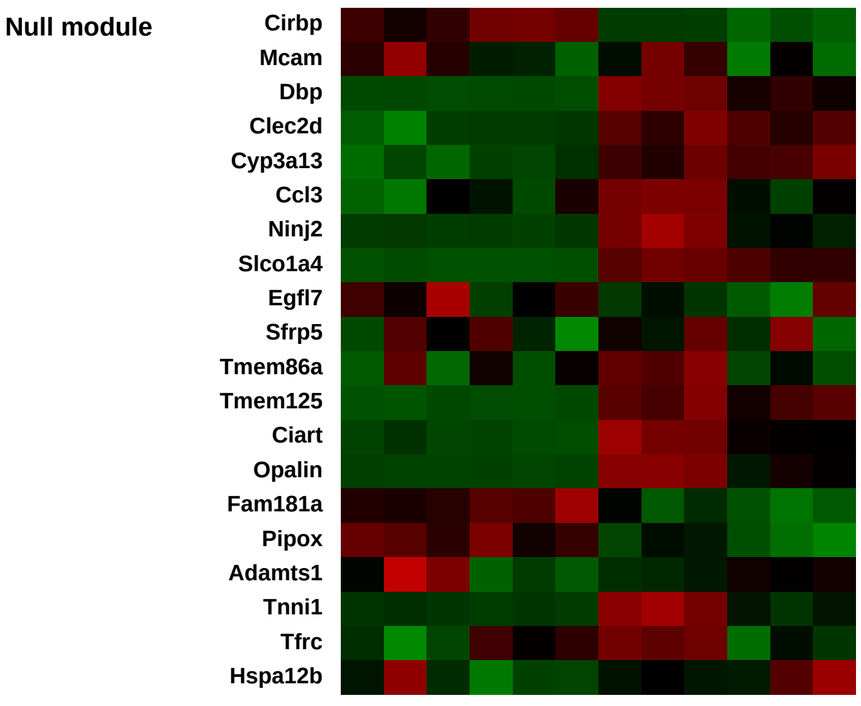

GEO Series "GSE46496" Expression Profiles

Num of samples in this series: 9

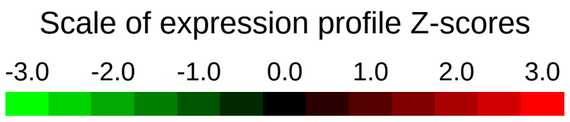

GEO Link:	http://www.ncbi.nlm.nih.gov/geo/query/acc.cgi?acc=GSE46496
Status:	Public on Jun 07 2013
Title:	Atrial Identity Is Determined by A COUP-TFII Regulatory Network (RNA)
Organism:	Mus musculus
Experiment type:	Expression profiling by array
Platform:	GPL1261
Pubmed ID:	23725765
Summary & Design:	**Summary:** Atria and ventricles exhibit distinct molecular profiles that produce structural and functional differences between the two cardiac compartments. However, factors that determine these differences remain largely undefined. Cardiomyocyte-specific COUP- TFII ablation produces ventricularized atria that exhibit ventricle-like action potentials, increased cardiomyocyte size, and development of extensive T-tubules. We used microarrays to examine the molecular profile of cardiomyocyte-specific COUP-TFII knockout adult atria in comparison with that of normal atria. **Overall design:** We extracted RNA from mutant right atria, control right atria and control ventricles from 2 months old adult mice, followed by gene expression profiling using Affymetrix microarrays.

Background corr dist: KL-Divergence = 0.0268, L1-Distance = 0.0394, L2-Distance = 0.0028, Normal std = 0.6869

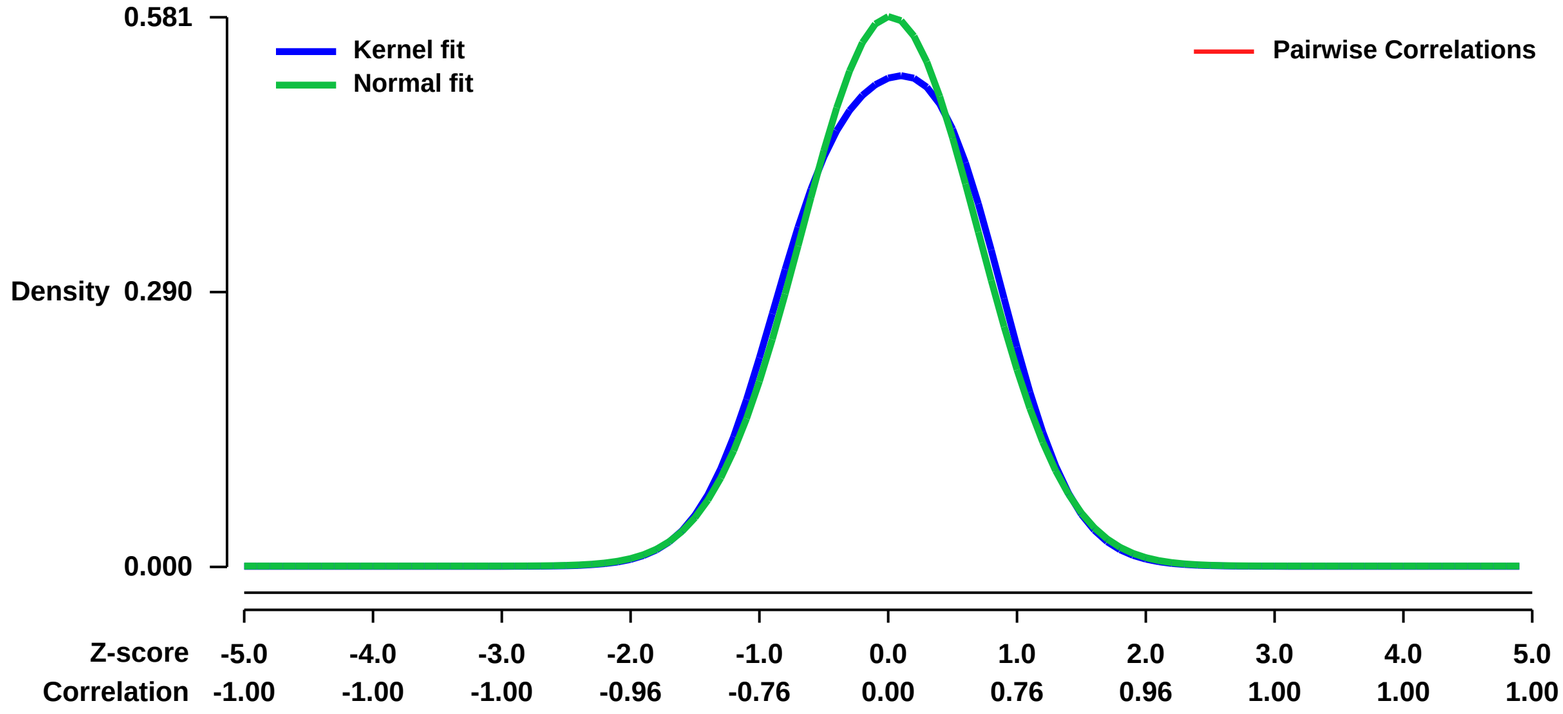

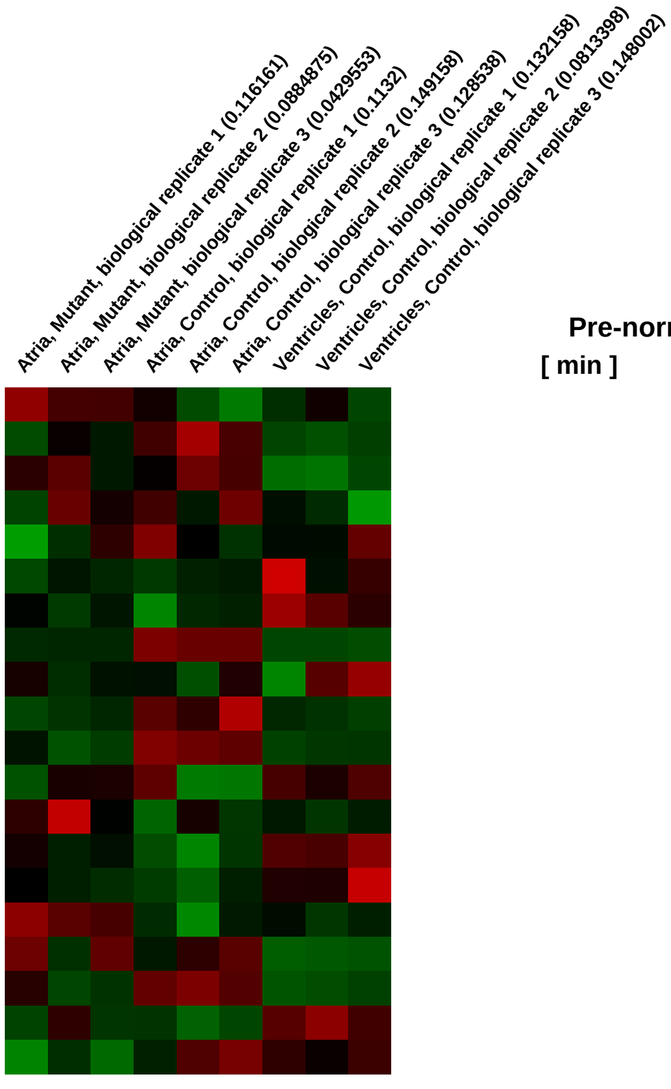

GEO Series "GSE4656" Expression Profiles

Num of samples in this series: 7

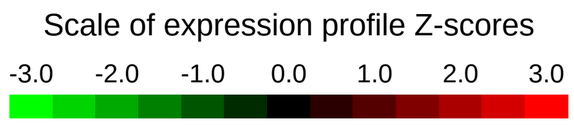

GEO Link:	http://www.ncbi.nlm.nih.gov/geo/query/acc.cgi?acc=GSE4656
Status:	Public on Mar 11 2007
Title:	day3 brown fat from wt compared to day3 from Gyk ko
Organism:	Mus musculus
Experiment type:	Expression profiling by array
Platform:	GPL1261
Pubmed ID:	17406644
Summary & Design:	**Summary:** **Glycerol kinase (GK) is at the interface of fat and carbohydrate metabolism and has been implicated in insulin resistance and type 2 diabetes mellitus (T2DM). To define GKâ s role in insulin resistance, we examined gene expression in brown adipose tissue in a glycerol kinase (Gyk) knockout (KO) mouse model using microarray analysis. Global gene expression profiles of KO mice were distinct from wild type (WT) with 668 genes that were differentially expressed. These included genes involved in lipid metabolism, carbohydrate metabolism, insulin signaling, and insulin resistance. Real-Time (RT) PCR analysis confirmed the differential expression of selected genes involved in lipid and carbohydrate metabolism. PathwayAssist analysis confirmed direct and indirect connections between GK and genes in lipid metabolism, carbohydrate metabolism, insulin signaling, and insulin resistance. Network Component Analysis (NCA) showed that the transcription factors, peroxisome proliferator-activated receptor gamma (PPAR-¿‡), sterol regulatory element binding factor 1 (SREBP-1), SREBP-2, signal transducer and activator of transcription 3 (STAT3), STAT5, trans-acting transcription factor 1 (SP1), CCAAT/enhancer binding protein alpha (CEBP-¿–), cAMP responsive element binding protein 1 (CREB), glucocorticoid receptor (GR), and PPAR-¿– have altered activity in the KO mice. NCA also revealed the individual contribution of these transcription factors on the expression of genes altered in the microarray data. This study elucidates the transcription network of Gyk and further confirms a role for Gyk, a simple Mendelian disorder, in insulin resistance and T2DM, a common complex genetic disorder.** **Keywords: genotype state analysis** **Overall design:** **7 samples are analyzed; 3 wildtype and 4 KO. the WT samples are used as control and KO samples are used as the experimental group.**

Background corr dist: KL-Divergence = 0.0613, L1-Distance = 0.0172, L2-Distance = 0.0003, Normal std = 0.5265

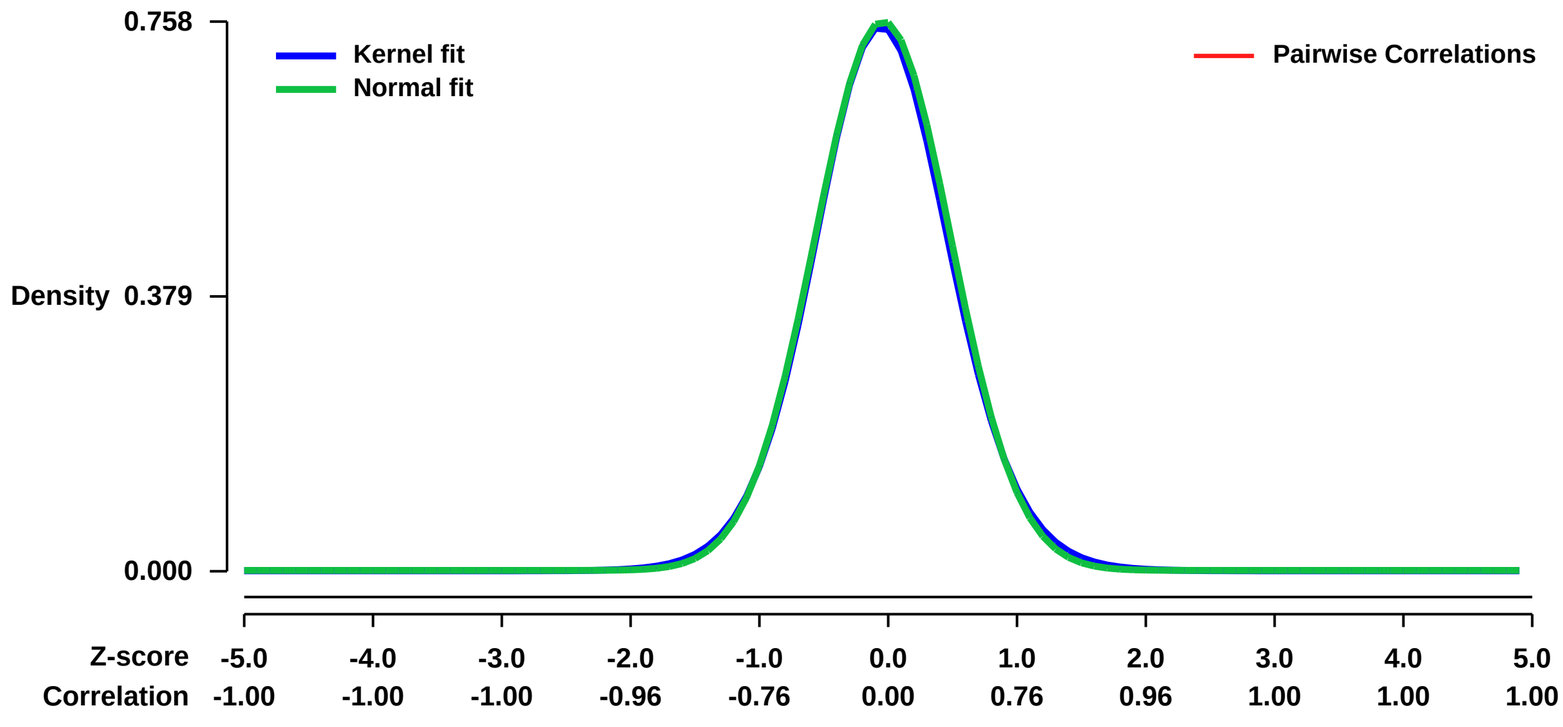

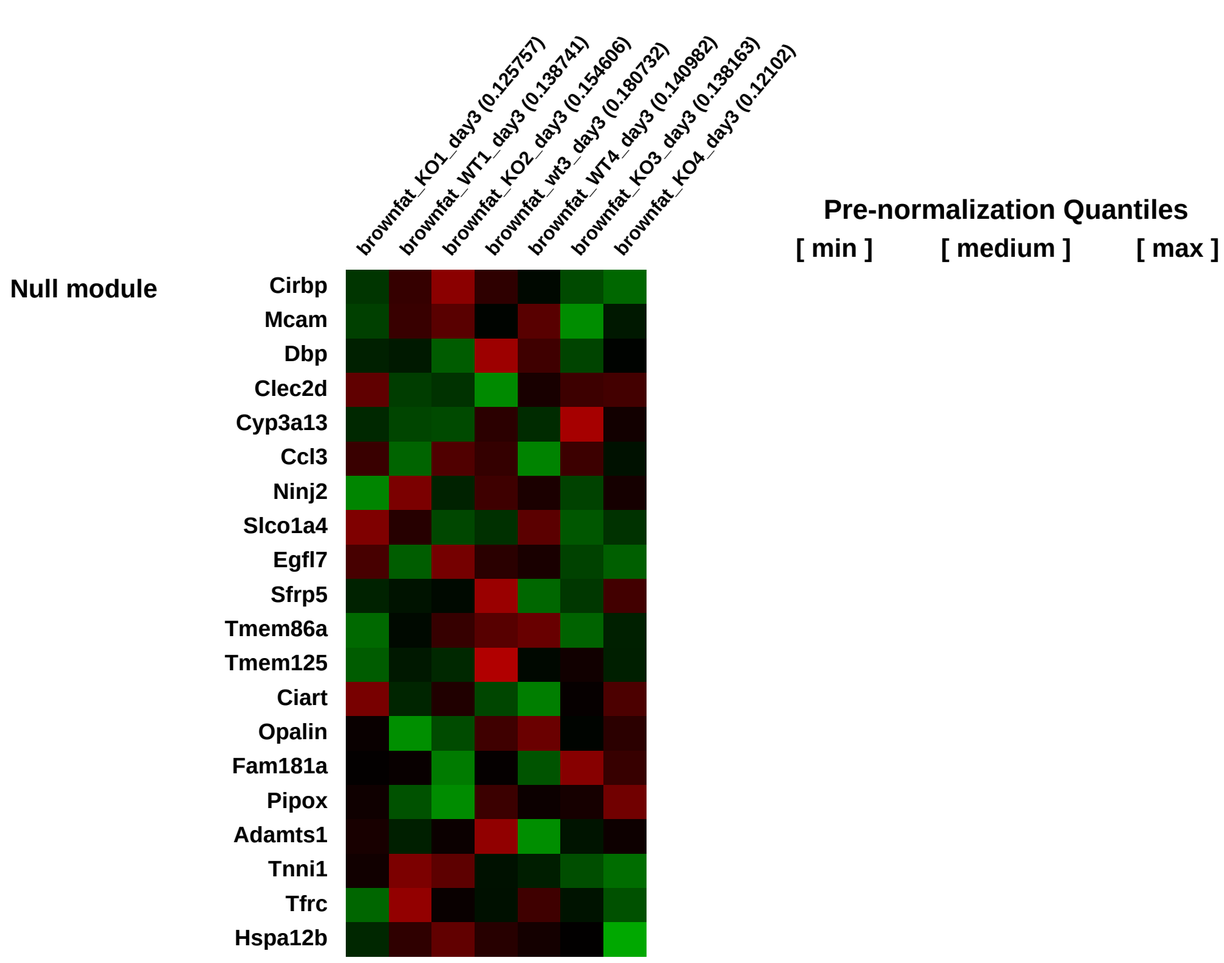

GEO Series "GSE4658" Expression Profiles

Num of samples in this series: 6

Scale of expression profile Z-scores

-3.0 -2.0 -1.0 0.0 1.0 2.0 3.0

GEO Link:	http://www.ncbi.nlm.nih.gov/geo/query/acc.cgi?acc=GSE4658
Status:	Public on Dec 31 2006
Title:	static vs simulated microgravity
Organism:	Mus musculus
Experiment type:	Expression profiling by array
Platform:	GPL1261
Pubmed ID:	17243119
Summary & Design:	**Summary:** The below table includes a smaller list of data that was analyzed by dChip and filtered by pvalue such that a file with about 4600 genes was obtained, which allowed for ease of use from 40,000 genes. **Keywords: static vs simulated microgravity** **Overall design:** The total RNA was extracted from 2T3 pre-osteoblast cells exposed to static or simulated microgravity (Rotating Wall Vessel) conditions. The RNA was then sent to Affymetrix microarray core facility at Baylor College of Medicine (Houston, TX) for microarray analysis.

Background corr dist: **KL-Divergence = 0.0342, L1-Distance = 0.0397, L2-Distance = 0.0022, Normal std = 0.6845**

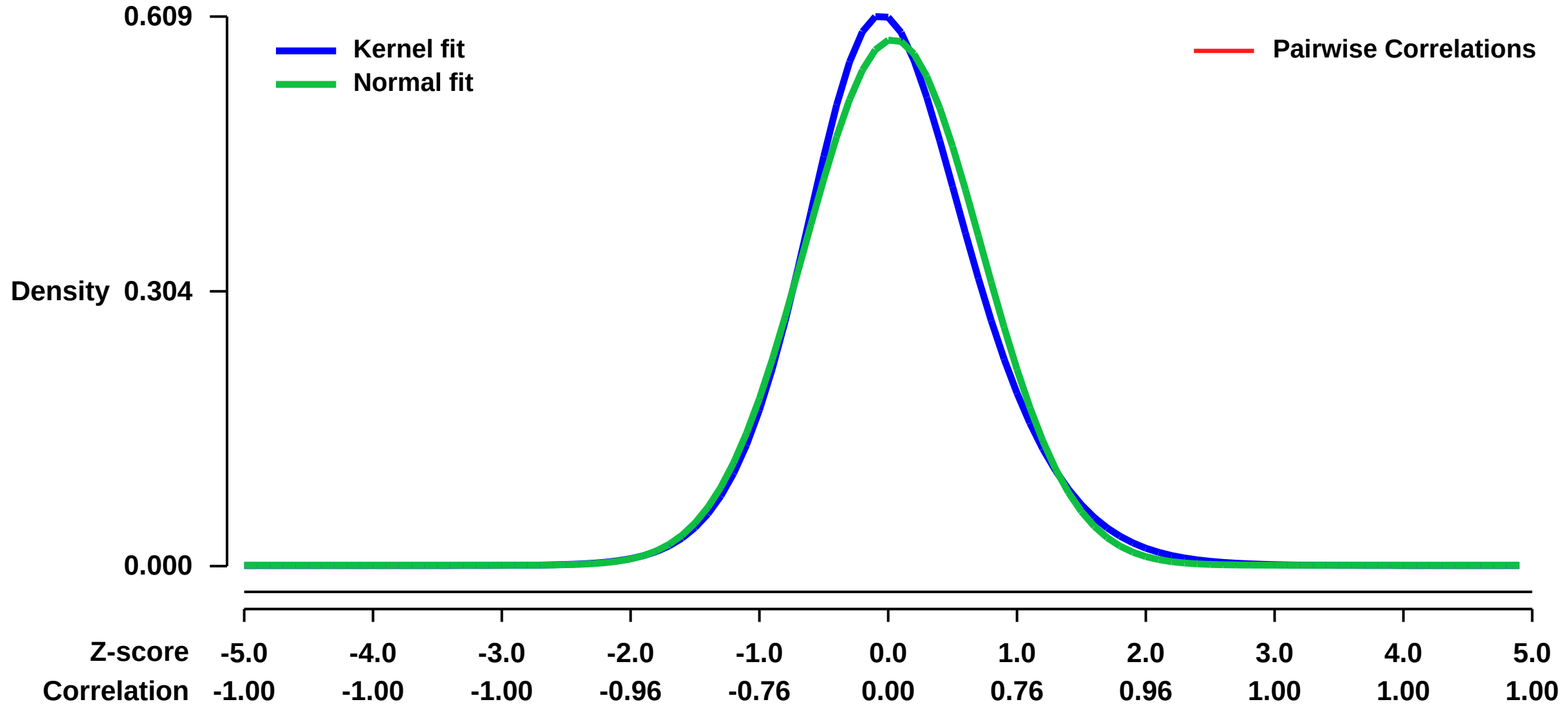

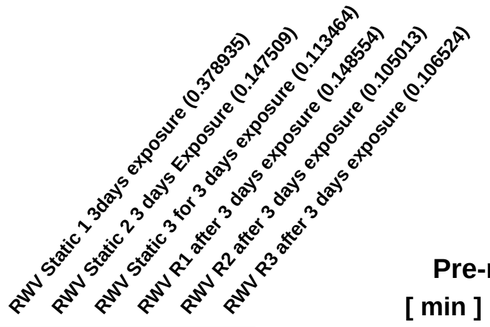

Pre-normalization Quantiles

[min] [medium] [max]

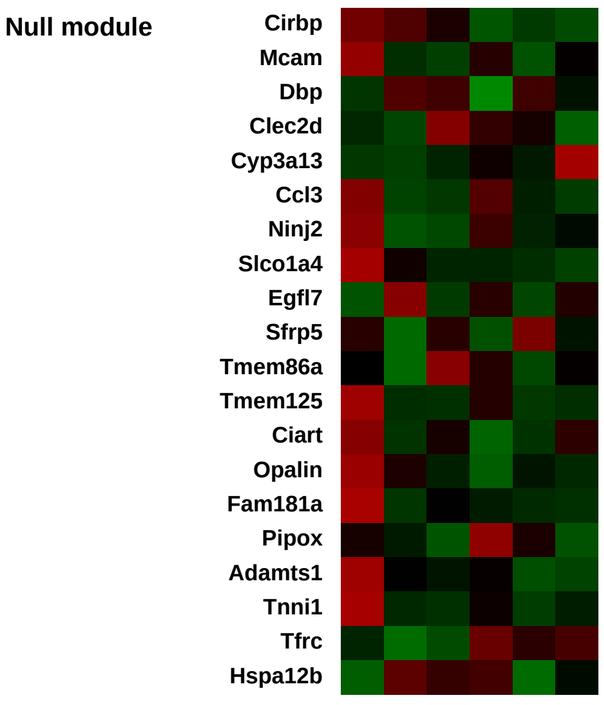

GEO Series "GSE46600" Expression Profiles

Num of samples in this series: 44

Scale of expression profile Z-scores

-3.0 -2.0 -1.0 0.0 1.0 2.0 3.0

GEO Link:	http://www.ncbi.nlm.nih.gov/geo/query/acc.cgi?acc=GSE46600
Status:	Public on Jun 20 2014
Title:	Transcriptome and Molecular Pathways Analysis of CD4 T-Cells from Young NOD Mice
Organism:	Mus musculus
Experiment type:	Expression profiling by array
Platform:	GPL1261
Pubmed ID:	24918037
Summary & Design:	**Summary:** Type 1 diabetes is a multigenic disease caused by T-cell mediated destruction of the insulin producing ˛†-cells. Although conventional (targeted) approaches of identifying causative genes have advanced our knowledge of this disease, many questions remain unanswered. Using a whole molecular systems study, we unraveled the genes/molecular pathways that are altered in CD4 T-cells from young NOD mice prior to insulitis (lymphocytic infiltration into the pancreas). Many of the CD4 T-cell altered genes lie within known diabetes susceptibility regions (Idd), including several genes in the diabetes resistance region Idd13 and two genes (Khdrbs1 and Ptp4a2) in the CD4 T-cell diabetogenic activity region Idd9/11. Alterations involved apoptosis/cell proliferation and metabolic pathways (predominant at 2 weeks), inflammation and cell signaling/activation (predominant at 3 weeks), and innate and adaptive immune responses (predominant at 4 weeks). We identified several factors that may regulate these abnormalities: IRF-1, HNF4A, TP53, BCL2L1 (lies within Idd13), IFNG, IL4, IL15, and prostaglandin E2, which were common to all 3 ages; AR and IL6 to 2 and 4 weeks; and Interferon (IFN-I) and IRF-7 to 3 and 4 weeks. Others were unique to the various ages (e. g. MYC, JUN, and APP to 2 weeks; TNF, TGFB1, NFKB, ERK, and p38MAPK to 3 weeks; and IL12 and STAT4 to 4 weeks). Our data suggest that diabetes resistance genes in Idd13 and Idd9/11, and BCL2L1, IL6-AR and IFNG-IRF-1-IFN-I/IRF-7-IL12 pathways play an important role in CD4 T-cells in the early pathogenesis of autoimmune diabetes. Thus, the alternative approach of investigation at the molecular systems level has captured new information, which combined with validation studies, offers the opportunity to test hypotheses on the role played by the genes/molecular pathways identified in this study, to understand better the mechanisms of autoimmune diabetes in CD4 T-cells, and to develop new therapeutic strategies for the disease. **Overall design:** CD4 T-cells were purified from spleen leukocytes collected from 2-, 3- and 4-week old NOD mice and two age-matched control strains, NOR, and C57BL/6, (n=5 for each strain and each age group; except NOD2wk). NOR is an insulitis- and diabetes-free control strain that shares shares ~88% of its genome with NOD mice, including the diabetogenic H2g7 MHC haplotype and several important non-MHC T1D susceptibility loci. C57BL/6 is also a diabetes-resitant strain, but it is more genetically distantly related to NOD.

Background corr dist: KL-Divergence = 0.4129, L1-Distance = 0.0601, L2-Distance = 0.0093, Normal std = 0.2468

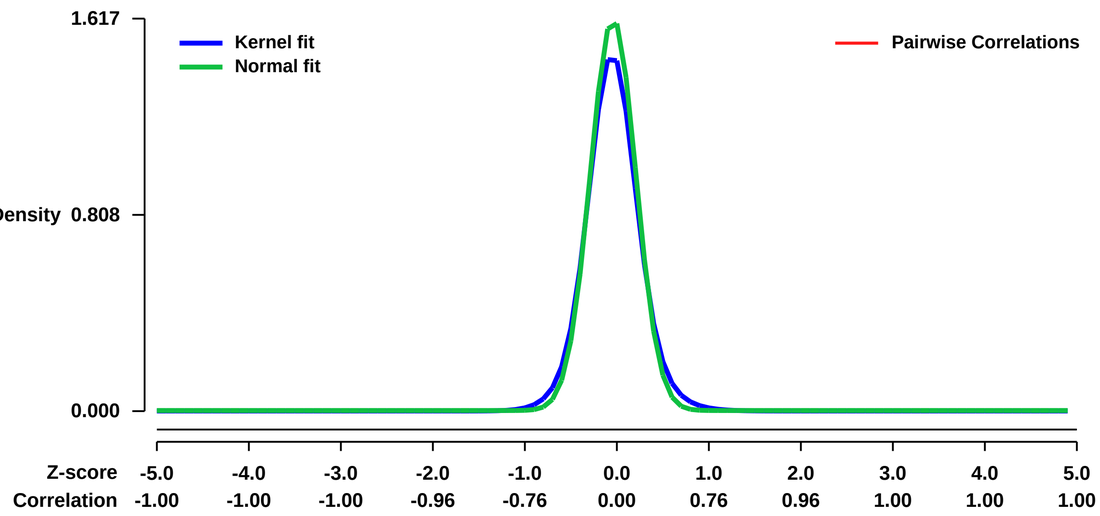

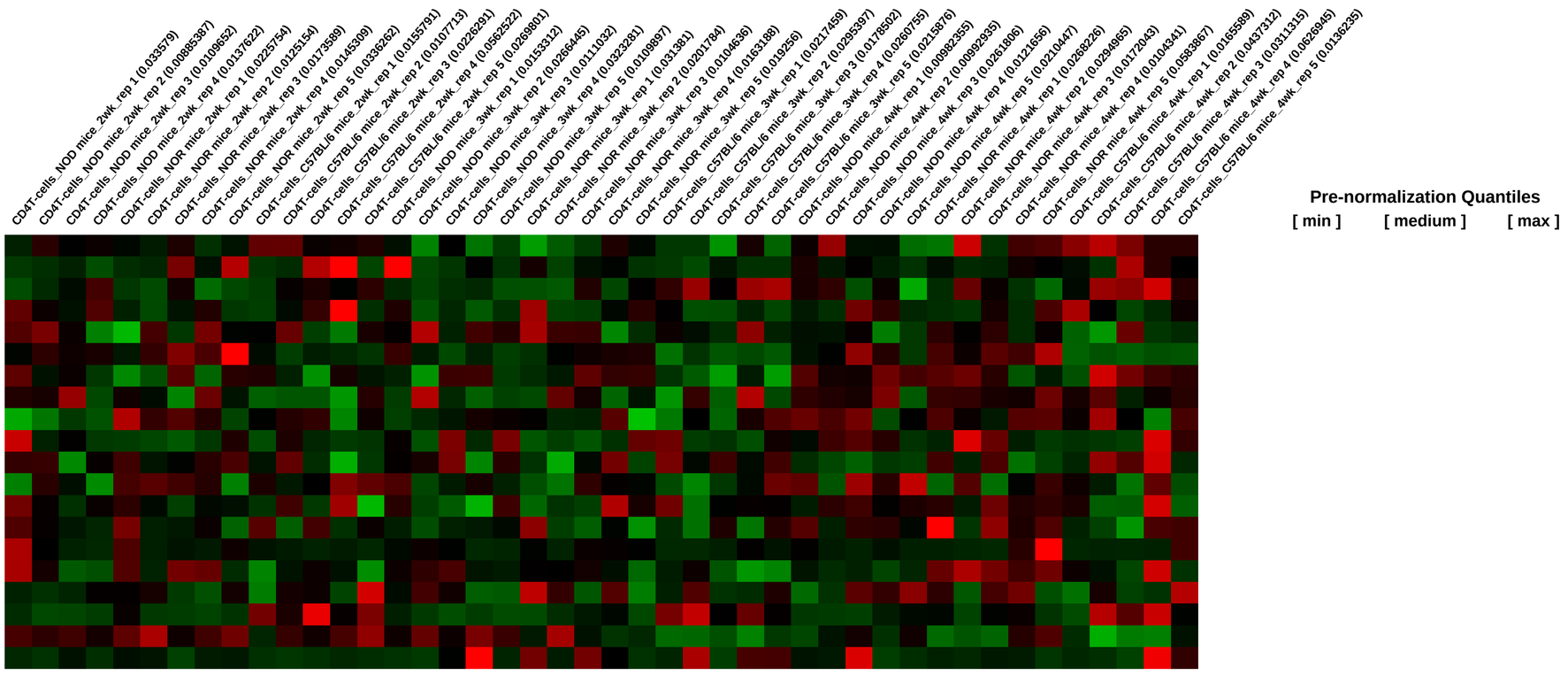

GEO Series "GSE46606" Expression Profiles

Num of samples in this series: 30

Scale of expression profile Z-scores

-3.0 -2.0 -1.0 0.0 1.0 2.0 3.0

GEO Link:	http://www.ncbi.nlm.nih.gov/geo/query/acc.cgi?acc=GSE46606
Status:	Public on May 04 2013
Title:	Transcriptional regulation of germinal center B and plasma cell fates by dynamical control of IRF4 (expression)
Organism:	Mus musculus
Experiment type:	Expression profiling by array
Platform:	GPL1261
Pubmed ID:	23684984
Summary & Design:	**Summary:** Temporal analysis of B cell activation in vitro using CD40L and IL-2/4/5 cytokines in wild type Irf4+/+ B cells or in mutant Irf4-/- B cells harboring a tet-inducible allele of Irf4. IRF4 expression was restored, or not, in the Irf4-/- background by culturing in the presence of low or high concentrations of doxycycline. The results provide insight in the role of IRF4 expression levels in coordinating different programs of B cell differentiation. **Overall design:** Resting mature peripheral primary B cells were enriched from the spleens of Irf4+/+ or Irf4-inducible mice on the Irf4-/- background. We sought to compare gene expression profiles of wild type and Irf4 mutant B cells in response to mitogens that promote the differentiation of the B cells into plasma cells and cells that have undergone class switch recombination. Day 0 samples represent RNA analysis of unstimulated cells, whereas Day 1 and Day 3 samples represent analysis of stimulated cells in culture. For stimulation, cells were cultured with insect cell purified CD40L and IL-2/4/5 cytokines for the indicated days. In the case of doxycycline-mediated rescue of IRF4 expression, doxycycline was added at predefined low and high concentrations that yield low or high numbers of plasma cells, respectively (see Molecular Systems Biology 7:495). Each replicate represents analysis of B cells from an individual mouse. Of the three replicates in each group, two were performed in parallel and one was performed at a different time. All cells were lysed using Trizol and total RNA was purified according to manufacturer's suggestions. The high quality of the RNA was confirmed using Agilent Bioanalyzer 2100 system. 250ng of RNA was then processed into biotinylated cRNA according to standard procedures and used to hybridize to Affymetrix 430 2.0 arrays. Signal intensities were normalized using the D-Chip algorithm (PM-only model) and the output was used to quantify differential gene expression between groups.

Background corr dist: KL-Divergence = 0.0934, L1-Distance = 0.0402, L2-Distance = 0.0024, Normal std = 0.4712

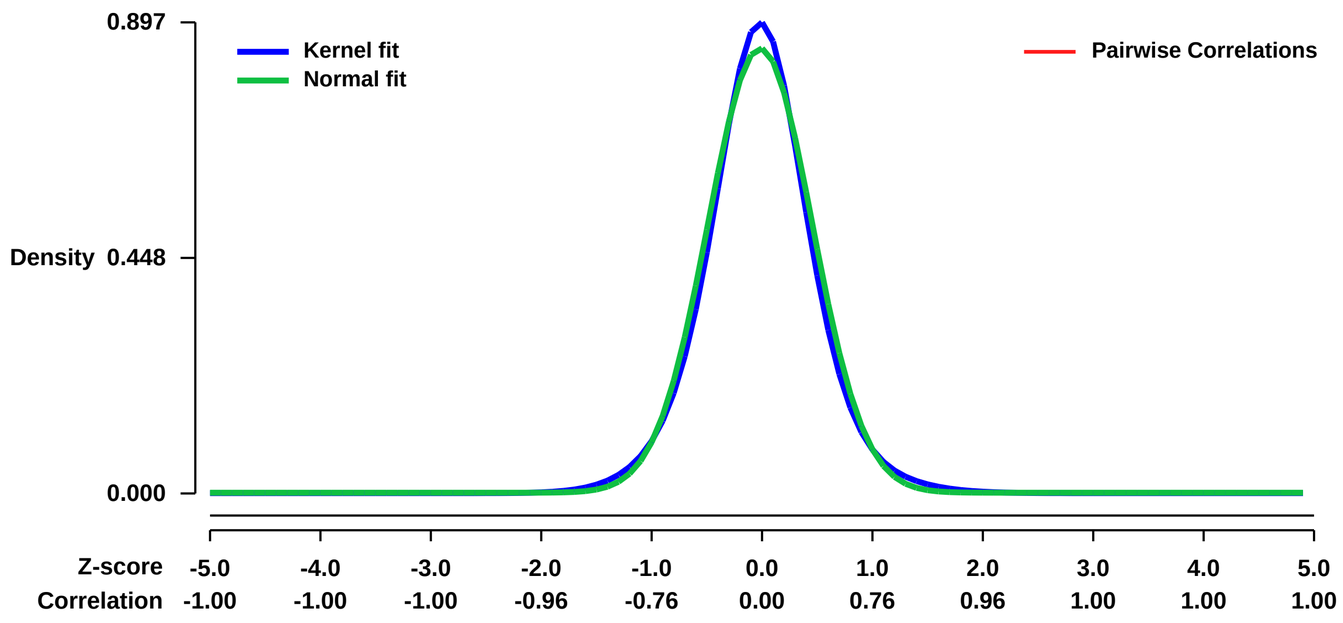

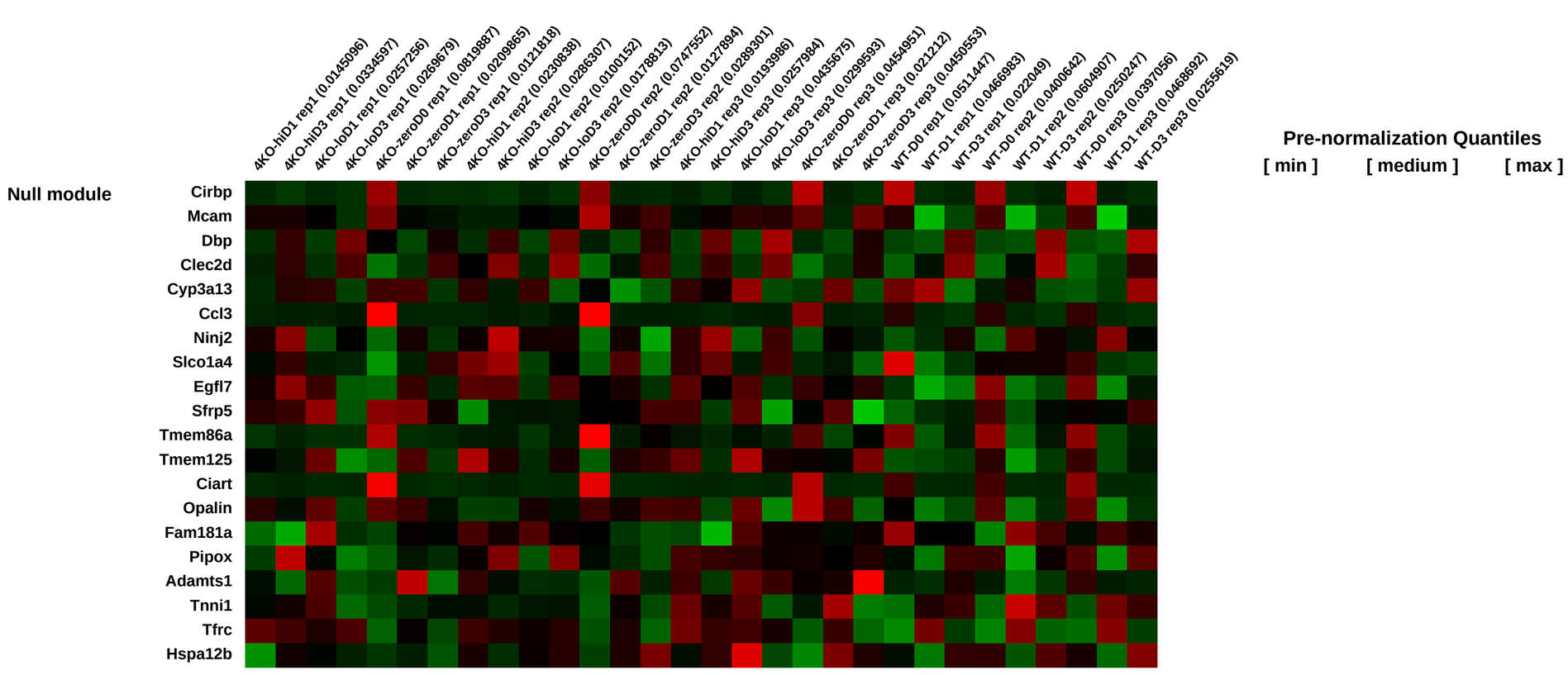

GEO Series "GSE46646" Expression Profiles

Num of samples in this series: 12

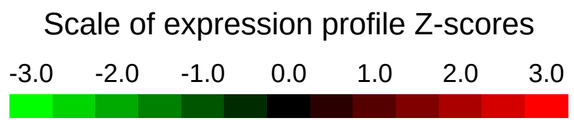

GEO Link:	http://www.ncbi.nlm.nih.gov/geo/query/acc.cgi?acc=GSE46646
Status:	Public on Dec 13 2013
Title:	IQGAP2 knockout model of hepatocellular carcinoma
Organism:	Mus musculus
Experiment type:	Expression profiling by array
Platform:	GPL1261
Pubmed ID:	23951254
Summary & Design:	**Summary:** Whole body knockout mice lacking IQ-motif containing GTPase-activating protein 2 (IQGAP2) develop spontaneous hepatocellular carcinoma (HCC) at the age of 12 months and older (Schmidt et al., 2008). Hepatic transcript expression profiles were obtained for IQGAP2 knockout and wild-type control mice of two age groups, 6- and 24-month-old. Liver samples from 24-month-old IQGAP2 knockout mice were HCC tumors, livers from all other groups were tumor-free. Results provide insights into the potential role of IQGAP2 as a liver-specific tumor suppressor. **Overall design:** Transcript profiles of four groups of mouse livers (N = 3 in each group) were compared using Affymetrix GeneChip´fi Mouse Genome 430 2.0 Array. The groups included livers from 6- and 24-month-old wild-type (WT) mice and 6- and 24-month-old (KO) Iqgap2-/- mice.

Background corr dist: KL-Divergence = 0.1090, L1-Distance = 0.0294, L2-Distance = 0.0016, Normal std = 0.4252

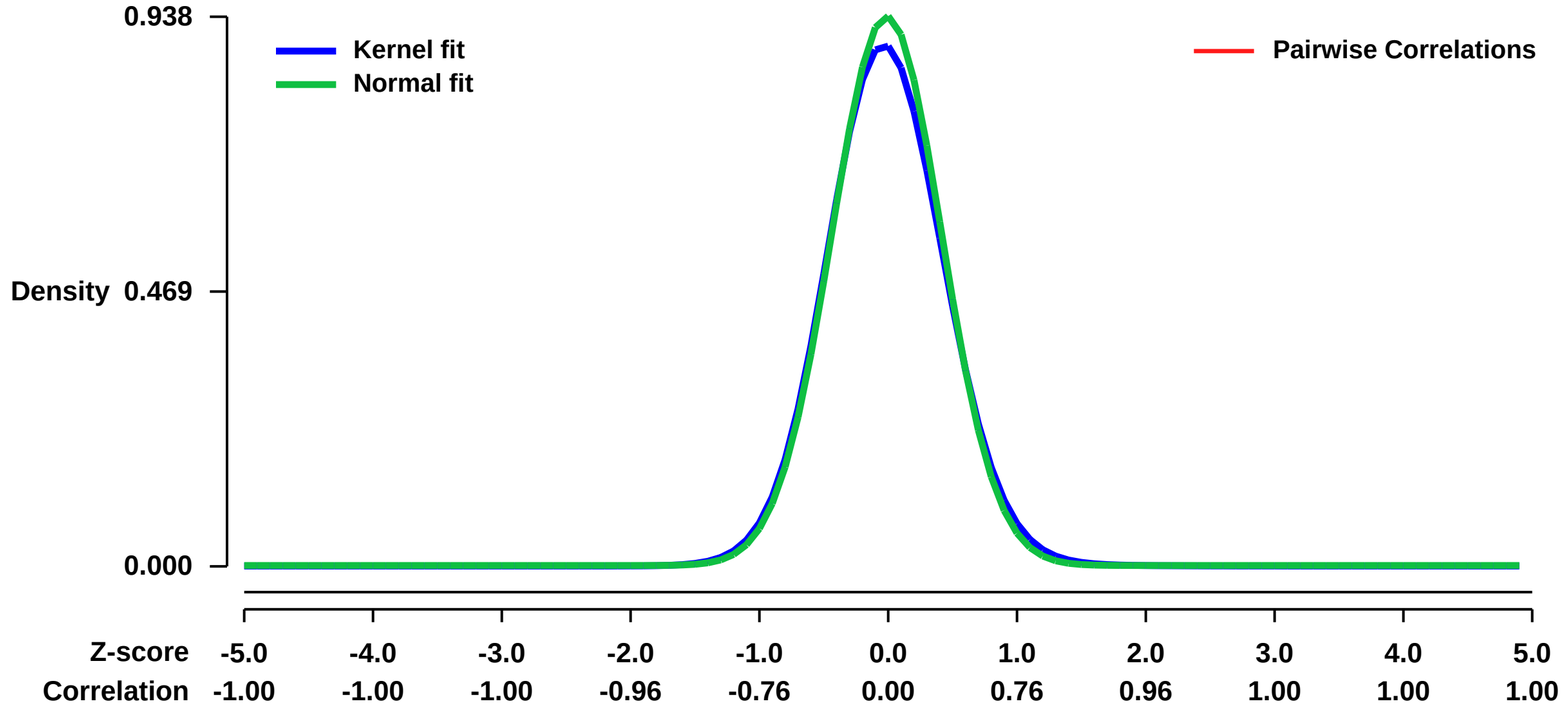

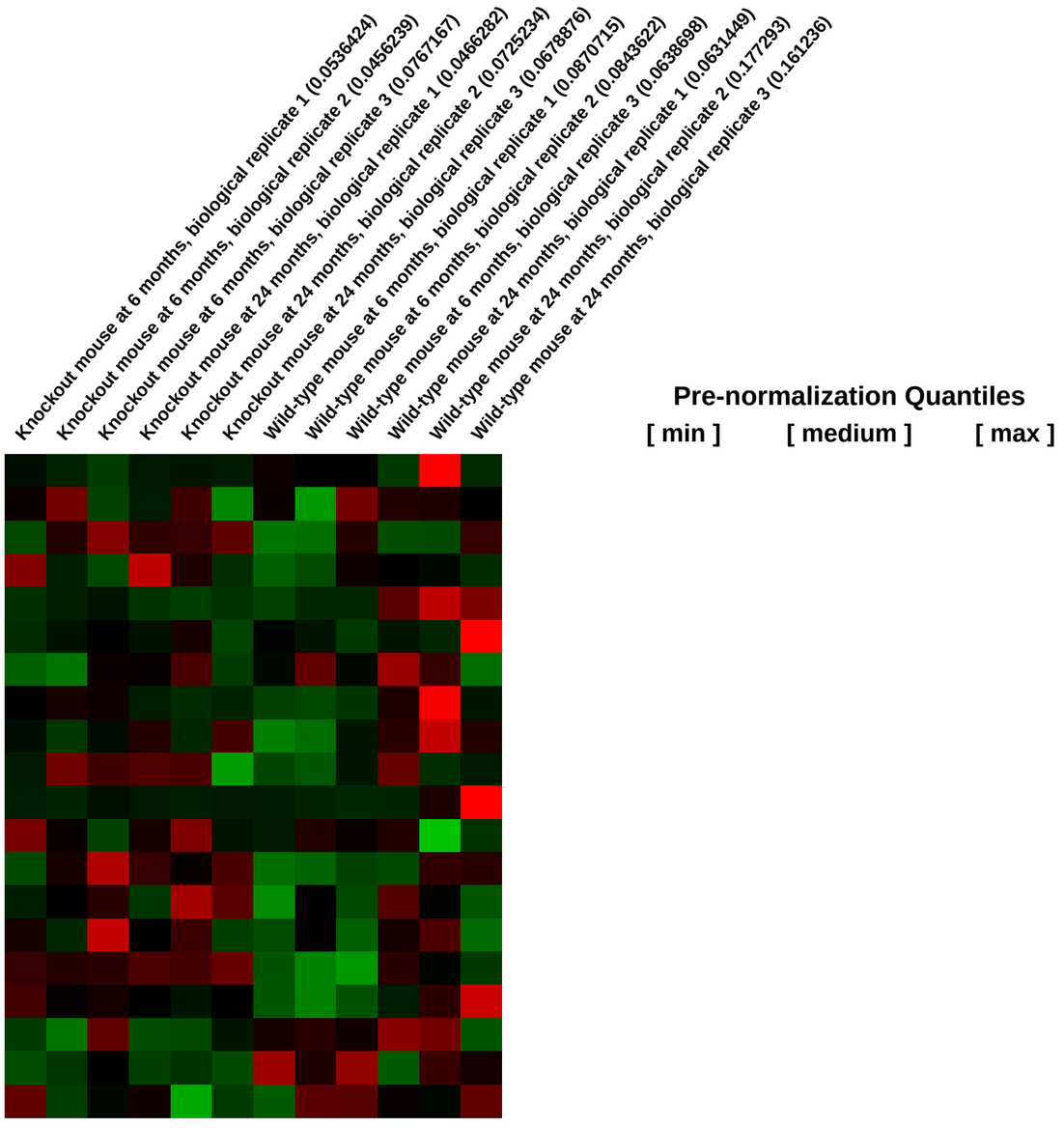

GEO Series "GSE4671" Expression Profiles

Num of samples in this series: 28

Scale of expression profile Z-scores

-3.0 -2.0 -1.0 0.0 1.0 2.0 3.0

GEO Link:	http://www.ncbi.nlm.nih.gov/geo/query/acc.cgi?acc=GSE4671
Status:	Public on Jul 28 2006
Title:	Microarray Analysis of the Delipidation of White Adipose Tissue of Mice Fed Conjugated Linoleic Acid
Organism:	Mus musculus
Experiment type:	Expression profiling by array
Platform:	GPL1261
Pubmed ID:	16868072
Summary & Design:	**Summary:** The white adipose tissue (WAT) rapidly loses mass when mice are fed a diet containing trans-10, cis-12 conjugated linoleic acid (t10c12 CLA). A microarray analysis of WAT due to CLA feeding was performed to better define the processes and genes involved. WAT weight decreased by ca. 80% over 17 days of feeding a 0.5% t10c12 CLA diet. The lipid volume decreased by 90% and the number of adipocytes and total cells were reduced by15% and 47%, respectively. Microarray profiling of replicated pools of control and treated mice (n=140) at seven time points over the 17day feeding indicated between 2798 to 4318 genes showed mRNA changes of 2-fold or more. Transcript levels for genes of glucose and fatty acid import or biosynthesis were significantly reduced. A prolific inflammation response was indicated by the 2 to100-fold induction of many cytokine transcripts, including those for IL-6, IL1?, TNF ligands, and CXC family members We used microarrays to characterize transcriptome changes in mouse adipose tissue due to feeding trans-10 cis-12 linoleic acid . **Keywords:** time course **Overall design:** Mice were fed either diet with 0.5 % CLA or control diet, and the retroperitoneal fat pad mRNA surveyed by high density oligonucleotide array expression profiling. Microarray profiling of replicated pools of control and treated mice (n=140) at seven time points (day 1, 2, 3, 4, 10, 17) over the 17day feeding indicated between 2798 to 4318 genes showed mRNA changes of 2-fold or more.

Background corr dist: KL-Divergence = 0.1498, L1-Distance = 0.0280, L2-Distance = 0.0012, Normal std = 0.3767

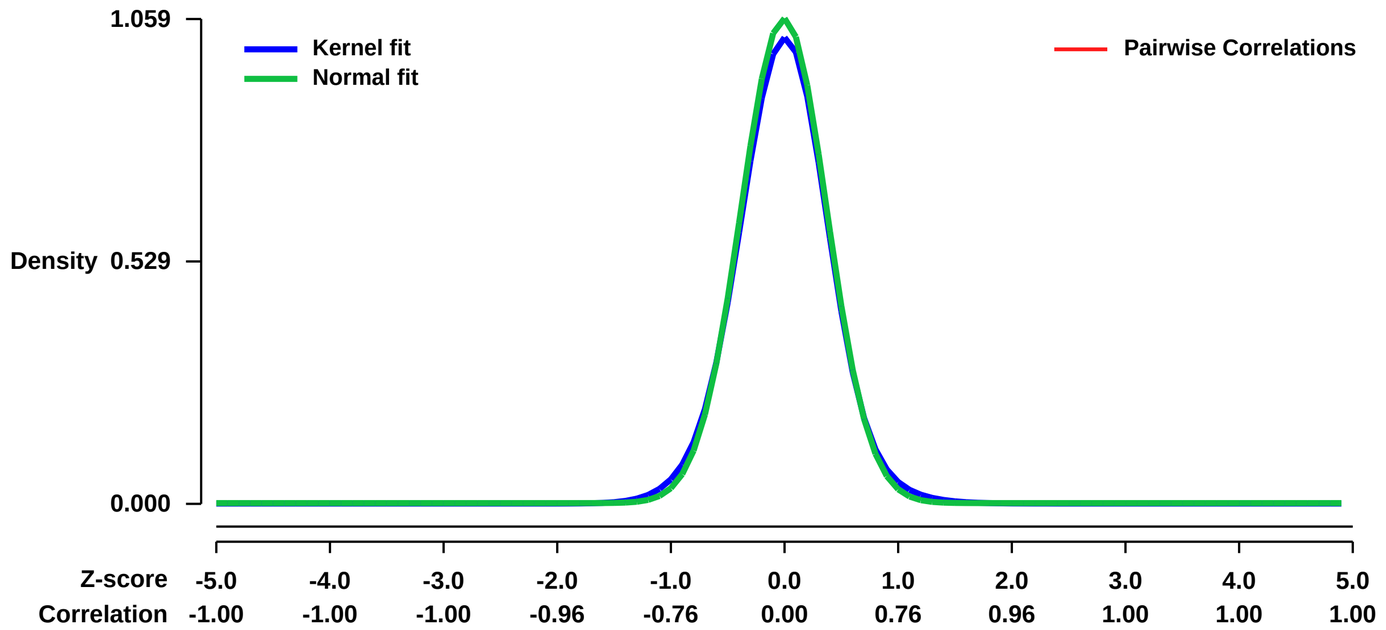

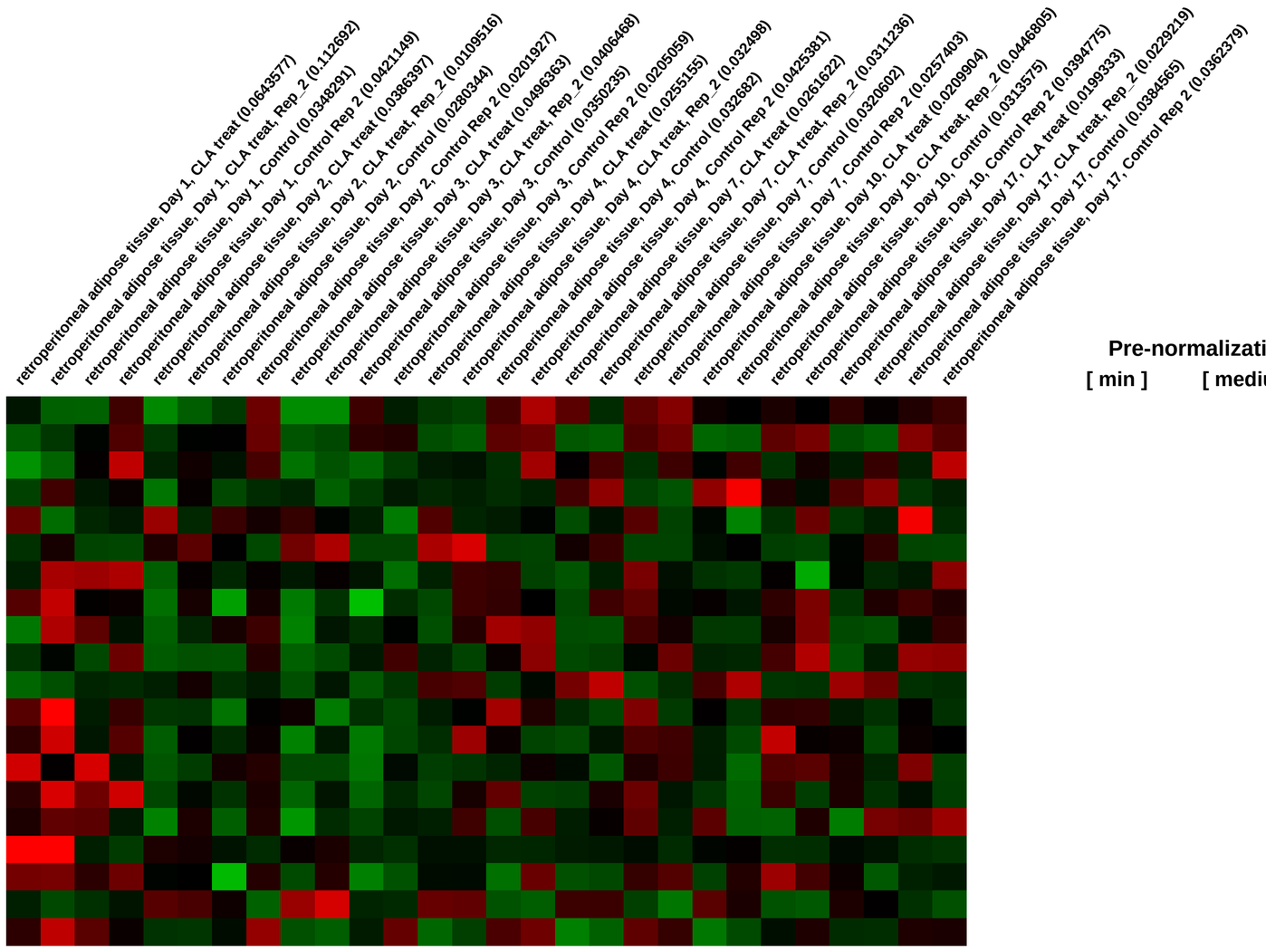

GEO Series "GSE46722" Expression Profiles

Num of samples in this series: 6

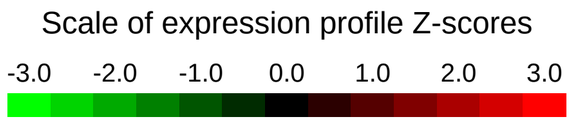

GEO Link:	http://www.ncbi.nlm.nih.gov/geo/query/acc.cgi?acc=GSE46722
Status:	Public on Jul 01 2013
Title:	Expression data from adult LSK Hes1-GFP positive and adult LSK Hes1-GFP negative
Organism:	Mus musculus
Experiment type:	Expression profiling by array
Platform:	GPL1261
Pubmed ID:	23791481
Summary & Design:	**Summary:** Notch signaling defines a conserved, fundamental pathway, responsible for determination in metazoan development and is widely recognized as an essential component of lineage specific differentiation and stem cell self-renewal in many tissues including the hematopoietic system. Until recently, the majority of studies in the hematopoietic system focused on Notch signaling in lymphocyte differentiation and knowledge of individual Notch receptor roles in early hematopoiesis has been limited due to a paucity of genetic tools available To fate-map Notch receptor expression and pathway activity in the hematopoietic system we used tamoxifen-inducible CreER knock-in mice for individual Notch receptors in combination to a novel Notch reporter strain (Hes1GFP) and a conditional gain of function allele of Notch2 receptor (Rosa-lsl-ICN2). **Overall design:** Bone marrow lineage negative, cKit+, Sca1+ cells were sorted from Hes-GFP mice for RNA extraction and hybridization on Affymetrix microarrays

Background corr dist: KL-Divergence = 0.0508, L1-Distance = 0.0373, L2-Distance = 0.0021, Normal std = 0.5892

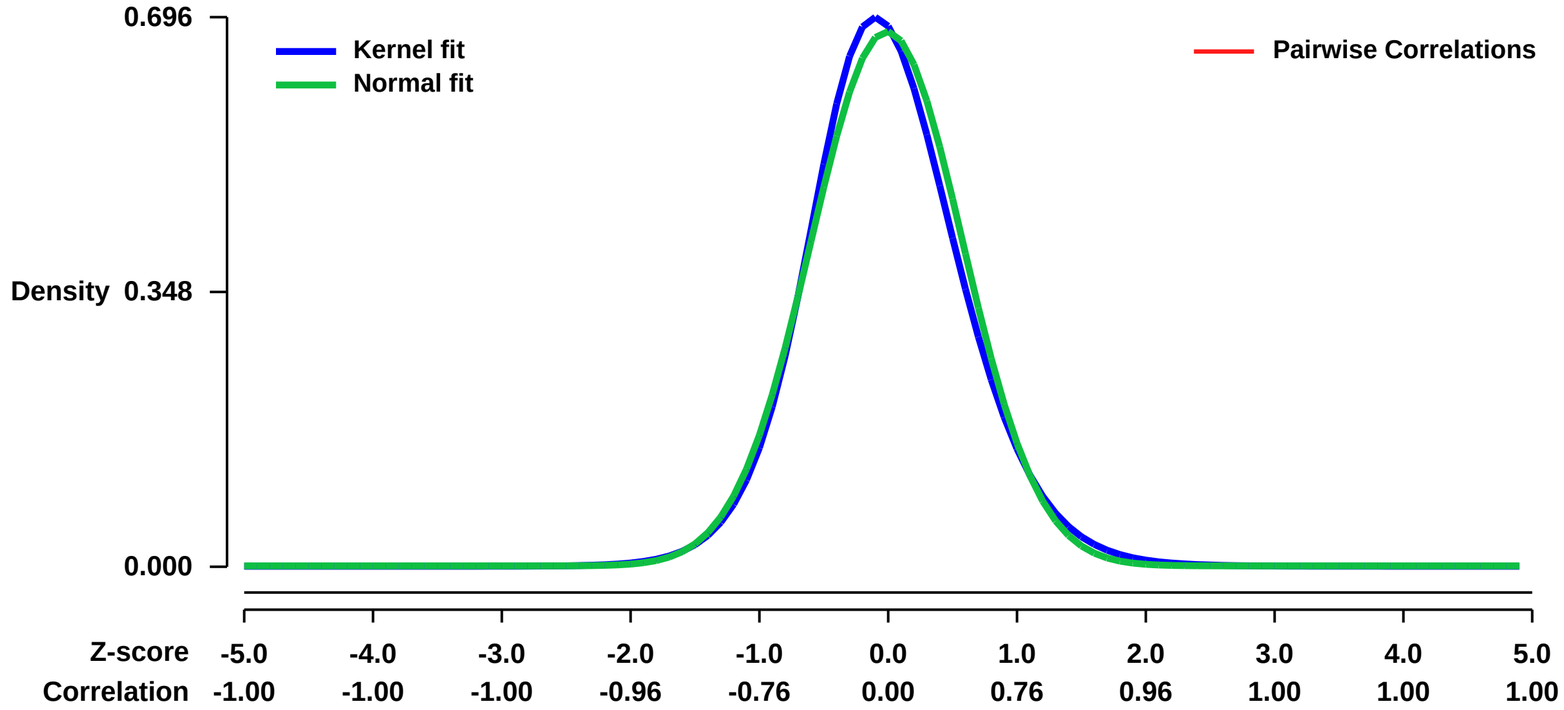

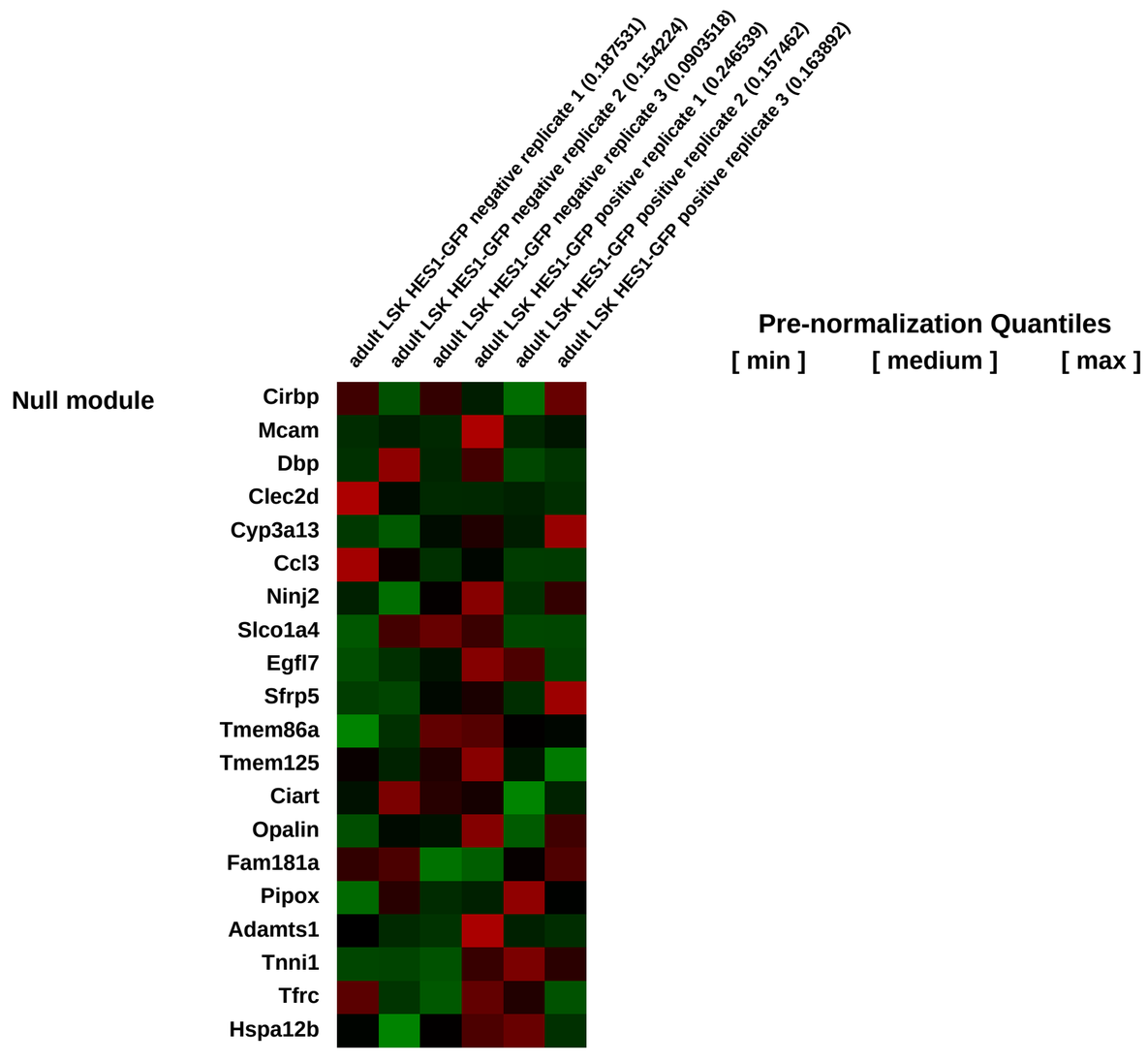

GEO Series "GSE46723" Expression Profiles

Num of samples in this series: 6

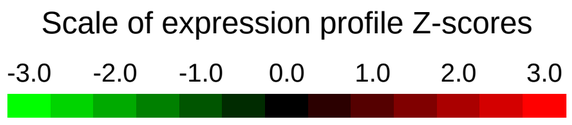

GEO Link:	http://www.ncbi.nlm.nih.gov/geo/query/acc.cgi?acc=GSE46723
Status:	Public on Jul 01 2013
Title:	Expression data from adult Myeloerythroid Progenitors (MP) Hes1-GFP positive and adult Myeloerythroid Progenitors (MP) Hes1-GFP negative
Organism:	Mus musculus
Experiment type:	Expression profiling by array
Platform:	GPL1261
Pubmed ID:	23791481
Summary & Design:	**Summary:** Notch signaling defines a conserved, fundamental pathway, responsible for determination in metazoan development and is widely recognized as an essential component of lineage specific differentiation and stem cell self-renewal in many tissues including the hematopoietic system. Until recently, the majority of studies in the hematopoietic system focused on Notch signaling in lymphocyte differentiation and knowledge of individual Notch receptor roles in early hematopoiesis has been limited due to a paucity of genetic tools available To fate-map Notch receptor expression and pathway activity in the hematopoietic system we used tamoxifen-inducible CreER knock-in mice for individual Notch receptors in combination to a novel Notch reporter strain (Hes1GFP) and a conditional gain of function allele of Notch2 receptor (Rosa-lsl-ICN2). **Overall design:** Bone marrow lineage negative, cKit+, Sca1- cells were sorted from Hes-GFP mice for RNA extraction and hybridization on Affymetrix microarrays

Background corr dist: KL-Divergence = 0.0189, L1-Distance = 0.0122, L2-Distance = 0.0002, Normal std = 0.7520

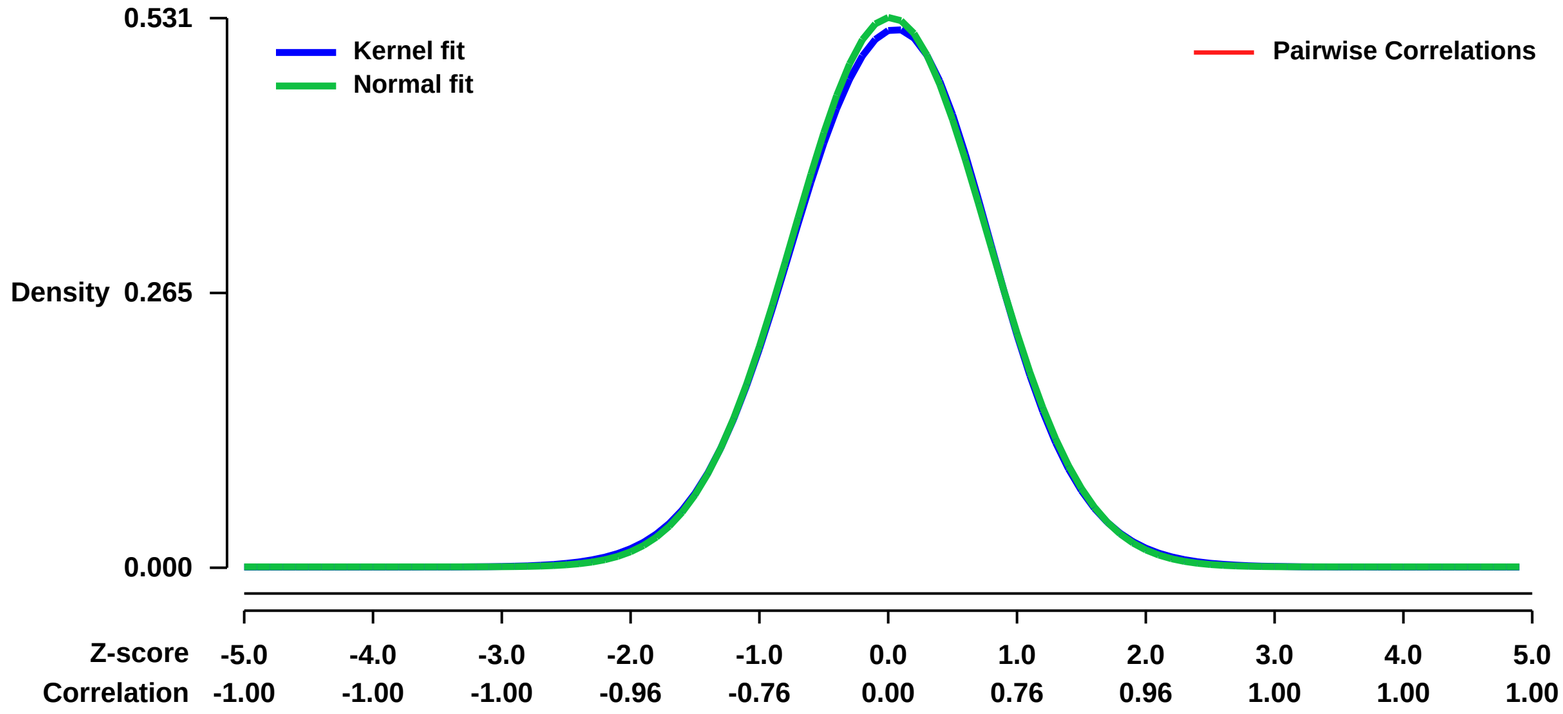

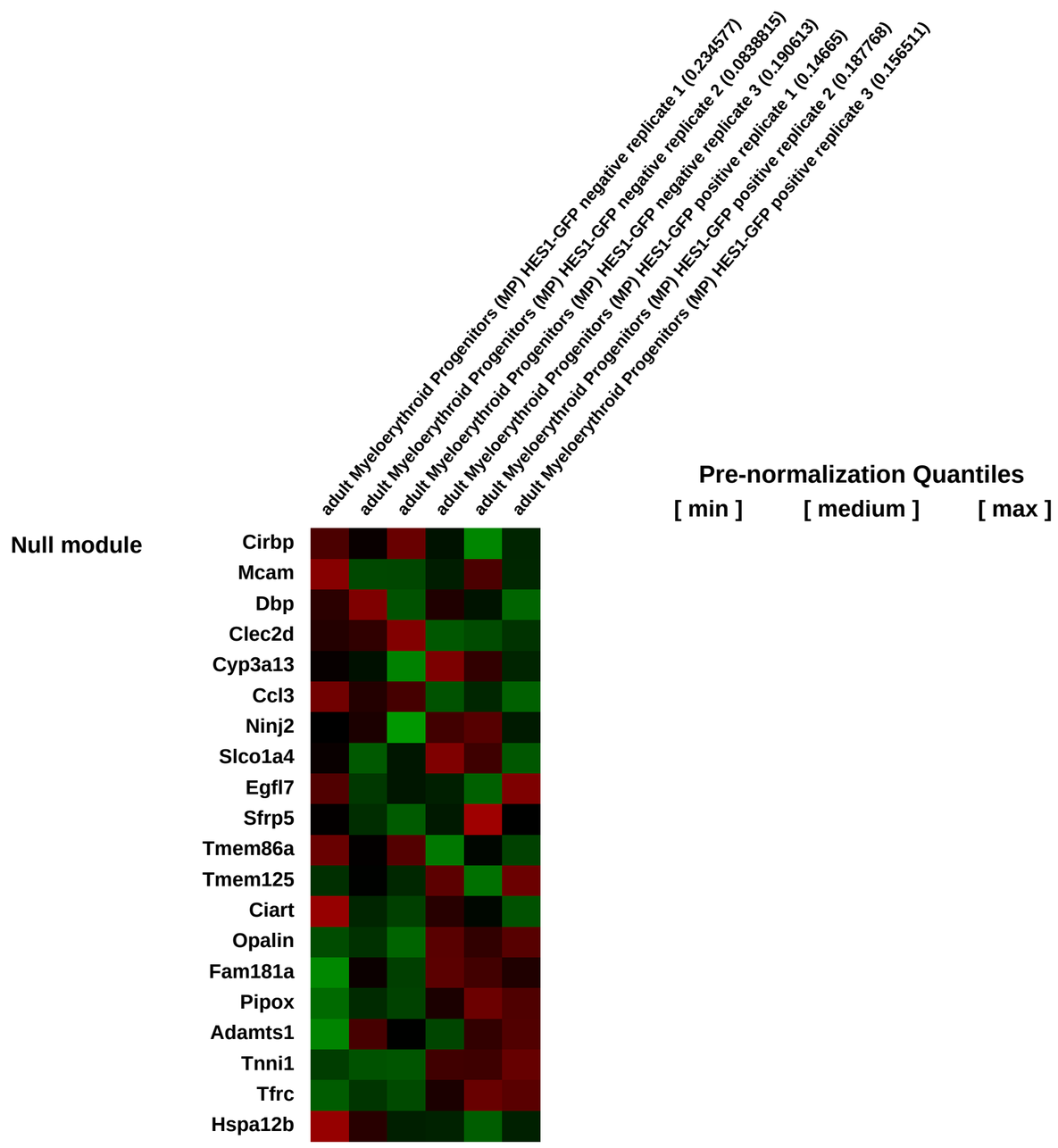

GEO Series "GSE46724" Expression Profiles

Num of samples in this series: 6

Scale of expression profile Z-scores

-3.0 -2.0 -1.0 0.0 1.0 2.0 3.0

GEO Link:	http://www.ncbi.nlm.nih.gov/geo/query/acc.cgi?acc=GSE46724
Status:	Public on Jul 01 2013
Title:	Expression data from adult Myeloerythroid Progenitors (MP) ICN2 positive and adult Myeloerythroid Progenitors (MP) ICN2 negative
Organism:	Mus musculus
Experiment type:	Expression profiling by array
Platform:	GPL1261
Pubmed ID:	23791481
Summary & Design:	**Summary:** Notch signaling defines a conserved, fundamental pathway, responsible for determination in metazoan development and is widely recognized as an essential component of lineage specific differentiation and stem cell self-renewal in many tissues including the hematopoietic system. Until recently, the majority of studies in the hematopoietic system focused on Notch signaling in lymphocyte differentiation and knowledge of individual Notch receptor roles in early hematopoiesis has been limited due to a paucity of genetic tools available To fate-map Notch receptor expression and pathway activity in the hematopoietic system we used tamoxifen-inducible CreER knock-in mice for individual Notch receptors in combination to a novel Notch reporter strain (Hes1GFP) and a conditional gain of function allele of Notch2 receptor (Rosa-lsl-ICN2). **Overall design:** Bone marrow lineage negative, cKit+, Sca1- cells were sorted from Rosa-lsl-ICN2 Mx1-cre+ mice or Mx1-cre+ littermates for RNA extraction and hybridization on Affymetrix microarrays

Background corr dist: KL-Divergence = 0.0317, L1-Distance = 0.0230, L2-Distance = 0.0005, Normal std = 0.6657

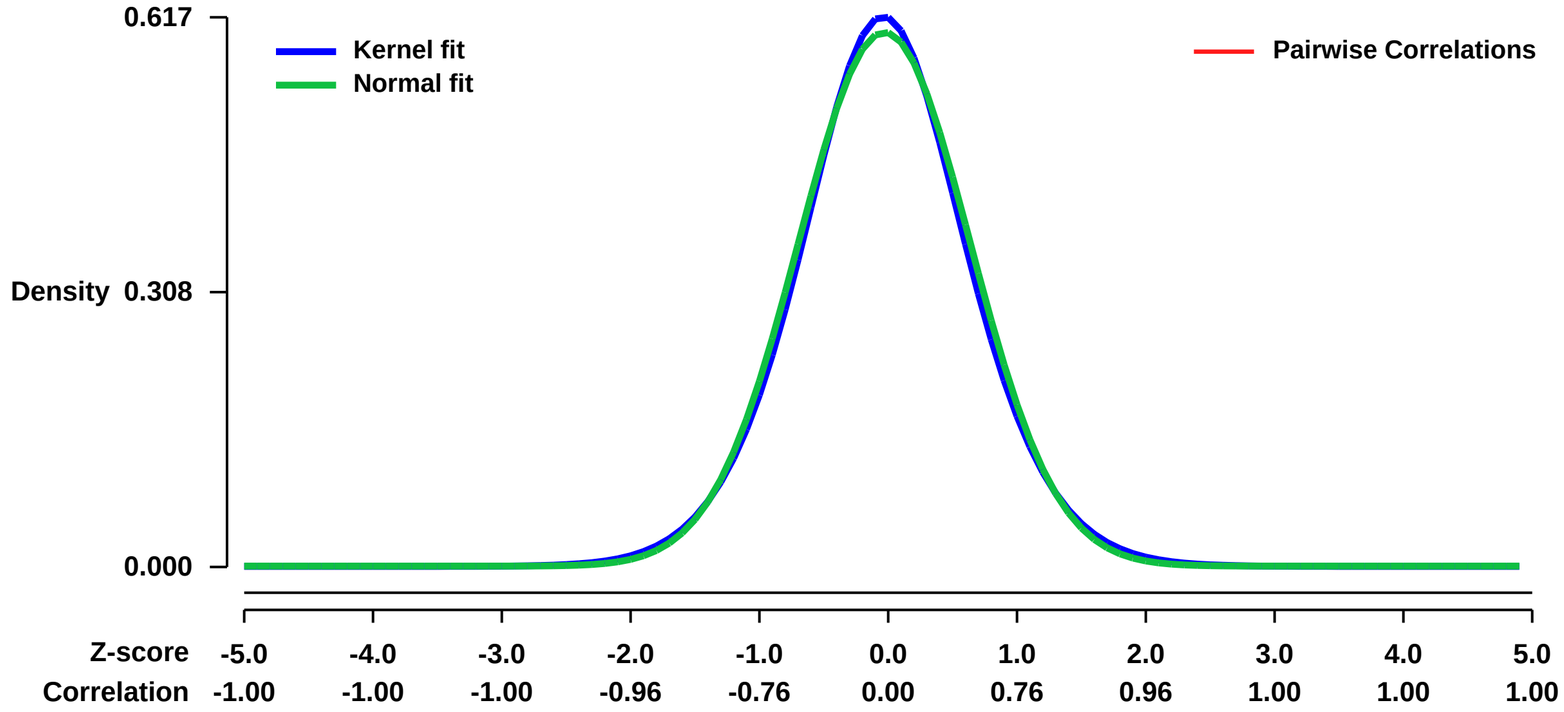

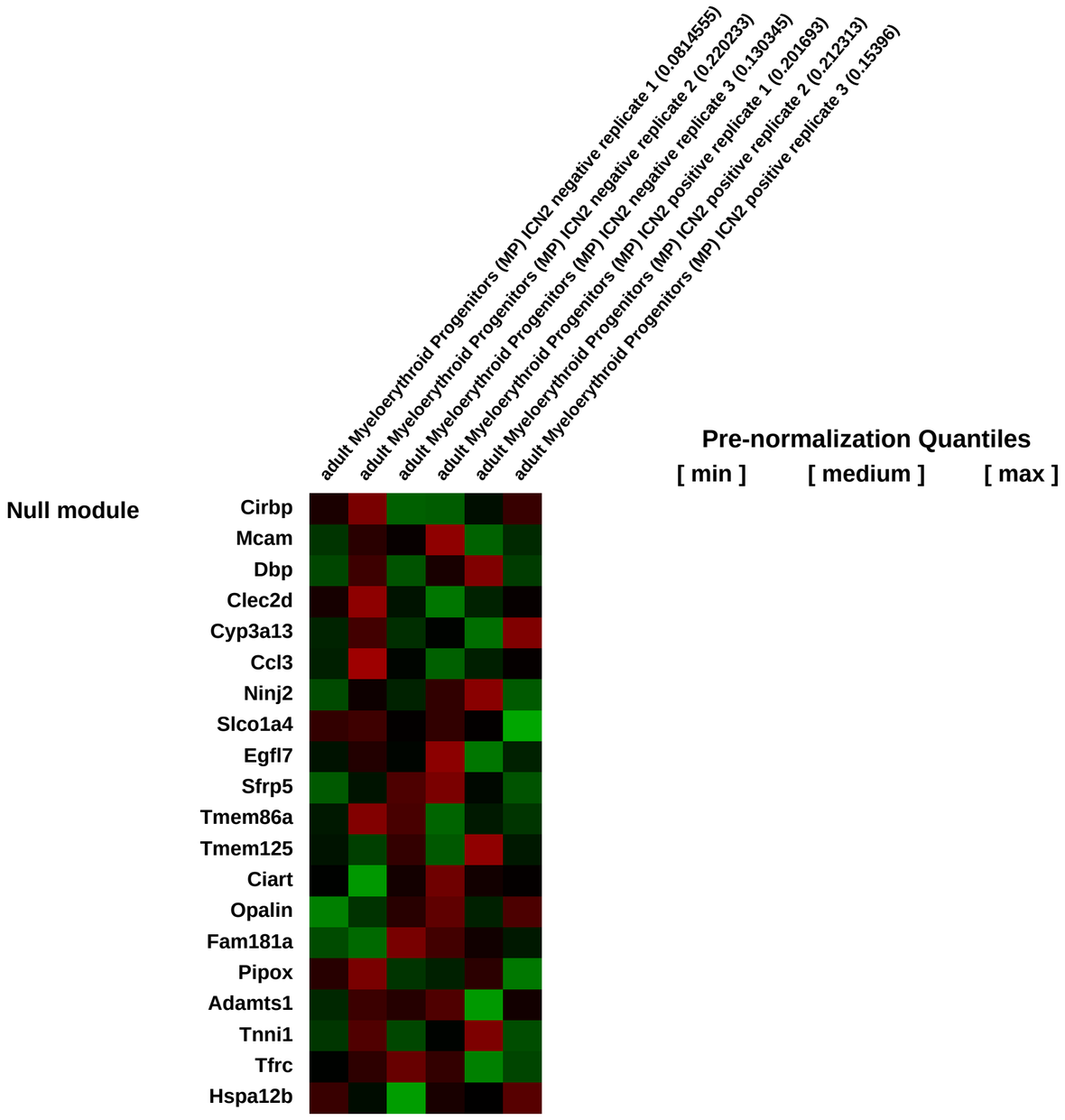

GEO Series "GSE46797" Expression Profiles

Num of samples in this series: 6

Scale of expression profile Z-scores

-3.0 -2.0 -1.0 0.0 1.0 2.0 3.0

GEO Link:	http://www.ncbi.nlm.nih.gov/geo/query/acc.cgi?acc=GSE46797
Status:	Public on May 10 2013
Title:	Expression data from c-Myc+ Notch1 T-ALL initiating cells
Organism:	Mus musculus
Experiment type:	Expression profiling by array
Platform:	GPL1261
Pubmed ID:	23791182
Summary & Design:	**Summary:** Missense FBXW7 mutations are prevalent in various tumors, including T-cell acute lymphoblastic leukemia (T-ALL). To study the effects of such lesions, we generated animals carrying regulatable Fbxw7 mutant alleles. We show here that these mutations specifically bolster cancer-initiating cell activity in collaboration with Notch1 oncogenes, but spare normal hematopoietic stem cell function. We were also able to show that FBXW7 mutations specifically affect the ubiquitylation and half-life of c-Myc protein, a key T-ALL oncogene. Using animals carrying c-Myc fusion alleles, we connected Fbxw7 function to c-Myc abundance and correlated c-Myc expression to leukemia-initiating activity. **Overall design:** Three independent Notch1 T-ALL were derived on c-Myc-GFP background and sorted from the spleen of leukemic mice on the basis of GFP expression for RNA extraction and hybridization on Affymetrix microarrays

Background corr dist: KL-Divergence = 0.0376, L1-Distance = 0.0289, L2-Distance = 0.0011, Normal std = 0.6371

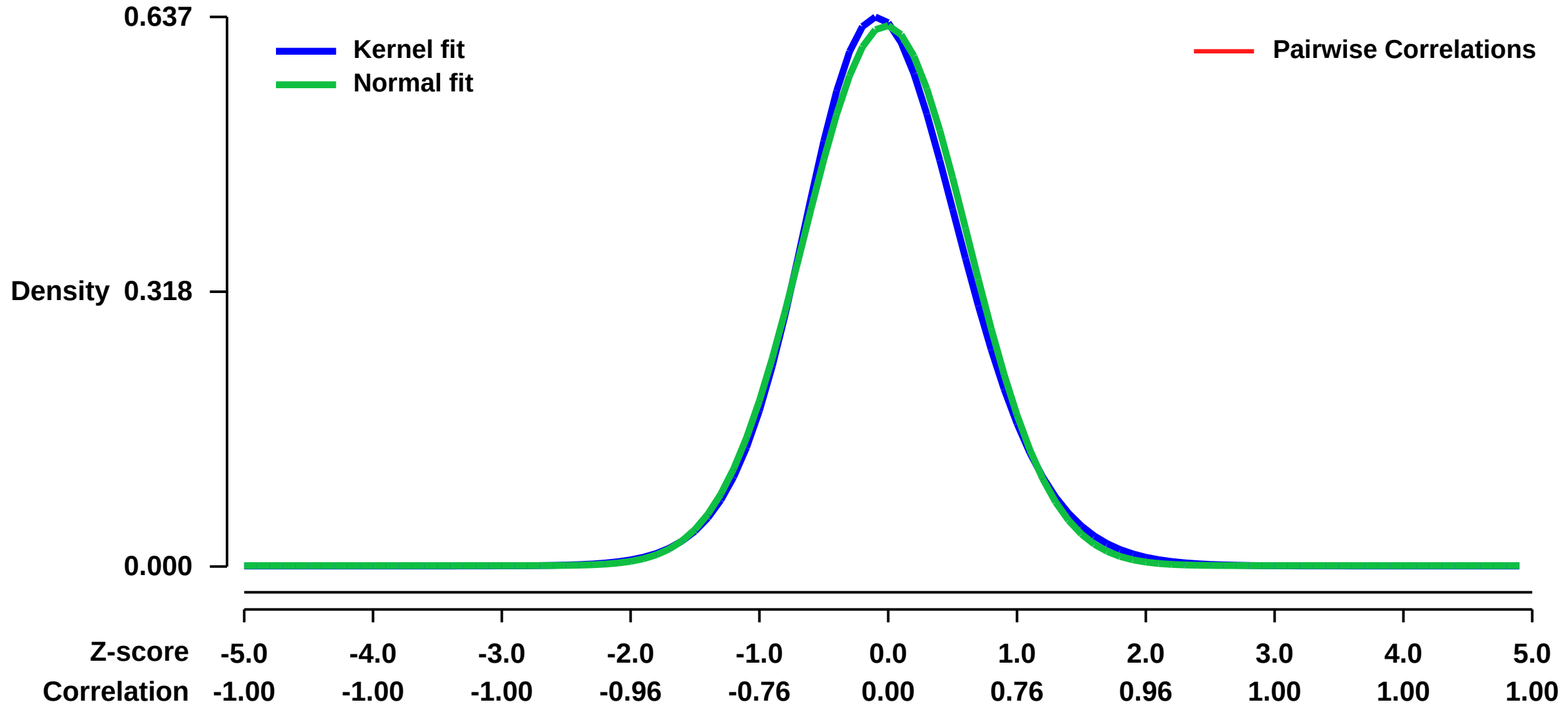

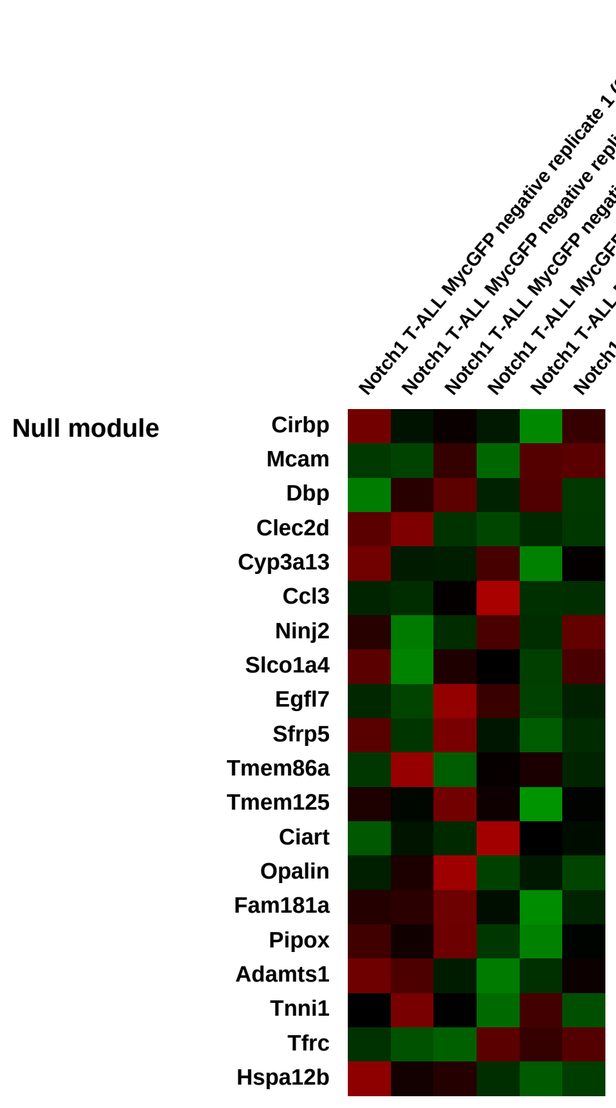

GEO Series "GSE46869" Expression Profiles

Num of samples in this series: 6

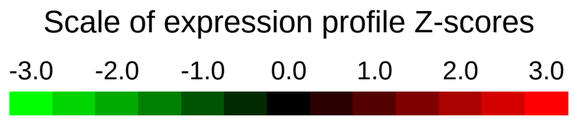

GEO Link:	http://www.ncbi.nlm.nih.gov/geo/query/acc.cgi?acc=GSE46869
Status:	Public on May 02 2014
Title:	Gene expression profiles of PIK3CA knockdown by shRNA in lung cancer cells
Organism:	Mus musculus
Experiment type:	Expression profiling by array
Platform:	GPL1261
Pubmed ID:	24762440
Summary & Design:	**Summary:** To gain insight into EMT-independent biological processes through which PI3K promotes invasion, RNA samples from 344SQ_p110‸–shRNA cells and 344SQ_scr cells were subjected to global transcriptional profiling. **Overall design:** Two group comparison

Background corr dist: KL-Divergence = 0.0368, L1-Distance = 0.0279, L2-Distance = 0.0008, Normal std = 0.6524

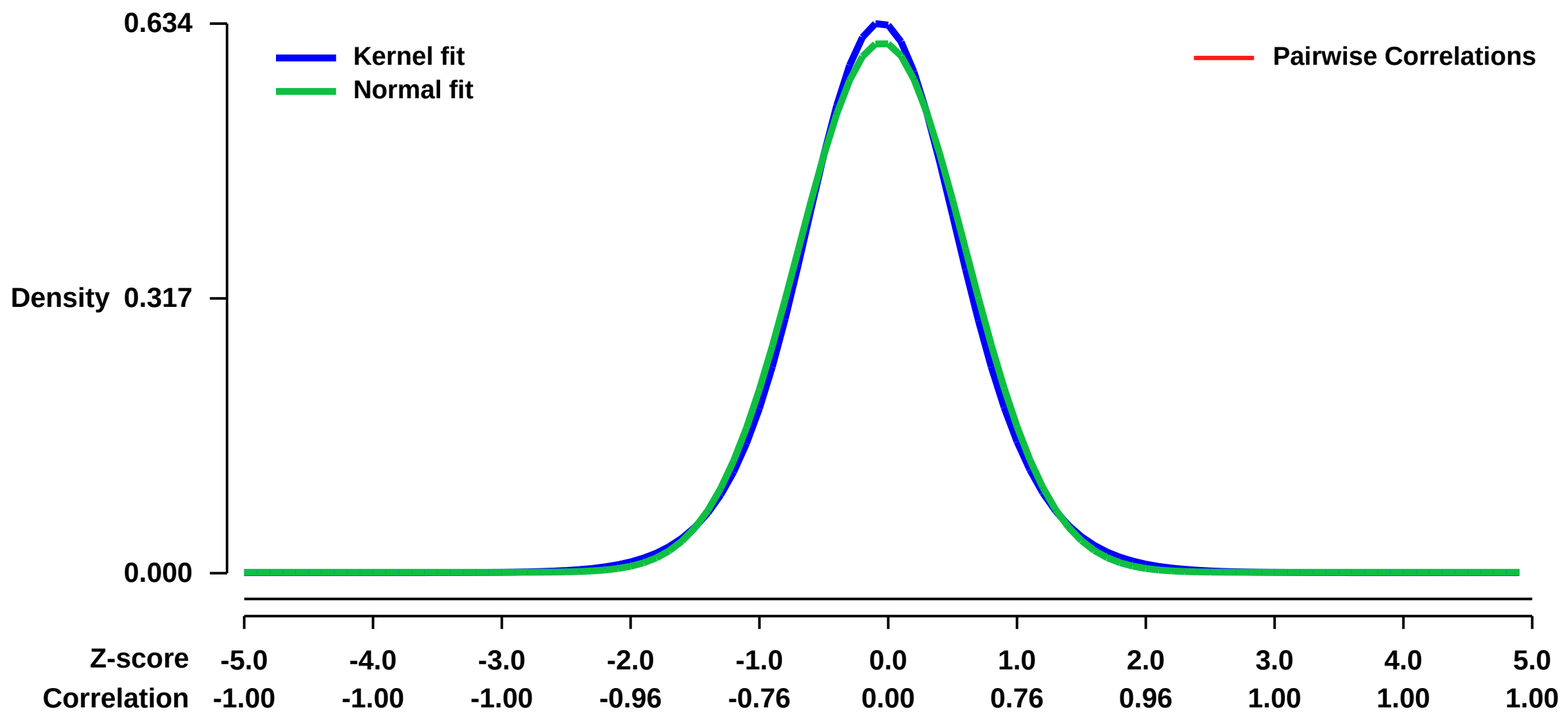

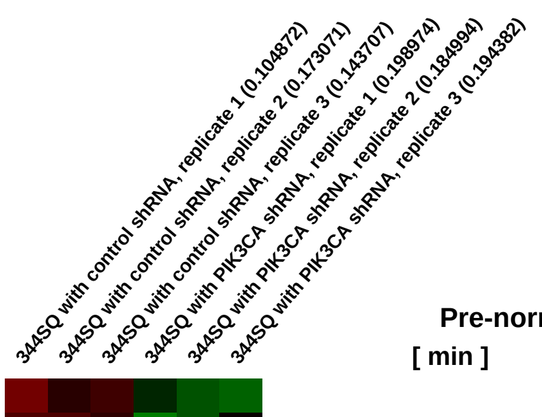

Pre-normalization Quantiles

[min] [medium] [max]

Null module

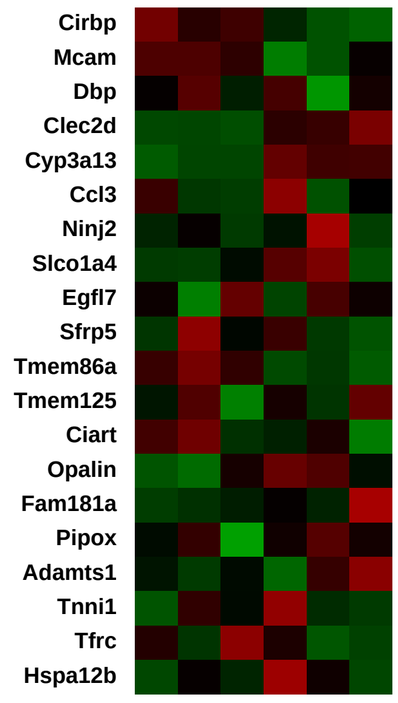

GEO Series "GSE46871" Expression Profiles

Num of samples in this series: 6

Scale of expression profile Z-scores

-3.0 -2.0 -1.0 0.0 1.0 2.0 3.0

GEO Link:	http://www.ncbi.nlm.nih.gov/geo/query/acc.cgi?acc=GSE46871
Status:	Public on May 14 2013
Title:	Hippocampal gene expression profiling of a model of Alzheimer‘s Disease upon treatment with the ACE inhibitor captopril
Organism:	Mus musculus
Experiment type:	Expression profiling by array
Platform:	GPL1261
Pubmed ID:	23959119
Summary & Design:	**Summary:** Extracellular senile plaques of amyloid beta (Abeta) are a pathological hallmark in brain of patients with Alzheimer‘s Disease (AD). Abeta is generated by the amyloidogenic processing of the amyloid precursor protein (APP). Concomitant to Abeta load, AD brain is characterized by an increase in protein level and activity of the angiotensin-converting enzyme (ACE). ACE inhibitors are a widely used class of drugs with established benefits for patients with cardiovascular disease. However, the role of ACE and ACE inhibition in the development of Abeta plaques and the process of AD-related neurodegeneration is not clear since ACE was reported to degrade Abeta. To investigate the effect of ACE inhibition on AD-related pathomechanisms, we used Tg2576 mice with neuron-specific expression of APPSwe as AD model. From 12 months of age, substantial Abeta plaque load accumulates in the hippocampus of Tg2576 mice as a brain region, which is highly vulnerable to AD-related neurodegeneration. The effect of central ACE inhibition was studied by treatment of 12 month-old Tg2576 mice for six months with the brain penetrating ACE inhibitor captopril. At an age of 18 months, hippocampal gene expression profiling was performed of captopril-treated Tg2576 mice relative to untreated 18 month-old Tg2576 controls with high Abeta plaque load. As an additional control, we used 12 month-old Tg2576 mice with low Abeta plaque load. Whole genome microarray gene expression profiling revealed gene expression changes induced by the brain-penetrating ACE inhibitor captopril, which could reflect the neuro-regenerative potential of central ACE inhibition. **Overall design:** Microarray gene expression profiling was performed of hippocampi isolated from aged, 18 month-old Tg2576 (APPSwe-transgenic) AD mice with high Abeta plaque load relative to age-matched Tg2576 mice, which were treated for 6 months with the centrally active ACE inhibitor captopril. Another study group consisted of 12 month-old Tg2576 mice with low Abeta plaque load. In total, three study groups were analyzed, i.e. (i) 18 month-old untreated Tg2576 mice with high Abeta plaque load, (ii) age-matched Tg2576 mice treated for 6 months with the brain-penetrating ACE inhibitor captopril (20 mg/kg body weight/day in drinking water), and (iii) untreated 12 month-old Tg2576 mice with low Abeta plaque load reflecting the time point when captopril treatment was initiated. Two biological replicates were made of each group, and total hippocampal RNA of four mice was pooled for one gene chip.

Background corr dist: KL-Divergence = 0.0289, L1-Distance = 0.0256, L2-Distance = 0.0007, Normal std = 0.6941

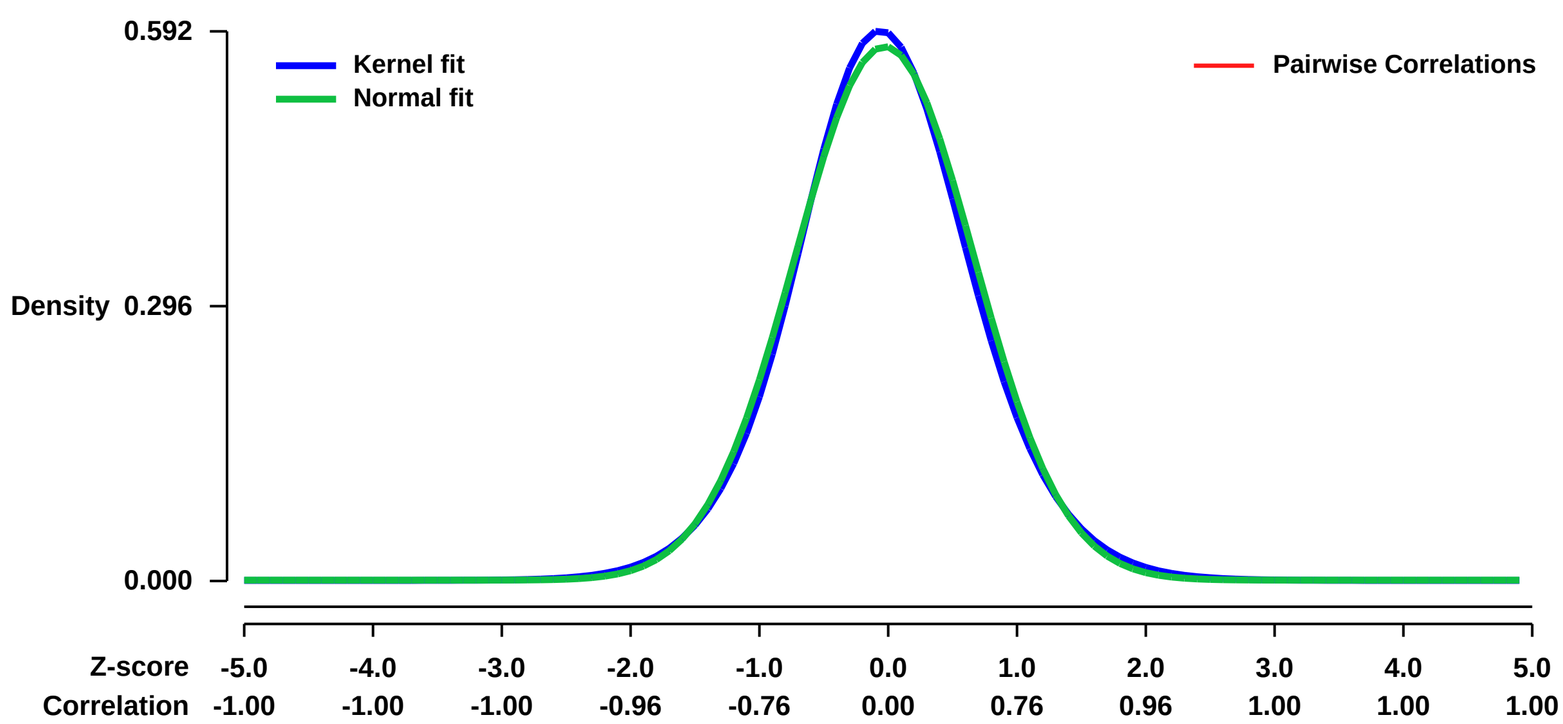

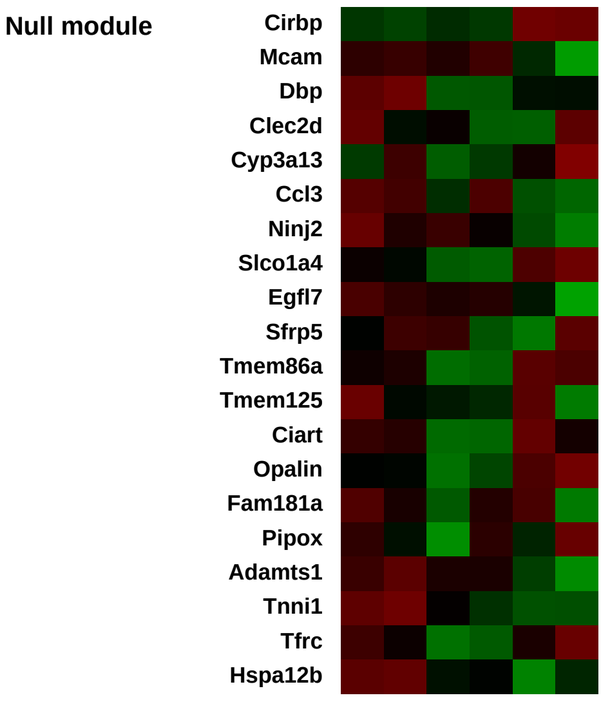

GEO Series "GSE4694" Expression Profiles

Num of samples in this series: 6

Scale of expression profile Z-scores

-3.0 -2.0 -1.0 0.0 1.0 2.0 3.0

GEO Link:	http://www.ncbi.nlm.nih.gov/geo/query/acc.cgi?acc=GSE4694
Status:	Public on Apr 30 2006
Title:	Expression data from myogenesis
Organism:	Mus musculus
Experiment type:	Expression profiling by array
Platform:	GPL1261
Pubmed ID:	17062158
Summary & Design:	**Summary:** During muscle differentiation, myogenesis sepcific genes are differentially regulated, including Lamins that function at least in maintenance of nuclear architecture and regulation of gene expression. We used microarrays to detail the global changes of gene expression in lamins and nuclear envelope assoicated proteins during myogenesis. Keywords: comparative, myogenesis **Overall design:** C2C12 were cultured either in 20% serum (undifferentiated) or in 2% horse serum (differentiated). Differentiated C2C12 cells were harvested on day 6 after induction of myogenesis in low serum. Affymetirx microarray raw data were further processed by GCRMA to globally normalized signal values and then subjected to analysis of Bayesian regularized t-test. Gene expression, that has a p-value less than 0.05 in the t-test and has more than 1.5 fold change, was considered siginificant.

Background corr dist: KL-Divergence = 0.0380, L1-Distance = 0.0307, L2-Distance = 0.0010, Normal std = 0.6550

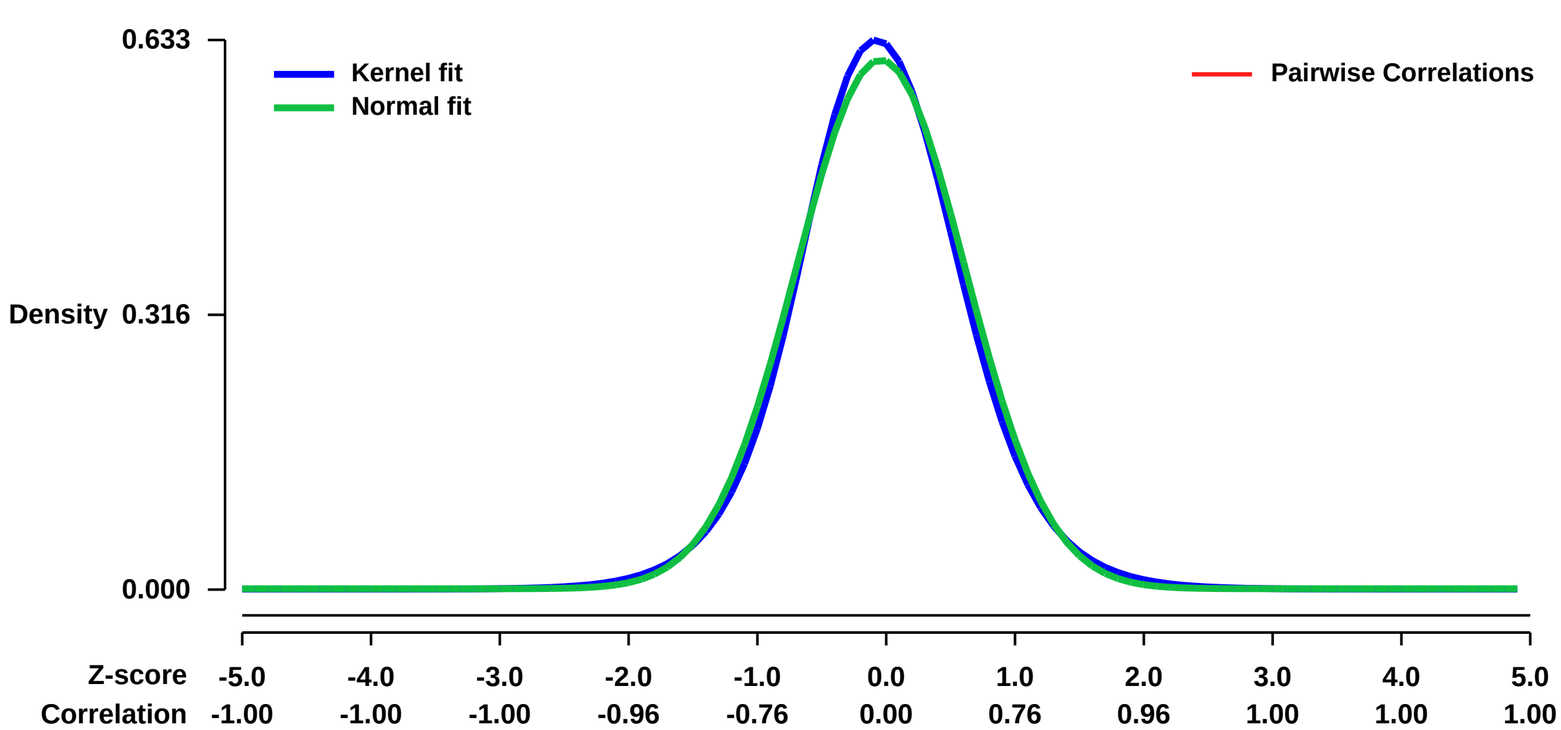

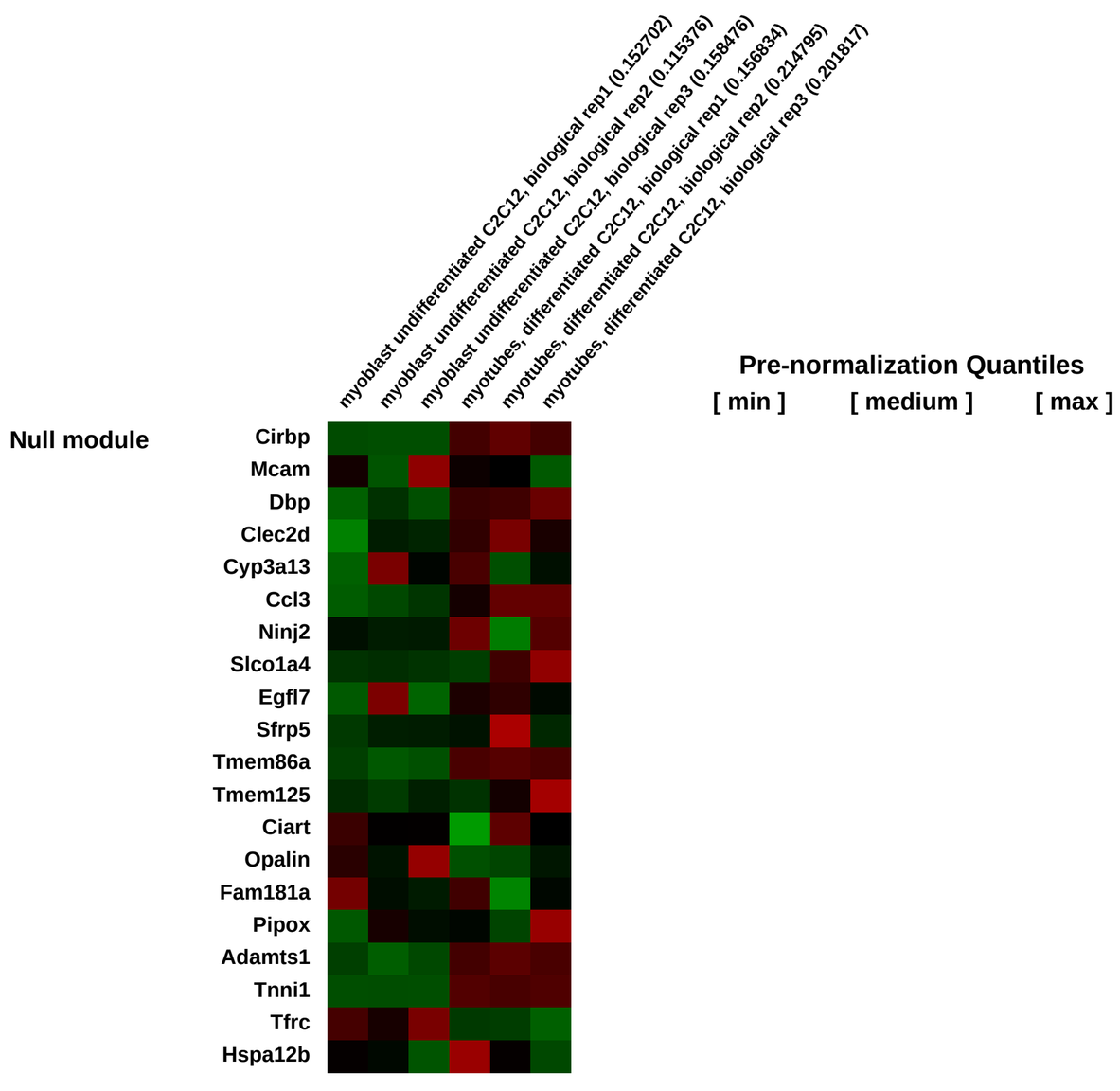

GEO Series "GSE4695" Expression Profiles

Num of samples in this series: 6

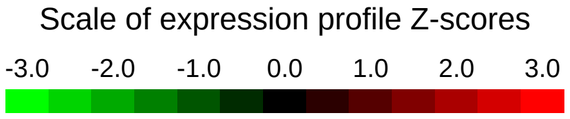

GEO Link:	http://www.ncbi.nlm.nih.gov/geo/query/acc.cgi?acc=GSE4695
Status:	Public on Apr 25 2006
Title:	Changes in gene expression in dermal fibroblasts following exposure to Et1 peptide
Organism:	Mus musculus
Experiment type:	Expression profiling by array
Platform:	GPL1261
Pubmed ID:	16870175
Summary & Design:	**Summary:** To determine if aberrant activation of endothelin-1 (Et1) could lead to the dysregulation of many downstream genes, we exposed fibroblasts to exogenous ET1 peptide and assayed for transcriptional changes by microarray. Mouse dermal fibroblasts were treated with exogenous Et1 peptide for 24 hours. ET1 treatment resulted in significant expression changes â primarily downregulation â of a number of genes. In particular, Tgf‚†2 and Tgf‚†3 were among the downregulated genes, which in turn alter the expression status of their many target genes. These data suggest that the stable silencing of Et1 is important for the phenotypic stability of dermal fibroblasts, and perhaps many other cell types as well. **Keywords:** endothelin-1; Et1; dermal fibroblast **Overall design:** Three separate biological replicates were derived for both control and treated samples. The primary dermal fibroblasts were derived by explant procedure from the skin of mouse pups aged 0-3 days. By passage 5, cells were split to two separate cultures-- one with 100nM synthetic Et1 peptide added to the medium (treated) and the other with nothing added (control). Cells were exposed to Et1 for 24 hrs, then treated and control populations were harvested for total RNA.

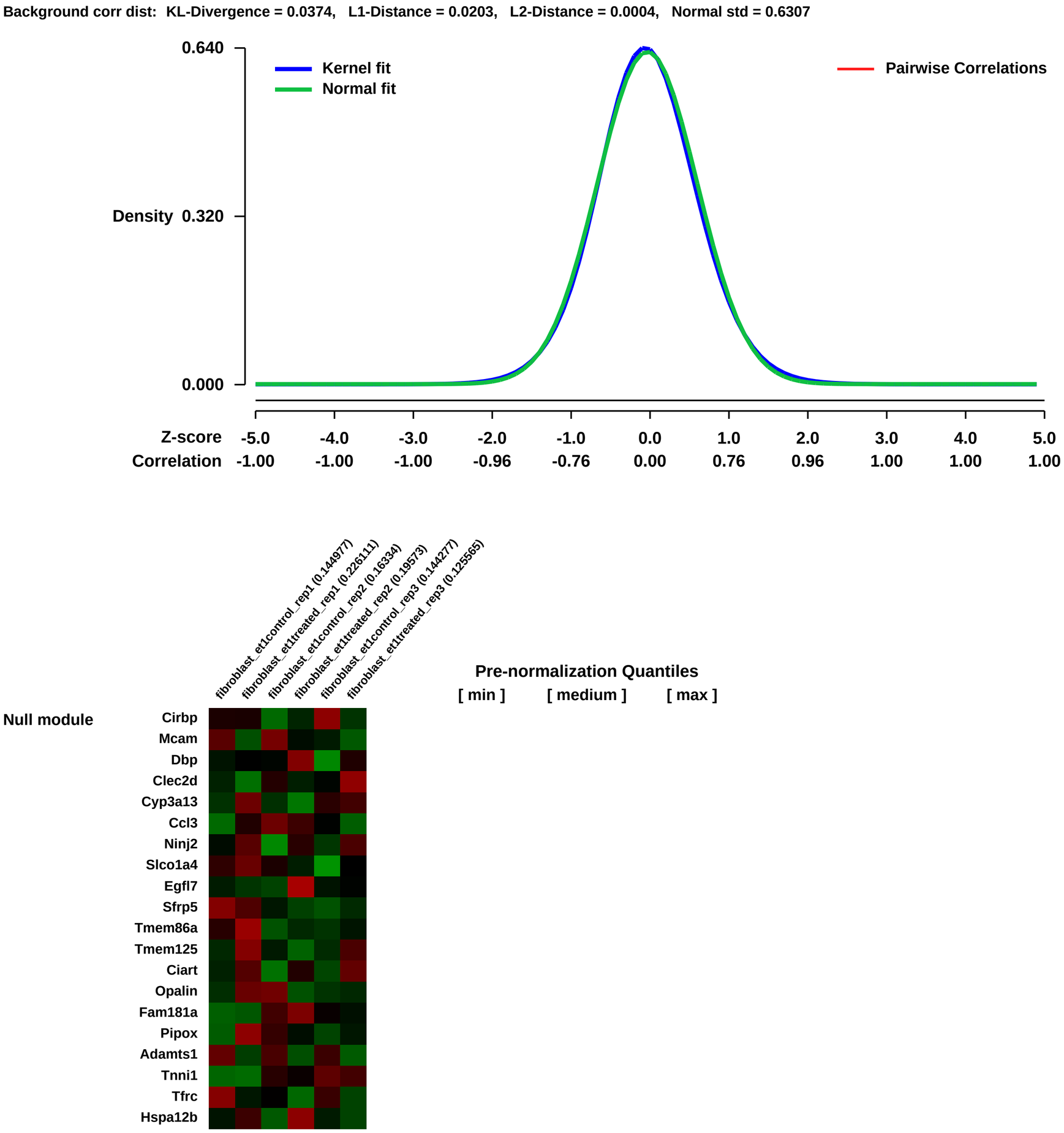

GEO Series "GSE46970" Expression Profiles

Num of samples in this series: 15

Scale of expression profile Z-scores

-3.0 -2.0 -1.0 0.0 1.0 2.0 3.0

GEO Link:	http://www.ncbi.nlm.nih.gov/geo/query/acc.cgi?acc=GSE46970
Status:	Public on Jun 18 2013
Title:	Gene expression of 4, 5, and 6 days differentiated Flk1+ WT ES cells, and of 6 days differentiated Flk1+ Runx1-/- and Tal-1-/- ES cells
Organism:	Mus musculus
Experiment type:	Expression profiling by array
Platform:	GPL1261
Pubmed ID:	19265543
Summary & Design:	**Summary:** **In order to identify genes that are activated in differentiating WT ESCs, but are missing in Tal-1-/- and Runx1-/- ESCs, and which might be involved in the generation of definitive hematopoietic progenitors and their specification thereafter, we performed microarray analyses on purified Flk-1+ cells, differentiated from these ESCs for 4, 5, and 6 days â in vitroâ .** **Overall design:** **Gene-expression profiling of three biological replicates was performed at days 4, 5, and 6 during the differentiation process of WT J1 ESCs (9 samples), and at day 6 during the differentiation process of either Runx1-/- J1 or Tal-1-/- J1 ESCs (3 samples each). Total RNA was extracted using the RNeasy Mini kit (Qiagen). The integrity and amount of isolated RNA was assessed for each sample using an Agilent 2100 Bioanalyzer (Agilent, Waldbronn, Germany) and a NanoDrop ND-1000 spectrophotometer (NanoDrop Technologies, Wilmington, DE). Complementary DNA was synthesized from 3-5 ¸…g total RNA, using reagents recommended in the technical manual GeneChip Expression Analysis (Affymetrix, Santa Clara, CA). The in vitro transcription, necessary for the synthesis of biotinylated complementary RNA (cRNA) was performed using the Enzo RNA Transcript Labeling kit (Affymetrix). Fifteen micrograms of fragmented cRNA of each sample were hybridized to nine Mouse Genome 430-2 arrays (Affymetrix). Hybridization was performed in a Hybridization Oven 640, and chips were washed and stained in the Fluidics Station 400 (both Affymetrix), according to procedure 2 as described in the technical manual. Finally, the arrays were scanned with a GeneChip Scanner 3000 using the GCOS software, both Affymetrix. All relevant GCOS data of quality checked microarrays were analyzed with High Performance Chip Data Analysis (HPCDA, unpublished), using the BioRetis database (www.bioretis-analysis.de), as described and validated previously (55). Used query parameters for database filtering process was described earlier several times (56). For hierarchical cluster analysis, we used the program Genes@Work (57) with gene vectors for normalization and Pearson w/mean for similarity measure. As cluster type, we used center of mass.**

Background corr dist: KL-Divergence = 0.1350, L1-Distance = 0.0345, L2-Distance = 0.0023, Normal std = 0.3999

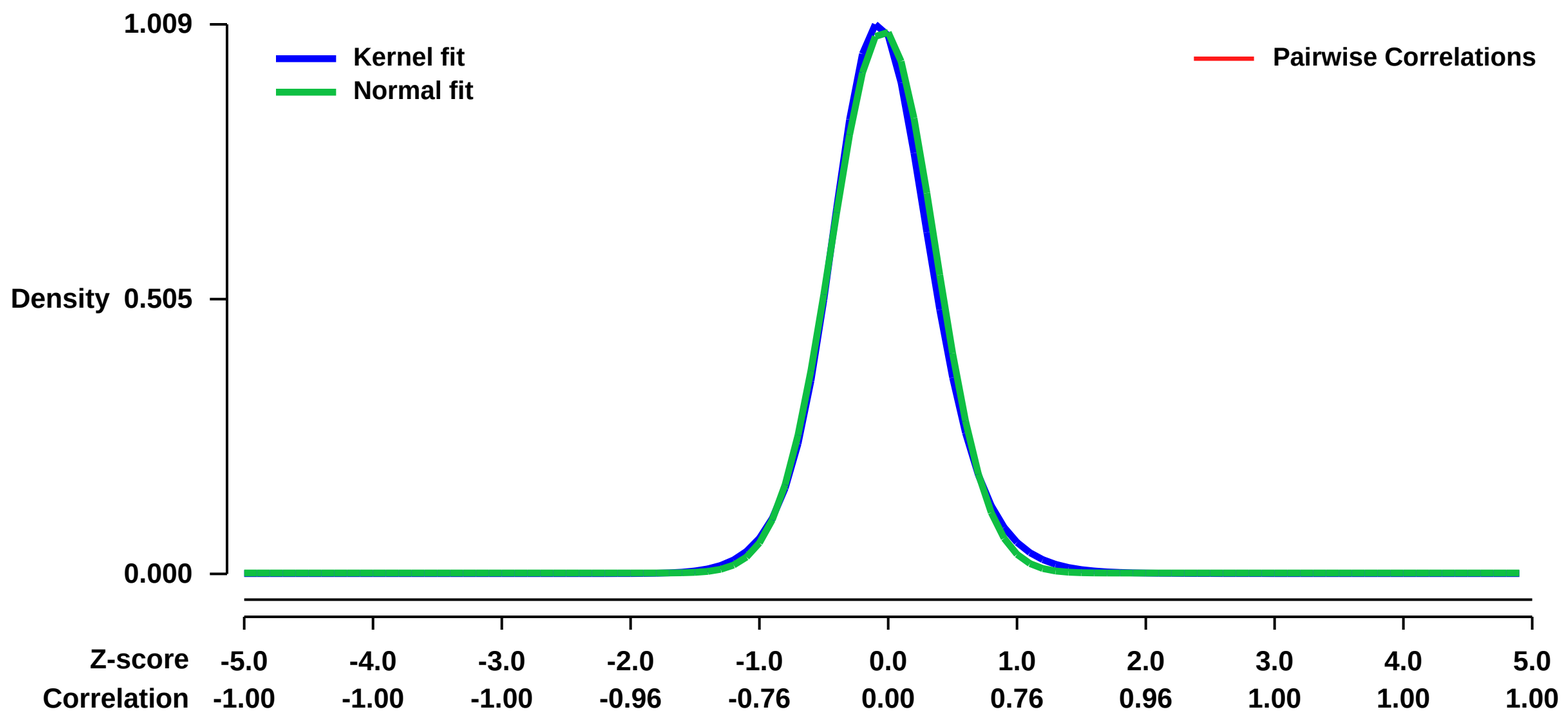

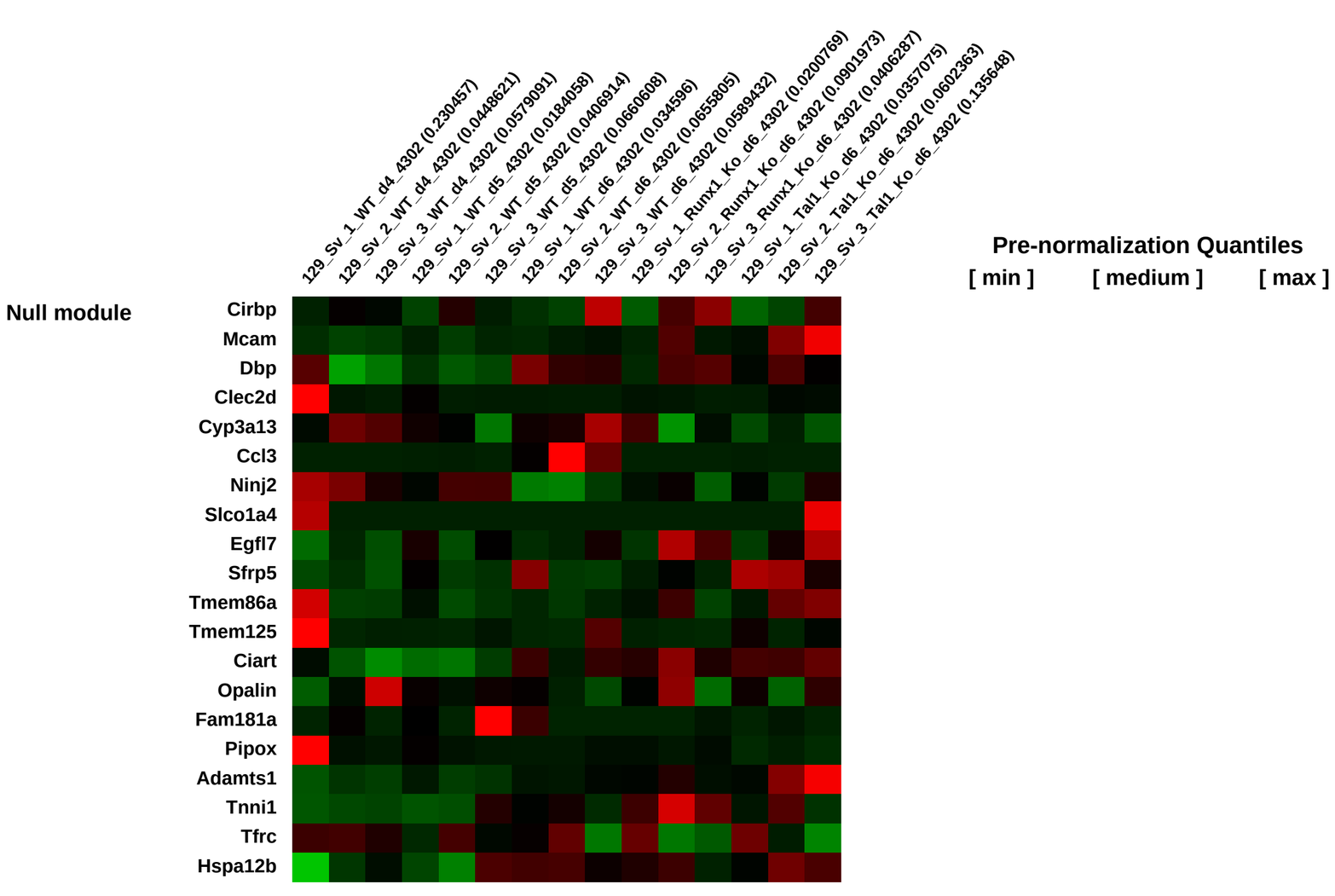

GEO Series "GSE47049" Expression Profiles

Num of samples in this series: 6

Scale of expression profile Z-scores

-3.0 -2.0 -1.0 0.0 1.0 2.0 3.0

GEO Link:	http://www.ncbi.nlm.nih.gov/geo/query/acc.cgi?acc=GSE47049
Status:	Public on May 09 2014
Title:	Expression data from wild type and Gata6-deficient tissue resident peritoneal macrophages
Organism:	Mus musculus
Experiment type:	Expression profiling by array
Platform:	GPL1261
Pubmed ID:	24762537
Summary & Design:	**Summary:** Tissue resident macrophages are notoriously heterogeneous, exhibiting discrete phenotypes as a consequence of tissue- and micro-anatomical niche-specific functions, but the molecular basis for this is not understood. We resolved a restricted transcriptional profile for the self-renewing population of peritoneal resident macrophages, which is expressed during homeostasis and inflammation and distinct from other Mˆ . Prominent within this profile was the expression of Gata6. This study represents a characterisation of the role of Gata6 in peritoneal resident macrophage phenotype. We used microarrays to determine the patterns of gene expression in peritoneal resident Mˆ in the absence of GATA-6 against wild type. **Overall design:** Conditional 'floxed' Gata6 deficient sex-matched mice between 7 weeks old were compared against wild type

Background corr dist: KL-Divergence = 0.0407, L1-Distance = 0.0228, L2-Distance = 0.0006, Normal std = 0.6176

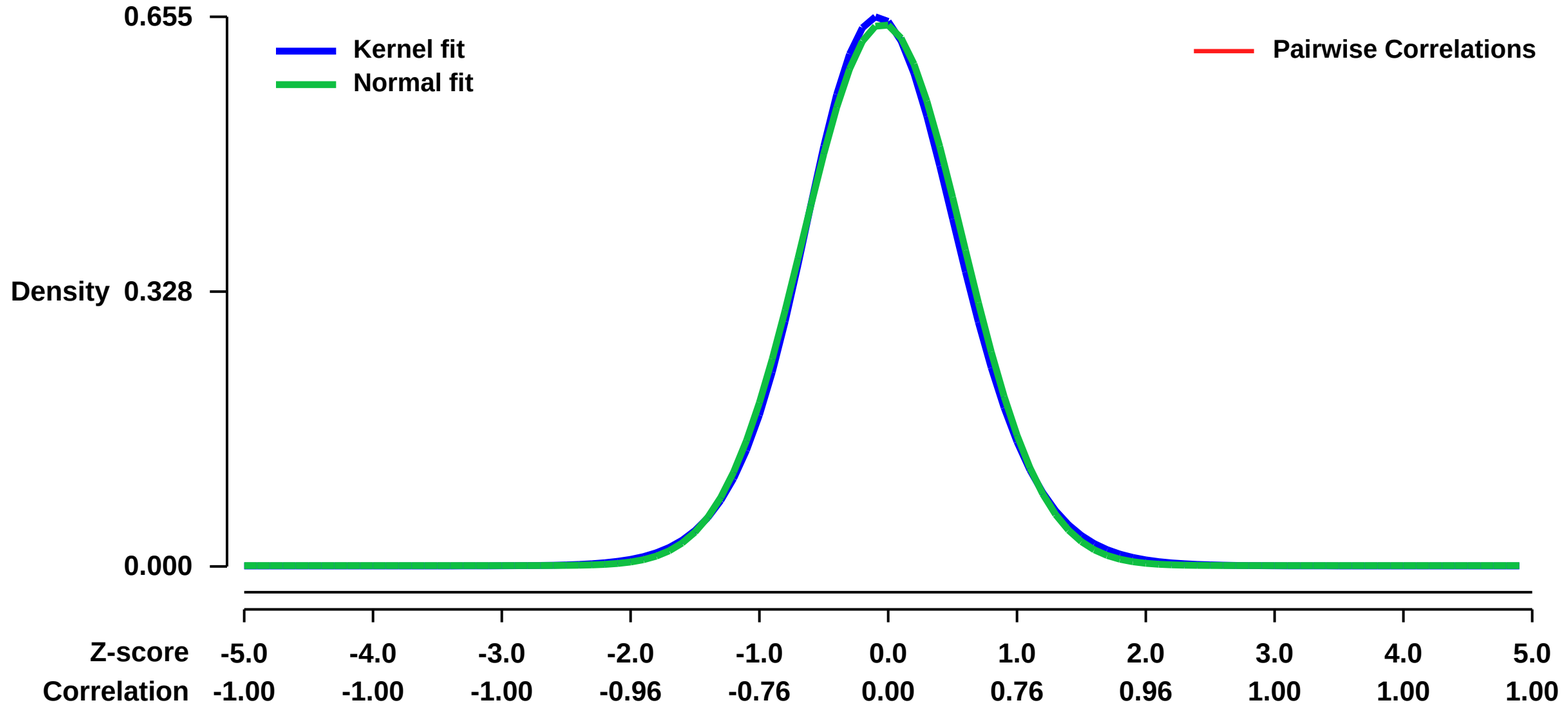

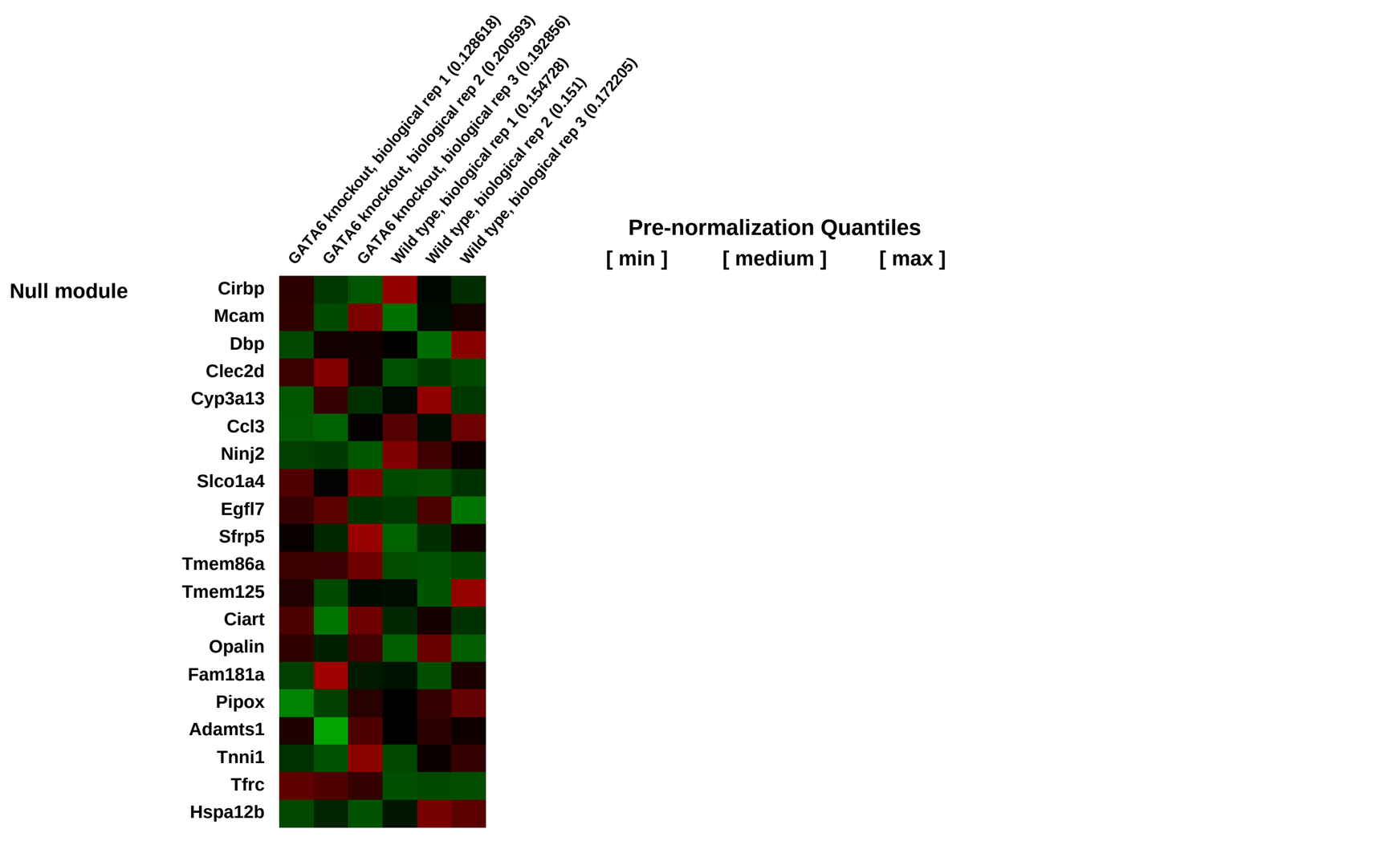

GEO Series "GSE47065" Expression Profiles

Num of samples in this series: 8

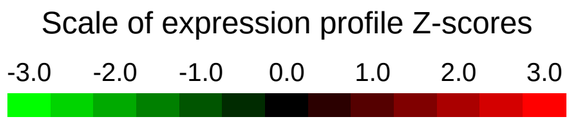

GEO Link:	http://www.ncbi.nlm.nih.gov/geo/query/acc.cgi?acc=GSE47065
Status:	Public on May 18 2013
Title:	Gene expression profiling of IR-/-, IGF-1R-/- (dKO) newborn epidermis.
Organism:	Mus musculus
Experiment type:	Expression profiling by array
Platform:	GPL1261
Pubmed ID:	23906066
Summary & Design:	**Summary:** Analysis of newborn mouse epidermis lacking the expression of Insulin receptor (IR) and Insulin like growth factor 1 receptor (IGF-1R). Results show that IR/IGF-1R signalling control epidermal morphogenesis. **Overall design:** RNA was isolated from newborn mouse epidermis.Gene expression profiling was on on Affymetrix 430-2.0 platform.

Background corr dist: KL-Divergence = 0.0742, L1-Distance = 0.0224, L2-Distance = 0.0008, Normal std = 0.4920

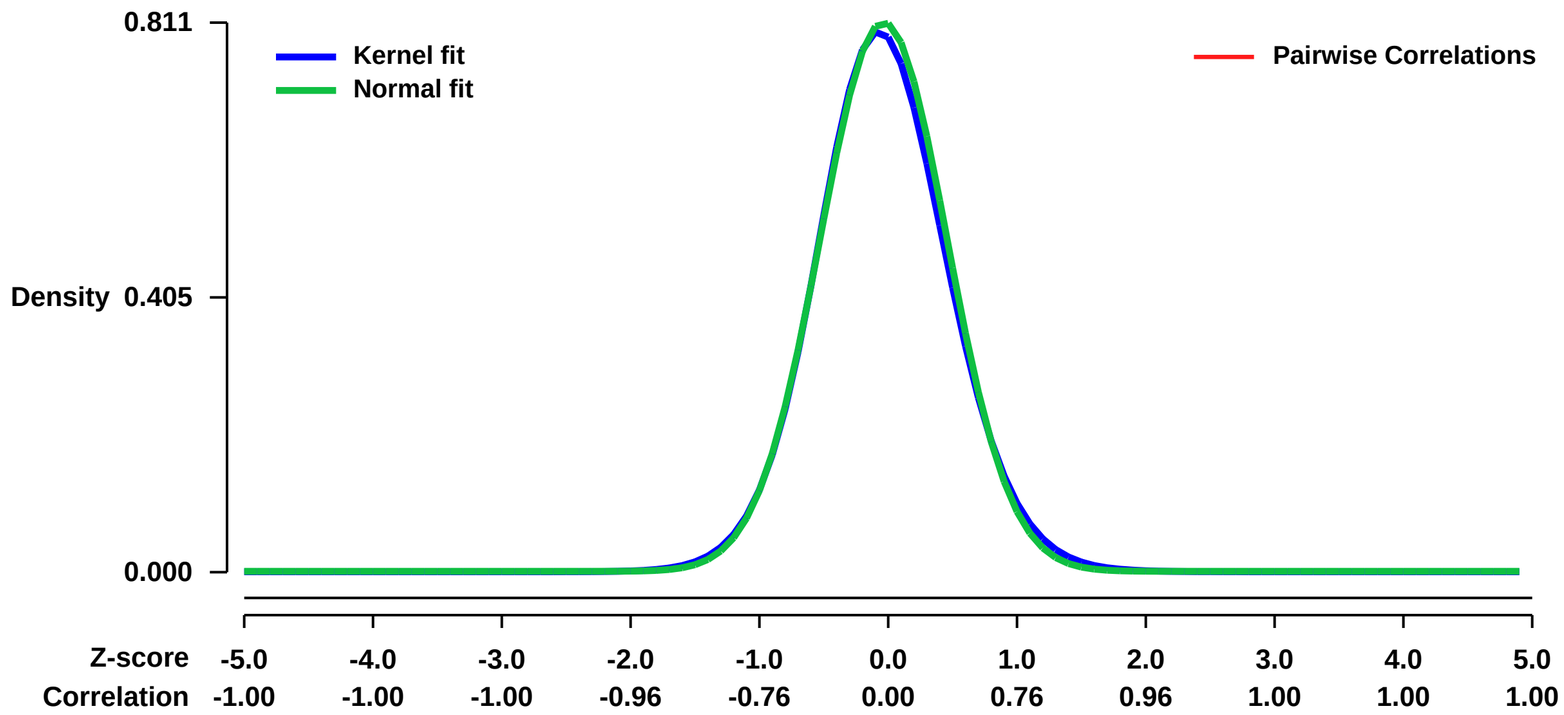

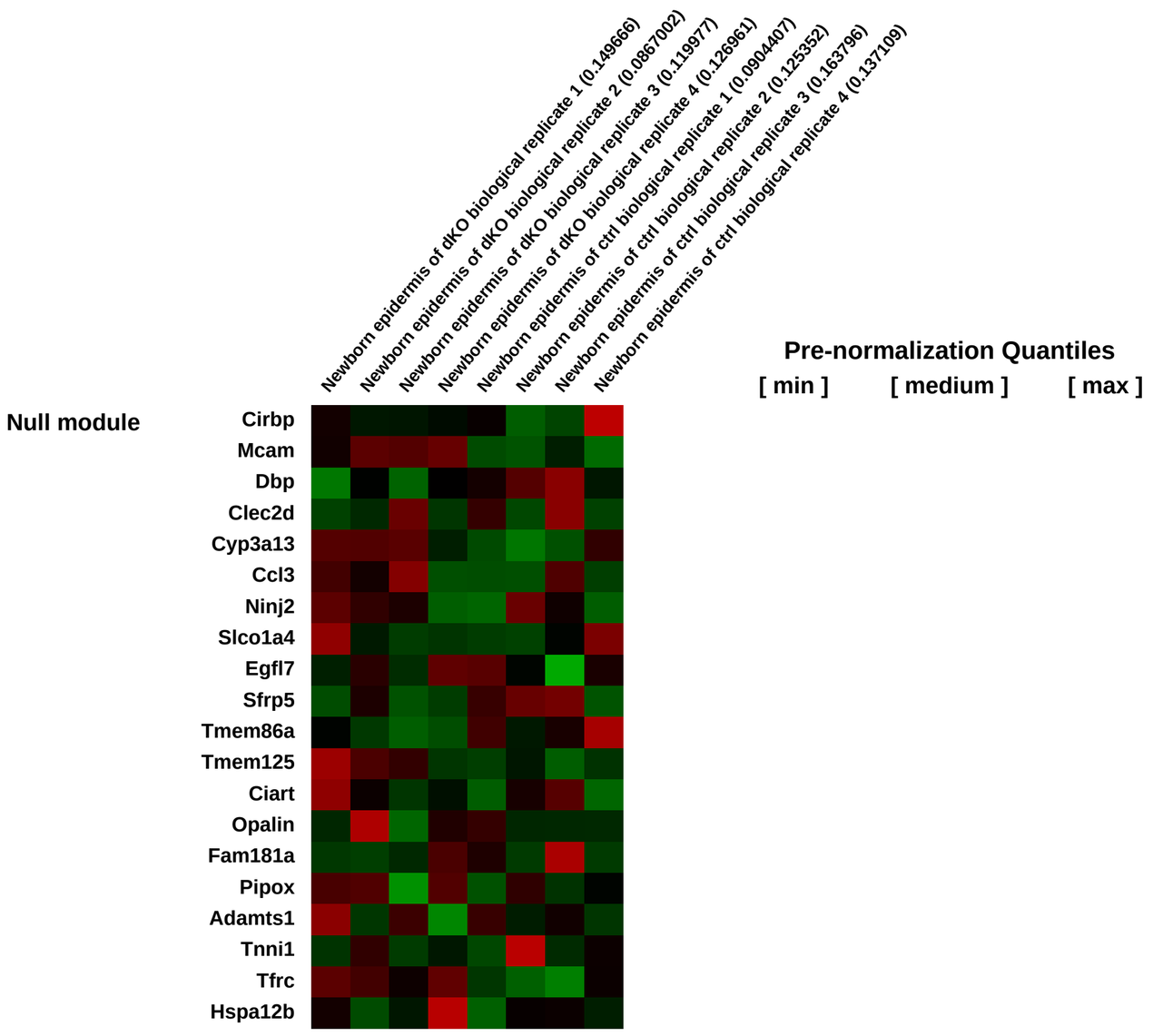

GEO Series "GSE4712" Expression Profiles

Num of samples in this series: 21

Scale of expression profile Z-scores

-3.0 -2.0 -1.0 0.0 1.0 2.0 3.0

GEO Link:	http://www.ncbi.nlm.nih.gov/geo/query/acc.cgi?acc=GSE4712
Status:	Public on Oct 24 2006
Title:	Edema Toxin-treated Macrophage Study
Organism:	Mus musculus
Experiment type:	Expression profiling by array
Platform:	GPL1261
Pubmed ID:	16846716
Summary & Design:	**Summary:** Edema toxin (EdTx), which is a combination of edema factor and a binding moiety (protective antigen), is produced by Bacillus anthracis, the etiological agent of anthrax. EdTx is an adenylyl cyclase enzyme that converts adenosine triphosphate to adenosine-3â ,5â -monophosphate, resulting in interstitial edema seen in anthrax patients. We used GeneChip analysis to examine global transcriptional profiles of EdTx-treated RAW 264.7 murine macrophage-like cells at 3 and 6 hr. **Keywords: Toxin response** **Overall design:** RAW 264.7 cells were treated with EdTx (2.5 ´µg/ml of protective antigen and 0.625 ´µg/ml of Edema factor), PA (2.5 ´µg/ml), or LPS (1 ng/mL) for 0, 3, and 6 hr. Each experiment was performed in triplicate, generating a total of 21 arrays (biological replciates).

Background corr dist: KL-Divergence = 0.2004, L1-Distance = 0.0429, L2-Distance = 0.0041, Normal std = 0.3331

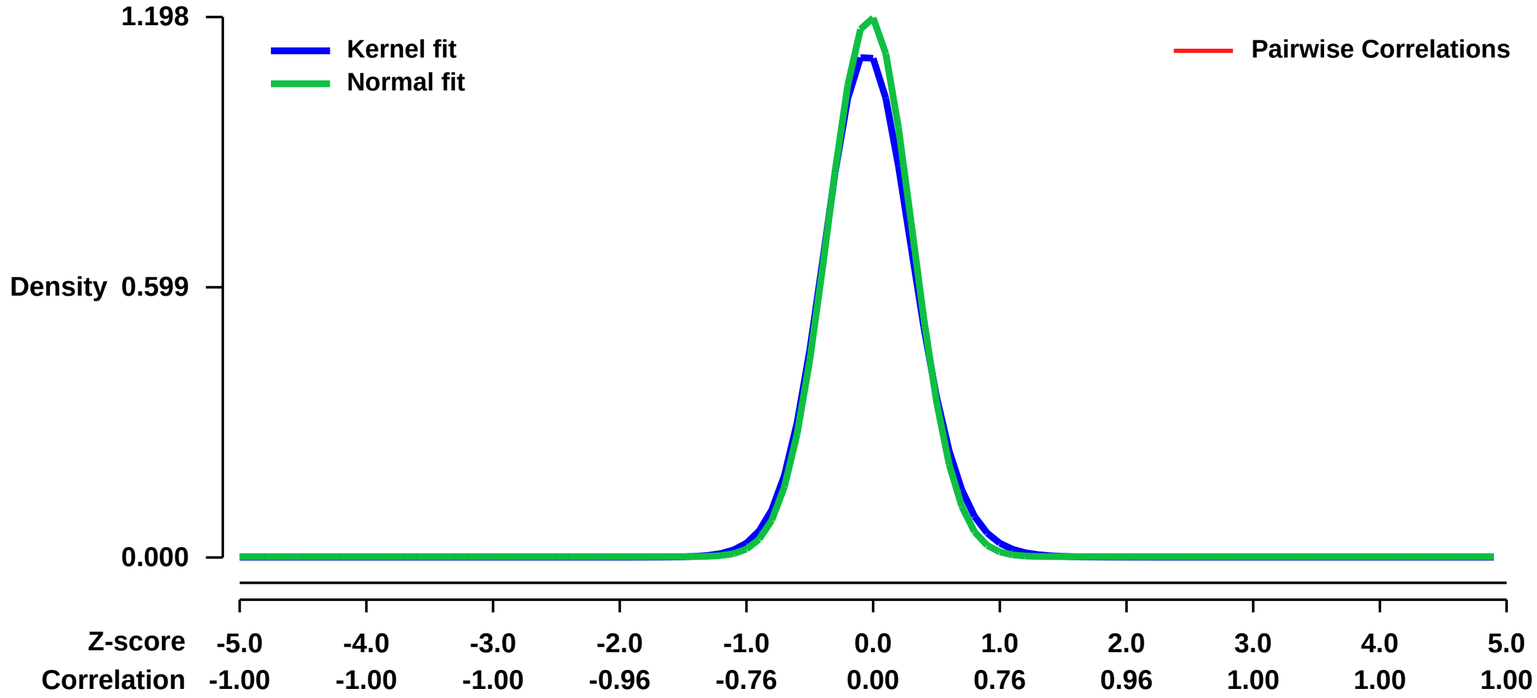

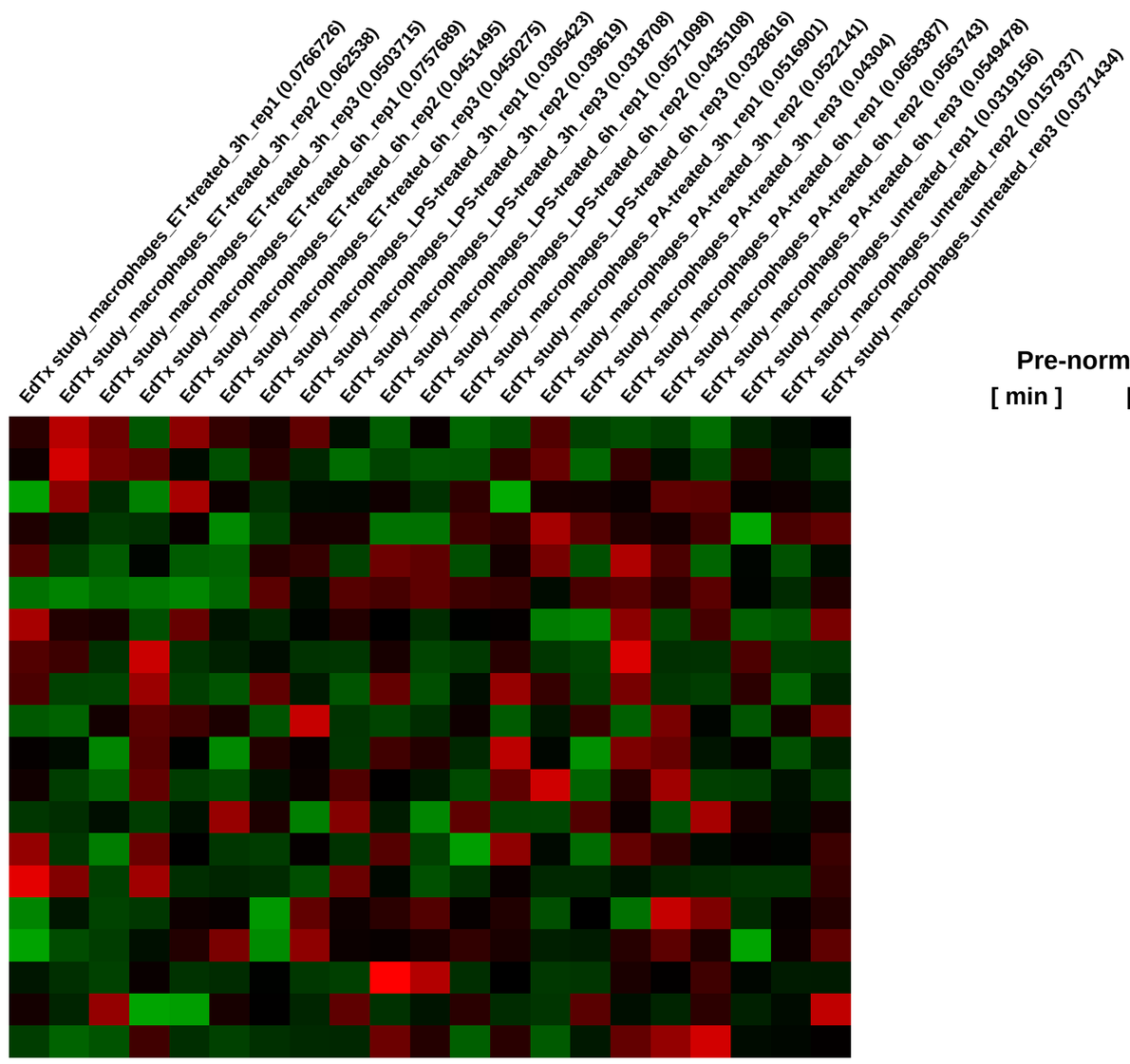

GEO Series "GSE4718" Expression Profiles

Num of samples in this series: 6

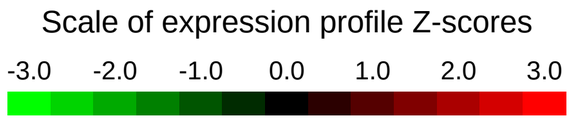

GEO Link:	http://www.ncbi.nlm.nih.gov/geo/query/acc.cgi?acc=GSE4718
Status:	Public on Apr 27 2006
Title:	Improved DNA methylation analysis via enrichment of demethylated cells expressing an X-inactivated GFP transgene
Organism:	Mus musculus
Experiment type:	Methylation profiling by array
Platform:	GPL1261
Pubmed ID:	17068962
Summary & Design:	**Summary:** **The demethylating drug 5-aza-2â -deoxycytidine (5-aza-2dC) is frequently used to investigate the** **effect of global DNA demethylation on gene expression in cultured mammalian cells. Here, we utilize a novel method that uses the reactivation of an X-inactivated GFP transgene as a marker to enrich for cells that have undergone drug-induced demethylation. By combining it with microarray gene expression profiling, we demonstrate the methodâ s utility in identifying genes activated by global DNA demethylation.** **Keywords: 5-aza-2'-deoxycytidine; methylation; dermal fibroblast; X-linked GFP** **Overall design:** **Laboratory. Male transgenic animals were bred to wildtype BL6 female mice to obtain females that were heterozygous for the transgene. Dermal fibroblasts were obtained from explant cultures of neonatal female mice from these crosses. The cells were then sorted using FACS to obtain only GFP-nonexpressing cells. These cells represent the population with the GFP transgene on the inactive X chromosome. The GFP-silent cells were treated with the demethylating drug 5-aza-2'-deoxycytidine. This drug does not affect all cells and uses a passive form of demethylation that results in a heterogenous population of unaffected and demethylated cells. A portion of the cells affected by demethylation activate the inactive GFP transgene by demethylating the inactive X chromosome. The GFP-active and GFP-inactive cells were sorted by FACS and assayed by microarray to determine what genes were affected by demethylation. Also the microarray results indicated if sorting for GFP-active cells enriches for cells affected by the drug.**

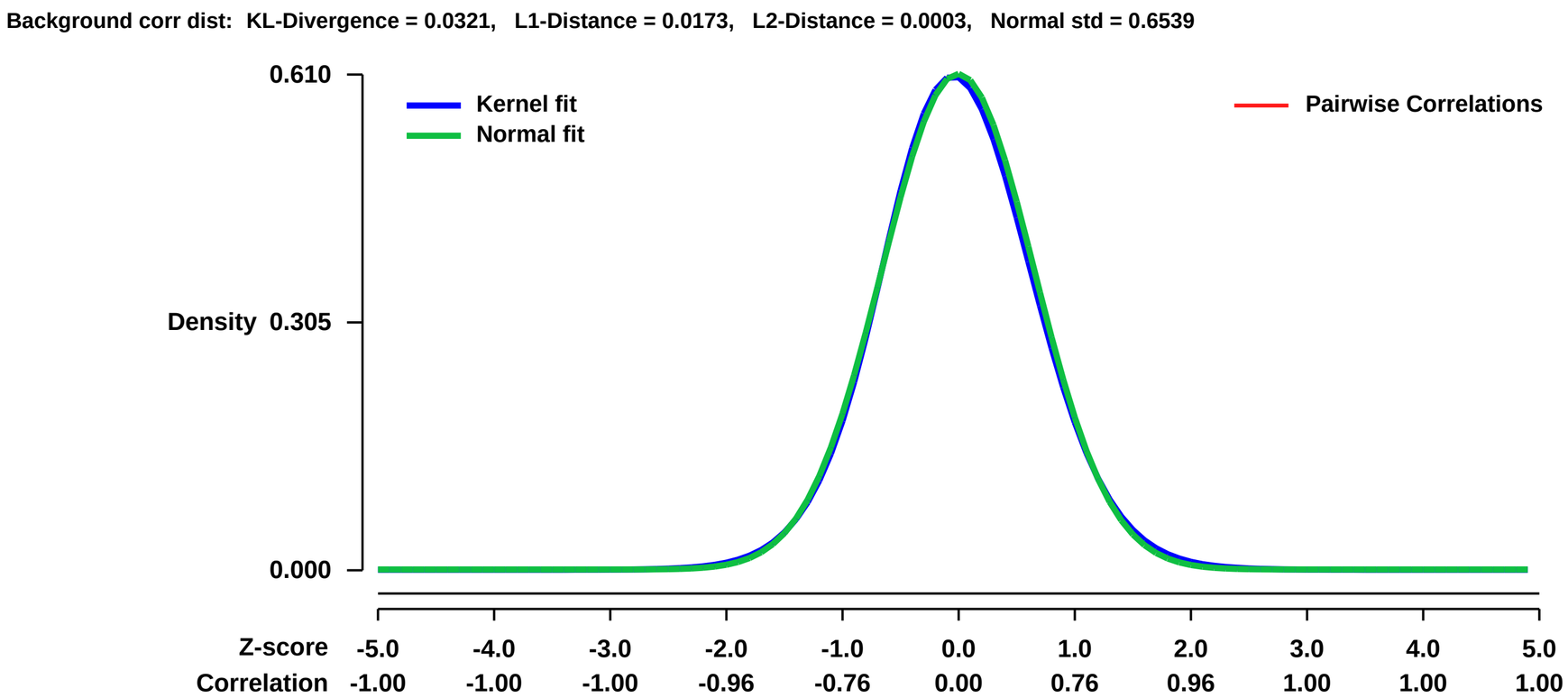

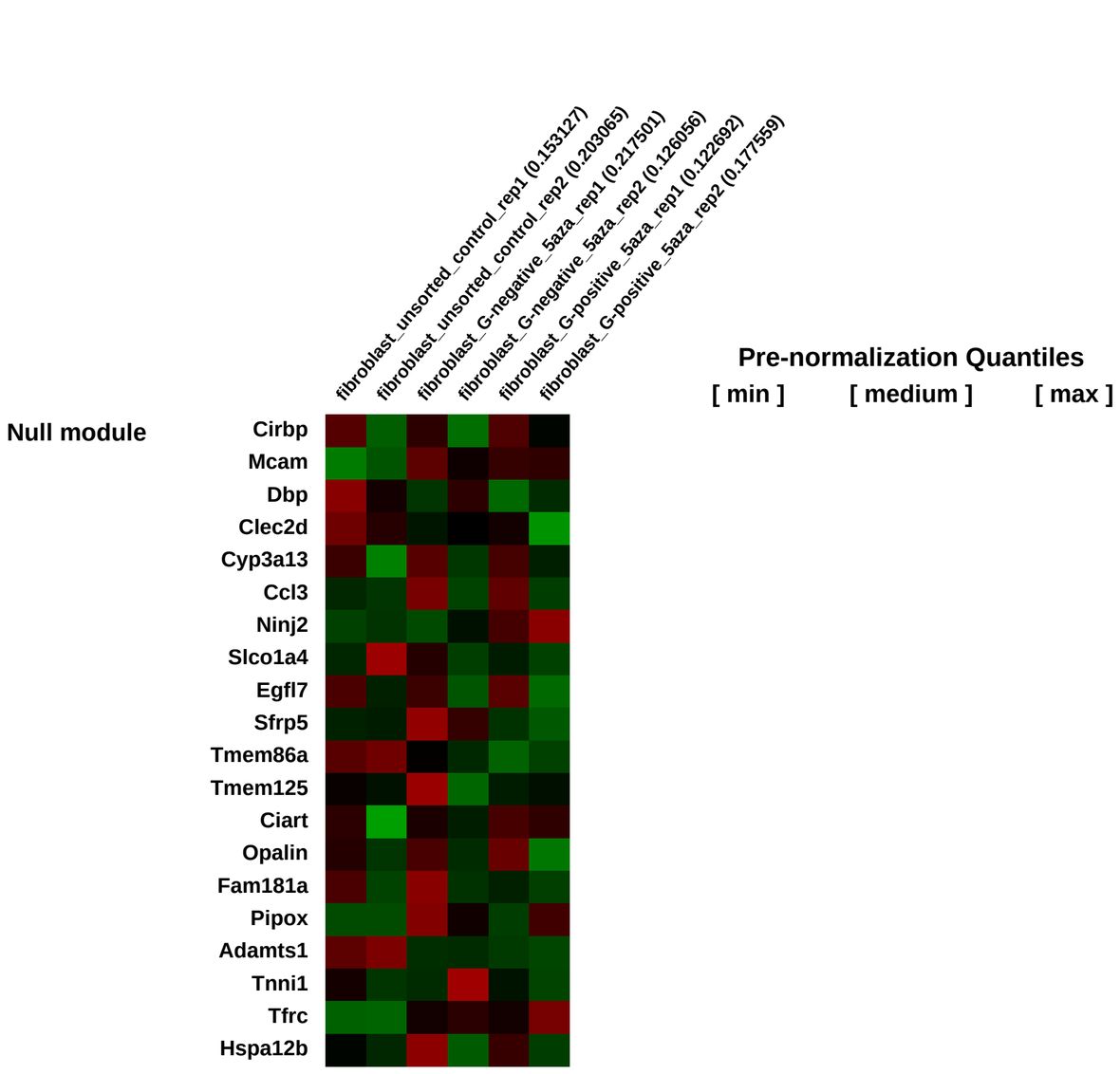

GEO Series "GSE47196" Expression Profiles

Num of samples in this series: 6

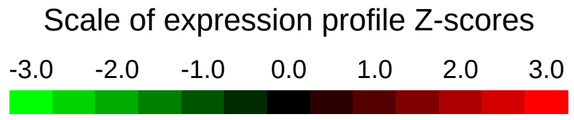

GEO Link:	http://www.ncbi.nlm.nih.gov/geo/query/acc.cgi?acc=GSE47196
Status:	Public on May 23 2013
Title:	Immunoglobulin-like domain receptor 1 mediates fat-stimulated cholecystokinin secretion.
Organism:	Mus musculus
Experiment type:	Expression profiling by array
Platform:	GPL1261
Pubmed ID:	23863714
Summary & Design:	**Summary:** Cholecystokinin (CCK) is a satiety hormone produced by discrete enteroendocrine cells scattered among absorptive cells of the small intestine. CCK is released into blood following a meal; however, the mechanisms inducing hormone secretion are largely unknown. Ingested fat is the major stimulant of CCK secretion. We recently identified a novel member of the lipoprotein remnant receptor family known as immunoglobulin-like domain containing receptor 1 (ILDR1) in intestinal CCK cells and postulated that this receptor conveyed the signal for fat-stimulated CCK secretion. In the intestine, ILDR1 is expressed exclusively in CCK cells. Orogastric administration of fatty acids elevated blood levels of CCK in wild type but not ILDR1-deficient mice, although the CCK secretory response to trypsin inhibitor was retained. The uptake of fluorescently labeled lipoproteins in ILDR1-transfected CHO cells and release of CCK from isolated intestinal cells required a unique combination of fatty acid plus HDL. CCK secretion secondary to ILDR1 activation is associated with increased [Ca2+]i consistent with regulated hormone release. These findings demonstrate that ILDR1 regulates CCK release through a mechanism dependent on fatty acids and lipoproteins and that absorbed fatty acids regulate gastrointestinal hormone secretion. **Overall design:** GFP positive cells from CCK-EGFP transgenic mice were isolated by FACS and the expression profile was compared with an equal number of non-fluorescent intestinal cells.

Background corr dist: KL-Divergence = 0.0167, L1-Distance = 0.0318, L2-Distance = 0.0015, Normal std = 0.7899

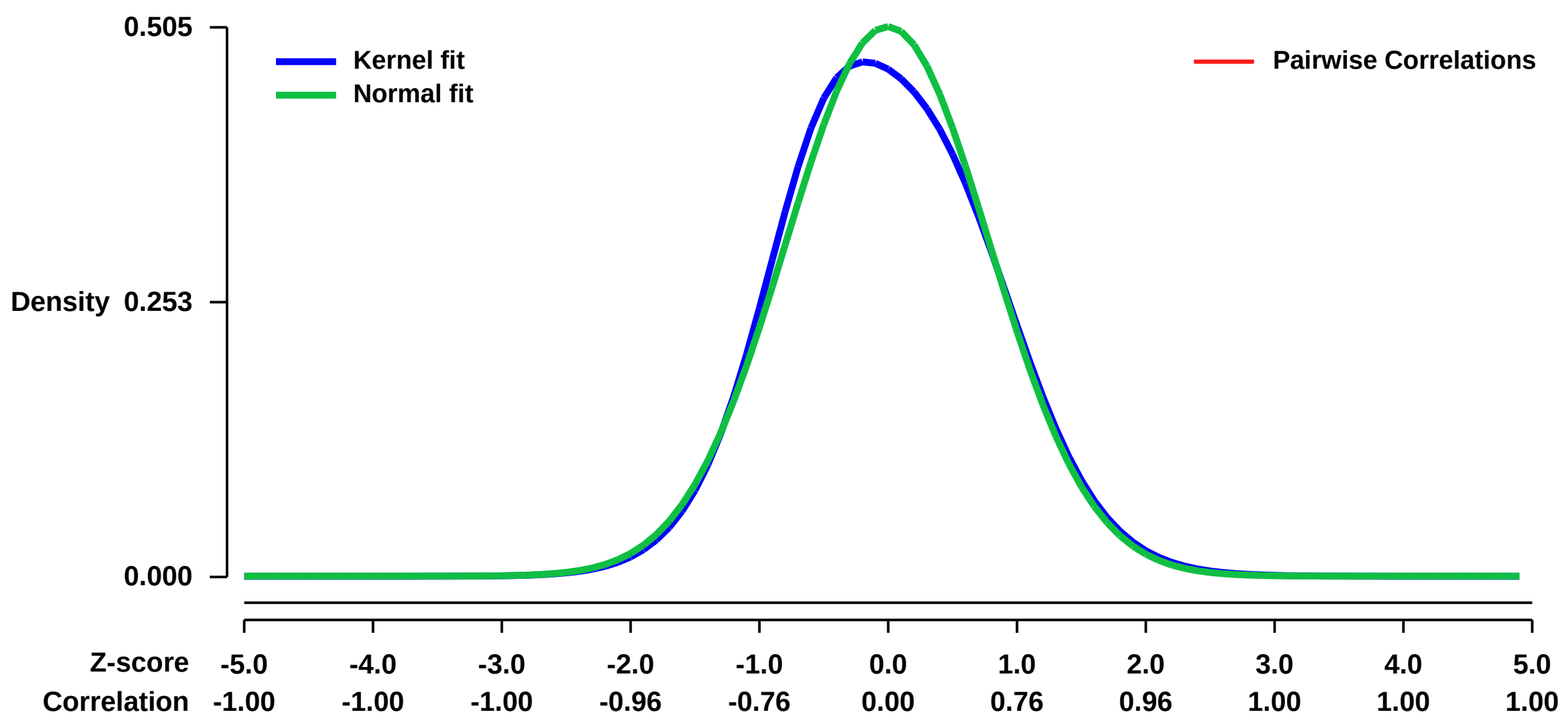

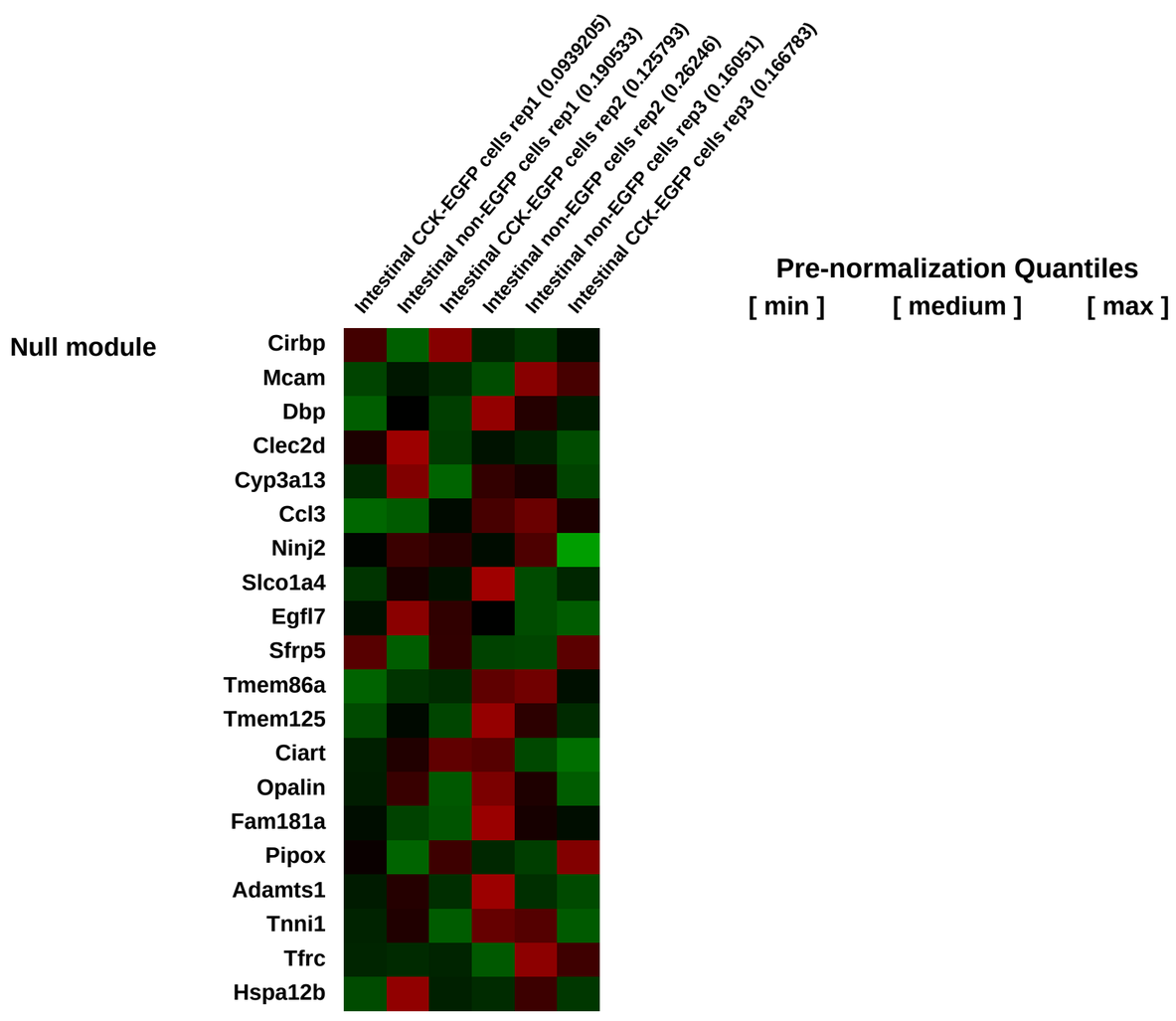

GEO Series "GSE47205" Expression Profiles

Num of samples in this series: 10

Scale of expression profile Z-scores

-3.0 -2.0 -1.0 0.0 1.0 2.0 3.0

GEO Link:	http://www.ncbi.nlm.nih.gov/geo/query/acc.cgi?acc=GSE47205
Status:	Public on May 24 2013
Title:	MLL regulated genes in LSK/CD48- hematopoietic stem cells
Organism:	Mus musculus
Experiment type:	Expression profiling by array
Platform:	GPL1261
Pubmed ID:	23744037
Summary & Design:	**Summary:** The histone methyltransferase mixed lineage leukemia (MLL) is essential to maintain hematopoietic stem cells and is a leukemia protooncogene. Although Hox genes are well-characterized targets of MLL and MLL fusion oncoproteins, the range of Mll-regulated genes in normal hematopoietic cells remains unknown. Here we identify and characterize part of the Mll-transcriptional network in hematopoietic stem cells with an integrated approach by using conditional loss-of-function models, genomewide expression analyses, chromatin immunoprecipitation, and functional rescue assays. The Mll-dependent transcriptional network extends well beyond the previously appreciated Hox targets, is comprised of many characterized regulators of self-renewal, and contains target genes that are both dependent and independent of the MLL cofactor, Menin. Interestingly, Prdm16 emerged as a target gene that is uniquely effective at partially rescuing Mll-deficient hematopoietic stem and progenitor cells. This work highlights the tissue-specific nature of regulatory networks under the control of MLL/Trithorax family members and provides insight into the distinctions between the participation of MLL in normal hematopoiesis and in leukemia. We used microarrays to determine the gene expression profiles of HSCs upon conditional deletion of Mll. **Overall design:** LSK/CD48- HSCs were sorted from 5 pI:pC injected MllF/F control mice or 5 pI:pC injected Mx1-cre;MllF/F mice 6 days after the initial injection. Total RNA was purified from 1,500 to 10,000 sorted cells, amplified, labeled, fragmented and hybridized to GeneChip Mouse Genome 430 2.0 arrays from Affymetrix.

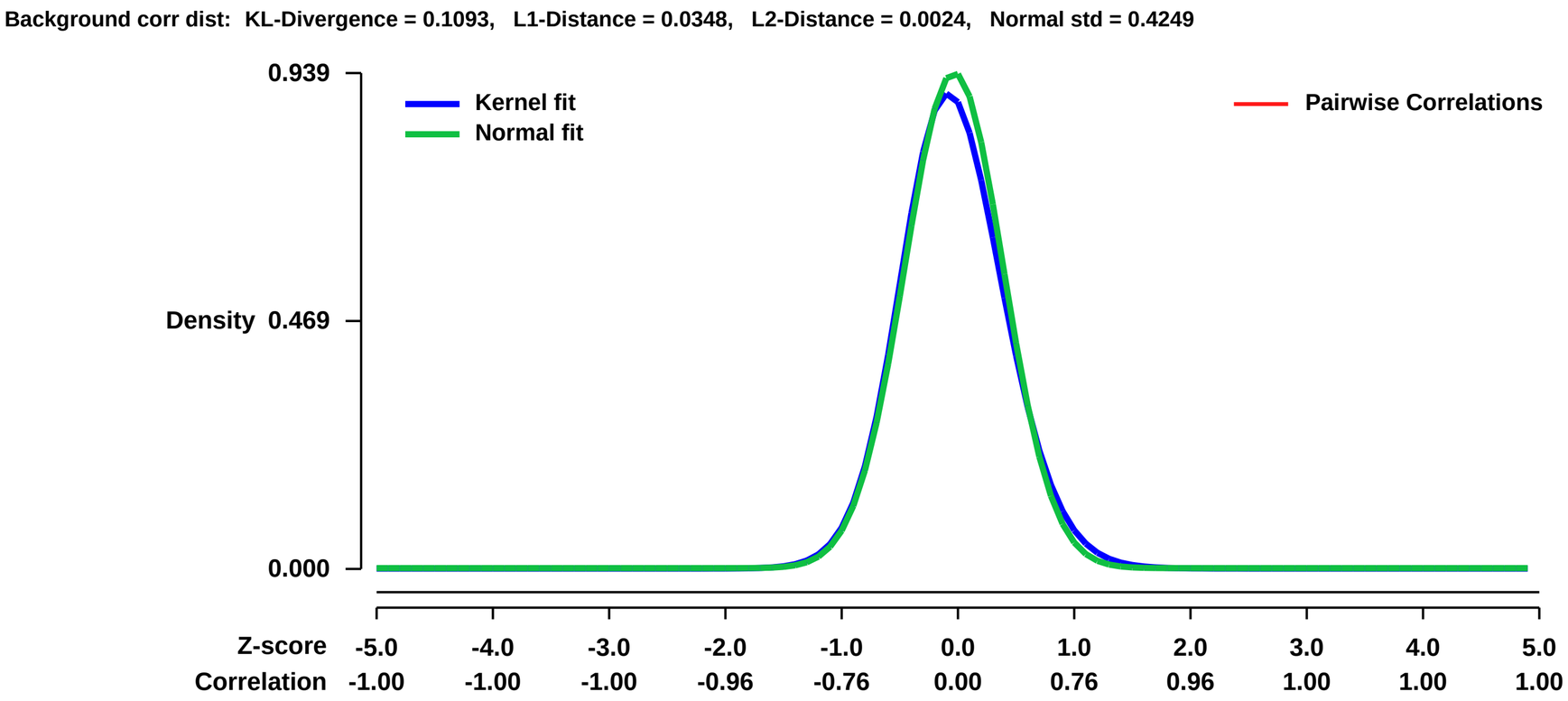

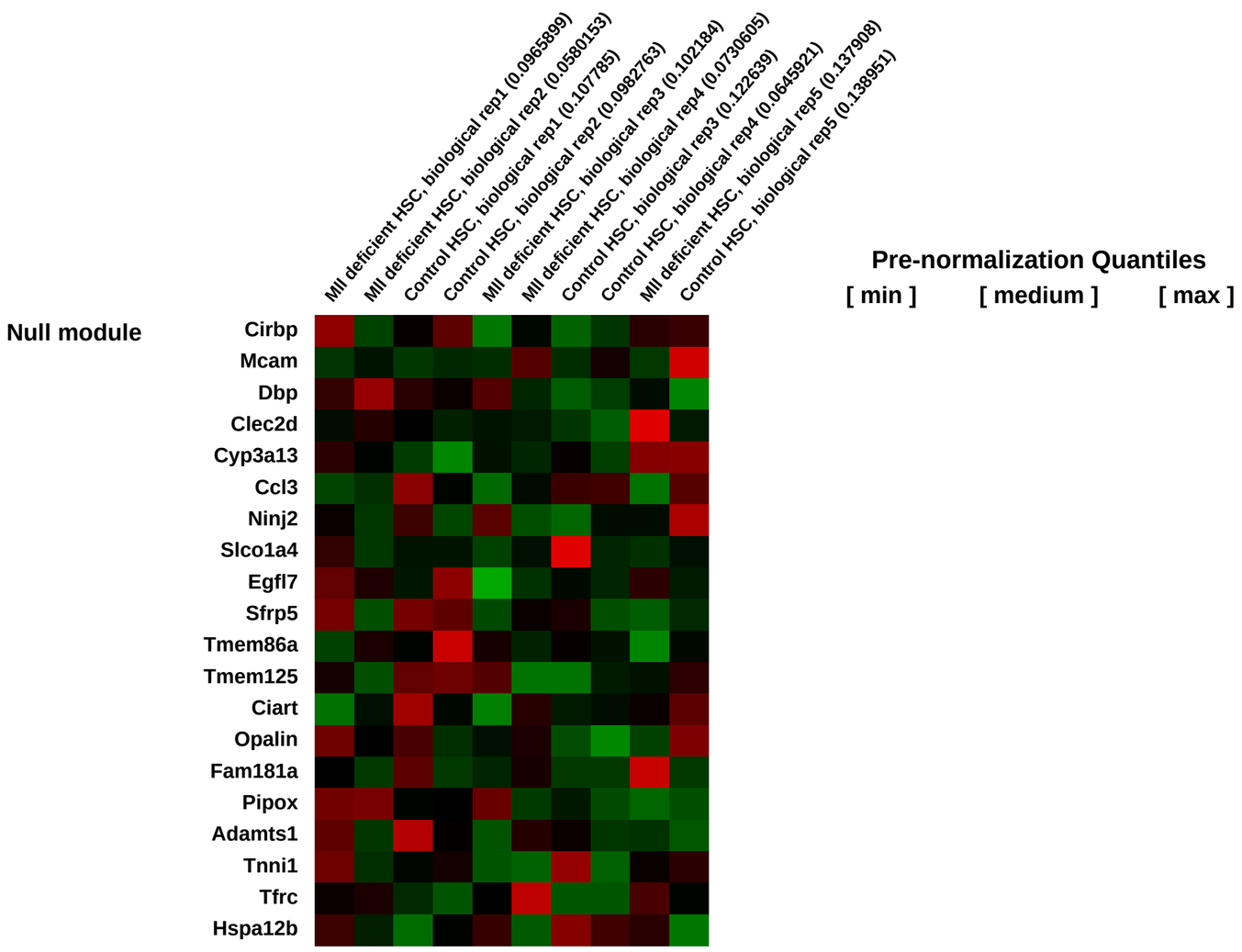

GEO Series "GSE4739" Expression Profiles

Num of samples in this series: 19

Scale of expression profile Z-scores

-3.0 -2.0 -1.0 0.0 1.0 2.0 3.0

GEO Link:	http://www.ncbi.nlm.nih.gov/geo/query/acc.cgi?acc=GSE4739
Status:	Public on Jun 15 2006
Title:	Temporal control of gene expression by ERK MAP kinase during cell cycle progression from G0/G1 to S phase
Organism:	Mus musculus
Experiment type:	Expression profiling by array
Platform:	GPL1261
Pubmed ID:	19160492
Summary & Design:	**Summary:** The ERK family of MAP kinase plays a critical role in growth factor-stimulated cell cycle progression from G0/G1 to S phase. But, how sustained activation of ERK promotes G1 progression has remained unclear. Here, our systematic analysis on the temporal program of ERK-dependent gene expression shows that sustained activation of ERK is required for induction and maintenance of the decreased expression levels of a set of genes. Moreover, our cell biological analysis reveals that these ERK-dependent downregulated genes have the ability to block S phase entry. Cessation of ERK activation at mid or late G1 leads to a rapid increase of these anti-proliferative genes and results in the inhibition of S phase entry. These findings uncover an important mechanism by which the duration of ERK activation regulates cell cycle progression through dynamic changes in gene expression, and identify novel ERK target genes crucial for the regulation of cell cycle progression. **Keywords:** time course **Overall design:** time points: 0h, 1h, 4h, 7h, 12h

Background corr dist: KL-Divergence = 0.2379, L1-Distance = 0.0474, L2-Distance = 0.0052, Normal std = 0.3097

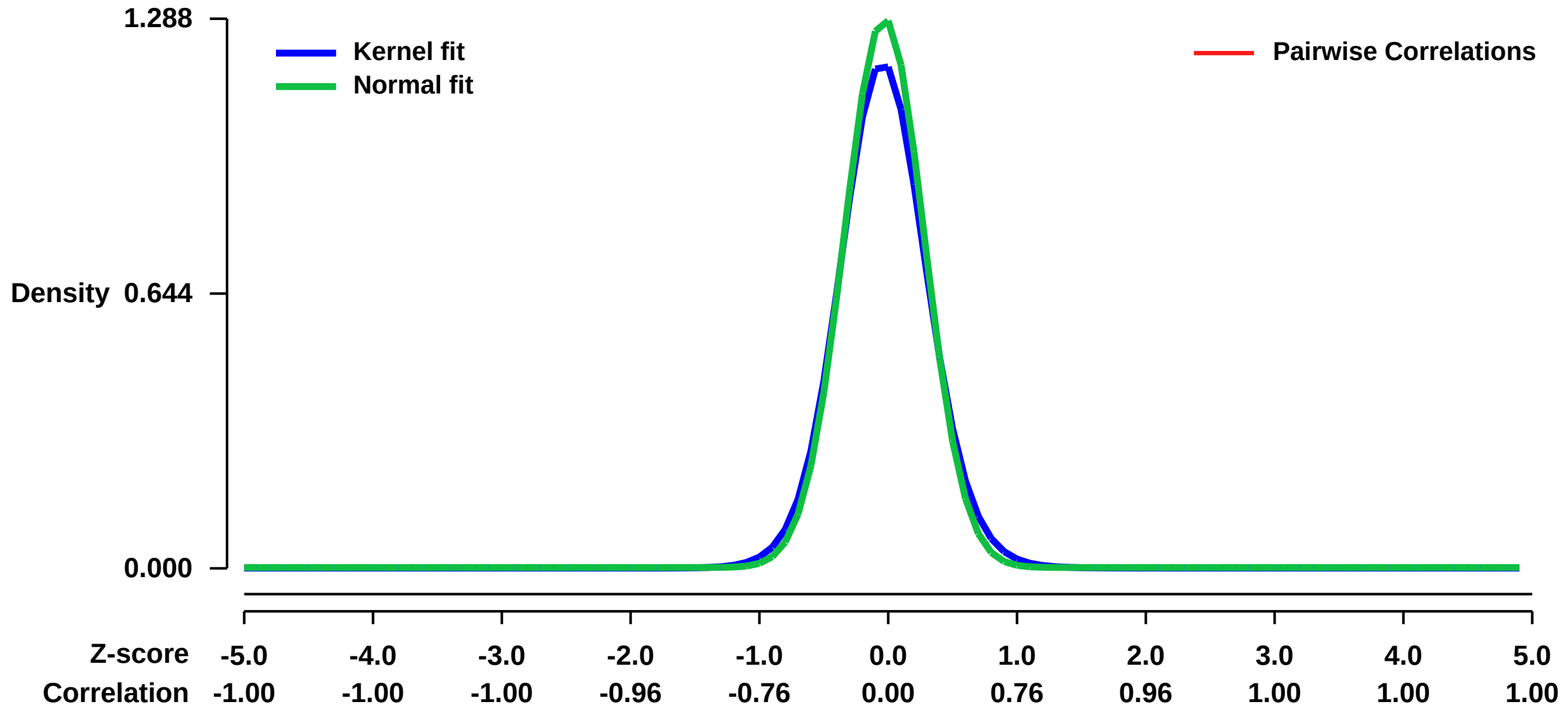

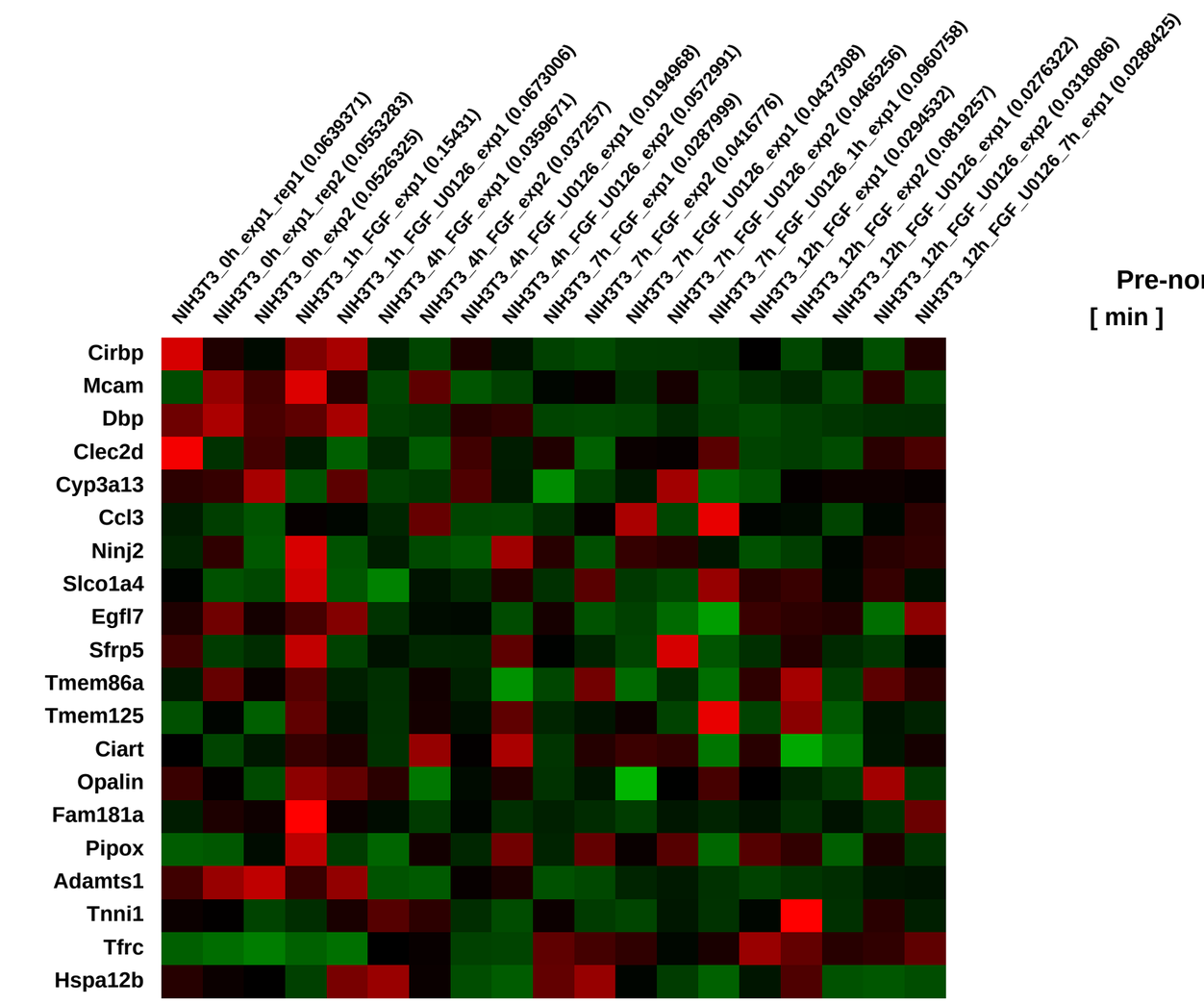

GEO Series "GSE47402" Expression Profiles

Num of samples in this series: 6

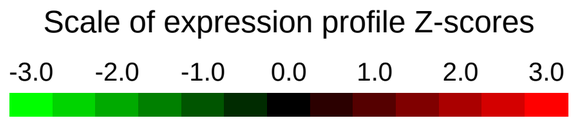

GEO Link:	**http://www.ncbi.nlm.nih.gov/geo/query/acc.cgi?acc=GSE47402**
Status:	**Public on Jun 30 2013**
Title:	**Runx1 deficiency effect on MLL-ENL cells**
Organism:	**Mus musculus**
Experiment type:	**Expression profiling by array**
Platform:	**GPL1261**
Pubmed ID:	**23979164**
Summary & Design:	**Summary:** **To identify the target genes of Runx1 in MLL fusion leukemia, we performed microarray analysis using control and Runx1-deficient MLL-ENL leukemia cells.** **Overall design:** **Runx1 intact and excised bone marrow cells were transduced with MLL-ENL and transplanted into congenic mice. Leukemic cells were harvested from moribund mice, and gene expression was compared using 3 independent leukemia cells for each genotype.**

Background corr dist: **KL-Divergence = 0.0413, L1-Distance = 0.0212, L2-Distance = 0.0005, Normal std = 0.6105**

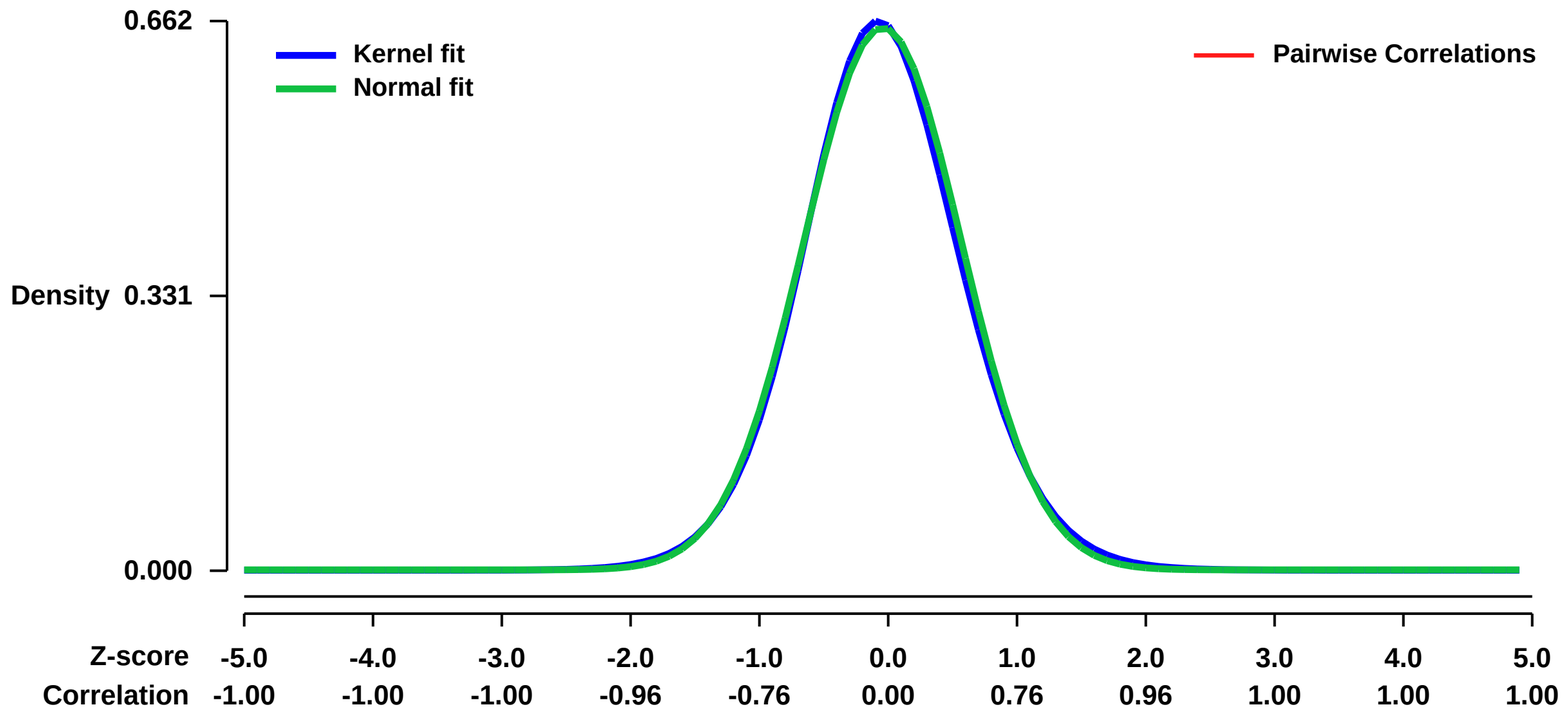

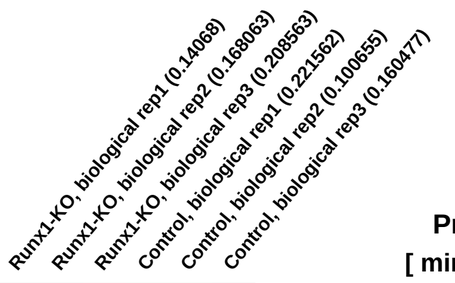

Pre-normalization Quantiles

[min] [medium] [max]

Null module

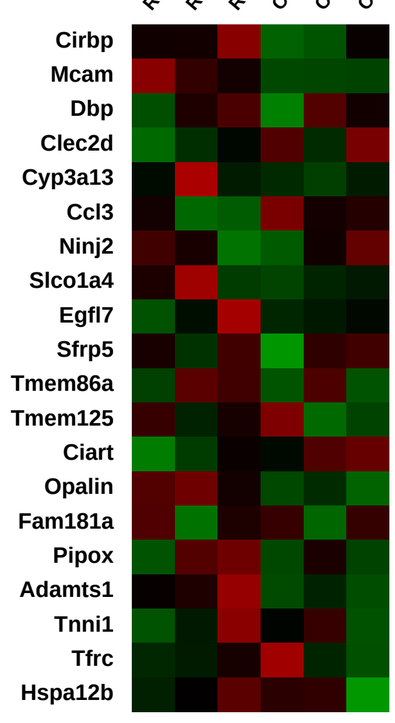

GEO Series "GSE47414" Expression Profiles

Num of samples in this series: 18

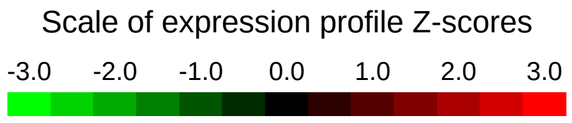

GEO Link:	http://www.ncbi.nlm.nih.gov/geo/query/acc.cgi?acc=GSE47414
Status:	Public on Jun 12 2013
Title:	Expression data from bone marrow macrophage derived from lean and obese mice after 1,4, and 24h exposition to P.gingivalis
Organism:	Mus musculus
Experiment type:	Expression profiling by array
Platform:	GPL1261
Pubmed ID:	
Summary & Design:	**Summary:** Obesity is a chronic inflammatory disease that weakens macrophage innate immune response to infections. Since M1 polarization is crucial during acute infectious diseases, we hypothesized that diet-induced obesity inhibits M1 polarization of macrophages in the response to bacterial infection. Using a computational approach in conjunction with microarray data, we identified switching genes that may differentially control the behavior of response pathways in macrophages from lean and obese mice. **Overall design:** Bone marrow macrophages (BMMϕ) from lean and obese mice were exposed to live Porphyromonas gingivalis (P. gingivalis) for three incubation times (1 h, 4 h and 24 h). cDNA from BMMϕ of lean and obese mice were hybridized on Affymetrix Mouse Genome 430 2.0 Arrays. Hybridization was performed on three replicates at each time point (18 arrays total).

Background corr dist: KL-Divergence = 0.0932, L1-Distance = 0.0325, L2-Distance = 0.0014, Normal std = 0.4688

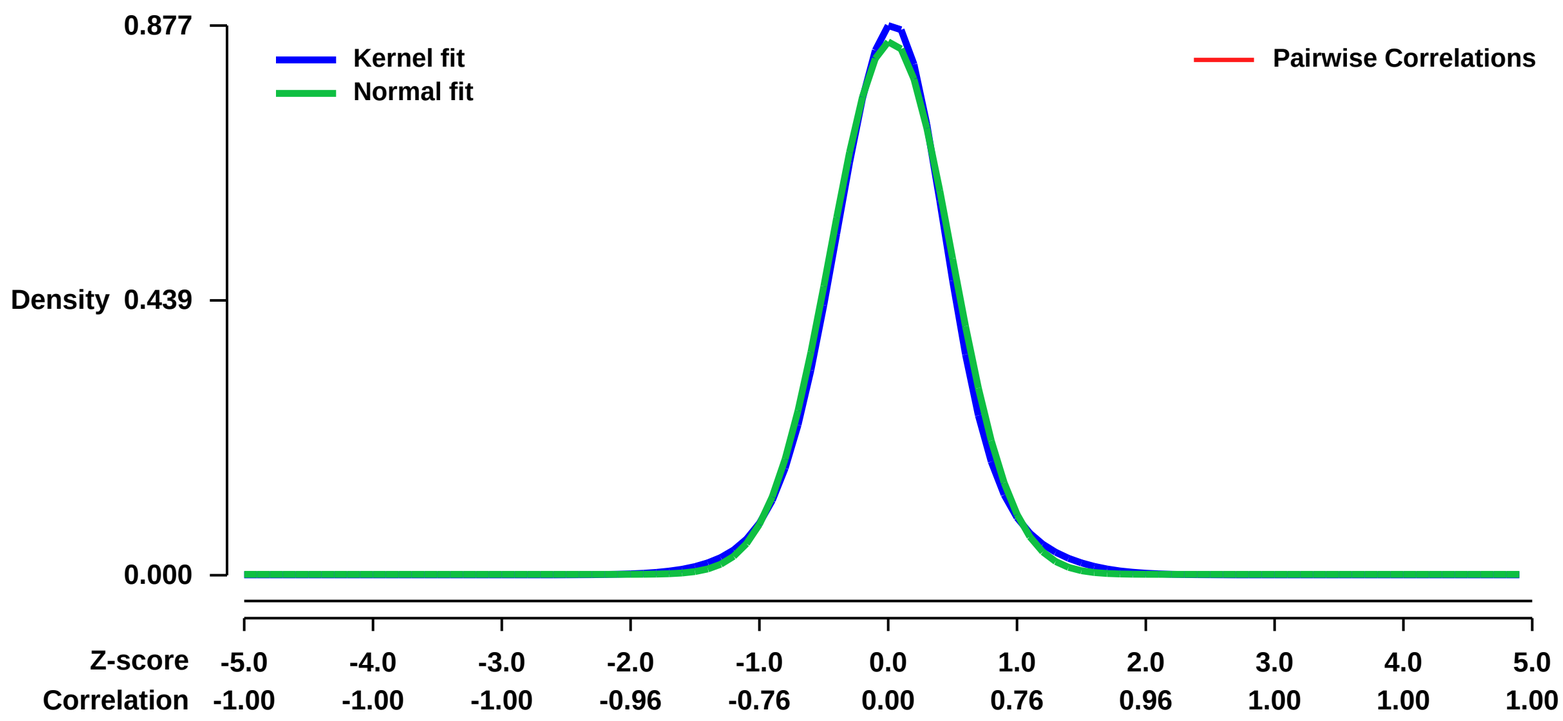

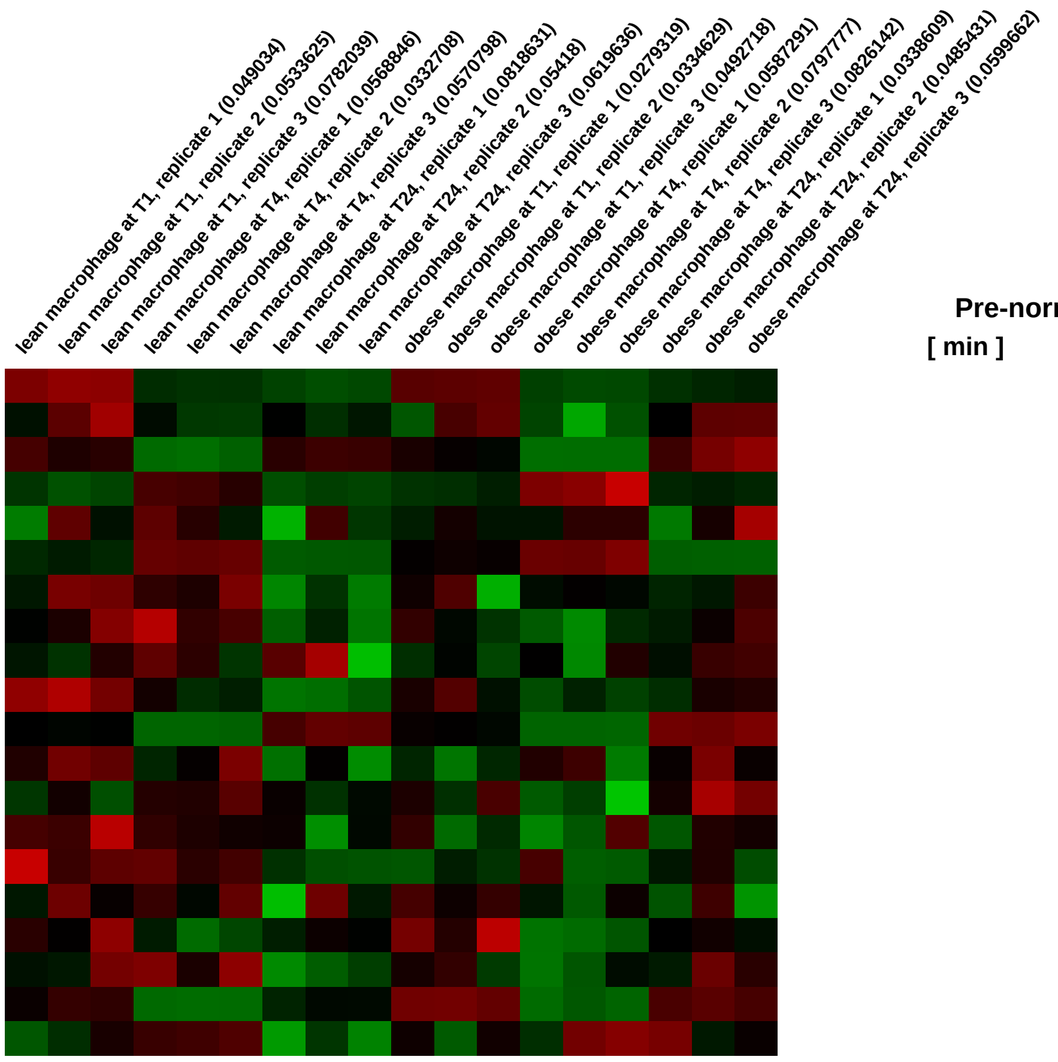

GEO Series "GSE47425" Expression Profiles

Num of samples in this series: 7

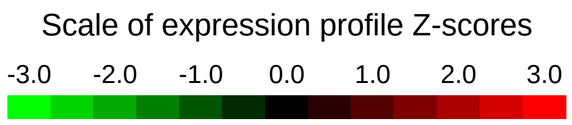

GEO Link:	**http://www.ncbi.nlm.nih.gov/geo/query/acc.cgi?acc=GSE47425**
Status:	**Public on Aug 26 2013**
Title:	**Lung transcript expression profile after Gata5 gene deletion**
Organism:	**Mus musculus**
Experiment type:	**Expression profiling by array**
Platform:	**GPL1261**
Pubmed ID:	**24199649**
Summary & Design:	**Summary:** **Gata5 is a zinc finger transcription factor that is expressed in embryonic pulmonary mesenchyme and becomes upregulated in the lungs, gut, and bladder during postnatal development. We used microarray to comapre gene expression profiles of mouse lung between Gata5 knockout and wild type mice. We hope to identify the differentially expressed genes that affected by Gata5 gene deletion and their functional clusters or pathways.** **The goal of this study is to identify the differentially expressed genes that affected by Gata5 gene deletion and their functional clusters or pathways.** **Overall design:** **Total RNA samples from three Gata5 KO and four wild type control mouse left lungs were extracted from the mouse lungs and profiled using Affymetrix GeneChip Mouse Genome 430 2.0 Array.**

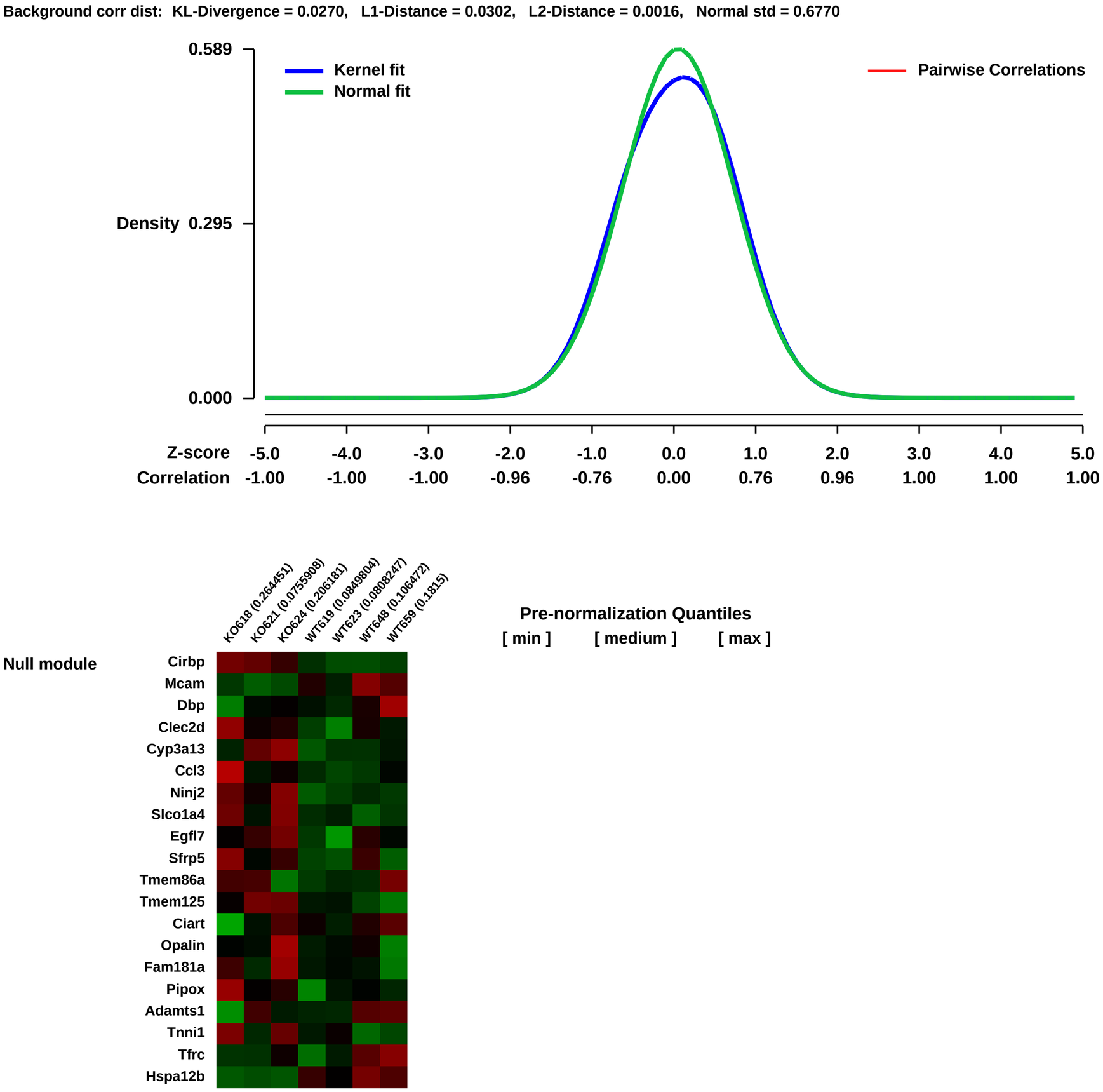

GEO Series "GSE4749" Expression Profiles

Num of samples in this series: 6

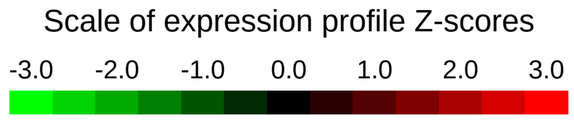

GEO Link:	http://www.ncbi.nlm.nih.gov/geo/query/acc.cgi?acc=GSE4749
Status:	Public on Feb 20 2008
Title:	Microarray based comparison of gene expression in stria vascularis of 129S6 mice lacking slc26a4 and wildtype controls
Organism:	Mus musculus
Experiment type:	Expression profiling by array
Platform:	GPL1261
Pubmed ID:	17187680
Summary & Design:	**Summary:** To see for differential expression of genes in the stria vascularis of wild type and pendrin knockout mice **Keywords: Knockout vs Control** **Overall design:** Six samples in total of stria vascularis RNA were analyzed. Triplicates from wild type and pendrin knockout mice were run and analyzed.

Background corr dist: KL-Divergence = 0.0292, L1-Distance = 0.0187, L2-Distance = 0.0004, Normal std = 0.6723

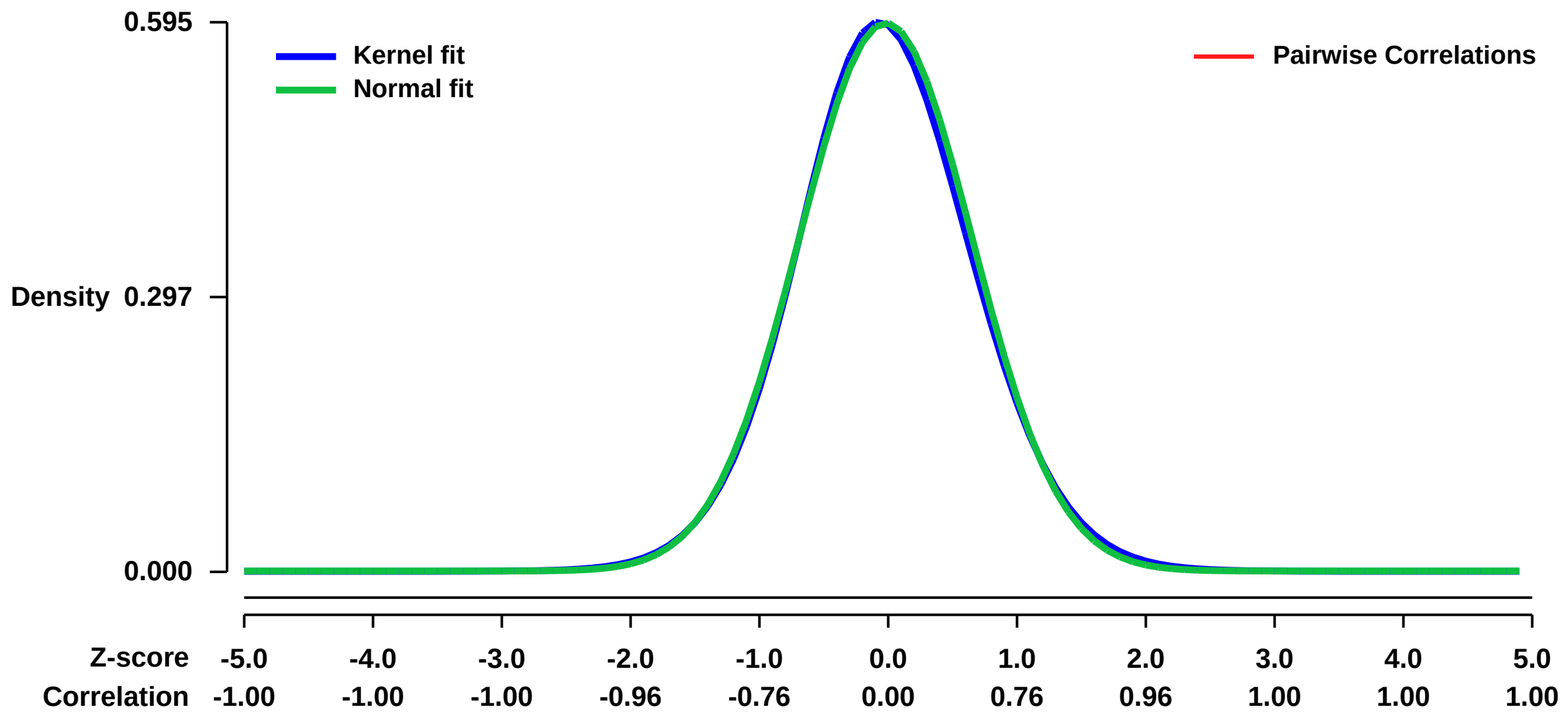

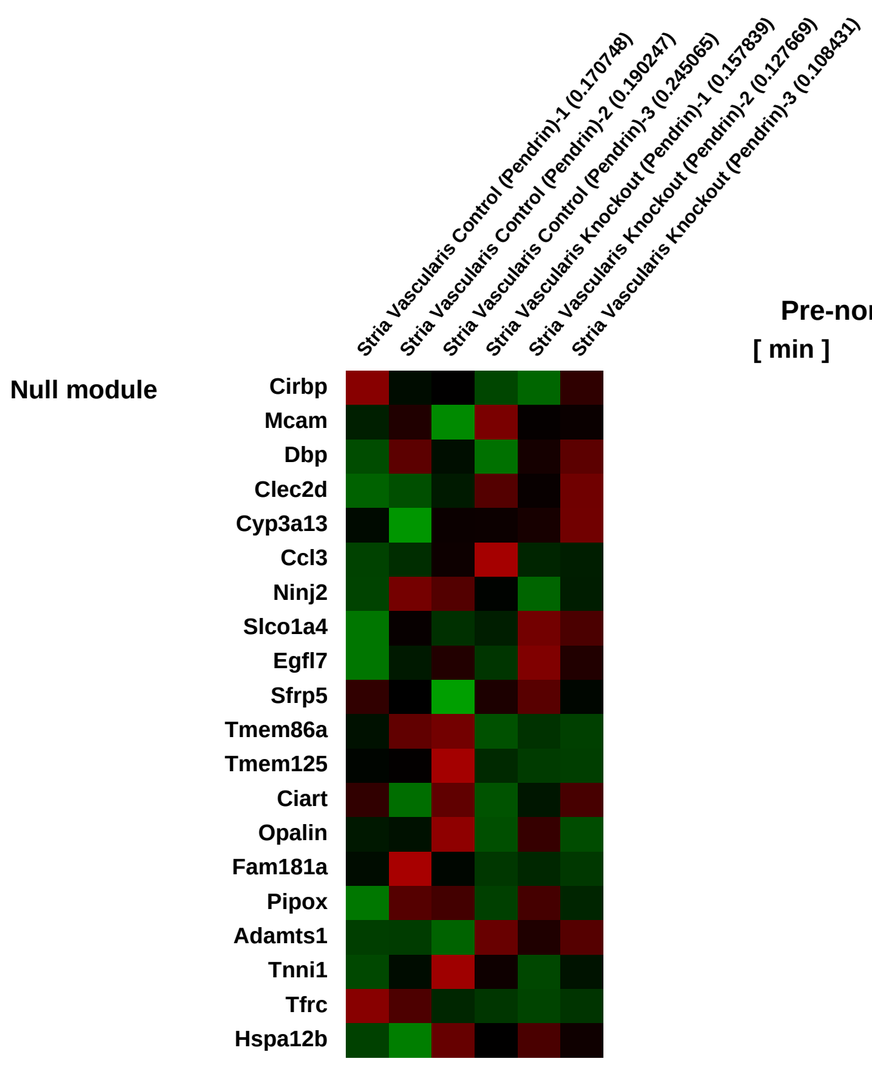

GEO Series "GSE4752" Expression Profiles

Num of samples in this series: 6

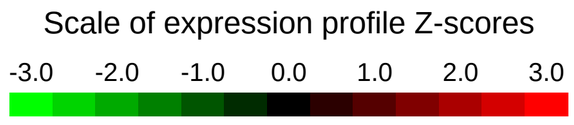

GEO Link:	**http://www.ncbi.nlm.nih.gov/geo/query/acc.cgi?acc=GSE4752**
Status:	**Public on May 02 2006**
Title:	**tourt-affy-mouse-243760**
Organism:	**Mus musculus**
Experiment type:	**Expression profiling by array**
Platform:	**GPL1261**
Pubmed ID:	

Summary & Design:

Summary:
The early growth response (Egr) family of transcriptional regulators consists of four closely related molecules (Egr1-4) that regulate target genes involved in cellular growth and differentiation. In the brain, Egr transcription factors have a critical role in learning and memory processing, presumably by regulating effector target genes that alter synaptic efficacy or mediate structural changes in neurons. Previous work suggests that Egr1 and Egr3 are the most important synaptic activity induced Egr molecules in the brain and they appear to have redundant regulatory function. How Egr transcriptional regulators influence learning and memory processing in the brain is unknown because target genes regulated by them have not been identified. Using Affymetrix microarray analysis and Egr loss-of-function mice, we will begin to characterize the gene regulatory networks modulated by Egr transcription factors in the brain. We anticipate that basic mechanisms related to transcriptional control of learning and memory related plasticity and the identification of plasticity effector molecules that may be involved in synaptic dysfunction associated with degenerative diseases or brain injury will result from these studies.

To identify Egr transcription factor target gene regulation in brain: Target genes regulated by Egr transcription factors have not been identified in the brain, yet the transcription factors are essential for normal learning and memory processes. Using Egr1/3 double knockout and wild type littermate mice, we will compare gene expression profiles from somatosensory cortex to identify genes that are deregulated in Egr1/3 dKO brains.

Egr1 and Egr3 gene expression is coupled to synaptic N-methyl D-aspartate (NMDA) receptor activation, mitogen activated protein kinase (MAPK) signaling engaged by NMDA receptor activation and long term synaptic potentiation (LTP). Previous studies have demonstrated defects in late phase LTP, long-term memory in hippocampal dependent tasks and reconsolidation of memories in Egr1-deficient mice, but the target effector molecules regulated by Egr transcription factors are not known. We hypothesize that it will be possible to identify Egr dependent target genes by using Affymetrix microarray analysis to compare gene expression from wild type cerebral cortex that has high levels of Egr protein expression with gene expression in cortex from Egr1/3 double knockout mice.

Egr1 and Egr3 are highly expressed in mouse cortex and hippocampus twenty one days after birth because of the large amount of maternal stimulation they receive prior to weaning. We will compare the gene expression profile in somatosensory cortex from P21 wild type mice to that of P21 Egr1/3 dKO mice. We will perform microarray analysis using the Mouse 430 2.0 gene array with RNA samples from 3 wild type and 3 1/3 dKO brains (6 arrays total). Differentially regulated genes (up-regulated and down-regulated) will be identified from the list of genes with significantly altered expression greater than or equal to 2-fold by paired T test. Interesting genes will be validated by real-time PCR in wild type and 1/3 dKO brains. Our main goal is to identify genes that are directly regulated by Egr3. Recognizing that both direct and indirect target genes may be identified in the list of differentially expressed genes, real-time PCR validated target genes will be further screened using chromatin immunoprecipitation coupled with PCR (ChIP-PCR) to determine whether Egr1 and/or Egr3 are bound to potential regulatory regions of the putative target genes.

Keywords: other

Overall design:

Background corr dist: KL-Divergence = 0.0459, L1-Distance = 0.0191, L2-Distance = 0.0004, Normal std = 0.5886

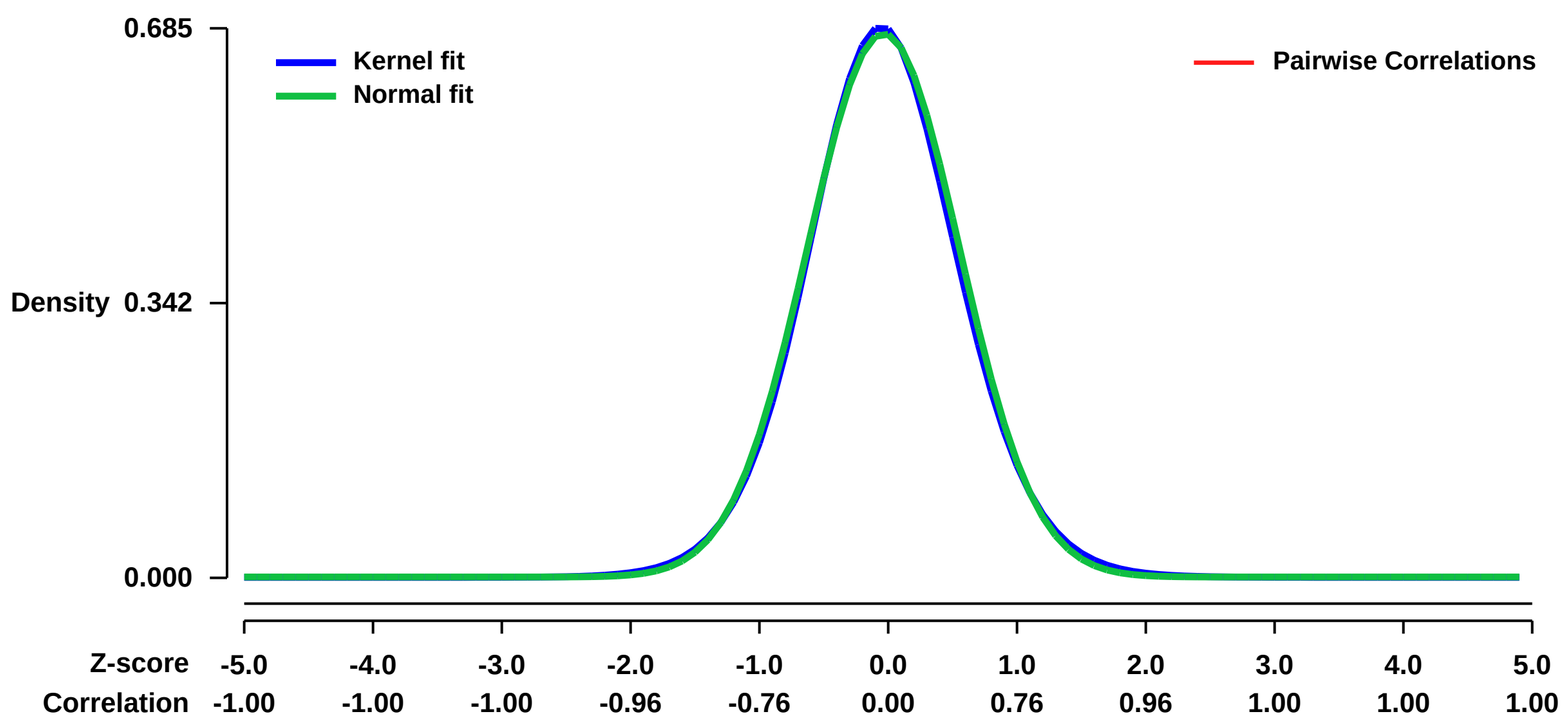

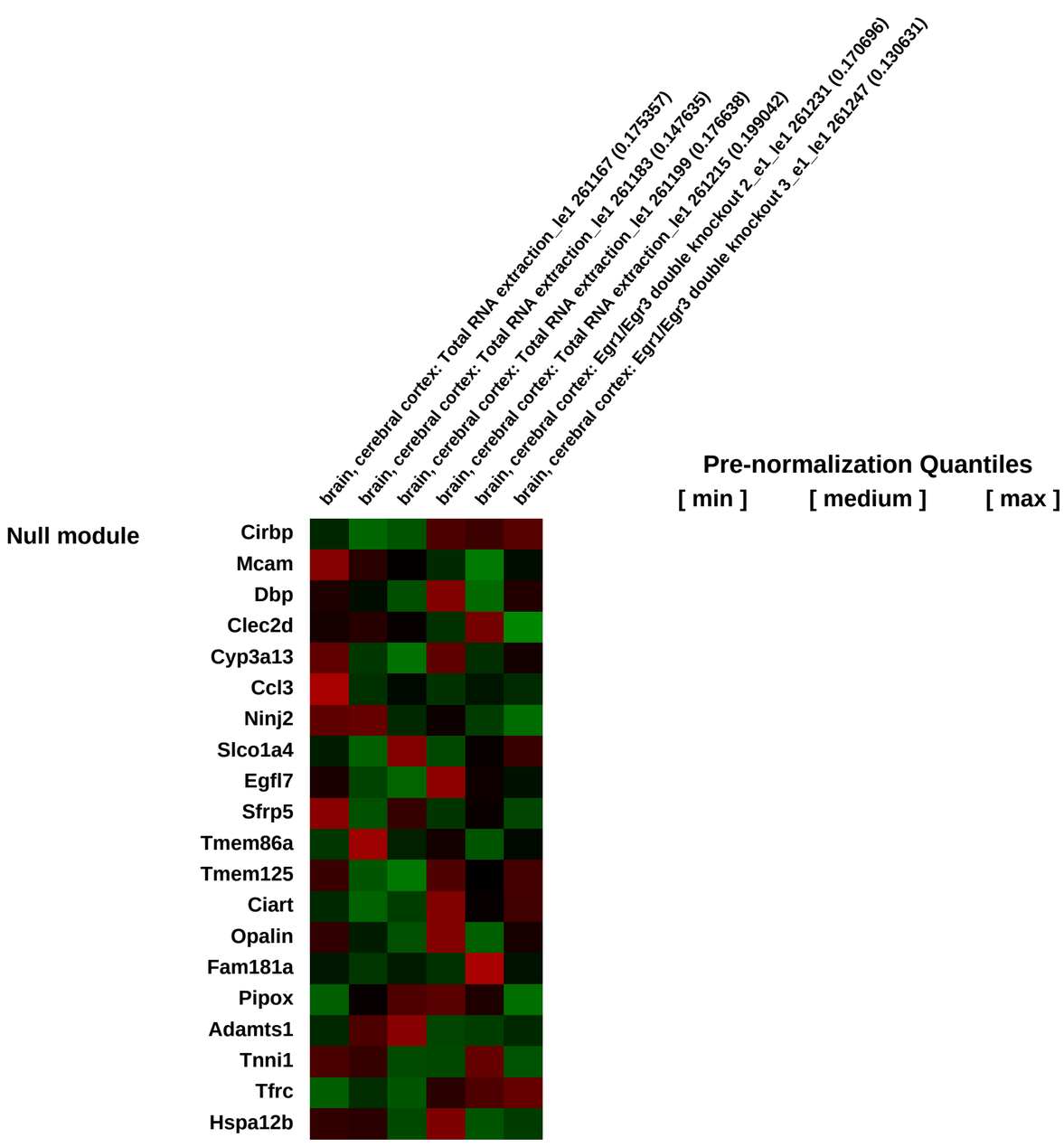

GEO Series "GSE4756" Expression Profiles

Num of samples in this series: 8

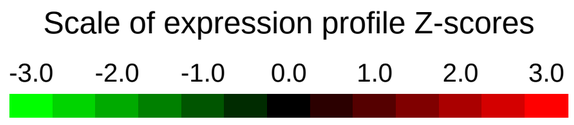

GEO Link:	**http://www.ncbi.nlm.nih.gov/geo/query/acc.cgi?acc=GSE4756**
Status:	**Public on May 02 2006**
Title:	**ruiz-affy-mouse-243540**
Organism:	**Mus musculus**
Experiment type:	**Expression profiling by array**
Platform:	**GPL1261**
Pubmed ID:	
Summary & Design:	**Summary:** **The retinal degeneration slow gene (rds/peripherin), is essential for normal photoreceptor (rods and cones) outer segment structure in the neurosensory retina. Our rds animal model, are stable transgenic mice that carry a null mutation (complete lost of function) in the rds gene. Those animals become blind, mimicking a human form of retinitis pigmentosa. In our experience we have observed dramatic levels of photoreceptor rescue after subretinal injection of those animals with a ciliary neurotrophic factor (CNTF) inserted into a recombinant Adeno-associate virus (rAAV) vector. However, this cell rescue is accompanied by changes in photoreceptor nuclear morphology, attenaution of the electroretinogram and evetually Apoptosis. By using Microarray analysis we hope to identify genes whose expression or lack thereof brings the cell to the brink of suicide. Identification of these genes will suggest therapeutic targets for the future.** **We will determine gene expression patterns in the retina of rds mice non-injected and injected with CNTF/rAAV virus after 60 days of injection.** **Our working hypothesis is that the injected CNTF/rAAV vector induces the expression of genes that somehow partially restores the photoreceptor morphology of rds mice. Paradoxically, it also has a negative effect on the phisiology of these cells (ERG). The up or down regulation of genes in different areas of the neurosensory retina collected by Laser Capture Microdissection will give us an insight on the relevance of candidate genes responsible for this phenomenon.** **We will use rds mice at age P25 and inject their rigth eye with CNTF/AVV virus (2.68x e13 particles/ml) and use the left eye as a control. Injection is performed via subretinal. Retinas will be collected at age P90 post injection. RNA will be extracted and processed accordingly for MIcroarray analysis.** **Keywords: dose response** **Overall design:**

Background corr dist: KL-Divergence = 0.0571, L1-Distance = 0.0213, L2-Distance = 0.0006, Normal std = 0.5396

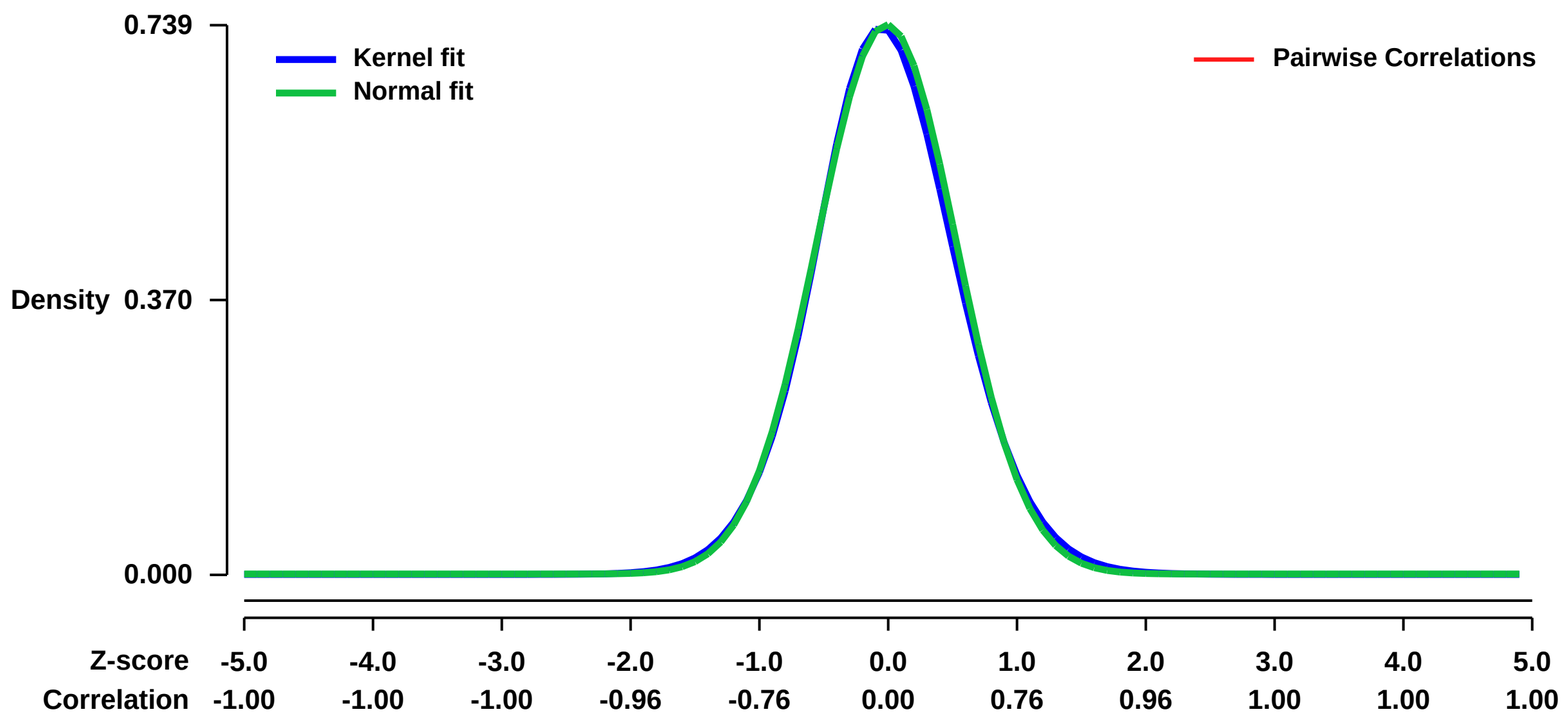

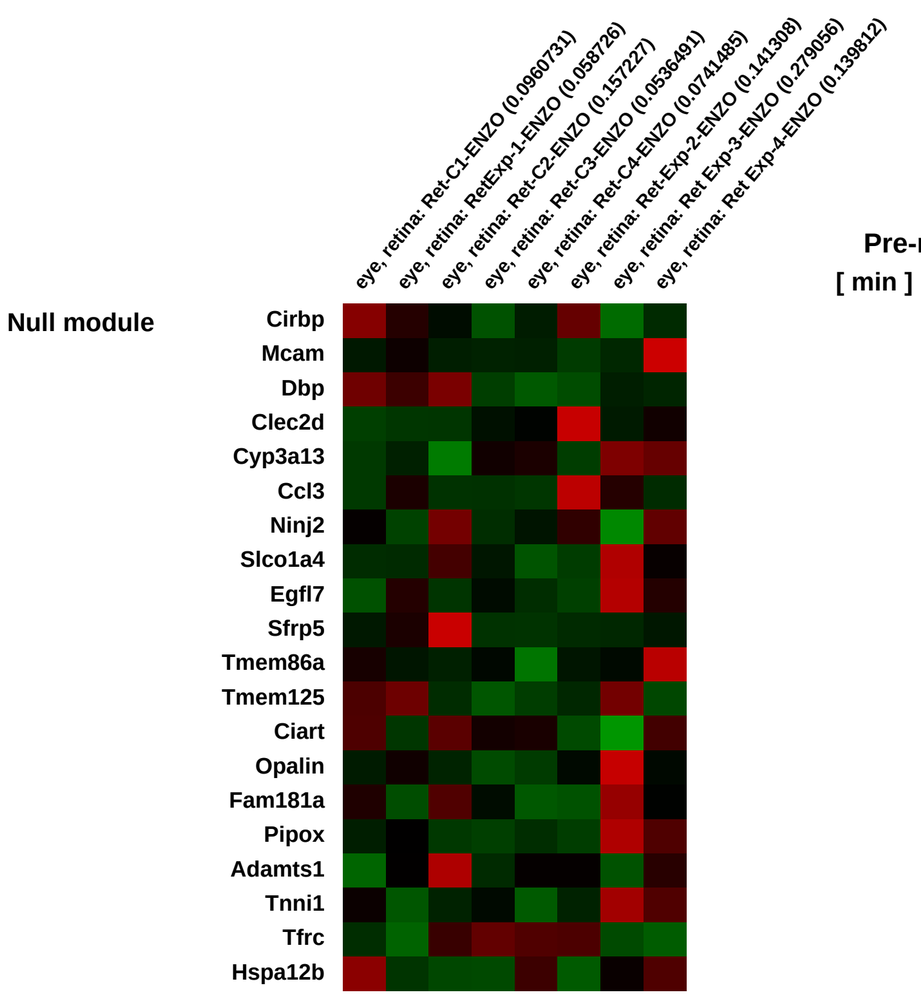

GEO Series "GSE4758" Expression Profiles

Num of samples in this series: 24

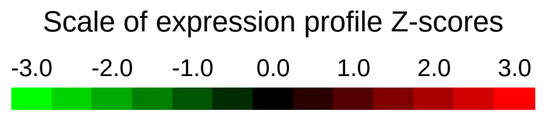

GEO Link:	**http://www.ncbi.nlm.nih.gov/geo/query/acc.cgi?acc=GSE4758**
Status:	**Public on May 02 2006**
Title:	**conra-affy-mouse-89474**
Organism:	**Mus musculus**
Experiment type:	**Expression profiling by array**
Platform:	**GPL1261**
Pubmed ID:	
Summary & Design:	**Summary:** **Parkinsonâ s disease (PD) and Dementia with Lewy bodies (DLB) are the two most common examples of synucleinopathies, i.e. human disorders that display intracellular deposition of the Alpha-synuclein (aSYN) protein. The two forms of aSYN deposits, intracellular Lewy bodies and Lewy neurites, are in the PD brain primarily found in the substantia nigra whereas in DLB brains they are diffusely spread in cortical and limbic areas. We are currently analyzing the protective effects on aSYN pathology by the molecular chaperone hsp70 in mice overexpressing wildtype human aSYN. Moreover, transgenic mice overexpressing hsp70 have been cross-bred with the aSYN mouse line. Intriguingly, the aSYN / hsp70 double transgenics display a pronounced reduction in biochemically assessed aSYN aggregation. Gene expression of these mice will not only provide insight into the disease mechanisms of aSYN pathology but its prevention by the overexpression of hsp70, leading to new potential avenues of treatment.** **Project 1: To investigate and compare alterations in gene expression profiles of brains from wild-type mice and mice overexpressing wildtype human aSYN, human hsp70 and aSYN / hsp70, respectively.** **The comparison of the expression profiles of the groups of mice: aSYN, Hsp70, aSYN/ Hsp70 and non-transgenic littermates will help to identify the genes that are involved in the mediation of aggregation toxicity of aSYN expression as well as the genes that may mediate an attenuation of aSYN pathology in hsp70-coexpressors.** **Project 1: Selection of animals Mice of 4 month old (n=6) of age of each background (aSYN, Hsp70, aSYN/ Hsp70 and non-transgenic littermates) will be used for RNA-extraction for a total of 24 mice. Preparation of samples For the proposed experiments, we will use the recommended procedures, as outlined by the consortium, for extracting and purifying RNA from whole brain homogenate. Briefly, RNA will be extracted by the trizol method and purified by using the RNeasy MinElute Cleanup (QIAGEN Inc., USA). RNA labeling and hybridization procedures will be carried out by the microarray consortium. SPECIAL NOTE: The samples will be sent upon availability. Gene Expression Microarray Analysis Six mice will be included in each group per timepoint to generate statistically testable data and limit the possible confound of individual mouse gene expression variations. The genome expression will be evaluated through the use of the GeneChip´fi Mouse Genome 430 2.0 Array (Affymetrix) for each individual mouse constituting a total of 24 arrays for the proposed study. Gene expression data interpretation will be assisted by the Microarray Consortium Center bioinformatics core.** **Keywords: time-course** **Overall design:**

Background corr dist: KL-Divergence = 0.2005, L1-Distance = 0.0460, L2-Distance = 0.0046, Normal std = 0.3320

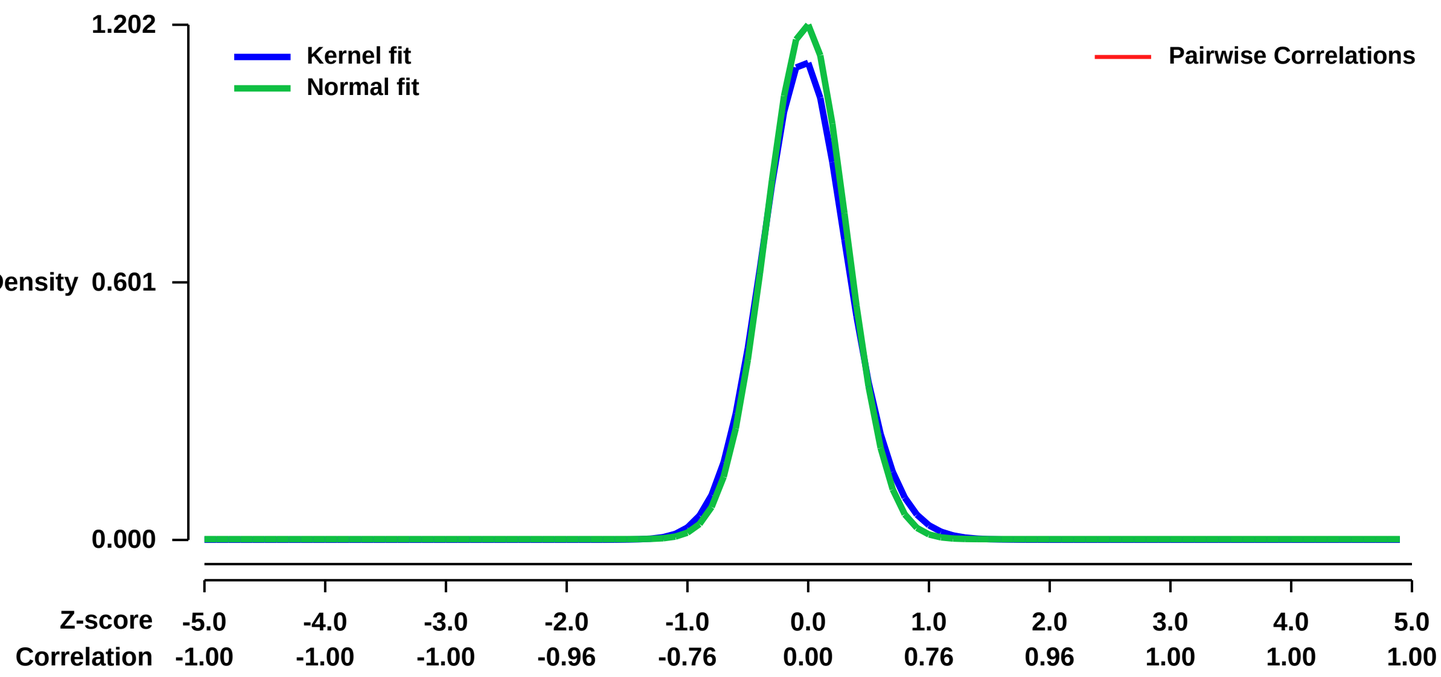

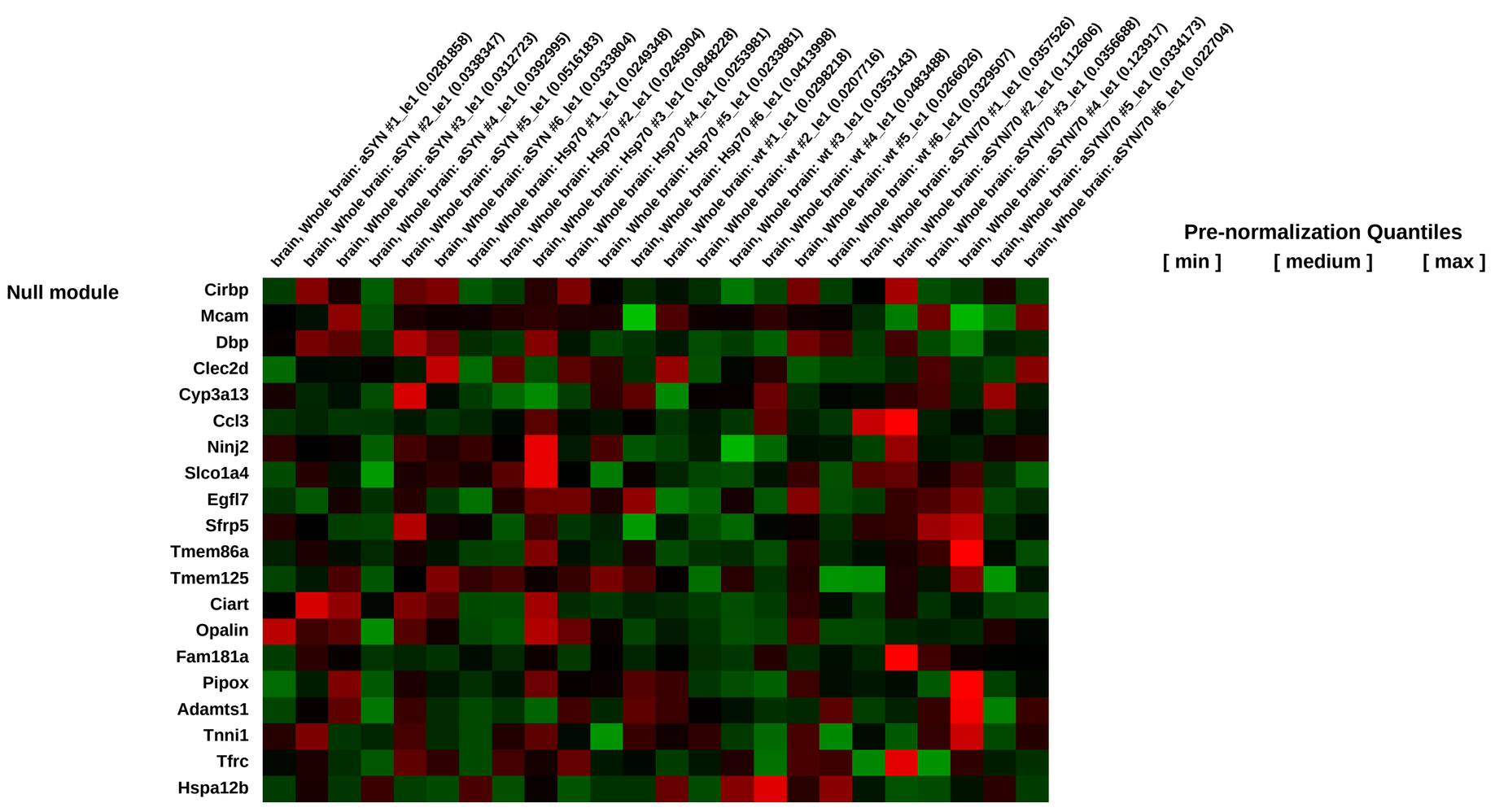

GEO Series "GSE47607" Expression Profiles

Num of samples in this series: 12

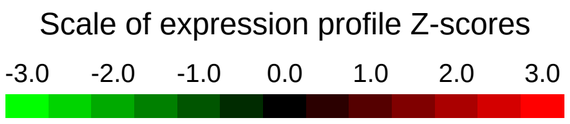

GEO Link:	http://www.ncbi.nlm.nih.gov/geo/query/acc.cgi?acc=GSE47607
Status:	Public on Jun 11 2014
Title:	Environmental factors transmitted by aryl hydrocarbon receptor influence severity of psoriatic skin inflammation [Affymetrix]
Organism:	Mus musculus
Experiment type:	Expression profiling by array
Platform:	GPL1261
Pubmed ID:	24909886
Summary & Design:	**Summary:** Environmental stimuli are known to contribute to psoriasis pathogenesis and that of other autoimmune diseases, but the mechanism is unknown. Here we show that the aryl hydrocarbon receptor (AhR), a transcription factor that senses environmental stimuli, modulates pathology in psoriasis. AhR-activating ligands reduced inflammation in the lesional skin of psoriasis patients, whereas AhR antagonists upregulated inflammation. Similarly, AhR signaling via the endogenous FICZ ligand reduced the inflammatory response in the imiquimod-induced model of psoriasis and AhR deficient mice exhibited a substantial exacerbation of the disease, compared to AhR sufficient controls. Non-haematopoietic cells, in particular keratinocytes, were responsible for this hyper-inflammatory response, which involved increased reactivity to IL-1beta and upregulation of AP-1 family members of transcription factors. Thus, our data suggest a critical role for AhR in the regulation of inflammatory responses and open the possibility for novel therapeutic strategies in chronic inflammatory disorders. **Overall design:** Total RNA obtained from skin explants taken from AhR heterozygous or knock-out mice treated pericutaneously with imiquimod for 0 and 2d.

Background corr dist: KL-Divergence = 0.0682, L1-Distance = 0.0241, L2-Distance = 0.0009, Normal std = 0.4997

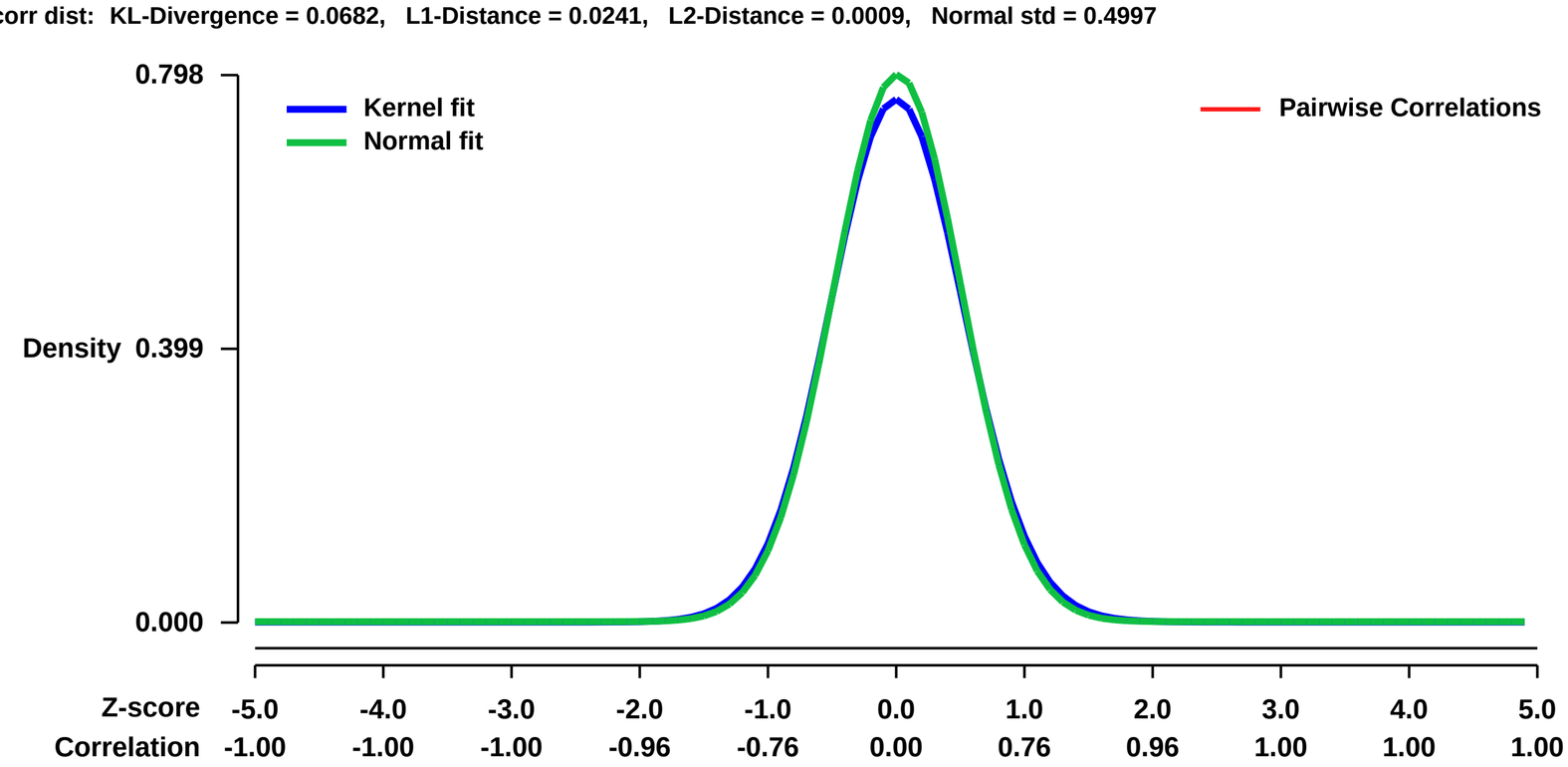

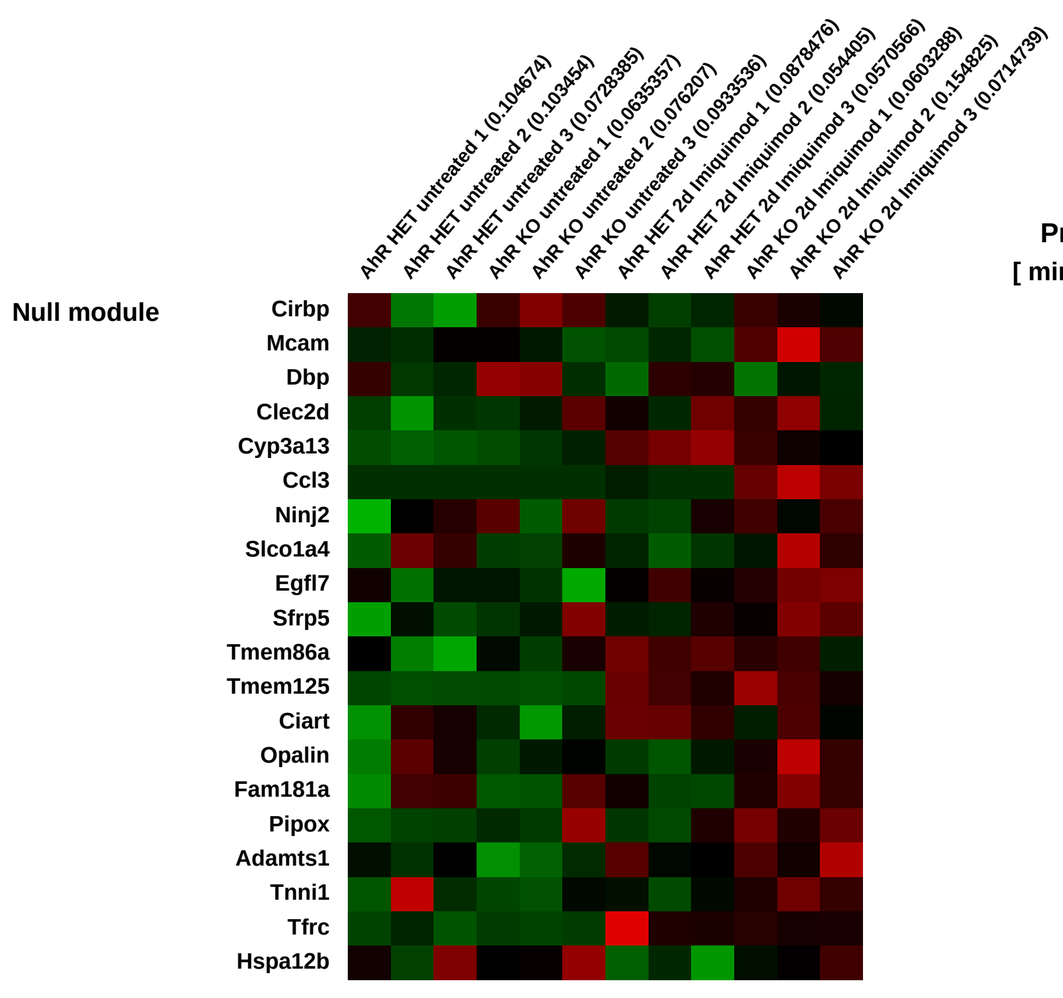

GEO Series "GSE47643" Expression Profiles

Num of samples in this series: 12

Scale of expression profile Z-scores

-3.0 -2.0 -1.0 0.0 1.0 2.0 3.0

GEO Link:	http://www.ncbi.nlm.nih.gov/geo/query/acc.cgi?acc=GSE47643
Status:	Public on Jun 05 2013
Title:	Gene expression of in vitro cultivated preB cells before and after 8, 16 and 24 hours induction of miR-221
Organism:	Mus musculus
Experiment type:	Expression profiling by array
Platform:	GPL1261
Pubmed ID:	23716169
Summary & Design:	**Summary:** PreB cells were analyzed for differences in gene expression before and after the overexpression of miR-221. In order to dissect possible targets for the miR-221, gene expression profiles of preB cells un-induced or induced for the miR-221 expression after 8, 16 and 24 hours were compared. All induction time-points, e.g. after 8, 16 and 24 hours were compared to un-induced preB cells and to each other group. **Overall design:** After total RNA extraction, reverse transcription, cDNA extraction, the biotinylated cRNA was transcribed, fragmented, and 15 ´µg cRNA hybridized in triplicates for each of the four groups to the 12 GeneChip arrays: Group1, un-induced preB cells, Group2, preB cells induced for miR-221 expression after 8h, Group3, preB cells induced for miR-221 expression after 16h, Group4, preB cells induced for miR-221 expression after 24h.

Background corr dist: KL-Divergence = 0.1416, L1-Distance = 0.0249, L2-Distance = 0.0012, Normal std = 0.3853

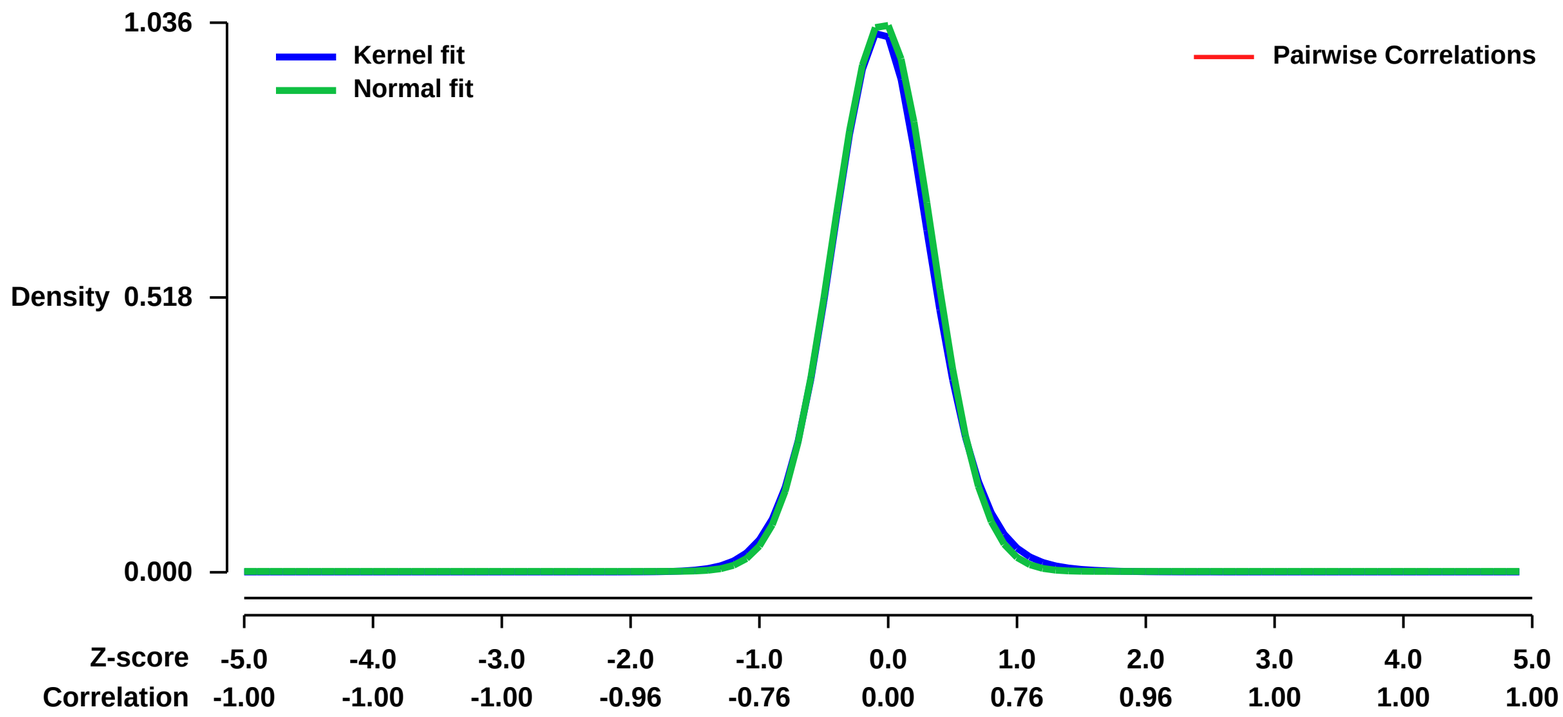

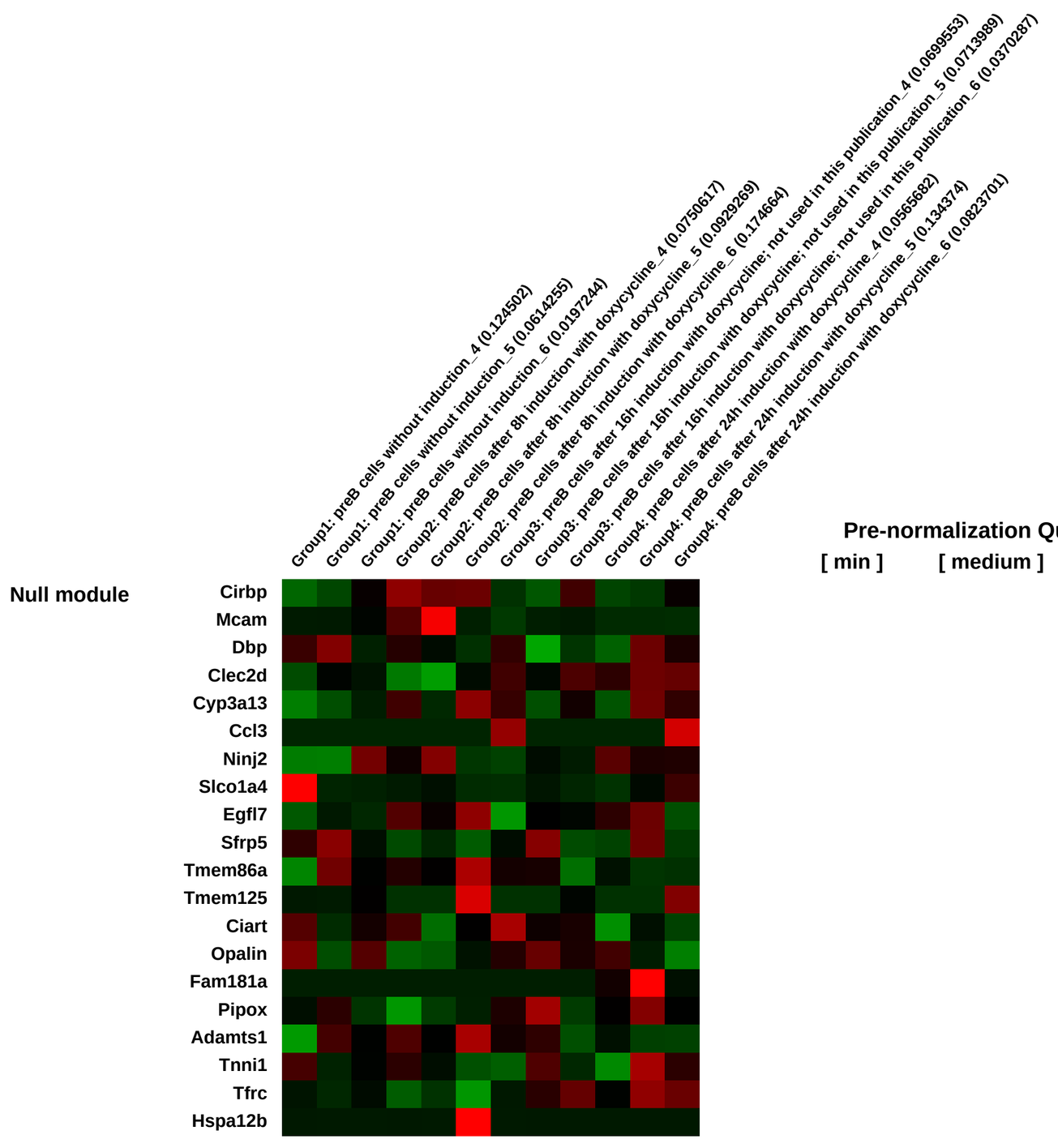

GEO Series "GSE4765" Expression Profiles

Num of samples in this series: 6

Scale of expression profile Z-scores

-3.0 -2.0 -1.0 0.0 1.0 2.0 3.0

GEO Link:	**http://www.ncbi.nlm.nih.gov/geo/query/acc.cgi?acc=GSE4765**
Status:	**Public on Nov 03 2006**
Title:	**SM by NZB Female Liver Gene Expression**
Organism:	**Mus musculus**
Experiment type:	**Expression profiling by array**
Platform:	**GPL1261**
Pubmed ID:	
Summary & Design:	**Summary:** **3 x 3 comparison of the inbred strains SM/J and NZB/BinJ.** **Keywords: Comparitive mRNA** **Overall design:** **Simple comparison of native untreated gene expression profiles of female 8wk old SM mice (x3) by female 8wk old NZB mice (x3)**

Background corr dist: **KL-Divergence = 0.0199, L1-Distance = 0.0258, L2-Distance = 0.0010, Normal std = 0.7416**

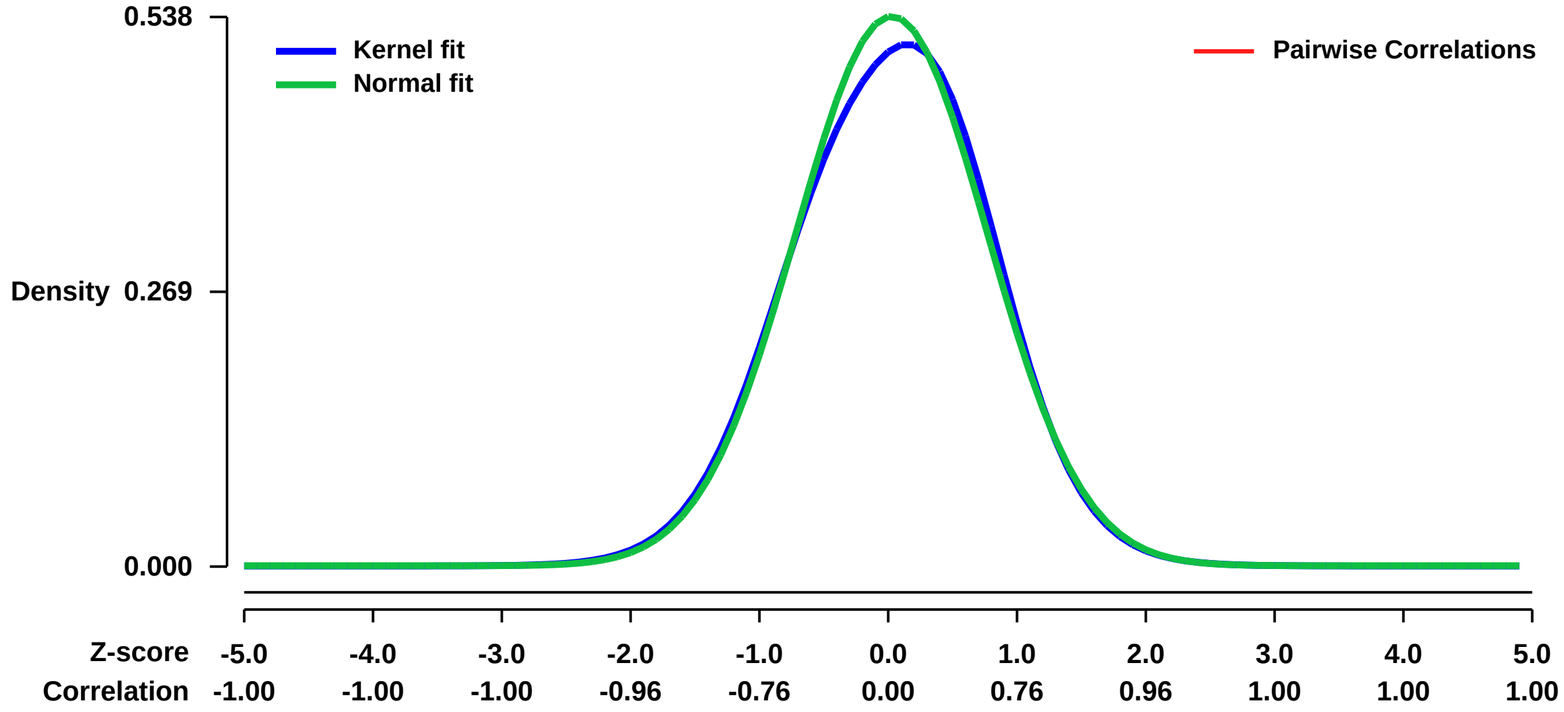

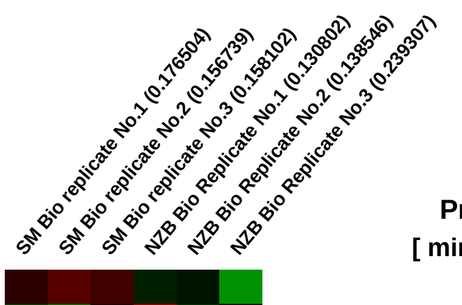

Pre-normalization Quantiles

[min] [medium] [max]

Null module

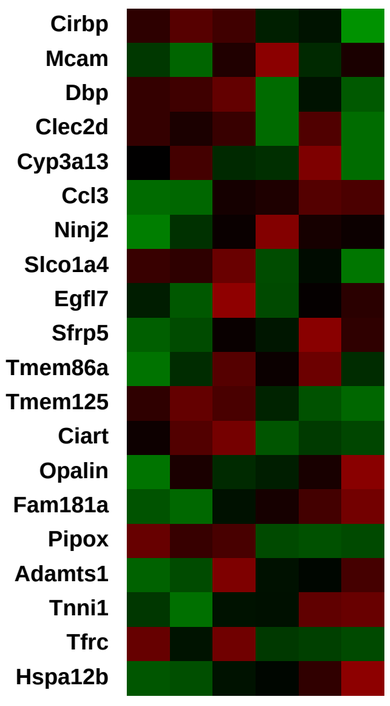

GEO Series "GSE47694" Expression Profiles

Num of samples in this series: 10

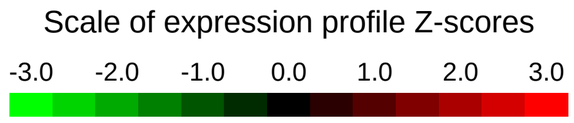

GEO Link: http://www.ncbi.nlm.nih.gov/geo/query/acc.cgi?acc=GSE47694

Status: Public on Jul 01 2013

Title: Regulation of Mouse Lens Development and Gene Expression by Krˆ…ppel-Like Factor 4

Organism: Mus musculus

Experiment type: Expression profiling by array

Platform: GPL1261

Pubmed ID:

Summary & Design:

Summary:
Conditional disruption of Klf4 in the ectoderm-derived tissues of the eye results in defective cornea, conjunctiva and the lens.

Expression of Klf4 is first detected in the embryonic day-12 (E12) mouse lens, peaks at E16, and declines thereafter.

Lenses from Mice which were conditional null for Klf4 (Klf4CN) were characterized by morphology and transcriptome.

Overall design:
Wild type and Klf4-conditional null mouse lens gene expression at embryonic day 16.5 (E16.5) and postnatal day 56 (PN56) was surveyed using Affymetrix mouse whole genome 430 2 arrays.

Background corr dist: **KL-Divergence = 0.0301, L1-Distance = 0.0216, L2-Distance = 0.0005, Normal std = 0.6597**

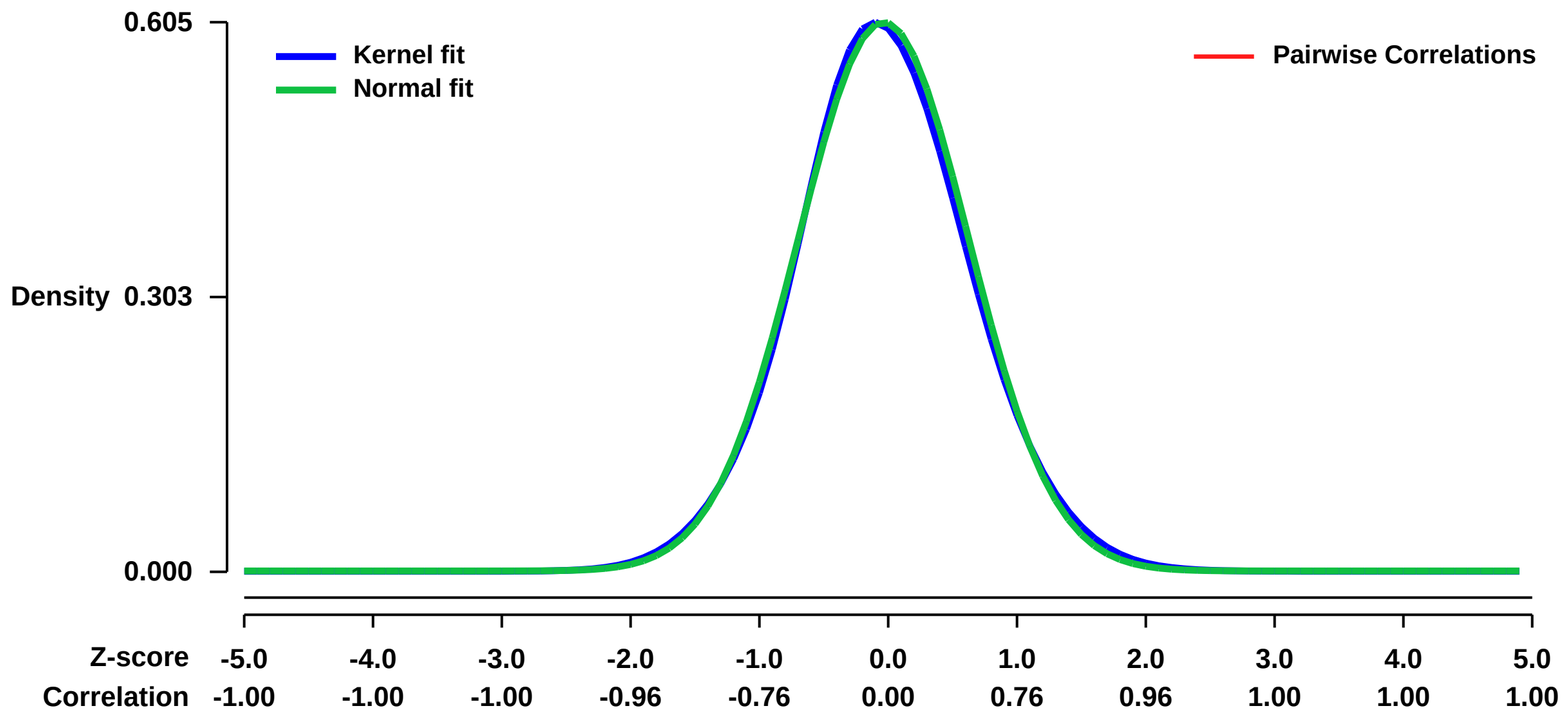

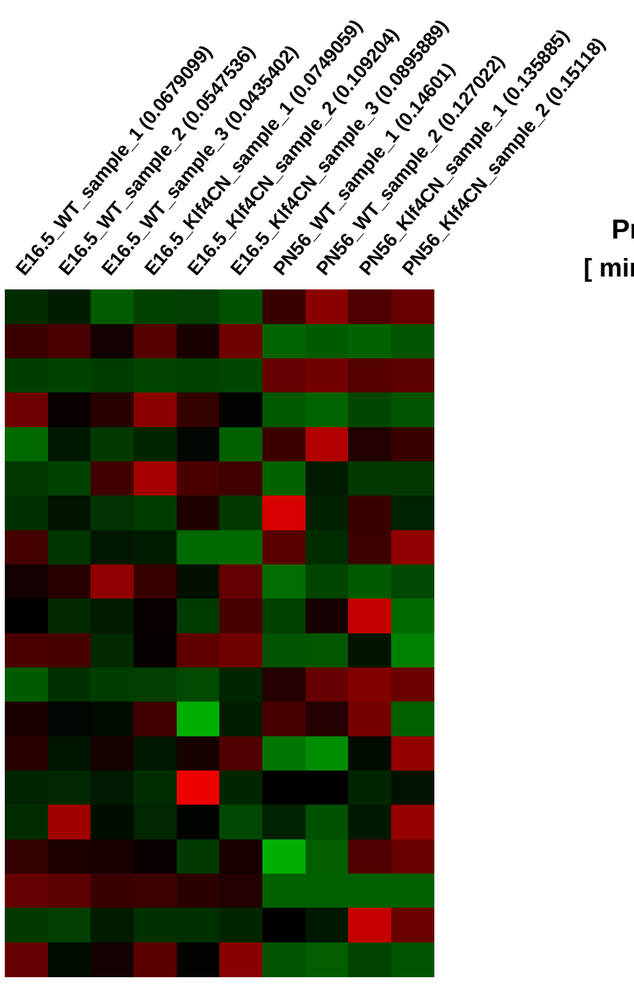

GEO Series "GSE4774" Expression Profiles

Num of samples in this series: 15

Scale of expression profile Z-scores

-3.0 -2.0 -1.0 0.0 1.0 2.0 3.0

GEO Link:	http://www.ncbi.nlm.nih.gov/geo/query/acc.cgi?acc=GSE4774
Status:	Public on Jun 06 2006
Title:	ruben-affy-mouse-187820
Organism:	Mus musculus
Experiment type:	Expression profiling by array
Platform:	GPL1261
Pubmed ID:	18697905
Summary & Design:	**Summary:** The Dlx homeobox genes have central roles in controlling patterning and differentiation of the brain and craniofacial primordia. In the brain, loss of Dlx function results in defects in the production, migration and differentiation of GABAergic neurons, that can lead to epilepsy. In the branchial arches, loss of Dlx function leads to craniofacial malformations that include trigeminal axon pathfinding defects. To determine how these genes function, we wish to identify the transcriptional circuitry that lies downstream of these transcription factors by comparing gene expression in wild type with Dlx mutant CNS and craniofacial tissues. 1) Compare gene expression in the maxillay branch of the first branchial arch (BA) of E10.5 wild type and Dlx2 -/- mutants. 2) Compare gene expression in the maxillary branch of the first BA of E10.5 wild type and Dlx1/2 -/- mutants. 3) Compare gene expression in wild type maxillary and mandibular branchial arches. 4) Compare gene expressionin mandibular branch of Dlx5/6 -/- mutants with wild type mandibular branch. The Dlx transcription factors are essential for controlling patterning of the brain and craniofacial primordia. In the brain, they control differentiation of GABAergic neurons of the basal ganglia. In the branchial arches, they control regional patterning. I hypothesize that there will be some conserved and some divergent mechanisms that the Dlx genes use in controlling brain and craniofacial development. We have already performed array analyses on Dlx function in the developing basal ganglia (with TGEN) by comparing expressed genes in wild type and Dlx1/2 mutants. Here we will compare gene expression in the brachial arches of wild type and Dlx mutant mice. 1) Generate E10.5 mouse embryos that are either wild type, Dlx2-/-, Dlx1/2 -/- or Dlx5/6 -/-. 2) Determine genotype by PCR. 3) Dissect branchial arches from the different genotypes. 4) Separate maxillary and mandibular branch of each branchial arch. 5) Prepare total RNA from the specimens. Obtain sufficient tissue to obtain 10 ug of total RNA - based on previous experience we anticipate that this will require ~ 10 branchial arches. We will pool the tissue from different embryos of the same genotype. 6) Send total RNA to TGEN for probe preparation, hybridization and array result analysis. **Keywords:** other **Overall design:**

Background corr dist: KL-Divergence = 0.2115, L1-Distance = 0.0476, L2-Distance = 0.0052, Normal std = 0.3241

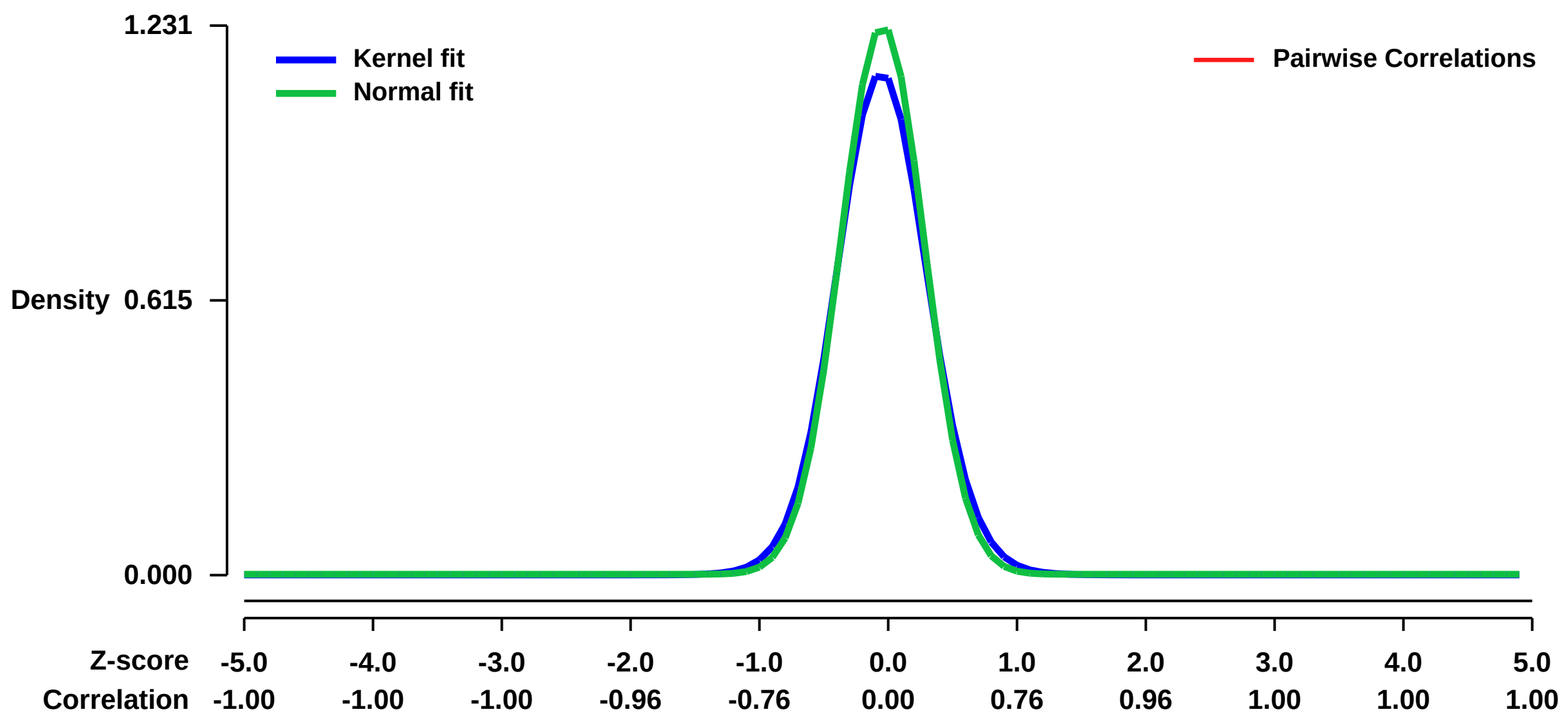

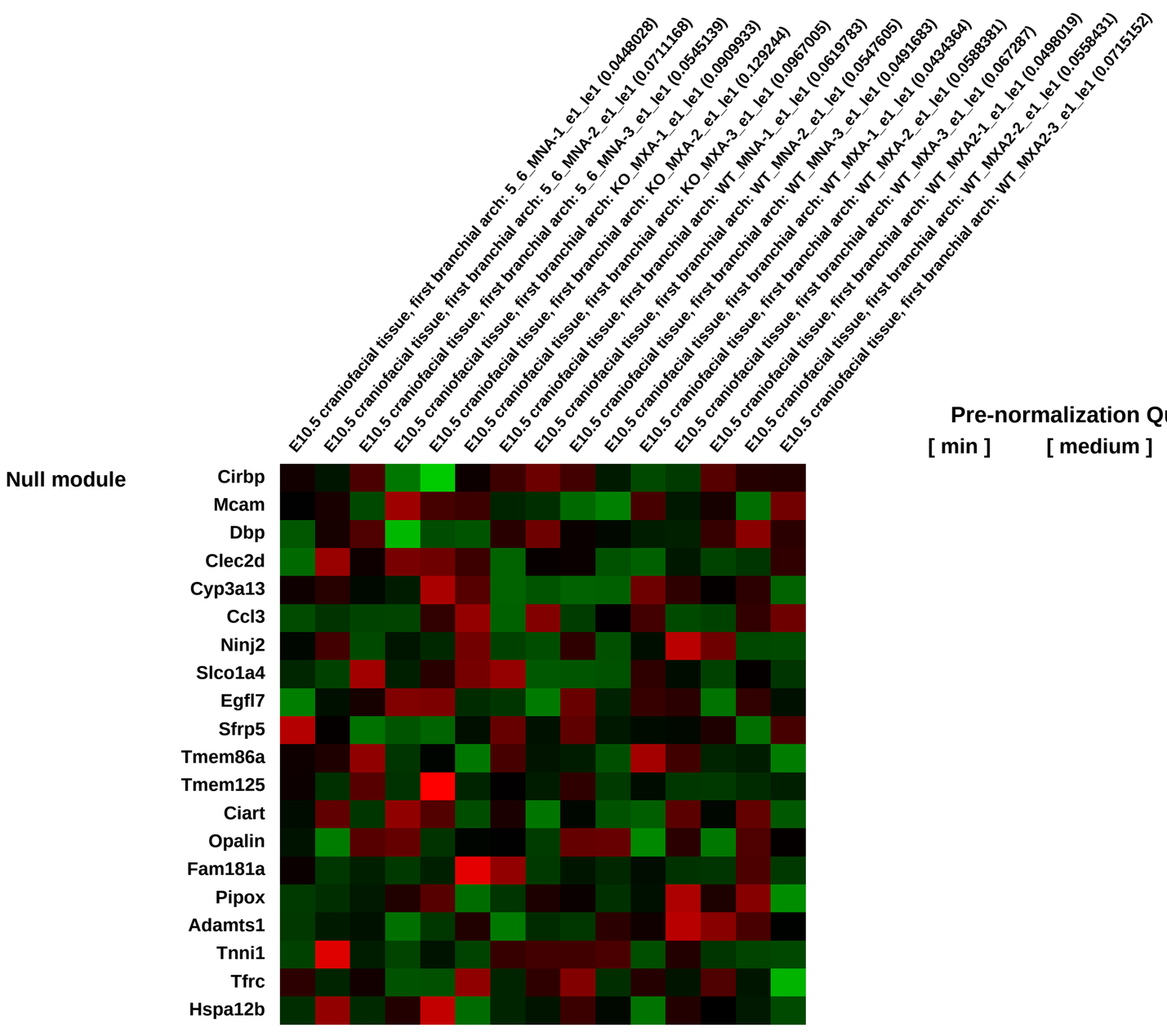

GEO Series "GSE47772" Expression Profiles

Num of samples in this series: 24

Scale of expression profile Z-scores

-3.0 -2.0 -1.0 0.0 1.0 2.0 3.0

GEO Link:	http://www.ncbi.nlm.nih.gov/geo/query/acc.cgi?acc=GSE47772
Status:	Public on Oct 01 2013
Title:	Expression data from subpopulations of Apc1638N/+ intestinal adeno tumors versus Apc1638N/+ / KRAS v12G intestinal adenocarcinomas tumors
Organism:	Mus musculus
Experiment type:	Expression profiling by array
Platform:	GPL1261
Pubmed ID:	24069241
Summary & Design:	**Summary:** Constitutive activation of the Wnt pathway leads to adenoma formation, an obligatory step towards intestinal cancer. In view of the established role of Wnt in regulating stemness, we attempted the isolation of cancer stem cells (CSCs) from Apc- and Apc/KRAS-mutant intestinal tumours. Whereas CSCs are present in malignant Apc/KRASâ mutant carcinomas, they appear to be very rare (<10-6) in the benign Apcâ mutant adenomas. In contrast, the Lin-CD24hiCD29+ subpopulation of adenocarcinoma cells appear to be enriched in CSCs with increased levels of active ï ¢-catenin. Expression profiling analysis of the CSC-enriched subpopulation confirmed their enhanced Wnt activity and revealed additional differential expression of other signalling pathways, growth factor binding proteins, and extracellular matrix components. As expected, genes characteristic of the Paneth cell lineage (e.g. defensins) are co-expressed together with stem cell genes (e.g. Lgr5) within the CSC-enriched subpopulation. This is of interest as it may indicate a cancer stem cell niche role for tumor-derived Paneth-like cells, similar to their role in supporting Lgr5+ stem cells in the normal intestinal crypt. Overall, our results indicate that oncogenic KRAS activation in Apc-driven tumours results in the expansion of the CSCs compartment by increasing b-catenin intracellular stabilization. **Overall design:** To identify molecular differences between stem-like and more differentiated (bulk) tumour cells from Apc1638N/+ and Apc1638N/+/KRASV12G intestinal adenomas and adenocarcinomas, we isolated total RNA from 104 Lin-CD24hiCD29+, Lin-CD24medCD29+/Lin-CD24loCD29+ and Lin- (bulk) tumour cells from 5 individual mice of each genotype (Apc1638N/+ and Apc1638N/+/KRASV12G). Total RNA samples were then employed to hybridize oligonucleotide microarrays (Affymetrix Mouse Genome 430A 2.0 Array) according to conventional protocols.

Background corr dist: KL-Divergence = 0.2441, L1-Distance = 0.0549, L2-Distance = 0.0075, Normal std = 0.3060

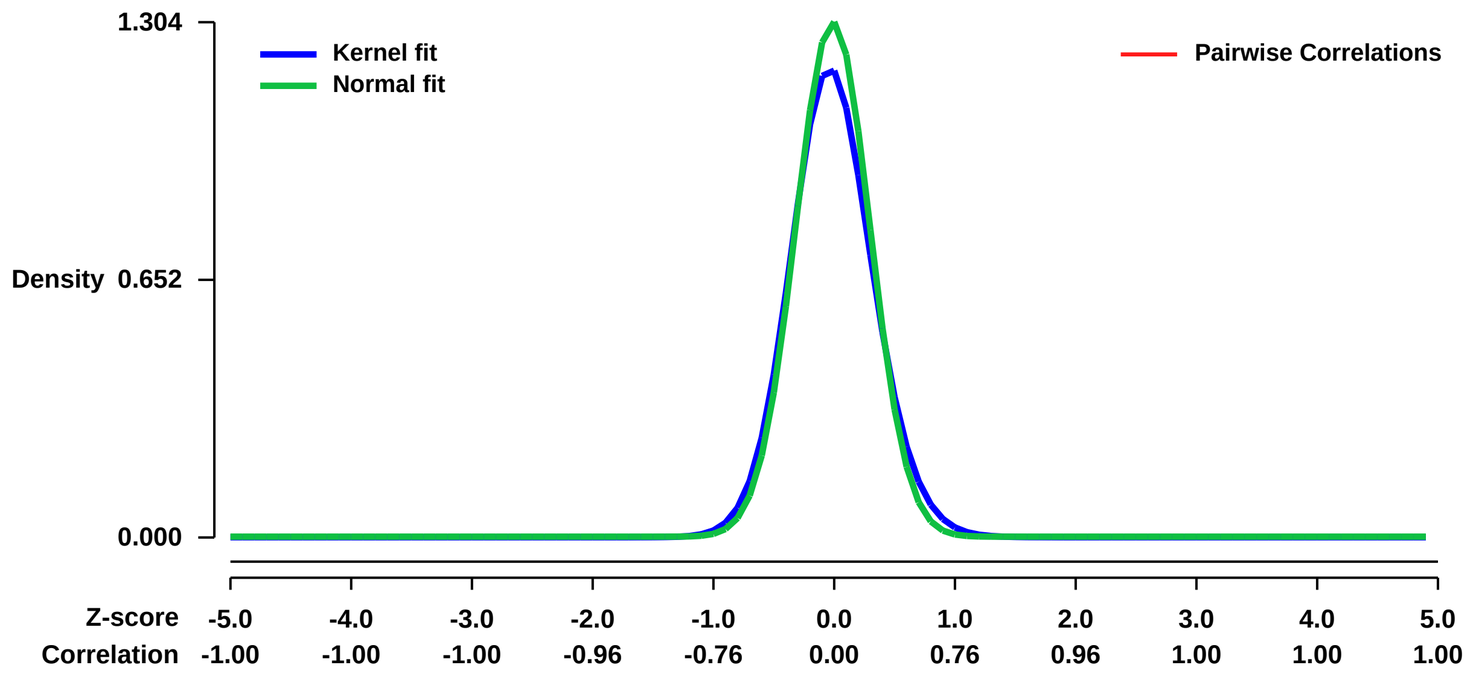

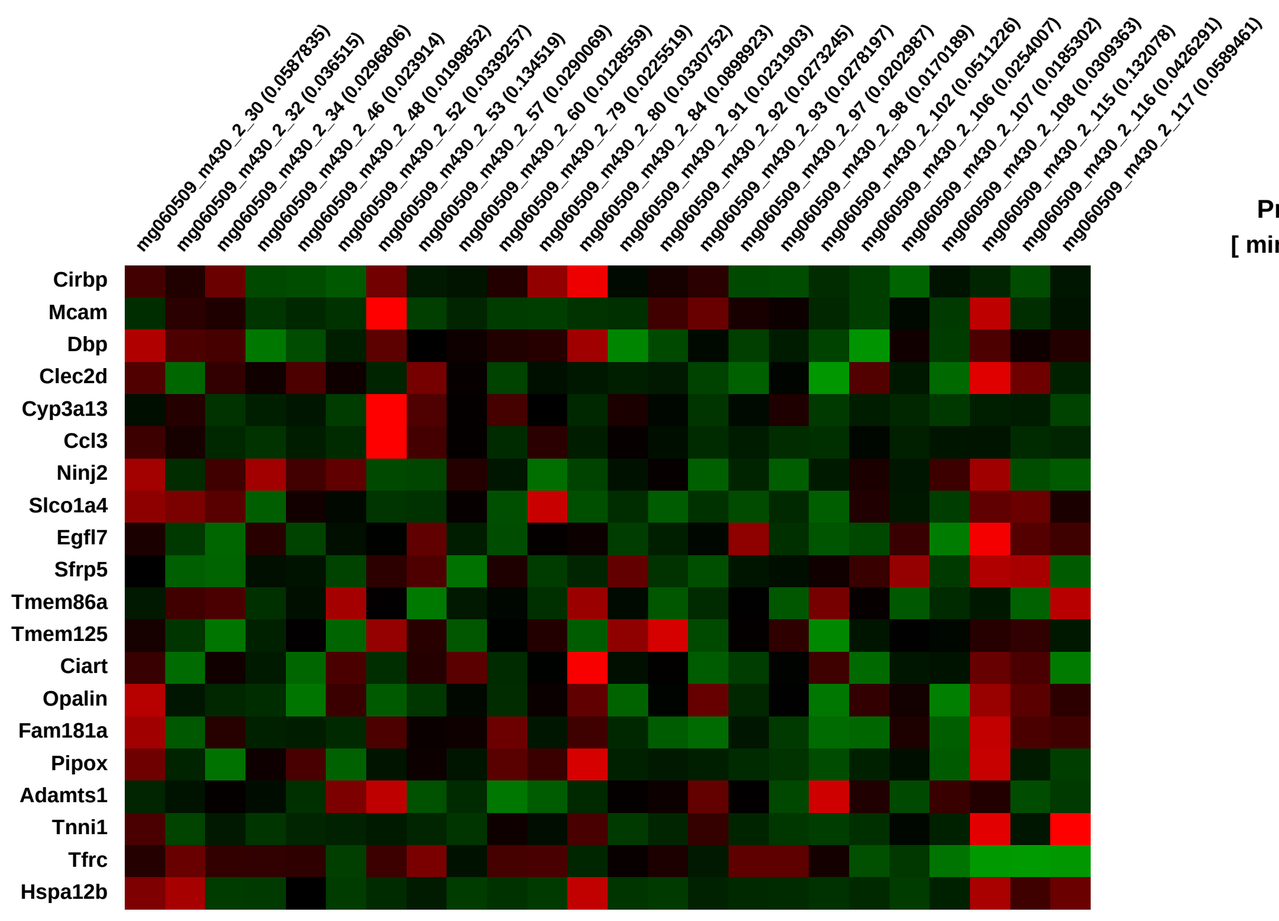

GEO Series "GSE47777" Expression Profiles

Num of samples in this series: 8

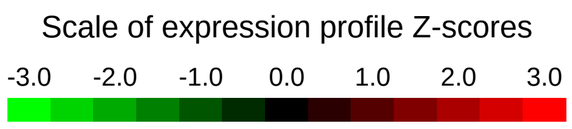

GEO Link:	http://www.ncbi.nlm.nih.gov/geo/query/acc.cgi?acc=GSE47777
Status:	Public on Jun 30 2013
Title:	Whole genome expression data comparison between WT and Cebpg-/- MEFs.
Organism:	Mus musculus
Experiment type:	Expression profiling by array
Platform:	GPL1261
Pubmed ID:	23775115
Summary & Design:	**Summary:** C/EBP‚† is an important regulator of oncogene-induced senescence (OIS). Here we show that C/EBP‚‡, a heterodimeric partner of C/EBP‚† whose biological functions are not well understood, inhibits cellular senescence. Cebpg-/- MEFs proliferated poorly, entered senescence prematurely, and expressed a pro-inflammatory gene signature, including elevated levels of senescence-associated secretory phenotype (SASP) genes whose induction by oncogenic stress requires C/EBP‚†. The senescence-suppressing activity of C/EBP‚‡ required its ability to heterodimerize with C/EBP‚†. Covalently linked C/EBP‚† homodimers (‚†~‚†) inhibited the proliferation and tumorigenicity of RasV12-transformed NIH3T3 cells, activated SASP gene expression, and recruited the CBP co-activator in a Ras-dependent manner, whereas ‚‡~‚† heterodimers lacked these capabilities and efficiently rescued proliferation of Cebpg-/- MEFs. C/EBP‚† depletion partially restored growth of C/EBP‚‡-deficient cells, indicating that the increased levels of C/EBP‚† homodimers in Cebpg-/- MEFs inhibit proliferation. The proliferative functions of C/EBP‚‡ are not restricted to fibroblasts, as hematopoietic progenitors from Cebpg-/- bone marrow also displayed impaired growth. Furthermore, high CEBPG expression correlated with poorer clinical prognoses in several human cancers, and C/EBP‚‡ depletion decreased proliferation and induced senescence in lung tumor cells. Our findings demonstrate that C/EBP‚‡ neutralizes the cytostatic activity of C/EBP‚† through heterodimerization, which prevents senescence and suppresses basal transcription of SASP genes. **Overall design:** Mouse embryonic fibroblasts were isolated at E13.5 and propagated. At passage 3 cells were plated with equal density and collected 48 hours later.

Background corr dist: KL-Divergence = 0.0549, L1-Distance = 0.0186, L2-Distance = 0.0005, Normal std = 0.5405

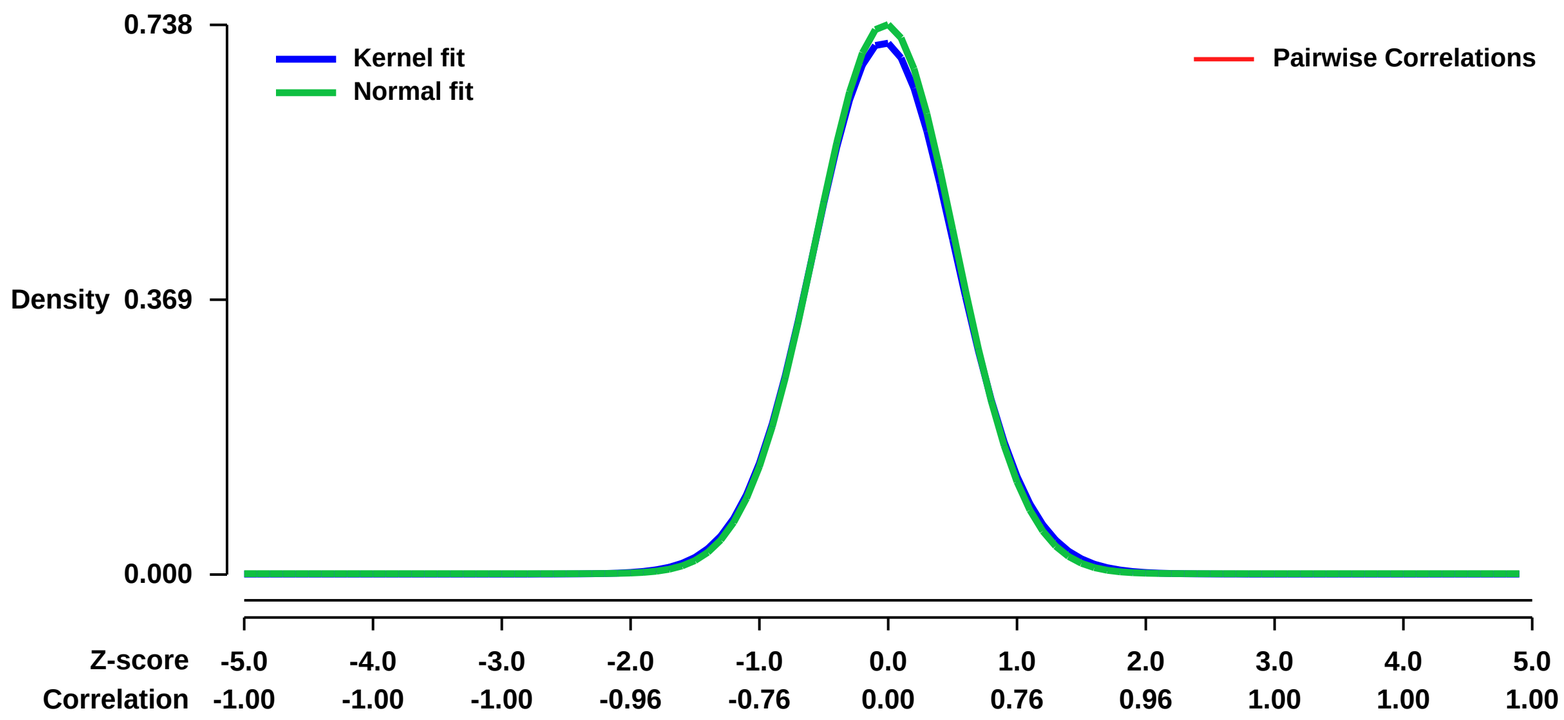

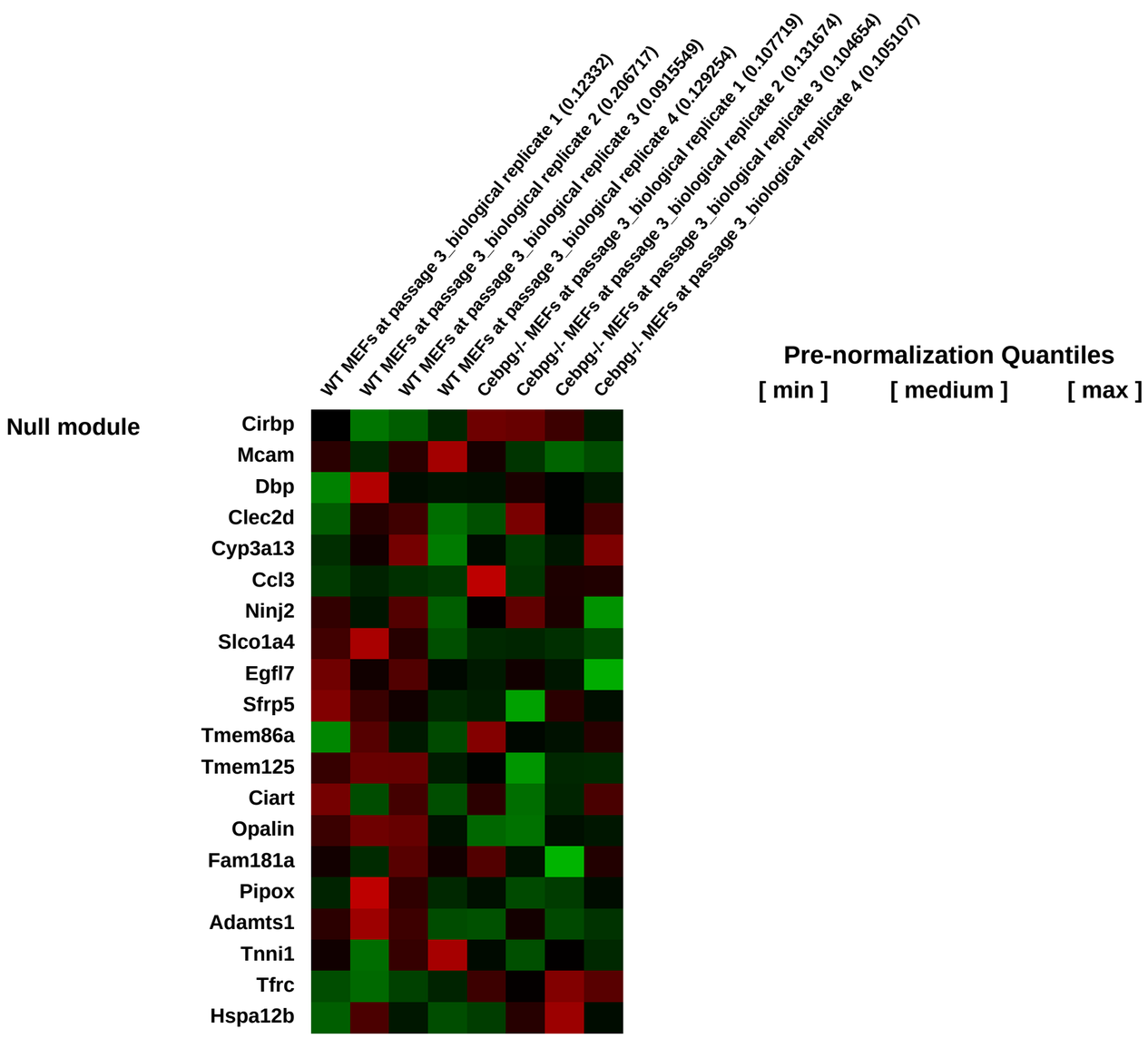

GEO Series "GSE47811" Expression Profiles

Num of samples in this series: 12

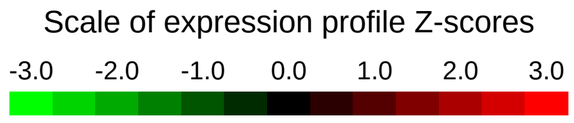

GEO Link:	http://www.ncbi.nlm.nih.gov/geo/query/acc.cgi?acc=GSE47811
Status:	Public on Jun 12 2013
Title:	Pancreatic cancer biomarkers in mouse saliva
Organism:	Mus musculus
Experiment type:	Expression profiling by array
Platform:	GPL1261
Pubmed ID:	23880764
Summary & Design:	**Summary:** This is a pilot study. We are trying to detect potential salivary biomarkers in mice with a pancreatic tumor. Global gene expression profiling has shown great promise in high-throughput biomarker discovery for early disease detection in body fluids such as saliva, which is accessible, cost-effective, and non-invasive. However, this goal has not been fully realized because saliva, like many clinical samples, contains partially fragmented and degraded RNAs that are difficult to amplify and detect with prevailing technologies. Here, using nanogram scale salivary RNA as a proof-of-principle example, we describe our progress with a novel poly-A tail independent mRNA amplification strategy combined with the Affymetrix GeneChip Exon arrays. We defined a Salivary Exon Core Transcriptome (SECT) with highly similar expression profiles in healthy individuals verified by quantitative PCR. Informatics analysis of SECT provided important mechanistic insight to their potential origin and function. Finally we demonstrated the diagnostic potential of true exon level expression profiling approach with salivary exon biomarkers that accurately discriminated gender in healthy individuals. Recent studies have demonstrated that discriminatory salivary biomarkers can be readily detected upon the development of systemic diseases such as pancreatic cancer, breast cancer, lung cancer and ovarian cancer. However, the utility of salivary biomarkers for the detection of systemic diseases has been undermined due to the absence of biological and mechanistic rationale why distal diseases from the oral cavity would lead to the development of discriminatory biomarkers in saliva. Here, we examine the hypothesis that pancreatic tumor-derived exosomes are mechanistically involved in the development of pancreatic cancer-discriminatory salivary transcriptomic biomarkers. We first developed a pancreatic cancer mouse model that yielded discriminatory salivary biomarkers by implanting the mouse pancreatic cancer cell line Pan02 into the pancreas of the syngeneic host C57BL/6. The role of pancreatic cancer-derived exosomes in the development of discriminatory salivary biomarkers was then tested by engineered a Pan02 cell line that is suppressed for exosome biogenesis, implanted into the C56BL/6 mouse and examine if the discriminatory salivary biomarker profile was ablated or disrupted. Suppression of exosome biogenesis results in the ablation of discriminatory salivary biomarker development. This study supports that tumor-derived exosomes provide a mechanism in the development of discriminatory biomarkers in saliva and distal systemic diseases. **Overall design:** We analyzed saliva from 6 healthy mice and 6 mice with a pancreatic tumor using the Affymetrix Mouse Exon Genome 430 2.0 platform. Array data was processed by dChip. No techinical replicates were performed.

Background corr dist: KL-Divergence = 0.1253, L1-Distance = 0.0807, L2-Distance = 0.0154, Normal std = 0.4325

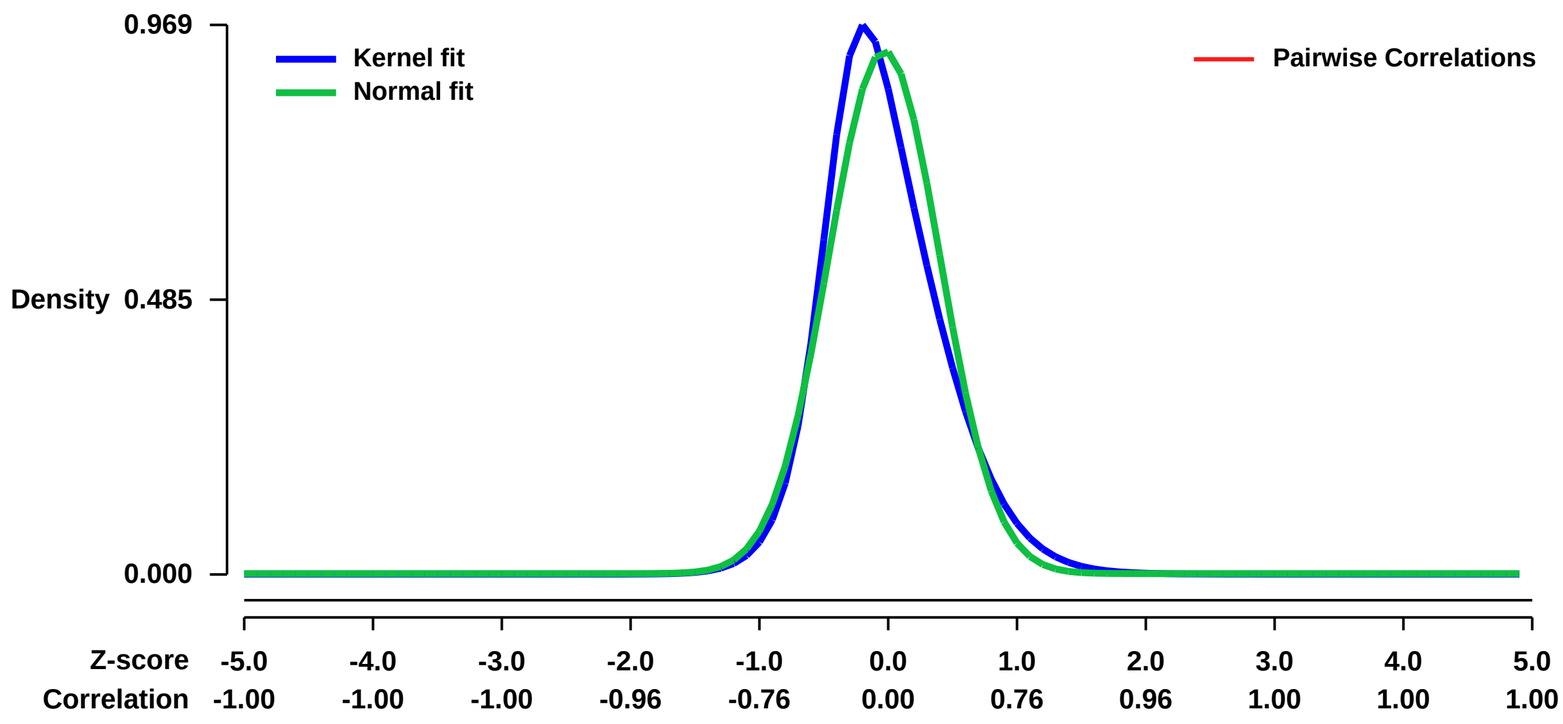

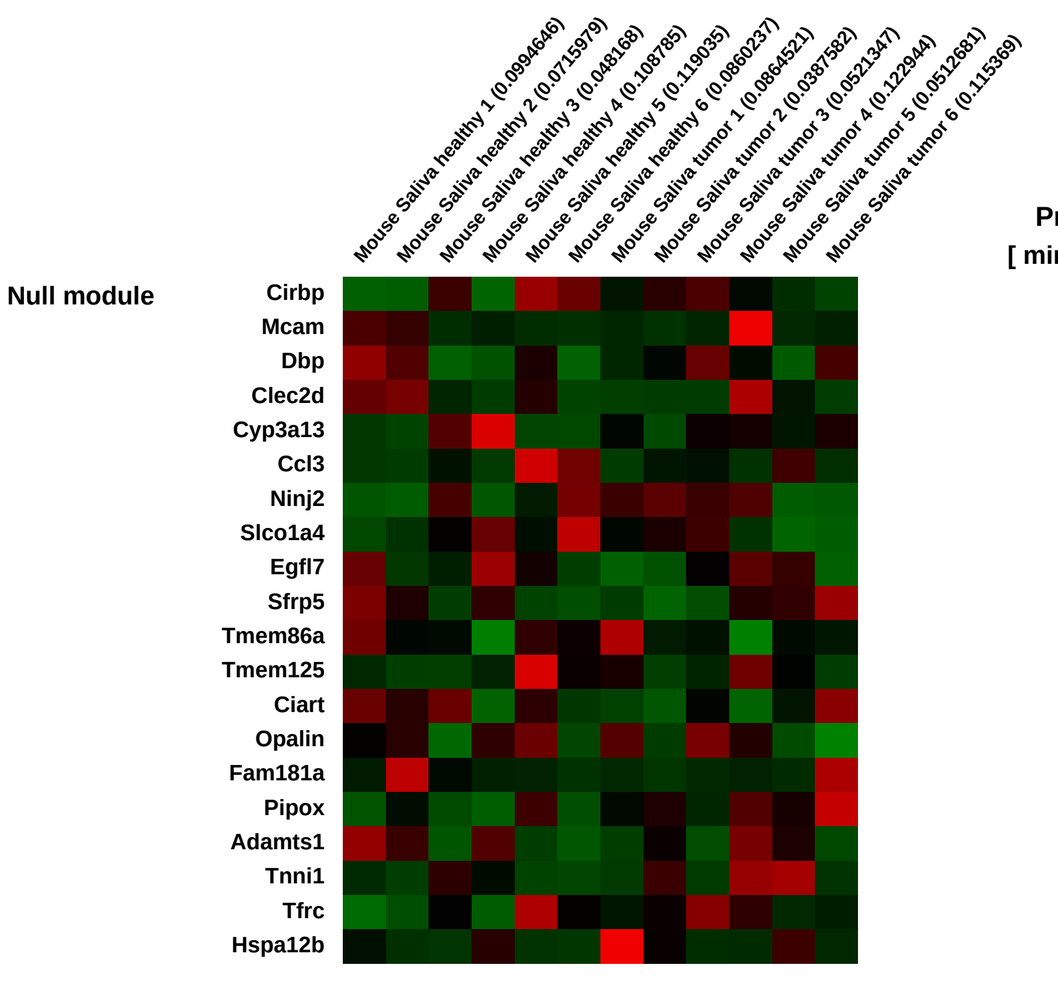

GEO Series "GSE4786" Expression Profiles

Num of samples in this series: 9

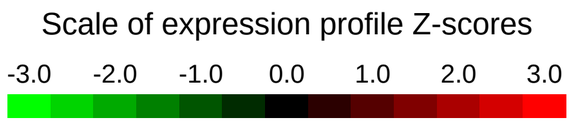

GEO Link:	http://www.ncbi.nlm.nih.gov/geo/query/acc.cgi?acc=GSE4786
Status:	Public on May 01 2007
Title:	Caloric restriction suppresses apoptotic cell death in the mammalian cochlea and leads to prevention of presbycusis
Organism:	Mus musculus
Experiment type:	Expression profiling by array
Platform:	GPL1261
Pubmed ID:	16890326
Summary & Design:	**Summary:** Presbycusis is characterized by an age-related progressive decline of auditory function, and arises mainly from the degeneration of hair cells or spiral ganglion (SG) cells in the cochlea. Here we show that caloric restriction suppresses apoptotic cell death in the mouse cochlea and prevents late onset of presbycusis. Caloric restricted mice, which maintained body weight at the same level as that of young control (YC) mice, retained normal hearing and showed no cochlear degeneration. CR mice also showed significantly fewer TUNEL-positive staining cells and fewer cleaved caspase-3-positive staining cells relative to middle-age control (MC) mice. Microarray analysis revealed that CR down-regulated the expression of 28 proapoptotic genes, including Bak and Bim. Taken together, our findings suggest that loss of critical cells through apoptosis is an important mechanism of presbycusis in mammals, and that CR or staying lean can retard this process by suppressing apoptosis in the inner ear tissue. **Keywords:** Effect of aging, effect of caloric restriction, time course, disease state analysis **Overall design:** Quality control measures were not used. No replicates were done. Dye swap was not used.

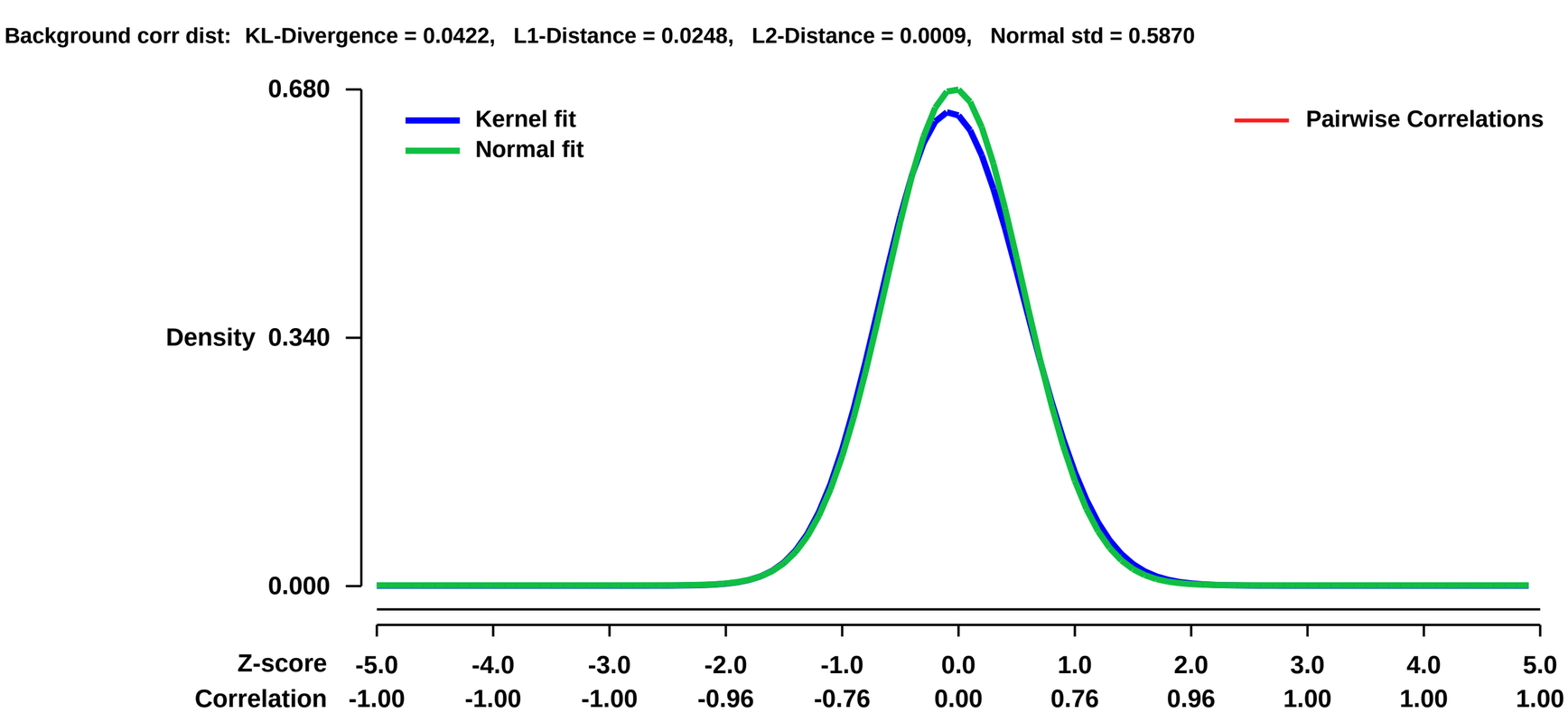

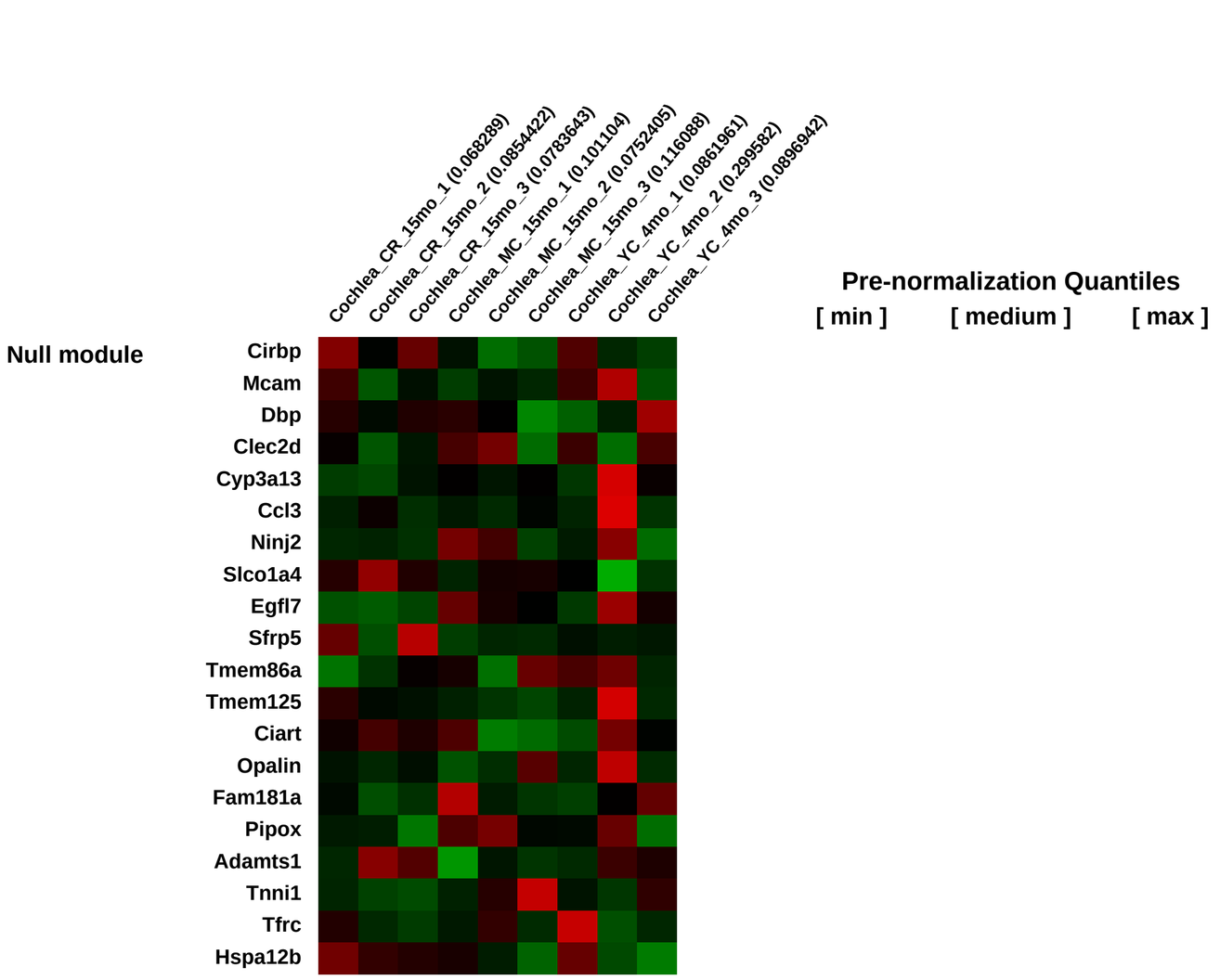

GEO Series "GSE47872" Expression Profiles

Num of samples in this series: 6

Scale of expression profile Z-scores

-3.0 -2.0 -1.0 0.0 1.0 2.0 3.0

GEO Link:	http://www.ncbi.nlm.nih.gov/geo/query/acc.cgi?acc=GSE47872
Status:	Public on Mar 26 2014
Title:	Integrated analysis identifies key determinants of embryonic stem cell identity and homeostasis
Organism:	Mus musculus
Experiment type:	Expression profiling by array
Platform:	GPL1261
Pubmed ID:	24711389
Summary & Design:	**Summary:** Despite RNAi-based screens to uncover genes controlling embryonic stem cell (ESC) identity, the pluripotency network remains poorly characterized, as does the precise molecular mechanisms underlying the balance between self-renewal and differentiation. Here we carried out a systematic meta-analysis of published gene expression data to rank-order genes based on their likelihood of regulating ESC identity. Not only did our analysis correctly rank known pluripotency-associated genes atop the list, but it also helped unearth many novel determinants of ESC identity including several components of functionally distinct complexes, as determined using RNAi. We focus on our top-hit Nucleolin, and characterize its mechanistic role in the maintenance of ESC homeostasis by shielding from differentiation-inducing redox imbalance-induced oxidative stress. Notably, we identify a conceptually novel mechanism involving a Nucleolin-dependent bistable switch regulating the homeostatic balance between self-renewal and differentiation in ESCs. Our gene ranks represent a rich and valuable resource for uncovering novel ESC regulators. **Overall design:** Microarray gene expression profiling in E14Tg2a mESCs after transfection with indicated siRNAs: Ncl siRNA #1 (Invitrogen, 17975-MSS206961) Ncl siRNA #2 (Invitrogen, 17975-MSS275939), and Control siRNA duplex targeting firefly luciferase.

Background corr dist: KL-Divergence = 0.0151, L1-Distance = 0.0201, L2-Distance = 0.0004, Normal std = 0.8200

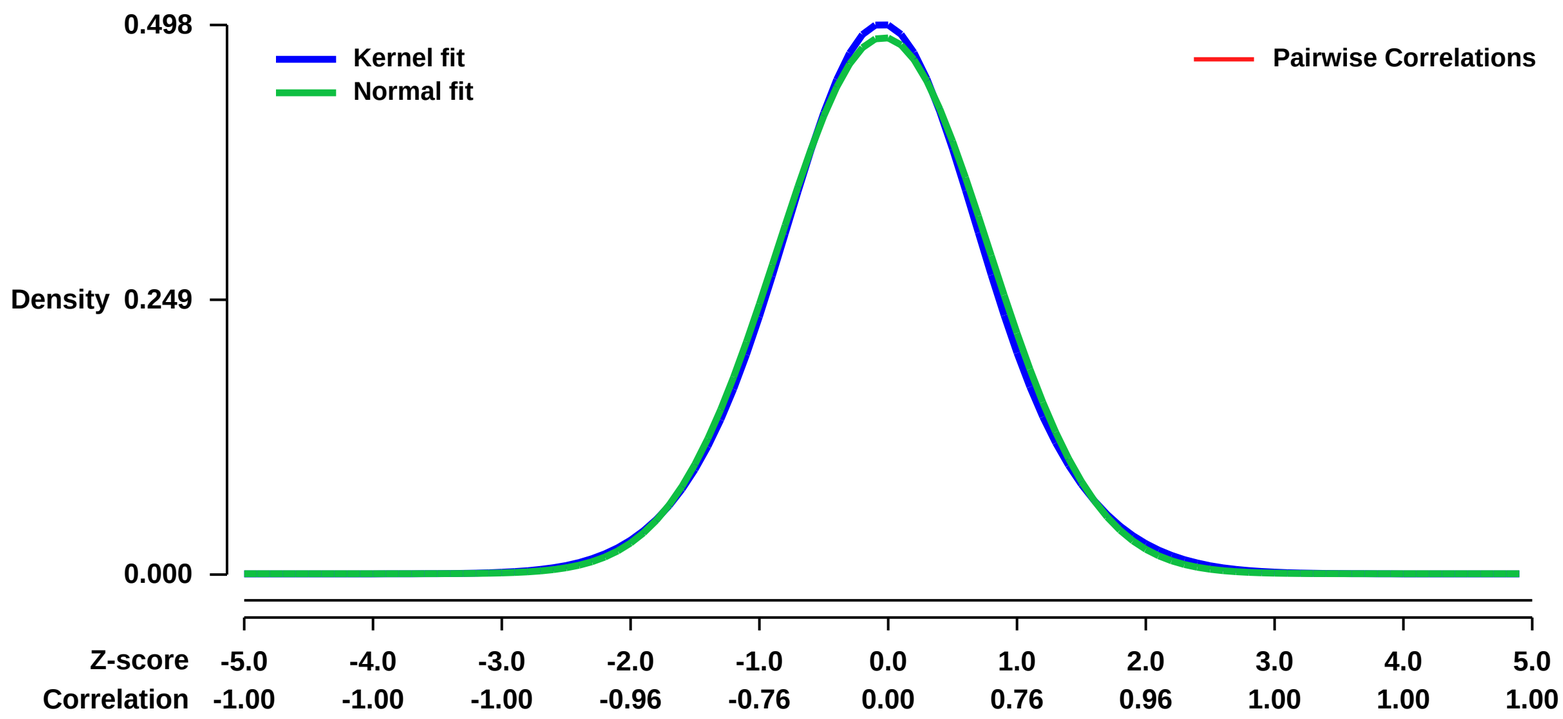

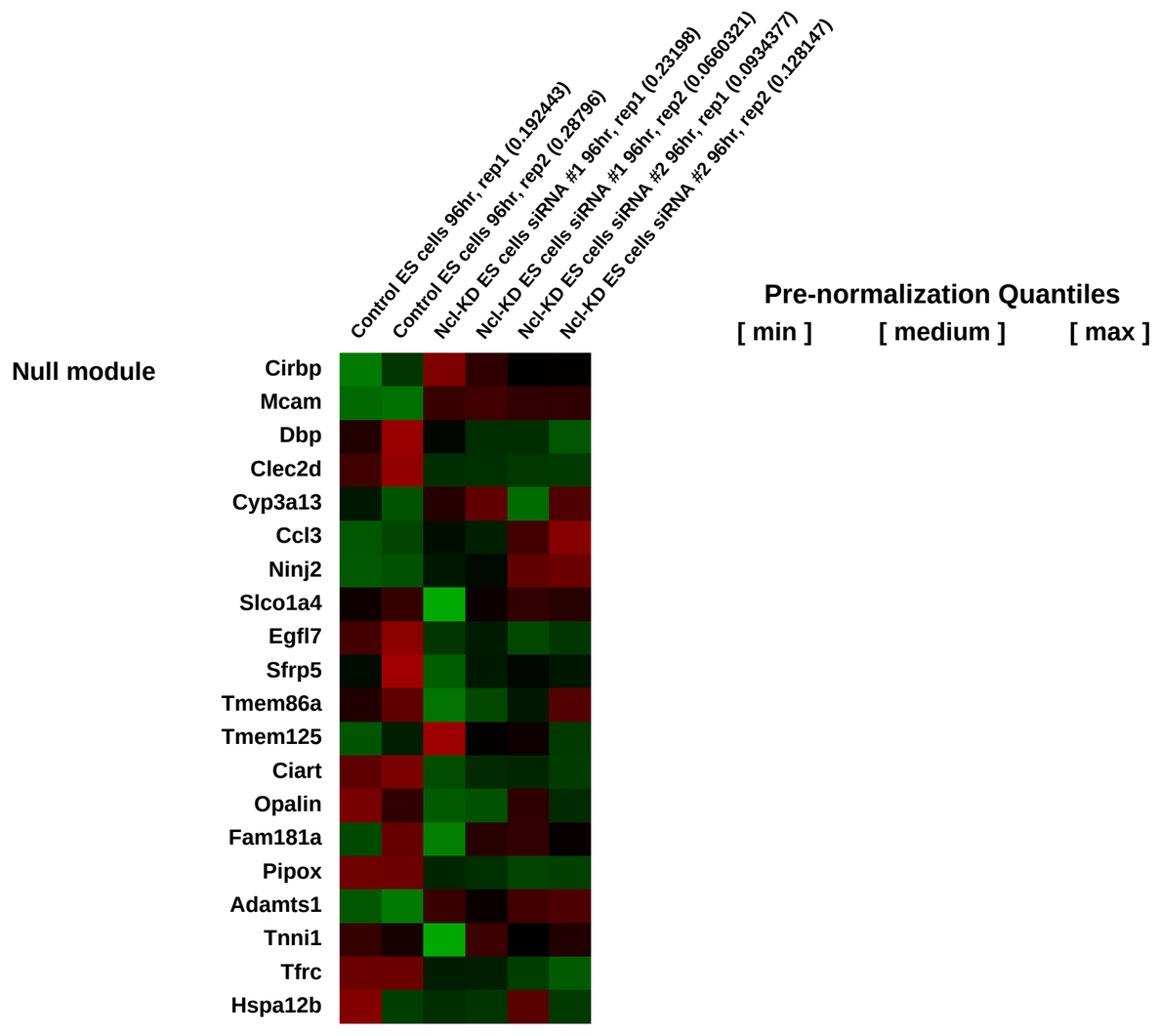

GEO Series "GSE47959" Expression Profiles

Num of samples in this series: 8

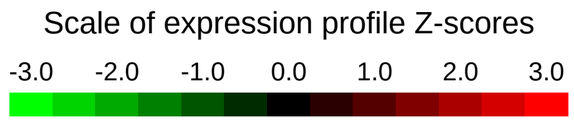

GEO Link:	http://www.ncbi.nlm.nih.gov/geo/query/acc.cgi?acc=GSE47959
Status:	Public on Jul 25 2014
Title:	NKT-10 cells represent a novel invariant NKT cell subset with regulatory characteristics
Organism:	Mus musculus
Experiment type:	Expression profiling by array
Platform:	GPL1261
Pubmed ID:	25061873
Summary & Design:	**Summary:** We compared splenic Va14i NKT cells from C57BL/6 control mice and from mice injected 4 weeks earlier intravenously with 4ug/mouse of the iNKT cell antigen alpha-galactosylceramide (aGalCer). These mice were either left unstimulated or were stimulated with 1ug/mouse aGalCer i.v.. All mice were female and 8 weeks of age at the beginning of the experiment. Va14i NKT cells were enriched via magnetic selection and cell sorted for TCRb+ CD1d/aGalCer-tetramer+. Total RNA were prepared using a Qiagen RNeasy mini kit. IVT probe generation and hybridization to Affymetrix Mouse Genome 430 2.0 arrays was carried out by the Veterans Medical Research Foundation GeneChipTM Microarray located at UCSD. **Overall design:** Group 1 (Ctr_unstim) = iNKT cells from C57BL/6 control mice and left unstimulated / Group 2 (Ctr_stim) = iNKT cells from C57BL/6 control mice and injected 1h before purification with 1ug aGalCer i.v. / Group 3 (Pre_unstim) = iNKT cells from C57BL/6 mice injected 4weeks earlier with 4ug aGalCer i.v. and left unstimulated / Group 4 (Pre_stim) = iNKT cells from C57BL/6 mice injected 4weeks earlier with 4ug aGalCer i.v. and injected 1h before purification with 1ug aGalCer i.v. / Sample were prepared in duplicates in two independent experiments.

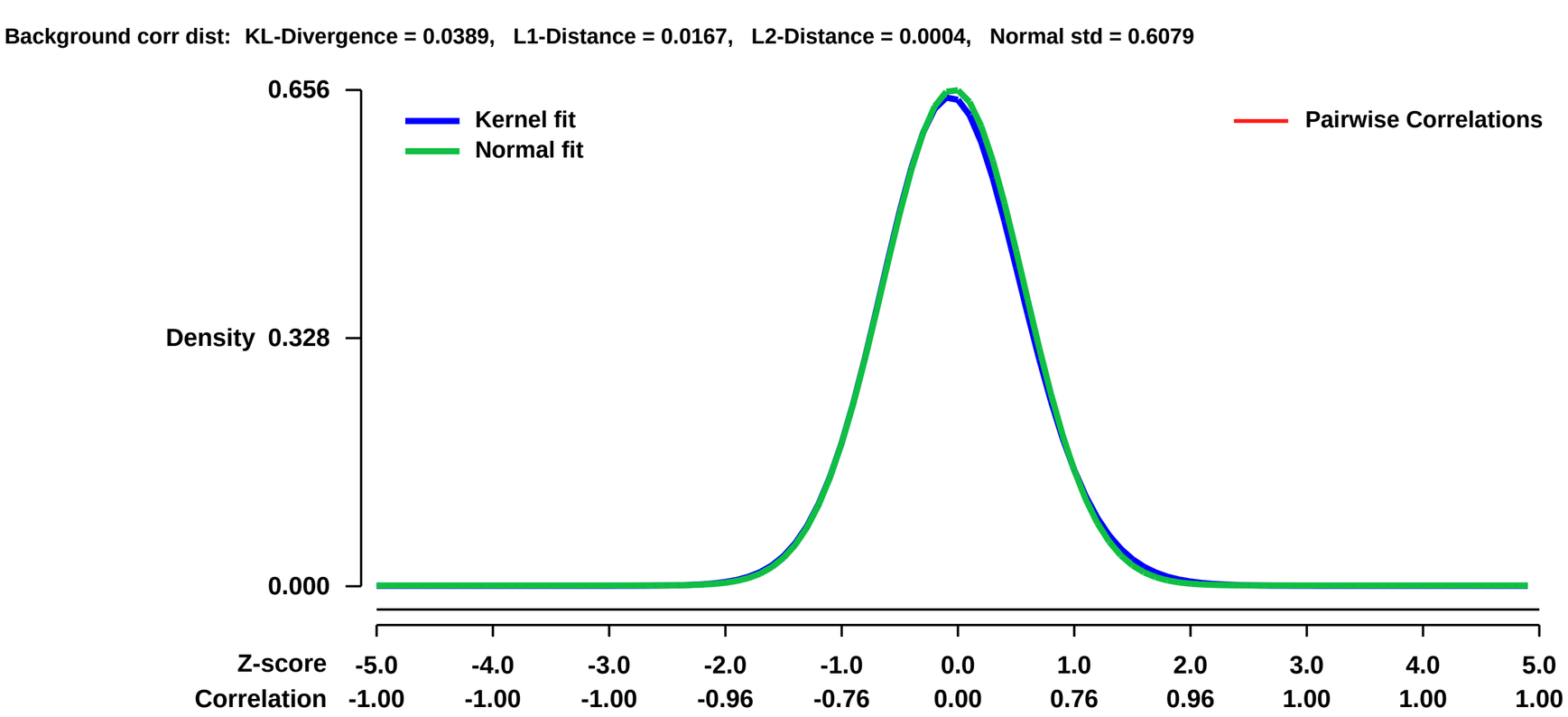

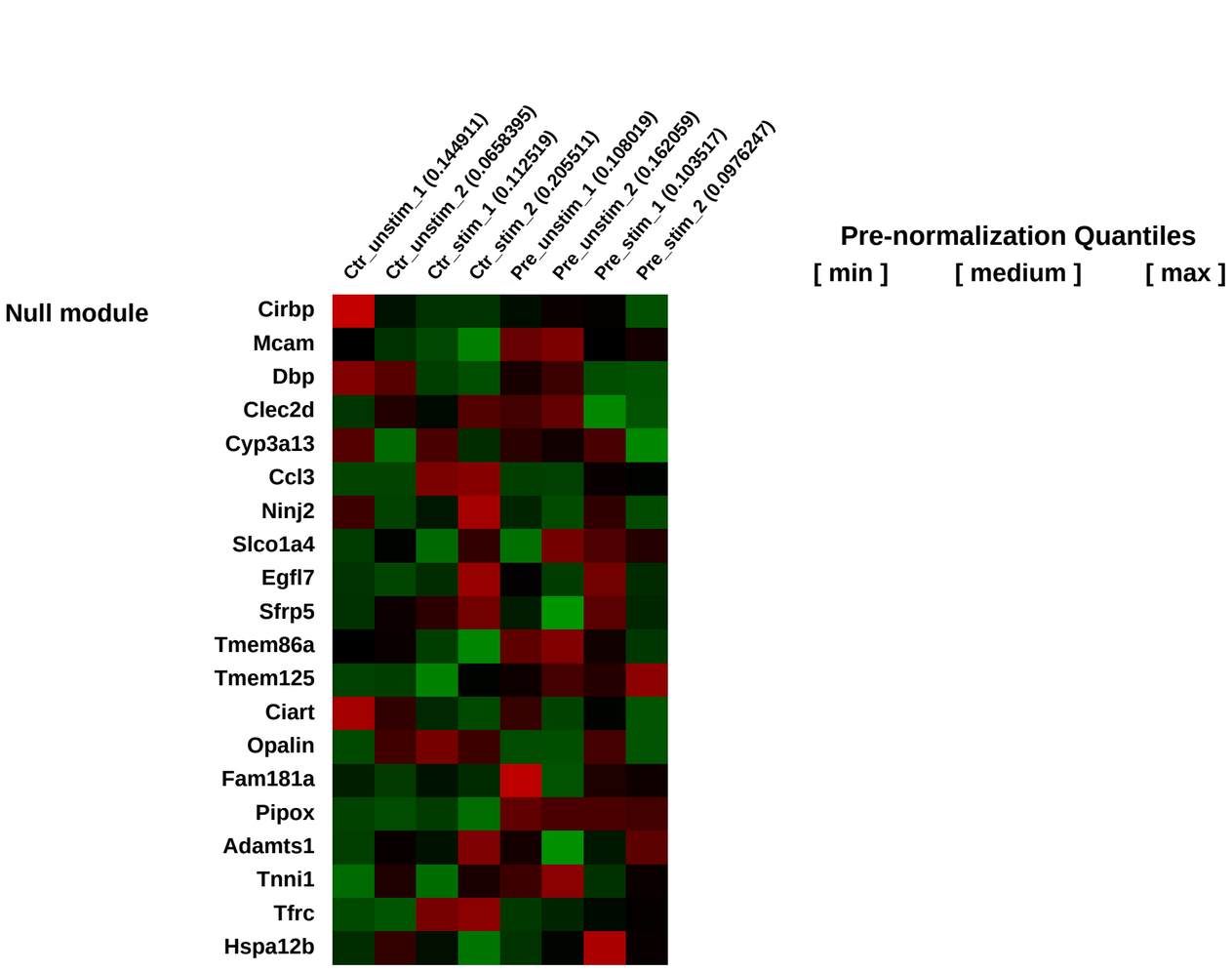

GEO Series "GSE4799" Expression Profiles

Num of samples in this series: 15

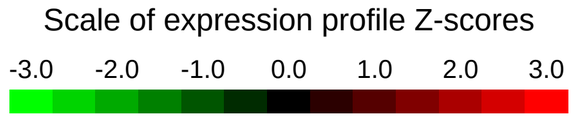

GEO Link:	http://www.ncbi.nlm.nih.gov/geo/query/acc.cgi?acc=GSE4799
Status:	Public on May 11 2006
Title:	GDNF-regulated gene expression in cultured mouse spermatogonial stem cells
Organism:	Mus musculus
Experiment type:	Expression profiling by array
Platform:	GPL1261
Pubmed ID:	16740658
Summary & Design:	**Summary:** GDNF-regulated gene expression was studied in cultures of actively self-renewing spermatogonial stem cells established from 6 day old male mice. GDNF is the essential growth factor regulating mouse spermatogonial stem cell self-renewal. Using a serum-free chemically defined culture system that supports mouse spermatogonial stem cell self-renewal for extended periods of time, GDNF-regulated genes were identified using microarray profiling. **Keywords: GDNF withdrawal and time-course replacement** **Overall design:** Established cultures of highly enriched self-renewing spermatogonial stem cells were subjeted to withrawal of GDNF and GFRalpha1 for 18-hr followed by replacement of the growth factors for 2, 4, and 8-hr. Gene expression was studied using microarray profiling prior to withdrawal, after withdrawal and at each time-point of GDNF/GFRalpha1 replacement.

Background corr dist: KL-Divergence = 0.1956, L1-Distance = 0.0445, L2-Distance = 0.0044, Normal std = 0.3346

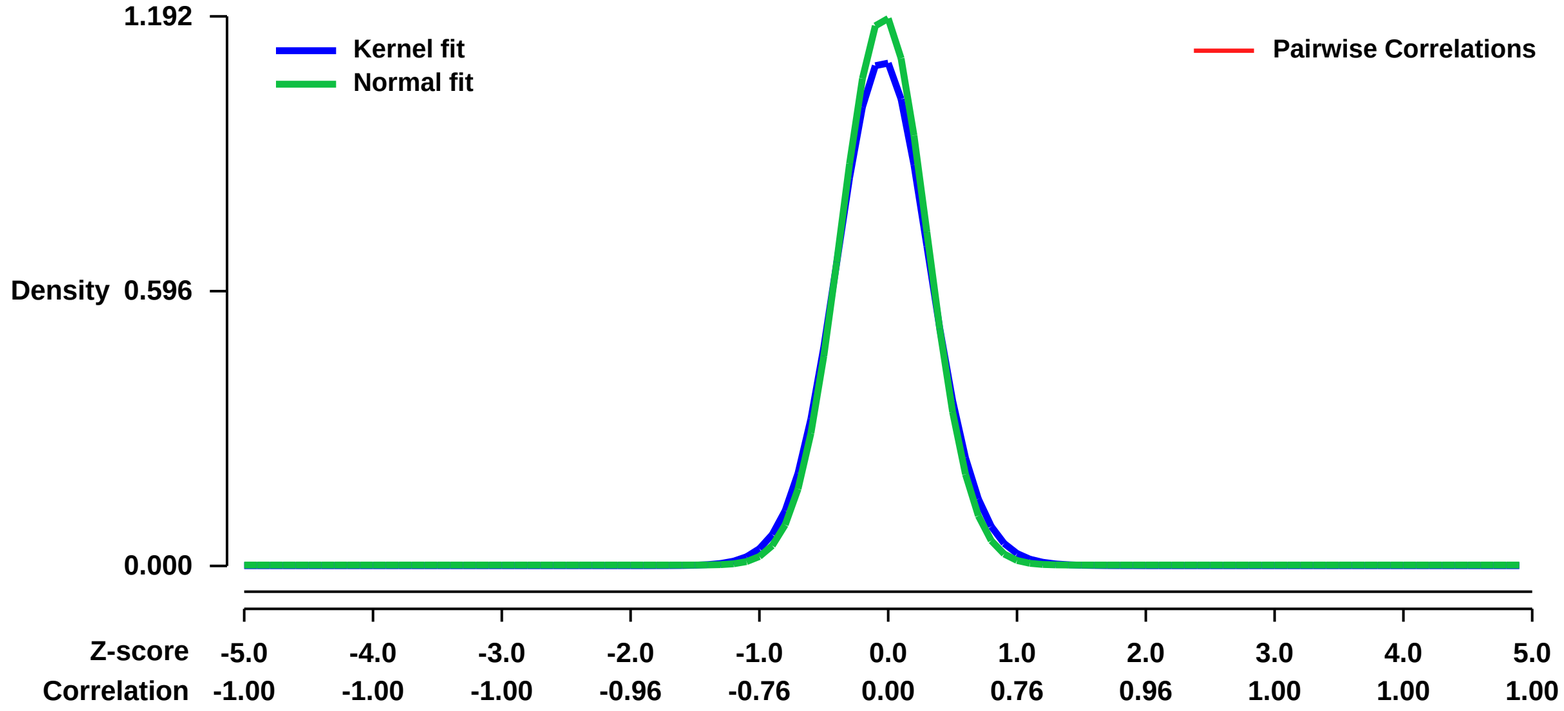

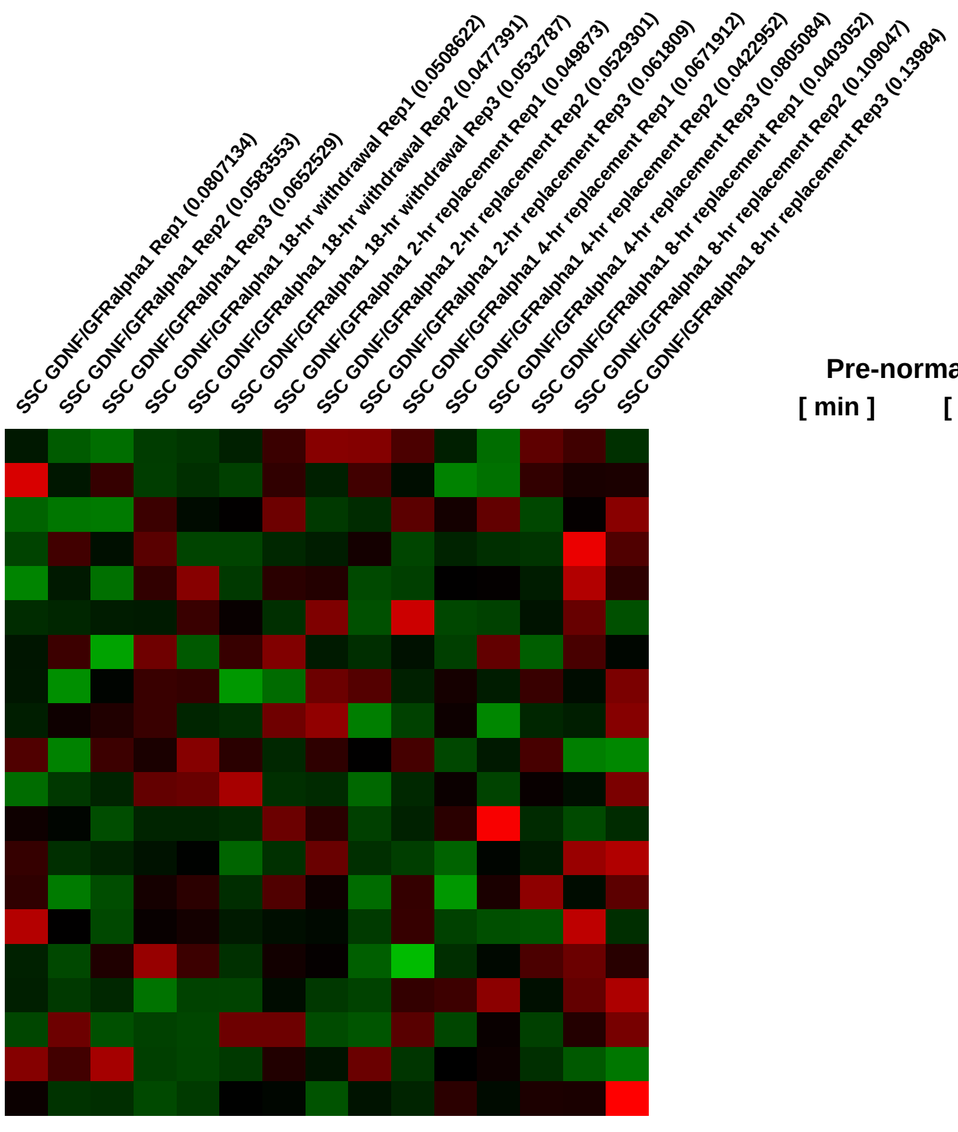

GEO Series "GSE48004" Expression Profiles

Num of samples in this series: 6

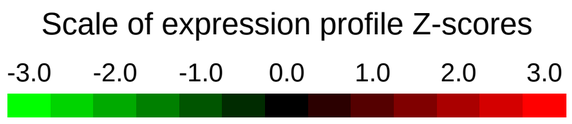

GEO Link:	http://www.ncbi.nlm.nih.gov/geo/query/acc.cgi?acc=GSE48004
Status:	Public on Aug 21 2013
Title:	Targeted disruption of Hotair leads to homeotic transformation and de-repression of imprinted genes [Microarray Analysis]
Organism:	Mus musculus
Experiment type:	Expression profiling by array
Platform:	GPL1261
Pubmed ID:	24075995
Summary & Design:	**Summary:** Long noncoding RNAs (lncRNAs) are thought to be prevalent regulators of gene expression, but the consequences of lncRNA inactivation in vivo are mostly unknown. Here we show that targeted deletion of mouse Hotair lncRNA leads to de-repression of hundreds of genes, resulting in homeotic transformation of the spine and malformation of metacarpal-carpal bones. RNA-seq and conditional inactivation reveal an ongoing requirement of Hotair to repress HoxD genes and multiple imprinted loci such as Dlk1-Meg3 and Igf2-H19. Hotair binds to both Polycomb repressive complex 2 that methylates histone H3 at lysine 27 (H3K27) and Lsd1 complex that demethylates histone H3 at lysine 4 (H3K4) in vivo. Hotair inactivation causes coordinate H3K27me3 loss and H3K4me3 gain at select target genes throughout the genome. These results reveal a shared regulatory mechanism to enforce silent chromatin state at Hox and imprinted genes via Hotair lncRNA. **Overall design:** Microarray analysis was performed on triplicate samples with Affymetrix GeneChip Mouse Genome 430 2.0 Array for both wildtype and Hotair Knockout.

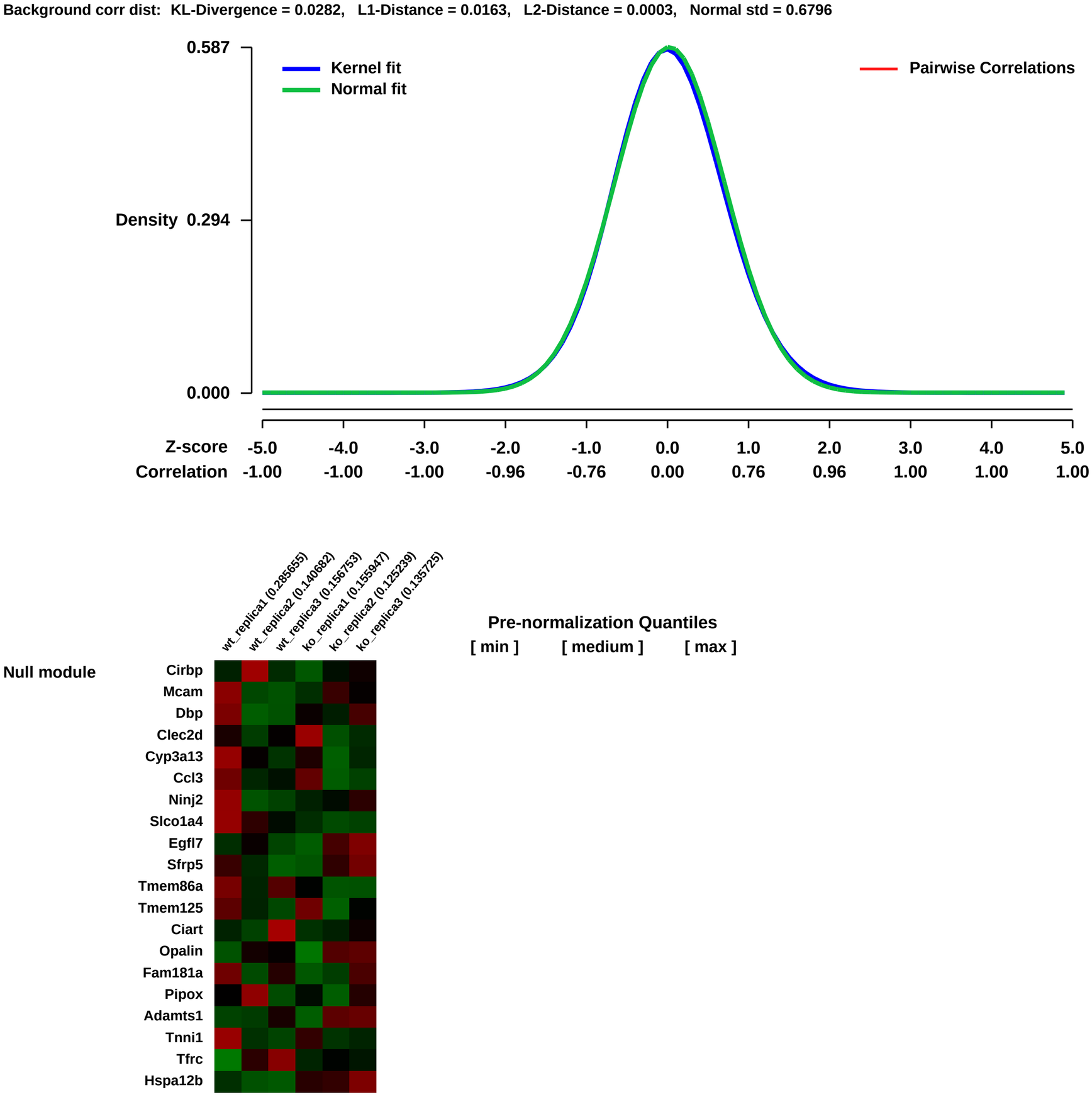

GEO Series "GSE4816" Expression Profiles

Num of samples in this series: 12

Scale of expression profile Z-scores

-3.0 -2.0 -1.0 0.0 1.0 2.0 3.0

GEO Link:	**http://www.ncbi.nlm.nih.gov/geo/query/acc.cgi?acc=GSE4816**
Status:	**Public on May 12 2006**
Title:	**Gene expression profiles of the P1 bladder isolated from SMAA or SMAGA (Acta2 or Actg2) transgenic and wild type mice. (GUDMAP Series ID: 2)**
Organism:	**Mus musculus**
Experiment type:	**Expression profiling by array**
Platform:	**GPL1261**
Pubmed ID:	
Summary & Design:	**Summary:** **The long term objective is to create an encyclopedia of the expression levels of all genes in multiple components of the developing bladder. The central thesis is straightforward. The combination of laser capture microdissection (LCM) plus microarray analysis offers a powerful, efficient and effective method for the creation of a global gene expression atlas of the developing bladder. Microarrays with essentially complete genome coverage can be used to quantitate expression levels of every gene in laser capture microdissected components of the developing bladder. The ensuing rapid read-out provides an expression atlas that is more sensitive, more economical and more complete than would be possible by in situ hybridizations alone. As a first step we sought to determine if expression of the reporter gene (EGFP or EYFP) used to identify smooth muscle cells altered the gene expression profile of the bladder.** **Keywords: Comparison of postnatal day 1 bladders.** **Overall design:** **Postnatal day 1 bladders were isolated from transgenic and wild-type mice to determine the effects of transgene expression on the gene expression profile in the bladder.**

Background corr dist: KL-Divergence = 0.1519, L1-Distance = 0.0383, L2-Distance = 0.0029, Normal std = 0.3705

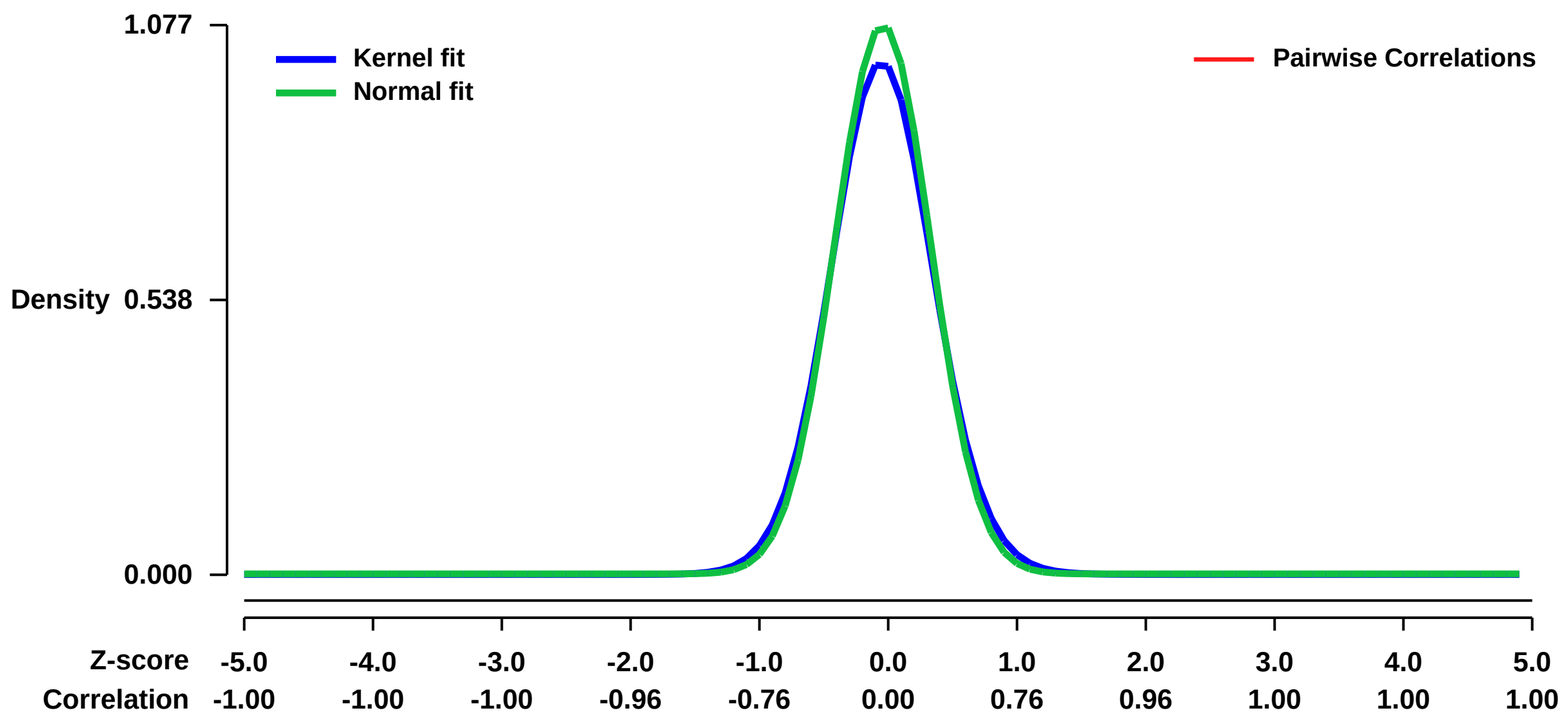

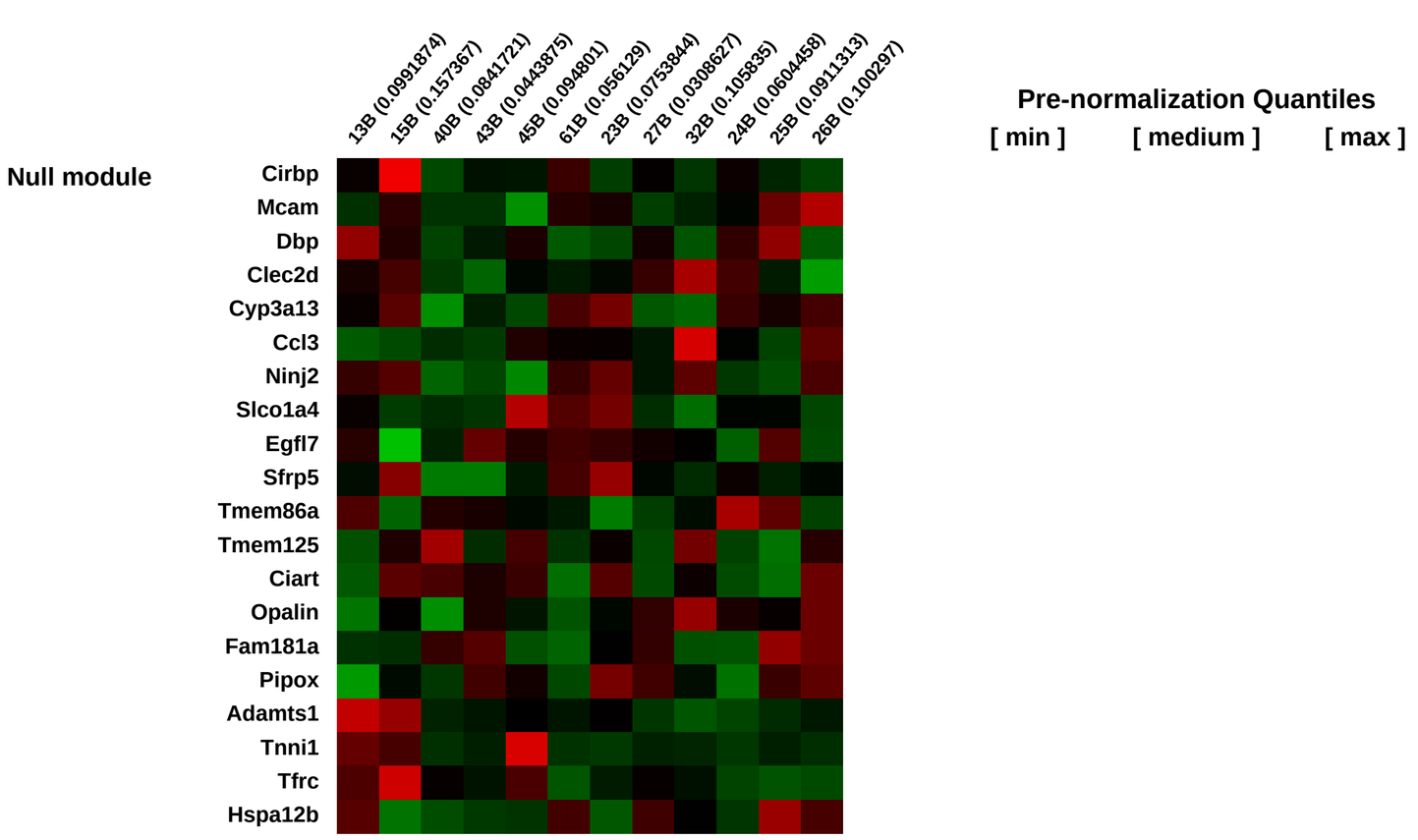

GEO Series "GSE4818" Expression Profiles

Num of samples in this series: 21

Scale of expression profile Z-scores

-3.0 -2.0 -1.0 0.0 1.0 2.0 3.0

GEO Link:	**http://www.ncbi.nlm.nih.gov/geo/query/acc.cgi?acc=GSE4818**
Status:	**Public on May 12 2006**
Title:	**Gene expression profiling of whole testes in embryonic (gestational day 11, 12, 14, 16 & 18) and postnatal day 2 mice. (GUDMAP Series ID: 3)**
Organism:	**Mus musculus**
Experiment type:	**Expression profiling by array**
Platform:	**GPL1261**
Pubmed ID:	
Summary & Design:	**Summary:** **The overall objective of this proposal is to map the temporal and spatial dynamics of gene expression in the fetal mouse testis at key developmental timepoints. Urogenital tract malformations are the most common birth defects in males and their incidence together with other male reproductive health concerns such as reduced fertility and testicular cancer are reportedly on the rise in the human population. To better understand the impact of genetic factors and environmental influences on testicular development, it is important to first understand normal gene expression patterns and signaling cascades within the fetal testis during development. The goal of this study is to identify cell-specific genes that can be used as biomarkers for key differentiation events.** **Keywords: developmental time course** **Overall design:** **Day to day comparison in whole testes throughout development with triplicates at each time point. Each sample is a pair of testes from a single animal and each animal is taken from a different dam.**

Background corr dist: KL-Divergence = 0.1571, L1-Distance = 0.0451, L2-Distance = 0.0046, Normal std = 0.4081

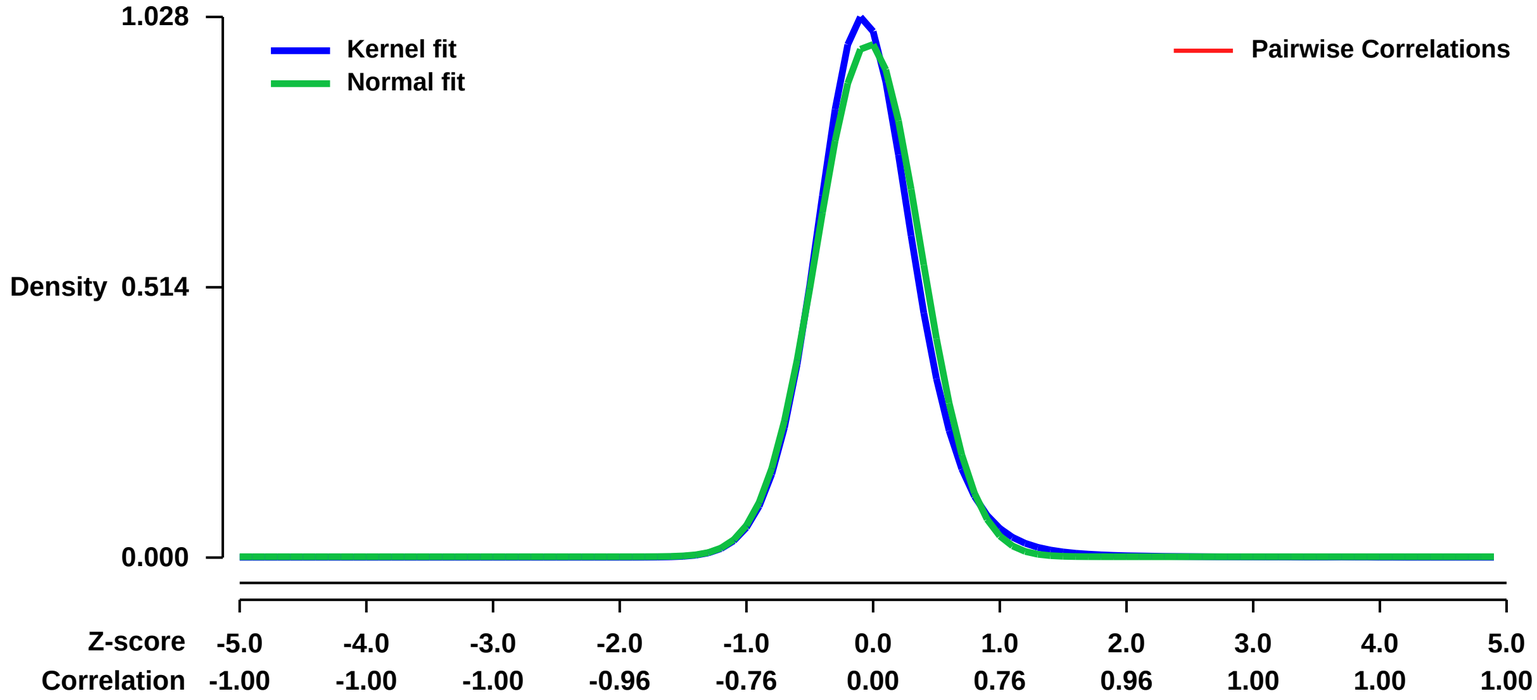

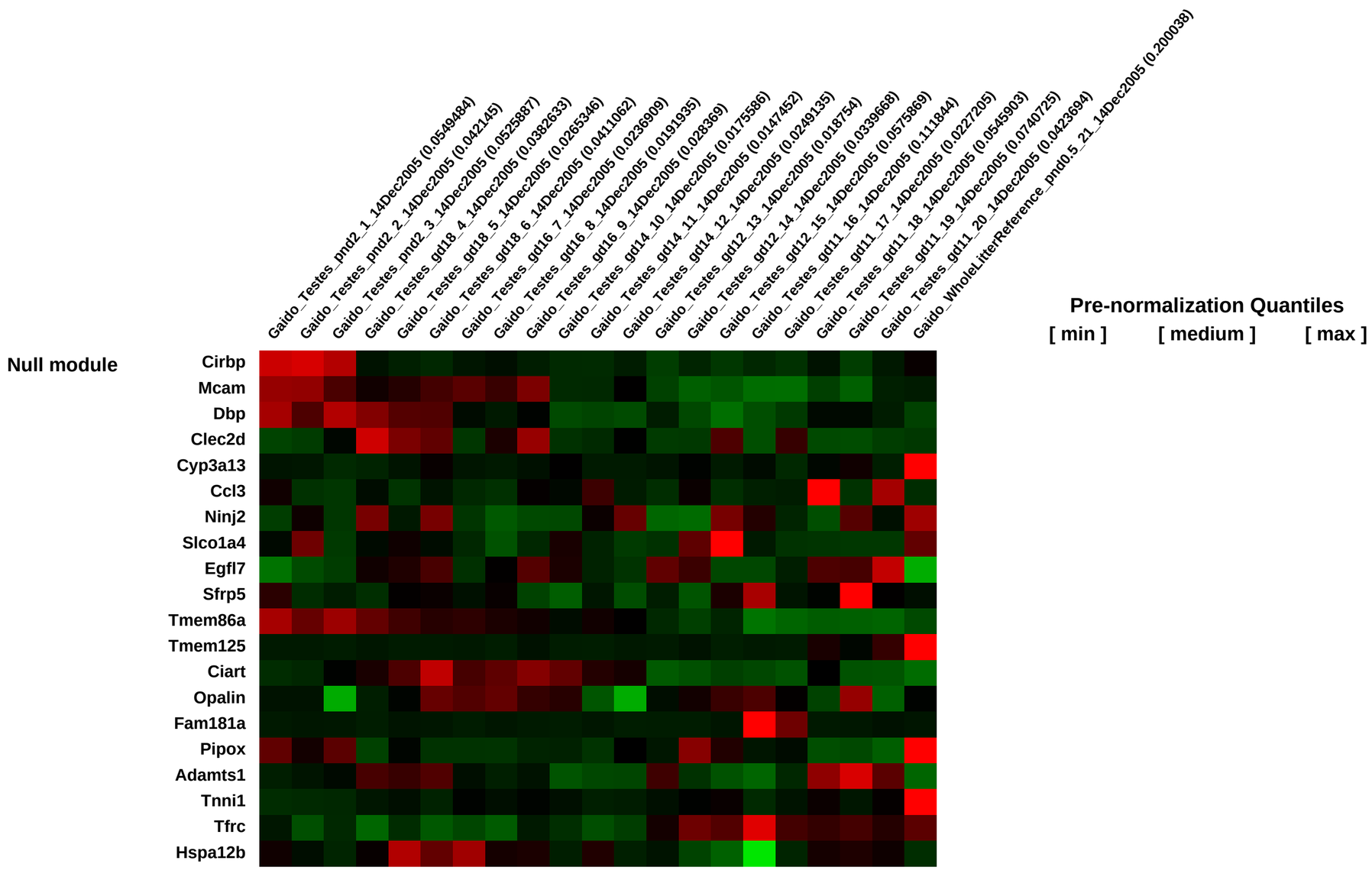

GEO Series "GSE48261" Expression Profiles

Num of samples in this series: 14

Scale of expression profile Z-scores

-3.0 -2.0 -1.0 0.0 1.0 2.0 3.0

GEO Link:	http://www.ncbi.nlm.nih.gov/geo/query/acc.cgi?acc=GSE48261
Status:	Public on Mar 20 2014
Title:	Gene expression in mouse hematopoietic stem and multi-potent progenitor cells with temporally defined divisional histories
Organism:	Mus musculus
Experiment type:	Expression profiling by array
Platform:	GPL1261
Pubmed ID:	24749072
Summary & Design:	**Summary:** Homeostatic hematopoietice stem cells (HSCs) with greater divisional history lose repopulating potential after very few cell divisions. Divisional history overrides both phenotype and immediate quiescence in determining functional activity. In GFP label retaining system GFP is progressively diluted when cells proceed through a cascade of divisions. We used a GFP label retaining system and performed microarray expression analyses to track the changes in the gene expression profile of bone marrow (BM) LSK cells that relates to divisional history during homeostasis. **Overall design:** Chromatins are dynamically labeled in a double transgenic mouse (huCD34-tTA X Tet-O-H2B-GFP) by the expression of GFP tagged Histone2B. The expression is driven by a human CD34 promoter active specifically in all bone marrow (BM) hematopoietic stem and multi-potent progenitor cells. This is a pulse/chase Tet-off system where cells constantly label with GFP. Upon administration of Doxycyclin (Dox) to GFP labeled animals, further labeling is stopped during the chase period. With each round of cell division, the newly synthesized endogenous H2B will dilute H2B-GFP by one-half, whereas cells that donâ t divide will retain GFP labeling. Therefore, the level of GFP reflects how many times cells have divided over the period of Dox treatment (chase). Animals were treated with Dox for 12 weeks starting at the age of 6-8 weeks. After chase, BM Lineage negative, Sca1+, Kit+ (LSK) cells with varying GFP levels were sorted for mRNA extraction. GFP levels were ranked from 0 to 4 based on the kinetic analysis of GFP fully labeled LSK cells and obvious peaks in the GFP histogram of LSK cells after Dox treatment. There is approximately 1-2 cell divisions between each level of GFP.

Background corr dist: KL-Divergence = 0.0810, L1-Distance = 0.0924, L2-Distance = 0.0149, Normal std = 0.5480

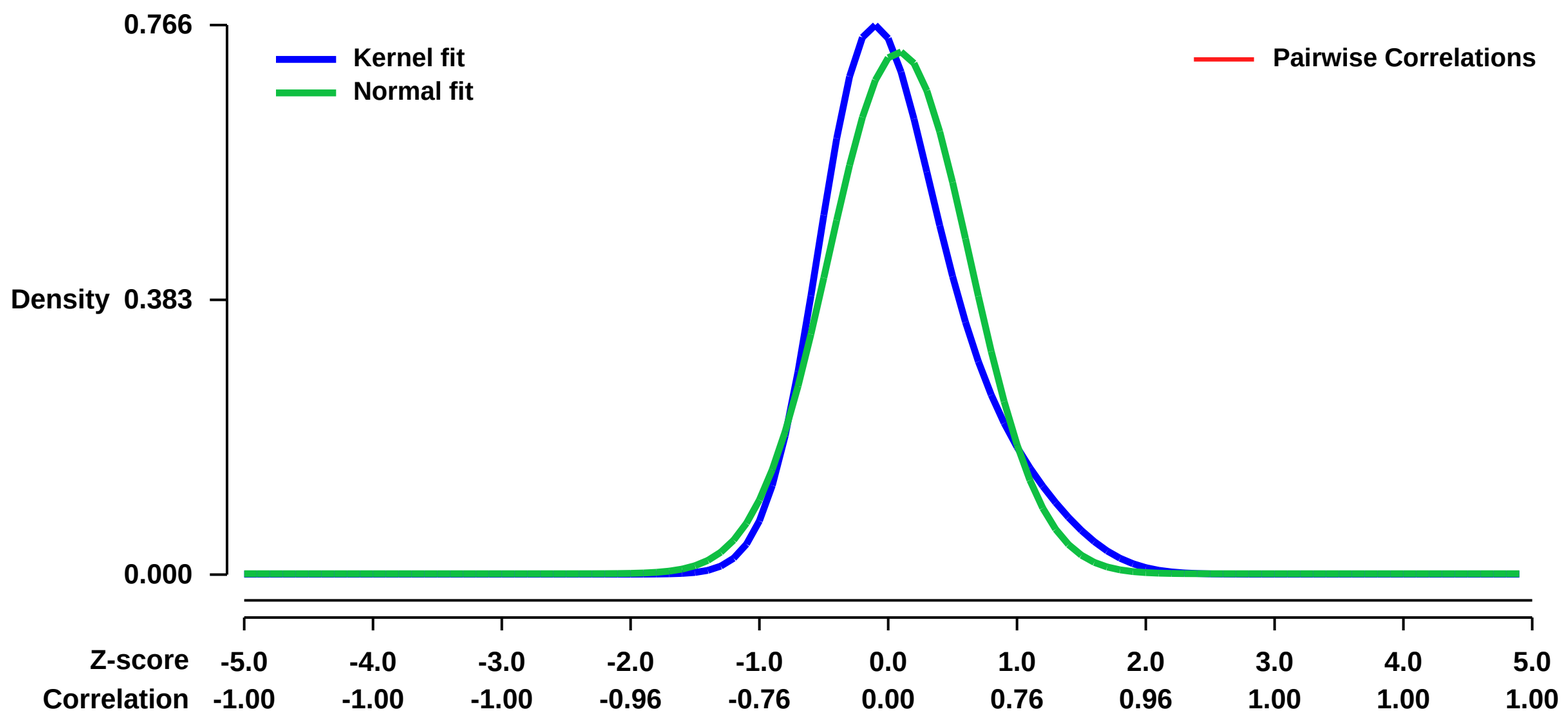

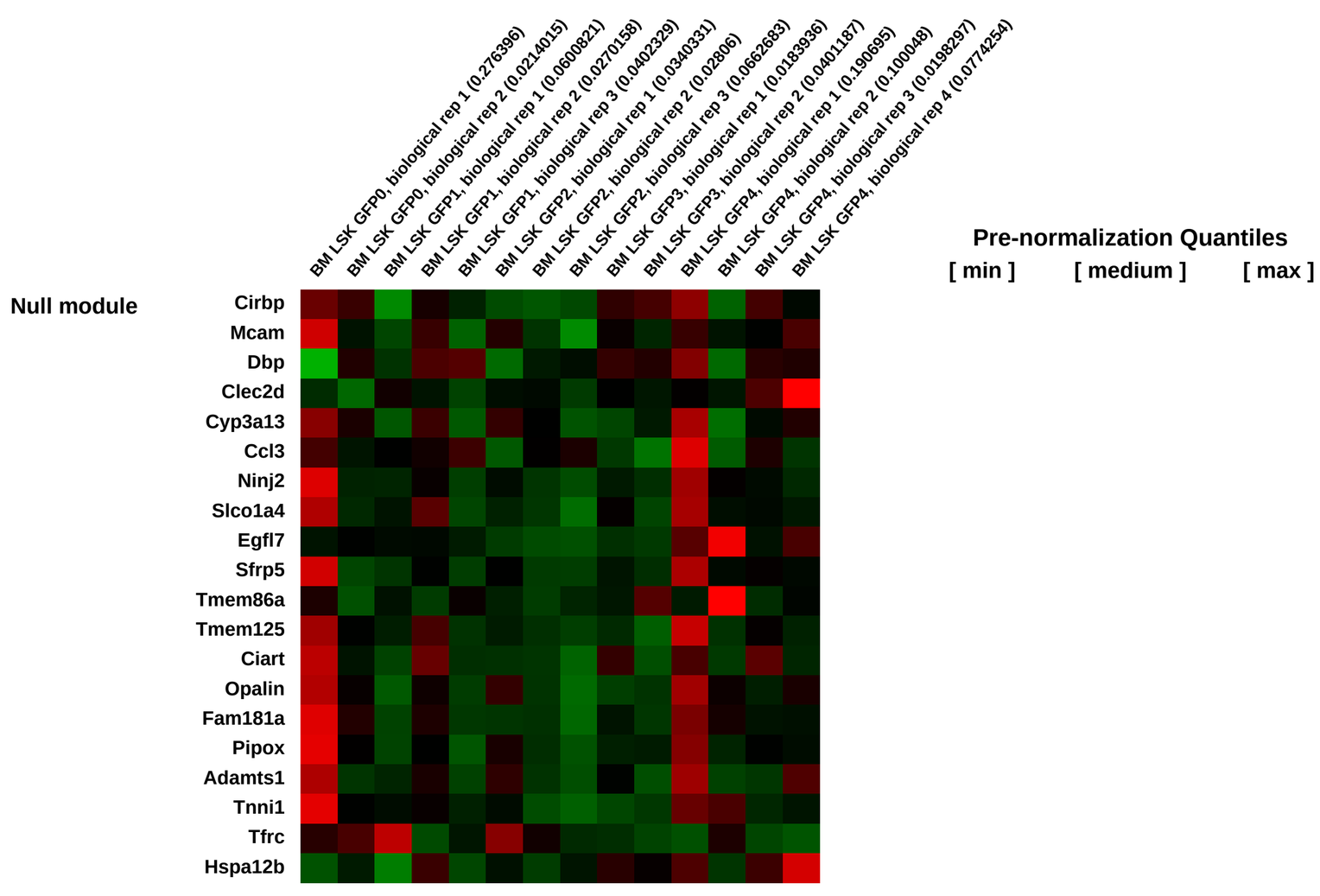

GEO Series "GSE48338" Expression Profiles

Num of samples in this series: 8

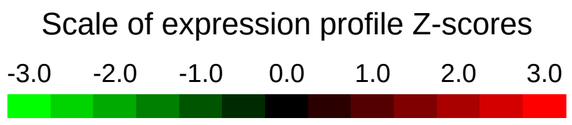

GEO Link:	http://www.ncbi.nlm.nih.gov/geo/query/acc.cgi?acc=GSE48338
Status:	Public on Jun 03 2014
Title:	Tpl2 promotes chemokine/chemokine receptor expression and macrophage migration during acute inflammation
Organism:	Mus musculus
Experiment type:	Expression profiling by array
Platform:	GPL1261
Pubmed ID:	24713702
Summary & Design:	**Summary:** In autoimmune diseases, accumulation of activated leukocytes correlates with inflammation and disease progression, and therefore, disruption of leukocyte trafficking is an active area of research. The protein kinase Tpl2 (MAP3K8) regulates leukocyte inflammatory responses and is also being investigated for therapeutic inhibition during autoimmunity. Herein, we addressed the contribution of Tpl2 to the regulation of macrophage chemokine and chemokine receptor expression and subsequent migration in vivo using a mouse model of Tpl2 ablation. We found that gene expression of the chemokine ligands CCL2, CCL7, CXCL2, and CXCL3 as well as the chemokine receptors CCR1 and CCR5 were reduced in macrophages from the bone marrow and peritoneal cavities of tpl2-/- mice following stimulation with LPS. LPS stimulation repressed chemokine receptor expression of CCR1, CCR2 and CCR5. Notably, LPS-induced repression of CCR1 and CCR5 was significantly enhanced in Tpl2-deficient macrophages and was observed to be dependent upon Erk activation and independent of PI3K and mTOR signaling. Consistent with alterations in chemokine and chemokine receptor expression, tpl2-/- macrophages were defective in trafficking to the peritoneal cavity following thioglycollate-induced inflammation. Overall, this study demonstrates a Tpl2-dependent mechanism for macrophage expression of both chemokine receptors and their ligands and provides further insight into how Tpl2 inhibition may disrupt inflammatory networks in vivo. **Overall design:** microarray was used to profile the genome-wide expression patterns in Tpl2 wild-type and deficient macrophage.

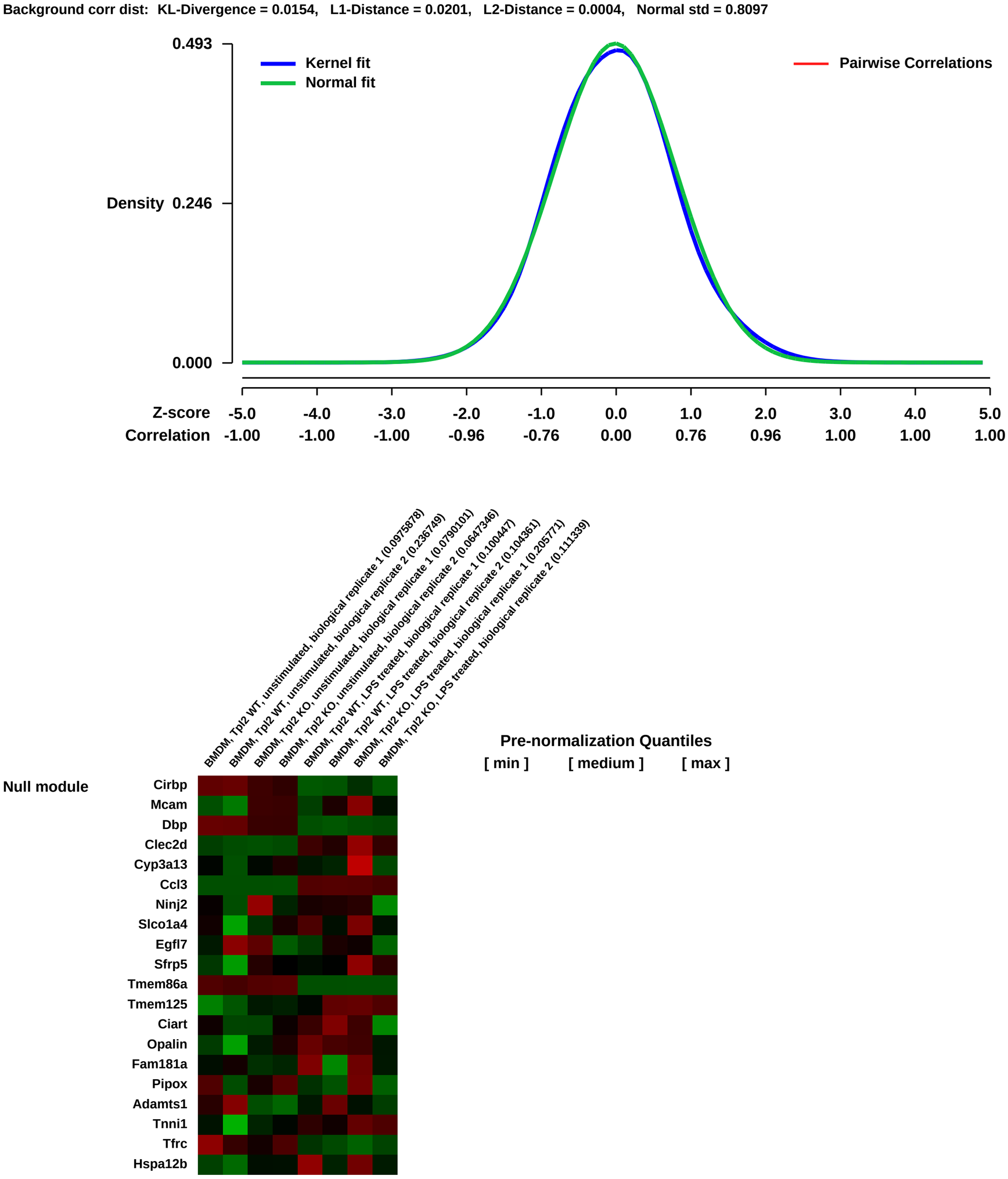

GEO Series "GSE48369" Expression Profiles

Num of samples in this series: 36

Scale of expression profile Z-scores

-3.0 -2.0 -1.0 0.0 1.0 2.0 3.0

GEO Link:	http://www.ncbi.nlm.nih.gov/geo/query/acc.cgi?acc=GSE48369
Status:	Public on Aug 20 2013
Title:	Expression data of sleeping, waking, and sleep deprived in adult heterozygous Cnp â eGFP-L10a mice
Organism:	Mus musculus
Experiment type:	Expression profiling by array
Platform:	GPL1261
Pubmed ID:	24005282
Summary & Design:	**Summary:** Transcriptomic studies revealed that hundreds of mRNAs show differential expression in the brains of sleeping versus awake rats, mice, flies, and sparrows. Although these results have offered clues regarding the molecular consequences of sleep and sleep loss, their functional significance thus far has been limited. This is because the previous studies pooled transcripts from all brain cells, including neurons and glia. In the following experiment, we studied the specific effects of sleep and wake conditions on glia cells of mouse cerebral cortex using the genetically targeted translating ribosome affinity purification (TRAP) methodology. We used bacterial artificial chromosome (BAC) transgenic mice expressing EGFP tagged ribosomal protein L10a in oligodendrocytes which constitute a defined cellular population of the mouse brain. Using this approach, we could extract only the oligodendrocitic mRNAs, and only those already committed to be translated into proteins (L10a is part of the translational machinery). **Overall design:** Six mice for each vigilant state group (sleep (S), waking (W), and sleep deprivation (SD)) were considered. For each animal, one forebrain sample was immediately processed. Samples were immunoprecipitated to isolate oligodendrocytes. The precipitated portion formed the bound sample (IP) containing olidodendrocytes and the remaining part formed the unbound sample (UB) containing all the remaining cell types (neurons and other glia cells). Then, both IP and UB samples were processed and RNA was extracted.

Background corr dist: KL-Divergence = 0.0780, L1-Distance = 0.0388, L2-Distance = 0.0022, Normal std = 0.4968

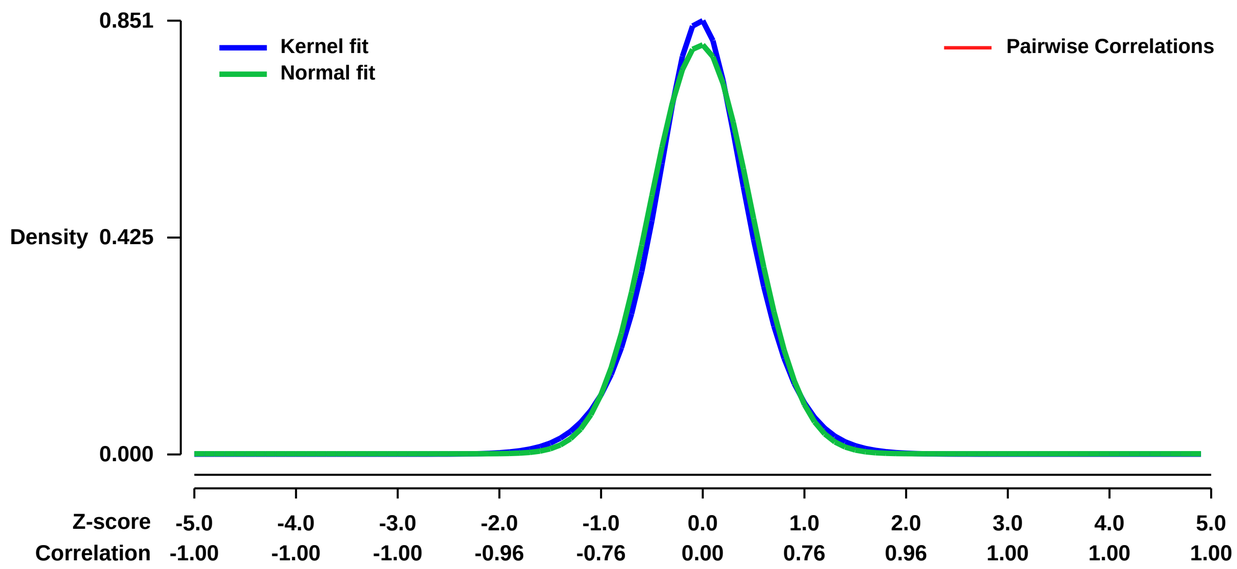

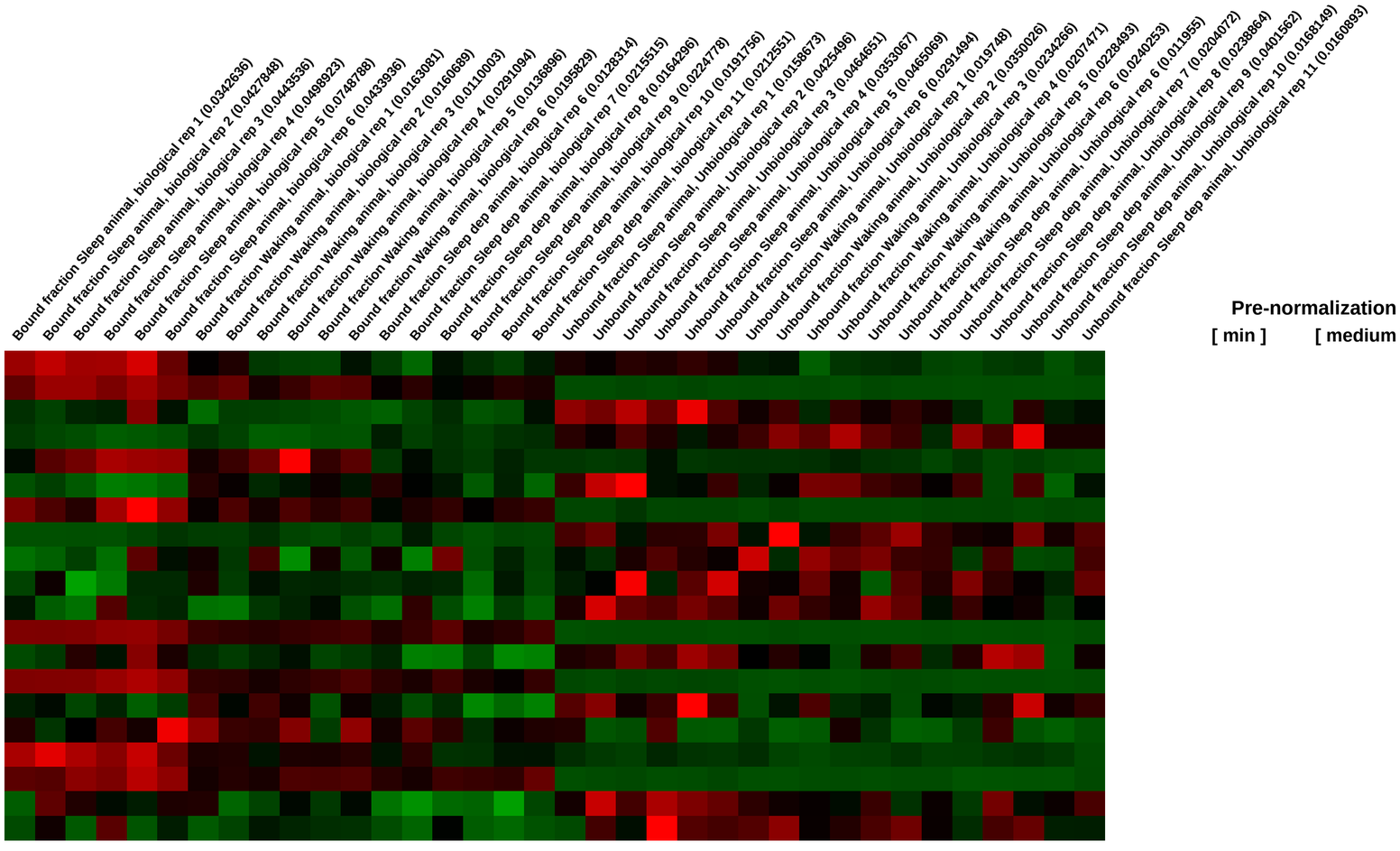

GEO Series "GSE48397" Expression Profiles

Num of samples in this series: 10

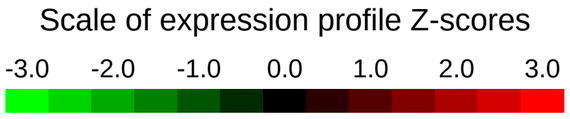

GEO Link:	http://www.ncbi.nlm.nih.gov/geo/query/acc.cgi?acc=GSE48397
Status:	Public on Jul 10 2013
Title:	Expression data from (mouse) normal lung fibroblasts and carcinoma-associated fibroblasts
Organism:	Mus musculus
Experiment type:	Expression profiling by array
Platform:	GPL1261
Pubmed ID:	22962265
Summary & Design:	**Summary:** Cancer-associated fibroblasts (CAFs) have been reported to support tumor progression by a variety of mechanisms. However, their role in the progression of non-small cell lung cancer (NSCLC) remains poorly defined. In addition, the extent to which specific proteins secreted by CAFs contribute directly to tumor growth is unclear. To study the role of CAFs in NSCLC, a cross-species functional characterization of mouse and human lung CAFs was performed, including gene expression analysis comparing normal mouse lung fibroblasts (NFs) and mouse lung CAFs to seek for differentially-expressed secreted proteins. Gene expression microarrays were used to identify transcriptomic changes between NFs and CAFs that may contribute to their different tumor-enhancing capacity. **Overall design:** NFs and CAFs were grown in vitro for RNA extraction and hybridization on mouse 430_2 Affymetrix microarrays

Background corr dist: KL-Divergence = 0.0594, L1-Distance = 0.0233, L2-Distance = 0.0009, Normal std = 0.5290

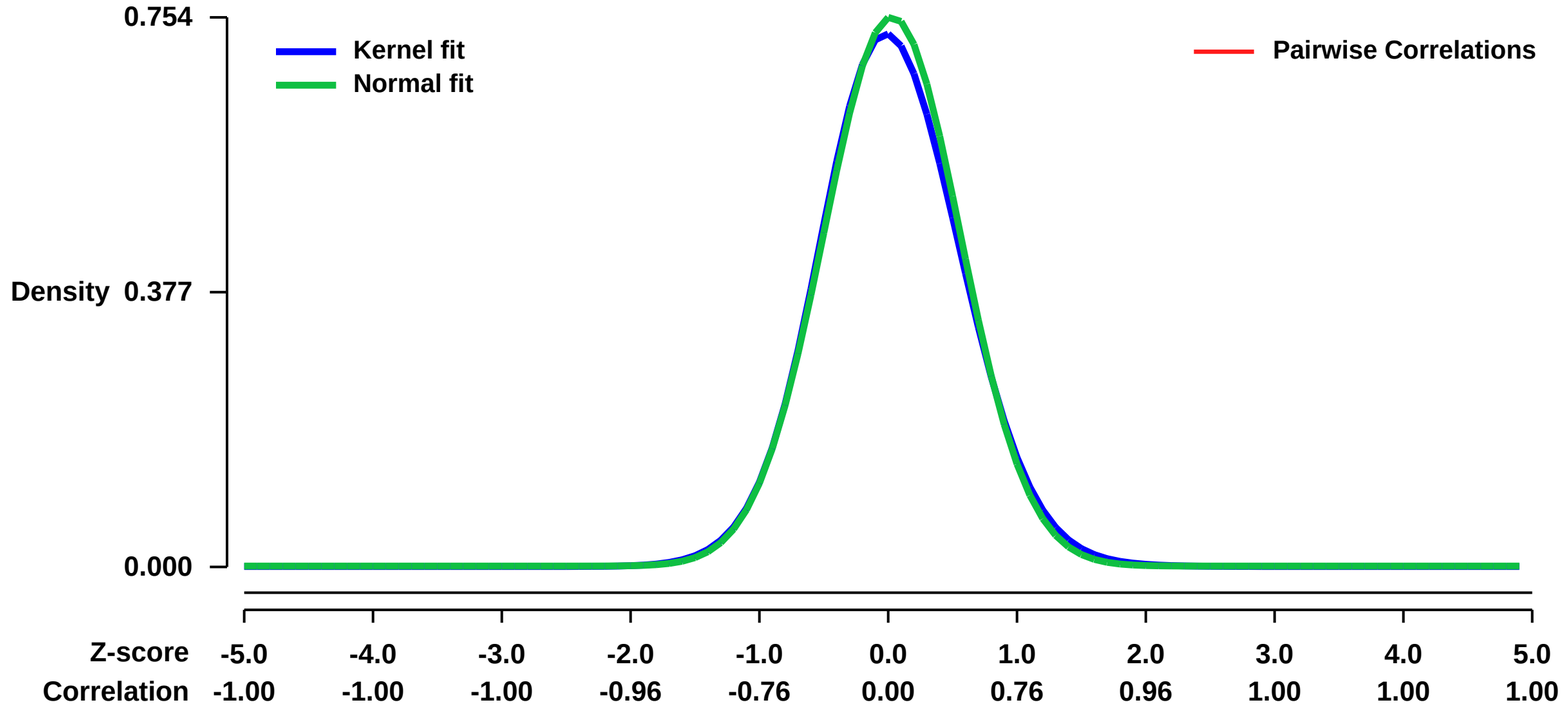

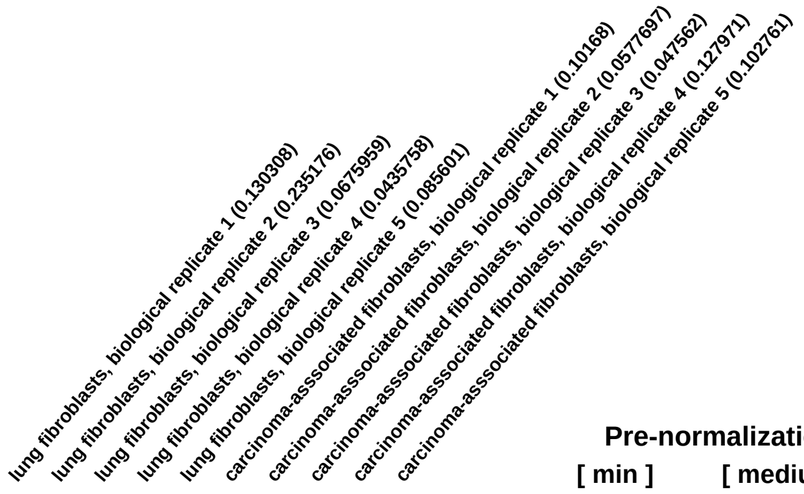

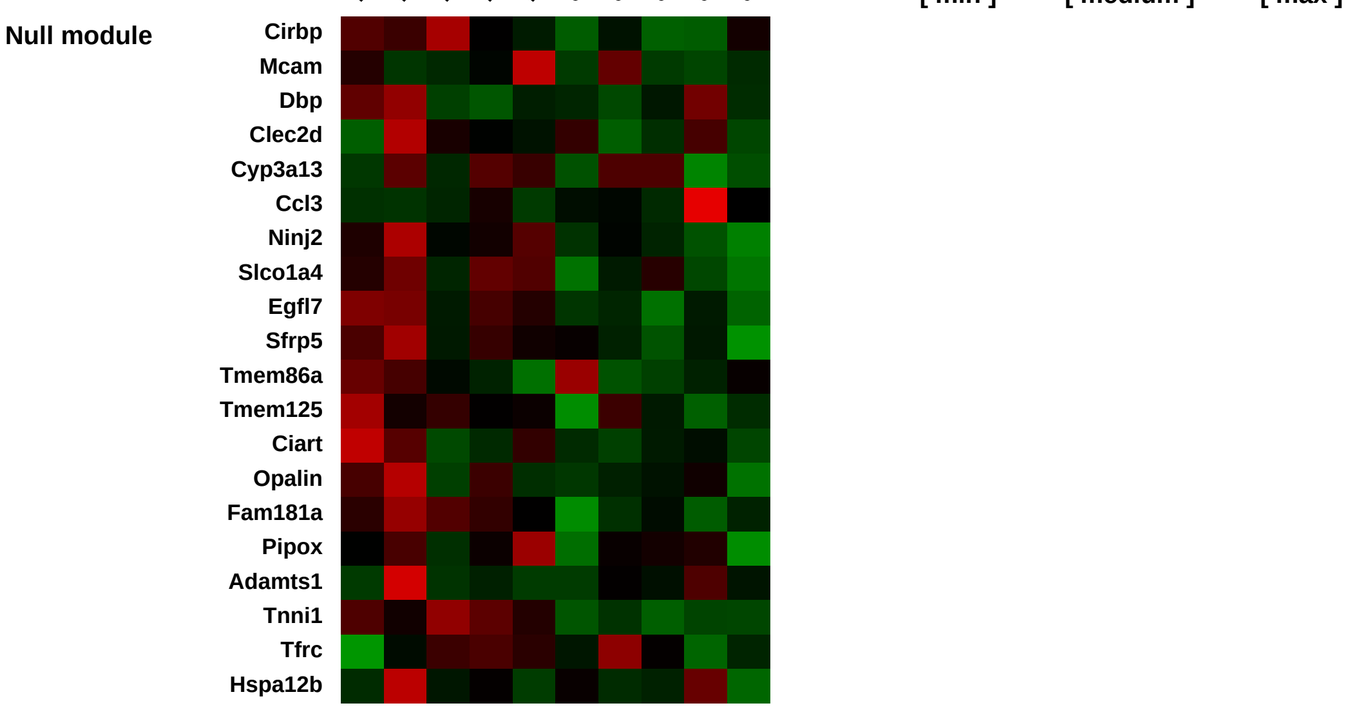

GEO Series "GSE48522" Expression Profiles

Num of samples in this series: 11

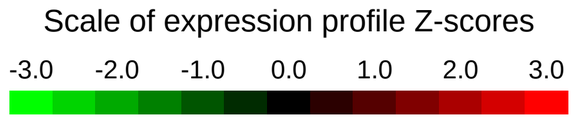

GEO Link:	http://www.ncbi.nlm.nih.gov/geo/query/acc.cgi?acc=GSE48522
Status:	Public on Jan 26 2014
Title:	Akt signalling leads to stem cell activation and promotes tumour development in epidermis.
Organism:	Mus musculus
Experiment type:	Expression profiling by array
Platform:	GPL1261
Pubmed ID:	24504902
Summary & Design:	**Summary:** A permantly active form of the oncogene Akt was expressed in the keratinocytes of the basal proliferative layer of the epidermis. Stem cells of the hair follicle expressing the cell surface marker CD34 were isolated. RNA form the CD34(+) and CD34(-) keratinocytes was extracted and and hybridized to Mouse Genome 430 2.0 Affymetrix arrays. **Overall design:** Gene expression was compared between CD34(+) hair follicle stem cells and CD34(-) cells isolates from the back skin of K5-myrAkt transgenic mice.

Background corr dist: KL-Divergence = 0.0750, L1-Distance = 0.0312, L2-Distance = 0.0018, Normal std = 0.4914

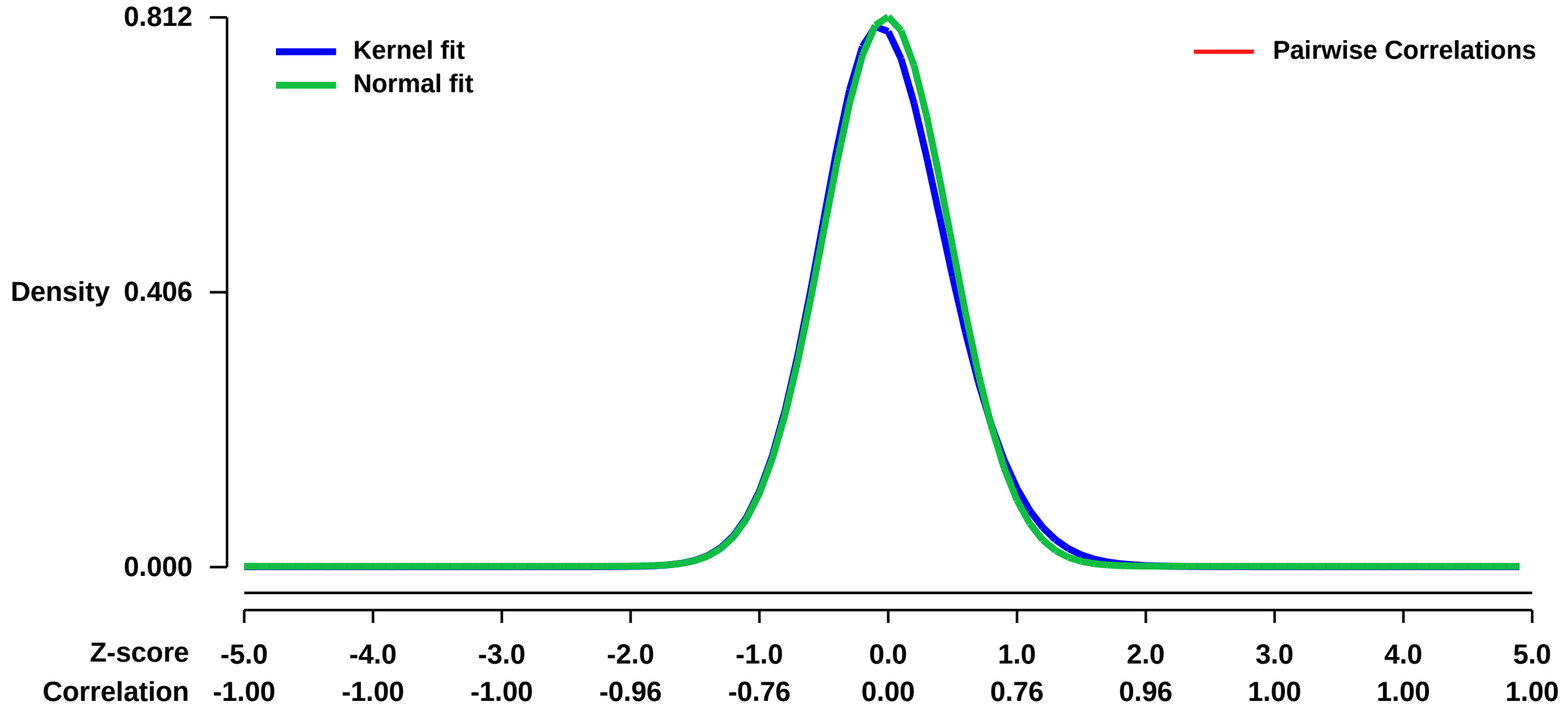

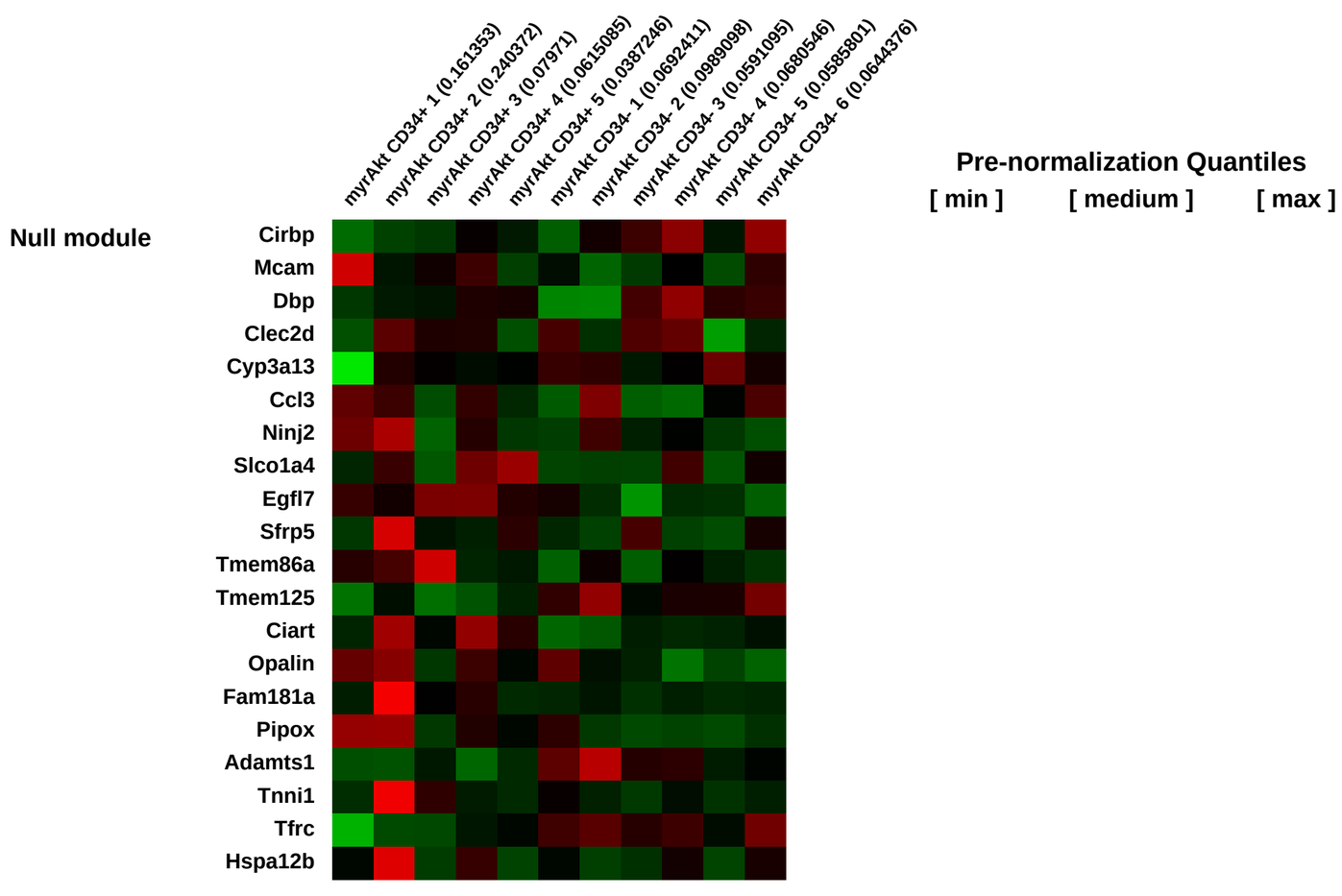

GEO Series "GSE48622" Expression Profiles

Num of samples in this series: 16

Scale of expression profile Z-scores

-3.0 -2.0 -1.0 0.0 1.0 2.0 3.0

GEO Link:	http://www.ncbi.nlm.nih.gov/geo/query/acc.cgi?acc=GSE48622
Status:	Public on Jul 10 2013
Title:	Transcriptional Profiling of Neuronal APP/APLP2 Double-Conditional Knockout Mice.
Organism:	Mus musculus
Experiment type:	Expression profiling by array
Platform:	GPL1261
Pubmed ID:	20855613
Summary & Design:	**Summary:** Gene expression analysis of 2-month-old APP/APLP2 double-conditional Knockout (N-dCKO) mice and littermate APLP2 knockout controls, APP knockout and wildtype controls. **Overall design:** Mouse hippocampus were dissected for RNA extraction and hybridization on Affymetrix microarrays.

Background corr dist: KL-Divergence = 0.2702, L1-Distance = 0.0634, L2-Distance = 0.0108, Normal std = 0.2920

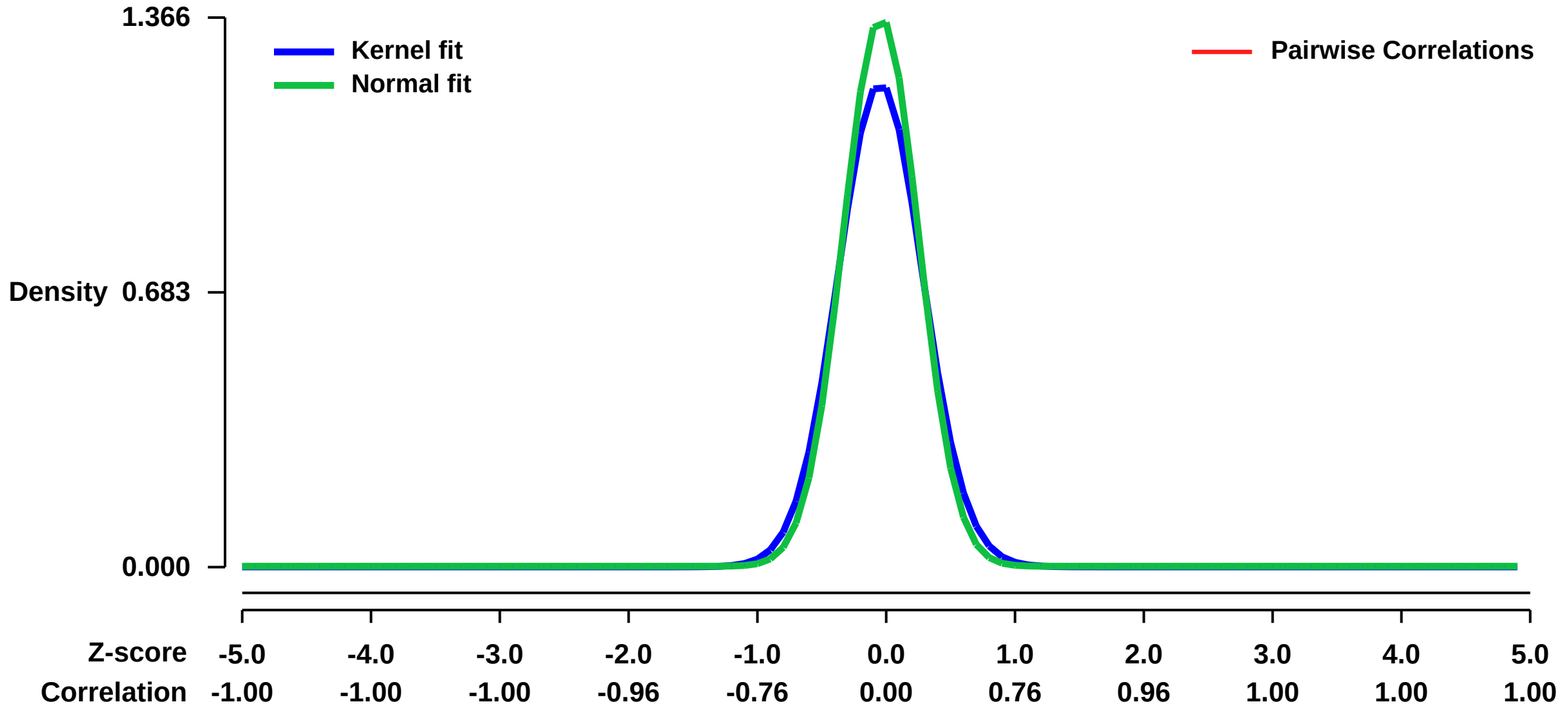

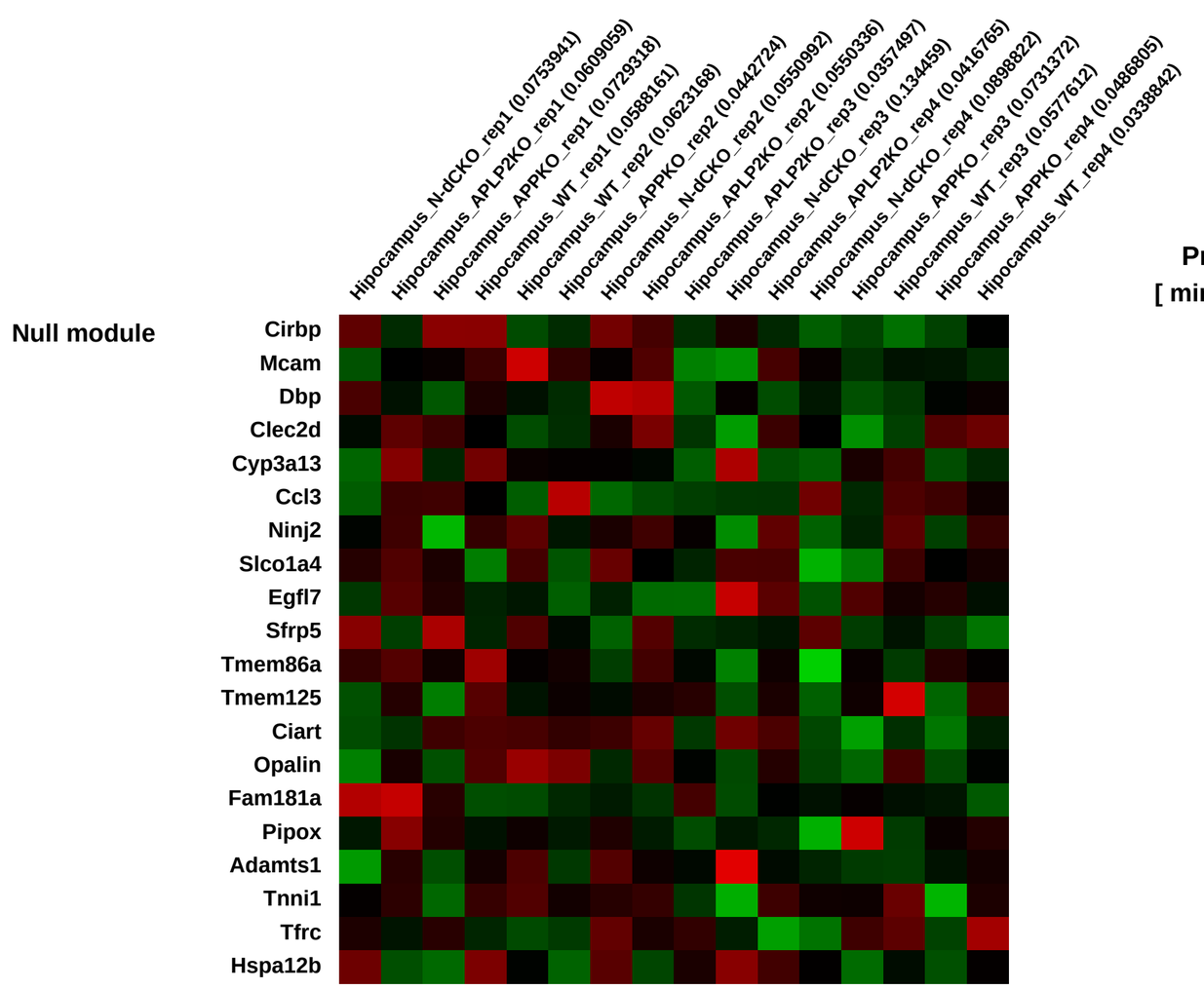

GEO Series "GSE4866" Expression Profiles

Num of samples in this series: 10

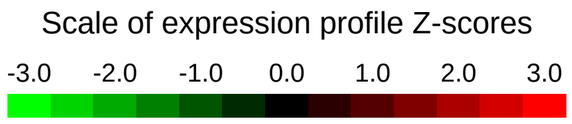

GEO Link:	http://www.ncbi.nlm.nih.gov/geo/query/acc.cgi?acc=GSE4866
Status:	Public on May 18 2007
Title:	The role of mtDNA mutations in age-related hearing loss in mice carrying a mutator DNA polymerase gamma
Organism:	Mus musculus
Experiment type:	Expression profiling by array
Platform:	GPL1261
Pubmed ID:	17363114
Summary & Design:	**Summary:** Mitochondrial DNA (mtDNA) mutations may contribute to aging and age-related disorders. Previously, we created mice expressing a proofreading-deficient version of the mtDNA polymerase gamma (Polg) which accumulate age-related mtDNA mutations and display premature aging. Here we performed microarray gene expression profiling to identify mtDNA mutation-responsive genes in the cochlea of aged mitochondrial mutator mice. Age-related accumulation of mtDNA mutations was associated with transcriptional alternations consistent with reduced inner ear function, mitochondrial dysfunction, neurodegeneration, and reduced cell structural modulation. Hearing assessment and histopathological results confirmed that aged PolgD257A/D257A (D257A) mice exhibited moderate hearing loss and severe cochlear degenerations. Age-related accumulation of mtDNA mutations also resulted in alternations in gene expression consistent with induction of apoptosis, proteolysis, stress response, and reduced DNA repair. TUNEL (Terminal deoxynucleotidyl transferase-mediated dUTP nick-end labeling) assay confirmed that the cochleae from aged D257A mice showed significantly more TUNEL positive cells compared to wild-type (WT) mice. The levels of cleaved caspase-3 were also found to increase in the cochleae of aged D257A mice. These observations provide evidence that age-related accumulation of mtDNA mutations is associated with apoptotic cell death in aged cochlea. Our results provide the first global view of molecular events associated with mtDNA mutations in postmitotic tissue, and suggest that apoptosis is the major mechanism of mtDNA mediated cell death in the development of age-related hearing disorder. **Keywords:** disease state analysis **Overall design:** Affymetrix standard spike controls were used in all experiments (eukaryotic hybridization control kit). Quality control measures were not used. No replicates were done. Dye swap was not used.

Background corr dist: KL-Divergence = 0.0920, L1-Distance = 0.0291, L2-Distance = 0.0015, Normal std = 0.4506

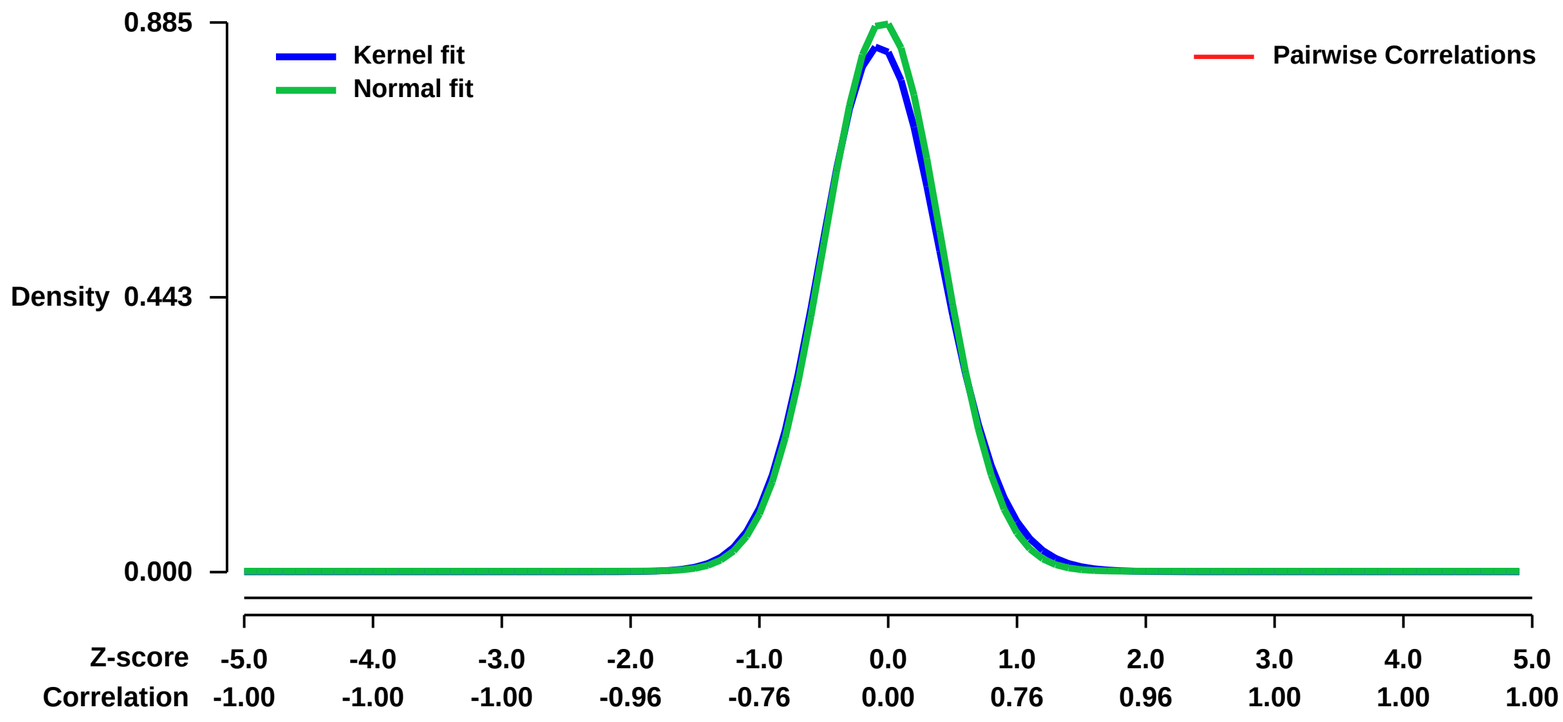

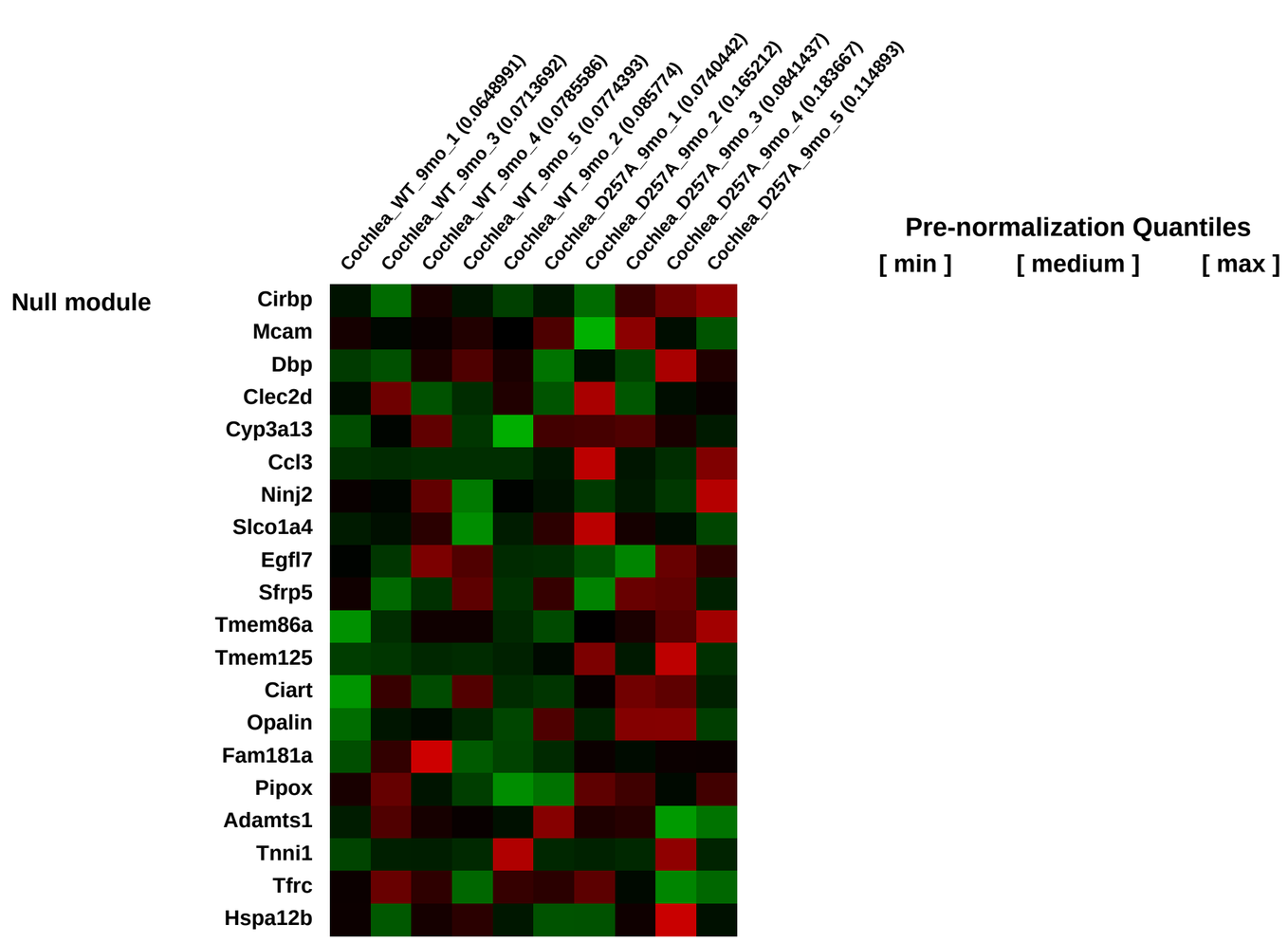

GEO Series "GSE48790" Expression Profiles

Num of samples in this series: 8

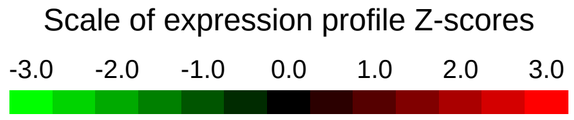

GEO Link:	**http://www.ncbi.nlm.nih.gov/geo/query/acc.cgi?acc=GSE48790**
Status:	**Public on Jul 12 2013**
Title:	**Expression data from GTF2i mutated ES cells**
Organism:	**Mus musculus**
Experiment type:	**Expression profiling by array**
Platform:	**GPL1261**
Pubmed ID:	**23831514**
Summary & Design:	**Summary:** **Data present the expression analysis of different mouse ES cell line with altered expression of GTF2I.** **Overall design:** **We used microarrays to detail the global programme of gene expression underlying altered expression of GTF2I and identified distinct classes of deregulated genes**

Background corr dist: **KL-Divergence = 0.0303, L1-Distance = 0.0391, L2-Distance = 0.0018, Normal std = 0.6989**

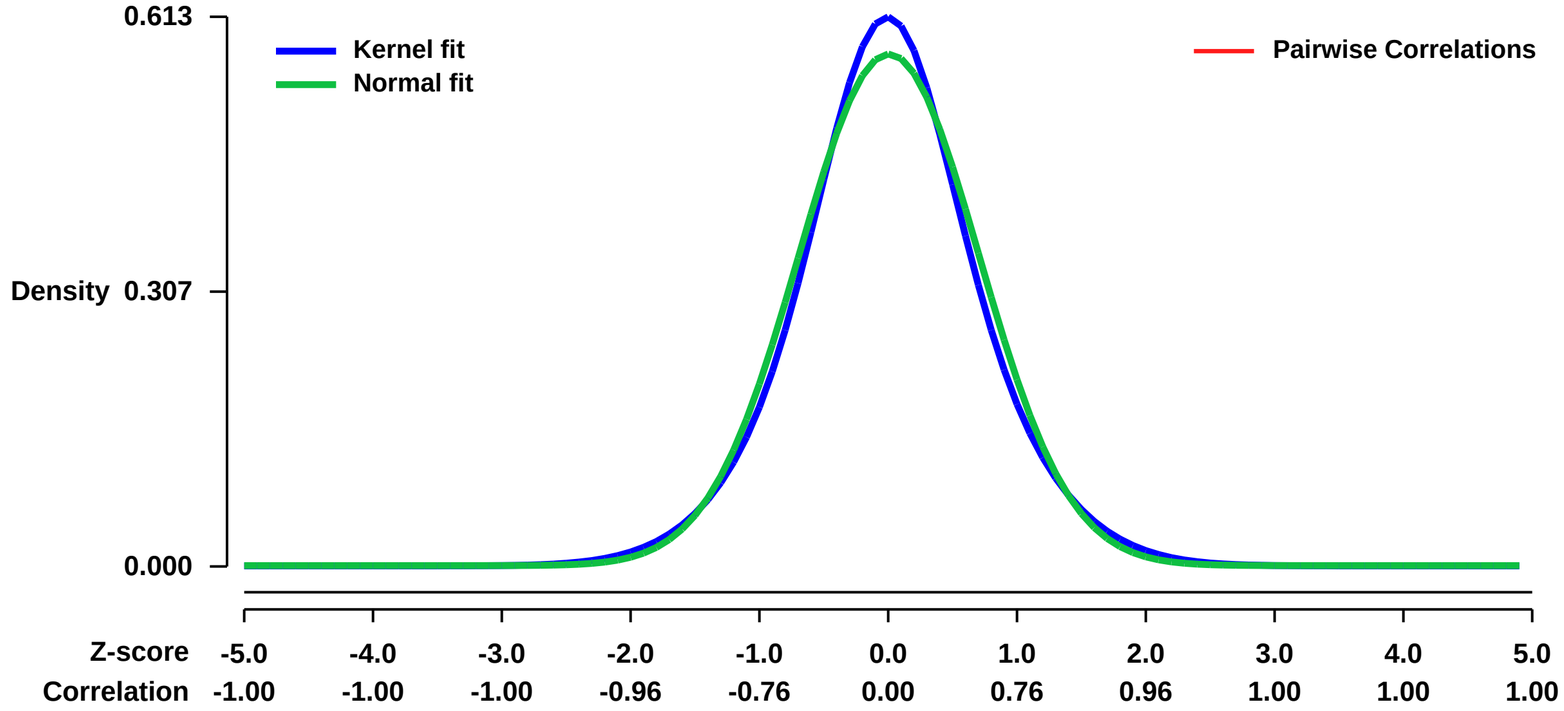

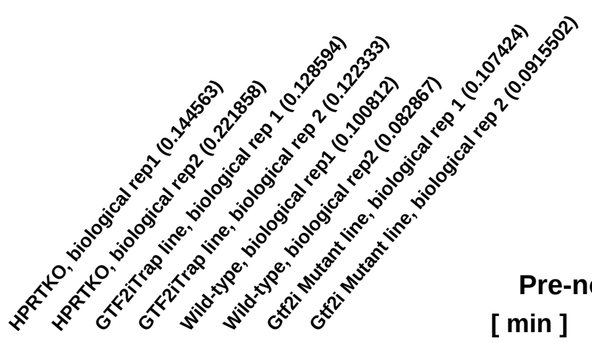

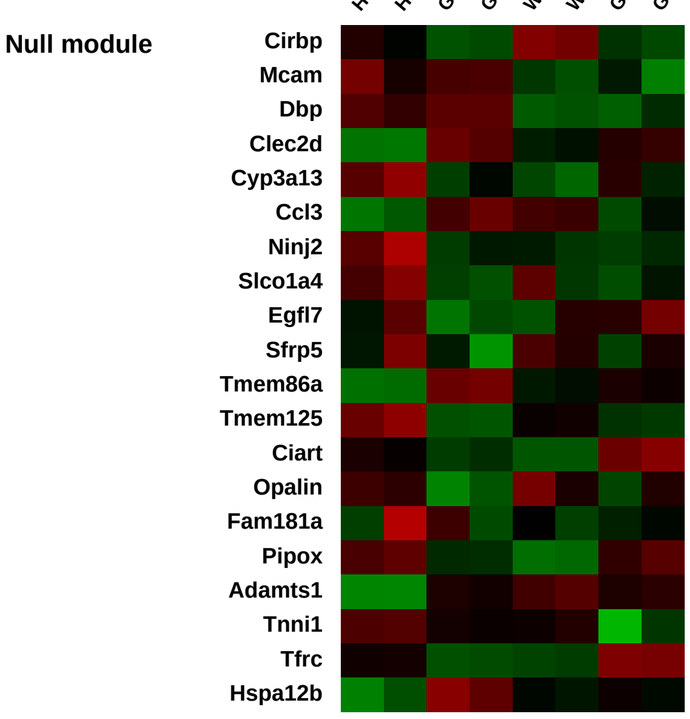

GEO Series "GSE48884" Expression Profiles

Num of samples in this series: 12

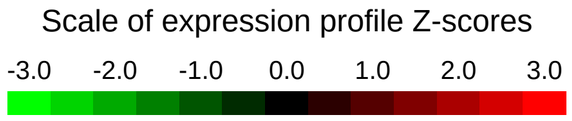

GEO Link:	http://www.ncbi.nlm.nih.gov/geo/query/acc.cgi?acc=GSE48884
Status:	Public on Jul 16 2013
Title:	Cyclin D1 determines estrogen depependent signaling in mouse mammary gland.
Organism:	Mus musculus
Experiment type:	Expression profiling by array
Platform:	GPL1261
Pubmed ID:	23864650
Summary & Design:	**Summary:** Ovariectomized virgin Ccnd1-/- and Ccnd1+/+ mice (5 weeks of age) were allowed to recuperate for 2 weeks. The mice were assigned to either replacement pellets containing E2 (0.75 mg, 60-day release) or pellet containing placebo. Mice were sacrificed at day 7 after pellet implantation. RNA extracted from mammary glands (3 each group) was labeled and used to probe Affymetrix 430_2.0 arrays. **Overall design:** Six separate control Ccnd1+/+ C57BL/6 were compared to six Ccnd1-/- C57BL/6 mice. 3 mice in each group treated with placebo and three mice treated with E2

Background corr dist: KL-Divergence = 0.0851, L1-Distance = 0.0269, L2-Distance = 0.0012, Normal std = 0.4687

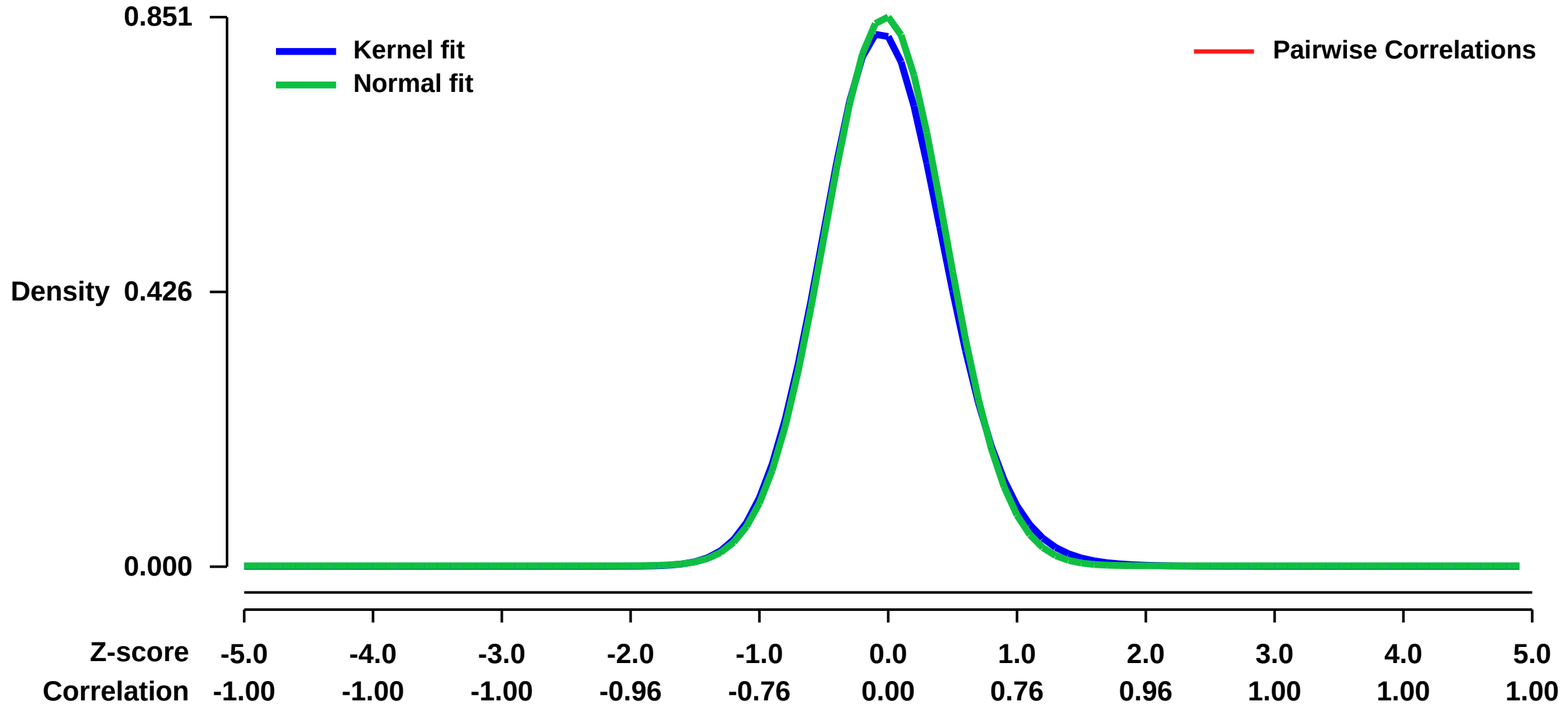

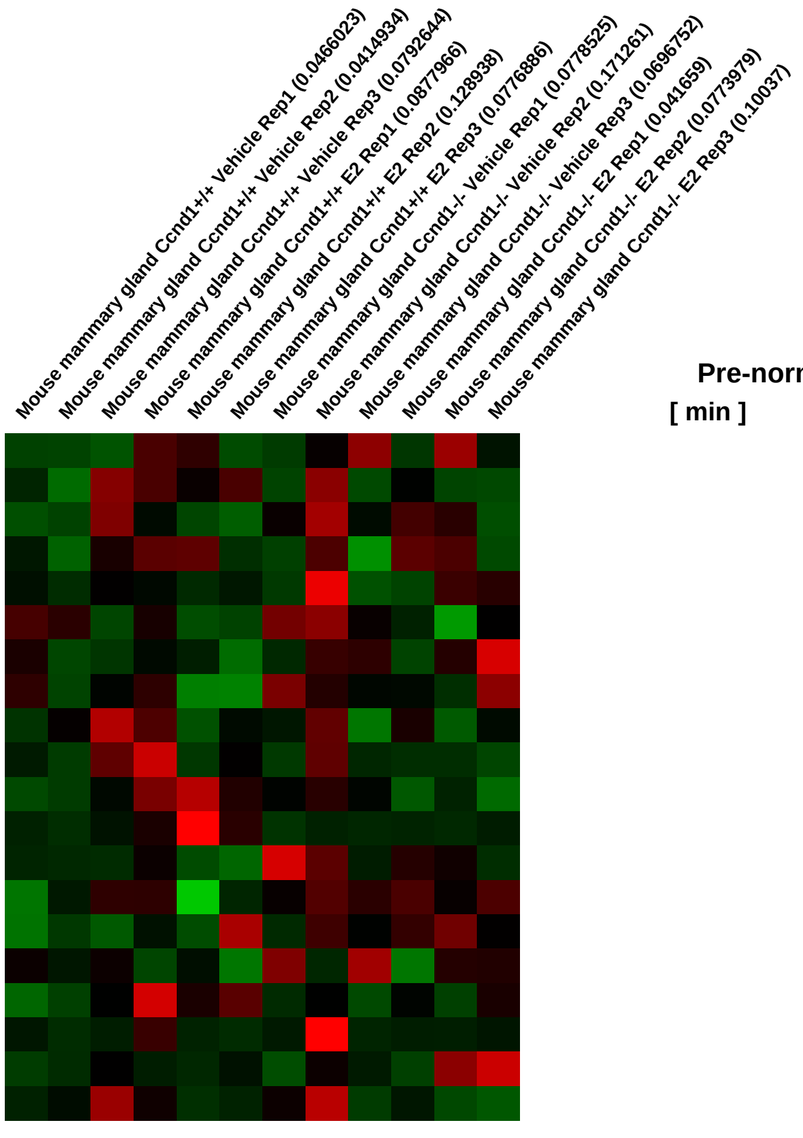

GEO Series "GSE48932" Expression Profiles

Num of samples in this series: 12

Scale of expression profile Z-scores

-3.0 -2.0 -1.0 0.0 1.0 2.0 3.0

GEO Link:	**http://www.ncbi.nlm.nih.gov/geo/query/acc.cgi?acc=GSE48932**
Status:	**Public on Sep 04 2013**
Title:	**Analysis of gene expression changes induced in wild-type or Atf6a-/- mice by treatment with tunicamycin for 8h**
Organism:	**Mus musculus**
Experiment type:	**Expression profiling by array**
Platform:	**GPL1261**
Pubmed ID:	**24069029**
Summary & Design:	**Summary:** **Protein misfolding stress in the endoplasmic reticulum (ER) leads to dysregulation of lipid metabolism in the liver, and ER stress is associated with human diseases that are accompanied by hepatic lipid accumulation, including obesity, alcoholism, and viral hepatitis; yet the pathways leading from ER stress to the regulation of lipid metabolism are poorly understood. Working exclusively in vivo, we used a â bottom-upâ approach to infer pathways in the genetic regulation of lipid metabolism by the UPR.** **We used a functional genomics to link gene expression patterns taken from microarray data to the severity and persistence of ER stress, using mice lacking the UPR signaling molecule ATF6¸–. This approach revealed that functionally related genes clustered into a small number of distinct expression profiles, and that lipid oxidation and efflux were targets for coordinated transcriptional suppression during ER stress.Our results establish a framework for hepatic gene regulation during ER stress.** **Overall design:** **Atf6a-/- or +/+ mice of variable age and gender were injected intraperitoneally with 2 mg/kg tunicamycin or vehicle. 3 separate mice were used in each group. 8h after injection, mice were sacrificed and total RNA was prepared from resected livers.**

Background corr dist: KL-Divergence = 0.0464, L1-Distance = 0.0564, L2-Distance = 0.0064, Normal std = 0.5923

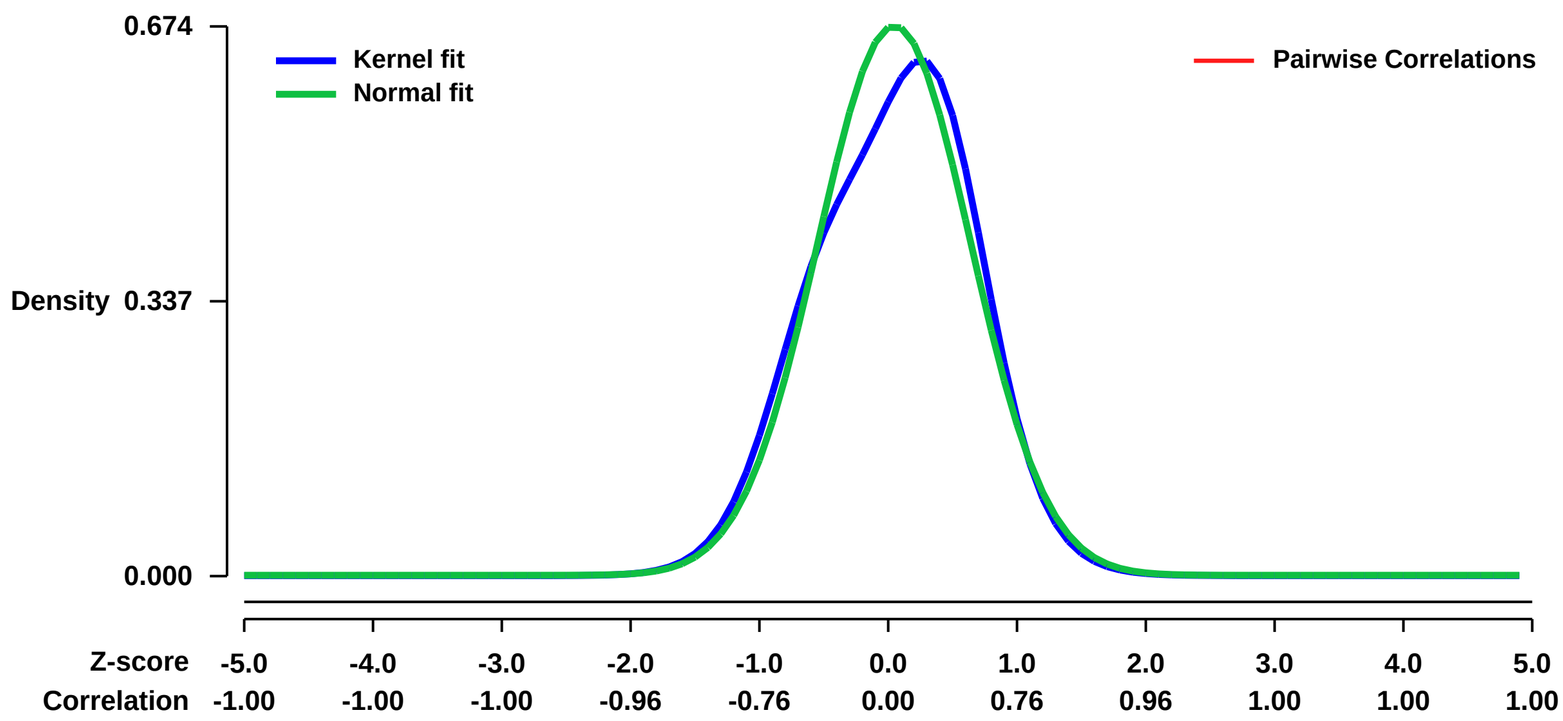

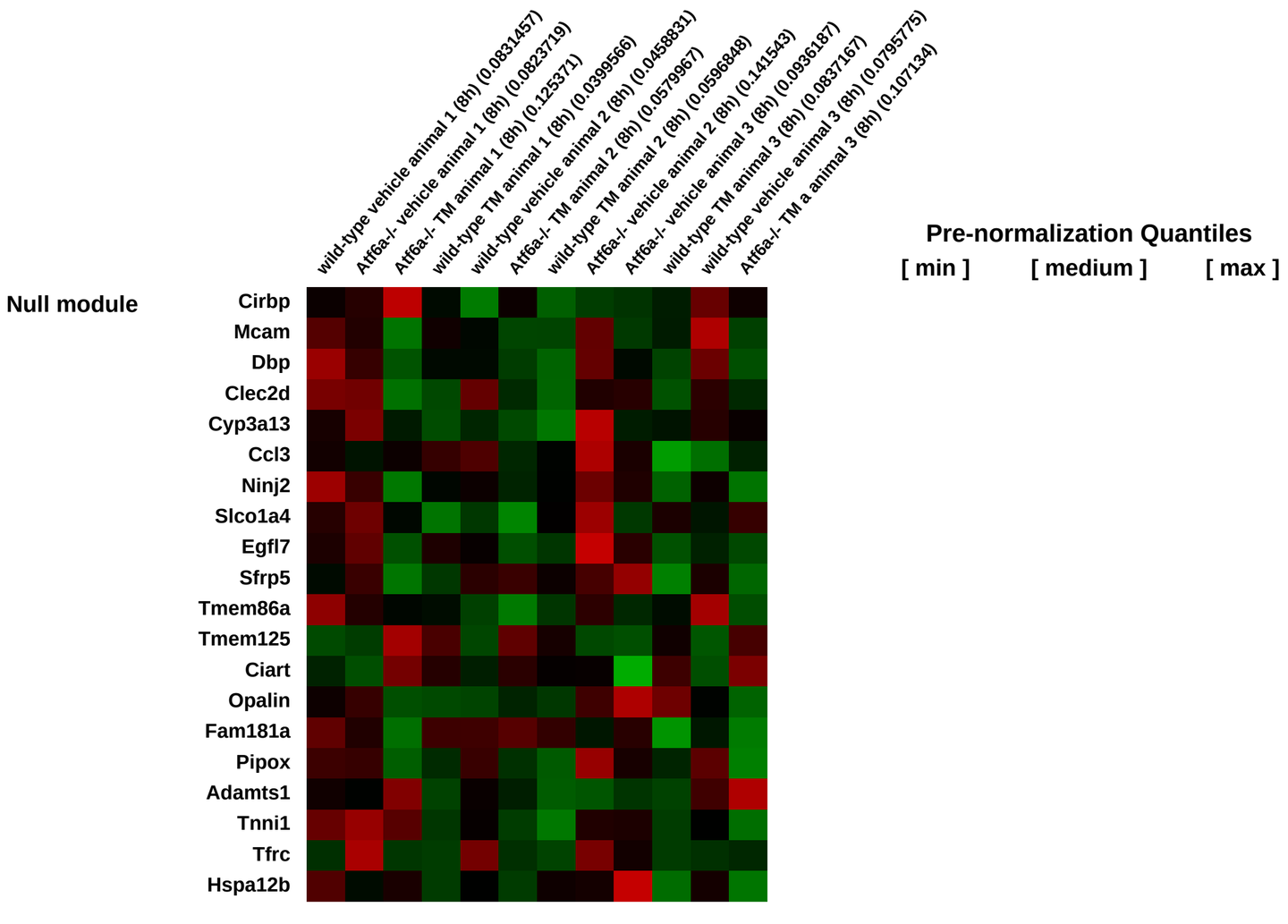

GEO Series "GSE48935" Expression Profiles

Num of samples in this series: 12

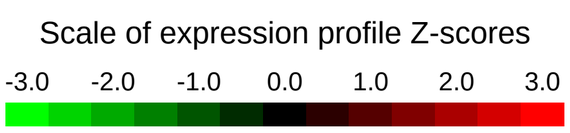

GEO Link:	**http://www.ncbi.nlm.nih.gov/geo/query/acc.cgi?acc=GSE48935**
Status:	**Public on Sep 04 2013**
Title:	**Analysis of gene expression changes induced in wild-type or Atf6a-/- mice by treatment with tunicamycin for 34h**
Organism:	**Mus musculus**
Experiment type:	**Expression profiling by array**
Platform:	**GPL1261**
Pubmed ID:	**24069029**
Summary & Design:	**Summary:** **Protein misfolding stress in the endoplasmic reticulum (ER) leads to dysregulation of lipid metabolism in the liver, and ER stress is associated with human diseases that are accompanied by hepatic lipid accumulation, including obesity, alcoholism, and viral hepatitis; yet the pathways leading from ER stress to the regulation of lipid metabolism are poorly understood. Working exclusively in vivo, we used a â bottom-upâ approach to infer pathways in the genetic regulation of lipid metabolism by the UPR.** **We used a functional genomics to link gene expression patterns taken from microarray data to the severity and persistence of ER stress, using mice lacking the UPR signaling molecule ATF6¸–. This approach revealed that functionally related genes clustered into a small number of distinct expression profiles, and that lipid oxidation and efflux were targets for coordinated transcriptional suppression during ER stress.Our results establish a framework for hepatic gene regulation during ER stress.** **Overall design:** **Atf6a-/- or +/+ mice of variable age and gender were injected intraperitoneally with 1 mg/kg tunicamycin or vehicle. 3 separate mice were used in each group. 34h after injection, mice were sacrificed and total RNA was prepared from resected livers.**

Background corr dist: KL-Divergence = 0.0722, L1-Distance = 0.0377, L2-Distance = 0.0019, Normal std = 0.5191

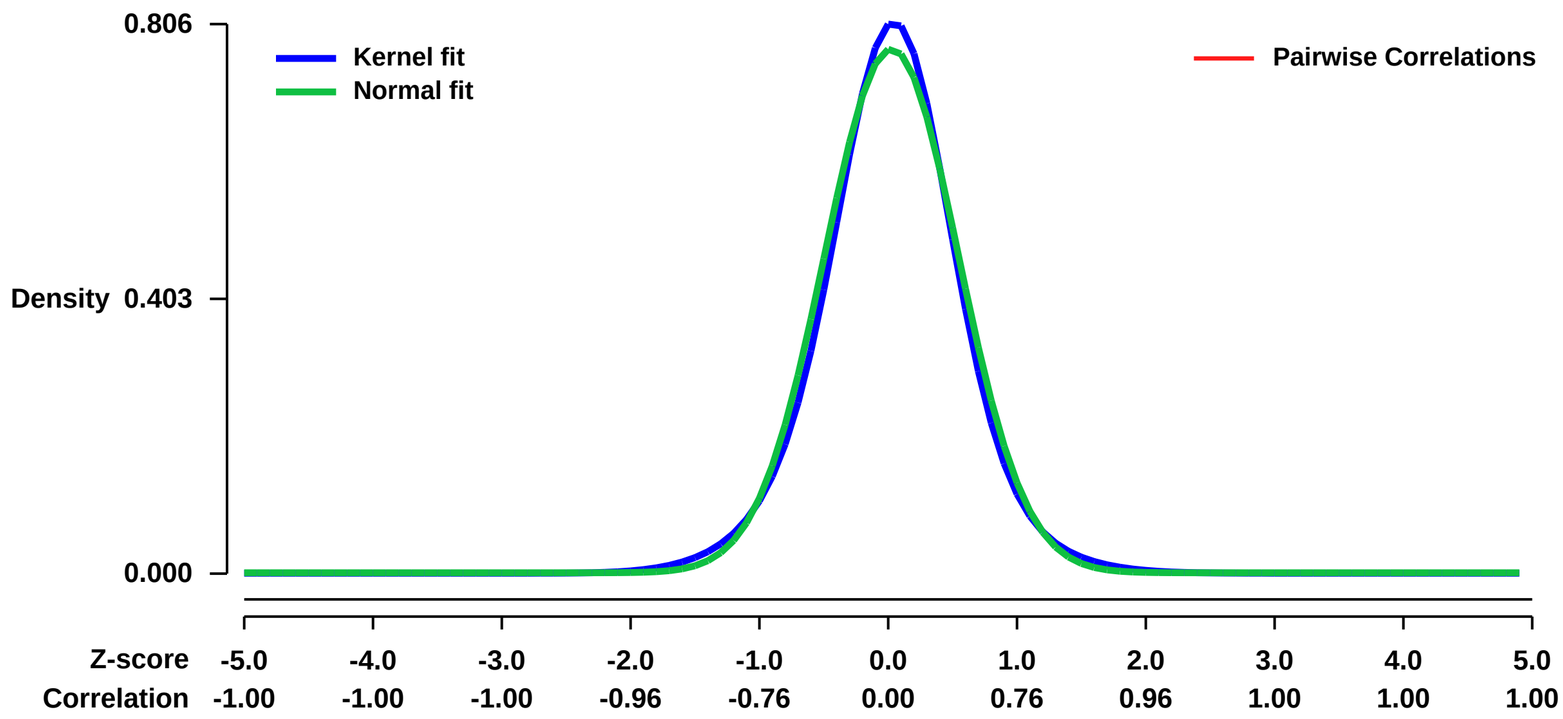

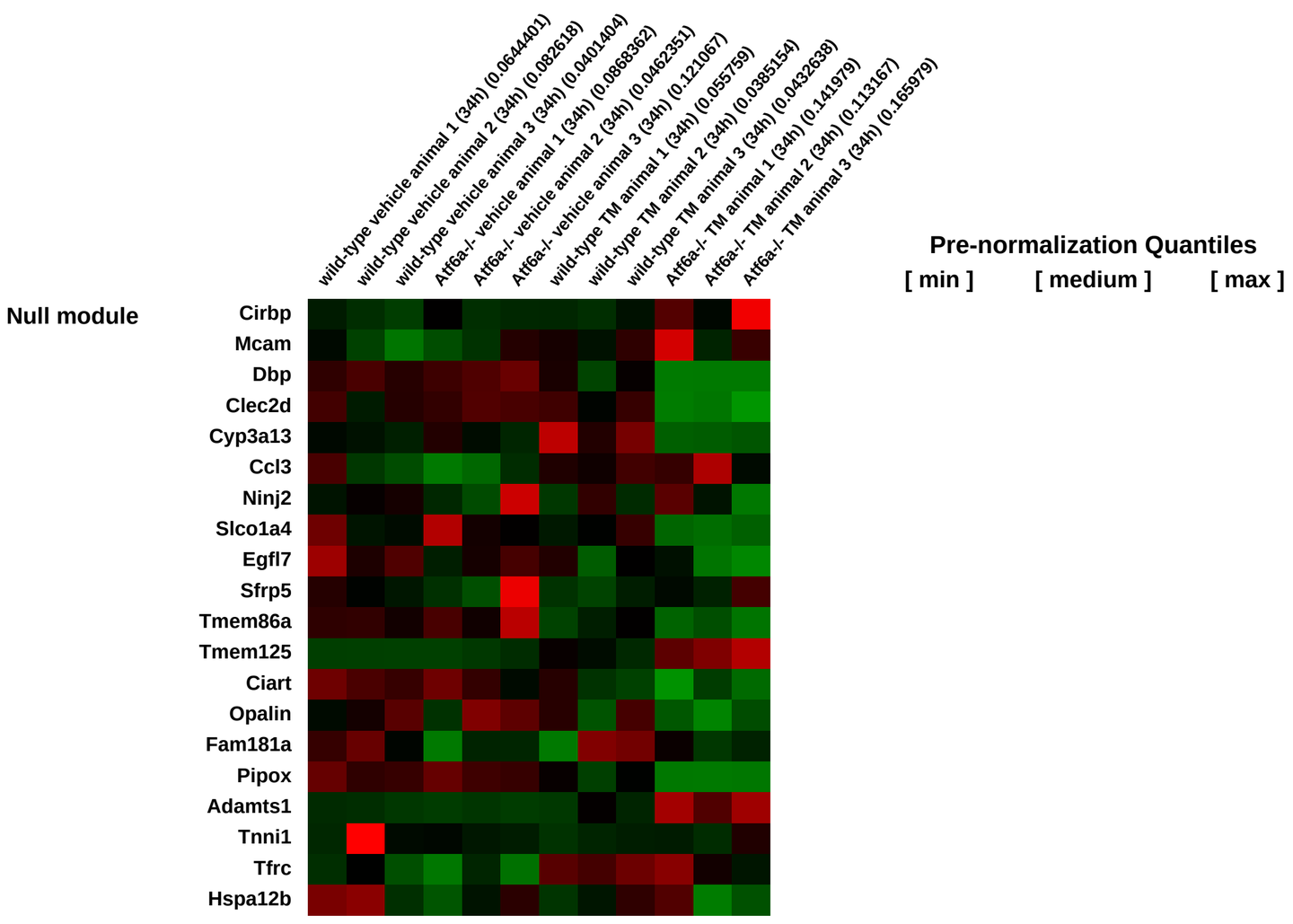

GEO Series "GSE49030" Expression Profiles

Num of samples in this series: 24

Scale of expression profile Z-scores

-3.0 -2.0 -1.0 0.0 1.0 2.0 3.0

GEO Link:	http://www.ncbi.nlm.nih.gov/geo/query/acc.cgi?acc=GSE49030
Status:	Public on Oct 23 2013
Title:	Genome-wide profiling of the activity-dependent hippocampal transcriptome
Organism:	Mus musculus
Experiment type:	Expression profiling by array
Platform:	GPL1261
Pubmed ID:	24146943
Summary & Design:	**Summary:** Activity-dependent gene expression is central for sculpting neuronal connectivity in the brain. Despite the importance for synaptic plasticity, a comprehensive analysis of the temporal changes in the transcriptomic response to neuronal activity is lacking. In a genome wide survey we identified genes that were induced at 1, 4, 8, or 24 hours following neuronal activity in the hippocampus. **Overall design:** 3 month old male mice were injected with kainic acid or isotonic saline solution. Animals were sacrificed by cervical luxation 1, 2, 4, 8, or 24 h after onset of the first seizure, and RNA was extracted from the hippocampal region.

Background corr dist: KL-Divergence = 0.1663, L1-Distance = 0.0450, L2-Distance = 0.0044, Normal std = 0.3569

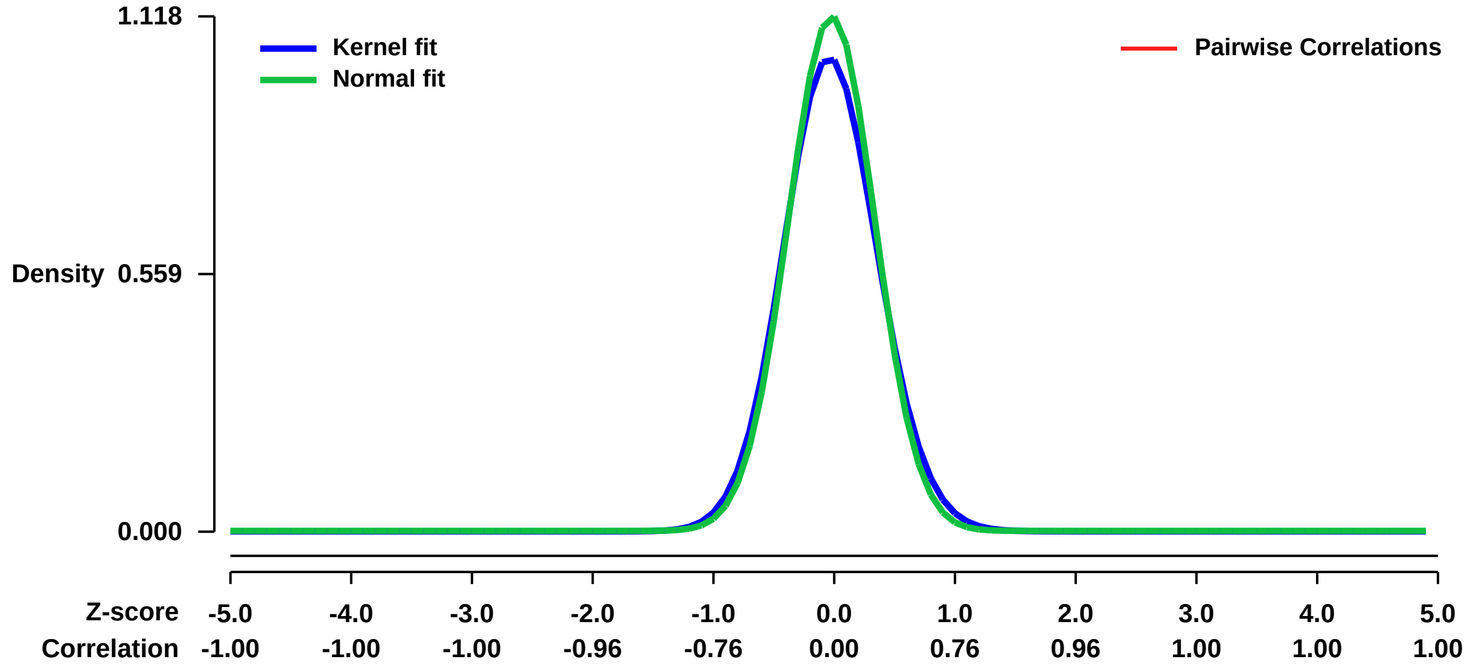

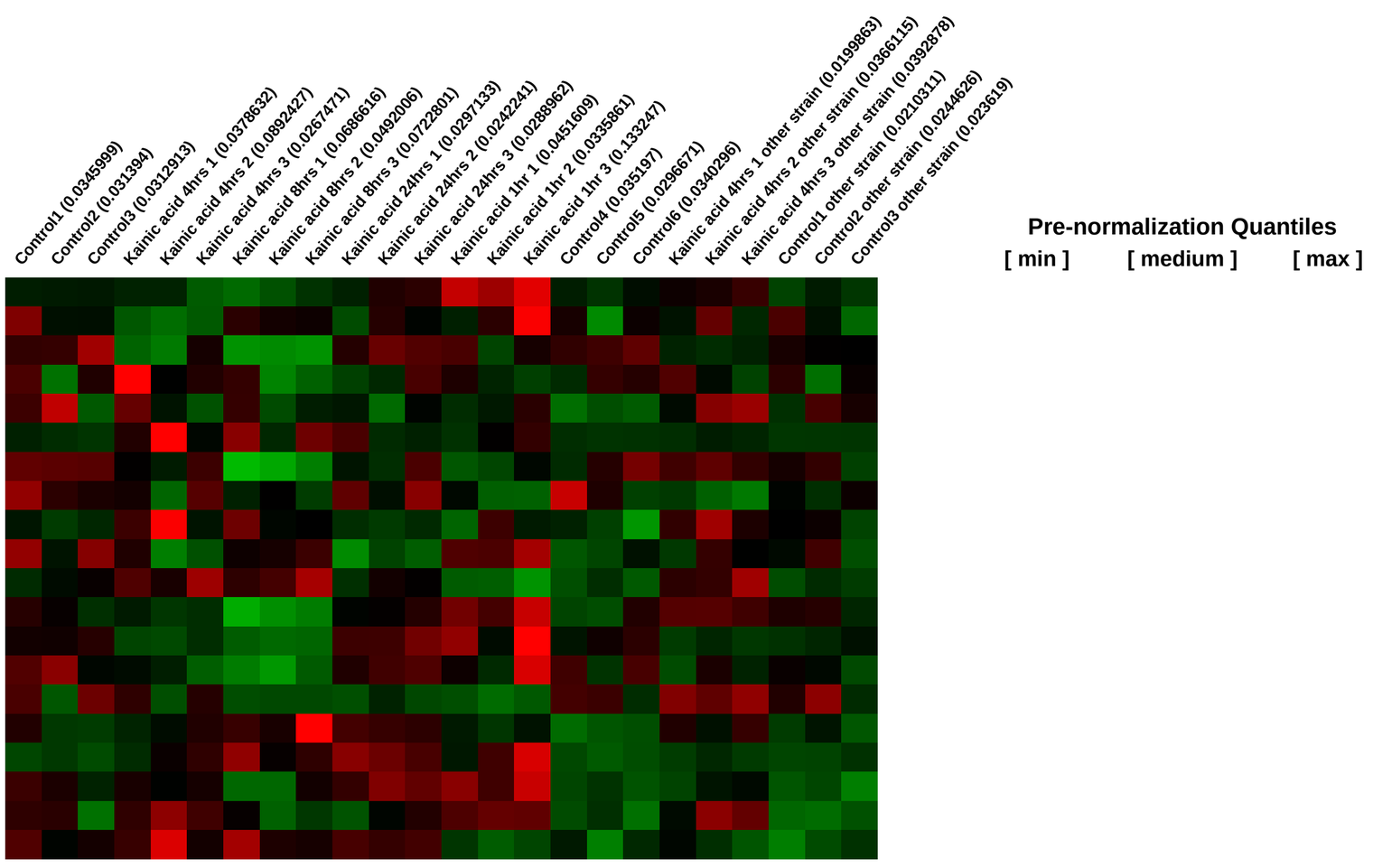

GEO Series "GSE49122" Expression Profiles

Num of samples in this series: 14

Scale of expression profile Z-scores

-3.0 -2.0 -1.0 0.0 1.0 2.0 3.0

GEO Link:	http://www.ncbi.nlm.nih.gov/geo/query/acc.cgi?acc=GSE49122
Status:	Public on Jul 23 2013
Title:	Otitis Media Impact on Inner Ear
Organism:	Mus musculus
Experiment type:	Expression profiling by array
Platform:	GPL1261
Pubmed ID:	24124478
Summary & Design:	**Summary:** **Objective: Otitis media is known to alter expression of cytokine and other genes in the mouse middle ear and inner ear. However, whole mouse genome studies of gene expression in otitis media have not previously been undertaken. Ninety-nine percent of mouse genes are shared in the human, so these studies are relevant to the human condition.** **Methods: To assess inflammation-driven processes in the mouse ear, gene chip analyses were conducted on mice treated with trans-tympanic heat-killed Hemophilus influenza using untreated mice as controls. Middle and inner ear tissues were separately harvested at 6 hours, RNA extracted, and samples for each treatment processed on the Affymetrix 430 2.0 Gene Chip for expression of its 34,000 genes.** **Results: Statistical analysis of gene expression compared to control mice showed significant alteration of gene expression in 2,355 genes, 11% of the genes tested and 8% of the mouse genome. Significant middle and inner ear upregulation (fold change >1.5, p<0.05) was seen in 1,081 and 599 genes respectively. Significant middle and inner ear downregulation (fold change <0.67, p<0.05) was seen in 978 and 287 genes respectively. While otitis media is widely believed to be an exclusively middle ear process with little impact on the inner ear, the inner ear changes noted in this study were numerous and discrete from the middle ear responses. This suggests that the inner ear does indeed respond to otitis media and that its response is a distinctive process. Numerous new genes, previously not studied, are found to be affected by inflammation in the ear.** **Conclusion: Whole genome analysis via gene chip allows simultaneous examination of expression of hundreds of gene families influenced by inflammation in the middle ear. Discovery of new gene families affected by inflammation may lead to new approaches to the study and treatment of otitis media.** **Overall design:** **There are 6 control samples and 8 samples trans-tympanically injected with H flu 10e9 for 6 hours. Each sample is a pool of 4 animals**

Background corr dist: KL-Divergence = 0.0179, L1-Distance = 0.0166, L2-Distance = 0.0003, Normal std = 0.7467

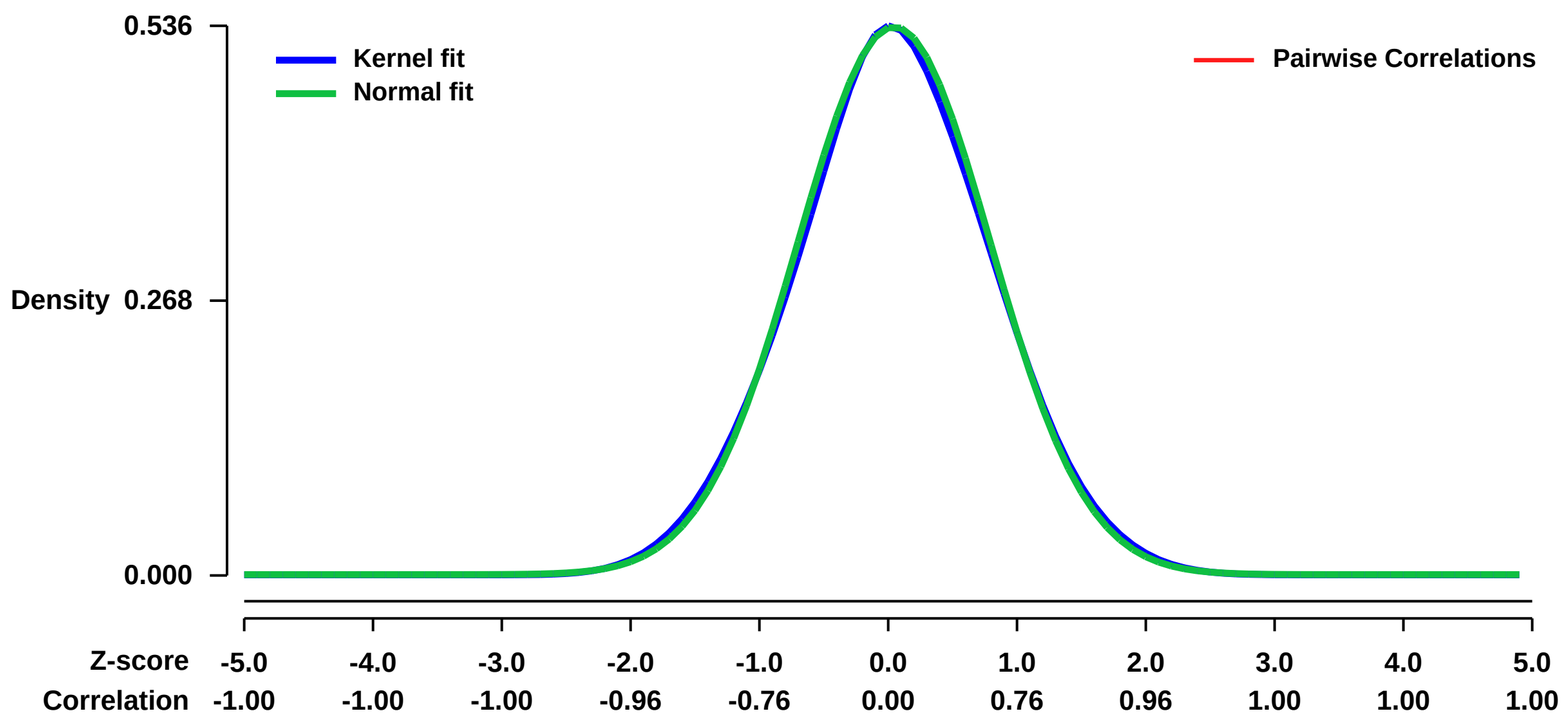

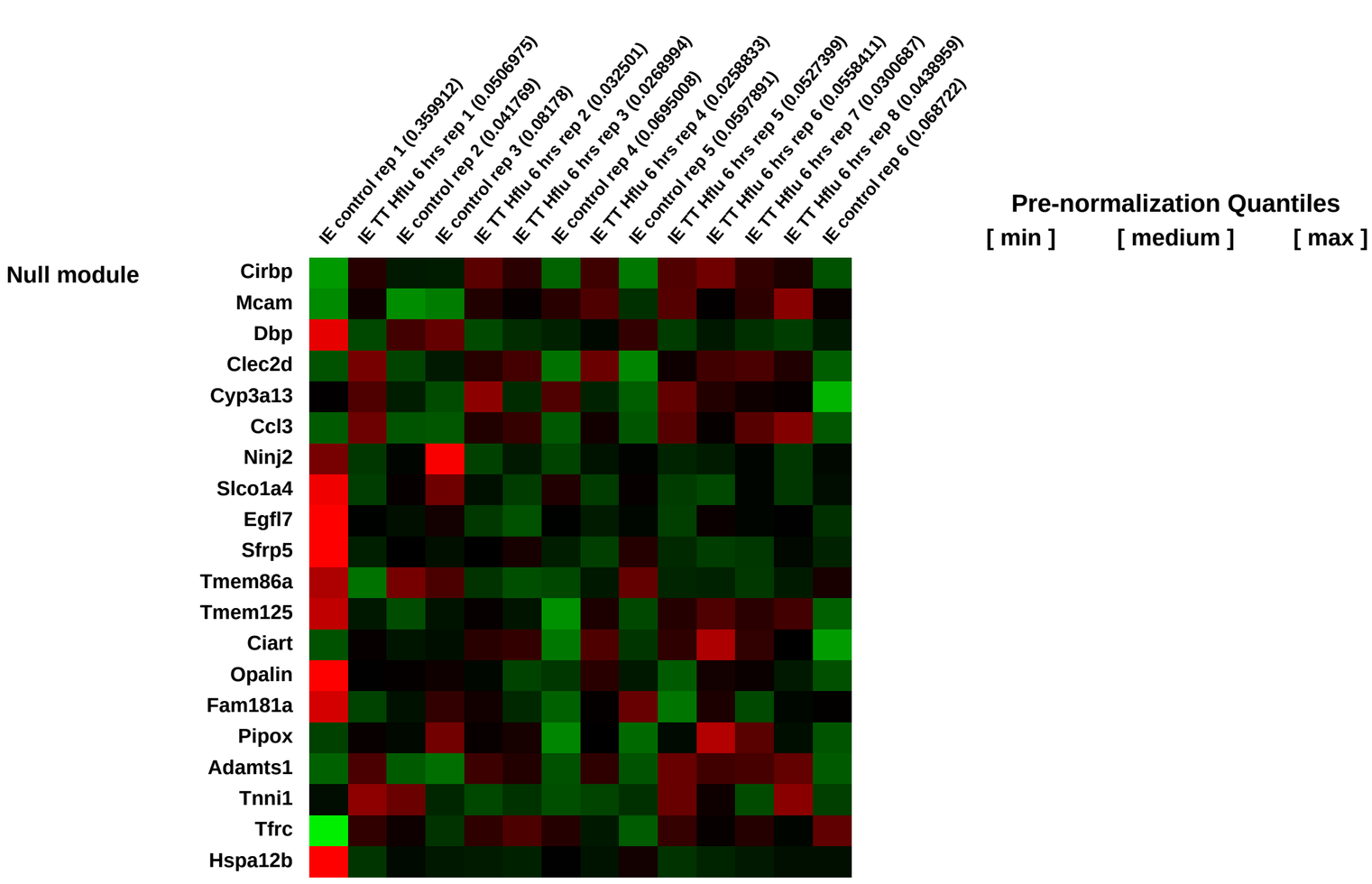

GEO Series "GSE49128" Expression Profiles

Num of samples in this series: 17

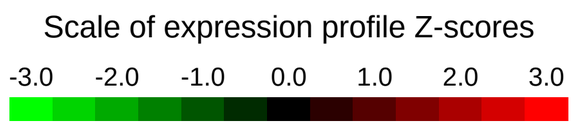

GEO Link:	http://www.ncbi.nlm.nih.gov/geo/query/acc.cgi?acc=GSE49128
Status:	Public on Jul 23 2013
Title:	Otitis Media Impact on Middle Ear
Organism:	Mus musculus
Experiment type:	Expression profiling by array
Platform:	GPL1261
Pubmed ID:	24124478

Summary & Design:

Summary:
Objective: Otitis media is known to alter expression of cytokine and other genes in the mouse middle ear and inner ear. However, whole mouse genome studies of gene expression in otitis media have not previously been undertaken. Ninety-nine percent of mouse genes are shared in the human, so these studies are relevant to the human condition.

Methods: To assess inflammation-driven processes in the mouse ear, gene chip analyses were conducted on mice treated with trans-tympanic heat-killed Hemophilus influenza using untreated mice as controls. Middle and inner ear tissues were separately harvested at 6 hours, RNA extracted, and samples for each treatment processed on the Affymetrix 430 2.0 Gene Chip for expression of its 34,000 genes.

Results: Statistical analysis of gene expression compared to control mice showed significant alteration of gene expression in 2,355 genes, 11% of the genes tested and 8% of the mouse genome. Significant middle and inner ear upregulation (fold change >1.5, p<0.05) was seen in 1,081 and 599 genes respectively. Significant middle and inner ear downregulation (fold change <0.67, p<0.05) was seen in 978 and 287 genes respectively. While otitis media is widely believed to be an exclusively middle ear process with little impact on the inner ear, the inner ear changes noted in this study were numerous and discrete from the middle ear responses. This suggests that the inner ear does indeed respond to otitis media and that its response is a distinctive process. Numerous new genes, previously not studied, are found to be affected by inflammation in the ear.

Conclusion: Whole genome analysis via gene chip allows simultaneous examination of expression of hundreds of gene families influenced by inflammation in the middle ear. Discovery of new gene families affected by inflammation may lead to new approaches to the study and treatment of otitis media.

Overall design:
There are 8 control samples and 9 samples trans-tympanically injected with H flu 10e9 for 6 hours. Each sample is from a single animal.

Background corr dist: KL-Divergence = 0.1073, L1-Distance = 0.0314, L2-Distance = 0.0014, Normal std = 0.4348

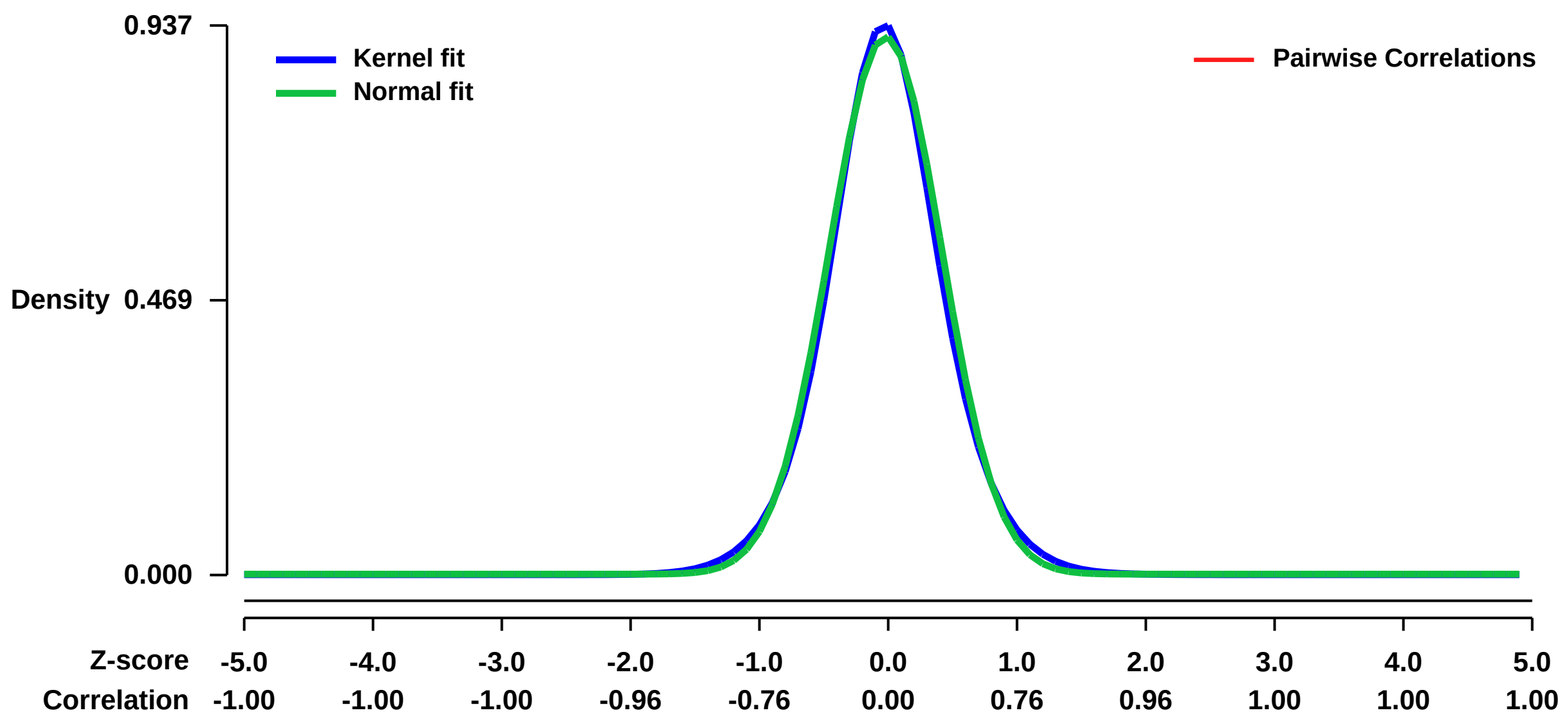

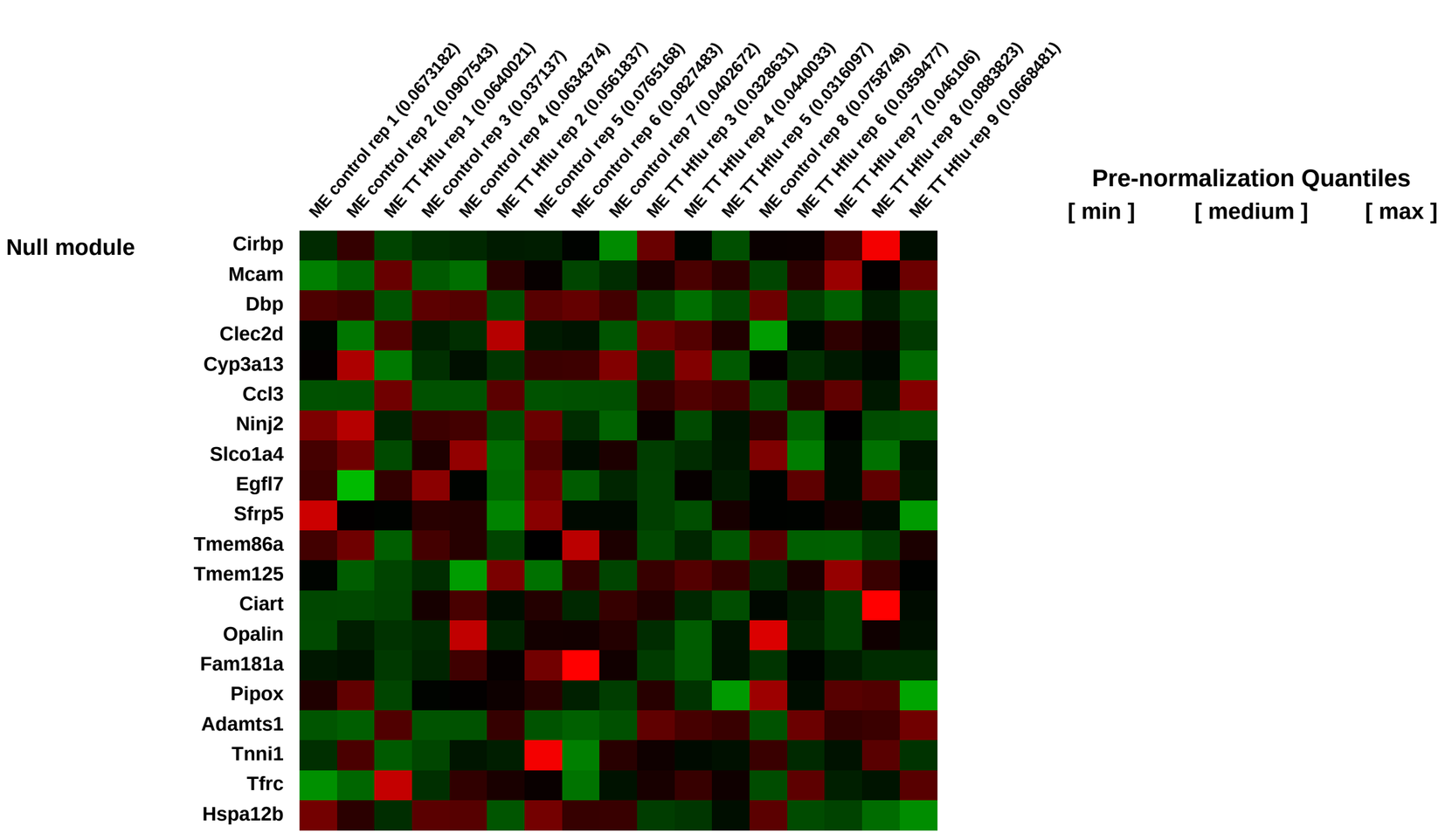

GEO Series "GSE49237" Expression Profiles

Num of samples in this series: 8

Scale of expression profile Z-scores

-3.0 -2.0 -1.0 0.0 1.0 2.0 3.0

GEO Link:	http://www.ncbi.nlm.nih.gov/geo/query/acc.cgi?acc=GSE49237
Status:	Public on Dec 31 2013
Title:	Analysis of TBR1 downnstream target genes in embryonic forebrains
Organism:	Mus musculus
Experiment type:	Expression profiling by array
Platform:	GPL1261
Pubmed ID:	24441682
Summary & Design:	**Summary:** **TBR1 is a forebrain specific T-box transcription factor. Tbr1-/- mice have been characterized by defective axonal projections from cerebral cortex and abnormal neuronal migration of cerebral cortex and amygdala.** **To investigate how TBR1 regulates neural development, the gene expression profile of Tbr1-/- brains was compared with WT littermates.** **Overall design:** **Total RNAs purified from forebrains at embryonic day 16.5 were hybridized on Affymetrix microarrays**

Background corr dist: KL-Divergence = 0.0472, L1-Distance = 0.0231, L2-Distance = 0.0006, Normal std = 0.5812

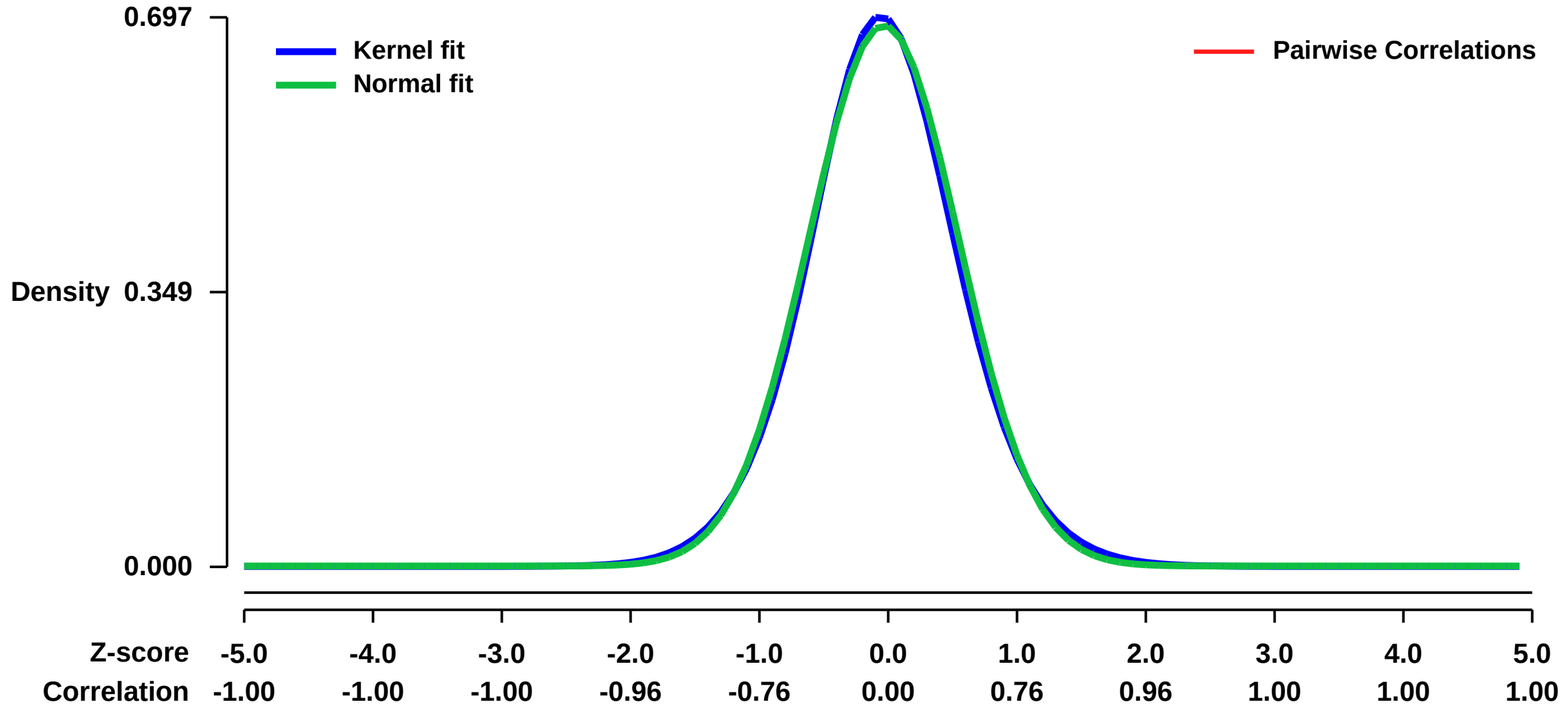

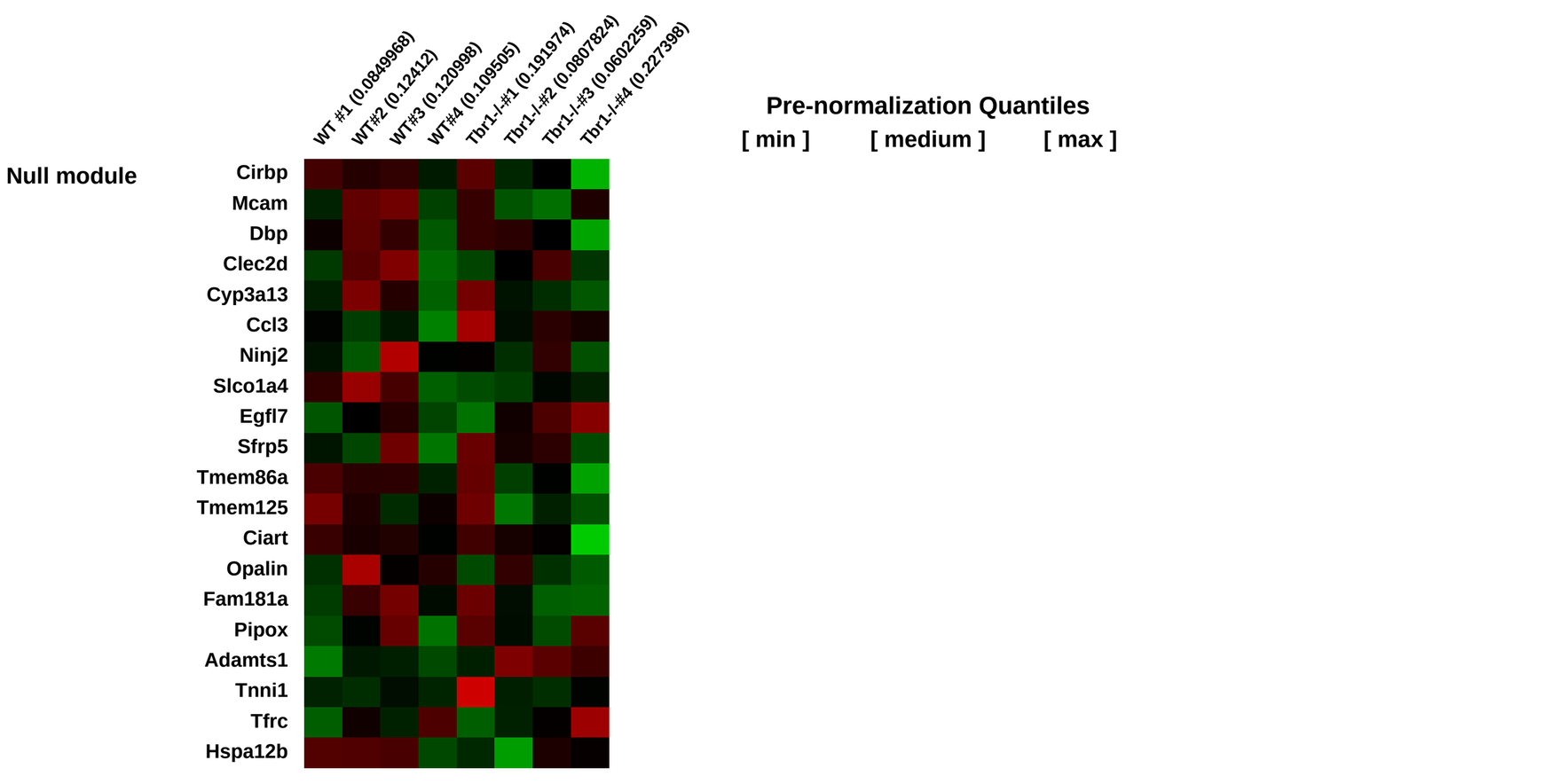

GEO Series "GSE49248" Expression Profiles

Num of samples in this series: 12

Scale of expression profile Z-scores

-3.0 -2.0 -1.0 0.0 1.0 2.0 3.0

GEO Link:	http://www.ncbi.nlm.nih.gov/geo/query/acc.cgi?acc=GSE49248
Status:	Public on Jul 02 2014
Title:	KrasG12D partially compensates for the loss of beta-catenin in MLL-AF9 AML
Organism:	Mus musculus
Experiment type:	Expression profiling by array
Platform:	GPL1261
Pubmed ID:	24189294
Summary & Design:	**Summary:** The Wnt/beta-catenin pathway is required for the development of leukemia stem cells in MLL-AF9 AML. We evaluated the dependance on beta-catenin for KrasG12DMLL-AF9 leukemia. **Overall design:** Lin-Kit+ bone marrow cells obtained from mice transplanted with primary MLL-AF9 leukemia cells and KRasG12DMLL-AF9 leukemia cells were assessed for gene expression in the presence or absence of beta-catenin

Background corr dist: KL-Divergence = 0.1418, L1-Distance = 0.0367, L2-Distance = 0.0025, Normal std = 0.3804

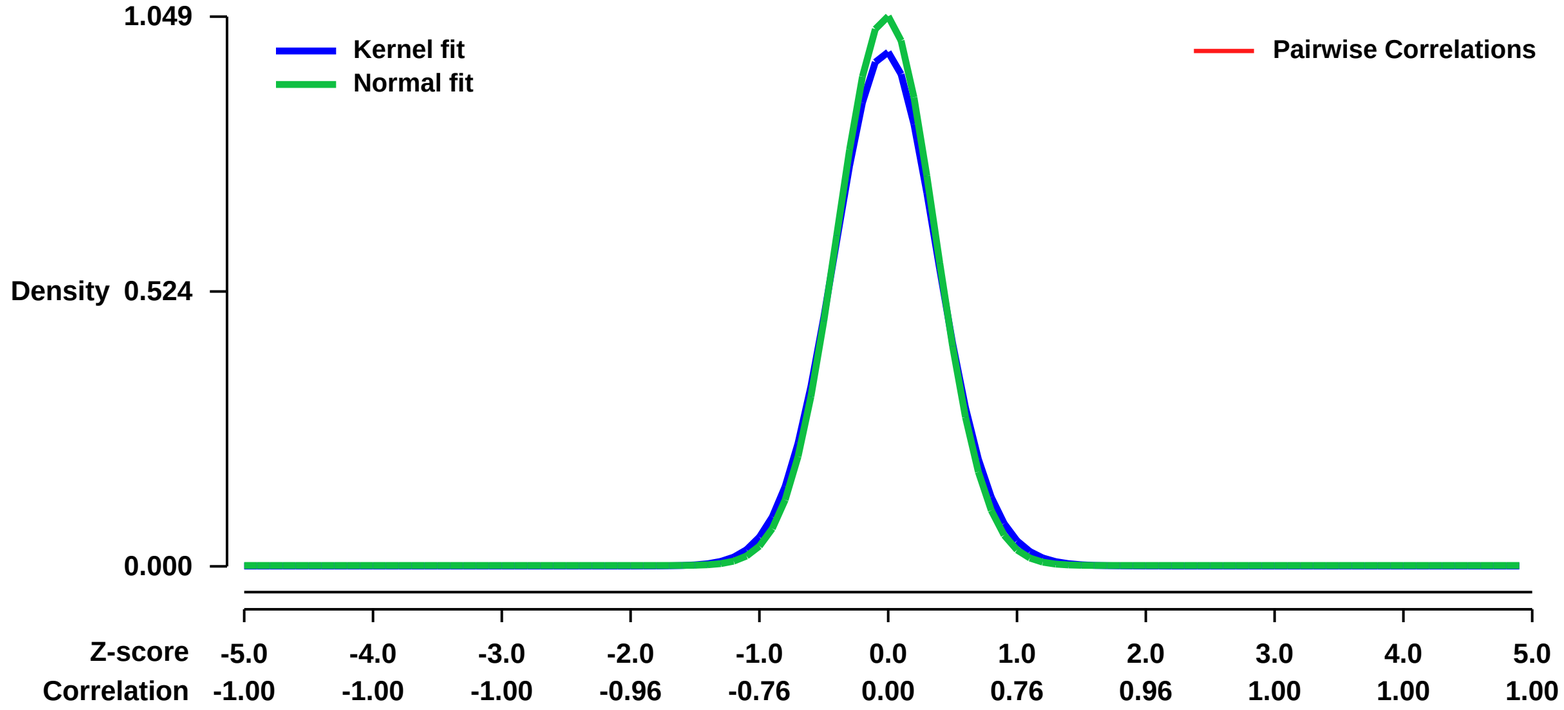

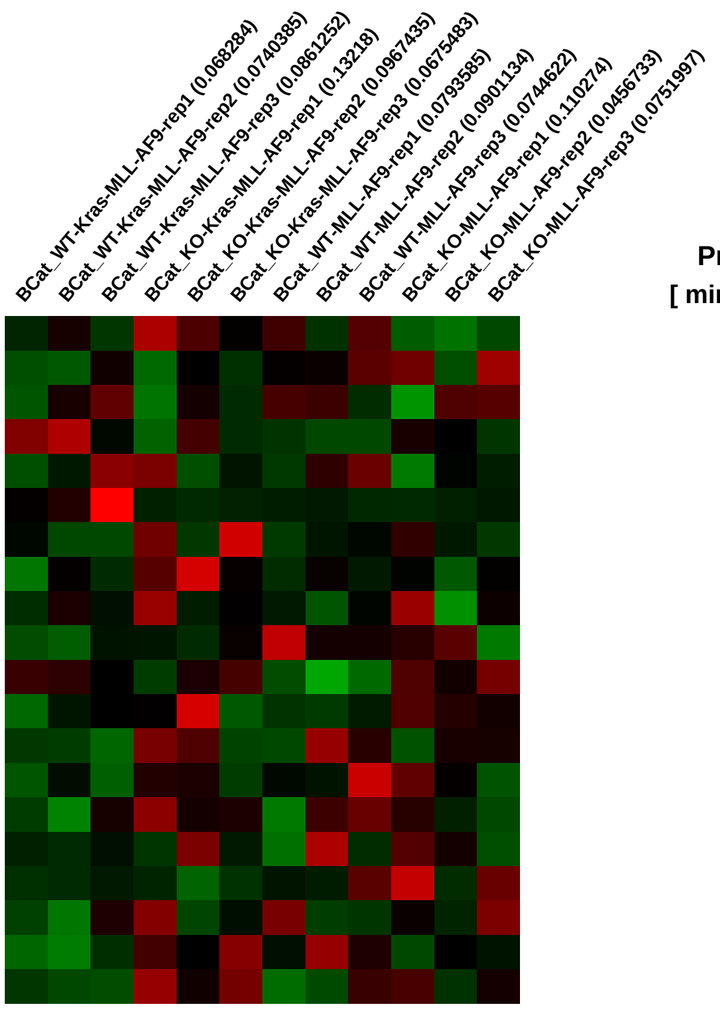

GEO Series "GSE4926" Expression Profiles

Num of samples in this series: 12

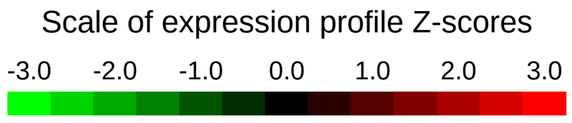

GEO Link:	http://www.ncbi.nlm.nih.gov/geo/query/acc.cgi?acc=GSE4926
Status:	Public on Mar 01 2008
Title:	Gene expression profiling of a mouse model of islet dysmorphogenesis
Organism:	Mus musculus
Experiment type:	Expression profiling by array
Platform:	GPL1261
Pubmed ID:	18297134
Summary & Design:	**Summary:** In the past decade, several transcription factors critical for pancreas development have been identified. Despite this success, many of the cell surface and extracellular factors necessary for proper islet morphogenesis and function remain uncharacterized. Previous studies have shown that transgenic over-expression of the transcription factor HNF6 specifically in the pancreatic endocrine cell lineage resulted in the disruption of islet morphogenesis, including dysfunctional endocrine cell sorting, increased islet size, and failure of islets to migrate away from the ductal epithelium. We exploited the dysmorphic islets in pdx1PBHnf6 animals as a tool to identify factors important for islet morphogenesis. Genome-wide microarray analysis was used to identify differences in the gene expression profiles of late gestation and early postnatal pancreas tissue from wild type and pdx1PBHnf6 animals. We report the identification of genes with an altered expression in HNF6 Tg animals and highlight factors with potential importance in islet morphogenesis. **Keywords:** disease state analysis, developmental stage analysis **Overall design:** Whole genome microarray analysis was used to identify differences in the gene expression profiles of late gestation and early postnatal pancreas tissue from wild type (WT) animals and HNF6 transgenic animals at a time when the events of normal islet morphogenesis are occurring (e18.5 and postnatal day 1). RNA was isolated from individual pancreata at the appropriate developmental stage. Highly pure samples were pooled according to their genotype (3-5 animals per pool) in order to obtain an adequate quantity of RNA for Affymetrix GeneChip analysis. Twelve samples were run in total, 3 replicates each of 4 groups: embryonic day 18.5, wild type mouse; embryonic day 18.5, HNF6 Transgenic mouse; post-natal day 1, wild type mouse; post-natal day 1, HNF6 Transgenic mouse.

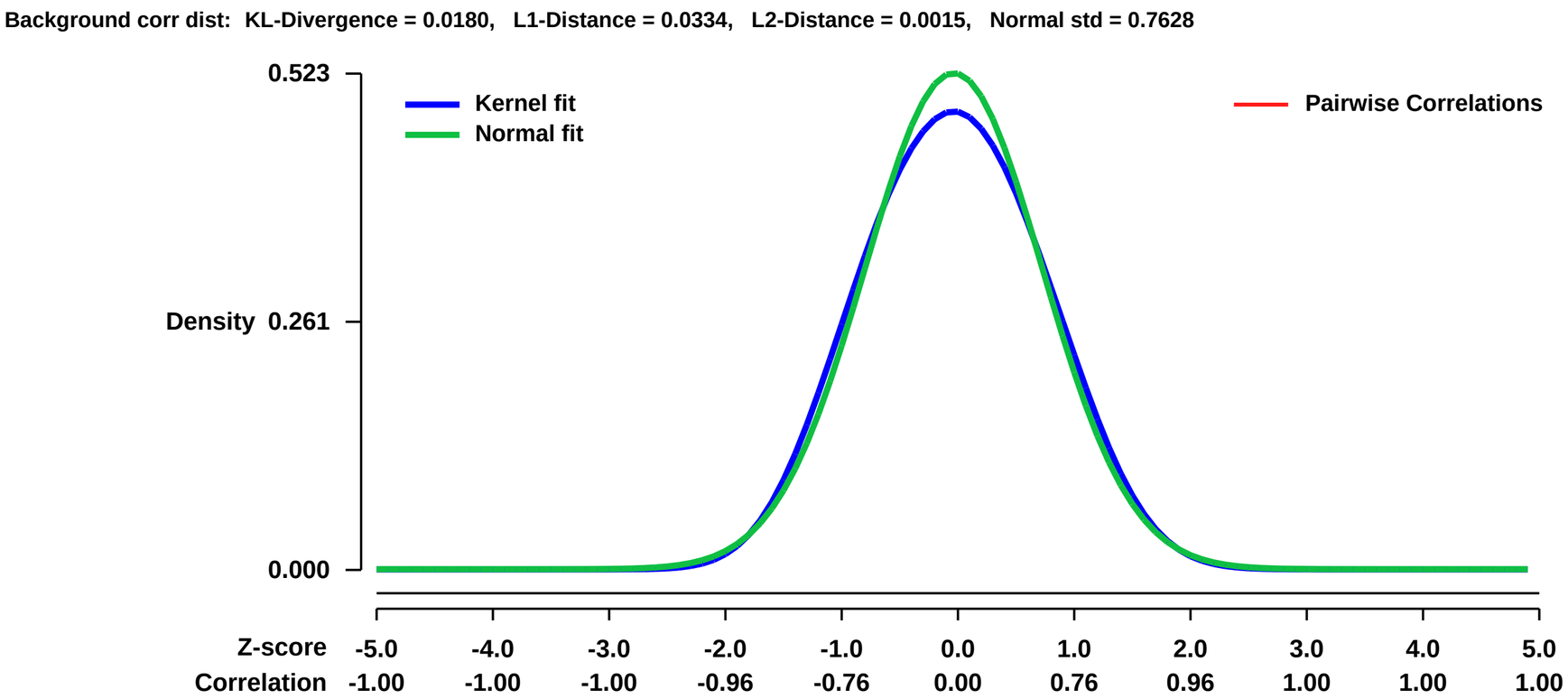

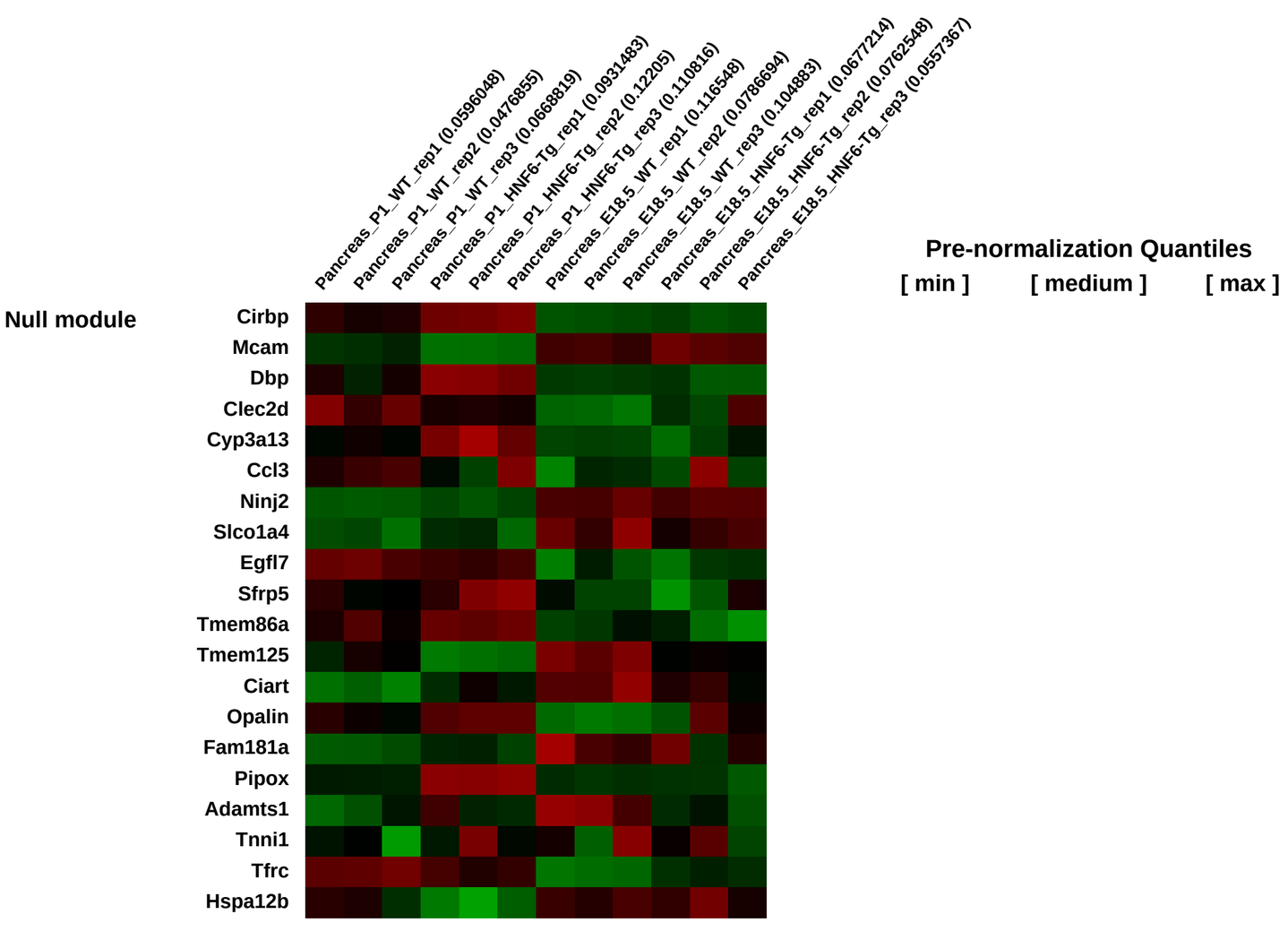

GEO Series "GSE4927" Expression Profiles

Num of samples in this series: 6

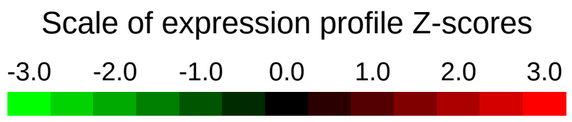

GEO Link:	http://www.ncbi.nlm.nih.gov/geo/query/acc.cgi?acc=GSE4927
Status:	Public on Apr 30 2007
Title:	Effect of OMP on gene expression in the olfactory epithelium
Organism:	Mus musculus
Experiment type:	Expression profiling by array
Platform:	GPL1261
Pubmed ID:	17444493
Summary & Design:	**Summary:** OMP is expressed only in mature olfactory sensory neurons, arguing that its function is specially suited to the needs of OSNs. However none of the properties of OMP suggest any direct role in regulating gene expression in OSNs. Our data confirms that gene expression in the olfactory epithelium of mice lacking OMP is indistinguishable from mice expressing OMP. We used affymerix M430v2.0 gene chips to cover as much of genome as possible and observed no statistically significant differences in mRNA abundance between the two genotypes.These results imply that OMPs ability to regulate signal transduction with in OSNs has little effect on gene expression and that its ability to promote mitosis in neighbouring cells (under culture conditions) is insufficiently active under normal laboratory housing conditions to generate detectable differences in gene expression patterns. **Keywords:** genetic modification **Overall design:** The overall design of the experiment is to undertand the effect of OMP (olfactory marker protein) on gene expression in the olfactory epithelium. We isolated the olfactory epithelium from homozygous and heterozygous OMP-GFP mice, extracted the RNA and hybridized on to the mouse expression set 430 2.0 Chip.

Background corr dist: KL-Divergence = 0.0486, L1-Distance = 0.0184, L2-Distance = 0.0003, Normal std = 0.5777

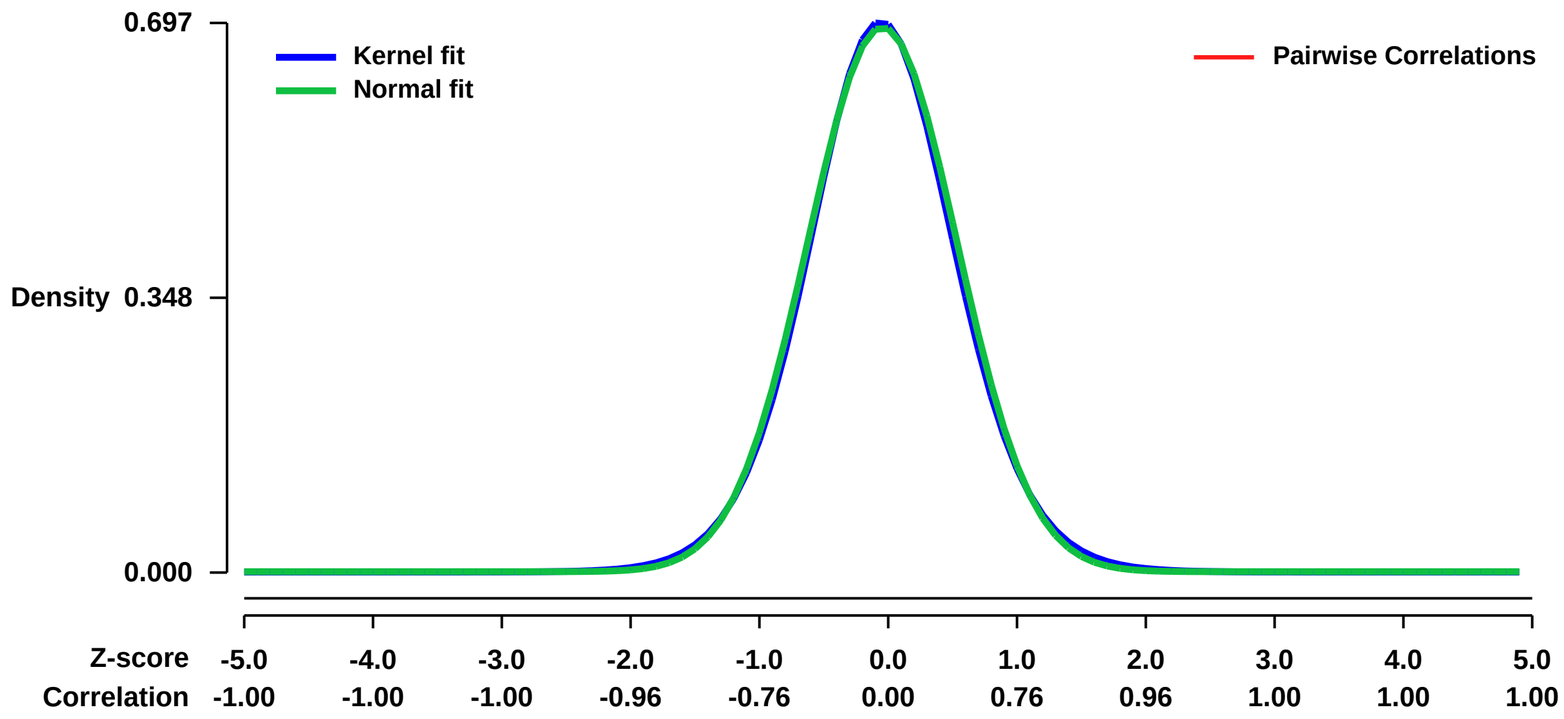

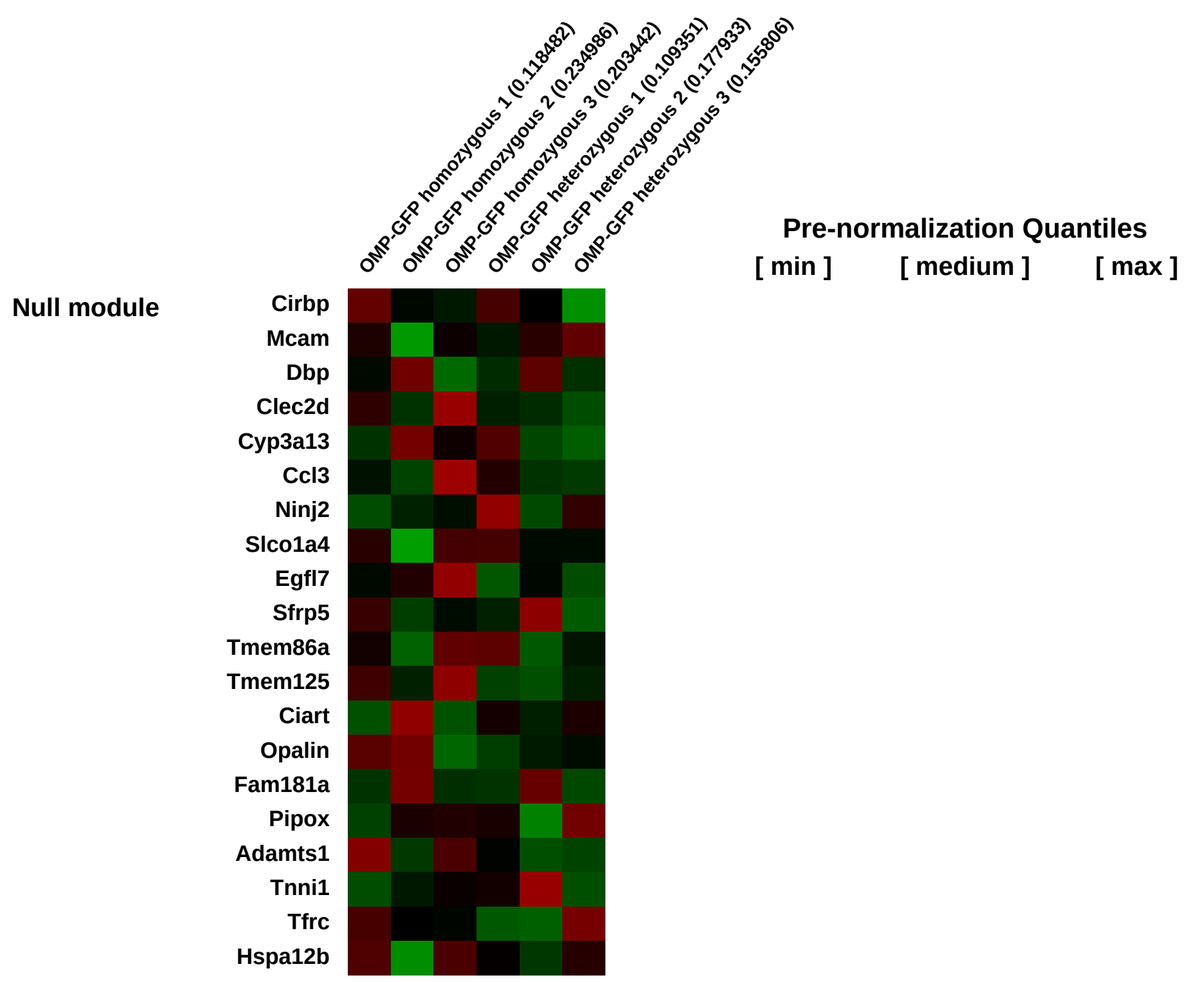

GEO Series "GSE49283" Expression Profiles

Num of samples in this series: 12

Scale of expression profile Z-scores

-3.0 -2.0 -1.0 0.0 1.0 2.0 3.0

GEO Link:	http://www.ncbi.nlm.nih.gov/geo/query/acc.cgi?acc=GSE49283
Status:	Public on Jul 27 2013
Title:	Translational activation of developmental mRNAs during neonatal mouse testis development
Organism:	Mus musculus
Experiment type:	Expression profiling by array
Platform:	GPL1261
Pubmed ID:	23926285
Summary & Design:	**Summary:** The sequence of gene regulatory events that drive neonatal germ cell development in the mammalian testis is not yet clear. We assessed changes in mRNA utilization in the neonatal testis at 1 and 4 dpp, times when the testis contains quiescent gonocytes (1 dpp) and proliferating spermatogonia (4 dpp). There are not thought to be major changes in the nature or number of somatic cells over that interval. We used microarrays to detail the global expression levels of mRNA distribution between non-translating mRNAs and efficiently translating mRNAs during testis development at 1 dpp and 4 dpp **Overall design:** Extracts of mouse testes from 1 dpp and 4 dpp CD-1 mice were fractionated over a sucrose gradient in triplicate. Gradients were fractionated using an ISCO gradient fractionation system equipped with a UA-6 detector. The position of the 80S peak defined the boundary between translating and non-translating mRNAs. Pooled non-polysomal (non-translating; fractions 1-3) and heavy polysomal (efficiently translating, fractions 7-13) RNAs were isolated from sucrose gradient fractions for hybridization on Affymetrix 420 2.0 microarrays.

Background corr dist: KL-Divergence = 0.0491, L1-Distance = 0.0591, L2-Distance = 0.0063, Normal std = 0.5856

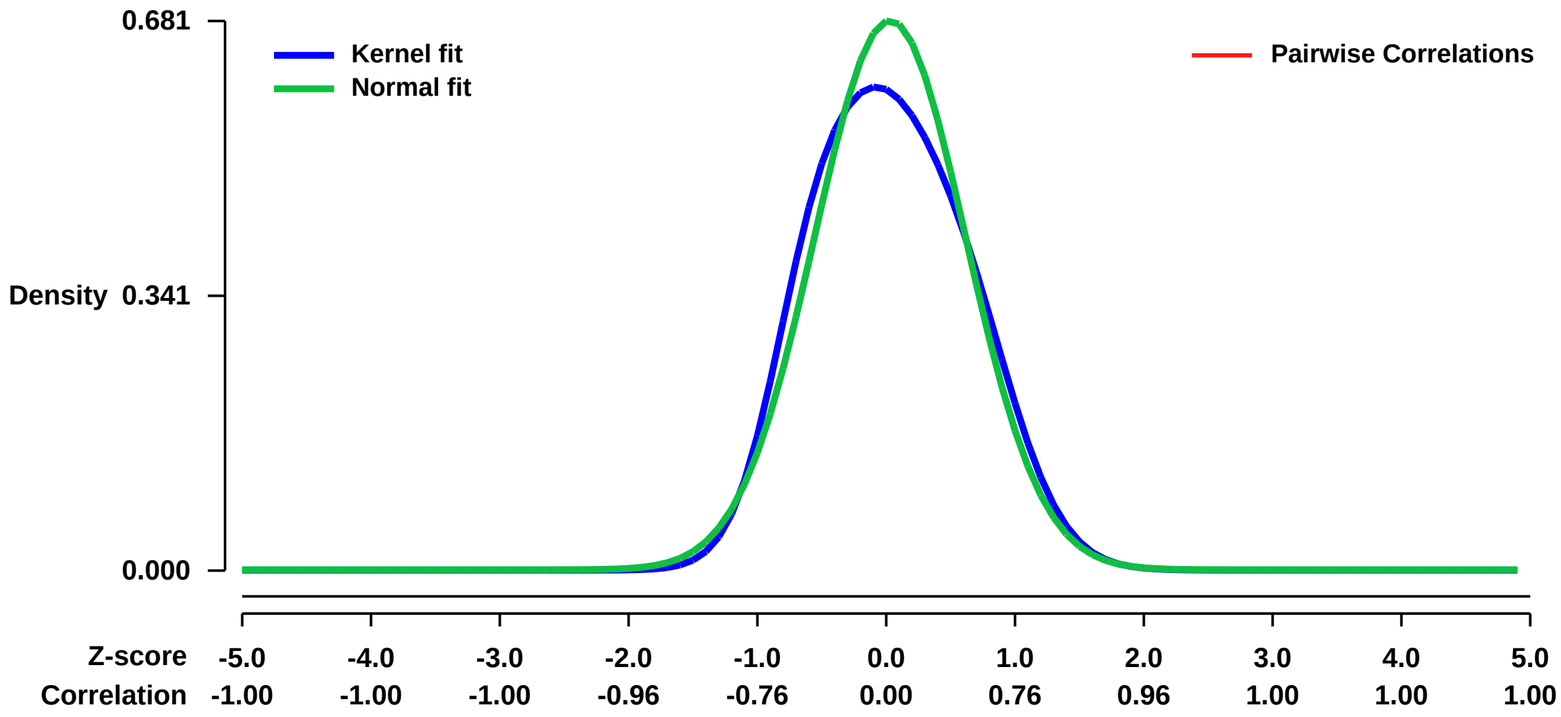

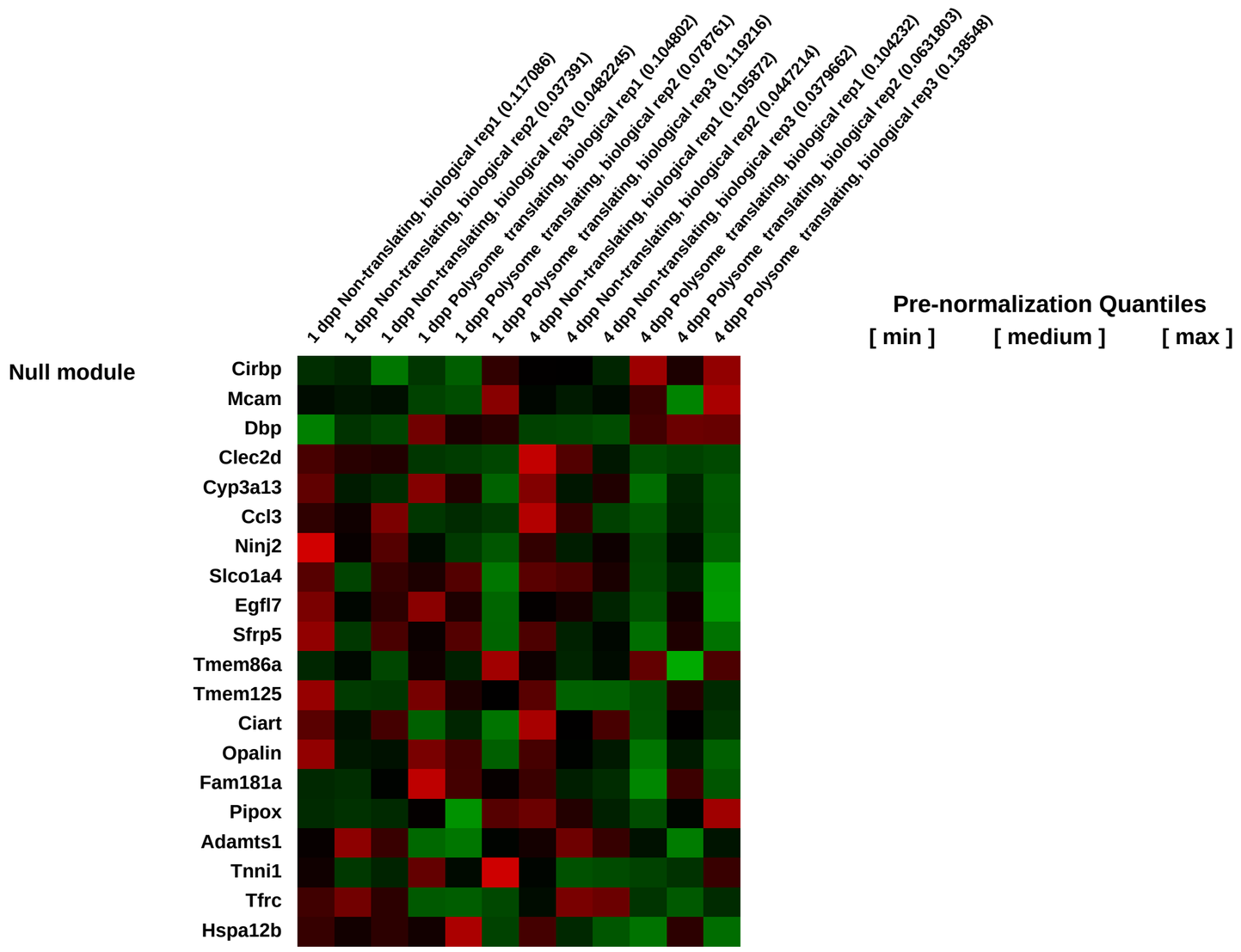

GEO Series "GSE49346" Expression Profiles

Num of samples in this series: 6

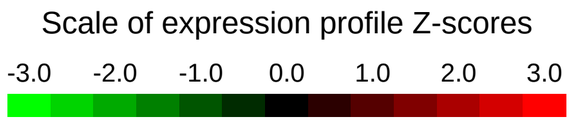

GEO Link:	http://www.ncbi.nlm.nih.gov/geo/query/acc.cgi?acc=GSE49346
Status:	Public on Mar 07 2014
Title:	Expression data from adult ATII and E18 Bipotent progenitor cells in the mouse lung
Organism:	Mus musculus
Experiment type:	Expression profiling by array
Platform:	GPL1261
Pubmed ID:	24499815
Summary & Design:	**Summary:** **Alveoli are thin-walled sacs that serve as the gas exchange units of the lung. They are affected in devastating lung diseases including COPD, Idiopathic Pulmonary Fibrosis, and the major form (adenocarcinoma) of lung cancer, the leading cause of cancer deaths. The alveolar epithelium is composed of two morphologically distinct cell types: alveolar type (AT) 1 cells, exquisitely thin cells across which oxygen diffuses to reach the blood, and AT2 cells, specialized surfactant-secreting cells. Classical studies suggested that AT1 cells arise from AT2 cells during development and following injury, but more recent studies suggest other sources. Here we use histological and marker analysis, lineage tracing, and clonal analysis in mice to identify alveolar progenitor and stem cells and map their locations and potential in vivo. The results show that AT1 and AT2 cells arise independently during development from a bipotential progenitor. After birth, new AT1 cells derive from rare, long-lived, self-renewing AT2 cells, each producing a slowly expanding clonal focus of regenerated alveoli contiguous with the founder AT2 cell. This stem cell function of AT2 cells is broadly activated by diffuse AT1 cell injury, and AT2 self-renewal can be induced in vitro by EGF ligands and permanently activated in vivo by AT2 cell-specific targeting of the oncogenic KrasG12D allele, efficiently transforming AT2 cells into monoclonal adenomatous tumors that rapidly enlarge and prove fatal. Thus, there is a developmental switch in alveolar progenitor cells after birth, when mature AT2 cells function as facultative stem cells that contribute to local alveolar renewal, repair, and cancer. We propose that short-range signals from dying AT1 cells regulate AT2 stem cell activity: a signal transduced by EGFR-KRAS controls AT2 self-renewal and is hijacked during oncogenic transformation, and a separate signal controls reprogramming to AT1 cell fate.** **Overall design:** **To compare expression between ATII and E18 BP populations, RNA was isolated from either population purified by FACS. Two populations are analyzed with 3 biological replicates per population.**

Background corr dist: KL-Divergence = 0.0359, L1-Distance = 0.0425, L2-Distance = 0.0025, Normal std = 0.6765

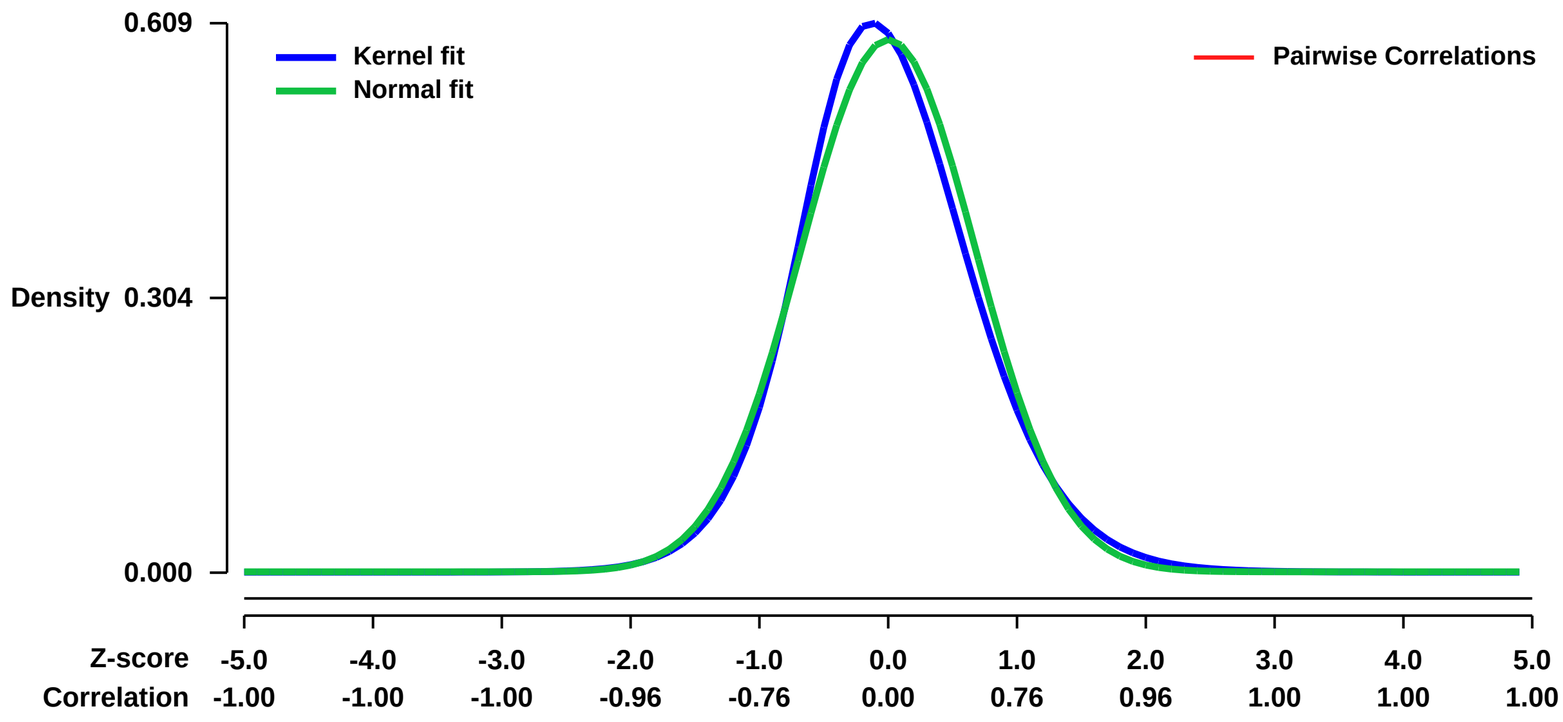

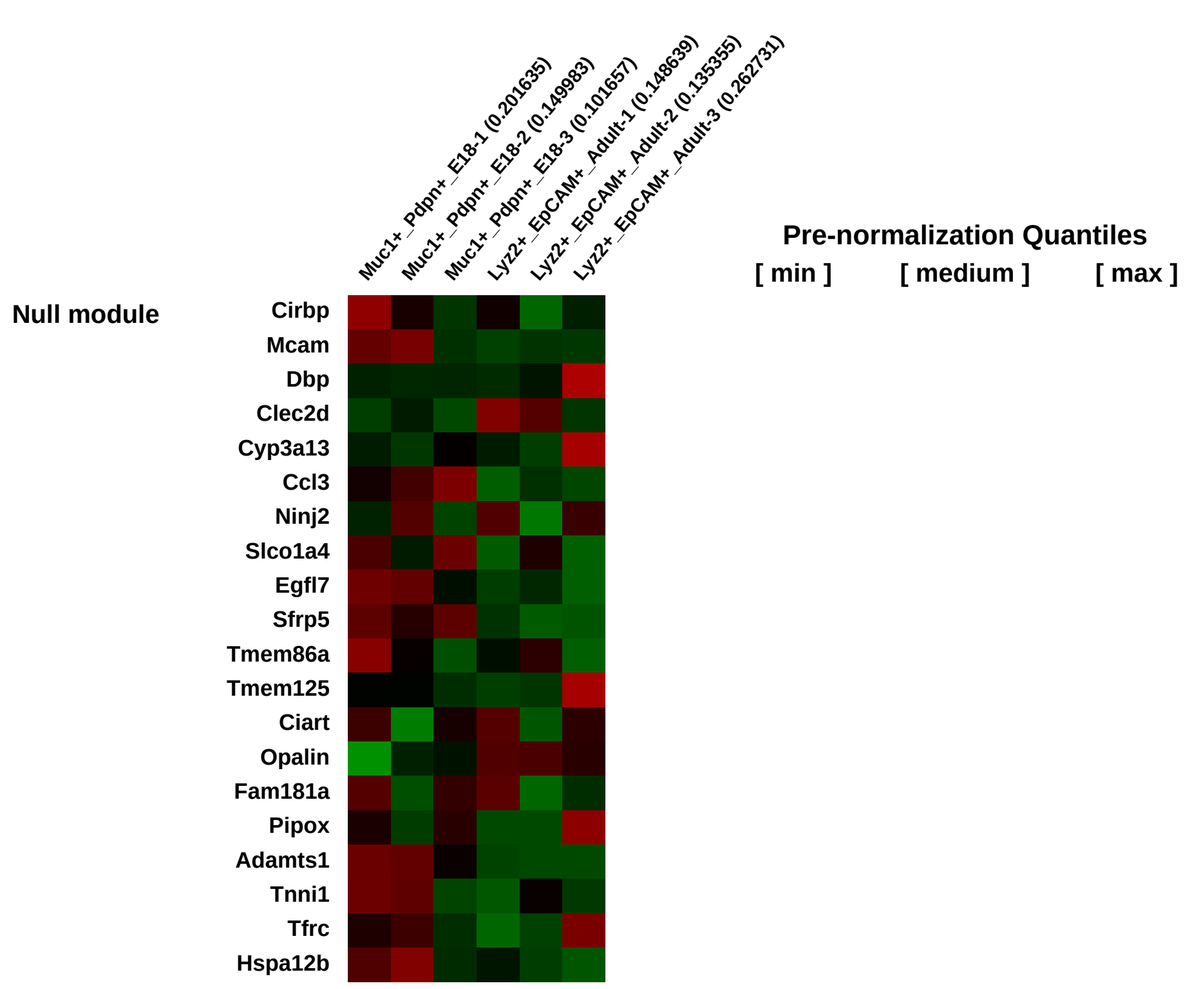

GEO Series "GSE49351" Expression Profiles

Num of samples in this series: 6

Scale of expression profile Z-scores

-3.0 -2.0 -1.0 0.0 1.0 2.0 3.0

GEO Link:	http://www.ncbi.nlm.nih.gov/geo/query/acc.cgi?acc=GSE49351
Status:	Public on Jul 31 2013
Title:	Microarray gene expression profiling of transgenic mice with myocardium-specific over-expression of fatty acid synthase (FASN)
Organism:	Mus musculus
Experiment type:	Expression profiling by array
Platform:	GPL1261
Pubmed ID:	
Summary & Design:	**Summary:** The fatty acid synthase (FASN) is the major fat synthesizing enzyme. FASN is an indispensable enzyme because mice with genetic deletion of Fasn are not viable. Apart from its physiological function, previous studies indicated that FASN could also exert a pathophysiological role, in the heart, because patients with heart failure showed up-reguation of FASN. To investigate the in vivo function of FASN up-regulation in the heart, we generated mice with myocardium-specific expression of FASN under control of the alpha-MHC promoter. Two different founder lines were generated with high and low FASN over-expression. Microarray gene expression profiling of heart tissue was performed of heart tissue from transgenic mice with high and low FASN expression **Overall design:** Microarray gene expression profiling was performed with heart tissue isolated from three study groups: (i) Transgenic mice with high cardiac FASN expression, (ii) transgenic mice with low cardiac FASN expression, and (iii) B6 control mice.

Background corr dist: KL-Divergence = 0.0393, L1-Distance = 0.0214, L2-Distance = 0.0005, Normal std = 0.6240

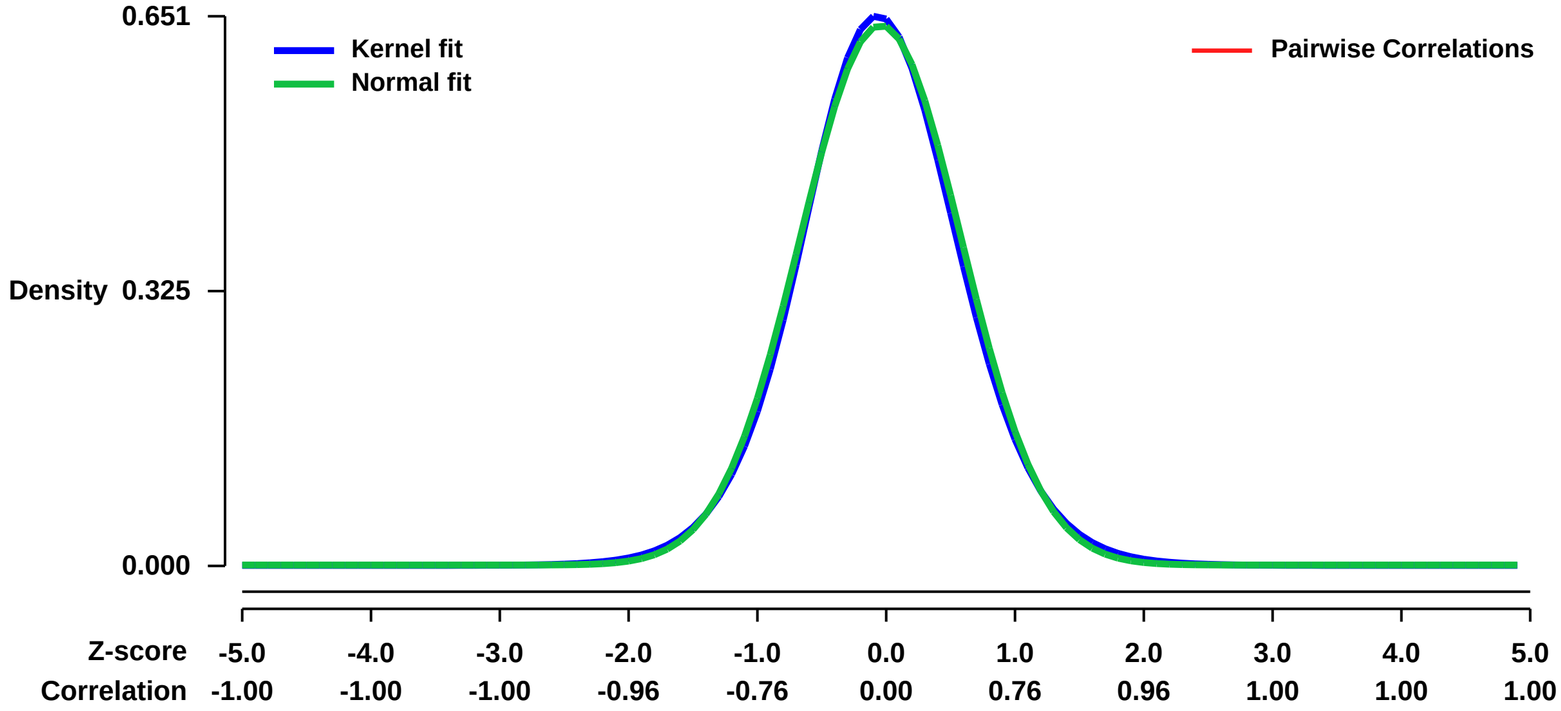

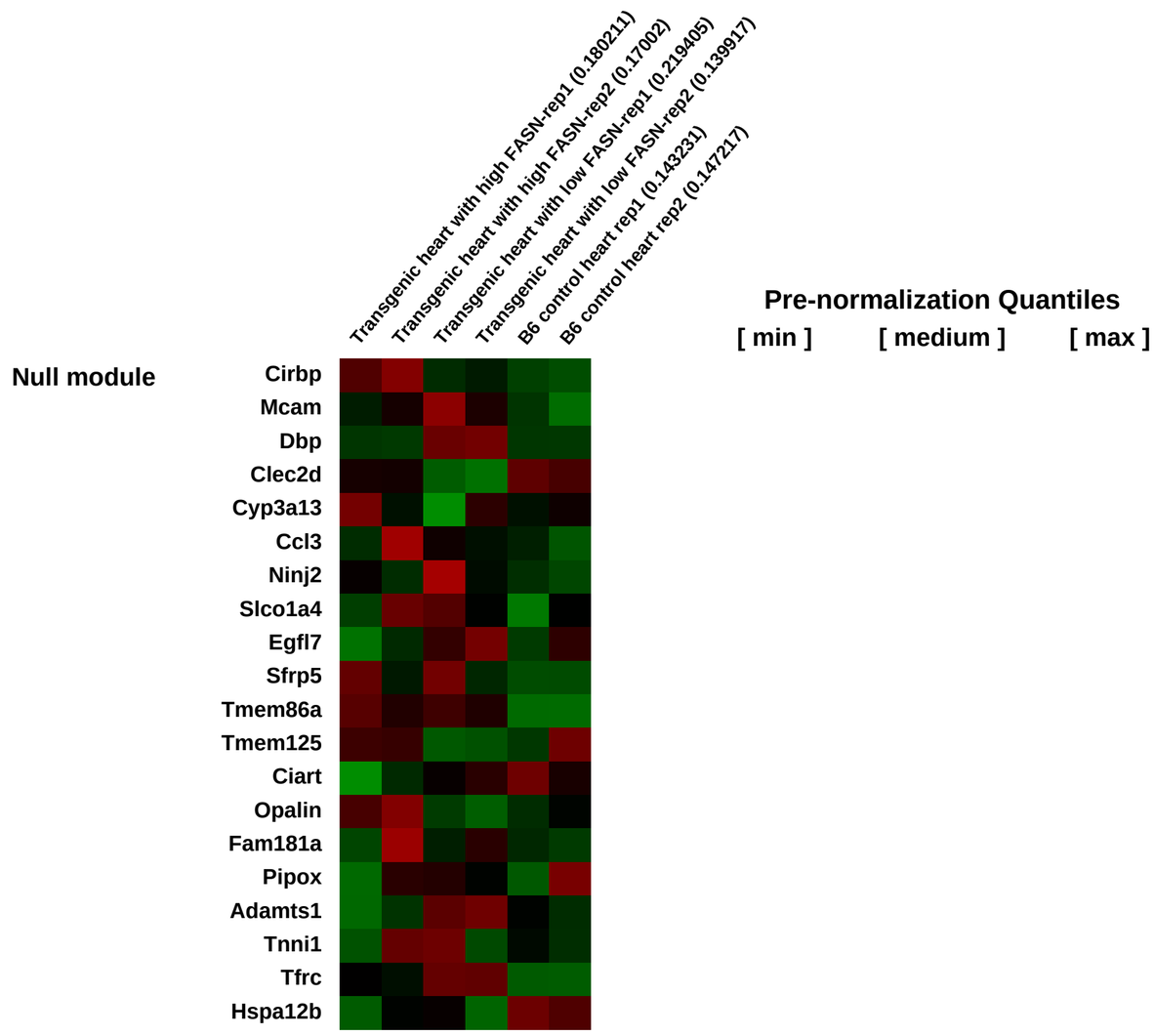

GEO Series "GSE4936" Expression Profiles

Num of samples in this series: 8

Scale of expression profile Z-scores

-3.0 -2.0 -1.0 0.0 1.0 2.0 3.0

GEO Link:	http://www.ncbi.nlm.nih.gov/geo/query/acc.cgi?acc=GSE4936
Status:	Public on Apr 20 2007
Title:	Transcriptional Profiling of Hh-Treated Embryoid Bodies
Organism:	Mus musculus
Experiment type:	Expression profiling by array
Platform:	GPL1261
Pubmed ID:	17442700
Summary & Design:	**Summary:** This experiment was specifically designed to measure neural targets of Shh signaling, we sought to profile the genes upregulated by Hh signaling in the ventral neural tube to obtain a valid dataset. To obtain ventral-specific markers, we generated retinoic acid-treated EBs grown in the presence or absence of HH-Ag. We did not observe induction of ventral Hh markers in RA-treated constitutive Gli1FLAG EBs and used these for the control, baseline set. The presence of FoxA2, Nkx2.9 and Nkx6.1 amongst the top 10 genes based on expression levels suggests that profiling significantly enriches for Hh-dependent cell types. As expected, the benchmark standard Gli1 was not up-regulated in our array, since it is constitutively expressed in the control as well. Keywords: neural progenitors, embryoid bodies, differentiation, Hedgehog, retinoic acid Overall design: There are a total of 8 samples. Four biological replicates of Retinoic-acid treated EBs (Baseline) and 4 additional biological samples of retinoic acid + Hh-Ag treated EBs (induced sample).

Background corr dist: KL-Divergence = 0.0856, L1-Distance = 0.0227, L2-Distance = 0.0007, Normal std = 0.4632

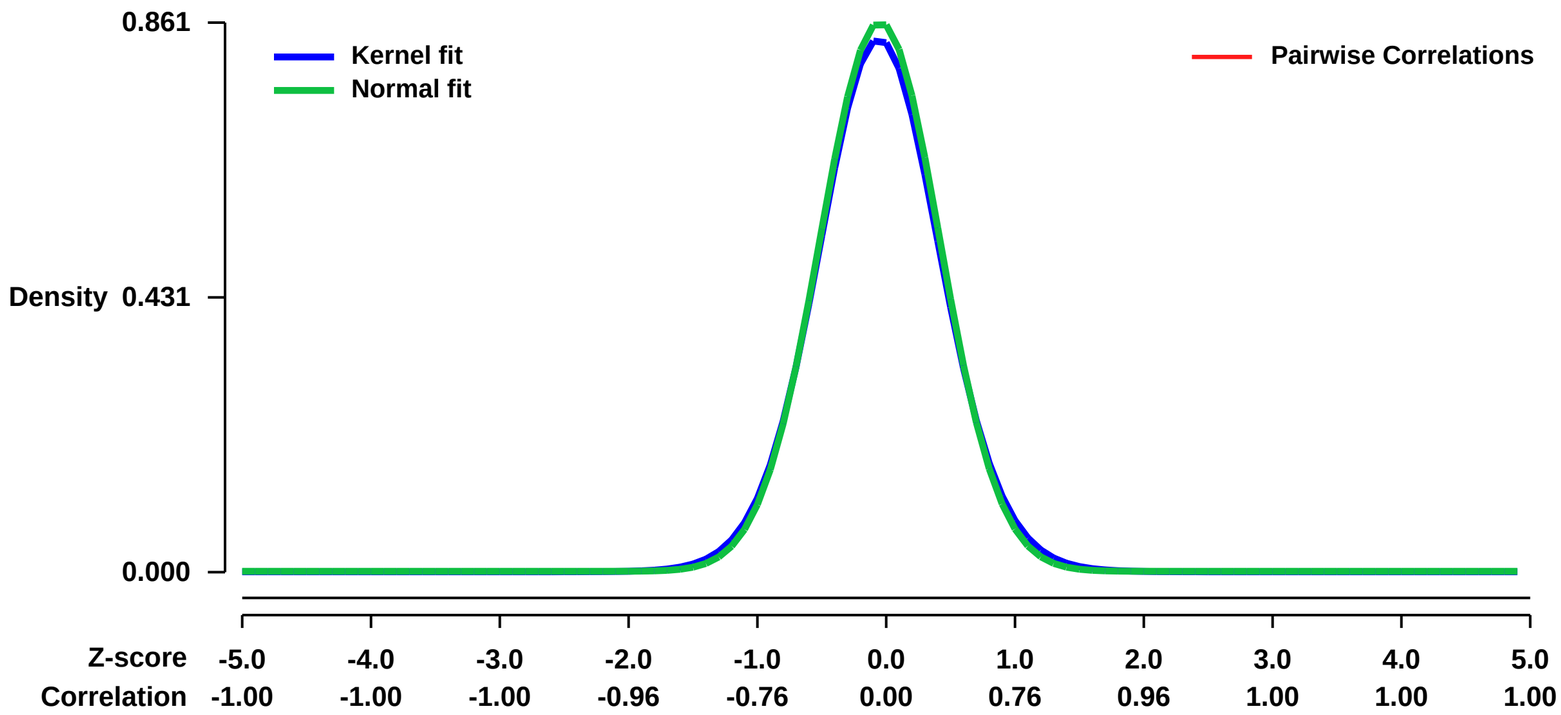

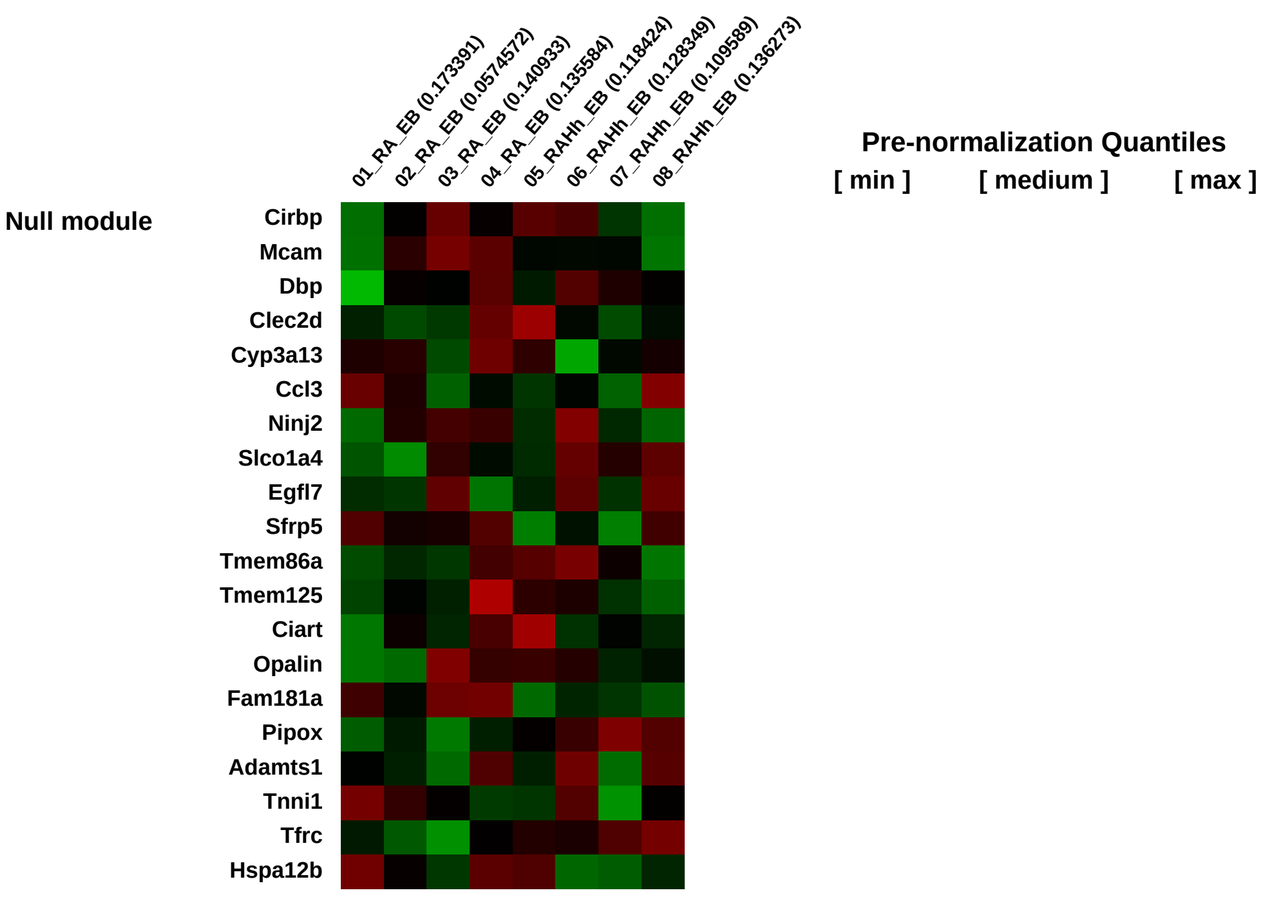

GEO Series "GSE49689" Expression Profiles

Num of samples in this series: 23

Scale of expression profile Z-scores

-3.0 -2.0 -1.0 0.0 1.0 2.0 3.0

GEO Link:	http://www.ncbi.nlm.nih.gov/geo/query/acc.cgi?acc=GSE49689
Status:	Public on Dec 11 2013
Title:	A Mesodermal Factor, T (BRACHYURY), specifies mouse germ cell fate by directly activating germline determinants.
Organism:	Mus musculus
Experiment type:	Expression profiling by array
Platform:	GPL1261
Pubmed ID:	24331926
Summary & Design:	**Summary:** The germ cell lineage ensures reproduction and heredity in metazoans. Primordial germ cells (PGCs) in mice are induced in pluripotent epiblast cells by BMP4 and WNT3, yet their mechanism of action remains elusive. Here, using in vitro PGC specification system, we show that WNT3, but not BMP4, induces many transcription factors associated with mesoderm in epiblast-like cells (EpiLCs) through beta-CATENIN. Among these, T (BRACHYURY), a classical and conserved mesodermal factor, was essential for robust activation of Blimp1 and Prdm14, two of the germline determinants. T, but not SMAD1 or beta-CATENIN/TCF1, binds distinct regulatory elements of both Blimp1 and Prdm14, and directly up-regulates these genes without BMP4 and WNT3. Without BMP4, a program induced by WNT3 prevents T from activating Blimp1 and Prdm14, demonstrating that BMP4 is permissive for PGC specification. These findings establish a fundamental role of a mesodermal gene in PGC specification, a potentially evolutionarily conserved mechanism across metazoans. **Overall design:** Wnt3 (+/+) and Wnt3 (-/-) mouse embryonic stem cells (mESCs) bearing the BV transgenes expressing membrane-targeted Venus under the control of Blimp1 regulatory elements (Blimp1-mVenus: BV; PMID 18583473) were established and maintained. Epiblast-like cells (EpiLCs) were then induced from the established ES lines, followed by the cytokine stimulation (No cytokines [negative control], BMP4, Wnt3a, BMP4+Wnt3a) for different periods (0h, 12h, 24h, 36h).

Background corr dist: KL-Divergence = 0.2220, L1-Distance = 0.0407, L2-Distance = 0.0033, Normal std = 0.3199

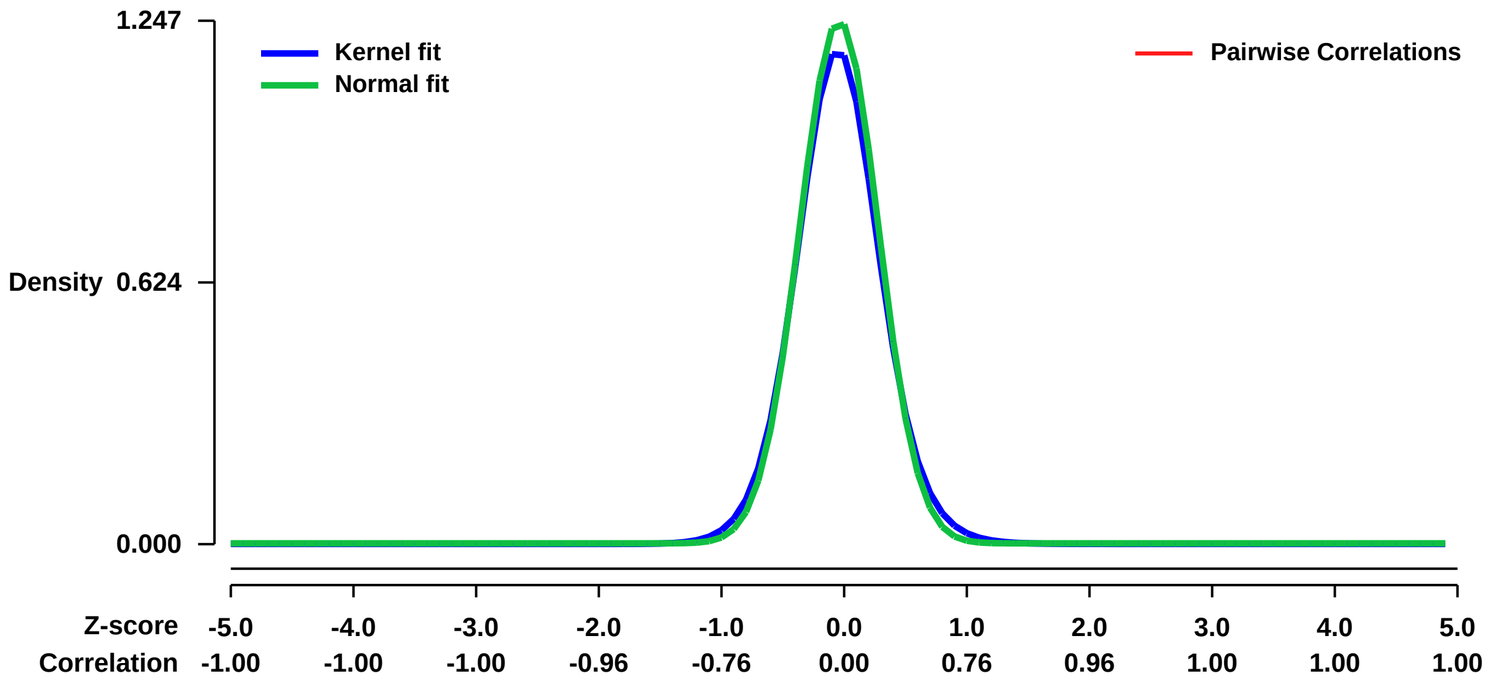

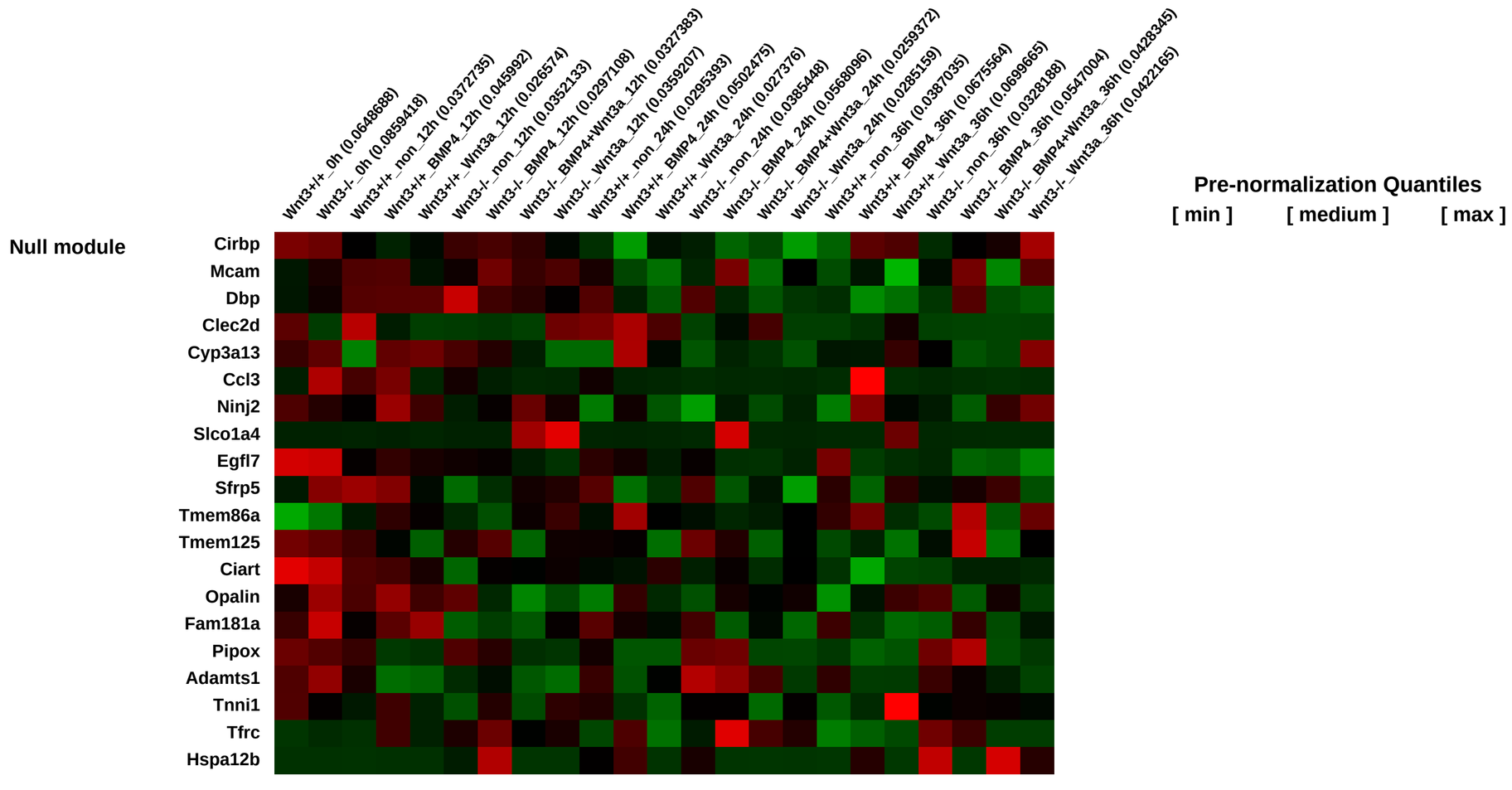

GEO Series "GSE49814" Expression Profiles

Num of samples in this series: 8

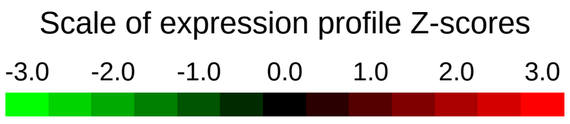

GEO Link:	http://www.ncbi.nlm.nih.gov/geo/query/acc.cgi?acc=GSE49814
Status:	Public on Oct 21 2013
Title:	Genome-wide cheater screen reveals safeguards for cell cooperation during embryogenesis
Organism:	Mus musculus
Experiment type:	Expression profiling by array
Platform:	GPL1261
Pubmed ID:	24030493

Summary & Design:

Summary:
Ensuring cooperation among formerly autonomous cells has been a central challenge in the evolution of multicellular organisms. One solution is monoclonality, but this option does not eliminate genetic and epigenetic variability, leaving room for exploitative behavior. We therefore hypothesized that embryonic development must be protected by robust regulatory mechanisms that prevent aberrant clones from superseding wild-type cells. Using a genome-wide screen in murine induced pluripotent stem cells, we identified a network of genes (centered on p53, topoisomerase 1, and olfactory receptors) whose downregulation caused the cells to replace wild-type cells, both in vitro and in the mouse embryoâ without perturbing normal development. These genes thus appear to fulfill an unexpected role in fostering cell cooperation.

Overall design:
We mixed knockdown (Top1 or p53) and mock embryonic stem cells and collected mRNA on day 4 of coculture, while cells were in the growth phase. These conditions allowed direct comparisons within a single cell type rather than a mixture of different cell types as seen under differentiation conditions. To extract information specific to cell cooperation as opposed to canonical p53 and Top1 functions, we compared results obtained from our mixed (1:4) culture with those obtained after mixing mRNA (also 1:4) from p53- or Top1-knockdown cells and mock cells that were grown homotypically.

Background corr dist: KL-Divergence = 0.0856, L1-Distance = 0.0220, L2-Distance = 0.0007, Normal std = 0.4642

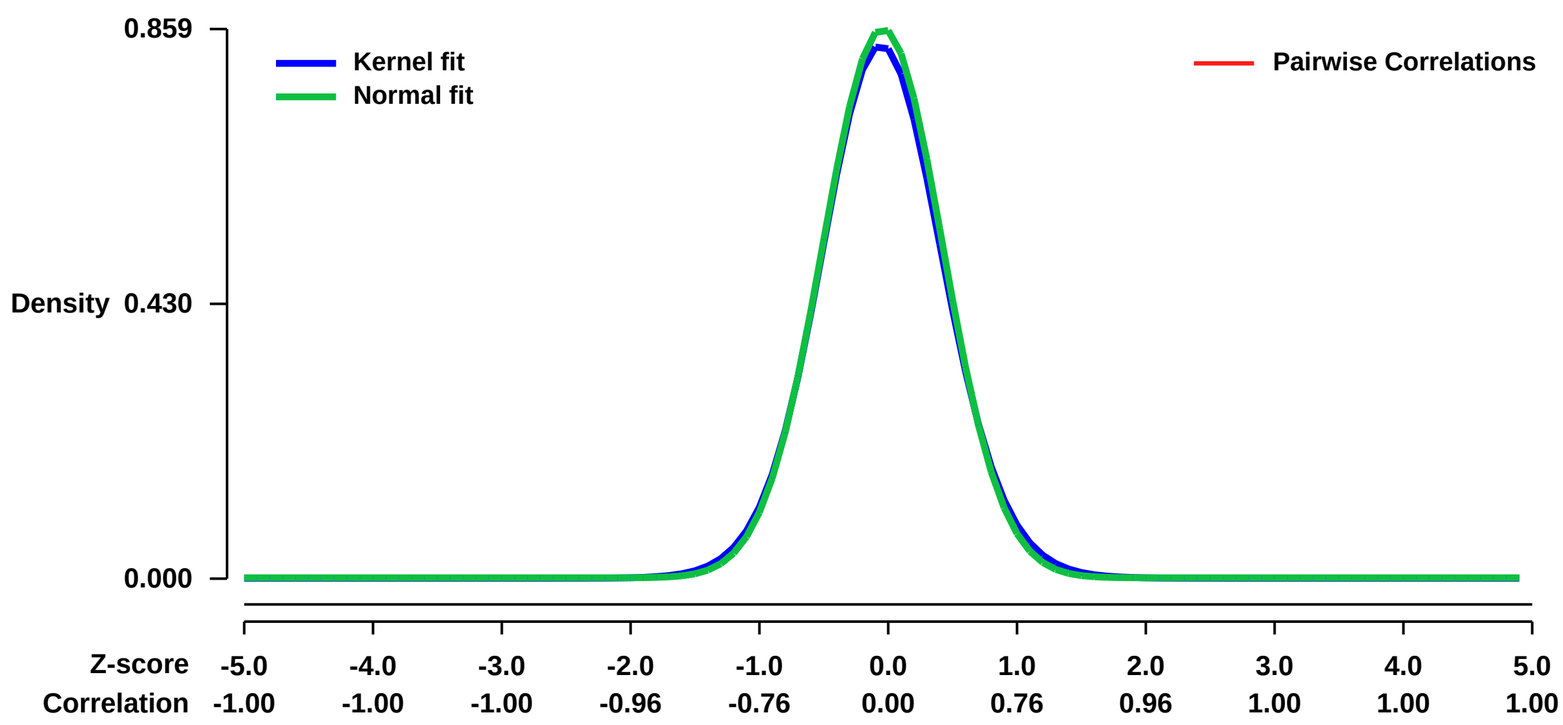

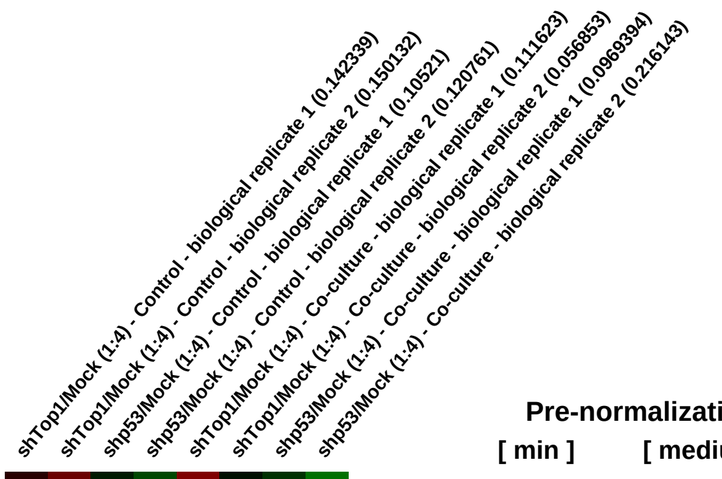

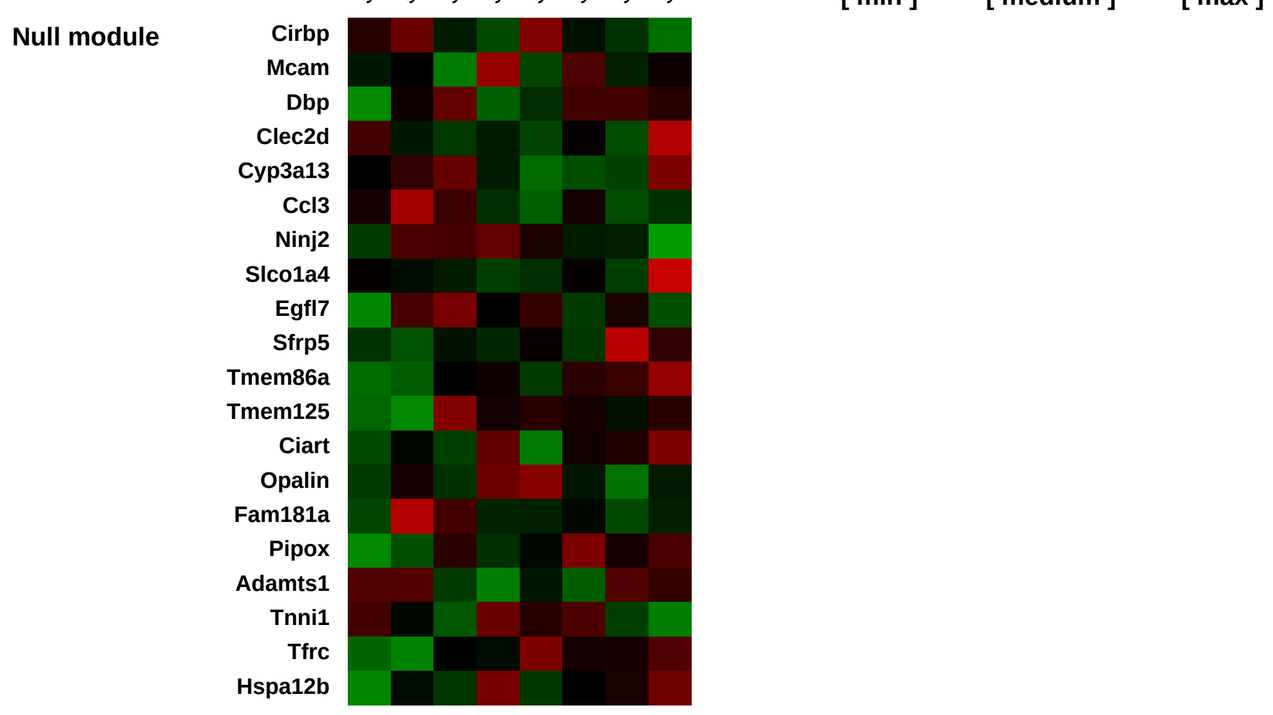

GEO Series "GSE50059" Expression Profiles

Num of samples in this series: 8

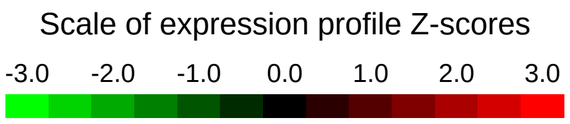

GEO Link:	http://www.ncbi.nlm.nih.gov/geo/query/acc.cgi?acc=GSE50059
Status:	Public on Jan 01 2014
Title:	Endothelin2 signaling in the neural retina promotes the endothelial tip cell state and inhibits angiogenesis
Organism:	Mus musculus
Experiment type:	Expression profiling by array
Platform:	GPL1261
Pubmed ID:	24043815
Summary & Design:	**Summary:** Endothelin signaling is required for neural crest migration and homeostatic regulation of blood pressure. Here we report that constitutive over-expression of Endothelin-2 (Edn2) in the mouse retina perturbs vascular development by inhibiting endothelial cell (EC) migration across the retinal surface and subsequent EC invasion into the retina. Developing endothelial cells exist in one of two states: tip cells at the growing front, and stalk cells in the vascular plexus behind the front. This division of endothelial cell states is one of the central organizing principle of angiogenesis. In the developing retina, Edn2 over-expression leads to over-production of endothelial tip cells by both morphologic and molecular criteria. Spatially localized over-expression of Edn2 produces a correspondingly localized endothelial response. Edn2 over-expression in the early embryo inhibits vascular development at mid-gestation, but Edn2 over-expression in developing skin and brain has no discernable effect on vascular structure. Inhibition of retinal angiogenesis by Edn2 requires expression of Endothelin receptor A (Ednra) but not Ednrb in the neural retina. Taken together, these observations imply that the neural retina responds to Edn2 by synthesizing one or more factors that promote the endothelial tip cell state and inhibit angiogenesis. The response to Edn2 is sufficiently potent that it over-rides the activities of other homeostatic regulators of angiogenesis, such as vascular endothelial growth factor. **Overall design:** Z/Edn2 females were crossed to Six3-Cre; Six3-Cre males. Postnatal P8 pups were genotyped for the Z/Edn2 allele by detection of Laz-Z activity in tail clips. Retinas from 2 - 3 pups were pooled for each data point.

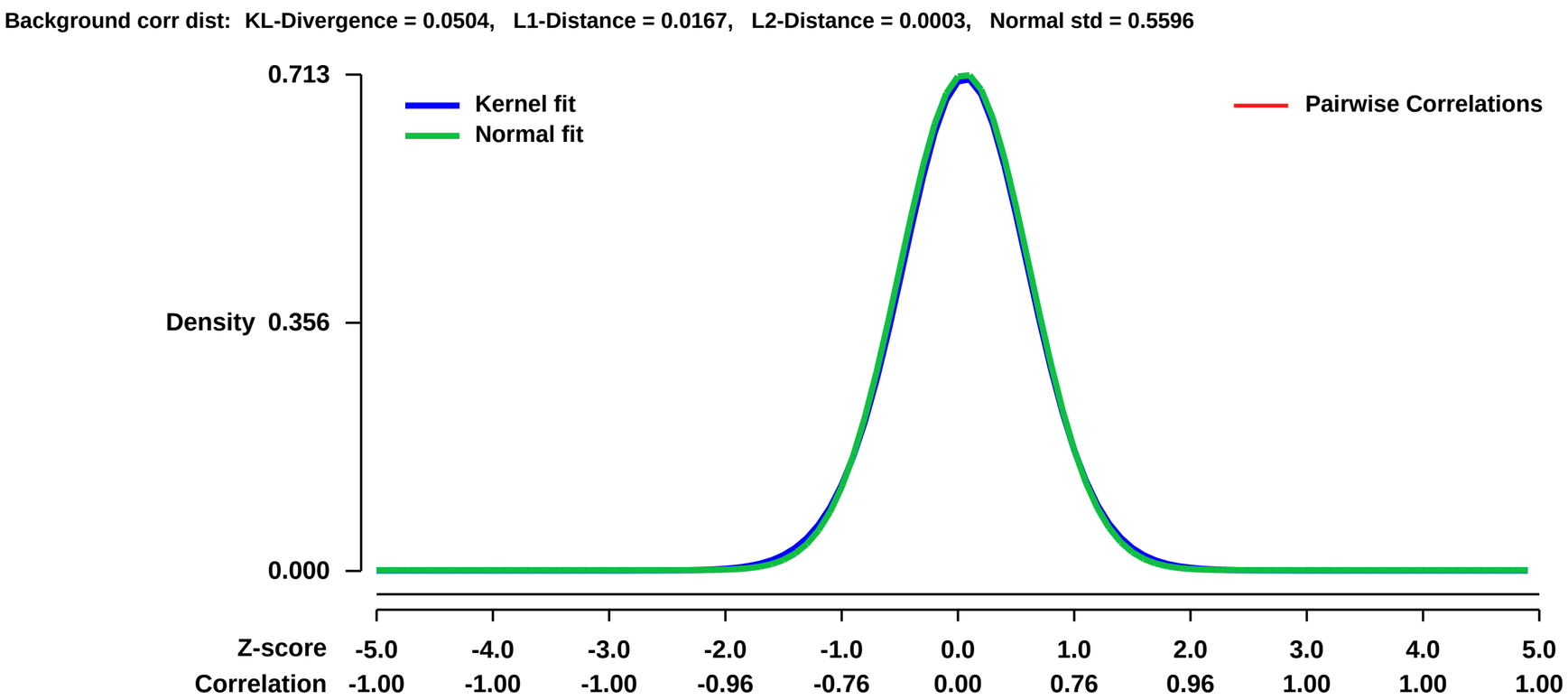

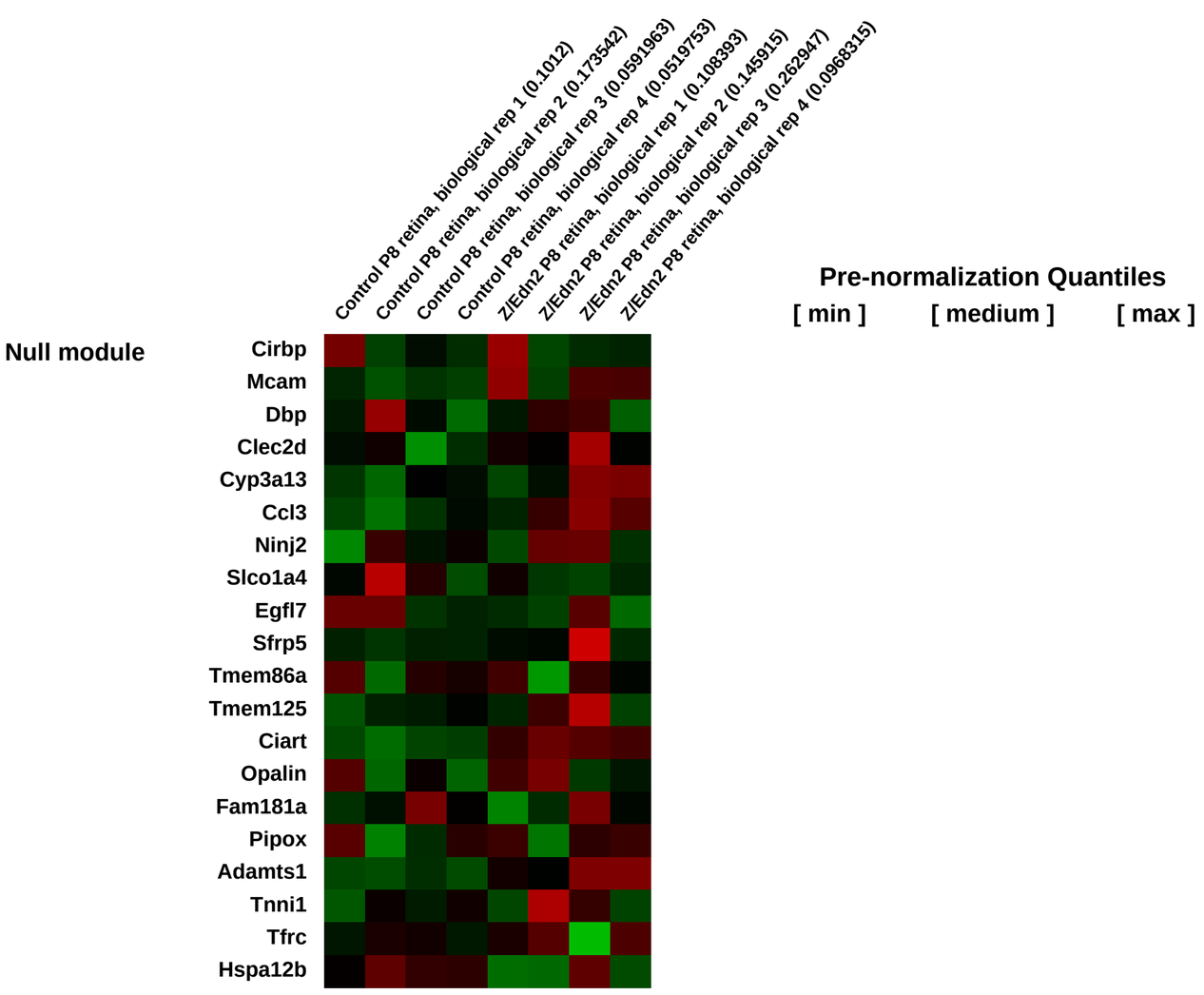

GEO Series "GSE5011" Expression Profiles

Num of samples in this series: 10

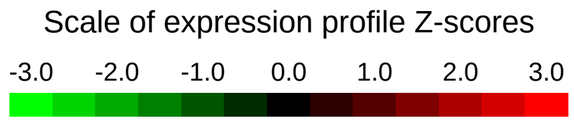

GEO Link: http://www.ncbi.nlm.nih.gov/geo/query/acc.cgi?acc=GSE5011

Status: Public on Jun 06 2006

Title: oksen-affy-mouse-212956

Organism: Mus musculus

Experiment type: Expression profiling by array

Platform: GPL1261

Pubmed ID:

Summary & Design:

Summary:
Experimental autoimmune encephalomyelitis (EAE) is an autoimmune inflammatory disease of the CNS that is mediated by T cells and macrophages and represents the paradigmatic model for multiple sclerosis (MS). In EAE, therapeutic approaches targeting T cells have been successfully utilized leading to immunosuppression or tolerance. It has been recently shown that mesenchimal stem cells (MSC) isolated from C57BL/6J mice are an effective treatment of EAE induced by the encephalitogenic peptide pMOG 35-55. In this project we aim to track and evaluate the molecular changes the MSC acquire through several in-vitro passages that determine their therapeutic potential. Elucidation of the molecular pathways involved in this process will allow us to formulate better models of disease progression and curative strategies.

Specific aim:The specific aim of this proposal is to dissect the molecular pathways that mesenchimal stem cells undergo during in-vitro treatment and confer them the therapeutic potential to cure EAE. To accomplish this aim, we will purify and grow murine MSC under the same conditions used for therapy as described in Zappia et al (In press. Brain, 2005) and obtain samples at several stages of the culture. RNA will be purified from each sample and profiled using Affymetrix microarrays. Initial bioinformatics analysis will include data transformation, normalization and filtering. A second stage analysis will involve time-series analysis by ANOVA and dynamic events modeling using neural networks.

Stem cells are now viewed as potential source of cells for almost any tissue due to their postulated capacity to give rise to virtually any type of cell. Among them, mesenchymal stem cells (MSC), can extensively proliferate in vitro and differentiate under appropriate conditions in bone, cartilage, and other mesenchymal tissues. It has been also reported that MSC can differentiate into other cells types including neuroectodermal cells. Furthermore, upon tissue injury MSC have been shown to migrate into the damaged brain. These results suggest that MSC could provide an ideal cell source for repair of injured organs including the central nervous system (CNS). In addition to their plasticity, MSC have been recently demonstrated to suppress several T lymphocyte activities thus exerting an immunoregulatory capacity both in vitro and in vivo. The mechanisms mediating such effect are only partially understood. We hypothesize that an analysis of how MSC acquire their therapeutic potential in vitro by expression profiling in a time series fashion will allow us to dissect the involved mechanisms.

Before arriving to our lab in UCSF, samples will be processed as follows: Bone marrow from 6-8 weeks old C57BL/6J mice will be flushed out of tibias and femurs. After two washings by centrifugation at 1500 rpm for 5 min in PBS (Sigma Chemical Co., St. Louis, MO, USA), cells will be plated in 75 cm2 tissue culture flasks at the concentration of 0.3-0.4 x 106 cells/cm2 utilizing Murine Mesencult as medium (Stem Cell Technologies Inc., Vancouver, BC, Canada). Cells will be kept in a humidified 5% CO2 incubator at 37˚C for about 4-5 weeks, when only adherent cells will be collected following 10 min incubation at 37˚C with 0.05% trypsin solution containing 0.02% EDTA. After the first cut and for the subsequent 4 or 5 passages, cells will be plated in 25 cm2 flasks at 1.2-2.0 x 104cells/cm2 . For the following passages cells will routinely seeded at 4-10 x 103cells/cm2 reaching confluence only after 4-5 days. Cells will be collected at selected timepoints and immersed in TRizol reagent and shipped to UCSF. For the initial stage of this project cell will be collected at the following 5 time points:

T0: Bone marrow aspirates (uncultured)

T1: pre-mesenchymal stem cells (some cut before the population completely subtracted of Hematopoietic stem cells)

T2: Mesenchymal stem cells (in vitro assessed, functionally and phenotipically)

T3: Mesenchymal stem cells biological active in vivo

T4: Mesenchymal stem cells at the passage in vitro next to the one active in vivo

T5: Mesenchymal stem cells no more active in vitro neither in vivo

Once in our lab, RNA will be extracted using the Trizol reagent (Invitrogen) and further purified by the RNeasy kit (Qiagen). Sample labeling will be performed according to the array manufacturer (Affymetrix) instructions. Subject to initial results, we plan to add intermediate timepoints in subsequent stages.

Keywords: time-course

Overall design:

Background corr dist: KL-Divergence = 0.1086, L1-Distance = 0.0338, L2-Distance = 0.0023, Normal std = 0.4283

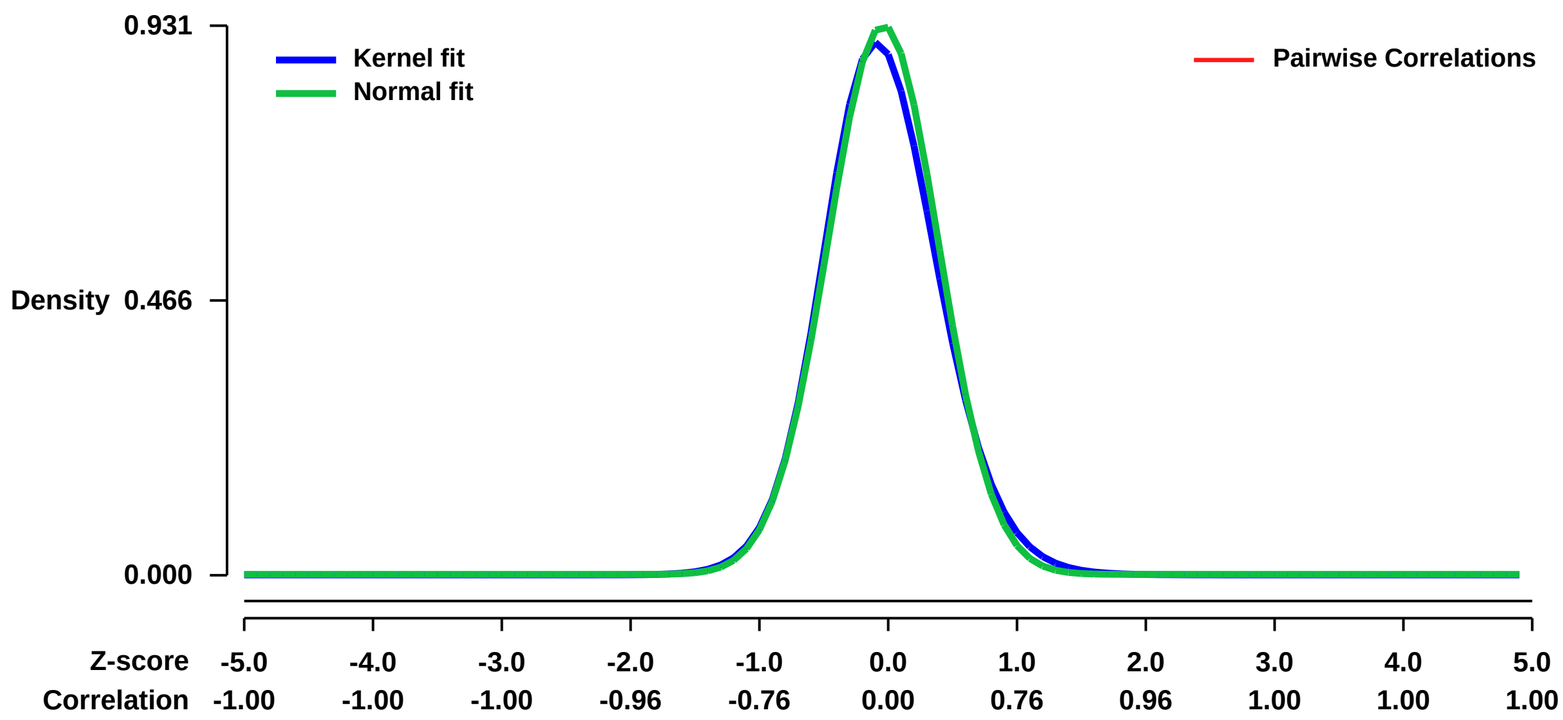

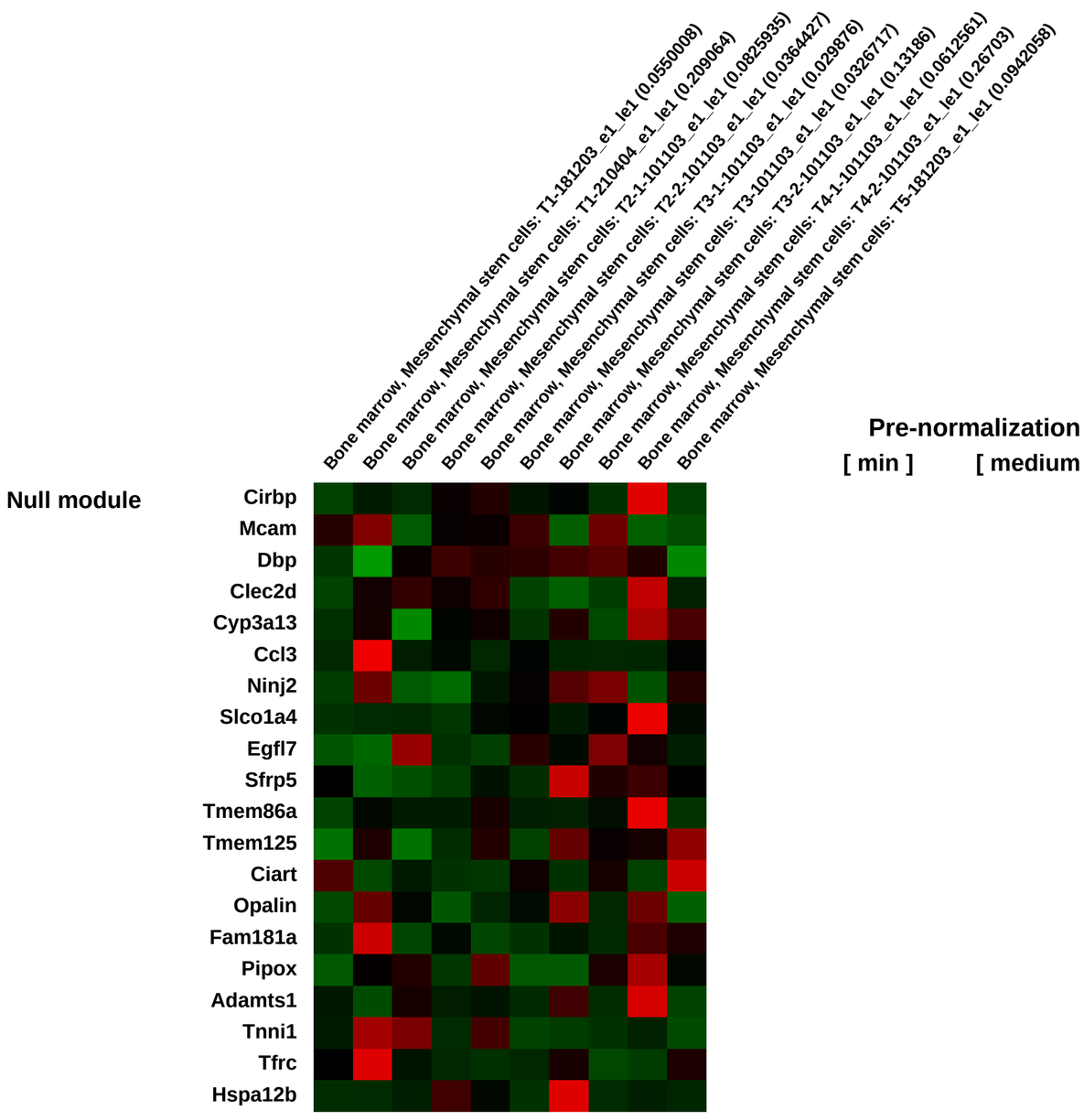

GEO Series "GSE50122" Expression Profiles

Num of samples in this series: 10

Scale of expression profile Z-scores

-3.0 -2.0 -1.0 0.0 1.0 2.0 3.0

GEO Link:	http://www.ncbi.nlm.nih.gov/geo/query/acc.cgi?acc=GSE50122
Status:	Public on Nov 18 2013
Title:	Runx3 function in splenic NK cells (IL-2 or IL-15)
Organism:	Mus musculus
Experiment type:	Expression profiling by array
Platform:	GPL1261
Pubmed ID:	24236182
Summary & Design:	**Summary:** NK cells are innate immune cells that recognize and kill foreign, virally-infected and tumor cells without the need for prior immunization. NK expansion following viral infection is IL-2 or IL-15-dependent. **Overall design:** To identify Runx3 responsive genes, NK cells were isolated from spleen of WT and Runx3-/- mice . Ten samples (5 WT and 5 Runx3-/-) of freshly isolated NK cells were separately obtained from individual mice. Cells were cultured for 7 days with IL-2 or IL-15.

Background corr dist: KL-Divergence = 0.0244, L1-Distance = 0.0693, L2-Distance = 0.0057, Normal std = 0.8495

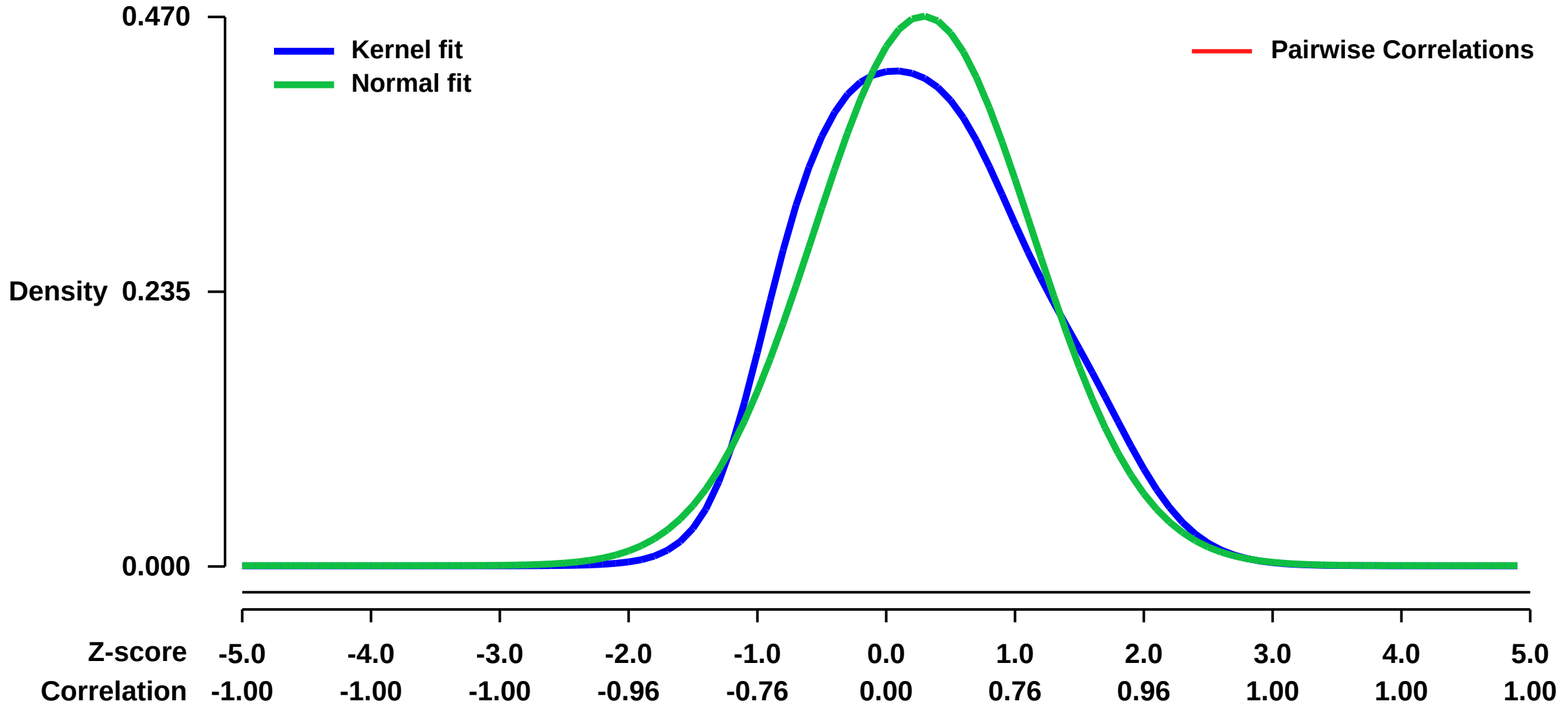

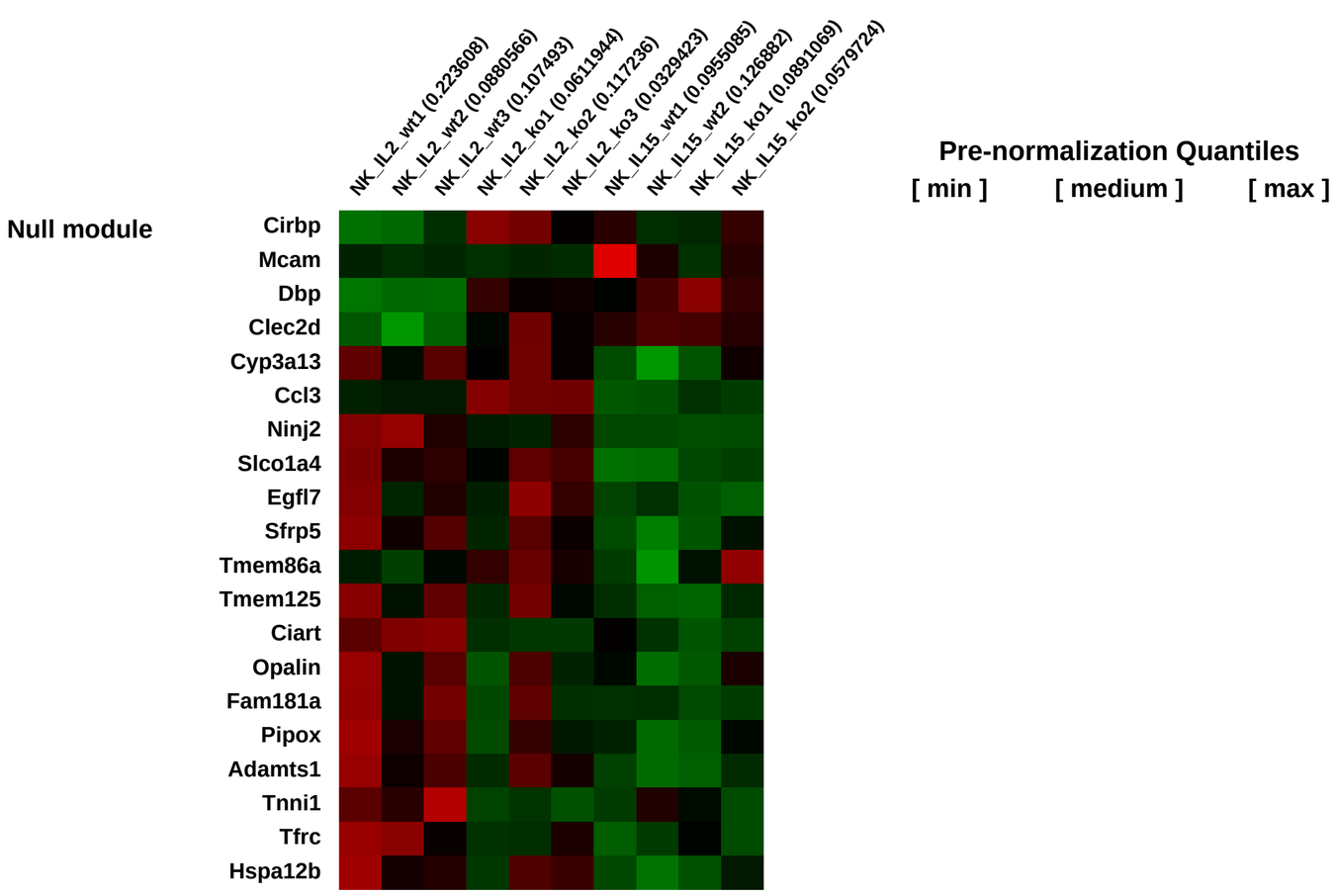

GEO Series "GSE50123" Expression Profiles

Num of samples in this series: 6

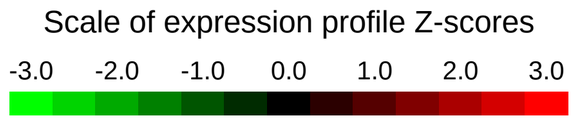

GEO Link:	**http://www.ncbi.nlm.nih.gov/geo/query/acc.cgi?acc=GSE50123**
Status:	**Public on Nov 18 2013**
Title:	**Runx3 function in splenic NK cells**
Organism:	**Mus musculus**
Experiment type:	**Expression profiling by array**
Platform:	**GPL1261**
Pubmed ID:	**24236182**
Summary & Design:	**Summary:** **NK cells are innate immune cells that recognize and kill foreign, virally-infected and tumor cells without the need for prior immunization. NK expansion following viral infection is IL-2 or IL-15-dependent.** **Overall design:** **To identify Runx3 responsive genes, NK cells were isolated from spleen of WT and Runx3-/- mice . Six samples (3 WT and 3 Runx3-/-) of freshly isolated NK cells (resting) were separately obtained from individual mice.**

Background corr dist: **KL-Divergence = 0.0470, L1-Distance = 0.0852, L2-Distance = 0.0114, Normal std = 0.6857**

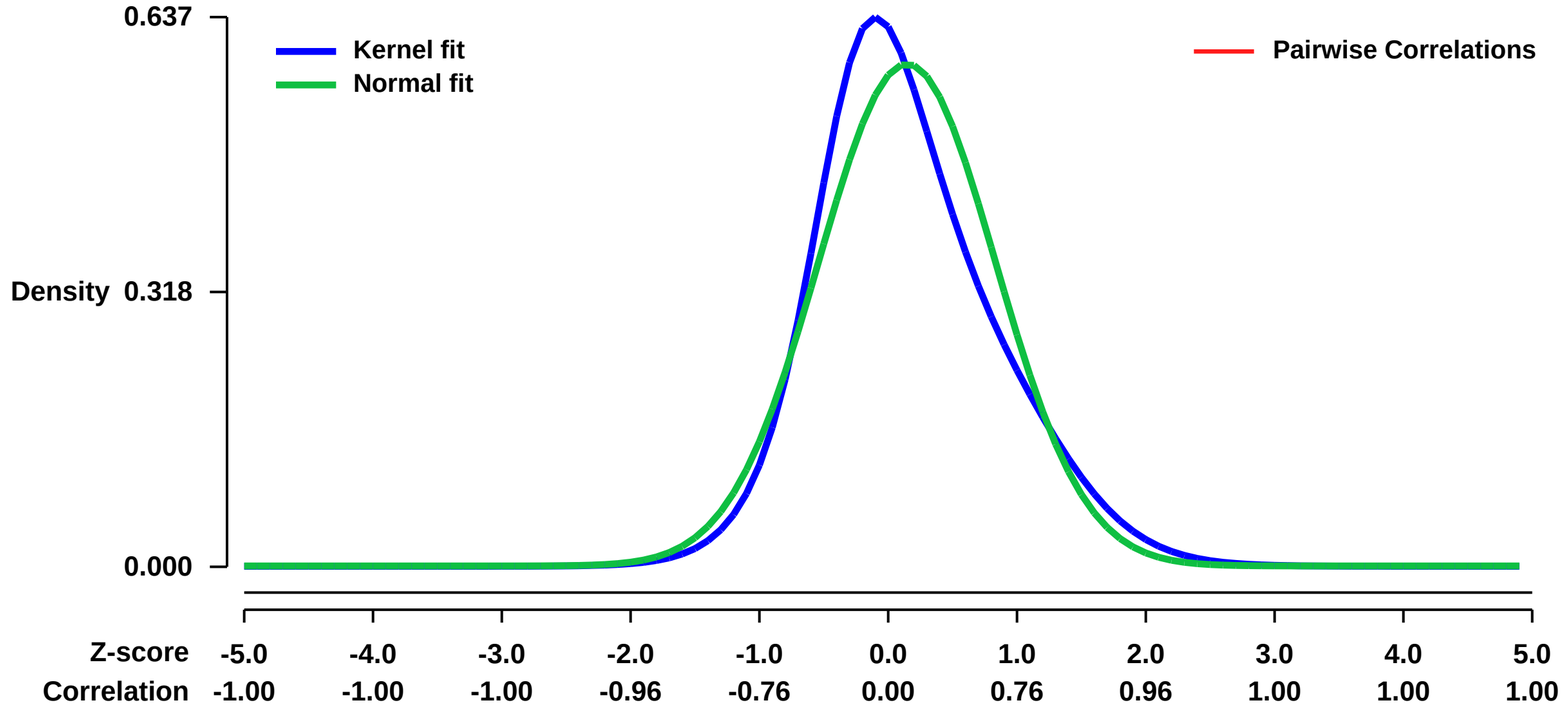

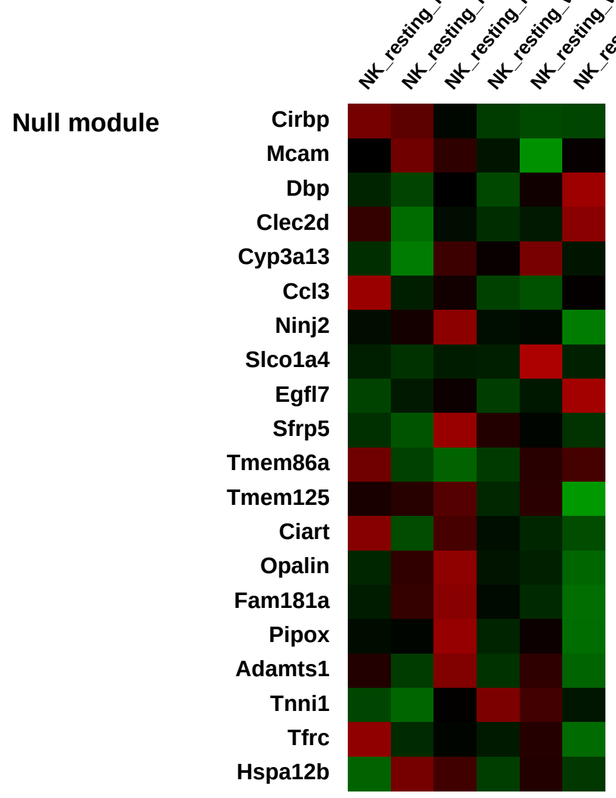

GEO Series "GSE5035" Expression Profiles

Num of samples in this series: 12

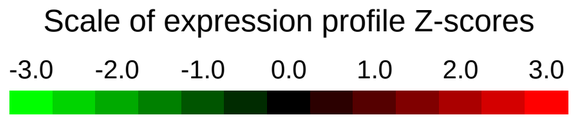

GEO Link:	**http://www.ncbi.nlm.nih.gov/geo/query/acc.cgi?acc=GSE5035**
Status:	**Public on Jun 09 2006**
Title:	**zhang-affy-arabi-50806**
Organism:	**Mus musculus**
Experiment type:	**Expression profiling by array**
Platform:	**GPL1261**
Pubmed ID:	

Summary & Design:

Summary:
In our original grant we proposed to use the NR3B-null mouse model to study the role of NR3B subunit in motor neuron function. We have now successfully generated NR3B null mice. Interestingly, NR3B-null mice invariably die at age P4-P8. Our preliminary examination indicates that the motor strength of these mice is severely impaired prior to death. As we continue to explore the cause of death in NR3B null mice, we propose to conduct gene profiling experiments to search for transcription changes in the brain related to ablation of the NR3B gene. We would like to use the facility provided by the NINDS/NIMH Microarray Consortium to identify true outlier genes that show abnormal expression patterns in these mice. Analysis of these outlier genes will help to identify changes in networks and pathways that may cause the death of NR3B-null mice. These studies will further help to elucidate the functional role of NR3B in motor neurons.

We will compare samples from the hindbrain and spinal cord of wild type and NR3B null mice to identify true outlier genes that show abnormal expression patterns, which may be implicated in the death of NR3B-null mice

We hypothesize that genes with their transcription level changing significantly by ablation of NR3B will be associated with the molecular mechanism underlying the death of motor neurons in NR3B null mice.

As NR3B is expressed primarily in the hindbrain and spinal cord, we will first collect and analyze the hindbrain and spinal cord samples from NR3B null mice and wild-type controls in triplicate at two time points (P0 and P5). Total RNA from total 12 samples will be purified. Extracted RNAs will be treated for with DNase I to remove contaminating genomic DNA. The purified RNA will be sent to the NINDS/NIMH Microarray Consortium to generate biotin-labeled probe according to the Affymetrix protocol. These probes will be used to hybridize the GeneChip Mouse Genome 430 2.0 Array. The hybridization, scanning, and initial data analysis of these GeneChips will be conducted by the Consortium staff. We will analyze the collected data further after data collection. We will use computer software, GeneSpring (Silicon Genetics, Redwood City, CA), to analyze data from microarray experiments. We will first identify genes that show significant changes between wild-type and NR3B null mice by applying ANOVA analysis to sample groups of different ages. The genes identified in this manner will then be subjected to hierarchical (Gene tree) and nonhierarchical (K-means) cluster analysis, in order to group them according to similar expression patterns. Another clustering method, the self-organizing map, will be used to determine whether one gene cluster is a variant of another. Finally, the Principal Components Analysis (PCA) will be employed to analyze large sample groups, which may include experimental variability with respect to age, anatomical location and genotype. We will determine from these analysis whether further experiments are needed using different array platforms, such as Agillent Oligo Array.

Keywords: time-course

Overall design:

Background corr dist: KL-Divergence = 0.1035, L1-Distance = 0.0235, L2-Distance = 0.0007, Normal std = 0.4373

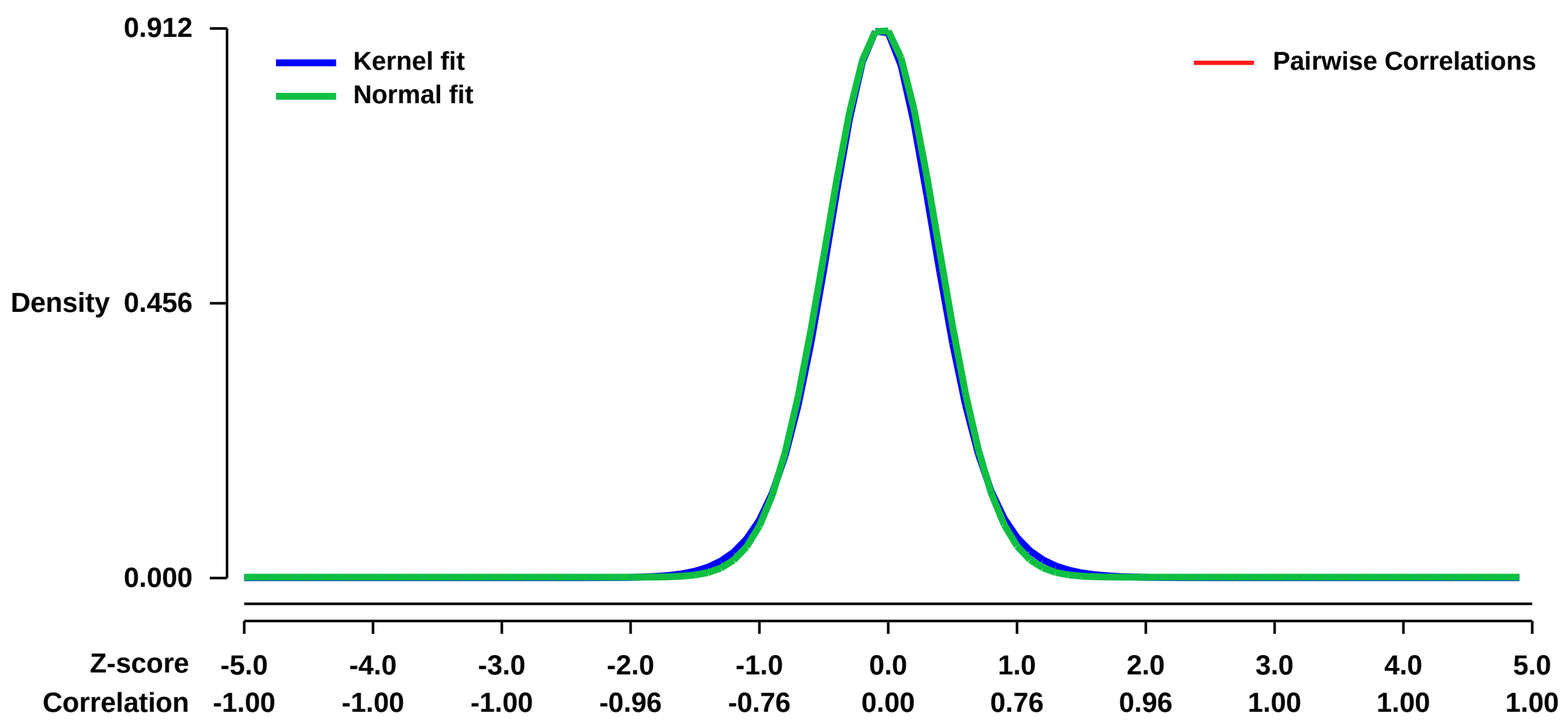

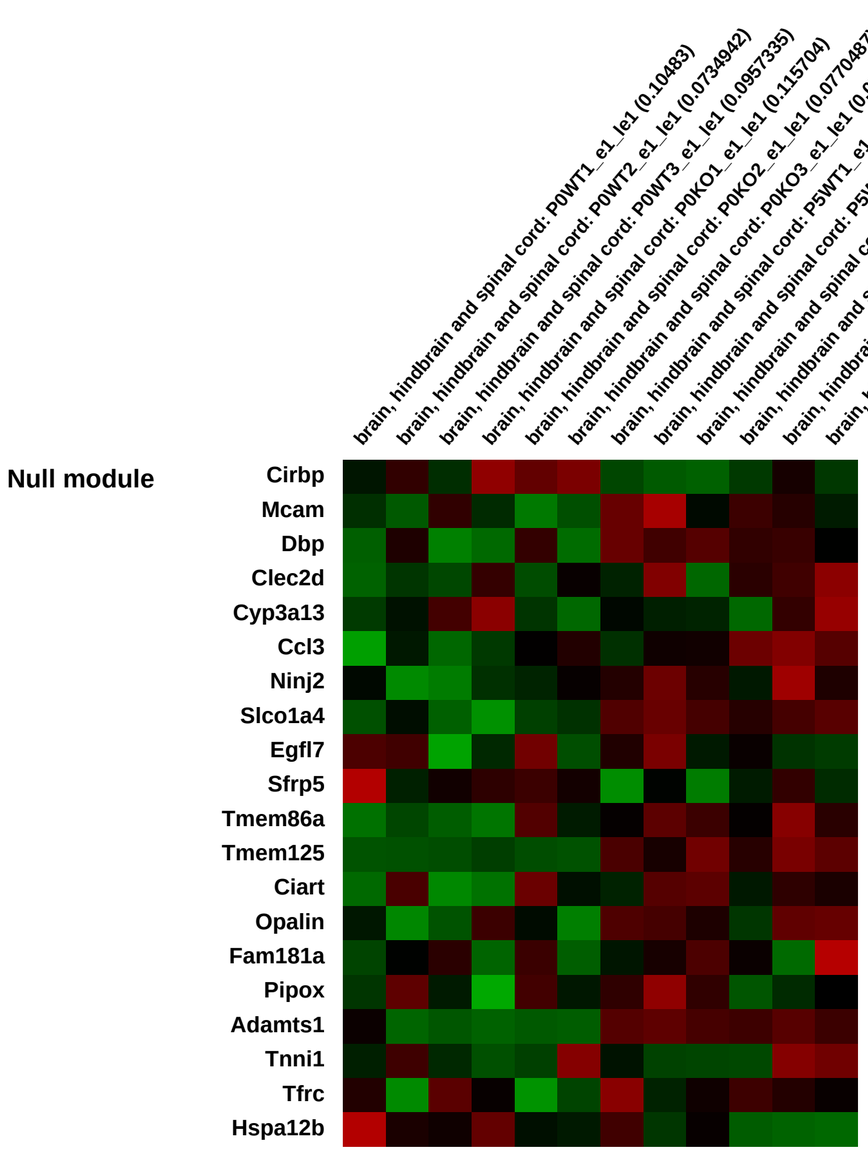

GEO Series "GSE5038" Expression Profiles

Num of samples in this series: 9

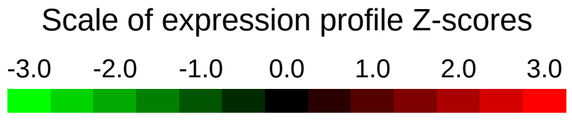

GEO Link:	**http://www.ncbi.nlm.nih.gov/geo/query/acc.cgi?acc=GSE5038**
Status:	**Public on Jun 09 2006**
Title:	**zhang-affy-mouse-308606**
Organism:	**Mus musculus**
Experiment type:	**Expression profiling by array**
Platform:	**GPL1261**
Pubmed ID:	

Summary & Design:

Summary:
In our original grant we proposed to use the NR3B-null mouse model to study the role of NR3B subunit in motor neuron function. We have now successfully generated NR3B null mice. Interestingly, NR3B-null mice invariably die at age P4-P8. Our preliminary examination indicates that the motor strength of these mice is severely impaired prior to death. As we continue to explore the cause of death in NR3B null mice, we propose to conduct gene profiling experiments to search for transcription changes in the brain related to ablation of the NR3B gene. We have used the facility provided by the NINDS/NIMH Microarray Consortium to identify genes that show abnormal expression patterns in these mice. We would like to compare these changes with that opccured in SOD1 mice, a mouse model of motor neuron diseases. Analysis of these genes will help to identify changes in networks and pathways that may cause the death of NR3B-null mice. These studies will further help to elucidate the functional role of NR3B in motor neurons.

We will compare samples from motor neurons of wild type and SOD1 mice to identify genes that show abnormal expression patterns, which may be implicated in the death of SOD1 mice and shared with the same changes in NR3B-null mice.

We hypothesize that genes with their transcription level changing significantly in SOD1 mutant mice will be associated with the molecular mechanism underlying the death of motor neurons.

We like to compare motor neuron and spinal cord smaples from SOD1 mice at the age prior to the disease onset. Total RNA from total 9 samples will be purified, each from ~200 motor neurons obtained by Laser Capture Microdissection and the total spinal cord. Extracted RNAs will be subjected to one or two rounds of amplification and the obtained cRNA will be biotinylated. The purified cRNA will be sent to the NINDS/NIMH Microarray Consortium be used to hybridize the GeneChip Mouse Genome 430 2.0 Array. The hybridization, scanning, and initial data analysis of these GeneChips will be conducted by the Consortium staff. We will analyze the collected data further after data collection. We will first identify genes that show significant changes between wild-type and SOD1 mice and then compare that with the result from NR3B null mice.

Keywords: other

Overall design:

Background corr dist: **KL-Divergence = 0.0309, L1-Distance = 0.0667, L2-Distance = 0.0062, Normal std = 0.7668**

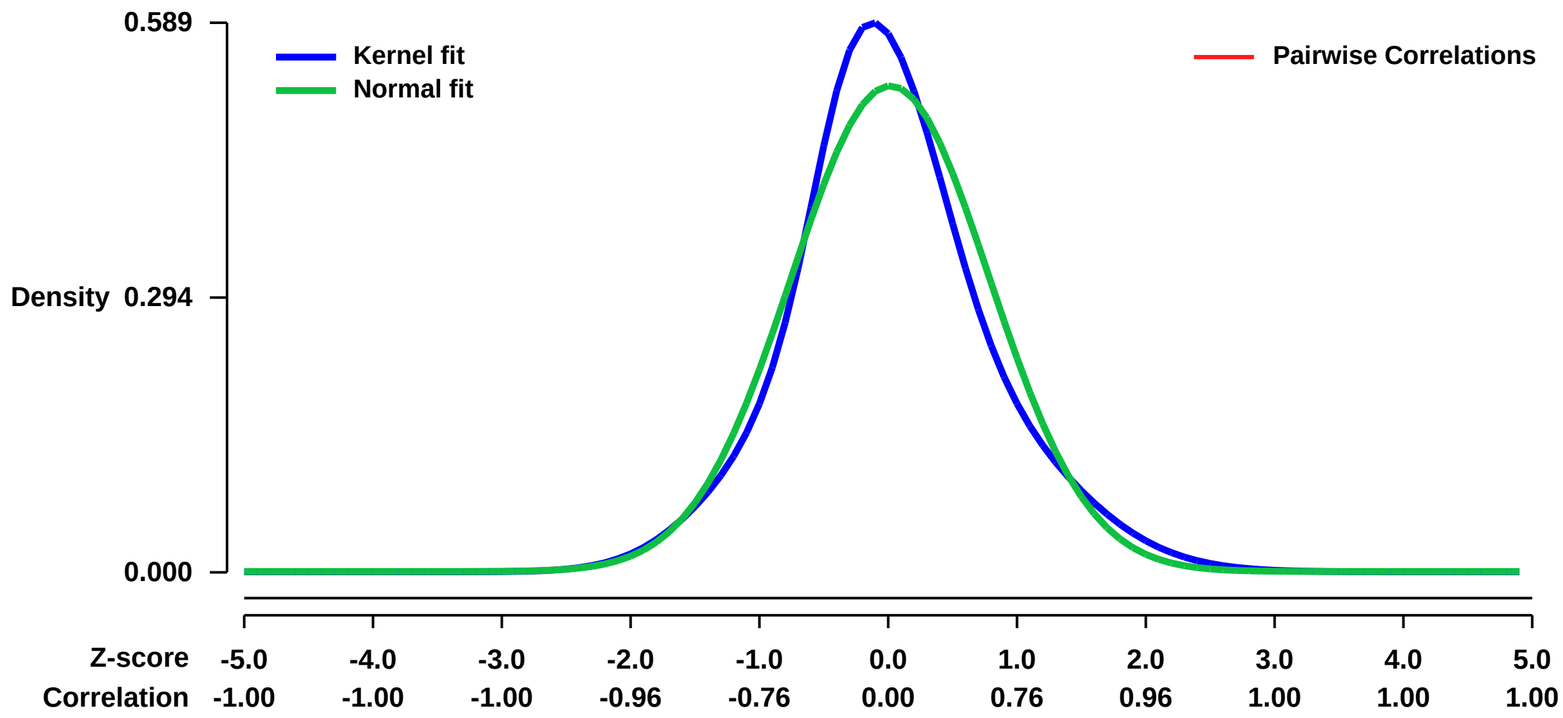

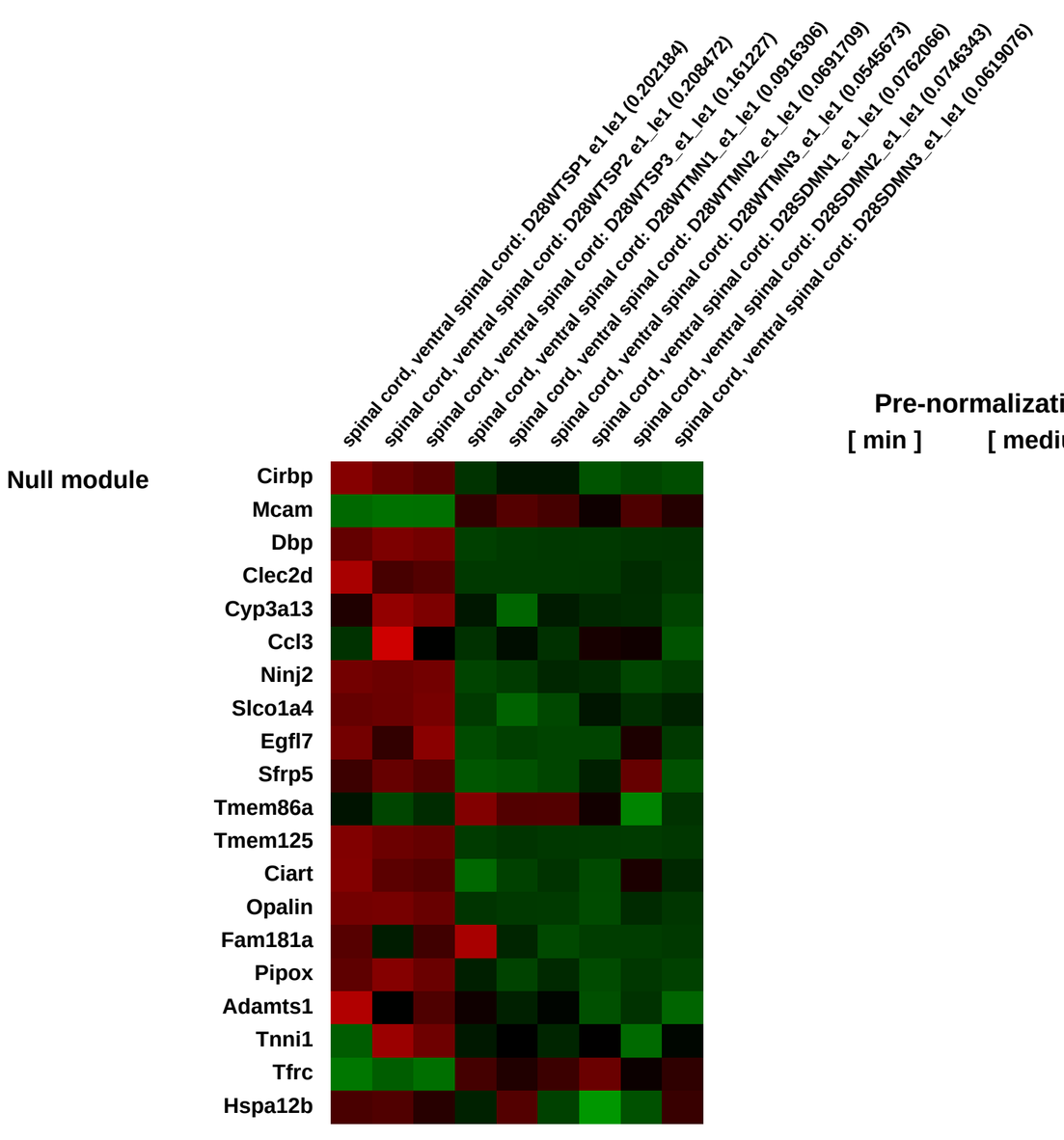

GEO Series "GSE5041" Expression Profiles

Num of samples in this series: 8

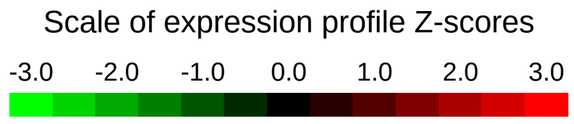

GEO Link:	http://www.ncbi.nlm.nih.gov/geo/query/acc.cgi?acc=GSE5041
Status:	Public on Jul 06 2006
Title:	Expression of the brown fat thermogenic gene program requires PGC-1alpha
Organism:	Mus musculus
Experiment type:	Expression profiling by array
Platform:	GPL1261
Pubmed ID:	16679291
Summary & Design:	**Summary:** To investigate the specific role of PGC-1 coactivators in brown fat cells, we generated immortal preadipocyte lines from the brown adipose tissue of mice lacking PGC-1alpha. We could then efficiently knockdown PGC-1beta expression by shRNA expression. Loss of PGC-1alpha did not alter brown fat differentiation but severly reduced the induction of thermogenic genes. In order to assess the specific requirement for PGC-1$_c$– in the global transcriptional response to cAMP, we used Affymetrix arrays to compare the sets of genes induced in response to a 4 hr dbcAMP treatment in differentiated wt and KO cells. This analysis revealed that 88 genes were induced more than 3-fold in the wt cells; of these, 54 (61% of total) were similarly increased in both wt and KO. However, 28 genes (32% of total) were decreased by at least 50% in the KO cells compared to wt cells. These data were confirmed by quantitative PCR for a subset of genes. These data indicate that PGC-1$_c$– is required for proper expression of approximately one third of the genes induced in response to cAMP in brown fat cells, but this set of sensitive genes is enriched in those involved in adaptative thermogenesis. **Keywords: thermogenic gene program** **Overall design:** WT and PGC-1alpha KO brown preadipocytes were differentiated into mature brown adipocytes for seven days. Cells were then treated with dibutyryl cAMP for four hours. Two replicates were made for each condition: WT non treated, WT treated with cAMP, KO non treated, KO treated with cAMP.

Background corr dist: KL-Divergence = 0.0435, L1-Distance = 0.0186, L2-Distance = 0.0004, Normal std = 0.5959

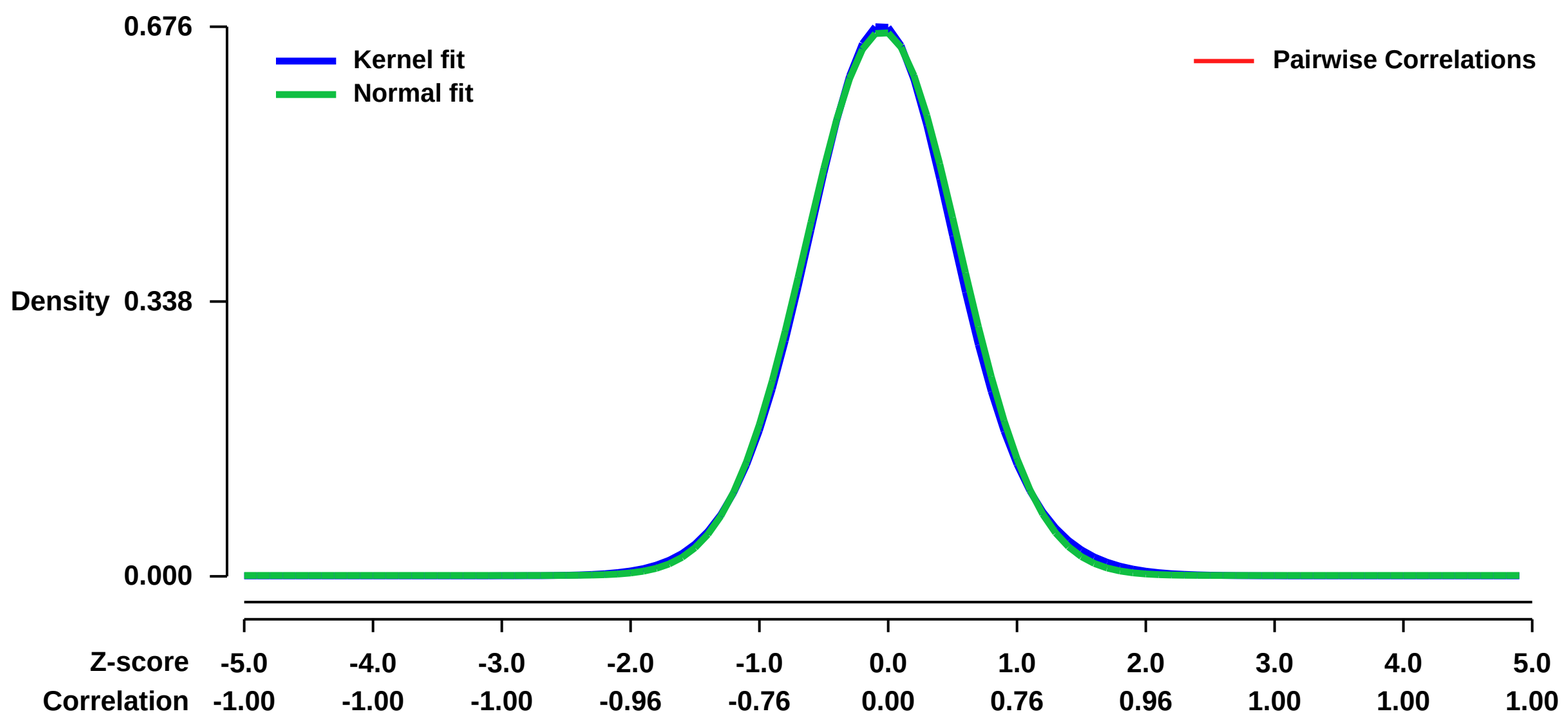

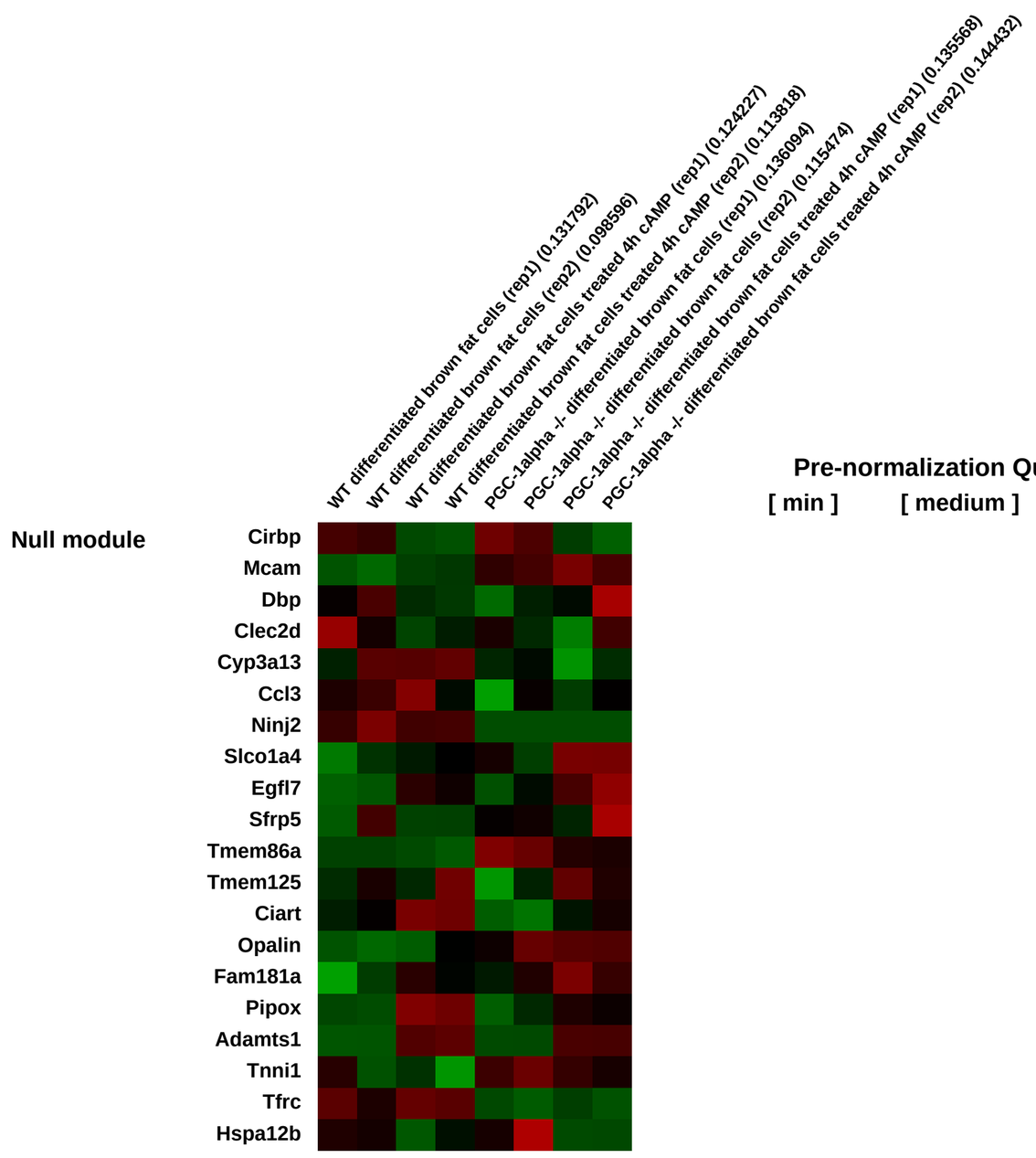

GEO Series "GSE50426" Expression Profiles

Num of samples in this series: 6

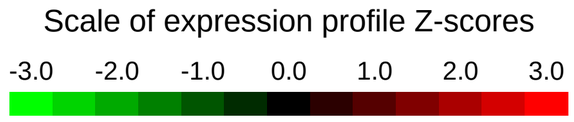

GEO Link:	**http://www.ncbi.nlm.nih.gov/geo/query/acc.cgi?acc=GSE50426**
Status:	**Public on Jan 01 2014**
Title:	**Expression Data from E16.5 hearts from WT and FOG-2R3K5A siblings**
Organism:	**Mus musculus**
Experiment type:	**Expression profiling by array**
Platform:	**GPL1261**
Pubmed ID:	
Summary & Design:	**Summary:** **Heart development is modulated by FOG-2/NuRD interactions. FOG-2R3K5A is unable to recuit the NuRD complex and this results in cardiac defects such as ASD, VSD, and thin ventricular walls** **We used microarrays to detail the changes in gene expression in FOG-2R3K5A hearts to determine misexpression of genes that may be causing the observed phenotypes.** **Overall design:** **Whole hearts from E16.5 Wild-type and FOG-2R3K5A siblings were processed for RNA extraction and hybridization on Affymetrix microarrays. We used three biological replicates of each genotype.**

Background corr dist: **KL-Divergence = 0.0394, L1-Distance = 0.0184, L2-Distance = 0.0003, Normal std = 0.6170**

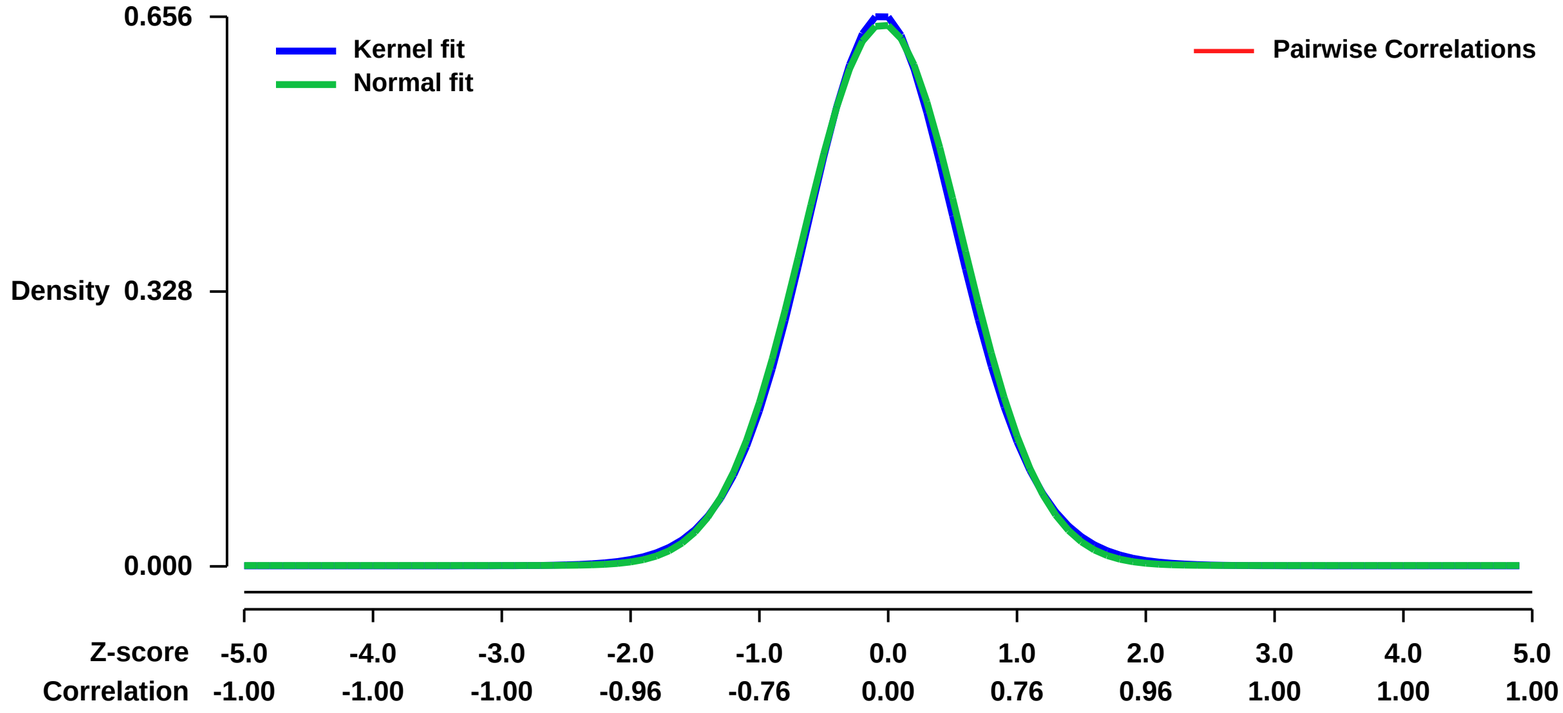

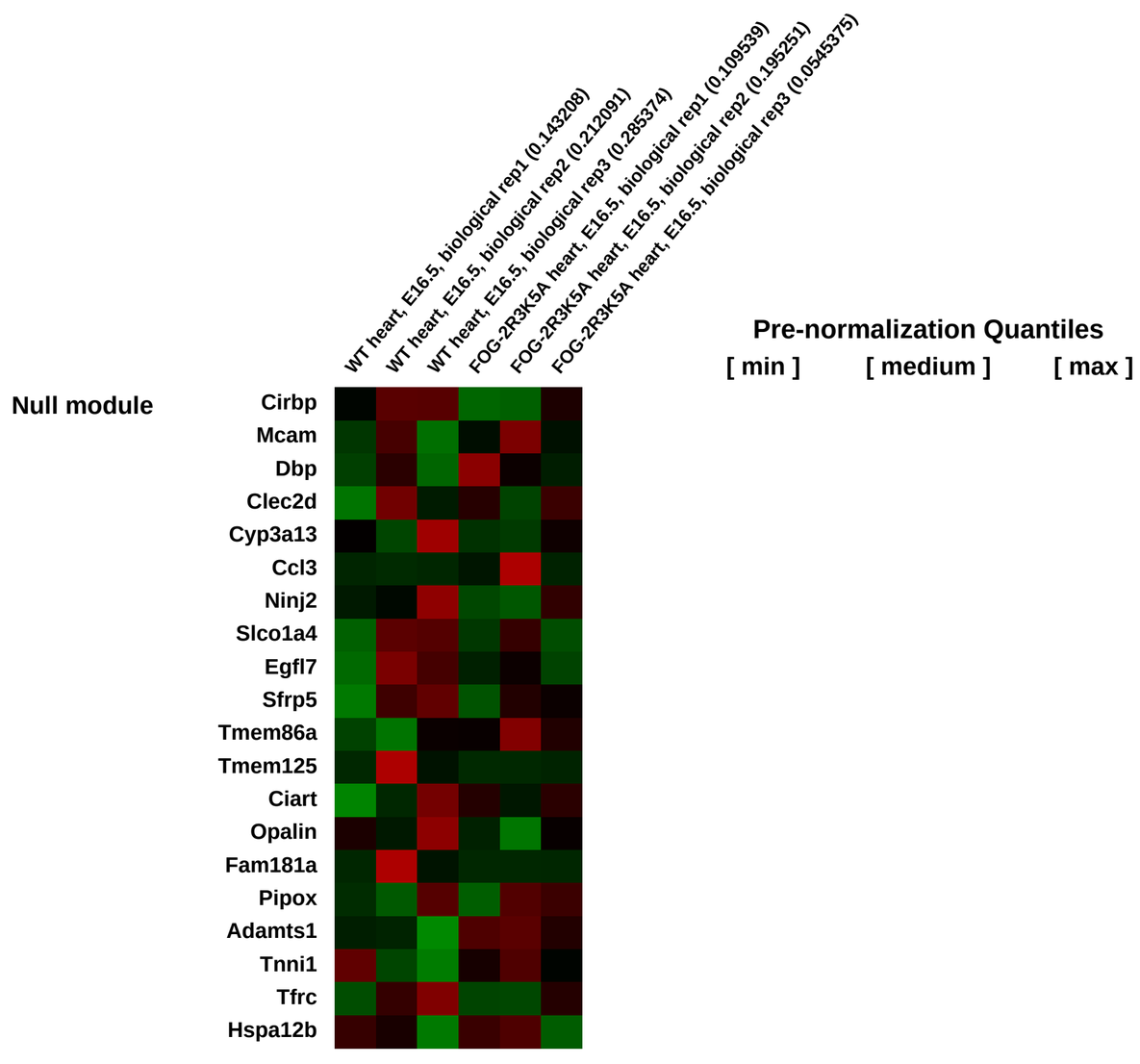

GEO Series "GSE50439" Expression Profiles

Num of samples in this series: 15

Scale of expression profile Z-scores

-3.0 -2.0 -1.0 0.0 1.0 2.0 3.0

GEO Link:	http://www.ncbi.nlm.nih.gov/geo/query/acc.cgi?acc=GSE50439
Status:	Public on Mar 01 2014
Title:	Examining efficiency of enrichment of kidney pericyte-specific messages by TRAP (Translating Ribosome Affinity Purification)
Organism:	Mus musculus
Experiment type:	Expression profiling by array
Platform:	GPL1261
Pubmed ID:	24652793
Summary & Design:	**Summary:** The long term goal is to define the transcriptional changes that accompany pericyte-to-myofibroblast transition in fibrotic kidney disease. Medullary pericytes are identified by their expression of a eGFPL10a fusion protein whose expression is driven by a Col1a1 promoter. Pericyte-specific RNA is generated by eGFP-affinity purification of polysomes from medullary lysates and then subject to microarray analysis. **Overall design:** Col1a1-eGFPL10a mice were subject to Sham or unilateral ureteral obstruction surgery. Sham kidneys were collected at day 0, and UUO kidneys were collected at day 2 or day 5 for TRAP.

Background corr dist: KL-Divergence = 0.1276, L1-Distance = 0.0385, L2-Distance = 0.0032, Normal std = 0.4031

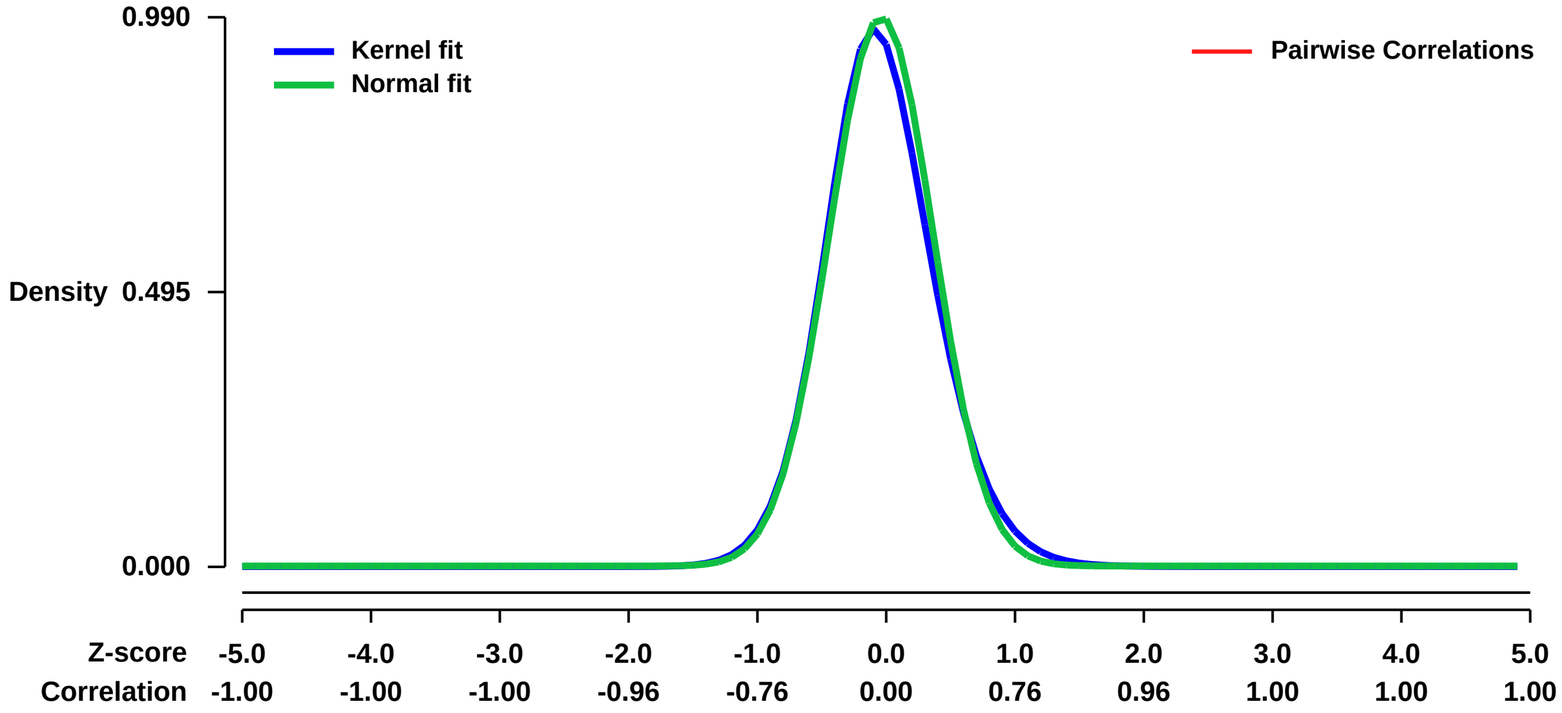

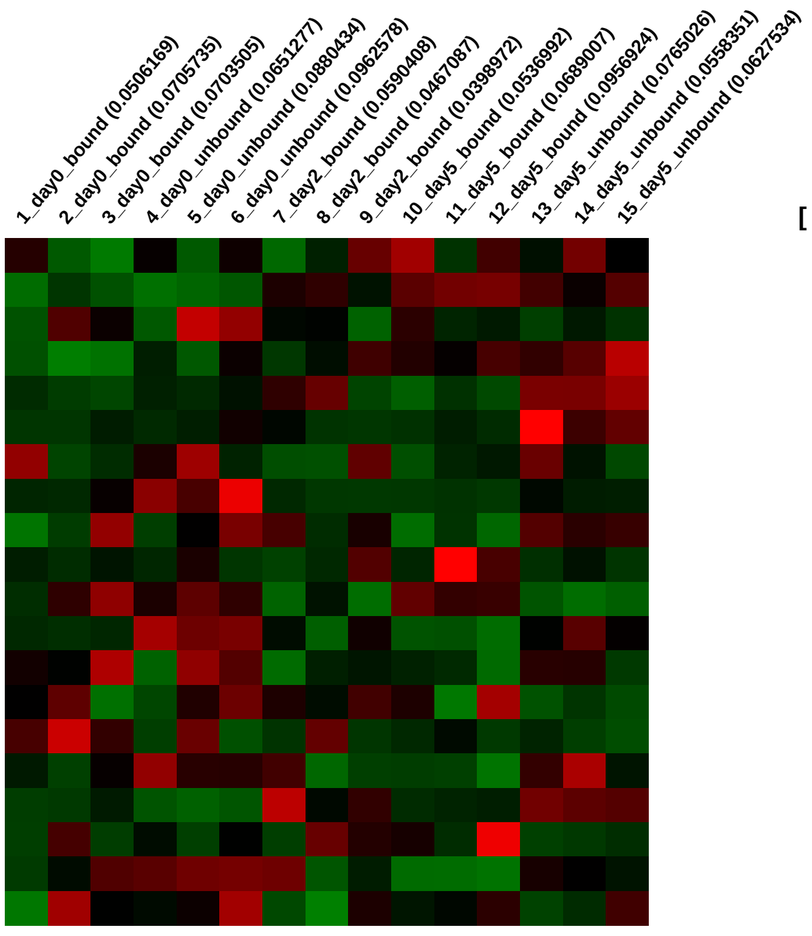

GEO Series "GSE50603" Expression Profiles

Num of samples in this series: 12

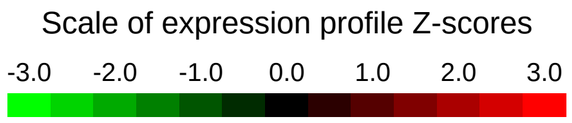

GEO Link:	**http://www.ncbi.nlm.nih.gov/geo/query/acc.cgi?acc=GSE50603**
Status:	**Public on Sep 05 2013**
Title:	**Effect of L-Proline on mouse embryonic stem cells (ESCs)**
Organism:	**Mus musculus**
Experiment type:	**Expression profiling by array**
Platform:	**GPL1261**
Pubmed ID:	**24319666**
Summary & Design:	**Summary:** **We found that the non-essential amino acid L-Proline (L-Pro) acts as a signaling molecule that promotes the conversion of embryonic stem cells (ESCs) into mesenchymal-like, spindle-shaped, highly motile, invasive pluripotent stem cells. This embryonic stem cell-to-mesenchymal-like transition (esMT) is accompanied by a genome-wide remodeling of the transcriptome** **We used microarrays to elucidate whether a diverse transcriptional program is the basis of the morphological and motility differences between ESCs and L- Proline treated ESCs (PiCs)** **Overall design:** **Total RNA was extracted from Control (ESCs) and L-Proline treated mouse embryonic stem cells (PiCs) and hybridized on Affimetrix microarrays.**

Background corr dist: **KL-Divergence = 0.0532, L1-Distance = 0.0337, L2-Distance = 0.0015, Normal std = 0.5680**

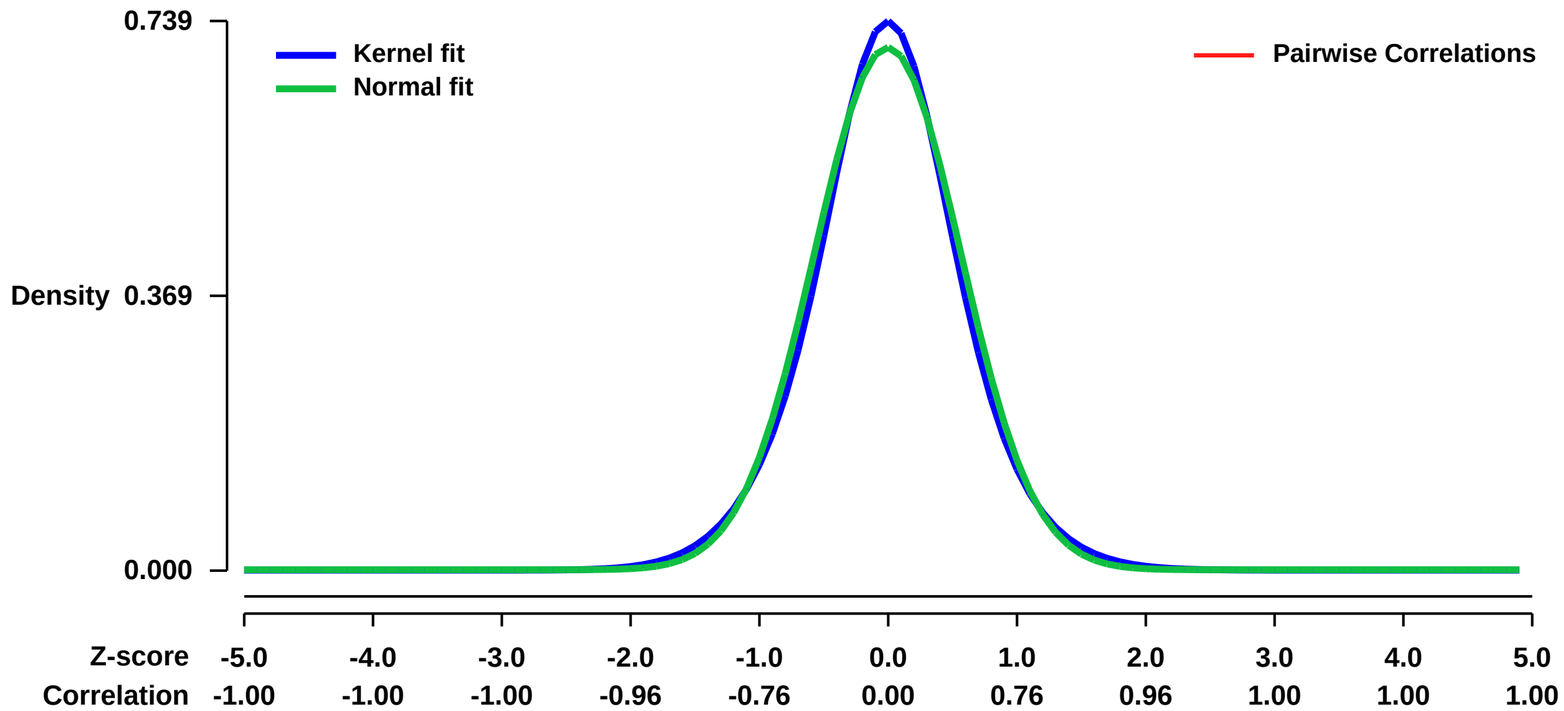

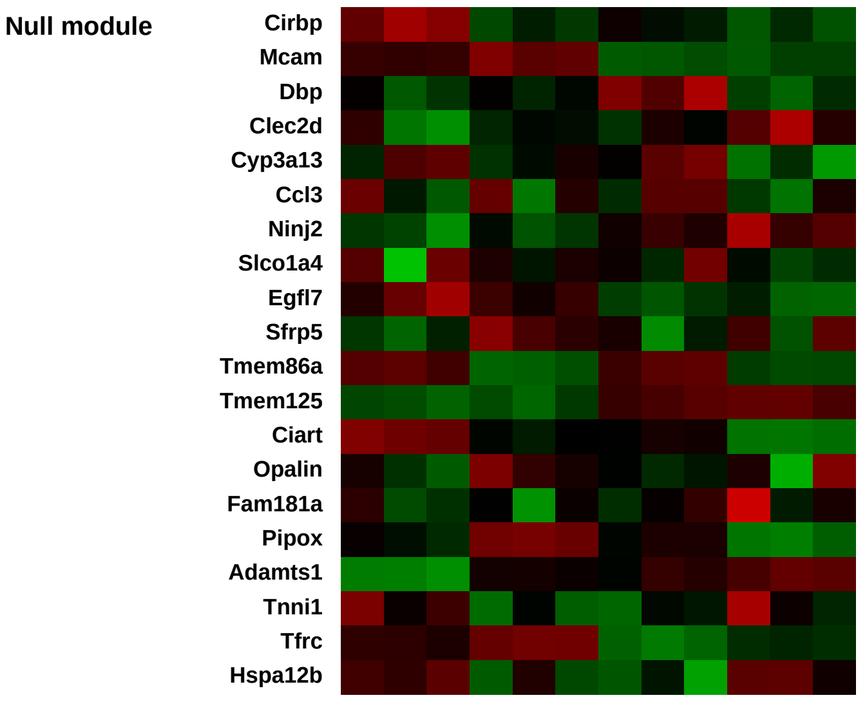

GEO Series "GSE50687" Expression Profiles

Num of samples in this series: 38

Scale of expression profile Z-scores

-3.0 -2.0 -1.0 0.0 1.0 2.0 3.0

GEO Link:	http://www.ncbi.nlm.nih.gov/geo/query/acc.cgi?acc=GSE50687
Status:	Public on Jan 31 2014
Title:	Expression data from testes of the mouse X-chromosome substitution strains
Organism:	Mus musculus
Experiment type:	Expression profiling by array
Platform:	GPL1261
Pubmed ID:	24743563
Summary & Design:	**Summary:** To investigate the evolutionary divergence of transcriptional regulation between the mouse subspecies, we performed transcriptome analysis by microarray on testes from the X-chromosome substitution strain, which carries different subspecies-derived X chromosome on the host subspecies genome. Transcription profiling showed that large-scale aberrations in gene expression were occurred on the introgressed X chromosome. This improper expression was restored by introducing chromosome 1 from the same donor strain as the X chromosome, suggesting that the genetic incompatibility between trans-acting regulatory gene(s) on chromosome 1 and X-linked downstream genes might be a cause of the misregulation. **Overall design:** Testes were collected from 5- and 7-day-old males for RNA extraction and the microarray experiments were performed by using Affymetrix microarrays. Testes from three different males for each strain were tested independently. Tested males are from control C57BL/6J (B6) strain, MSM strain, X-chromosome substitution strain (B6-ChrXMSM), partial X-chromosome substitution strain 1 (B6-ChrXTMSM), partial X-chromosome substitution strain 2 (XS39-tel), and restored (B6-ChrXTMSM X B6-Chr1MSM) F1.

Background corr dist: KL-Divergence = 0.1752, L1-Distance = 0.0398, L2-Distance = 0.0028, Normal std = 0.3593

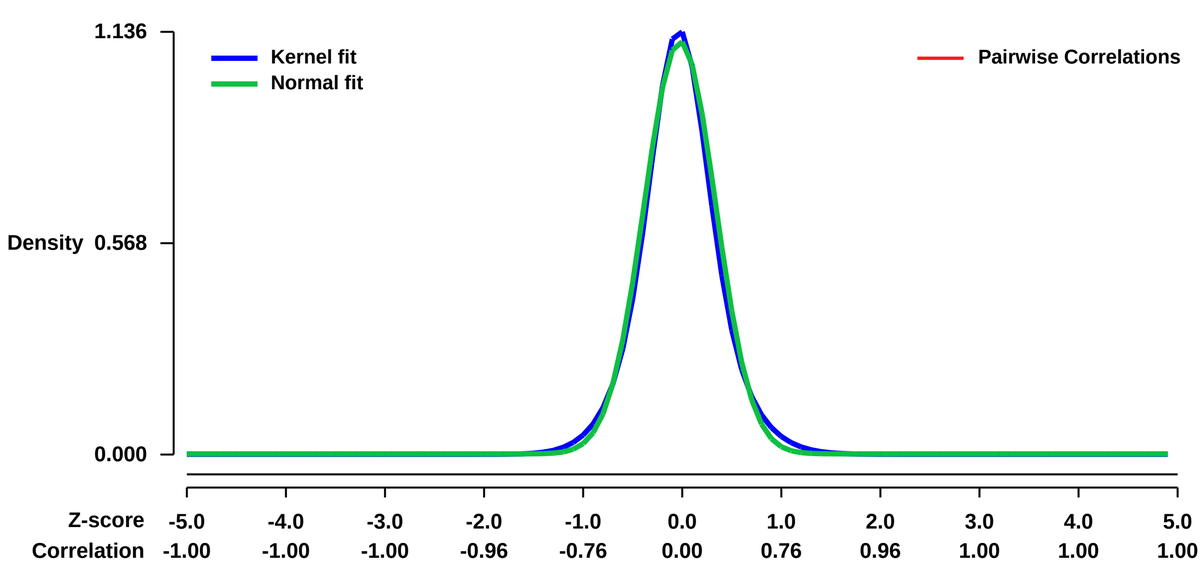

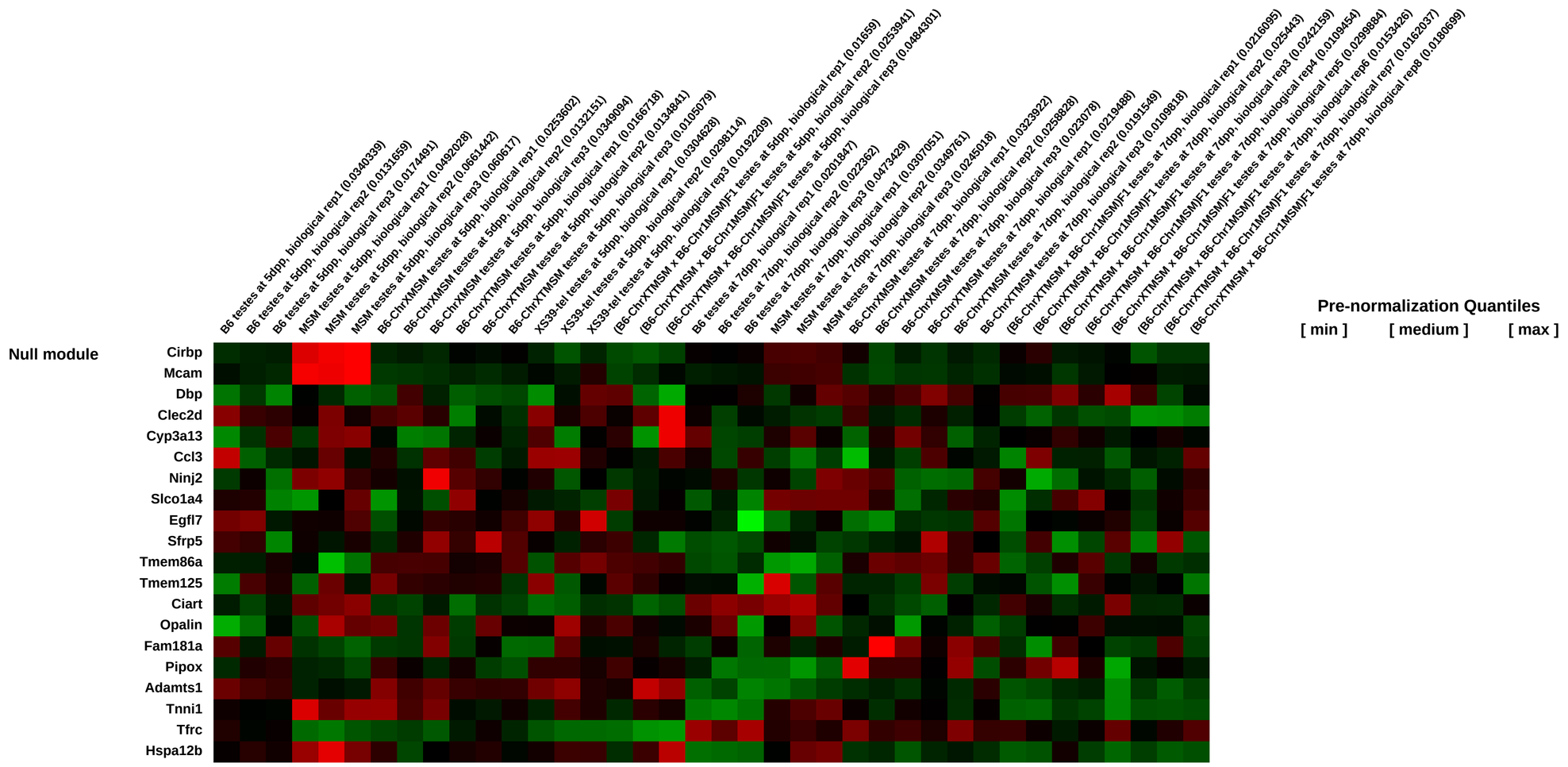

GEO Series "GSE50789" Expression Profiles

Num of samples in this series: 96

Scale of expression profile Z-scores

-3.0 -2.0 -1.0 0.0 1.0 2.0 3.0

GEO Link: http://www.ncbi.nlm.nih.gov/geo/query/acc.cgi?acc=GSE50789
Status: Public on Sep 26 2013
Title: Gene expression in mouse liver in response to short-term calorie restriction
Organism: Mus musculus
Experiment type: Expression profiling by array
Platform: GPL1261
Pubmed ID:
Summary & Design:

Summary:
The effect of a short-term calorie restricted diet was evaluated in six strains of mice

The dietary intervention was initiated at 8 weeks of age and continued until 22 weeks of age

Overall design:
Tissues were collected from mice at 22 weeks of age; there were 96 microarrays used in total: for each of the 6 strains of mice, there were 8 control-fed mice and 8 calorie restricted mice (one individual mouse per microarray)

Background corr dist: KL-Divergence = 0.2595, L1-Distance = 0.0730, L2-Distance = 0.0155, Normal std = 0.3052

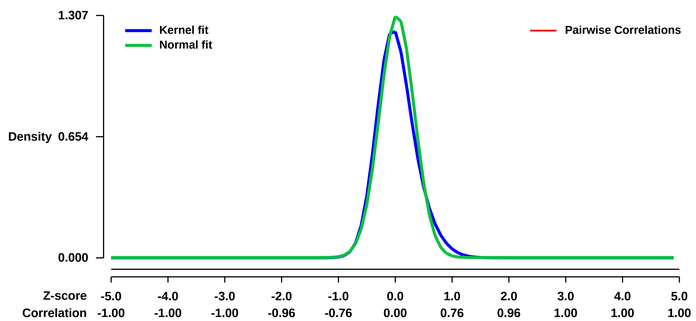

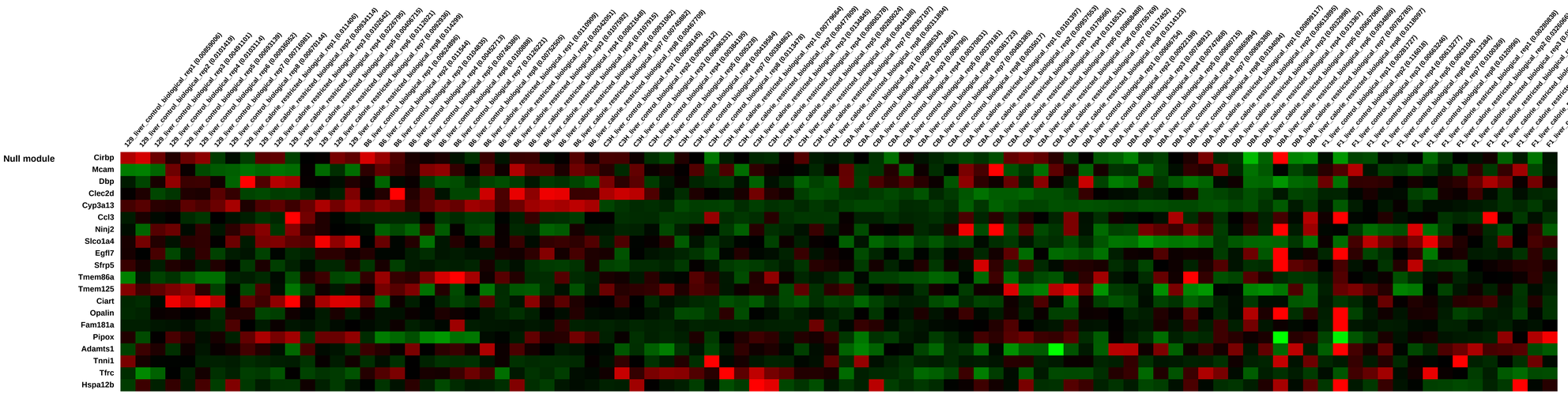

GEO Series "GSE50813" Expression Profiles

Num of samples in this series: 24

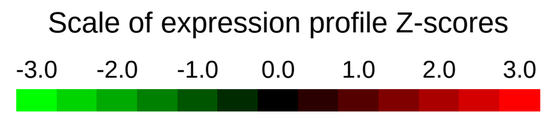

GEO Link:	**http://www.ncbi.nlm.nih.gov/geo/query/acc.cgi?acc=GSE50813**
Status:	**Public on Dec 31 2013**
Title:	**Prevention of mammary tumor progression by silencing HoxA1 via intraductal injection of nanoparticle-formulated siRNA**
Organism:	**Mus musculus**
Experiment type:	**Expression profiling by array**
Platform:	**GPL1261**
Pubmed ID:	**24382894**
Summary & Design:	**Summary:** **Silencing HoxA1 in vivo by intraductal delivery of nanoparticle-formulated siRNA reduced mammary tumor incidence by 75% , reduced cell proliferation, and prevented loss of ER and PR expression.** **Overall design:** **8 week wild type FVB mouse whole mammary gland and 8week to 20 week transgenic FVB C3(1)-SV40Tag mouse whole mammary gland**

Background corr dist: **KL-Divergence = 0.1026, L1-Distance = 0.0245, L2-Distance = 0.0008, Normal std = 0.4380**

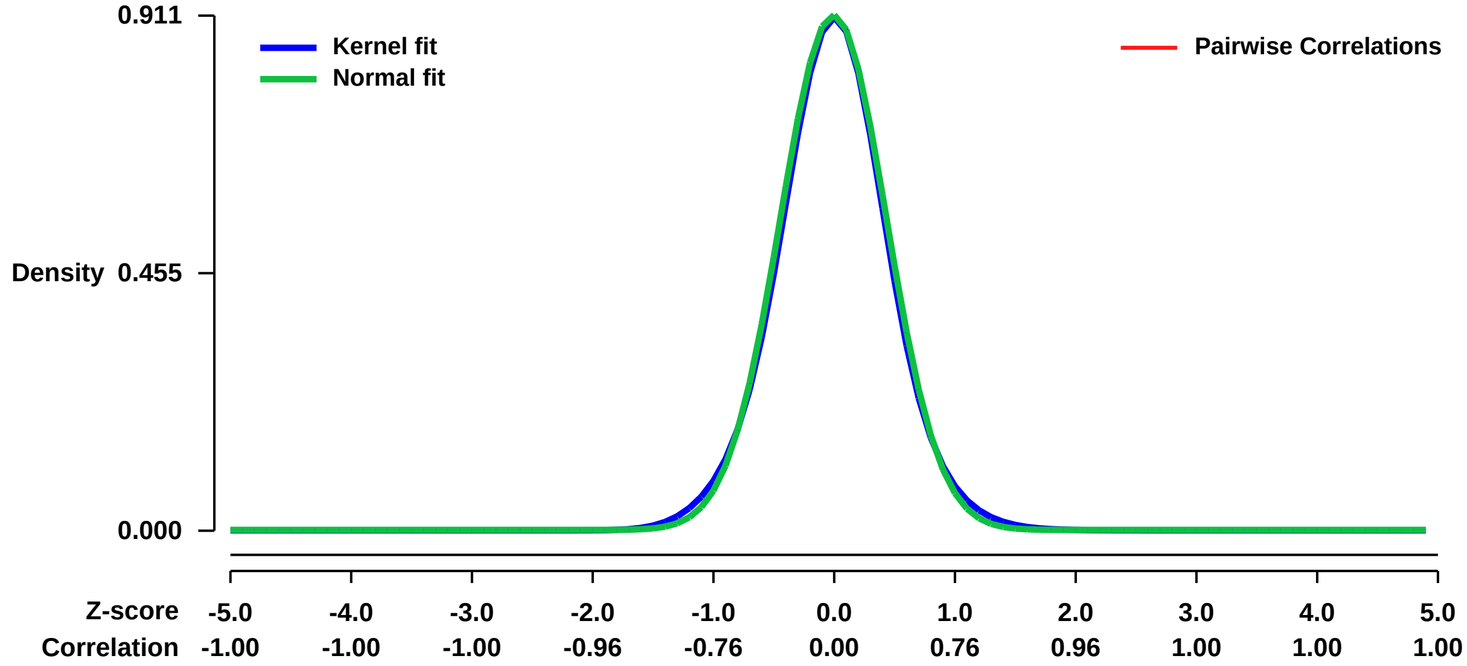

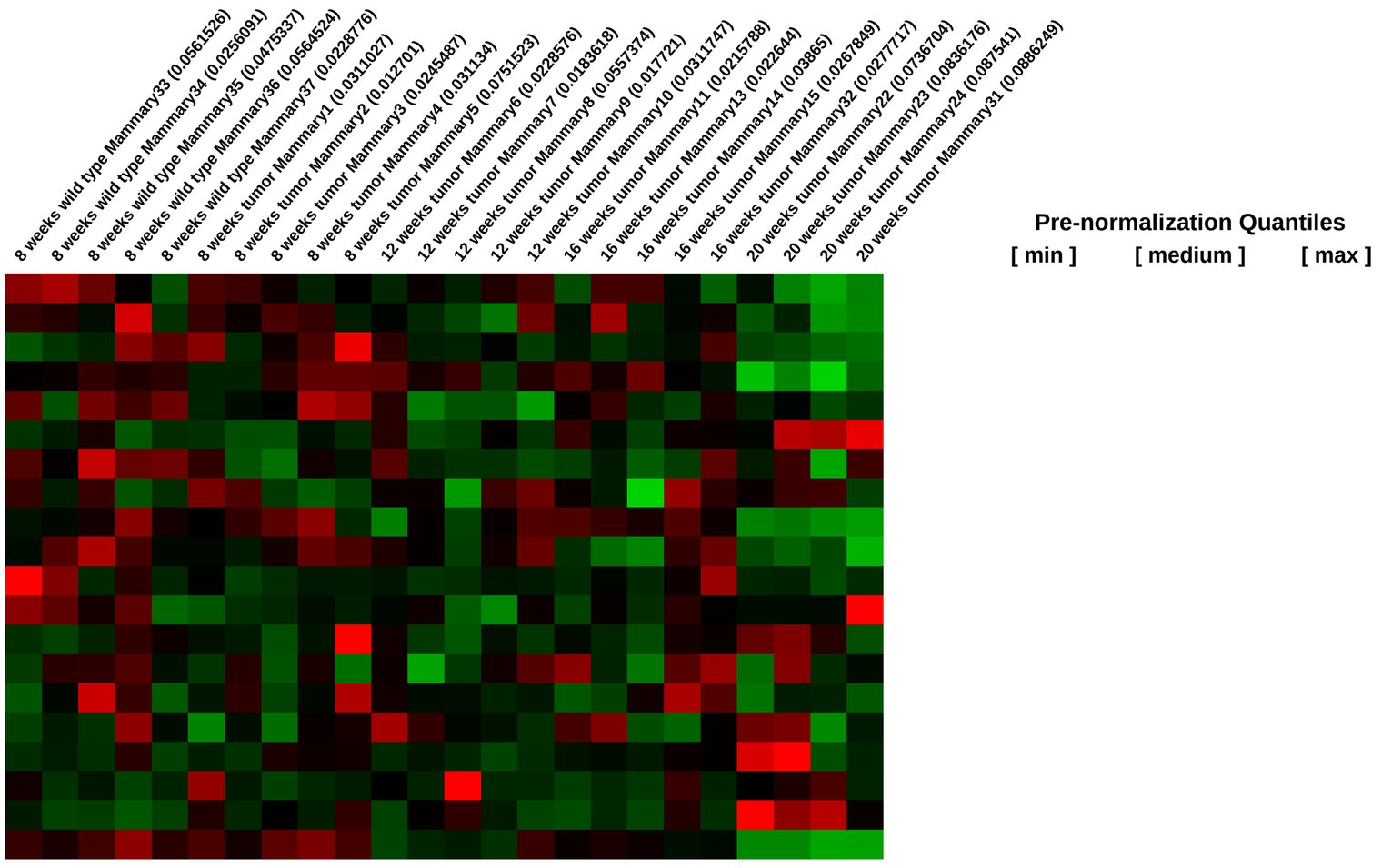

GEO Series "GSE50821" Expression Profiles

Num of samples in this series: 14

Scale of expression profile Z-scores

-3.0 -2.0 -1.0 0.0 1.0 2.0 3.0

GEO Link:	http://www.ncbi.nlm.nih.gov/geo/query/acc.cgi?acc=GSE50821
Status:	Public on May 08 2014
Title:	Restoring Systemic GDF11 Levels Reverses Age-Related Dysfunction in Mouse Skeletal Muscle
Organism:	Mus musculus
Experiment type:	Expression profiling by array
Platform:	GPL1261
Pubmed ID:	24797481
Summary & Design:	**Summary:** In this study, we investigated signaling pathways in Skeletal muscle precursors that are altered with aging and age-related deficits in muscle regenerative potential. We performed fluorescence activated cell sorting (FACS) to obtain highly purified skeletal muscle satellite cells from young, middle-aged and old mice. Parabiosis experiments indicate that impaired regeneration in aged mice is reversible by exposure to a young circulation, suggesting that young blood contains humoral ""rejuvenating"" factors that can restore regenerative function. Here, we demonstrate that the circulating protein growth differentiation factor 11 (GDF11) is a rejuvenating factor for skeletal muscle. Supplementation of systemic GDF11 levels, which normally decline with age, by heterochronic parabiosis or systemic delivery of recombinant protein, reversed functional impairments and restored genomic integrity in aged muscle stem cells (satellite cells). Increased GDF11 levels in aged mice also improved muscle structural and functional features and increased strength and endurance exercise capacity. These data indicate that GDF11 systemically regulates muscle aging and may be therapeutically useful for reversing age-related skeletal muscle and stem cell dysfunction. **Overall design:** We used Affymetrix Mouse Genome array to identify global transcriptional changes associated with age in skeletal muscle precursors.

Background corr dist: KL-Divergence = 0.1316, L1-Distance = 0.0442, L2-Distance = 0.0043, Normal std = 0.3912

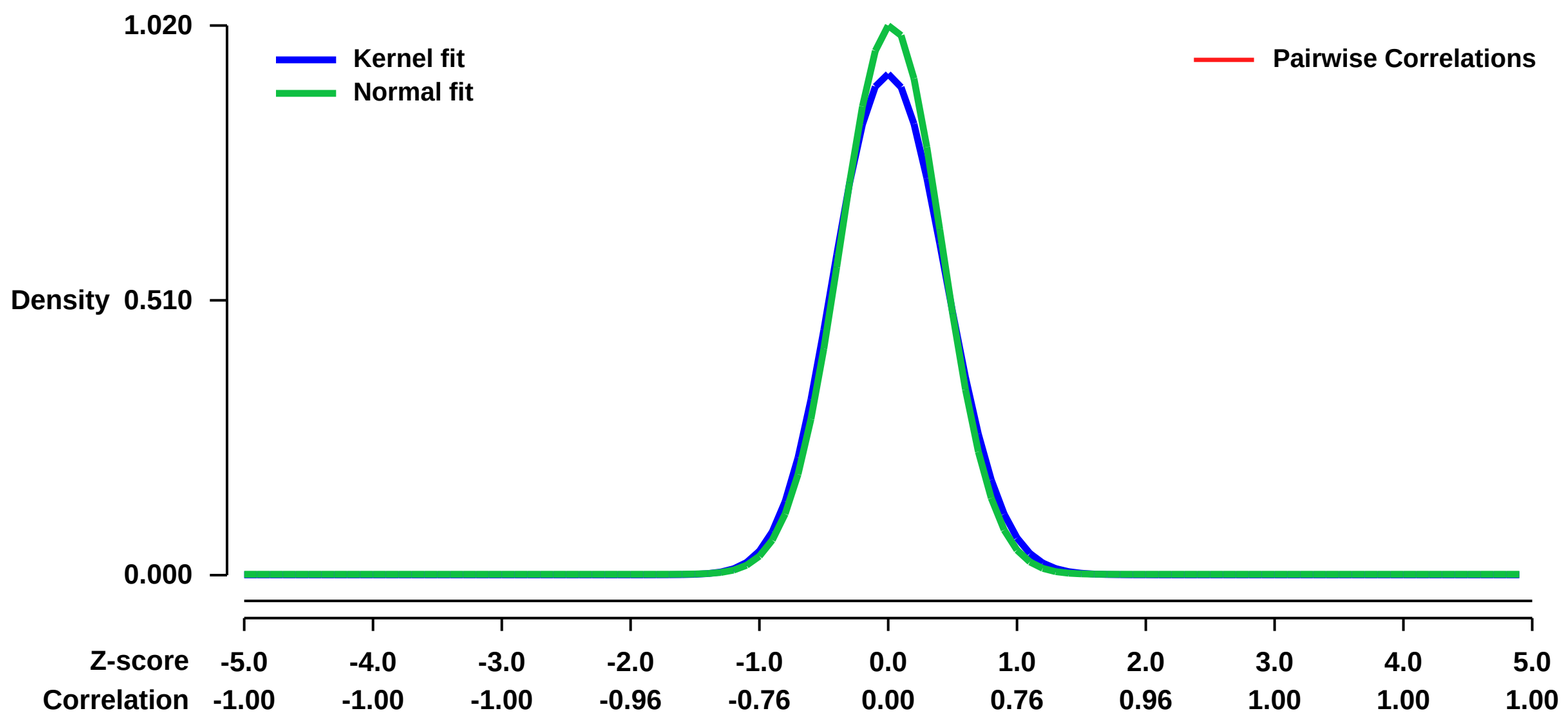

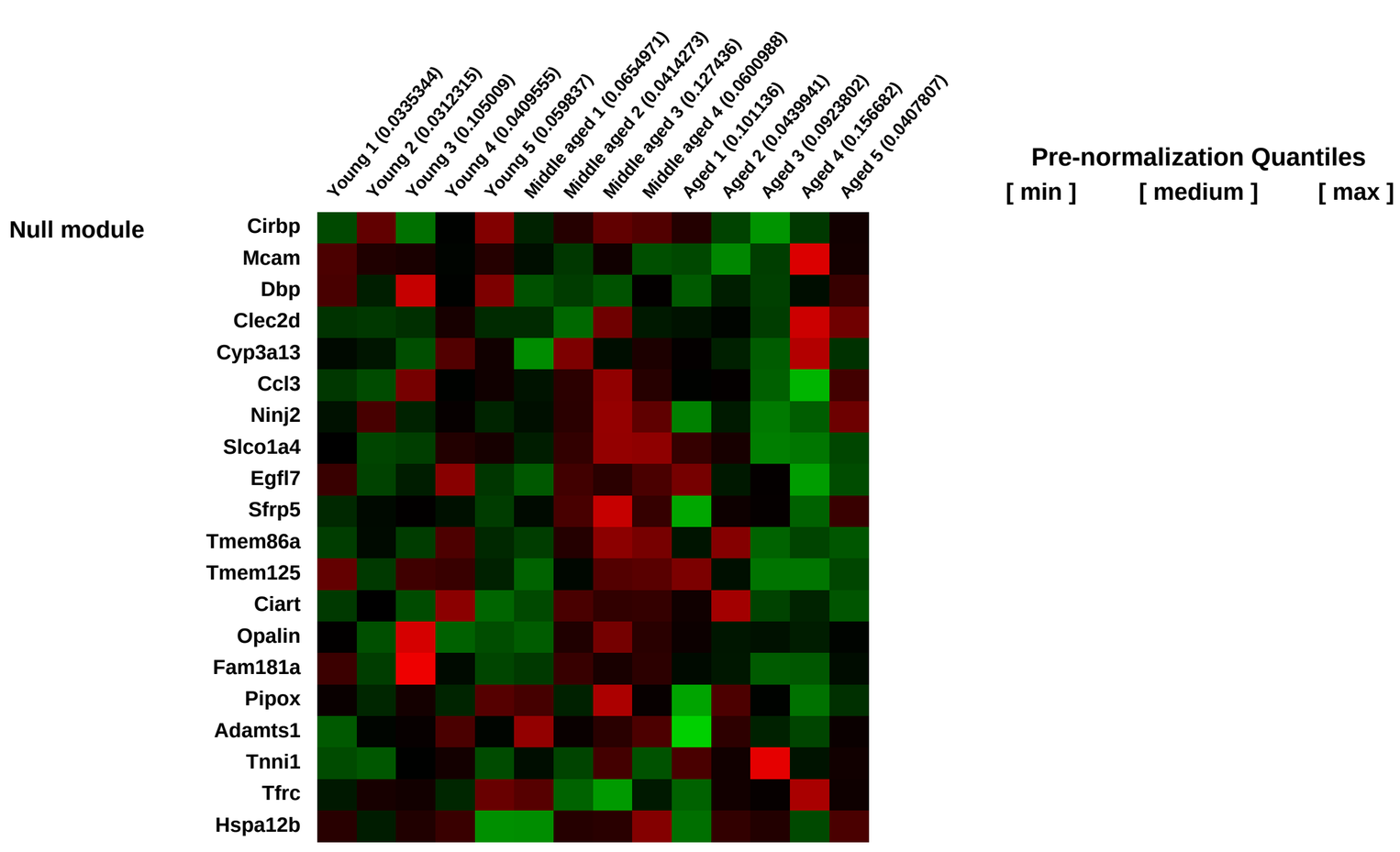

GEO Series "GSE50822" Expression Profiles

Num of samples in this series: 12

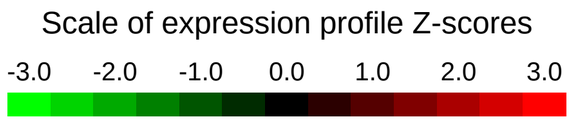

GEO Link:	http://www.ncbi.nlm.nih.gov/geo/query/acc.cgi?acc=GSE50822
Status:	Public on Dec 31 2013
Title:	Differential neuronal targeting of a new and 2 known calcium channel ¸†4 subunit splice variants correlates with their regulation of gene expression
Organism:	Mus musculus
Experiment type:	Expression profiling by array
Platform:	GPL1261
Pubmed ID:	24453333
Summary & Design:	**Summary:** The ¸† subunits of voltage-gated calcium channels regulate surface expression and gating of CaV1 and CaV2 ¸–1 subunits, and thus contribute to neuronal excitability, neurotransmitter release and calcium-induced gene regulation. In addition certain ¸† subunits are targeted into the nucleus, where they directly interact with the epigenetic machinery. Whereas their involvement in this multitude of functions is reflected by a great molecular heterogeneity of ¸† isoforms derived from four genes and abundant alternative splicing, little is known about the roles of individual ¸† variants in specific neuronal functions. In the present study, an alternatively spliced ¸†4 subunit lacking the variable N-terminus (¸†4e) is identified. It is highly expressed in mouse cerebellum and cultured cerebellar granule cells (CGC) and modulates P/Q-type calcium currents in tsA cells and CaV2.1 surface expression in neurons. Compared to the other two known full-length ¸†4 variants (¸†4a, ¸†4b) ¸†4e is most abundantly expressed in the distal axon, but lacks nuclear targeting properties. To examine the importance of nuclear targeting of ¸†4 subunits for transcriptional regulation, we performed whole genome expression profiling of CGCs from lethargic mice individually reconstituted with ¸†4a, ¸†4b, and ¸†4e. Notably, the number of genes regulated by each ¸†4 splice variant correlated with the rank order of their nuclear targeting properties (¸†4b> ¸†4a> ¸†4e). Together these findings support isoform-specific functions of ¸†4 splice variant in neurons, with ¸†4b playing a dual role in channel modulation and gene regulation, while the newly detected ¸†4e variant serves exclusively in calcium channel-dependent functions. We used microarrays to identify gene expression changes caused by ¸†4 splice variants (¸†4a, ¸†4b and ¸†4e) of the voltage gated calcium channel in cultured cerebellar granule cells of lethargic mice **Overall design:** Cultured cerebellar granule cells from lethargic (129/SvJ background) mice reconstituted with the ¸†4 splice variants (¸†4a, ¸†4b and ¸†4e) were compared to eGFP transfected controls

Background corr dist: KL-Divergence = 0.0838, L1-Distance = 0.0264, L2-Distance = 0.0011, Normal std = 0.4649

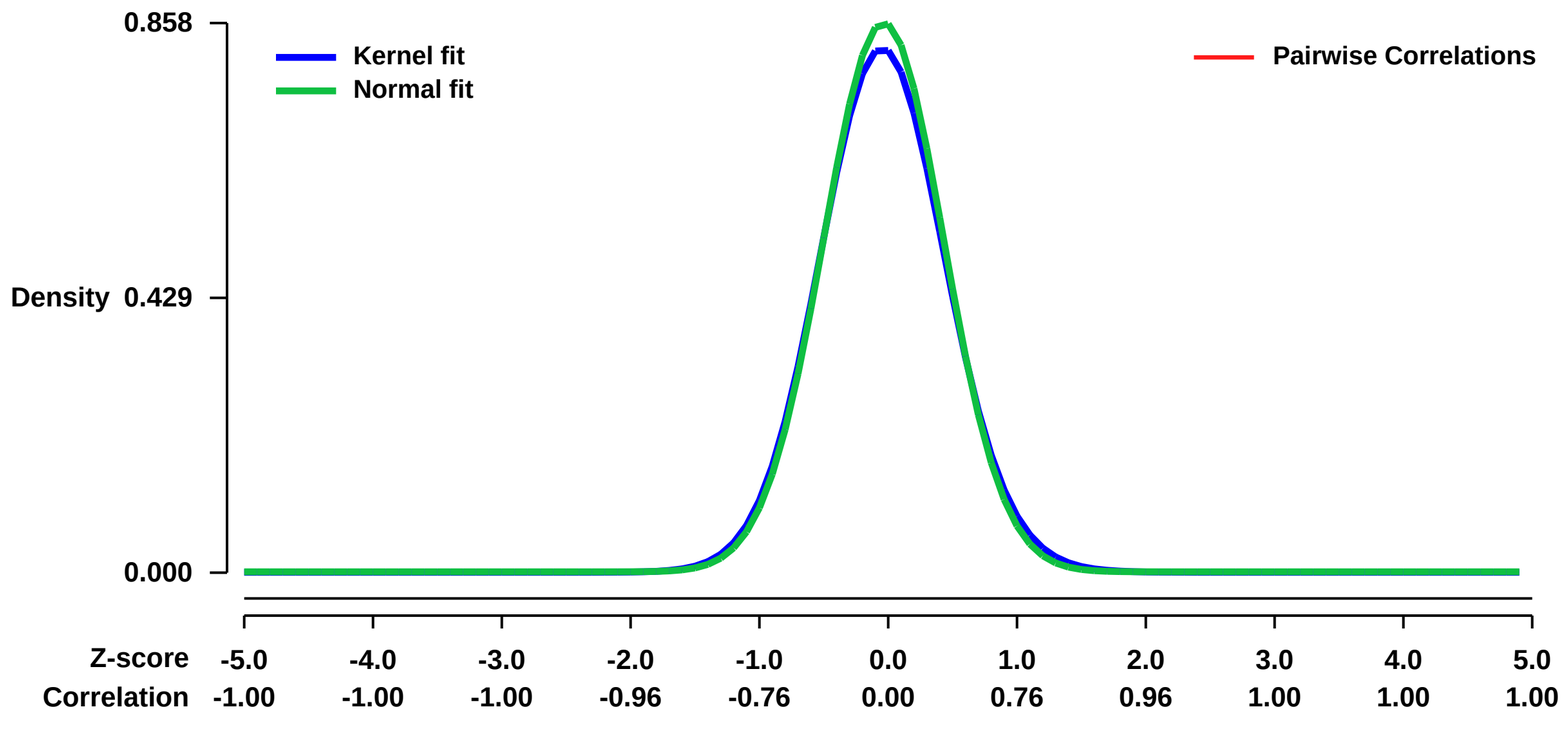

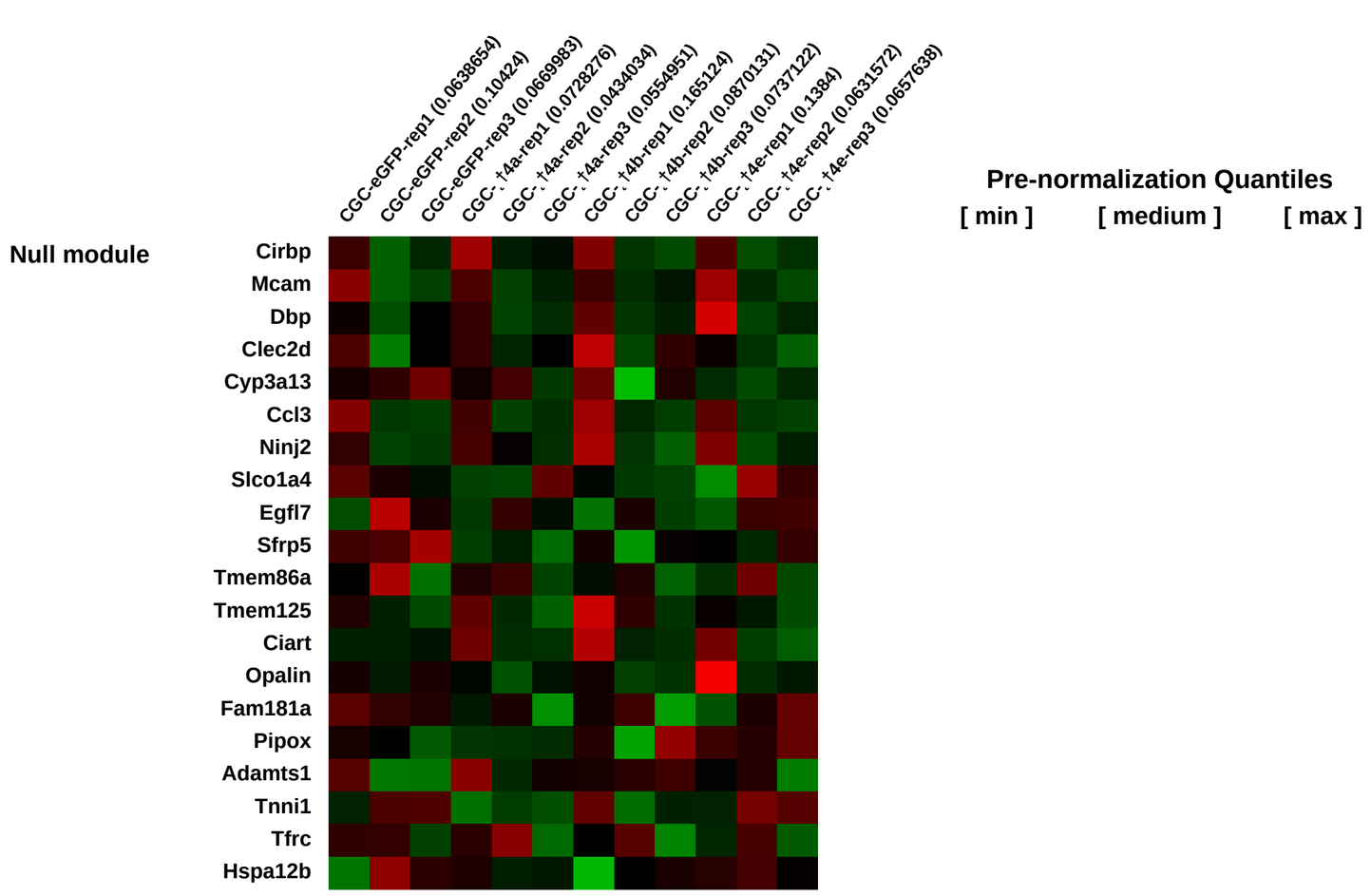

GEO Series "GSE50824" Expression Profiles

Num of samples in this series: 19

Scale of expression profile Z-scores

-3.0 -2.0 -1.0 0.0 1.0 2.0 3.0

GEO Link:	http://www.ncbi.nlm.nih.gov/geo/query/acc.cgi?acc=GSE50824
Status:	Public on Sep 13 2013
Title:	The identification and tumorigenecity of neuronal progenitors in developing cerebellum
Organism:	Mus musculus
Experiment type:	Expression profiling by array
Platform:	GPL1261
Pubmed ID:	24141309
Summary & Design:	**Summary:** It is generally believed that cerebellar granule neurons originate exclusively from granule neuron precursors (GNPs) in the external germinal layer (EGL). Here we identify a rare population of neuronal progenitors in the developing cerebellum that expresses Nestin. Although Nestin is widely considered a marker for multipotent stem cells, these Nestin-expressing progenitors (NEPs) are committed to the granule neuron lineage. Unlike conventional GNPs, which reside in the outer EGL and proliferate extensively, NEPs reside in the deep part of the EGL and are quiescent. Expression profiling reveals that NEPs are distinct from GNPs, and in particular, express markedly reduced levels of genes associated with DNA repair. Consistent with this, upon aberrant activation of Sonic hedgehog (Shh) signaling, NEPs exhibit more severe genomic instability and give rise to tumors more efficiently than GNPs. These studies identify a novel progenitor for cerebellar granule neurons and a novel cell of origin for medulloblastoma. **Overall design:** 4 samples of Nestin expressing progenitors (NEPs), 4 samples of Math1 positive cells (GNPs) and 3 samples of Neural stem cells (CD133+ NSCs) were used for microarray analysis to determine the distinct genetic profile of NEPs. 4 samples of NEP-derived tumor and 4 samples of GNP-derived tumor were used to determine the similarity of those tumors by microarray analysis.

Background corr dist: KL-Divergence = 0.1108, L1-Distance = 0.0321, L2-Distance = 0.0019, Normal std = 0.4402

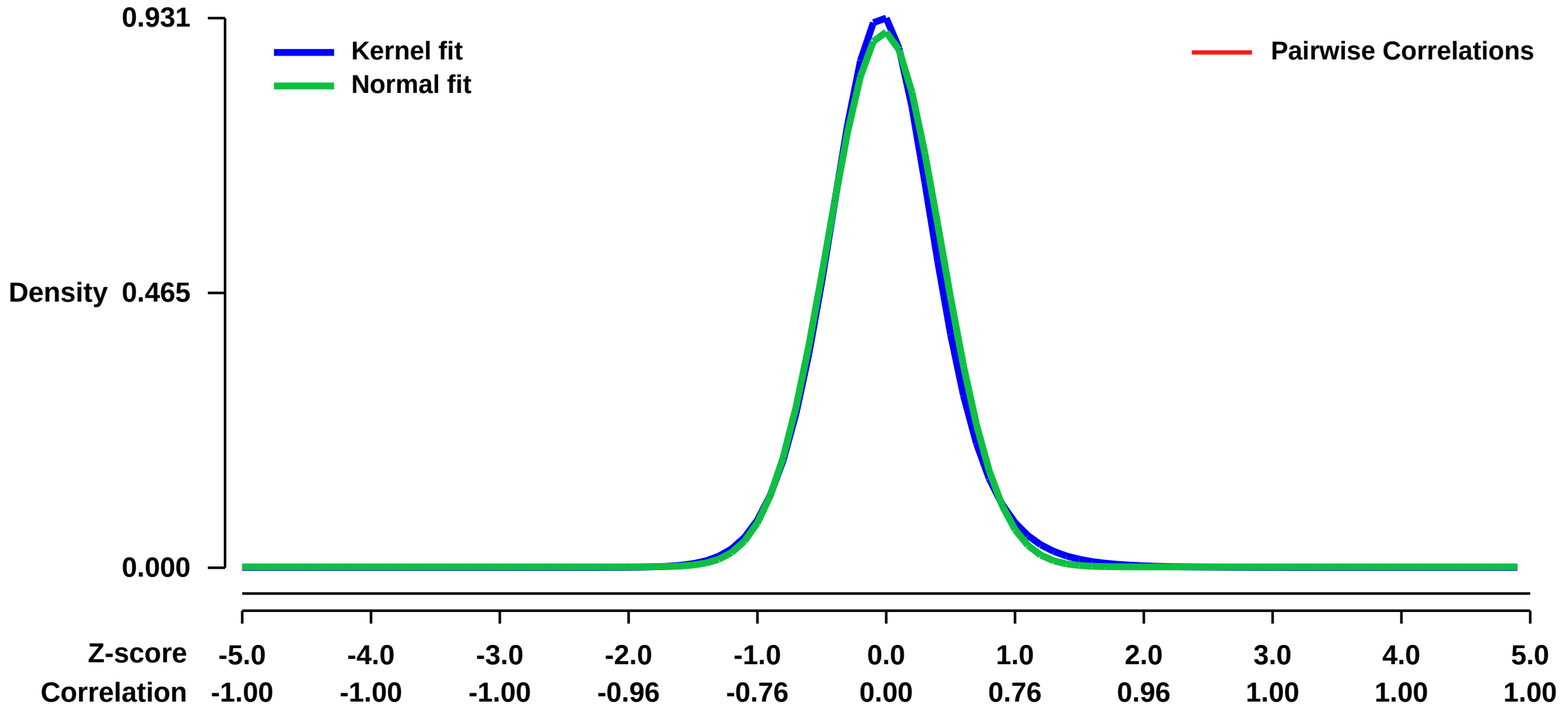

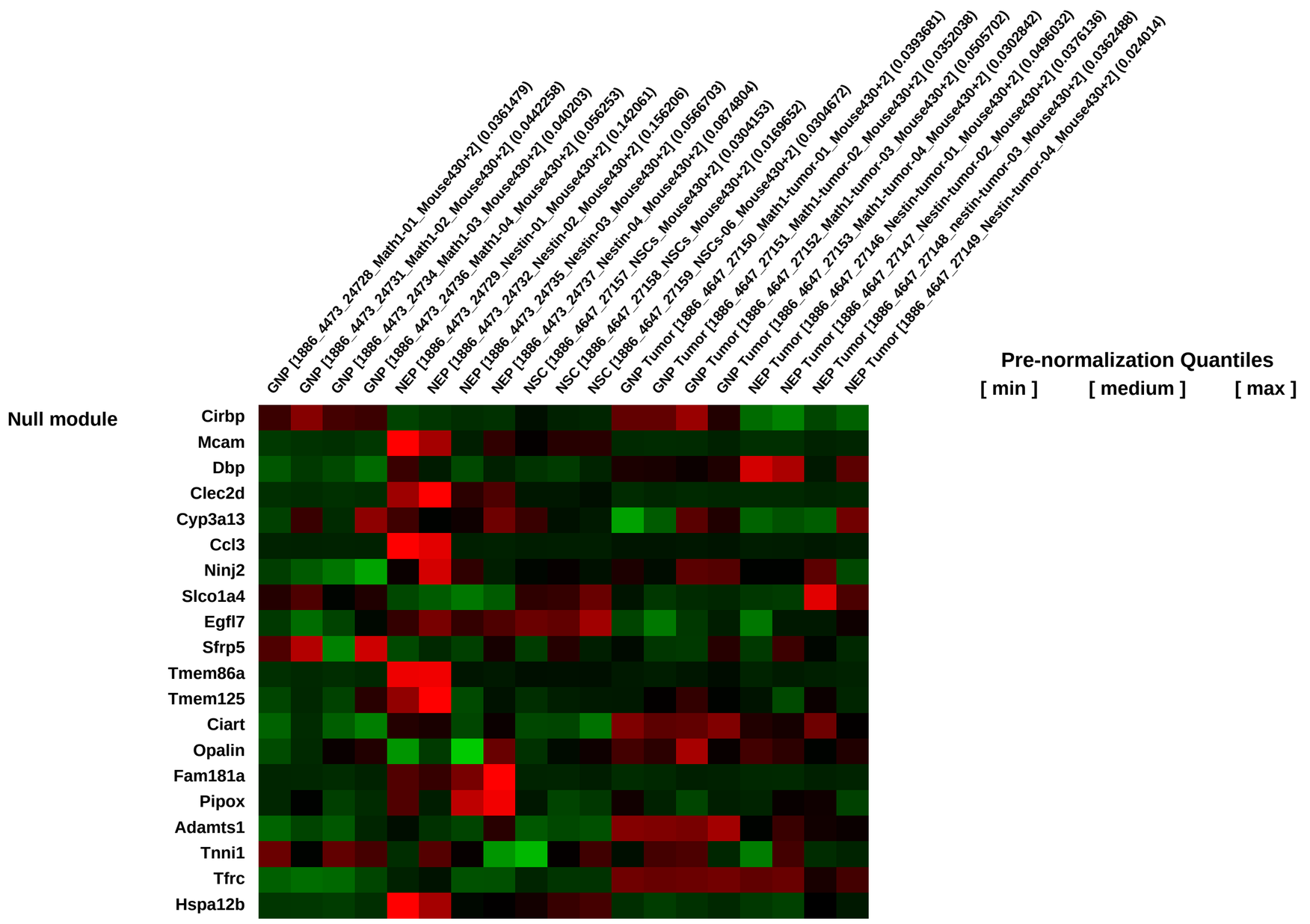

GEO Series "GSE50865" Expression Profiles

Num of samples in this series: 12

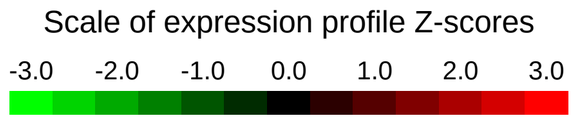

GEO Link:	http://www.ncbi.nlm.nih.gov/geo/query/acc.cgi?acc=GSE50865
Status:	Public on Sep 13 2013
Title:	Expression Data For BRD4 Inhibition
Organism:	Mus musculus
Experiment type:	Expression profiling by array
Platform:	GPL1261
Pubmed ID:	24373973
Summary & Design:	**Summary:** BRD4 Inhibition of spindle cell malignant peripheral nerve sheath tumor (sMPNST) tumor cells **Overall design:** Cells were treated with Brd4 shRNA (3 days) or 500 nM JQ1 (2 days) before RNA isolation

Background corr dist: KL-Divergence = 0.1079, L1-Distance = 0.0335, L2-Distance = 0.0015, Normal std = 0.4420

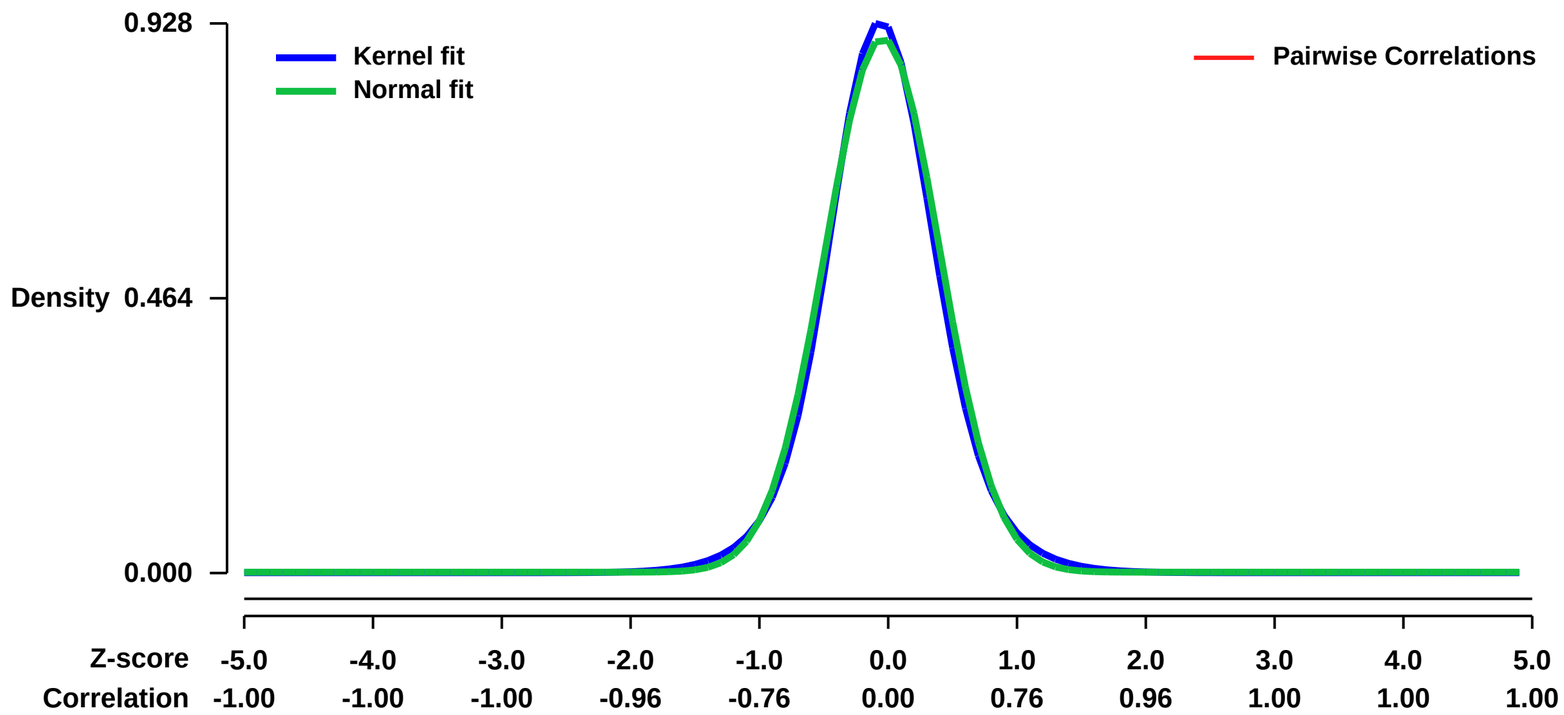

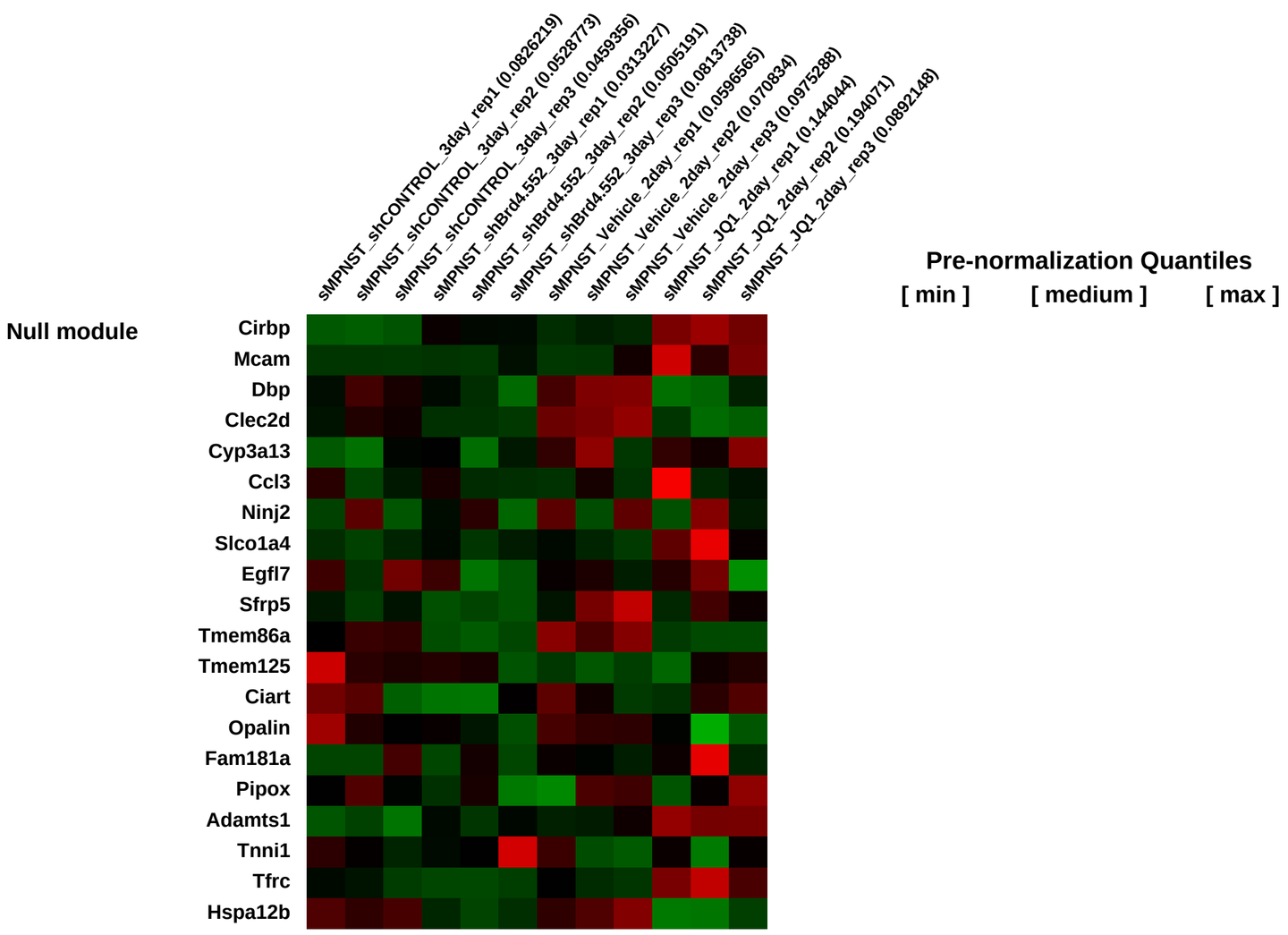

GEO Series "GSE50933" Expression Profiles

Num of samples in this series: 10

Scale of expression profile Z-scores

-3.0 -2.0 -1.0 0.0 1.0 2.0 3.0

GEO Link:	http://www.ncbi.nlm.nih.gov/geo/query/acc.cgi?acc=GSE50933
Status:	Public on Nov 19 2013
Title:	Essential functions for ID proteins at multiple checkpoints in natural killer T cell development
Organism:	Mus musculus
Experiment type:	Expression profiling by array
Platform:	GPL1261
Pubmed ID:	24244015
Summary & Design:	**Summary:** Thymic iNKT cell development is divided into four stages (stage 0-3) that are characterised, in C57BL/6 mouse strain, by the differential expression of surface markers, such as CD24, CD44 and NK1.1. During transition from immature to mature iNKT cell subsets, gene expression is tightly regulated. Here, we used microarray analysis to detail the influence of the transcriptional regulator ID3 during iNKT cell maturation in the thymus. **Overall design:** Stage 1 (Tet+CD24-CD44-NK1.1-) and Stage 2 (Tet+CD24-CD44+NK1.1-) iNKT cells from WT and Id3KO thymi were FACS sorted for RNA extraction and Affymetrix hybridisation.

Background corr dist: KL-Divergence = 0.1233, L1-Distance = 0.0324, L2-Distance = 0.0018, Normal std = 0.4019

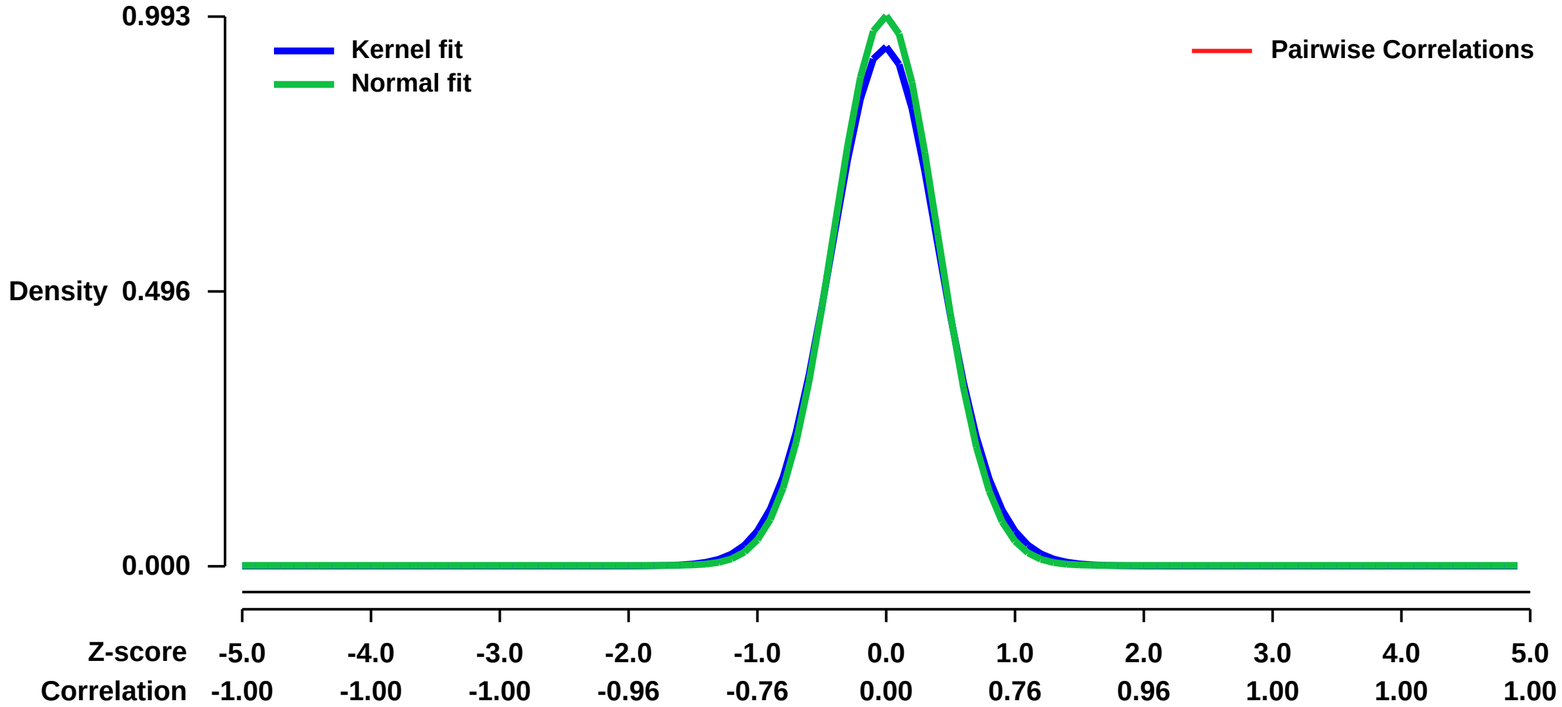

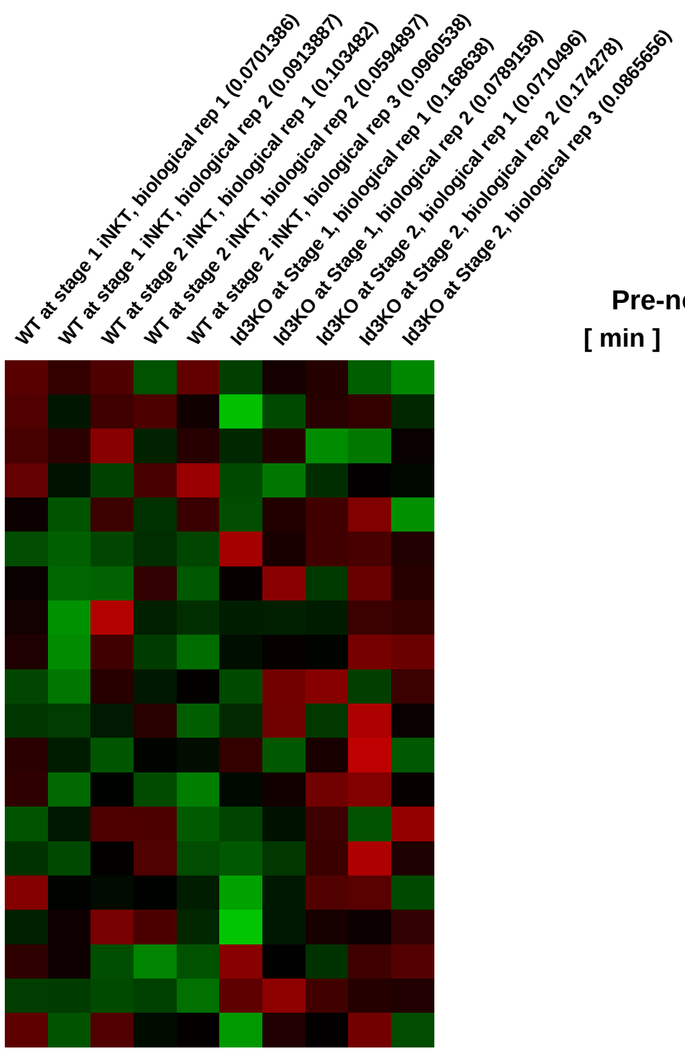

GEO Series "GSE50950" Expression Profiles

Num of samples in this series: 15

Scale of expression profile Z-scores

-3.0 -2.0 -1.0 0.0 1.0 2.0 3.0

GEO Link: http://www.ncbi.nlm.nih.gov/geo/query/acc.cgi?acc=GSE50950

Status: Public on Sep 18 2013

Title: Expression data from adult Shh-responding astroglia cells in mice

Organism: Mus musculus

Experiment type: Expression profiling by array

Platform: GPL1261

Pubmed ID:

Summary & Design:

Summary:
Sonic hedgehog (Shh) signals via Gli transcription factors to promote maintenance and proliferation of neural stem cells in the adult mouse forebrain. We have analyzed the gene expression pattern in neurogenic Shh-responding astroglia (= neural stem cells) in the subventicular zone of the lateral ventricle and dentate gyrus of the hippocampus in comparison to the non-neurogenic Shh-responding glia (=Bergman glia) in the cerebellum to identify the genes specifically involved in neurogenic function downstream of Shh signaling.

In this dataset, we include the expression data obtained from FACS-sorted Gli1+ GFAP+ cells from microdissected SVZ, hippocampus and cerebellum. GFAP expression is based on hGFAP-GFP reporter line and Gli1 expression is lineage marked using Gli1-CreER;ROSA26-tdTomato mice.

Overall design:
15 Total samples were analyzed. We compared expression levels of SVZ vs. Cerebellum, Hippocampus vs. Cerebelllum to identify genes which had more than 4 fold change in expression levels with p < 0.01. From this narrowed list, we compared between SVZ and Hippocampus to identify the common genes up and down regulated. In addition, we also identified commonly expressed genes in hippocampus and SVZ at high level.

Background corr dist: KL-Divergence = 0.1189, L1-Distance = 0.0684, L2-Distance = 0.0115, Normal std = 0.4285

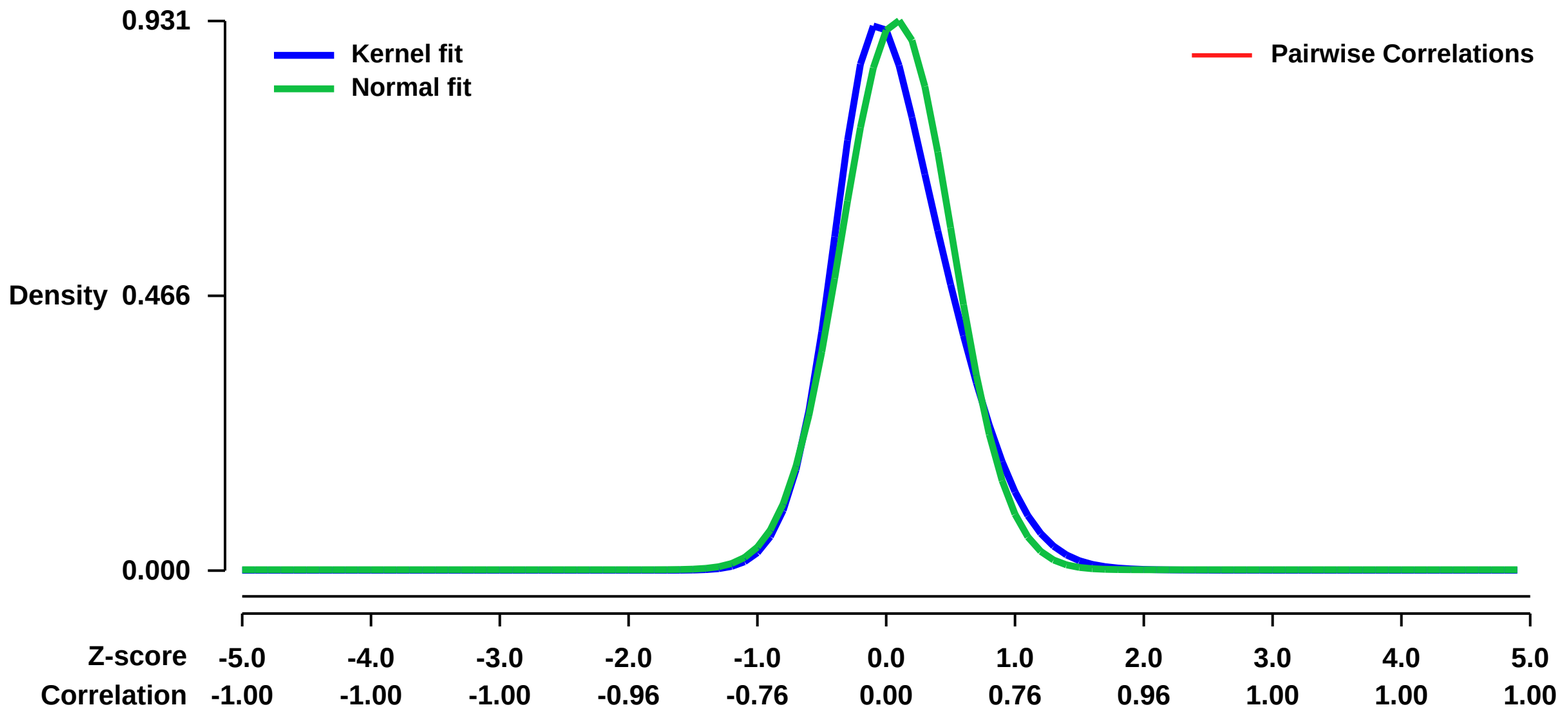

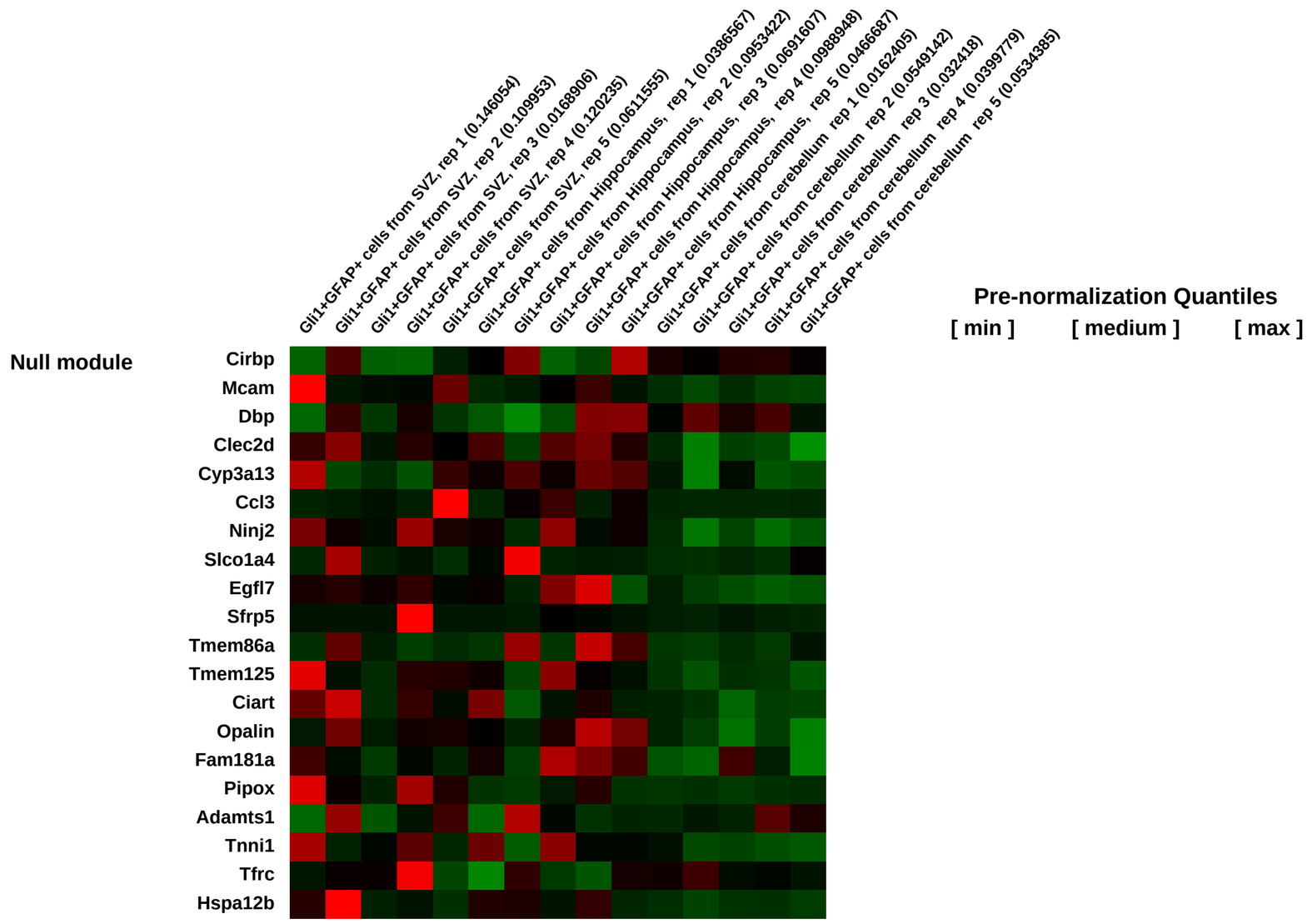

GEO Series "GSE51075" Expression Profiles

Num of samples in this series: 12

Scale of expression profile Z-scores

-3.0 -2.0 -1.0 0.0 1.0 2.0 3.0

GEO Link:	http://www.ncbi.nlm.nih.gov/geo/query/acc.cgi?acc=GSE51075
Status:	Public on Sep 22 2013
Title:	Transcriptional responses of murine macrophages to the adenylate cyclase toxin of Bordetella pertussis
Organism:	Mus musculus
Experiment type:	Expression profiling by array
Platform:	GPL1261
Pubmed ID:	17890046
Summary & Design:	**Summary:** Three different recombinant forms of CyaA were used to investigate transcriptional responses of murine bone marrow-derived macrophages (BMDMs) using Affymetrix Mouse Genome Genechips. These forms were enzymically active, invasive CyaA, nonenzymically active, invasive CyaA (CyaA*) and non-enzymically active, non-invasive CyaA (proCyaA*). BMMs, treated with 20 ng/ml of CyaA for 24 h, showed over 1000 significant changes in gene transcription compared with control cells. CyaA caused an increase in transcription of many inflammatory genes and genes associated with various signalling cascades such as those involved in cyclic AMP-dependent protein kinase A signalling. Most strikingly, CyaA caused down-regulation of numerous genes involved in cell proliferation. CyaA* at 20 ng/ml significantly up-regulated the transcription of only twelve genes after 24 h whereas proCyaA* at this concentration significantly increased the transcription of only two genes. **Overall design:** The effect of administration of three different recombinant forms of pertussis toxin to mouse bone marrow derived macrophages are compared with a vehicle only contol 24 hours after treatment in technical triplicate measurements

Background corr dist: KL-Divergence = 0.0967, L1-Distance = 0.0706, L2-Distance = 0.0078, Normal std = 0.5189

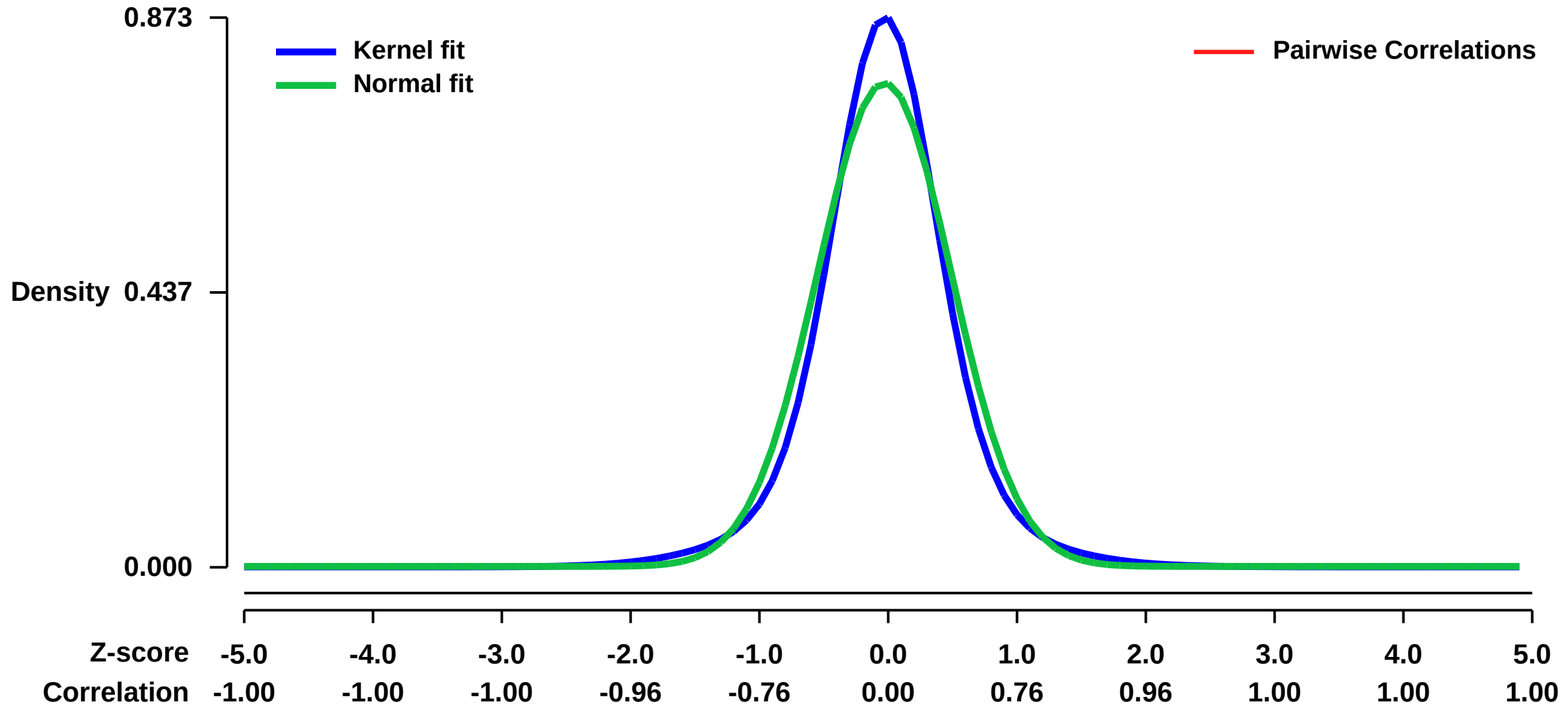

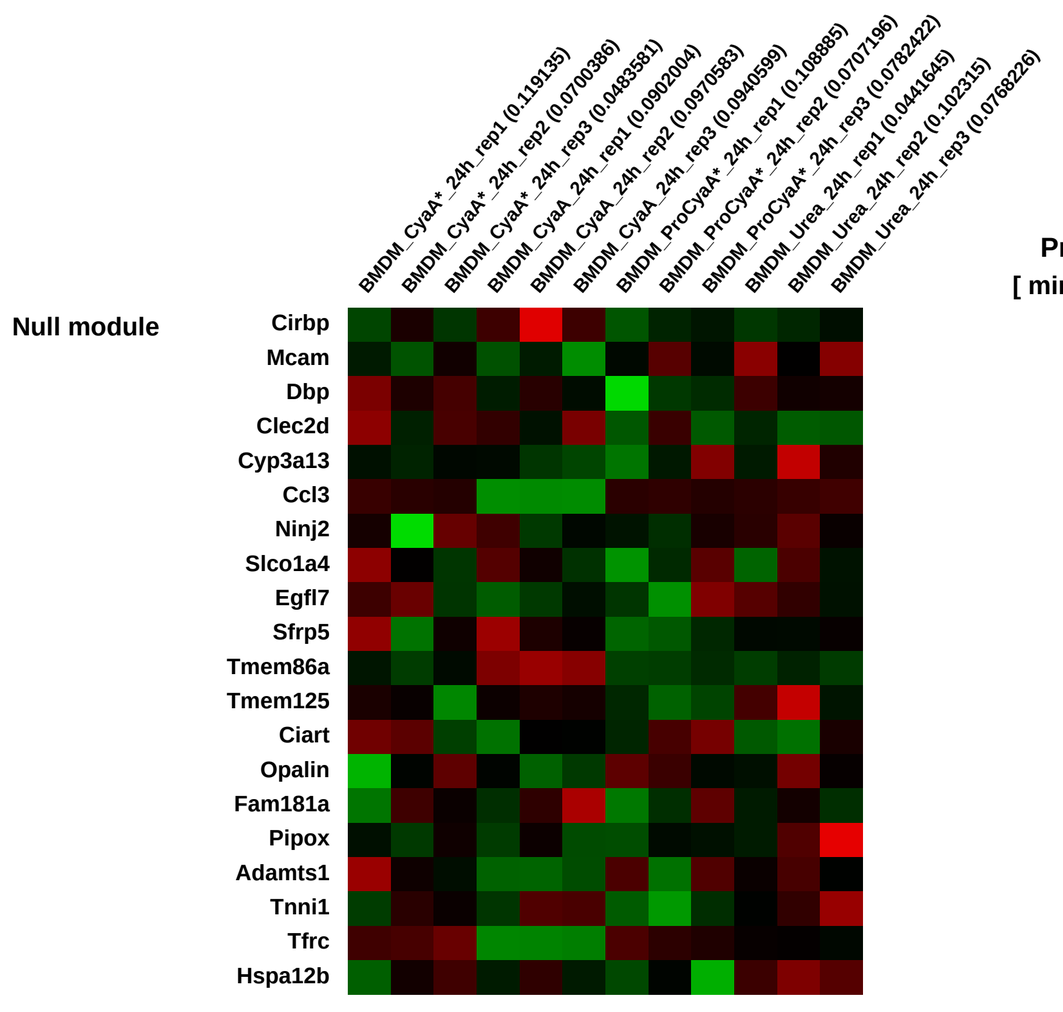

GEO Series "GSE51108" Expression Profiles

Num of samples in this series: 6

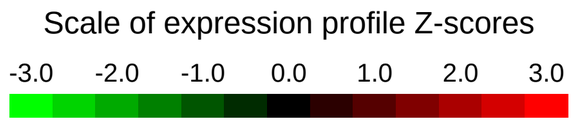

GEO Link:	http://www.ncbi.nlm.nih.gov/geo/query/acc.cgi?acc=GSE51108
Status:	Public on Nov 18 2013
Title:	Gene expression in liver tissue from Ghrh-KO and normal (wild-type) mice
Organism:	Mus musculus
Experiment type:	Expression profiling by array
Platform:	GPL1261
Pubmed ID:	24175087
Summary & Design:	**Summary:** The hypothalamus has recently emerged as a key regulator of metabolism and aging in mammals. We have examined the impact of targeted disruption of hypothalamic hypophysiotropic peptide: Growth Hormone-releasing Hormone (GHRH) in mice on longevity, and the putative mechanisms of delayed aging. GHRH knockout (KO) mice are remarkably long-lived and in comparison to genetically normal (wild type) animals exhibiting major shifts in the expression of genes related to xenobiotic detoxification, stress resistance, and insulin signaling. These mutant mice also have increased adiponectin levels and alterations in glucose homeostasis consistent with the removal of the counter-insulin effects of GH. While these effects overlap with those of caloric restriction (CR), we show that effects of CR and the GHRH mutation are additive, with lifespan of GHRH-KO mutants further increased by CR. We conclude that GHRH-KO mice feature perturbations in a network of signaling pathways related to stress resistance, metabolic control and inflammation, and therefore provide a new model that can be used to explore links between GHRH repression, downregulation of the somatotropic axis, and extended longevity. **Overall design:** Hepatic tissue was obtained from 3 Ghrh-KO mice and 3 control (wild-type) mice (males). Expression in each sample was profiled using Affymetrix Mouse Genome 430 2.0 arrays.

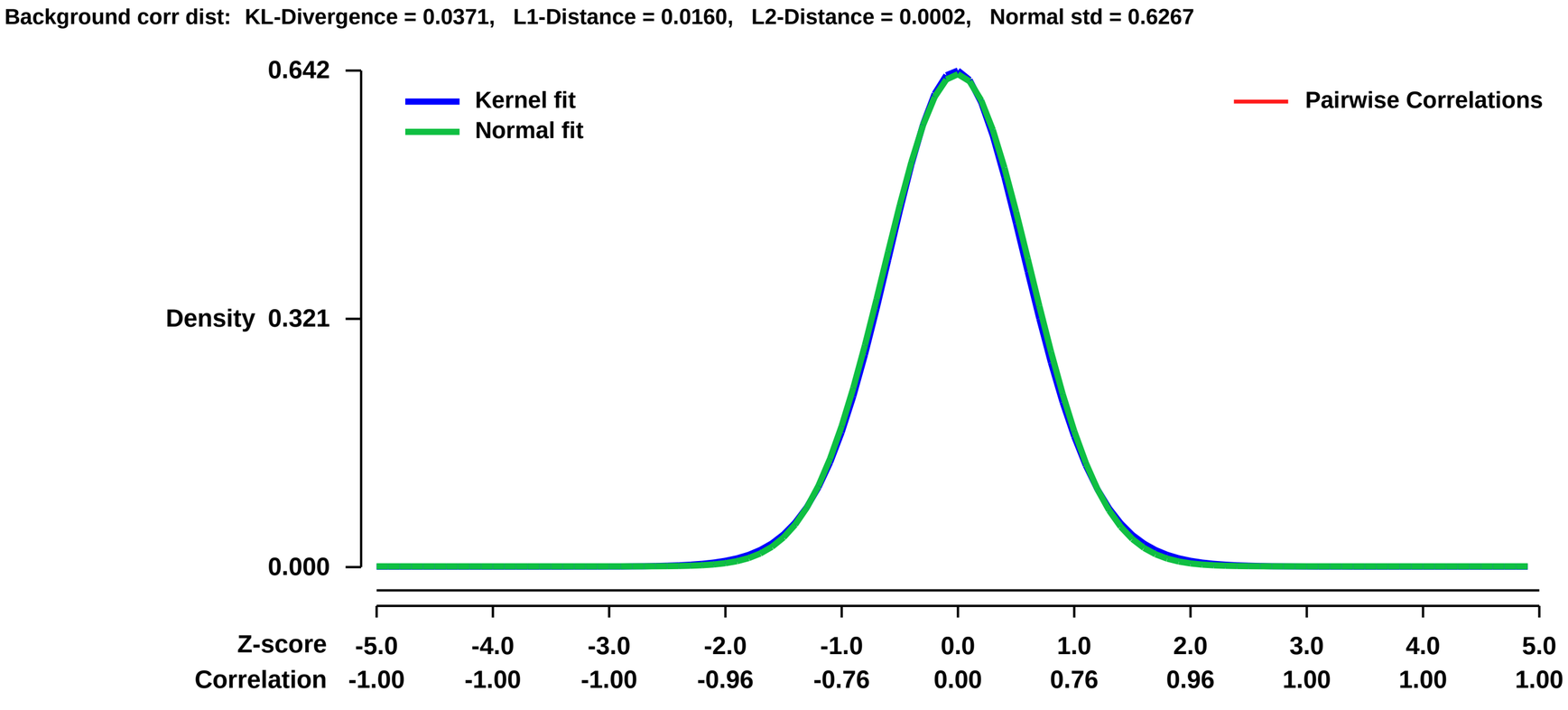

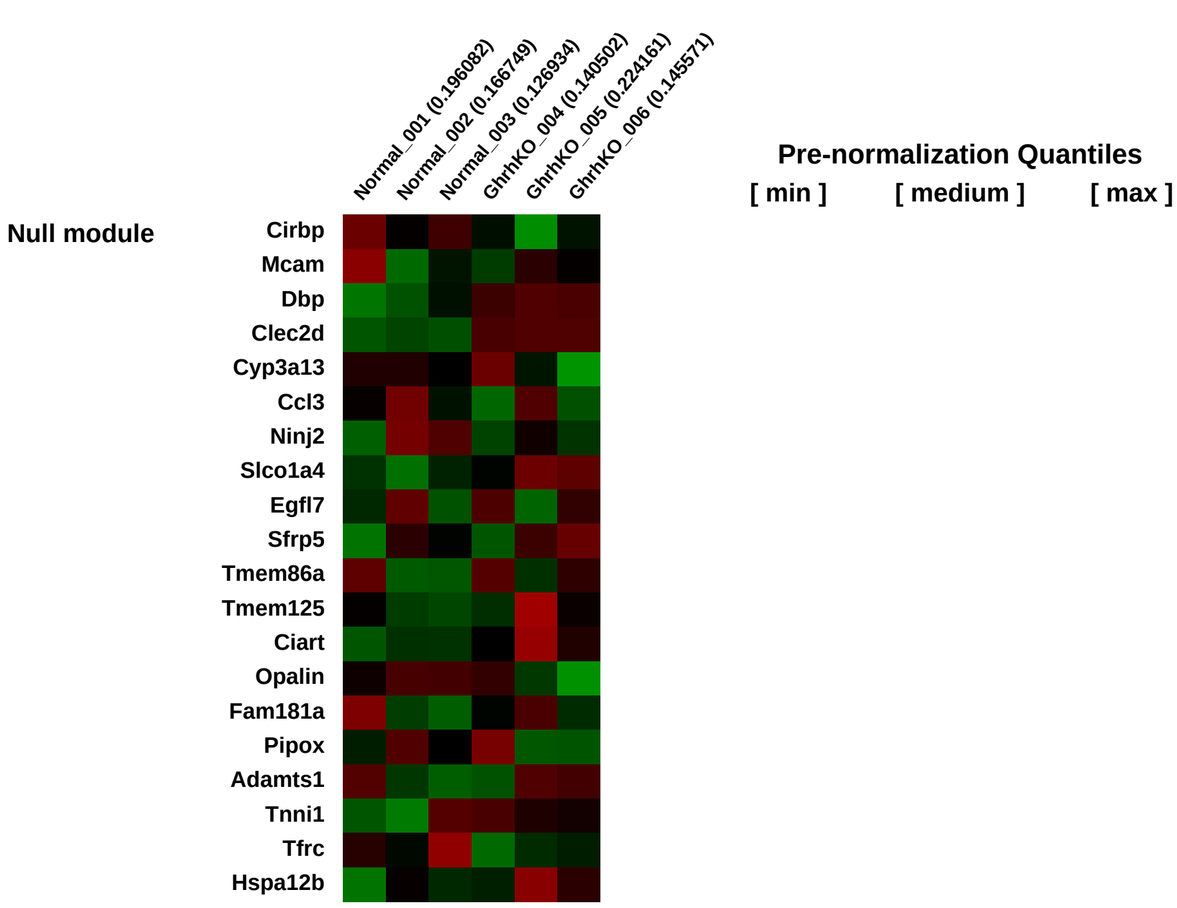

GEO Series "GSE5124" Expression Profiles

Num of samples in this series: 6

Scale of expression profile Z-scores

-3.0 -2.0 -1.0 0.0 1.0 2.0 3.0

GEO Link:	http://www.ncbi.nlm.nih.gov/geo/query/acc.cgi?acc=GSE5124
Status:	Public on Aug 28 2006
Title:	Hoxb1 gene expressing Hox-A1 protein: Altered transcriptional profile in rhombomere 4 at E10.5
Organism:	Mus musculus
Experiment type:	Expression profiling by array
Platform:	GPL1261
Pubmed ID:	16890163
Summary & Design:	**Summary:** This study analyzed mRNA profiles in rhombomere 4 of E10.5 mouse knock-in embryos expressing either normal endogenous Hox-B1 protein or the paralogous Hox-A1 protein from the Hoxb1 locus. The Hox-A1 protein was found to be detectably less efficacious than Hox-B1 in promoting neurogenesis in the basal plate of rhombomere 4 and its transcriptional profile shared several similarities with the Hoxb1 mutant. Keywords: gene swap, knock-in, hindbrain development, rhombomere 4 **Overall design:** GFP-positive cells were FACS-sorted from dissected hindbrains of entire litters of E10.5 mouse embryos expressing either normal endogenous Hox-B1 protein or the paralogous Hox-A1 protein from the Hoxb1 locus, either one tagged with IRES-tauGFP. Three independent biological replicates of each genotype were analyzed. Total RNA was isolated, amplified and hybridized to Affymetrix Mouse Genome 430 2.0 Arrays.

Background corr dist: KL-Divergence = 0.0481, L1-Distance = 0.0204, L2-Distance = 0.0005, Normal std = 0.5814

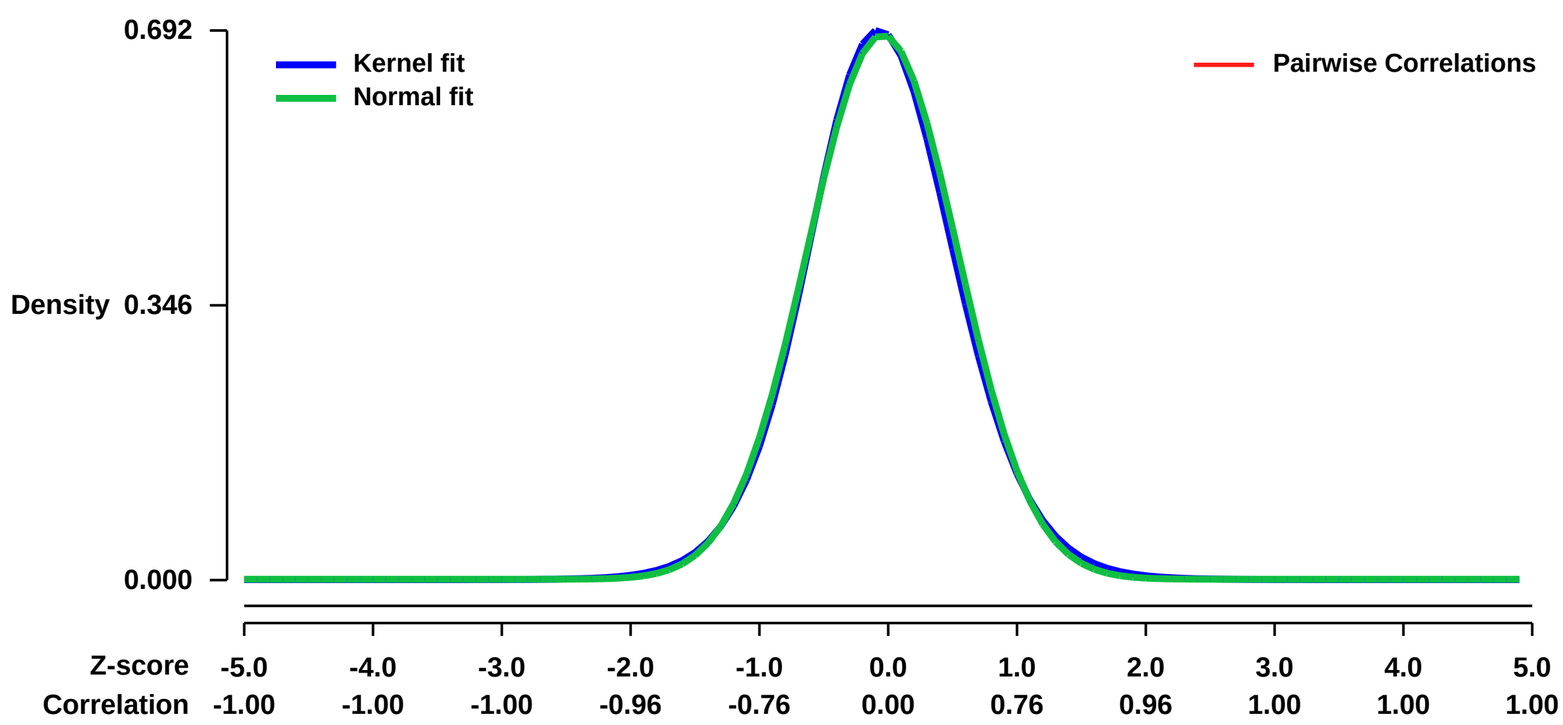

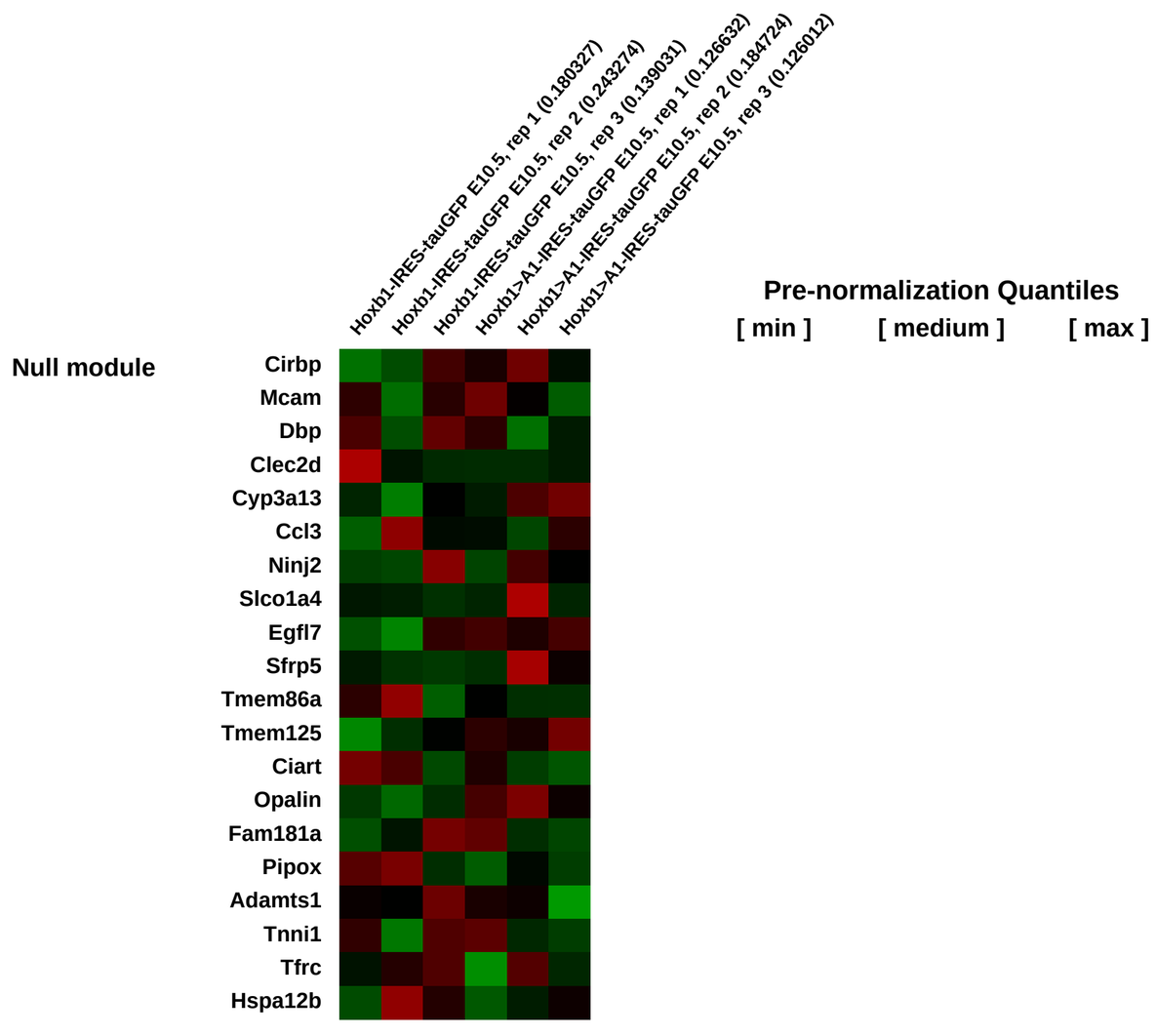

GEO Series "GSE51243" Expression Profiles

Num of samples in this series: 7

Scale of expression profile Z-scores

-3.0 -2.0 -1.0 0.0 1.0 2.0 3.0

GEO Link:	http://www.ncbi.nlm.nih.gov/geo/query/acc.cgi?acc=GSE51243
Status:	Public on Sep 28 2013
Title:	Comparison of the transcriptome of TEL-JAK2- versus activated NOTCH1 (ICN1)-induced T cell acute lymphoblastic leukemias (mouse)
Organism:	Mus musculus
Experiment type:	Expression profiling by array
Platform:	GPL1261
Pubmed ID:	24268771
Summary & Design:	**Summary:** The TEL-JAK2 fusion oncogene and the ICN1 activated allele of NOTCH1 are the result of specific chromosomal translocations in T cell acute lymphoblastic leukemia (T-ALL). Mouse models of these diseases (TEL-JAK2 transgenic mice; Carron C. et al. Blood (2000); a bone marrow transplantation model for ICN1-induced T-ALL) were used to compare the transcriptional program specific to each oncoprotein in mouse models of these leukemias. Tumor load was >50% leukemic cells in all selected organs. **Overall design:** Leukemic cells were collected from the thymus of terminally-ill TEL-JAK2 leukemic mice and bone marrow of terminally-ill ICN1 leukemic mice. RNA was extracted from each sample and processed for hybridization to Affymetrix arrays.

Background corr dist: KL-Divergence = 0.0331, L1-Distance = 0.0151, L2-Distance = 0.0003, Normal std = 0.6426

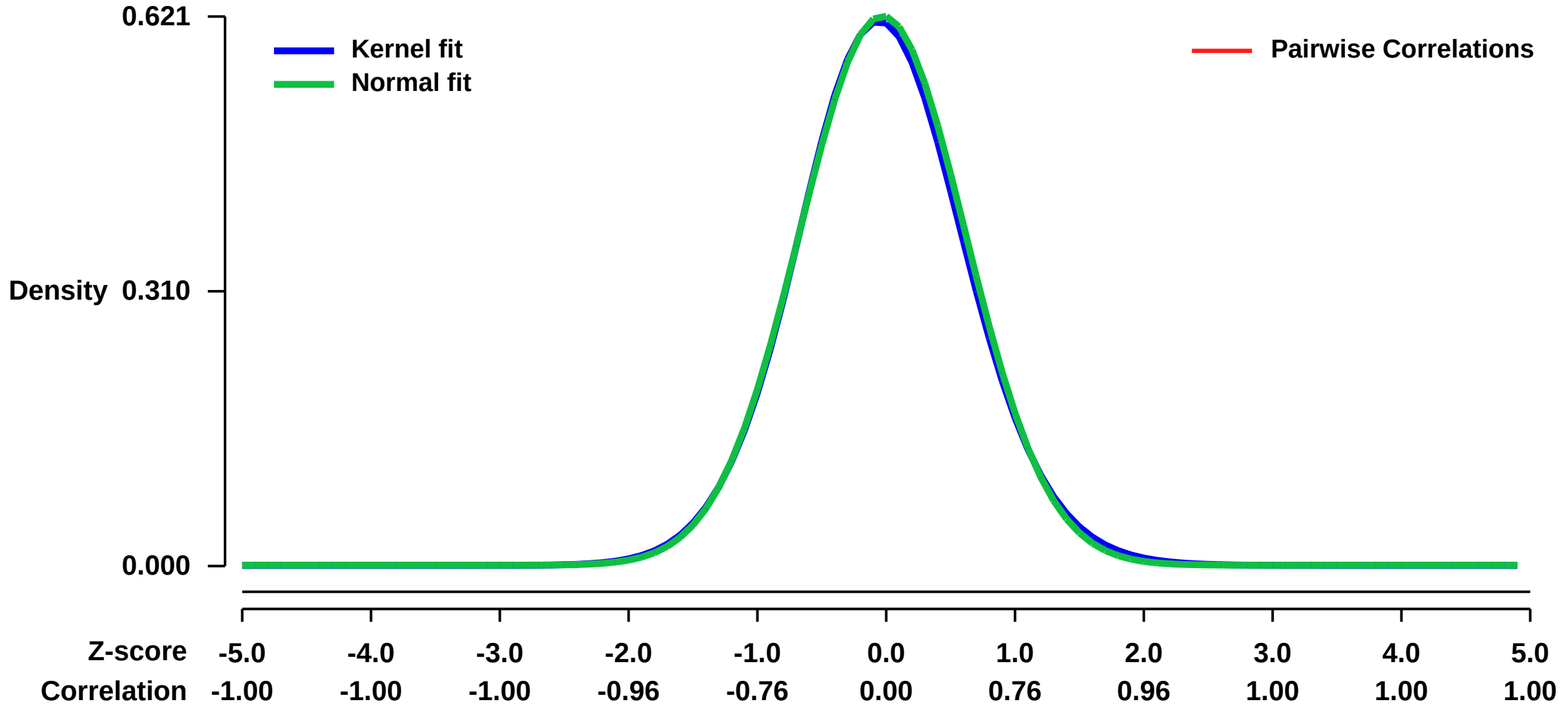

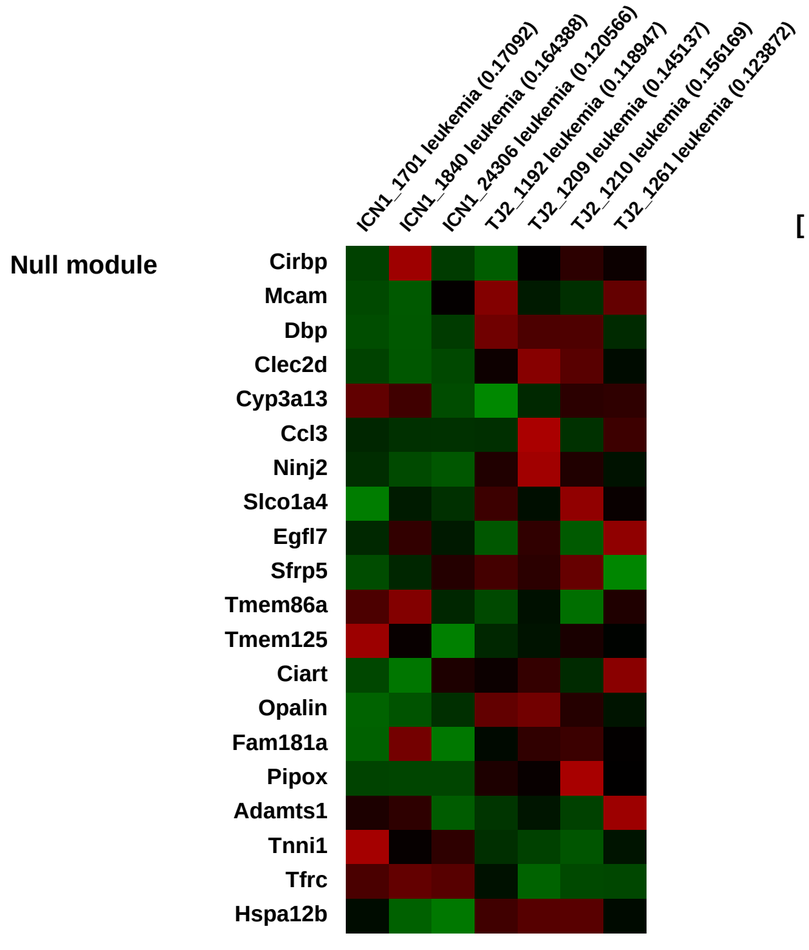

GEO Series "GSE5127" Expression Profiles

Num of samples in this series: 18

Scale of expression profile Z-scores

-3.0 -2.0 -1.0 0.0 1.0 2.0 3.0

GEO Link:	http://www.ncbi.nlm.nih.gov/geo/query/acc.cgi?acc=GSE5127
Status:	Public on Sep 01 2006
Title:	Gene Expression Biomarkers for Predicting Lung Tumors in Two-Year Rodent Bioassays
Organism:	Mus musculus
Experiment type:	Expression profiling by array
Platform:	GPL1261
Pubmed ID:	17114358
Summary & Design:	**Summary:** Two-year rodent bioassays play a central role in evaluating both the carcinogenic potential of a chemical and generating quantitative information on the dose-response behavior for chemical risk assessments. The bioassays involved are expensive and time-consuming, requiring nearly lifetime exposures (two years) in mice and rats and costing $2 to $4 million per chemical. Since there are approximately 80,000 chemicals registered for commercial use in the United States and 2,000 more are added each year, applying animal bioassays to all chemicals of concern is clearly impossible. To efficiently and economically identify carcinogens prior to widespread use and human exposure, alternatives to the two-year rodent bioassay must be developed. In this study, animals were exposed for 13 weeks to two chemicals that were positive for lung tumors in the two-year rodent bioassay, two chemicals that were negative for tumors, and two vehicle controls. Gene expression analysis was performed on the lungs of the animals to assess the potential for identifying gene expression biomarkers that can predict tumor formation in a two-year bioassay following a 13 week exposure. **Keywords:** toxicology, chemical carcinogenesis, lung **Overall design:** Five week old female B6C3F1 mice were exposed for 13 weeks to the following treatments: 1) 1,5-Naphthalenediamine, CAS No. 2243-62-1, feed, 2000 ppm, positive lung carcinogen; 2) 2,3-Benzofuran, CAS No. 271-89-6, gavage, 240 mg/kg, positive lung carcinogen; 3) N-(1-naphthyl)ethylenediamine dihydrochloride, CAS No. 1465-25-4, feed, 2000 ppm, negative lung carcinogen; 4) Pentachloronitrobenzene, CAS No. 82-68-8, feed, 8187 ppm, negative lung carcinogen; 5) Feed control; 6) Corn oil gavage control. Feed animals were exposed 7 days/week and gavage animals were exposed 5 days/week (5 ml/kg). Microarray analysis was performed on the lungs of three mice per treatment group.

Background corr dist: KL-Divergence = 0.1443, L1-Distance = 0.0395, L2-Distance = 0.0032, Normal std = 0.3779

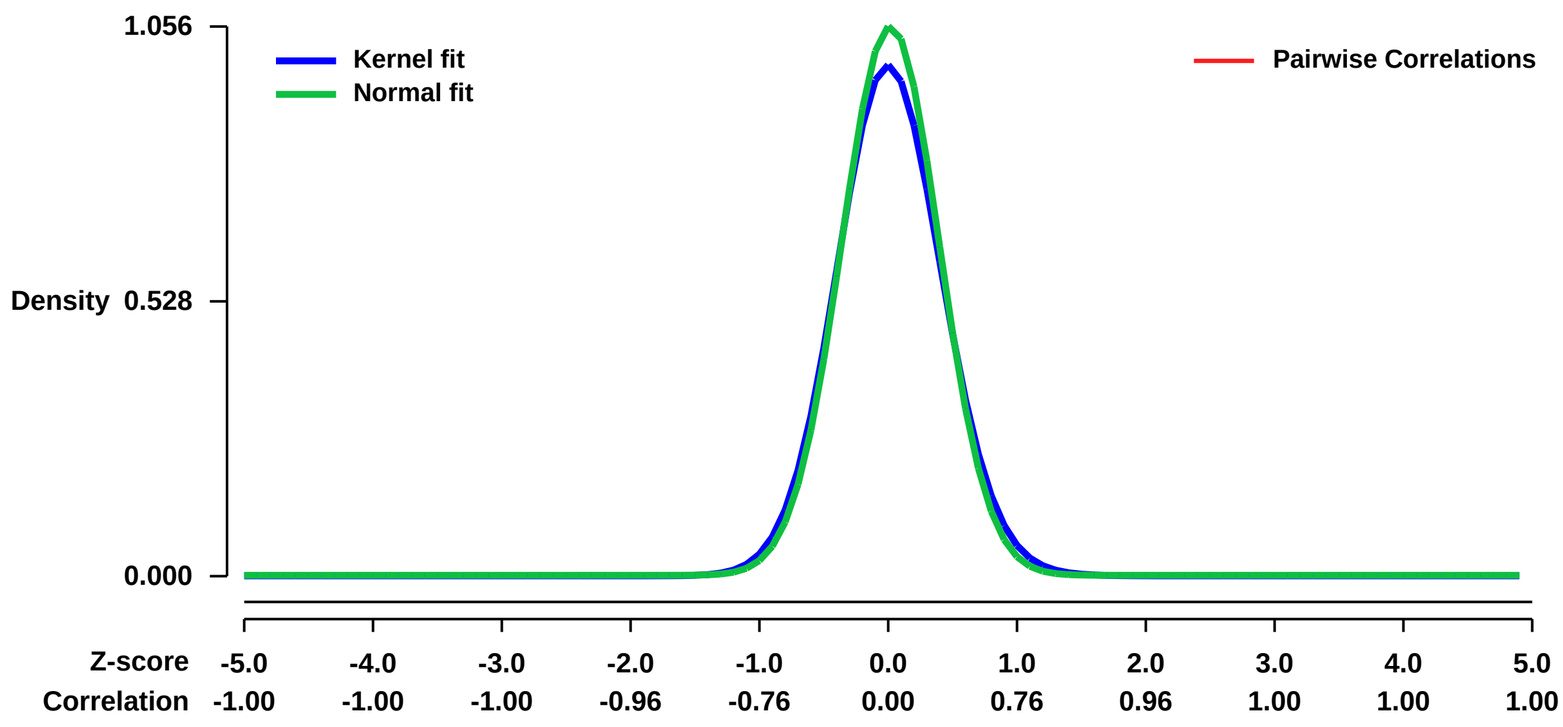

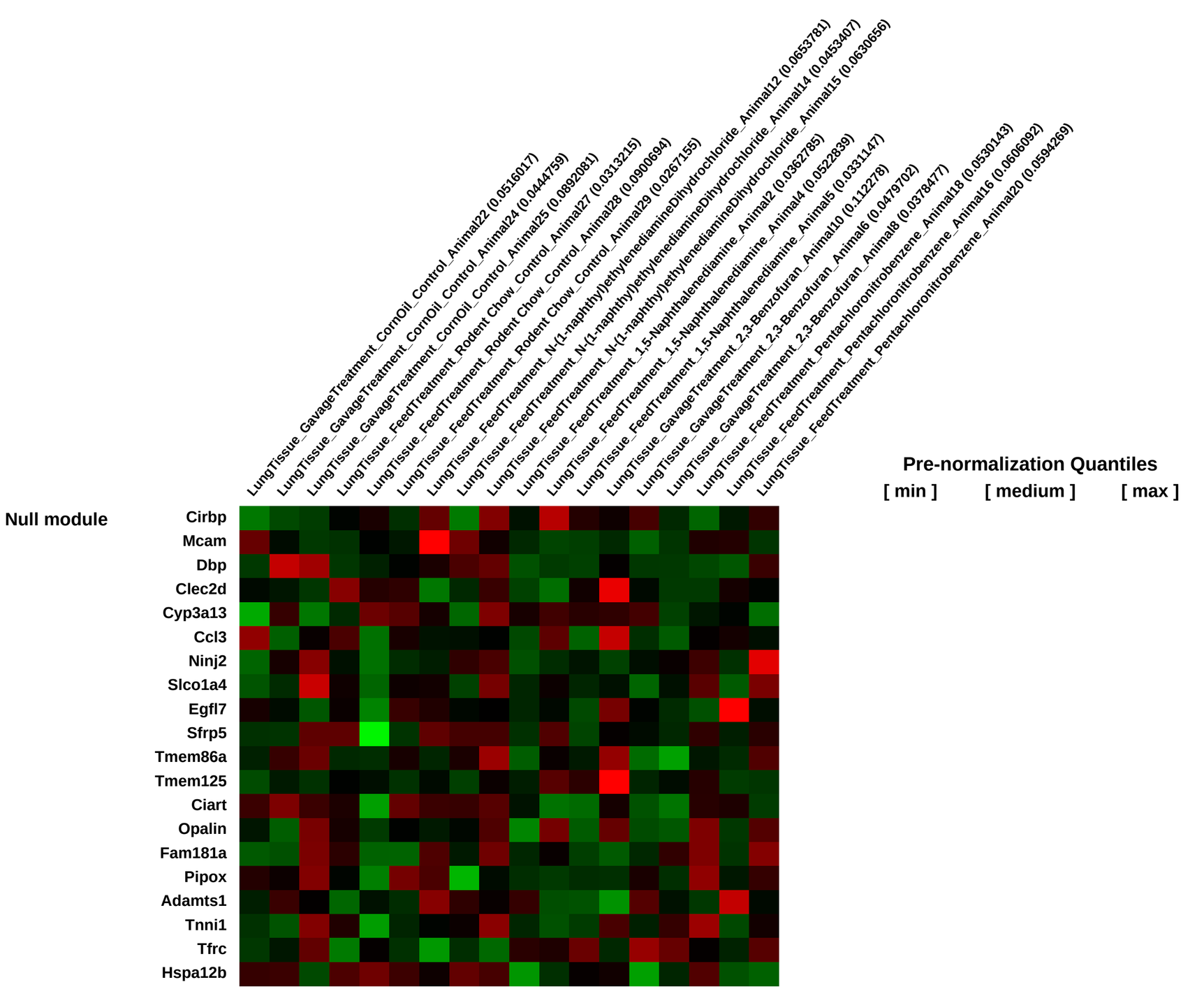

Null module

GEO Series "GSE5128" Expression Profiles

Num of samples in this series: 18

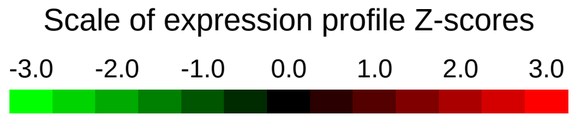

GEO Link:	http://www.ncbi.nlm.nih.gov/geo/query/acc.cgi?acc=GSE5128
Status:	Public on Sep 01 2006
Title:	Gene Expression Biomarkers for Predicting Liver Tumors in Two-Year Rodent Bioassays
Organism:	Mus musculus
Experiment type:	Expression profiling by array
Platform:	GPL1261
Pubmed ID:	17114358
Summary & Design:	**Summary:** Two-year rodent bioassays play a central role in evaluating both the carcinogenic potential of a chemical and generating quantitative information on the dose-response behavior for chemical risk assessments. The bioassays involved are expensive and time-consuming, requiring nearly lifetime exposures (two years) in mice and rats and costing $2 to $4 million per chemical. Since there are approximately 80,000 chemicals registered for commercial use in the United States and 2,000 more are added each year, applying animal bioassays to all chemicals of concern is clearly impossible. To efficiently and economically identify carcinogens prior to widespread use and human exposure, alternatives to the two-year rodent bioassay must be developed. In this study, animals were exposed for 13 weeks to two chemicals that were positive for liver tumors in the two-year rodent bioassay, two chemicals that were negative for liver tumors, and two vehicle controls. Gene expression analysis was performed on the livers of the animals to assess the potential for identifying gene expression biomarkers that can predict tumor formation in a two-year bioassay following a 13 week exposure. **Keywords:** toxicology, chemical carcinogenesis, liver **Overall design:** Five week old female B6C3F1 mice were exposed for 13 weeks to the following treatments: 1) 1,5-Naphthalenediamine, CAS No. 2243-62-1, feed, 2000 ppm, positive liver carcinogen; 2) 2,3-Benzofuran, CAS No. 271-89-6, gavage, 240 mg/kg, positive liver carcinogen; 3) N-(1-naphthyl)ethylenediamine dihydrochloride, CAS No. 1465-25-4, feed, 2000 ppm, negative liver carcinogen; 4) Pentachloronitrobenzene, CAS No. 82-68-8, feed, 8187 ppm, negative liver carcinogen; 5) Feed control; 6) Corn oil gavage control. Feed animals were exposed 7 days/week and gavage animals were exposed 5 days/week (5 ml/kg). Microarray analysis was performed on the livers of three mice per treatment group.

Background corr dist: KL-Divergence = 0.0940, L1-Distance = 0.0565, L2-Distance = 0.0073, Normal std = 0.4505

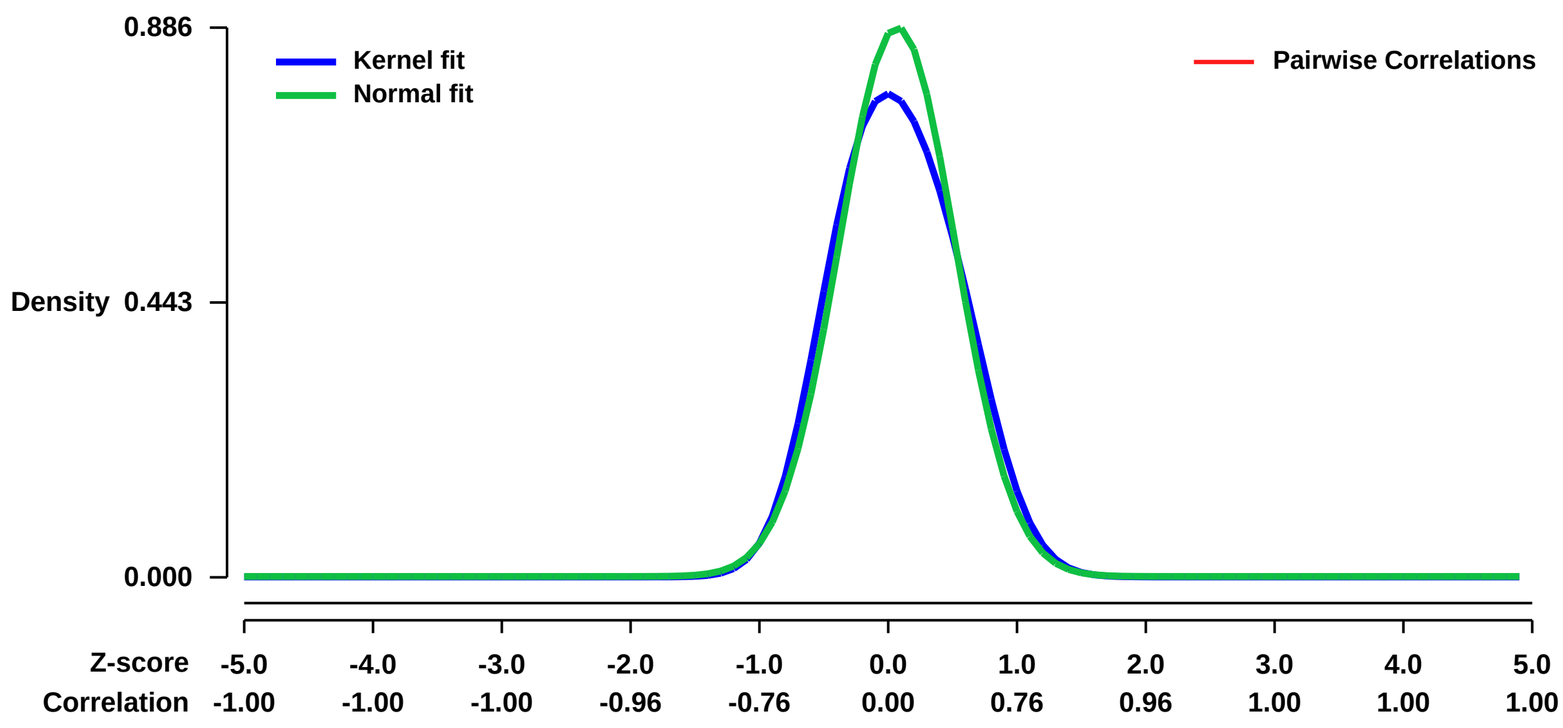

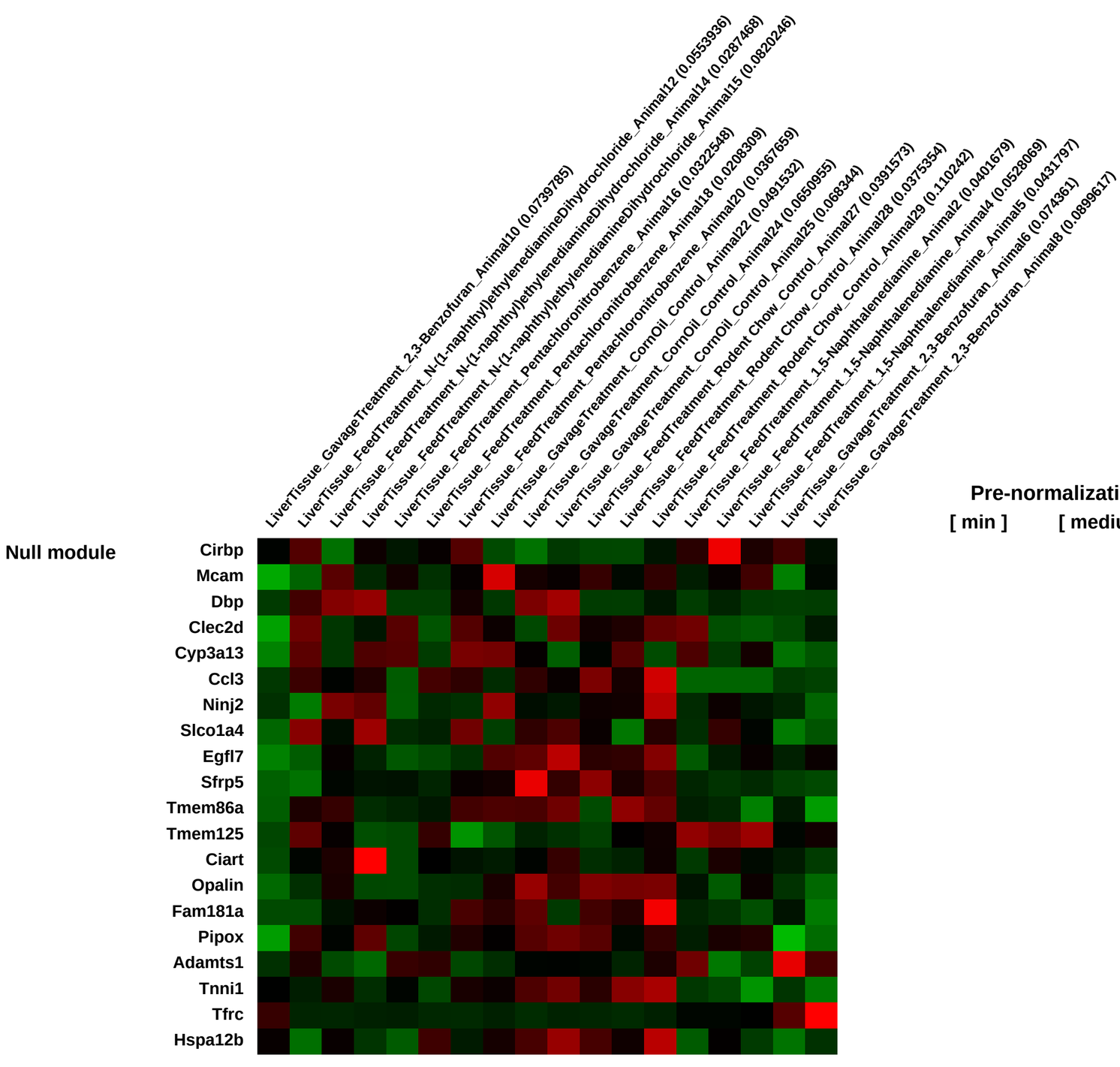

GEO Series "GSE51285" Expression Profiles

Num of samples in this series: 36

Scale of expression profile Z-scores

-3.0 -2.0 -1.0 0.0 1.0 2.0 3.0

GEO Link: http://www.ncbi.nlm.nih.gov/geo/query/acc.cgi?acc=GSE51285

Status: Public on Sep 30 2013

Title: Expression and Metabolic Profiles in a Panel of Five Neural Tube Defect Mouse Models

Organism: Mus musculus

Experiment type: Expression profiling by array

Platform: GPL1261

Pubmed ID:

Summary & Design:

Summary:
Neural tube defects (NTDs) are serious birth defects with an estimated worldwide incidence of 1 per 1,000 live births. The multifactorial nature of NTDs in humans has made it difficult to elucidate pathogenesis mechanisms. However, a strong relationship has been established between folate-homocysteine metabolism and NTD risk. Prevention of a substantial proportion of fetal NTDs can be achieved through maternal folic acid (FA) supplementation. However the mechanism by which FA exerts its beneficial effect remains unclear. METHODS: To improve our understanding of the underlying mechanisms of NTD pathogenesis and the ways in which folate exerts its beneficial effect, we analyzed mRNA profiles as well as folate and vitamin B12 levels in five NTD mouse mutants whose response to dietary FA was previously established. RESULTS: Differentially expressed genes representing the effect of each NTD-causing mutation were identified and associated with biologic pathways. Interestingly, the panel of NTD mutants collectively revealed pathways related to two nuclear receptors, retinoid X receptor (RXR) and pregnane X receptor (PXR), suggesting that these pathways may be related to a shared mechanism of NTD development. Moreover, the NTD-causing mutations that were associated with FA responsiveness had expression profiles that were related to folate-homocysteine metabolic pathways. These pathways were not strongly associated with mutants that do not respond to FA supplementation, implying that FA may be beneficial when the NTD mutation affects pathways related to folate-homocysteine metabolism.

Overall design:
5 groups of NTD mutants were studied. From each mutant group Heterozygous (test) and wild-type (control) female pups were used for this study at 6-8 weeks of age. 4 biological replicates were used for each of the test and control groups of each mutant. All mice used for the experiments were fasted 4-5 hours before dissection. A total of 36 samples were analyzed.

Background corr dist: KL-Divergence = 0.4270, L1-Distance = 0.0761, L2-Distance = 0.0177, Normal std = 0.2414

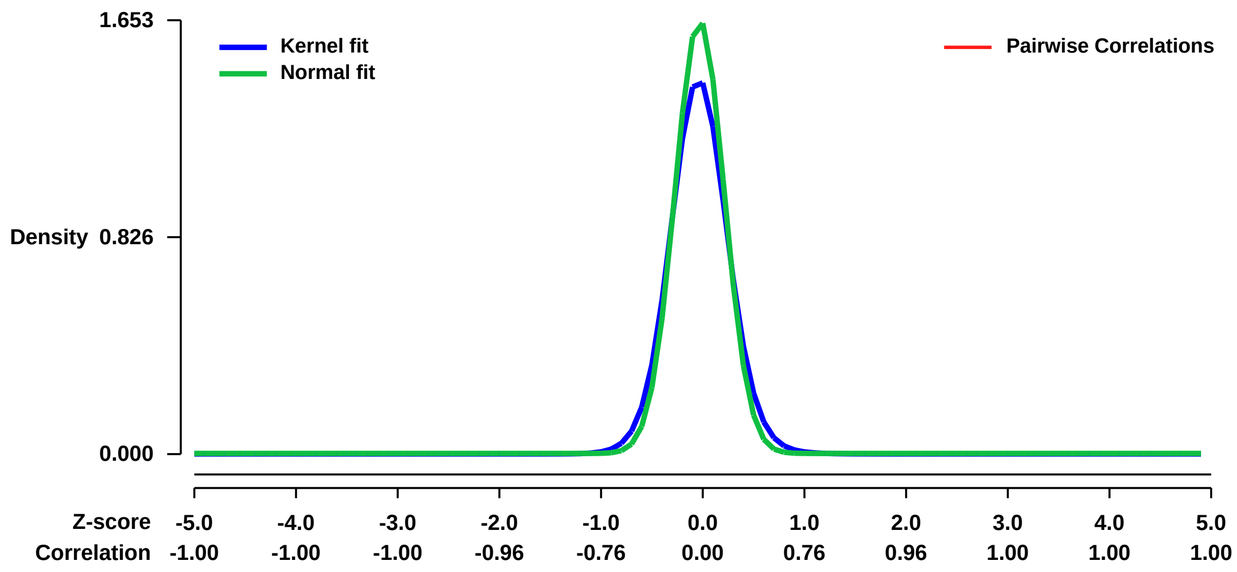

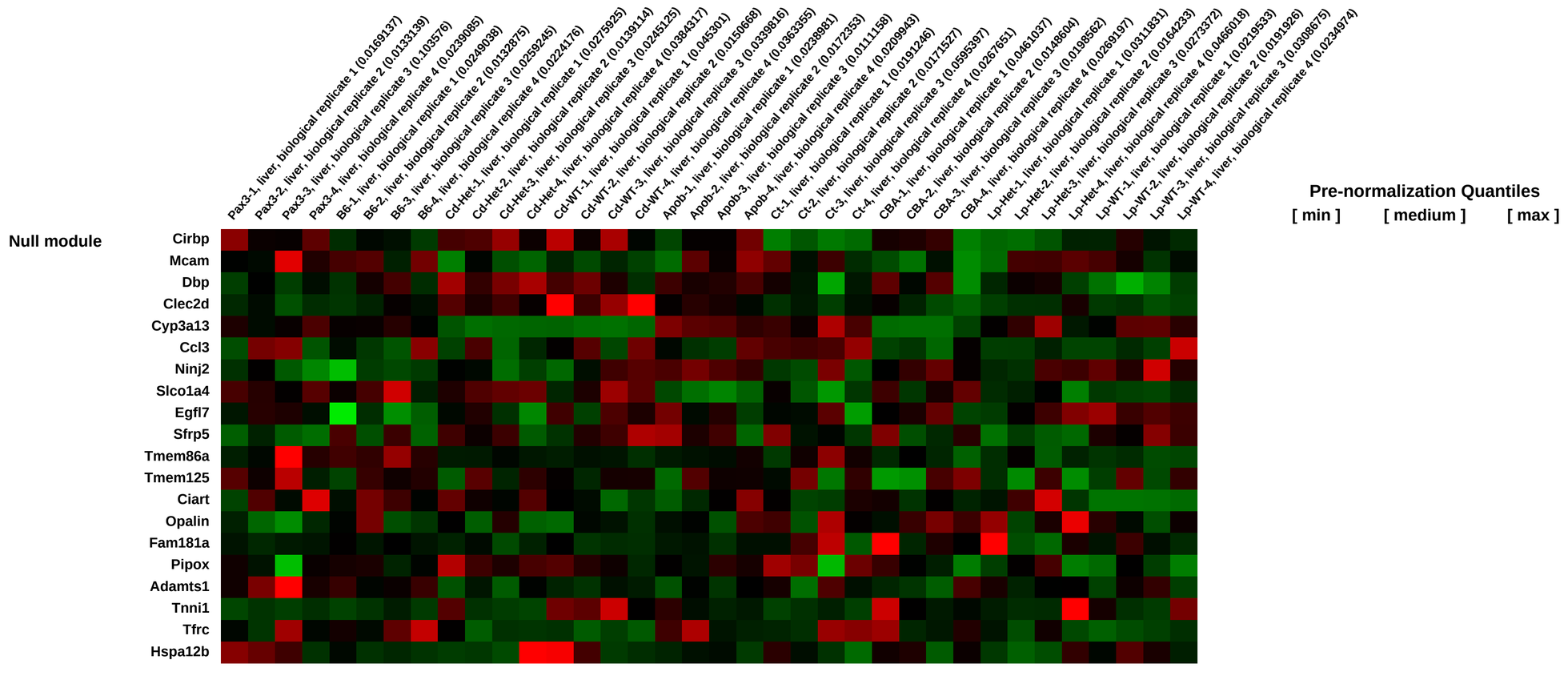

GEO Series "GSE51355" Expression Profiles

Num of samples in this series: 16

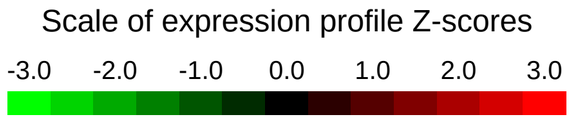

GEO Link:	**http://www.ncbi.nlm.nih.gov/geo/query/acc.cgi?acc=GSE51355**
Status:	**Public on Feb 10 2014**
Title:	**Metabolic programs orchestrated by the activated Ha-ras and ˛†-catenin oncoproteins in mouse liver tumors [mRNA]**
Organism:	**Mus musculus**
Experiment type:	**Expression profiling by array**
Platform:	**GPL1261**
Pubmed ID:	
Summary & Design:	**Summary:** **The process of hepatocarcinogenesis in the diethylnitrosamine (DEN) initiation/phenobarbital (PB) promotion mouse model involves the selective clonal outgrowth of cells harboring oncogene mutations in Ha-ras, B-raf, or Ctnnb1. Here, we have characterized mouse liver tumors harboring either Ctnnb1 or Ha-ras mutations via integrated molecular profiling at the transcriptional and translational and post-translational levels. In addition, metabolites of the intermediary metabolism were quantified by high resultion 1H magic angle nuclear magnetic resonance (HR-MAS NMR). We have identified tumor characteristic genotype-specific differences in mRNA and miRNA expression, protein levels, and post-translational modifications and in metabolite levels that facilitate the molecular and biochemical stratification of tumor phenotypes. Bioinformatic integration of these data at the pathway level led to novel insights into tumor genotype-specific aberrant cell signaling and in particular to a better understanding of alterations in pathways of the cell intermediary metabolism, which are driven by the constitutive activation of the ˛†-Catenin and Ha-ras oncoproteins in tumors of the two genotypes.** **Overall design:** **Male C3H/HeJ mice received a single i.p. injection of DEN (10 or 90´µg/g body weight) at 2, or 6 weeks of age. After a treatment-free interval of 2 weeks, the C3H/HeJ mice were either kept on a diet containing 0.05% PB or on a PB-free control diet for 28 to 36 weeks before they were sacrificed. Ha-ras- or Ctnnb1-mutated tumors and control tissues were isolated and either flash frozen in liquid nitrogen and stored at -80´℃, or prepared for immunohistochemistry.**

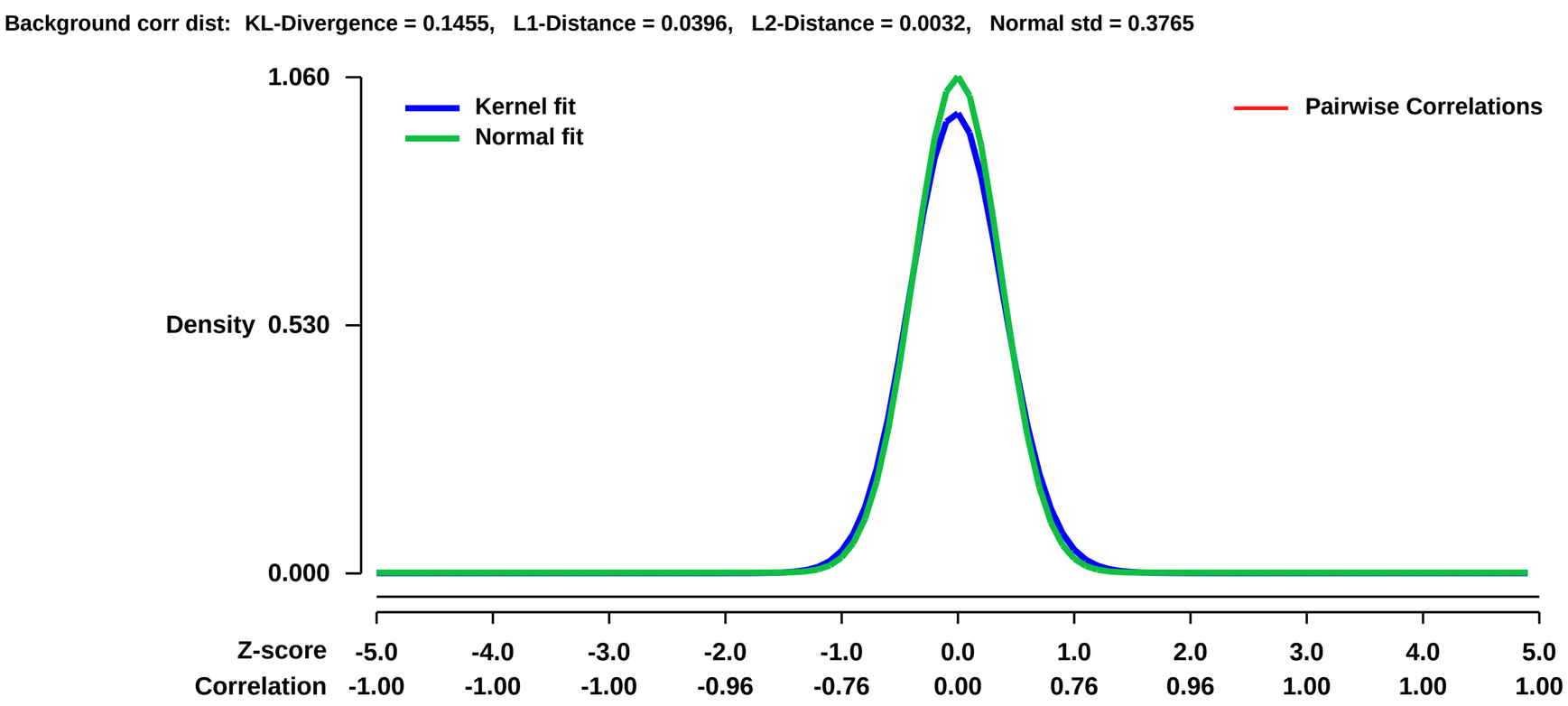

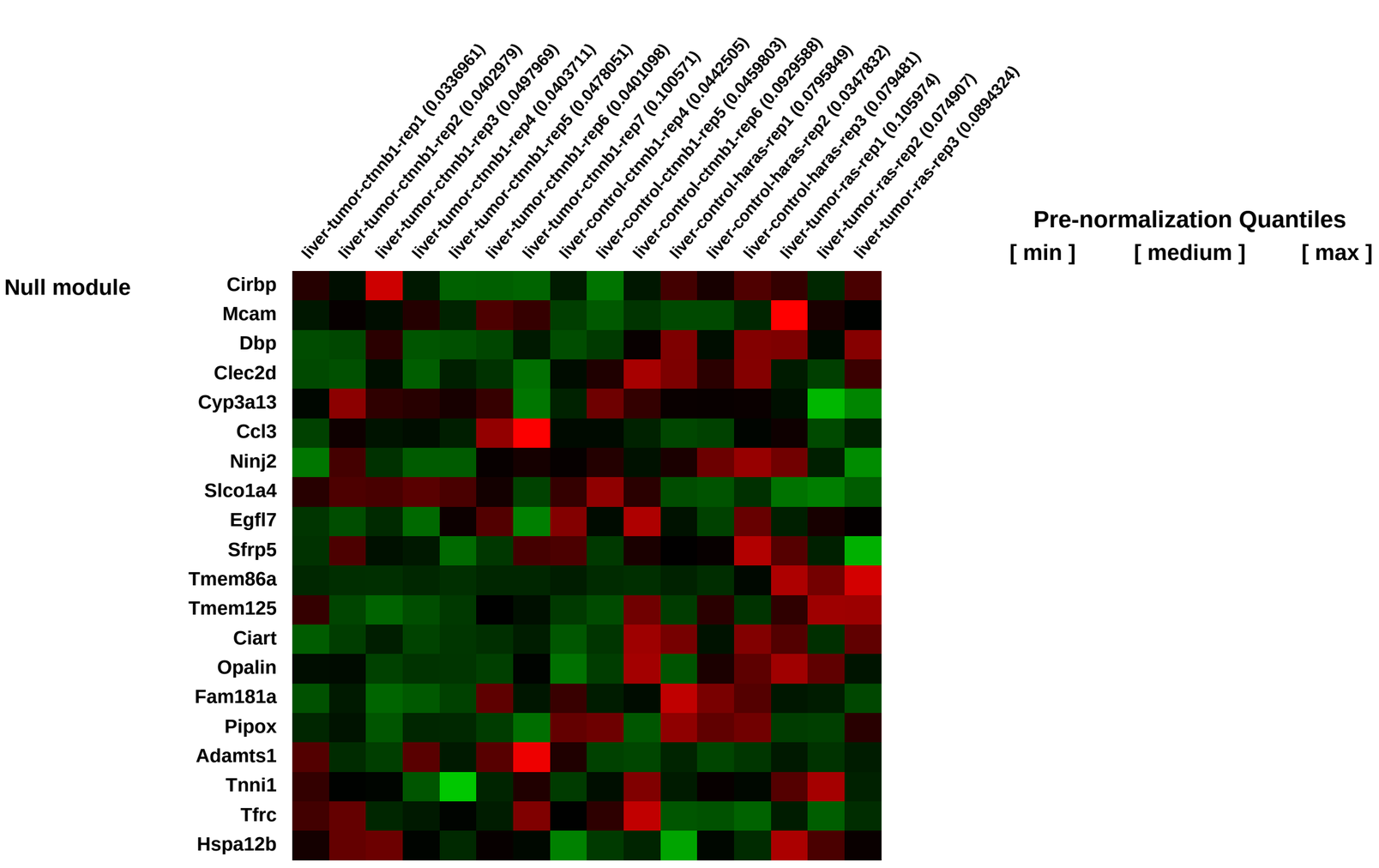

GEO Series "GSE51385" Expression Profiles

Num of samples in this series: 8

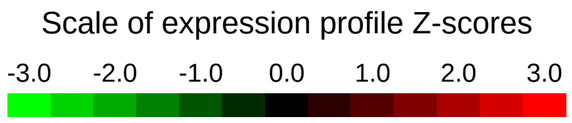

GEO Link:	http://www.ncbi.nlm.nih.gov/geo/query/acc.cgi?acc=GSE51385
Status:	Public on Oct 18 2013
Title:	Expression profiling of ProB and PreB cells in Ebf1 heterozygous mouse bone marrow
Organism:	Mus musculus
Experiment type:	Expression profiling by array
Platform:	GPL1261
Pubmed ID:	24078629
Summary & Design:	**Summary:** Loss of one allele of Ebf1 impairs pre-B cell (B220+CD19+CD43low/negIgM-) expansion. In order to better understand the underlying cause of the reduced pre-B cell compartment in Ebf1+/- mice, we sorted pro-B (B220+CD19+CD43highIgM-) as well as pre-B cells from Wt and Ebf1 heterozygote mutant mice and performed Affymetrix based microarray gene expression analysis. While the overall gene expression patterns as well as Pax5 expression in Wt and Ebf1 pro-B cells were similar, gene set enrichment (GSE) analysis of the microarray data suggested a reduced expression of cell division (p<0.001) and mitosis (p<0.001) genes in the Ebf1+/- pre-B cells as compared to their Wt counterparts. This in combination with rather normal expression of B-lineage genes in Ebf1+/- pre-B cells opens for the possibility that the phenotypic loss of pre-B cells in Ebf1+/- mice could be a result of reduced expansion of progenitors rather than by a differentiation block. **Overall design:** RNA was extracted from 20,000 or 25000 purified adult bone marrow cells using the RNAeasy microkit. RNA was labeled and amplified by dual amplification and hybridized to Affymetrix microarray MOE430_2, according to AffymetrixTM GeneChip Expression Analysis Technical Manual. Probe level expression values were calculated using the RMA algorithm.

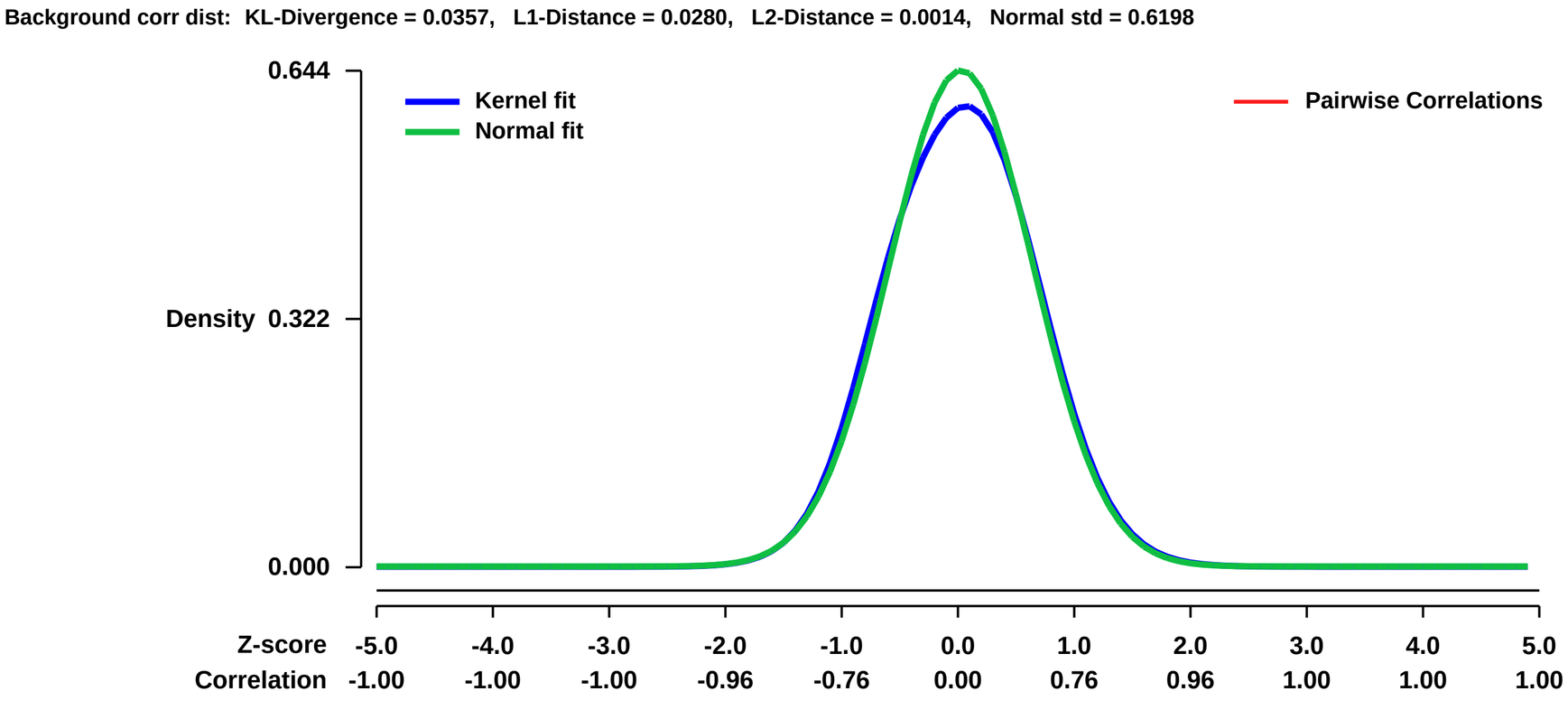

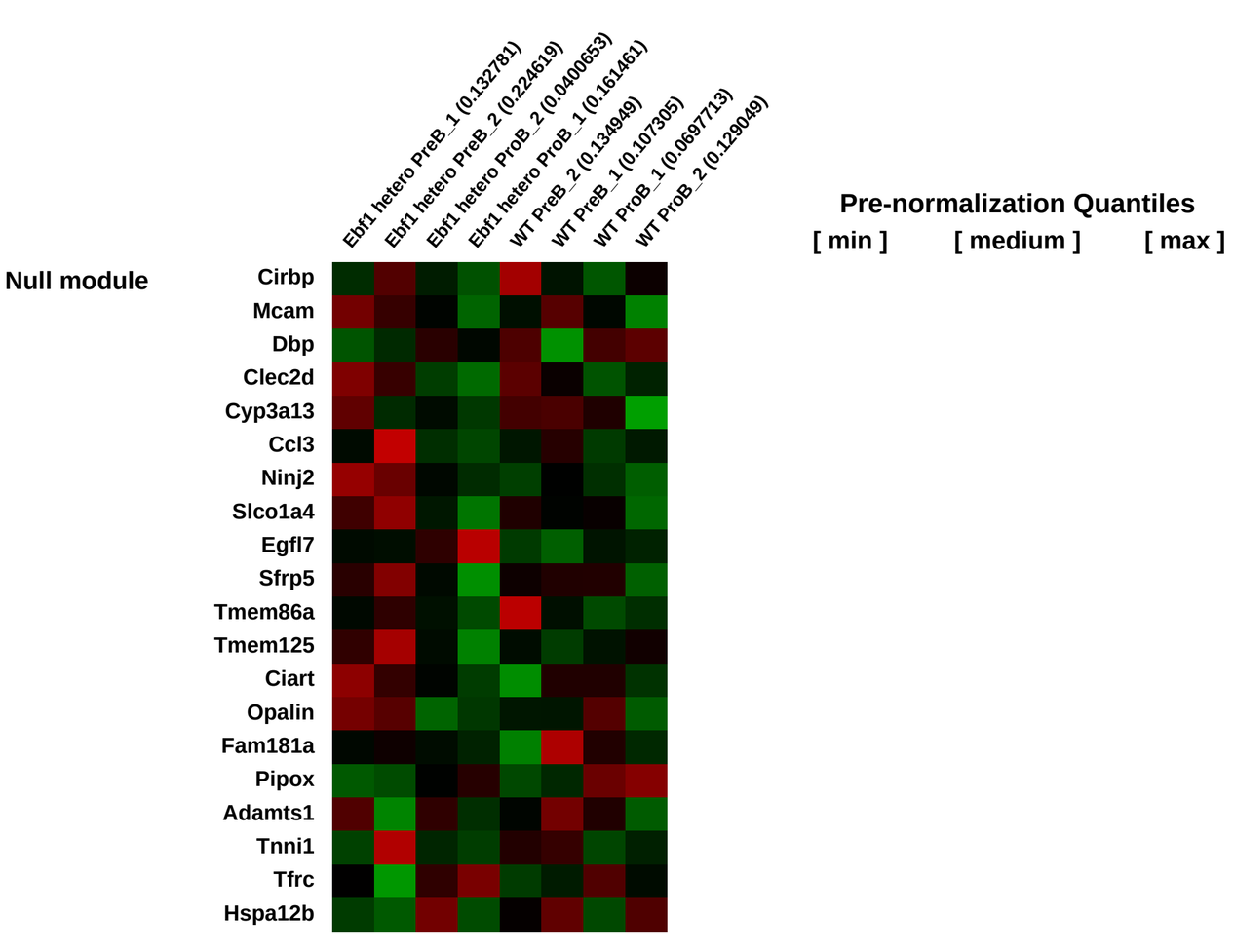

GEO Series "GSE5140" Expression Profiles

Num of samples in this series: 13

Scale of expression profile Z-scores

-3.0 -2.0 -1.0 0.0 1.0 2.0 3.0

GEO Link:	**http://www.ncbi.nlm.nih.gov/geo/query/acc.cgi?acc=GSE5140**
Status:	**Public on Jun 13 2007**
Title:	**Creatine increases health and life span in mice**
Organism:	**Mus musculus**
Experiment type:	**Expression profiling by array**
Platform:	**GPL1261**
Pubmed ID:	**17416441**
Summary & Design:	**Summary:** **Here we show that oral creatine (Cr) supplementation leads to increased life span in mice. Treated mice showed improved neurobehavioral performance, decreased accumulation of the aging pigment lipofuscin and upregulation of â anti-agingâ genes in brain. As Cr is virtually free of adverse effects, it may be a promising food supplement for healthy aging in man.** **Keywords: creatine, life span, neurobehavioural performance, microarray, oxidative stress, aging** **Overall design:** **6 biological replicates for creatine-treated mice, 7 biological replicates for untreated mice.**

Background corr dist: **KL-Divergence = 0.1947, L1-Distance = 0.0477, L2-Distance = 0.0052, Normal std = 0.3346**

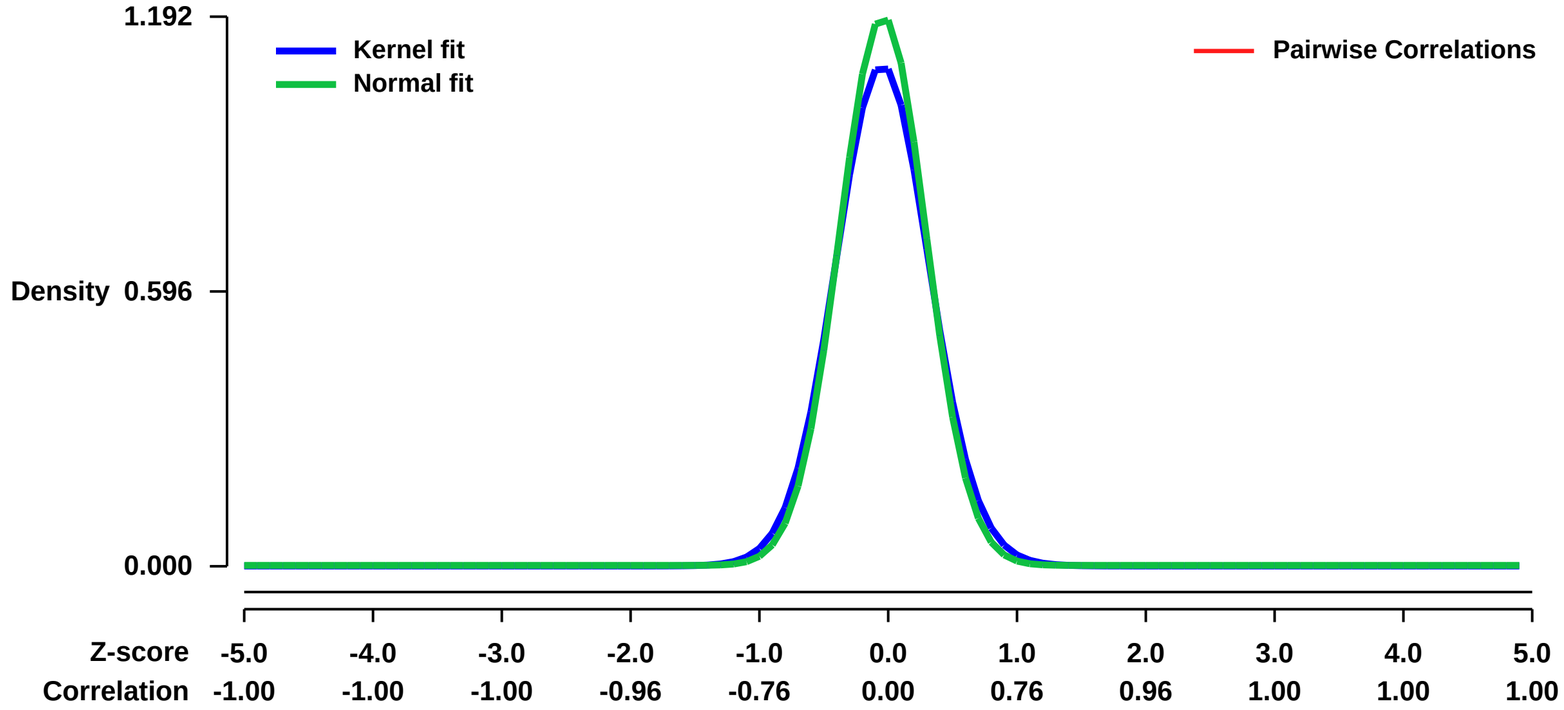

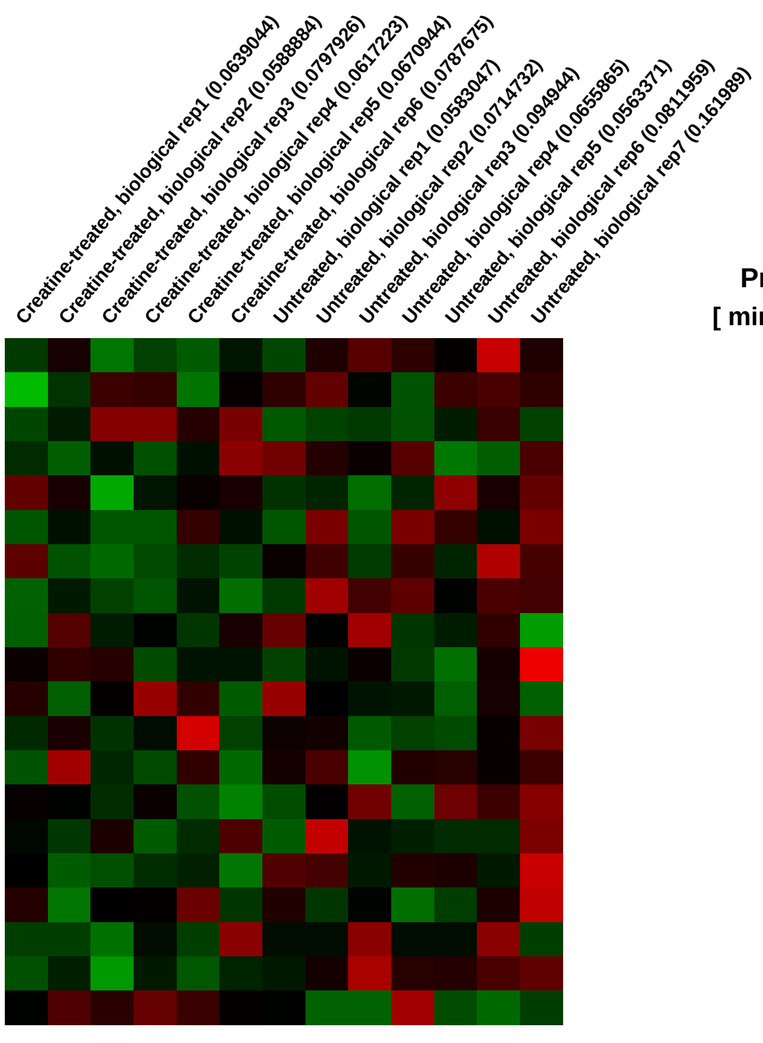

GEO Series "GSE51417" Expression Profiles

Num of samples in this series: 60

Scale of expression profile Z-scores

-3.0 -2.0 -1.0 0.0 1.0 2.0 3.0

GEO Link:	http://www.ncbi.nlm.nih.gov/geo/query/acc.cgi?acc=GSE51417
Status:	Public on Apr 15 2014
Title:	Comparative Iron Oxide Nanoparticle Cellular Dosimetry and Response in Mice by the Inhalation and Liquid Cell Culture Exposure Routes
Organism:	Mus musculus
Experiment type:	Expression profiling by array
Platform:	GPL1261
Pubmed ID:	
Summary & Design:	**Summary:** To identify the molecular impact of SPIO nanoparticle inhalation exposure on lung tissue. Transcriptional responses were measured by global microarray analysis of mouse lung. **Overall design:** Male Balb/c mice were exposed to aerosolized SPIO nanoparticles using a nano-aerosol generation and inhalation system . Exposure was performed using two groups of 30 male Balb/c mices (60 total). One group of 30 was exposed to aerosolized SPIO nanopartic

Background corr dist: KL-Divergence = 0.3759, L1-Distance = 0.0792, L2-Distance = 0.0189, Normal std = 0.2550

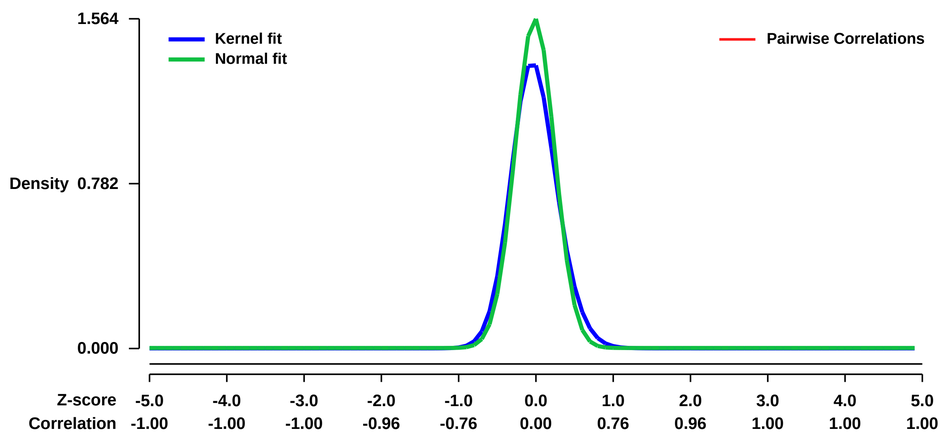

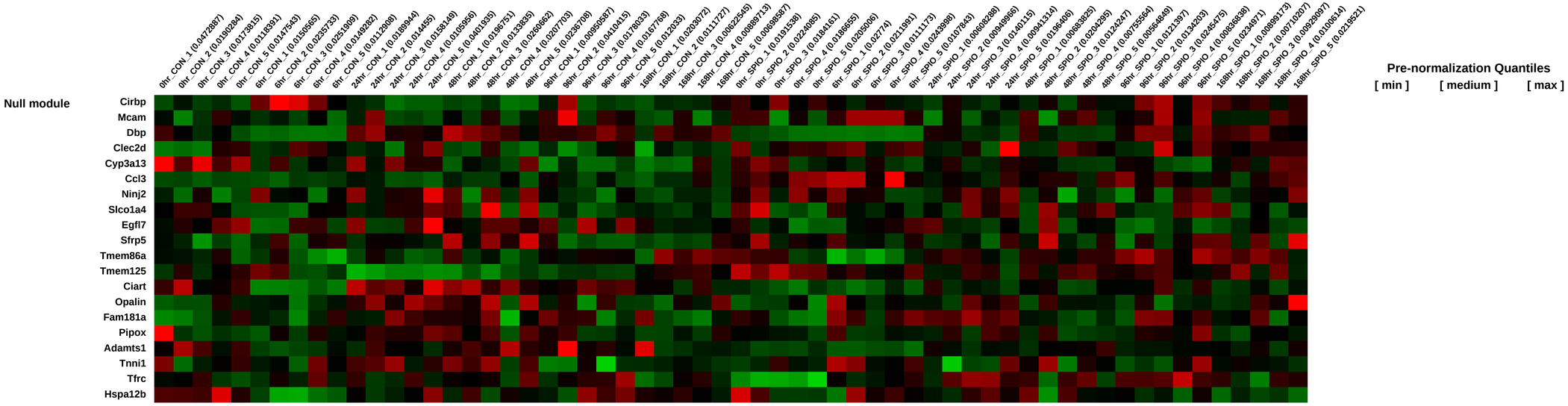

GEO Series "GSE51422" Expression Profiles

Num of samples in this series: 6

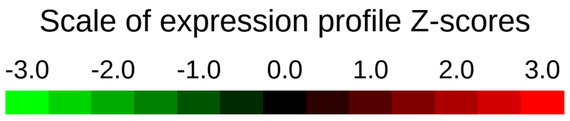

GEO Link:	http://www.ncbi.nlm.nih.gov/geo/query/acc.cgi?acc=GSE51422
Status:	Public on Oct 25 2013
Title:	Gene Expression in wild type and CCR5 knockout mice with lung metastasis
Organism:	Mus musculus
Experiment type:	Expression profiling by array
Platform:	GPL1261
Pubmed ID:	24197118
Summary & Design:	**Summary:** We have shown that C57BL/6J CCR5 knockout mice develop 30.4% ´– 8.6% fewer B16 F10 lung nodules compared to wild type mice after the intravenous injection of 100,000 B16 F10 cells. We sought to understand this phenomenon by comparing gene expression in the lungs of these mice at 6, 24, and 48 hours after tumor injection. **Overall design:** There were 6 groups or conditions (CCR5 - 6 hours, WT - 6 hours, CCR5 - 24 hours, WT - 24 hours, CCR5 - 48 hours, WT - 48 hour); each group had 4 to 5 mice. All of the mice were injected with 100,000 B16 F10 melanoma cells by tail vein. At the designated time, the mice were anesthetized with Avertin and their lungs were perfused with PBS. After this, the lungs were harvested and snap frozen in liquid nitrogen. They were kept at minus 80 degrees C until processing. mRNA was extracted as described below and equivalent amounts of mRNA (by weight) was pooled by group.

Background corr dist: KL-Divergence = 0.0292, L1-Distance = 0.0121, L2-Distance = 0.0001, Normal std = 0.6672

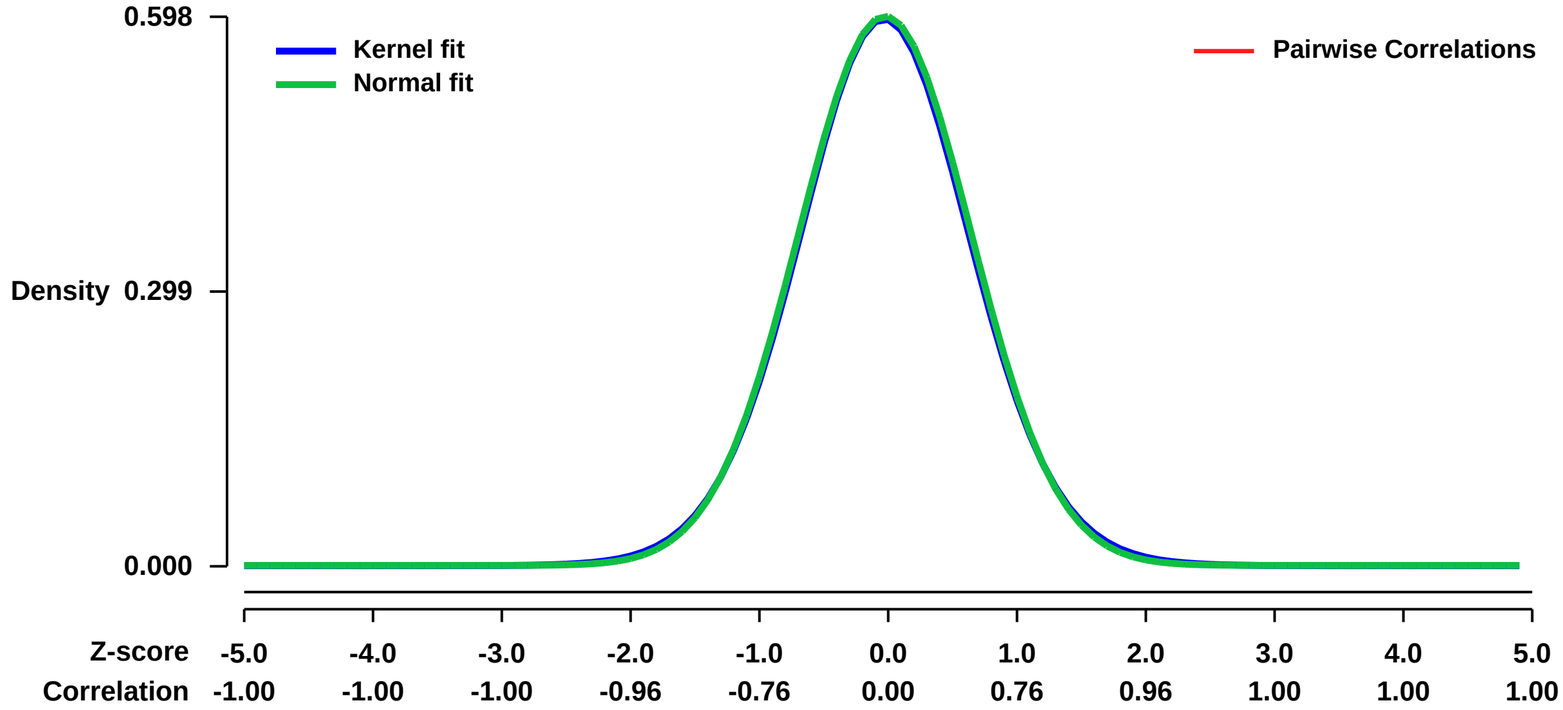

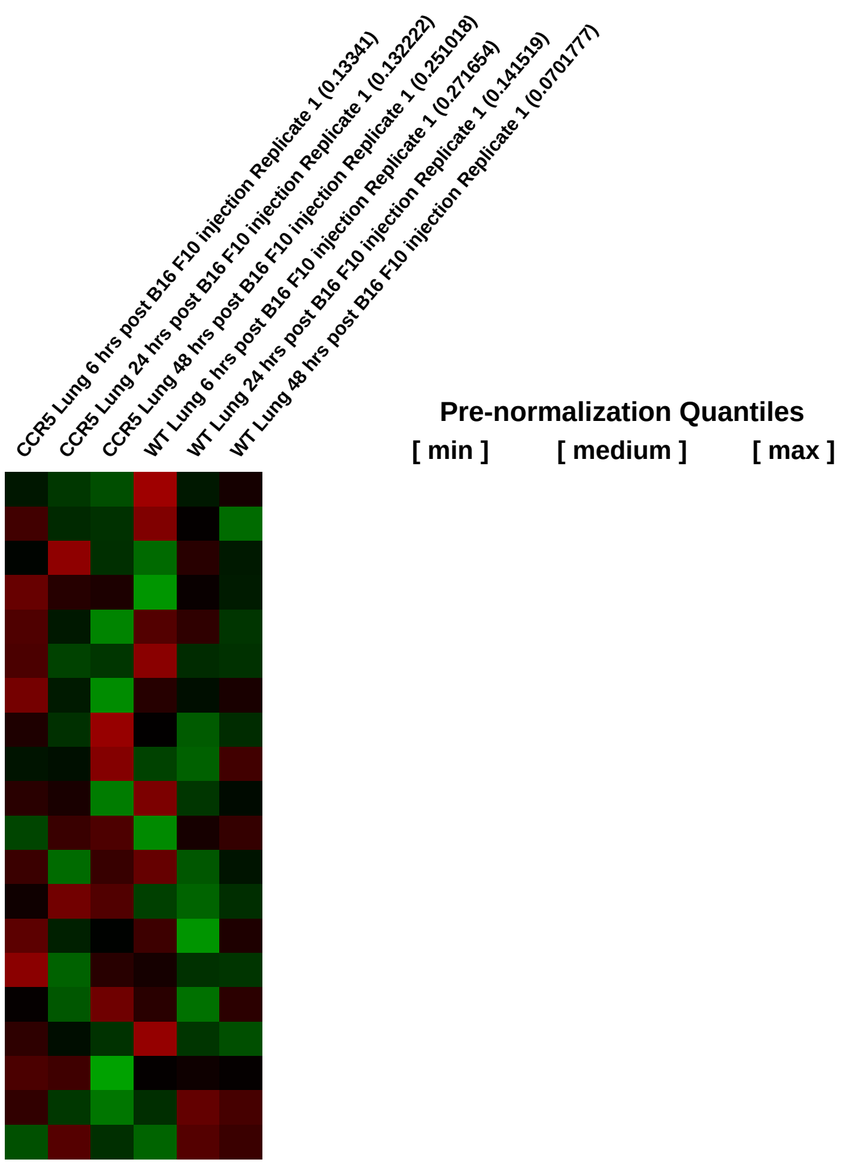

GEO Series "GSE51432" Expression Profiles

Num of samples in this series: 15

Scale of expression profile Z-scores

-3.0 -2.0 -1.0 0.0 1.0 2.0 3.0

GEO Link:	http://www.ncbi.nlm.nih.gov/geo/query/acc.cgi?acc=GSE51432
Status:	Public on May 28 2014
Title:	¸†-Cryptoxanthin suppresses inflammatory gene expression in diet-induced nonalcoholic steatohepatitis in mice
Organism:	Mus musculus
Experiment type:	Expression profiling by array
Platform:	GPL1261
Pubmed ID:	24858832
Summary & Design:	**Summary:** To evaluate the effect of ¸†-cryptoxanthin on diet-induced NASH, we fed a high-cholesterol and high-fat diet (CL diet) with or without 0.003% ¸†-cryptoxanthin to C56BL/6J mice for 12 weeks. After feeding, ¸†-cryptoxanthin attenuated fat accumulation, increases in Kupffer and activated stellate cells, and fibrosis in CL diet-induced NASH in the mice. Comprehensive gene expression analysis showed that although ¸†-cryptoxanthin histochemically reduced steatosis, it was more effective in inhibiting inflammatory gene expression change in NASH. ¸†-Cryptoxanthin reduced the alteration of expression of genes associated with cell death, inflammatory responses, infiltration and activation of macrophages and other leukocytes, quantity of T cells, and free radical scavenging. However, it showed little effect on the expression of genes related to cholesterol and other lipid metabolism. The expression of markers of M1 and M2 macrophages, T helper cells, and cytotoxic T cells was significantly induced in NASH and reduced by ¸†-cryptoxanthin. ¸†-Cryptoxanthin suppressed the expression of lipopolysaccharide (LPS)-inducible and/or TNF¸–-inducible genes and the antioxidant enzyme glutathione peroxidase 1 in NASH. Thus, ¸†-cryptoxanthin suppresses inflammation and the resulting fibrosis probably by primarily suppressing the increase and activation of macrophages and other immune cells. Reducing oxidative stress is likely to be a major mechanism of inflammation and injury suppression in the livers of mice with NASH. **Overall design:** Eight-week old male C57BL/6J mice were fed for 12 weeks on a CRF-1 standard chow (control), a high-cholesterol and high-fat diet (CL diet; 38.23% CRF-1, 60% cocoa butter, 1.25% cholesterol, 0.5% sodium cholate) or a CL diet containing 0.003% ¸†-cryptoxanthin.

Background corr dist: KL-Divergence = 0.2148, L1-Distance = 0.0482, L2-Distance = 0.0053, Normal std = 0.3222

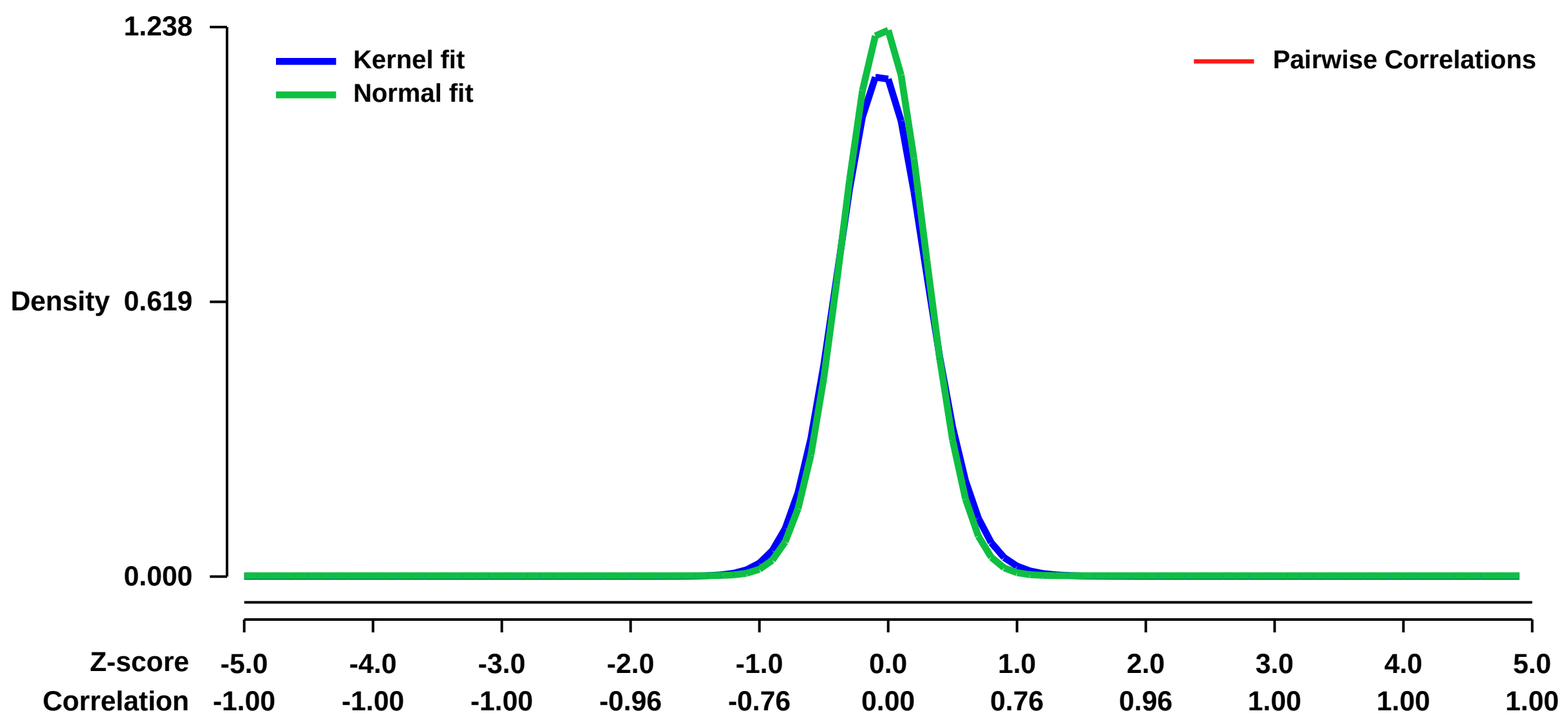

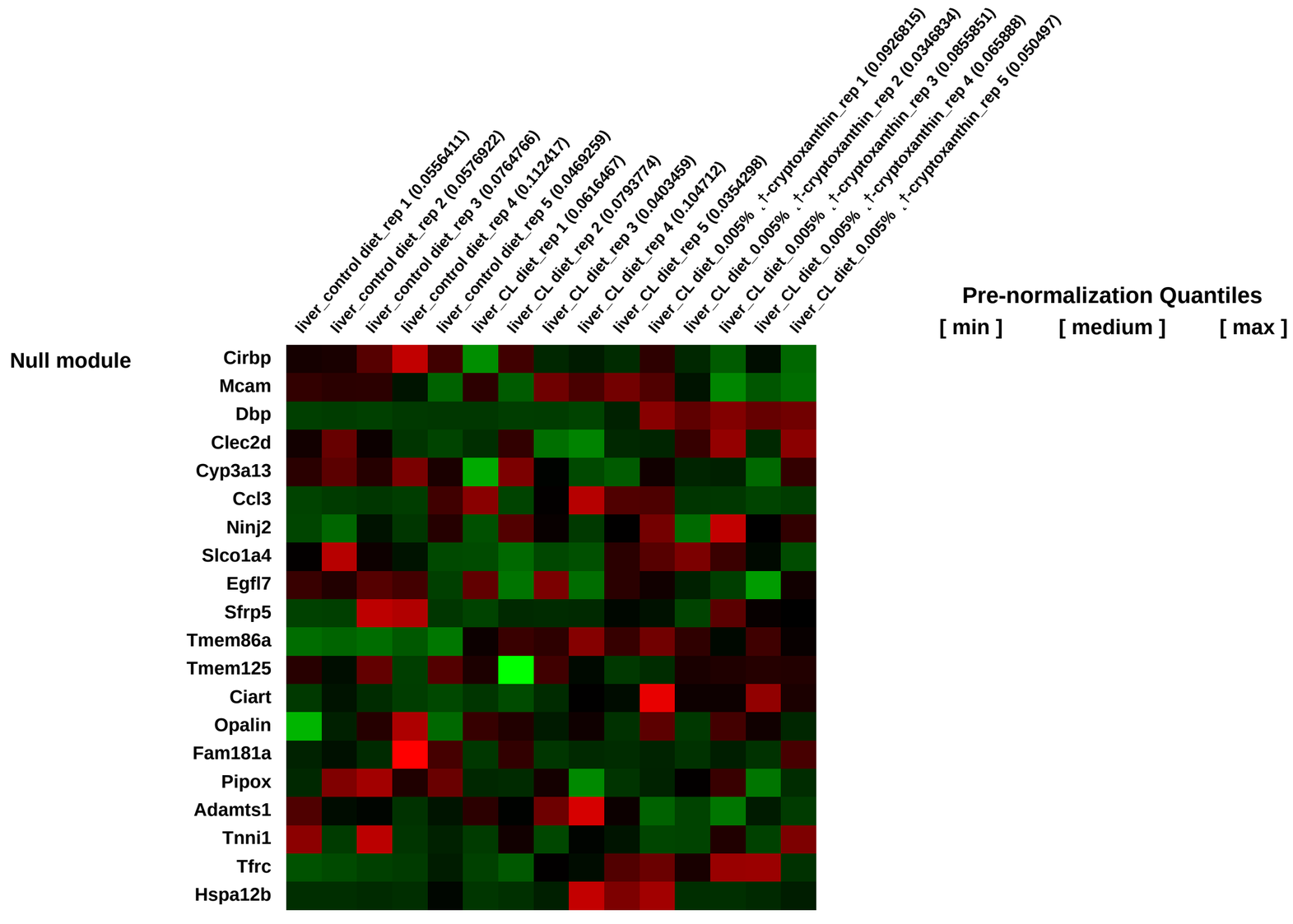

GEO Series "GSE51608" Expression Profiles

Num of samples in this series: 6

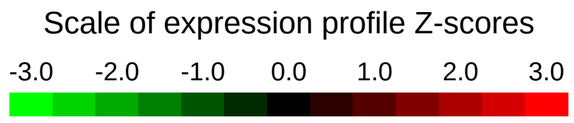

GEO Link:	http://www.ncbi.nlm.nih.gov/geo/query/acc.cgi?acc=GSE51608
Status:	Public on Oct 24 2013
Title:	Expression profiling of Ebf2- and Ebf2- stromal cells in mouse bone marrow
Organism:	Mus musculus
Experiment type:	Expression profiling by array
Platform:	GPL1261
Pubmed ID:	23184664
Summary & Design:	**Summary:** To identify the true molecular features of the Ebf2+ cells, we performed microarray analysis of freshly sorted CD45-TER119-Ebf2+ and Ebf2- cells. This allowed for the detection of 1968 genes that were 2-fold differentially expressed in Ebf2+ and Ebf2- cells. Among these, 1075 genes were upregulated and 893 genes including Ebf2, were downregulated in the Ebf2- as compared to the Ebf2+ cells. These include Nov, Fmod, Ndn, Dcn, Ctgf, Angiopoietin like-1(Angptl1), Fn1 and Jag1, some of which has been reported to be expressed in culture-selected MSCs. Furthermore, consistent with antigen expression analysis by FACS, the Ebf2+ cells highly expressed transcripts of Pdgfra, Pdgfrb, Sca1/Ly6a, Thy1 and Itga7 and Itgav, that have been suggested to be linked to MSCs. Nestin was mainly expressed in the Ebf2+ cells whereas it was hardly detectable in the Ebf2- cells. Altogether, molecularly, the Ebf2+ cells displayed features of a MSC. Ebf2 expression is not restricted to committed osteoblast progenitor cells but rather marks a multipotent mesenchymal progenitor cell population in adult mouse BM. These cells do not appear to be completely overlapping with the previous reported MSC populations. The findings provide new insights into the in vivo cellular identity and molecular properties of BM mesenchymal stem and progenitor cells. **Overall design:** RNA was extracted from 1,000 or 2000 purified adult bone marrow cells using the RNAeasy microkit. RNA was labeled and amplified by dual amplification and hybridized to Affymetrix microarray MOE430_2, according to AffymetrixTM GeneChip Expression Analysis Technical Manual. Probe level expression values were calculated using the RMA algorithm.

Background corr dist: KL-Divergence = 0.0181, L1-Distance = 0.0273, L2-Distance = 0.0011, Normal std = 0.7703

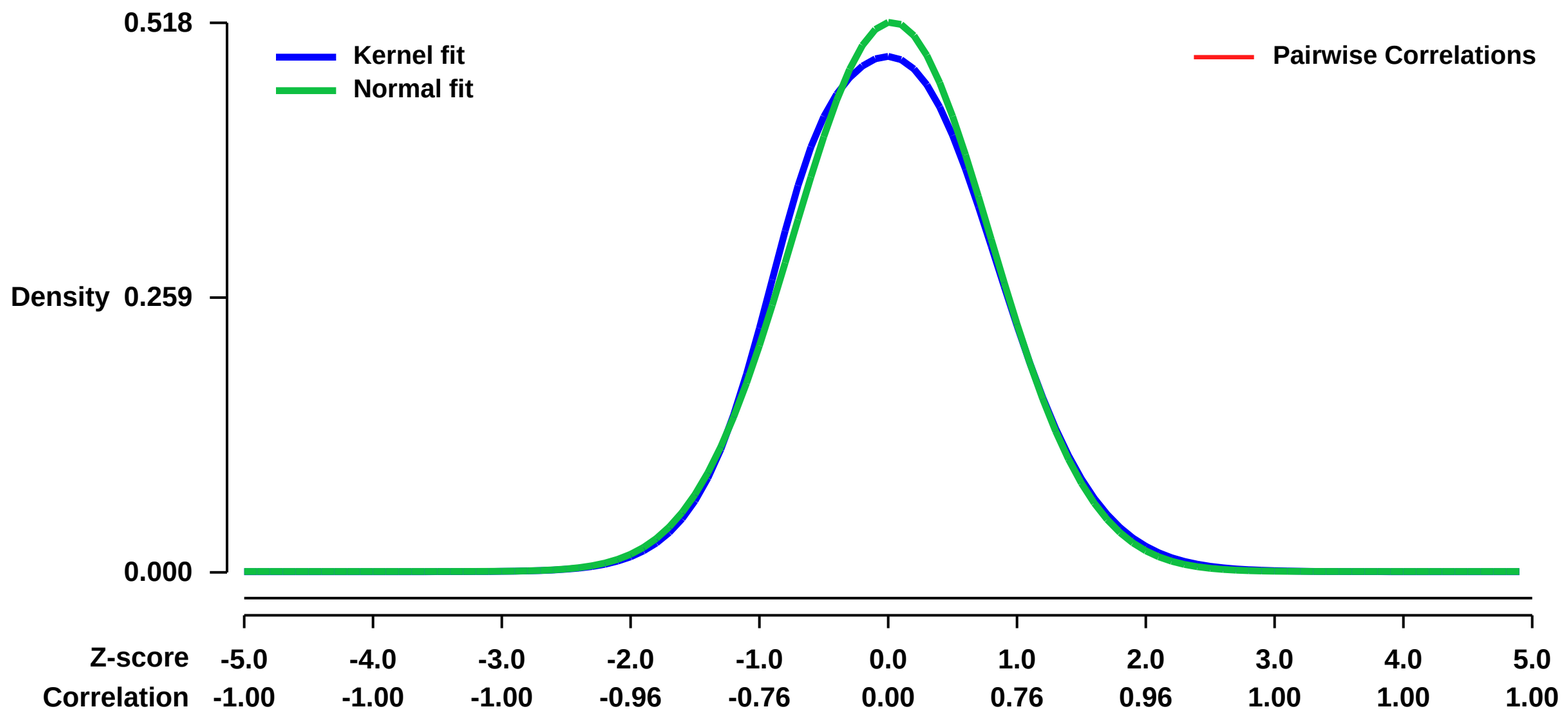

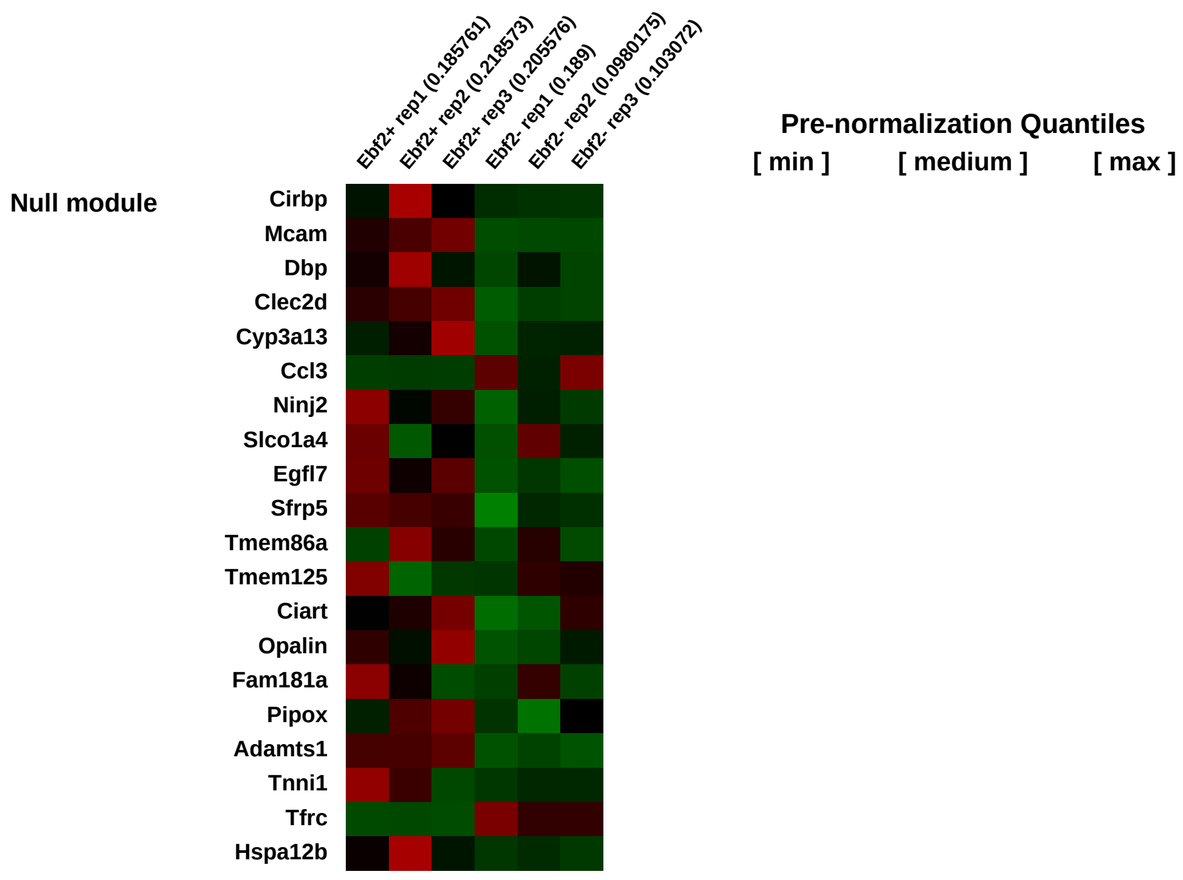

GEO Series "GSE51628" Expression Profiles

Num of samples in this series: 15

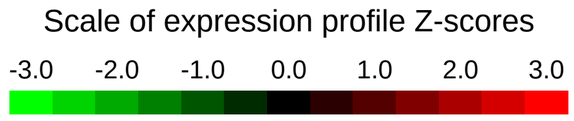

GEO Link:	**http://www.ncbi.nlm.nih.gov/geo/query/acc.cgi?acc=GSE51628**
Status:	**Public on Oct 24 2013**
Title:	**Effects of acute Notch activation on the mammary epithelial compartment in vivo**
Organism:	**Mus musculus**
Experiment type:	**Expression profiling by array**
Platform:	**GPL1261**
Pubmed ID:	
Summary & Design:	**Summary:** **Notch signaling is widely implicated in mouse mammary gland development and tumorigenesis. To investigate the effects of acute activation of Notch signaling in the mammary epithelial compartment, we generated bi-transgenic MMTV-rtTA; TetO-NICD1 (MTB/TICNX) mice that conditionally express a constitutively active NOTCH1 intracellular domain (NICD1) construct in the mammary epithelium upon doxycycline administration.** **Overall design:** **Two timepoints (48h and 96h) of doxycycline induction in TetO-NICD1 (TICNX; control) and MMTV-rtTA; TetO-NICD1 (MTB/TICNX) mice with 3-4 replicates per timepoint**
Background corr dist:	**KL-Divergence = 0.0788, L1-Distance = 0.0320, L2-Distance = 0.0014, Normal std = 0.4893**

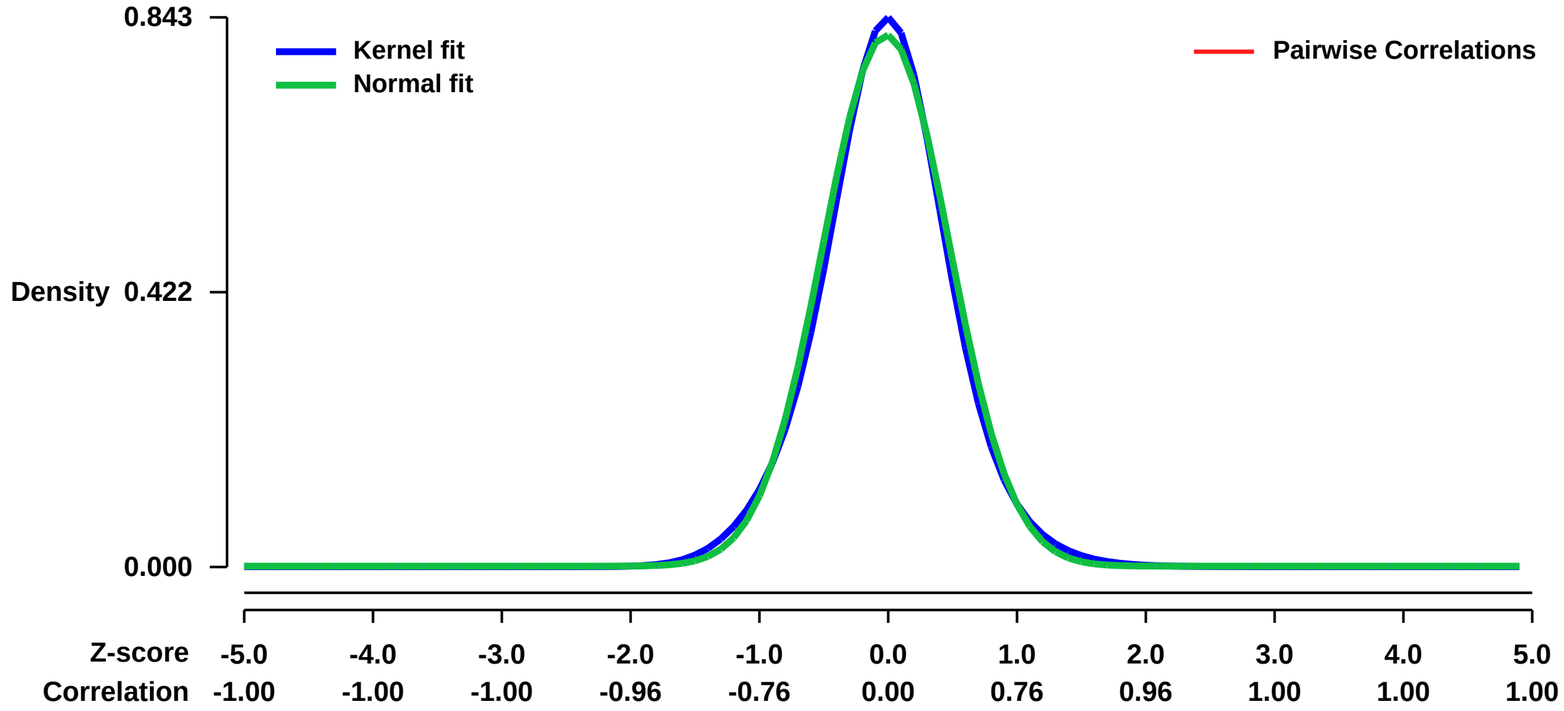

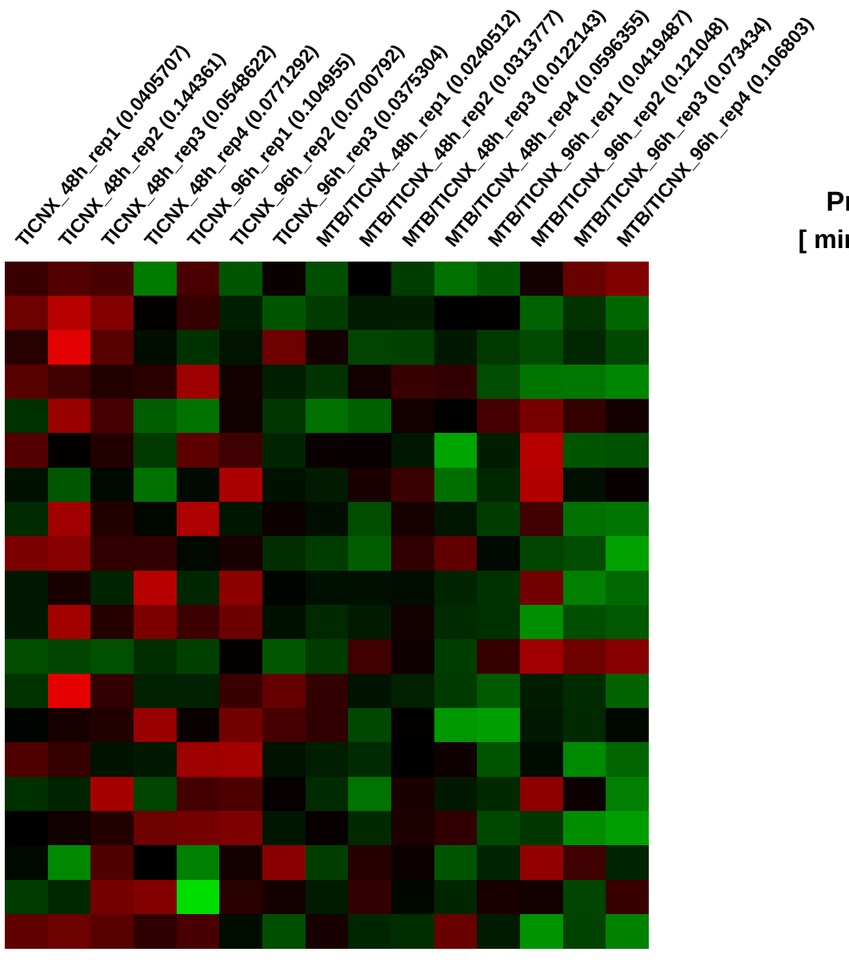

GEO Series "GSE51678" Expression Profiles

Num of samples in this series: 13

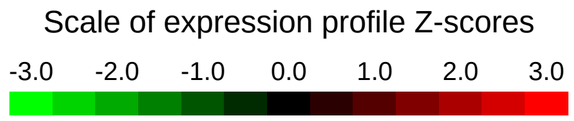

GEO Link:	**http://www.ncbi.nlm.nih.gov/geo/query/acc.cgi?acc=GSE51678**
Status:	**Public on Jun 23 2014**
Title:	**Microarray profiling of STEP knockout mouse striatum**
Organism:	**Mus musculus**
Experiment type:	**Expression profiling by array**
Platform:	**GPL1261**
Pubmed ID:	
Summary & Design:	**Summary:** **STEP (striatal-enriched tyrosine phosphatase) is a brain-specific phosphatase named for its robust expression in striatum. Brains from homozygous and heterozygous STEP knockout mice and wild-type littermates were harvested, and striatum microdissected. RNA was extracted and hybridized to Affymetrix 230_2 microarray chips.** **Overall design:** **n=4-5 per group. Wild-type littermates were compared with STEP +/- and -/-**

Background corr dist: **KL-Divergence = 0.1091, L1-Distance = 0.0348, L2-Distance = 0.0022, Normal std = 0.4212**

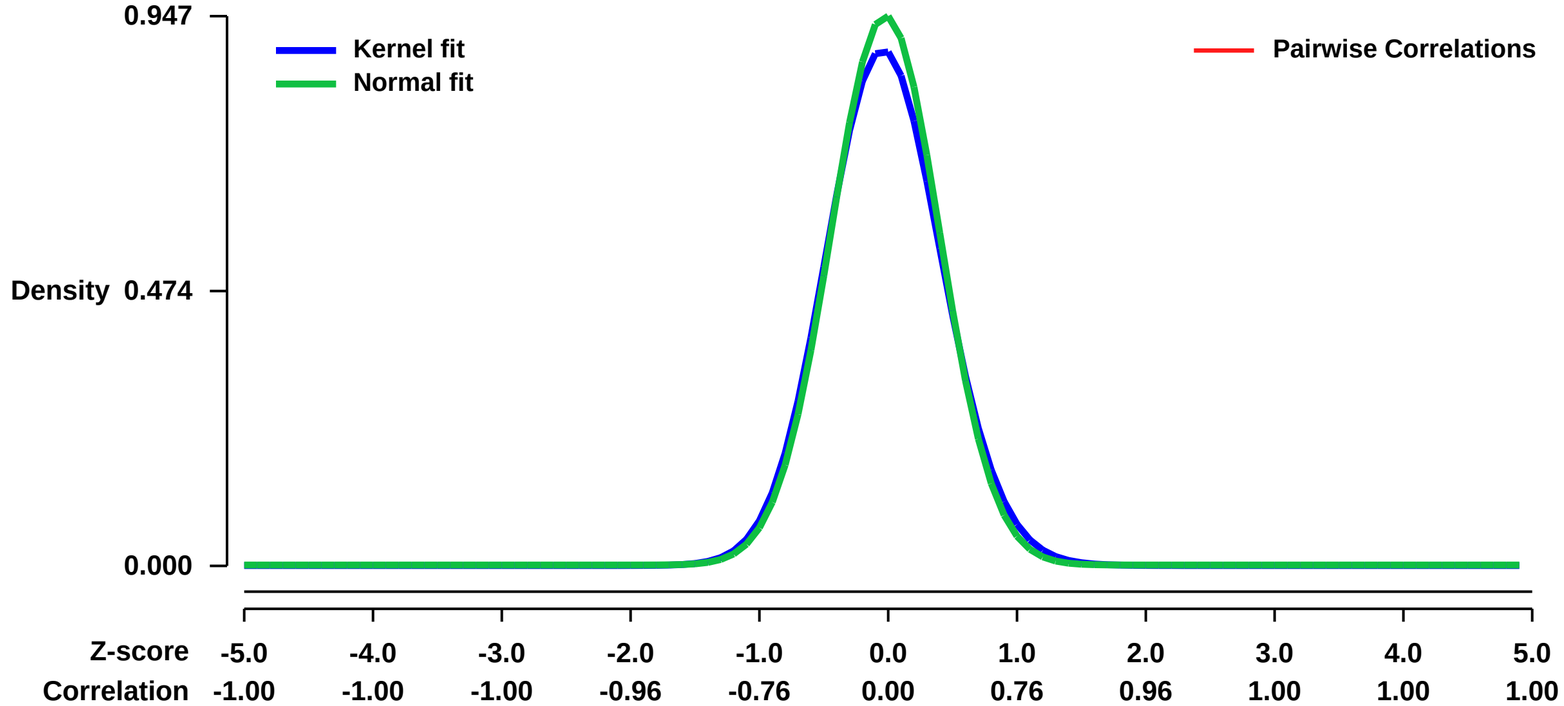

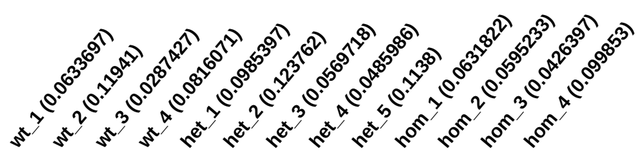

Pre-normalization Quantiles

[min] [medium] [max]

Null module

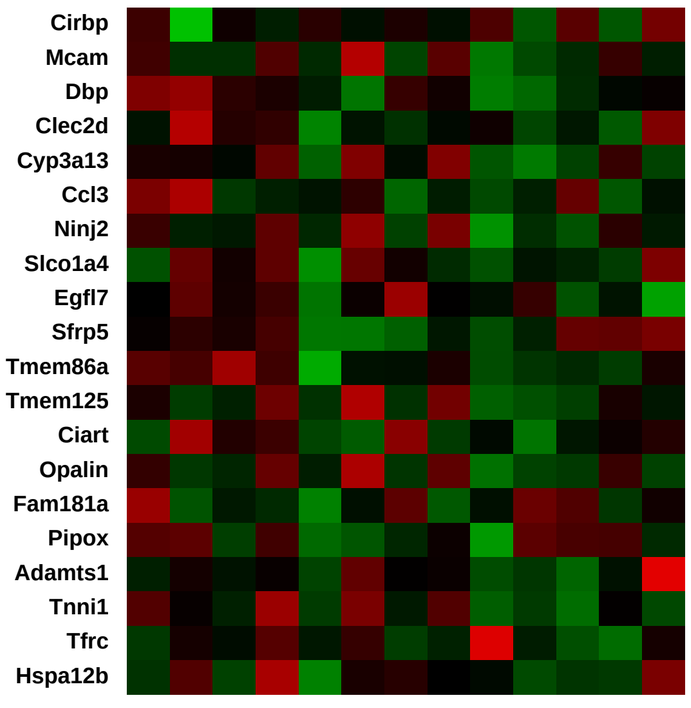

GEO Series "GSE51686" Expression Profiles

Num of samples in this series: 9

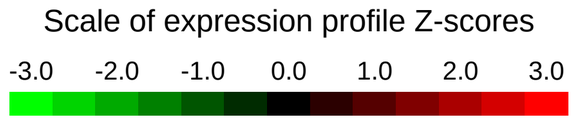

GEO Link:	**http://www.ncbi.nlm.nih.gov/geo/query/acc.cgi?acc=GSE51686**
Status:	**Public on Oct 25 2013**
Title:	**Fracture healing in osteoporotic mice**
Organism:	**Mus musculus**
Experiment type:	**Expression profiling by array**
Platform:	**GPL1261**
Pubmed ID:	
Summary & Design:	**Summary:** **Genome-wide comparative gene expression analysis of callus tissue of osteoporotic mice (Col1a1-Krm2 and Lrp5-/-) and wild-type were performed to identify candidate genes that might be responsible for the impaired fracture healing observed in Col1a1-Krm2 and Lrp5-/- mice.** **Overall design:** **To investigate bone healing in osteoporosis, we performed fracture healing studies in wild-type mice (C57BL/6 genetic background) and the low bone mass strains Col1a1-Krm2 and Lrp5-/- (Schulze et al., 2010; Kato et al., 2002). Osteotomy was set in femora of female mice and stabilized by a semi-rigid fixator to allow fast bone healing (R^¶ntgen et al., 2010). 21 days post surgery we analyzed the fracture calli by biochemical/histological methods, as well as micro-computed tomography, and observed impaired fracture healing in Col1a1-Krm2 and Lrp5-/- mice in comparison to wild-type. To identify genes that may be responsible for the impaired healing in osteoporotic mice, we performed microarray analysis of three independent callus samples of each genotype. The callus tissue was taken 10 days after surgery, because extensive bone formation took place at this point.**

Background corr dist: KL-Divergence = 0.0680, L1-Distance = 0.0239, L2-Distance = 0.0009, Normal std = 0.5035

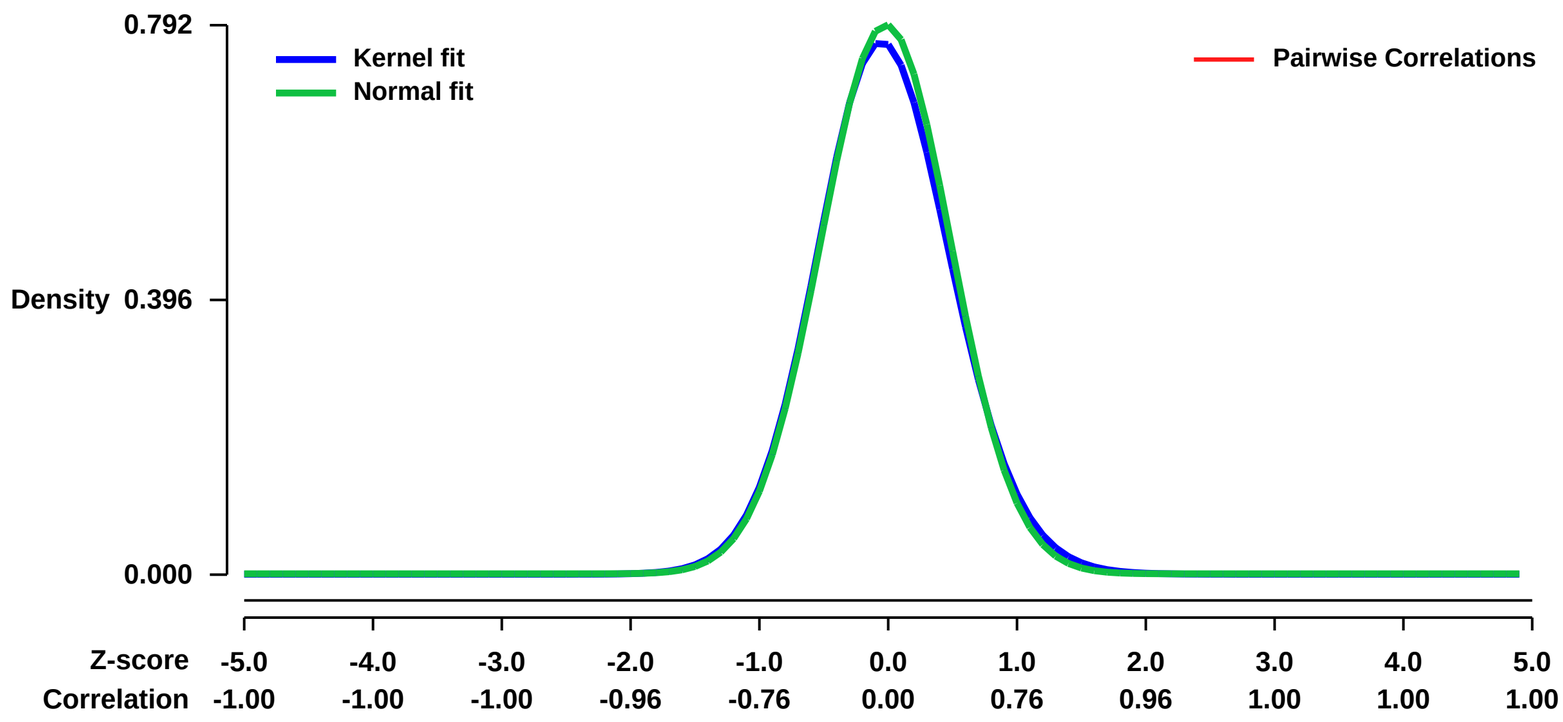

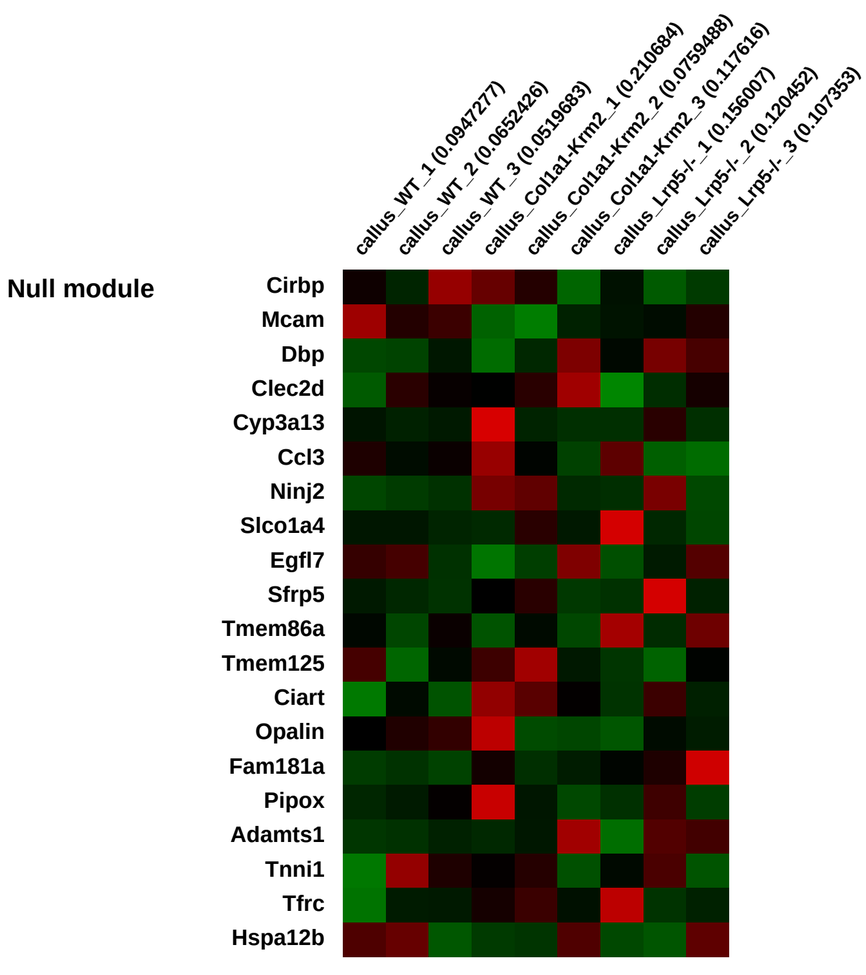

GEO Series "GSE51883" Expression Profiles

Num of samples in this series: 30

Scale of expression profile Z-scores

-3.0 -2.0 -1.0 0.0 1.0 2.0 3.0

GEO Link:	http://www.ncbi.nlm.nih.gov/geo/query/acc.cgi?acc=GSE51883
Status:	Public on Jan 28 2014
Title:	Effect of Mirn378 overexpression on gene expression during C2C12 myogenic and BMP2-induced osteogenic differentiation
Organism:	Mus musculus
Experiment type:	Expression profiling by array
Platform:	GPL1261
Pubmed ID:	
Summary & Design:	**Summary:** **Background: MicroRNAs (miRNAs) are a family of small, non-coding single-stranded RNA molecules involved in post-transcriptional regulation of gene expression. As such, they are believed to play a role in regulating the step-wise changes in gene expression patterns that occur during cell fate specification of multipotent stem cells. Here, we have studied whether terminal differentiation of C2C12 myoblasts is indeed controlled by lineage-specific changes in miRNA expression.** **Results: Using a previously generated RNA polymerase II (Pol-II) ChIP-on-chip dataset, we show differential Pol-II occupancy at the promoter regions of six miRNAs during C2C12 myogenic versus BMP2-induced osteogenic differentiation. Overexpression of one of these miRNAs, miR-378, enhances Alp activity, calcium deposition and mRNA expression of osteogenic marker genes in the presence of BMP2.** **Conclusions: Our results demonstrate a previously unknown role for miR-378 in promoting BMP2-induced osteogenic differentiation. #!#** **Overall design:** **Stable C2C12 cell lines C2C12-pMirn0 and C2C12-pMirn378 were generated by lentiviral transduction of C2C12 myoblasts with a Mirn378-overexpression construct and its parent vector, respectively. C2C12-pMirn0 and C2C12-pMirn378 cells were plated at 2.5 x 10^4 cells/cm2 (day -1), cultured for 1 day in DMEM 10%NCS, then (d0) treated with or without 300 ng/ml bone morphogenetic protein 2 (BMP2) for 6 days. RNA was extracted on d0, d3 and d6 and hybridized to GeneChip Mouse Genome 430 2.0 array (Affymetrix).**

Background corr dist: KL-Divergence = 0.1521, L1-Distance = 0.0728, L2-Distance = 0.0106, Normal std = 0.4058

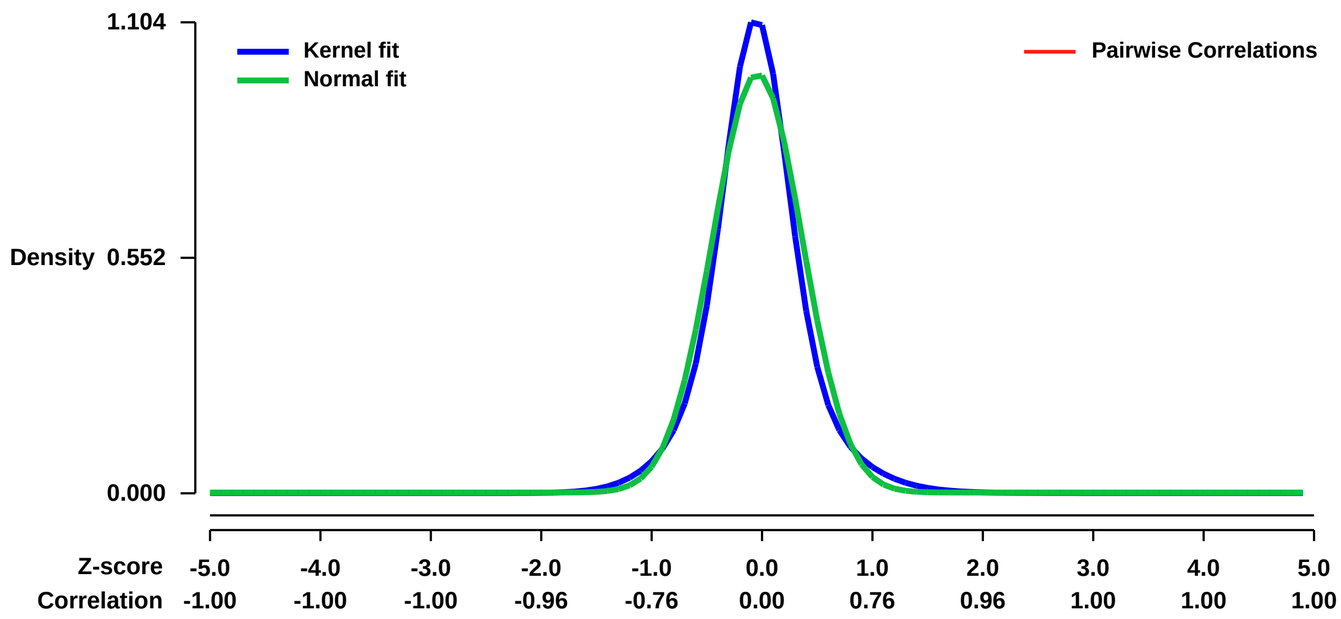

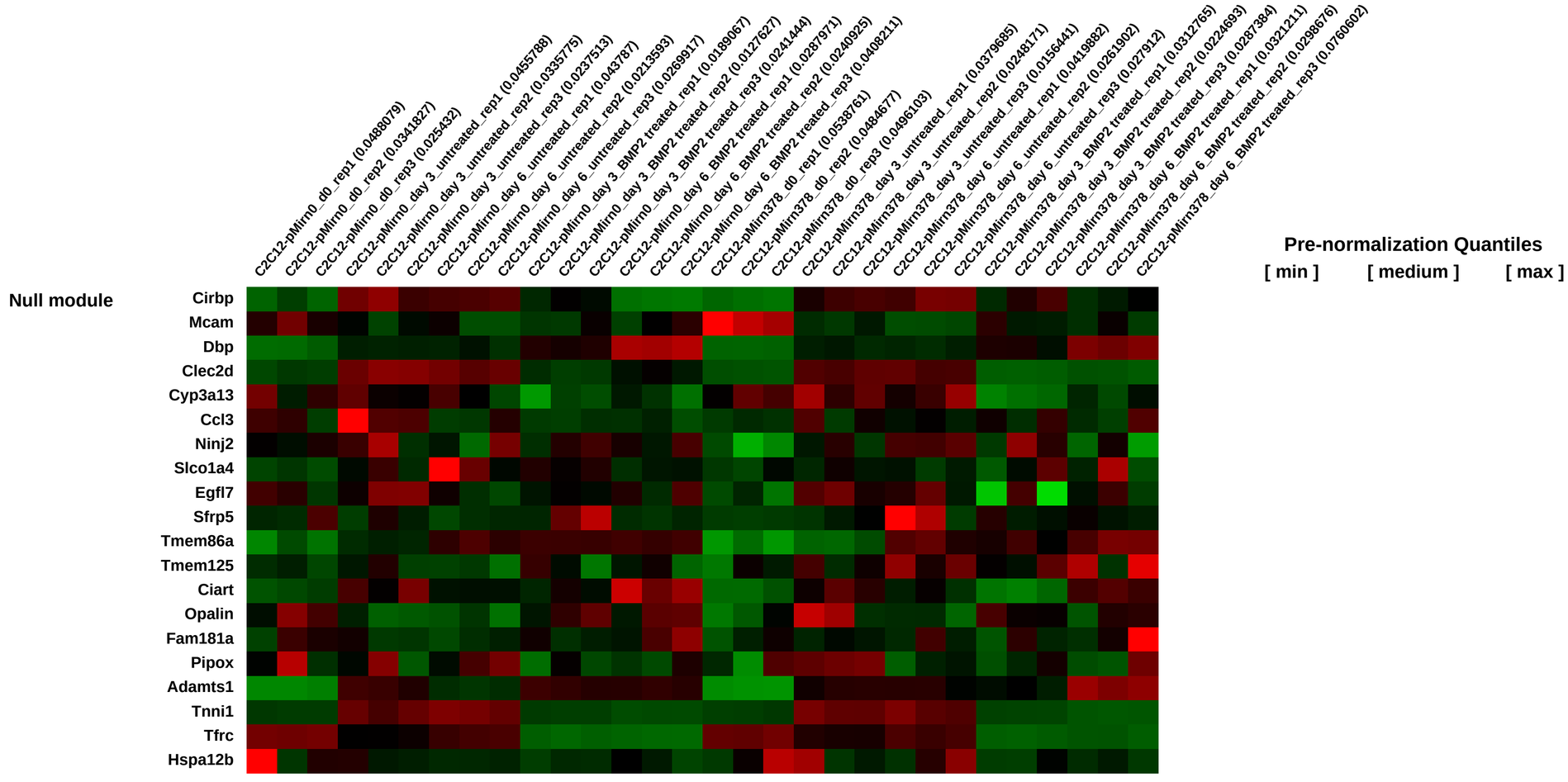

GEO Series "GSE51927" Expression Profiles

Num of samples in this series: 59

Scale of expression profile Z-scores

-3.0 -2.0 -1.0 0.0 1.0 2.0 3.0

GEO Link:	http://www.ncbi.nlm.nih.gov/geo/query/acc.cgi?acc=GSE51927
Status:	Public on Oct 30 2013
Title:	Expression analysis of murine primary and derived orthotopic SEOC tumors
Organism:	Mus musculus
Experiment type:	Expression profiling by array
Platform:	GPL1261
Pubmed ID:	24748377
Summary & Design:	**Summary:** We previously generated genetically engineered mouse (GEM) models based on perturbation of Tp53, Rb with or without Brca1 or Brca2 that develop serous epithelial ovarian cancer (SEOC) closely resembling the human disease on histologic and molecular levels. We have adapted these GEM models to orthotopic allografts that uniformly develop tumors with short latency in immunocompetent recipients and are ideally suited for routine preclinical studies. To monitor passaged tumors at the molecular level, we analyzed transcriptional profiles of a set of primary SEOC and matching derived passaged tumors. We have merged this dataset with previously published (doi: 10.1158/0008-5472.CAN-11-3834; PMID 22617326) dataset of murine primary ovarian tumors from our GEM models (GSE46169) and merged and compared them to expression profiles of human dataset published previously (doi: 10.1038/nature10166). The high mortality rate from ovarian cancers can be attributed to late-stage diagnosis and lack of effective treatment. Despite enormous effort to develop better targeted therapies, platinum-based chemotherapy still remains the standard of care for ovarian cancer patients, and resistance occurs at a high rate. One of the rate limiting factors for translation of new drug discoveries into clinical treatments has been the lack of suitable preclinical cancer models with high predictive value. We previously generated genetically engineered mouse (GEM) models based on perturbation of Tp53, Rb with or without Brca1 or Brca2 that develop serous epithelial ovarian cancer (SEOC) closely resembling the human disease on histologic and molecular levels. Here, we describe an adaptation of these GEM models to orthotopic allografts that uniformly develop tumors with short latency and are ideally suited for routine preclinical studies. **Overall design:** RNA was isolated from flash frozen ovarian tumors using Trizol and Qiagen RNeasy columns

Background corr dist: KL-Divergence = 0.3139, L1-Distance = 0.0666, L2-Distance = 0.0122, Normal std = 0.2763

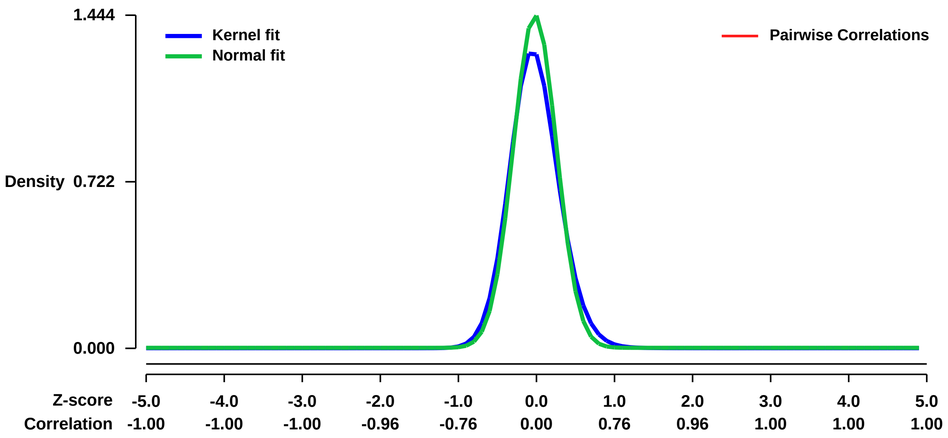

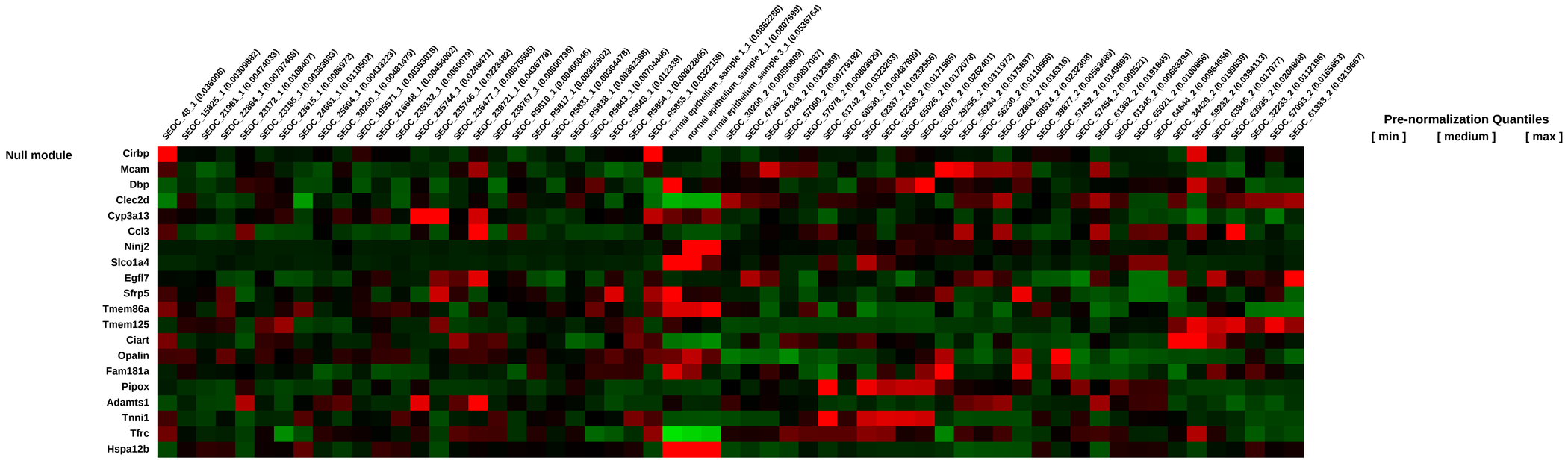

GEO Series "GSE51932" Expression Profiles

Num of samples in this series: 8

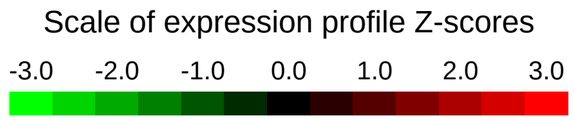

GEO Link:	http://www.ncbi.nlm.nih.gov/geo/query/acc.cgi?acc=GSE51932
Status:	Public on Nov 22 2013
Title:	Expression data from murine irf4-/- and irf4+/+ mature B cells purified by magnetic cell separation
Organism:	Mus musculus
Experiment type:	Expression profiling by array
Platform:	GPL1261
Pubmed ID:	24323359
Summary & Design:	**Summary:** Gene expression profiling of murine irf4-/- and irf4+/+ splenic B cells identifies genes regulated by the transcription factor IRF4 in quiescent mature B cells. **Overall design:** B cells from 12-week old irf4-/- and irf4+/+ littermate mice were isolated by magnetic depletion of non-B cells from splenic mononuclear cells. RNA was isolated. Labeled cRNA was hybridized to microarrays and genes specifically expressed in irf4-/- vs. irf4+/+ samples.

Background corr dist: KL-Divergence = 0.0828, L1-Distance = 0.0205, L2-Distance = 0.0007, Normal std = 0.4714

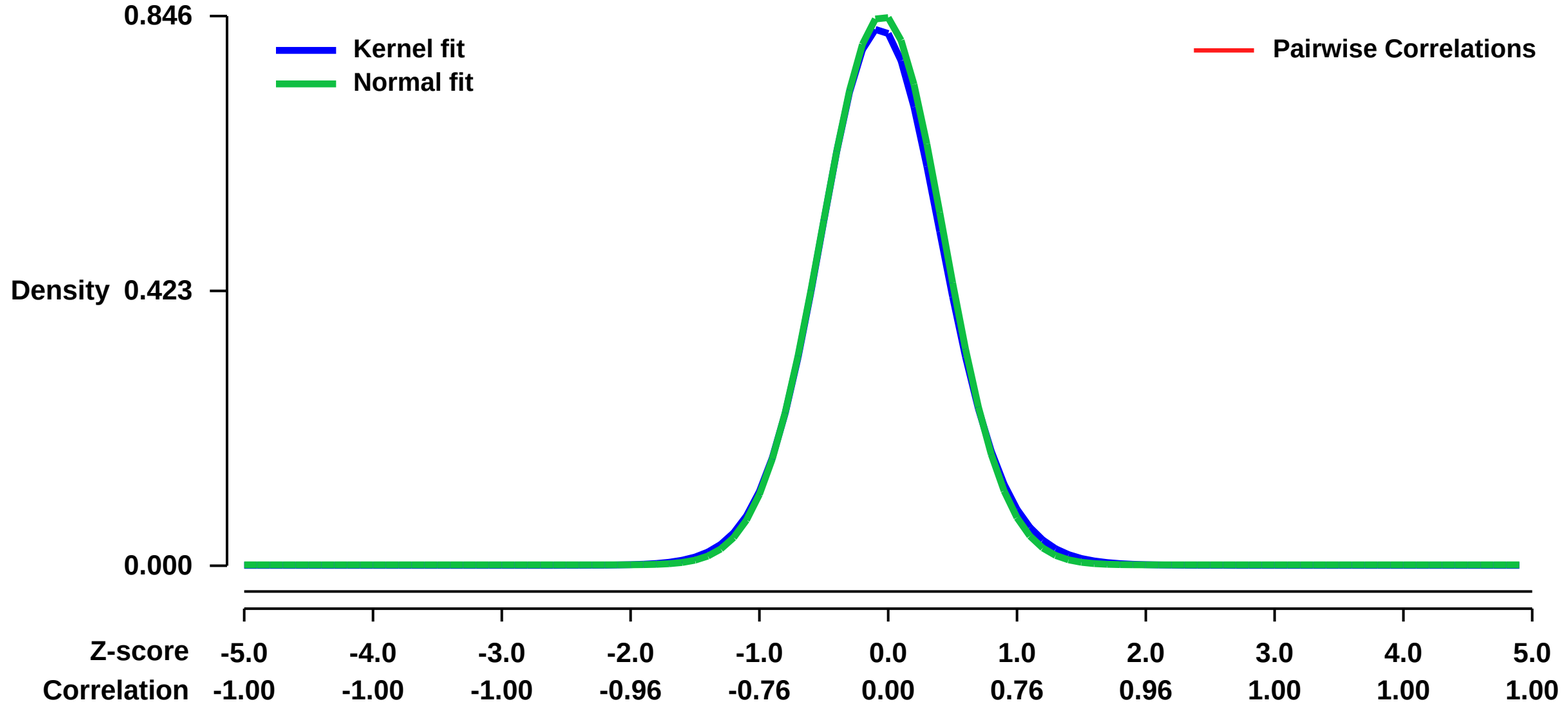

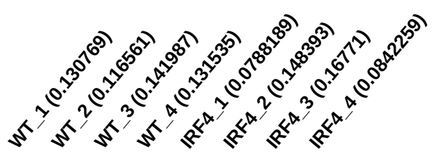

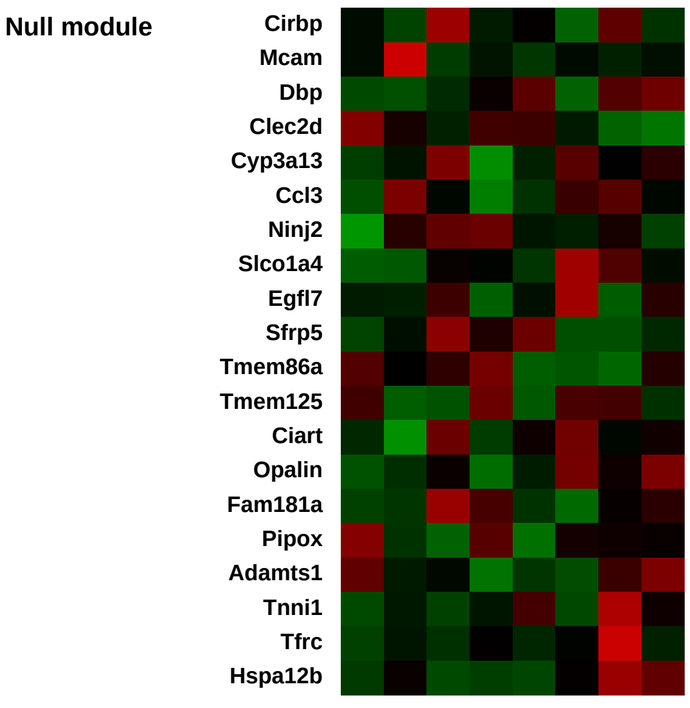

GEO Series "GSE5202" Expression Profiles

Num of samples in this series: 12

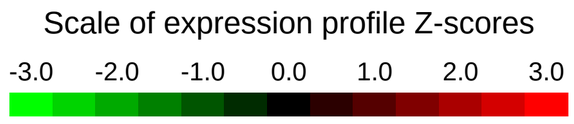

GEO Link:	http://www.ncbi.nlm.nih.gov/geo/query/acc.cgi?acc=GSE5202
Status:	Public on Jun 30 2006
Title:	Expression data from B. melitensis infected mouse macrophages
Organism:	Mus musculus
Experiment type:	Expression profiling by array
Platform:	GPL1261
Pubmed ID:	16926395
Summary & Design:	**Summary:** **Facultative intracellular Brucella infect and survive inside macrophages, and the outcome of macrophage-Brucella interaction is a basis for establishment of a chronic Brucella infection. The majority of Brucella are killed at the early infection stage. A subpopulation of virulent Brucella strains is instead trafficked to an intracellular replicative phagosome, and are resistant to further attack and begin to multiply dramatically. Virulent Brucella also inhibit macrophage apoptosis that in turn favors pathogen survival and replication.** **We used the Affymetrix mouse GeneChip 430 2.0 array to analyze mouse macrophage gene expression profiles during the time course of virulent B. melitensis strain 16M infection.** **Keywords: time course** **Overall design:** **Murine J774.A1 macrophage cells were infected with B. melitensis strain 16M at a MOI of 200:1. Brucella cultures derived from different Brucella colonies were used to infect different groups of macrophage cells to reflect independent infections. Following 4 h incubation, the cells were washed with PBS and treated with 50 ug/ml gentamicin to kill extracellular Brucella. At 0 h (no Brucella infection), 4 h, 24 h, and 48 h post-infection, cells were individually collected, and total RNA was isolated. The Affymetrix mouse GeneChip 430 2.0 array was used for microarray hybridization. Microarray intensity data were obtained by using Affymetrix GCOS software and further analyzed by GeneSpring and other software programs.**

Background corr dist: **KL-Divergence = 0.1187, L1-Distance = 0.0258, L2-Distance = 0.0010, Normal std = 0.4112**

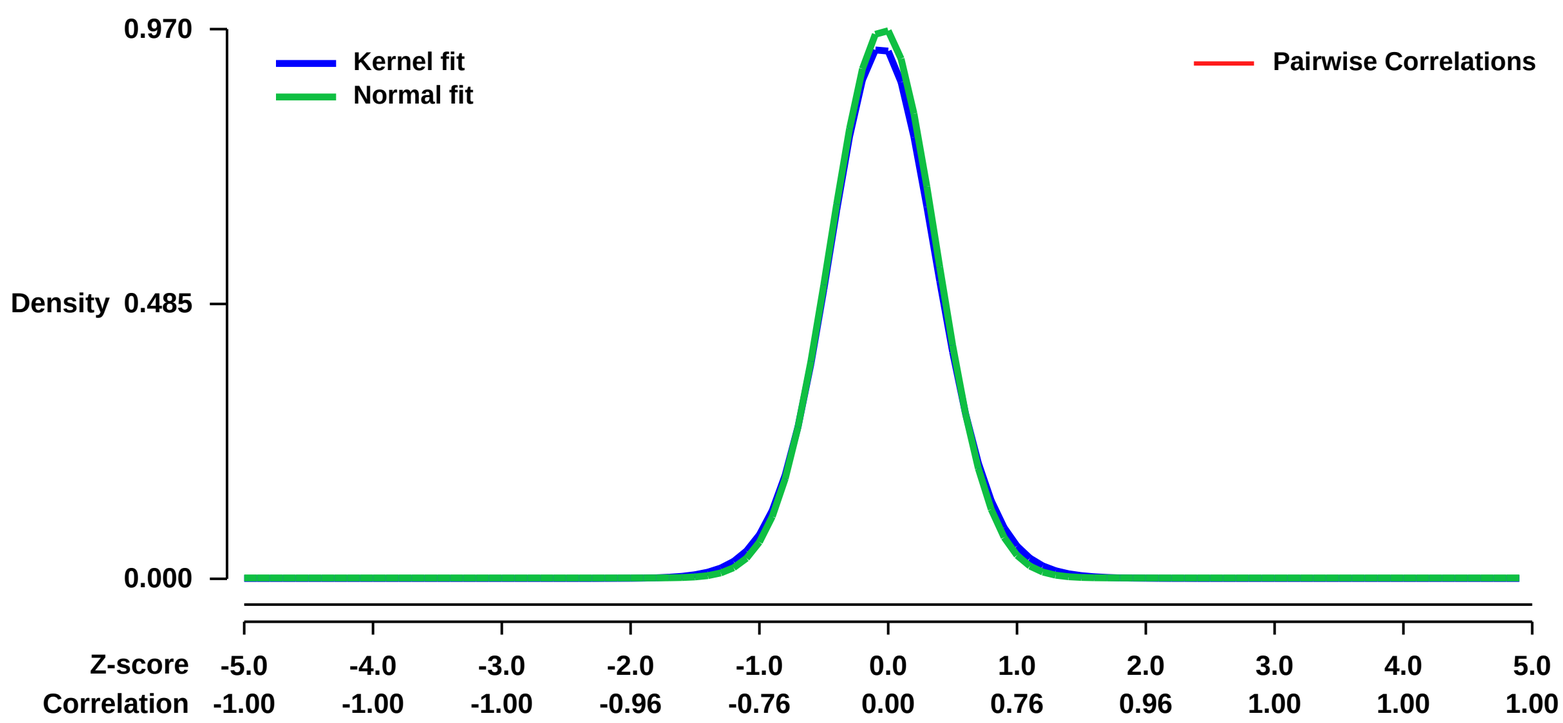

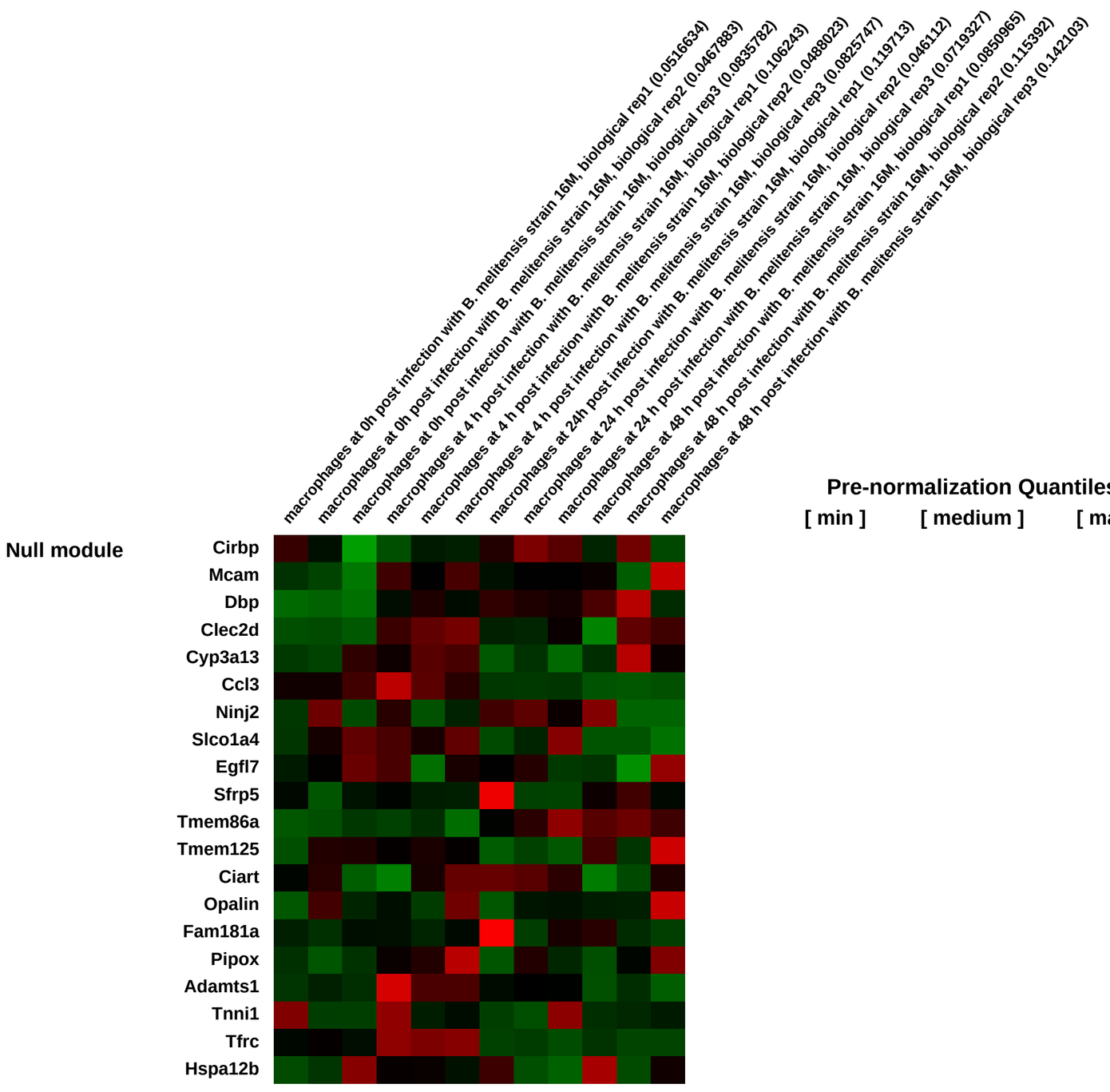

GEO Series "GSE52022" Expression Profiles

Num of samples in this series: 8

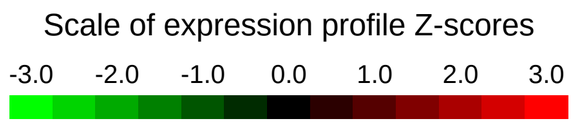

GEO Link:	**http://www.ncbi.nlm.nih.gov/geo/query/acc.cgi?acc=GSE52022**
Status:	**Public on Dec 01 2013**
Title:	**Genome wide analysis of transcriptome and microRNAs in early stage of Alzheimerâ s disease (mRNA)**
Organism:	**Mus musculus**
Experiment type:	**Expression profiling by array**
Platform:	**GPL1261**
Pubmed ID:	
Summary & Design:	**Summary:** **We addressed the integrated analysis of mRNA and miRNA expression levels of Tg6799 AD model mice at 4 month and 8 months of age. Total 8 gene cluster modules for co-expression network were predicted from transcriptome data and 6 modules were show relation with AD or aging. We constructed early stage AD network using data integration between mRNA and miRNA profiles and predicted miRNAs strongly involved in module regulation. We found that ARRDC3 showed AD mutation dependent changes of expression and was related metabolic dysfunction in early stage AD.** **These results demonstrate that candidate genes on the simultaneous profiling of mRNA and miRNA expressions in genome wide can be used for the understanding of non-coding RNA related gene expression in early stage AD. We suggested that our results could be future candidate to be developed as early biomarkers in progressive AD pathology. This result can be used for the further application in neurodegenerative diseases.** **Overall design:** **Tg6799 transgenic mice were purchased from The Jackson Laboratory (USA) and were housed under a 12h light-dark cycle with free access to food and water. Female Tg6799 mice are maintained until 4 months and 8 months of age (for littermate control: LM and mutant subjects: MT). RNA samples were isolated from hippocampus of mice using TRI-Reagent (Sigma-Aldrich, St. Louis, MO) according to the manufacturerâ s instructions. Gene expression was analyzed with GeneChip´fi Mouse Genome 430 2.0 Arrays (Affymetrix, Santa Clara, CA), which is comprised of over 45,000 probe sets representing approximately 28,700 well-characterized mouse genes. The Ion Total RNA-Seq Kit v2 (Lifetechnologies, USA) was used for the preparation of micro RNA libraries according to the manufacturer's instructions. Total numbers of subject used are as followed: 1) LM 4 months : MT 4 months : LM 8 months : MT 8 months (2:4:2:4) for screening mRMA and miRNA, 2) LM 4 months : MT 4 months : LM 8 months : MT 8 months (4:4:4:4) for expression verification. Tg6799 transgenic mice were purchased from The Jackson Laboratory (USA) and were housed under a 12h light-dark cycle with free access to food and water. Female Tg6799 mice are maintained until 4 months and 8 months of age (for littermate control: LM and mutant subjects: MT). RNA samples were isolated from hippocampus of mice using TRI-Reagent (Sigma-Aldrich, St. Louis, MO) according to the manufacturerâ s instructions. Gene expression was analyzed with GeneChip´fi Mouse Genome 430 2.0 Arrays (Affymetrix, Santa Clara, CA), which is comprised of over 45,000 probe sets representing approximately 28,700 well-characterized mouse genes. The Ion Total RNA-Seq Kit v2 (Lifetechnologies, USA) was used for the preparation of micro RNA libraries according to the manufacturer's instructions. Total numbers of subject used are as followed: 1) LM 4 months : MT 4 months : LM 8 months : MT 8 months (2:4:2:4) for screening mRMA and miRNA, 2) LM 4 months : MT 4 months : LM 8 months : MT 8 months (4:4:4:4) for expression verification.**

Background corr dist: KL-Divergence = 0.0823, L1-Distance = 0.0215, L2-Distance = 0.0006, Normal std = 0.4710

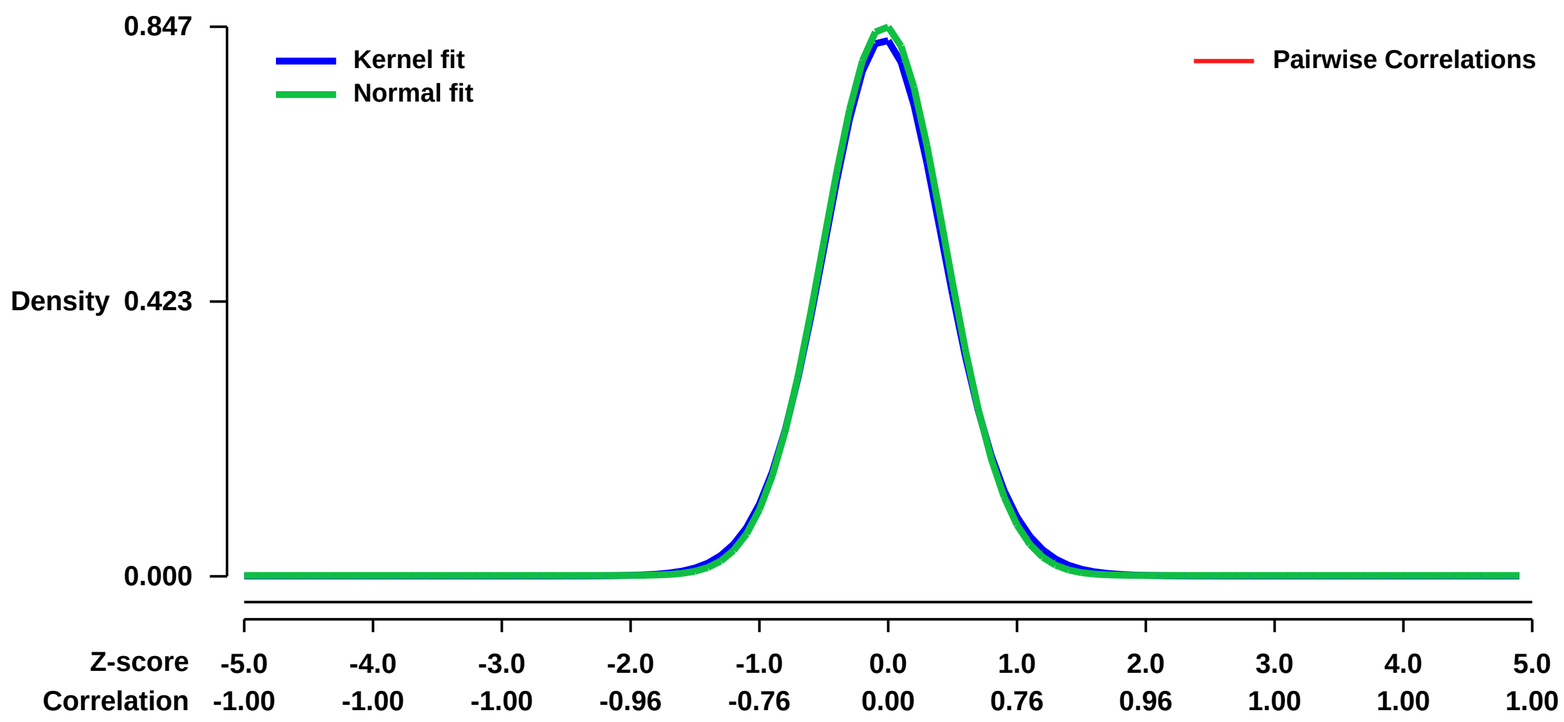

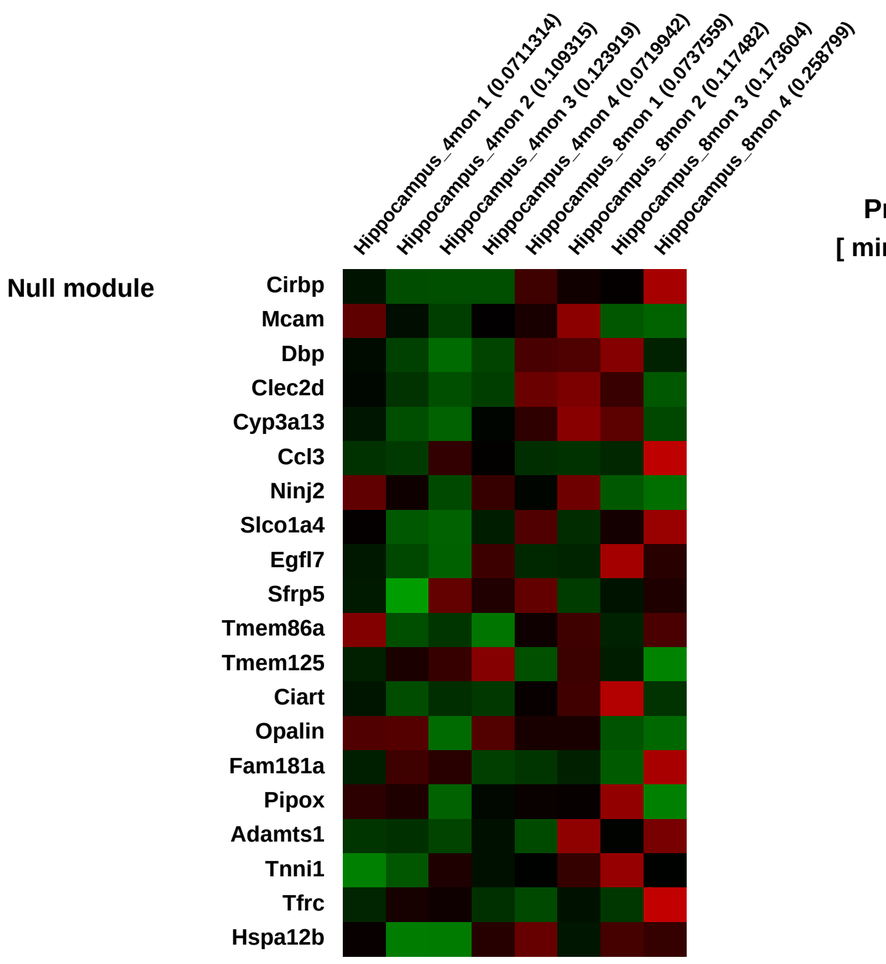

GEO Series "GSE52075" Expression Profiles

Num of samples in this series: 9

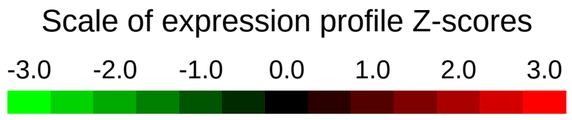

GEO Link:	http://www.ncbi.nlm.nih.gov/geo/query/acc.cgi?acc=GSE52075
Status:	Public on Nov 11 2013
Title:	Expression data of the endothelial-to-hematopoietic transition in E8.5 concepti
Organism:	Mus musculus
Experiment type:	Expression profiling by array
Platform:	GPL1261
Pubmed ID:	24326267
Summary & Design:	**Summary:** During development a specialised subset of endothelial cells, the haemogenic endothelium, undergo an endothelial-to-haematopoietic transition. This process critically involves the transcription factor Runx1. Here we have isolated a specific subpopulation of endothelial cells using a Runx1 enhancer-reporter transgenic mouse line (23GFP). We have compared the gene expression profile of this population to non-23GFP expressing endothelial cells and CD41 expressing haematopoietic progenitor cells to assess whether 23GFP expression marks a biologically distinct subset of endothelium. We used affymetrix microarrays to detail the global programme of gene expression underlying the different populations and identified a distinct expression profile of the 23GFP expressing endothelium. **Overall design:** 23GFP transgenic mouse embryos were dissected free of the ectoplacental cone at embryonic day E8.5, pooled, and sorted into 23GFP- and 23GFP+ endothelial (VE-Cad+ Ter119- CD45- CD41-) and CD41+ haematopoietic cells (VE-Cad+ Ter119-CD45-CD41+23GFP+) cells by FACS. Triplicate samples for each cell population were analysed. cDNA synthesis, fragmentation, and hybridisation were performed by the Stanford Protein and Nucleic Acid Facility.

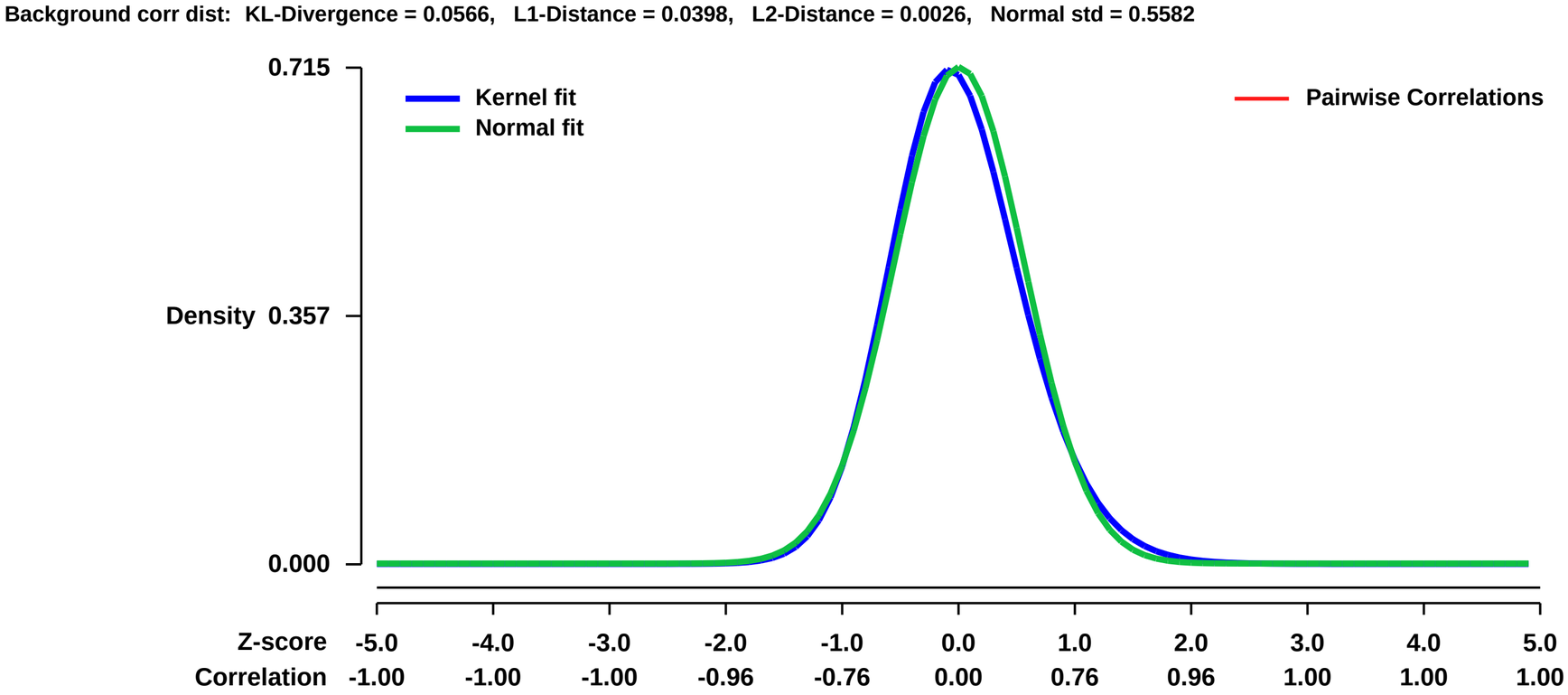

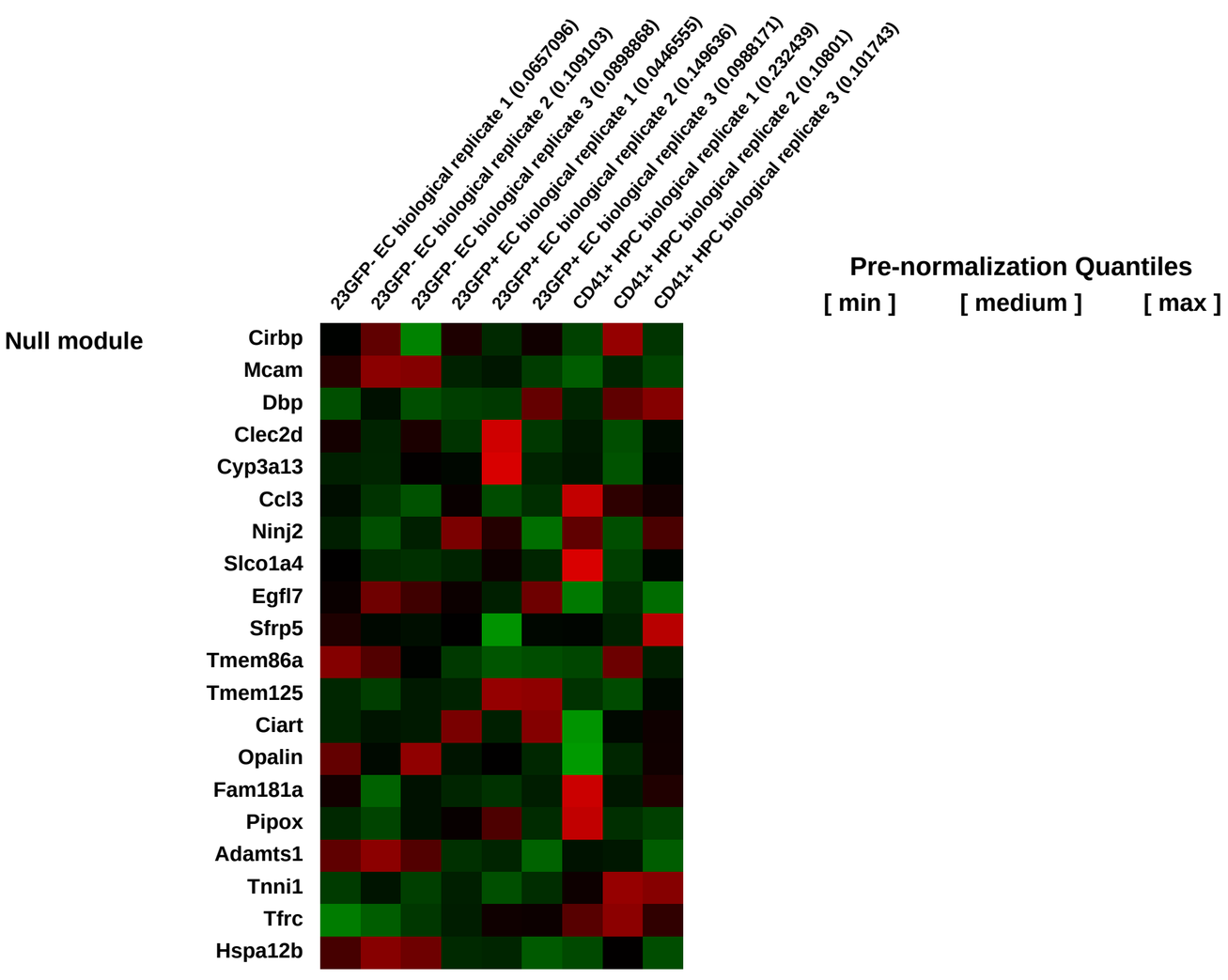

GEO Series "GSE52101" Expression Profiles

Num of samples in this series: 17

Scale of expression profile Z-scores

-3.0 -2.0 -1.0 0.0 1.0 2.0 3.0

GEO Link:	**http://www.ncbi.nlm.nih.gov/geo/query/acc.cgi?acc=GSE52101**
Status:	**Public on Dec 17 2013**
Title:	**Transcript abundance comparison between BALB/c ears inoculated with Leishmania mexicana and Leishmania mexicana plus promastigote secretory gel (PSG)**
Organism:	**Mus musculus**
Experiment type:	**Expression profiling by array**
Platform:	**GPL1261**
Pubmed ID:	
Summary & Design:	**Summary:** **To determine the modulation of gene expression of Leishmania mexicana(M379)-inoculated BALB/c ears in the presence of promastigote secretory gel (PSG)** **Overall design:** **A genome-wide transcriptional analysis was performed by comparing the gene expression profiles of Leishmania mexicana- inoculated BALB/c ears and Leishmania mexicana plus PSG BALB/c ears. Leishmania mexicana amastigotes were purified from mouse cutaneous lesions and transformed in vitro in metacycic promastigotes (MT). After 6, 24 and 48 hours, ears were collected and processed for RNA extraction. Three Biological replicates per condition were run.**

Background corr dist: **KL-Divergence = 0.0239, L1-Distance = 0.0741, L2-Distance = 0.0075, Normal std = 0.9021**

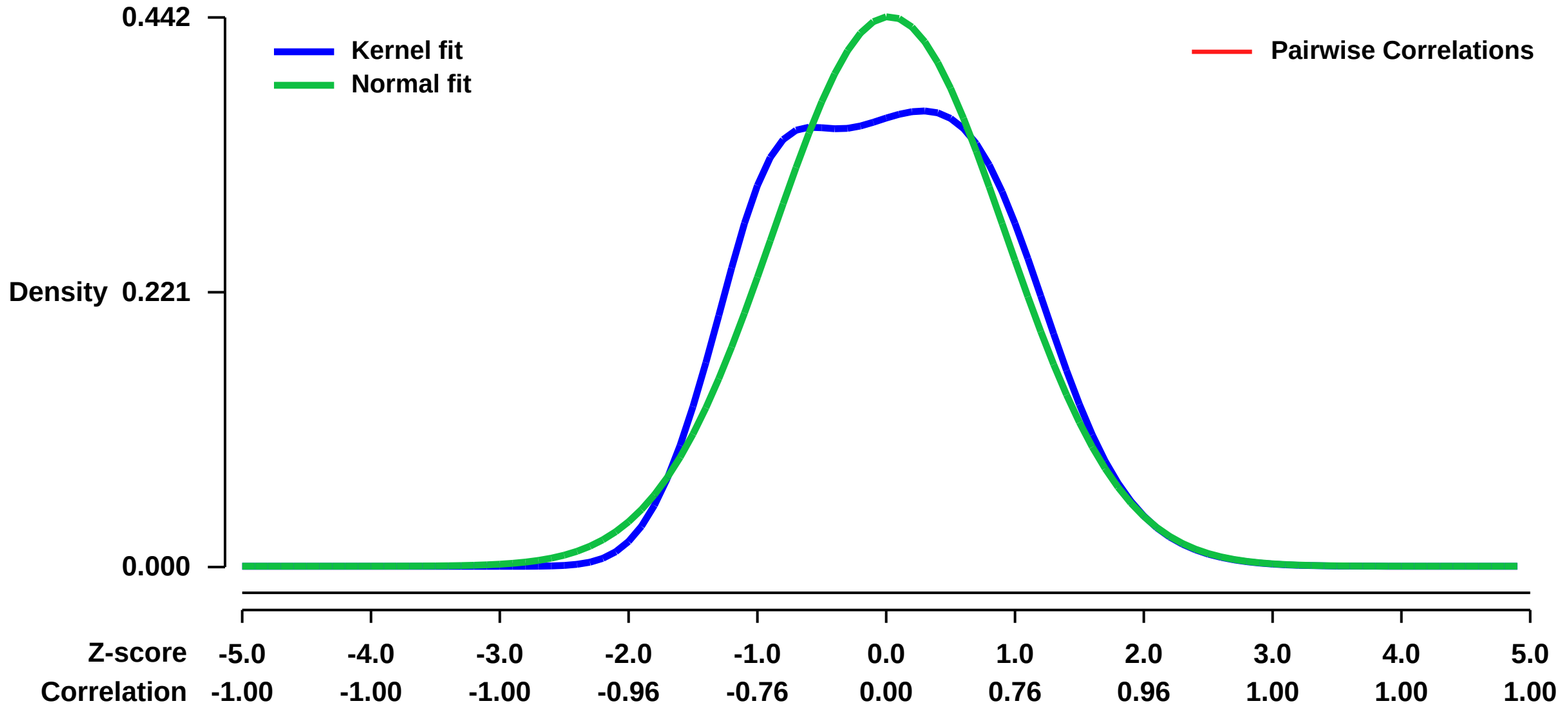

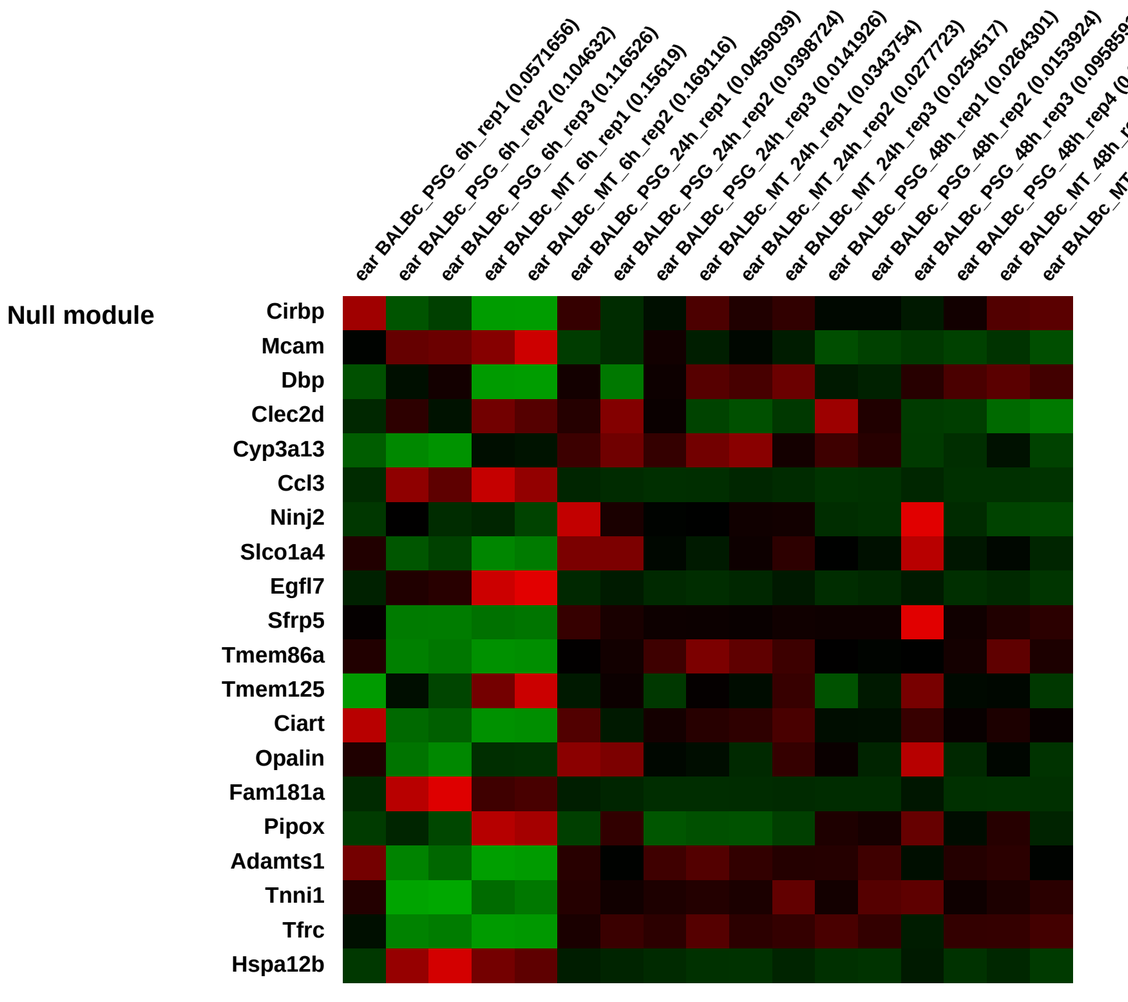

Pre-normalization Quantiles

[min] [medium] [max]

GEO Series "GSE52220" Expression Profiles

Num of samples in this series: 6

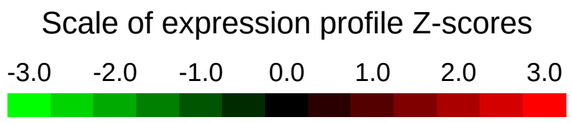

GEO Link:	http://www.ncbi.nlm.nih.gov/geo/query/acc.cgi?acc=GSE52220
Status:	Public on Nov 09 2013
Title:	Expression data from E11.5 mouse branchial arch 1 (BA1) - comparison between Ezh2lox/lox and Wnt1Cre Ezh2lox/lox embryos
Organism:	Mus musculus
Experiment type:	Expression profiling by array
Platform:	GPL1261
Pubmed ID:	24496623
Summary & Design:	**Summary:** Conditional ablation of Ezh2 in the neural crest lineage results in loss of the neural crest-derived mesenchymal derivatives. In this data sheet we determine gene expression analysis in Ezh2lox/lox and Wnt1Cre Ezh2lox/lox in E11.5 mouse BA1 cells. **Overall design:** Conditional ablation of Ezh2 in the neural crest lineage was achieved by crossing Wnt1creEzh2lox/wt mice with Ezh2lox/lox mouse lines. We analyzed a total of 6 samples including 3 biological replicates from Ezh2lox/lox embryos and 3 biological replicates from Wnt1cre Ezh2lox/lox embryos.

Background corr dist: KL-Divergence = 0.0375, L1-Distance = 0.0159, L2-Distance = 0.0002, Normal std = 0.6257

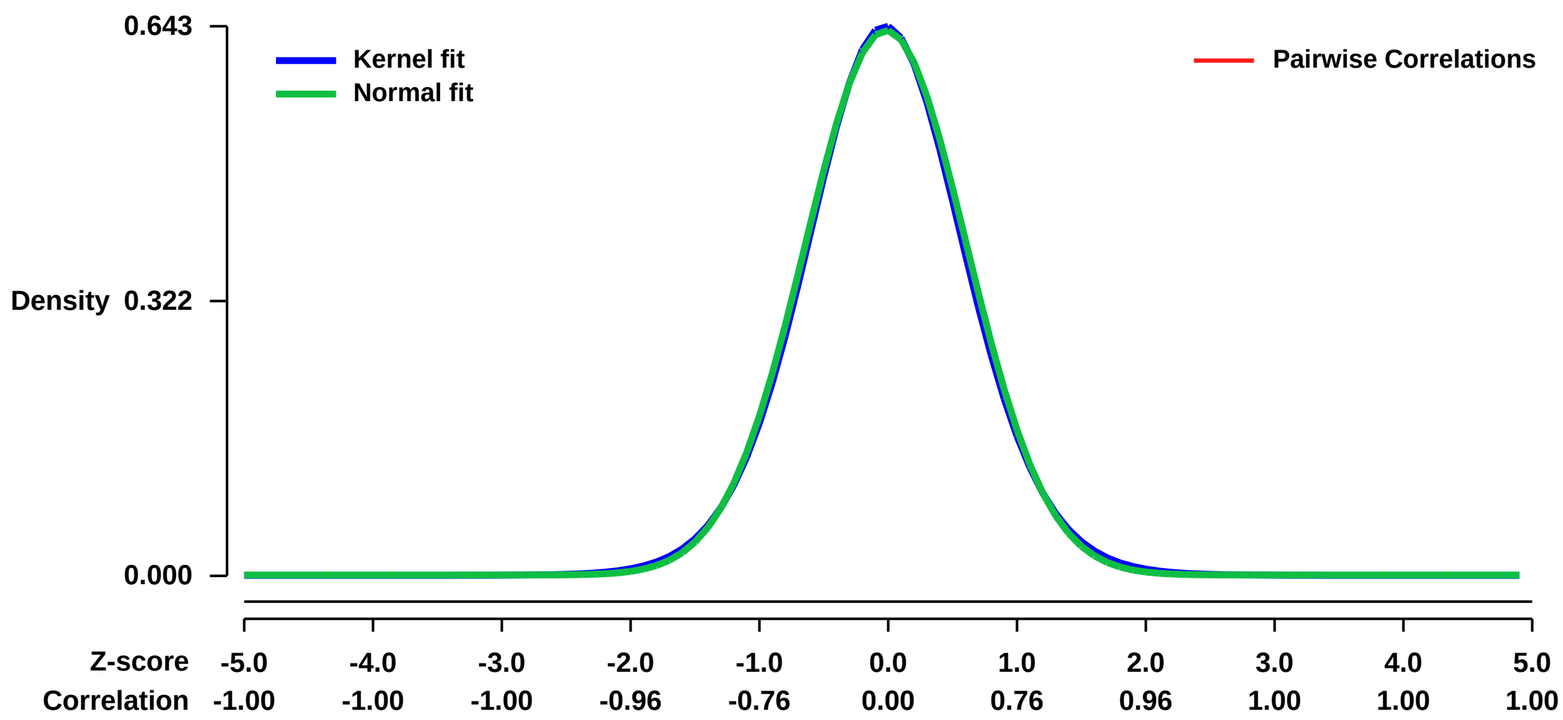

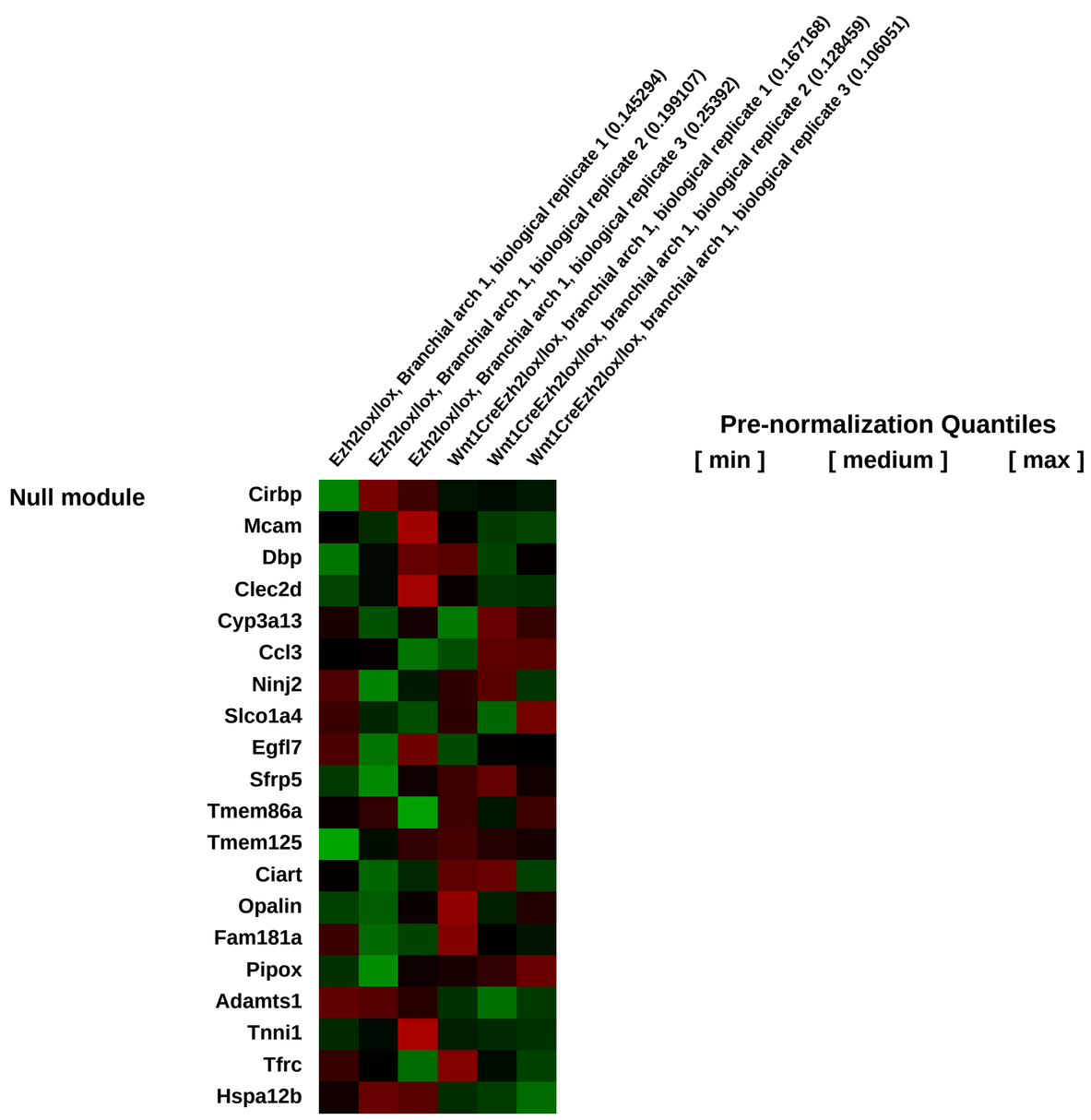

GEO Series "GSE5232" Expression Profiles

Num of samples in this series: 6

Scale of expression profile Z-scores

-3.0 -2.0 -1.0 0.0 1.0 2.0 3.0

GEO Link: http://www.ncbi.nlm.nih.gov/geo/query/acc.cgi?acc=GSE5232
Status: Public on Jul 05 2006
Title: Expression data from Lbeta T2 cells upon activin treatment
Organism: Mus musculus
Experiment type: Expression profiling by array
Platform: GPL1261
Pubmed ID:

Summary & Design:

Summary:
The primary response of Lbeta T 2cells upon activin treatment at 1hr, 2hr, and 6hr is the significant up-regulation of FSHbeta subunit. Affymetrix genearray missed this important information due to cross-hybridization of its probes with other genes and chromosome segments.

Activin modulates a network of genes and signaling pathways to exert a variety of functions.

Keywords: time course

Overall design:
Subconfluent Lbeta T2 cells were seeded in cell culture flasks for 16 hours in phenol-free, serum-free medium, and then treated with either vehicle or activin A (30ng/ml). At 1hr, 2hr, or 6hr after treatment, total RNA was isolated using RNeasy Mini Kit. Integrity of RNA was evaluated with an Agilent 2100 Bioanalyzer, and purity/concentration was determined using a GeneSpec III before target preparationi and hybridizations.

Background corr dist: KL-Divergence = 0.0477, L1-Distance = 0.0179, L2-Distance = 0.0003, Normal std = 0.5807

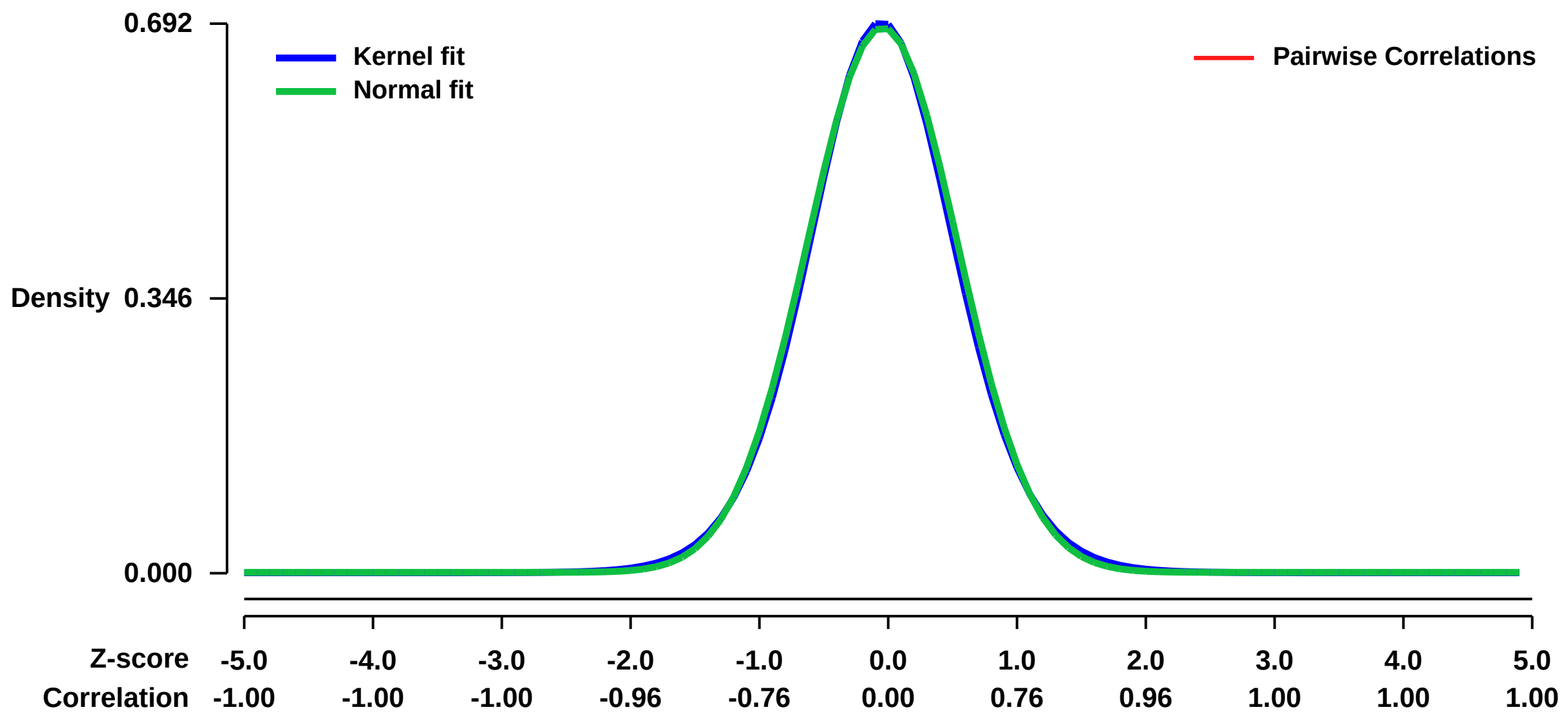

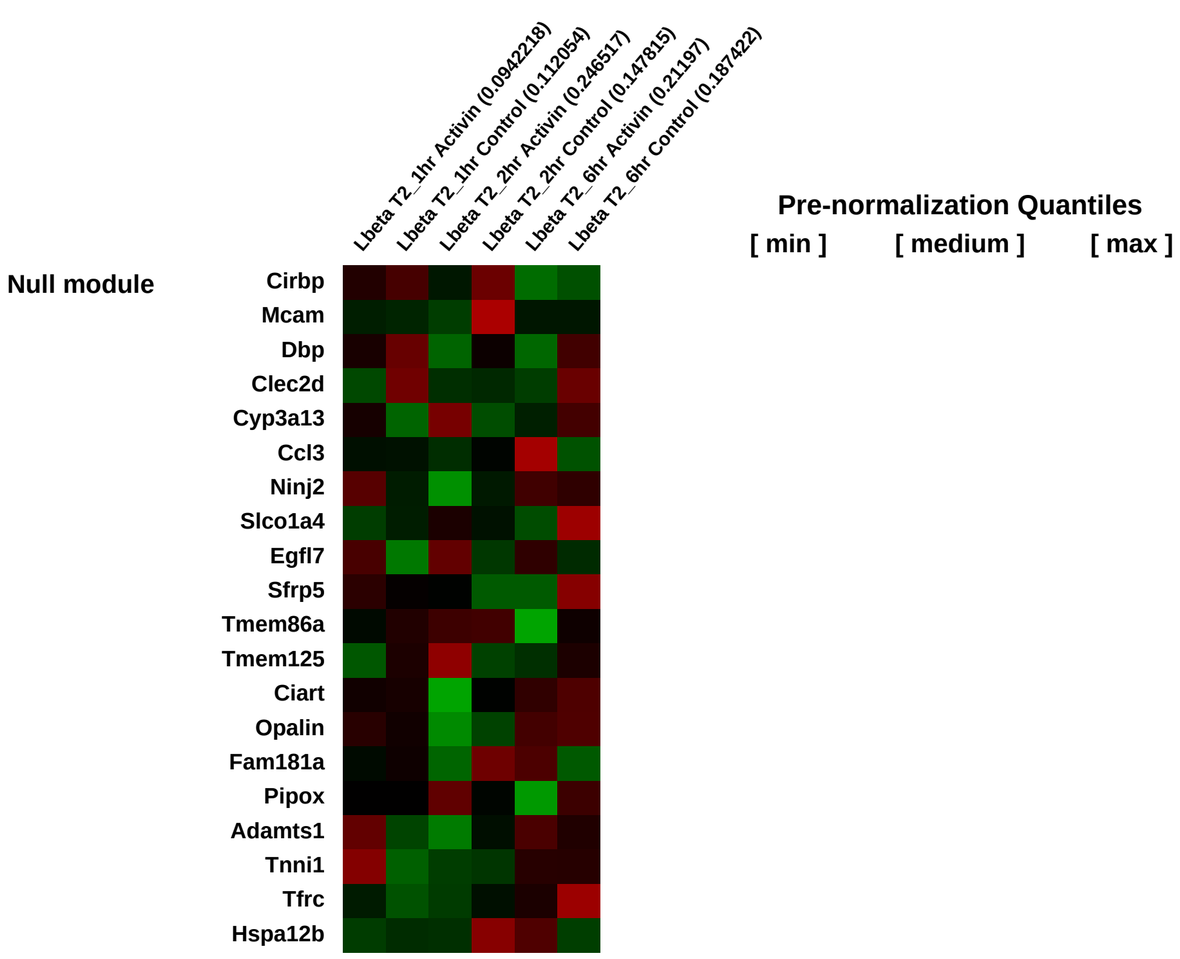

GEO Series "GSE52338" Expression Profiles

Num of samples in this series: 12

Scale of expression profile Z-scores

-3.0 -2.0 -1.0 0.0 1.0 2.0 3.0

GEO Link: http://www.ncbi.nlm.nih.gov/geo/query/acc.cgi?acc=GSE52338

Status: Public on Nov 14 2013

Title: Expression data from peritoneal macrophages stimulated with trehalose-6,6'-dimycolate (TDM)

Organism: Mus musculus

Experiment type: Expression profiling by array

Platform: GPL1261

Pubmed ID:

Summary & Design:

Summary:
Macrophage-inducible C-type lectin (Mincle, Clec4e) is a pathogen sensor that recognizes pathogenic fungi and Mycobactrium tuberculosis. We perfomed microarray analysis using peritoneal macrophages stimulated with TDM, a mycobacterial cell wall glycolipid that is known to be a Mincle ligand.

Many chemokine and cytokine genes were upregulated in wildtype macrophages stimulated with TDM. Upregulation of these genes were completely abolishd in Mincle KO macrophages.

Overall design:
Peritoneal macrophages from WT and Mincle KO mice were stimulated with TDM or vehicle for 24 h (3 samples each). Microarray analysis was performed using Affymetrix Mouse 430 2.0.

Background corr dist: KL-Divergence = 0.1547, L1-Distance = 0.0266, L2-Distance = 0.0011, Normal std = 0.3748

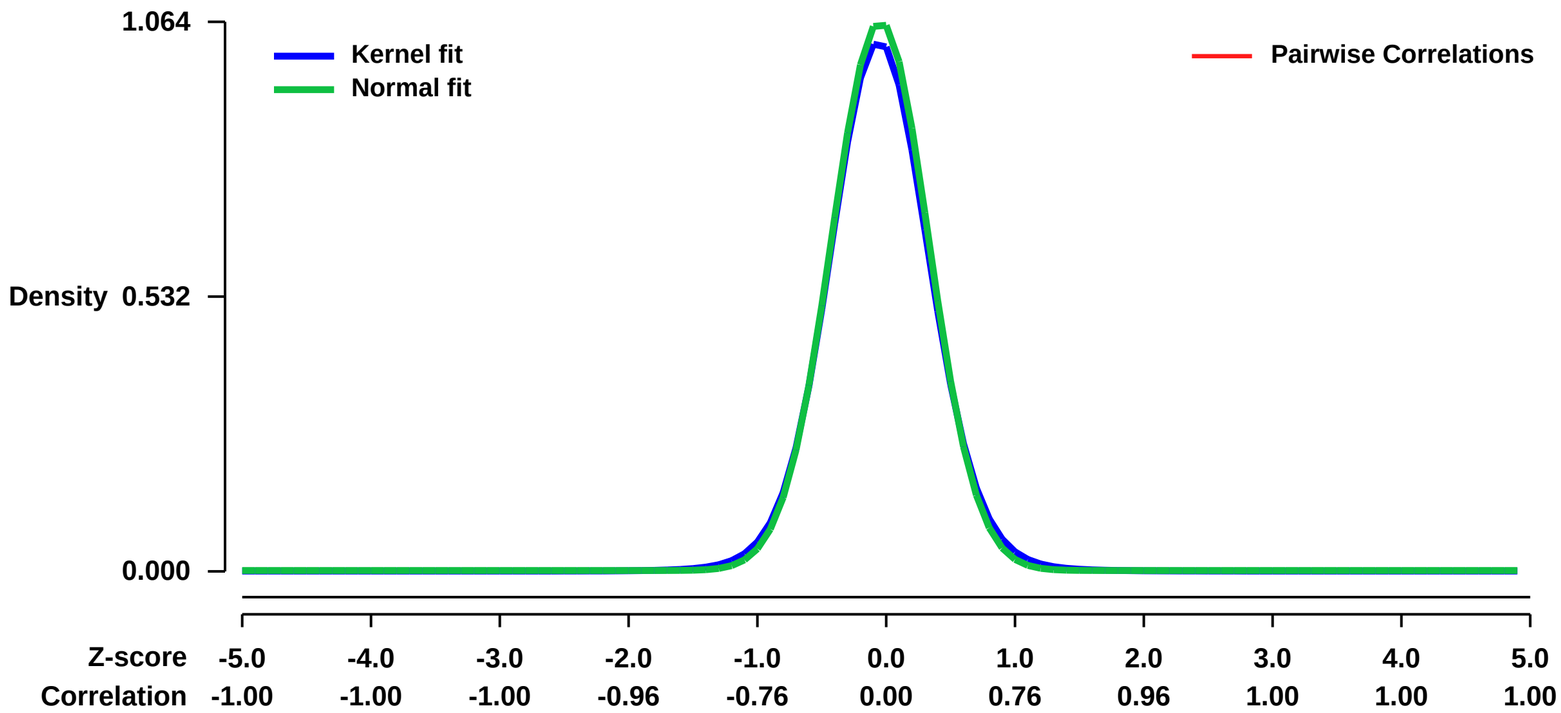

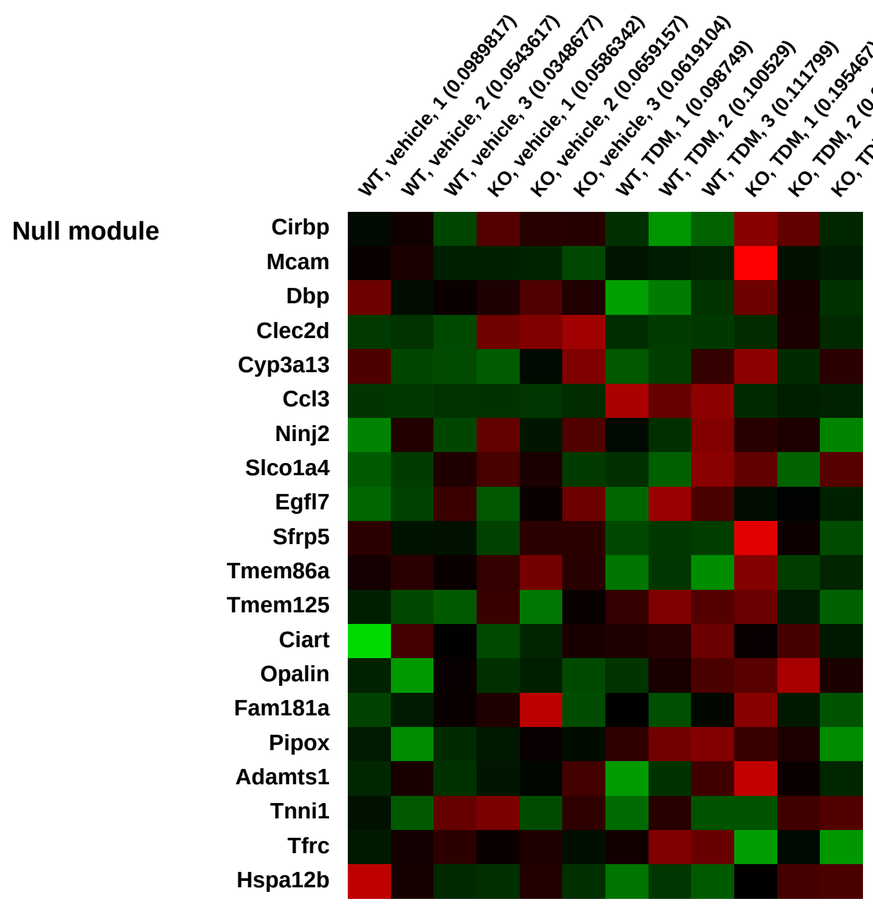

Pre-normalization Quantiles

[min] [medium] [max]

GEO Series "GSE52357" Expression Profiles

Num of samples in this series: 8

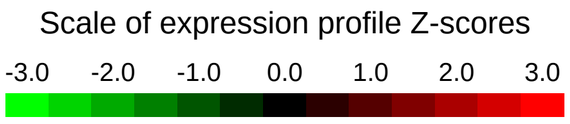

GEO Link: http://www.ncbi.nlm.nih.gov/geo/query/acc.cgi?acc=GSE52357

Status: Public on Jun 18 2014

Title: Gene expression profiling of the mandibular arch from Alk5 mutant mouse models

Organism: Mus musculus

Experiment type: Expression profiling by array

Platform: GPL1261

Pubmed ID:

Summary & Design:

Summary:
The overall goal of this project is to investigate the role of TGF-beta signaling in tissue-tissue interactions between myogenic precursors of craniofacial muscles and cranial neural crest cells (CNCCs). Here, we conducted gene expression profiling of the mandibular arch from mice at embryonic day E11.5 with a CNCC-specific conditional inactivation of the TGF-beta receptor type 1 gene Alk5. These mice provide a model of microglossia as well as disrupted extraocular and masticatory muscle development, which are congenital birth defects commonly observed in several syndromic conditions.

Overall design:
To investigate the adverse effects of dysfunctional TGF-beta signaling on tissue-tissue interactions between CNCCs and myogenic precursors of craniofacial muscles, we analyzed mandibular arch tissue of mice with a CNCC-specific conditional inactivation of Alk5 (Wnt1-Cre; Alk5 fl/fl). We performed microarray analyses of the mandibular arch of Alk5 fl/fl control mice and Wnt1-Cre; Alk5 fl/fl mutant mice, collected at embryonic day E11.5 (n=4 per group).

Background corr dist: KL-Divergence = 0.0293, L1-Distance = 0.0380, L2-Distance = 0.0021, Normal std = 0.6790

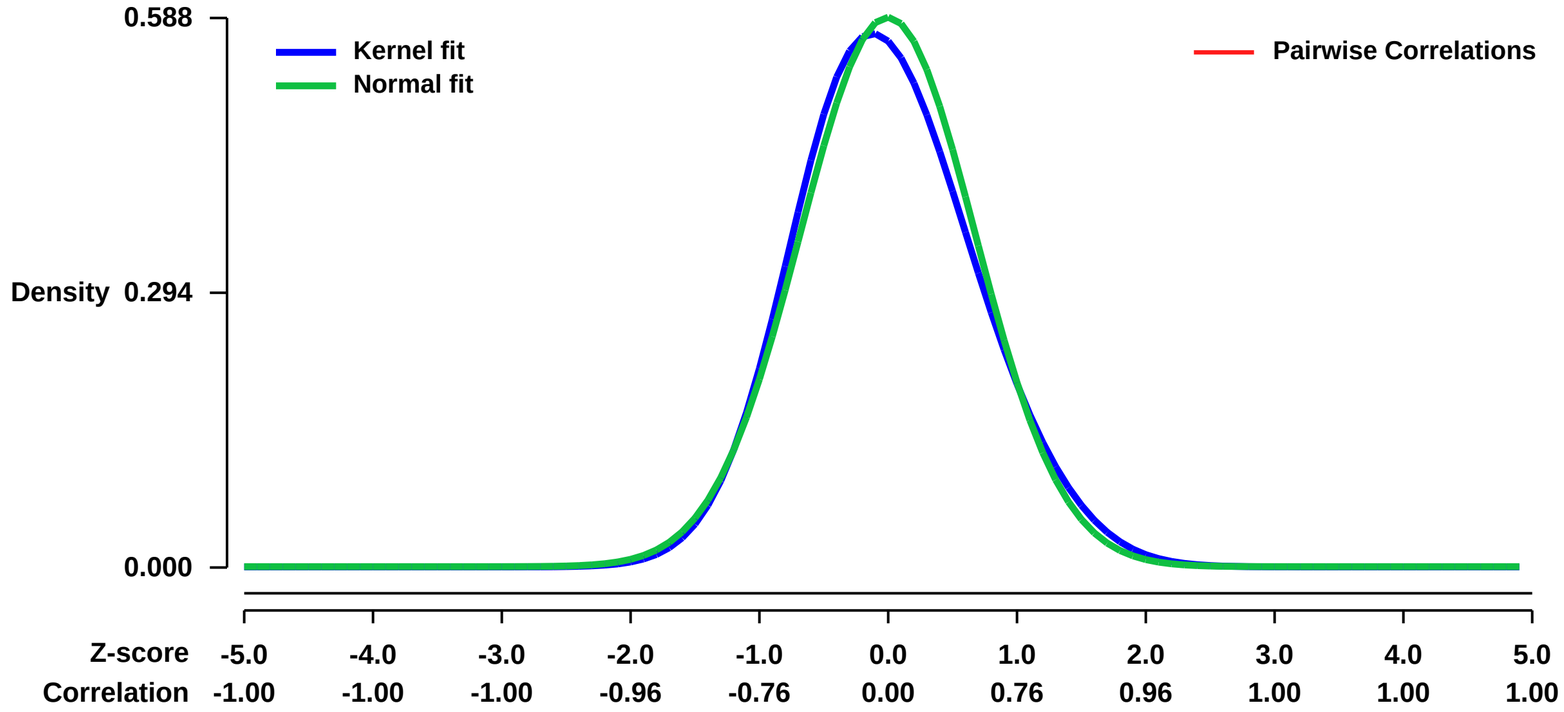

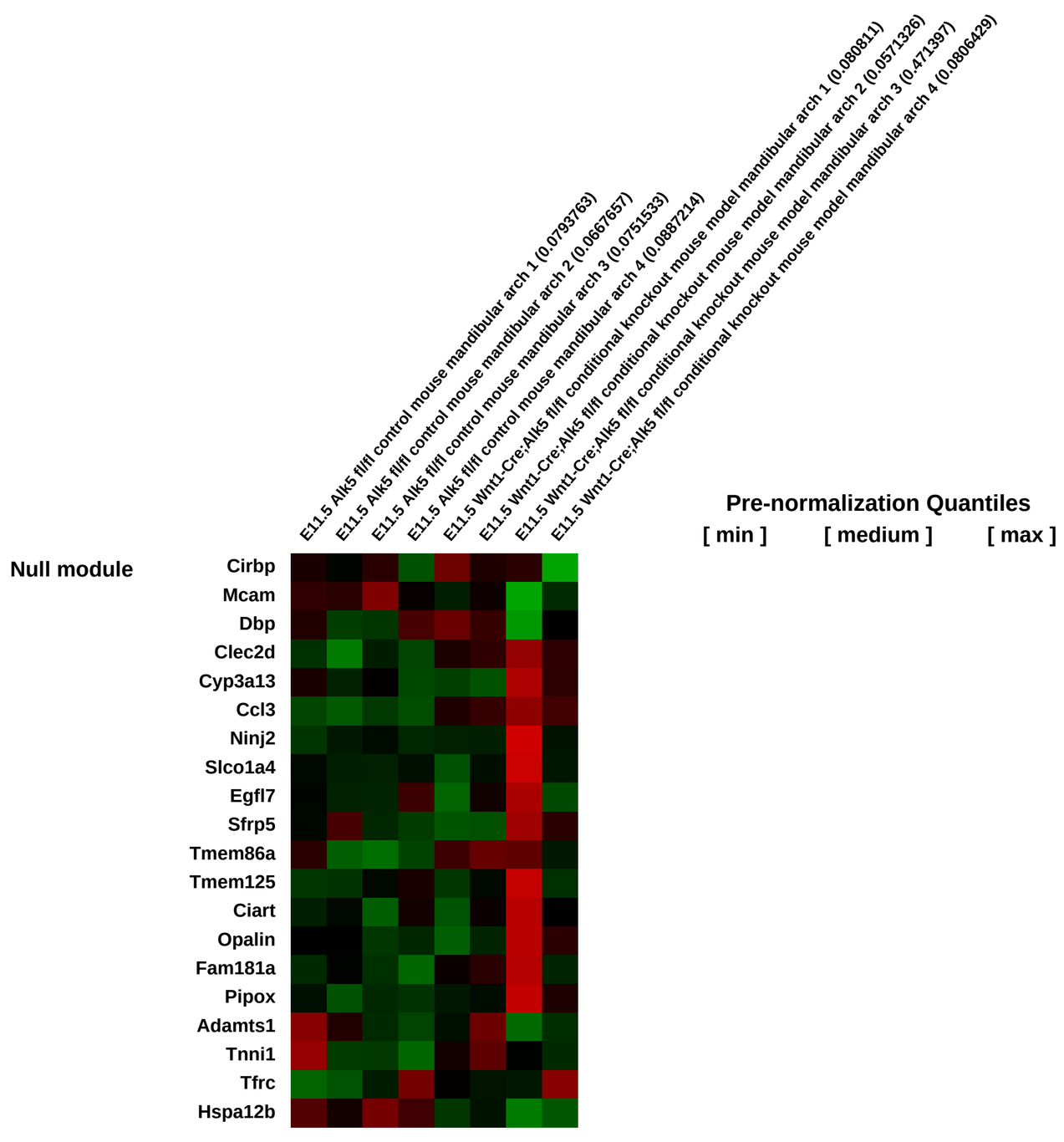

GEO Series "GSE52358" Expression Profiles

Num of samples in this series: 8

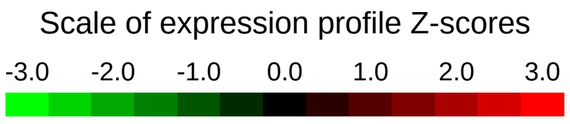

GEO Link:	**http://www.ncbi.nlm.nih.gov/geo/query/acc.cgi?acc=GSE52358**
Status:	**Public on Jun 18 2014**
Title:	**Gene expression profiling of the tongue bud from Alk5 mutant mouse models**
Organism:	**Mus musculus**
Experiment type:	**Expression profiling by array**
Platform:	**GPL1261**
Pubmed ID:	
Summary & Design:	**Summary:** **The overall goal of this project is to investigate the role of TGF-beta signaling in tissue-tissue interactions between myogenic precursors of craniofacial muscles and cranial neural crest cells (CNCCs). Here, we conducted gene expression profiling of the tongue bud from mice at embryonic day E13.5 with a CNCC-specific conditional inactivation of the TGF-beta receptor type 1 gene Alk5. These mice provide a model of microglossia as well as disrupted extraocular and masticatory muscle development, which are congenital birth defects commonly observed in several syndromic conditions.** **Overall design:** **To investigate the adverse effects of dysfunctional TGF-beta signaling on tissue-tissue interactions between CNCCs and myogenic precursors of craniofacial muscles, we analyzed tongue bud tissue of mice with a CNCC-specific conditional inactivation of Alk5 (Wnt1-Cre; Alk5 fl/fl). We performed microarray analyses of the tongue bud of Alk5 fl/fl control mice and Wnt1-Cre; Alk5 fl/fl mutant mice, collected at embryonic day E13.5 (n=4 per group).**

Background corr dist: **KL-Divergence = 0.0605, L1-Distance = 0.0184, L2-Distance = 0.0004, Normal std = 0.5241**

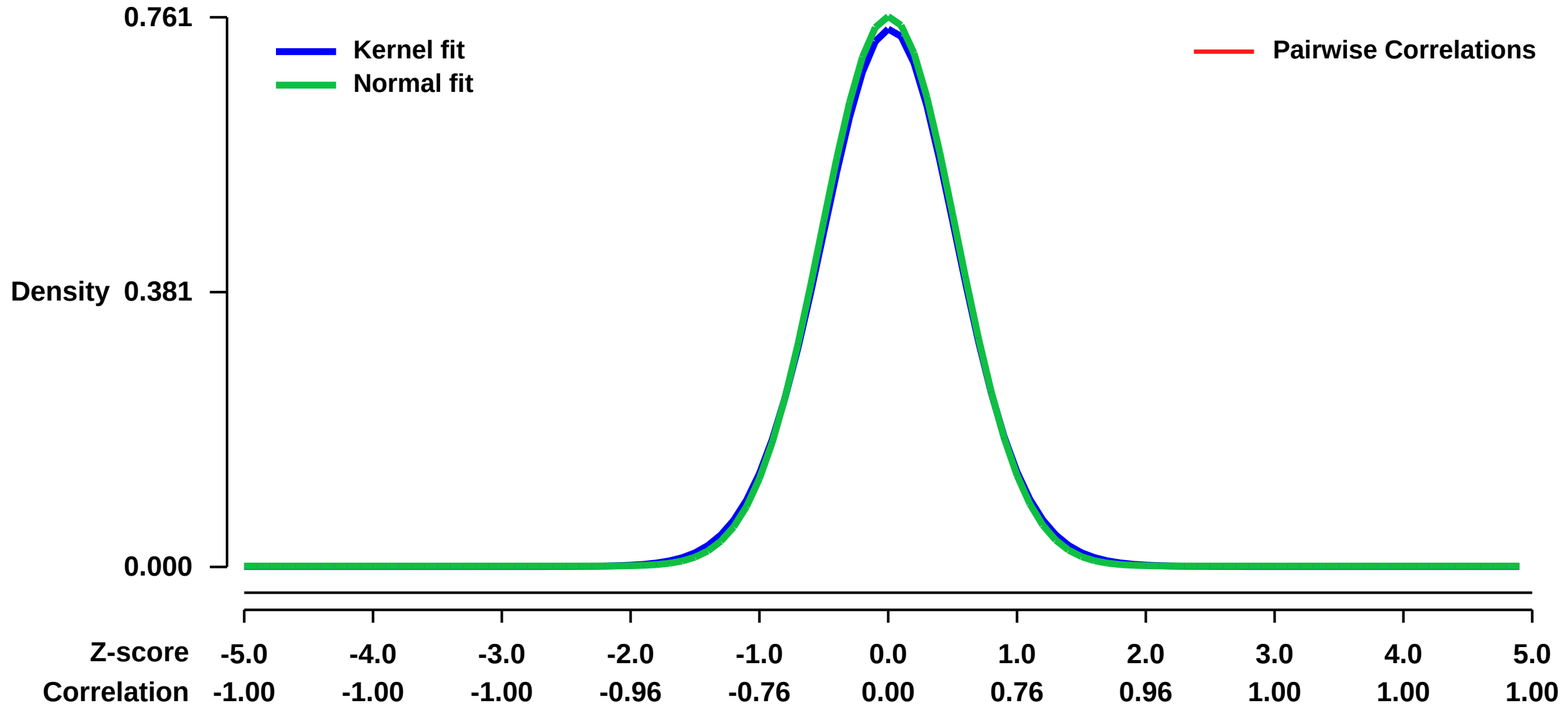

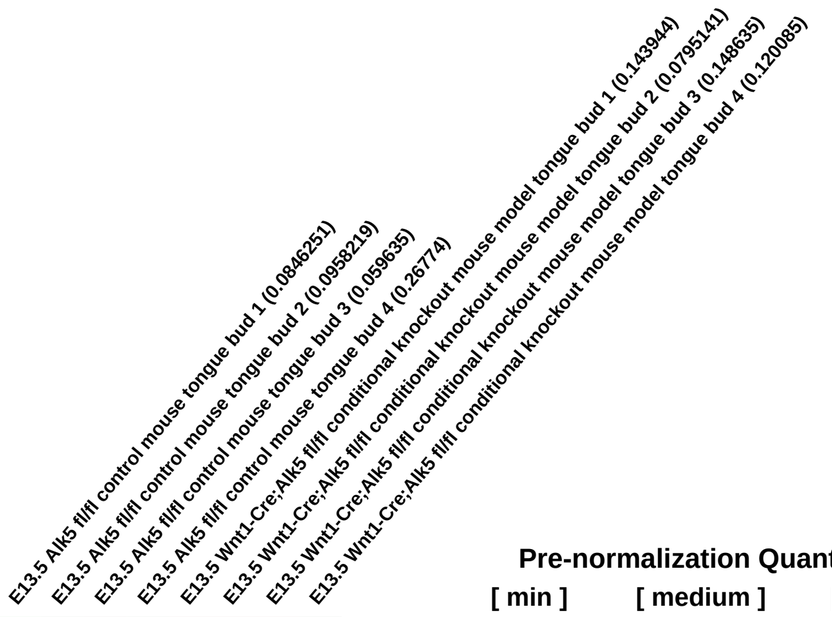

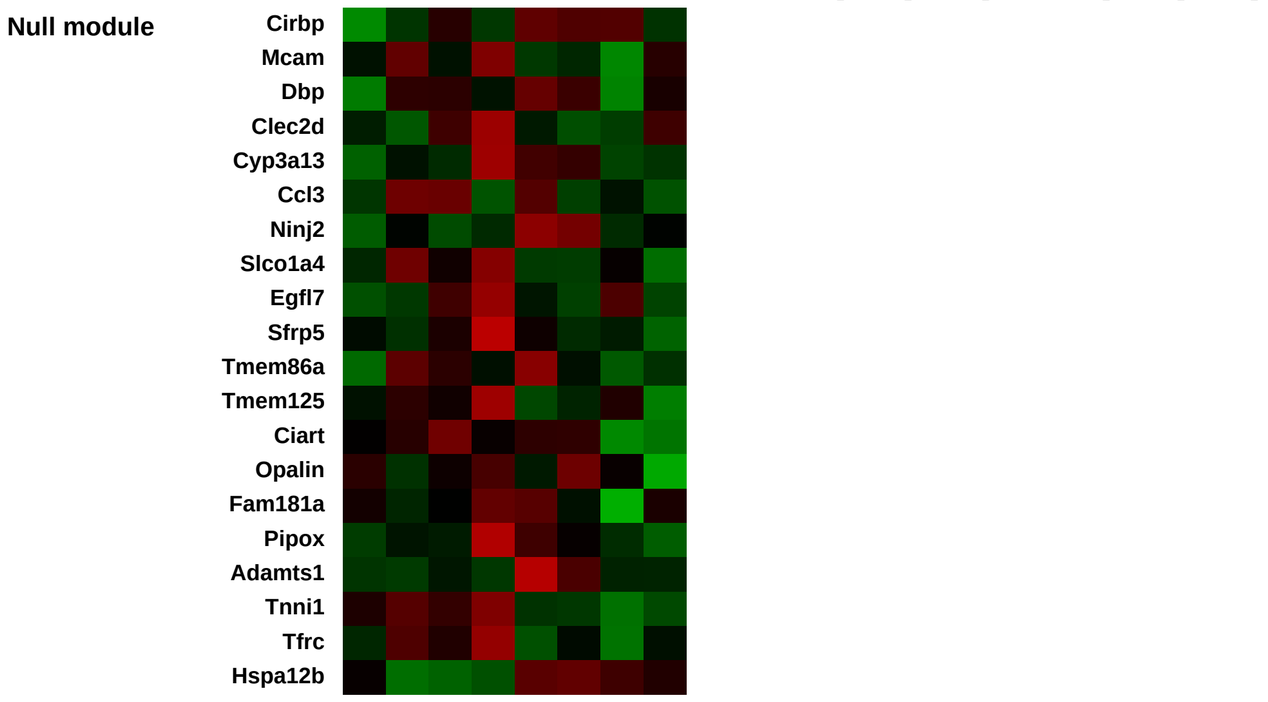

GEO Series "GSE5241" Expression Profiles

Num of samples in this series: 9

Scale of expression profile Z-scores

-3.0 -2.0 -1.0 0.0 1.0 2.0 3.0

GEO Link:	http://www.ncbi.nlm.nih.gov/geo/query/acc.cgi?acc=GSE5241
Status:	Public on Jan 31 2008
Title:	Liver toxicity of dichloroacetyl chloride and dichloroacetic anhydride in female MRL +/+ mice
Organism:	Mus musculus
Experiment type:	Expression profiling by array
Platform:	GPL1261
Pubmed ID:	18293905
Summary & Design:	**Summary:** Dichloroacetyl chloride (DCAC) is a metabolic intermediate of trichloroethene (TCE), an industrial chemical and ubiquitous environmental contaminant. TCE and its metabolites have been implicated in the induction of organ-specific and systemic autoimmunity, in the acceleration of autoimmune responses, and in the development of liver toxicity. In humans, effects of environmental toxicants are often multifactorial and detected only after long-term exposure. Therefore, we developed a small-animal model to determine mechanisms by which DCAC and related acylating agents affect liver disease. Autoimmune-prone female MRL +/+ mice were injected i.p. with 0.2 mmole/kg of DCAC or the acylating agent dichloroacetic anhydride (DCAA) in corn oil twice weekly for six weeks. We then determined changes in the liver transcriptome using microarray gene expression analysis. After exposure to DCAC or DCAA, we observed changes in liver gene expression consistent with inflammatory processes. Both toxicants up-regulated expression of acute phase response and inflammatory genes. Further, metallothionein genes were strongly up-regulated, indicating effects of the toxicants on zinc ion homeostasis and stress responses. In addition, DCAC and DCAA induced up-regulation of several genes indicative of tumorogenesis. Microarray gene expression analysis using a restricted set of genes could be a valuable tool to screen for early changes in liver function following suspected exposure to environmental toxicants. Keywords: Response to acylating agents; inflammatory response; disease state analysis. **Overall design:** Samples: Livers from three mice per group were independently processed. The integrity of the RNA samples was tested using an Agilent 2100 Bioanalyzer and RNA 6000 LabChip´fi kit (Agilent Technologies, Palo Alto, CA). Only RNA samples without signs of degradation were used. Comprehensive gene expression profiles were analyzed.

Background corr dist: KL-Divergence = 0.0831, L1-Distance = 0.0387, L2-Distance = 0.0023, Normal std = 0.5130

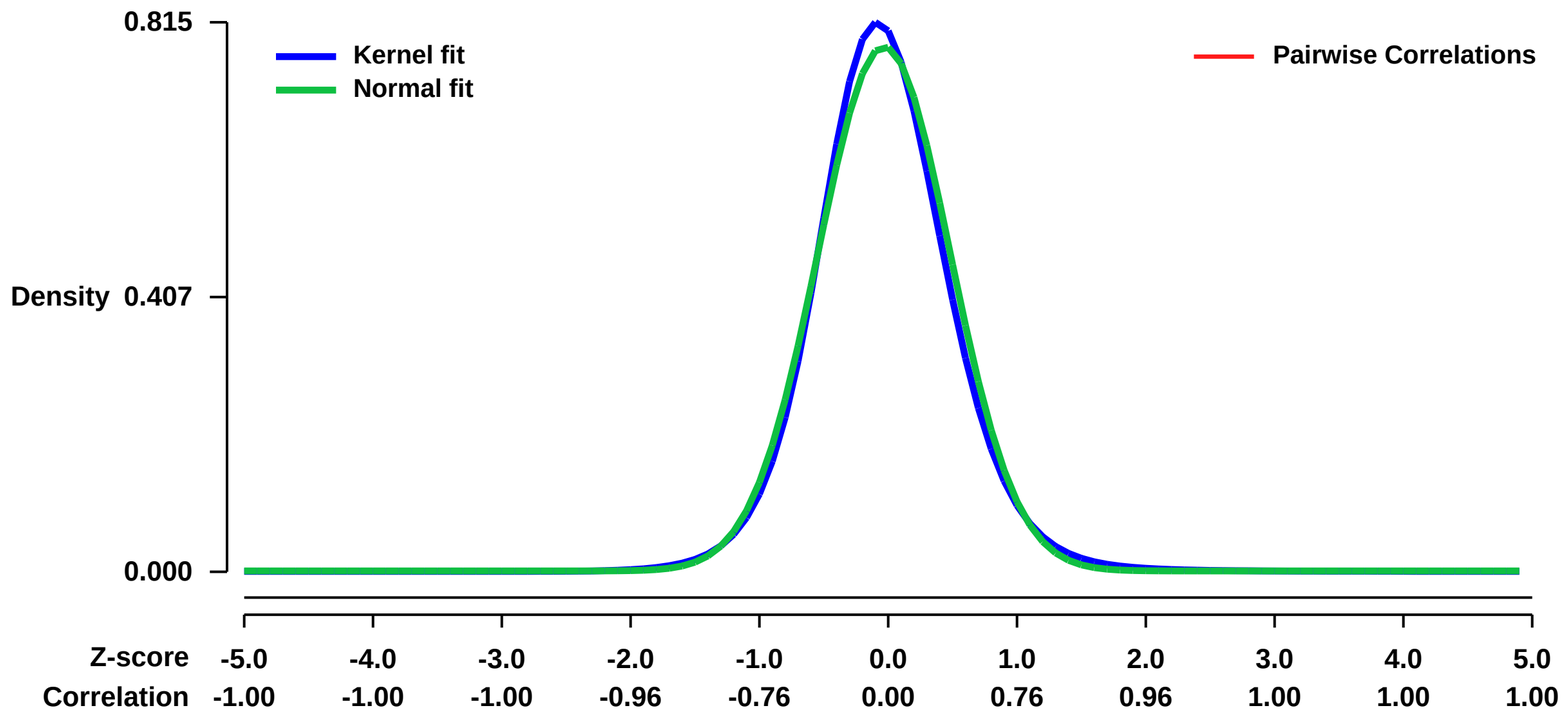

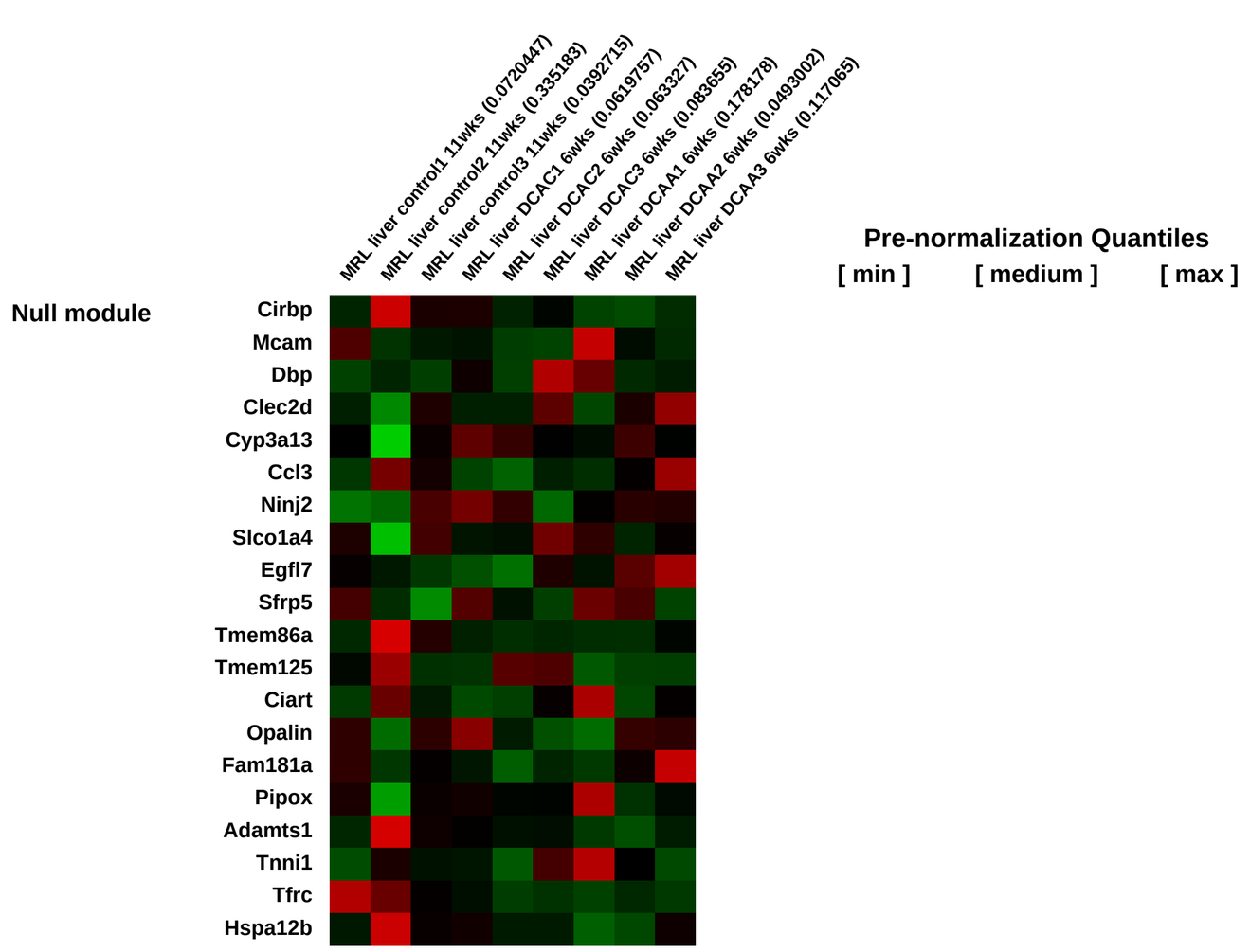

GEO Series "GSE5245" Expression Profiles

Num of samples in this series: 16

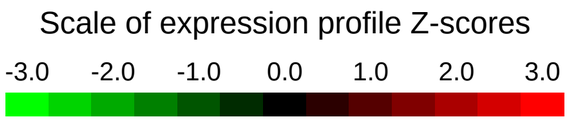

GEO Link:	**http://www.ncbi.nlm.nih.gov/geo/query/acc.cgi?acc=GSE5245**
Status:	**Public on Apr 03 2008**
Title:	**Profiling of CD4+ T cells responding to transient or persistent antigen presented by dendritic cells in vivo**
Organism:	**Mus musculus**
Experiment type:	**Expression profiling by array**
Platform:	**GPL1261**
Pubmed ID:	**17881563**
Summary & Design:	**Summary:** **These experiments were done to compare the gene expression profiles in CD4+ T cells responding to antigen presented by dendritic cells transiently or persistently. Some treatments include the activation of the dendritic cells by CD40 engagement.** **Keywords: immune response** **Overall design:** **2-4x106 lymph node cells from AND TCR-transgenic animals that expressed the congenic marker CD90.1 were transferred into double-transgenic (Ii-rTA/TIM) recipient animals that expressed the corresponding peptide from moth cytochrome c under a doxycycline-controllable promoter and were FACS-sorted 60 hours later. Recipients expressed the antigen not at all (â ctrlâ), transiently (â shortâ) or throughout the experiment (â longâ) due to different doxycycline treatment protocols. A second variable tested was the activation status of the dendritic cells: recipients were either injected by the stimulatory antibody FGK45.5 targeting CD40 (â FGKâ) or PBS (â PBSâ).**

Background corr dist: **KL-Divergence = 0.0477, L1-Distance = 0.0650, L2-Distance = 0.0079, Normal std = 0.5996**

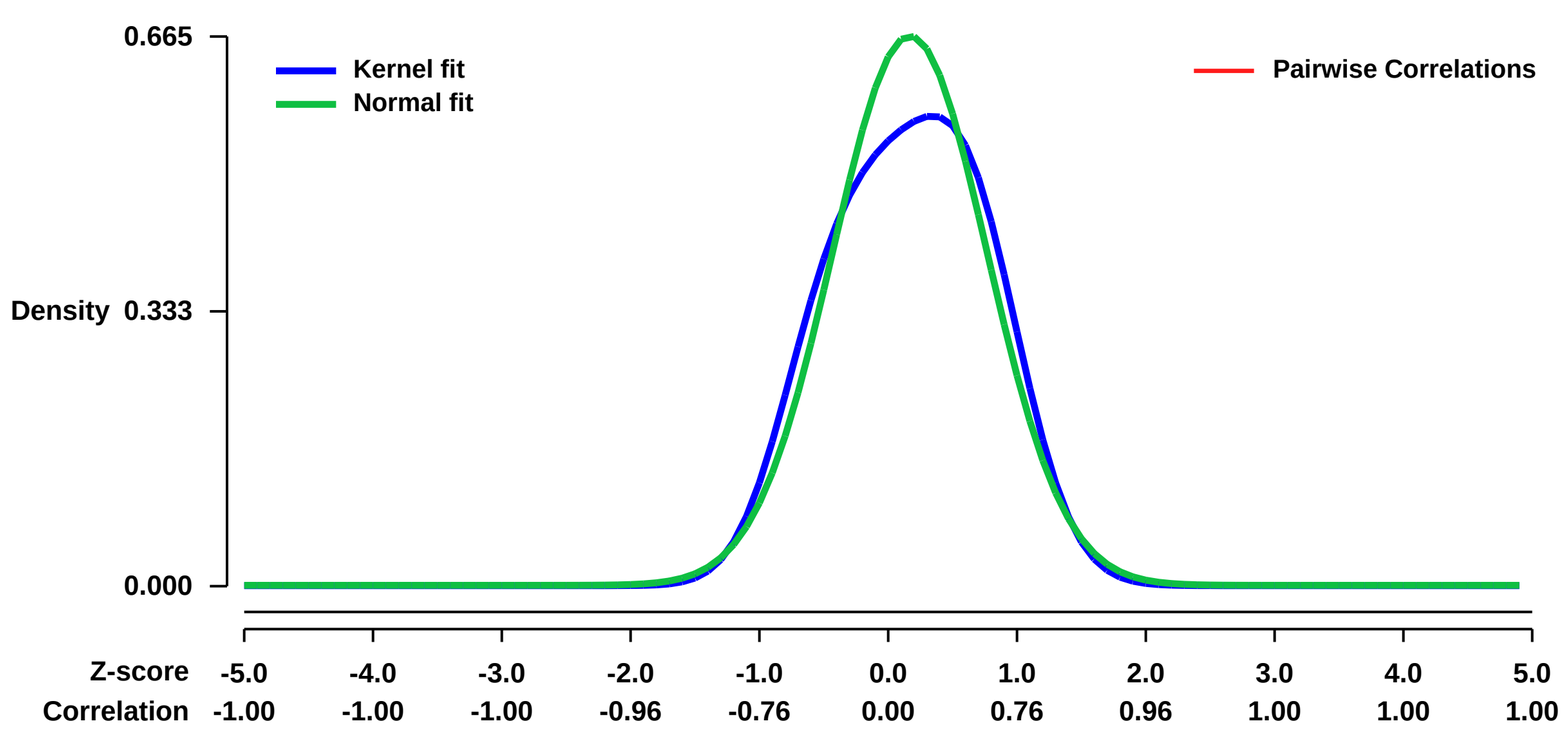

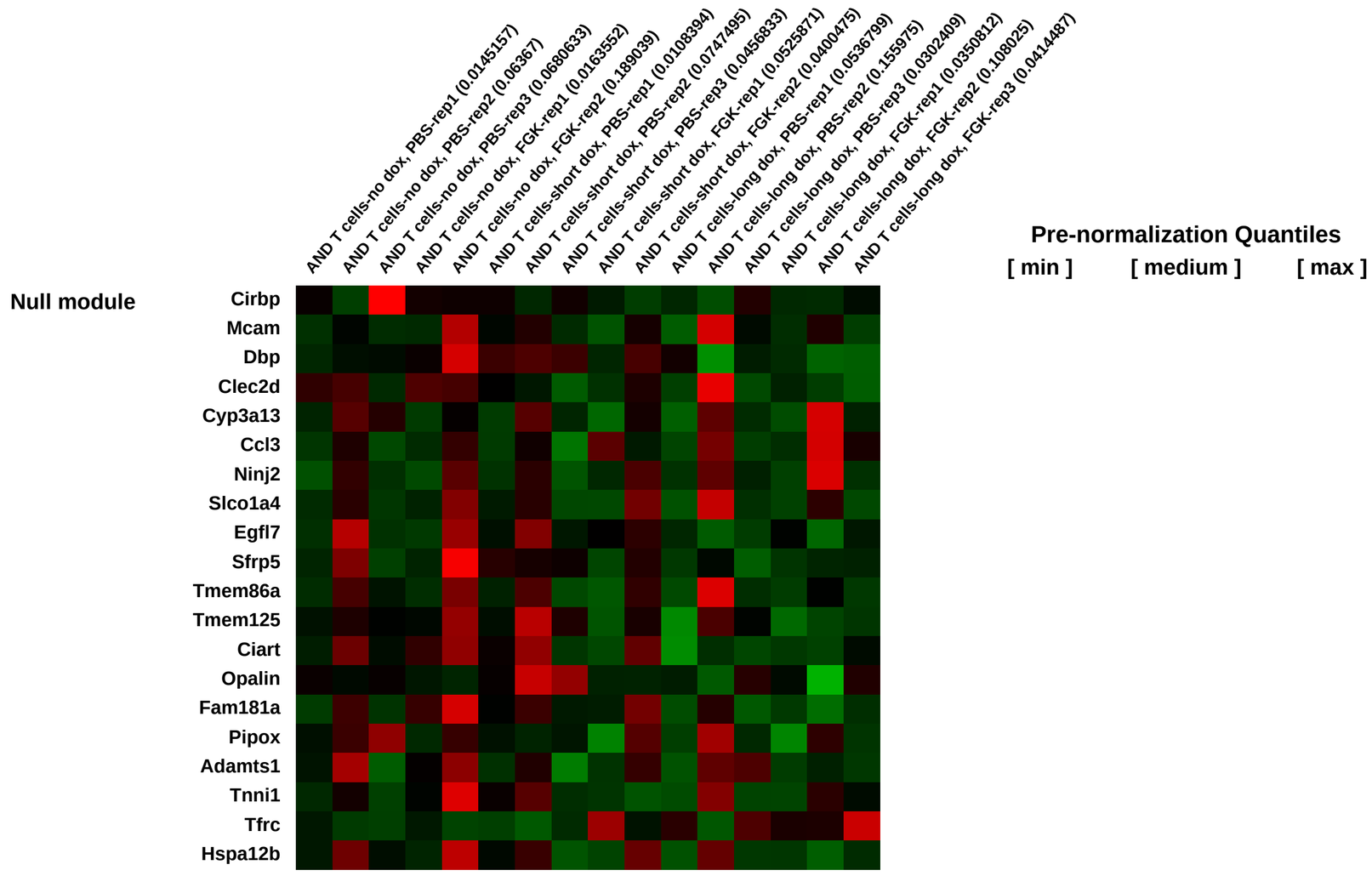

GEO Series "GSE52542" Expression Profiles

Num of samples in this series: 9

Scale of expression profile Z-scores

-3.0 -2.0 -1.0 0.0 1.0 2.0 3.0

GEO Link:	http://www.ncbi.nlm.nih.gov/geo/query/acc.cgi?acc=GSE52542
Status:	Public on Nov 21 2013
Title:	VEGF Isoform Transcriptome Changes in the E9.5 Murine Forebrain
Organism:	Mus musculus
Experiment type:	Third-party reanalysis
Platform:	GPL1261
Pubmed ID:	24124161
Summary & Design:	**Summary:** Regulation of neural stem cell (NSC) fate decisions is critical during the transition from a multicellular mammalian forebrain neuroepithelium to the multilayered neocortex. Forebrain development requires coordinated vascular investment alongside NSC differentiation. Vascular endothelial growth factor A (Vegf) has proven to be a pleiotrophic gene whose multiple protein isoforms regulate a broad range of effects in neurovascular systems. To test the hypothesis that the Vegf isoforms (120, 164, and 188) are required for normal forebrain development, we analyzed the forebrain transcriptome of mice expressing specific Vegf isoforms, Vegf120, VegfF188, or a combination of Vegf120/188. Transcriptome analysis identified differentially expressed genes in embryonic day (E) 9.5 forebrain, a time point preceding dramatic neuroepithelial expansion and vascular investment in the telencephalon. Meta-analysis identified gene pathways linked to chromosome-level modifications, cell fate regulation, and neurogenesis that were altered in Vegf isoform mice. **Overall design:** This study comprises of new samples and reanalysis of Samples from GSE30767 and GSE8091.

Background corr dist: KL-Divergence = 0.0176, L1-Distance = 0.0390, L2-Distance = 0.0022, Normal std = 0.7805

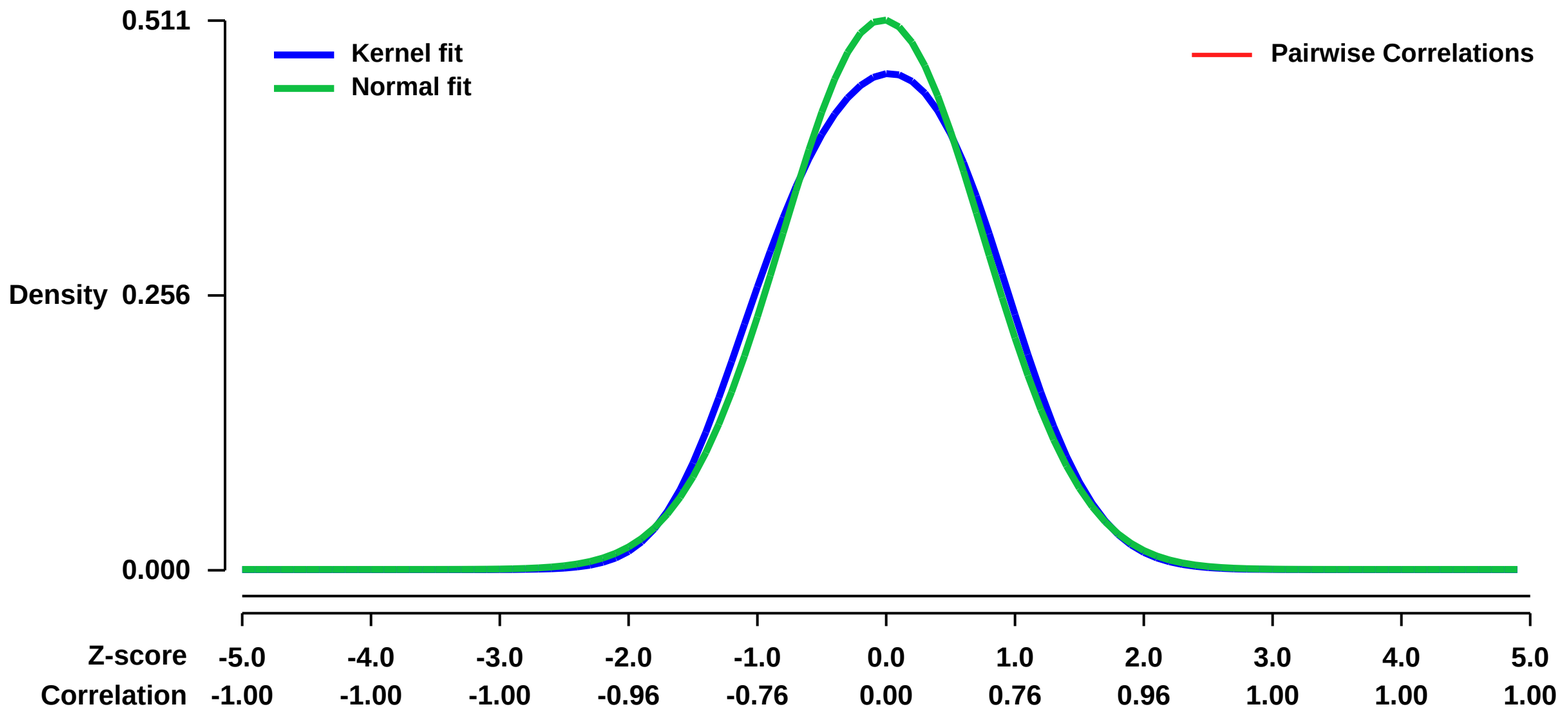

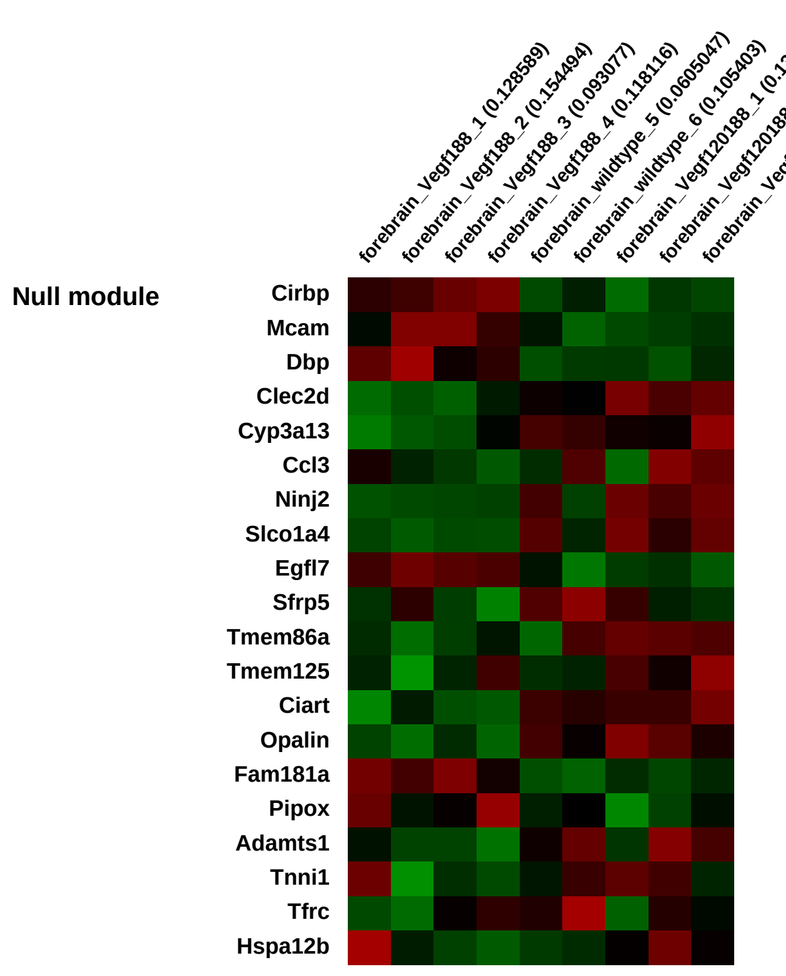

Pre-normalization Quantiles

[min] [medium] [max]

GEO Series "GSE52550" Expression Profiles

Num of samples in this series: 12

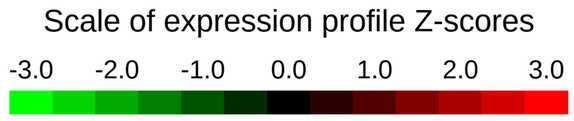

GEO Link:	**http://www.ncbi.nlm.nih.gov/geo/query/acc.cgi?acc=GSE52550**
Status:	**Public on Dec 05 2013**
Title:	**Progressive loss of PGC-1alpha expression in aging muscle potentiates glucose intolerance and systemic inflammation**
Organism:	**Mus musculus**
Experiment type:	**Expression profiling by array**
Platform:	**GPL1261**
Pubmed ID:	**24280126**
Summary & Design:	**Summary:** **Decreased mitochondrial mass and function in muscle of diabetic patients is associated with low PGC-1alpha, a transcriptional coactivator of the mitochondrial gene program. To investigate whether reduced PGC-1alpha and oxidative capacity in muscle directly contributes to age-related glucose intolerance, we compared the genetic signatures and metabolic profiles of aging mice lacking muscle PGC-1alpha. Microarray analysis revealed that a significant proportion of PGC-1alpha-dependent changes in gene expression overlapped with age-associated effects, and aging muscle and muscle lacking PGC-1alpha shared gene signatures of impaired electron transport chain activity and TGFbeta signalling.** **Overall design:** **Gastrocnemius muscle mRNA from young (10 week old) and old (24 month old) wild-type and knock-out (muscle-specific PGC-1alpha, myogenin-cre) C57Bl/6N/6J/129 mice**

Background corr dist: **KL-Divergence = 0.1012, L1-Distance = 0.0285, L2-Distance = 0.0014, Normal std = 0.4339**

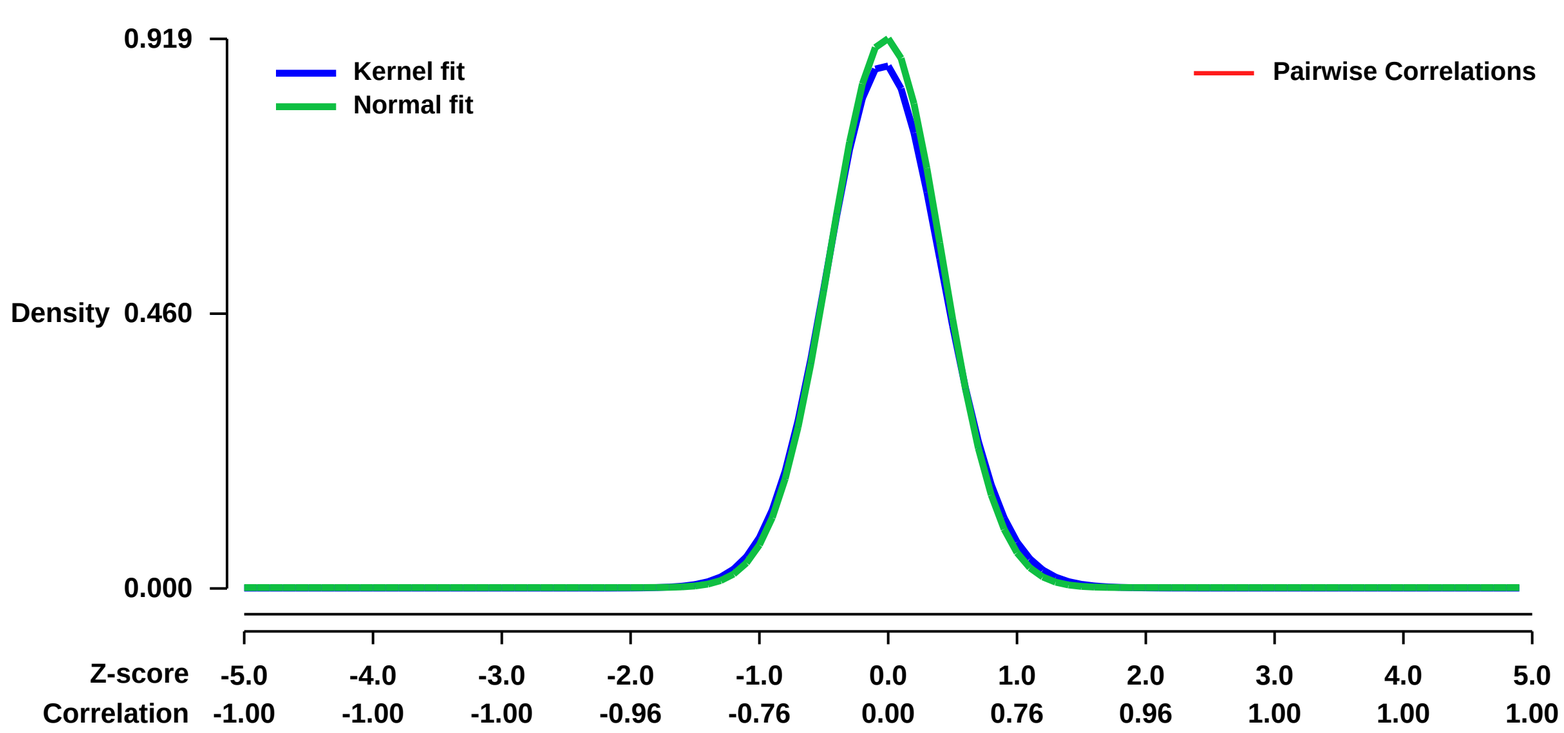

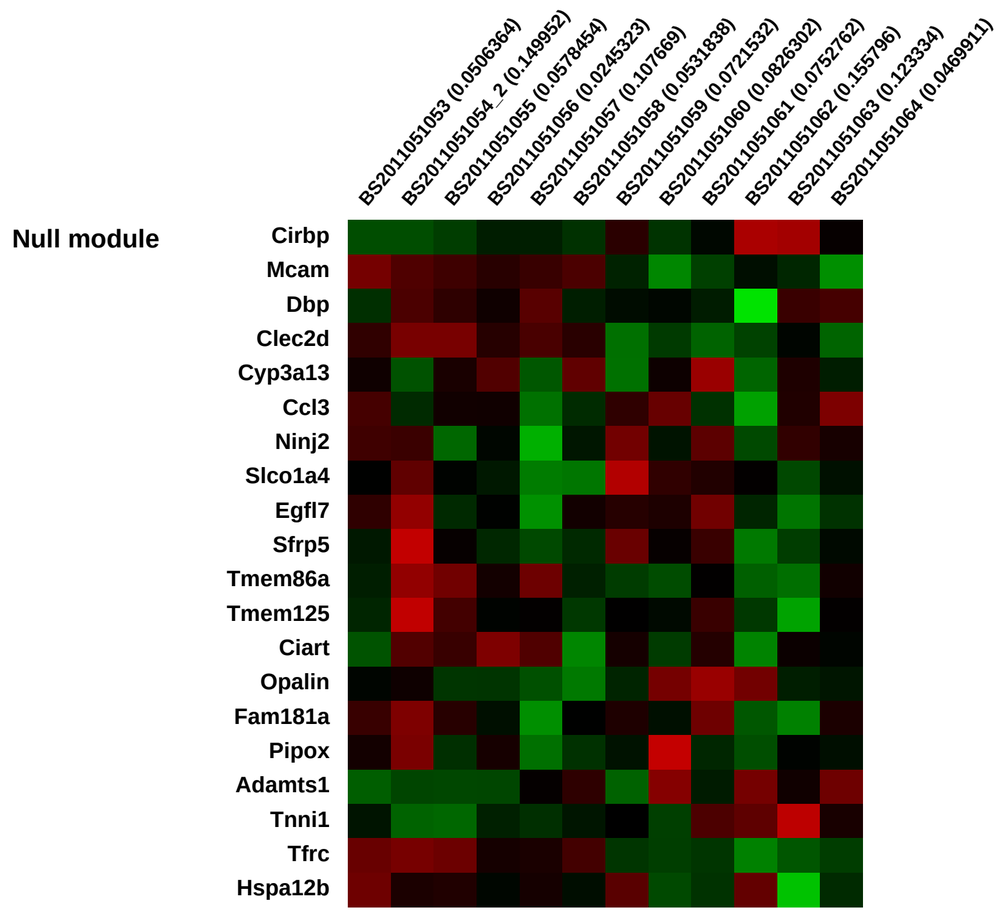

GEO Series "GSE5298" Expression Profiles

Num of samples in this series: 8

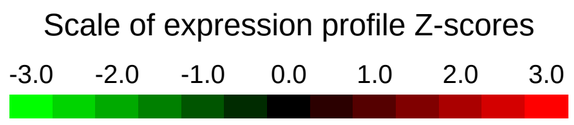

GEO Link:	http://www.ncbi.nlm.nih.gov/geo/query/acc.cgi?acc=GSE5298
Status:	Public on Jul 14 2006
Title:	Development of heart valves requires Gata4 expression in endothelial-derived cells
Organism:	Mus musculus
Experiment type:	Expression profiling by array
Platform:	GPL1261
Pubmed ID:	16914500

Summary & Design:

Summary:
Cardiac malformations due to aberrant development of the atrioventricular (AV) valves are among the most common forms of congenital heart disease. At localized swellings of extracellular matrix known as the endocardial cushions, the endothelial lining of the heart undergoes an epithelial to mesenchymal transition (EMT) to form mesenchymal progenitors of the AV valves. Further growth and differentiation of these mesenchymal precursors results in formation of portions of the atrial and ventricular septae, and generation of thin, pliable valves. The transcription factor Gata4 is expressed in the endothelium and mesenchyme of the AV valves. Using a Tie2-Cre transgene, we selectively inactivated Gata4 within endothelial-derived cells. Mutant endothelium failed to undergo EMT, resulting in hypocellular cushions. Mutant cushions had decreased levels of Erbb3, an EGF-family receptor essential for EMT in the atrioventricular cushions. In Gata4 mutant embryos, Erbb3 downregulation was associated with impaired activation of Erk, which is also required for EMT. Expression of a Gata4 mutant protein defective in interaction with Friend of Gata (FOG) cofactors rescued the EMT defect, but resulted in decreased proliferation of mesenchyme and hypoplastic cushions that failed to septate the ventricular inlet. We demonstrate two novel functions of Gata4 in development of the AV valves. First, Gata4 functions as an upstream regulator of an Erbb3-Erk pathway necessary for EMT, and second, Gata4 acts to promote cushion mesenchyme growth and remodeling.

Keywords: genetic modification

Overall design:
For RNA analysis, four mutant and four control RNA samples were prepared (Pico-Pure RNA Isolation Kit, Arcturus), each consisting of 10 microdissected AVCs. Probe was prepared from 50 ng total RNA using an isothermal amplification protocol (NuGen), and hybridized to Affymetrix Mouse 430 2.0 microarrays. Two control samples were excluded because of excessive noise.

Background corr dist: KL-Divergence = 0.0176, L1-Distance = 0.0303, L2-Distance = 0.0014, Normal std = 0.7687

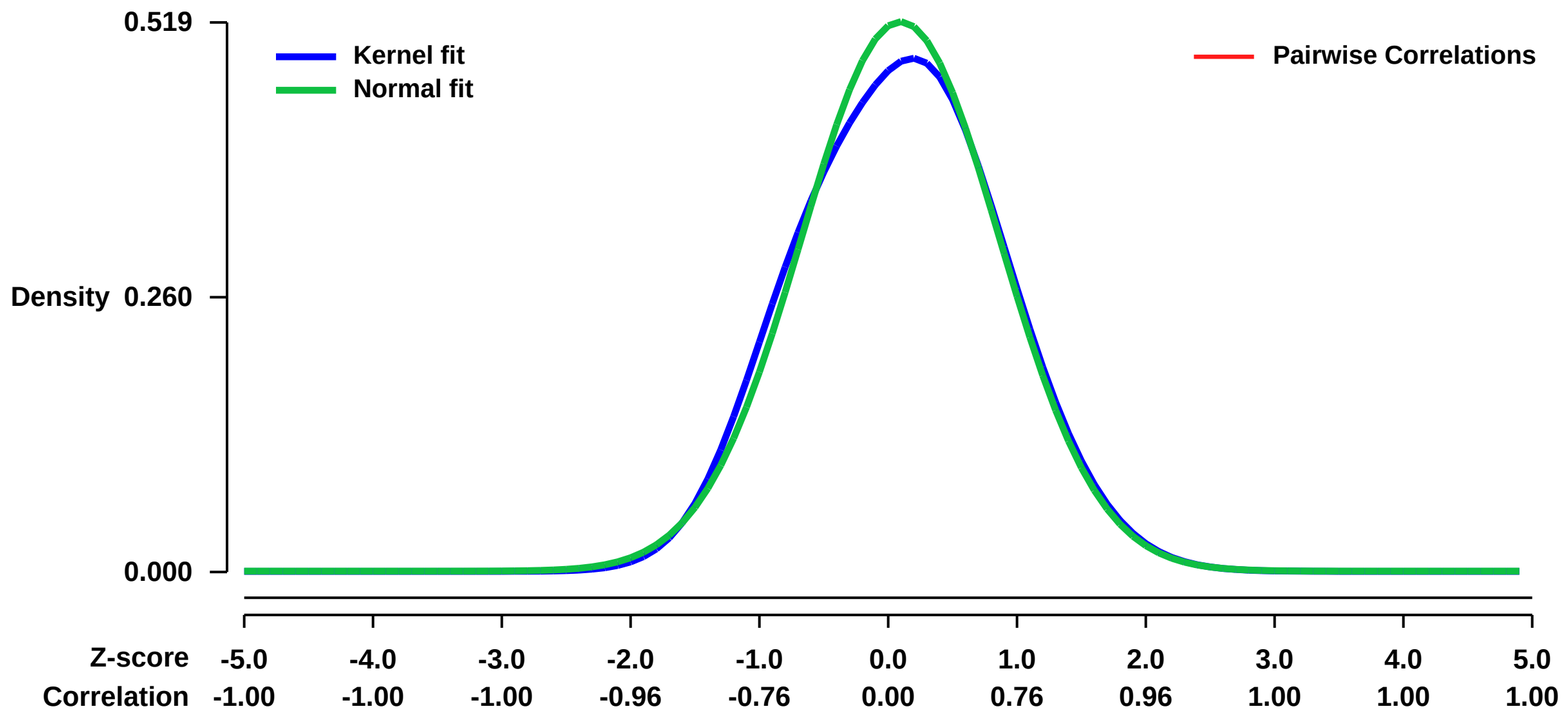

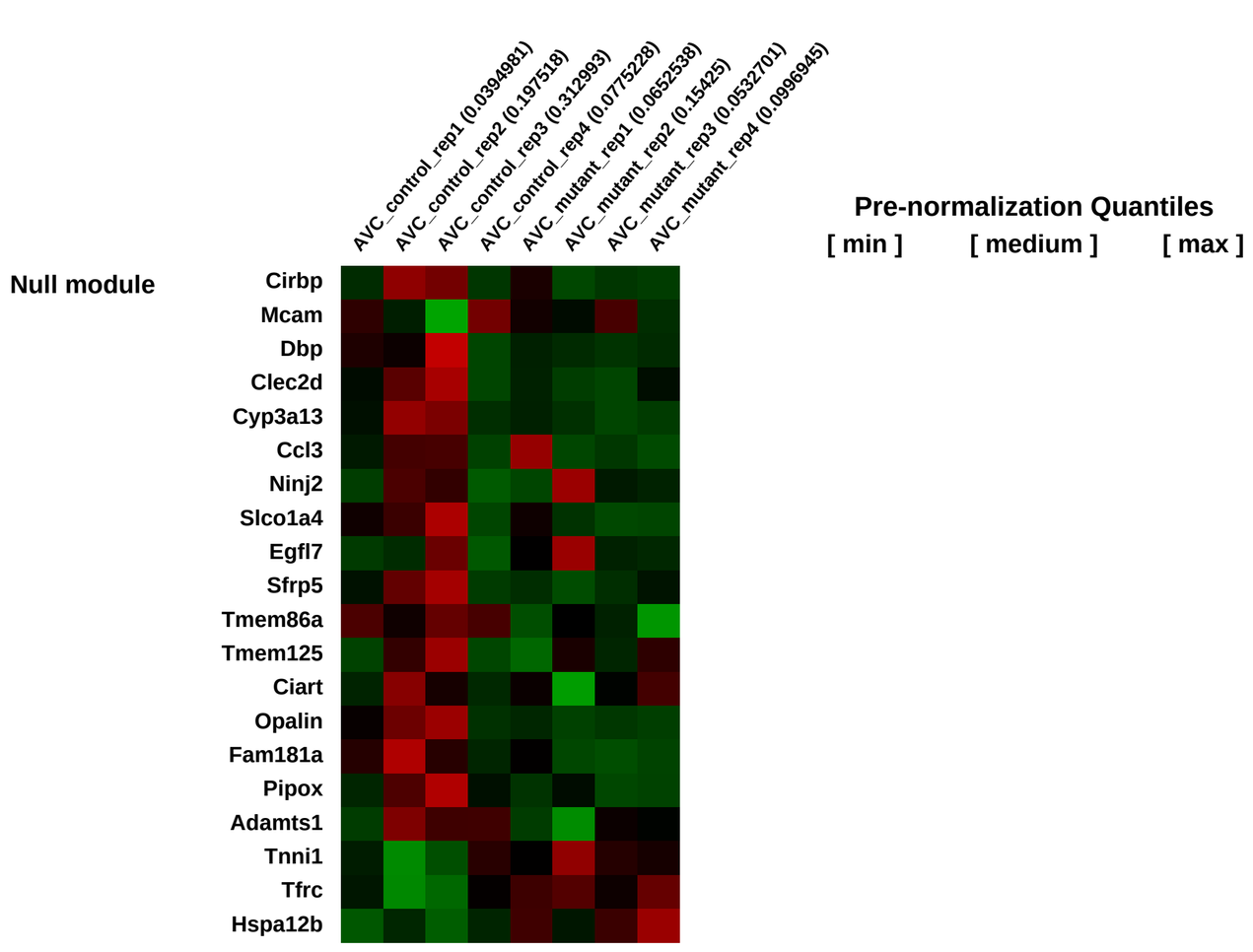

GEO Series "GSE5309" Expression Profiles

Num of samples in this series: 7

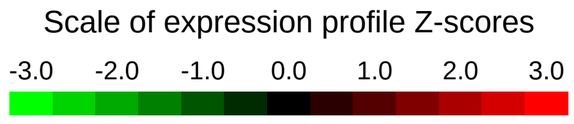

GEO Link:	http://www.ncbi.nlm.nih.gov/geo/query/acc.cgi?acc=GSE5309
Status:	Public on Jul 15 2006
Title:	Transcriptional Profiling of Mammary Gland Side Population Cells
Organism:	Mus musculus
Experiment type:	Expression profiling by array
Platform:	GPL1261
Pubmed ID:	16282442

Summary & Design:

Summary:
Similar to the bone marrow, the mammary gland contains a distinct population of Hoechst-effluxing side population cells, MG-SPs. To better characterize MG-SPs, their microarray gene profiles were compared to the remaining cells, which retain Hoechst dye (MG-NSPs). For analysis, gene ontology (GO) that describes genes in terms of biological processes and ontology traverser (OT) that performs enrichment analysis were utilized. OT showed that MG-SP specific genes were enriched in the GO categories of cell cycle regulation and checkpoints, multi-drug resistant transporters, organogenesis, and vasculogenesis. The MG-NSP upregulated genes were enriched in the GO category of cellular organization and biogenesis which includes basal epithelial markers, p63, smooth muscle actin (SMA), myosin, alpha-6 integrin, cytokeratin (CK) 14, as well as luminal markers, CK8 and CD24. Additional studies showed that a higher percentage of MG-SPs exist in the G1 phase of the cell cycle compared to the MG-NSPs. G1 cell cycle block of MG-SPs may be explained by higher expression of cell cycle negative regulatory genes such as TGF-beta2 (transforming growth factor-beta2), IGFBP-5 (insulin like growth factor binding protein-5), P18 INK4C and Wnt-5a (wingless-5a). Accordingly, a smaller percentage of MG-SPs expressed nuclear b-catenin, possibly as a consequence of the higher expression of Wnt-5a. In conclusion, microarray gene profiling suggests that MG-SPs are a lineage deficient mammary gland sub-population expressing key genes involved in cell cycle regulation, development and angiogenesis.

Supplemental File Descriptions:

Table 1 is a list of 1632 Genes differentially expressed by MG-SP and MG-NSP; Criteria for comparison included 1.2-fold difference in expression levels, false discovery rate (FDR) 9.4%, P value less than 0.05.

Table 2 is a list of 771 Genes differentially expressed by MG-SP and MG-NSP; Criteria for comparison included 1.5-fold difference in expression levels, FDR 3.4%, P value less than 0.05.

Table 3 is a list of 335 Genes differentially expressed by MG-SP and MG-NSP; Criteria for comparison included 2-fold difference in expression levels, FDR 0%, P value less than 0.05.

Table 4 is a list of 90 Genes differentially expressed by MG-SP and MG-NSP; Criteria for comparison included 2-fold difference in expression levels, FDR 0%, P value less than 0.01.

Keywords: Normal C57BL/6 Mammary Gland Epithelial Cells

Overall design:
Gene expression profiles were obtained by hybridizing amplified RNA from four replicate MG-SP and MG-NSP samples to Affymetrix 430 2.0 microarray chips. To isolate MG-SP and MG-NSPs, mammary gland cells were stained using the Hoechst dye 33342 and fluorescence displayed at two wavelength emissions, blue and red. The MG-SP and MG-NSP regions were indicated by trapezoids on the left (R1) and right (R2), respectively. We and others have previously shown that the R1 region is composed of side population cells since verapamil blocks their appearance. The cells in each region (R1 and R2) were sorted, their RNA isolated and amplified by two rounds of in vitro amplification and applied to Affymetrix chips. Hybridization, scanning, and production of raw data files were performed according to the Affymetrix standard protocols. Normalization and model-based expression measurements were performed with dChip. Two of the chips were eliminated from further analysis due to the high percentage of probe sets called an array outlier after model based expression analysis by dChip (Not included). The genes were filtered to eliminate those with very low expression values in most samples. From 45,000 probe sets, 16,744 probe sets were retained and used for further analysis. For normalization purposes and to allow for data comparison with other centers, universal mouse reference RNA (Stratagene) was hybridized to two chips. All other arrays were normalized to one of the universal mouse reference RNA arrays expressing average intensity closest to the median intensity of all chips (Stratagene Ref 2).

Background corr dist: KL-Divergence = 0.0531, L1-Distance = 0.0342, L2-Distance = 0.0017, Normal std = 0.5752

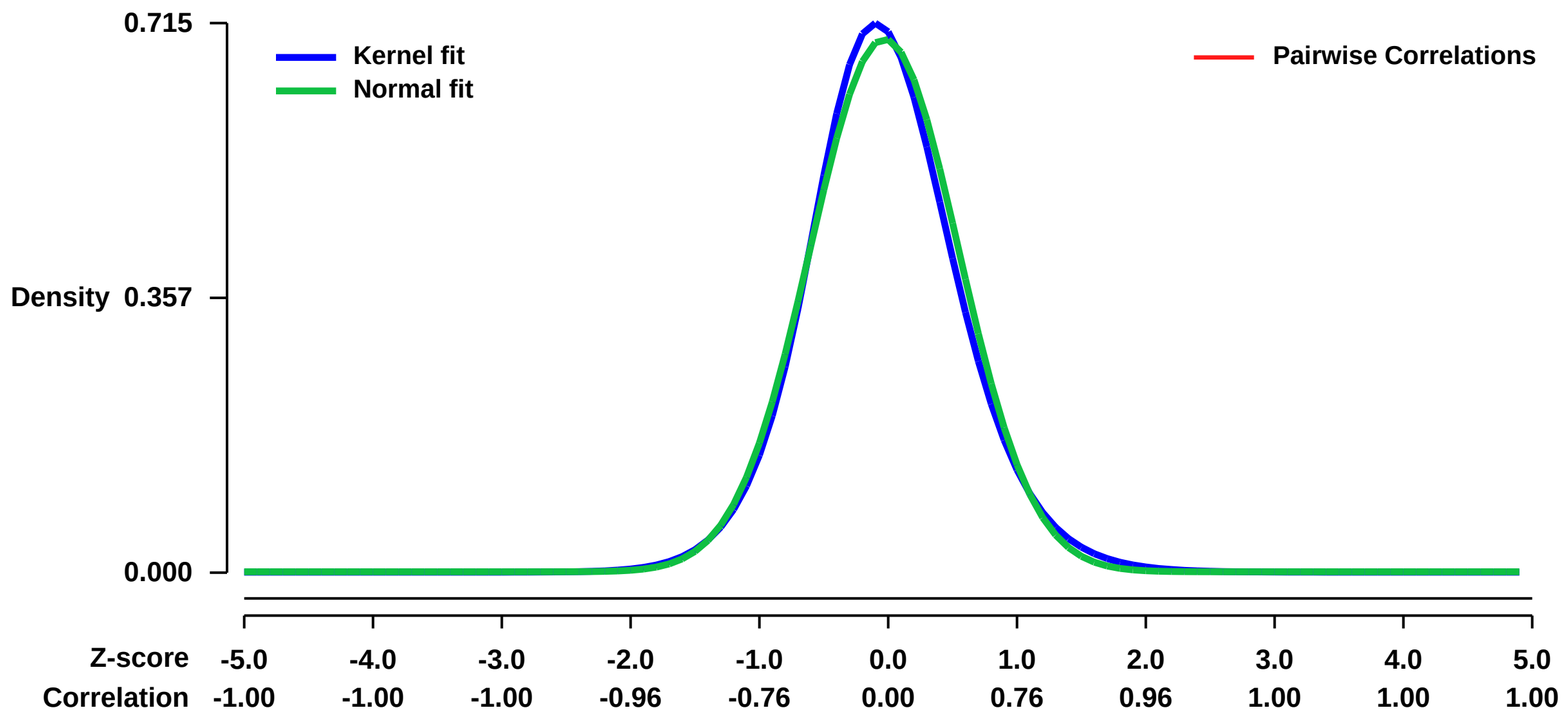

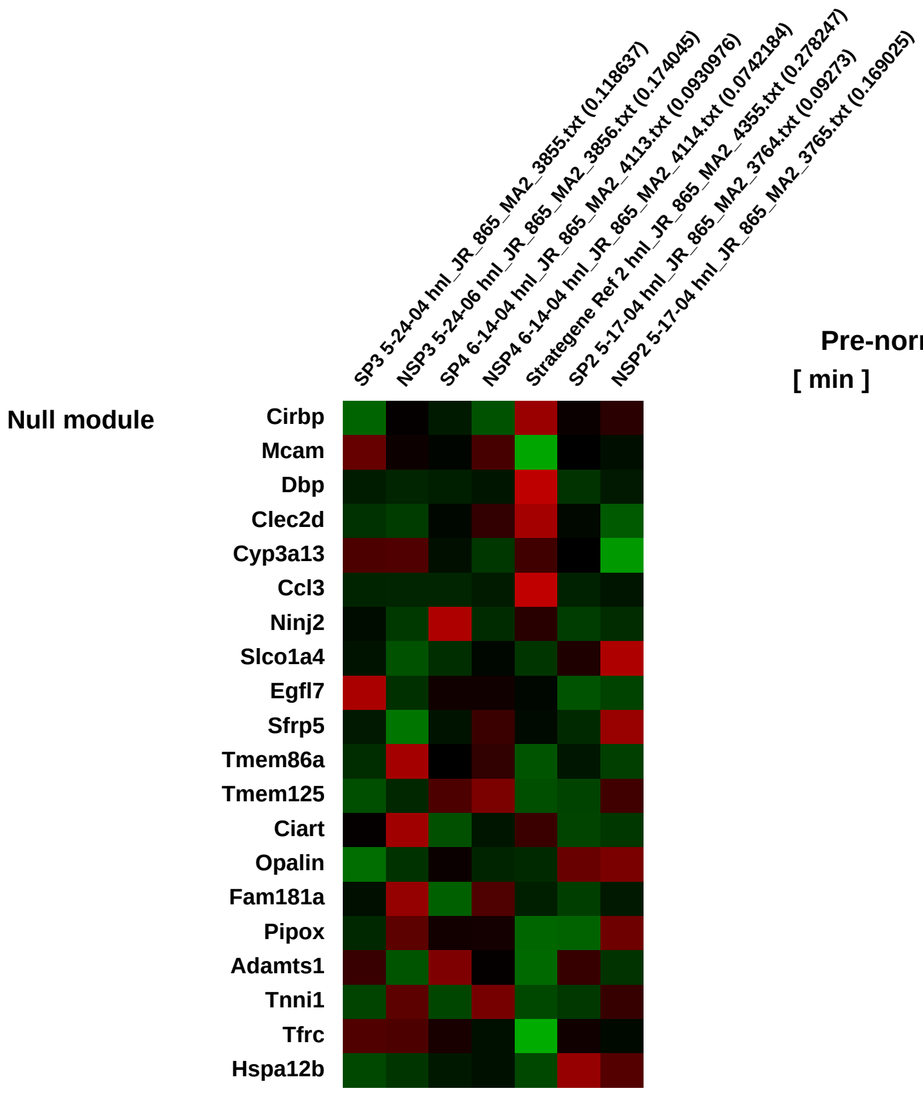

GEO Series "GSE5313" Expression Profiles

Num of samples in this series: 6

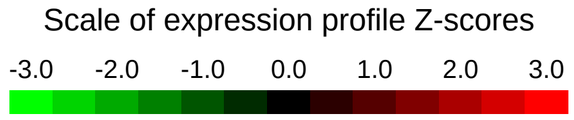

GEO Link:	http://www.ncbi.nlm.nih.gov/geo/query/acc.cgi?acc=GSE5313
Status:	Public on Dec 02 2006
Title:	Comparative analysis of gene expression in A/J CB versus DBA/2J
Organism:	Mus musculus
Experiment type:	Expression profiling by array
Platform:	GPL1261
Pubmed ID:	17098806
Summary & Design:	**Summary:** We hypothesize that gene expression in the CBs of these two strains of mice are divergent thus contributing to the disparity in the phenotypes. More specifically, (1) genes related to CB function are expressed less in the A/J mice compared to DBA/2J mice; (2) gene expression levels of morphogenic and trophic factors of the CB maybe significantly lower in the A/J mice than the DBA/2J mice. In order to test these hypotheses, we utilized microarray analysis to examine transcriptional differences between CBs of both strains of mice. **Keywords: comparative expression profiling** **Overall design:** . This study utilizes microarray analysis to test these hypotheses. Three sets of CBs were harvested from both strains. RNA was isolated and used for global gene expression profiling (Affymetrix Mouse 430 2.0 array). Statistically significant gene expression was determined as a minimum 6 counts of 9 pairwise comparisons, minimum 1.5-fold change, and p < 0.05.

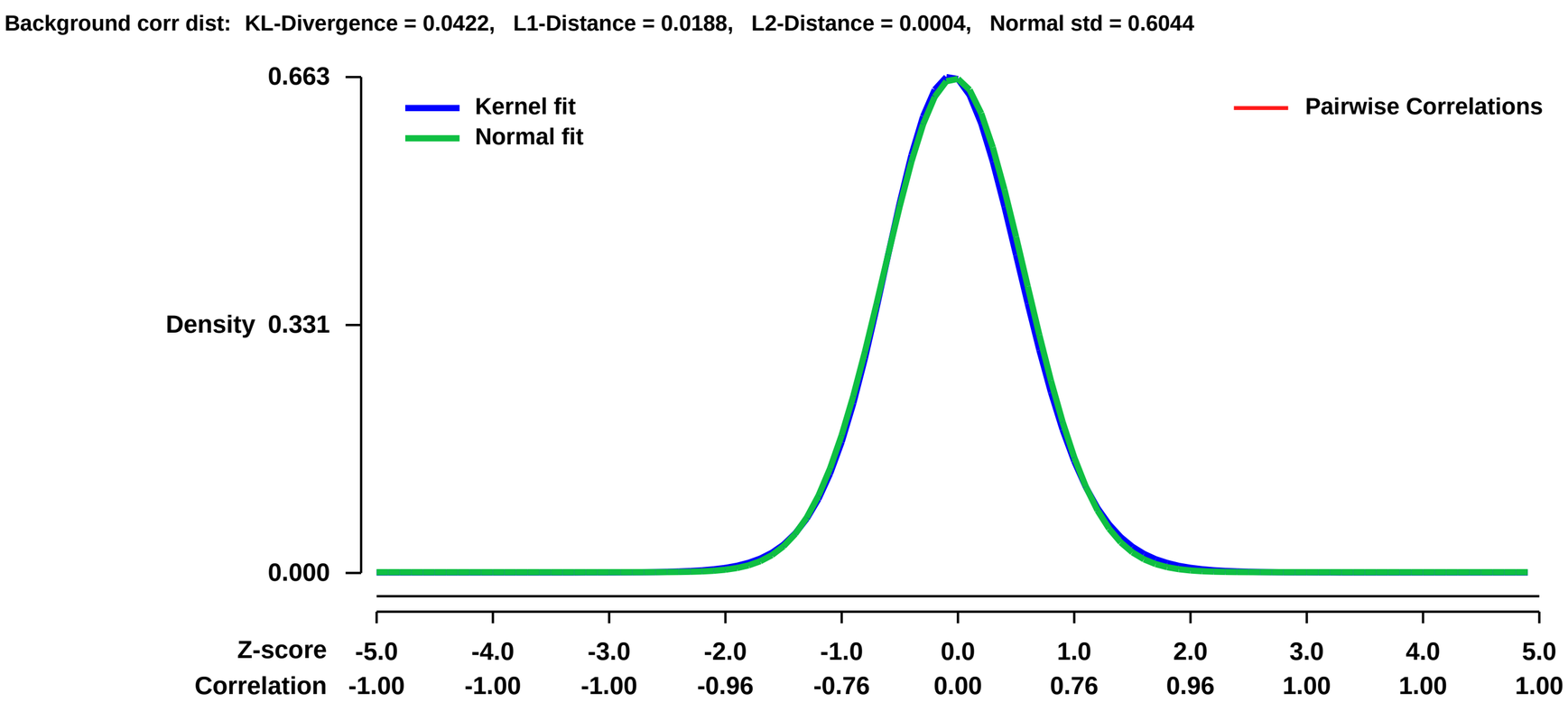

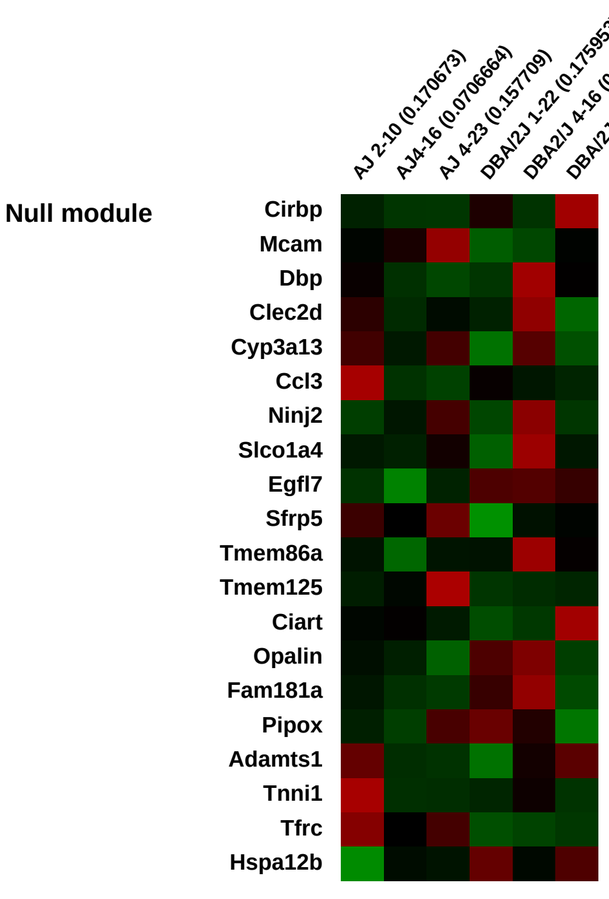

GEO Series "GSE53131" Expression Profiles

Num of samples in this series: 15

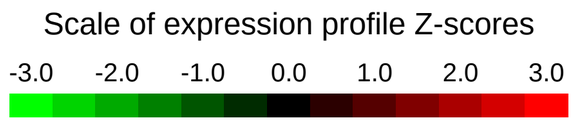

GEO Link:	**http://www.ncbi.nlm.nih.gov/geo/query/acc.cgi?acc=GSE53131**
Status:	**Public on Dec 10 2013**
Title:	**Expression data from livers of C57BL/6J mice fed a high-fat diet and coffee**
Organism:	**Mus musculus**
Experiment type:	**Expression profiling by array**
Platform:	**GPL1261**
Pubmed ID:	
Summary & Design:	**Summary:** **The present study was conducted to evaluate the effects of the intake of three types of coffee (caffeinated, decaffeinated, and green unroasted coffee) on the livers of C57BL/6J mice fed a high-fat diet, and to extensively elucidate the physiological responses to coffee intake by analysing the findings obtained from a comprehensive transcriptomic analysis using DNA microarrays.** **The present study was conducted to evaluate the effects of the intake of three types of coffee (caffeinated, decaffeinated, and green unroasted coffee) on the livers of C57BL/6J mice fed a high-fat diet, and to extensively elucidate the physiological responses to coffee intake by analysing the findings obtained from a comprehensive transcriptomic analysis using DNA microarrays.** **Overall design:** **Briefly, 7-week-old male C57BL/6J mice purchased from Charles River Laboratories Japan (Yokohama) were divided into the following five groups. The normal diet group (ND group) was fed D12450B (10 kcal% fat, Research Diets, New Brunswick, NJ, USA). The high-fat diet group (HF group) was fed D12492 (60 kcal% fat, Research Diets, New Brunswick, NJ, USA). The caffeinated coffee group (HFCC group) was fed a high-fat diet containing 2% caffeinated freeze-dried coffee. The decaffeinated coffee group (HFDC group) was fed a high-fat diet containing 2% decaffeinated freeze-dried coffee. The green unroasted coffee group (HFGC group) was fed a high-fat diet containing 2% unroasted caffeinated freeze-dried coffee. The mice had ad libitum access to their diets and drinking water. After 9 weeks, mice were sacrificed and the livers were subjected to the Affymrtix DNA microarray experiment.**

Background corr dist: KL-Divergence = 0.1748, L1-Distance = 0.0409, L2-Distance = 0.0034, Normal std = 0.3502

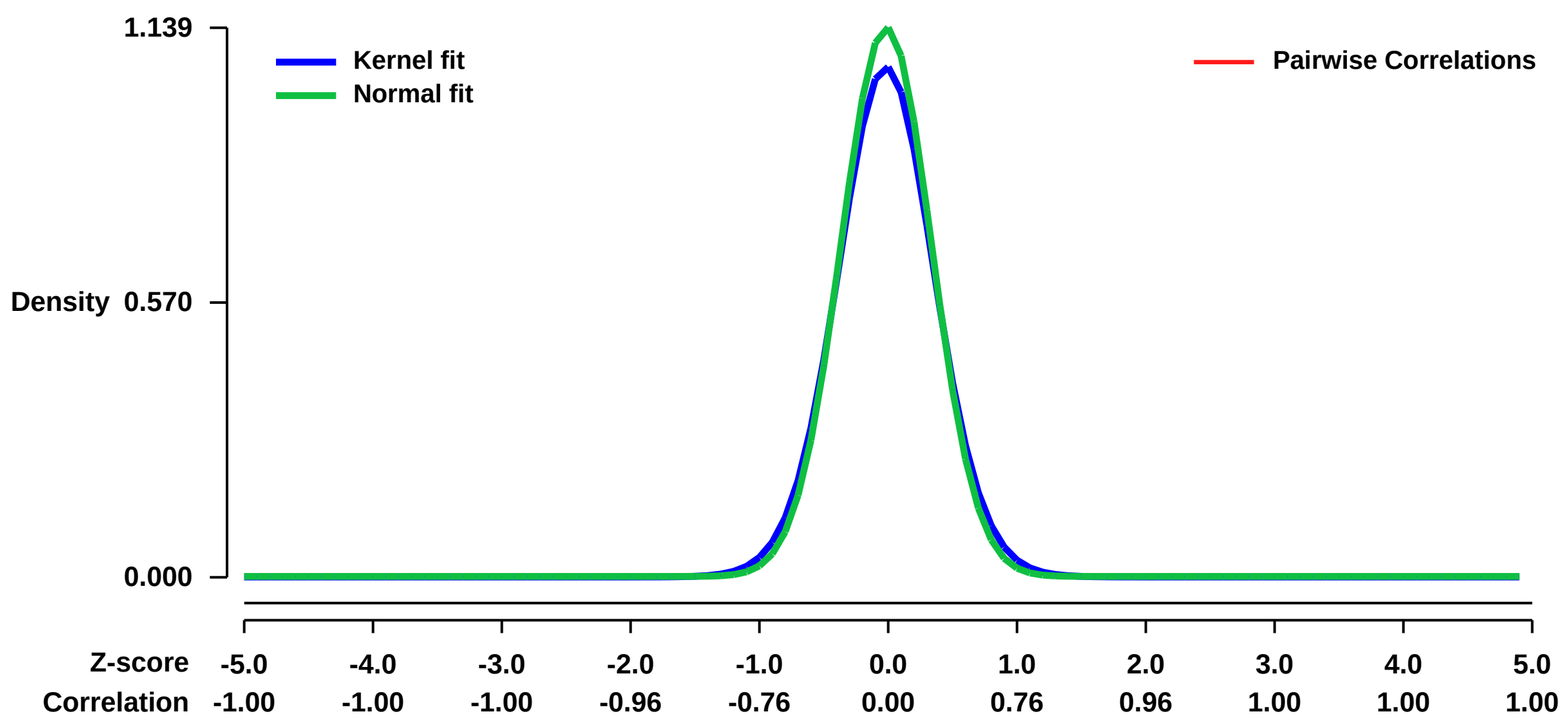

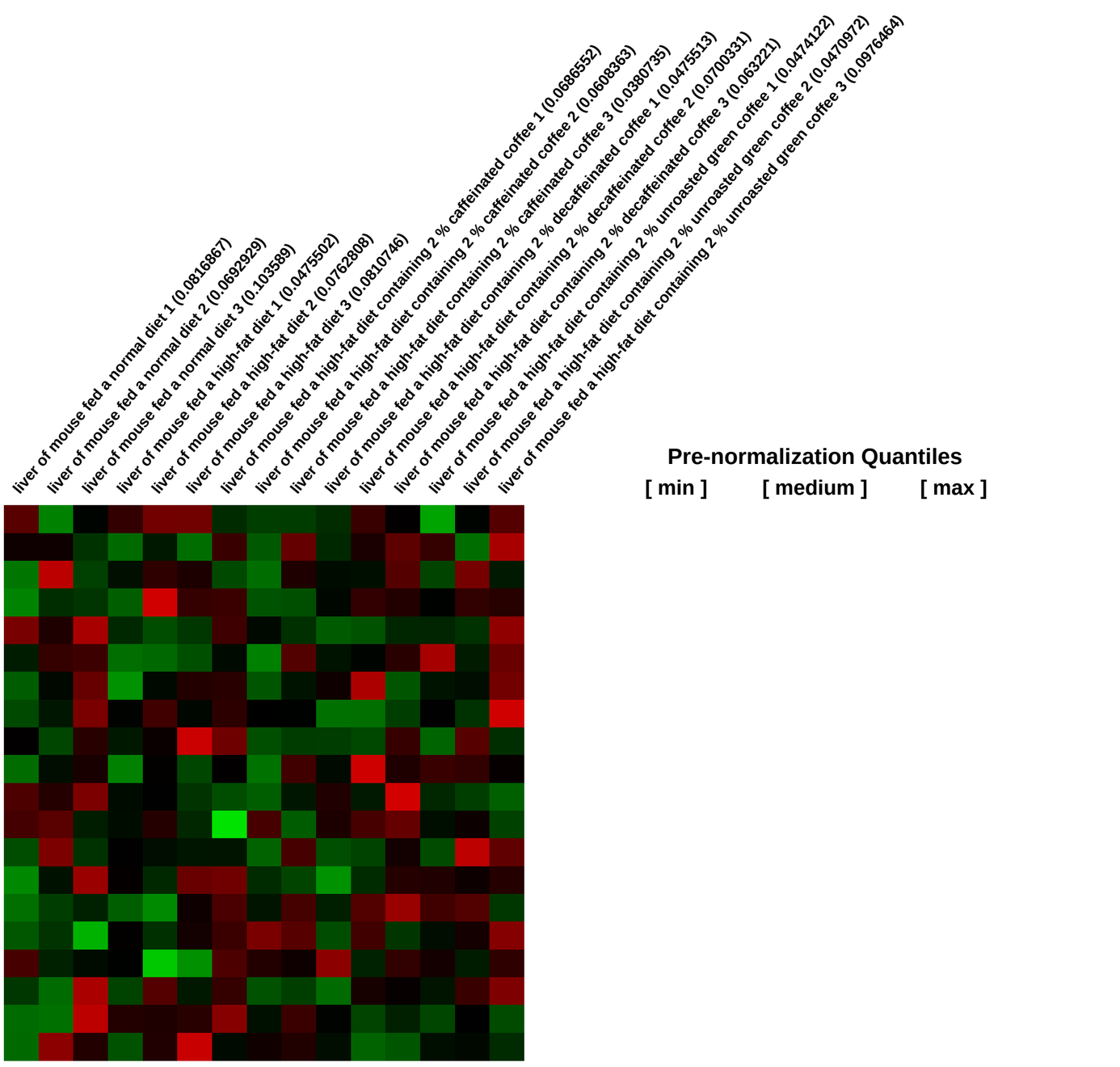

GEO Series "GSE5324" Expression Profiles

Num of samples in this series: 48

Scale of expression profile Z-scores

-3.0 -2.0 -1.0 0.0 1.0 2.0 3.0

GEO Link:	http://www.ncbi.nlm.nih.gov/geo/query/acc.cgi?acc=GSE5324
Status:	Public on Oct 17 2006
Title:	TTP mRNA targets identified by global analysis of stabilized transcripts in TTP-deficient fibroblasts
Organism:	Mus musculus
Experiment type:	Expression profiling by array
Platform:	GPL1261
Pubmed ID:	17030620
Summary & Design:	**Summary:** Tristetraprolin (TTP) is a tandem CCCH zinc finger protein that was identified through its rapid induction by mitogens in fibroblasts. Studies of TTP-deficient mice, and cells derived from them, showed that TTP could bind to certain AU-rich elements in mRNAs, leading to increases in the rates of mRNA deadenylation and destruction. Known physiological target mRNAs for TTP include tumor necrosis factor alpha (TNF), granulocyte macrophage colony stimulating factor (GM-CSF) and interleukin 2 beta (IL2 beta). Here we used microarray analysis of RNA from wild-type and TTP-deficient fibroblast cell lines to identify transcripts with different decay rates, after serum stimulation and actinomycin D treatment. Of 250 mRNAs apparently stabilized in the absence of TTP, 23 contained conserved TTP binding sites; 10 of these were shown by secondary analyses to be stabilized. The most dramatically affected transcript encoded the protein Ier3, recently implicated in the physiological control of blood pressure. The Ier3 transcript contained several conserved TTP binding sites that could bind TTP directly, and conferred TTP sensitivity to the mRNA in cell transfection studies. These studies have identified several new, physiologically relevant TTP target transcripts in fibroblasts; these target mRNAs encode proteins from a variety of functional classes. **Keywords:** mRNA degradation, time course, knockout experiment **Overall design:** 90 min and another sample taken, after which 5 …g/ml actinomycin D was added; samples for RNA analysis were then removed at 30, 60, 90 and 120 min after actinomycin D treatment. In all experiments, each sample represented three combined 100 mm dishes of cells.

Background corr dist: KL-Divergence = 0.1605, L1-Distance = 0.0418, L2-Distance = 0.0041, Normal std = 0.3654

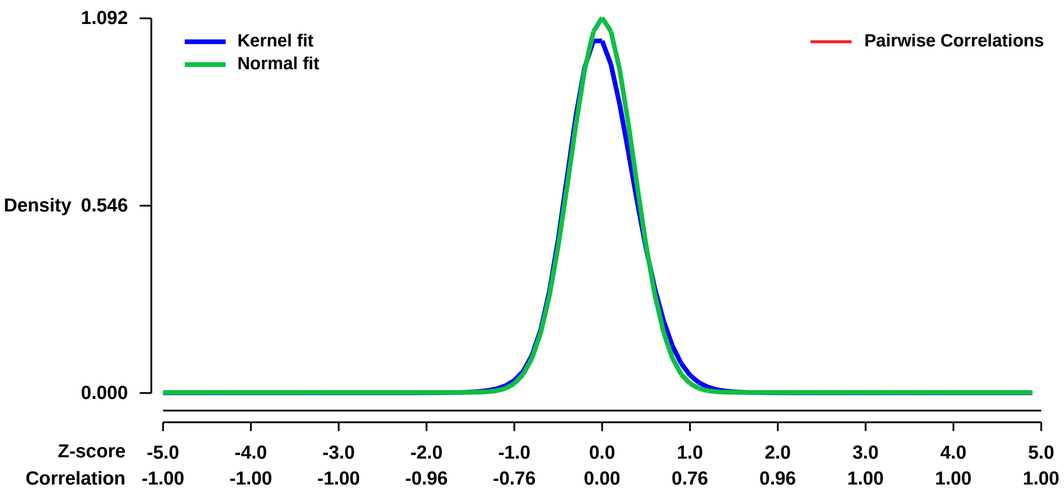

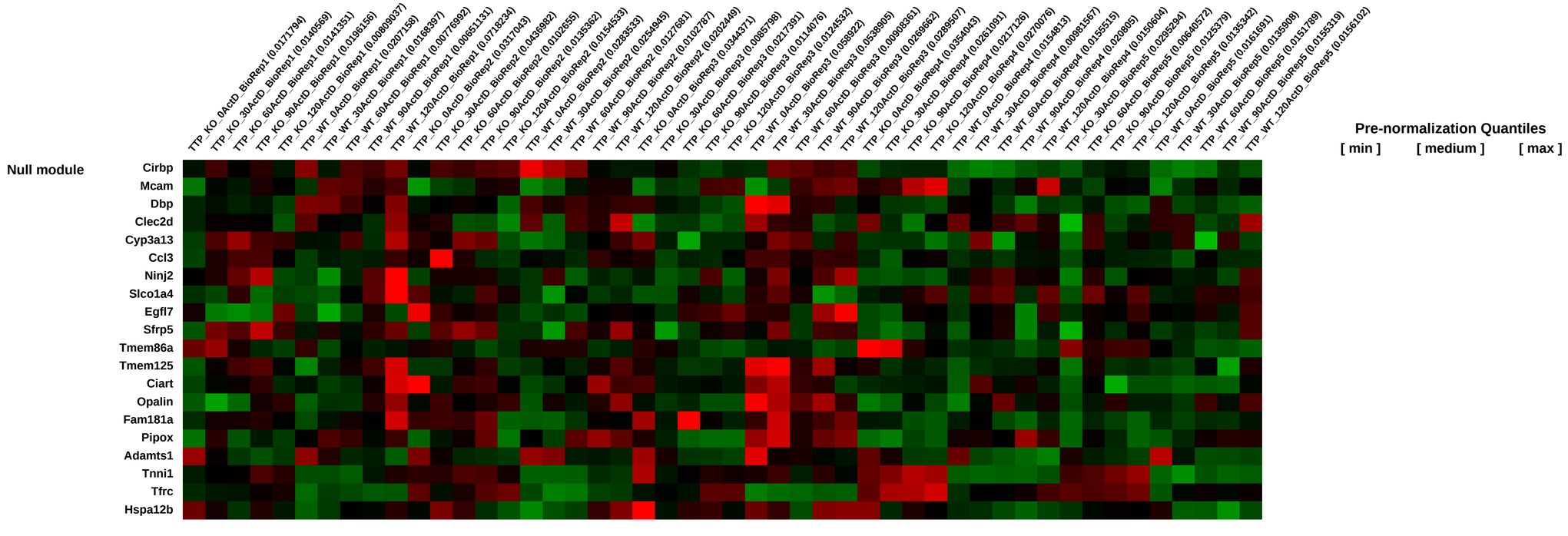

GEO Series "GSE5332" Expression Profiles

Num of samples in this series: 12

Scale of expression profile Z-scores

-3.0 -2.0 -1.0 0.0 1.0 2.0 3.0

GEO Link:	http://www.ncbi.nlm.nih.gov/geo/query/acc.cgi?acc=GSE5332
Status:	Public on Dec 01 2007
Title:	mTOR pathway controls mitochondrial gene expression and respiration through the YY1/PGC-1alpha transcriptional complex
Organism:	Mus musculus
Experiment type:	Expression profiling by array
Platform:	GPL1261
Pubmed ID:	18046414
Summary & Design:	**Summary:** Mitochondrial oxidative function is tightly controlled to maintain energy homeostasis in response to nutrient and hormonal signals. An important cellular component in the energy sensing response is the target of rapamycin (TOR) kinase pathway; however whether and how mTOR controls mitochondrial oxidative activity is unknown. Here, we show that mTOR kinase activity stimulates mitochondrial gene expression and oxidative function. In skeletal muscle cells and TSC2-/- MEFs, the mTOR inhibitor rapamycin largely decreased gene expression of mitochondrial transcriptional regulators such as PGC-1alpha and the transcription factors ERRalpha and NRFs. As a consequence, mitochondrial gene expression and oxygen consumption were reduced upon mTOR inhibition. Using computational genomics, we identified the transcription factor YY1 as a common target of mTOR and PGC-1alpha that controls mitochondrial gene expression. Inhibition of mTOR resulted in a failure of YY1 to interact and be coactivated by PGC-1alpha. Notably, knock-down of YY1 in skeletal muscle cells caused a significant decrease in mRNAs of mitochondrial regulators and mitochondrial genes that resulted in a decrease in respiration. Moreover, YY1 was required for rapamycin-dependent repression of mitochondrial genes. Thus, we have identified a novel mechanism in which a nutrient sensor (mTOR) balances energy metabolism via transcriptional control of mitochondrial oxidative function. These results have important implications for our understanding of how these pathways might be altered in metabolic diseases and cancer. **Keywords:** comparative genomics, drug treatment response **Overall design:** Data were analyzed by RMA (with default settings) in BioConductor 1.2 -- one batch for the Rapamycin vs. Vehicle, and another batch for the PGC vs GFP.

Background corr dist: KL-Divergence = 0.0285, L1-Distance = 0.0213, L2-Distance = 0.0006, Normal std = 0.6590

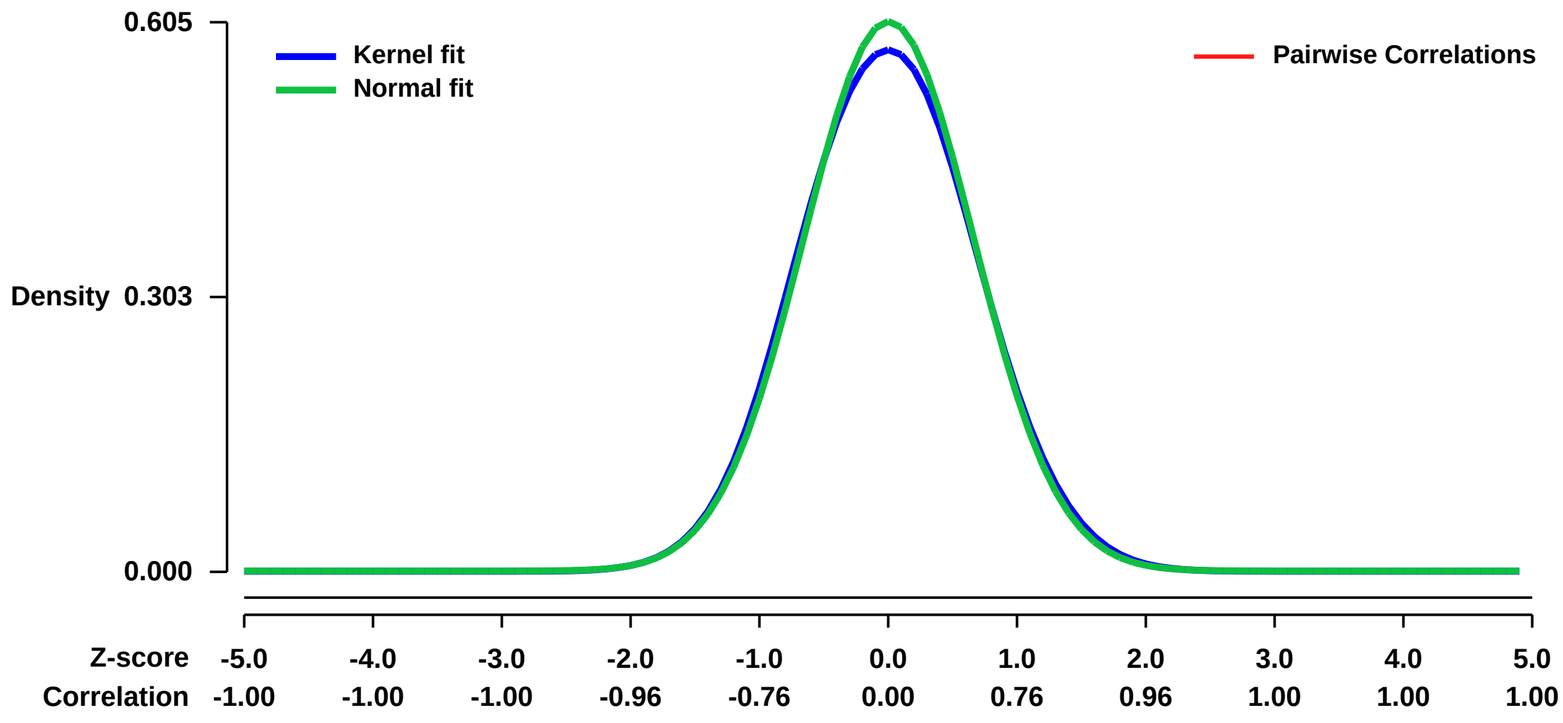

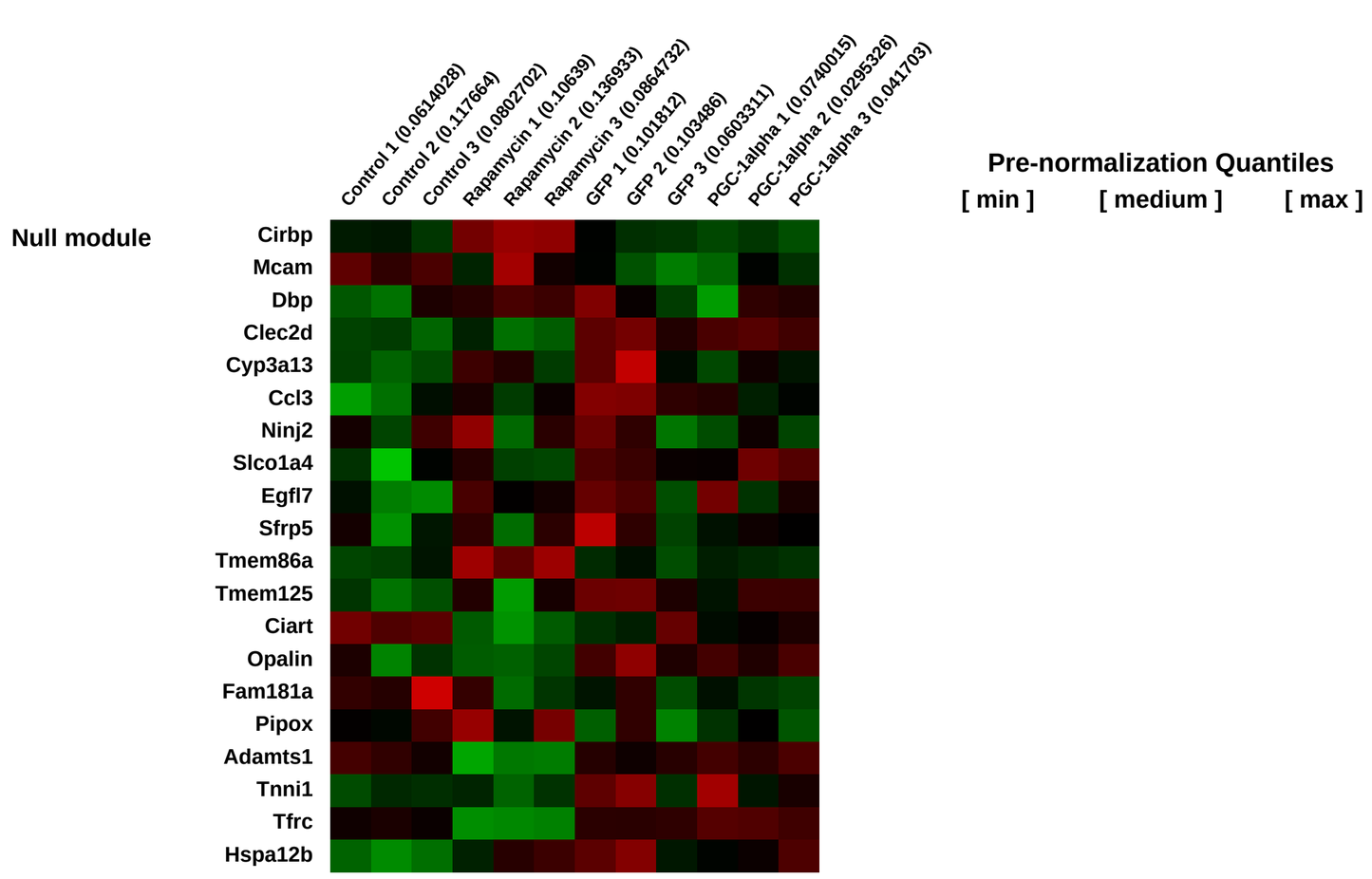

GEO Series "GSE5333" Expression Profiles

Num of samples in this series: 16

Scale of expression profile Z-scores

-3.0 -2.0 -1.0 0.0 1.0 2.0 3.0

GEO Link:	**http://www.ncbi.nlm.nih.gov/geo/query/acc.cgi?acc=GSE5333**
Status:	**Public on Jul 22 2006**
Title:	**Gene expression profiling of whole epididymis in embryonic (gestational day 12, 14, 16 & 18) and postnatal day 2 mice. (GUDMAP Series ID: 4)**
Organism:	**Mus musculus**
Experiment type:	**Expression profiling by array**
Platform:	**GPL1261**
Pubmed ID:	
Summary & Design:	**Summary:** **The overall objective of this proposal is to map the temporal and spatial dynamics of gene expression in the fetal mouse testis at key developmental timepoints. Urogenital tract malformations are the most common birth defects in males and their incidence together with other male reproductive health concerns such as reduced fertility and testicular cancer are reportedly on the rise in the human population. To better understand the impact of genetic factors and environmental influences on testicular development, it is important to first understand normal gene expression patterns and signaling cascades within the fetal testis during development. The goal of this study is to identify cell-specific genes that can be used as biomarkers for key differentiation events.** **Keywords: developmental time course** **Overall design:** **Day to day comparison in whole epididymus throughout development with triplicates at each time point. Each sample is a pair of epididymus from a single animal and each animal is taken from a different dam.**

Background corr dist: **KL-Divergence = 0.1487, L1-Distance = 0.0469, L2-Distance = 0.0047, Normal std = 0.4166**

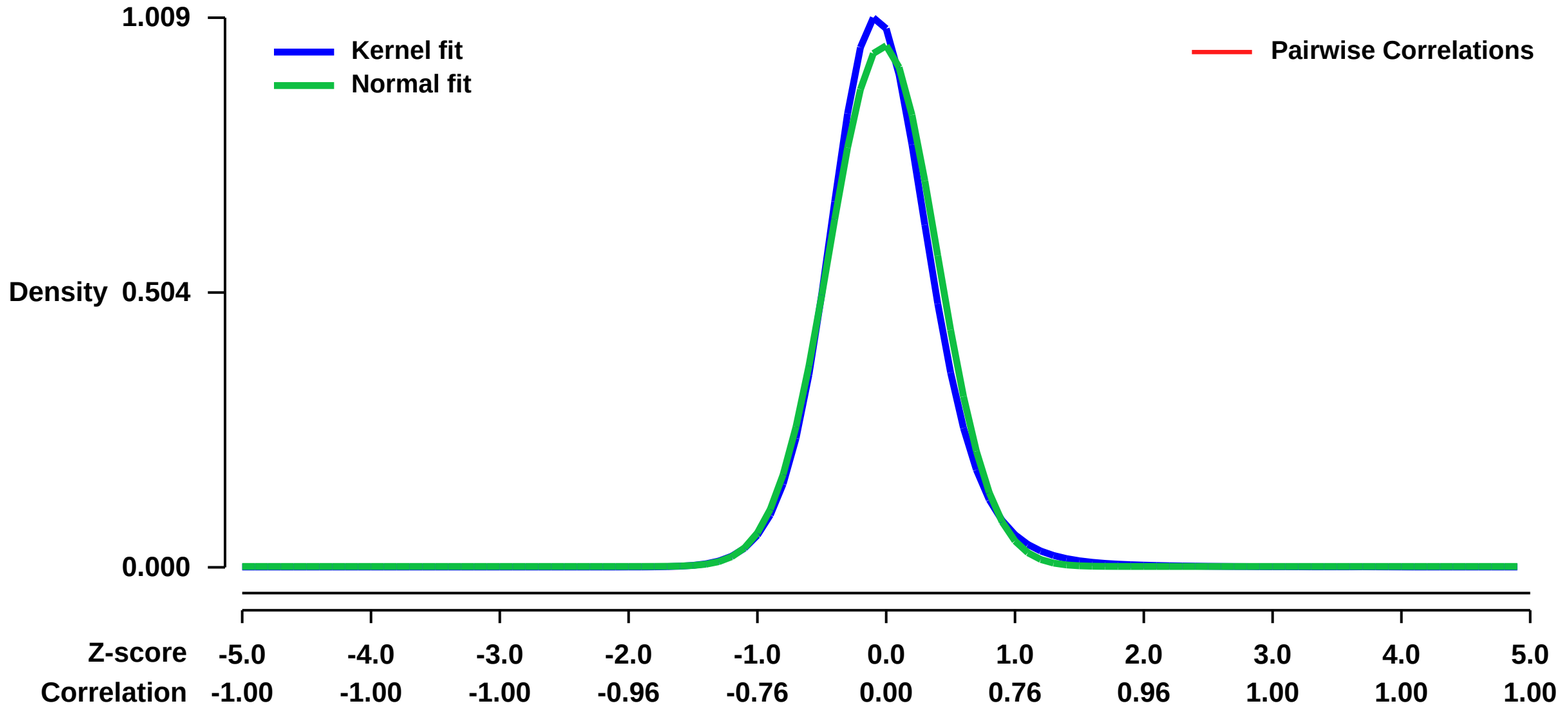

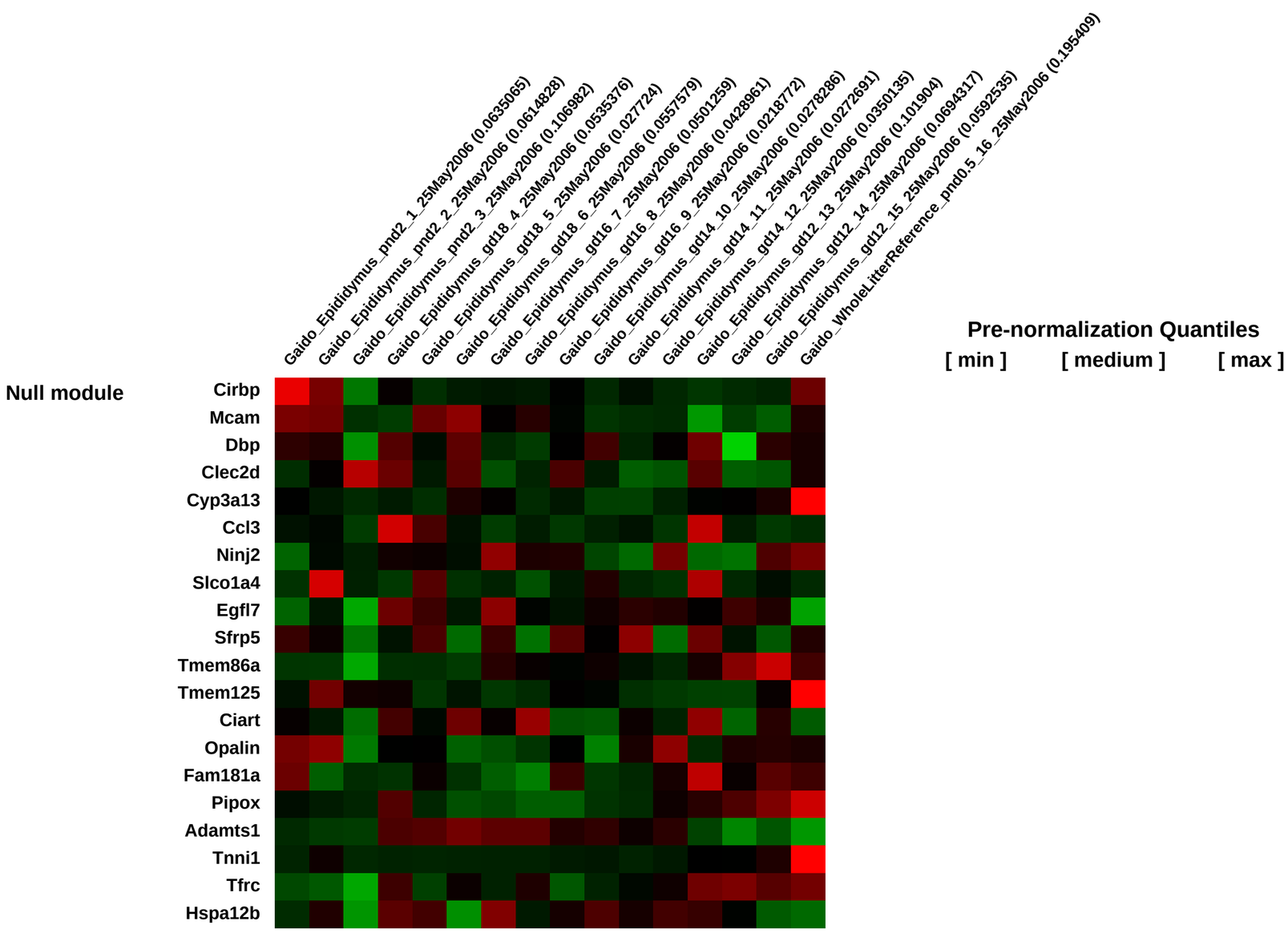

GEO Series "GSE5334" Expression Profiles

Num of samples in this series: 19

Scale of expression profile Z-scores

-3.0 -2.0 -1.0 0.0 1.0 2.0 3.0

GEO Link:	**http://www.ncbi.nlm.nih.gov/geo/query/acc.cgi?acc=GSE5334**
Status:	**Public on Jul 22 2006**
Title:	**Gene expression profiling of whole ovary in embryonic (gestional day 11, 12, 14, 16 & 18) and postnatal day 2 mice. (GUDMAP Series ID: 5)**
Organism:	**Mus musculus**
Experiment type:	**Expression profiling by array**
Platform:	**GPL1261**
Pubmed ID:	
Summary & Design:	**Summary:** **The overall objective of this proposal is to map the temporal and spatial dynamics of gene expression in the fetal mouse testis at key developmental timepoints. Urogenital tract malformations are the most common birth defects in males and their incidence together with other male reproductive health concerns such as reduced fertility and testicular cancer are reportedly on the rise in the human population. To better understand the impact of genetic factors and environmental influences on testicular development, it is important to first understand normal gene expression patterns and signaling cascades within the fetal testis during development. The goal of this study is to identify cell-specific genes that can be used as biomarkers for key differentiation events.** **Keywords: developmental time course** **Overall design:** **Day to day comparison in whole ovary throughout development with triplicates at each time point. Each sample is a pair of ovaries from a single animal and each animal is taken from a different dam (with the exception of gd11 sample numbers 18 and 19 which come from the same dam).**

Background corr dist: **KL-Divergence = 0.1760, L1-Distance = 0.0465, L2-Distance = 0.0050, Normal std = 0.3897**

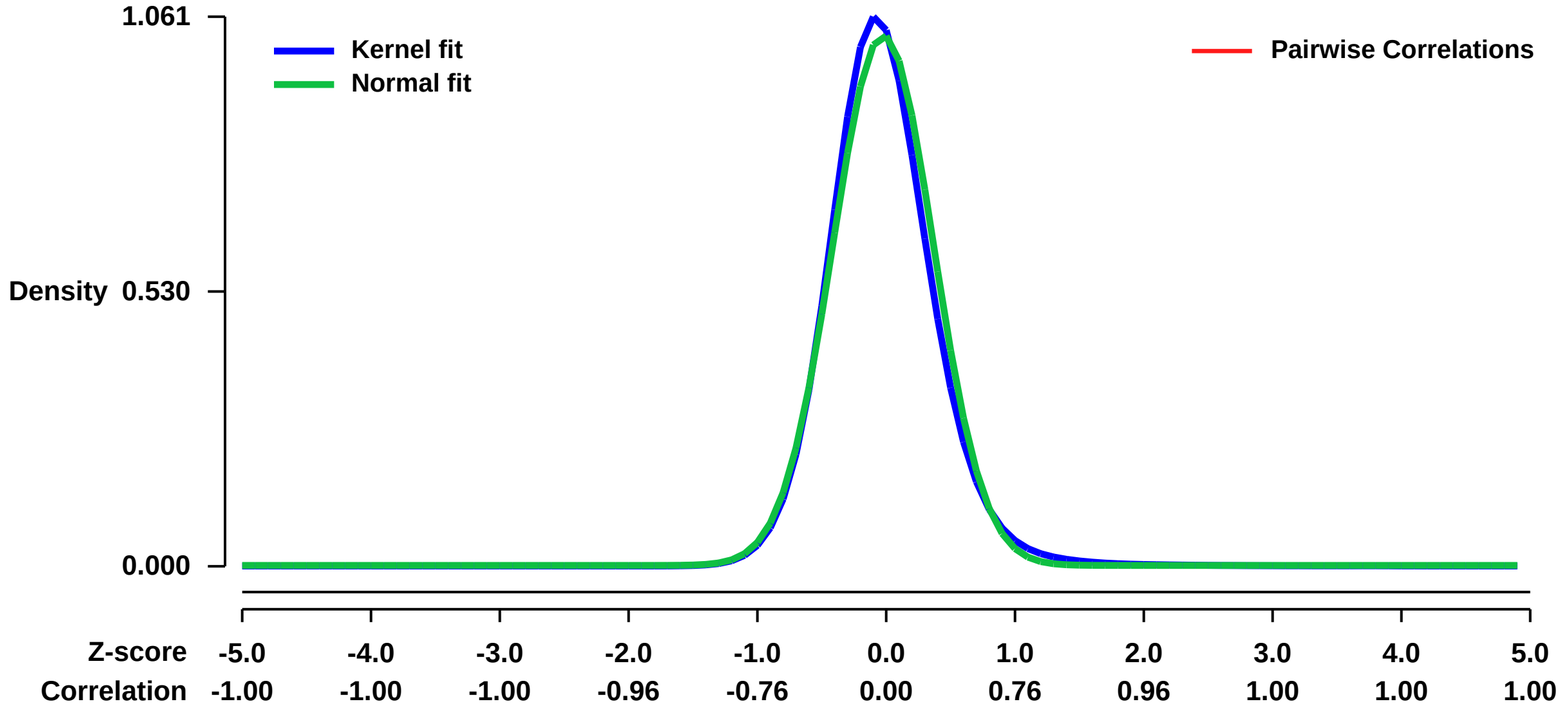

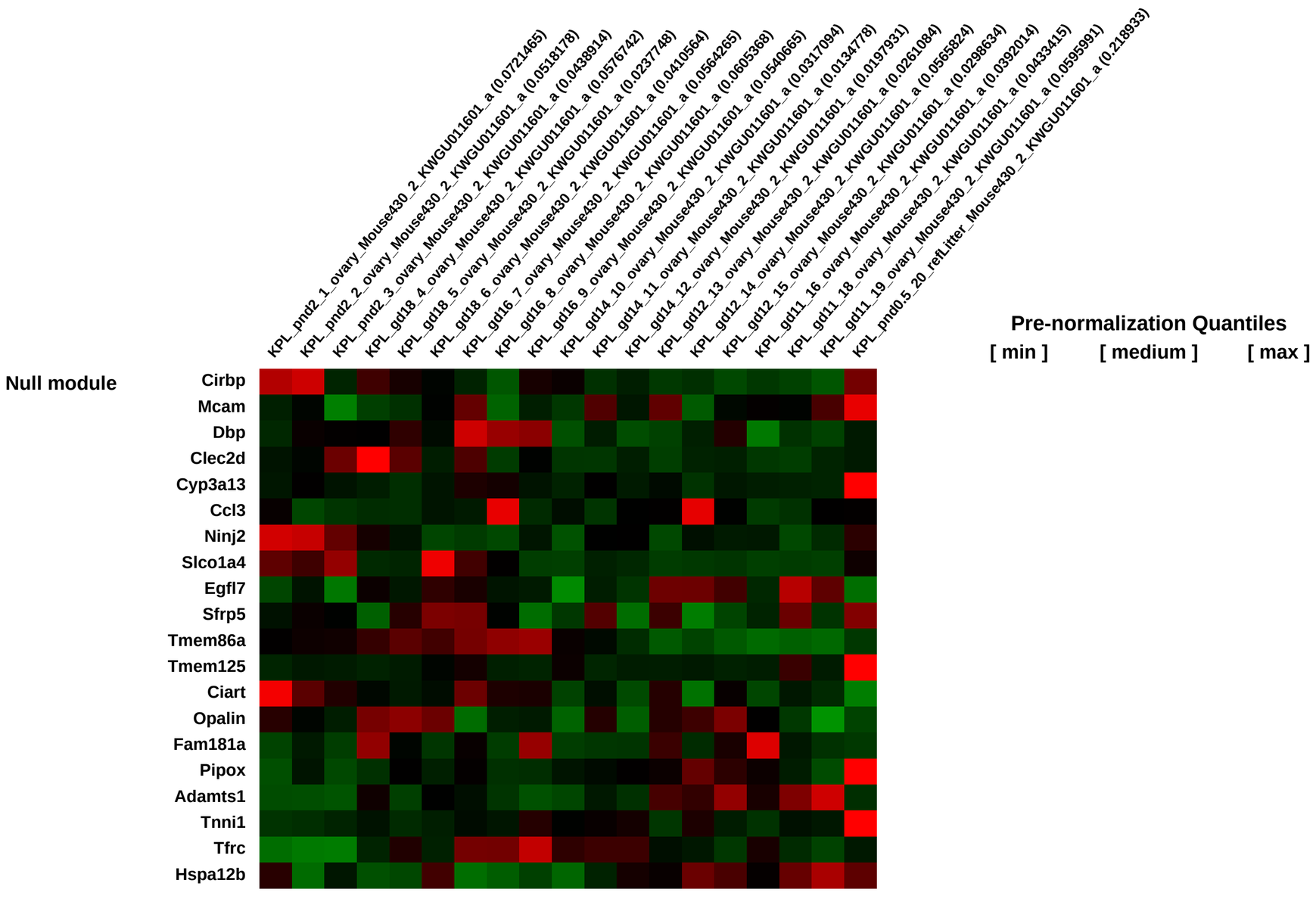

GEO Series "GSE53403" Expression Profiles

Num of samples in this series: 16

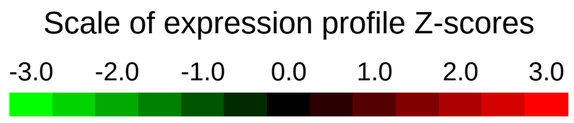

GEO Link:	http://www.ncbi.nlm.nih.gov/geo/query/acc.cgi?acc=GSE53403
Status:	Public on Dec 18 2013
Title:	Expression data from mouse adipose tissue macrophage
Organism:	Mus musculus
Experiment type:	Expression profiling by array
Platform:	GPL1261
Pubmed ID:	24315368
Summary & Design:	**Summary:** In mammals, expansion of adipose tissue mass induces accumulation of adipose tissue macrophages (ATMs). We isolated CD11c- (FB) and CD11c+ (FBC) perigonadal ATMs from SVCs of lean (C57BL/6J Lep +/+) and obese leptin-deficient (C57BL/6J Lep ob/ob) mice. We used expression microarrays to generate transcription profiles of perigonadal ATMs from lean (C57BL/6J Lep +/+) and obese (C57BL/6J Lep ob/ob) mice. Profiling purified FBs and FBCs, we identified 521 transcripts whose expression was differentially (nominal p-value < 0.01) expressed between FBs from lean and obese mice and 1509 genes whose expression was differentially (nominal p-value <0.01) expressed between FBC from lean and obese mice **Overall design:** RNA was isolated from sorted FBC (F4/80+, CD11b+, CD11c+) cells and FB (F4/80+, CD11b+, CD11c-) cells and using RNeasy micro-kits (Qiagen), using a PicoPure RNA isolation kit then amplified two-rounds. Labeled cRNA Mouse Genome 430 2.0 arrays (purified FB and FBC adipose tissue macrophages. There was a total of sixteen samples. FB and FBC populations were isolated from 4 lean and 4 obese mice.

Background corr dist: KL-Divergence = 0.1867, L1-Distance = 0.0454, L2-Distance = 0.0047, Normal std = 0.3432

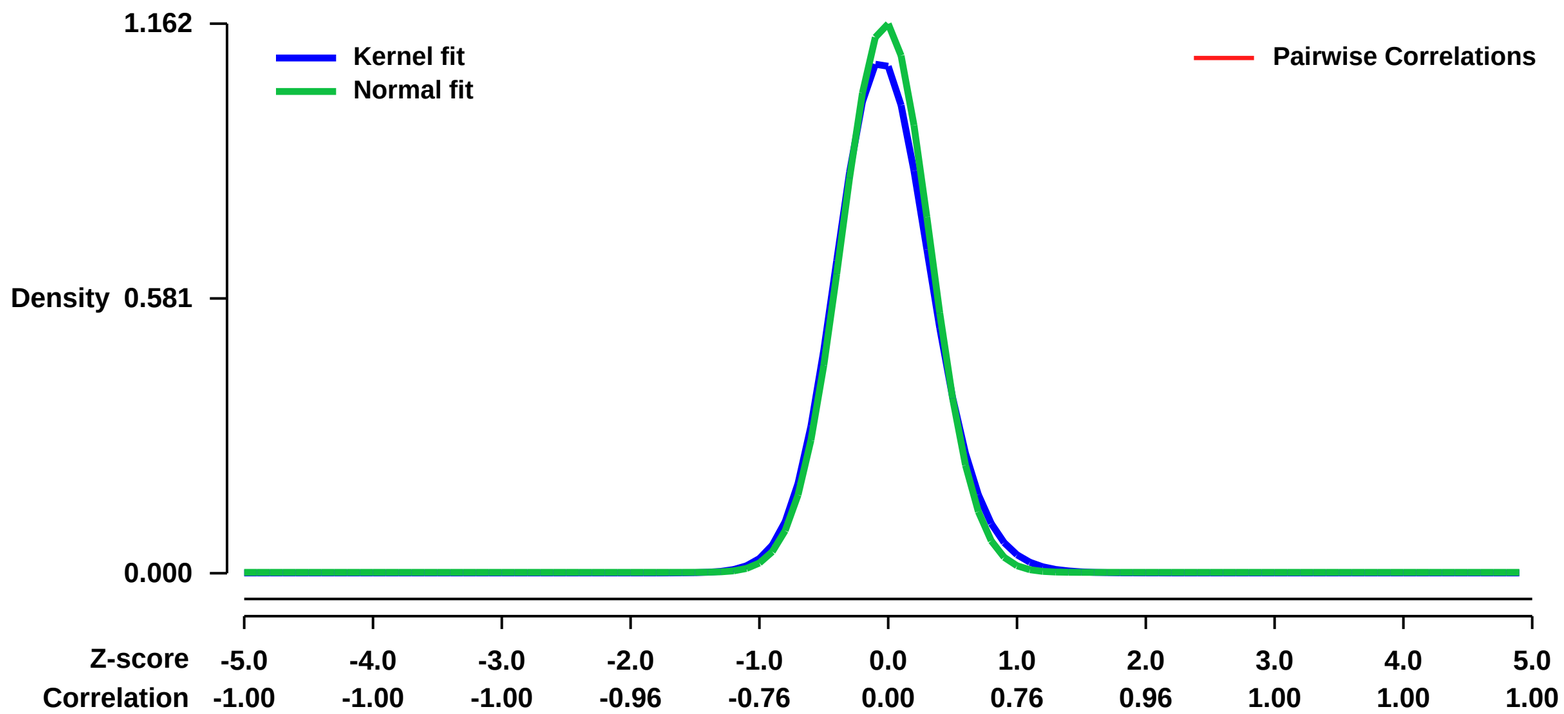

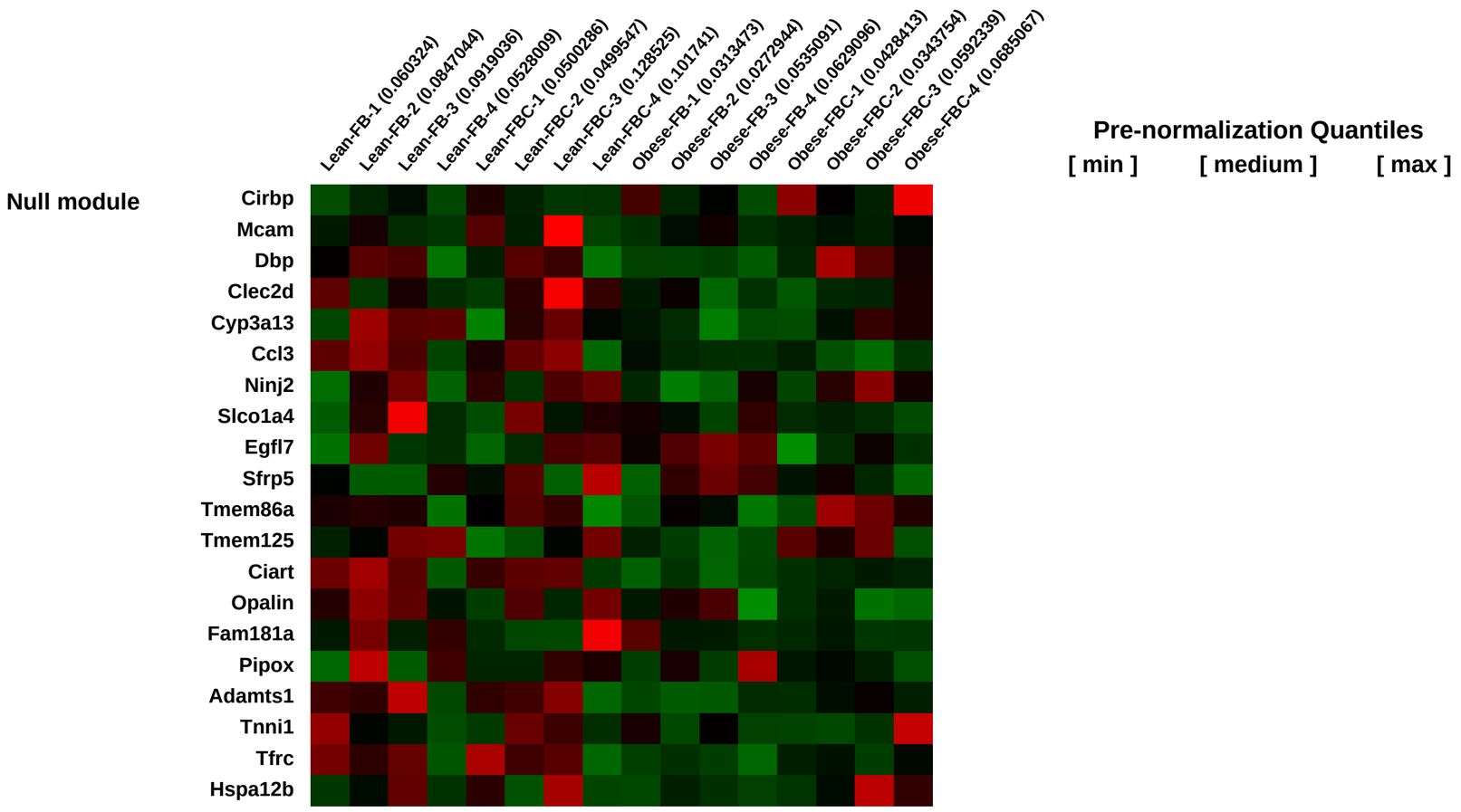

GEO Series "GSE53480" Expression Profiles

Num of samples in this series: 16

Scale of expression profile Z-scores

-3.0 -2.0 -1.0 0.0 1.0 2.0 3.0

GEO Link:	**http://www.ncbi.nlm.nih.gov/geo/query/acc.cgi?acc=GSE53480**
Status:	**Public on Dec 19 2013**
Title:	**Expression data from Tg4510 and Wild-type mice after AAVTFEB injection**
Organism:	**Mus musculus**
Experiment type:	**Expression profiling by array**
Platform:	**GPL1261**
Pubmed ID:	
Summary & Design:	**Summary:** **We used microarrays to detail the global programme of gene expression after 4 months of TFEB overexpression in the brain.** **Overall design:** **Groups of Tg4510 and Wild-type mice were injected at P0 in the brain. Those groups of mice and the respectively controls were sacrificed and analyzed after 4 months from the injection. RNA extraction from the hippocampus and hybridization on Affymetrix microarrays was done.**

Background corr dist: **KL-Divergence = 0.1843, L1-Distance = 0.0396, L2-Distance = 0.0031, Normal std = 0.3439**

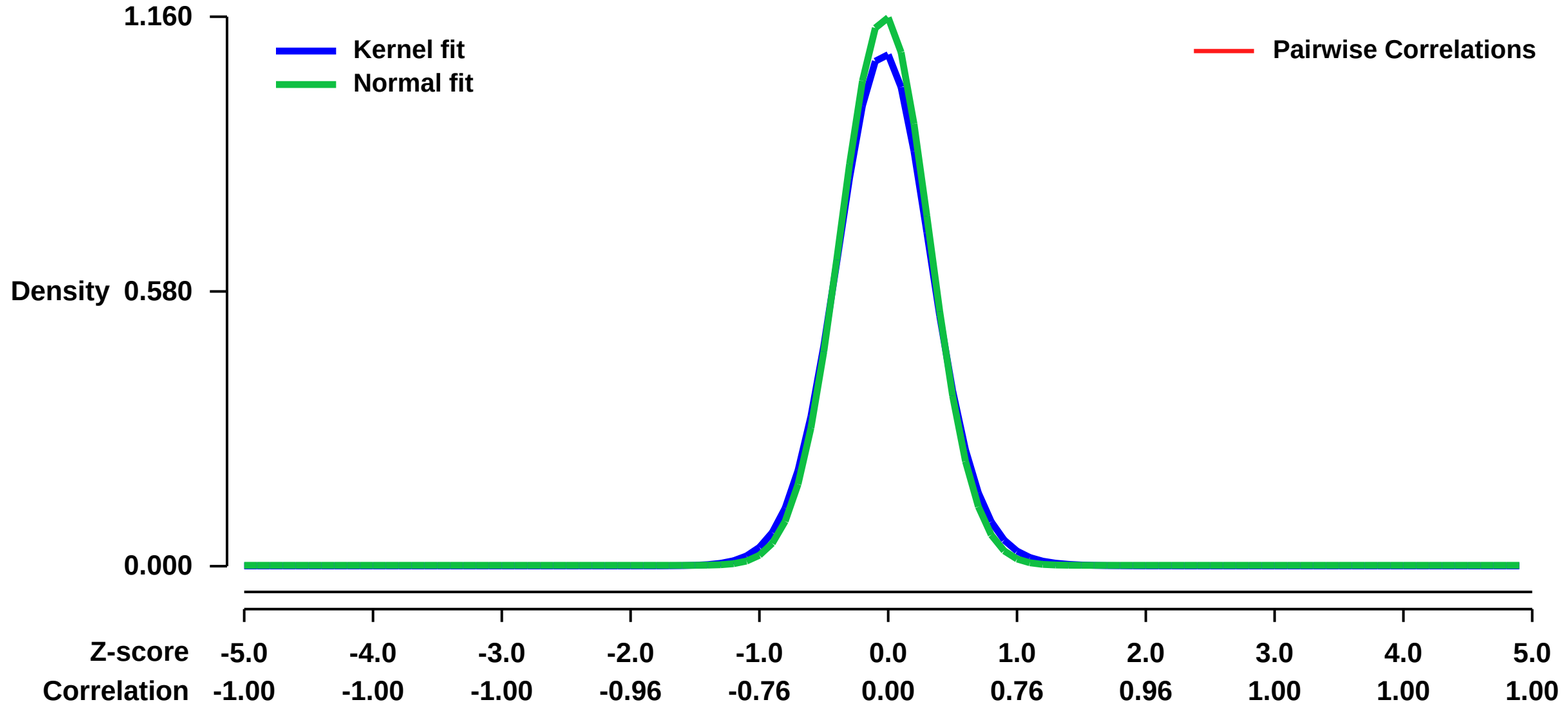

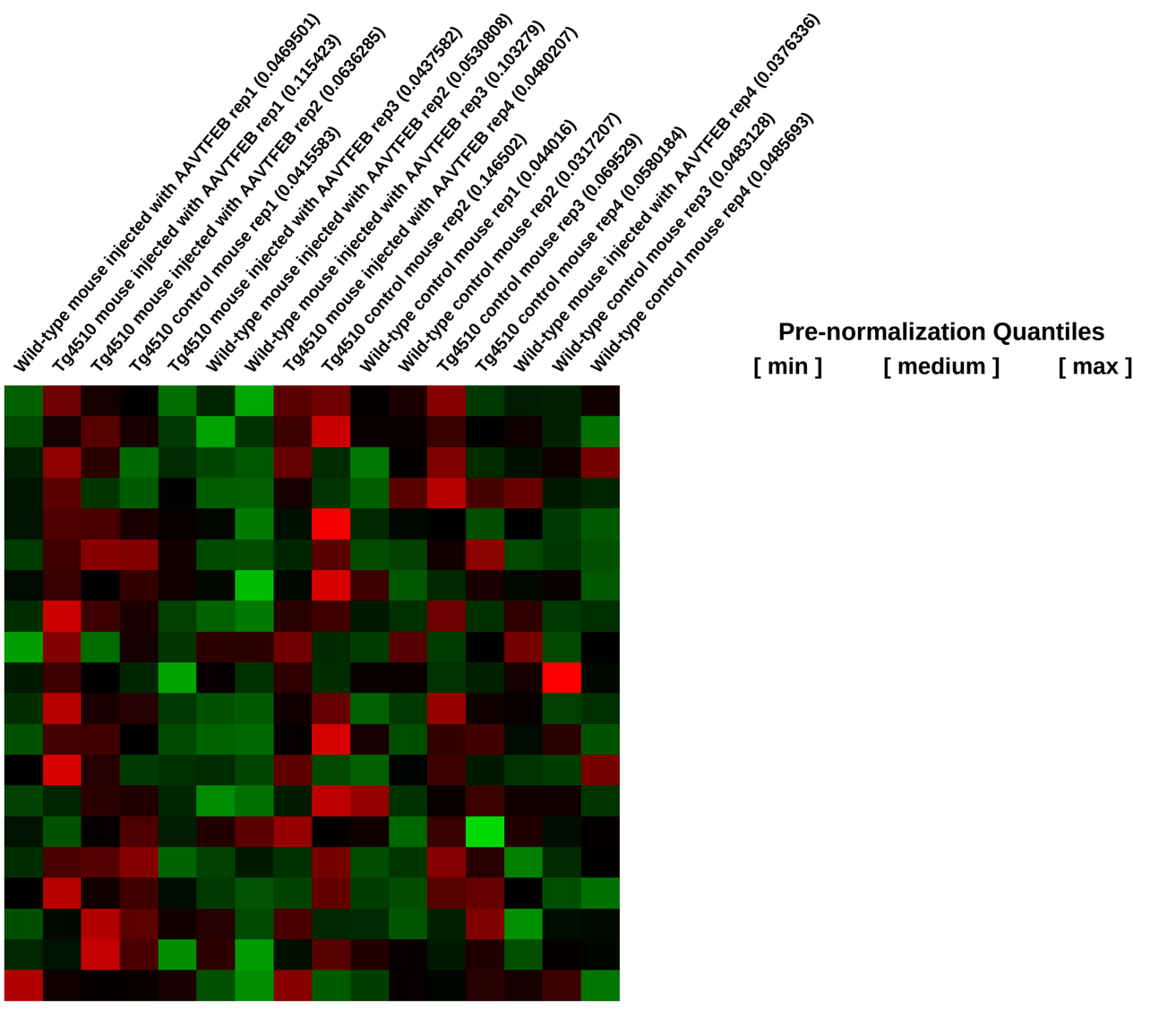

GEO Series "GSE53590" Expression Profiles

Num of samples in this series: 8

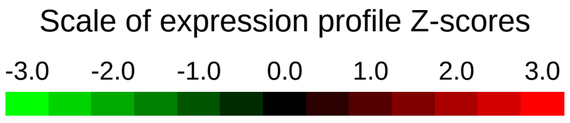

GEO Link: http://www.ncbi.nlm.nih.gov/geo/query/acc.cgi?acc=GSE53590

Status: Public on Dec 24 2013

Title: Dietary fat disturbance of of gut microbial diurnal patterns uncouples host metabolic networks.

Organism: Mus musculus

Experiment type: Expression profiling by array

Platform: GPL1261

Pubmed ID:

Summary & Design:

Summary:
Diet-induced obesity (DIO) is rapidly becoming a global health problem, particularly as Westernization of emerging nations continues. Currently, one third of adult Americans are considered obese and, if current trends continue, >90% of US citizens are predicted to be affected by 2050. However, efforts to fight this epidemic have not yet produced sound solutions for prevention or treatment. Our studies reveal a balanced and chronobiological relationship between food consumption, daily variation in gut microbial evenness and function, basomedial hypothalamic circadian clock (CC) gene expression, and key hepatic metabolic regulatory networks , including CC and nuclear receptors (NR), that is are essential for metabolic homeostasis. â Westernâ diets high in saturated fats dramatically alter diurnal variation in microbial composition and function, which in turn lead to uncoupling of the hepatic CC and NR networks from central CC control in ways that offset the timing and types of regulatory factors directing metabolic function. These signals include microbial metabolites such as short chain fatty acids (SCFAs) and hydrogen sulfide (H2S) that can directly regulate or disrupt metabolic networks of the hepatocyte. Our study therefore provides insights into the complex and dynamic relationships between diet, gut microbes, and the host that are critical for maintenance of health. Perturbations of this constellation of processes, in this case by diet-induced dysbiosis and its metabolomic signaling, can potentially promote metabolic imbalances and disease. This knowledge opens up many possibilities for novel therapeutic and interventional strategies to treat and prevent DIO, ranging from the manipulation of gut microbial function to pharmacological targeting of host pathways to restore metabolic balance.

Overall design:
Mice were raised under germ-free or specific pathogen-free condition, or germ-free followed by conventionization. Liver tissues were harvested for total RNA isolation and hybridization on Affymetrix microarrays

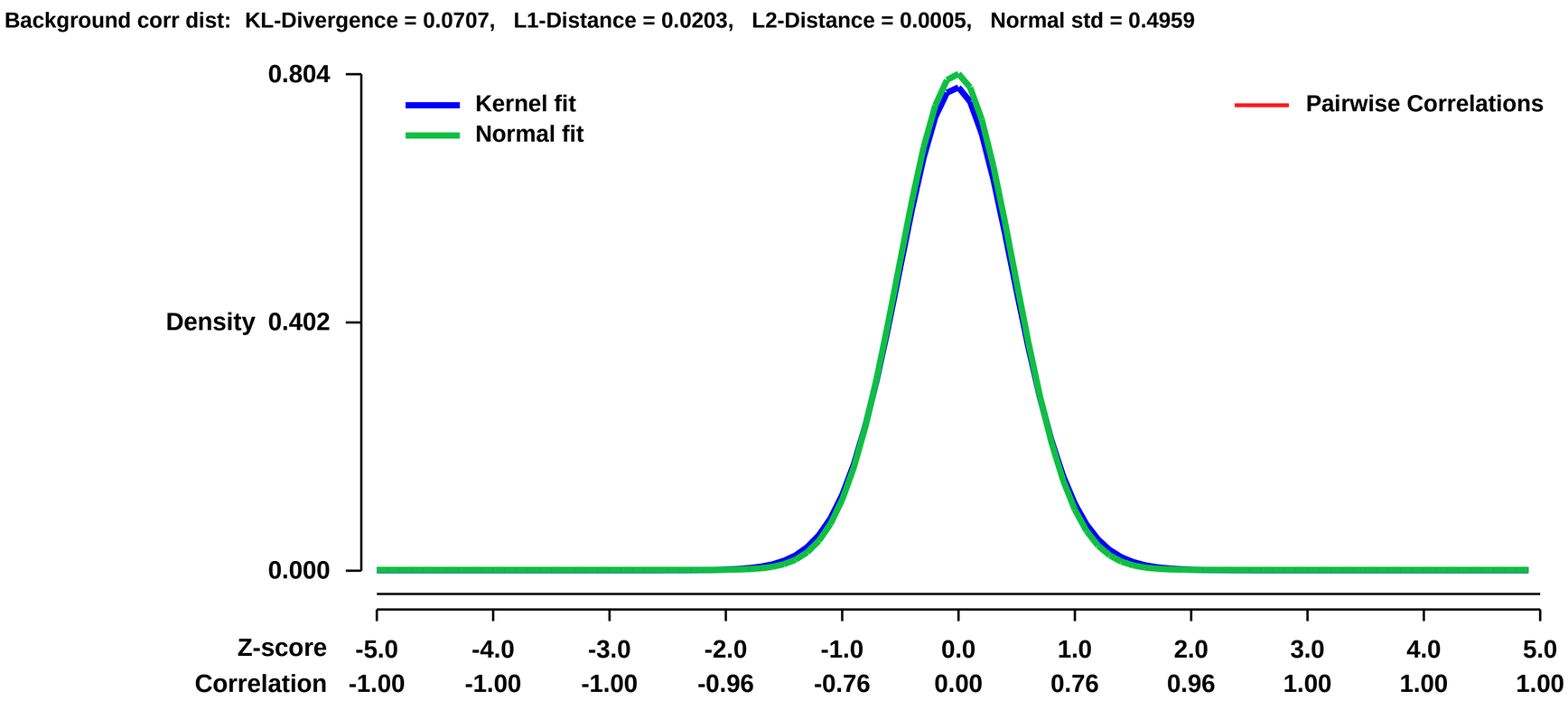

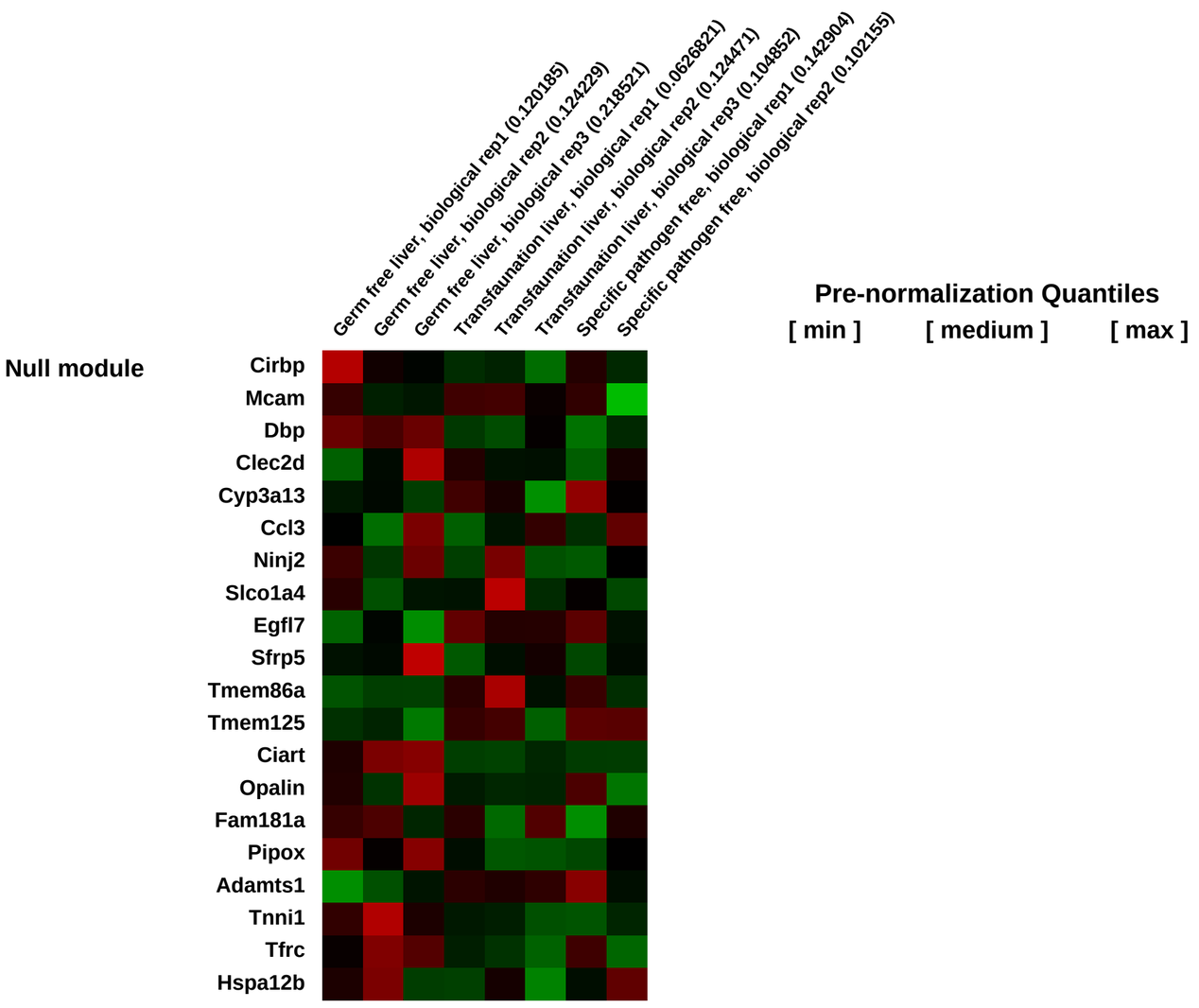

GEO Series "GSE5371" Expression Profiles

Num of samples in this series: 8

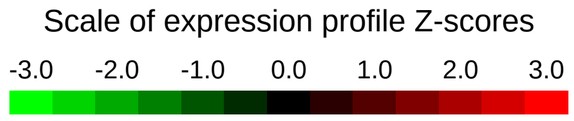

GEO Link:	**http://www.ncbi.nlm.nih.gov/geo/query/acc.cgi?acc=GSE5371**
Status:	**Public on Jul 21 2006**
Title:	**Maternal BRG1 regulates zygotic genome activation in the mouse**
Organism:	**Mus musculus**
Experiment type:	**Expression profiling by array**
Platform:	**GPL1261**
Pubmed ID:	**16818606**
Summary & Design:	**Summary:** **Embryos were collected at 2 cell stage. cRNA from four biological replicates of each were generated and the expression profiles were determined using Affymetrix MOE430 v2.** **Keywords: repeat** **Overall design:** **4 embryo at 2 cell stage biological replicates were analyzed**

Background corr dist: **KL-Divergence = 0.0503, L1-Distance = 0.0327, L2-Distance = 0.0016, Normal std = 0.5980**

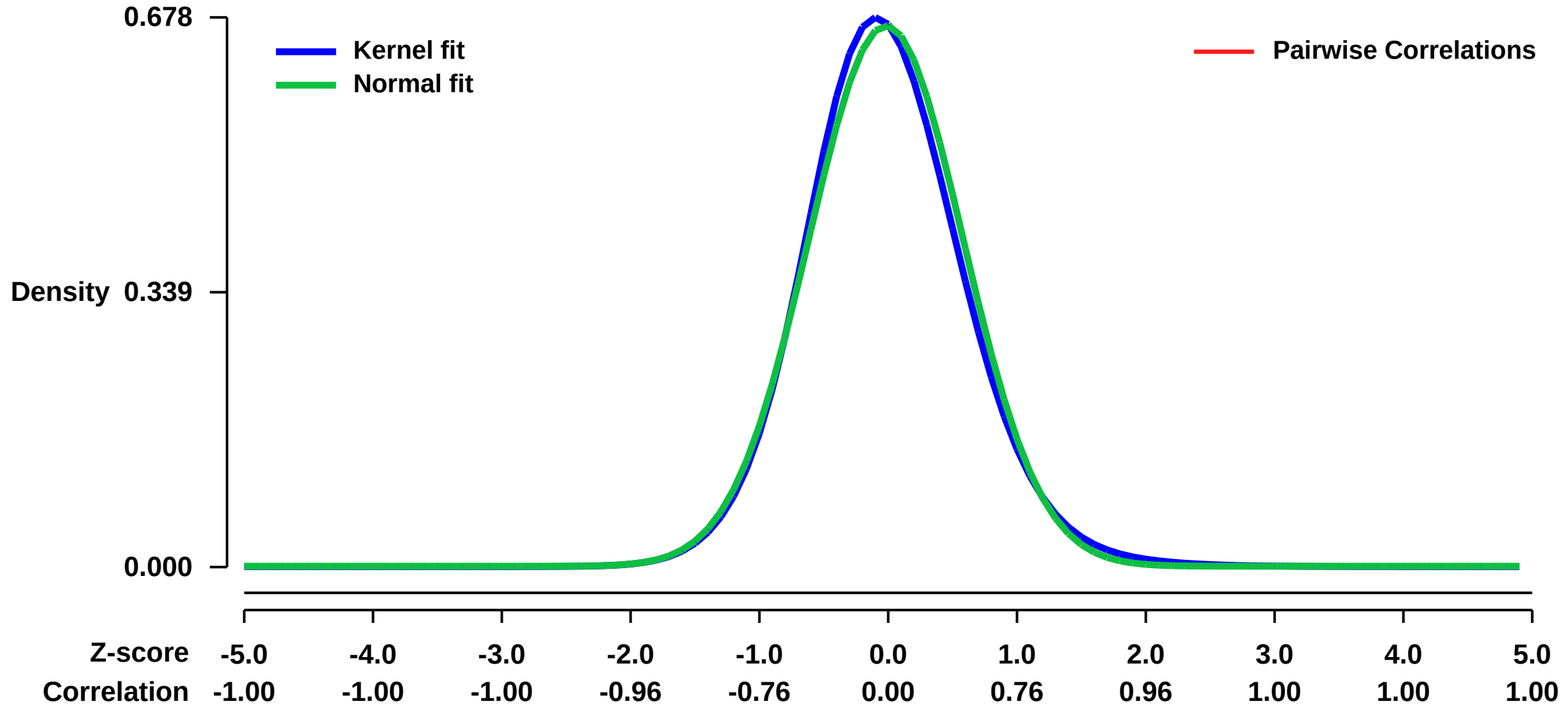

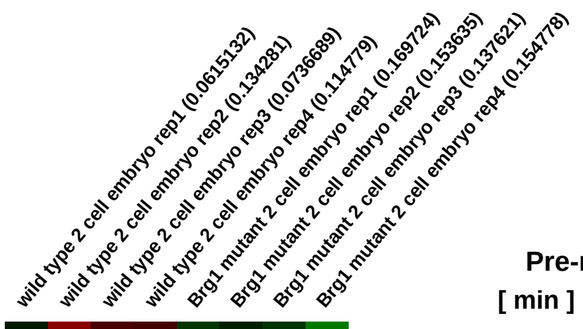

Pre-normalization Quantiles

[min] [medium] [max]

Null module

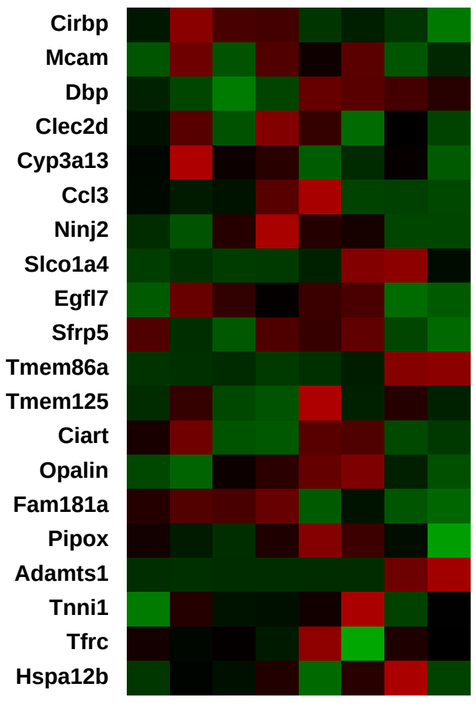

GEO Series "GSE53834" Expression Profiles

Num of samples in this series: 18

Scale of expression profile Z-scores

-3.0 -2.0 -1.0 0.0 1.0 2.0 3.0

GEO Link:	**http://www.ncbi.nlm.nih.gov/geo/query/acc.cgi?acc=GSE53834**
Status:	**Public on Jan 07 2014**
Title:	**Gene expression profiles in the liver of AIM+/+ and AIM-/- mice fed a high-fat diet**
Organism:	**Mus musculus**
Experiment type:	**Expression profiling by array**
Platform:	**GPL1261**
Pubmed ID:	
Summary & Design:	**Summary:** **Expression of genes related to fibrosis was assessed in the liver of AIM+/+ and AM-/- mice fed a high-fat diet (HFD) for various period. Overall, there was no significant difference in the magnitude of expression of fibrosis-related genes during the steatosis progression.** **Overall design:** **AIM+/+ and AIM-/- mice were fed an HFD for 0, 12 or 20 weeks. Liver samples were homogenized with Trizol, and total RNA was extracted according to the manufacturer's instructions. Microarray experiments were performed using Mouse Genome 430 2.0 Arrays (Affymetrix).**

Background corr dist: **KL-Divergence = 0.2329, L1-Distance = 0.0488, L2-Distance = 0.0055, Normal std = 0.3118**

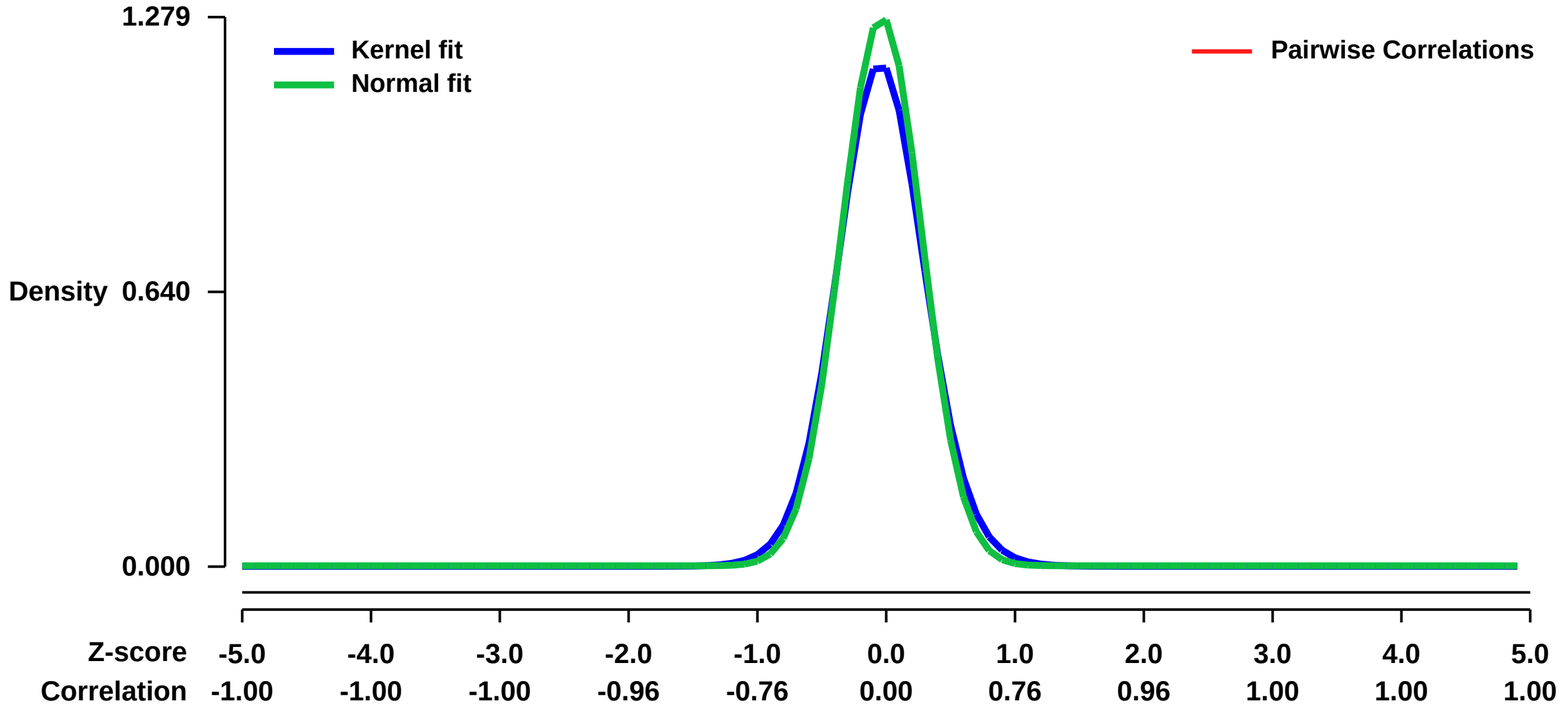

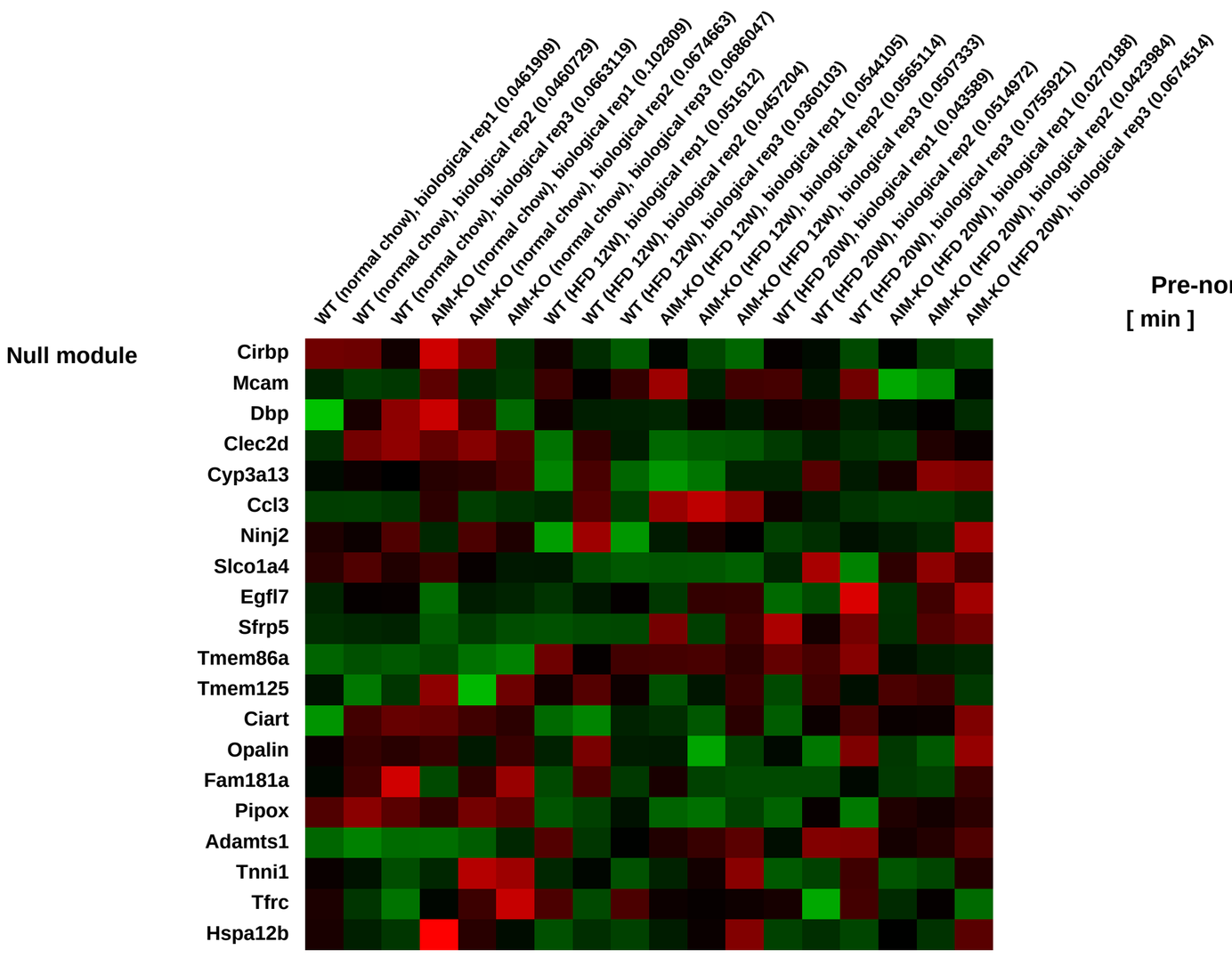

GEO Series "GSE53916" Expression Profiles

Num of samples in this series: 6

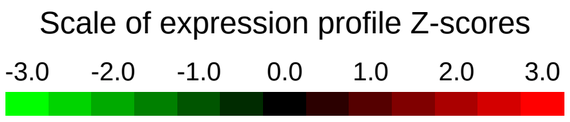

GEO Link:	http://www.ncbi.nlm.nih.gov/geo/query/acc.cgi?acc=GSE53916
Status:	Public on Feb 17 2014
Title:	Expression data from mouse bone marrow cells expressing renin driven expression of green fluorescent protein.
Organism:	Mus musculus
Experiment type:	Expression profiling by array
Platform:	GPL1261
Pubmed ID:	24549417
Summary & Design:	**Summary:** Local renin antiotensin systems have been identified for many extra-renal sites. Bone marrow has been proposed as one such site, although the nature of the renin-expressing cell type(s) has not been established. Affymetrix microarrays were used to characterize the expression profile of renin-expressing GFP positive cells. **Overall design:** Green fluorescent protein positive cells were sorted from whole bone marrow collected from adult transgenic mice. Bone marrow from several mice was collected and pooled on the day of a FACS sort. A portion of this was reserved for RNA extraction while the remainder was sorted. RNA was prepared with Trizol. Bone marrow collection and sorting was performed 3 times so that microarrays could be run in triplicate.

Background corr dist: KL-Divergence = 0.0206, L1-Distance = 0.0262, L2-Distance = 0.0007, Normal std = 0.7706

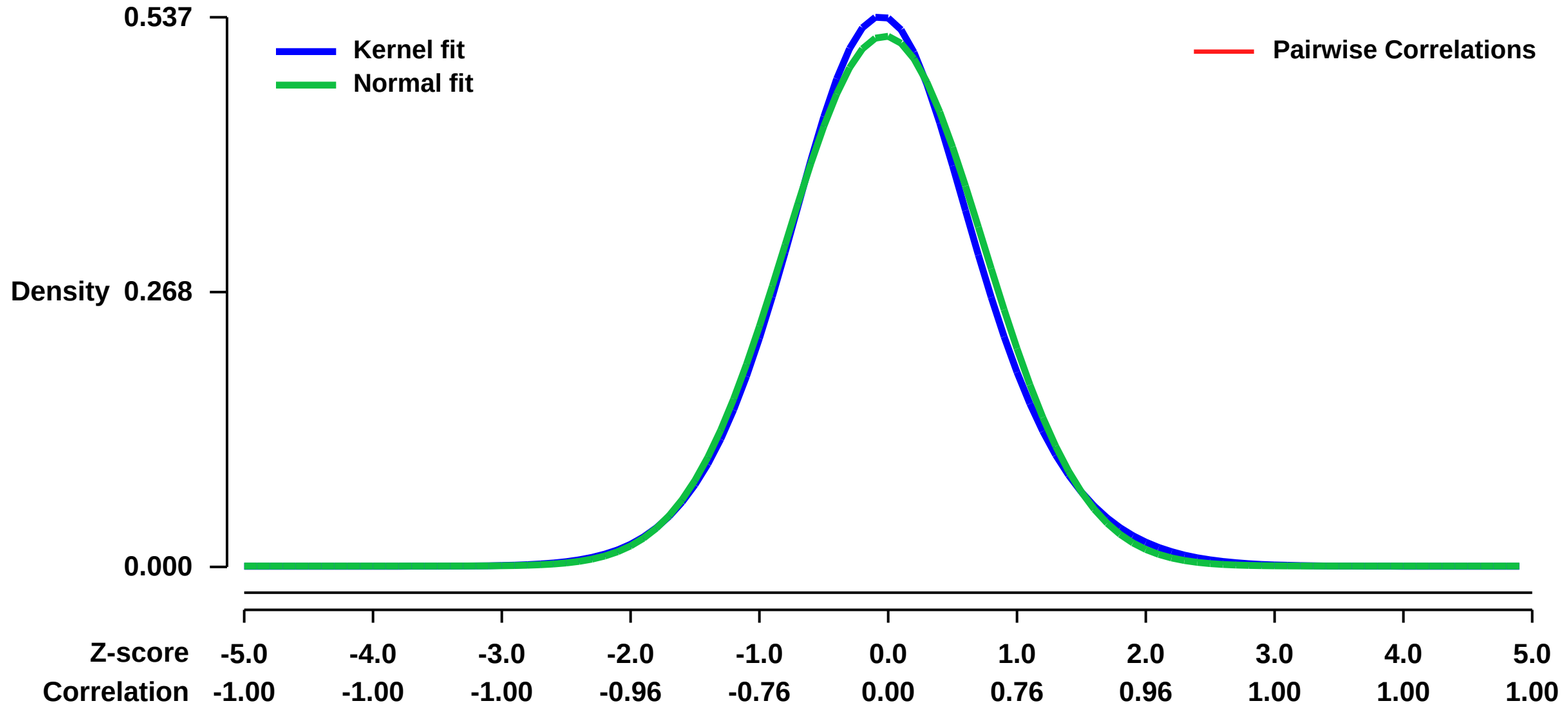

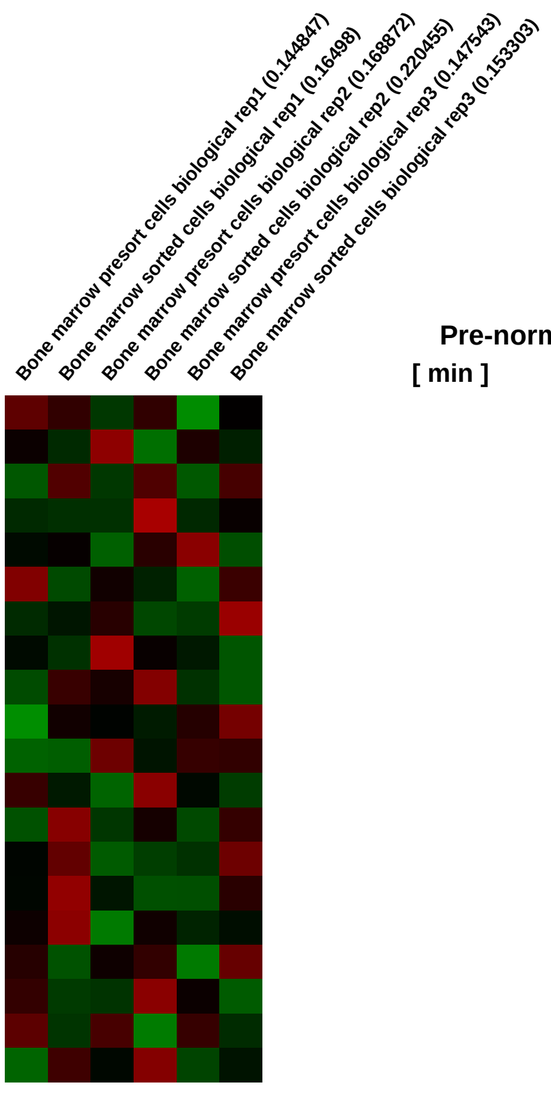

GEO Series "GSE53946" Expression Profiles

Num of samples in this series: 6

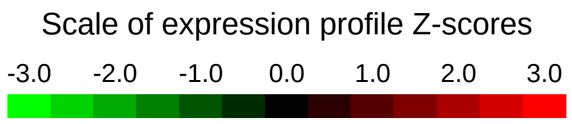

GEO Link:	http://www.ncbi.nlm.nih.gov/geo/query/acc.cgi?acc=GSE53946
Status:	Public on Jan 10 2014
Title:	Affymetrix gene expression of Transitional Type-1 B-cells from Wild-type (CBA), Xid and Btk KO mice
Organism:	Mus musculus
Experiment type:	Expression profiling by array
Platform:	GPL1261
Pubmed ID:	16764821
Summary & Design:	**Summary:** Splenic Transitional Type-1 B-cells from CBA wild-type mice, X-linked immunodeficiency mice and Bruton's tyrosine kinase knock-out mice. Two replicates where run on Affymetrix 420 2.0 arrays for CBA wild-type, Xid samples and the Btk KO samples. Bruton's tyrosine kinase (Btk) is a cytoplasmic tyrosine kinase important for B-lymphocyte maturation. Mutations in Btk give rise to the primary immunodeficiency disease X-linked agammaglobulinemia (XLA) in man and X-linked immunodeficiency (Xid) in mice. Recent studies have subdivided the mouse immature, or transitional, B-cells into two distinct subsets according to their respective surface markers. Transitional type 1 (T1) and transitional type 2 (T2) cells are also located in distinct anatomic locations. Based on a limited number of markers it has previously been reported that the earliest phenotypic sign of Btk deficiency is manifested at the T2 stage in mice. Here, we report on distinct genome-wide transcriptomic signature differences found in T1 B-lymphocytes from Btk-defective compared to normal mice and demonstrate that Btk deficiency is visible already at this stage. **Overall design:** 2 replicates of T1 B-cells from CBA (WT), Xid samples and the Btk KO samples

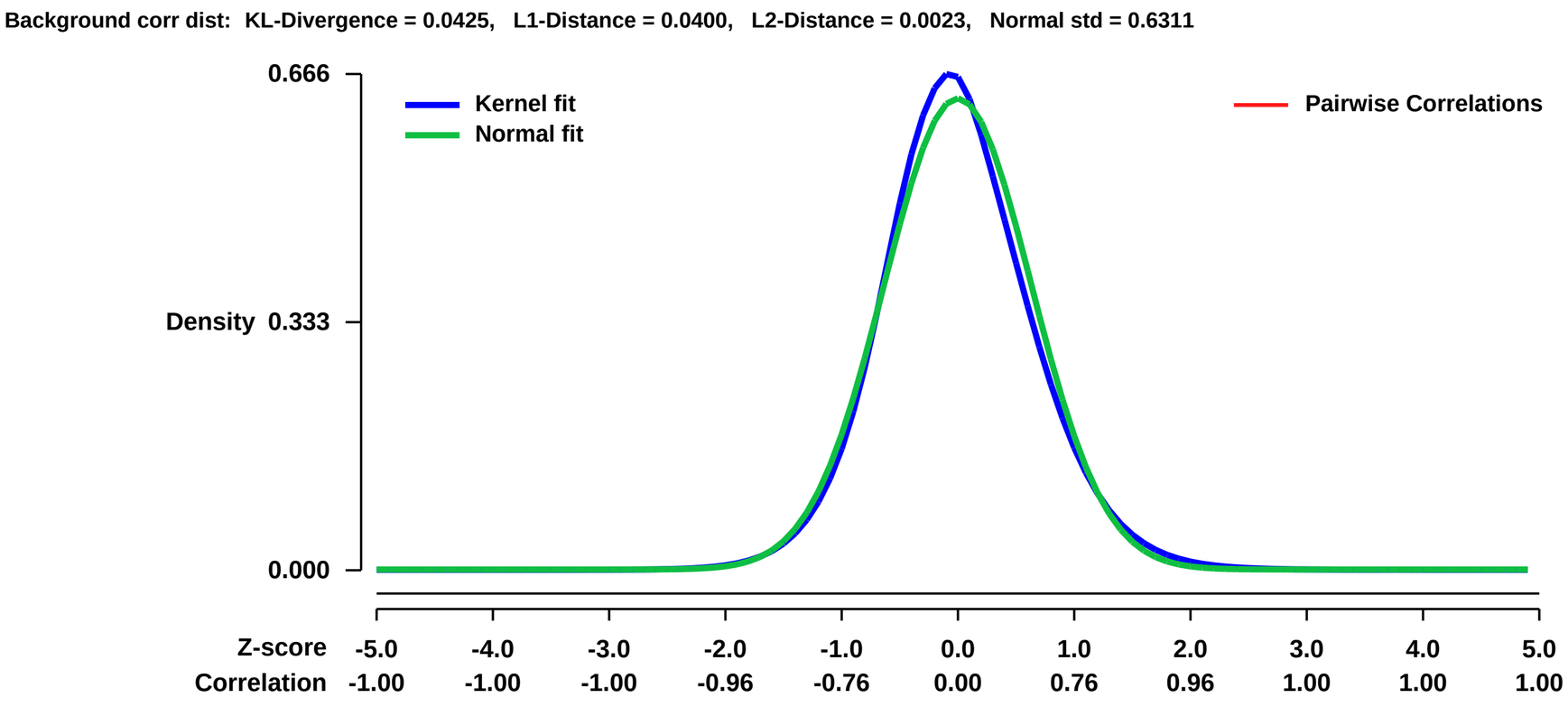

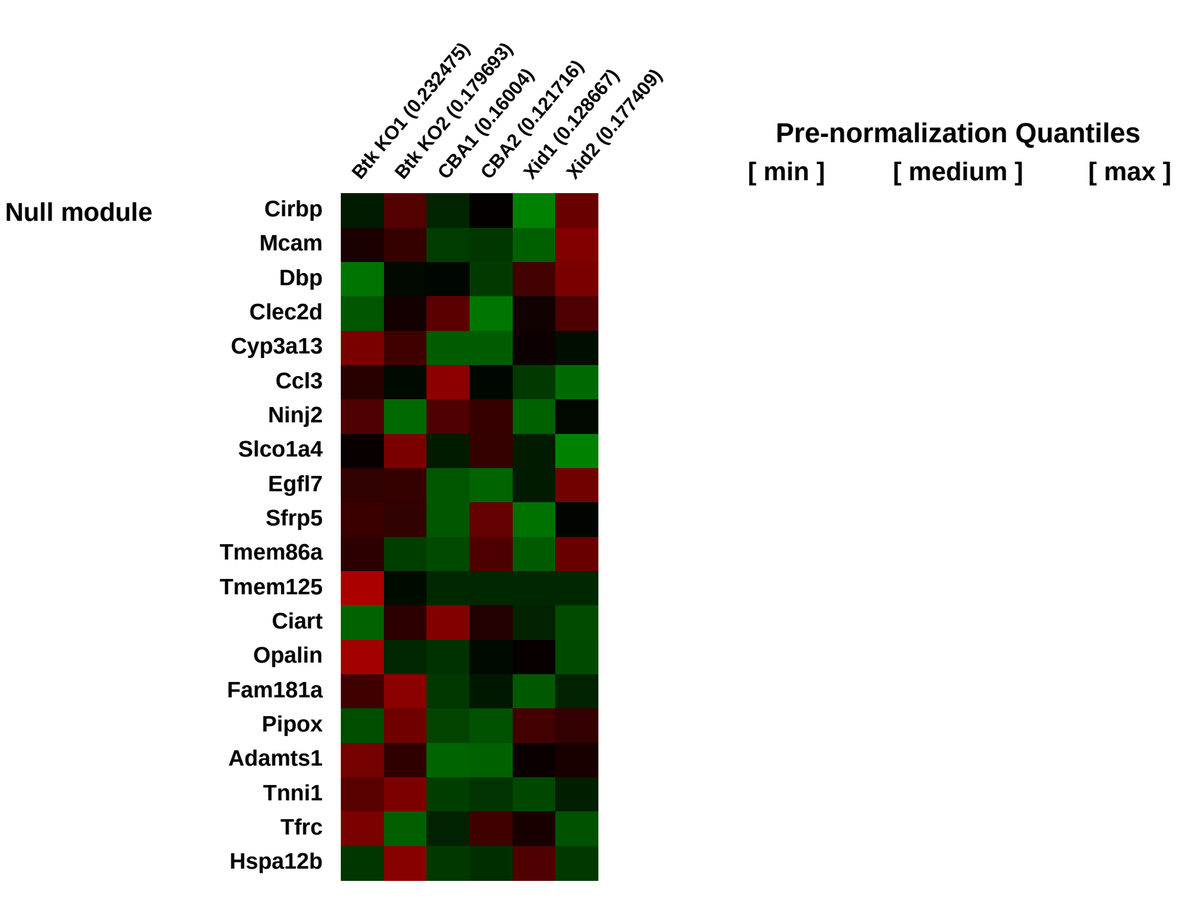

GEO Series "GSE53951" Expression Profiles

Num of samples in this series: 10

Scale of expression profile Z-scores

-3.0 -2.0 -1.0 0.0 1.0 2.0 3.0

GEO Link:	http://www.ncbi.nlm.nih.gov/geo/query/acc.cgi?acc=GSE53951
Status:	Public on Jan 10 2014
Title:	Gene expression after type-I interferon treatment in primary neurons, primary fibroblasts and L929 cells
Organism:	Mus musculus
Experiment type:	Expression profiling by array
Platform:	GPL1261
Pubmed ID:	24453359
Summary & Design:	**Summary:** Microarray expression profilling of mouse primary mixed cortical/hippocampal neurons, primary fibroblasts and L929 cells to compare ISGs signature in disctinct cell types **Overall design:** Primary mixed cortical/hippocampal neurons, primary fibroblasts (MEFs) and L929 cells were mock-treated or treated with 5U/mL of IFN-beta and RNA was harvested after 24 hours. For neurons and fibroblast, 2 samples were analyzed for each condition.

Background corr dist: KL-Divergence = 0.0405, L1-Distance = 0.0863, L2-Distance = 0.0101, Normal std = 0.7845

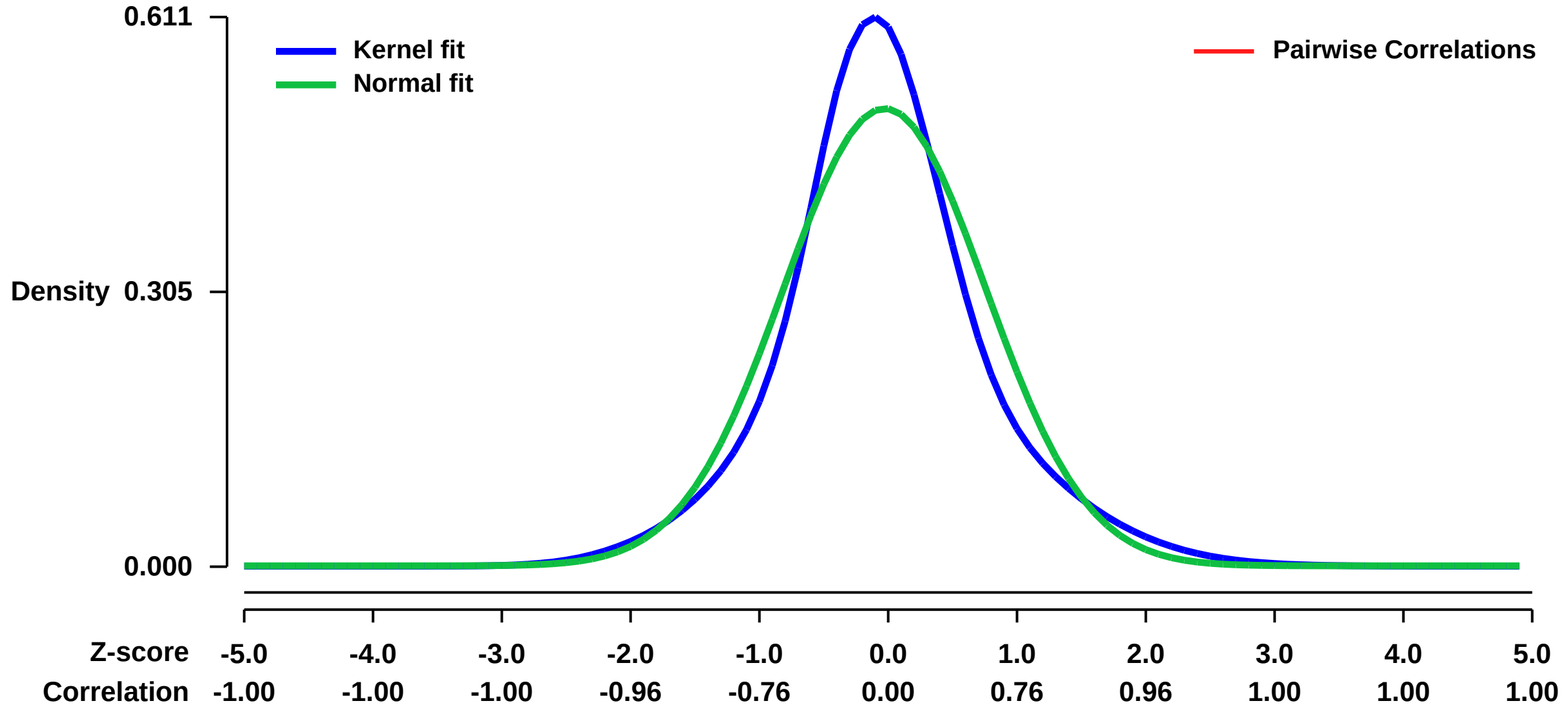

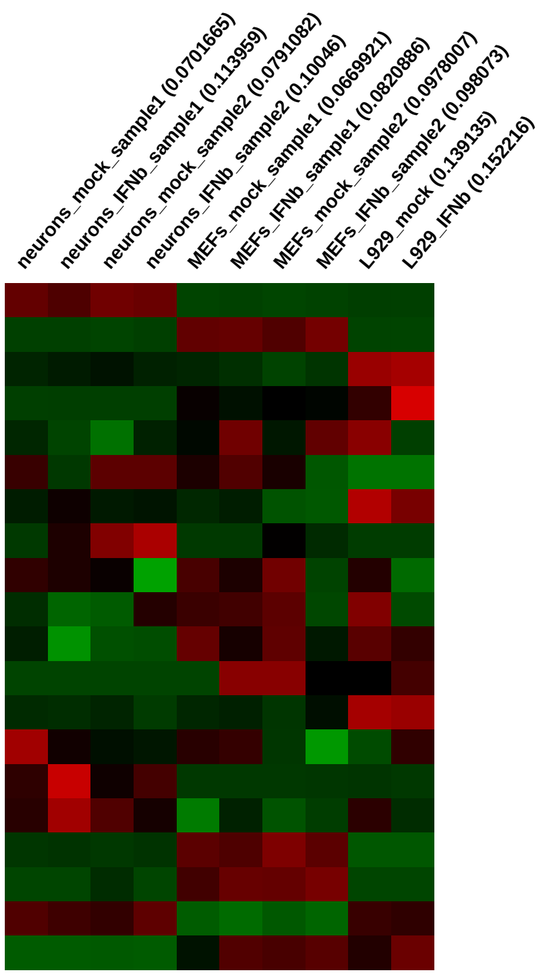

GEO Series "GSE53986" Expression Profiles

Num of samples in this series: 16

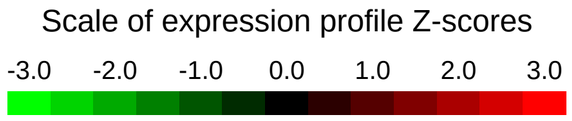

GEO Link:	**http://www.ncbi.nlm.nih.gov/geo/query/acc.cgi?acc=GSE53986**
Status:	**Public on Mar 31 2014**
Title:	**NRROS negatively regulates ROS in phagocytes during host defense and autoimmunity**
Organism:	**Mus musculus**
Experiment type:	**Expression profiling by array**
Platform:	**GPL1261**
Pubmed ID:	**24739962**
Summary & Design:	**Summary:** **Production of reactive oxygen species (ROS) is one of the important antimicrobial mechanisms of phagocytic cells. Enhanced oxidative burst requires these cells to be primed with agents such as IFNg and LPS with a synergistic effect of these agents on the level of the burst. However, excessive ROS generation will lead to tissue damage and has been implicated in a variety of inflammatory and autoimmune disease. Therefore, this process needs to be tightly regulated. In order to understand the genes regulating this process, we will treat bone marrow derived macrophages with above mentioned priming agents and study the gene expression.** **We used microarrays to determine the changes in gene expression that occur in bone marrow derived macrophages after treatment with IFNg, LPS, or a combination of IFNg and LPS** **Overall design:** **Four condition experiment; Biological replicates: four replicates per condition**

Background corr dist: KL-Divergence = 0.1364, L1-Distance = 0.0322, L2-Distance = 0.0018, Normal std = 0.3981

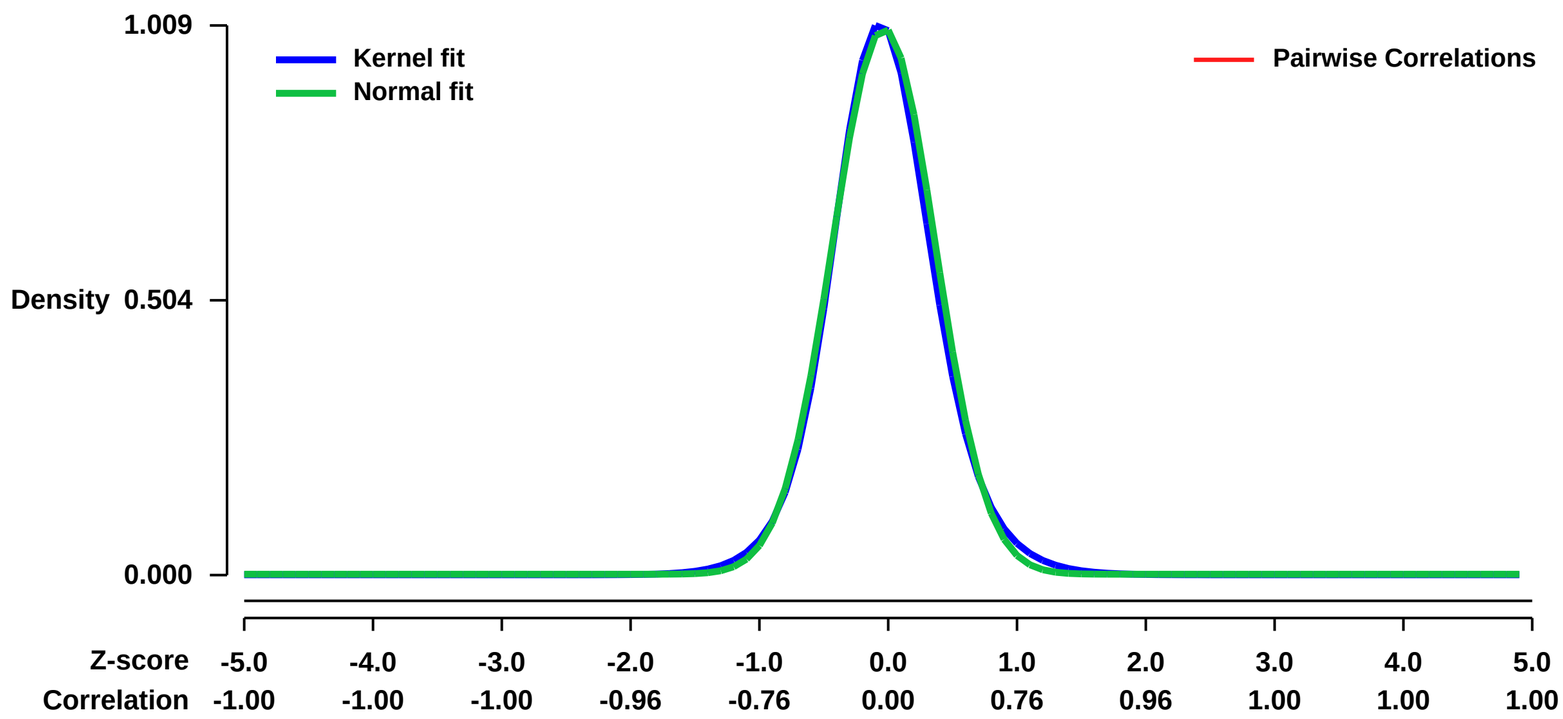

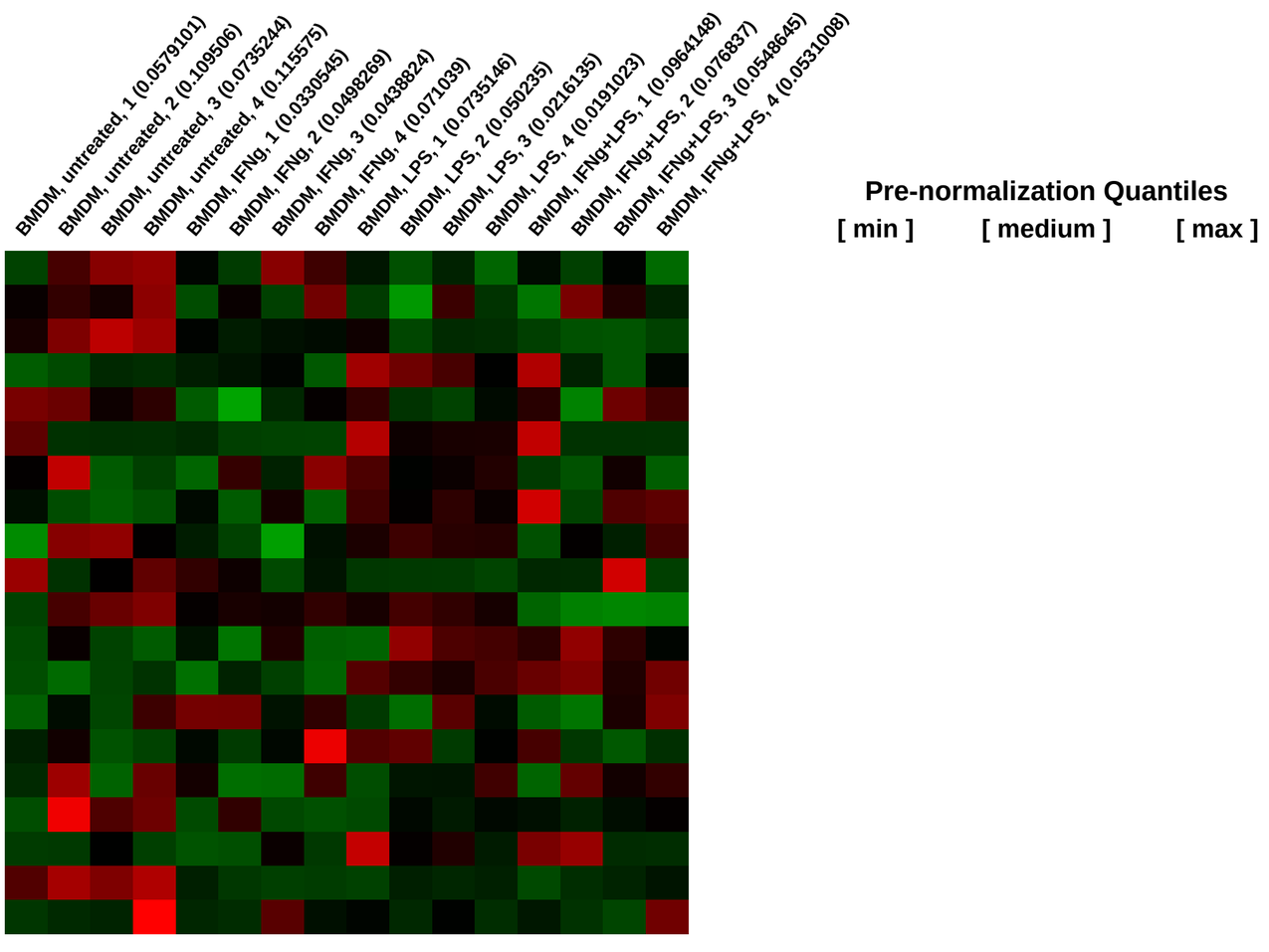

GEO Series "GSE54056" Expression Profiles

Num of samples in this series: 12

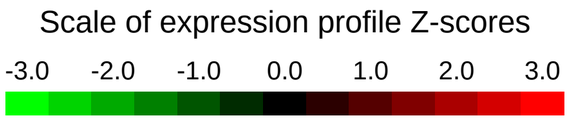

GEO Link:	http://www.ncbi.nlm.nih.gov/geo/query/acc.cgi?acc=GSE54056
Status:	Public on Mar 06 2014
Title:	Expression data from adult mouse normal and damaged retina from B6 and 129 mouse strains
Organism:	Mus musculus
Experiment type:	Expression profiling by array
Platform:	GPL1261
Pubmed ID:	24747725
Summary & Design:	**Summary:** Retinal damage causes proliferation of Muller glia, but the degree of proliferation depends on mouse strains. Muller glial proliferation was significantly promoted by the addition of GSK3 inhibitor in 129, but not in B6. We used retinal explant culture as a model for retinal damage which caused preferential photoreceptor death in a few days. We used microarrays to detail the global programme of gene expression regulating the proliferative potential of Muller glia after retinal damage. **Overall design:** Total RNA from intact whole retina, retinal tissue cultured for three days, and retinal tissue cultured with chir99021 for three days was used. Retinal tissues from 10 weeks old mice were used.

Background corr dist: KL-Divergence = 0.0576, L1-Distance = 0.0272, L2-Distance = 0.0009, Normal std = 0.5454

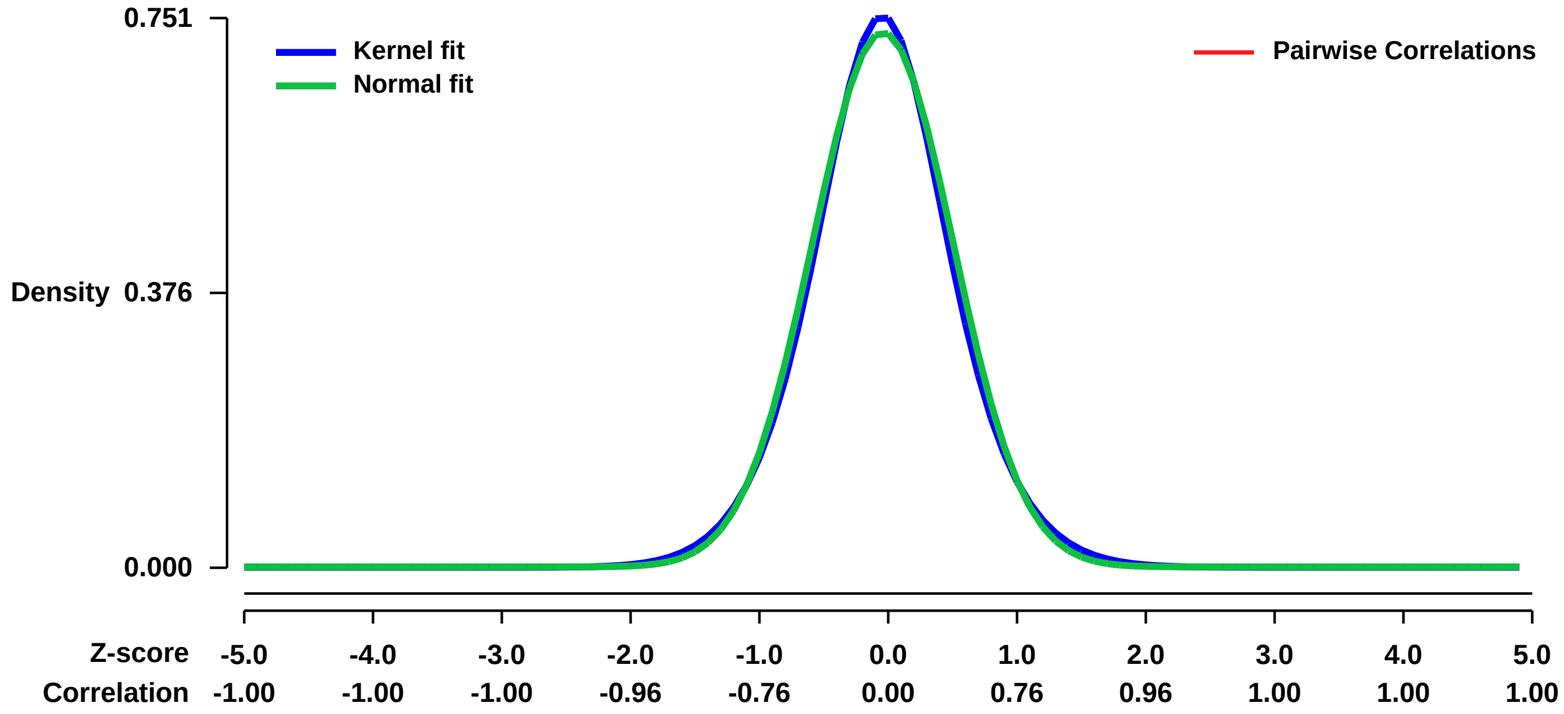

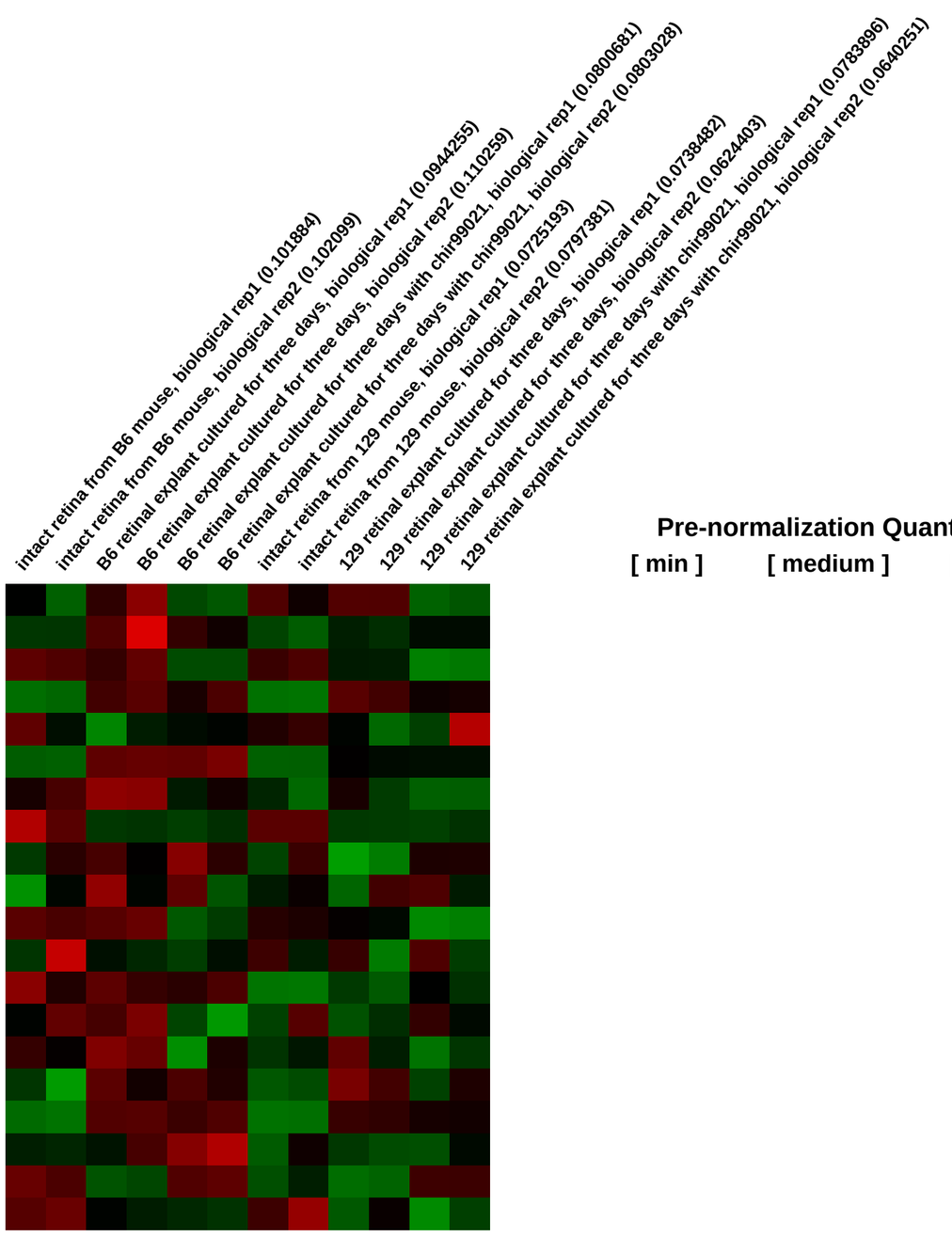

GEO Series "GSE54207" Expression Profiles

Num of samples in this series: 9

Scale of expression profile Z-scores

-3.0 -2.0 -1.0 0.0 1.0 2.0 3.0

GEO Link:	**http://www.ncbi.nlm.nih.gov/geo/query/acc.cgi?acc=GSE54207**
Status:	**Public on Jan 18 2014**
Title:	**Expression data from mouse limb tendon cells during development.**
Organism:	**Mus musculus**
Experiment type:	**Expression profiling by array**
Platform:	**GPL1261**
Pubmed ID:	
Summary & Design:	**Summary:** **We have undertaken a screen of mouse limb tendon cells in order to identify molecular pathways involved in tendon development. Mouse limb tendon cells were isolated based on Scleraxis (Scx) expression at different stages of development: E11.5, E12.5 and E14.5** **Microarray comparisons were carried out between tendon progenitor and differentiated stages.** **Overall design:** **Forelimbs from E11.5, E12.5 and E14.5 Scx-GFP embryos were collected and dissociated with trypsin to obtain cell suspensions. Scx-positive tendon cells were isolated by FACS. RNA was extracted and Fragmented biotin-labelled cRNA samples were hybridized on Affymetrix Gene Chip Mouse Genome 430 2.0 arrays.**

Background corr dist: **KL-Divergence = 0.0661, L1-Distance = 0.0279, L2-Distance = 0.0010, Normal std = 0.5212**

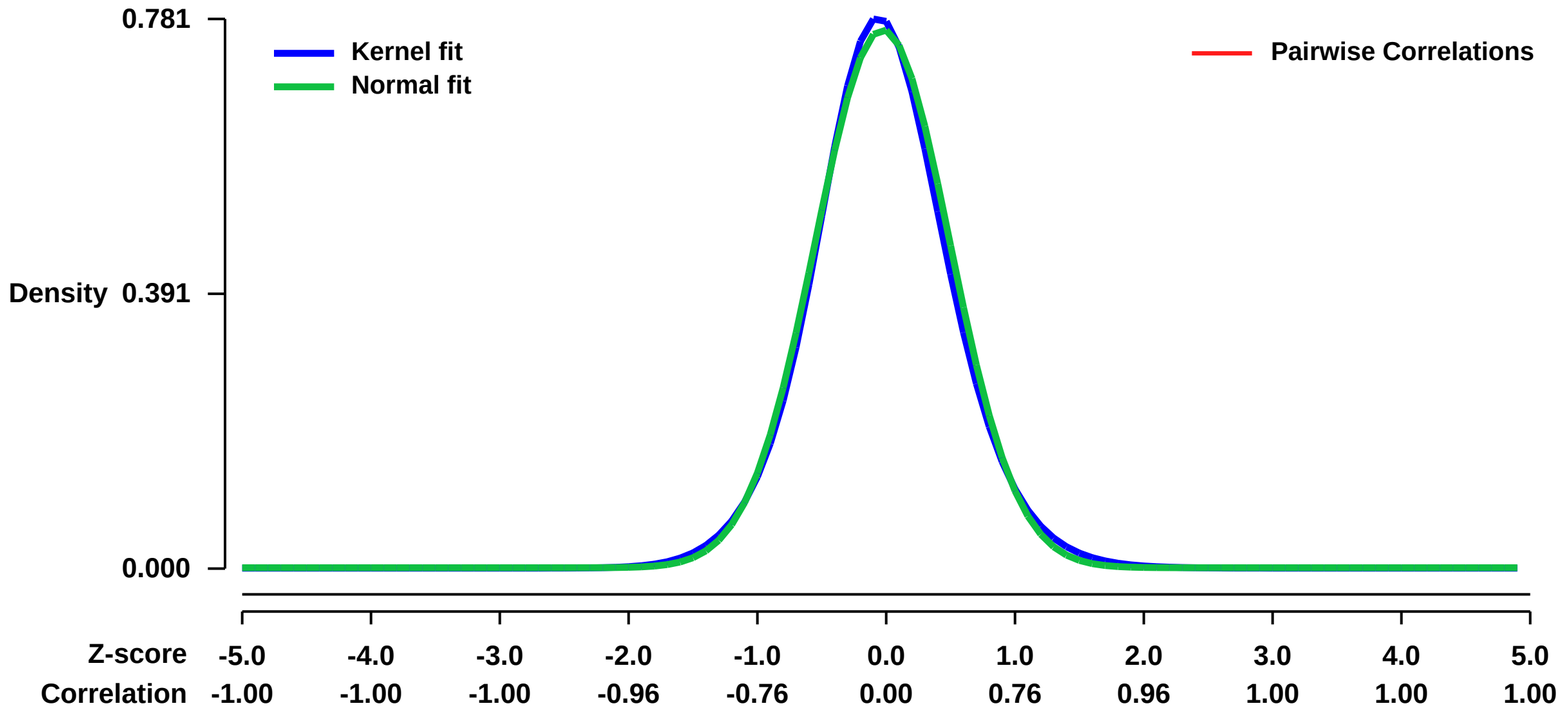

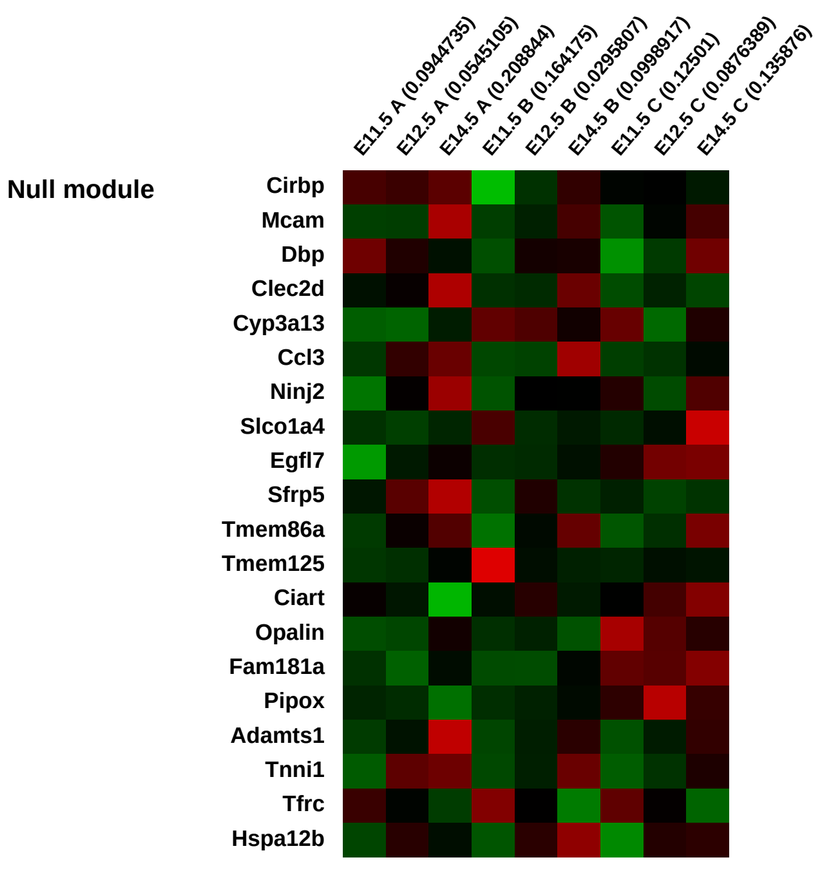

GEO Series "GSE54285" Expression Profiles

Num of samples in this series: 12

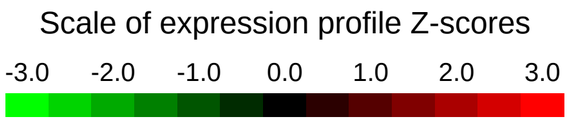

GEO Link:	http://www.ncbi.nlm.nih.gov/geo/query/acc.cgi?acc=GSE54285
Status:	Public on Jan 23 2014
Title:	Analysis of impact of Toxoplasma effector MAF1 during Type II infection in WT MEFs and during Type I infection in WT and MAVS KO MEFs
Organism:	Mus musculus
Experiment type:	Expression profiling by array
Platform:	GPL1261
Pubmed ID:	24781109
Summary & Design:	**Summary:** The goals of the microarray experiment were to determine the role of MAF1, the Toxoplasma gondii mediator of host mitochondrial association, on host cell gene expression by comparing infection of WT cells with Type II and Type II:MAF1 parasites. We also explored the role of MAF1 on host cell gene expression by comparing profiles of WT and MAVS KO MEFs infected with Type I and Type Imaf1KO parasites. We used microarrays to detail the global programme of gene expression underlying cellularisation and identified distinct classes of up-regulated genes during this process. **Overall design:** WT MEFs were infected with Type II and Type II:MAF1 parasites at an MOI of 5. At 8 hpi RNA was harvested using TriZol. The Affymetrix IVT (16h) express kit was used for cDNA synthesis and labeling.

Background corr dist: KL-Divergence = 0.0168, L1-Distance = 0.0175, L2-Distance = 0.0003, Normal std = 0.7584

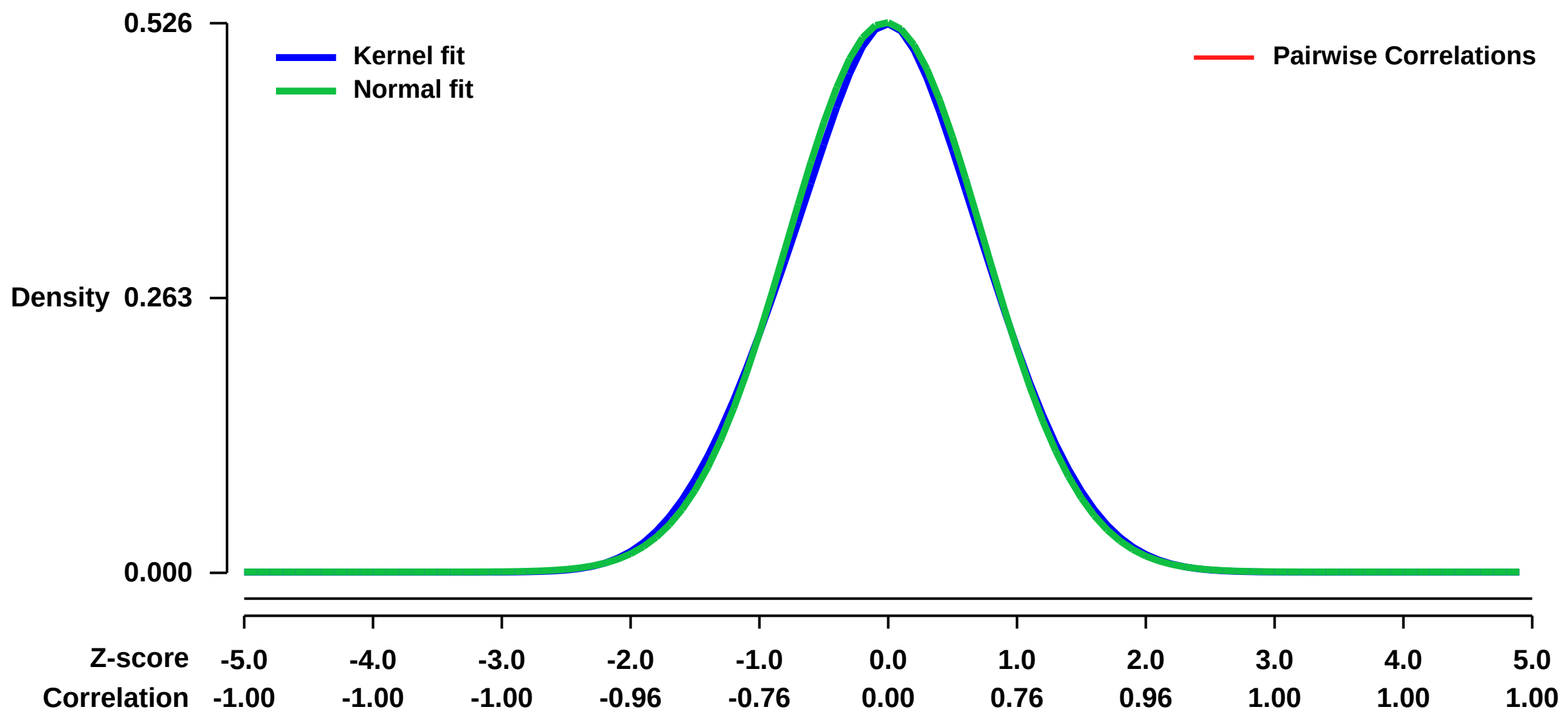

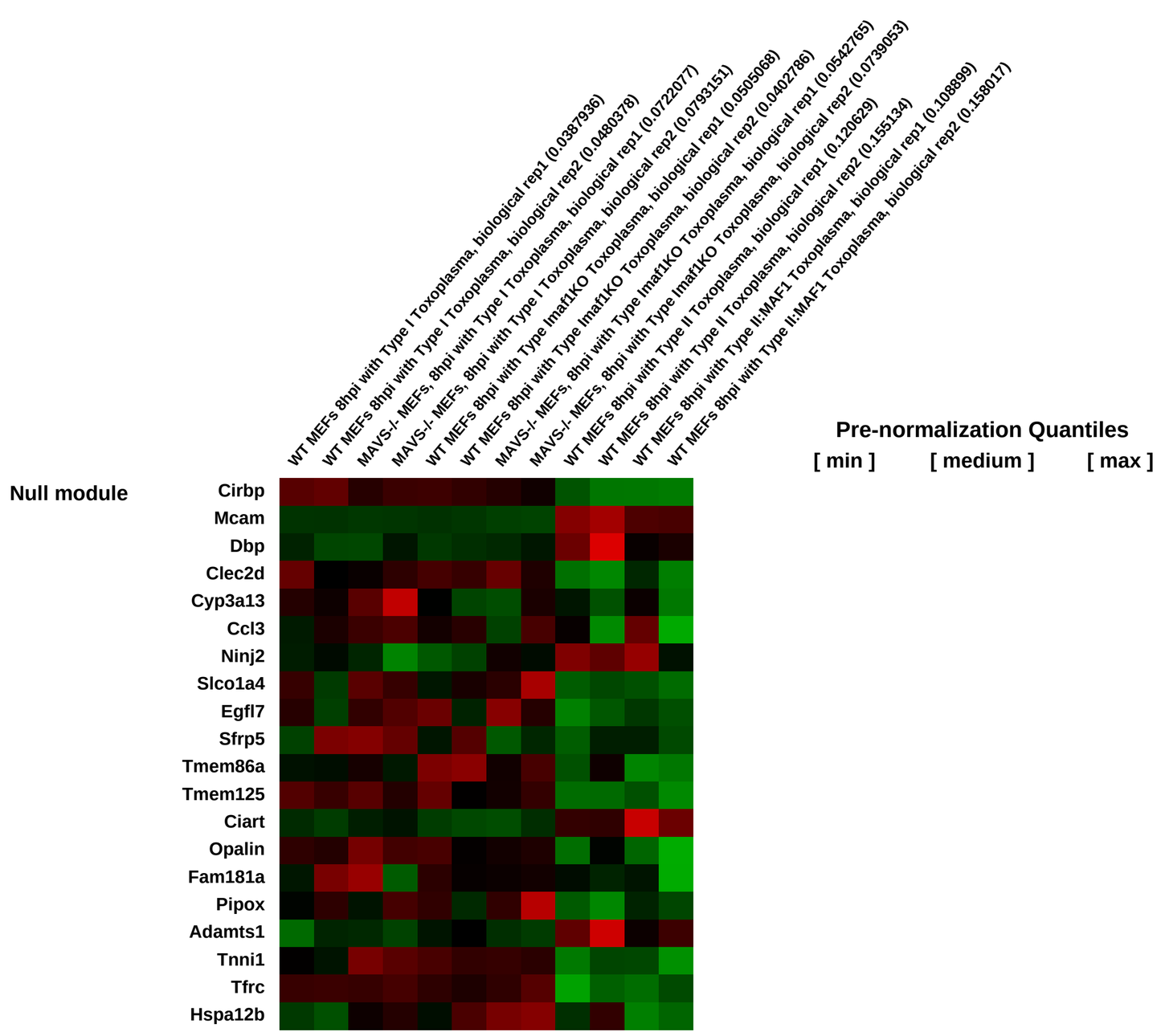

GEO Series "GSE54581" Expression Profiles

Num of samples in this series: 21

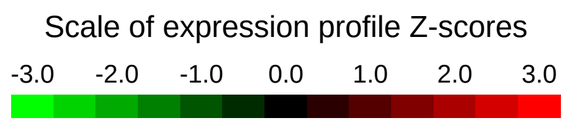

GEO Link:	http://www.ncbi.nlm.nih.gov/geo/query/acc.cgi?acc=GSE54581
Status:	Public on Jun 02 2014
Title:	Selective mRNA translation during eIF2 phosphorylation induces expression of IBTKalpha
Organism:	Mus musculus
Experiment type:	Expression profiling by array
Platform:	GPL1261
Pubmed ID:	24648495
Summary & Design:	**Summary:** **Disruption of protein folding in the endoplasmic reticulum triggers the Unfolded Protein Response (UPR), a transcriptional and translational control network designed to restore protein homeostasis. Central to the UPR is PERK phosphorylation of the alpha subunit of eIF2 (eIF2~P), which represses global translation coincident with preferential translation of mRNAs, such as ATF4 and CHOP, that serve to implement the UPR transcriptional regulation. In this study, we used sucrose gradient ultracentrifugation and a genome-wide microarray approach to measure changes in mRNA translation during ER stress. Our analysis suggests that translational efficiencies vary across a broad range during ER stress, with the majority of transcripts being either repressed or resistant to eIF2~P, while a notable cohort of key regulators are subject to preferential translation. From this latter group, we identify IBTKa as being subject to both translation and transcriptional induction during eIF2~P in both cell lines and a mouse model of ER stress. Translational regulation of IBTKalpha mRNA involves the stress-induced relief of two inhibitory uORFs in the 5'-leader of the transcript. Depletion of IBTKalpha by shRNA reduced viability of cultured cells coincident with increased caspase 3/7 cleavage, suggesting that IBTKalpha is a key regulator in determining cell fate during the UPR.** **We used a genome-wide microarray approach to determine how individual mRNAs were differentially translated during endoplasmic reticulum stress.** **Overall design:** **Please note that the treatment plus fractionation based on association with different numbers of ribosomes did yield different populations of mRNAs, which resulted in considerable variation in normalized data across the samples.**

Background corr dist: KL-Divergence = 0.1148, L1-Distance = 0.0307, L2-Distance = 0.0019, Normal std = 0.4200

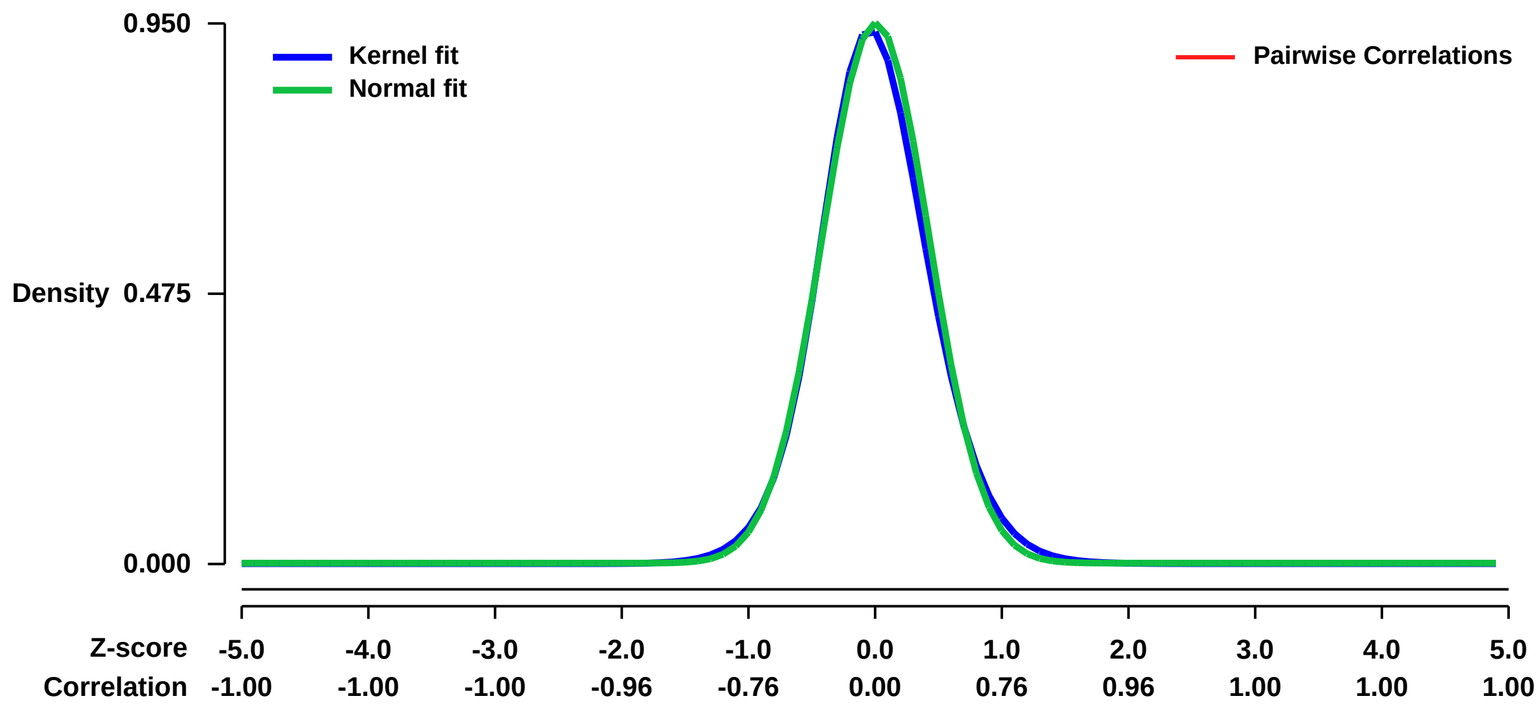

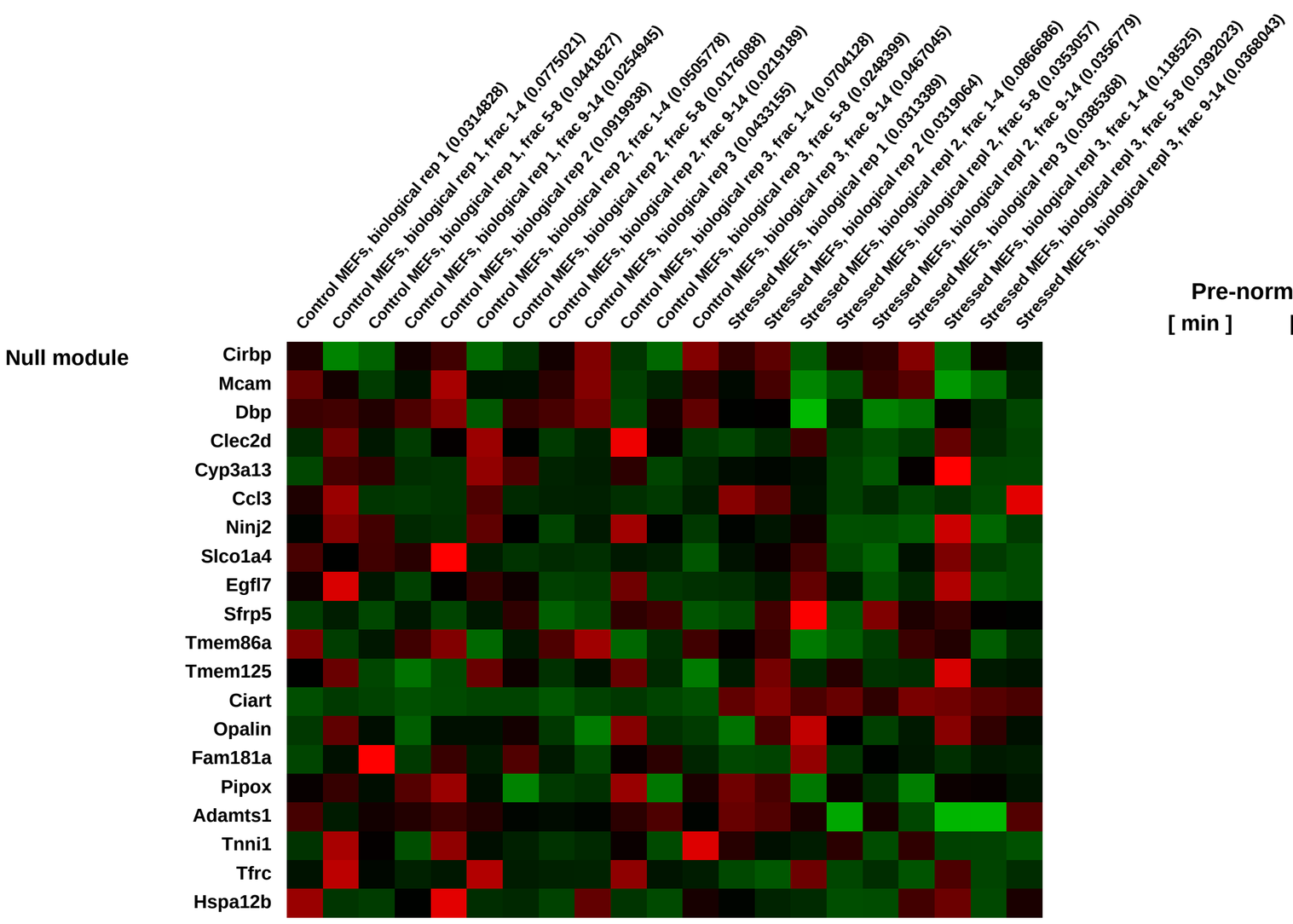

GEO Series "GSE54653" Expression Profiles

Num of samples in this series: 6

Scale of expression profile Z-scores

-3.0 -2.0 -1.0 0.0 1.0 2.0 3.0

GEO Link:	http://www.ncbi.nlm.nih.gov/geo/query/acc.cgi?acc=GSE54653
Status:	Public on May 07 2014
Title:	Expression data from quiescent and activated neural stem cells from the adult mouse V-SVZ niche
Organism:	Mus musculus
Experiment type:	Expression profiling by array
Platform:	GPL1261
Pubmed ID:	
Summary & Design:	**Summary:** RNA was purified from GFAP::GFP+CD133+ and GFAP::GFP+CD133+EGFR+ cells isolated from the adult mouse V-SVZ niche (GFAP::GFP mice, Jackson Mice Stock number 003257) **Overall design:** 6 samples consisting of two conditions of three biological replicates each were analyzed

Background corr dist: KL-Divergence = 0.0262, L1-Distance = 0.0342, L2-Distance = 0.0016, Normal std = 0.7186

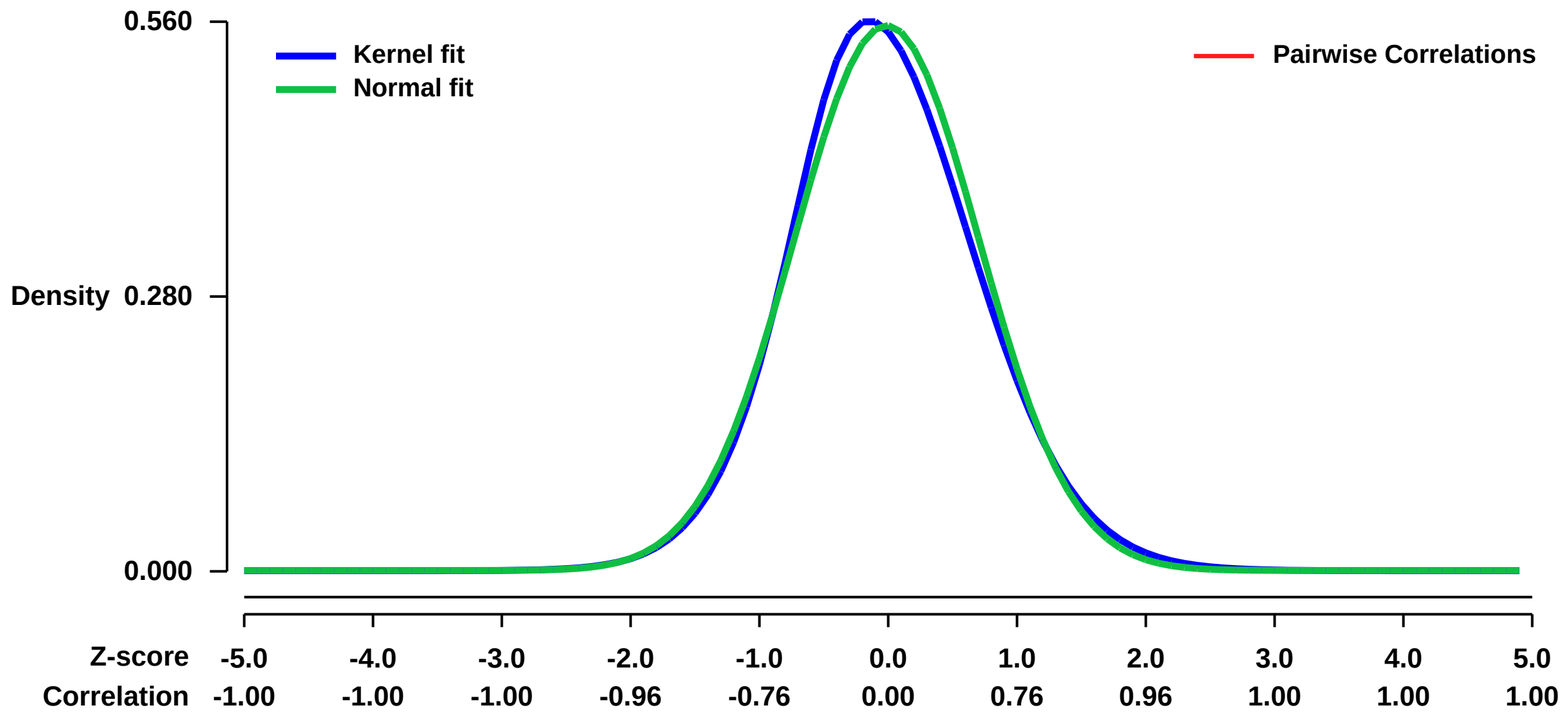

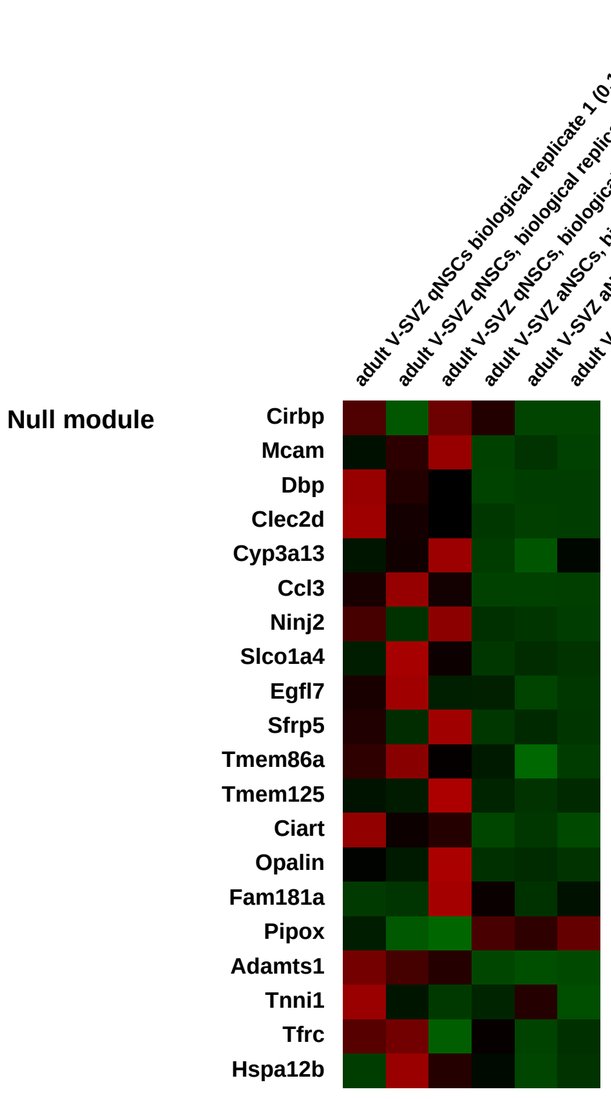

GEO Series "GSE54656" Expression Profiles

Num of samples in this series: 27

Scale of expression profile Z-scores

-3.0 -2.0 -1.0 0.0 1.0 2.0 3.0

GEO Link:	http://www.ncbi.nlm.nih.gov/geo/query/acc.cgi?acc=GSE54656
Status:	Public on Feb 05 2014
Title:	G9a influences neuronal subtype specification in striatum
Organism:	Mus musculus
Experiment type:	Expression profiling by array
Platform:	GPL1261
Pubmed ID:	24584053
Summary & Design:	**Summary:** Cocaine-mediated repression of the histone methyltransferase (HMT) G9a has recently been implicated in transcriptional, morphological, and behavioral responses to chronic cocaine administration. Here, using a ribosomal affinity purification approach, we find that G9a repression by cocaine occurs in both Drd1 (striatonigral)- and Drd2 (striatopallidal)-expressing medium spiny neurons (MSNs). Conditional knockout and overexpression of G9a within these distinct cell types, however, reveals divergent behavioral phenotypes in response to repeated cocaine treatment. Our studies further indicate that such developmental deletion of G9a selectively in Drd2 neurons results in the unsilencing of transcriptional programs normally specific to striatonigral neurons, and the acquisition of Drd1-associated projection and electrophysiological properties. This partial striatopallidal to striatonigral â switchingâ phenotype in mice indicates a novel role for G9a in contributing to neuronal subtype identity, and suggests a critical function for cell-type specific histone methylation patterns in the regulation of behavioral responses to environmental stimuli. **Overall design:** Polyribosome associated mRNAs from 2-5 month old, age and sex matched Drd1-Cre; Drd1-TRAP; G9afl/fl and Drd1-TRAP; G9afl/fl, Drd2-Cre; Drd2-TRAP; G9afl/fl and Drd2-TRAP; G9afl/fl mice (n = 2-4 mice/genotype/drug treatment, 2 hours after the last of eight repeated cocaine injections of 20 mg/kg/day) were obtained as previously described. EGFP labeled ribosomes and associated mRNAs were immunoprecipitated using a mix of two monoclonal anti-GFP antibodies (50 ¸…g of clones #19C8 and #19F7 for each IP, available at Sloan-Kettering Monoclonal Antibody Facility). Purified mRNA was amplified and processed for microarray and qPCR analysis using the Affymetrix two-cycle cDNA Synthesis kit (Affymetrix) as previously described. Affymetrix Mouse Genome 430 2.0 arrays were used in all experiments. Information regarding the array design and features can be found at www.affymetrix.com. Mouse Genome 430 2.0 arrays were scanned using the GeneChip Scanner 3000 (Affymetrix) and globally scaled to 150 using the Affymetrix GeneChip Operating Software (GCOS v1.4).

Background corr dist: KL-Divergence = 0.1756, L1-Distance = 0.0521, L2-Distance = 0.0065, Normal std = 0.3487

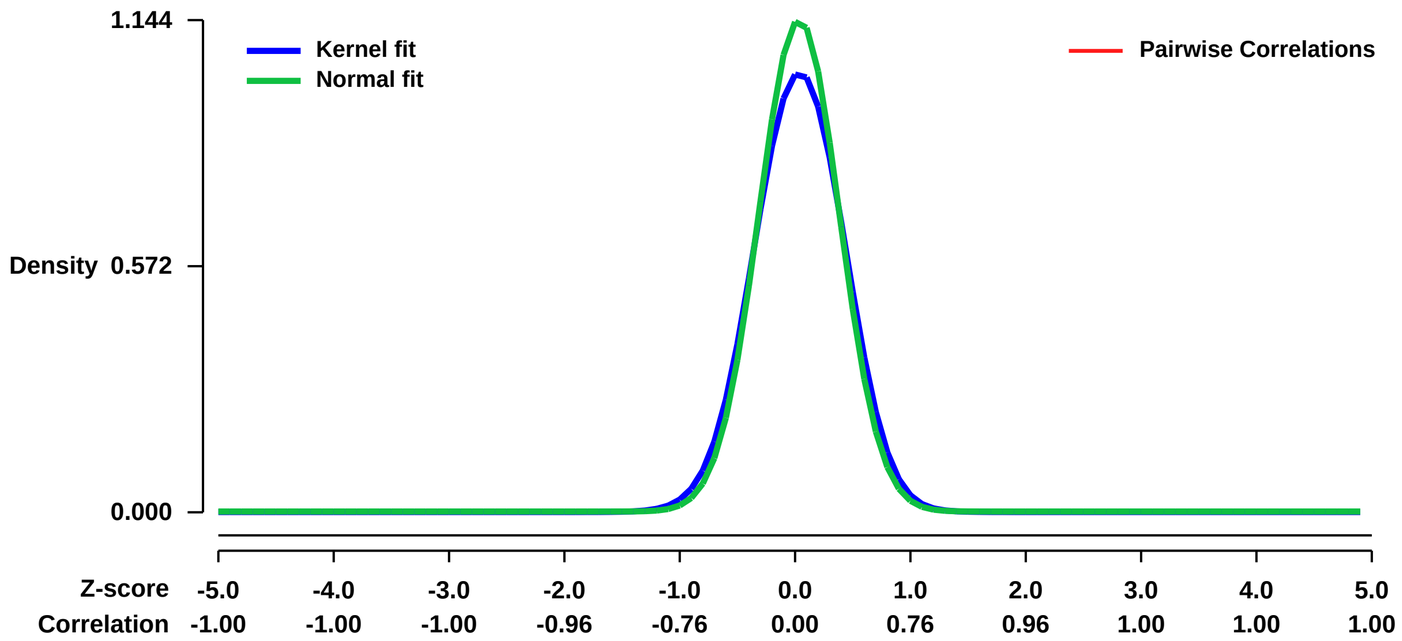

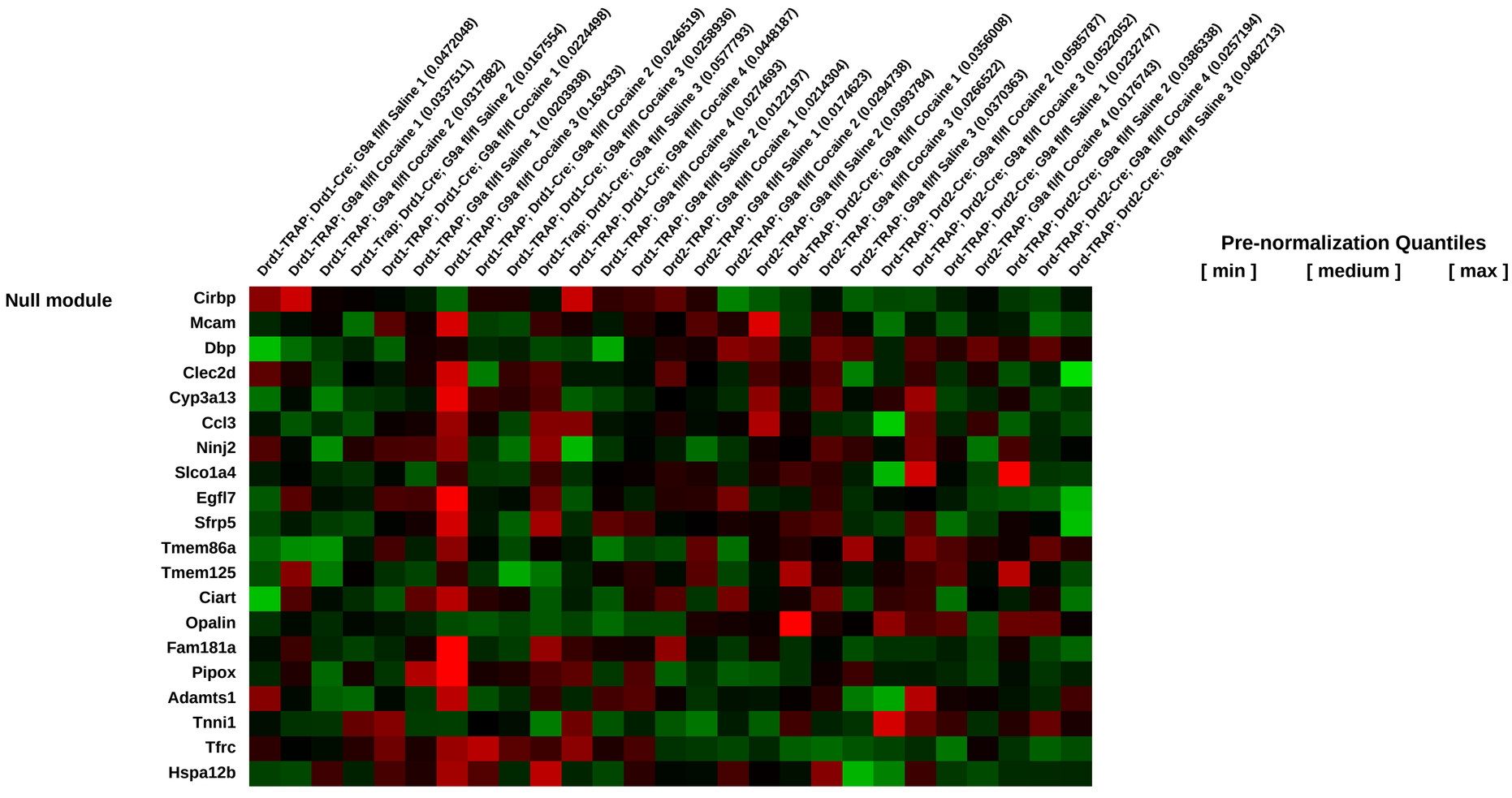

GEO Series "GSE54678" Expression Profiles

Num of samples in this series: 6

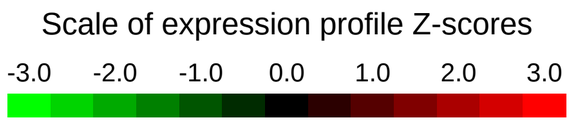

GEO Link:	**http://www.ncbi.nlm.nih.gov/geo/query/acc.cgi?acc=GSE54678**
Status:	**Public on Jun 30 2014**
Title:	**A pivotal role of SRC-2 in Metastatic and Castration Resistant Prostate Cancer**
Organism:	**Mus musculus**
Experiment type:	**Expression profiling by array**
Platform:	**GPL1261**
Pubmed ID:	
Summary & Design:	**Summary:** **SRC-2 is frequently amplified or overexpressed in metastatic prostate cancer patients. In this study, we used genetically engineered mice, overexpressing SRC-2 specifically in the prostate epithelium as a mouse model to examine the role of SRC-2 in prostate tumorigenesis. Over-expression of SRC-2 in PTEN heterozygous mice accelerates PTEN mutation induced tumor progression and develops a metastasis-prone cancer.** **We used microarrays to examine the molecular profile of prostate-specific SRC-2 overexpression adult dorsal-lateral prostate in comparison with that of control PTENF/+ heterozygous deletion mice.** **Overall design:** **total RNA was extracted from dorsal-lateral prostate of 7 months old-PTEN flox/+ control and PTEN flox/+; Rosa26-SRC-2 OE/+ adult mice, followed by gene expression profiling using Affymetrix microarrays. Each sample contains pooled prostate RNA from 3 mice.**

Background corr dist: **KL-Divergence = 0.0300, L1-Distance = 0.0202, L2-Distance = 0.0004, Normal std = 0.6761**

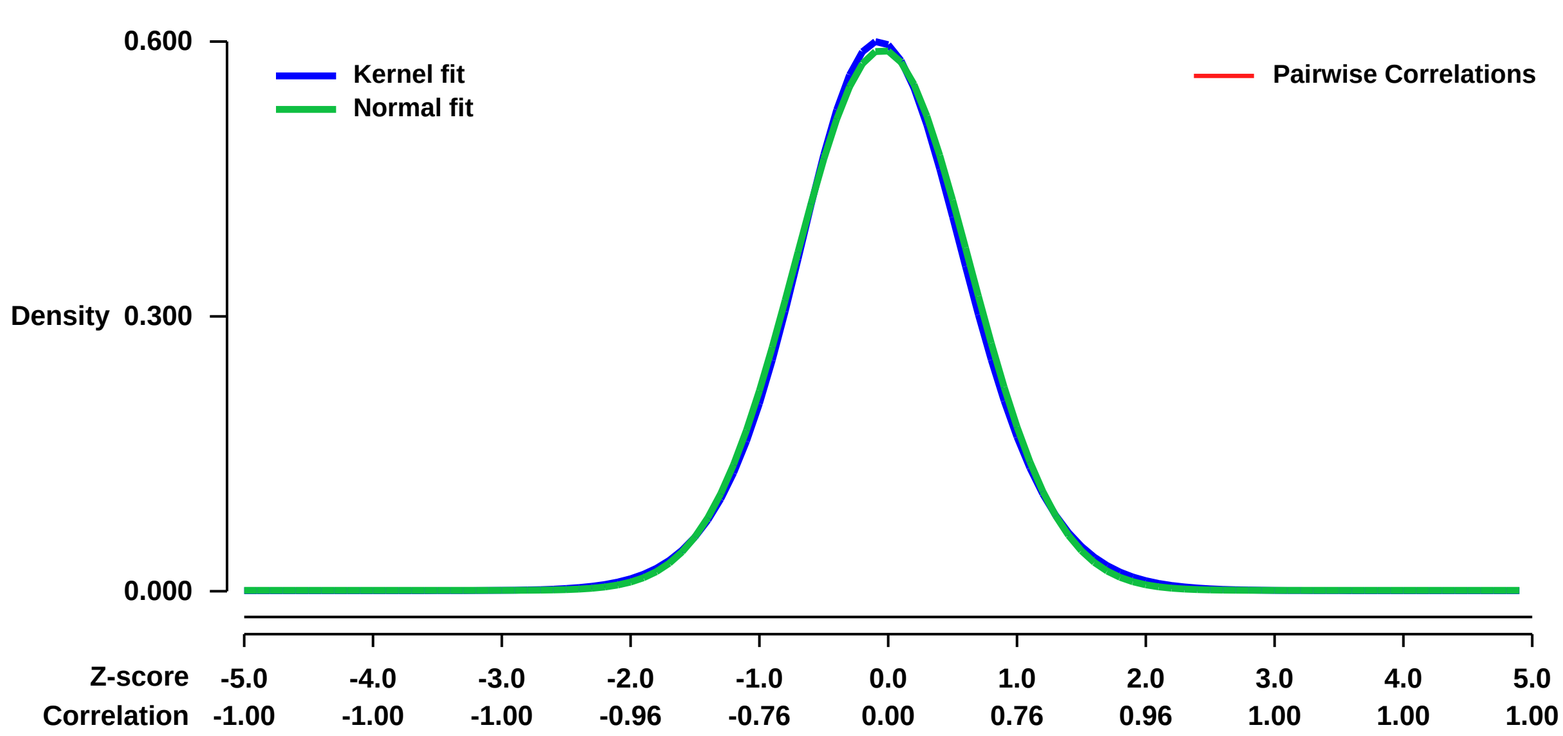

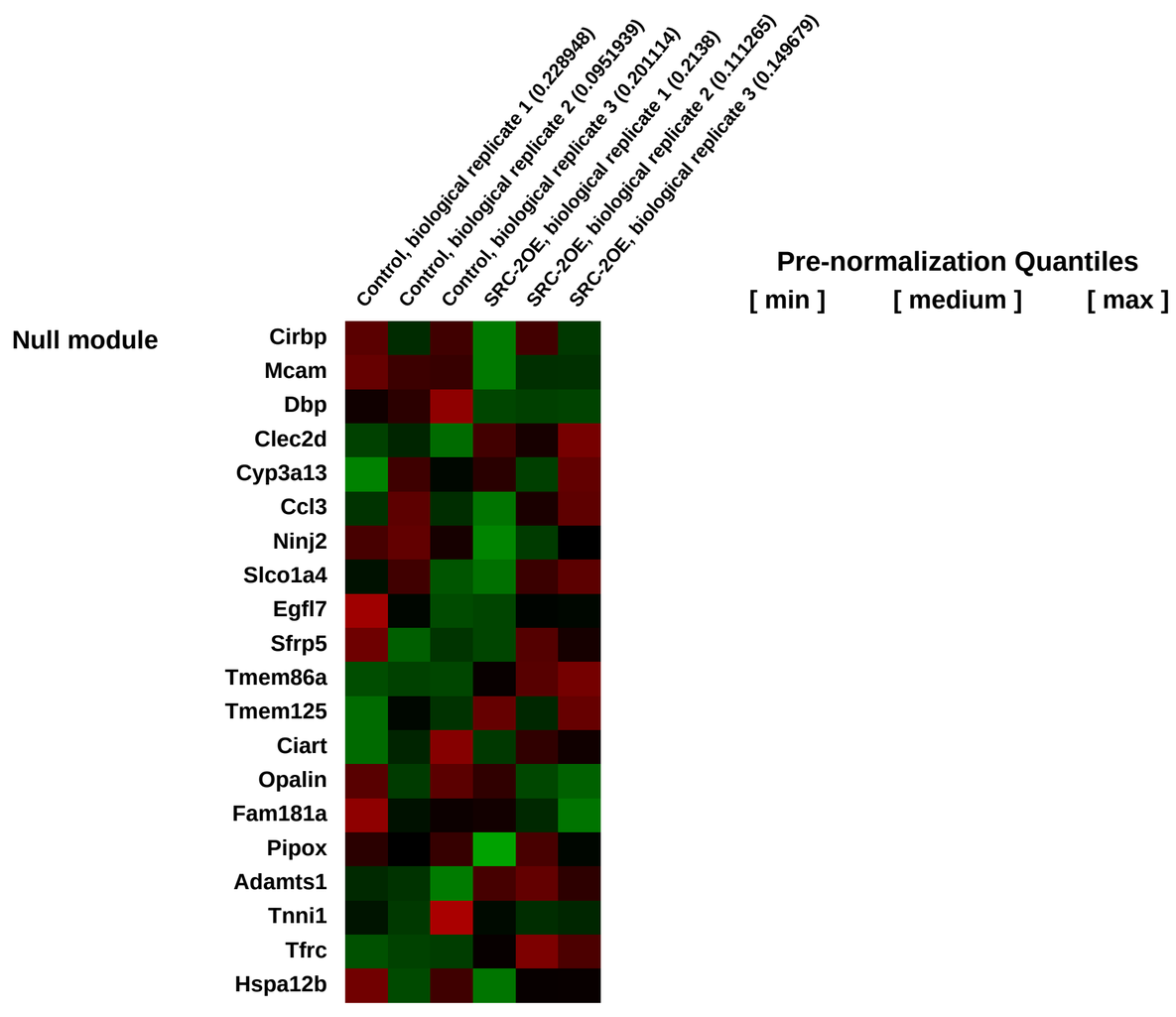

GEO Series "GSE54774" Expression Profiles

Num of samples in this series: 12

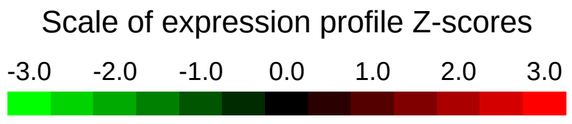

GEO Link:	**http://www.ncbi.nlm.nih.gov/geo/query/acc.cgi?acc=GSE54774**
Status:	**Public on Jun 01 2014**
Title:	**Expression data from mice on a high fat, high carbohydrate diet treated with exenatide**
Organism:	**Mus musculus**
Experiment type:	**Expression profiling by array**
Platform:	**GPL1261**
Pubmed ID:	

Summary & Design:

Summary:
The present study was constructed to confirm previous findings that mice on a high fat diet (HFD) treated by subcutaneous injection with exenatide (EXE) at 3´¡g/kg once daily for 6 weeks develop exocrine pancreatic injury (Rouse et al. 2014). The present study included 12 weeks of EXE exposure at multiple concentrations (3, 10, or 30 ¸…g/kg) with multiple endpoints (histopathology evaluations, immunoassay for cytokines, immunostaining of the pancreas, serum chemistries and measurement of trypsin, amylase, and, lipase, and gene expression profiles). Time- and dose-dependent exocrine pancreatic injury was observed in mice associated with EXE exposure in a HFD environment. The time- and dose-dependent morphological changes identified in the pancreas involved acinar cell injury and death (autophagy, apoptosis, necrosis, and atrophy), cell adaptations (hypertrophy and hyperplasia), and cell survival (regeneration) accompanied with varying degrees of inflammatory response leading to secondary injury in pancreatic blood vessels, ducts, and adipose tissues. Gene expression profiles supported the presence of increased signaling for cell survival and altered lipid metabolism. The potential for EXE to cause acute or early chronic pancreatic injury was identified in a HFD environment. In human disease, the influence of pancreatitis risk factors or pre-existing chronic pancreatitis on this injury potential requires further investigation.

Overall design:
Male C57BL/6 mice 6 to 8 weeks of age were purchased from Harlan Laboratories (Frederick, MD). Mice were housed individually in an environmentally controlled room (18´℃â 21´℃, 40%â 70% relative humidity) with a twelve-hour light/dark cycle. Mice were initially fed Certified Purina Rodent Chow #5002 (Ralston Purina Co., St. Louis, MO) providing 63% of calories through carbohydrates, 24% from protein, and 13% from fat. Per the experimental design, mice were subsequently placed on a Teklad Custom Research Diet, TD.06415 (Harlan, Frederick, MD), providing 45% of calories through fats (36% saturated, 47% monounsaturated, 17% polyunsaturated), 36% from carbohydrates, and 19% from protein. Water and food were available ad libitum. Thorough out the experiment all mice were weighed weekly and dosing adjusted accordingly for each mouse. A cohort of eighty 6 to 8 week-old male C57BL6 mice were received from Harlan Laboratories. The cohort represented experimental time point of 12 weeks. The cohort was further divided into 4 exenatide (EXE) treatment groups (0, 3, 10, or 30 ¸…g/kg) of 20 mice each. Initially, all mice were placed on HFD for six weeks without additional treatment and were then maintained on HFD for an additional 12 weeks while receiving daily subcutaneous injections of saline or EXE (Creative Peptides, Shirley, NY; 3, 10, or 30¸…g/kg). At the 12 week timepoint, twenty-four hours following their final dose, the mice from the treatment cohort were anesthetized with isoflurane and euthanized by exsanguination with collection of blood for serum harvest. The pancreas from 12 mice in each cohort was preserved in 10% formalin for histology processing. The pancreas from 5 mice in each cohort was placed in RNAlater (Life Technologies, Grand Island, NY) for subsequent RNA extraction and the pancreas from 3 mice in each cohort was immediately frozen in liquid nitrogen and then stored at -80´℃. Pancreas tissue was resected, preserved in RNALater, and stored at -80 C. After thawing, 2.5 mg of each sample were processed using miRNeasy Mini Kits (Cat # 217004) (Qiagen, Valencia, CA). Samples were homogenized in 700 uL of Qiazol Lysis Reagent (Qiagen), for 5 minutes at 50 hz in a TissueLyser LT (Qiagen), and processed using the automated purification of total RNA on a Qiacube (Qiagen), using the â Purification of total RNA, including small RNAs, from animal tissues & cells (aqueous phase), version 2 (April 2010)â standard protocol, as described in the miRNeasy Mini Handbook (1073008 07/2012) & http://www.qiagen.com/QIAcube/Standard/ProtocolView.aspx?StandardProtocolID=847.Mean yield per 2.5 mg of pancreas tissue was approximately 35 ug, determined by NanoDrop spectrophotometer (Thermo Scientific, Wilmington, DE). Average RIN values were approximately 5.4 +/- 1.4, as assayed by a 2100 Bioanalyzer Instrument (Agilent Technologies, Santa Clara, CA), using an Agilent RNA 6000 Nano Kit (cat # 5067-1511). This RIN mean was consistent with our previous experiences in RNA extraction from murine pancreatic tissue. The isolated RNA was labeled and gene expression analysis performed by Expression Analysis, Inc. (Durham, NC). The 3 samples with the highest RIN from each treatment group were used to probe treatment effect on gene expression. Total RNA samples (100 ng) were converted into cDNA using Ovation WGA FFPE System (NuGEN, Part No. 6200). The second strand cDNA is then purified with Agencourt RNAClean beads and followed by SPIA amplification. Amplified SPIA cDNA product is purified using Agencourt RNAClean beads and quantitated using a NanoDrop ND-8000 spectrophotometer. Target preparation was performed using 4 ¸…g of amplified cDNA and the NuGEN FL-Ovation cDNA Biotin Module V2. Fragmented and biotin-labeled target was hybridized to Affymetrix GeneChip Mouse Genome 430 2.0 microarrays. Raw gene expression data were first analyzed using ArrayTrack bioinformatics tool with robust multichip average algorithm and quantile normalization. Differentially expressed genes were defined by p < 0.05 and fold change > 1.3 in Welch t-test comparing treatment and control groups. Expression data were then imported to Ingenuity Pathway Analysis (IPA) tool for further analyses of pathway, biofunction, and toxicity using general and pancreas-specific knowledge bases.

Background corr dist: **KL-Divergence = 0.1265, L1-Distance = 0.0189, L2-Distance = 0.0006, Normal std = 0.4217**

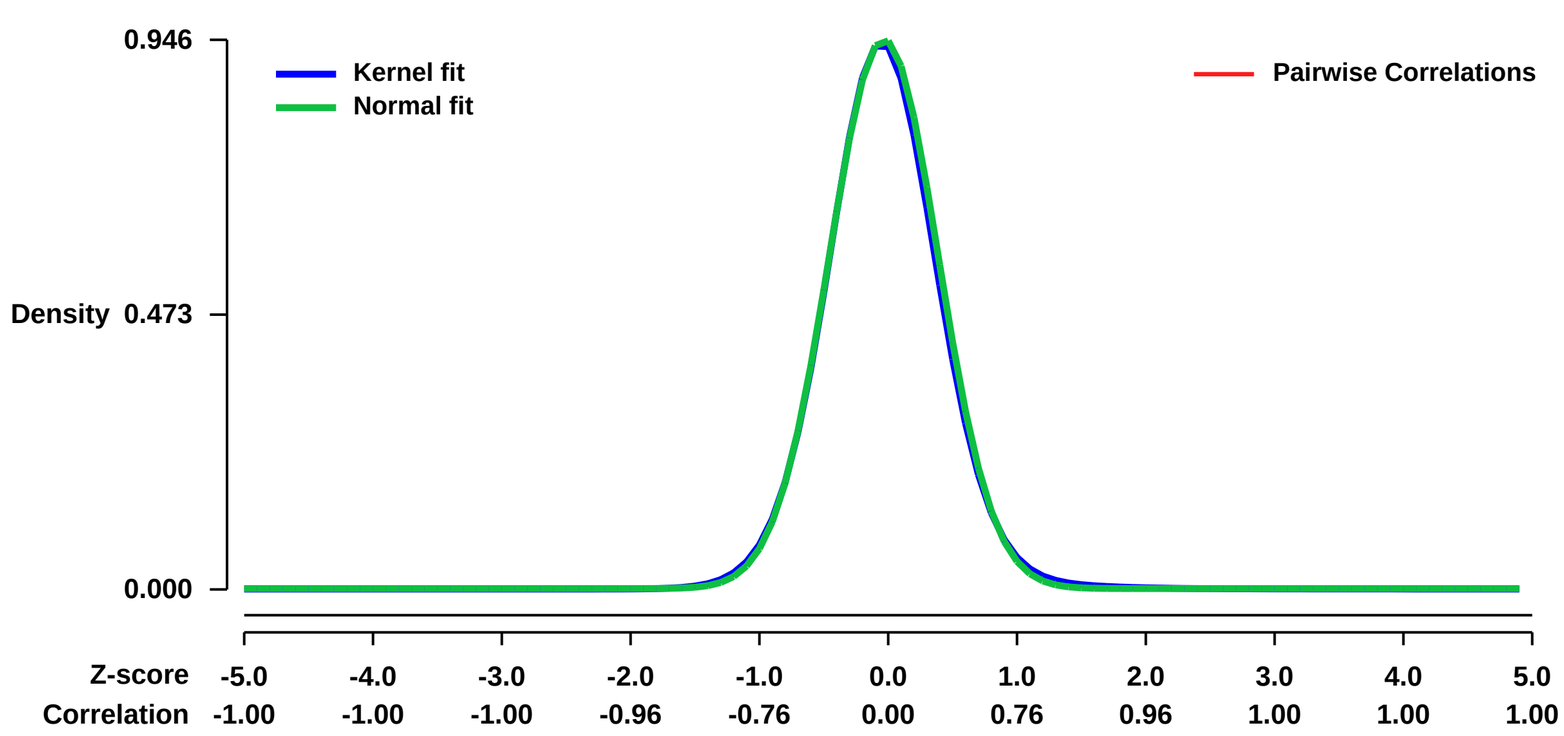

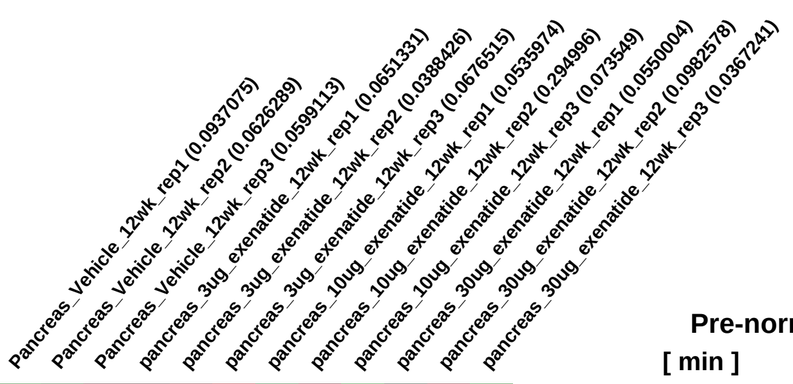

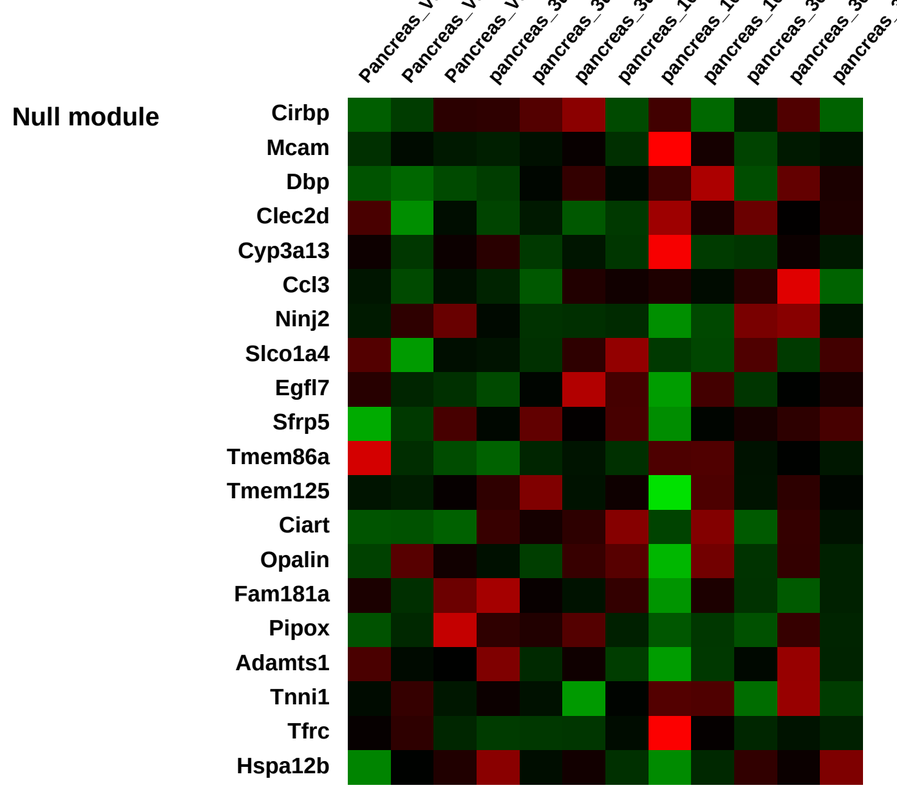

GEO Series "GSE54785" Expression Profiles

Num of samples in this series: 6

Scale of expression profile Z-scores

-3.0 -2.0 -1.0 0.0 1.0 2.0 3.0

GEO Link:	http://www.ncbi.nlm.nih.gov/geo/query/acc.cgi?acc=GSE54785
Status:	Public on Feb 08 2014
Title:	The acetylome regulators Hdac1 and Hdac2 differently modulate intestinal epithelial cell dependent homeostatic responses in experimental colitis
Organism:	Mus musculus
Experiment type:	Expression profiling by array
Platform:	GPL1261
Pubmed ID:	24525021
Summary & Design:	**Summary:** Histone deacetylases (Hdac) remove acetyl groups from proteins, influencing global and specific gene expression. Hdacs control inflammation, as shown by Hdac inhibitor-dependent protection from DSS-induced murine colitis. While tissue-specific Hdac knockouts show redundant and specific functions, little is known of their intestinal epithelial cell (IEC) role. We have shown previously that dual Hdac1/Hdac2 IEC-specific loss disrupts cell proliferation and determination, with decreased secretory cell numbers and altered barrier function. We thus investigated how compound Hdac1/Hdac2 or Hdac2 IEC-specific deficiency alters the inflammatory response. Floxed Hdac1 and Hdac2 and villin-Cre mice were interbred. Compound Hdac1/Hdac2 IEC-deficient mice showed chronic basal inflammation, with increased basal Disease Activity Index (DAI) and deregulated Reg gene colonic expression. DSS-treated dual Hdac1/Hdac2 IEC-deficient mice displayed increased DAI, histological score, intestinal permeability and inflammatory gene expression. In contrast to double knockouts, Hdac2 IEC-specific loss did not affect IEC determination and growth, nor result in chronic inflammation. However, Hdac2 disruption protected against DSS colitis, as shown by decreased DAI, intestinal permeability and caspase-3 cleavage. Hdac2 IEC-specific deficient mice displayed increased expression of IEC gene subsets, such as colonic antimicrobial Reg3b and Reg3g mRNAs, and decreased expression of immune cell function-related genes. Our data show that Hdac1 and Hdac2 are essential IEC homeostasis regulators. IEC-specific Hdac1 and Hdac2 may act as epigenetic sensors and transmitters of environmental cues and regulate IEC-mediated mucosal homeostatic and inflammatory responses. Different levels of IEC Hdac activity may lead to positive or negative outcomes on intestinal homeostasis during inflammation **Overall design:** Total RNAs from the colon of three control and three Hdac2 IEC-specific knockout mix background (CD-1/129/C57BL/6) mice were isolated with the Rneasy kit (Qiagen, Mississauga, ON, Canada).

Background corr dist: KL-Divergence = 0.0343, L1-Distance = 0.0202, L2-Distance = 0.0004, Normal std = 0.6501

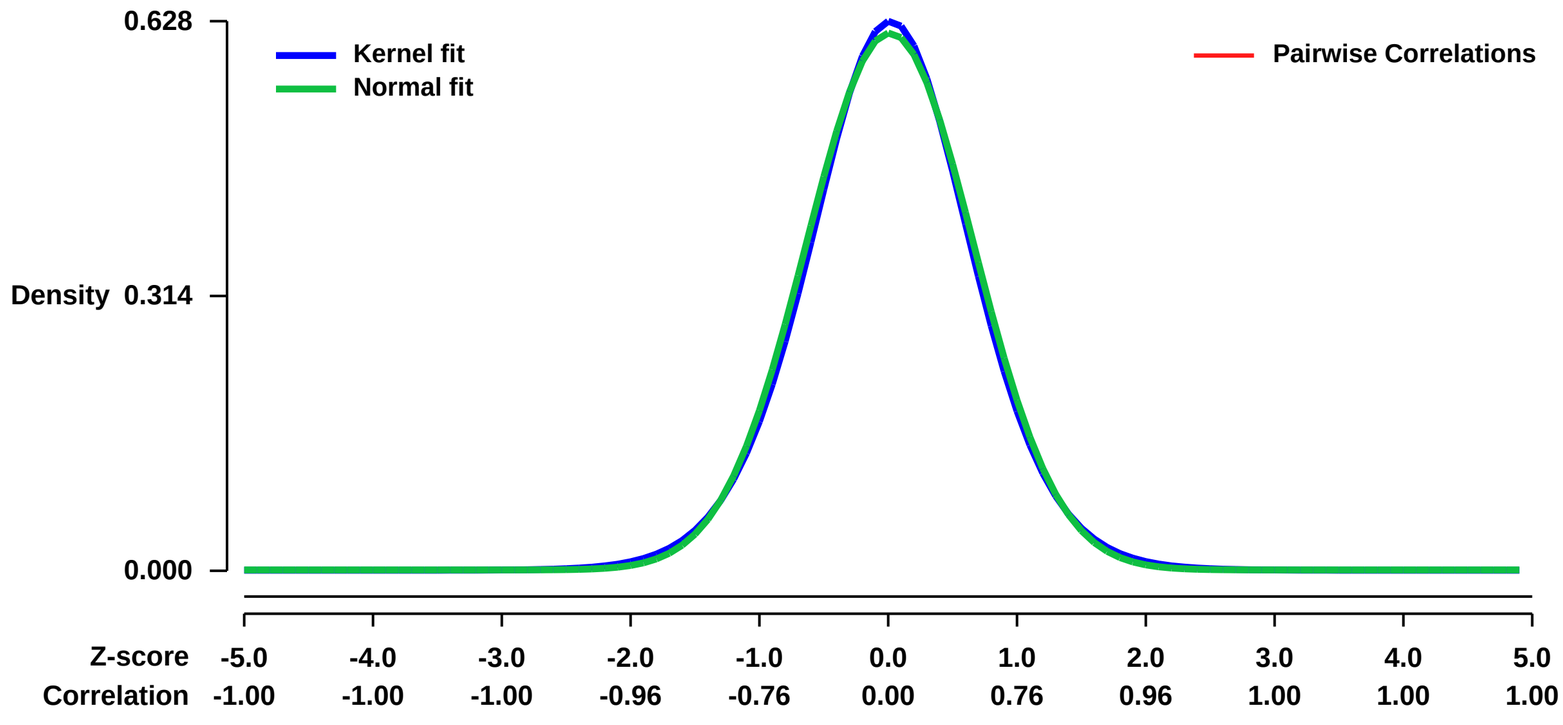

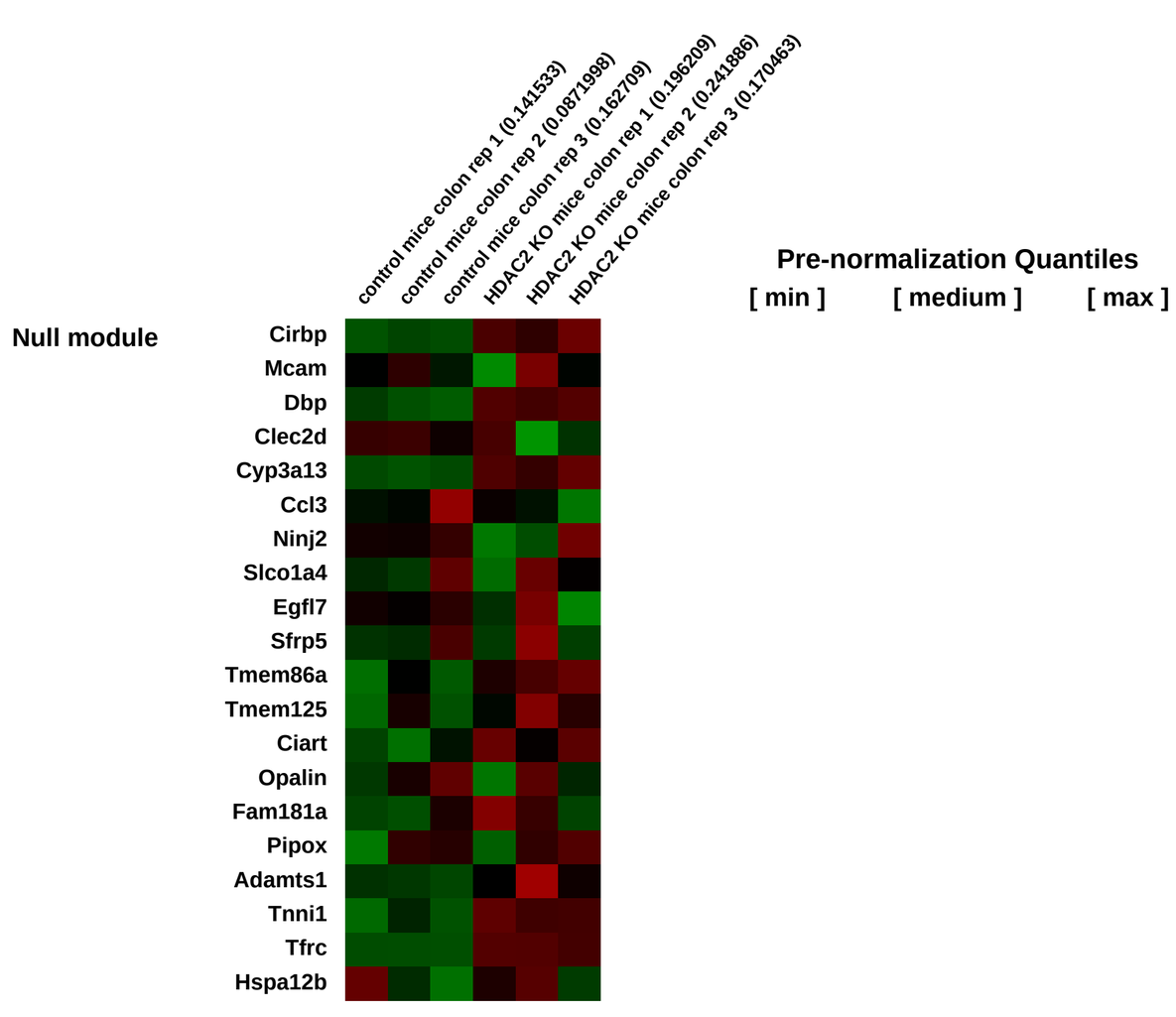

GEO Series "GSE5497" Expression Profiles

Num of samples in this series: 6

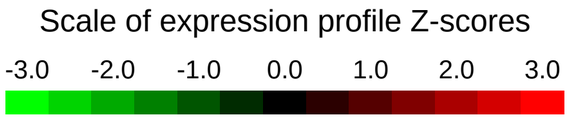

GEO Link:	http://www.ncbi.nlm.nih.gov/geo/query/acc.cgi?acc=GSE5497
Status:	Public on Aug 12 2006
Title:	Pyruvate induces mitochondrial biogenesis by a PGC-1alpha independent mechanism
Organism:	Mus musculus
Experiment type:	Expression profiling by array
Platform:	GPL1261
Pubmed ID:	17182725
Summary & Design:	**Summary:** The present study examines the impact of altering energy provision on mitochondrial biogenesis in muscle cells. C2C12 myoblasts were chronically treated with supraphysiological levels of sodium pyruvate for 72 hr. Treated cells exhibited increased mitochondrial protein expression, basal respiratory rate and maximal oxidative capacity. The increase in mitochondrial biogenesis was independent of increases in PGC-1alpha and PGC-1alpha mRNA expression. To further assess whether PGC-1alpha expression was necessary for pyruvate action, cells were infected with adenovirus containing shRNA for PGC-1alpha prior to treatment with pyruvate. Despite a 70% reduction in PGC-1alpha mRNA the effect of pyruvate was preserved. Furthermore, pyruvate induced mitochondrial biogenesis in primary myoblasts from PGC-1alpha null mice. These data suggest that regulation of mitochondrial biogenesis by pyruvate in myoblasts is independent of PGC-1alpha, suggesting the existence of a novel energy-sensing pathway regulating oxidative capacity. **Keywords:** basal state versus treatment at one time point **Overall design:** C2C12 myoblasts were incubated with either basal media or basal media supplemented with 50 mM sodium pyruvate for 72 hr. Total RNA was extracted using TRIzol and GeneChip experiment was conducted using Gene Chip Mouse Genome 430 2.0 Expression Array. A Gene Chip analysis for each condition was performed in triplicate.

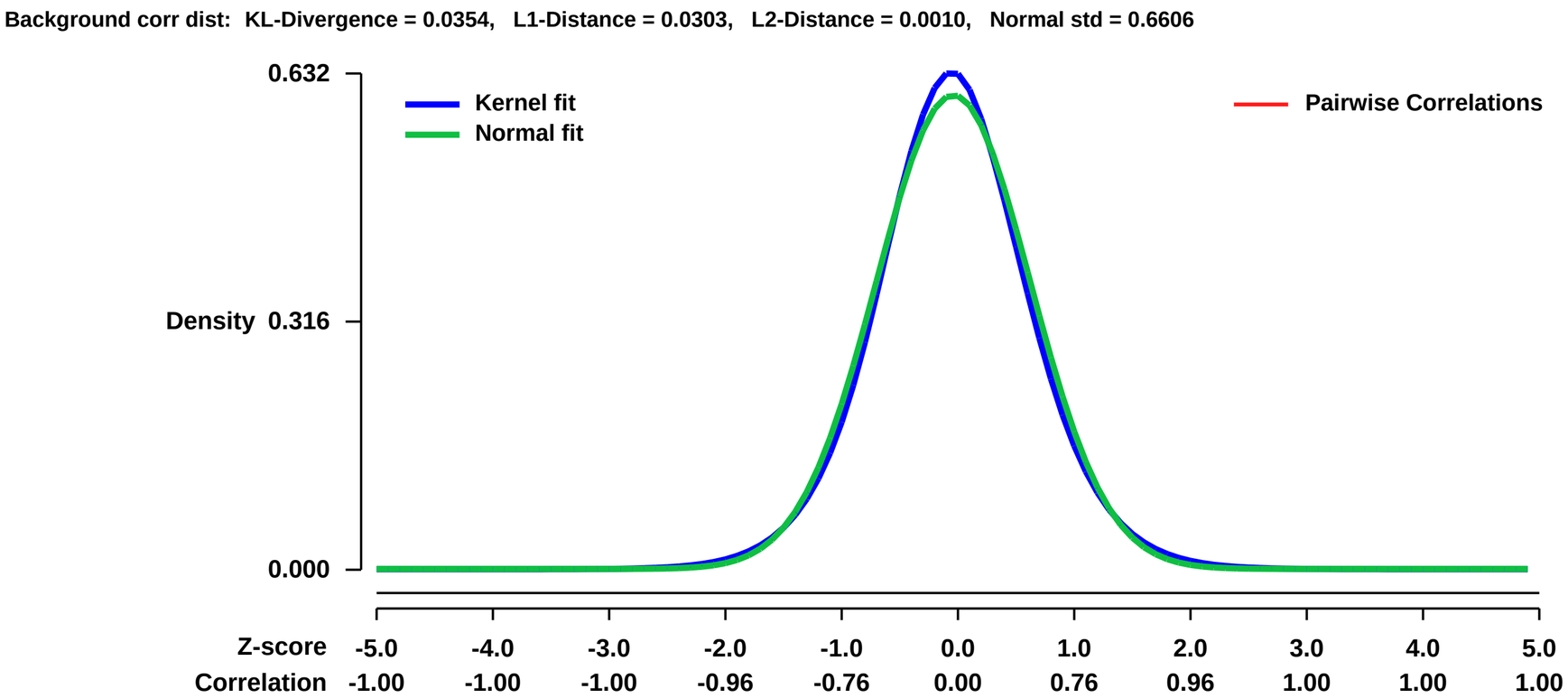

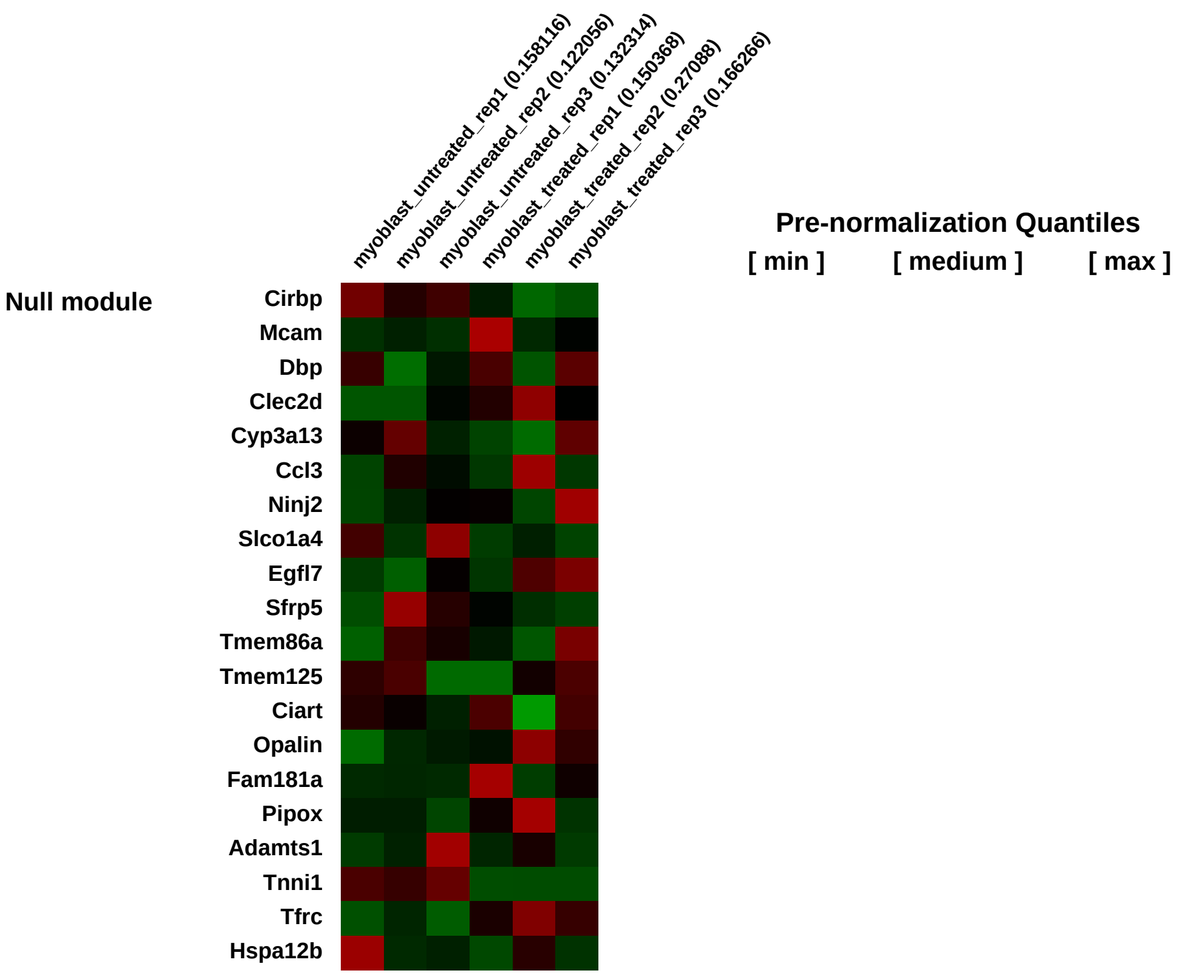

GEO Series "GSE54976" Expression Profiles

Num of samples in this series: 17

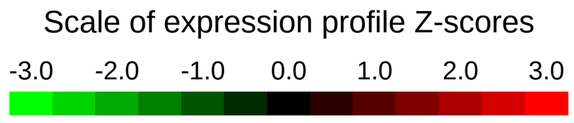

GEO Link:	**http://www.ncbi.nlm.nih.gov/geo/query/acc.cgi?acc=GSE54976**
Status:	**Public on Feb 14 2014**
Title:	**Gene expression in thymi of Tcf1 -/-, Tcf +/- or Tcf1 -/- mice with tumor.**
Organism:	**Mus musculus**
Experiment type:	**Expression profiling by array**
Platform:	**GPL1261**
Pubmed ID:	**23185135**

Summary & Design:

Summary:
The HMG-box factor Tcf1 is required during T-cell development in the thymus and mediates the nuclear response to Wnt signals. Tcf1â /â mice have previously been characterized and show developmental blocks at the CD4â CD8â double negative (DN) to CD4+CD8+ double positive transition. Due to the blocks in T-cell development, Tcf1â /â mice normally have a very small thymus. Unexpectedly, a large proportion of Tcf1â /â mice spontaneously develop thymic lymphomas with 50% of mice developing a thymic lymphoma/leukemia at the age of 16 wk. These lymphomas are clonal, highly metastatic, and paradoxically show high Wnt signaling when crossed with Wnt reporter mice and have high expression of Wnt target genes Lef1 and Axin2. In wild-type thymocytes, Tcf1 is higher expressed than Lef1, with a predominance of Wnt inhibitory isoforms. Loss of Tcf1 as repressor of Lef1 leads to high Wnt activity and is the initiating event in lymphoma development, which is exacerbated by activating Notch1 mutations. Thus, Notch1 and loss of Tcf1 functionally act as collaborating oncogenic events. Tcf1 deficiency predisposes to the development of thymic lymphomas by ectopic up-regulation of Lef1 due to lack of Tcf1 repressive isoforms and frequently by cooperating activating mutations in Notch1. Tcf1 therefore functions as a T-cellâ specific tumor suppressor gene, besides its established role as a Wnt responsive transcription factor. Thus, Tcf1 acts as a molecular switch between proliferative and repressive signals during T-lymphocyte development in the thymus.

Using the Tcf1â /â ¸ VII/¸ VII knockout mouse (Verbeek et al. Nature 1995), thymocytes of 17 mice (5 control Tcf+/-, 4 Tcf-/- and 8 Tcf-/- with thymic lymphoma) were homogenized for RNA isolation using Qiagen RNeasy minicolumns. The quantity and quality of total RNA was determined using spectrophotometry (Nanodrop) and an Agilent Bioanalyzer. One ´µg of RNA was used to generate cRNA using Affymetrix One cycle cDNA synthesis kit (Affymetrix, Santa Clara, CA, USA), after which the samples were biotinylated using an Affymetrix IVT labeling kit (Affymetrix). The samples were hybridized overnight at 42´℃ to GeneChip mouse genome 430 2.0 Arrays (Affymetrix). Washing and staining steps were performed on a Fluidics station 450, and the Genechips were scanned using a GeneChip scanner 3000 (Affymetrix) at the Department of Immunology, Erasmus Medical Center. Raw data were normalized and summarized using Robust Multichip Average (RMA) method.

Overall design:
The experiment consists of 5 control Tcf+/- thymi, 4 Tcf-/- thymi and 8 Tcf-/- thymus samples with thymic lymphoma.

Background corr dist: KL-Divergence = 0.0678, L1-Distance = 0.0800, L2-Distance = 0.0128, Normal std = 0.5432

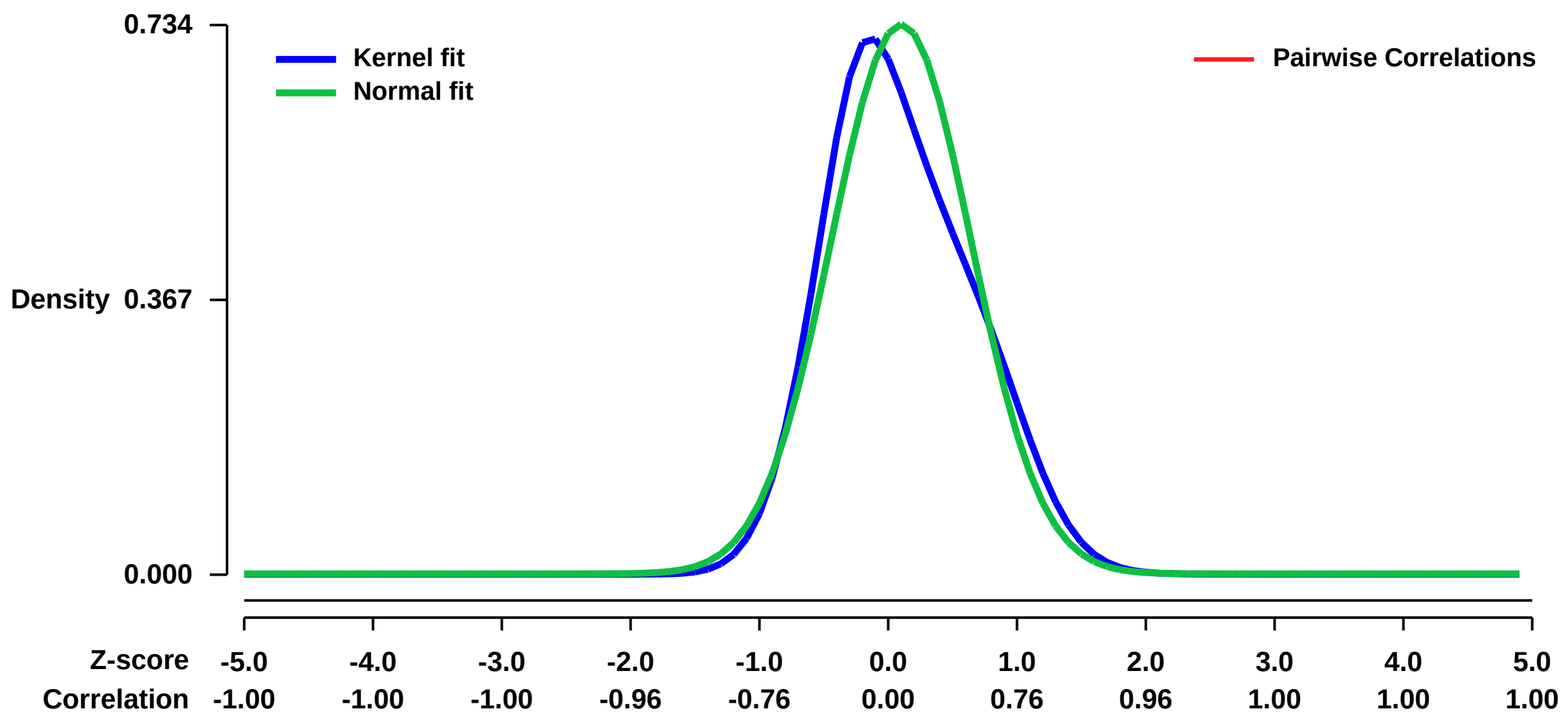

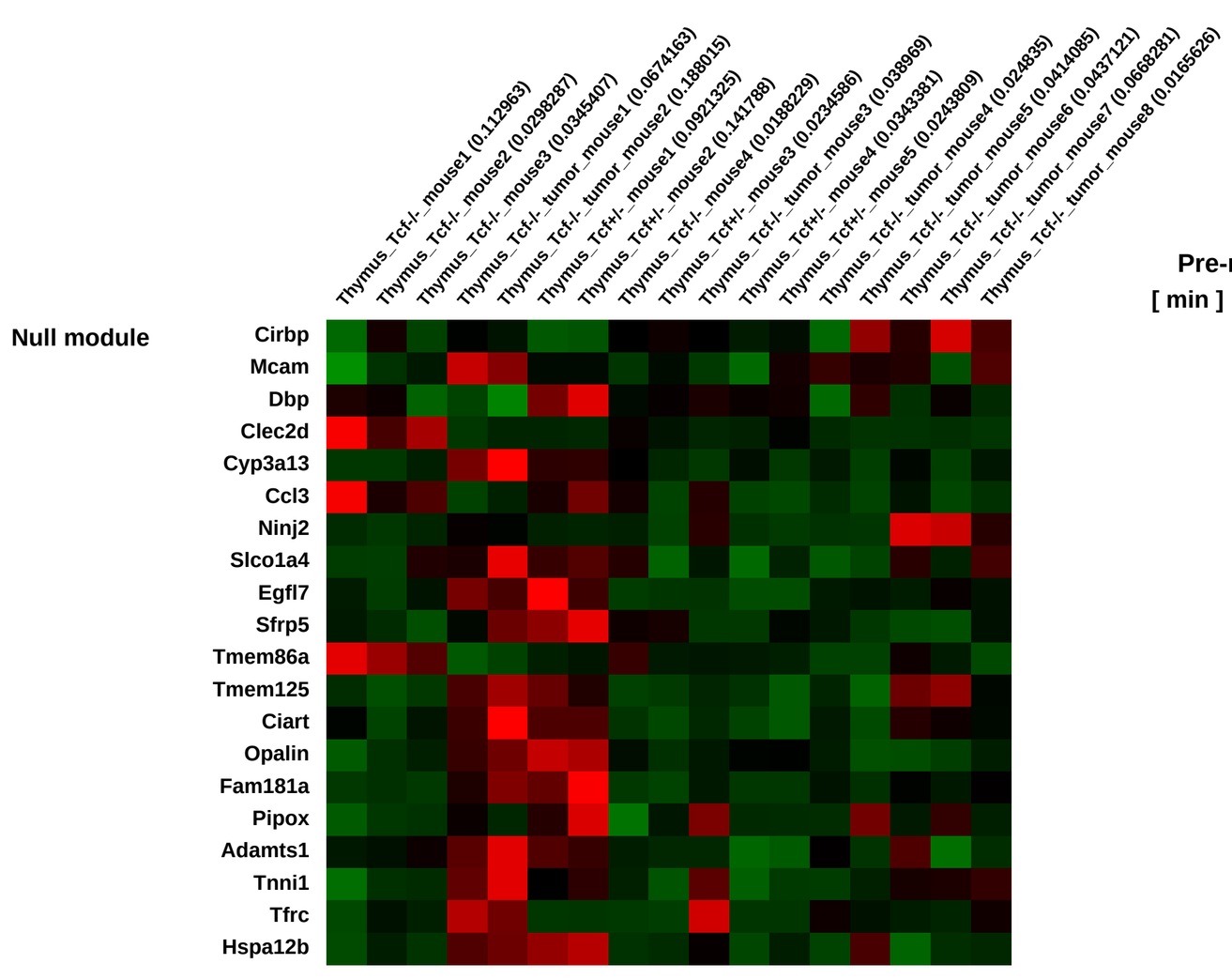

GEO Series "GSE55002" Expression Profiles

Num of samples in this series: 6

Scale of expression profile Z-scores

-3.0 -2.0 -1.0 0.0 1.0 2.0 3.0

GEO Link:	http://www.ncbi.nlm.nih.gov/geo/query/acc.cgi?acc=GSE55002
Status:	Public on Feb 14 2014
Title:	Transcription array by profiling in WT and SRC-2 null mouse liver
Organism:	Mus musculus
Experiment type:	Expression profiling by array
Platform:	GPL1261
Pubmed ID:	16423883
Summary & Design:	**Summary:** The molecular targets of SRC-2 regulation in the murine liver stimulate fatty acid degradation and glycolytic pathway while fatty acid, cholesterol, and steroid biosynthetic pathways are down-regulated. **Overall design:** A genomic approach using microarray analysis was employed to identify the subsets of genes that are altered in the liver of SRC-2-/- mice.

Background corr dist: KL-Divergence = 0.0418, L1-Distance = 0.0178, L2-Distance = 0.0003, Normal std = 0.6064

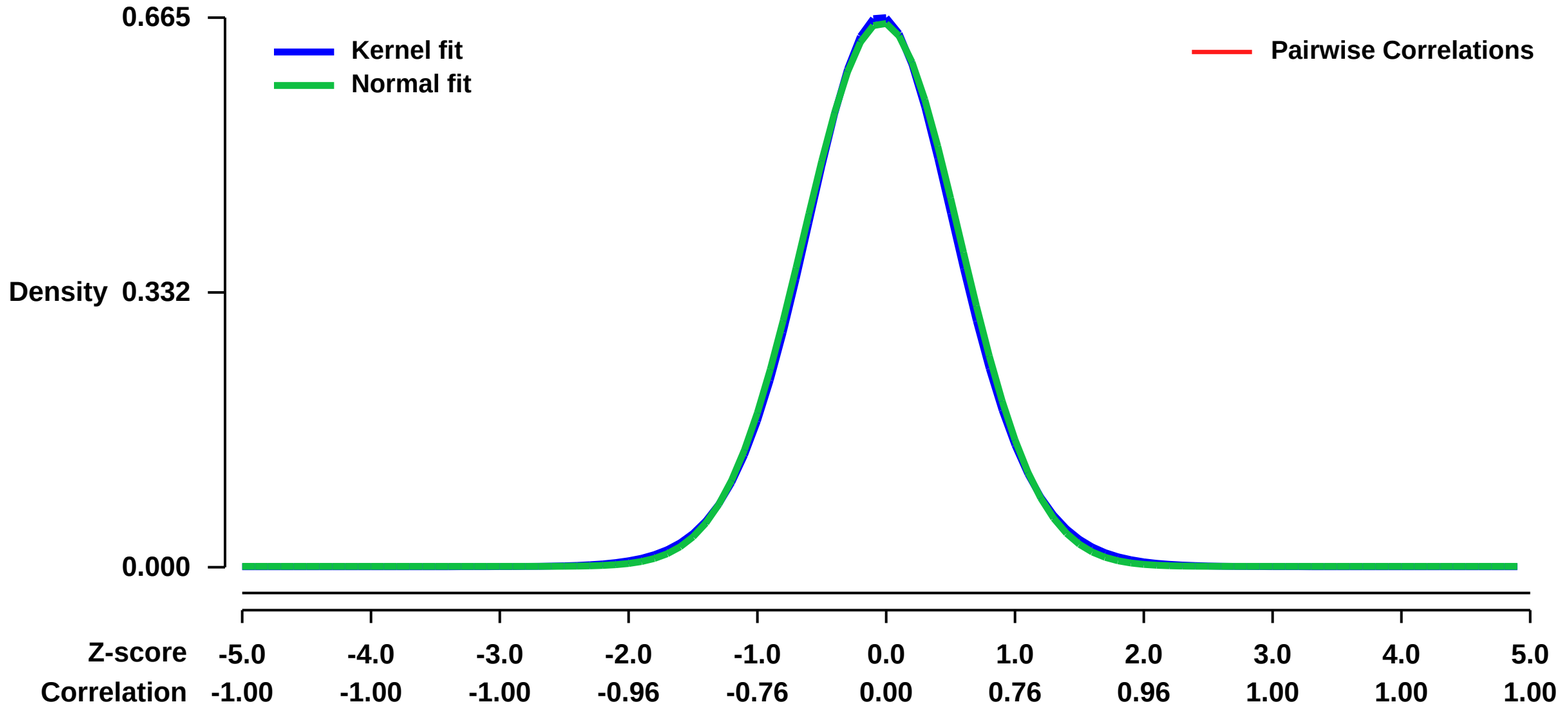

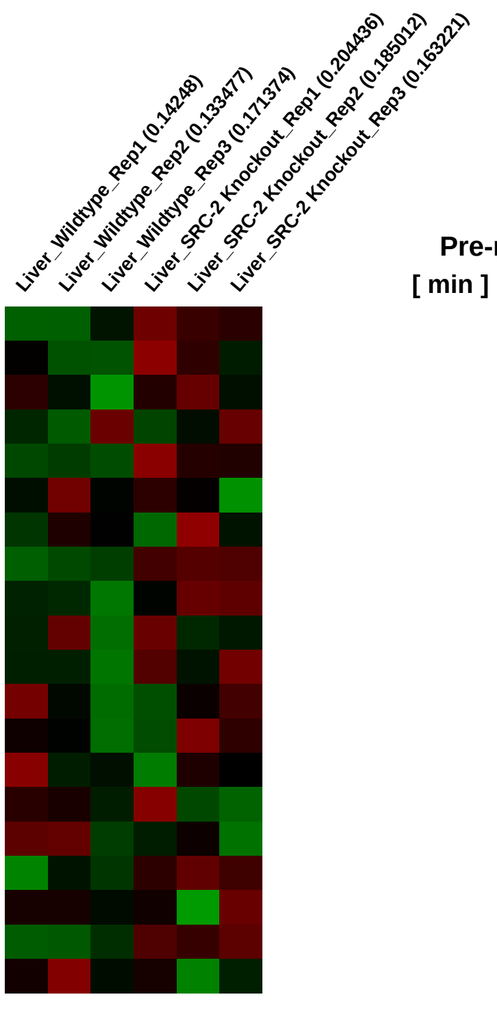

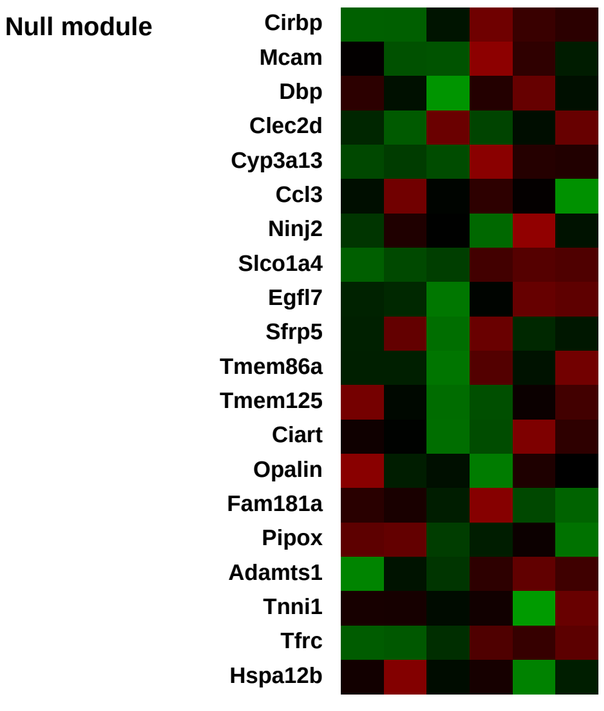

GEO Series "GSE55003" Expression Profiles

Num of samples in this series: 12

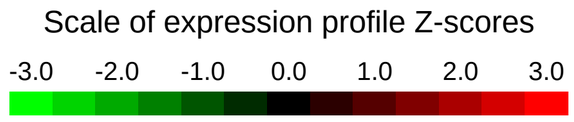

GEO Link:	**http://www.ncbi.nlm.nih.gov/geo/query/acc.cgi?acc=GSE55003**
Status:	**Public on Feb 18 2014**
Title:	**Expression profiling by array in livers of Nrf2 null mice administered CDDO-IM**
Organism:	**Mus musculus**
Experiment type:	**Expression profiling by array**
Platform:	**GPL1261**
Pubmed ID:	
Summary & Design:	**Summary:** **Nrf2 null mice administered CDDO-IM** **Overall design:** **Nrf2 null mice treated with CDDO-IM**

Background corr dist: **KL-Divergence = 0.0863, L1-Distance = 0.0388, L2-Distance = 0.0031, Normal std = 0.4590**

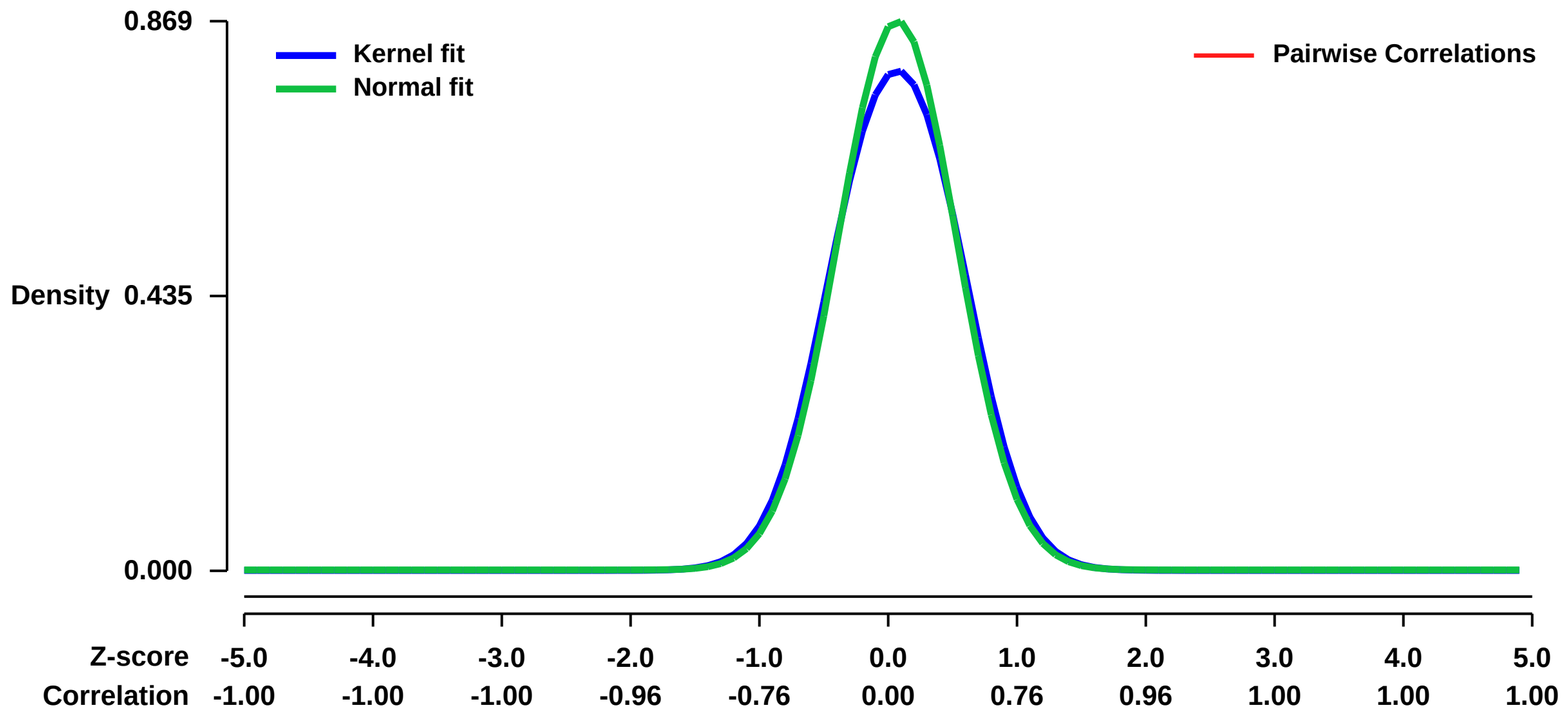

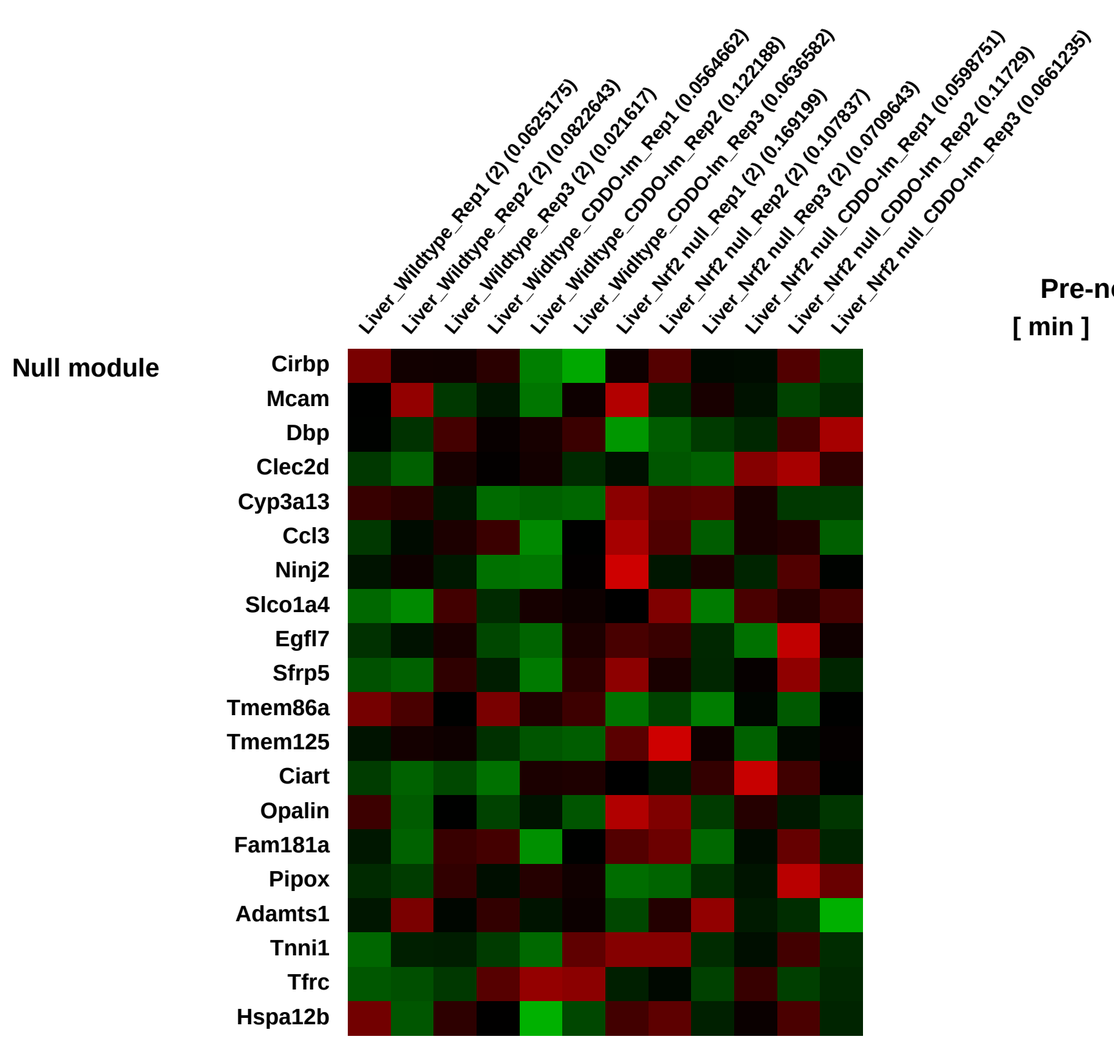

GEO Series "GSE55028" Expression Profiles

Num of samples in this series: 6

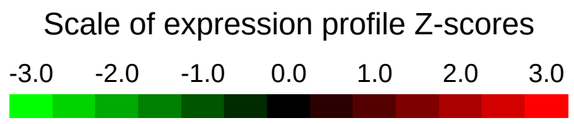

GEO Link:	**http://www.ncbi.nlm.nih.gov/geo/query/acc.cgi?acc=GSE55028**
Status:	**Public on Apr 01 2014**
Title:	**CMPF alters expression of genes related to metabolism in isolated mouse islets**
Organism:	**Mus musculus**
Experiment type:	**Expression profiling by array**
Platform:	**GPL1261**
Pubmed ID:	
Summary & Design:	**Summary:** **CMPF is elevated in diabetes and is associated with impaired insulin secretion. We used microarrays to determine the effect of CMPF on gene expression in isolated islets.** **Overall design:** **Isolated islets from male CD1 mice were treated for 24h with vehicle control or 200uM CMPF.**

Background corr dist: **KL-Divergence = 0.0294, L1-Distance = 0.0116, L2-Distance = 0.0001, Normal std = 0.6652**

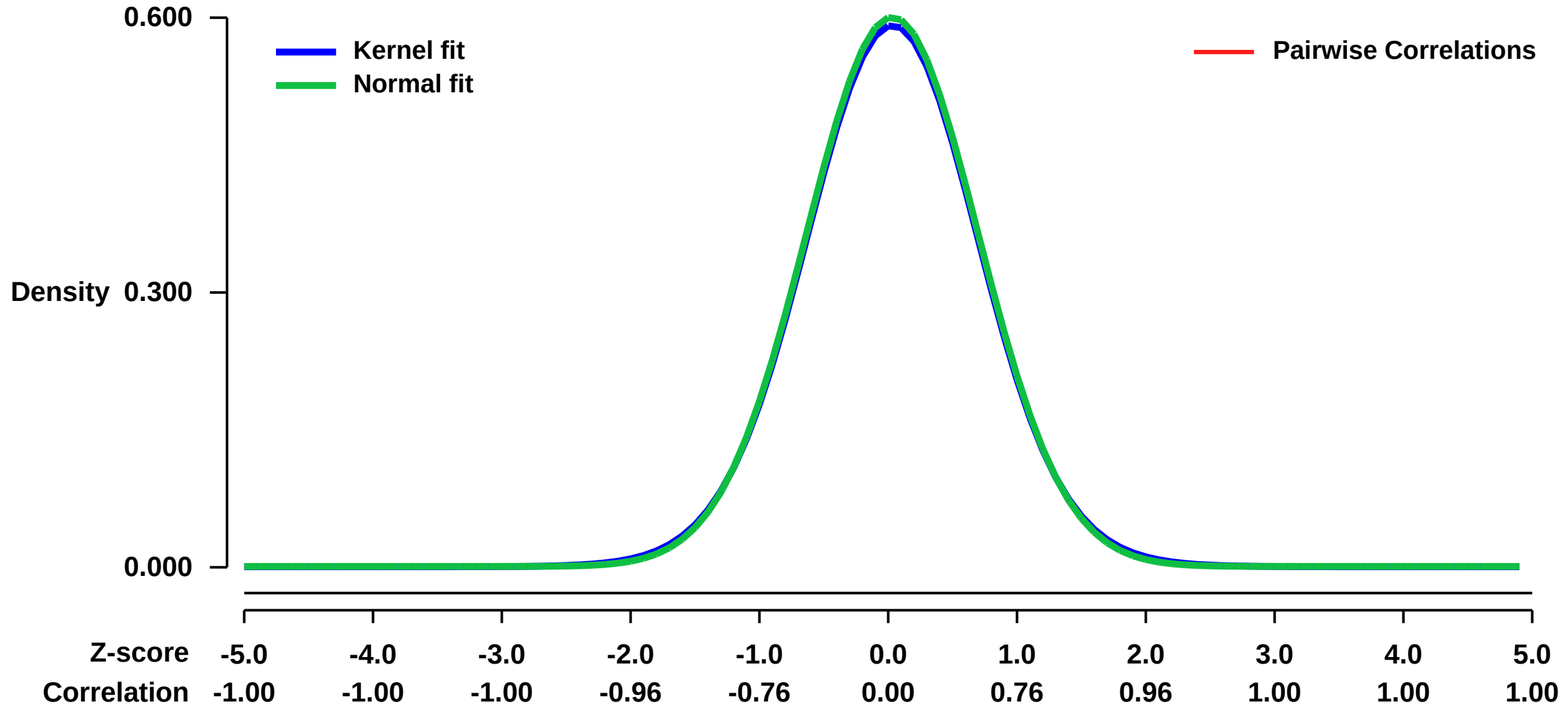

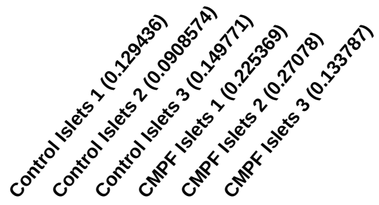

Pre-normalization Quantiles

[min] [medium] [max]

Null module

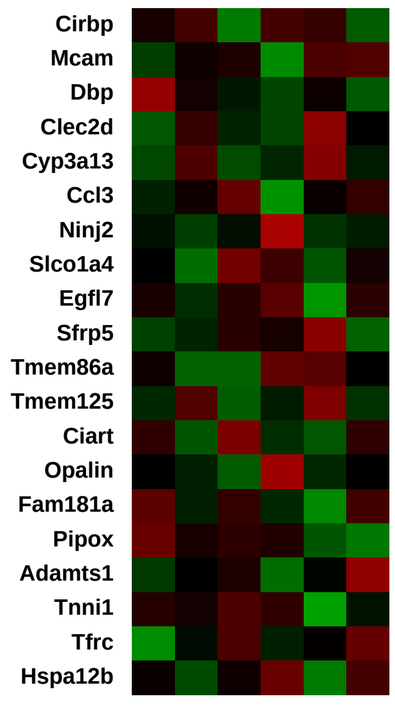

GEO Series "GSE55162" Expression Profiles

Num of samples in this series: 8

Scale of expression profile Z-scores

-3.0 -2.0 -1.0 0.0 1.0 2.0 3.0

GEO Link:	http://www.ncbi.nlm.nih.gov/geo/query/acc.cgi?acc=GSE55162
Status:	Public on Feb 20 2014
Title:	Age-related changes in the cellular composition and epithelial organization of the mouse trachea
Organism:	Mus musculus
Experiment type:	Expression profiling by array
Platform:	GPL1261
Pubmed ID:	24675804
Summary & Design:	**Summary:** We report here senescent changes in the structure and organization of the mucociliary pseudostratified epithelium of the mouse trachea and the main stem bronchi. We confirm previous reports of the graduate appearance of age-related, gland-like structures (ARGLS) in the submucosa, espeically in the intercartilage regions and carina. Immunohistochemistry shows these structures contain ciliated and secretory cells and Krt5+ basal cells, but not the myoepithelial cells or ciliated ducts typical of normal submucosal glands. Data suggests they arise de novo by budding from teh surface epithelium rather than by delayted growth of small or cryptic submucosal glands. In old mice the surface epithelium contains fewer cells per unit length than in young mice and the proportion of Krt5+, p63+ basal cells is reduced in both males and females. However, there appears to be no significant difference in the ability of basal stem cells isolated from individual young and old mice to form clonal tracheospheres in culture or in the ability of the pithelium to repair after damage by inhaled sulfur dioxide. Gene expression analysis by Affymetrix microarray and quantitative PCR, as well as immunohistochemistry and flow sorting studies, are consistent with low-grade chronic inflammation in the tracheas of old versus young mice. The significance of these changes for ARGL formation are not clear since several treatments that induce acute inflammation in young mice did not result in budding of the surface epithelium. **Overall design:** Total RNA from distal tracheas and carinas of four young (2 month) and four older (14 month) C57Bl/6 female mice was extracted using QIAshredder and RNeasy Micro Kits (QIAGEN). The quality was checked with a 2100 Bioanalyzer (Agilent Technologies). Total RNA was processed using Ambion MessageAmpTM Premier by the Duke Microarray Facility. Standard Affymetrix protocols and Affymetrix GeneChip´fi Mouse Genome 430 2.0 Array chips were used to generate .cel files.

Background corr dist: KL-Divergence = 0.0838, L1-Distance = 0.0224, L2-Distance = 0.0006, Normal std = 0.4668

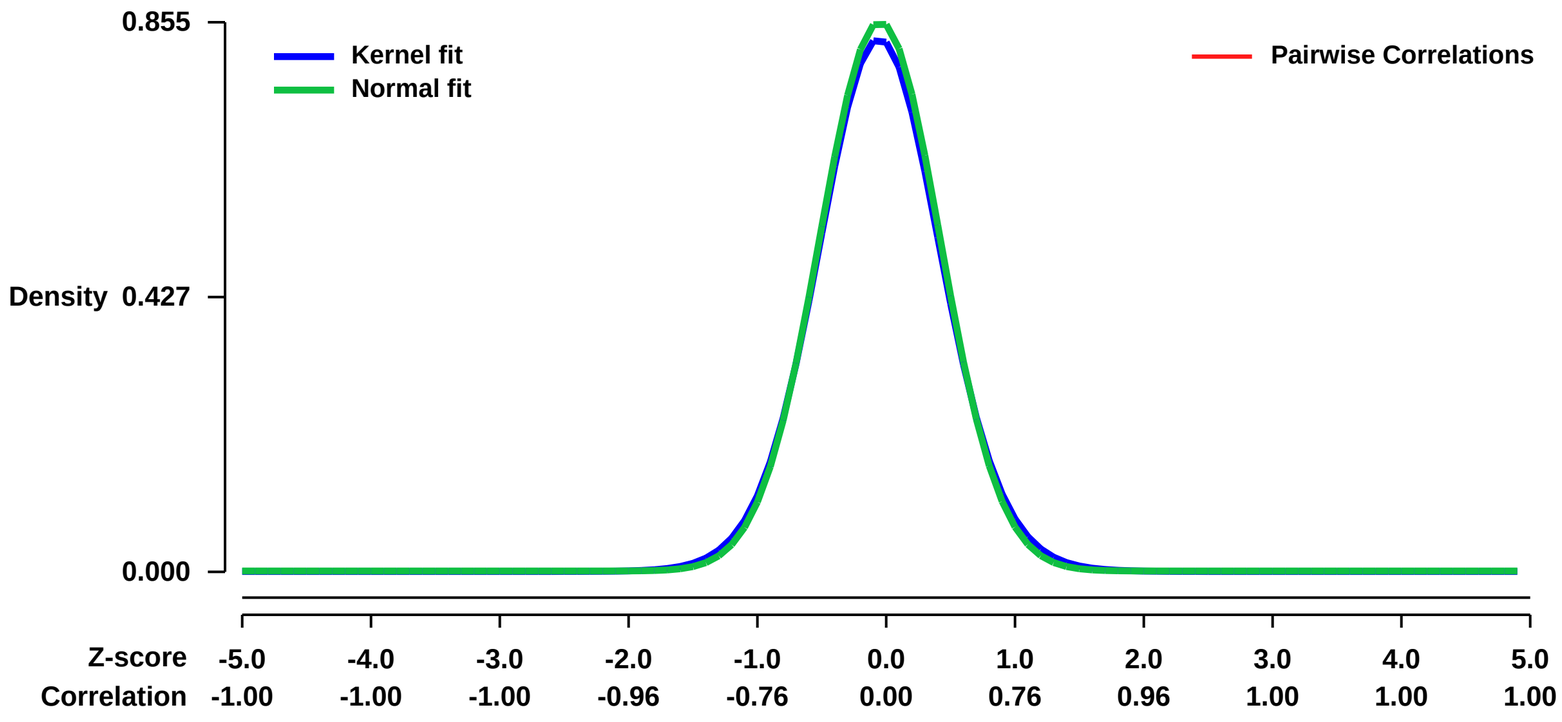

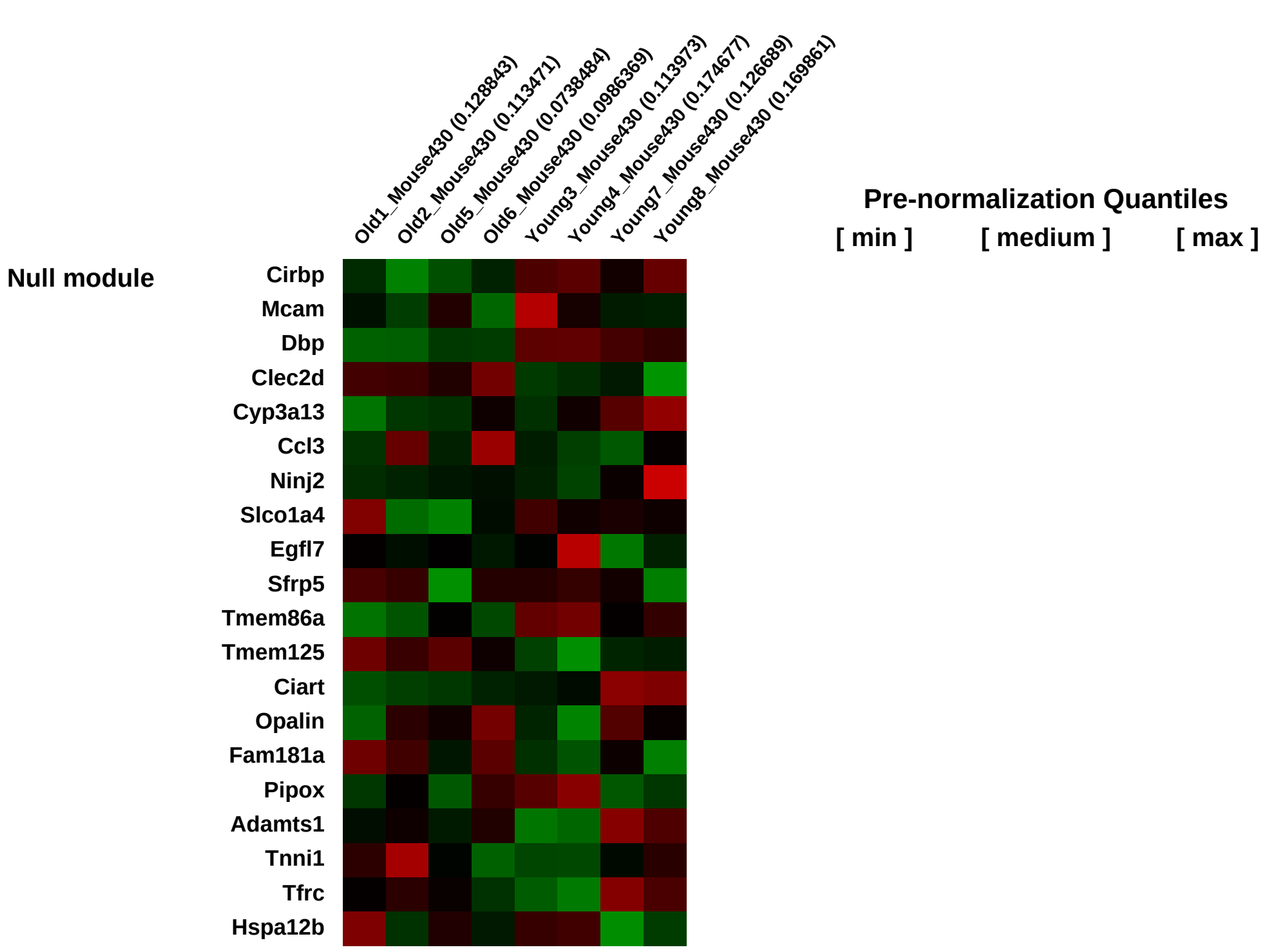

GEO Series "GSE55238" Expression Profiles

Num of samples in this series: 28

Scale of expression profile Z-scores

-3.0 -2.0 -1.0 0.0 1.0 2.0 3.0

GEO Link:	http://www.ncbi.nlm.nih.gov/geo/query/acc.cgi?acc=GSE55238
Status:	Public on Feb 21 2014
Title:	Host Responses to Sepsis Vary in Different Low-Lethality Murine Models
Organism:	Mus musculus
Experiment type:	Expression profiling by array
Platform:	GPL1261
Pubmed ID:	
Summary & Design:	**Summary:** **The CS and CLP murine models of intra-abdominal sepsis have unique transcriptomic respones 2 hrs, 1 and 3 days after sepsis** **Overall design:** **Infection protocol: Used the Cecal Ligation and Puncture (CLP) model and Cecal Slurry (CS) method in young mice.**

Background corr dist: **KL-Divergence = 0.0772, L1-Distance = 0.0719, L2-Distance = 0.0112, Normal std = 0.5033**

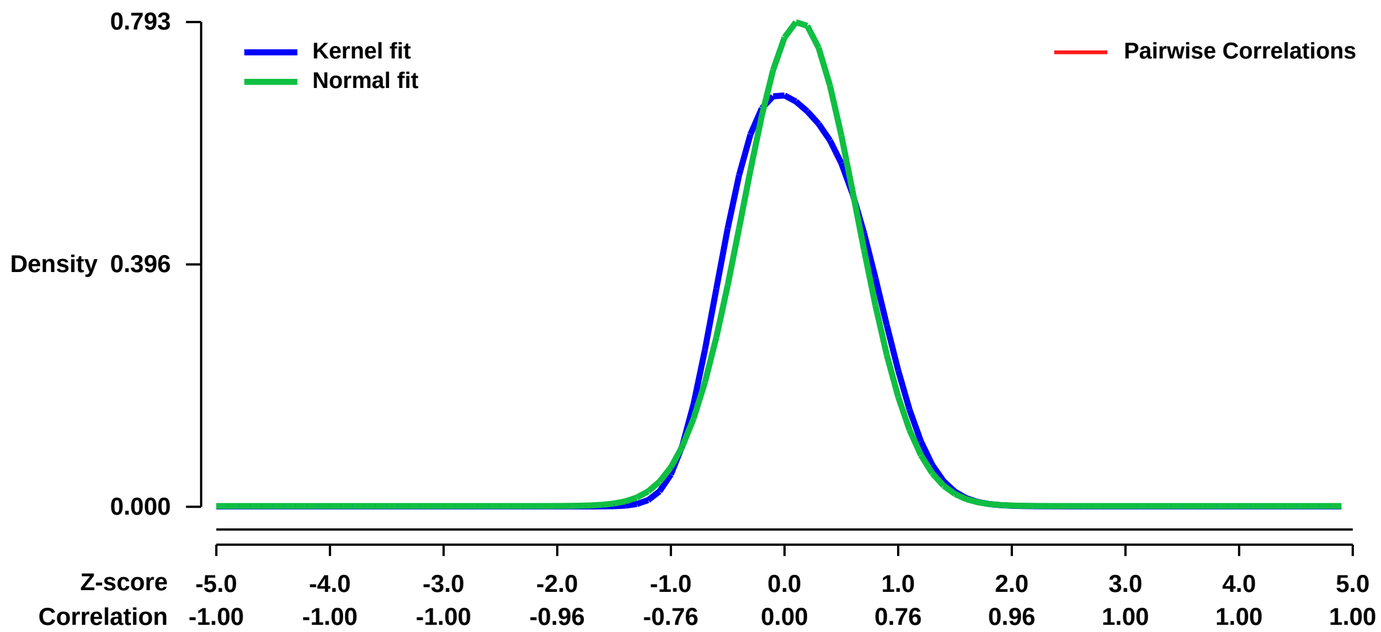

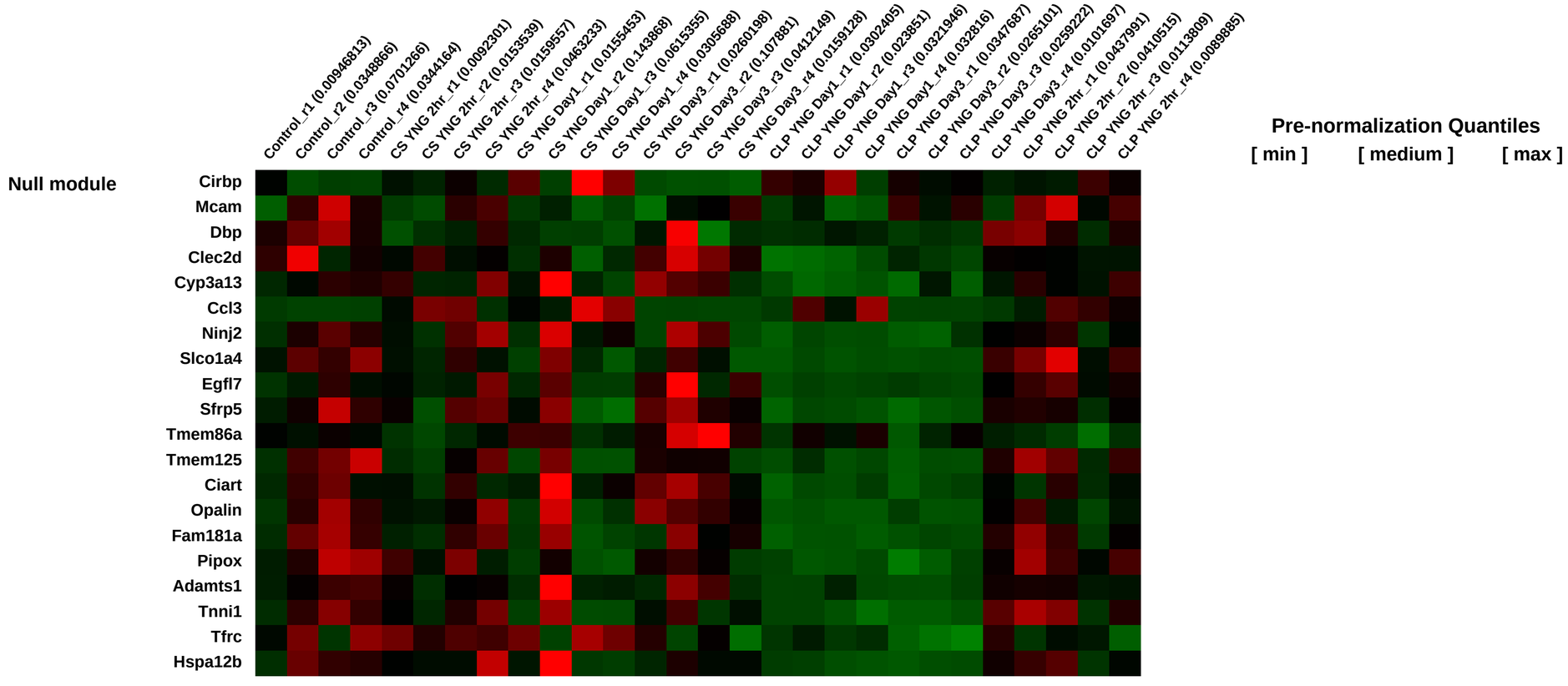

GEO Series "GSE55356" Expression Profiles

Num of samples in this series: 6

Scale of expression profile Z-scores

-3.0 -2.0 -1.0 0.0 1.0 2.0 3.0

GEO Link:	**http://www.ncbi.nlm.nih.gov/geo/query/acc.cgi?acc=GSE55356**
Status:	**Public on Jul 01 2014**
Title:	**p38a-dependent gene expression in the colonic mucosa**
Organism:	**Mus musculus**
Experiment type:	**Expression profiling by array**
Platform:	**GPL1261**
Pubmed ID:	
Summary & Design:	**Summary:** **Gene expression in the colonic mucosa of wild-type and p38a-knockout intestinal epithelial cells (IECs) were compared.** **C57BL/6 wild-type mice, and intestinal epithelial cell-specific p38a-knockout mice on a C57BL/6 background were used for isolation of colonic mucosa** **Overall design:** **Gene expression in each genotype was analyzed in triplicate.**

Background corr dist: **KL-Divergence = 0.0251, L1-Distance = 0.0199, L2-Distance = 0.0005, Normal std = 0.7025**

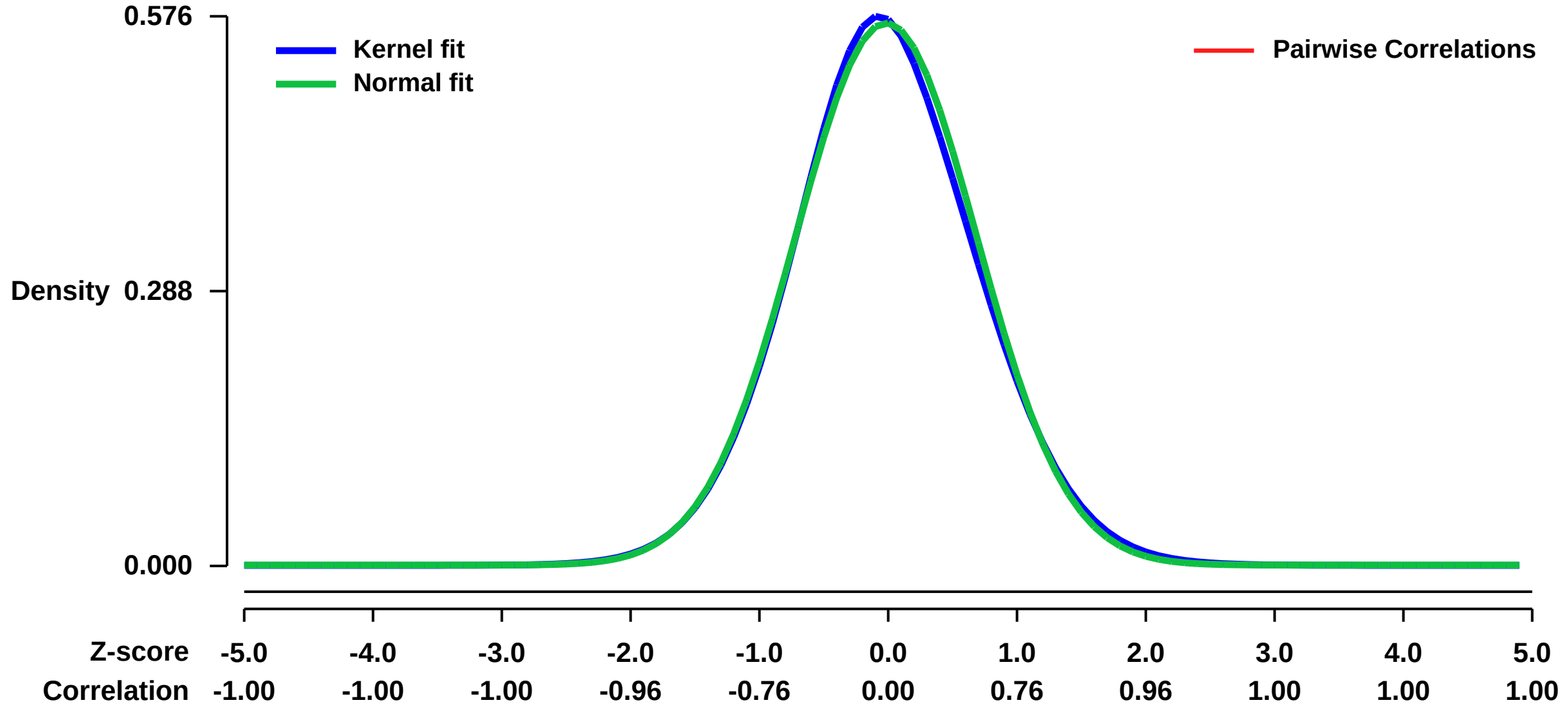

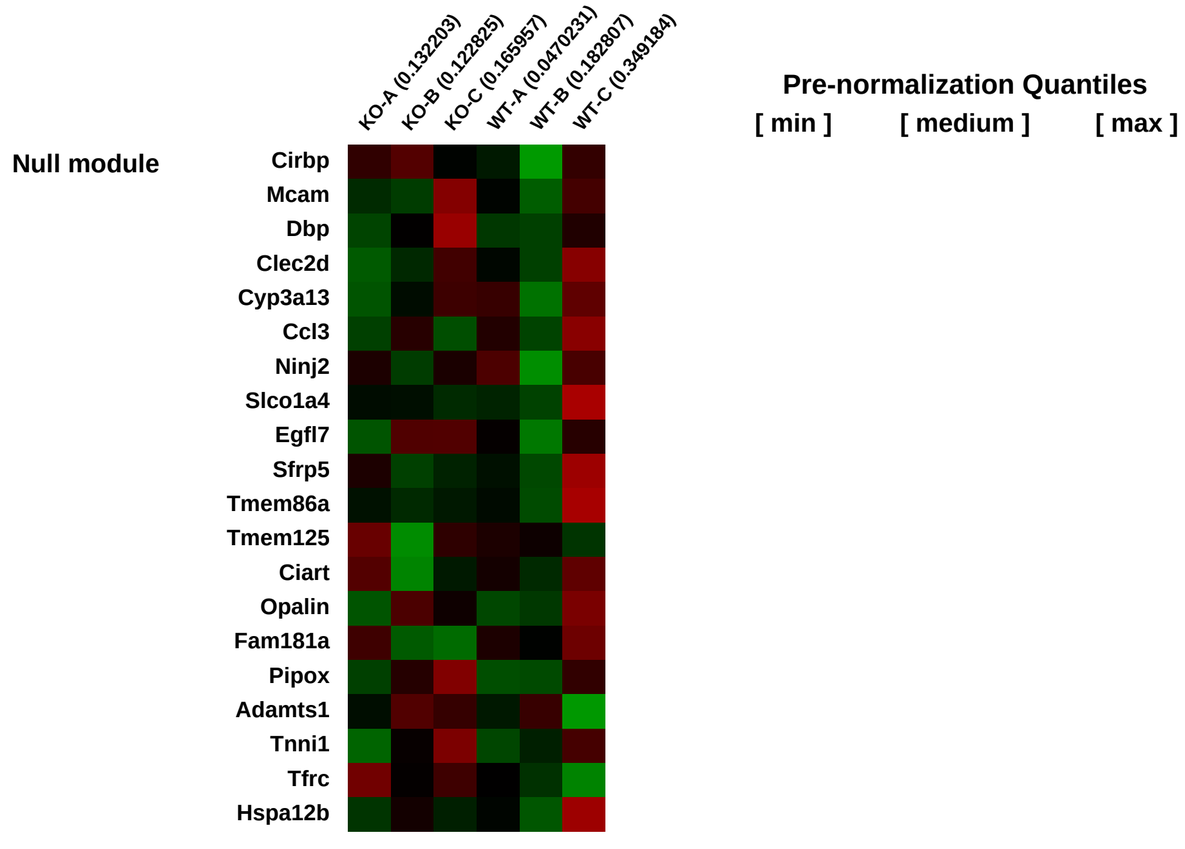

GEO Series "GSE55607" Expression Profiles

Num of samples in this series: 18

Scale of expression profile Z-scores

-3.0 -2.0 -1.0 0.0 1.0 2.0 3.0

GEO Link:	http://www.ncbi.nlm.nih.gov/geo/query/acc.cgi?acc=GSE55607
Status:	Public on Mar 06 2014
Title:	A mouse model of HIES reveals pro and anti-inflammatory functions of STAT3
Organism:	Mus musculus
Experiment type:	Expression profiling by array
Platform:	GPL1261
Pubmed ID:	24632714
Summary & Design:	**Summary:** Mutations of STAT3 underlie the autosomal dominant form of hyper-immunoglobulin E syndrome (HIES). STAT3 has critical roles in immune cells and thus, hematopoietic stem cell transplantation (HSCT), might be a reasonable therapeutic strategy in this disease. However, STAT3 also has critical functions in non-hematopoietic cells and dissecting the protean roles of STAT3 is limited by the lethality associated with germline deletion of Stat3. Thus, predicting the efficacy of HSCT for HIES is difficult. To begin to dissect the importance of STAT3 in hematopoietic and non-hematopoietic cells as it relates to HIES, we generated a mouse model of this disease. We found that these transgenic mice recapitulate multiple aspects of HIES, including elevated serum IgE and failure to generate Th17 cells. We found that these mice were susceptible to bacterial infection that was partially corrected by HSCT using wild type bone marrow, emphasizing the role played by the epithelium in the pathophysiology of HIES. **Overall design:** The effect of IL-6 and IL-10 on BM-DC gene expression was investigated in cell derived from wild type or mut-Stat3 mice

Background corr dist: KL-Divergence = 0.0380, L1-Distance = 0.0921, L2-Distance = 0.0112, Normal std = 0.7946

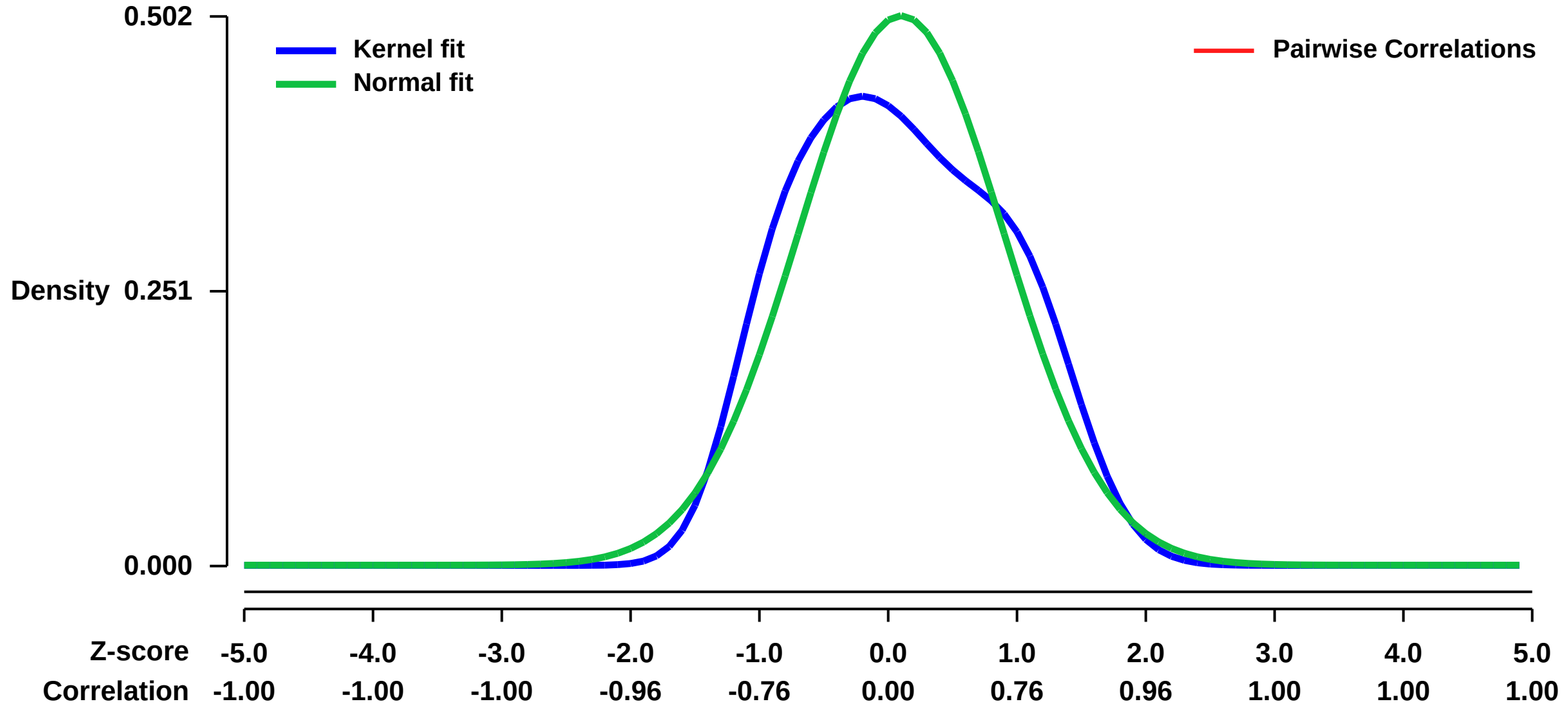

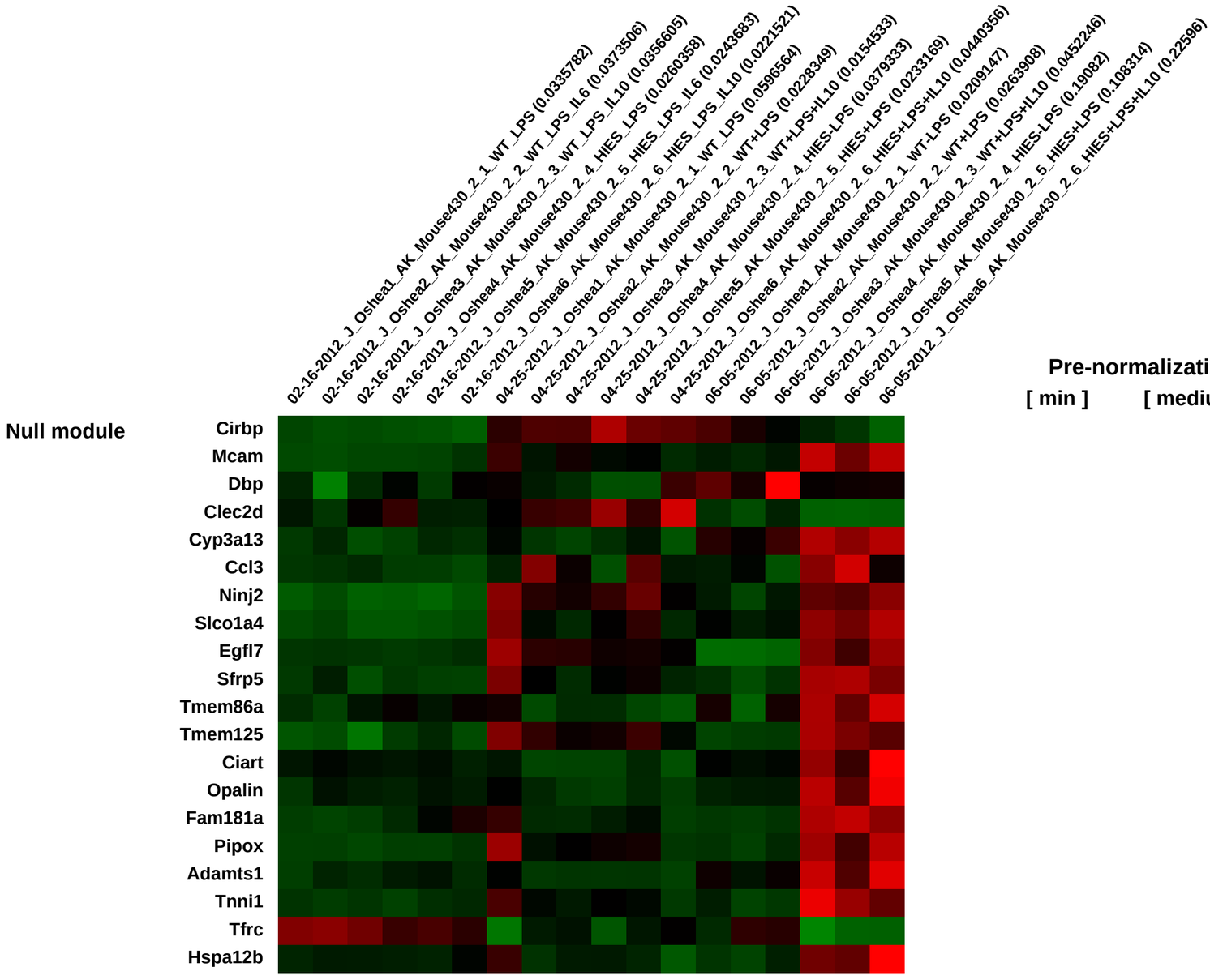

GEO Series "GSE5562" Expression Profiles

Num of samples in this series: 9

Scale of expression profile Z-scores

-3.0 -2.0 -1.0 0.0 1.0 2.0 3.0

GEO Link:	http://www.ncbi.nlm.nih.gov/geo/query/acc.cgi?acc=GSE5562
Status:	Public on Sep 01 2006
Title:	Gene expression profiling in small intestine of mice administered lactoperoxidase
Organism:	Mus musculus
Experiment type:	Expression profiling by array
Platform:	GPL1261
Pubmed ID:	17827675
Summary & Design:	**Summary:** Lactoperoxidase (LPO) is a component of milk and other external secretions. Recently, we found antiinflammatory effect of orally administered LPO in mouse model of influenza virus-induced pneumonia. In order to study influence of bovine LPO on the digestive tract as its possible target organ, we performed comprehensive gene expression analysis of the mouse small intestine using GeneChip microarray to compare the effect of LPO with that of water or bovine serum albumin (BSA). We observed that 3 h after single ingestion of LPO the levels of 78 gene expression are upregulated and those of 9 gene expressions are downregulated. Within most changed genes, 5 upregulated and 1 downregulated genes such as FK506 binding protein 5 (FKBP5) and serum/glucocorticoid regulated kinase (SGK) are known to be transcriptionally modulated by glucocorticoid. This result suggests that ingested LPO modulates gene expressions in the small intestine in a glucocorticoid-like manner and this activity may link to its systemic antiinflammatory effects. **Keywords:** treatment comparison **Overall design:** Mice were orally administered 200 microL of water (n=3), bovine serum albumin (BSA, 2.5 g/kg body weight, n=3), or bovine lactoperoxidase (LPO, 2.5 g/kg body weight, n=3). Three hours after administration, comprehensive gene expressions of jejunum detached payer's patch were analysed for comparison of LPO administration with water or BSA administration.

Background corr dist: KL-Divergence = 0.1144, L1-Distance = 0.0288, L2-Distance = 0.0014, Normal std = 0.4149

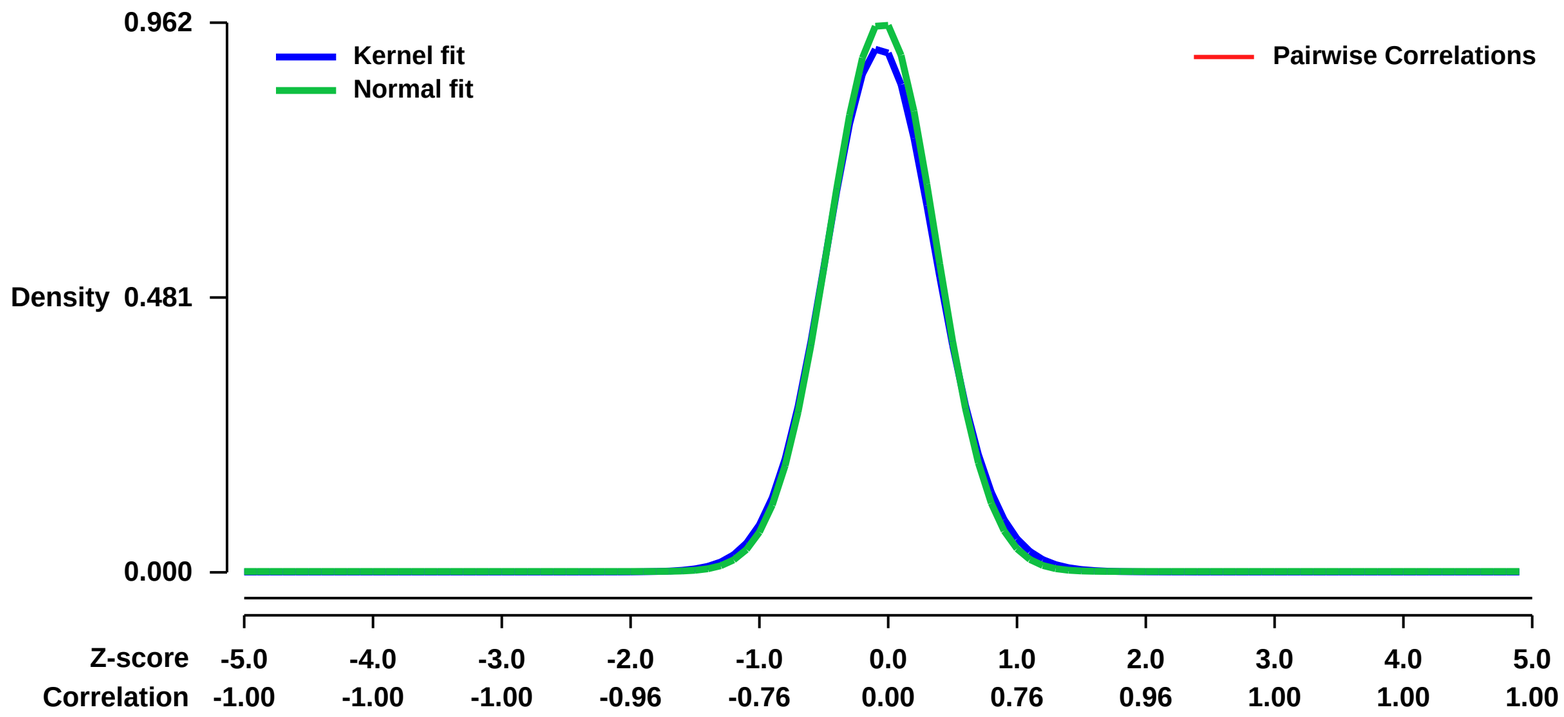

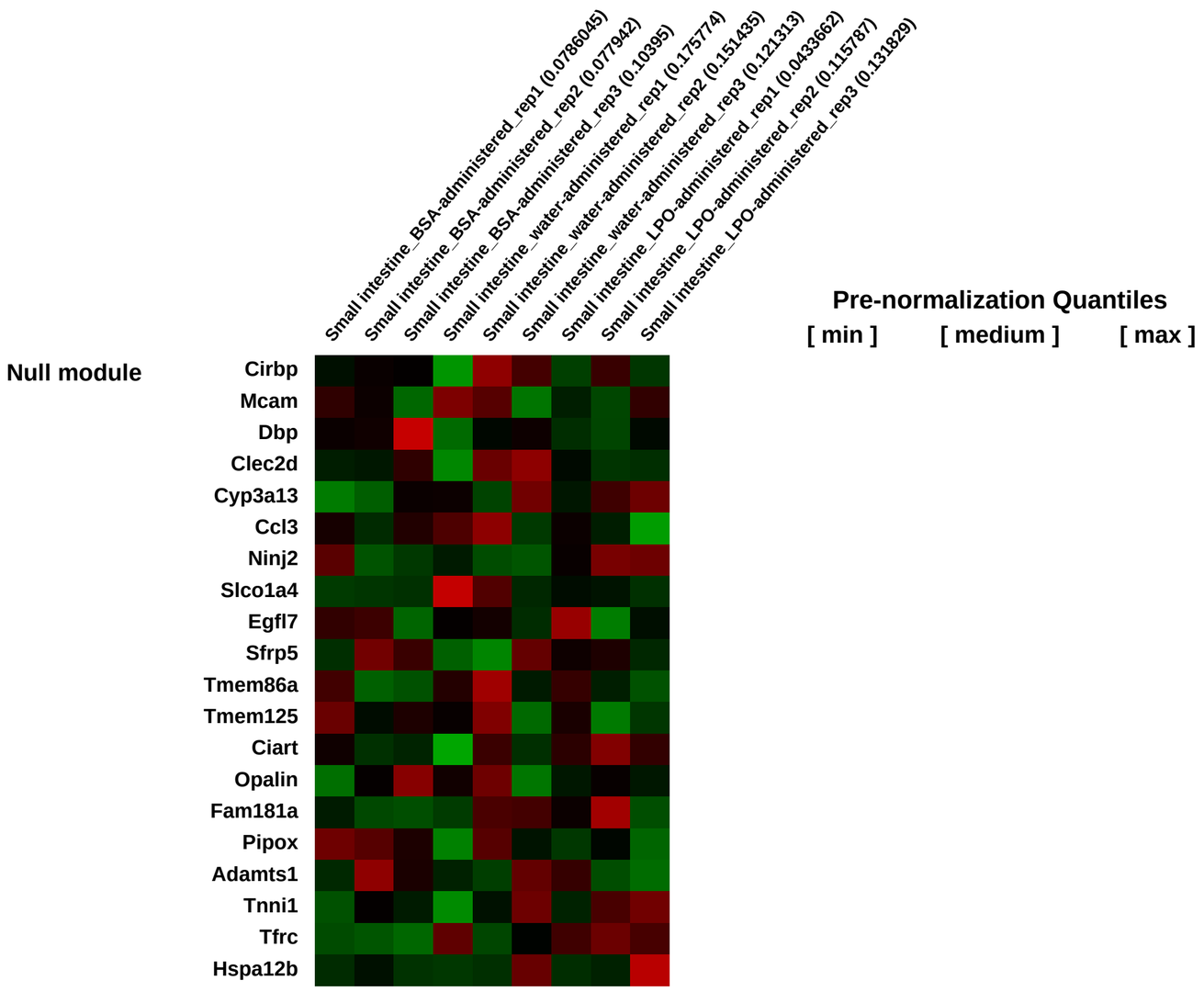

GEO Series "GSE55622" Expression Profiles

Num of samples in this series: 22

Scale of expression profile Z-scores

-3.0 -2.0 -1.0 0.0 1.0 2.0 3.0

GEO Link:	http://www.ncbi.nlm.nih.gov/geo/query/acc.cgi?acc=GSE55622
Status:	Public on Jun 26 2014
Title:	Cytoplasmic YAP and TAZ are intrinsic components of the b-catenin destruction complex
Organism:	Mus musculus
Experiment type:	Expression profiling by array
Platform:	GPL1261
Pubmed ID:	
Summary & Design:	**Summary:** To investigate the role of YAP/TAZ as b-catenin inhibitors, we compared the expression profiles of Rex1GFPd2 ES cells transfected with siControl#1, siControl#2, siYAP/TAZ#1, siYAP/TAZ#2 and cultured in 2i medium or PD-only medium **Overall design:** We collected RNA from Rex1GFPd2 embryonic stem (ES) cells transfected with siControl#1, siControl#2, siYAP/TAZ#1, siYAP/TAZ#2. Cells were maintained in 2i medium (2i=PD0325901+CHIR99021) or switched to PD (PD0325901)-only medium after 24 hours from siRNA transfection. Cells were harvested 72 hours post-siRNA transfection. Samples were then processed for total RNA extraction and hybridization on Affymetrix microarrays.

Background corr dist: KL-Divergence = 0.0811, L1-Distance = 0.0749, L2-Distance = 0.0091, Normal std = 0.5416

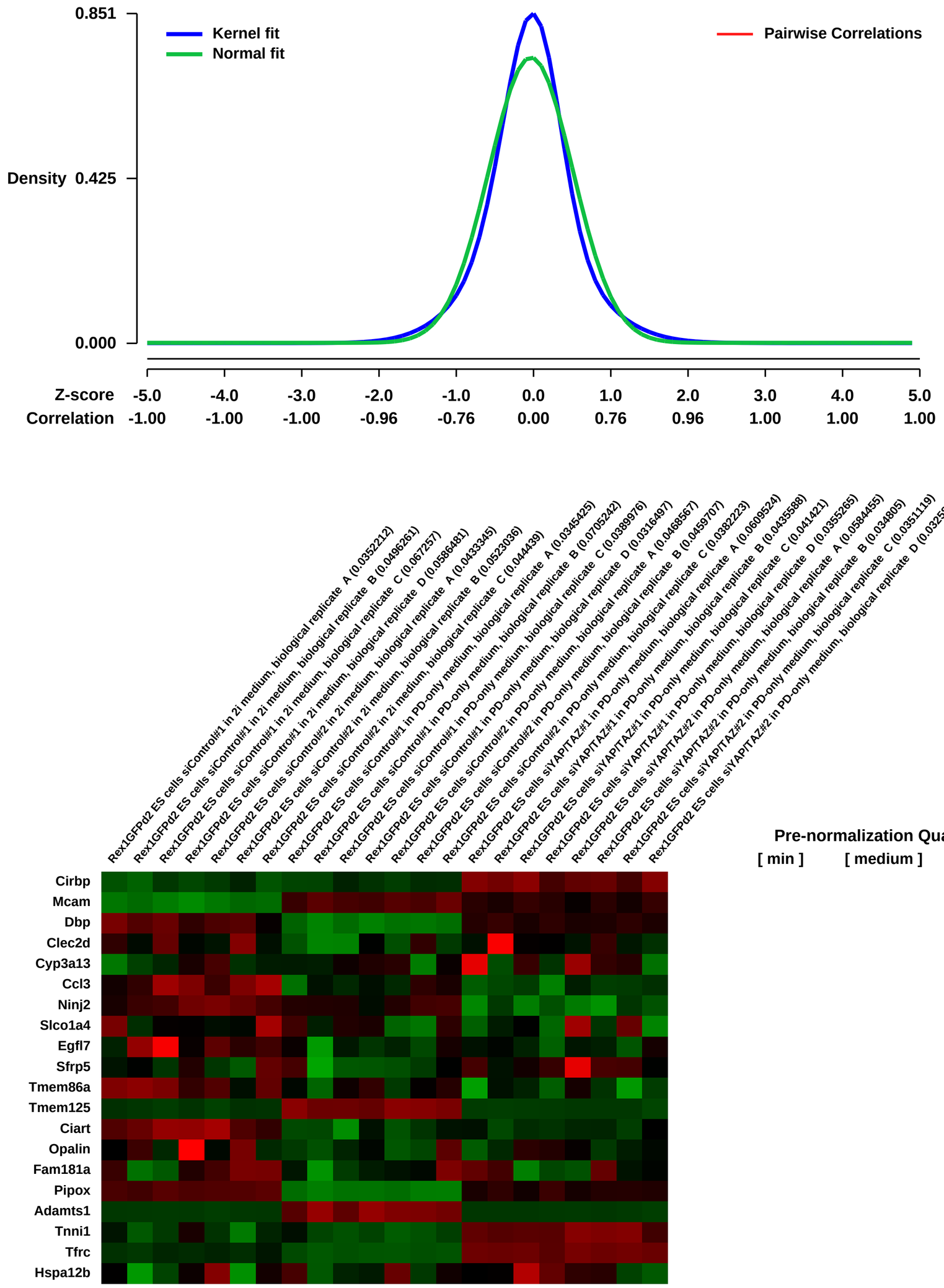

GEO Series "GSE55705" Expression Profiles

Num of samples in this series: 10

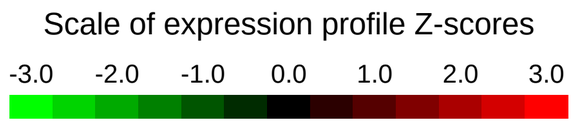

GEO Link:	**http://www.ncbi.nlm.nih.gov/geo/query/acc.cgi?acc=GSE55705**
Status:	**Public on Apr 12 2014**
Title:	**Inflammation induced repression of Foxp3-bound chromatin in regulatory T cells [microarray]**
Organism:	**Mus musculus**
Experiment type:	**Expression profiling by array**
Platform:	**GPL1261**
Pubmed ID:	
Summary & Design:	**Summary:** **The transcription factor Foxp3 is indispensable for the ability of regulatory T (Treg) cells to suppress fatal inflammation. Here, we characterized the role of Foxp3 in chromatin remodeling and regulation of gene expression in actively suppressing Treg cells in an inflammatory setting. Although genome-wide Foxp3 occupancy of DNA regulatory elements was similar in resting and in vivo activated Treg cells, Foxp3-bound enhancers were poised for repression only in activated Treg cells. Following activation, Foxp3-bound sites showed reduced chromatin accessibility and selective H3K27 tri-methylation, which was associated with Ezh2 recruitment and downregulation of nearby gene expression. Thus, Foxp3 poises its targets for repression by facilitating formation of repressive chromatin in regulatory T cells upon their activation in response to inflammatory cues.** **The supplementary file GSE55705_dt_expr.txt is a matrix for Treg expression data from platform GPL1261 that includes co-normalized data from GSE40685.** **Overall design:** **array expression**

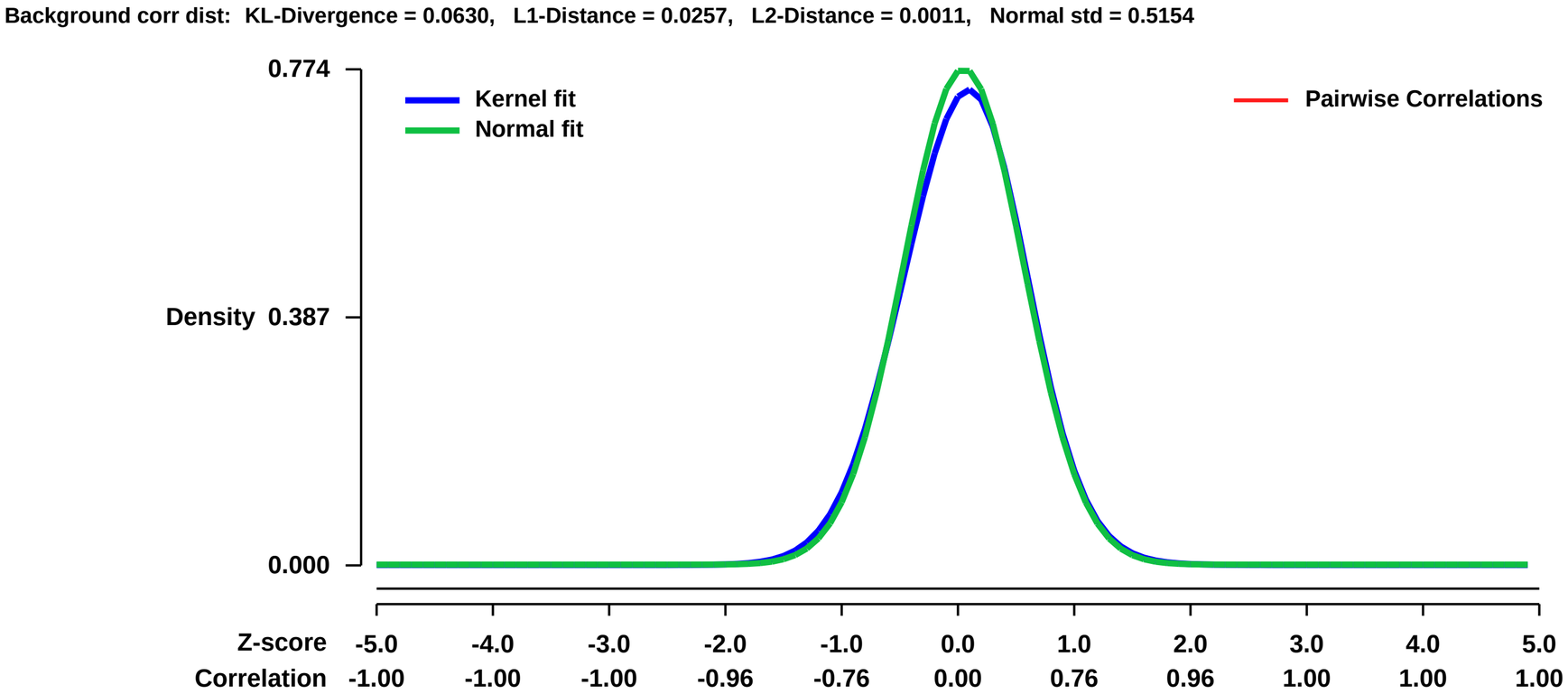

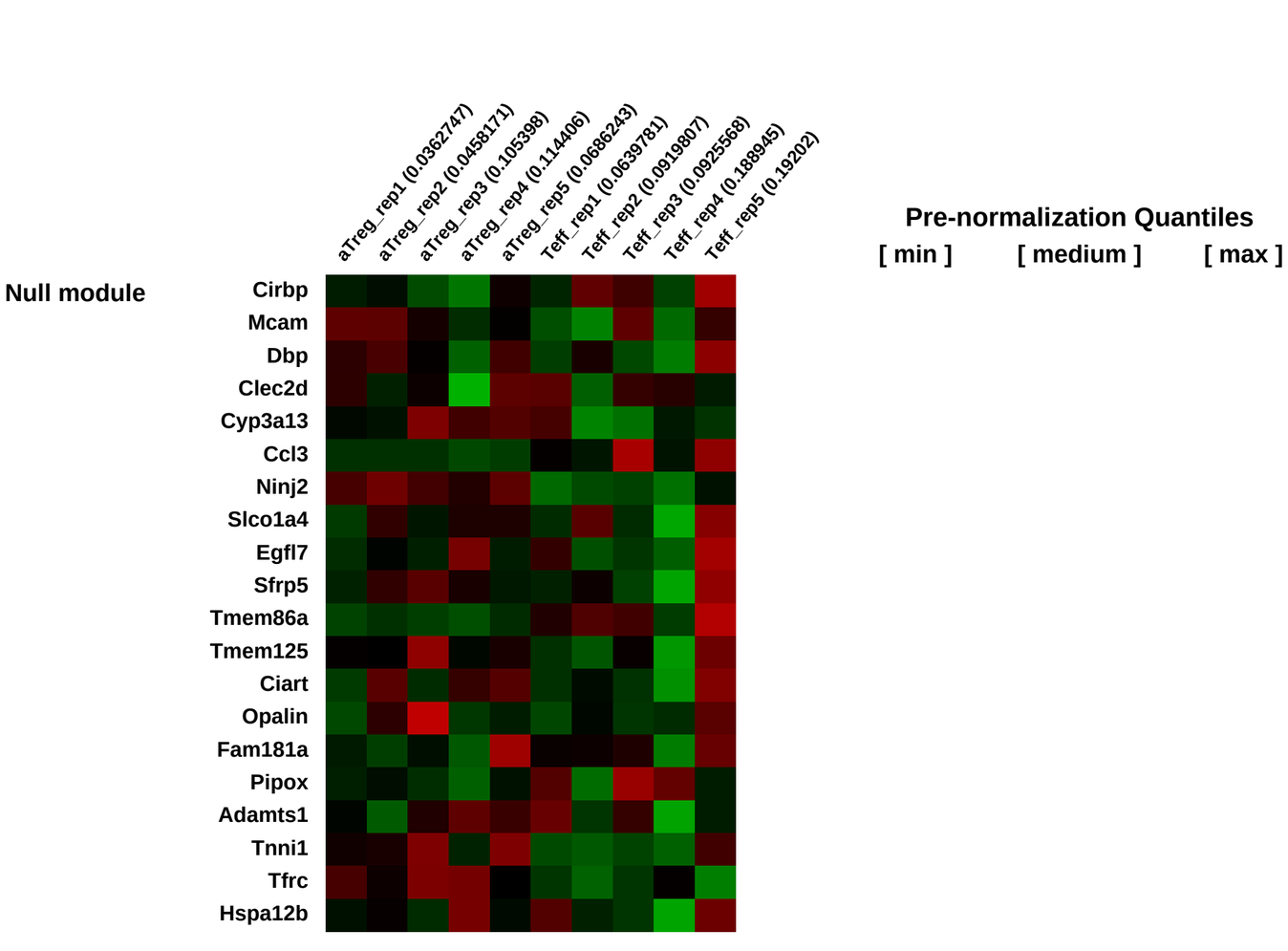

GEO Series "GSE55733" Expression Profiles

Num of samples in this series: 24

Scale of expression profile Z-scores

-3.0 -2.0 -1.0 0.0 1.0 2.0 3.0

GEO Link:	**http://www.ncbi.nlm.nih.gov/geo/query/acc.cgi?acc=GSE55733**
Status:	**Public on Mar 17 2014**
Title:	**Acute Effects Caused by the Rodent Non-Genotoxic Carcinogen Diethylhexylphthalate**
Organism:	**Mus musculus**
Experiment type:	**Expression profiling by array**
Platform:	**GPL1261**
Pubmed ID:	
Summary & Design:	**Summary:** **Acute effects caused by the non-genotoxic carcinogen and peroxisome proliferator (PP) diethylhexylphthalate (DEHP) in the mouse liver** **Overall design:** **Mice (n = 6) were dosed by oral gavage (10 ml/kg body weight) with the non-genotoxic carcinogen diethylhexylphthalate (DEHP), every 24 h for 3 days (1150 mg/kg/day), or with an equivalent volume of vehicle control (corn oil).**

Background corr dist: **KL-Divergence = 0.2626, L1-Distance = 0.0668, L2-Distance = 0.0121, Normal std = 0.2957**

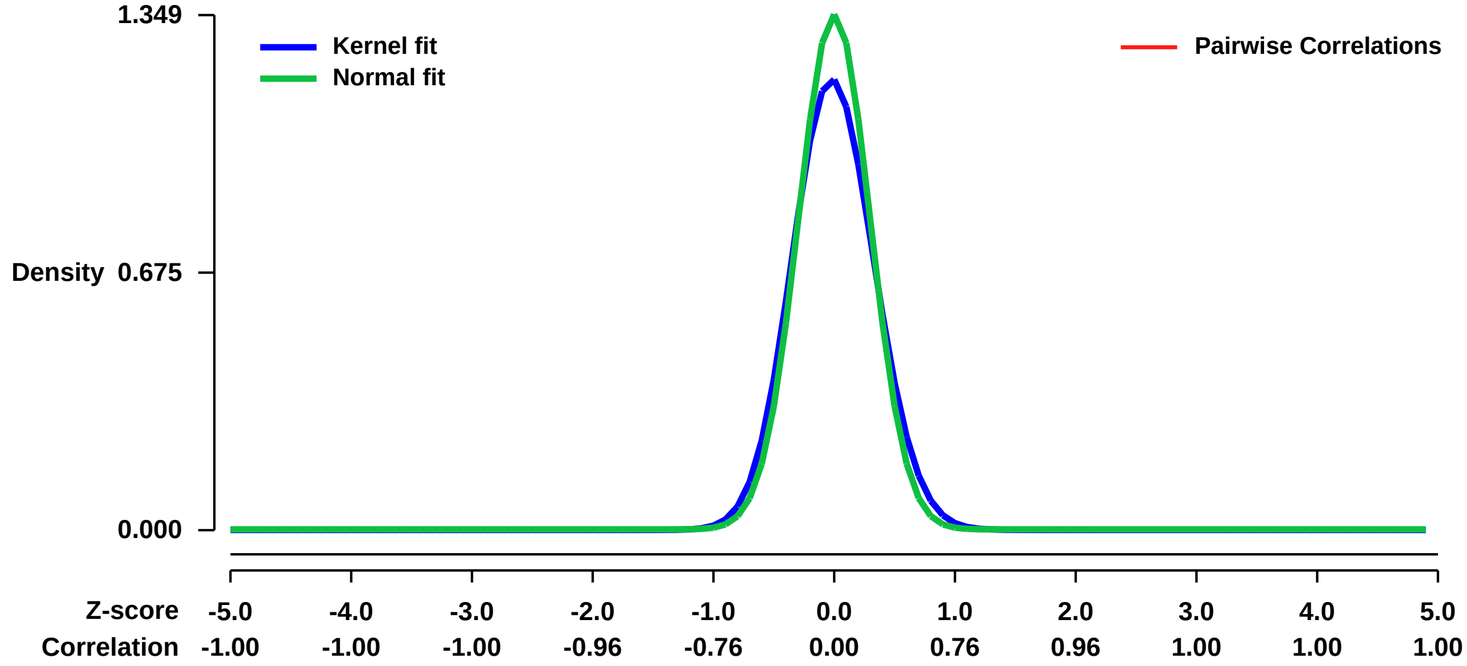

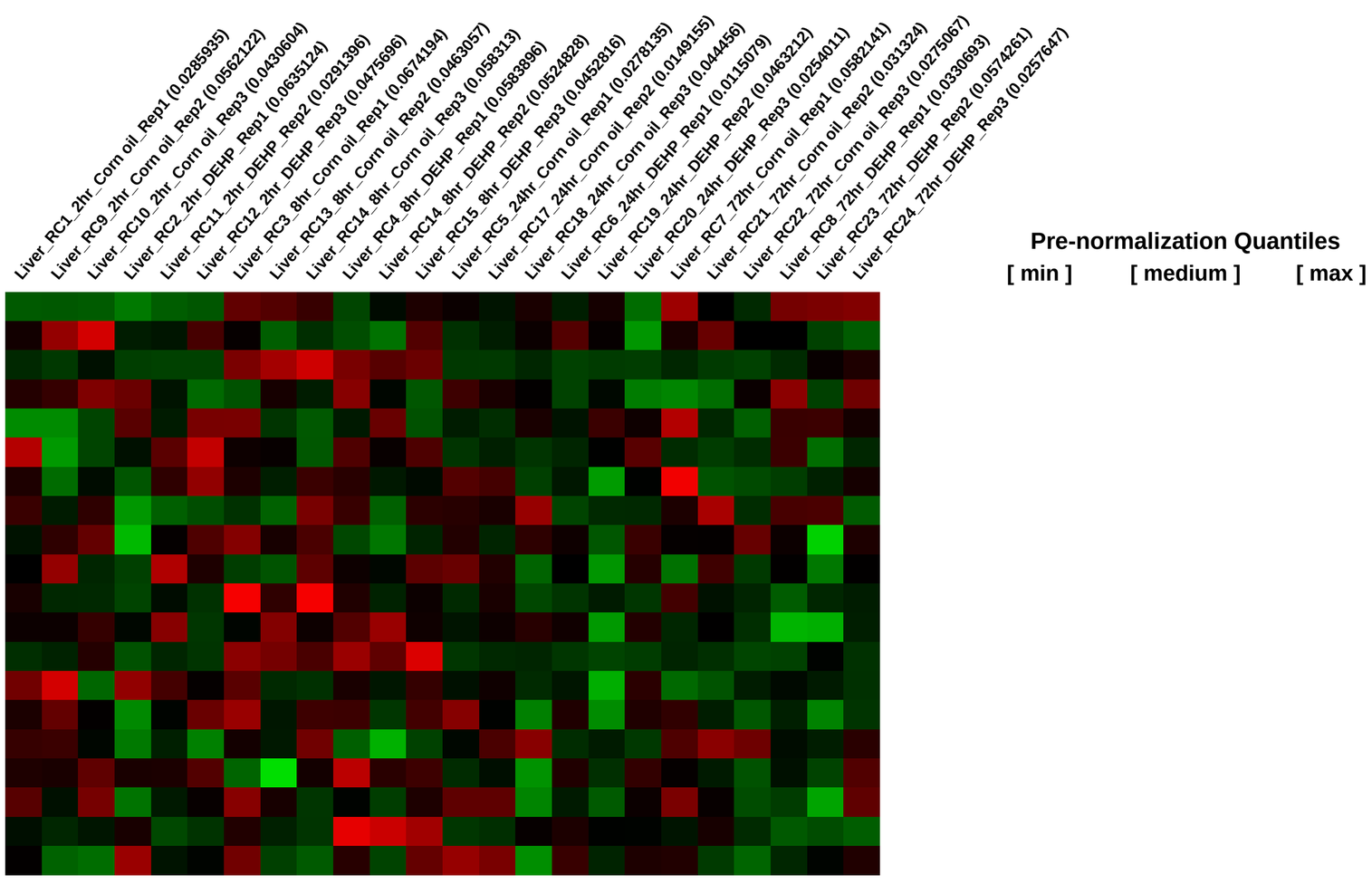

Null module

GEO Series "GSE55738" Expression Profiles

Num of samples in this series: 6

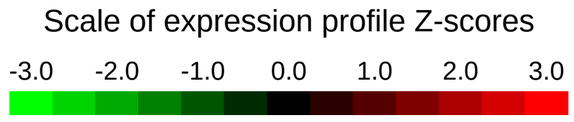

GEO Link: http://www.ncbi.nlm.nih.gov/geo/query/acc.cgi?acc=GSE55738

Status: Public on Jun 08 2014

Title: Expression data from chemically-induced skin papillomas (benign tumours)

Organism: Mus musculus

Experiment type: Expression profiling by array

Platform: GPL1261

Pubmed ID:

Summary & Design:

Summary:
Cancer stem cells (CSCs) have been reported in various cancers including skin squamous cell carcinoma (SCC). The molecular mechanisms regulating tumour initiation and stemness are still poorly characterized. Here, we found that Sox2, a transcription factor expressed in various types of embryonic and adult stem cells (SCs), was the most upregulated transcription factor in CSCs of squamous skin tumours. Sox2 is absent in normal epidermis and begins to be expressed in the vast majority of mouse and human pre-neoplastic skin tumours and continues to be expressed in a heterogeneous manner in invasive mouse and human SCCs. In contrast to other SCCs, in which Sox2 is frequently genetically amplified, the expression of Sox2 in mouse and human skin SCCs is transcriptionally regulated. Conditional deletion of Sox2 in the mouse epidermis dramatically decreases skin tumour formation following chemical induced carcinogenesis. Using Sox2-GFP knockin mice, we showed that Sox2 expressing cells in invasive SCC are greatly enriched in tumour propagating cells (TPCs) that further increase upon serial transplantations. Lineage ablation of Sox2 expressing cells within primary benign and malignant SCCs leads to tumour regression, consistent with the critical role of Sox2 expressing cells in tumour maintenance. Conditional Sox2 deletion in pre-existing skin papilloma and SCC leads to their regression and decreases their ability to be propagated upon transplantation into immunodeficient mice, supporting the essential role of Sox2 in regulating CSC functions. Transcriptional profiling of Sox2-GFP expressing CSC and upon Sox2 deletion uncovered a gene network regulated by Sox2 in primary tumour cells in vivo. Chromatin immunoprecipitation identified several direct Sox2 target genes controlling tumour stemness, survival, proliferation, adhesion, invasion, and paraneoplastic syndrome. Altogether, our study demonstrates that Sox2, by marking and regulating the functions of skin tumour initiating cells and CSCs, establishes a continuum between tumour initiation and progression in primary skin tumours.

We used microarrays to profile tumour epithelial cells upon Sox2 deletion to uncover a gene network regulated by Sox2 in primary tumour cells in vivo.

Overall design:
Microarray analysis was performed on FACS isolated Epcam+ a6+ TECs from 3 different biological experiments following TAM administration to K14CREER:SOX2fl/fl and control mice. Total RNA was analysed using Mouse whole genome 430 2.0 array from Affymetrix.

Background corr dist: KL-Divergence = 0.0382, L1-Distance = 0.0141, L2-Distance = 0.0002, Normal std = 0.6180

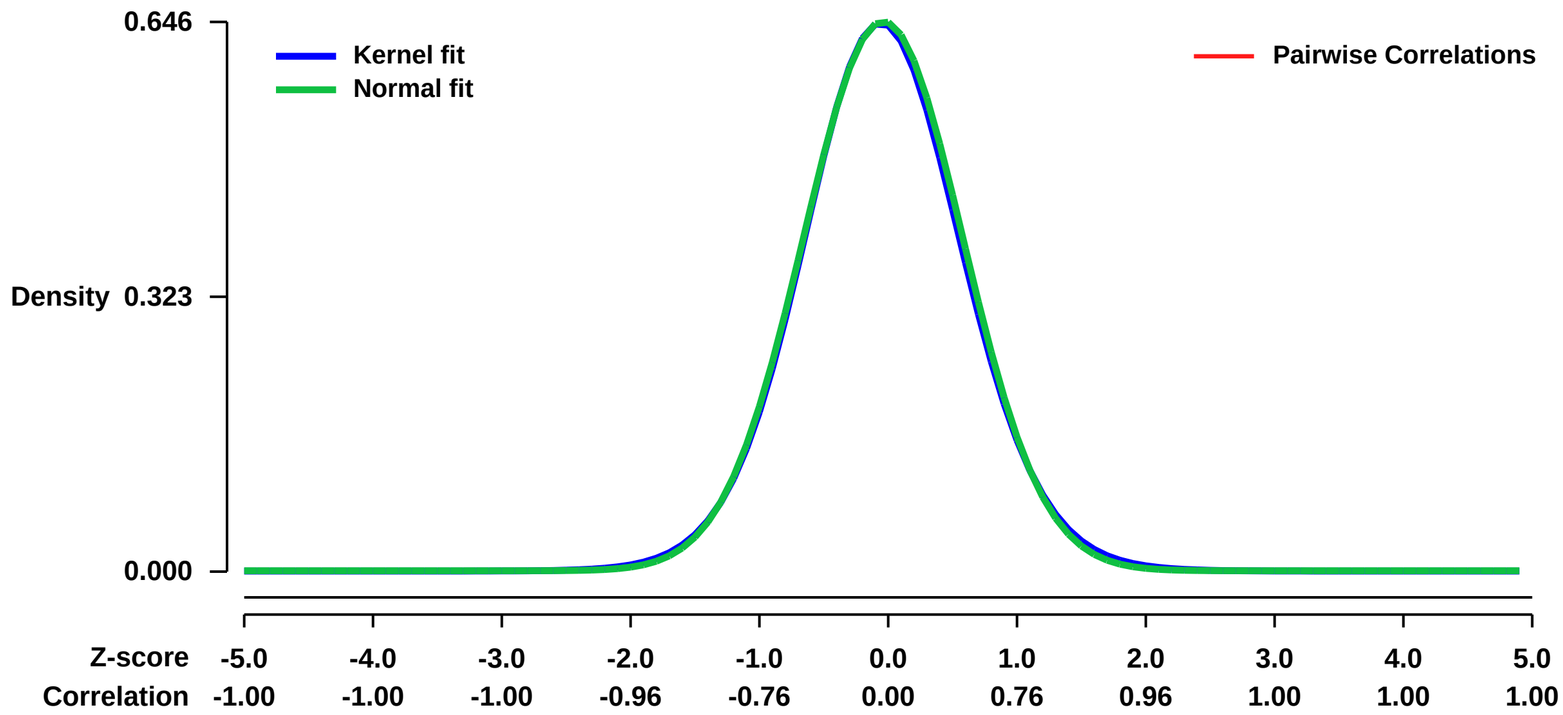

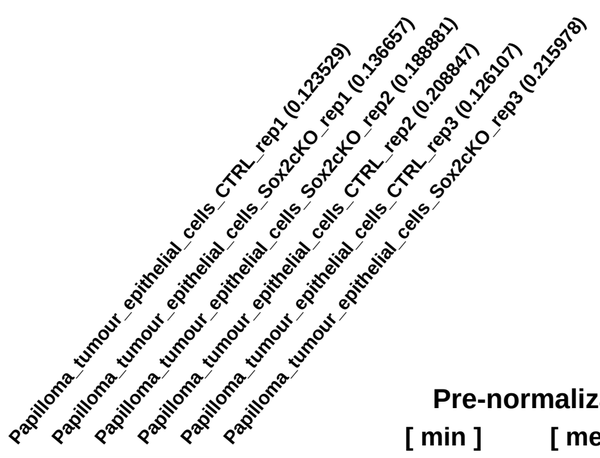

Pre-normalization Quantiles

[min] [medium] [max]

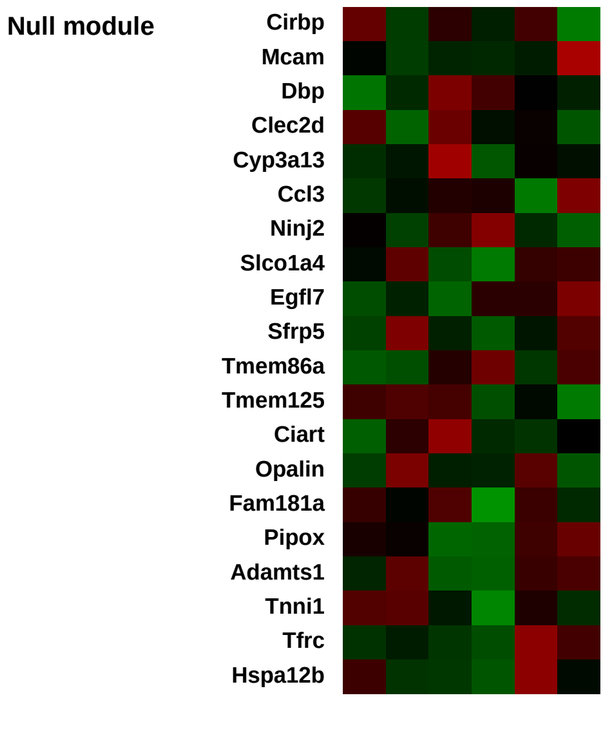

GEO Series "GSE55756" Expression Profiles

Num of samples in this series: 47

Scale of expression profile Z-scores

-3.0 -2.0 -1.0 0.0 1.0 2.0 3.0

GEO Link:	http://www.ncbi.nlm.nih.gov/geo/query/acc.cgi?acc=GSE55756
Status:	Public on Mar 17 2014
Title:	Transcription profiling of mouse liver by array
Organism:	Mus musculus
Experiment type:	Expression profiling by array
Platform:	GPL1261
Pubmed ID:	
Summary & Design:	**Summary:** PPAR$_{\alpha}$--null and wild-type male mice treated with PFHxS or PFNA **Overall design:** PPAR$_{\alpha}$--null and wild-type male mice at 6-9 months of age were dosed by gavage for 7 consecutive days with either 0, 3, or 10 mg/kg´ PFHxS, or 1 or 3 mg/kg PFNA (#394459, Sigma-Aldrich, St, Louis, MO) in water.´ PFHxS was kindly provided by 3M Corp (St. Paul, MN).´ Four biological replicates consisting of individual animals were included in each dose group.´ Dose levels reflected exposures that produce hepatomegaly in adult mice without inducing overt toxicity.

Background corr dist: KL-Divergence = 0.3832, L1-Distance = 0.0705, L2-Distance = 0.0143, Normal std = 0.2527

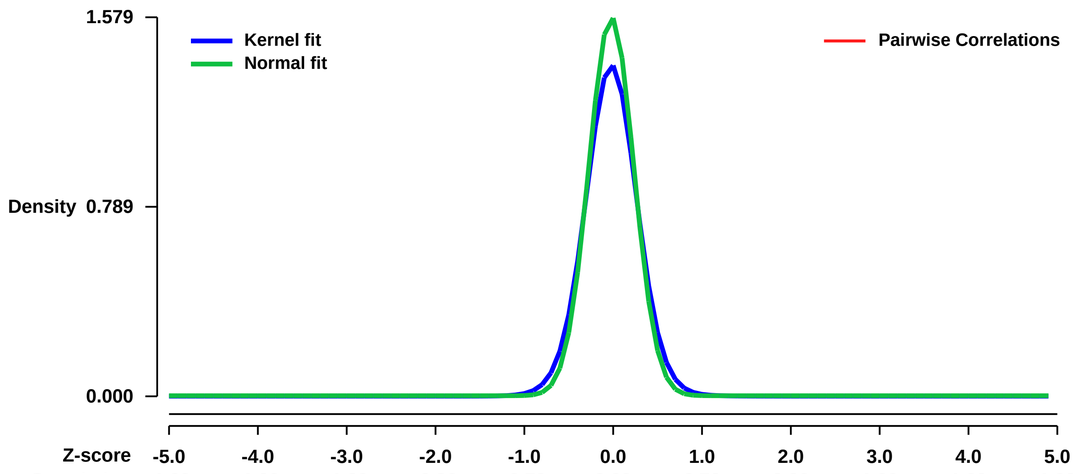

Z-score	-5.0	-4.0	-3.0	-2.0	-1.0	0.0	1.0	2.0	3.0	4.0	5.0
Correlation	-1.00	-1.00	-1.00	-0.96	-0.76	0.00	0.76	0.96	1.00	1.00	1.00

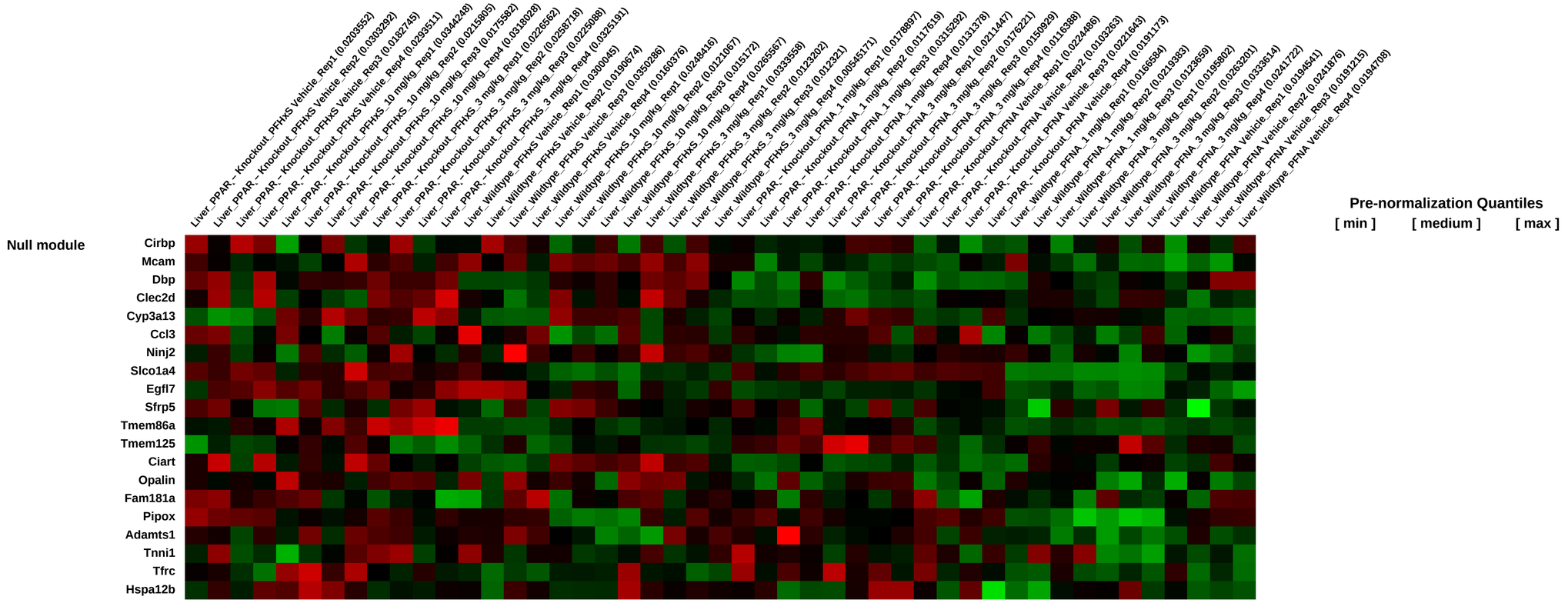

GEO Series "GSE55855" Expression Profiles

Num of samples in this series: 6

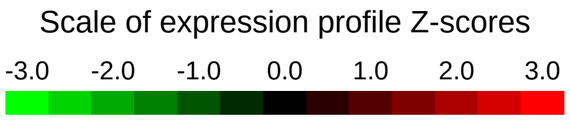

GEO Link:	**http://www.ncbi.nlm.nih.gov/geo/query/acc.cgi?acc=GSE55855**
Status:	**Public on Mar 13 2014**
Title:	**Effect of CSF1R inhibition in tumor macrophages on gene expression in metastatic epithelial cells**
Organism:	**Mus musculus**
Experiment type:	**Expression profiling by array**
Platform:	**GPL1261**
Pubmed ID:	
Summary & Design:	**Summary:** **Metastasis is the primary cause of mortality in breast cancer patients. Tumor associated macrophages (TAMs) are active collaborators in mediating several steps of the tumor metastatic cascade, but the molecular details governing this collaboration remain ill-defined. Colony Stimulating Factor 1 (CSF1), a factor critical for macrophage differentiation and survival, functions to recruit TAMs to the primary tumor site, and anti-CSF1 therapies are in clinical trials.In this study, we tested the effect of inhibiting CSF1 signaling in macrophages on gene expression in metastatic tumor cells in mouse models of breast cancer metastasis. Tumor cells were sorted from lung metastases from control and CSF1R inhibitor treated mice. Several pro-tumor processes were significantly affected by CSF1R inhibitor treatment, including angiogenesis and tumor cell proliferation. In addition, a 29 gene signature derived from this data could retrospectively predict survival in a cohort of luminal B breast cancer patients. Collectievly, our results highlight the utility of employing CSF1R inhibitors for the treatment of metastatic breast cancer.** **Overall design:** **GFP tagged MVT1 metastatic mammary tumor cells were injected intravenously into FVB/N mice. Mice were gavaged with the CSF1R inhibitor GW2580 or vehicle starting one week post injection. GFP tagged tumor cells were sorted from metastatic tumor bearing lungs 1 and 2 weeks post injection from 2 vehicle treated mice for each. These are denoted 1_week_WT and 2_week_WT respectively. GFP tagged tumor cells were simultaneously sorted from mice gavaged with GW2580. These samples are denoted 2_week_GW. RNA was extracted and gene expression profiling was performed using the Affymetrix Mouse Genome 430 2.0 Array platform.**

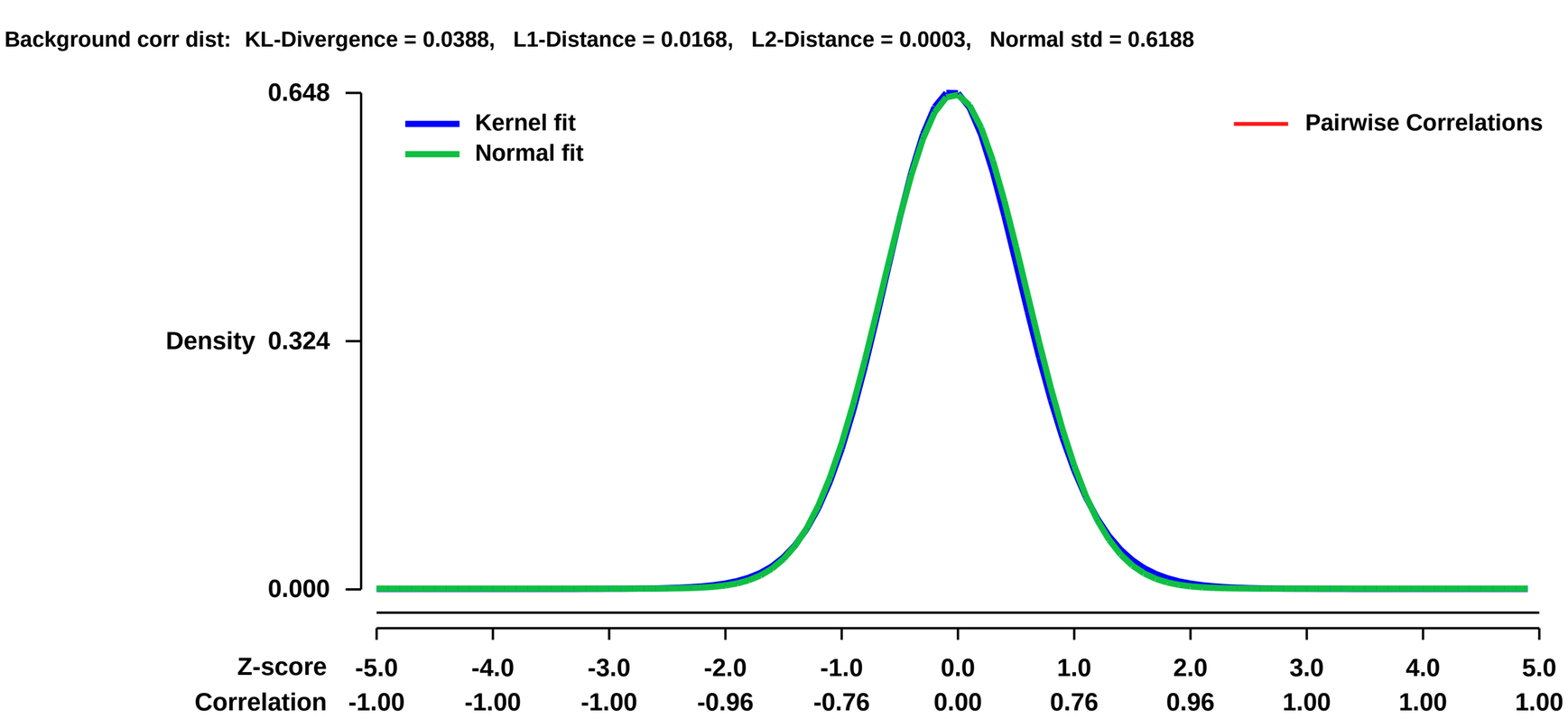

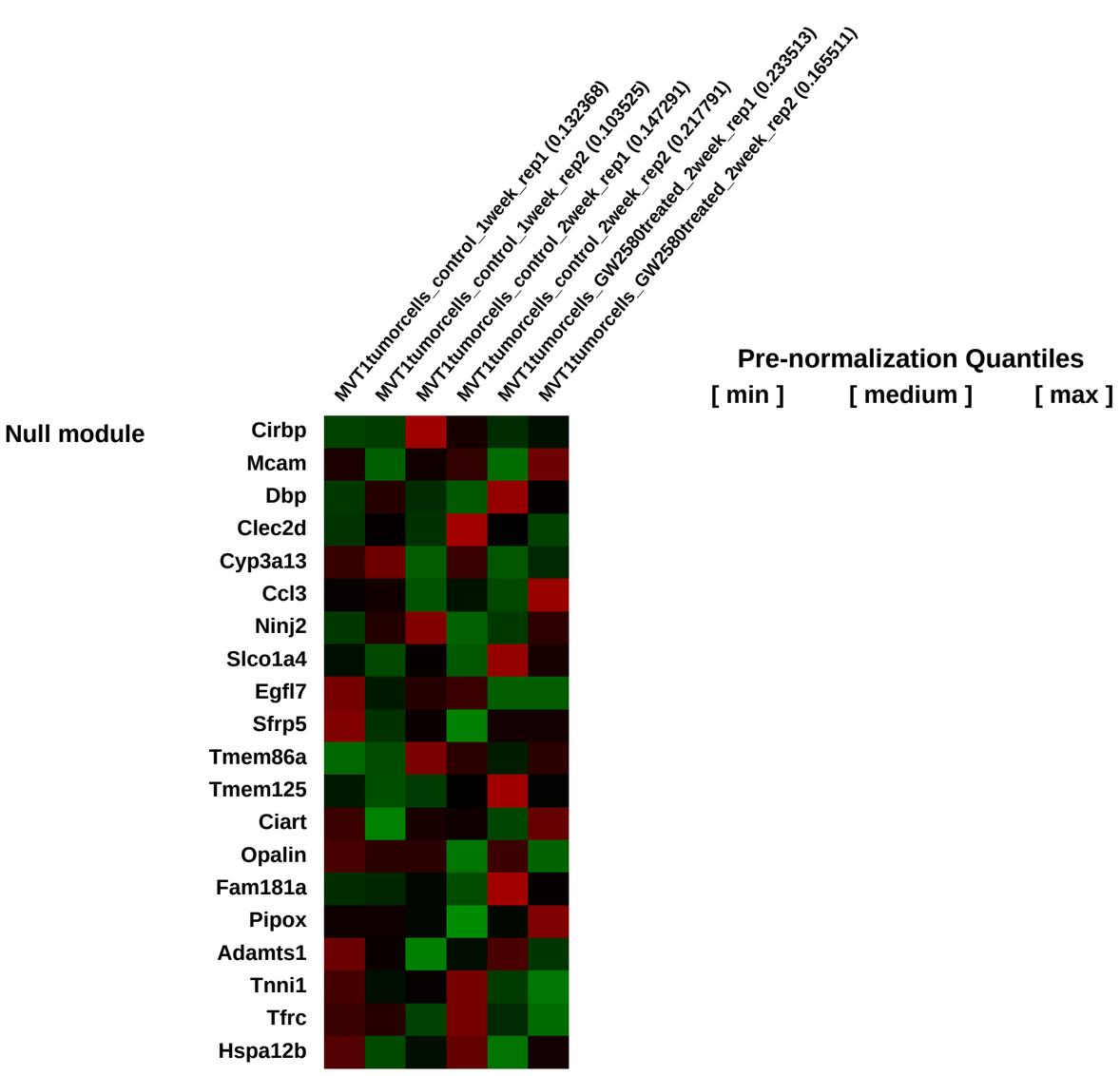

GEO Series "GSE5587" Expression Profiles

Num of samples in this series: 6

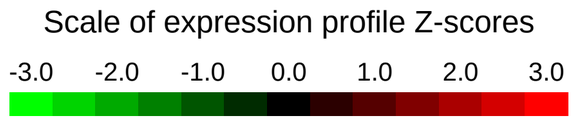

GEO Link:	http://www.ncbi.nlm.nih.gov/geo/query/acc.cgi?acc=GSE5587
Status:	Public on Aug 24 2006
Title:	tourt-affy-arabi-307860
Organism:	Mus musculus
Experiment type:	Expression profiling by array
Platform:	GPL1261
Pubmed ID:	17513727

Summary & Design:

Summary:
The Early Growth Response (Egr) family of transcription factors consists of 4 members (Egr1-4) that are expressed in a wide variety of cell types. A large body of evidence point to a role for Egr transcription factors in growth, survival, and differentiation. A major unanswered question is whether Egr transcription factors serve similar functions in diverse cell types by activating a common set of target genes. Signal transduction cascades in neurons and lymphocytes show striking parallels. Activation of either cell type activates the Ras-MAPK pathway and, in parallel, leads to increases in intracellular calcium stimulating the calcineurin-NFAT pathway. In both cell types, the strength of the activation signal affects the cellular outcomes and very strong stimuli lead to cell death. Notably both these pathways converge on the induction of Egr genes. We believe that downstream targets of Egr transcription factors in lymphocytes may also be activated by Egr factors in activated neurons. There is precedence for common target gene activation in these two cell types: apoptosis in both activated T cells and methamphetamine stimulated neurons occurs via FasL induction by NFAT transcription factors. We propose to use developing T lymphocytes (thymocytes) as a model system for discovery of Egr-dependent target genes for several reasons. First, we have observed a prominent survival defect in thymocytes from mice deficient in both Egr1 and Egr3 (1/3 DKO) and a partial differention block in the immature double negative (DN) stage. In addition, thymocytes are an easily manipulatable cell type, and the DN subpopulation affected in 1/3 DKO mice can be isolated to very high purity. We anticipate that 1/3 DKO thymocytes will provide an excellent experimental system that will provide insight into Egr-dependent transcription in neuronal development, activation, and death.

To identify Egr transcription factor target genes in developing thymocytes. Egr1/3 DKO mice show a profound defect in thymocyte survival and differentiation, but the target genes downstream of Egr1 and Egr3 are unknown. Using Egr1/3 double knockout and wild type littermate mice, we will compare gene expression profiles from DN thymocytes to identify genes that are deregulated in Egr1/3 DKO cells.

Egr1 and Egr3 expression is necessary for the proper survival and differentiation of developing thymocytes. We hypothesize that we will be able to identify crucial target genes of Egr1 and Egr3 by comparing gene expression profiles from wild type and 1/3 DKO thymocytes.

Egr1 and Egr3 are first expressed in the immature double negative (DN) thymocytes. We will isolate DN thymocytes by FACS sorting which allows isolation of cell populations of >99% purity. We will perform microarray analysis using the Mouse 430 2.0 gene array with thymocyte RNA samples from 3 wild type and 3 1/3 DKO mice (6 arrays total). Differentially regulated genes (up-regulated and down-regulated) will be identified from the list of genes with significantly altered expression greater than or equal to 2-fold by paired T test. Interesting genes will be validated by real-time PCR in wild type and 1/3 DKO thymocytes. Recognizing that both direct and indirect target genes may be identified in the list of differentially expressed genes, real-time PCR validated target genes will be further screened using chromatin immunoprecipitation coupled with PCR (ChIP-PCR) to determine whether Egr1 and/or Egr3 are bound to potential regulatory regions of the putative target genes.

Keywords: other

Overall design:

Background corr dist: KL-Divergence = 0.0424, L1-Distance = 0.0270, L2-Distance = 0.0009, Normal std = 0.6121

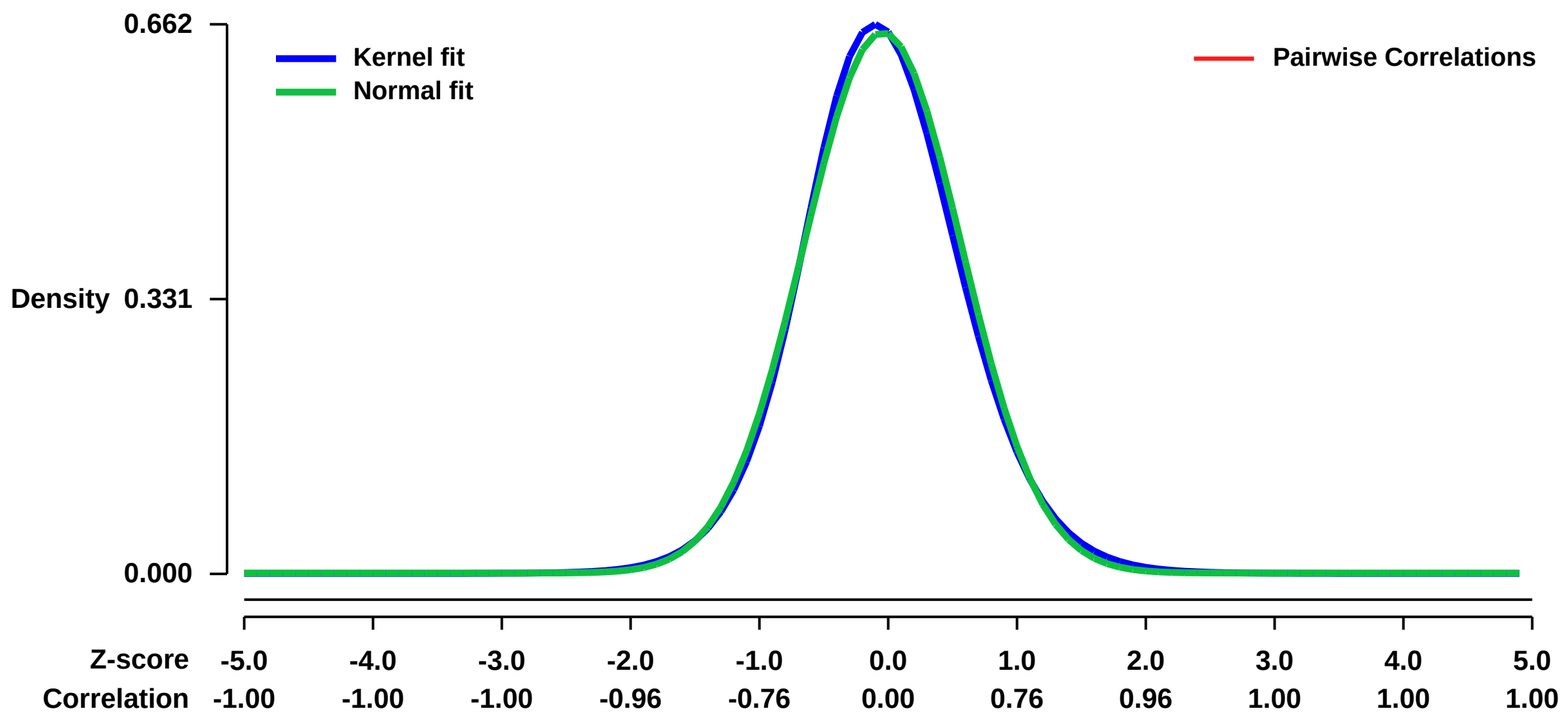

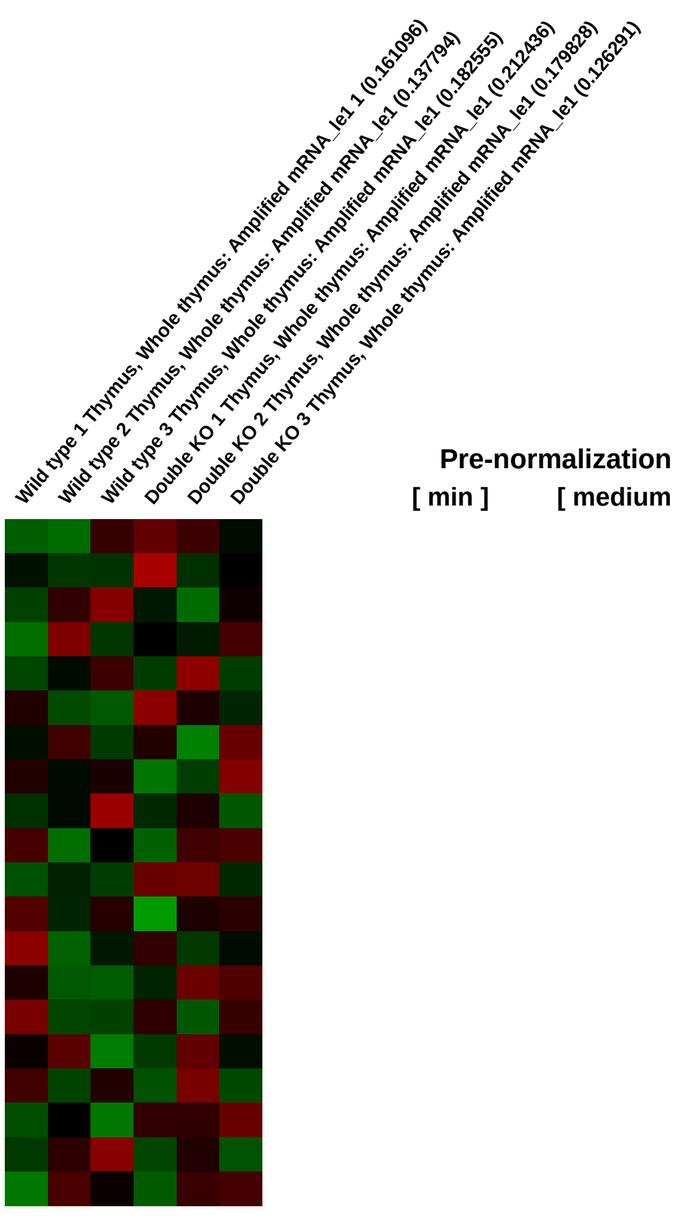

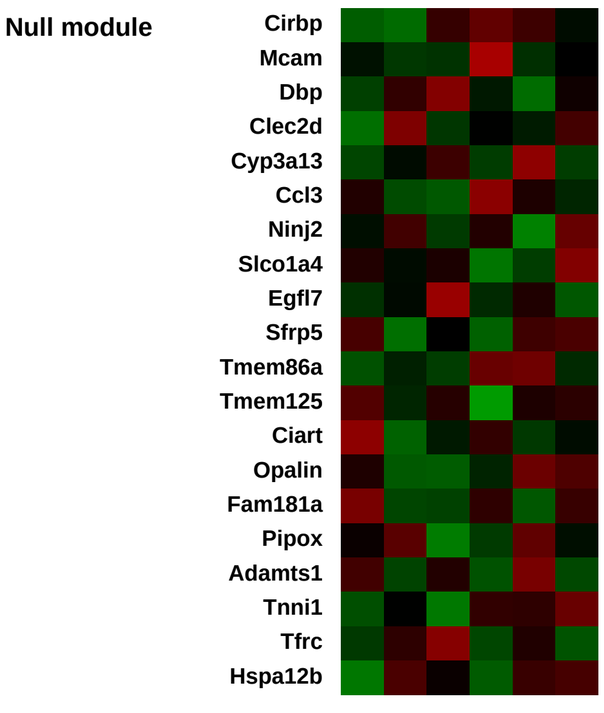

GEO Series "GSE56162" Expression Profiles

Num of samples in this series: 18

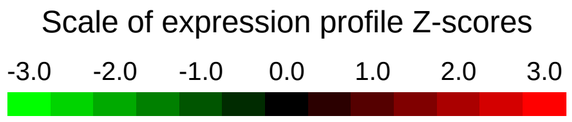

GEO Link:	http://www.ncbi.nlm.nih.gov/geo/query/acc.cgi?acc=GSE56162
Status:	Public on Jun 30 2014
Title:	Differential effects of maternal high protein diets on liver transcriptomes
Organism:	Mus musculus
Experiment type:	Expression profiling by array
Platform:	GPL1261
Pubmed ID:	
Summary & Design:	**Summary:** The objective of this study was to test if maternal high protein diet during pregnancy or lactation, imposes different transient or persistently imprinted effects on the liver transcriptome of offspring **Overall design:** Livers from 4 to 5 animals (one animal per litter) at days 21 and 150 of of each dietary group were combined to 3 pools each, and processed for microarray analysis.

Background corr dist: KL-Divergence = 0.2001, L1-Distance = 0.0369, L2-Distance = 0.0028, Normal std = 0.3341

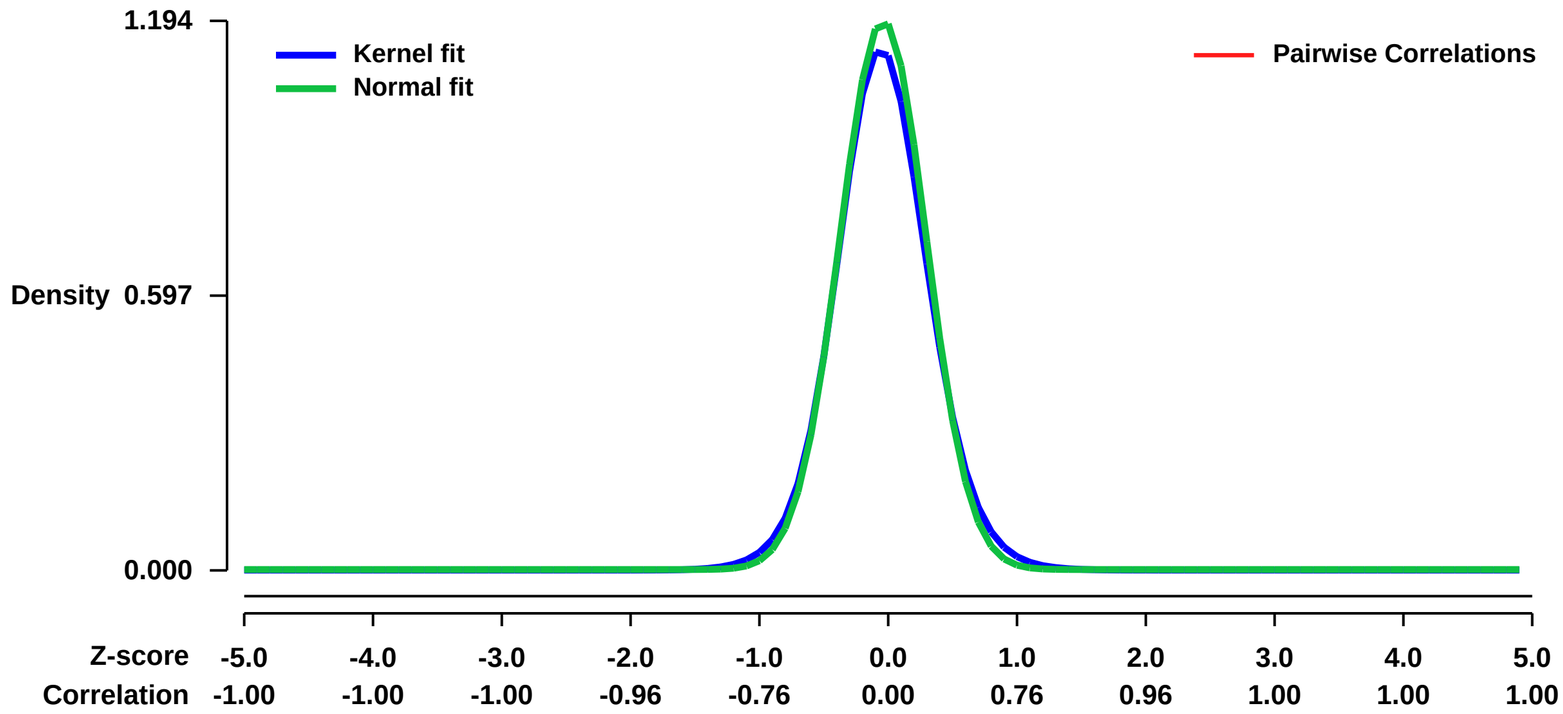

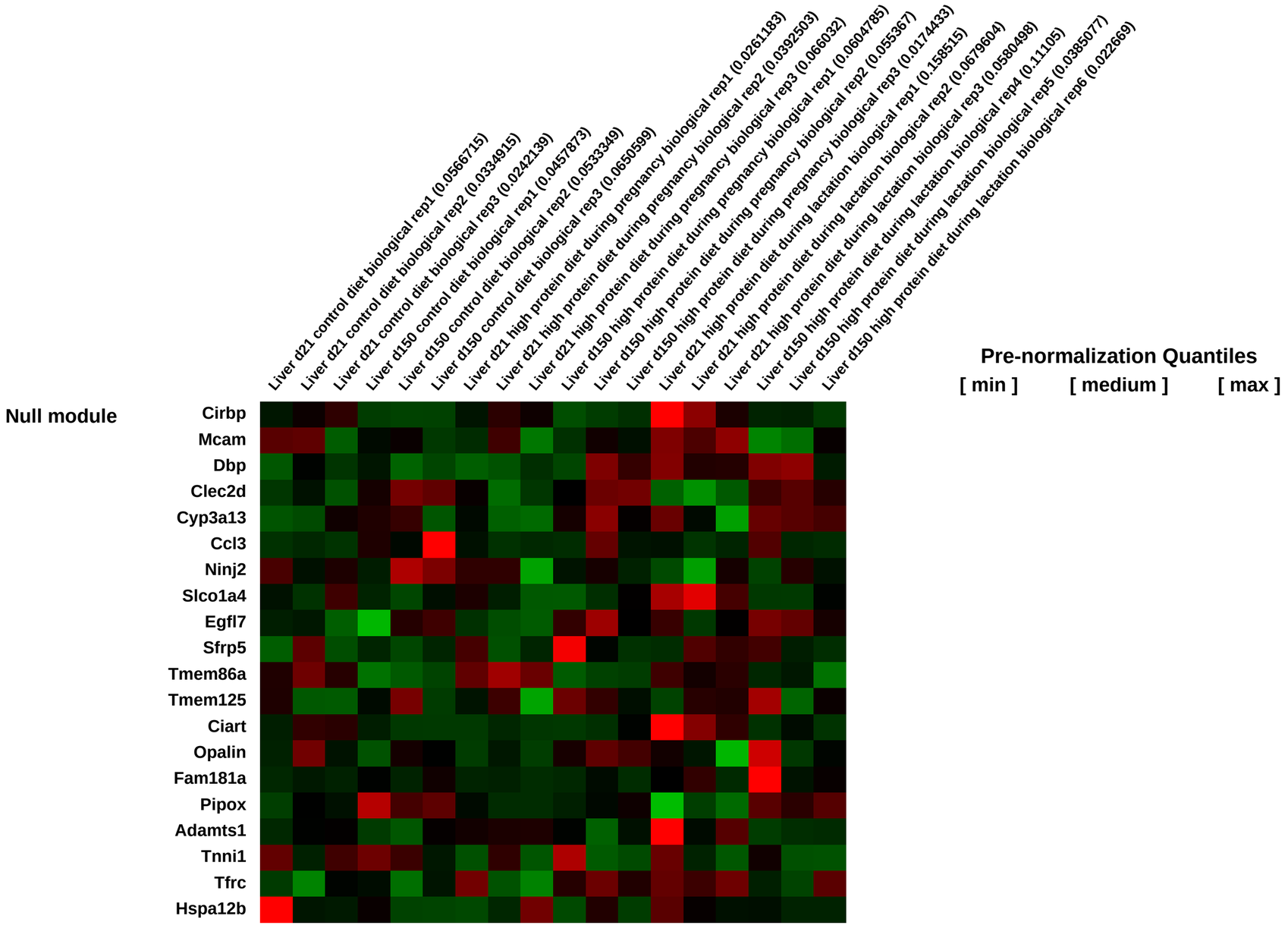

GEO Series "GSE56321" Expression Profiles

Num of samples in this series: 12

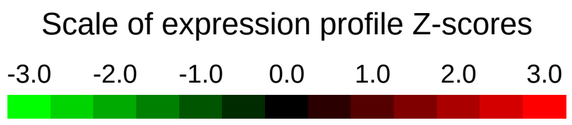

GEO Link:	http://www.ncbi.nlm.nih.gov/geo/query/acc.cgi?acc=GSE56321
Status:	Public on Mar 28 2014
Title:	SIRT4 KO livers microarray
Organism:	Mus musculus
Experiment type:	Expression profiling by array
Platform:	GPL1261
Pubmed ID:	24043310
Summary & Design:	**Summary:** Sirtuins are a family of protein deacetylases, deacylases, and ADP-ribosyltransferases that regulate life span, control the onset of numerous age-associated diseases, and mediate metabolic homeostasis. We have uncovered a novel role for the mitochondrial sirtuin SIRT4 in the regulation of hepatic lipid metabolism during changes in nutrient availability. We show that SIRT4 levels decrease in the liver during fasting and that SIRT4 null mice display increased expression of hepatic peroxisome proliferator activated receptor (PPAR) target genes associated with fatty acid catabolism. Accordingly, primary hepatocytes from SIRT4 knockout (KO) mice exhibit higher rates of fatty acid oxidation than wild-type hepatocytes, and SIRT4 overexpression decreases fatty acid oxidation rates. The enhanced fatty acid oxidation observed in SIRT4 KO hepatocytes requires functional SIRT1, demonstrating a clear cross talk between mitochondrial and nuclear sirtuins. Thus, SIRT4 is a new component of mitochondrial signaling in the liver and functions as an important regulator of lipid metabolism. **Overall design:** SIRT4 knockout (KO) and wild-type (WT) littermates (male; n 6 per genotype; 7- to 8-month-old littermates) were sacrificed after a 16-h overnight fast. Samples were individually hybridized on Affymetrix Mouse Genome 430 2.0 GeneChips by the Biopolymers Facility (Harvard Medical School).

Background corr dist: KL-Divergence = 0.1803, L1-Distance = 0.0453, L2-Distance = 0.0044, Normal std = 0.3452

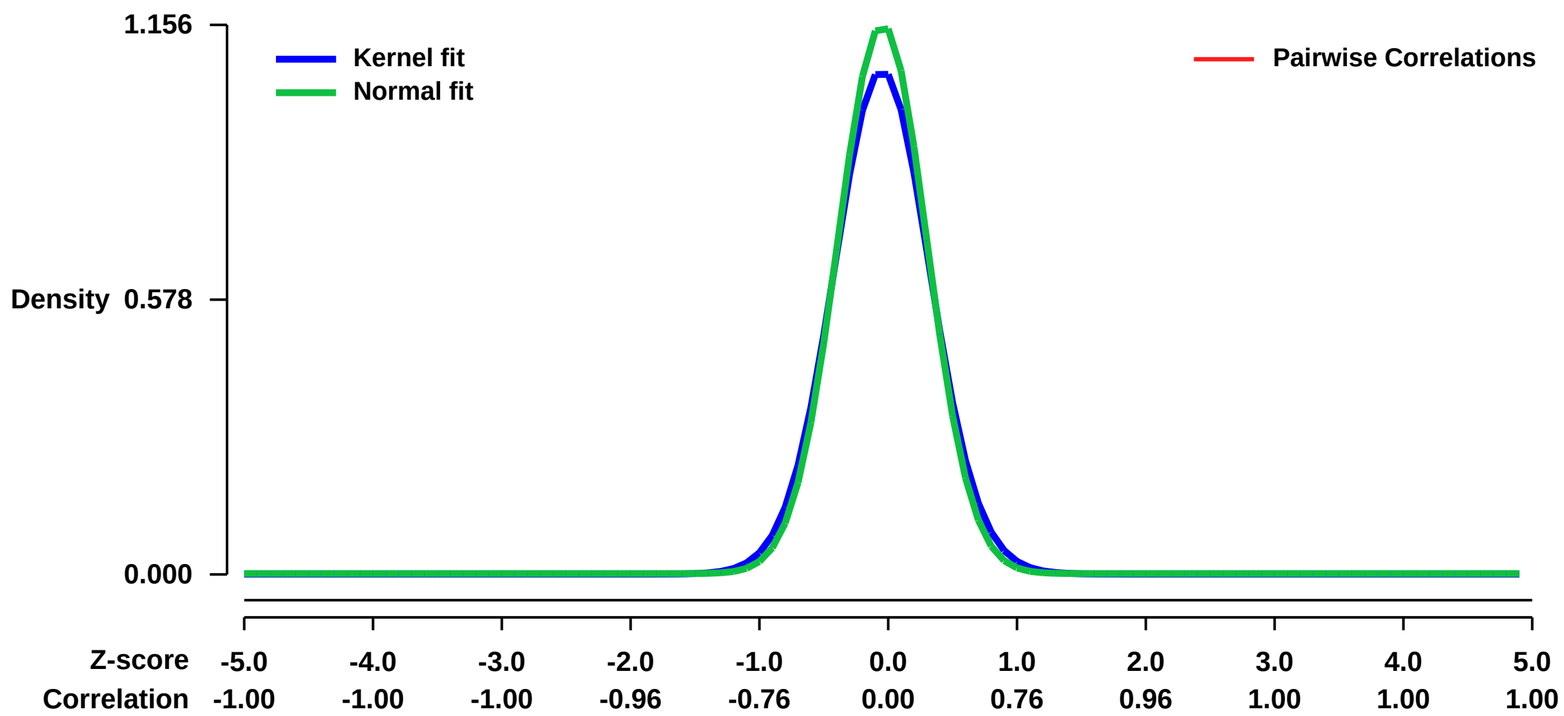

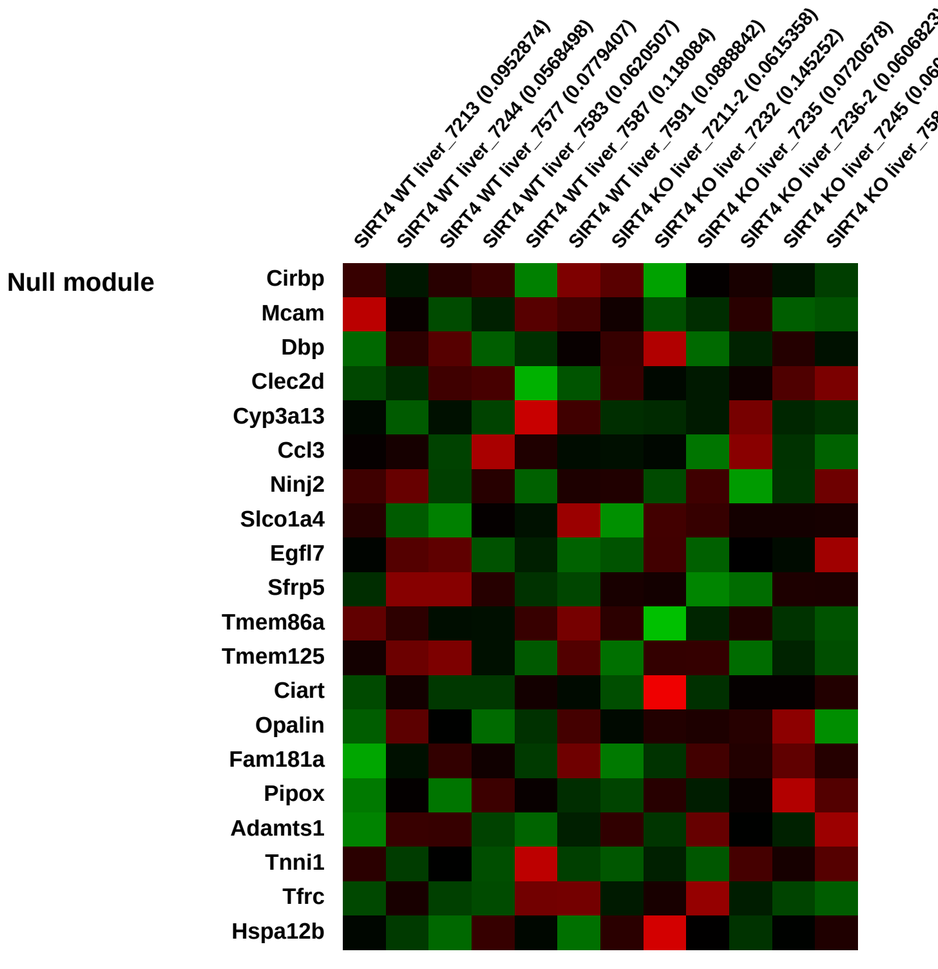

GEO Series "GSE56482" Expression Profiles

Num of samples in this series: 8

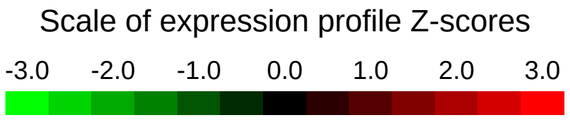

GEO Link:	**http://www.ncbi.nlm.nih.gov/geo/query/acc.cgi?acc=GSE56482**
Status:	**Public on Jul 04 2014**
Title:	**Expression Data comparing Gene Expression in 27-day old testes of wild-type and Brwd1-/- mice**
Organism:	**Mus musculus**
Experiment type:	**Expression profiling by array**
Platform:	**GPL1261**
Pubmed ID:	
Summary & Design:	**Summary:** **Brwd1-/- mice are infertile with post-meiotic defects in the male. BRWD1 contains bromodomains and may function as a transcriptional regulator important for post-meiotic development in the male germline.** **This microarray compares post-meiotic gene expression between WT and mutant mice.** **Overall design:** **We collected total RNA from testes of 27-day old WT and Brwd1-/- (MT) mice. At this age, germ cells have completed meiosis and are mid-way in post-meiotic development. Any gene expression changes in spermatids would be apparent at this time-point. We decided to do this with 4 WT and 4 Brwd1-/- mice.**

Background corr dist: **KL-Divergence = 0.0388, L1-Distance = 0.0285, L2-Distance = 0.0010, Normal std = 0.6239**

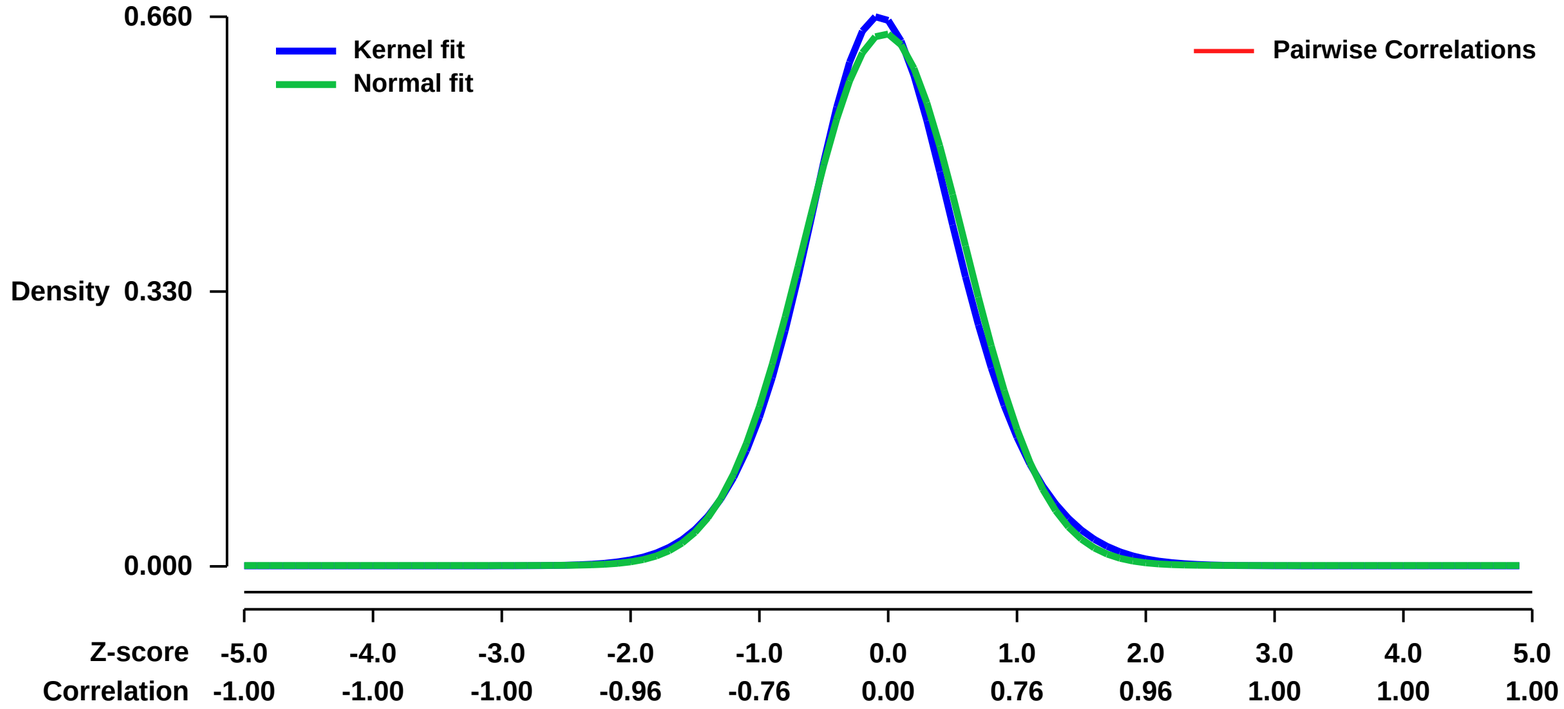

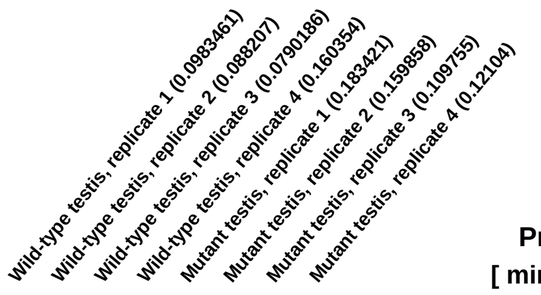

Pre-normalization Quantiles

[min] [medium] [max]

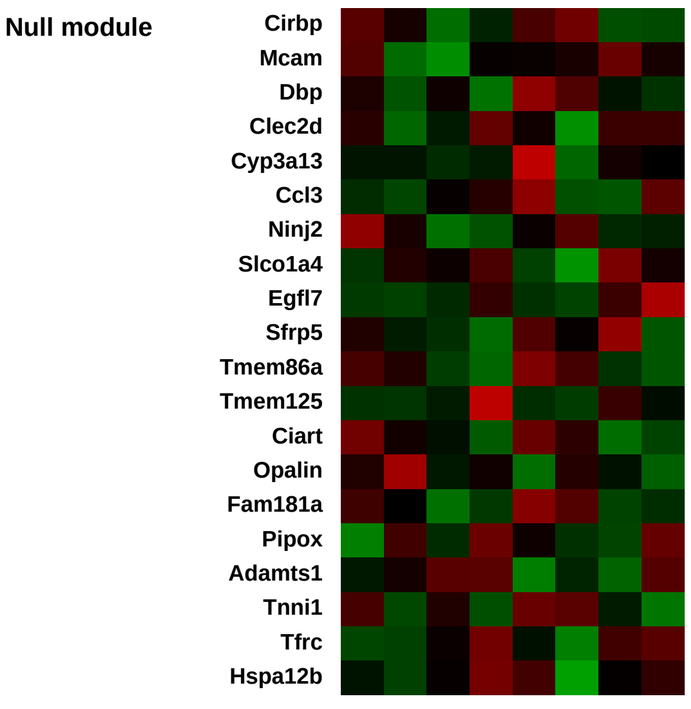

GEO Series "GSE56492" Expression Profiles

Num of samples in this series: 12

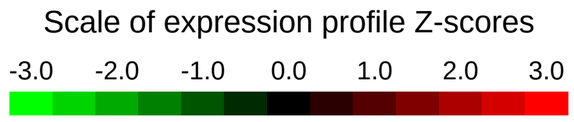

GEO Link:	**http://www.ncbi.nlm.nih.gov/geo/query/acc.cgi?acc=GSE56492**
Status:	**Public on Apr 15 2014**
Title:	**Identification of targets regulated by MLL1 in response to HSP90 inhibitors**
Organism:	**Homo sapiens**
Experiment type:	**Expression profiling by array**
Platform:	**GPL1261**
Pubmed ID:	
Summary & Design:	**Summary:** **MLL1 WT or KO MEF with and without HSP90 inhibitor treatment** **Overall design:** **MEF cells were seeded in 6-well plates for 3d with 100ng/ml doxycycline prior to treatment with 0.1% DMSO or 100nM AUY922 for 3h**

Background corr dist: **KL-Divergence = 0.0311, L1-Distance = 0.0822, L2-Distance = 0.0115, Normal std = 0.7736**

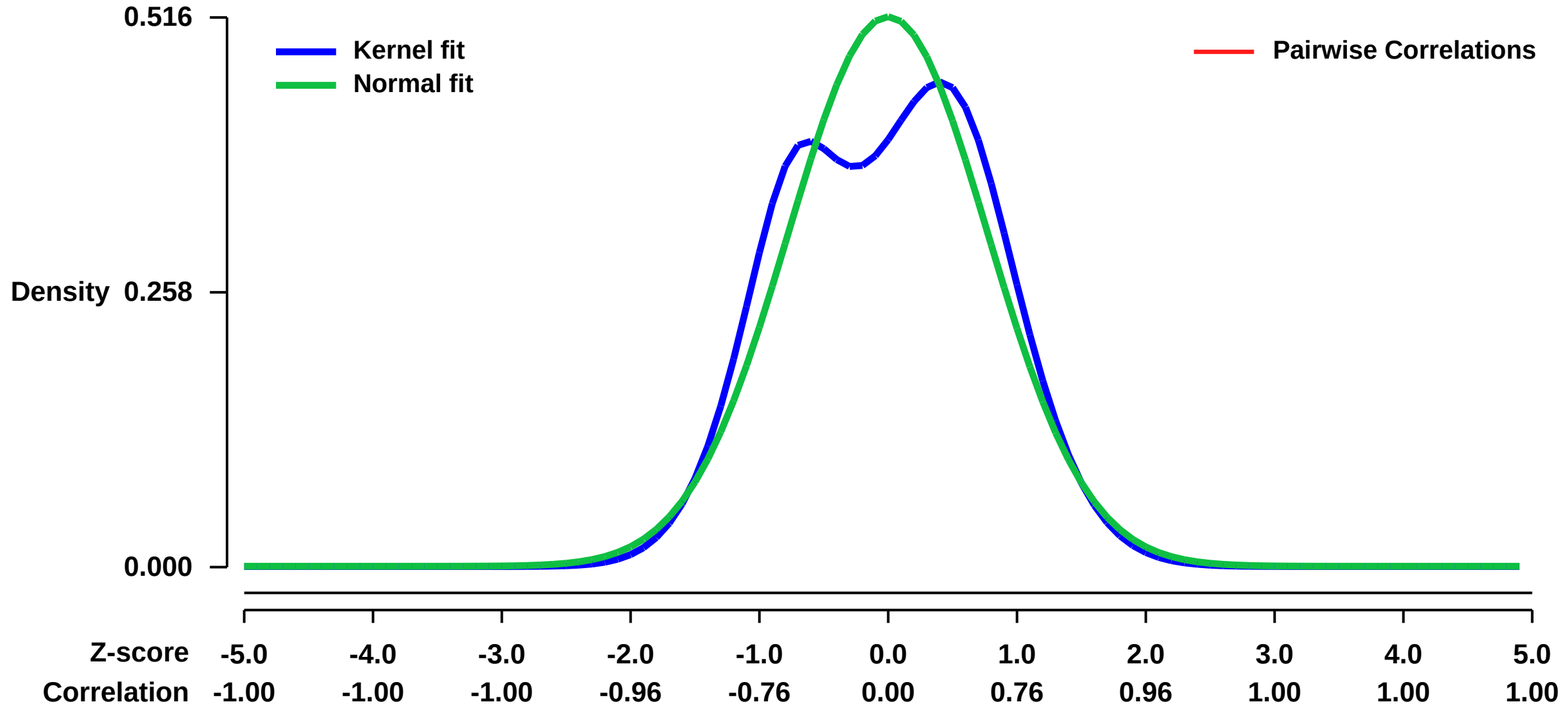

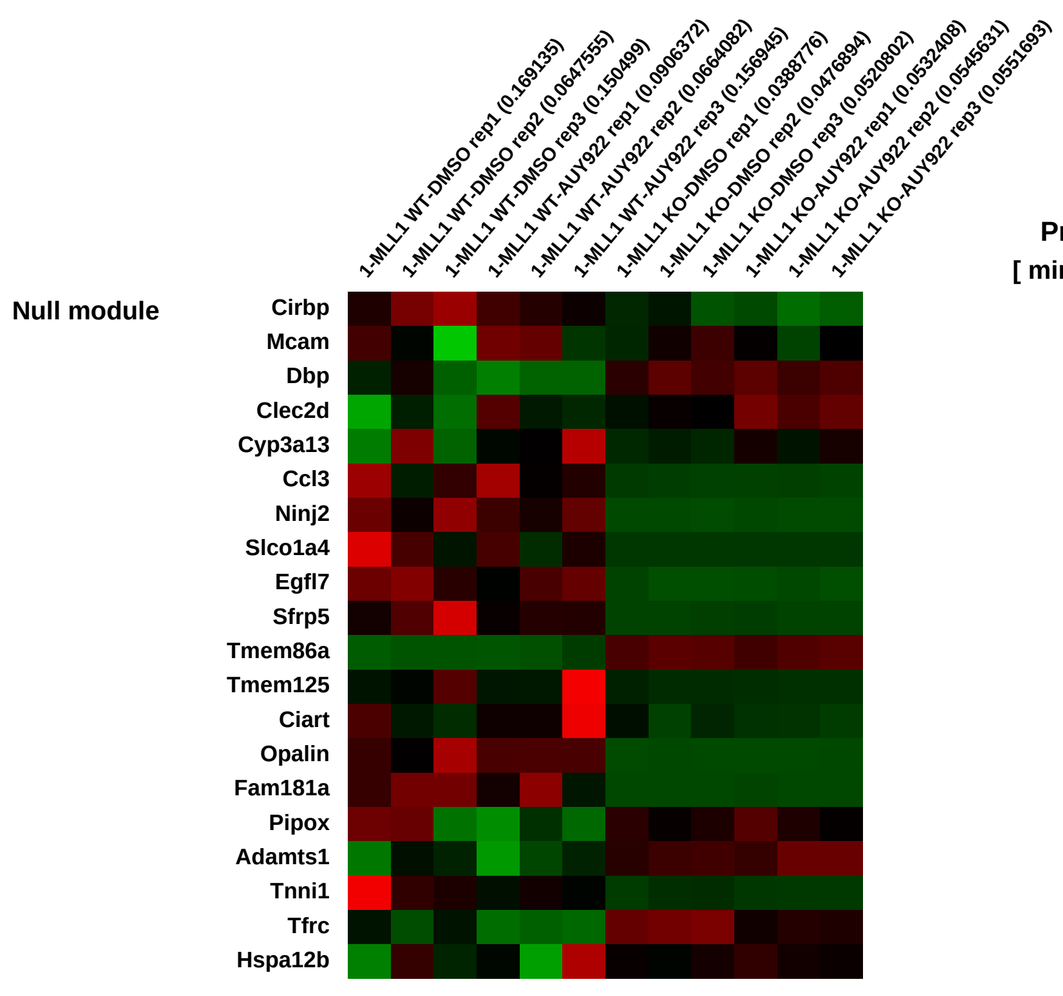

GEO Series "GSE56534" Expression Profiles

Num of samples in this series: 32

Scale of expression profile Z-scores

-3.0 -2.0 -1.0 0.0 1.0 2.0 3.0

GEO Link:	http://www.ncbi.nlm.nih.gov/geo/query/acc.cgi?acc=GSE56534
Status:	Public on Jun 01 2014
Title:	Infection of macrophages by Toxoplasma Progeny from a Type II x Type III cross
Organism:	Mus musculus
Experiment type:	Expression profiling by array
Platform:	GPL1261
Pubmed ID:	
Summary & Design:	**Summary:** Infection of RAW264.7 cells for 24 hours with 32 Toxoplasma Progeny from a Type II x Type III cross To measure changes in gene expression induced in macropahges upon Toxoplasma infection, we infected RAW 264.7 macrophages in cell culture with one of 32 Toxoplasma parasite progeny from a Type II x Type III cross. RNA was harvested 24 hours post infection. **Overall design:** Cells were infected with Toxoplasma parasites, in vitro

Background corr dist: KL-Divergence = 0.1124, L1-Distance = 0.0430, L2-Distance = 0.0039, Normal std = 0.4154

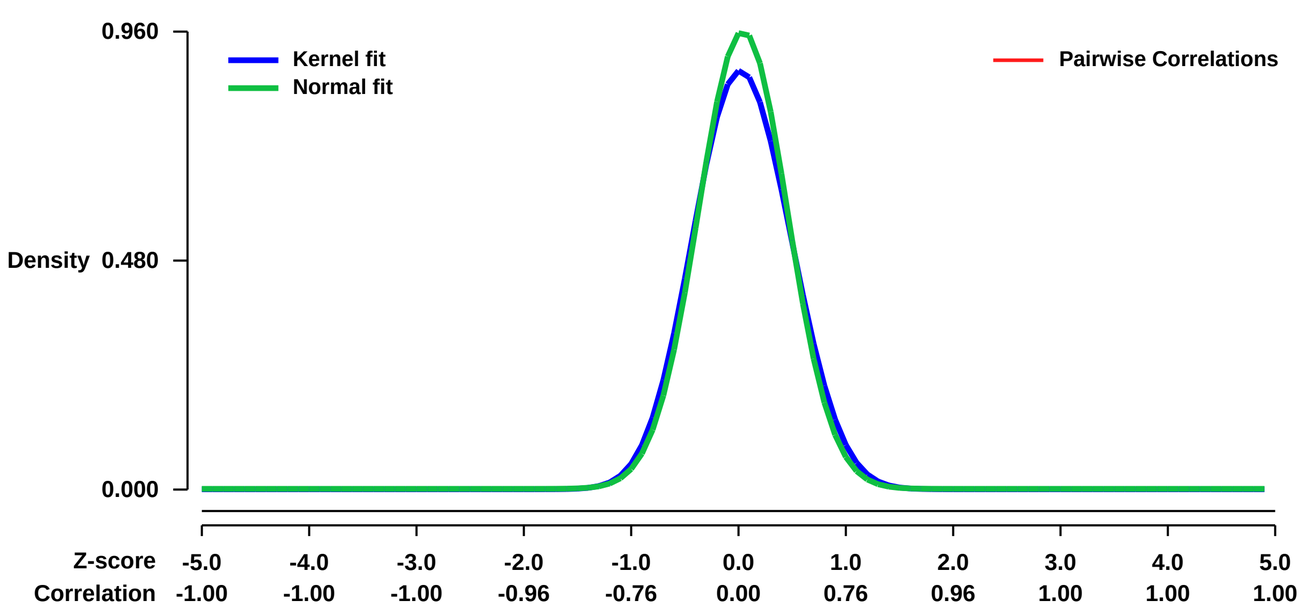

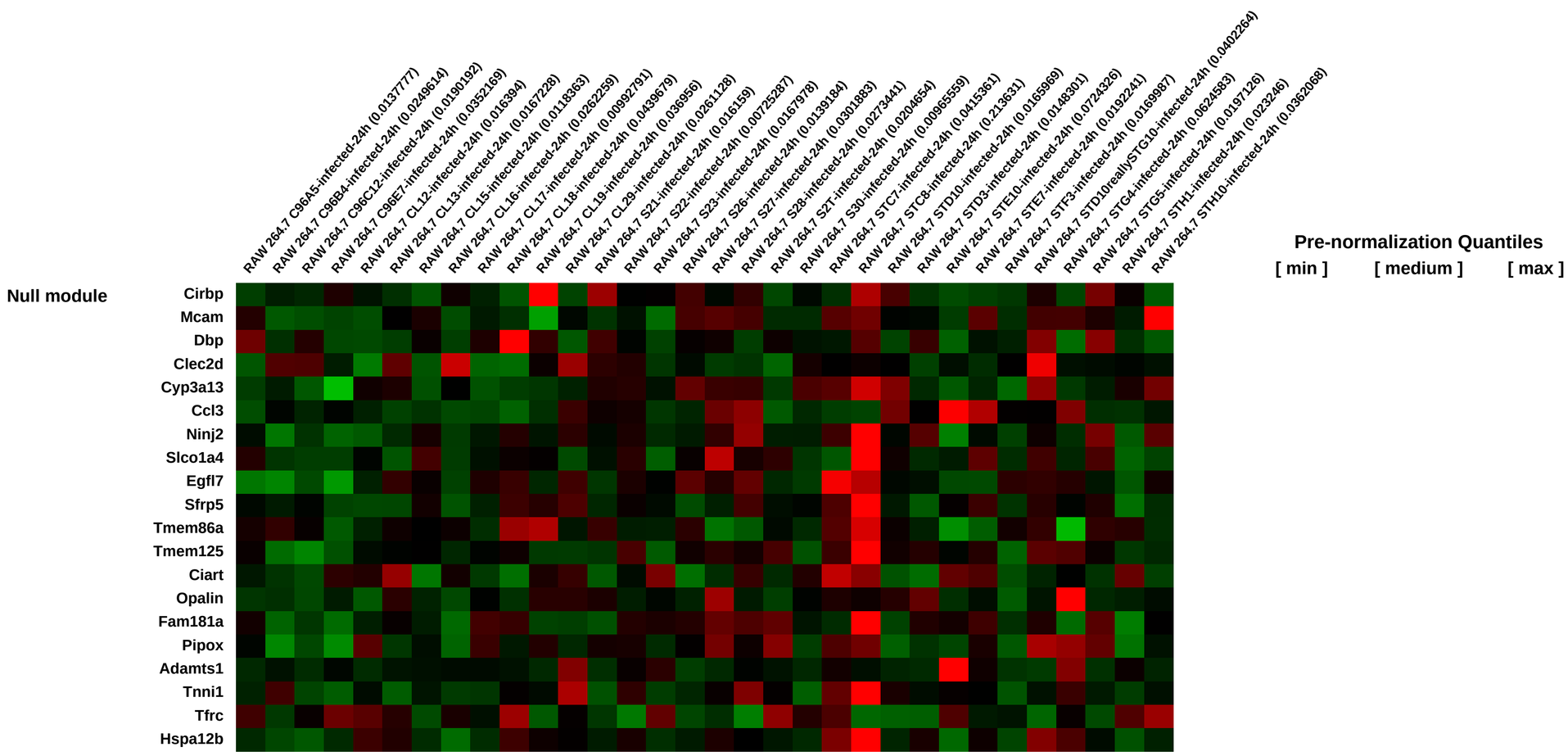

GEO Series "GSE56542" Expression Profiles

Num of samples in this series: 8

Scale of expression profile Z-scores

-3.0 -2.0 -1.0 0.0 1.0 2.0 3.0

GEO Link:	**http://www.ncbi.nlm.nih.gov/geo/query/acc.cgi?acc=GSE56542**
Status:	**Public on Apr 07 2014**
Title:	**Expression data from CD4+ T cells of germ free mice, SPF IQI mice and SPF C57BL/6 mice depletd with Uhrf1 (by Cd4Cre-Uhrf1flox/flox)**
Organism:	**Mus musculus**
Experiment type:	**Expression profiling by array**
Platform:	**GPL1261**
Pubmed ID:	
Summary & Design:	**Summary:** **Commensal bacteria shapes gut immune system. Colonization bacteria increase the frequency of regulatory T cells, however, the molecular mechanisms has not yet been unknown. To reveal the mechanism, we isolated Treg cells and Non-Treg cells and performed the global expression analysis.** **Overall design:** **Colonic lamina propria cells were isolated from mice described above. Treg cells and Non-Treg cells (also called as Tconv cells) were sorted by FACS AriaIII**

Background corr dist: **KL-Divergence = 0.0404, L1-Distance = 0.0306, L2-Distance = 0.0014, Normal std = 0.6162**

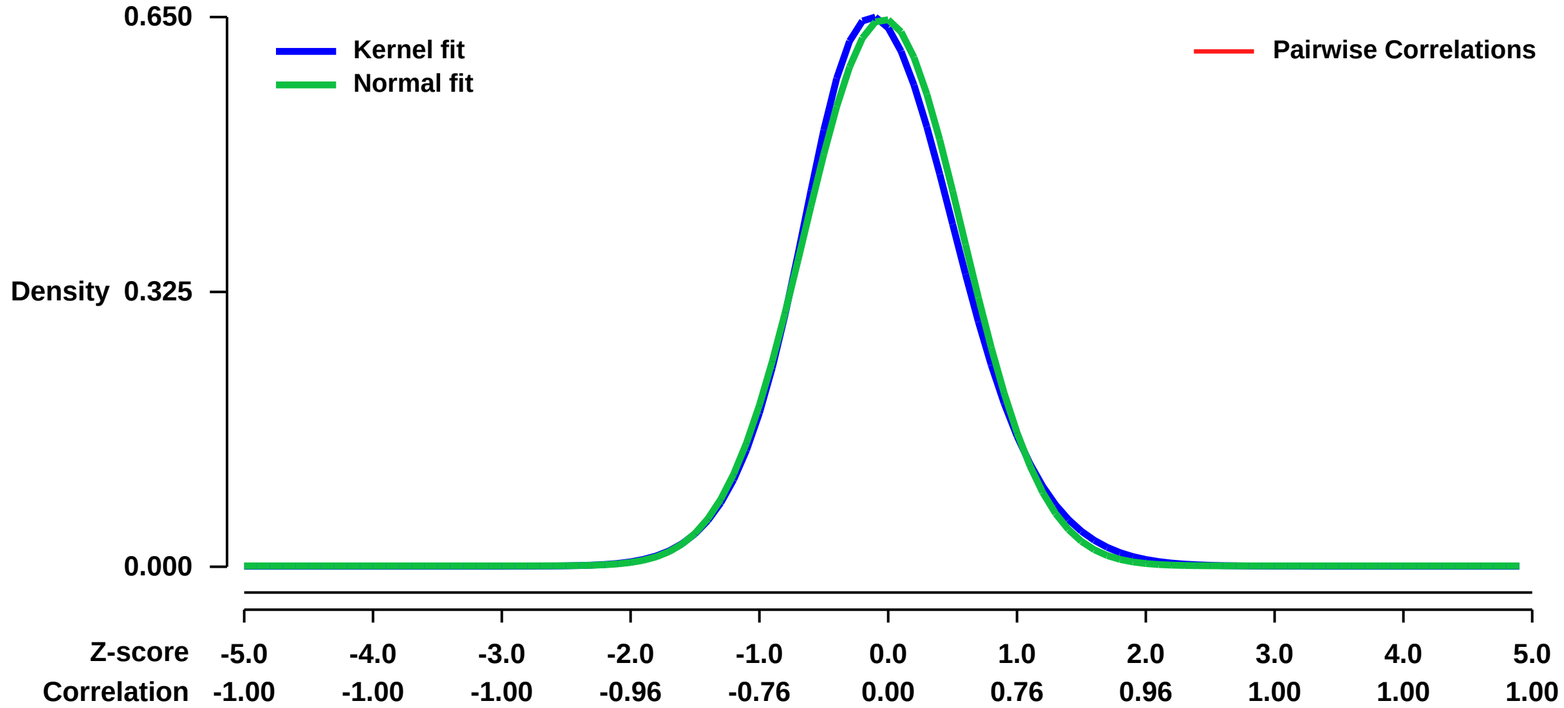

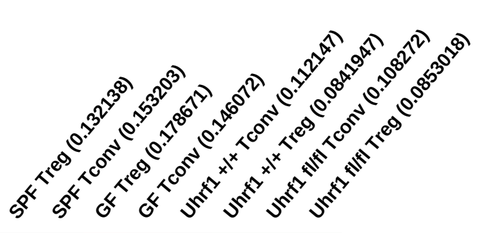

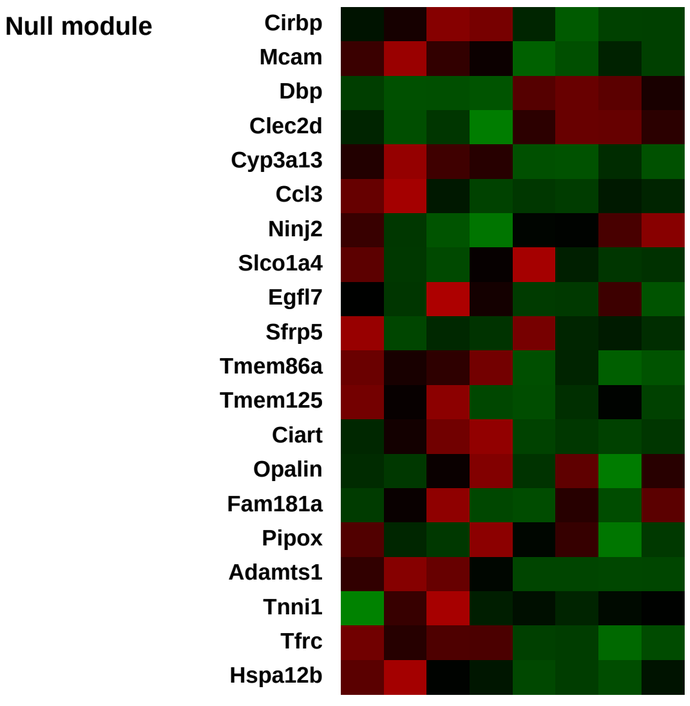

GEO Series "GSE5715" Expression Profiles

Num of samples in this series: 10

Scale of expression profile Z-scores

-3.0 -2.0 -1.0 0.0 1.0 2.0 3.0

GEO Link:	http://www.ncbi.nlm.nih.gov/geo/query/acc.cgi?acc=GSE5715
Status:	Public on May 21 2007
Title:	Intestinal Phenotype of Variable Weight Cystic Fibrosis Knockout Mice
Organism:	Mus musculus
Experiment type:	Expression profiling by array
Platform:	GPL1261
Pubmed ID:	17615178
Summary & Design:	**Summary:** Cystic fibrosis transmembrane conductance regulator (Cftr) knockout mice present the clinical features of low body weight and intestinal disease permitting an assessment of the interrelatedness of these phenotypes in a controlled environment. To identify intestinal alterations which affect body weight in CF mice the histological phenotypes of crypt-villus axis height, goblet cell hyperplasia, and mast cell infiltrate were measured, cardiac blood samples assessed, and gene expression profiling of the ileum was completed for 12 week old (C57BL/6xBALB) F2 Cftrtm1UNC and non-CF mice presenting a range of body weight. Crypt-villus axis height decreased with increasing weight in CF, but not control, mice. Goblet cell hyperplasia and mast cell infiltration in the submucosa and muscularis externa layers of the CF intestine, were identified to be independent of bodyweight. Blood triglyceride levels were found to be significantly lower in CF mice than control mice (p = 3.02 x 10-5) but were not dependent on CF mouse body weight. By expression profiling, genes of DNA replication and lipid metabolism were among those altered in CF mice relative to non-CF controls; and no differences in gene expression were measured between samples from CF mice in the 25th and 75th percentile for weight. This study indicates that the absence of Cftr leads to altered morphology in the CF intestine the extent of which is correlated with body weight in CF mice while CF related changes in blood triglyceride levels and in the intestinal gene expression profile were not dependent on body weight in this model. **Keywords:** disease state analysis **Overall design:** B6xBALB F2 mice gene expression was collected for nine CF-/- mice and 6 controls. Differential expression was analyzed between the groups

Background corr dist: KL-Divergence = 0.0959, L1-Distance = 0.0285, L2-Distance = 0.0013, Normal std = 0.4421

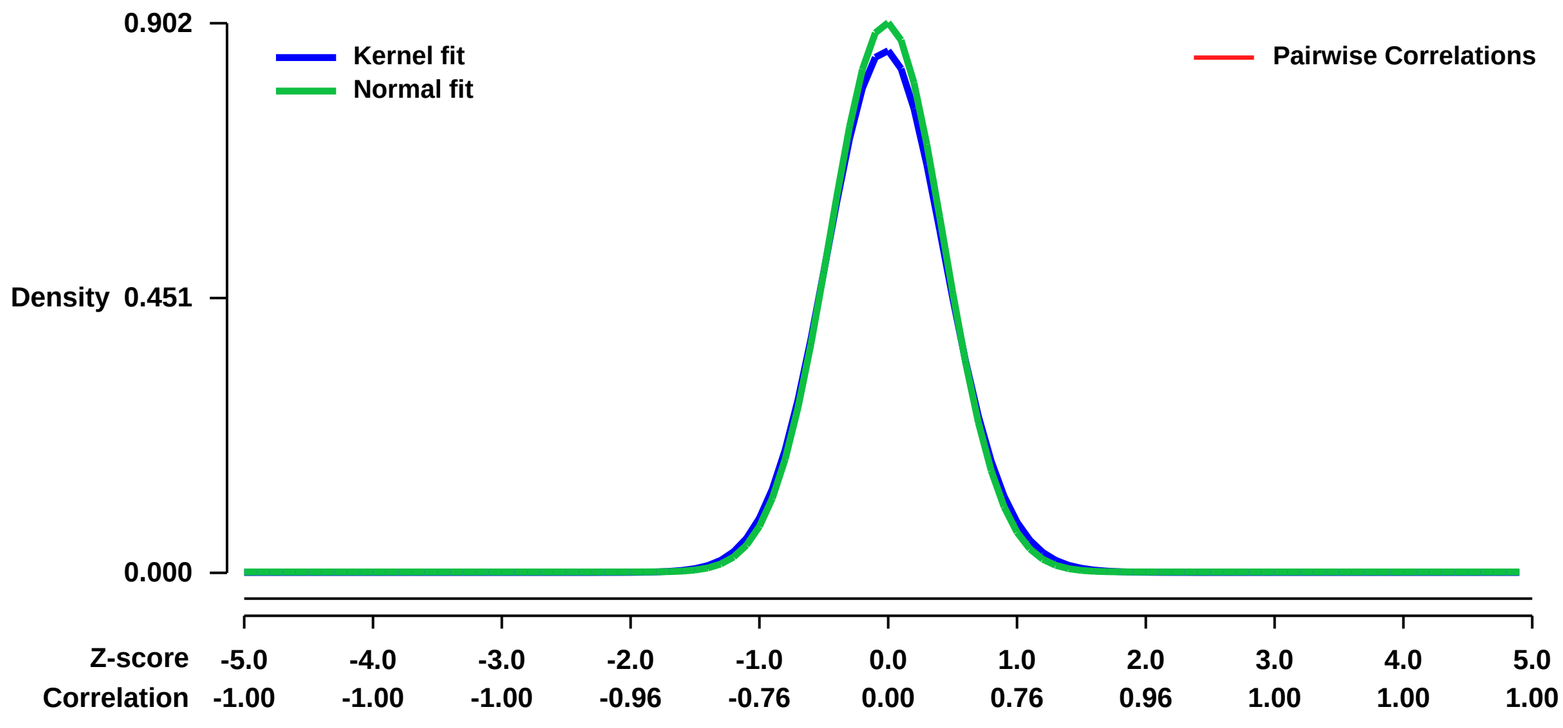

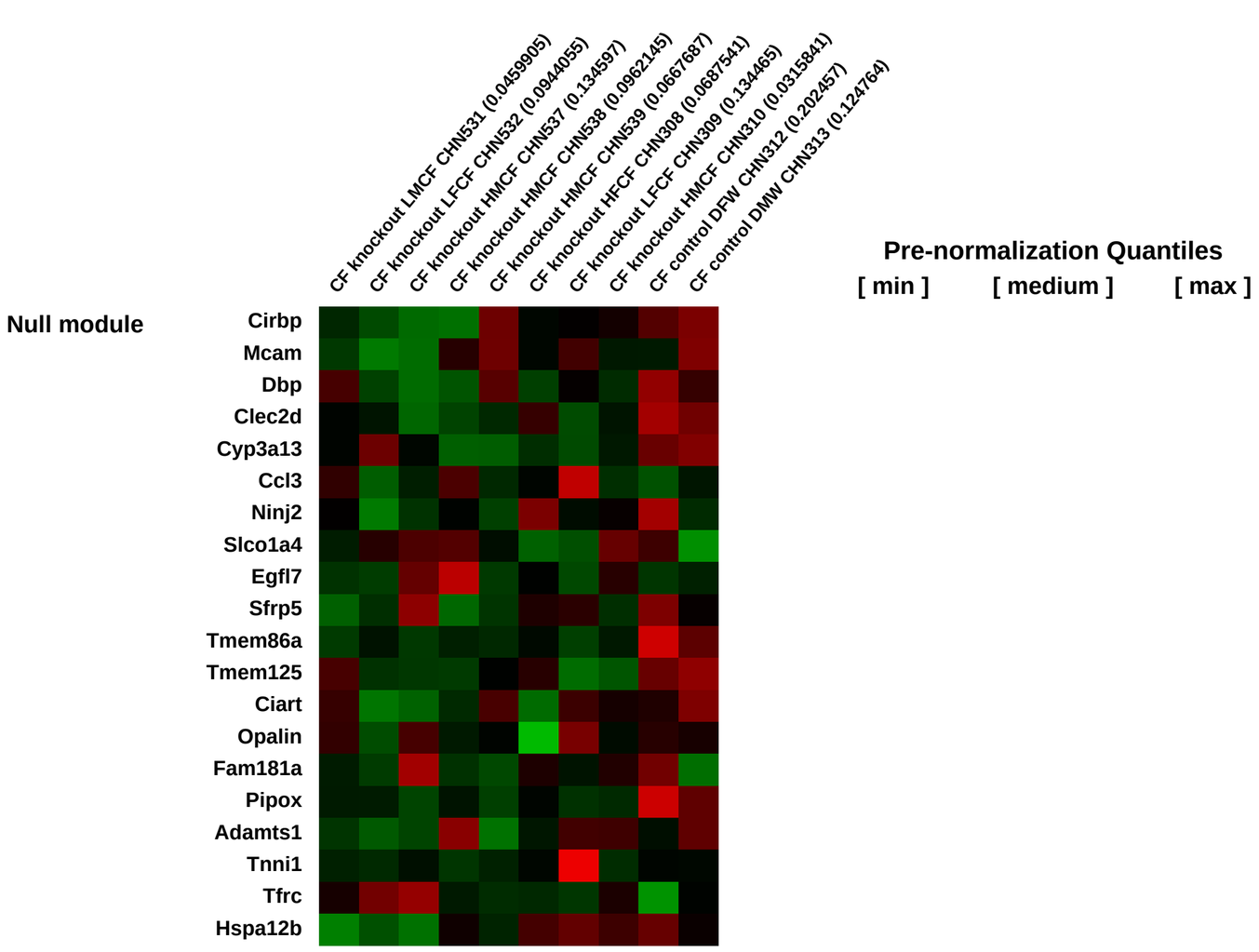

GEO Series "GSE57425" Expression Profiles

Num of samples in this series: 6

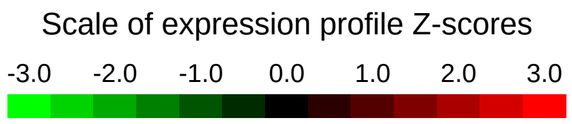

GEO Link:	**http://www.ncbi.nlm.nih.gov/geo/query/acc.cgi?acc=GSE57425**
Status:	**Public on May 09 2014**
Title:	**Gene expression data of livers from C57BL/6 fed a normal diet or high-fat-diet**
Organism:	**Mus musculus**
Experiment type:	**Expression profiling by array**
Platform:	**GPL1261**
Pubmed ID:	
Summary & Design:	**Summary:** **Obesity is tightly associated with an increased risk of nonalcoholic fatty liver disease (NAFLD). However, the molecular mechanisms of obesity-induced fatty liver remain largely unknown.In order to identify genes that are potentially involved in dysfunctional hepatic lipid homeostasis in obesity, we performed a clustering analysis of Affymetrix arrays,which revealed that a number of mRNAs were dys-regulated in the livers of mice fed a high-fat diet (HFD), compared with mice fed a normal chow diet (ND).** **Overall design:** **To identify genes that are potentially involved in dysfunctional hepatic lipid homeostasis in obesity, male C57BL/6 mice aged 8 weeks were fed a normal diet (ND) or high-fat-diet (HFD) containing 60 Kcal% of fat for 12 weeks. Then mice were sacrificed and total RNAs were isoloated from hepatic tissues. Affymetrix array hybridisation and scanning were performed using Mouse Genome 430 2.0 chips.Total RNA samples obtained from six mice per group (ND and HFD) and pooled by each of the two were used for microarray analysis.**

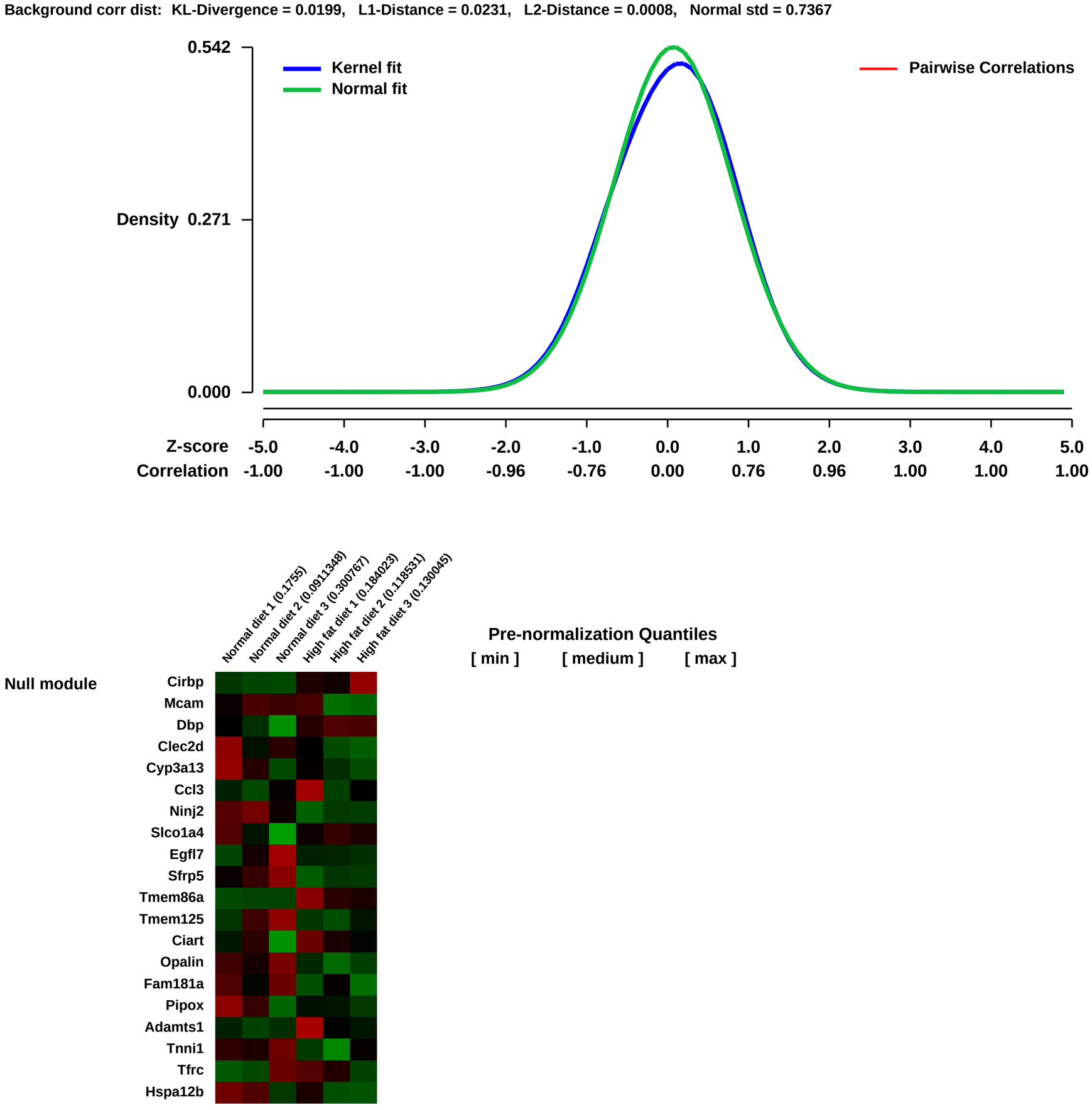

GEO Series "GSE57469" Expression Profiles

Num of samples in this series: 6

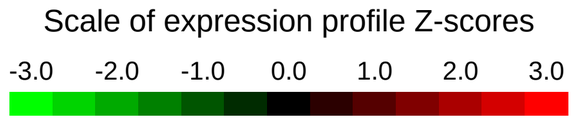

GEO Link:	**http://www.ncbi.nlm.nih.gov/geo/query/acc.cgi?acc=GSE57469**
Status:	**Public on May 09 2014**
Title:	**Expression data from common myeloid progenitor cells (CMP) of C57BL6 mouse**
Organism:	**Mus musculus**
Experiment type:	**Expression profiling by array**
Platform:	**GPL1261**
Pubmed ID:	
Summary & Design:	**Summary:** **Common myeloid progenitor cells from murine bone marrow were sorted according to ROS content using FACS with H2-DCFDA staining.** **We compared gene expression profile between CMP with low-ROS levels and those with high-ROS levels.** **Overall design:** **We analysed function of ROS in differentiation step from CMP to MEP.**

Background corr dist: **KL-Divergence = 0.0403, L1-Distance = 0.0192, L2-Distance = 0.0004, Normal std = 0.6122**

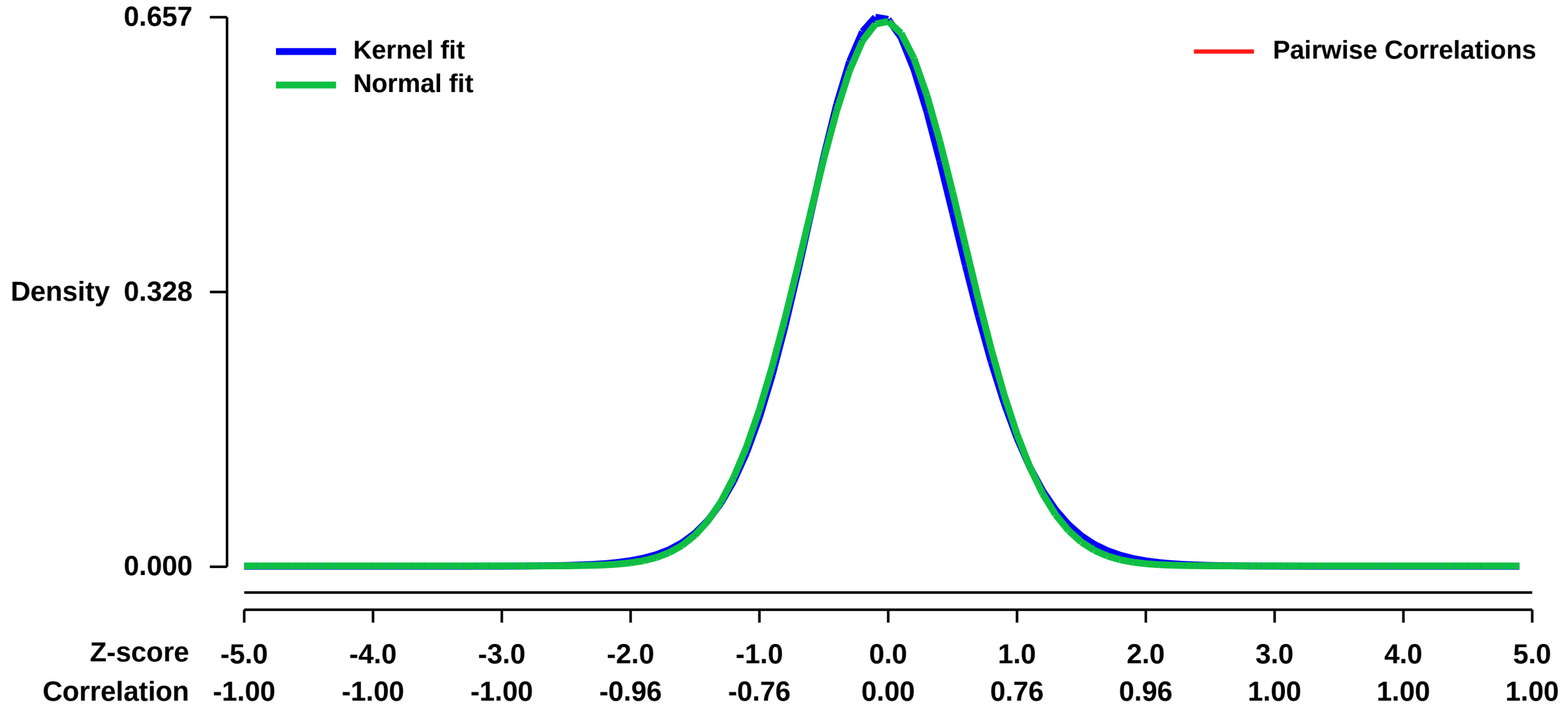

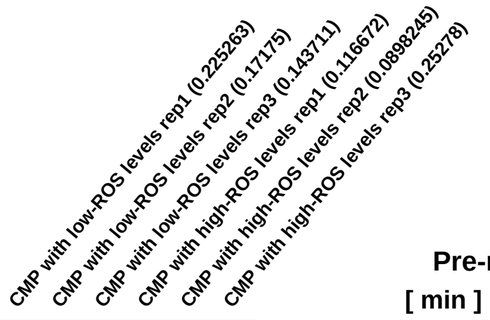

Pre-normalization Quantiles

[min] [medium] [max]

Null module

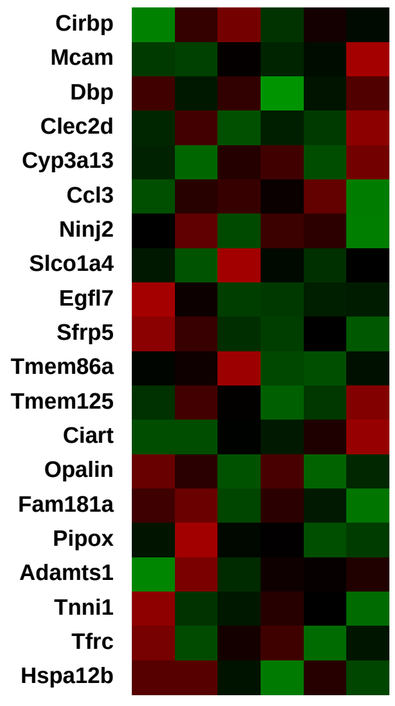

GEO Series "GSE57543" Expression Profiles

Num of samples in this series: 6

Scale of expression profile Z-scores

-3.0 -2.0 -1.0 0.0 1.0 2.0 3.0

GEO Link: http://www.ncbi.nlm.nih.gov/geo/query/acc.cgi?acc=GSE57543
Status: Public on May 13 2014
Title: Expression data from B6 mouse miR-142 KO and WT T cells
Organism: Mus musculus
Experiment type: Expression profiling by array
Platform: GPL1261
Pubmed ID:

Summary & Design:

Summary:
T cells are critical for modulating immune responses. miRNAs are small, noncoding RNAs and play a significant role in T cell responses. miR-142 is a hematopoietic specific miRNA. To explore the potential role of miR-142 in regulating T cell responses, we generated mutant mice bearing a targeted deletion of the miR-142 gene.

We used microarrays to detail the global programme of gene expression underlying the profile changes between miR-142 KO and WT T cell and identified distinct classes of up-regulated genes during this process.

Overall design:
miR-142 KO mice and WT littermates (biological triplicates) matched with age and sex were selected. T cells were purified from spleens by negative selection and processed for RNA isolation and hybridization on Affymetrix microarrays.

Background corr dist: KL-Divergence = 0.0094, L1-Distance = 0.0206, L2-Distance = 0.0006, Normal std = 0.8842

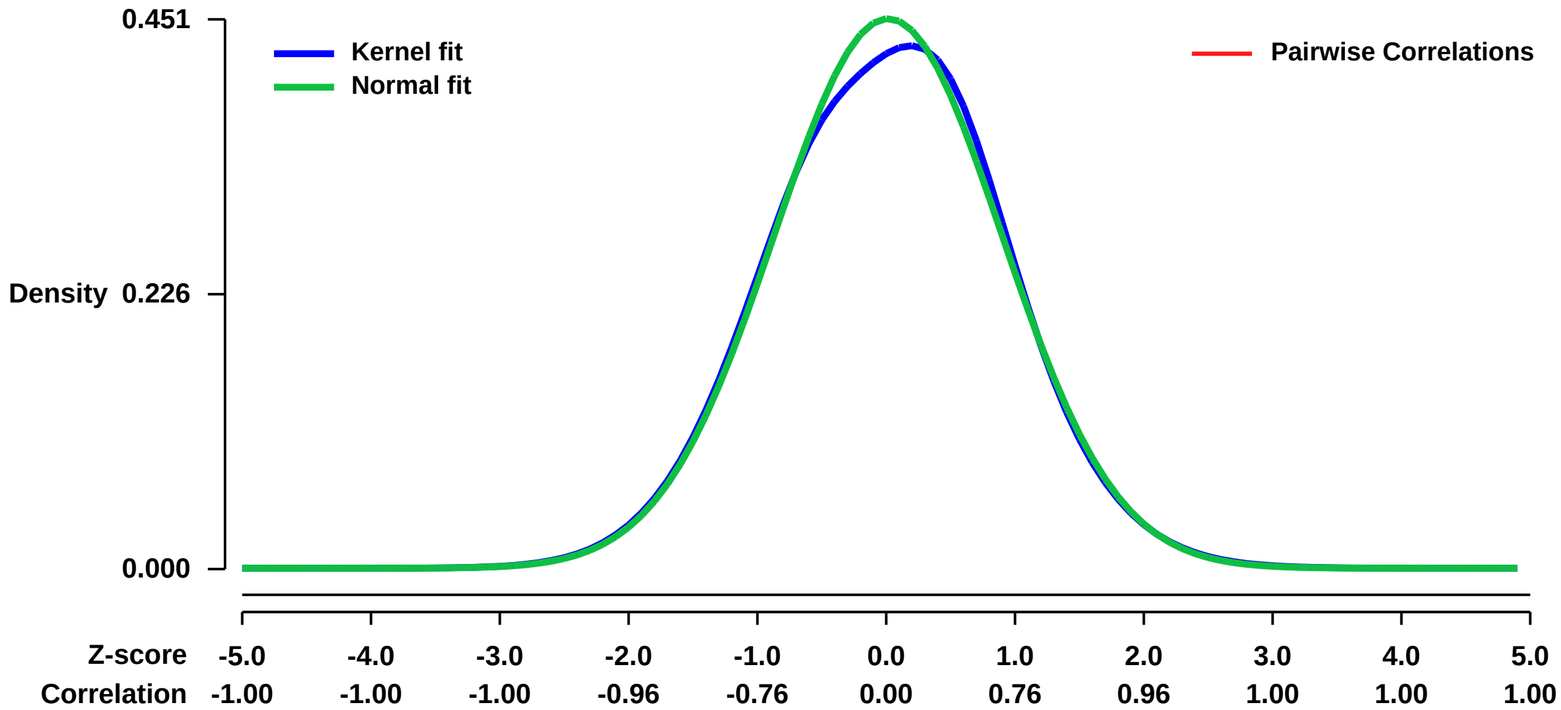

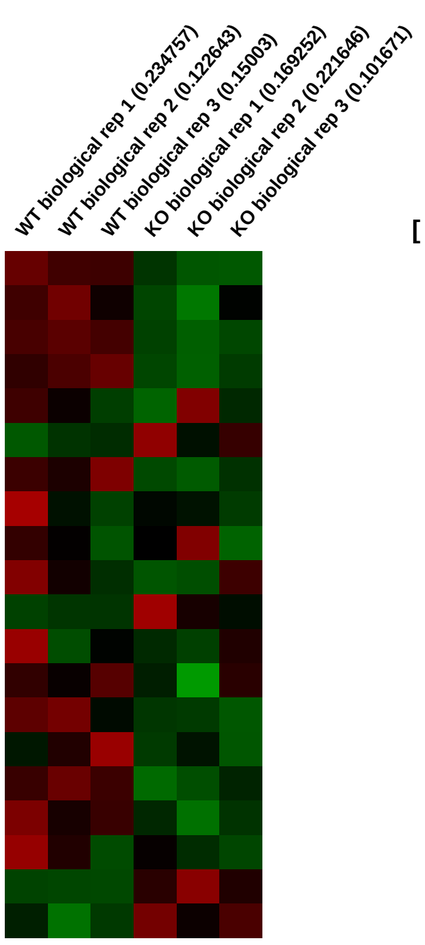

GEO Series "GSE5763" Expression Profiles

Num of samples in this series: 9

Scale of expression profile Z-scores

-3.0 -2.0 -1.0 0.0 1.0 2.0 3.0

GEO Link:	http://www.ncbi.nlm.nih.gov/geo/query/acc.cgi?acc=GSE5763
Status:	Public on Sep 10 2006
Title:	Expression data from mouse brain region bed nucleus of the stria terminalis, nucleus accumbens, and dorsal striatum.
Organism:	Mus musculus
Experiment type:	Expression profiling by array
Platform:	GPL1261
Pubmed ID:	17911379
Summary & Design:	**Summary:** To identify distinct transcriptional patterns between the major subcortical dopamine targets commonly studied in addiction we studied differences in gene expression between the bed nucleus of the stria terminalis (BNST), nucleus accumbens (NAc), and dorsal striatum (dStr) using microarray analysis. We first tested for differences in expression of genes encoding transcripts for common neurotransmitter systems as well as calcium binding proteins routinely used in neuroanatomical delineation of brain regions. This a priori method revealed differential expression of corticotropin releasing hormone (Crh), the GABA transporter (Slc6a1), and prodynorphin (Pdyn) mRNAs as well as several others. Using a gene ontology tool, functional scoring analysis, and Ingenuity Pathway Analysis, we further identified several physiological pathways that were distinct among these brain regions. These two different analyses both identified calcium signaling, G15 coupled protein receptor signaling, and adenylate cyclase-related signaling as significantly different among the BNST, NAc, and dStr. These types of signaling pathways play important roles in, amongst other things, synaptic plasticity. Investigation of differential gene expression revealed several instances that may provide insight into reported differences in synaptic plasticity between these brain regions. The results support other studies suggesting that crucial pathways involved in neurotransmission are distinct among the BNST, NAc, and dStr, and provide insight into the potential use of pharmacological agents that may target region-specific signaling pathways. Further, these studies provide a framework for future mouse-mouse comparisons of transcriptional profiles after behavioral/pharmacological manipulation. **Keywords:** Tissue type comparison **Overall design:** The genome-wide geen expression of mouse brain region bed nucleus of the stria terminalis, nucleus accumbens, and dorsal striatum were analyzed by Affymetrix Mouse430_2 chip. The expression and functional profiles were compared between these 3 tissues and cross-validated from independant data published before.

Background corr dist: KL-Divergence = 0.0578, L1-Distance = 0.0190, L2-Distance = 0.0004, Normal std = 0.5281

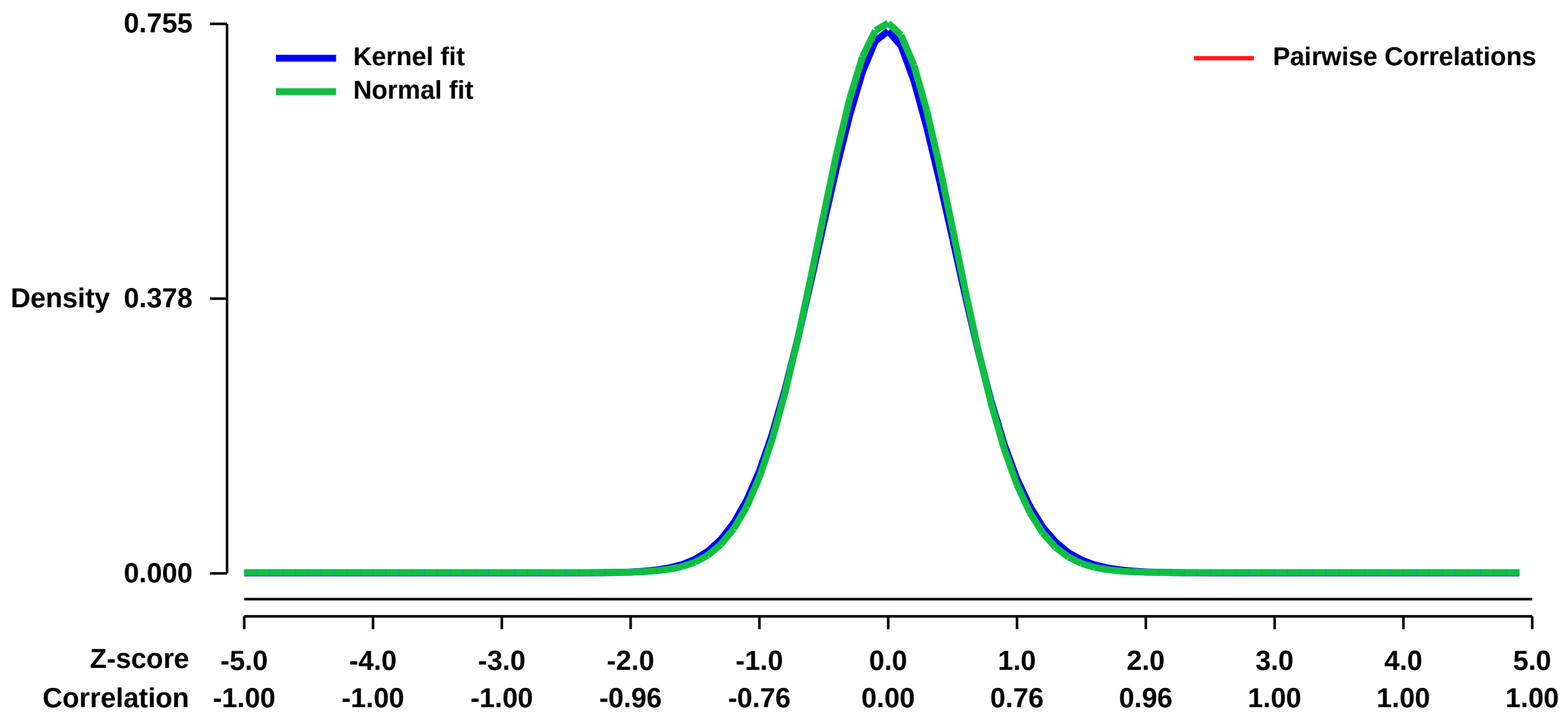

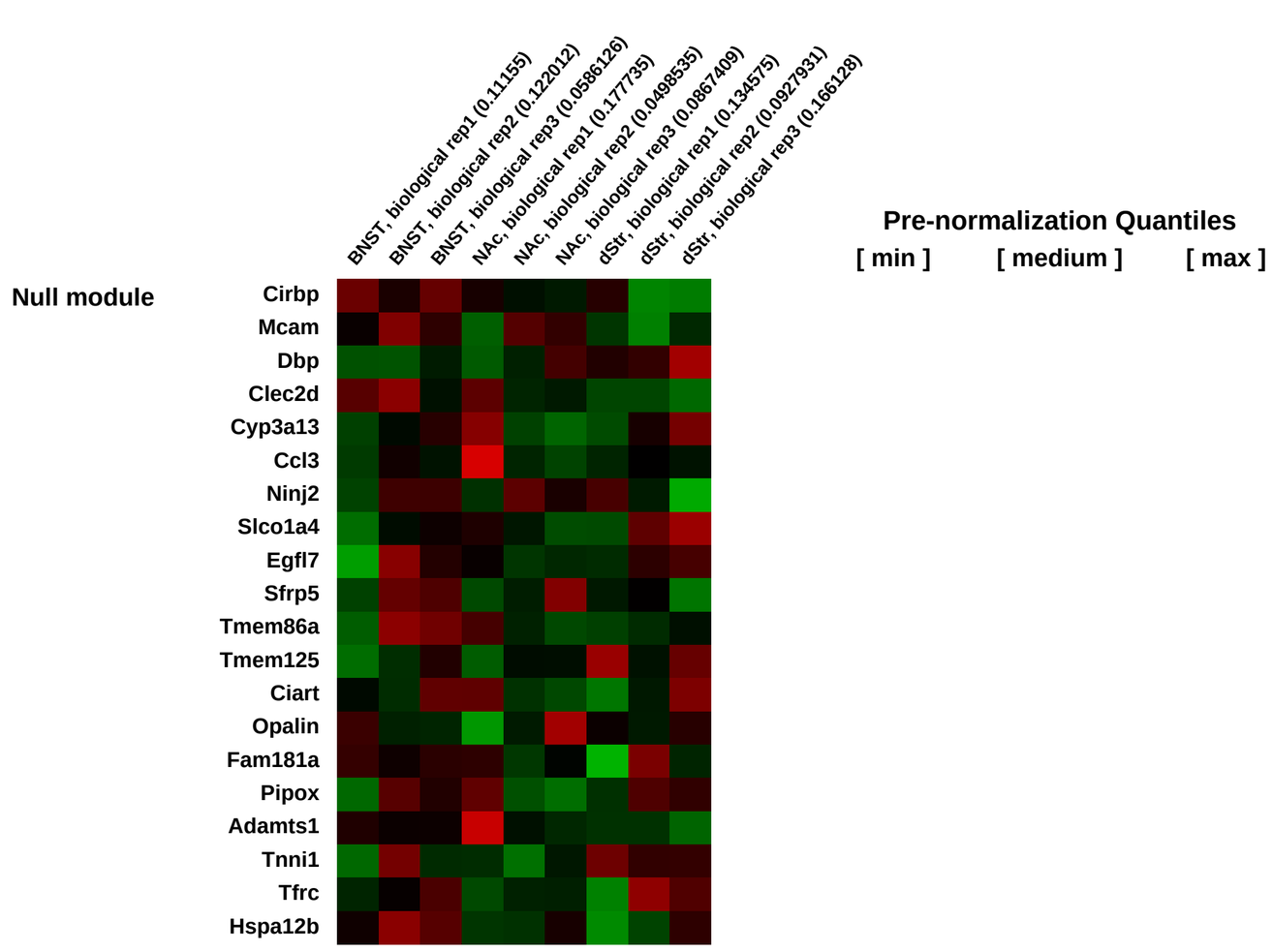

GEO Series "GSE57797" Expression Profiles

Num of samples in this series: 23

Scale of expression profile Z-scores

-3.0 -2.0 -1.0 0.0 1.0 2.0 3.0

GEO Link:	**http://www.ncbi.nlm.nih.gov/geo/query/acc.cgi?acc=GSE57797**
Status:	**Public on Jul 13 2014**
Title:	**Expression data from the subclones of Lewis Lung Carcinoma (LLC) cells**
Organism:	**Mus musculus**
Experiment type:	**Expression profiling by array**
Platform:	**GPL1261**
Pubmed ID:	
Summary & Design:	**Summary:** **Medium conditioned by LLC cells stimulates thermogenic gene expression when added onto primary adipocytes. We generated single cell colonies from parental LLC cells. Media conditioned by the subclones stimulated thermogenic gene expression in primary adipocytes at varying degrees.** **Subclones 2, 3, 6 and 28 produce significantly larger amount of thermogenic activity than the subclones 18, 19, 23 and 24. We compared gene expression profiles of these subclones to identify secreted factors enriched in the more thermogenic clones.** **Overall design:** **LLC subclones were cultured under conditioned medium preparation conditiones and total RNA was extracted from biological replicates.**

Background corr dist: KL-Divergence = 0.2154, L1-Distance = 0.0344, L2-Distance = 0.0019, Normal std = 0.3269

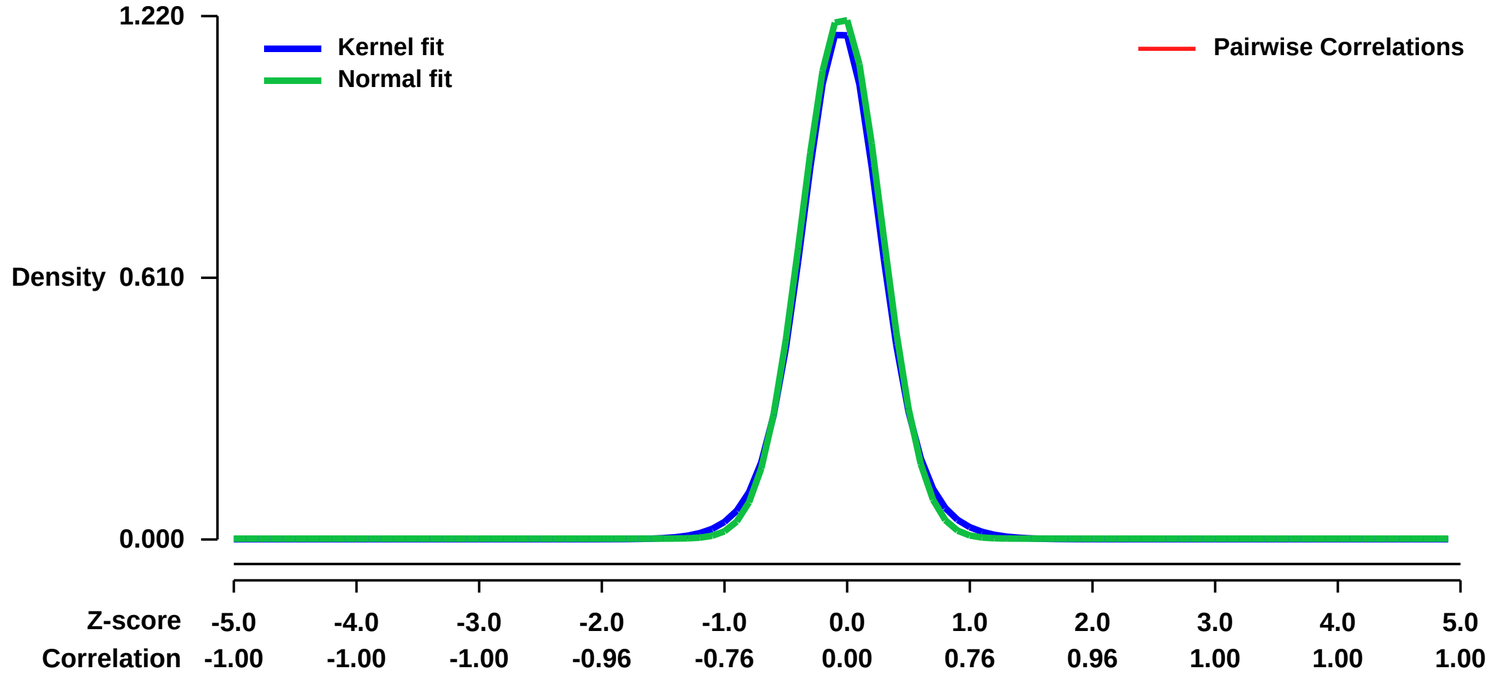

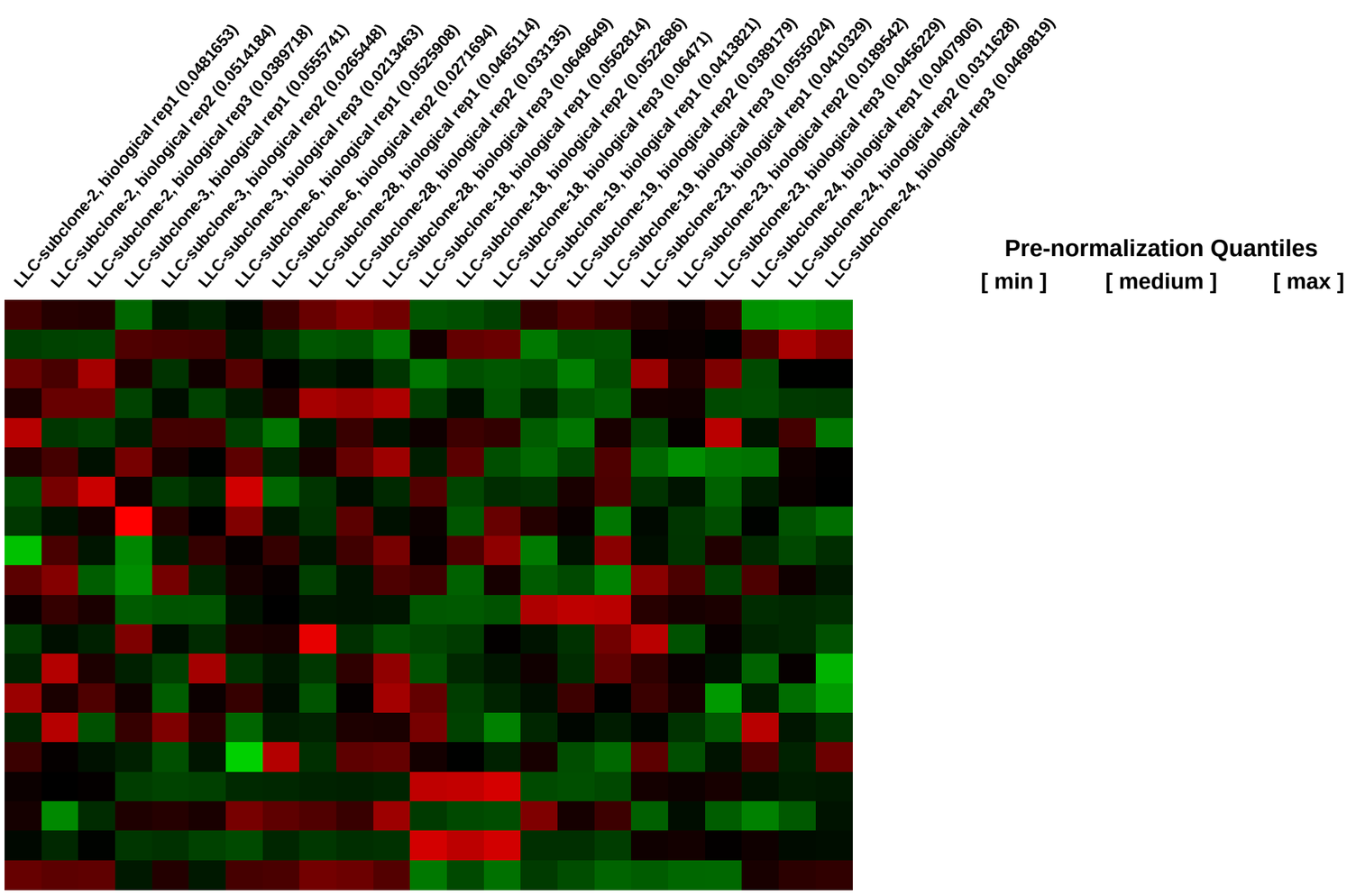

GEO Series "GSE5786" Expression Profiles

Num of samples in this series: 6

Scale of expression profile Z-scores

-3.0 -2.0 -1.0 0.0 1.0 2.0 3.0

GEO Link:	http://www.ncbi.nlm.nih.gov/geo/query/acc.cgi?acc=GSE5786
Status:	Public on Oct 05 2006
Title:	Gene Expression Profiling of PGC-1a KO mouse striata
Organism:	Mus musculus
Experiment type:	Expression profiling by array
Platform:	GPL1261
Pubmed ID:	17018277
Summary & Design:	**Summary:** Huntingtonâ s Disease (HD) is an inherited neurodegenerative disease caused by a glutamine repeat expansion in huntingtin protein. Transcriptional deregulation and altered energy metabolism have been implicated in HD pathogenesis. We report here that mutant huntingtin causes disruption of mitochondrial function by inhibiting expression of PGC-1a, a transcriptional coactivator that regulates several metabolic processes including mitochondrial biogenesis and respiration. Mutant huntingtin represses PGC-1a gene transcription by associating with the promoter and interfering with the CREB/TAF4-dependent transcriptional pathway critical for the regulation of PGC-1a gene expression. Crossbreeding of PGC-1a knockout mice with HD knock-in mice leads to increased neurodegeneration of striatal neurons and motor abnormalities in the HD mice. Importantly, expression of PGC-1a partially reverses the toxic effects of mutant huntingtin in cultured striatal neurons. Moreover, lentiviral-mediated delivery of PGC-1a in the striatum provides neuroprotection in the transgenic HD mice. These studies suggest a key role for PGC-1a in the control of energy metabolism in the early stages of HD pathogenesis. **Keywords:** PGC-1a, striatum **Overall design:** Total RNA was extracted from striata of 3 pgc1¸– KO mice and 3 littermate controls using the RNeasy Mini Kit (Qiagen) according to manufacturerâ s protocol. Samples were analyzed using RNA 6000 Nano LabChip kit on a 2100 Bioanalyzer (Agilent Technologies) to ensure integrity of RNA.

Background corr dist: KL-Divergence = 0.0498, L1-Distance = 0.0184, L2-Distance = 0.0004, Normal std = 0.5732

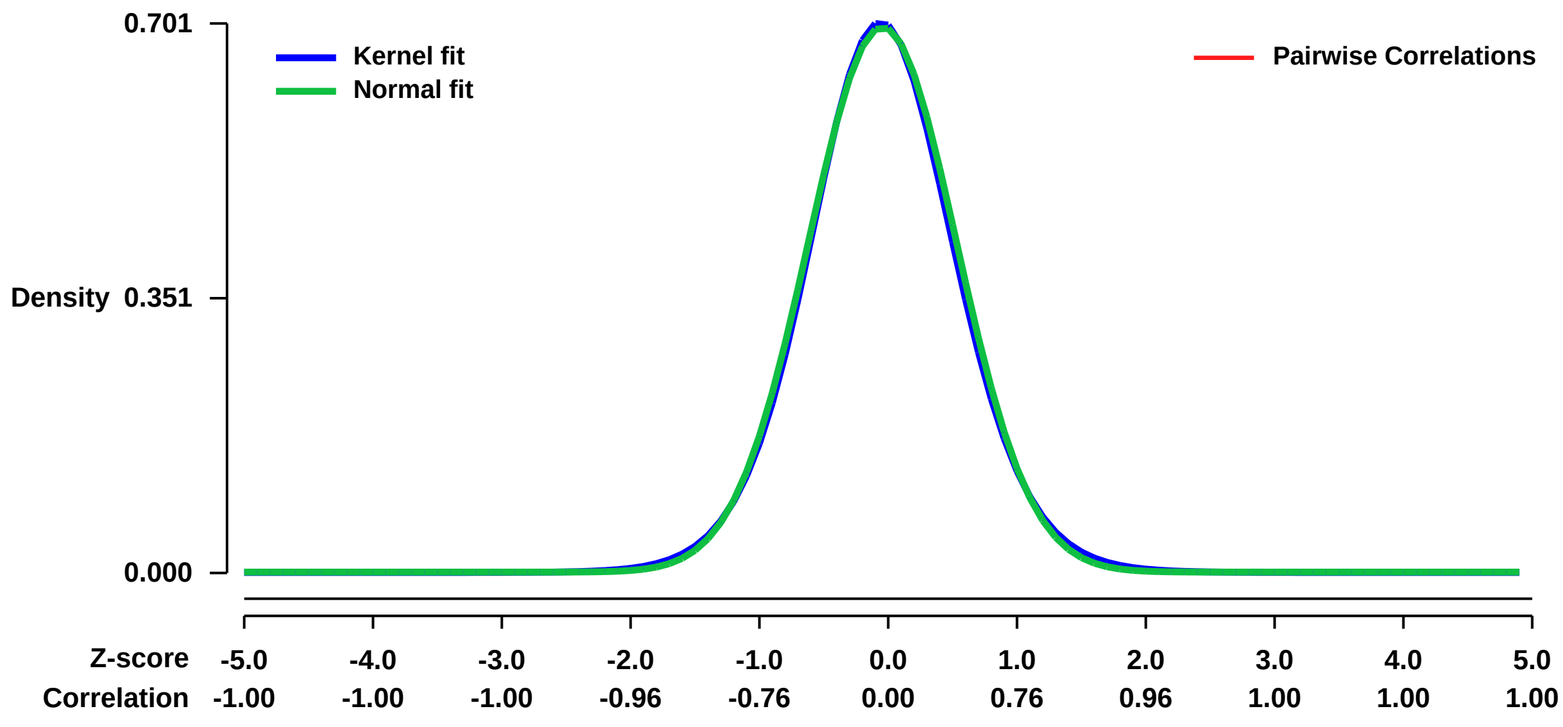

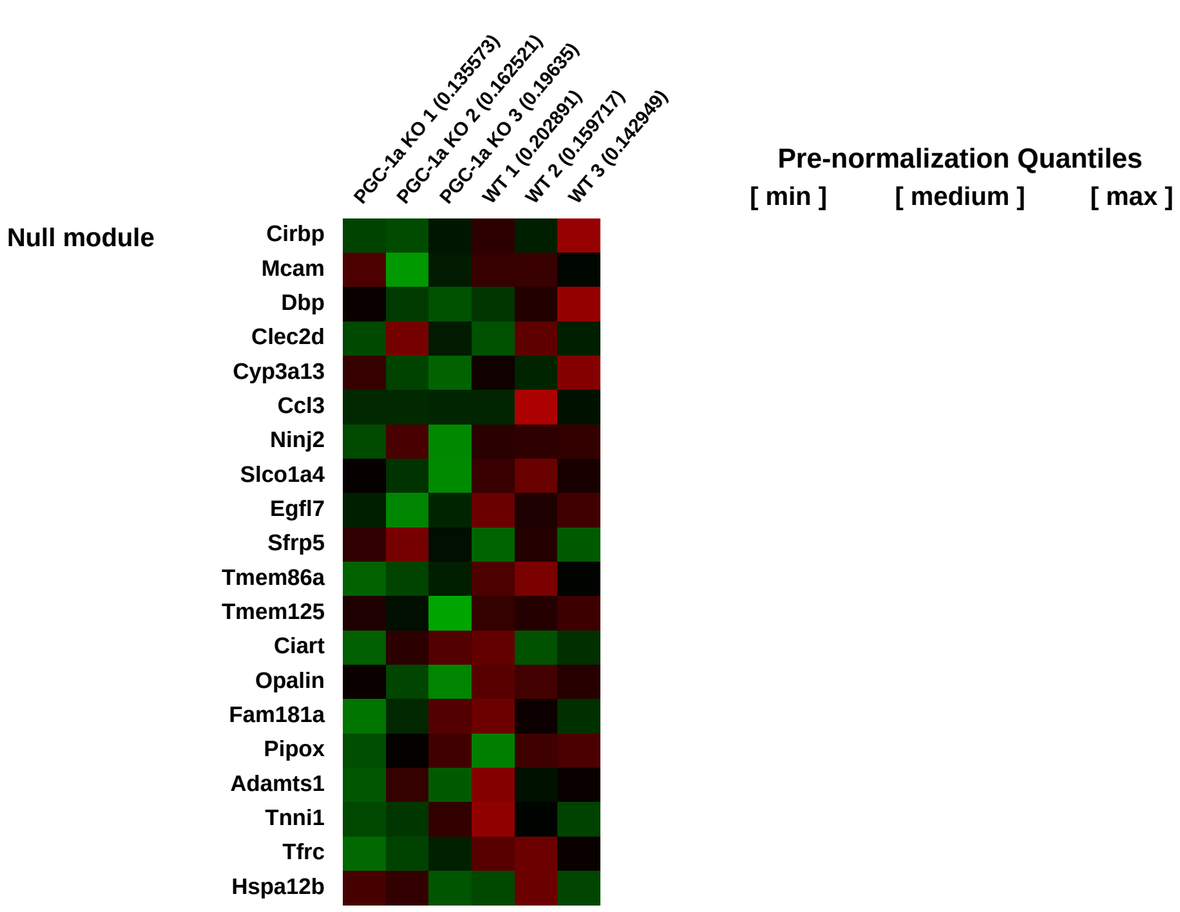

GEO Series "GSE5800" Expression Profiles

Num of samples in this series: 6

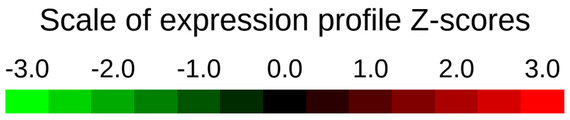

GEO Link:	http://www.ncbi.nlm.nih.gov/geo/query/acc.cgi?acc=GSE5800
Status:	Public on Oct 01 2006
Title:	Expression data from mouse IRF6 null and wt skin
Organism:	Mus musculus
Experiment type:	Expression profiling by array
Platform:	GPL1261
Pubmed ID:	17041601
Summary & Design:	**Summary:** Transcription factor paralogs may share a common role (e.g. Hox) in staged or overlapping expression in specific tissues. In other examples, members have distinct roles in a range of embryologic, differentiation or response pathways (e.g. Tbx, Pax). For the Interferon Regulatory Factor (IRF) family of transcription factors, mice deficient in Irf1, Irf2, Irf3, Irf4, Irf5, Irf7, Irf8 or Irf9, have defects in the immune response but display no embryologic abnormalities. Mice deficient for Irf6 have not been reported, but in humans, mutations in IRF6 cause two Mendelian orofacial clefting syndrome, and genetic variation in IRF6 confers risk for isolated cleft lip and palate. Mice deficient for Irf6 have abnormal skin, limb and craniofacial development. Histological and gene expression analyses indicate that the primary defect is in keratinocyte differentiation and proliferation. This study describes a novel role for an IRF family member in epidermal development. **Keywords:** Comparison of tissue from two genotypes **Overall design:** Skin from E17.5 mice was removed and flash frozen for RNA extraction and hybridization on Affymetrix microarrays.

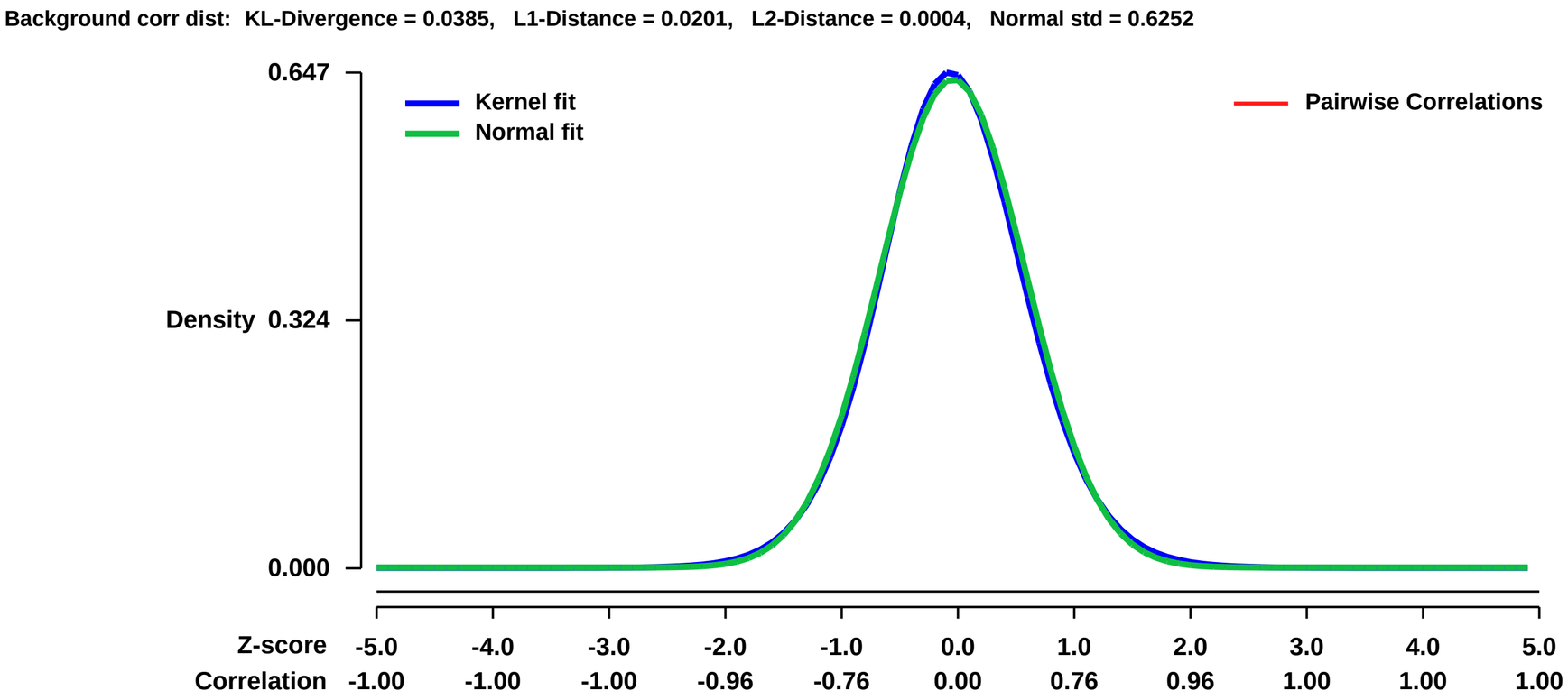

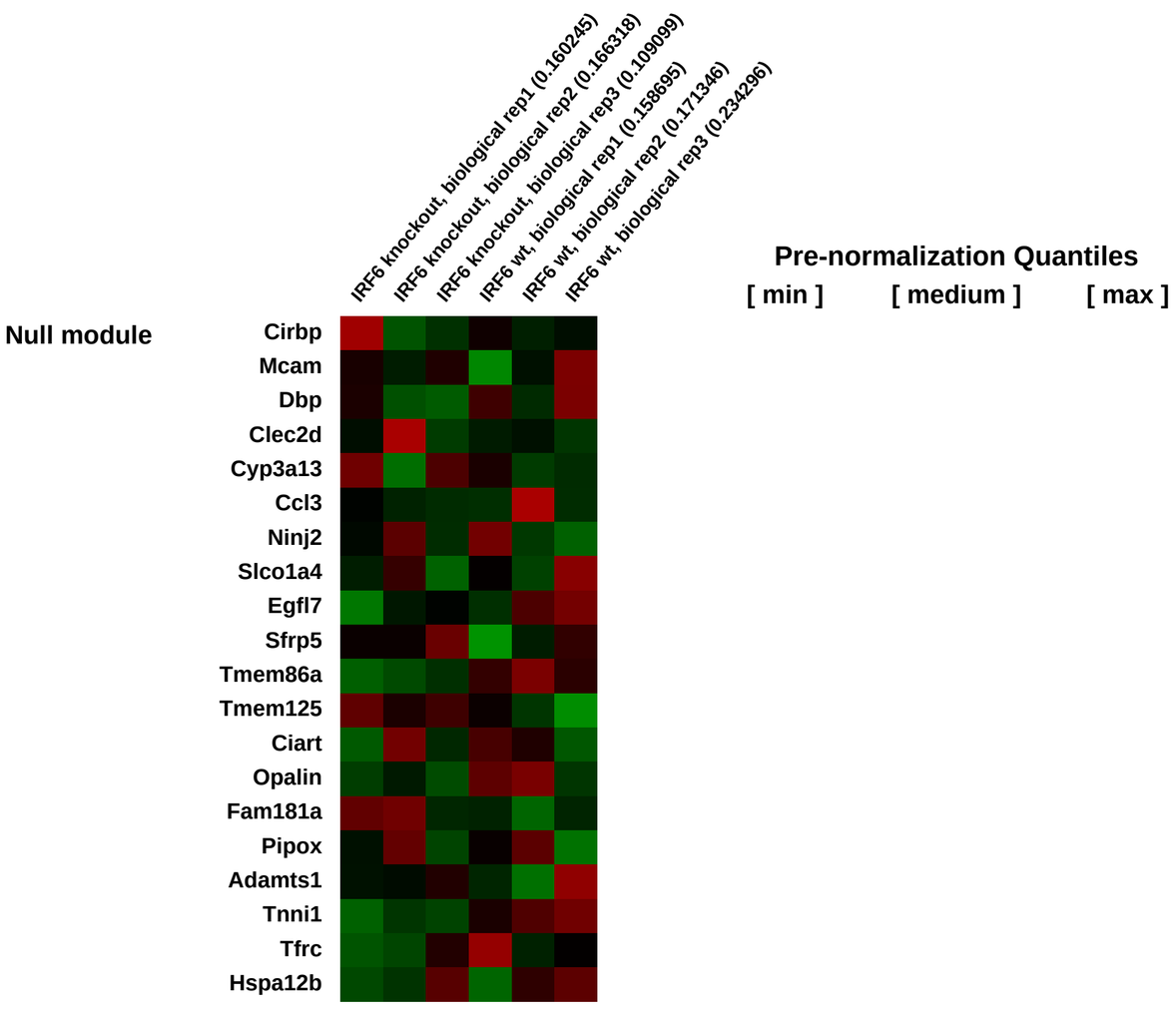

GEO Series "GSE5817" Expression Profiles

Num of samples in this series: 21

Scale of expression profile Z-scores

-3.0 -2.0 -1.0 0.0 1.0 2.0 3.0

GEO Link:	http://www.ncbi.nlm.nih.gov/geo/query/acc.cgi?acc=GSE5817
Status:	Public on Sep 12 2006
Title:	marsh-affy-mouse-232749
Organism:	Mus musculus
Experiment type:	Expression profiling by array
Platform:	GPL1261
Pubmed ID:	18799476
Summary & Design:	**Summary:** Malformations of cortical development are the underlying eitiology of many cases of Mental Retardation and Epilepsy. Subtle, below the resolution of current MRI, cortical dysplasias are probably involved in many cases of MR, Epilepsy and Autism for which no diagnosis can currently be made. Therefore, understanding the process of cortical development will be vital in diagnosing and eventual treatment of many patients with these conditions. More specifically, the cortex forms from two major populations of neuroblasts which reach their final destination in the cortex by differerent mechanisms. One is radial migration from ventricular neuroblasts to the cortical plate. These cells are excititory projection neurons and glia. The second pathway is from the ventral ganglionic eminences and tangential migration of the interneuronal population of primarily inhibitory neurons. Much less is known about the control of the latter process, and many of these currently undiagnosed subtle malformations may stem from abnormalities of this tangential migration. This project focuses on the understanding the control of the tangentially migrating inhibitory interneurons. We aim to uncover the transcriptional differences between two distinct neuronal populations, GFP positive cells in the ganglionic emience and GFP positive cells within the cortical plate, in order to understand the genetic control of tangential migration. We will acomplish this aim by targeting two different labeled transcripts againts the affymetrix mouse genome arrays. We hypothesis that there will be distinct differences in mRNA transcription profiles between the ganglionic eminence and cortical plate within developing interneurons. The differences in transcript profiles will be genes that regulate the migration and differentiation of these developing neurons. Transgenic mice have been generated which express green flourscent protien (GFP) based on the activity of the Dlx 5-6 promotor. Dlx 5-6 are highly regulated genes, and are expressed only in developing interneurons with in the embryonic brain. The expression of this gene begins at around E8 within the medial and lateral ganglionic eminence (GE) and then remain present as cells born within these regions migrate out into the developing cortex. Therefore, we can take advantage of these mice by harvesting embryos at a midpoint in their development (E13.5-14.5) and dissect out GFP positive cells from the ganglionic eminence and from the cortical plate. In order to obtain enough cells to extract sufficent mRNA, we have choosen to perform microdisction of the entire GE and entire cortical plate then break up the tissue into single cell suspension and Florescent activated cell sort (FACs) the populations of GFP + and GFP - cells. We then will extract the total RNA from the GFP postive cell populations using a Trizol based method and purify the RNA with a Quiagen column purification method. The purified RNA will then be amplified using the Affymetrix 1 or 2 round T7 based amplification procedure in order to generate the microgram quantities of labelled cRNA. The labelled biotin cRNA will be sent to the microarray consortium for hybridization againt the Affy mouse genome chip. Three embryos will be pooled in order to obtain sufficent RNA and 6 GFP positive GE and cortical plate samples will be used. The six replicates will be obtained from at least 3 different pregnant mice. **Keywords:** other **Overall design:**

Background corr dist: KL-Divergence = 0.1016, L1-Distance = 0.0943, L2-Distance = 0.0158, Normal std = 0.5231

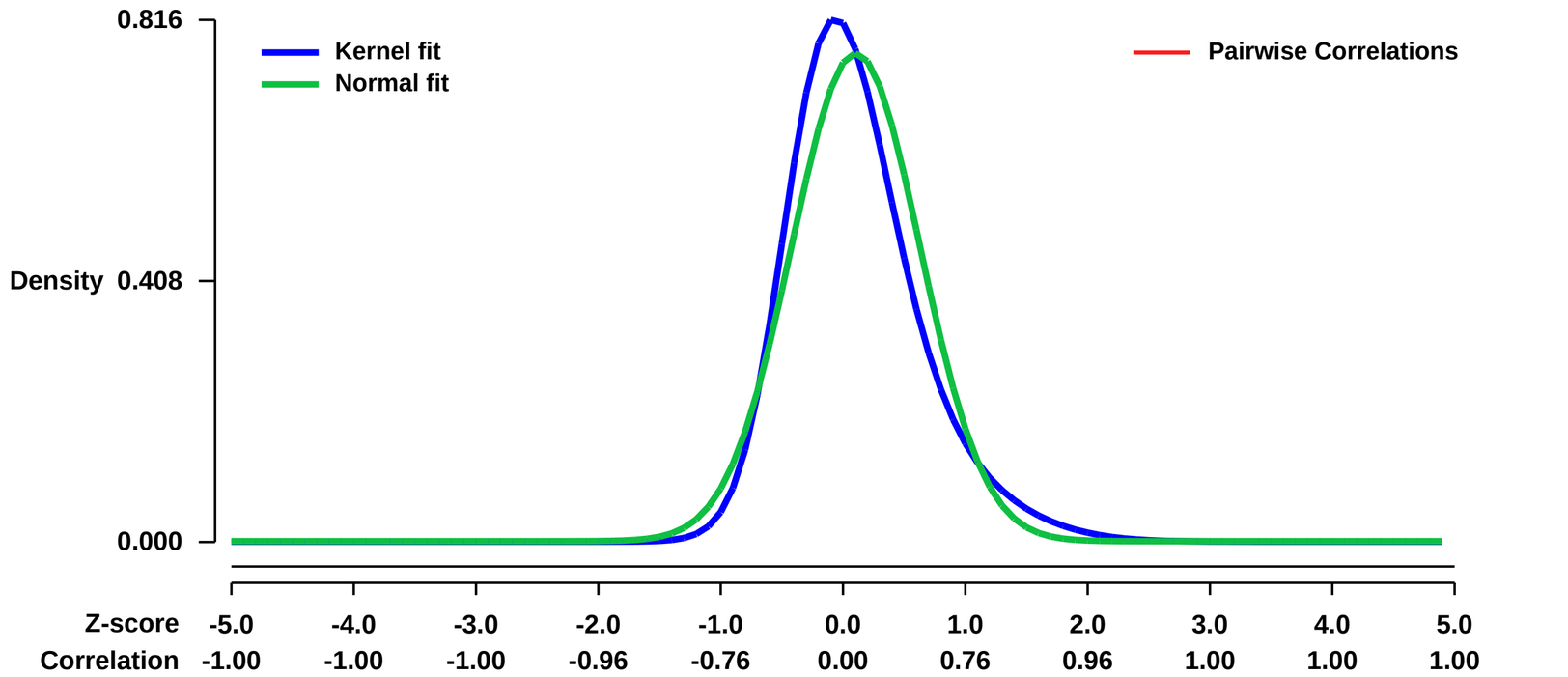

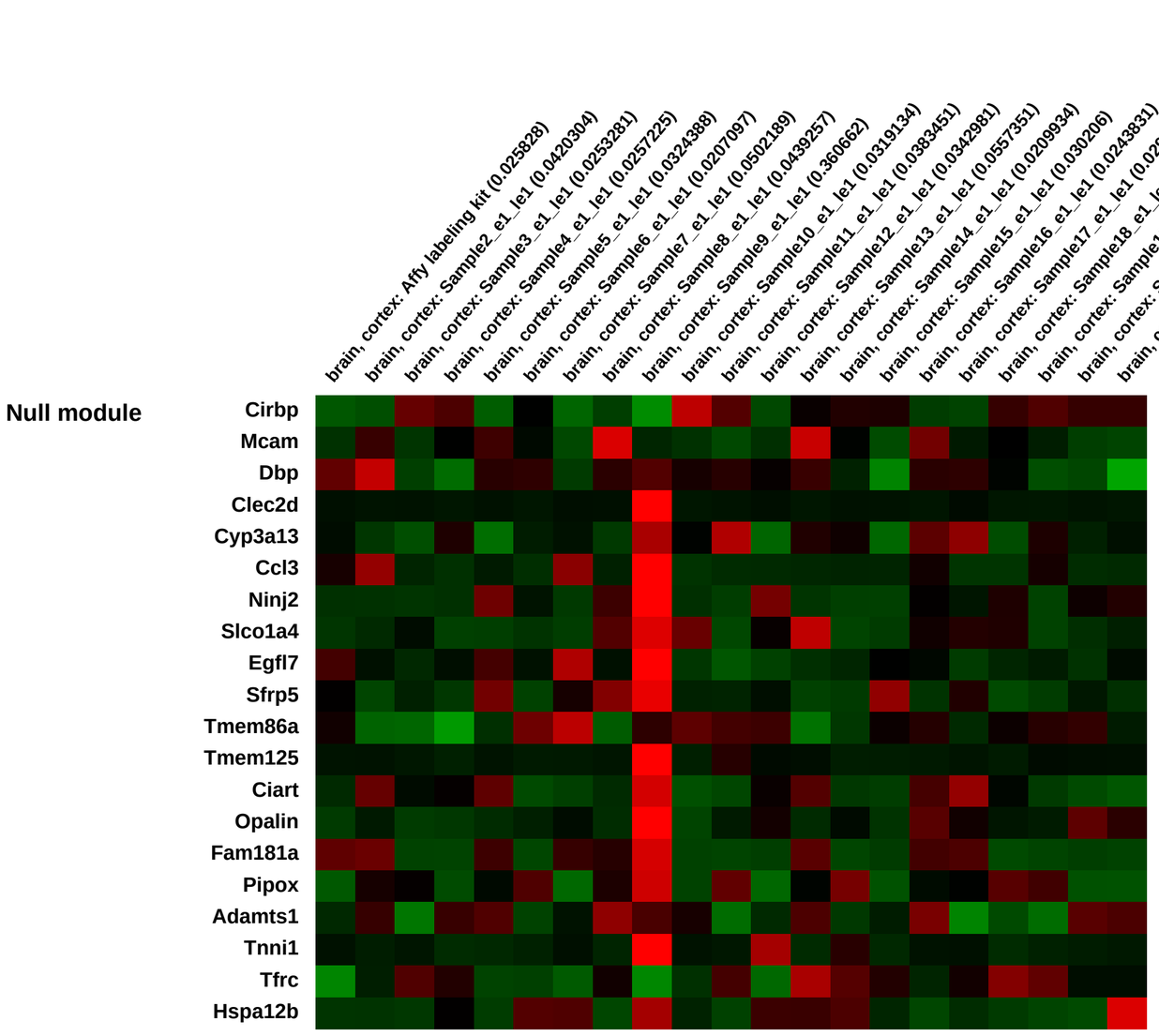

GEO Series "GSE58193" Expression Profiles

Num of samples in this series: 9

Scale of expression profile Z-scores

-3.0 -2.0 -1.0 0.0 1.0 2.0 3.0

GEO Link:	http://www.ncbi.nlm.nih.gov/geo/query/acc.cgi?acc=GSE58193
Status:	Public on Jun 04 2014
Title:	Characterizing the profiles of Ebf1 in mouse fat cells.
Organism:	Mus musculus
Experiment type:	Expression profiling by array
Platform:	GPL1261
Pubmed ID:	24174531
Summary & Design:	**Summary:** gene expression data from mouse adipocyte, with and without Ebf1 knock-down **Overall design:** To ascertain the functional targets of Ebf1 in adipocytes, we depleted Ebf1 from mature 3T3-L1 cells by transducing them with lentivirus harboring one of two different Ebf1-specific hairpins or a scrambled control. We then performed expression profiling using Affymetrix arrays with triplicate samples for each hairpin.

Background corr dist: KL-Divergence = 0.0645, L1-Distance = 0.0174, L2-Distance = 0.0003, Normal std = 0.5180

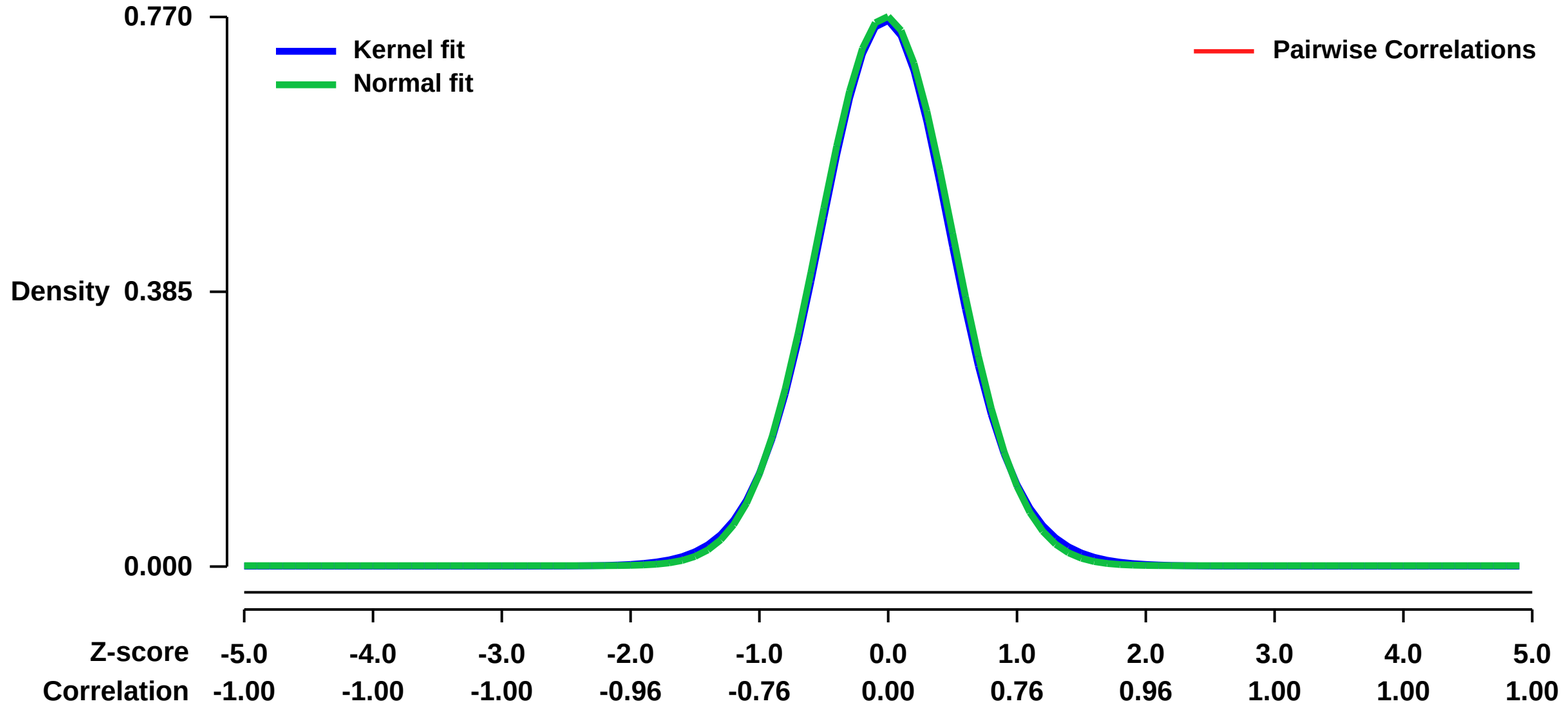

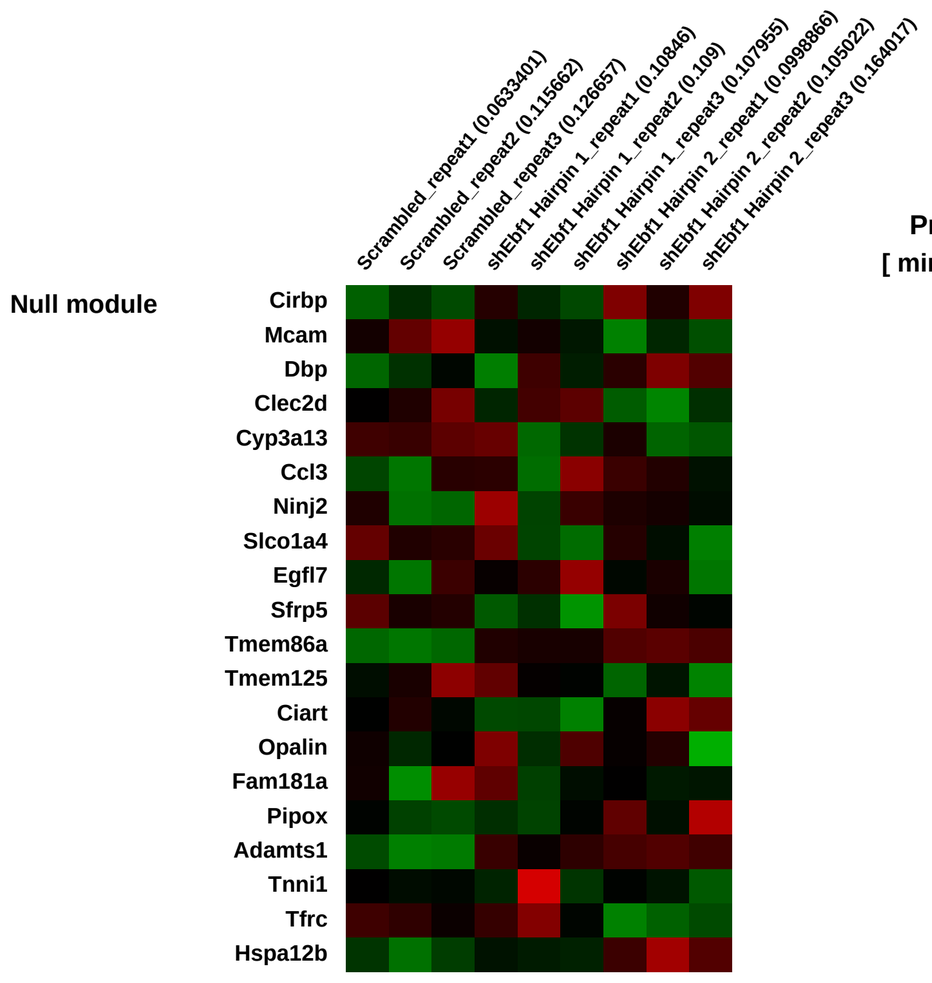

GEO Series "GSE58214" Expression Profiles

Num of samples in this series: 6

Scale of expression profile Z-scores

-3.0 -2.0 -1.0 0.0 1.0 2.0 3.0

GEO Link:	**http://www.ncbi.nlm.nih.gov/geo/query/acc.cgi?acc=GSE58214**
Status:	**Public on Jun 06 2014**
Title:	**Expression data from liver of Retnla transgenic (Tg) and non-transgenic (non-Tg) mice.**
Organism:	**Mus musculus**
Experiment type:	**Expression profiling by array**
Platform:	**GPL1261**
Pubmed ID:	
Summary & Design:	**Summary:** **We found that Retnla-Tg mice had significantly lower serum cholesterol levels than non-Tg mice on a high-fat diet (HFD). To explore the molecular mechanisms underlying the cholesterol-lowering effects of Retnla under hyperlipidemic conditions, we subjected age- and sex-matched Retnla-Tg and non-Tg mice to a HFD for 4 weeks.** **Using a microarray approach, we analyzed the hepatic gene expression profiles related to cholesterol metabolism, including catabolism, biosynthesis, and transport.** **Overall design:** **Total RNA was extracted from livers of Retnla-Tg and non-Tg mice after feeding with a HFD for four weeks, and transcriptional profiling was performed on individual samples using Affymetrix Mouse Genome chips (MG 430 2.0 array).**

Background corr dist: **KL-Divergence = 0.0480, L1-Distance = 0.0213, L2-Distance = 0.0005, Normal std = 0.5825**

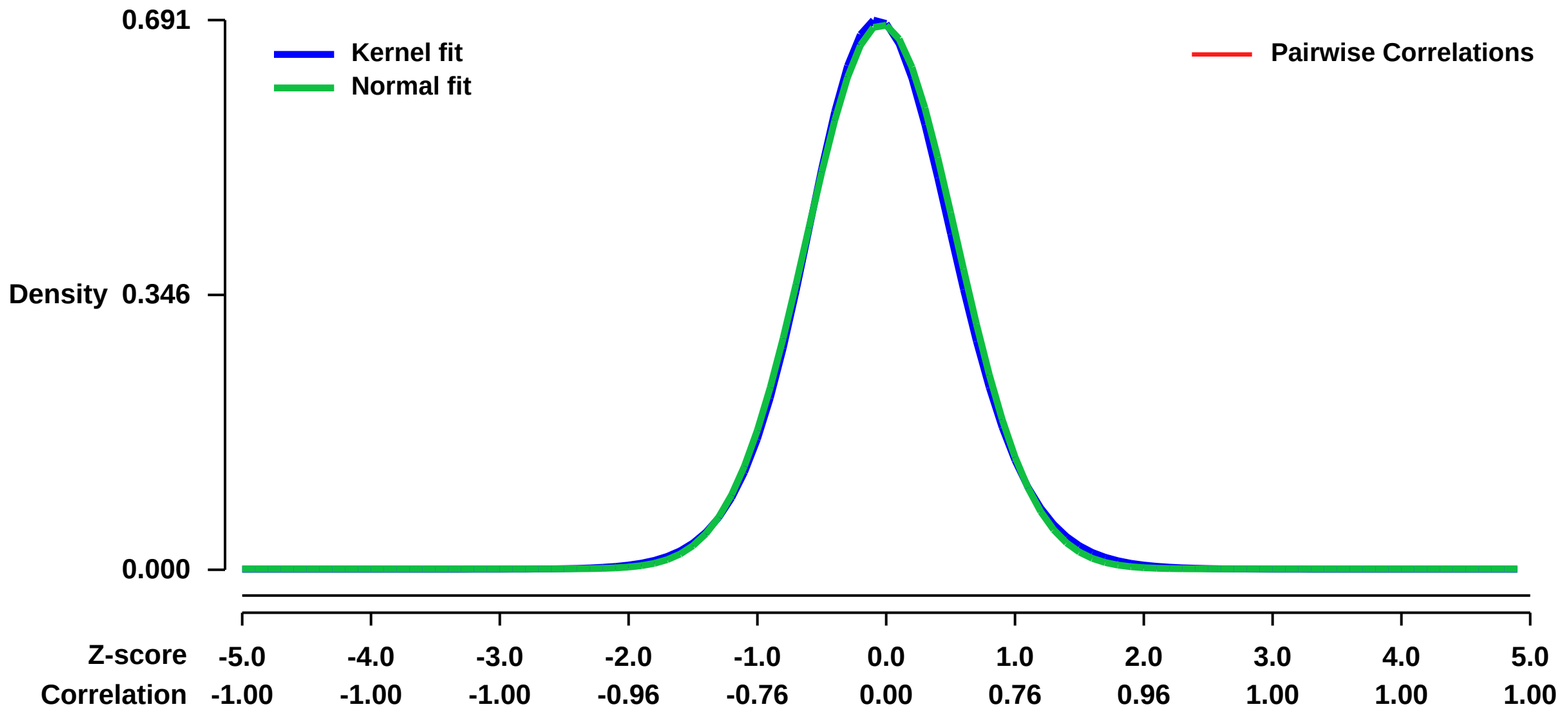

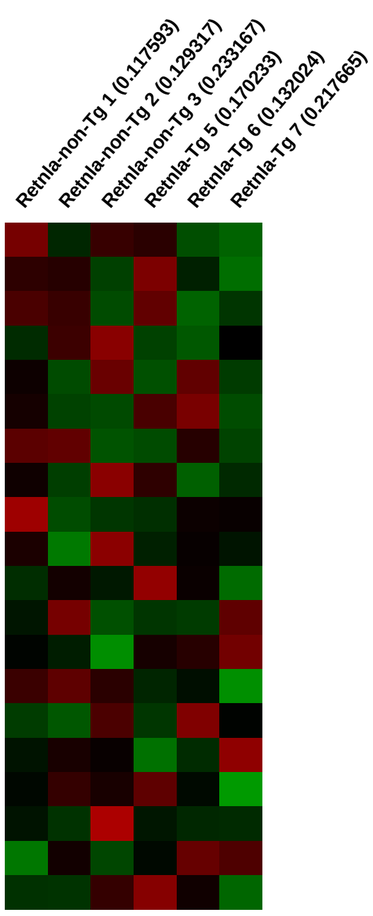

GEO Series "GSE58262" Expression Profiles

Num of samples in this series: 18

Scale of expression profile Z-scores

-3.0 -2.0 -1.0 0.0 1.0 2.0 3.0

GEO Link:	**http://www.ncbi.nlm.nih.gov/geo/query/acc.cgi?acc=GSE58262**
Status:	**Public on Jun 06 2014**
Title:	**Impact of gamma chain cytokines on the differentiation of recently antigen-activated CD8 T cells**
Organism:	**Mus musculus**
Experiment type:	**Expression profiling by array**
Platform:	**GPL1261**
Pubmed ID:	
Summary & Design:	**Summary:** **Analysis of how different gamma chain family cytokines influence CD8 T cell differentiation.** **Overall design:** **Naˆflve CD8 T cells were isolated from the spleens OT-I Thy1.1 TCR Tg mice. Whole splenocytes from wild-type C57BL/6 mice were used as stimulator cells. Purified naˆflve wild-type OT-I (1ˆ 106/well) were stimulated with OVA peptide (SIINFEKL) pulsed (5 ´µg/ml) and irradiated (2,000 rads) syngeneic splenocytes (6ˆ 106/well) in 24-well plates. Forty-eight hours later, activated OT-I T cells were harvested and viable cells were enriched over a Ficoll-paque gradient and washed with cRPMI prior to being reseeded in cRPMI (5ˆ 105 cells/ml) and treated with the media supplemented with various ¸‡c cytokines (IL-2, IL-4, IL-7, IL-15 and IL-21). Experimental samples were treated with 100 ng/ml of their respective gamma chain cytokine and incubated at 37´”C for 24 hours. RNA was isolated using either the RNeasy Mini kit, or a combination of TRIzol reagent and the Direct-zol RNA miniprep kit, all following manufacturer protocols. Two biological replicates for mRNA analysis were prepped using the RNeasy kit. The third replicate was prepped using the Trizol/Direct-zol approach. The quality and quantity of RNA samples was further analyzed on the Bioanalyzer. Labeled target cDNA was prepared from total RNA samples using the Ambion MessageAmp Premier protocol (3â IVT assay). Each sample target was hybridized to a Mouse 430 2.0 GeneChip array. Image processing and expression analysis were performed using Affymetrix GeneChip Command Console (AGCC) v. 3.1.1 and Affymetrix Expression Console v.1.1 software, respectively. Data from all biological replicates and conditions was imported into the Affymetrix Expression Console and normalized (RMA). RNA processing and microarray hybridization were performed by the Oregon Health & Science University Gene Microarray Shared Resource core facility in Portland, Oregon.**

Background corr dist: KL-Divergence = 0.0628, L1-Distance = 0.0441, L2-Distance = 0.0034, Normal std = 0.5375

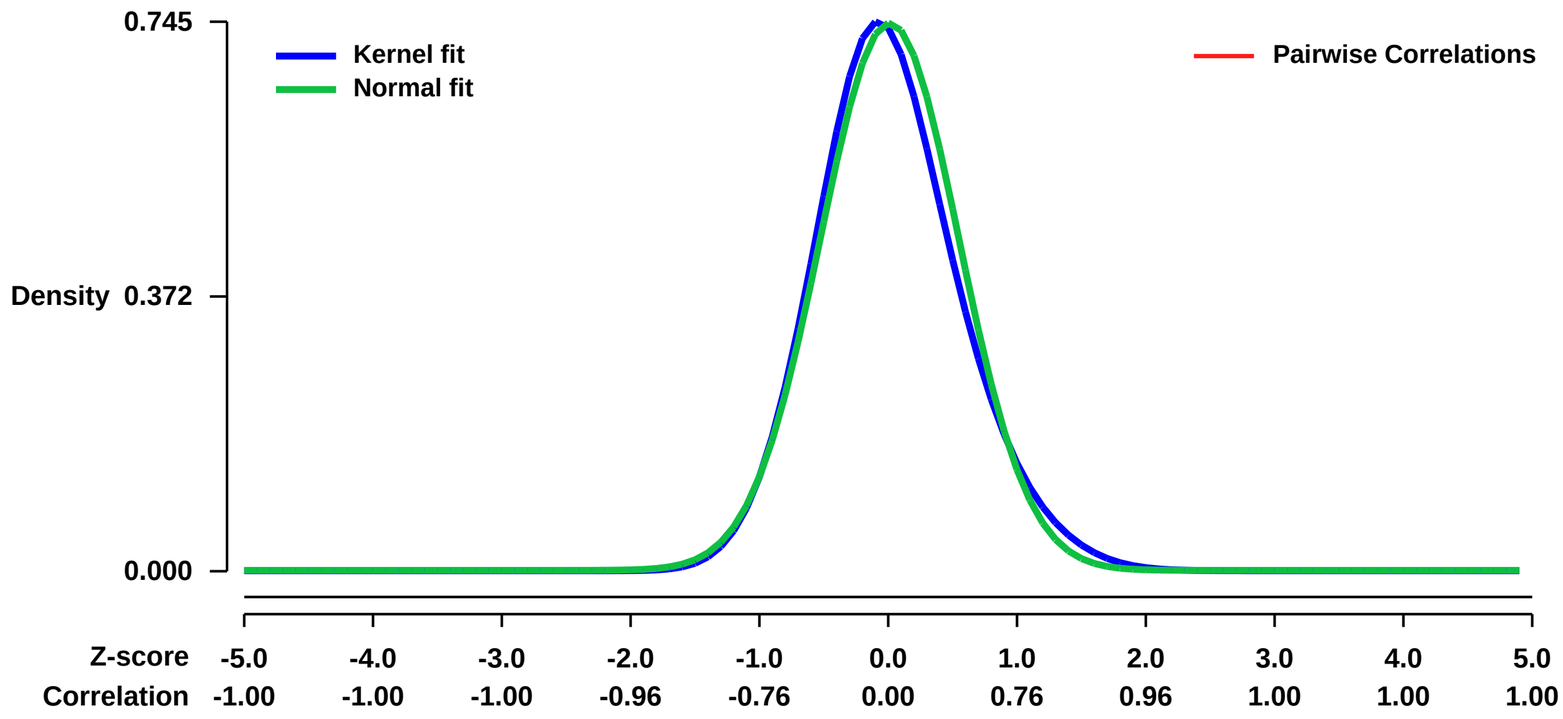

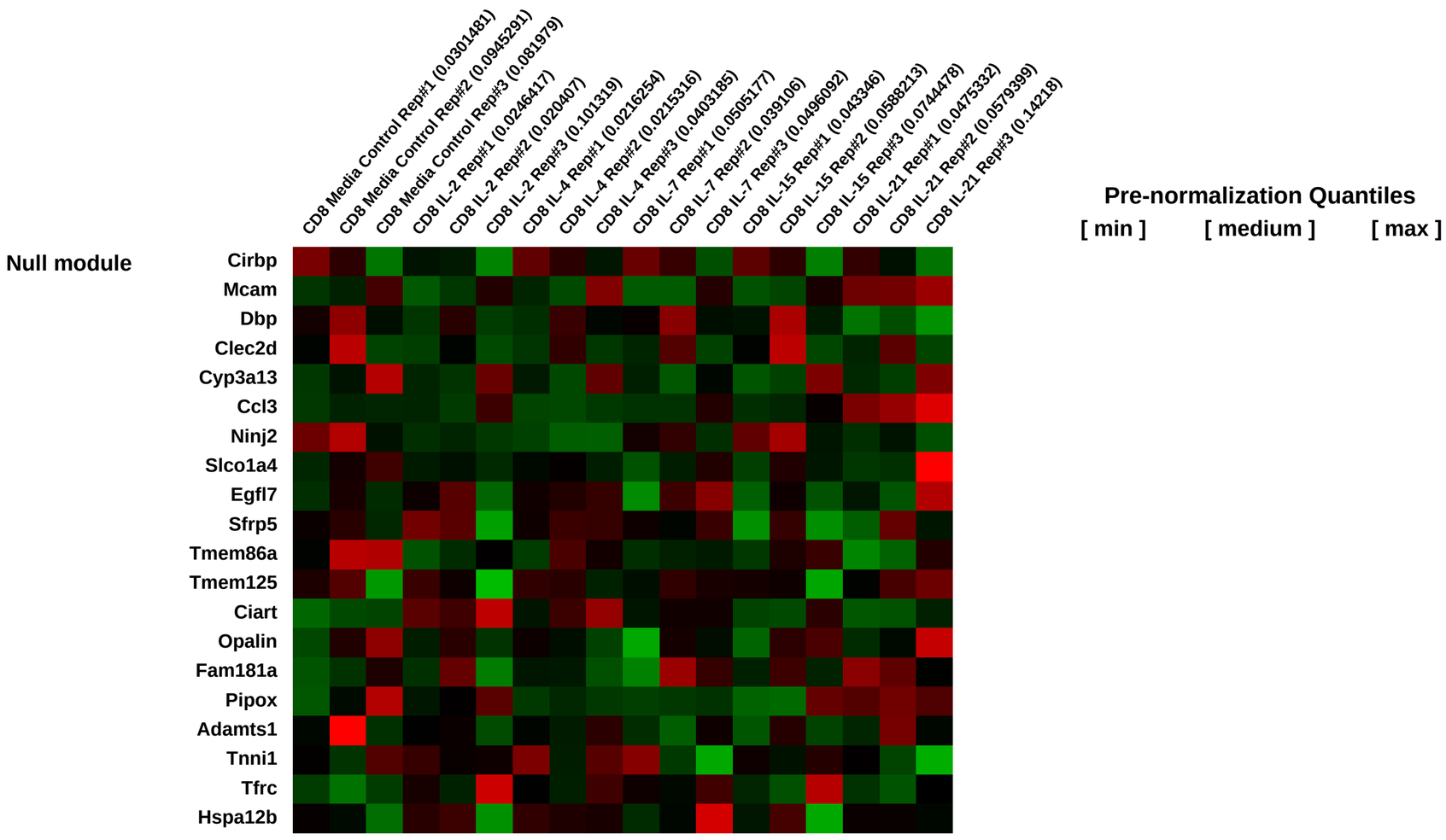

GEO Series "GSE58296" Expression Profiles

Num of samples in this series: 9

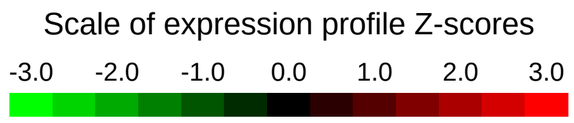

GEO Link:	**http://www.ncbi.nlm.nih.gov/geo/query/acc.cgi?acc=GSE58296**
Status:	**Public on Jun 09 2014**
Title:	**Expression data from intestinal organoids altered for Tgfbeta signaling**
Organism:	**Mus musculus**
Experiment type:	**Expression profiling by array**
Platform:	**GPL1261**
Pubmed ID:	
Summary & Design:	**Summary:** **We treated intestinal organoids continuously for 5 days with or without TgfbR1/2 inhibitor (LY2109761) or Tgfb1 ligand** **Overall design:** **Organoids were continuously treated for 5 days, then RNA was extracted and hybridized to Affymetrix Mouse Genome 430 2.0**

Background corr dist: **KL-Divergence = 0.0550, L1-Distance = 0.0401, L2-Distance = 0.0021, Normal std = 0.5732**

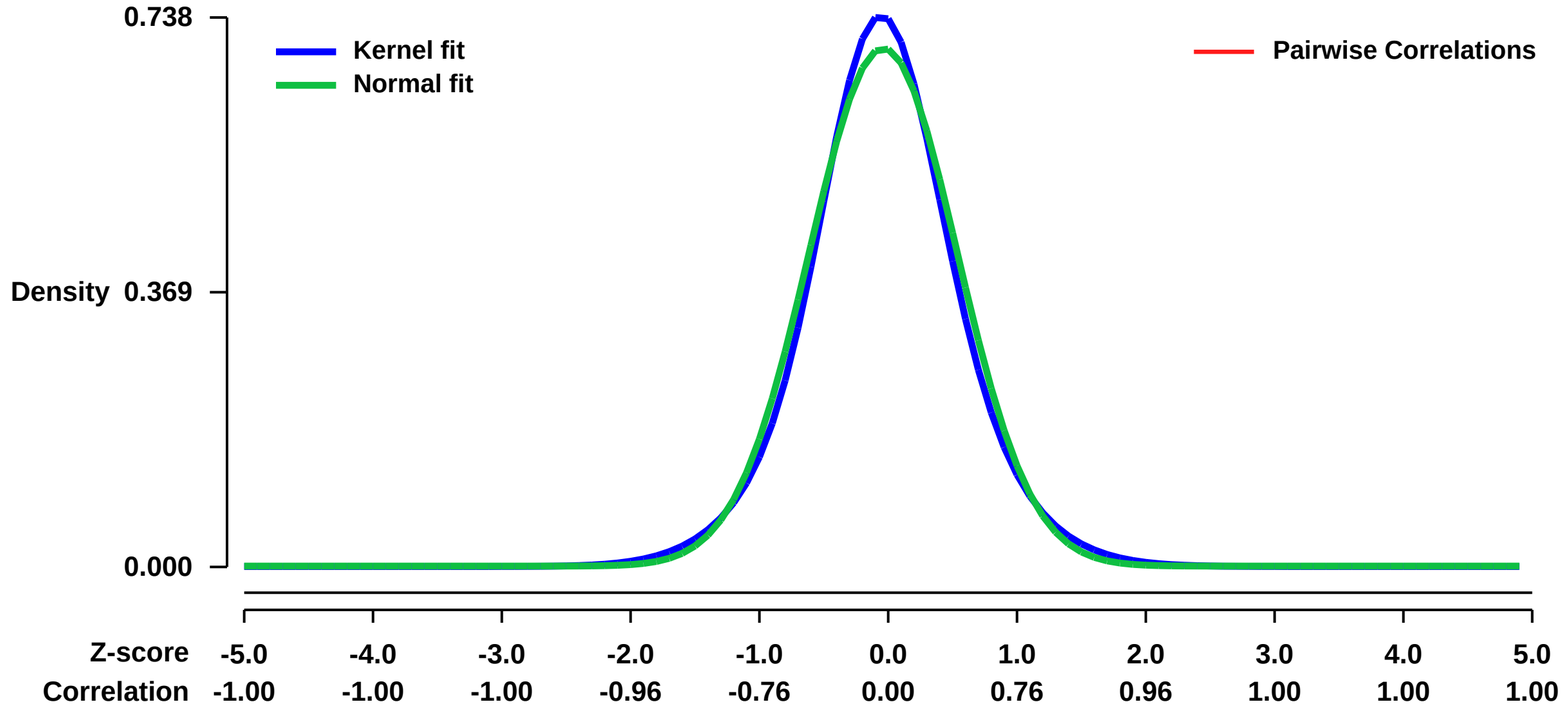

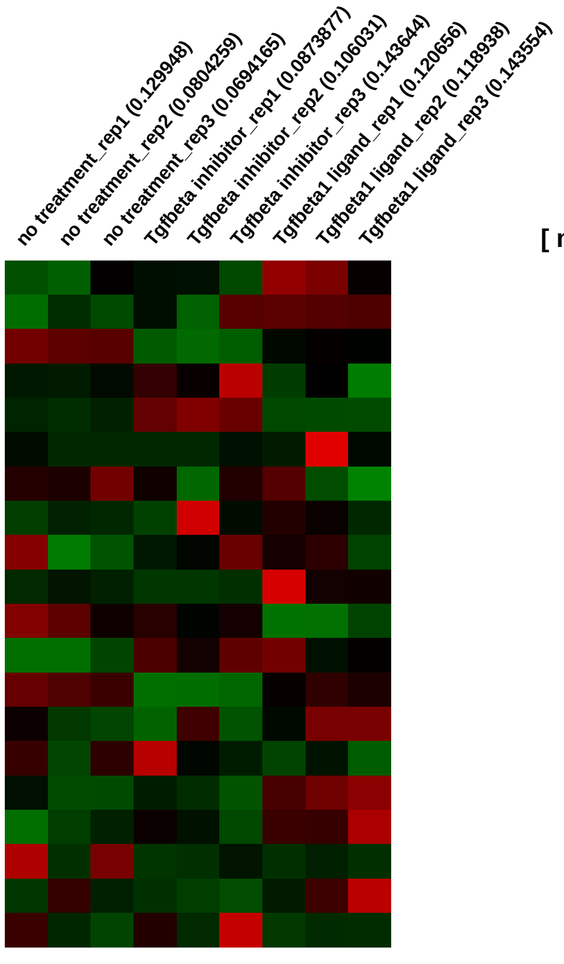

GEO Series "GSE58368" Expression Profiles

Num of samples in this series: 15

Scale of expression profile Z-scores

-3.0 -2.0 -1.0 0.0 1.0 2.0 3.0

GEO Link: http://www.ncbi.nlm.nih.gov/geo/query/acc.cgi?acc=GSE58368
Status: Public on Jun 11 2014
Title: Linking Notch signaling to ischemic stroke
Organism: Mus musculus
Experiment type: Expression profiling by array
Platform: GPL1261
Pubmed ID:

Summary & Design:

Summary:
Using a hitherto uncharacterized knockout mouse model of Notch 3, a Notch signaling receptor paralogue highly expressed in vascular SMCs, we uncover a striking susceptibility to ischemic stroke upon challenge. Cellular and molecular analyses of vascular SMCs derived from these animals associate Notch 3 activity to the expression of specific gene targets, whereas genetic rescue experiments unambiguously link Notch 3 function in vessels to the ischemic phenotype.

Overall design:
Microarray Studies. Biotinylated cRNA samples from freshly sorted brain SMCs (four Notch 3 +/â mice and five Notch 3 â /â mice) were fragmented before hybridization (15 ¿…g each) onto mouse 430 2.0 Affymetrix chips. The chips were washed, stained by using strepavidin-phycoerytrin, and scanned the next day as described in ref. 24. For data normalization, all probe sets were scaled to a target intensity of 150. Microarray data analysis was performed by using Rosetta Resolver. All cells were from 10- to 12-week-old male mice.
Gene Ontology Analyses. PANTHER software was used to define over- and underrepresented functions in the list of signature genes found by microarray analysis (25). P values were calculated by using binomial statistics.

Background corr dist: KL-Divergence = 0.0540, L1-Distance = 0.0336, L2-Distance = 0.0015, Normal std = 0.5673

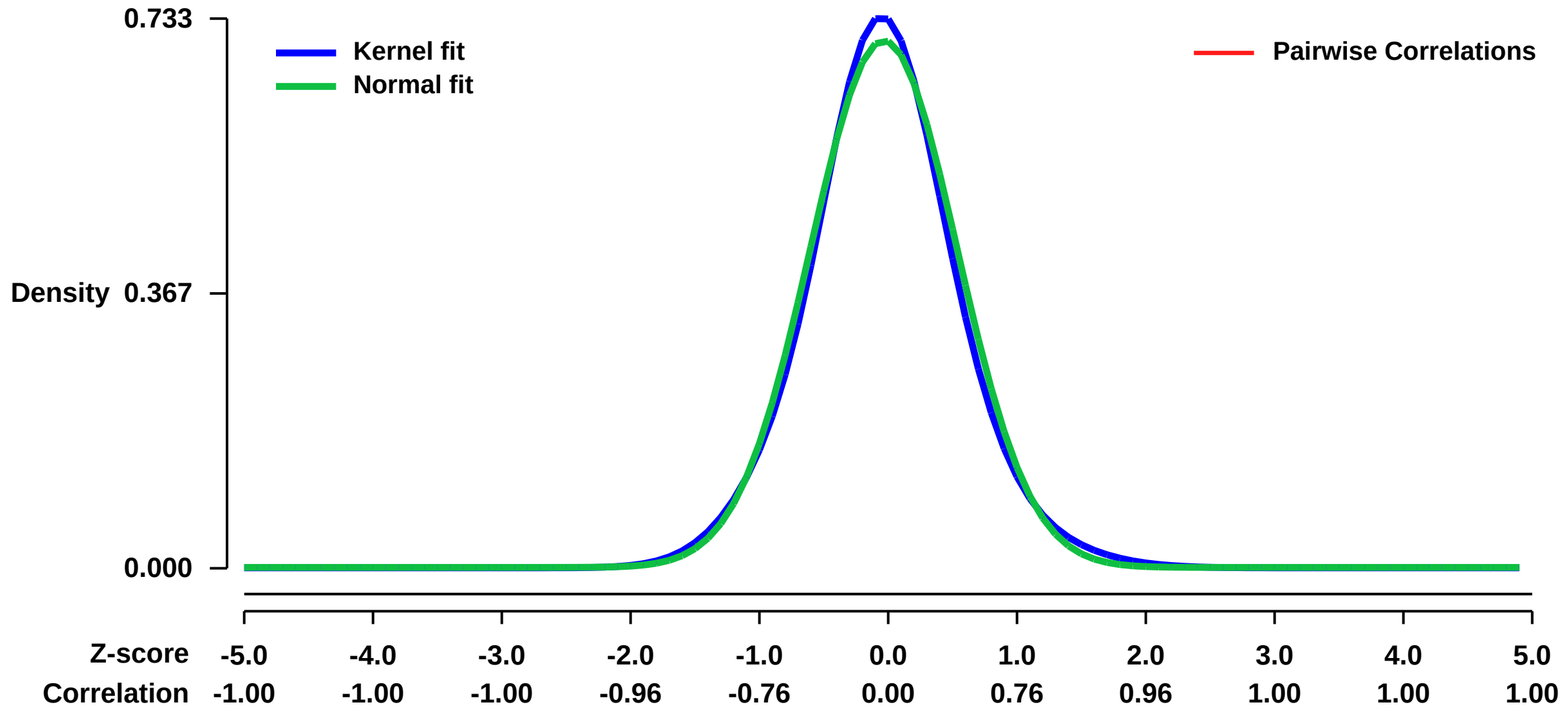

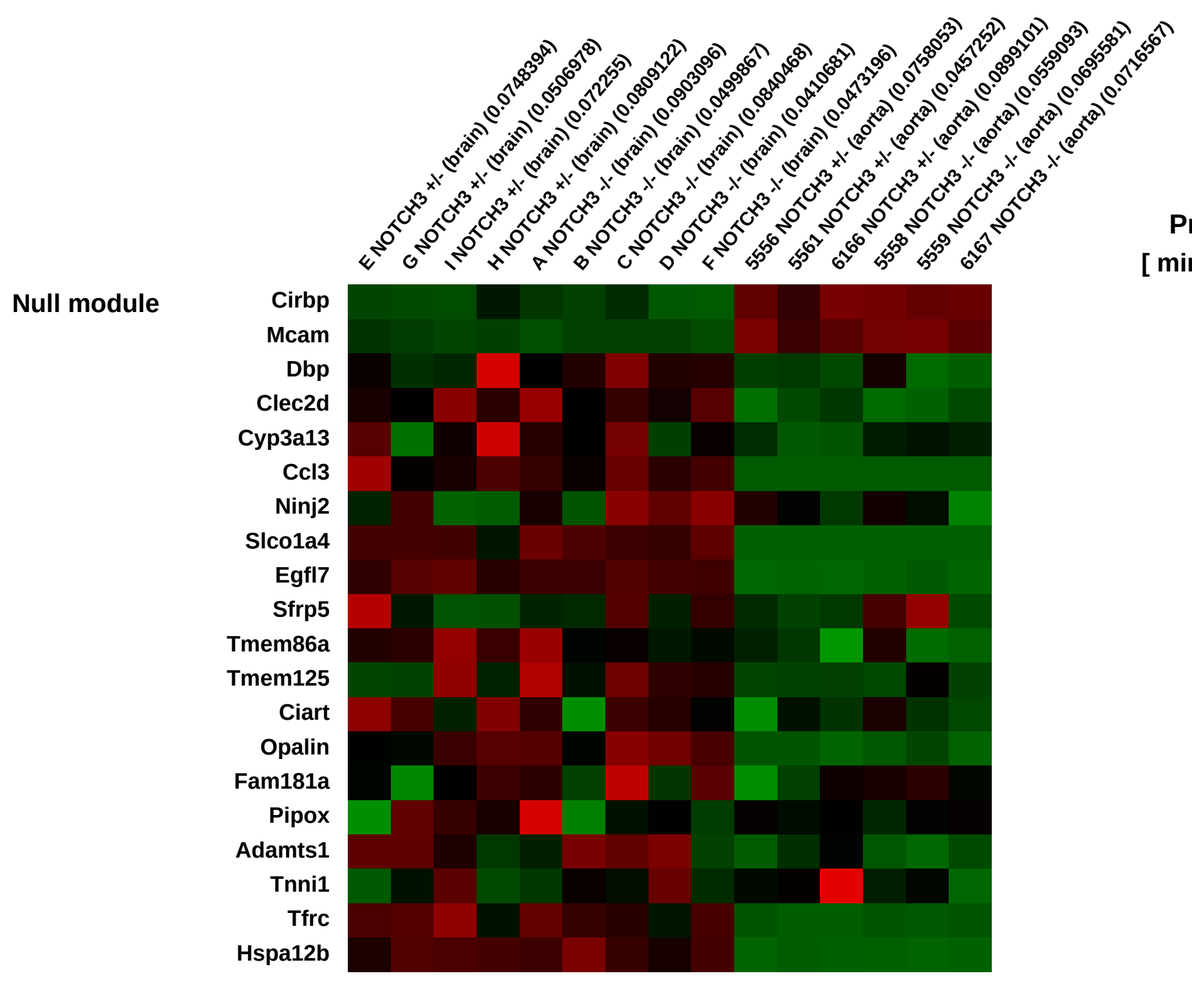

GEO Series "GSE5841" Expression Profiles

Num of samples in this series: 6

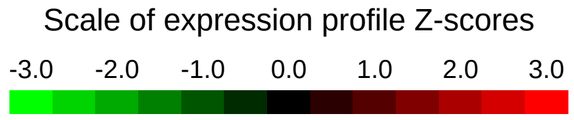

GEO Link:	http://www.ncbi.nlm.nih.gov/geo/query/acc.cgi?acc=GSE5841
Status:	Public on Nov 19 2010
Title:	Differential gene expression in mouse skNAC knockout heart at E11.5
Organism:	Mus musculus
Experiment type:	Expression profiling by array
Platform:	GPL1261
Pubmed ID:	21071677
Summary & Design:	**Summary:** Targeted deletion of skNAC in mice resulted in early embryonic lethality with cardiac defects. In order to investigate the molecular mechanism of the cardiac defect, we designed the microarray comparing gene expression of the mutant E11.5 heart to wild type E11.5 heart. **Keywords: genetic modification in mouse** **Overall design:** 3 for each genotypes, comparing Littermates of E11.5, total RNA (500ng) from ventricles, Affymetrix GeneChip Mouse Genome 430 2.0 Array

Background corr dist: KL-Divergence = 0.0415, L1-Distance = 0.0183, L2-Distance = 0.0004, Normal std = 0.6077

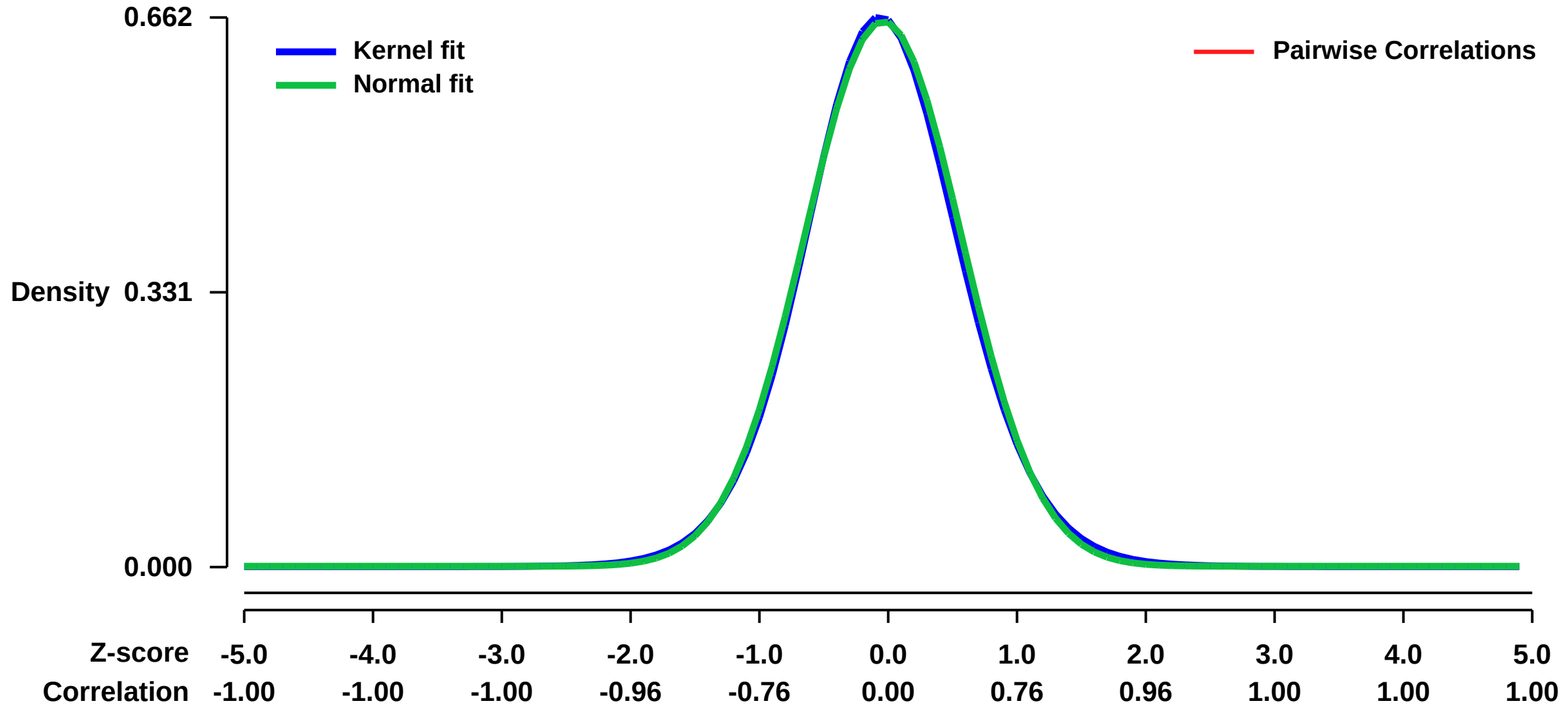

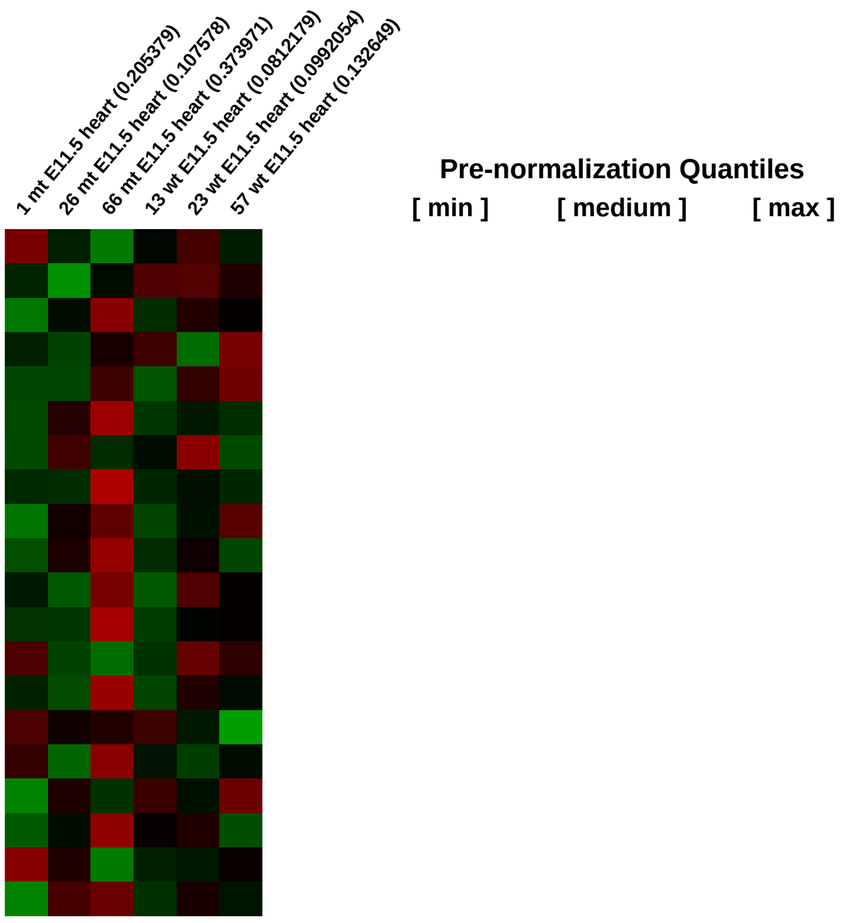

GEO Series "GSE5861" Expression Profiles

Num of samples in this series: 6

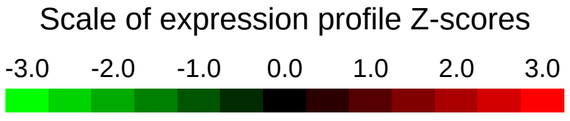

GEO Link:	http://www.ncbi.nlm.nih.gov/geo/query/acc.cgi?acc=GSE5861
Status:	Public on Sep 19 2006
Title:	Searching for Brca1 regulated X-linked genes
Organism:	Mus musculus
Experiment type:	Expression profiling by array
Platform:	GPL1261
Pubmed ID:	17350580
Summary & Design:	**Summary:** We compared the expression levels of X-linked genes in the mammary glands of Brca1 D11/D11;p53+/- mutant and control (p53+/-) mice at three different stages of the mammary cycle: virgin, pregnant day 16.5, and lactation day 1, using a cDNA microarray. In about 690 X-linked genes that are expressed at these three stages of mammary cycle of development, we found 16 X-linked genes showed altered expression levels in Brca1 D11/D11;p53+/- mammary glands in comparison with controls at all three time points. Among them, 9 genes were up-regulated and 7 were down-regulated. This result indicates that mutation of Brca1 could affect expression of a few X-linked genes in mammary tissues. However, this was unlikely caused by failure of X chromosome inactivation, as seven of them were down-regulated, and Xist RNA was expressed in all the Brca1 mutant mammary tissues. Keywords: BRCA1 mutation analysis Overall design: Mutations in breast cancer associated gene-1 (BRCA1) are associated with hereditary breast and ovarian cancers. BRCA1 encodes a tumor suppressor protein that functions in DNA repair, transcriptional regulation, chromatin remodeling, centrosome duplication and checkpoint control, etc.. We were interested in fishing out the genes regulated by Brca1. Three pairs of mammary glands from Brca1 D11/D11;p53+/- mutant and control (p53+/-) mice at three different stages of the mammary cycle were analyzed by microarray for gene expression levels.

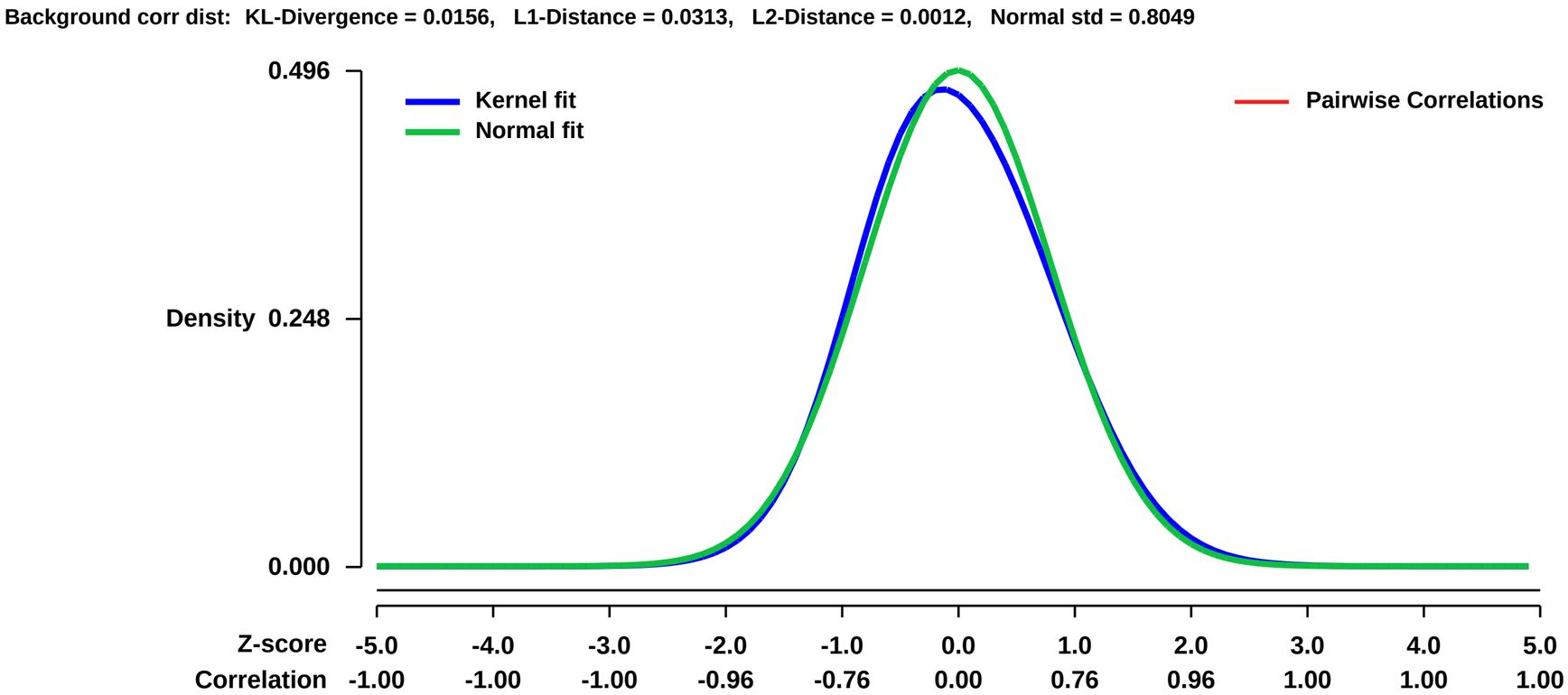

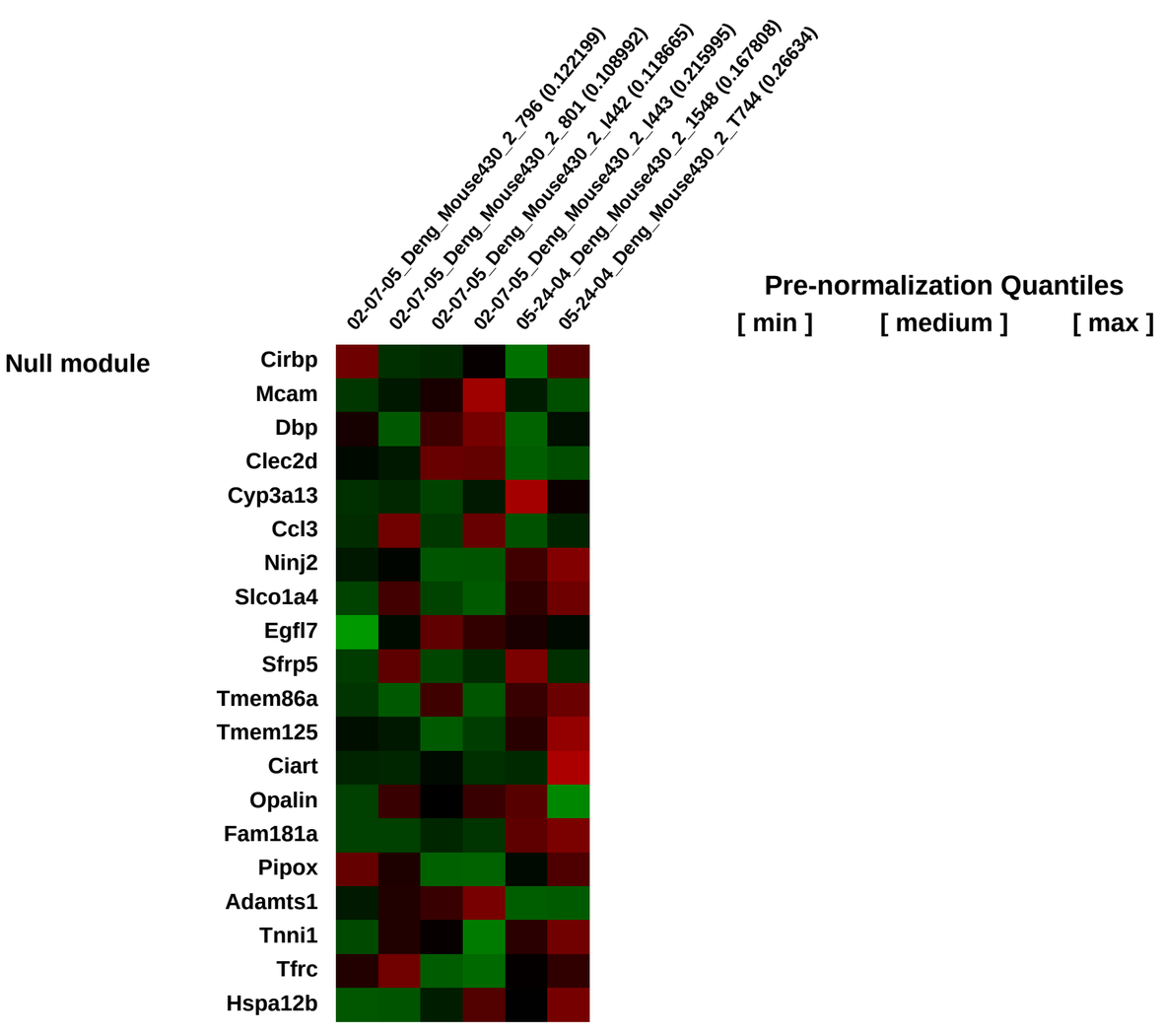

GEO Series "GSE59202" Expression Profiles

Num of samples in this series: 8

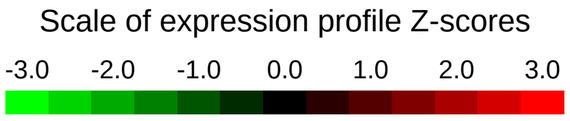

GEO Link:	**http://www.ncbi.nlm.nih.gov/geo/query/acc.cgi?acc=GSE59202**
Status:	**Public on Jul 09 2014**
Title:	**Fluorochrome-based definition of naturally occurring Foxp3+ regulatory T cells of intra- and extrathymic origin**
Organism:	**Mus musculus**
Experiment type:	**Expression profiling by array**
Platform:	**GPL1261**
Pubmed ID:	
Summary & Design:	**Summary:** **Here, we report on experiments in double-transgenic mice, in which RFP is expressed in all Foxp3+ Treg cells, whereas Foxp3-dependent GFP expression is exclusively confined to intrathymically induced Foxp3+ Treg cells. This novel molecular genetic tool enabled us to faithfully track and characterize naturally induced Treg cells of intrathymic (RFP+GFP+) and extrathymic (RFP+GFPâ) origin in otherwise unmanipulated mice.** **These experiments directly demonstrate that extrathymically induced Treg cells substantially contribute to the overall pool of mature Foxp3+ Treg cells residing in peripheral lymphoid tissues of steady-state mice. Furthermore, we provide evidence that intra- and extrathymically induced Foxp3+ Treg cells represent distinct phenotypic and functional sublineages.** **Overall design:** **CD4+CD25+ RFP+GFP- and CD4+CD25+ RFP+GFP+ T cells from pooled lymph nodes and pooled spleens of 20 mice were FACS sorted for RNA extraction and hybridization on Affymetrix microarrays in duplicates.**

Background corr dist: **KL-Divergence = 0.0598, L1-Distance = 0.0245, L2-Distance = 0.0007, Normal std = 0.5412**

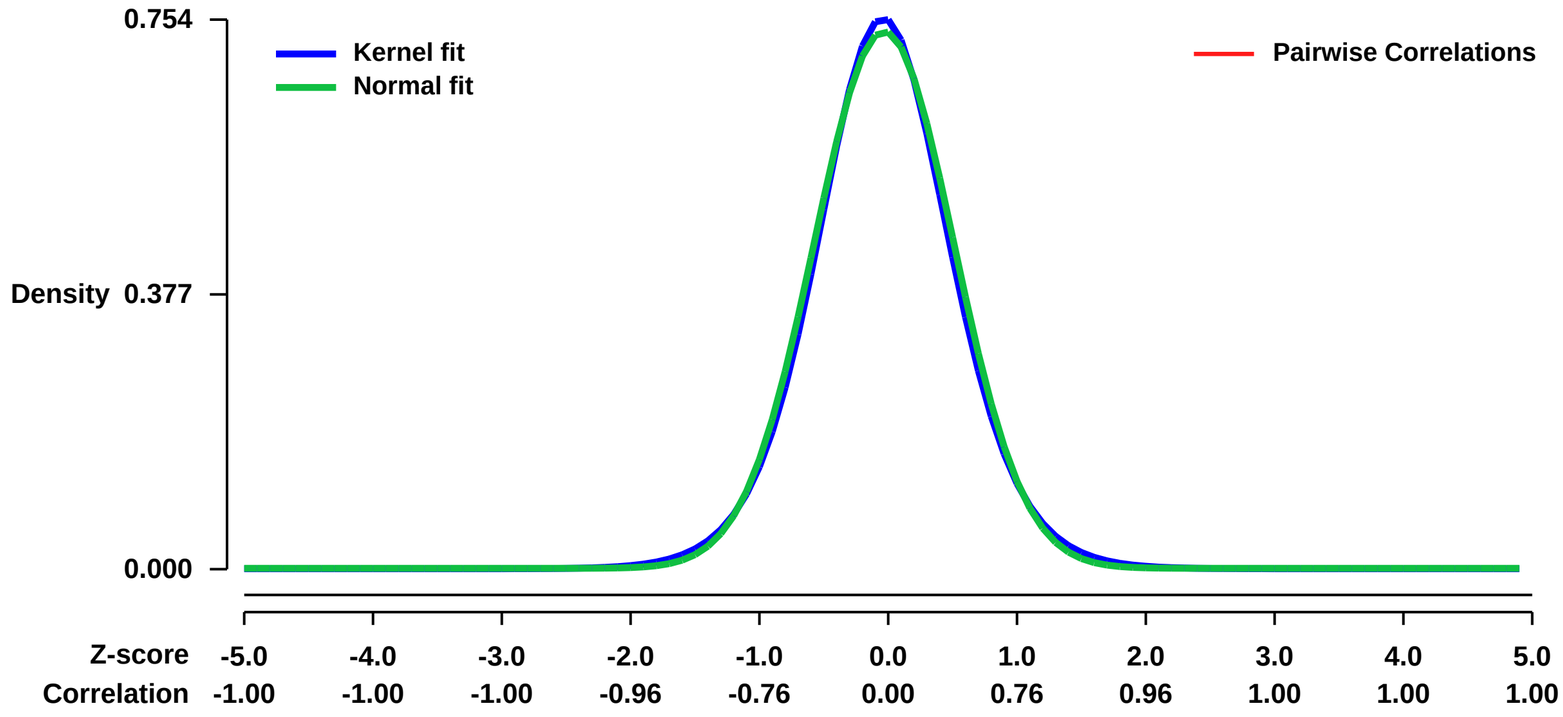

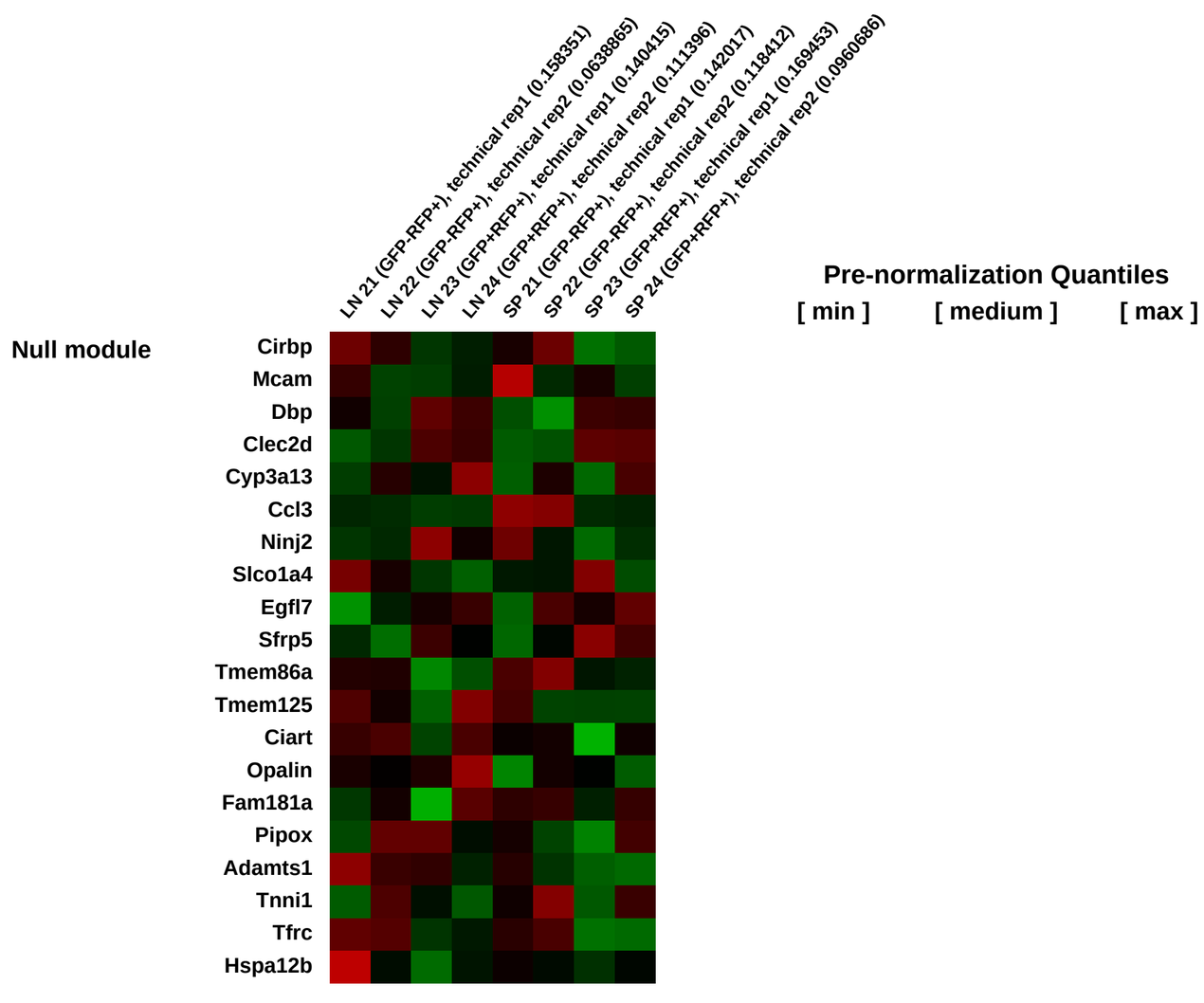

GEO Series "GSE5921" Expression Profiles

Num of samples in this series: 6

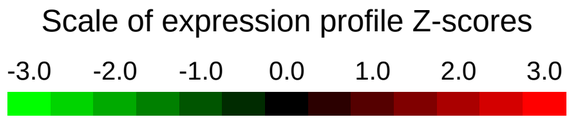

GEO Link:	http://www.ncbi.nlm.nih.gov/geo/query/acc.cgi?acc=GSE5921
Status:	Public on Sep 26 2007
Title:	Differential expression of BMP4-regulated genes associated with commitment of C3H10T1/2 cells into adipocytes
Organism:	Mus musculus
Experiment type:	Expression profiling by array
Platform:	GPL1261
Pubmed ID:	17204246
Summary & Design:	**Summary:** C3H10T1/2 stem cells are committed to the adipocyte lineage by treatment with BMP-4 and grown to postconfluence. When subjected to our standard differentiation protocol, the committed cells differentiate into adipocytes in a manner indistinguishable from that of 3T3-L1 preadipocytes. In contrast, C3H10T1/2 cells not committed with BMP-4 remain undifferentiated despite treatment with differentiation inducers. The molecular basis of the commitment process, however, has not been elucidated. Since postconfluent uncommitted and committed C3H10T1/2 cells respond differently to the differentiation inducers, it was reasoned that the two cell types differed at the gene expression level. Therefore, we undertook microarray gene expression profiling to detect changes between the two cell populations at postconfluence to identify expressed genes that may be responsible for the dramatic change in phenotype. **Keywords: control vs treated** **Overall design:** C3H10T1/2 cells were plated and treated with 50 ng/ml BMP4 and grown to postconfluence. Control samples were treated in the same manner were not given BMP4. Total RNA was collected at postconfluence. There were 3 replicates each for control and treated cells.

Background corr dist: KL-Divergence = 0.0414, L1-Distance = 0.0193, L2-Distance = 0.0004, Normal std = 0.6115

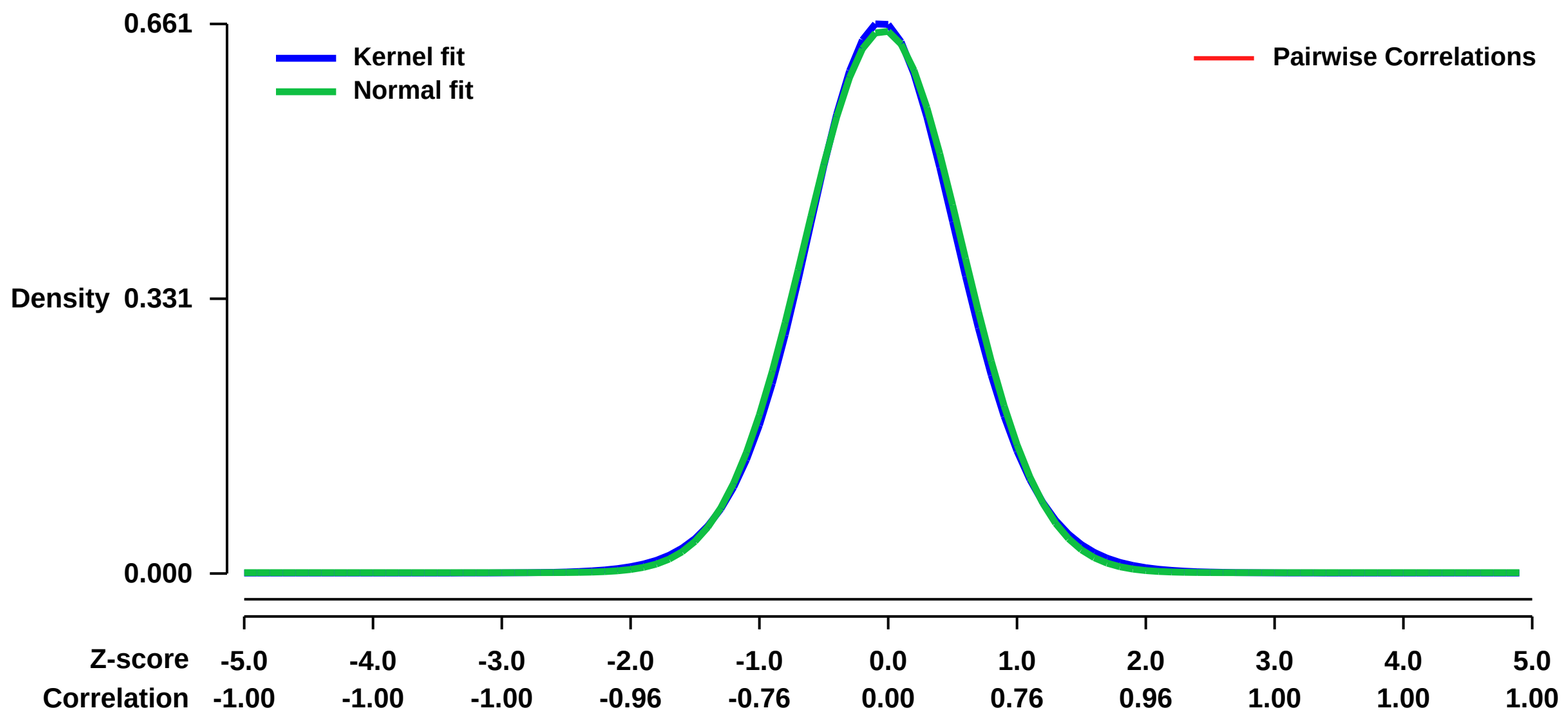

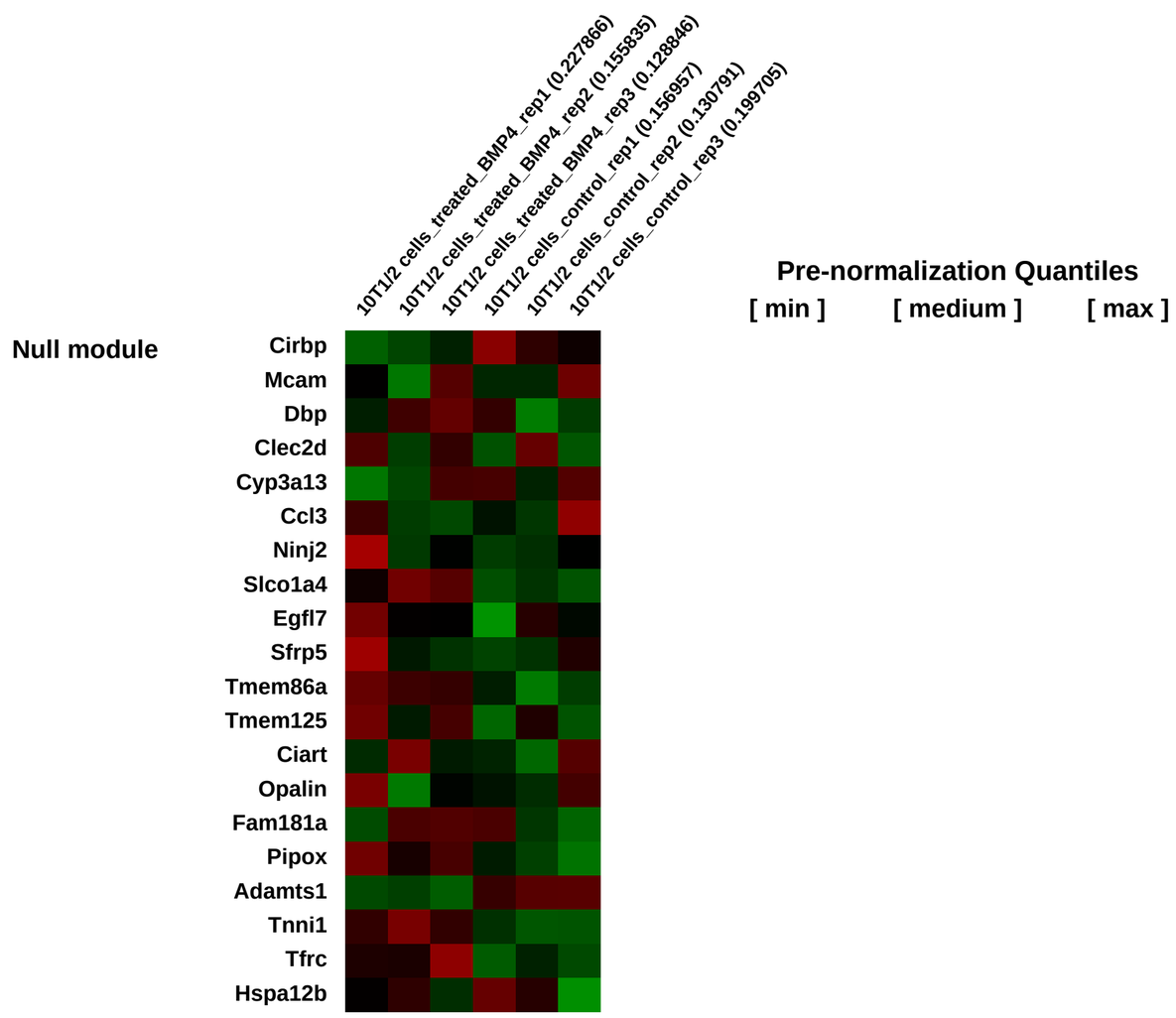

GEO Series "GSE59319" Expression Profiles

Num of samples in this series: 6

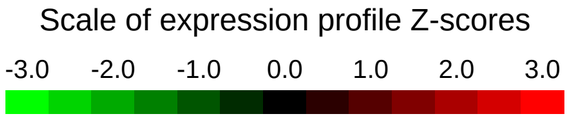

GEO Link:	http://www.ncbi.nlm.nih.gov/geo/query/acc.cgi?acc=GSE59319
Status:	Public on Jul 11 2014
Title:	Expression data of LPS-stimulated macrophages in wild-type and LysM-Cre+;Akirin2fl/fl mice
Organism:	Mus musculus
Experiment type:	Expression profiling by array
Platform:	GPL1261
Pubmed ID:	
Summary & Design:	**Summary:** Akirin2 is an evolutionally conserved nuclear protein involved in the regulation of a set of inflammatory gene expression in various cell types. We used microarrays to examine the effect of Akirin2 deficiency in LPS-inducible gene expression in macrophages **Overall design:** Peritoneal macrophages from wild-type and LysM-Cre+;Akirin2fl/fl mice were stimulated with LPS for 0, 2 and 4 hours, followed by RNA extraction and microarray analysis.

Background corr dist: KL-Divergence = 0.0412, L1-Distance = 0.0187, L2-Distance = 0.0004, Normal std = 0.6094

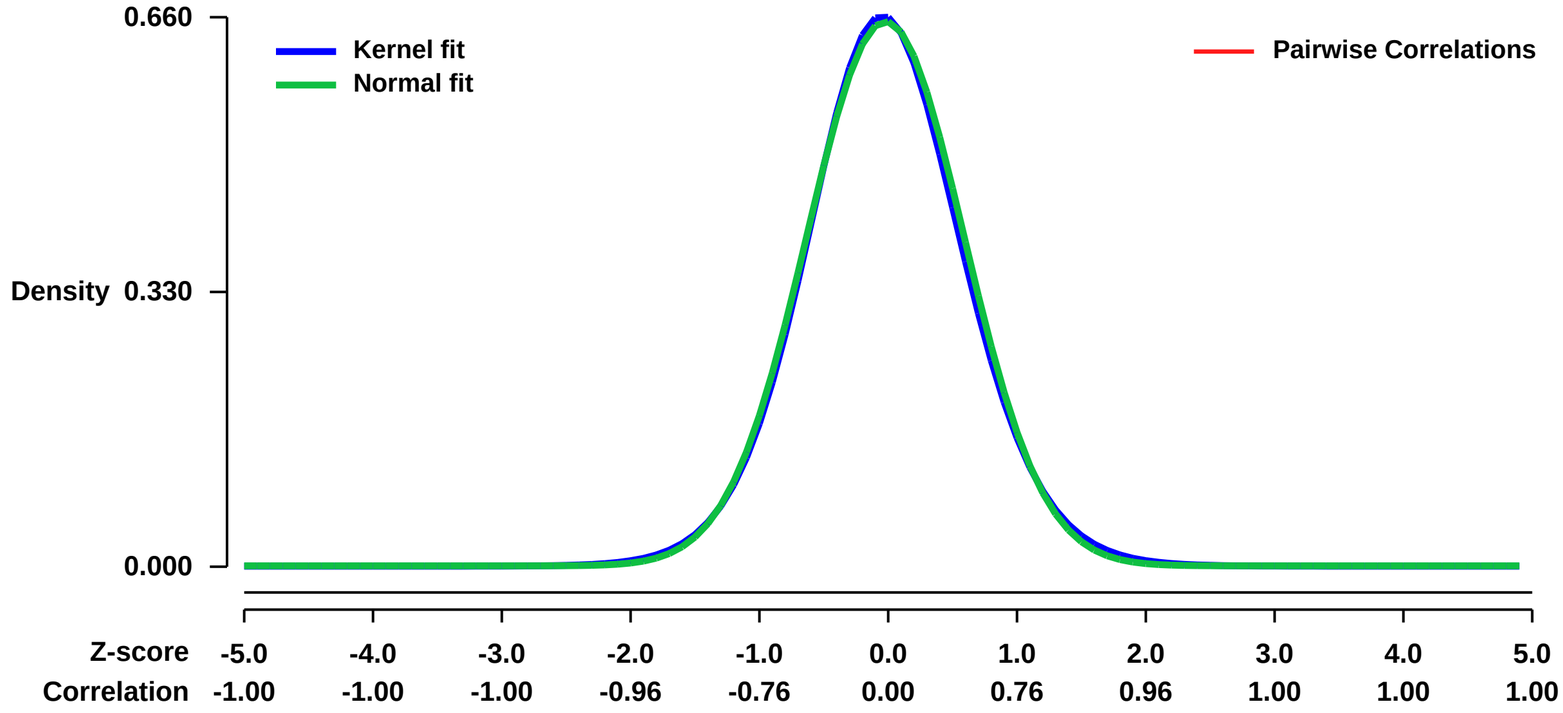

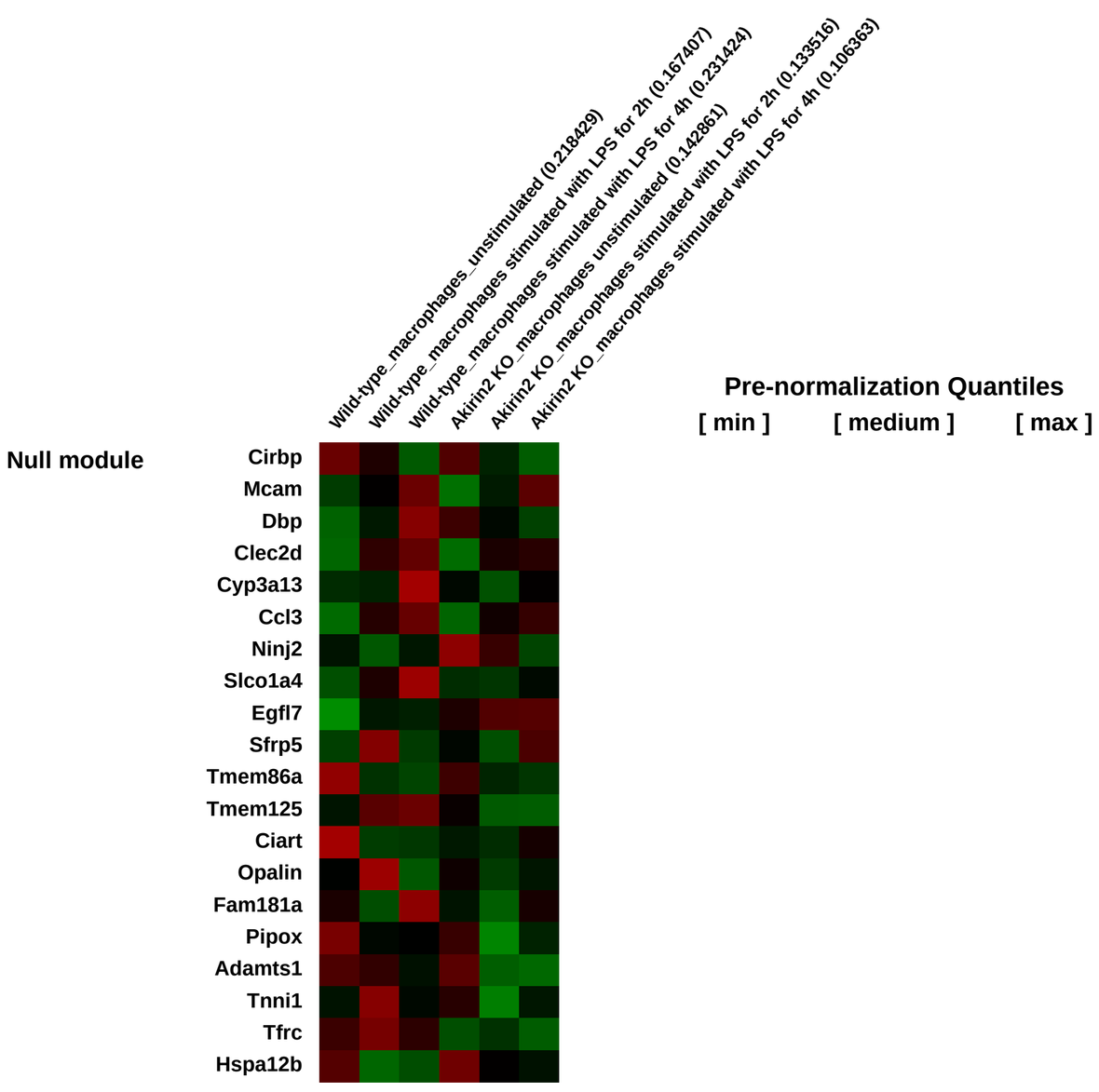

GEO Series "GSE5959" Expression Profiles

Num of samples in this series: 6

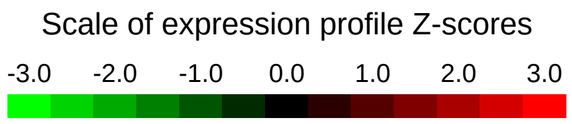

GEO Link:	http://www.ncbi.nlm.nih.gov/geo/query/acc.cgi?acc=GSE5959
Status:	Public on Oct 29 2006
Title:	Expression differences in the liver of a congenic mouse with low serum IGF-1
Organism:	Mus musculus
Experiment type:	Expression profiling by array
Platform:	GPL1261
Pubmed ID:	17584978
Summary & Design:	**Summary:** Several studies have shown that bone mineral density (BMD), a clinically measurable predictor of osteoporotic fracture, is the sum of genetic and environmental influences. In addition, serum IGF-1 levels have been correlated to both BMD and fracture risk. We previously identified a Quantitative Trait Locus (QTL) for Bone Mineral Density (BMD) on mouse Chromosome (Chr) 6 that overlaps a QTL for serum IGF-1. The B6.C3H-6T (6T) congenic mouse is homozygous for C57BL/6J (B6) alleles across the genome except for a 30 cM region on Chr 6 that is homozygous for C3H/HeJ (C3H) alleles. This mouse was created to study biology behind both the BMD and the serum IGF-1 QTLs and to identify the gene(s) underlying these QTLs. Female 6T mice have lower BMD and lower serum IGF-1 levels at all ages measured. As the liver is the major source of serum IGF-1, we examined differential expression in the livers of fasted female B6 and 6T mice by microarray. **Keywords:** Genetic variation **Overall design:** The experimental design of this experiment was a simple two-factor experiment, with three biological replicates of each factor (in this case mouse strain, B6.C3H-6T vs. C57BL/6J). Each sample represented one mouse; no samples were pooled. No technical replicated were done.

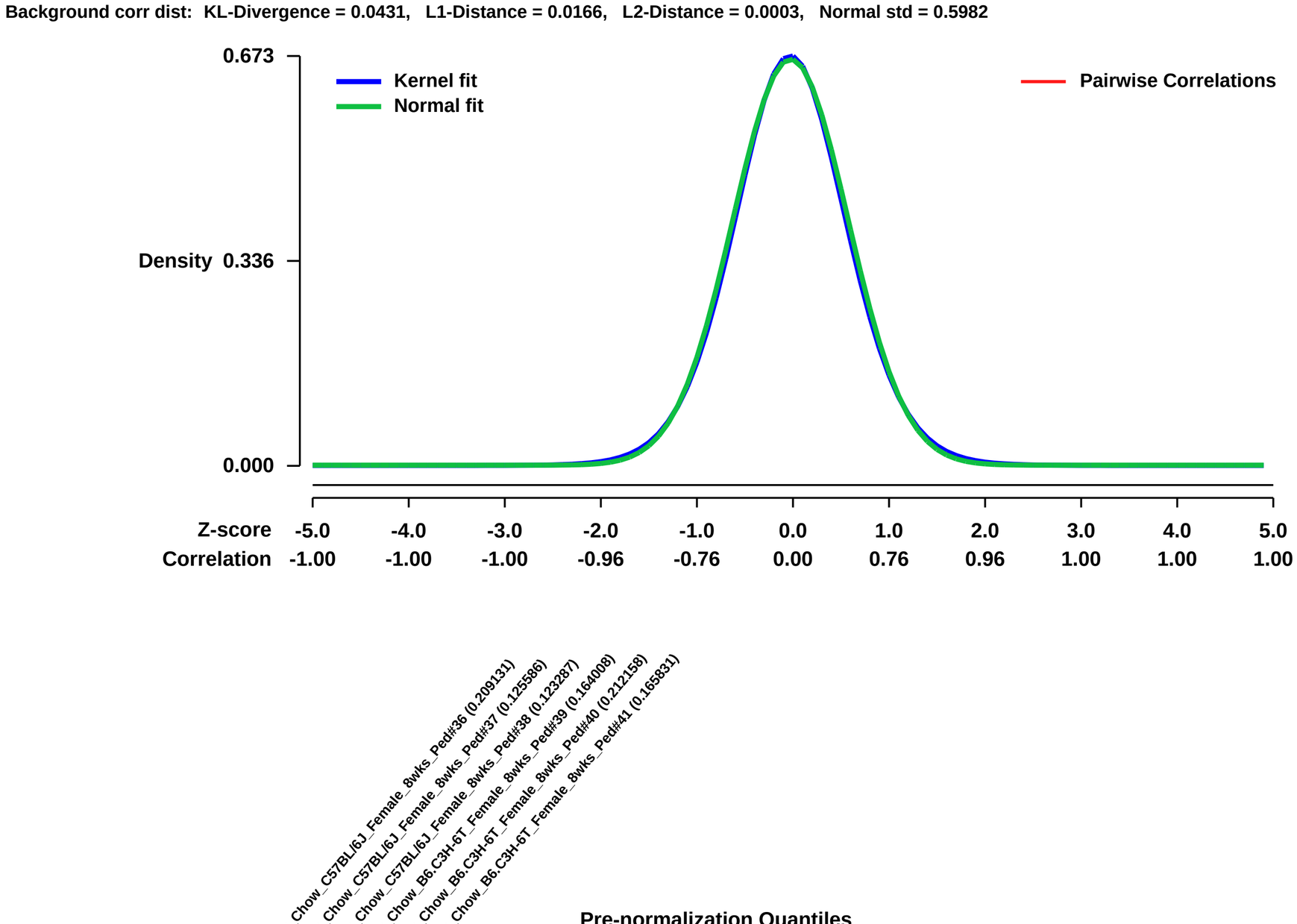

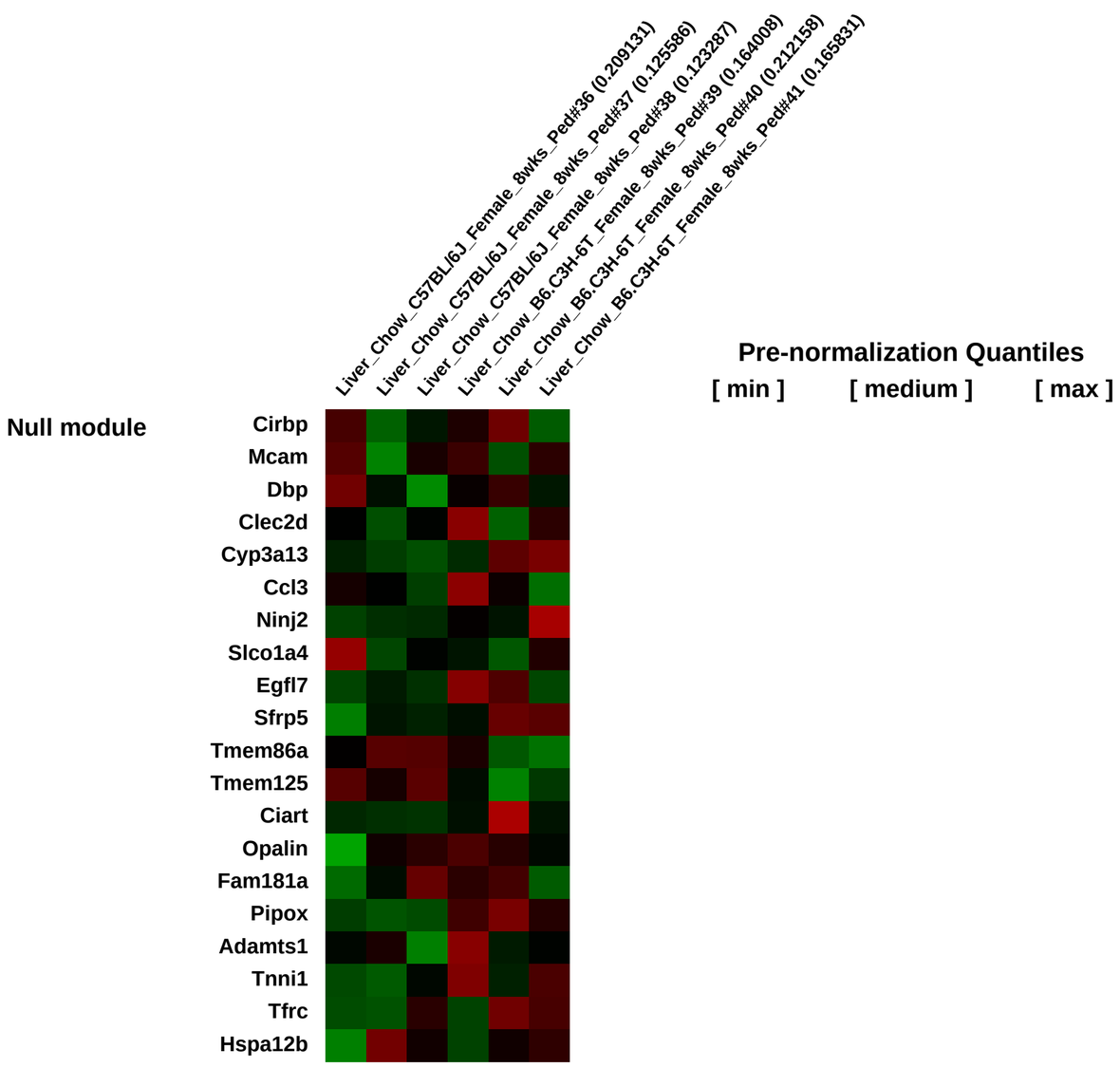

GEO Series "GSE59672" Expression Profiles

Num of samples in this series: 12

Scale of expression profile Z-scores

-3.0 -2.0 -1.0 0.0 1.0 2.0 3.0

GEO Link:	http://www.ncbi.nlm.nih.gov/geo/query/acc.cgi?acc=GSE59672
Status:	Public on Jul 23 2014
Title:	Expression data from DOX(doxorubicin) -treated wild type or CHIP knockout C57BL/6J mice at day 5
Organism:	Mus musculus
Experiment type:	Expression profiling by array
Platform:	GPL1261
Pubmed ID:	
Summary & Design:	**Summary:** The clinical application of doxorubicin as a broad-spectrum anti-tumor antibiotic is limited greatly by its cardiotoxicity. Various mechanisms have been studied, but little is known about whether genes or pathways relevant with energy metabolism contributes to doxorubicin-induced cardiomyopathy or not. We used microarrays to detail the global expression profiling of acute cardiomyopathy induced by doxorubicin in wild type or CHIP knockout C57BL/6J mice and discovered distinct classes of changed genes during this process. **Overall design:** The whole hearts were selected for RNA extraction and hybridization on Affymetrix microarrays at day 5 after a single intraperitoneal injection of doxorubicin at a dose of 15 mg/kg.

Background corr dist: KL-Divergence = 0.1136, L1-Distance = 0.0306, L2-Distance = 0.0016, Normal std = 0.4148

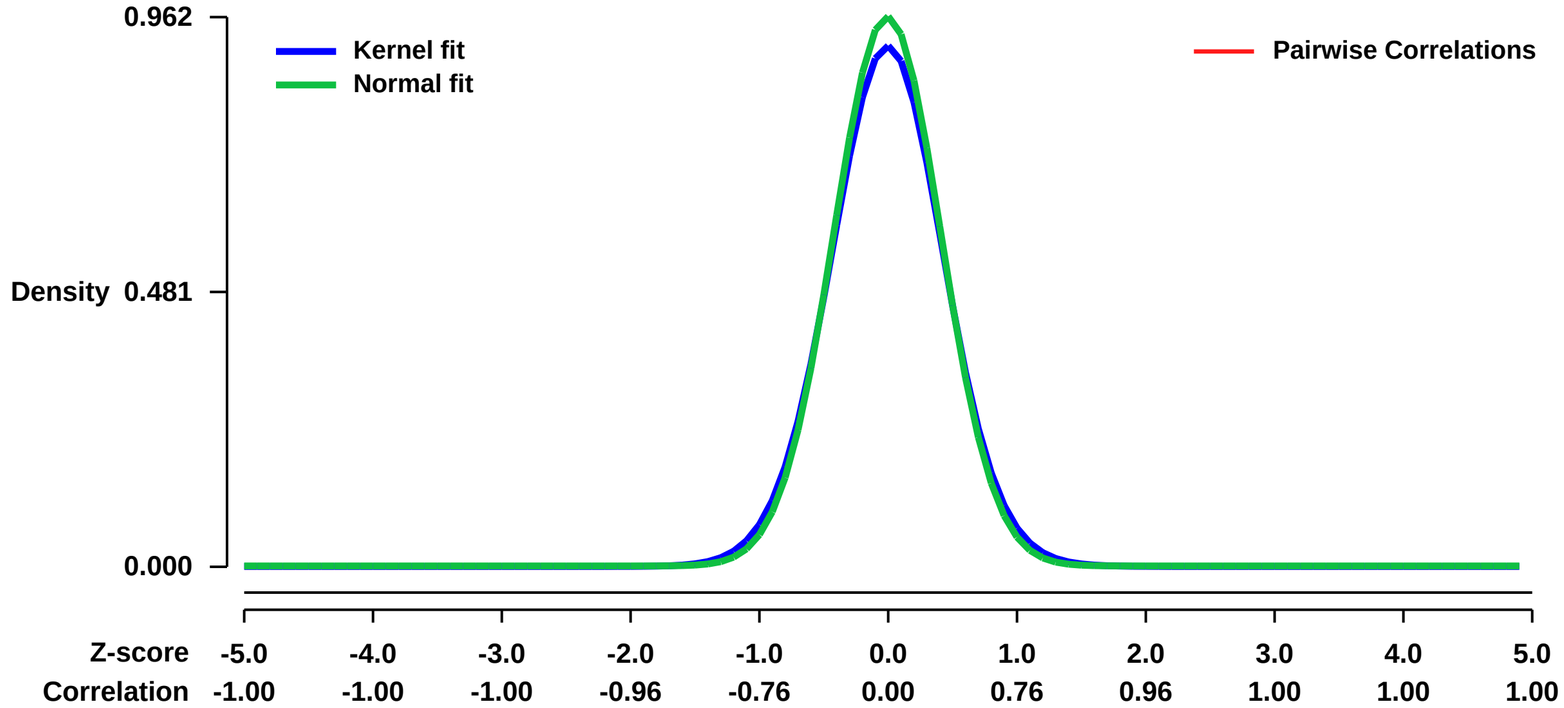

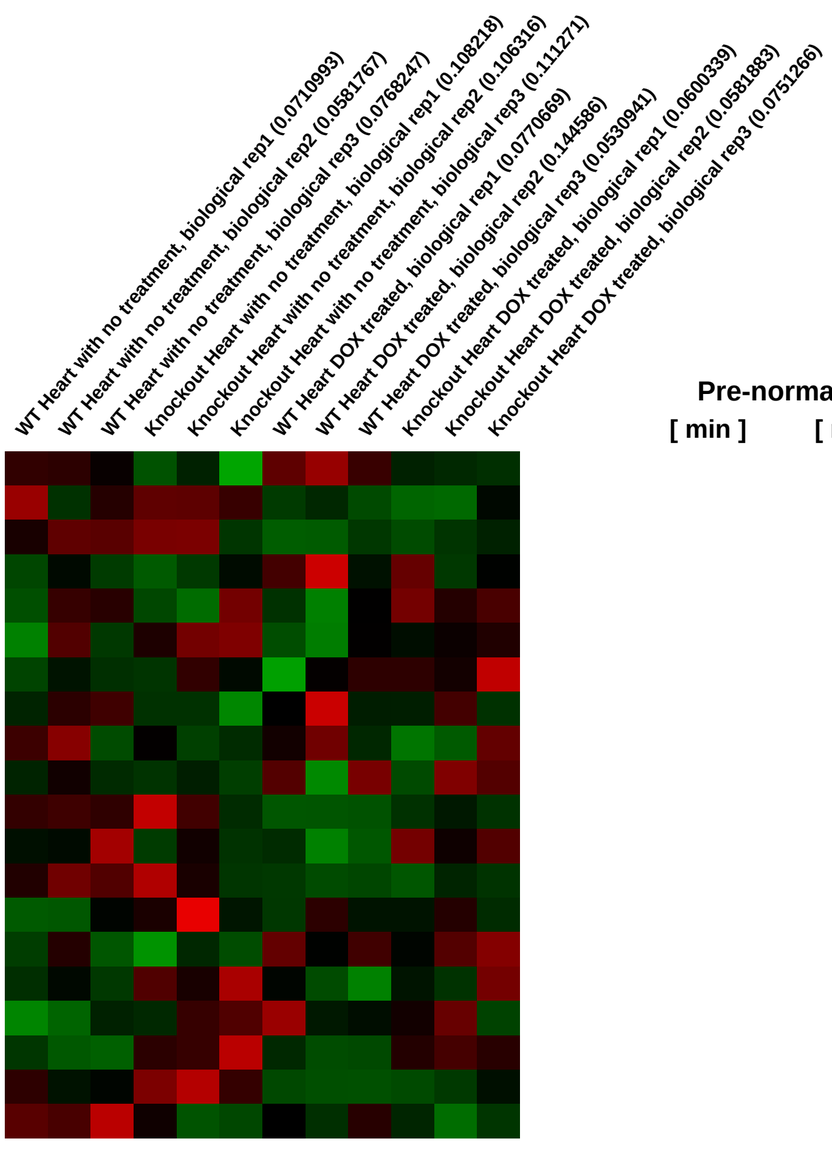

GEO Series "GSE5976" Expression Profiles

Num of samples in this series: 12

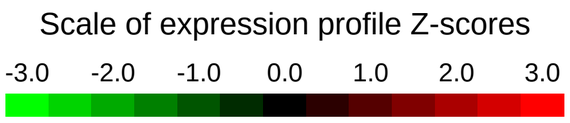

GEO Link:	**http://www.ncbi.nlm.nih.gov/geo/query/acc.cgi?acc=GSE5976**
Status:	**Public on Jul 01 2008**
Title:	**Mesp1-induced gene expression changes**
Organism:	**Mus musculus**
Experiment type:	**Expression profiling by array**
Platform:	**GPL1261**
Pubmed ID:	**18593559**
Summary & Design:	**Summary:** **During gastrulation, cells of the prospective mesoderm ingress through the primitive streak and acquire fates based on complex spatial and temporal cues. Progenitors of the cardiogenic mesoderm are first found at E6.5 in the posterior lateral epiblast and subsequently migrate laterally and anteriorly to form the cardiac crescent at E7.5, when regionalized cell fates are first delineated . Lineage tracing and heterotopic transplantation studies suggest that precursors in the earliest heart field possess potential to generate myocardium, endocardium, and pericardium. The mechanisms by which inductive signals in the primitive streak effect the development of this pancardiac progenitor field, however, remain poorly understood** **In mice, the earliest restricted progenitors of the cardiovascular system are marked by expression of the basic helix-loop-helix transcription factor, Mesp1. We therefore use microarray analysis to determine the early and intermediate effects of transiently forced Mesp1 expression during ES cell differentiation.** **Keywords: time course** **Overall design:** **ES cells bearing a targeted, doxycycline inducible Mesp1 transgene were differentiated in the absence or presence of DKK1 from day 0-4, either with or without transient doxycycline treatment from day 2-4.**

Background corr dist: KL-Divergence = 0.0893, L1-Distance = 0.0268, L2-Distance = 0.0010, Normal std = 0.4657

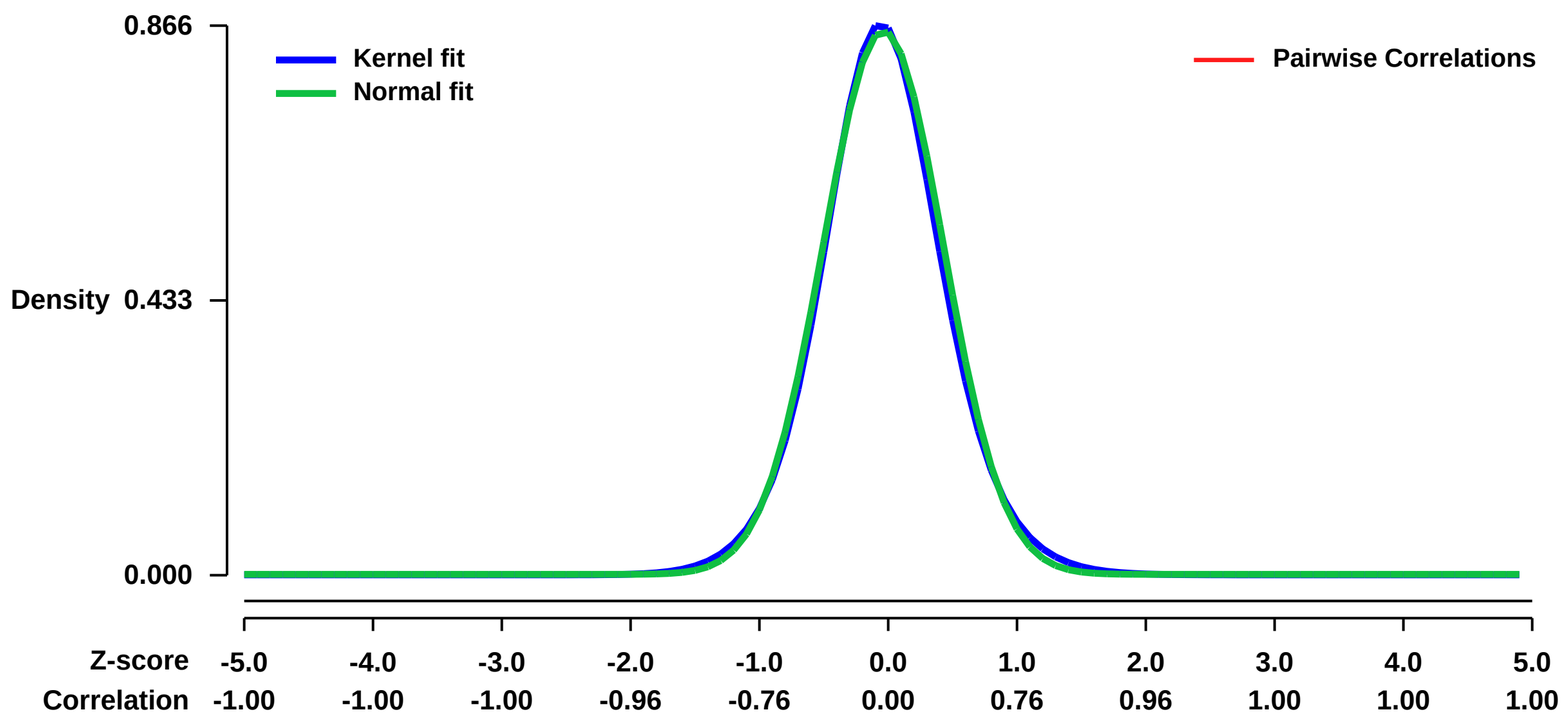

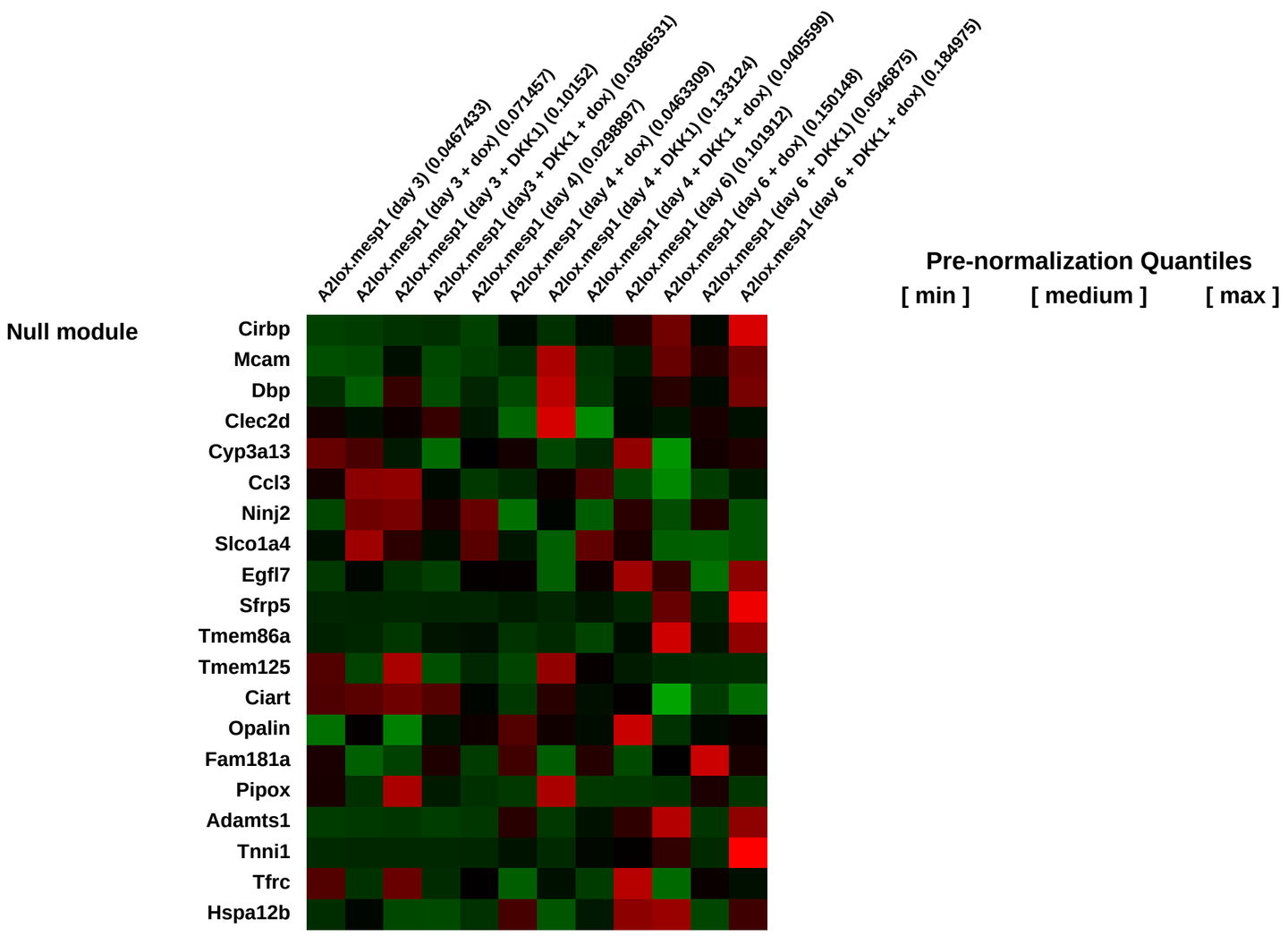

GEO Series "GSE6030" Expression Profiles

Num of samples in this series: 6

Scale of expression profile Z-scores

-3.0 -2.0 -1.0 0.0 1.0 2.0 3.0

GEO Link:	http://www.ncbi.nlm.nih.gov/geo/query/acc.cgi?acc=GSE6030
Status:	Public on Oct 13 2007
Title:	Pineal gland gene expression of 129 Wt P0 mice versus NeuroD1 pineal gene expression at P0
Organism:	Mus musculus
Experiment type:	Expression profiling by array
Platform:	GPL1261
Pubmed ID:	17630985
Summary & Design:	**Summary:** This study determines pineal gland gene expression levels in the NeuroD1 knockout mouse at postnatal day zero. Comparison was performed against pineal gland gene expression levels in 129 wildtype mice also disected at P0. Keywords: Comparison of wildtype versus transgenic pineal gland gene expression **Overall design:** Triplicate arrays were run for wildtype and the homozygous animals.

Background corr dist: KL-Divergence = 0.0386, L1-Distance = 0.0276, L2-Distance = 0.0010, Normal std = 0.6292

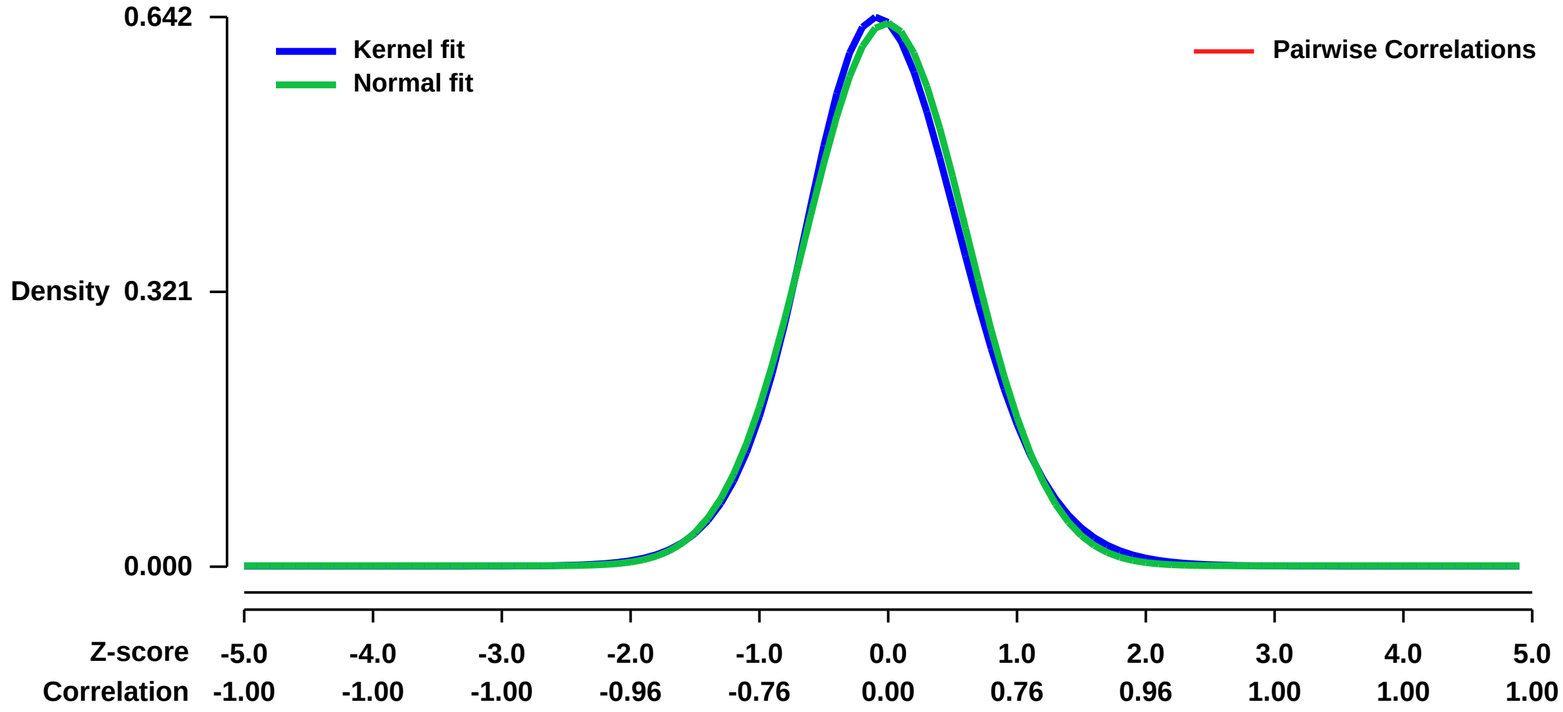

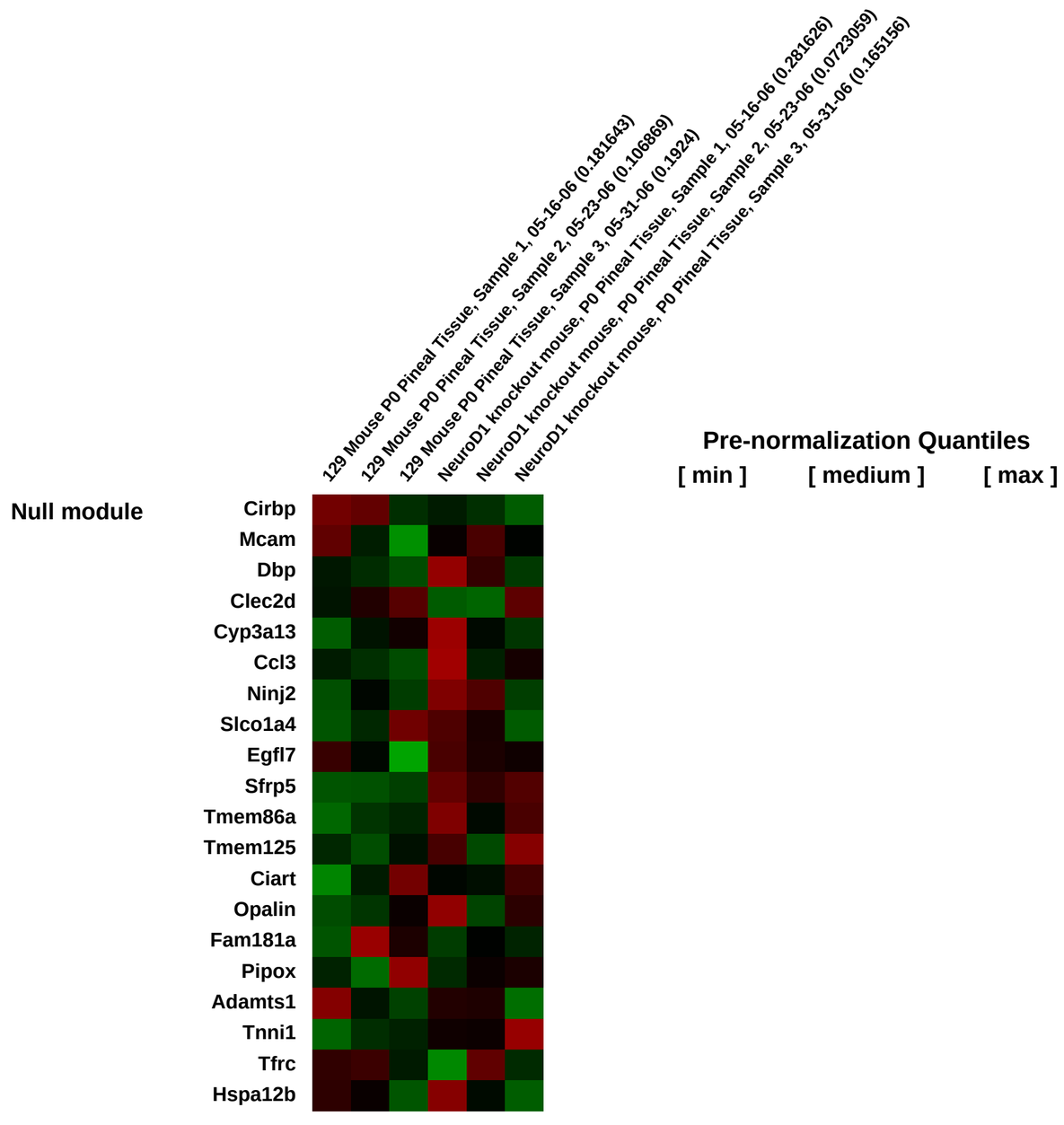

GEO Series "GSE6055" Expression Profiles

Num of samples in this series: 8

Scale of expression profile Z-scores

-3.0 -2.0 -1.0 0.0 1.0 2.0 3.0

GEO Link:	http://www.ncbi.nlm.nih.gov/geo/query/acc.cgi?acc=GSE6055
Status:	Public on Dec 14 2006
Title:	Gene Expression Profiling Reveals Unique Pathways Associated with Differential Severity of Lyme Arthritis
Organism:	Mus musculus
Experiment type:	Expression profiling by array
Platform:	GPL1261
Pubmed ID:	17114465
Summary & Design:	**Summary:** **Keywords: disease state analysis, time course** **Overall design:** **Expression profiling of ankle tissues of C3H, C57BL/6, and C57BL/6-IL10-/- mice infected with B. burgdorfer (0, 1, 2, and 4 weeks post-infection)**

Background corr dist: **KL-Divergence = 0.0594, L1-Distance = 0.0221, L2-Distance = 0.0005, Normal std = 0.5419**

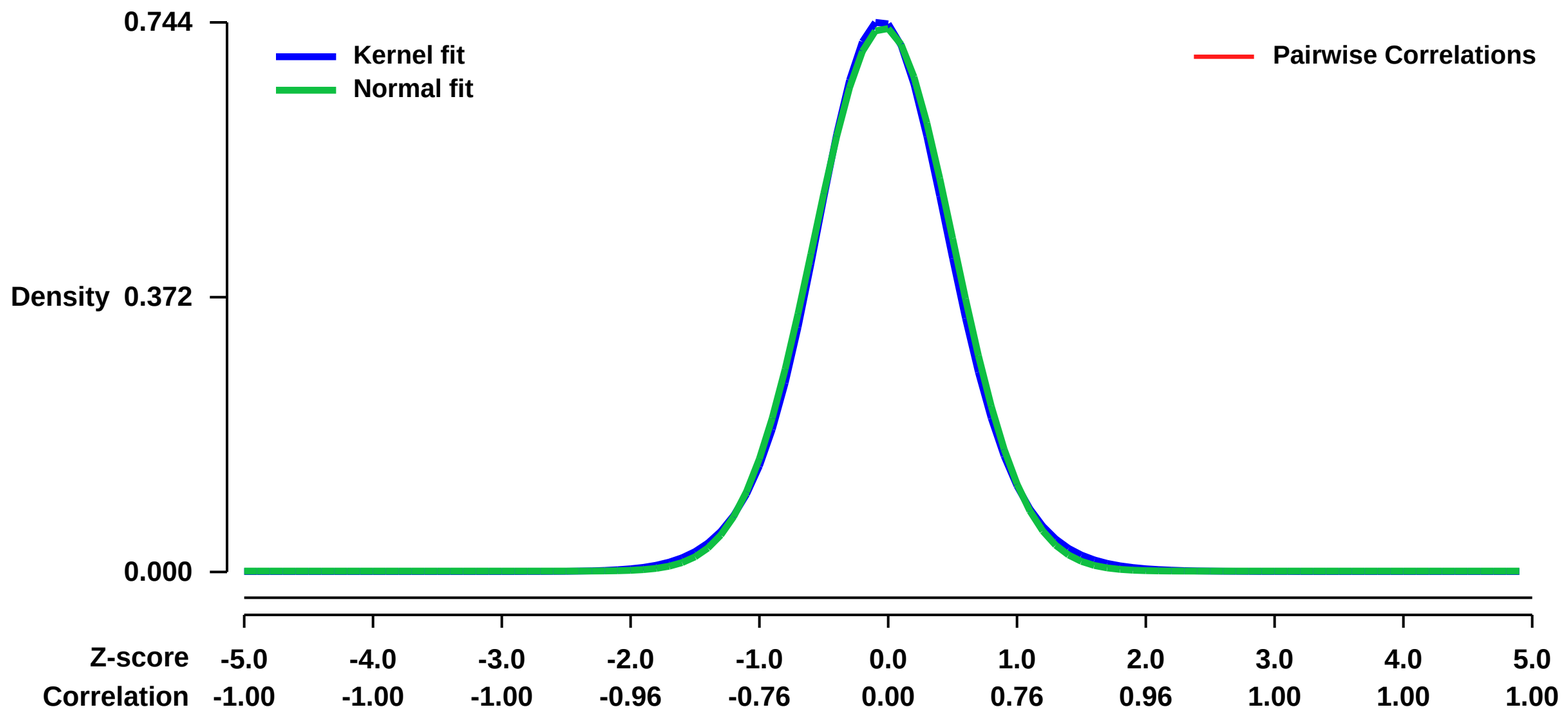

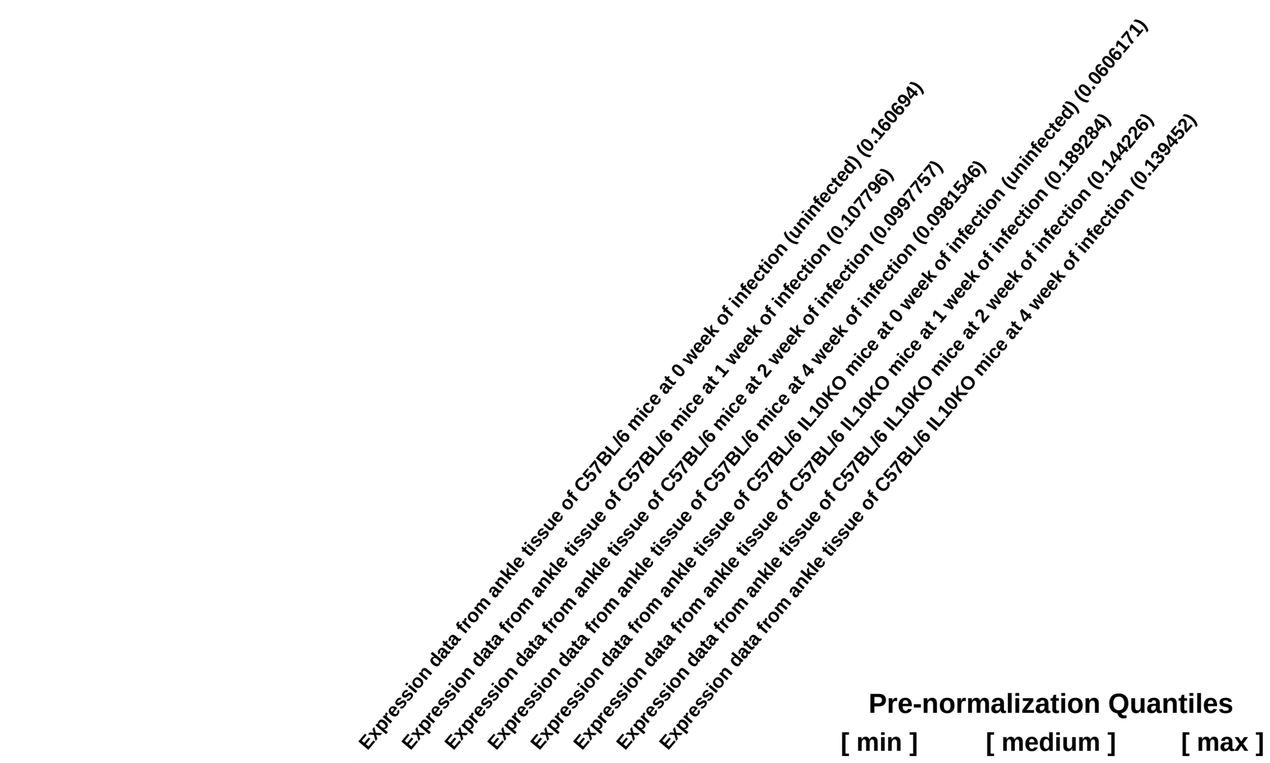

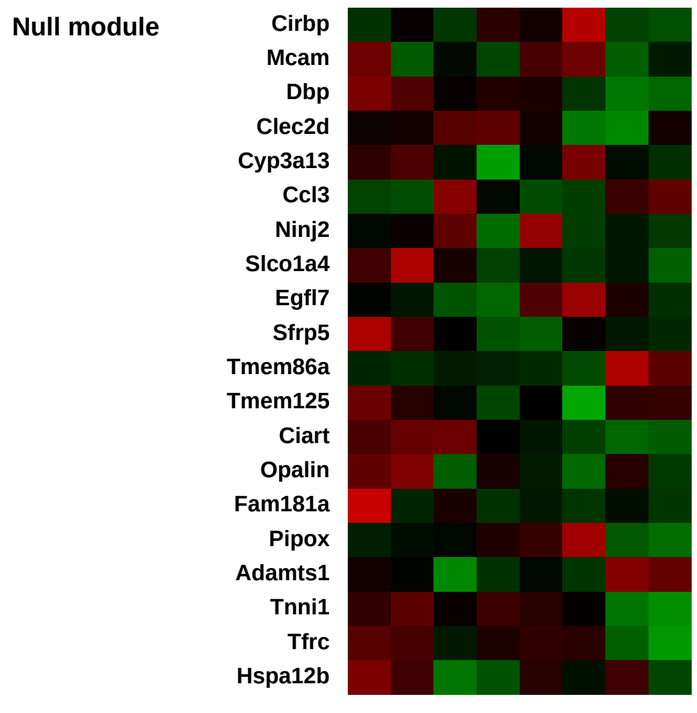

GEO Series "GSE6065" Expression Profiles

Num of samples in this series: 100

Scale of expression profile Z-scores

-3.0 -2.0 -1.0 0.0 1.0 2.0 3.0

GEO Link: http://www.ncbi.nlm.nih.gov/geo/query/acc.cgi?acc=GSE6065
Status: Public on Oct 21 2006
Title: Murine host cell response to Aeromonas infection
Organism: Mus musculus
Experiment type: Expression profiling by array
Platform: GPL1261
Pubmed ID: 17897183

Summary & Design:

Summary:
Aims: To assess the virulence of multiple Aeromonas spp. using two models, a neonatal mouse assay and a mouse intestinal cell culture.

Methods and Results: Transcriptional responses to both infection models were evaluated using microarrays. After artificial infection with a variety of Aeromonas spp., mRNA extracts from the two models were processed and hydridized to murine microarrays to determine host gene response. Definition of virulence was determined based on host mRNA production in murine neonatal intestinal tissue and mortality of infected animals. Infections of mouse intestinal cell cultures were then performed to determine whether this simpler model system's mRNA responses correlated to neonatal results and therefore be predictive of virulence of Aeromonas spp. Virulent aeromonads up-regulated transcripts in both models including multiple host defense gene products (chemokines, regulation of transcription and apoptosis, cell signaling). Avirulent species exhibited little or no host response in neonates. Mortality results correlated well with both bacterial dose and average fold change of up-regulated transcripts in the neonatal mice.

Conclusions: Cell culture results were less discriminating but showed promise as potentially being able to be predictive of virulence. Jun oncogene up-regulation in murine cell culture is potentially predictive of Aeromonas virulence.

Significance and Impact of the Study: Having the ability to determine virulence of waterborne pathogens quickly would potentially assist public health officials to rapidly assess exposure risks.

Keywords: Aeromonas; Virulence; Gene expression; Host response

Overall design:
Two infection models were assessed, live, whole animals (neonatal Swiss Webster mice) and a murine small intestinal cell culture. Biological replicates (n=5) were infected with different Aeromonas species/strains and compared to uninfected controls.

Background corr dist: KL-Divergence = 0.0734, L1-Distance = 0.0755, L2-Distance = 0.0103, Normal std = 0.5327

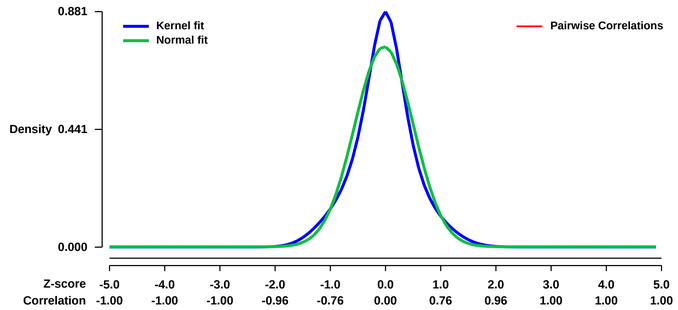

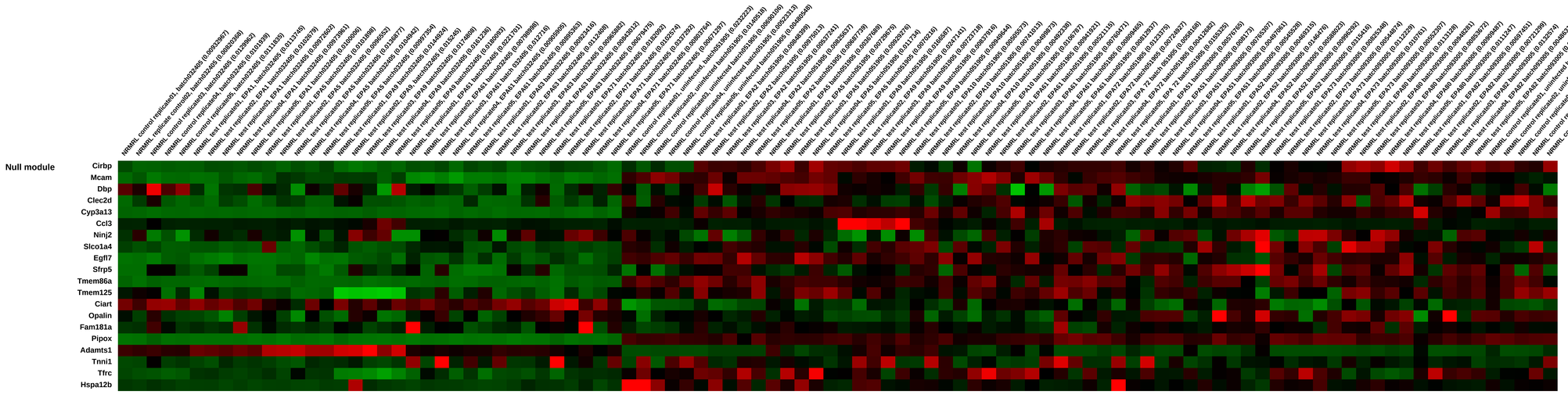

GEO Series "GSE6084" Expression Profiles

Num of samples in this series: 12

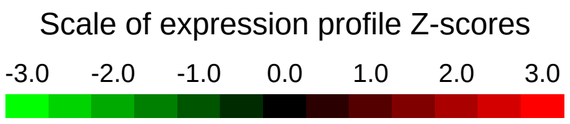

GEO Link:	**http://www.ncbi.nlm.nih.gov/geo/query/acc.cgi?acc=GSE6084**
Status:	**Public on Jan 10 2009**
Title:	**Expression data from Murine T cell in response to cycloheximide treatment**
Organism:	**Mus musculus**
Experiment type:	**Expression profiling by array**
Platform:	**GPL1261**
Pubmed ID:	
Summary & Design:	**Summary:** **Cycloheximide has been used for inhibiting protein synthesis in order to identify IL-2 direct targeted genes in T cells, but the effects of cycloheximide itself on genomewide genes are not well defined** **We conducted a global analysis of cycloheximide regulated genes in mouse T cell line CTLL-2 using Affymetrix mouse genome array, and identified 213 genes differentially expressed (?1.5-fold change) in response to cycloheximide 30min after adding cylcoheximide to T cells cultured without IL-2 for 14 hours. These genes involve in a number biological processes.** **Keywords: stress response** **Overall design:** **Murine cytotoxic T lymphocyte cell line CTLL-2, derived from a C57BL/6 mouse, is an IL-2 dependent cell line. Cells were cultured in D10 medium in an incubator with 5% CO2 at 37oC to mid-log phase (~2 X 105 cells/mL), and collected by centrifugation, washed with phosphate buffered saline (PBS) (Invitrogen), resuspended at 1 X 106 cells/mL in the medium without IL-2 (IL-2 starvation) and cultured for 14 hours (No IL-2 stimulation, T0, 5 reps), followed by adding cycloheximide (20 ?g/mL) for 30min (T4-CHX, 4 reps). Total RNA were extracted from the cells and was hybridized on Affymetrix GeneChip Mouse Genome 430 2.0 Array.**

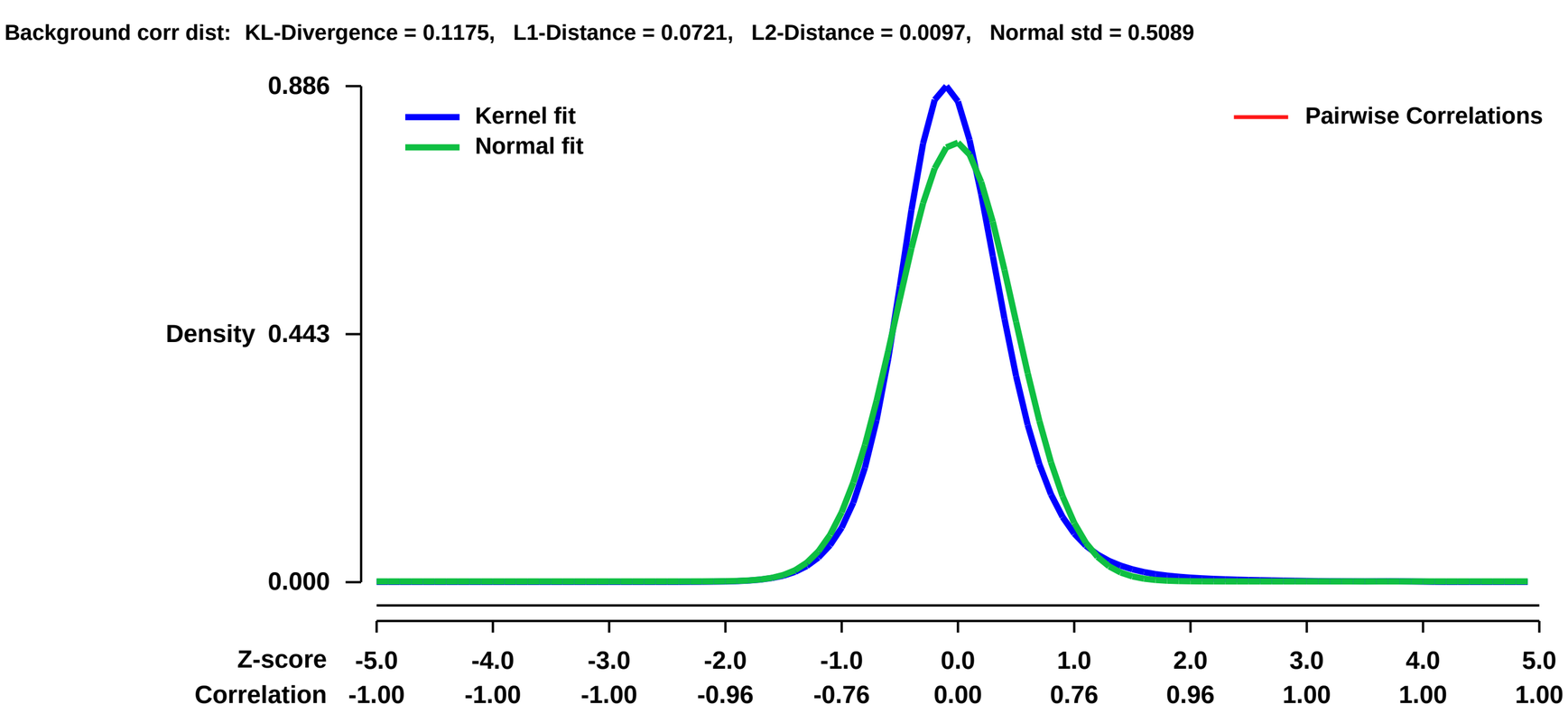

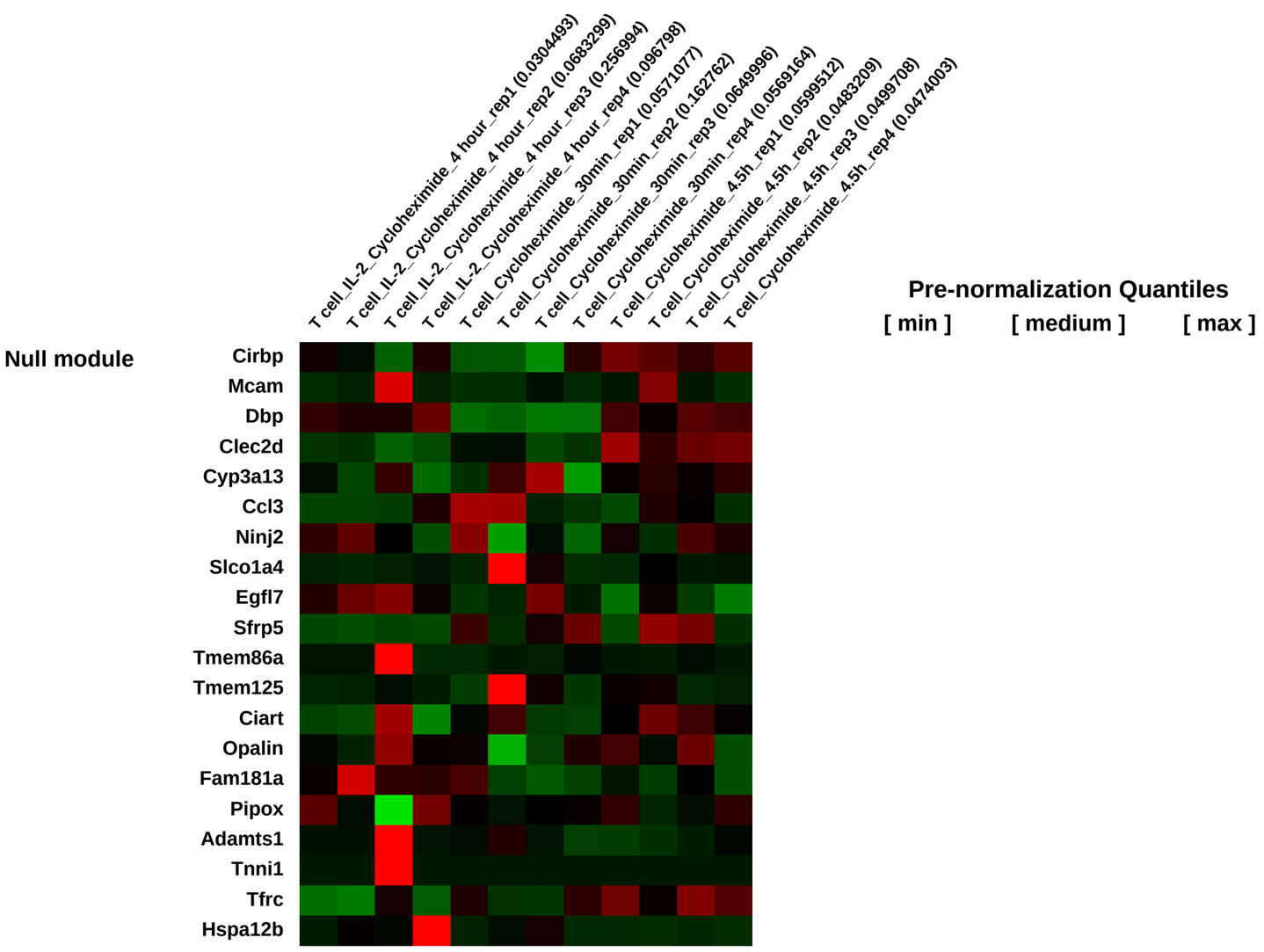

GEO Series "GSE6116" Expression Profiles

Num of samples in this series: 70

Scale of expression profile Z-scores

-3.0 -2.0 -1.0 0.0 1.0 2.0 3.0

GEO Link:	http://www.ncbi.nlm.nih.gov/geo/query/acc.cgi?acc=GSE6116
Status:	Public on Feb 14 2007
Title:	Transcriptional Biomarkers to Predict Female Mouse Lung Tumors in Rodent Cancer Bioassays - A 13 Chemical Training Set
Organism:	Mus musculus
Experiment type:	Expression profiling by array
Platform:	GPL1261
Pubmed ID:	17311802
Summary & Design:	**Summary:** The primary goal of toxicology and safety testing is to identify agents that have the potential to cause adverse effects in humans. Unfortunately, many of these tests have not changed significantly in the past 30 years and most are inefficient, costly, and rely heavily on the use of animals. The rodent cancer bioassay is one of these safety tests and was originally established as a screen to identify potential carcinogens that would be further analyzed in human epidemiological studies. Today, the rodent cancer bioassay has evolved into the primary means to determine the carcinogenic potential of a chemical and generate quantitative information on dose-response behavior in chemical risk assessments. Due to the resource-intensive nature of these studies, each bioassay costs $2 to $4 million and takes over three years to complete. Over the past 30 years, only 1,468 chemicals have been tested in a rodent cancer bioassay. By comparison, approximately 9,000 chemicals are used by industry in quantities greater than 10,000 lbs and nearly 90,000 chemicals have been inventoried by the U.S. Environmental Protection Agency as part of the Toxic Substances Control Act. Given the disparity between the number of chemicals tested in a rodent cancer bioassay and the number of chemicals used by industry, a more efficient and economical system of identifying chemical carcinogens needs to be developed. **Keywords: toxicology, chemical carcinogenesis, lung** **Overall design:** Five-week old female B6C3F1 mice were exposed for 13 weeks in the following dose groups: 1) 1,5-Naphthalenediamine, CAS No. 2243-62-1, feed, 2000 ppm, positive lung carcinogen; 2) 2,3-Benzofuran, CAS No. 271-89-6, gavage, 240 mg/kg, positive lung carcinogen; 3) 2,2-Bis(bromomethyl)-1,3-propanediol, CAS No. 3296-90-0, feed, 1250 ppm, positive lung carcinogen; 4) N-Methylolacrylamide, CAS No. 924-42-5, gavage (water), 50 mg/kg, positive lung carcinogen; 5) 1,2-Dibromoethane, CAS No. 106-93-4, gavage (corn oil), 62 mg/kg, positive lung carcinogen; 6) Coumarin, CAS No. 91-64-5, gavage (corn oil), 200 mg/kg, positive lung carcinogen; 7) Benzene, CAS No. 71-43-2, gavage (corn oil), 100 mg/kg, positive lung carcinogen; 8) N-(1-naphthyl)ethylenediamine dihydrochloride, CAS No. 1465-25-4, feed, 2000 ppm, negative lung carcinogen; 9) Pentachloronitrobenzene, CAS No. 82-68-8, feed, 8187 ppm, negative lung carcinogen; 10) 4-Nitroanthranilic acid, CAS No. 619-17-0, feed, 10000 ppm, negative lung carcinogen; 11) 2-Chloromethylpyridine hydrochloride, CAS No. 6959-47-3, gavage (water), 250 mg/kg, negative lung carcinogen; 12) Diazinon, CAS No. 333-41-5, feed, 200 ppm, negative lung carcinogen; 13) Malathion, CAS No. 121-75-5, feed, 16000 ppm, negative lung carcinogen; 14) Corn oil control, gavage; 15) Water control, gavage; 16) Rodent diet control, feed. Feed animals were exposed 7 days/week and gavage animals were exposed 5 days/week (5 ml/kg). After 13 weeks, animals were euthanized and lungs were collected. The right lobe was used for microarray analysis. Microarray analysis was performed on the lungs of three to four mice per treatment group.

Background corr dist: KL-Divergence = 0.0952, L1-Distance = 0.0327, L2-Distance = 0.0020, Normal std = 0.4508

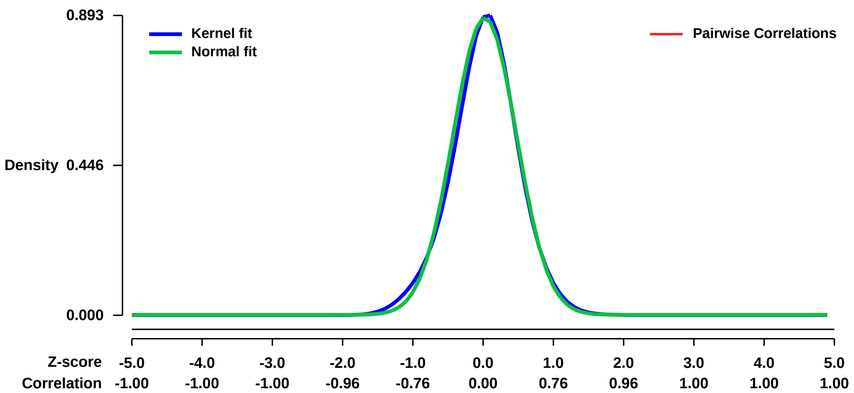

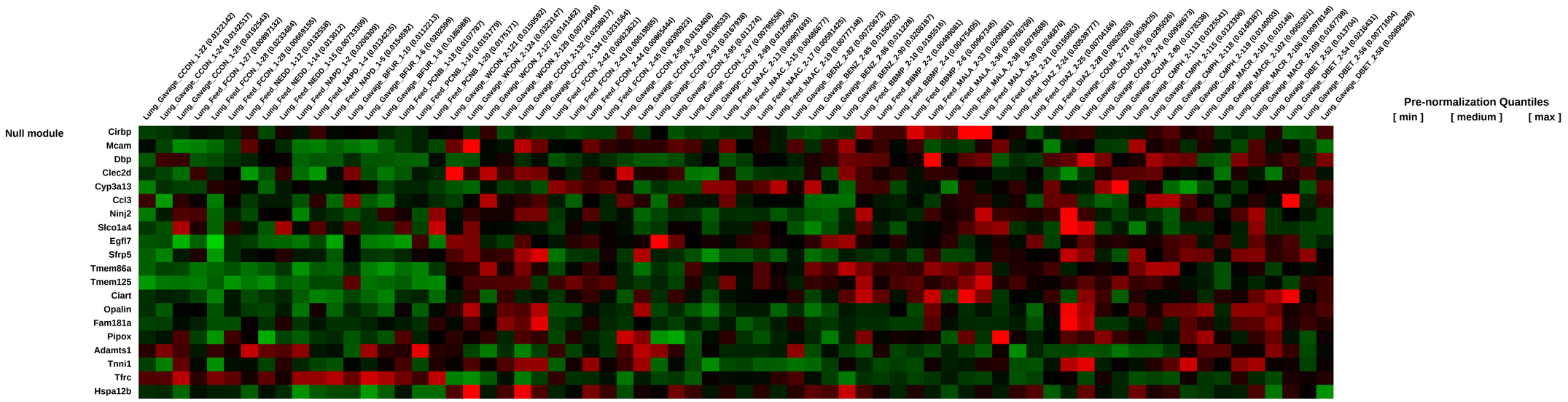

GEO Series "GSE6134" Expression Profiles

Num of samples in this series: 7

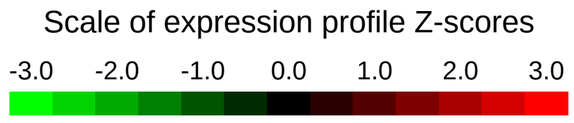

GEO Link:	http://www.ncbi.nlm.nih.gov/geo/query/acc.cgi?acc=GSE6134
Status:	Public on Aug 08 2007
Title:	Offsprings of crosses between hypercholesterolemic and normocholesterolemic parents LUMC-HKG-ApoE-Atherosclerosis
Organism:	Mus musculus
Experiment type:	Expression profiling by array
Platform:	GPL1261
Pubmed ID:	17656671
Summary & Design:	**Summary:** Enhanced prenatal fatty streak formation in human fetuses has been associated with maternal hypercholesterolemia. However, the possible roles of maternal genetic background and in utero environment on development of atherosclerosis in adult life have not been unraveled. We generated genetically identical heterozygous apoE-deficient mice offspring with a different maternal background to study the intrauterine effect of maternal genotype and associated hypercholesterolemia on the developing vascular system. As read out for increased atherosclerosis development in adult life, a constrictive collar was placed around the carotid artery to induce lesion formation. A significant increase in endothelial cell activation and damage was detected in the carotid arteries of heterozygous apoE-deficient fetuses with apoE-deficient mothers compared with offspring from wild type mothers, but no fatty streak formation was observed. Postnatally, all carotid arteries revealed normal morphology. In adult offspring with maternal apoE-deficiency, the constrictive collar resulted in severe lesion (9/10) development compared with no to only minor lesions (2/10) in offspring of wild type mothers. Microarray analysis showed no effect of maternal apoE-deficiency on gene expression in adult offspring. We conclude that maternal apoE-deficiency not only affects fetal arteries, but also increases the susceptibility for development of collar-induced atherosclerosis in adult life. **Keywords: Atheroslcersosis development** **Overall design:** Crossing of hypercholesterolemic female with normocholesterolemic male and vice versa, determination of susceptabilioty to atherosclerosis in offspring

Background corr dist: KL-Divergence = 0.0638, L1-Distance = 0.0198, L2-Distance = 0.0006, Normal std = 0.5205

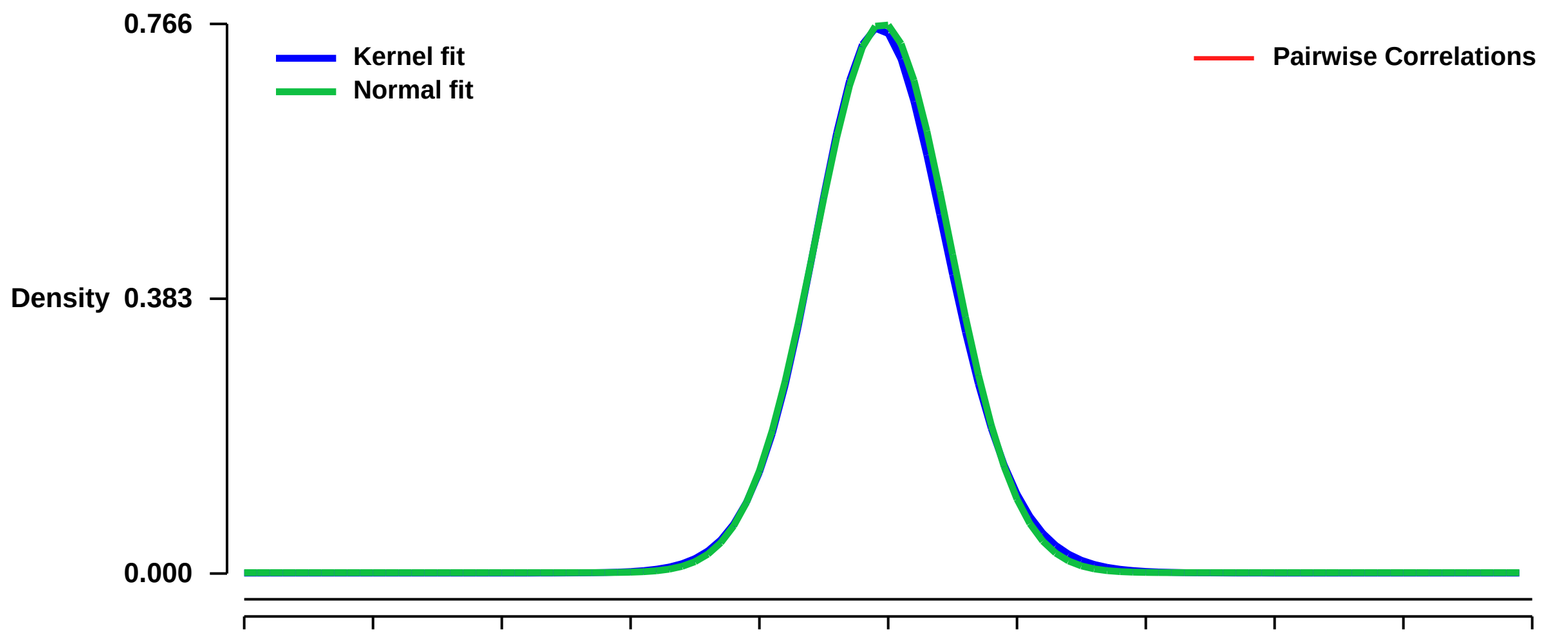

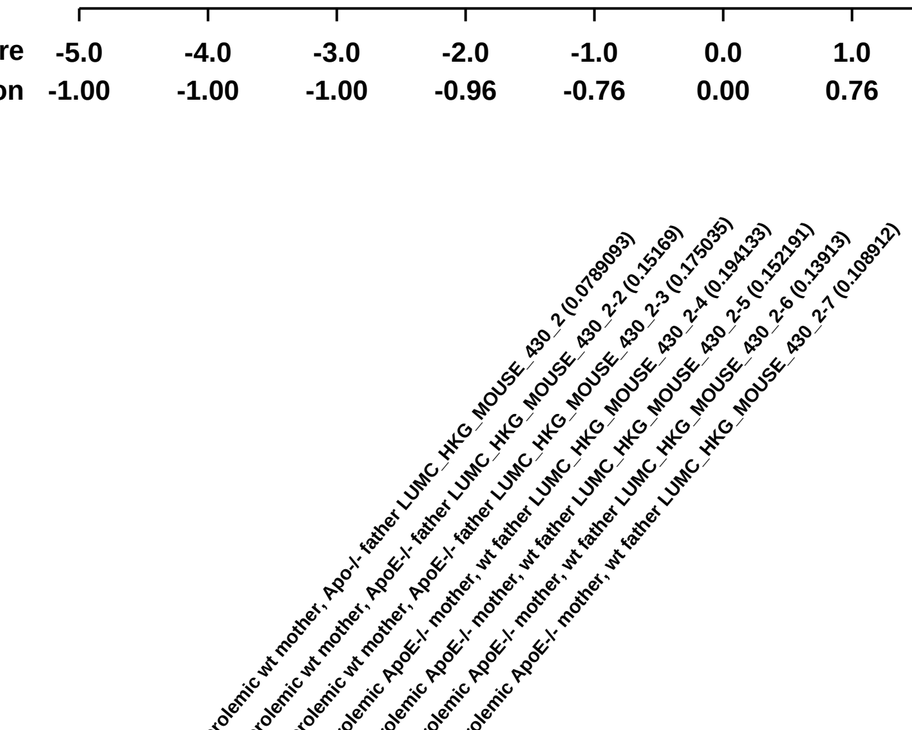

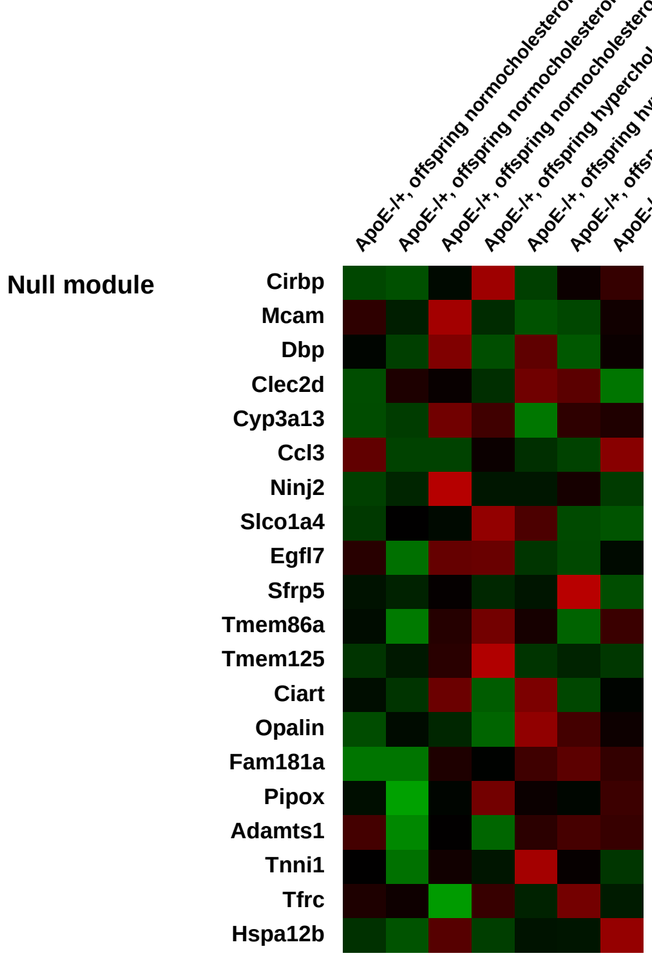

GEO Series "GSE6196" Expression Profiles

Num of samples in this series: 9

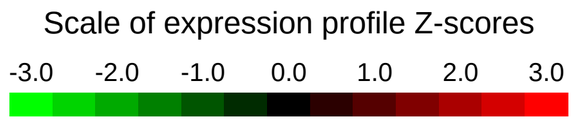

GEO Link:	**http://www.ncbi.nlm.nih.gov/geo/query/acc.cgi?acc=GSE6196**
Status:	**Public on Mar 21 2009**
Title:	**Mouse Reissner's Membrane Gene Expression studies**
Organism:	**Mus musculus**
Experiment type:	**Expression profiling by array**
Platform:	**GPL1261**
Pubmed ID:	**19144862**
Summary & Design:	**Summary:** **The goal was to screen for the expressed genes in Reissner's membrane (RM) that are related to ion transport and its regulation. The objectives were 1) to determine whether short-term incubation altered the transcriptome and 2) to discover which genes changed expression levels in response to glucocorticoids.** **Keywords: drug response** **Overall design:** **RM was dissected free-hand from mouse cochleae and either immediately subjected to RNA extraction or incubated for 24 as explants. Two series of samples were incubated in the presence or absence of dexamethasone (100 nM) and samples of RM were pooled to obtain sufficient material for gene array analysis. The pooled samples were used to hybridize 3 gene array chips for each biological sample.**

Background corr dist: **KL-Divergence = 0.0363, L1-Distance = 0.0602, L2-Distance = 0.0046, Normal std = 0.7133**

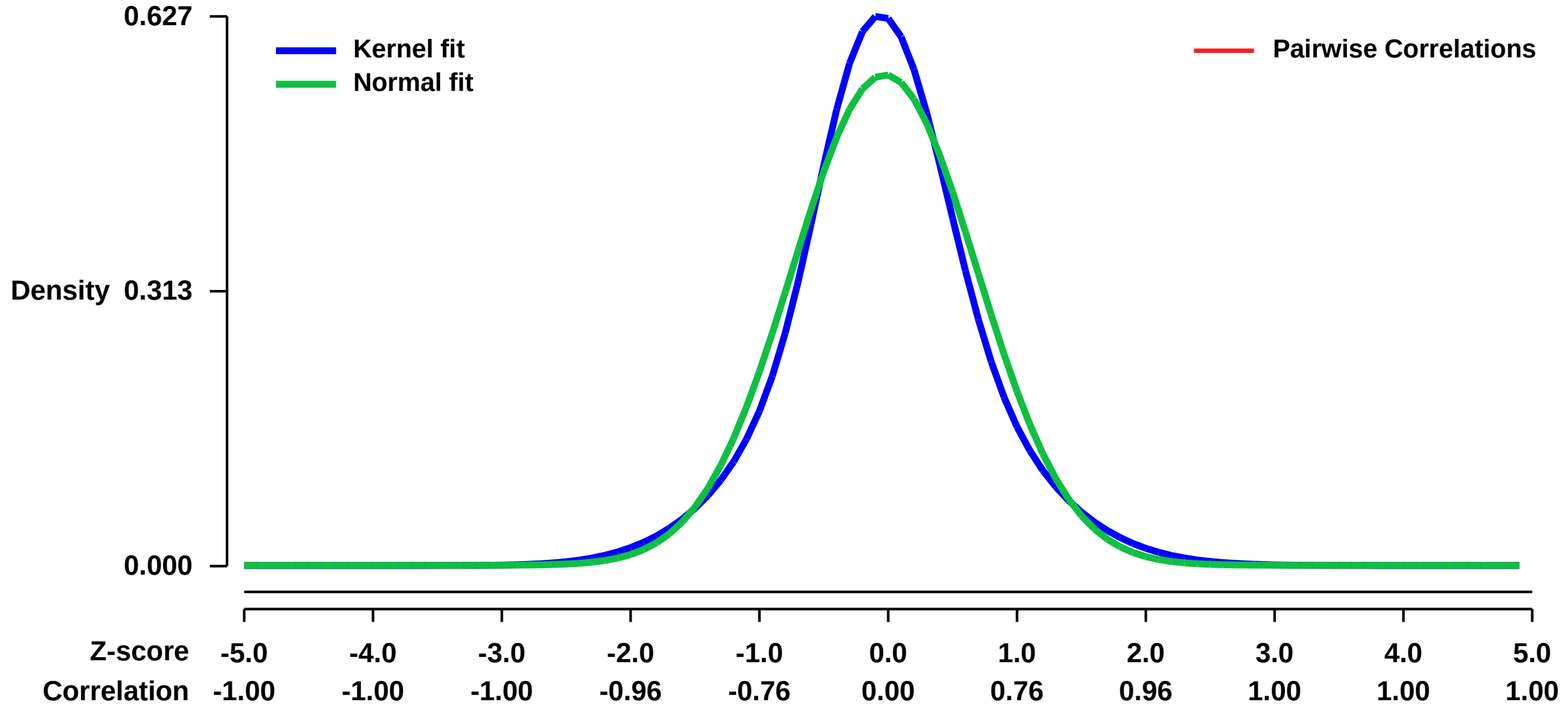

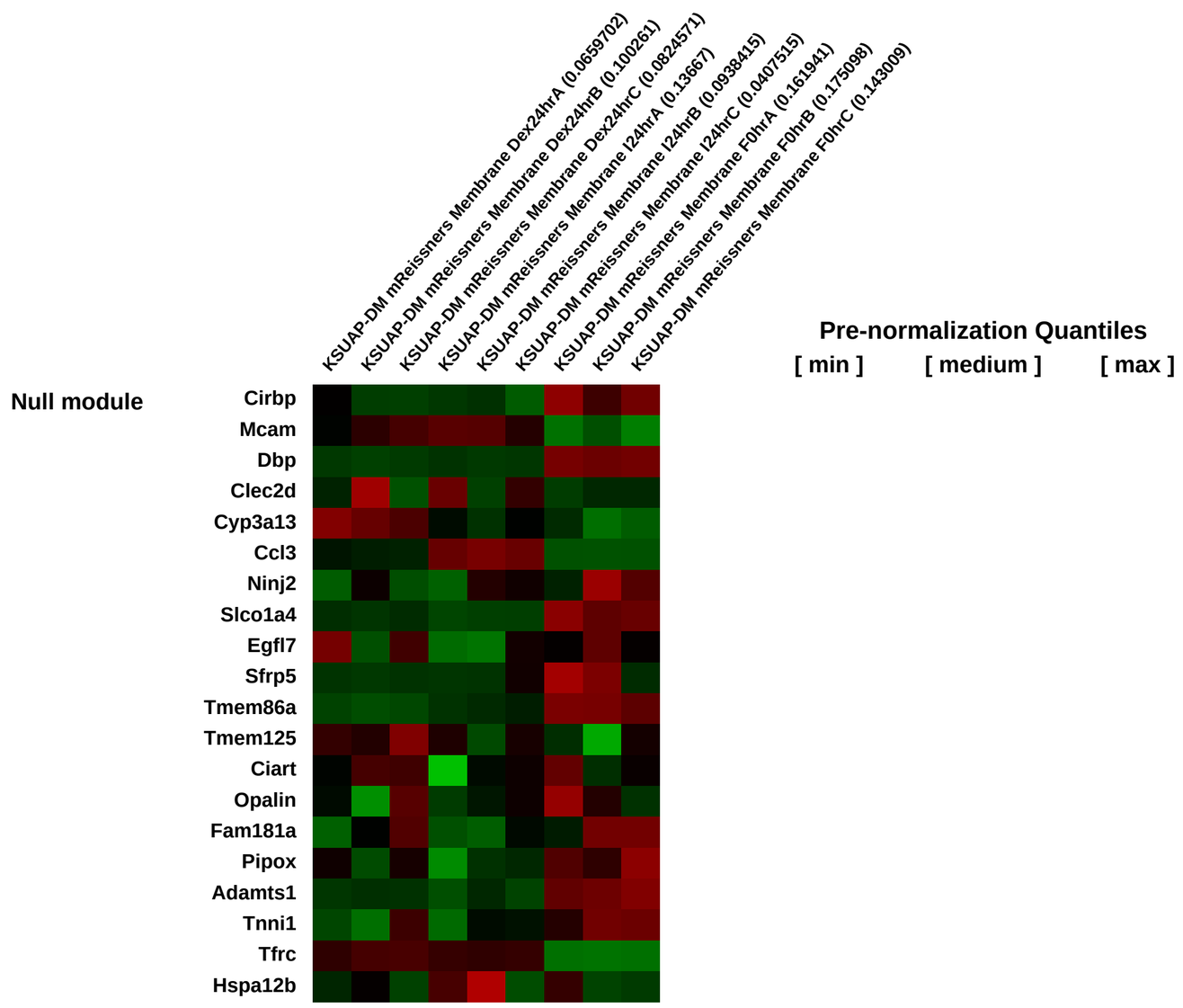

GEO Series "GSE6285" Expression Profiles

Num of samples in this series: 24

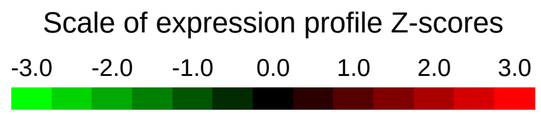

GEO Link:	http://www.ncbi.nlm.nih.gov/geo/query/acc.cgi?acc=GSE6285
Status:	Public on Jan 15 2008
Title:	Expression data from brains of mice fed four different diets
Organism:	Mus musculus
Experiment type:	Expression profiling by array
Platform:	GPL1261
Pubmed ID:	18231591
Summary & Design:	**Summary:** Beyond the DNA sequence difference between humans and closely related apes, there are large differences in the environments that these species experience. One prominent example for this is diet. The human diet diverges from those of other primates in various aspects, such as having a high calorie and protein content, as well as being cooked. Here, we used a laboratory mouse model to identify gene expression differences related to dietary differences. **Keywords: diet** **Overall design:** We fed four groups of six genetically identical 8-week-old female NMR1 mice one of four diets ad libidum: (1) a diet consisting of vegetables, fruit and yogurt identical to the diet fed to chimpanzees in our ape facility (’Chimpanzee’); (2) a diet consisting exclusively of McDonalds. fast food (’FastFood’); (3) a diet consisting of cooked food eaten by our staff in the Institute cafeteria (’HumanCafe’); (4) the mouse pellet diet on which they were raised (’Pellet’). At the end of a 2-week period, mice were euthanized by cervical dislocation and both liver and brain (right cerebral hemisphere) tissue were dissected. RNA was extracted from the 24 liver and brain samples as per established lab protocols and processed in two batches (containing equal numbers of individuals from all groups).

Background corr dist: KL-Divergence = 0.0423, L1-Distance = 0.0996, L2-Distance = 0.0129, Normal std = 0.8226

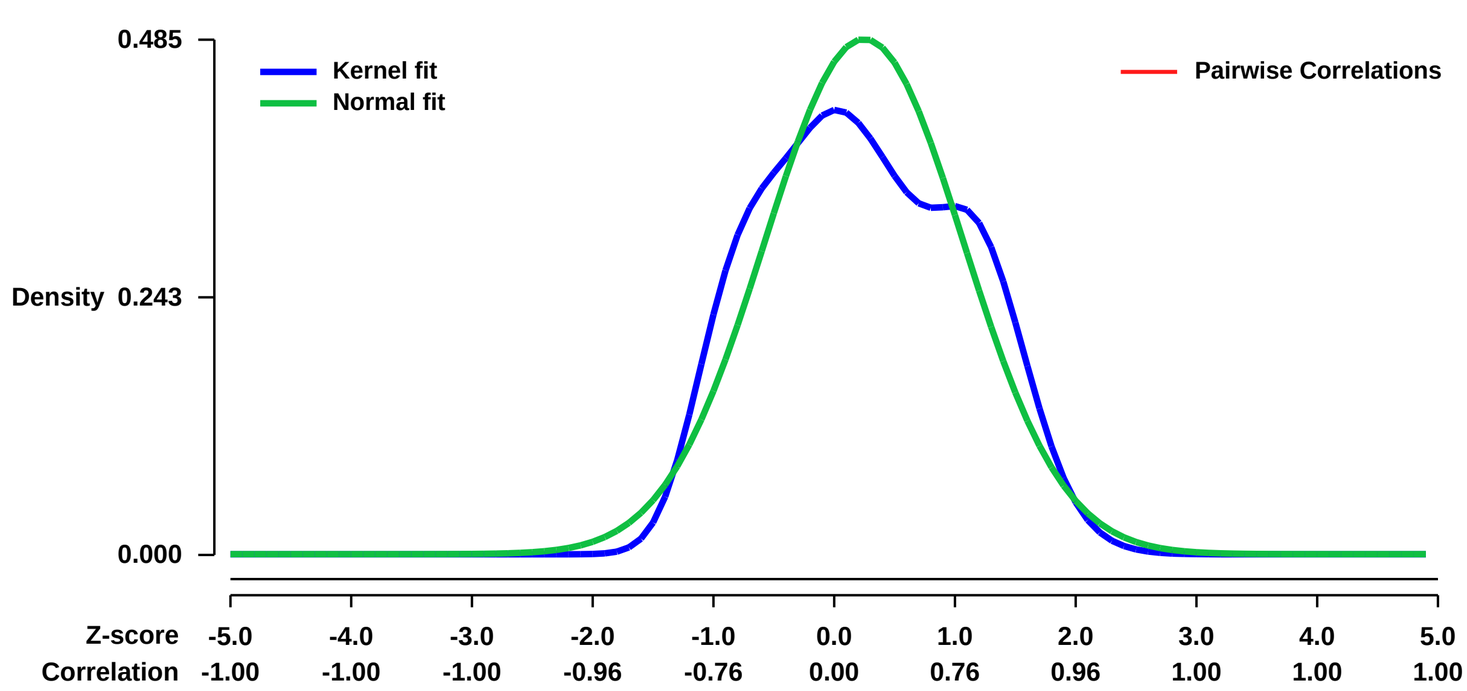

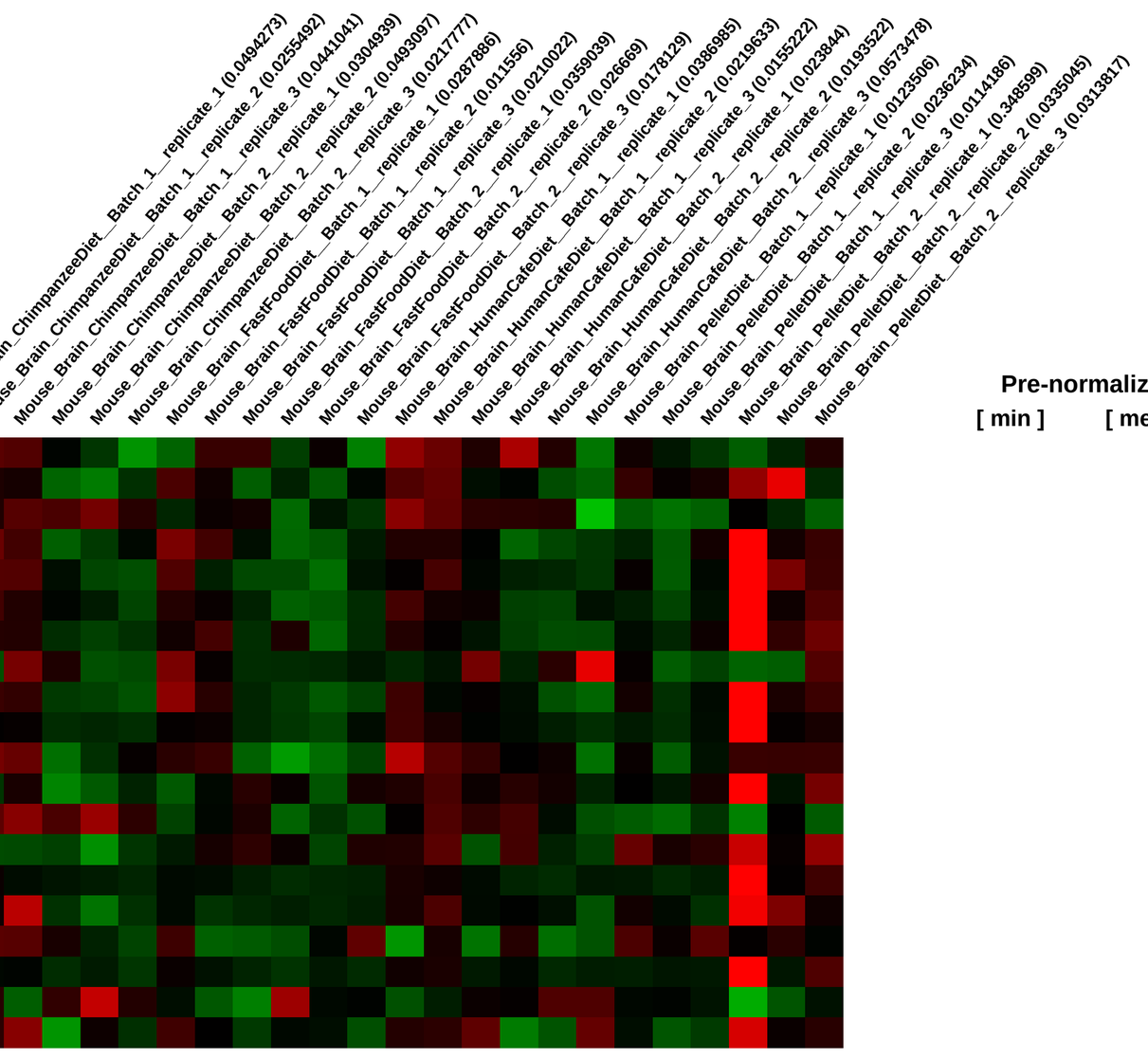

Pre-normalization Quantiles

[min] [medium] [max]

GEO Series "GSE6383" Expression Profiles

Num of samples in this series: 6

Scale of expression profile Z-scores

-3.0 -2.0 -1.0 0.0 1.0 2.0 3.0

GEO Link:	http://www.ncbi.nlm.nih.gov/geo/query/acc.cgi?acc=GSE6383
Status:	Public on Mar 12 2007
Title:	Mouse small intestine epithelium vs. mesenchyme
Organism:	Mus musculus
Experiment type:	Expression profiling by array
Platform:	GPL1261
Pubmed ID:	17299133
Summary & Design:	**Summary:** During organogenesis of the intestine, reciprocal crosstalk between the endodermally-derived epithelium and the underlying mesenchyme is required for regional patterning and proper differentiation. Though both of these tissue layers participate in patterning, the mesenchyme is thought to play a prominant role in the determination of epithelial phenotype during development and in adult life. However, the molecular basis of this instructional dominance is unclear. In fact, surprisingly little is known about the cellular origins of many of the critical signaling molecules and the gene transcriptional events that they impact. Here, we profile genes that are expressed in separated mesenchymal and epithelial compartments of the perinatal mouse intestine. The data indicate that the vast majority of soluble modulators of signaling pathways such as Hedgehog, Bmp, Wnt, Fgf and Igf are expressed predominantly or exclusively by the mesenchyme, accounting for its ability to dominate instructional crosstalk. We also catalog the most highly enriched transcription factors in both compartments and find evidence for a major role for Hnf4alpha and Hnf4 gamma in the regulation of epithelial genes. Finally, we find that while epithelially enriched genes tend to be highly tissue-restricted in their expression, mesenchymally-enriched genes tend to be broadly expressed in multiple tissues. Thus, the unique tissue-specific signature that characterizes the intestinal epithelium is instructed and supported by a mesenchyme that itself expresses genes that are largely non-tissue specific. **Keywords: comparative genomic hybridization: epithelium vs. mesenchyme** **Overall design:** Mouse small intestine (E18.5) is separated to epithelium and mesenchyme. Total RNA is extracted from epithelium and mesenchyme. There are 6 samples in this microarray experiment: 3 for epithelium and 3 for mesenchyme. Samples are hybridized the affymetrix Mouse Genome 430 2.0 Array. We compare the gene expression between epithelium and mesenchyme to study the gene expression profiles in these two compartments.

Background corr dist: KL-Divergence = 0.0057, L1-Distance = 0.0149, L2-Distance = 0.0002, Normal std = 0.9832

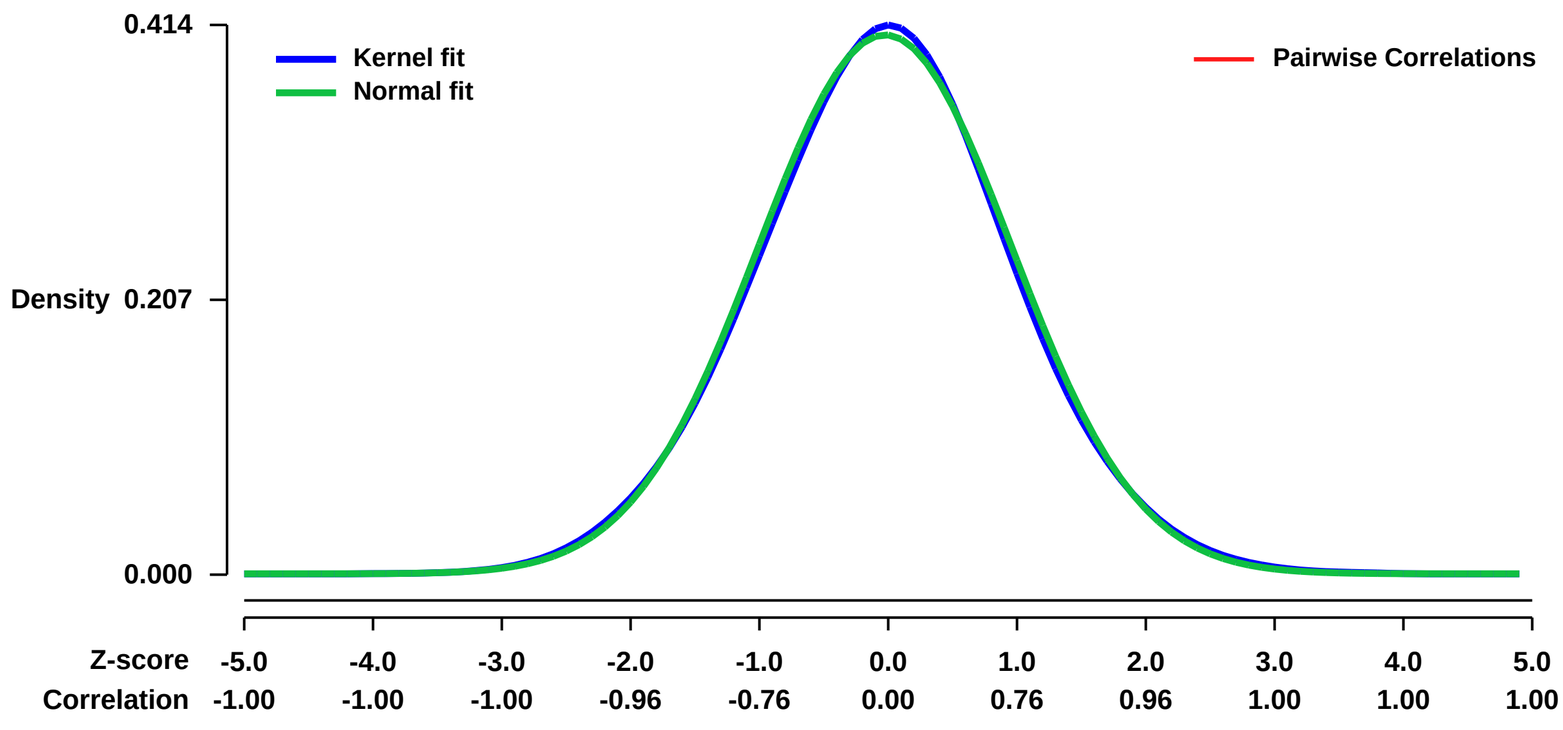

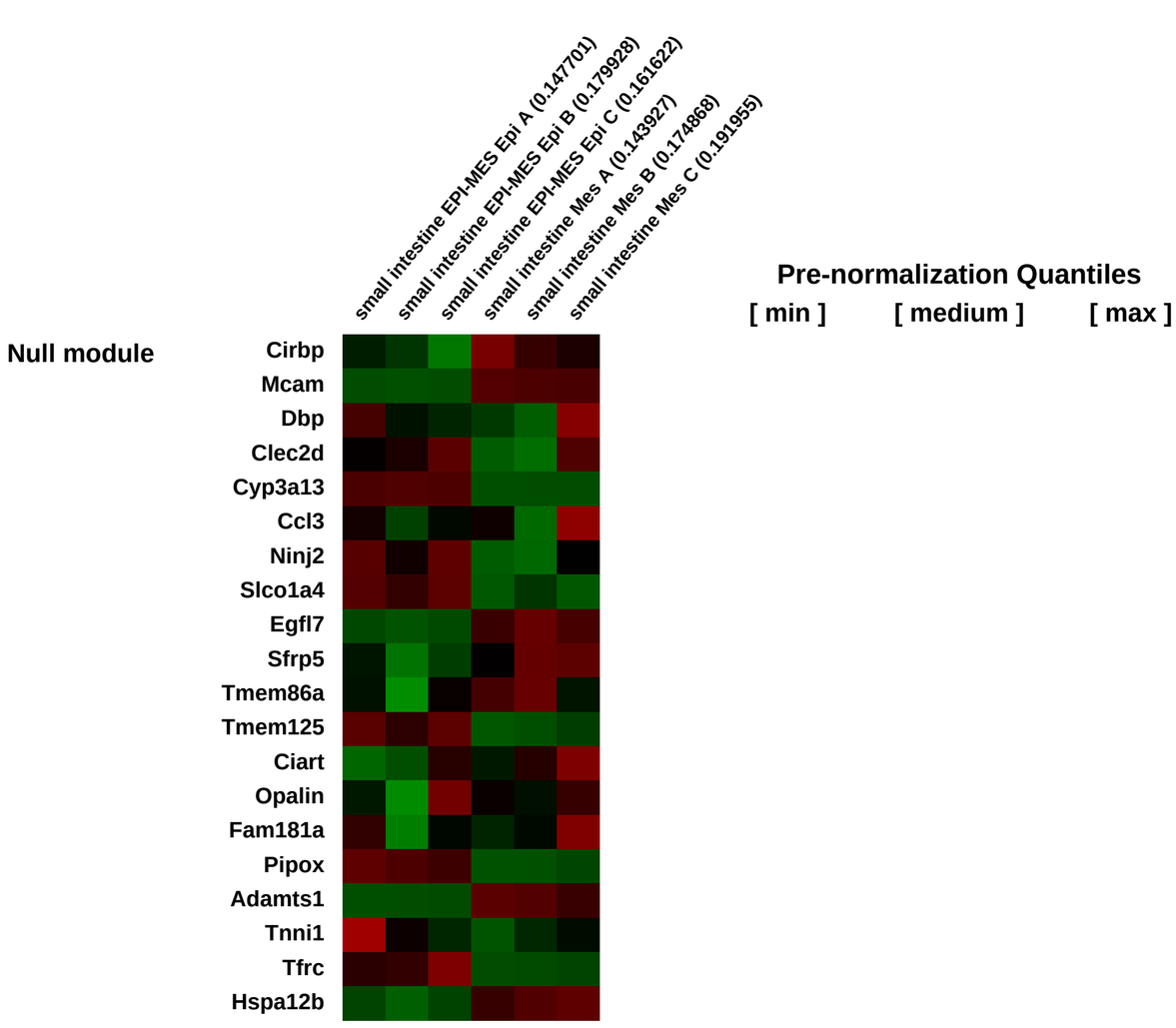

GEO Series "GSE6466" Expression Profiles

Num of samples in this series: 7

Scale of expression profile Z-scores

-3.0 -2.0 -1.0 0.0 1.0 2.0 3.0

GEO Link: http://www.ncbi.nlm.nih.gov/geo/query/acc.cgi?acc=GSE6466

Status: Public on Dec 08 2006

Title: Gene expression profiles of P1 and adult bladders isolated from SMGA (Actg2) transgenic mice. (GUDMAP Series ID: 11)

Organism: Mus musculus

Experiment type: Expression profiling by array

Platform: GPL1261

Pubmed ID:

Summary & Design:

Summary:
The long term objective is to create an encyclopedia of the expression levels of all genes in multiple components of the developing bladder. The central thesis is straightforward. The combination of microdissected and laser capture microdissection (LCM) plus microarray analysis offers a powerful, efficient and effective method for the creation of a global gene expression atlas of the developing urogenital system. Microarrays with essentially complete genome coverage can be used to quantitate expression levels of every gene. The ensuing rapid read-out provides an expression atlas that is more sensitive, more economical and more complete than would be possible by in situ hybridizations alone. The data submitted here represents the gene expression profiles of the adult and postnatal day 1 bladder.

Keywords: Gene expression comparison between postnatal day 1 and adult bladders

Overall design:
Bladders, from postnatal day 1 and adult transgenic mice in which EGFP is driven by a SMGA promoter/EGFP, were isolated by dissection and total RNA was extracted and underwent 2-round amplification (Epicentre´fi Biotechnologies) for gene expression analysis using the Affymetrix MOE430 microarray chip

Background corr dist: KL-Divergence = 0.0589, L1-Distance = 0.0444, L2-Distance = 0.0030, Normal std = 0.6024

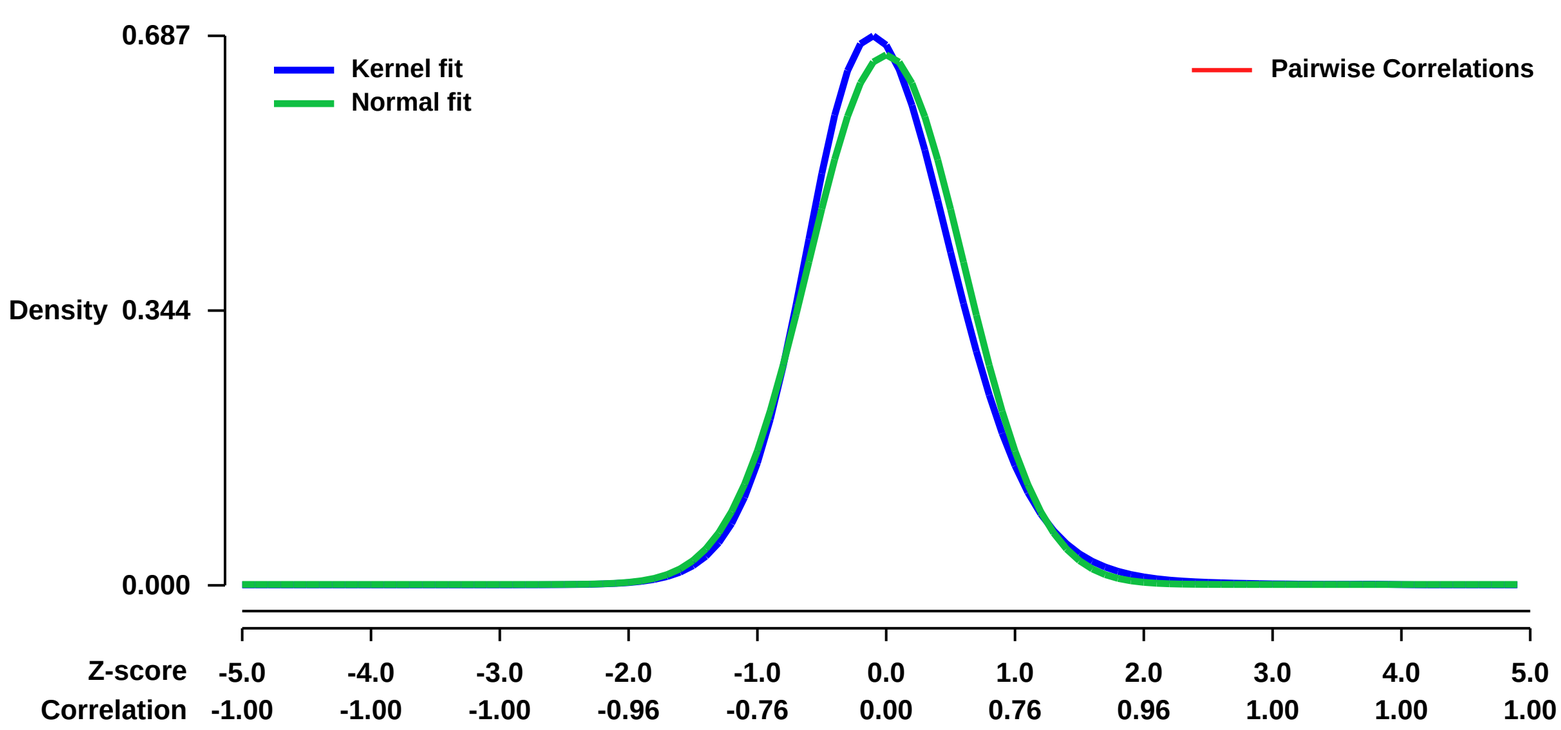

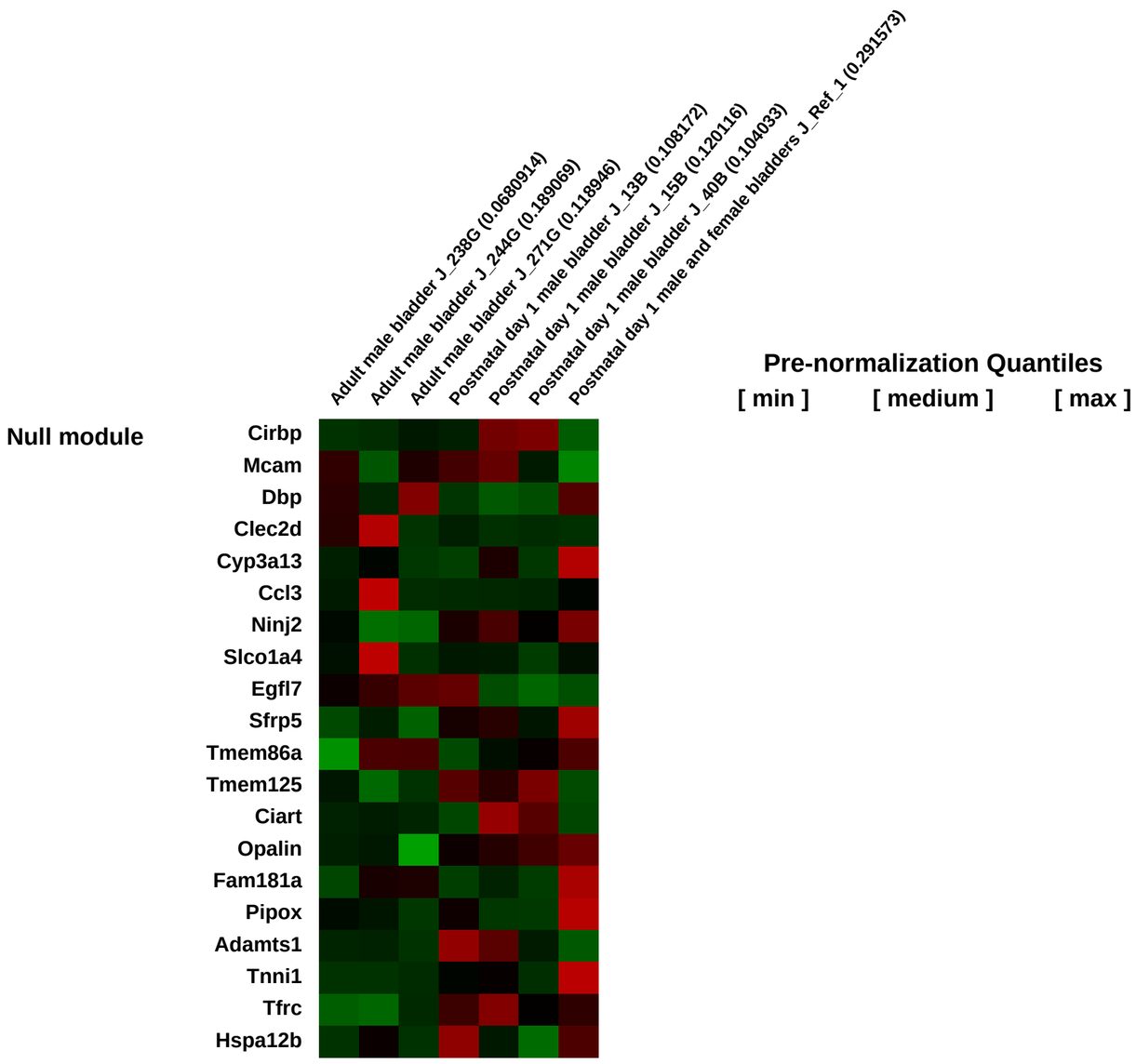

GEO Series "GSE6482" Expression Profiles

Num of samples in this series: 9

Scale of expression profile Z-scores

-3.0 -2.0 -1.0 0.0 1.0 2.0 3.0

GEO Link:	http://www.ncbi.nlm.nih.gov/geo/query/acc.cgi?acc=GSE6482
Status:	Public on Jan 01 2007
Title:	mECK36: a cell and animal model of virally induced Kaposi's sarcoma
Organism:	Mus musculus
Experiment type:	Expression profiling by array
Platform:	GPL1261
Pubmed ID:	17349582
Summary & Design:	**Summary:** Transfection of a Kaposi's sarcoma (KS) herpesvirus (KSHV) Bacterial Artificial Chromosome (KSHVBac36) into mouse bone marrow endothelial lineage cells generated a cell (mECK36) that induced KS-like tumors in mice. mECK36 formed KSHV-harboring vascularized spindle-cell sarcomas that were LANA+ and displayed a KSHV and host transcriptomes reminiscent of KS tumors. **Keywords: Cell type comparison** **Overall design:** There are three biological replicates per sample. Tumors (mKS) were compared the the human KS signature. mECK36 and mEC-V were compared to putative BM lineage cells.

Background corr dist: KL-Divergence = 0.0664, L1-Distance = 0.0251, L2-Distance = 0.0010, Normal std = 0.5172

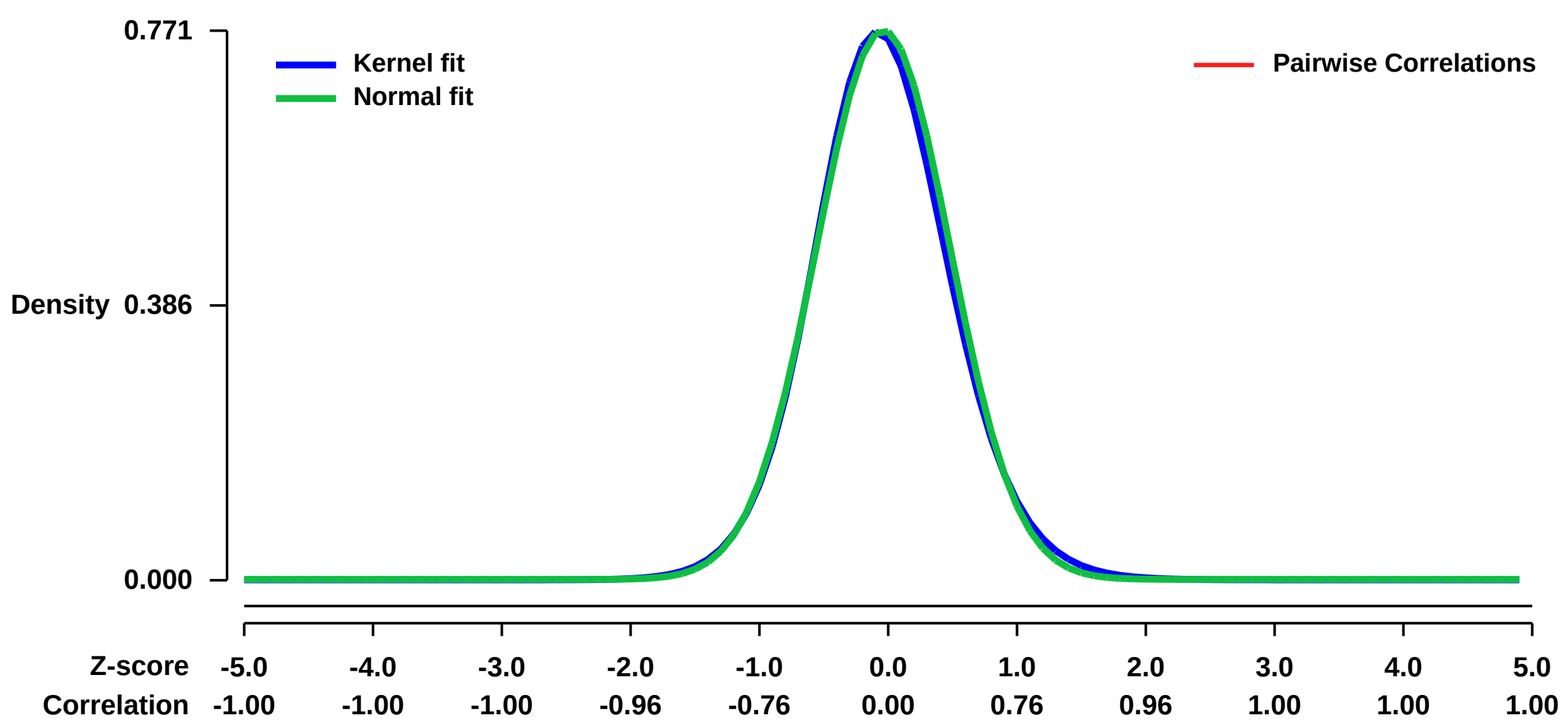

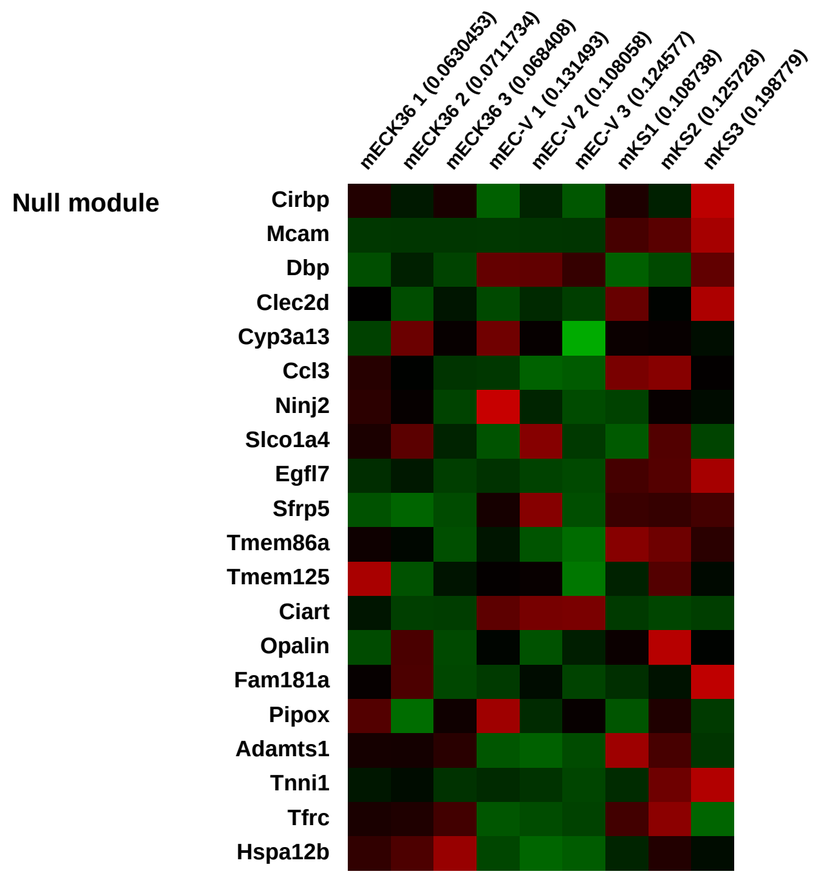

GEO Series "GSE6485" Expression Profiles

Num of samples in this series: 6

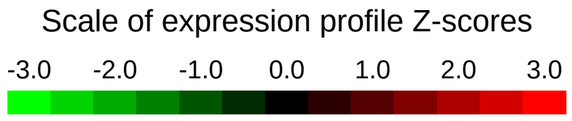

GEO Link:	http://www.ncbi.nlm.nih.gov/geo/query/acc.cgi?acc=GSE6485
Status:	Public on Dec 06 2007
Title:	Expression data from olfactory epithelium of Harlequin mutant mice compared to littermate controls
Organism:	Mus musculus
Experiment type:	Expression profiling by array
Platform:	GPL1261
Pubmed ID:	17868149
Summary & Design:	**Summary:** Microarray analysis of gene expression in the olfactory epithelium of Harlequin mouse as a model of oxidative-stress induced neurodegeneration of olfactory sensory neurons **Keywords: comparison of gene expression level in unperturbed tissue of mutant vs. control mouse** **Overall design:** Olfactory epithelium from Harlequin mutant mice and littermate control mice was microdissected for RNA extraction and hybridization on Affymetrix microarrays. We compared levels of gene expression in 6-month old mice to begin to identify mechanisms of oxidative-stress induced neurodegeneration and to correlate the cellular changes that we observed in the olfactory epithelium by using histology and immunohistochemistry with gene expression changes.

Background corr dist: KL-Divergence = 0.0482, L1-Distance = 0.0186, L2-Distance = 0.0004, Normal std = 0.5794

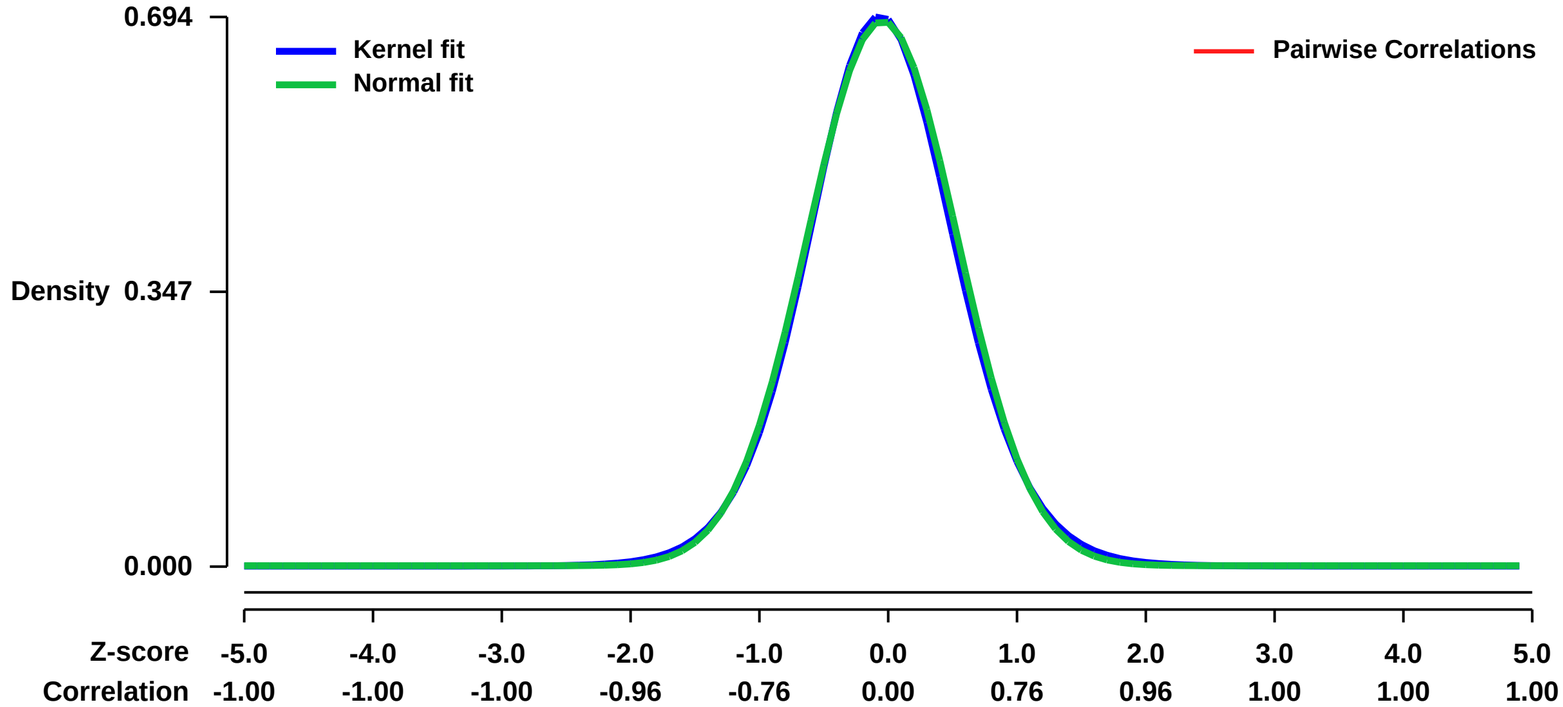

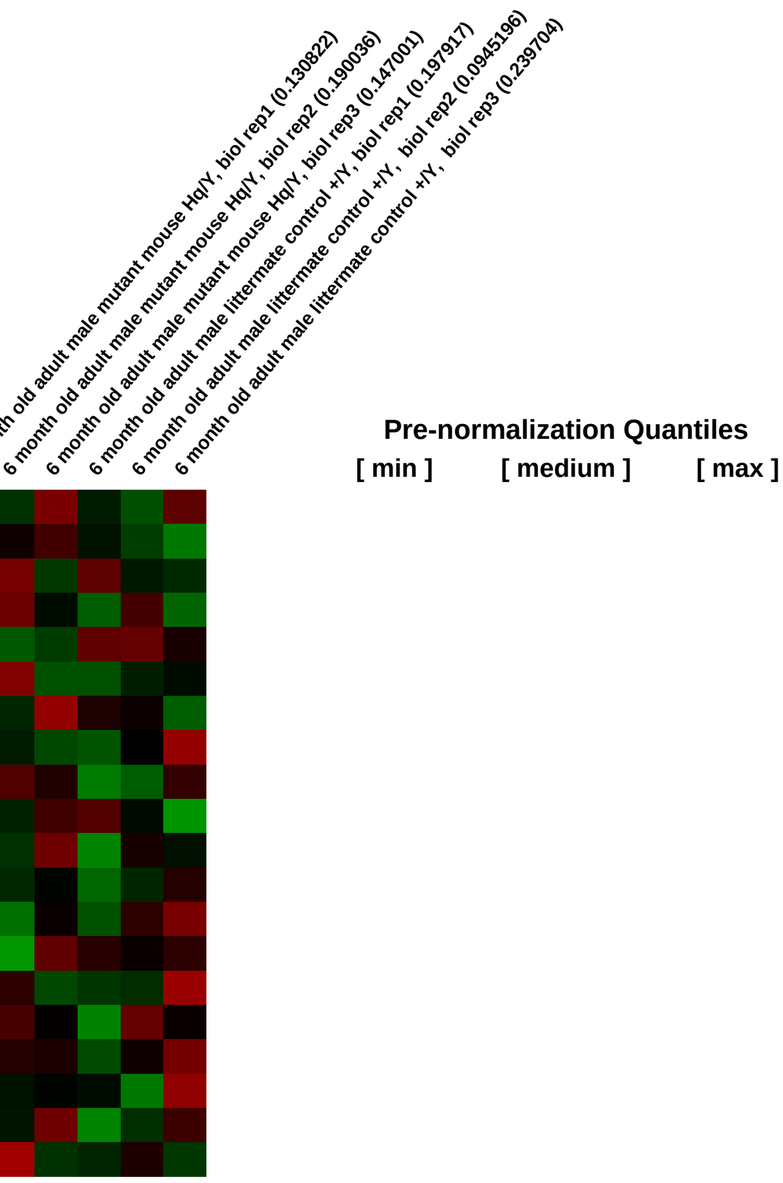

GEO Series "GSE6487" Expression Profiles

Num of samples in this series: 30

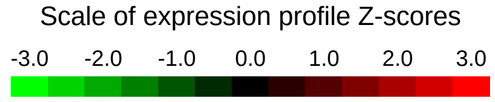

GEO Link:	http://www.ncbi.nlm.nih.gov/geo/query/acc.cgi?acc=GSE6487
Status:	Public on Dec 13 2006
Title:	Myogenesis MyoD
Organism:	Mus musculus
Experiment type:	Expression profiling by array
Platform:	GPL1261
Pubmed ID:	17965412
Summary & Design:	**Summary:** The transcription factor MyoD can coax na?e fibroblasts or otherwise committed cells to adopt the skeletal muscle phenotype by activating the muscle gene expression program. Activation of muscle gene expression occurs in quantal steps with not all the target genes of MyoD being activated at the same time. Some genes are induced in the initial phases, others at later stages despite the fact that MyoD is present throughout the differentiation process. MyoD is post-translationally modified by phosphorylation, ubiquitination, and acetylation. Here, we have employed a model system in which MyoD and its non-acetylatable version were inducibly expressed in mouse embryonic fibroblasts derived from mice to investigate how MyoD acetylation may contribute to differential gene activation. **Keywords: Time-Series** **Overall design:** Mouse embryos fibroblasts (MEFs) obtained from MyoD-/-/Myf5-/- animals will be transduced with retroviruses expressing a estrogen receptor hormone binding domain fused to either mouse MyoD wild type (ER-MyoD wt) or MyoD bearing three point mutations at lysine residues 99, 102, and 104 that render it no longer acetylatable (ER-MyoD RRR). A retrovirus without the ER-MyoD insert was also employed as negative control.</p> Aim 2. We will compare genome-wide expression profiling of MEFs transduced with either ER-MyoD wt or ER-MyoD RRR cultured in the presence of a medium that promotes skeletal muscle differentiation (DM) supplemented with beta-estradiol for 0, 6, 12, and 24 hours, respectively.

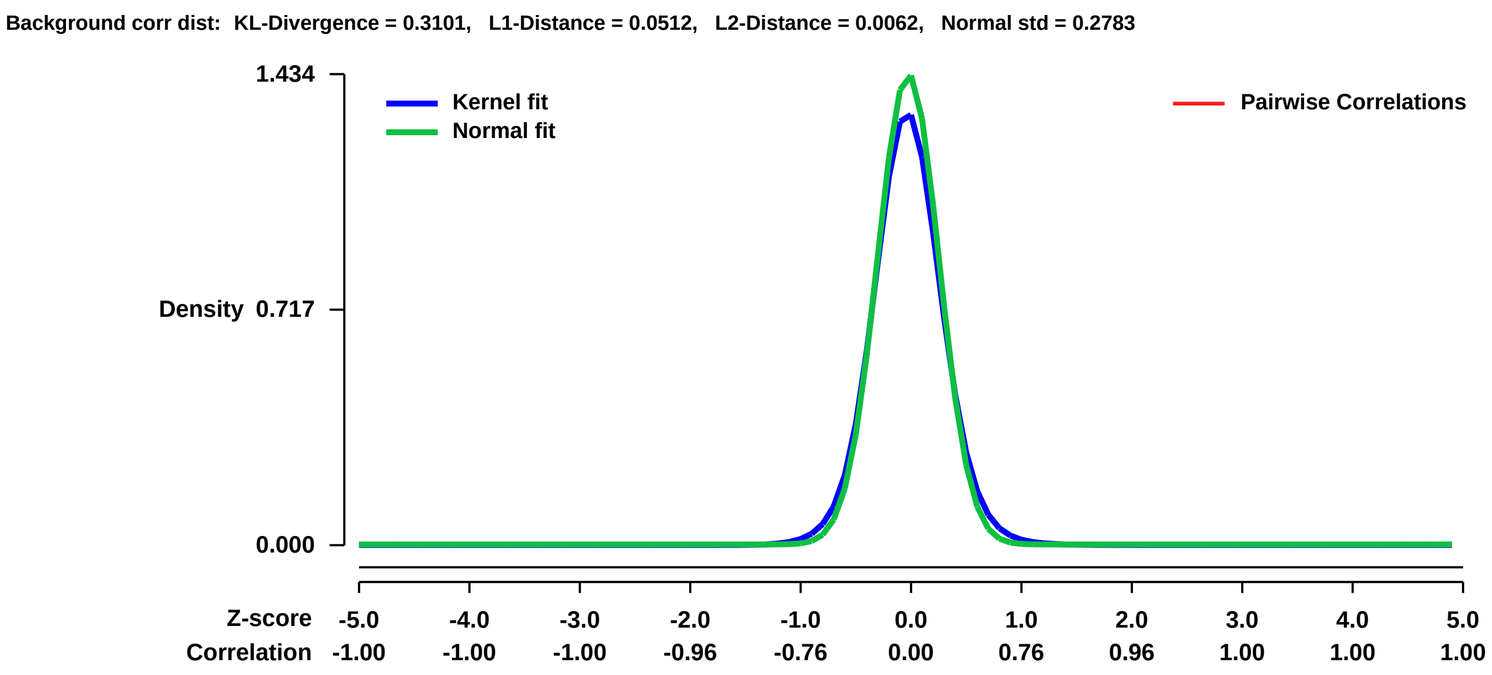

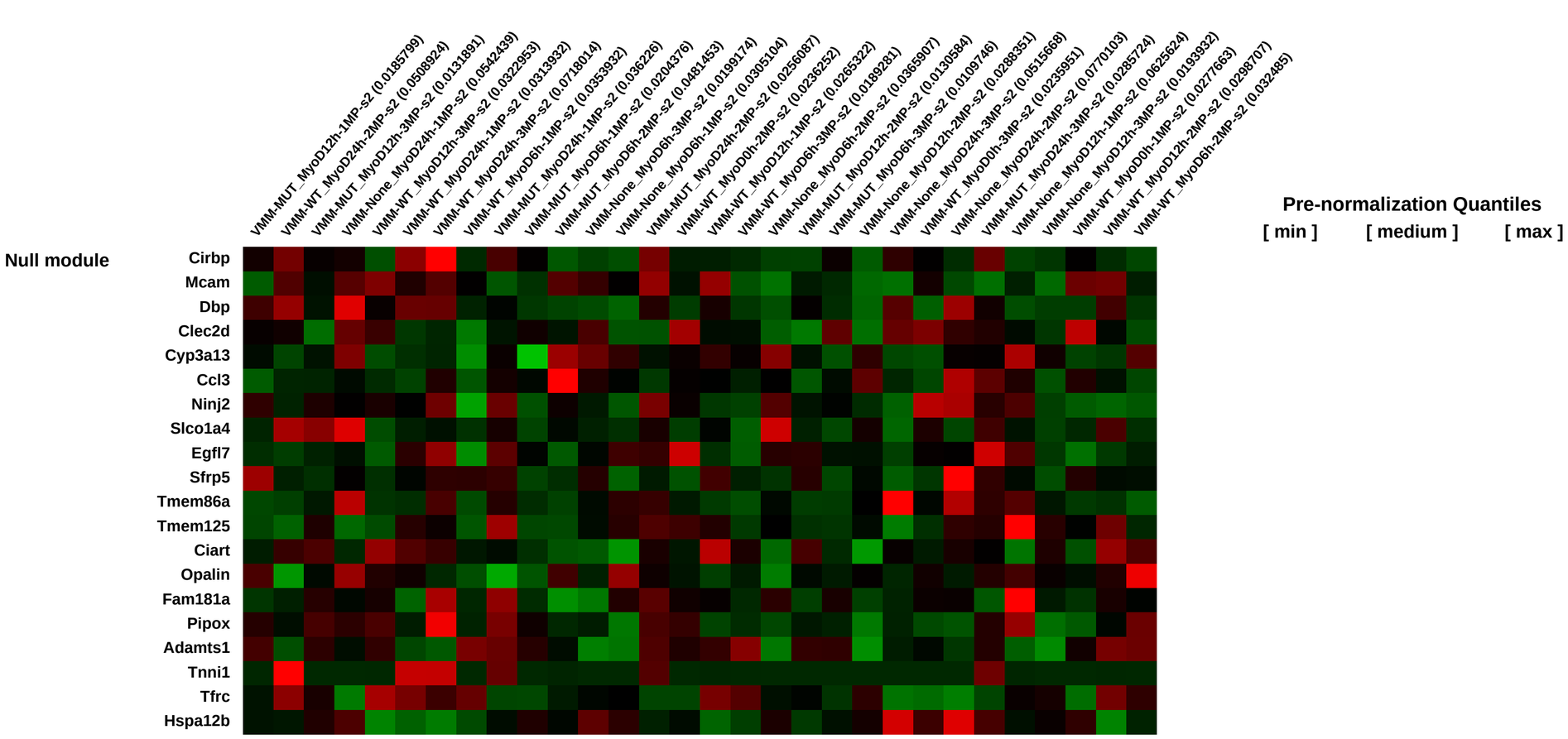

GEO Series "GSE6514" Expression Profiles

Num of samples in this series: 90

Scale of expression profile Z-scores

-3.0 -2.0 -1.0 0.0 1.0 2.0 3.0

GEO Link:	http://www.ncbi.nlm.nih.gov/geo/query/acc.cgi?acc=GSE6514
Status:	Public on Feb 11 2007
Title:	Gene expression in the mouse brain during spontaneous sleep and prolonged wakefulness
Organism:	Mus musculus
Experiment type:	Expression profiling by array
Platform:	GPL1261
Pubmed ID:	17698924
Summary & Design:	**Summary:** These studies address temporal changes in gene expression during spontaneous sleep and extended wakefulness in the mouse cerebral cortex, a neuronal target for processes that control sleep; and the hypothalamus, an important site of sleep regulatory processes. We determined these changes by comparing expression in sleeping animals sacrificed at different times during the lights on period, to that in animals sleep deprived and sacrificed at the same diurnal time. **Keywords:** gene expression, temporal changes, brain, behavior, sleep, **Overall design:** Experiments were performed on male mice (C57/BL6), 10 weeks of age ´–1 week. Animals were housed in a light/dark cycle of 12 hrs, in a pathogen free, temperature- and humidity-controlled room (22´°C and 45-55%, respectively) with water available ad libitum. Food was accessible for 12 hrs only during the active period. Animals were subjected to 14 days of acclimatization during which a nighttime feeding pattern was established. This was done to avoid differential food intake between mice that were subsequently sleep deprived during the lights on period and those allowed to sleep. Mice were sacrificed following 3, 6, 9 and 12 hrs of total sleep deprivation (n=5 at each time point). Deprivation was initiated at lights-on, and performed through gentle handling. Sleeping animals, which were left undisturbed, were sacrificed at the same diurnal time points as sleep deprived mice (n=5 at each time point). An additional control group of mice were sacrificed at time zero, i.e., at the time of lights-on (n=5). All mice were behaviorally monitored using the AccuScan infrared monitoring system that detects movement when the mouse crosses electronic beams (Columbus Instruments). Mice were sacrificed by cervical dislocation. Brain sectioning was performed according to the mouse brain atlas of Franklin and Paxinos . The primary and secondary motor areas (M1 and M2) of the cerebral cortex and broadly defined regions and zones of the hypothalamus were sampled. RNA was isolated with Trizol (Invitrogen) and further purified using RNeasy columns (Qiagen) as per the manufacturer's instructions.

Background corr dist: KL-Divergence = 0.4027, L1-Distance = 0.0528, L2-Distance = 0.0064, Normal std = 0.2506

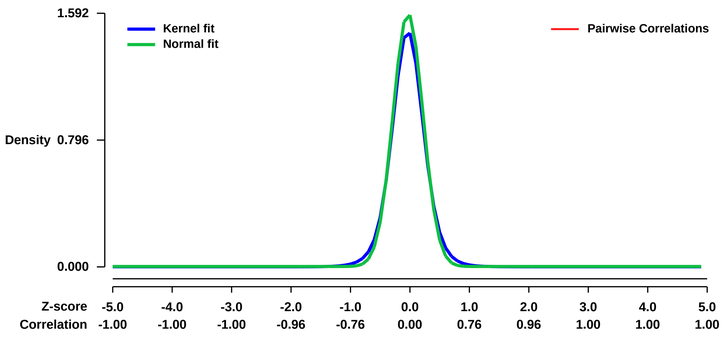

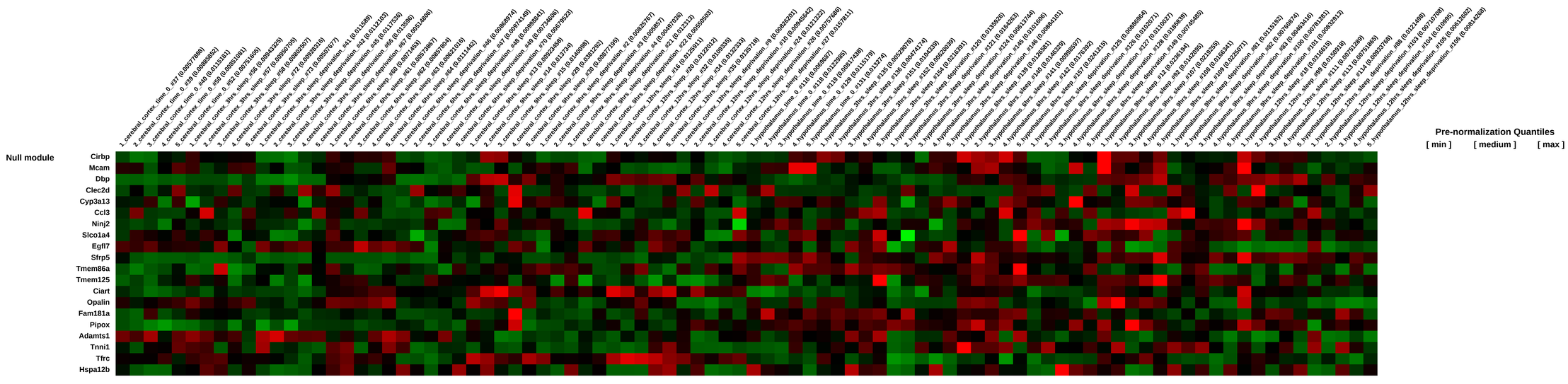

GEO Series "GSE6526" Expression Profiles

Num of samples in this series: 16

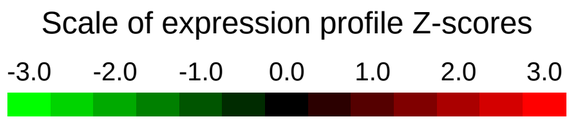

GEO Link:	http://www.ncbi.nlm.nih.gov/geo/query/acc.cgi?acc=GSE6526
Status:	Public on Mar 01 2007
Title:	Expression time course data HEY2 KO and WT MASMC treated with PDGF
Organism:	Mus musculus
Experiment type:	Expression profiling by array
Platform:	GPL1261
Pubmed ID:	17327490
Summary & Design:	**Summary:** **The cardiovascular restricted transcription factor CHF1/Hey2 has been previously shown to regulate the smooth muscle response to growth factors. To determine how CHF1/Hey2 affects the smooth muscle response to growth factors, we performed a genomic screen for transcripts that are differentially expressed in wild type and knockout smooth muscle cells after stimulation with platelet derived growth factor.** **We screened 45101 probes representing more than 39,000 transcripts derived from at least 34,000 genes, at eight different time points. We analyzed the expression data utilizing an algorithm based on Bayesian statistics to derive the best polynomial clustering model to fit the expression data. We found that in a total of 9827 transcripts the normalized ratio of knockout to wild type expression diverged more than 3 fold from baseline in at least one time point, and these transcripts separated into 17 distinct clusters. Further analysis of each cluster revealed distinct alterations in gene expression patterns for immediate early genes, transcription factors, matrix metalloproteinases, signaling molecules and other molecules important in vascular biology.** **Keywords: time course** **Overall design:** **WT and Hey2 knockout mouse aortic smooth muscle cells were treated in parallel with PDGF and harvested at successive time points for RNA extraction and hybridization on Affymetrix microarrays. We sought to identify differentially expressed transcripts through Bayesian statistical methods that would explain the differential response to PDGF observed in vitro.**

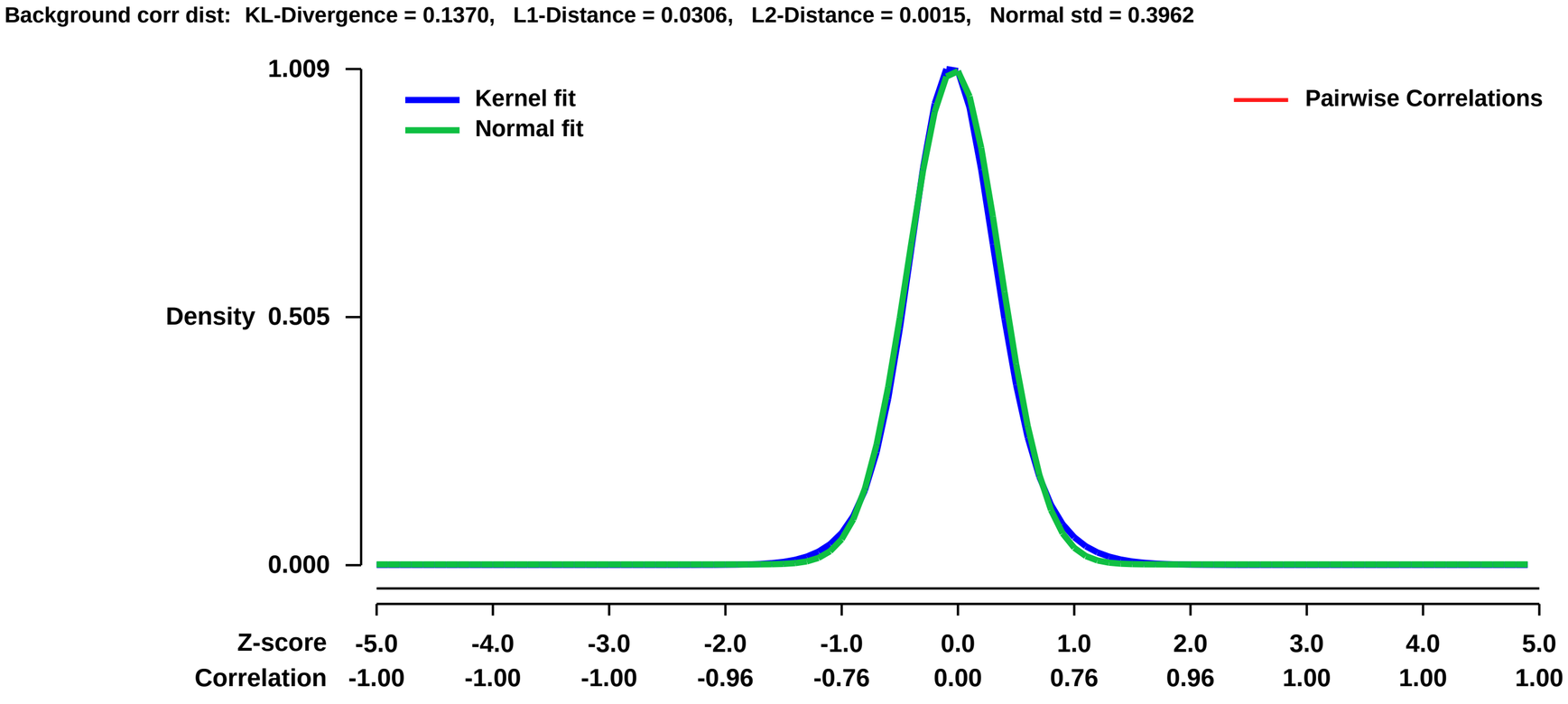

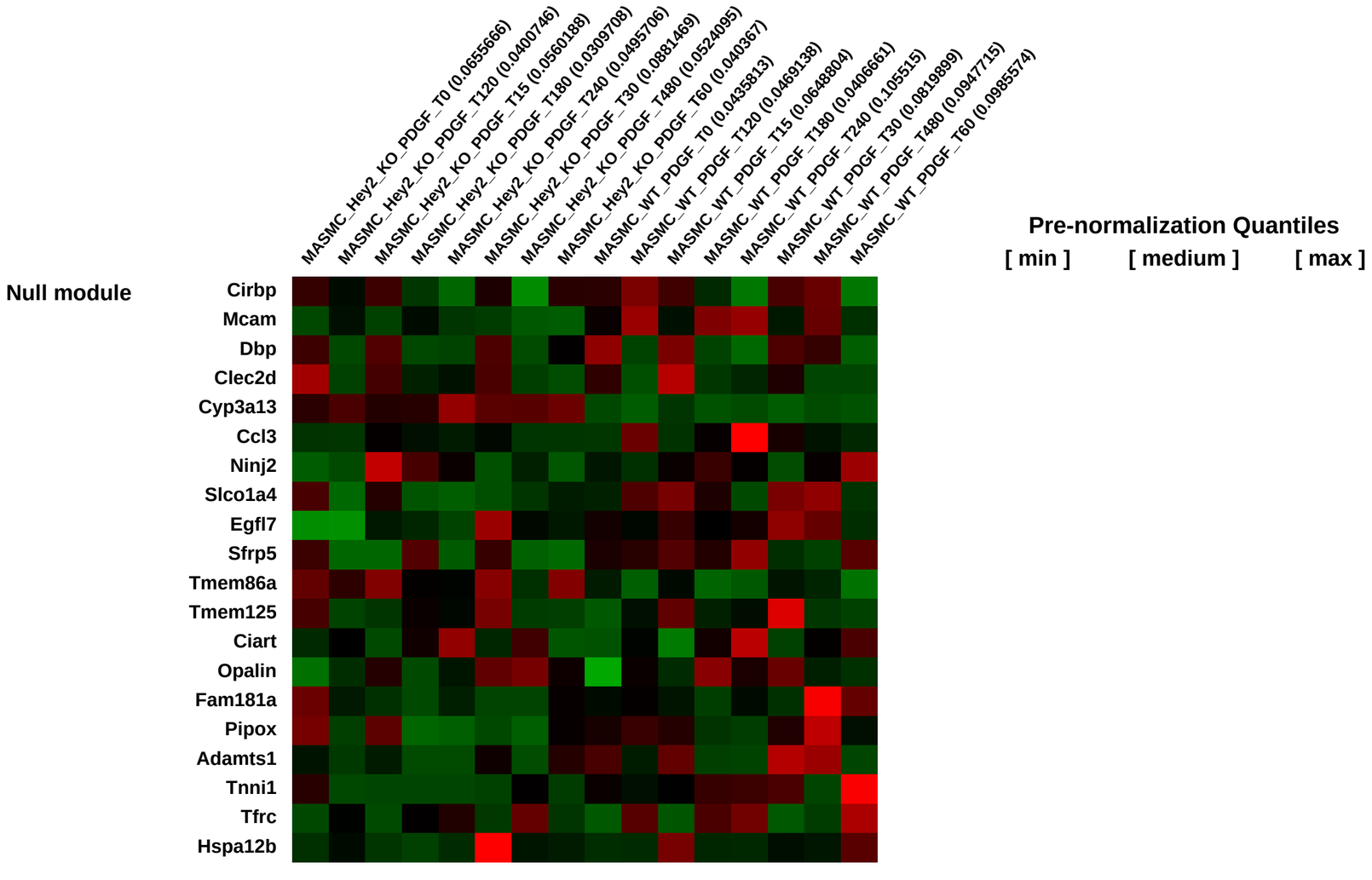

GEO Series "GSE6540" Expression Profiles

Num of samples in this series: 12

Scale of expression profile Z-scores

-3.0 -2.0 -1.0 0.0 1.0 2.0 3.0

GEO Link:	http://www.ncbi.nlm.nih.gov/geo/query/acc.cgi?acc=GSE6540
Status:	Public on Dec 14 2007
Title:	Expression data from olfactory epithelium of Lip-C-treated mice compared to Lip-O-treated control mice
Organism:	Mus musculus
Experiment type:	Expression profiling by array
Platform:	GPL1261
Pubmed ID:	17848607
Summary & Design:	**Summary:** Microarray analysis of gene expression in the olfactory epithelium of macrophage depleted mice to study the role of macrophages in regulating neurodegeneration, neuroprotection, and neurogenesis of olfactory sensory neurons **Keywords: comparison of gene expression level in sham and 48 hr OBX Lip-O mice versus Lip-C mice** **Overall design:** Olfactory epithelium from LIp-C-treated and Lip-O-treated mice was microdissected for RNA extraction and hybridization on Affymetrix microarrays. We compared levels of gene expression in macrophage-depleted and non-depleted sham and 48 hr OBX mice using a 2x2 ANOVA and pairwise comparisons to identify molecular mechanisms of macrophage-mediated neurodegeneration, neuroprotection, and neurogenesis and to validate the gene expression patterns using real-time RT-PCR and immunohistochemistry

Background corr dist: KL-Divergence = 0.1195, L1-Distance = 0.0264, L2-Distance = 0.0010, Normal std = 0.4100

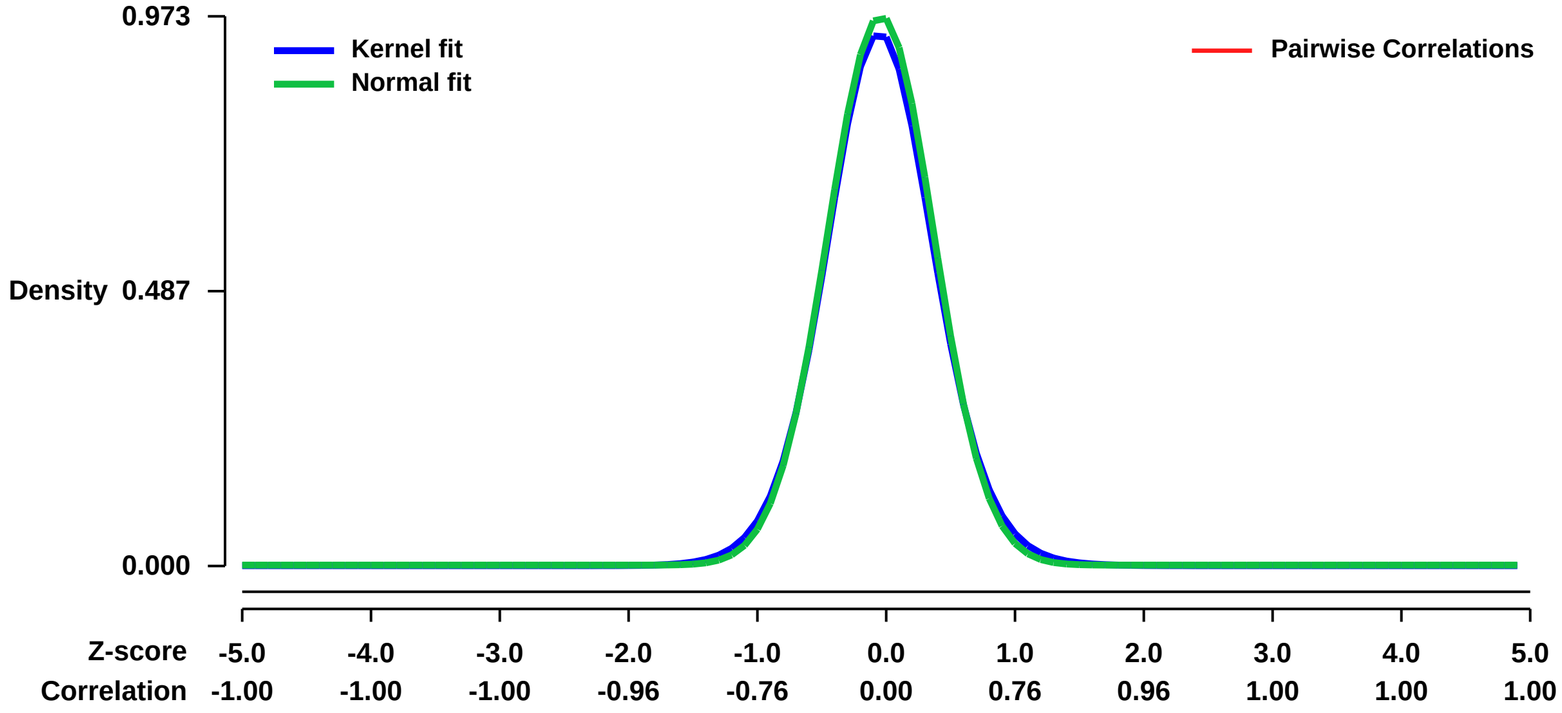

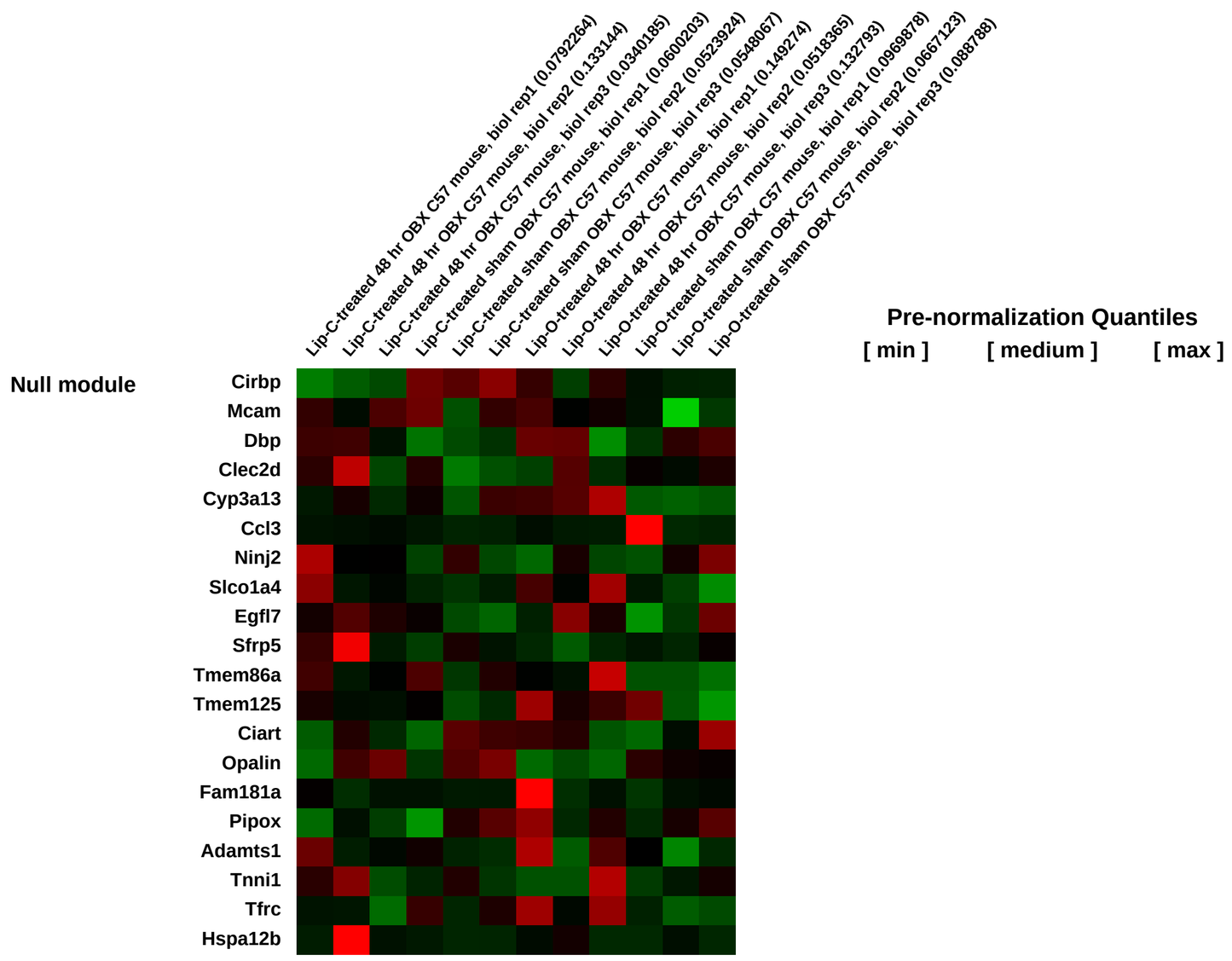

GEO Series "GSE6591" Expression Profiles

Num of samples in this series: 15

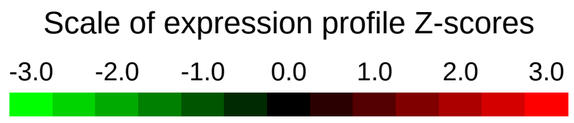

GEO Link:	**http://www.ncbi.nlm.nih.gov/geo/query/acc.cgi?acc=GSE6591**
Status:	**Public on Aug 31 2007**
Title:	**Comparative analysis of gene expression in C57BL/6J and DBA/2J aging lungs.**
Organism:	**Mus musculus**
Experiment type:	**Expression profiling by array**
Platform:	**GPL1261**
Pubmed ID:	**17726092**
Summary & Design:	**Summary:** **We hypothesize that gene expression in the aging lungs of these two strains of mice are divergent thus contributing to the disparity in the phenotypes. More specifically, (1) Aging DBA/2J mice compared to aging C57BL/6 mice are known to be accelerated in their lung physiology and morphometry; (2) C57BL/6J are known to have longer natural longevity than DBA/2J mice. In order to test these hypotheses at the gene expression level, we utilized microarray analysis to examine transcriptional differences between aging lungs of both strains of mice.** **Keywords: comparative expression profiling** **Overall design:** **This study utilizes microarray analysis to test these hypotheses. Three sets of lungs were harvested from both strains at each time point (C57BL/6J: 2, 18, AND 26 mos; DBA/2J: 2 and 18 mos). RNA was isolated and used for global gene expression profiling (Affymetrix Mouse 430 2.0 array). Statistically significant gene expression was determined as a minimum 6 counts of 9 pairwise comparisons, minimum 1.5-fold change, and p < 0.05. Further, Absolute | FC - FC SEM | >= 1.5.**

Background corr dist: KL-Divergence = 0.1652, L1-Distance = 0.0405, L2-Distance = 0.0034, Normal std = 0.3584

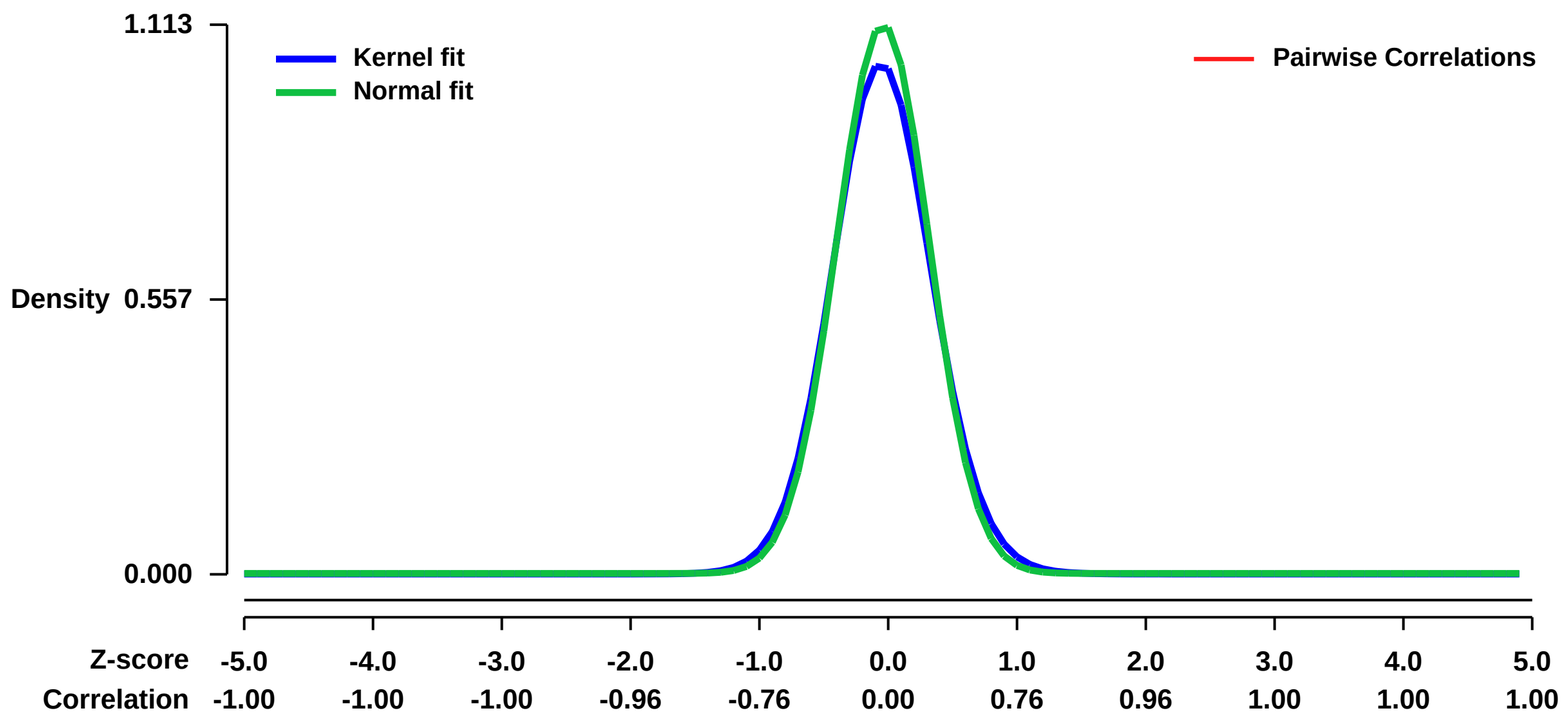

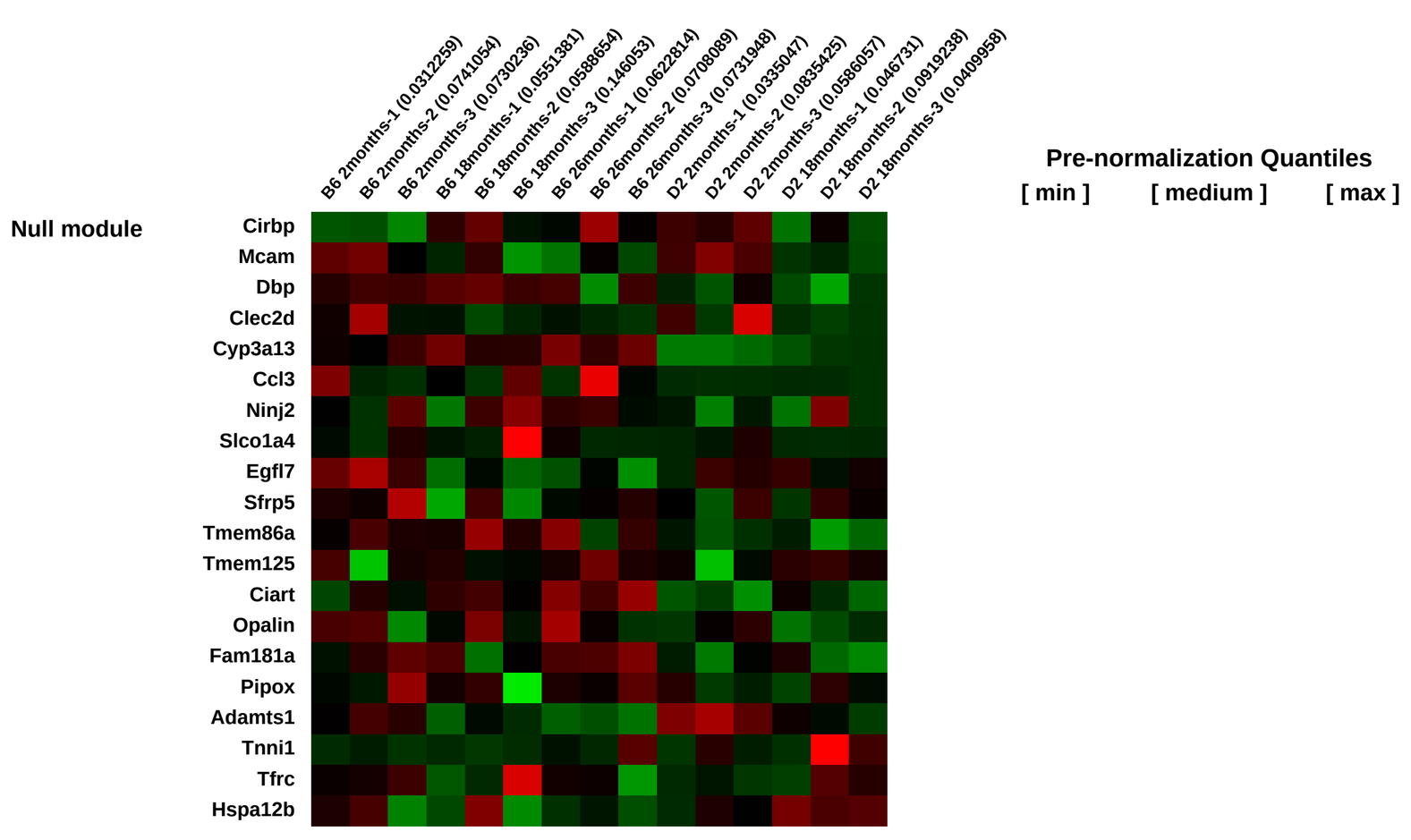

GEO Series "GSE6632" Expression Profiles

Num of samples in this series: 6

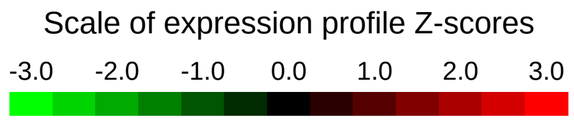

GEO Link:	http://www.ncbi.nlm.nih.gov/geo/query/acc.cgi?acc=GSE6632
Status:	Public on Oct 06 2007
Title:	Hepatocellular carcinoma follows loss of liver-gender specificity in mice
Organism:	Mus musculus
Experiment type:	Expression profiling by array
Platform:	GPL1261
Pubmed ID:	18089782
Summary & Design:	**Summary:** We are investigating hepatic transcriptional responses associated with castration and tumorigenic hepatitis induced by Helicobacter hepaticus infection in mature male A/JCr mice Microarray data demonstrated a global loss of gender-dimorphic gene expression regulation in mice with chronic hepatitis and liver cancer Keywords: dose **Overall design:** Male A/JCr mice were inoculated with H. hepaticus or vehicle at 4 weeks; some underwent castration at 1 year, and all were necropsied at 21 months

Background corr dist: KL-Divergence = 0.0381, L1-Distance = 0.0232, L2-Distance = 0.0006, Normal std = 0.6377

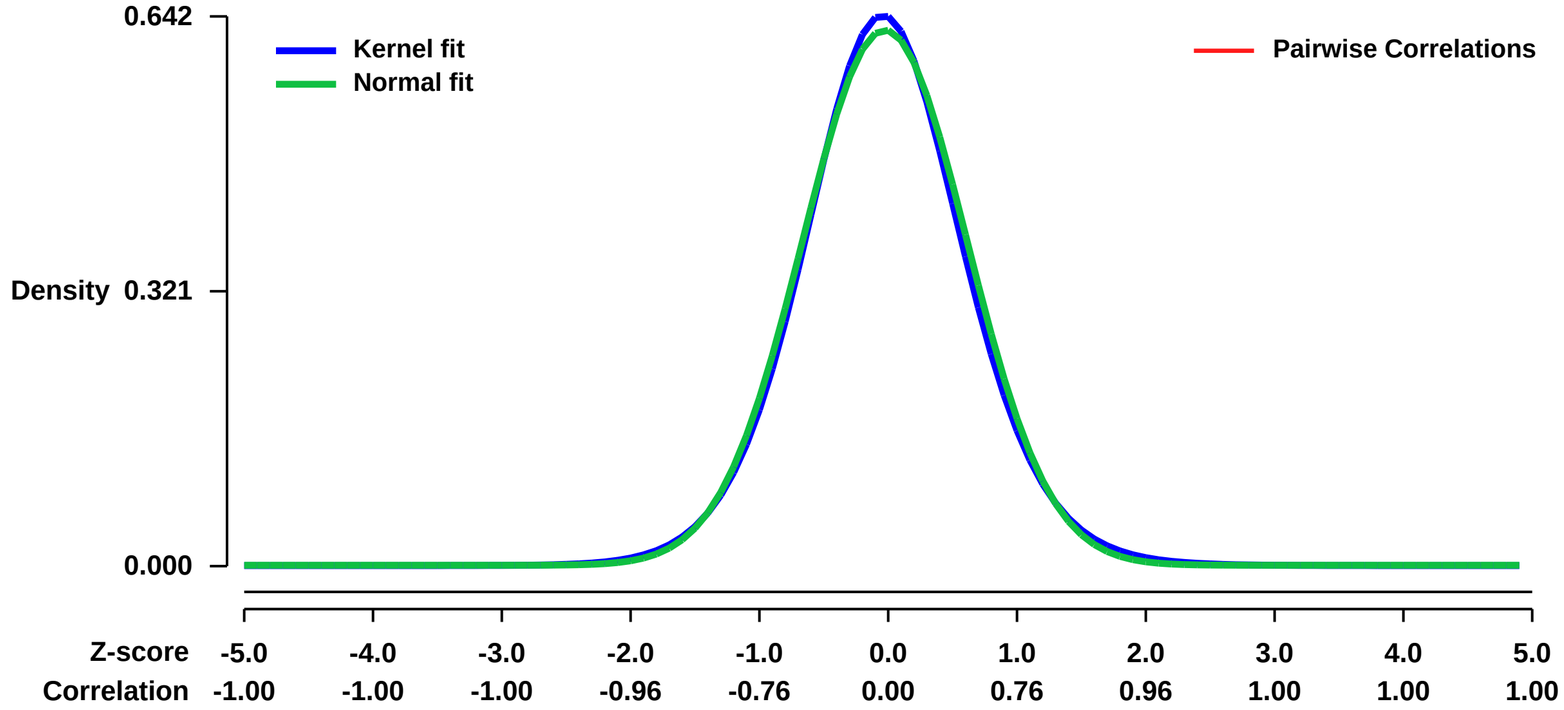

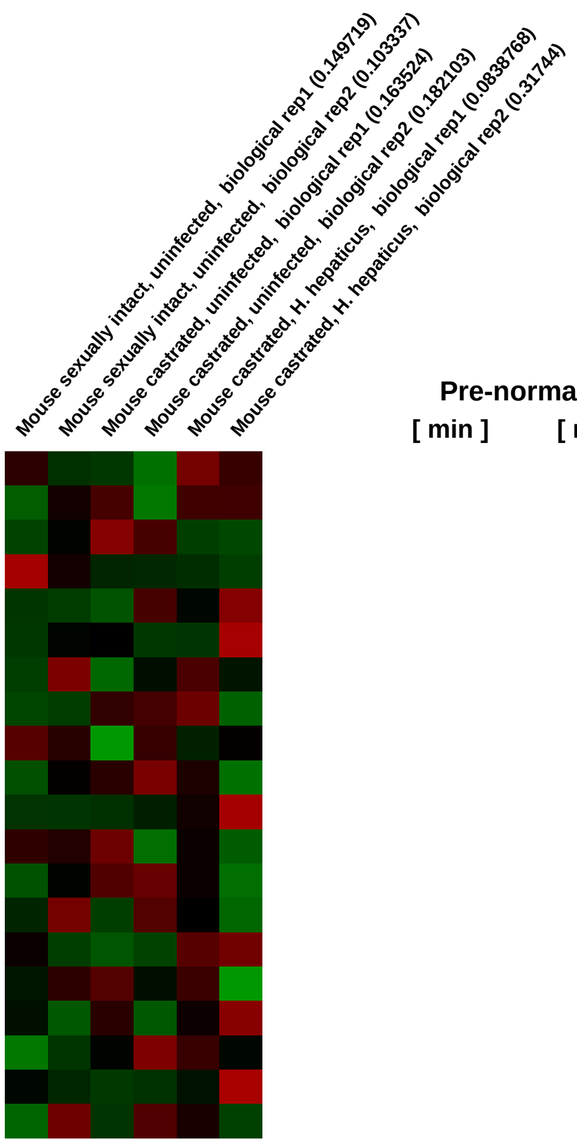

GEO Series "GSE6674" Expression Profiles

Num of samples in this series: 15

Scale of expression profile Z-scores

-3.0 -2.0 -1.0 0.0 1.0 2.0 3.0

GEO Link:	**http://www.ncbi.nlm.nih.gov/geo/query/acc.cgi?acc=GSE6674**
Status:	**Public on Dec 01 2007**
Title:	**Gene expression program of AM-14 B cells stimulated through the B cell receptor (BCR) and/or Toll-like receptors (TLR)**
Organism:	**Mus musculus**
Experiment type:	**Expression profiling by array**
Platform:	**GPL1261**
Pubmed ID:	**18025183**
Summary & Design:	**Summary:** **We have previously shown that rheumatoid factors (RF) produced by Fas-deficient autoimmune-prone mice typically bind autologous IgG2a with remarkably low affinity. Nevertheless, B cells representative of this RF population proliferate vigorously in response IgG2a/chromatin immune complexes through a mechanism dependent on the sequential engagement of the BCR and Toll-like receptor 9 (TLR9). To more precisely address the role of both receptors in this response, we analyzed the signaling pathways activated in AM14 B cells stimulated with these complexes. We found that the BCR not only serves to direct the chromatin complex to an internal compartment where it can engage TLR9 but also transmits a suboptimal signal that in combination with the signals emanating from TLR9 leads to NF?B activation and proliferation. Importantly, engagement of both receptors leads to the upregulation of a group of gene products, not induced by the BCR or TLR9 alone, that include IL-2. These data indicate that autoreactive B cells, stimulated by a combination of BCR and TLR9 ligands, acquire functional properties that may contribute to the activation of additional cells involved in the autoimmune disease process.** **Keywords: cell stimulation** **Overall design:** **15 Samples, 3 replicates for each treatment**

Background corr dist: KL-Divergence = 0.1169, L1-Distance = 0.0268, L2-Distance = 0.0011, Normal std = 0.4129

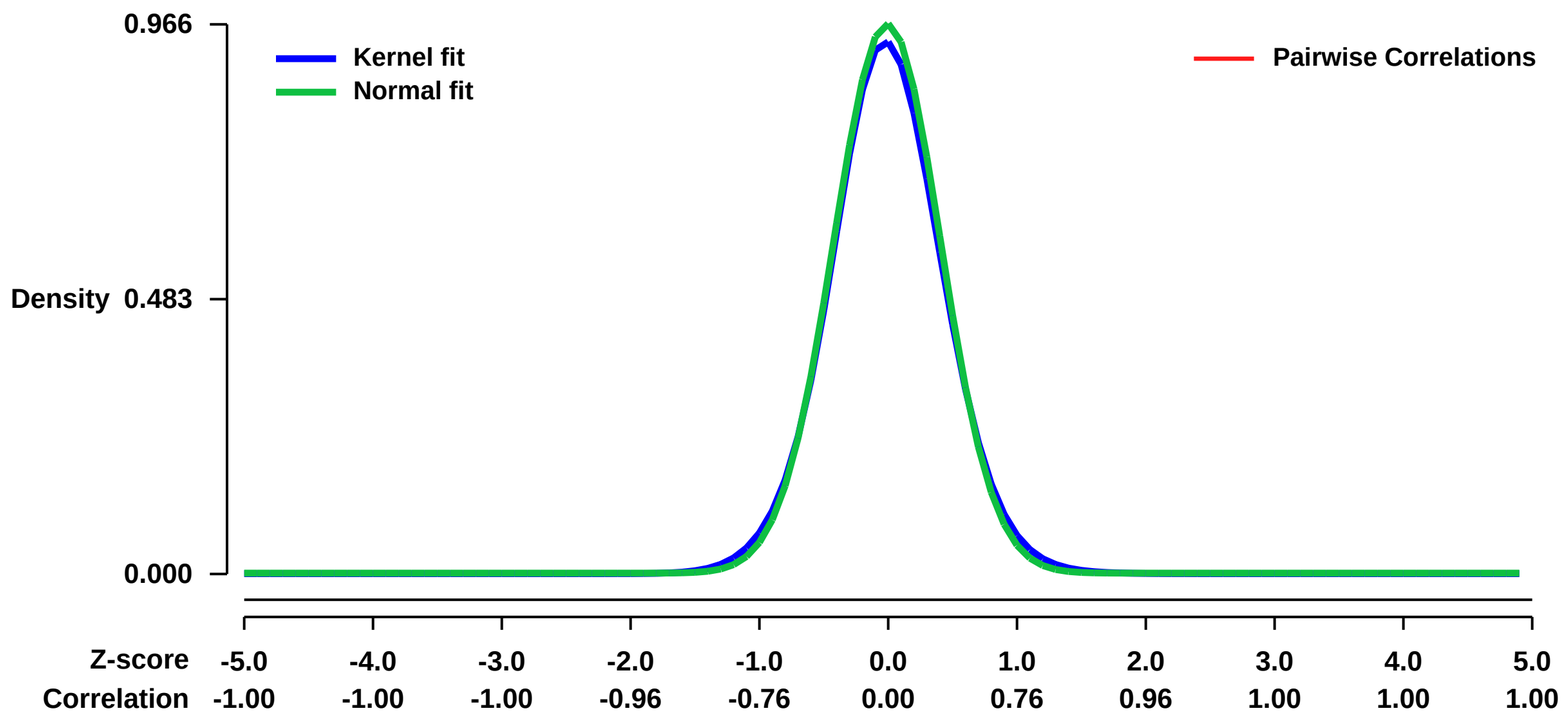

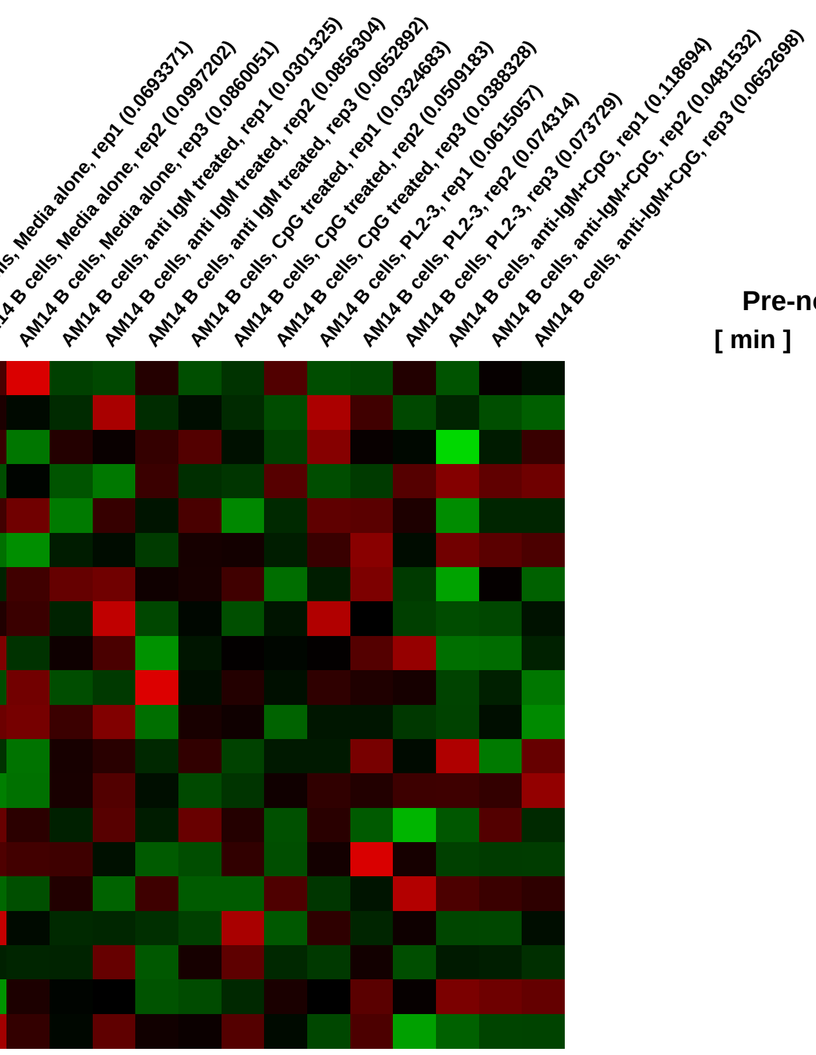

GEO Series "GSE6675" Expression Profiles

Num of samples in this series: 8

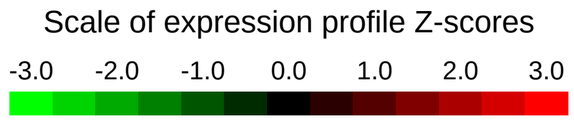

GEO Link:	http://www.ncbi.nlm.nih.gov/geo/query/acc.cgi?acc=GSE6675
Status:	Public on Jan 09 2007
Title:	Astroglial gene expression program elicited by fibroblast growth factor-2 mande-affy-mouse-307080
Organism:	Mus musculus
Experiment type:	Expression profiling by array
Platform:	GPL1261
Pubmed ID:	

Summary & Design:

Summary:
Astroglia, the star-shaped cells found throughout the central nervous system are the most numerous cell type in the brain. The astroglial response to injury, generically termed reactive astrogliosis, is classically defined by cellular hypertrophy and process extension, increased glial filament production, and some degree of proliferation. Astrogliosis and its functional outcomes, glial scar formation and neuroinflammation, are often viewed as detrimental to recovery. However, increasing evidence points to neuroprotective roles of reactive astroglia in the setting of brain injury. Therapeutic modulation of this double-edged sword will require detailed knowledge of mechanisms by which specific signals induce detrimental and beneficial phenotypes.

This proposal is is a logical extension of a published, peer reviewed study (Heffron DS and Mandell JW, Opposing roles of ERK and p38 MAP kinases in FGF2-induced astroglial process extension. Mol Cell Neurosci 2005, 28:779-90). The downstream gene expression changes underlying these pathway-specific responses are largely unknown. The data generated from the proposed project will delineate pathway-specific gene expression responses of astroglia to fibroblast growth factors. This information will allow a rational approach to pharmacological approaches to modulate reactive astrogliosis in brain and spinal cord injury.

Determine the astroglial gene expression program elicited by fibroblast growth factor-2, and dissect specific contributions of the ERK and p38 MAP kinase pathways using highly specific pharmacological inhibitors.

FGF2, acting via two distinct intracellular signaling pathways, ERK- and p38 MAPK, leads to pathway-specific gene expression changes in astrocytes which promote the morphological plasticity (ERK-dependent) and pro-inflammatory properties (p38-dependent) of reactive astroglia.

Cell culture

Neonatal primary astrocyte cultures are prepared exactly as previously described (Heffron and Mandell, 2005), using slight modifications of established protocols (McCarthy and de Vellis, 1980).

Astrocytes prepared with these methods comprised greater than 95% of cell cultures as determined by GFAP staining. Microglia are present as a contaminating cell type at a percentage of 3.6 ´– 0.9% as determined by CD11B staining.

For process induction experiments, cells are trypsinized and replated in DMEM with 1% fetal bovine serum. This low serum concentration is necessary for good adhesion of the cells. Pharmacological inhibitors are dissolved in DMSO and added 2 h later. P38 MAP kinase inhibitors SB202190 (Calbiochem) and the MEK inhibitor U0126 (Promega) are used at 20 ´µM. We previously determined that the inactive analog of SB 202190, SB202474 (Calbiochem) had no effects on pathway activation or astrocyte morphology. Therefore, the inactive drug analog will not be used in the array experiments.

Final DMSO concentration in the drug treatments and vehicle controls is 0.2%. Human recombinant FGF2 (obtained from the National Cancer Institute Preclinical Repository) is used at 25 ng/ml, based on extensive dose/response analyses in our published work.

Keywords: fibroblast growth factor-2 treatment

Overall design:

Background corr dist: KL-Divergence = 0.0599, L1-Distance = 0.0210, L2-Distance = 0.0005, Normal std = 0.5359

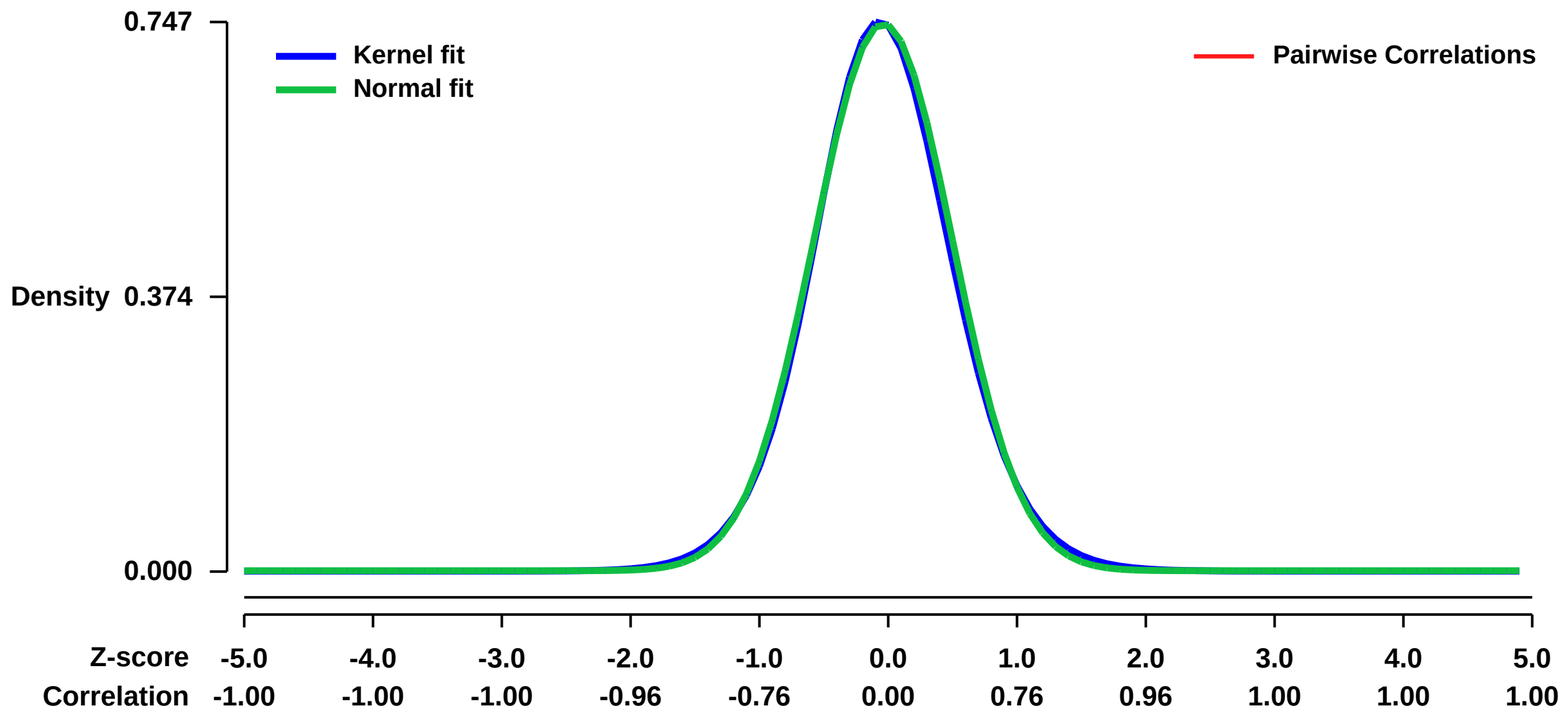

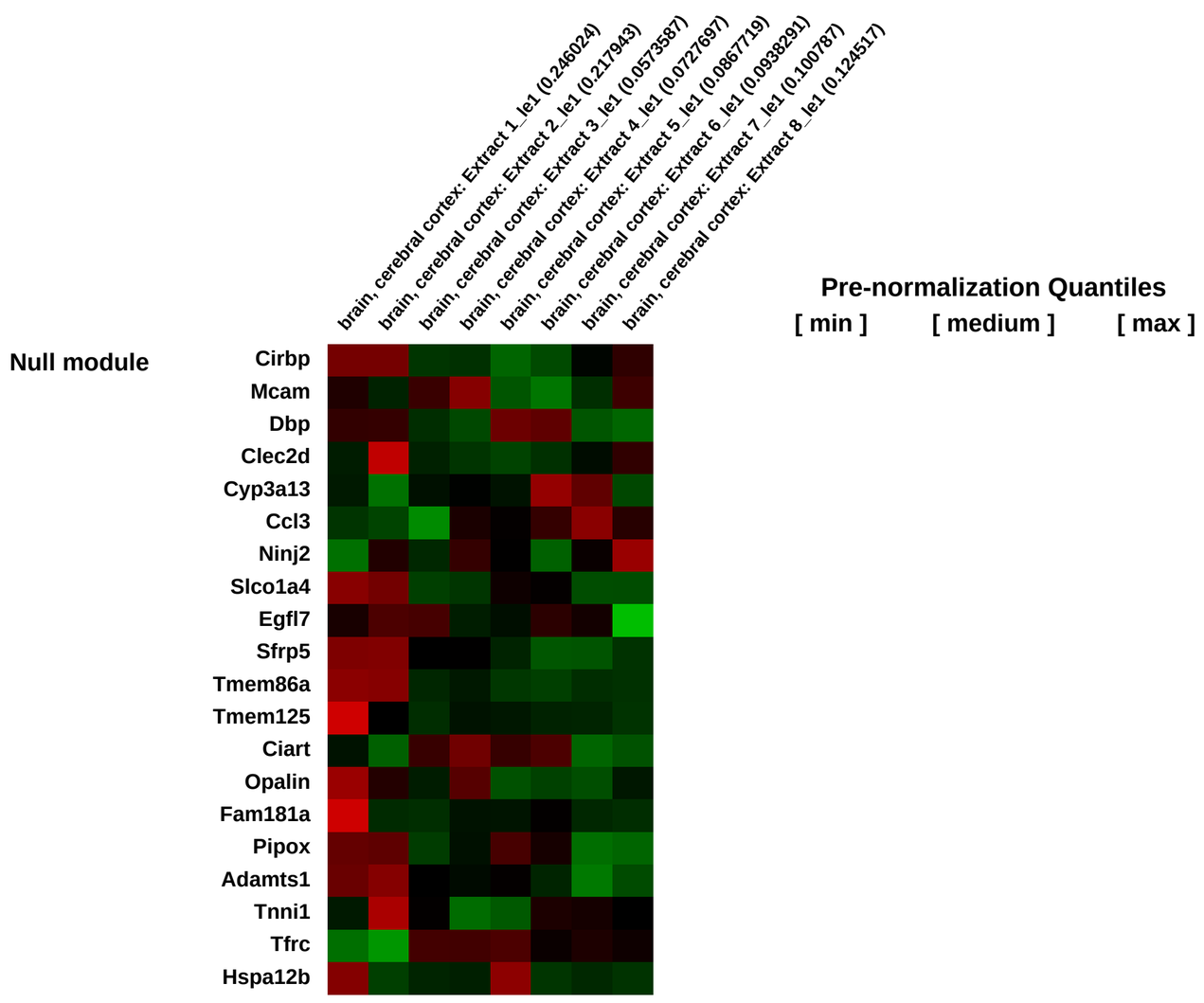

GEO Series "GSE6676" Expression Profiles

Num of samples in this series: 8

Scale of expression profile Z-scores

-3.0 -2.0 -1.0 0.0 1.0 2.0 3.0

GEO Link:	http://www.ncbi.nlm.nih.gov/geo/query/acc.cgi?acc=GSE6676
Status:	Public on Jan 09 2007
Title:	Comparison of corneas from wildtype mice to those from mice under the influence of high doses of TGF-beta russe-affy-mouse-372894
Organism:	Mus musculus
Experiment type:	Expression profiling by array
Platform:	GPL1261
Pubmed ID:	
Summary & Design:	**Summary:** Characteristic structural details of the cornea are transparency, the absence of blood vessels, and the presence of numerous sensory nerve endings. The corneal epithelium is one of the most densely innervated tissues of the body. The characteristics of the cornea are established during fetal development, and are lost in adult life when the cornea regenerates after injury. The common reaction of the cornea to injury is the formation of opaque scars, the ingrowth of blood vessels, and distinct changes in the innervation pattern. Scar formation of the cornea is critically modulated by the expression of transforming growth factor-beta (TGF-beta). To identify genes that are important for corneal transparency, dense innervation and absence of blood vessels by comparing corneas from wildtype mice with those that are under the influence of high doses of TGF-beta. Transparency, dense innervation, and absence of blood vessels in the cornea all depend on the expression of a critical set of genes that are not expressed when TGF-beta is present. Mice were generated that overexpress TGF-beta under control of a strong lens-specific promoter. These mice developed opaque corneas that are vascularized and lack sensory nerves. In addition, these corneas were densely populated with cells expressing neural cell adhesion protein. RNA was isolated from corneas of transgenic animals and wildtype littermates in order to analyze differentially expressed genes and to identify those that are only expressed in transparent, avascular, and densely innervated wildtype corneas. Keywords: TGF-beta overexpression Overall design:

Background corr dist: KL-Divergence = 0.0715, L1-Distance = 0.0250, L2-Distance = 0.0011, Normal std = 0.5009

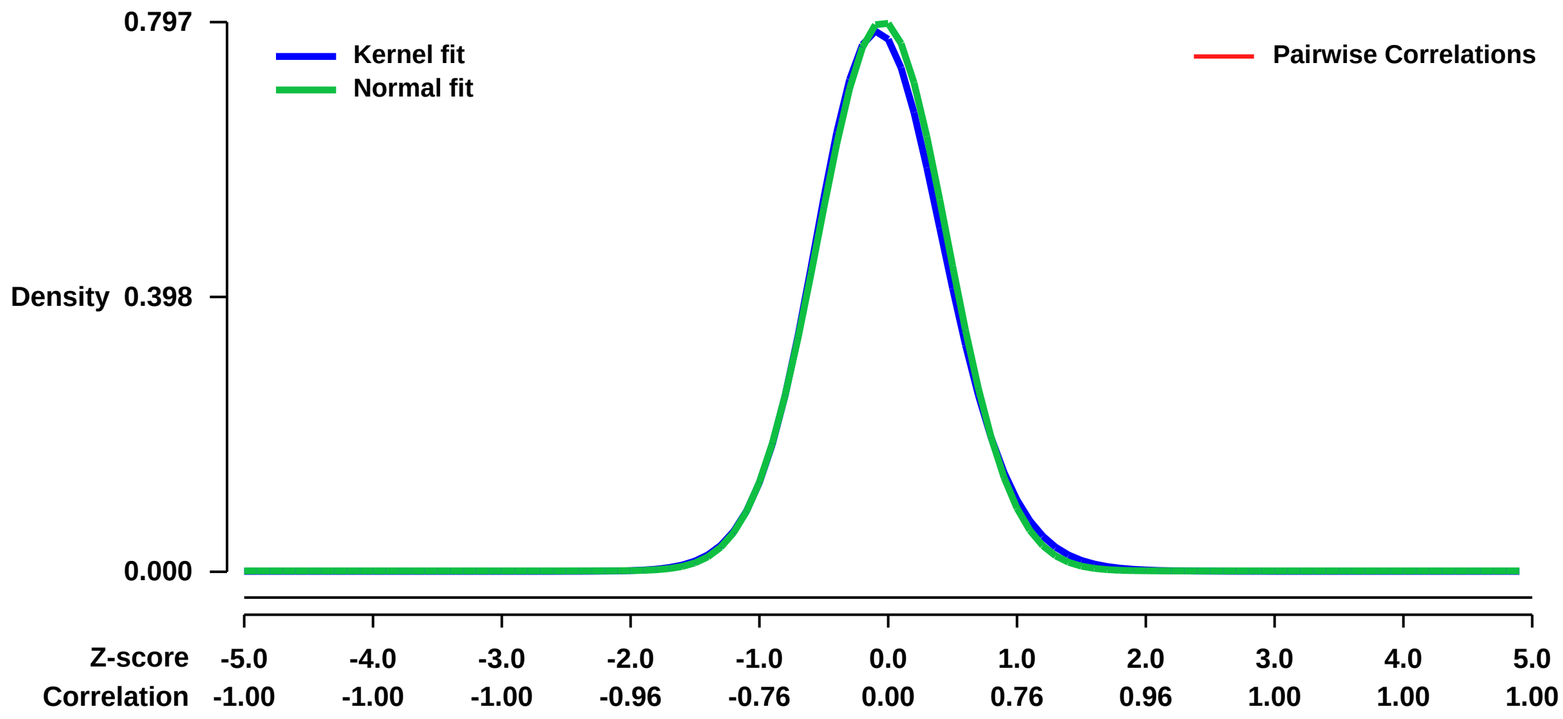

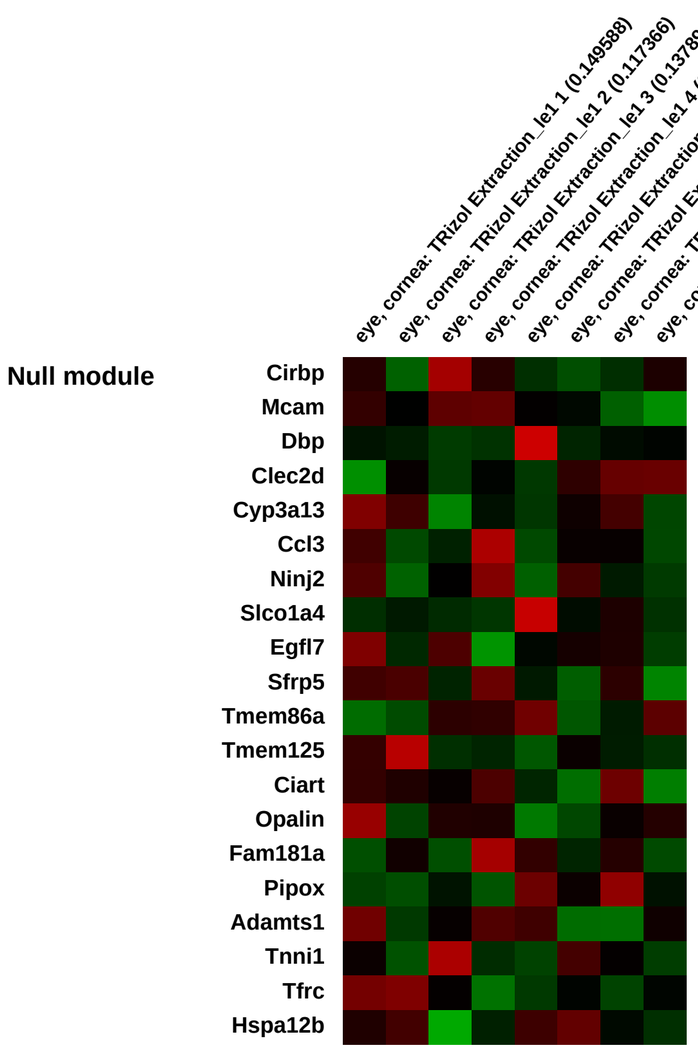

GEO Series "GSE6678" Expression Profiles

Num of samples in this series: 18

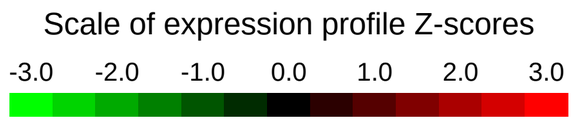

GEO Link:	**http://www.ncbi.nlm.nih.gov/geo/query/acc.cgi?acc=GSE6678**
Status:	**Public on Jan 09 2007**
Title:	**Palmitoyl protein thioesterase-1 knockout mice hofma-affy-mouse-370000**
Organism:	**Mus musculus**
Experiment type:	**Expression profiling by array**
Platform:	**GPL1261**
Pubmed ID:	
Summary & Design:	**Summary:** **Infantile neuronal ceroid lipofuscinosis (aka infantile Batten disease) is a severe neurodegenerative disorder of early childhood characterized by cortical atrophy, blindness and seizures, leading to premature death in the first decade. The disorder is caused by deficiency in a soluble lysosomal enzyme, palmitoyl protein thioesterase-1 (PPT1). PPT1 knockout mice faithfully reproduce the features of the human disease, with motor deterioration, blindness, seizures, and death before 10 months of age. The progression of events leading from enzyme deficiency to organ failure is poorly defined. The neuronal ceroid lipofuscinoses are of particular interest because of the similarities between the accumulated material and lipofuscin that is associated with normal aging.** **We will determine changes in gene expression that occur during the course of neurodegeneration in PPT1 knockout as compared to control mice.** **Gene expression profiling of brain tissue from PPT1 knockout mice as compared to normal controls will provide insights into the mechanism of neurodegeneration. Comparison of this profile with gene expression profiles associated with normal aging may provide insights into the contribution of lipofuscin to aging and neurodegeneration.** **PPT1 knockout mice on a C57BL/6 background will be sacrificed under CO2 and whole brains removed and frozen under liquid nitrogen. Three mice will be used for each time point. Data points will be collected at 3 months, 5 months and 8 months of age. Normal age- and sex-matched C57BL/6 mice will be used as controls.** **Keywords: gene knockout** **Overall design:**

Background corr dist: **KL-Divergence = 0.2682, L1-Distance = 0.0557, L2-Distance = 0.0079, Normal std = 0.2938**

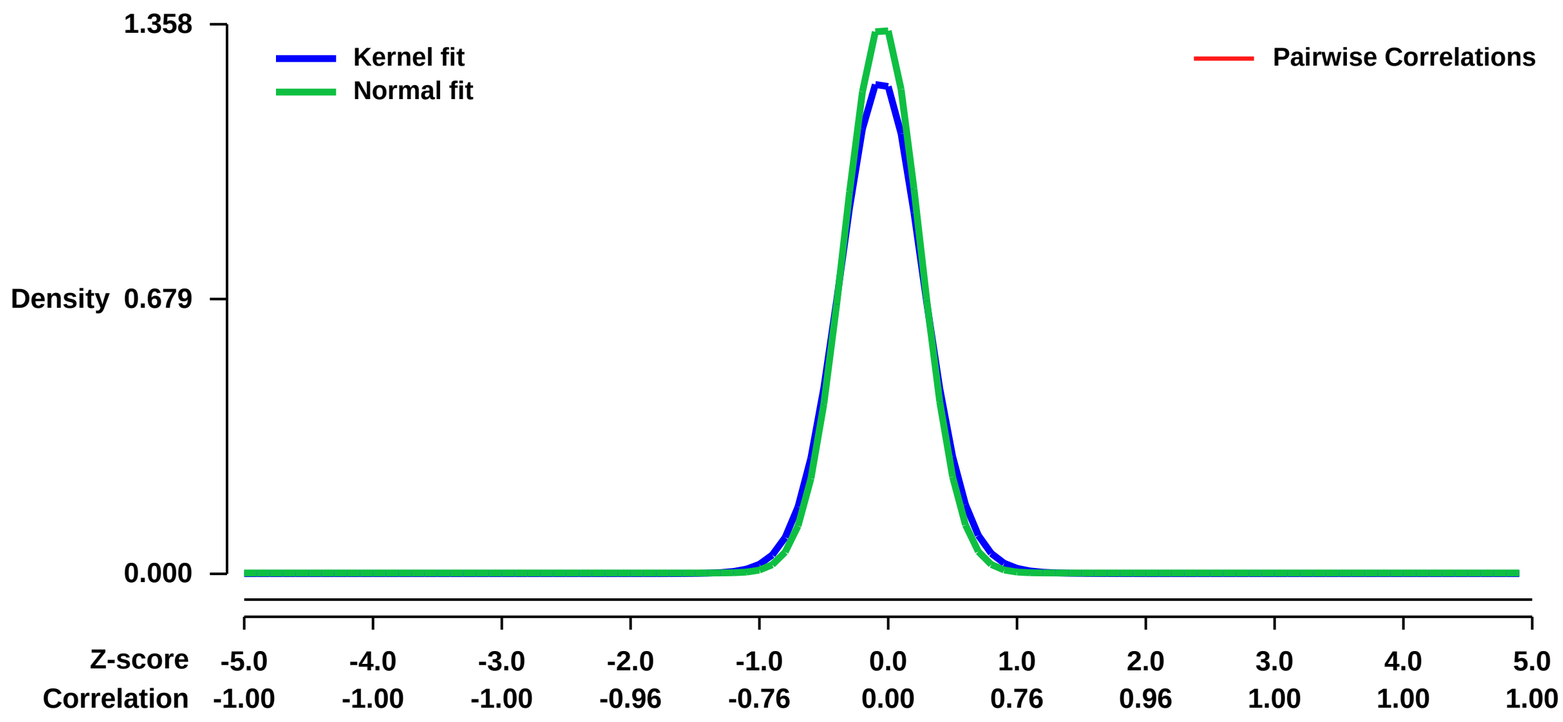

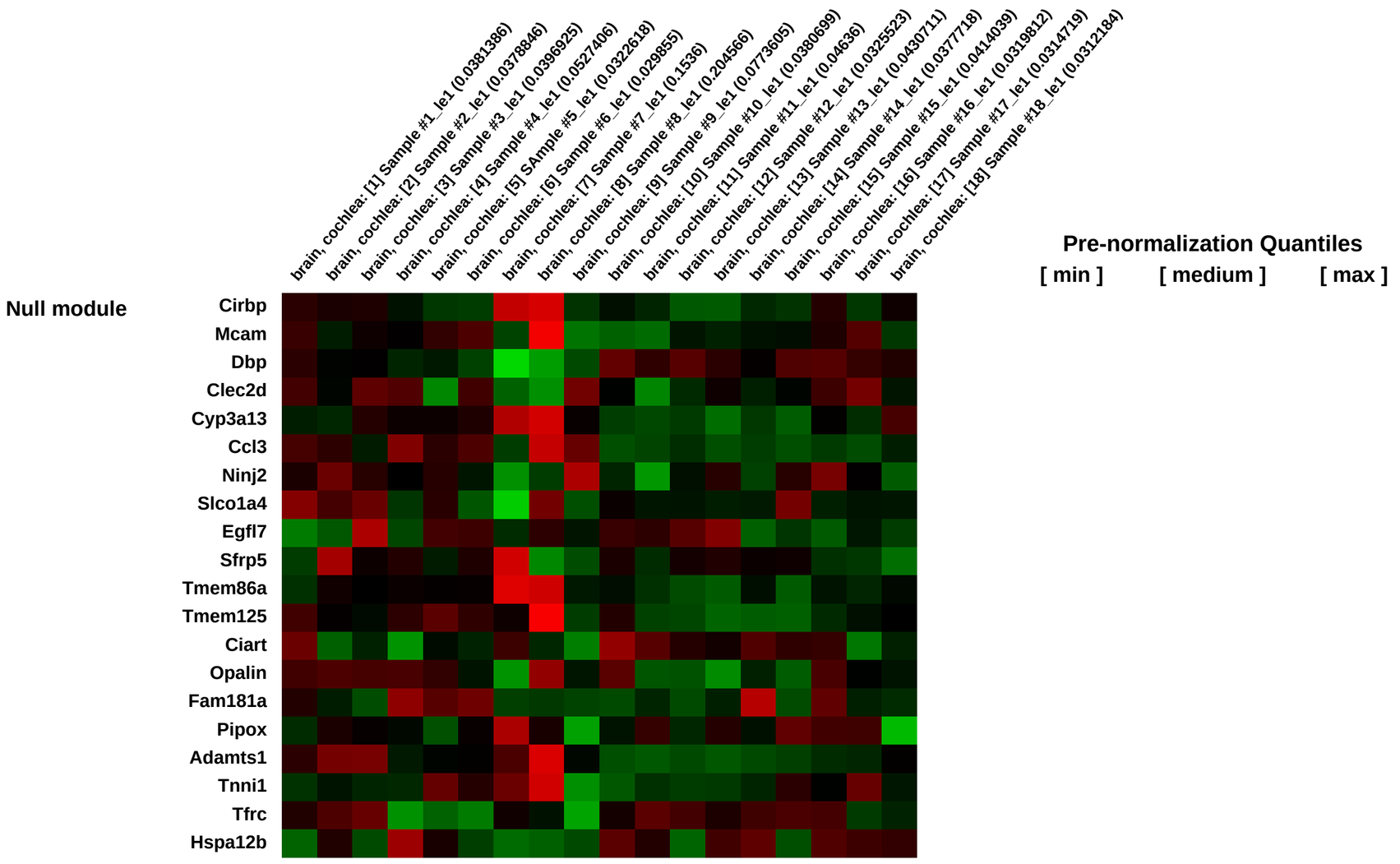

GEO Series "GSE6765" Expression Profiles

Num of samples in this series: 9

Scale of expression profile Z-scores

-3.0 -2.0 -1.0 0.0 1.0 2.0 3.0

GEO Link:	http://www.ncbi.nlm.nih.gov/geo/query/acc.cgi?acc=GSE6765
Status:	Public on Jan 20 2007
Title:	Aeromonas caviae infection, 24 hours
Organism:	Mus musculus
Experiment type:	Expression profiling by array
Platform:	GPL1261
Pubmed ID:	20130691
Summary & Design:	**Summary:** Aeromonas caviae has been associated with human gastrointestinal disease. Strains of this species typically lack virulence factors (VFs) such as enterotoxins and hemolysins that are produced by other human pathogens of the Aeromonas genus. Microarray profiling of murine small intestinal extracts, 24 hours after oral infection with an A. caviae strain, provides evidence of a Th1 type immune response. A large number of gamma-interferon (¸‡-IFN) induced genes are up-regulated as well as several tumor necrosis factor-alpha (TNF-¸–) transcripts. A. caviae has always been considered an opportunistic pathogen because it lacks obvious virulence factors. This current effort suggests A. caviae colonizes murine intestinal tract and causes what has been described by others as a dysregulatory cytokine response leading to an irritable bowel-like syndrome. This response would explain why a number of diarrheal waterborne outbreaks have been attributed to A. caviae even though it lacks obvious enteropathogenic properties. **Keywords:** Aeromonas caviae, infection, disease mechanism, TH1 resposne **Overall design:** Biological replicates (n=5), controls are uninfected mice, test replicates are infected with organism

Background corr dist: KL-Divergence = 0.0980, L1-Distance = 0.0252, L2-Distance = 0.0010, Normal std = 0.4406

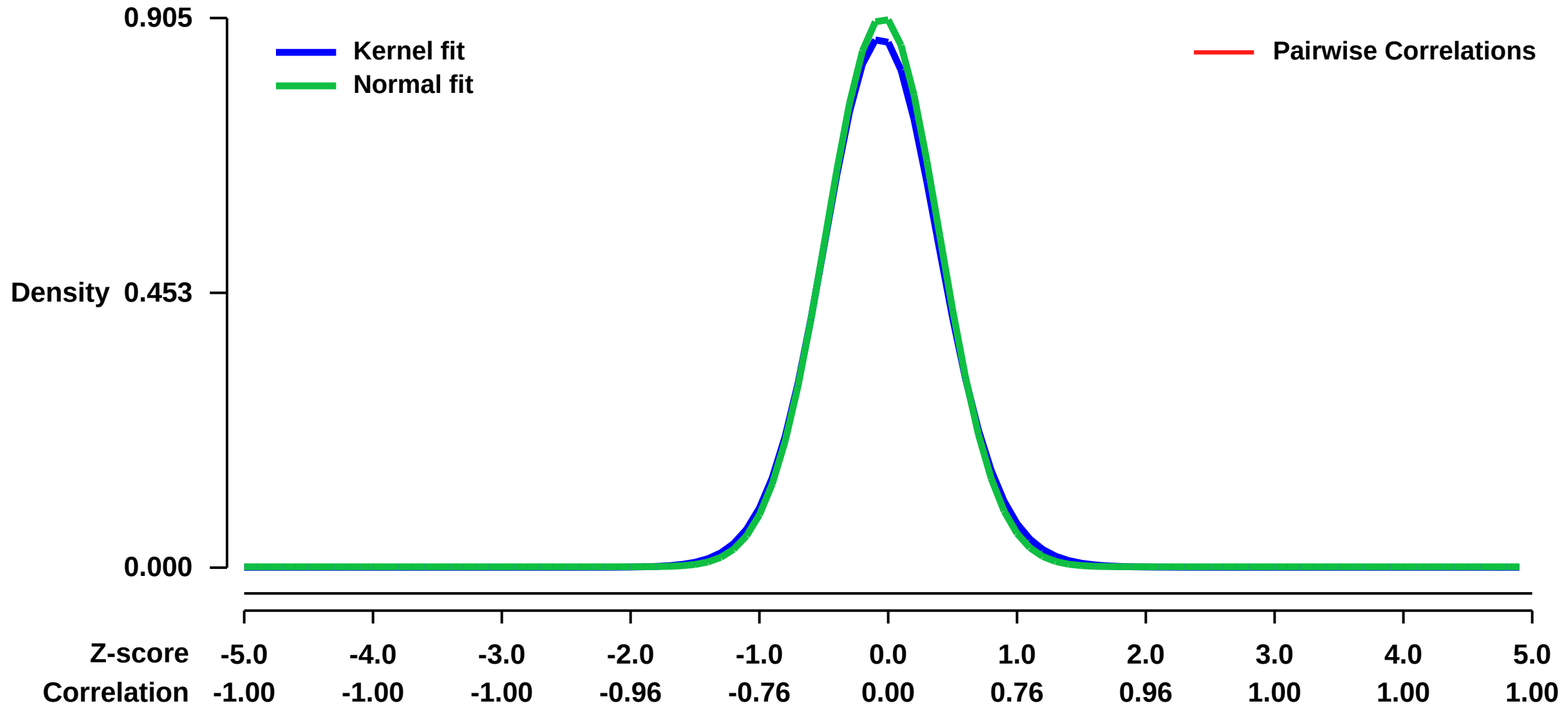

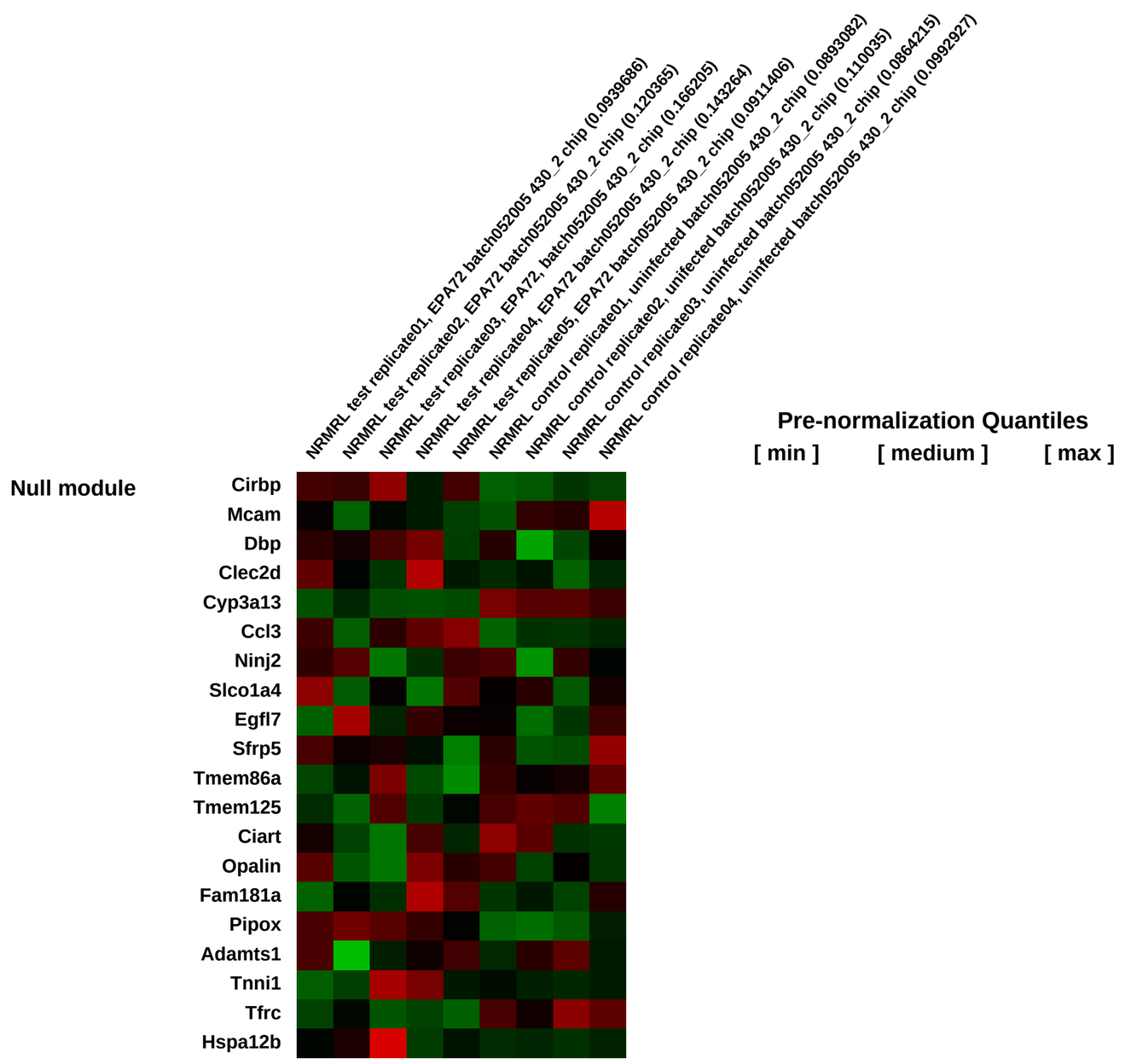

GEO Series "GSE6837" Expression Profiles

Num of samples in this series: 8

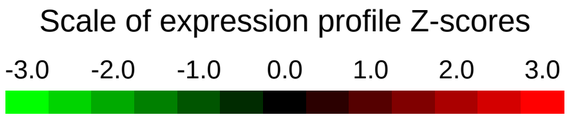

GEO Link:	http://www.ncbi.nlm.nih.gov/geo/query/acc.cgi?acc=GSE6837
Status:	Public on Jan 31 2007
Title:	Expression data from wild type (wt) and Ikbke knockout (Ikke) embryonic fibroblasts (EF)
Organism:	Mus musculus
Experiment type:	Expression profiling by array
Platform:	GPL1261
Pubmed ID:	17332413
Summary & Design:	**Summary:** WT and Ikbke-/- EF cells were stimulated with recombinant interferon beta for 6 hours. Cells lacking IKKe kinase show a defect in a subset of interferon stimulated gene transcription **Keywords: comparative study** **Overall design:** WT and Ikbke cells were either stimulated and left untreated to compare their response to interferon.

Background corr dist: KL-Divergence = 0.0231, L1-Distance = 0.0545, L2-Distance = 0.0038, Normal std = 0.8315

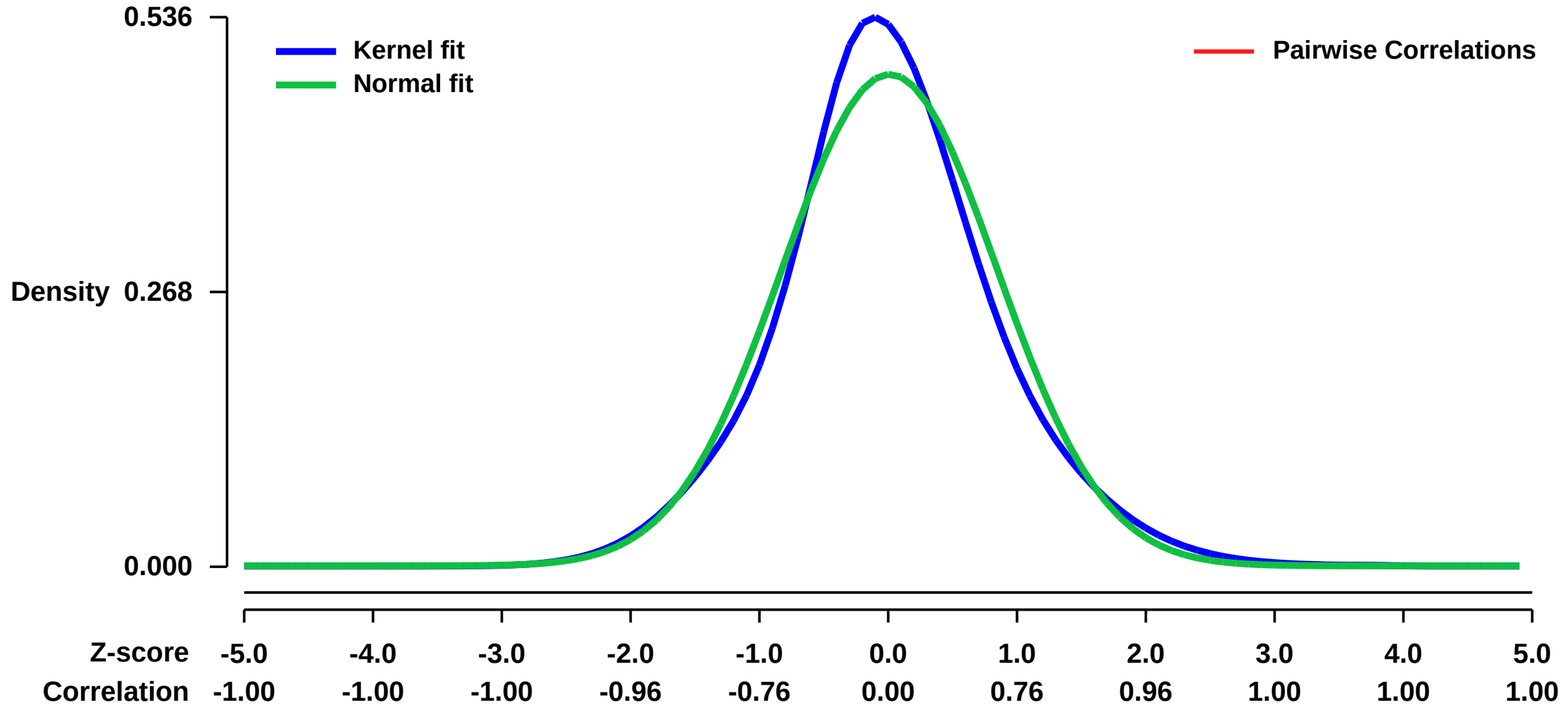

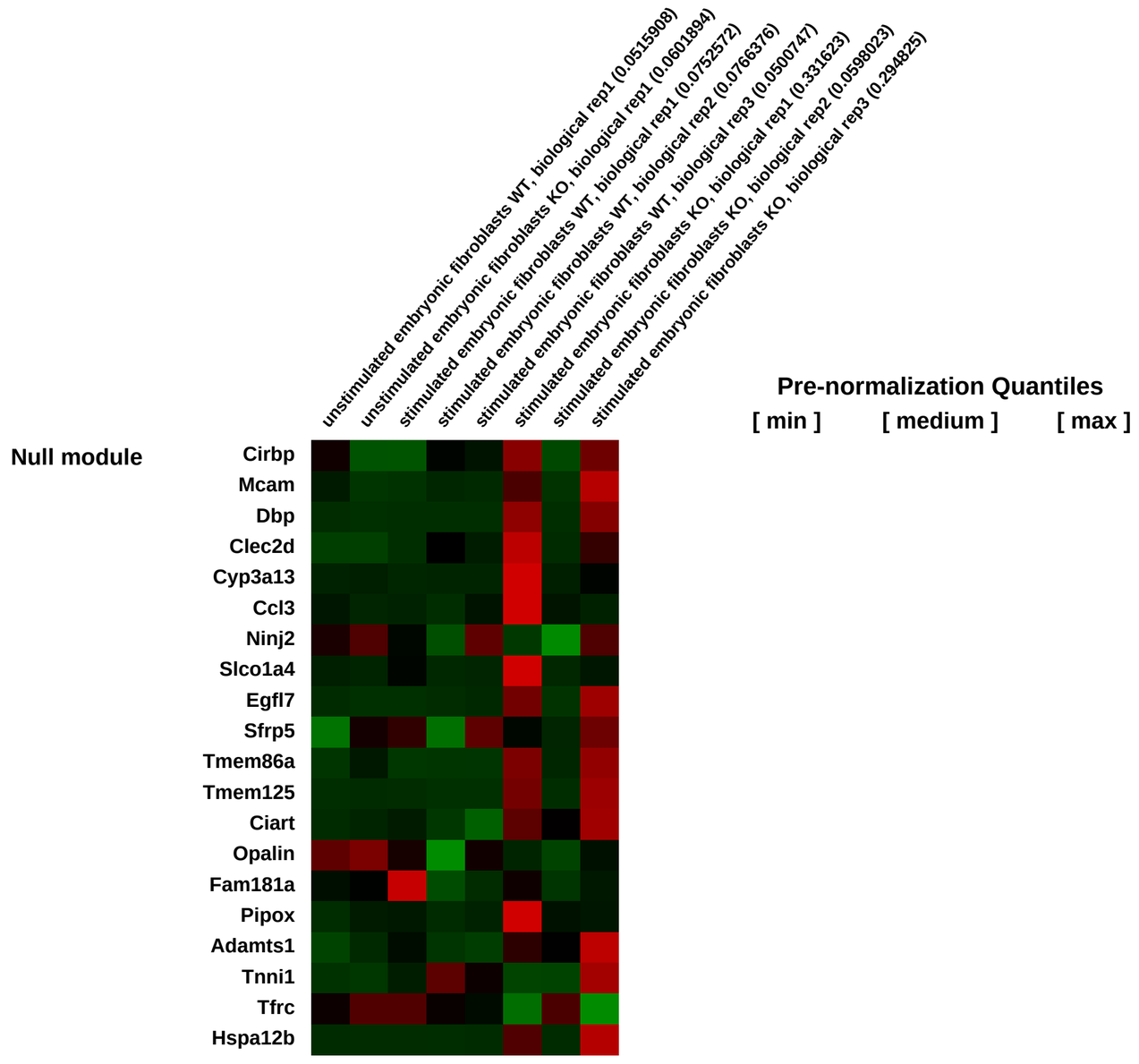

GEO Series "GSE6846" Expression Profiles

Num of samples in this series: 6

Scale of expression profile Z-scores

-3.0 -2.0 -1.0 0.0 1.0 2.0 3.0

GEO Link:	http://www.ncbi.nlm.nih.gov/geo/query/acc.cgi?acc=GSE6846
Status:	Public on Aug 24 2007
Title:	Gene Expression and Biological Processes Influenced By Deletion of Stat3 in pulmonary Alveolar Type II Cells
Organism:	Mus musculus
Experiment type:	Expression profiling by array
Platform:	GPL1261
Pubmed ID:	18070348
Summary & Design:	**Summary:** Deletion of Stat3 induced genes influencing protein metabolism, transport, chemotaxis and apoptosis and decreased the expression of genes mediating lipid synthesis and metabolism. Srebf1 and 2, key regulators of fatty acid and steroid biosynthesis, were decreased in Stat3D/D mice. Stat3 influenced both pro- and anti-apoptotic pathways, regulating and maintaining the balance between a subset of pro- and anti-apoptotic genes that determine cell death or survival. Akt, a known target of Stat3, participates in many Stat3 mediated pathways including Jak-Stat signaling, apoptosis, the MAPK signaling, cholesterol and fatty acid biosynthesis. Deletion of Stat3 from type II epithelial cells altered the expression of genes regulating diverse cellular processes, including cell growth and apoptosis, lipid biosynthesis and metabolism. Stat3 regulates cell formation through a complex regulatory network that likely enhances alveolar epithelial cell survival and surfactant/lipid synthesis, necessary for the protection of the lung during injury. Keywords: genotype comparison **Overall design:** To better understand the roles and molecular mechanisms by which Stat3 influences gene expression in lung, the effect of cell-selective deletion of Stat3 (Stat3D/D) on genome wide mRNA expression profiles was determined in murine type II alveolar epithelial cells. Differentially expressed genes were identified from Affymetrix Murine GeneChips analysis and subjected to gene ontology classification promoter analysis, pathway mapping and literature mining.

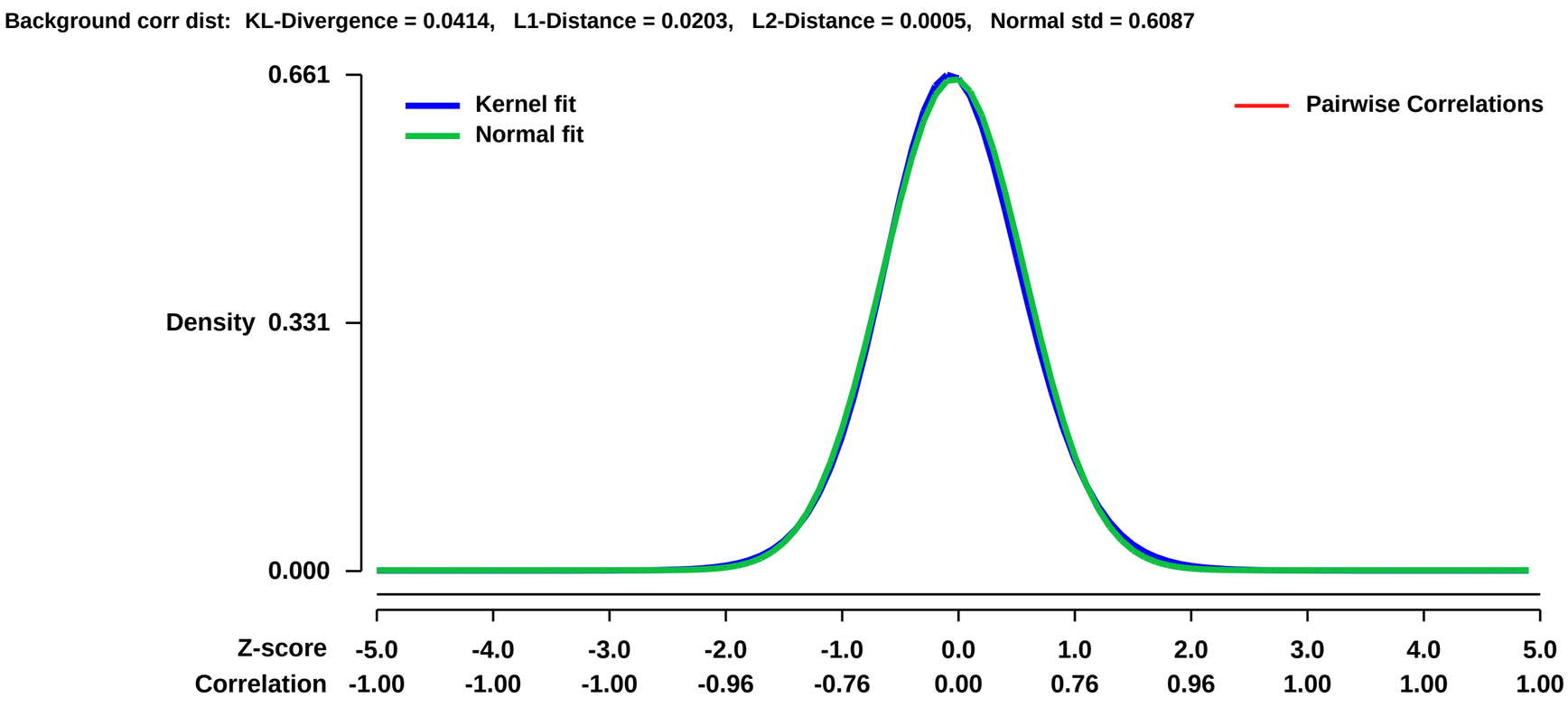

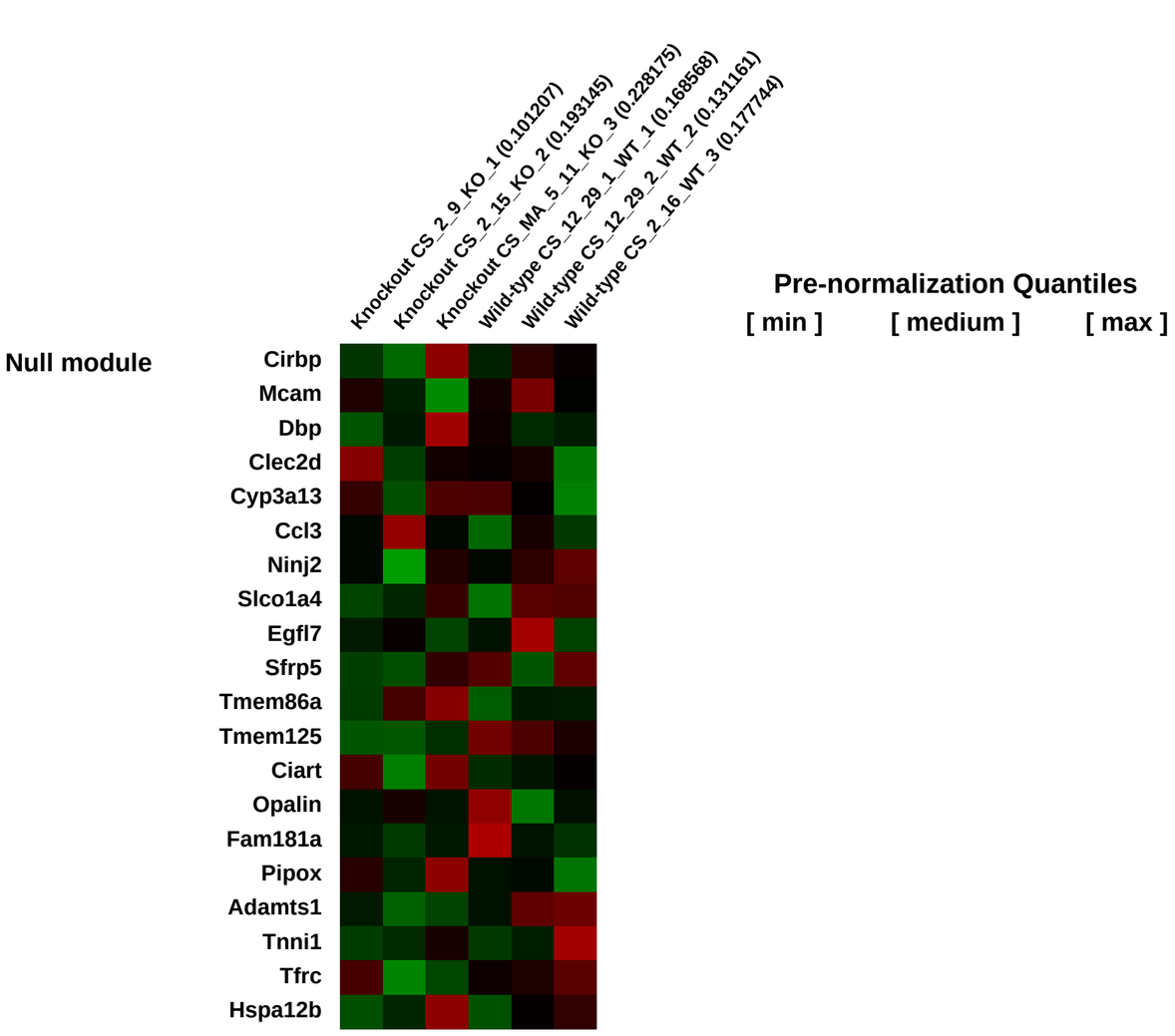

GEO Series "GSE6850" Expression Profiles

Num of samples in this series: 10

Scale of expression profile Z-scores

-3.0 -2.0 -1.0 0.0 1.0 2.0 3.0

GEO Link:	http://www.ncbi.nlm.nih.gov/geo/query/acc.cgi?acc=GSE6850
Status:	Public on Jun 15 2007
Title:	A dominant negative form of cJun affects genes that have opposing effects on lipid homeostasis in mice
Organism:	Mus musculus
Experiment type:	Expression profiling by array
Platform:	GPL1261
Pubmed ID:	17456467
Summary & Design:	**Summary:** cJun is a transcription factor activated by phosphorylation by SAPK/JNK MAP kinase pathway that has been linked to atherosclerosis. Adenovirus mediated gene transfer of a dominant negative form of cJun in C57BL/6 mice increased greatly the apolipoprotein E (ApoE) mRNA and plasma apoE levels and induced dyslipidmia, characterized by increased plasma cholesterol, triglyceride and VLDL levels and accumulation of discoidal HDL particles. Unexpectedly, infection of ApoE-/- mice with adenovirus expressing dn-cJun reduced by 50% plasma cholesterol, suggesting that the dn-cJun affected other genes that control plamsa cholesterol. To determine the molecular pathways implicated in this process we performed whole genome expression profiling using total RNA from the liver of infected ApoE-/- mice. **Keywords:** disease **Overall design:** We extracted total RNA from 5 ApoE-/- mice infected with an adenovirus expressing dominant negative cJun and 5 ApoE-/- mice infected with a control adenovirus expressing GFP. Each RNA sample was hybridized to a different Affymetrix 430 2.0 array.

Background corr dist: KL-Divergence = 0.1286, L1-Distance = 0.0328, L2-Distance = 0.0020, Normal std = 0.3960

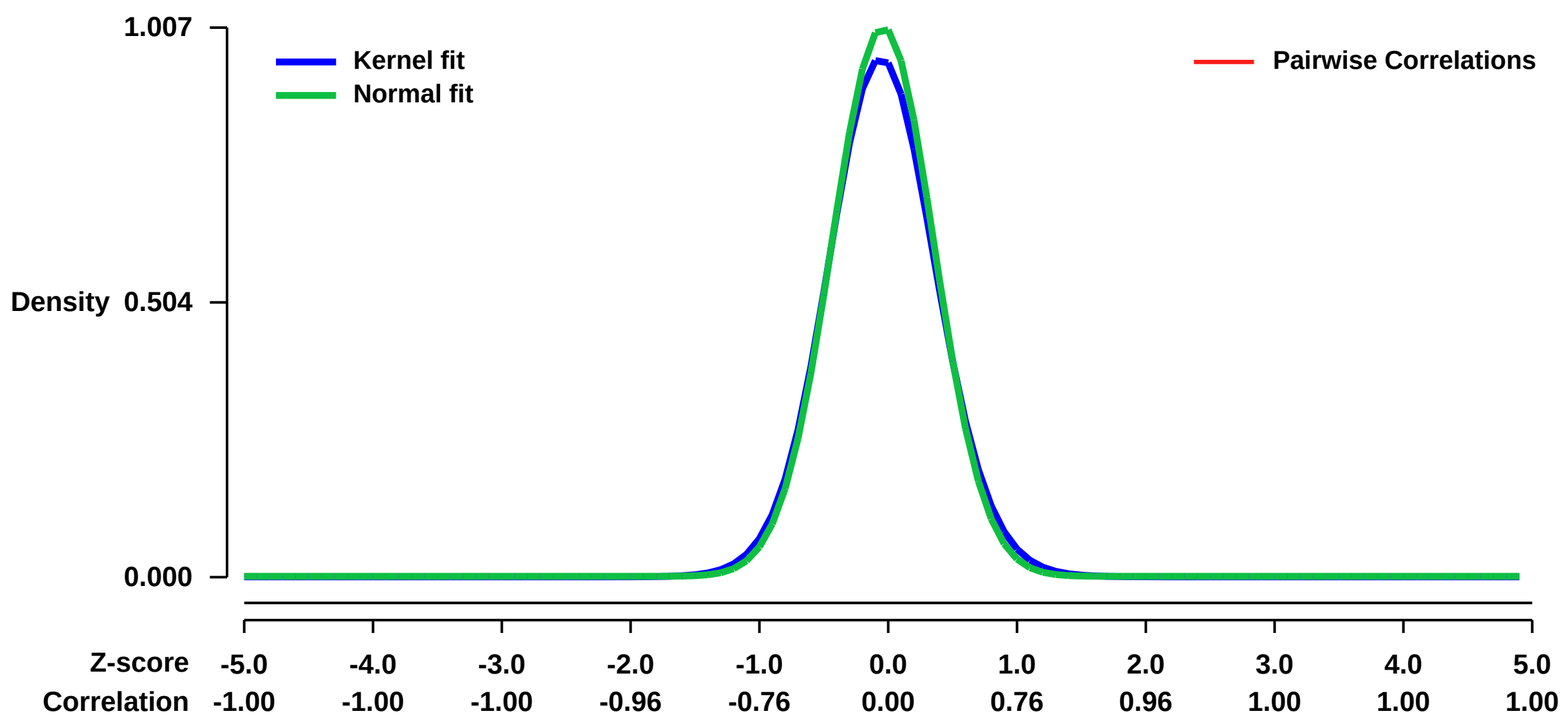

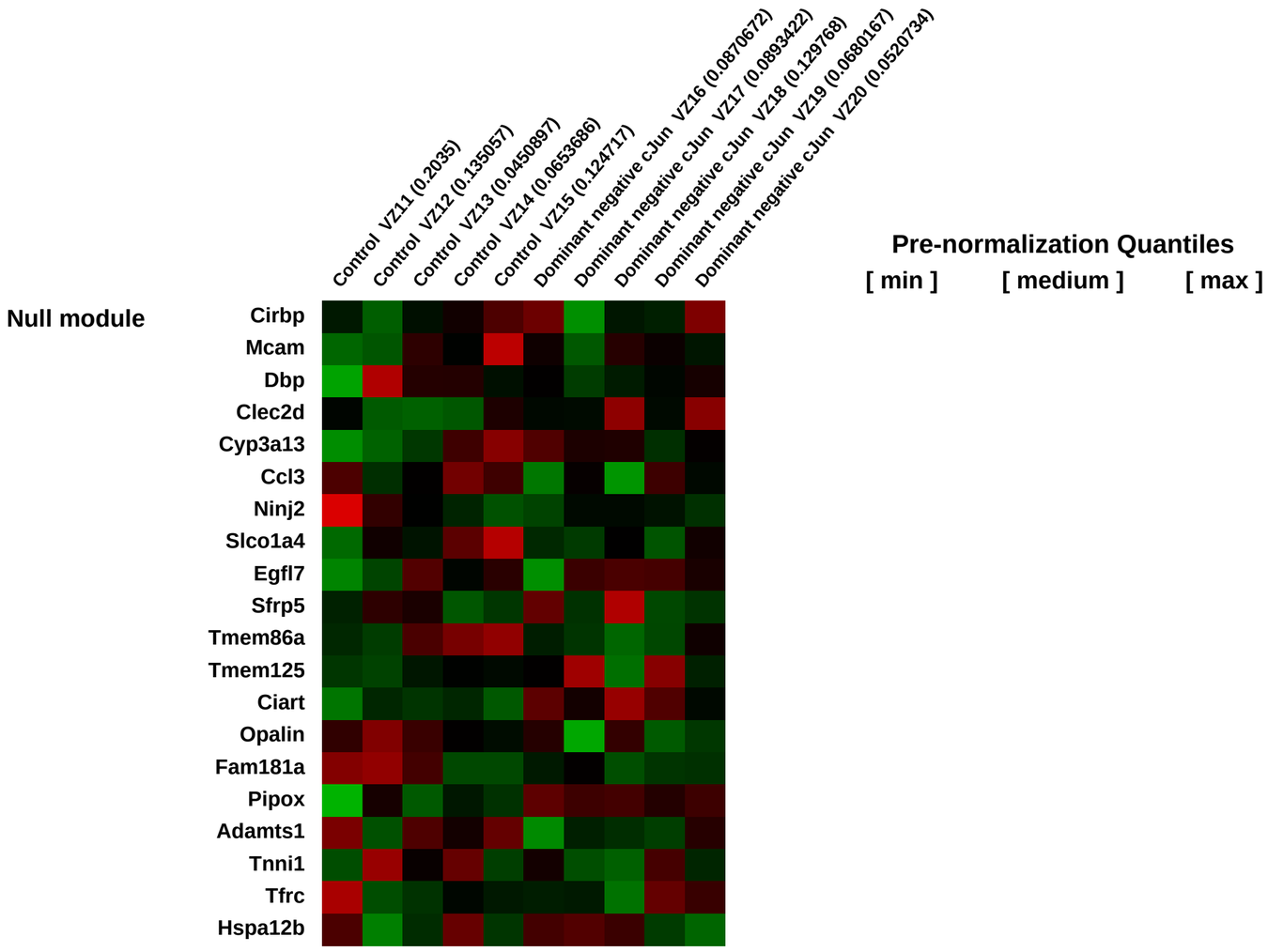

GEO Series "GSE6858" Expression Profiles

Num of samples in this series: 16

Scale of expression profile Z-scores

-3.0 -2.0 -1.0 0.0 1.0 2.0 3.0

GEO Link:	http://www.ncbi.nlm.nih.gov/geo/query/acc.cgi?acc=GSE6858
Status:	Public on Apr 23 2007
Title:	Expression data from experimental murine asthma
Organism:	Mus musculus
Experiment type:	Expression profiling by array
Platform:	GPL1261
Pubmed ID:	17437023
Summary & Design:	**Summary:** Experimental asthma was induced in BALB/c mice by sensitization and challenge with the allergen ovalbumin. Control groups received PBS. To investigate the innate immune component of experimental asthma, we also analyzed recombinase activating gene (RAG) deficient mice following exposure to ovalbumin and control PBS **Keywords: case control** **Overall design:** Each experimental group was exposed to ovalbumin or control PBS. At day 22, 1 day after completion of the allergen exposure, whole lungs were harvested, total mRNA prepared, and gene expression determined by hybridization to Affymetrix microarrays.

Background corr dist: KL-Divergence = 0.1222, L1-Distance = 0.0416, L2-Distance = 0.0036, Normal std = 0.4289

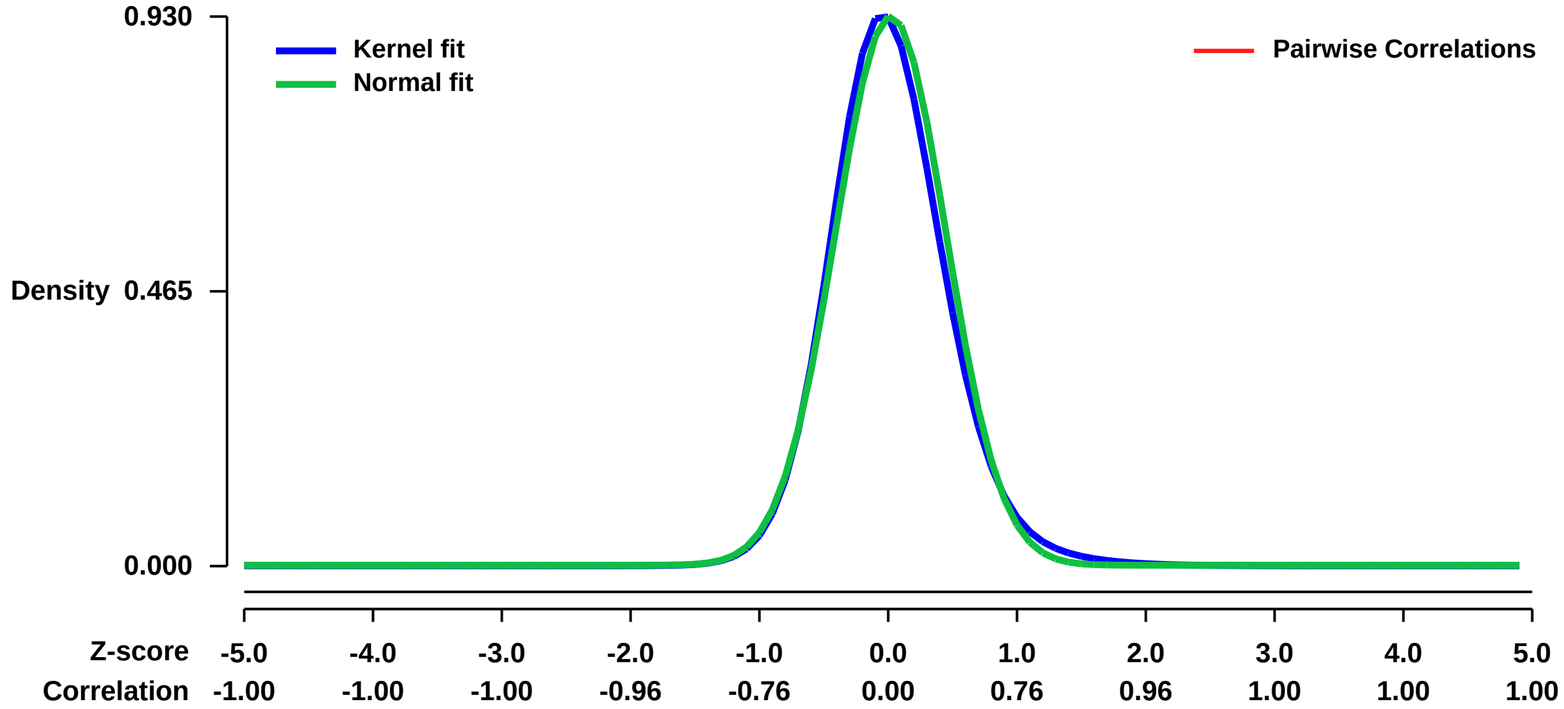

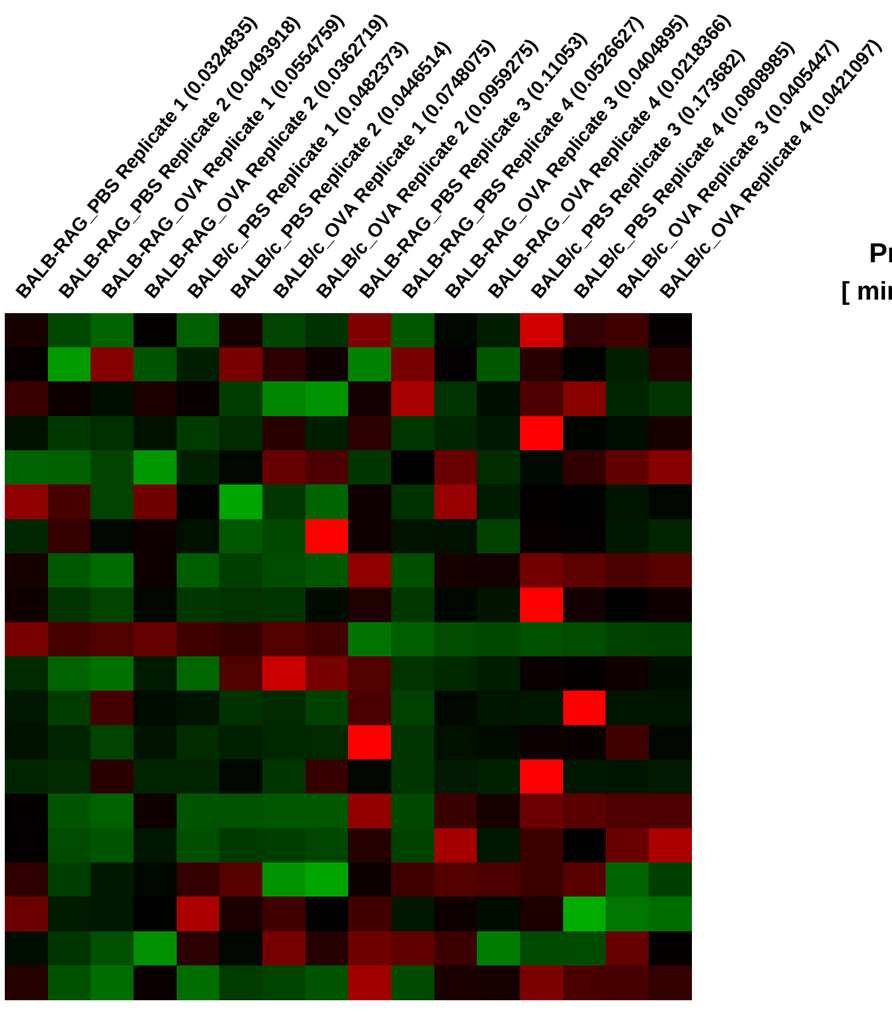

GEO Series "GSE6867" Expression Profiles

Num of samples in this series: 6

Scale of expression profile Z-scores

-3.0 -2.0 -1.0 0.0 1.0 2.0 3.0

GEO Link:	http://www.ncbi.nlm.nih.gov/geo/query/acc.cgi?acc=GSE6867
Status:	Public on Jan 26 2007
Title:	Expression data in the absence of Notch1 in hair follicles
Organism:	Mus musculus
Experiment type:	Expression profiling by array
Platform:	GPL1261
Pubmed ID:	17611229
Summary & Design:	**Summary:** Notch1 deficient hair matrix keratinocytes have lower mitotic rates, resulting in smaller follicles with fewer cells. In addition, the ratio of melanocytes to keratinocytes is greatly reduced. Microarray was performed to study downstream mechanism of Notch1-deficiency **Keywords: genetic modification** **Overall design:** Microarray was first performed using HF_emN1-1 and HF_anN1-1 samples. Later, HF_emN1-2, HF_anN1-2, HF_WT-1, and HF_WT-2 were used to perform another set of microarray. anN1s and WTs were used as wild-type controls.

Background corr dist: KL-Divergence = 0.0385, L1-Distance = 0.0217, L2-Distance = 0.0005, Normal std = 0.6256

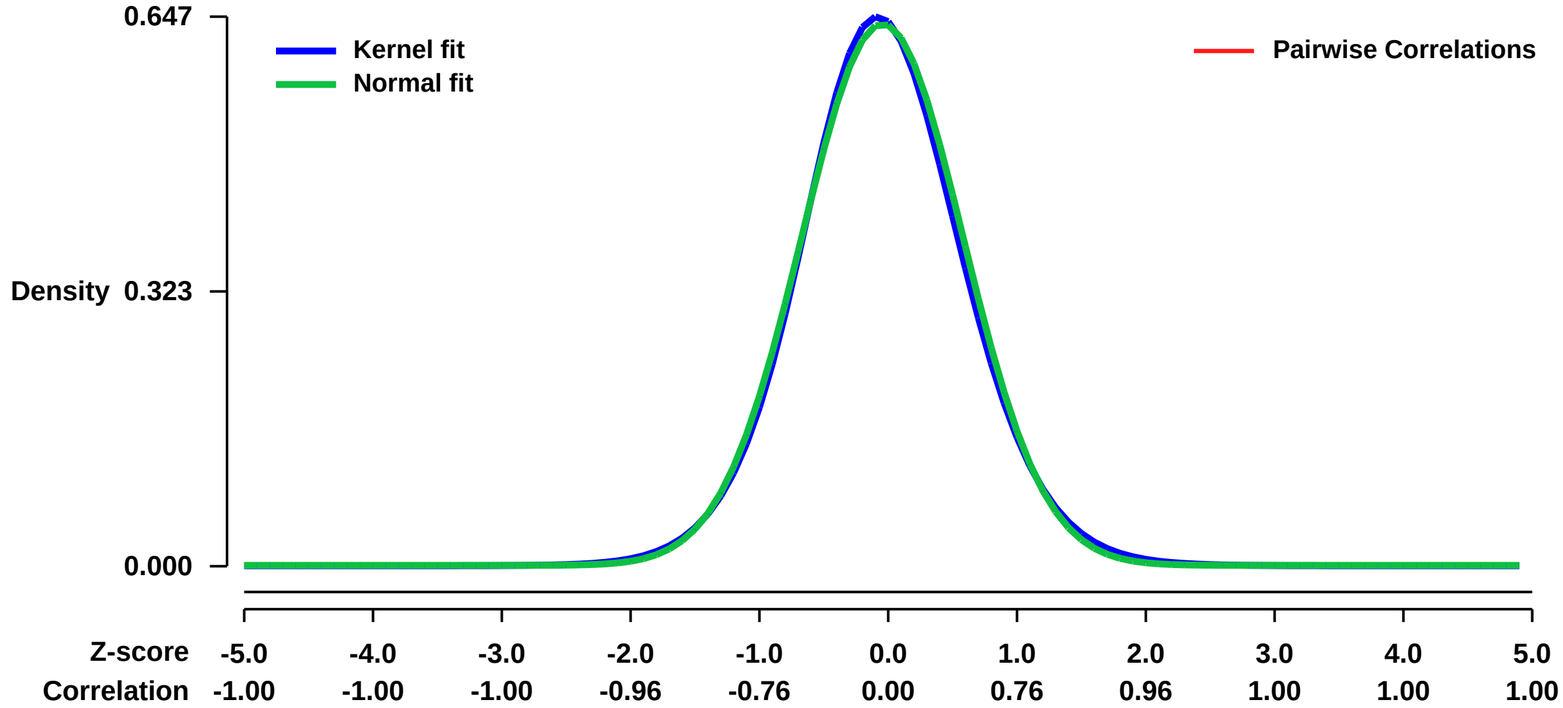

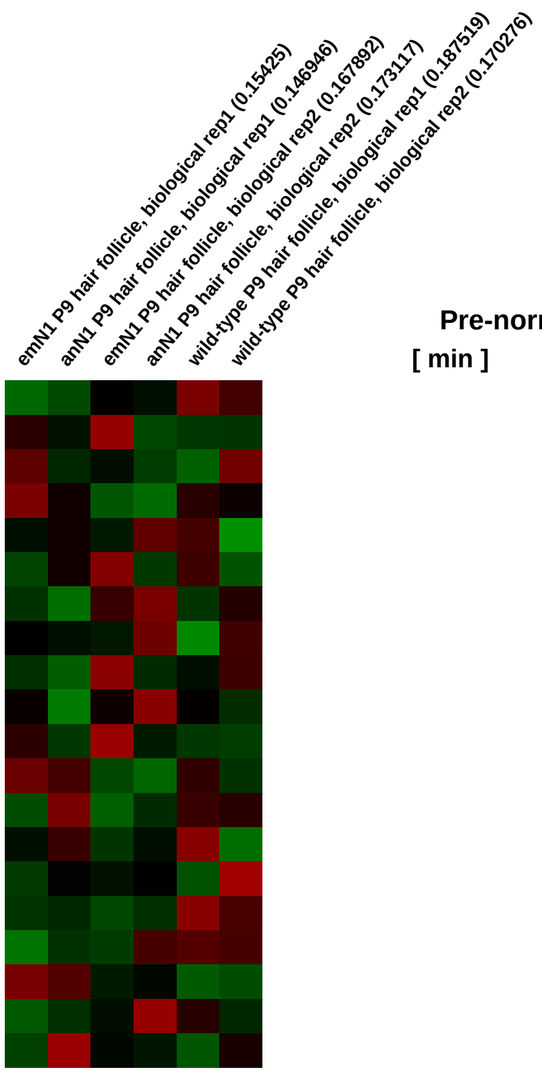

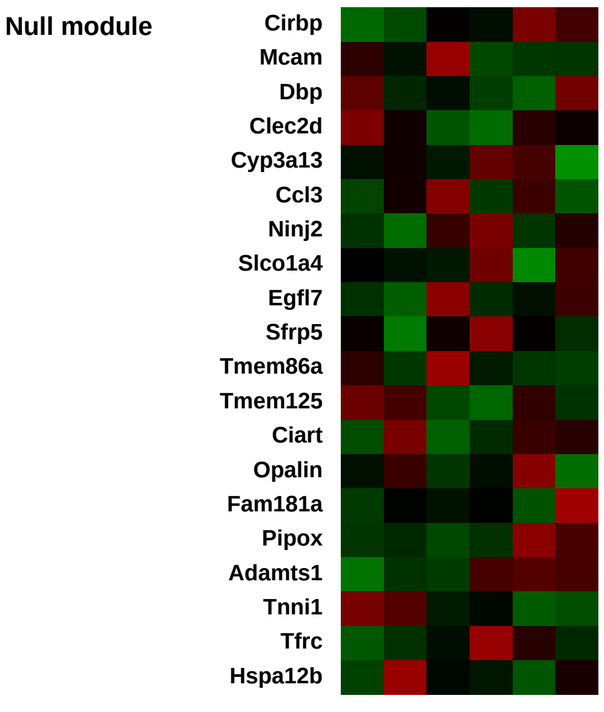

GEO Series "GSE6875" Expression Profiles

Num of samples in this series: 8

Scale of expression profile Z-scores

-3.0 -2.0 -1.0 0.0 1.0 2.0 3.0

GEO Link:	http://www.ncbi.nlm.nih.gov/geo/query/acc.cgi?acc=GSE6875
Status:	Public on Jan 26 2007
Title:	Development of Regulatory T cell Precursors in the Absence of a Functional Foxp3 Protein
Organism:	Mus musculus
Experiment type:	Expression profiling by array
Platform:	GPL1261
Pubmed ID:	17273171
Summary & Design:	**Summary:** To analyze gene expression in in regulatory T cell precursors that develop in the absence of a functional Foxp3 protein as compared to that of normal regulatory T cells **Keywords: Cell type comparison** **Overall design:** Murine wild-type and mutant (delta) Foxp3 alleles were tagged with EGFP reporters. CD4 positive T cells expressing the respective tagged Foxp3 allele (Foxp3/EGFP and delta Foxp3/EGFP) were isolated from hemizygous male mice by cell sorting using FACS. CD4 positive cells that did not express the EGFP tag were a isolated. Total RNA was prepared and used in the array studies.

Background corr dist: KL-Divergence = 0.0619, L1-Distance = 0.0225, L2-Distance = 0.0006, Normal std = 0.5327

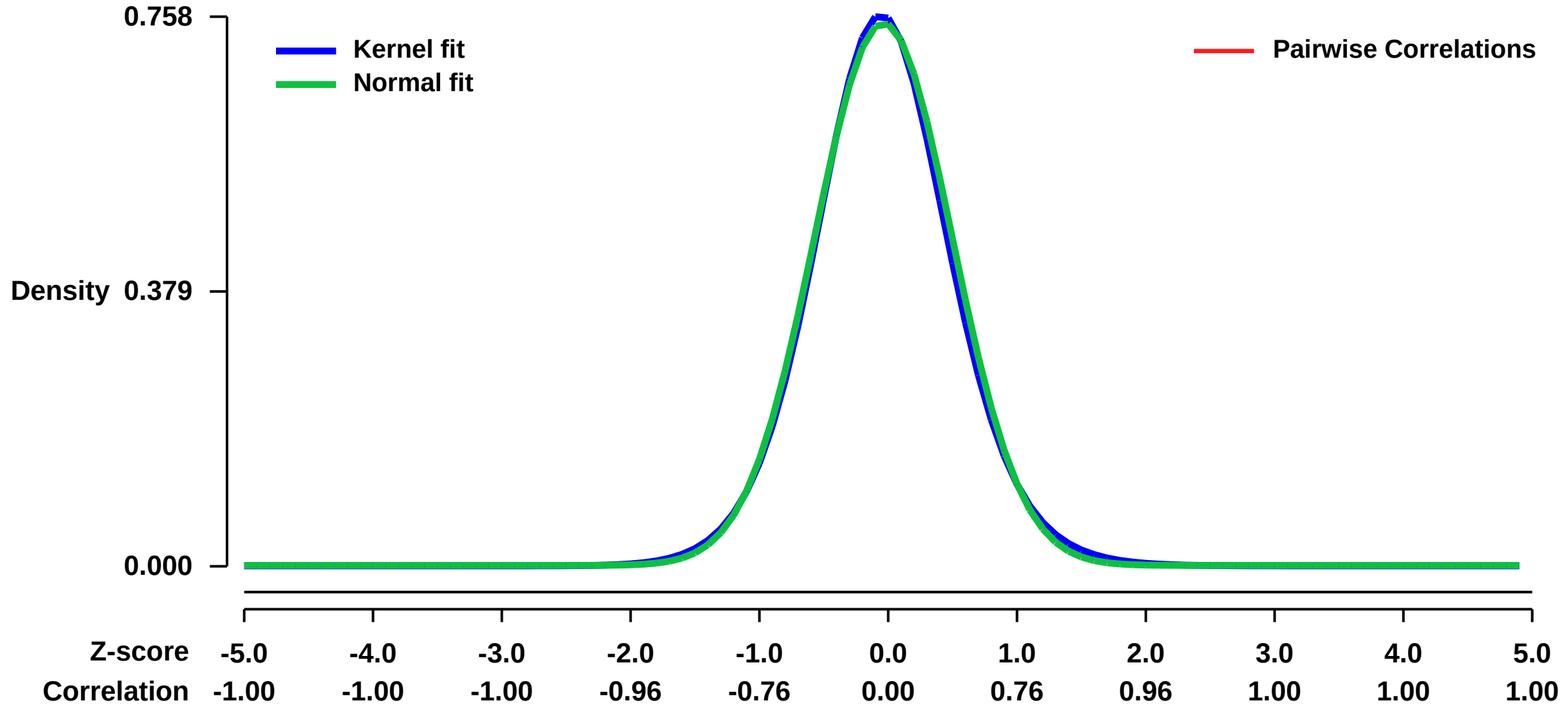

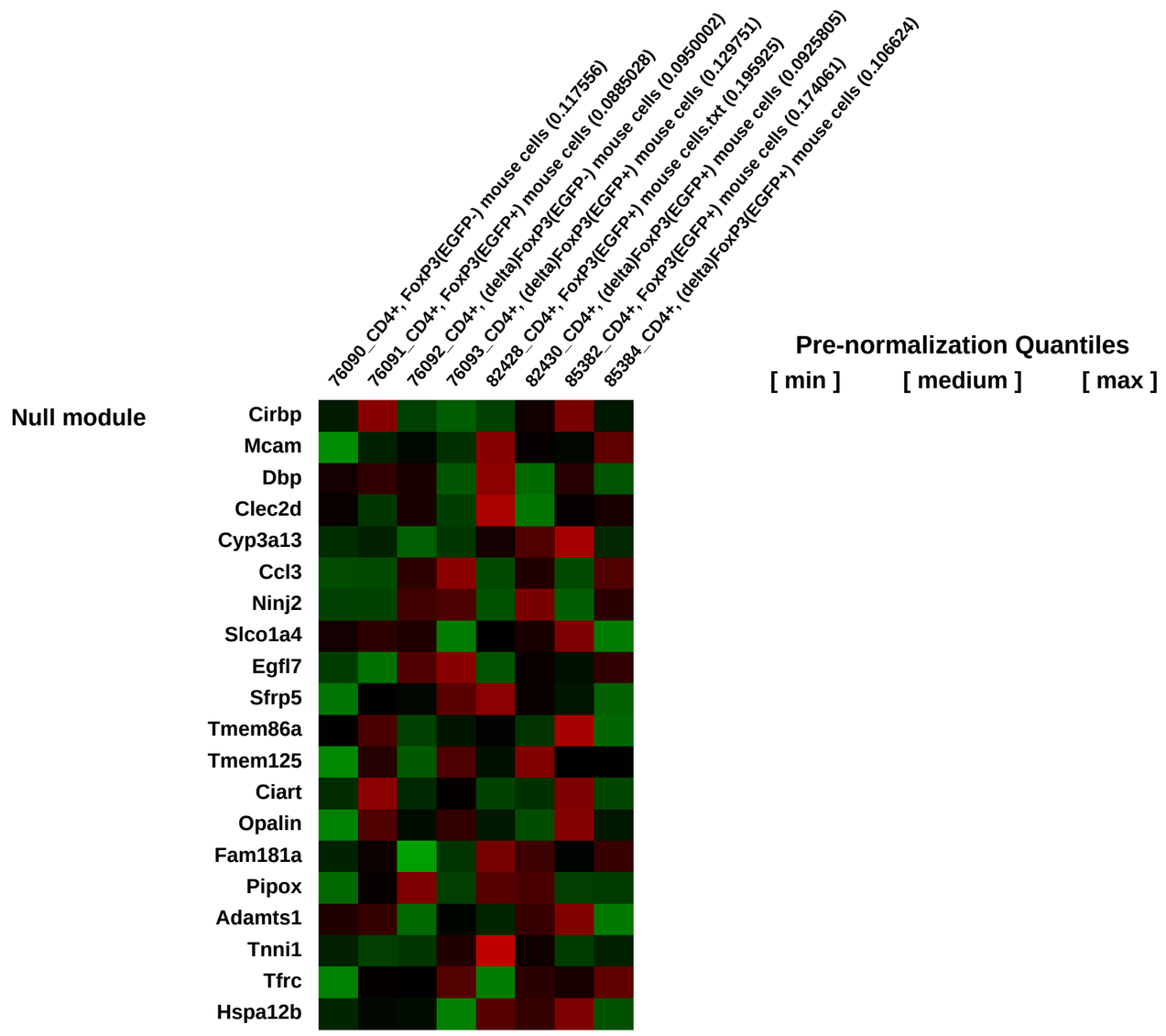

GEO Series "GSE6881" Expression Profiles

Num of samples in this series: 10

Scale of expression profile Z-scores

-3.0 -2.0 -1.0 0.0 1.0 2.0 3.0

GEO Link:	http://www.ncbi.nlm.nih.gov/geo/query/acc.cgi?acc=GSE6881
Status:	Public on Feb 05 2007
Title:	Embryonic Testis Developmental Time Course
Organism:	Mus musculus
Experiment type:	Expression profiling by array
Platform:	GPL1261
Pubmed ID:	15496517
Summary & Design:	**Summary:** Time course of gene expression in the murine embryonic testis from the time of the indifferent gonad (11.5dpc) to birth (18.5dpc) **Keywords: Time Course** **Overall design:** Independent embryonic testis preps were used for array analysis. Duplicates were provided for each sample.

Background corr dist: KL-Divergence = 0.0763, L1-Distance = 0.0229, L2-Distance = 0.0009, Normal std = 0.4853

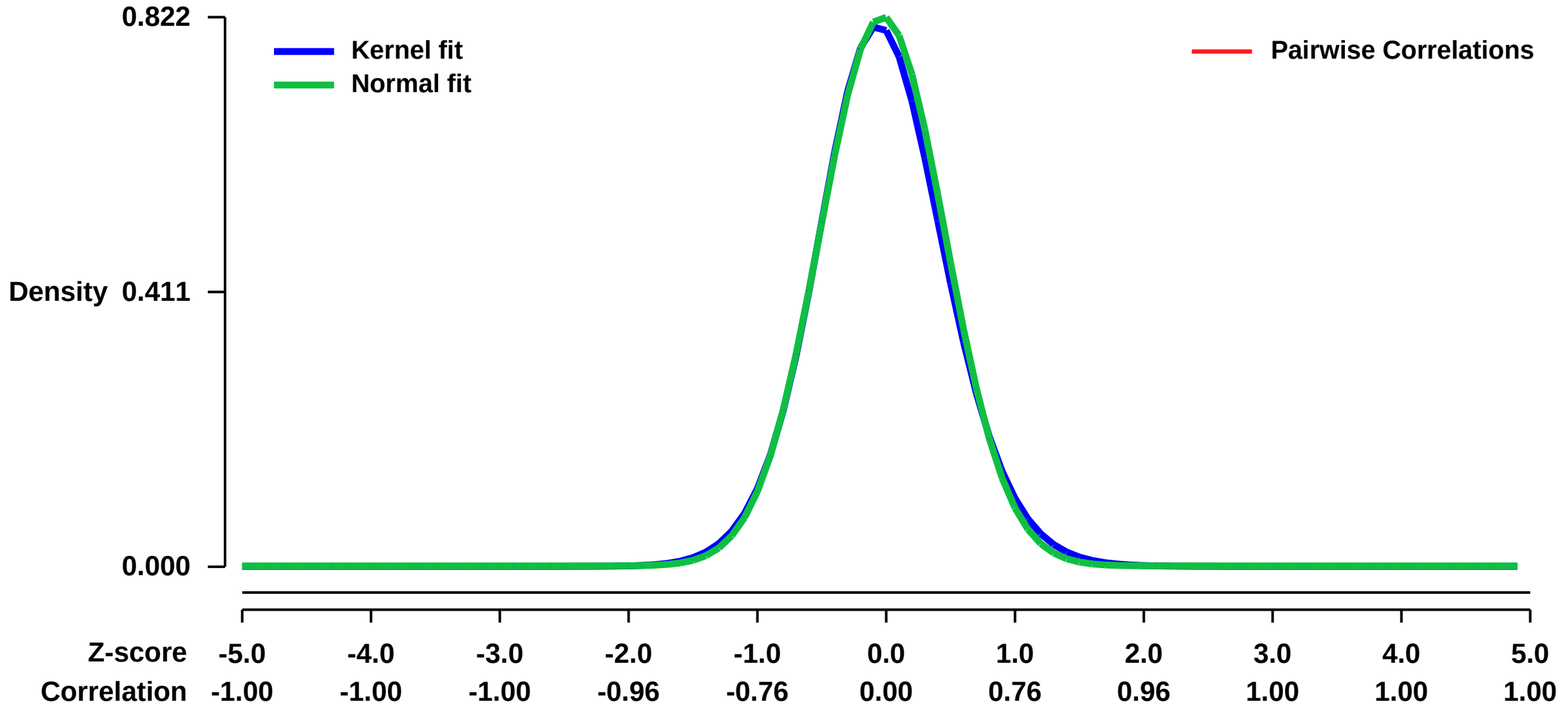

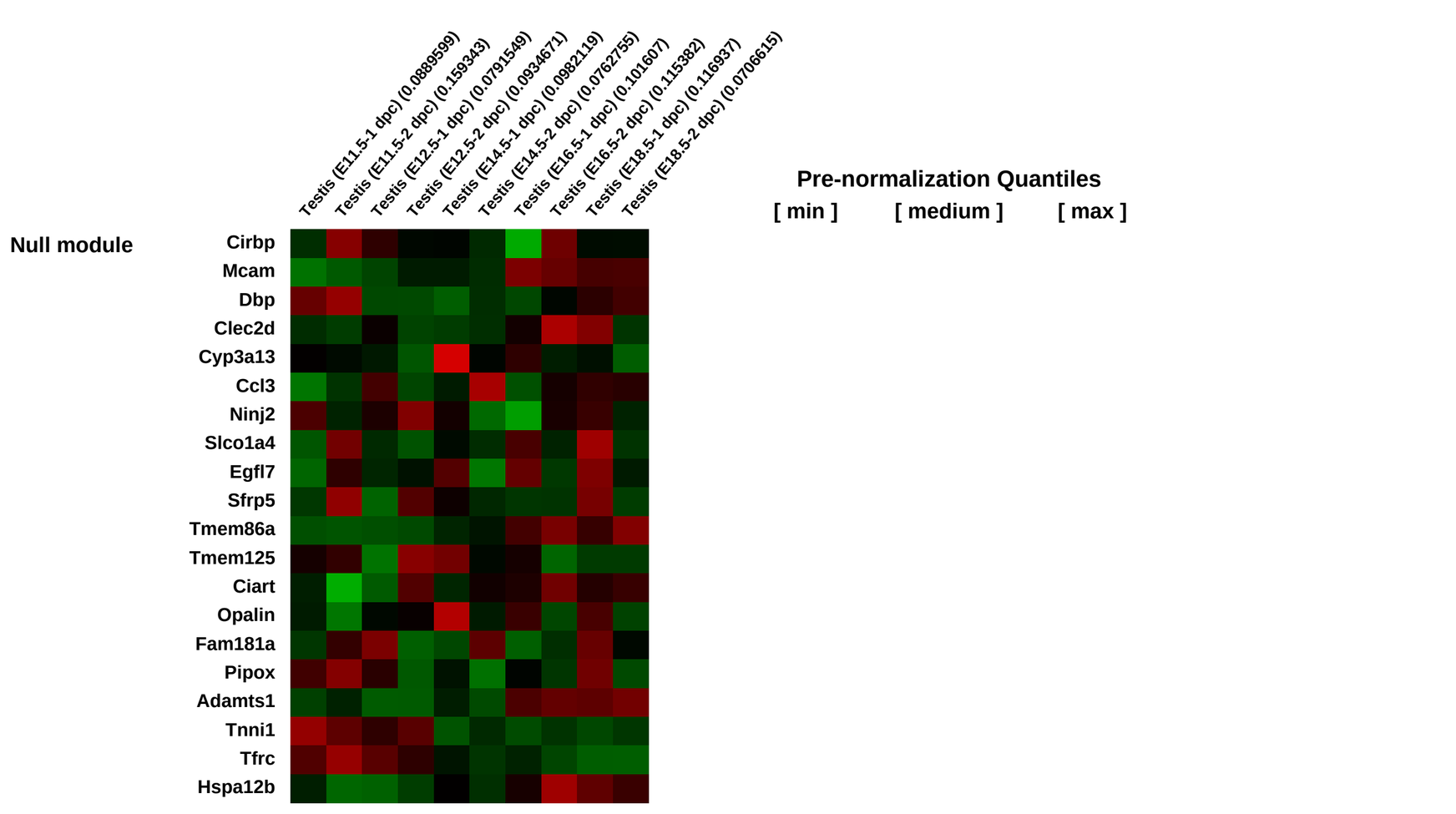

GEO Series "GSE6882" Expression Profiles

Num of samples in this series: 10

Scale of expression profile Z-scores

-3.0 -2.0 -1.0 0.0 1.0 2.0 3.0

GEO Link:	http://www.ncbi.nlm.nih.gov/geo/query/acc.cgi?acc=GSE6882
Status:	Public on Feb 05 2007
Title:	Embryonic Ovary Developmental Time Course
Organism:	Mus musculus
Experiment type:	Expression profiling by array
Platform:	GPL1261
Pubmed ID:	15496517
Summary & Design:	**Summary:** Time course of gene expression in the murine embryonic ovary from the time of the indifferent gonad (11.5dpc) to birth (18.5dpc) **Keywords: Time course** **Overall design:** Independent embryonic ovary preps were used for array analysis. Duplicates were provided for each sample.

Background corr dist: KL-Divergence = 0.0405, L1-Distance = 0.0692, L2-Distance = 0.0059, Normal std = 0.7288

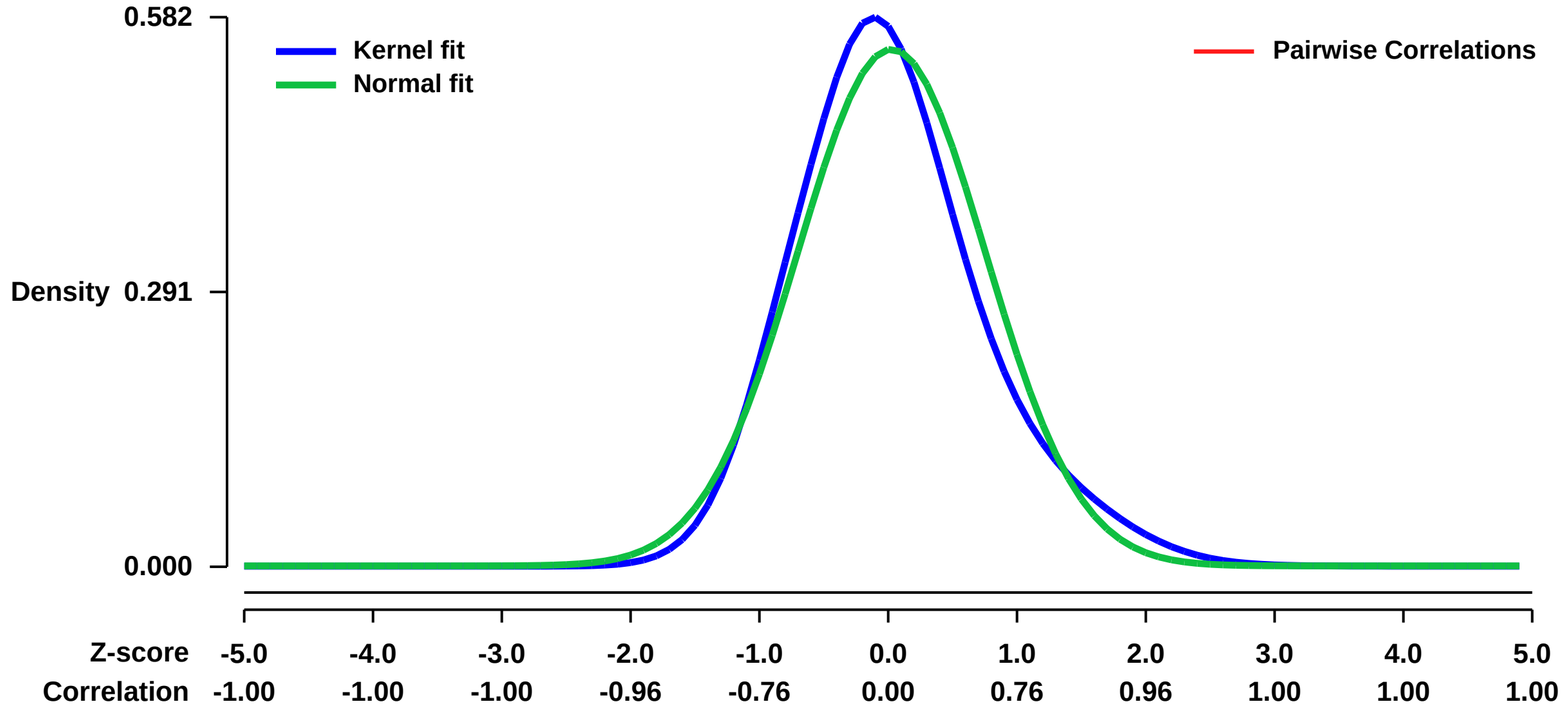

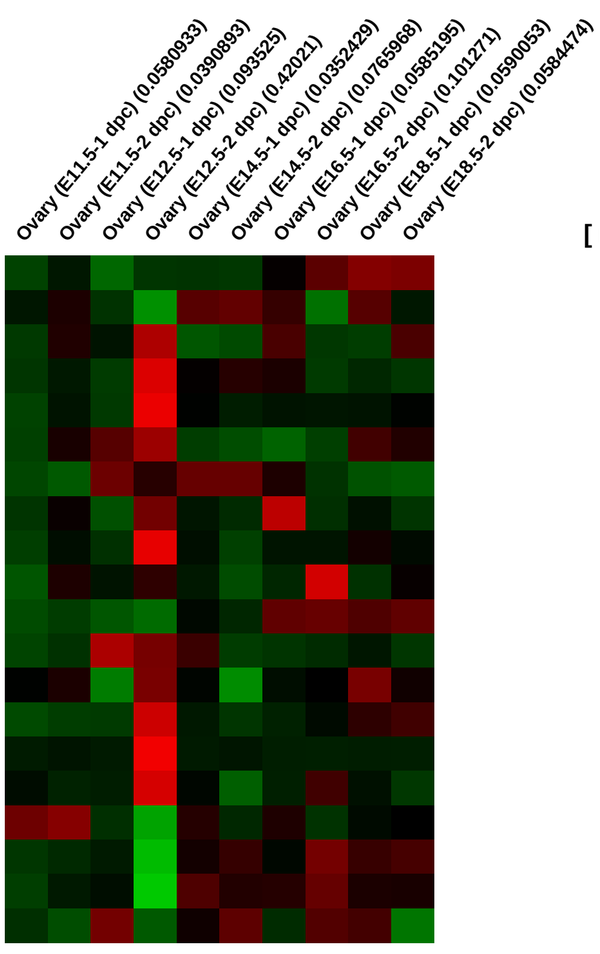

GEO Series "GSE6903" Expression Profiles

Num of samples in this series: 6

Scale of expression profile Z-scores

-3.0 -2.0 -1.0 0.0 1.0 2.0 3.0

GEO Link:	**http://www.ncbi.nlm.nih.gov/geo/query/acc.cgi?acc=GSE6903**
Status:	**Public on Aug 03 2007**
Title:	**Expression data from high-fat diet feeded WT and LIGHT Tg mice**
Organism:	**Mus musculus**
Experiment type:	**Expression profiling by array**
Platform:	**GPL1261**
Pubmed ID:	**17431181**
Summary & Design:	**Summary:** **effect of over-expression LIGHT on T cells for the liver gene expression** **We used microarrays to detail the global programme of gene expression underlying WT and LIGHT Tg liver** **Keywords: genetic difference** **Overall design:** **mice were selected at 4-8 wks old after 2 weeks HFD feeding for RNA extraction and hybridization on Affymetrix microarrays. The total liver were used.**

Background corr dist: KL-Divergence = 0.0282, L1-Distance = 0.0173, L2-Distance = 0.0003, Normal std = 0.6803

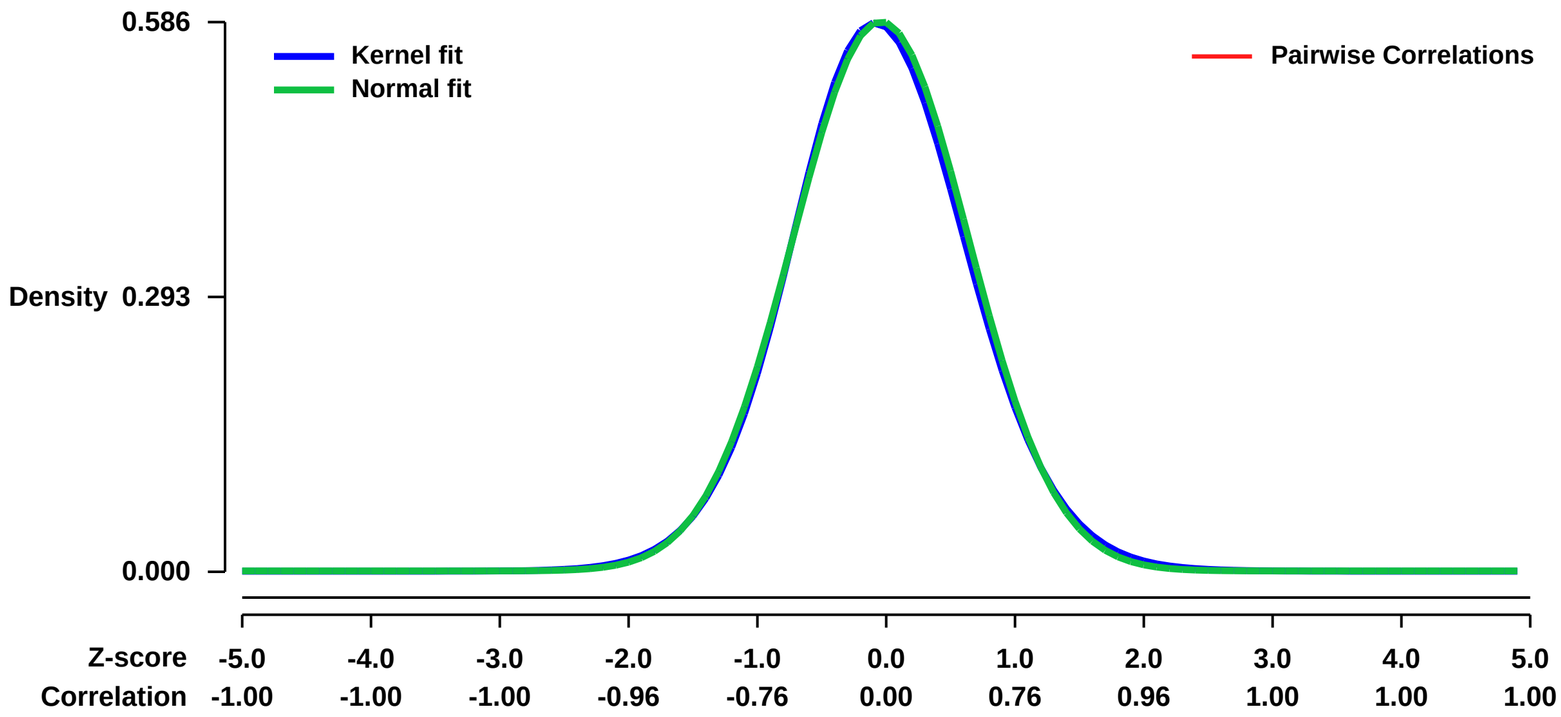

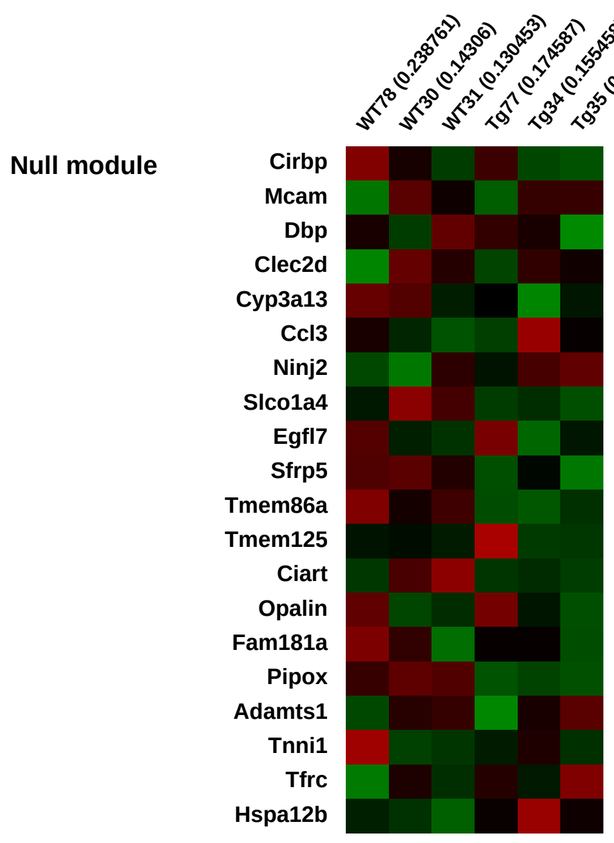

GEO Series "GSE7012" Expression Profiles

Num of samples in this series: 13

Scale of expression profile Z-scores

-3.0 -2.0 -1.0 0.0 1.0 2.0 3.0

GEO Link:	http://www.ncbi.nlm.nih.gov/geo/query/acc.cgi?acc=GSE7012
Status:	Public on May 01 2007
Title:	Identif. of oscillatory genes in somitogenesis from functional genomic analysis of C2C12 myoblast line
Organism:	Mus musculus
Experiment type:	Expression profiling by array
Platform:	GPL1261
Pubmed ID:	17362910
Summary & Design:	**Summary:** During somitogenesis, oscillatory expression of genes in the notch and wnt signaling pathways plays a key role in regulating segmentation. These oscillations in expression levels are elements of a species-specific developmental mechanism. To date, the periodicity and components of the human clock remain unstudied. Here we show that a human mesenchymal stem/stromal cell (MSC) model can be induced to display oscillatory gene expression. We observed that the known cycling gene HES1 oscillated with a 5 hour period, consistent with available data on the rate of somitogenesis in humans. We also observed cycling of Hes1 expression in mouse C2C12 myoblasts with a period of 2 hours, consistent with previous in vitro and embryonic studies. Furthermore, we used microarray and quantitative PCR (Q-PCR) analysis to identify additional genes that display oscillatory expression both in vitro and in mouse embryos. We confirmed oscillatory expression of the notch pathway gene Maml3 and the wnt pathway gene Nkd2 by whole mount in situ hybridization analysis and Q-PCR. Expression patterns of these genes were disrupted in Wnt3atm1Amc mutants but not in Dll3pu mutants. Our results demonstrate that human and mouse in vitro models can recapitulate oscillatory expression observed in embryo and that a number of genes in multiple developmental pathways display dynamic expression in vitro. **Keywords: time series** **Overall design:** Synchronization of C2C12 myoblasts was carried out as follows: T-25 cm flasks were set up in parallel. These cells were grown to 90% confluence in DMEM supplemented with 5% FBS then incubated in DMEM with only 0.2% FBS for 24 hours, and returned to DMEM supplemented with FBS. Samples were collected every 30 min. for 8 hours.

Background corr dist: KL-Divergence = 0.1130, L1-Distance = 0.0298, L2-Distance = 0.0017, Normal std = 0.4214

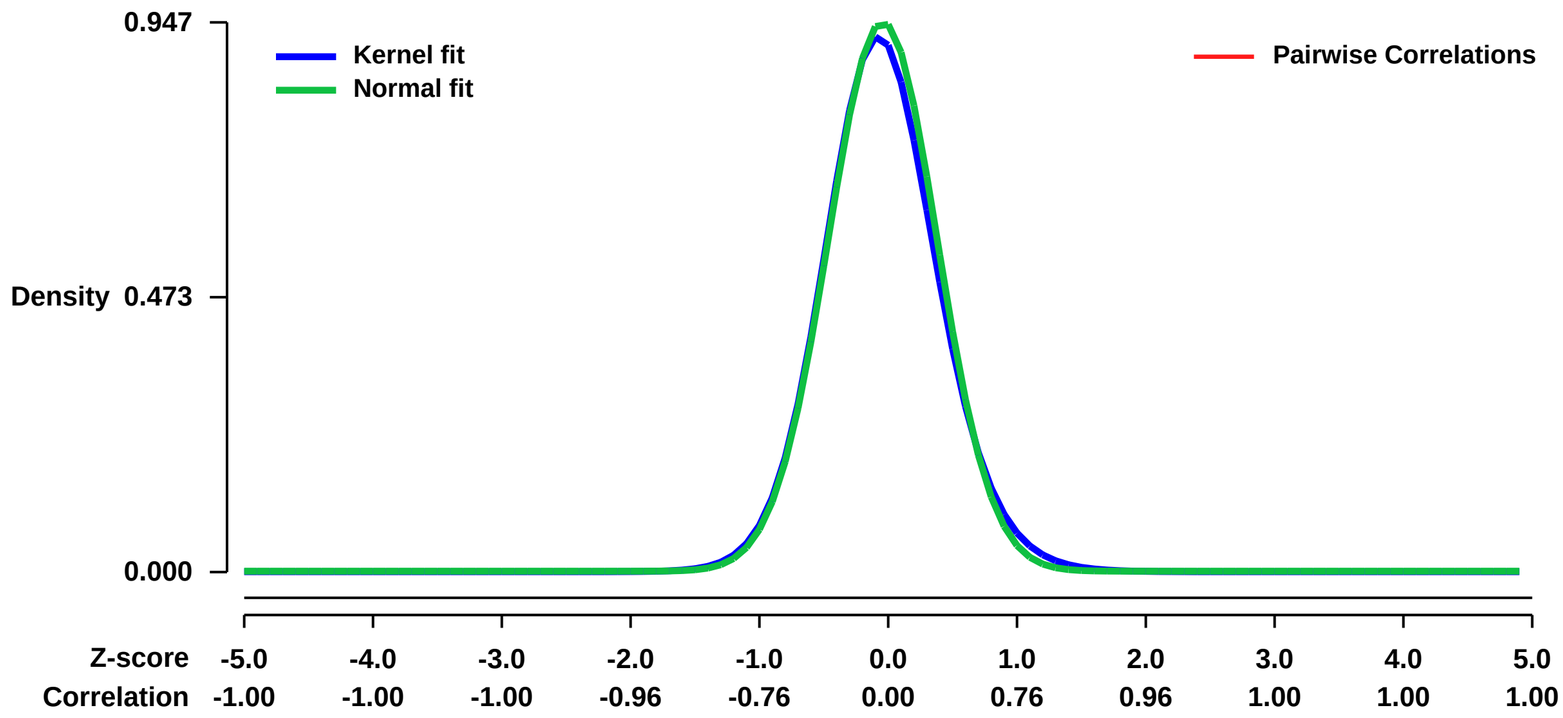

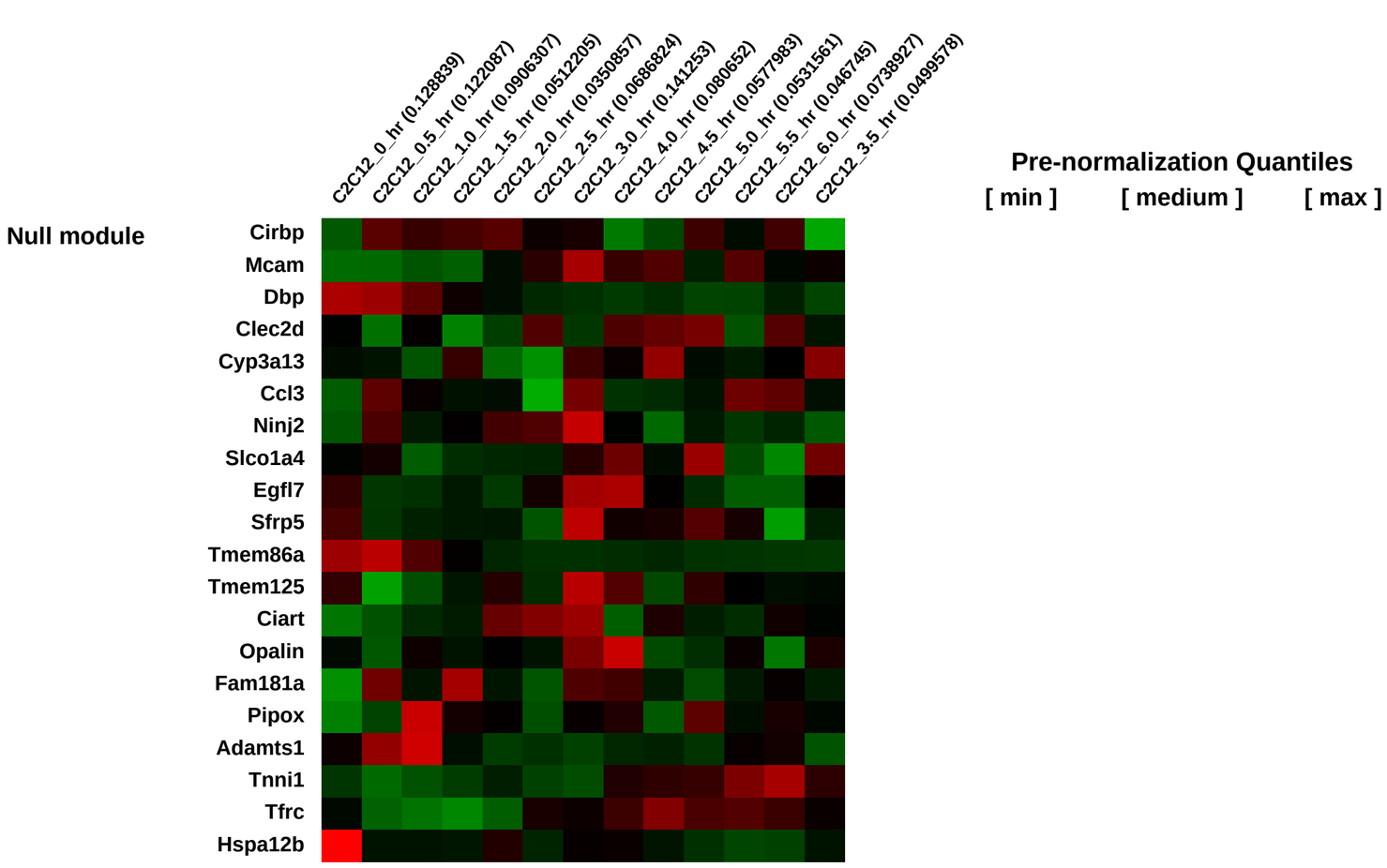

GEO Series "GSE7020" Expression Profiles

Num of samples in this series: 8

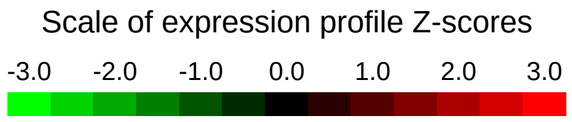

GEO Link:	http://www.ncbi.nlm.nih.gov/geo/query/acc.cgi?acc=GSE7020
Status:	Public on Feb 14 2007
Title:	The molecular consequences of Nix ablation on apoptosis and erythropoiesis
Organism:	Mus musculus
Experiment type:	Expression profiling by array
Platform:	GPL1261
Pubmed ID:	17420462
Summary & Design:	**Summary:** Normal erythropoiesis requires a critical balance between proapoptotic and antipaoptotic pathways. Bcl-xl, an antiapoptotic protein is induced at end-stages of differentiation of erythroid precursors in response to erythropoietin. The details of the proapoptotic pathway and the critical proapoptotic proteins inhibited by Bcl-xl in erythropoiesis are not well understood. We employed gene targeting to ablate Nix, a proapoptotic BH3-domain only Bcl2 family protein, which is known to be transcriptionally induced during erythropoiesis. Nix null mice exhibited reticulocytosis and thrombocytosis in the peripheral blood; and profound splenomegaly with erythroblastosis in the spleen and bone marrow despite normal erythropoietin levels and blood oxygen tension. In vivo apoptosis was diminished in erythroblast precursors from Nix null spleens. To define the molecular consequences of Nix ablation on apoptosis and erythropoiesis, we conducted a detailed comparative analysis of gene expression in spleens from 8 week old Nix null mice and wild type controls. Of 45,101 genes analyzed, 514 were significantly upregulated and 386 down-regulated in Nix-/- splenocytes. Functional cluster analysis delineated the ten most highly regulated gene sets, revealing increased levels of cell cycle and erythroid genes, with decreased levels of cell death and B-cell genes. **Keywords: strain comparison** **Overall design:** In the study, we hybridized RNA from 8 week old spleens of wild type (WT) control and Nix null mice (Nix-/-) to Affymetrix MOE430A GeneChip´fi arrays containing 45,101 well characterized mouse genes/ESTs.

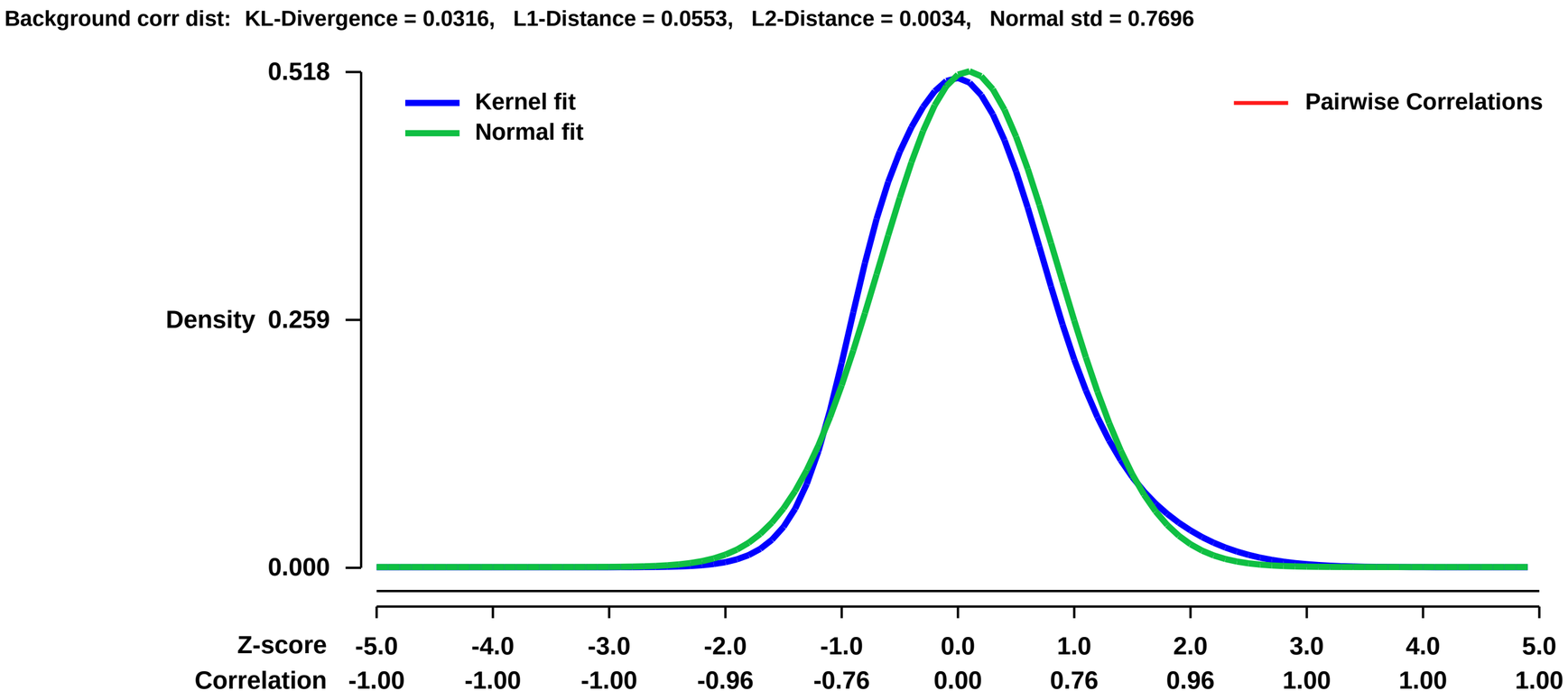

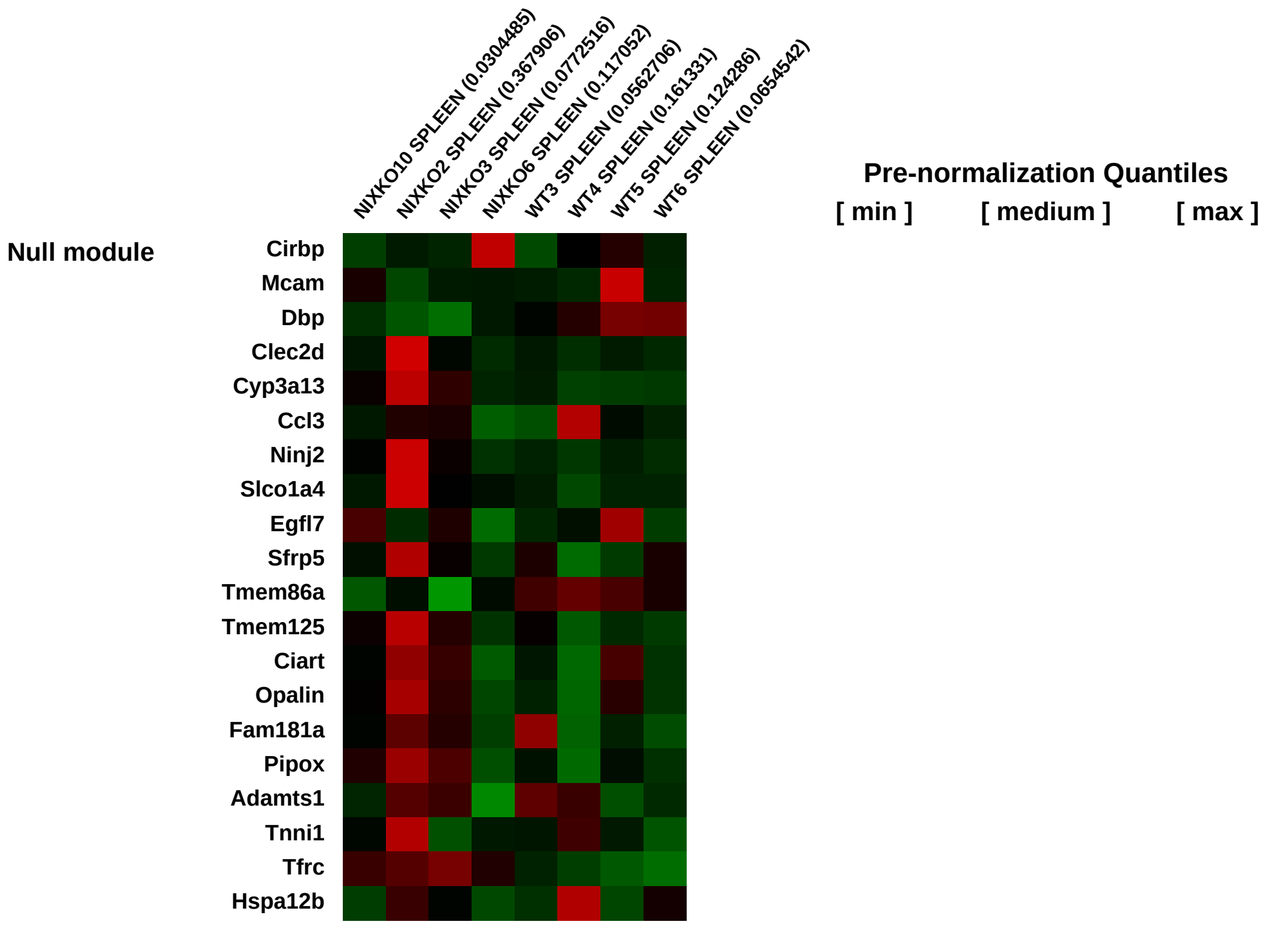

GEO Series "GSE7111" Expression Profiles

Num of samples in this series: 6

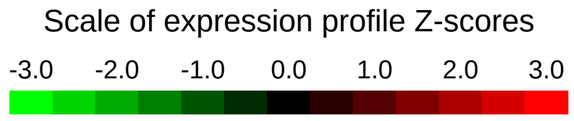

GEO Link:	**http://www.ncbi.nlm.nih.gov/geo/query/acc.cgi?acc=GSE7111**
Status:	**Public on Dec 25 2012**
Title:	**Resveratrol treatment of 3T3-L1 cells**
Organism:	**Mus musculus**
Experiment type:	**Expression profiling by array**
Platform:	**GPL1261**
Pubmed ID:	
Summary & Design:	**Summary:** **Murine 3T3-L1 progenitor adipocytes cell cultures, treated and untreated (Control) with resveratrol before the induction of differentiation and the effects on adipogenesis and insulin signaling was investigated.** **Keywords: Treatment response** **Overall design:** **3 Replicates of treated and untreated (Control) cell cultures**

Background corr dist: **KL-Divergence = 0.0438, L1-Distance = 0.0219, L2-Distance = 0.0005, Normal std = 0.6019**

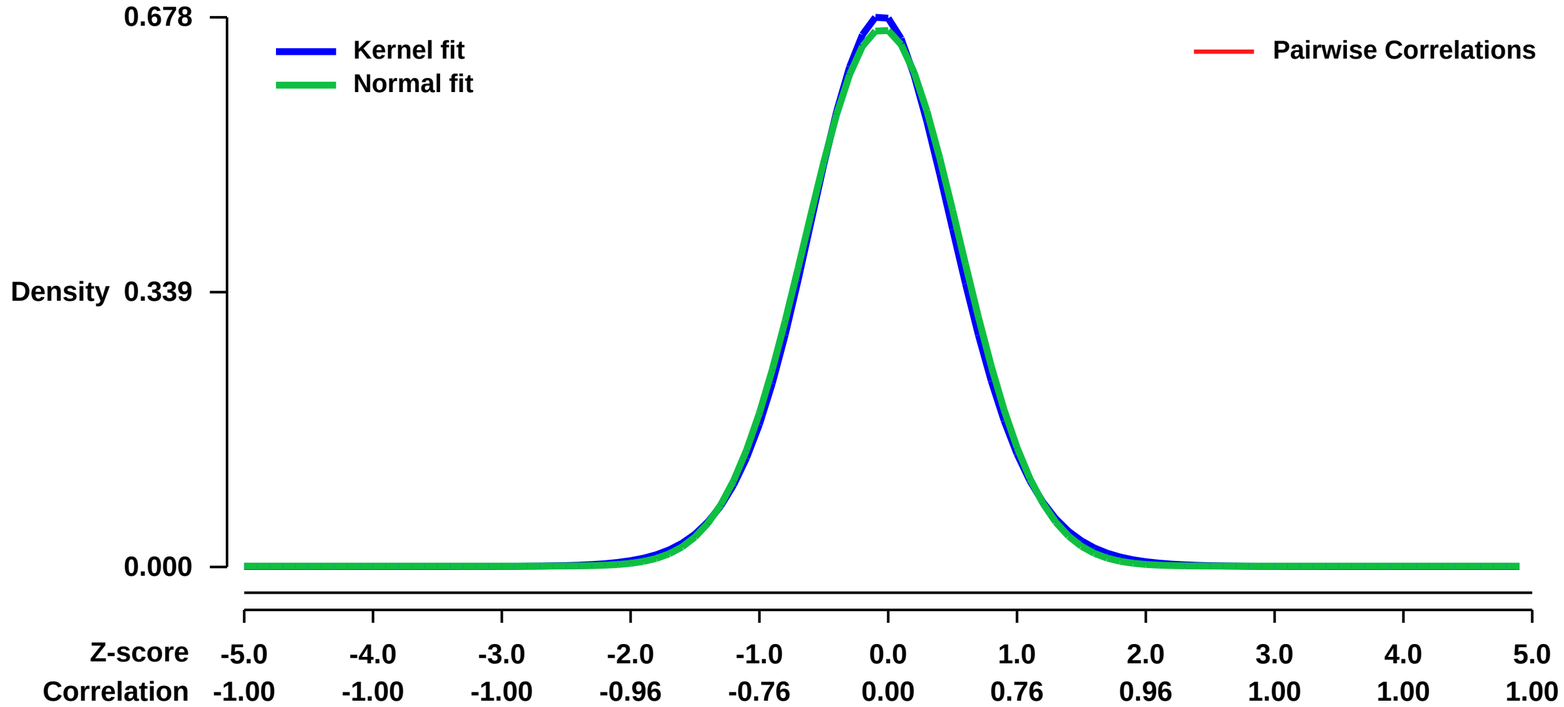

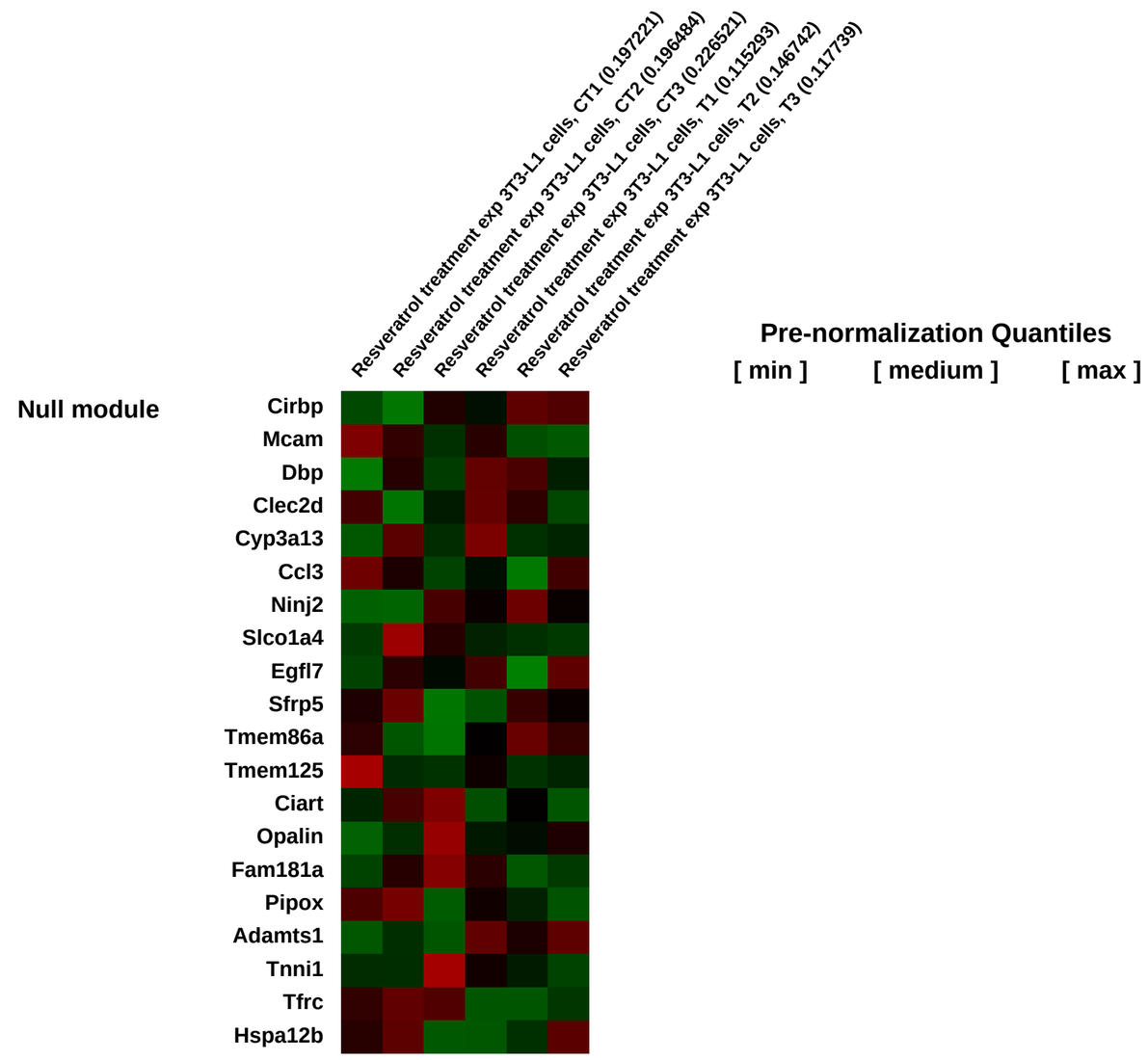

GEO Series "GSE7141" Expression Profiles

Num of samples in this series: 6

Scale of expression profile Z-scores

-3.0 -2.0 -1.0 0.0 1.0 2.0 3.0

GEO Link:	http://www.ncbi.nlm.nih.gov/geo/query/acc.cgi?acc=GSE7141
Status:	Public on Jan 01 2008
Title:	mRNA expression analysis of undifferentiated Dicer +/- (D4) and Dicer -/- (27H10) embryonic cell lines
Organism:	Mus musculus
Experiment type:	Expression profiling by array
Platform:	GPL1261
Pubmed ID:	18311153
Summary & Design:	**Summary:** We have analyzed the transcript expression levels in Dicer heterozygous and Dicer knock-out embryonic stem (ES) cells in order to identify which transcripts are regulated by RNAi pathway in mouse ES cells. **Keywords: Cell type comparison of cell line with or without knock-out** **Overall design:** Two cell lines were analysed in an undifferentiated state. Triplicates of both cell lines were analyzed.

Background corr dist: KL-Divergence = 0.0260, L1-Distance = 0.0446, L2-Distance = 0.0022, Normal std = 0.7653

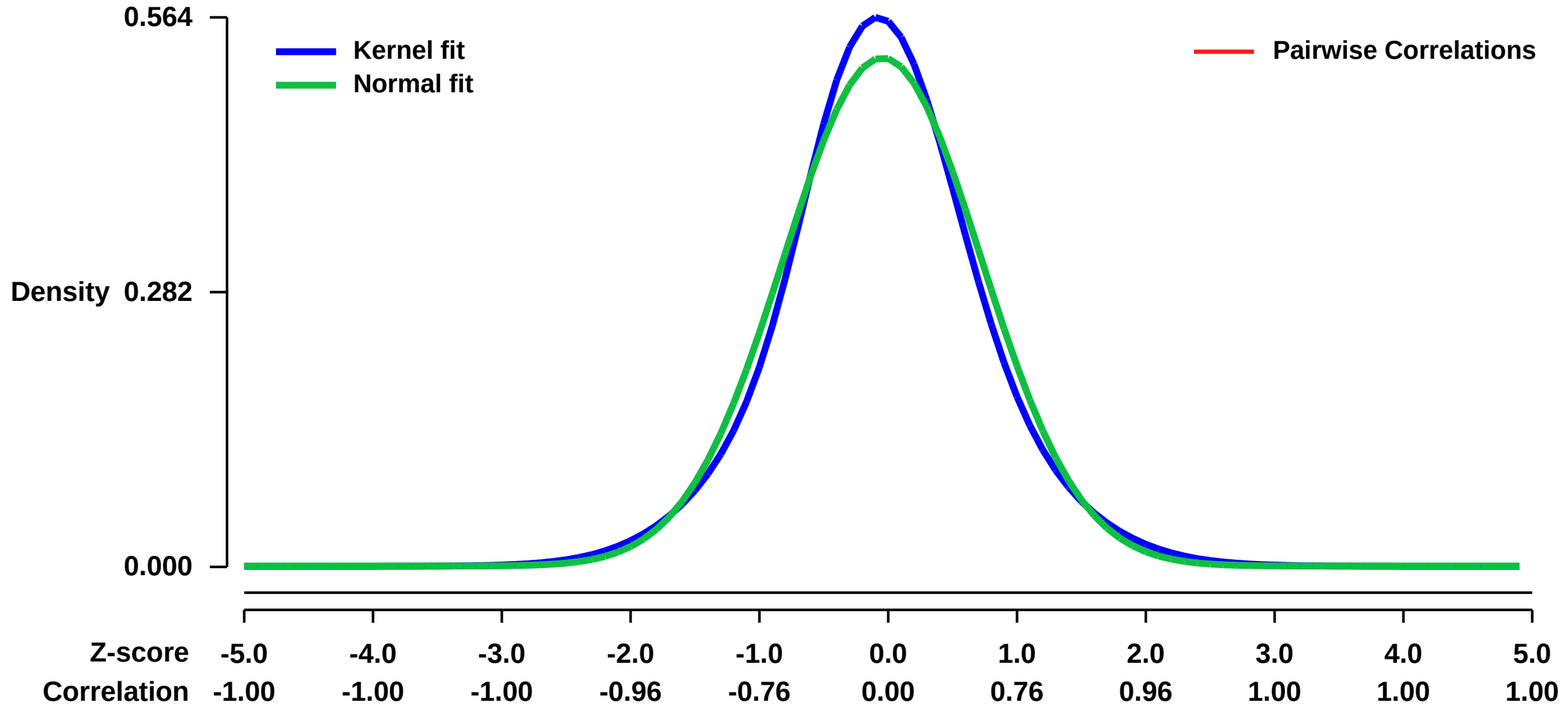

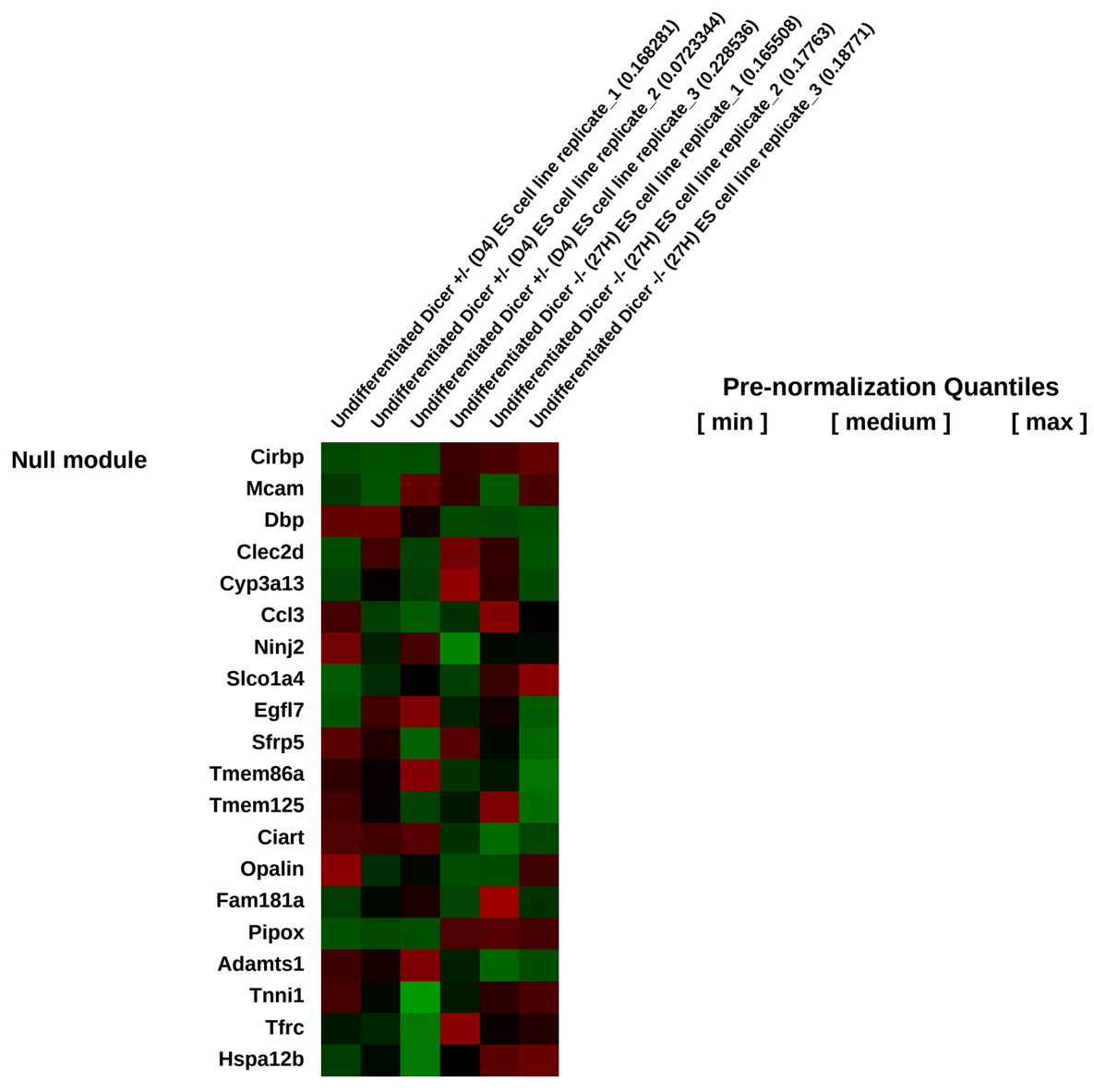

GEO Series "GSE7155" Expression Profiles

Num of samples in this series: 9

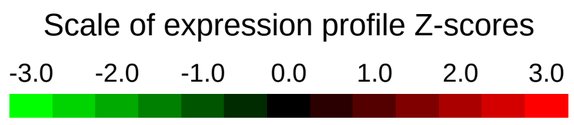

GEO Link:	http://www.ncbi.nlm.nih.gov/geo/query/acc.cgi?acc=GSE7155
Status:	Public on Jul 30 2007
Title:	Expression data from adult laboratory mouse brain hemispheres
Organism:	Mus musculus
Experiment type:	Expression profiling by array
Platform:	GPL1261
Pubmed ID:	17936574
Summary & Design:	**Summary:** Inbred congenic strain B6.C6.132.54/Vad was created using C57BL/6ByJ background and BALB/cJ donor strains. Flanking background markers at chr. 6: 75.9 Mb (rs4226008, NCBI Mouse Build 36 / dbSNP Build 126) and 122.3 Mb (rs3023093), and limiting donor markers at 81.9 Mb (rs4226024) and at 91.8 Mb (rs3712161) defined the introgressed region. We concluded the segment size must be between 9.9 Mb and 46.4 Mb. In a Quantitative Trait Gene identification study we compared brain (without cerebellum) gene expression between progenitors and congenics. Such comparisons can facilitate identification of cis-regulated genes and to establish genetic control of a complex phenotype whose expression is associated with the introgressed chromosome segment. We used microarrays to detail the global programme of gene expression underlying cellularisation and identified distinct classes of up-regulated genes during this process. **Keywords:** strain comparison **Overall design:** Experiments were carried out in three batches. In each batch 10 animals per strain were used. After processing each hemisphere separately, 10 hemispheres were pooled for one high-density oligonucleotide microarray (Mouse Genome 430 2.0, Affymetrix, Santa Clara, CA). For each strain 3 oligonucleotide microarrays were used (n=3). We used adult, untreated, male mice (n=30, 90 mice in toto).

Background corr dist: KL-Divergence = 0.0759, L1-Distance = 0.0218, L2-Distance = 0.0007, Normal std = 0.4870

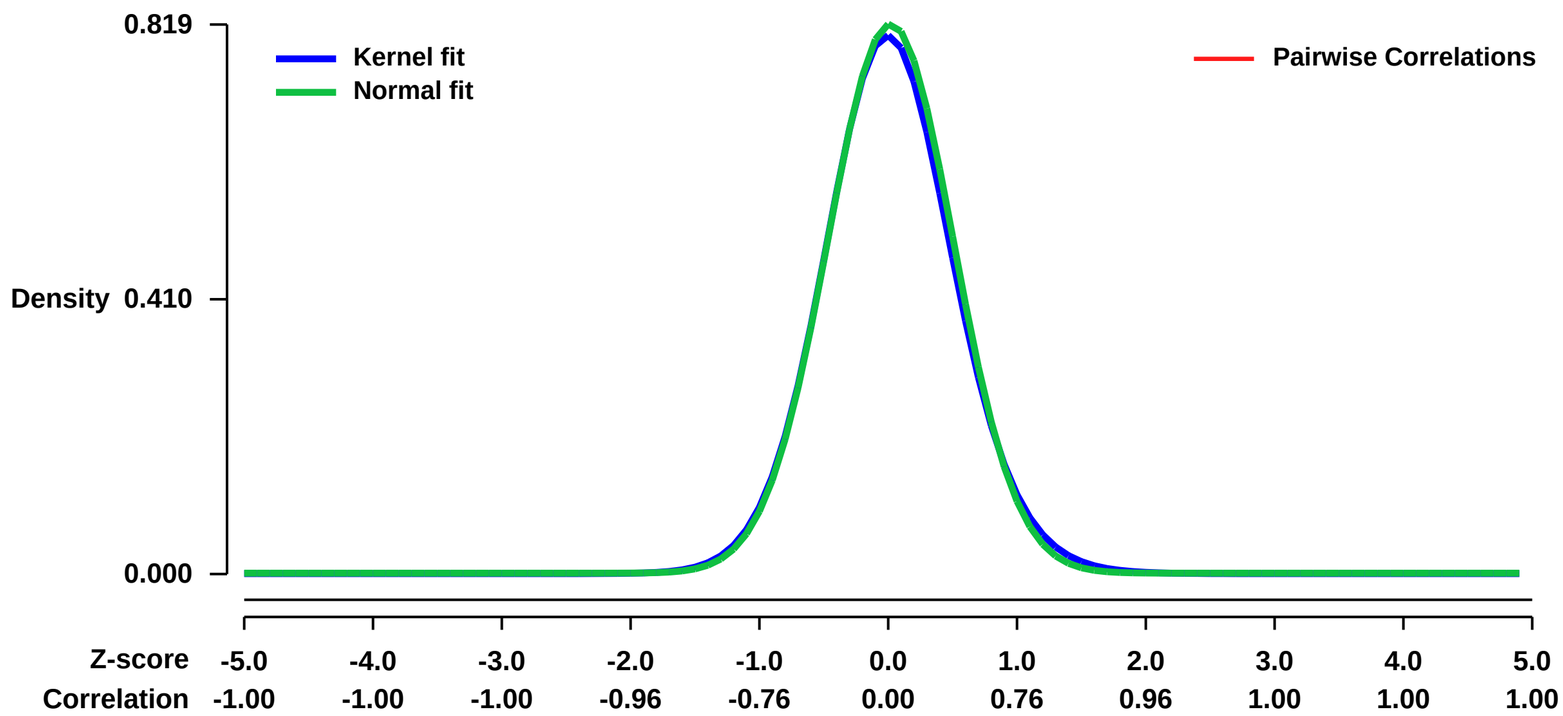

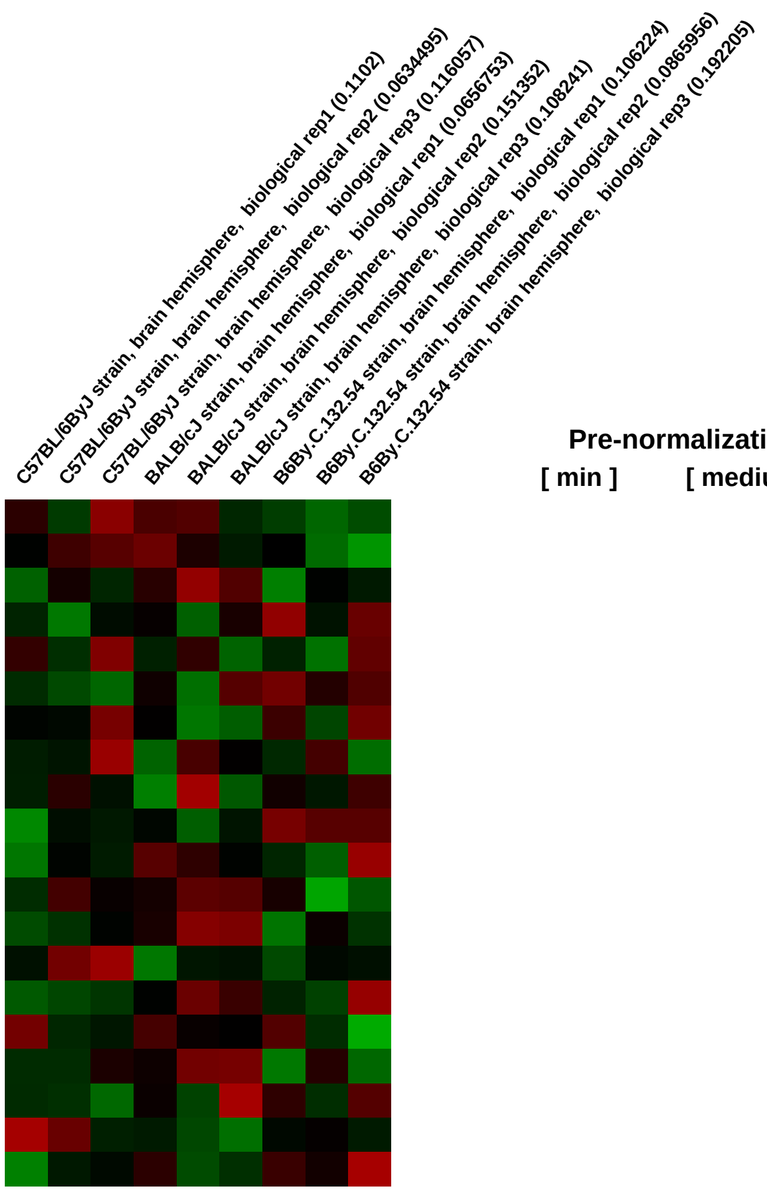

GEO Series "GSE7196" Expression Profiles

Num of samples in this series: 6

Scale of expression profile Z-scores

-3.0 -2.0 -1.0 0.0 1.0 2.0 3.0

GEO Link:	http://www.ncbi.nlm.nih.gov/geo/query/acc.cgi?acc=GSE7196
Status:	Public on Mar 08 2007
Title:	Differential gene expression between WT and ERRa-null hearts
Organism:	Mus musculus
Experiment type:	Expression profiling by array
Platform:	GPL1261
Pubmed ID:	17488637
Summary & Design:	**Summary:** Total RNA was isolated from 3 WT and 3 ERRa null hearts and independent hybridizations were performed using MOE430 2.0 microarrays. Expression profiling was conducted to determine changes in gene expression in hearts lacking ERRa. The expression of genes involved in heart and muscle development, muscle contraction, lipid metabolism, OxPhos, protein metabolism and transcription were affected by the loss of ERRa. **Keywords: microarray and genetic modification** **Overall design:** 3 hearts from WT and 3 hearts from ERRa-null mice were used in the study. The expression of genes in the ERRa KO hearts were compared to the reference WT hearts.

Background corr dist: KL-Divergence = 0.0468, L1-Distance = 0.0226, L2-Distance = 0.0006, Normal std = 0.5889

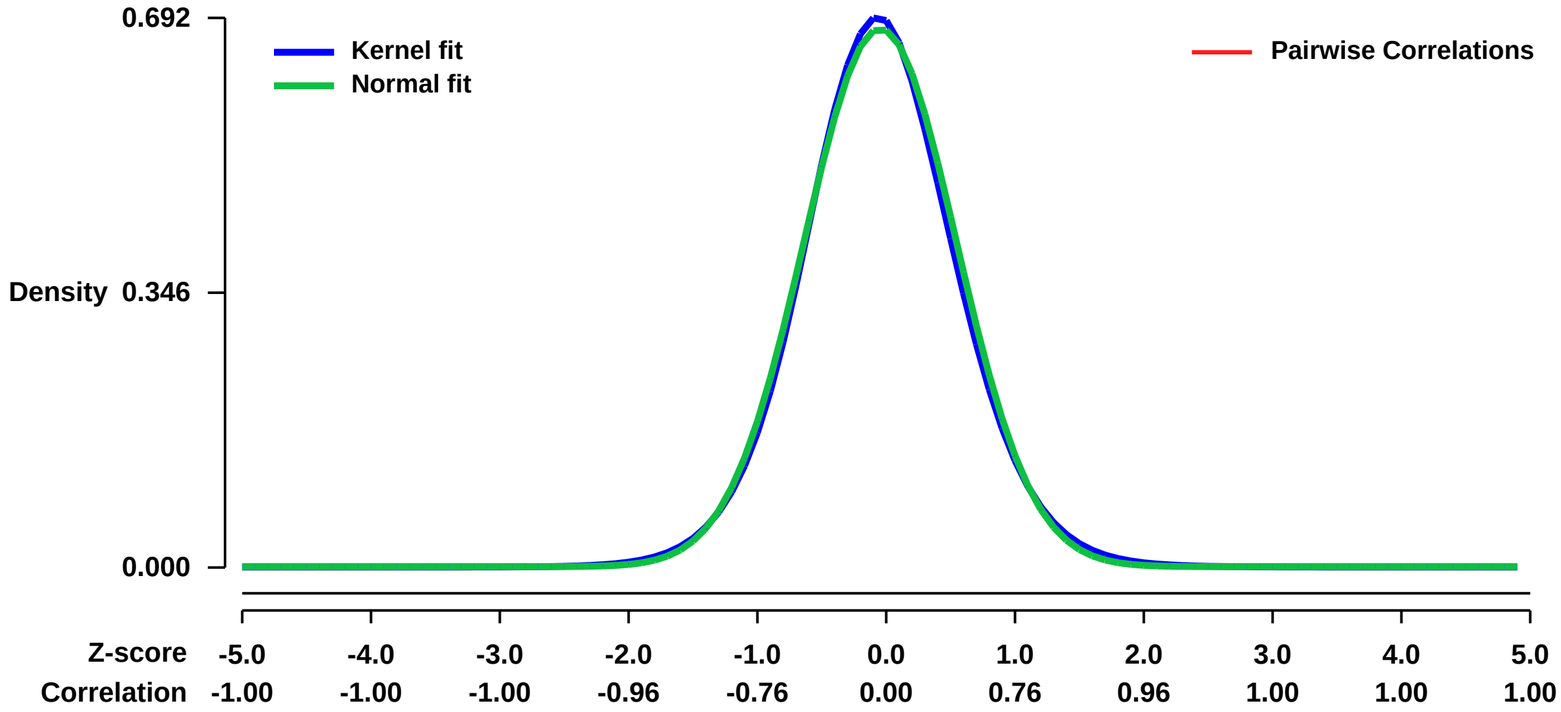

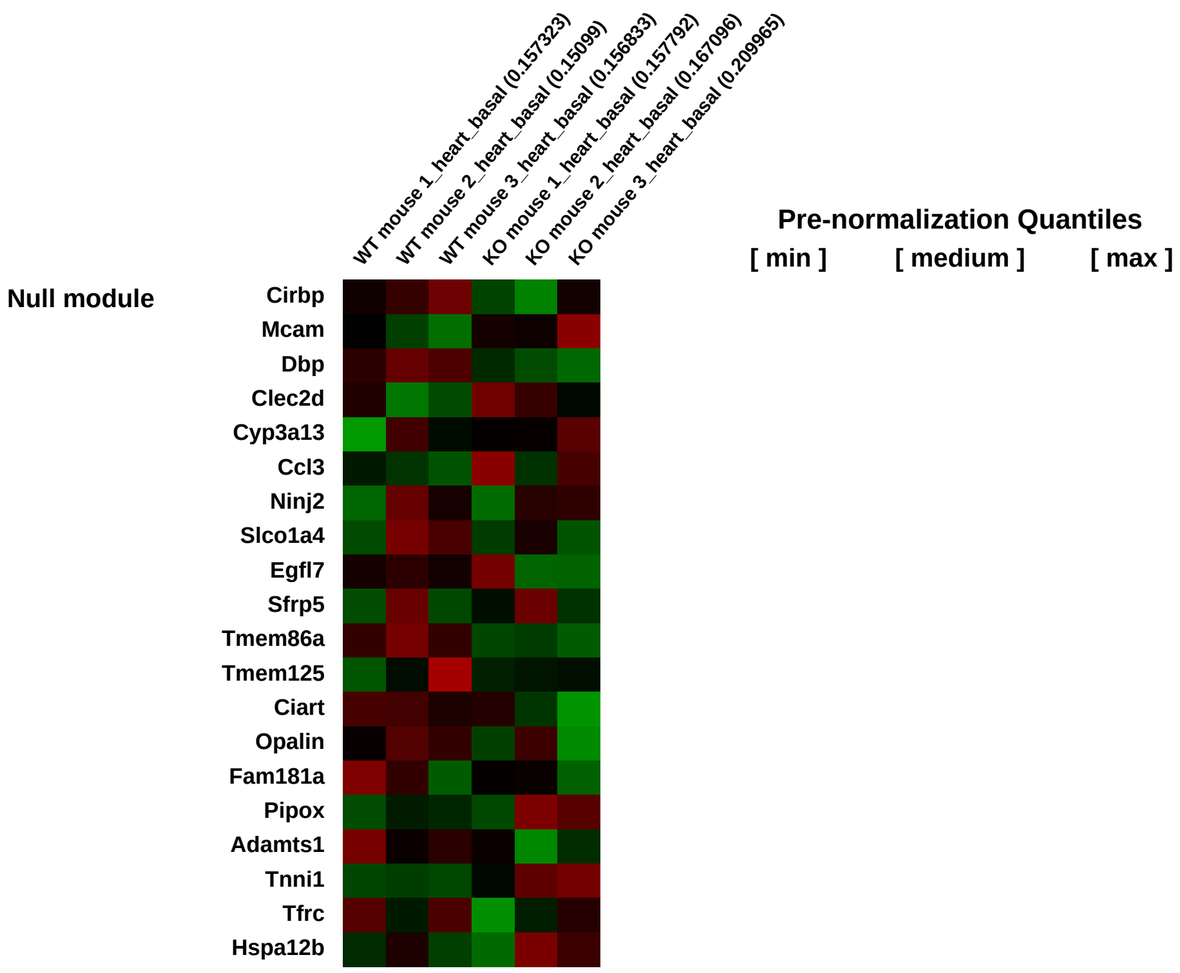

GEO Series "GSE7225" Expression Profiles

Num of samples in this series: 9

Scale of expression profile Z-scores

-3.0 -2.0 -1.0 0.0 1.0 2.0 3.0

GEO Link:	http://www.ncbi.nlm.nih.gov/geo/query/acc.cgi?acc=GSE7225
Status:	Public on Oct 22 2007
Title:	Identification and characterization of the changed transcripts in cumulus cells of Bmp15-/- and Bmp15-/-Gdf9+/--DM mice.
Organism:	Mus musculus
Experiment type:	Expression profiling by array
Platform:	GPL1261
Pubmed ID:	21047911
Summary & Design:	**Summary:** Mouse oocytes control cumulus cell metabolic processes that are deficient in the oocytes themselves and this delegation is necessary for oocyte development. Oocyte-derived bone morphogenetic factor 15 (BMP15) and growth differentiation factor 9 (GDF9) appear to be key regulators of follicular development. The effect of these factors on cumulus cell function before the preovulatory surge of luteinizing hormone (LH) was assessed by analysis of the transcriptomes of cumulus cells from wildtype (WT), Bmp15-/-, and Bmp15-/- Gdf9+/- double mutant (DM) mice using microarray analysis. The biological themes associated with the most highly-affected transcripts were identified using bioinformatic approaches, IPA and GenMAPP/MAPPFinder. There were 5,332, 7,640, and 2,651 transcripts identified to be significantly changed in the comparisons of Bmp15-/- vs. WT, DM vs. WT, and DM vs. Bmp15-/- respectively by the criteria of FC (fold change) p <0.01. Among theses changed transcripts, 744 were commonly changed in all three pair-wise comparisons, and hence were considered to be the most highly affected transcripts by mutation of Bmp15 and Gdf9. IPA Analyses revealed that metabolism was the major theme associated with the most highly-changed transcripts: glycolysis and sterol biosynthesis were the two most significantly affected pathways. Most of the transcripts encoding enzymes for sterol biosynthesis were down-regulated in both mutant cumulus cells and in WT cumulus cell after oocytectomy. Similarly, there was a reduction of de novo-synthesized cholesterol in these cumulus cells. This suggests that oocytes regulate cumulus cell metabolism, particularly sterol biosynthesis, by promoting the expression of corresponding transcripts. Furthermore, in WT-mice, Mvk, Pmvk, Fdps, Sqle, Cyp51, Sc4mol, and Ebp, which encode enzymes in the sterol biosynthetic pathway, were found to be expressed robustly in cumulus cells, but expression was barely detectable in oocytes. Levels of de novo-synthesized cholesterol were significantly higher in cumulusâ enclosed oocytes than denuded oocytes. These results indicate that mouse oocytes are deficient in their ability to synthesize cholesterol and require cumulus cells to provide them with products of the sterol biosynthetic pathway. Oocyte-derived BMP15 and GDF9 may promote this metabolic pathway in cumulus cells as compensation for their own deficiencies. **Keywords:** Gdf9, Bmp15, cumulus cells, transcriptome, metabolism, sterol biosynthesis, genotype comparison, microarray, ingenuity pathways analyses. **Overall design:** GC_430_2_GES05_0169_033105_1.CEL

Background corr dist: KL-Divergence = 0.0629, L1-Distance = 0.0203, L2-Distance = 0.0005, Normal std = 0.5154

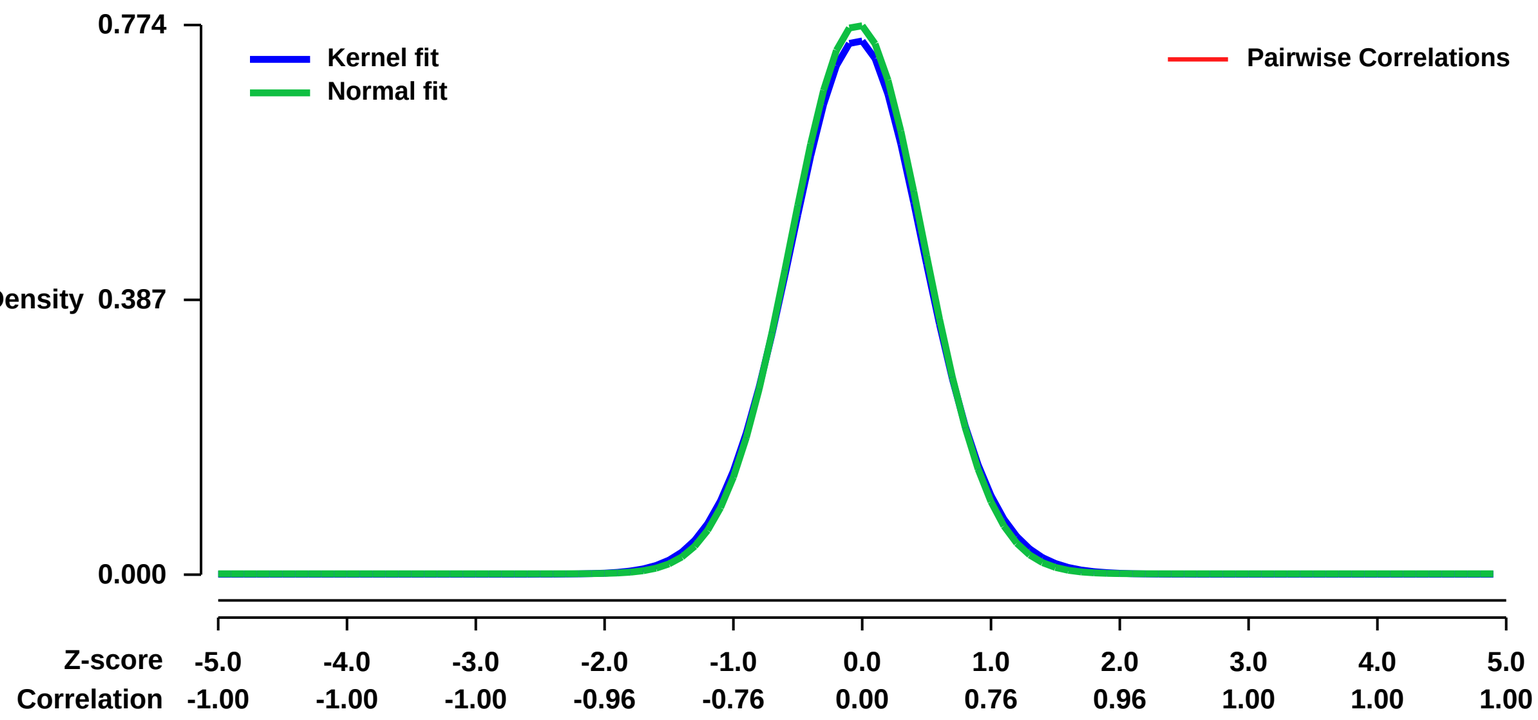

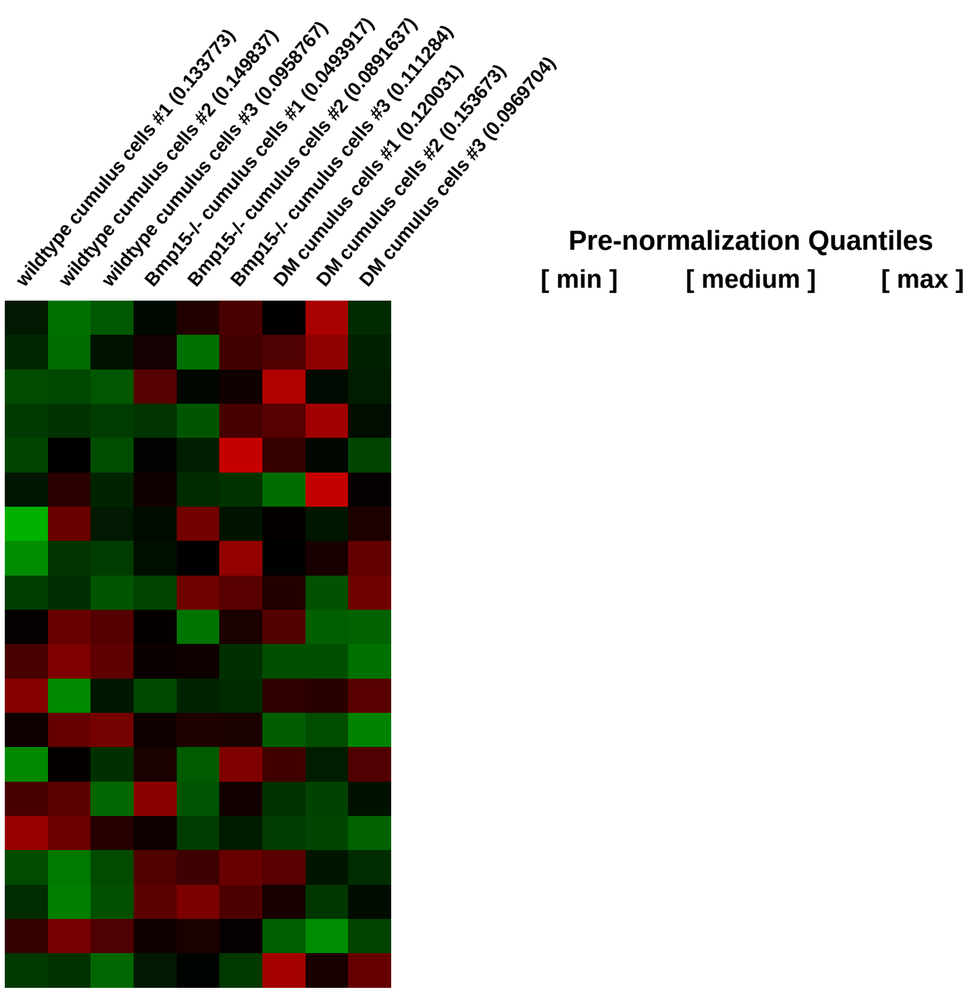

GEO Series "GSE7257" Expression Profiles

Num of samples in this series: 9

Scale of expression profile Z-scores

-3.0 -2.0 -1.0 0.0 1.0 2.0 3.0

GEO Link:	http://www.ncbi.nlm.nih.gov/geo/query/acc.cgi?acc=GSE7257
Status:	Public on Apr 10 2007
Title:	Laser capture-microarray analysis of Lim1 mutant kidney development.
Organism:	Mus musculus
Experiment type:	Expression profiling by array
Platform:	GPL1261
Pubmed ID:	17610272
Summary & Design:	**Summary:** The Lim1 gene has essential functions during several stages of kidney development. In particular, a tissue specific knockout in the early metanephric mesenchyme results in the formation of the earliest nephron precursor, the renal vesicle, but failure of this structure to progress to the next stage, the comma shaped body. To better understand the molecular nature of this developmental arrest we used a laser capture microdissection-microarray strategy to examine the perturbed gene expression pattern of the mutant renal vesicles. Among the genes found differently expressed were Chrdl2, an inhibitor of BMP signaling, the pro-apoptotic factor Bmf, as well as myob5, an atypical myosin which modulates chemokine and transferring signaling, and pdgfr1, which is important in epithelial folding. Of particular interest, the microarray data indicated that the Dkk1 gene, which encodes an inhibitor of Wnt signaling, was downregulated nine fold in mutants. This was confirmed by in situ hybridizations. It is interesting to note that Lim1 and Dkk1 mutant mice have striking similarities in phenotype. These results suggest that the Dkk1 gene might be a key downstream effector of Lim1 function. **Keywords:** Lim1 mutant, kidney development, gene expression profile comparison **Overall design:** We compared gene expression profiles of wild type and mutant Lim1 renal vesicles, which were isolated from E12.5 kidneys by laser capture microdissection. Nine biological independent samples were examined, with four mutant and five wild type. Each sample included approximately 30-50 renal vesicles. Detailed protocols are described at GUDMAP.org

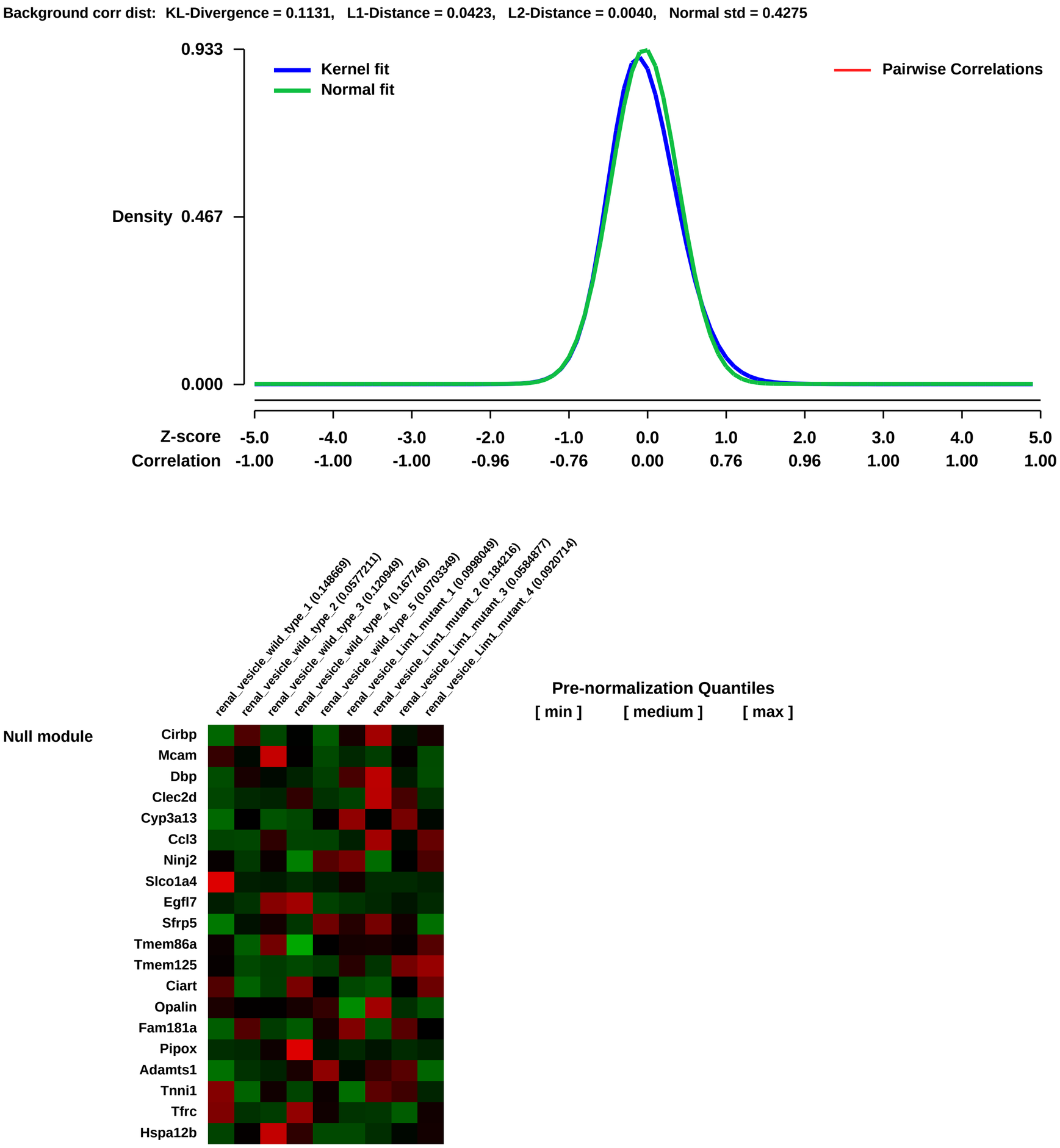

GEO Series "GSE7258" Expression Profiles

Num of samples in this series: 17

Scale of expression profile Z-scores

-3.0 -2.0 -1.0 0.0 1.0 2.0 3.0

GEO Link:	http://www.ncbi.nlm.nih.gov/geo/query/acc.cgi?acc=GSE7258
Status:	Public on Feb 20 2008
Title:	Expression data of bronchoalveolar lavage cells from control or urethane treated AJ mice
Organism:	Mus musculus
Experiment type:	Expression profiling by array
Platform:	GPL1261
Pubmed ID:	18172294
Summary & Design:	**Summary:** AJ mouse is susceptible to lung carcinogenesis from urethane treatment and is a good model for human adenocarcinoma. We completed a study using microarray analysis of bronchoalveolar lavage cells from control or urethane treated mice. A unique macrophage expression signature in the lung tumor microenvironment was able to correctly classify the lavage samples. **Keywords:** AJ mouse control and urethane treatment carcinogenesis protocol **Overall design:** RNA from bronchoalveolar lavage cells of age matched untreated AJ mice controls (C) or from urethane treated (T) AJ mice was prepared. Datasets were accurately classified using a unique macrophage gene expression signature derived from the tumor microenvironment.

Background corr dist: KL-Divergence = 0.1136, L1-Distance = 0.0400, L2-Distance = 0.0032, Normal std = 0.4166

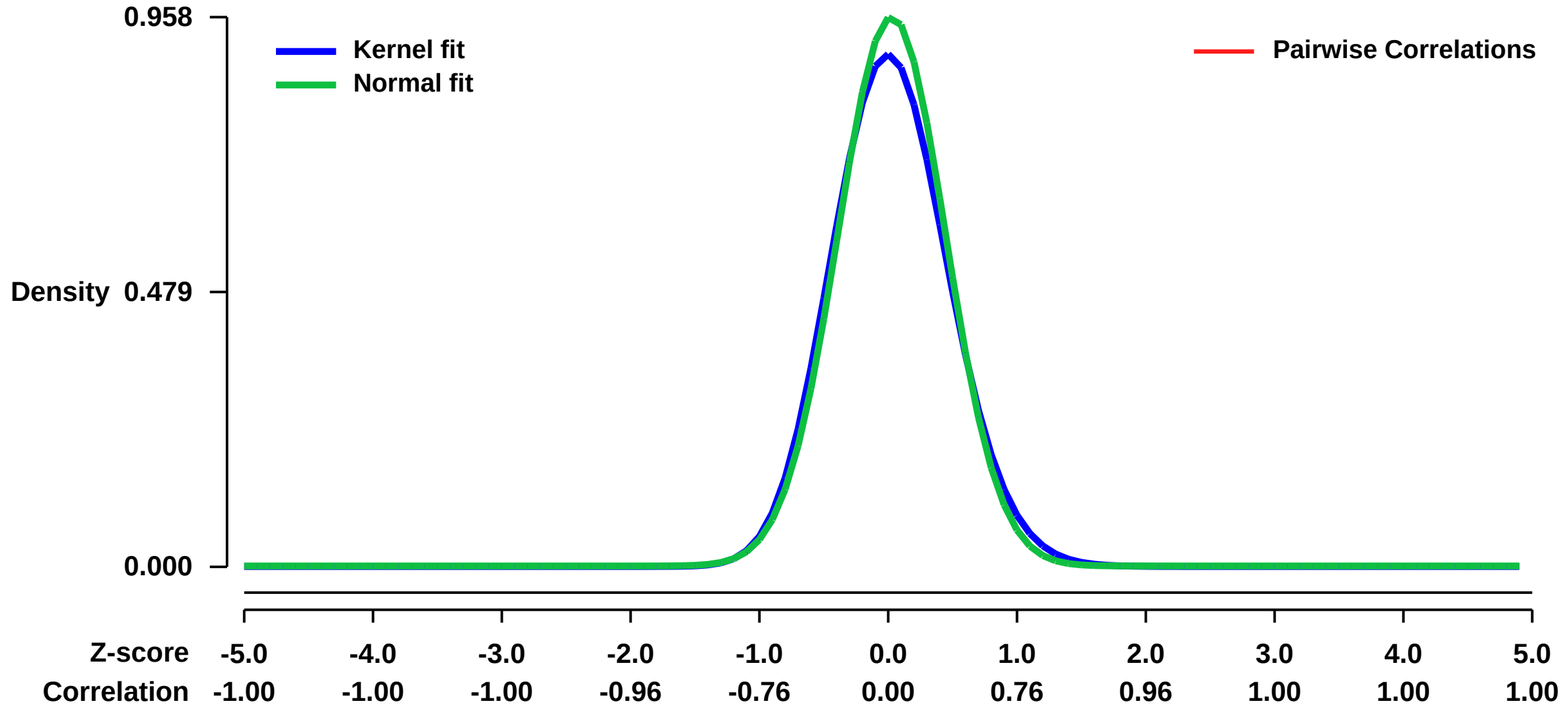

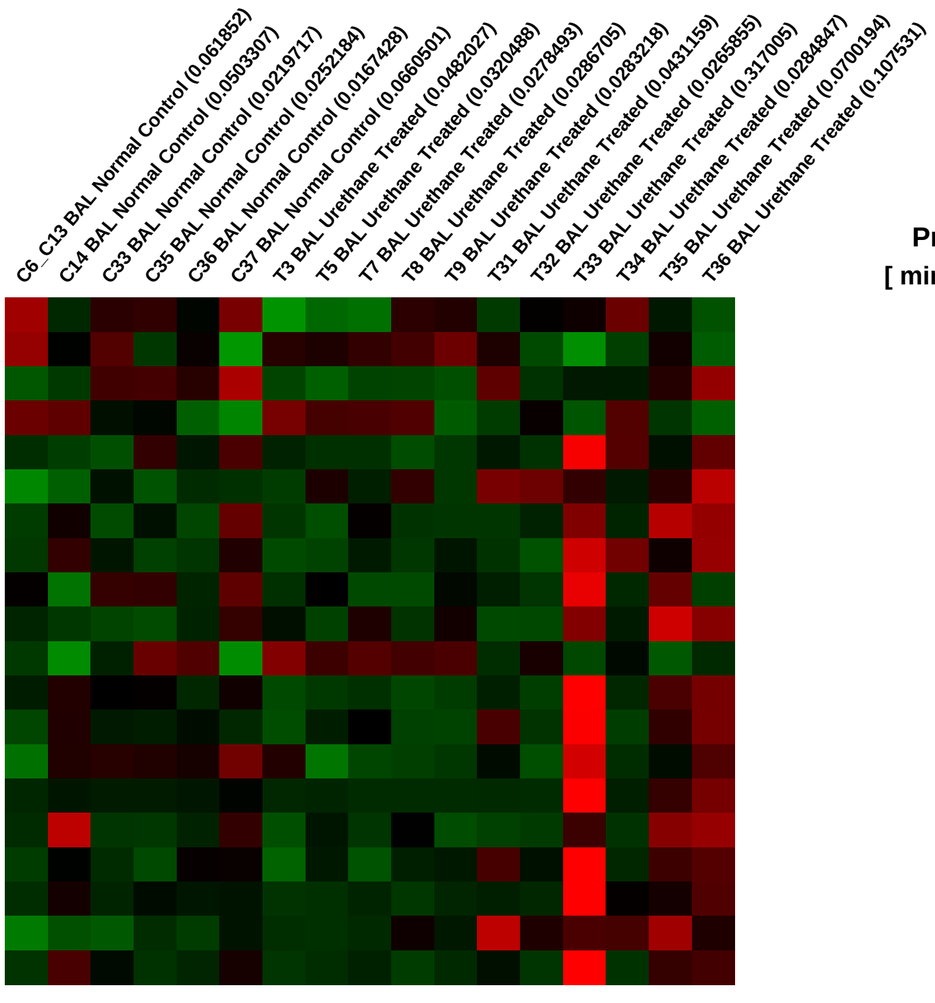

Null module

GEO Series "GSE7275" Expression Profiles

Num of samples in this series: 8

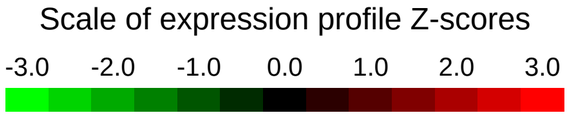

GEO Link:	**http://www.ncbi.nlm.nih.gov/geo/query/acc.cgi?acc=GSE7275**
Status:	**Public on Sep 05 2007**
Title:	**Evaluation of murine mast cells derived exosomal RNA versus their parental cells MC/9.**
Organism:	**Mus musculus**
Experiment type:	**Expression profiling by array**
Platform:	**GPL1261**
Pubmed ID:	**17486113**
Summary & Design:	**Summary:** **Exosomes are vesicles of endocytic origin released by many types of cells into the extracellular environment. In an attempt to further examine the exosome-mediated cellular communication, we show that exosomes from a mouse mast cell line (MC/9), exosomes from primary bone marrow derived mast cells, and exosomes from a human mast cell line (HMC-1) contain RNA but not DNA.** **Microarray assessments of exosome-derived RNA revealed that these vesicles contain mRNA from approximately 1200 genes, many of which are unique and not present in the cytoplasmic RNA pool in the donor cell.** **Keywords: Exosomal RNA versus their parental cells, MC/9** **Overall design:** **Exosomes were prepared from the supernatant of MC/9 cells by differential centrifugations and filtration. RNA was isolated from the exosomes and their parental cells using Trizo. The microarray experiments were performed by SweGene (www.swegene.org/) according to Affymetrix microarray DNA chip analysis. The experiment was performed in quadruple samples. ExoRNA1, ExoRNA2, ExoRNA3, and ExoRNA4 for the exosomes samples and Mast_cells1, Mast_cells2, Mast_cells3, and Mast_cells4 for the MC/9 cells.**

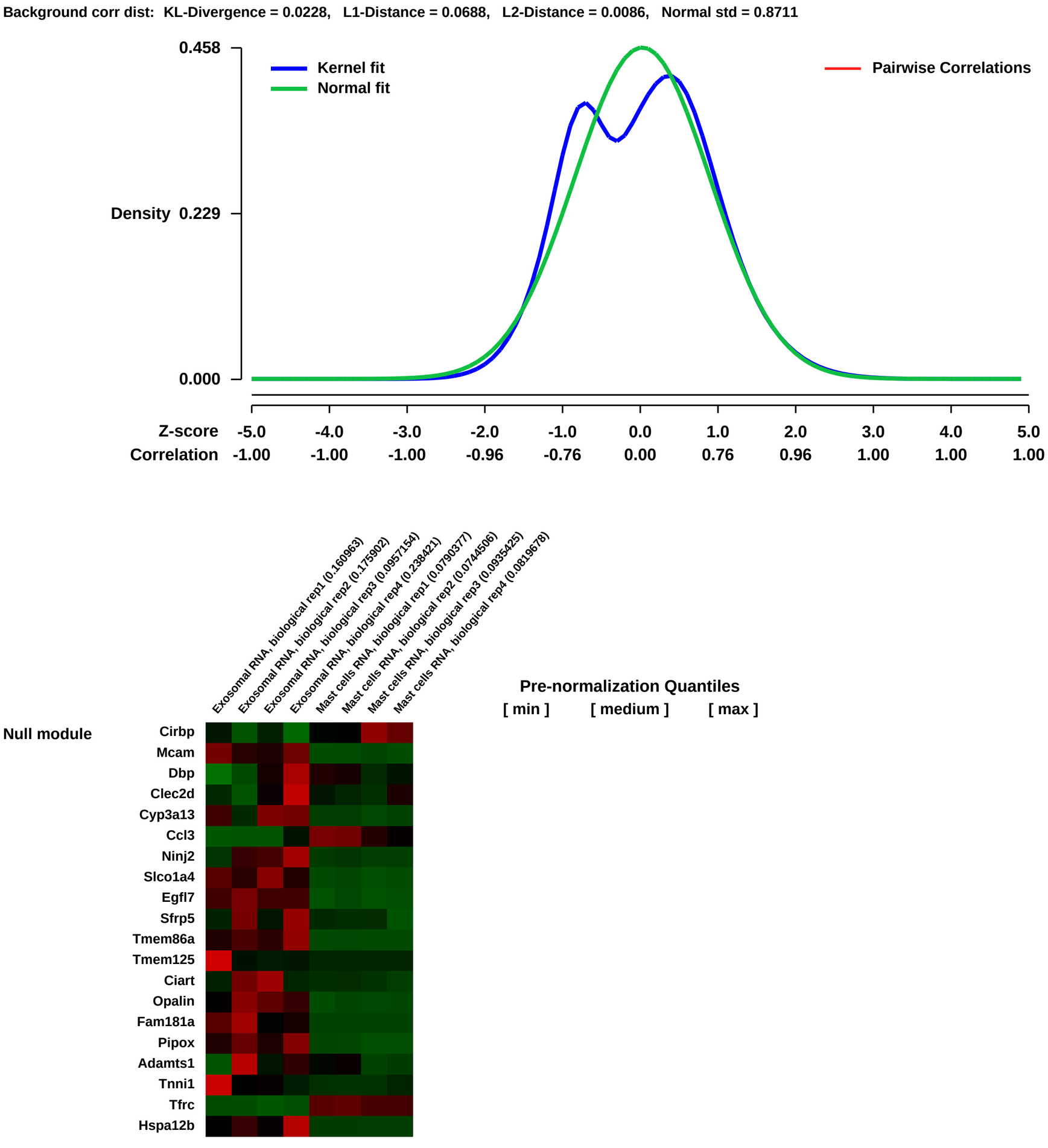

GEO Series "GSE7309" Expression Profiles

Num of samples in this series: 12

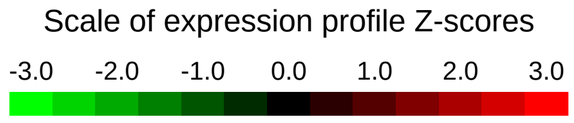

GEO Link:	http://www.ncbi.nlm.nih.gov/geo/query/acc.cgi?acc=GSE7309
Status:	Public on Jun 04 2007
Title:	Requirement for ERK MAP kinase in mouse preimplantation development
Organism:	Mus musculus
Experiment type:	Expression profiling by array
Platform:	GPL1261
Pubmed ID:	17611221

Summary & Design:

Summary:
Preimplantation development is a crucial step for successful implantation and pregnancy. Although both compaction and blastocyst formation have been extensively studied, mechanisms regulating early cell division stages before compaction have remained unclear. Here, we show that ERK MAP kinase function is required for early embryonic cell division and normal cell-cell adhesion before compaction. Our analysis demonstrates that inhibition of ERK activation in the late 2-cell stage embryos leads to a reversible arrest in G2 phase in the 4-cell stage. The G2 arrested, 4-cell stage embryos show weakened cell-cell adhesion as compared to control embryos. Remarkably, microarray analyses show that most of the programmed changes of upregulated and downregulated gene expression during the 4- to 8-cell stages normally proceed in the 4-cell stage-arrested embryos, except for a portion of the genes whose expression profiles closely parallel the stages of embryonic development when arrested in G2 and released to resume development. These parallel genes include the genes encoding intercellular adhesion molecules, whose expression is found to be positively regulated by the ERK pathway. We also show that while ERK inactivation in the 8-cell stage embryos does not lead to cell division arrest, it does cause cell division arrest when cadherin-mediated cell-cell adhesion is disrupted. These results demonstrate an essential role of ERK function in the G2/M transition and the expression of adhesion molecules during the 2-cell to 8-cell stage embryos, and suggest a loose parallelism between the gene expression programs and the developmental stages before compaction.

Keywords: preimplantation development

Overall design:
We examined expression profiles of genes during early cell division stages in mouse preimplantation development. We performed the genome-wide analysis by using Affymetrix GeneChip oligonucleotide microarrays, and examined the effect of the ERK pathway inhibitor U0126 on the expression profiles. Two independent experiments were carried out. We collected embryos at six points as follows; control embryos at day 1.5 (cont. 1.5, 2-cell stage), day 2.5 (cont. 2.5, 4- to 8-cell), and day 3.5 (cont. 3.5, morula to blastocyst), and the U0126-treated embryos at day 2.5 (U2.5, 4-cell arrested), embryos released from the U0126-induced arrest at day 3.5 (U3.5, 8-cell) and at day 4.5 (U4.5, morula to blastocyst). Hybridization was carried out with the Mouse Genome 430 2.0 array following Affymetrix instructions. Hybridized arrays were scanned using an Affymetrix GeneChip Scanner. Expression analysis was performed using GeneChip Operating Software v. 1.2 (GCOS) and GeneSpring 7.3.

Background corr dist: KL-Divergence = 0.1006, L1-Distance = 0.0712, L2-Distance = 0.0102, Normal std = 0.4923

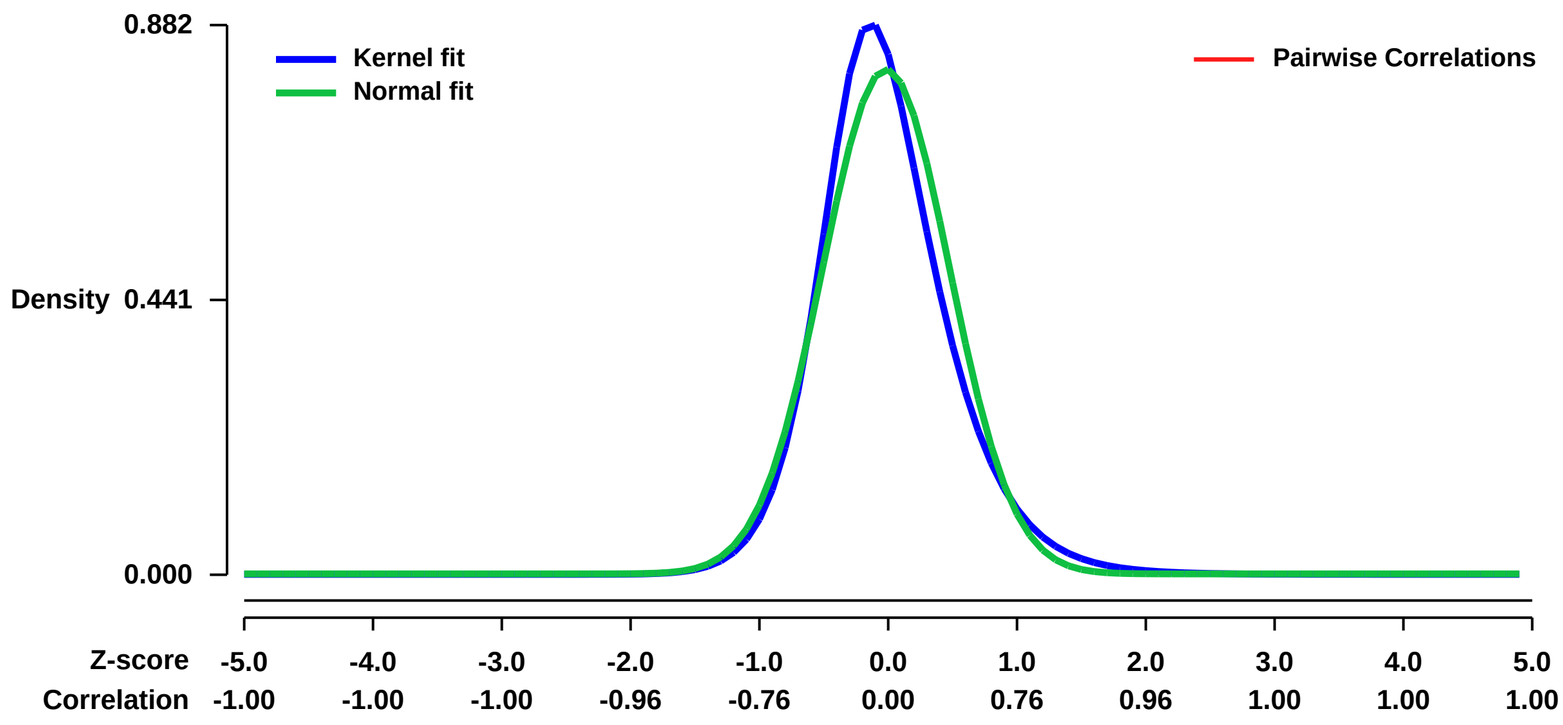

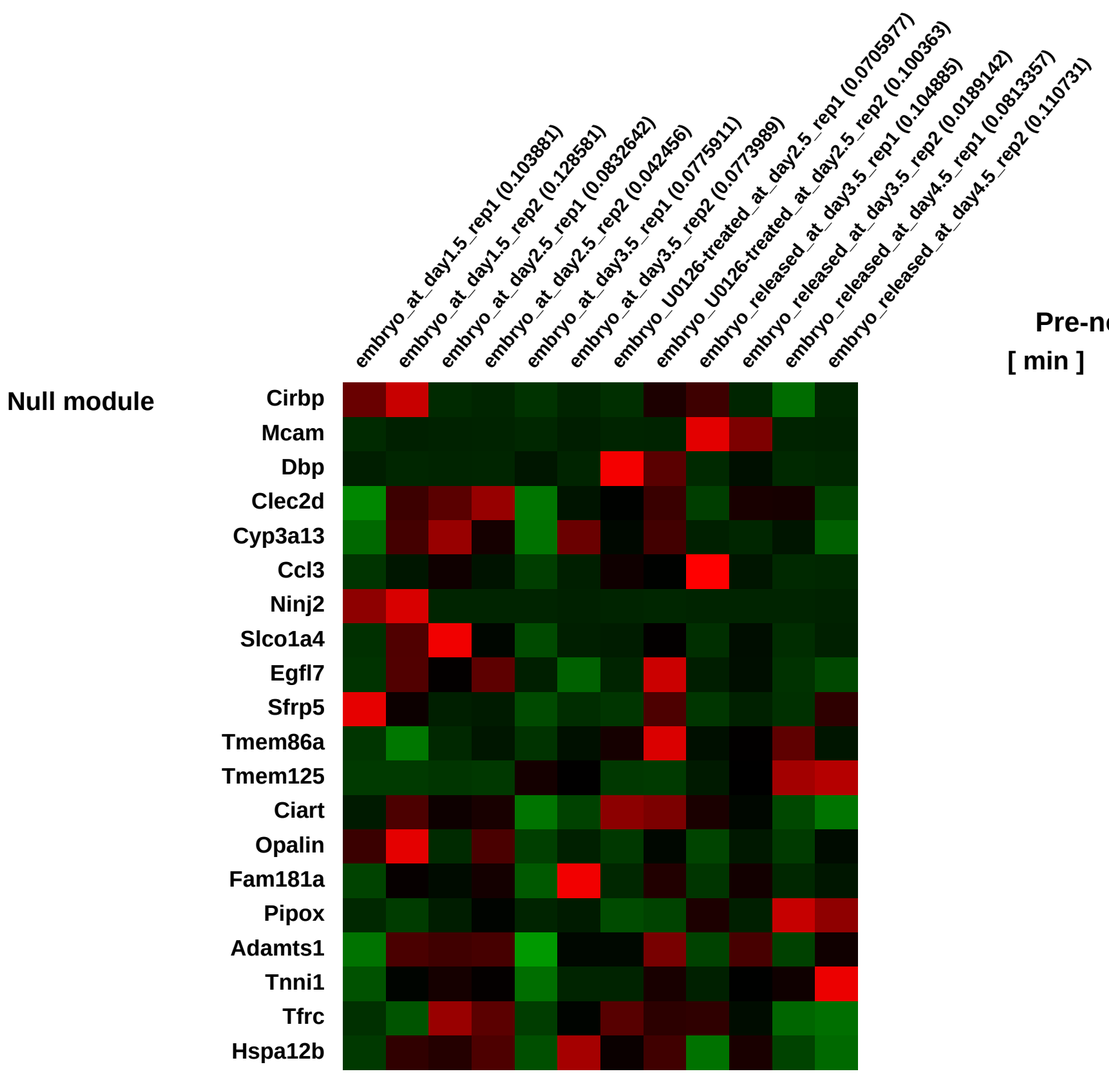

GEO Series "GSE7310" Expression Profiles

Num of samples in this series: 10

Scale of expression profile Z-scores

-3.0 -2.0 -1.0 0.0 1.0 2.0 3.0

GEO Link:	http://www.ncbi.nlm.nih.gov/geo/query/acc.cgi?acc=GSE7310
Status:	Public on Jan 01 2008
Title:	Comparison analysis of 2 week old C57BL6J lung exposed to 2 weeks of cigarette smoke compared to age-matched controls
Organism:	Mus musculus
Experiment type:	Expression profiling by array
Platform:	GPL1261
Pubmed ID:	17975176
Summary & Design:	**Summary:** We hypothesize that gene expression in the cigarette smoke (CS) exposed neonatal lung and age-matched controls will be divergent. CS exposed lung will have divergence of immune response genes and structural genes. The lungs of (6) 2 week old neonatal mice exposed to 2 weeks of CS were compared to the lung of (4) 2 week old age-matched control mice. We utilized microarray analysis to examine transcriptional differences between smoke exposed neonatal lung and age-matched controls. **Keywords: comparative expression profiling** **Overall design:** This study utilizes microarray analysis to test these hypotheses. Six sets of lungs were harvested from CS exposed mice and four sets of lungs were harvested from age-matched control mice. RNA was isolated and used for global gene expression profiling (Affymetrix Mouse 430 2.0 array). Statistically significant gene expression was determined as a minimum 6 counts of 9 pairwise comparisons, minimum 1.5-fold change, and p < 0.05. Further, Absolute | FC - FC SEM | >= 1.5.

Background corr dist: KL-Divergence = 0.0562, L1-Distance = 0.0341, L2-Distance = 0.0021, Normal std = 0.5400

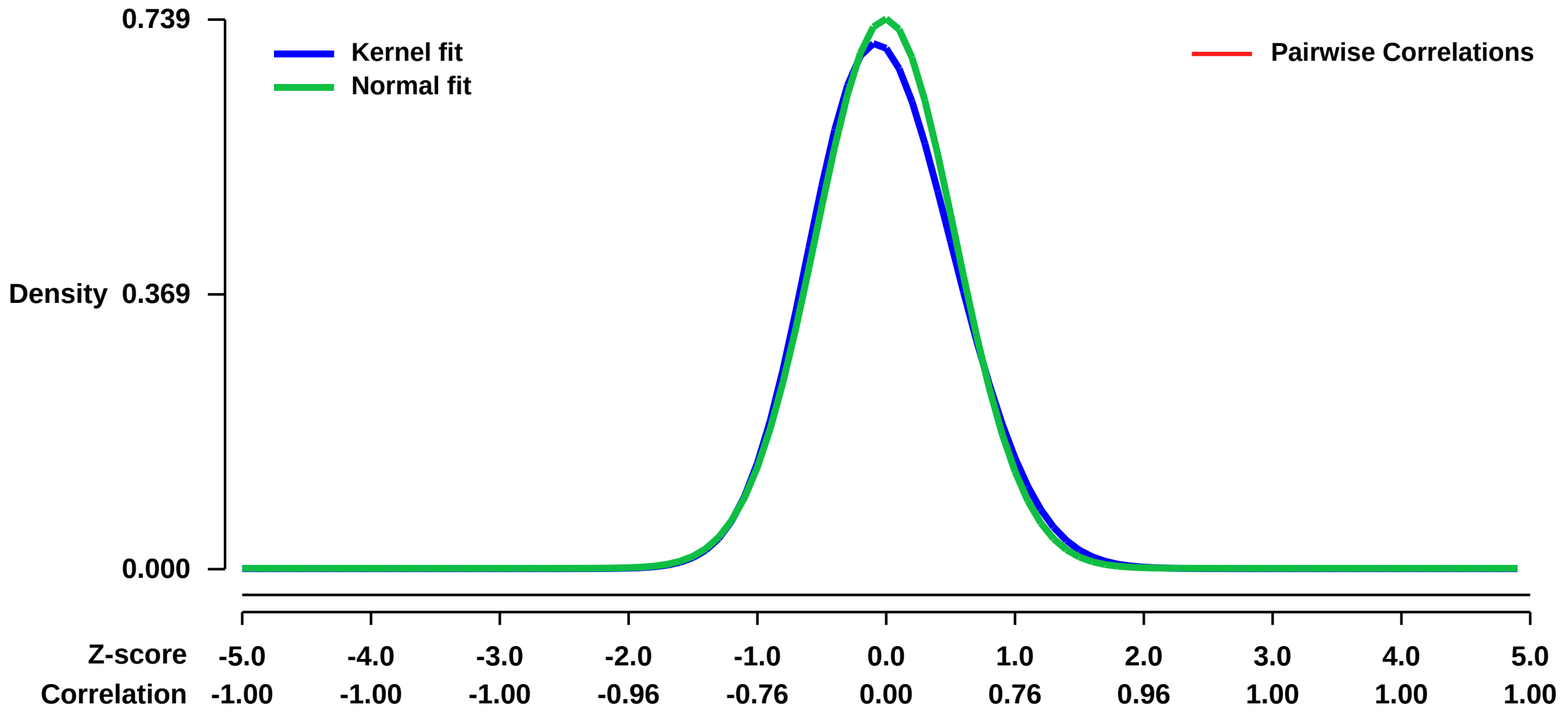

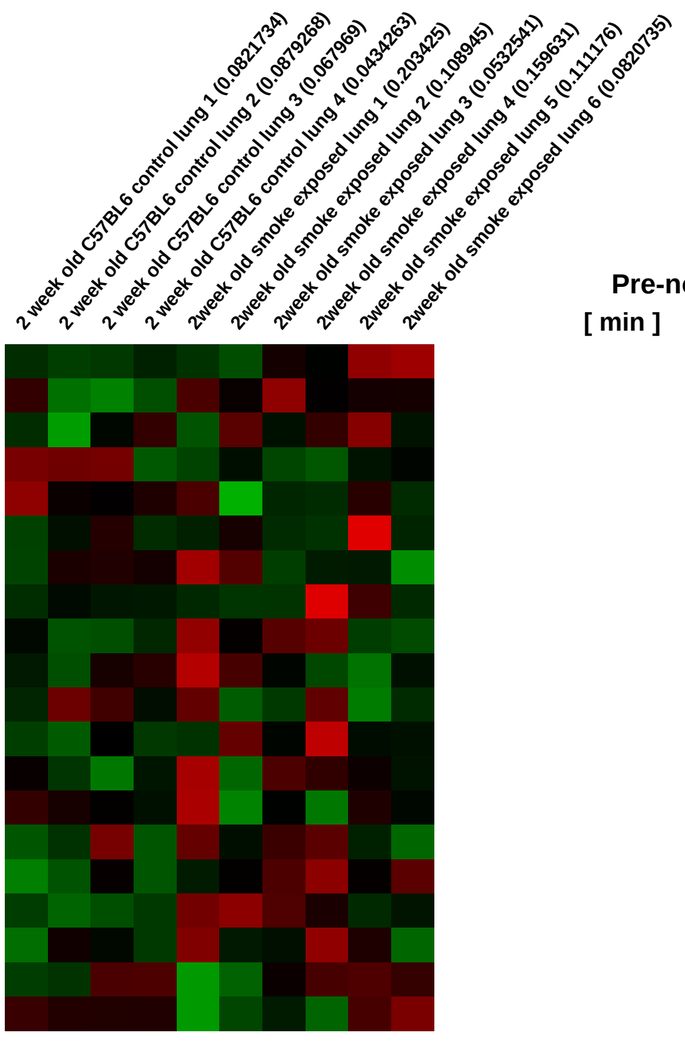

GEO Series "GSE7324" Expression Profiles

Num of samples in this series: 10

Scale of expression profile Z-scores

-3.0 -2.0 -1.0 0.0 1.0 2.0 3.0

GEO Link: http://www.ncbi.nlm.nih.gov/geo/query/acc.cgi?acc=GSE7324

Status: Public on Mar 21 2007

Title: Structural basis for recognition of SMRT/N-CoR by the MYND domain and its contribution to AML1/ETO's activity

Organism: Mus musculus

Experiment type: Expression profiling by array

Platform: GPL1261

Pubmed ID:

Summary & Design:

Summary:
To examine the effects of disrupting the AML1/ETO MYND-SMRT interaction with the W692A substitution on AML1/ETO function, the global gene expression profile of mouse bone marrow LSK cells transduced with GFP was compared to that of cells transduced with either wild-type AML1/ETO or AML1/ETO harboring the W692A substitution in the MYND domain. Three independent biological replicates were assessed for both the control (GFP/MigR1) and AML1/ETO (intact MYND-SMRT interaction) conditions, whereas four independent biological replicates were assessed for the W692A (disrupted MYND-SMRT interaction) condition. The three GFP replicates were used to establish a baseline signal for comparison to both the AML1/ETO and W692A samples.

Keywords: genetic modification

Overall design:
Global gene expression profiles of FACS-sorted Lin-Sca1+cKit+ mouse bone marrow cells transduced with empty vector (GFP-MigR1), AML1/ETO, or AML1/ETO with the W692A substitution (W692A).

Background corr dist: KL-Divergence = 0.0891, L1-Distance = 0.0209, L2-Distance = 0.0006, Normal std = 0.4614

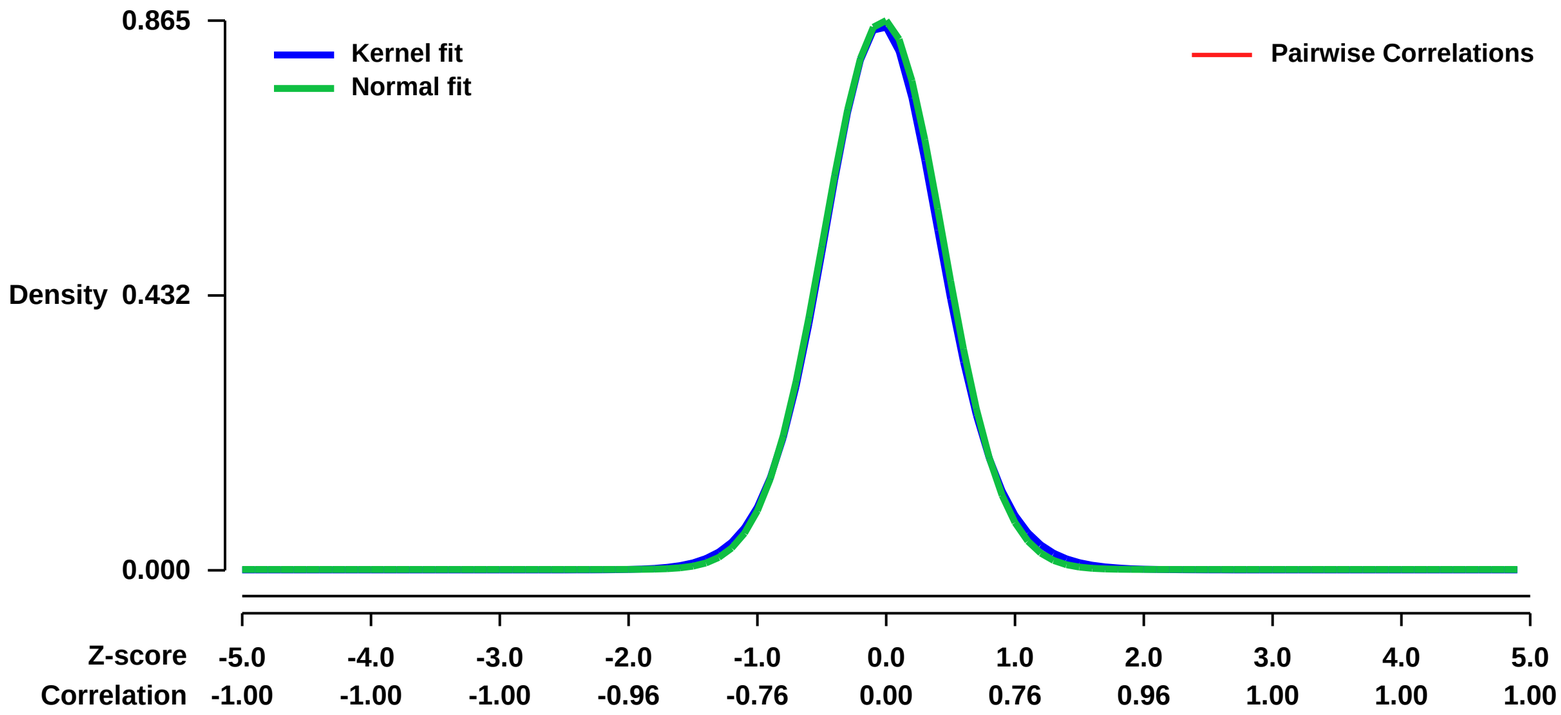

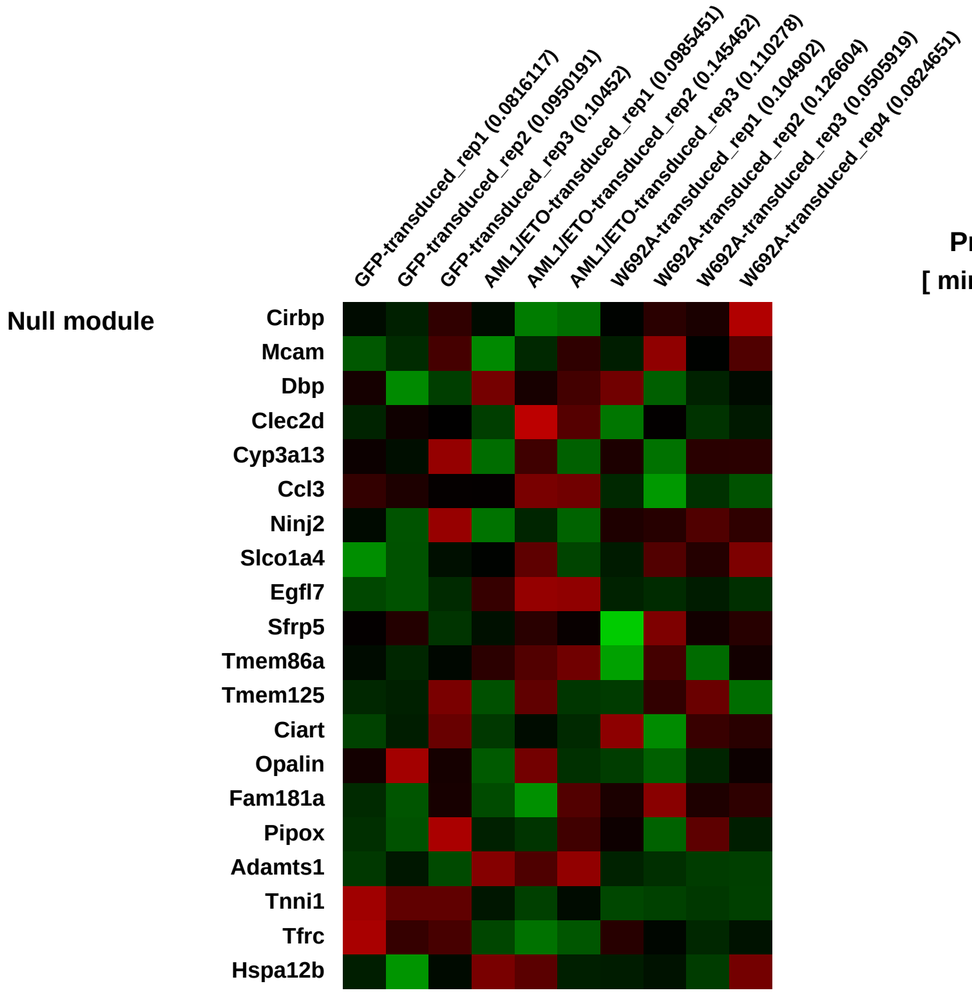

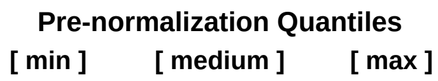

GEO Series "GSE7333" Expression Profiles

Num of samples in this series: 6

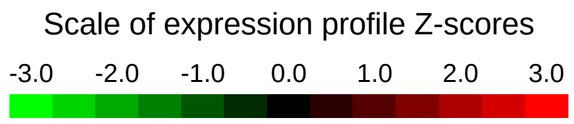

GEO Link:	**http://www.ncbi.nlm.nih.gov/geo/query/acc.cgi?acc=GSE7333**
Status:	**Public on Mar 29 2007**
Title:	**miR-1-2 knockout versus wild-type hearts**
Organism:	**Mus musculus**
Experiment type:	**Expression profiling by array**
Platform:	**GPL1261**
Pubmed ID:	**17397913**
Summary & Design:	**Summary:** **microarray was done on Heart tissue from ko and wt** **MicroRNAs (miRNAs) are genomically encoded small RNAs used by organisms to regulate the dosage of proteins generated from messenger RNA transcripts. The in vivo requirement of specific miRNAs in mammals is unknown, and reliable prediction of mRNA targets remains problematic. Here, we show that miRNA biogenesis in the mouse heart is essential for cardiogenesis. Furthermore, targeted deletion of the muscle-specific miRNA, miR-1-2, revealed numerous functions in the heart, including regulation of cardiac morphogenesis, electrical conduction, and cell cycle control. Analyses of miR-1 complementary sequences in mRNAs upregulated upon miR-1-2 deletion revealed an enrichment of miR-1 ""seed matches"" and a strong tendency for potential miR-1 binding sites to be located in physically accessible regions. These findings indicate that subtle alteration of miRNA dosage can have profound consequences in mammals and demonstrate the utility of mammalian loss-of-function models in revealing physiologic miRNA targets.** **Keywords: miRNA** **Overall design:** **Heart tissues from 3 wild type and 3 miR-1-2 knockout mice at postnatal days 10 were used and total RNA was extracted by Trizol. Expression level was compared between wild type and miR-1-2 knockout mice. The affy package from R/Bioconductor was used to generate RMA values.**

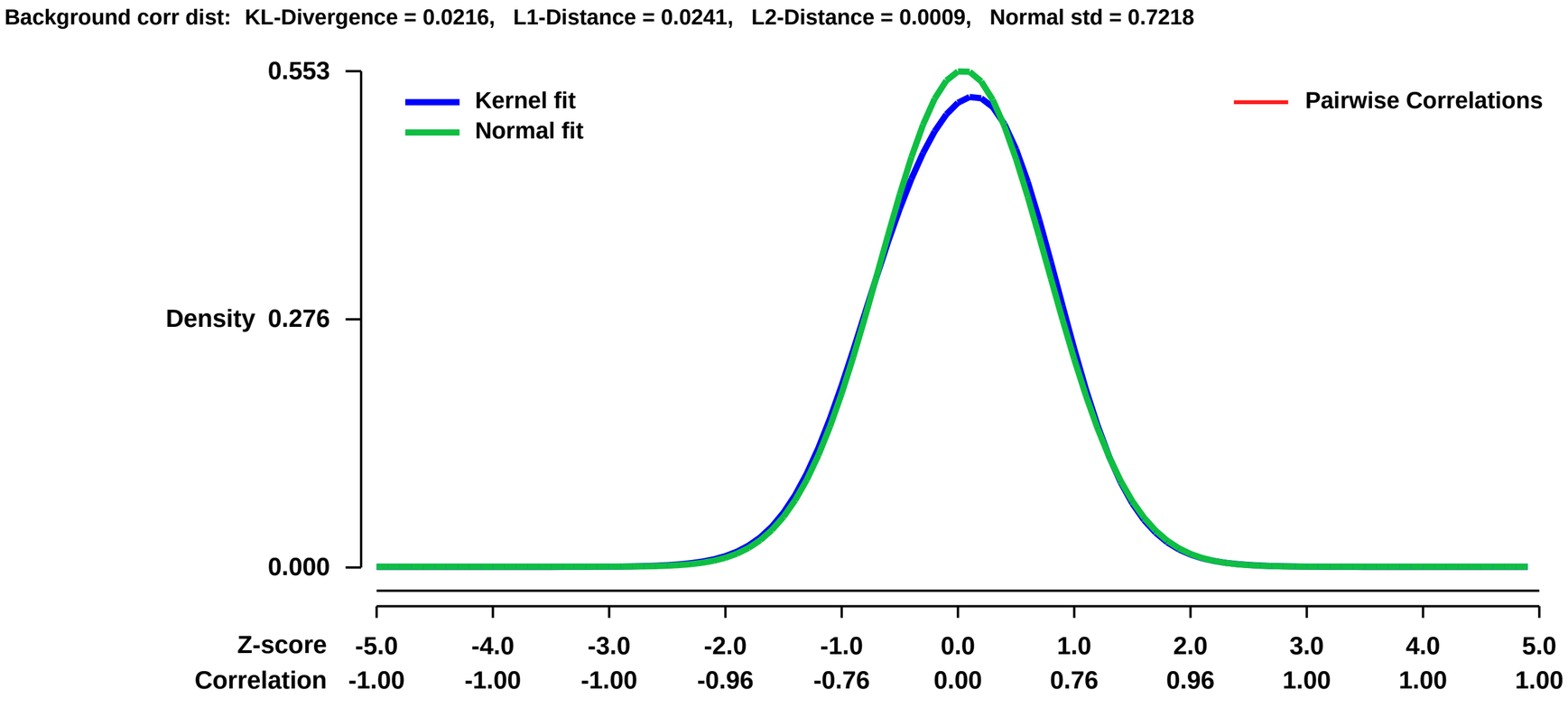

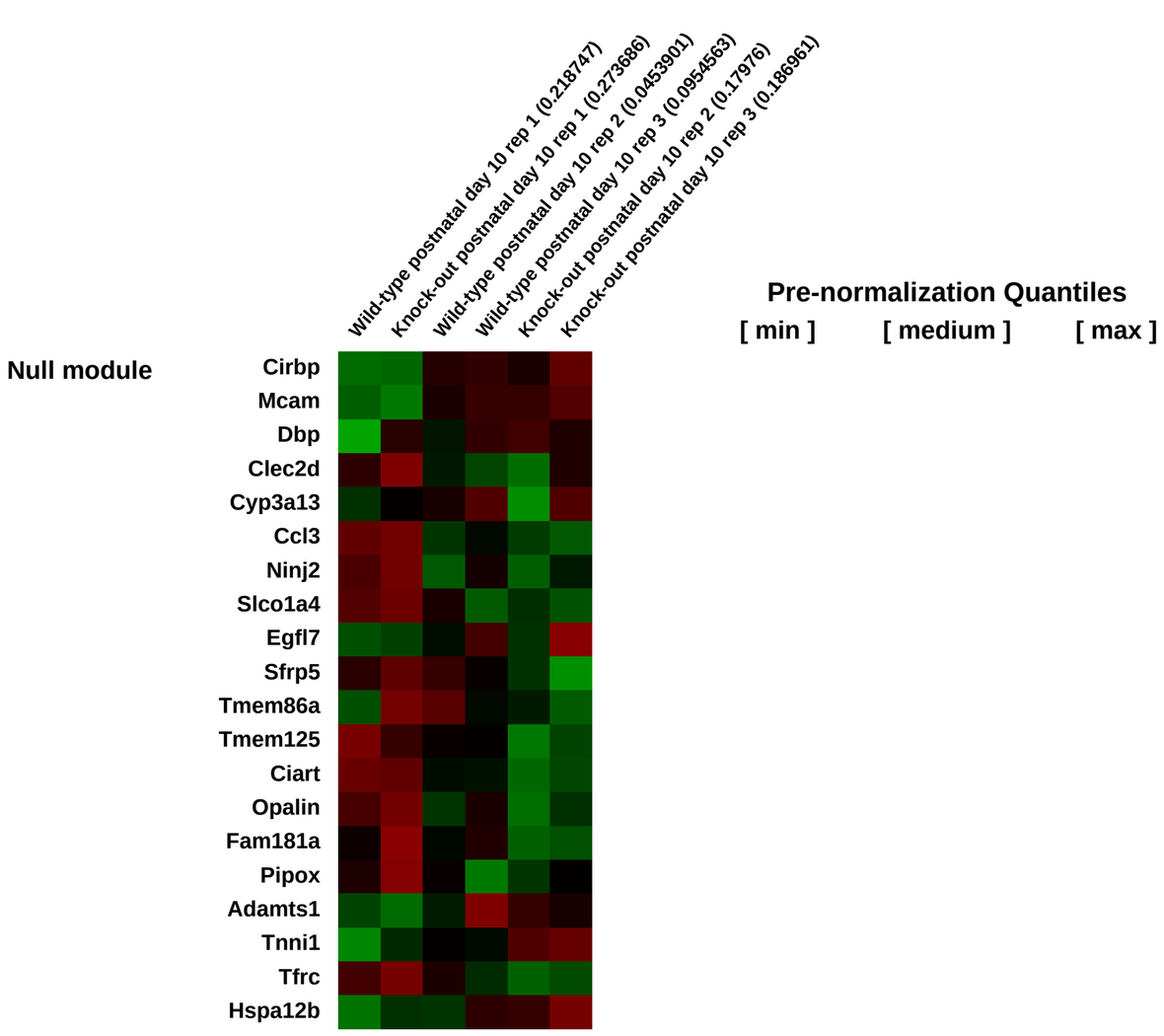

GEO Series "GSE7342" Expression Profiles

Num of samples in this series: 12

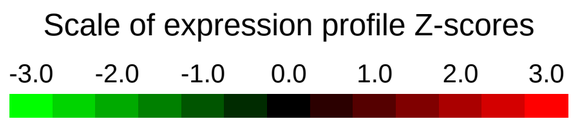

GEO Link:	http://www.ncbi.nlm.nih.gov/geo/query/acc.cgi?acc=GSE7342
Status:	Public on Mar 23 2007
Title:	Expression data from p38 knock out versus wild type fetal liver
Organism:	Mus musculus
Experiment type:	Expression profiling by array
Platform:	GPL1261
Pubmed ID:	17468757
Summary & Design:	**Summary:** The mitogen-activated protein kinase (MAPK) p38alpha controls inflammatory responses and cell proliferation. Using mice carrying conditional p38alpha alleles, we investigated its function in postnatal development and tumorigenesis. When p38alpha is specifically deleted in the mouse embryo, fetuses develop to term but die shortly after birth, likely due to lung dysfunction. Fetal hematopoietic cells and embryonic fibroblasts deficient in p38alpha display increased proliferation, resulting from sustained activation of the c-Jun N-terminal kinase (JNK)/c-Jun pathway. Importantly, in chemical-induced liver cancer development, mice with liver-specific deletion of p38alpha show enhanced hepatocyte proliferation and tumor development that also correlates with JNK/c-Jun upregulation. Furthermore, increased proliferation of p38alpha-deficient hepatocytes and tumor cells is suppressed by inactivation of JNK or c-Jun. These results reveal a novel mechanism whereby p38alpha negatively regulates cell proliferation through antagonizing the JNK/c-Jun pathway in multiple cell types and in liver cancer development. We used microarrays to identifiy differental regulated genes by p38alpha in fetal liver cells **Keywords:** time course **Overall design:** Wild type and p38 deficient fetal liver cell were used for RNA extraction and hybridization on Affymetrix microarrays.

Background corr dist: KL-Divergence = 0.0482, L1-Distance = 0.0409, L2-Distance = 0.0034, Normal std = 0.5674

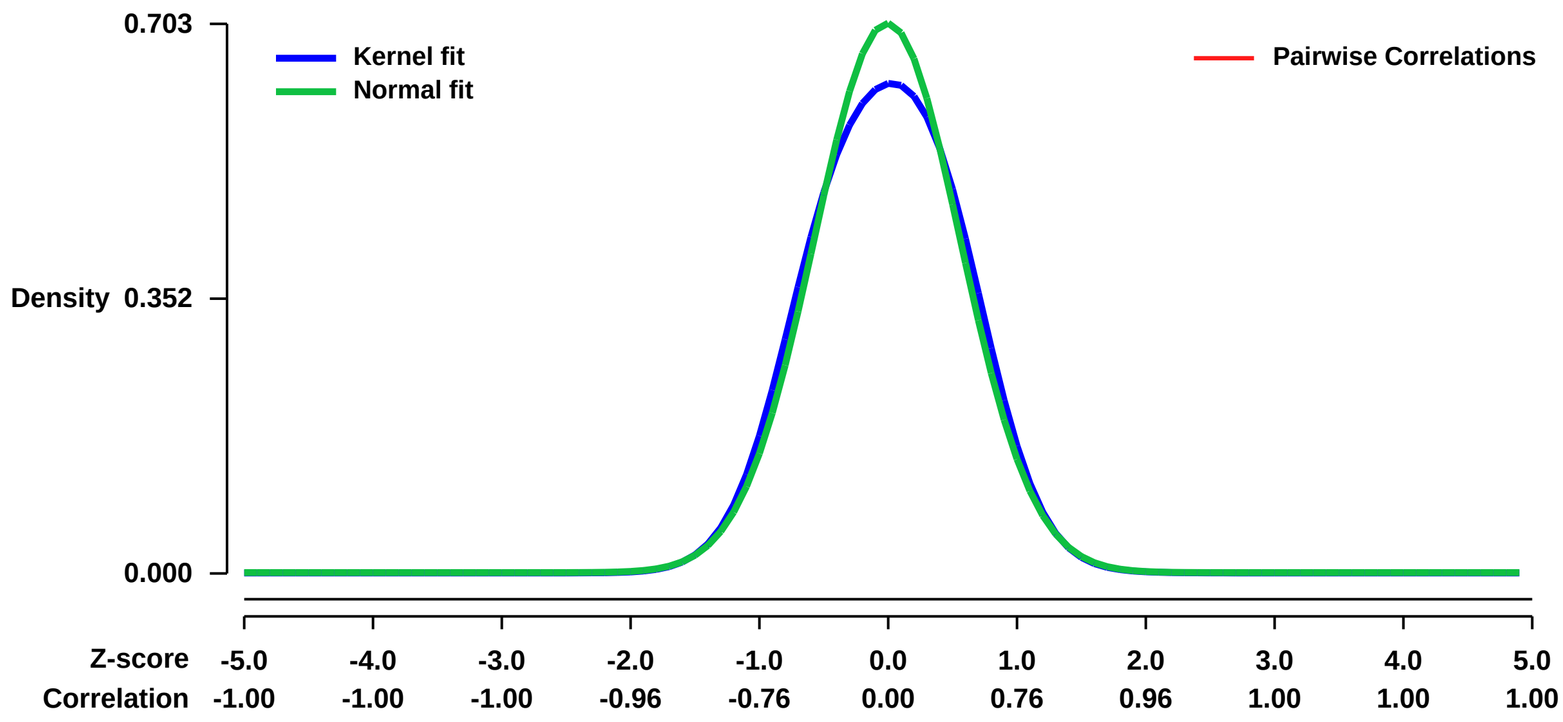

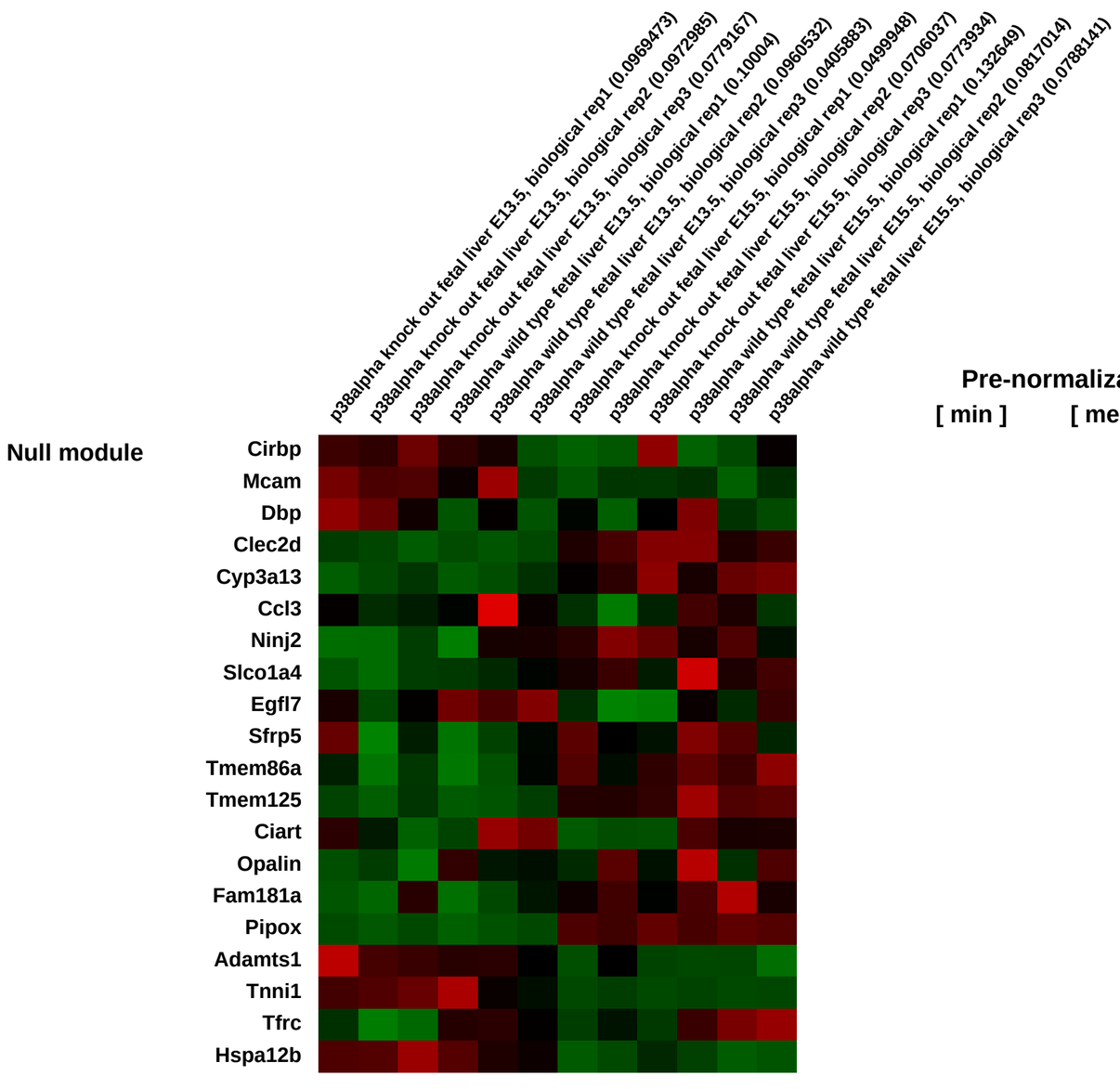

GEO Series "GSE7381" Expression Profiles

Num of samples in this series: 6

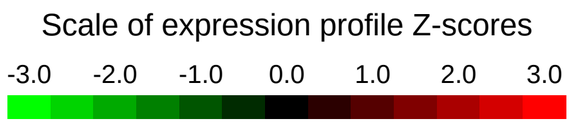

GEO Link:	http://www.ncbi.nlm.nih.gov/geo/query/acc.cgi?acc=GSE7381
Status:	Public on Apr 12 2007
Title:	Expression profiling of back skin of Get1 and control mice at e18.5
Organism:	Mus musculus
Experiment type:	Expression profiling by array
Platform:	GPL1261
Pubmed ID:	16949565
Summary & Design:	**Summary:** **Defective permeability barrier is an important feature of many skin diseases and causes mortality in premature infants. To investigate the control of barrier formation, we characterized the epidermally expressed Grainyhead-like epithelial transactivator (Get-1)/Grhl3, a conserved mammalian homologue of Grainyhead, which plays important roles in cuticle development in Drosophila. Get-1 interacts with the LIM-only protein LMO4, which is co-expressed in the developing mammalian epidermis. The epidermis of Get-1(-/-) mice showed a severe barrier function defect associated with impaired differentiation of the epidermis, including defects of the stratum corneum, extracellular lipid composition and cell adhesion in the granular layer. The Get-1 mutation affects multiple genes linked to terminal differentiation and barrier function, including most genes of the epidermal differentiation complex. Get-1 therefore directly or indirectly regulates a broad array of epidermal differentiation genes encoding structural proteins, lipid metabolizing enzymes and cell adhesion molecules. Although deletion of the LMO4 gene had no overt consequences for epidermal development, the epidermal terminal differentiation defect in mice deleted for both Get-1 and LMO4 is much more severe than in Get-1(-/-) mice with striking impairment of stratum corneum formation. These findings indicate that the Get-1 and LMO4 genes interact functionally to regulate epidermal terminal differentiation.** **Keywords: knockout and wildtype mice comparison** **Overall design:** **The same region of the mouse back skin was excised from three Get1 +/+ and three Get1 â /â mice at e18.5.**

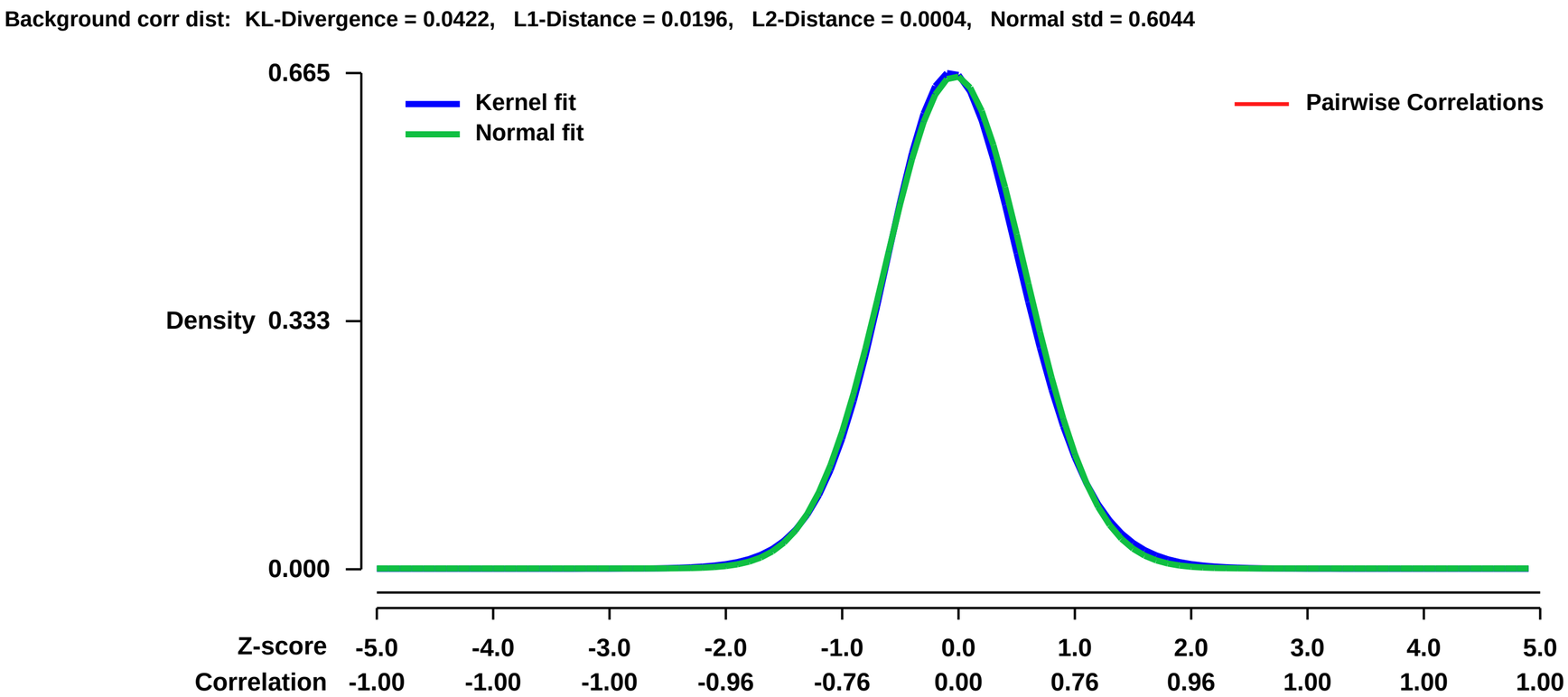

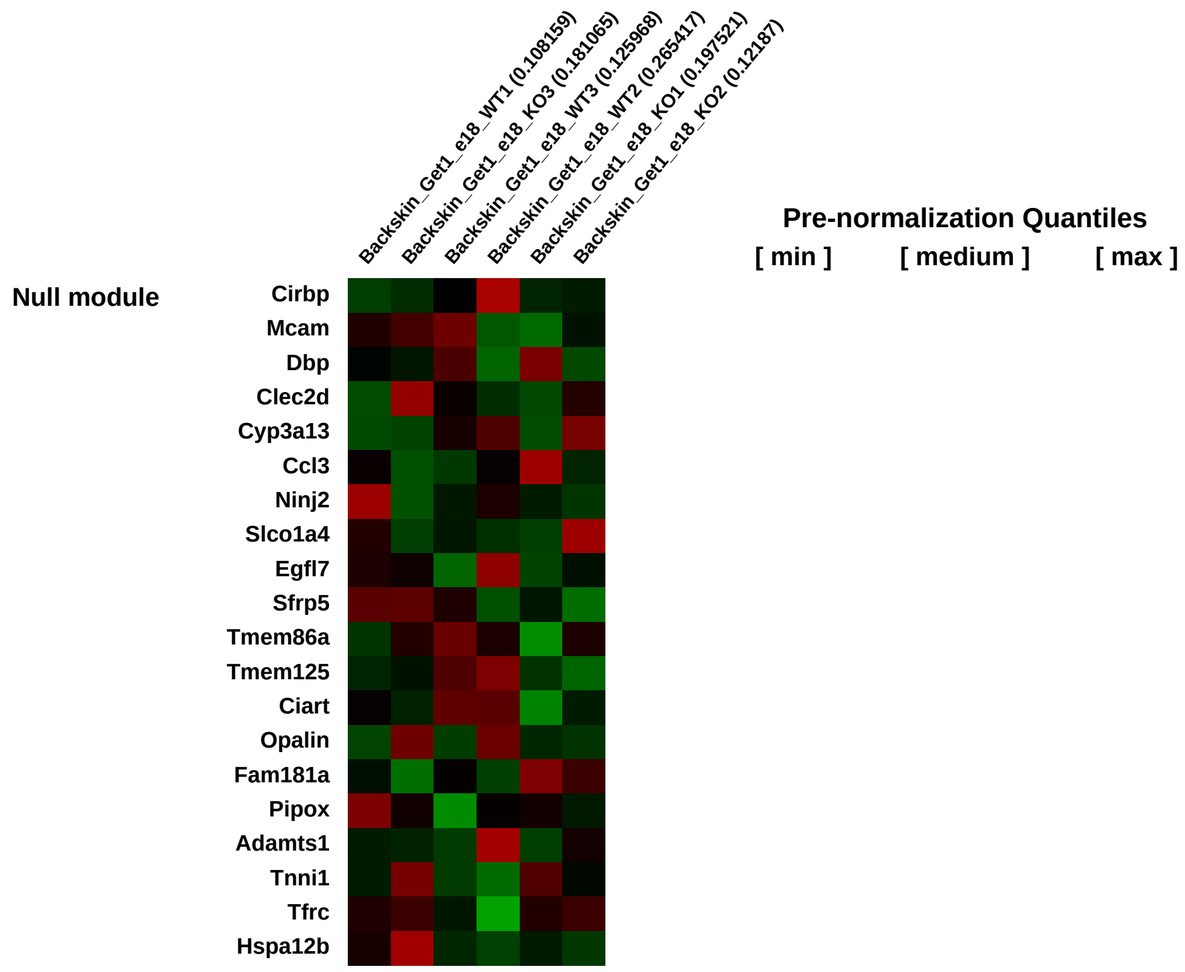

GEO Series "GSE7424" Expression Profiles

Num of samples in this series: 8

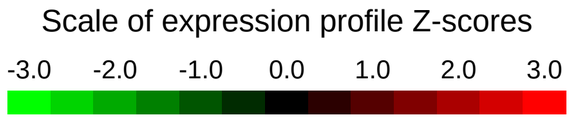

GEO Link:	http://www.ncbi.nlm.nih.gov/geo/query/acc.cgi?acc=GSE7424
Status:	Public on Apr 03 2007
Title:	Intragraft gene expression profile associated with the induction of tolerance
Organism:	Mus musculus
Experiment type:	Expression profiling by array
Platform:	GPL1261
Pubmed ID:	18267024
Summary & Design:	**Summary:** Xenotransplantation holds the promise of providing an unlimited supply of donor organs for terminal patients with organ failure. The gal carbohydrate results in rejection of wild type pig grafts, however, chimerism established by expression of the GalT gene prior to transplantation in GalT knockout mice results in tolerance to Gal+ heart grafts. We used microarrays in order to further understand the early events that occur within grafts that demonstrate tolerance. Keywords: transplntation tolerance **Overall design:** The GalT BMT recipient is a GalT knockout mouse which recieved GalT gene transduced allo-bone marrow cells transplantation after sublethal irradiation. A heart of wild type C57BL/6 was heterotopically transplanted into the recipient after GalT BMT. Syngeneic Control recipient is a wild type C57BL/6 transplanted a heart of wild C57BL/6.

Background corr dist: KL-Divergence = 0.0600, L1-Distance = 0.0214, L2-Distance = 0.0007, Normal std = 0.5344

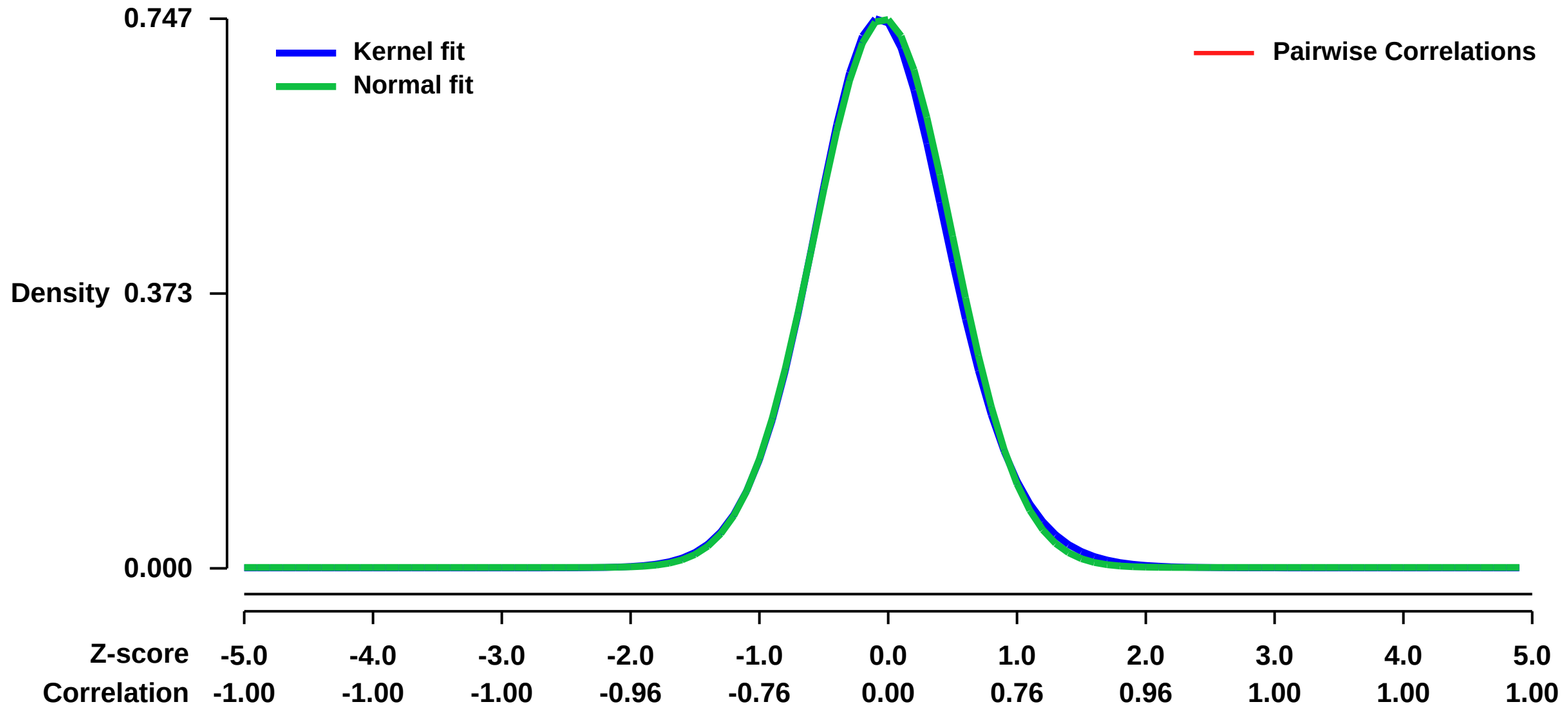

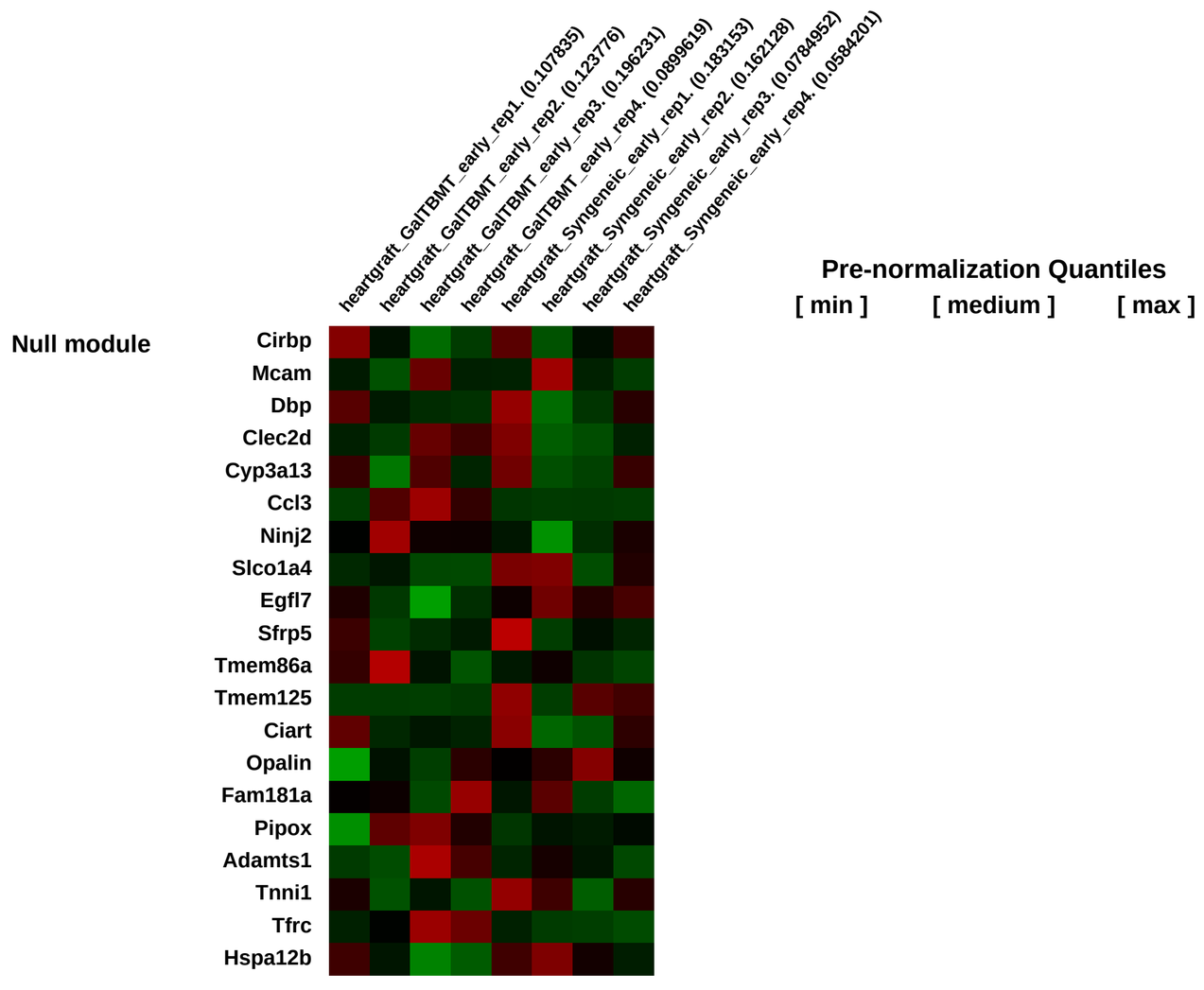

GEO Series "GSE7430" Expression Profiles

Num of samples in this series: 12

Scale of expression profile Z-scores

-3.0 -2.0 -1.0 0.0 1.0 2.0 3.0

GEO Link:	http://www.ncbi.nlm.nih.gov/geo/query/acc.cgi?acc=GSE7430
Status:	Public on Apr 04 2007
Title:	Investigate the role of Wnt/beta-catenin signaling in development of the exocrine pancreas
Organism:	Mus musculus
Experiment type:	Expression profiling by array
Platform:	GPL1261
Pubmed ID:	17222338
Summary & Design:	**Summary:** beta-catenin is an essential mediator of canonical Wnt signaling and a central component of the cadherin-catenin epithelial adhesion complex. Dysregulation of beta-catenin expression has been described in pancreatic neoplasia. Newly published studies have suggested that beta-catenin is critical for normal pancreatic development although these reports reached somewhat different conclusions. In addition, the molecular mechanisms by which loss of beta-catenin affects pancreas development are not well understood. The goals of this study then were; 1] to further investigate the role of beta-catenin in pancreatic development using a conditional knockout approach and 2] to identify possible mechanisms by which loss of beta-catenin disrupts pancreatic development. A Pdx1-cre mouse line was used to delete a floxed beta-catenin allele specifically in the developing pancreas, and embryonic pancreata were studied by immunohistochemistry and microarray analysis. **Keywords:** Time course **Overall design:** In the study, we hybridized RNA from Embryonic day 14.6 and 16.5 pancreas of wild type (WT) control and Pdx1Cre/+; beta-cateninflox/flox´ beta-catenin null in the pancreas) embryonic pancreas to Affymetrix MOE430 2.0 GeneChipˆ´fi arrays containing 45,101 well characterized mouse genes/ESTs.

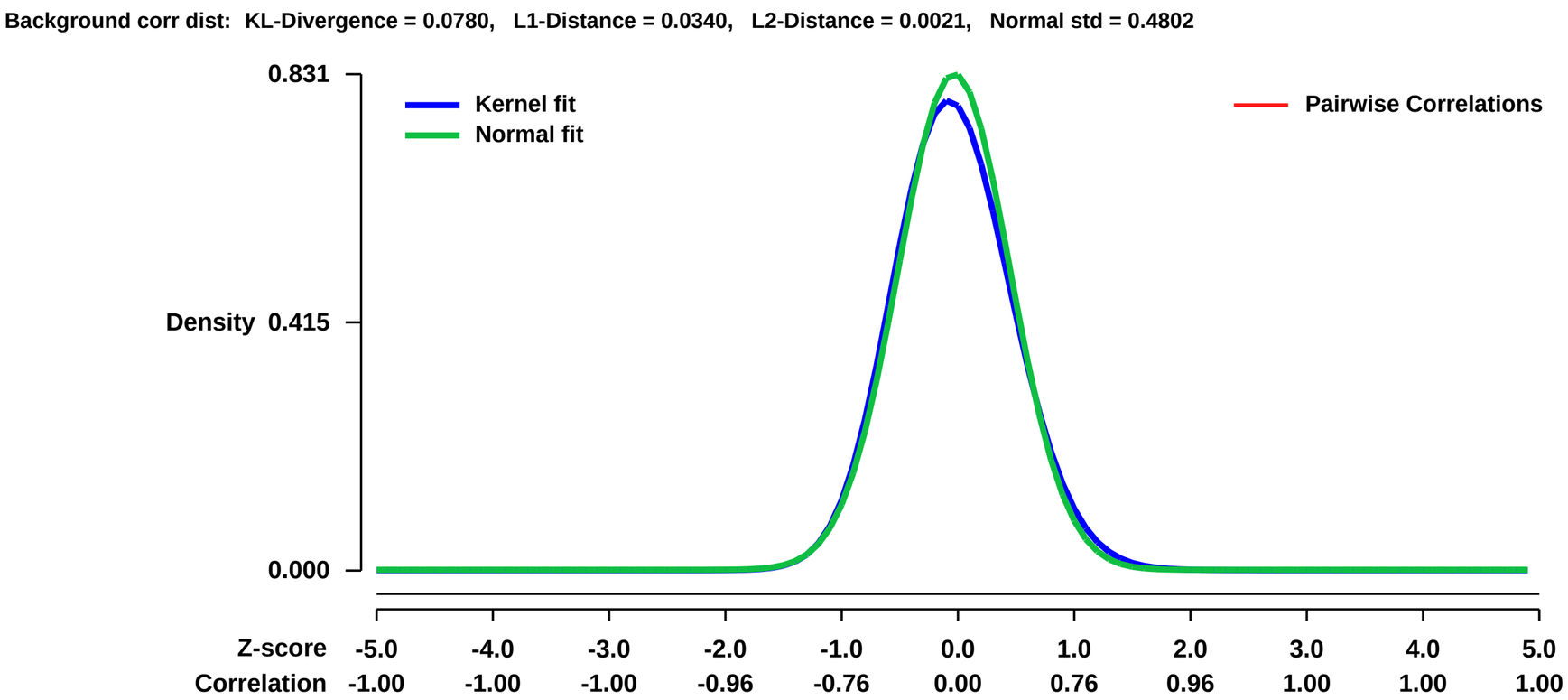

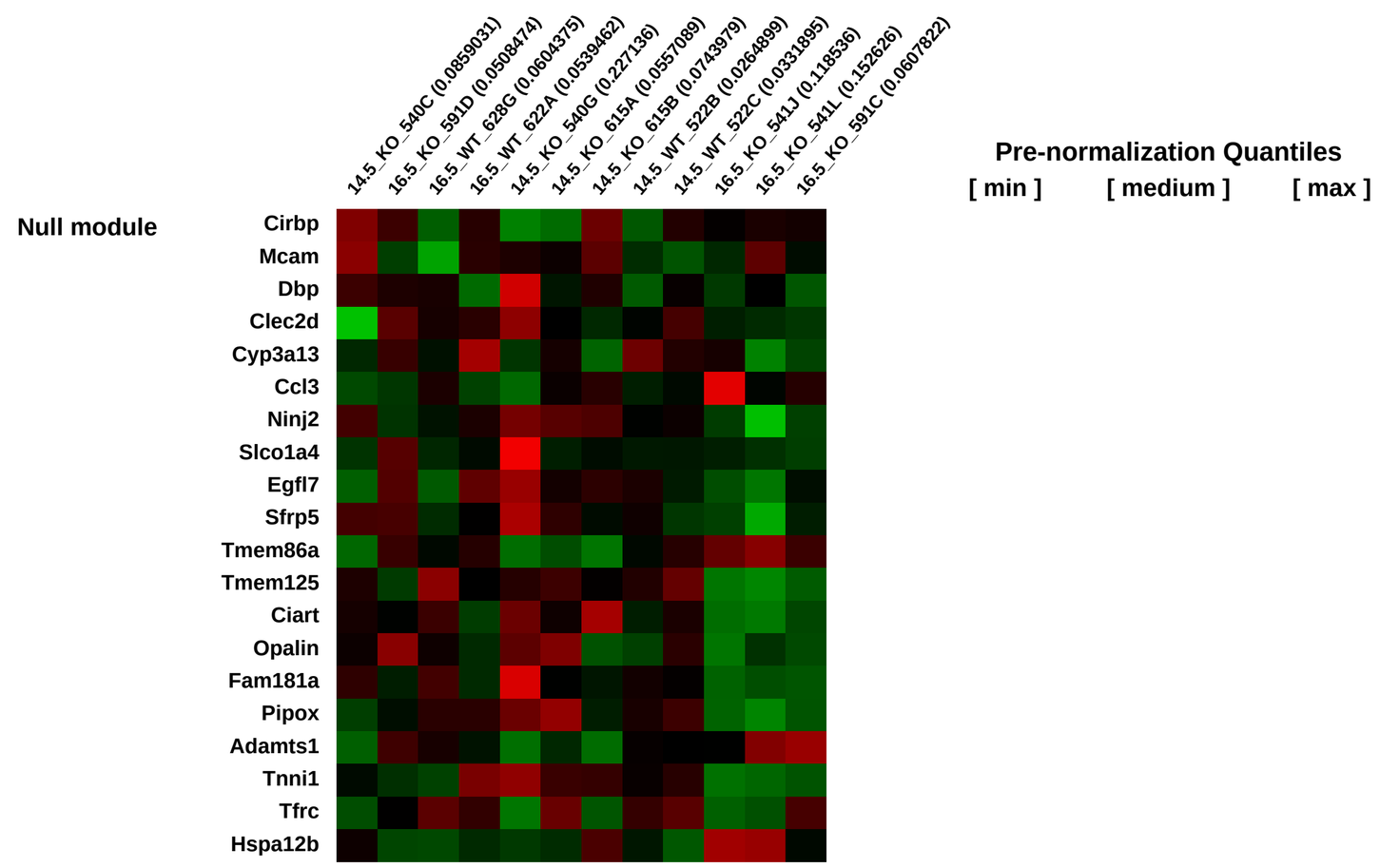

GEO Series "GSE7475" Expression Profiles

Num of samples in this series: 16

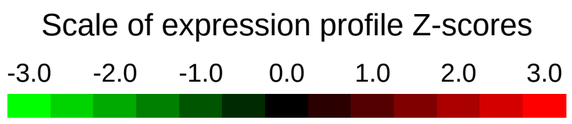

GEO Link:	http://www.ncbi.nlm.nih.gov/geo/query/acc.cgi?acc=GSE7475
Status:	Public on Jun 30 2007
Title:	Inflammatory response to titanium dioxide particles exposure is enhanced during pregnancy
Organism:	Mus musculus
Experiment type:	Expression profiling by array
Platform:	GPL1261
Pubmed ID:	17656681
Summary & Design:	**Summary:** Rationale: Maternal immune responses can promote allergy development in offspring. Pilot data show that neonates of mother mice exposed during pregnancy to air pollution particles have increased allergic susceptibility. Objective: We investigated whether inflammatory response to titanium dioxide (TiO2) particles earlier considered immunologically â inertâ is enhanced during pregnancy. Methods: Pregnant BALB/c mice (or non-pregnant controls) received particle suspensions intranasally at day 14 of pregnancy. Lung inflammatory responses were evaluated 19 and 48 h after exposure. Results: Pregnant mice showed robust and persistent acute inflammatory responses after exposure to TiO2, while non-pregnant females had the expected minimal responses. Genomic profiling identified genes differentially expressed in pregnant lungs exposed to TiO2. Neonates of mothers exposed to TiO2 (but not PBS) developed increased susceptibility to allergens. Conclusion: Pregnancy enhances lung inflammatory responses to otherwise relatively innocuous inert particles. **Keywords:** Particles exposure, pregnancy vs normal **Overall design:** 4 samples were analyzed in each of 4 groups: Normal PBS, Normal TiO2, Pregnant PBS and Pregnant TiO2, for a total of 16 samples.

Background corr dist: KL-Divergence = 0.2293, L1-Distance = 0.0543, L2-Distance = 0.0071, Normal std = 0.3130

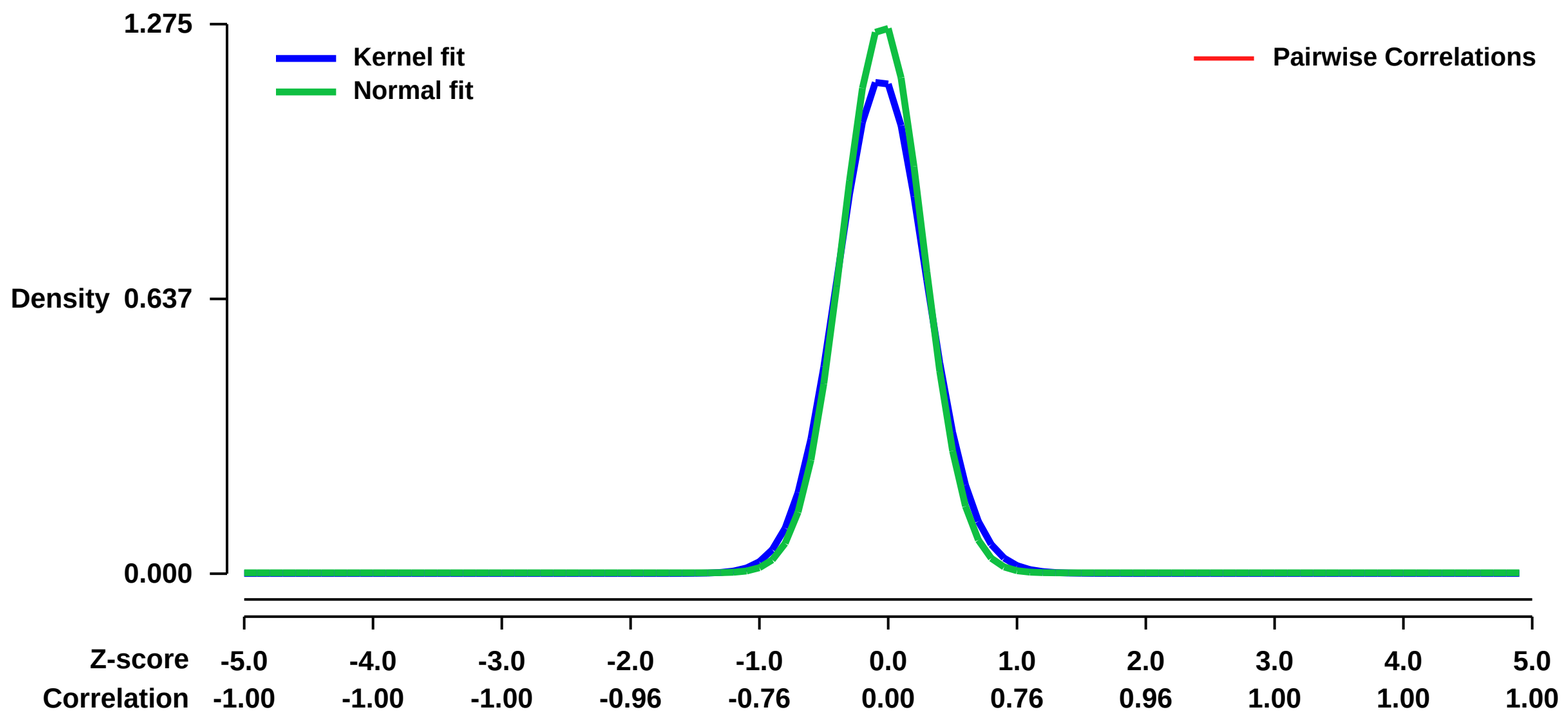

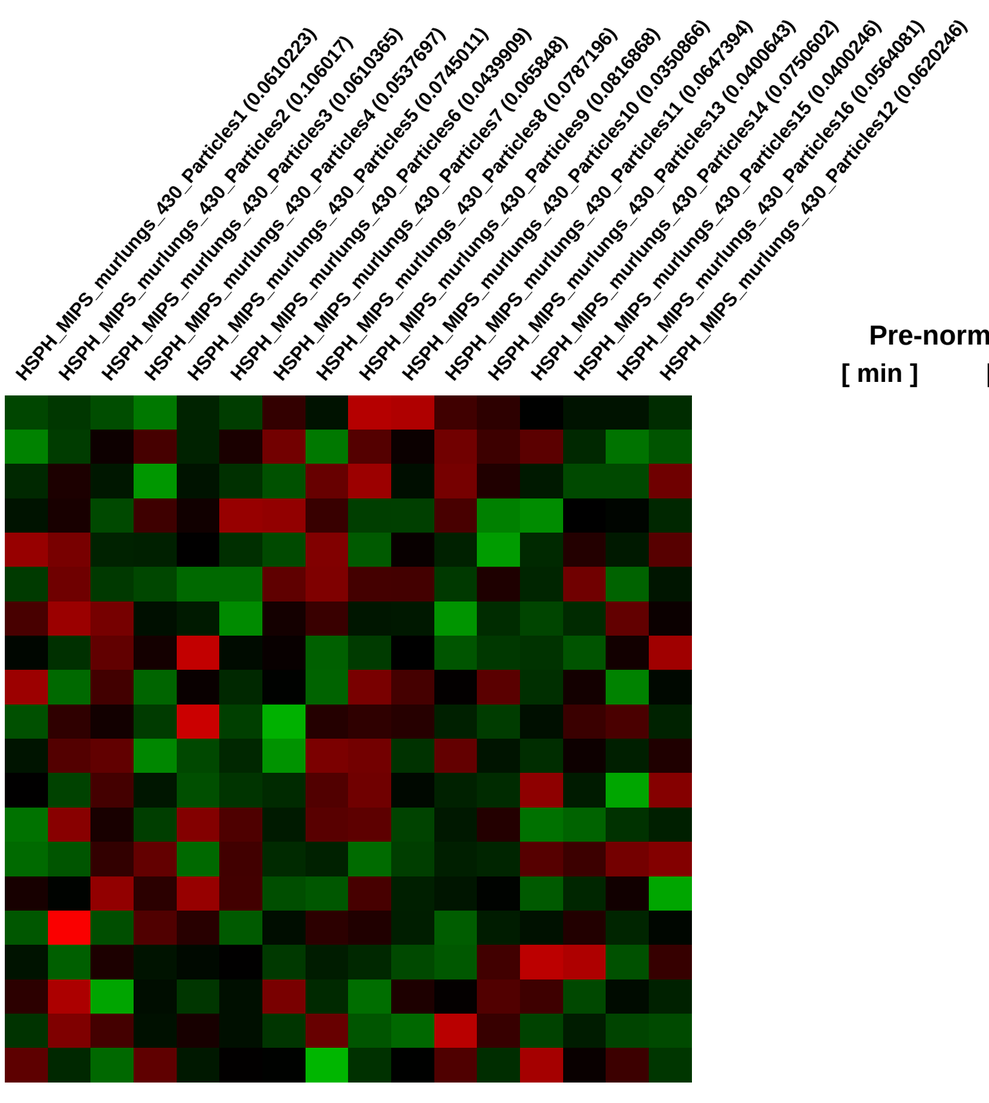

GEO Series "GSE7503" Expression Profiles

Num of samples in this series: 6

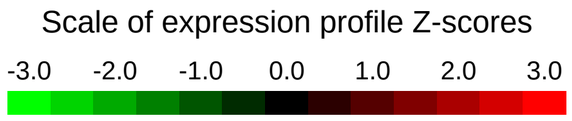

GEO Link:	**http://www.ncbi.nlm.nih.gov/geo/query/acc.cgi?acc=GSE7503**
Status:	**Public on Aug 01 2007**
Title:	**Effects of JNK on TGF-beta responses of mouse B lymphoma derived A20 cells**
Organism:	**Mus musculus**
Experiment type:	**Expression profiling by array**
Platform:	**GPL1261**
Pubmed ID:	
Summary & Design:	**Summary:** **TGF-beta plays multiple functions in a board range of cellular responses such as proliferation, differentiation, motility and survival by activating several cellular signaling pathways, including Smads and MAP kinases (Erk, JNK and p38). In particular, TGF-beta can activate pro- or anti-apoptotic signals depending on the target cells. We found that blockage of JNK activation sensitized mouse B lymphoma derived A20 cells to TGF-beta-induced apoptosis. These results suggest that TGF-beta activate JNK to inhibit the activation of death signal that is simultaneously activated by TGF-beta.** **We used microarrays to gain insight into the effects of JNK inhibition on gene expression in TGF-b-stimulated A20 cells and identified JNK-dependent TGF-beta inducible genes.** **Keywords: time course** **Overall design:** **The following six samples were prepared: untreated A20 cells (non-stimulated, DMSO): A20 cells cultured with SP600125 for 24 h (non-stimulated, SP600125): A20 cells stimulated with TGF-beta for 12 h (TGF-beta 12 h, DMSO) and 24 h (TGF-beta 24 h, DMSO): and A20 cells stimulated with TGF-beta in the presence of SP600125 for 12 h (TGF-beta 12 h, SP600125) and 24 h (TGF-beta 24 h, SP600125), respectively. Total RNA was prepared and hybridized to the Affymetrix Mouse Genome 430 2.0 array. Genes whose expression was increased by more than 2-fold at either 12 or 24 h after TGF-beta stimulation were identified as TGF-beta inducible genes. Amongst them, we identified genes whose induction levels were reduced by more than 75% by co-treatment with the JNK inhibitor SP600125.**

Background corr dist: KL-Divergence = 0.0429, L1-Distance = 0.0241, L2-Distance = 0.0007, Normal std = 0.6069

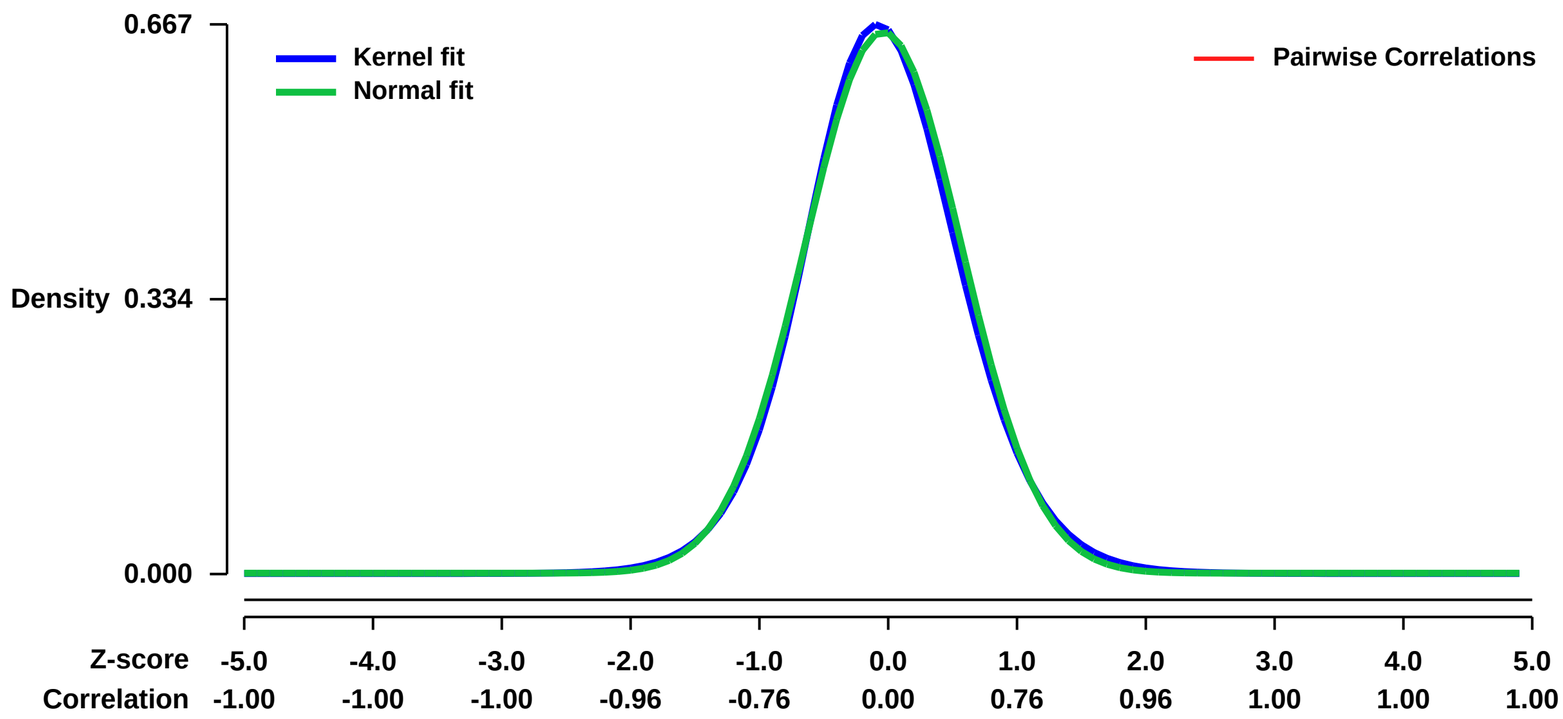

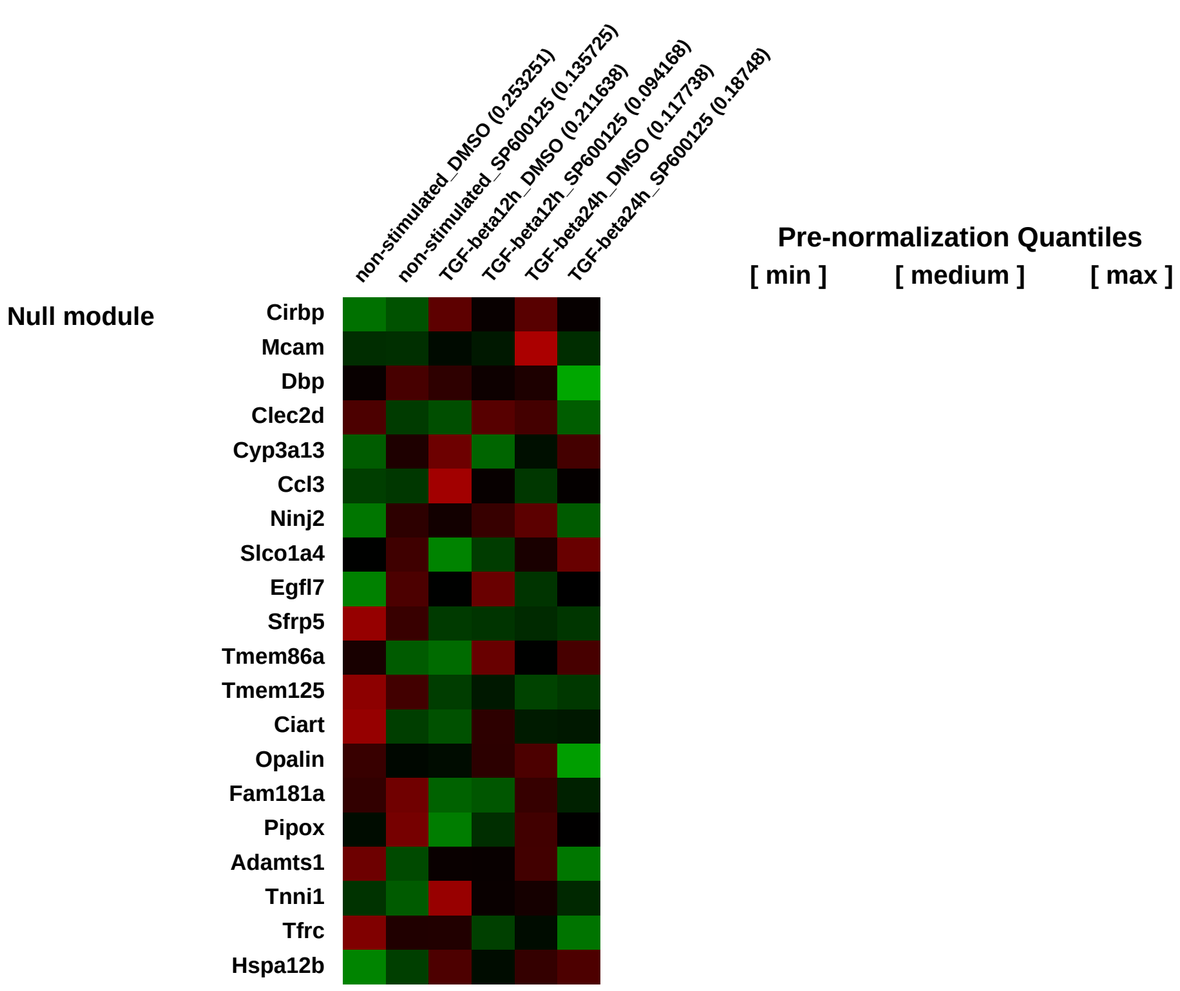

GEO Series "GSE7596" Expression Profiles

Num of samples in this series: 6

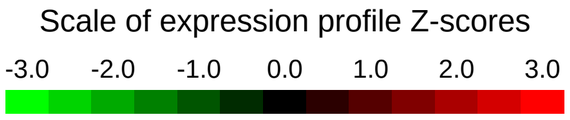

GEO Link:	http://www.ncbi.nlm.nih.gov/geo/query/acc.cgi?acc=GSE7596
Status:	Public on Feb 15 2008
Title:	AKT regulates de novo induction of Foxp3
Organism:	Mus musculus
Experiment type:	Expression profiling by array
Platform:	GPL1261
Pubmed ID:	18283119
Summary & Design:	**Summary:** The CD4+Foxp3+ regulatory T cells play an essential role in maintaining tolerance via their suppressive function on conventional T cells. The intracellular signaling pathways that regulate Foxp3 expression are largely unknown. In this study we describe a novel inhibitory role for AKT in regulating de novo induction of Foxp3 both in vivo and in vitro. A constitutively active allele of AKT significantly diminished TGF-ˆ¢ induced Foxp3 induction via a rapamycin-sensitive pathway, establishing a role for the AKT-mTOR axis in Treg cells. Moreover, the observed impairment in Foxp3 induction was paralleled by a selective downmodulation of the imparted Treg transcriptional signature highlighting the importance of the balance of intracellular signals in Treg differentiation . Our results provide a basis for further elucidation of molecular mechanisms that regulate Foxp3 induction and identify AKT as an important negative regulator of this process. **Keywords: Cell population comparison** **Overall design:** All gene expression profiles were obtained from highly purified T cell populations sorted by flow cytometry. To reduce variability, cells from multiple mice were pooled for sorting, and three replicates were generated for all groups. RNA from 0.5-2.5 x 105 cells was amplified, labeled, and hybridized to Affymetrix M430v2 microarrays. Raw data were preprocessed with the RMA algorithm in GenePattern, and averaged expression values were used for analysis.

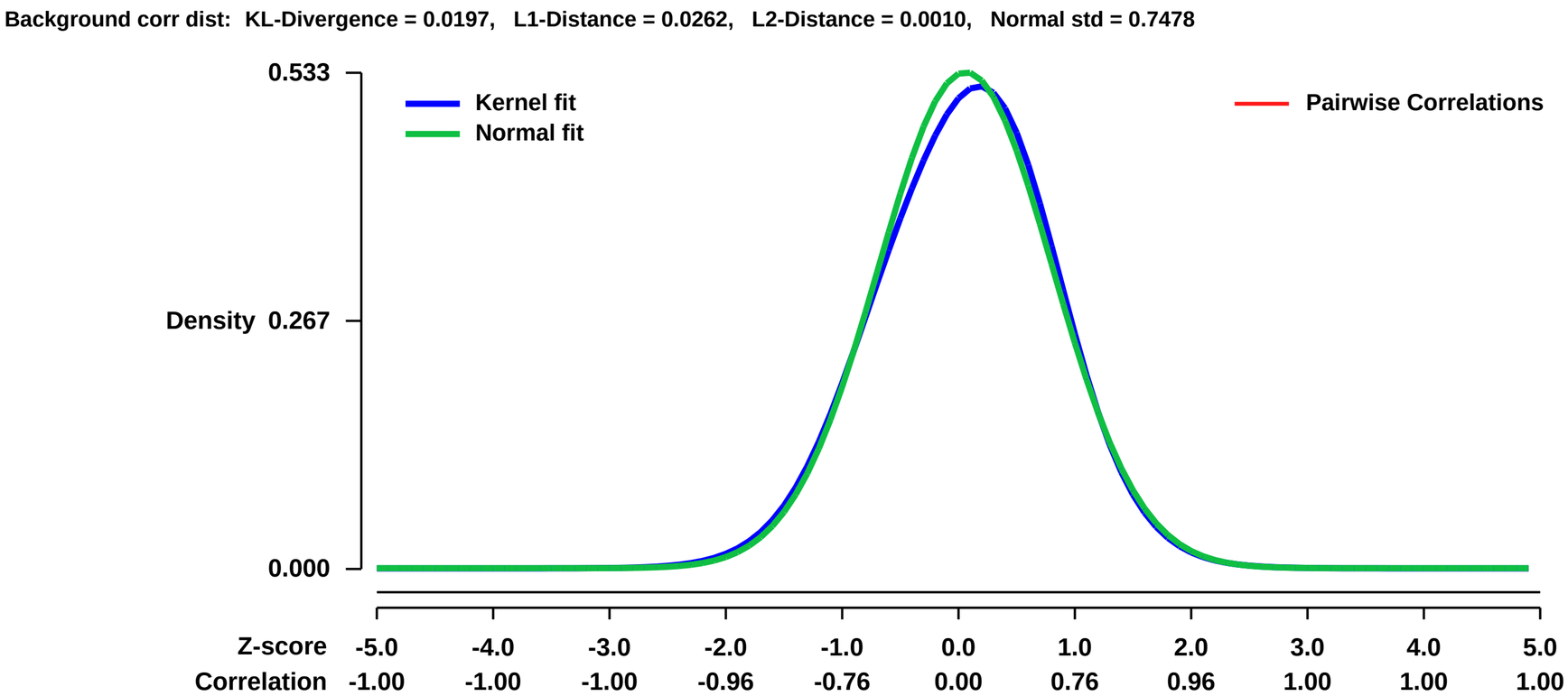

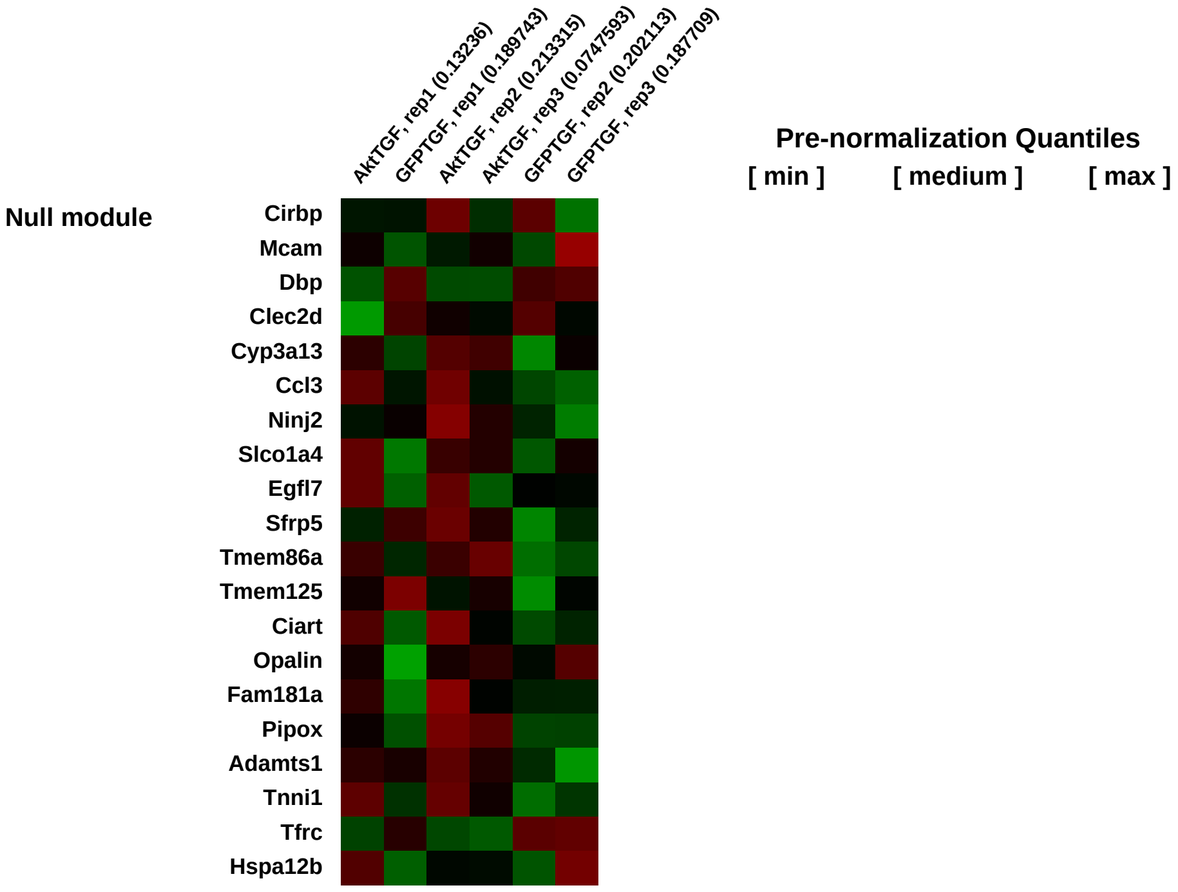

GEO Series "GSE7598" Expression Profiles

Num of samples in this series: 8

Scale of expression profile Z-scores

-3.0 -2.0 -1.0 0.0 1.0 2.0 3.0

GEO Link:	http://www.ncbi.nlm.nih.gov/geo/query/acc.cgi?acc=GSE7598
Status:	Public on Jan 01 2008
Title:	Identification and characterization of genes expressed in the mouse ZPA using a novel microarray approach
Organism:	Mus musculus
Experiment type:	Expression profiling by array
Platform:	GPL1261
Pubmed ID:	17911046
Summary & Design:	**Summary:** Comparing gene expression of cells from the E10.5 limb bud ZPA and the rest of the E10.5 limb bud from Shhgfpcre heterozygotes separated by FACS. **Keywords: comparison, cell-type comparison, experiemental versus control** **Overall design:** 8 samples, 4 ZPA and 4 rest of the limb

Background corr dist: **KL-Divergence = 0.0410, L1-Distance = 0.0441, L2-Distance = 0.0031, Normal std = 0.6311**

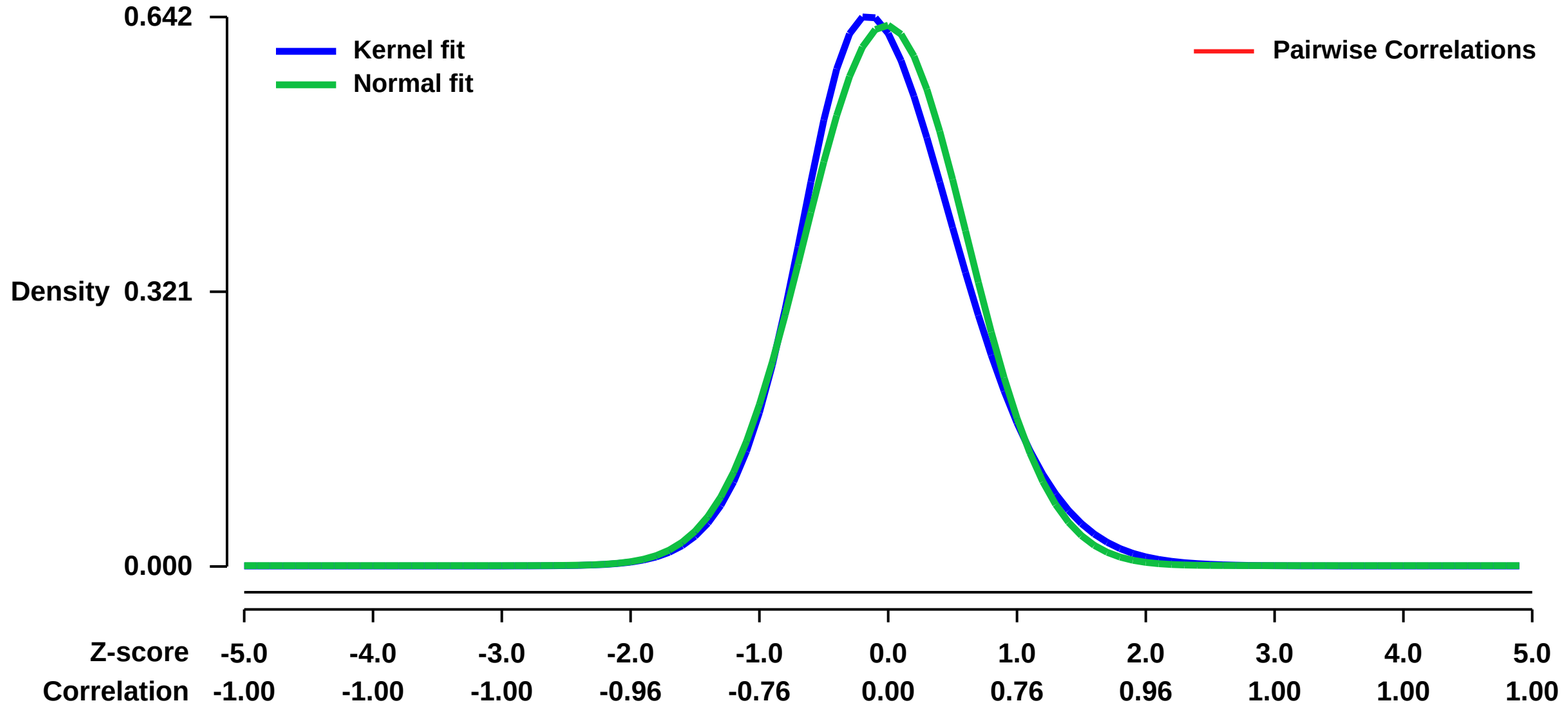

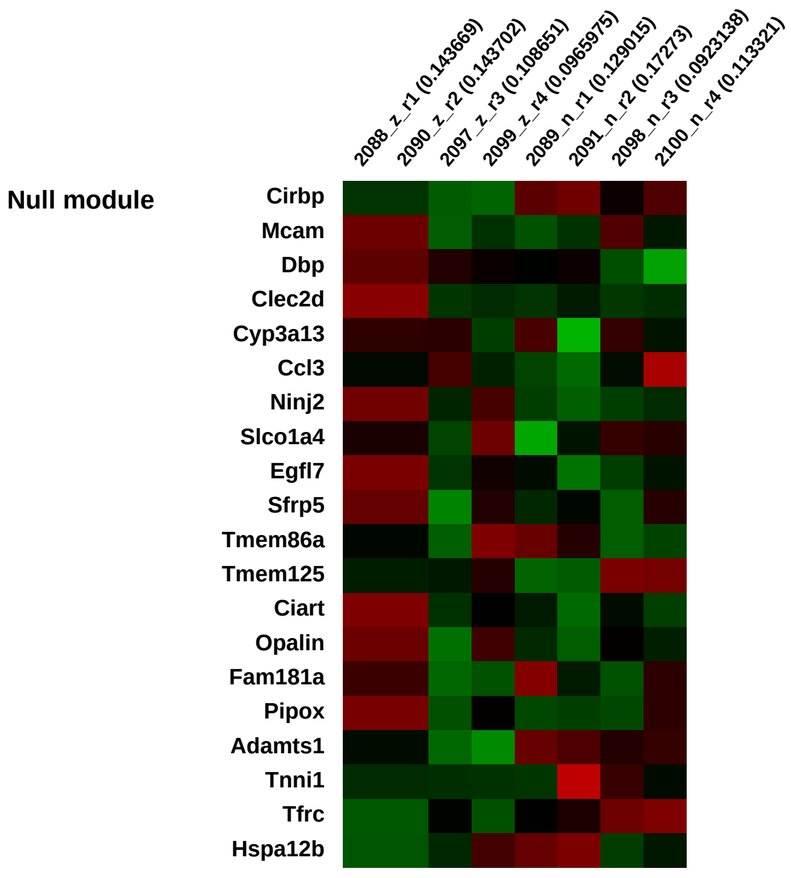

GEO Series "GSE7605" Expression Profiles

Num of samples in this series: 18

Scale of expression profile Z-scores

-3.0 -2.0 -1.0 0.0 1.0 2.0 3.0

GEO Link:	http://www.ncbi.nlm.nih.gov/geo/query/acc.cgi?acc=GSE7605
Status:	Public on Nov 01 2007
Title:	Expression in Kir6.1-deficient heart following LPS challenge
Organism:	Mus musculus
Experiment type:	Expression profiling by array
Platform:	GPL1261
Pubmed ID:	18026101
Summary & Design:	**Summary:** KATP opposes depolarization of cells in the heart, smooth muscle, and other tissues by permitting the efflux of potassium ions and this efflux is evidently required to prevent unopposed vasoconstriction and insufficiency of coronary artery blood flow triggered by one or more cytokines induced in response to LPS. The cytokine(s) involved must elicit a dysfunctional response in the Kir6.1-deficient environment, and to gain further insight into the effects of the mutation, we examined the transcriptional status of whole heart, isolated from normal C57BL/6J mice or KcnJ8Md/Md mice, before and after injection of 1 ¸…g of LPS **Keywords:** Time course, stress response, disease state analysis, genetic modification **Overall design:** 3 mice per genotype were injected with 0.5 ug LPS in PBS or with PBS alone and hearts were collected after 30 min or 3 h.

Background corr dist: KL-Divergence = 0.0549, L1-Distance = 0.0384, L2-Distance = 0.0029, Normal std = 0.5407

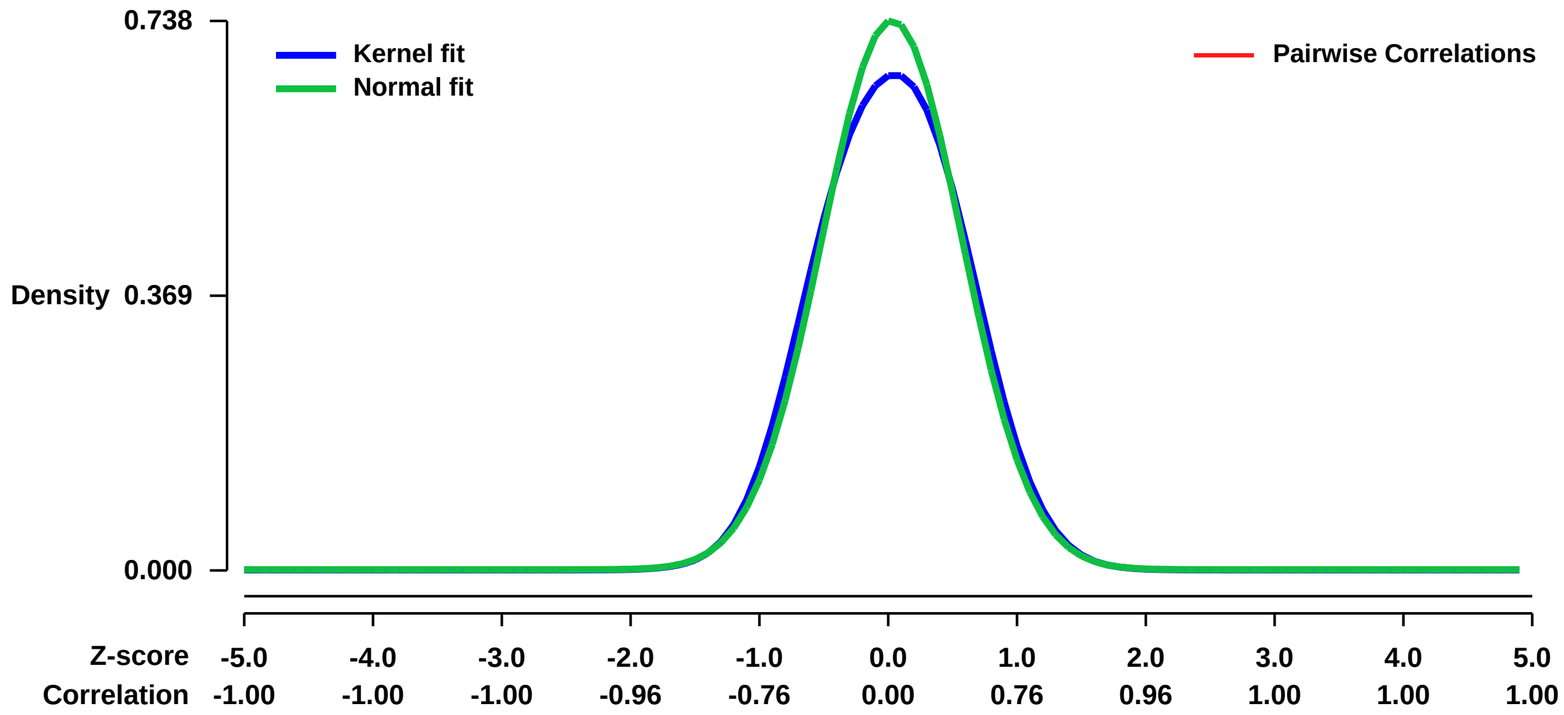

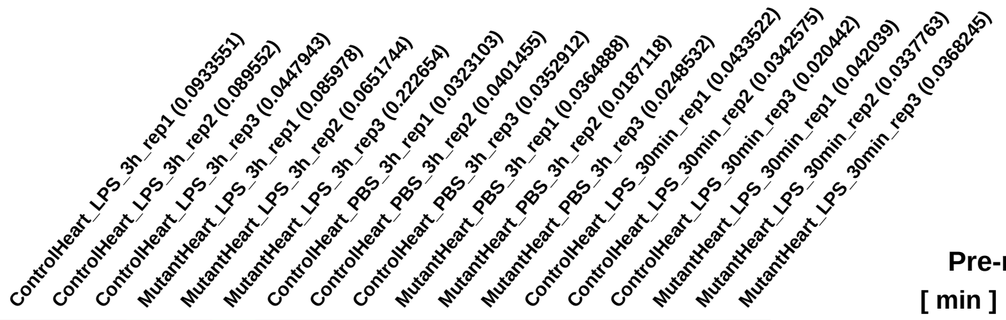

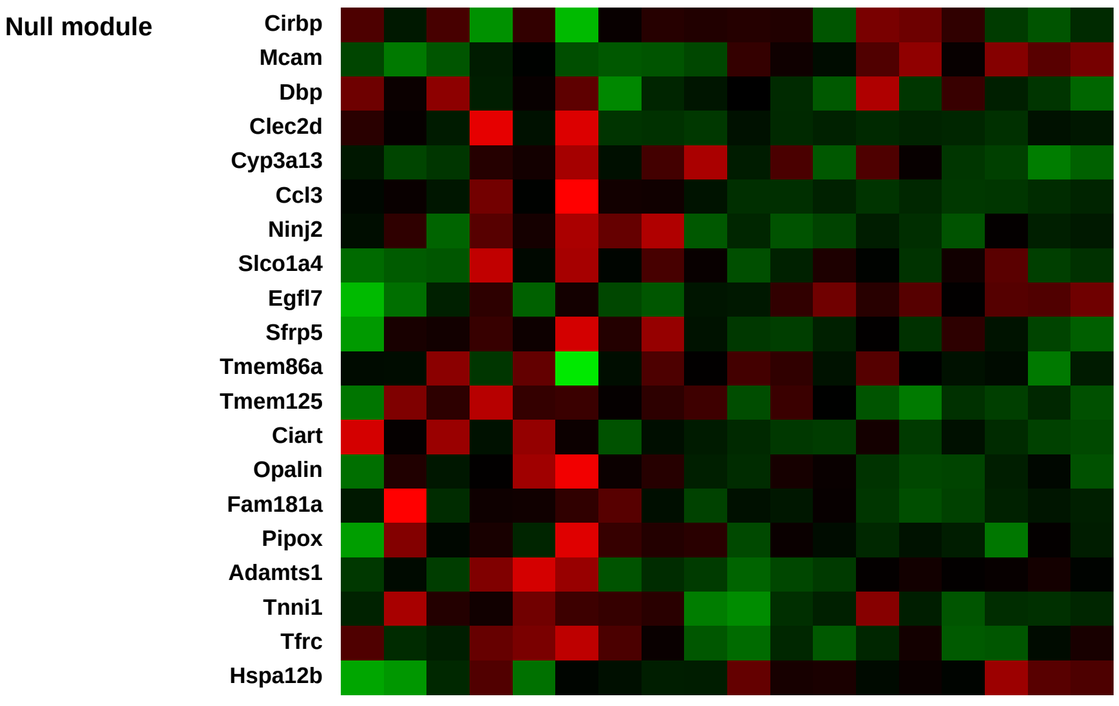

GEO Series "GSE7657" Expression Profiles

Num of samples in this series: 12

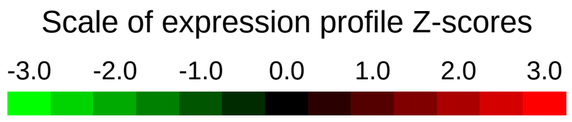

GEO Link:	**http://www.ncbi.nlm.nih.gov/geo/query/acc.cgi?acc=GSE7657**
Status:	**Public on May 01 2008**
Title:	**Identification of phase-specific arthritis-related genes in mice**
Organism:	**Mus musculus**
Experiment type:	**Expression profiling by array**
Platform:	**GPL1261**
Pubmed ID:	
Summary & Design:	**Summary:** **Rheumatoid arthritis (RA), one of the most common polygenic diseases, is characterized by a chronic, progressive inflammation mainly in joints and has an unknown etiology. Numerous studies have revealed the significance of cytokines TNF and IL-1 in the onset and progression of RA. Due to the complexity of interactions among different cytokines and immune cells, little is known about the precise molecular mechanisms underlying RA. In this study, oligonucleotide microarray analysis and a mouse model of RA, IL-1 receptor antagonist deficient mice were used to address this issue. Two hundred and ninety transcripts were found to be dysregulated greater than or equal to 2-fold in the diseased mice. Phase-specific gene expression changes were identified, including early increase and late decrease of heat shock protein coding genes and Cyr61. Moreover, common gene expression changes were also observed, especially the upregulation of paired-Ig-like receptor A (Pira) in both early and late phases of arthritis. We conclude that common and distinct gene expression change patterns that were identified globally may represent novel opportunities for better control of RA through early diagnosis and development of alternative therapeutic strategies.** **Keywords: Time course** **Overall design:** **Six wild-type and 6 Il1rn deficient BALB/c mice at 1 month and 4 month (3 for each time point) were used for microarray analysis of splenic gene expression profiling.**

Background corr dist: KL-Divergence = 0.0960, L1-Distance = 0.0243, L2-Distance = 0.0010, Normal std = 0.4471

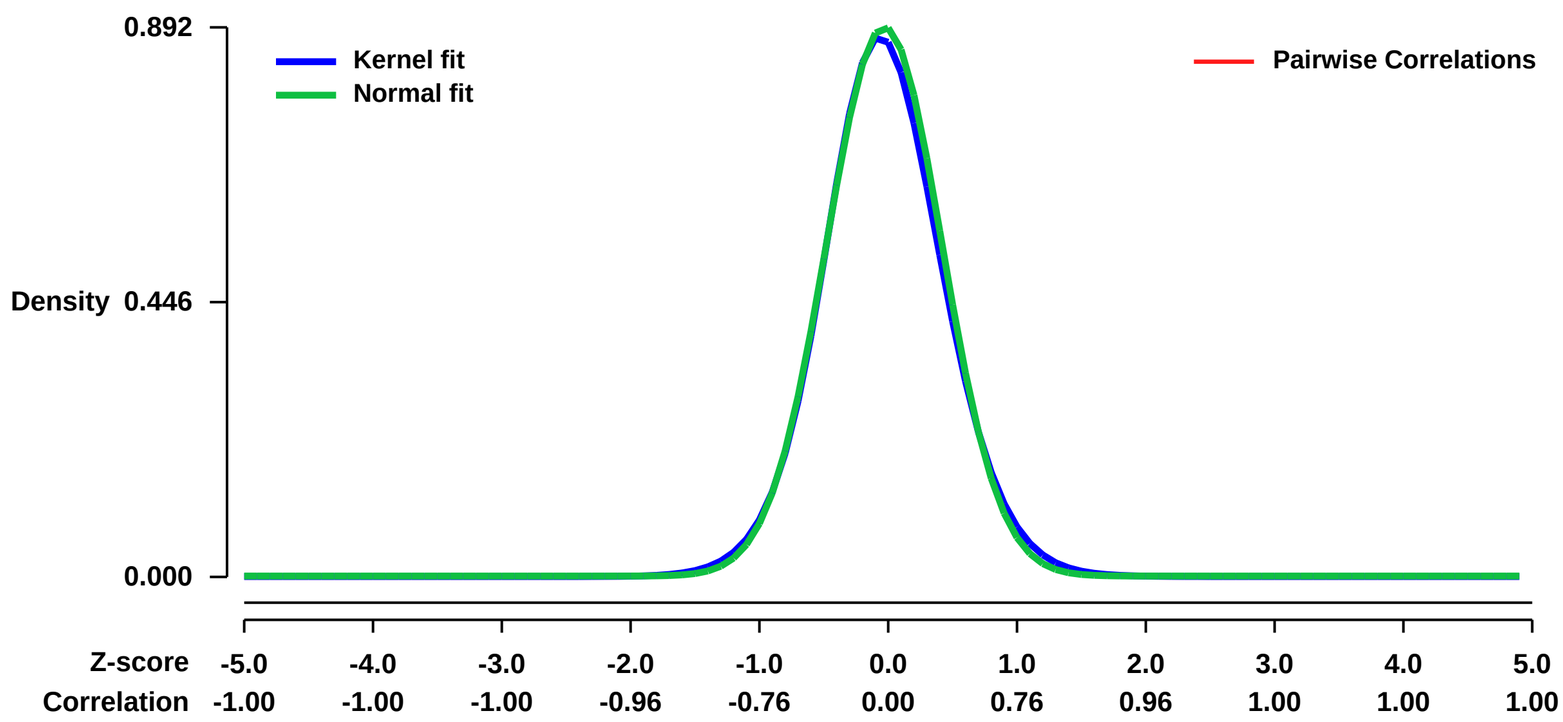

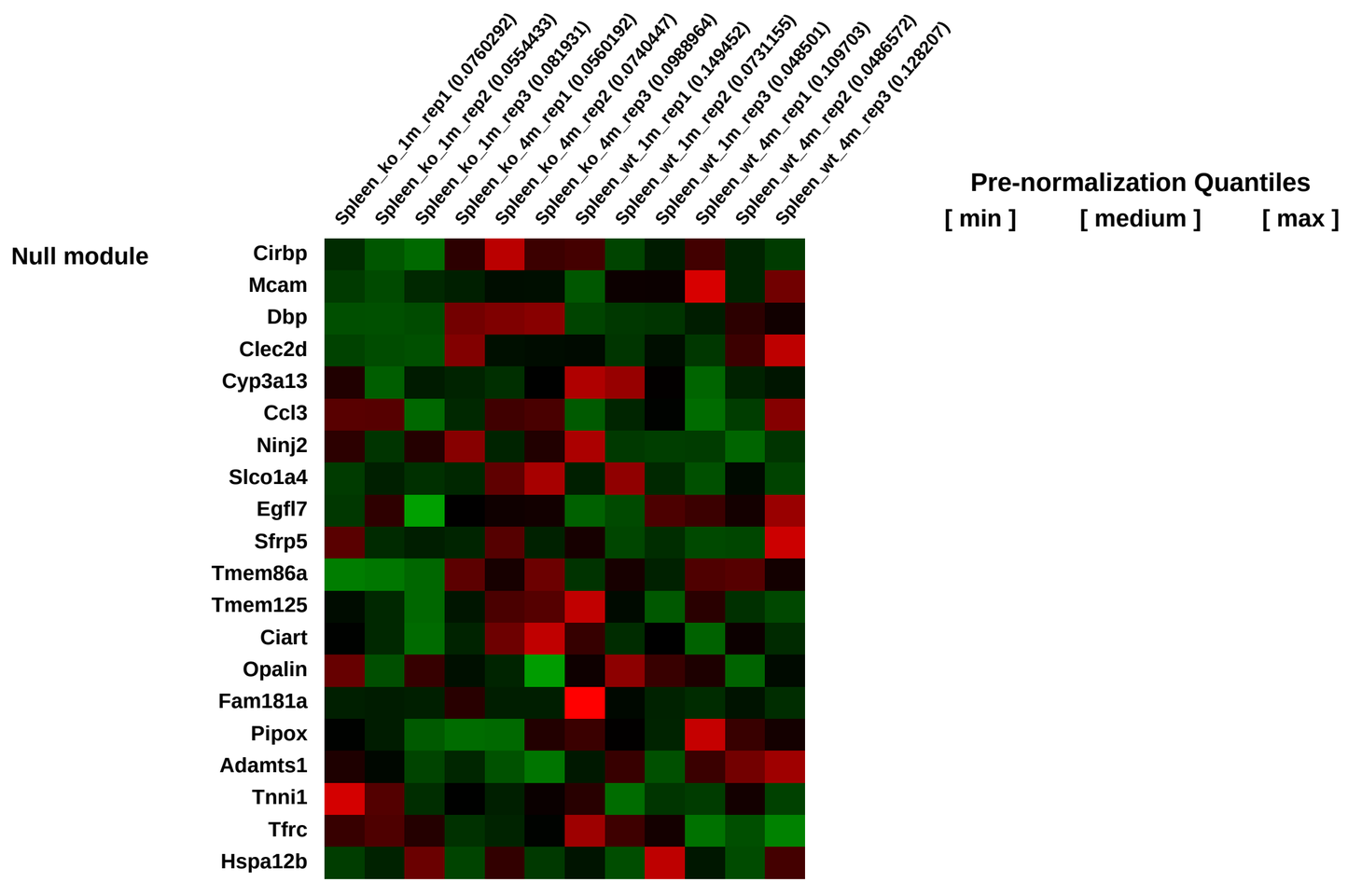

GEO Series "GSE7676" Expression Profiles

Num of samples in this series: 10

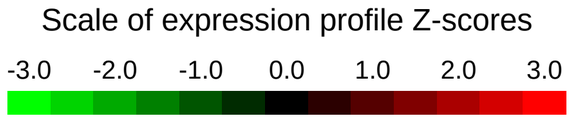

GEO Link:	**http://www.ncbi.nlm.nih.gov/geo/query/acc.cgi?acc=GSE7676**
Status:	**Public on Jun 30 2008**
Title:	**Changes in gene expression following Protocadherin 12 knockout**
Organism:	**Mus musculus**
Experiment type:	**Expression profiling by array**
Platform:	**GPL1261**
Pubmed ID:	**18477666**
Summary & Design:	**Summary:** **Protocadherin 12 (Pcdh12) is a transmembrane adhesive protein with homophilic adhesive properties and expressed in endothelial cells, the glycogen trophoblast cells of the placenta, and the mesangial cells of kidney glomeruli. Pcdh12-deficient mice are alive although they show alterations in placenta development.** **To reveal Pcdh12-associated pathways, 45,000 - Affymetrix probe arrays were used on Pcdh12 knockout and control placentas.** **Keywords: Comparative gene knockout results** **Overall design:** **To identify genes whos expression was modified by Pcdh12 deficiency, we examined global gene expression profiles of whole E12.5 knockout placentas (Pcdh12 -l-) and their wild-type (WT â Pcdh12+l+) littermates, using the Affymetrix Murine Genome 430 2.0 microarrays. Gestation day 12 was chosen as it is the period at which placentas already formed distinct layers, but organogenesis is still very active. Total RNA was extracted from five Pcdh12 knockout embryos and five normal placentas. RNA were tested for integrity on Agilent 2100 BioAnalyzer, prior to cRNA synthesis and chip hybridization (performed by the Institute of Genetics and Molecular and Cellular Biology, Strasbourg, France).**

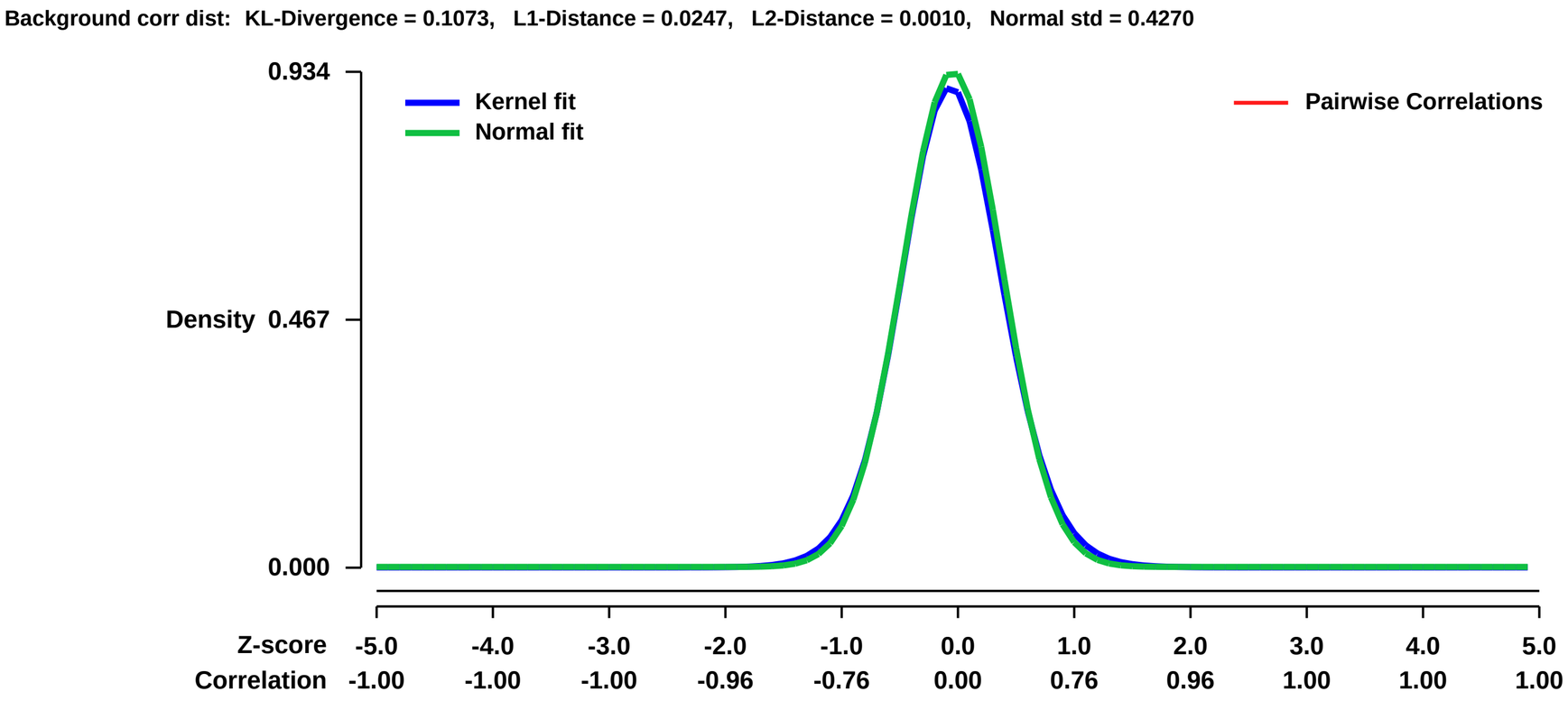

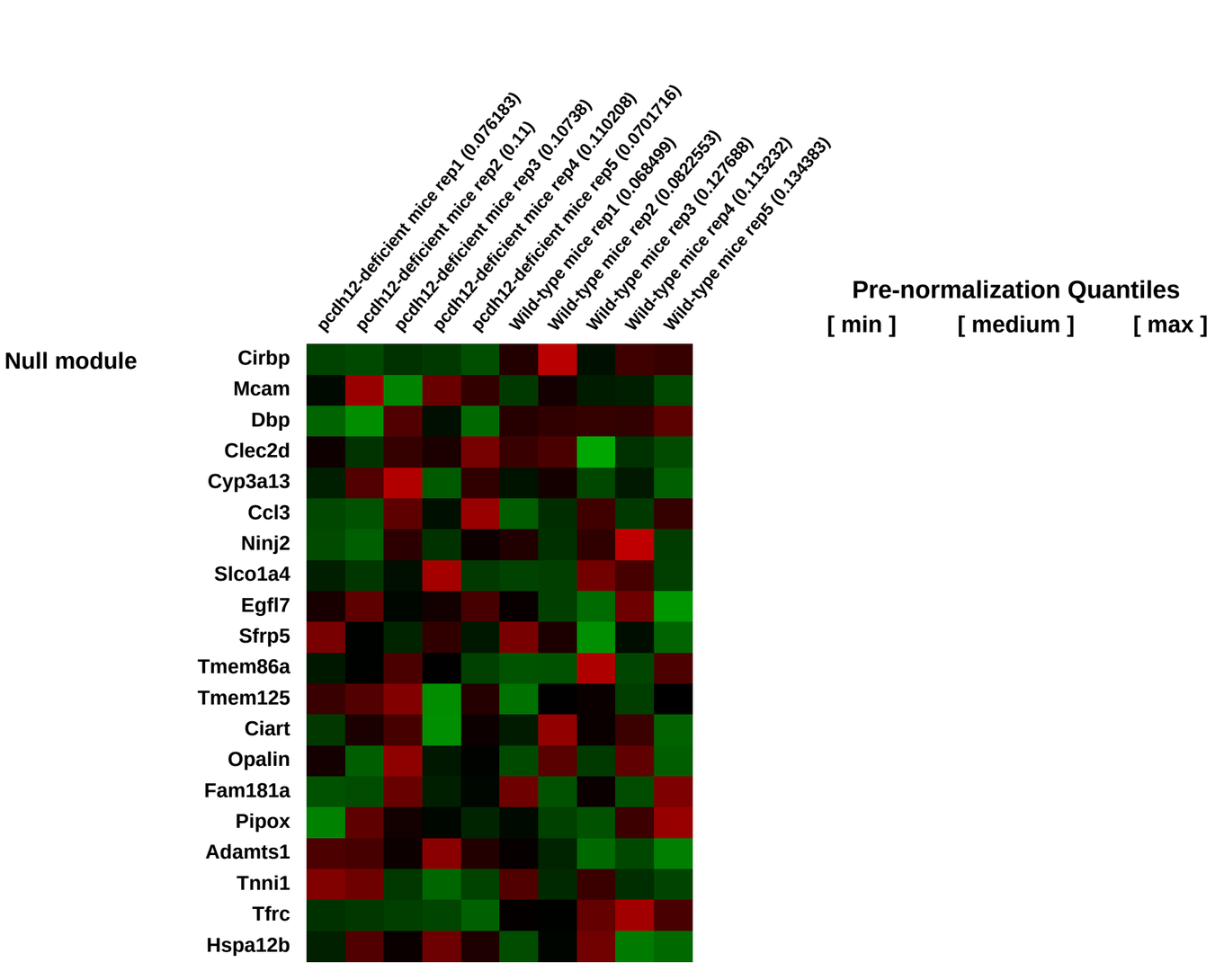

GEO Series "GSE7694" Expression Profiles

Num of samples in this series: 12

Scale of expression profile Z-scores

-3.0 -2.0 -1.0 0.0 1.0 2.0 3.0

GEO Link:	http://www.ncbi.nlm.nih.gov/geo/query/acc.cgi?acc=GSE7694
Status:	Public on Jun 11 2007
Title:	Cannabinoid receptor double knockout mice (Cnr1 -/- /Cnr2 -/-) in CHS model
Organism:	Mus musculus
Experiment type:	Expression profiling by array
Platform:	GPL1261
Pubmed ID:	17556587
Summary & Design:	**Summary:** We evaluated cutaneous contact hypersensitivity (CHS) in Cnr1-/-/Cnr2-/- animals using the obligate contact allergen 2,4-dinitrofluorobenzene (DNFB), which generates a specific cutaneous T-cell mediated allergic response upon repeated allergen contact. Allergic contact dermatitis affects about 5% of men and 11% of women in industrialized countries and is one of the leading causes for occupational diseases. In an animal model for cutaneous contact hypersensitivity we show that mice lacking both known cannabinoid receptors display exacerbated allergic inflammation. In contrast, fatty acid amide hydrolase deficient mice, which have increased levels of the endocannabinoid anandamide, displayed reduced allergic responses in the skin. Cannabinoid receptor antagonists exacerbated whereas receptor agonists attenuated allergic inflammation. These results demonstrate a protective role of the endocannabinoid system in contact allergy in the skin, and suggest a novel target for therapeutic intervention. **Keywords: Strain (Wt versus Ko) and disease state (DNFB treated versus control).** **Overall design:** Three wildtype mice (Wt) and three Cnr1-/-/Cnr2-/- (Ko) mice were used. Contact hypersensitivity was determined always at the right ears, which therefore were treated with DNFB (Tr). Left ears of mice were kept untreated and served as control ears (C). A total of 12 hybridizations were performed (2 strains x 2 treatments X 3 biological replicates) in this experiment.

Background corr dist: KL-Divergence = 0.0647, L1-Distance = 0.0516, L2-Distance = 0.0039, Normal std = 0.5463

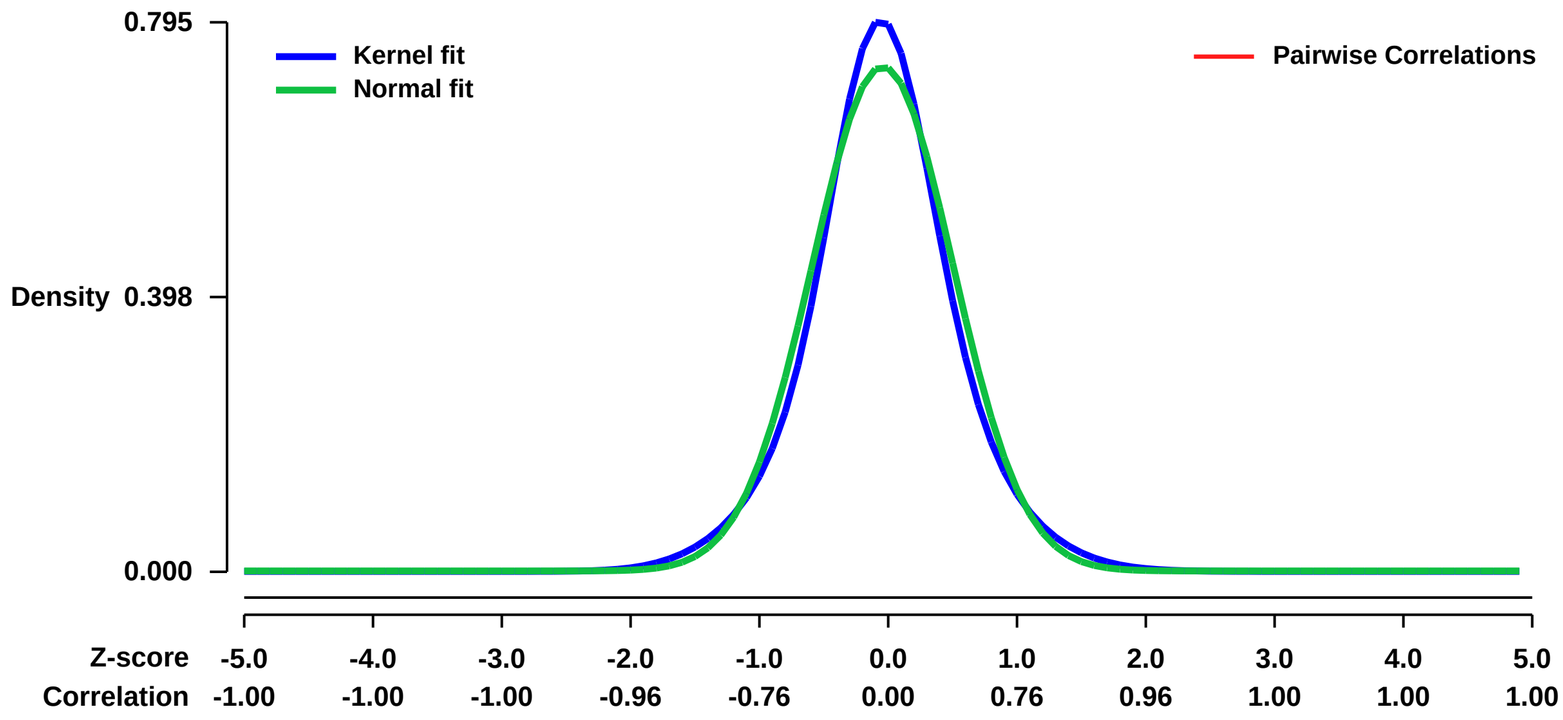

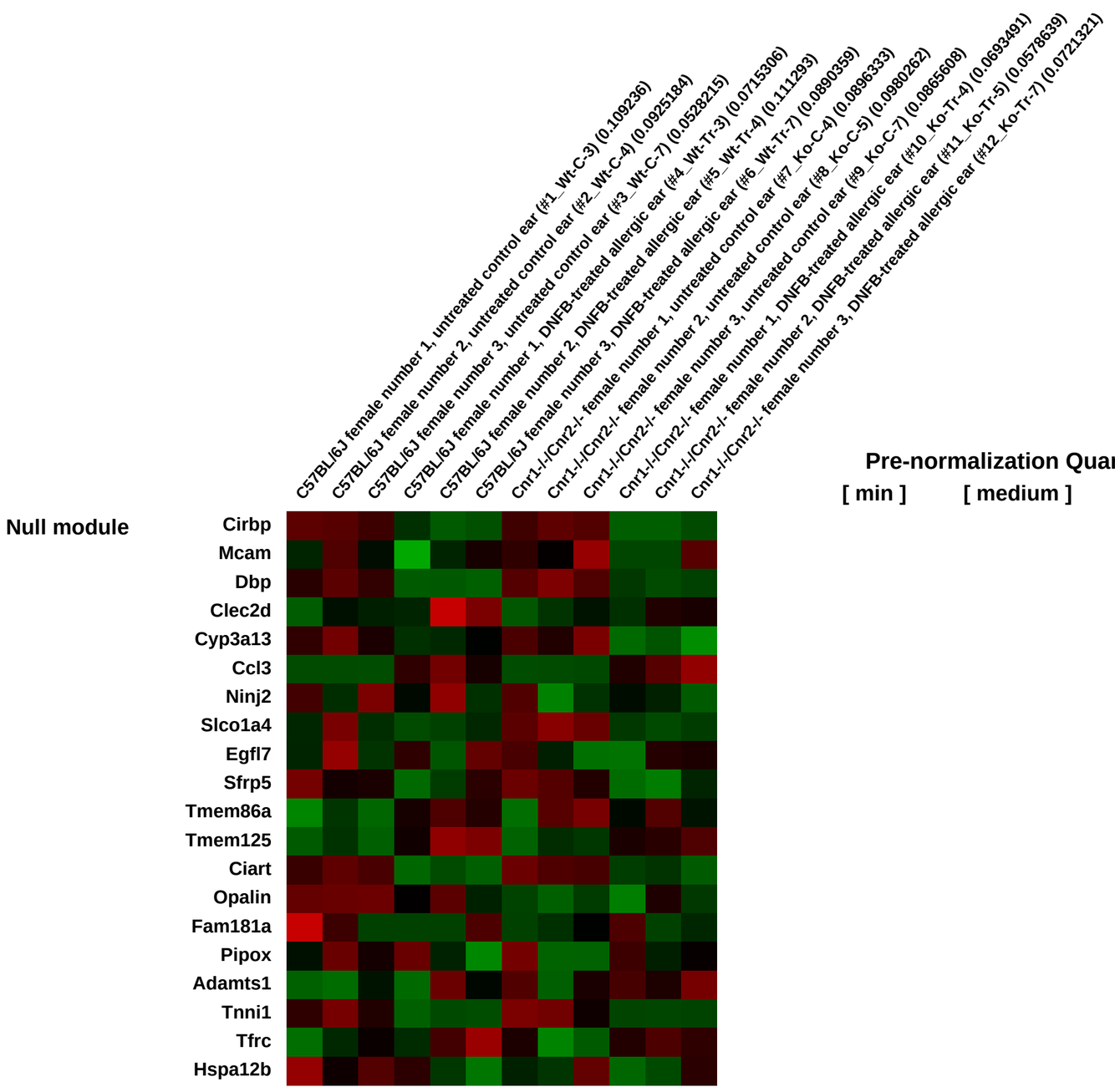

GEO Series "GSE7699" Expression Profiles

Num of samples in this series: 6

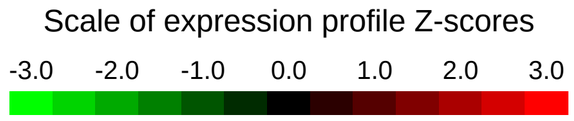

GEO Link:	http://www.ncbi.nlm.nih.gov/geo/query/acc.cgi?acc=GSE7699
Status:	Public on May 04 2007
Title:	A high fat, ketogenic diet induces a unique metabolic state in mice.
Organism:	Mus musculus
Experiment type:	Expression profiling by array
Platform:	GPL1261
Pubmed ID:	17299079
Summary & Design:	**Summary:** Analysis of liver gene transcription during feeding of a ketogenic diet. Ketogenic diets may alter physiologic and metabolic profiles in a direction that favors weight loss. C57BL/6J mice were maintained for six weeks on either chow or ketogenic diet. Mice eating KD had lower weights, 90% reduction in insulin levels and increased energy expenditure compared to animals fed chow. Despite consumpiton of a very high fat diet serum lipids remained normal. Here we show that consumption of KD shifted liver metabolism to drastically increased fatty acid oxidation. Concurrently, expression of genes involved in fatty acid synthesis were markedly suppressed. **Keywords: Hepatic profile** **Overall design:** Eight week old C57BL/6 mice were fed either chow (Labdiet 5008, Pharmserv) or KD (F3666, Bio-Serv) for six weeks. Livers were harvested in the morning in ad lib fed animals. Total RNA from 2-3 animals in each group was used for Affymetrix analysis.

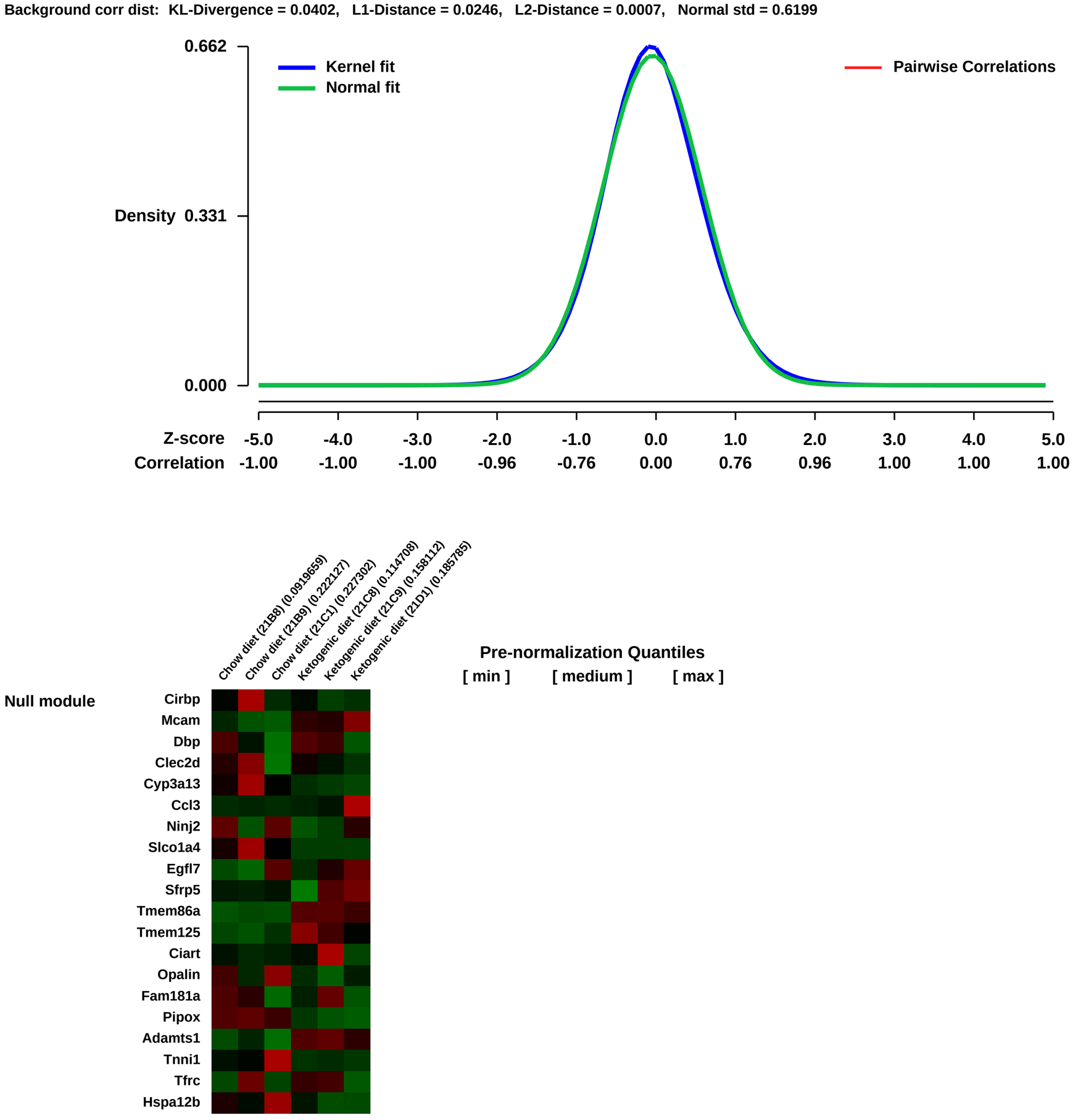

GEO Series "GSE7705" Expression Profiles

Num of samples in this series: 10

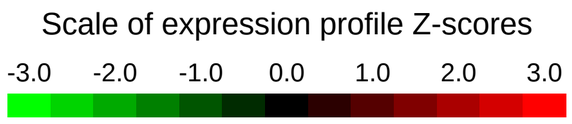

GEO Link:	**http://www.ncbi.nlm.nih.gov/geo/query/acc.cgi?acc=GSE7705**
Status:	**Public on May 01 2008**
Title:	**Microarray analysis of CD4+T cells in murine arthritis**
Organism:	**Mus musculus**
Experiment type:	**Expression profiling by array**
Platform:	**GPL1261**
Pubmed ID:	
Summary & Design:	**Summary:** **Although activated CD4+ T cell-driven overproduction of cytokines, especially TNF and IL1, is generally regarded as the major factor in the development of rheumatoid arthritis (RA), little is known about the precise role of CD4+ T cells in the initiation and progression of this disease. In this study, this issue was addressed using a time-course microarray analysis in a mouse model of RA, Il1rn deficient mice.No obvious cytokine gene expression changes reflecting T cell activation was observed in CD4+ T cells in the Il1rn deficient mice during the course of spontaneous arthritis. On the contrast, majority of dysregulated genes were those predominantly expressed in myeloid lineage cells, suggesting T cell reprogramming involvement in arthritis development. Distinct gene expression patterns were identified for different stages of disease, including downregulated expression of immunoglobulin heavy chain constant region genes and increased expression of inflammatory genes in the early phase, and downregulation of MHC class II genes in the late phase. The common changes occurred in both early and late phases included upregulation of Arl2bp and Mfap1, which are involved in the regulation of cytoskeletal dynamics.** **Keywords: Time course** **Overall design:** **Two KO mice and three WT mice for each time point (1 month and 4 month) were used for this study.**

Background corr dist: KL-Divergence = 0.0808, L1-Distance = 0.0282, L2-Distance = 0.0010, Normal std = 0.4856

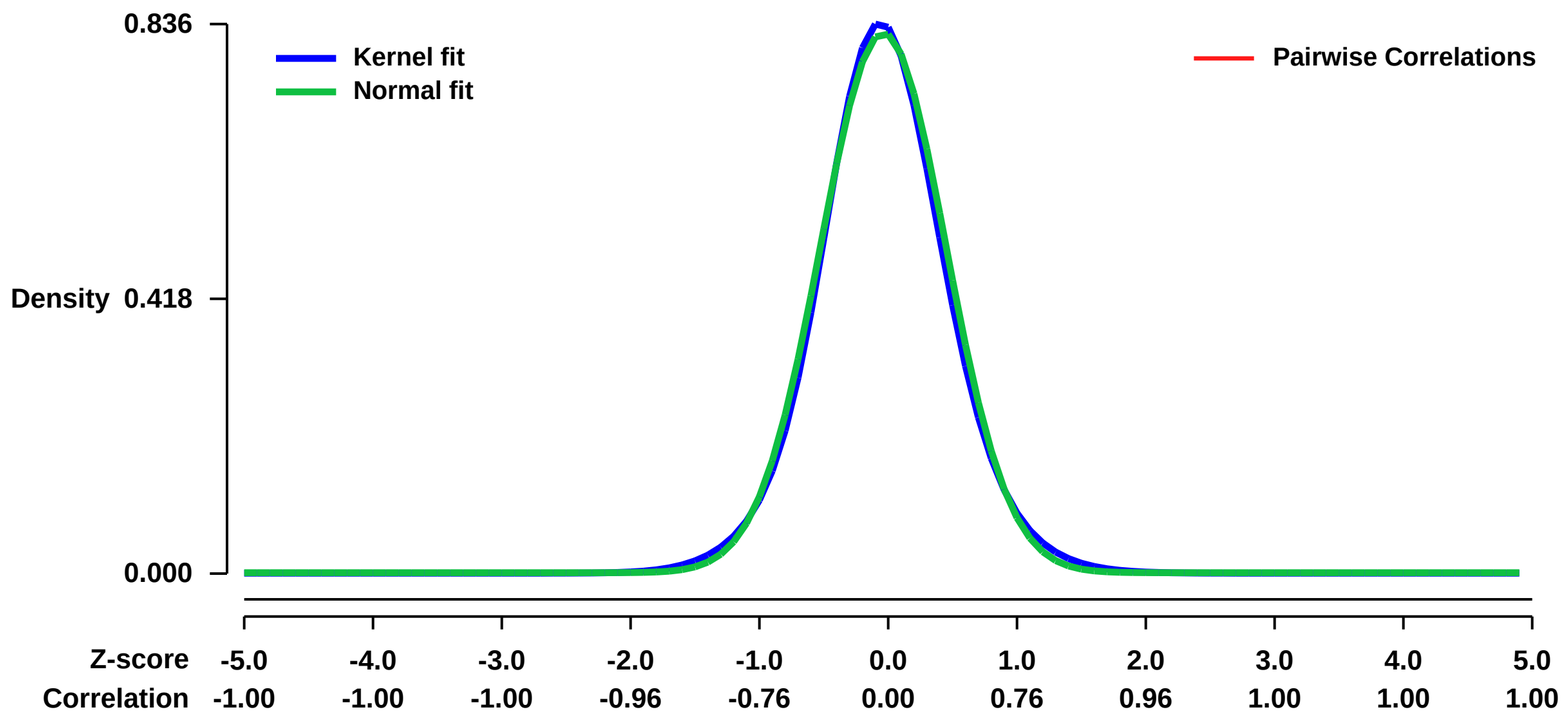

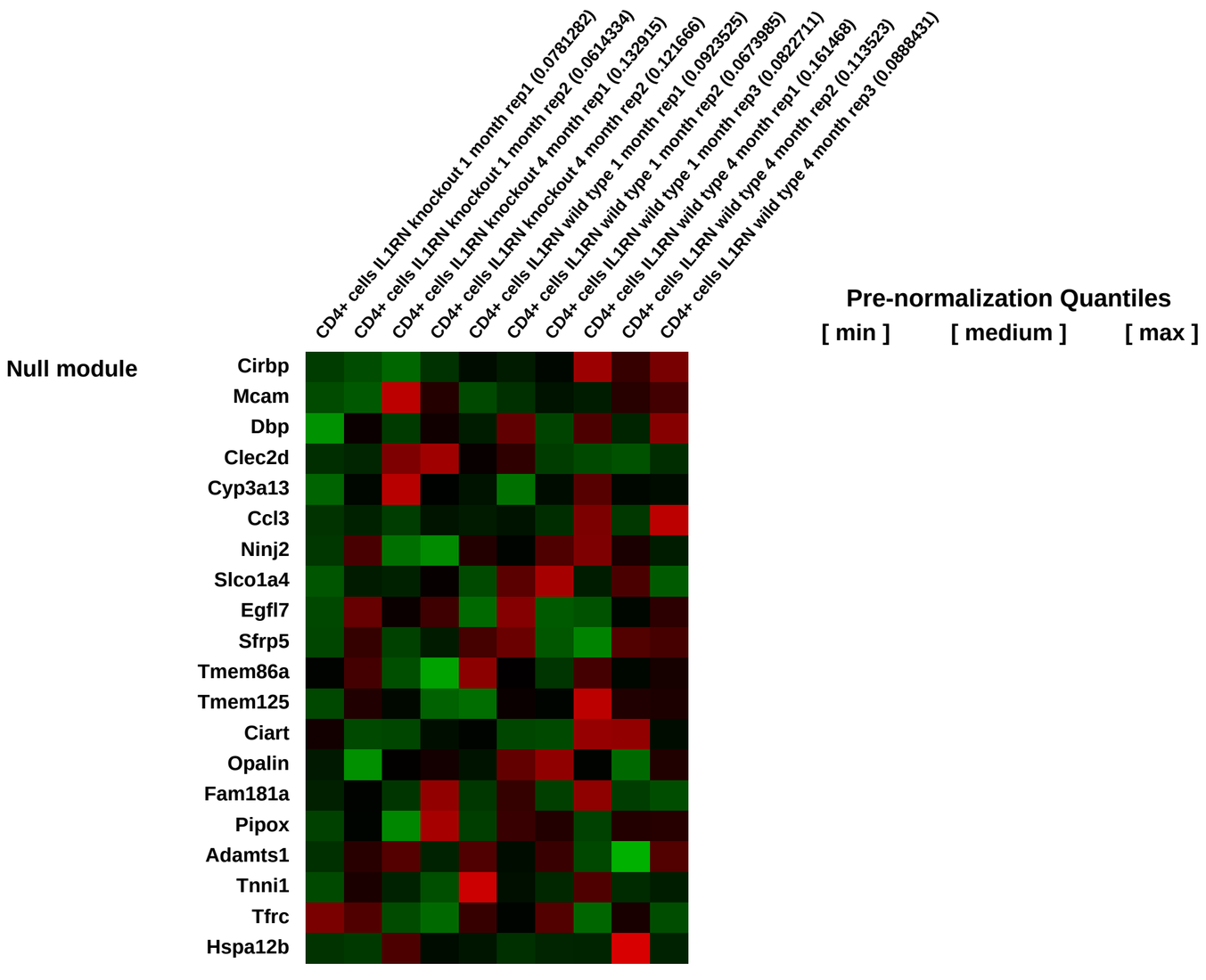

GEO Series "GSE7767" Expression Profiles

Num of samples in this series: 6

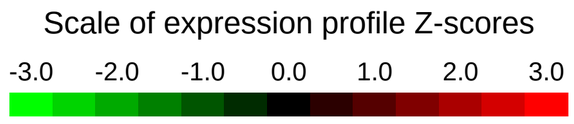

GEO Link:	http://www.ncbi.nlm.nih.gov/geo/query/acc.cgi?acc=GSE7767
Status:	Public on Jul 15 2007
Title:	Differential transcription of ip Chlamydia infected C57BL6J and DBA2J mice
Organism:	Mus musculus
Experiment type:	Expression profiling by array
Platform:	GPL1261
Pubmed ID:	17641048

Summary & Design:

Summary:
C57BL/6J mice were 105-fold more resistant to Chlamydia psittaci infection than DBA/2J mice by LD100 determinations. Linkage analysis using BXD recombinant inbred strains revealed a single effector locus at a 1.5 Mbp region on chromosome 11 encoding a cluster of three p47GTPases (Irgb10, Igtp, and Iigp2). Western blots of infected tissue showed that Irgb10 was elevated in resistant mice and one of the two possible Iigp2 protein isoforms was preferentially expressed in susceptible mice. The BXD39 strain, susceptible at Irgb10 and resistant at Iigp2, had an intermediate phenotype, implicating the non-redundant role of these p47GTPases. C57BL/6J and DBA/2J exhibited a difference in IFNg dependent chlamydial control, which was reversible by Iigp2 siRNA knockdown. Microarrays of infected peritoneal lavage revealed >10 fold up regulation of neutrophil recruiting chemokines in susceptible mice and >100 fold increase in macrophage differentiation genes in resistant mice, indicating that susceptibility pattern involves stimulation of different inflammatory cell recruiting pathways. Massive neutrophil recruitment was seen in susceptible mice by histology and flow cytometry, and neutrophil chemokine receptor (CXCR2) knockout mice on a susceptible background survived lethal challenge confirming that neutrophil recruitment was required for susceptibility. Congenic Igtp knockout mice also susceptible at Irgb10 and Iigp2 on a resistant background recruited neutrophils and succumbed to infection. We conclude that Irgb10 and Iigp2 act together to confer differential susceptibility against murine chlamydial infection. Results indicate that these p47GTPases have cell autonomous effects, which results in vastly different inflammatory stimulation leading to either recovery or death.

Keywords: Comparative disease state analysis

Overall design:
C57BL/6J and DBA2J mice (4 mice each) were infected I.p. with 10E4 IFU of Chlamydia psittaci then peritoneal lavage was collected on day 3 post infection. Cells were centrifuged then treated with Trizol for total RNA extraction.

Background corr dist: KL-Divergence = 0.0126, L1-Distance = 0.0218, L2-Distance = 0.0006, Normal std = 0.8222

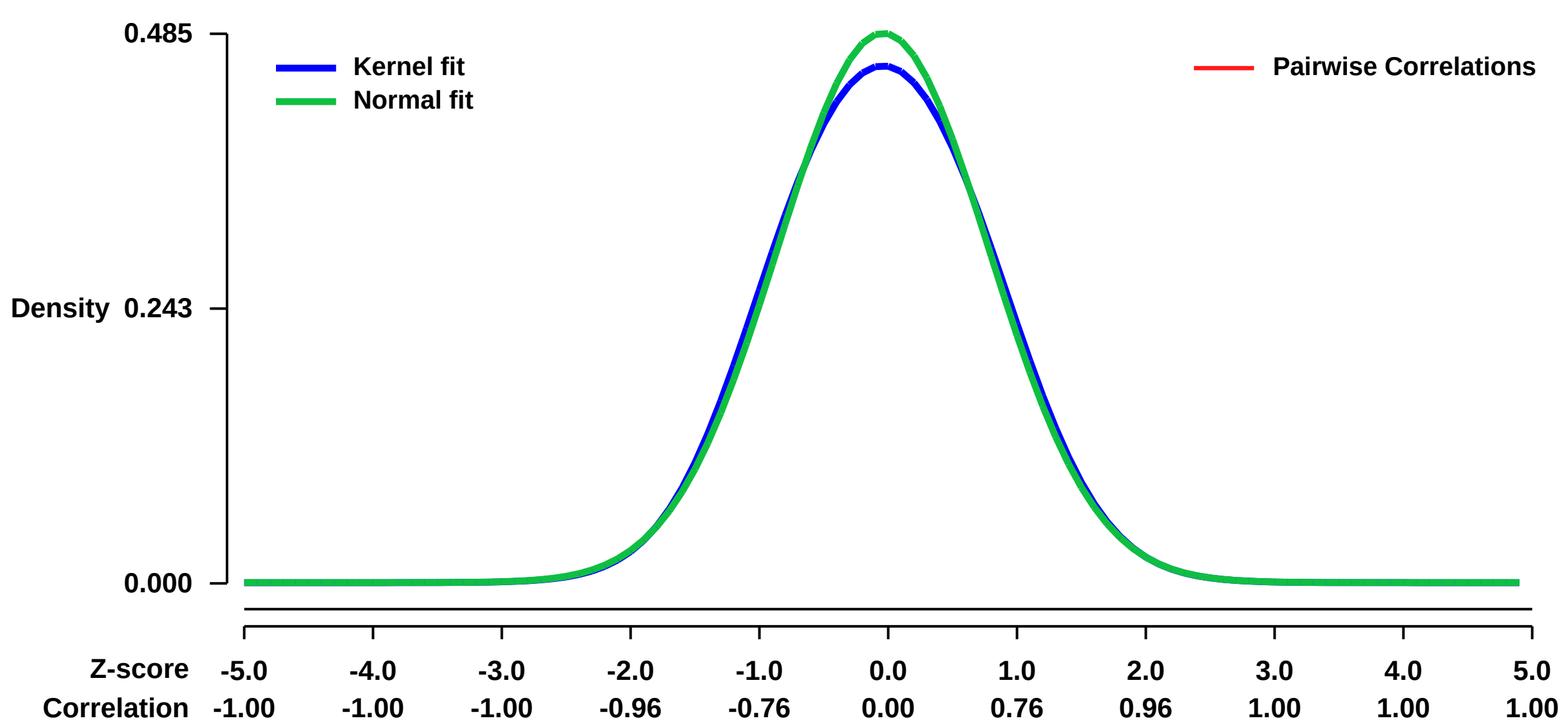

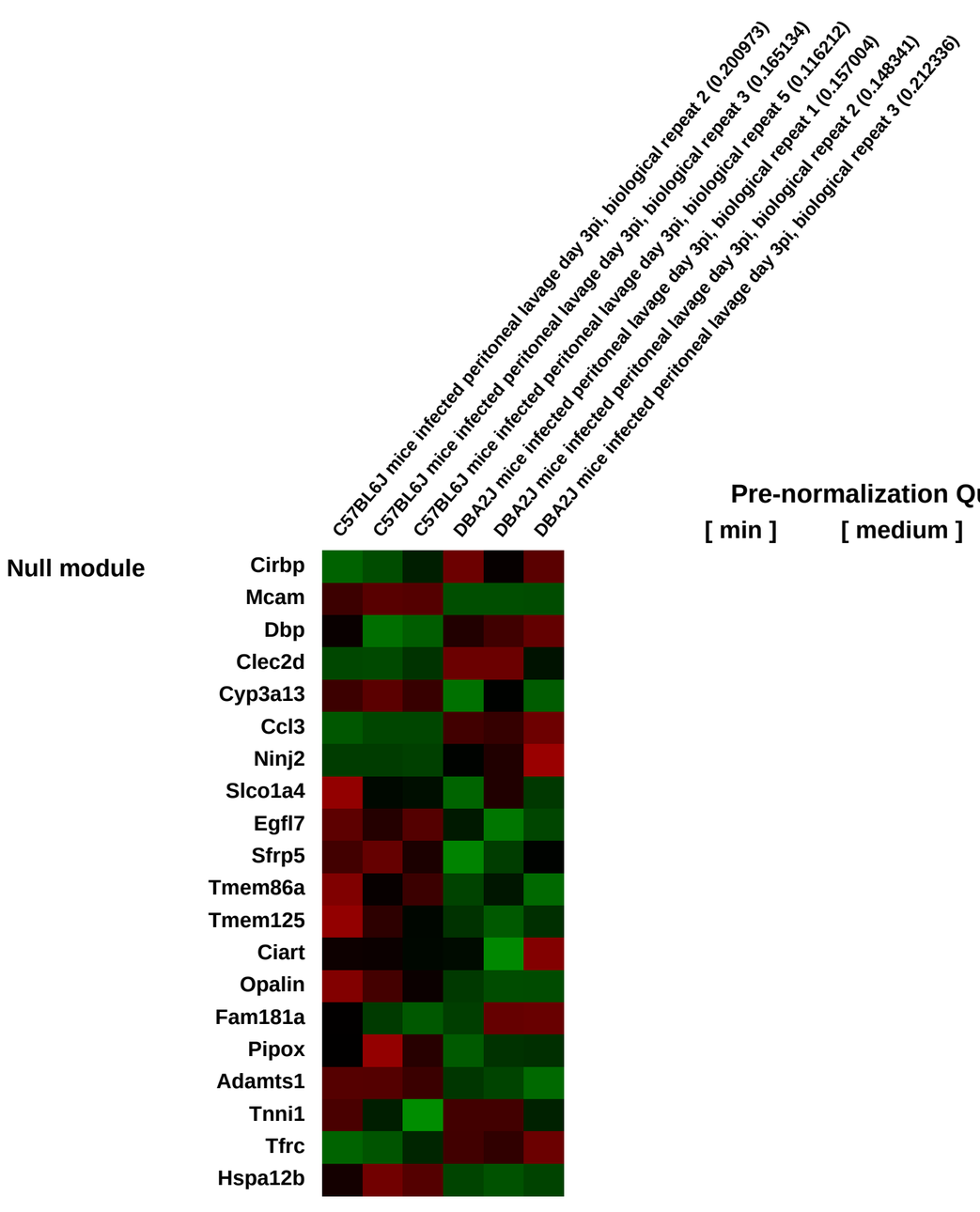

GEO Series "GSE7784" Expression Profiles

Num of samples in this series: 12

Scale of expression profile Z-scores

-3.0 -2.0 -1.0 0.0 1.0 2.0 3.0

GEO Link:	http://www.ncbi.nlm.nih.gov/geo/query/acc.cgi?acc=GSE7784
Status:	Public on May 17 2007
Title:	Expression profiling of double negative thymocytes
Organism:	Mus musculus
Experiment type:	Expression profiling by array
Platform:	GPL1261
Pubmed ID:	17911620
Summary & Design:	**Summary:** In order to understand the molecular mechanisms of DN thymocyte development, it may be also of use to clarify how these developmental processes are regulated in terms of their entire gene expression, to which cell differentiation is ultimately ascribed. In the current study, we approached this issue by investigating gene expression profiles in discrete subsets of DN thymocytes under development, in which DN2, DN3, and DN4 thymocytes were sorted and subjected to expression profiling analysis with high-density oligonucleotide microarrays. Keywords: developmental stages **Overall design:** The DN2, DN3, and DN4 populations were FACS-sorted from DN thymocytes harvested from four C57BL/6 mice and analyzed by Affymetrix´fi Mouse Genome 430 2.0 Array´fi for gene expression. Four independent experiments were performed using 16 mice.

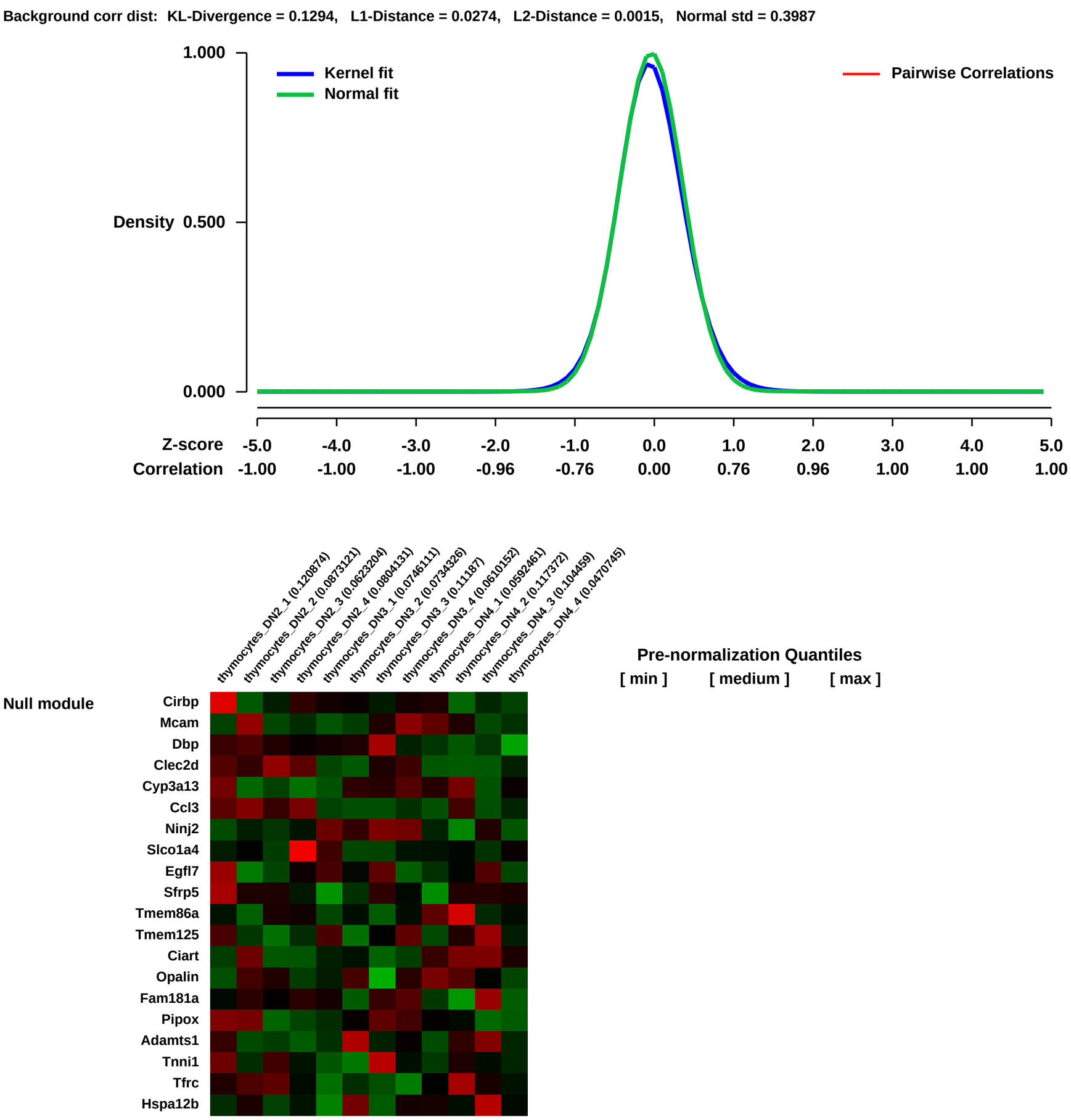

GEO Series "GSE7798" Expression Profiles

Num of samples in this series: 16

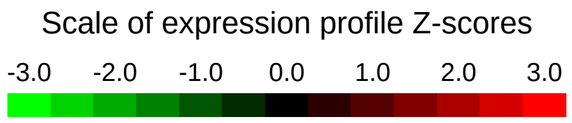

GEO Link:	http://www.ncbi.nlm.nih.gov/geo/query/acc.cgi?acc=GSE7798
Status:	Public on Jun 01 2007
Title:	Osteoclastic estrogen receptor alpha mediates the osteoprotective estrogen action through Fas ligand signaling
Organism:	Mus musculus
Experiment type:	Expression profiling by array
Platform:	GPL1261
Pubmed ID:	17803905
Summary & Design:	**Summary:** Estrogen clearly prevents osteoporotic bone loss by attenuating bone resorption. The molecular basis of how this is accomplished, however, remains elusive. Here we report a critical role of osteoclastic ERa in mediating estrogen action on bone in females. We selectively ablated ERa in differentiated osteoclasts (ERa dOc/dOc). ERa dOc/dOc females, but not males, exhibited clear trabecular bone loss, similar to the osteoporotic bone phenotype in post-menopausal women. Recovery of bone loss by estrogen treatment of the ovariectomized ERa dOc/dOc females was ineffective in the trabecular areas of the long bones and lumbar vertebral bodies. Osteoclastic apoptosis, induced by estrogen, occurred simultaneously with up-regulation of Fas ligand (FasL) expression in intact trabecular bones of ERa +/+mice, but not in ERa dOc/dOc mice. ERa was also required for similar effects of estrogen and tamoxifen in cultured osteoclasts. These findings suggest that the osteoprotective actions of estrogen and SERMS are mediated at least in part through osteoclastic ERa in trabecular bone; and the life span of mature osteoclasts is regulated through activation of the Fas/FasL system. **Keywords:** Study about estrogen response of osteoclast-specific estrogen receptor alpha mice **Overall design:** Wild type and osteoclast-specific Estrogen Receptor alpha knock-out mice were ovariectomized. The number of both genotypes of mice was eight. The mice of each genotypes were divided to vehicle control and estrogen treated group. Four hours after chemical treatment, the distal 5 mm of the left femurs were harvested after sacrificing by cervical dislocation and total RNAs were purified for Affymetix GeneChip microarray analysis without pooling. Therefore, this experiment consists of four groups with four replicates per group.

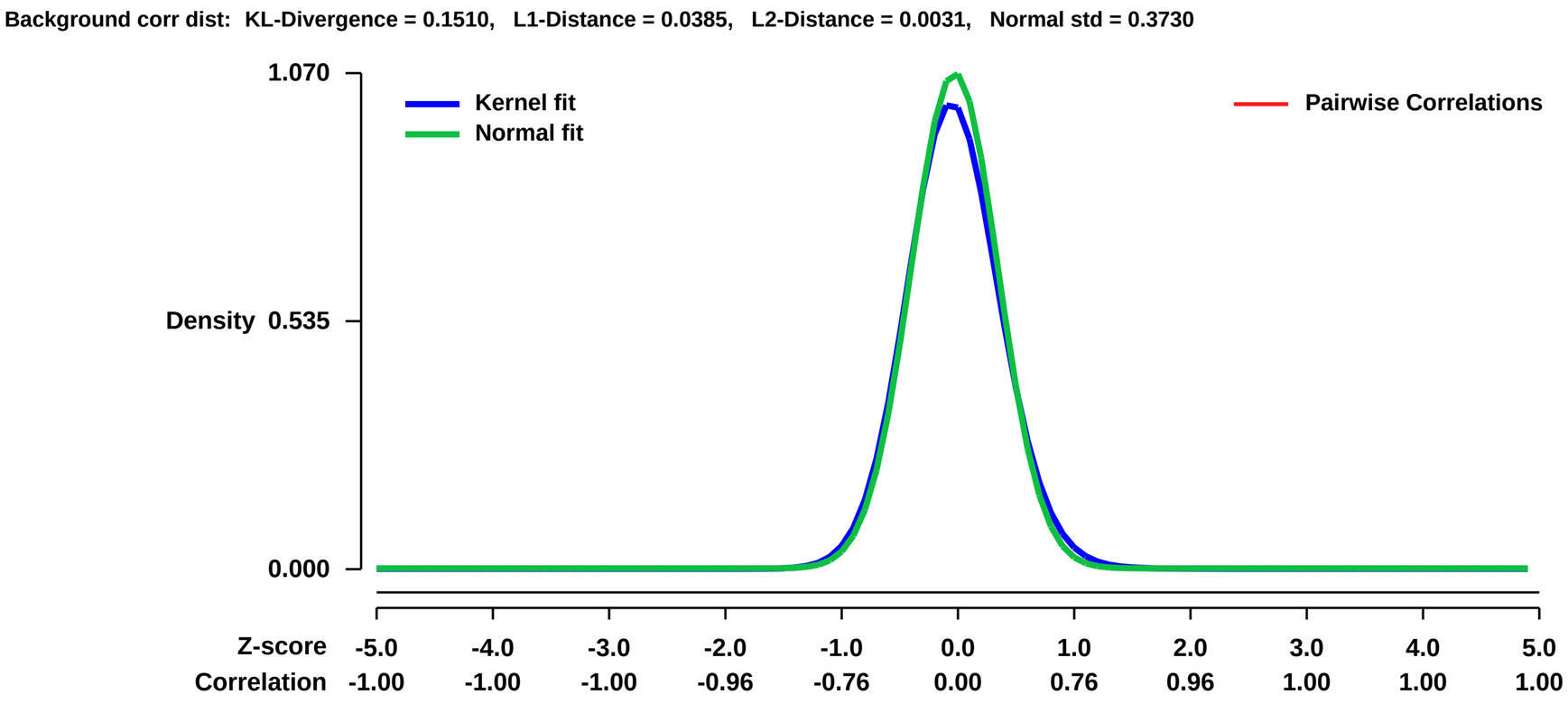

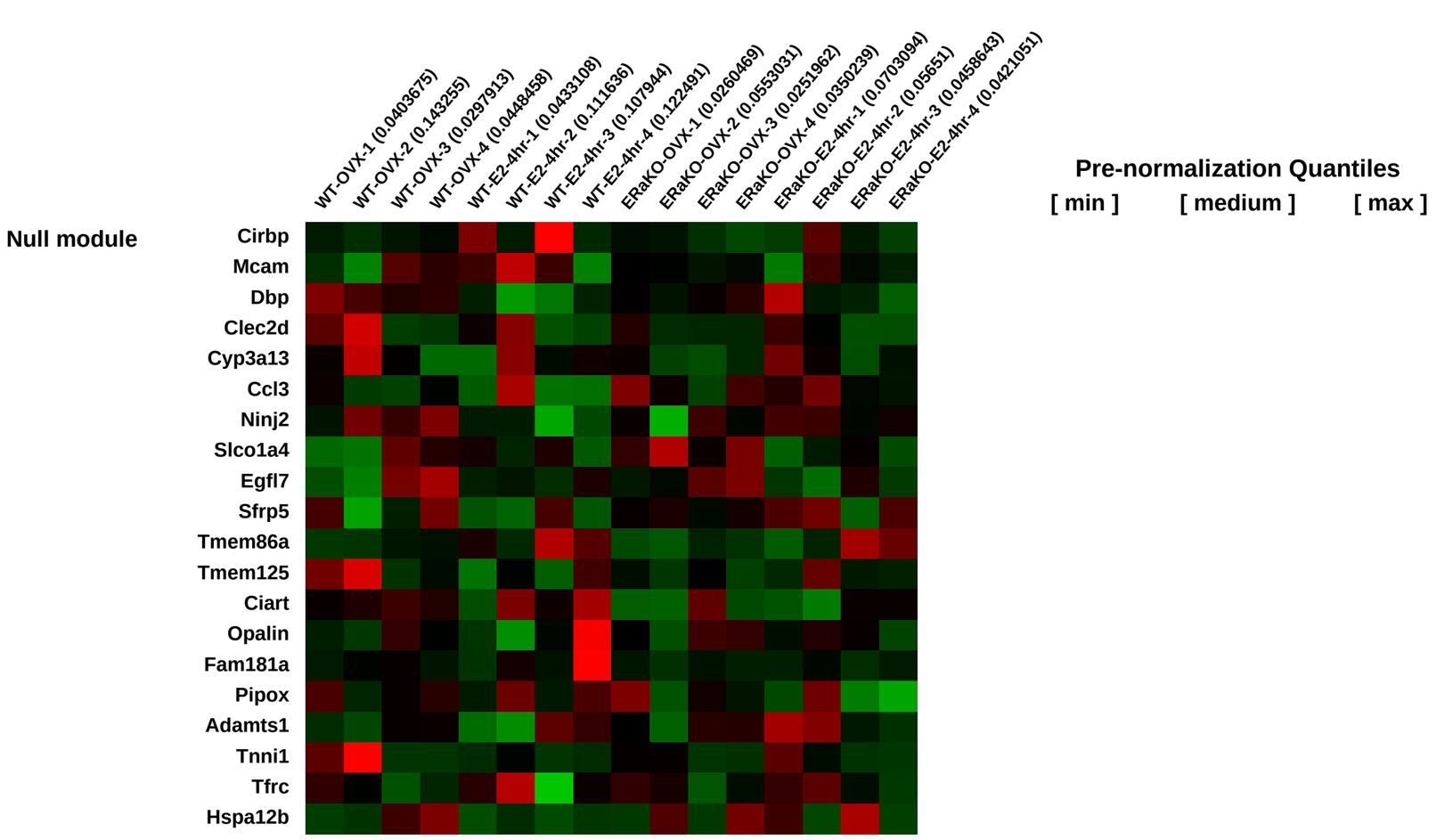

GEO Series "GSE7810" Expression Profiles

Num of samples in this series: 9

Scale of expression profile Z-scores

-3.0 -2.0 -1.0 0.0 1.0 2.0 3.0

GEO Link:	http://www.ncbi.nlm.nih.gov/geo/query/acc.cgi?acc=GSE7810
Status:	Public on May 18 2007
Title:	Comparative analysis of gene expression WT and Nrf2-/- mice Type II cells
Organism:	Mus musculus
Experiment type:	Expression profiling by array
Platform:	GPL1261
Pubmed ID:	17895394
Summary & Design:	**Summary:** We hypothesize that gene expression in the Type II cells of Nrf2+/+ and Nrf2-/- mice are divergent thus contributing the cell growth. More specifically, type II cells from Nrf2-/- mice have increased reactive oxygen species that cause the impaired cell growth. In order to test these hypotheses at the gene expression level, we utilized microarray analysis to examine transcriptional differences between Nrf2+/+ and Nrf2-/- cells. **Keywords: comparative expression profiling** **Overall design:** . This study utilizes microarray analysis to test these hypotheses. Three sets of type II cells were isolated from lungs from both Nrf2+/+ and Nrf2-/- mice and grown for 5 days. RNA was isolated and used for global gene expression profiling (Affymetrix Mouse 430 2.0 array). Statistically significant gene expression was determined as a minimum 6 counts of 9 pairwise comparisons, minimum 1.5-fold change, and p < 0.05. Further, Absolute | FC - FC SEM | >= 1.5.

Background corr dist: KL-Divergence = 0.0624, L1-Distance = 0.0171, L2-Distance = 0.0003, Normal std = 0.5241

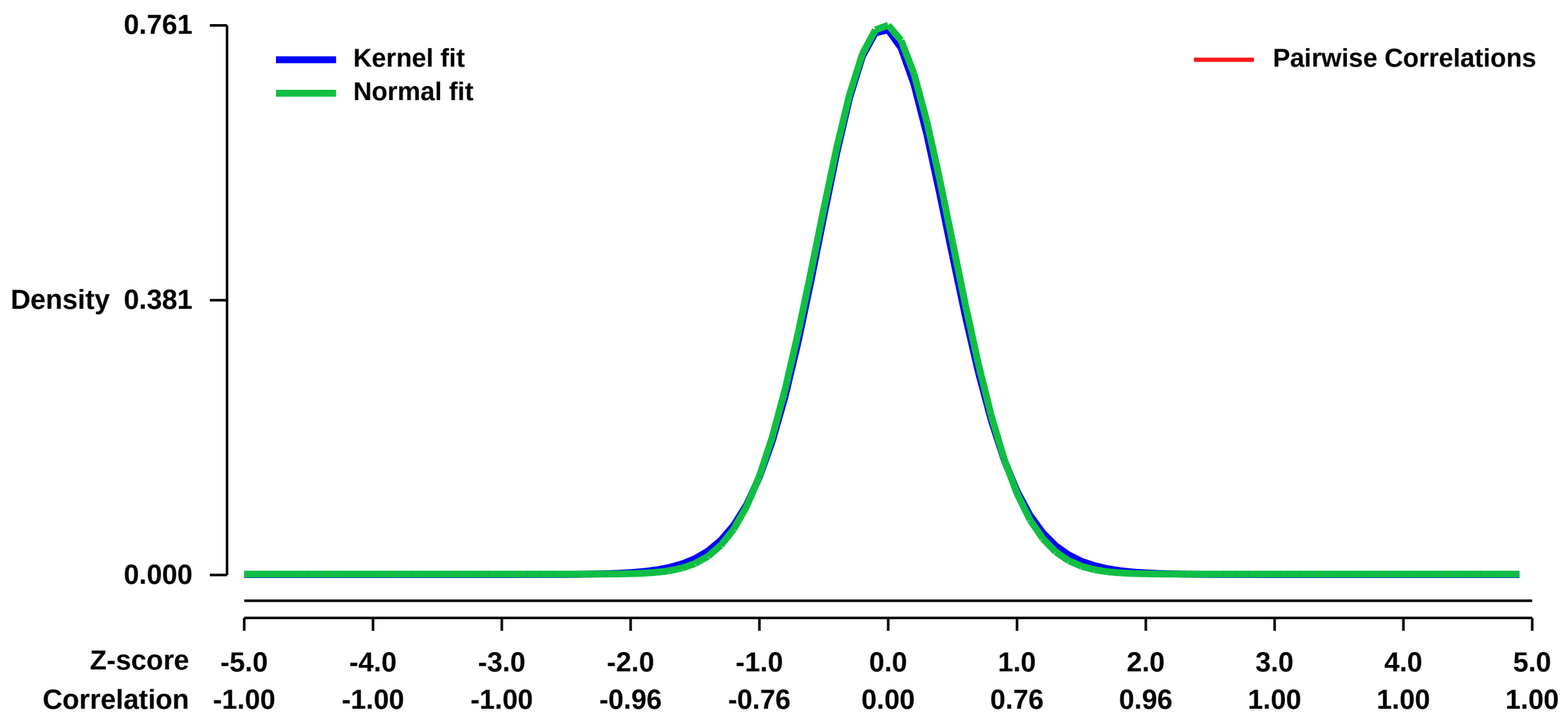

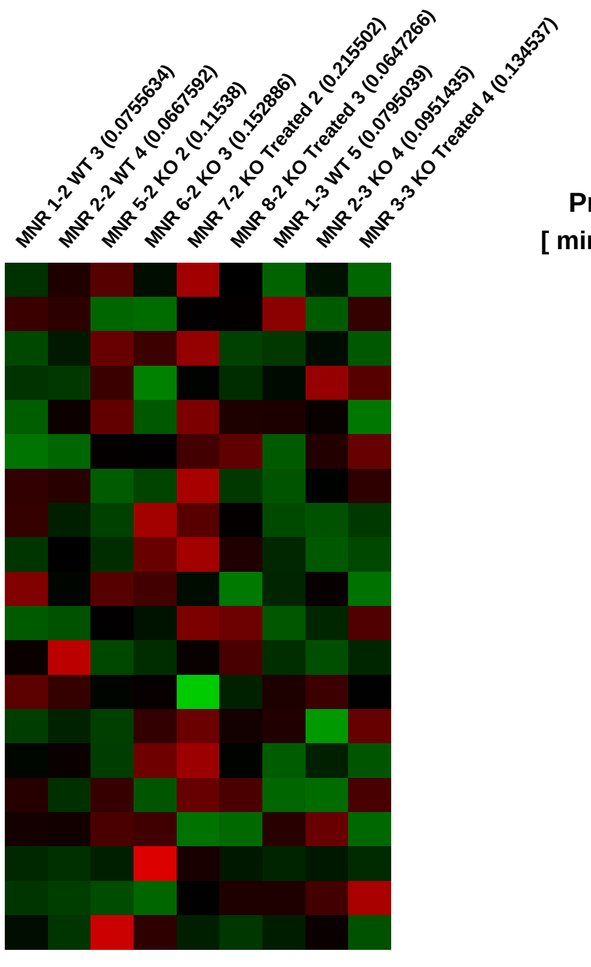

GEO Series "GSE7823" Expression Profiles

Num of samples in this series: 9

Scale of expression profile Z-scores

-3.0 -2.0 -1.0 0.0 1.0 2.0 3.0

GEO Link:	http://www.ncbi.nlm.nih.gov/geo/query/acc.cgi?acc=GSE7823
Status:	Public on May 18 2007
Title:	Murine Pulmonary Response to Chronic Hypoxia is Strain Specific
Organism:	Mus musculus
Experiment type:	Expression profiling by array
Platform:	GPL1261
Pubmed ID:	18600498
Summary & Design:	**Summary:** 6-8 week old BL6, FVB/N and SV129 mouse strains were kept in normoxia or hypobaric hypoxia for 4 weeks and then phenotyped by echocardiogram and right ventricular heart catheterization, followed by tissue collection. In addition, Affymetrix expression analysis was conducted in a paired fashion. **Keywords: Differential response to hypoxia by strain** **Overall design:** This series actually includes another 12 arrays. However, the others had technical difficulties and so aren't really appropriate for general distribution.

Background corr dist: KL-Divergence = 0.0874, L1-Distance = 0.0272, L2-Distance = 0.0013, Normal std = 0.4774

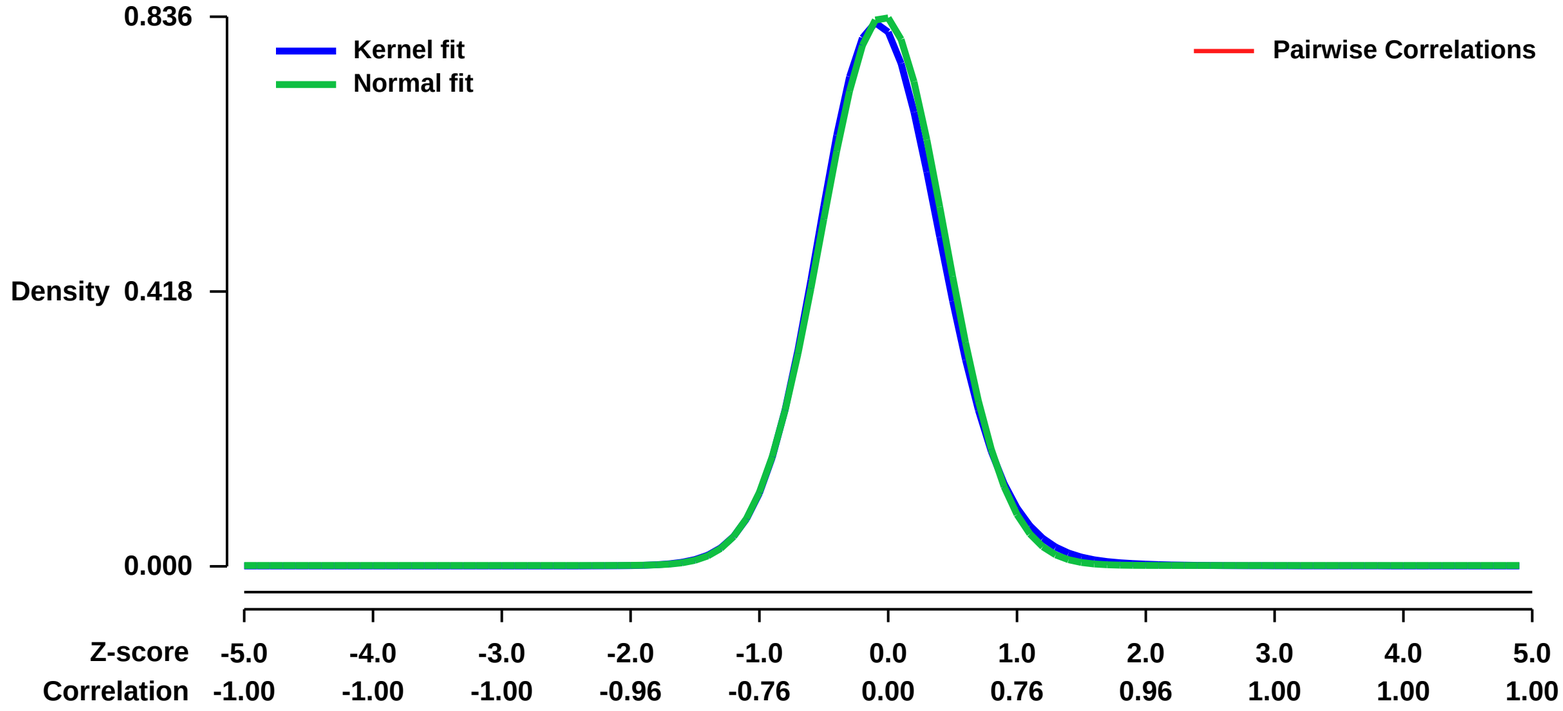

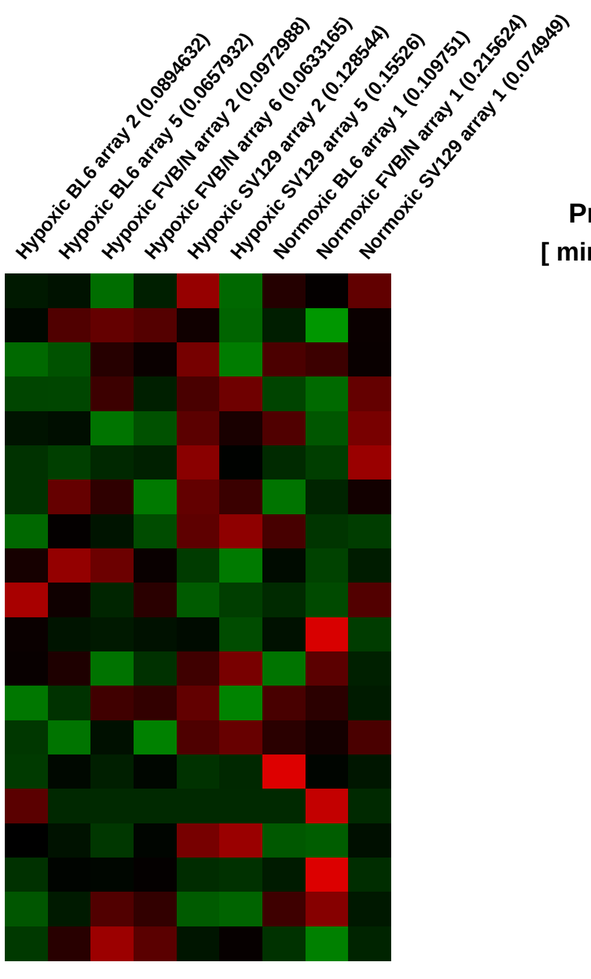

GEO Series "GSE7831" Expression Profiles

Num of samples in this series: 14

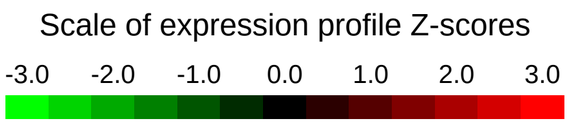

GEO Link:	http://www.ncbi.nlm.nih.gov/geo/query/acc.cgi?acc=GSE7831
Status:	Public on Dec 13 2007
Title:	Expression data from immature pDC and pDC activated with CpG 1826 and influenza virus PR8
Organism:	Mus musculus
Experiment type:	Expression profiling by array
Platform:	GPL1261
Pubmed ID:	18029397
Summary & Design:	**Summary:** CpG 1826 binds to Toll-like receptor (TLR)9, whereas influenza virus PR8 activates pDC via TLR7. Differential stimulation of pDCs is expected to result in unique activation mechanism(s) leading to a different phenotypically and functionally matured pDC We used microarrays to detail the global programme of gene expression underlying the maturation process of pDC activated with CpG 1826 and influenza virus PR8. We identified a distinct expression profile of upregulated immunomediators. Keywords: time course **Overall design:** Sorted pDCs were cultured for 1h and 4hs in medium control or with 5 ´µg/ml CpG 1826 or 300 HAU/ml purified influenza A/PR/8 virus. The first experiment (e1) included pDC in media and stimulated with CpG for 4h. In two other independent experimental batches (e2 and e3), we obtained samples of sorted pDC cultured in medium alone (med), and with CpG or PR8 (flu) for 1h and 4h. RNA extraction was performed using the RNeasy Kit (Qiagen) and hybridization on Affymetrix microarrays was performed using standard protocols. We sought to obtain homogeneous populations of pDCs at different time points under defined activation conditions in order to decipher the temporal resolution of expression profiles during the process of their maturation.

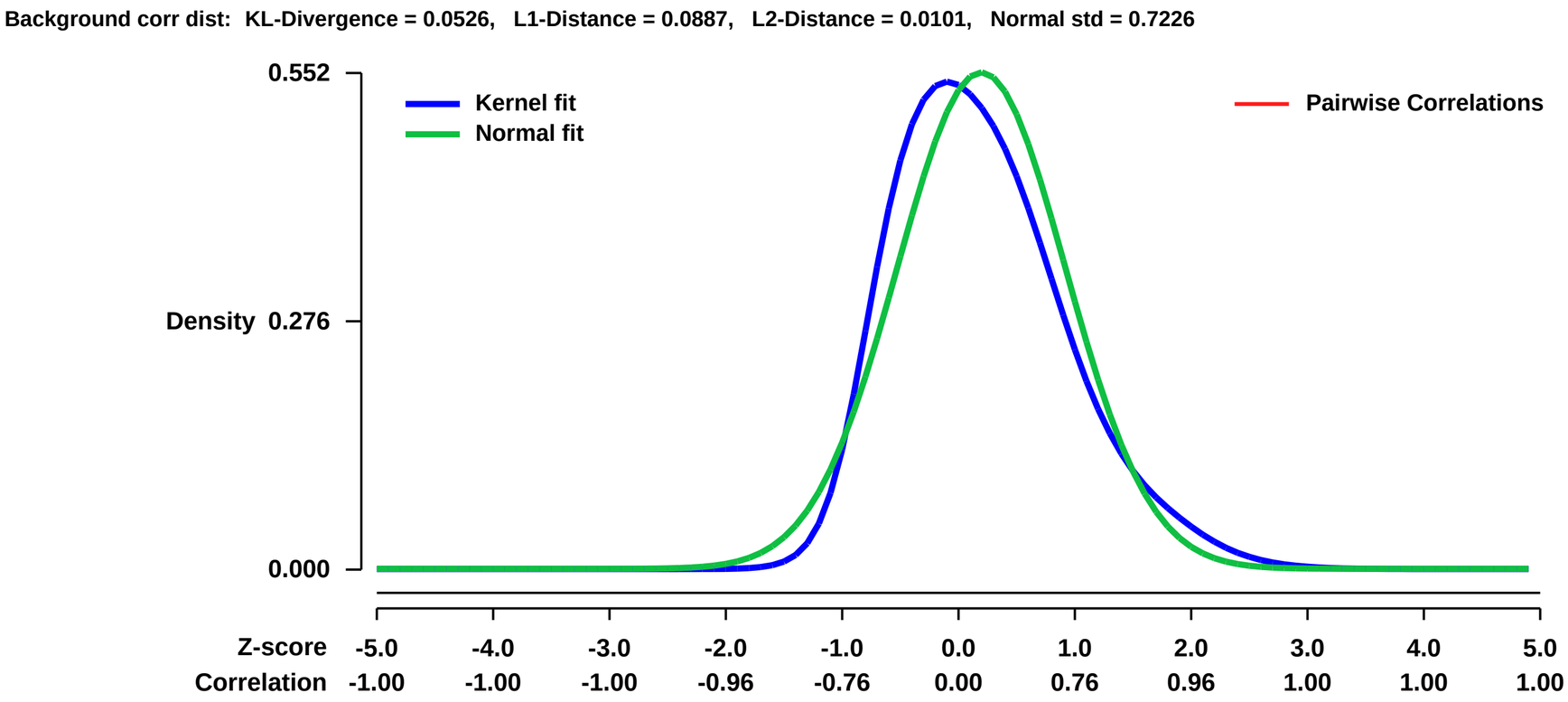

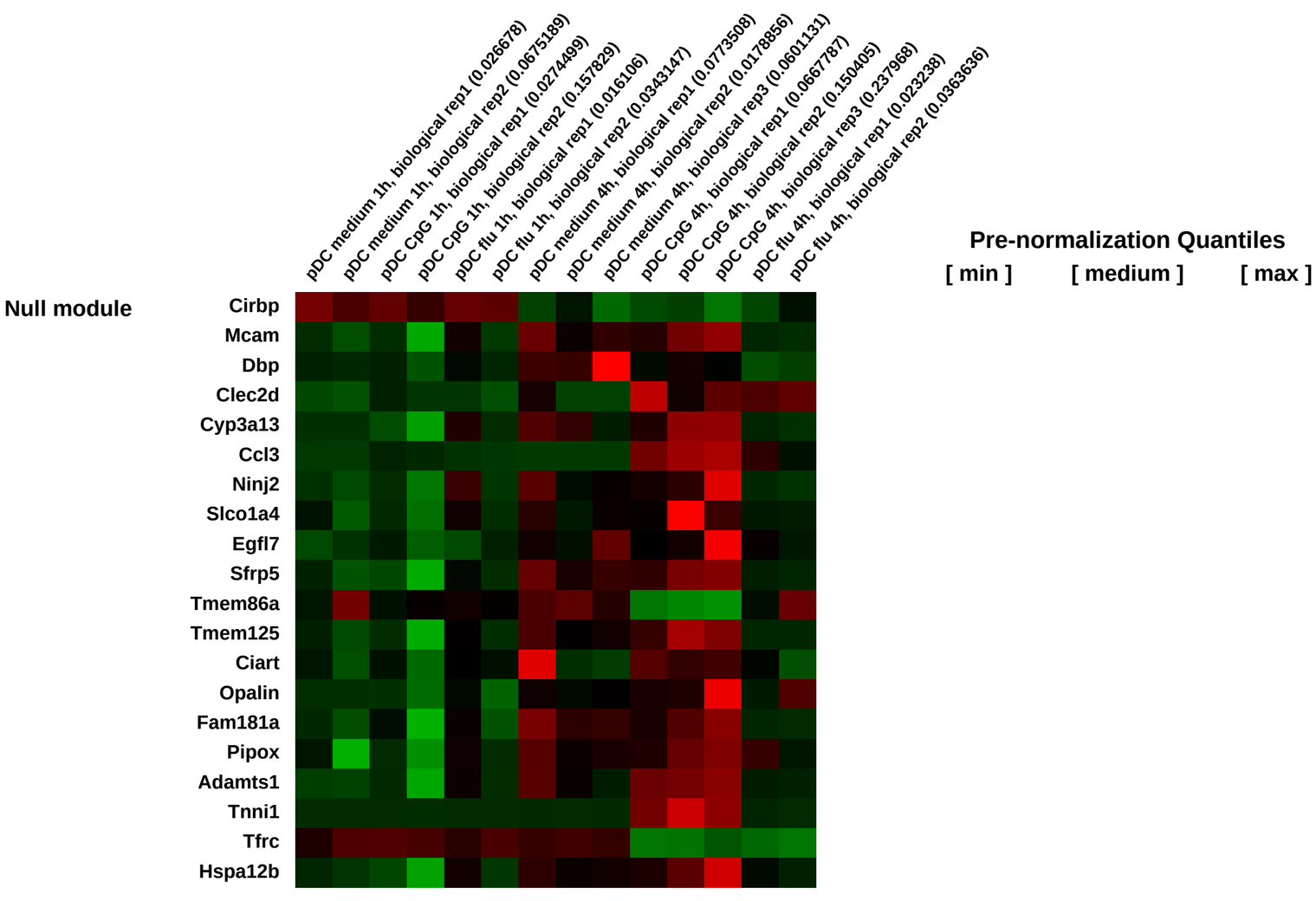

GEO Series "GSE7875" Expression Profiles

Num of samples in this series: 16

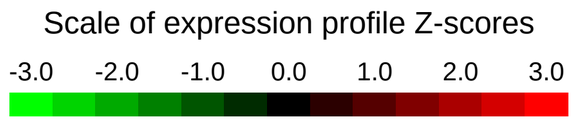

GEO Link:	http://www.ncbi.nlm.nih.gov/geo/query/acc.cgi?acc=GSE7875
Status:	Public on Oct 03 2007
Title:	Deletion of PKBalpha/Akt1 affects thymic development
Organism:	Mus musculus
Experiment type:	Expression profiling by array
Platform:	GPL1261
Pubmed ID:	17912369
Summary & Design:	**Summary:** The thymus constitutes the primary lymphoid organ for the majority of T cells. The phosphatidyl-inositol 3 kinase (PI3K) signaling pathway is involved in lymphoid development. Defects in single components of this pathway prevent thymocytes from progressing beyond early T cell developmental stages. Protein kinase B (PKB) is the main effector of the PI3K pathway. To determine whether PKB mediates PI3K signaling in early T cell development, we characterized PKB knockout thymi. Our results reveal a significant thymic hypocellularity in PKBalpha-/- neonates and an accumulation of early thymocyte subsets in PKBalpha-/- adult mice. The latter finding is specifically attributed to the lack of PKBalpha within the lymphoid component of the thymus. Microarray analyses show that the absence of PKBalpha in early thymocyte subsets modifies the expression of genes known to be involved in pre-TCR signaling, in T cell activation, and in the transduction of interferon-mediated signals. This report highlights the specific requirements of PKBalpha for thymic development. **Keywords:** Genetic modification **Overall design:** Early thymocyte subsets (DN3 and ISP8) were sorted by FACS from 4 PKBalpha-/- / PKBalpha+/+ mouse littermate pairs. The same number of DN3 or ISP8 cells was sorted (7 000 to 25 000 cells) within a PKBalpha-/- / PKBalpha+/+ pair. Four replicates per condition were then analysed (4xPKBalpha-/- DN3, 4xPKBalpha+/+ DN3, 4xPKBalpha-/- ISP8, 4xPKBalpha+/+ ISP8). Total RNA was extracted using PicoPureTM RNA isolation kit (Arcturus, Sunnyvale, CA, USA) and RNA quality was controlled using the 2100 Bioanalyser (Agilent Technologies, Santa Clara, CA, USA). Total RNA was amplified and labeled using the Affymetrix 2-cycle 3â labelling kit according to manufacturerâ s instructions. After fragmentation, 10 ug cRNA was hybridised to mouse genome 430 2.0 GeneChips (Affymetrix, Santa Clara, CA). The supplementary file represents the expression values estimated using the GC-RMA function provided by Refiner 3.1 (Genedata, Basel, Switzerland) for each of the samples.

Background corr dist: KL-Divergence = 0.1420, L1-Distance = 0.0394, L2-Distance = 0.0024, Normal std = 0.3992

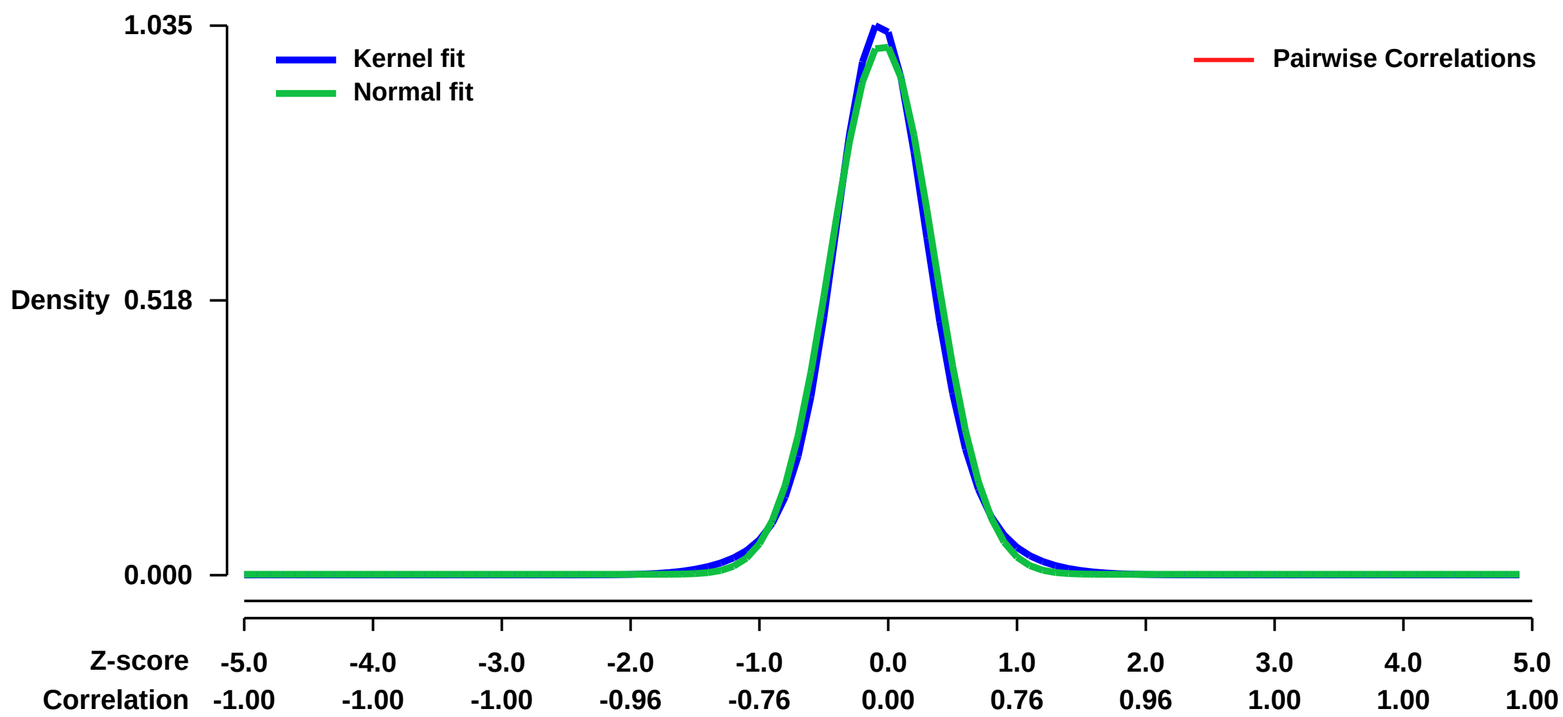

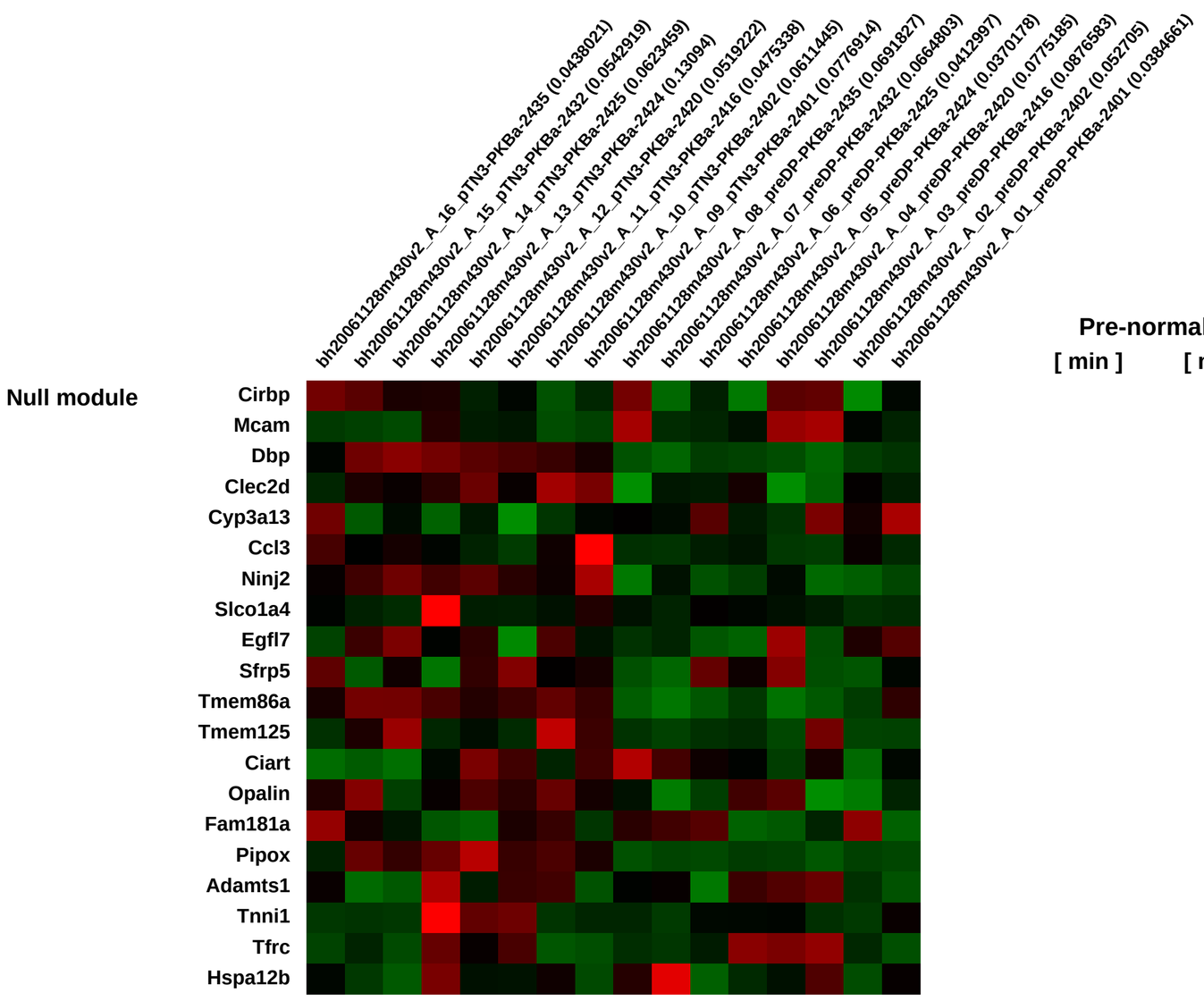

GEO Series "GSE7958" Expression Profiles

Num of samples in this series: 12

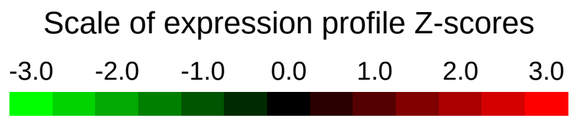

GEO Link:	http://www.ncbi.nlm.nih.gov/geo/query/acc.cgi?acc=GSE7958
Status:	Public on Jul 01 2007
Title:	Striatal gene expression data from 3- and 18-month-old Q92 mice and control mice.
Organism:	Mus musculus
Experiment type:	Expression profiling by array
Platform:	GPL1261
Pubmed ID:	17519223
Summary & Design:	**Summary:** Achieving a mechanistic understanding of disease and initiating preclinical therapeutic trials necessitate the study of huntingtin toxicity and its remedy in model systems. To allow the engagement of appropriate experimental paradigms, Huntingtonâ s disease (HD) models need to be validated in terms of how they recapitulate a particular aspect of human disease. In order to examine transcriptome-related effects of mutant huntingtin, we compared striatal mRNA profiles from seven genetic mouse models of disease to that of postmortem human HD caudate using microarray analysis. Transgenic models expressing short N-terminal fragments of mutant huntingtin (R6/1 and R6/2 mice) exhibited the most rapid effects on gene expression, consistent with previous studies. Although changes in the brains of knock-in models of HD took longer to appear, 15-month and 22-month CHL2Q150/Q150, 18-month HdhQ92/Q92 and 2-year-old YAC128 animals also exhibited significant HD-like mRNA signatures. When the affected genes were compared across models, a robust concordance was observed. Importantly, changes concordant across multiple lines mice were also in excellent agreement with the mRNA changes seen in human HD caudate. Although it was expected that the expression of full-length huntingtin transprotein might result in unique gene expression changes compared to those caused by expression of an N-terminal huntingtin fragment, no discernable differences between full-length and fragment models were detected. There was, however, an overall concordance between transcriptomic signature and disease stage. We thus conclude that the transcriptional changes of HD can be modelled in several available lines of transgenic mice, comprising lines expressing both N-terminal and full-length mutant huntingtin proteins. The combined analysis of mouse and human HD transcriptomes provides an important chronology of mutant huntingtin's gene expression effects. **Keywords:** genetic modification **Overall design:** Striatal samples from 6 Q92 mutant mice (3 3-month-old and 3 18-month-old) and 6 age-matched wild-type mice.

Background corr dist: KL-Divergence = 0.1336, L1-Distance = 0.0375, L2-Distance = 0.0027, Normal std = 0.3898

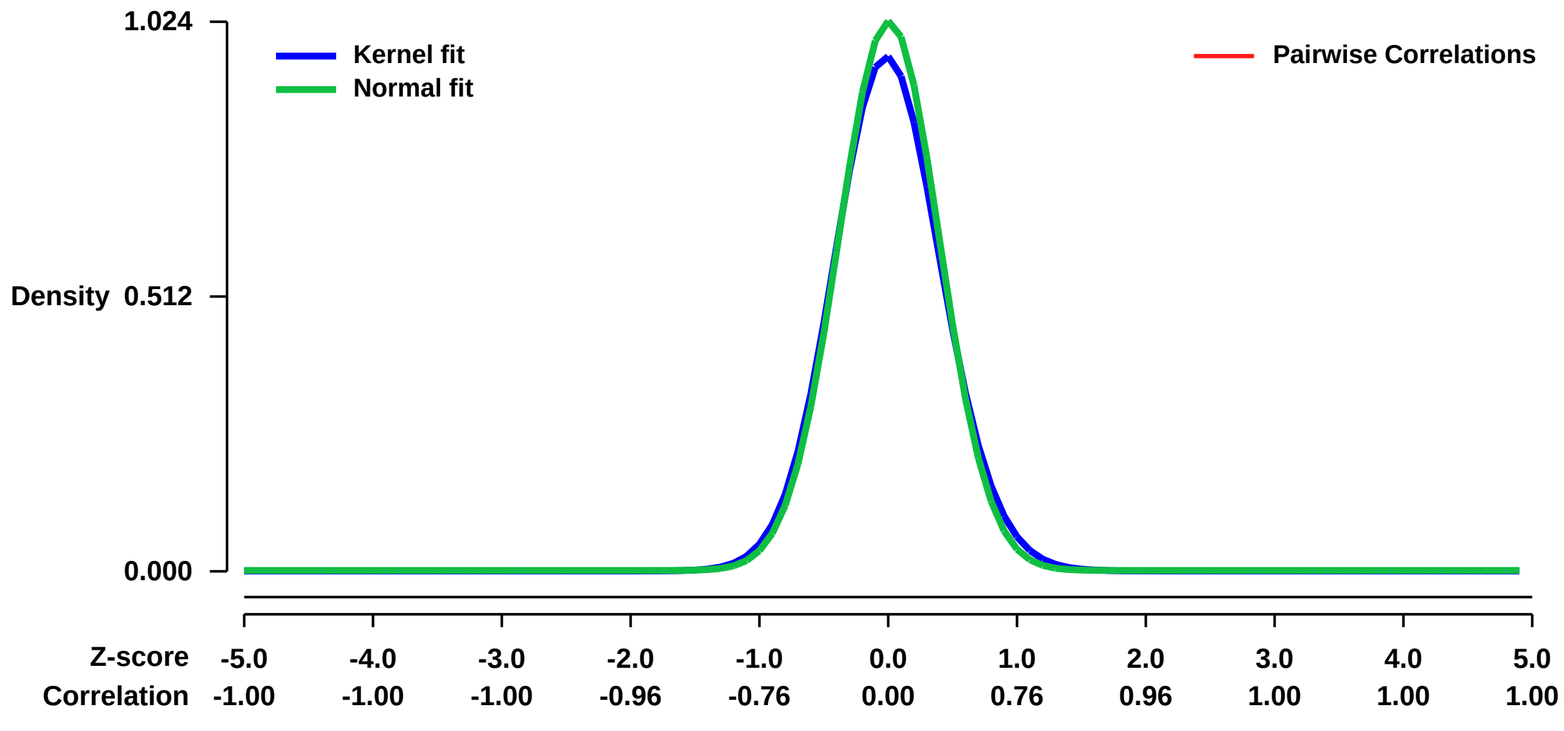

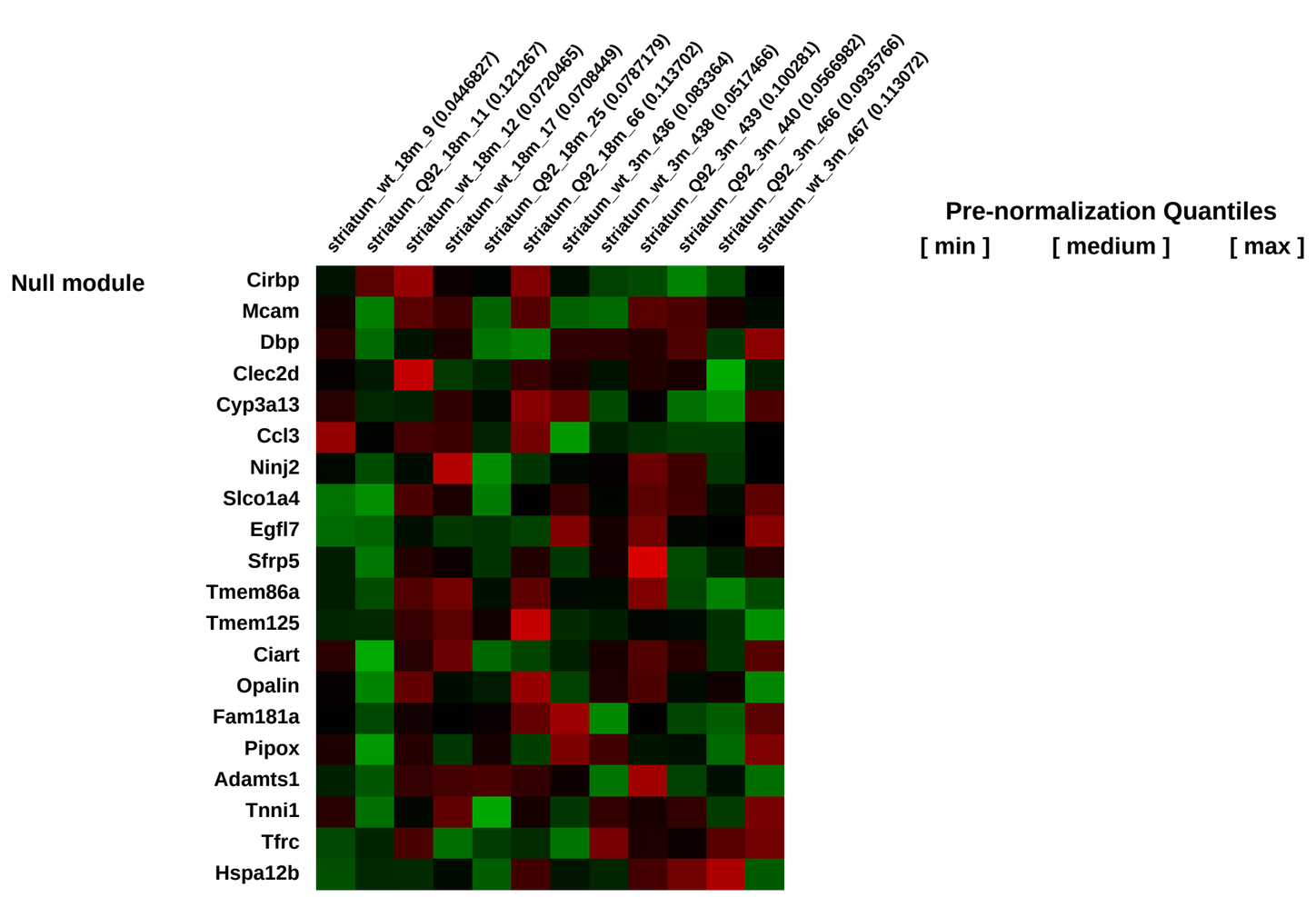

GEO Series "GSE8065" Expression Profiles

Num of samples in this series: 18

Scale of expression profile Z-scores

-3.0 -2.0 -1.0 0.0 1.0 2.0 3.0

GEO Link:	http://www.ncbi.nlm.nih.gov/geo/query/acc.cgi?acc=GSE8065
Status:	Public on Jun 12 2007
Title:	Gene expression during early postnatal development of the small intestine
Organism:	Mus musculus
Experiment type:	Expression profiling by array
Platform:	GPL1261
Pubmed ID:	18388184
Summary & Design:	**Summary:** It was the purpose to analyse the changes in gene expression which occur in the mouse small intestine from the pre-weaning to the post-weaning stage. The gene expression was accordingly followed from postnatal day 4 to postnatal day 32. **Keywords: Time-course** **Overall design:** 6 time-points were defined corresponding to postnatal day 4, 7, 9, 11, 24 and 32. Ileal samples were taken from individual mice at each time-point. All layers of the small intestine were included in the sample. Three samples from individual mice were analysed by hybridization to Affymetrix GeneChips.

Background corr dist: KL-Divergence = 0.0658, L1-Distance = 0.0198, L2-Distance = 0.0006, Normal std = 0.5101

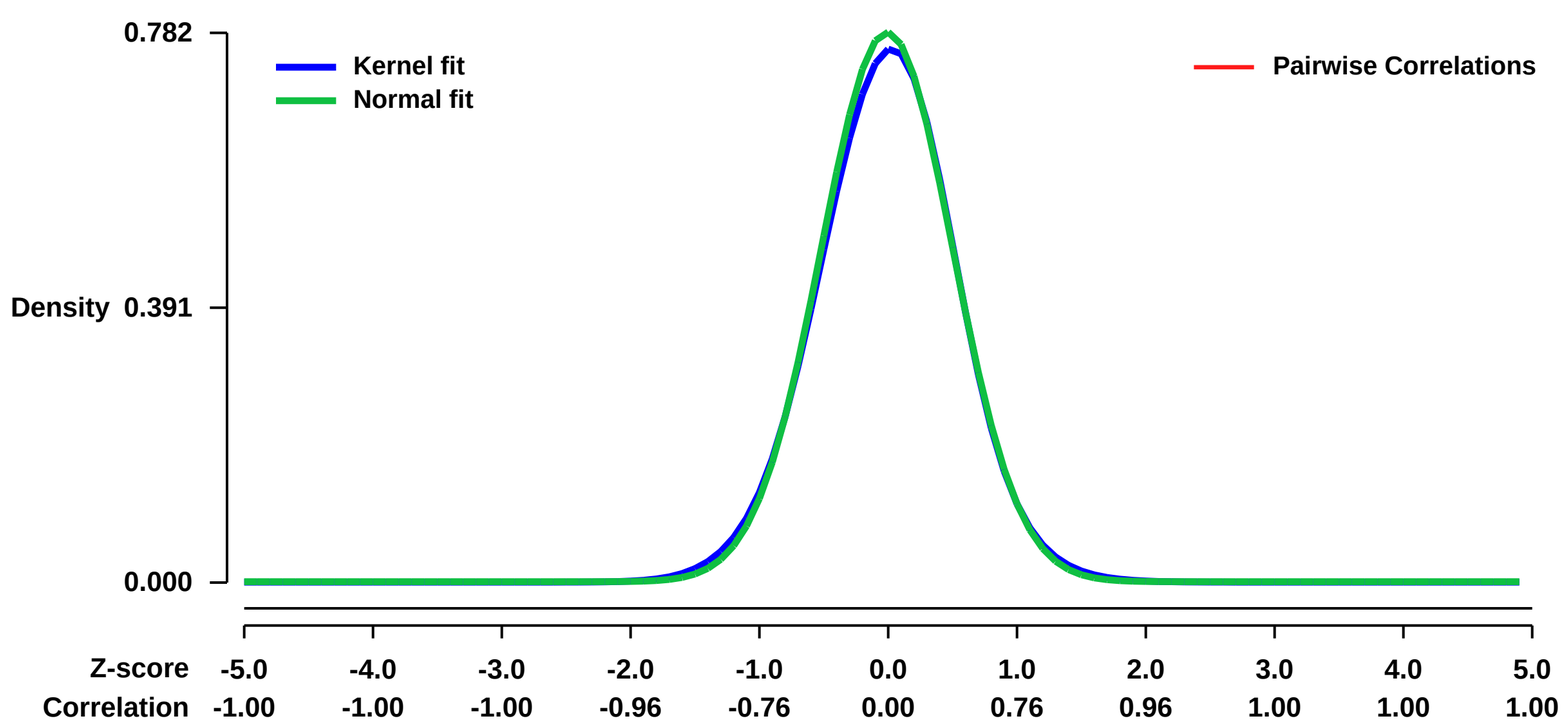

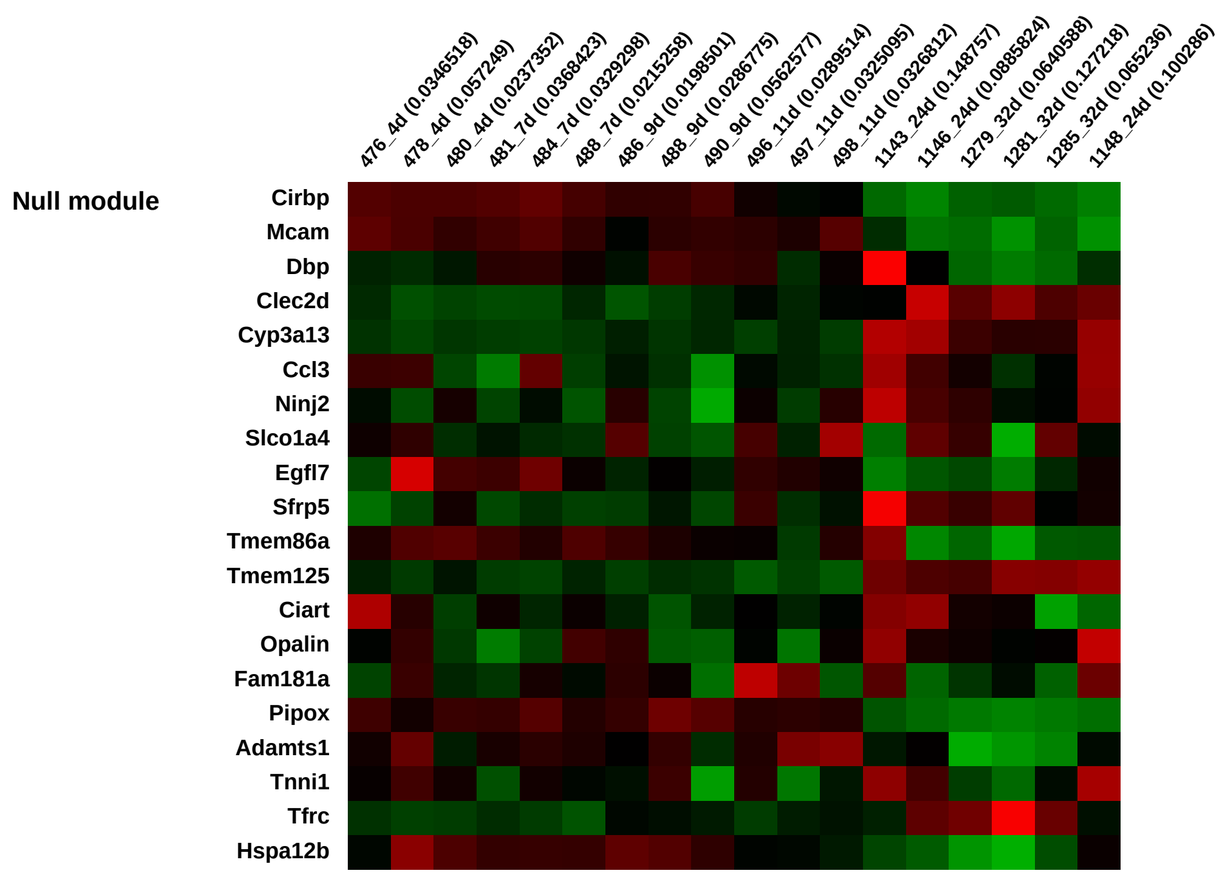

GEO Series "GSE8091" Expression Profiles

Num of samples in this series: 16

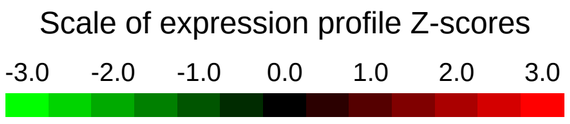

GEO Link:	http://www.ncbi.nlm.nih.gov/geo/query/acc.cgi?acc=GSE8091
Status:	Public on May 29 2008
Title:	Transcriptome and proteome analysis of early embryonic mouse brain development
Organism:	Mus musculus
Experiment type:	Expression profiling by array
Platform:	GPL1261
Pubmed ID:	18283662
Summary & Design:	**Summary:** Embryonic mouse brain development involves a sequential differentiation of multipotent progenitor cells into neurons and glia. Using microarrays and large 2-D electrophoresis, we investigated the transcriptome and proteome of mouse brains at embryonic days 9.5, 11.5 and 13.5. During this developmental period, neural progenitor cells shift from proliferation to neuronal differentiation. As expected, we detected numerous expression changes between the time points investigated but interestingly, the rate of alteration was about 10% to 13% of all proteins and mRNAs during every two days of development. Furthermore, up- and downregulation was balanced. This was confirmed for two additional stages of development, embryonic day 16 and 18. We hypothesize that during embryonic development, the rate of protein expression alteration is rather constant due to a limitation of cellular resources such as energy, space and free water. The similar complexity found at the transcriptome and proteome level at all stages suggests, that changes in relative concentration of gene products rather than an increased number of gene products dominate throughout cellular differentiation. We found that metabolism and cell cycle related gene products were downregulated in expression when precursor cells switched from proliferation to neuronal differentiation (day 9.5 to 11.5), whereas neuron specific gene products were upregulated. A detailed analysis revealed their implication in differentiation related processes such as rearrangement of the actin cytoskeleton as well as Notch and Wnt signaling pathways. **Keywords:** time course, development, transcriptome, proteome **Overall design:** E13.5: 6 biological replicates

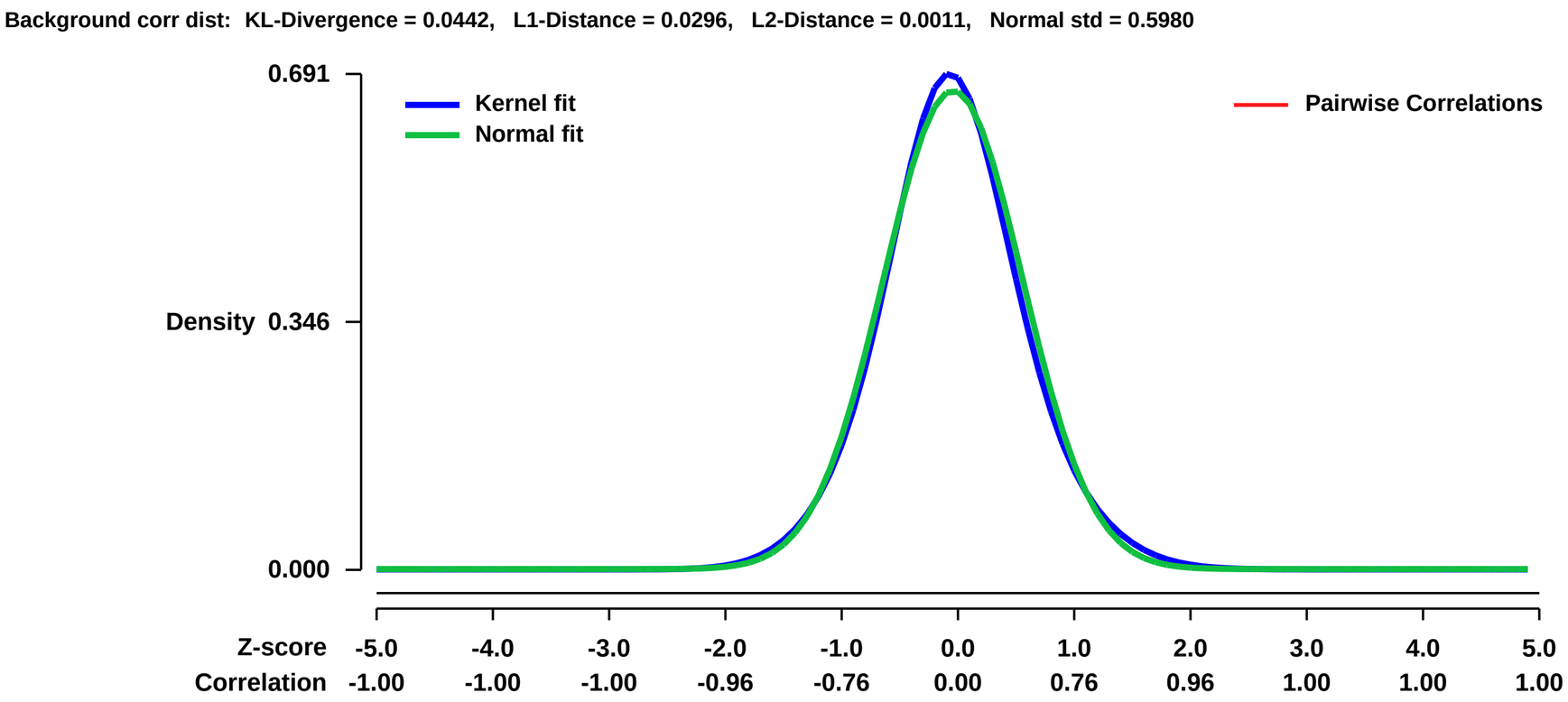

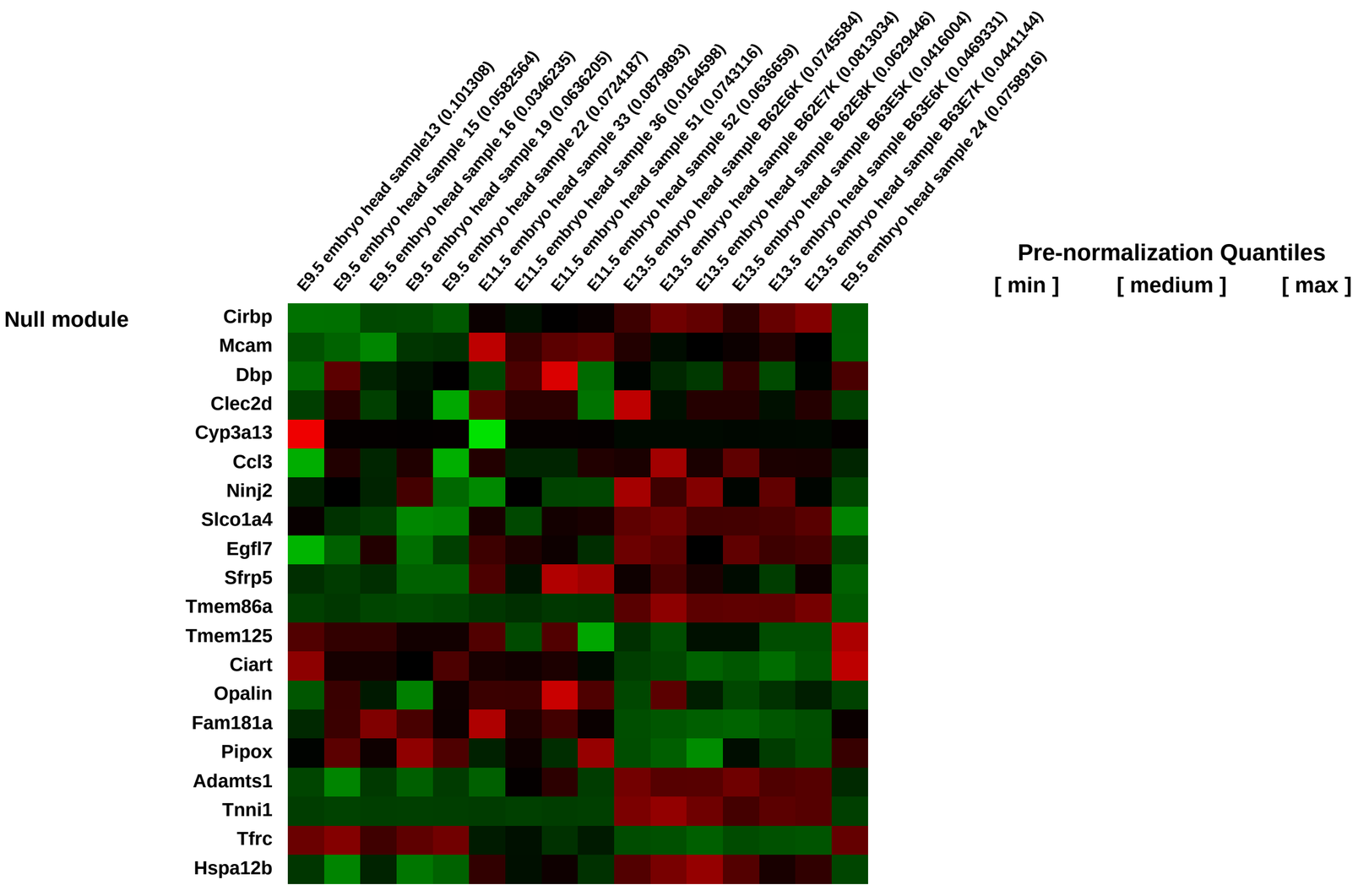

GEO Series "GSE8150" Expression Profiles

Num of samples in this series: 20

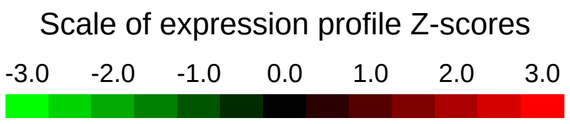

GEO Link:	http://www.ncbi.nlm.nih.gov/geo/query/acc.cgi?acc=GSE8150
Status:	Public on Aug 31 2007
Title:	Age-related transcriptional changes and the effect of dietary supplementation of vitamin E in the mouse brain
Organism:	Mus musculus
Experiment type:	Expression profiling by array
Platform:	GPL1261
Pubmed ID:	17316780
Summary & Design:	**Summary:** We established the transcriptional profile of brain aging and examine the global effects of vitamin E supplementation on age-related alterations in expression in the aged mouse brain. **Keywords: expression profiling** **Overall design:** Gene expression profiles were obtained from the neocortex tissues of 5-month-old controls, 30-month-old controls and 30-month old B6C3F1 mice with middle age-onset supplementation of ¸–-tocopherol or a mixture of ¸–- and ¸‡-tocopherol (500mg/kg of each tocopherol).

Background corr dist: KL-Divergence = 0.2537, L1-Distance = 0.0569, L2-Distance = 0.0081, Normal std = 0.3000

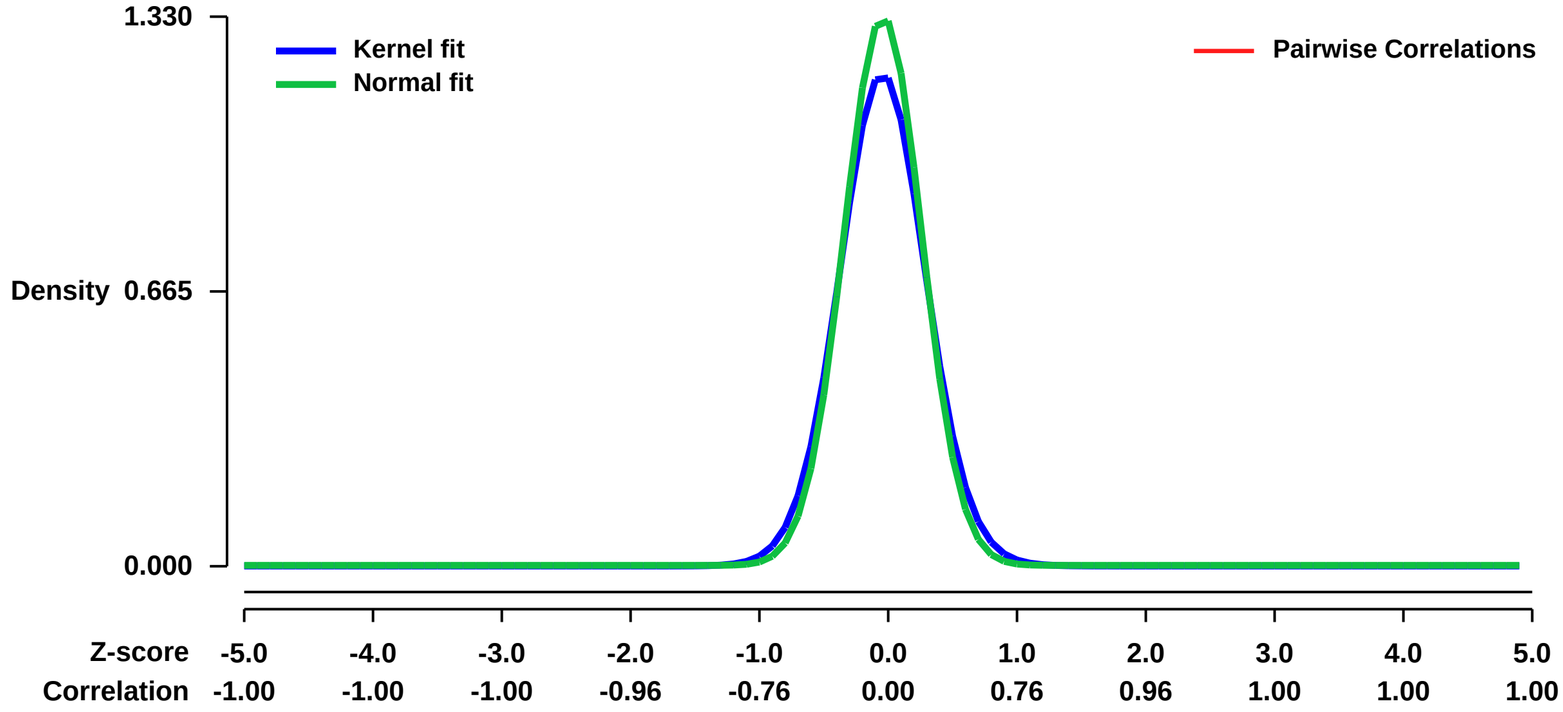

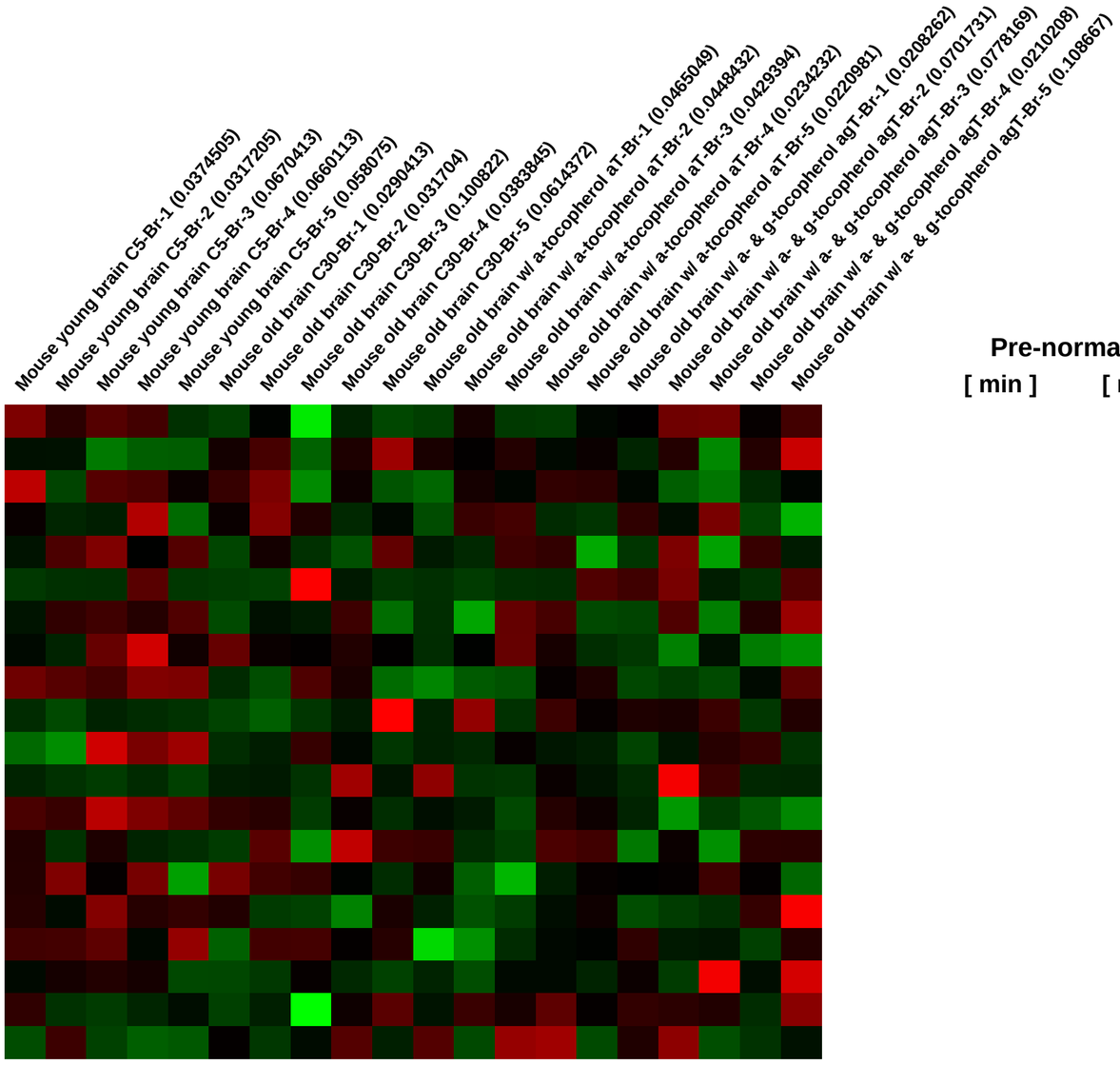

GEO Series "GSE8156" Expression Profiles

Num of samples in this series: 6

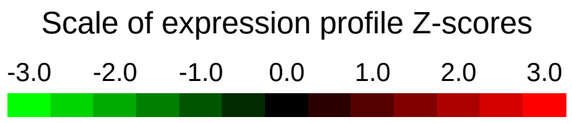

GEO Link:	http://www.ncbi.nlm.nih.gov/geo/query/acc.cgi?acc=GSE8156
Status:	Public on Jun 15 2008
Title:	Smad1/5/8 mutant granulosa cell tumor gene expression
Organism:	Mus musculus
Experiment type:	Expression profiling by array
Platform:	GPL1261
Pubmed ID:	17967875
Summary & Design:	**Summary:** The objective of this study was to understand the gene expression changes during granulosa cell tumor development in Smad1/5/8 mutant ovaries. **Keywords:** Microarray analysis, gene expression **Overall design:** Three independent mouse mutant granulosa cell tumors were compared to three wild type granulosa cells samples.

Background corr dist: KL-Divergence = 0.0332, L1-Distance = 0.0254, L2-Distance = 0.0008, Normal std = 0.6596

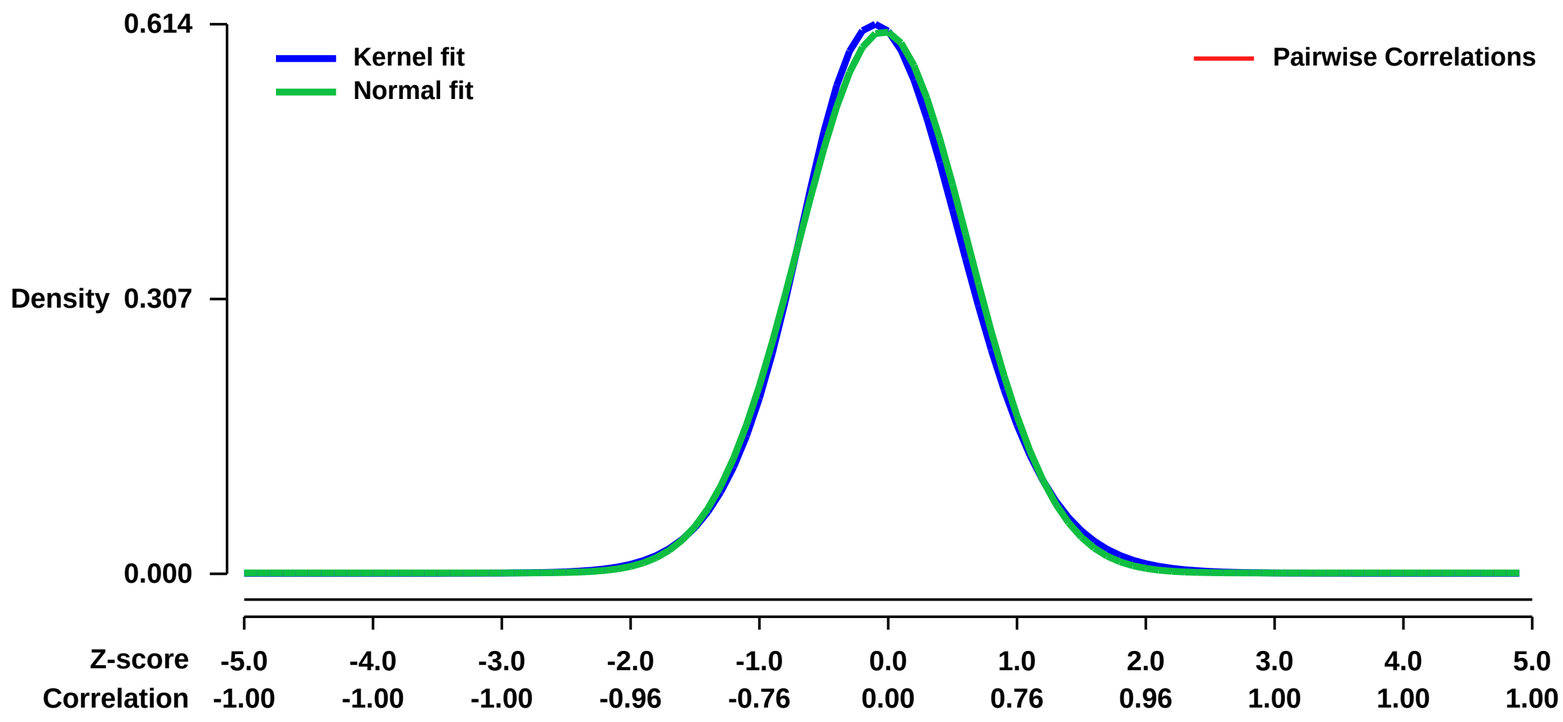

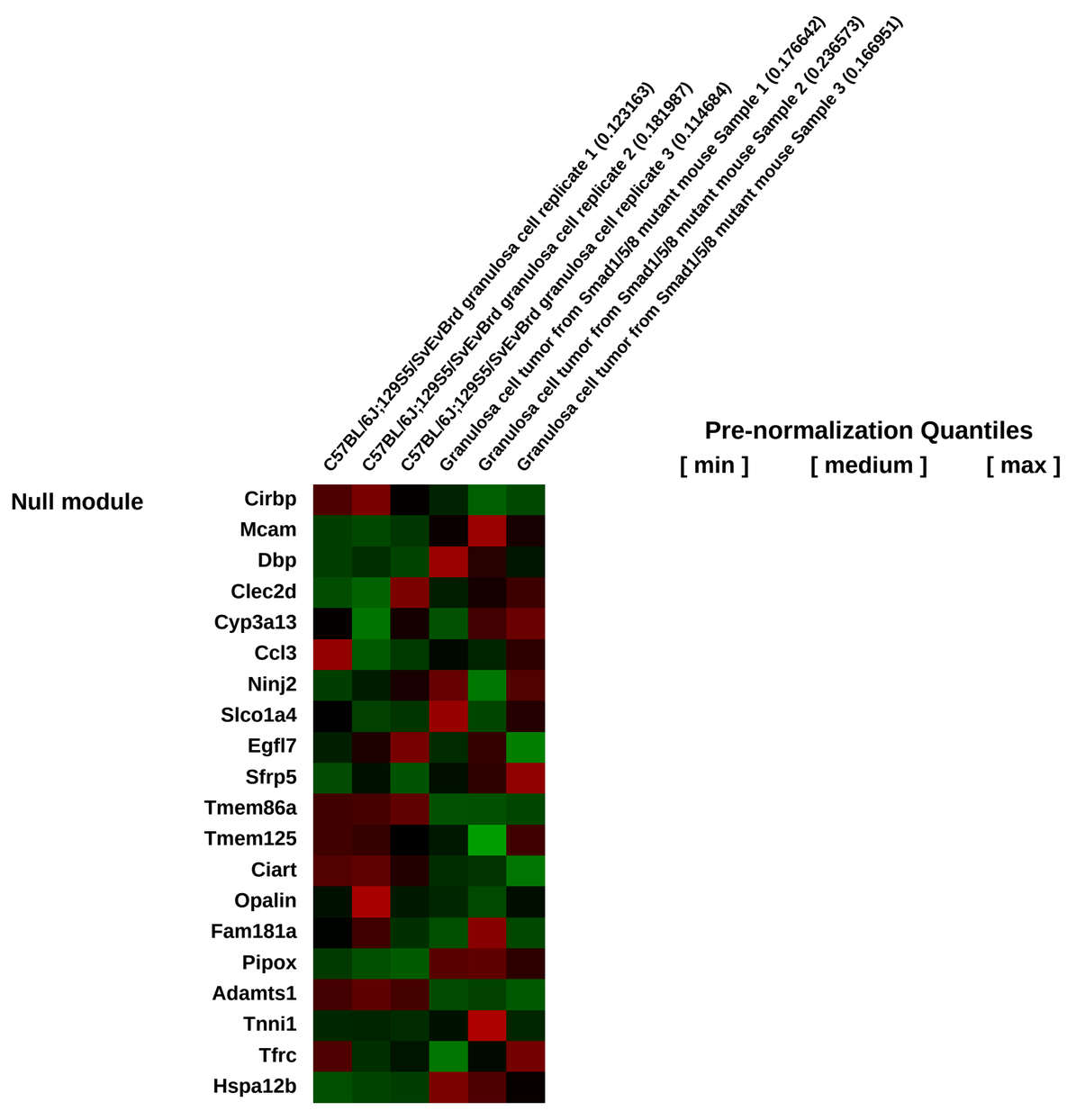

GEO Series "GSE8199" Expression Profiles

Num of samples in this series: 9

Scale of expression profile Z-scores

-3.0 -2.0 -1.0 0.0 1.0 2.0 3.0

GEO Link:	http://www.ncbi.nlm.nih.gov/geo/query/acc.cgi?acc=GSE8199
Status:	Public on Jul 10 2007
Title:	E18.5 Estrogen-related Receptor gamma Knockout Mouse Heart
Organism:	Mus musculus
Experiment type:	Expression profiling by array
Platform:	GPL1261
Pubmed ID:	17618853
Summary & Design:	**Summary:** **3 ventricles from E18.5 male mice were pooled for each array. Three arrays per genotype.** **Title: ERR‚Ä° Directs and Maintains the Transition to Oxidative Metabolism in the Post-Natal Heart** **Abstract: At birth the heart undergoes a critical metabolic switch to transition from a predominant dependence on carbohydrates during fetal life to a greater dependence on postnatal oxidative metabolism. This remains the principle metabolic state throughout life; although pathologic conditions such as heart failure and cardiac hypertrophy reactivate components of the fetal genetic program to increase carbohydrate utilization. Disruption of the ERR‚Ä° gene, which is expressed at high levels in the fetal and postnatal mouse heart, blocks this switch resulting in lactatemia, electrocardiographic (ECG) abnormalities and death during the first week of life. Genomic ChIP-on-chip and expression analysis at E18.5 clearly identifies ERR‚Ä° as both a direct and indirect regulator of a nuclear-encoded mitochondrial genetic network that coordinates the postnatal metabolic transition. These findings reveal an unexpected and essential molecular genetic component of the oxidative metabolic gene program in the heart and highlight ERR‚Ä° in the study of cardiac hypertrophy and failure.** **Keywords: ChIP-on-chip, electrocardiography, fetal gene program, OXPHOS, PGC-1a, sodium current, Single time point (E18.5) to compare genotype differences** **Overall design:** **Fetal mice were collected by caesarean secation. Hearts were stored in RNALater (Qiagen)**

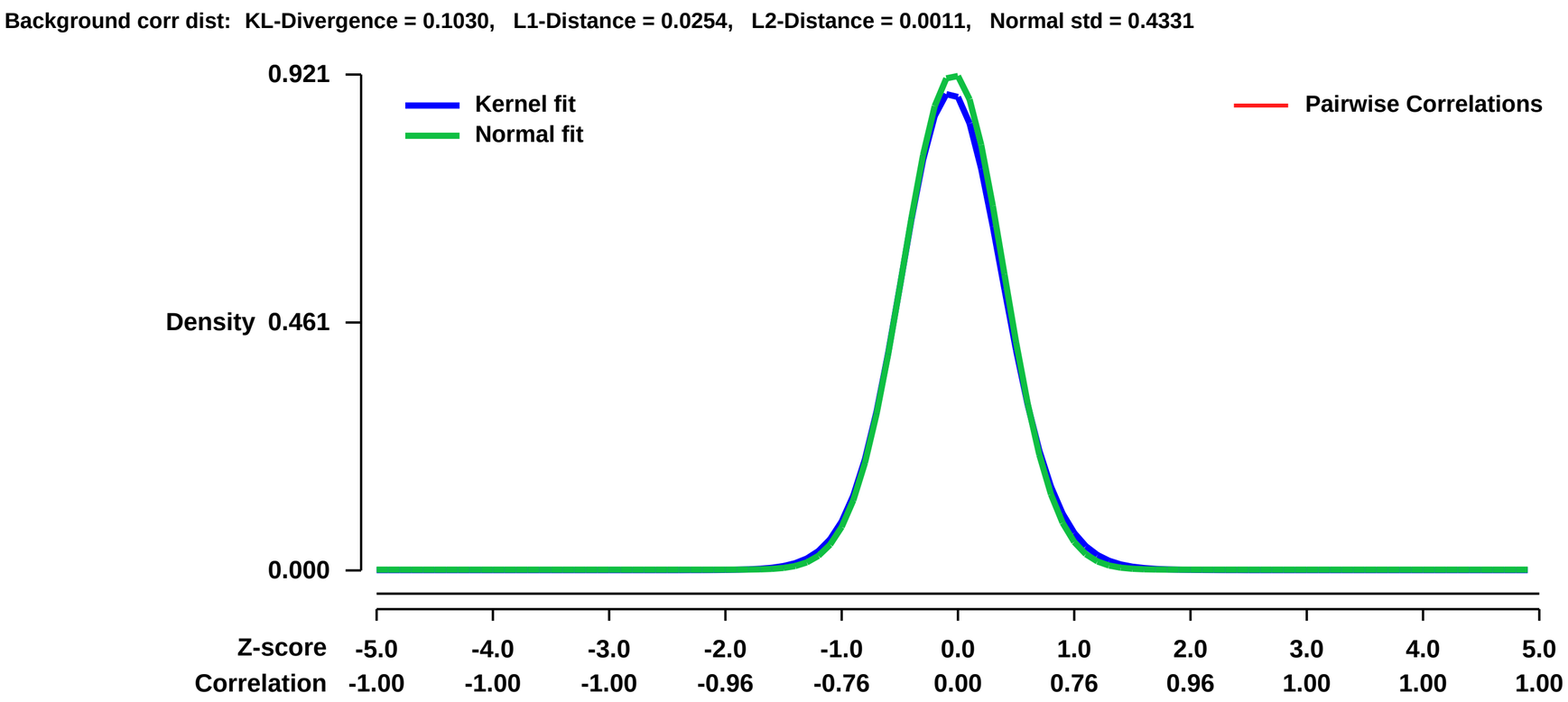

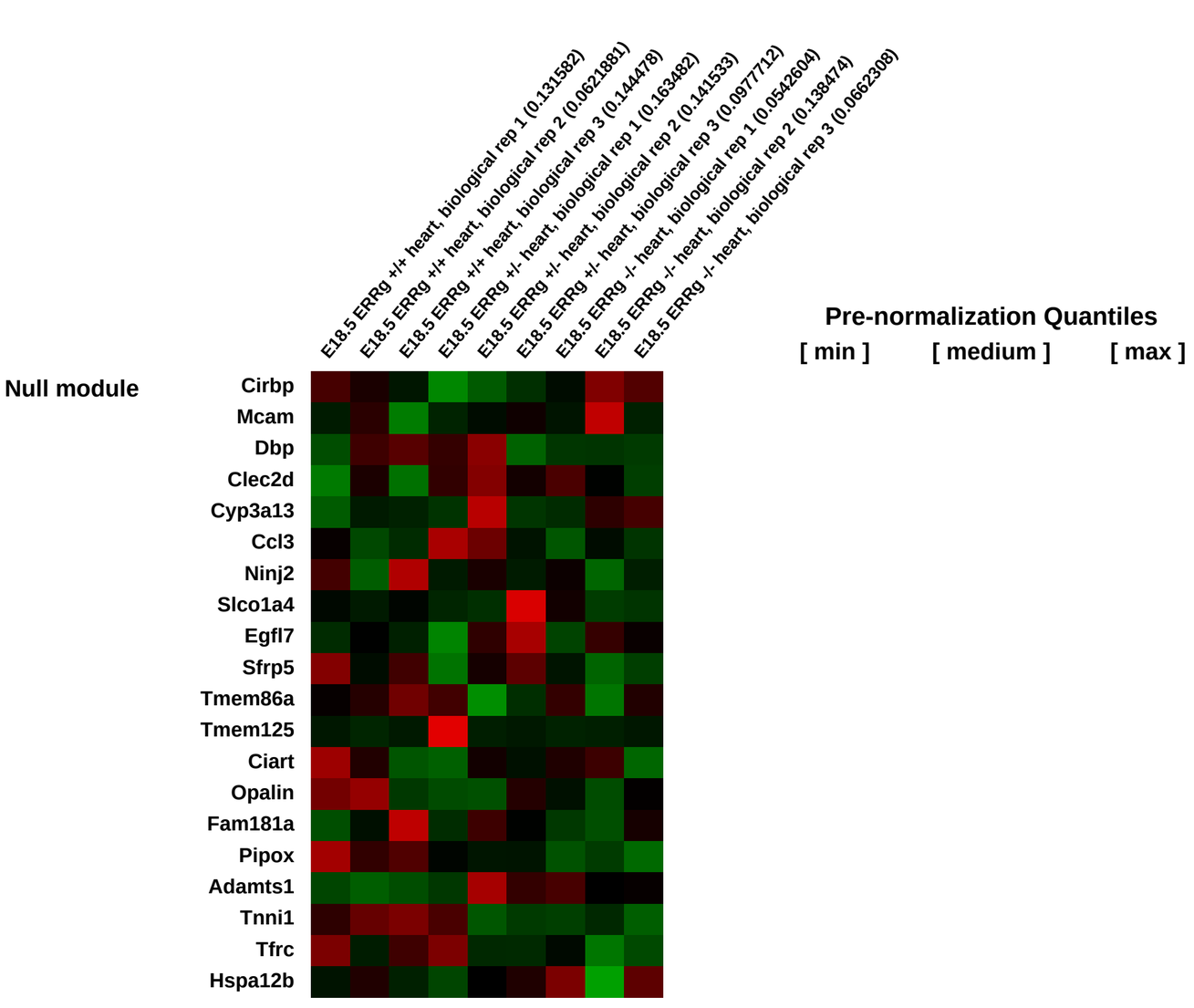

GEO Series "GSE8295" Expression Profiles

Num of samples in this series: 16

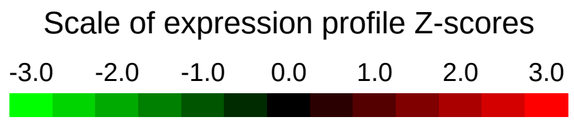

GEO Link:	http://www.ncbi.nlm.nih.gov/geo/query/acc.cgi?acc=GSE8295
Status:	Public on Jul 24 2007
Title:	Comprehensive analysis of PPARα–-dependent regulation of hepatic lipid metabolism by expression profiling - 4
Organism:	Mus musculus
Experiment type:	Expression profiling by array
Platform:	GPL1261
Pubmed ID:	18288265
Summary & Design:	**Summary:** PPARα– is a ligand-activated transcription factor involved in the regulation of nutrient metabolism and inflammation. Although much is already known about the function of PPARα– in hepatic lipid metabolism, many PPARα–-dependent pathways and genes have yet to be discovered. In order to obtain an overview of PPARα–-regulated genes relevant to lipid metabolism, and to probe for novel candidate PPARα– target genes, livers from several animal studies in which PPARα– was activated and/or disabled were analyzed by Affymetrix GeneChips. Numerous novel PPARα–-regulated genes relevant to lipid metabolism were identified. Out of this set of genes, eight genes were singled out for study of PPARα–-dependent regulation in mouse liver and in mouse, rat, and human primary hepatocytes, including thioredoxin interacting protein (Txnip), electron-transferring-flavoprotein α† polypeptide (Etfb), electron-transferring-flavoprotein dehydrogenase (Etfdh), phosphatidylcholine transfer protein (Pctp), endothelial lipase (EL, Lipg), adipose triglyceride lipase (Pnpla2), hormone-sensitive lipase (Lipe), and monoglyceride lipase (Mgll). Using an in silico screening approach, one or more PPAR response elements (PPREs) were identified in each of these genes. Since Pnpla2, Lipe, and Mgll contribute to hepatic triglyceride hydrolysis, gene regulation was studied under conditions of elevated hepatic lipids. In wild-type mice fed a high fat diet, the decrease in hepatic lipids following treatment with the PPARα– agonist Wy14643 was paralleled by significant up-regulation of Pnpla2, Lipe, and Mgll, suggesting that induction of triglyceride hydrolysis may contribute to the anti-steatotic role of PPARα–. Our study illustrates the power of transcriptional profiling to uncover novel PPARα–-regulated genes and pathways in liver. **Keywords:** identification of target genes **Overall design:** Five microgram total RNA was labelled according to the ENZO-protocol, fragmented and hybridized according to Affymetrix's protocols.

Background corr dist: KL-Divergence = 0.1374, L1-Distance = 0.0285, L2-Distance = 0.0011, Normal std = 0.4050

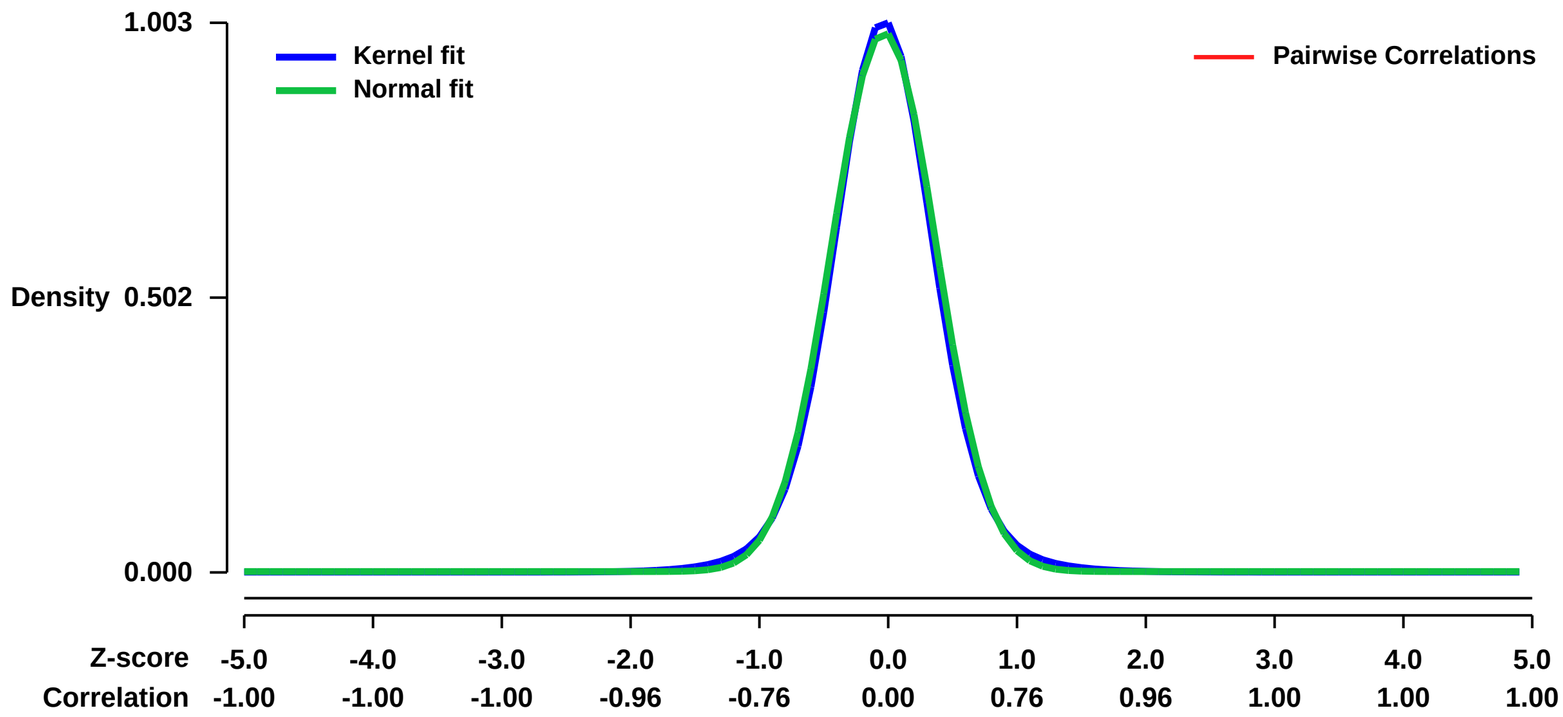

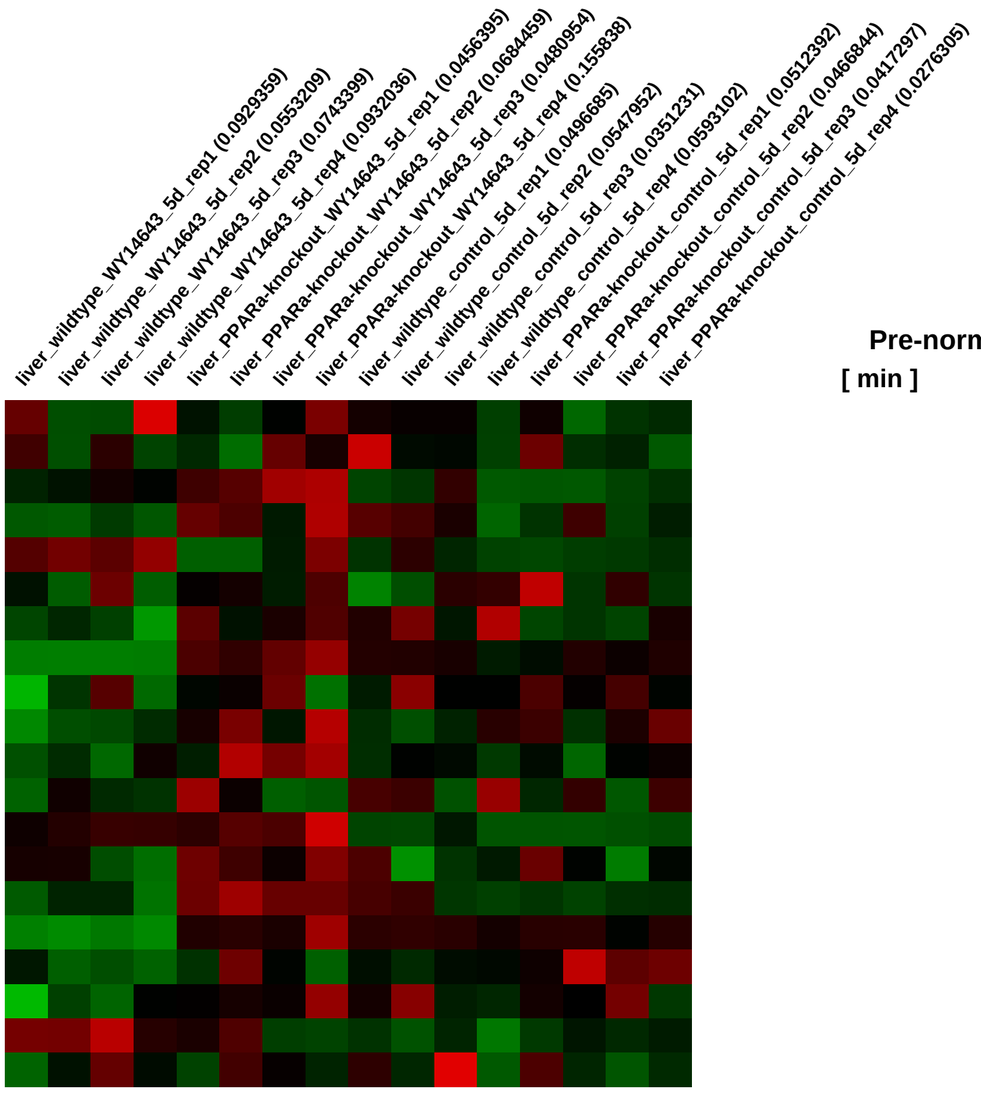

GEO Series "GSE8312" Expression Profiles

Num of samples in this series: 6

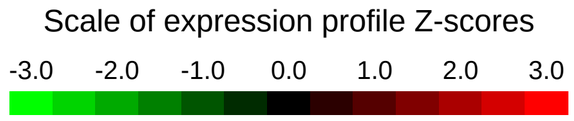

GEO Link:	http://www.ncbi.nlm.nih.gov/geo/query/acc.cgi?acc=GSE8312
Status:	Public on Dec 23 2007
Title:	Enhancing integrin alpha7 expression effect on myoblast transcription
Organism:	Mus musculus
Experiment type:	Expression profiling by array
Platform:	GPL1261
Pubmed ID:	18045857
Summary & Design:	**Summary:** Analysis of C2C12 myoblast induced with tetracycline to enhance integrin alpha7 expression. Integrin alpha7 is the major laminin binding integrin in muscle cells. Enhancing its expression has been demonstrated to alleviate pathology in a murine model of Duchenne muscular dystrophy. Results of this study provide insights into the effects of increasing integirn alpha7 expression on muscle cells and possible side effects associate with enhancing integrin alpha7 in muscle cells. **Keywords:** comparitive of integrin lapha7 induced and non-induced c2C12 myobalst **Overall design:** Triplicate biological smaples for each condition(induced and non-induced) C2C12 myoblast were used.

Background corr dist: KL-Divergence = 0.0480, L1-Distance = 0.0208, L2-Distance = 0.0005, Normal std = 0.5830

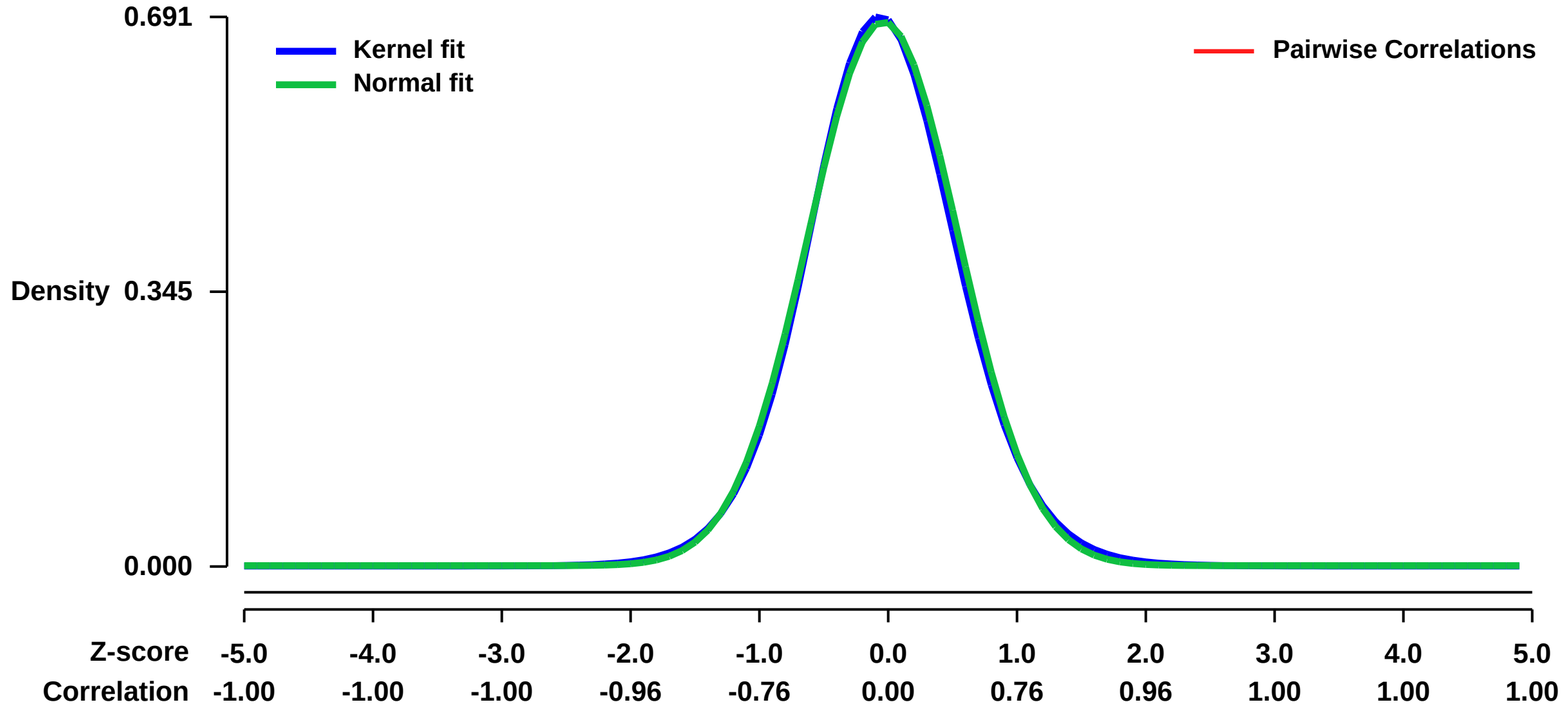

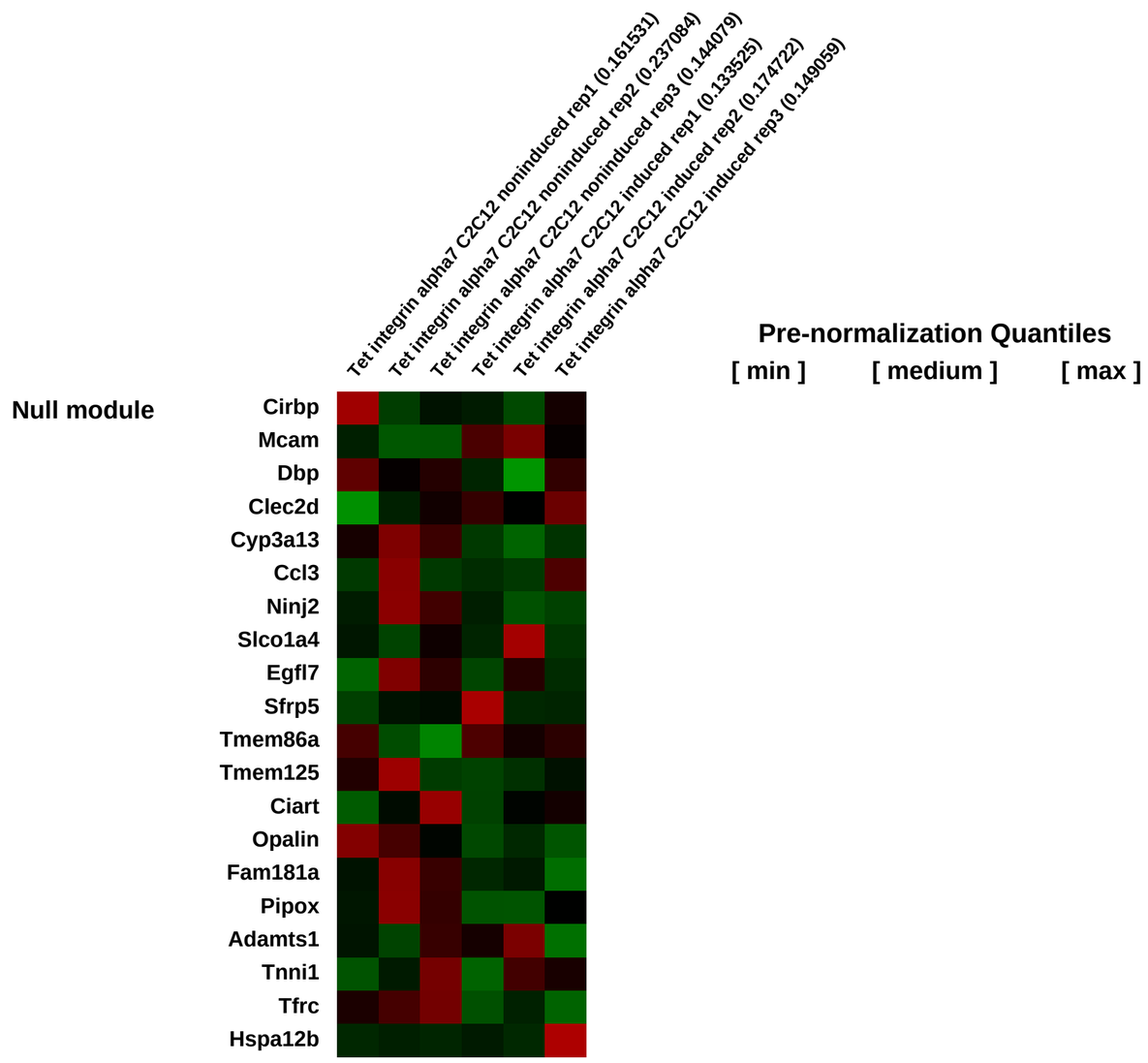

GEO Series "GSE8313" Expression Profiles

Num of samples in this series: 6

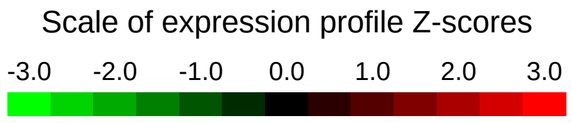

GEO Link:	http://www.ncbi.nlm.nih.gov/geo/query/acc.cgi?acc=GSE8313
Status:	Public on Dec 23 2007
Title:	integrin alpha7 overexpression effects on skeletal muscle transcriptions
Organism:	Mus musculus
Experiment type:	Expression profiling by array
Platform:	GPL1261
Pubmed ID:	18045857
Summary & Design:	**Summary:** Analysis of integrin alpha7 transgenic mice skeletal muscle transcription profiles comparing to wild type controls. Integrin alpha7 is the major laminin binding integrin in muscle cells. Enhancing its expression has been demonstrated to alleviate pathology in a murine model of Duchenne muscular dystrophy. Results of this study provide insights into the effects of increasing integrin alpha7 expression on skeletal muscle transcription and physiology in vivo. This analysis also evaluates any potential possible side effects associate with enhancing integrin alpha7 in skeletal muscle. **Keywords:** transgenic mice comparision to wild type controls **Overall design:** Equal amount of total RNA from six animals of each genotype were pooled to generate a biological replicate. Total of three biological replicates were used. Together, 18 mice of each genotype were used in this analysis.

Background corr dist: KL-Divergence = 0.0494, L1-Distance = 0.0189, L2-Distance = 0.0004, Normal std = 0.5755

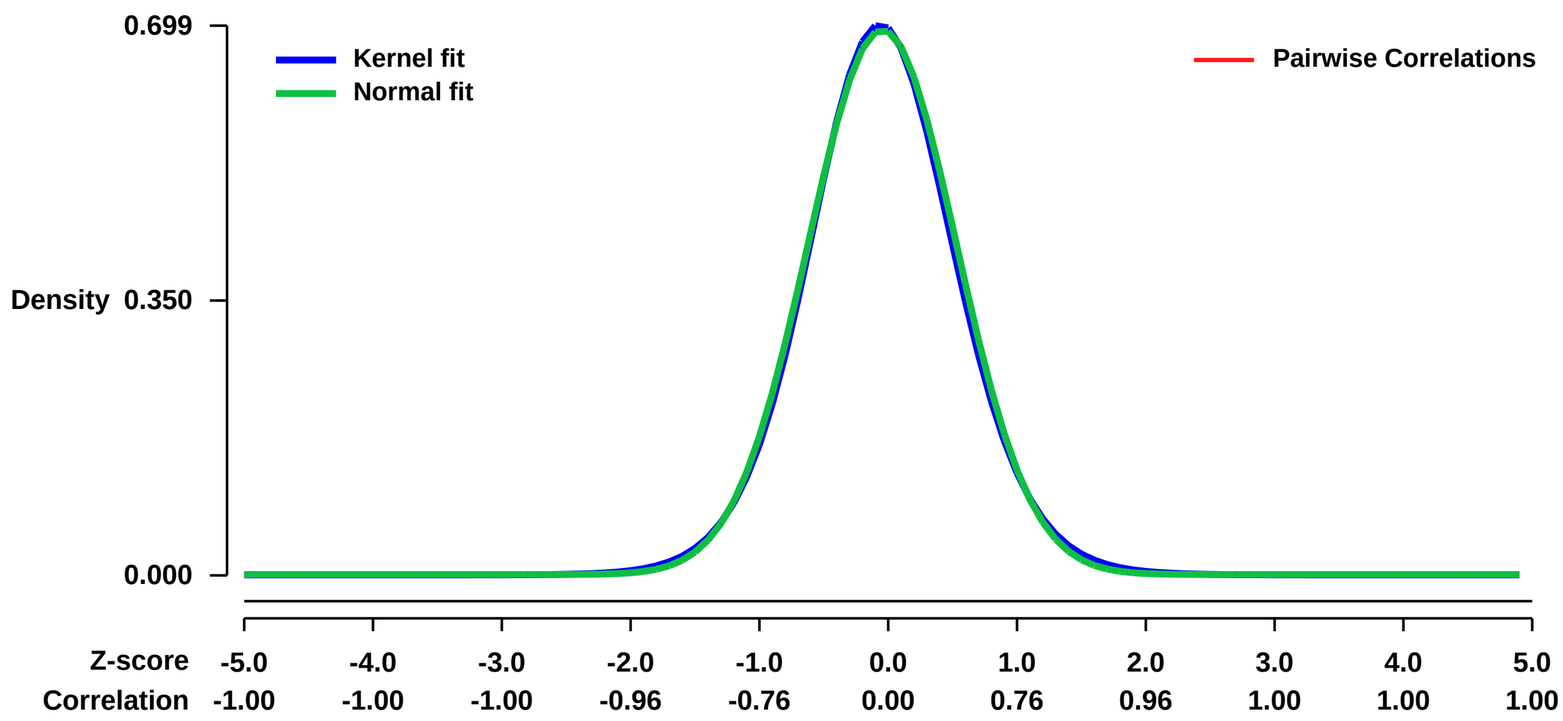

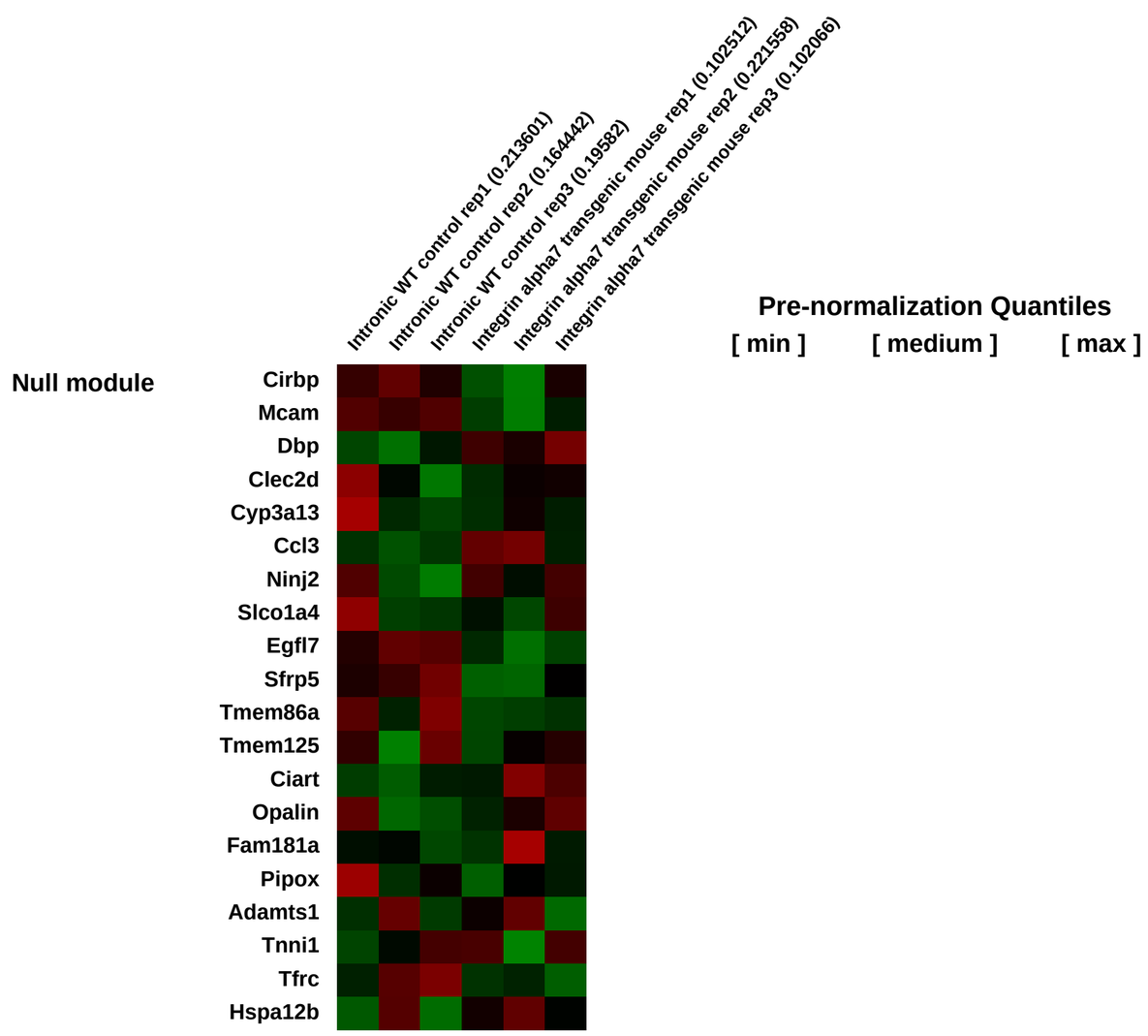

GEO Series "GSE8349" Expression Profiles

Num of samples in this series: 10

Scale of expression profile Z-scores

-3.0 -2.0 -1.0 0.0 1.0 2.0 3.0

GEO Link:	http://www.ncbi.nlm.nih.gov/geo/query/acc.cgi?acc=GSE8349
Status:	Public on Mar 25 2008
Title:	Microarray platform comparison study of hippocampal gene expression in DCLK1 transgenic and wild-type mice
Organism:	Mus musculus
Experiment type:	Expression profiling by array
Platform:	GPL1261
Pubmed ID:	18927111
Summary & Design:	**Summary:** The aim of the present study was to compare, on a statistical basis, the performance of different microarray platforms to detect differences in gene expression in a realistic and challenging biological setting. Gene expression profiles in the hippocampus of five wild-type and five transgenic ¸·C-doublecortin-like kinase mice were evaluated with five microarray platforms: Applied Biosystems, Affymetrix, Agilent, Illumina and home-spotted oligonucleotide arrays. We observed considerable overlap between the different platforms, the overlap being better detectable with significance level-based ranking than with a p-value based cut-off. Confirming the qualitative agreement between platforms, Pathway analysis consistently demonstrated aberrances in GABA-ergic signalling in the transgenic mice, even though pathways were represented by only partially overlapping genes on the different platforms. **Keywords:** microarray platform comparison **Overall design:** Illumina_raw_data.csv contains the raw data for GSM206887 to GSM206896. In these files, the sample identifiers are included in the column headers.

Background corr dist: KL-Divergence = 0.0755, L1-Distance = 0.0346, L2-Distance = 0.0023, Normal std = 0.4822

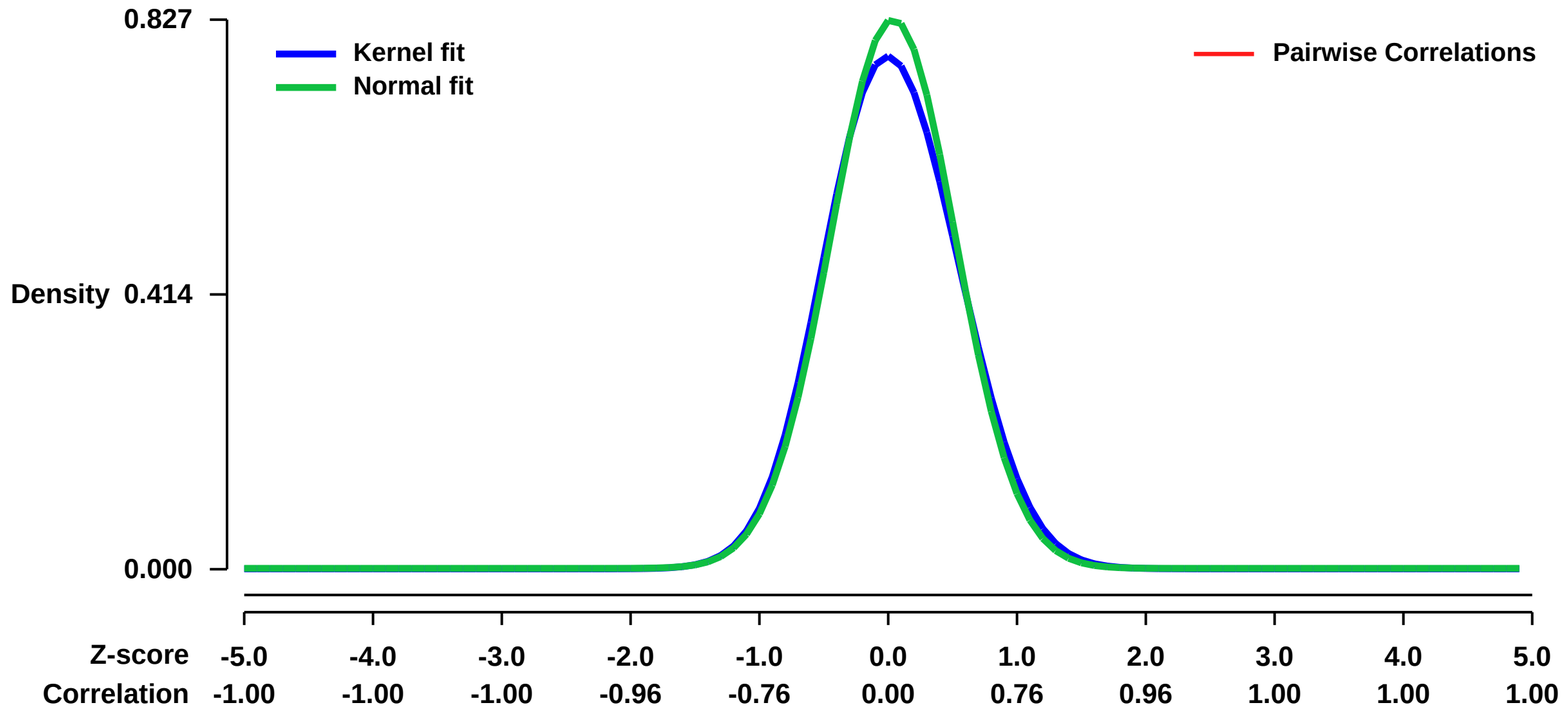

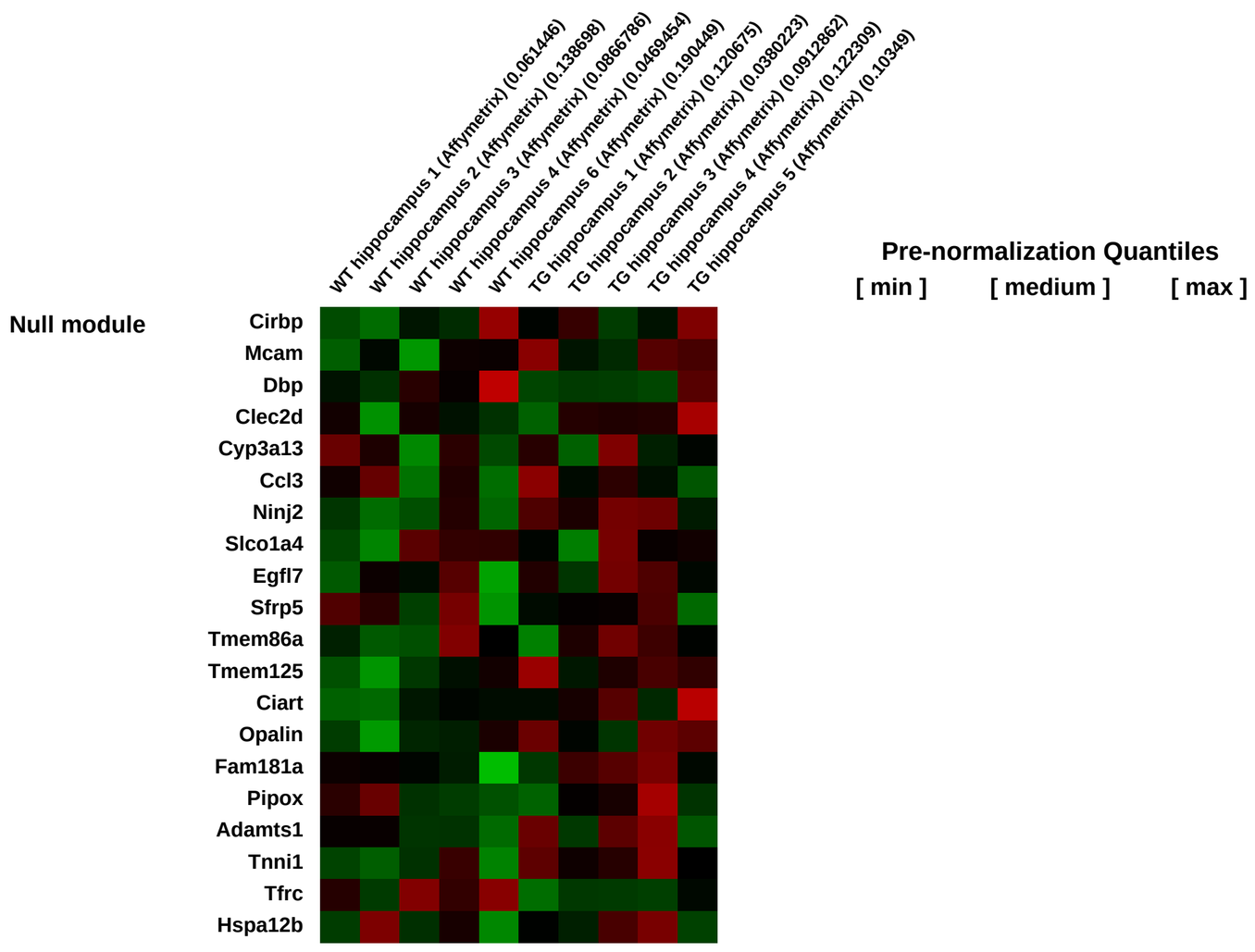

GEO Series "GSE8357" Expression Profiles

Num of samples in this series: 6

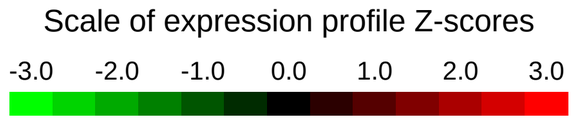

GEO Link:	**http://www.ncbi.nlm.nih.gov/geo/query/acc.cgi?acc=GSE8357**
Status:	**Public on Dec 31 2007**
Title:	**Functional analysis of exon 2 of p130Cas in fibroblasts derived from exon 2-specific knockout mice.**
Organism:	**Mus musculus**
Experiment type:	**Expression profiling by array**
Platform:	**GPL1261**
Pubmed ID:	
Summary & Design:	**Summary:** **p130Cas (Cas, Crk-associated substrate) is an adaptor molecule composed of an N-terminal Src homology 3 (SH3) domain, a substrate domain (SD), and a C-terminal Src binding domain (SBD). The SH3 domain of Cas has been shown to associate with various signaling molecules, including focal adhesion kinase (FAK), but its role in cellular function remains unclear. To address this issue, we established and analyzed primary fibroblasts derived from mice expressing a truncated Cas lacking the exon 2 encoding the SH3 domain (Cas exon 2â /â). In comparison to wild-type (Cas exon 2+/+) cells, Cas exon 2â /â primary fibroblasts showed delayed migration in wound healing and reduced spreading on fibronectin (FN), which would be due to reduced complex formation of Cas exon 2â /â with FAK and CrkII and also to impaired localization of Cas exon 2â /â to focal adhesions on FN. In addition, to analyze downstream signaling pathway regulated by Cas exon 2, we compared gene expression profiles between Cas exon 2+/+ and Cas exon 2â /â cells by a microarray analysis. Interestingly, we found that Cas exon 2-deficiency upregulated expression of CXC Chemokine Receptor-4 (CXCR4), CC Chemokine Receptor-5 (CCR5), and thrombospondin 4, which are implicated in cell motility and adhesion. These results define the role of Cas SH3-encoding exon in cell motility, FAK/Cas/CrkII complex formation, recruitment of Cas to focal adhesions, and regulation of cell adhesion-associated gene expression in primary fibroblasts.** **Keywords: SH3-encoding exon, p130Cas** **Overall design:** **RNA samples extracted from Cas exon 2+/+, Cas exon 2+/â , and Cas exon 2â /â fibroblasts (12.5dpc, two embryos for each genotype) were labeled and hybridized on Affymetrix microarray. Gene expression patterns of Cas exon 2â /â fibroblasts were compared with those of Cas exon 2+/+ and Cas exon 2+/â cells.**

Background corr dist: KL-Divergence = 0.0415, L1-Distance = 0.0221, L2-Distance = 0.0005, Normal std = 0.6121

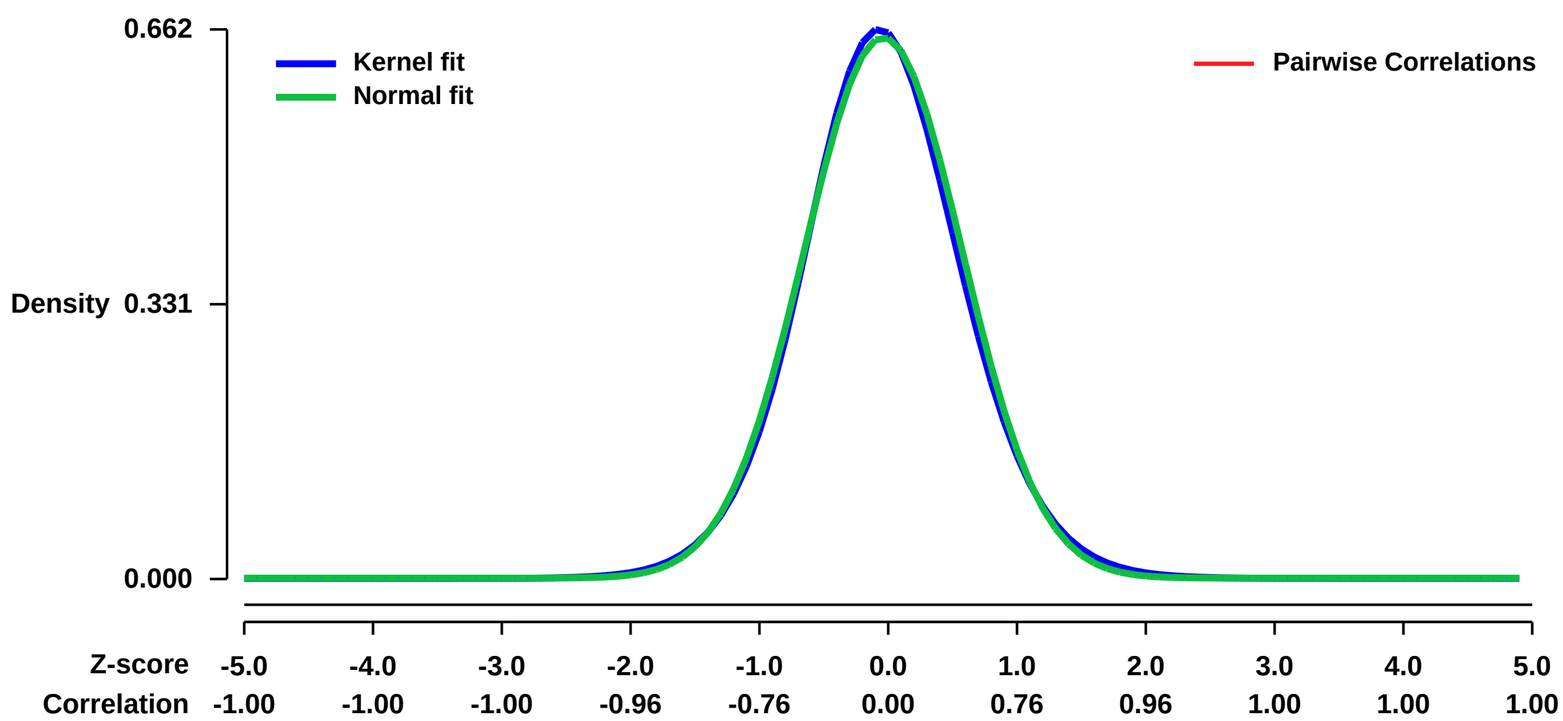

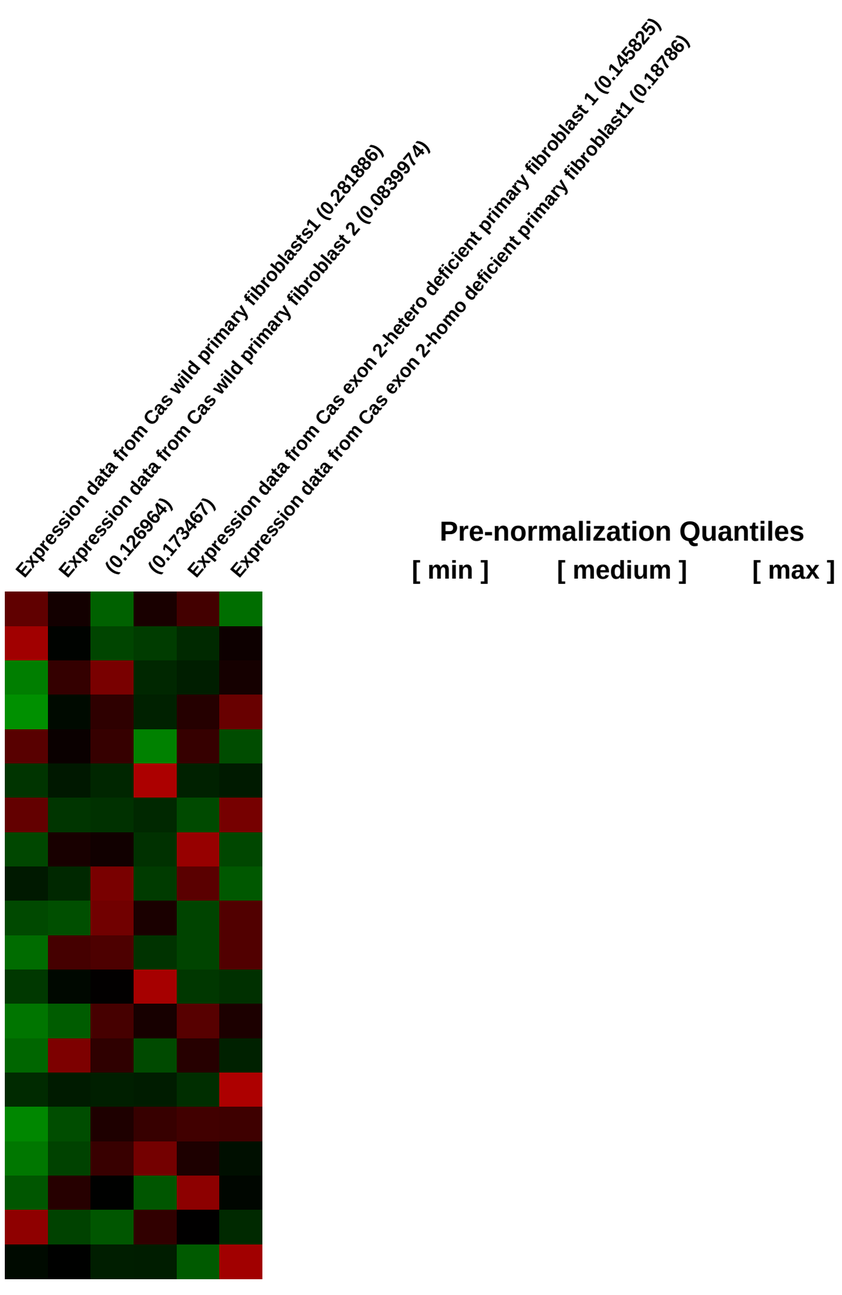

GEO Series "GSE8367" Expression Profiles

Num of samples in this series: 12

Scale of expression profile Z-scores

-3.0 -2.0 -1.0 0.0 1.0 2.0 3.0

GEO Link:	http://www.ncbi.nlm.nih.gov/geo/query/acc.cgi?acc=GSE8367
Status:	Public on Dec 31 2009
Title:	Sustained L-type Calcium Channel Blockade Alters Gene Regulation in the Adult Mouse Ventricle
Organism:	Mus musculus
Experiment type:	Expression profiling by array
Platform:	GPL1261
Pubmed ID:	
Summary & Design:	**Summary:** **Objective: L-type calcium channels (LTCC) homeostatically regulate calcium on a beat by beat basis, but also provide Ca that over long time scales may contribute to transcriptional regulation. We previously showed that sustained LTCC blockade (CCB) elicits LTCC remodeling in ventricular cardiac myocytes (CM). Here we hypothesize that sustained CCB has broad effects on the expression of genes involved in calcium handling. Methods and Results: Therefore, we subjected adult mice to sustained CCB for 24 hours and performed gene expression profiling. In comparison to vehicle-only control animals, 231 genes were up-regulated, and 111 genes were down-regulated by sustained LTCC blockade (p <0.01). Gene ontology analysis suggested that the CaMKIIdelta signaling pathway was up-regulated in these cells. Unexpectedly, phosphorylation of phospholamban (PLN) at threonine17 (Thr17), an index of CaMKIIdelta activity, was not changed by sustained CCB; however, the degree of phosphorylation of the neighboring PLN-Ser16 substrate site for PKA was significantly reduced by sustained CCB compared to control. Gene expression profiling suggested no change in PKA, but it showed that protein phosphatase 2A (PP2A) mRNA increased, and immunoblots demonstrated that PP2Ac-alpha protein was significantly increased by sustained CCB. Consistent with elevated PP2Ac-alpha protein expression LTCC exhibited decreased phosphorylation of the C-terminal Ser1928 PKA substrate site. Conclusions: We conclude that sustained CCB elicits a spectrum of transcriptional events, including compensatory up-regulation of LTCC and PP2Ac-alpha. Although this study is restricted to mouse, these results suggest the new hypothesis that clinically-relevant sustained LTCC blockade in humans results in changes in gene regulation in the heart.** **Keywords: L-type calcium channel, calcium channel blockade, verapamil** **Overall design:** **Left ventricular free wall from female mice was rapidly excised and either snap frozen at -80oC or used immediately for RNA isolation. Three VER treated mice and 3 vehicle treated mice were used to generate RNA for microarray. Total RNA was isolated using the RNAqueous -4PCR kit (Ambion) and quantitated spectrophotometrically at 260nm. Contaminating genomic DNA was eliminated by DNase treatment (Ambion). RNA quality was assessed using the Agilent 2100 Bioanalyzer. Microarray data was obtained using the Affymetrix 430 V2 GeneChip (representing 45,101 probe sets), in accordance with the manufacturerâ s specifications.**

Background corr dist: **KL-Divergence = 0.1573, L1-Distance = 0.0392, L2-Distance = 0.0031, Normal std = 0.3657**

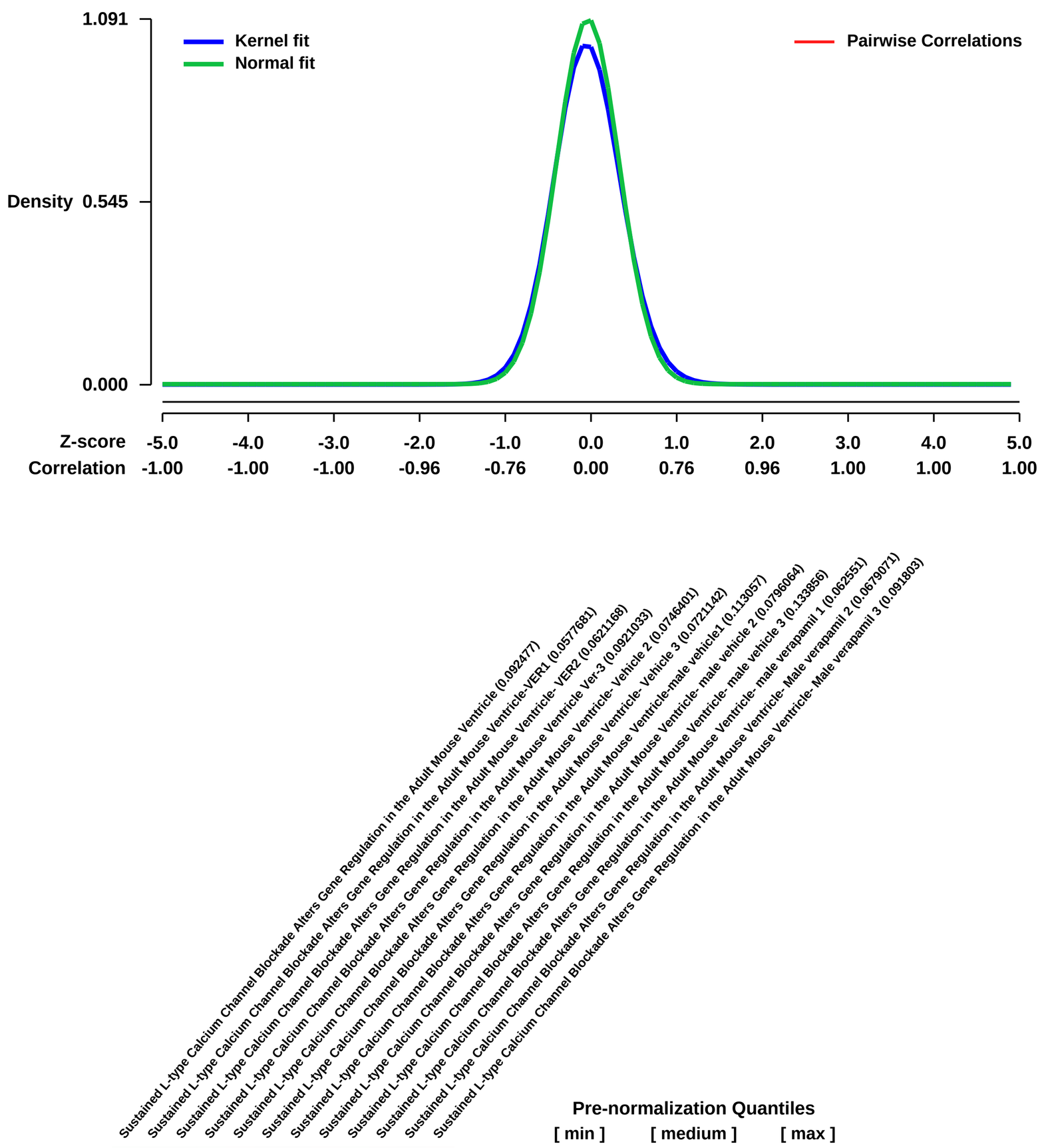

GEO Series "GSE8407" Expression Profiles

Num of samples in this series: 17

Scale of expression profile Z-scores

-3.0 -2.0 -1.0 0.0 1.0 2.0 3.0

GEO Link:	http://www.ncbi.nlm.nih.gov/geo/query/acc.cgi?acc=GSE8407
Status:	Public on Aug 01 2007
Title:	Elucidation of the phenotypic, functional and molecular topography of a myeloerythroid progenitor cell hierarchy
Organism:	Mus musculus
Experiment type:	Expression profiling by array
Platform:	GPL1261
Pubmed ID:	18371379
Summary & Design:	**Summary:** The major myeloid blood cell lineages, including erythrocytes, platelets, granulocytes and macrophages, are generated from hematopoietic stem cells (HSC) by differentiation through a series of increasingly more committed progenitor cells. Precise phenotypic identification and functional characterization of such intermediate progenitors has important consequences for understanding fundamental differentiation processes and is clinically relevant since such events become dysregulated in various disease settings, including leukemia. While previous studies have suggested a hierarchy for myeloid differentiation involving a common progenitor through which all myeloid lineages are derived, several recent studies have suggested that such a developmental intermediate might not be an absolute requirement. Here, we evaluated the functional in vitro and in vivo potentials of a range of prospectively isolated myeloid precursors with differential expression of CD150, Endoglin and CD41. Our studies reveal a complex hierarchy of myeloerythroid progenitors with distinct and developmentally restricted lineage potentials. Global gene expression signatures of these cellular subsets revealed expression patterns consistent with their functional capacities, while hierarchical clustering analysis provides details on their lineage relationships. These data challenge existing models of hematopoietic differentiation, by suggesting that progenitors of the innate and adaptive immune system in the adult separate late, and to a large extent, following the divergence of megakaryocytic/erythroid potential. **Keywords:** global gene expression profiling of prospectively isolated murine bone marrow progenitor subset by usage of affymetrix **Overall design:** RNA was extracted from purified adult BM subsets using RNeasy mRNA purification kit (Qiagen). Subsequent handling was performed at the SweGene Affymetrix unit at Lund University (http://www.swegene.org/microarray). Briefly, RNA (arrays in triplicate for all progenitor fractions except for pre MegE for which 5 arrays were produced) was labeled and amplified according to AffymetrixTM; Small Sample Labelling Protocol v.2, with the exception that the second round of in vitro transcription (IVT) was performed using AffymetrixTM GeneChipTM Expression 3â amplification kit. Hybridization and washing was performed according to AffymetrixTM GeneChipTM Expression analysis technical manual. Chips were scanned using an AffymetrixTM GeneChipTM Scanner 3000 and scaled to a median intensity of 100. For subsequent analysis, probe level expression values were extracted using RMA (Irizarry et al., 2003) and subsequent analyses was performed using dChip software (http://biosun1.harvard.edu/complab/dchip/) following filtering (0.5<SD/mean<1,000).

Background corr dist: KL-Divergence = 0.0647, L1-Distance = 0.0781, L2-Distance = 0.0127, Normal std = 0.5494

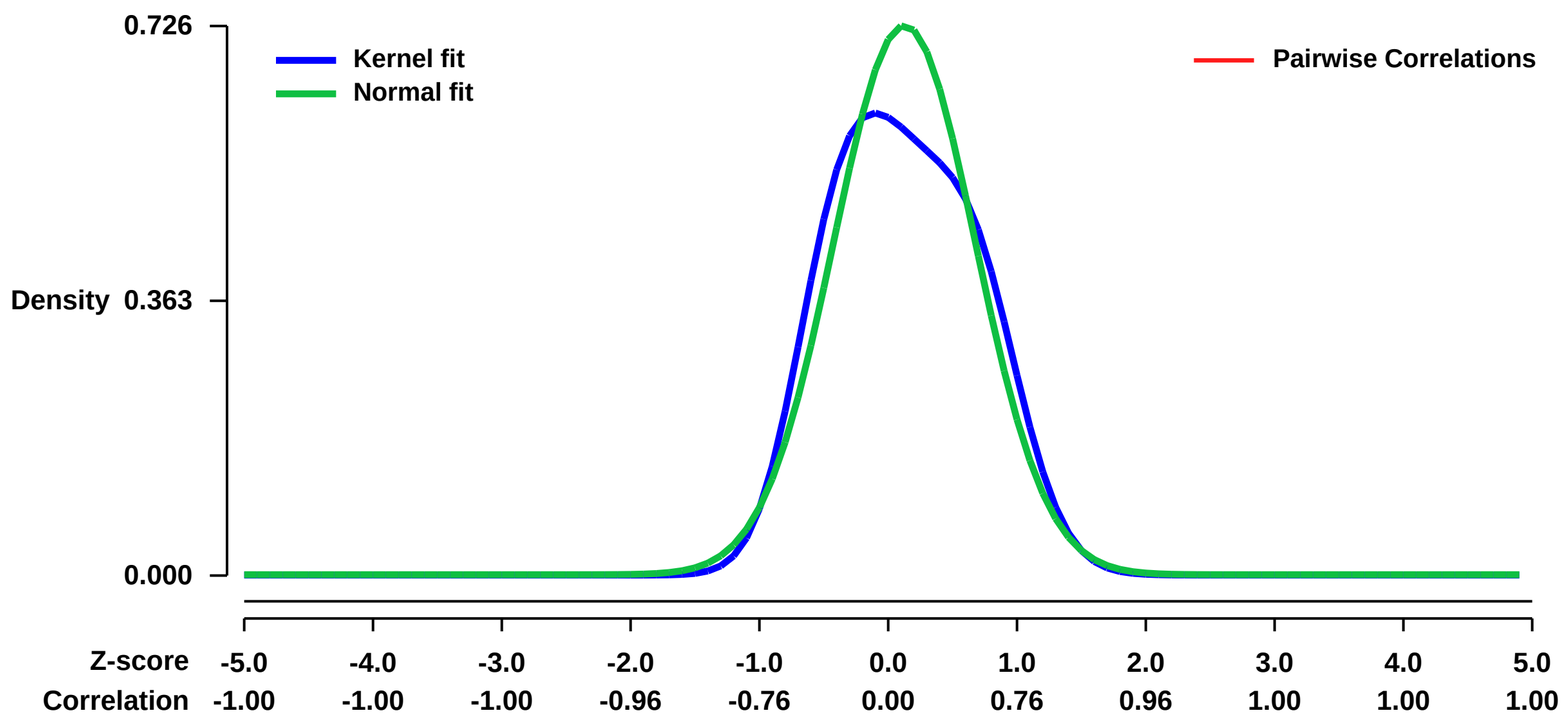

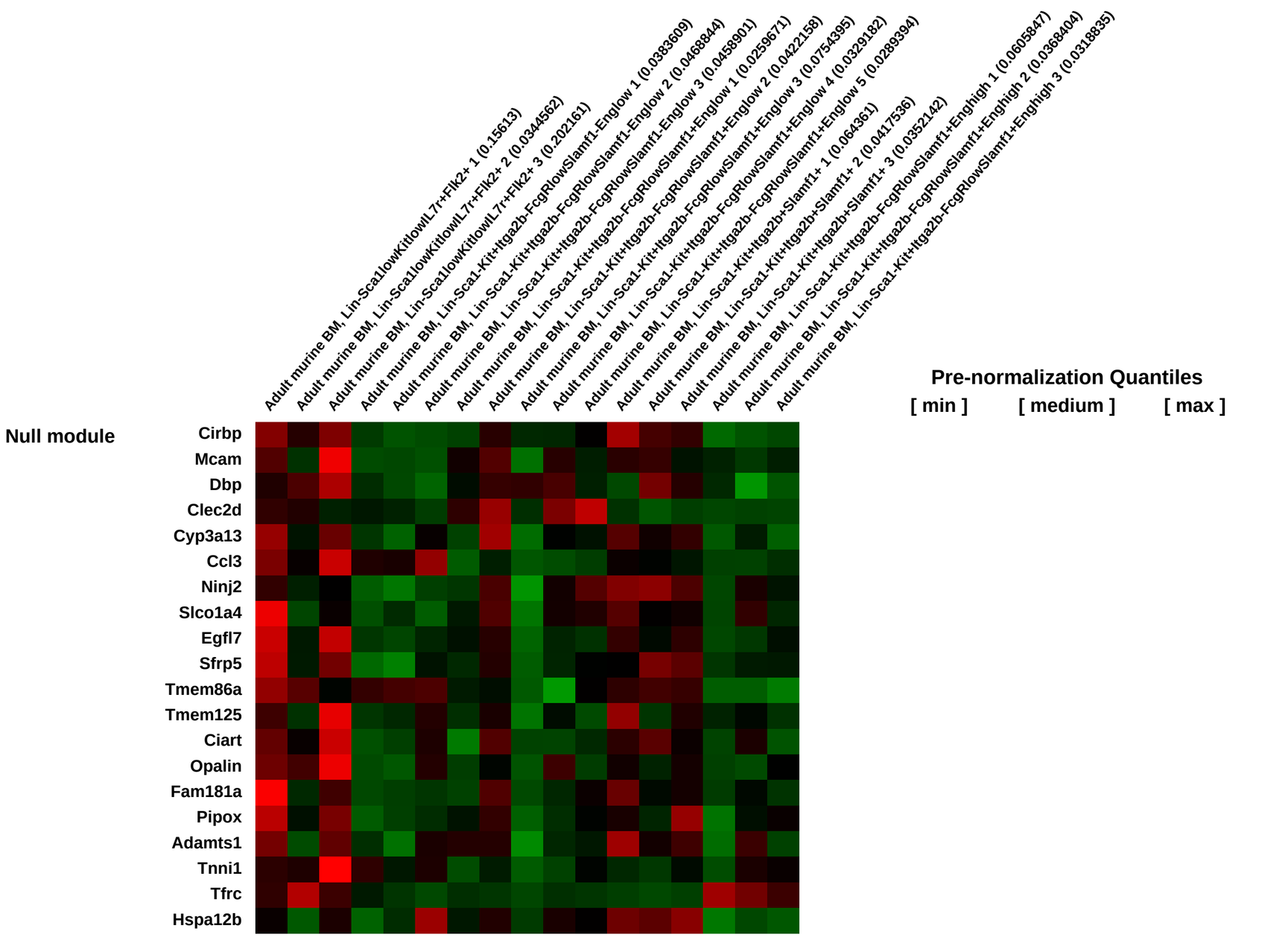

GEO Series "GSE8431" Expression Profiles

Num of samples in this series: 12

Scale of expression profile Z-scores

-3.0 -2.0 -1.0 0.0 1.0 2.0 3.0

GEO Link:	http://www.ncbi.nlm.nih.gov/geo/query/acc.cgi?acc=GSE8431
Status:	Public on Dec 18 2007
Title:	Microarray screening of RARgamma responsive genes in F9 teratocarcinoma cells
Organism:	Mus musculus
Experiment type:	Expression profiling by array
Platform:	GPL1261
Pubmed ID:	18164278
Summary & Design:	**Summary:** We compared the differentially expressed genes between the F9 Wt cells and F9 RAR gamma knock out cells before and after RA treatment. 3 replicates for each conditions. We also identified the RA responsive genes in the F9 Wt cells. Keywords: mutant type **Overall design:** F9 wt cells and F9 RAR gamma knock out cells are treated with RA (1 uM) or ethanol for 24 hours. 3 replicates for each condition.

Background corr dist: KL-Divergence = 0.0991, L1-Distance = 0.0302, L2-Distance = 0.0018, Normal std = 0.4467

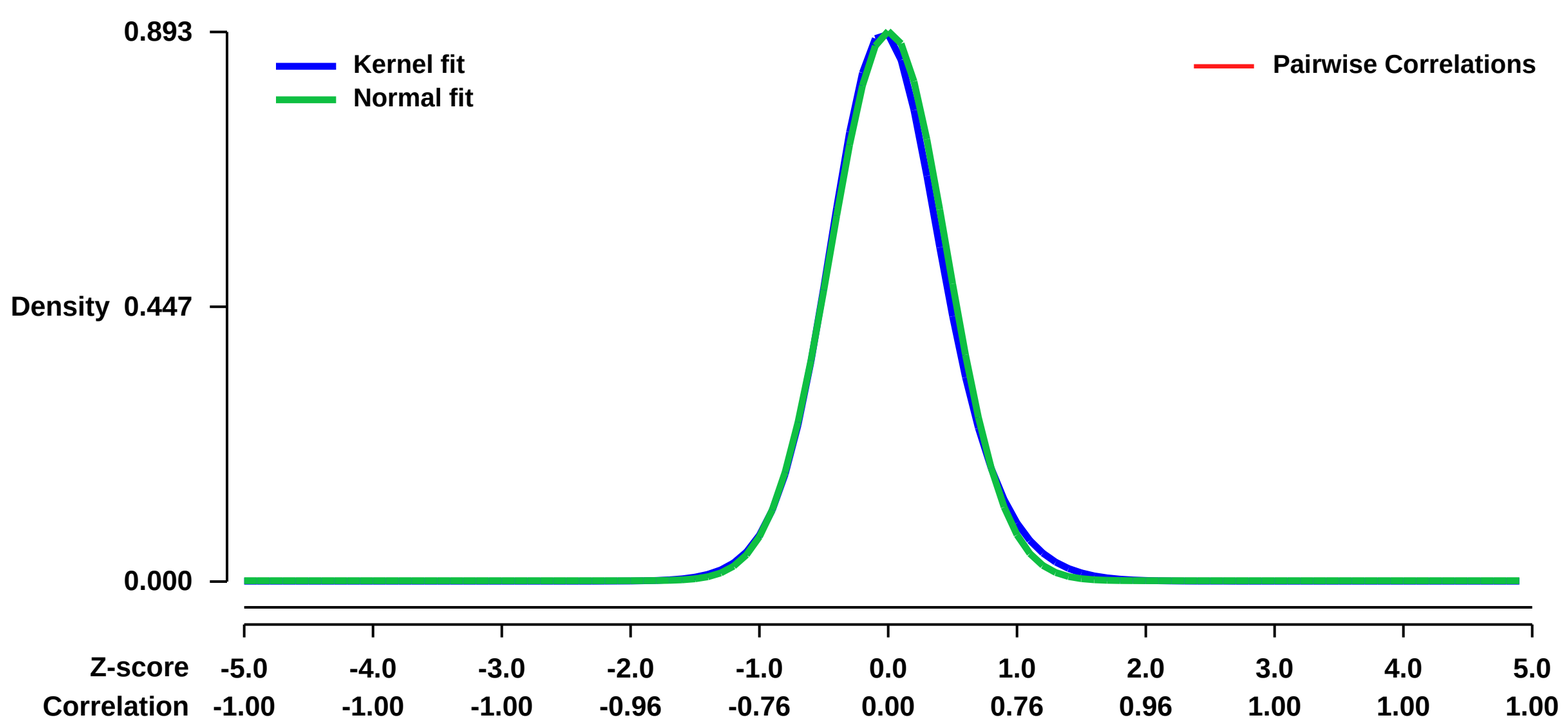

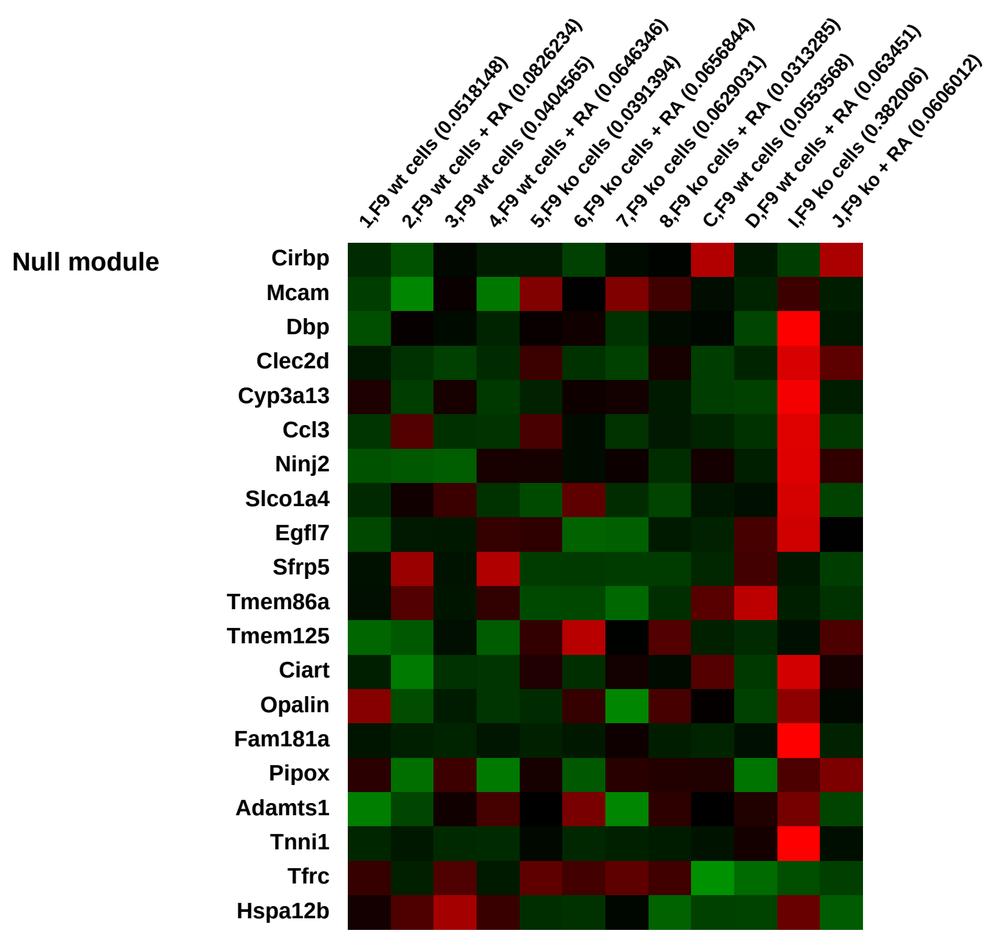

GEO Series "GSE8434" Expression Profiles

Num of samples in this series: 6

Scale of expression profile Z-scores

-3.0 -2.0 -1.0 0.0 1.0 2.0 3.0

GEO Link:	http://www.ncbi.nlm.nih.gov/geo/query/acc.cgi?acc=GSE8434
Status:	Public on Aug 01 2007
Title:	Transcriptional regulation by Errb (Nr3b2) in stria vascularis
Organism:	Mus musculus
Experiment type:	Expression profiling by array
Platform:	GPL1261
Pubmed ID:	17765677
Summary & Design:	**Summary:** Transcriptional profiles were compared in microdissected lateral walls of the inner ears from Errb mutant mice and wild type littermate controls. The goal is to identify transcriptional targets of Errb and candidate genes for inner ear diseases. **Keywords: genetic mutant analysis** **Overall design:** Errb mutant mice were generated by conditional knock-out strategy. Inner ears from 10 mice were pooled for each sample and 3 replicates of wild type and mutant samples were analyzed.

Background corr dist: **KL-Divergence = 0.0097, L1-Distance = 0.0148, L2-Distance = 0.0002, Normal std = 0.8623**

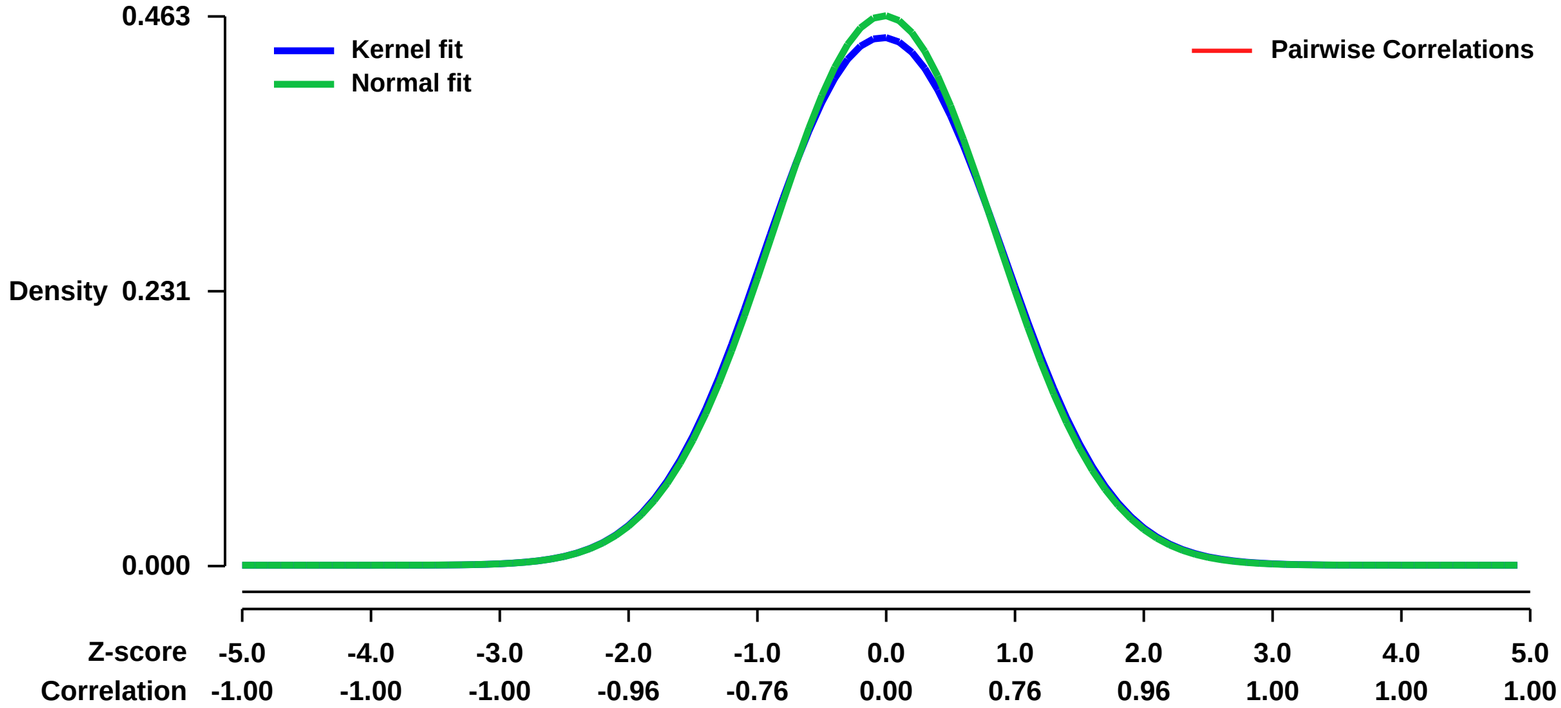

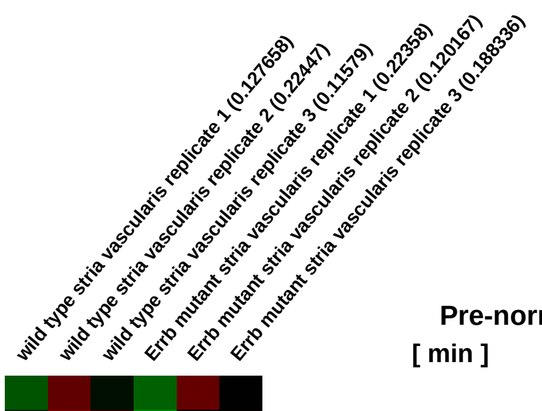

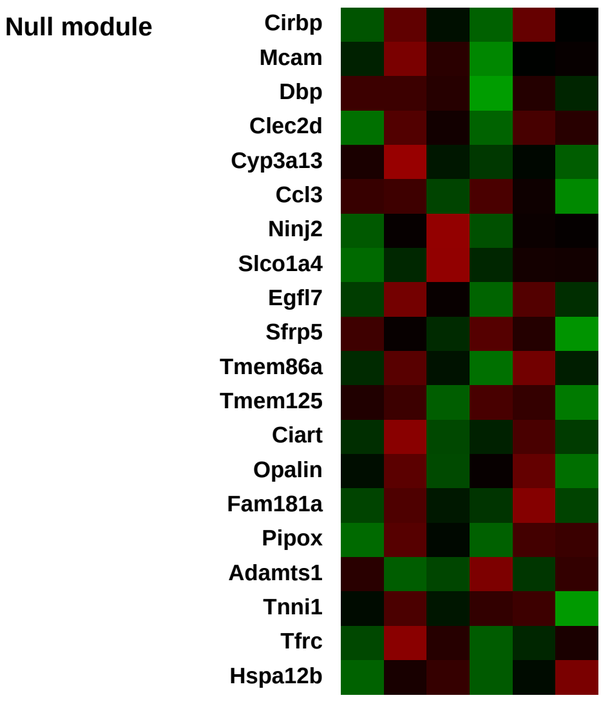

GEO Series "GSE8498" Expression Profiles

Num of samples in this series: 6

Scale of expression profile Z-scores

-3.0 -2.0 -1.0 0.0 1.0 2.0 3.0

GEO Link:	http://www.ncbi.nlm.nih.gov/geo/query/acc.cgi?acc=GSE8498
Status:	Public on Aug 04 2007
Title:	The MicroRNA miR-124 Promotes Neuronal Differentiation by Triggering Brain-Specific Alternative Pre-mRNA Splicing
Organism:	Mus musculus
Experiment type:	Expression profiling by array
Platform:	GPL1261
Pubmed ID:	17679093
Summary & Design:	**Summary:** Both microRNAs and alternative pre-mRNA splicing have been implicated in the development of the nervous system (NS), but functional interactions between these two pathways are poorly understood. We demonstrate that the neuron-specific microRNA miR-124a directly targets PTBP1/PTB/hnRNPI mRNA, which encodes a global repressor of alternative pre-mRNA splicing in non-neuronal cells. Among the targets of PTBP1 is a critical cassette exon in the pre-mRNA of PTBP2/nPTB/brPTB, an NS-enriched PTBP1 homolog. When this exon is skipped, PTBP2 mRNA is subject to nonsense-mediated decay. During neuronal differentiation, miR-124a reduces PTBP1 levels leading to the accumulation of correctly spliced PTBP2 mRNA and a dramatic increase in PTBP2 protein. These events culminate in the transition from non-NS to NS-specific alternative splicing patterns. We also present evidence that miR-124a plays a key role in the differentiation of progenitor cells to mature neurons. Thus, miR-124a promotes NS development at least in part by regulating an intricate network of NS-specific alternative splicing. We used microarrays to detail the global programme of gene expression of CAD cells over-expressing miR-124a-2. Keywords: treatment versus control **Overall design:** Expression data from CAD cells transfected with plasmid expressing miR-124a-2.

Background corr dist: KL-Divergence = 0.0253, L1-Distance = 0.0120, L2-Distance = 0.0002, Normal std = 0.6906

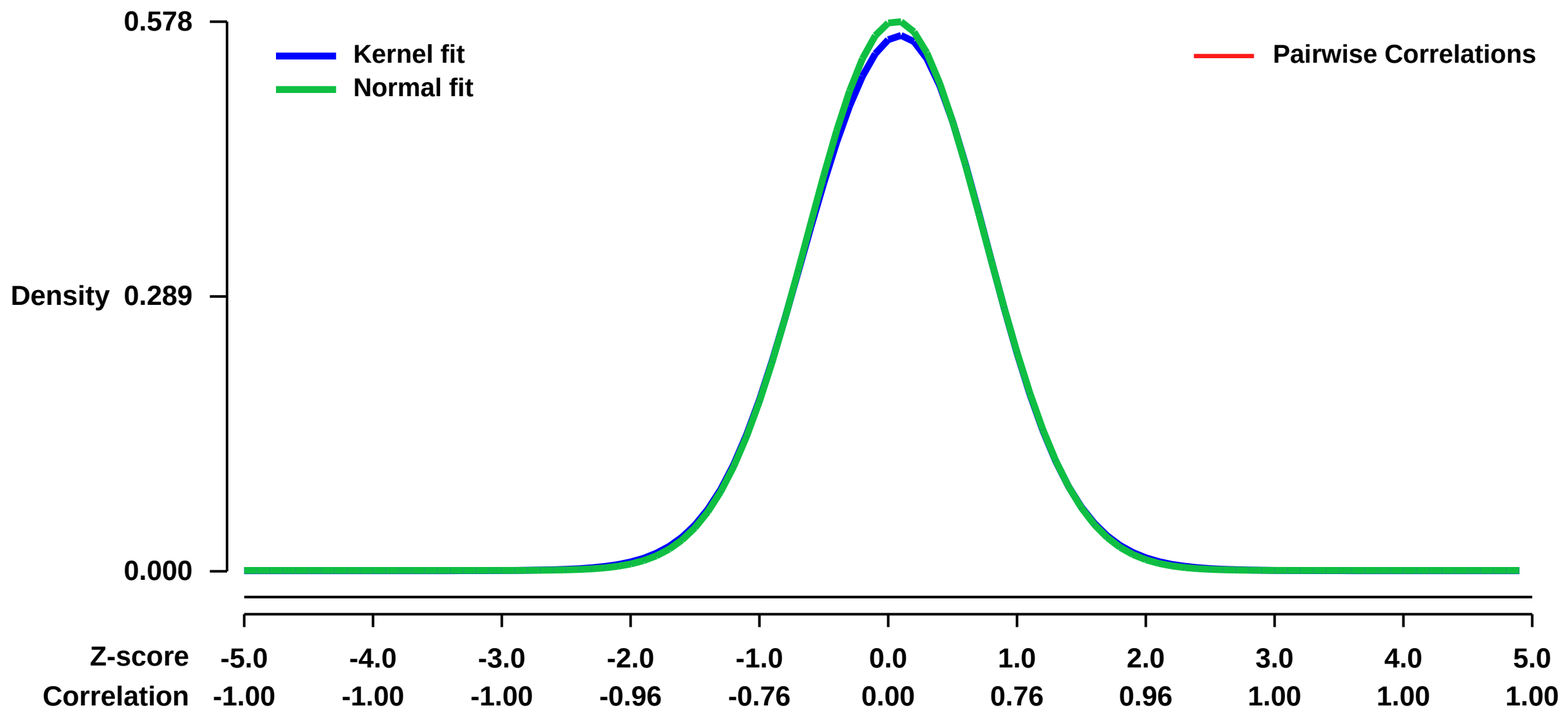

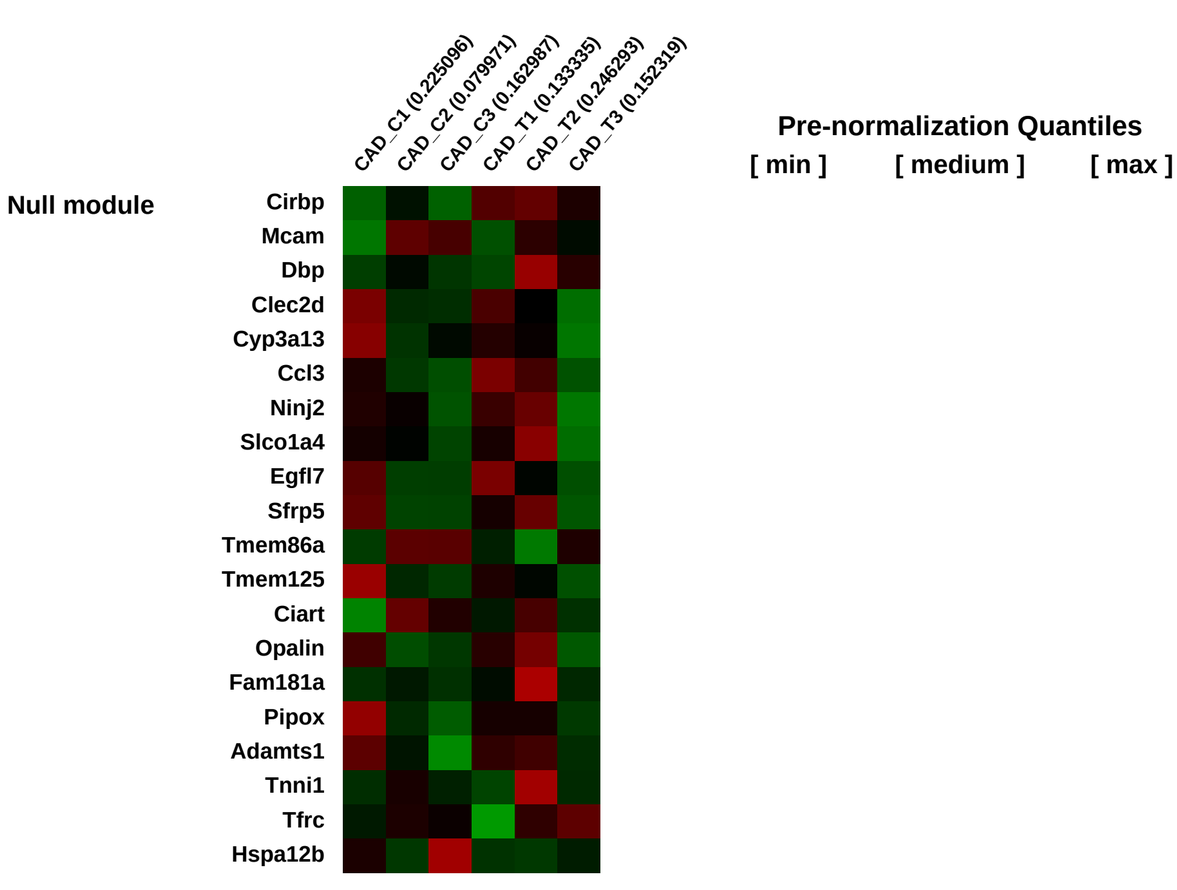

GEO Series "GSE8503" Expression Profiles

Num of samples in this series: 6

Scale of expression profile Z-scores

-3.0 -2.0 -1.0 0.0 1.0 2.0 3.0

GEO Link:	http://www.ncbi.nlm.nih.gov/geo/query/acc.cgi?acc=GSE8503
Status:	Public on Jan 01 2008
Title:	mRNA expression analysis of undifferentiated Dicer -/- (27H10) embryonic stem cells after miRNA transfection
Organism:	Mus musculus
Experiment type:	Expression profiling by array
Platform:	GPL1261
Pubmed ID:	18311153
Summary & Design:	**Summary:** We have analyzed the transcript expression levels in Dicer knock-out embryonic stem (ES) cells 24 hours after transfection with either control siRNA agains Renilla luciferase or miRNA Mimics (Dharmacon) of mmu-miR-290 cluster members in order to identify primary targets of miR-290 cluster miRNAs. **Keywords:** Comparison of effect of two different transfections on transcriptome of Dicer-KO ES cells **Overall design:** Cell were analysed 24h after transfections in an undifferentiated state. Triplicates of both transfections were analyzed.

Background corr dist: KL-Divergence = 0.0399, L1-Distance = 0.0219, L2-Distance = 0.0005, Normal std = 0.6216

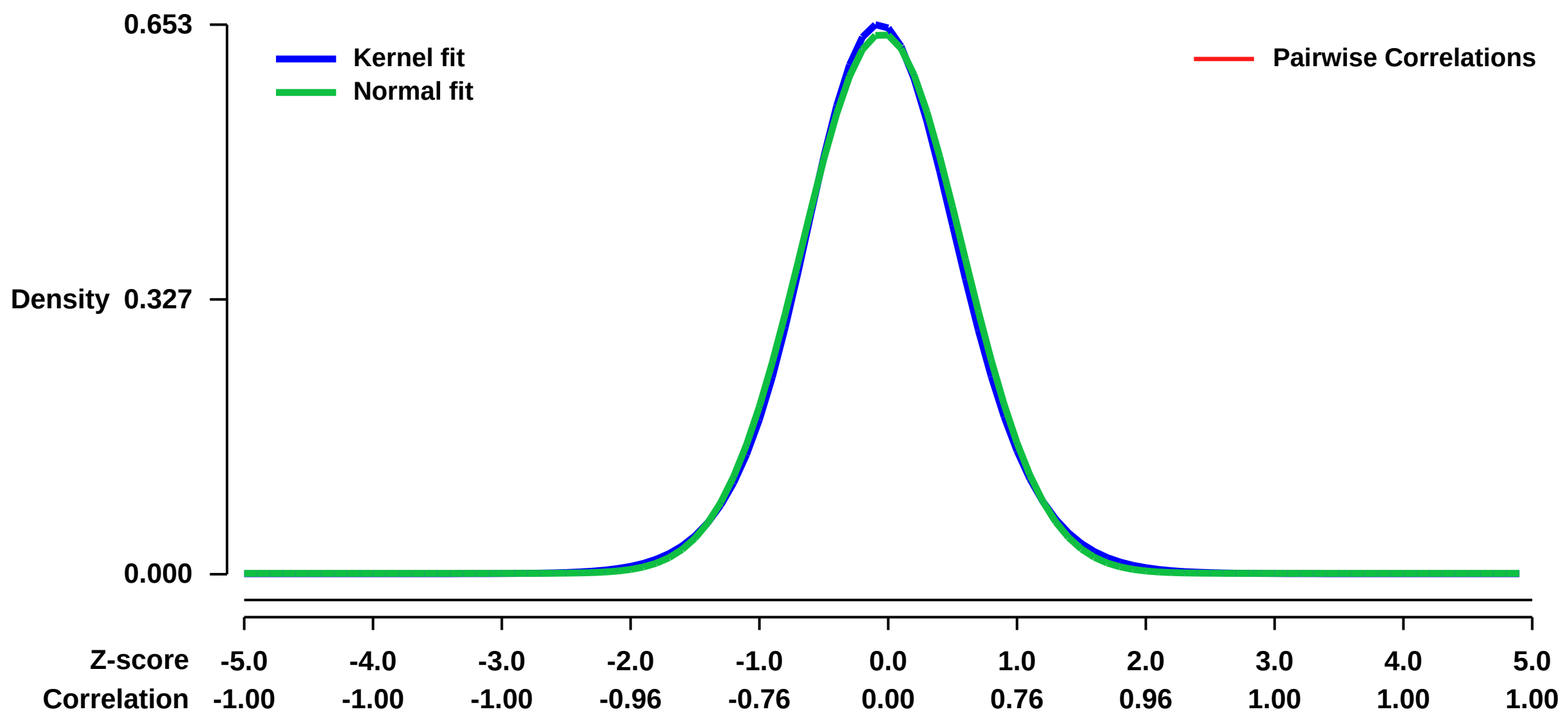

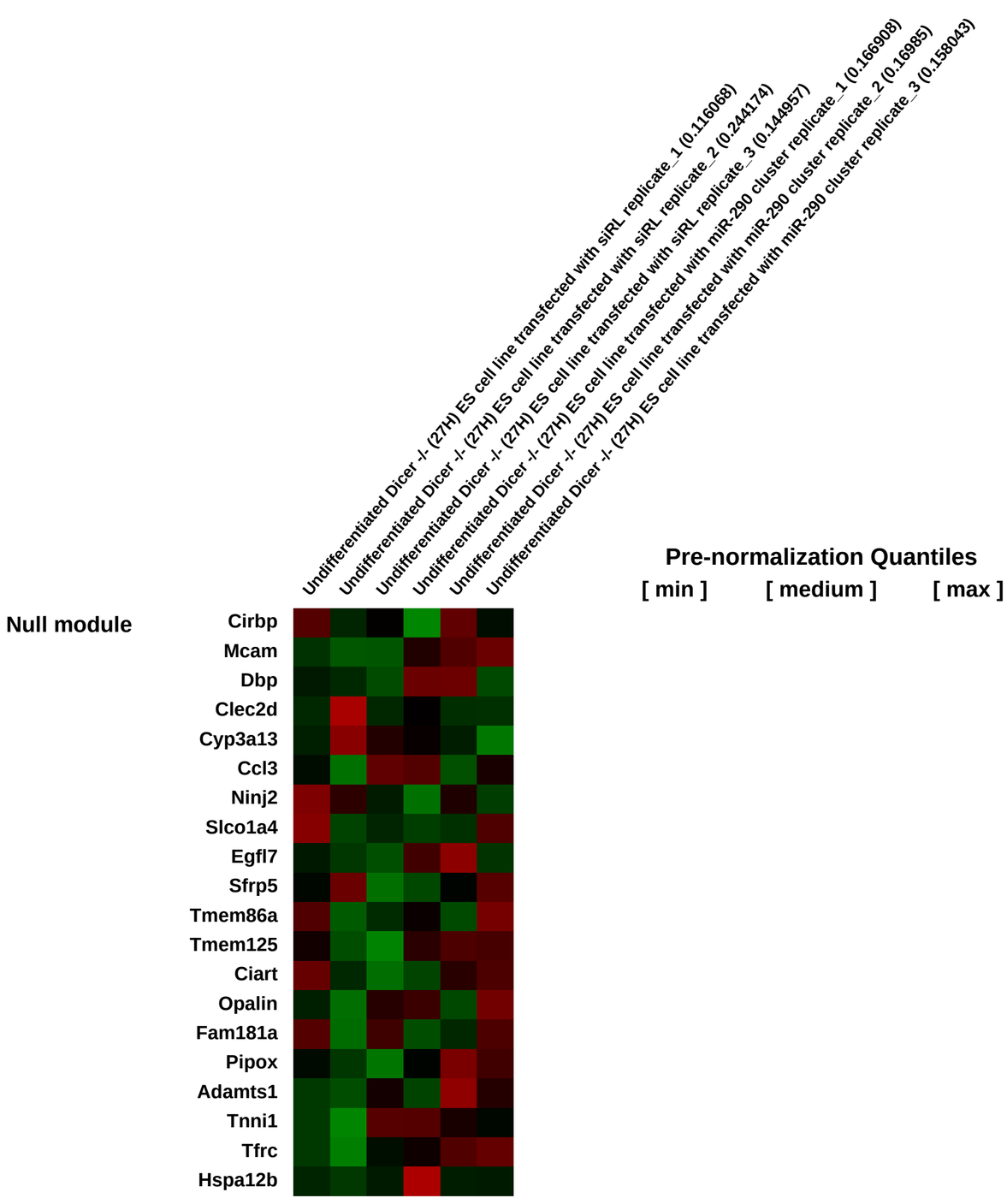

GEO Series "GSE8512" Expression Profiles

Num of samples in this series: 207

Details of this dataset are not shown due to large number of samples and the page size limit.

Find details in http://www.ncbi.nlm.nih.gov/geo/query/acc.cgi?acc=GSE8512

Background corr dist: KL-Divergence = 0.6663, L1-Distance = 0.0976, L2-Distance = 0.0324, Normal std = 0.1991

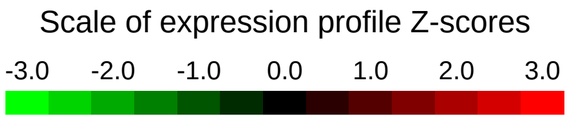

GEO Series "GSE8555" Expression Profiles

Num of samples in this series: 8

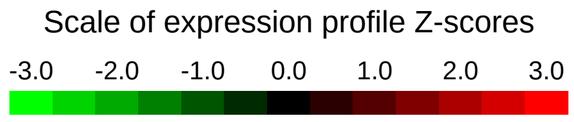

GEO Link:	http://www.ncbi.nlm.nih.gov/geo/query/acc.cgi?acc=GSE8555
Status:	Public on Jul 25 2007
Title:	Genome-wide analysis of Phgdh inactivation in murine embryonic head
Organism:	Mus musculus
Experiment type:	Expression profiling by array
Platform:	GPL1261
Pubmed ID:	18228065
Summary & Design:	**Summary:** **D-3-Phosphoglycerate dehydrogenase (Phgdh; EC 1.1.1.95) is a necessary enzyme for de novo L-serine biosynthesis via the phosphorylated pathway. We demonstrated previously that Phgdh is expressed exclusively by neuroepithelium and radial glia in developing mouse brain and later mainly by astrocytes. Mutations in the human PHGDH gene cause serine deficiency disorders (SDD) associated with severe neurological symptoms such as congenital microcephaly, psychomotor retardation, and intractable seizures. We recently demonstrated that genetically engineered mice, in which the gene for Phgdh has been disrupted, have significantly decreased levels of serine and glycine, and exhibit malformation of brain such as microcephaly. The Phgdh null (KO) embryos exhibit lethal phenotype after gestational day 14, indicating that the phosphorylated pathway is essential for embryogenesis, especially for brain development. It is worth noting that the Phgdh knockout (KO) embryos primarily displayed microcephaly, which is the most conspicuous phenotype of patients with SDD. Thus, Phgdh KO mice are a useful animal model for studying the effect of diminished L-serine levels on development of the central nervous system and other organs. To better understand the mechanism underlying the molecular pathogenesis of SDD, we sought to examine whether gene expression is altered in the Phgdh KO mouse model. We identify genes that have altered expression in the head of the Phgdh KO embryos using the GeneChip array. Some of the genes identified by this method belong in functional categories that are relevant to the biochemical and morphological aberrations of the Phgdh deletion.** **Keywords: genetic modification** **Overall design:** **RNA of 4 biological replicates was hybridized to Affymetrix Mouse Genome 430 2.0 arrays. Five microgram total RNA was labelled according to the ENZO-protocol, fragmented and hybridized according to Affymetrix's protocols.**

Background corr dist: **KL-Divergence = 0.0229, L1-Distance = 0.0165, L2-Distance = 0.0003, Normal std = 0.6997**

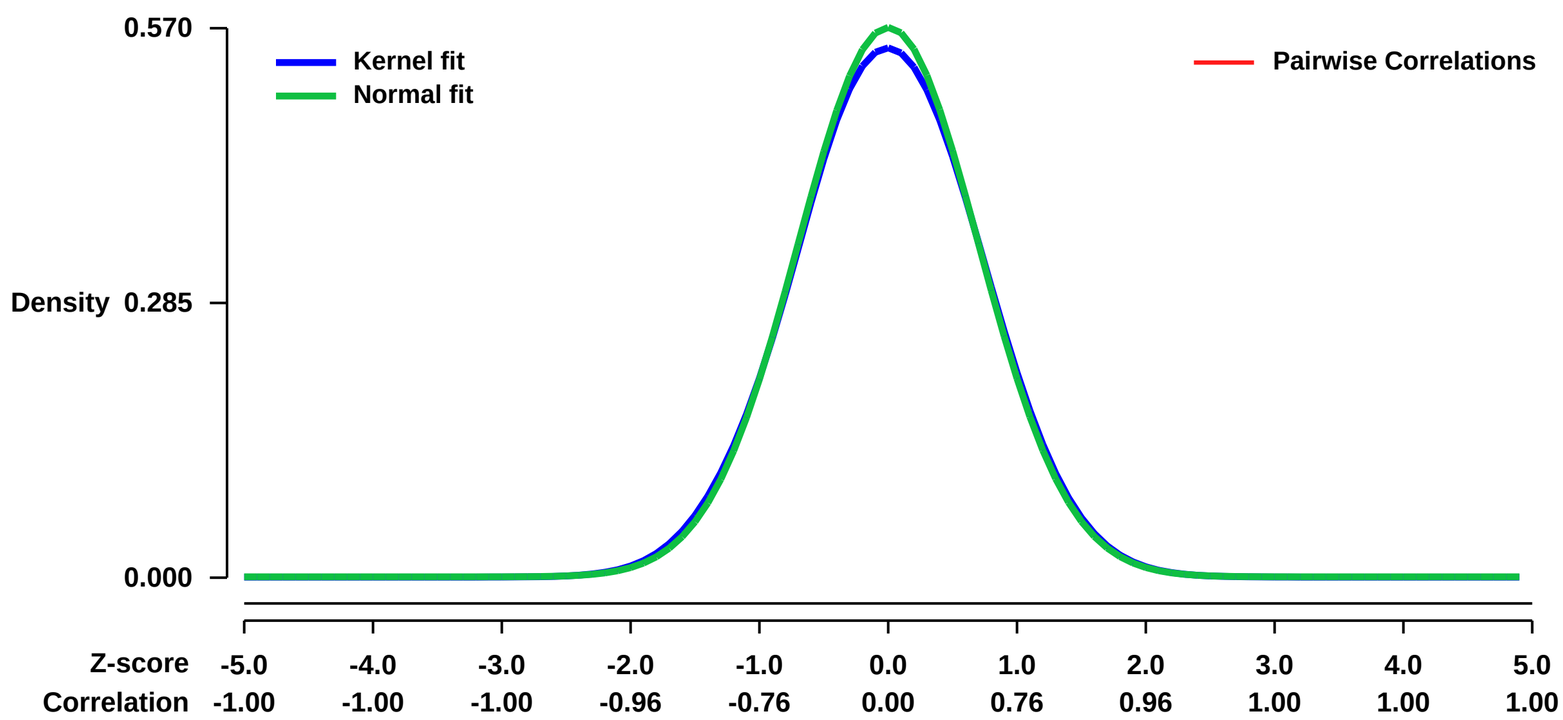

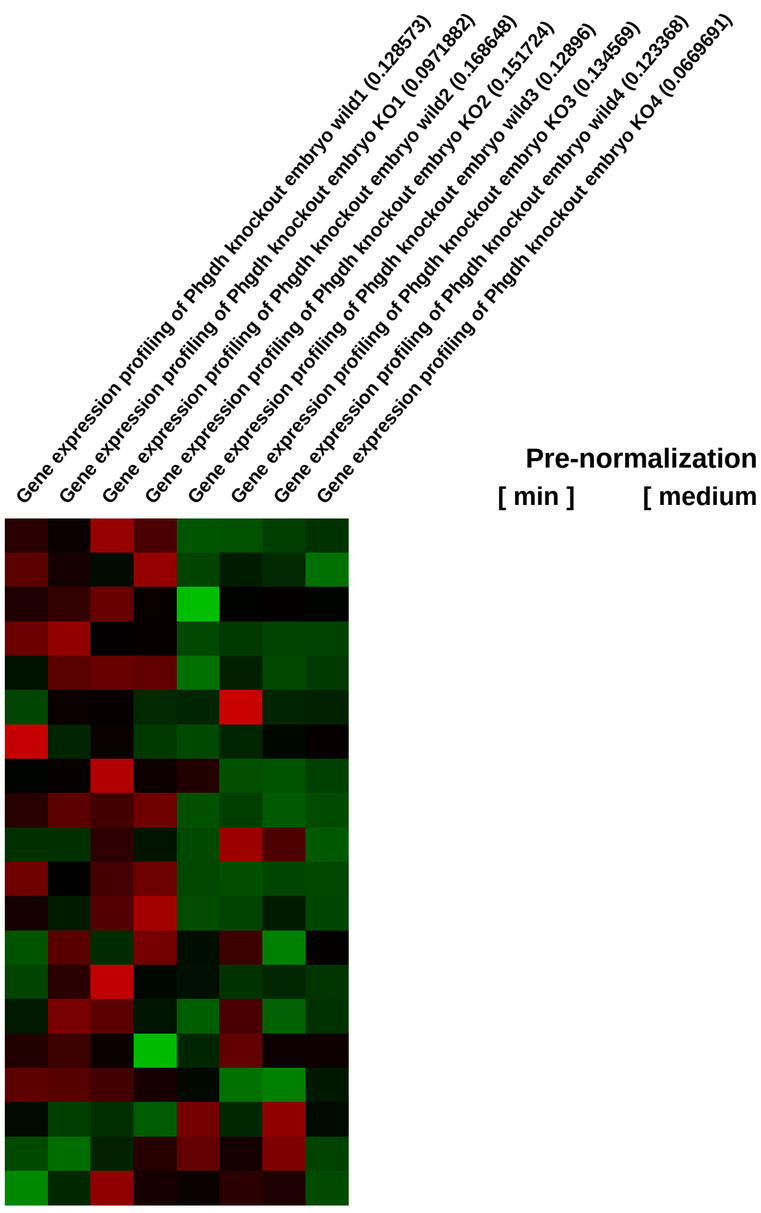

GEO Series "GSE8564" Expression Profiles

Num of samples in this series: 20

Scale of expression profile Z-scores

-3.0 -2.0 -1.0 0.0 1.0 2.0 3.0

GEO Link:	http://www.ncbi.nlm.nih.gov/geo/query/acc.cgi?acc=GSE8564
Status:	Public on Jul 22 2008
Title:	Analysis of Aire effects on individual mice of different genetic backgrounds
Organism:	Mus musculus
Experiment type:	Expression profiling by array
Platform:	GPL1261
Pubmed ID:	18838677
Summary & Design:	**Summary:** We compared gene expression profiles of aire-deficient and wild-type littermate thymic medullary epithelial cells. This was done in order to determine whether Aire's effects differed among strains, and also among individuals of the same strain. **Keywords: genetic modification** **Overall design:** Individual thymi were digested with collagenase, dispase and DNAse, and meduallary epithelial cells with the phenotype CD45-G8.8+Ly51intMHCclasssIIhi were isolated by FACS.

Background corr dist: KL-Divergence = 0.1413, L1-Distance = 0.0434, L2-Distance = 0.0041, Normal std = 0.3817

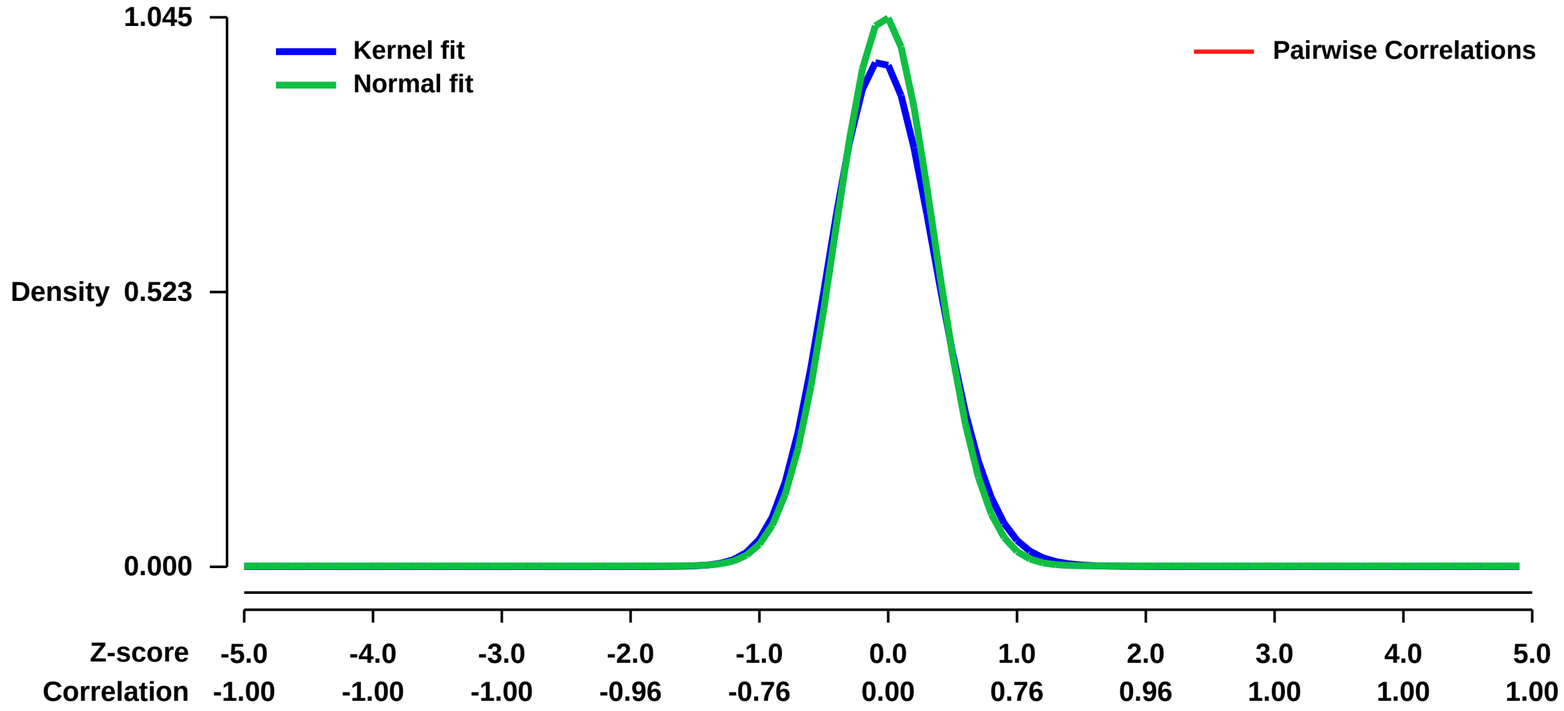

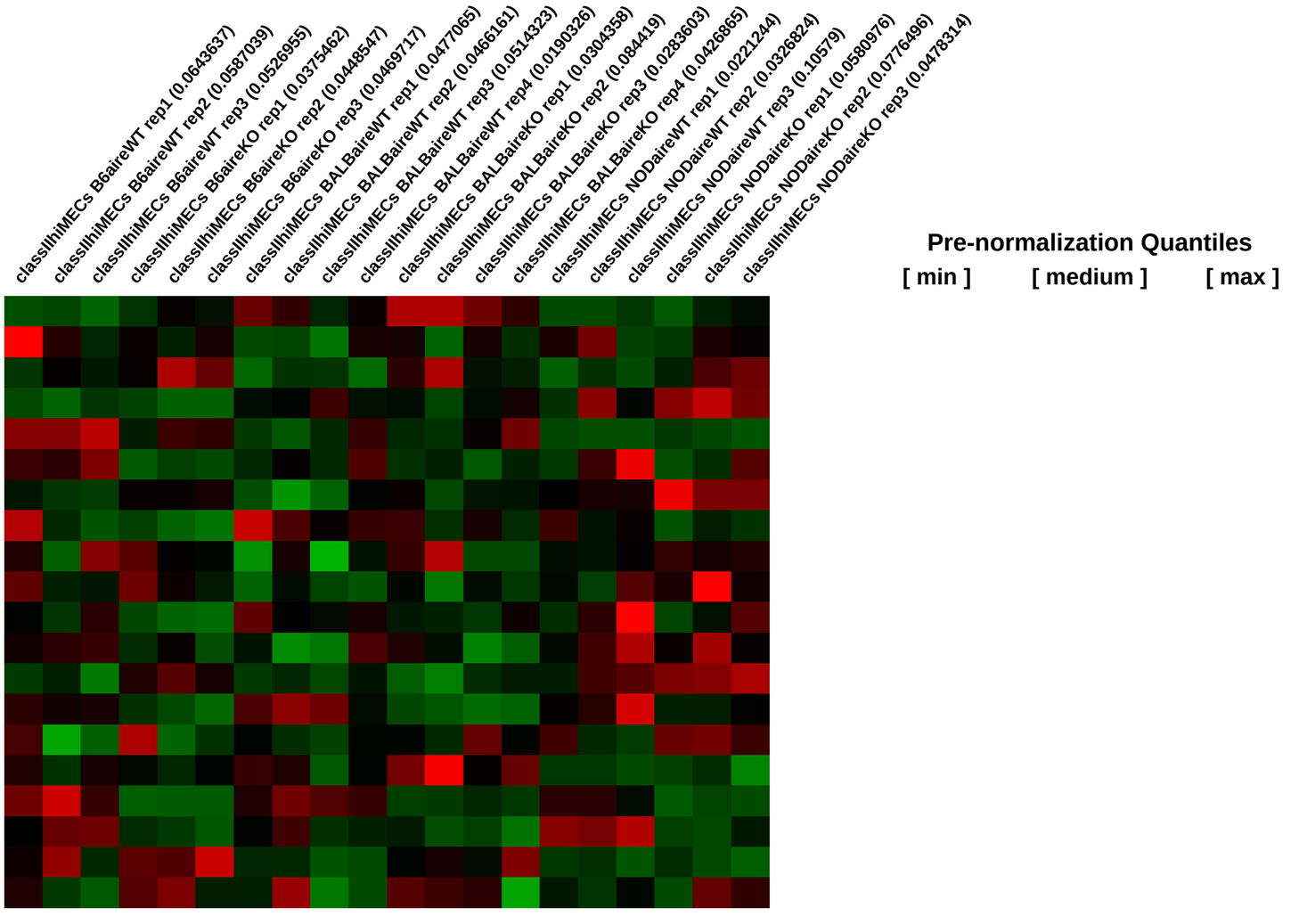

GEO Series "GSE8621" Expression Profiles

Num of samples in this series: 12

Scale of expression profile Z-scores

-3.0 -2.0 -1.0 0.0 1.0 2.0 3.0

GEO Link:	http://www.ncbi.nlm.nih.gov/geo/query/acc.cgi?acc=GSE8621
Status:	Public on Aug 10 2007
Title:	LPS tolerance in macrophages
Organism:	Mus musculus
Experiment type:	Expression profiling by array
Platform:	GPL1261
Pubmed ID:	18086374
Summary & Design:	**Summary:** Among the multiple mechanisms that control the intensity and duration of macrophage activation, the development of a state of refractoriness to a second stimulation in cells treated with LPS has long been recognized. Release of inhibitory cytokines and alterations in intracellular signaling pathways may be involved in the development of LPS tolerance. Although a number of molecules have been implicated, a detailed picture of the molecular changes in LPS tolerance is still missing. We have used a genome-wide gene expression analysis approach to (i) define which fraction of LPS target genes are subject to tolerance induction and (ii) identify genes that are expressed at high levels in tolerant macrophages. Our data show that in LPS tolerant macrophages the vast majority of LPS-induced gene expression is abrogated. The extent of tolerance induction varies for individual genes, and a small subset appears to be excepted. Compared to other negative control mechanisms of macrophages, e.g. IL-10-induced deactivation, LPS-tolerance inhibits a much wider range of transcriptional targets. Some previously described negative regulators of TLR-signaling (e.g. IRAK-M) were confirmed as expressed at higher levels in LPS-tolerant macrophages. In addition, we discuss other potential players in LPS tolerance identified in this group of genes. **Keywords:** pre and restimulation with LPS, tolerance induction **Overall design:** Cells were either prestimulated (1_X) or not (0_X) for 18h with 100 ng/ml LPS. Media was exchanged and after 2h rest, cells either restimulated (X_1) or not (X_0) with again 100 ng/ml LPS. This resulted in 4 experimental conditions: 0_0, 0_1, 1_0 and 1_1. There were 3 biological replicates done, resulting in 12 arrays altogether.

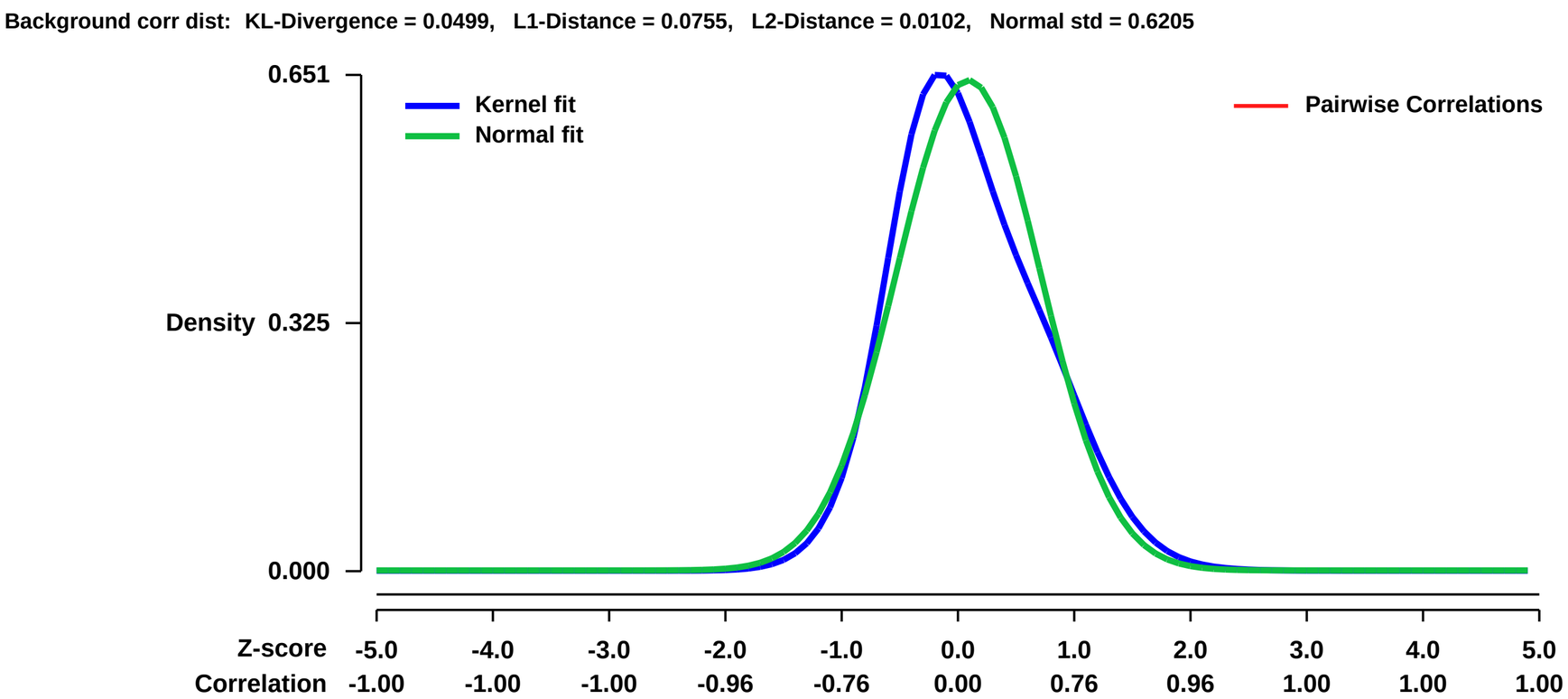

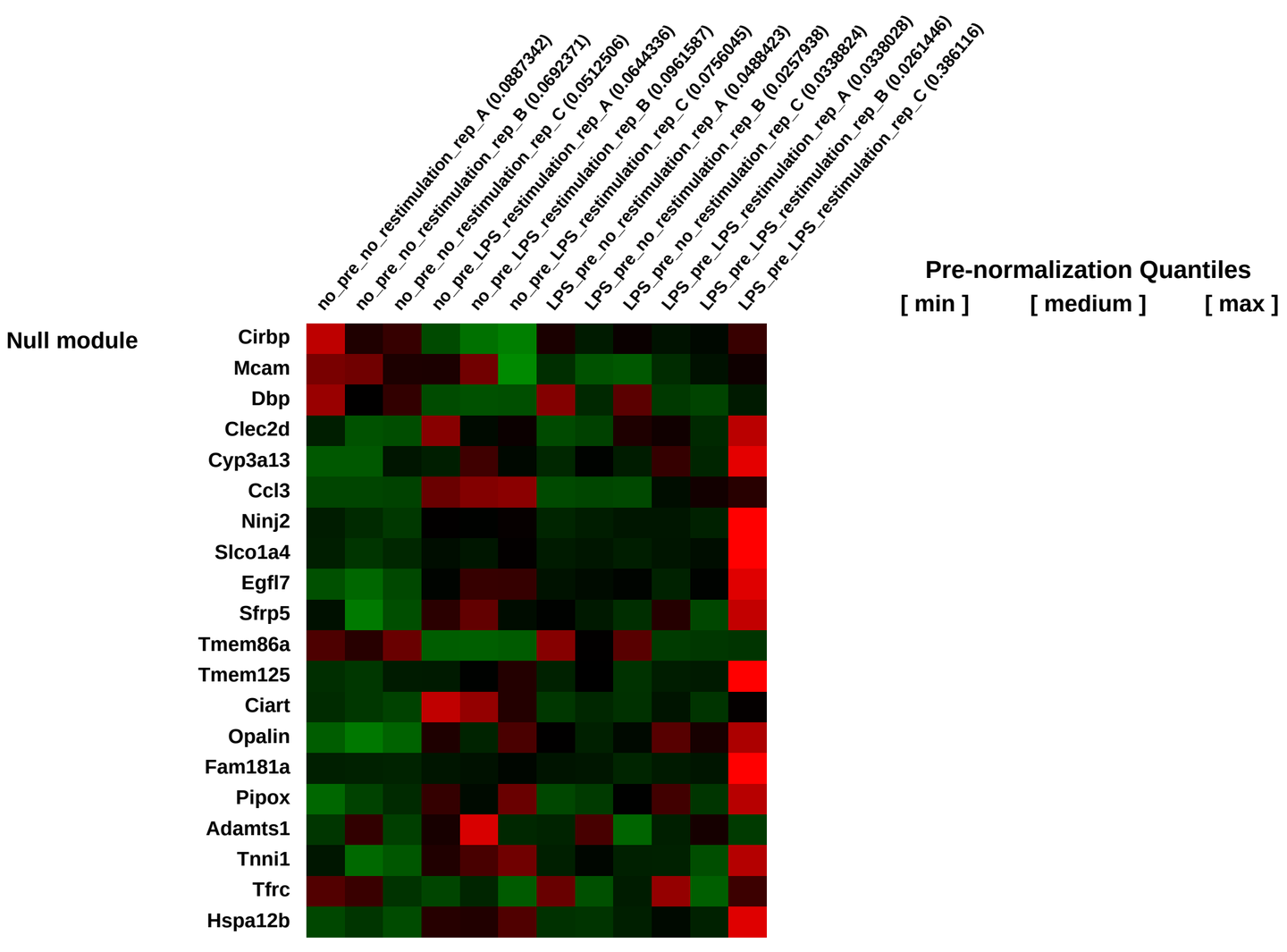

GEO Series "GSE8660" Expression Profiles

Num of samples in this series: 6

Scale of expression profile Z-scores

-3.0 -2.0 -1.0 0.0 1.0 2.0 3.0

GEO Link:	http://www.ncbi.nlm.nih.gov/geo/query/acc.cgi?acc=GSE8660
Status:	Public on Aug 01 2008
Title:	C-terminal diversity within the p53 family accounts for differences in DNA binding and transcriptional activity
Organism:	Mus musculus
Experiment type:	Expression profiling by array
Platform:	GPL1261
Pubmed ID:	18267967
Summary & Design:	**Summary:** The p53 family is known as a family of transcription factors with functions in tumor suppression and development. Whereas the central DNA binding domain is highly conserved among the three family members p53, p63 and p73, the C-terminal domains (CTDs) are diverse and subject to alternative splicing and post-translational modification. Here we demonstrate that the CTDs strongly influence DNA binding and transcriptional activity. While p53 and the p73 isoform p73gamma have basic CTDs and form weak sequence-specific protein-DNA complexes, the major p73 isoforms alpha, beta and delta have neutral CTDs and bind DNA strongly. A basic CTD has been previously shown to enable sliding along the DNA backbone and to facilitate the search for binding sites in the complex genome. Our experiments, however, reveal that a basic CTD also reduces protein-DNA complex stability, intranuclear mobility, promoter occupancy in vivo, transgene activation and induction of cell cycle arrest or apoptosis. A basic CTD in p53 and p73gamma therefore provides both positive and negative regulatory functions presumably to enable rapid switching of protein activity in response to stress. In contrast, most p73 isoforms exhibit constitutive DNA binding activity consistent with a predominant role in developmental control. **Keywords:** Adenoviros, p73 / p53 **Overall design:** Infection of H1299 cell with different p73/p53 constructs by adenoviral system

Background corr dist: KL-Divergence = 0.0374, L1-Distance = 0.0263, L2-Distance = 0.0008, Normal std = 0.6403

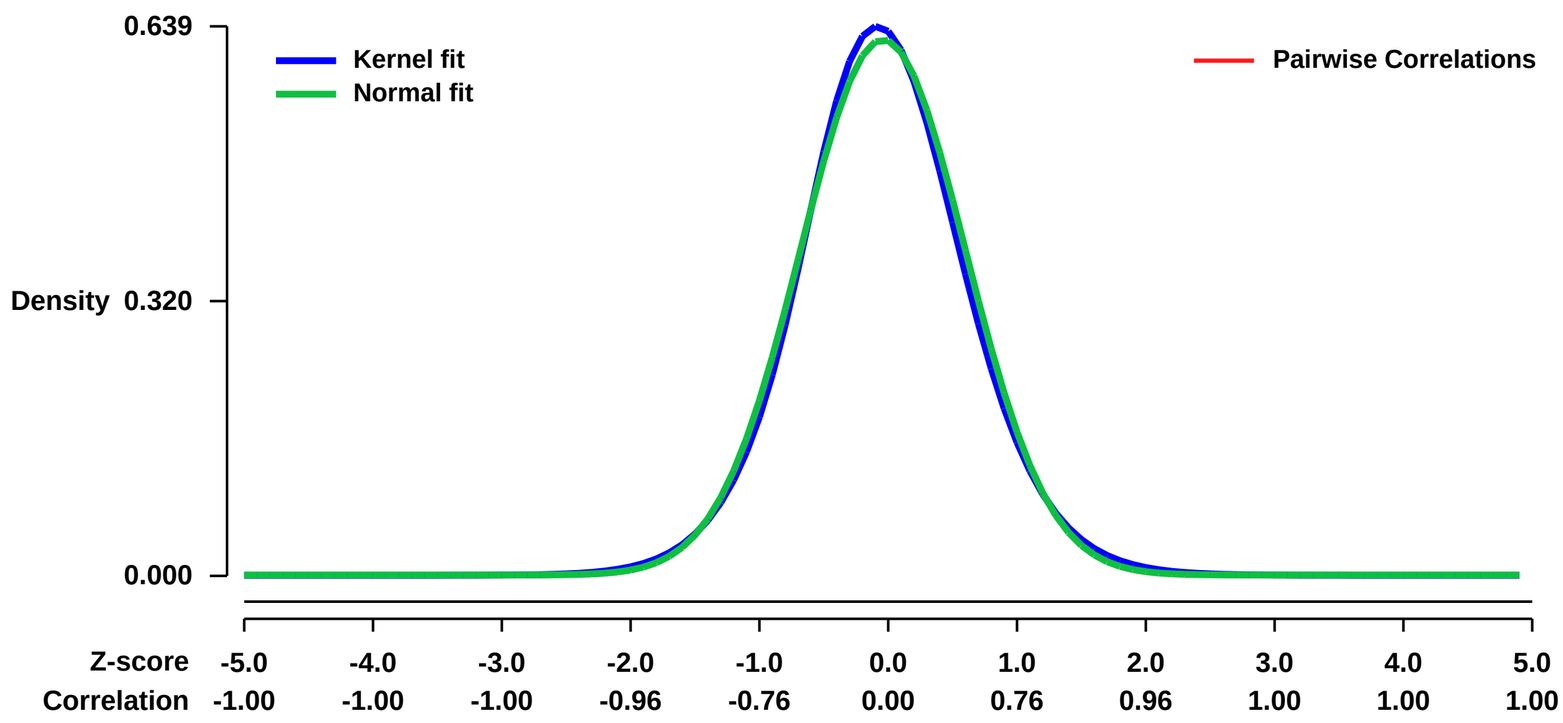

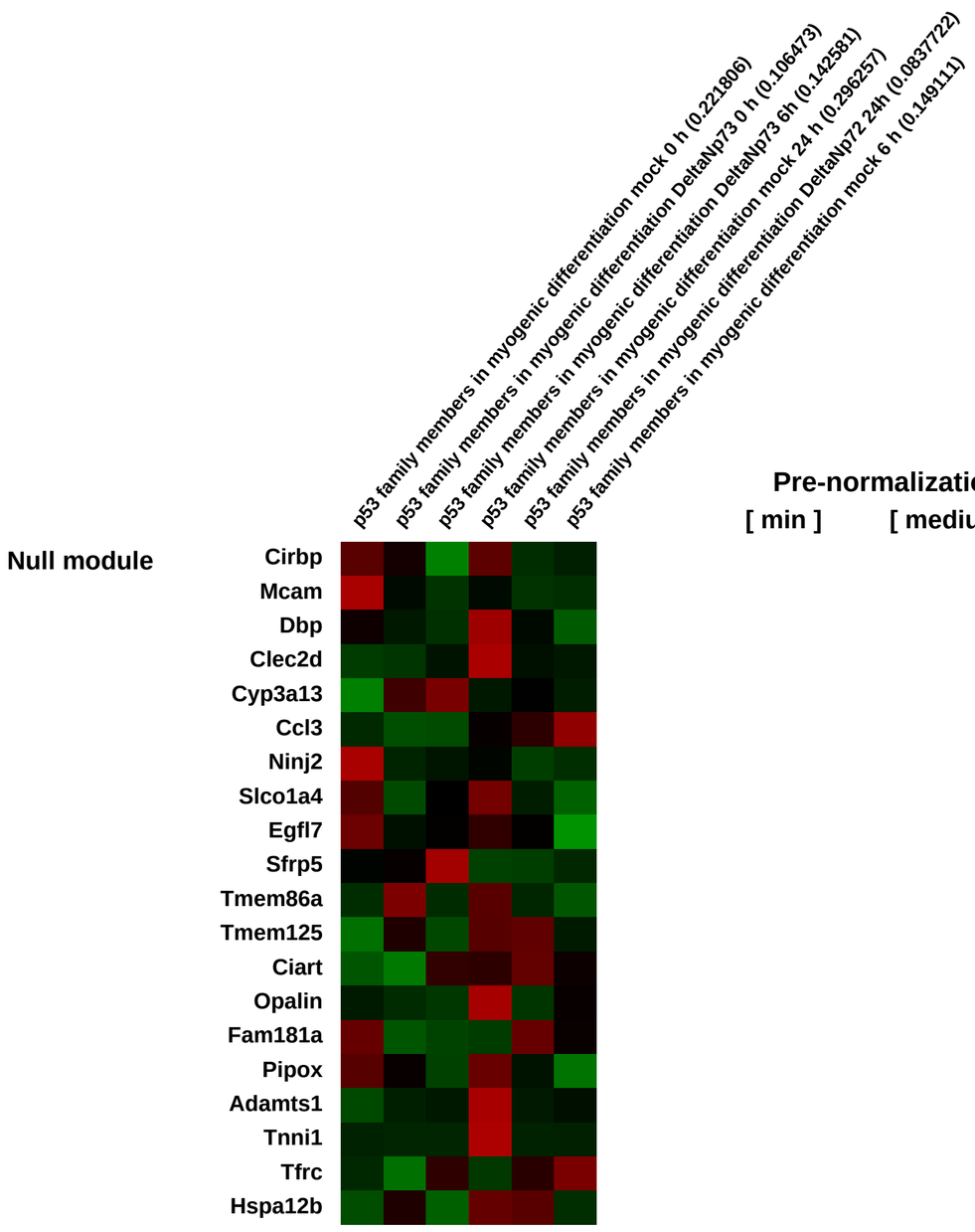

GEO Series "GSE8678" Expression Profiles

Num of samples in this series: 6

Scale of expression profile Z-scores

-3.0 -2.0 -1.0 0.0 1.0 2.0 3.0

GEO Link:	http://www.ncbi.nlm.nih.gov/geo/query/acc.cgi?acc=GSE8678
Status:	Public on Aug 23 2007
Title:	Gene expression data from sorted IL-7Rhi/lo effector CD8 T cells on day 6/7 after LCMV armstrong infection
Organism:	Mus musculus
Experiment type:	Expression profiling by array
Platform:	GPL1261
Pubmed ID:	20921525
Summary & Design:	**Summary:** At the peak of the CD8 T cell response to acture viral and bacterial infections, expression of the Interleukin-7 Receptor (IL-7R) marks Memory Precursor Effector CD8 T Cells (MPECs) from other Short-Lived Effector CD8 T cells (SLECs), which are IL-7Rlo. This study was designed to determine the gene expression differences between these two subsets of effector CD8 T cells. **Keywords: expression comparison** **Overall design:** This study compared IL-7Rhi and IL-7Rlo LCMV-specific P14 Transgenic CD8 T cells, sorted from LCMV armstrong infected recipient mice 6/7 days after infection. Data includes 3 independent replicates for the IL-7Rhi and IL-7Rlo groups.

Background corr dist: KL-Divergence = 0.0428, L1-Distance = 0.0228, L2-Distance = 0.0006, Normal std = 0.6086

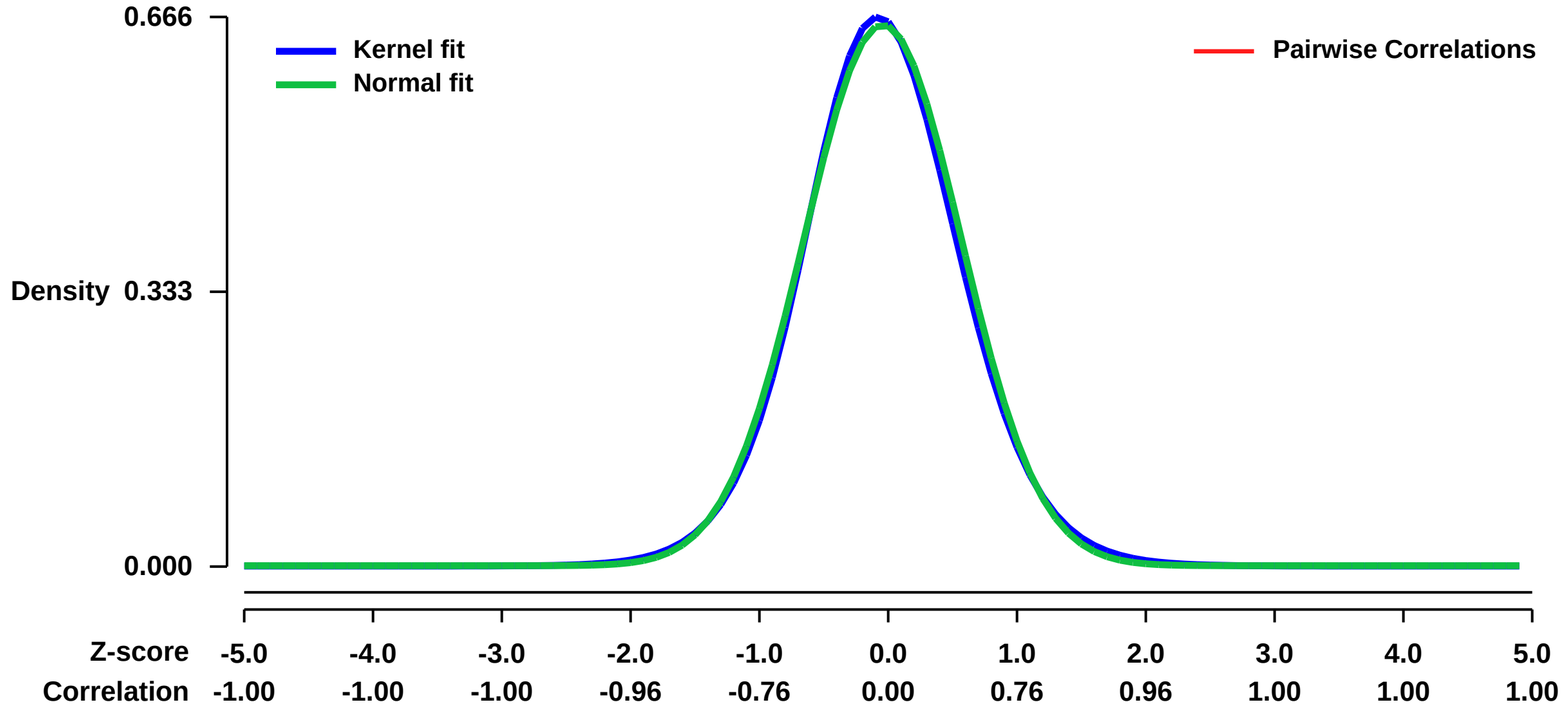

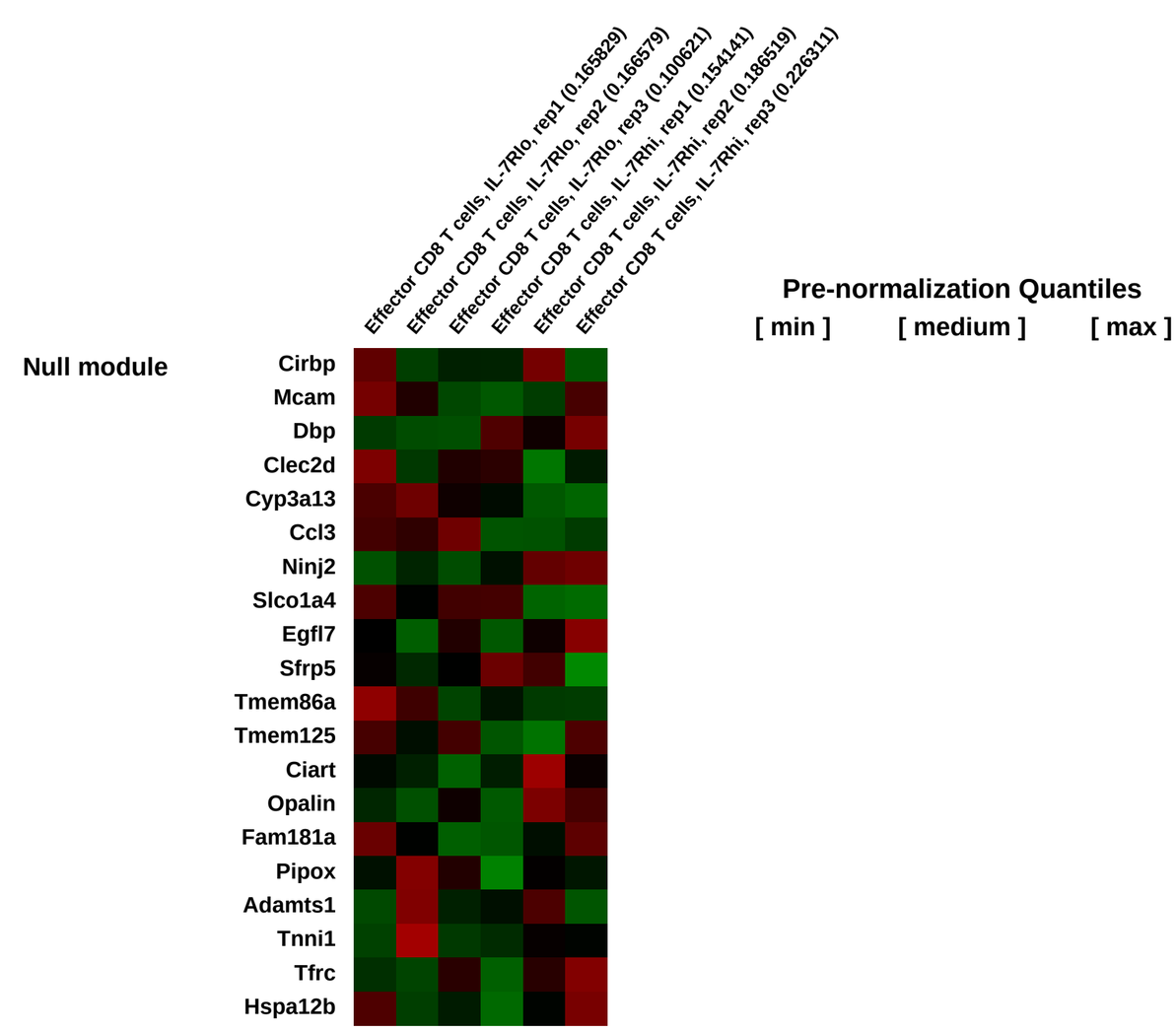

GEO Series "GSE8679" Expression Profiles

Num of samples in this series: 12

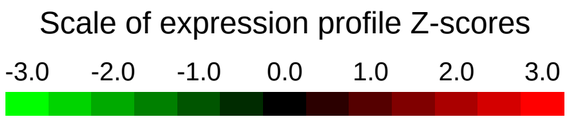

GEO Link:	http://www.ncbi.nlm.nih.gov/geo/query/acc.cgi?acc=GSE8679
Status:	Public on Jan 11 2008
Title:	Gene expression in mouse white adipose tissue
Organism:	Mus musculus
Experiment type:	Expression profiling by array
Platform:	GPL1261
Pubmed ID:	17878318
Summary & Design:	**Summary:** Trans-10, Cis-12 conjugated linoleic acid (t10c12 CLA) causes fat loss in mouse white adipose tissue (WAT). The early transcriptome changes in WAT were analyzed using high-density microarrays to better characterize the signaling pathways responding to t10c12 CLA. Their gene expression responses between 4 to 24 hr after treatment showed a common set of early gene expression changes indicative of an integrated stress response (ISR). **Keywords: control/treatment time course** **Overall design:** Mouse WAT RNA for each time point was isolated from two control and two treatment samples for analysis on four microarrays. The two control and two treatment samples consisted of RP tissues from 5 pooled mice for each sample, requiring a total of twenty mice for the four samples taken at each time point.

Background corr dist: KL-Divergence = 0.1214, L1-Distance = 0.0366, L2-Distance = 0.0027, Normal std = 0.4127

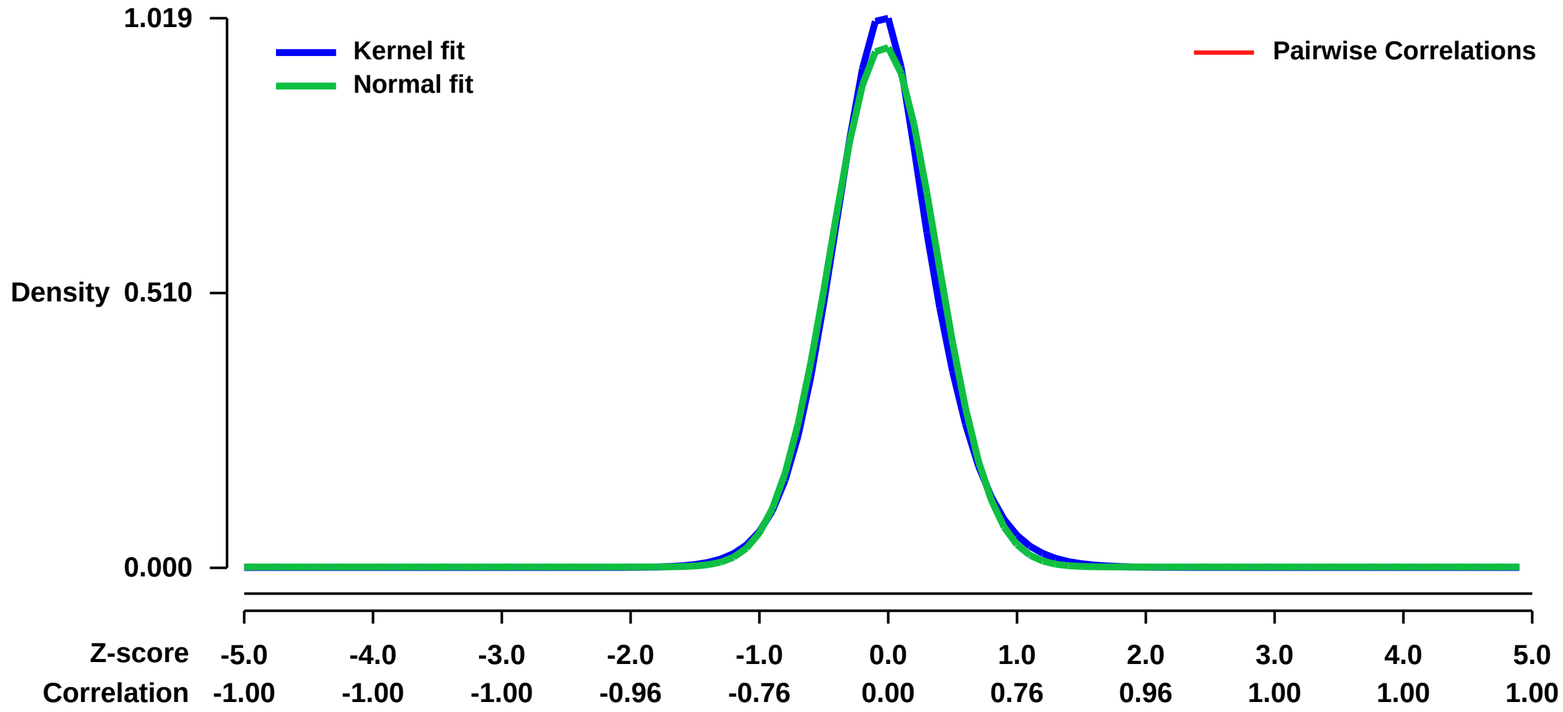

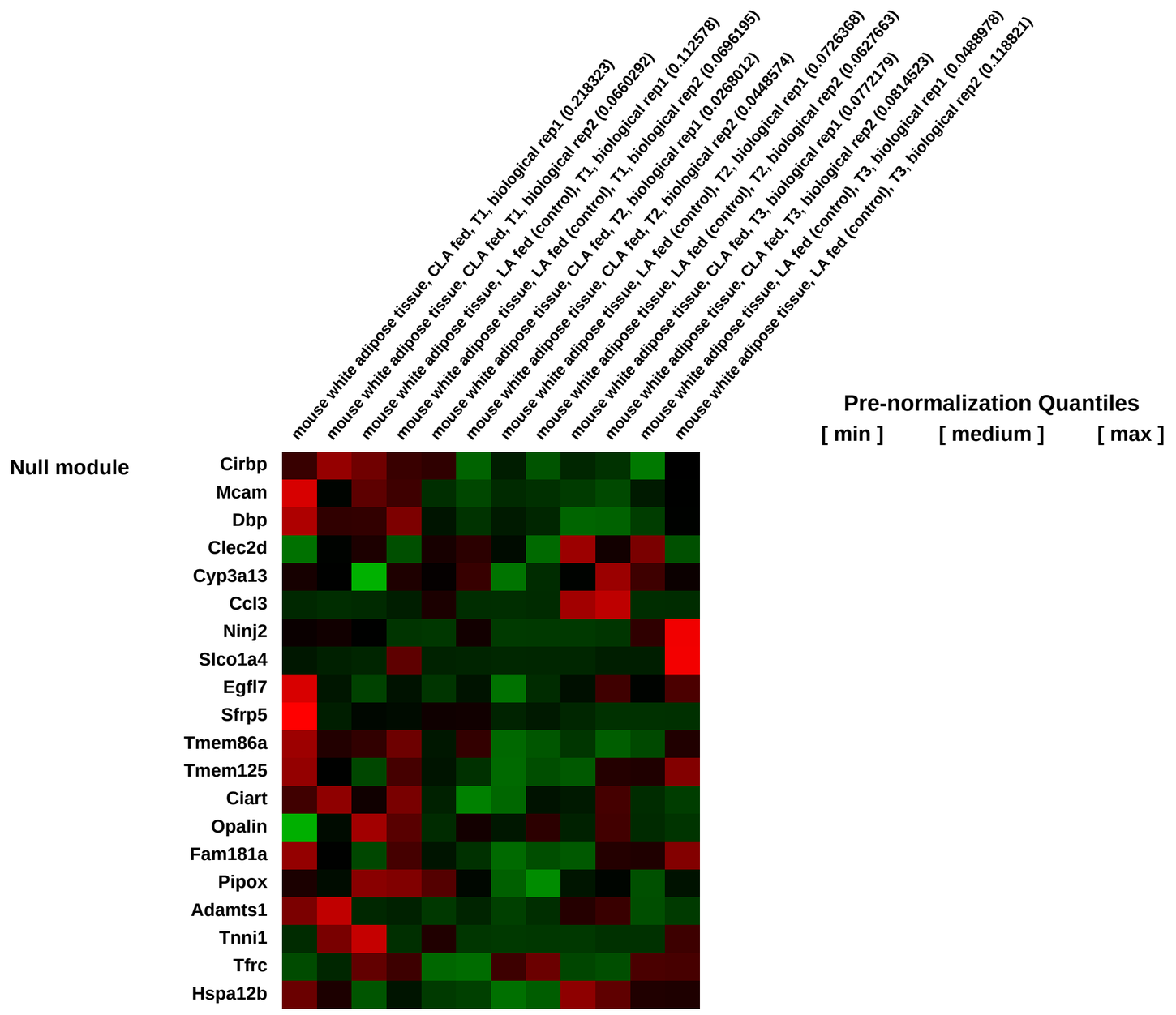

GEO Series "GSE8681" Expression Profiles

Num of samples in this series: 25

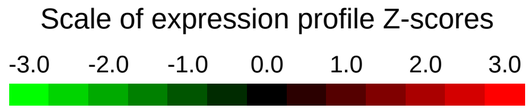

GEO Link:	http://www.ncbi.nlm.nih.gov/geo/query/acc.cgi?acc=GSE8681
Status:	Public on Jan 11 2008
Title:	Gene expression in mouse 3T3-L1 adipocyte tissue culture treated with CLA
Organism:	Mus musculus
Experiment type:	Expression profiling by array
Platform:	GPL1261
Pubmed ID:	17878318
Summary & Design:	**Summary:** Trans-10, Cis-12 conjugated linoleic acid (t10c12 CLA) causes fat loss in mouse 3T3-L1 adipocyte tissue culture. The early transcriptome changes were analyzed using high-density microarrays to better characterize the signaling pathways responding to t10c12 CLA. Their gene expression responses between 4 to 24 hr after treatment showed a common set of early gene expression changes indicative of an integrated stress response (ISR). **Keywords: control/treatment time course** **Overall design:** Mouse 3T3-L1 RNA for each time point was isolated from control and treatment samples for analysis on microarrays with two to four biological reps.

Background corr dist: KL-Divergence = 0.1410, L1-Distance = 0.0407, L2-Distance = 0.0032, Normal std = 0.3886

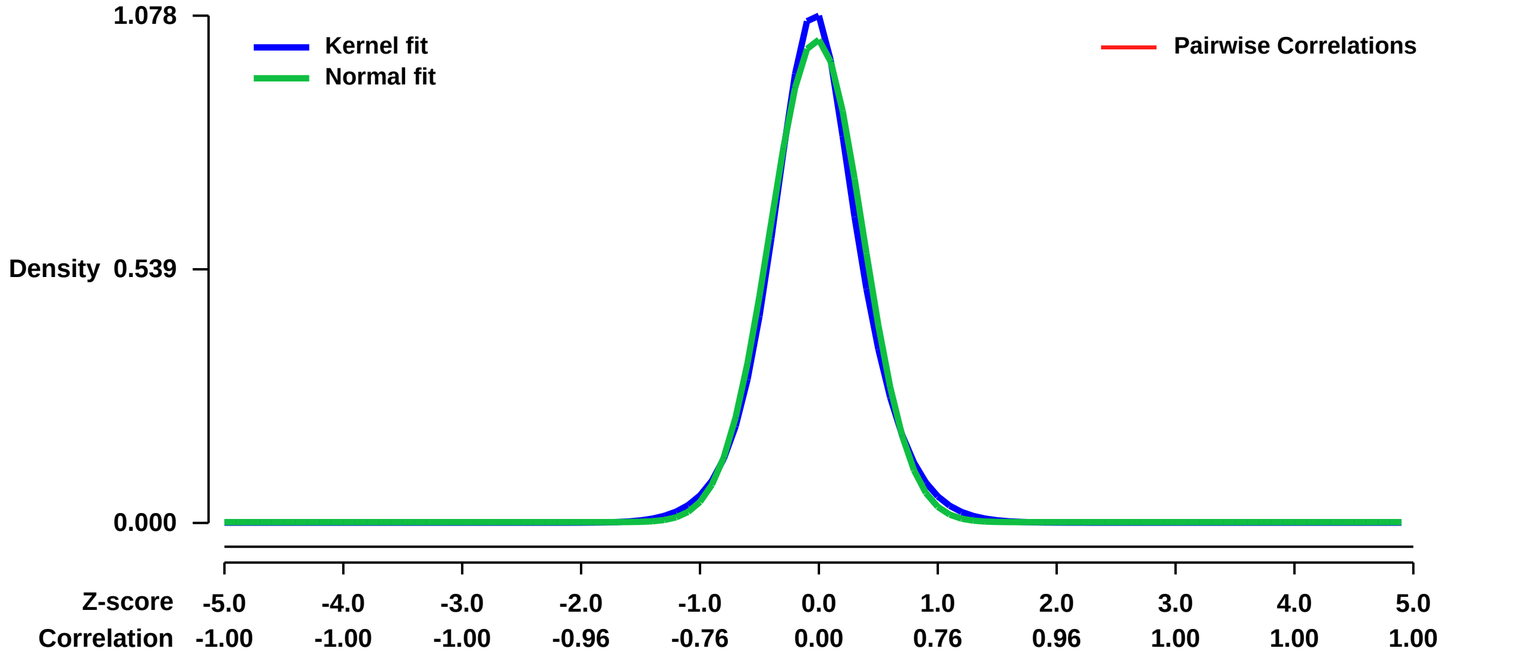

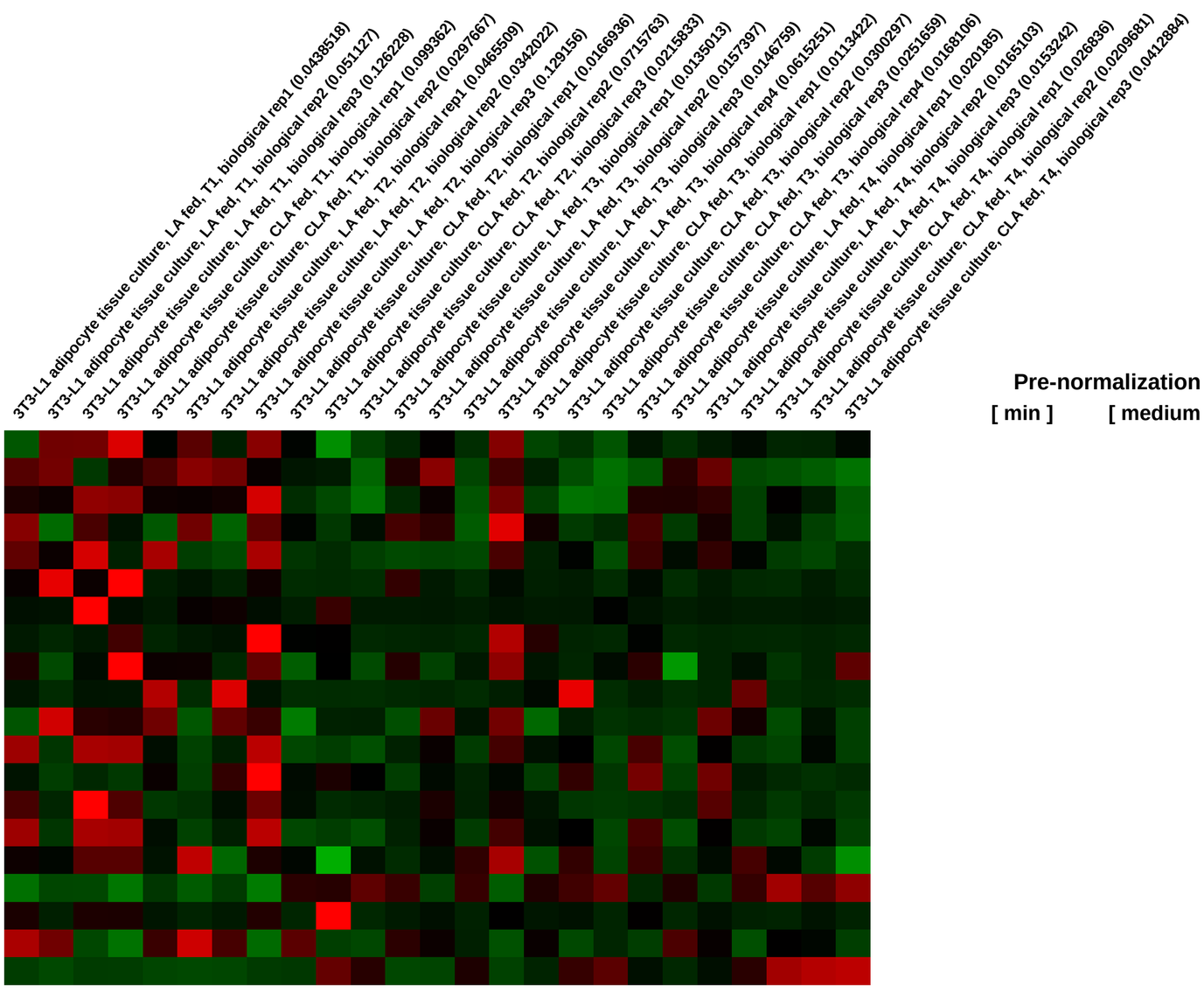

GEO Series "GSE8682" Expression Profiles

Num of samples in this series: 8

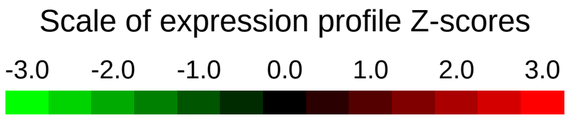

GEO Link:	http://www.ncbi.nlm.nih.gov/geo/query/acc.cgi?acc=GSE8682
Status:	Public on Jan 11 2008
Title:	Gene expression in mouse 3T3-L1 adipocyte tissue culture treated with tunicamycin
Organism:	Mus musculus
Experiment type:	Expression profiling by array
Platform:	GPL1261
Pubmed ID:	17878318
Summary & Design:	**Summary:** Tunycamcin induces UPR/ISR and Inflammation in mouse 3T3-L1 adipocyte tissue culture. The early transcriptome changes were analyzed using high-density microarrays to better characterize the signaling pathways responding to tunicamycin, to be compared with similar experiments with CLA as the treatment. Their gene expression responses between 4 to 12 hr after treatment showed a common set of early gene expression changes indicative of a UPR/Inflammation stress response. **Keywords: control/treatment time course** **Overall design:** Mouse 3T3-L1 RNA for each time point was isolated from control and treatment samples for analysis on microarrays with two biological reps.

Background corr dist: KL-Divergence = 0.0724, L1-Distance = 0.0702, L2-Distance = 0.0125, Normal std = 0.5281

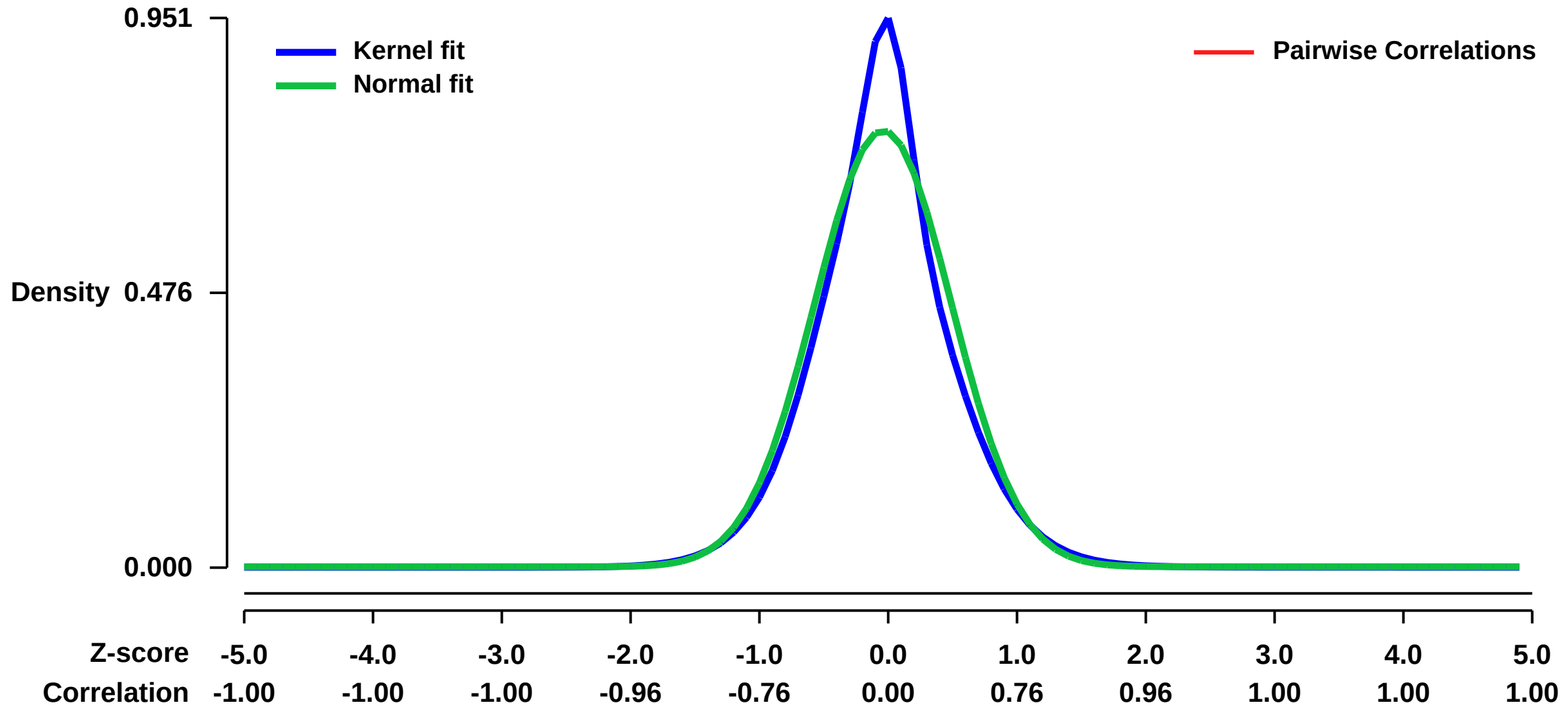

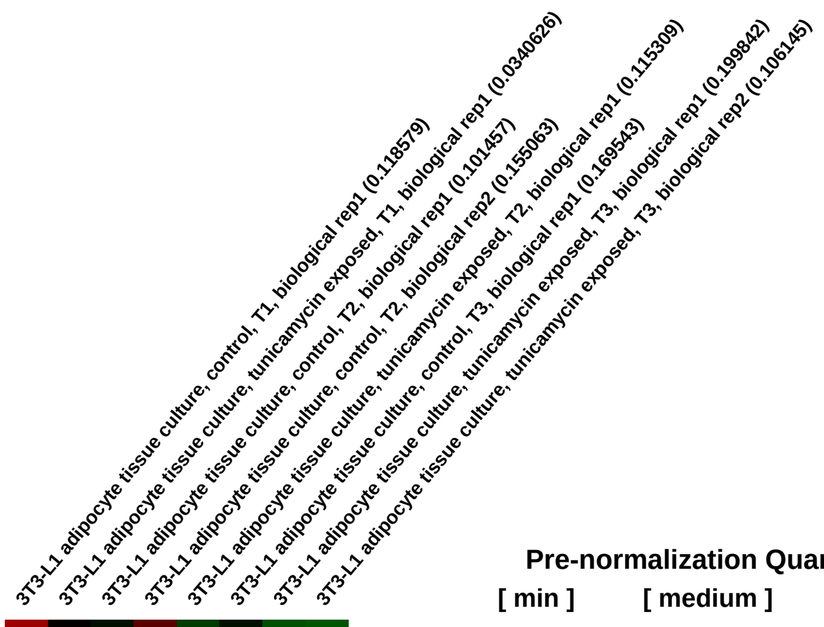

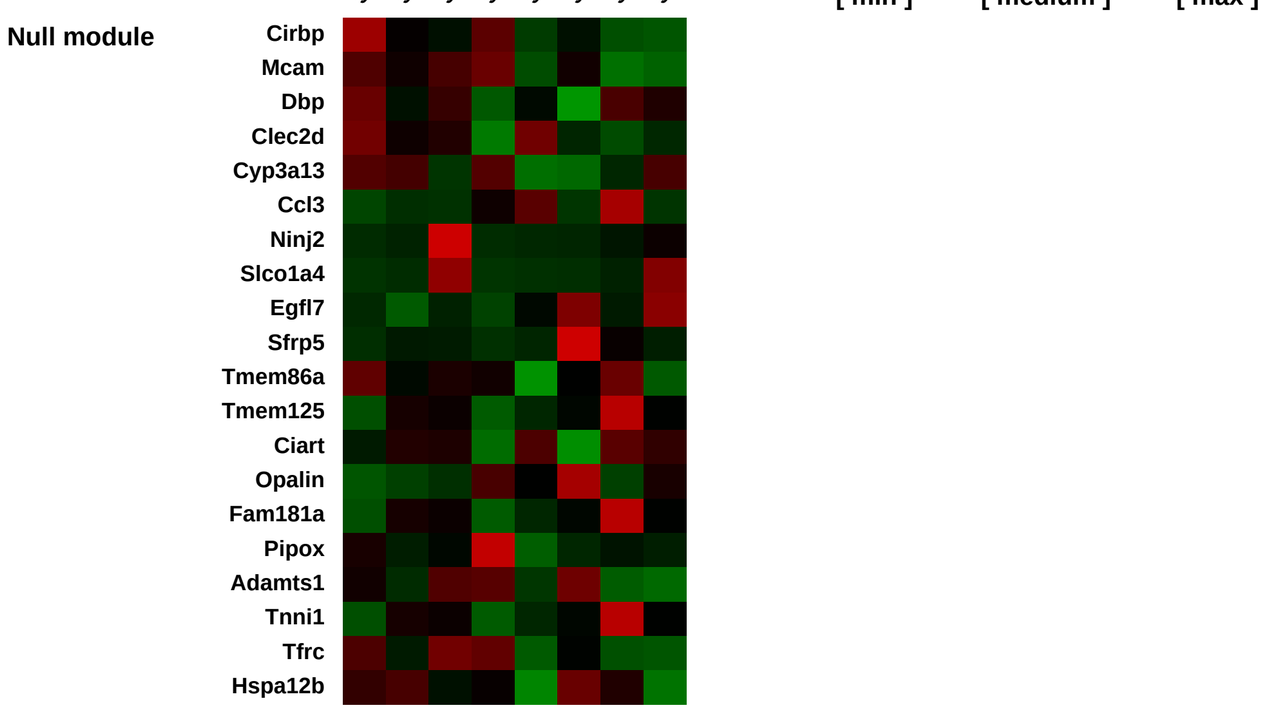

GEO Series "GSE8683" Expression Profiles

Num of samples in this series: 11

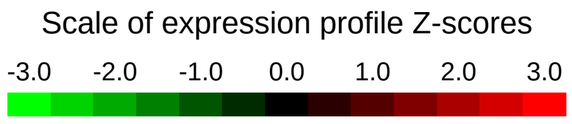

GEO Link:	**http://www.ncbi.nlm.nih.gov/geo/query/acc.cgi?acc=GSE8683**
Status:	**Public on Jan 11 2008**
Title:	**Gene expression in 3T3-L1 mouse tissue (preadipocytes) treated with Trans-10,Cis-12 conjugated linoleic acid(t10c12 CLA)**
Organism:	**Mus musculus**
Experiment type:	**Expression profiling by array**
Platform:	**GPL1261**
Pubmed ID:	**17878318**
Summary & Design:	**Summary:** **Trans-10, Cis-12 conjugated linoleic acid (t10c12 CLA) causes fat loss in mouse white adipose tissue (WAT) and 3T3-L1 adipocyte tissue culture; however in preadipocyte tissue (this series) the UPS/ISR and fat loss is not detected. The early transcriptome changes in 3T3-L1 preadipocyte tissue culture were analyzed using high-density microarrays to better characterize the signaling pathways responding to t10c12 CLA. Their gene expression responses between 4 to 12 hr after treatment do not show a set of genes indicative of an integrated stress response (ISR).** **Keywords: control/treatment time course** **Overall design:** **Mouse 3T3-L1 RNA for each time point was isolated from two control (LA) and two treatment (CLA) samples for analysis on four microarrays.**

Background corr dist: **KL-Divergence = 0.0965, L1-Distance = 0.0724, L2-Distance = 0.0128, Normal std = 0.4696**

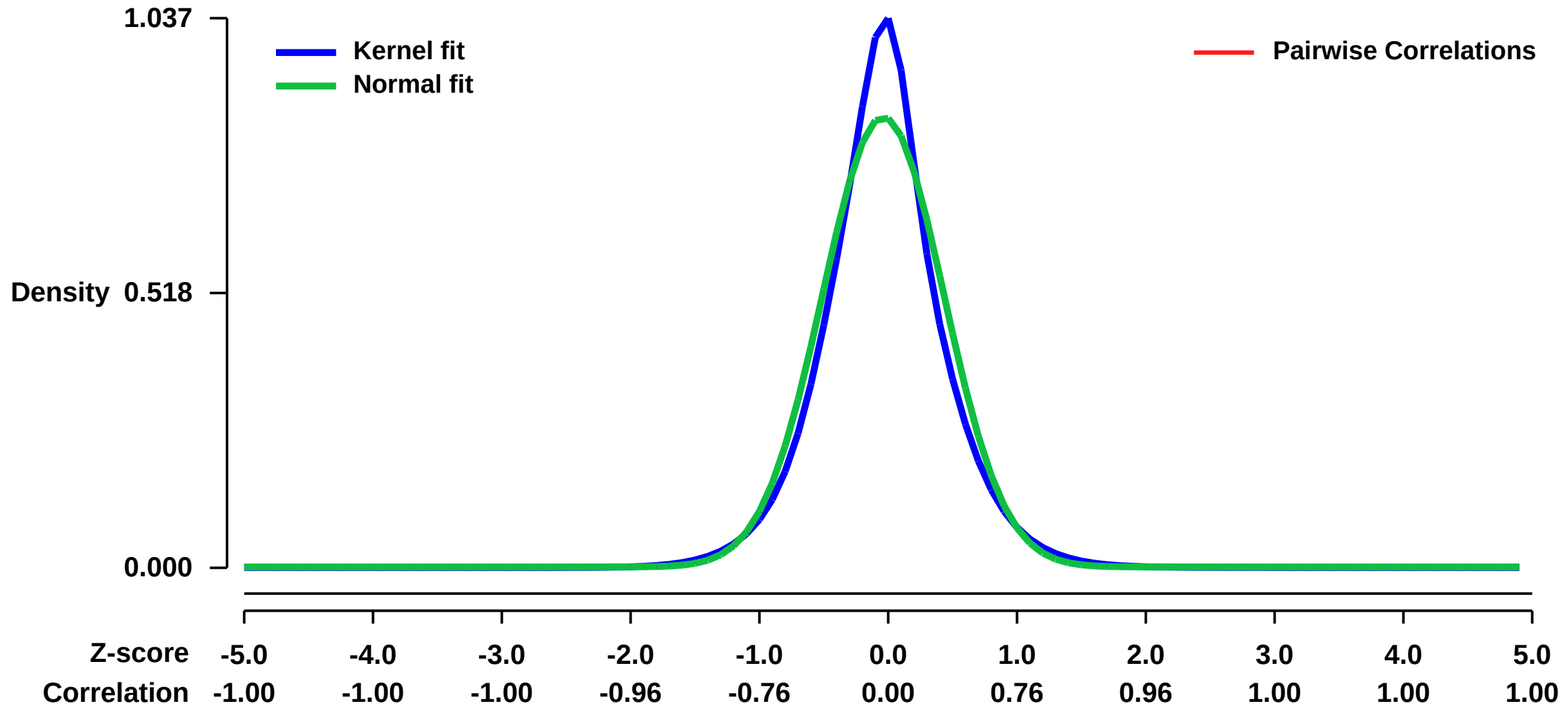

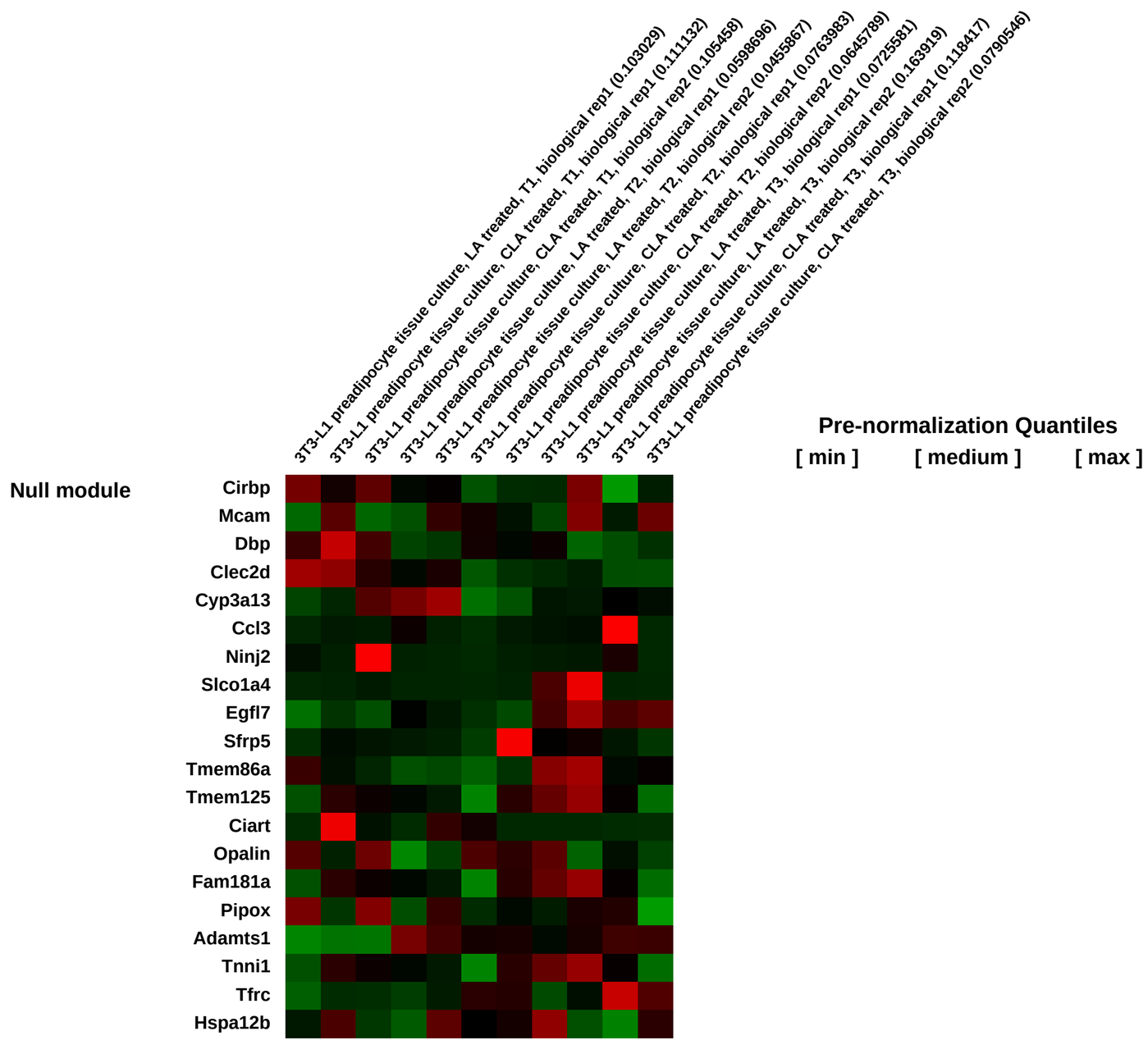

GEO Series "GSE8684" Expression Profiles

Num of samples in this series: 10

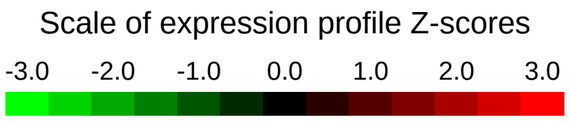

GEO Link:	http://www.ncbi.nlm.nih.gov/geo/query/acc.cgi?acc=GSE8684
Status:	Public on Jan 11 2008
Title:	Gene expression in mouse 3T3-L1 adipocyte tissue culture treated with cis-9,trans-11 conjugated linoleic acid(c9t11 CLA)
Organism:	Mus musculus
Experiment type:	Expression profiling by array
Platform:	GPL1261
Pubmed ID:	17878318
Summary & Design:	**Summary:** Trans-10, Cis-12 conjugated linoleic acid (t10c12 CLA) causes fat loss in mouse 3T3-L1 adipocyte tissue culture; however cis-9, trans-11 CLA does not (this series). The early transcriptome changes were analyzed using high-density microarrays to better characterize the signaling pathways responding to c9t11 CLA. Their gene expression responses between 8 to 12 hr after treatment showed no gene expression changes indicative of an integrated stress response (ISR). **Keywords: control/treatment time course** **Overall design:** Mouse 3T3-L1 RNA for each time point was isolated from control and treatment samples for analysis on microarrays; there are four biological reps for the controls for each timepoint, and only one rep for the treatment.

Background corr dist: KL-Divergence = 0.0618, L1-Distance = 0.0610, L2-Distance = 0.0079, Normal std = 0.5509

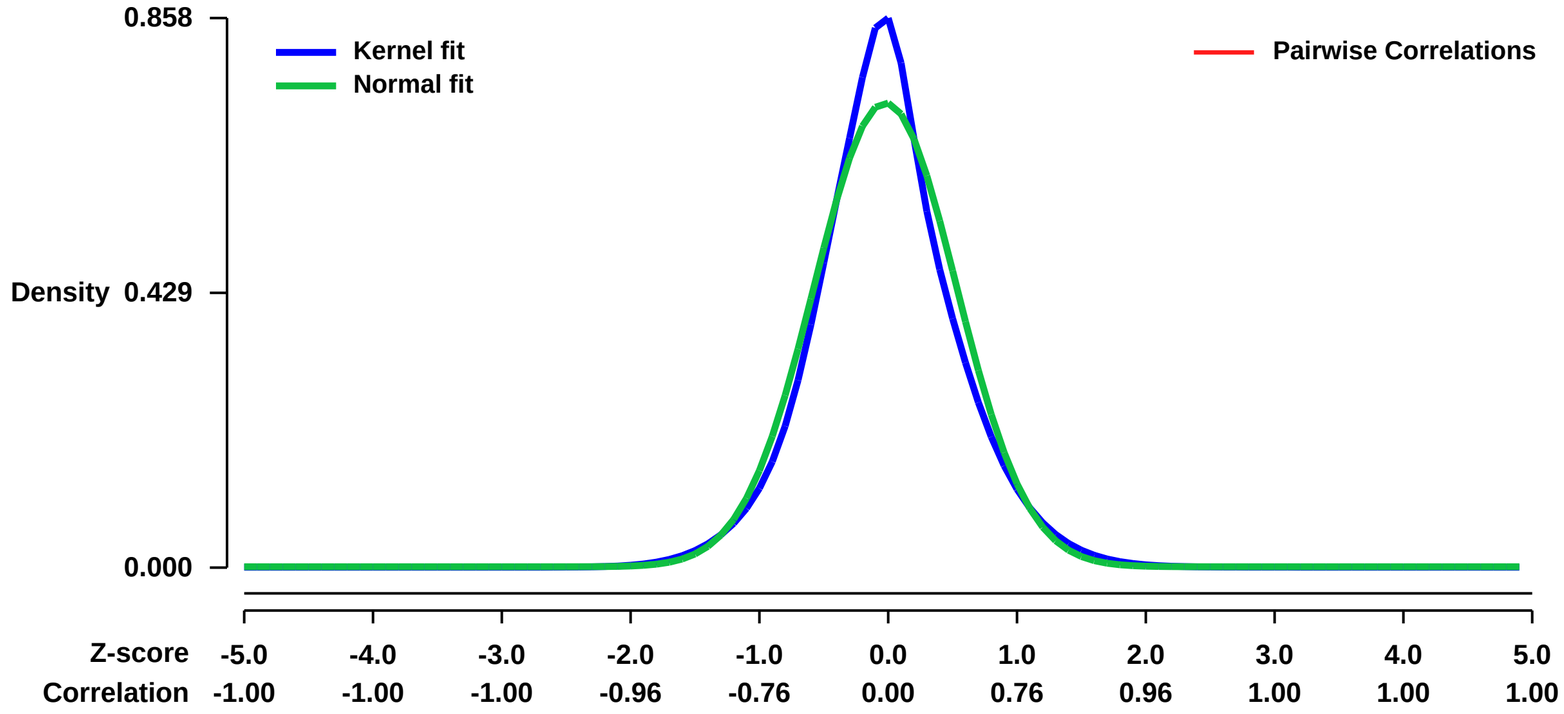

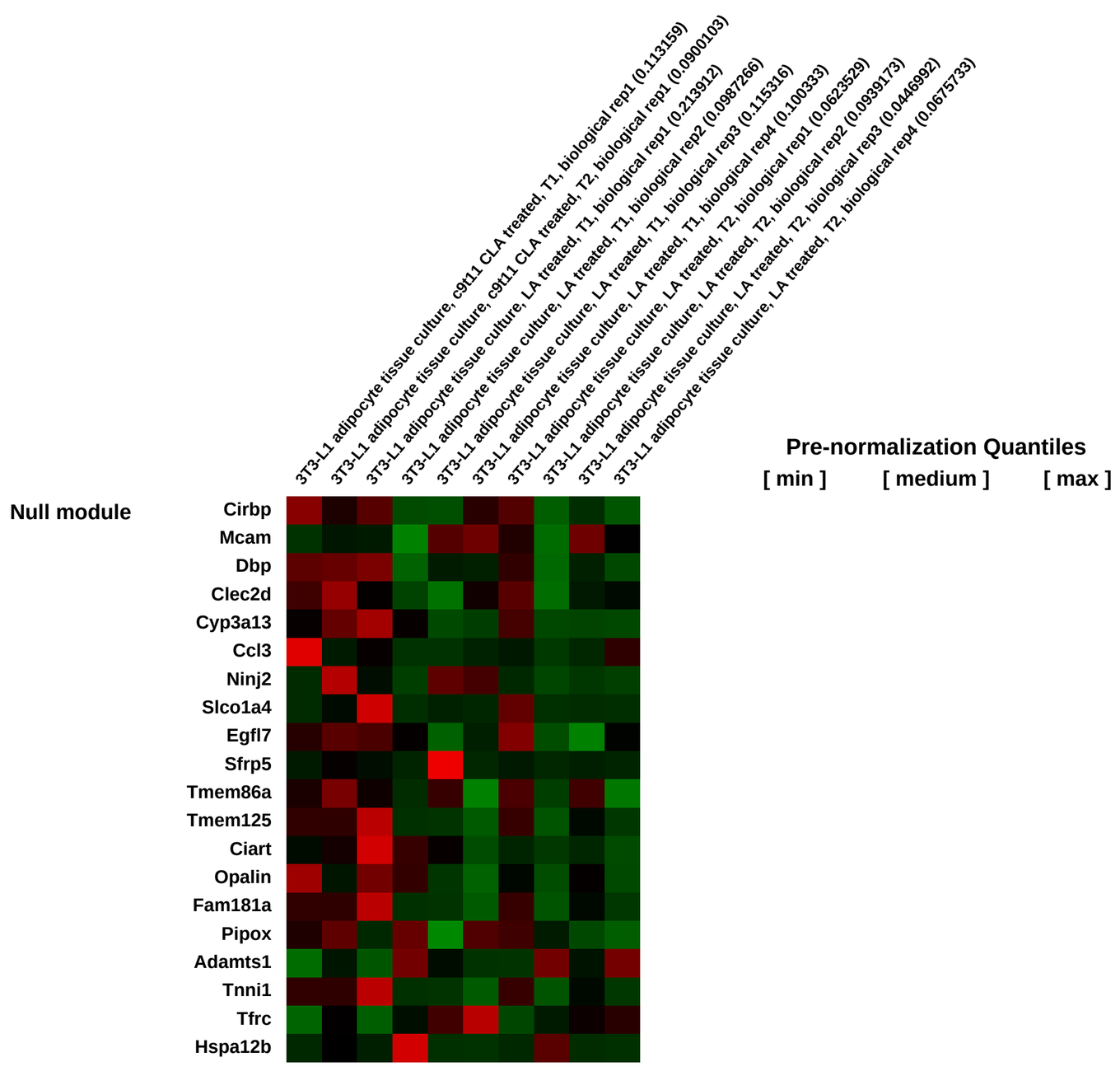

GEO Series "GSE8726" Expression Profiles

Num of samples in this series: 7

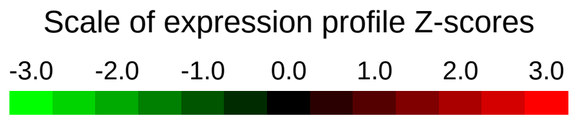

GEO Link:	**http://www.ncbi.nlm.nih.gov/geo/query/acc.cgi?acc=GSE8726**
Status:	**Public on Aug 06 2008**
Title:	**Expression Data from Sod2-/- and Sod2+/+ Mouse Erythroblasts.**
Organism:	**Mus musculus**
Experiment type:	**Expression profiling by array**
Platform:	**GPL1261**
Pubmed ID:	

Summary & Design:

Summary:
The mitochondrial superoxide dismutase (SOD2) is a major antioxidant protein which detoxifies superoxide anion radicals generated by mitochondrial respiration (Weisiger and Fridovich, J. Biol. Chem. 1973). We designed a model of oxidative stress-induced anemia caused by SOD2-deficiency (Friedman et al. J. Exp. Med. 2001). Our previous work showed that mice reconstituted with SOD2-deficient hematopoietic stem cells develop an anemia with striking similarity to human sideroblastic anemia (SA) (Friedman et al. Blood 2004; Martin et al. Exp Hematol 2005). Our overall goal was to define early events in the pathogenesis of SOD2-deficiency SA and, in particular, to identify genes involved in the response of erythroid progenitors to oxidative stress. We compared gene expression of sorted TER-119+ CD71+ erythroblasts from SOD2-/- (’KO’) versus Sod2+/+ (’WT’) hematopoietic stem cell recipients using cDNA microarrays.

Samples used in this study were re-hybridized with GLYCOv2 oligonucleotide arrays. GLYCOv2 oligonucleotide arrays are custom Affymetrix GeneChip arrays (Affymetrix, Santa Clara, CA) designed for the Functional Glycomics Gateway, collaboration between the Consortium for Functional Glycomics (CFG, http://www.functionalglycomics.org/) and Nature Publishing Group. A complete description of the array can be found at http://www.functionalglycomics.org/static/consortium/resources/resourcecoree.shtml . Hybridization results and quality control details can be found at https://www.functionalglycomics.org/glycomics/publicdata/microarray.jsp , by clicking on the â Raw Dataâ icon link for microarray experiment â Jeff Friedman 1: Sod2 KO anemic miceâ . Briefly but importantly, one Sod2-/- sample, which was prepared separately, and whose GAPDH 3’/5’ ratio was off range, was legitimately removed from the analysis of the GLYCOv2 and 430 2.0 arrays.

Keywords: Genotype comparison, genetic modification

Overall design:
We sorted Sod2-/- and Sod2+/+ size-matched mouse erythroblasts based on the expression of two developmental surface markers, CD71 and TER-119. Total RNA from 4 biological replicates per genotype were extracted and hybridized on 8 Affymetrix Mouse Genome 430 2.0 arrays (Affymetrix, Santa Clara, CA). After quality controls (see scan protocol), analysis was performed with GeneSifter (VizX Labs, Seattle, WA) using 4 Sod2+/+ (control samples, WT) and 3 Sod2-/- (KO) replicates.

Background corr dist: KL-Divergence = 0.0320, L1-Distance = 0.0795, L2-Distance = 0.0104, Normal std = 0.7538

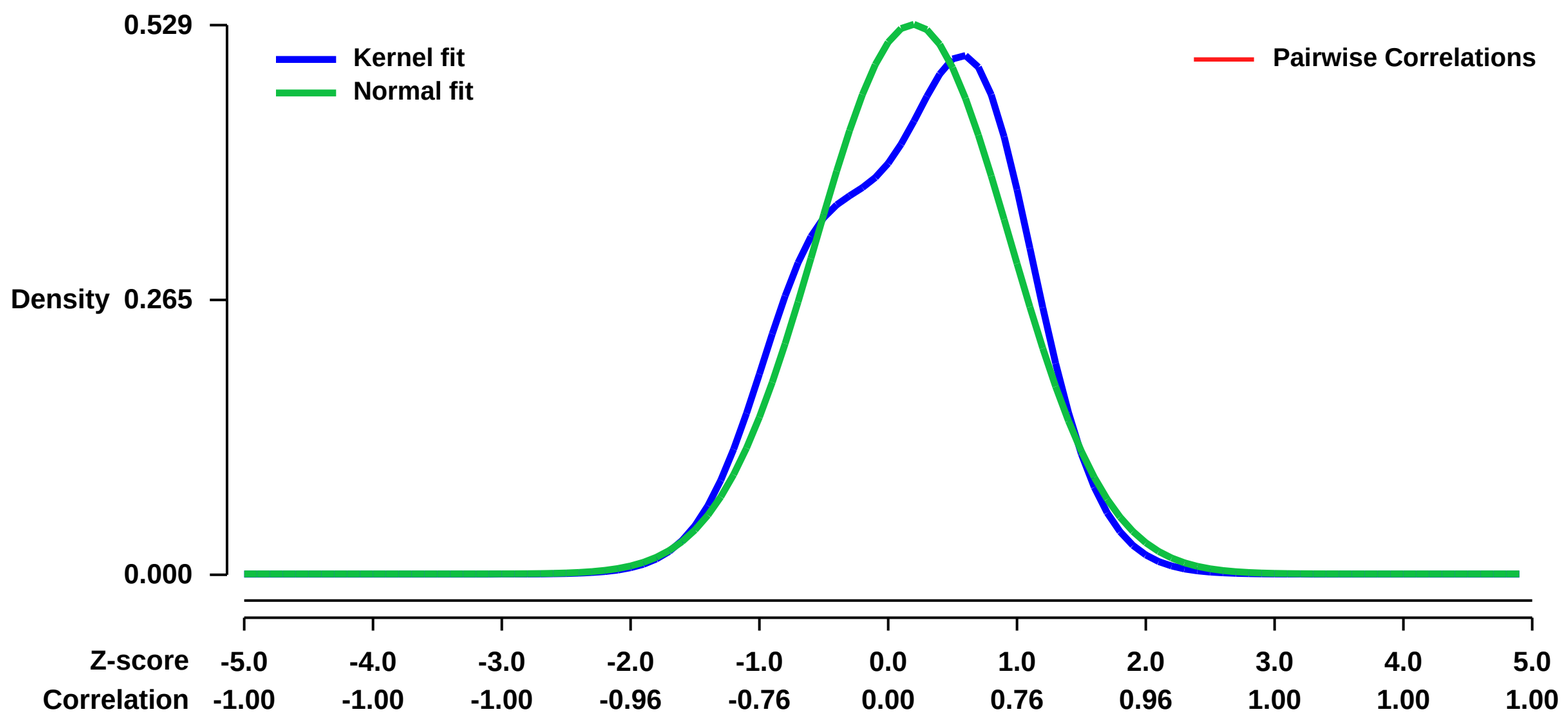

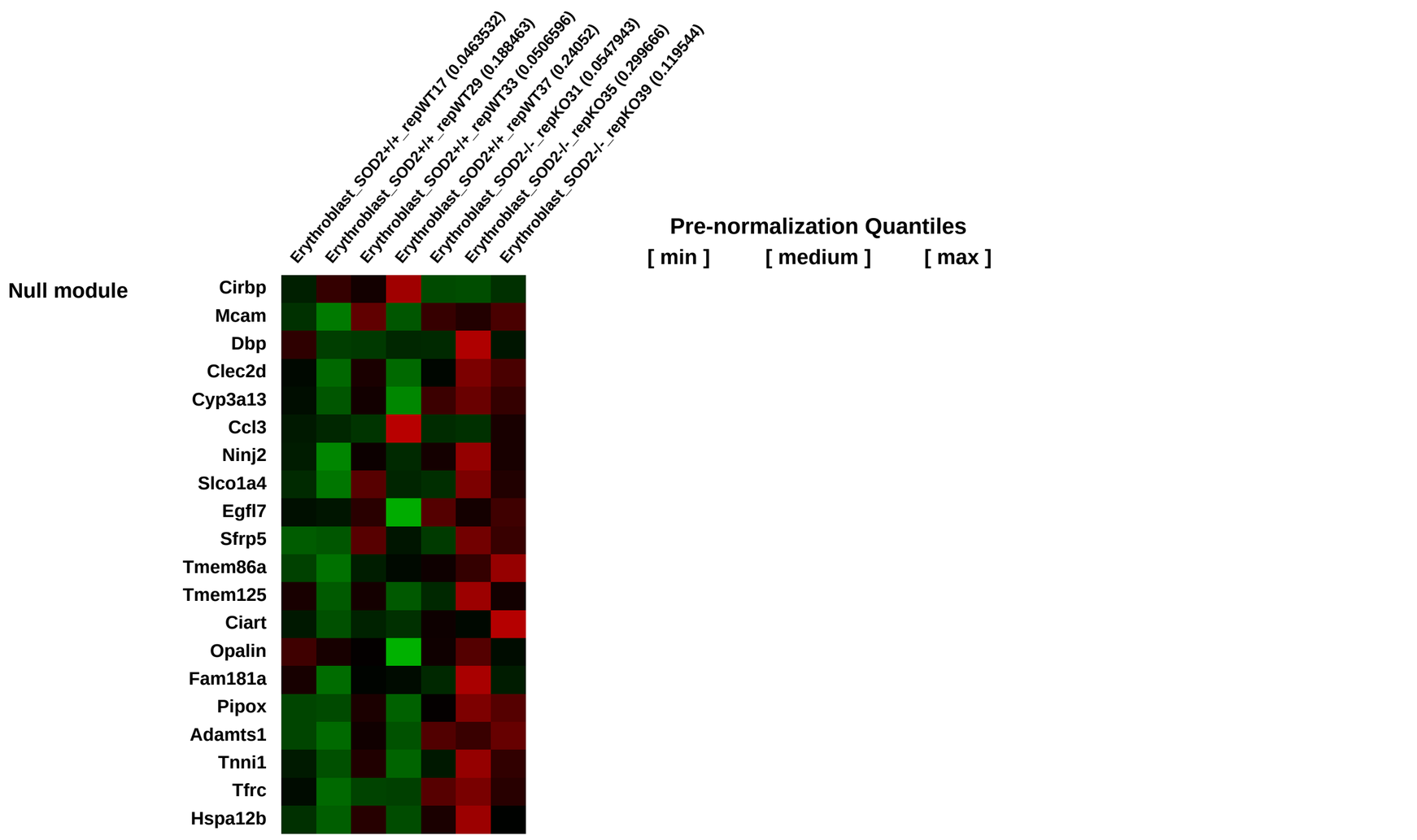

GEO Series "GSE8733" Expression Profiles

Num of samples in this series: 24

Scale of expression profile Z-scores

-3.0 -2.0 -1.0 0.0 1.0 2.0 3.0

GEO Link:	**http://www.ncbi.nlm.nih.gov/geo/query/acc.cgi?acc=GSE8733**
Status:	**Public on Aug 10 2007**
Title:	**Folate deficiency enhances arsenic effects on ODC mouse skin gene expression**
Organism:	**Mus musculus**
Experiment type:	**Expression profiling by array**
Platform:	**GPL1261**
Pubmed ID:	**17928125**
Summary & Design:	**Summary:** **We demonstrate that expression of key markers of keratinocyte differentiation is suppressed by exposure to sodium arsenite. Folate deficiency exacerbates this effect. In addition, cancer-related cell movement genes, and growth and proliferation genes are altered. Several redox-sensitive transcription factors are implicated in mediating these gene expression changes due to arsenic treatment and folate deficiency.** **Keywords: gene expression/microarray** **Overall design:** **K6/ODC mice were maintained on either a folate deficient or folate sufficient diet and exposed to 0, 1, or 10 ppm sodium arsenite in the drinking water for 30 days. Total RNA was isolated from skin samples and gene expression analyzed using Affymetrix Mouse 430 2.0 GeneChips. Data from 24 samples, with four mice in each of the six treatment groups, were analyzed.**

Background corr dist: **KL-Divergence = 0.1869, L1-Distance = 0.0446, L2-Distance = 0.0043, Normal std = 0.3409**

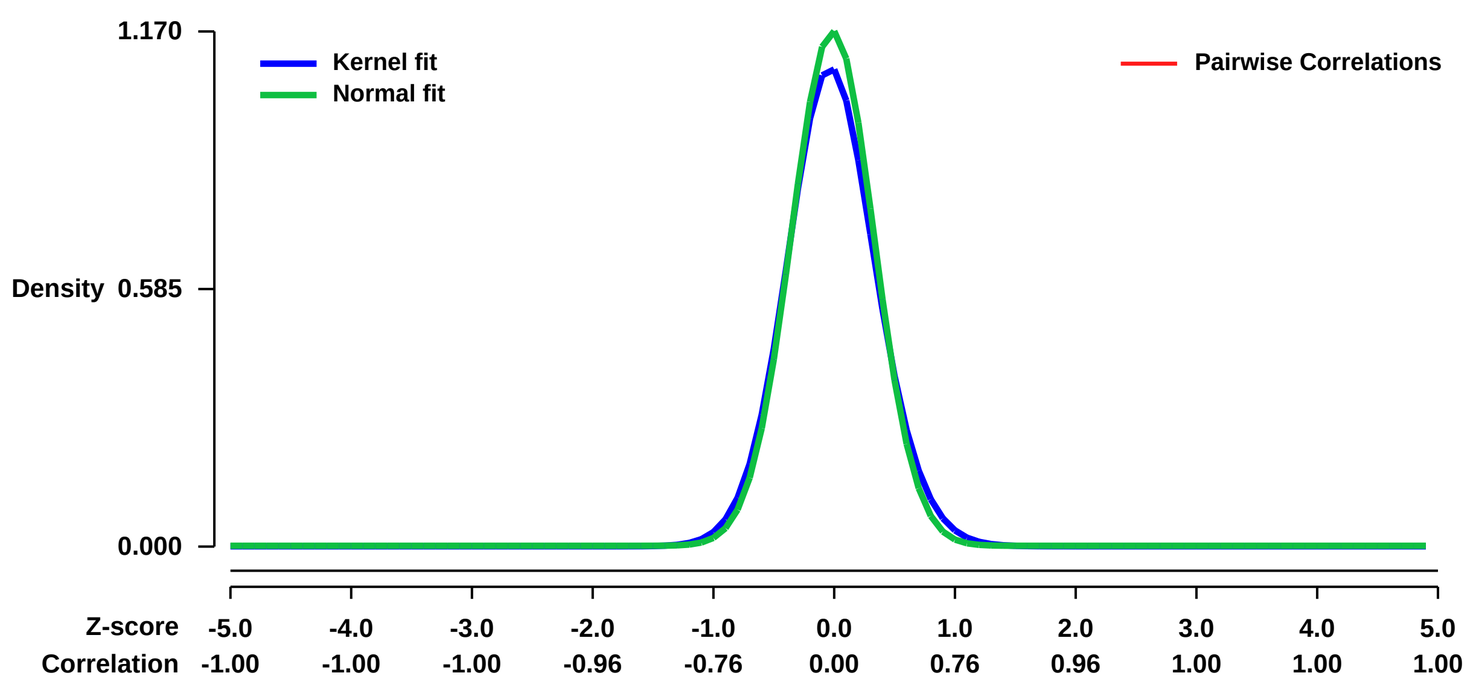

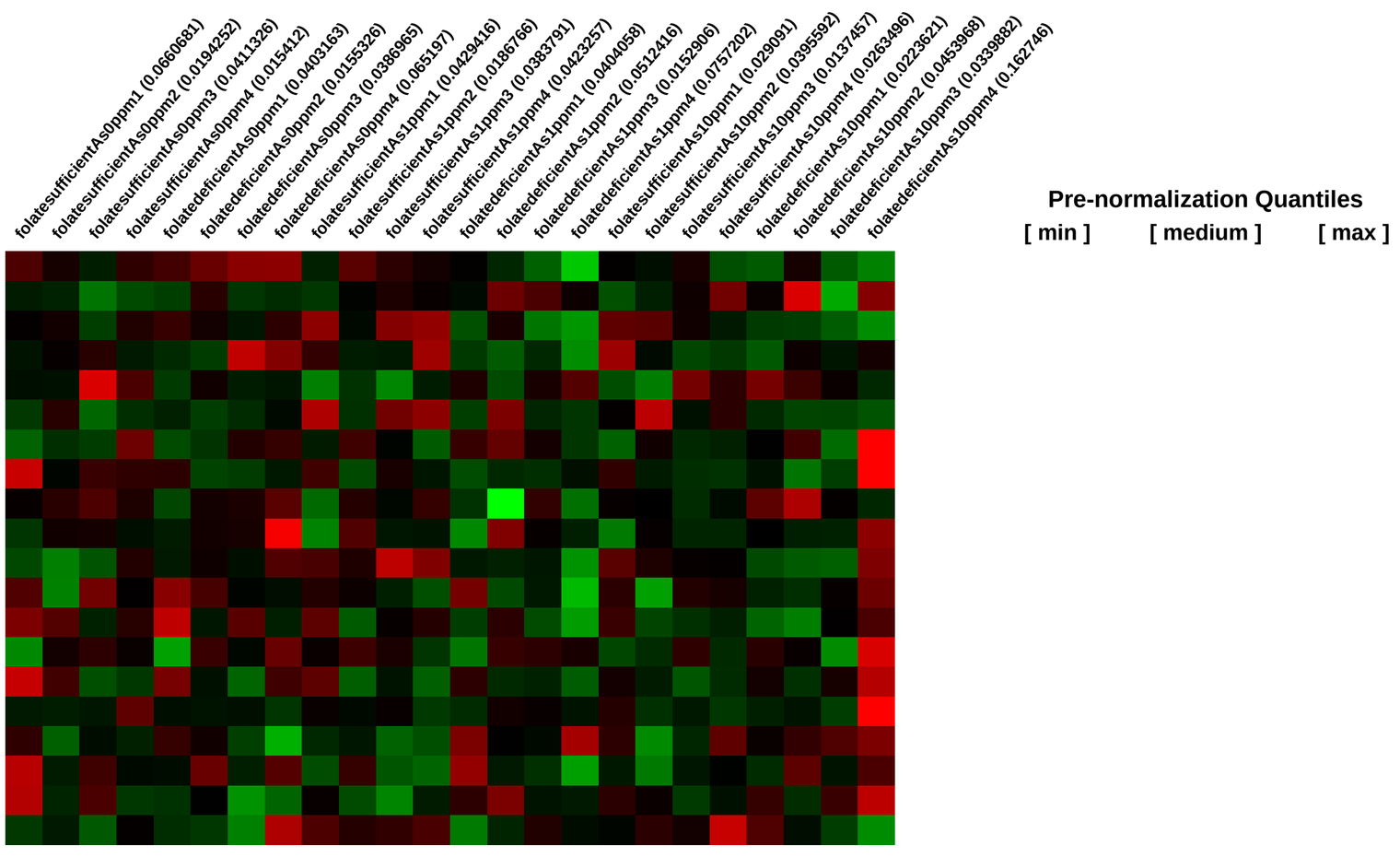

GEO Series "GSE8836" Expression Profiles

Num of samples in this series: 56

Scale of expression profile Z-scores

-3.0 -2.0 -1.0 0.0 1.0 2.0 3.0

GEO Link:	http://www.ncbi.nlm.nih.gov/geo/query/acc.cgi?acc=GSE8836
Status:	Public on Dec 01 2007
Title:	CLL in Em-TCL1 mice provides a biologically relevant model to unravel and reverse immune deficiency in human cancer.
Organism:	Mus musculus
Experiment type:	Expression profiling by array
Platform:	GPL1261
Pubmed ID:	19332800
Summary & Design:	**Summary:** Immune deficiency is common in cancer, but the biological basis for this and ways to reverse it remains elusive. Here we present a mouse model of B cell chronic lymphocytic leukemia (CLL) that recapitulates changes in the non-malignant circulating T cells seen in patients with this illness.1 To validate this model, we examined changes in T cell gene expression, protein expression and function in Em-TCL1 transgenic mice as they developed CLL 2,3 and demonstrate that development of CLL in these transgenic mice is associated with changes in impaired T cell function and in gene expression in CD4 and CD8 T cells similar to those observed in patients with this disease. Infusion of CLL cells into non-leukemia bearing Em-TCL1 mice rapidly induces these changes, demonstrating a causal relationship between leukemia and the induction of T cell changes. This model allows dissection of the molecular changes induced in CD4 and CD8 T cells by interaction with leukemia cells and further supports the concept that cancer results in complex abnormalities in the immune microenvironment. Gene expression profiling was performed to determine whether Em-TCL1 murine model of chronic lymphocytic leukemia (CLL) mimics T cell defects induced by CLL cells in patients with CLL. Keywords: comparative gene expression profiling analysis. **Overall design:** CD4 T cells and CD8 T cells were obtained from spleens of B6C3 and Em-TCL1 transgenic murine model of CLL or from peripheral blood mononuclear cells of previously untreated patients with CLL and healthy individuals (Pubmed ID: 15965501). Gene expression profiling was performed using total RNA and the data were analysed to compare gene expression profile of CLL to healthy within or between the species.

Background corr dist: KL-Divergence = 0.4566, L1-Distance = 0.0842, L2-Distance = 0.0228, Normal std = 0.2347

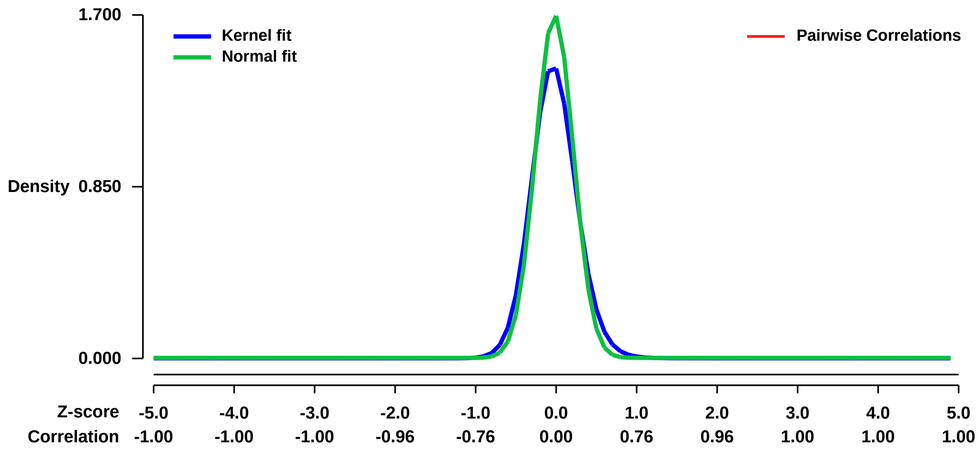

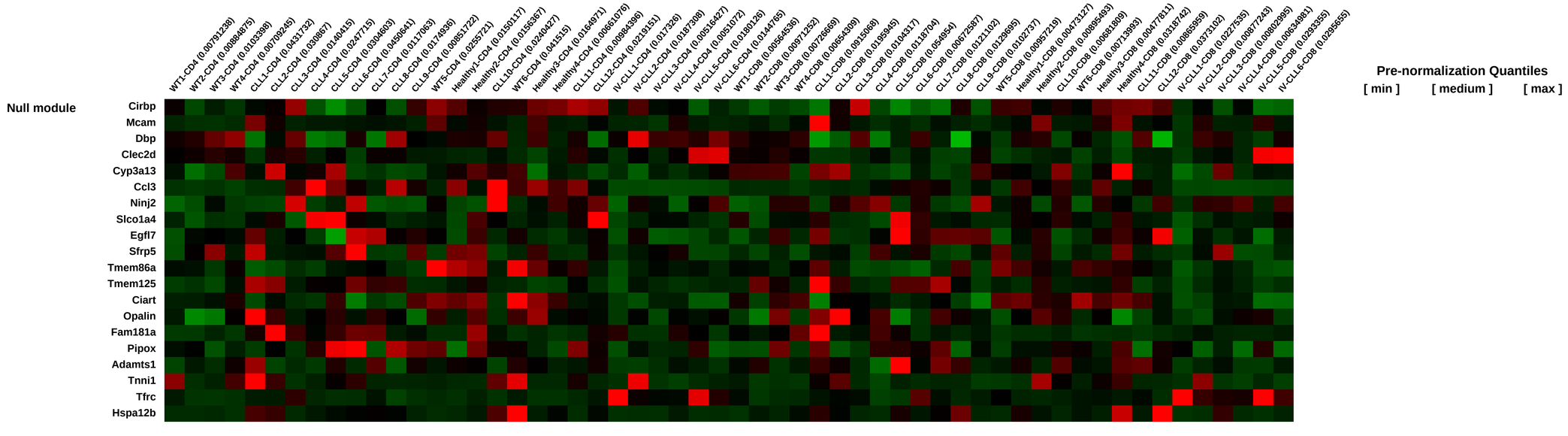

GEO Series "GSE8863" Expression Profiles

Num of samples in this series: 18

Scale of expression profile Z-scores

-3.0 -2.0 -1.0 0.0 1.0 2.0 3.0

GEO Link:	**http://www.ncbi.nlm.nih.gov/geo/query/acc.cgi?acc=GSE8863**
Status:	**Public on Jun 27 2008**
Title:	**Mouse mammary tumor-initiating cells**
Organism:	**Mus musculus**
Experiment type:	**Expression profiling by array**
Platform:	**GPL1261**
Pubmed ID:	**18559513**
Summary & Design:	**Summary:** **Using a syngeneic p53 null mouse mammary gland tumor model that closely mimics human breast cancer, we have identified by limiting dilution transplantation as well as in vitro mammosphere and clonogenic assays a Lin-CD29HighCD24High subpopulation of tumor-initiating cells. Differentially expressed genes in the Lin-CD29HighCD24High mouse mammary gland tumor-initiating cell population include those involved in DNA damage response and repair, as well as genes involved in epigenetic regulation previously shown to be critical for stem cell self-renewal.** **Keywords: tumor-initiating cells** **Overall design:** **12 samples (RNA of 4 subpopulations based on expression of CD29 and CD24 for each tumor of 3) were included in the identification of differentially expressed genes of tumor-initiating cells. 5 samples (RNA of subpopulations based on expression of CD29 and CD24 of normal mammary epithelial cells) were included in the normal group analysis. Reference RNA was used to normalize all samples.**

Background corr dist: KL-Divergence = 0.2376, L1-Distance = 0.0592, L2-Distance = 0.0094, Normal std = 0.3138

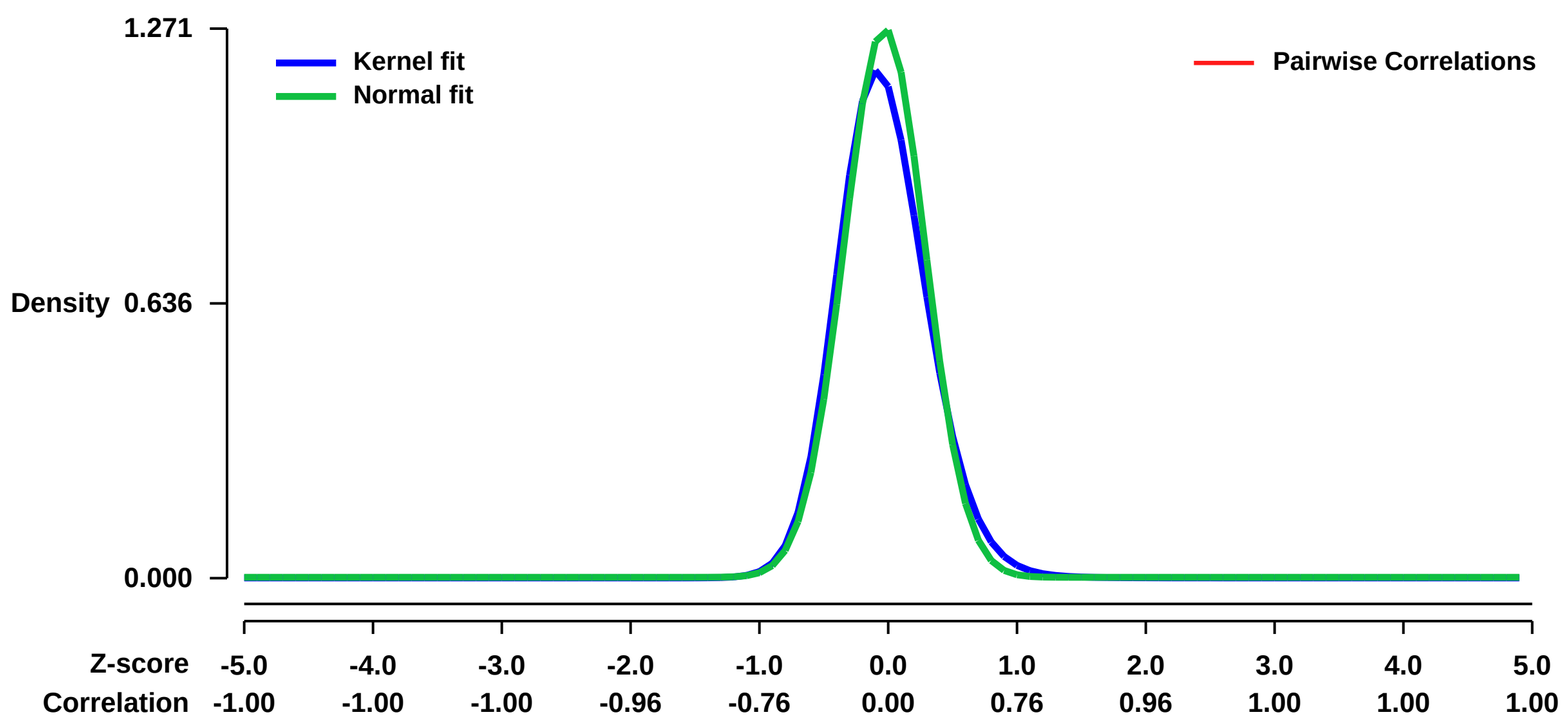

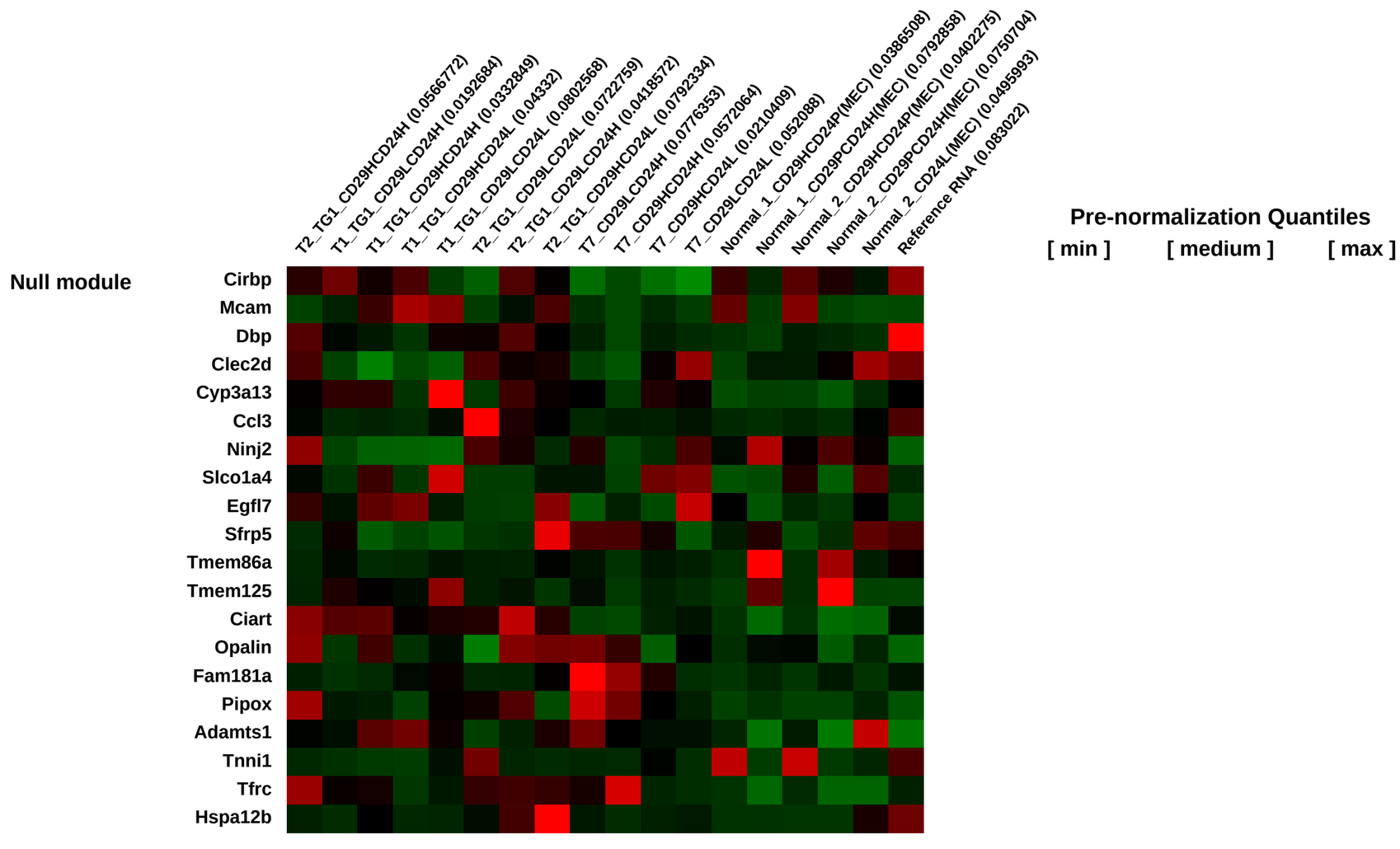

GEO Series "GSE8949" Expression Profiles

Num of samples in this series: 20

Scale of expression profile Z-scores

-3.0 -2.0 -1.0 0.0 1.0 2.0 3.0

GEO Link:	http://www.ncbi.nlm.nih.gov/geo/query/acc.cgi?acc=GSE8949
Status:	Public on Dec 12 2007
Title:	Gene expression changes in mouse aorta during activation of or interference with PPAR gamma signaling.
Organism:	Mus musculus
Experiment type:	Expression profiling by array
Platform:	GPL1261
Pubmed ID:	20018933
Summary & Design:	**Summary:** Ligand-mediated activation of the nuclear hormone receptor PPAR gamma lowers blood pressure and improves glucose tolerance in humans. Two naturally occurring mutations (P467L, V290M) in the ligand binding domain of PPAR gamma have been described in humans that lead to severe insulin resistance and hypertension. Experimental evidence suggests that these mutant versions of PPAR gamma act in a dominant negative fashion. To better understand the molecular mechanisms underlying PPAR gamma action in the vasculature, we determined the gene expression patterns in mouse aorta in response to activation or interference with the PPAR gamma signaling pathway. **Keywords: time course, dose response** **Overall design:** To assess the response to PPAR gamma interference, we used adult mice containing a dominant negative form of PPAR gamma. These mice have a targeted P465L mutation, which is equivalent to the P467L mutant, described in human patients. Wild-type littermates were used as the genetic control. The PPAR gamma signaling pathway was activated by administration of rosiglitazone for either 2 or 14 days to adult mice (C57BL/6J strain) at a dose of 3 or 10 mg/kg/day via the food. Control mice were fed standard mouse chow. For the microarray hybridizations, 2-3 biological replicates from each experimental group were used. Biological replicates were RNA pooled from 8 different mouse aortas. All the microarray procedures were conducted at the University of Iowa DNA Core facility using standard Affymetrix protocols. In brief, approximately 3 ug of total RNA was used as input to a one-step amplification procedure to generate biotin-labeled RNA fragments for hybridization to the Affymetrix GeneChip Mouse Genome 430 2.0 array.

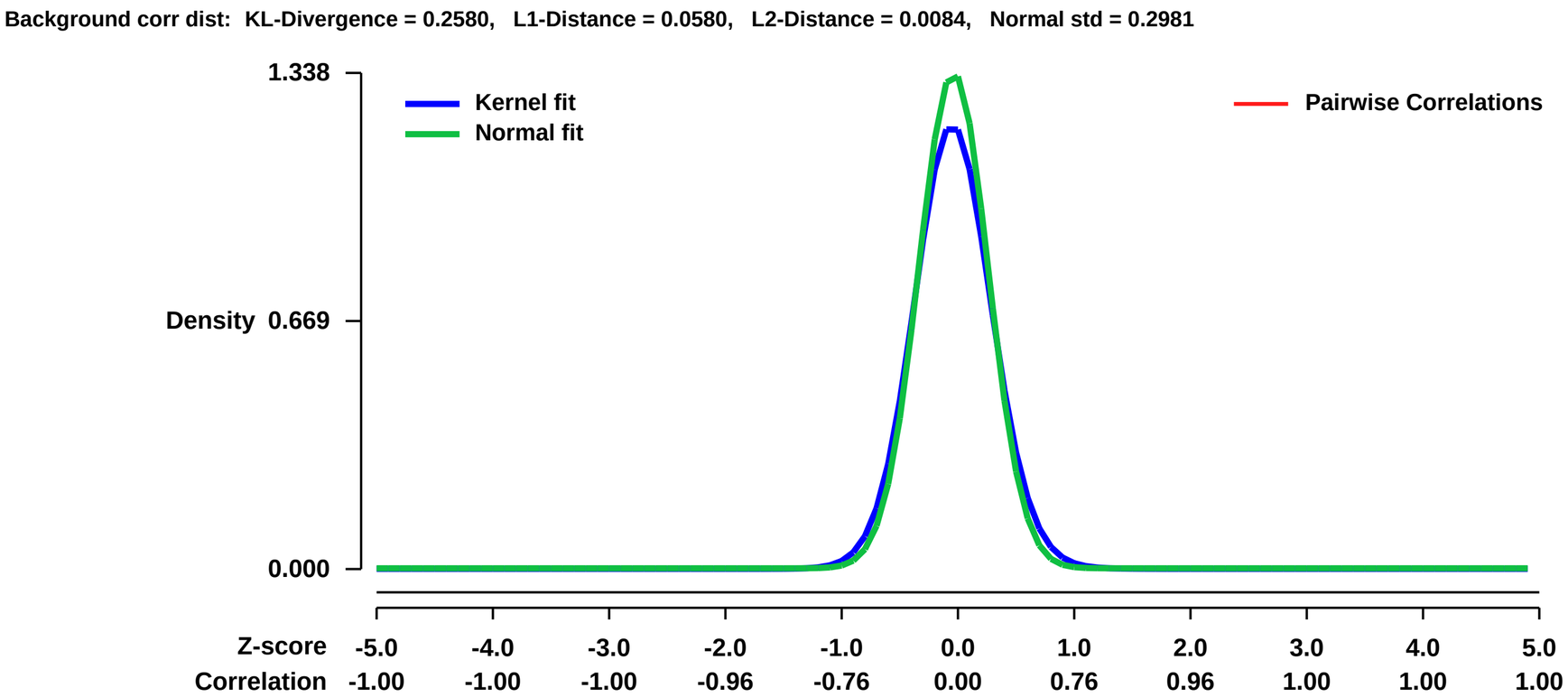

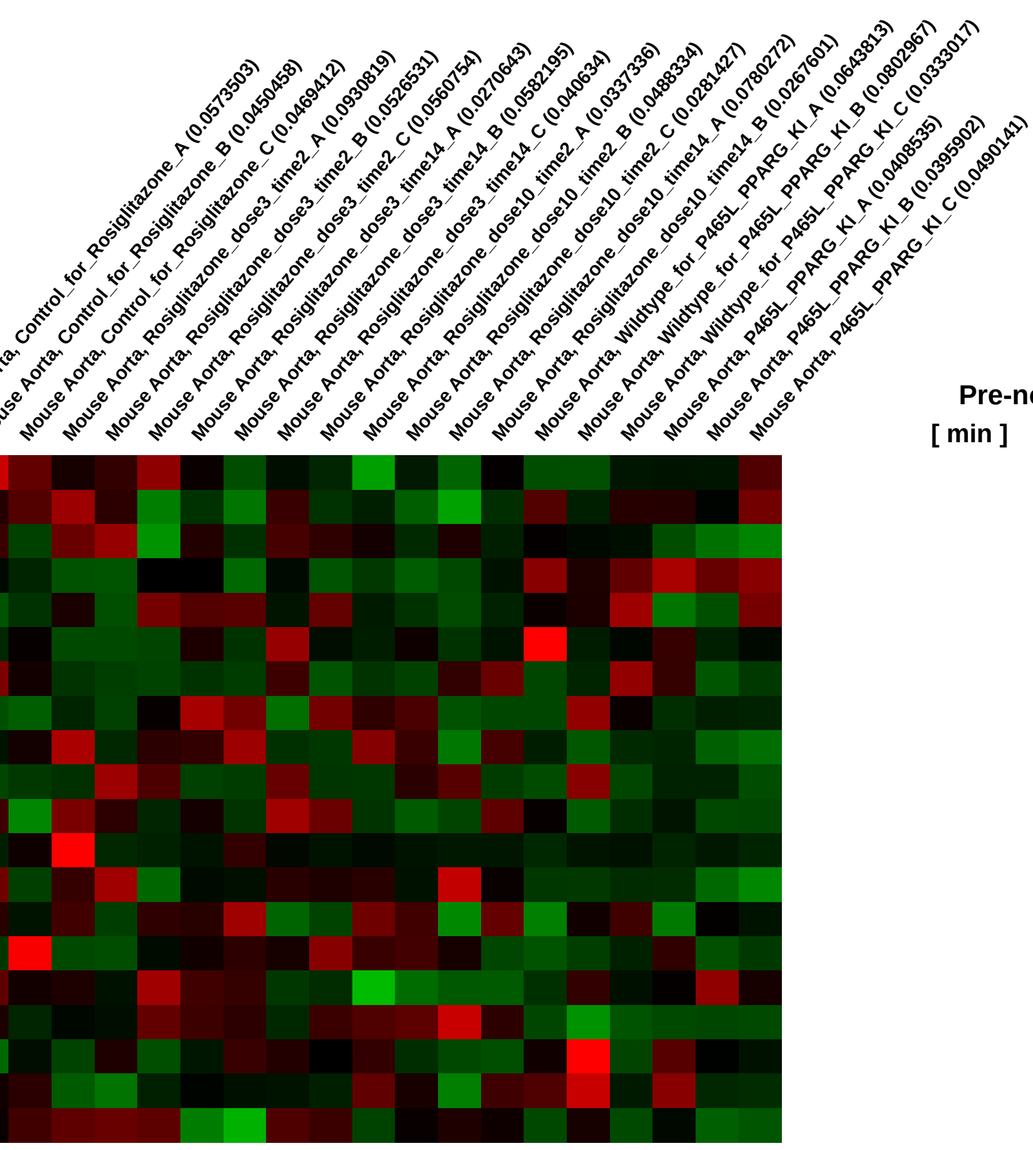

GEO Series "GSE8960" Expression Profiles

Num of samples in this series: 18

Scale of expression profile Z-scores

-3.0 -2.0 -1.0 0.0 1.0 2.0 3.0

GEO Link:	http://www.ncbi.nlm.nih.gov/geo/query/acc.cgi?acc=GSE8960
Status:	Public on Sep 01 2008
Title:	The TLR2/NOD2/RICK signaling axis regulates stimulus-specific IL-10 production
Organism:	Mus musculus
Experiment type:	Expression profiling by array
Platform:	GPL1261
Pubmed ID:	18549453
Summary & Design:	**Summary:** Recognition and response to gram-positive bacteria by macrophages and dendritic cells is mediated in part through TLR2. We found that that Streptococcus pneumoniae cell wall fragments, containing primarily peptidoglycan and teichoic acids, induced prodigious secretion of IL-10 from macrophages and dendritic cells and was dependent on TLR2 and NOD2, a cytoplasmic CARD-NACHT-LRR protein encoded by Card15. IL-10 secretion in response to cell walls was also dependent on RICK/RIP2, a kinase associated with NOD2, and MYD88 but independent of the ERK/p38 pathway. The reduction of IL-10 secretion by cell wall-activated NOD2-deficient myeloidâ derived cells translated into downstream effects on IL-10 target gene expression and elevations in subsets of pro-inflammatory cytokine expression normally restrained by autocrine/paracrine effects of IL-10. Since NOD2 is linked to aberrant immune responses in Crohnâ s Disease patients bearing mutations in CARD15, the temporal and quantitative effects of the TLR2/NOD/RICK pathway on IL-10 secretion may affect homeostatic control of immune responses to gram-positive bacteria. **Keywords:** immune response simulated pathogen response **Overall design:** KO mice were treated with a cel wall extract and evaluated for immune response 1 hr and 4 hrs after treatment

Background corr dist: KL-Divergence = 0.1989, L1-Distance = 0.0359, L2-Distance = 0.0026, Normal std = 0.3354

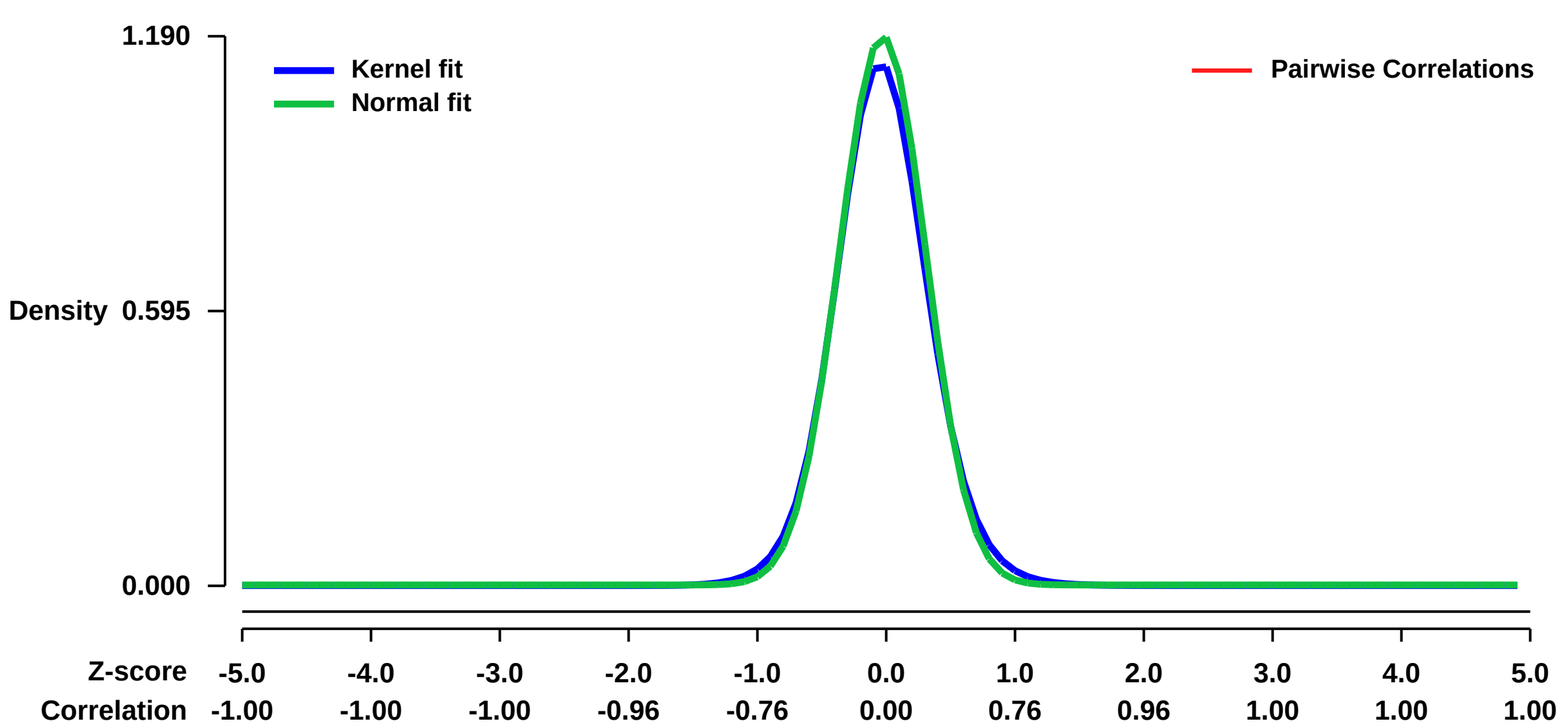

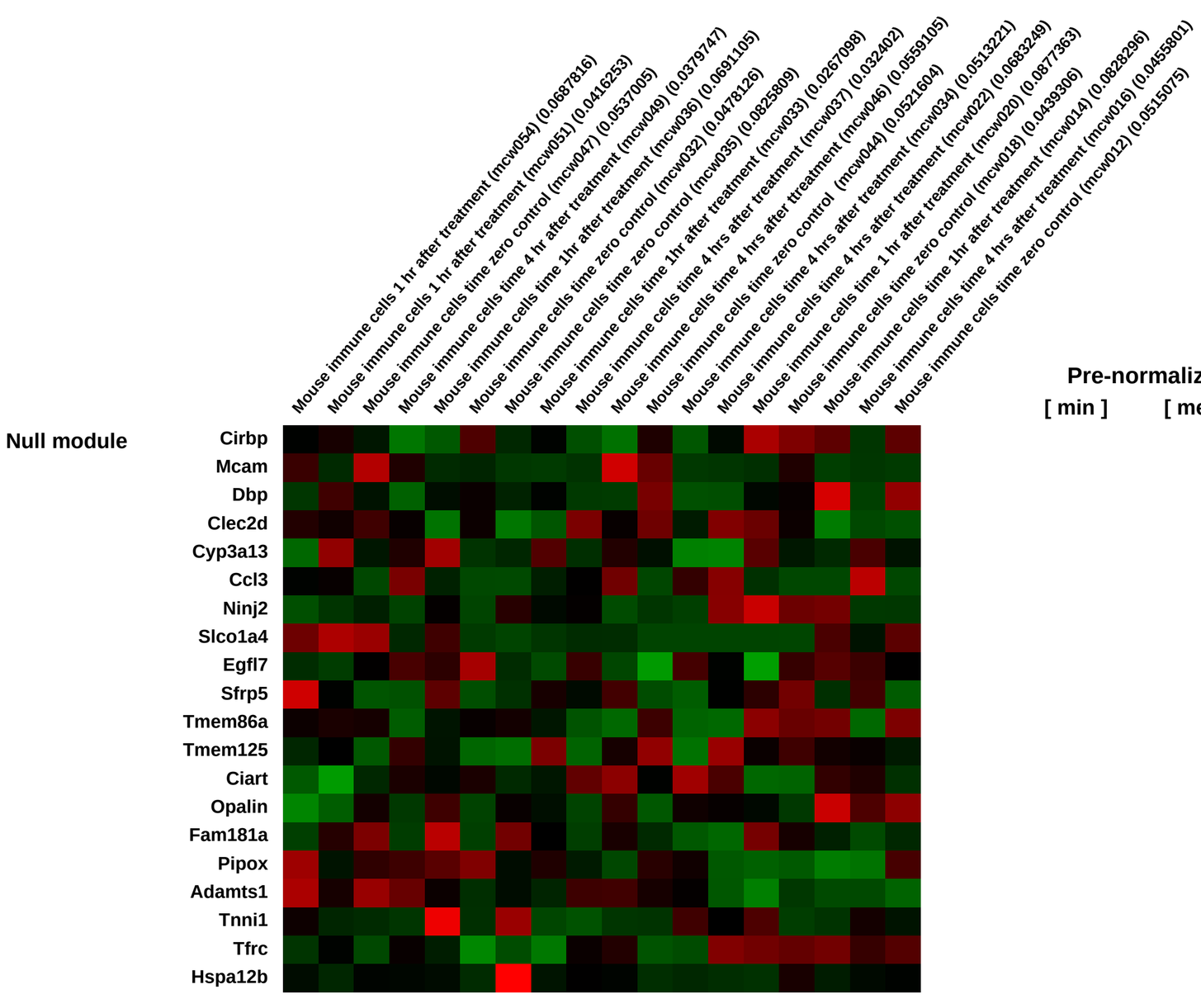

GEO Series "GSE8966" Expression Profiles

Num of samples in this series: 12

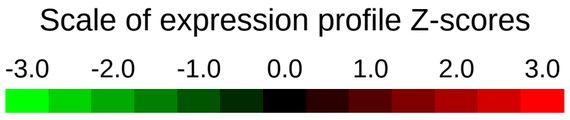

GEO Link:	http://www.ncbi.nlm.nih.gov/geo/query/acc.cgi?acc=GSE8966
Status:	Public on Aug 17 2009
Title:	Liver Transcriptome Profiles Associated with Strain-Specific Ehrlichia chaffeensisâ induced Hepatitis
Organism:	Mus musculus
Experiment type:	Expression profiling by array
Platform:	GPL1261
Pubmed ID:	19001077
Summary & Design:	**Summary:** Infection of humans with Ehrlichia chaffeensis, the etiologic agent of human monocytic ehrlichiosis, can cause hepatitis of varying severity. When the three human isolates of E. chaffeensis, each belongs to different geno-groups, are inoculated into severe combined immunodeficiency mice, the severity of clinical signs and bacterial burden detected in the liver are strain Wakulla>Liberty>Arkansas. Disseminated and granulomatous inflammation is evident in the liver of mice infected with strains Wakulla and Arkansas, respectively, but not in mice infected with strain Liberty. In this paper, we used microarray analysis to define transcriptional profiles characteristic to the histopathological features in the mouse liver. Cytokine and chemokine profiles were strikingly different among three strains of E. chaffeensis: IFN-¿‡, CCL5, CXCL1, CXCL2, CXCL7 and CXCL9 were highly up-regulated with strain Arkansas, TNF-¿–, CCL2, CCL3, CCL5, CCL6, CCL12, CCL20, CXCL2, CXCL7, CXCL9 and CXCL13 were highly up-regulated with strain Wakulla. With strain Liberty, only CXCL13 was highly up-regulated. In the livers infected with the Arkansas strain, monocytes/macrophages and NK cells were enriched in the granulomas and increase of NK cell-marker mRNAs was detected. Livers infected with the Wakulla strain displayed infiltration of significantly more neutrophils and increase of neutrophil-marker mRNAs. Genes up-regulated commonly in the liver infected with the three stains are other host innate immune and inflammatory response genes including several acute phase proteins. Genes down-regulated commonly are related to host physiologic functions. The results suggest that marked modulation of host cytokine and chemokine profiles by E. chaffeensis strains underlie the distinct host liver disease. **Overall design:** Three mice were examined for each of the 4 groups.

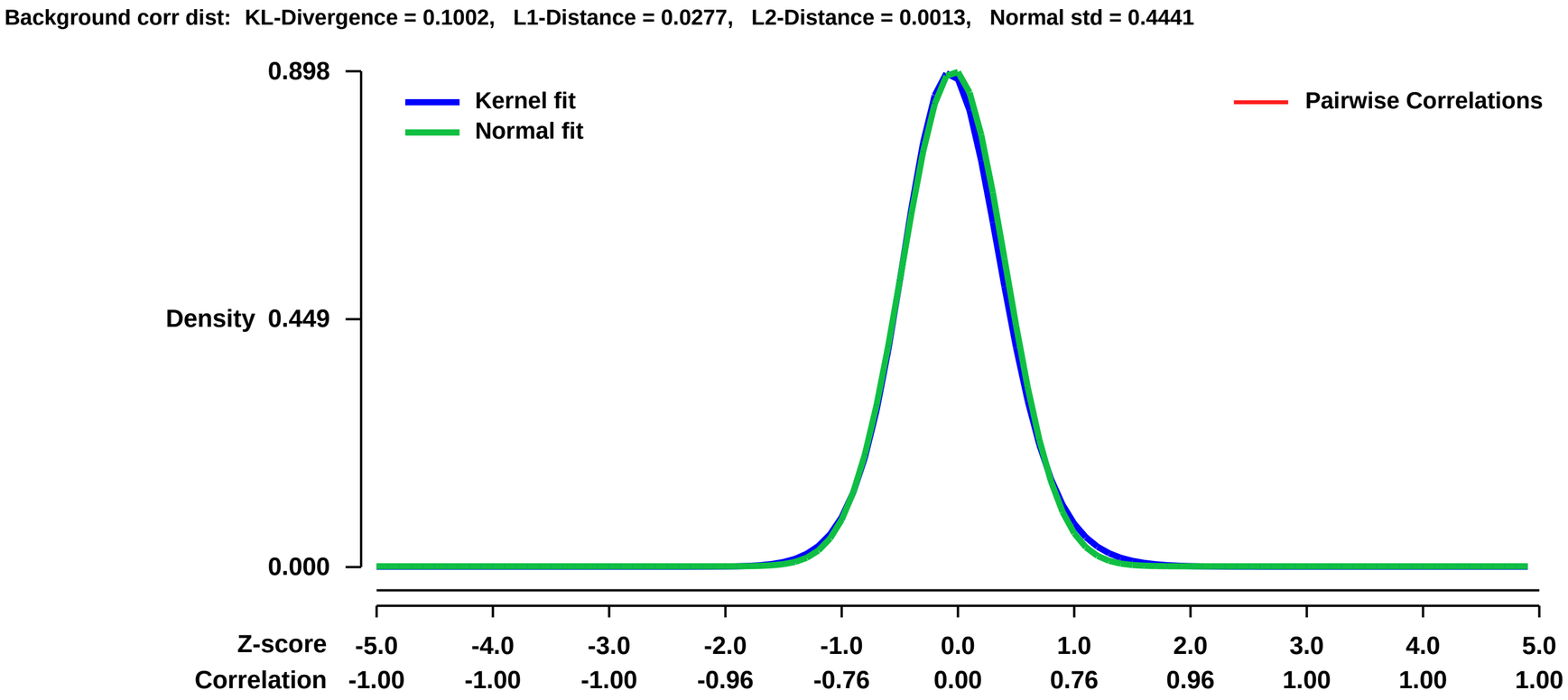

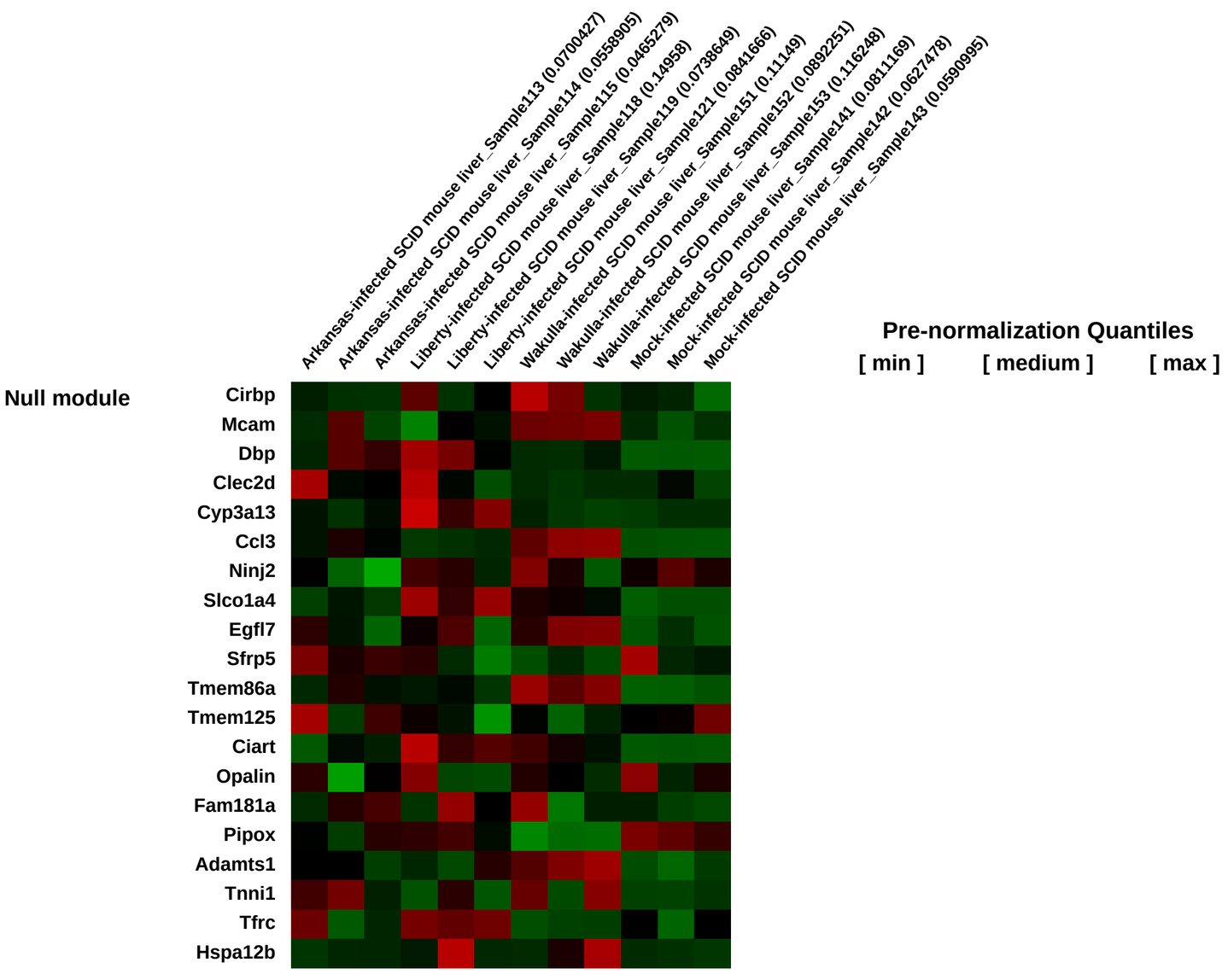

GEO Series "GSE8969" Expression Profiles

Num of samples in this series: 6

Scale of expression profile Z-scores

-3.0 -2.0 -1.0 0.0 1.0 2.0 3.0

GEO Link:	http://www.ncbi.nlm.nih.gov/geo/query/acc.cgi?acc=GSE8969
Status:	Public on Jan 15 2008
Title:	Impaired liver regeneration in Nrf2 knockout mice caused by ROS-mediated insulin/IGF-1 resistance
Organism:	Mus musculus
Experiment type:	Expression profiling by array
Platform:	GPL1261
Pubmed ID:	18059474
Summary & Design:	**Summary:** The liver is frequently challenged by surgery-induced metabolic overload, viruses, or toxins, which induce the formation of reactive oxygen species. To determine the effect of oxidative stress on liver regeneration and to identify the underlying signalling pathways, we studied liver repair in mice lacking the Nrf2 transcription factor. In these animals, expression of several cytoprotective enzymes was reduced in hepatocytes, resulting in oxidative stress. As a consequence, tissue damage was aggravated, and liver regeneration after partial hepatectomy was delayed. Using in vitro and in vivo studies we identified oxidative stress-induced insulin/insulin-like growth factor resistance as the underlying mechanism. This deficiency impaired the activation of p38 mitogen-activated kinase, Akt kinase, and downstream targets after hepatectomy, resulting in enhanced death and delayed proliferation of hepatocytes. Our results reveal novel roles of Nrf2 in the regulation of growth factor signalling and in tissue repair. In addition, they provide new insight into the mechanisms underlying oxidative stress-induced defects in liver regeneration and thus offer new avenues to improve regeneration in patients with acute or chronic liver damage. **Keywords:** genetic modification, wilde type (wt) vs. knock out (k.o.) liver samples **Overall design:** Livers from Nrf2 k.o. and wt mice; 3 hybridizations per genoype: RNA samples were pooled from 3 individual animals

Background corr dist: KL-Divergence = 0.0490, L1-Distance = 0.0223, L2-Distance = 0.0006, Normal std = 0.5784

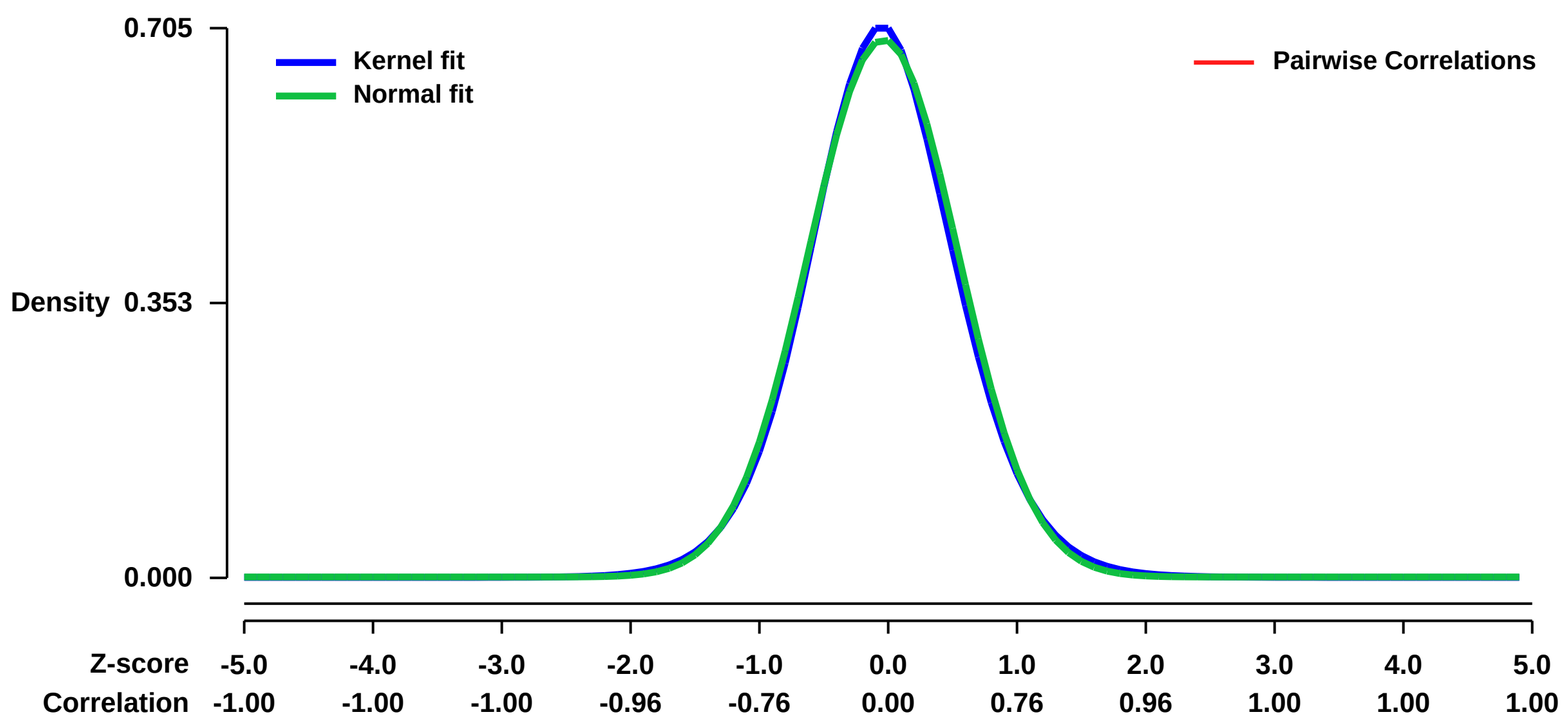

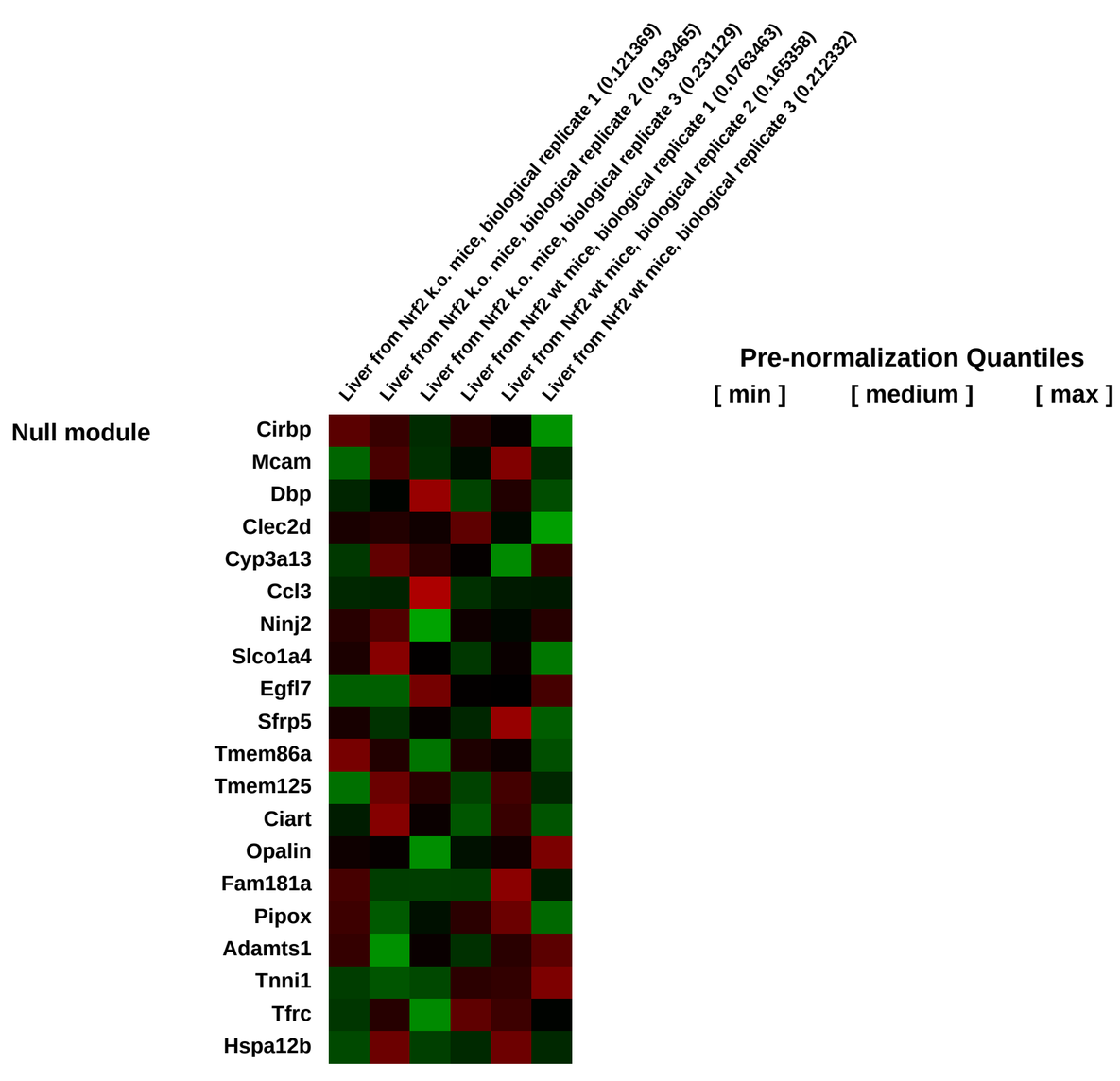

GEO Series "GSE9010" Expression Profiles

Num of samples in this series: 10

Scale of expression profile Z-scores

-3.0 -2.0 -1.0 0.0 1.0 2.0 3.0

GEO Link:	http://www.ncbi.nlm.nih.gov/geo/query/acc.cgi?acc=GSE9010
Status:	Public on Sep 11 2007
Title:	HOXB4 target genes in adult hematopoietic stem and progenitor cells (HSC/HPCs)
Organism:	Mus musculus
Experiment type:	Expression profiling by array
Platform:	GPL1261
Pubmed ID:	17940039
Summary & Design:	**Summary:** HOXB4 mediates expansion of adult and embryo-derived hematopoietic stem cells (HSCs) when expressed ectopically. To define the underlying molecular mechanisms, we performed gene expression profiling in combination with subsequent functional analysis using enriched adult HSCs expressing inducible HOXB4. A substantial number of the identified HOXB4 target genes are involved in signaling pathways important for controlling self-renewal, maintenance and differentiation of stem cells. Functional assays performed on selected pathways confirmed the biological coherence of the array results. HOXB4 activity protected adult HSCs from the detrimental effects mediated by the proinflammatory cytokine TNF-alpha. Furthermore, we demonstrate that HOXB4 activity and FGF-signaling are intertwined. HOXB4-mediated expansion of adult HSCs was enhanced by specific and complete inhibition of FGF-receptors. Based on our results we propose that HOXB4 governs pivotal cell-intrinsic pathways involved in the regulation of cell cycle, differentiation and apoptosis. Our results strongly suggest that HOXB4 modulates the response of HSCs to multiple extrinsic signals in a concerted manner, thereby shifting the balance towards stem cell self-renewal. **Keywords:** plus/minus induction of HOXB4 activity by treatment with 4-hydroxytamoxifen (TMX) **Overall design:** To understand the mechanisms of HOXB4 activity, we wished to identify target genes of HOXB4 in adult hematopoietic stem and progenitor cells (HSC/HPCs). We thus transduced murine HSC/HPCs with a retroviral vector that co-expresses EGFP and a tamoxifen-inducible form of HOXB4 (HOXB4-ER). Upon addition of 4-hydroxytamoxifen (TMX), the HOXB4-ER fusion protein translocates from the cytoplasm to the nucleus, consequently being capable of modulating gene expression. Transduced cell populations were expanded for 14 days in the presence of TMX. Thereafter, HOXB4-ER+LSK (GFP+ , lineage negative, Sca1+, ckit+) cells were flow cytometrically isolated and cultivated either with or without TMX for 1 or 4 hours. Inactivation of HOXB4 activity by TMX withdrawal was intended to mimic the naturally occurring down-regulation of HOXB4 in differentiating stem cells. RNA was prepared after the aforementioned times and the transcriptional profiles of HOXB4-ER+LSK +/- TMX analyzed using the Affymetrixâ¢ platform. As a control, profiling was also performed with LSK cells expressing unmodified constitutively active HOXB4 (HOXB4const) ´– TMX, to exclude changes in gene expression due to unknown effects of tamoxifen itself. RNAs from adult LSK cells were processed for use on Affymetrix GeneChips Mouse Genome 430 2.0. All quality parameters for the arrays were confirmed to be in the recommended range.

Background corr dist: KL-Divergence = 0.0863, L1-Distance = 0.0379, L2-Distance = 0.0029, Normal std = 0.4736

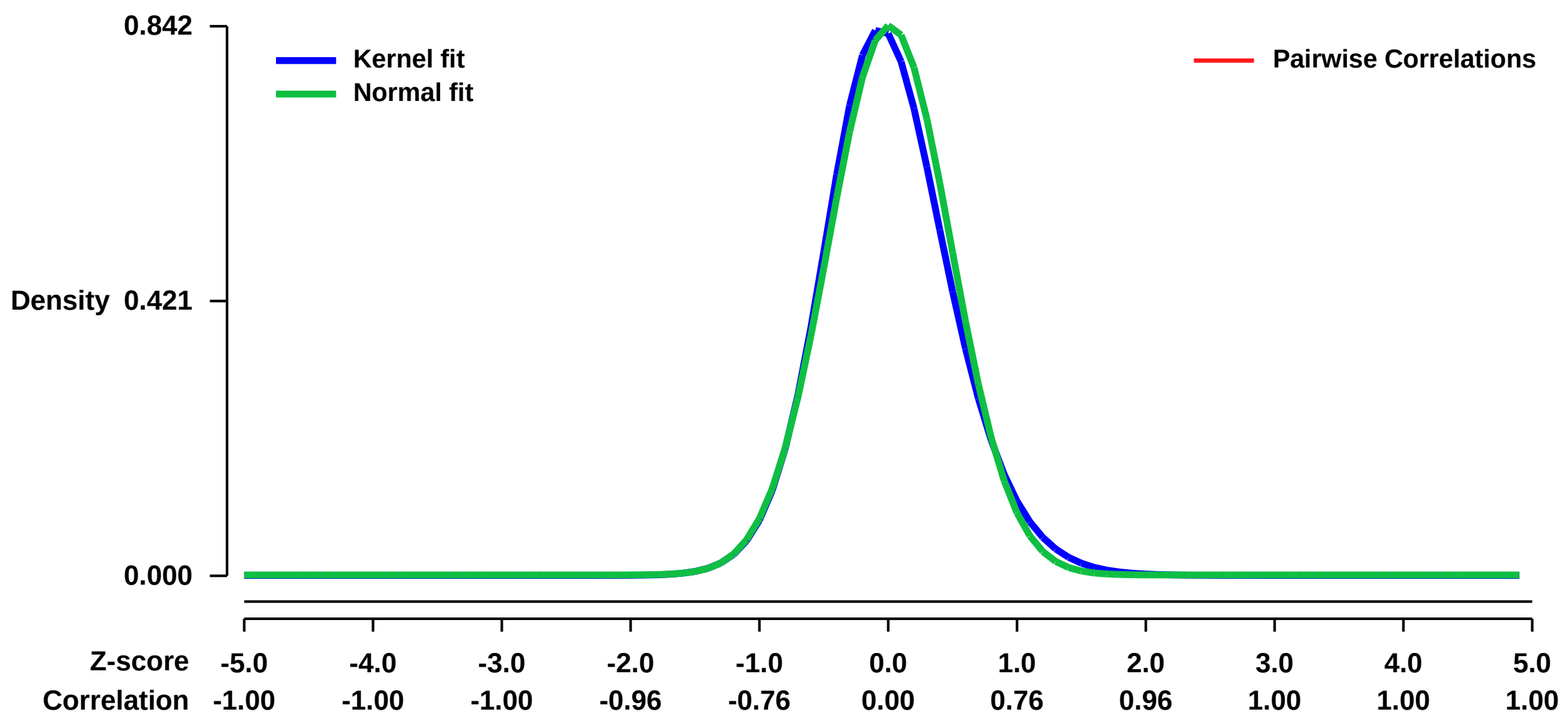

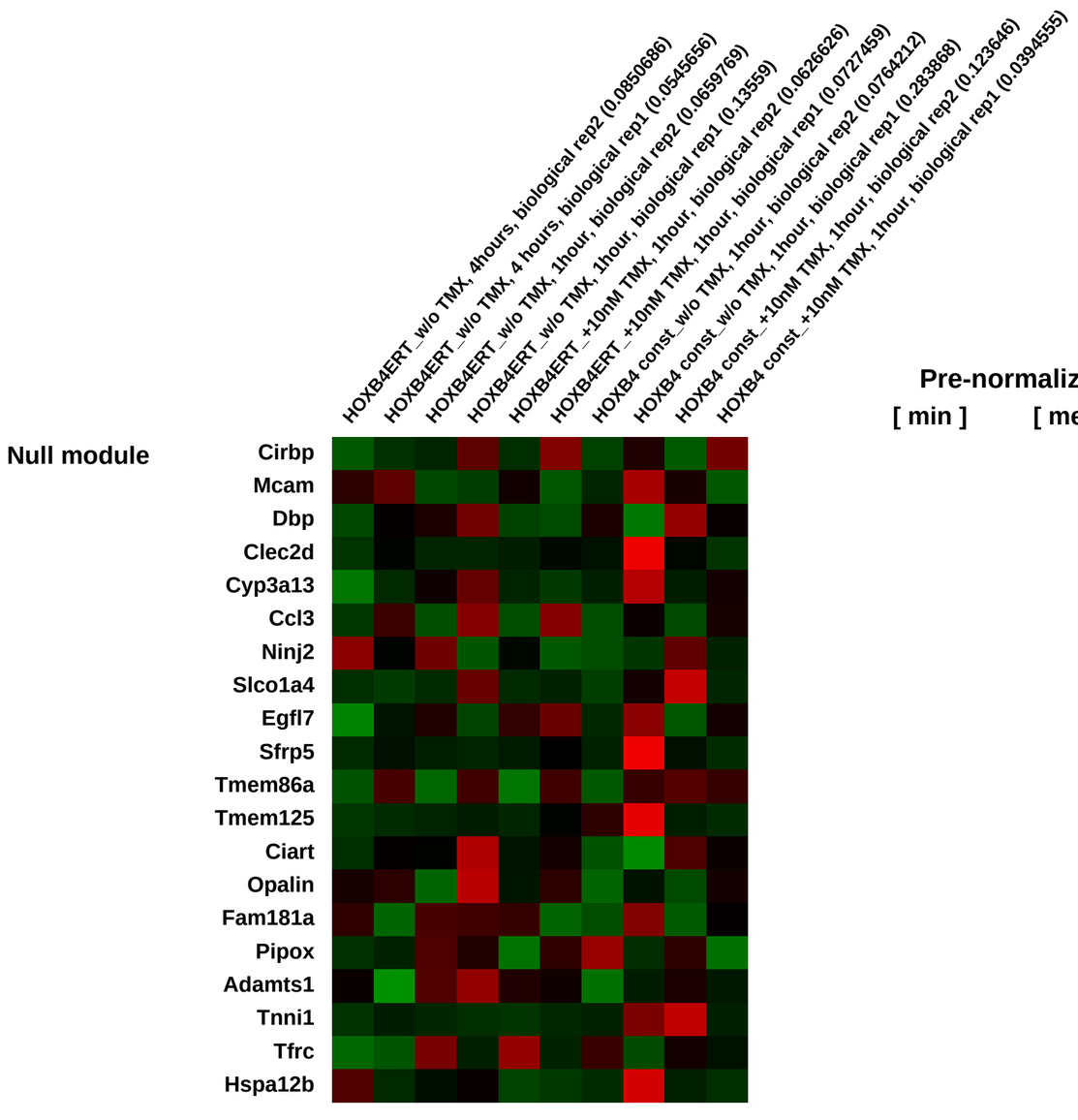

GEO Series "GSE9012" Expression Profiles

Num of samples in this series: 10

Scale of expression profile Z-scores

-3.0 -2.0 -1.0 0.0 1.0 2.0 3.0

GEO Link:	http://www.ncbi.nlm.nih.gov/geo/query/acc.cgi?acc=GSE9012
Status:	Public on Nov 19 2007
Title:	Expression data from spontaneous liver tumors of Trim24/TIF1a-null mice.
Organism:	Mus musculus
Experiment type:	Expression profiling by array
Platform:	GPL1261
Pubmed ID:	18026104
Summary & Design:	**Summary:** The transcriptional coregulator Trim24 (formerly known as TIF1a) functions in mice as a liver-specific tumor suppressor. Mice carrying a null mutation in the Trim24 gene all develop hepatocellular carcinoma (HCC). We used microarrays to identify the alterations in gene expression patterns associated with loss of Trim24 and consequent HCC development. Keywords: normal-tumor comparison **Overall design:** Five independent liver tumor (HCC) samples taken from five Trim24 knockout (KO) mice and five normal liver tissue samples taken from wild-type (WT) littermate controls were used for RNA extraction and hybridization on Affymetrix microarrays.

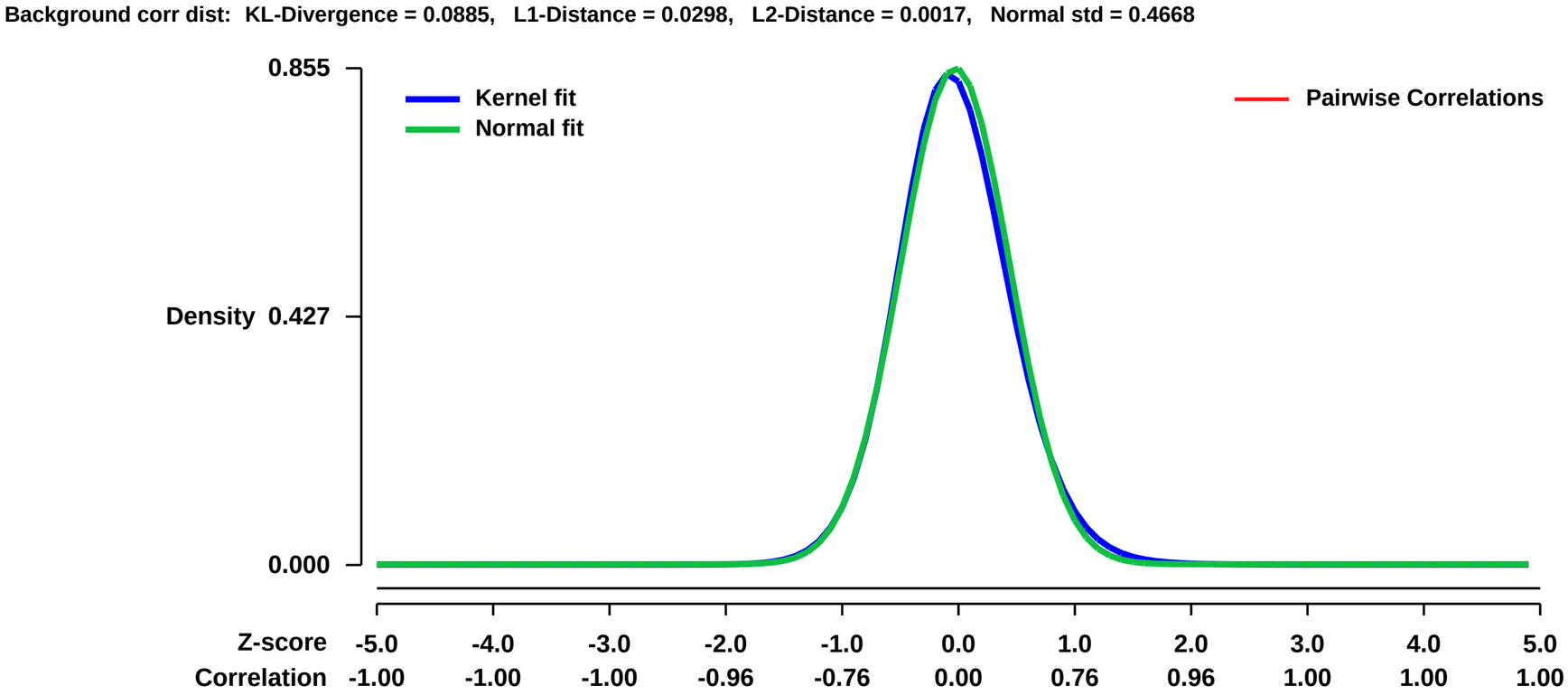

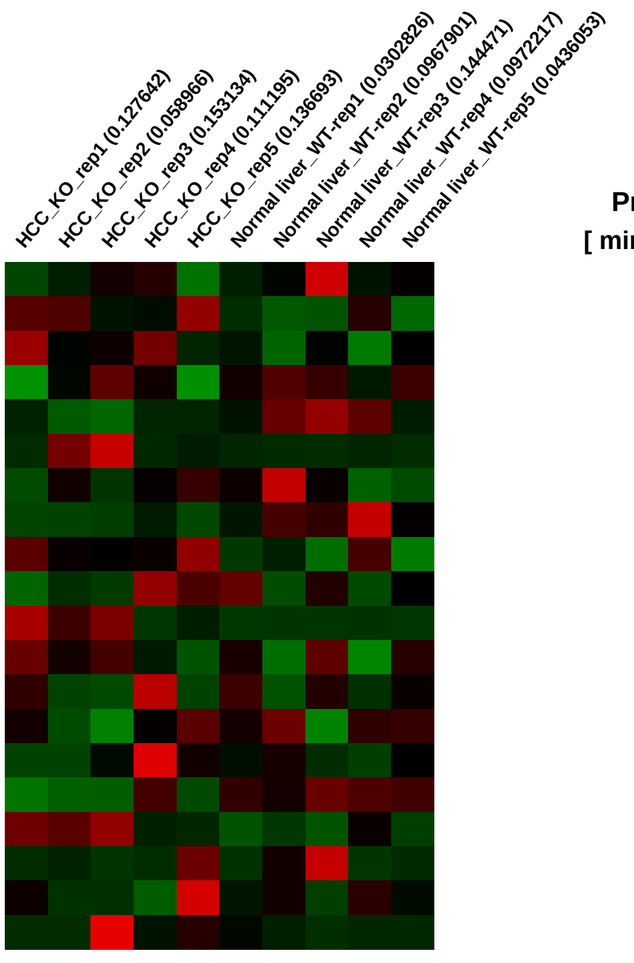

GEO Series "GSE9018" Expression Profiles

Num of samples in this series: 9

Scale of expression profile Z-scores

-3.0 -2.0 -1.0 0.0 1.0 2.0 3.0

GEO Link:	**http://www.ncbi.nlm.nih.gov/geo/query/acc.cgi?acc=GSE9018**
Status:	**Public on Dec 27 2007**
Title:	**IgA impact on distal small intestine after colonization with B. thetaiotaomicron**
Organism:	**Mus musculus**
Experiment type:	**Expression profiling by array**
Platform:	**GPL1261**
Pubmed ID:	**18005754**
Summary & Design:	**Summary:** **Wildtype B6, Rag1-/- B6 and Rag1-/- B6 mice harboring the 225.4 IgA producing hybridoma were colonized for 10 days with Bacteroides thetaiotaomicron** **Keywords: RNA Expression Array** **Overall design:** **Distal small intestine segments were snap frozen immediately after the mice were sacrificed, and small intestine divided into 16 equal segments, segments 10, 11, 12 and 14 were pooled and RNA extracted.**

Background corr dist: **KL-Divergence = 0.0788, L1-Distance = 0.0223, L2-Distance = 0.0008, Normal std = 0.4803**

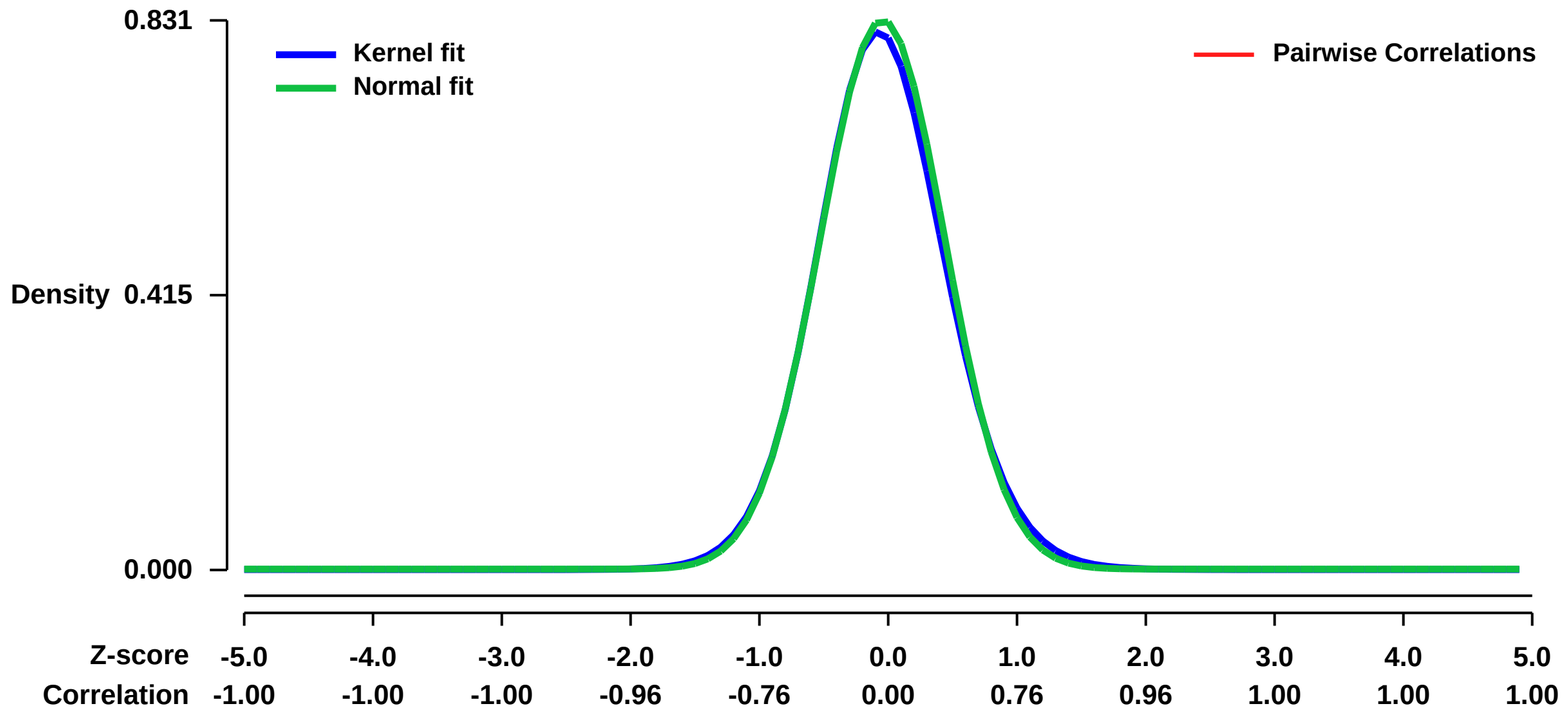

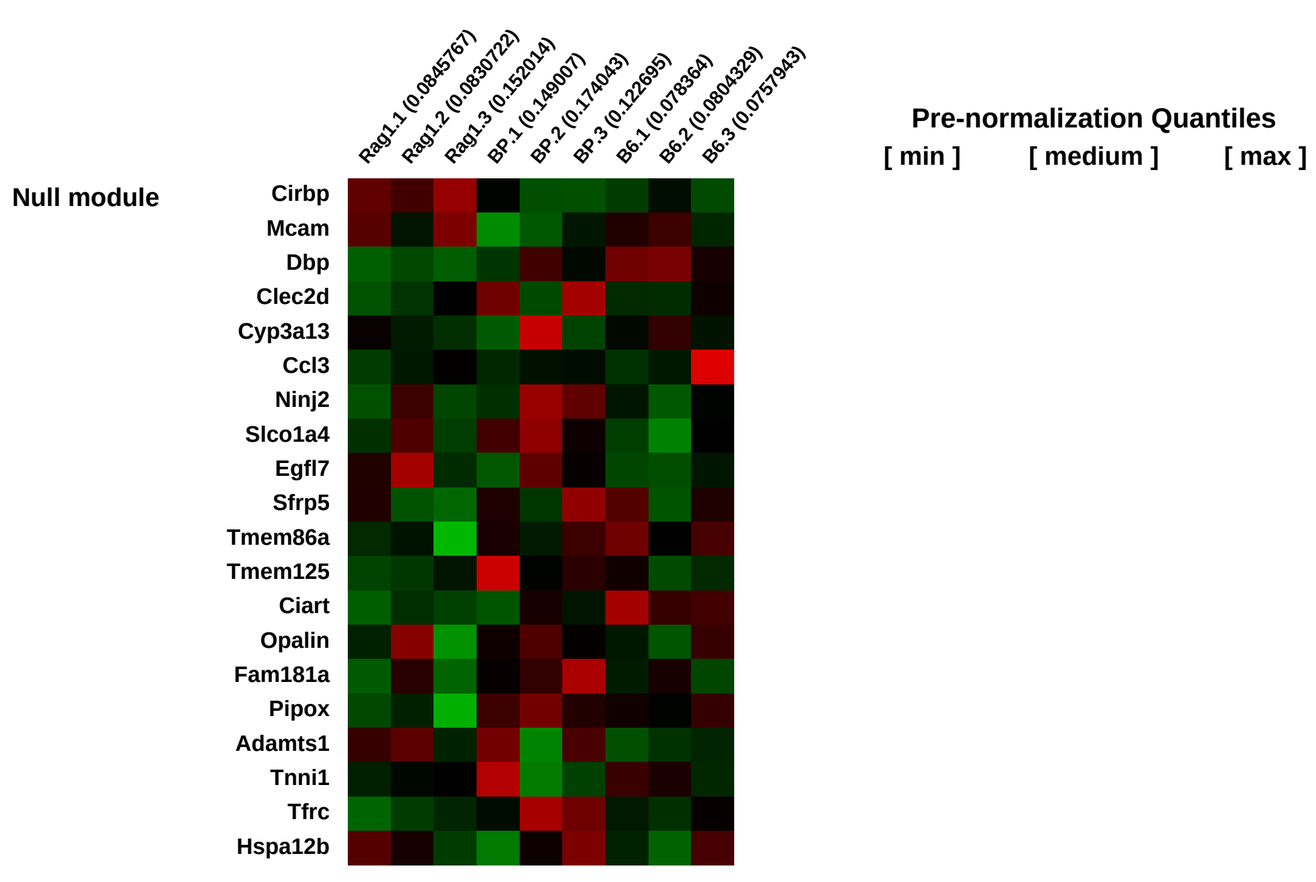

GEO Series "GSE9037" Expression Profiles

Num of samples in this series: 12

Scale of expression profile Z-scores

-3.0 -2.0 -1.0 0.0 1.0 2.0 3.0

GEO Link:	http://www.ncbi.nlm.nih.gov/geo/query/acc.cgi?acc=GSE9037
Status:	Public on Jun 25 2008
Title:	response to LPS of WT and IRAK4 kinase dead mouse bone marrow macrophages
Organism:	Mus musculus
Experiment type:	Expression profiling by array
Platform:	GPL1261
Pubmed ID:	18266302
Summary & Design:	**Summary:** **IRAK-4 is an essential component of the signal transduction complex downstream of the IL-1- and Toll-like receptors. Though regarded as the first kinase in the signaling cascade, the role of IRAK-4 kinase activity versus its scaffold function is still controversial. In order to investigate the role of IRAK-4 kinase function in vivo, â knock-inâ mice were generated by replacing the wild type IRAK-4 gene with a mutant gene encoding kinase deficient IRAK-4 protein (IRAK-4 KD). Analysis of bone marrow macrophages obtained from WT and IRAK-4 KD mice with a number of experimental techniques demonstrated that the IRAK-4 KD cells greatly lack responsiveness to stimulation with the Toll-like receptor 4 (TLR4) agonist LPS. One of the techniques used, microarray analysis, identified IRAK-4 kinase-dependent LPS response genes and revealed that the induction of LPS-responsive mRNAs was largely ablated in IRAK-4 KD cells. In summary, our results suggest that IRAK-4 kinase activity plays a critical role in TLR4-mediated induction of inflammatory responses.** **Keywords: genetic modification, strain comparison, cell stimulation, time course, anti-bacterial response, innate immune response, inflammatory response** **Overall design:** **The response of mouse bone marrow macrophages from WT and IRAK4 kinase dead animals to stimulation with LPS at two time points was determined. There were 12 samples in total, 6 from WT and 6 from IRAK4 kinase dead cells; for each strain there were 3 conditions: growth for 4 hours without stimulation (the strain-specific control), growth for 1 hour with stimulation, and growth for 4 hours with stimulation; for each condition there were two biological replicates.**

Background corr dist: KL-Divergence = 0.1460, L1-Distance = 0.0329, L2-Distance = 0.0021, Normal std = 0.3783

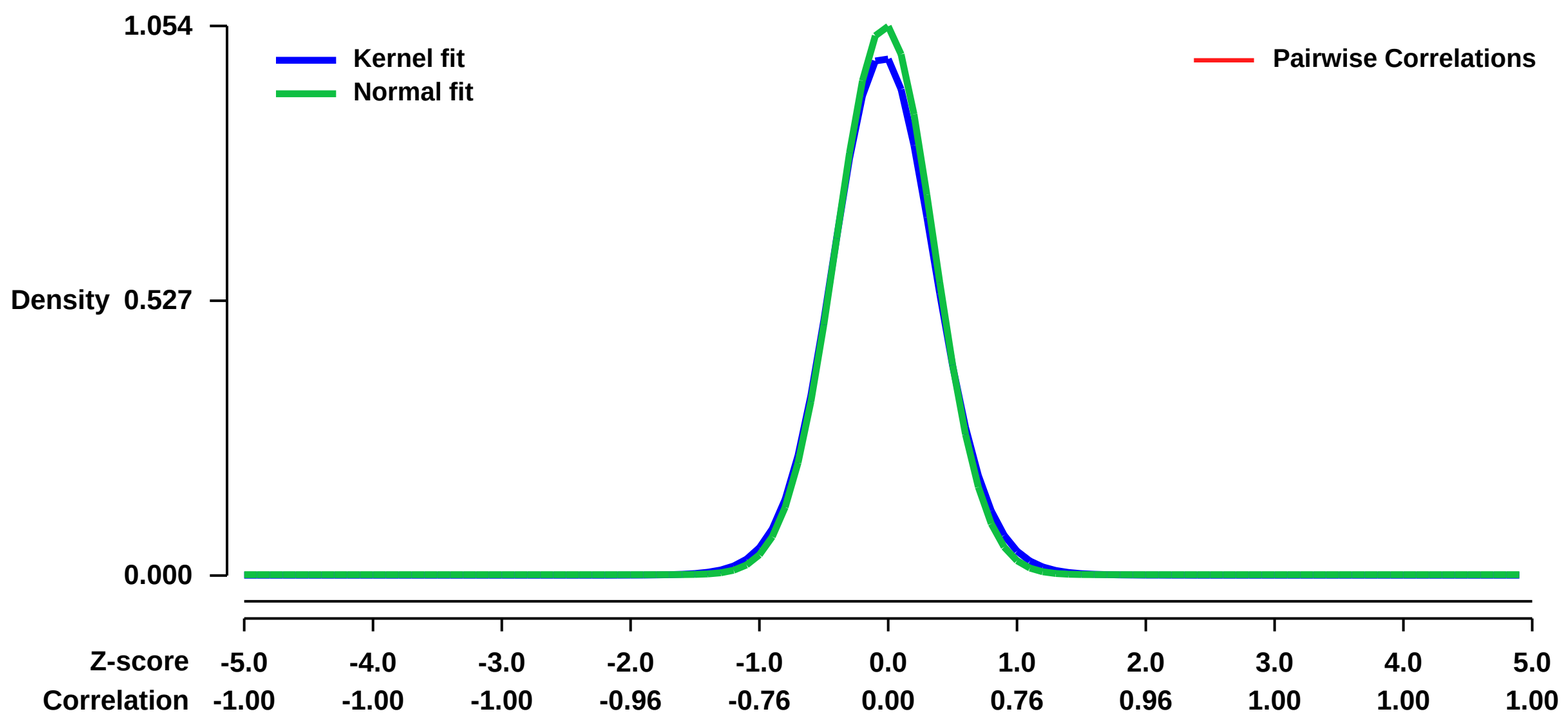

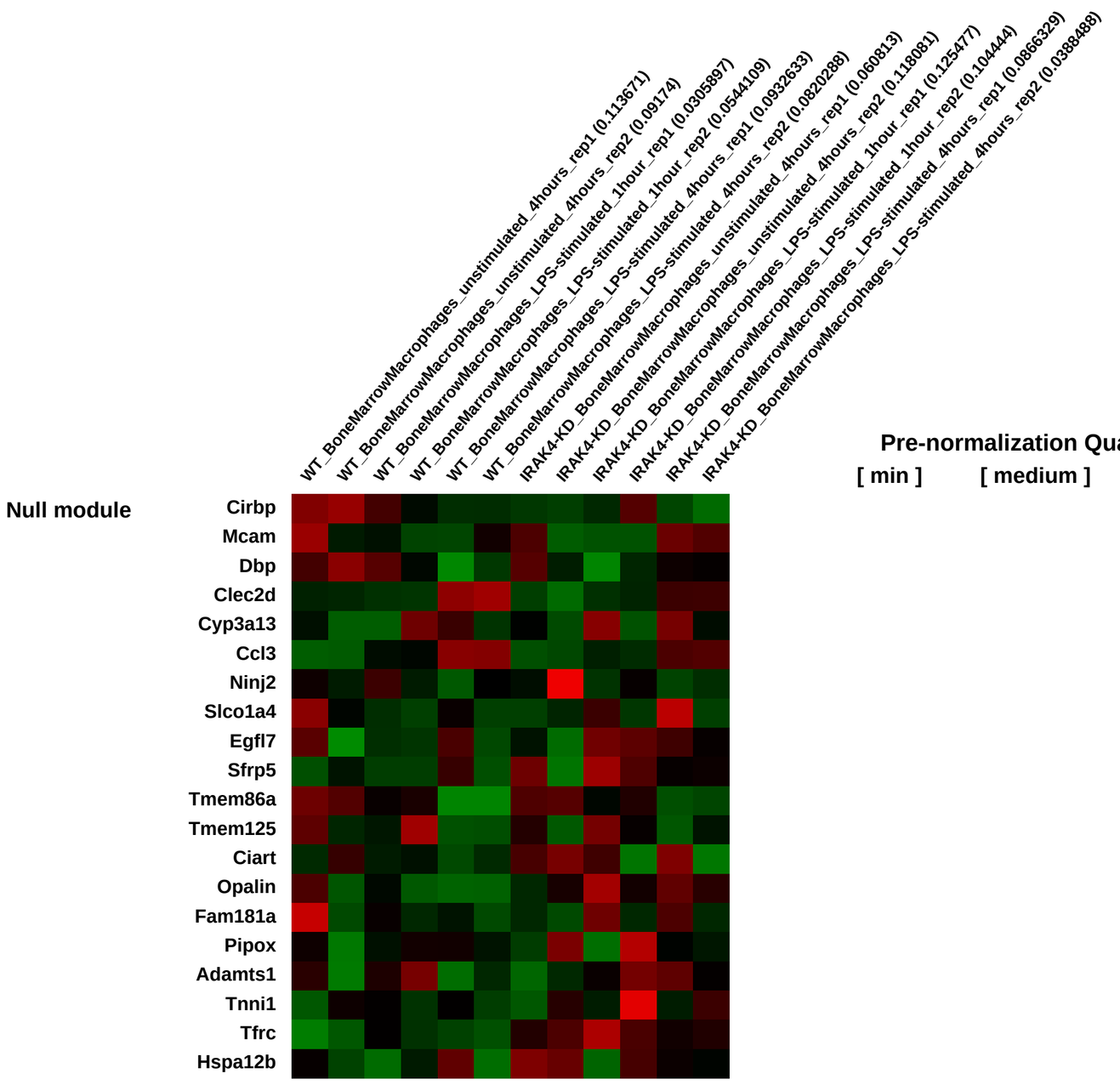

GEO Series "GSE9043" Expression Profiles

Num of samples in this series: 6

Scale of expression profile Z-scores

-3.0 -2.0 -1.0 0.0 1.0 2.0 3.0

GEO Link: http://www.ncbi.nlm.nih.gov/geo/query/acc.cgi?acc=GSE9043
Status: Public on Aug 24 2011
Title: Dap12 microglia
Organism: Mus musculus
Experiment type: Expression profiling by array
Platform: GPL1261
Pubmed ID:

Summary & Design:

Summary:
Polycystic lipomembranous osteodysplasia with sclerosing leukoencephalopathy (PLOSL) is an inherited brain and bone disease. It manifests as dementia and bone fractures. The PLOSL phenotype is caused by loss-of-function mutations in one of the two genes encoding the components of the DAP12/TREM2 receptor complex. The DAP12/TREM2 complex is expressed in cells of the myeloid lineage, including microglia in the central nervous system (CNS). The molecular mechanisms producing the CNS phenotype of PLOSL remain largely unknown. To gain insight into dysfunctional CNS pathways behind PLOSL, we performed genome-wide expression analysis of Dap12 (Tyrobp)-deficient mouse microglial cells.

Keywords: knock-out response

Overall design:
Transcript profiles of three wild type and three Dap12-deficient primary microglial cultures were analyzed.

Background corr dist: KL-Divergence = 0.0465, L1-Distance = 0.0288, L2-Distance = 0.0011, Normal std = 0.5993

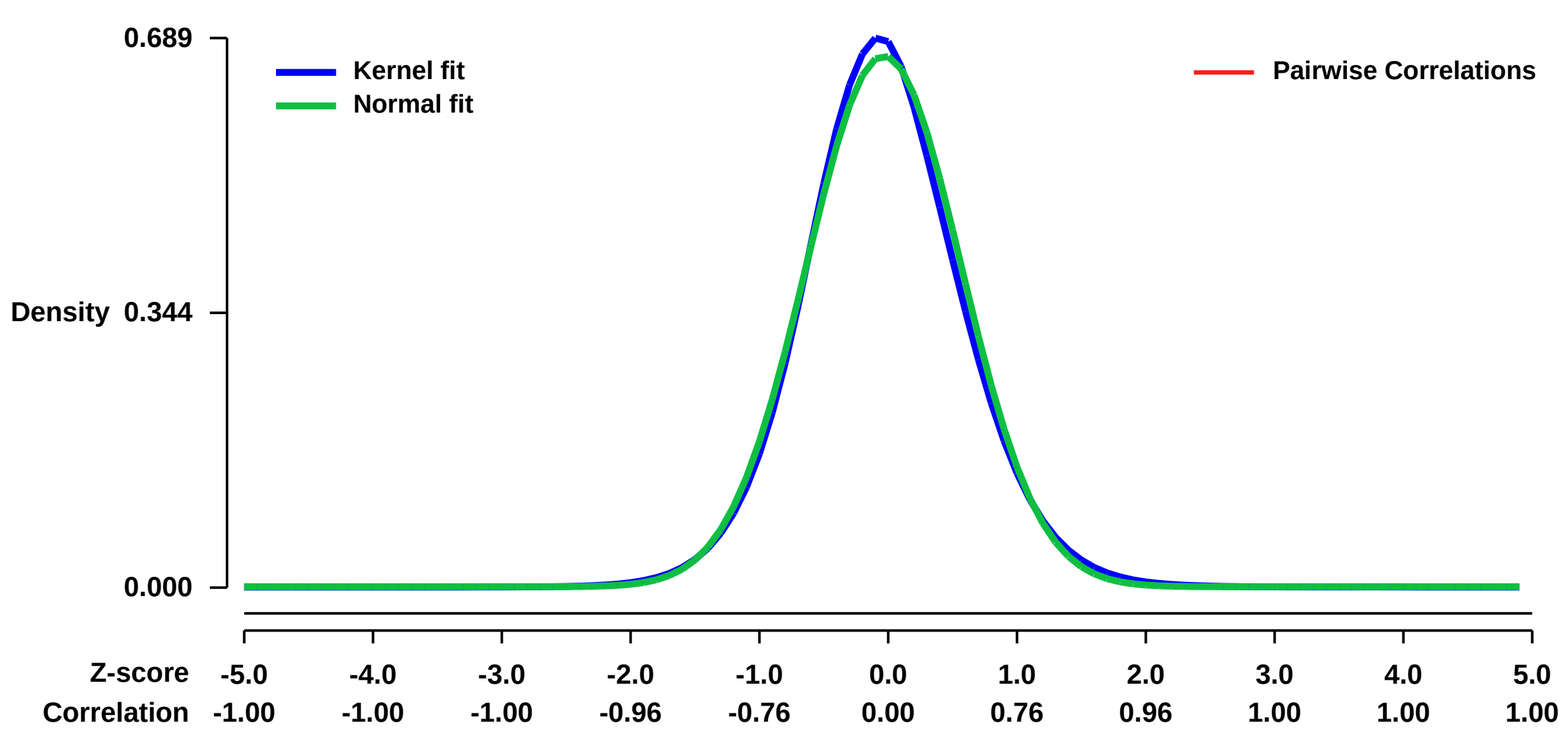

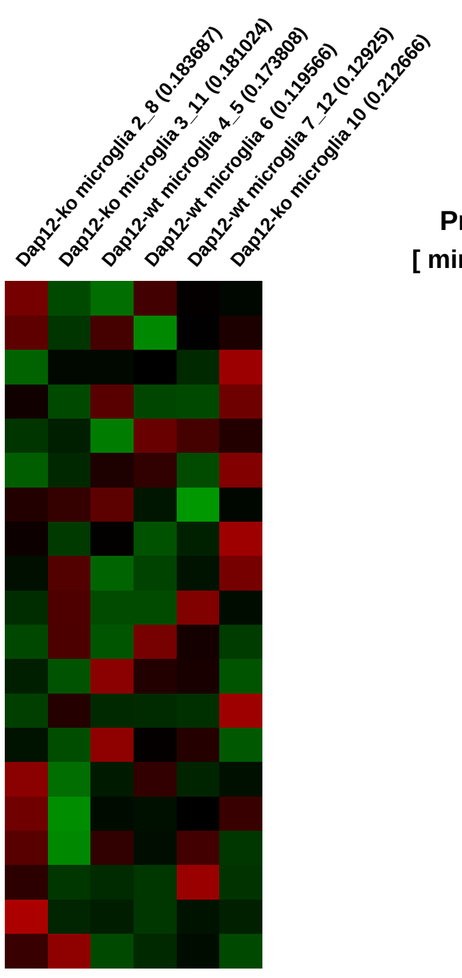

GEO Series "GSE9044" Expression Profiles

Num of samples in this series: 6

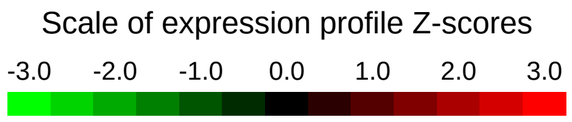

GEO Link:	**http://www.ncbi.nlm.nih.gov/geo/query/acc.cgi?acc=GSE9044**
Status:	**Public on Sep 19 2007**
Title:	**HOXB4 target genes in ES cell-derived embryoid bodies (EBs)**
Organism:	**Mus musculus**
Experiment type:	**Expression profiling by array**
Platform:	**GPL1261**
Pubmed ID:	**17940039**
Summary & Design:	**Summary:** **To unravel the molecular mechanism by which HOXB4 promotes the expansion of early hematopoietic progenitors within differentiating ES cells, we analzed the gene expression profiles of embryoid bodies (EBs) in which transcription of HOXB4 had been induced or not induced. A substantial number of the identified HOXB4 target genes are involved in signaling pathways important for controlling self-renewal, maintenance and differentiation of stem cells. Furthermore, we demonstrate that HOXB4 activity and FGF-signaling are intertwined. HOXB4-mediated expansion of ES cell-derived early progenitors was enhanced by specific and complete inhibition of FGF-receptors. In contrast, the expanding activity of HOXB4 on hematopoietic progenitors in day4-6 embryoid bodies was blunted in the presence of basic FGF (FGF2) indicating a dominant negative effect of FGF-signaling on the earliest hematopoietic cells. Taken together, we show that modulation of FGF signaling is an essential feature of HOXB4 activity in the context of embryonic hematopoiesis.** **Keywords: plus/minus induction of HOXB4 gene expression by treatment with doxycycline (Dox)** **Overall design:** **Biological replicates: 3**

Background corr dist: KL-Divergence = 0.0351, L1-Distance = 0.0254, L2-Distance = 0.0008, Normal std = 0.6458

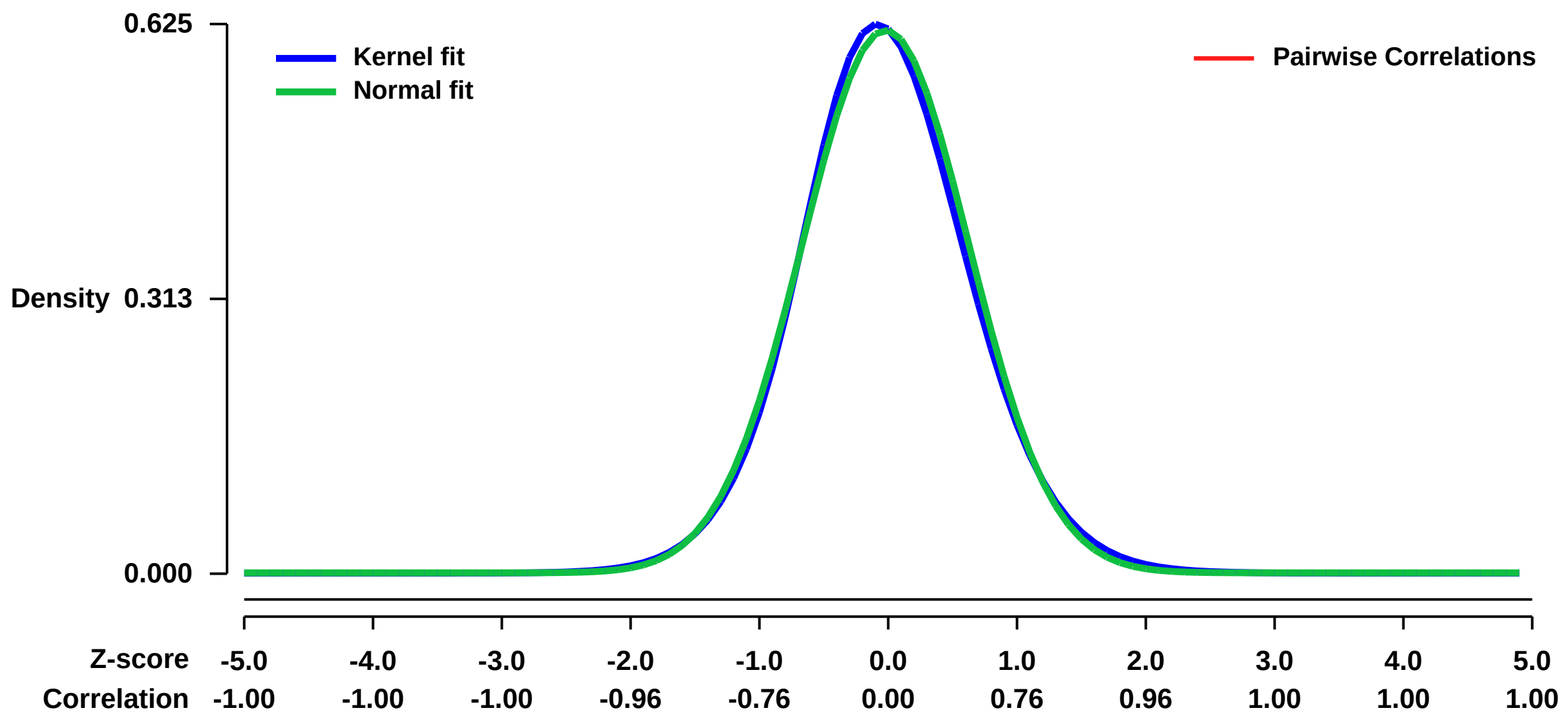

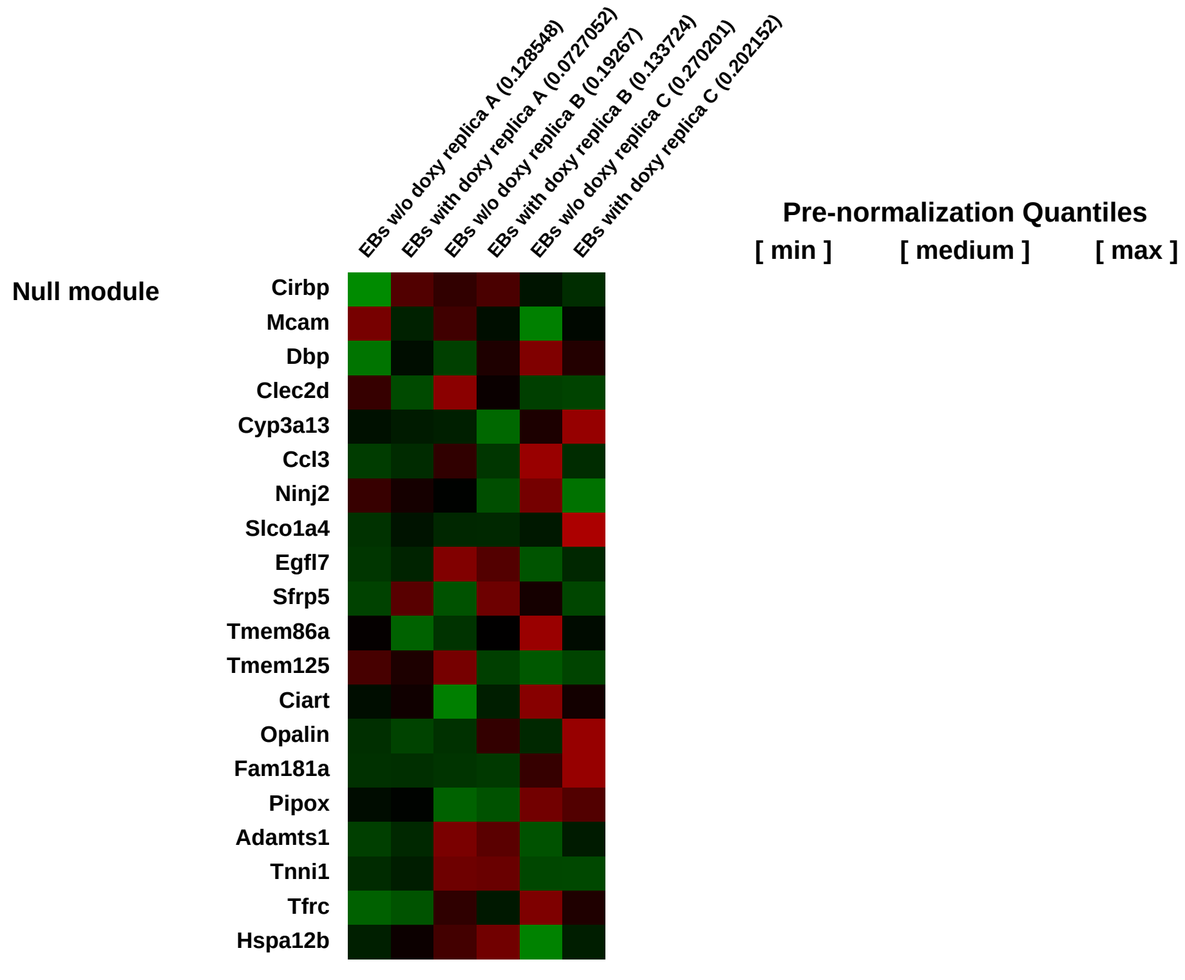

GEO Series "GSE9061" Expression Profiles

Num of samples in this series: 6

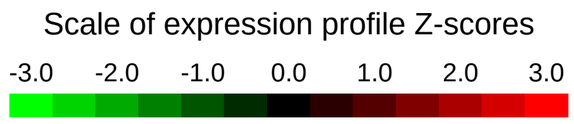

GEO Link:	**http://www.ncbi.nlm.nih.gov/geo/query/acc.cgi?acc=GSE9061**
Status:	**Public on Aug 24 2011**
Title:	**Dap12-deficient mouse brain (1 month)**
Organism:	**Mus musculus**
Experiment type:	**Expression profiling by array**
Platform:	**GPL1261**
Pubmed ID:	
Summary & Design:	**Summary:** **Polycystic lipomembranous osteodysplasia with sclerosing leukoencephalopathy (PLOSL) is an inherited brain and bone disease. It manifests as dementia and bone fractures. The PLOSL phenotype is caused by loss-of-function mutations in one of the two genes encoding the components of the DAP12/TREM2 receptor complex. The DAP12/TREM2 complex is expressed in cells of the myeloid lineage, including microglia in the central nervous system (CNS). The molecular mechanisms producing the CNS phenotype of PLOSL remain largely unknown. To gain insight into dysfunctional CNS pathways behind PLOSL, we performed genome-wide expression analysis of Dap12 (Tyrobp)-deficient mouse brain. In Dap12-deficient mice, we observed alterations in several pathways involved in synaptic function. In agreement with the myelin loss in PLOSL patients, we also saw changes in transcript levels of genes encoding myelin components.** **Keywords: knockout response** **Overall design:** **Transcript profiles of the midbrain (diencephalon and basal ganglia) of three Dap12-knockout and three heterozygous mice were analyzed.**

Background corr dist: KL-Divergence = 0.0275, L1-Distance = 0.0302, L2-Distance = 0.0012, Normal std = 0.7023

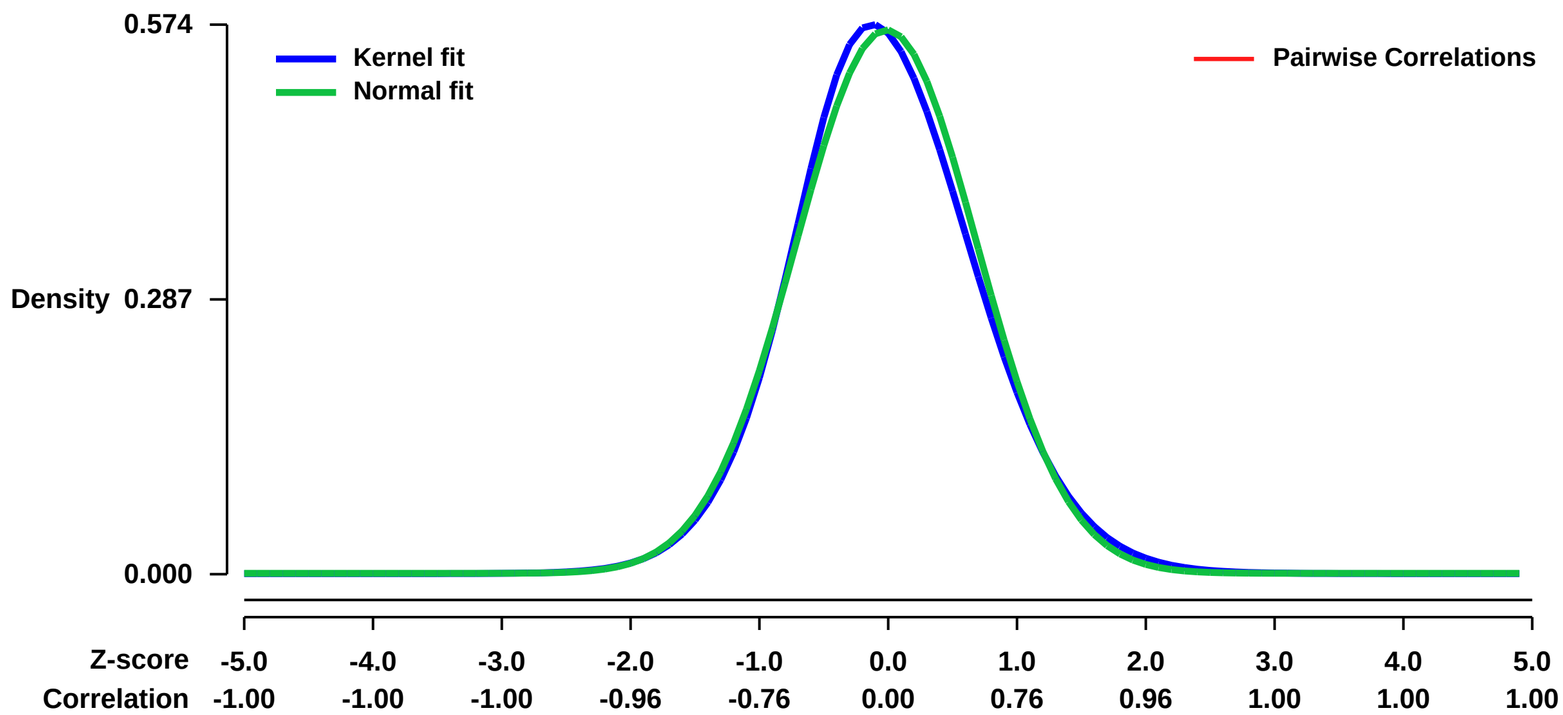

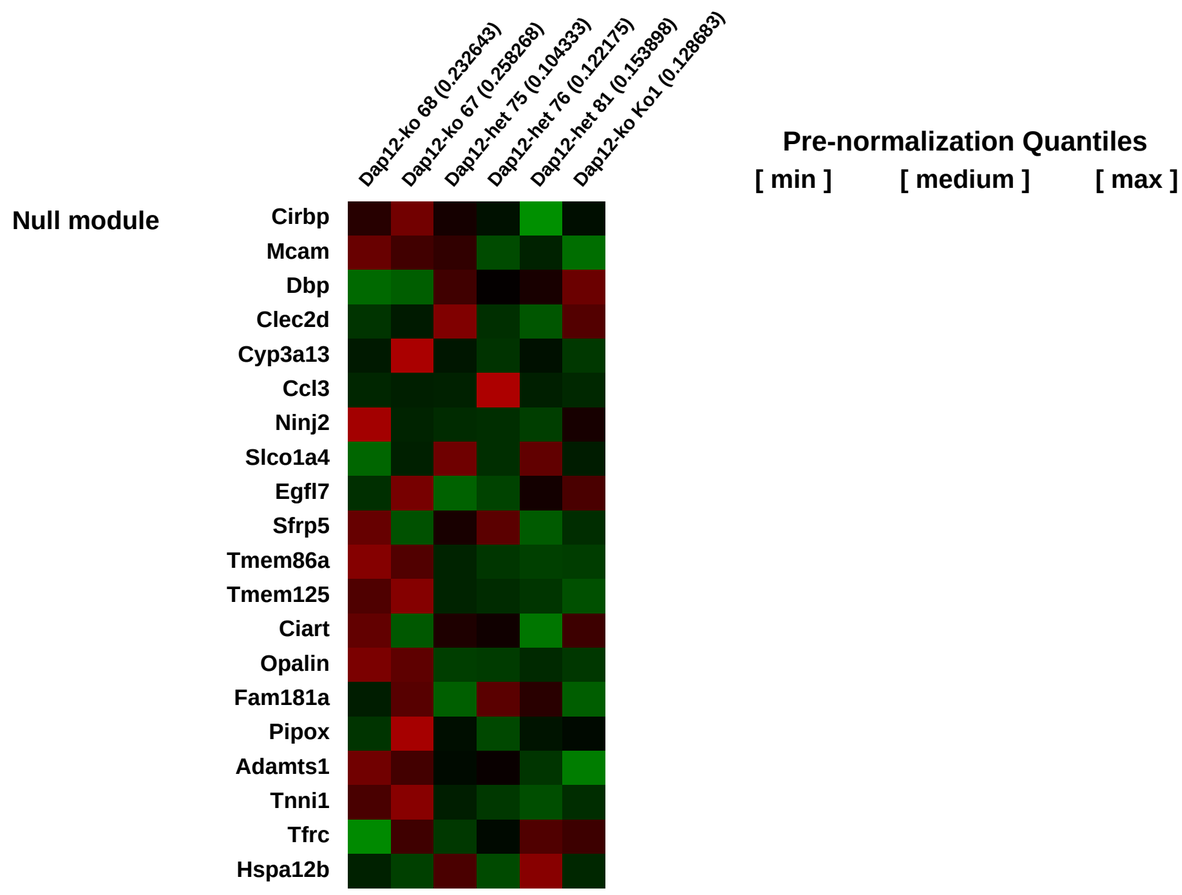

GEO Series "GSE9123" Expression Profiles

Num of samples in this series: 8

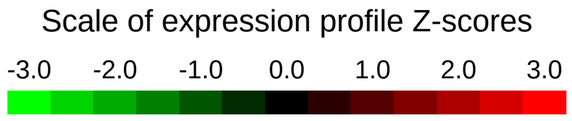

GEO Link:	http://www.ncbi.nlm.nih.gov/geo/query/acc.cgi?acc=GSE9123
Status:	Public on Sep 22 2007
Title:	transcription factor PlagL2 regulates steps in chylomicron metabolism
Organism:	Mus musculus
Experiment type:	Expression profiling by array
Platform:	GPL1261
Pubmed ID:	17983586
Summary & Design:	**Summary:** Enterocytes assemble dietary lipids into chylomicron particles that are taken up by intestinal lacteal vessels and peripheral tissues. Although chylomicrons are known to assemble in part within membrane secretory pathways, the modifications required for efficient vascular uptake are unknown. We report that the transcription factor Pleomorphic adenoma gene-like 2 (PLAGL2) is essential for this aspect of dietary lipid metabolism. PlagL2-/- mice die from post-natal wasting owing to failure of fat absorption. Lipids modified in the absence of PlagL2 exit from enterocytes but fail to enter interstitial lacteal vessels. Dysregulation of enterocyte genes closely linked to intracellular membrane transport identified candidate regulators of critical steps in chylomicron assembly. PlagL2 thus regulates essential and poorly understood aspects of dietary lipid absorption and its deficiency represents an authentic animal model with implications for amelioration of obesity or the metabolic syndrome. **Keywords:** gene expression profiling analysis **Overall design:** Total RNA was extracted from 4 knockout and 4 wild-type mouse small intestines at 18.5 dpc using the Macherey-Nagel Nucleospin kit. cRNA synthesis and labeling, hybridization to Affymetrix (Santa Clara, CA) MOE430 2.0 expression arrays, and data acquisition occurred on the Affymetrix GeneChip Instrument System.

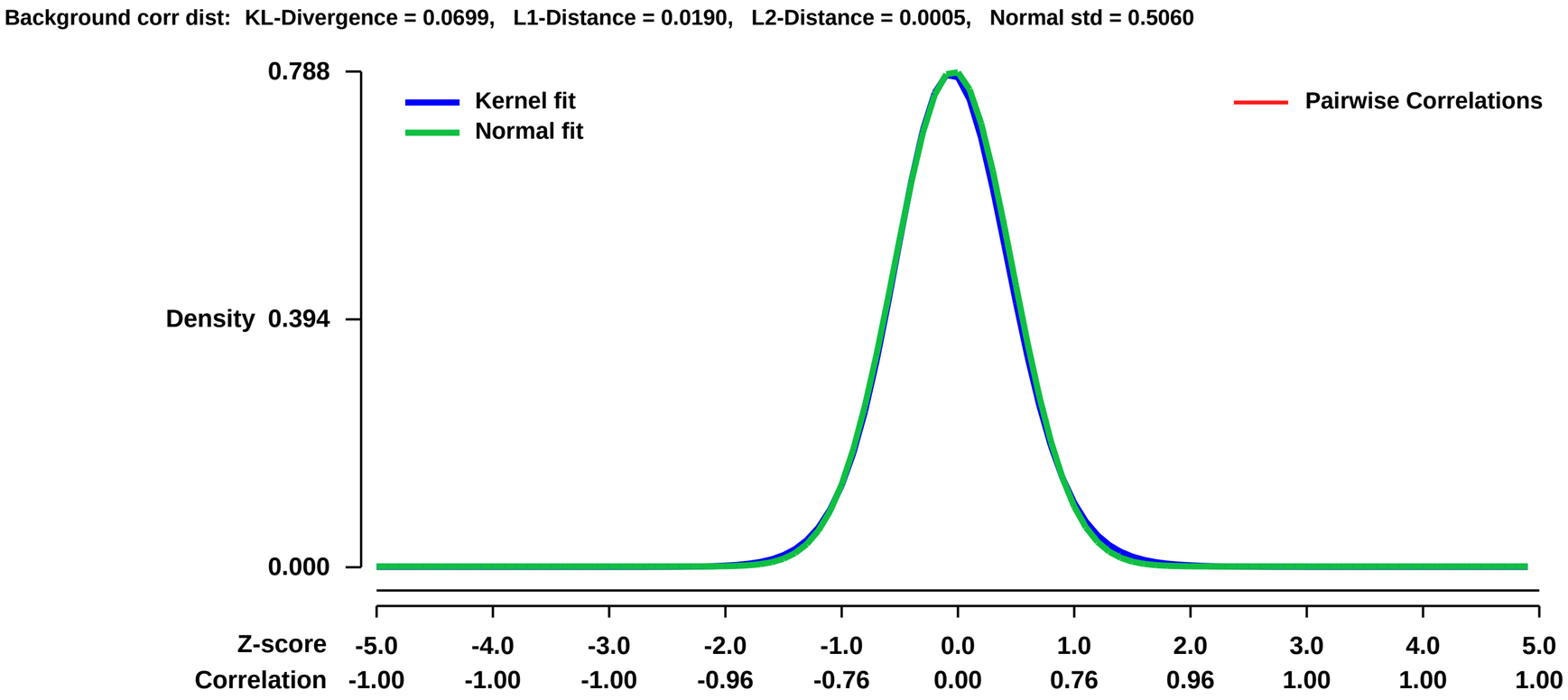

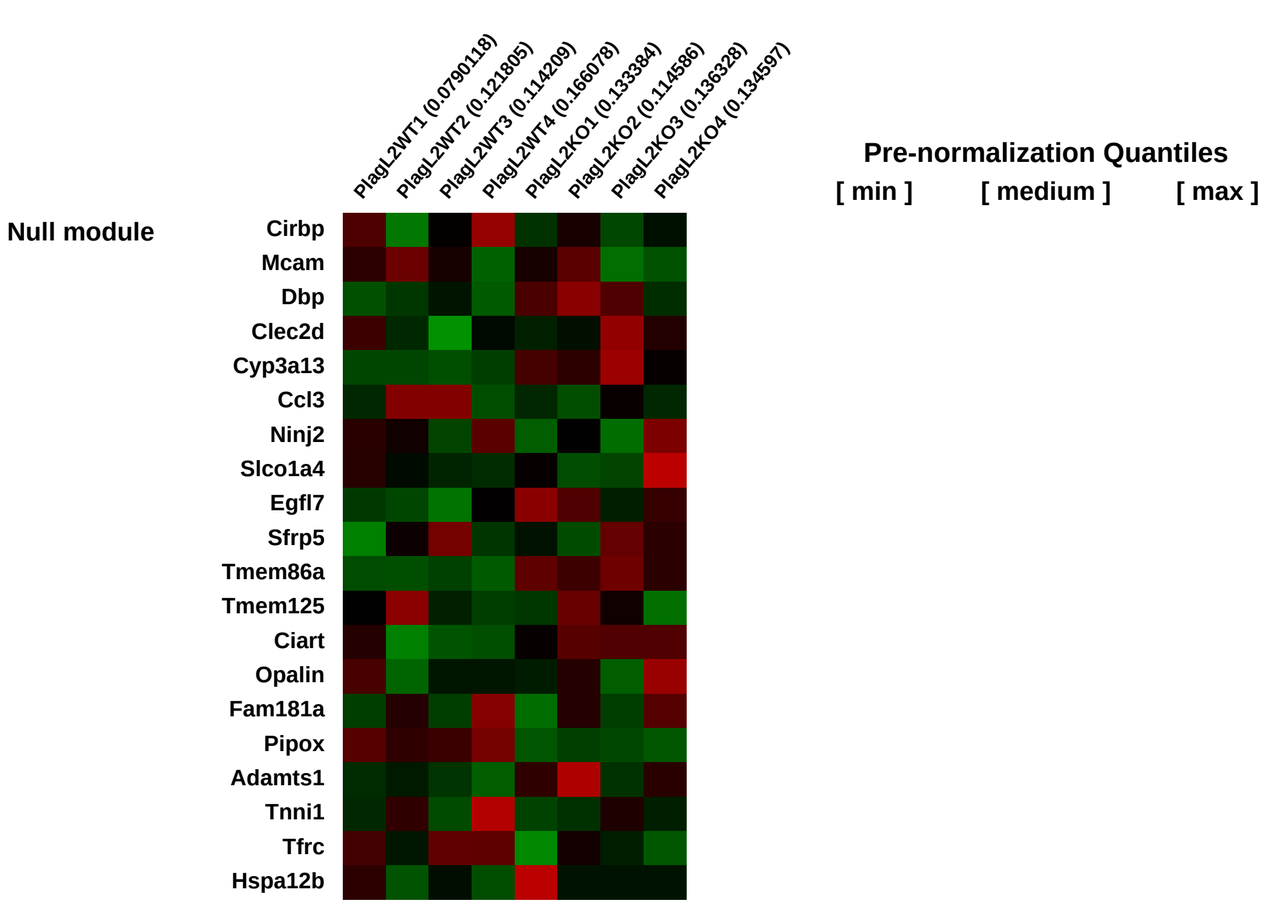

GEO Series "GSE9124" Expression Profiles

Num of samples in this series: 6

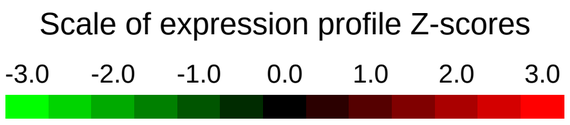

GEO Link:	http://www.ncbi.nlm.nih.gov/geo/query/acc.cgi?acc=GSE9124
Status:	Public on Nov 01 2007
Title:	Gene expression profiling of E12.5 wildtype- and Sp3 null hearts
Organism:	Mus musculus
Experiment type:	Expression profiling by array
Platform:	GPL1261
Pubmed ID:	17923686
Summary & Design:	**Summary:** Mice lacking the zinc finger transcription factor Specificity protein 3 (Sp3) die prenatally in the C57Bl/6 background. To elucidate the cause of mortality we analyzed the potential role of Sp3 in embryonic heart development. Sp3 null hearts display defective looping at E10.5, and at E14.5 the Sp3 null mutants have developed a range of severe cardiac malformations. In an attempt to position Sp3 in the cardiac developmental hierarchy, we analysed the expression patterns of >15 marker genes in Sp3 null hearts. Expression of Cardiac ankyrin repeat protein (Carp) was downregulated prematurely after E12.5, while expression of the other marker genes was not affected. ChIP analysis revealed that Sp3 is bound to the Carp promoter region in vivo. Microarray analysis indicates that small molecule metabolism and cell-cell interactions are the most significantly affected biological processes in E12.5 Sp3 null myocardium. Since the epicardium showed distension from the myocardium, we studied expression of Wt1, a marker for epicardial cells. Wt1 expression was diminished in epicardium-derived cells in the myocardium of Sp3 null hearts. We conclude that Sp3 is required for normal cardiac development, and suggest that it has a crucial role in myocardial differentiation. (**Keywords:** Transcription factors, Sp3, knockout mice, cardiac malformations, E12.5 **Overall design:** Hearts were dissected from E12.5 wildtype (n=3) and Sp3 knockout (n=3) fetuses. Total RNA was isolated from individual hearts; 5¸…g was used for labelling and hybridization to 430 2.0 Gene Chips (a total of 6).

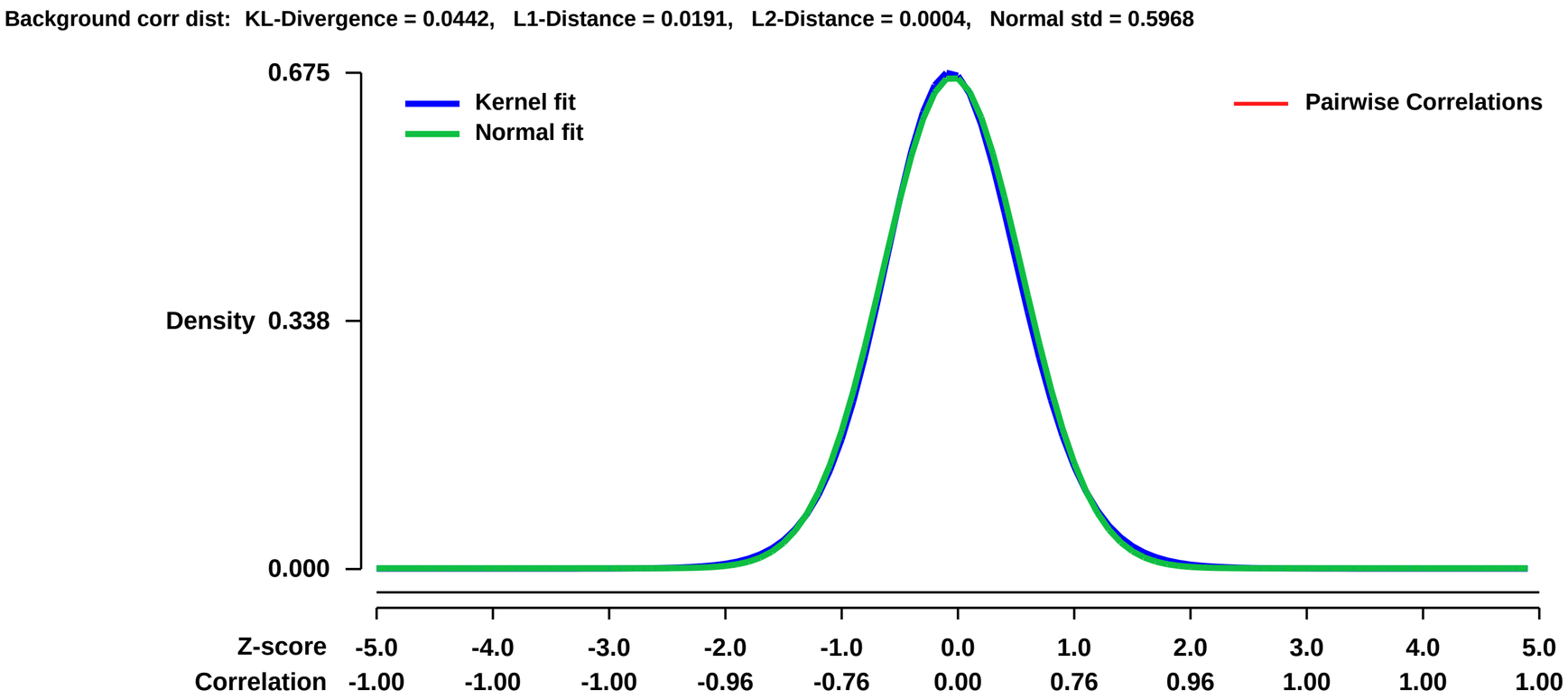

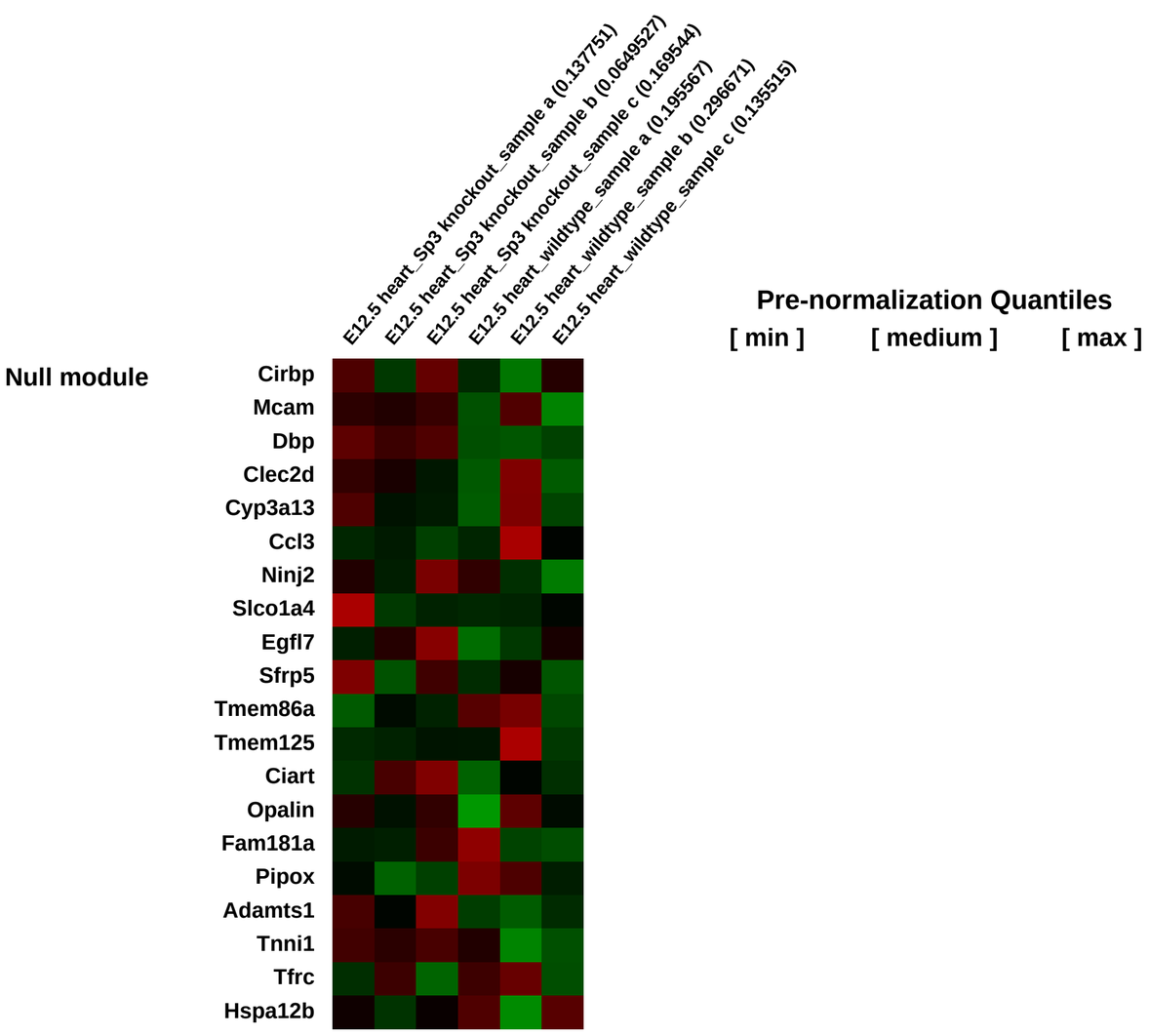

GEO Series "GSE9130" Expression Profiles

Num of samples in this series: 6

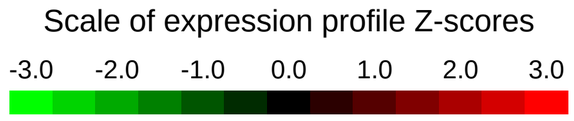

GEO Link:	**http://www.ncbi.nlm.nih.gov/geo/query/acc.cgi?acc=GSE9130**
Status:	**Public on Sep 22 2007**
Title:	**aP2-nSREBP1c_white_Adipose_Tissue_expression_differentials**
Organism:	**Mus musculus**
Experiment type:	**Expression profiling by array**
Platform:	**GPL1261**
Pubmed ID:	**17921248**
Summary & Design:	**Summary:** **Identifying gene expression changes in adipose tissue of lipodystrophic aP2-nSREBP1c trangenic mice** **Keywords: Genetic modification** **Overall design:** **RNA from epididymal white adipose pads of three 10-week-old aP2-nSREBP1c transgenic males and three litter-matched WT controls was analyzed by MOE430v2.0 GeneChipâ¢ arrays, one mouse per array.**

Background corr dist: **KL-Divergence = 0.0222, L1-Distance = 0.0289, L2-Distance = 0.0009, Normal std = 0.7553**

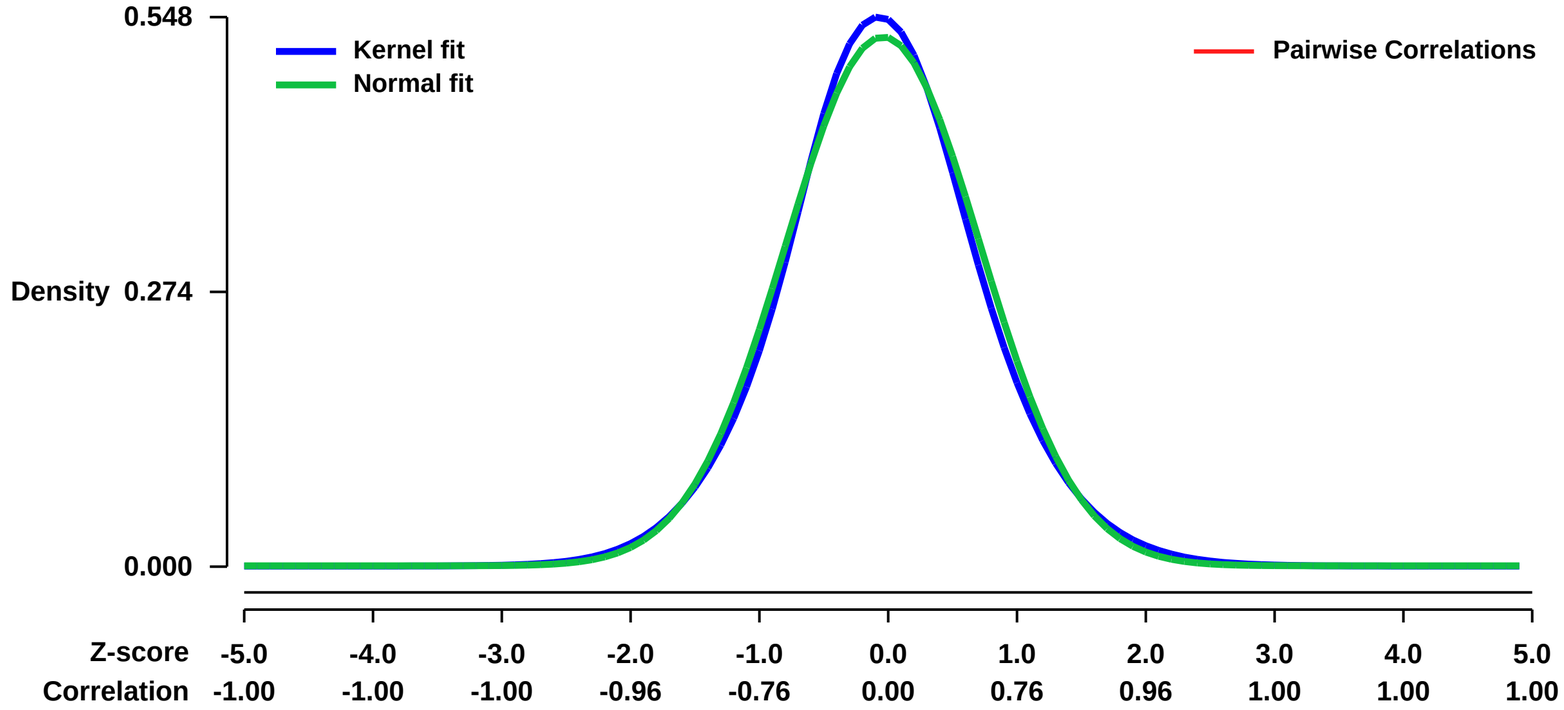

Pre-normalization Quantiles

[min] [medium] [max]

Null module

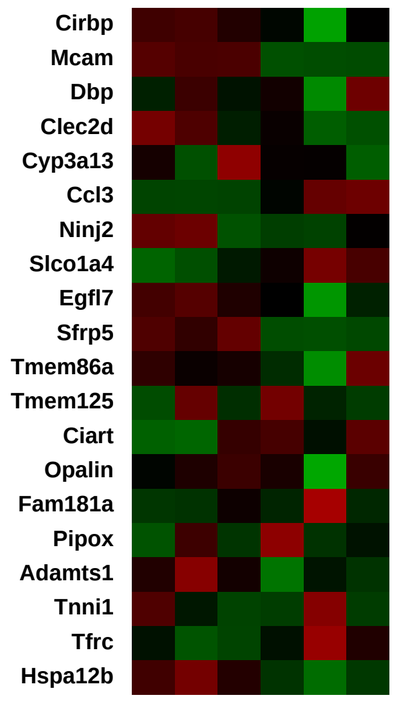

GEO Series "GSE9131" Expression Profiles

Num of samples in this series: 6

Scale of expression profile Z-scores

-3.0 -2.0 -1.0 0.0 1.0 2.0 3.0

GEO Link:	**http://www.ncbi.nlm.nih.gov/geo/query/acc.cgi?acc=GSE9131**
Status:	**Public on Sep 22 2007**
Title:	**Pparg<ldi/+> white Adipose Tissue expression differentials**
Organism:	**Mus musculus**
Experiment type:	**Expression profiling by array**
Platform:	**GPL1261**
Pubmed ID:	**17921248**
Summary & Design:	**Summary:** **Identifying gene expression changes in adipose tissue of lipodystrophic Pparg<ldi/+> targeted mice** **Keywords: Genetic modification** **Overall design:** **RNA from epididymal white adipose pads of three 10-week-old Pparg<ldi/+> males and three litter-matched WT controls was analyzed by MOE430v2.0 GeneChipâ¢ arrays, one mouse per array.**

Background corr dist: **KL-Divergence = 0.0333, L1-Distance = 0.0274, L2-Distance = 0.0008, Normal std = 0.6683**

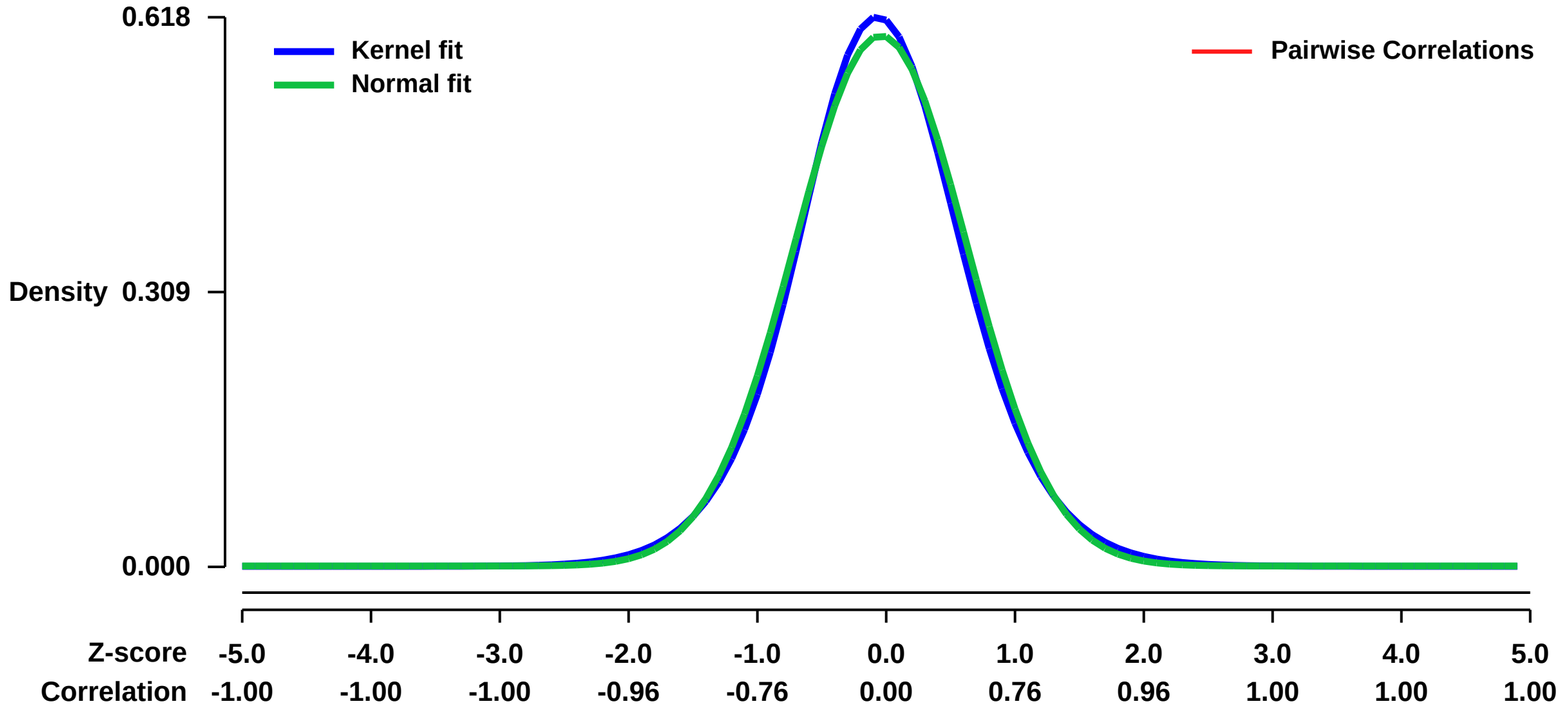

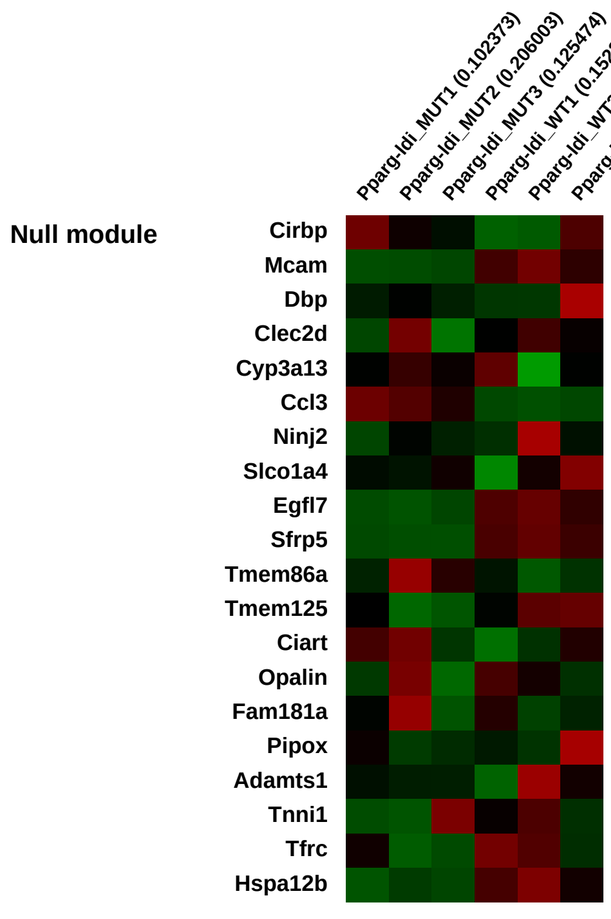

GEO Series "GSE9146" Expression Profiles

Num of samples in this series: 27

Scale of expression profile Z-scores

-3.0 -2.0 -1.0 0.0 1.0 2.0 3.0

GEO Link:	http://www.ncbi.nlm.nih.gov/geo/query/acc.cgi?acc=GSE9146
Status:	Public on Apr 04 2008
Title:	Irradiation response in PKBalpha MEF
Organism:	Mus musculus
Experiment type:	Expression profiling by array
Platform:	GPL1261
Pubmed ID:	18439899
Summary & Design:	**Summary:** MEF proficient or deficient in PKBalpha, or PKBalpha knockout MEF where PKBalpha expression was reconstituted by stable transfection were subjected to 10Gy gamma-IR treatment. 4 or 24 hours after treatment, gene expression changes were analyzed. **Keywords: genotype0-specific stress response in PKBalpha MEF** **Overall design:** three biological replicates were included in the experiment for each condition analyzed. overall, 27 samples were included in the study. the reference samples were untreated MEF of each respective genotype.

Background corr dist: KL-Divergence = 0.2065, L1-Distance = 0.0377, L2-Distance = 0.0026, Normal std = 0.3367

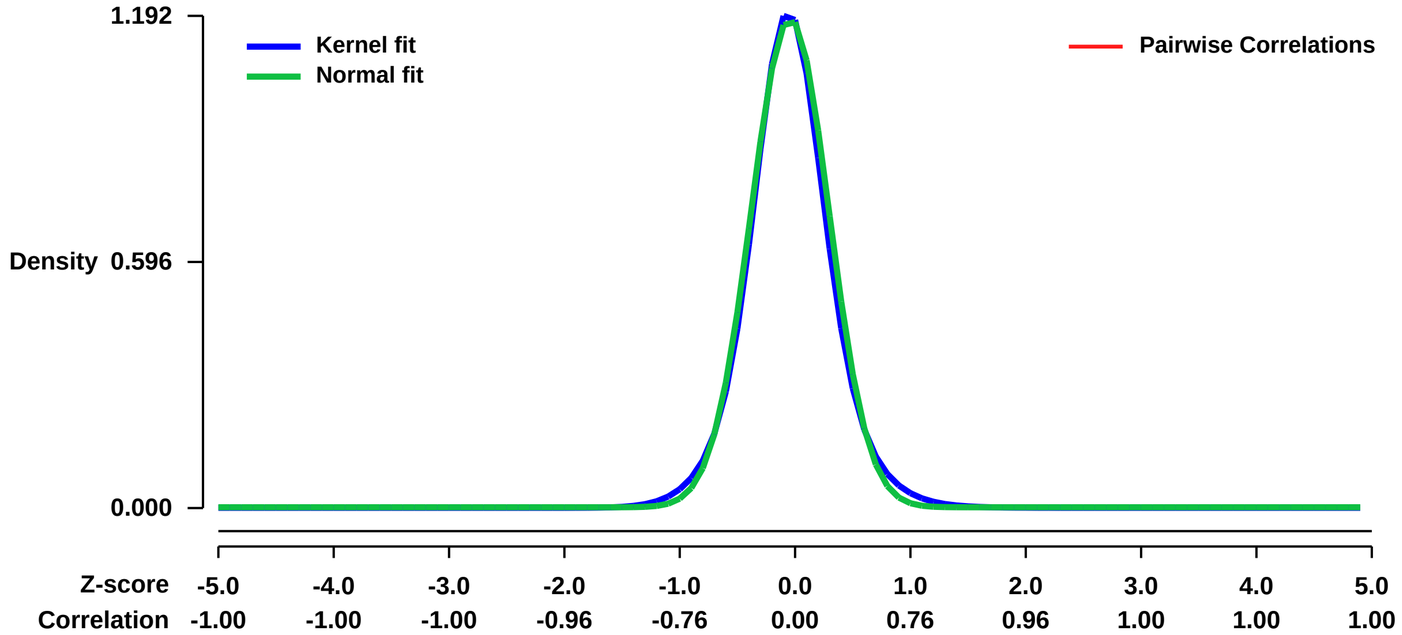

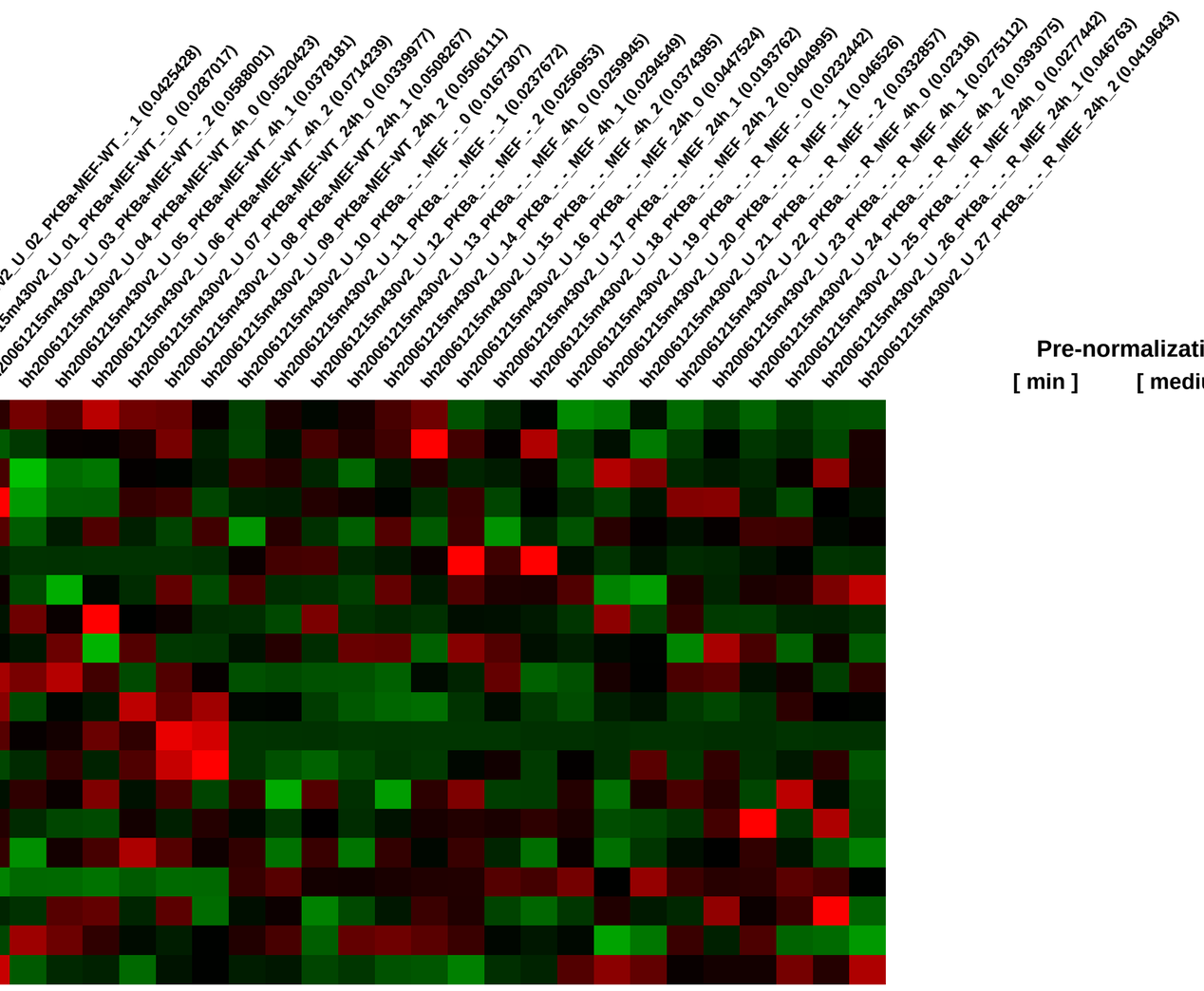

GEO Series "GSE9161" Expression Profiles

Num of samples in this series: 9

Scale of expression profile Z-scores

-3.0 -2.0 -1.0 0.0 1.0 2.0 3.0

GEO Link:	http://www.ncbi.nlm.nih.gov/geo/query/acc.cgi?acc=GSE9161
Status:	Public on Jan 07 2008
Title:	Expression profiling of cyclin D1 splice variants cyclin D1a and D1b in mouse 3T3 cells.
Organism:	Mus musculus
Experiment type:	Expression profiling by array
Platform:	GPL1261
Pubmed ID:	18180298
Summary & Design:	**Summary:** Cyclin D1 is an important cell cycle regulator but in cancer its overexpression also increases cellular migration mediated by p27KIP1 stabilization and RhoA inhibition. Recently, a common polymorphism at the exon 4-intron 4 boundary of the human cyclin D1 gene within a splice donor region was associated with an altered risk of developing cancer. Altered RNA splicing caused by this polymorphism gives rise to a variant cyclin D1 isoform termed cyclin D1b, which has the same N-terminus as the canonical cyclin D1a isoform but a distinct C-terminus. Analysis was performed of mouse cyclin D1 knockout 3T3 cells infected with splice variants of cyclin D1. 3T3 cells transduced with retroviral vectors expressing each cyclin D1 isoform were processed for expression analysis. Keywords: Cancer associated risk factor **Overall design:** Three Mouse Embryonic Fibroblasts cell lines obtained from littermate cyclin D1 knockout E14 embyos were serial passaged to obtain cyclin D1 knockout (D1KO) 3T3 cells. Each of the D1KO 3T3 cell lines were infected using the Murine Stem Cell Virus (MSCV) expressing splice variants of cyclin D1; cyclin D1a/ cyclin D1b or GFP control to give triplicate sample sets. 7 days post infection total RNA from each sample was extracted using Trizol and further purified using Qiagenâ s RNeasy Kit. Preparation of biotinylated cRNA and hybridization to oligonucleotide arrays (Affymetrix mouse genome genechip 430 2.0) were performed in conjuction with Pestell lab and the Nucleic Acid Core Facility at Thomas Jefferson University. Mouse 430 2.0 genechip contains 39,000 transcripts. Gene chips were scanned and analyzed using Robust Multi-array Average (RMA) algorithm.

Background corr dist: KL-Divergence = 0.0683, L1-Distance = 0.0192, L2-Distance = 0.0006, Normal std = 0.5072

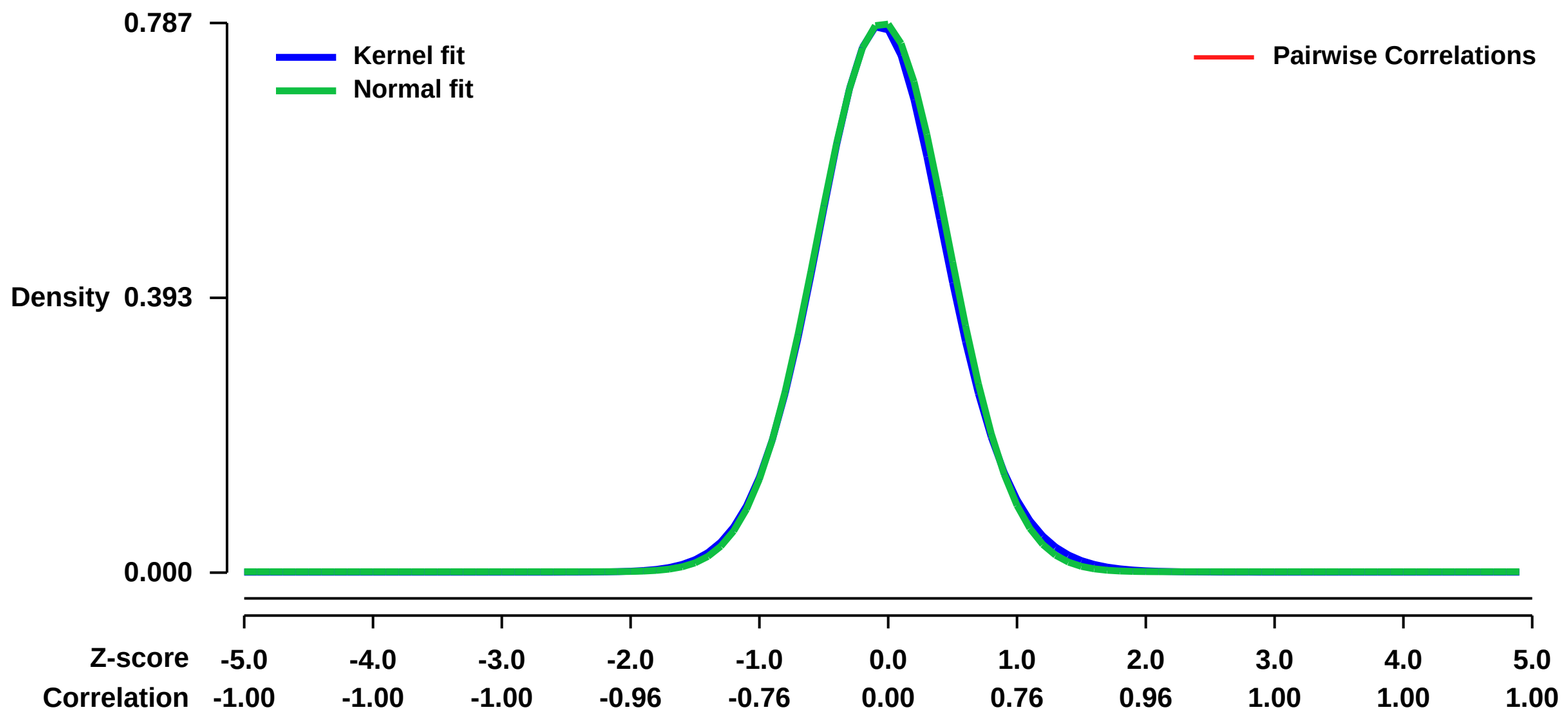

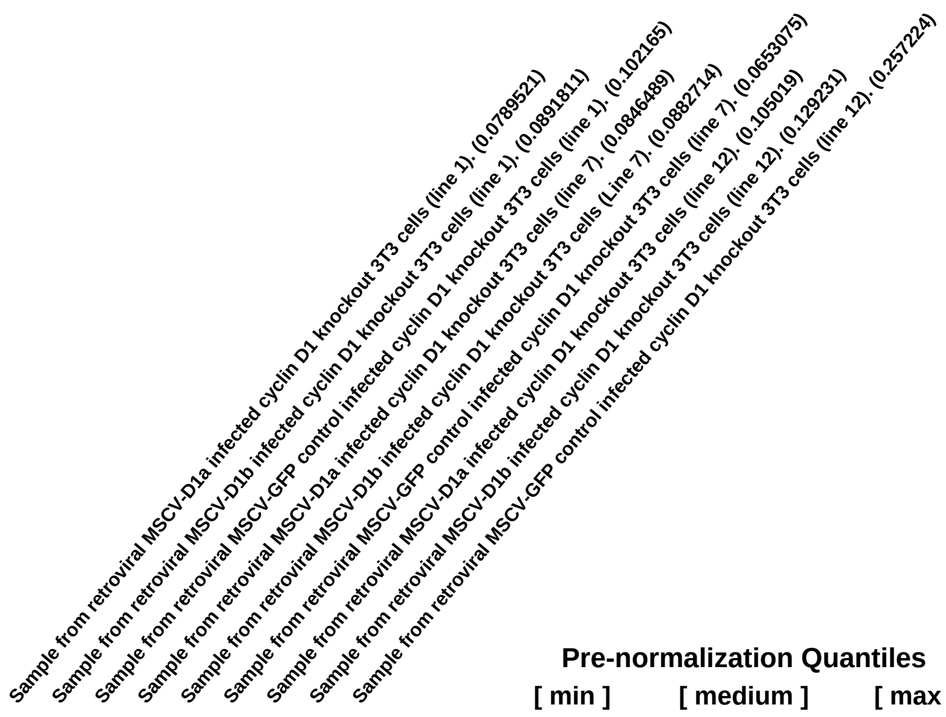

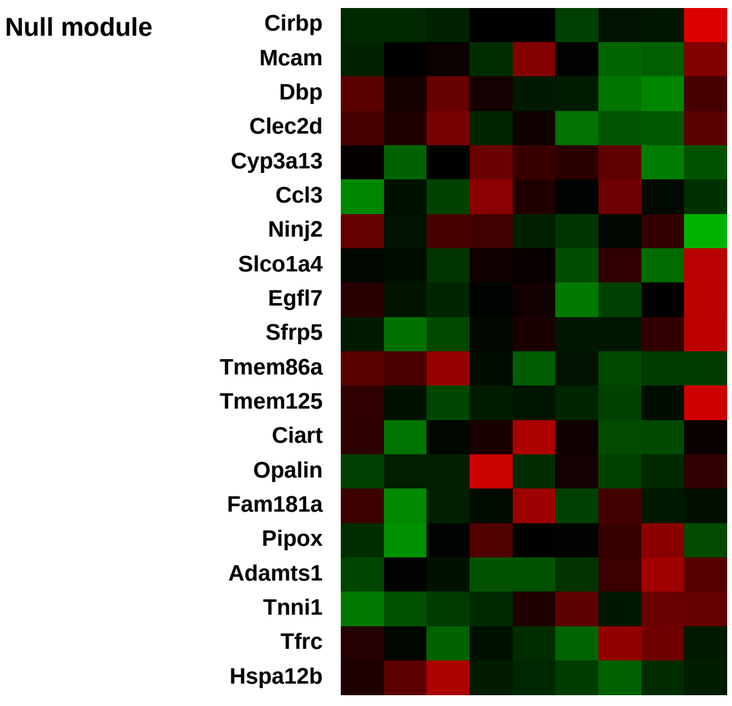

GEO Series "GSE9249" Expression Profiles

Num of samples in this series: 28

Scale of expression profile Z-scores

-3.0 -2.0 -1.0 0.0 1.0 2.0 3.0

GEO Link: http://www.ncbi.nlm.nih.gov/geo/query/acc.cgi?acc=GSE9249

Status: Public on Nov 01 2007

Title: Gene expression analysis of B-NHL from ¸»MYC, ¸»MYC/Í´µHABCL6, ¸»MYC/AIDKO and ¸»MYC/Í´µHABCL6/AIDKO mouse models

Organism: Mus musculus

Experiment type: Expression profiling by array

Platform: GPL1261

Pubmed ID: 18066064

Summary & Design:

Summary:
Most human B cell lymphomas (B-NHL) are derived from germinal centers (GCs), the structure where B-cells undergo class switch recombination (CSR) and somatic hypermutation (SHM) and are selected for high-affinity antibody production. The pathogenesis of B-NHL is associated with distinct genetic lesions, including chromosomal translocations and aberrant somatic hypermutation, which appear to arise from mistakes occurring during CSR and SHM. To ascertain the role of CSR and SHM in lymphomagenesis, we crossed three oncogene-driven (MYC, BCL6, MYC/BCL6) mouse models of B cell lymphoma with mice lacking activation-induced cytidine deaminase (AID), the enzyme required for both processes.

We show that AID deficiency prevents BCL6-dependent, GC-derived B-NHL, while it has no impact on the formation of MYC-driven, pre-GC lymphomas. Accordingly, abrogation of AID is associated with the disappearance of both CSR- and SHM-mediated structural alterations, including cMYC-IgH chromosomal translocations and aberrant SHM. These results demonstrate that AID is required for GC-derived lymphomagenesis, providing direct support to the notion that errors in AID-mediated antigen-receptor gene modification events represent major contributors to the pathogenesis of human B-NHL.

Keywords: Phenotypic characterization of tumors developing in oncogene-driven mouse models of lymphomas

Overall design:
Nodal B-NHL from 5 MYC, 7 MYC/AIDKO, 12 MYC/HABCL6 and 6 MYC/HABCL6/AIDKO mice were analyzed in this study. Total RNA was extracted from frozen tumor biopsies and processed according to Affymetrix standard protocols

Background corr dist: KL-Divergence = 0.3116, L1-Distance = 0.0597, L2-Distance = 0.0098, Normal std = 0.2778

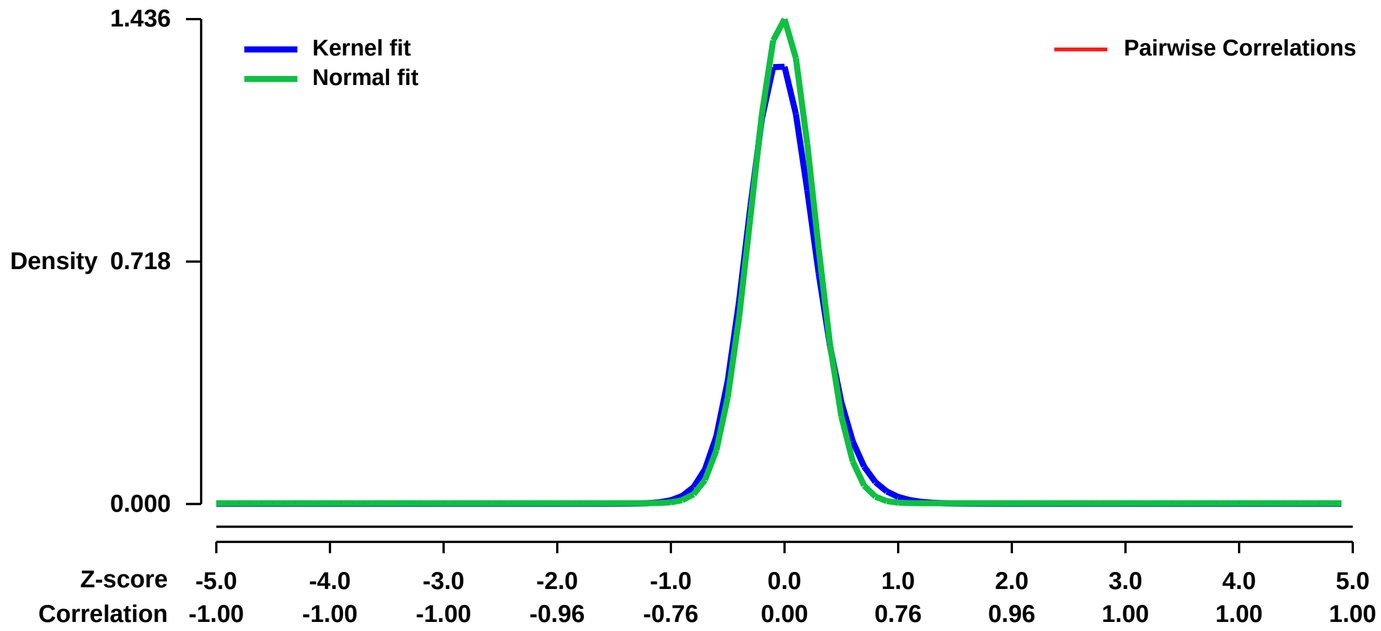

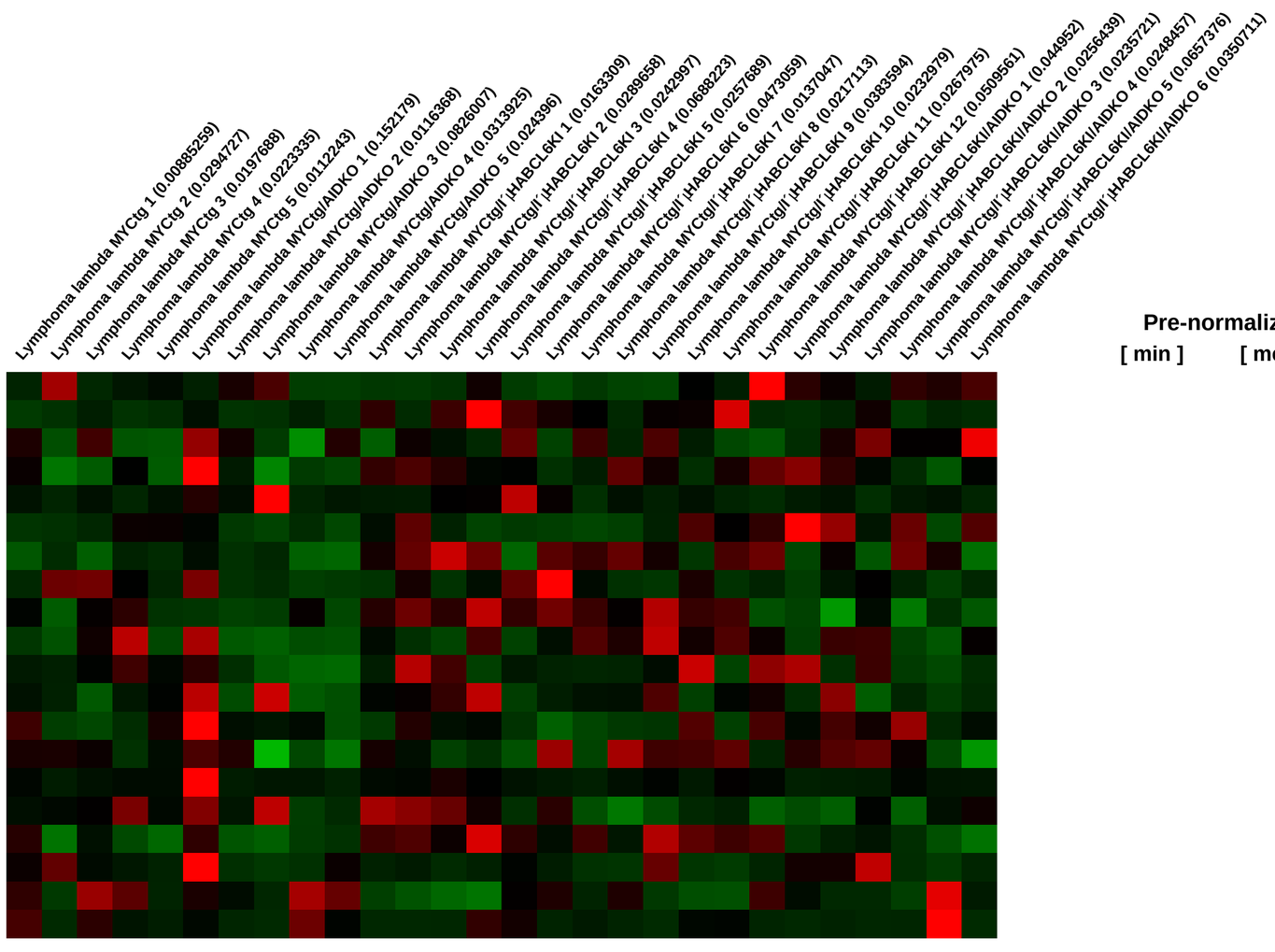

GEO Series "GSE9287" Expression Profiles

Num of samples in this series: 8

Scale of expression profile Z-scores

-3.0 -2.0 -1.0 0.0 1.0 2.0 3.0

GEO Link: http://www.ncbi.nlm.nih.gov/geo/query/acc.cgi?acc=GSE9287
Status: Public on Dec 15 2009
Title: Differential gene expression in wild-type versus Yaa mutant mouse spleen cells
Organism: Mus musculus
Experiment type: Expression profiling by array
Platform: GPL1261
Pubmed ID:

Summary & Design:

Summary:
T cells from many patients with systemic lupus erythematosus are hypoproliferative in response to TCR ligation. This defect is mediated, at least in part, through down regulation of the TCR zeta chain. Investigation of this phenomenon in lupus-prone mice revealed that the hypoproliferative T cell phenotype apparent in BXSB males is mediated

in part by the Yaa locus. The BXSB model of lupus is a recombinant inbred strain that was originally derived from a cross between a male SB/LE mouse and a female C57BL/6 mouse. BXSB is unique among lupus-prone mouse strains, in that males carry an autoimmune accelerating factor on the Y chromosome, termed Yaa, which accelerates disease onset in male BXSB mice so that fatal glomerulonephritis occurs around 6 months of age. It was recently reported that the Yaa locus is a translocation of a short stretch of genes including that encoding Toll-like

receptor 7 (Tlr-7) from the X to the Y chromosome, leading to a two-fold over expression of a subset of these genes, including Tlr-7, and hypersensitivity of Yaa+ cells to TLR-7 agonists.

To more fully understand the functional significance of the Yaa gene and how it plays a part in the modulation of CD4+ T cell responses, we performed microarray analysis using Affymetrix 430 2.0 arrays on spleens from B6 male B6.Yaa male samples. The analysis revealed an enhanced signature of innate immunity, including increased expression not only of Tlr7 and Tlr8, in line with reports that the Yaa locus leads to a duplication of the murine Tlr7 and Tlr8 genes , but also of Tlr2, Tlr5, Cd14, Lbp, C2, C3 and genes for several heat-shock proteins. T cells from B6.Yaa mice also displayed decreased TCR¸¶ expression. Interestingly, cell surface levels of the inhibitory molecule B7-H1 were increased on B6.Yaa B cells and monocytes/macrophages. In line with increased TLR-7 expression reported in B6.Yaa mice, the TLR-7 agonist imiquimod increased B7-H1 expression on normal B cells. Restoration of proliferation in co-cultures of B6 T cells and B6.Yaa APC with B7-H1 blocking Ab demonstrated a mechanistic contribution of B7-H1 up-regulation to Yaa-mediated APC-dependent T cell hypoproliferation. In addition, T cell hypoproliferation was induced in normal B6 T cells in vitro by the application of imiquimod. However, this defect was not mediated by B7-H1 or secreted factors but was independent of APC and mediated through direct imiquimod stimulation of T cells themselves. We postulate that excessive TLR-7 stimulation in Yaa+ mice mediates T cell hypoproliferation in part through up-regulation of B7-H1 and possibly also through direct T cell-mediated effects.

Keywords: differential gene expression, RNA, spleen, C57Bl/6J, B6.SB-Yaa/J, male, wild type, Yaa

Overall design:
RNA was separately extracted, labeled, and hybridized from each animal.

Background corr dist: KL-Divergence = 0.0581, L1-Distance = 0.0301, L2-Distance = 0.0011, Normal std = 0.5502

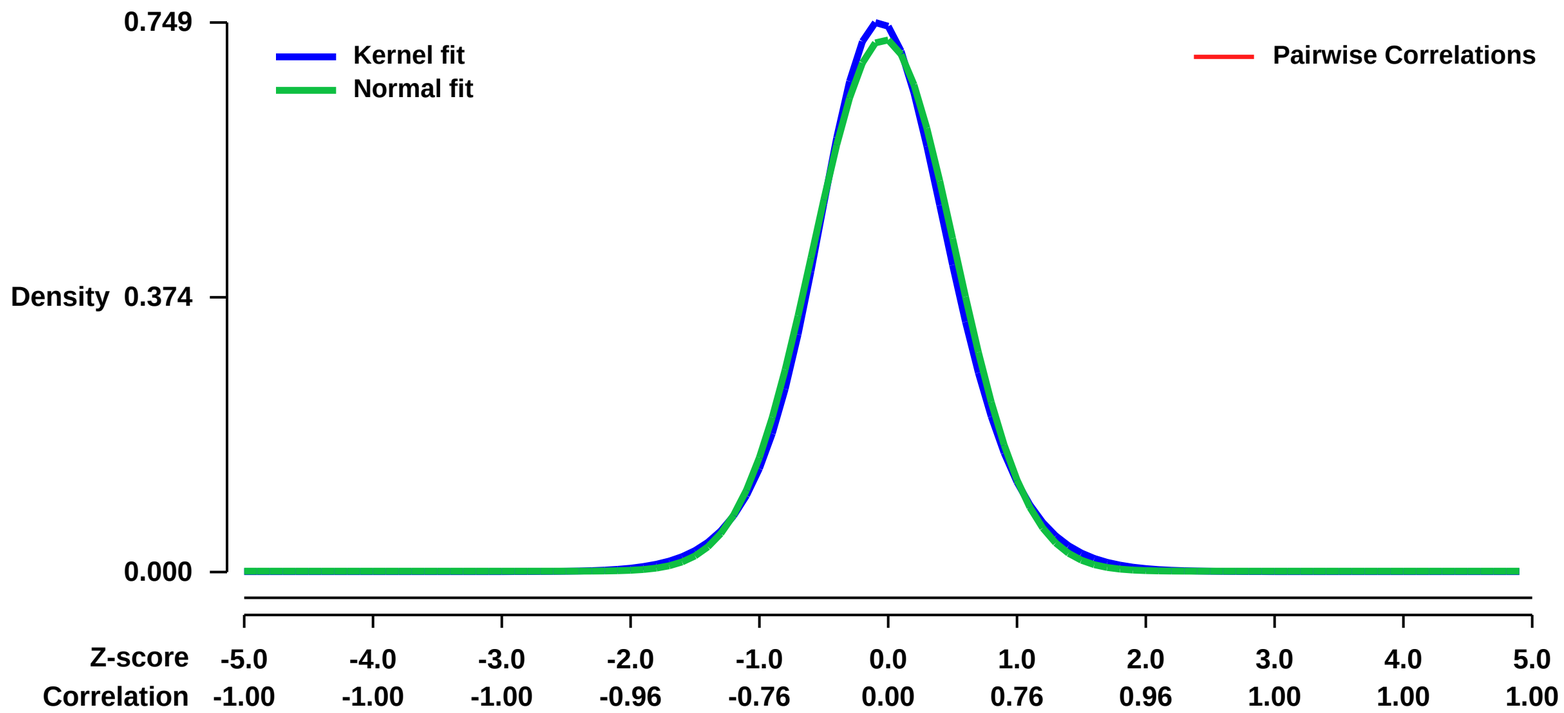

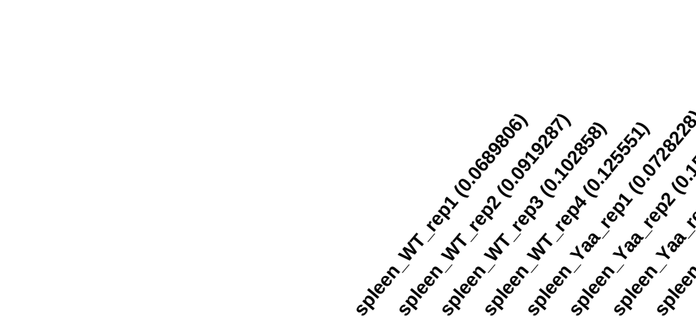

GEO Series "GSE9294" Expression Profiles

Num of samples in this series: 12

Scale of expression profile Z-scores

-3.0 -2.0 -1.0 0.0 1.0 2.0 3.0

GEO Link:	**http://www.ncbi.nlm.nih.gov/geo/query/acc.cgi?acc=GSE9294**
Status:	**Public on Oct 09 2008**
Title:	**EOM and TA Sp cell comparison**
Organism:	**Mus musculus**
Experiment type:	**Expression profiling by array**
Platform:	**GPL1261**
Pubmed ID:	**19116248**
Summary & Design:	**Summary:** **Using Affymetrix GeneChips, we analyzed expression profiles of SP cells from EOM and TA. 348 differentially expressed transcripts defined the EOM-SP transcriptome: 229 upregulated in EOM-SP and 119 in TA-SP.** **Keywords: Expression Profiling** **Overall design:** **Six independently separated EOM and six TA SP cell preparations were used for microarray analysis using the Affymetrix´fi Mouse 430 ver 2.0 GeneChip arrays.**

Background corr dist: KL-Divergence = 0.0728, L1-Distance = 0.0522, L2-Distance = 0.0052, Normal std = 0.5125

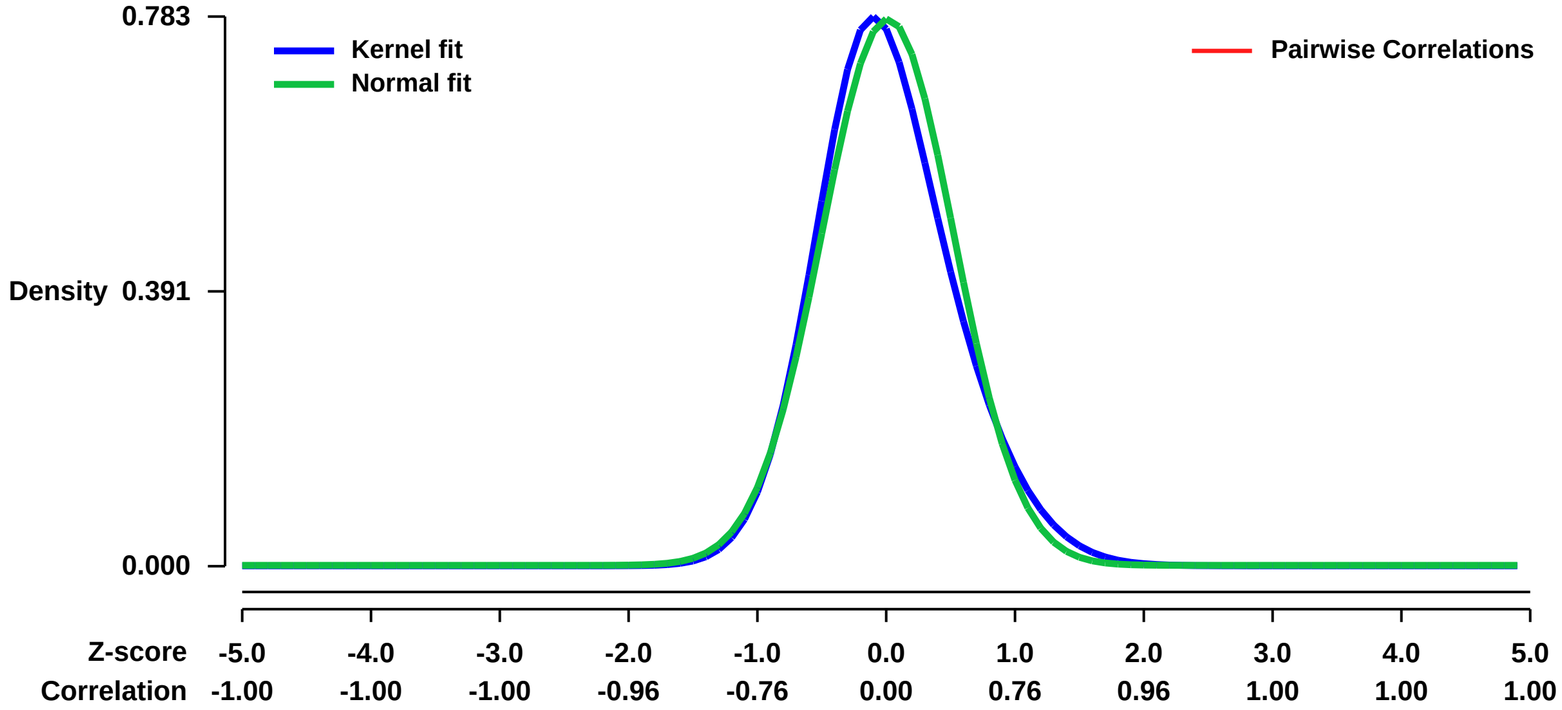

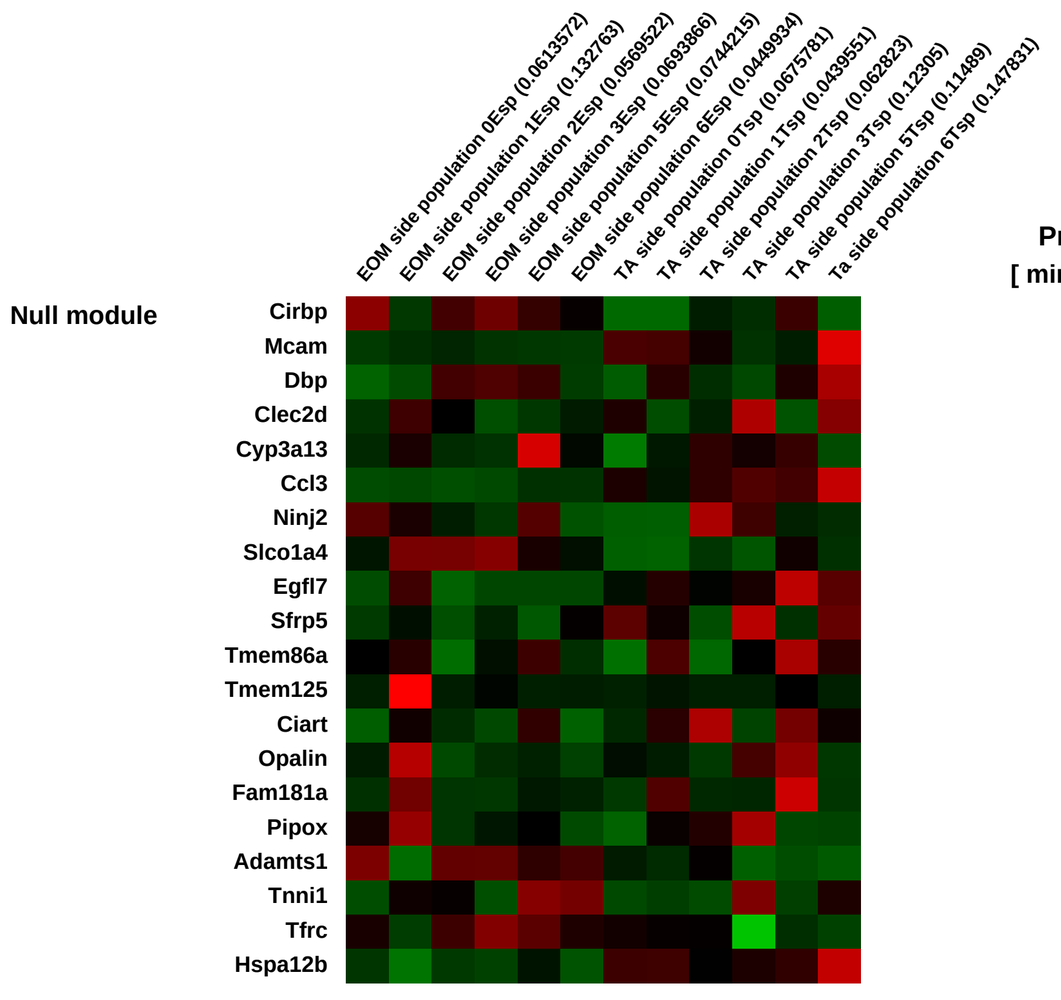

GEO Series "GSE9297" Expression Profiles

Num of samples in this series: 27

Scale of expression profile Z-scores

-3.0 -2.0 -1.0 0.0 1.0 2.0 3.0

GEO Link:	**http://www.ncbi.nlm.nih.gov/geo/query/acc.cgi?acc=GSE9297**
Status:	**Public on Nov 01 2008**
Title:	**Genomic profile of IL10-/- knocked out colitis model**
Organism:	**Mus musculus**
Experiment type:	**Expression profiling by array**
Platform:	**GPL1261**
Pubmed ID:	
Summary & Design:	**Summary:** **Objetives: study and characterization of the IL10-/- knocked out colitis model in mice at genomic level and the study of the influence of bacteria in the development of the disease.** **Keywords: Differentially expressed genes analysis** **Overall design:** **RNA was extracted from homogenized full-thickness colonic tissues in Trizol´fi reagent (Invitrogen) and purified with RNeasy affinity columns (Qiagen), according to manufacturer´·s protocol. The microarray analysis was performed by Progenika Biopharma (Bilbao, Spain) on GeneChip´fi Rat Genome 230 2.0 Array (Affymetrix). All sample labeling (biotin), hybridization, staining and scanning procedures were carried out using Affimetrix, standard protocols (www.affymetrix.com). Normalization was carried out using Bioconductor sofware (affyPLM package).**

Background corr dist: **KL-Divergence = 0.1442, L1-Distance = 0.0387, L2-Distance = 0.0024, Normal std = 0.3895**

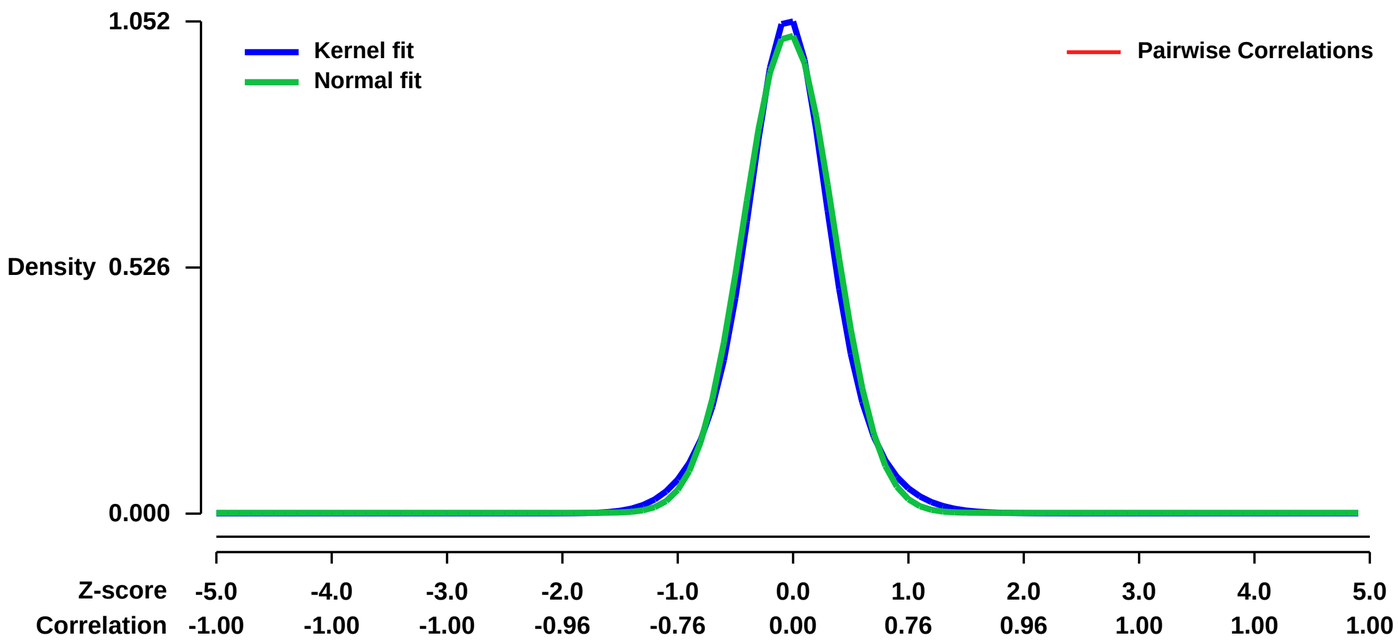

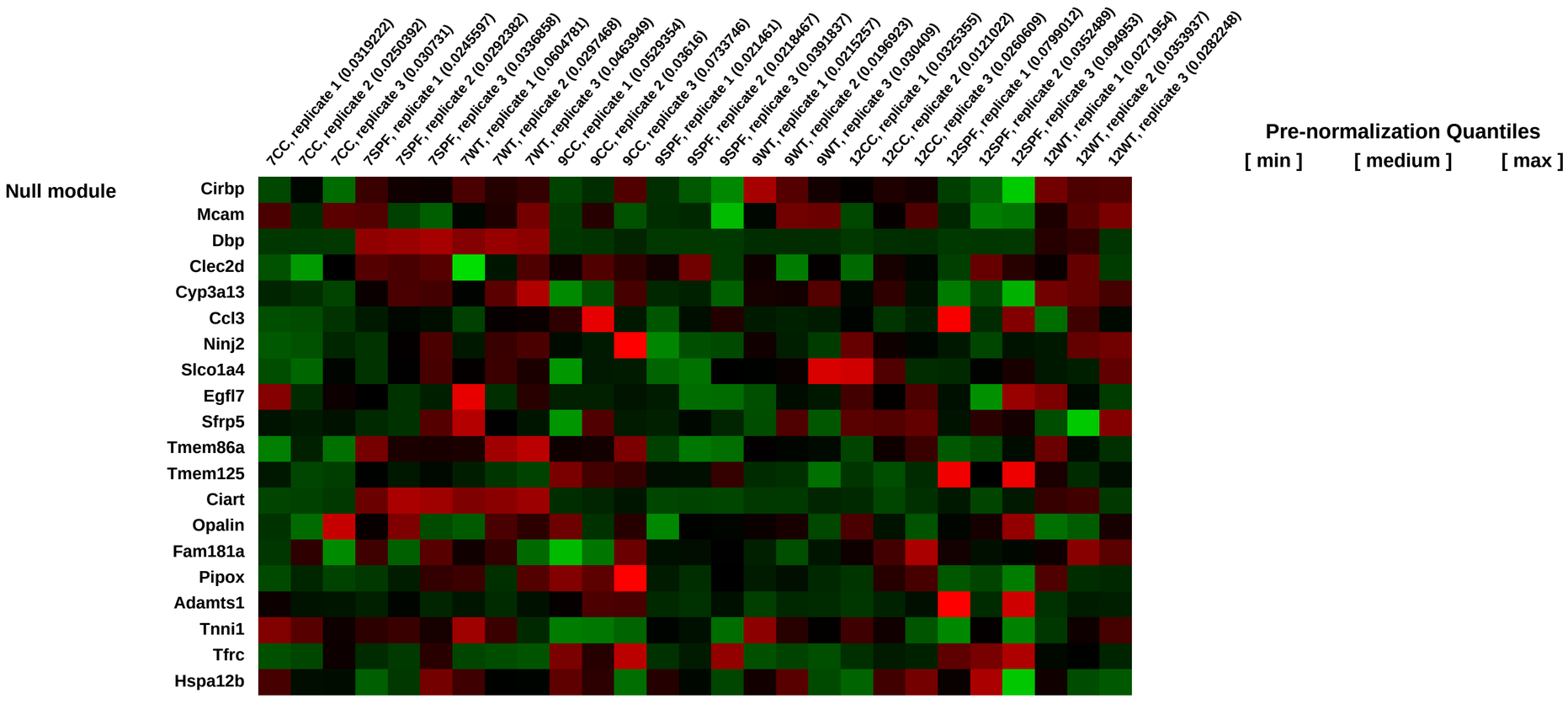

GEO Series "GSE9312" Expression Profiles

Num of samples in this series: 6

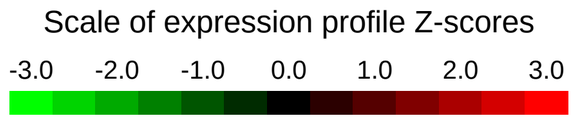

GEO Link:	**http://www.ncbi.nlm.nih.gov/geo/query/acc.cgi?acc=GSE9312**
Status:	**Public on Apr 12 2008**
Title:	**MIA overexpression**
Organism:	**Mus musculus**
Experiment type:	**Expression profiling by array**
Platform:	**GPL1261**
Pubmed ID:	
Summary & Design:	**Summary:** **In experiments using tissue recombinants and mesenchyme-free culture, we have demonstrated that the entire embryonic respiratory tract epithelium, from the trachea to the distal lung tips, exhibits substantial plasticity in its eventual phenotype that is dependent on the inductive cues it receives from its associated mesenchyme. This observation led us to speculate that the differences between embryonic trachea and lung are defined by limited subset of genes, and that the molecular comparison of these two tissues might provide new information on genes that are important for both lung and trachea development. Microarray experiments designed to identify genes differentially expressed in the E11.5 lung and trachea showed that melanoma inhibitory activity (Mia1) was expressed only in the lung. Mia1 was abundantly expressed during early lung development, but was virtually absent by the end of gestation. Bitransgenic mice expressing MIA under the control of the SFTPC promoter after E16.5, the age when Mia1 is normally silenced, died from respiratory failure at birth with morphologically immature lungs associated with reduced levels of saturated phosphatidylcholine and mature SP-B. Microarray analysis showed significant reductions expression of Sftpa, Sftpb, Abca3, Aqp5, Lzp-s, Scd2, and Aytl2 in lungs misexpressing MIA.** **Keywords: genotype comparison** **Overall design:** **To assess the effect of misexpressing MIA on overall lung gene expression, we analyzed RNA from day E18.5 lungs of bitransgenic and control littermates by microarray (Affymetrix MOE430 chip).**

Background corr dist: KL-Divergence = 0.0335, L1-Distance = 0.0178, L2-Distance = 0.0003, Normal std = 0.6480

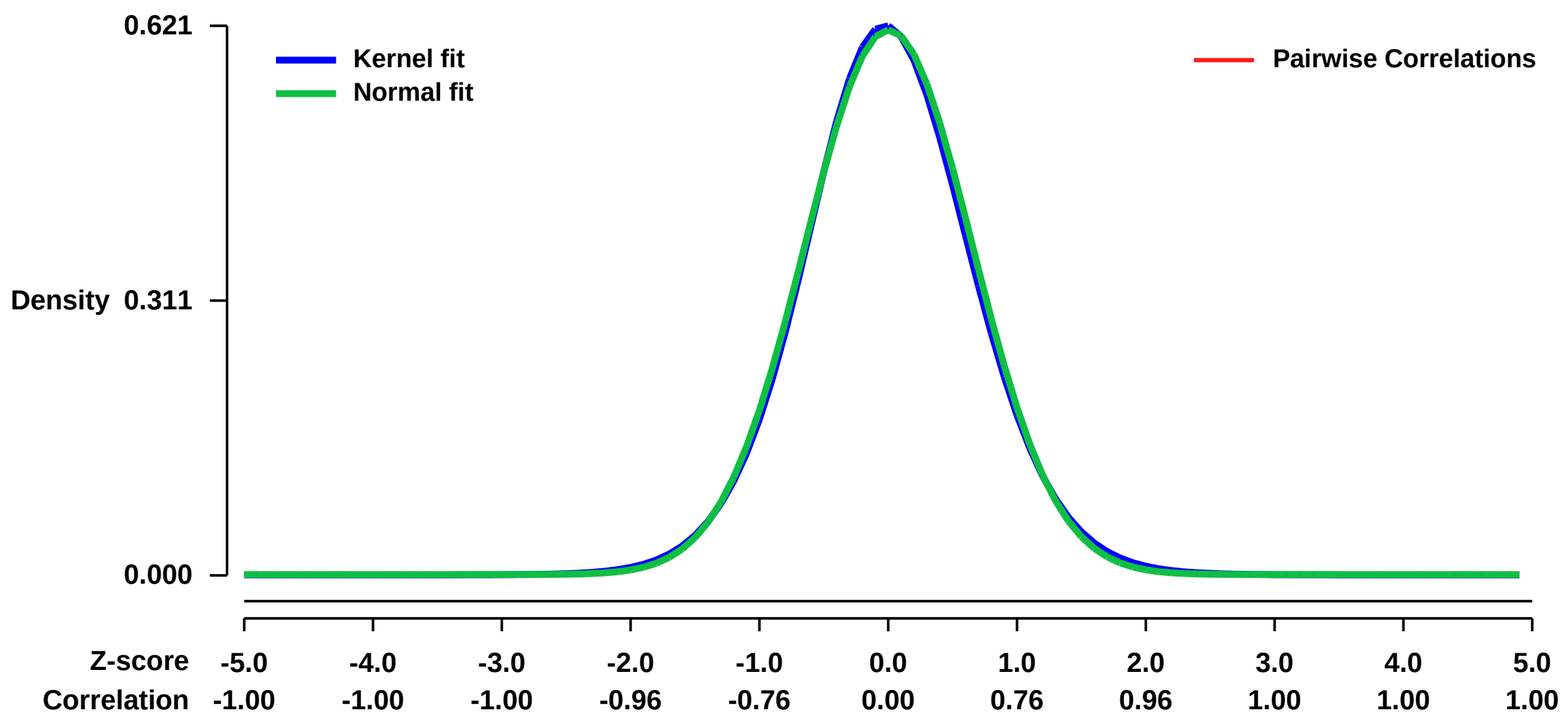

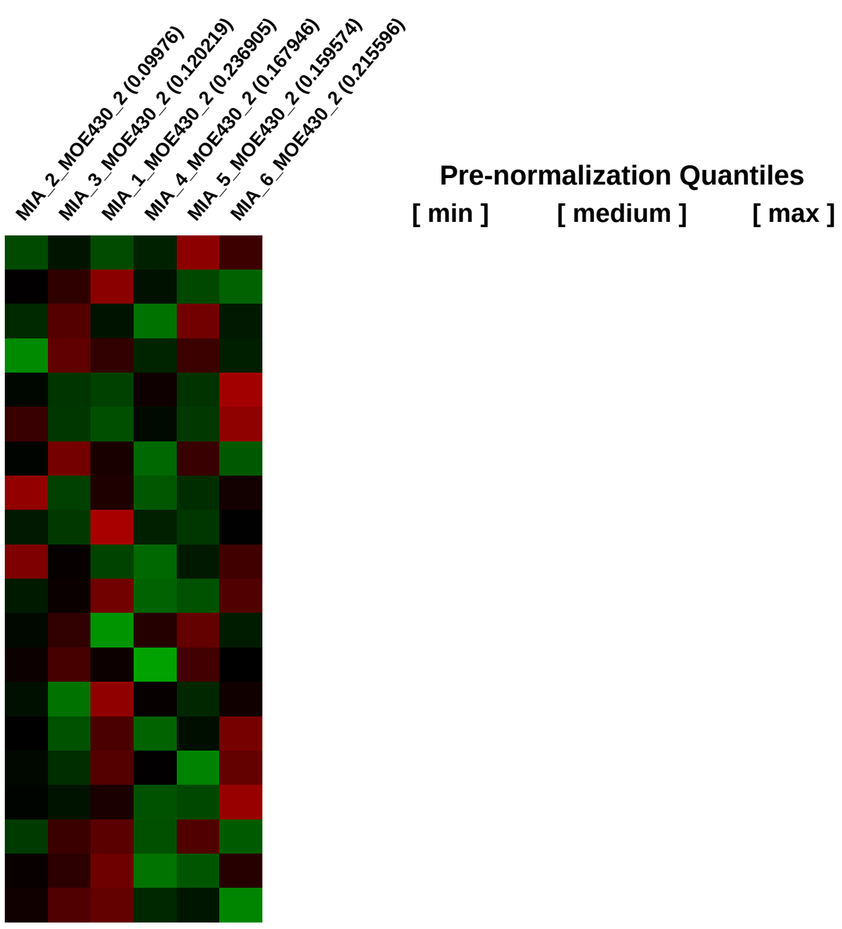

GEO Series "GSE9330" Expression Profiles

Num of samples in this series: 8

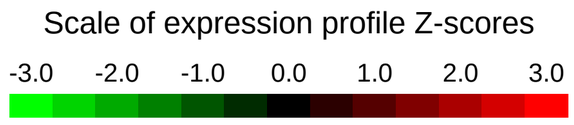

GEO Link:	http://www.ncbi.nlm.nih.gov/geo/query/acc.cgi?acc=GSE9330
Status:	Public on Dec 15 2007
Title:	Expression data from wild type and Ctip2-/- (Bcl11b) mutant mouse striatum at P0
Organism:	Mus musculus
Experiment type:	Expression profiling by array
Platform:	GPL1261
Pubmed ID:	18199763

Summary & Design:

Summary:
Striatal medium spiny neurons (MSN) are critically involved in motor control, and their degeneration is a principal component of Huntingtonâ s disease. We find that the transcription factor Ctip2 (also known as Bcl11b) is central to MSN differentiation and striatal development. Within the striatum, it is expressed by all MSN, while it is excluded from essentially all striatal interneurons. In the absence of Ctip2, MSN do not fully differentiate, as demonstrated by dramatically reduced expression of a large number of MSN markers, including DARPP-32, FOXP1, Chrm4, Reelin, MOR1, GluR1, and Plexin-D1. Furthermore, MSN fail to aggregate into patches, resulting in severely disrupted patch-matrix organization within the striatum. Finally, heterotopic cellular aggregates invade the Ctip2-/- striatum suggesting a failure by MSN to repel these cells in the absence of Ctip2. In order to investigate the molecular mechanisms that underlie Ctip2-dependent differentiation of MSN and that underlie the patch-matrix disorganization in the mutant striatum, we directly compared gene expression between wild type and mutant striatum at P0. Because CTIP2-expressing MSN constitute 90-95% of the neurons within the striatum, we reasoned that we should be able to detect changes in medium spiny neuron gene expression in Ctip2 null mutants. We microdissected out small regions of striatum at matched locations in wild type and Ctip2-/- mutant littermates at P0 and investigated gene expression with Affymetrix microarrays. We selected the 153 most significant genes and further analyzed them to identify a smaller set of genes of potentially high biological relevance. In order to verify the microarray data and define the distribution of the identified genes in the striatum, we performed in situ hybridization or immunohistochemistry for 12 selected genes: Plexin-D1, Ngef, Nectin-3, Kcnip2, Pcp4L1, Neto1, Basonuclin 2, Fidgetin, Semaphorin 3e, Secretagogin, Unc5d, and Neurotensin. We find that all these genes are either specifically downregulated (Plexin-D1, Ngef, Nectin-3 Kcnip2, Pcp4L1, Neto1), or upregulated (Basonuclin 2, Fidgetin, Semaphorin 3e, Secretagogin, Unc5d, Neurotensin), in the Ctip2-/- striatum, confirming and extending the microarray results. Together, these data indicate that Ctip2 is a critical regulator of MSN differentiation, striatal patch development, and the establishment of the cellular architecture of the striatum.

Keywords: mutant analysis

Overall design:
Matched regions of striatum from wild type and Ctip2-/- mice were obtained via 500 ´µm diameter punch biopsies performed in the center of the developing striatum in acutely sectioned 300 ´µm coronal slices of the brain at postnatal day 0 (P0). Sections were matched rostro-caudally between wild type and null mutant tissue, and fiduciary landmarks were used to assure reproducible microdissection of comparable regions. RNA was extracted using the StrataPrep Total RNA Mini Kit (Stratagene, La Jolla, CA), and RNA quality was assayed using a bioanalyzer (Agilent Technologies, Paola Alto, CA). To ensure reproducibility and biological significance, microarrays were performed with RNA samples from three independent wild type, one heterozygote, and four Ctip2-/- mice (biological replicates). Microarray data were normalized using the RMA function within Bioconductor (Irizarry et al., 2003). Statistical significance of gene expression differences between wild type and knockout was determined using Statistical Analysis of Micrarrays (SAM) (Tusher et al., 2001). Using a SAM d-score cutoff of > 2 or < -2, we selected the 153 most significant genes and further analyzed them to identify a smaller set of genes of potentially high biological relevance.

Background corr dist: KL-Divergence = 0.0229, L1-Distance = 0.0600, L2-Distance = 0.0051, Normal std = 0.7875

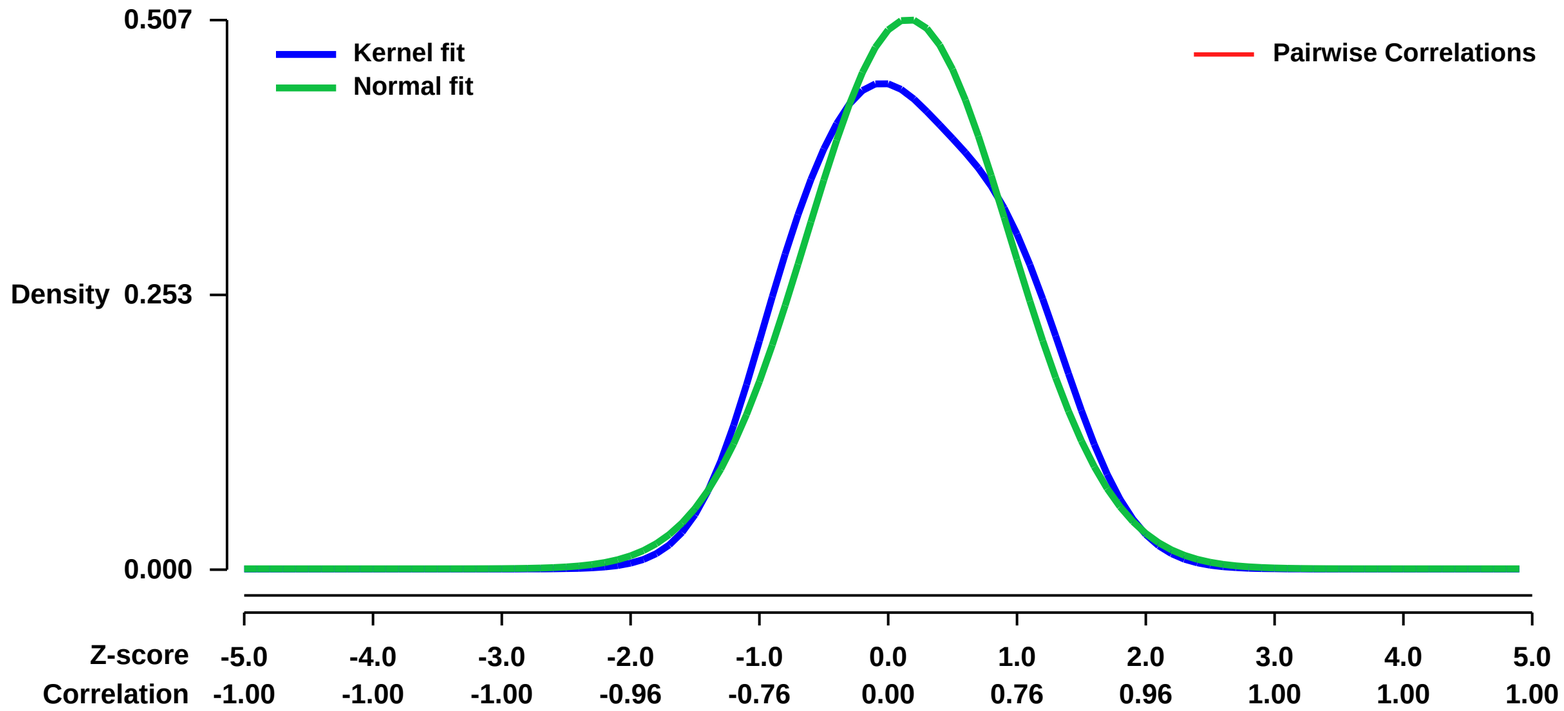

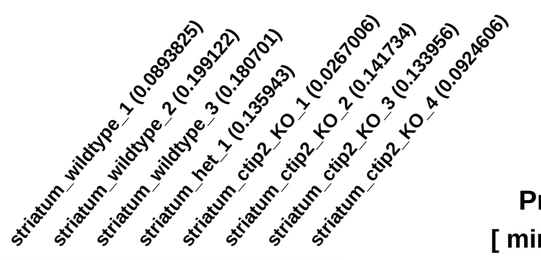

Pre-normalization Quantiles
[min] [medium] [max]

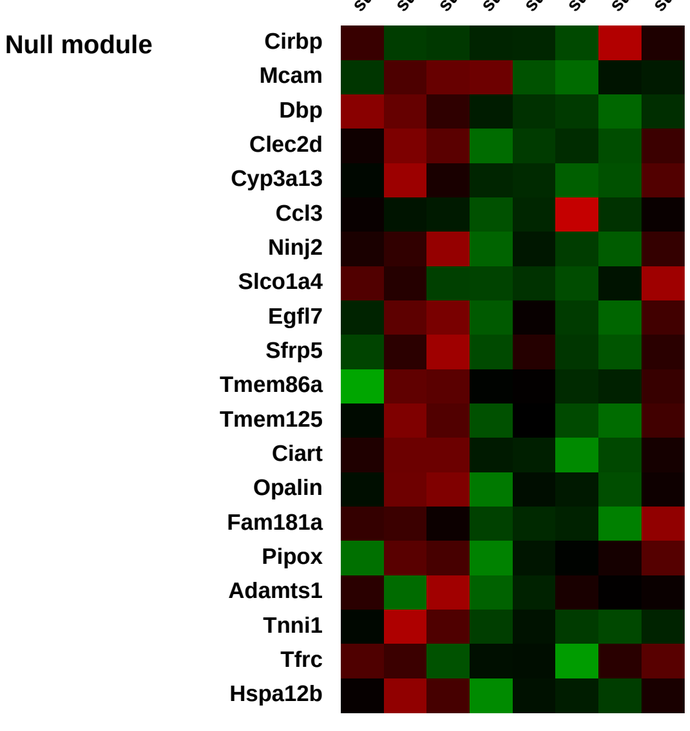

GEO Series "GSE9368" Expression Profiles

Num of samples in this series: 12

Scale of expression profile Z-scores

-3.0 -2.0 -1.0 0.0 1.0 2.0 3.0

GEO Link:	http://www.ncbi.nlm.nih.gov/geo/query/acc.cgi?acc=GSE9368
Status:	Public on Nov 01 2007
Title:	Mouse lung with recombinant human soluble PBEFtreatment and ventilator-induced lung injury: age 8-12wks
Organism:	Mus musculus
Experiment type:	Expression profiling by array
Platform:	GPL1261
Pubmed ID:	18658108
Summary & Design:	**Summary:** We have previously demonstrated that pre-B-cell colony enhancing factor (PBEF) ais a biomarker in sepsis and sepsis-induced acute lung injury (ALI) with genetic variants conferring ALI susceptibility118. In the current study, we explored the mechanistic participation of PBEF in ALI and ventilator-induced associated lung injury (VIALI). Initial in vitro studies and demonstrated rhPBEF aas a direct rat neutrophil chemotactic factor in vitro producing marked in vivo increases in BAL leukocytes (PMNs) in vivo following (intratracheal injection (,IT) in C57B6 mice. These latter changes were accompanied by increased BAL levels of the PMN chemoattractants (, KC and MIP2), and modest changes in lung vascular and but were not associated with significant increasesin alveolar permeability. We next explored the potential synergism between rhPBEF administration (IT) and a mechanical ventilation model of modest VILI lung injury (4 hours, 30 ml/kg tidal volume). We and observed dramatic synergistic increases in BAL PMNs, and both BAL protein and cytokine levels (IL-6, TNF-?, KC). Gene expression profiling Microarray analysis further supported a major role for PBEF in the induction of gene modules associated with ALI and VALI (NFkB pathway, leukocyte extravasation, apoptosis, toll receptor signaling). Finally, we exposed wild type and heterozygous PBEF+/- mice (targeted deletion of a single PBEF allele deletion) to a model of severe VILImechanical ventilation-induced lung injury (4 hours, 40 ml/kg tidal volume). PBEF+/- mice were significantly protected from VIALI-associated increases in BAL protein and BAL IL-6 levels and exhibited significantly reduced expression of ALI-associated gene expression modules. Together, these results indicate that PBEF is a key inflammatory mediator intimately involved in both the development and severity of ventilator-induced ALI. We used microarrays to detail the global programme of gene expression induced by rhPBEF treatment and VALI. **Keywords:** response to treatment and/or stress **Overall design:** animals were treated by PBS, rhPBEF (IT administration), VILI (4 hours, 30 ml/kg tidal volume), or both.

Background corr dist: KL-Divergence = 0.1051, L1-Distance = 0.0265, L2-Distance = 0.0010, Normal std = 0.4288

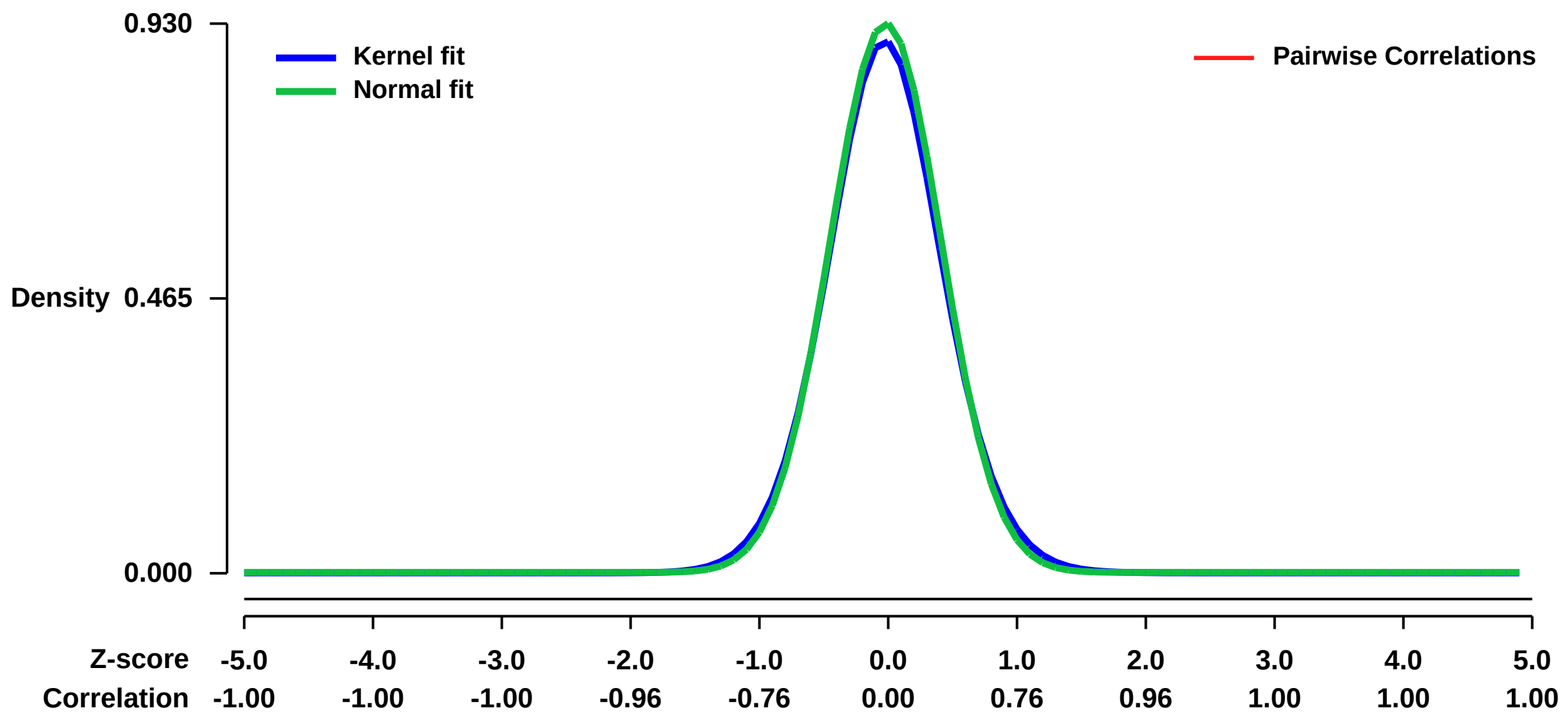

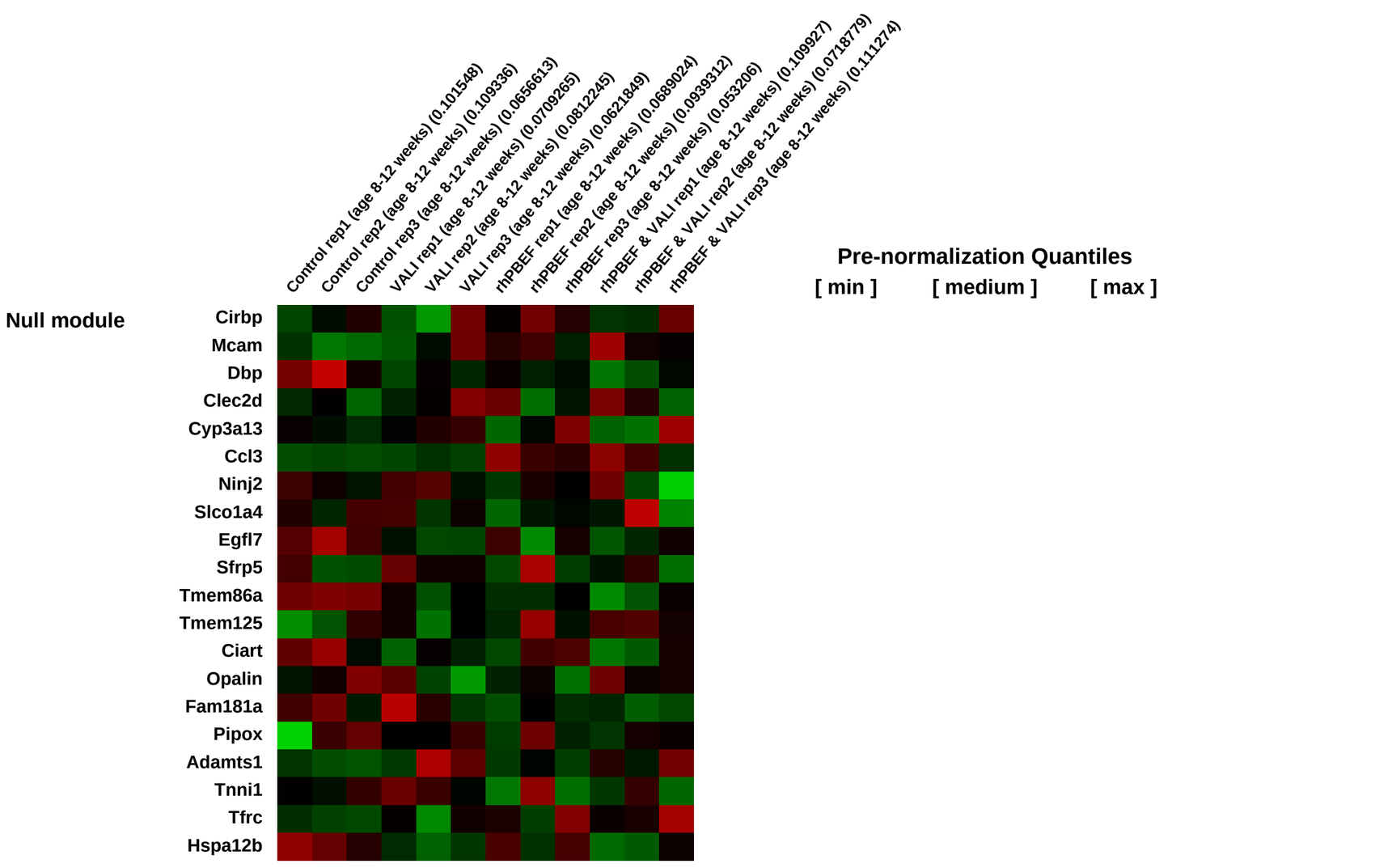

GEO Series "GSE9400" Expression Profiles

Num of samples in this series: 8

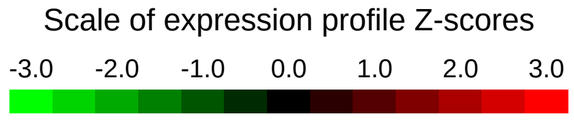

GEO Link:	**http://www.ncbi.nlm.nih.gov/geo/query/acc.cgi?acc=GSE9400**
Status:	**Public on Oct 10 2009**
Title:	**Hypoxic gene regulation on mice Quadriceps muscle**
Organism:	**Mus musculus**
Experiment type:	**Expression profiling by array**
Platform:	**GPL1261**
Pubmed ID:	
Summary & Design:	**Summary:** **To address whether hypoxia contributes to muscle patho-physiology, normal, adult C57 mice were exposed to chronic, normobaric and hypobaric hypoxic environments for 2 weeks in order to simulate levels of hypoxaemia reported in DMD patients with advanced respiratory insufficiency. Control mice were maintained under normoxic conditions. Control and experimental mice were studied.** **Keywords: Hypoxia effect, Comparison type** **Overall design:** **Fifteen micrograms labeled cRNA of hypoxic or normoxic QF muscle was fragmented, and 10¿…g was hybridized to Affymetrix´fi Mouse 430 ver 2.0 GeneChip arrays for 18â 24h (Affymetrix Inc.). Each microarray was washed and stained with streptavidinâ phycoerythrin and scanned at a 6-¿…m resolution with Agilent model G2500A GeneArray scanner A visual quality control measurement was performed to ensure proper hybridization after each chip was scanned.**

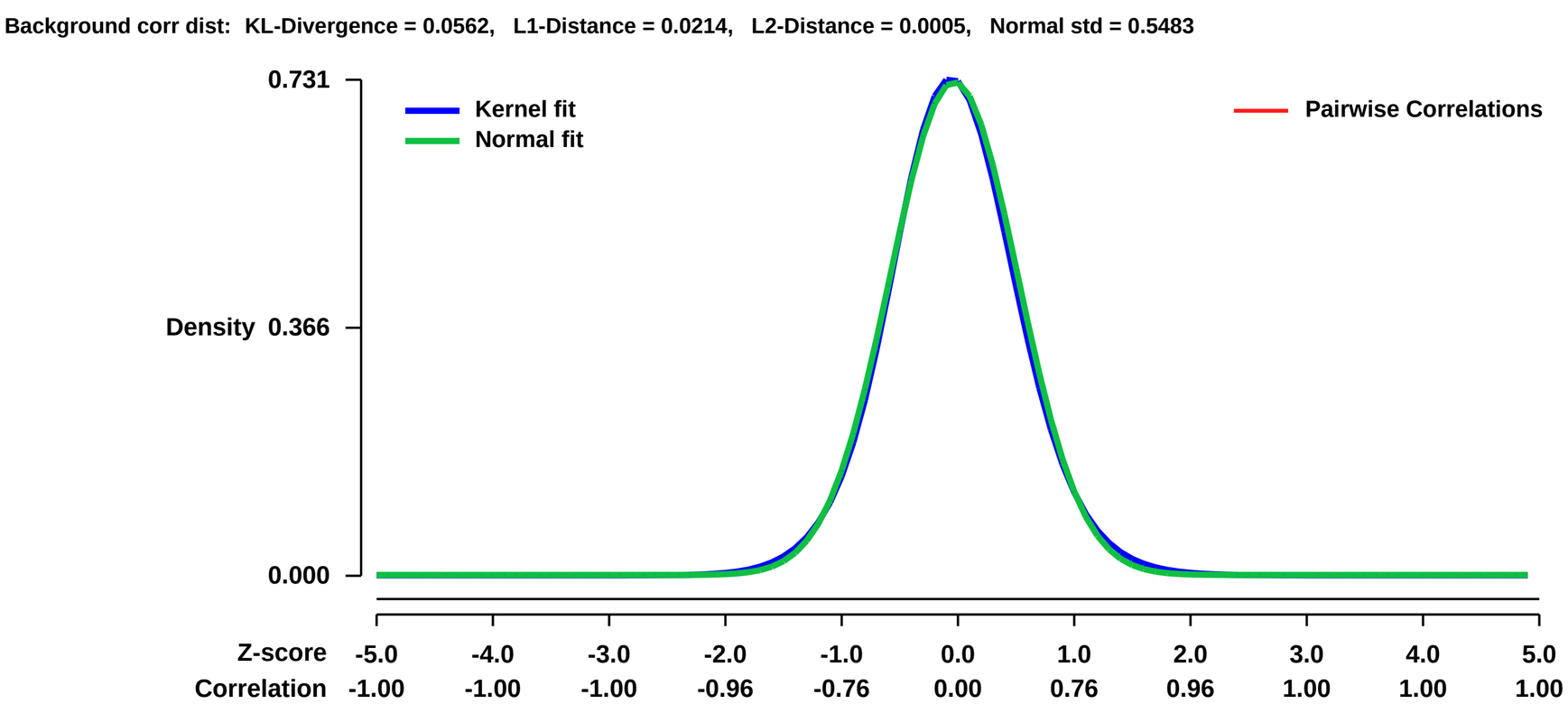

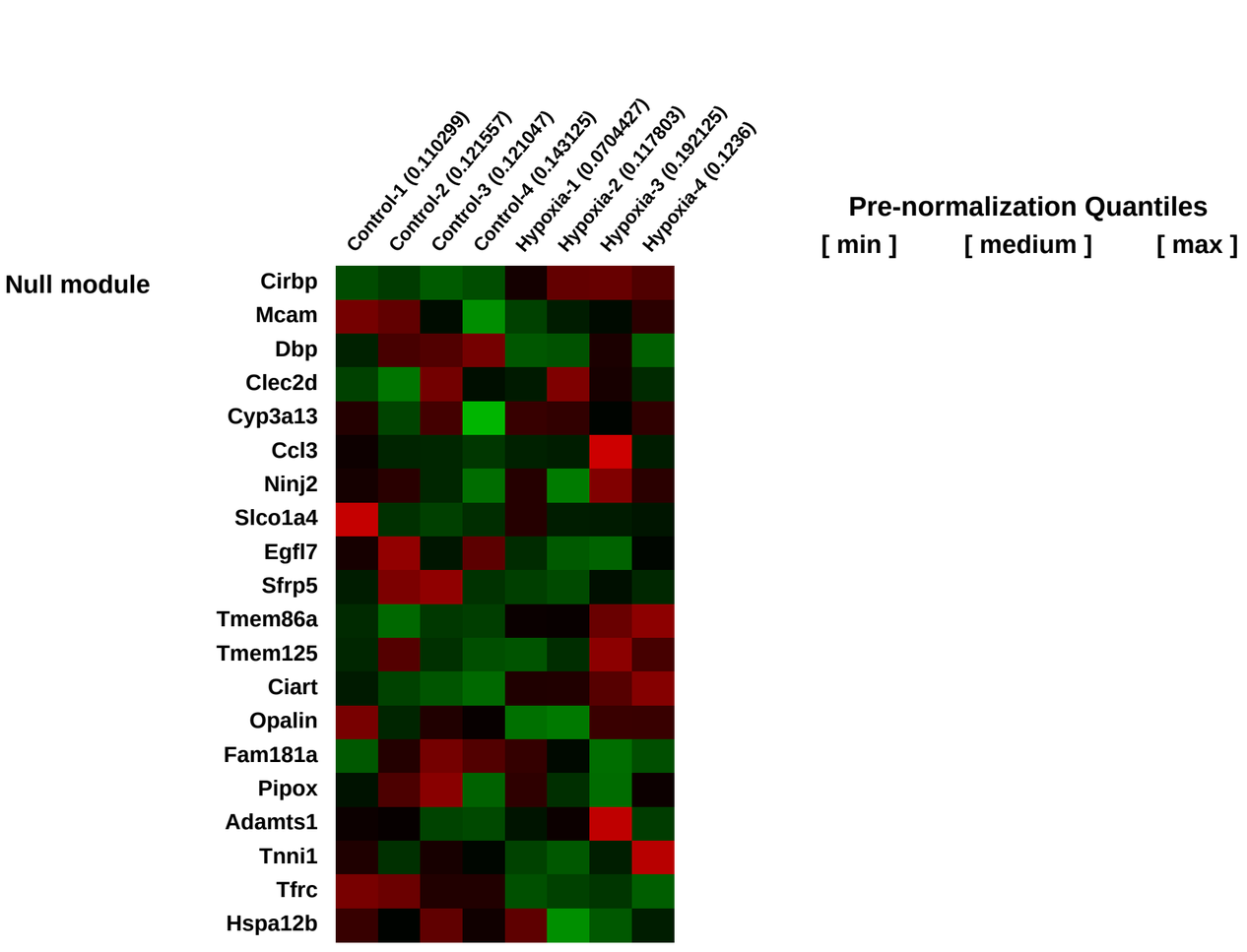

GEO Series "GSE9441" Expression Profiles

Num of samples in this series: 36

Scale of expression profile Z-scores

-3.0 -2.0 -1.0 0.0 1.0 2.0 3.0

GEO Link:	http://www.ncbi.nlm.nih.gov/geo/query/acc.cgi?acc=GSE9441
Status:	Public on Dec 07 2007
Title:	The effect of sleep deprivation on gene expression in the brain and the liver of three inbred mouse strains
Organism:	Mus musculus
Experiment type:	Expression profiling by array
Platform:	GPL1261
Pubmed ID:	18077435
Summary & Design:	**Summary:** These studies adress differential changes in gene expression between 6h sleep deprived and control mice in the brain and the liver. We profiled gene expression in three different inbred strains to understand the influence of genetic background. **Keywords: brain, genetic background, sleep deprivation** **Overall design:** Experiments were performed on male mice (C57BL/6J (B6), AKR/J (AK), DBA/2J (D2)), 12-13 weeks of aged, purchased from Jackson Laboratory. Animals were housed in a light/dark cycle of 24 hrs with water and food available ad libitum. Mice of the 3 inbred strains were sleep deprived for 6h starting at light onset (ZT0) and sacrificed together with their home-cage controls at ZT6 (n=9 / strain =3 / condition =2 / tissues =2; total = 108 mice).

Background corr dist: KL-Divergence = 0.0092, L1-Distance = 0.0360, L2-Distance = 0.0014, Normal std = 0.9491

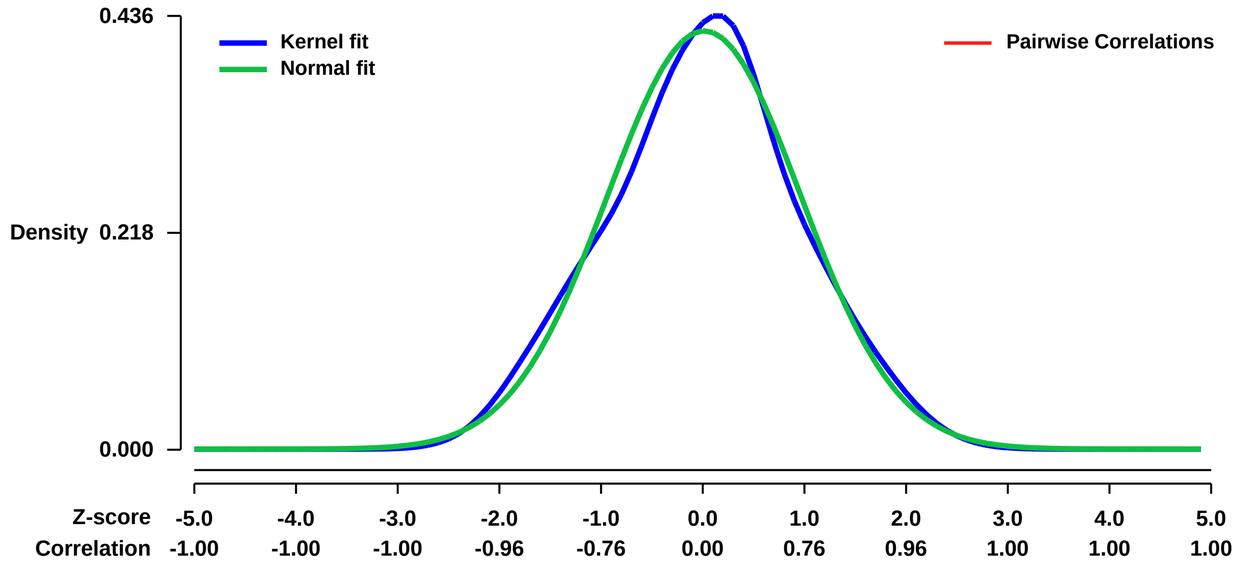

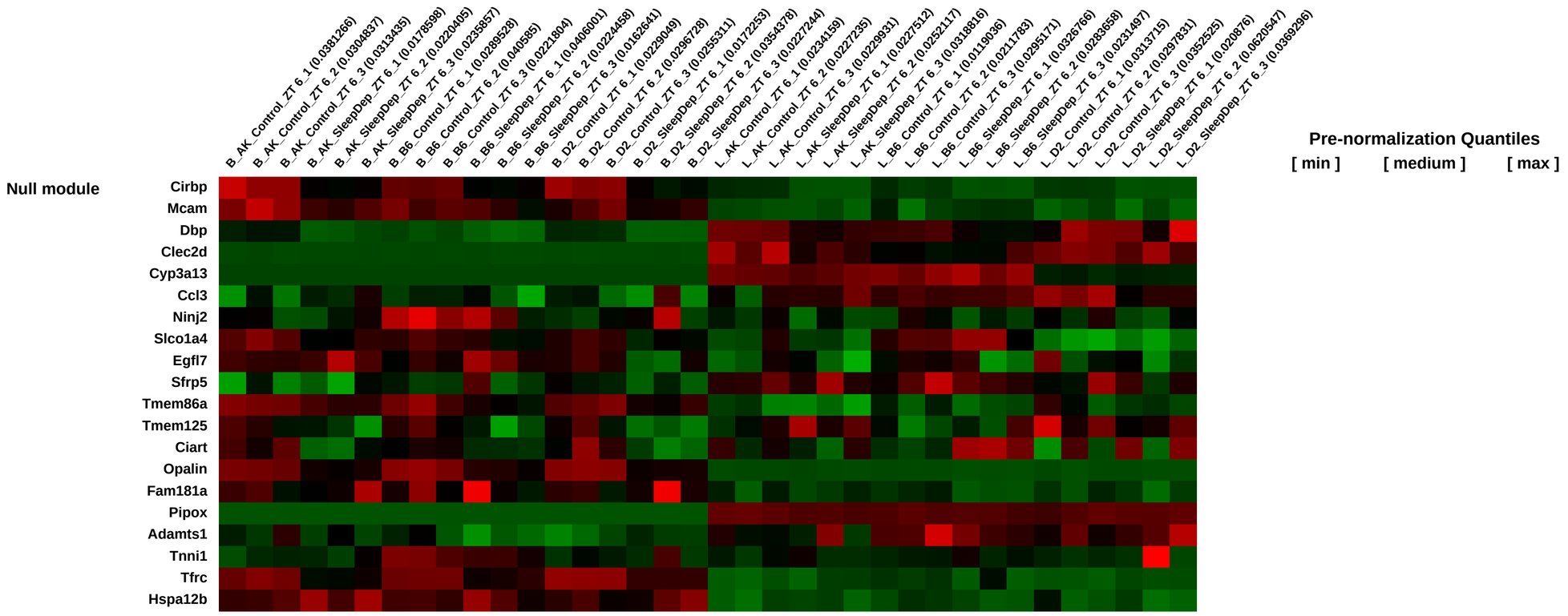

GEO Series "GSE9442" Expression Profiles

Num of samples in this series: 71

Scale of expression profile Z-scores

-3.0 -2.0 -1.0 0.0 1.0 2.0 3.0

GEO Link: http://www.ncbi.nlm.nih.gov/geo/query/acc.cgi?acc=GSE9442
Status: Public on Dec 07 2007
Title: Molecular correlates of sleep deprivation in the brain of three inbred mouse strains in an around-the-clock experiment
Organism: Mus musculus
Experiment type: Expression profiling by array
Platform: GPL1261
Pubmed ID: 18077435

Summary & Design:

Summary:
These studies adress differential changes in gene expression between sleep deprived and control mice. We profiled gene expression at four time points across the 24H Light/Dark cycle to take into account circadian influences and used three different inbred strains to understand the influence of genetic background.

Keywords: brain, circadian, genetic background, sleep deprivation

Overall design:
Experiments were performed on male mice (AKR/J (A), C57BL/6J (B), DBA/2J (D)), 12-13 weeks of age, purchased from Jackson Laboratory. Animals were housed in a light/dark cycle of 24 hrs with water and food available ad libitum. Mice of the 3 inbred strains were sleep deprived for 6h starting at light onset (ZT0), at the middle of the light (ZT6), at the beginning of the dark (ZT12), or at the middle of the dark (ZT18) period, and sacrificed together with their home-cage controls (n=9 / strain =3 / time =4 / condition =2; total =216 mice).

Background corr dist: KL-Divergence = 0.5365, L1-Distance = 0.0827, L2-Distance = 0.0223, Normal std = 0.2191

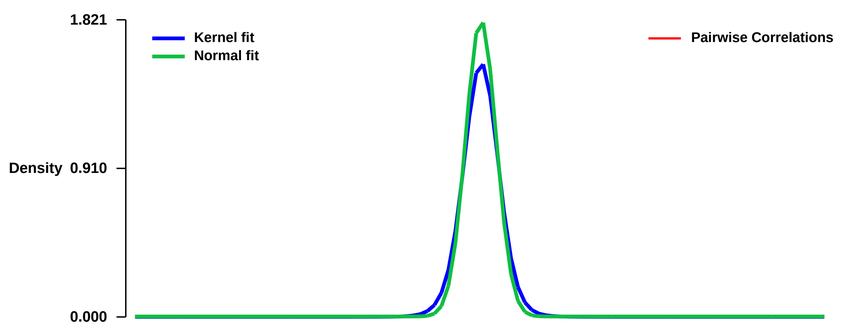

Z-score	-5.0	-4.0	-3.0	-2.0	-1.0	0.0	1.0	2.0	3.0	4.0	5.0
Correlation	-1.00	-1.00	-1.00	-0.96	-0.76	0.00	0.76	0.96	1.00	1.00	1.00

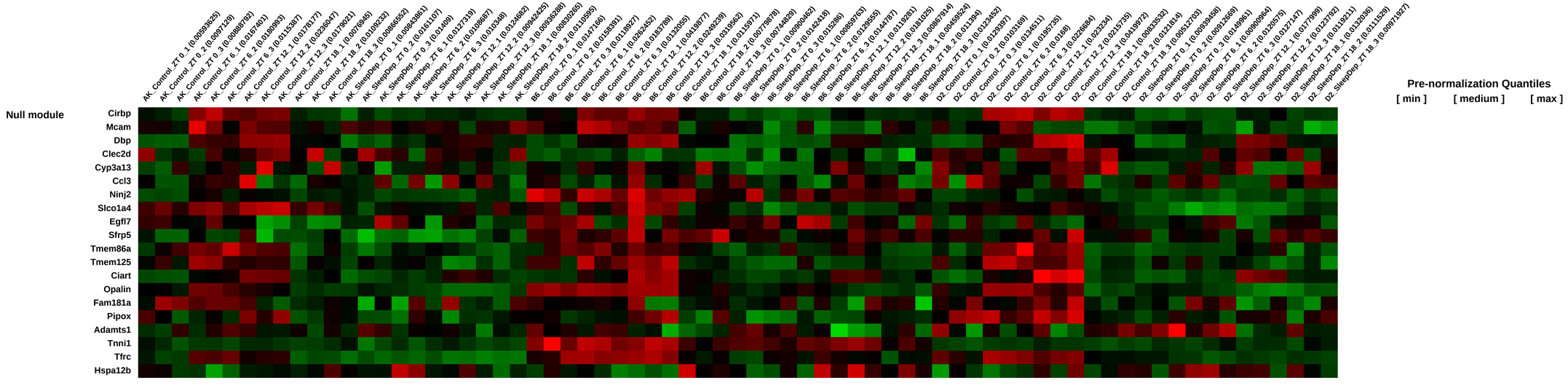

GEO Series "GSE9509" Expression Profiles

Num of samples in this series: 18

Scale of expression profile Z-scores

-3.0 -2.0 -1.0 0.0 1.0 2.0 3.0

GEO Link:	http://www.ncbi.nlm.nih.gov/geo/query/acc.cgi?acc=GSE9509
Status:	Public on Dec 01 2007
Title:	A transcriptional repressor and co-repressor induced by the STAT3-regulated anti-inflammatory signaling pathway.
Organism:	Mus musculus
Experiment type:	Expression profiling by array
Platform:	GPL1261
Pubmed ID:	18025162
Summary & Design:	**Summary:** IL-10 regulates anti-inflammatory signaling via the activation of STAT3, which in turn controls the induction of a gene expression program whose products execute inhibitory effects on pro-inflammatory mediator production. Here we show that IL-10 induces the expression of an ETS family transcriptional repressor, ETV3 and a helicase family co-repressor, SBNO2 (Strawberry notch homolog 2) in mouse and human macrophages. IL-10-mediated induction of ETV3 and SBNO2 expression was dependent upon both STAT3, and co-stimulus through the TLR pathway. We also observed that ETV3 expression was strongly induced by the STAT3 pathway induced by IL-10 but not STAT3 signaling activated by IL-6, which cannot activate the anti-inflammatory signaling pathway. ETV3 and SBNO2 specifically repressed NF-kB-mediated transcription and can physically interact. Collectively our data suggest that ETV3 and SBNO2 are components of the pathways that contribute to the downstream anti-inflammatory effects of IL-10. We compared expression profiles of macrophages isolated from IL-10 -/- mice. Macrophages were treated with either LPS or LPS plus IL-10. Treatment times were 10, 20 and 30 minutes. Keywords: time-course, treatment response, gene expression analysis **Overall design:** Mouse IL-10 -/- macrophages were isolated and purified and set up in culture medium containing LPS or LPS plus IL-10. A total of 18 samples were analyzed. This set contains three replicates of each treatment condition where treatment (LPS versus LPS plus IL-10) and time (10min, 20min and 30min) were varied.

Background corr dist: KL-Divergence = 0.1615, L1-Distance = 0.0290, L2-Distance = 0.0013, Normal std = 0.3670

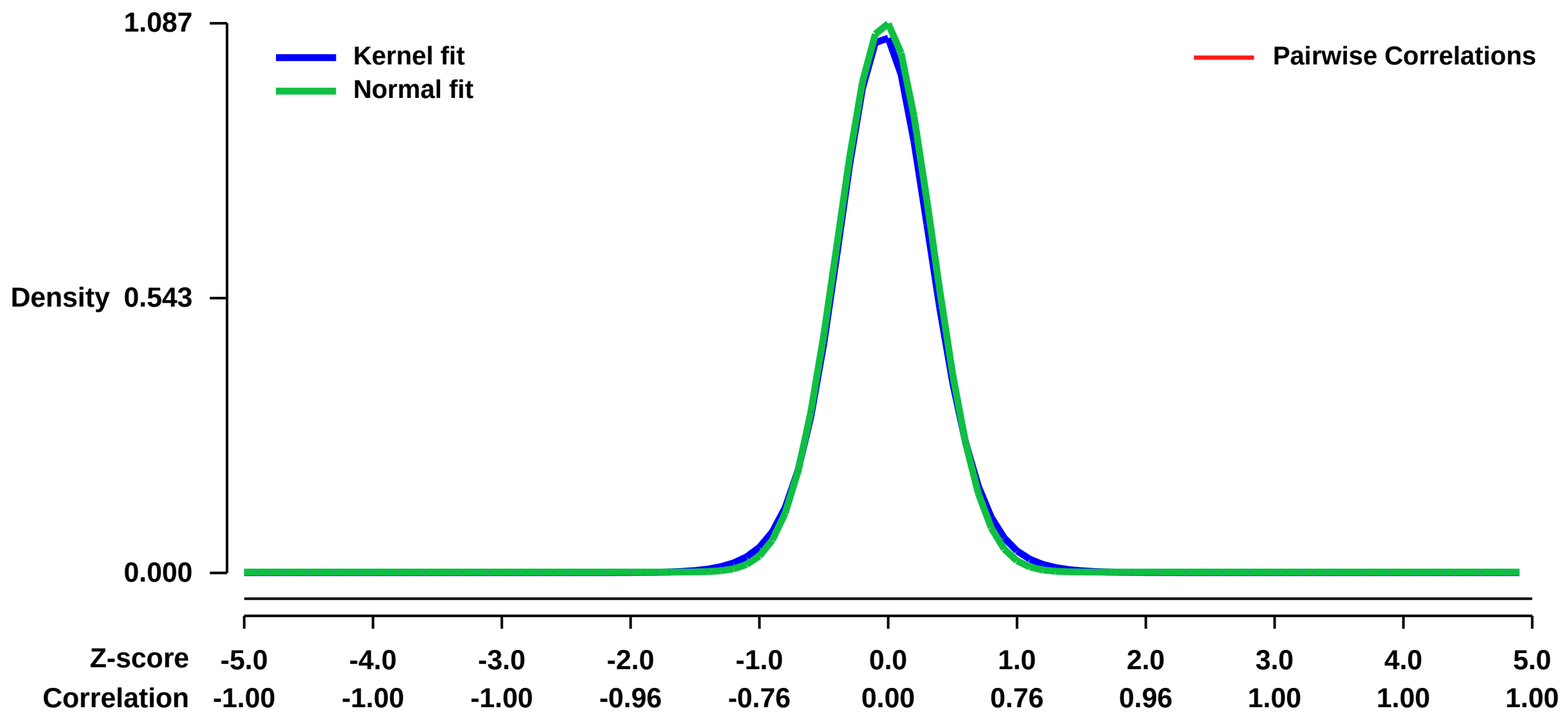

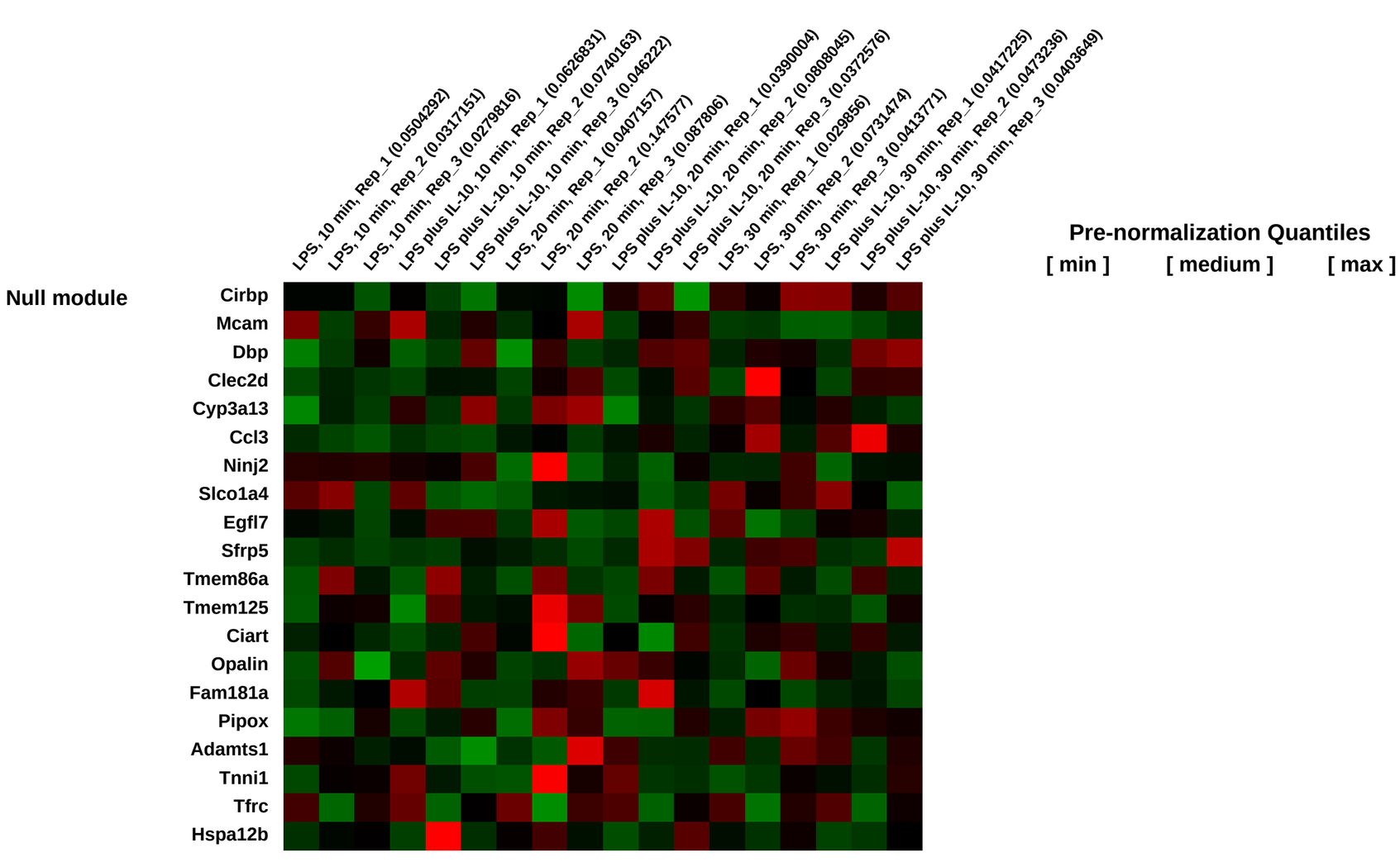

GEO Series "GSE9533" Expression Profiles

Num of samples in this series: 35

Scale of expression profile Z-scores

-3.0 -2.0 -1.0 0.0 1.0 2.0 3.0

GEO Link:	http://www.ncbi.nlm.nih.gov/geo/query/acc.cgi?acc=GSE9533
Status:	Public on May 22 2008
Title:	PPARalpha-mediated effects of dietary lipids on intestinal barrier gene expression
Organism:	Mus musculus
Experiment type:	Expression profiling by array
Platform:	GPL1261
Pubmed ID:	18489776
Summary & Design:	**Summary:** **Background: The selective absorption of nutrients and other food constituents in the small intestine is mediated by a group of transport proteins and metabolic enzymes, often collectively called â intestinal barrier proteinsâ . An important receptor that mediates the effects of dietary lipids on gene expression is the peroxisome proliferator-activated receptor alpha (PPARˆ±), which is abundantly expressed in enterocytes. In this study we examined the effects of acute nutritional activation of PPARˆ± on expression of genes encoding intestinal barrier proteins. To this end we used triacylglycerols composed of identical fatty acids in combination with gene expression profiling in wild-type and PPARˆ±-null mice. Treatment with the synthetic PPARˆ± agonist WY14643 served as reference.** **Results: We identified 74 barrier genes that were PPARˆ±-dependently regulated 6 hours after activation with WY14643. For eicosapentaenoic acid (EPA), docosahexaenoic acid (DHA) and oleic acid (OA) these numbers were 46, 41, and 19, respectively. The overlap between EPA-, DHA-, and WY14643-regulated genes was considerable, whereas OA treatment showed limited overlap. Functional implications inferred form our data suggested that nutrient-activated PPARˆ± regulated transporters and phase I/II metabolic enzymes were involved in a) fatty acid oxidation, b) cholesterol, glucose, and amino acid transport and metabolism, c) intestinal motility, and d) oxidative stress defense.** **Conclusion: We identified intestinal barrier genes that were PPARˆ±-dependently regulated after acute activation by fatty acids.This knowledge provides a better understanding of the impact dietary fat has on the barrier function of the gut, identifies PPARˆ± as an important factor controlling this key function, and underscores the importance of PPARˆ± for nutrient-mediated gene regulation in intestine.** **Keywords: metabolic state analysis** **Overall design:** **Pure bred wild-type (129S1/SvImJ) and PPARˆ±-null (129S4/SvJae) mice were treated for 6 hours with the synthetic triacylglycerols triolein [oleic acid (OA, C18:1)], trieicosapentaenoin [eicosapentaenoic acid (EPA, C20:5)] or tridocosahexaenoin [ocosahexaenoic acid (DHA, C22:6)], or the potent PPARˆ± agonist WY14,643. Two weeks before the start of the experiment, mice were put on a modified AIN76A diet, in which corn oil was replaced by olive oil. At the day of the experiment mice were fasted for four hours. At 9 AM mice were dosed by oral gavage with 400 ´µl of a 0.1% WY14643 suspension in 0.5% carboxymethyl cellulose, or 400 ´µl of the synthetic triacylglycerols. Six hours after the gavage the mice were anaesthetized, small intestines were removed, flushed with ice-cold PBS and remaining fat and pancreatic tissue was carefully removed. Total RNA was then isolated. RNA of 4-5 biological replicates was hybridized to Affymetrix 430-2.0 plus arrays. Five microgram total RNA was labelled according to the ENZO-protocol, fragmented and hybridized according to Affymetrix's protocols.**

Background corr dist: **KL-Divergence = 0.3720, L1-Distance = 0.0584, L2-Distance = 0.0087, Normal std = 0.2574**

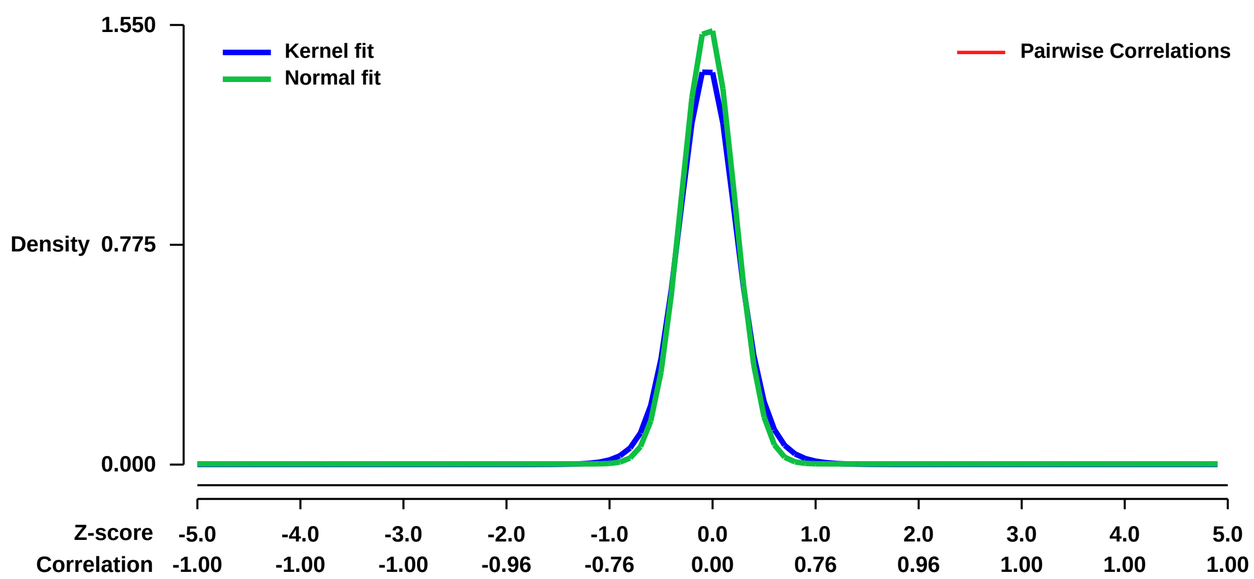

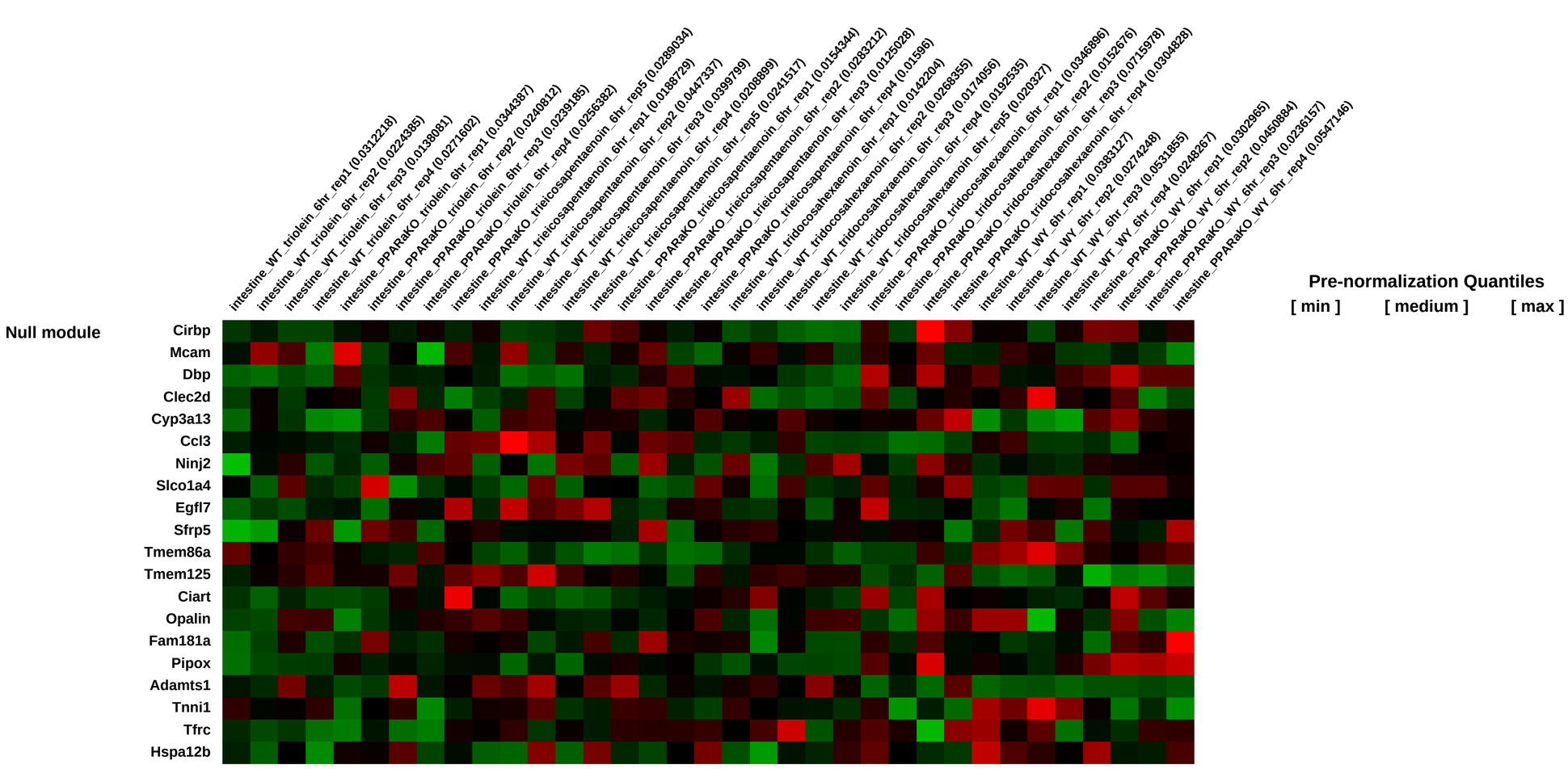

GEO Series "GSE9545" Expression Profiles

Num of samples in this series: 11

Scale of expression profile Z-scores

-3.0 -2.0 -1.0 0.0 1.0 2.0 3.0

GEO Link:	http://www.ncbi.nlm.nih.gov/geo/query/acc.cgi?acc=GSE9545
Status:	Public on Aug 24 2009
Title:	Gene Expression Profiles Associated with Ethanol-Induced Teratogenic Effects in a C57BL/6 Mouse Embryo Culture Model
Organism:	Mus musculus
Experiment type:	Expression profiling by array
Platform:	GPL1261
Pubmed ID:	18366608
Summary & Design:	**Summary:** **Mouse model for Fetal Alcohol Syndrome. Embryos exposed to alcohol in controlled environment to assess teratogenic effects.** **Fetal Alcohol Syndrome (FAS) is a leading developmental disorder. To date, a holistic view of molecular gene changes is largely unexplored. Using microarray analysis of whole embryo mouse culture with strict-control over alcohol-level, we found, directly related alcohol-metabolism, a reduction of retinol binding protein 1(Rbp1), and a, de novo expression of aldehyde dehydrogenase 1B1 (ALDH1B1). Remarkably, four key hemopoiesis genes (glycophorin A, adducin 2, beta-2 microglobulin, and ceruloplasmin) became absent, and many histone variants genes were reduced. Hypothesis-driven informatics analysis and intersection analysis of two independent experiments indicated that the altered genes are involved in cell growth, hemopoiesis, histone modification, eye and heart development, and a collective reduction in expression of growth factor genes (Igf1, Efemp1, Tieg, and Edil3) and neural specification genes (neurogenin, Sox 5, bHLHb5). Down-regulated neural specification phenotypes further supported the above findings. Further more, the gene expression profile indicated distinct subgroups which overlapped with the teratogenesis of the open- and the closed-neural tubes known in FAS. In summary, our data reveal genes alteration with causal potential for dysmorpology (e.g. retinoic acid, neuronal specification, and neurotrophic factors, and epigenetics related histone genes) and those downstream responsive genes related to alcohol metabolism, and developmental teratogenesis.** **Keywords: comparison of gene expression profiles for treated vs. control** **Overall design:** **Comparison of whole embryo gene expression after exposure to ethanol for 46 hours. Note 2 independent experiments completed.**

Background corr dist: KL-Divergence = 0.1510, L1-Distance = 0.0385, L2-Distance = 0.0030, Normal std = 0.3711

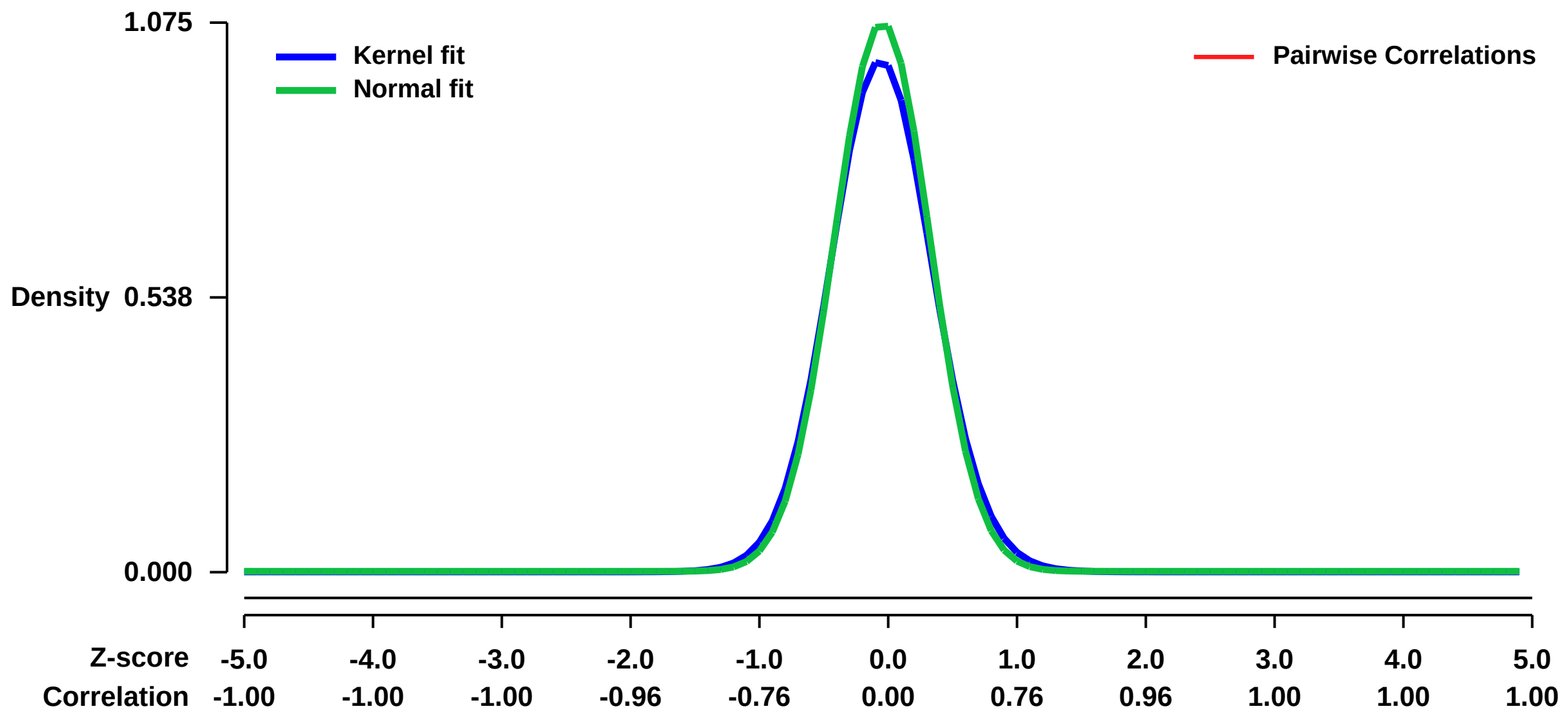

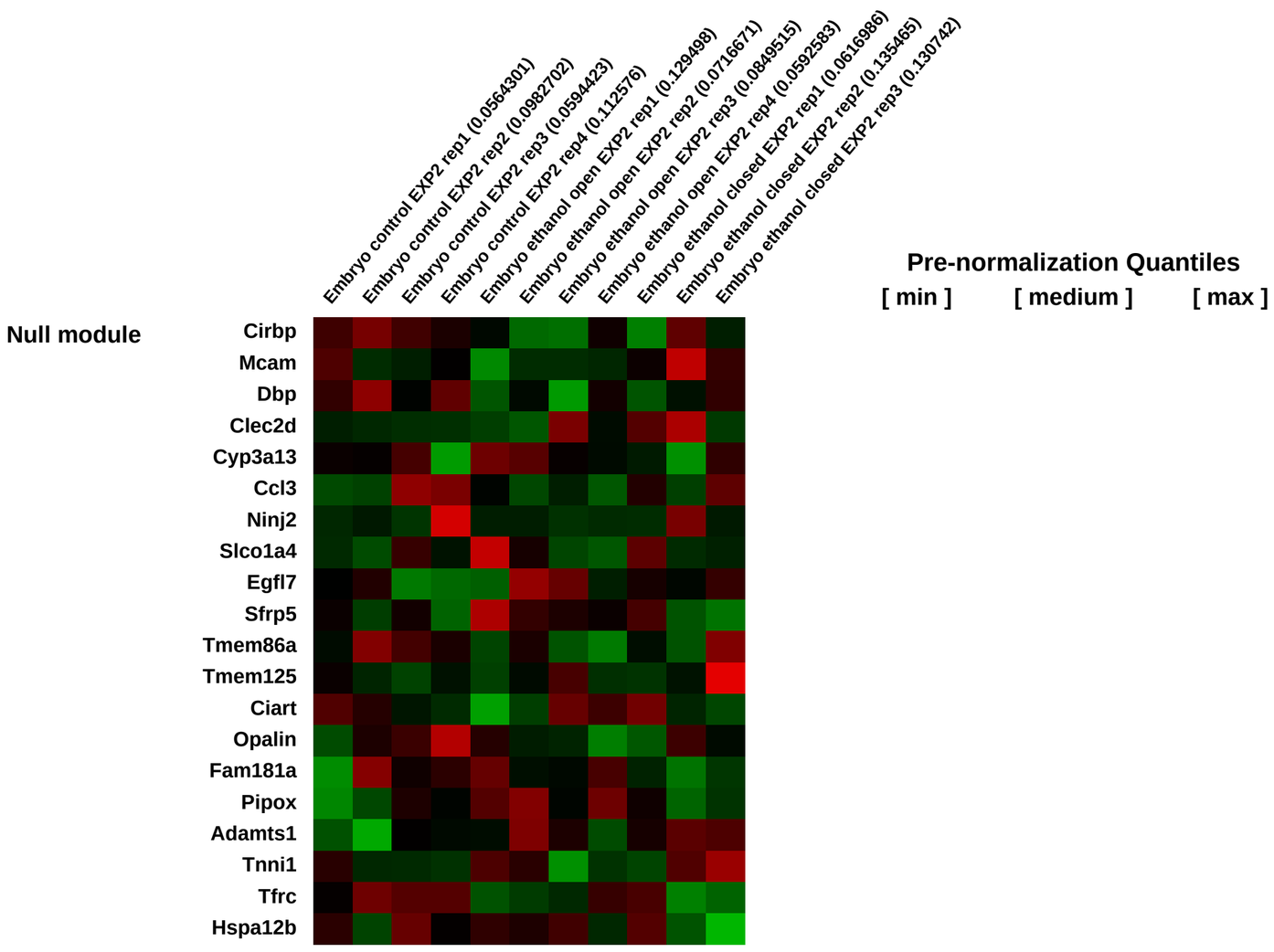

GEO Series "GSE9630" Expression Profiles

Num of samples in this series: 59

Scale of expression profile Z-scores

-3.0 -2.0 -1.0 0.0 1.0 2.0 3.0

GEO Link:	http://www.ncbi.nlm.nih.gov/geo/query/acc.cgi?acc=GSE9630
Status:	Public on Nov 17 2007
Title:	Expression data from mouse liver
Organism:	Mus musculus
Experiment type:	Expression profiling by array
Platform:	GPL1261
Pubmed ID:	18396267
Summary & Design:	**Summary:** Exposure to high levels of arsenic in drinking water is associated with several types of cancers including lung, bladder and skin, as well as vascular disease and diabetes. Drinking water standards are based primarily on epidemiology and extrapolation from higher dose experiments, rather than measurements of phenotypic changes associated with chronic exposure to levels of arsenic similar to the current standard of 10ppb, and little is known about the difference between arsenic in food as opposed to arsenic in water. Measurement of phenotypic changes at low doses may be confounded by the effect of laboratory diet, in part because of trace amounts of arsenic in standard laboratory chows, but also because of broad metabolic changes in response to the chow itself. Finally, this series contrasts 8hr, 1mg/kg injected arsenic with the various chronic exposures, and also contrasts the acute effects of arsenic, dexamethasone or their combination. Male C57BL/6 mice were fed on two commercially available laboratory diets (LRD-5001 and AIN-76A) were chronically exposed, through drinking water or food, to environmentally relevant concentrations of sodium arsenite, or acutely exposed to dexamethasone. **Keywords:** dose response **Overall design:** Another group animals, fed on the AIN 76A diet, was IP injected with dexamethasone (1 mg/kg), sodium arsenite (1mg/kg), both dexamethosone and arsenite, or saline alone.

Background corr dist: KL-Divergence = 0.2465, L1-Distance = 0.0752, L2-Distance = 0.0169, Normal std = 0.3041

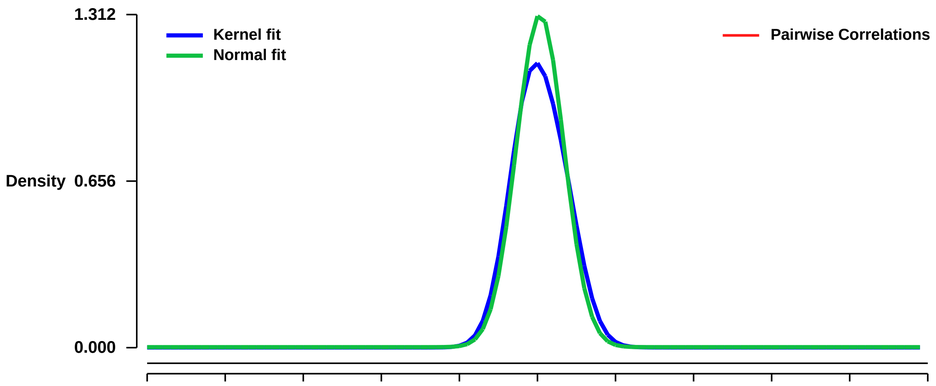

Z-score	-5.0	-4.0	-3.0	-2.0	-1.0	0.0	1.0	2.0	3.0	4.0	5.0
Correlation	-1.00	-1.00	-1.00	-0.96	-0.76	0.00	0.76	0.96	1.00	1.00	1.00

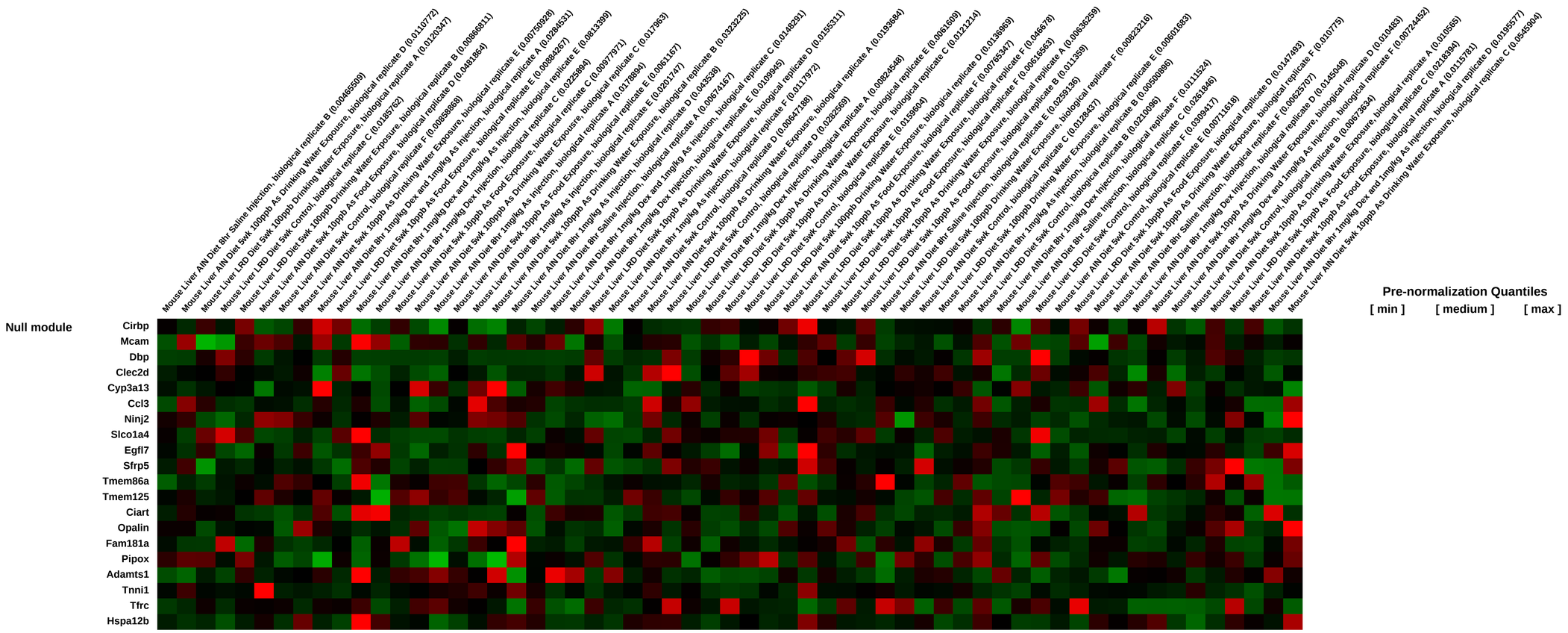

GEO Series "GSE9652" Expression Profiles

Num of samples in this series: 11

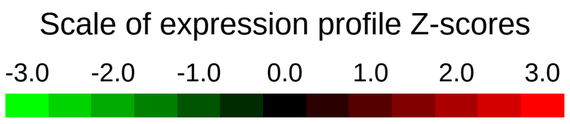

GEO Link:	http://www.ncbi.nlm.nih.gov/geo/query/acc.cgi?acc=GSE9652
Status:	Public on Jul 01 2008
Title:	GATA4 is a direct activator of Cyclin D2 and is required for proliferation in 2nd heart field-derived myocardium
Organism:	Mus musculus
Experiment type:	Expression profiling by array
Platform:	GPL1261
Pubmed ID:	18591257
Summary & Design:	**Summary:** The second heart field (SHF) comprises a population of mesodermal progenitor cells that are added to the nascent linear heart to give rise to the majority of the right ventricle, interventricular septum, and outflow tract of mammals and birds. The zinc finger transcription factor GATA4 functions as an integral member of the cardiac transcription factor network in the SHF and its derivatives. In addition to its role in cardiac differentiation, GATA4 is also required for cardiomyocyte replication, although the transcriptional targets of GATA4 required for proliferation have not been previously identified. In the present study, we disrupted Gata4 function exclusively in the SHF and its derivatives. Gata4 SHF knockout mice die by embryonic day 13.5 and exhibit hypoplasia of the right ventricular myocardium and interventricular septum and display profound ventricular septal defects. Loss of Gata4 function in the SHF results in decreased myocyte proliferation in the right ventricle, and we identify numerous cell cycle genes that are dependent on Gata4 by microarray analysis. We show that Gata4 is required for Cyclin D2 expression in the right ventricle and that the Cyclin D2 promoter is bound and activated by GATA4 via three consensus GATA binding sites. These findings establish Cyclin D2 as a direct transcriptional target of GATA4 and support a model in which GATA4 controls cardiomyocyte proliferation by coordinately regulating numerous cell cycle genes. **Keywords: genetic modification** **Overall design:** 170 n=3), and Gata4flox/flox; Nkx2-5Cre/+ (Gata4 CKONkx, n=5).

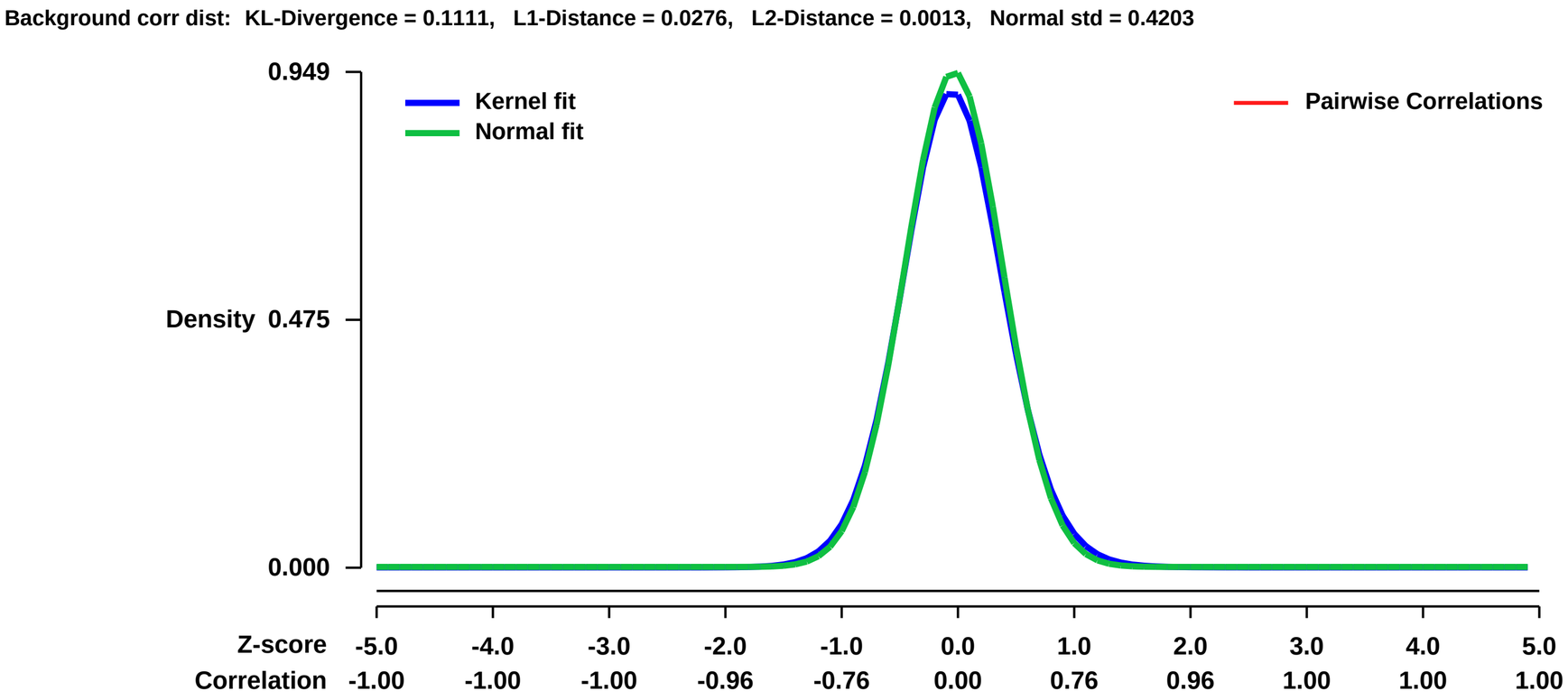

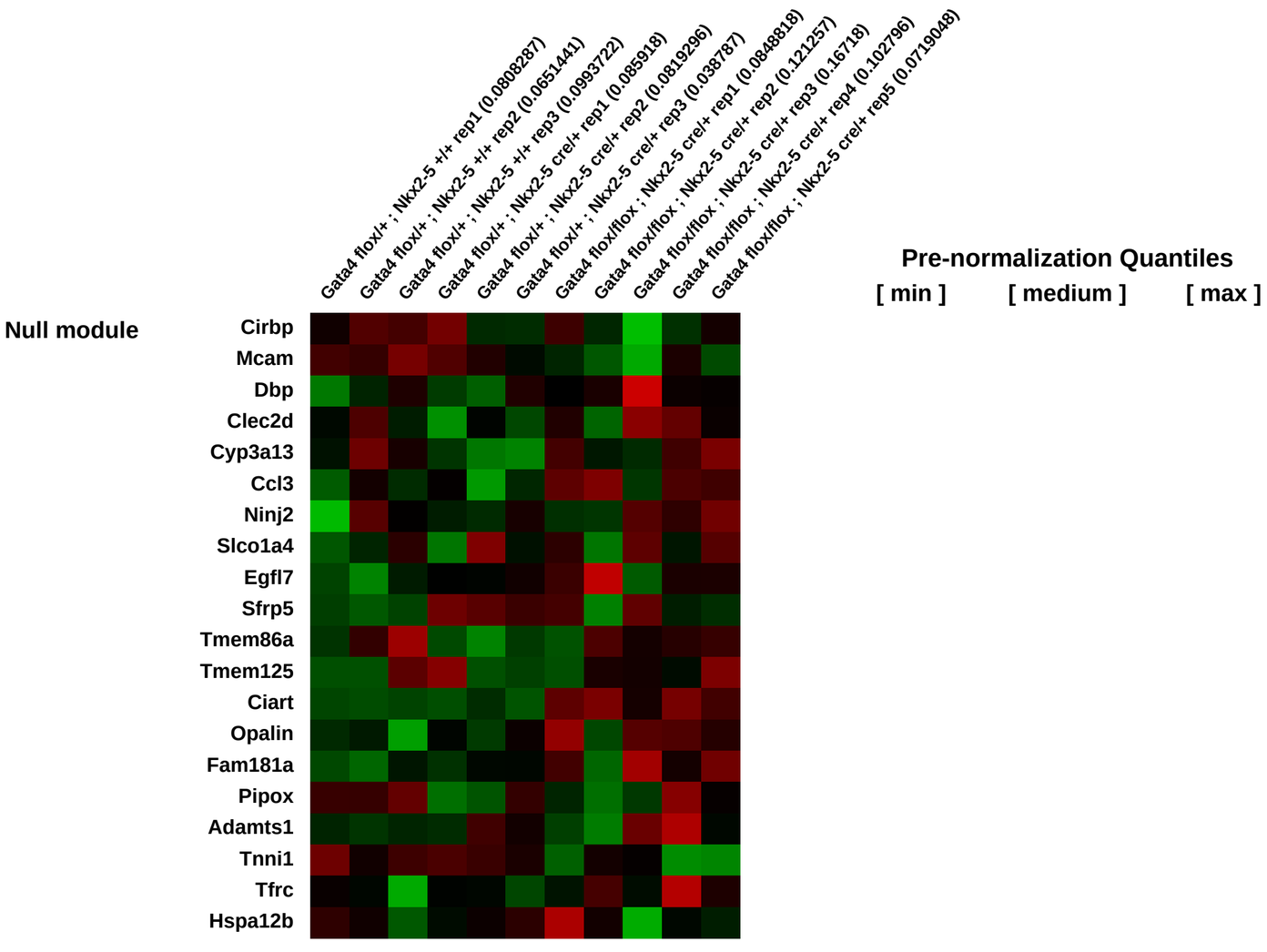

GEO Series "GSE9711" Expression Profiles

Num of samples in this series: 6

Scale of expression profile Z-scores

-3.0 -2.0 -1.0 0.0 1.0 2.0 3.0

GEO Link:	**http://www.ncbi.nlm.nih.gov/geo/query/acc.cgi?acc=GSE9711**
Status:	**Public on Jul 11 2008**
Title:	**Expression comparison between wild-type and transgenic mouse lenses**
Organism:	**Mus musculus**
Experiment type:	**Expression profiling by array**
Platform:	**GPL1261**
Pubmed ID:	
Summary & Design:	**Summary:** **The vertebrate ocular lens consists of two basic cell types: the lens fibers, highly specialized cells that make up the bulk of the lens and are the basis for its unique optical characteristics, and the epithelial cells that cover the anterior hemisphere and acts as a stem cell population for progenitors of new fibers. The forkhead transcription factor FoxE3 is essential for maintenance, proliferation and survival of the epithelial cells, and silencing of the FoxE3 gene coincides with the cell cycle arrest that marks initiation of fiber cell differentiation. Here we have used transgenic ectopic expression of murine Foxe3 in fiber cells to investigate the consequences of persistent Foxe3 expression during fiber differentiation. Microarray transcript profiling showed that ectopic Foxe3 caused a general increase in mRNAs which are normally enriched in epithelial cells, consistent with an epithelialization of the transgenic fibers.** **Keywords: Genetic modification** **Overall design:** **Whole lenses from P2 animals were dissected and genotyped. 12 lenses from each genotype were used for RNA extraction and hybridization to Affymetrix arrays. Total of 3 replicates/genotype.**

Background corr dist: KL-Divergence = 0.0358, L1-Distance = 0.0146, L2-Distance = 0.0002, Normal std = 0.6368

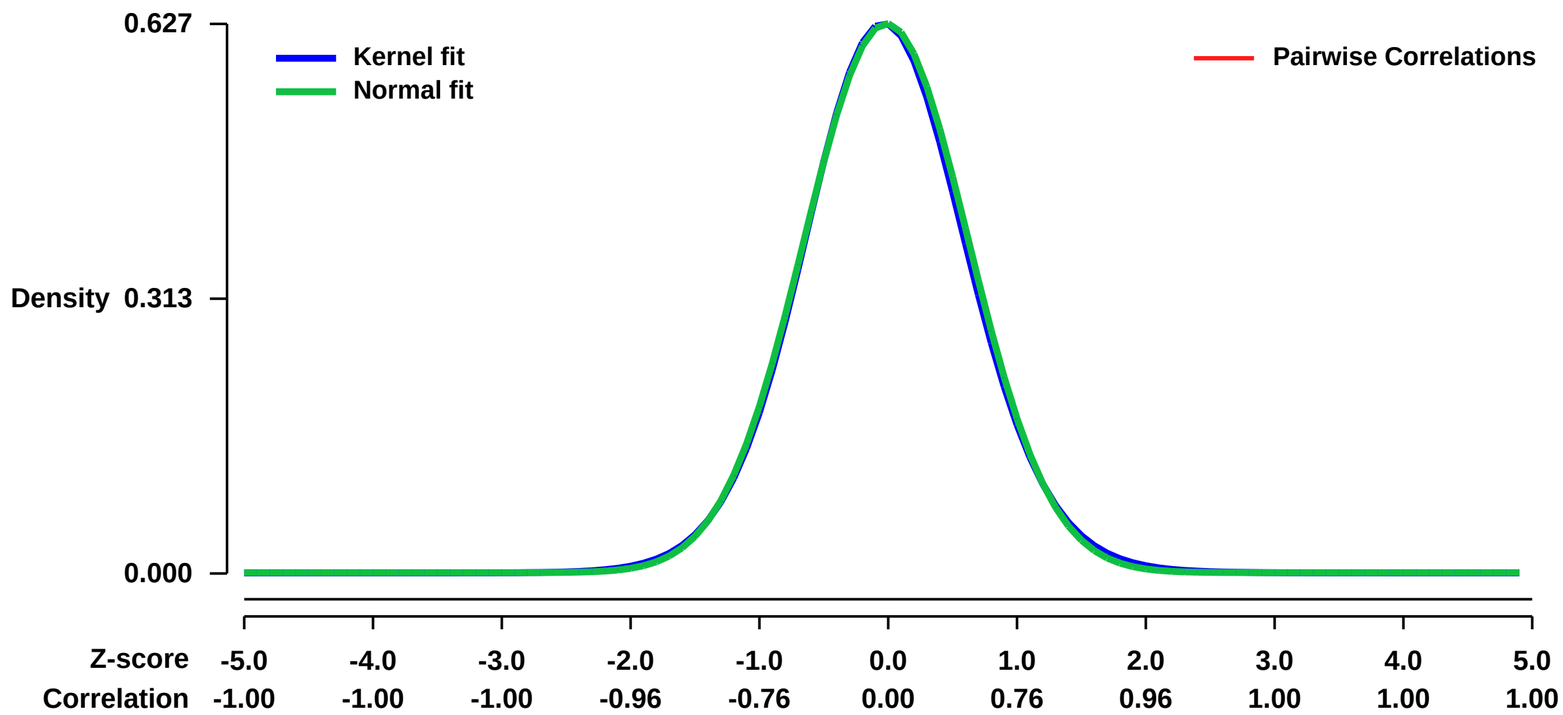

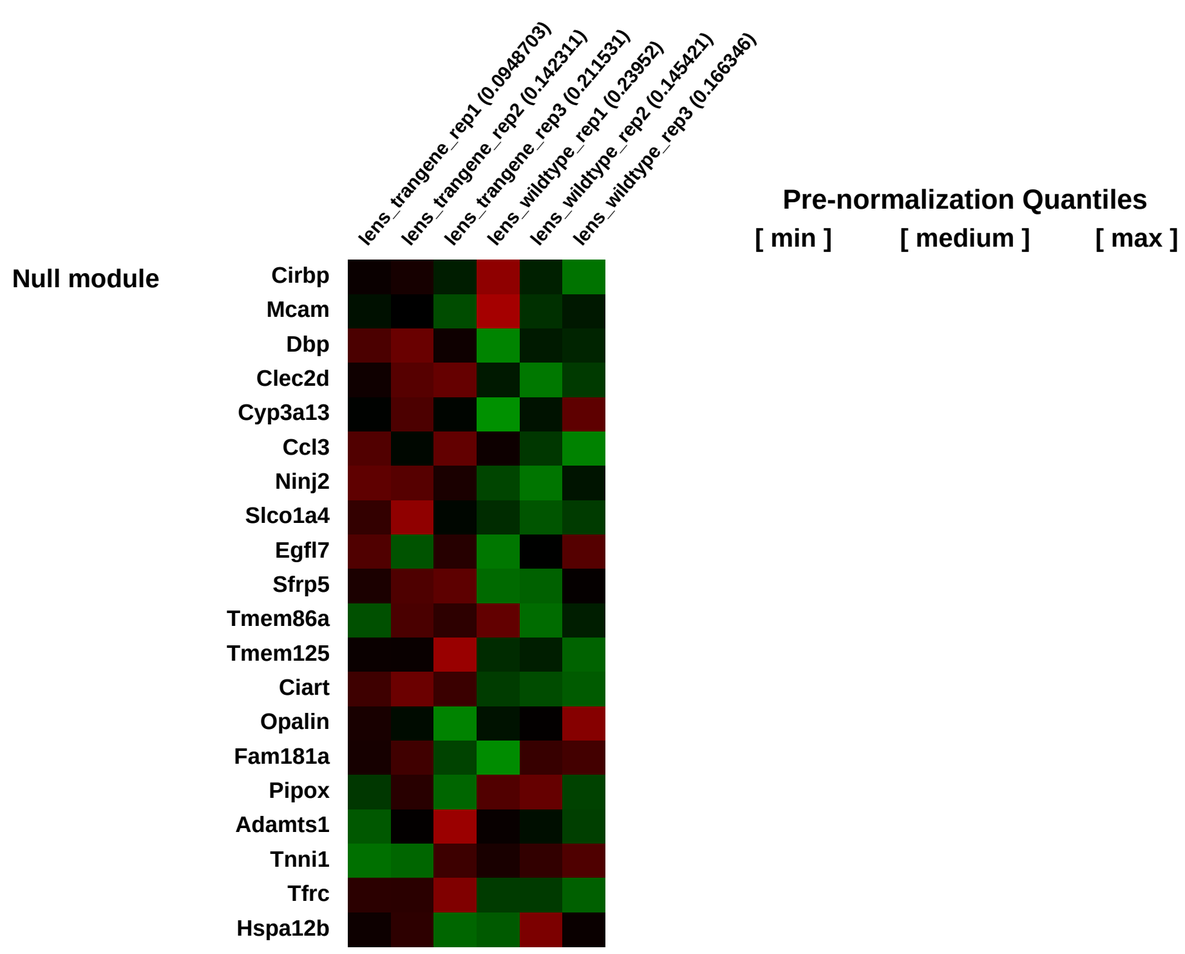

GEO Series "GSE9717" Expression Profiles

Num of samples in this series: 6

Scale of expression profile Z-scores

-3.0 -2.0 -1.0 0.0 1.0 2.0 3.0

GEO Link:	http://www.ncbi.nlm.nih.gov/geo/query/acc.cgi?acc=GSE9717
Status:	Public on Feb 14 2008
Title:	Rb Intrinsically Promotes Erythropoiesis by Coupling Cell Cycle Exit with Mitochondrial Biogenesis
Organism:	Mus musculus
Experiment type:	Expression profiling by array
Platform:	GPL1261
Pubmed ID:	18258751
Summary & Design:	**Summary:** Regulation of the cell cycle is intimately linked to erythroid differentiation, yet how these processes are coupled is not well understood. To gain insight into this coordinate regulation, we examined the role that the retinoblastoma protein (Rb), a central regulator of the cell cycle, plays in erythropoiesis. We found that Rb serves a cell-intrinsic role and its absence causes ineffective erythropoiesis, with a differentiation block at the transition from early to late erythroblasts. Unexpectedly, in addition to a failure to properly exit the cell cycle, mitochondrial biogenesis fails to be upregulated concomitantly, contributing to this differentiation block. The link between erythropoiesis and mitochondrial function was validated by inhibition of mitochondrial biogenesis. Erythropoiesis in the absence of Rb resembles the human myelodysplastic syndromes, where defects in cell cycle regulation and mitochondrial function frequently occur. Our work demonstrates how these seemingly disparate pathways play a role in coordinately regulating cellular differentiation. Keywords: disease state analysis Overall design: Microarray expression analysis from sorted CD71+/Ter-119+ bone marrow erythroid progenitors of Rb-null animals and controls. The Rb-null genotype was EpoR-GFPcre/+; Rb fl/fl and the control genotype was EpoR-GFPcre/+; Rb fl/+. We have analyzed 3 Rb-null datasets and 3 control datasets.

Background corr dist: KL-Divergence = 0.0253, L1-Distance = 0.0283, L2-Distance = 0.0011, Normal std = 0.7113

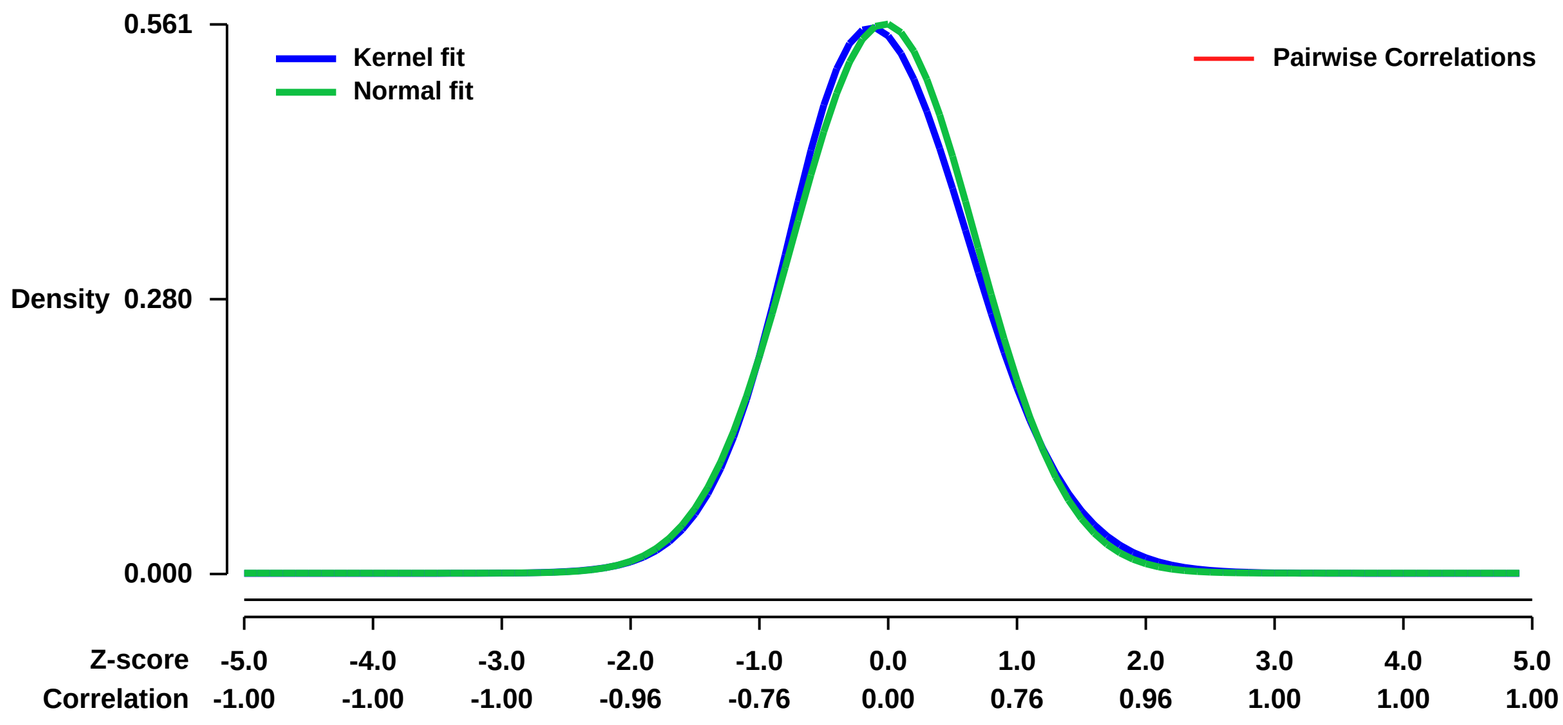

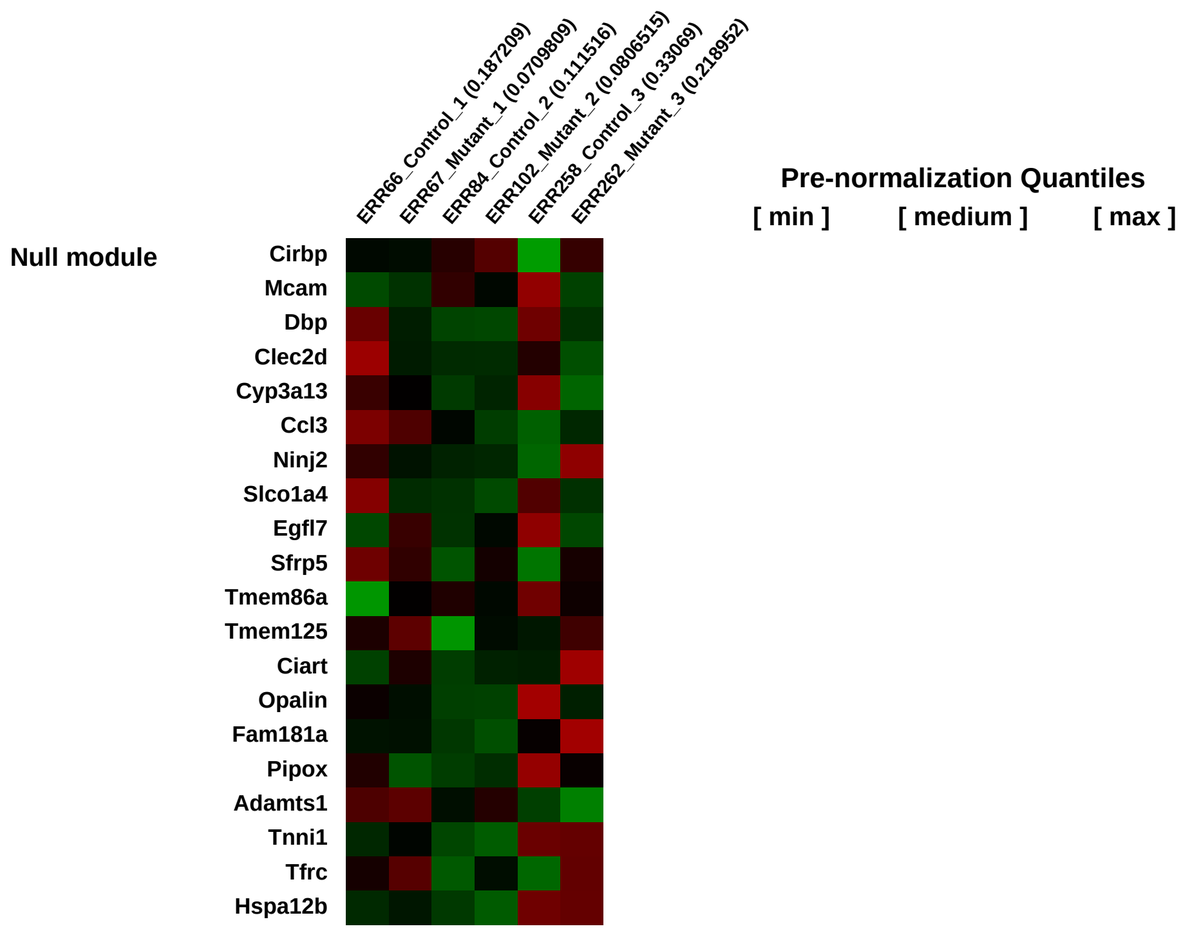

GEO Series "GSE9725" Expression Profiles

Num of samples in this series: 16

Scale of expression profile Z-scores

-3.0 -2.0 -1.0 0.0 1.0 2.0 3.0

GEO Link:	http://www.ncbi.nlm.nih.gov/geo/query/acc.cgi?acc=GSE9725
Status:	Public on Dec 13 2007
Title:	Gene expression data after acute withdrawal of TERT in mouse skin
Organism:	Mus musculus
Experiment type:	Expression profiling by array
Platform:	GPL1261
Pubmed ID:	18208333
Summary & Design:	**Summary:** TERT is an essential protein component of telomerase, a ribonuclearprotein complex that protects chromosomal ends. Ectopic expression of TERT in mouse skin activates hair follicle stem cells and induces active growth phase of hair cycles, called anagen. This activity of TERT is independent of its reverse transcriptase function, indicating that this is a non-telomeric function of TERT. We performed time-course microarray analysis using conditional bi-transgenic mice (iK5-TERT) to understand the mechanism of this novel non-telomeric function of TERT. Keywords: Time course, 2 cohorts (control, experimental) **Overall design:** Hair follicles of iK5-TERT mice at postnatal day 60 is in TERT-induced anagen. To those mice, we injected either PBS, to maintain TERT transgene expression, or doxycycline, to rapidly extinguish transgene expression. We then took time-course dorsal skin biopsies (0,6,12,24 hr) of these mice and analyzed differential gene expressions using Affymetrix Genechips and various bioinformatic tools, including SAM, to discover TERT-regulated genes.

Background corr dist: KL-Divergence = 0.1451, L1-Distance = 0.0302, L2-Distance = 0.0014, Normal std = 0.3801

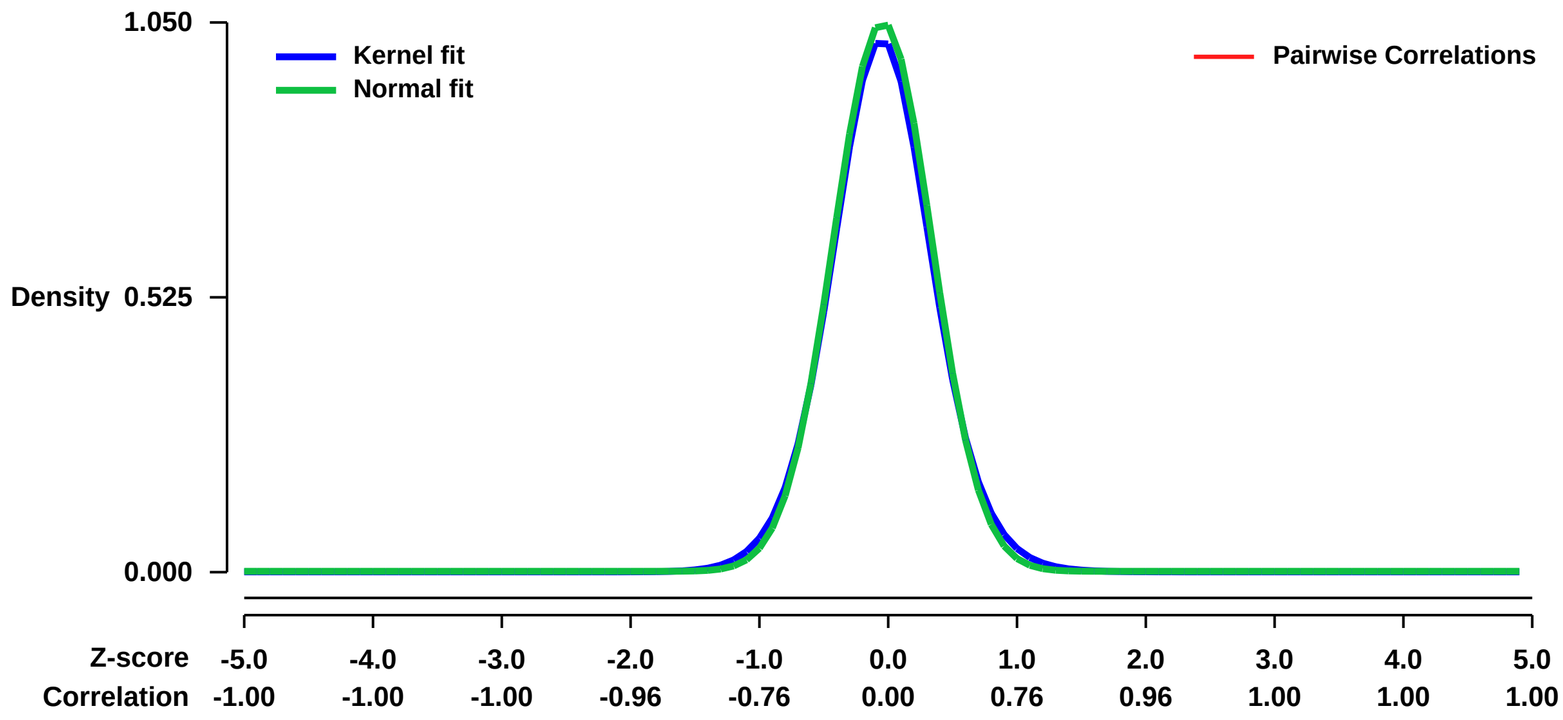

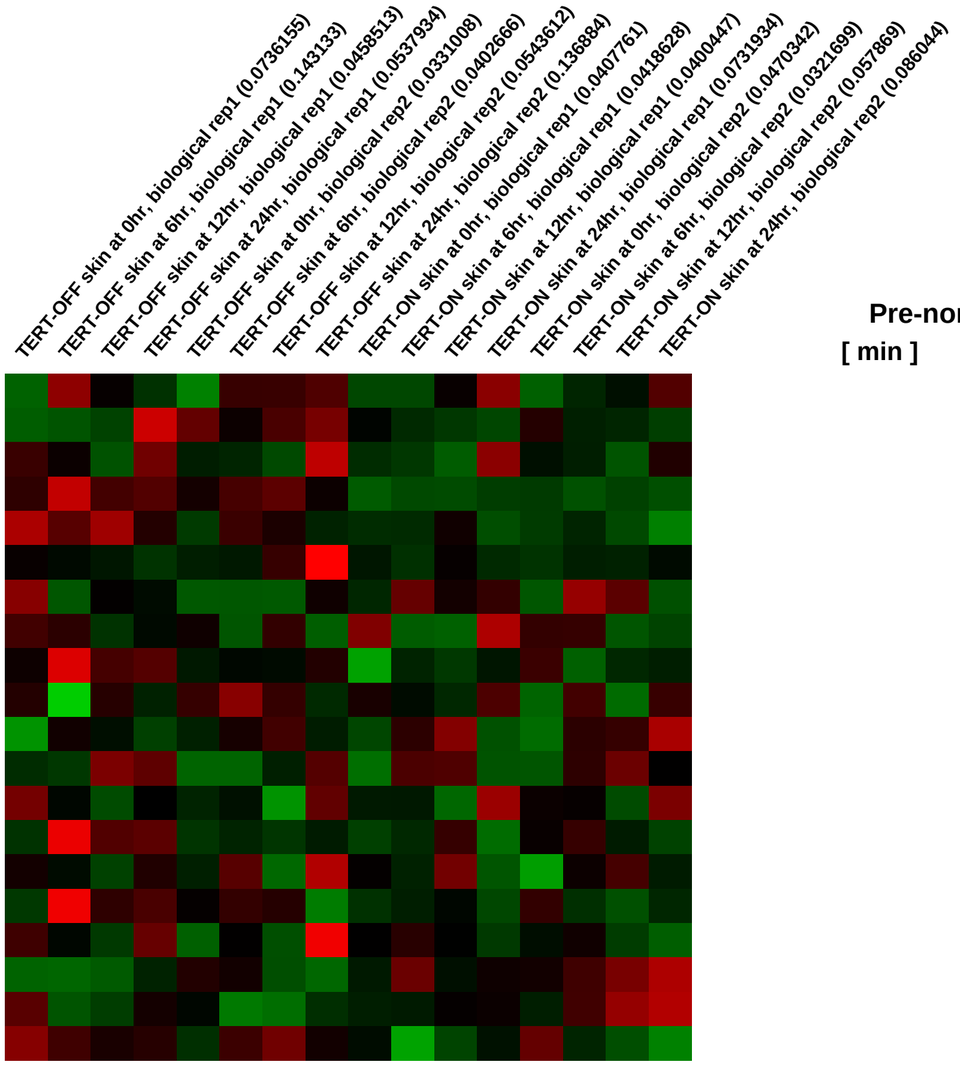

GEO Series "GSE9735" Expression Profiles

Num of samples in this series: 9

Scale of expression profile Z-scores

-3.0 -2.0 -1.0 0.0 1.0 2.0 3.0

GEO Link:	**http://www.ncbi.nlm.nih.gov/geo/query/acc.cgi?acc=GSE9735**
Status:	**Public on Nov 29 2008**
Title:	**B6_IL1218_WAP**
Organism:	**Mus musculus**
Experiment type:	**Expression profiling by array**
Platform:	**GPL1261**
Pubmed ID:	
Summary & Design:	**Summary:** **Dataset of IL-12+IL-18 trated and Yersinia enterocolitica infected C57BL/6 NK cells** **Keywords: infection response** **Overall design:** **3 conditions, 3 biological replicates each**

Background corr dist: **KL-Divergence = 0.0617, L1-Distance = 0.0954, L2-Distance = 0.0121, Normal std = 0.7100**

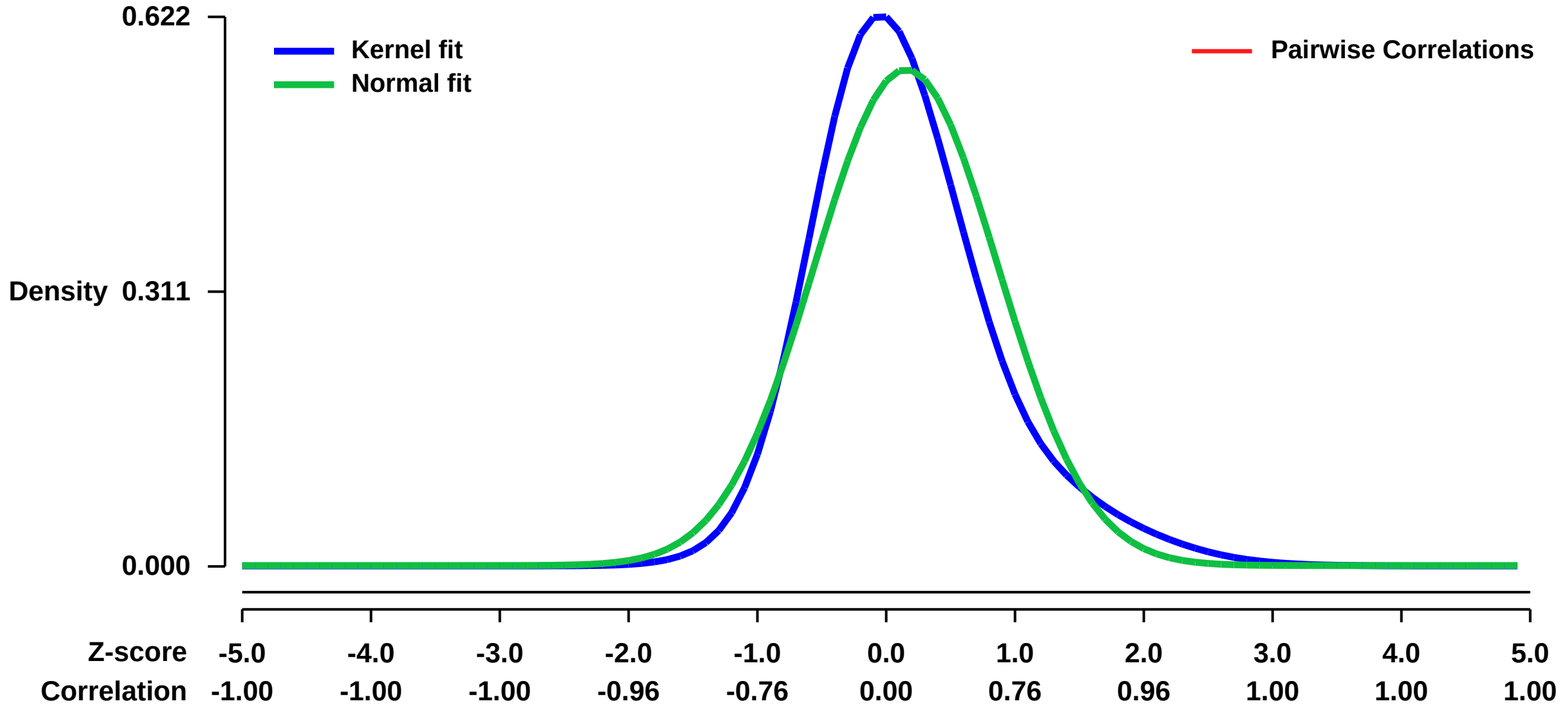

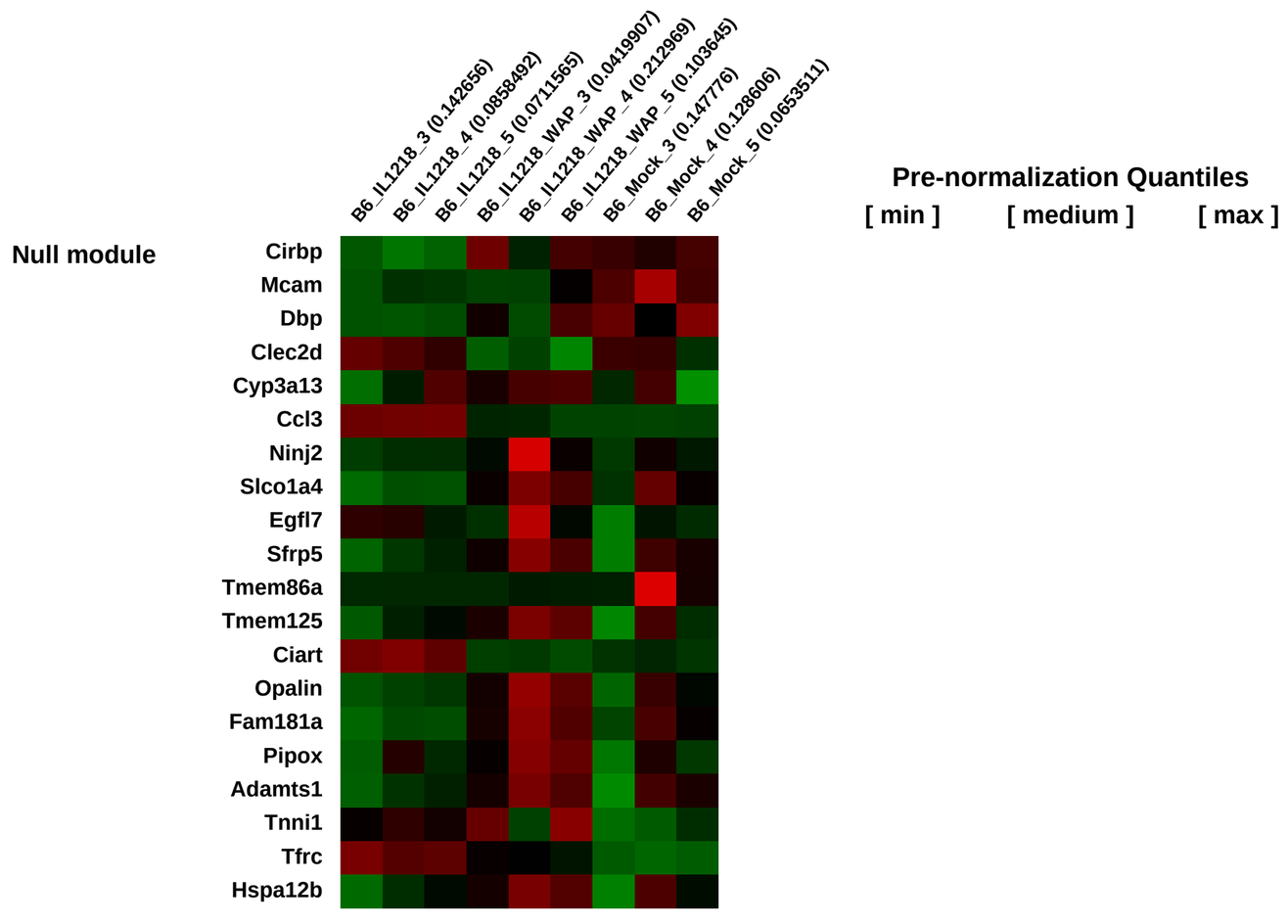

GEO Series "GSE9743" Expression Profiles

Num of samples in this series: 12

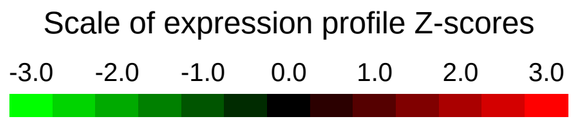

GEO Link:	http://www.ncbi.nlm.nih.gov/geo/query/acc.cgi?acc=GSE9743
Status:	Public on May 30 2008
Title:	The in vivo effect of actin cytoskeletal abnormalities on gene expression
Organism:	Mus musculus
Experiment type:	Expression profiling by array
Platform:	GPL1261
Pubmed ID:	18381839
Summary & Design:	**Summary:** Remodeling of the actin cytoskeleton through actin dynamics (assembly and disassembly of filamentous actin) is known to be essential for numerous basic biological processes. In addition, recent in vitro studies provided evidence that actin dynamics participate in the control of gene expression. A spontaneous mouse mutant, corneal disease 1 (corn1), is deficient for a regulator of actin dynamics, destrin (DSTN; also known as actin depolymerizing factor or ADF), and develops epithelial hyperproliferation and neovascularization in the cornea. Dstncorn1 mice exhibit the actin dynamics defect in the corneal epithelial cells as evidenced by increased filamentous actin, offering an in vivo model to investigate the physiological significance of the transcriptional regulation by actin dynamics. To examine the effect of the Dstncorn1 mutation on gene expression, we performed a microarray analysis using the cornea from Dstncorn1 and wild-type control mice. A dramatic alteration of gene expression was observed in the Dstncorn1 cornea, with 1,226 annotated genes differentially expressed. Functional annotation of these genes revealed that most significantly enriched functional categories are associated with actin and/or cytoskeleton. Among genes that belong to these categories, a considerable number of serum response factor (SRF) target genes were found, indicating the existence of the actin-SRF pathway of transcriptional regulation in vivo. A comparative study using an allelic mutant strain, Dstncorn1-2J, with milder corneal phenotypes also suggested that the severity of the actin dynamics defect correlates with the level of gene expression changes. Our study provides evidence that actin dynamics have a strong impact on gene expression in vivo. **Keywords:** Comparative gene expression **Overall design:** Microarray analysis was performed in triplicate with RNA from each genotype, A. BY H2bc H2-T18f/SnJ (A. BY wild-type), A. BY H2bc H2-T18f/SnJ-Dstncorn1/J (Dstncorn1), C57BL/6J (B6 wild-type), C57BL/6JSmn-Dstncorn1-2J/J (Dstncorn1-2J), and C.129S2(B6)-Il8rbtm1Mwm/J (Il8rb-/-), hybridized to three Affymetrix MG 430 2.0 arrays.

Background corr dist: KL-Divergence = 0.0655, L1-Distance = 0.0932, L2-Distance = 0.0099, Normal std = 0.8050

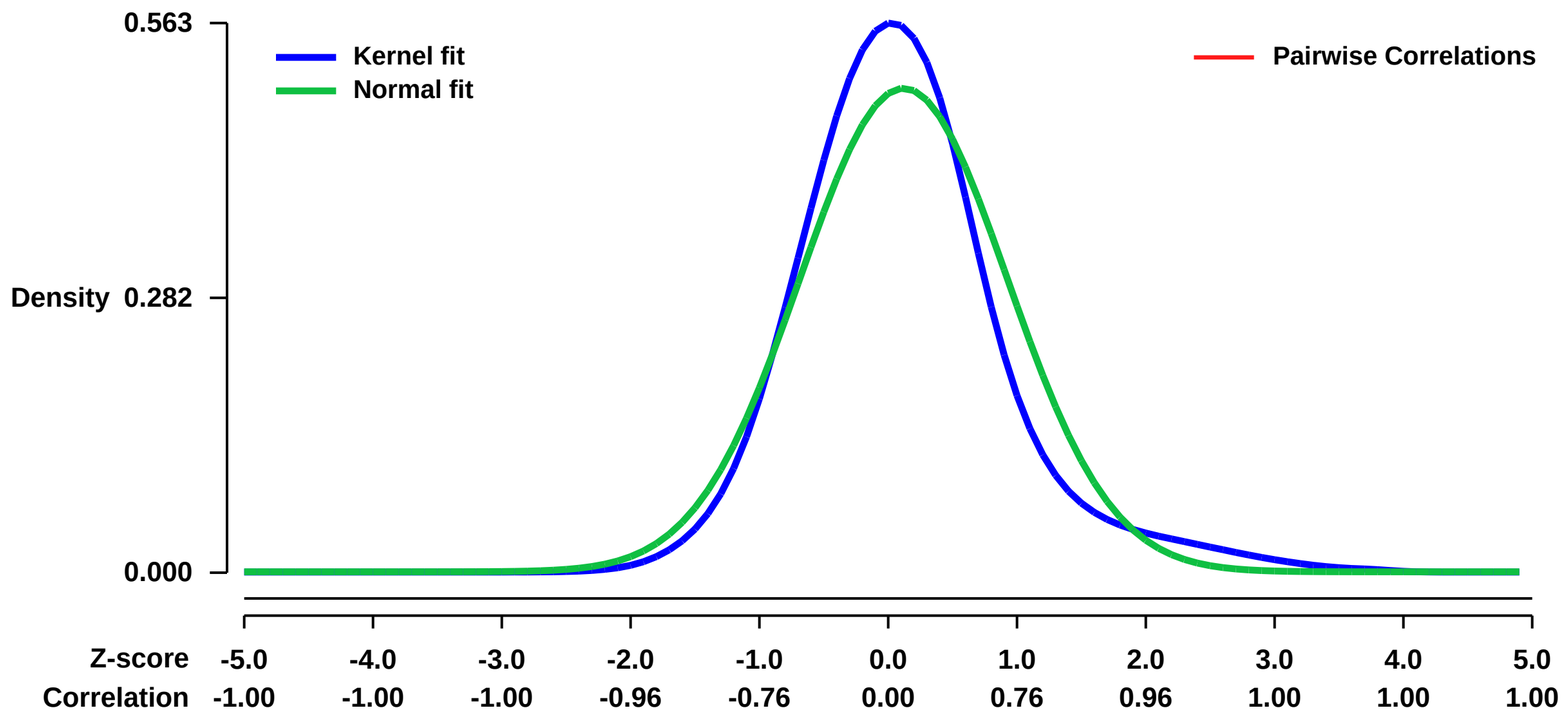

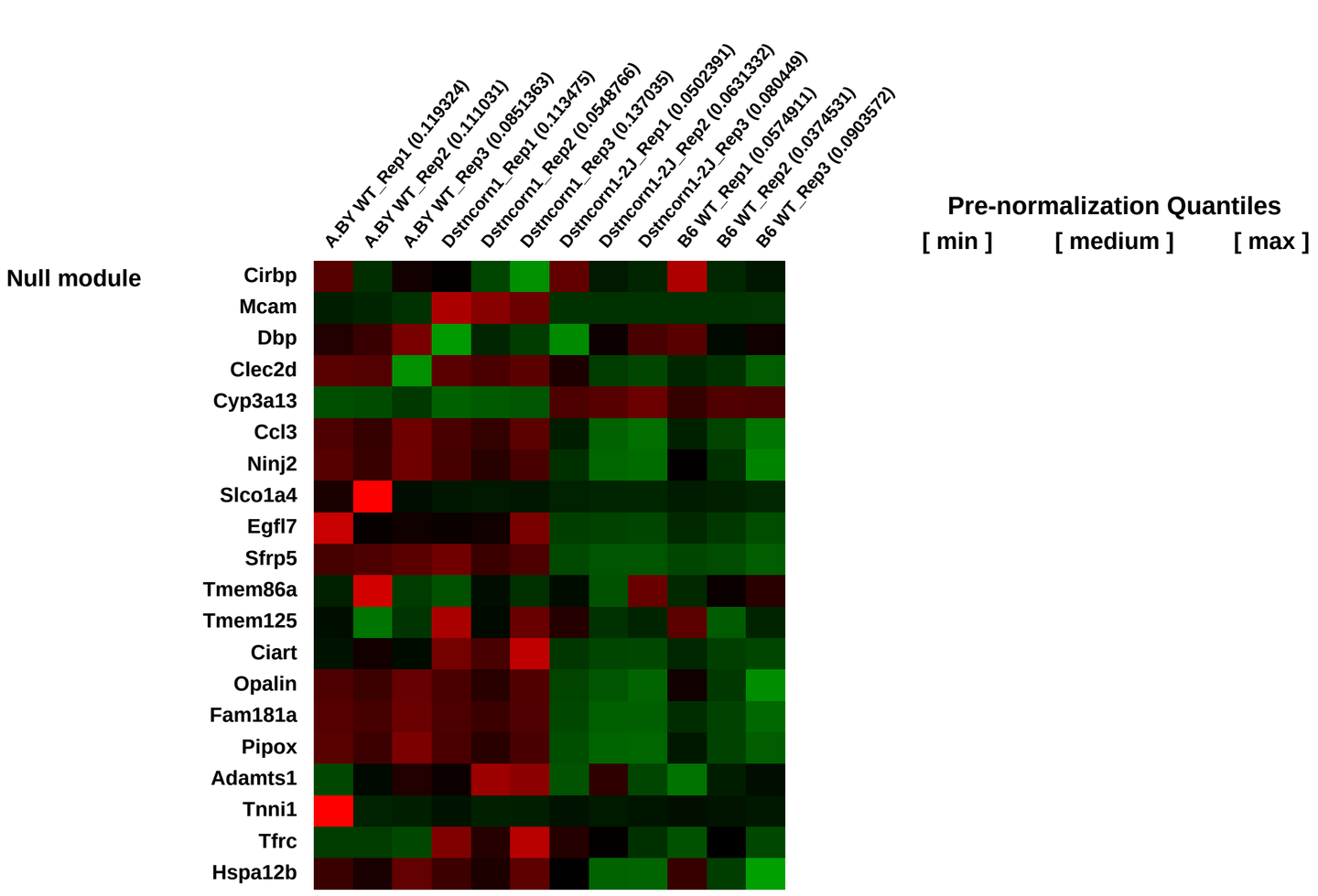

GEO Series "GSE9760" Expression Profiles

Num of samples in this series: 12

Scale of expression profile Z-scores

-3.0 -2.0 -1.0 0.0 1.0 2.0 3.0

GEO Link:	http://www.ncbi.nlm.nih.gov/geo/query/acc.cgi?acc=GSE9760
Status:	Public on Dec 04 2007
Title:	Embryonic stem cells with expanded CAG repeats (lorin-affy-mouse-501743)
Organism:	Mus musculus
Experiment type:	Expression profiling by array
Platform:	GPL1261
Pubmed ID:	
Summary & Design:	**Summary:** **Huntington´ s disease (HD) is a devastating neurodegenerative disease, with out effective treatment. Despite significant advances, our understanding of how an expanded CAG repeat in the amino terminus of the large ubiquitously expressed HD gene product remains incomplete. Augmented adult neurogenesis in response to acute and chronic injury, including Huntington´ s disease, has been demonstrated, but its role development, disease, and recovery is largely unknown, as are the factors controlling it. The HD gene product, huntingtin (htt) is know to interact with a number of transcription factors which subsequently influence gene expression. Understanding the factors involved in controlling neurogenesis in response to disease would bridge a significant knowledge gap and have tremendous therapeutic potential.** **We propose to identify transcripts responsible for CAG repeat facilitated neurogenesis.** **Our hypothesis is that expanded CAG repeats in the Huntington´ s disease gene facilitates neurogenesis by altering transcription of genes critical in neurogenesis.** **We have developed a model in which mouse embryonic stem cells (ESC) with expanded CAG repeats have facilitated neurogenesis. In this model more ESC with expanded CAG repeats transition to neuronal precursors and then develop into mature neurons more rapidly than control ESC. We propose to compare the gene expression profiles between ESC with expanded CAG repeats and control ESCs on days 4 and 6 of neuronal differentiation. Initial studies indicate that key transcriptional differences are occurring at these time points. Control ECS and a an ESC line with150 CAG repeats will be differentiated in triplicate, and RNA isolated form each replicate. It is anticipated that comparison of gene expression between the control and CAG repeat lines at each time point will identify transcripts involved in CAG repeat facilitated neurogenesis. Observed differences at day 4 may be more relevant to the transition from ESC to neuronal precursor whereas differences at day 6 may be more relevant to the neuronal precursor to neuron transition.** **Keywords: time-course** **Overall design:**

Background corr dist: **KL-Divergence = 0.0981, L1-Distance = 0.0297, L2-Distance = 0.0012, Normal std = 0.4524**

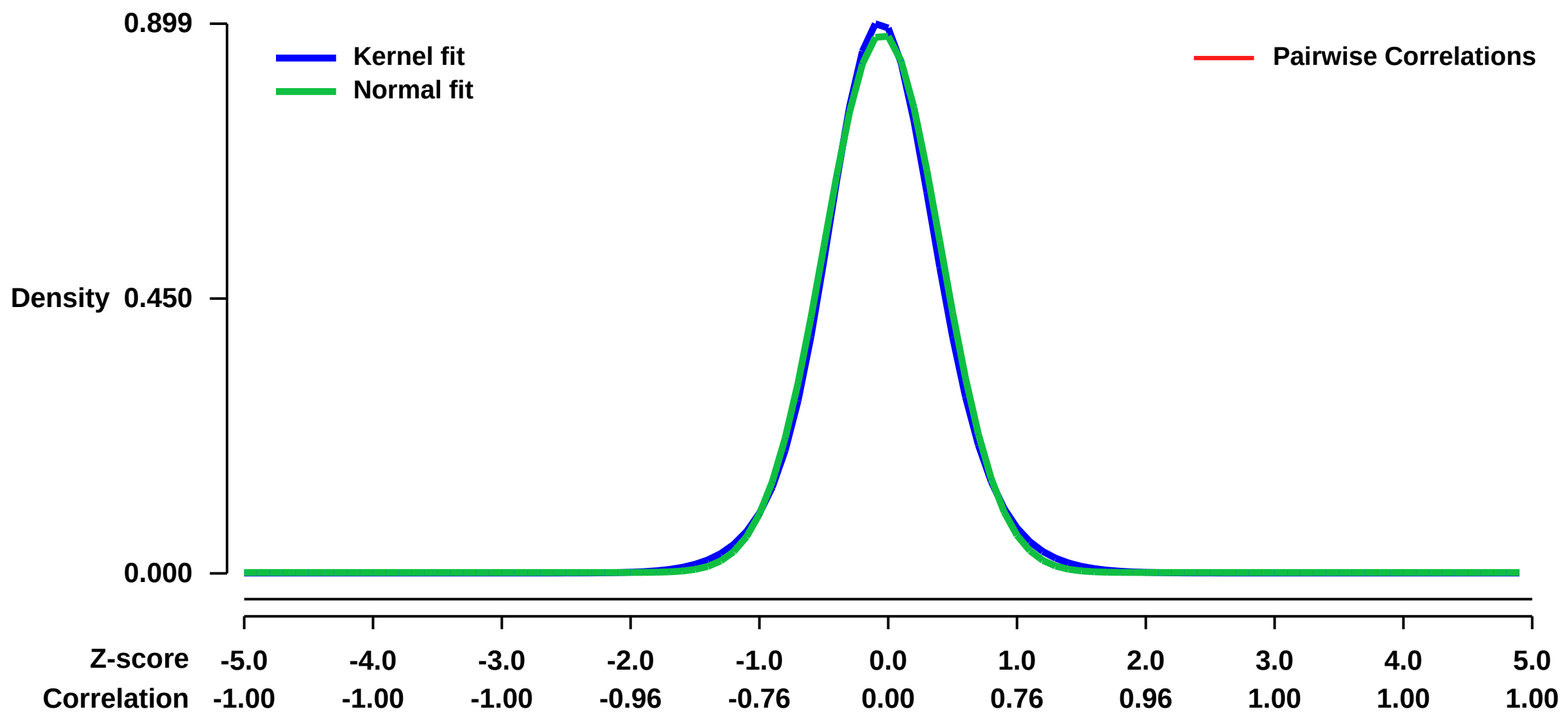

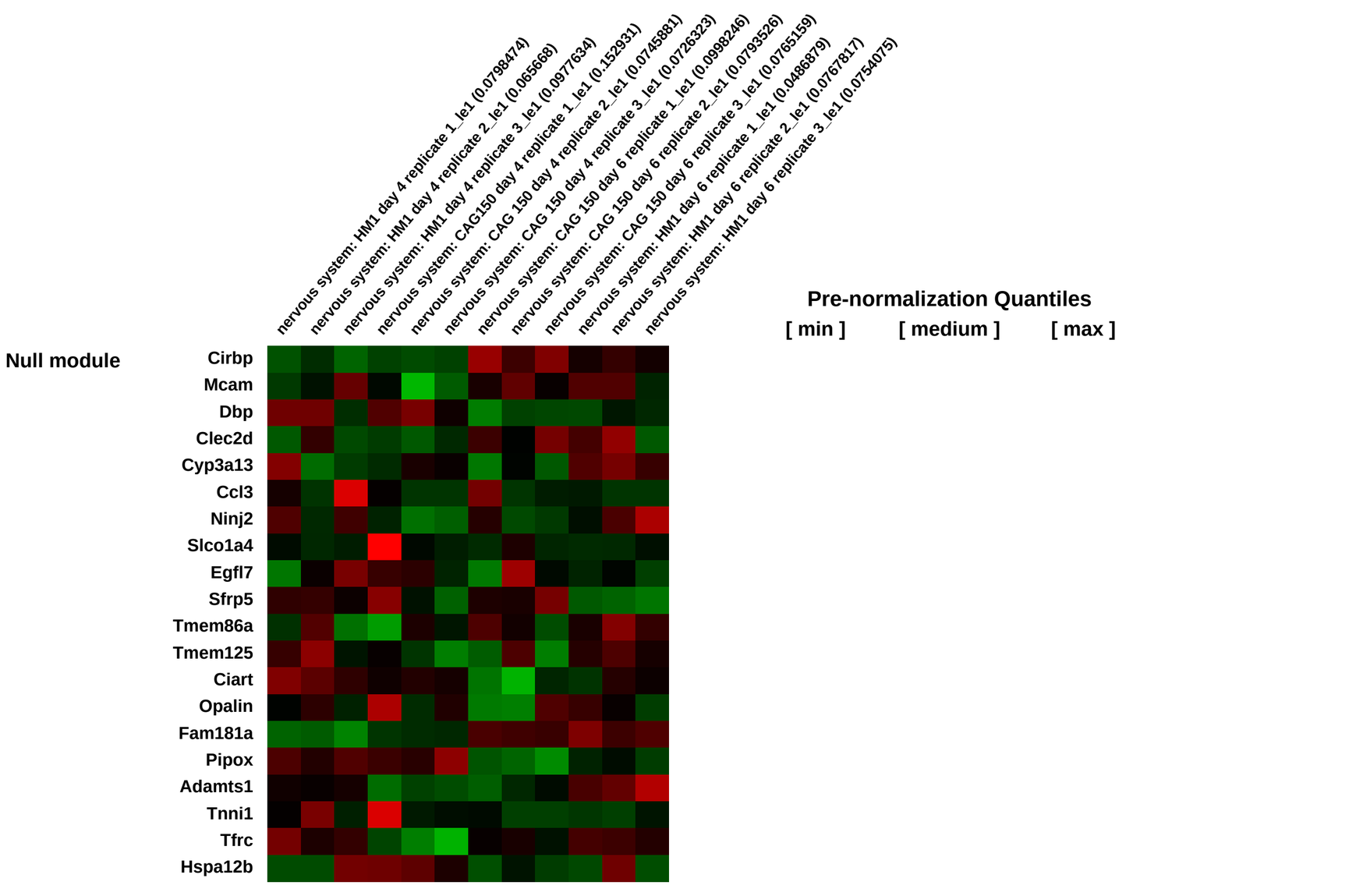

GEO Series "GSE9763" Expression Profiles

Num of samples in this series: 20

Scale of expression profile Z-scores

-3.0 -2.0 -1.0 0.0 1.0 2.0 3.0

GEO Link: http://www.ncbi.nlm.nih.gov/geo/query/acc.cgi?acc=GSE9763

Status: Public on Dec 04 2007

Title: Transformed glial progenitor cells (prosc-affy-mouse-450860)

Organism: Mus musculus

Experiment type: Expression profiling by array

Platform: GPL1261

Pubmed ID:

Summary & Design:

Summary:
The goals of this research are three-fold: (i) One is to identify genetic changes associated with tumorgenesis that interfere with the ability of transformed glial cells to differentiate. This is connected with (ii) our analysis of the regulation of differentiation in normal glial progentor cells, as only by understanding this in normal cells can we understand what is occurring when differentiation fails in transformed versions of the same cells. (iii) The third is to identify the molecular basis for the greater resistance of transformed glial progenitor cells to chemotherapeutic agents as compared with normal glial progenitor cells. Thus, analysis of the populations provided will yield data crucial to two of our central areas of research, as awarded by NINDS in ""Oligodendrocytes & precursors: toxicity of chemotherapy"" (5R01NS044701), and ""Low-level toxicant perturbation of neural cell function"" (1R01ES012708).

Our ability to work with essentially unlimited numbers of primary progenitor cells and transformed derivatives of these cells offers one of the few systems in which side-by-side comparison of normal and transformed cells at both the biochemical and molecular levels is possible. Using defined cell populations, expression profiles will be compared to reveal changes in cell type specific markers and regulatory factors associated with transformation. In addition, retention of markers despite transformation may enable identification of new markers useful in the diagnosis of glial tumors.

Transformation of glial progenitor cells is associated both with loss of the proteins required for normal differentiation and with an inability to normally activate proteins that function in differentiation control. By side-by-side analysis of gene expression in normal and transformed glial progenitor cells, and analysis of the response to inducers of differentiation in each these populations, we will identify candidate regulators critical in the control of normal differentiation. Identification of these regulators will also provide clues as to overcome the blockade of differentiation that occurs in glial cancers (which represent the majority of adult brain tumors).

RNA will be isolated from two separate preparations of glial progenitors. Preparation of purified populations has been described in multiple of our previous publications (Mayer, M. et al. (1994) Development 120, 142-153; Mayer-Prˆ¶schel, M. et al. (1997) Neuron 19, 773-785; Rao, M. and Mayer-Prˆ¶schel, M. (1997) Dev. Biology 188, 48-63). Total RNA from purified cell cultures will be extracted in a two step process. RNA will first be extracted by dounce homogenization in phenol/guanidine isothiocyonate solution (Trizol, Invitrogen, California) followed by isopropanol precipitation. Contaminating traces of DNA and protein will then be removed by silica-based affinity chromatography and Dnase treatment (NucleoSpin RNA Purification system, Clontech, California). Depending on the cell type, 5x105 cells will typically yield 5-15´µg of high quality RNA (OD260/280=2.1 at pH7.5). In order to determine purity and molecular weight distribution, samples will be routinely tested on a Agilent Bioanalyzer. cDNA will be generated from total RNA and then be submitted to one round of amplification and labeling using the messageAmp system (Ambion). Probes are then hybridized to the Affymerix Rat 230 (A/B or 2.0) GeneChip expression array. Array data will be processed using the Micro Array Suite 5.0 (MAS, Affymetrix). .Cel files containing normalized, relative expression data for all genes tested will be used for downstream statistical analysis.

Keywords: other

Overall design:

Background corr dist: KL-Divergence = 0.1052, L1-Distance = 0.0572, L2-Distance = 0.0056, Normal std = 0.4613

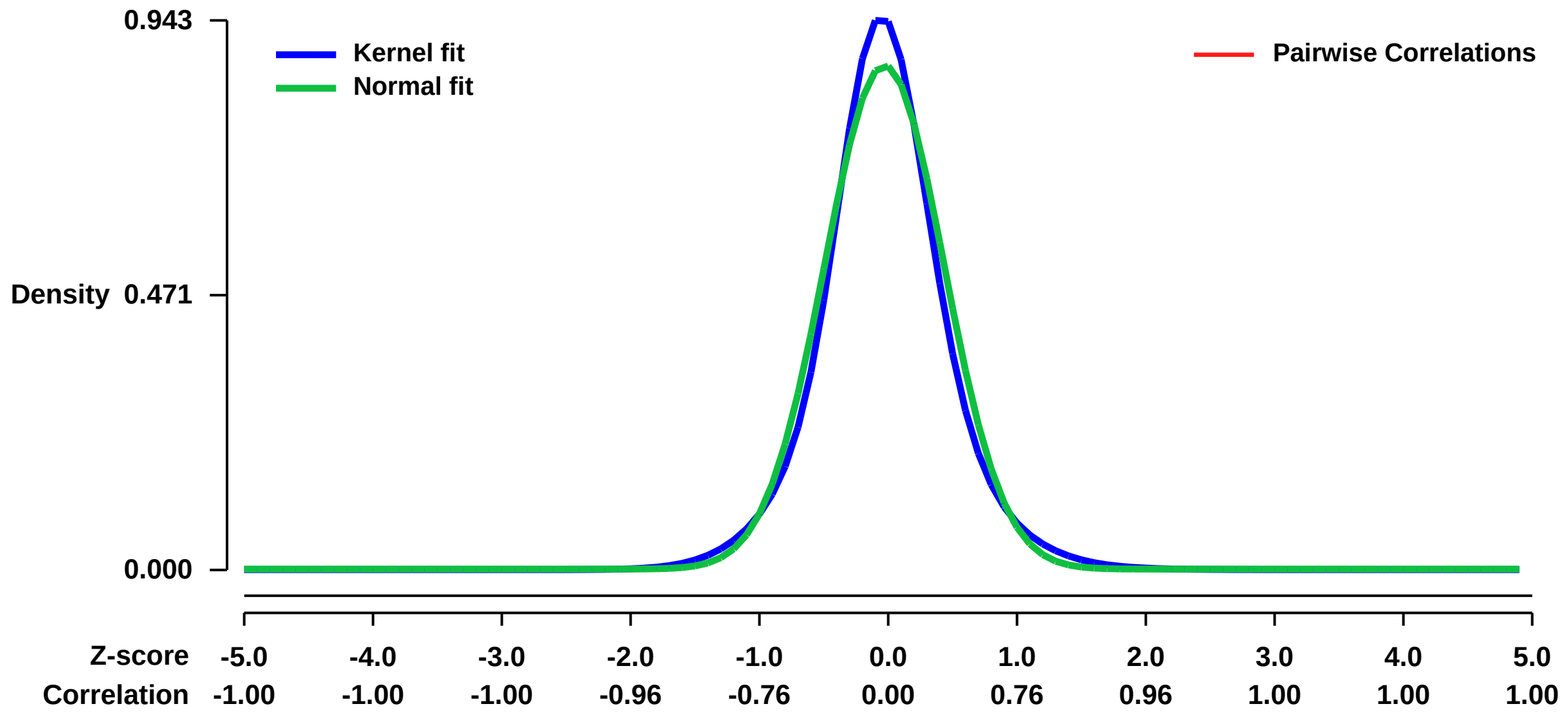

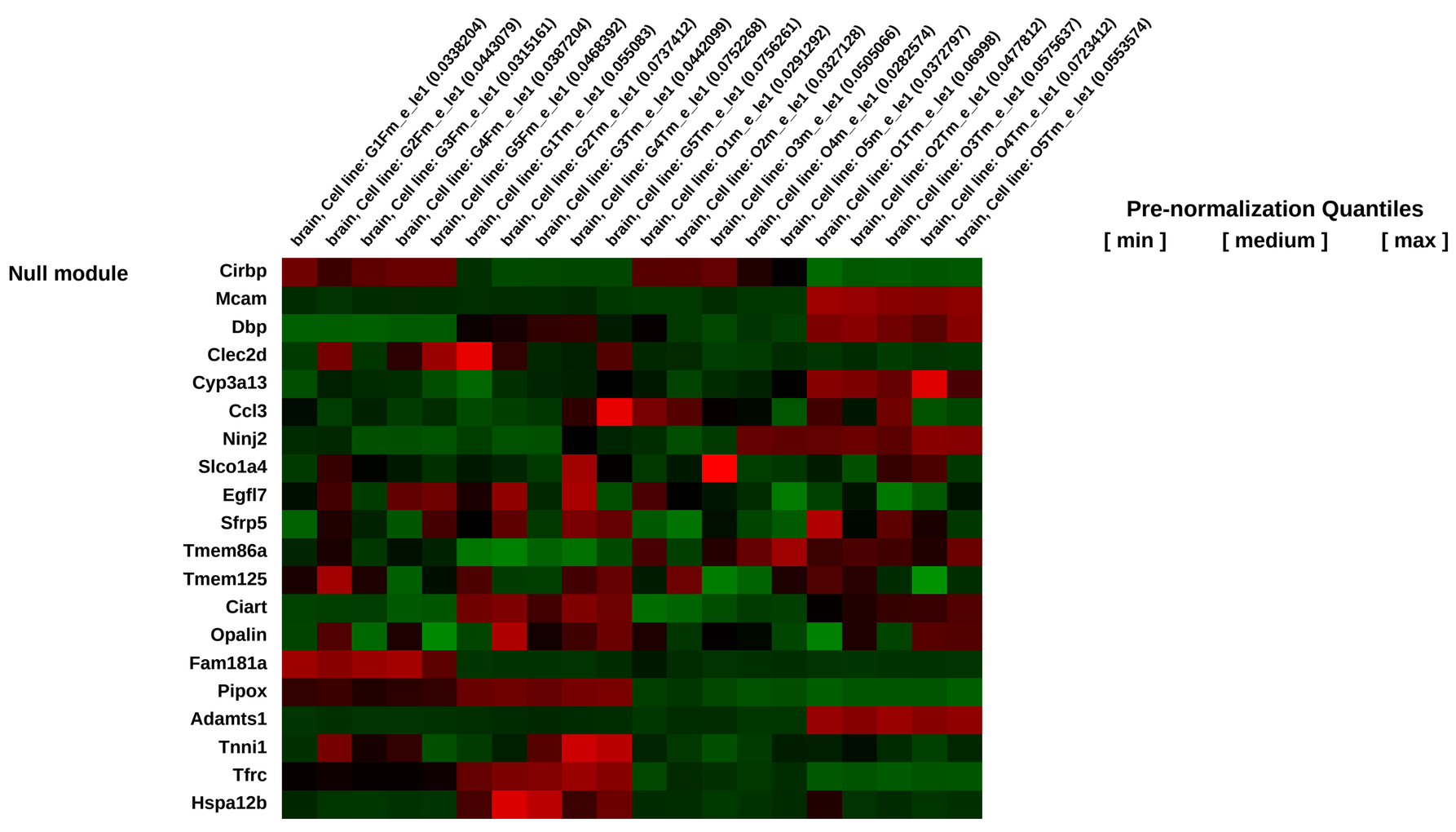

GEO Series "GSE9803" Expression Profiles

Num of samples in this series: 9

Scale of expression profile Z-scores

-3.0 -2.0 -1.0 0.0 1.0 2.0 3.0

GEO Link:	http://www.ncbi.nlm.nih.gov/geo/query/acc.cgi?acc=GSE9803
Status:	Public on Dec 17 2007
Title:	Striatal gene expression data from 12 weeks-old R6/2 mice and control mice (set 1)
Organism:	Mus musculus
Experiment type:	Expression profiling by array
Platform:	GPL1261
Pubmed ID:	17519223
Summary & Design:	**Summary:** To test the hypotheses that mutant huntingtin protein length and wild-type huntingtin dosage have important effects on disease-related transcriptional dysfunction, we compared the changes in mRNA in seven genetic mouse models of Huntington's disease (HD) and postmortem human HD caudate. Transgenic models expressing short N-terminal fragments of mutant huntingtin (R6/1 and R6/2 mice) exhibited the most rapid effects on gene expression, consistent with previous studies. Although changes in the brains of knock-in and full-length transgenic models of HD took longer to appear, 15- and 22-month CHL2(Q150/Q150), 18-month Hdh(Q92/Q92) and 2-year-old YAC128 animals also exhibited significant HD-like mRNA signatures. Whereas it was expected that the expression of full-length huntingtin transprotein might result in unique gene expression changes compared with those caused by the expression of an N-terminal huntingtin fragment, no discernable differences between full-length and fragment models were detected. In addition, very high correlations between the signatures of mice expressing normal levels of wild-type huntingtin and mice in which the wild-type protein is absent suggest a limited effect of the wild-type protein to change basal gene expression or to influence the qualitative disease-related effect of mutant huntingtin. The combined analysis of mouse and human HD transcriptomes provides important temporal and mechanistic insights into the process by which mutant huntingtin kills striatal neurons. In addition, the discovery that several available lines of HD mice faithfully recapitulate the gene expression signature of the human disorder provides a novel aspect of validation with respect to their use in preclinical therapeutic trials. **Keywords:** genetic modification **Overall design:** Striatal samples from 4 R6/2 mutant mice (12 weeks-old) and 5 age-matched wild-type mice.

Background corr dist: KL-Divergence = 0.0775, L1-Distance = 0.0213, L2-Distance = 0.0006, Normal std = 0.4814

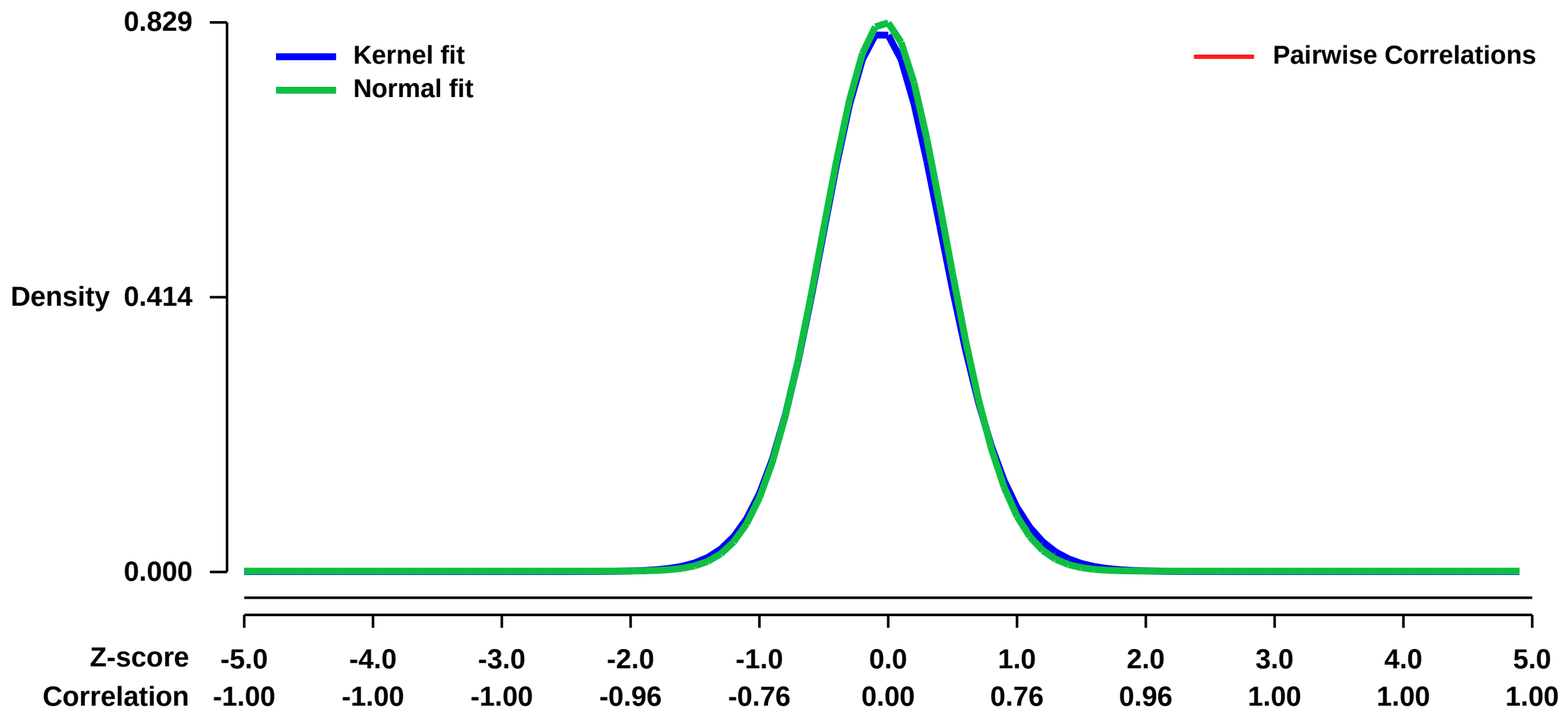

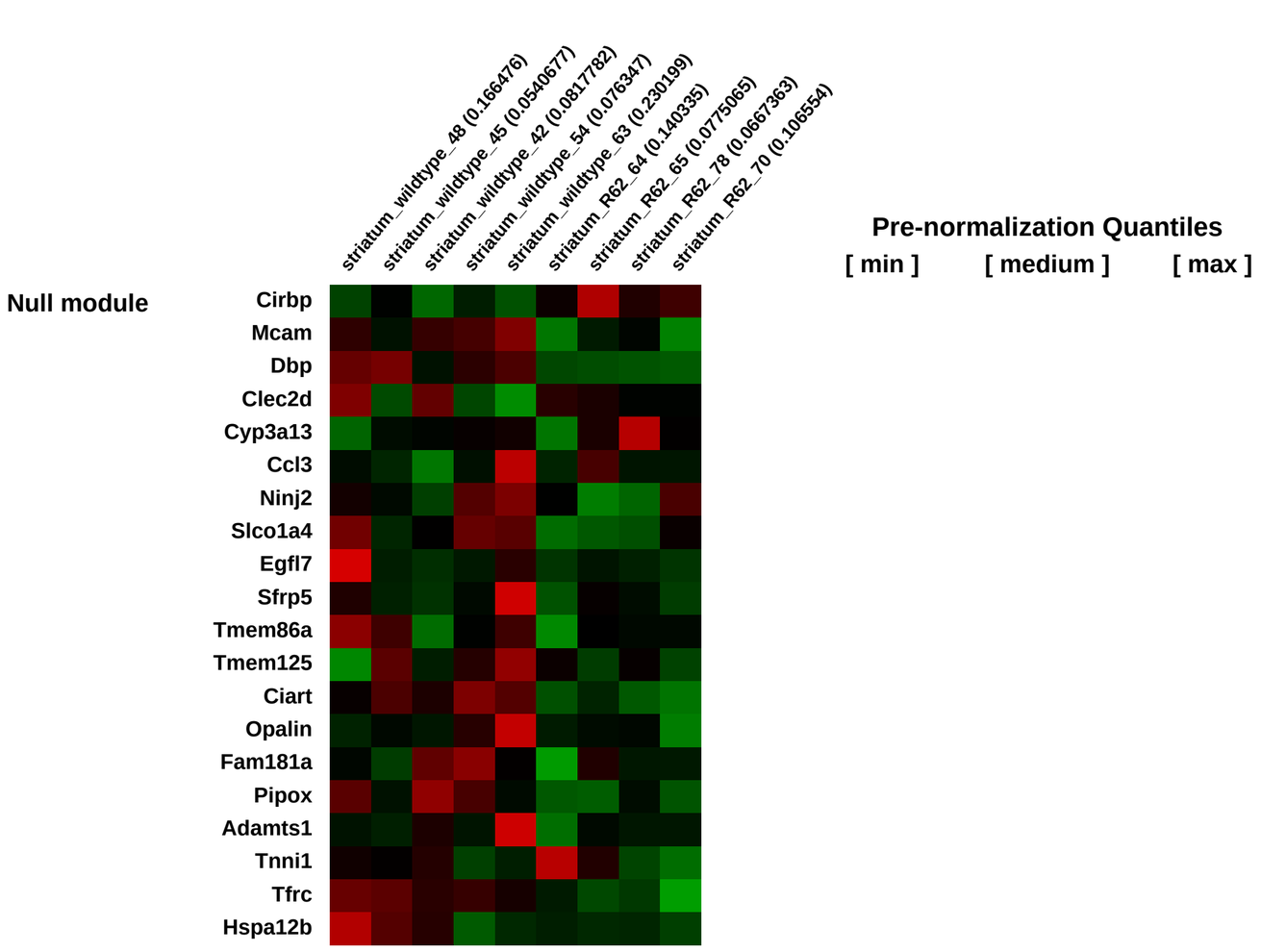

GEO Series "GSE9804" Expression Profiles

Num of samples in this series: 9

Scale of expression profile Z-scores

-3.0 -2.0 -1.0 0.0 1.0 2.0 3.0

GEO Link:	http://www.ncbi.nlm.nih.gov/geo/query/acc.cgi?acc=GSE9804
Status:	Public on Dec 17 2007
Title:	Striatal gene expression data from 12 weeks-old R6/2 mice and control mice (set 2)
Organism:	Mus musculus
Experiment type:	Expression profiling by array
Platform:	GPL1261
Pubmed ID:	17519223
Summary & Design:	**Summary:** To test the hypotheses that mutant huntingtin protein length and wild-type huntingtin dosage have important effects on disease-related transcriptional dysfunction, we compared the changes in mRNA in seven genetic mouse models of Huntington's disease (HD) and postmortem human HD caudate. Transgenic models expressing short N-terminal fragments of mutant huntingtin (R6/1 and R6/2 mice) exhibited the most rapid effects on gene expression, consistent with previous studies. Although changes in the brains of knock-in and full-length transgenic models of HD took longer to appear, 15- and 22-month CHL2(Q150/Q150), 18-month Hdh(Q92/Q92) and 2-year-old YAC128 animals also exhibited significant HD-like mRNA signatures. Whereas it was expected that the expression of full-length huntingtin transprotein might result in unique gene expression changes compared with those caused by the expression of an N-terminal huntingtin fragment, no discernable differences between full-length and fragment models were detected. In addition, very high correlations between the signatures of mice expressing normal levels of wild-type huntingtin and mice in which the wild-type protein is absent suggest a limited effect of the wild-type protein to change basal gene expression or to influence the qualitative disease-related effect of mutant huntingtin. The combined analysis of mouse and human HD transcriptomes provides important temporal and mechanistic insights into the process by which mutant huntingtin kills striatal neurons. In addition, the discovery that several available lines of HD mice faithfully recapitulate the gene expression signature of the human disorder provides a novel aspect of validation with respect to their use in preclinical therapeutic trials. **Keywords:** genetic modification **Overall design:** Striatal samples from 5 R6/2 mutant mice (12 weeks-old) and 4 age-matched wild-type mice.

Background corr dist: KL-Divergence = 0.0684, L1-Distance = 0.0199, L2-Distance = 0.0005, Normal std = 0.5033

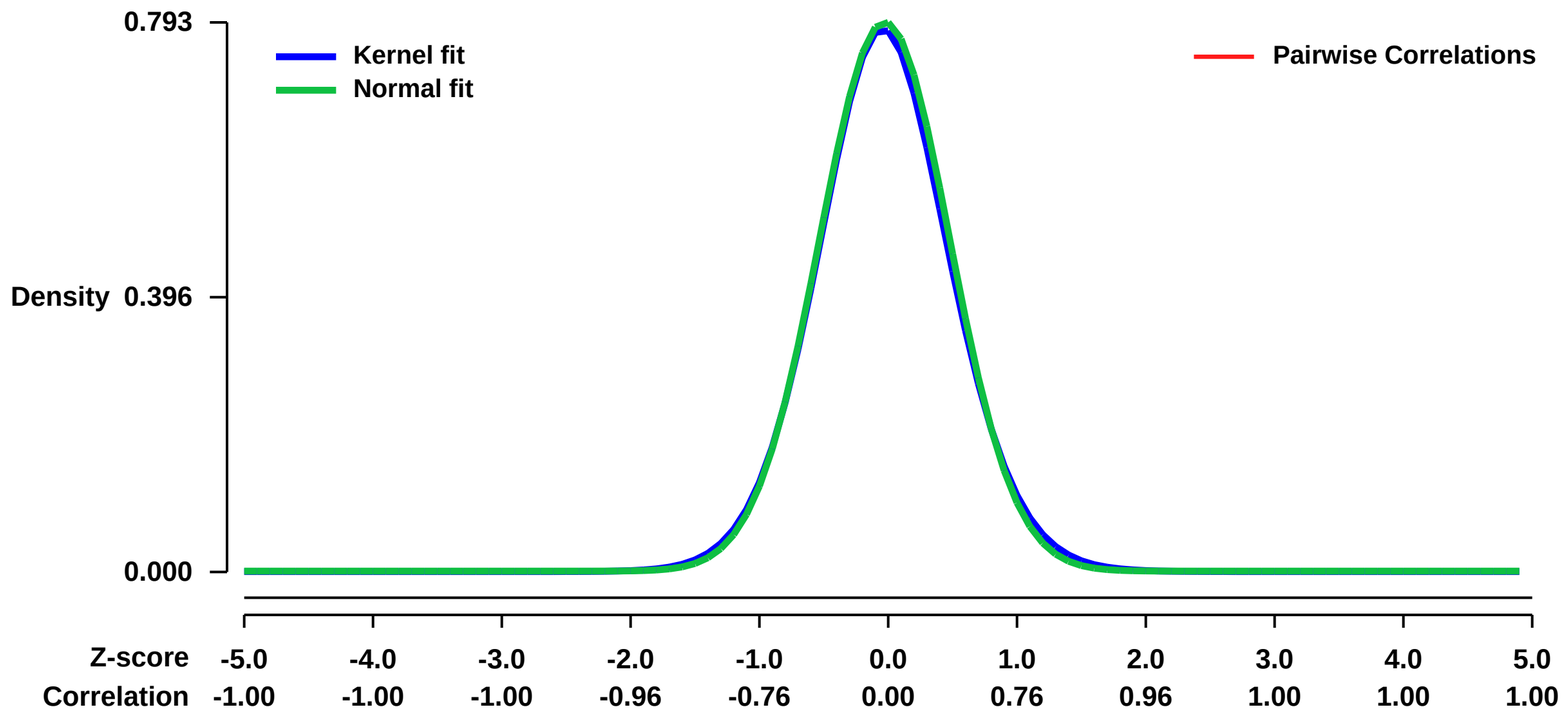

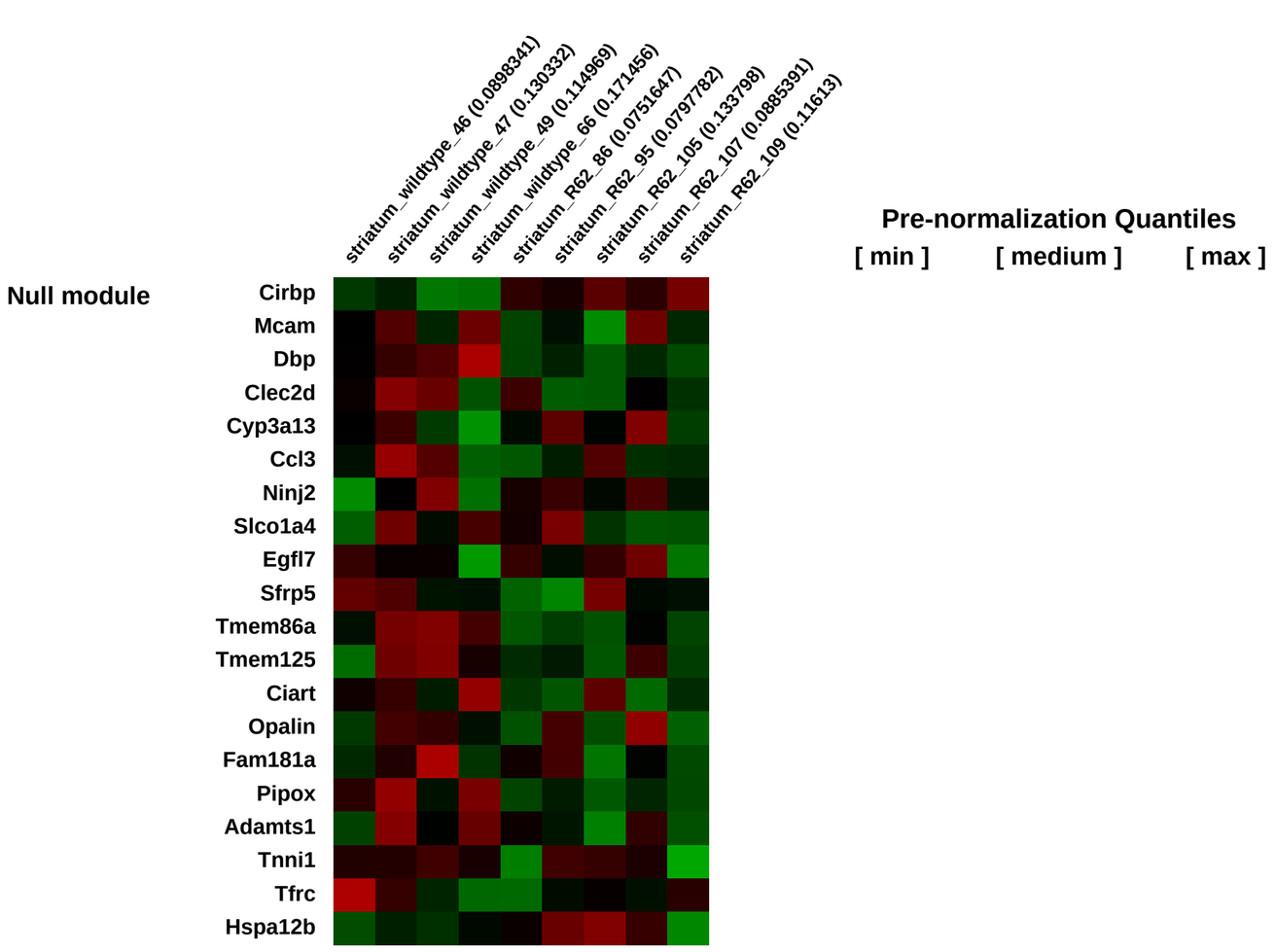

GEO Series "GSE9809" Expression Profiles

Num of samples in this series: 10

Scale of expression profile Z-scores

-3.0 -2.0 -1.0 0.0 1.0 2.0 3.0

GEO Link:	http://www.ncbi.nlm.nih.gov/geo/query/acc.cgi?acc=GSE9809
Status:	Public on Dec 01 2008
Title:	Expression data from GNMT knockout mice
Organism:	Mus musculus
Experiment type:	Expression profiling by array
Platform:	GPL1261
Pubmed ID:	19035462
Summary & Design:	**Summary:** We report that 7 of 7 female Gnmt-/- mice developed hepatocellular carcinoma (HCC), the most common form of liver cancer, at the mean age of 16.1 months. In contrast, only one-third (2/6) of male Gnmt-/- mice had HCC, the remaining had either premature death or liver necrosis. Microarray analysis showed that genes involved in the following pathways were deregulated in different stages of tumorigenesis: S-adenosylmethionine (SAM)-dependent methyltransferases, metabolism, signal transduction, cell proliferation, cell adhesion and immune responses. This study reveals that GNMT plays an important role in the prevention of hapatotumorigenesis through regulating DNA methylaiton and oxidative stress signaling pathways. We postulate that GNMT is a stress-responsive protein and its expression may account for the gender difference of the susceptibility to liver cancer. Keywords: Gnmt knockout **Overall design:** Liver tissues from wild-type or Gnmt knockout mice at young ages, devoloping dysplasia nodules or HCC were used for RNA extraction and hybridization on Affymetrix microarrays. For 11 weeks old mice, total RNA were mixed in equal proportion from 3 mice.

Background corr dist: KL-Divergence = 0.1128, L1-Distance = 0.0327, L2-Distance = 0.0021, Normal std = 0.4199

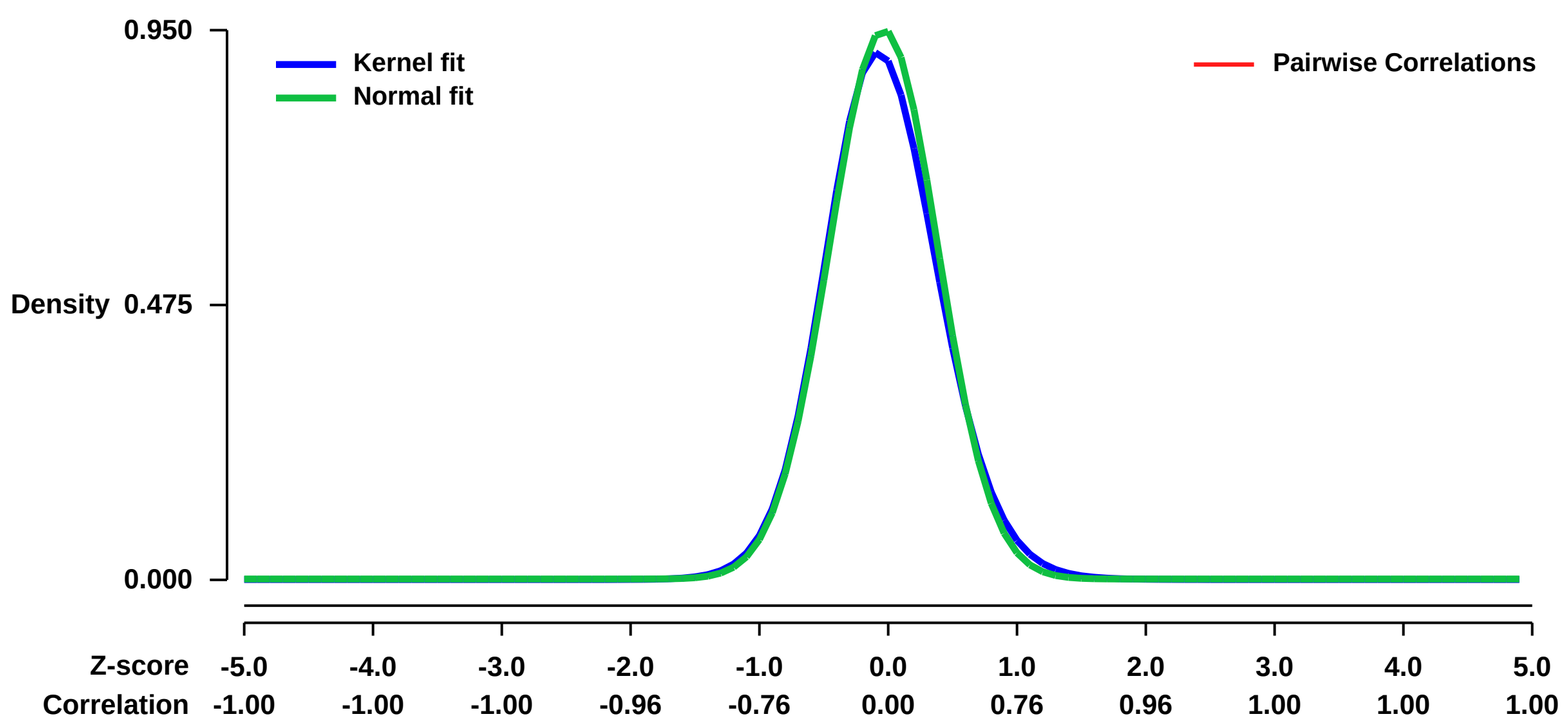

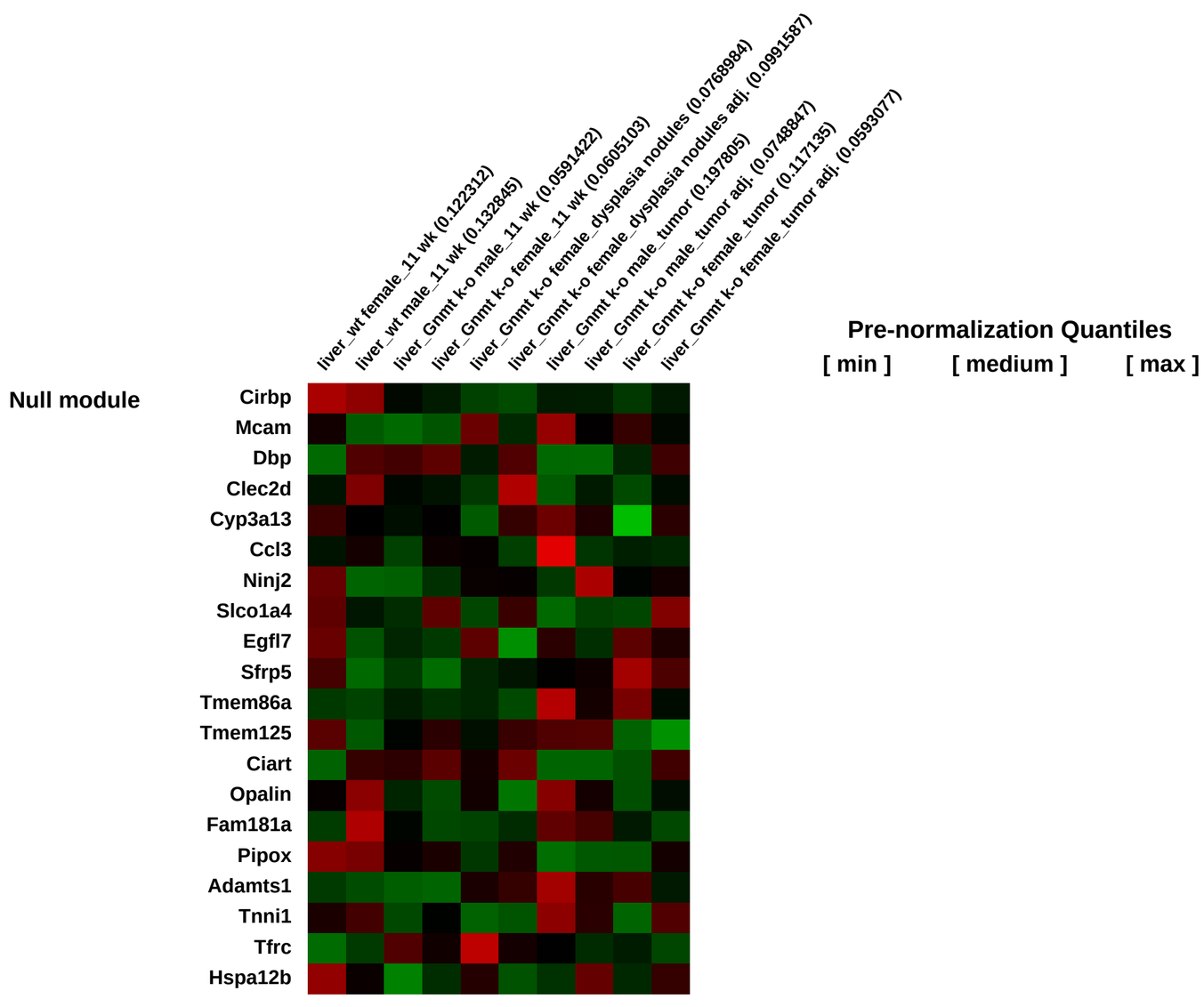

GEO Series "GSE9878" Expression Profiles

Num of samples in this series: 6

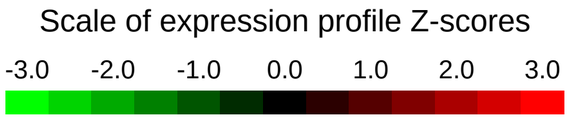

GEO Link:	http://www.ncbi.nlm.nih.gov/geo/query/acc.cgi?acc=GSE9878
Status:	Public on Dec 15 2007
Title:	Gene expression analysis of Pax5-/- proB cells transduced with control or EBF retrovirus.
Organism:	Mus musculus
Experiment type:	Expression profiling by array
Platform:	GPL1261
Pubmed ID:	18176567
Summary & Design:	**Summary:** We have determined that sustained expression of EBF suppresses alternate lineage genes independently of Pax5. Keywords: Transcription factor EBF restricts alternate lineage options and promotes B cell fate commitment independently of Pax5. **Overall design:** Pax5-/- pro-B cells transduced with control or EBF retrovirus. Transduced cells were FACS sorted based on GFP expression and total RNA was isolated. RNA isolated from control or EBF transduced cells was analyzed using the Affymetrix Rat 230A microarrays.

Background corr dist: KL-Divergence = 0.0260, L1-Distance = 0.0124, L2-Distance = 0.0002, Normal std = 0.6863

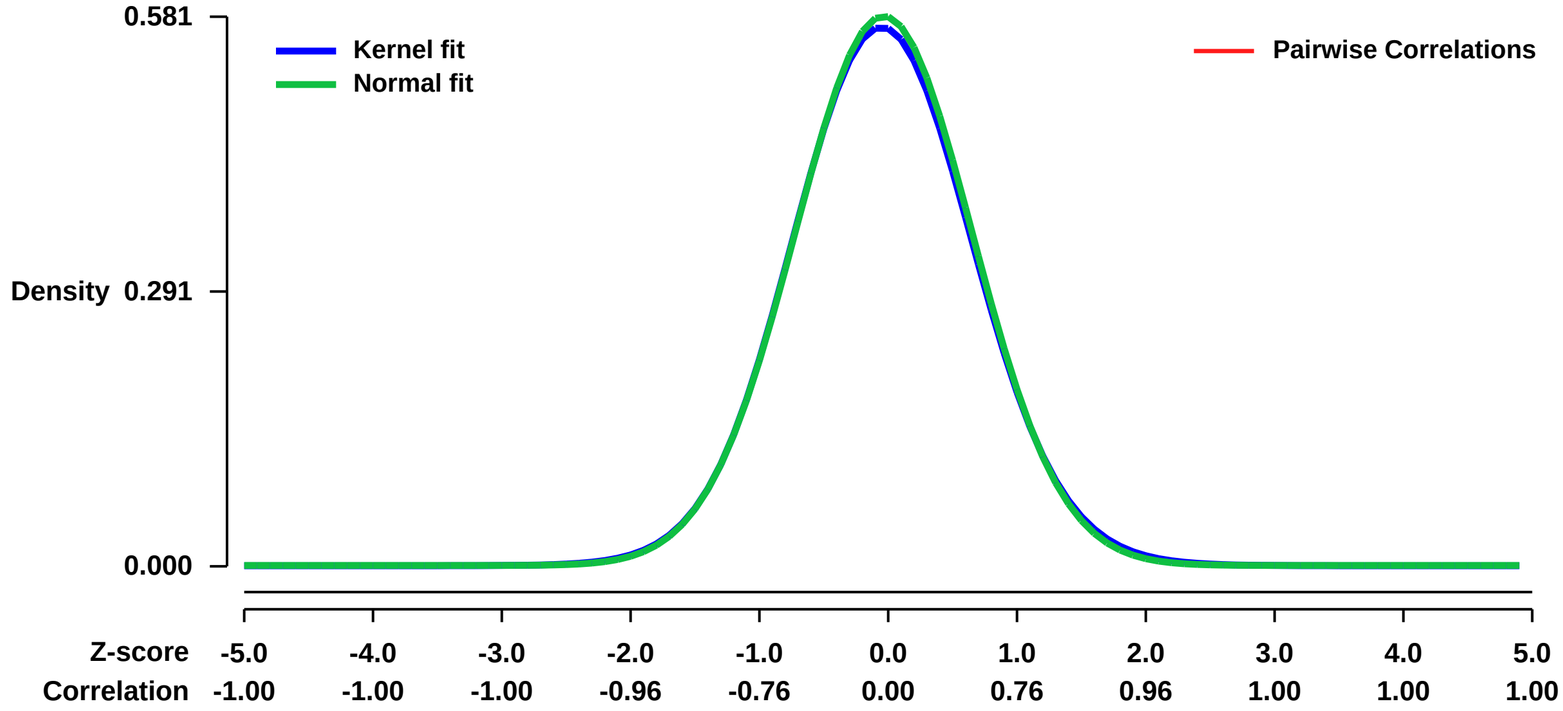

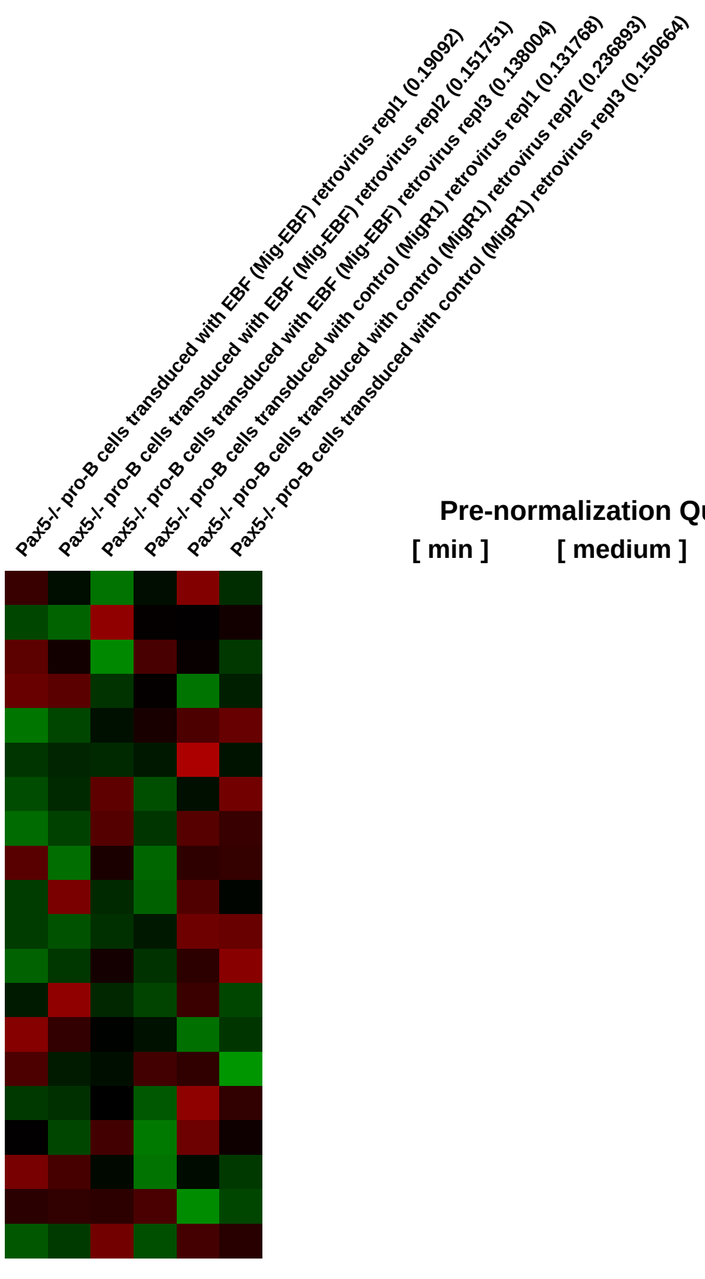

GEO Series "GSE9913" Expression Profiles

Num of samples in this series: 9

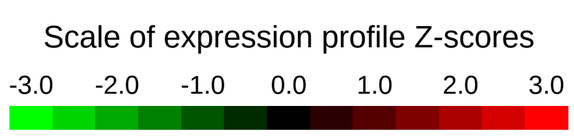

GEO Link:	http://www.ncbi.nlm.nih.gov/geo/query/acc.cgi?acc=GSE9913
Status:	Public on Mar 01 2008
Title:	Intestinal gene expression in ENU mutagenesis mouse strains with missense mutations in Muc2 mucin and ER stress
Organism:	Mus musculus
Experiment type:	Expression profiling by array
Platform:	GPL1261
Pubmed ID:	18318598

Summary & Design:

Summary:
Background

MUC2 mucin produced by intestinal goblet cells is the major component of the intestinal mucus barrier. MUC2 homo-oligomerizes intracellularly into large secreted polymers which give mucus its viscous properties. The inflammatory bowel disease (IBD) ulcerative colitis is characterized by depleted goblet cells and a reduced mucus layer, whereas goblet cells and the mucus layer are increased in the other major inflammatory bowel disease, Crohnâ s disease.

Methods and Findings

By murine N-ethyl-N-nitrosourea-mutagenesis we identified two distinct non-complementing missense mutations in Muc2 exons encoding N- and C-terminal homo-oligomerization domains causing an ulcerative colitis-like phenotype. Both strains developed mild spontaneous distal intestinal inflammation, chronic diarrhea, rectal bleeding and prolapse, increased susceptibility to acute and chronic colitis induced by a luminal toxin, aberrant Muc2 biosynthesis, smaller goblet cell thecae (less stored mucin) and a diminished mucus barrier. Enhanced local production of IL-1beta, TNF-alpha and IFN-gamma was seen in the distal colon. The number of leukocytes within mesenteric lymph nodes was increased five-fold and leukocytes cultured in vitro produced both Th1 and Th2 cytokines (IFN-gamma, TNF-alpha and IL-13). Intestinal permeability was increased and the luminal bacterial flora were more heavily coated with immunoglobulin as occurs in IBD. This pathology was accompanied by accumulation of the Muc2 precursor and ultrastructural and biochemical evidence of endoplasmic reticulum (ER) stress in goblet cells, activation of the unfolded protein response, and altered intestinal expression of genes involved in ER stress, inflammation, apoptosis and wound repair. Expression of mutated Muc2 oligomerization domains in vitro demonstrated that aberrant Muc2 oligomerization underlies the ER stress. These models show that mutations in Muc2 oligomerization domains can lead to aberrant assembly of the Muc2 complex leading to ER stress, a depleted mucus barrier and intestinal inflammation. In ulcerative colitis we demonstrate similar accumulation of non-glycosylated MUC2 precursor in goblet cells together with ultrastructural and biochemical evidence of ER stress even in non-inflamed intestinal tissue.

Conclusions

The observations that mucin misfolding and ER stress lead directly to intestinal inflammation and that ER stress and goblet cell pathology occur in ulcerative colitis suggest that ER stress-related mucin depletion could be a fundamental component of the pathogenesis of colitis.

Keywords: Single gene, multiple mutant comparison

Overall design:
3 individual mice from the Eeyore, Winnie or Wild-type strains were compared as groups. An Affymetrix ID was compared between groups if the ID was Present within two of the three mice within each grouping. IDs were compared by calculating the log2 of Group One average signal divided by Group 2 average signal.

Background corr dist: KL-Divergence = 0.0799, L1-Distance = 0.0215, L2-Distance = 0.0007, Normal std = 0.4781

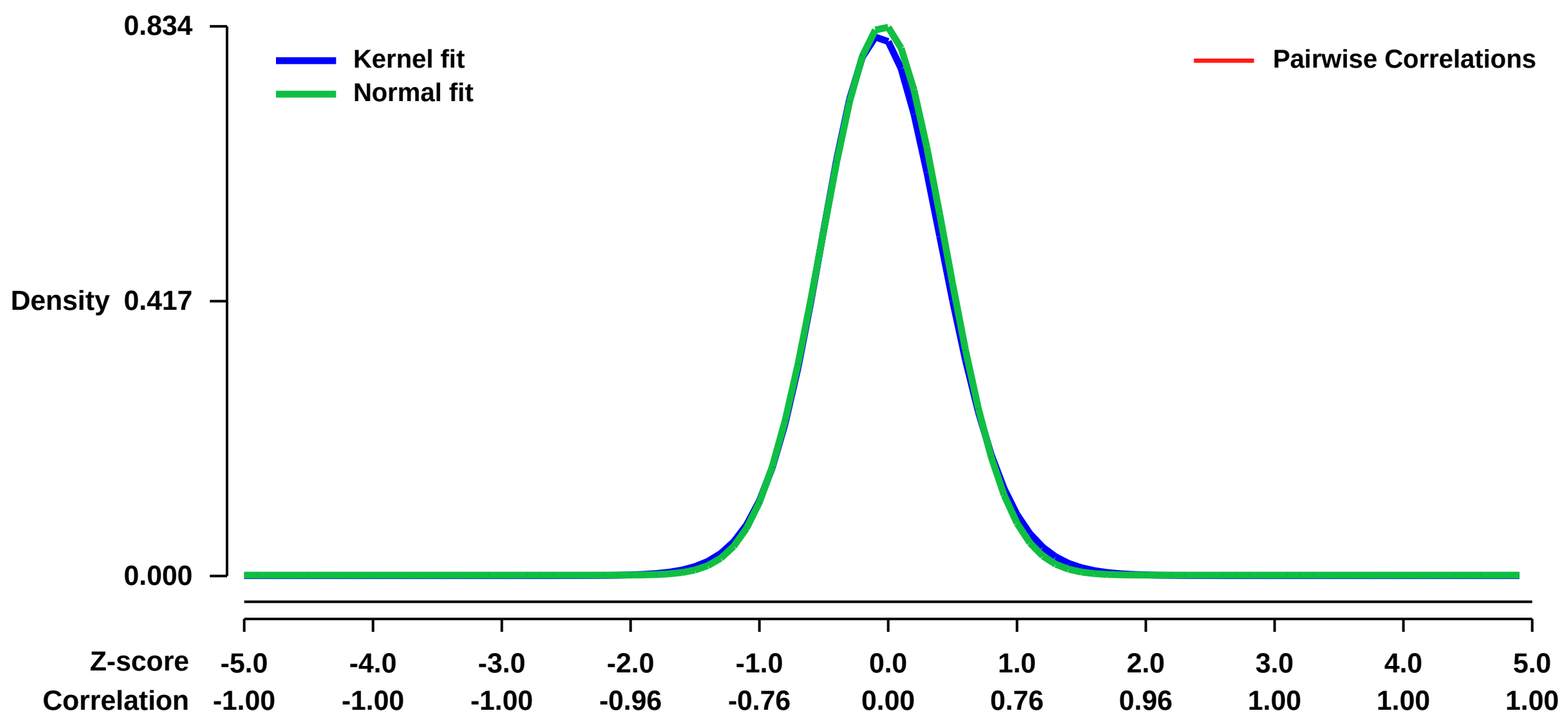

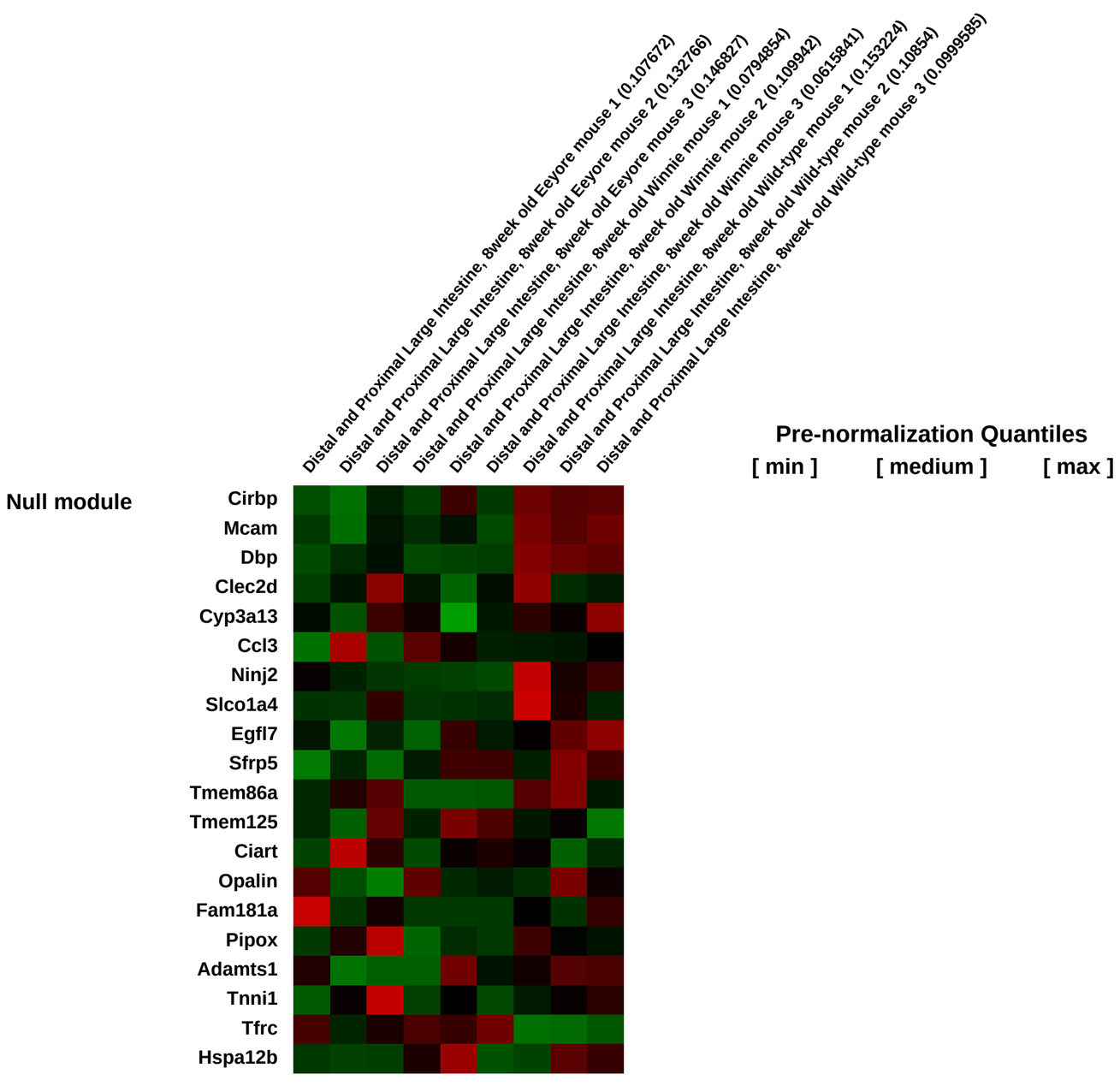

GEO Series "GSE9975" Expression Profiles

Num of samples in this series: 36

Scale of expression profile Z-scores

-3.0 -2.0 -1.0 0.0 1.0 2.0 3.0

GEO Link:	http://www.ncbi.nlm.nih.gov/geo/query/acc.cgi?acc=GSE9975
Status:	Public on Sep 30 2009
Title:	newly transcribed RNA (nt-RNA) for IFN alpha and gamma time course
Organism:	Mus musculus
Experiment type:	Expression profiling by array
Platform:	GPL1261
Pubmed ID:	18658122
Summary & Design:	**Summary:** Expression data from NIH-3T3 cells treated with mock, 100 U/ml IFN alpha or 100 U/ml gamma for 1 or 3h on nt-RNA labeled for 30-60 min at different times of interferon treatment Differential gene expression caused by IFN alpha or gamma was analyzed in newly transcribed RNA (nt-RNA) of NIH-3T3 cells treated for 1 or 3 h. RNA was labeled for 30 to 60 min and separated from total cellular RNA (tc-RNA) following Trizol RNA preparation and thiol-specific biotinylation We used microarrays to analyze the effects of IFNalpha and gamma treatment in newly transcribed RNA (nt-RNA) Keywords: time course **Overall design:** NIH-3T3 cells (5th to 15th passage after thawing) were split 24 h before start of the experiment. When starting the experiment 80% confluency was reached. The experiment was started by applying fresh, prewarmed, CO2-equilibrated medium containing either mock, 100U/ml IFN alpha or 100 U/ml IFN gamma. Labeling was either started simultaneously, 30 or 150 minutes later.

Background corr dist: KL-Divergence = 0.0632, L1-Distance = 0.0569, L2-Distance = 0.0049, Normal std = 0.5658

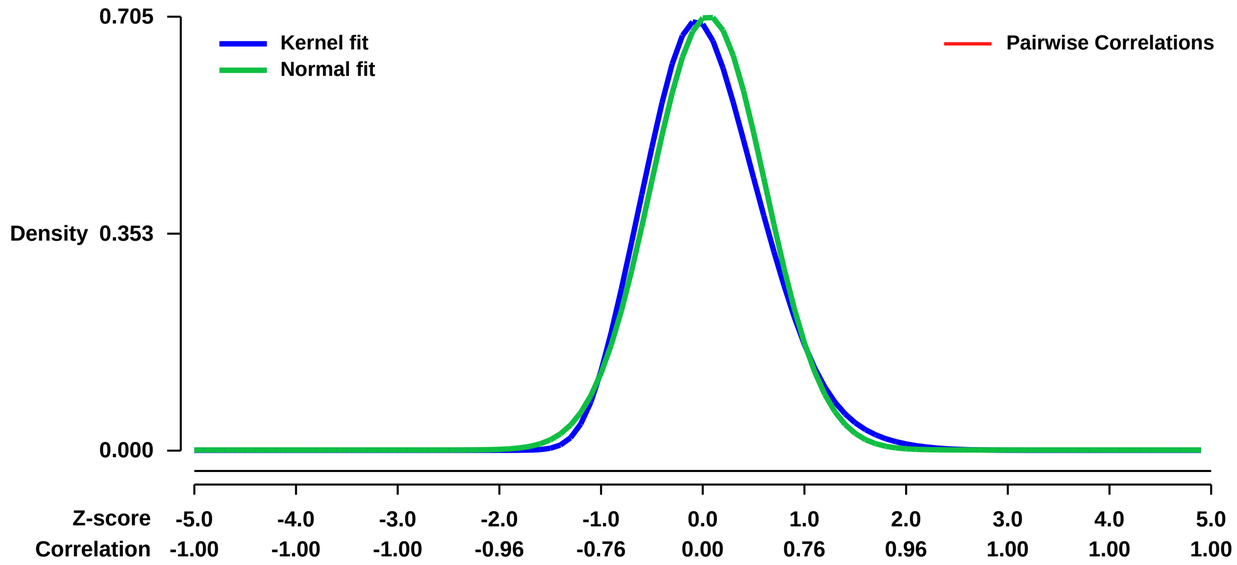

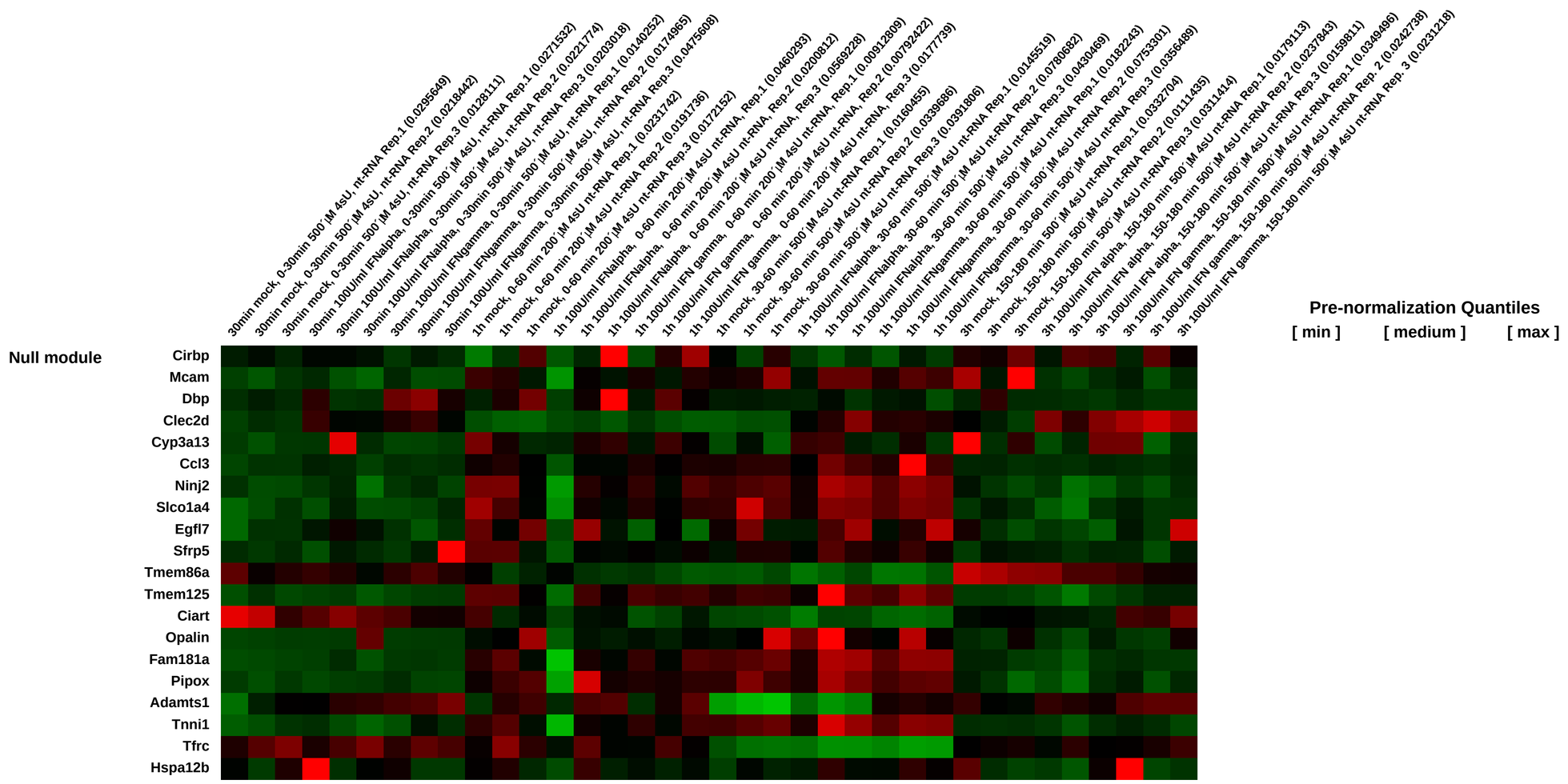

GEO Series "GSE9977" Expression Profiles

Num of samples in this series: 24

Scale of expression profile Z-scores

-3.0 -2.0 -1.0 0.0 1.0 2.0 3.0

GEO Link:	http://www.ncbi.nlm.nih.gov/geo/query/acc.cgi?acc=GSE9977
Status:	Public on Sep 30 2009
Title:	Expression data from NIH-3T3 cells treated with mock, 100 U/ml IFN alpha or 100 U/ml gamma for 1or 3h
Organism:	Mus musculus
Experiment type:	Expression profiling by array
Platform:	GPL1261
Pubmed ID:	18658122
Summary & Design:	**Summary:** Differential gene expression caused by 1h and 3h of IFN alpha or gamma treatment was analyzed in total cellular RNA of NIH-3T3 cells compared to mock We used microarrays to analyze the effects of 1 and 3h of IFNalpha and gamma treatment in total cellular RNA Keywords: time course in total cellular RNA (tc-RNA) **Overall design:** NIH-3T3 cells (5th to 15th passage after thawing) were split from confluent plates 24h before start of the experiment. At the begin of the experiment about 80% confluency was reached. The experiment was started by applying fresh, prewarmed, CO2-equilibrated medium containing either mock, 100U/ml IFN alpha or 100 U/ml IFN gamma. Labeling was either started together with addition of IFN for 60 minutes or for 30 minutes starting 150 minutes after begin of treatment.

Background corr dist: KL-Divergence = 0.0343, L1-Distance = 0.0629, L2-Distance = 0.0042, Normal std = 0.7786